CELL BIOLOGY

A LABORATORY HANDBOOK

Third Edition
Volume 1

Editor-in-chief
Julio E. Celis, Institute of Cancer Biology, *Danish Cancer Society, Copenhagen, Denmark*

Associate Editors
Nigel P. Carter, *The Sanger Center, Wellcome Trust, Cambridge, UK*
Kai Simons, *Max-Planck Institute of Molecular Cell Biology and Genetics, Dresden, Germany*
J. Victor Small, *Austrian Academy of Sciences, Salzburg, Austria*
Tony Hunter, *The Salk Institute, La Jolla, California, USA*
David M. Shotten, *University of Oxford, UK*

CELL BIOLOGY

A LABORATORY HANDBOOK

Third Edition
Volume 1

Edited by

Julio E. Celis
Institute of Cancer Biology, Danish Cancer Society,
Copenhagen, Denmark

ELSEVIER
ACADEMIC
PRESS

AMSTERDAM • BOSTON • HEIDELBERG • LONDON
NEW YORK • OXFORD • PARIS • SAN DIEGO
SAN FRANCISCO • SINGAPORE • SYDNEY • TOKYO

Elsevier Academic Press
30 Corporate Drive, Suite 400, Burlington, MA 01803, USA
525 B Street, Suite 1900, San Diego, California 92101-4495, USA
84 Theobald's Road, London WC1X 8RR, UK

This book is printed on acid-free paper.

Copyright © 2006, Elsevier Inc. All rights reserved.

No part of this publication may be reproduced or transmitted in any form or by any means, electronic or mechanical, including photocopy, recording, or any information storage and retrieval system, without permission in writing from the publisher.

Permissions may be sought directly from Elsevier's Science & Technology Rights Department in Oxford, UK: phone: (+44) 1865 843830, fax: (+44) 1865 853333, E-mail: permissions@elsevier.co.uk. You may also complete your request on-line via the Elsevier homepage (http://elsevier.com), by selecting "Customer Support" and then "Obtaining Permissions."

Library of Congress Cataloging-in-Publication Data
Application Submitted

British Library Cataloguing in Publication Data
A catalogue record for this book is available from the British Library

ISBN 13: 978-0-12-164731-5
ISBN 10: 0-12-164731-5
Set ISBN 13: 978-0-12-164730-8
Set ISBN 10: 0-12-164730-7

For all information on all Elsevier Academic Press publications
visit our Web site at www.books.elsevier.com

Printed in China
05 06 07 08 09 10 9 8 7 6 5 4 3 2 1

Working together to grow
libraries in developing countries
www.elsevier.com | www.bookaid.org | www.sabre.org
ELSEVIER BOOK AID International Sabre Foundation

Contents of Volume 1

Contents of other Volumes

VOLUME 2

PART A. ORGANELLES AND CELLULAR STRUCTURES

Section 1. Isolation: Plasma Membrane, Organelles, and Cellular Structures

PART F. CYTOGENETICS AND *IN SITU* HYBRIDIZATION

Section 14. Cytogenetics

Section 15. *In Situ* Hybridization

PART G. GENOMICS

Section 16. Genomics

PART H. TRANSGENIC, KNOCKOUTS, AND KNOCKDOWN METHODS

Section 17. Transgenic, Knockouts and Knockdown Methods

Section 13. Protein/DNA Interactions

Section 14. Protein Degradation

Section 15. Mass Spectrometry: Protein Identification and Interactions

Contributors

Numbers in parenthesis indicate the volume (bold face) and page on which the authors' contribution begins.

Mads Aaboe (**4**: 83) Clinical Biochemical Department, Molecular Diagnostic Laboratory, Aarhus University Hospital, Skejby, Brendstrupgaardvej, Aarhus N, DK-8200, DENMARK

Tanja Aarvak (**1**: 239) Dynal Biotech ASA, PO Box 114, Smestad, N-0309, NORWAY

Harindra R. Abeysinghe (**3**: 345) Department of Pathology and Laboratory Medicine, University of Rochester School of Medicine, 601 Elmwood Ave., Rm 1-6337, Rochester, NY 14642

Ruedi Aebersold (**4**: 437) The Institute for Systems Biology, 1441 North 34th Street, Seattle, WA 98103-8904

Ueli Aebi (**3**: 233, 241) ME Muller Institute for Microscopy, Biozentrum, University of Basel, Klingelbergstr. 50/70, Basel, CH-4056, SWITZERLAND

Cheol-Hee Ahn (**4**: 29) School of Materials Science and Engineering, Seoul National University, Seoul, 151-744, SOUTH KOREA

Natalie G. Ahn (**4**: 443) Department of Chemistry & Biochemistry, University of Colorado, 215 UCB, Boulder, CO 80309

Ramiro Alberio (**4**: 45) School of Biosciences, University of Nottingham, Sutton Bonington, Loughborough, Leics, LE12 5RD, UNITED KINGDOM

Donna G. Albertson (**3**: 445) Cancer Research Institute, Department of Laboratory Medicine, The University of California, San Francisco, Box 0808, San Francisco, CA 94143-0808

Heiner Albiez (**1**: 291) Department of Biology II, Ludwig-Maximilians University of Munich, Munich, GERMANY

Terence Allen (**3**: 325) CRC Structural Cell Biology Group, Paterson Institute for Cancer Research, Christie Hospital NHS Trust, Wilmslow Road, Withington, Manchester, M20 4BX, UNITED KINGDOM

Noona Ambartsumian (**1**: 363) Department of Molecular Cancer Biology, Danish Cancer Society, Institute of Cancer Biology, Strandboulevarden 49, Copenhagen, DK-2100, DENMARK

Øystein Åmellem (**1**: 239) Immunosystems, Dynal Biotech ASA, PO Box 114, Smestad, N-0309, NORWAY

Patrick Amstutz (**1**: 497) Department of Biochemistry, University of Zürich, Winterthurerstr. 190, Zurich, CH-8057, SWITZERLAND

Jens S. Andersen (**4**: 427) Protein Interaction Laboratory, University of Southern Denmark—Odense, Campusvej 55, Odense M, DK-5230, DENMARK

Mads Hald Andersen (**1**: 97) Tumor Immunology Group, Institute of Cancer Biology, Danish Cancer Society, Strandboulevarden 49, Copenhagen, DK-2100, DENMARK

Helena Andersson (**4**: 63) Bioscience at Novum, Karolinska Institutet, Halsovagen 7-9, Huddinge, SE-141 57, SWEDEN

Peter W. Andrews (**1**: 183) Department of Biomedical Science, The University of Sheffield, Rm B2 238, Sheffield, S10 2TN, UNITED KINGDOM

Elsa Anes (**2**: 57) Faculdade de Farmacia, Universidade de Lisboa, Av. Forcas Armadas, Lisboa, 1649-019, PORTUGAL

James M. Angelastro (**1**: 171) Department of Pathology and Center for Neurobiology and Behavior, Columbia University College of Physicians

and Surgeons, 630 West 168th Street, New York, NY 10032

Sergey V. Anisimov (**4**: 103) Molecular Cardiology Unit, National Institute on Aging, NIH, 5600 Nathan Shock Drive, Baltimore, MD 21224

Celia Antonio (**2**: 379) Department of Biochemistry & Molecular Biophysics, College of Physicians & Surgeons, Columbia University, 701 W 168ST HHSC 724, New York, NY 69117

Shigehisa Aoki (**1**: 411) Department of Pathology & Biodefence, Faculty of Medicine, Saga University, Nebeshima 5-1-1, Saga, 849-8501, JAPAN

Ron D. Appel (**4**: 207) Swiss Institute of Bioinformatics, CMU, Rue Michel Servet 1, Geneva 4, CH-1211, SWITZERLAND

Rolf Apweiler (**4**: 469) EMBL Outstation, European Bioinformatics Institute, Wellcome Trust Genome Campus, Hinxton, Cambridge, CB10 1SD, UNITED KINGDOM

Nobukazu Araki (**2**: 147) Department of Histology and Cell Biology, School of Medicine, Kagawa University, Mki, Kagawa, 761-0793, JAPAN

Christopher M. Armstrong (**4**: 295) Dana Faber Cancer Institute, Harvard University, 44 Binney Street, Boston, MA 02115

Anthony J. Ashford (**2**: 155) Antibody Facility, Max Planck Institute of Molecullar Cell Biology and Genetics, Pfotenhauerstrsse 108, Dresden, D-01307, GERMANY

Daniel Axelrod (**3**: 19) Dept of Physics & Biophysics Research Division, University of Michigan, Ann Arbor, MI 48109-1055

Sheree Bailey (**1**: 475) Dept of Immunology, Allergy and Arthritis, Flinders Medical Centre and Flinders University, Bedford Park, Adelaide, SA, 5051, SOUTH AUSTRALIA

Nathalie Q. Balaban (**2**: 419) Department of Physics, The Hebrew University-Givat Ram, Racah Institute, Jerusalem, 91904, ISRAEL

William E. Balch (**2**: 209) Department of Cell and Molecular Biology, The Scripps Research Institute, 10550 North Torrey Pines Road, La Jolla, CA 92037

Debabrata Banerjee (**1**: 315) Department of Medicine, Cancer Institute of New Jersey, 195 Little Albany Street, New Brunswick, NJ 08903

Jiri Bartek (**4**: 253) Department of Cell Cycle and Cancer, Danish Cancer Society, Strandboulevarden 49, Copenhagen, DK-2100, DENMARK

Werner Baschong (**3**: 5) ME Muller Institute for Microscopy, Biozentrum, University of Basel, Klingelbergstrasse 50/70, Basel, CH-4056, SWITZERLAND

Philippe I. H. Bastiaens (**3**: 153) Cell Biology and Cell Biophysics Program, European Molecular Biology Laboratory, Meyerhofstrasse 1, Heidelberg, 69117, GERMANY

Jürgen C. Becker (**1**: 103) Department of Dermatology, University of Würzburg, Sanderring 2, Würzburg, 97070, GERMANY

Martin Béhé (**4**: 149) Department of Nuclear Medicine, Philipp's-University of Marburg, Baldingerstraße, Marburg/Lahn, D-35043, GERMANY

Thomas M. Behr (**4**: 149) Department of Nuclear Medicine, Philipp's-University of Marburg, Baldingerstraße, Marburg, D-35043, GERMANY

Stefanie Benesch (**2**: 399) Department of Cell Biology, Gesellschaft fur Biotechnoogische Forschung, Mascheroder Weg 1, Braunschweig, D-38124, GERMANY

Aaron Bensimon (**3**: 429) Laboratoire de Biophysique de l'ADN, Departement des Biotechnologies, Institut Pasteur, 25 rue du Dr. Roux, Paris Cedex 15, F-75724, FRANCE

John J. M. Bergeron (**2**: 41) Department of Anatomy and Cell Biology, Faculty of Medicine, McGill University, STRATHCONA Anatomy & Dentistry Building, Montreal, QC, H3A 2B2, CANADA

Michael W. Berns (**3**: 351) Beckman Laser Institute, University of California, Irvine, 1002 Health Sciences Road E, Irvine, CA 92697-1475

Joseph R. Bertino (**1**: 315) The Cancer Institute of New Jersey, 195 Little Albany Street, New Brunswick, NJ 08901

Paulo Bianco (**1**: 79) Dipartimento di Medicina Sperimentale e Patologia, Universita 'La Sapienza', Viale Regina Elena 324, Roma, I-00161, ITALY

Hans Kaspar Binz (**1**: 497) Department of Biochemistry, University of Zürich, Winterthurerstr. 190, Zürich, CH-8057, SWITZERLAND

R. Curtis Bird (**1**: 247) Department of Pathobiology, Auburn University, Auburn, AL 36849

Mina J. Bissell (**1**: 139) Life Sciences Division, Lawrence Berkeley National Laboratory, 1 Cyclotron Road, Bldg 83-101, Berkeley, CA 94720

Stephanie Blackwood (**3**: 445) Cancer Research Institute, University of California San Francisco, PO Box 0808, San Francisco, CA 94143-0808

Blagoy Blagoev (**4**: 427) Protein Interaction Laboratory, University of Southern Denmark—Odense, Campusvej 55, Odense M, DK-5230, DENMARK

Kenneth R. Boheler (**4**: 103) Laboratory of Cardiovascular Science, National Institute on Aging, NIH, 5600 Nathan Shock Drive, Baltimore, MD 21224-6825

Michelle A. Booden (**1**: 345) Lineberger Comprehensive Cancer Center, University of North Carolina at Chapel Hill, Chapel Hill, NC 27599-7295

Gary G. Borisy (**3**: 277) Department of Cell and Molecular Biology, Northwestern University Medical School, Chicago, IL 6011-3072

Elliot Botvinick (**3**: 351) Beckman Laser Institute, University of California, Irvine, 1002 Health Sciences Road, East, Irvine, CA 92697-1475

Gérard Bouchet (**4**: 207) Swiss Institute of Bioinformatics (SIB), CMU, rue Michel-Servet 1, Genève 4, CH-1211, SWITZERLAND

Rosemary Boyle (**4**: 437) The Institute for Systems Biology, 1441 North 34th St., Seattle, WA 98109

Susanne Brandfass (**1**: 563) Department of Biochemistry and Cell Biology, Max Planck Institute of Biophysical Chemistry, Am Faßberg 11, Gottingen, D-37077, GERMANY

Pascal Braun (**4**: 73) Department of Chemistry and Chemical Biology, Harvard University, 12 Oxford Street, Cambridge, MA 02138

Steven A. Braut (**4**: 121) Department of Anatomy and Structural Biology, Golding # 601, Albert Einstein College of Medicine of Yeshiva University, 1300 Morris Park Avenue, Bronx, NY 10461

Alvis Brazma (**4**: 95) EMBL Outstation—Hinxton, European Bioinformatics Institute, Wellcome Trust Genome Campus, Hinxton, Cambridge, CB10 1SD, UNITED KINGDOM

J. David Briley (**3**: 471) Department of Genomic Sciences, Glaxo Wellcome Research and Development, 5 Moore Drive, Research Triangle Park, NC 27709-3398

Simon Broad (**1**: 133) Keratinocyte Laboratory, London Research Institute, 44 Lincoln's Inn Fields, London, WC2A 3PX, UNITED KINGDOM

Nicholas H. Brown (**3**: 77) Wellcome Trust/Cancer Research UK Institute and Departmentt of Anatomy, University of Cambridge, Tennis Court Road, Cambridge, CB2 1QR, UNITED KINGDOM

Heather L. Brownell (**2**: 329, 341) Office of Technology Licensing and Industry Sponsored Research, Harvard Medical School, 25 Shattuck Street, Gordon Hall of Medicine, Room 414, Boston, MA 02115

Damien Brunner (**3**: 69) Cell Biology and Cell Biophysics Programme, European Molecular Biology Laboratory, Meyerhofstrasse 1, Heidelberg, D-69117, GERMANY

Suzannah Bumpstead (**3**: 463) Genotyping / Chr 20, The Wellcome Trust Sanger Institute, The Wellcome Trust Genome Campus, Hinxton, Cambridge, CB10 1SA, UNITED KINGDOM

Deborah C. Burford (**3**: 403) Wellcome Trust, Sanger Institute, The Wellcome Trust Genome Campus, Hinxton, Cambridge, CB10 1SA, UNITED KINGDOM

Gerald Burgstaller (**2**: 161) Department of Cell Biology, Institute of Molecular Biology, Austrian Academy of Sciences, Billrothstrasse 11, Salzburg, A-5020, AUSTRIA

Ian M. Caldicott (**1**: 157)

Angelique S. Camp (**1**: 457) Gene Therapy Centre, University of North Carolina at Chapel Hill, 7119 Thurston-Bowles (G44 Wilson Hall), Chapel Hill, NC 27599-7352

Keith H. S. Campbell (**4**: 45) School of Biosciences, Sutton Bonington, Loughborough, Leics, LE12 5RD, UNITED KINGDOM

Yihai Cao (**1**: 373) Microbiology & Tumor Biology Center, Karolinska Institute, Room: Skrivrum (G415), Box 280, Stockholm, SE-171 77, SWEDEN

Maria Carmo-Fonseca (**2**: 277, **3**: 419) Institute of Molecular Medicine, Faculty of Medicine, University of Lisbon, Av. Prof. Egas Moniz, Lisbon, 1649-028, PORTUGAL

T. Carneiro (**3**: 419) Faculty of Medicine, Institute of Molecular Medicine, University of Lisbon, Av. Prof. Egas Moniz, Lisboa, 1649-028, PORTUGAL

Nigel P. Carter (**2**: 133) The Wellcome Trust, Sanger Institute, The Wellcome Trust, Genome Campus, Hinxton, Cambridge, CB10 1SA, UNITED KINGDOM

Célia Carvalho (**3**: 419) Faculty of Medicine, Institute of Molecular Medicine, University of Lisbon, Av. Prof. Egas Moniz, Lisboa, 1649-028, PORTUGAL

Lucy A. Carver (**2**: 11) Cellular and Molecular Biology Program, Sidney Kimmel Cancer Center, 10835 Altman Row, San Diego, CA 92121

Doris Cassio (**1**: 231, **3**: 387) INSERM U-442: Signalisation cellulaire et calcium, Bat 443, Universite Paris-Sud, Street George Clemenceau Pack, 444, Orsay, Cedex, F-91405, FRANCE

Chris Catton (**3**: 207) Department of Zoology, University of Oxford, South Parks Road, Oxford, OX1 3PS, UNITED KINGDOM

Julio E. Celis (**1**: 527, **4**: 69, 165, 219, 243, 289) Danish Cancer Society, Institute of Cancer Biology and Danish Centre for Translational Breast Cancer Research, Strandboulevarden 49, Copenhagen O, DK-2100, DENMARK

Pierre Chambon (**3**: 501) Institut de Génétique et de Biologie Moléculaire et Cellulaire, 1 rue Laurent Fries, B.P.10142, Illkirch CEDEX, F-67404, FRANCE

Francis Ka-Ming Chan (**2**: 355) Department of Pathology, University of Massachusetts Medical School, Room S2-125, 55 Lake Avenue North, Worcester, MA 01655

Ming-Shien Chang (**3**: 87) Department of Physics, Duke University, 107 Physics Bldg, Durham, NC 27708-1000

Samit Chatterjee (**2**: 241) Margaret M. Dyson Vision Research Institute, Department of Ophthalmology, Weill Medical College of Cornell University, 1300 York Avenue, New York, NY 10021

Sandeep Chaudhary (**1**: 121) Veterans Affairs Medical Center, San Diego (V111G), 3350 La Jolla Village Drive, San Diego, CA 92161

Jingwen Chen (**3**: 471) Department of Genomic Sciences, Glaxo Wellcome Research and Development, 5 Moore Drive, Research Triangle Park, NC 27709

Yonglong Chen (**1**: 191) Institute for Biochemistry and Molecular Cell Biology, University of Goettingen, Justus-von-Liebig-Weg 11, Göttingen, D-37077, GERMANY

Yong Woo Cho (**4**: 29) Akina, Inc., Business & Technology Center, 1291 Cumberland Ave., #E130, West Lafayette, IN 47906

Juno Choe (**1**: 269) Institute for Systems Biology, 1441 N. 34th St, Seattle, WA 98103

Claus R. L. Christensen (**1**: 363) Department of Molecular Cancer Biology, Danish Cancer Society, Institute of Cancer Biology, Strandboulevarden 49, Copenhagen, DK-2100, DENMARK

Theodore Ciaraldi (**1**: 121) Veterans Affairs Medical Center, University of California, San Diego, 9500 Gilman Drive, La Jolla, CA 92093-9111

Aaron Ciechanover (**4**: 351) Center for Tumor and Vascular Biology, The Rappaport Faculty of Medicine and Research Institute, Technion-Israel Institute of Technology, POB 9649, Efron Street, Bat Galim, Haifa, 31096, ISRAEL

Mark S. F. Clarke (**2**: 233, **4**: 5) Department of Health and Human Performance, University of Houston, 3855 Holman Street, Garrison—Rm 104D, Houston, TX 77204-6015

Martin Clynes (**1**: 335) National Institute for Cellular Biotechnology, Dublin City University, Glasnevin, Dublin, 9, IRELAND

Philippe Collas (**1**: 207) Institute of Medical Biochemistry, University of Oslo, PO Box 1112 Blindern, Oslo, 0317, NORWAY

Kristen Correia (**4**: 35) Krumlauf Lab, Stowers Institute for Medical Research, 1000 East 50th Street, Kansas City, MO 64110

Pascale Cossart (**2**: 407) Unite des Interactions Bacteries-Cellules/Unité INSERM 604, Institut Pasteur, 28, rue du Docteur Roux, Paris Cedex 15, F-75724, FRANCE

Thomas Cremer (**1**: 291) Department of Biology II, Ludwig-Maximilians University of Munich, Munich, 80333, GERMANY

Robert A. Cross (**2**: 371) Molecular Motors Group, Marie Curie Research Institute, The Chart, Oxted, Surrey, RH8 0TE, UNITED KINGDOM

Matthew E. Cunningham (**1**: 171) Hospital for Special Surgery, New York Hospital, 520 E. 70th Street, New York, NY 10021

Noélia Custódio (**3**: 419) Faculty of Medicine, Institute of Molecular Medicine, University of Lisbon, Av. Prof. Egas Moniz, Lisboa, 1649-028, PORTUGAL

Zbigniew Darzynkiewwicz (**1**: 279) The Cancer Research Institute, New York Medical College, 19 Bradhurst Avenue, Hawthorne, NY 10532

Ilan Davis (**3**: 187) Wellcome Trust Centre for Cell Biology, Institute of Cell and Molecular Biology, The University of Edinburgh, Michael Swann Building, The King's Buildings, Mayfield Road, Edinburgh, EH9 3JR, SCOTLAND

Stephen C. De Rosa (**1**: 257) Vaccine Research Center, National Institutes of Health, 40 Convent Dr., Room 5610, Bethesda, MD 20892-3015

Nicholas M. Dean (**3**: 523) Functional Genomics, GeneTrove, GeneTrove (a division of Isis Isis Pharmaceuticals, Inc.), 2292 Faraday Avenue, Carlsbad, CA 92008

Anne Dell (**4**: 415) Department of Biological Sciences, Biochemistry Building, Imperial College of Science, Technology & Medicine, Biochemistry Building, London, SW7 2AY, UNITED KINGDOM

Panos Deloukas (**3**: 463) The Wellcome Trust, Sanger Institute, Hinxton, Cambridge, CB10 1SA, UNITED KINGDOM

Nicolas Demaurex (**3**: 163) Department of Cell Physiology and Metabolism, University of Geneva Medical Center, 1 Michel-Servet, Geneva, CH-1211, SWITZERLAND

Chris Denning (**4**: 45) Division of Animal Physiology, School of Biosciences, Institute of Genetics Room C15, University of Nottingham, Queens Medical Centre, Nottingham, NG7 2UH, UNITED KINGDOM

Ami Deora (**2**: 241) Margaret M. Dyson Vision Research Institute, Department of Ophthalmology, Weill Medical College of Cornell University, 1300 York Avenue, New York, NY 10021

Julien Depollier (**4**: 13) Centre de Recherche en Biochimie Macromoléculaire (UPR 1086), Centre National de la Recherche Scientifique (CNRS), 1919 Route de Mende, Montpellier Cedex 5, F-34293, FRANCE

Channing J. Der (**1**: 345) Department of Pharmacology, University of North Carolina at Chapel Hill, Lineberger Comprehensive Cancer Center, Chapel Hill, NC 27599

Bart Devreese (**4**: 259) Department of Biochemistry, Physiology and Microbiology, University of Ghent, K.L. Ledeganckstraat 35, Ghent, B-9000, BELGIUM

Alberto Diaspro (**3**: 201) Department of Physics, University of Genoa, Via Dodecaneso 33, Genoa, I-16146, ITALY

James Fred Dice (**4**: 345) Department Physiology, Tufts University School of Medicine, 136 Harrison Ave, Boston, MA 02111

Thomas J. Diefenbach (**4**: 307) Department of Physiology, Tufts University School of Medicine, 136 Harrison Avenue, Boston, MA 02111

Chris Dinant (**2**: 121) Biomolecular Sciences, UMIST, PO Box 88, Manchester, M60 1QD, UNITED KINGDOM

Da-Qiao Ding (**3**: 171) Structural Biology Section and CREST Research Project, Kansai Advanced Research Center, Communications Research Laboratory, 588-2 Iwaoka, Iwaoka-cho, Nishi-ku, Kobe, 651-2492, JAPAN

Gilles Divita (**4**: 13) Centre de Recherche en Biochimie Macromoléculaire (UPR 1086), Centre National de la Recherche Scientifique (CNRS), 1919 Route de Mende, Montpellier Cedex 5, F-34293, FRANCE

Eric P. Dixon (**1**: 483) TriPath Oncology, 4025 Stirrup Creek Drive, Suite 400, Durham, NC 27703

Bernhard Dobberstein (**2**: 215) Zentrum fur Molekulare Biologie, Universitat Heidelberg, Im Neuenheimer Feld 282, Heidelberg, D-69120, GERMANY

Lynda J. Donald (**4**: 457) Department of Chemistry, University of Manitoba, Room 531 Parker Building, Winnipeg, MB, R3T 2N2, CANADA

Wolfgang R. G. Dostmann (**2**: 299) Department of Pharmacology, University of Vermont, Health Science Research Facility 330, Burlington, VT 05405-0068

Adam Douglass (**3**: 129) Department of Cellular and Molecular Pharmacology, The University of California, San Francisco, School of Medicine, Medical Sciences Building, Room S1210, 513 Parnassus Avenue, San Francisco, CA 94143-0450

Kate Downes (**3**: 463) Genotyping / Chr 20, The Wellcome Trust, Sanger Institute, The Wellcome Trust Genome Campus, Hinxton, Cambridge, CB10 1SA, UNITED KINGDOM

Harry W. Duckworth (**4**: 457) Department of Chemistry, University of Manitoba, Room 531 Parker Building, Winnipeg, MB, R3T 2N2, CANADA

Derek M. Dykxhoorn (**3**: 511) CBR Institute for Biomedical Research, Harvard Medical School, 200 Longwood Ave, Boston, MA 02115

Lars Dyrskjøt (**4**: 83) Clinical Biochemical Department, Molecular Diagnostic Laboratory, Aarhus University Hospital, Skejby, Brendstrupgaardvej, Aarhus N, DK-8200, DENMARK

Christoph Eckerskorn (**4**: 157) Protein Analytics, Max Planck Institute for Biochemistry, Klopferspitz 18, Martinsried, D-82152, GERMANY

Glenn S. Edwards (**3**: 87) Department of Physics, Duke University, 221 FEL Bldg, Box 90305, Durham, NC 27708-0305

Andreas A. O. Eggert (**1**: 103) Department of Dermatology, Julius-Maximillians University, Josef-Schneider-Str. 2, Würzburg, 97080, GERMANY

Maria Ekström (**4**: 63) Bioscience at Novum, Karolinska Institutet, Huddinge, SE-141 57, SWEDEN

Andreas Engel (**3**: 317) Maurice E. Müller Institute for Microscopy at the Biozentrum, University of Basel, Klingelbergstrasse 70, Basel, CH-4056, SWITZERLAND

Anne-Marie Engel (**1**: 353) Bartholin Institutte, Bartholinsgade 2, Copenhagen K, DK-1356, DENMARK

José A. Enríquez (**2**: 69) Department of Biochemistry and Molecular and Cellular Biology, Universidad de Zaragoza, Miguel Servet, 177, Zaragoza, E-50013, SPAIN

Rachel Errington (**1**: 305) Department of Medical Biochemistry and Immunology, University of Wales College of Medicine, Heath Park, Cardiff, CF14 4XN, UNITED KINGDOM

Virginia Espina (**3**: 339) Microdissection Core Facility, Laboratory of Pathology, National Cancer Institute, 9000 Rockville Pike, Building 10, Room B1B53, Bethesda, MD 20892

H. Dariush Fahimi (**2**: 63) Department of Anatomy and Cell Biology II, University of Heidelberg, Im Neuenheimer Feld 307, Heidelberg, D-69120, GERMANY

Federico Federici (**3**: 201) Department of Physics, University of Genoa, Via Dodecaneso 33, Genoa, I-16146, ITALY

Daniel L. Feeback (**2**: 233, **4**: 5) Space and Life Sciences Directorate, NASA-Johnson Space Center, 3600 Bay Area Blvd, Houston, TX 77058

Patricio Fernández-Silva (**2**: 69) Dept of Biochemistry and Molecular and Cellular Biology, Univeridad de Zaragoza, Miguel Servet 177, Zaragoza, E-50013, SPAIN

Erika Fernández-Vizarra (**2**: 69) Dept of Biochemistry and Molecular and Cellulary Biology, Universidad de Zaragoza, Miguel Servet, 177, Zaragoza, E-50013, SPAIN

Patrick F. Finn (**4**: 345) Department of Physiology, Tufts University School of Medicine, 136 Harrison Ave, Boston, MA 02111

Kevin L. Firth (**2**: 329, **2**: 341) ASK Science Products Inc., 487 Victoria St, Kingston, Ontario, K7L 3Z8, CANADA

Raluca Flükiger-Gagescu (**2**: 27) Unitec—Office of Technology Transfer, University of Geneva and University of Geneva Hospitals, 24, Rue Général-Dufour, Geneva 4, CH-1211, SWITZERLAND

Leonard J. Foster (**4**: 363, 427) Protein Interaction Laboratory, University of Southern Denmark, Odense, Campusvej 55, Odense M, DK-5230, DENMARK

Dimitrios Fotiadis (**3**: 317) M. E. Müller Institute for Microscopy at the Biozentrum, University of Basel, Klingelbergstrasse 70, Basel, CH-4056, SWITZERLAND

Patrick L. T. M. Frederix (**3**: 317) M. E. Müller Institute for Microscopy at the Biozentrum, University of Basel, Klingelbergstrasse 70, Basel, CH-4056, SWITZERLAND

Marcus Frohme (**4**: 113) Functional Genome Analysis, German Cancer Research Center, Deutsches Krebsforschungszentrum, Im Neuenheimer Feld 580, Heidelberg, D-69120, GERMANY

Masanori Fujimoto (**4**: 197) Department of Biochemistry and Biomolecular Recognition, Yamaguchi University School of Medicine, 1-1-1, Minami-kogushi, Ube, Yamaguchi, 755-8505, JAPAN

Margarida Gama-Carvalho (**2**: 277) Faculty of Medicine, Institute of Molecular Medicine, University of Lisbon, AV. Prof. Egas Moniz, Lisbon, 1649-028, PORTUGAL

Henrik Garoff (**1**: 419, **4**: 63) Unit for Cell Biology, Center for Biotechnology. Karolinska Institute, Huddinge, SE-141 57, SWEDEN

Susan M. Gasser (**2**: 359) Friedrich Miescher Institute fr Biomedical Research, Maulbeerstrasse 66, Basel, CH-1211, SWITZERLAND

Kristine G. Gaustad (**1**: 207) Institute of Medical Biochemistry, University of Oslo, PO Box 1112 Blindern, Oslo, 0317, NORWAY

Benjamin Geiger (**2**: 419) Dept. of Molecular Cell Biology, Weizman Institute of Science, Wolfson Building, Rm 617, Rehovot, 76100, ISRAEL

Kris Gevaert (**4**: 379, **4**: 457) Dept. Medical Protein Research, Flanders Interuniversity Institute for Biotechnology, Faculty of Medicine and Health Sciences, Ghent University, Instituut Rommelaere—Blok D, Albert Baertsoenkaai 3, Gent, B-9000, BELGIUM

Jilur Ghori (**3**: 463) Genotyping / Chr 20, The Wellcome Trust, Sanger Institute, The Wellcome Trust, Genome Campus, Hinxton, Cambridge, CB10 1SA, UNITED KINGDOM

Alasdair J. Gibb (**1**: 395) Department of Pharmacology, University College London, Gower Street, London, WC1E GBT, UNITED KINGDOM

Mario Gimona (**1**: 557, **2**: 161, **4**: 145) Department of Cell Biology, Institute of Molecular Biology, Austrian Academy of Sciences, Billrothstrasse 11, Salzburg, A-5020, AUSTRIA

David A. Glesne (**1**: 165) Biosciences Division, Argonne National Laboratory, 9700 South Cass Avenue, Argonne, IL 60439-4844

Martin Goldberg (**3**: 325) Science Laboratories, University of Durham, South Road, Durham, DH1 3LE, UNITED KINGDOM

Kenneth N. Goldie (**3**: 267) Structural and Computational Biology Programme, EMBL, Meyerhofstrasse 1, Heidelberg, D-69117, GERMANY

Jon W. Gordon (**3**: 487) Geriatrics and Adult Development, Mount Sinai School of Medicine, One Gustave L. Levy Place, New York, NY 10029

Angelika Görg (**4**: 175) Fachgebiet Proteomik, Technische Universität München, Am Forum 2, Freising Weihenstephan, D-85350, GERMANY

Martin Gotthardt (**4**: 149) Department of Nuclear Medicine, Philipp's-University of Marburg, Baldingerstraße, Marburg/Lahn, D-35043, GERMANY

Frank L. Graham (**1**: 435) Department of Biology, McMaster University, Life Sciences Building, Room 430, Hamilton, Ontario, L8S 4K1, CANADA

Claude Granier (**1**: 519) UMR 5160, Faculté de Pharmacie, 15 Av. Charles Flahault, Montpellier Cedex 5, BP 14491, 34093, FRANCE

Lloyd A. Greene (**1**: 171) Department of Pathology and Center for Neurobiology and Behavior, Columbia University, College of Physicians and Surgeons, 630 W. 168th Street, New York, NY 10032

Susan M. Gribble (**3**: 403) Sanger Institute, The Wellcome Trust, The Wellcome Trust Genome Campus, Hinxton, Cambridge, CB10 1SA, UNITED KINGDOM

Gareth Griffiths (**2**: 57, **3**: 299) Department of Cell Biology, EMBL, Postfach 102209, Heidelberg, D-69117, GERMANY

Sergio Grinstein (**3**: 163) Cell Biology Program, Hospital for Sick Children, 555 University Avenue, Toronto, Ontario, M5G 1X8, CANADA

Pavel Gromov (**1**: 527, **4**: 69, 165, 243, 289) Institute of Cancer Biology and Danish Centre for Translational Breast Cancer Research, Danish Cancer Society, Strandboulevarden 49, Copenhagen, DK-2100, DENMARK

Irina Gromova (**4**: 219) Department of Medical Biochemistry and Danish Centre for Translational Breast Cancer Research, Danish Cancer Society, Strandboulevarden 49, Copenhagen, DK-2100, DENMARK

Dale F. Gruber (**1**: 33) Cell Culture Research and Development, GIBCO/Invitrogen Corporation, 3175 Staley Road, Grand Island, NY 14072

Markus Grubinger (**4**: 145) Institute of Physics and Biophysics, University of Salzburg, Hellbrunnerstr. 34, Salzburg, A-5020, AUSTRIA

Jean Gruenberg (**2**: 27, 201) Department of Biochemistry, University of Geneva, 30, quai Ernest Ansermet, Geneva 4, CH-1211, SWITZERLAND

Stephanie L. Gupton (**3**: 137) 10550 North Torrey Pines Road, CB 163, La Jolla, CA 92037

Cemal Gurkan (**2**: 209) Department of Cell and Molecular Biology, The Scripps Research Institute, 10550 North Torrey Pines Road, La Jolla, CA 92037

Martin Guttenberger (**4**: 131) Zentrum für Molekulariologie der Pflanzen, Universitat Tübingen, Entwicklungsgenetik, Auf der Morgenstelle 3, Tübingen, D-72076, GERMANY

Thomas Haaf (**3**: 409) Institute for Human Genetics, Johannes Gutenberg-Universität Mainz, 55101, Mainz, D-55131, GERMANY

Christine M. Hager-Braun (**1**: 511) Health and Human Services, NIH National Institute of Environmental Health Sciences, MD F0-04, PO Box 12233, Research Triangle Park, NC 27709

Anne-Mari Håkelien (**1**: 207) Institute of Medical Biochemistry, Institute of Medical Biochemistry, University of Oslo, PO Box 1112 Blindern, Oslo, 0317, NORWAY

Fiona C. Halliday (**1**: 395) GlaxoSmithKline, Greenford, Middlesex, UB6 OHE, UNITED KINGDOM

Gerald Hammond (**2**: 223) Molecular Neuropathobiology Laboratory, Cancer Reasearch UK London Research Institute, 44 Lincoln's Inn Fields, London, WC2A 3PX, UNITED KINGDOM

Klaus Hansen (**4**: 253)

Hironobu Harada (**1**: 367) Department of Neurosurgery, Ehime University School of Medicine, Shitsukawa, Toon-shi, Ehime, 791-0295, JAPAN

Robert J. Hay (**1**: 43, 49, 573) Viitro Enterprises Incorporated, 1113 Marsh Road, PO Box 328, Bealeton, VA 22712

Izumi Hayashi (**1**: 151) National Medical Center and Beckman Research Institute, Division of Neurosciences, City of Hope, 1500 E. Duarte Rd, Duarte, CA 91010-3000

Timothy A. Haystead (**4**: 265) Department of Pharmacology and Cancer Biology, Duke University Medical Center, Box 3813 Med Ctr, Durham, NC 27710

Rebecca Heald (**2**: 379) Molecular and Cell Biology Department, University of California, Berkeley, Berkeley, CA 94720-3200

Florence Hediger (**2**: 359) Department of Molecular Biology, University of Geneva, 30, Quai Ernest Ansermet, Geneva, CH-1211, SWITZERLAND

Rainer Heintzmann (**3**: 29) Randall Division of Cell and Molecular Biophysics, King's College London, Guy's Campus, London, SE1 1UL, UNITED KINGDOM

Frederic Heitz (**4**: 13) Centre de Recherche en Biochimie Macromoléculaire (UPR 1086), Centre National de la Recherche Scientifique (CNRS), 1919 Route de Mende, Montpellier Cedex 5, F-34293, FRANCE

Johannes W. Hell (**2**: 85) Department of Pharmacology, University of Iowa, 2152 Bowen Science Building, Iowa City, IA 52242

Kai Hell (**4**: 269) Adolf-Butenandt-Institut fur Physiologische Chemie, Lehrstuhl: Physiologische Chemie, Universitat Munchen, Butenandtstr. 5, Gebäude B, Munchen, D-81377, GERMANY

Robert R. Henry (**1**: 121) Veterans Affairs Medical Center, San Diego (V111G), 3350 La Jolla Village Drive, San Diego, CA 92161

Johan Hiding (**2**: 45) Göteborg University, Institute of Medical Biochemistry, PO Box 440, Göteborg, SE-403-50, SWEDEN

Yasushi Hiraoka (**3**: 171) Structural Biology Section and CREST Research Project, Kansai Advanced Research Center, Communications Research Laboratory, 588-2 Iwaoka, Iwaoka-cho, Nishi-ku, Kobe, 651-2492, JAPAN

Mary M. Hitt (**1**: 435) Department of Pathology & Molecular Medicine, McMaster University, 1200 Main Street West, Hamilton, Ontario, L8N 3Z5, CANADA

Julie Hodgkinson (**3**: 307) School of Crystallography, Birkbeck College, Unversity of London, Malet Street, London, WC1E 7HX, UNITED KINGDOM

Klaus P. Hoeflich (**2**: 307) Division of Molecular and Structural Biology, Ontario Cancer Institute, Department of Medical Biophysics, University of Toronto, 610 University Avenue, 7-707A, Toronto, Ontario, M5G 2M9, CANADA

Tracy L. Hoffman (**1**: 21) ATCC, P.O. Box 1549, Manassas, VA 20108

Jörg D. Hoheisel (**4**: 113) Functional Genome Analysis, German Cancer Research Center, Deutsches Krebsforschungszentrum, Im Neuenheimer Feld 580, Heidelberg, D-69120, GERMANY

Thomas Hollemann (**1**: 191) Institute for Biochemistry and Molecular Cell Biology, University of Goettingen, Justus-von-Liebig-Weg 11, Göttingen, D-37077, GERMANY

Caterina Holz (**4**: 57) PSF biotech AG, Huebnerweg 6, Berlin, D-14059, GERMANY

Akira Honda (**2**: 299) Department of Pharmacology, University of Vermont, Health Science Research Facility 330, Burlington, VT 05405-0068

Masanori Honsho (**2**: 5) Max Planck Institute of Molecular Cell Biology and Genetics, Pfotenhauerstrasse 108, Dresden, D-01307, GERMANY

Andrew N. Hoofnagle (**4**: 443) School of Medicine, University of Colorado Health Sciences Center, Denver, CO 80262

Eliezer Huberman (**1**: 165) Gene Expression and Function Group, Argonne National Laboratory, 9700 South Cass Avenue, Argonne, IL 60439-4844

M. Shane Hutson (**3**: 87) Department of Physics, Duke University, 107 Physics Bldg, Durham, NC 27708-1000

Andreas Hüttmann (**1**: 115) Abteilung für Hämatologie, Universitäkrankenhaus Essn, Hufelandstr. 55, Essen, 45122, GERMANY

Anthony A. Hyman (**2**: 155) Max Planck Institute of Molecular Cell Biology and Gene Technology, Pfotenhauerstrasse 108, Dresden, D-01307, GERMANY

Sherrif F. Ibrahim (**1**: 269) Institute for Systems Biology, 1441 N. 34th St, Seattle, WA 98103

Kazuo Ikeda (**1**: 151) National Medical Center and Beckman Research Institute, Division of Neurosciences, City of Hope, 1500 East Duarte Road, Duarte, CA 91010-3000

Elina Ikonen (**2**: 181) The LIPID Cell Biology Group, Department of Biochemistry, The Finnish National Public Health Institute, Mannerheimintie 166, Helsinki, FIN-00300, FINLAND

Pranvera Ikonomi (**1**: 49) Director, Cell Biology, American Type Culture Collection (ATCC), 10801 University Blvd., Manassas, VA 20110-2209

Mitsuhiko Ikura (**2**: 307) Division of Molecular and Structural Biology, Ontario Cancer Institute, Department of Medical Biophysics, University of Toronto, 610 University Avenue 7-707A, Toronto, Ontario, M5G 2M9, CANADA

Arup Kumar Indra (**3**: 501) Institut de Génétique et de Biologie Moléculaire et Cellulaire (IGBMC), 1 rue Laurent Fries, B.P.10142, Illkirch CEDEX, F-67404, FRANCE

Takayoshi Inoue (**4**: 35) National Institute for Neuroscience, 4-1-1 Ogawahigashi, Kodaira, Tokyo, 187-8502, JAPAN

Kumiko Ishii (**2**: 139) Supra-Biomolecular System Research Group, RIKEN (Institute of Physical and Chemical Research), 2-1, Hirosawa, Wako-shi, Saitama, 351-0198, JAPAN

Dean A. Jackson (**2**: 121) Department of Biomolecular Sciences, UMIST, PO Box 88, Manchester, M60 1QD, UNITED KINGDOM

Reinhard Jahn (**2**: 85) Department of Neurobiology, Max-Planck-Institut for Biophysical Chemistry, Am Faßberg 11, Gottingen, D-37077, GERMANY

Kim D. Janda (**1**: 491) Department of Chemistry, BCC-582, The Scripps Research Institute, 10550 N. Torrey Pines Road, La Jolla, CA 92037

Harry W. Jarrett (**4**: 335) Department of Biochemistry, University of Tennessee Health Sciences Center, Memphis, TN 38163

Daniel G. Jay (**4**: 307) Dept. Physiology, Tufts University School of Medicine, 136 Harrison Avenue, Boston, MA 02111

David W. Jayme (**1**: 33) Cell Culture Research and Development, GIBCO/Invitrogen Corporation, 3175 Staley Road, Grand Island, NY 14072

Ole Nørregaard Jensen (**4**: 409) Protein Research Group, Department of Biochemistry and Molecular Biology, University of Southern Denmark, Campusvej 55, Odense M, DK-5230, DENMARK

Jae Hyun Jeong (**4**: 29) Department of Chemical & Biomolecular Engineering, Center for Ultramicrochemical Process Systems, Korea Advanced Institute of Science and Technology, Daejeon, 305-701, SOUTH KOREA

Jeff A. Jones (**2**: 233) Space and Life Sciences Directorate, NASA-Johnson Space Center, TX 77058

Gloria Juan (**1**: 279) Research Pathology Division, Room S-830, Memorial Sloan-Kettering Cancer Center, 1275 York Avenue, New York, NY 10021

Melissa S. Jurica (**2**: 109) Molecular, Cell & Developmental Biology, Center for Molecular Biology of RNA, UC Santa Cruz, 1156 High Street, Santa Cruz, CA 95064

Eckhart Kämpgen (**1**: 103) Department of Dermatology, Friedrich Alexander University, Hartmannstr. 14, Erlangen, D-91052, GERMANY

Roger Karlsson (**2**: 165) Department of Cell Biology, The Wenner-Gren Institute, Stockholm University, Stockholm, S-10691, SWEDEN

Fredrik Kartberg (**2**: 45) Göteborg University, Institute of Medical Biochemistry, PO Box 440, Gothenburg, SE, 403-50, SWEDEN

Irina N. Kaverina (**3**: 111) Institute of Molecular Biotechnology, Austrian Academy of Sciences, Dr. Bohrgasse 3-5, Vienna, A-1030, AUSTRIA

Ralph H. Kehlenbach (**2**: 267) Hygiene-Institut-Abteilung Virologie, Universitat Heidelberg, Im Neuenheimer Feld 324, Heidelberg, D-69120, GERAMNY

Daniel P. Kiehart (**3**: 87) Department of Biology, Duke University, B330g Levine Sci Bldg, Box 91000, Durham, NC 27708-1000

Katherine E. Kilpatrick (**1**: 483) Senior Research Investigator, TriPath Oncology, 4025 Stirrup Creek Drive, Suite 400, Durham, NC 27703

Jong-Duk Kim (**4**: 29) Department of Chemical & Biomolecular Engineering, Center for Ultramicrochemical Process Systems, Korea Advanced Institute of Science and Technology, Daejeon, 305-701, SOUTH KOREA

Maurice Kléber (**1**: 69) Institute of Cell Biology, Department of Biology, Swiss Federal Institute of Technology, ETH—Hönggerberg, Zurich, CH-8093, SWITZERLAND

Toshihide Kobayashi (**2**: 139) Supra-Biomolecular System Research Group, RIKEN (Institute of Physical and Chemical Research) Frontier Research System, 2-1, Hirosawa, Wako-shi, Saitama, 351-0198, JAPAN

Stefan Kochanek (**1**: 445) Division of Gene Therapy, University of Ulm, Helmholtz Str. 8/I, Ulm, D-89081, GERMANY

Anna Koffer (**2**: 223) Physiology Department, University College London, 21 University Street, London, WC1E 6JJ, UNITED KINGDOM

Antonius Koller (**4**: 383) Department of Cell Biology, Torrey Mesa Research Institute, 3115 Merryfield Row, San Diego, CA 92121

Erich Koller (**3**: 523) Functional Genomics, GeneTrove, Isis Pharmaceuticals, Inc., 2292 Faraday Ave., Carlsbad, CA 92008

Robert L. Kortum (**1**: 215) The Eppley Institute for Research in Cancer, The University of Nebraska Medical Center, 986805 Nebraska Medical Center, Omaha, NE 68198-6805

Irina Kratchmarova (**4**: 427) Protein Interaction Laboratory, University of Southern Denmark—Odense, Campusvej 55, Odense M, DK-5230, DENMARK

Geri E. Kreitzer (**2**: 189) Cell and Developmental Biology, Weill Medical College of Cornell University, LC-300, New York, NY 10021

Florian Kreppel (**1**: 445) Division of Gene Therapy, University of Ulm, Helmholtz Str. 8/I, Ulm, D-89081, GERMANY

Mogens Kruhøffer (**4**: 83) Molecular Diagnostic Laboratory, Clinical Biochemical Department, Aarhus University Hospital, Skejby, Brendstrupgaardvej, Aarhus N, DK-8200, DENMARK

Robb Krumlauf (**4**: 35) Stowers Institute for Medical Research, 1000 East 50th Street, Kansas City, MO 64110

Michael Kühl (**1**: 191) Development Biochemistry, University of Ulm, Albert-Einstein-Allee 11, Ulm, D-89081, GERMANY

Mark Kühnel (**2**: 57) Department of Cell Biology, EMBL, Postfach 102209, Heidelberg, D-69117, GERMANY

Anuj Kumar (**3**: 179) Dept. of Molecular, Cellular, and Developmental Biology and Life Sciences Institute, University of Michigan, 210 Washtenaw Avenue, Ann Arbor, MI 48109-2216

Thomas Küntziger (**1**: 207) Institute of Medical Biochemistry, Institute of Medical Biochemistry, University of Oslo, PO Box 1112 Blindern, Oslo, 0317, NORWAY

Yasuhiro Kuramitsu (**4**: 197) Department of Biochemistry and Biomolecular Recognition, Yamaguchi University School of Medicine, 1-1-1 Minami-kogushi, Ube, Yamaguchi, 755-8505, JAPAN

Sergei A. Kuznetsov (**1**: 79) Craniofacial and Skeletal Disease Branch, NIDCR, NIH, Department of Health and Human Services, 30 Convent Drive MSC 4320, Bethesda, MD 20892

Joshua Labaer (**4**: 73) Harvard Institute of Proteomics, 320 Charles Street, Boston, MA 02141-2023

Frank Lafont (**2**: 181) Department of Biochemistry, University of Geneva, 30, quai Ernest-Ansermet 1211, Geneva 4, CH-1211, SWITZERLAND

Yun Wah Lam (**2**: 103, 115) Wellcome Trust Biocentre, MSI/WTB Complex, University of Dundee, Dow Street, Dundee, DD1 5EH, UNITED KINGDOM

Angus I. Lamond (**2**: 103, 115) Wellcome Trust Biocentre, MSI/WTB Complex, University of Dundee, Dow Street, Dundee, DD1 5EH, UNITED KINGDOM

Lukas Landmann (**3**: 5) Institute for Anatomy (LL), Anatomisches Institut, University of Basel, Pestalozzistrasse 20, Basel, CH-4056, SWITZERLAND

Helga B. Landsverk (**1**: 207) Institute of Medical Biochemistry, Institute of Medical Biochemistry, University of Oslo, PO Box 1112 Blindern, Oslo, 0317, NORWAY

Christine Lang (**4**: 57) Department of Microbiology and Genetics, Berlin University of Technology, Gustav-Meyer-Allee 25, Berlin, D-13355, GERMANY

Paul LaPointe (**2**: 209) Department of Cell and Molecular Biology, The Scripps Research Institute, 10550 North Torrey Pines Road, La Jolla, CA 92037

Martin R. Larsen (**4**: 371) Department of Biochemistry and Molecular Biology, University of Southern Denmark, Campusvej 55, Odense M, DK-5230, DENMARK

Pamela L. Larsen (**1**: 157) Department of Cellular and Structural Biology, University of Texas Health Science Center at San Antonio, San Antonio, TX 78229-3900

Eugene Ngo-Lung Lau (**1**: 115) Leukaemia Foundation of Queensland Leukaemia Research Laboratories, Queensland Institute of Medical Research, Royal Brisbane Hospital Post Office, Brisbane, Queensland, Q4029, AUSTRALIA

Sabrina Laugesen (**4**: 371) Department of Biochemistry and Molecular Biology, University of Southern Denmark, Campusvej 55, Odense M, DK-5230, DENMARK

Daniel Laune (**1**: 519) Centre de Pharmacologie et Biotechnologie pour la Santé, CNRS UMR 5160, Faculté de Pharmacie, Avenue Charles Flahault, Montpellier Cedex 5, F-34093, FRANCE

Andre Le Bivic (**2**: 241) Groupe Morphogenese et Compartimentation Membranaire, UMR 6156, IBDM, Faculte des Sciences de Luminy, case 907, Marseille cedex 09, F-13288, FRANCE

Ronald Lebofsky (**3**: 429) Laboratoire de Biophysique de l'ADN, Departement des Biotechnologies, Institut Pasteur, 25 rue du Dr. Roux, Paris Cedex 15, F-75724, FRANCE

Chuan-PU Lee (**2**: 259) The Department of Biochemistry and Molecular Biology, Wayne State University School of Medicine, 4374 Scott Hall, 540 E. Canfield, Detroit, MI 48201

Eva Lee (**1**: 139) Life Sciences Division, Lawrence Berkeley National Laboratory, 1 Cyclotron Road, Bldg 83-101, Berkeley, CA 94720

Joon-Hee Lee (**4**: 45) School of Biosciences, University of Nottingham, Sutton Bonington, Loughborough, Leics, LE12 5RD, UNITED KINGDOM

Kwangmoon Lee (**1**: 215) The Eppley Institute for Research in Cancer, The University of Nebraska Medical Center, 986805 Nebraska Medical Center, Omaha, NE 68198-6805

Thomas Lee (**4**: 443) Dept of Chemistry and Biochemistry, Univ of Colorado, 215 UCB, Boulder, CO 80309-0215

Margaret Leversha (**3**: 395) Memorial Sloan Kettering Cancer Center, 1275 York Avenue, New York, NY 10021

Jeffrey M. Levsky (**4**: 121) Department of Anatomy and Structural Biology, Golding # 601, Albert Einstein College of Medicine of Yeshiva University, 1300 Morris Park Avenue, Bronx, NY 10461

Alexandre Lewalle (**3**: 37) Randall Centre, New Hunt's House, Guy's Campus, London, SE1 1UL, UNITED KINGDOM

Chung Leung Li (**1**: 115) Experimental Haematology Laboratory, Stem Cell Program, Institute of Zoology/Genomics Research Center, Academia Sinica, Nankang 115, Nankang, Taipei, 11529, R.O.C.

LiQiong Li (**3**: 345) Department of Pathology and Laboratory Medicine, University of Rochester School of Medicine, 601 Elmwood Ave., Rm 1-6337, Rochester, NY 14642

Mei Li (**3**: 501) Institut de Génétique et de Biologie Moléculaire et Cellulaire (IGBMC), 1 rue Laurent Fries, B.P.10142, Illkirch CEDEX, F-67404, FRANCE

Siming Li (**4**: 295) Dana Faber Cancer Institute, Harvard University, 44 Binney Street, Boston, MA 02115

Lih-huei Liaw (**3**: 351) Beckman Laser Institute, University of California, Irvine, 1002 Health Sciences Road E, Irvine, CA 92697-1475

Antonietta M. Lillo (**1**: 491) Department of Chemistry, BCC-582, The Scripps Research Institute, 10550 N. Torrey Pines Road, La Jolla, CA 92037

Uno Lindberg (**2**: 165) Department of Cell Biology, Stockholm University, The Wenner-Gren Institute, Stockhólm, S-10691, SWEDEN

Christian Linden (**1**: 103) Department of Virology, Julius-Maximillins University, Versbacher Str. 7, Würzburg, D-97080, GERMANY

Robert Lindner (**2**: 51) Department of Cell Biology in the Center of Anatomy, Hannover Medical School, Hannover, D-30625, GERMANY

Lance A. Liotta (**3**: 339) Chief, Laboratory of Pathology, National Cancer Institute Building 10, Room 2A33, 9000 Rockville Pike, Bethesda, MD 20892

Adam J. Liska (**4**: 399) Max Planck Institute of Molecular Cell Biology and Genetics, Pfotenhauerst 108, Dresden, D-01307, GERMANY

Hong Liu (**1**: 139) Life Sciences Division, Lawrence Berkeley National Laboratory, 1 Cyclotron Road, Bldg 83-101, Berkeley, CA 94720

Silvia Lommel (**2**: 399) Department of Cell Biology, German Research Center for Biotechnology (GBF), Mascheroder Weg 1, Braunschweig, D-38124, GERMANY

Giuseppe S. A. Longo-Sorbello (**1**: 315) Centro di Riferimento Oncologico, Ospedale "S. Vincenzo", Taormina, Contradra Sirinam, 08903, ITALY

Lovisa Lovmar (**3**: 455) Department of Medical Sciences, Uppsala University, Akademiska sjukhuset, Uppsala, SE-75185, SWEDEN

Eugene Lukanidin (**1**: 363) Department of Molecular Cancer Biology, Institute of Cancer Biology, Danish Cancer Society, Strandboulevarden 49, Copenhagen, DK-2100, DENMARK

Jiri Lukas (**4**: 253) Department of Cell Cycle and Cancer, Danish Cancer Society, Strandboulevarden 49, Copenhagen, DK-2100, DENMARK

Peter J. Macardle (**1**: 475) Department of Immunology, Allergy and Artritis, Flinders Medical Centre and Flinders University, Bedford Park, Adelaie, SA, 5051, SOUTH AUSTRALIA

Peder S. Madsen (**4**: 69) Institute of Medical Biochemistry, University of Aarhus, Ole Worms Alle, Building 170, Aarhus C, DK-8000, DENMARK

Nils E. Magnusson (**4**: 83) Clinical Biochemical Department, Molecular Diagnostic Laboratory, Aarhus University Hospital, Skejby, Brendstrupgaardvej, Aarhus N, DK-8200, DENMARK

Asami Makino (**2**: 139) Supra-Biomolecular System Research Group, RIKEN (Institute of Physical and Chemical Research) Frontier Research System, 2-1, Hirosawa, Wako-shi, Saitama, 351-0198, JAPAN

G. Mike Makrigiorgos (**3**: 477) Department of Radiation Oncology, Dana Farber-Brigham and Women's Cancer Center, 75 Francis Street, Level L2, Boston, MA 02215

Matthias Mann (**4**: 363, 427) Protein Interaction Laboratory, University of Southern Denmark, Odense, Campusvej 55, Odense M, DK-5230, DENMARK

Edward Manser (**4**: 285) Glaxo-IMCB Group, Institute of Molecular and Cell Biology, Singapore, 117609, SINGAPORE

Ahmed Mansouri (**3**: 491) Department of Molecular Cell Biology, Max-Planck-Institute of Biophysical Chemistry, Am Fassberg 11, Göttingen, D-37077, GERMANY

Alan D. Marmorstein (**2**: 241) Cole Eye Institute, Weill Medical College of Cornell Cleveland Clinic, 9500 Euclid Avenue, i31, Cleveland, OH 44195

Bruno Martoglio (**2**: 215) Institute of Biochemistry, ETH Zentrum, Building CHN, Room L32.3, Zurich, CH-8092, SWITZERLAND

Susanne E. Mason (**1**: 407) Department of Physiology, University of Maryland School of Medicine, 655 W. Baltimore St., Baltimore, MD 21201

Stephen J. Mather (**1**: 539) Dept of Nuclear Medicine, St Bartholomews Hospital, London, EC1A 7BE, UNITED KINGDOM

Arvid B. Maunsbach (**3**: 221, 289) Department of Cell Biology, Institute of Anatomy, Aarhus University, Aarhus, DK-8000, DENMARK

William Hayes McDonald (**4**: 391) Department of Cell Biology, The Scripps Research Institute, 10550 North Torrey Pines Rd, La Jolla, CA 92370

Kathleen M. McKenzie (**1**: 491) Department of Chemistry, BCC-582, The Scripps Research Institute, 10550 N. Torrey Pines Road, La Jolla, CA 92037

Alexander D. McLellan (**1**: 103) Department of Microbiology & Immunology, University of Otago, PO Box 56, 720 Cumberland St, Dunedin, NEW ZEALAND

Scott W. McPhee (**1**: 457) Department of Surgery, University of Medicine and Dentistry of New Jersey, Camden, NJ 08103

Jill Meisenhelder (**4**: 139) Molecular and Cell Biology Laboratory, The Salk Institute, 10010 North Torrey Pines Road, La Jolla, CA 92037

Paula Meleady (**1**: 13) National Institute for Cellular Biotechnology, Dublin City University, Glasnevin, Dublin, 9, IRELAND

Nicholas T. Mesires (**4**: 345) Department of Physiology, Tufts University School of Medicine, 136 Harrison Ave, Boston, MA 02111

Daniel Metzger (**3**: 501) Institut de Génétique et de Biologie Moléculaire et Cellulaire (IGBMC), Institut Clinique de la Souris (ICS), 1 rue Laurent Fries, B.P.10142, Illkirch CEDEX, F-67404, FRANCE

Martina Mirlacher (**3**: 369) Division of Molecular Pathology, Institue of Pathology, University of Basel, Schonbeinstrasse 40, Basel, CH-4031, SWITZERLAND

Suchareeta Mitra (**4**: 335) Department of Biochemistry, University of Tennessee Health Sciences Center, Memphis, TN 38163

Atsushi Miyawaki (**2**: 317) Laboratory for Cell Function and Dynamics, Advanced Technology Center, Brain Science Institute, Institute of Physical and Chemical Research (RIKEN), 2-1 Horosawa, Wako, Saitama, 351-0198, JAPAN

Dejana Mokranjac (**4**: 269) Adolf-Butenandt-Institut fur Physiologische Chemie, Lehrstuhl: Physiologische Chemie, Universitat Munchen, Butenandtstr. 5, Gebäude B, Munchen, D-81377, GERMANY

Peter L. Molloy (**4**: 325) CSIRO Molecular Science, PO Box 184, North Ryde, NSW, 1670, AUSTRALIA

Richard A. Moravec (**1**: 25) Promega Corporation, 2800 Woods Hollow Road, Madison, WI 53711-5399

José M. A. Moreira (**1**: 527) Institute of Cancer Biology and Danish Centre for Translational Breast Cancer Research, Danish Cancer Society, Strandboulevarden 49, Copenhagen O, DK-2100, DENMARK

May C. Morris (**4**: 13) Centre de Recherche en Biochimie Macromoléculaire (UPR 1086), Centre National de la Recherche Scientifique (CNRS), 1919 Route de Mende, Montpellier Cedex 5, F-34293, FRANCE

Robert A. Moxley (**4**: 335) Department of Biochemistry, University of Tennessee Health Sciences Center, Memphis, TN 38163

Anne Muesch (**2**: 189) Margaret M. Dyson Vision Research Institute, Department of Opthalmology, Weill Medical College of Cornell University, New York, NY 10021

Peggy Müller (**1**: 325) Zentrum für Angewandte Medizinische und Humanbiologische Forschung, Labor für Molekulare Hepatologie der Universitätsklinik und Polikinik für Innere Medizin I, Martin Luther University Halle-Wittenburg, Heinrich-Damerow-Street 1, Saale, Halle, D-06097, GERMANY

Steve Murray (**3**: 325) CRC Structural Cell Biology Group, Paterson Institute for Cancer Research, Christie Hospital NHS Trust, Wilmslow Road, Withington, Manchester, M20 4BX, UNITED KINGDOM

Connie Myers (**1**: 139) Life Sciences Division, Lawrence Berkeley National Laboratory, 1 Cyclotron Road, Bldg 83-101, Berkeley, CA 94720

Kazuyuki Nakamura (**4**: 197) Department of Biochemistry and Biomolecular Recognition, Yamaguchi University School of Medicine, 1-1-1 Minami-kogushi, Ube, Yamaguchi, 755-8505, JAPAN

Maithreyi Narasimha (**3**: 77) Wellcome Trust/Cancer Research UK Institute and Dept of Anatomyaraki, University of Cambridge, Tennis Court Road, Cambridge, CB2 1QR, UNITED KINGDOM

Dobrin Nedelkov (**4**: 279) Intrinsic Bioprobes, Inc., 625 S. Smith Road, Suite 22, Tempe, AZ 85281

Randall W. Nelson (**4**: 279) Intrinsic Bioprobes Inc., 625 S. Smith Road, Suite 22, Tempe, AZ 85281

Frank R. Neumann (**2**: 359) Department of Molecular Biology, University of Geneva, 30, Quai Ernest Ansermet, Geneva, CH-1211, SWITZERLAND

Walter Neupert (**4**: 269) Adolf-Butenandt-Institut fur Physiologische Chemie, Lehrstuhl: Physiologische Chemie, Universitat Munchen, Butenandtstr. 5, Gebäude B, Munchen, D-81377, GERMANY

Axl Alois Neurauter (**1**: 239) Immunosystem R & D, Dynal Biotech ASA, PO Box 114, Smestad, N-0309, NORWAY

Phillip Ng (**1**: 435) Dept of Molecular and Human Genetics, Baylor College of Medicine, One Baylor Plaza, Houston, TX 77030

Garth L. Nicolson (**1**: 359) The Institute for Molecular Medicine, 15162 Triton Lane, Huntington Beach, CA 92649-1041

Trine Nilsen (**4**: 275) Department of Biochemistry, Institute for Cancer Research, The Norwegian Radium Hospital, Montebello, Oslo, N-0310, NORWAY

Tommy Nilsson (**2**: 45) Göteborg University, Institute of Medical Biochemistry, PO Box, Göteborg, SE-403 50, SWEDEN

Lars Norderhaug (**1**: 239) Dynal Biotech ASA, PO Box 114, Smestad, N-0309, NORWAY

Robert O'Connor (**1**: 5, 13, 335) National Institute for Cellular Biotechnology, Dublin City University, Glasnevin, Dublin, 9, IRELAND

Lorraine O'Driscoll (**1**: 5, 335) National Institute for Cellular Biotechnology, Dublin City University, Glasnevin, Dublin, 9, IRELAND

Martin Offterdinger (**3**: 153) Cell Biology and Cell Biophysics Program, European Molecular Biology Laboratory, Meyerhofstrasse 1, Heidelberg, D-69117, GERMANY

Philip Oh (**2**: 11) Cellular and Molecular Biology Program, Sidney Kimmel Cancer Center, 10835 Altman Row, San Diego, CA 92121

Takanori Ohnishi (**1**: 367) Department of Neurosurgery, Ehime University School of Medicine, Shitsukawa, Toon-shi, Ehime, 791-0295, JAPAN

Sjur Olsnes (**4**: 19, 275) Department of Biochemistry, The Norwegian Radium Hospital, Montebello, Oslo, 0310, NORWAY

Shao-En Ong (**4**: 427) Protein Interaction Laboratory, University of Southern Denmark—Odense, Campusvej 55, Odense M, DK-5230, DENMARK

Akifumi Ootani (**1**: 411) Department of Internal Medicine, Faculty of Medicine, Saga University, Nebeshima 5-1-1, Saga, 849-8501, JAPAN

Valerio Orlando (**4**: 317) Dulbecco Telethon Institute, Institute of Genetics & Biophysics CNR, Via Pietro Castellino 111, Naples, I-80131, ITALY

Torben Faeck Ørntoft (**4**: 83) Clinical Biochemical Department, Molecular Diagnostic Laboratory, Aarhus University Hospital, Skejby, Brendstrupgaardvej 100, Aarhus N, DK-8200, DENMARK

Mary Osborn (**1**: 549, 563) Department of Biochemistry and Cell Biology, Max Planck Institute of Biophysical Chemistry, Am Faßberg 11, Gottingen, D-37077, GERMANY

Lawrence E. Ostrowski (**2**: 99) Cystic Fibrosis/Pulmonary Research and Treatment Centre, University of North Carolina at Chapel Hill, Thurston-Bowles Building, Chapel Hill, NC 27599-7248

Hendrik Otto (**2**: 253) Institut für Biochemie und Molekularbiologie, Universität Freiburg, Hermann-Herder-Str. 7, Freiburg, D-79104, GERMANY

Kerstin Otto (**1**: 103) Department of Dermatology, Julius-Maximillians University, Josef-Schneider-Str. 2, Würzburg, 97080, GERMANY

Michel M. Ouellette (**1**: 215) Department of Biochemistry and Molecular Biology, Eppley Institute for Research in Cancer, The University of Nebraska Medical Center, 986805 Nebraska Medical Center, Omaha, NE 68198-6805

Jacques Paiement (**2**: 41) Département de pathologie et biologie cellulaire, Université de Montréal, Case postale 6128, Succursale "Centre-Ville", Montreal, QC, H3C 3J7, CANADA

Patricia M. Palagi (**4**: 207) Swiss Institute of Bioinformatics, CMU, 1 Michel Servet, Geneva 4, CH-1211, SWITZERLAND

Kinam Park (**4**: 29) Department of Pharmaceutics and Biomedical Engineering, Purdue University School of Pharmacy, 575 Stadium Mall Drive, Room G22, West Lafayette, IN 47907-2091

Helen Parkinson (**4**: 95) EMBL Outstation—Hinxton, European Bioinformatics Institute, Wellcome Trust Genome Campus, Hinxton, Cambridge, CB10 1SD, UNITED KINGDOM

Richard M. Parton (**3**: 187) Wellcome Trust Centre for Cell Biology, Institute of Cell and Molecular Biology The University of Edinburgh, Michael Swann Building, The King's Buildings, Mayfield Road, Edinburgh, EH9 3JR, SCOTLAND

Bryce M. Paschal (**2**: 267) Center for Cell Signaling, University of Virginia, 1400 Jefferson Park Avenue, West Complex Room 7021, Charlottesville, VA 22908-0577

Wayne F. Patton (**4**: 225) Perkin-Elmer LAS, Building 100-1, 549 Albany Street, Boston, MA 02118

Staffan Paulie (**1**: 533) Mabtech AB, Box 1233, Nacha Strand, SE-131 28, SWEDEN

Rainer Pepperkok (**3**: 121) Cell Biology and Cell Biophysics Programme, European Molecular Biology Laboratory (EMBL), Meyerhofstrasse 1, Heidelberg, D-69117, GERMANY

Xomalin G. Peralta (**3**: 87) Department of Physics, Duke University, 107 Physics Bldg, Durham, NC 27708-1000

Martha Perez-Magallanes (**1**: 151) National Medical Center and Beckman Research Institute, Division of Neurosciences, City of Hope, 1500 E. Duarte Rd, Duarte, CA 91010

Stephen P. Perfetto (**1**: 257) Vaccine Research Center, National Institutes of Health, 40 Convent Dr., Room 5509, Bethesda, MD 20892-3015

Hedvig Perlmann (**1**: 533) Department of Immunology, Stockholm University, Biology Building F5, Top floor, Svante Arrhenius väg 16, Stockholm, SE-10691, SWEDEN

Peter Perlmann (**1**: 533) Department of Immunology, Stockholm University, Biology Building F5, Top floor, Svante Arrhenius väg 16, Stockholm, SE-10691, SWEDEN

Timothy W. Petersen (**1**: 269) Institute for Systems Biology, 1441 N. 34th St, Seattle, WA 98103

Patti Lynn Peterson (**2**: 259) Department of Neurology, Wayne State University School of Medicine, 5L26 Detroit Receiving Hospital, Detroit Medical Center, Detroit, MI 48201

Nisha Philip (**4**: 265) Department of Pharmacology and Cancer Biology, Duke University, Research Dr. LSRC Rm C115, Box 3813, Durham, NC 27710

Thomas Pieler (**1**: 191) Institute for Biochemistry and Molecular Cell Biology, University of Goettingen, Humboldtallee 23, Göttingen, D-37073, GERMANY

Daniel Pinkel (**3**: 445) Department of Laboratory Medicine, University of California San Francisco, Box 0808, San Francisco, CA 94143-0808

Javier Pizarro Cerdá (**2**: 407) Unite des Interactions Bacteries-Cellules/Unité INSERM 604, Institut Pasteur, 28, rue du Docteur Roux, Paris Cedex 15, F-75724, FRANCE

Andreas Plückthun (**1**: 497) Department of Biochemistry, University of Zürich, Winterthurerstrasse 190, Zürich, CH-8057, SWITZERLAND

Helen Plutner (**2**: 209) Department of Cell and Molecular Biology, The Scripps Research Institute, 10550 North Torrey Pines Road, La Jolla, CA 92037

Piotr Pozarowski (**1**: 279) Brander Cancer Research Institute, New York Medical College, Valhalla, NY 10595

Johanna Prast (**1**: 557) Institute of Molecular Biology, Austrian Academy of Sciences, Billrothstrasse 11, Salzburg, A-5020, AUSTRIA

Brendan D. Price (**3**: 477) Department of Radiation Oncology, Dana Farber-Brigham and Women's Cancer Center, 75 Francis Street, Level L2, Boston, MA 02215

Elena Prigmore (**3**: 403) Sanger Institute, The Wellcome Trust, The Wellcome Trust Genome Campus, Hinxton, Cambridge, CB10 1SA, UNITED KINGDOM

Gottfried Proess (**1**: 467) Eurogentec S.A., Liege Science Park, 4102 Seraing, B-, BELGIUM

David M. Prowse (**1**: 133) Centre for Cutaneous Research, Barts and The London Queen Mary's School of Medicine and Dentistry, Institute of Cell and Molecular Science, 2 Newark Street, Whitechapel London, WC2A 3PX, UNITED KINGDOM

Manuela Pruess (**4**: 469) EMBL outstation—Hinxton, European Bioinformatic Institute, Welcome Trust Genome Campus, Hinxton, Cambridge, CB10 1SD, UNITED KINGDOM

Eric Quéméneur (**4**: 235) Life Sciences Division, CEA Valrhô, BP 17171 Bagnols-sur-Cèze, F-30207, FRANCE

Leda Helen Raptis (**2**: 329, 341) Department of Microbiology and Immunology, Queen's University, Room 716 Botterell Hall, Kingston, Ontario, K7L3N6, CANADA

Anne-Marie Rasmussen (**1**: 239) Dynal Biotech ASA, PO Box 114, Smestad, N-0309, NORWAY

Andreas S. Reichert (**4**: 269) Department of Physiological Chemistry, University of Munich, Butenandtstr. 5, München, D-81377, GERMANY

Siegfreid Reipert (**3**: 325) Ordinariat II, Institute of Biochemistry and Molecular Biology, Vienna Biocenter, Dr. Bohr-Gasse 9, Vienna, A-1030, AUSTRIA

Guenter P. Resch (**3**: 267) Institute of Molecular Biology, Dr. Bohrgasse 3-5, Vienna, A-1030, AUSTRIA

Katheryn A. Resing (**4**: 443) Dept of Chemistry and Biochemistry, University of Colorado, 215 UCB, Boulder, CO 80309-0215

Donald L Riddle (**1**: 157) Division of Biological Sciences, University of Missouri, 311 Tucker Hall, Columbia, MO 65211

Mara Riminucci (**1**: 79) Department of Experimental Medicine, Universita' dell' Aquilla, Via Vetoio, Coppito II, L'Aquila, I-67100, ITALY

Terry L. Riss (**1**: 25) Promega Corporation, 2800 Woods Hollow Road, Madison, WI 53711-5399

Pamela Gehron Robey (**1**: 79) Craniofacial and Skeletal Disease Branch, NIDCR, NIH, Department of Health and Human Services 30 Convent Dr, MSC 4320, Bethesda, MD 20892-4320

Linda J. Robinson (**2**: 201)

Philippe Rocca-Serra (**4**: 95) EMBL Outstation—Hinxton, European Bioinformatics Institute, Wellcome Trust Genome Campus, Hinxton, Cambridge, CB10 1SD, UNITED KINGDOM

Alice Rodriguez (**3**: 87) Department of Biology, Duke University, Durham, NC 27708-1000

Enrique Rodriguez-Boulan (**2**: 189, 241) Margaret M Dyson Vision Research Institute, Department of Opthalmology, Weill Medical College of Cornell University, New York, NY 10021

Mario Roederer (**1**: 257) ImmunoTechnology Section and Flow Cytometry Core, Vaccine Research Center, National Institute for Allergy and Infectious Diseases, National Institutes of Health, 40 Convent Dr., Room 5509, Bethesda, MD 20892-3015

Peter Roepstorff (**4**: 371) Department of Biochemistry and Molecular Biology, University of Southern Denmark, Campusvej 55, Odense M, DK-5230, DENMARK

Manfred Rohde (**2**: 399) Department of Microbial Pathogenicity, Gesellschaft fur Biotechnoogische Forschung, Mascheroder Weg 1, Braunschweig, D-38124, GERMANY

Norbert Roos (**3**: 299) Electron Microscopical Unit for Biological Sciences, University of Oslo, Blindern, Oslo, 0316, NORWAY

Sabine Rospert (**2**: 253) Institut für Biochemie und Molekularbiologie, Universität Freiburg, Hermann-Herder-Str. 7, Freiburg, D-79104, GERMANY

Klemens Rottner (**3**: 111) Cytoskeleton Dynamics Group, German Research Centre for Biotechnology (GBF), Mascheroder Weg 1, Braunschweig, D-38124, GERMANY

Line Roy (**2**: 41) Department of Anatomy and Cell Biology, Faculty of Medicine, McGill University, STRATHCONA Anatomy & Dentistry Building, Montreal, QC, H3A 2B2, CANADA

Sandra Rutherford (**3**: 325) CRC Structural Cell Biology Group, Paterson Institute for Cancer Research, Christie Hospital NHS Trust, Wilmslow Road, Withington, Manchester, M20 4BX, UNITED KINGDOM

Beth Rycroft (**1**: 395) Department of Pharmacology, University College London, Gower Street, London, WC1E GBT, UNITED KINGDOM

Patrick Salmon (**1**: 425) Department of Genetics and Microbiology, Faculty of Medicine, University of Geneva, CMU-1 Rue Michel-Servet, Geneva 4, CH-1211, SWITZERLAND

Paul M. Salvaterra (**1**: 151) National Medical Center and Beckman Research Institute, Division of Neurosciences, City of Hope, 1500 E. Duarte Rd, Duarte, CA 91010-3000

R. Jude Samulski (**1**: 457) Gene Therapy Centre, Department of Pharmacology, University of North Carolina at Chapel Hill, 7119 Thurston Bowles, Chapel Hill, NC 27599-7352

Susanna-Assunta Sansone (**4**: 95) EMBL Outstation—Hinxton, European Bioinformatics Institute, Wellcome Trust Genome Campus, Hinxton, Cambridge, CB10 1SD, UNITED KINGDOM

Ugis Sarkan (**4**: 95) EMBL Outstation—Hinxton, European Bioinformatics Institute, Wellcome Trust Genome Campus, Hinxton, Cambridge, CB10 1SD, UNITED KINGDOM

Moritoshi Sato (**2**: 325) Department of Chemistry, School of Science, University of Tokyo, 7-3-1 Hongo, Bunkyo-Ku, Tokyo, 113-0033, JAPAN

Guido Sauter (**3**: 369) Institute of Pathology, University of Basel, Schonbeinstrasse 40, Basel, CH-4003, SWITZERLAND

Carolyn L. Sawyer (**2**: 299) Department of Pharmacology, University of Vermont, Health Science Research Facility 330, Burlington, VT 05405-0068

Guray Saydam (**1**: 315) Department of Medicine, Section of Hematology, Ege University Hospital, Bornova Izmir, 35100, TURKEY

Silvia Scaglione (**3**: 201) BIOLab, Department of Informatic, Systemistic and Telematic, University of Genoa, Viale Causa 13, Genoa, I-16145, ITALY

Lothar Schermelleh (**1**: 291, 301) Department of Biology II, Biocenter of the Ludwig-Maximilians University of Munich (LMU), Großhadernerstr. 2, Planegg-Martinsried, 82152, GERMANY

Gudrun Schiedner (**1**: 445) CEVEC Pharmaceuticals GmbH, Gottfried-Hagen-Straße 62, Köln, D-51105, GERMANY

David Schieltz (**4**: 383) Department of Cell Biology, Torrey Mesa Research Institute, 3115 Merryfield Row, San Diego, CA 92121

Jan E. Schnitzer (**2**: 11) Sidney Kimmel Cancer Center, 10835 Altman Row, San Diego, CA 92121

Morten Schou (**1**: 353) Bartholin Institute, Bartholinsgade 2, Copenhagen K, DK-1356, DENMARK

Sebastian Schuck (**2**: 5) Max Planck Institute of Molecular Cell Biology and Genetics, Pfotenhauerstrasse 108, Dresden, D-01307, GERMANY

Herwig Schüler (**2**: 165) Department of Cell Biology, The Wnner-Gren Institute, Stockholm University, Stockholm, S-10691, SWEDEN

Michael Schuler (**3**: 501) Institut de Génétique et de Biologie Moléculaire et Cellulaire (IGBMC), 1 rue Laurent Fries, B.P.10142, Illkirch CEDEX, F-67404, FRANCE

Ulrich S. Schwarz (**2**: 419) Theory Division, Max Planck Institute of Colloids and Interfaces, Potsdam, 14476, GERMANY

Antonio S. Sechi (**2**: 393) Institute for Biomedical Technology-Cell Biology, Universitaetsklinikum Aachen, RWTH, Pauwelsstrasse 30, Aachen, D-52057, GERMANY

Richard L. Segraves (**3**: 445) Comprehensive Cancer Center, University of California San Francisco, Box 0808, 2400 Sutter N-426, San Francisco, CA 94143-0808

James R. Sellers (**2**: 387) Cellular and Motility Section, Laboratory of Molecular Cardiology, National Heart, Lung and Blood Institute (NHLBI), National Institutes of Health, 10 Center Drive, MSC 1762, Bethesda, MD 20892-1762

Nicholas J. Severs (**3**: 249) Cardiac Medicine, National Heart and Lung Institute, Imperial College, Faculty of Medicine, Royal Brompton Hospital, Dovehouse Street, London, SW3 6LY, UNITED KINGDOM

Jagesh Shah (**3**: 351) Laboratory of Cell Biology, Ludwig Institute for Cancer Research, University of California, 9500 Gilman Drive, MC 0660, La Jolla, CA 92093-0660

Norman E. Sharpless (**1**: 223) The Lineberger Comprehensive Cancer Center, The University of North Carolina School of Medicine, Lineberger Cancer Center, CB# 7295, Chapel Hill, NC 27599-7295

Andrej Shevchenko (**4**: 399) Max Planck Institute for Molecular Cell Biology and Genetics, Pfotenhauerstrasse 108, Dresden, D-01307, GERMANY

David M. Shotton (**3**: 207, 249, 257) Department of Zoology, University of Oxford, South Parks Road, Oxford, OX1 3PS, UNITED KINGDOM

David I. Shreiber (**1**: 379) Department of Biomedical Engineering, Rutgers, the State University of New Jersey, 617 Bowser Road, Piscataway, NJ 08854-8014

Snaevar Sigurdsson (**3**: 455) Department of Medical Sciences, Uppsala University, Akademiska sjukhuset, Uppsala, SE-751 85, SWEDEN

Stephen Simkins (**1**: 483) TriPath Oncology, 4025 Stirrup Creek Drive, Suite 400, Durham, NC 27703

Ronald Simon (**3**: 369) Division of Molecular Pathology, Institute of Pathology, University of Basel, Schonbeinstrasse 40, Basel, CH-4031, SWITZERLAND

Kai Simons (**1**: 127, **2**: 5, 181) Max Planck Institute of Molecular Cell Biology and Genetics, Pfotenhauerstrasse 108, Dresden, D-01307, GERMANY

Jeremy C. Simpson (**3**: 121) Cell Biology and Cell Biophysics Programme, European Molecular Biology Laboratory (EMBL), Meyerhofstrasse 1, Heidelberg, D-69117, GERMANY

Robert H. Singer (**4**: 121) Department of Anatomy and Structural Biology, Golding # 601, Albert Einstein College of Medicine of Yeshiva University, 1300 Morris Park Avenue, Bronx, NY 10461

Mathilda Sjöberg (**1**: 419) Department of Biosciences at Novum, Karolinska Instituet, Huddinge, SE-141-57, SWEDEN

Camilla Skiple Skjerpen (**4**: 275) Department of Biochemistry, Institute for Cancer Research, The Norwegian Radium Hospital, Montebello, Oslo, N-0310, NORWAY

John Sleep (**3**: 37) Randall Division, Guy's Campus, New Hunt's House, London, SE1 1UL, UNITED KINGDOM

J. Victor Small (**1**: 557) Department of Cell Biology, Institute of Molecular Biology, Austrian Academy of Sciences, Billrothstrasse 11, Salzburg, A-5020, AUSTRIA

Joél Smet (**4**: 259) Department of Pediatrics and Medical Genetics, University Hospital, De Pintelaan 185, Ghent, B-9000, BELGIUM

Kim Smith (**3**: 381) Director of Cytogenetic Services, Oxford Radcliffe NHS Trust, Headington, Oxford, OX3 9DU, UNITED KINGDOM

Paul J. Smith (**1**: 305) Dept of Pathology, University of Wales College of Medicine, Heath Park, Cardiff, CF14 4XN, UNITED KINGDOM

Antoine M. Snijders (**3**: 445) Comprehensive Cancer Center, Cancer Research Institute, The University of California, San Francisco, Box 0808, 2340 Sutter Street N-, San Fransisco, CA 94143-0808

Michael Snyder (**3**: 179) Department of Molecular, Cellular and Developmental Biology, Yale University, P. O. Box 208103, Kline Biology Tower, 219 Prospect St., New Haven, CT 06520-8103

Irina Solovei (**1**: 291) Department of Biology II, Anthropology & Human Genetics, Ludwig-Maximilians University of Munich, Munich, GERMANY

Marion Sölter (**1**: 191) Institute for Biochemistry and Molecular Cell Biology, University of Goettingen, Justus-von-Liebig-Weg 11, Göttingen, D-37077, GERMANY

Lukas Sommer (**1**: 69) Institute of Cell Biology, Department of Biology, Swiss Federal Institute of Technology, ETH—Hönggerberg, Zurich, CH-8093, SWITZERLAND

Simon Sparks (**3**: 207) Department of Zoology, University of Oxford, South Parks Road, Oxford, OX1 3PS, UNITED KINGDOM

Kenneth G. Standing (**4**: 457) Department of Physics and Astronomy, University of Manitoba, 510 Allen Bldg, Winnipeg, MB, R3T 2N2, CANADA

Walter Steffen (**3**: 37, 307) Randall Division, Guy's Campus, New Hunt's House, London, SE1 1UL, UNITED KINGDOM

Theresia E. B. Stradal (**3**: 111) Department of Cell Biology, German Research Centre for Biotechnology (GBF), Mascheroder Weg 1, Braunschweig, D-38124, GERMANY

Per Thor Straten (**1**: 97) Tumor Immunology Group, Institute of Cancer Biology, Danish Cancer Society, Strandboulevarden 49, Copenhagen, DK-2100, DENMARK

Hajime Sugihara (**1**: 411) Department of Pathology & Biodefence, Faculty of Medicine, Saga University, Nebeshima 5-1-1, Saga, 849-8501, JAPAN

Chung-Ho Sun (**3**: 351) Beckman Laser Institute, University of California, Irvine, 1002 Health Sciences Road E, Irvine, CA 92697-1475

Mark Sutton-Smith (**4**: 415) Department of Biological Sciences, Imperial College of Science, Technology and Medicine, Biochemistry Building, London, SW7 2AY, UNITED KINGDOM

Tatyana M. Svitkina (**3**: 277) Department of Cell and Molecular Biology, Northwestern University Medical School, Chicago, IL 60611

Ann-Christine Syvänen (**3**: 455) Department of Medical Sciences, Uppsala University, Forskningsavd 2, ing 70, Uppsala, SE-751 85, SWEDEN

Masako Tada (**1**: 199) ReproCELL Incorporation, 1-1-1 Uchisaiwai-cho, Chiyoda-ku, Tokyo, 100-0011, JAPAN

Takashi Tada (**1**: 199) Stem Cell Engineering, Stem Cell Research Center, Institute for Frontier Medical Sciences, Kyoto University, 53 Kawahara-cho Shogoin, Sakyo-ku, Kyoto, 606-8507, JAPAN

Angela Taddei (**2**: 359) Department of Molecular Biology, University of Geneva, 30, Quai Ernest Ansermet, Geneva 4, CH-1211, SWITZERLAND

Tomohiko Taguchi (**2**: 33) Department of Cell Biology, Yale University School of Medicine, 333 Cedar Street, PO Box 208002, New Haven, CT 06520-8002

Kazusuke Takeo (**4**: 197) Department of Biochemistry and Biomolecular Recognition, Yamaguchi University School of Medicine, 1-1-1, Minami-kogushi, Ube, Yamaguchi, 755-8505, JAPAN

Nobuyuki Tanahashi (**2**: 91) Laboratory of Frontier Science, Core Technology and Research Center, The Tokyo Metropolitan Institute of Medical Sciences, 3-18-22 Honkomagome, Bunkyo-ku, Tokyo, 113-8613, JAPAN

Keiji Tanaka (**2**: 91) Laboratory of Frontier Science, Core Technology and Research Center, The Tokyo Metropolitan Institute of Medical Sciences, 3-18-22 Honkomagome, Bunkyo-ku, Tokyo, 133-8613, JAPAN

Chi Tang (**2**: 121) Dept of Biomolecular Sciences, UMIST, PO Box 88, Manchester, M60 1QD, UNITED KINGDOM

Kirill V. Tarasov (**4**: 103) Molecular Cardiology Unit, National Institute on Aging, NIH, 5600 Nathan Shock Drive, Baltimore, MD 21224

J. David Taylor (**3**: 471) Department of Genomic Sciences, Glaxo Wellcome Research and Development, 5 Moore Drive, Research Triangle Park, NC 27709-3398

Nancy Smyth Templeton (**4**: 25) Department of Molecular and Cellular Biology & the Center for Cell and Gene Therapy, Baylor College of Medicine, One Baylor Plaza, Alkek Bldg., Room N1010, Houston, TX 77030

Kenneth K. Teng (**1**: 171) Department of Medicine, Wiell Medical of Cornell University, 1300 York Ave., Rm-A663, New York, NY 10021

Patrick Terheyden (**1**: 103) Department of Dermatology, Julius-Maximillians University, Josef-Schneider-Str. 2, Würzburg, D-97080, GERMANY

Scott M. Thompson (**1**: 407) Department of Physiology, University of Maryland School of Medicine, 655 W. Baltimore St., Baltimore, MD 21201,

John F. Timms (**4**: 189) Department of Biochemistry and Molecular Biology, Ludwig Institute of Cancer Research, Cruciform Building 1.1.09, Gower Street, London, WC1E 6BT, UNITED KINGDOM

Shuji Toda (**1**: 411) Department of Pathology & Biodefence, Faculty of Medicine, Saga University, Nebeshima 5-1-1, Saga, 849-8501, JAPAN

Yoichiro Tokutake (**3**: 87) Department of Physics, Duke University, 107 Physics Bldg, Durham, NC 27708-1000

Evi Tomai (**2**: 329) Department of Microbiology and Immunology, Queen's University, Room 716 Botterell Hall, Kingston, Ontario, K7L3N6, CANADA

Kenneth B. Tomer (**1**: 511) Mass Spectrometry, Laboratory of Structural Biology, National Institute of Environmental Health Sciences NIEH/NIH, 111 Alexander Drive, PO Box 12233, Research Triangle Park, NC 27709

Derek Toomre (**3**: 19) Department of Cell Biology, Yale University School of Medicine, SHM-C227/229, PO Box 208002, 333 Cedar Street, New Haven, CT 06520-8002

Sharon A. Tooze (**2**: 79) Secretory Pathways Laboratory, Cancer Research UK London Research Institute, 44 Lincoln's Inn Fields, London, WC2A 3PX, UNITED KINGDOM

David Tosh (**1**: 177) Centre for Regenerative Medicine, Department of Biology and Biochemistry, University of Bath, Claverton Down, Bath, BA2 7AY, UNITED KINGDOM

Yusuke Toyama (**3**: 87) Department of Physics, Duke University, 107 Physics Bldg, Box 90305, Durham, NC 27708-0305

Robert T. Tranquillo (**1**: 379) Department of Biomedical Engineering and Department of Chemical Engineering and Materials Science, University of Minnesota, Biomedical Engineering, 7-112 BSBE. 312 Church St SE, Minneapolis, MN 55455

Signe Trentemølle (**4**: 165) Institute of Cancer Biology and Danish Centre for Translational Breast Cancer Research, Danish Cancer Society,

Strandboulevarden 49, Copenhagen, DK-2100, DENMARK

Didier Trono (**1**: 425) Department of Genetics and Microbiology, Faculty of Medicine, University of Geneva, CMU-1 Rue Michel-Servet, Geneva 4, CH-1211, SWITZERLAND

Kevin Truong (**2**: 307) Division of Molecular and Structural Biology, Ontario Cancer Institute, Department of Medical Biophysics, University of Toronto, 610 University Avenue, 7-707A, Toronto, Ontario, M5G 2M9, CANADA

Jessica K. Tyler (**2**: 287) Department of Biochemistry and Molecular Genetics, University of Colorado Health Sciences Center at Fitzsimons, PO Box 6511, Aurora, CO 80045

Aylin S. Ulku (**1**: 345) Department of Pharmacology, University of North Carolina at Chapel Hill, Lineberger Comprehensive Cancer Center, Chapel Hill, NC 27599-7295

Yoshio Umezawa (**2**: 325) Department of Chemistry, The School of Science, University of Tokyo, 7-3-1 Hongo, Bunkyo-ku, Tokyo, 113-0033, JAPAN

Ronald Vale (**3**: 129) Department of Cellular and Molecular Pharmacology, The Howard Hughes Medical Institute, The University of California, San Francisco, N316, Genentech Hall, 1600 16th Street, San Francisco, CA 94107

Jozef Van Beeumen (**4**: 259) Department of Biochemistry, Physiology and Microbiology, University of Ghent, K.L. Ledeganckstraat 35, Ghent, B-9000, BELGIUM

Rudy N. A. van Coster (**4**: 259) Department of Pediatrics and Medical Genetics, University Hospital, University of Ghent, De Pintelaan 185, Ghent, B-9000, BELGIUM

Ger van den Engh (**1**: 269) Institute for Systems Biology, 1441 North 34th Street, Seattle, WA 98103-8904

Peter van der Geer (**4**: 139) Department of Chemistry and Biochemistry, University of California, San Diego, 9500 Gilman Dr., La Jolla, CA 92093-0601

Joël Vandekerckhovr (**4**: 379, 457) Department of Medical Protein Research, Flanders Interuniversity Institute for Biotechnology, KL Ledeganckstraat 35, Gent, B-9000, BELGIUM

Charles R. Vanderburg (**4**: 5) Department of Neurology, Massachusetts General Hospital, 114 Sixteenth Street, Charlestown, MA 02129

John Venable (**4**: 383) Department of Cell Biology, Scripps Research Institute, 10550 North Torrey Pines Road, La Jolla, CA 92037

Isabelle Vernos (**2**: 379) Cell Biology and Cell Biophysics Programme, European Molecular Biology Laboratory, Meyerhofstrasse 1, Heidelberg, D-69117, GERMANY

Peter J. Verveer (**3**: 153) Cell Biology and Cell Biophysics Program, European Molecular Biology Laboratory, Meyerhofstrasse 1, Heidelberg, D-69117, GERMANY

Marc Vidal (**4**: 295) Cancer Biology Department, Dana-Farber Cancer Institute, 44 Binney Street, Boston, MA 02115

Emmanuel Vignal (**2**: 427) Department Genie, Austrian Academy of Sciences, Billrothstrasse 11, Salzbourg–Autriche, A-520, 5020, AUSTRIA

Sylvie Villard (**1**: 519) Centre de Pharmacologie et Biotechnologie pour la Santé, CNRS—UMR 5094, Faculté de Pharmacie, Avenue Charles Flahault, Montpellier Cedex 5, F-34093, FRANCE

Hikka Virta (**1**: 127) Department of Cell Biology, European Molecular Biology Laboratory, Cell Biology Programme, Heidelberg, D-69012, GERMANY

Alfred Völkl (**2**: 63) Department of Anatomy and Cell Biology II, University of Heidelberg, Im Neuenheimer Feld 307, Heidelberg, D-69120, GERMANY

Sonja Voordijk (**4**: 207) Geneva Bioinformatics SA, Avenue de Champel 25, Geneva, CH-1211, SWITZERLAND

Adina Vultur (**2**: 329, 341) Department of Microbiology and Immunology, Queen's University, Room 716 Botterell Hall, Kingston, Ontario, K7L3N6, CANADA

Teruhiko Wakayama (**1**: 87) Center for Developmental Biology, RIKEN, 2-2-3 Minatojima-minamimachi, Kobe, 650-0047, JAPAN

Daniel Walther (**4**: 207) Swiss Institute of Bioinformatics (SIB), CMU, rue Michel-Servet 1, Genève 4, 1211, SWITZERLAND

Gang Wang (**3**: 477) Department of Radiation Oncology, Dana Farber-Brigham and Women's Cancer Center, 75 Francis Street, Level L2, Boston, MA 02215

Nancy Wang (**3**: 345) Department of Pathology and Laboratory Medicine, University of Rochester School of Medicine, 601 Elmwood Ave., Rm 1-6337, Rochester, NY 14642

Xiaodong Wang (**2**: 209) Department of Cell and Molecular Biology, The Scripps Research Institute, 10550 North Torrey Pines Road, La Jolla, CA 92037

Yanzhuang Wang (**2**: 33) Department of Cell Biology, Yale University School of Medicine, 333 Cedar Street, PO BOX 208002, New Haven, CT 06520-8002

Yu-Li Wang (**3**: 107) Department of Physiology, University of Massachusetts Medical School, 377 Plantation St., Rm 327, Worcester, MA 01605

Graham Warren (**2**: 33) Department of Cell Biology, Yale University School of Medicine, 333 Cedar Street, PO Box 208002, New Haven, CT 06520-8002

Clare M. Waterman-Storer (**3**: 137) 10550 North Torrey Pines Road, CB 163, La Jolla, CA 92037

Jennifer C. Waters (**3**: 49) Department of Cell Biology, Department of Systems Biology, Harvard Medical School, 240 Longwood Ave, Boston, MA 02115

Fiona M. Watt (**1**: 133) Keratinocyte Laboratory, London Research Institute, 44 Lincoln's Inn Fields, London, WC2A 3PX, UNITED KINGDOM

Gerhard Weber (**4**: 157) Protein Analytics, Max Planck Institute for Biochemistry, Klopferspitz 18, Martinsried, D-82152, GERMANY

Peter J. A. Weber (**4**: 157) Proteomics Division, Tecan Munich GmbH, Feldkirchnerstr. 12a, Kirchheim, D-, 85551, GERMANY

Paul Webster (**3**: 299) Electron Microscopy Laboratory, House Ear Institute, 2100 West Third Street, Los Angeles, CA 90057

Jürgen Wehland (**2**: 399) Department of Cell Biology, Gesellschaft fur Biotechnoogische Forschung, Mascheroder Weg 1, Braunschweig, D-38124, GERMANY

Dieter G. Weiss (**3**: 57) Institute of Cell Biology and Biosystems Technology, Department of Biological Sciences, Universitat Rostock, Albert-Einstein-Str. 3, Rostock, D-18051, GERMANY

Walter Weiss (**4**: 175) Fachgebiet Proteomik, Technische Universität Muenchen, Am Forum 2, Freising Weihenstephan, D-85350, GERMANY

Adrienne R. Wells (**3**: 87) Department of Biology, Duke University, Durham, NC 27708-1000

Jørgen Wesche (**4**: 19) Department of Biochemistry, The Norwegian Radium Hospital, Montebello, Oslo, 0310, NORWAY

Pamela Whittaker (**3**: 463) Genotyping / Chr 20, The Wellcome Trust Sanger Institute, The Wellcome Trust Genome Campus, Hinxton, Cambridge, CB10 1SA, UNITED KINGDOM

John Wiemann (**3**: 87) Department of Biology, Duke University, B330g Levine Sci Bldg, Box 91000, Durham, NC 27708-1000

Sebastian Wiesner (**2**: 173) Dynamique du Cytosquelette, Laboratoire d'Enzymologie et Biochimie Structurales, UPR A 9063 CNRS, Building 34, Bat. 34, avenue de la Terrasse, Gif-sur-Yvette, F-91198, FRANCE

Ilona Wolff (**1**: 325) Prodekanat Forschung, Medizinnishce Fakultät, Martin Luther University Halle-Wittenburg, Magdeburger Str 8, Saale, Halle, D-06097, GERMANY

Ye Xiong (**2**: 259) The Department of Biochemistry and Molecular Biology, Wayne State University School of Medicine, 4374 Scott Hall, 540 E. Canfield, Detroit, MI 48201

David P. Yarnall (**3**: 471) Department of Metabolic Diseases, Glaxo Wellcome Inc, 5 Moore Drive, Research Triangle Park, NC 27709-3398

Hideki Yashirodas (**2**: 91) Laboratory of Frontier Science, Core Technology and Research Center, The Tokyo Metropolitan Institute of Medical Sciences, 3-18-22 Honkomagome, Bunkyo-ku, Tokyo, 133-8613, JAPAN

John R. Yates III (**4**: 383, 391) Department of Cell Biology, Scripps Research Institute, 10550 North Torrey Pines Road, La Jolla, CA 92037

Charles Yeaman (**2**: 189) Department of Cell and Developmental Biology, Weill Medical College of Cornell University, New York, NY 10021

Robin Young (**2**: 41) Département de pathologie et biologie cellulaire, Université de Montréal, Case postale 6128, Succursale "Centre-Ville", Montreal, QC, H3C 3J7, CANADA

Christian Zahnd (**1**: 497) Department of Biochemistry, Univerisity of Zürich, Winterthurerstr. 190, Zürich, CH-8057, SWITZERLAND

Zhuo-shen Zhao (**4**: 285) Glaxo-IMCB Group, Institute of Molecular and Cell Biology, Singapore, 117609, SINGAPORE

Huilin Zhou (**4**: 437) Department of Cellular and Molecular Medicine, Ludwig Institute for Cancer Research, University of California, San Diego, 9500 Gilman Drive, CMM-East, Rm 3050, La Jolla, CA 92093-0660

Timo Zimmermann (**3**: 69) Cell Biology and Cell Biophysics Programme, EMBL, Meyerhofstrasse 1, Heidelberg, D-69117, GERMANY

Chiara Zurzolo (**2**: 241) Department of Cell Biology and Infection, Pasteur Institute, 25,28 rue du Docteur Roux, Paris, 75015, FRANCE

Preface

Scientific progress often takes place when new technologies are developed, or when old procedures are improved. Today, more than ever, we are in need of complementary technology platforms to tackle complex biological problems, as we are rapidly moving from the analysis of single molecules to the study of multifaceted biological problems. The third edition of *Cell Biology: A Laboratory Handbook* brings together 236 articles covering novel techniques and procedures in cell and molecular biology, proteomics, genomics, and functional genomics. It contains 165 new articles, many of which were commissioned in response to the extraordinary feedback we received from the scientific community at large.

As in the case of the second edition, the *Handbook* has been divided in four volumes. The first volume covers tissue culture and associated techniques, viruses, antibodies, and immunohistochemistry. Volume 2 covers organelles and cellular structures as well as assays in cell biology. Volume 3 includes imaging techniques, electron microscopy, scanning probe and scanning electron microscopy, microdissection, tissue arrays, cytogenetics and in situ hybridization, genomics, transgenic, knockouts, and knockdown methods. The last volume includes transfer of macromolecules, expression systems, and gene expression profiling in addition to various proteomic technologies. Appendices include representative cultured cell lines and their characteristics, Internet resources in cell biology, and bioinformatic resources for in silico proteome analysis. The Handbook provides in a single source most of the classical and emerging technologies that are essential for research in the life sciences. Short of having an expert at your side, the protocols enable researchers at all stages of their career to embark on the study of biological problems using a variety of technologies and model systems. Techniques are presented in a friendly, step-by-step fashion, and gives useful tips as to potential pitfalls of the methodology.

I would like to extend my gratitude to the Associate Editors for their hard work, support, and vision in selecting new techniques. I would also like to thank the staff at Elsevier for their constant support and dedication to the project. Many people participated in the realization of the *Handbook* and I would like to thank in particular Lisa Tickner, Karen Dempsey, Angela Dooley, and Tari Paschall for coordinating and organizing the preparation of the volumes. My gratitude is also extended to all the authors for the time and energy they dedicated to the project.

Julio E. Celis
Editor

PART

A

CELL AND TISSUE CULTURE: ASSORTED TECHNIQUES

SECTION

1

General Techniques

CHAPTER

1

Setting up a Cell Culture Laboratory

Robert O'Connor and Lorraine O'Driscoll

I. INTRODUCTION

Over the past three decades, the continuous culture of eukaryotic cells has become a mainstay technique in many different forms of biological, biochemical, and biomedical experimentation. While at first, to the uninitiated, the techniques, methodology, and equipment can appear daunting, clear specification of the experimental requirements can help make choices straightforward. This article does not purport to be an exhaustive guide but rather aims to prompt the researcher to plan and make choices appropriate to their experimental, environmental, and financial resources.

II. WHERE TO START

Cell culture needs a commitment of energy and resources to be undertaken in a professional manner for any continuous period. Therefore, the biggest decision to be made before going down this experimental road is whether there will be an ongoing need for culture facilities or whether for short periods of work it might be more economical to collaborate with an established laboratory or sub contract work. Assuming that there is an agreed need to set up a cell culture facility, there are several *fundamental considerations*.

A. Environment

Purpose-built facilities are optimal for ergonomic and experimental reasons but often this choice is not available. Small cell culture facilities can be engineered (with inherent limitations) without making significant modifications to laboratory rooms. Before going into the detailed choices available, it is perhaps timely to go through some of the basics.

There are two fundamental considerations that govern most choices available to the would-be cell culture researcher: contamination and safety.

The fundamentals of cell culture owe much to the basic methodologies developed by microbiologists over the last two centuries. However, microorganisms reproduce several orders of magnitude more rapidly than eukaryotic cells and, in direct competition, bacteria and fungi will rapidly reproduce more biomass than eukaryotic cells. Eukaryotic cells are also very sensitive to the primary and secondary metabolic products of microbes. Bacteria and fungi are therefore the biggest problem, for those growing eukaryotic cells. As mentioned in the article by *Meleady and O'Connor*, there is also potential for cross contamination of one cell line by another if proper procedures are not observed (a major problem with the first cultured human cell lines).

Eukaryotic cells can potentially harbour subcellular microbes that could cause disease to human beings or animals. More specifically, most human cell cultures are derived from human cancers. Being derived from human beings who could be harbouring several known (and potentially, as yet, unknown) pathogens, appropriate steps must be taken to ensure that cells do not pose a risk of passing disease on to human beings, including the researcher or others including visitors or cleaning staff. In practice, the majority of pathogenic organisms are quite fragile and do not survive well under general culture conditions. The risk of disease is therefore greatest when working with primary biological material, i.e., material recently removed from

Copyright 2006, Elsevier Science (USA).
All rights reserved.

another (human) being. However, one should assume that any eukaryotic cells could potentially harbour microbes and/or viruses (including oncogenic viruses) and/or prion-contaminated material. As a general rule, taking the maximum amount of reasonable precautions (in procedures and equipment) gives the best margin of protection for staff, provides peace of mind for operators, and limits the culpability of supervisors/managers. The Centers for Disease Control (CDC) in the United States stipulate that general cell cultures should be undertaken in biosafety level 2 containment facilities (CDC, 1999).

B. Location

Having briefly outlined these fundamentals, it should be clear that correctly locating a cell culture facilities is of paramount importance. The *working environment* needs to be clean, free from dust, and easy to disinfect. The immediate area should have limited/restricted access, with no passing traffic. Consideration should be given to proper ergonomics in the area, e.g., correct heights of equipment, nothing requiring bending down, suitable chairs, and so on, to reduce the chance of chronic or acute injuries to staff (see the excellent laboratory website by the NIH for further details, specifications, and illustrations). Thought should also be given to how large and often heavy equipment, particularly laminar flow cabinets, can be brought in and out without major disruptions. If a building is being planned, this may include provisions for large lifts with fully opening doors or direct door access to higher floors with high loading equipment. Door openings need to be extra wide, typically at least 1 m full clearance, and corners designed that large equipment can get by. Provision must also be made for the movement and storage of consumables and bulk items. In practice, it is usually better to pool certain sets of equipment together in individual rooms, e.g., several biosafety cabinets being located with an incubator and other ancillary equipment. This reduces the overall equipment/cost necessary and can also make for a more "communal" working environment. Quarantine areas are an obvious exception to this suggestion.

C. Gases

Many cell cultures can be maintained in HEPES-buffered medium, which utilises carefully controlled incubators that do not need a separate carbon dioxide gas supply. However, some cells do not grow optimally in HEPES and need the buffering provided by the equilibrium of 5% CO_2 with bicarbonate in medium. This can be important for some specific cell lines, primary culture, and hybridoma work (Freshney, 2000). At a minimum, such incubators should have two separate CO_2 sources supplying them. Direct connection of a single cylinder means that the incubators are vulnerable every time a cylinder is changed and cylinders may fail to provide an adequate pressure of gas as they near an empty state. Cylinder changeover units permit, for example, one main line of gas and one backup cylinder, which means that incubators can be left for weeks or months (depending on use) without needing gas replacement and, when cylinders are replaced, there is no interruption in supply to the incubator (see NTC services website). Cylinders in a laboratory environment must always be fully fixed to an immovable object to lessen the risk of them toppling and doing serious injury and damage. Appropriate automatic changeover units can also be incorporated into external supplies of CO_2. It is always better not to have large cylinders of gas in a culture room for safety, practical, and aesthetic reasons. Building regulations in some areas may also legislate against the use of large cylinders in enclosed rooms.

D. Ventilation

Ventilation and airflow in the cell culture environment are critical to operation. At its simplest, there must be no disruption to the laminar airflow pattern in the biological safety cabinet and no undue circulation of dust and dirt that could occur with, for example, significant staff movement around the unit or location near drafts or vents. Ideally, there should be no openable windows; if so, they should be sealed to prevent drafts, insects, and dust entering (Freshney, 2000). However, in a purpose-built facility, if possible, it is ergonomically and aesthetically desirable that there be a source of natural light. When planning, one should also make provisions in case there is a need to fumigate the room or equipment (Doyle, 1998). Cabinets will usually need to be fumigated in advance of any filter changes, although this can now usually be performed on single cabinets (using a cabinet bag system) rather than whole rooms.

Clearly, whatever the room design, there must be some replenishment of air in a room and such ventilation must not interfere with the operation of the cabinet. If liquid nitrogen is being utilised in the same location as the cabinet, the ventilation must be adequate to remove the continuous evaporation of liquid and the ventilation/air space sufficient to ensure that if there is an acute spillage of liquid or a rupture of the vacuum vessel, there will still be sufficient oxygen concentration to support life and permit evacuation, i.e., that instant evaporation of all the liquid nitrogen

will not reduce the oxygen concentration below 14%. If this cannot be guaranteed at all times, oxygen monitoring and alarm equipment will be required (Angerman, 1999).

High efficiency particulate air (HEPA) filtration within the safety cabinet will ensure a good quality working environment. However, if the air around the unit is dusty, the cabinet filters will age and clog quite rapidly. HEPA filtration is a statistical process (99.999%–99.97% efficient depending on the manufacturer) and unduly contaminated air may also reduce the air quality inside the cabinet. HEPA filtration of air into a cell culture room should improve operation and cabinet filter longevity and is also a requirement of biocontainment-classified rooms. However, if the room itself is not maintained properly, expensively ducted HEPA-filtered air may merely be clean air being utilised to circulate dust and microbes. Depending on the biocontainment level required for operation, HEPA filtration may also be required on exhaust vents for a cell culture room (class 2+ biocontainment and above).

In larger cell culture facilities, careful balancing of air pressures in culture and anterooms may be useful or may be required for operation to appropriate biocontainment levels, specifically the positive and negative air pressures required for class 2 and greater biocontainment (CDC, 1999). Balancing and filtration require careful installation and validation from the outset and continued regular maintenance and monitoring to ensure appropriate function. Ventilation systems will also need to be tied into building fire management systems with, for example, automatic smoke dampeners to prevent the ventilation system from fanning or spreading smoke and fire.

E. Basic Cell Culture Requirements

To perform a basic range of cell culture procedures for any prolonged period the following list of equipment is required (Freshney, 2000).

Laminar flow cabinet
Incubator
Centrifuge
Refrigerator
Freezer
Microscope
Haemocytometer
Pipette boy
Micropipette

Outside immediate culture environment

Autoclave
Selection of appropriate consumables and cultureware
General laboratory facilities for the storage of chemicals, provision of standard reagents such as clean water, and controlled temperature water baths

F. Ideal Layout

1. Purpose-Built Facility

There are significant advantages in having the resources to custom design and implement a *purpose-built facility*. A purpose-built facility should be strongly considered (and will likely be more economical in the long term) if cell culture is performed on a significant scale (involving many researchers) for an established organisation and/or if this work is likely to be undertaken on a commercial basis. Aside from the support departments, which are mentioned later, the standard accepted laboratory scheme for cell culture involves a general laboratory room, an anteroom (physically and methologically separating the general laboratory area from the cell culture room), and a specific, self contained, cell culture room.

2. Equipment

a. Biosafety Cabinets. While basic cell culture can be performed with sterile equipment and good techniques, there is no question that the development of modern biological cabinets has greatly facilitated routine culture procedures and the prolonged manipulation of cells required for many experimental procedures. Laminar flow cabinets come in many sizes, capacities, and with several variants appropriate for different types of cell culture. Most manufacturers have excellent technical schematics describing the appropriate operation, dimensions, and so on. For examples, see the websites by Heto-Holten or Baker. Any laminar flow cabinet should be designed to an internationally recognised specification and biological safety standard appropriate to the work being undertaken or likely to be performed in at least the next 5 years. [See CDC (1995, 2000) and the list of international specifications in the Appendix for further details.] Laminar flow cabinets represent a significant investment and will usually give decades of service if adequately maintained. A careful choice is therefore important. The precise operation of a laminar flow cabinet is beyond the scope of this review except to say that they fundamentally consist of a large air-pumping motor, pumping air through a HEPA filter onto a working surface (CDC, 2000). Cabinet HEPA filters are designed to remove particulates (from proportionately large dust down to submicroscopic viral particles). Forcing large volumes of air through these filters needs large motors, which inherently imply significant

weight in their own right, and a heavy chassis to support this weight and to prevent vibration. Before locating/installing, one therefore needs to consider how the unit is to be placed in the required position. Typical weights can vary from 200 kg for new models to an excess of 500 kg for older units (which may still be very usable). More modern concrete-fabricated buildings will usually be designed to take the weight of one or more cabinets on a limited floor space, but this may need to be checked with an appropriate engineer and will certainly cause limitations in many lighter prefabricated or older buildings. A clear path from the point where a delivery vehicle may drop off the cabinet to its final resting place is required. Doors will need to be wide enough for the delivery pallet or, at least, the unpacked unit. Lift size and weight restrictions may be a particular problem, as can sharp corners on the route. Lift specifications should always be in excess of the largest envisaged unit that they might be expected to transport. In addition or if an appropriate lift cannot be provided, direct access to corridors on upper floors should be provided so that low loaders or cranes can directly insert heavy equipment to each floor of the building. Although one should plan for the unit to be in place for many years, one should also consider possibilities of bringing in new units and/or removing units as a particular group of scientists may expand or move their operation. Careful planning is therefore essential. Some manufacturers also have built-in modifications or supply units in subsections, which allow their units to take up a smaller space during movement than required for the operational unit.

Which Unit to Purchase/Use? Several international bodies have developed standard specifications for laminar flow cabinets (*see specification list in Appendix*). General cell culture requires a class II cabinet for an adequate protection of cells and operator (see Section A). These units recirculate HEPA-filtered air and exhaust a portion of that air back into the room through a HEPA filter. Where hazardous agents may be used, higher specification units such as external venting cabinets may be required (e.g. class II type B2/B3). These require very specific and costly exhaust ducting (CDC, 2000).

A careful choice of cabinet size should be made. In our centre, many researchers prefer a 4-ft (1.2 m)-wide laminar with plenty of space between the inner top of the cabinet and the work surface. Smaller cabinets may suit more restricted spaces but also restrict the amount of work that can be undertaken in comfort inside. Larger units may be useful for bulkier operations such as batch media production. The operator should be able to get their legs fully under the working space to permit appropriate posture and to reduce stretching and bending, which can cause repetitive strain injuries. The unit and the culture room should be well lit with low flicker lighting of an appropriate intensity (preferably supplemented with natural light). The motor size of safety cabinets causes the units to give off a significant amount of heat. A very significant heat load may be generated in areas where there are several (non-ducted) units in a confined space with incubators. The air-handling system must be able to cope with such a loading and maintain the temperature at a comfortable level. Optional extras, such as ultraviolet lights, are often dispensable and may have limitations or be inappropriate. If laboratory benches are used to support the cabinet, they must be sufficiently sturdy to support the full weight of the unit for the duration of use. Legs must also be sufficiently broadly spaced to prevent any risk of toppling.

b. Incubators. Most mammalian cells are maintained at 37°C, whereas insect cell cultures typically grow at 28°C. As mentioned previously, there may also be a need for a regulated use of CO_2 and possibly other gas mixtures in the cabinet. Many different-sized *incubators* are available to suit the needs and requirements of the researcher. Temperature control and accuracy usually to 0.1°C is an obvious requirement, and units that have heated doors and glass inner doors, permitting limited observation without letting all the heat out, are preferable. In our laboratory, units of 200- to 300-liter internal capacity are capable of supporting the culture output of several researchers. Roller bottle and spinner flask culture vessels may also require special incubators or adapters. The incubator should ideally be located close to the laminar cabinet to reduce temperature changes, which could affect cultured cells. General cell culture incubators require the ambient temperature to be usually 5–10°C colder than the target temperature. If the ambient temperature is too close to the target temperature, standard units can overheat, making temperature control in the room critically important for reliable operation. The incubator should also be at standing height to prevent the need for bending down. Temperature-controlled warm rooms may be useful in specific circumstances; however, larger incubators and particularly warm rooms are very difficult to maintain at a homogeneous temperature all through the space, which can adversely affect growth.

All internal surfaces should be polished metal and accessible for cleaning purposes. Any surface or component that cannot be cleaned but is inside the air

space of the incubator is likely to see significant microbial growth as residue builds up. Where vented culture flasks and CO_2 are being used, the unit must also have a bath of clean water inside and the incubator must monitor relative humidity. Vented flasks and other unsealed culture vessels, such as 96-well culture plates, will rapidly dry out if humidity drops.

Most units available now are very straightforward to calibrate the level of CO_2 and temperature. Sensors that use infrared measurement of CO_2 are the easiest to calibrate as opposed to older electrochemical sensors. It is advisable to periodically check the calibration of such equipment using external measuring devices.

c. Centrifuges. Many different models of centrifuge are available for cell culture. For ergonomic reasons, the unit should be located near the biosafety cabinet and at an appropriate height. All *centrifuges* will vibrate to some degree, and measures should be taken to ensure that such vibrations cannot damage other equipment, cause unnecessary noise, or allow the centrifuge to creep and potentially fall. The centrifuging of tubes containing media and cells can induce aerosols, and all centrifuges used for cell culture and biological procedures must have some form of seal either above the rotor head or over the buckets, which prevents aerosol leaking, particularly where tubes may rupture or leak during operation. A common operational centrifugation rate is appproximately 110×*g*, and units must capable of fractions and low multiples of this rate to cope with different research requirements. Temperature control, particularly the ability to spin at refrigerated temperatures, can be a very useful add on to standard units. The buckets in the rotor should have adapters that snugly fit the standard consumables used for culture in that facility, e.g., 25- and 50-ml universal tubes. Control of the acceleration and deceleration rates can also be useful when working with certain very sensitive cell lines.

d. Refrigerator/Freezer Units. Storage of media, media components, buffers, and so on needs *refrigeration and freezing facilities*. Domestic-type units are often used for this purpose; however, domestic units can have limitations in their ability to maintain a steady temperature and must also never be used if flammable liquids are to be stored inside (an externally thermostat-controlled unit must be used for such purposes). It can also be useful if the door has a lockable latch, as this can help ensure that the unit is closed properly after every use. In practice, careful monitoring of the storage and use of refrigerators/freezers are necessary to prevent space wastage. Fridges and freezers should be cleaned out regularly. When this is not done, it is common to see gradual increases in the number of such units, which can greatly add to heat loads in the laboratory. In larger scale facilities, it may be prudent to combine the use of fridges/freezers with longer term, volume storage in central cold/freezer rooms. In such laboratories it may also be useful to use cooling/freezing units that have condenser units located outside the laboratory. Although not usually required for cell culture operations, freezers that can operate below –60°C, usually –80°C, are often necessary for the storage of molecular biological enzymes and reagents.

e. Liquid Nitrogen. Maintenance of cultured cells for any prolonged period requires that cell stocks can be kept well below the glass temperature of water (approximately –60°C). In practice, *liquid nitrogen storage* is often a convenient general storage environment for stocks of cultured cells. However, electrical freezers operating at –120°C can perform a similar function. Liquid nitrogen boils at –196°C, and because the resultant nitrogen gas is an asphyxiant in high concentrations, proper handling and ventilation procedures are necessary (*see article by Meleady and O'Connor*). Proper inherently safe methods for transport and storage must be used to get the liquid gas into the cell storage containers. As the storage vessels usually require topping up at least once a week (more regularly as the containers age), the route from the gas delivery/production area to the laboratory must be as short as possible and the surface and equipment appropriate for the transport involved. Storage of cells by multiple users for prolonged periods necessitates careful inventory management to ensure that cells are maintained optimally and economically. It is good practice to have two independently stored stocks of cells: one vessel containing master stocks of important cells and the other, in the laboratory environment, containing working stocks.

Modern incubators, refrigerators, freezers, and liquid nitrogen vessels typically have alarms that can be set if parameters, such as temperature, drop below a critical values. However, such alarms are only of use if there is someone nearby to hear them. Where critical or expensive procedures are being utilised, it is wise to have such equipment linked into a monitoring system that can alert a researcher day or night. Consideration should also be given to the provision of a backup electricity generator that can automatically restore supply for a finite period in the event of an electrical blackout.

f. Autoclave. Modern single-use plastic consumables have reduced the dependence on a laboratory *autoclave* for sterilising equipment and reagents; however, an appropriately sized, robust autoclave is still vital for continued cell culture work. Although appropriately sourced plastic consumables and presterilised reagents can eliminate the potential for contamination, there can still be huge cost savings by utilising specific pieces of glass equipment that can be repetitively autoclaved, used, and recycled, particularly reagent and media bottles, and by sterilising one's own general reagents, such as water and phosphate-buffered saline. Small autoclaves can generate significant amounts of foul odour, steam, and heat and should not be used in a general laboratory environment. Because of the biohazardous nature of cell culture, autoclaving of all materials and reagents that come into contact with cells is also required. For larger facilities, it is strongly recommended to have a centralised autoclave facility away from an individual laboratory. A distinction of clean and waste autoclaves is necessary to prevent cross contamination, particularly of odours and volatile substances. A backup autoclave is also good insurance against maintenance and unanticipated downtime. As such facility autoclaves are large, need regular maintenance and inspection, and can have a limited life span, provision for easy access and removal/replacement is advisable. The operational characteristics of the autoclave should also be regularly checked with spore strips, for example, to validate that the autoclave is operating effectively.

3. General Environmental Recommendations

Ideally, there should be a limited facility for the temporary storage of small amounts of culture consumables next to the biosafety cabinet. However, cardboard can be a significant source of fungal spores, and large-scale storage in the culture area causes clutter. Consumables are best stored in a central location, and if cell culture is being undertaken on a larger scale, it is far more economical to bulk purchase supplies and distribute them as necessary to each laboratory. Provision also needs to be made for the storage of flammable materials, especially disinfectant alcohols, which are used for local disinfection and "swabbing" (disinfectant wiping of consumables and reagents as they enter the working space inside safety cabinets).

Ideally, all flooring, walls, and other surfaces in the culture environment should be readily accessible, chemically resistant, nonadsorbent, and easy to clean. Shelves should not be used, and open flat surfaces should be minimised as these will need to be cleaned and can be a source for the buildup of dirt and dust. Walls should be smooth skimmed and coated with epoxy paint. The floor should also be resistant and bonded to the wall so that there are no crevices or corners that cannot be cleaned and any spillages can be easily isolated and cleaned. Sinks, coat hooks, and so on should all be kept in an anteroom and not in the culture room.

Regular training, standard operating procedures, and centralised management of all aspects of cell culture, particularly technique and safety, ensure that there is an economical, continuously monitored, high standard of operation. The function of vital equipment should be continuously monitored and recorded. Particular attention should be paid to the monitoring of environmental microbial levels throughout the facility. For example, "settle" plates should be periodically left in laminar flow cabinets to check for sterility, as well as in all laboratory areas to validate the cleanliness of such areas.

The microbial quality of cell stocks should also be monitored as part of this process. All cells coming into a facility, regardless of the source, especially if supplied by noncommercial sources, should be quarantined and initially cultured in isolation from the general culture environment. *Mycoplasma* is the main microbial contaminant of concern because such contamination can go unnoticed for long periods and is very easy to pick up and cross contaminate stocks of cells. Ideally, a facility should have provision for routine *Mycoplasma* detection. Experience and expertise are required to do this job reliably, and where such expertise is not available in-house, commercial testing facilities exist.

Industrial disinfectants such as Virkon and/or Tego need to be employed (at recommended dilutions) as part of the routine cleaning of equipment and areas, in addition to diluted industrial methylated spirits or isopropyl alcohol, which is used for local disinfection and "swabbing."

Other Areas. A successful laboratory will have a two-way flow of people and materials. To manage and control these, it is useful to have a centrally located reception area to administer all incoming deliveries of consumables, cells, chemicals, and so on. Provision needs to made for effective communication within the organisation, including phone access in all but the most specialist of rooms, internet, and e-mail access and storage of records and scientific literature. If the unit is fully self-contained, the human environment must also be considered with an adequate provision of locker and toilet facilities and appropriate locations for taking breaks and eating completely away from the laboratory.

III. SUMMARY

The reader will note the preference in this text for larger centralised, purpose-built facilities. In individual situations, it may be appropriate to represent the areas mentioned in a smaller more general way; however, even at its simplest, maintenance of a small cell culture environment necessitates that time be spent validating and monitoring the quality of that environment and the various flow paths contained therein. This obviously reduces the time available for research. However, in larger facilities, such critical validatory tasks can become specific jobs enabling the researcher to concentrate with confidence on biological research. Where such facilities are properly established, it is common that they continue to expand. The final thought in setting up a cell culture environment is to look as much as possible to the future and to allow for changes in use and facility expansion from the very start.

APPENDIX

The following relevant international standards are used for biosafety cabinets.

American National Standards Institute (National Sanitation Foundation). NSF/ANSI—49 (1992). Class II (Laminar Flow) Biohazard Cabinetry. Now superseded by NSF/ANSI49 (2002) and NSF/ANSI 49-02e (2002).

Australian standards AS2252.1, Biological Safety Cabinets (Class I) for personal protection (1980). AS2252.2 Biological Safety Cabinets (Class II) for personal protection (1981). Standards Association of Australia.

Canadian Standards Association, CSA Z316.3-95 (1995). Biological Containment Cabinets: Installation and Field Testing.

European standard EN12469:2000 (2000). Performance criteria for microbiological safety cabinets. Supersedes EU member state standards such as BS 5726 (British), DIN 12950 (German), and NF X44-201 (French).

Japanese Industrial Standard JIS K 3800 (JACA) for Class II biological safety cabinets.

South African standards, SABS 0226:2001 (2001). The installation, postinstallation tests, and maintenance of microbiological safety cabinets (2001) and VC 8041:2001, microbiological safety cabinets (Classes I, II, and III) (2001).

References

Angerman, D. (1999). "Handbook of Compressed Gases," 4th Ed. Kluwer Academic, New York.

Baker Biosafety cabinet website. http://bakercompany.com/products/ 161 Gatehouse Road, Sanford, Maine 04073 USA.

CDC (1995). "Biosafety Cabinets; Primary Containment for Biohazards: Selection, Installation and Use of Biological Safety Cabinets," 1st Ed. U.S. Department of Health and Human Services Public Health Service Centers for Disease Control and Prevention and National Institutes of Health. U.S. Government Printing Office, Washington. Web edition http://www.niehs.nih.gov/odhsb/biosafe/bsc/bsc.htm

CDC (1999). U.S. Department of Health and Human Services Public Health Service Centers for Disease Control and Prevention and National Institutes of Health. "Biosafety in Microbiological and Biomedical Laboratories," 4th Ed. U.S. Government Printing Office, Washington. Web edition http://www.cdc.gov/od/ohs/biosfty/bmbl4/bmbl4toc.htm. See also the CDC Office of Health and Safety biosafety general website: http://www.cdc.gov/od/ohs/biosfty/biosfty.htm

CDC (2000). "Primary Containment for Biohazards: Selection, Installation and Use of Biological Safety Cabinets." U.S. Department of Health and Human Services Public Health Service Centers for Disease Control and Prevention and National Institutes of Health. U.S. Government Printing Office, Washington. Web edition http://www.cdc.gov/od/ohs/biosfty/bsc/bsc.htm

Doyle, A. (1998). "Cell and Tissue Culture: Laboratory Procedures" (A. Doyle, J. B. Griffiths, and D. G. Newell, eds.), Chap. 1. Wiley, Chichester.

Freshney, R. I. (2000). "Culture of Animal Cells: A Manual of Basic Technique," 4th Ed. Wiley-Liss, New York.

Heto Holten Biosafety cabinet website. http://www.heto-holten.com/prod-holten.htm. Heto-Holten now part of Jouan Nordic, Gydevang 17–19, DK-3450, Allerød, Denmark.

National Institutes of Health (NIH) laboratory safety website http://www.nih.gov/od/ors/ds/ergonomics/lab3.html

NTC services limited. Northern Technical & Chemical Services. Unit D44, Brunswick Business Centre, Liverpool, L3 4BD.UK. http://www.merseyworld.com/ntcs/

CHAPTER

2

General Procedures for Cell Culture

Paula Meleady and Robert O'Connor

I. INTRODUCTION

A. Background

Mammalian cell culture emerged as a valuable research tool in the 1950s when the first cell line, HeLa, was successfully cultured from a human cervical cancer (Gey *et al*., 1952). However, it is only since the mid-1980s that reproducible and reliable large-scale culture of mammalian cells has been achieved. The development of cell culture led to new experimental approaches to cellular physiology in which isolated, functionally differentiated cells could be maintained in culture under conditions that allowed direct manipulations of the environment and measurement of the resulting changes in the function of a single cell type. Today many aspects of research and development involve the use of animal cells as *in vitro* model systems, substrates for viruses, and in the production of diagnostic and therapeutic products in the pharmaceutical industry.

The process of initiating a culture from cells, tissues, or organs taken directly from an animal and cultured either as an explant culture or following dissociation into a single cell suspension by enzyme digestion is known as primary culture. Certain primary cultures may be passaged for a finite number of population doublings before senescence occurs, but usually the number of doublings is limited in adult-derived or differentiated cell types. However, these cells are still invaluable as they retain many of the differentiated characteristics of the cell *in vivo*. After a number of subcultures a cell line will either die out, referred to as a finite cell line (and is usually diploid), or a population of cells can transform to become a continuous cell line. Lines of transformed cells can also be obtained from normal primary cell cultures by infecting them with oncogenic viruses or treating them with carcinogenic chemicals. It is often very difficult to obtain a normal human cell line from a culture of normal tissue. In contrast, neoplasms from humans have been generated into many cell lines. It appears that the possession of a cancerous phenotype allows the easier adaptation to cell culture, which may be due in part to the fact that cancer cells are aneuploid. Transformed cell lines have the advantage of almost limitless availability; however, they often retain very little of the original *in vivo* characteristics.

Cell cultures *in vitro* take one or two forms, either growing in suspension (as single cells or small clumps) or as an adherent monolayer attached to the surface of the tissue culture flask. It is necessary that cell culture medium is produced so that it mimics the physiological conditions within tissues. *In vitro* growth of cell lines requires a sterile environment in which all the nutrients for cellular metabolism can be provided in a readily accessible form at the optimal pH and temperature for growth. Media formulations vary in complexity and have been developed to support a wide variety of cell types, including Eagle's minimum essential medium (MEM), Dulbecco's modified Eagle's medium (DMEM), RPMI 1640, and Ham's F12. Cell culture media essentially consist of a number of factors required for the growth of the cells, including amino acids (essential and nonessential), lipids (essential fatty acids, glycerides, etc.), trace elements, vitamins, and cofactors. Carbohydrates such as glucose or fructose are usually added as an energy source. Other essential components include inorganic salts, which provide buffering capacity and osmotic balance (260–320 mOsm/kg) to counteract the effects of carbon

Copyright 2006, Elsevier Science (USA).
All rights reserved.

dioxide and lactic acid produced during cellular metabolism. The pH of medium should ideally be between 7.2 and 7.4 (however, fibroblasts prefer a pH range of 7.4–7.7 whereas transformed cells prefer a pH range of 7.0–7.4). When phenol red is included in the medium, the medium turns purple above pH 7.6 and yellow below pH 7.0. Buffering of culture media is usually provided by sodium bicarbonate and cells are usually maintained in vented tissue culture flasks in an atmosphere of 5% CO_2. Synthetic buffers such as HEPES can also help maintain correct pH levels in closed, nonvented tissue culture flasks, although it may be toxic to some cell types. Serum, which is a complex mixture of albumins, growth promoters, and growth inhibitors, may also be incorporated into the growth medium at concentrations from 5 to 20%, although certain production processes and experimental procedures require the use of serum-free conditions. The majority of cell lines require the addition of serum to defined culture medium to stimulate growth and cell division but can be subject to significant biological variation. The most common source is bovine and this may be of adult, newborn, or foetal origin.

A number of other books give more detailed and comprehensive treatment of procedures for mammalian cell culture and the reader is recommended to refer to these books for additional information (Doyle *et al*., 1998; Freshney, 1992, 2000; Shaw, 1996).

B. General Safety when Working with Mammalian Cells in Culture

In general, because of the potential risks that may be associated with material of biological origin, standard and specific laboratory regulations should always be adhered to.

- Antibodies, sera, and cells (particularly but not exclusively those of human and nonhuman primate origin) may pose a potential threat of infection or other biological hazard (e.g., prion disease).
- Many animal cells contain C-type particles, which may be retrovirus related. All such materials may harbour pathogens and should be handled as potentially infectious material in accordance with local guidelines.
- Laboratory coats are essential. The Howie-type coat is the only recommended coat for biological work. Coats should be used only in the culture area and should be laundered frequently.
- Protective glasses should be worn at all times while contact lenses should never be worn in the laboratory area.
- No eating, drinking, or smoking should be permitted.
- No mouth pipetting of any solutions.
- Operators must make sure that any cuts, especially on the hands, are covered. Wearing gloves is strongly recommended, particularly for manipulations involving cells and biological material. Gloves should be of a standard appropriate to the risk of the agent being handled. Nitrile gloves may provide superior protection with lower allergy potential than traditional latex gloves.
- Thorough washing of hands before and after cell work with appropriate laboratory soap is essential.
- Immunisation against hepatitis B may be recommended if working with primary human material. In certain countries, where tuberculosis (TB) vaccination is not a standard (or staff are employed from such countries and where the material being handled may have a TB hazard) BCG vaccination may also be recommended (Richmond and McKinney, 1999). However, this should be at the discretion of the individual operator, and regular follow-up and paperwork, including titre estimation, are necessary to have an effective vaccination policy.
- To comply with current safety regulations, a cell culture laboratory should be fully ventilated, preferably with high efficiency particulate air (HEPA) filters on the inlets, and equipped with HEPA-filtered workstations where the airflow is directed away from the operator. A class II (type A) downflow recirculating laminar flow biological safety cabinet will provide a safe working environment for standard hazard material and should be checked yearly (or as recommended by manufacturer) for containment, airflow velocity, and efficiency. A horizontal flow cabinet should never be used, as it can, even in the absence of viruses, possibly increase exposure to allergens.
- In addition to standard alcohol-based disinfection for routine work and introduction of consumables, primary equipment and work areas should be regularly disinfected with laboratory disinfectants, e.g., Virkon, Tego, or equivalent. Manufacturer guidelines should be followed as some disinfectants may corrode materials.

II. MATERIALS AND INSTRUMENTATION

A. Materials

The following are from Sigma Aldrich: DMEM (Cat. No. D5648), Ham's F12 (Cat. No. N2650), RPMI (Cat.

No. R6504), $NaHCO_3$ (Cat. No. S5761), HEPES (Cat. No. H4034), dimethyl sulphoxide (DMSO, Cat. No. D5879), foetal calf serum (FCS, Cat. No. F7524), EDTA (Cat. No. E5134), soybean trypsin inhibitor (Cat. No. T6522), haemocytometers (Neubauer improved chamber) (Cat. No. Z35, 962–9), and replacement coverslips (Cat. No. Z37, 535–7).

The following are from Invitrogen (GIBCO brand): 200 m*M* (100×) L-glutamine (Cat. No. 25030-024), penicillin/streptomycin (5000 IU/500 µg/ml) (Cat. No. 15070-063), 2.5% trypsin (10×) (Cat. No. 15090-046), and Trypan blue (Cat. No. 15250-061).

The following are from Corning (Costar brand): 10-ml (Cat. No. 4101CS) and 25-ml (Cat. No. 4251) pipettes, 25-cm^2 (Cat. No. 3055) and 75-cm^2 (Cat. No. 3375) nonvented tissue culture flasks, and 25-cm^2 (Cat. No. 3056) and 75-cm^2 (Cat. No. 3376) vented tissue culture flasks.

The following are from Greiner: 30-ml (Cat. No. 2011-51) and 50-ml (Cat. No. 210161G) sterile containers/centrifuge tubes, cryovials (Cat. No. 122278G), and autoclave bags (Cat. No. Bag1).

The following are from Millipore: 0.22-µm low protein-binding filters for small volumes (Cat. No. SLGVR25KS) and 0.22-µm filters for large volumes (Cat. No. SPGPM10RJ).

Phosphate-buffered saline (PBS) (Cat. No. BR14A) is from Oxoid. Laboratory disinfectants such as Virkon (Cat. No. CL900.05) and Tego (Cat. No. 2000) are from Antec and Goldschmidt, respectively.

B. Instrumentation

Automatic pipette aids (Accu-jet, Model No. Z33,386–7) are from Sigma Aldrich, the inverted microscope with phase-contrast optics (Model No. DM 1L) is from Leica Microsystems, and the centrifuge is from Eppendorf (Model No. 5810). The 37°C incubator (Model No. 310) is from Thermo Forma. The laminar flow cabinet (Model No. NU-425-600) is from Nuaire.

Other standard laboratory apparatus includes refrigerators, –20°C and –80°C freezers, and a liquid nitrogen freezer. Clean autoclaves should be available for solutions, glassware, and other items that require sterilisation by moist heat. A separate waste autoclave should be available for general biological laboratory waste, including plastics and waste media. Dishwashers should also be available to ensure thorough cleaning of all glassware used in cell culture procedures.

III. PROTOCOLS

A. Good Practice and Safety Considerations

Equipment in the designated area for cell culture should be kept to the minimum required for the job. There should be proper entry facilities and internal surfaces must be easy to clean and dust free. When setting up a cell culture laboratory the following equipment is essential:

- Class II downflow recirculating laminar flow cabinet
- Low-speed biological centrifuge
- CO_2 incubator
- Inverted microscope with phase-contrast capabilities
- Refrigeration and freezing facilities
- Cell storage (liquid nitrogen) facilities

Prevention of contamination by bacteria, fungi (especially yeast), mycoplasma, or viruses is absolutely necessary in cell culture. Good laboratory practice requires that the following standard procedures are followed:

- Cell culture should be performed in a designated area that is easy to clean and free from clutter. Equipment used should broadly be designated for that purpose to prevent potential chemical or biological contamination by or due to other laboratory processes and operation. Ensure that all equipment are cleaned and serviced regularly.
- Cell culture by definition involves the handling of biological material. As such, all biological material can potentially harbour infective agents. Therefore, routine precautions to prevent infection should be exercised. Waste media and items coming into contact with biological material should be disinfected; autoclaving is probably the most broadly useful method. Where material of primary origin is in use and in the absence of specific legal guidelines, validation of the inactivation of biological material is vital.
- Although the majority of common culture lines are characterised as biosafety level 1, the Centers for Disease Control and Prevention (CDC) in the United States suggest that handling procedures be of biosafety level 2 standard, where material is of mixed origin, including some primary material. Biosafety level 2 or 2+ will be mandatory unless prior knowledge indicates the need for even higher standards of safe handling (Richmond and McKinney, 1999).
- It is important that cell lines are obtained from a reputable source, preferably the laboratory of origin or an established cell repository (e.g., ATCC or ECACC).

Cells from all sources should be handled in quarantine until all quality control checks are completed, particularly microbial (and especially *Mycoplasma*) contamination should be checked.

- Only sterile, wrapped items (i.e., pipettes, culture flasks) should enter the room, and discarded media and waste should be removed each day. All used materials should be disposed of safely, efficiently, and routinely in accordance with local regulatory requirements. Keep cardboard packaging to a minimum in all cell culture areas.
- Stock cultures of two cell lines should never be worked on at the same time in a laminar flow cabinet. When working with different cell lines, a thorough cleaning of surfaces with a suitable disinfectant is required and a minimum of 15 min between handling different cell lines is essential to prevent cross contamination. Use of pipettes, medium/waste bottles, and so on for more than one cell line is another possible source of cross contamination and must be avoided.
- When setting up a large frozen stock line, aliquots should be thawed to test for viability, growth, and absence of contamination (including *Mycoplasma*). They should also be characterised and authenticated by some appropriate criteria (e.g., DNA fingerprinting and cytogenetic analysis), both for comparison to the parent cell line and as a standard for comparison of future stocks.
- It is advisable not to use antibiotics continuously in culture medium as this will inevitably lead to the appearance of antibiotic-resistant strains.
- Quality control all of the reagents used in tissue culture to ensure all materials used provide reproducible growth characteristics and are free from contamination prior to use with cells.
- Ensure laboratory coats are changed regularly.
- A disinfectant, e.g., 70% isopropyl alcohol [or alternatives such as 70% industrial methylated spirits (IMS) or ethanol] should be used liberally to disinfectant work surfaces, bottles, plastics, and so on.
- Cell culture is often combined with other methodologies, including chemical and drug methodologies. These may necessitate additional consideration of the chemical/toxicological hazards involved (e.g., use of cytotoxic laminar flow cabinets, cytoguards).

B. Subculturing Cells

In order to maintain cell cultures in optimum conditions it is essential to keep cells in the log phase of growth as far as it is practicable. There are two general types of culture method appropriate for adherent and suspension cells.

1. Subculturing Adherent Cells

Adherent cells (usually of epithelial, endothelial, and fibroblastic origin) will continue to grow *in vitro* until either they have covered the surface available for growth or they have depleted the nutrients in the surrounding medium. Cells kept for prolonged periods in the stationary phase of growth will lose plating efficiency and may become senescent, lose viability and other characteristics, or even die. The frequency of subculture is dependent on a number of factors, including inoculation density, growth rate, plating efficiency, and saturation density. These factors will vary between cell lines.

Protocol 1. Subculturing of Adherent Cells

The following procedure is described for the adherent cell line A549 (human lung adenocarcinoma, purchased from the ATCC) of epithelial origin, which can be subcultured indefinitely. These cells can be grown in HEPES-buffered medium and can therefore be routinely grown in nonvented tissue culture flasks in a normal 37°C incubator.

Media and Solutions

100× L-glutamine stock (200 mM): Thaw stock solution and aliquot into sterile 5-ml amounts and store at –20°C.

100× penicillin/streptomycin solution: Aliquot stock solution into sterile 5-ml amounts and store at –20°C.

FCS: Thaw stock solution and aliquot into sterile 20- to 50-ml amounts and store at –20°C.

1× phosphate-buffered saline (PBS): Add 1 tablet to 500 ml of ultrapure water, according to manufacturer's instructions, and autoclave. Store sterile solution at 4°C.

1% EDTA solution: Add 1 g of EDTA to 100 ml of ultrapure water and autoclave. Store sterile solution at 4°C.

0.25% trypsin/EDTA solution: Thaw the 2.5% (10×) stock trypsin solution. To 440 ml of sterile PBS solution, add 10 ml of sterile 1% EDTA and 50 ml of 2.5% trypsin stock solution. Mix resultant solution by gentle inversion and aliquot into sterile 20 ml amounts. Store aliquots at –20°C.

1× DMEM: Prepare 1× DMEM from 10× powder according to the manufacturer's instructions, supplement the medium with $NaHCO_3$ and HEPES (adjust pH to 7.2–7.4), and filter sterilise using a 0.22-µm filter capable of handling large volumes or, alternatively, purchase premade 1× medium from a relevant supplier. Store basal media at 4°C.

1× Ham's F12: Prepare 1× Ham's F12 from 10× powder according to the manufacturer's instructions, supplement the medium with $NaHCO_3$ and HEPES (adjust pH to 7.2–7.4), and filter sterilise using a 0.22-µm filter capable of handling large volumes or, alternatively, purchase premade 1× medium from a relevant supplier. Store basal media at 4°C.

Complete DMEM/Ham's F12 1:1 medium: To prepare 100 ml of complete medium, mix 47 ml of 1× DMEM with 47 ml of 1× Ham's F12 and supplement with 5 ml of FCS and 1 ml of 100× L-glutamine. One milliliter of antibiotic solution (e.g., 100× penicillin/streptomycin solution) may also be supplemented to the medium if absolutely necessary.

Procedure

1. Examine the condition of the cells using an inverted microscope with phase-contrast capabilities. Ensure that the cells are healthy and subconfluent (i.e., in the exponential phase of growth) and free of contamination.

2. Sanitise the laminar flow cabinet by wiping the surface of the working area with 70% IMS (or equivalent alternative). Wipe the surfaces of any materials prior to starting work, including gloves, media bottles, and pipettes.

3. Remove the spent growth medium from the flask using a pipette and wash the monolayer with a sufficient volume of prewarmed trypsin/EDTA solution (0.25% trypsin/EDTA solution in PBS) to ensure the removal of all media from the flask.

4. Add an appropriate volume of the 0.25% trypsin/ EDTA solution to the flask (2 ml for a 25-cm^2 flask, 4 ml for a 75-cm^2 flask, 7–8 ml for a 175-cm^2 flask) and incubate at 37°C to allow the cells to detach from the inside surface of the flask (the length of time depends on the cell line, but usually this will occur within 2–10 min). Examine the cells with an inverted microscope to ensure all the cells are detached and in suspension. Gently tap the flask with the palm of the hand a couple of times to release any remaining detached cells.

5. Inactivate the trypsin by adding an equal volume of serum-containing (complete) media to the flask.

6. Remove the cell suspension from the flask and place in to a sterile container. Centrifuge typically at 1000 rpm for 5 min.

7. Pour off the supernatant from the container and resuspend the pellet in complete medium. Perform a viable cell count (see article by Hoffman) and reseed a flask with an aliquot of cells at the required density. The size of culture flask used depends on the number of cells required. An appropriate volume of complete medium is added to the flask (5–7 ml for a 25-cm^2 flask, 10–15 ml for a 75-cm^2 flask, or 20–30 ml for a 175-cm^2 flask). A cell count may not always be necessary if the cell line has a known split ratio (refer to ATCC or ECACC data sheets for the required seeding density). Label each flask with cell line name, passage number, and date.

Notes

- It is recommended to prepare fresh complete medium 1 week in advance of use, which gives time for a 5-day sterility check.
- L-Glutamine is more labile in cell culture solution than any other amino acid and the rate of degradation is dependent on storage temperatures, age of product, and pH. It is usually added in excess to culture medium, as it can be a limiting factor during cell growth. However, the degradation of L-glutamine causes a buildup of ammonia, which can have a detrimental effect on some culture suspensions. It is important to be very cautious when exceeding the formulated level of L-glutamine originally in the medium. Its degradation occurs at a faster rate at 37°C compared to 4°C; therefore it is recommended to keep medium containing L-glutamine at 4°C.
- To maintain serum-free conditions for specific cultures, trypsin may be neutralised with soybean trypsin inhibitor where an equal volume of inhibitor at a concentration of 1 mg/ml is added to the trypsinised cells. Cells can then be processed as described in steps 6 and 7 described earlier. For more details, refer to the article by Gayme and Gruber.
- An alternative to proteases is cell-scraping methods.
- Although most cells will detach in the presence of trypsin alone, EDTA is added to enhance the activity of the enzyme.
- Cells should only be exposed to trypsin long enough to detach the cells. Prolonged exposure can damage surface receptors on cells.

2. *Subculturing Suspension Cells*

Once established in culture, many tumour cell lines do not produce attachment factors and remain in suspension either as single cells or as clumps of cells. Examples of this cell type are lymphoblasts and cells of haematopoietic origin. Lymphoblastoids and many other tumour cell lines do not require a surface on which to grow and therefore do not require proteases such as trypsin for subculturing. Nonadherent cells may be subcultured by a number of methods, including subculture by direct dilution and subculture by sedimentation followed by dilution. The disadvantage of subculturing suspension cells by dilution is that

during growth, cells produce metabolic by-products, which become toxic if allowed to accumulate in the medium. Initially, sufficient waste metabolites will be removed by diluting cell cultures, allowing growth to continue but the viability of the cells will gradually decline after a few subcultures. Surviving cells may also undergo selection pressures, resulting in altered characteristics. Subculture by sedimentation overcomes this problem of toxic metabolites but one must be careful not to overdilute the cells, which will increase the lag phase of the cells and may prevent them from dividing and also removes any growth factors produced by the cells.

Protocol 2. Subculture of Suspension Cells by Sedimentation

The following procedure is described for the human haematopoietic cell line HL60 (purchased from the ATCC), which can be subcultured indefinitely in suspension culture. HL60 cells cannot be grown in medium containing HEPES as a buffering agent. These cells need to be grown in vented tissue culture flasks in an atmosphere of 5% CO_2. HEPES is known to be toxic to some cell lines, so this needs to be checked before culturing the cell line of interest.

Media and Solutions

1× RPMI: Prepare 1× RPMI from 10× powder according to the manufacturer's instructions and supplement the medium with $NaHCO_3$ (adjust pH to 7.2–7.4) and filter sterilise using a 0.22 µm filter capable of handling large volumes or, alternatively, purchase premade 1× medium from a relevant supplier. Store basal media at 4°C.

Complete RPMI medium: To prepare 100 ml of complete medium, aliquot 89 ml of 1× RPMI and supplement with 10 ml of FCS and 1 ml of 100× L-glutamine. One milliliter of antibiotic solution (e.g., 100× penicillin/streptomycin) may also be supplemented to the medium if absolutely necessary.

Procedure

1. Examine the cultures microscopically for signs of cell deterioration and high-density growth. Cells in the exponential phase of growth will appear bright, round, and refractile, whereas dying cultures show cell lysis and shrunken cells. Hybridomas may be sticky and adhere loosely to the surface of the flask. These may require a gentle tap to the flask to detach the cells into suspension. Examination of the colour of the media may also indicate the growth stage of the cells (pH indicator in media).

2. Remove a volume of the cells for a viable cell count (refer to the article by Hoffman for details). The viability of suspension cell cultures should not be allowed to fall below 90%.

3. Transfer the cells to a sterile container and centrifuge the cells at 1000 rpm for 5 min to form a pellet.

4. Discard the supernatant and resuspend the pellet with fresh media.

5. Set up the required number of vented tissue culture flasks and add an appropriate volume of prewarmed growth medium to the flasks. Add the appropriate number of cells to the flasks and incubate the flasks at 37°C in a CO_2 incubator. Refer to data sheets for recommended seeding densities of the cell line of interest (a typical growing density range for many suspension cells is 10^5–10^6 cells/ml).

C. Cryopreservation of Cells

Cell lines can change properties over time such as growth rate, antigen expression, and isoenzyme profile. It is therefore essential to set up a large frozen stock of each cell line, i.e., a working cell bank, and to work only within a defined number of cell doublings (or passages at a defined dilution/split ratio). A 10-passage period is satisfactory for many cell lines to maintain characteristic profiles.

1. Good Practice and Safety Considerations

Liquid nitrogen is the main refrigerant used for the long-term storage of biological material on a laboratory scale. The nitrogen boils above –196°C (–320°F) and thus the liquid is intensely cold and can pose several forms of safety hazard (Angerman, 1999).

- Cold of this magnitude will almost instantly burn skin and tissue. Such burns will also be produced by contact with material that has been exposed to liquid nitrogen. In some cases, items may actually adhere to skin and tissue that they contact, exacerbating burn damage.
- Liquid nitrogen can only be transported and stored in appropriately insulated containers. Most materials become extremely brittle in contact with such temperatures. For small quantities, special polystyrene containers can be used for transport. For larger quantities, purpose-built vacuum-insulated dewars are vital.
- The constant boiling of liquid nitrogen, particularly the instantaneous boiling that can occur if objects at room temperature are encountered, necessitates that all exposed areas of skin are covered. Hands, in particular, will need specific thermal-insulating gloves designed for low temperatures and these must never be used if damp or wet. The face should also be protected by a full face visor. This becomes particularly

important when cryovials are being removed from liquid phase storage. The liquid gas can enter such vials during storage. The gas phase of nitrogen occupies approximately 700-fold the space of the liquid. Hence boiling of the liquid in a closed vial generates unbearable pressure that can result in explosive projections.

• The huge expansion of liquid nitrogen also causes boiling of the liquid to displace air if ventilation is insufficient. As nitrogen is an asphyxiant gas, careful consideration must be given to storage and transport. Ventilation must be adequate at all times to prevent buildup of the boiled gas produced under normal storage and the amount of gas that could be immediately produced in the event of a vessel rupture. Storage of large liquid nitrogen volumes needs specialist attention, including automatic oxygen level monitoring in the area. There have unfortunately been notable cases of death by asphyxiation where storage and monitoring have not been appropriate.

DMSO, which is often used in cryopreservation, must be handled with care. The chemical is flammable, although high temperatures are required to generate a risk of explosion. DMSO readily permeates some types of gloves and the skin. In itself DMSO is not hugely toxic to the body; however, DMSO may carry other chemicals and allergens through the skin barrier (Freshney, 2000).

2. *Cryopreservation of Adherent and Suspension Cells*

It is impractical to maintain cell lines in culture indefinitely as cell cultures will undergo genetic drift with continuous passage and risk losing their differentiated characteristics. It therefore becomes necessary to store cell stocks for future use and as a backup in case of contamination or alterations in the characteristics of the cells. There should be a limit placed on the number of passages any cell line can undergo before being discarded and replaced with new cells from the cryopreserved stock (e.g., a limit of 10 passages). Nearly all cell lines can be cryopreserved indefinitely in liquid nitrogen at –196°C. The cryopreservation process is based on slow freeze and fast thaw, together with a high protein concentration (foetal calf serum) and the presence of a cryopreservative agent that increases membrane permeability (e.g., DMSO or glycerol).

Cryopreservatives may be classed as being penetrative or nonpenetrative. Penetrative cryopreservatives, such as DMSO and glycerol, protect the cells against freezing damage caused by intracellular ice crystals and osmotic effects. Nonpenetrative cryopreservatives, such as serum, protect the cells from damage by extracellular ice crystals. Cells should only be cryopreserved when in the exponential phase of growth to increase the chances of good recovery. It is important to check each batch of cryopreserved vials for viability, sterility, and maintenance of specific cell characteristics.

Protocol 3. Cryopreservation of Adherent and Suspension Cells

Media and Solutions

2× freezing medium (20% DMSO): To prepare 20 ml of freezing medium, add 4 ml of DMSO to 16 ml of FCS. Filter sterilise the solution using a 0.22-µm low-protein-binding filter. Aliquot the final solution into 5-ml amounts and store at –20°C.

Procedure

1. Check cultures using an inverted microscope to assess the degree of cellular growth and to ensure that the cells are free of contamination. Adherent or suspension cells are harvested for cryopreservation in the exponential phase of growth (refer to Protocols 1 and 2) and are counted as described in the article by Hoffman. Ideally, the cell viability should be greater than 90% in order to achieve a good recovery after freezing.
2. Thaw the 2× freezing medium and leave at 4°C until required.
3. Resuspend the cells in a suitable volume of serum. Slowly, in a dropwise manner, add an equal volume of the cold 20% DMSO/serum solution (or alternative freezing medium) to the cell suspension while at the same time gently swirling the cell suspension to allow the cells to adapt to the presence of DMSO. Note that DMSO is toxic to cells if added too quickly. The final concentration of DMSO should be 10%.
4. Place a total volume of 1 ml of this suspension, which ideally should contain between 5×10^6 and 1×10^7 cells, into each cryovial. Ensure that each cryovial is clearly marked with the cell line name, passage number, and date of freezing.
5. Place these vials in the vapour phase of a liquid nitrogen container, which is equivalent to a temperature of –80°C for a minimum of 3 h (or overnight).
6. Remove the vials from the vapour phase of the liquid nitrogen container and transfer them to the liquid phase for storage (–196°C).

Notes

• DMSO is a good universal cryoprotectant and most cell lines can be frozen down in a final concen-

tration of 5–10% DMSO. However, it may not be suitable for every cell line

i. Alternative freeze medium (e.g., glycerol): check the suitability on individual cell lines.
ii. It may have differentiation effects on certain cell lines (Freshney, 2000).

• Programmable freezers: the European Collection of Animal Cell Cultures (ECACC) recommends a cooling rate of –3°C per minute for most cell types.

• With serum-free conditions, nonpenetrative cryoprotectants such as methylcellulose and polyvinylpyrollidone (Merten *et al*., 1995; Ohno *et al*., 1988) can be used as alternatives to serum to maintain serum-free conditions (Keenan *et al*., 1998).

Protocol 4. Thawing of Cryopreserved Cells

1. Aliquot a volume of 9 ml of medium to a sterile container. Remove the cryopreserved cells from the liquid nitrogen and thaw at 37°C. It is important to thaw the cryopreserved cells rapidly to ensure minimal damage to the cells by the thawing process and the cryopreservation agent DMSO, which is toxic above 4°C.

2. Allow the contents to thaw until a small amount of ice remains in the cryovial.

3. Wipe the outside of the cryovial with a tissue moistened with 70% IMS (or alternative) and transfer the cell suspension to the previously aliquoted media.

4. Centrifuge the resulting cell suspension at 1000 rpm for 5 min to remove the cryoprotectant. Remove the supernatant and resuspend the pellet in fresh culture medium.

5. Assess the viability of the cells as described in the article by Hoffman to ensure that the viability is above 90%.

6. Add cells to an appropriately sized tissue culture flask (usually a 25- or 75-cm^2 flask) with a suitable volume of growth medium. Allow adherent cells to attach overnight and refeed the next day to remove any dead or floating cells. It is advisable to start cultures at between 30 and 50% of their final maximum cell density as this allows the cells rapidly to condition the medium and enter the exponential phase of growth.

IV. COMMENTS

• The procedures described in this article are applicable to many different continuous cell lines. However, some specialised cell types require special conditions for growth and differentiation (e.g., defined media, growth factors, coated flasks/plates) and are described elsewhere within this volume.

• A number of other basic cell culture procedures are also applicable to this article but are described elsewhere. These include cell counting (Hoffman) proliferation assays (Riss and Moravec), cell line authentication (Hay), and testing of cell cultures for microbial and viral contamination, including *Mycoplasma* (Hay and Ikonomi).

References

Angerman, D. (ed.) (1999). "*Handbook of Compressed Gases: Compressed Gas Association*," 4th Ed. Kluwer Academic, New York.

Doyle, A., Griffiths, J. B., and Newell, D. G. (eds.) (1998). "*Cell and Tissue Culture: Laboratory Procedures*." Wiley, New York.

Freshney, R. I. (ed.) (1992). "*Animal Cell Culture, a Practical Approach*," 2nd Ed. IRL Press, Oxford.

Freshney, R. I. (ed.) (2000). "*Culture of Animal Cells: A Manual of Basic Techniques*," 4th Ed. Wiley-Liss, New York.

Gey, G., Coffman, W. D., and Kubiech, M. T. (1952). *Cancer Res.* **12**, 264.

Keenan, J., Meleady, P., and Clynes, M. (1998). Serum-free media. *In* "*Animal Cell Culture Techniques*" (M. Clynes, ed.), pp. 54–66. Springer-Verlag, New York.

Merten, O. W., Peters, S., and Couve, E. (1995). A simple serum free freezing medium for serum free cultured cells. *Biologicals* **23**, 186–189.

Ohno, T., Kurita, K., Abe, S., Eimori, N., and Ikawa, Y. (1988). A simple freezing medium for serum-free cultured cells. *Cytotechnology* **1**, 257–260.

Richmond, J. Y., and McKinney, R. W. (eds.) (1999). "Biosafety in Microbiological and Biomedical Laboratories." U.S. Department of Health and Human Services, Public Health Service Centers for Disease Control and Prevention and National Institutes of Health. 4th Ed. U.S. Government Printing Office, Washington. 1999 Web edition: http://www.cdc.gov/od/ohs/biosfty/bmbl4/bmbl4toc.htm.

Shaw, A. J. (ed.) (1996). "*Epithelial Cell Culture: A Practical Approach*." IRL Press, Oxford.

CHAPTER

3

Counting Cells

Tracy L. Hoffman

I. INTRODUCTION

Cell culture is the technique of growing cell lines or dissociated cells extracted from normal tissues or tumors. The *cell count* measures the status of the culture at a given time and is essential when subculturing or assessing the effects of experimental treatments on cells. The cell count can be expressed as the number of cells per milliliter of medium (for suspension cultures) or per centimeter squared area of attachment surface (for monolayer cultures).

II. MATERIALS AND INSTRUMENTATION

Dulbecco's phosphate-buffered salire (PBS; DPBS) and *exclusion dyes* are available from ATCC (DPBS, Cat. No. 30-2200; 0.1% erythrosin B stain solution, Cat. No. 30-2404; 0.4% trypan blue stain solution, Cat. No. 30-2402). Citric acid and crystal violet are available from Sigma Chemical Co. (citric acid, Cat. No. C-0759; crystal violet, Cat. No. C-0775). The hemocytometer set and tally counter can be obtained from VWR (double Neubauer chamber and cover glass, Cat. No. 15170-173 or Bright-Line chamber with Neubauer ruling and cover glass, Cat. No. 15170-172; tally counter, Cat. No. 15173-252).

The Innovatis "Cedex" cell analysis system and associated reagents are available within the United States from Biomedical Resources International, Inc. (Cedex System, Cat. No. 702 00 00 00; 20-position automatic sampler, Cat. No. AS20, autosampler cups, Cat. No. 600 05 00 00; detergent concentrate, Cat. No. 702.00.125 or 702.00.250; density reference beads, Cat. No. 7 60 00 00 17). The Vi-CELL cell viability analyzer is available from Beckman Coulter (1-position carousel model, Part No. 6605617; 12-position carousel model, Part No. 6605587). The NucleoCounter mammalian cell counting system is available from New Brunswick Scientific (NucleoCounter, Cat. No. M1293-0000; NucleoCassettes, Cat. No. M1293-0100; starter kit, Cat. No. M1293-0020).

III. PROCEDURES

Cell culture measurements can be divided into three major categories: (1) visual methods using light microscopy and a hemocytometer; (2) indirect visual methods, which count cell nuclei using light microscopy and a hemocytometer; and (3) electronic systems, which automate the visual method.

A. Visual Methods

This procedure is taken from those of Absher (1973), Freshney (2000), Merchant *et al.* (1964), and Phillips (1973).

The most practical method for routine determination of the number of cells that are in suspension or that can be put into suspension is a direct count in a *hemocytometer*. The hemocytometer is a modified glass slide engraved with two counting chambers of known area. Each chamber grid is composed of nine squares (subgrids), with each square being 1 mm^2 (see Fig. 1). The hemocytometer is supplied with a glass coverslip of precise thickness that is supported 0.100 mm above the ruled area.

Copyright 2006, Elsevier Science (USA).
All rights reserved.

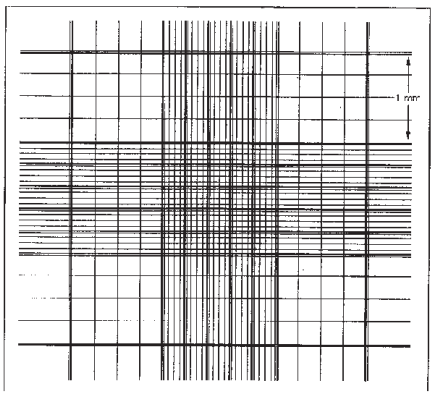

FIGURE 1 Schematic of one chamber grid of a hemocytometer with Neubauer ruling.

When the coverslip is positioned correctly, the volume of liquid over each square (subgrid) is a known constant, 0.1 mm^3 or 1.0×10^{-4} mL. If cells are counted in each of the corner squares and in the central squares of each of the two chamber grids, a total volume of 1×10^{-3} mL ($10 \times 0.1\,mm^3 = 1.0\,mm^3$) will have been examined, and the cells per milliliter (concentration) of the sample added to the hemocytometer can be determined by multiplying the count by 1000. It should be noted that when cells are diluted in stain or buffer during preparation, then multiplication by the appropriate dilution factor is also required to obtain the concentration of the sample. *Determination of viability* with the hemocytometer method involves the dye exclusion test. This test relies on the ability of living cells to exclude certain stains from crossing the cell membrane. Dead cells are permeable and will take up the stain.

1. Dilution of Cell Suspension

a. Place 0.3 mL of sterile DPBS into a polypropylene tube capable of holding at least a 1.0-mL volume.

b. Aseptically collect a sample from the suspension culture or detached monolayer culture. Prior to collection, mix the cell culture to be counted by pipetting up and down two to five times.

c. Transfer 0.1 mL of the mixed culture sample to the tube containing the DPBS (Step 1a). Mix by pipetting up and down two to five times.

d. Add 0.1 mL exclusion dye (0.1% erythrosin B or 0.4% trypan blue) to the tube containing the cell suspension (step 1c). Mix by pipetting up and down two to five times.

2. Use of Hemocytometer and Counting of Cells

a. Obtain a hemocytometer and coverslip from storage (70% alcohol bath). Wipe both pieces dry and put coverslip in place. With a Pasteur pipette or pipetman and pipette tip, introduce enough homogeneous stained cell suspension (Step 1d) to the V-shaped filling troughs for each of the two chambers to fill the hemocytometer.

b. Place the hemocytometer on the microscope stage and focus with an objective that will permit one subgrid (one of the nine squares) to be visible (usually 100 × magnification).

c. Using a tally counter with at least two registers, count viable (nonstained) cells and nonviable (stained) cells in each grid by counting cells in each of 10 subgrids (5 subgrids per chamber grid). The subgrids to be counted are the 4 outer, corner subgrids and the middle subgrid in each of the two chambers.

d. Remove cells from hemocytometer and return it to storage.

3. Calculation of Cell Count

a. Calculate the viable cell concentration using the formula $C = N \times D \times 10^3$, where C is the viable cells/mL, N is the number of viable cells counted in 10 subgrids (1.0 mm^3), D is the dilution factor, and 10^3 is the hemocytometer correction factor.

b. Calculate percentages cell viability using the formula $V = N/T \times 100\%$, where V is the percentage viability, N is the number of viable cells counted per 10 subgrids (1 mm^3), and T is the number of total cells counted per 10 subgrids (1 mm^3).

B. Indirect Visual Methods

This procedure is modified from that of Patterson (1979).

Some adherent cells, such as human diploid cells, are difficult to count directly. In such cases, a procedure can be used to stain and count cell nuclei rather than the cells themselves.

1. Preparation of Solutions

a. Prepare 0.1 *M* citric acid by dissolving 1.9212 g in 100 mL distilled water.

b. Prepare 0.1 *M* citric acid containing 0.01% (w/v) crystal violet by dissolving 0.005 g crystal violet (also known as basic violet 3 or gentian violet; C.I.42555) in 50 mL of the 0.1 *M* citric acid (prepared in step B1b)

2. Procedure

a. Aseptically transfer a sample from the suspension culture or detached monolayer culture containing approximately 5×10^5 cells to a centrifuge tube. Prior to collection, mix cell culture to be counted by pipetting up and down two to five times.

b. Centrifuge at 500 ± 50 *g* for 5 to 10 min.

c. Decant the supernatant. Add 1.0 mL 0.1 *M* citric acid solution to the cell pellet. Mix well and incubate at 35° to 37°C for 1 to 2 h.

d. Separate nuclei by violent shaking followed by centrifugation at 1000 ± 100 *g* for 20 to 25 min.

e. Discard supernatant. Resuspend the cell pellet in 0.5 to 1.0 mL citric acid-crystal violet solution.

3. Use of Hemocytometer and Counting of Cells

a. Obtain a hemocytometer and coverslip from storage (70% alcohol bath). Wipe both pieces dry and put coverslip in place. With a Pasteur pipette or pipetman and pipette tip, introduce enough homogeneous stained cell suspension (step 1d) to the V-shaped filling troughs for each of the two chambers to fill the hemocytometer.

b. Place the hemocytometer on the microscope stage and focus with an objective that will permit one subgrid (one of the nine squares) to be visible (usually 100X magnification).

c. Using a tally counter, count stained nuclei in each grid by counting nuclei in each of 10 subgrids (5 subgrids per chamber grid). The subgrids to be counted are the 4 outer, corner subgrids and the middle subgrid in each of the two chambers.

d. Remove cells from hemocytometer and return it to storage.

4. Calculation of Cell Count

Calculate the cell concentration using the formula $C = N \times D \times 10^3$, where C is the cells/mL, N is the number of nuclei counted in 10 subgrids (1.0 mm^3), D is the dilution factor, and 10^3 is the hemocytometer correction factor.

C. Electronic Systems

The visual method can be user dependent, tedious, and time-consuming. Over the course of the last few years, systems that eliminate these problems through the automation of the process have become available commercially. There are two major types of system: (1) those that use trypan blue to arrive at a viable cell count and (2) those that use propidium iodide (PI) for counting cell nuclei.

1. Automated Trypan Blue Method

Both the Cedex system (Innovatis) and the Vi-CELL system (Beckman Coulter) incorporate image analysis technology and fluidics management to automate the mixing, staining, and hemocytometer counting process. As a result, the staining process is executed with high precision and reproducibility. Automation of the sample preparation process eliminates human errors in connection with pipette handling.

a. Set up the system with the appropriate reagents following the manufacturer's instructions.

b. Calibrate the system as per the manufacturer's schedule and instructions.

c. Aseptically collect a sample from the suspension culture or detached monolayer culture. Prior to collection, mix the cell culture to be counted by pipetting up and down two to five times. Transfer at least 1.0 mL to a sample cup.

d. Load sample cup onto the unit.

e. Log in pertinent information about the sample and initiate the counting sequence.

f. When the count cycle is complete (typically about 3 min), the viable cell density, total cell density, and percentage viability will appear on the screen. The results can then be printed and saved as appropriate.

g. After use, the sample cup(s) can be disposed of as biological waste. The system flow path is flushed and cleaned automatically, following each count, as part of the count cycle.

2. Automated Propidium Iodide Method

Similar to the Cedex and Vi-CELL systems, the NucleoCounter mammalian cell counting system (New Brunswick Scientific) also incorporates image analysis technology and fluidics management to automate the mixing, staining, and hemocytometer counting process. Unlike these systems, however, the NucleoCounter stains nuclei rather than intact cells. Because of this, two separate counts are needed to obtain culture viability.

a. Aseptically collect two samples from the suspension culture or detached monolayer culture. Prior to collection, mix the cell culture to be counted by pipetting up and down two to five times.

b. Pretreat the first sample with lysis and stabilization buffers following the manufacturer's instructions. Load the pretreated sample into the NucleoCassette. Place into the unit and press "run."

c. A total cell count will be displayed when the run is complete (typically about 30 s).

d. Load the second, untreated sample into another NucleoCassette. Place into the unit and press "run."

e. A total cell count will be displayed when the run is complete (typically about 30 s).

f. Divide the total count obtained from the pretreated sample (step C2b) by the total count obtained from the untreated sample (step C2d) and multiply by 100% to obtain the percentage viability of the culture.

g. After use, the NucleoCassette(s) can be disposed of as biological waster, with the PI dye safely enclosed. The system itself requires no cleaning.

IV. PITFALLS

A. The visual method is best applied when only a few samples are to be counted. If numerous cultures are to be counted on a routine basis, electronic systems should be considered.

B. The dye exclusion test gives information about the integrity of the cell membrane, but does not necessarily indicate how the cell is functioning.

C. Trypan blue has a greater affinity for serum proteins than for cellular protein. It is recommended that cells be suspended in DPBS or serum-free medium before counting when using this exclusion dye. When using trypan blue as the exclusion dye, mix the sample well and allow it to stand for 5 to 10 min prior to performing the cell count.

D. Among the major errors in all visual counts are:

1. *Nonuniform cell suspensions*. The total volume over a chamber grid is assumed to be a random sample. This assumption is invalid unless the cell suspension is uniform and free of cell clumps. Also, cells settle from suspensions rapidly. A uniform suspension can only be obtained if cells are mixed thoroughly before sampling.
2. *Improper filling of chamber grids*. The chamber must be filled by capillary action, without overflowing. Both pipettes and the hemocytometer set must be scrupulously clean.
3. *Failure to adopt a routine method for counting cells in contact with boundary lines*. All such conventions are arbitrary, but are essential to obtain reproducible results by counting comparable areas. The most commonly used method is to count only those cells that touch the left and/or upper boundary lines. Those cells that touch the right and/or lower boundary lines are not counted.
4. *Statistical error*. The cell sample should be diluted so that no fewer than 10 and no more than 50 cells are over each 1-mm^2 square. Because the cells follow a Poisson distribution in the hemocytometer chamber grids, the count error will be approximated by the square root of the count. Using the best techniques, an experienced individual can generally obtain counts with a total error of 10 to 15% (Absher, 1973).

E. The dynamic range for the Cedex and Vi-CELL systems is 1×10^4 to 1×10^7 cells/mL. For the NucleoCounter, it is 5×10^3 to 4×10^6, with the optimum being 10^5 to 2×10^6 cells/mL. Samples should be diluted or concentrated as appropriate and rerun if the values reported by the system fall outside these ranges.

F. Due to the small bore of the flow cell path in the Cedex and Vi-CELL systems, routine maintenance of the instruments as outlined by the manufacturer is critical. Failure to perform routing priming and/or flushing could result in clogging.

References

Absher, M. (1973). Hemocytometer counting. *In "Tissue Culture: Methods and Applications"* (P. F. Kruse, Jr., and M. K. Patterson, Jr., eds.), pp. 395–397. Academic Press, New York.

Freshney, R. I. (2000) Quantitation. *In "Culture of Animal Cells: A Manual of Basic Technique,"* 4th Ed., pp. 309–312. Wiley-Liss, New York.

Merchant, D. J., Kahn, R. H., and Murphy, W. H., Jr. (1964). *"Handbook of Cell and Organ Culture,"* 2nd Ed., pp. 155–157. Burgess, Minneapolis.

Patterson, M. K. (1979). Measurement of growth and viability of cells in culture. *In "Cell Culture"* (W. B. Jakoby and I. H. Pastan, eds.), pp. 141–149, Academic Press, New York.

Phillips, H. J. (1973). Dye exclusion test for cell viability. *In "Tissue Culture: Methods and Applications"* (P. F. Kruse, Jr., and M. K. Patterson, Jr., eds.), pp. 406–408. Academic Press, New York.

CHAPTER

4

Cell Proliferation Assays: Improved Homogeneous Methods Used to Measure the Number of Cells in Culture

Terry L. Riss and Richard A. Moravec

I. INTRODUCTION

Over the last decade several improvements have been made in assay technology to enable miniaturization and more efficient measurement of the number of cells present in microwell plates. A variety of different methods have been optimized for convenient use in multiwell formats, making it easier to do large numbers of assays. The most significant improvement in efficiency has been the development of homogeneous "add, mix, and measure" assay formats compatible with robotic automation for high-throughput screening (HTS) of test compounds.

Making a choice among available assay formats often depends on the preference for which marker is measured or the level of sensitivity required. Homogeneous assays are now available to measure total cell number, viable cell number, the number of dead cells present in a population, or the number of cells undergoing apoptosis. For many experimental systems the most useful information is the number of viable cells at the end of a treatment period. The parameter used most conveniently to determine the number of viable cells in culture is measurement of an indicator of active metabolism.

This article describes four options for measuring cell number that are based on assaying different aspects of cellular metabolism. The example assays chosen include ATP quantitation, tetrazolium reduction using [3-(4,5-dimethylthiazol-2-yl)-5-(4-sulfophenyl)-2*H*-tetrazolium, inner salt (MTS), resazurin reduction, and total lactate dehydrogenase (LDH) activity measurement. The four examples are all homogeneous methods sensitive enough to detect cell numbers typically used in automated high-throughput 96- and 384-well plate formats. The methods are equally suitable for measuring just a few samples processed manually. In addition, all of these assays have been shown to be reproducible and exhibit good *Z′*-factor values (Zhang *et al*., 1999) desirable for automated HTS applications. Each assay has its own set of advantages and disadvantages that contribute to the decision of which one to choose.

II. MATERIALS

RPMI 1640 culture medium containing 15 m*M* HEPES (Cat. No. R-8005), 2-mercaptoethanol (Cat. No. M-7154), trypan blue solution (0.4% Cat. No. T-8154), and phenazine ethosulfate (PES; Cat. No. P-4544) are from Sigma. Fetal bovine serum (Cat. No. SH30070) is from Hyclone. Ninety-six-well plates with opaque white walls and clear bottoms (Cat. No. 3610) are from Corning.

The CellTiter-Glo luminescent cell viability assay (Cat. No. G7571) for determining ATP content, the CytoTox-ONE homogeneous membrane integrity

Copyright 2006, Elsevier Science (USA).
All rights reserved.

assay (Cat. No. G7891) for determining total LDH activity, the CellTiter 96 AQ_{ueous} one solution cell proliferation assay (Cat. No. G3580) for measuring MTS tetrazolium reduction, the CellTiter-Blue cell viability assay (Cat. No. G8080) for measuring resazurin reduction, and recombinant human interleukin (IL)-6 (Cat. No. G5541) are from Promega.

III. INSTRUMENTATION

The Model MTS-4 plate shaker obtained from IKA Works, Inc. is used to mix the contents of the 96-well plates. Absorbance is recorded using a Molecular Devices V_{max} plate reader spectrophotometer. Luminescence is recorded using a Dynex MLX plate-reading luminometer. Fluorescence is recorded using a Labsystems Fluoroscan Ascent fluorescence plate reader fitted with a 560 (excitation) and 590 (emission) filter pair.

IV. PROCEDURES

The assay plates for all four procedures are prepared in an identical manner using stock cultures of the IL-6-dependent B9 hybridoma cell line. B9 cells are cultured in RPMI 1640 containing 15 m*M* HEPES and 50 µ*M* 2-mercaptoethanol supplemented with 10% fetal bovine serum (assay medium) and 2 ng/ml of IL-6 (specific activity 168 U/ng protein, assigned by direct comparison to the interim reference standard #88/514 from the National Institute of Biologic Standards and Controls). Cell cultures are maintained at densities between 2×10^4 and 3×10^5/ml in a humidified chamber at 37°C with 5% CO_2.

Stock cultures of cells used to prepare the proliferation assay are seeded at 2×10^4/ml in standard T-75 flasks containing assay medium supplemented with 2 ng/ml IL-6 and are allowed to expand for 3 days. Cells are harvested using centrifugation (4 min at 200 *g*) and washed twice using assay medium without IL-6. Cells are suspended in assay medium without IL-6, treated with trypan blue solution, counted using a hemocytometer, and adjusted to 6.25×10^4 viable cells/ml. Eighty microliters of cell suspension (5000 cells) is dispensed into each well of multiple 96-well clear-bottom white opaque walled plates with replicates of four for each sample.

Serial two-fold dilutions of IL-6 are prepared in assay medium without IL-6 so 20-µl/well additions would contain a final concentration range of 0–2.0 ng/ml. An equivalent volume of assay medium without IL-6 is added to sets of negative control wells. Assay plates are cultured for 72 h at 37°C with 5% CO_2 before processing with each of the cell number assays.

A. MTS Tetrazolium Reduction Assay

Viable cells reduce tetrazolium compounds into intensely colored formazan products that can be detected as an absorbance change with a spectrophotometer. The amount of formazan color produced is directly proportion to the number of viable cells in standard culture conditions. Cells rapidly lose the ability to reduce tetrazolium compounds shortly after death, which enables tetrazolium reduction to be used as an indicator of viable cell number. The first MTT tetrazolium reduction cell proliferation assay was described two decades ago (Mosmann, 1983). Upon cellular reduction, the MTT tetrazolium reagent results in the formation of a formazan precipitate and requires the addition of a solubilizing agent to generate a solution suitable for recording absorbance.

The chemical properties of the MTS tetrazolium compound provide an improvement over the MTT assay. The formazan product resulting from bioreduction of MTS is directly soluble in cell culture medium, thus eliminating the solubilization step required for the MTT assay. The chemical properties of MTS that contribute to the formation of a soluble formazan product also restrict entry of MTS into viable cells. As a result, cell-permeable, electron-coupling agents (such as PES) are used in combination with MTS to shuttle in and out of cells to pick up reducing equivalents from molecules such as NADH. The reduced PES can move from the cytoplasm into the culture medium and reduce MTS into the soluble formazan product.

The combination of MTS + PES provides an assay that requires only a single reagent addition to the cell culture wells and results in a homogeneous "add, incubate, and measure" assay format. An additional advantage of using aqueous soluble tetrazolium assays is that data can be recorded from the same plate at various intervals after the addition of MTS + PES, which simplifies the optimization of the incubation period during characterization of the effects of particular compounds on cells (Fig. 1). The sensitivity of the MTS assay is dependent on cell type, but it is usually adequate for detecting the number of cells used commonly in microwell plates. Typically, the MTS assay can detect fewer than 1000 viable cells/well in the 96-well plate format or fewer than 250 cells/well in 384-well plates. For additional background information, refer to Promega Technical Bulletin #245.

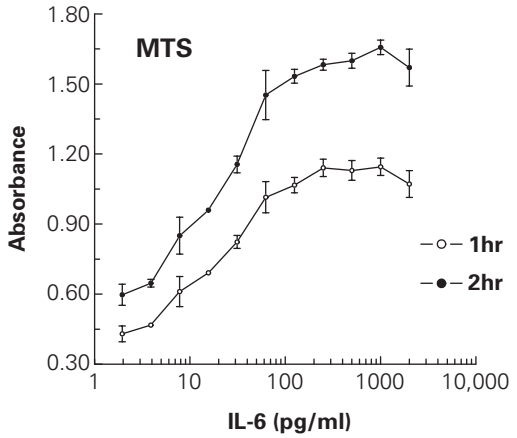

FIGURE 1 The effect of different concentrations of IL-6 on cell number was determined by measuring MTS reduction to the colored formazan product. Absorbance at 490 nm was recorded after 1 h of incubation with the MTS + PES reagent. Plates were returned to the cell culture incubator for an additional hour before recording the 490-nm absorbance after a total of 2 h of incubation. The 490-nm absorbance from control wells of cells without IL-6 (not shown on the log scale) was 0.39 for 1 h of incubation and 0.54 for 2 h of incubation. Values represent the mean ± standard deviation from four replicate wells.

Steps

1. Warm the CellTiter 96 AQ_{ueous} one solution reagent to 37°C. (*Note*: The reagent contains 2 mg/ml MTS tetrazolium and 300 µM PES electron transfer reagent in a solution of phosphate-buffered saline. This solution is photolabile and should be stored protected from light.)
2. Remove the multiwell assay plate from the cell culture incubator and transfer to a laminar flow hood.
3. Add 20 µl of CellTiter 96 AQ_{ueous} one solution reagent to the culture medium in each well using a multichannel pipette and aseptic conditions.
4. Mix the contents of the culture wells using a plate shaker to ensure uniform suspension of MTS reagent in the culture medium.
5. Return assay plate to a 37°C cell culture incubator for a period of 1 to 4 h, depending on the number and metabolic activity of cells being used.
6. Transfer assay plate to a multiwell plate-reading spectrophotometer, shake plate for 10 s (using the instrument's on-board plate shaking function) to ensure a uniform solution in the assay wells, and record absorbance at 490 nm.
7. Plot 490 nm absorbance vs cell number.

B. ATP Assay

The measurement of ATP has become widely accepted as a valid indicator of the number of viable cells present in culture (Ekwall *et al*., 2000). Under cell culture experimental conditions that do not alter metabolism drastically, the amount of ATP is directly proportional to the number of viable cells (Crouch *et al*., 1993). Historically, sample preparation for ATP assays has been a multistep process requiring inactivation of endogenous ATPases (known to interfere with measurement of ATP) and neutralization of the acidic extract prior to addition to a luciferase-containing reaction mixture (Lundin *et al*., 1986; Stanley, 1986). Firefly luciferase purified from *Photinus pyralis* has been used most often as a reagent for ATP assays (Lundin *et al*., 1986; Crouch *et al*., 1993). Unfortunately, the native form of luciferase has only moderate stability *in vitro* and is sensitive to its chemical environment, e.g., pH and detergents, thus limiting its usefulness for developing a robust homogeneous ATP assay.

A stable form of luciferase has been developed from a different firefly, *Photuris pennsylvanica*, using an approach of directed evolution to select for characteristics that improve performance in ATP assays. The development strategy included selection for increased thermostability and resistance to degradation products of luciferin, which inhibit luciferase activity. The unique characteristics of this mutant (Luc*Ppe2*^{m}) enabled design of a homogeneous single-step reagent approach for performing ATP assays on cultured cells that overcomes the problems caused by factors such as ATPases that reduce the level of ATP in cell extracts. The CellTiter-Glo reagent is physically robust and provides a sensitive and stable luminescent output that is ideal for automated HTS cell proliferation and cytotoxicity assays. The homogeneous "add, mix, and measure" format results in cell lysis, inhibition of endogenous ATPases, and generation of a luminescent signal proportional to the amount of ATP present. In addition, the CellTiter-Glo assay conditions generate a "glow-type" luminescent signal, having a half-life of greater than 5 h, providing flexibility for recording data.

For most situations, the ATP assay is the method of choice because it has a simple homogeneous "add–mix–measure" procedure, it provides the quickest way to collect data (i.e., it avoids the 1- to 4-h incubation step required for tetrazolium or resazurin assays), and it has the best detection sensitivity among all the available methods. The ATP-based detection of cells has been shown to be more sensitive than other methods (Petty *et al*., 1995). Assay sensitivity and range of responsiveness are typically between 50 and 50,000 cells/well in 96-well plates, but sensitivities of as few as 4 cells/well have been achieved using 384-well plates. For additional background information, refer to Promega Technical Bulletin #288.

Preparation of CellTiter-Glo Reagent

1. Allow a vial of the lyophilized substrate and a bottle of frozen assay buffer to equilibrate to ambient temperature (22°C).
2. Add 10 ml of assay buffer to the substrate to reconstitute the lyophilized cake and form the CellTiter-Glo reagent and mix gently to dissolve. The reagent is a buffered solution containing detergents to lyse cells, ATPase inhibitors to stabilize the ATP released from the lysed cells, luciferin as a substrate, and luciferase to generate a bioluminescent signal proportional to the amount of ATP present in the cell lysate.

Steps

1. Remove the multiwell assay plate from the cell culture incubator and equilibrate to ambient temperature for approximately 20–30 min. (*Note*: Transferring eukaryotic cells from 37°C to ambient temperature for the length of time required for temperature equilibration has little affect on cell viability or ATP content.)
2. Add a volume of CellTiter-Glo reagent equal to the volume of cell culture medium present in each well using a multichannel pipette. (*Note*: For 384-well plates containing 25 µl of culture medium, add 25 µl of reagent.)
3. Mix the contents of the assay wells to ensure uniform distribution of the reagent in the culture medium and to speed cell lysis.
4. Allow the assay plate to stand at ambient temperature for 10 min.
5. Record luminescence using a multiwell plate-reading luminometer.
6. Plot luminescence vs cell number (Fig. 2).

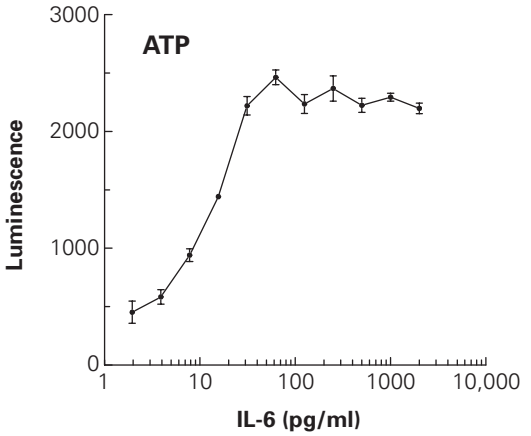

FIGURE 2 The effect of different concentrations of IL-6 on cell number was determined by measuring the total amount of ATP. Luminescence was recorded 10 min after addition of the CellTiter-Glo reagent. The luminescence of control wells of cells without IL-6 (not shown on the log scale) was 260 relative light units. Values represent the mean ± standard deviation from four replicate wells.

C. LDH Assay

Lactate dehydrogenase is a cytoplasmic enzyme that has been used as a marker of cell damage *in vitro* because the enzymatic activity is relatively stable in cell culture medium and can be measured easily after leakage out of cells with a compromised membrane (i.e., nonviable cells). The LDH assay is performed most commonly as a cytotoxicity assay by measuring the enzymatic activity from a sample of culture medium removed from the treated population of cells. Most assay methods require transfer of an aliquot of culture medium (without cells) into a separate assay vessel because the reagent formulation would damage living cells, resulting in the release of additional LDH (Korzeniewski and Callewaert, 1983). Reactions often proceed for 30 min and result in a colorimetric signal (Decker and Lohmann-Matthes, 1988).

Recent improvements in LDH assay performance have been accomplished by using more sensitive fluorescent reporter molecules and by formulating the assay reagents in a physiologically balanced buffer that is not harmful to viable cells. These improvements enabled the development of a rapid homogeneous cytotoxicity assay format to detect the number of damaged cells directly in cell culture wells containing a mixed population of viable and nonviable cells. The reagent used to perform the coupled enzymatic assay is a buffered solution containing lactate as a substrate and NAD^+ as a cofactor to drive the LDH reaction. The reagent also contains the enzyme diaphorase to catalyze the NADH-driven reduction of resazurin into the fluorescent resorufin product.

As illustrated in the following example procedure, the total number of cells in culture (i.e., viable and nonviable) also can be estimated using an LDH assay by measuring total enzymatic activity from the entire population of cells. The cytotoxicity assay format is modified to detect total LDH in cultures by including a cell lysis step in the procedure utilizing a detergent that is compatible with the LDH assay chemistry. The detection sensitivity and linear range of the fluorescent LDH assay are typically 800–50,000 cells/well in the 96-well plate format, with sensitivity improving to 200 cell/well in 384-well plates. For additional background information, refer to Promega Technical Bulletin #306.

Preparation of CytoTox-ONE Reagent

1. Allow a vial of the lyophilized substrate and a bottle of frozen assay buffer to equilibrate to ambient temperature (22°C).
2. Add 11 ml of assay buffer to the substrate to reconstitute the lyophilized cake and form the CytoTox-ONE reagent and mix gently to dissolve. Protect the reagent from direct light.

Steps

1. Remove the multiwell assay plate from the cell culture incubator.
2. Add 2 µl of the lysis solution component of the kit (i.e., 9% Triton X-100) to each 100 µl of culture medium to lyse the cells and release LDH into the surrounding medium. (*Note*: If it is inconvenient to pipette very small volumes, a 1:5 dilution of lysis solution may be prepared using water so 10 µl can be dispensed into each well.)
3. Shake the plate for approximately 10 s to ensure uniform distribution of the contents of the wells and to ensure complete cell lysis.
4. Equilibrate the plate to ambient temperature (approximately 20–30 min).
5. Add a volume of CytoTox-ONE reagent equal to the volume of cell culture medium present in each well using a multichannel pipette. (*Note*: For 384-well plates containing 25 µl of culture medium, add 25 µl of reagent to each well.)
6. Mix the contents of the assay wells for 30 s to ensure uniform distribution of the reagent in the culture medium.
7. Allow the assay plate to incubate at ambient temperature for 10–15 min for the LDH reaction to proceed.
8. Add 50 µl to each well of the stop solution [3% (w/v) sodium dodecyl sulfate] provided as a component of the CytoTox-ONE assay kit. (*Note*: Add 12.5 µl stop solution for the 384-well plate format containing 25 µl of cells in culture medium and 25 µl of CytoTox-ONE reagent.)
9. Record the fluorescence of resorufin using a multiwell plate reading fluorometer fitted with a filter set for 560-nm excitation and 590-nm emission wavelengths. (*Note*: The spectra of resorufin will enable a variety of filter sets to be used. Data can be collected using excitation filters in the range of 530–570 nm and emission filters in the range of 580–620 nm.)
10. Plot fluorescence vs cell number (Fig. 3).

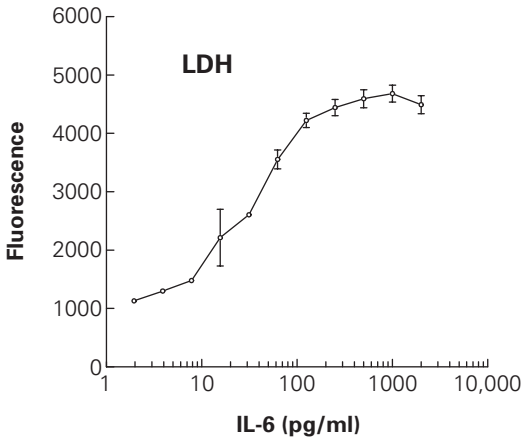

FIGURE 3 The effect of different concentrations of IL-6 on cell number was determined by measuring the total amount of LDH from the lysed population of cells. Cells were lysed by the addition of 2 µl/well of 10% (v/v) Triton X-100 in phosphate-buffered saline prior to addition of the CytoTox-ONE reagent. The reaction was stopped by addition of the stop solution, and fluorescence (560 excitation/590 emission) was recorded. The fluorescence value of control wells of cells without IL-6 (not shown on the log scale) was 1081 relative fluorescence units. Values represent the mean ± standard deviation from four replicate wells.

D. Resazurin Reduction Assay

Resazurin is a redox dye that can be reduced by cultured cells to form resorufin. Resazurin is dark blue and has little intrinsic fluorescence until it is reduced to the pink resorufin product. The spectral properties of resorufin allow the molecule to be detected using either fluorescence or absorbance; however, fluorescence is the preferred method because it provides greater sensitivity.

The resazurin reduction assay is based on the ability of metabolically active living cells to convert a redox dye (resazurin) into a fluorescent end product (resorufin). Resazurin can enter living cells where it becomes reduced, and the resazurin product, which is also permeable, can be found in the cell culture medium (O'Brien *et al.*, 2000). The specific cellular mechanisms responsible for the reduction of resazurin are unknown (Gonzales and Tarloff, 2001), but probably involve reactions generating reducing equivalents such as NADH. Nonviable cells lose metabolic capacity rapidly and do not reduce resazurin to generate a fluorescent signal. The resazurin substrate is soluble in phosphate-buffered saline compatible with preparation of a reagent for direct addition to cell cultures. The homogeneous assay procedure involves addition of a single resazurin-containing reagent directly to cells cultured in serum-supplemented medium. After an incubation step, data are recorded using either a plate-reading fluorometer (preferred method) or a spectrophotometer. The reagent is generally nontoxic to cells, allowing extended incubation periods in some

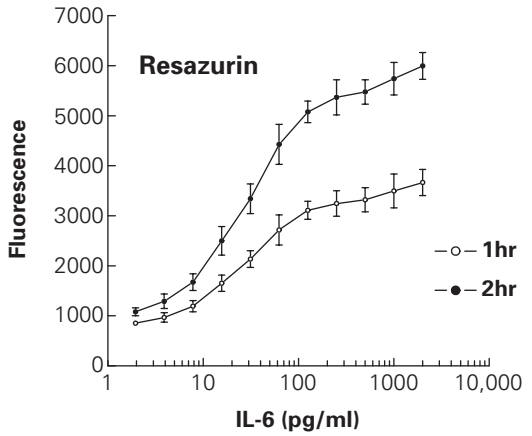

FIGURE 4 The effect of different concentrations of IL-6 on cell number was determined by measuring the ability of viable cells to reduce resazurin into the fluorescent resorufin. Fluorescence was recorded after 1 h of incubation with the CellTiter-Blue reagent. Plates were returned to the cell culture incubator for an additional hour before recording fluorescence a second time after a total of 2 h of incubation. The average fluorescence from control wells of cells without IL-6 (not shown on the log scale) was 814 for 1 h of incubation and 1017 for 2 h of incubation. Values represent the mean ± standard deviation from four replicate wells.

situations. Fluorescence data can be recorded at various intervals after the addition of resazurin, which simplifies optimization of the incubation period during characterization of the effects of particular compounds on cells (Fig. 4). Longer incubation periods may result in increased detection sensitivity; however, there may be a loss in the linear range of response. Assay sensitivity and range depend on cell type and metabolic capacity, but are typically between 200 and 50,000 cells/well in 96-well plates. For additional background information, refer to Promega Technical Bulletin #317.

Steps

1. Thaw CellTiter-Blue reagent containing resazurin and warm to 37°C.
2. Remove the multiwell assay plate from the cell culture incubator and transfer to a laminar flow hood.
3. Add 20 µl CellTiter-Blue reagent to each well containing 100 µl culture medium using a multichannel pipette and aseptic conditions. (*Note*: For 384-well plates containing 25 µl of culture medium, add 5 µl/well of CellTiter-Blue reagent.)
4. Mix the contents of the assay wells for 10 s to ensure uniform distribution of the reagent in the culture medium.
5. Return assay plate to a 37°C cell culture incubator for a period of 1 to 4 h to develop the fluorescent resorufin product.
6. Record the fluorescence of resorufin using a multiwell plate-reading fluorometer fitted with a filter set for 560-nm excitation and 590-nm emission wavelengths. (*Note*: The spectra of resorufin will enable a variety of filter sets to be used. Data can be collected using excitation filters in the range of 530–570 nm and emission filters in the range of 580–620 nm.)
7. Plot fluorescence vs cell number.

V. COMMENTS

Each assay format has its own set of advantages and disadvantages. The tetrazolium assay is currently the most widely used method of estimating the number of viable cells in multiwell plates and is the most often cited in the scientific literature. The resazurin reduction assay is functionally similar to the tetrazolium assay, except it has the optional advantage of using fluorescent detection methods. In contrast to the tetrazolium and resazurin reduction assays that require 1–4 h of incubation to obtain meaningful results, data from ATP and LDH assays can be obtained after a 10-min incubation. The ATP and LDH assays lyse cells and thus provide "a snapshot" of the condition of the cells at time of lysis. This advantage provides a quicker assay and avoids any toxic effects of the assay reagents that may occur during the incubation period. For many applications, the ATP assay may be the best choice. It is the most sensitive, provides results faster than any of the other assays, and is the easiest to use. However, one of the limitations of the ATP assay is that it requires a multiwell plate-reading luminometer that may not be available in all laboratories. The choice of which particular assay format to use may depend on the availability of instruments to record data, the detection sensitivity required, the number of samples to be measured, and whether total cell number, viable cell number, or nonviable cell number is chosen as an end point for measurement.

Multiplexing of two assays to gather more than one type of data from the same experimental well may help eliminate the possibility of artifacts. For example, an LDH cytotoxicity assay and an ATP viability assay can be done using the same sample of cells. A small aliquot of culture supernatant can be used for estimating the number of dead cells by measuring the amount of LDH released into the culture medium. Because the sample of cells remains intact, an ATP assay (or any of the other methods) can be used to measure viable or total cell number.

VI. PITFALLS

Temperature is a factor that affects the performance of the aforementioned assays because of its effect on enzymatic rates. It is critical to run the assays at a uniform temperature to ensure reproducibility across a single plate or among stacks of several plates. For assays developed at room temperature, it is important to ensure adequate equilibration of samples after the removal of assay plates from a 37°C incubator to avoid differential temperature gradients resulting in "edge effects." Stacking large numbers of assay plates together in close proximity should be avoided to ensure complete temperature equilibration.

Proper negative and positive controls are required to test whether compounds being measured have an effect on the assay chemistry or result in artifacts. For example, strong reducing compounds may interfere with procedures using redox dyes such as the tetrazolium or resazurin reduction assays. Culture medium supplemented with pyruvate will slow the rate of the LDH reaction and thus will require longer incubation periods to generate an adequate fluorescent signal in the CytoTox-ONE assay. In addition, different animal sera have different amounts of LDH activity that will influence background fluorescence. To correct for many of these factors, use of a "no treatment" negative control and a positive control to show maximum effect on each multiwell plate is recommended for all assays.

References

CellTiter 96 AQ_{ueous} One Solution Cell Proliferation Assay *Technical Bulletin* #TB245, Promega Corporation.

CellTiter-Blue Cell Viability Assay *Technical Bulletin* #TB317, Promega Corporation.

CellTiter-Glo Luminescent Cell Viability Assay *Technical Bulletin* #TB288, Promega Corporation.

Cory, A. H., *et al*. (1991). Use of an aqueous soluble tetrazolium/formazan assay for cell growth assays in culture. *Cancer Commun.* **3**(7), 207–212.

Crouch, S. P., *et al*. (1993). The use of ATP bioluminescence as a measure of cell proliferation and cytotoxicity. *J. Immunol. Methods* **160**, 81–88.

CytoTox-ONE Homogeneous Membrane Integrity Assay *Technical Bulletin* #TB306, Promega Corporation.

Decker, T., and Lohmann-Matthes, M. L. (1988). A quick and simple method for the quantitation of lactate dehydrogenase release in measurements of cellular cytotoxicity and tumor necrosis factor (TNF) activity. *J. Immunol. Methods* **115**, 61–69.

Ekwall, B., *et al*. (2000). MEIC Evaluation of acute systemic toxicity. VIII. Multivariat partial least squares evaluation, including the selection of a battery of cell line tests with a good prediction of human acute lethal peak blood concentrations for 50 chemicals. *Altern. Lab. Anim.* **28**(Suppl. 1), 201–234.

Gonzales, R. J., and Tarloff, J. B. (2001). Evaluation of hepatic subcellular fractions for Alamar Blue and MTT reductase activity. *Toxicol In Vitro* **15**, 257–259.

Korzeniewski, C., and Callewaert, D. M. (1983). An enzyme-release assay for natural cytotoxicity. *J. Immunol. Methods* **64**, 313–320.

Lundin, A., *et al*. (1986). Estimation of biomass in growing cell lines by ATP assay. *Methods Enzymol.* **133**, 27–42.

Mosmann, T. (1983). Rapid colorimetric assay for cellular growth and survival: Application to proliferation and cytotoxicity assay. *J. Immunol. Methods* **65**, 55–63.

O'Brien, J., *et al*. (2000). Investigation of the Alamar Blue (resazurin) fluorescent dye for the assessment of mammalian cell cytotoxicity. *Eur. J. Biochem.* **267**, 5421–5426.

Petty, R. D., *et al*. (1995). Comparison of MTT and ATP-based assays for measurement of viable cell number. *J. Biolumin. Chemilumin.* **10**, 29–34.

Stanley, P. E. (1986).Extraction of adenosine triphosphate from microbial and somatic cells. *Methods Enzymol.* **133**, 14–22.

Zhang, H.-U., *et al*. (1999). A simple statistical parameter for use in evaluation and validation of high throughput screening assays. *J. Biomol. Screen.* **4**, 67–73.

CHAPTER

5

Development of Serum-Free Media: Optimization of Nutrient Composition and Delivery Format

David W. Jayme and Dale F. Gruber

I. INTRODUCTION

In a previous edition, we introduced many of the basic formulation concerns to be considered when developing a serum-free basal medium (Jayme and Gruber, 1998). Since that publication, societal and safety concerns have prompted additional scientific requirements that ultimately impact the construction of serum-free medium. Safety concerns, to be discussed at some length later in this article, now recommend all medium components to be animal-origin free (Jayme, 1999). Consistent with these guidelines, every medium constituent must document a traceable history free of primary or secondary contact with animal-origin products. These regulatory requirements apply to all scales of production from developmental to production formats, and are also extended to bioreactor supplementation and to downstream purification processes. This article reviews the impetus for these new requirements and improvements in serum-free medium development consistent with these directives.

Although many practitioners of tissue culture consider their field to be an art, others characterize it as a science. Both positions may be appropriate, considering the circumstances surrounding the ontogeny of medium development. The advantages of cultivating cells and tissues in a defined nutrient medium were first recognized over eighty years ago. However, since its inception, maturation of the tissue culture field may be characterized as a series of fits and starts predicated mostly upon perceived societal, economic, or experimental needs of the time. Tissue culture has now inarguably gained legitimacy as a research tool and has enabled many scientific investigations to reach successful conclusions. Yet investigators have continued to press for more fully defined cell cultivation environments. Theoretically, a fully defined cell culture medium system would eliminate confounding variables and allow the most accurate assessment and description of dependent variables. Although relatively simple in both concept and statement, practical elimination of tissue culture variables has proved to be no trivial undertaking. As the field has matured and cell-based applications have become more complex, there has been a transition from simple salt solutions to simple basal media and to more complex, nutrient enhanced media, all of which required some level of supplementation by animal sera.

The ultimate goal—to eliminate serum and develop effective serum-free or even protein-free or chemically defined media—proved more challenging. Merely eliminating the serum additive proved ineffective due to the broad diversity of serum functions within a cell culture environment. The presumptive serum-free medium formulation must contain all requisite materials to support the synthesis of new cells (proliferation), as well as all the vitamins, minerals, energy substrates, lipids, and inorganic ions essential to maintain all normal and/or genetically engineered physiological functions.

As such, the field of tissue culture may be generally described as always being in the discovery mode. As

Copyright 2006, Elsevier Science (USA).
All rights reserved.

specific cellular requirements are identified, appropriate changes are made in media formulae to support that particular cellular function. Certain cell types, important to a thorough understanding of normal and dysfunctional physiology, have been nutritionally fastidious and difficult to propagate *in vitro*. Often, these cell types were more effectively cultured and more persistently retained differentiated cellular function in the absence of serum. Finally, the target end point evolved from supporting cell proliferation or increasing total biomass to optimizing the bioreactor yield of a biomolecule (monoclonal antibody, recombinant protein, virus) of interest.

Innovations in proteomics, gene therapy, and bio- and chemoinformatics have also added momentum to serum-free medium development. Societal issues, such as the global concerns regarding bioterrorism (e.g., anthrax, smallpox), immunodeficiency virus (HIV), and transmissible spongioform encephalopathy (prion) contamination, have prompted an amalgamation of scientific and regulatory positions. Public attention has focused on practices relevant to pharmaceutical and vaccine development. As the entire body of tissue culture knowledge focused on these biotechnology applications, analytical techniques facilitated acceleration in the design and development of numerous next-generation serum-free media. As biotechnology era products matured from discovery phases through production and advanced clinical trials and, eventually, into commercialization phases, more regulatory fervor has been engendered, encompassing all portions of cell culture from cell growth and expansion to gene amplification and expression, and biological product harvest and purification.

A. History

In its infancy (1950s), tissue culture was conducted primarily in glass vessels, the matrix of choice at that time. Commensurate with increased popularity in the 1960s, tissue culture systems scaled up to larger formats to include microcarrier and stir tank reactor formats and practices. Although representing a significant step in scale, the tissue culture field nonetheless languished under the daunting sterility practices and requirements associated with reuseable glass vessels. In the 1970s, sterile disposable plastic culture flasks were developed and, after 30 years, remain the mainstay of today's practitioners. In the 1980s, the tissue culture landscape was transfigured by the introduction of tissue culture-derived bioproducts into the commercial marketplace. In the 1990s, tissue culture expanded directly into therapeutic products, including skin replacement for burn patients, cartilage for focal articular surface repair, and experimental cell and gene therapy regimens.

During the last decade and in parallel to the maturation of tissue culture there has been explosive growth in the knowledge and practices pertaining to molecular and cellular biology. As pathological situations have been ascribed to the presence or absence of specific genes or proteins, the fields of genomics and proteomics have assumed both academic and therapeutic importance. The desire to produce specific proteins in culture evoked the ability to select, clone, and express the gene encoding that specific target protein of interest. Once gene expression for the specific protein was verified in a stable cell bank, it became the responsibility of the process development function to maximize product yield through optimized upstream and downstream activities. Optimization of the *in vitro* cultivation conditions typically involves a careful balance between maintaining the narrowly defined *in vivo* environment of normal cells and perturbing that environment (physicochemically and nutritionally) to stress the cells into differentially producing copious quantities of the desired bioproduct.

B. Serum as a Culture Additive

This audience is familiar with the evolution of tissue culture beginning with simple salt solutions to simple and more complex media formulations supplemented with serum, extracts, hydrolysates, or peptones. Technical considerations and disadvantages to the use of serum in cell culture applications have been reviewed previously (Jayme and Greenwold, 1991) and included physiological variability, quality control complexity, cellular specificity, downstream processing artifacts, adventitious agent contamination, cost and availability, growth inhibitors, and proteolytic enzyme activity (Freshney, 2000).

A curious paradox concerning the use of serum as a cell culture additive is that cells cannot proliferate in serum alone. The specialized microenvironment required by cultured cells is mimicked *in vitro* by replacing serum with a mixture of metabolic precursors, macromolecules, and biophysical elements (Ham, 1982; Bottenstein *et al*., 1979). Serum functions in cell culture (Freshney, 2000; Jayme and Blackman, 1985) and factors to consider in selecting serum for specific applications (Hamilton and Jayme, 1998) have been reviewed previously.

C. Regulatory Impacts

In 2001, the council of Europe adopted regulation (EC) 999/2001 known as the transmissible spongiform

encephalopathies (TSE) regulation. Its purpose was to establish principles and guidelines to minimize the risk of transmission of a TSE via human or veterinary medicinal products. This regulation applied to all materials used in the preparation of active and excipient substances and included all source materials and reagents (including culture medium) used in production of an end product. The U.S. Food and Drug Administration (FDA), although not in regulation form as yet, issued letters (1991, 1993, and 1996) and a guidance document (1997), issuing strong recommendations toward the reduction or elimination of all animal-origin components used in the manufacture of FDA-regulated products. These strong regulatory positions have resulted in concerted efforts toward the elimination of serum and other animal-derived factors (e.g., serum albumin, transferrin) and performance qualification of substitute serum-free formulations.

II. CURRENT ISSUES IN NUTRIENT MEDIUM DEVELOPMENT

Failure in transitioning to a presumptive serum-free medium may be attributable to a variety of factors, including ineffective cellular adaptation and cultivation protocols or suboptimal nutrient composition. Three general approaches may be implemented to achieve a serum-free culture environment: (1) replacing serum with recombinant cytokines and with nonanimal transport or adhesion factors necessary for proliferation or production; (2) adapting or genetically modifying parental cells to reduce or eliminate their requirement for serum specific factors; or (3) developing or supplementing a basal formulation with low molecular weight constituents to yield an enriched, protein-free, biochemically defined nutrient medium optimized for the target application.

A useful exercise at the outset is an analysis of the primary motivation for eliminating serum (Jayme and Greenwold, 1991). Is it because serum is ill-defined and variable from lot to lot so that you are uncertain of all factors that impact your culture environment? Are you concerned with cost and availability of qualified serum additives that "work" in your system? Is your cell type unable to grow with serum supplementation because of overgrowth by contaminating fibroblasts or inhibitory or differentiating serum factors? Does serum contain other elements that mask or inhibit a normal biological function you desire to study? Are you concerned with potential adventitious contaminants or degradative enzymes? Is your project exclusively a laboratory research study or will its results ultimately be transferred to pilot or production-scale environments for diagnostic or biopharmaceutical applications? Results from this self-directed analysis may lead the investigator along different paths toward the development and optimization of serum-free culture medium (Waymouth, 1984; Jayme, 1991).

This section, focuses exclusively on three categories: (1) problematic constituents of basal nutrient media, (2) manufacturing process issues and, (3) concerns regarding cell maintenance under serum-free conditions. We will comment on several emerging trends in a subsequent section.

A. Nutrient Medium Constituents

1. Raw Material Definition and Standardization

Efforts to design effective serum-free formulations are often thwarted by the improper selection of basal components. In many instances, compendial specifications do not exist for certain medium ingredients. Unlike many constituents of classical medium formulations that may have compendial specifications for pharmaceutical use, novel growth and attachment additives frequently used as components of serum-free media remain unstandardized. Some additives are quantitated based upon protein content, whereas others are described in units of activity determined by bioassay performance results. Although percentage purity is frequently reported, there may be substantial variation among suppliers regarding the percentage and type of impurity. The presence or absence as raw material contaminants of certain micronutrients or cytotoxic elements may be amplified under serum-free cultivation conditions.

Some serum-free media formulations contain substantial levels of ill-defined hydrolysates, peptones, or extracts that exhibit lot-to-lot variability in biochemical composition and biological performance properties. For example, plant hydrolysates exhibit variable performance as a function of inherent seasonal growth variations, maturity at harvest, mechanism of harvest, or processing differences. These same additives may also create regulatory concerns regarding adventitious contaminants if primary or secondary processing involved contact with animal-origin materials. If possible without compromising biological activity, substitution of protein-free or chemically defined formulations devoid of macromolecular constituents may offer both technical and regulatory benefits. Protein additives to serum-free media should be synthetic in origin or be treated by processes validated to

eliminate adventitious contaminants. Ensure that all medium components will be available from at least one reliable supplier at a cost and consistent quality commensurate with projected application needs.

Even where such compendial descriptions exist, specifications and analytical tests may vary significantly among global sources and suppliers. Despite efforts toward international harmonization of specifications, there remain United States (USP), European, and Japanese pharmacopoeias and an U.S. National Formulary (NP). The USP contains legally recognized standards of identity, strength, quality, purity, packaging, storage, and labeling. The NF includes standards for excipients, botanicals, and other "nondrug" ingredients that could feasibly be present in media formulations. Although there are similarities among the three international pharmacopoeias, there remain procedural or reporting differences in component identification, strength, stability, sterility, or endotoxin determination that may lend themselves to significant formulation or performance differences within serum-free culture environments.

2. Water

An often overlooked and undervalued component is water, the principal constituent of liquid cell culture medium. Given the wide variation in source materials, processing and storage methods, and quality parameters, water could readily qualify as a key variable component of the cell culture environment. Without the protective benefits of elevated serum proteins, variations in water quality could introduce variables that critically impact serum-free cultures, such as beneficial or cytotoxic trace metals, organic materials, bioburden, or bacterial endotoxin. The effects of these various contaminants will vary by cell type and by concentration, but each must be rigorously considered, controlled, and evaluated for effect. A useful guideline might be for investigators to use water that meets "water for injection" (WFI) standards to minimize these variables. We recommend that WFI should be produced fresh using validated procedures and should conform to published quality standards and specifications established through a routine testing program (Freshney, 2000).

3. Dissociating Enzymes

Trypsin is the most common enzyme used for tissue disaggregation or dissociation, as it is well tolerated by a wide range of cell culture applications. However, with the transition to serum-free culture environments without animal-origin constituents, the origin of trypsin materials is problematic. Trypsin is a naturally occurring protein in the pancreas of most mammals. The traditional sources of trypsin have been bovine or porcine pancreatic tissues, neither of which is acceptable under the current regulatory definitions as primarily and secondarily animal-origin free. Raw materials are routinely treated with gamma irradiation to destroy parvovirus and other likely adventitious contaminants.

Various protease alternatives to pancreatic trypsin have been commercialized from fungal, plant, and other nonanimal sources. These dissociating enzyme preparations appear to function equivalently to serine proteases derived from animal tissues and may exhibit other practical advantages for small-scale and production-scale cell culture applications. It is anticipated that these nonanimal trypsin substitutes will reduce the risk of introducing adventitious virus to adherent cultures and will serve as a superior alternative to porcine trypsin for regulated applications.

B. Manufacturing Process Issues

1. Storage and Stability

The functional shelf life of a particular nutrient medium may vary, depending on the professional perspective. A quality assurance professional with an analytical chemistry background might be challenged by the reality that medium formulations do not exhibit a "potency" analogous to a pharmaceutical agent. Nutrient media are formulated to deliver a reasonably homogeneous range of 30–70 different constituents. However, process variables, such as formulation water temperature, speed and duration of mixing, and filtration media, will differentially impact the postprocessing active concentration of the various ingredients.

The postfiltration stability of medium constituents is also highly variable. Some ingredients, such as ascorbic acid, break down quite rapidly in aqueous medium, whereas other components are quite stable with refrigerated storage. Most nutrient media formulated without glutamine and stored in the dark at 2–8°C should perform stably for 6–12 months. Once L-glutamine or other relatively unstable constituents have been added to the medium, performance should be monitored for individual applications. Spontaneous deamidation of glutamine to yield pyroglutamate and ammonia can be problematic due both to glutamine limitation and to sensitivity of serum-free cultures to ammonia.

Perhaps the most reliable determinations of medium shelf life are derived from cell-specific applications. Such analysis should not be limited to the observation of cellular growth kinetics, but should also include the investigation of biological function, as the

production of biomolecules and other cellular functions may be impaired earlier than the proliferative rate.

2. *Light Sensitivity*

Deterioration of tissue culture medium components by exposure to high-intensity light has been documented since the late 1970s (Wang, 1976; Wang and Nixon, 1978; Spierenburg *et al*., 1984; Parshad and Sanford, 1977). Fluorescent lighting caused the deterioration of riboflavin, tryptophan (Wang, 1976; Lee and Rogers, 1988), and HEPES buffer (Zigler *et al*., 1985; Lepe-Zuniga *et al*., 1987) in medium. Riboflavin (vitamin B_2) is broken down by visible and ultraviolet light exposures below 540 nm. These photo effects on riboflavin and HEPES are mediated through the generation of superoxide radicals. These free radicals are relatively short lived, but are highly reactive and deleterious to most hydrocarbon moieties in their immediate vicinity, particularly ringed heterocycles. The resultant peroxides are also cytotoxic, particularly in serum-free environments. Of course, cell types exhibit varying sensitivities to light-induced medium cytotoxicity (Spierenburg *et al*., 1984), but it is generally recommended that medium, chemstocks, and cell cultures be protected from light to minimize the possibility of deleterious photo effects.

3. *Lipid Delivery Mechanisms*

Lipids play an integral cellular role in signal transduction, cellular communication, and intermediary metabolism. Lipids are an essential, albeit underinvestigated, ingredient of serum-free medium formulations. From a medium development perspective, lipids present unique challenges (Darfler, 1990; Gorfien *et al*., 2000).

Traditionally, lipid constituents were obtained from animal sources, similar to the lipid elements present in human intravenous feeding solutions. Sourcing biologically active sterols from nonanimal sources to meet customer and regulatory requirements was problematic due to biochemical differences that resulted in a significant loss of bioactivity. Traditionally, ovine cholesterol derived from lanolin has been the primary sterol additive source for cell culture. Synthetic cholesterol and plant-derived sterols have exhibited encouraging performance as substitutes for ovine cholesterol in serum-free culture.

The ability to solubilize lipids in aqueous medium and to maintain them stably following filter sterilization has raised additional challenges. Historically, lipid delivery was accomplished through attachment to albumin or other serum-derived proteins. With the demand to eliminate animal-derived proteins, ethanol dissolution was initially investigated, but it proved less desirable due to limited lipid dissolution capacity and stability. Pluronic-based microemulsions overcame some of these issues (Stanton, 1957; Schmolka, 1977), but the production scale was limited by the capacity of the microfluidization apparatus. Pluronic-based emulsions also exhibited variable stability, and sterile filtration of single-strength nutrient medium following the addition of concentrated lipid emulsion effectively removed all supplemental lipid. Advances in cyclodextrin-based technology appear to have overcome many of these practical limitations to lipid delivery (Walowitz *et al*., 2003).

4. *Vendor Audits*

As noted earlier, under serum-free or protein-free environments, cultured cells are exquisitely sensitive to fluctuations in medium quality associated with any component of the manufacturing conversion process. Absent the protective and detoxifying contribution of serum proteins, raw material impurities may exert a greater impact on culture performance. Manufacturing protocols should be consistent with current good manufacturing practices (cGMP). Prompted by quality compliance and regulatory issues, most media manufacturers have instituted a raw material qualification program, including routine vendor audits to assess and control the quality and consistency of individual medium components. Quality documentation for all raw materials and process components should be carefully scrutinized during routine audits of nutrient medium suppliers to ensure compliance with appropriate standards and specifications.

C. Cell Maintenance under Serum-Free Cultivation Condition

Unique constraints exist for cell cultivation in serum-free environments that have been reviewed exhaustively elsewhere (Bottenstein *et al*., 1979; Ham, 1982; Jayme and Blackman, 1985). Three critical elements are noted briefly here.

1. *Adaptation*

Experimental procedures for adapting cultures to serum-free medium have been described previously (Jayme and Gruber, 1998). Our global interactions with investigators attempting to transition to serum-free culture suggest that many failures may be attributed to inadequate or inappropriate efforts to adapt cells to a novel exogenous environment. Key concerns include the growth state of the cellular inoculum, cell seeding density, subcultivation techniques, and biophysical attributes of the cell culture system.

Typically, cultures may be transitioned from serum-supplemented medium to serum-free medium over a period of 3–6 weeks, following a weaning protocol that sequentially adapts cells in a proportionate mixture of conditioned and fresh media over a period of multiple subcultures. Following adaptation, cells should be recloned in serum-free medium to establish both master and working cell banks. Adapted cell banks should be verified for consistent biological performance properties and absence of adventitious agents for cGMP applications.

2. Cryopreservation and Recovery

Two principal criteria for successful cell cryopreservation and recovery are to initiate the freeze with a healthy cell population and to ensure that both cryopreservation and recovery procedures minimize cellular insult. Log-phase cultures should be maintained with normal proliferative characteristics for a minimum of three passages in the selected serum-free medium prior to cryopreservation.

Because historical cryopreservation protocols included serum or albumin in the freezing medium, we are frequently asked if the addition of animal origin proteins is required. Our experience indicates that it is not necessary to include these additives to achieve high viability recovery of cryopreserved cells. Cells previously adapted to serum-free medium conditions have been cryopreserved successfully in a formulation consisting of equal portions of conditioned and fresh medium, supplemented with 5–10% (v/v) dimethyl sulfoxide (DMSO) as a cryoprotectant. The cryoprotectant agent is necessary to minimize the disruption of cellular and organellar membranes by ice crystals that form during freezing. To accommodate cell-specific variations, titration of DMSO may be required to determine the optimal cryoprotectant concentration for viable cell recovery.

Recovery protocols remain controversial and may vary by cell type as alternative optimization schedules are developed. A generally recommended procedure is a rapid thawing of cryovials in a 37°C water bath and an immediate dilution of cryoprotectant by inoculating cells into prewarmed nutrient medium. During recovery from a cryopreserved state, cells are particularly sensitive to mechanical disruption. Consequently, vigorous trituration, centrifugation, and other physical stresses should be avoided or minimized. When cellular recovery is evidenced by adequate observable increases in cell density, spin down cells gently and remove as much as possible of the medium containing the residual cryoprotectant and replace on a volume-for-volume basis with fresh prewarmed medium.

3. Adherent Cultures

Attachment-dependent cultures pose additional challenges to the development of serum-free media. Many adherent cell types have the capacity to deposit complex extracellular matrices, utilizing exogenous attachment factors and synthesized glycosaminoglycans for cell-to-matrix attachment purposes. In serum-supplemented medium, such attachment factors (e.g., fibronectin, vitronectin) were contributed by the serum additive. Within a serum-free environment, there are three general approaches to improving cell attachment: (1) selection or genetic modification of the cell line to augment native adherence, (2) modification of substratum properties to facilitate attachment and spreading (Griffith, 2000; Han and Hubbell 1996), and (3) nutrient medium supplementation with attachment-promoting factors or precursors. Although some progress has been made with medium modification, many potential factors are commercially unattractive from cost and animal origin perspectives and from their propensity to adsorb to container surfaces.

III. EMERGING TRENDS

We have chosen to focus on four trends that are exerting a significant impact on the development of serum-free culture environments: (1) format options for delivering nutrient medium, (2) outsourcing of biological production activities, (3) alimentation options to improve bioreactor productivity, and (4) expanded cell culture applications.

A. Format Evolution

To achieve production-scale economies, biotechnology manufacturers have transitioned to larger and more efficient bioreactors. Previous nutrient medium format options were limited to single-strength liquid medium in bulk containers or to ball-milled powder configurations. However, both of these historical options presented technical and logistical challenges for large-scale biological production applications.

Development of liquid media concentrates (50× subgroupings) facilitated stable solubilization of complex constituents of serum-free medium into a format that was readily reconstituted in either batch or continuous mode to yield production volumes of nutrient medium (Jayme *et al*., 1992). Liquid media concentrates have been utilized commercially for vaccine and recombinant protein. Combining this technology with an in-line mixing device facilitated commercial production of >30,000 liter batches of liquid

medium dispensed directly into bulk containers from common ingredients (Jayme *et al*., 1996).

To minimize the shipment of water, many production-scale applications prefer a dry format, but encounter performance variations, incomplete solubilization, and hygienic concerns with the hydration of serum-free formulations produced as a ball-milled powder. Milling within a stainless steel hammer mill (FitzMill) overcame technical concerns regarding thermal inactivation of heat-labile components and regulatory concerns regarding sanitization associated with ceramic ball-milling processes.

A novel approach to producing a dry-form nutrient medium was introduced by the application of fluid bed granulation to serum-free formulations, yielding a granular medium format (Fike *et al*., 2001). This alternative approach, termed advanced granulation technology (AGT), resulted in the homogeneous distribution of trace elements and labile components onto granules that dispersed and dissolved rapidly within a medium formulation tank. Upon hydration, medium granules yield a single-strength nutrient medium with superior biological performance relative to the ball-milled powder format of the identical formulation and with specified pH and osmolality without requirement for manual titration (Radominski *et al*., 2001).

B. Outsourcing

Given the extended developmental lead time and associated expense from identifying a lead candidate, through process development, clinical investigation and regulatory submission, and eventually culminating in an approved biological product, many companies are choosing to defer capital investment in production capacity or hiring of manufacturing personnel pending regulatory approval and commercial success. Such companies may develop mutually beneficial partnerships with contract manufacturing organizations with the ability to produce gram-to-kilogram quantities of a biological product.

Similarly, many companies have identified core competencies that they uniquely possess and have chosen to outsource noncritical capabilities, finding it financially advantageous to hire, buy, or acquire source technology. Various instances of consolidation within the biotechnology industry have resulted in acquisition by the pharmaceutical industry of entrepreneurial firms with intellectual property assets. Other biotechnology companies have opted to outsource significant requirements to contract research organizations. Others have chosen to defer capital investment in media or buffer kitchens or cell banking capabilities by contracting these ancillary services or purchasing ready-to-use materials.

C. Bioreactors

Inevitably, the transition from bench-scale shake flasks or spinner cultures to pilot or production-scale stirred tank or airlift bioreactors encounters various scale-up challenges. In addition to the classical engineering issues of agitation, gas transfer, and control of temperature and pH, there may be qualitative or quantitative adjustments in nutrient formulation or delivery schedule. Nutrient medium qualified for the batch culture of specific cells may benefit from additional optimization if cultures are to be expanded in a bioreactor that has a linear nutrient flow, such as a hollow fiber or horizontal plate-style bioreactor. Variations in nutrient consumption kinetics dependent on the bioreactor environment, such as mechanical stress, dissolved oxygen content, and gas sparging, may profoundly impact cellular energetics and predispose cells to alternative metabolic pathways that alter cell functionality or product quality.

To extend bioreactor longevity and provide more consistent product quality, process development groups often augment traditional batch bioreactor regimens by supplementing exhausted nutrients in fed-batch or perfusion mode (Mahadevan *et al*., 1994). While a concentrated nutrient feed cocktail may be developed solely by eliminating inorganic salts and buffering components from the base medium, superior cell viability and biological productivity may be achievable through analysis of spent medium (Fike *et al*., 1993). Determination of component exhaustion kinetics by quantitative analysis of spent medium produced by high-density cultures can yield valuable information regarding metabolite reduction or enrichment to optimize culture productivity. Nutrient modifications derived from iterative analysis, resulting either in adjustment of the initial formulation or inperiodic or continuous addition of concentrated nutrient supplements, have resulted in enhanced bioreactor longevity and specific productivity (Jayme, 1991). Although initially more laborious, this method often yields a simple, customized nutrient cocktail that permits optimized adjustment of individual nutrients and avoids inhibitory effects resulting from excessive additives or metabolic by-products.

D. Applications to Cell Therapy and Tissue Engineering

Tissue engineering applies engineering and life sciences techniques to develop biological substitutes that

restore, maintain, or improve tissue or organ function. Integration of biomaterials and biological scaffolding (Griffith, 2000; Han and Hubbell, 1996) with a suitable cell type(s) and a bathing nutrient fluid can expand progenitor cells along a desirable lineage or repopulate a deficient tissue with healthy cells possessing the desired biological function. Cells may be obtained from autologous, allogeneic, or xenogeneic sources or be derived from immortalized cell lines or stem cell progenitors. Given the intended therapeutic application, nutrient media for each specialized application will ultimately need to be acceptable by both technical and regulatory criteria.

IV. CONCLUSIONS

The justifications for eliminating serum from cell culture are numerous, and serum-free media have now been developed for a broad array of biotechnological applications. The past few years have addressed regulatory concerns regarding the potential contamination of biopharmaceuticals by adventitious agents introduced via medium constituents of animal origin or defects in the manufacturing process. Eliminating all animal-origin components has proved daunting, but numerous protein-free nutrient formulations have been specifically designed and developed to eliminate questionable components without sacrificing biological performance. Coincident to the removal of animal-origin components has been the concomitant increase in the biochemical definition of medium composition. Biochemical definition will ultimately translate to enhanced production consistency for prospective biopharmaceuticals synthesized in animal cell-based bioreactors and for biomaterials designed for tissue repair or regeneration, drug delivery, or genetic therapy. Defined serum-free nutrient media and scaffolding matrices compatible with technical and regulatory requirements are under active investigation for the three-dimensional regeneration of bone, ligaments, skin, blood vessels, nerves, and organ functions. These applications extend into many of today's problematic areas, such as arthritis, diabetes, cancer, cardiovascular disease, congenital defects, or sports injuries.

Over the past decade, a striking series of trends has transformed the landscape of tissue culture. The electronic availability of information and data has reduced response times and established new international standards. Biotechnology and tissue culture have become globalized in both needs and concerns. The synergy of molecular biology techniques into functional genomics and proteomics has revolutionized and condensed the developmental pipeline for cell-based products. Enhanced social and safety consciousness has redefined our fundamental responsibility for generating products and research capabilities that will meet global criteria for scientific, economic, regulatory, and ethical acceptability.

References

Bottenstein, J., Hayashi, I., Hutchings, S., Masui, H., Mather, J., McClure, D. B., Ohasa, S., Rizzino, A., Sato, G., Serrero, G., Wolfe, R., and Wu, R. (1979). The growth of cells in serum-free hormone-supplemented media. *Methods Enzymol.* **LVIII**, 94–109.

Darfler, F. J. (1990). Preparation and use of lipid microemulsions as nutritional supplements for culturing mammalian cells. *In Vitro* **26**, 779–783.

Fike, R., Dadey, B., Hassett, R., Radominski, R., Jayme, D., and Cady, D. (2001). Advanced granulation technology (AGT): An alternate format for serum-free, chemically-defined and protein-free cell culture media. *Cytotechnology* **36**, 33–39.

Fike, R., Kubiak, J., Price, P., and Jayme, D. (1993). Feeding strategies for enhanced hybridoma productivity: Automated concentrate supplementation. *BioPharm*. **6**(8), 49–54.

Freshney, R. I. (2000). "Culture of Animal Cells: A Manual of Basic Technique," 4th Ed. Wiley-Liss, New York.

Gorfien, S. F., Paul, B., Walowitz, J., Keem, R., Biddle, W., and Jayme, D. (2000). Growth of NS0 cells in protein-free, chemically-defined medium. *Biotechnol. Prog.* **16**(3), 682–687.

Griffith, L. G. (2000). Polymeric biomaterials. *Acta Mater.* 48, 263–277.

Ham, R. G. (1982). Importance of the basal nutrient medium in the design of hormonally defined media. *In* "*Growth of Cells in Hormonally Defined Media*" (G. H. Sato, A. B. Pardee, and D. A. Sirbasku, eds.), pp. 39–60. Cold Spring Harbor Laboratory, New York.

Hamilton, A. O., and Jayme, D. W. (1998). Fetal bovine serum lot testing. *In* "*Cell Biology: A Laboratory Handbook*" (J. E. Celis, ed.), Vol. 1, pp. 27–34. Academic Press, New York.

Han, D. K., and Hubbell, J. A. (1996). Lactide-based poly(ethylene glycol) polymer networks for scaffolds in tissue engineering. *Macromolecules* **29**, 5233–5235.

Jayme, D. W. (1991). Nutrient optimization for high density biological production applications. *Cytotechnology* **5**, 15–30.

Jayme, D. W. (1999). An animal origin perspective of common constituents of serum-free medium formulations. *Dev. Biol. Stand.* **99**, 181–187.

Jayme, D. W., and Blackman, K. E. (1985). Review of culture media for propagation of mammalian cells, viruses and other biologicals. *In* "*Advances in Biotechnological Processes*" (A. Mizrahi and A. L. van Wezel, eds.), Vol. 5, pp. 1–30. Al. R. Liss, New York.

Jayme, D. W., DiSorbo, D. M., Kubiak, J. M., and Fike, R. M. (1992). Use of nutrient medium concentrates to improve bioreactor productivity. *In* "*Animal Cell Technology: Basic and Applied Aspects*" (H. Murakami, S. Shirahata, and H. Tachibana, eds.), Vol. 4, pp. 143–148. Kluwer, New York.

Jayme, D. W., and Greenwold, D. J. (1991). Media selection and design: Wise choices and common mistakes. *Bio/Technology* **9**, 716–721.

Jayme, D. W., and Gruber, D. F. (1998). Development of serum-free media and methods for optimization of nutrient composition. *In* "*Cell Biology: A Laboratory Handbook*" (J. E. Celis, ed.), Vol. 1, pp. 19–26, Academic Press, New York.

Jayme, D. W., Kubiak, J. M., Battistoni, and Cady, D. J. (1996). Continuous, high capacity reconstitution of nutrient media from concentrated intermediates. *Cytotechnology* **22**, 255–261.

Lee, M. G., and Rogers, C. M. (1988). Degradation of tryptophan in aqueous solution. *J. Parenteral Sci. Tech.* **42**, 20–22.

Lepe-Zuniga, J. L., Zigler, J. S., Jr., and Gery, I. (1987). Toxicity of light exposed HEPES media. *J. Immunol. Methods* **103**, 145.

Mahadevan, M. D., Klimkowsky, J. A., and Deo, Y. M. (1994). Media replenishment: A tool for the analysis of high-cell density perfusion systems. *Cytotechnology* **14**, 89–96.

Parshad, R., and Sanford, K. K. (1977). Proliferative response of human diploid fibroblasts to intermittent light exposure. *J. Cell Physiol.* **92**, 481–485.

Radominski, R., Hassett, R., Dadey, B., Fike, R., Cady, D., and Jayme, D. (2001). Production-scale qualification of a novel cell culture medium format. *BioPharm* **14**(7), 34–39.

Schmolka, I. R. (1977). A review of block polymer surfactants. *J. Am. Oil Chem. Soc.* **54**, 110–116.

Spierenburg, G. T., Oerlemans, F. T., van Laarhoven, J. P., and de Bruyn, C. H. (1984). Phototoxicity of N-2-hydroxyethylpiperazine-N2-ethanesulfonic acid-buffered culture media for human leukemic cell lines. *Cancer Res.* **44**, 2253–2254.

Stanton, W. B. (1957). Polymeric nonionic surfactants. *Soap Chem. Spec.* **33**, 47–49.

Walowitz, J. L., Fike, R. M., and Jayme, D. W. (2003). Efficient lipid delivery to hybridoma culture by use of cyclodextrin in a novel granulated dry-form medium technology. *Biotechnol. Prog.*

Wang, R. J. (1976). Effect of room fluorescent light on the deterioration of tissue culture medium. *In Vitro* **12**, 19–22.

Wang, R. J., and Nixon B. T. (1978). Identification of hydrogen peroxide as a photoproduct toxic to human cells in tissue culture medium irradiated with daylight fluorescent light. *In Vitro* **14**, 715–722.

Waymouth, C. (1984). Preparation and use of serum-free culture media. *In "Methods for Preparation of Media, Supplements, and Substrata for Serum-Free Animal Cell Culture,"* pp. 23–68. A. R. Liss, New York.

Zigler, J. S., Jr., Lepe-Zuniga, J. L., Vistica, B., and Gery, I. (1985). Analysis of the cytotoxic effects of light-exposed HEPES-containing culture medium. *In Vitro Cell Dev. Biol.* **21**, 282–287.

CHAPTER

6

Cell Line Authentication

Robert J. Hay

I. INTRODUCTION

This article provides a strategy and summarizes steps for the authentication of cell line stocks. It serves as a preface for the following article and for others in this series offering detail on the characterization of cells and cell lines. For those working with serially propagated cells, it is absolutely critical that quality control tests be applied periodically. Rationale and pertinent key references are included here.

Literally hundreds of instances of cross-contamination in cell culture systems have been documented (Nelson-Rees, 1978: Nelson-Rees *et al.*, 1981.; Hukku *et al.*, 1984; MacLeod *et al.*, 1999). Many others have gone unreported. The novice technician or student using cell culture techniques soon is made painfully aware of the potential for bacterial and fungal infection. Generally, however, one must be alerted to the more insidious problems of animal cell cross-contaminations, the presence of mycoplasma, and especially the potential for latent or otherwise inconspicuous viral infection. The financial losses in research and production efforts resulting from the use of contaminated cell lines are certainly equivalent to many millions of dollars. Accordingly, frequent reiteration of the details of cell culture contaminations and of precautionary steps to avoid and detect such problems clearly is warranted.

This article includes a review of quality control steps applied to authenticate cell lines, i.e., to ensure absence of microbial, viral, and cellular contamination, as well as potential tests to verify the identity of human cells. The approach suggested has been developed during the establishment of a national cell repository. Specific rationales for applying the tests indicated are included in this volume and are discussed in more detail elsewhere (Hay *et al.*, 2000).

Most established cell lines have been characterized by the originator and collaborators well beyond the steps essential for quality control. Specific details are provided in subsequent chapters of this series and include, for example, phase-contrast and ultrastructural morphologies; detailed cytogenetic analysis; definition of protooncogene, oncogene, or oncogene product presence, nature, and location; detailed evaluation of intermediate-filament proteins; and demonstration of tissue-specific antigens or production of other specific products. These characterizations obviously increase the value of each line for research and for production work. However, cell resource organizations need not repeat all of these tests before distributing the stock cultures. Decisions must be made to establish the most acceptable authentication steps, consistent with maintaining the lowest possible cost, to provide a high-quality cell stock. Authentication can be considered the act of confirming or verifying the identity and critical feature of a specific line, whereas characterization is the definition of the many traits of the cell line, some of which may be unique and also may serve to identify or reauthenticate that line specifically. Essential steps for quality control will vary with the type of cell resource constructed. Minimal descriptive data frequently will be supplemented with a much broader characterization base for each particular cell line.

II. SEED STOCK CONCEPT

Definitions of public repository seed stocks may vary from those used for specific applications such as

Copyright 2006, Elsevier Science (USA).
All rights reserved.

the production of vaccines or other biologicals. A scheme illustrating the steps involved in developing seed stocks is presented as Fig. 1.

Generally, starter cultures or ampules are obtained from the originator, and progeny are propagated according to the instructions to yield the first "token" freeze. Cultures derived from such token material are then tested for bacterial, fungal, and mycoplasmal contamination. The species of each cell line is verified. These quality control steps are the minimum ones that must be performed before eventual release of a line. If these steps confirm that further efforts are warranted, the material is expanded to produce the seed and distribution stocks. Note that, under ideal conditions, additional major quality control and characterization efforts are applied to cell populations from seed stock ampules. Test results refer to *specific numbered stocks*. The distribution stock consists of ampules that are distributed on request to investigators. The reference seed stock, however, is retained to generate further distribution stocks as the initial distribution stock becomes depleted. The degree of characterization applied to master cell banks or master working cell banks in production facilities is generally most rigorous. The seed stock here, like the master cell bank, is used as a reservoir to replenish depleted distribution lots over the years. By adherence to this principle, one can avoid problems associated with genetic instability, cell line selection, or transformation.

III. MICROBIAL CONTAMINATION

Microbial contamination in cell culture systems remains a serious problem. Cryptic contaminants, even of readily isolatable bacteria and fungi, are missed by many laboratories. The American Type Culture Collection (ATCC) still receives cultures, even for the patent depository, that contain yeast, filamentous fungi, and/or mycoplasma contaminants.

A. Bacteria and Fungi

Microscopic examination is not sufficient for the detection of gross contaminations; even some of these cannot be detected readily by simple observations. Therefore, an extensive series of culture tests is also required to provide reasonable assurance that a cell line stock or medium is free of fungi and bacteria. Details are given in the following article.

B. Mycoplasma Infection

Contamination of cell cultures by mycoplasma can be a much more insidious problem than that created by the growth of bacteria or fungi. Although the presence of some mycoplasma species may be apparent because of the degenerative effects induced, other mycoplasma metabolize and proliferate actively in the

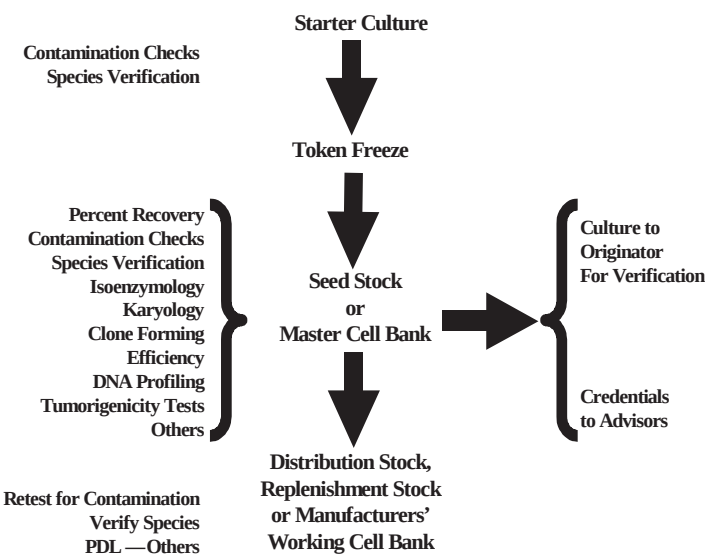

FIGURE 1 Accessioning Scheme.

culture without producing any overt morphological change in the contaminated cell line. Thus, cell culture studies relating to metabolism, surface receptors, virus–host interactions, and so forth are certainly suspect to interpretation, if not negated in interpretation entirely, when conducted with cell lines that harbor mycoplasma. The seriousness of these problems has been documented through published data from testing services and cell culture repositories.

The high incidence of mycoplasma contamination from human operators is supported by the fact that *Mycoplasma orale* and others of human origin (*Mycoplasma hominus*, *M. salivarium*, *and M. fermentas)* are among those most frequently isolated. In the study of Del Giudice and Gardella (1984) of the 34,697 lines tested, 3955 (11%) were positive; 36% of these isolates were mycoplasmas of human origin. A high incidence of isolation of *Mycoplasma hyorhinus* was noted that may have resulted from using contaminated sera or by culture-to-culture spread in laboratories working with infected biologicals. After a more recent study, Uphoff *et al.* (1992) reported that 84 (33%) of 253 cell lines submitted for their developing cell repository in Germany were infected with mycoplasma. Data showing that these are not unusual findings are presented in Table I. Results from seven laboratories published since 1980 indicate clearly that mycoplasma infection is still a very major problem in the cell culture field. Some 5 to 20% of cultures tested were positive. This is the range even today.

Protocols to test for mycoplasma infection are included in the following chapter.

Four general recommendations can be offered to avoid the problem. The implementation of an effective regimen to monitor cell lines for mycoplasma is one critical step. Quarantining all new, untested lines and the use of mechanical pipetting aids are others. Most experts also strongly suggest that the use of antibiotics be eliminated when possible. Antibiotic-free systems permit overgrowth by bacteria and fungi to provide ready indication whenever a lapse in aseptic technique occurs. When a primary tissue is used, e.g., a human tumor sample, antibiotics may be employed initially, but after the primary population has been grown out and cyropreserved, reconstituted cells may be propagated further in antibiotic-free medium.

TABLE I Mycoplasma Infection of Cell Lines (1982–2002)

Reference test laboratory	Percentage positive	Total
McGarrity (1982)	4.7	16,197
Del Giudice and Gardella (1984)	11.4	34,697
Uphoff *et al.* (1992)	33	233
Takeuch *et al.* (1993)	21	2,332
Lundin and Lincoln (1994)	10.2	1,000
Hay *et al.* (1996b)	15.5	5,362
Uphoff and Drexler (2002)	17	549

C. Viruses

Verification of the absence of viruses in cell lines is recognized as a most significant problem. That these may coexist as noncytopathic entities (e.g., the c-type retroviruses) or in a latent form (e.g., papilloma viruses and some herpes viruses) compounds difficulties in detection. Judicious choices are necessary not only to select appropriate methods available for recognizing viruses associated with cell lines, but also to identify the offending species. The nature of the cell resource, its users, and budget available, plus the intended purposes for which the lines will be needed, all affect decisions on testing. More complete detail and protocols are provided in the following article.

IV. CELLULAR CROSS-CONTAMINATION

Wherever cells are grown in culture, serious risk exists for the inadvertent addition and subsequent overgrowth by cells of another individual or species. One most certainly cannot rely on morphologic criteria alone to recognize or identify cell lines. Data-documenting problems have been collected over the years by groups offering identification services for cell culture laboratories in the United States and elsewhere.

In one study, 466 lines from 62 laboratories were examined. Of these, 75 (16%) were found to be identified incorrectly. A total of 43 lines (9%) were not of the species expected, whereas 32 lines (7%) were either incorrect mixtures of two or more lines or were not the individual line as stated (Nelson-Rees, 1978). Hukku *et al.* (1984) examined 275 lines over a period of 18 months. Results of their analyses are summarized in Table II. A total of 96 lines (35%) were not as indicated by the donor laboratories. For purported human lines, 36% were not as expected, 25% were a different species, and 11% a different human individual. More recently, Drexler *et al.* (1994), while developing a resource of cell lines, reported that 10% of those provided by outside investigators contained cells different from those expected, probably due to misidentification or cross-contamination.

TABLE II Summary of Cell Line Cross-Contamination[a]

Reported cell species	Cultures received	Interspecies	Intraspecies	Percentage of total
Human	160	40 (25%)	18 (11%)	36
Others	115	38	—	33
Total	275	78	18	35

[a] Adapted from Hukku *et al.* (1984)

To minimize the risk of cellular cross-contamination, culture technicians require a laminar flow hood for ideal operation. These individuals must be instructed periodically to work with only one cell line at any given time, use one reservoir of medium for each line, and avoid introducing pipettes that have been used to dispense or mix cells into any medium reservoir. Technicians must be reminded repeatedly to legibly label each and every cell culture with designations, passages, and dates. Labels of differing colors can be used to more readily distinguish one cell line from another during expansion.

Technicians must also be instructed to allow at least 5 min of hood clearance time, with ultraviolet lights and blower on, between cell lines when working on more than one line during a particular period. The inner surfaces of each hood should be swabbed with 70% ethanol between such uses.

The studies outlined earlier illustrate the severity of the problem of cellular cross-contamination and provide a strong rationale for vigilance in careful handling, characterization, and authentication of cell lines.

A. Species Verification

Species of origin can be determined for cell lines by a variety of immunological tests, by isoenzymology, and/or by cytogenetics (Nelson-Rees, 1978; Hukku *et al.*, 1984; Hay *et al.*, 2000). The indirect fluorescent antibody-staining technique is used in many laboratories to verify the species of a cell line (for details, see Hay *et al.*, 1992). Isozyme analyses performed on homogenates of cell lines from over 25 species have demonstrated the utility of these biochemical characteristics for species verification (O'Brien *et al.*, 1977). By determining the mobilities of three isozyme systems—glucose-6-phosphate dehydrogenase, lactic acid dehydrogenase, and nucleoside phosphorylase—using vertical starch gel electrophoresis, the species of origin of cell lines can be identified with a high degree of certainty. Alternatively, a standardized kit employing agarose gels and stabilized reagents may be obtained for this purpose (AuthentiKit, Innovative Chemistry, Inc., Marshfield, MA).

Karyologic techniques have long been used informatively to monitor for interspecies contamination among cell lines. In many instances, the chromosomal constitutions are so dramatically different that even cursory microscopic observations are adequate. In others, for example, in comparisons among cell lines from closely related primates, careful evaluation of banded preparations is required (Nelson-Rees, 1981; Hukku *et al.*, 1984). Cytogenetics has the advantage of detecting even very minor contaminants, on the order of 1% or less in some circumstances. Furthermore, it can provide precise identification of specific lines in cases where marker chromosomes are known or detected (e.g., Drexler *et al.*, 2002). However, cytogenetic analyses are time-consuming and interpretation requires a high degree of skill. The karyotype is constructed by cutting chromosomes from a photomicrograph and arranging them according to arm length, position of centromere, presence of secondary constrictions, and so forth. Automated analytical systems are available but expensive. The "Atlas of Mammalian Chromosomes" (Hsu and Benirschke, 1967–1975) illustrates examples of conventionally stained preparations from over 550 species. Detailed protocols are available elsewhere (Hay *et al.*, 2000).

B. Intraspecies Cross-Contamination

With the dramatic increase in numbers of cell lines being developed, especially from human tissues, the risk of intraspecies cross-contamination rises proportionately. The problem is especially acute in laboratories requiring work with the many different cell lines of human and murine origin available today.

Methods for verifying cell line species employing enzyme mobility studies have been mentioned. Using similar technology, but with different enzyme systems, one can also screen for intraspecies cellular cross-contamination. Cell lines from various individuals of the same species often show different codominant alleles for a given enzyme locus, the products of which are polymorphic and electrophoretically resolvable. In most cases, the phenotype for these allelic enzymes (allozymes) is extremely stable. Consequently, when

allozyme phenotypes are determined over a suitable spectrum of loci, they can be used effectively to provide an allozyme genetic signature for each line under study (O'Brien *et al*., 1977; Hukku *et al*., 1984).

The application of recombinant DNA technology and cloned DNA probes to identify and quantitate allelic polymorphisms provides additional powerful means for cell line identification. These polymorphisms can be recognized as extremely useful markers, even if they are not expressed through transcription and translation to yield structural enzymatically active proteins.

Hybridization probes to regions of the human genome that are highly variable have been produced for DNA profiling applications, including cell line individualization. Profiles derived from human cell lines can be interpreted best using scanning devices as the patterns are complicated. For protocols and examples, see Jeffreys *et al.* (1985), Gilbert *et al.* (1990), and Hay *et al.* (1996, 2000).

Original procedures included fingerprints using larger (10–20 bp) minisatellite DNA and Southern blotting. With application of the polymerase chain reaction (PCR), loci can be typed in hours rather than days. Smaller microsatellite (2–6 bp) loci have been identified as well. Edwards *et al.* (1992) demonstrated the usefulness of these "short tandem repeat" (STR) loci in recognizing individuals at the DNA level. One significant advantage of STR loci over minisatellite repeats is their small size. The small size of STR loci allows multiplex PCR reactions to be developed in which many loci are examined simultaneously in a single reaction. Commercially available multiplexed STR systems are available for routine screening of new cell lines for authenticity as well as for validating any subsequent distribution of replenishment cell lines. More detail on STR profiling of human DNA cell lines is available elsewhere (Hay *et al*., 2000). A comprehensive database can be accessed via the ATCC website at http://www.atcc.org/cultures/str.cfm. STR loci are among the most informative polymorphic markers in the genome. The profiling process used at ATCC involves simultaneous amplification of eight STR loci and the amelogenin gene in a multiplex PCR reaction (Promega PowerPlex 1.2 system). This allows for discrimination of fewer than 1 in 10^8 individuals. The amplicons are separated by electrophoresis and are analyzed using Genotyper 2.0 software from Applied Biosystems. Each peak in the resulting electropherogram represents an allele that is alphanumerically scored and entered into our database.

The classical method for intraspecies cell line individualization involves karyotype analysis after treatment with trypsin and Giemsa stain (Giemsa or G-banding). The banding patterns made apparent by this technique are characteristic for each chromosome pair and permit recognition, by an experienced cytogeneticist, of even comparatively minor inversions, deletions, or translocations. Many lines retain multiple marker chromosomes, readily recognizable by this method, that identify the cells specifically and positively (Chen *et al.* 1987; Drexler *et al.* 2002). If readily recognized marker chromosomes are present, contaminations at less than 1% can be recognized with careful scrutiny. This technique even permits discrimination among lines from the same individual that cannot be identified as different by DNA. These lines have similar marker chromosomes, indicating a common source, but each also has markers unique in type and copy number. In contrast, Gilbert *et al.* (1990) noted no distinct differences among the nine HeLa derivatives examined using the minisattelite probe 33.6 after *Hae*III designation. Metabolic differences among the HeLa derivatives (Nelson-Rees *et al*., 1980) will ultimately be traced to genetic differences among the lines, as reflected by the unique cytogenetic profiles. On this basis, the importance of documenting the precise cytogenetics of cell lines used for production purposes is very clear. Protocols are provided elsewhere in this series.

V. ORIGIN AND FUNCTION

The markers used for verification of the source tissues for cell lines are probably as numerous as the types of metazoan cells. Major methods of demonstration include an analysis of fine structure, immunological tests for cytoskeletal and tissue-specific proteins, and, of course, an extremely broad range of biochemical tests for specific functional traits of tissue cells. Ultrastructural features such as desmosomes or Weibel–Palade bodies identify epithelia and endothelia, respectively. The nature of intermediate-filament proteins, demonstrated using monoclonal antibodies, permits differentiation among epithelial subtypes, mesenchymal, and neurological cells. Tissue- and tumor-specific antigens can be used when reagents are reliable and available. In addition, tissue-specific biochemical reactions or syntheses may be used for absolute identification if these features are retained by the cell line in question. One excellent example is the cell line NCI-H820 (ATCC—HTB 181) isolated from a metastic lesion of a human papillary lung adenocarcinoma. Cells of this line reportedly retain multilamellar bodies suggestive of type 2 pneumocytes and express the three surfactant-associated proteins SP-A

(constitutively), SP-B, and SP-C (after dexamethasone stimulation; A. Gazdar, personal communication). For more examples, see other articles of this series and Hay (1992).

VI. CONCLUSIONS

The overall utility of any bank of cultured cell lines depends on the degree of characterization of the holdings that has been performed by the originators, the banking agency, and other individuals within the scientific community. Ready availability at a reasonable cost of the lines and such data, as well as the ability to track distribution of the biologicals, are additional critical considerations. Documenting the verification of species and identity of each cell line, when possible, is considered essential. Freedom from bacterial, fungal, and mycoplasmal infection must be assured. However, from the cell banking perspective, applying all possible characterizations to every seed or master cell stock developed is neither essential nor practical. At ATCC, for example, screens for particular viruses have been applied when a specific program support is available for such testing. Similarly, the definition of ultrastructural features, tumorigenicity, and functional traits, for example, is performed with appropriate external support and adequate rationale. The central responsibility is to produce reference stocks, authenticated and well characterized for multiple purposes, and to return to those preparations over the years for the development of working stocks for distribution or other specific applications. Each replacement distribution stock requires reauthentication prior to distribution to intended users.

References

Chen, T. R. (1988). Re-evaluation of HeLa, HeLaS3 and Hep-2 karyotypes. *Cytogenet. Cell Genet.* **48**, 19–24.

Chen, T. R., Drabkowski, D., Hay, R. J., Macy, M. L., and Peterson, W., Jr. (1987). WiDr is a derivative of another colon adenocarcinoma cell line, HT-29. *Cancer Genet. Cytogenet.* **27**, 125–134.

Del Giudice, R. A., and Gardella, R. S. (1984). Mycoplasma infection of cell culture: Effects, incidence and detection. *In* "*In Vitro* Monograph 5: Uses and Standardization of Vertebrate Cell Cultures," pp. 104–115. Tissue Culture Association, Gaithersburg, MD.

Drexler, H. G., Gignac, S. M., Minowada, J. (1994). Hematopoietic cell lines. *In* "*Atlas of Human Tumor Cell Lines* (R. J. Hay, R. Gazdar, and J. G. Park, eds.), pp. 213–250. Academic Press, Orlando.

Drexler H. G., Quentmeier, H., Dirks, W. G., Uphoff, C. C., and MacLeod, R. A. (2002). DNA profiling and cytogenetic analysis of cell line WSU-CLL reveal cross-contamination with cell line REH (pre B-ALL). *Leukemia* 1868–70.

Edwards, A., Hammond, H. A., Jin, L., Caskey, C. T., and Chakraborty, R. (1992). Genetic variation at five trimeric and tetrameric tandem repeat loci in four human population groups. *Genomics* 241–253.

Gilbert, D.A, Reid, Y. A., Gail, M. H., Pee, D., White, C., Hay, R. J., and O'Brien, S. J. (1990). Application of DNA fingerprints for cell line individualization. *Am. J. Hum. Genet.* **47**, 499–514.

Hay, R. J. (1992). Cell line preservation and characterization. *In* "*Animal Cell Culture: A Practical Approach*" (R. I. Freshney, ed.), 2nd Ed., pp.95–148. IRL Press, New York.

Hay, R. J., Caputo, J., and Macy, M. L. (1992). "ATCC Quality Control Methods for Cell Lines," 2nd Ed. ATCC, Rockville, MD.

Hay, R. J., Reid, Y. A., McClintock. P. R., Chen, T. R., and Macy, M. L. (1996). Cell line banks and their role in cancer research. *J. Cell Biochem. Suppl.* **27**, 1–22.

Hay, R. J., Reid, Y. A., and Miranda, M. (1996b). Advances in methodologies for cell line authentication. *In* "*Culture Collections to Improve the Quality of Life*" (R. A. Sampson, J. A. Staplers, D. vander Mei, and A. H. Stouthamer, eds.), pp. 131–137. CVS, Baarm, The Netherlands.

Hay, R. J., Cleland, M. M., Durkin, S., and Reid, Y. A. (2000). Cell line preservation and authentication *In* "*Animal Cell Culture: A Practical Approach*" (J. R. W. Masters, ed.), 3rd Ed., pp. 69–103. Oxford University Press, New York.

Hsu, T. C., and Benirschke, K. (1967–1975). "At Atlas of Mammalian Chromosomes." Springer-Verlag, New York.

Hukku, B., Halton, D. M., Mally, M., and Peterson, W. D., Jr. (1984). Cell characterization by use of multiple genetic markers. *In* "*Eukaryotic Cell Cultures*" (R. T. Acton and J. D., Lynn, eds.), pp. 13–31. Plenum, New York.

Jeffreys, A. J., Wilson, L., and Thein, S. L. (1985). Hypervariable minisatellite regions in human DNA. *Nature* **314**, 67–73.

Lundin, D. J., and Lincoln, C. K. (1994). Mycoplasmal testing of cell cultures by a combination of direct culture and DNA-fluorochrome staining. *In Vitro* **30A**, 111.

MacLeod R. A. F., Dirks, W. G., Kaufmann, M., Matsuo Y., Milch, H., and Drexler, H. G. (1999). Widespread intraspecies cross-contamination of human tumor cell line arising at source. *Int. J. Cancer* **83**:555–563.

McGarrity, G. J. (1982). Detection of mycoplasmal infection of cell cultures. *Adv. Cell Culture* **2**, 9–131.

Nelson-Rees, W. A. (1978). The identification and monitoring of cell line specificity. *Progr. Clin. Biol. Res.* **20**, 25–79.

Nelson-Rees, W. A., Daniels, D. W., and Flandermeyer, R. R. (1981). Cross-contamination of cell lines. *Science* **212**, 446–452.

Nelson-Rees, W. A., Hunter, L., Darlington, G. J., and O'Brien, S. J. (1980). Characteristics of HeLa strains: Permanent vs. variable features. *Cytogenet. Cell Genet.* **27**, 216–231.

O'Brien, S. J., Kleiner, G., Olson, R., and Shannon, J. E. (1977). Enzyme polymorphisms as genetic signatures in human cell culture. *Science* **195**, 1345–1348.

Reid, Y. A., Gilbert, D. A., and O'Brien, S. J. (1990). The use of DNA hypervariable probes for human cell line identification. *Am. Type Cult. Collect. Newslett.* **10**(4), 1–3.

Reid, Y. A., and Lou, X. (1993). The use of PCR-amplified hypervariable regions for the identification and characterization of human cell lines. *In Vitro* **29A**, 120A.

Takeuchi, M., Yoshida, T., Satoh, M., Kuno, H., and Ohno, T. (1993). Survey of mycoplasmal contamination in animal cell lines collected by three cell banks in Japan. *Bull. JFCC* **9**, 13–18.

Uphoff, C. C., Brauer, S., Grunicke, D., Gignae, S. M., MacLeod, R. A. F., Quentmeier, H., Steube, K., Tummler, M., Voges, M., Wagner, B., and Drexler, H. G. (1992). Sensitivity and specificity of the different mycoplasma detection assays. *Leukemia* **6**, 335–341.

Uphoff, C. C., and Drexler, H. G. (2002). Detection of mycoplasma in leukemia-lymphoma cell lines using polymerase chain reaction. *Leukemia* **16**, 289–293.

CHAPTER

7

Detection of Microbial and Viral Contaminants in Cell Lines

Robert J. Hay and Pranvera Ikonomi

I. INTRODUCTION

The presence of microbial contaminants—bacteria, fungi, mycoplasma, or protozoa—in cell cultures seriously compromises virtually all research or production work involving culture technology. Although many contamination events are overt and readily apparent, others are insidious and more difficult to detect. Similarly, viral infection may be obvious if cytopathogenesis is affected, but many viruses do not induce a drastic alteration in host cells and some are present in latent forms.

This article provides representative test protocols suitable for detecting most microbes and many viruses that might be expected in cell culture systems. The perspective is that of staff operating a national cell culture resource.

II. MATERIALS

The following media and reagents are from Difco: Bacto Sabouraud dextrose-broth (Cat. No: 0382-1); Bacto fluid thioglycollate medium (Cat. No. 0256-01); beef extract (Cat. No. 0131); brain–heart infusion (BHI) broth (Cat. No. 0037-016); neopeptone (Cat. No. B119); proteose peptone (Cat. No. 3); YM broth (Cat. No. 0711-01); nutrient broth (Cat. No. 003-01); Bacto yeast extract (Cat. No. 012701); trypsin, 1:250 Difco certified (Cat. No. 0152-15); and blood agar base (Cat. No. 0045-01). Trypticase soy broth powder (Cat. No. 01-162), trypticase (Cat. No. B11770), mycoplasma broth base (Cat. No. 11458), and mycoplasma agar base (Cat. No. 11456) are from Becton-Dickinson Microbiology Systems (formerly BBL). Fresh defibrinated rabbit blood (Cat. No. 82-8614) and sheep blood are from Editek, and North American Biologicals provided Diamond's TP-S-1 broth base powder (Cat. No. 73-9502) and Diamond's TP-S-1 vitamin solution (40X, Cat. No. 72-2315). American Hoechst is the source of bisbenzamide fluorochrome stain (Cat. No. 33217), and oil-free, dry annealed aluminum foil is from Reynolds Aluminum (Cat. No. 1235-0). Unless specified otherwise, cell culture media (various) and sera are from ATCC, Sigma, GIBCO-BRL, or Hyclone.

Template-primers poly(rA) · poly(dT)$_{12–18}$ (Cat. No. 7878) and poly(dA)–poly(dT)$_{12–18}$ (Cat. No. 7868) are from P-L Biochemicals, and [*methyl*-^{3}H]thymidine triphosphate ([3H]TTP, carrier-free, specific activity 50–60 Ci/mmol, 1.0 mCi/ml, Cat. No. NET 221X) is from Dupont New England Nuclear. The scintillation counter fluid (Betafluor, Cat. No. LS-151) was purchased from National Diagnostics.

The following items are required in screening for c-type viruses such as HIV and HTLV:

Rneasy minikit, Qiagen (Cat. No. 74104)
SuperScript double-stranded cDNA synthesis kit, Invitrogen (Cat. No. 11917-010)
Platinum Taq DNA polymerase, Invitrogen (Cat. No. 0966034)
Sybr Green I, Molecular Probes, Inc. (Cat. No. S7563)
DNA standard and HIV and HTLV positive cell lines, ATCC (Cat. No. 53069 CRL-8993 and CRL 8543)

Standards, primers, and probes:

A pUC18 vector containing a 9.9-kb insert from HIV-standard DNA is used as standard DNA for HIV (ATCC, Manassas, VA, ATCC No. 53069). For GAPDH and HTLV, polymerase chain reaction

Copyright 2006, Elsevier Science (USA).
All rights reserved.

(PCR) products containing the primer and probe sequence for both targets have been cloned into the pUC18 vector.

Primers and probes include:

HIV	Forward primer	5′ TCCACCTATCCCAG TAGGAGAAAT 3′
	Reverse primer	5′ GGTCCTTGTCTTAT GTCCAGAATG 3′
	TaqMan probe	5′ GATTAAATAAAATAG TAAGAATGTATAGC 3′
HTLV	Forward primer	5′ CAATCACTCATACA ACCCCCAA 3′
	Reverse primer	5′ CTGGAAAAGACAGG GTTGGG 3′
	TaqMan probe	5′ TCCTCCAGGCCATG CGCAAATACTCG 3′

In most cases, Sigma or VWR supplied general laboratory chemicals and solvents plus such items as instruments and bacteriological or cell culture glass- and plasticware.

The following additional specialty items are required: Leighton tubes (Cat. No. 3393) from Costar; cellulose filters, 0.45 and 0.22 µm (Cat. Nos. HATF 14250 and GSTF 14250, respectively) from Millipore; GasPak anaerobic systems (Cat. No. 60465) from Becton-Dickinson Microbiology Systems; embryonated chicken eggs from SPAFAS; egg candlers (Cat. No. C6372N-50001) from Nasco; egg drills, cutters, and moto tool (Cat. No. 9826-00) from Cole-Parmer; stainless-steel sterilizing pans (Cat. No. 2065-5) from Orem; and adjustable microliter pipettes and Pipetman (Cat. No. P-20 D/P-200D) from Rainin. Reference microbes, cell lines, and viruses are from the American Type Culture Collection (ATCC): *Pseudomonas aeruginosa* (e.g., ATCC 14502), *Micrococcus salivarious* (e.g., ATCC 14344), *Escherichia coli* (e.g., ATCC 4157), *Bacteroides distasonis* (e.g., ATCC 8503), *Penicillium notatum* (e.g., ATCC 8537), *Aspergillus niger* (e.g., ATCC 34467), *Candida albicans* (e.g., ATCC 10231), influenza virus (e.g., ATCC VR-95 or VR-810), Newcastle disease virus (e.g., ATCC VR-108 or VR-109), and Rous sarcoma virus (e.g., ATCC VR-140 or VR-724). The Gen-Probe kit is available from Fisher (Cat. No. GP1591) and the mycoplasma PCR kit is from ATCC (Cat. No. 90-1001K).

III. PROCEDURES

A. Bacteria and Fungi

Tests for sterility are performed routinely at ATCC on all culture media used, on cultures submitted from the community, on cultures at various stages during the accessioning process, and on all seed and distribution freezes. *Pseudomonas* species, micrococci, and *E. coli* are common bacterial isolates, whereas *Penicillium*, *Aspergillus*, and *Candida* species are common fungal and yeast contaminants.

1. Preparation of Media Solutions

1. *Sabouraud dextrose broth:* Dissolve 30 g dehydrated powder in 1000 ml distilled water and dispense 10-m1 aliquots into each of one hundred 16 × 150-mm test tubes. Cap each tube loosely and sterilize in an autoclave for 15 min at 15 lb pressure (121°C) on slow exhaust. After removing the tubes from the autoclave, press down caps securely and store at room temperature until used. Caps of differing colors may be used to permit ready identification.

2. *Nutrient broth with 2% yeast extract:* Dissolve 8 g of nutrient broth powder plus 20 g of Bacto yeast extract in 1000 ml distilled water and dispense 10-ml aliquots into each of one hundred 16 × 150-mm test tubes. Cap each tube loosely, sterilize, and store as described for solution 1.

3. *Thioglycollate medium:* Suspend 29.8 g dehydrated powder in 1000 ml distilled water in a 3-liter flask and heat to boiling to dissolve the powder completely. Dispense 10-m1 aliquots of the thioglycollate medium into each of one hundred 16 × 150-mm test tubes; cap each tube loosely. Sterilize in the autoclave as described for solution 1. After removing the tubes from the autoclave, press down caps securely and store in the dark at room temperature. This medium changes color in processing. As it dissolves it turns red or gold depending on the amount of dissolved oxygen. After autoclaving it is clear and gold in color, like nutrient broth. After cooling, the top layer of medium oxidizes and the indicator in the upper portion of the tube turns pink or red. The fluid should not be used if the indicator has changed to a red color in the lower third of the tube.

4. *Trypticase soy broth:* Suspend 30 g powder in 1000 ml distilled water and mix thoroughly and warm gently until solution is complete. Dispense 10-ml aliquots of die trypticase soy booth into each of one hundred 16 × 150-mm test tubes; cap each tube loosely and sterilize and store as described for solution 1.

5. *BHI broth:* Suspend 37 g powder in 1000 ml of distilled water, dissolve completely, and dispense 10-ml aliquots of BHI into 16 × 150-mm test tubes. Cap each tube loosely. Sterilize in the autoclave for 15 min at 15 lb pressure on slow exhaust. After autoclaving, press down caps securely, cool, and store at 4°C.

6. *YM broth:* Dissolve 21 g powder in 1000 ml distilled water and dispense 10-ml aliquots of the broth into each of one hundred 16 × 150-mm test tubes; cap each tube loosely. Sterilize and store as described for solution 1.

7. *Blood agar plates:* Suspend 40 g blood agar base in 950 ml cold distilled water and heat to boiling to dissolve the powder completely. Sterilize in the autoclave for 15 min at 15 lb pressure on slow exhaust. When the sterile blood agar base is cooled to 50°C, add 5% (50 ml) of pretested, fresh, defibrinated rabbit blood and mix by swirling. Dispense aseptically to 9-cm plates and store at 4°C. The rabbit blood is pretested for sterility by inoculating 0.5-ml aliquots into BHI broth and YM broth and onto blood agar base plates with subsequent incubation at 25° and 37°C. Negative results in 48 to 72 h are usually sufficient to permit use of the tested fluid.

2. *Examination*

Steps

1. Using an inverted microscope, equipped with phase-contrast optics if possible, examine cell culture vessels individually. Scrutiny should be especially vigorous in cases where large-scale production is involved.

2. Check each culture first using low power. After moving the cultures to a suitable isolated area, remove aliquots of fluid from cultures that are suspect; retain these for further examination. Alternatively, autoclave and discard all such cultures.

3. Prepare wet mounts using drops of the test fluids and observe under high power.

4. Prepare smears, heat fix, and stain by any conventional method using filtered solutions.

5. Examine under oil immersion for microbial contaminants.

6. Consult Freshney (2000) for further details.

3. *Inoculation and Incubation of Test Samples*

Steps

1. After cryopreservng stocks of cells (Hay *et al.*, 2000), retrieve and thaw about 5% of the ampoules from liquid nitrogen or vapor storage. Pool and mix the contents of the ampoules from each cryopreserved lot using a sterile 1-ml disposable pipette. It is recommended that antibiotics not be included in media used to prepare stocks of cells for preservation. If antibiotics are used, the pooled suspension should be centrifuged at 2000 g for 20 min and the pellet should be resuspended in antibiotic-free medium. A series of three such washes with antibiotic-free medium prior to testing eliminates traces of antibiotics that could obscure contamination.

2. From each pool, inoculate each of the following with a minimum of 0.3 ml of the test cell suspension: (a) two blood agar plates, (b) two tubes of thioglycollate broth, (c) two tubes of trypticase soy broth, (d) two tubes of BHI broth, (e) two tubes of Sabouraud broth, (f) two tubes of YM broth, and (g) two tubes of nutrient broth with 2% yeast extract.

3. Incubate test plates and broths as follows. (a) Blood agar plates: one at 37°C under aerobic conditions and one at 37°C anaerobically (a BBL Gaspak anaerobic system is convenient for the latter). (b) Tubes of thioglycollate broth, trypticase soy broth, BHI broth, Sabouraud broth, YM broth, and nutrient broth with yeast extract: one each at 37°C and one each at 26°C under aerobic conditions. (c) Incubate and examine periodically for 14 days the tubes of thioglycollate, trypticase soy broth, BHI broth, and blood agar plates. (d) Observe the tubes of Sabouraud broth, YM broth, and nutrient broth with yeast extract for 21 days before concluding that the test is negative. Contamination is indicated if colonies appear on solid media or if any of the liquid media become turbid.

4. Repeat any components of the test series that are positive initially to confirm the presence of a contaminant.

5. Autoclave and discard any contaminated cultures or ampule lots.

Comments

Of the seven media employed, trypticase soy, BHI, blood agar, and thioglycollate are suitable for detecting a wide range of bacterial contaminants. Sabouraud broth, YM broth, and nutrient broth with yeast extract will support growth of fungal contaminants. Stock media and incubation conditions used can be tested with the following ATCC control strains: *P. aeruginosa*, *M. salivarius*, *E. coli*, *B. distasonis*, *P. notatum*, *A. niger*, and *C. albicans*. Table I summarizes this recommended test regimen.

Pitfalls

Although this test regimen permits detection of most common bacterial and fungal organisms that grow in cell cultures, we have experiences with at least one very fastidious bacterial strain that initially escaped observation. This was present in nine different cell cultures from a single clinical laboratory in the United States submitted for testing and expansion under a government contract. The organism grew extremely slowly but could be detected after 3 weeks of incubation with cell cultures without antibiotics and with no fluid changes. Samples so developed were inoculated into sheep blood agar plates and New York City broth (ATCC medium 1685). The organism could

TABLE I Suggested Regimen for Detecting Bacterial or Fungal Contamination

Test medium	Temperature (°C)	Gas phase	Observation time (days)
Blood agar with fresh defibrinated rabbit blood (5%)	37	Aerobic	14
	37	Anaerobic	14
Thioglycollate broth	37	Aerobic	14
	26		
Trypticase soy broth	37	Aerobic	14
	26		
Brain–heart infusion broth	37	Aerobic	14
	26		
Sabouraud broth	37	Aerobic	21
	26		
YM broth	37	Aerobic	21
	26		
Nutrient broth with 2% yeast extract	37	Aerobic	21

be observed during a subsequent 6-week incubation period at 37°C.

The bacteriology department at ATCC determined suitable culture conditions for this microorganism and tentatively identified it as a *Corynebacterium*. Antibiotic sensitivity tests revealed bacteriostasis with some compounds, but no bactericidal antibiotics have yet been found.

This incident emphasizes the critical importance of diligent testing of cell cultures for contaminant microorganisms. By combining protocols such as those described here with procedures discussed later (e.g., fluorescent or nucleic acid probes for mycoplasma and viruses), one can be more certain that clean cell cultures are available for experimentation.

B. Mycoplasma

Mycoplasmal contamination of cell cultures has been established as a common occurrence that is capable of altering normal cell structure and function. Mycoplasmas have been shown to inhibit cell metabolism and growth, alter nucleic acid synthesis, affect cell antigenicity, induce chromosomal alterations, interfere with virus replication, and mimic viral actions. Basically, the growth of mycoplasma in cell cultures can be detected either by a direct microbiological agar culture procedure or by indirect procedures using staining, biochemical methods, or nucleic acid hybridization techniques (McGarrity, 1982; Hay *et al*., 1989, 1992, 2000).

In testing cell cultures for contamination, both direct and indirect procedures should be employed. The indirect method employed most frequently at the ATCC was originally described by Chen (1977). It requires the bisbenzamide DNA fluorochrome staining procedure plus an indicator cell. This adaptation is described here with slight modifications.

Duplicate screening techniques are generally recommended for rigorous cell line testing. Alternative methods to those included here include nucleic acid hybridization and a new technique involving the polymerase chain reaction. Details are available elsewhere (Hu and Buck, 1993; ATCC website http://www.atcc.org).

In screening cell lines for mycoplasma contamination, it is important to include positive controls in order to be assured that the test systems being used are optimal. Special precautions, however, are necessary when working with such material. The handling of mycoplasma cultures should be done at the end of a particular test and, when possible, in an isolated area using a biohazard-type hood. All equipment used in manipulations involving control cultures should be collected and sterilized immediately by autoclaving. More detailed accounts of the measures necessary to detect and prevent the spread of contamination can be found elsewhere (Uphoff and Drexler, 2001; Freshney, 2000).

1. Direct Method

The procedures used in preparing and pretesting the following culture media should be standardized, and the final pH should be adjusted to 7.2 to 7.4. Both media are prepared in quantities to be utilized within 3 to 4 weeks. The quality of the major components of the media may vary from batch to batch in the degree of toxicity and in their ability to support the growth of mycoplasma. The growth-promoting properties of each new lot of freshly prepared broth and agar media

are determined by making inoculations using ATCC 23206, *Acholeplasma laidlauii*, and ATCC 23838, *Mycoplasma arginini*. In addition, the horse serum, like all sera employed for cell culture work, is screened for mycoplasmal contamination. Briefly, a 100-m1 aliquot of the serum being tested is used as the serum supplement for 400 ml of broth medium. The cultures are incubated aerobically at 37°C for 4 weeks and are observed for turbidity and change in pH. Subcultures to agar plates and inoculations onto Vero indicator cultures for the indirect test are performed weekly during the incubation period. In testing samples in which bacterial and/or fungal contaminations may be prevalent, penicillin and thallium acetate are added to the basic medium. Penicillin is added to the stock solution (step a below) to provide a final concentration of 500 U per milliliter. Thallium acetate is added to the basic media (step b below) to provide a final concentration of 1:2000.

Steps

a. Preparation of Stock Solution. To 900 ml freshly distilled water, add 50 g dextrose and 10 g L-arginine HC1. Mix the ingredients at 37°C until dissolved. Bring the final volume up to 1000-ml. Sterilize the solution by filtration using a 0.22-µm filter, dispense into 100-ml aliquots, and store at –70°C until needed.

b. Preparation of Mycoplasma Broth Medium. Add 14.7 g mycoplasma broth base and 0.02 g phenol red to 600 ml water, heat to dissolve. Sterilize the solution by autoclaving for 15 min at 121°C using a slow exhaust cycle and allow the broth mixture to cool to room temperature. Aseptically add 200 ml horse serum, 100 ml yeast extract (15%), and 100 ml thawed stock solution (step a). Mix the solution completely. Dispense 10-ml aliquots of the broth medium into sterile test tubes and cap. Store broth tubes at 5°C and use within 3 to 4 weeks.

c. Preparation of Mycoplasma Agar Medium. Add 23.8 g mycoplasma agar base to 600 ml water. To dissolve, bring solution to a boil and sterilize the solution by autoclaving for 15 min at 121°C using a slow exhaust cycle. Place the sterilized medium in a water bath at 50°C. Place 200 ml horse serum, 100 ml yeast extract (15%), and 100 ml stock solution (step a) in a water bath at 37°C. Allow the components to equilibrate at these respective temperatures. Aseptically add the horse serum, yeast extract, and stock solution to the medium; mix well. Proceed immediately to dispense 10-ml aliquots in 60 × 15-mm petri dishes. Add the fluid as quickly as possible in order to eliminate the problem of the agar solidifying before the medium is dispensed completely. Stack the agar plates into holding racks, wrap in autoclave bags to minimize dehydration, and store at 5°C. Use within 3 to 4 weeks.

NOTE This procedure involves a total incubation time of about 35 days for both broth and agar cultures. This schedule is advisable for detecting lower levels of mycoplasma contamination that otherwise might be scored as false negatives.

d. Inoculation of Test Sample. Select a cell culture that is near confluency and has not received a fluid renewal within the last 3 days. Remove and discard all but 3 to 5 ml of the culture medium. Scrape a portion of the cell monolayer into the remaining culture medium using a sterile disposable scraper. For suspension culture systems, take the test sample directly from a heavily concentrated culture that has not received a fresh medium supplement or renewal within the last 3 days. Samples for testing can also be taken directly from thawed ampules that have been stored in the frozen state.

Inoculate 1.0 ml of the test cell culture suspension into a mycoplasma broth culture. Inoculate 0.1 ml of the test sample onto an agar culture plate. Incubate the broth culture aerobically at 37°C. Observe daily for the development of turbidity and/or shift in pH. Incubate the agar plate anaerobically at 37°C in a humidified atmosphere of 5% CO_2–95% nitrogen. After 5 to 7 days of incubation, and again after 10 to 14 days, remove a 0.1-m1 sample from the broth culture and inoculate a new agar plate. Incubate these plates anaerobically at 37°C.

Microscopically examine the agar plates weekly for at least 3 weeks for mycoplasma colony formation and growth before considering them to be negative. Observe the plates at 100 to 300 magnification using an inverted microscope.

The positive differentiation of mycoplasma colonies on agar plates, as opposed to air bubbles, tissue culture cells, and pseudocolonies, can be accomplished by subculturing a small section (1 cm^2) of the suspicious area of the agar culture into a new broth culture (for examples, see Freshney, 2000).

2. *Indirect Method (Staining for DNA)*

The bisbenzamide stain concentrate (step a below) should be examined routinely for contamination. Sterilization by filtration diminishes the quality of fluorescence, and fresh stock needs to be prepared periodically. The pH of the mounting medium (step b below) is critical for optimal fluorescence and should also be monitored routinely.

Continuous cells lines, such as ATCC.CCL 81, Vero, African green monkey kidney or ATCC.CCL 96, 3T6 mouse fibroblast, have been used very effectively as indicator cells in the indirect DNA-staining procedure. The use of transformed cell lines is not recommended because they produce large amounts of nuclear background fluorescence, which interfere with the interpretation of the results.

Utilization of the indicator cell with the DNA-staining procedure provides two major advantages. First, the indicator cell line supports the growth of the more fastidious mycoplasma species. Second, both positive and negative control cultures are readily available for direct comparisons with the culture samples being tested.

Steps

a. Preparation of Stain Concentrate. To 100 ml of Hanks' balanced salt solution without sodium bicarbonate or phenol red, add 5.0 mg bisbenzamide fluorochrome stain and 10 mg thimerosol. Mix thoroughly using a magnetic stirrer for 30 to 45 min at room temperature. The stain is heat and light sensitive. Prepare the concentrate in a brown amber bottle wrapped completely in aluminum foil. Store aliquots at –20°C. These are stable for about 1 year.

b. Preparation of Mounting Medium. Combine 22.2 ml *0.1 M* citric acid, 27.8 ml 0.2 *M* disodium phosphate, and 50 ml glycerol and adjust pH of mixture to 5.5. Store in a cold room at 5°C.

c. Preparation of Indicator Cell Cultures and Inoculation of Test Samples. Aseptically place a glass coverslip (previously sterilized) into each 60 × 15-mm culture dish. Dispense 3 ml Eagle's minimum essential medium with Earle's salts, 100 U/ml penicillin, and 100 µ*g*/ml streptomycin plus 10% bovine calf serum into each culture dish. Make certain that each glass coverslip is totally submerged and not floating on top of the medium.

Prepare a single cell suspension of ATCC.CCL 81, the African green monkey kidney cell line Vero, in this medium at a concentration of 1.0×10^5 cells/ml. The 3T6 murine line (ATCC.CCL 96) can be used instead. Inoculate 1 ml of the cell suspension into each culture dish and incubate the cultures overnight in a 5% CO_2 95% air incubator at 37°C. Examine the cultures microscopically to verify that the cells have attached to the glass coverslip. Number the top of each culture dish for identification purposes to record the test sample inoculated. Add 0.5 ml of culture medium to each of two cultures for negative controls and 0.2 to 0.5 ml of each test sample to each of two culture dishes. Add 0.5 ml ATCC 29052, *M. hyorhinis*, to each of two cultures for positive controls. Alternatively, a known infected cell line can be used. Return the cultures to the CO_2 incubator and allow to incubate undisturbed for 6 days.

d. Fixing, Staining, and Mounting Coverslips. To prepare the staining solution:

1. Add 1.0 ml of stock concentration (step a) to 100 ml Hanks' balanced salt solution without sodium bicarbonate and phenol red.
2. Prepare in a brown amber bottle wrapped in aluminum foil.
3. Mix thoroughly for 30 to 45 min at room temperature using a magnetic stirrer.

Remove cultures from the incubator and aspirate the medium from each dish. Add 5 ml of a 1 : 3 mixture of acetic acid : methanol to each culture dish for 5 min. Do not allow the culture to dry between removal of the culture medium and addition of the fixative. Aspirate each culture dish and repeat the fixation step for 10 min. Aspirate the fixative and let the cultures air dry. Add 5 ml of the staining solution [step d (1–3)] to each culture dish; cover and let stand at room temperature for 30 min. Aspirate the stain and rinse each culture three times with 5 ml distilled water.

After the third rinse, aspirate well so that the glass coverslip is completely dry. Let air dry if necessary. Place a drop of mounting fluid (step b) on a clean glass slide. Use forceps to remove the glass coverslip containing the specimen from the culture dish and place face up on the top of the mounting fluid. Add a second drop of mounting fluid onto the top of the specimen coverslip and cover with a larger clean coverslip. Lower both coverslips onto the mounting fluid in such a way as to eliminate trapped air bubbles. Label each slide to identify the specimen being tested and record results.

Observe each specimen under oil immersion, including both the positive and the negative controls, by fluorescence microscopy at 500X. A blue glass excitation filter (BG12 for Zeiss microscopes) is used in combination with a No. 50 barrier filter. Small fluorescing particles indicate mycoplasmal DNA and infection.

Alternative molecular methods readily available in kit form should also be considered. The PCR-based method for mycoplasma detection (Harasawa *et al.*, 1993; Hu and Buck, 1993) in use at the ATCC requires primers based on the DNA sequences in 16S and 23S mycoplasmal rRNA. These amplify DNA from all of the common mycoplasma found in cell cultures to levels easily detected after gel electrophoresis and

ethidium bromide staining. Advantages of the method include speed and sensitivity, as well as the ability to detect and identify species of most of the common mycoplasma known to infect cell cultures. Furthermore, it does not suffer from interpretation difficulties associated with some of the Hoechst or DAPI-stained preparations. Levels of sensitivity compare favorably with the Hoechst stain. Sample sizes need consideration. Detailed methodologies are provided with the kits (see the ATCC website for more details).

C. Protozoa

The overall frequency of infection of cell cultures with protozoans is low but the incidence may be higher if one is working with tissues such as human clinical material and animal tissues such as kidney or colon. The small limax amoebae belonging to the *Acanthamoeba* (or *Hartmanella*) genus are ubiquitous in nature and have been isolated from cells and tissues in culture in a significant number of laboratories. Jahnes *et al*. (1957) first reported spontaneous contamination of monkey kidney cells in culture by such free-living amoebae. The organisms have also been detected as occasional contaminants in such diverse cell lines as dog lymphosarcoma (LS30), HeLa, chick embryo fibroblast-like, and Chang liver cells (Holmgren, 1973). In some cases, protozoans are demonstrably cytopathic in cell culture.

Observation, cytological examination, and attempts at isolation are required in the detection of protozoan contaminants. These techniques are suitable for detecting many of the most common flagellates and amoeboid protozoans, including species of the genera *Acanthamoeba*, *Giardia*, *Leishmania*, *Naegleria*, and *Trypanosoma* (for more details, see Hay *et al*., 1992).

1. Preparation of Solutions and Protozoan Media

Steps

1. *Trypsin-EDTA:* Combine 2.5 g trypsin (1:250 Difco certified), 0.3 g EDTA, 0.4 g KCl, 8.0 g NaCl, 1.0 g glucose, 0.58 g NaHCO3, and 0.01 g phenol red in 1 liter double-distilled water, sterilize by filtration (0.22-µm Millipore filter), and store at –40°C.

2. *Hanks' balanced salt solution without divalent cations:* Combine 8.0 g NaCl, 0.4 g KCl, 0.05 g Na_2HPO4, 0.06 g KH_2PO4, and 0.02 g phenol red in 50 ml double-distilled water to dissolve chemicals; then bring volume to 100 ml. Autoclave on slow exhaust for 15 min, adjust pH to 7.2 to 7.4 with sterile 0.4*N* NaOH, and store at 4°C.

3. *Giemsa stock solution:* For stock solution of stain, combine 40 ml glycerol, 65 ml absolute methanol, and 1.0 g Giemsa powder. Filter two or three times and store at 4°C.

4. *Price's buffer (I0X):* Combine 6.0 g Na_2HPO_4, 5.0 g KH_2P0_4, and 1.0 liter distilled water. Before use dilute buffer with distilled water to 1X.

5. *Price's Giemsa stain:* Dilute Giemsa stain stock 3:97 with 1X buffer. After staining, discard unused portion.

6. *ATCC medium No. 400, Diamond's TP-S-1 medium for axenic cultivation of Entamoeba (ATCC medium No. 400):* Dissolve one packet of Diamond's TP-S-1 broth base powder in 875 ml distilled water, adjust pH to 7.0 with 0.4*N* NaOH, and filter through Whatman No. 1 paper. Sterilize at 120°C for 15 min. Aseptically add 100 ml inactivated (56°C for 30 min) bovine serum and 25 ml Diamond's TP-S-1 vitamin solution (40X, North American Biologicals), and aseptically dispense 13 ml per sterile test tube. Some commercial lots of Diamond's TP-S-1 medium have been shown to be toxic to *Entamoeba*. *To* test for toxicity, subculture *Entamoeba* through three to five passages.

7. *Locke's solution:* Combine 8.0 g NaCl, 0.2 g NaCl, 0.2 $CaCl_2$, 0.3 g KH_2PO_4, 2.5 glucose, and 1.0 liter distilled water and autoclave the solution for 20 min at 121°C.

8. *Diphasic blood agar medium (ATCC medium No. 1011):* Infuse 25.0 g beef extract in 250 ml distilled water by bringing to a rapid boil for 2 to 3 min while stirring constantly. Filter through Whatman No. 2 filter paper and add 10.0 g Difco neopeptone, 2.5 g NaC_l, and 10.0 g agar. Heat to boiling and filter through Whatman No. 2 paper, make up volume to 500 ml with distilled water, and adjust pH to 7.2 to 7.4. Autoclave for 20 min at 121°C, cool mixture to 50°C, aseptically add 30% sterile, defibrinated rabbit blood (Editek) to whole mixture, and dispense in sterile tubes and slant. After the slants have set, cover with 3.0 ml sterile Locke's solution.

9. *PYb medium (ATCC medium No. 711):* Combine 1.0 g Difco proteose peptone, 1.0 g yeast extract, 20.0 g agar, and 900.0 ml distilled water. Prepare and sterilize separately each of the following stock solutions and add to the basal medium as indicated to avoid precipitation: $CaC1_2$ (0.05*M*), 4.0 ml; $MgSO_4 \cdot 7H_2O$ (0.4*M*), 2.5 ml; Na_2HPO_4 (0.25*M*), 8.0 ml; and KH_2PO_2 (0.25*M*), 32 ml. Make the volume to 1 liter, check that the pH is at 6.5, and sterilize by autoclaving for 25 min at 120°C. Pour into petri dishes and allow to solidify.

10. *Brain-heart infusion blood agar (ATCC medium No. 807):* For the agar component, dissolve 37.0 g Difco BHI broth and 18.0 g agar in 1 liter boiling water. Dispense 5.0 ml solution per tube (16 × 125 mm) and sterilize for 25 min at 121°C. Cool to 48°C. Add 0.5 ml per tube of sterile, defibrinated rabbit blood and slant. After slants

have set, cover with 0.5 ml BHI broth (1.0 liter distilled water and 37.0 g BHI broth) with sterilization by autoclaving at 121°C for 25 min.

11. *Leishmania medium (ATCC medium No. 811):* Combine 1.2 g sodium citrate, 1.0 g NaCl, and 90.0 ml distilled water. Dispense 1.0 ml per tube, autoclave for 25 min at 121°C, and cool. Add 1.0 ml defibrinated, lysed rabbit blood solution (prepare by mixing equal parts of whole rabbit blood and sterile distilled water and freezing and thawing twice).

12. *NTYG medium (ATCC medium No. 935):* Combine 5.0 g trypticase, 5.0 g yeast extract, 10.0 g glucose, and 1.0 liter distilled water. Dispense 10.0 ml per test tube and sterilize. Just before use, add 0.2 ml dialyzed, heat-activated bovine serum and 0.1 ml defibrinated sheep blood. Protozoan growth media retain stability for at least 3 months if maintained at 4°C, with the exception of ATCC medium 400, which maintains stability for 2 to 4 weeks.

2. Preparation of Cell Culture Samples for Inoculation into Protozoan Media

Steps

1. Rapidly thaw a frozen ampoule of the sample in a water bath at 37°C.
2. Aseptically open the ampoule. Continue to use sterile techniques.
3. Transfer 0.8 ml of the concentrated cell suspension from the ampoule into a T-25 flask. Save 0.2 ml of the suspension for Giemsa staining (step 3 below).
4. Add 7 ml of the appropriate cell culture medium to maintain the culture.
5. Incubate at 37°C until the monolayer becomes confluent (3 to 5 days depending on the cell line). Examine the culture microscopically during this incubation period for the presence of (a) movement (i.e., motile cells), (b) intracellular contaminants, and (c) cytopathology.
6. Transfer the supernate from the confluent test cell culture to a sterile 15-m1 plastic centrifuge tube and retain at room temperature for use in step 12.
7. Rinse the cell monolayer (T-25 flask, step 5) with 5 ml Ca"- and Mg"- free Hanks' saline and discard saline solution.
8. Add 2 ml 0.25% trypsin-EDTA solution to the T-25 flask and incubate at 37°C for 10 min.
9. Add 7 ml of cell culture medium to the T-25 flask and aspirate gently to obtain a single-cell suspension.
10. Dispense aliquots (0.5 ml) of the trypsinized single-cell suspension to the following ATCC protozoan growth media: (a) ATCC medium No. 400 (for *Entamoeba*, Giardia); (b) ATCC medium No. 711 with *Enterobacter aerogenes* (for *Acanthamoeba*) [use a wire loop to streak medium No. 711 with *E. aerogenes* (*ATCC* 15038) 48 h before use]; (c) ATCC medium Nos. 807, 811, and 1011 (for trypanosomatids); and (d) ATCC medium No. 935 (for *Naegleria*).
11. Incubate samples for 7 to 10 days at 35°C and examine microscopically for the presence of flagellate, cyst, and trophozoite forms of protozoa.
12. Prepare five wet mounts for each test cell monolayer using the supernate collected in step 6. Examine microscopically with phase contrast for the presence of motile and nonmotile protozoans.

3. Preparation of Culture Cells for Giemsa Staining

Steps

1. Aseptically add 1.5 ml of the appropriate culture medium to a sterile Leighton tube containing a coverslip.
2. Dispense 0.2 ml of the original cell suspension (sample preparation just earlier) into the Leighton tube and incubate at 37°C until the culture is confluent.
3. Remove the coverslip from the Leighton tube, fix with absolute methanol for 1 min, and airdry.
4. Stain for 10 min with Price's Giemsa, rinse with tap water, and mount the coverslip to a glass slide using Aquamount.
5. Examine the slide; use low power (20X) for scanning and high power (100X) for close examination.

Controls

It is recommended that positive controls be included. For example, if cultured cells of the upper respiratory tract are being used, *Acanthameba castellanii* (ATCC 30010) or *Naegleria lovaniensis* (ATCC 30569) can be used as positive controls. *A. castellanii* was isolated from human clinical material. *N. lovaniensis* strain TS, another nonpathogenic strain of amoebae, was isolated from a Vero cell culture at passage 120. *Entamoeba histolytica* (ATCC 30042), the common pathogen causing amoebic dysentery, or the nonpathogenic *Entamoeba invadens* (ATCC 30020) can be used for positive controls if cells are being isolated from the intestinal tract. *E. histolytica is* a human isolate, and *E. invadens* strain PZ is a snake isolate.

Comments

The methods described are suitable for the detection of most common protozoan genera (i.e., limax amoebae) that could survive in association with cells in culture. Because cysts and trophozoites closely resemble damaged tissue cells, their presence as occasional contaminants can remain unnoticed. However, cells in cultures infected productively with amoebae of the genus *Acanthamoeba* frequently become granular

and gradually progress to complete disintegration. The time elapsed depends on the inoculum size and whether cysts or the motile trophozoites predominate in the inoculum. The cytopathic effect of amoebic contaminants has been reported, and in some cases the responsible agent has been mistakenly identified as viral in origin. Therefore, frequent observation of the cell culture is particularly stressed when examining for parasitic protozoan contaminants.

The possible presence of other genera (i.e., *Entamoeba* or trypanosomatids) should be considered not only in experimental studies involving primary tissues, but also with work requiring development or utilization of cell lines. The only known case of an isolation other then an amoeboid protozoan occurred in the isolation of a trypanosomatid from liver tissue.

The particular animal and tissue employed provide valuable clues as to the type of protozoan contaminant, the specific media, and staining procedures required.

D. Viruses

Of the various tests applied for detection of adventitious agents associated with cultured cells, those for endogenous and contaminant viruses are the most problematical. Table II lists representative problem viruses. Development of an overt and characteristic cytopathogenic effect (CPE) will certainly provide an early indication of viral contamination; however, the absence of a CPE definitely does not indicate that the culture is virus free. In fact, persistent or latent infections may exist in cell lines and remain undetected until the appropriate immunological, cytological, ultrastructural, and/or biochemical tests are applied. Unfortunately, separate tests are necessary for each class of virus and for specific viruses. Additional host systems or manipulations, e.g., treatment with halogenated nucleosides, may be required for virus activation and isolation (Aaronson *et al*., 1971). Common screening methods or tests for specific virus classes are listed in Table III.

Without such screens, latent viruses and viruses that do not produce an overt CPE or hemadsorption will escape detection. Some of these could be potentially dangerous for the cell culture technician. For example, Hantaan virus, the causative agent of Korean hemorrhagic fever, replicates in tumor and other cell lines. Outbreaks of the disease in individuals exposed to infected colonies of laboratory rats have been reported separately in five countries. An incident of transmission during passage of a cell line was confirmed in Belgium. As a result of these findings, cell lines expanded in this laboratory were screened using an indirect immunofluorescent antibody assay (LeDuc *et al*., 1985) and were found to be negative.

Substantial concern over laboratory transmission of the human immunodeficiency viruses is also evident. Cases of probable infection during processing in U.S. laboratories have been described. One, for example, was presumed due to parenteral exposure and another to work with highly concentrated preparations (Weiss *et al*., 1988). In the latter circumstance, strict adherence to biosafety level *3* containment and practices is essential. A more detailed discussion of safety precautions for work with cell lines in general is provided elsewhere (Caputo, 1988).

ATCC cell lines from selected groups have been screened for HIV-1 using PCR amplification followed by a slot-blot test for envelope and GAG sequences (Ou *et al*., 1988). The oligonucleotide primer pairs SK *38/39* and SK *68/69 plus* SK *19* or SK 70 probes were used. Human cell lines of T-cell, monocyte–macrophage, brain and nervous system, B-cell, and gastrointestinal origin plus an array of other primate lines have been examined to date. Only those already known to be infected with HIV-1 have been positive. Additional viruses that could present a substantial health hazard to cell culture technicians include, for example, hepatitis and cytomegaloviruses. Rapid PCR-based tests for these have been described [e.g.,

TABLE II Representative Viruses of Special Concern in Cell Production Work

Human	Other
Human immunodeficiency viruses	Hantavirus
Human T-cell leukemia viruses	Lymphocytic choriomeningitis virus
Other endogenous retroviruses	Ectromelia virus
Hepatitis viruses	Murine hepatitis
Human herpesvirus 6	Simian viruses
Cytomegalovirus	Sendai virus
Human papillomavirus	Avian leukosis virus
Epstein–Barr virus	Bovine viral diarrhea virus

TABLE III Common Methods for Detection of Viruses in Cell Line Stocks[a]

Cytopathogenic effect observation	Reverse transcriptase assays
Chorioallantoic membrane inoculation	Nucleic acid hybridization
Hemagglutination	Fluorescent antibody staining
Hemadsorption	Electron microscopic fine structure
Cocultivation	Animal inoculation

[a] See IABS (1989) and Hsuing *et al*. (1994) for more details.

Ulrich *et al*. (1989) and Cassol *et al*. (1989), respectively].

Other viruses that may present problems generally in cell culture work include ectromelia virus, the causative agent of bovine viral diarrhea (BVDV), and Epstein–Barr virus (EBV). [See also Bolin *et al*. (1994), Harasawa *et al*. (1994), and Hay *et al*. (2000) for testing methodology and further discussion.]

It should be emphasized at the outset that the following protocols represent an expedient compromise established at ATCC to monitor for readily detectable viruses associated with cell lines. Egg inoculations plus select cocultivations and hemadsorption tests were included in addition to routine examinations for CPE using phase-contrast microscopy. Similar general tests are recommended by government agencies in cases where cell lines are to be used for biological production work (Code of Federal Regulations on Animals and Animal Products, 9 CFR *113.34-113.52*, revised Jan. 1, 1978; Code of Federal Regulations on Food and Drugs, Subchapter F on Biologics, *21* CFR *630.13* b-c, revised April 1, 1979; IABS, 1989; Lubiniecki and May, 1985). Procedures for reverse transcriptase assays to detect oncogenic viruses are also being applied at the ATCC for selected cell lines.

Because endogenous and most exogenous retroviruses produce no morphological transformation or cytopathology in infected cells, the production of such viruses by cell cultures is generally undetectable except by serological or biochemical means. At ATCC the concentration of particulate material from culture supernates and assay for viral RNA-directed DNA polymerase (RDDP) provide sensitive and reliable means for detecting retrovirus production by cultured cells.

One or more of the following procedures is currently being applied to all cell lines accessioned for the ATCC repository. Tests for specific viruses may be applied through collaborations as described earlier.

1. Examination of Established Cultures for Overt Cytopathogenic Effect or Foci

Steps

1. Hold each flask or bottle so that light is transmitted through the monolayer and look for plaques, foci, or areas that lack uniformity. If frozen stocks of cells are to be examined, pool and mix the contents of about *5%* of the ampoules from each lot using a syringe with a cannula. Establish cultures for morphological examinations and for tests in the following sections using progeny from such pooled populations.

2. Using an inverted microscope equipped with phase-contract optics wherever possible, examine cell culture vessels individually, paying special attention to any uneven areas in gross morphology observed in step 1. Check first using low power. If the cell line is suspect, subculture taking the appropriate safety precautions. Prepare coverslip cultures for further examination. Alternatively, autoclave and discard all suspect cultures. (Stainless-steel collection and sterilizing pans for this purpose can be obtained from the Orem Medical Company.)

3. Remove fluid from coverslip cultures that require additional study. Treat with neutral buffered formalin or other suitable fixative. Prepare a wet mount and examine under high power. [Consult Rovozzo and Burke (1973), Hsuing *et al*. (1994), and Yolken *et al*. (1999) for examples of cytopathogenic effects and further details.]

2. Application of the Hemadsorption Test

Steps

1. Establish test cultures in T-25 flasks using an inoculation density such that the monolayers become confluent in 48 to 72 h.

2. Prepare washed red blood cell suspensions on the day the test is to be performed. Pack the erythrocytes from 5 ml of the purchased suspensions by centrifugation at 100 *g* and resuspend in 35 ml Hanks' saline without divalent canons. Repeat three times and resuspend the final pellet to yield a 0.5% suspension (v/v) of red blood cells in saline.

3. Remove the culture fluid and rinse the test monolayers with 5 ml Hanks' saline minus divalent cations.

4. Add 0.5 ml each of the suspensions of chick, guinea pig, and human type O erythrocytes from step 2. Then place the flask with monolayer down at 4°C for 20 min.

5. Observe macroscopically and microscopically under low power for clumping and adsorption of red blood cells to the monolayer.

6. Repeat steps 2–4 on all test cultures not exhibiting hemadsorption before recording a negative result. [A suitable positive control can be established by infecting a flask of rhesus monkey kidney cells with 0.2 ml of undiluted ATCC VR-95 (influenza virus strain A/PR/8/34) 48 to 72 h before testing.]

3. Egg Preparation

Steps

1. Drill a small hole in the egg air sac (blunt end) using the electric drill (Cole-Parmer) and a 1/16-in. burr-type bit or an 18-gauge needle in this and subsequent operations; work with sterile instruments. Swab areas of the shell to be drilled with 70% ethanol before

and after each manipulation. The drill bits may be placed in 70% ethanol before use.

2. Using the candling lamp (Nasco), locate the area of obvious blood vessel development and, at a central point, carefully drill through the shell, leaving the shell membrane intact.

3. Place 2 or 3 drops of Hanks' saline on the side hole and carefully pick through the shell membrane with a 26-gauge syringe needle. The saline will seep in and over the chorioallantoic membrane (CAM) to facilitate its separation from the shell membrane.

4. Apply gentle suction to the hole in the air sac using a short piece of rubber tubing with one end to the mouth and the other pressed to the blunt end of the egg. Use the candling lamp to monitor formation of the artificial air sac over the CAM.

5. Seal both holes with squares of adhesive or laboratory tape and incubate the eggs horizontally at 37°C. Standard cell culture incubators and walk-in rooms are entirely adequate for egg incubations. High-humidity or air/CO_2 boxes are not satisfactory.

4. Egg Inoculations

Steps

1. Obtain suspensions of test cells in the appropriate growth medium and adjust the concentration such that 0.2 ml contains 0.5 to 1×10^7 cells.

2. Remove the seal from side holes in the embryonated eggs and inject 0.2 ml of the cell suspension onto the CAM of each of 5 to 10 eggs.

3. Using the candling lamp, examine the embryos 1 day after adding the cell suspension; discard any embryos that have died. Repeat the examination periodically for 8 to 9 days.

4. If embryos appear to be viable at the end of the incubation period, open the eggs over the artificial air sac and examine the CAM carefully for edema, foci, or pox. Check the embryo itself for any gross abnormalities such as body contortions or stunting.

5. In cases in which viral contamination is indicated, repeat steps 1–4 both with a second aliquot of the suspect cells and with fresh fluid samples from eggs in which the embryos have died or appear abnormal. Positive controls may be established by inoculating eggs with influenza virus, Newcastle disease virus, and/or Rous sarcoma virus.

5. Cocultivation Trials

Steps

1. Select two appropriate cell lines for cocultivation with each cell line to be tested. The lines chosen will depend on the species from which the test cell line originated. For example, for a human cell line, one could cocultivate with ATCC CCL 75 (WI-38), ATCC CCL 171 (MRC-5), or primary human embryonic kidney (HEK) cells. A cell line from a second species of choice in this example could be ATCC CCL 81 (Vero) originating from the African green monkey.

2. Inoculate a T-75 flask with 10^6 cells from each line in a total of 8 ml of an appropriate growth medium. In some cases, the inocula may have to be adjusted in an attempt to maintain both cell populations during the cocultivation period. For example, if a very rapidly proliferating line is cocultivated with a test line that multiplies slowly, the initial ratio of the former to the latter could be adjusted to 1:10. Similarly, the population that multiplies slowly might have to be reintroduced to the cocultivation flasks if it were being overgrown by the more rapidly dividing cells.

3. Change the culture fluid twice weekly and subcultivate the population as usual soon after it reaches confluence.

4. Examine periodically for CPE and hemadsorption over a 2- to 3-week period at minimum, using procedures described earlier.

Viral isolates may be identified through standard neutralization (hemadsorption inhibition, plaque inhibition, hemagglutination inhibition) or complement fixation tests. The ATCC virology department retains and distributes antisera to many viral serotypes, and identification can be accomplished readily.

6. Reverse Transcriptase Assays

Positive serological assays for retrovirus antigens in cells and cell packs indicate that a retrovirus genome is present, but these assays do not indicate whether release of progeny virus particles is occurring. It has been found that the concentration of particulate material from culture supernates and the assay for viral RDDP (Baltimore, 1970; Temin and Mizutani, 1970) provide a sensitive and reliable means for detecting retrovirus production by cultured cells.

a. Preparation of Cell Cultures. Cell cultures to be examined for the production of retrovirus should be cultured by the methods and in the media that are optimal for the particular cells. It is important that the cells be in good condition and not undergoing degeneration and autolysis.

Steps

1. When adherent cell cultures are about 50 to 60% confluent, or when suspension cultures are at a cell density about 50% of the maximum, completely replace the medium and reincubate the cultures.

2. Harvest fluid approximately 24 h after feeding.

b. Processing of Culture Fluid

Steps

1. Collect culture medium aseptically.
2. Clarify medium by centrifugation at 1000 to *3000 g* for 10 min at 4°C. Decant and save the clarified supernates and discard sedimented materials.
3. The clarified medium contains 0.15 *M* NaCl; add 5.0 *M* NaCl to a final concentration of 0.5 *M* NaCl. Calculate the volume of 5.0 *M* NaCl according to the formula $0.15(V_1) + 5.0(V_2) = 0.5\ (V_1 + V_2)$, where V_1 is the volume of clarified culture fluid and V_2 is the volume of 5.0 *M* NaCl to be added. Mix well. If the medium becomes cloudy after adding NaCl, centrifuge at *10,000 g* for 10 min and save the supernate.
4. To 2 volumes of clarified supernate containing 0.5 *M* NaCl, add 1 volume 30% PEG 6000 in 0.5 *M* NaCl. Mix well.
5. Allow precipitation to occur for at least 1 h while holding in wet ice. At this point samples may be held overnight at 4°C if necessary.
6. Centrifuge at 7000 *g* for 10 min.
7. Decant and discard the supernates.
8. Drain the pellets thoroughly while holding at 4°C.
9. Resuspend the pellets in 50% (v/v) buffer A [0.05 *M* Tris–HCl, pH 7.5, 0.1 *M* KCl, 0.5 m*M* EDTA, 10 m*M* dithiothreitol, 0.05% (v/v) Triton X-100, and 50% glycerol]. Care must be taken to ensure that pellets are completely resuspended.
10. Store resuspended pellets at –20°C. Aliquots are used for RDDP assays.

c. Assay of RNA-Directed DNA Polymerase Activity. This procedure is based on that of Gallagher and Gallo (1975).

Solutions

1. *Stock mix:* 0.5% (v/v) Triton X-100, 1.13 *M KCl*.
2. *Template-primer solutions (P-L Biochemicals).* Mix A: Combine 1 mg/ml poly(rA)–poly$(dT)_{12–18s}$ with 0.01 *M* Tris–HCl, pH 7.5, and 0.1 *M* NaCl. Mix B: Combine 1 mg/ml poly(dA)–poly$(dT)_{12–18}$ with 0.1 *M* NaCl and 0.01 *M* Tris–HCI, pH 7.5.
3. *Working mixtures of template-primer solutions: Mix* stock mix and template-primer solutions in 3:2 (v/v) ratio.
4. *Reaction cocktail:* Evaporate 250 µl [3H]TTP (carrier-free, New England Nuclear 221-X) to dryness under vacuum. Redissolve in 720/µl H_2O before adding the following components (volumes given are for 10 tubes): 1.0 *M* Tris–HCl, pH 7.8 (40 µl), 0.2 *M* dithiothreitol (40 µl), *0.01 M* $MnCl_2$ (50 µl). Add $MnCl_2$ last (just before initiating reactions).

Steps

1. Distribute culture medium concentrates and positive and negative control samples into siliconized 10 × 75-mm assay tubes. (a) For positive controls, use concentrates prepared from culture media of cell cultures known to be producing retroviruses. (b) For negative controls, use buffer A-glycerol (Table IV).
2. Add appropriate template-primer mix to each tube and mix with a vortex mixer. Hold tubes in wet ice for 15 min.
3. Initiate reactions by adding reaction cocktail to each tube and mixing. Allow reactions to proceed for 30 min in a 37°C water bath.
4. At the end of incubation period, remove tubes to an ice bath; terminate reactions by adding 25 µl 0.1 *M* EDTA per tube (Sethi and Sethi, 1975).

TABLE IV Contents of RNA-Directed Polymerase Assays for Three Samples

Tube No.	Medium concentrate	Sample volume	Mix A	Mix B	Cocktail
1	1	5 µl	10 µl	—	85 µl
2	1	5 µl	—	10 µl	85 µl
3	2	5 µl	10 µl	—	85 µl
4	2	5 µl	—	10 µl	85 µl
5	3	5 µl	10 µl	—	85 µl
6	3	5 µl	—	10 µl	85 µl
7	Negative control	5 µl[a]	10 µl	—	85 µl
8	Negative control	5 µl[a]	—	10 µl	85 µl
9	Positive control	5 µl[b]	10 µl	—	85 µl
10	Positive control	5 µl[b]	—	10 µl	85 µl

[a] Buffer A-glycerol (1:1) as used for resuspending PEG precipitates.
[b] PEG-precipitated particles from medium collected from known retrovrus (e.g., murine leukemia virus)-producing cells.

5. Spot 100 µl from each tube onto appropriately numbered DE-81 filters. Allow liquid to soak into filters.

6. Wash batches of filters with gentle manual swirling in at least 10 ml (per filter) of 5% (w/v) $Na_2HPO_4 \cdot 7H_2O$. Repeat for a total of six washes (Sethi and Sethi, 1975).

7. Wash twice with distilled H_2O and twice with 95% ethanol and arrange filters on cardboard covered with absorbent paper. Dry thoroughly under a heat lamp.

8. Place each filter in a separate numbered scintillation vial, add 10 ml PPO-POPOP scintillation cocktail (Betafluor) to the vial, and count in a liquid scintillation counter (Beckman LS-3133) using a tritium window.

Comments

A number of precautions must be observed in the interpretation of the results obtained in this assay. If the cultures to be tested are very heavy and undergoing autolysis, a large amount of cellular DNA-directed DNA polymerase may be associated with microsomal particles in the culture medium. These particles are concentrated by the polyethylene glycol procedure just as virus particles are. Because cellular DNA polymerases do not exhibit an absolute specificity for a DNA template, a certain level of [3H]TMP ([^{3}H]thymidylate) incorporation directed by an RNA template will result from cellular polymerase activity. If a high level of DNA-directed cellular polymerase activity is present in medium concentrates, the (sometimes high) degree of incorporation by these enzymes can mask true RDDP activity, which may be present. Consequently, it is important that media be collected from healthy, actively growing cultures.

It must be remembered that enzymes that catalyze the polymerization or terminal addition of [^{3}H]TMP with a poly(rA) · oligo(dT) template-primer are not exclusively viral (Harrison *et al*., 1976). poly(rA) DD–CC oligo(dT) is generally employed because the activity of retroviral RDDP is usually greater with that template-primer than it is when measured by the incorporation of dGMP (deoxyguanylate) directed by poly(rC) · oligo(dG1) or by methylated derivatives of the poly(rC) template; however, DNA synthesis directed by poly(rC) · oligo(dG) is more specific for viral enzyme. Consequently, medium concentrates that show incorporation of [^{3}H]TMP with the poly(rA) template should be tested for the incorporation of [^{3}H]dGMP directed by a poly(rC) template.

Incorporation of isotopic precursors into macromolecular form is generally detected by the precipitation of macromolecules with trichloroacetic acid after the enzymatic reaction is terminated. Although background levels of radioactivity may be somewhat higher by the use of adsorption to and elution from ion-exchange filter paper, the ion-exchange procedure obviates the need for a filtration manifold, which is generally employed for acid precipitation. Also, the batch method employed allows many more samples to be processed efficiently.

7. A Rapid PCR-Based Procedure for Detecting the Presence of HIV and HTLV RNA in ATCC Cell Lines

An additional high-throughput method has been adopted to screen for HIV and HTLV RNA in ATCC cell lines using quantitative PCR. Priorities include lines, which might be expected to support growth of these viruses, namely T cells, macrophages and monocytes, lines from the brain and nervous system, lines of gastrointestinal origin, selected human hybridomas, and others.

Steps

1. Total RNA is extracted from 10^6 cells of selected cell lines (Qiagen, Valencia, CA).

2. After quantitative and qualitative analyses using the Bioanalyser 2100, 500 ng of RNA is reverse transcribed in the presence of a mixture of random hexamers and oligo(dT). For real-time PCR (ABI PRISM 700, sequence detector, Foster City, CA), 12.5 ng of initial RNA (0.5 µl of cDNA reaction) is used.

3. Specific primers and TaqMan probes are used individually to measure levels of HIV-1, HTLV-1, and GAPDH transcripts. For HIV-1 and HTLV-1, the Sybr Green I dye assay is also used.

Notes and Results

Both the SybrGreenI dye (Molecular Probes, Eugene, OR) and TaqMan assays for HIV-1 and HTLV-1 show an amplification signal. GAPDH *transcripts*, used as an internal control, are detectable in all the cell lines tested. Every sample is run on triplicates, and an average is calculated. Absolute quantities of HIV, HTLV, and GADPH are calculated using the standard DNA method as described in User Bulletin 2 (PE Applied Biosystems, Foster City, CA).

We have used two different detection methods: Sybr Green I dye or the TaqMan probe method. Sybr Green I is a double-stranded DNA-binding dye, which, when added into the PCR mix, binds to the amplicon, the double-stranded DNA fragment produced during PCR. As the PCR progresses, more amplicons are created. Due to the binding of Sybr Green I dye to all double-stranded DNA, the increase in fluorescence is proportionate to the amount of PCR product. In addition to forward and reverse primers, TaqMan

technology uses a sequence-specific oligonucleotide labeled with fluorescent dye at the 5′ end and a quencher dye at the 3′ end. While the probe is intact, the proximity of the quencher dye reduces the fluorescence emitted by the reporter dye by fluorescence resonance energy transfer (FRET) through space. If the target sequence is present, the probe anneals downstream from one of the primer sites and is cleaved by the 5′ nuclease activity of *Taq* DNA polymerase during primer extension (Figs. 1A and 1B). The cleavage of the probe separates the reporter dye from the quencher dye, increasing the reporter dye signal (Fig. 1C). Additional cleavage of the probe occurs at every cycle, resulting in an increase of the fluorescent signal proportional to the amount of the amplicon. Thus the presence of the TaqMan probe enables detection of the specific amplicon as it accumulates during PCR cycles.

HIV- and HTLV-specific primers and probes were designed to avoid false-negative samples due to nucleotide variation in the target sequence (Desire 2001; Schutten, 2000; Bisset, 2001). Blast search of GenBank indicated that the probe and primer set used in these analyses will detect the majority of HIV-1 subtypes and HTLV-I. Total RNA was extracted from frozen cell pellets for all the cell lines used in the test. For CRL-8993, total RNA was used from both frozen and fresh cells as a comparison. During RNA extraction, DNase I was added to avoid contamination of RNA extracts with genomic DNA. Extracted RNA was evaluated using the 2100 Bioanalyzer (Agilent Technologies, Wilmington, DE). Although the amount of total RNA extracted from frozen cells is significantly lower than the total RNA extracted from fresh cells, the RNA extracted from frozen cells is sufficient for several RT-PCR assays and no RNA degradation was observed. Total RNA (300 ng) was reverse transcribed in a 20-µl reaction using Superscript (Invitrogen, Carlsbad, CA) and 1 µl of the cDNA product was used for real-time PCR. We have used both Sybr Green and TaqMan methods to quantitate and detect HIV-1 and HTLV-I viruses in human cell lines. For absolute quantitation, known amounts of plasmid DNA containing full-length or partial sequences of HIV and HTLV were used in parallel with the unknown templates. PCR was performed using the same set of primers and the TaqMan probe for both standard and sample cDNA. Amplification plots and standard curves were generated for HIV (Fig. 2A) and HTLV (data not shown). The absolute amounts of HIV and HTLV for each sample were calculated based on the standard curves (Figs. 2B and 2C). We have also analyzed levels of GAPDH as an endogenous control, and standard curves for GAPDH were generated using plasmid DNA containing a GAPDH cDNA (Fig. 3). Absolute amounts of GAPDH were also calculated based on the standard curve method.

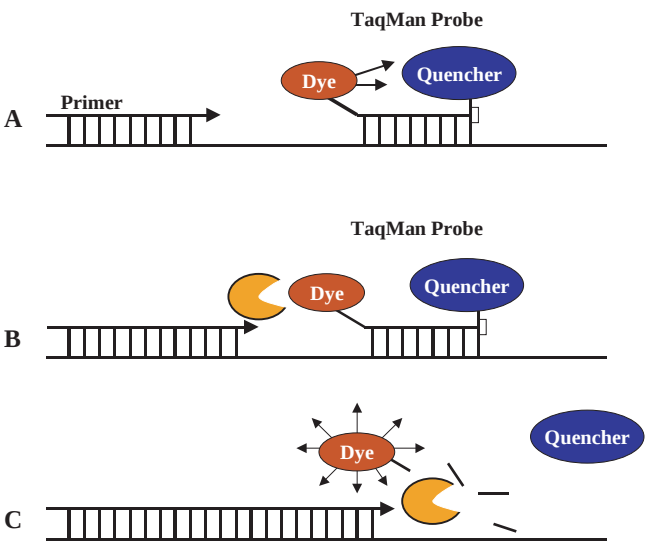

FIGURE 1 Description of 5′ nuclease assay. (A) Sequence-specific primers and dual-fluorescence TaqMan probe anneal to complementary sequences in the DNA template. Due to frequency resonance energy of transfer emission of the fluorescence dye (reporter) is reduced significantly by the presence of the proximal quencher. (B) Due to *Taq* polymerase activity, primer extension and synthesis of a complementary strand occur. (C) While extending, due to its 5′ nuclease activity, the *Taq* polymerase cleaves the TaqMan probe and enables the release of a fluorescent signal by the reporter.

Quantitation of copies of viral HIV and HTLV, as well as quantitation of endogenous GAPDH, is shown in Table V and Fig. 4. Sybr Green assays were run for the quantitation of HIV, HTLV, and GAPDH, analyses were performed using the standard curve method, and similar results were obtained (data not shown). Therefore, if primers are well designed and PCR conditions are such that do not generate nonspecific amplicons or primer dimers, testing for the presence of viral RNA using Sybr Green I dye could be less expensive and as effective as the TaqMan assay. As shown in Figs. 3 and 4, HIV and HTLV viral RNA was detected only in CRL-8993 and CRL-8543 cell lines. CRL-8993 is a lymphoid cell line reportedly positive for HIV, and CRL-8543 is also reported to contain HIV and HTLV viruses. CRL-8993 was used as a control, and total RNA was extracted from both fresh culture and frozen cells. As shown in Fig. 4, the difference in absolute copies of either GAPDH or HIV transcripts between the two RNA extracts is insignificant, suggesting that total RNA extracted from frozen cells could be used effectively for RT-PCR analyses.

In summary, we have established a quick and accurate method for the detection of HIV-1 and HTLV-I

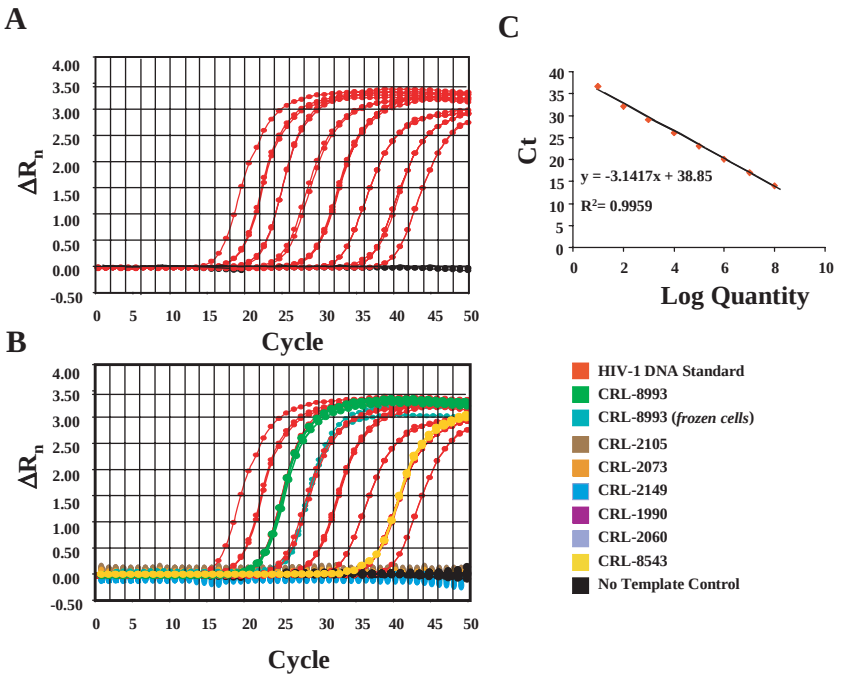

FIGURE 2 Real-time PCR assays for the detection and quantitation of HIV. Amplification plots (A) and standard curves (B) generated for the quantitation of HIV. (C) Amplification plots of unknown templates (total RNA from human cell lines).

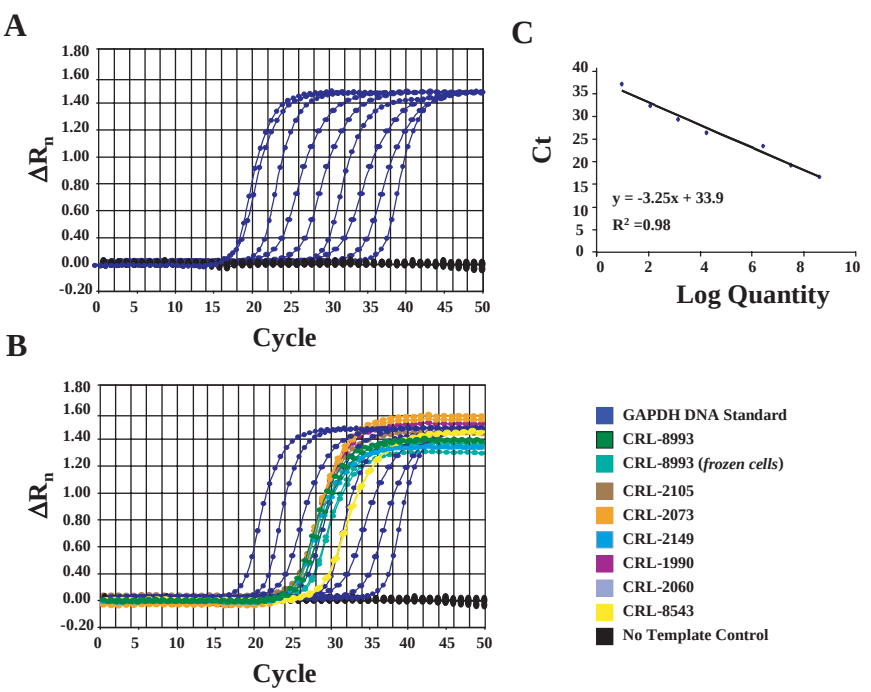

FIGURE 3 Real-time PCR assays for the quantitation of endogenous GAPDH transcripts as an internal control. Amplification plots (A) and standard curves (B) generated for the quantitation of GAPDH. (C) Amplification plots of endogenous GAPDH from each specific cell line.

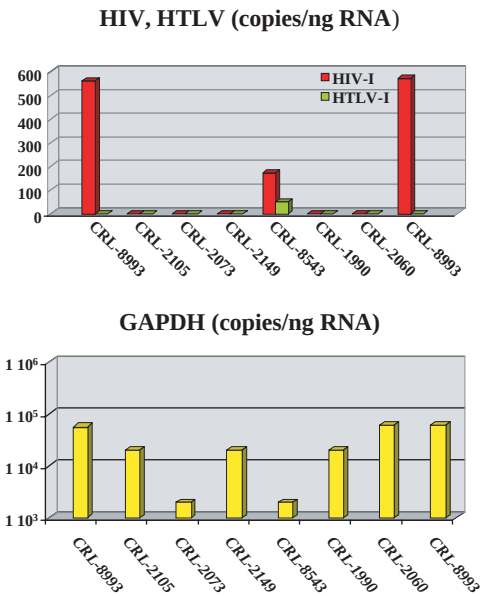

FIGURE 4 Detection and quantitation of HIV, HTLV, and GAPDH transcripts based on real-time PCR analyses.

TABLE V HIV and HTLV Contaminants in Selected Cell Lines[a]

Cell line	Designation	GAPDH	HIV	HTLV
CRL-8993	8E5(CEM)	82,000	560	0
CRL-2105	HH	20,000	0	0
CRL-2073	NCCIT	2,000	0	0
CRL-2149	SK-N-DZ	20,000	173	51
CRL-8543	H9/HTLV-111B	2,000	0	0
CRL-1990	J45–01	20,000	0	0
CRL-2060	PFSK-1	60,000	0	0
CRL-8993	8E5(CEM)	60,000	572	0

[a] Results are presented as copies of HIV and HTLV transcripts per nanogram of total RNA. Quantitation of GAPDH transcripts is also provided.

viruses. Given the high sensitivity of real-time PCR, very low amounts of total RNA are needed for PCR analyses. Therefore, RNA can be extracted directly from frozen cell pellets and particular cell lines can be tested for the presence of viral RNA prior to cultivation. Real-time PCR offers the possibility of detecting and quantitating as low as 10 copies of viral DNA.

IV. GENERAL COMMENTS

The microbial contamination and viral infection of cell lines are still extremely serious problems. Mycoplasmal infection has been especially well studied, and the incidence of problems has been documented through government-funded programs. Screening results reported within the past two decades showed that as many as 4 to 33% of cultures tested were infected with one or more species *of* mycoplasma (Hay *et al*., 1989). It *is absolutely imperative* that cell lines used in research or production work be tested routinely for such adventitious infection. The comparative cost in time and materials is extremely small. Rewards in terms *of* research or production reliability are substantial.

Testing for viral infection is more problematical in that it is expensive and multiple tests are required to provide even a limited degree of assurance on freedom from infection. We recommend consideration of screening on a case-by-case basis depending on anticipated use for the line, funding available, and a risk-versus-benefit analysis. Of course, a potential health hazard for cell culture technicians is a major concern.

Finally, it is also critically important to verify the identity of cell lines employed. Hukku *et al*. (1984) documented the incidence of cross-contamination of cell lines reporting misidentifications in excess of 35%.

Thus, a reasonably rigorous authentication pro-gram must include not only reliable tests to ensure an absence of microbial infections (including mycoplasma), but also cell species verification. Methods are detailed elsewhere (Hay *et al*., 2000, 1992) as are precautions required to avoid operator-induced contamination during routine processing (Hay, 1991).

References

Aaronson, S. A., Todaro, G. J., and Scolnick, E. M. (1971). Induction of murine C-type viruses from clonal lines of virus-free BALB/3T3 cells. *Science* **174**, 157–159.

Baltimore, D. (1970). RNA-dependent DNA polymerase in virions *of* RNA tumor viruses. *Nature* (*Lond*.) **226**, 1209–1211.

Bisset L. R. (2001). Quantification of *in vitro* retroviral replication using a one-tube real time RT-PCR system incorporating direct RNA preparation. *J. Virol. Methods*. **91**(2), 149–155.

Bolin, S. R., Ridpath, I. F., Black, J., Macy, M., and Roblin, R. (1994). Survey of cell lines in the American Type Culture Collection for bovine viral diarrhea virus. *J. Virol. Methods* **48**, 211–221.

Caputo, J. (1988). Biosafety procedures in cell cultures. *J. Tissue Cult Methods* **11**, 223–228.

Cassol, S. A., Poon, M.-C., Pal, R., Naylor, M. J., Culver-lames, J., Bowen, T. J., Russel, J. A., Krawetz, S. A., Pon, R. T., and Hoar, I. (1989). Primer mediated enzymatic amplification of cytomegalovirus (CMV) DNA. *J. Clin. Invest*. **83**, 1109–1115.

Chen, T. R. (1977). *In situ* demonstration *of* mycoplasma contamination in cell cultures by fluorescent Hoechst 33258 stain. *Exp. Cell Res*. **104**, 255–262.

Desire, N. (2001). Quantification of HIV type 1 proviral load by TaqMan real time PCR. *J. Clin. Microbiol*. **39**(4), 1303–1310.

Fogh, J. (1973). Contaminants demonstrated by microscopy of living tissue cultures or of fixed and stained tissue culture preparations.

In "*Contamination in Tissue Culture*" (J. Fogh, ed.), pp. 65–106. Academic Press, New York.

Freshney, R. I. (2000). "Culture of Animal Cells: A Manual of Basic Technique," 4th Ed., Wiley-Liss, New York.

Gallagher, R. E., and Gallo, R. C. (1975). Type C RNA tumor virus isolated from cultured human acute myelogenous leukemia cells. *Science* **187**, 350–353.

Harasawa, R., Kazumasa, H., Tanabe, H., Takada, Y., and Mizusawa, H. (1994). Detection of adventitious pestivirus in cell cultures by polymerase chain reaction using nested-pair primers. *Jpn. Tissue Cult. Assoc. J.* **12**, 215–220.

Harrison, T. A., Barr, R. D., McCaffrey, R. P., Sarna, G., Silverstone, A. F., Perry, S., and Baltimore, D. (1976). Terminal deoxynucleotidyl transferase in AKR leukemia cells and lack of relation of enzyme activity to cell cycle phase. *Biochem. Biophys. Res. Commun.* **69**, 63–67.

Hay, R. J. (1991). Operator-induced contamination in cell cultures systems. *Aeres-Sorono Symp. Dev. Biol. Stand.* **75**, 193–204.

Hay, R. J., Caputo, J., and Macy, M. (1992). "ATCC Quality Control Methods for Cell Lines," 2nd Ed. ATCC, Rockville, MD.

Hay, R. J., Cleland, M. M., Durkin, S., and Reid, Y. A. (2000). Cell Line Preservation and Authentication in "Animal Cell Culture" (J. R. W. Masters, ed.) Oxford Univ. Press, New York.

Hay, R. J., Macy, M. L., and Chen, T. R. (1989). Mycoplasma infection of cultured cells. *Nature* **339**, 487–488.

Holmgren, N. B. (1973). Contamination in tissue culture by parasites. *In* "*Contamination in Tissue Culture*" (J. Fogh, ed.), pp. 195–203. Academic Press, New York.

Hsiung, G. D., Fong, C. K. Y., and Landry, M. L. (1994). "Hsuing's Diagnostic Virology," 4th Ed. Yale Univ. Press, London.

Hu, M., and Buck, C. (1993). Application of polymerase chain reaction technique for detection of mycoplasma contamination. *J. Tissue Cult. Methods* **15**, 155–160.

Hukku, B., Halton, D. M., Mally, M., and Peterson, W. D., Jr. (1984). Cell characterization by use of multiple genetic markers in eukaryotic cell cultures. *In* "*Eukaryotic Cell Cultures, Basics and Applications*" (R. T. Acton and J. D. Lyn, eds.), pp. 13–31. Plenum Press, New York.

IABS (1989). "Continuous Cell Lines as Substrates for Biologicals." IABS Symposium on Developments in Biological Standardization, Vol. 70. Karger, Basel.

Jahnes, W. G., Fullmer, H. M., and Li, C. P. (1957). Free-living amoebae as contaminants in monkey kidney tissue culture. *Proc. Soc. Exp. Biol. Med.* **96**, 484–488.

LeDuc, J. W., Smith, G. A., Macy, M. L., and Hay, R. J. (1985). Certified cell lines of rat origin appear free of infection with hantavirus. *J. Infect. Dis.* **152**, 1081–1082.

Lubiniecki, A. S., and May, L. H. (1985). Cell bank characterization for recombinant DNA mammalian cell lines. *Dev. Biol. Stand.* **60**, 141–146.

McGarrity, G. J. (1982). Detection of mycoplasmal infection of cell cultures. *Adv. Cell Cult.* **2**, 99–131.

Ou, C.-Y., Kwok, S., Mitchell, S. W., Mack, D. H., Sninsky, J. J., Krebs, J. W., Feorino, P., Warfield, D., and Schochetman, G. (1988). DNA amplification for direct detection of HIV-1 in DNA of peripheral blood mononuclear cells. *Science* **239**, 295–297.

Rovozzo, G. C., and Burke, C. N. (1973). "A Manual of Basic Virological Techniques." Prentice-Hall, Englewood Cliff's, NJ.

Schutten, T. (2000). Development of real-time Q RT-PCR for detection of HIV-2 RNA in plasma. *J. Virol. Methods* **88**, 81–87.

Sethi, V. S., and Sethi, M. L. (1975). Inhibition of reverse transcriptase activity of RNA tumor viruses by fagaronine. *Biochem. Biophys. Res. Commun.* **63**, 1070–1076.

Temin, H. M., and Mizutani, S. (1970). RNA-dependent DNA polymerase in vMons of ROUS sarcoma virus. *Nature* (*Lond.*) **226**, 1211–1213.

Ulrich, P. P., Bhat, R. A., Seto, B., Mack, D., Sninsky, J., and Yvas, G. N. (1989). Enzymatic amplification of hepatitis B virus DNA in serum compared with infectivity testing in chimpanzees. *J. Infect. Dis.* **160**, 37–43.

Uphoff, C. C., and Drexler, H. G. (2001). Prevention of mycoplasma contamination in leukemia-lymphoma cell lines. *Hum. Cell* **14**, 244–247.

Weiss, S. H., Goedert, J. J., Gartner, S., Popovic, M., Waters, D., Markham, P., Veronese, F. M., Gail, M. H., Barkley, W. E, Gibbons, J., Gill, F. A., Leuther, M., Shaw, G. M., Gallo, R. C., and Blattner, W. A. (1988). Risk of human immunodeficiency virus (HIV-1) infection among laboratory workers. *Science* **239**, 68–71.

Yolken, R. H., Lennette, D. A., Smith, T. F., and Warner, J. L. (1999). "Manual of Clinical Microbiology," 7th Ed. ASM Press, Washington, DC.

SECTION

2

Culture of Specific Cell Types: Stem Cells

CHAPTER

8

Neural Crest Stem Cells

Maurice Kléber and Lukas Sommer

I. INTRODUCTION

Cellular diversity in the vertebrate peripheral nervous system is achieved by the differentiation of neural crest stem cells (NCSCs) in a spatially and temporally regulated fashion. During embryonic development, neural crest cells detach from the neuroepithelium of the dorsal neural tube and migrate to their sites of terminal differentiation (Le Douarin and Kalcheim, 1999). At least a subpopulation of these cells are multipotent and able to give rise to neuronal, glial, and nonneural derivatives, as has been shown by grafting experiments and by clonal analysis in culture and *in vivo* (Anderson *et al*., 1997; Ziller *et al*., 1983). Moreover, some crest cells display features of stem cells that not only generate multiple cell types, but also have the capacity to self-renew (Morrison *et al*., 1999; Stemple and Anderson, 1992). In migrating neural crest and in target tissues of the neural crest, multipotent crest cells coexist with cells that have a more restricted developmental potential (Sommer, 2001). Cell intrinsic differences between crest cells from different regions of the peripheral nervous system are involved in the generation of neural diversity. In addition, the decision of a NCSC to survive, self-renew, or differentiate depends on the combinatorial activity of multiple environmental signals (Sommer, 2001). To identify these signals, NCSCs have to be challenged by altering both their extracellular environment and their intrinsic genetic programs. This is facilitated greatly by the availability of neural crest culture systems. Because signals required to maintain undifferentiated, multipotent NCSCs for an extended period of time in culture have not yet been identified, various cell culture conditions have been established by different laboratories. This article describes methods for culturing rat and mouse neural crest stem cells, largely based on articles by Stemple and Anderson (1992) (rat NCSCs), Sommer *et al*. (1995) (mouse NCSCs), Greenwood *et al*. (1999) (culture conditions permissive for sensory neurogenesis), and Morrison *et al*. (1999) (postmigratory NCSCs).

II. MATERIALS AND INSTRUMENTATIONS

A. Instruments and Plasticware

Modular incubator chamber (Billups-Rothenberg Inc., www.brincubator.com); Dumont #3 and #5 forceps (Fine Science Tools, Cat. Nos. 11231-30 and 11251-10); Vannas style iris spring scissors (Fine Science Tools, Cat. No. 15000-02); cell culture dishes, 35 × 10-mm style (Corning Cat. No. 430165); 6-well cell culture dishes (Corning Cat. No. 430166); tissue culture dishes, 60 × 15-mm style (Nunclon DSI Cat. No. 064194); Omnifix, 50 ml (Braun Cat. No. 459785OF); Millex syringe-driven filter unit, 0.22 µm (Millipore Cat. No. SLGPO33RB); and Steritop 500 GP express plus membrane, 0.22 µm (Milipore Cat. No. SCGPT05RE).

B. General Buffers and Reagents

Hanks' balanced salts (HBSS) without Ca^{2+} and Mg^{2+}, 95.18 g (Amimed Cat. No. 3-02P30-M); Hanks' balanced salts without phenol red, 97.5 g (Amimed Cat. No. 3-02P32-M); phosphate-buffered saline (PBS) Dulbecco (D-PBS) 50l (Biochrom KG Cat. No. L-182-

Copyright 2006, Elsevier Science (USA).
All rights reserved.

50); formaldehyde solution, 250 ml (Fluka Cat. No. 47608); and potassium hydroxide (Fluka Cat. No. 60375).

C. Enzymes

Dispase 1 (neutral protease) 10 × 5 mg (Roche Cat. No. 1 284 908); collagenase types 1, 3, and 4 (Worthington Biochemical Coorporation); 0.25% trypsin–EDTA, 100 ml (Invitrogen-GIBCO Cat. No. 25200-056); 2.5% trypsin (10×), 100 ml (Invitrogen-GIBCO Cat. No. 25090-028); hyaluronidase type IV-S, 50 mg (Sigma H-4272); and deoxyribonuclease type 1 (Sigma Cat. No. D-4263).

D. Substrates

Fibronectin (0.1% solution), 5 mg (Sigma Cat. No. F1141), and poly-D-lysine (pDL), 5 mg, (Sigma Cat. No. P-7280).

E. Media Components

Dulbecco's modified Eagle medium (DMEM)-low glucose, 500 ml (Invitrogen-GIBCO Cat. No. 11880-028); DMEM, 500 ml (Invitrogen-GIBCO Cat. No. 41966-029); minimum essential medium (MEM), 500 ml (Invitrogen-GIBCO Cat. No. 31095-029); Leibovitz's L15 medium powder (Invitrogen-GIBCO Cat. No. 41300-021); dimethyl sulfoxide (DMSO) 251 (Aldrich Cat. No. 27,043-1); N2-supplement (100×), 5 ml (Invitrogen-GIBCO Cat. No. 17502-048); 2-mercaptoethanol (Sigma Cat. No. M-7522); B-27 supplement (50×), 10 ml (Invitrogen-GIBCO Cat. No.17504-048); forskolin, 10 mg (Sigma Cat. No. F-6886); fetal bovine serum (FBS), 500 ml (different suppliers); water, cell culture tested, 500 ml (Sigma Cat. No. W-3500); phenol red solution, 100 ml (Sigma Cat. No. P-0290); imidazole, 1 g (Sigma Cat. No. I-0250); hydrochloride acid solution, 100 ml (Sigma Cat. No. H-9892); sodium bicarbonate, 500 g (Sigma Cat. No. S-5761); dexamethasone, 25 mg (Sigma Cat. No. D-4902); bovine albumin crystalline, 5 g (Sigma Cat. No. A-4919); 99.5% glycerol, 500 ml (Invitrogen-GIBCO Cat. No. 15514-011); transferrin, holo, bovin plasma, 100 mg (Calbiochem Cat. No. 616420); putrescine (Sigma Cat. No. P-7505); (+/–)-α-tocopherol (vitamin E), 5 g (Sigma Cat. No. T-3251); insulin, 100 mg (Sigma Cat. No. I-6634); human epidermal growth factor (hEGF), 200 µg (R&D Systems Cat. No. 236-EG-200); human nerve growth factor (β-NGF) (R&D Systems Cat. No. 256-GF-100); selenious acid (Aldrich Cat. No. 22,985-7); basic fibroblast growth factor (bFGF), 25 µg (R&D Systems Cat. No. 233-FB-025); progesterone, 1 g (Sigma Cat. No. P-8783); human neurotrophin 3 (NT3), 10 µg (BioConcept Cat. No. 1 10 01862); human brain-derived neurotrophic factor (BDNF), 10 µg (BioConcept Cat. No. 1 10 11961); insulin-like growth factor (IGF1), 250 µg (R&D Systems Cat. No. 291-G1-250); and retinoic acid (Sigma Cat. No. R-2625).

F. Stable Vitamin Mix

Aspartic acid, 100 g (Sigma Cat. No. A-4534); L-glutamic acid, 100 g (Sigma Cat. No. G-8415); L-proline, 25 g (Sigma Cat. No. P-4655); L-cystine (Sigma Cat. No. C-7602); *p*-aminobenzoic acid (Aldrich Cat. No. 42,976-7); 3-aminoproprionic acid, 100 g (Sigma Cat. No. A-9920); vitamin B_{-12}, 1 g (Sigma Cat. No. V-6629); *myo*-inositol, 50 g (Sigma Cat. No. I-7508); choline chloride, 100 g (Sigma Cat. No. C-7527); fumaric acid, 100 g (Sigma Cat. No. F-8509); coenzyme A, 100 mg (Sigma Cat. No. C-4282); D-biotin (Sigma Cat. No. B-4639); and DL-α-lipoic acid, 5 g (Sigma Cat. No. T-1395).

G. 1:1:2

Dextrose [D-(+)-glucose] (Sigma Cat. No. G-7021); L-glutamine (Sigma Cat. No. G-6392); and penicillin–streptomycin, 100 ml (Invitrogen-GIBCO Cat. No. 15140-015).

H. Mix7

DL-β-Hydroxybutyric acid sodium salt (Sigma Cat. No. H-6501); cobalt chloride, 25 g (Sigma Cat. No. C-8661); oleic acid, 250 mg (Sigma Cat. No. O-7501); α-melanocyte-stimulating hormone (α-MSH), 5 mg (Sigma Cat. No. M-4135); $prostaglandin_{E1}$, 1 mg (Sigma Cat. No. P-5515); and 3,3',5- triiodo L-thyronine (T3), 100 mg (Sigma Cat. No. T-6397).

I. FVM

DMPH B grade (Calbiochem Cat. No. 31636); L-glutathione (Sigma Cat. No. G-6013); and L-ascorbic acid, 25 g (Sigma Cat. No. A-4544).

III. PROCEDURES

A. Solutions and Stocks

1. Chicken Embryo Extract (CEE)

Incubate white chicken eggs for 11 days at 38°C in a humidified atmosphere. Wash eggs with 70% ethanol, open the top of each shell, and remove the

embryos and place them into a petri dish containing MEM at 4°C. Macerate the embryos by pressing through a 50-ml syringe into a 50-ml centrifuge tube (Falcon) (approximately 25 ml of homogenate per tube). Add 25 ml of MEM per 25 ml of chicken homogenate. Shake the tubes at 4°C for 1 h. Add 100 µl (800 U) sterile hyaluronidase to 50 ml of chicken homogenate and centrifuge the mixture for 6 h at 30,000 *g* at 4°C. Collect the supernatant, filtrate through a 0.22-µm Steritop filter, and distribute in 5-ml aliquots. Store at –80°C until use.

2. Stable Vitamin Mix (SVM)

Collect 198 ml water into a detergent-free beaker. To the 198 ml water add 0.6 g aspartic acid, 0.6 g L-glutamic acid, 0.6 g L-proline, 0.6 g L-cystine, 0.2 g *p*-aminobenzoic acid, 0.2 g 3-aminoproprionic acid, 80 mg vitamin B_{-12}, 0.4 g *myo*-inositol, 0.4 g choline chloride, 1.0 g fumaric acid, and 16 mg coenzyme A. Suspend 0.4 mg D-biotin and 100 mg DL-α-lipoic acid in 10 ml water and add 2 ml of this solution to the solution in the beaker. Mix the solutions, prepare 1.5-ml aliquots and store at –20°C until use.

3. L-15CO2

Add 3.675 g L-15 powder, 0.019 g imidazole, and 1.6 ml SVM to 288 ml water in a 500-ml beaker. Mix the solution until dissolved and add 240 µl of 1 *M* HCl to adjust the pH between 7.35 and 7.40. In a 100-ml beaker, mix 0.8 g sodium bicarbonate, 120 µl phenol red, and 59 ml water. Apply CO_2 directly to this solution using a Pasteur pipette until it turns yellow and no further color change can be observed. Then mix the sodium bicarbonate solution with the L-15 solution and apply CO_2 again for a short time. Determine the pH, which should range between 7.15 and 7.25. Filter the solution through a 0.22-µm filter into a 500-ml tissue culture bottle and store at 4°C until use.

4. 1:1:2

Slowly dissolve 60 g dextrose in 160 ml water by stirring. Adjust the volume to 200 ml after dextrose is dissolved. Add 100 ml glutamine (200 m*M*) and 100 ml penicillin–streptomycin, filter the solution through a 0.22-µm filter, and distribute in 2-ml aliquots. Store at –20°C until use.

5. Fresh Vitamin Mix (FVM)

Dissolve 5 mg DMPH, 25 mg glutathione, and 500 mg L-ascorbic acid in 80 ml water by stirring. After all chemicals are dissolved, raise the pH to 5–6 with 1 *M* potassium hydroxide. Then adjust the volume to 100 ml, filter the solution through a 0.22 µm filter, and store in 550-µl aliquots at –20°C until use.

6. Mix7

Dissolve 630 mg DL-β-hydroxybutyrate in 10 ml water (1000× stock). Dissolve cobalt chloride to 10 mg/ml in water and then add 25 µl from that solution to 10 ml of $L15CO_2$ to obtain a stock of 25 µg/ml (1000×). Dissolve biotin to 10 mg/ml in DMSO and then dilute to 1 mg/ml in $L15CO_2$ (1000×). Dissolve oleic acid to 2.8 mg/ml in water and then add 37.5 µl of this to 10 ml of $L15CO_2$ to 10 µg/ml (1000×). Dissolve αMSH to 1 mg/ml in water and dilute to 0.1 mg/ml in $L15CO_2$ (1000×). Dissolve prostaglandin to 1 mg/ml in 95% ethanol and dilute 1:100 in $L15CO_2$ to 10 µg/ml (1000×). Dissolve T_3 to 10 mg/ml in DMSO and add 67.5 µl of this to 10 ml $L15CO_2$ to 67.5 µg/ml (1000×). Add 5 ml of each of the aforementioned solutions to 15 ml of $L15CO_2$, filter the solution through a 0.22-µm filter, and store in 550-µl aliquots at –20°C until use.

7. Additives

Dissolve most additives in H_2O, except for the following: dissolve retinoic acid to 17.5 mg/ml in DMSO and then dilute this solution 1:500 in equal volumes of 95% ethanol and $L15CO_2$ to 35 µg/ml (1000×). Dissolve vitamin E to 50 mg/ml in DMSO and dilute this 1:10 to 5 mg/ml (1000×). Dissolve 3.93 mg dexamethasone in 10 ml 95% ethanol to 1 mM stock; for use, dilute stock 1:100 in $L15CO_2$. Dissolve 50 mg insulin in 10 ml 5 m*M* HCl solution. Dissolve 31.5 mg progesterone in 10 ml 95% ethanol to 10 mM and dilute 1:100 in 95% ethanol to a 0.1 m*M* stock. Dissolve 100 mg transferrin in 2 ml 1× D-PBS. Dissolve 100 µg β-NGF in 2 ml $L15CO_2$(+1 mg/ml BSA) to 50 µg/ml. Dissolve 200 µg hEGF in 2 ml $L15CO_2$(+1 mg/ml BSA) to 100 µg/ml. Dissolve 25 µg bFGF in 1 ml $L15CO_2$(+1 mg/ml BSA) to 25 µg/ml. Dissolve 10 µg NT-3 in 400 µl $L15CO_2$ (+1 mg/ml BSA) to 25 µg/ml. Dissolve 10 µg BDNF in 400 µl $L15CO_2$(+1 mg/ml BSA) to 25 µg/ml. Dissolve 250 µg IGF-1 in 2 ml $L15CO_2$(+1 mg/ml BSA) to 125 µg/ml. Store these additives at –80°C until use. Dissolve 80 mg putrescine in 10 ml water to 8 mg/ml. Dissolve 1.29 g selenious acid in 10 ml water and dilute to a stock of 0.1 m*M*. Store these additives at 4°C until use.

B. Media

1. Standard Medium (SM)

To prepare 50 ml of defined medium (DM) (Stemple and Anderson, 1992) take 46.3 ml $L15CO_2$, 50 mg BSA (1 mg/ml), 2 ml 1:1:2, 500 µl FVM, 315 µl glycerol, 100 µl putrescine (16 µg/ml), 100 µl transferrin (100 µg/ml), 50 µl vitamin E (5 µg/ml), 50 µl EGF (100 ng/ml), 50 µl insulin (5 µg/ml), 20 µl NGF (20 ng/ml), 15 µl selenious acid (30 n*M*), 8 µl bFGF (4 ng/ml), 10 µl

progesterone (20 n*M*), 0.5 µl dexamethasone (100 n*M*), 500 µl Mix7. To prepare 50 ml standard medium, add to 45 ml DM 5 ml CEE and 50 µl retinoic acid (35 ng/ml). Filter the medium through a 0.22-µm filter and store at 4°C until use. (Final concentrations are in parentheses.)

A simplified SM has been used by Morrison and colleagues (Bixby *et al*., 2002; Morrison *et al*., 1999). To prepare 50 ml of standard medium take 38.9 ml DMEM low glucose, 2 ml 1:1:2, 25 µl retinoic acid (17.5 ng/ml), 500 µl N2 salt supplement (1%), 15 µl selenious acid, 1 ml B27 supplement (1:50), 2.5 µl 2-mercaptoethanol (50 µM), 8 µl IGF1 (20 ng/ml), and 7.5 ml CEE (15%). For SM1, add 40 µl bFGF (20 ng/ml). After 6 days of culture incubation, use SM2 to allow differentiation: reduce bFGF levels to 20 µl (10 ng/ml) and CEE to 500 µl (1%) and fill up to 50 ml with DMEM low glucose. Filter the medium through a 0.22-µm filter and store at 4°C until use.

Comment

In our hands, the simplified medium according to Morrison *et al*. (1999) was less efficient in supporting neural crest cultures than the more complex standard medium (Stemple and Anderson, 1992). To increase cell survival, IGF1 has been added in a more recent study by Bixby *et al*. (2002).

2. Medium Supporting Early Neural Crest Stem Cells and Sensory Neurogenesis (SN1 + SN2)

To prepare 50 ml of SN medium (Greenwood *et al*., 1999) take 47.1 ml L15CO_2, 50 mg BSA (1 mg/ml), 2 ml 1:1:2, 50 µl insulin (5 µg/ml), 100 µl putrescine (16 µg/ml), 10 µl progesterone (20 n*M*), 15 µl selenious acid (30 n*M*), 0.5 µl dexamethasone, 143 µl glycerol, 50 µl vitamin E (5 µg/ml), and 500 µl Mix7.

To culture NCSCs for 2–3 days, make SN1 by adding 20 µl bFGF (10 ng/ml) to SN. For further differentiation, use SN2, which is prepared by adding the following reagents to SN: 8 µl bFGF (4 ng/ml), 25 µl EGF (50 ng/ml), 25 µl retinoic acid (17.5 ng/ml), 25 µl NGF (25 ng/ml), 25 µl BDNF (12.5 ng/ml), 25 µl NT3 (12.5 ng/ml), and 250 µl CEE (0.05%). Filter the medium through a 0.22-µm filter and store at 4°C until use. In brackets, (Final concentrations are in parentheses.)

C. Isolation

1. Migratory Neural Crest Stem Cells from Neural Tube Explant Cultures

Mouse NCSCs are isolated at embryonic day 9 (E9) (Sommer *et al*., 1995), whereas rat NCSCs are isolated at E10.5 (Stemple and Anderson, 1992) (Fig. 1). The isolation of trunk neural crest is described here.

1. Sacrifice time-mated females by CO_2 asphyxiation in accordance with National Institutes of Health guidelines.
2. Remove the uterus into a 10-cm petri dish containing sterile HBSS without phenol red.
3. With a pair of fine spring scissors, cut an opening along the length of each uterus, being careful not to cut into the embryo and yolk sac.
4. Under a dissecting microscope, remove the embryos by squeezing the uterus gently with a Dumont #3 forceps while cutting the surface of the decidua and amnionic sac with another #3 forceps. After every embryo has been removed from the uterus, transfer the embryos to a new 10-cm petri dish containing sterile HBSS without phenol red.
5. Use an L-shaped electrolytically sharpened tungsten needle and a Dumont #5 forceps to dissect a block of tissue from a region corresponding to the region caudal to the heart to the most caudal somite. Pool and place the trunks into a new 3-cm petri dish. They can be stored for an hour at 4°C.
6. Prepare digestion mix using 12 ml HBSS without Ca^{2+} and Mg^{2+} and one vial (5 mg) of dispase 1. Distribute digestion mix to three 3-cm petri dishes. Transfer the trunks with a Pasteur pipette to the dispase mix and transfer them from the first to the second and then from the second to the third petri dish. Triturate slowly for 2 min at room temperature. Place the dish at 4°C for 6 min.
7. Triturate the trunks gently and patiently until the neural tubes are free of other tissues. Transfer every tube to DMEM+10% FBS to stop the digestion reaction. Then transfer the tubes to the appropriate media.
8. Coat 35-mm Corning tissue culture dishes with fibronectin (FN) as described later and preincubate with appropriate media. Withdraw media and plate three to four neural tubes directly onto the dish. Monitor each step carefully under a dissecting microscope.
9. Allow the tubes to attach for 30 min at 37°C in a 5% CO_2 atmosphere and then flood the dish gently with 1 ml medium. If the tubes do not attach, withdraw the media gently and repeat the step until the tube is properly attached to the dish. Incubate the dishes in medium appropriate to the experiment.

2. Isolation of Postmigratory Neural Crest Stem Cells

Postmigratory NCSCs from dorsal root ganglia (DRG) (Fig. 1), from sciatic nerve, and from gut have been isolated at various stages of development, both

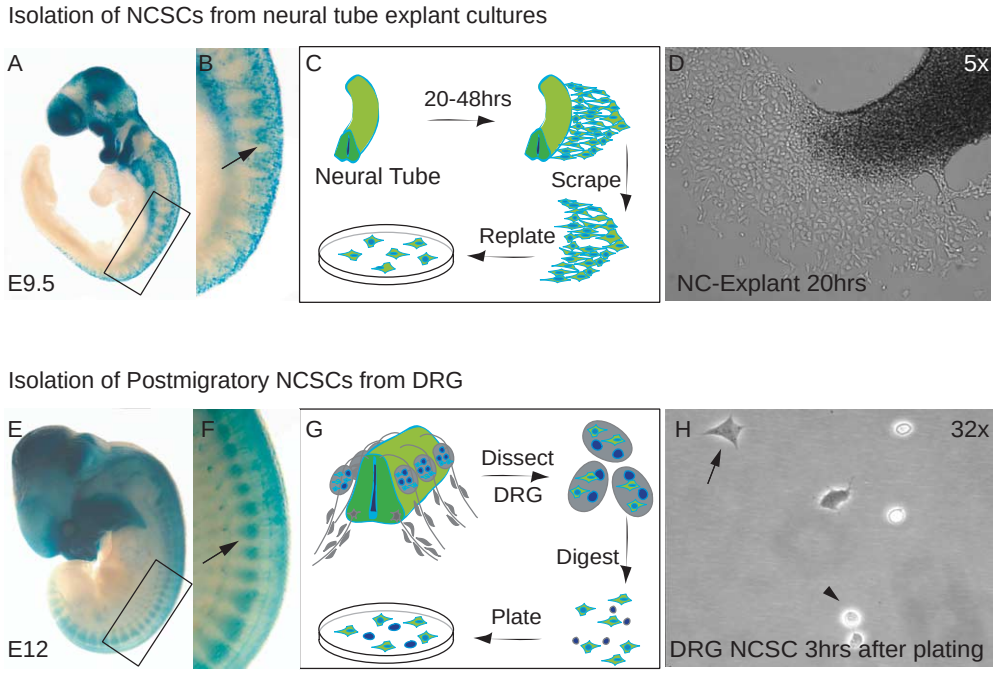

FIGURE 1 To illustrate the localization of migratory and postmigratory neural crest cells (arrows), X-gal staining was performed on mouse embryos at E9.5 (A) and at E12 (E), in which neural crest cells had been marked by Wnt1Cre-mediated recombination (Danielian *et al.*, 1998) of the ROSA26 reporter gene (Soriano, 1999). Boxes in A and E represent areas enlarged in B and F, respectively. (C) Scheme of the explant culture system of a trunk neural crest and (D) phase-contrast picture of a neural crest explant at 5× magnification. (G) Isolation scheme of postmigratory NCSCs from DRG and (H) phase-contrast picture of DRG-derived postmigratory NCSCs (arrow) and neuronal cells (arrowhead).

from mouse and from rat embryos (Bixby *et al.*, 2002; Hagedorn *et al.*, 1999; Lo and Anderson, 1995; Morrison *et al.*, 1999; Paratore *et al.*, 2002; Pomeranz *et al.*, 1993). Studies have also shown that NCSCs can be isolated from postnatal and adult gut (Kruger *et al.*, 2002). Note that the plating efficiency is very low for adult gut NCSCs.

a. NCSCs from Embryonic DRG.

1. Sacrifice time-mated females as described. After removal from the uterus, transfer the embryos to a new 10-cm petri dish containing sterile HBSS without phenol red.

2. Use an L-shaped electrolytically sharpened tungsten needle and a Dumont #5 forceps to dissect a block of tissue from a region rostral to the heart to the most caudal somite. Pool and place the trunks into a new 3-cm petri dish. They can be stored for an hour at 4°C.

3. Gently drive the tungsten needle between the cartilage primordium of the vertebral bodies and the neural tube while stabilizing the trunk with the forceps. Take care not to damage the neural tube. Dissect the cartilage primordium by pulling the needle ventrally. Tear apart the tissue lateral to the neural tube to display the ventral part of the neural tube.

4. Hold the neural tube with a Dumont #3 forceps and separate from dorsal muscle and epithelial tissue using another forceps.

5. Collect the DRGs, which remain attached to the neural tube, using the tungsten needle. Pool the DRGs in ice-cold HBSS without phenol red.

6. Centrifuge the DRGs for 2 min at 2000 rpm and withdraw the HBSS. Digest the DRGs by incubation in 0.25% trypsin and 3.5 mg collagenase type 1 in HBSS without Ca^{2+} and Mg^{2+} for 20 min at 37°C.

7. Stop the reaction by adding FBS to 10%, centrifuge the cells for 2 min at 2000 rpm, resuspend the cells in the appropriate medium, and plate the cells onto culture dishes that have been precoated with either fibronectin or pDL/fibronectin (see Section III,D,1).

b. Sciatic Nerve NCSCs.

1. Isolate embryos as described earlier.

2. Fix embryos on a wax support. Cut an opening dorsolateral to the hind limb, proximal to the spinal

cord. Nerve and nerve plexus are revealed underneath muscle tissue.

3. Fix the hind limb with a Dumont #5 forceps. With another #5 forceps, pull out sciatic nerve running into the hind limb. Dissect sciatic nerves into ice-cold HBSS without Ca^{2+} and Mg^{2+}. Centrifuge cells at 2000 rpm for 2 min, withdraw HBSS, and resuspend the pellet in a solution containing 0.025% trypsin and 1 mg/ml type 3 collagenase.

4. Incubate for 4 min at 37°C and then quench the digestion with 2 volumes of $L15CO_2$ containing 1 mg/ml BSA, penicillin/streptomycin, and 25 µg/ml deoxyribonuclease type 1.

5. Centrifuge the cells at 2000 rpm for 2 min and slowly triturate them in medium.

c. NCSCs from the Enteric Nervous System

1a. To prepare enteric NCSCs from embryos, dissect the entire gut distal to the stomach and digest in 1 mg/ml collagenase type I in HBSS without Ca^{2+} and Mg^{2+} for 20 min at 37°C. Preparations from older embryos are digested for 45 min in a solution that, in addition to the collagenase, contains 0.01% trypsin.

1b. Stop the digestion by adding FBS to 10%. Subsequently, centrifuge the cells for 2 min at 1800 rpm, triturate, and resuspend.

2a. To isolate and culture early postnatal gut NCSCs, separate the small intestine from the attached mesentry and place into ice-cold HBSS without Ca^{2+} and Mg^{2+}. Peel free the outer muscle/plexus layers of the underlying epithelium, mince, and dissociate in 0.025% trypsin/EDTA plus 1 mg/ml type 4 collagenase in HBSS without Ca^{2+} and Mg^{2+} for 8 min at 37°C. Quench the digestion with two volumes medium, centrifuge the cells, and triturate.

2b. Filter the cells through a nylon screen to remove clumps of cells and undigested tissue. Before plating, resuspend the cells in medium.

3. Flow Cytometry

Isolation of prospectively identified NCSCs by FACS avoids contamination by nonneural cells and allows enrichment of the NCSC population. Suspend dissociated cells in antibody-binding buffer, add the primary antibody (or mixture of antibodies) at the appropriate concentration, and incubate for 20–25 min on ice. Wash three times in antibody-binding buffer and incubate with fluorophore-conjugated secondary antibody. Wash cells and resuspend in buffer containing 2 µg/ml of the viability dye 7-aminoactinomycin D (7-AAD; Molecular Probes, Eugene, OR). This step allows exclusion of 7-AAD-positive dead cells during the FACS procedure. To isolate NCSCs from sciatic nerve, cells have been sorted that express the neurotrophin receptor p75 but not P0, a PNS myelin component (Morrison *et al*., 1999). For the isolation of gut NCSCs, a selection for p75/α4 integrin double-positive cells has been performed (Bixby *et al*., 2002; Kruger *et al*., 2002). Prior to and after sorting, it is recommended to keep tissue culture plates in sealed plastic bags gassed with 5% CO_2 to maintain the pH in the medium.

D. Culture of NCSCs

1. Substrate Preparation

Dishes coated with fibronectin: dilute 5 ml (one vial; 5 mg) fibronectin in 20 ml sterile 1× D-PBS. Apply 1 ml fibronectin to 35-mm Corning tissue culture dishes and withdraw it immediately and add the appropriate media. It is possible to reuse the fibronectin solution several times. Dishes coated with poly-D-lysine/fibronectin: resuspend 5 mg poly-D-lysine in 10 ml cell culture water. Rinse each 35 mm Corning tissue culture dish with 1 ml poly-D-lysine solution. Allow plates to air dry. Subsequently, wash twice with tissue culture water and air dry plates again. Apply fibronection to poly-D-lysine-coated plates as described earlier.

2. Culturing NCSCs from Neural Tube Explants in SM

In the absence of instructive growth factors (see Section III,D,5), the following conditions are permissive for the generation of autonomic neurons, peripheral glia, and nonneural smooth muscle-like cells. After neural tube isolation, the culture dishes are incubated at 37°C, 5% CO_2 and 20% O_2 (from air) for 24 h (rat neural crest) to 48 h (mouse neural crest) in SM. At this stage, most of the emigrated neural crest cells coexpress the transcription factor Sox10 and the low-affinity neurotrophin receptor p75 as markers for undifferentiated NCSCs (Paratore *et al*., 2001; Stemple and Anderson, 1992). For further incubation, it is possible to scrape away the neural tube from the neural crest cells that migrated onto the substrate using an L-shaped tungsten needle and an inverted phase-contrast microscope equipped with a 5 or 10× objective lens (Fig. 1). Differentiated cell types become apparent after a few days of culture in SM (Stemple and Anderson, 1992). Differentiation is promoted by the addition of 10% FBS and 5 µ*M* forskolin (Sommer *et al*., 1995).

Comments

In the presence of the neural tube and upon addition of NT3, BDNF, and LIF, the generation of sensory neurons is observed proximal to the neural tube, in addition to the autonomic neurons that are found

scattered throughout the outgrowth after 8 days in culture (Greenwood *et al*., 1999).

3. Culturing NCSCs from Neural Tube Explants in SN Medium

In the absence of instructive growth factors (see Section III,D,5), neural tube explants in SN medium consist of early NCSCs that can generate sensory neurons. After plating, neural tube explants are incubated in SN1 medium for 20 h. Outgrowth of NCSCs occurs during this period. To allow sensory neuronal differentiation, withdraw the SN1 medium from the plates after 48 h of explant incubation and add SN2 medium for another 2 days.

Comments

Twenty hours after having plated the isolated neural tubes, the early neural crest explants cultured in SN1 express neither the sensory marker Brn-3A nor NF160, whereas virtually all neural crest cells express p75 and Sox10 (Figs. 2A and 2B) (Hari *et al*., 2002). Sensory neurons obtained after prolonged incubation are characterized by coexpression of the POU domain transcription factor Brn-3A and NF160 (Fedtsova and Turner, 1995) (Figs. 2C and 2D).

4. Replating NCSCs from Neural Tube Explants and Cloning Procedure

Allow rat and mouse NCSCs to emigrate for 24 and 48 h, respectively. After scraping away the neural tubes, carefully wash plates once with DMEM. Detach the NCSCs by treatment with a 0.05% trypsin solution for 2 min at 37°C. Quickly resuspend the cells in DMEM+10% FBS to abolish the reaction. Centrifuge the cells at 2000 rpm for 2 min and resuspend the pellet in 1 ml fresh medium. Count the cells in a Neubauer counting chamber. Plate the cells at low density (100–300 cells/35-mm plate). Let the cells settle down for approximately 3 h. Single NCSCs are mapped by labeling the surface antigen p75 on living cells (Stemple and Anderson, 1992).

Staining is performed in SM for 30 min using a rabbit antimouse p75 antibody (1:300 dilution, Chemikon International). Wash the cells three times in DMEM and visualize the staining using a Cy3-coupled goat antirabbit IgG (Jackson Laboratories) in SM for 30 min at room temperature. Wash the cells three times in DMEM and add 1 ml fresh SM medium to each plate. Detect p75-expressing NCSCs with an inverted fluorescence microscope at 10× magnification. Mark single founder cells by inscribing them with a 3- to 4-mm circle using a grease pencil on the bottom of the dish.

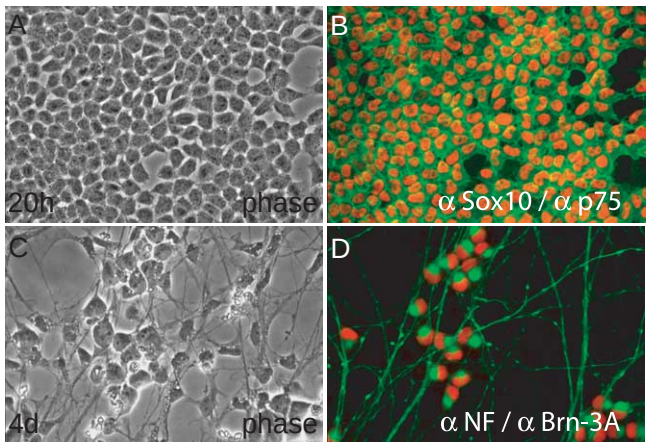

FIGURE 2 NCSCs are identified by coexpression of the transcription factor Sox10 and the low-affinity neurotrophin receptor p75 (B). Neural tube explant cultures cultured in SN conditions for 20 h were fixed with 3.7% formaldehyde in D-PBS for 10 min. Cells were treated for 10 min at room temperature with blocking buffer containing 10% goat serum, 0.3% Triton X-100, and 0.1% BSA in D-PBS and were stained with rabbit antimouse p75 (1:300 dilution, Chemikon International) for 1 h at room temperature and with the monoclonal anti-Sox10 antibody (1:10 dilution; Paratore *et al*., 2001) for 2 h at room temperature. Within 4 days in culture, neural crest cells differentiate into sensory neurons identified by coexpression of the POU transcription factor Brn-3A and NF160 (D). Immunocytochemistry with the polyclonal rabbit anti-Brn-3A antibody [1:300 dilution (Fedtsova and Turner, 1995)] and monoclonal anti-NF160 antibody NN18 (1:300 dilution, IgG, Sigma-Aldrich) were carried out at room temperature for 1 h. Immunostainings were visualized by incubation for 1 h at room temperature using the following secondary antibodies at 1:200 dilution: Cy3-conjugated goat antimouse IgG, Cy3-conjugated goat antirabbit IgG, FITC-coupled donkey antirabbit IgG (Jackson Immuno Research Laboratories), and FITC-coupled horse antimouse IgG (Vector Laboratories). (A and C) Corresponding phase-contrast pictures.

Comments

For reasons not entirely clear, mouse NCSCs display a low survival capacity at clonal density. Clonal experiments with mouse NCSCs are therefore only possible under certain conditions (such as in the presence of fetal bovine serum) (Paratore *et al*., 2001). In the rat, clonogenic culture systems allowed assessment of the state of commitment of neural crest cells by exposing individual cells to changing environmental cues. Using such experiments, instructive growth factors have been identified that are able to promote the differentiation of NCSCs to specific lineages *in vitro* (Morrison *et al*., 1999, 2000b; Shah *et al*., 1994, 1996). Bone morphogenic protein 2 (BMP2) promotes a neuronal and, to a lesser extent, a smooth muscle-like fate, whereas single neural crest cells are instructed by transforming growth factor-β (TGFβ) to adopt a non-neural fate. Furthermore, individual neural crest cells

choose a glial fate upon either Notch signal activation or treatment with GGF, an isoform of neuregulin 1 (NRG1). Finally, canonical Wnt signaling instructively promotes sensory neurogenesis in NCSCs (Lee et al., 2004). However, the response of NCSCs to instructive growth factors is modulated by short-range cell–cell interactions termed community effects and other signals (Hagedorn *et al*., 1999).

Moreover, serial subcloning experiments demonstrated the self-renewal capacity of NCSCs (Morrison *et al*., 1999; Stemple and Anderson, 1992). The signals promoting self-renewal and maintenance of NCSCs have not yet been discovered.

5. Culturing Postmigratory NCSCs

Cells are cultured either in 35-mm or in 6-well plates that have been precoated with poly-D-lysine and fibronectin (see earlier discussion). Both the traditional SM according to Stemple and Anderson (1992) and a simplified SM (Bixby *et al*., 2002; Morrison *et al*., 1999) have been used successfully to culture postmigratory NCSCs (Bixby *et al*., 2002; Hagedorn *et al*., 1999; Morrison *et al*., 1999). When using the simplified SM, incubate cells in SM1 for 6 days and then add SM2 for another 8 days to favor differentiation. For clonal analysis, directly plate cells at low density after dissociation of postmigratory neural crest target tissues (100–300 cells/35-mm plate; fewer than 30 cells per well of a 6-well plate).

Comments

Although neural crest cells isolated both from neural tube explant cultures and from various neural crest-derived tissues have been shown to be multipotent and responsive to instructive growth factors, cell-intrinsic differences between NCSCs from different origins affect fate decisions by changing the sensitivity of the cells to specific extracellular signals (Bixby *et al*., 2002; Kruger *et al*., 2002; Paratore *et al*., 2001; White *et al*., 2001).

6. Culturing NCSCs at Reduced Oxygen Levels

Reduced levels of oxygen have been shown to influence the survival, proliferation, and cell fate decision of neural stem cells (Morrison *et al*., 2000a). To culture neural tube explants at reduced oxygen levels, put all the dishes after neural tube isolation into a gas-tight modular incubator chamber and flush the chamber for 3–5 min with a custom gas mixture of 1% O_2, 6% CO_2, and balance N_2 to generate an actual O_2 level of 3–6%. The gas-tight chamber is housed inside a normal incubator. Once cultures are established in the reduced oxygen chamber, minimize the opening to avoid reperfusion.

Comment

We observed that in SN1 NCSCs appeared healthier after 20 h when cultured at reduced oxygen levels (M. Kléber *et al*., unpublished results). Moreover, culturing NCSCs at reduced oxygen levels in the presence of BMP-2 and forskolin revealed that low oxygen levels can influence cell fate (Morrison *et al*., 2000a).

IV. PITFALLS

1. In order to establish NCSC cultures, follow the instructions carefully. Note that small differences in concentrations of media ingredients may influence outgrowth, proliferation, survival, and differentiation of NCSCs.
2. Different batches of CEE and FBS might have different effects on the cultures. When using a new batch of CEE or FBS, always compare it to an older batch.
3. During isolation, triturate the neural tubes slowly and patiently. Rapid trituration can damage the neural tubes, which can impair efficient neural crest outgrowth.
4. Do not exceed the time of the digestion during isolation.
5. Always use fresh media. Media should not be stored for more than 1 week.

Acknowledgments

The protocols described here have been developed over a number of years. They represent the work of many people, mainly from the laboratories of Dr. David J. Anderson and Dr. Sean J. Morrison and from our own laboratory. We thank Dr. Ned Mantei and Hye-Youn Lee for help with the manuscript and thank Drs. Andrew McMahon, Philippe Soriano, Eric Turner, and Michael Wegner for tools used to prepare the figures.

References

Anderson, D. J., Groves, A., Lo, L., Ma, Q., Rao, M., Shah, N. M., and Sommer, L. (1997). Cell lineage determination and the control of neuronal identity in the neural crest. *Cold Spring Harb. Symp. Quant. Biol.* **62**, 493–504.

Bixby, S., Kruger, G. M., Mosher, J. T., Joseph, N. M., and Morrison, S. J. (2002). Cell-intrinsic differences between stem cells from different regions of the peripheral nervous system regulate the generation of neural diversity. *Neuron* **35**, 643–656.

Danielian, P. S., Muccino, D., Rowitch, D. H., Michael, S. K., and McMahon, A. P. (1998). Modification of gene activity in mouse embryos in utero by a tamoxifen-inducible form of Cre recombinase. *Curr. Biol.* **8**, 1323–1326.

Fedtsova, N. G., and Turner, E. E. (1995). Brn-3.0 expression identifies early postmitotic CNS neurons and sensory neural precursors. *Mech. Dev.* **53**, 291–304.

Greenwood, A. L., Turner, E. E., and Anderson, D. J. (1999). Identification of dividing, determined sensory neuron precursors in the mammalian neural crest. *Development* **126**, 3545–3559.

Hagedorn, L., Suter, U., and Sommer, L. (1999). P0 and PMP22 mark a multipotent neural crest-derived cell type that displays community effects in response to TGF-ß family factors. *Development* **126**, 3781–3794.

Hari, L., Brault, V., Kléber, M., Lee, H. Y., Ille, F., Leimeroth, R., Paratore, C., Suter, U., Kemler, R., and Sommer, L. (2002). Lineage-specific requirements of beta-catenin in neural crest development. *J. Cell Biol.* **159**, 867–880.

Kruger, G. M., Mosher, J. T., Bixby, S., Joseph, N., Iwashita, T., and Morrison, S. J. (2002). Neural crest stem cells persist in the adult gut but undergo changes in self-renewal, neuronal subtype potential, and factor responsiveness. *Neuron* **35**, 657–669.

Le Douarin, N. M., and Kalcheim, C. (1999). "The Neural Crest." *Cambridge Univ. Press, UK.*

Lee, H. Y., Kléber, M., Hari, L., Brault, V., Suter, U., Taketo, M. M., Kemler, R., and Sommer, L. (2004). Instructive Role of Wnt/β-Catenin in Sensory Fate Specification in Neural Crest Stem Cells. *Science*, **303**, 1020–1023.

Lo, L., and Anderson, D. J. (1995). Postmigratory neural crest cells expressing c-RET display restricted developmental and proliferative capacities. *Neuron* **15**, 527–539.

Morrison, S. J., Csete, M., Groves, A. K., Melega, W., Wold, B., and Anderson, D. J. (2000a). Culture in reduced levels of oxygen promotes clonogenic sympathoadrenal differentiation by isolated neural crest stem cells. *J. Neurosci.* **20**, 7370–7376.

Morrison, S. J., Perez, S. E., Qiao, Z., Verdi, J. M., Hicks, C., Weinmaster, G., and Anderson, D. J. (2000b). Transient Notch activation initiates an irreversible switch from neurogenesis to gliogenesis by neural crest stem cells. *Cell* **101**, 499–510.

Morrison, S. J., White, P. M., Zock, C., and Anderson, D. J. (1999). Prospective identification, isolation by flow cytometry, and *in vivo* self-renewal of multipotent mammalian neural crest stem cells. *Cell* **96**, 737–749.

Paratore, C., Goerich, D. E., Suter, U., Wegner, M., and Sommer, L. (2001). Survival and glial fate acquisition of neural crest cells are regulated by an interplay between the transcription factor Sox10 and extrinsic combinatorial signaling. *Development* **128**, 3949–3961.

Paratore, C., Hagedorn, L., Floris, J., Hari, L., Kléber, M., Suter, U., and Sommer, L. (2002). Cell-intrinsic and cell-extrinsic cues regulating lineage decisions in multipotent neural crest-derived progenitor cells. *Int. J. Dev. Biol.* **46**, 193–200.

Pomeranz, H. D., Rothman, T. P., Chalazonitis, A., Tennyson, V. M., and Gershon, M. D. (1993). Neural crest-derived cells isolated from gut by immunoselection develop neuronal and glial phenotypes when cultured on laminin. *Dev. Biol.* **156**, 341–361.

Shah, N., Groves, A., and Anderson, D. J. (1996). Alternative neural crest cell fates are instructively promoted by TGFß superfamily members. *Cell* **85**, 331–343.

Shah, N. M., Marchionni, M. A., Isaacs, I., Stroobant, P., and Anderson, D. J. (1994). Glial growth factor restricts mammalian neural crest stem cells to a glial fate. *Cell* **77**, 349–360.

Sommer, L. (2001). Context-dependent regulation of fate decisions in multipotent progenitor cells of the peripheral nervous system. *Cell Tissue Res.* **305**, 211–216.

Sommer, L., Shah, N., Rao, M., and Anderson, D. J. (1995). The cellular function of MASH1 in autonomic neurogenesis. *Neuron* **15**, 1245–1258.

Soriano, P. (1999). Generalized lacZ expression with the ROSA26 Cre reporter strain. *Nature Genet.* **21**, 70–71.

Stemple, D. L., and Anderson, D. J. (1992). Isolation of a stem cell for neurons and glia from the mammalian neural crest. *Cell* **71**, 973–985.

White, P. M., Morrison, S. J., Orimoto, K., Kubu, C. J., Verdi, J. M., and Anderson, D. J. (2001). Neural crest stem cells undergo cell-intrinsic developmental changes in sensitivity to instructive differentiation signals. *Neuron* **29**, 57–71.

Ziller, C., Dupin, E., Brazeau, P., Paulin, D., and Le Douarin, N. M. (1983). Early segregation of a neural precursor cell line in the neural crest as revealed by culture in a chemically defined medium. *Cell* **32**, 627–638.

CHAPTER

9

Postnatal Skeletal Stem Cells: Methods for Isolation and Analysis of Bone Marrow Stromal Cells from Postnatal Murine and Human Marrow

Sergei A. Kuznetsov, Mara Riminucci, Pamela Gehron Robey, and Paolo Bianco

I. INTRODUCTION

Skeletal stem cells are found among the adherent and clonogenic subset of bone marrow stromal cells. It is of utmost importance to realize that the very existence of a skeletal stem cell is established through a complex sequence of *ex vivo* isolation and expansion, and *in vivo* transplantation. Through the *ex vivo* expansion of a single cell-derived strain and the subsequent *in vivo* transplantation, a complete heterotopic bone/bone marrow organ, containing a hematopoiesis-supporting stroma, must be established in order to prove that the single, originally cloned cell was indeed a stem cell. In addition, stromal cells isolated from the heterotopic organ must be able to transfer the hematopoietic microenvironment and have the potential to establish bone tissue *in vivo* upon serial transplantation. *In vivo* transplantation of stroma cells from a variety of species usually does not lead to the formation of cartilage. This is due to the conditions of a relatively high oxygen tension established in open transplantation systems. Hence, the chondrogenic potential of the cell strain under examination must be probed separately using *in vitro* micromass cultures (Bianco and Robey, 2004).

It is also important to realize that monolayers of stromal cells, established through clonal or nonclonal cultures, are not per se homogeneous populations of "stem" cells, but an uncontrolled mixture of cells and progenitors of highly diverse differentiation potential. This is the natural consequence of the natural asymmetric kinetics of stromal stem cell growth in culture, which inherently leads to a progressive dilution of the original stem cells present in the explanted cells, unless some degree of expansion of the stem cells is allowed, during culture, through the stochastic reversal of asymmetric kinetics to symmetric expansion.

In vitro and *in vivo* assays are necessarily complementary to one another in the study of the biology and pathology of skeletal stem cells and cannot be sensibly used in isolation. Most *in vitro* assays of differentiation potential do not necessarily predict the behavior of the same test strain upon *in vivo* transplantation.

II. MATERIALS AND INSTRUMENTATION

Mice of any strain, including transgenic lines, can be used as a source of bone marrow stromal cells (BMSCs). Guinea pigs (Hartley Davis), used to create irradiated feeder cells, are obtained from Charles River Laboratories. Human bone fragments are collected as surgical waste, and human bone marrow aspirates are obtained from normal volunteers, both under internal review board-approved protocols for

Copyright 2006, Elsevier Science (USA).
All rights reserved.

the use of human subjects in research. For *in vivo* transplantation experiments, female Bg Nu/Nu-Xid mice, between 6 weeks and 6 months of age, are from Harlan. Standard tissue culture supplies (tubes, pipettes, dishes, flasks) and solutions [α-MEM, Coon's modified Ham's F-12, Hanks' balanced salt solution (HBSS), trypsin/EDTA, glutamine, penicillin–streptomycin] are not vendor specific. Cell strainers are from Becton–Dickinson (Cat. No. 2350). Lot-selected fetal bovine serum is obtained from a number of vendors (see Section V). Chondroitinase ABC is obtained from Seikagaku America (Cat. No. 100330-1A). Cloning cylinders were obtained from Sigma (Cat. No. C3983). Recombinant human TGFβ1 is obtained from Austral Biologics (Cat. No. GF-230-2). Hydroxyapatite/tricalcium ceramic, particle size 0.5–1 mm, is obtained from Zimmer by a material transfer agreement, and Gelfoam is from Upjohn (dental packs, size 4, 2×2 cm, Cat. No. NDC 0009-0396-04). Mouse fibrinogen and thrombin are from Sigma (Cat. Nos. F-4385 and T-8397, respectively). Ketamine hydrochloride, xylazine hydrochloride, and acepromazine (Cat. Nos. K2753, X1251, and A6908, respectively) are from Sigma. All other standard chemicals and reagents are from Sigma. Polymerase chain reaction is performed using a commercially available kit from Roche Diagnostics (Cat. No. 1 636 103). Standard equipment for use in dissection (scissors, forceps, blade knives) are sterilized by autoclaving prior to use and can be obtained from any vendor. Cell number enumeration is determined by use of a standard hemocytometer. Cell cultures are viewed by standard inverted and dissecting microscopes, and tissue sections are viewed by standard bright-field microscopes.

III. PROCEDURES

Bone marrow stromal cells can be prepared from bone specimens or bone marrow aspirates from any animal species using a variety of procedures. While there have been a number of modifications whereby single cell suspensions of marrow are subfractionated by density gradient centrifugation, the original assay described by Friedenstein (and described later) relies on the rapid adherence of BMSCs to plastic and avoids loss of these cells during fractionation (Friedenstein, 1980; Friedenstein *et al.*, 1992; Kuznetsov *et al.*, 1997a,b). When working with human cells, BMSCs can be isolated by FACS using the mouse monoclonal antibody Stro-1. However, there is significant contamination by hematopoietic cells such that adherence to tissue culture plastic is necessary to purify them further. It must also be noted that culture conditions must be optimized for each animal species that is used, particularly, in selecting appropriate lots of serum. The procedures presented here focus on the preparation of mouse and human cells in particular due to the fact that they are used most frequently, and to highlight some of the differences between establishing cultures from these two different species.

A. Collection and Preparation Single Cell Suspensions of Bone Marrow

Solutions

1. *Nutrient medium*: α-MEM
2. *Heparinized nutrient medium*: α-MEM containing 100 U/ml sodium heparin.

Steps

1. For preparation of mouse and guinea pig marrow, animals are euthanized by CO_2 inhalation in compliance with institutionally approved protocols for the use of animals in research. Femora, tibiae, and humeri are removed aseptically, and the entire bone marrow content of medullary cavities is flushed with nutrient medium and combined. From human surgical specimens, trabecular bone fragments are scraped with a steel blade into the nutrient medium and washed until the bone became marrow free. In other cases, a 0.5-ml aspirate is collected and mixed with 5 ml of ice-cold nutrient medium containing 100 U/ml sodium heparin. The cells are centrifuged at 135 *g* for 10 min, and the pellet is resuspended in fresh nutrient medium.

2. To prepare single cell suspensions (from all animal species), marrow preparations are pipetted up and down several times, passed through needles of decreasing diameter (gauges 16 and 20) to break up aggregates, and subsequently filtered through a cell strainer. Excessive pressure, both positive and negative, should be avoided while passing cell suspensions through the needles. Mononuclear cell concentrations are determined with a hemocytometer.

3. Guinea pig marrow suspensions, used as feeder cells in mouse cultures, are γ-irradiated with 6000 cGy to prevent the proliferation of adherent guinea pig cells.

B. Determination of Colony-Forming Efficiency (enumeration of CFU-F)

The concentration of CFU-F in bone marrow is usually expressed as the colony-forming efficiency (CFE), or number of BMSC colonies per 1×10^5 marrow nucleated cells in the original marrow cell suspension. In animals under physiological conditions, CFE

remains relatively stable; it is, however, somewhat age dependent and can be altered significantly by experimental procedures, such as acute bleeding, irradiation, or curettage (Friedenstein, 1976, 1990). In humans, CFE is also relatively constant; in normal bone marrow not diluted with peripheral blood, as occurs when aspirated, it is between 20 and 70 per 1×10^5 marrow cells (Kuznetsov and Gehron Robey, 1996).

Solutions

1. *Serum-containing medium (SM)*: SM consists of α-MEM, glutamine (2 m*M*), penicillin (100 U/ml), streptomycin sulfate (100 μg/ml), and 20% lot-selected fetal bovine serum.
2. *Hanks' balanced salt solution*
3. *100% methanol*
4. *Saturated methyl violet*

Steps

1. Mouse cells ($6–15 \times 10^5$ nucleated cells) or human cells ($1–6 \times 10^5$ nucleated cells) are plated into 25-cm^2 plastic culture flasks in 5 ml of SM. If significantly abnormal CFE can be expected, as in some human pathologies, numbers of nucleated cells per flask should be adjusted accordingly. In problematic cases, it is recommended that several groups of flasks, containing, for example, 1×10^4, 1×10^5, and 1×10^6 nucleated cells, are prepared.
2. After 2–3 hr of adhesion, unattached cells are removed by aspiration, and cultures are washed vigorously three times with SM. No more than several hundred nonadherent cells remain after the washing step.
3. Each flask receives 5 ml of SM. For mouse cultures, irradiated guinea pig feeder cells ($1.0–1.5 \times 10^7$ nucleated cells per flask) are added. If no more than 1×10^5 human cells per 25-cm^2 flask are plated, steps 2 and 3 can be omitted.
4. Cultivation is performed at 37°C in a humidified atmosphere of 5% CO_2 with air. On days 10–14, cultures are washed with HBSS, fixed with methanol, and stained with an aqueous solution of saturated methyl violet.
5. Colonies containing 30 or more cells are counted using a dissecting microscope, and colony-forming efficiency (number of colonies per 1×10^5 marrow cells plated) is determined (See Fig. 1A).

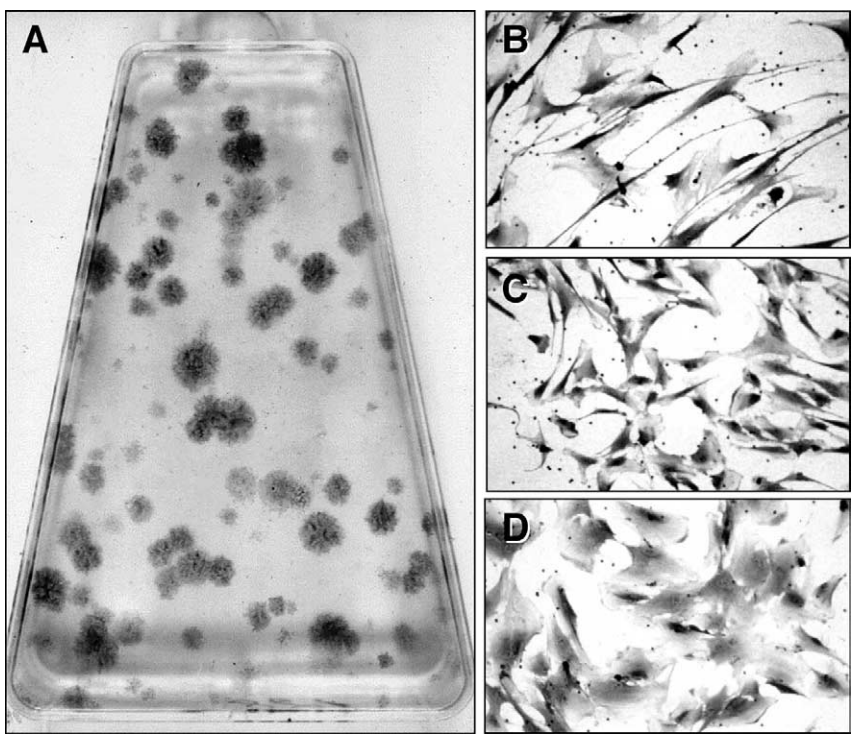

FIGURE 1 (A) When single cell bone marrow suspensions are plated at low density, the colony-forming unit-fibroblast present in the cell population adheres and forms colonies of bone marrow stromal cells. Their enumeration at low density is the basis of the colony-forming efficiency assay. Colonies are heterogeneous and grow at different rates, generating a broad range of colony sizes that are composed of cells with different morphologies, ranging from elongated, spindle-shaped cells (B), cells with a more compact morphology (C), and very flat and extended cells (D).

C. Preparation of Multicolony-Derived Strains of BMSCs

Solutions

1. *Hanks' balanced salt solution*
2. *Chondroitinase ABC*: Dissolve powdered chondroitinase ABC in HBSS to achieve a concentration of 20 mU/ml, aliquot, and store at −20°C.
3. *Serum-containing medium*: SM is prepared as described earlier.
4. *Trypsin/EDTA*: 0.05% trypsin with 0.53 m*M* EDTA
5. *Fetal bovine serum (FBS)*

Steps

1. Suspensions of mouse cells are prepared as described earlier. Contents of six mouse bones (two each of femora, tibiae, and humeri, approximately 6–8 $\times 10^7$ nucleated cells) are plated per 75-cm^2 flask. Suspensions from human surgical specimens are plated at 5×10^6 to 5×10^7 nucleated cells, and suspensions from aspirates are plated at 5×10^6 to 20×10^7 nucleated cells in 75-cm^2 flasks or 150-mm^2 dishes containing 30–50 ml of SM.

2. Cells are cultured at 37°C in a humidified atmosphere of 5% CO_2 with air, and medium is replaced on day 1 for human aspirates and at day 7 for all cultures. Passage generally is performed on days 12 to 14.

3. The resulting mouse cultures are passaged by (a) washing twice with HBSS, (b) incubating with chondroitinase ABC for 25–35 min at 37°C, (c) washing with HBSS, (d) treatment with trypsin/EDTA for 25–30 min at room temperature, (e) a second treatment with trypsin/EDTA for 25–30 min at 37°C, and (f) a final wash with SM. Steps b and c are omitted after passages greater than two. Human cultures are washed twice with HBSS and treated with two consecutive applications of trypsin/EDTA for 10 to 15 min each at room temperature, followed by a wash with SM.

4. Cold FBS is added to each fraction as collected (final concentration 1%) to inhibit enzymatic activity. Fractions are combined, pipetted vigorously to break up cell aggregates, and centrifuged at 135 *g* for 10 min, and the cell pellet is resuspended in fresh SM. Mouse cells are plated at 2–10 $\times 10^6$ cells per 75-cm^2 flask depending on hematopoietic cell numbers. The next passage is performed when cultures approach confluency. Human cells are plated at 2×10^6 cells per 75-cm^2 flask or 150-mm dish. Upon reaching approximately 70% confluency, cells are passaged using the same procedure.

D. Establishment of Single Colony-Derived Strains of BMSCs

While multicolony derived strains of BMSCs take on a homogeneous appearance after passaging, and their differentiation potential can be characterized en mass, examination of colonies that form when bone marrow suspensions are plated at low density (as in the CFE assay, Fig. 1A) shows a great deal of heterogeneity in the starting population. There is a marked difference in the growth rate of the colonies, as demonstrated by colonies of different size. Furthermore, colonies are formed by cells with varying morphologies, ranging from a long, spindle shape (Fig. 1B) to a more compact shape (Fig. 1C) and to a very flat and spread morphology (Fig. 1D). Based on this heterogeneity, a number of studies have focused on the characterization of single colony-derived strains, prepared as described later (Kuznetsov *et al*., 1997b), in order to better understand the hierarchy of BMSCs and their differentiation potential.

Solutions

1. *Serum-containing medium*: SM is prepared as described earlier.
2. *Hanks' balanced salt solution*
3. *Trypsin/EDTA*

Steps

1. Mouse cells, 6–15 $\times 10^5$ nucleated cells, are plated in 150-mm petri dishes in order to prepare single colony-derived strains. From human surgical specimens, 0.007–3.5 $\times 10^3$ nucleated cells/cm^2, and from aspirates, 0.14–14.0 $\times 10^3$ nucleated cells/cm^2, are plated in 150-mm dishes containing 30–50 ml of SM. Cells may also be plated by limiting dilution in 96-well microtiter plates.

2. After adhesion for 2–3 hr, cultures are washed vigorously, and irradiated guinea pig cells are added to mouse cultures as described earlier.

3. After 14 to 16 days, cultures are inspected visually, and well-separated colonies of perfectly round shape are identified for cloning. The medium is removed, cultures are washed with HBSS, and individual colonies are surrounded by a cloning cylinder attached to the dish with sterilized high vacuum grease.

4. Cells inside the cylinder are treated with two consecutive aliquots of trypsin/EDTA for 5–10 min each at room temperature. In both cases, the released cells are transferred to individual wells of 6-well plates containing SM.

5. Subsequent passage is performed before cells reach confluence, usually 5 to 10 days later. Each strain

is passaged consecutively to a 25-cm^2 flask (second passage) and to a 75-cm^2 flask (third passage).

E. Cartilage Formation by BMSCs in Micromass (Pellet) Cultures

Cartilage formation by BMSCs is generally performed *in vitro* using high-density "pellet" cultures, which generate a relatively anaerobic environment that is conducive for chondrogenesis, along with a chondrogenic medium. The following procedure is essentially as described by Johnstone *et al.* (1998), although it has been suggested that cells grown from day 0 with basic fibroblast growth factor (FGF-2) display more chondrogenic potential (Muraglia *et al.*, 2003).

Solution

1. *Chondrogenic medium*: Coon's modified Ham's F-12 medium is supplemented with $10^{-6}M$ bovine insulin, $8 \times 10^{-8}M$ human apo-transferrin, $8 \times 10^{-8}M$ bovine serum albumin, $4 \times 10^{-6}M$ linoleic acid, $10^{-3}M$ sodium pyruvate, 10 ng/ml rhTGFβ1, $10^{-7}M$ dexamethasone, $2.5 \times 10^{-4}M$ ascorbic acid, or media with similar formulation.

Steps

1. Either multicolony-derived or single colony-derived BMSCs (2.5×10^5) are centrifuged at 500 *g* in 15-ml polypropylene conical tubes in 5 ml of chondrogenic medium.
2. Cultures are incubated with caps partially unscrewed for 3 weeks at 37°C in 5% CO_2, with a medium change at 2- to 3-day intervals. Pellets should not be attached to the tubes.
3. At harvest, pellets are washed with phosphate-buffered saline (PBS), fixed in 4% neutral-buffered formaldehyde for 2 h, and embedded in paraffin for histological analysis (Figs. 3A and 3B).

F. Preparation of BMSC and Hydroxyapatite/Tricalcium Phosphate Constructs

In vivo transplantation of BMSCs has become the gold standard by which to measure their multipotentiality (see Fig. 2). In conjunction with hydroxyapatite/tricalcium phosphate (HA/TCP) or collagen sponges as described by Krebsbach *et al.* (1997), BMSCs have the ability to form bone, myelosupportive stroma, and adipocytes, thereby recreating an ectopic bone/marrow organ (ossicle) when transplanted subcutaneously into immunocompromised mice. It should be noted that while human BMSCs are not as sensitive to culture conditions as murine BMSCs, they are more sensitive to the substrates used for *in vivo* transplantation. To date, HA/TCP particles appear to provide the best substrate for ossicle formation by human BMSCs (Figs. 3C and 3D).

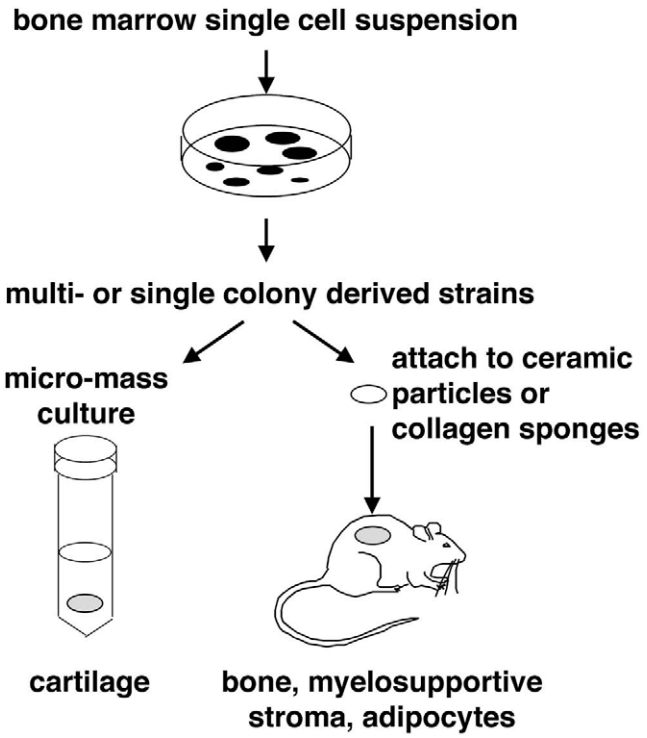

FIGURE 2 BMSC colonies can be passaged together to form multicolony-derived strains or isolated individually to form single colony-derived strains. Both types of cultures can be used to form cartilage in micromass (pellet) cultures in the presence of a chondrogenic medium and to demonstrate the ability to form bone, myelosupportive stroma, and adipocytes by *in vivo* transplantation in association with hydroxyapatite/tricalcium phosphate particles or collagen sponges.

Solutions

1. *Serum-containing medium*: SM is prepared as described earlier.
2. *Mouse fibrinogen*: Mouse fibrinogen is reconstituted in sterile PBS at 3.2 mg/ml, aliquoted, and kept at –80°C.
3. *Mouse thrombin*: Mouse thrombin is reconstituted in sterile 2% $CaCl_2$ at 25 U/ml, aliquoted, and kept at –80°C. (Because the salt is $CaCl_2 \cdot 2H_2O$, in order to prepare 2% solution, 2.65 g of the salt should be diluted in 100 ml of water.)

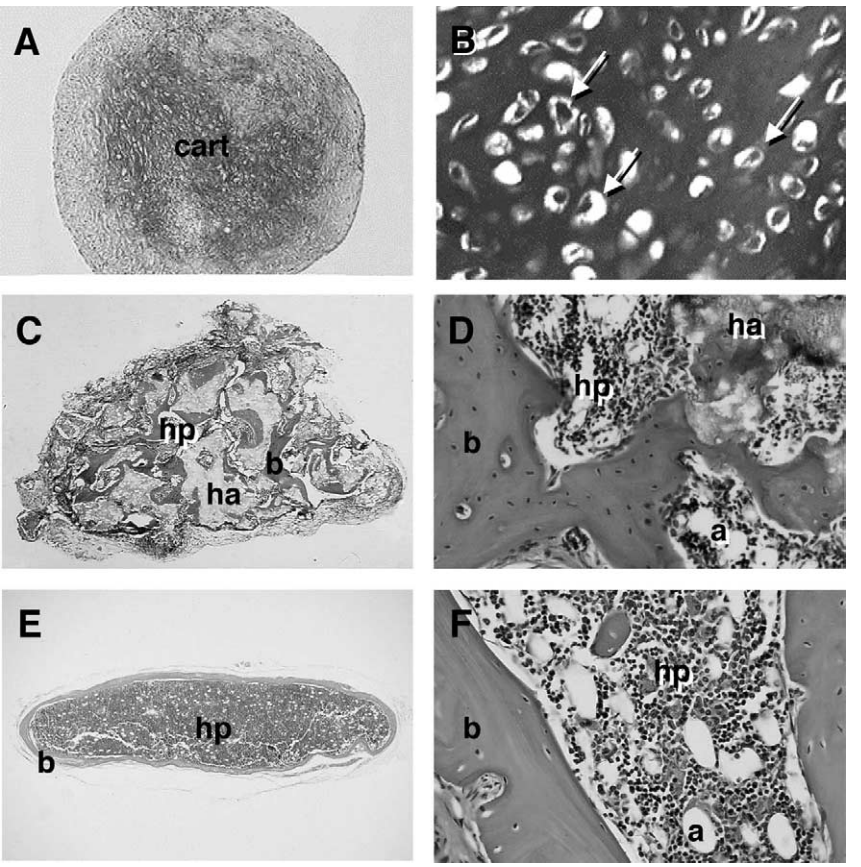

FIGURE 3 In micromass (pellet) cultures in chondrogenic medium, human BMSCs form a dense extracellular matrix that is metachromatic when stained with toluidine blue (A) and features chondrocyte-like cells embedded in this matrix (arrows in B). When transplanted in conjunction with hydroxyapatite/tricalcium phosphate particles (ha), human BMSCs form bone (b) that is actively deposited on the surface of the particles (C) and, with time, establish a fully functional hematopoietic marrow (hp), including adipocytes (a) as shown (D). Murine BMSCs are also able to form a cortex of bone (E) that surrounds a complete hematopoietic marrow with adipocytes when transplanted in collagen sponges (F).

Steps

1. Sterilization of HA/TCP particles is achieved by placing the particles into a glass bottle sealed with foil and heating at 220°C overnight (minimum 8 h). The particles are then aliquoted (40-mg/sterile round-bottomed centrifuge tube) in a hood using a sterile balance, sterile weighing spatula, and sterile filter paper.

2. Passaged BMSCs (see earlier discussion) are counted, pelleted at 135 g for 10 min, and resuspended in SM so that the volume in milliliters is equal to the number of transplants to be prepared.

3. HA/TCP powder is washed twice with SM, and the medium is discarded.

4. BMSCs designated for an individual transplant ($1–2 \times 10^6$ cells in 1 ml of SM) are transferred into a tube with HA/TCP powder. The powder is mixed with the cell suspension and is incubated at 37°C for 70–100 min with slow rotation (25 rpm).

5. Particles with adherent BMSCs are collected by a brief centrifugation (135 *g* for 1 min), and the supernatant is removed carefully.

6. Mouse fibrinogen (15 µl) is added to the cell/particle mixture, and the components are mixed gently. Mouse thrombin (15 µl) is added to the cell/particle mixture, and the components are mixed gently.

7. The tubes are left for a few minutes at room temperature. After a clot is formed, the cap is closed tightly to prevent the transplant from drying. The resulting fibrin clot with HA/TCP powder and BMSCs has the consistency of a gel; it can be easily taken out of the tube with a spatula and placed into a recipient animal as described later.

G. Preparation of BMSC and Collagen Sponge Constructs

Murine BMSCs generate complete ossicles in conjunction with HA/TCP and also when transplanted in collagen sponges (Gelfoam) (Figs. 3E and 3F), whereas human BMSCs only generate limited amounts of bone in the latter substrate.

Solution

1. *Serum-containing medium*: SM is prepared as described earlier.

Steps

1. Sterile Gelfoam sponges are cut into cubes of the desired size or into any other shape, placed into SM, and squeezed with forceps so that they regain their full size but with no air bubbles left inside.
2. BMSCs designated for individual transplants are transferred (1–2 $\times$ 10^6 cells/1 ml of SM) into an individual Eppendorf tube, pelleted at 135 *g* for 10 min, and most of the supernatant is discarded. The volume left should be smaller than the volume of the sponge (usually about 50 µl). The pellet is resuspended in this small volume.
3. Individual sponges are blotted between two sheets of sterile filter paper and are placed immediately into freshly resuspended cells in an Eppendorf tube where it expands, capturing the cell suspension. The tube is sealed tightly to prevent drying.
4. The sponges are incubated at 37°C for 90 min.
5. Sponges with cells are transplanted as described later.

H. *In Vivo* Transplantation of BMSC Constructs

Solutions

1. *Anesthesia*: Combine 225 µl ketamine, 69 µl of xylazine, 75 µl of acepromazine, and 231 µl of H_2O (total volume = 600 µl). Use 100 µl/mouse (25 g). If mice are smaller, less anesthesia should be used.
2. *Betadine*
3. *70% ethanol*

Steps

1. Anesthetize the mouse and clean the skin with betadine and 70% ethanol. A single 3-cm-longitudinal incision is made in the skin along the dorsal surface.
2. The tip of the dissecting scissors is used to make a pocket for the transplant by inserting the scissor subcutaneously and then opening the scissors approximately 1 cm. A sterile spatula is used to insert HA/TCP transplants, and forceps are used to insert collagen sponge transplants. The procedure is repeated twice on each side of the incision for a total of four pockets. The incision is closed with several autoclips. Autoclips are not removed due to the fact that it causes extensive bleeding in immunocompromised mice.
3. Transplants are harvested at various time points, fixed with 4% neutral-buffered formaldehyde overnight, decalcified, and embedded in paraffin for standard histological analyses.
4. Because both HA/TCP and collagen sponge transplants are open systems, there is no barrier to prevent host cells from invading transplants. Determination of cells of donor origin in transplants generated by murine cells requires that the donor bear a marker (e.g., lacZ, green fluorescent protein, or a transgene) (Krebsbach *et al*., 1997). When human cells are used, antibodies that recognize human proteins but not mouse analogs are commonly used (Krebsbach *et al*., 1997). *In situ* hybridization using human-specific Alu sequences as the probe has been particularly useful in characterizing transplants generated by human cells (Kuznetsov *et al*., 1997).

IV. COMMENTS

The methods of *ex vivo* expansion presented here are expressly for maintaining BMSCs in an uncommitted state. Subsequently, it is possible to demonstrate that these cells, either multicolony-derived or some single colony-derived strains, have the ability to generate multiple phenotypes. Their chondrogenic potential can be demonstrated *in vitro* by the establishment of high-density pellet cultures with a chondrogenic medium, and their ability to form bone, myelosupportive stroma, and adipocytes is best assessed by transplantation *in vivo*. These results demonstrate that a true postnatal stem cell exists within the population of BMSCs, with well-known implications in the emerging field of regenerative medicine. Furthermore, *in vivo* transplantation of BMSCs bearing gene defects, either occurring naturally or created by molecular engineering, provides the opportunity to study the specific role of a gene in the process of establishing a bone/marrow organ (Bianco and Robey, 1999).

While the differentiation capacity of BMSCs is best evaluated by *in vivo* transplantation, there are many methods for inducing an osteogenic phenotype *in vitro*. However, it must be noted that these methods result in the formation of a tissue that does not have the structural organization of bone that is formed *in vivo*; in many cases, mineralization is due to dystrophic

calcification as opposed to true bone formation. Adipogenesis can also be induced *in vitro* by a variety of different culture modifications (reviewed in Bianco *et al*., 1999), but again, the adipocytes that are formed tend to be multivacuolar (immature), whereas mature adipocytes in marrow are univacuolar. Nonetheless, cultures of BMSCs provide the opportunity to study the effects of extrinsic signals that cause these cells to shift from one phenotype to another and to analyze the resultant changes in the pattern of gene expression.

V. PITFALLS

1. The specific lot of fetal bovine serum used is critical not only for the determination of CFE, but also for the *ex vivo* expansion of BMSCs. It is not well recognized that fetal bovine serum must be tested extensively to select lots that are suitable for one animal species or another.

2. In murine BMSC cultures (and from other rodents), macrophages represent a major contaminant in the adherent population. In low-density cultures, clusters of macrophages are often mistaken by the untrained eye for a colony established by a CFU-F. In cultures established by high-density plating, ~11% of the adherent population are macrophages (as identified by α-naphthyl acetate esterase activity) at the second passage, and further passage or cell sorting is needed to eliminate them (Krebsbach *et al*., 1997). The contamination by macrophages in murine cultures not only has an impact on determination of CFE, but also on the interpretation of a variety of *in vitro* studies intending to determine the direct effect of factors on BMSCs and *in vivo* studies aimed at identifying where BMSCs engraft and what cell types they form after systemic injection.

3. In establishing BMSCs from bone marrow aspirates, the volume should not exceed 0.5 cc from any one site, or without repositioning the needle. Drawing larger volumes results in contamination of the marrow by peripheral blood, which influences the determination of CFE. Furthermore, peripheral blood has a negative influence on the growth of BMSCs.

References

Bianco, P., Riminucci, M., Kuznetsov, S., and Robey, P. G. (1999). *Crit. Rev. Eukaryot. Gene Expr.* **9**, 159–173.

Bianco, P., and Robey, P. (1999). *J. Bone. Miner. Res.* **14**, 336–341.

Bianco, P., and Robey, P. G. (2004). Skeletal stem cells. *In "Handbook of Adult and Fetal Stem Cells"* (R. P. Lanza, ed.). Academic Press, Sam Diegs.

Friedenstein, A. J. (1976). *Int. Rev. Cytol.* **47**, 327–359.

Friedenstein, A. J. (1980). *Hamatol. Bluttransfus.* **25**, 19–29.

Friedenstein, A. J. (1990). Osteogenic stem cells in bone marrow. *In "Bone and Mineral Research"* (J. N. M. Heersche, J. A. Kanis, eds.), pp. 243–72. Elsevier, New York.

Friedenstein, A. J., Latzinik, N. V., Gorskaya Yu, F., Luria, E. A., and Moskvina, I. L. (1992). *Bone Miner.* **18**, 199–213.

Johnstone, B., Hering, T. M., Caplan, A. I., Goldberg, V. M., and Yoo, J. U. (1998). *Exp. Cell Res.* **238**, 265–272.

Krebsbach, P. H., Kuznetsov, S. A., Satomura, K., Emmons, R. V., Rowe, D. W., and Robey, P. G. (1997). *Transplantation* **63**, 1059–1069.

Kuznetsov, S., and Gehron Robey, P. (1996). *Calcif. Tissue Int.* 59, 265–270.

Kuznetsov, S. A., Friedenstein, A. J., and Robey, P. G. (1997a). *Br. J. Haematol.* **97**, 561–570.

Kuznetsov, S. A., Krebsbach, P. H., Satomura, K., Kerr, J., Riminucci, M., *et al.* (1997b). *J. Bone Miner. Res.* **12**, 1335–1347.

Muraglia, A., Corsi, A., Riminucci, M., Mastrogiacomo, M., Cancedda, R., *et al.* (2003). *J. Cell Sci.* **116**, 2949–2955.

CHAPTER

10

Establishment of Embryonic Stem Cell Lines from Adult Somatic Cells by Nuclear Transfer

Teruhiko Wakayama

I. INTRODUCTION

Usually, embryonic stem (ES) cells are established from fertilized embryos. Recent studies have shown that it is possible to produce cloned embryos from adult somatic cell nuclei; even with a low success rate, some of those embryos can develop to full term (Wakayama *et al*., 1998, 2000a). Now, using this technique, it has become possible to create a new embryonic stem (ES) cell line via nuclear transfer (ntES cell line) from adult somatic cells (Munsie *et al*., 2000; Wakayama *et al*., 2001). These ntES cells differentiate not only all three embryonic germ layers *in vitro*, but also germ cells *in vivo*, and some ntES cell nuclei can develop to full term after a second nuclear transfer (Wakayama *et al*., 2001). The ntES cell techniques could be useful for research tools used in reprogramming, imprinting, and gene modification (Wakayama *et al*., 2002). "Whereas the ntES technique is expected to have applications in regenerative medicine without immune rejection, we demonstrated that it is also applicable to the preservation of genetic resources of mouse strains instead of an embryo, oocyte, or spermatozoon. At present, this technique is the only one available for the preservation of valuable genetic resources from mutant mouse without germ cells (Wakayama et al., 2005a,b)."

II. MATERIALS AND INSTRUMENTS

A. Mouse Cloning Medium

KSOM (long-term culture medium) from Specialty media (#MR-106-D). All others are obtained from Sigma unless otherwise mentioned. NaCl (S7653), KCl (P9327), $CaCl_2{\cdot}2H_2O$ (C5080), $MgSO_4{\cdot}7H_2O$ (M5921), KH_2PO_4 (P5379), D-glucose (G8769), $NaHCO_3$ (S5761), sodium lactate 60% (ml/liter) (L1375), HEPES·Na (H3784), EDTA·2Na (ED2SS), phenol red (P0290), cytochalasin B (C6762), $SrCl_2$ (S0390), polyvinylpyrrolidone (PVP; 360kD) (PVP-360), polyvinyl alcohol (PVA) (P8136), bovine serum albumin (BSA, A3311), dimethyl sulfoxide (DMSO, D8779), hyaluronidase (H4272), and mineral oil (M5310).

B. ES Cell Establishment and Medium Maintenance

Acidic tyrode solution (MR-004-D), DMEM (SLM-120-B), phosphate-buffered saline (PBS) Ca/Mg free (BSS-1006-B), 0.1% gelatin (ES-006-B), nucleosides (ES-008-CD), nonessential amino acid (TMS-001-C), 2-

Copyright 2006, Elsevier Science (USA).
All rights reserved.

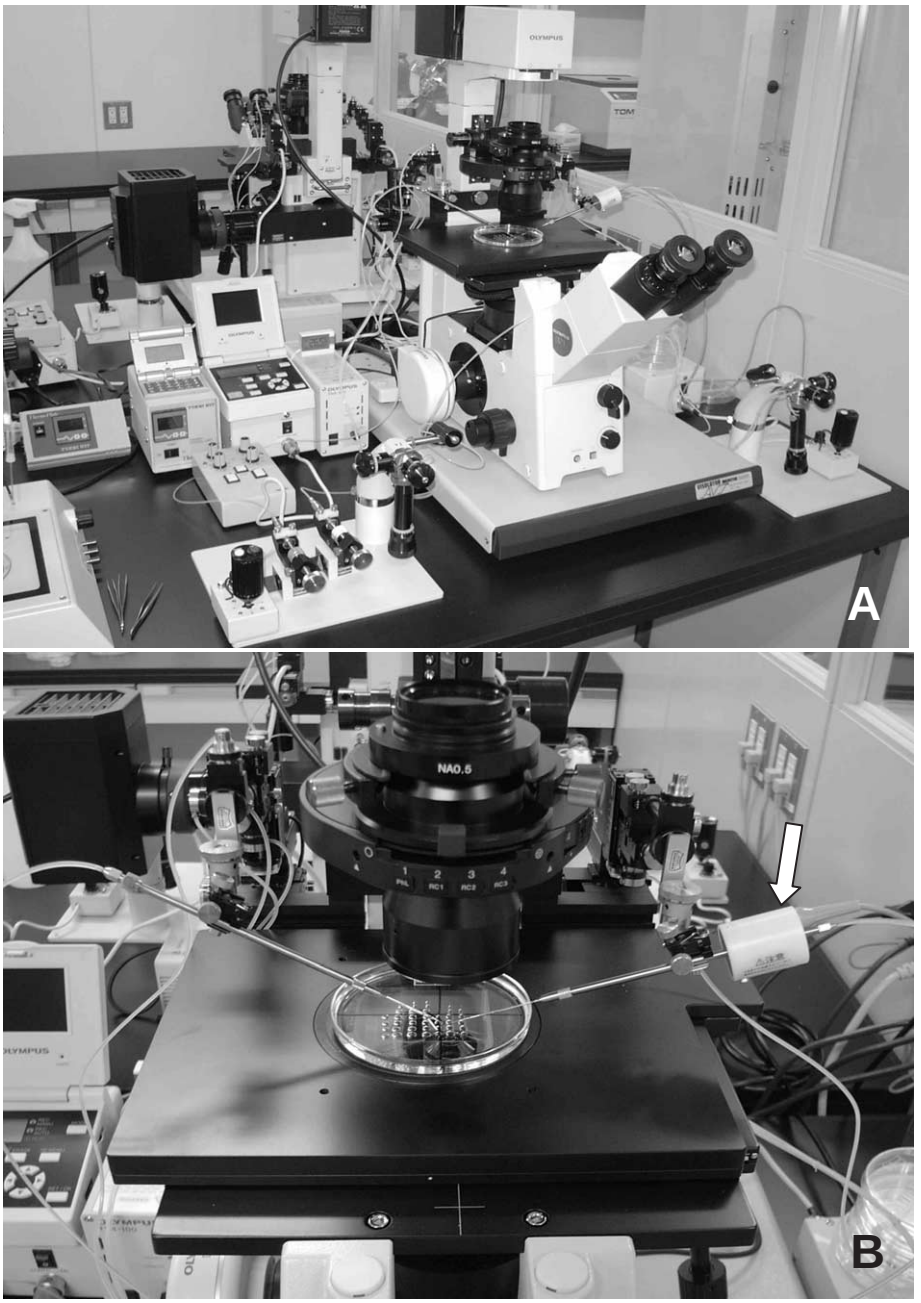

FIGURE 1 Micromanipulator and piezo system. (A) Equipment includes an inverted microscope with Hoffman optics, two injectors, air cushion, and warming plate on the stage of the microscope. (B) Piezo impact unit attached to the injection pipette holder (arrow).

mercaptoethanol (ES-007-E), penicillin–streptomycin solution (TMS-AB2-C), trypsin/EDTA solution (SM-2000-C), mitomycin C (Sigma, 0503): fetal calf serum (FCS, ES-009-B), KSR (invitrogen, 10828-028) and Lif (GIBCO #13275-029); Specialty media (http://www.specialitymedia.com) can provide most of these solutions.

C. Instruments

Inverted microscope with Hoffman optics is from Olympus (IX71) or Nikon (TE2000). Micromanipulator set is from Narishige (MMO-202ND) (Fig. 1A). Piezo impact drive system is from Prime Tech (PMM-150FU) (Fig. 1B). Pipette puller is from Sutter Instrument

TABLE I Formulations of Mouse Cloning Medium (mg/100 ml)[a]

Type of medium	CZB–HEPES Nuclear injection	CZB–PVP Donor cell diffusion	CZB–CB Oocyte enucleation	CZB–Sr Oocyte activation
NaCl	479	479	479	479
KCl	36	36	36	36
$CaCl_2 \cdot 2H_2O$	25	25	25	—
KH_2PO_4	16	16	16	16
$MgSO_4 \cdot 7H_2O$	29	29	29	29
D-Glucose	100	100	100	100
Sodium lactate 60% syrup	0.53 ml	0.53 ml	0.53 ml	0.53 ml
EDTA2Na	4	4	4	4
$NaHCO_3$	42	42	42	210
HEPESNa	520	520	520	—
Polyvinyl alcohol	10	10	10	10
Phenol red	1	1	1	1
Polyvinyl pyrrolidone		12000		
Cytochalasin B			0.5	
$SrCl_2$				2.7
BSA				500

[a] CZB medium is used with slight modifications for nuclear transfer.

Company (P-97). CO_2 incubator, centrifuge, pipettes, and tissue culture dishes/flasks are also needed.

III. PROCEDURES

A. Preparation of Medium

1. KSOM

Thaw the freezing KSOM medium inside a refrigerator overnight. After thawing, aliquot in 5-ml disposable tube and keep at 4°C. Make about 10 tubes and use a new tube every day. Tubes can be used 2 weeks after thawing.

2. CZB–HEPES (Embryo Handling and Nuclear Injection Medium)

Basically, the CZB medium (Chatot *et al*., 1990) is used with slight modifications during *in vitro* manipulations. As shown in Table I, all drugs must mix into 99 ml distilled water (finally becoming 100 ml). After everything is mixed adjust pH to about 7.4–7.6 using 1*N* HCl and 1*N* NaOH. Sterilize with 0.45-µm filters and aliquot into 5-ml tubes the same as KSOM.

3. CZB–PVP (Donor Cell Diffusion and Pipette-Washing Medium)

Add PVP in CZB–HEPES medium and keep in the refrigerator overnight and then filtrate and aliquot in a 1-ml tube.

4. CZB–CB (Oocyte Enucleation Medium)

Dissolve 1 mg cytochalasin B in 2 ml DMSO as stock solution (100 times concentration) and store at –20°C. Take 10 µl of this stock solution and mix with 990 µl of CZB–HEPES.

5. CZB–Sr (Oocyte Activation Medium)

As shown in Table I, this medium is similar to CZB but includes $SrCl_2$ and BSA instead of calcium and HEPES. After mixture, filtrate and aliquot in a 1-ml tube.

6. For ES Cell Establishment

All media can be obtained from Specialty media.

"After mixing all solutions, add FCS (for culture, 20%) or knockout serum (KSR; for ntES cell establishment, 20%) and filtrate."

B. Preparation of Micromanipulation Pipette and Manipulation Chamber

1. *Holding pipette*: The diameter of the outer pipette should be smaller than the oocyte. If the holding pipette is larger than the oocyte, you will lose the oocyte metaphase II spindle when the oocyte is caught by the holding pipette.

2. *Enucleation/injection pipette*: Break the tip of the pipette at flat, vertical and blunt ends using a microforge (Narishige Cat. No. MF-900) (Fig. 2A). A notched tip often kills the oocyte during enucleation and injection. The inner diameter of the enucleation pipette is about 8 µm and the injection pipette depends on the cell type (e.g., for cumulus cell: 5–6 µm, for fibroblast or ES cell: 6–7 µm, for G2/M phase cell: 7–8 µm).

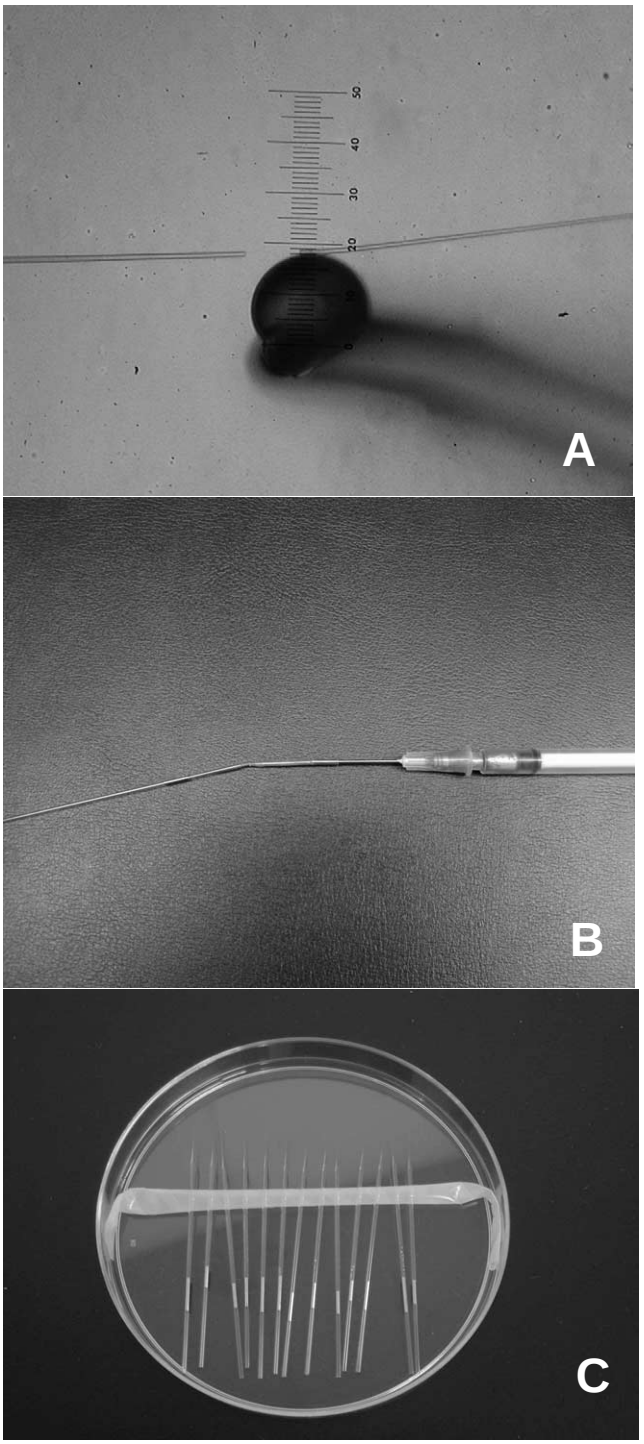

FIGURE 2 Injection pipette and storage. (A) Breaking the tip of a pipette using a microforge. The inner diameter of the tip depends on donor cell size. (B) Inject a small mount of mercury into the pipette using a 1-ml syringe with a 26-gauge needle. (C) Storage of the pipettes in a 10-cm dish. All pipettes are attached softly on sticky tape.

3. Bend the pipette very close to the tip at 15–20° by the microforge.

4. Load a small mount of mercury into the enucleation/injection pipette, which is not essential but enhances the piezo impact power and control (Fig. 2B).

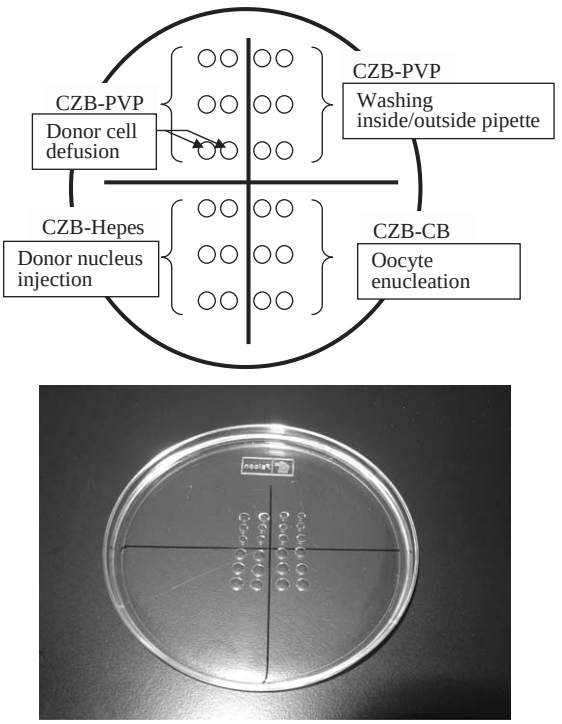

FIGURE 3 Manipulation chamber. Right above the line is CZB–PVP medium for washing pipettes. Right under the line is CZB–CB medium for oocyte enucleation. Left above the line is CZB–PVP medium. Top two drops and pick up nucleus are washing and last drop is donor cell diffusion. Left under the line is CZB–HEPES medium for donor nuclei injection into enucleated oocytes.

5. *Manipulation chamber*: As shown in Fig. 3, different media were put on the dish and then covered with mineral oil. This chamber can be use for both enucleation and injection.

6. Attach these pipettes to the pipette holder of the piezo impact drive unit of the micromanipulator (Fig. 1B).

7. Expel the air, oil, and mercury from the enucleation/injection pipette under CZB–PVP medium. Wash inside/outside of the pipette with the PVP medium, until inside wall of pipette becomes smooth. Without this washing, the enucleation/injection pipette becomes dirty quickly and needs to be changed.

C. Collection of Oocytes and Enucleation

1. Collect the oocyte/cumulus cell complex from ampullae of the oviduct 14–15 h after hCG injection and move that complex into hyaluronitase (0.1 %) containing CZB–HEPES medium. About 10 min later, pick up oocytes and keep in KSOM in the incubator.

2. Place about 20 oocytes into CZB–CB (enucleation medium) and keep in this medium at least 5 min before starting enucleation.

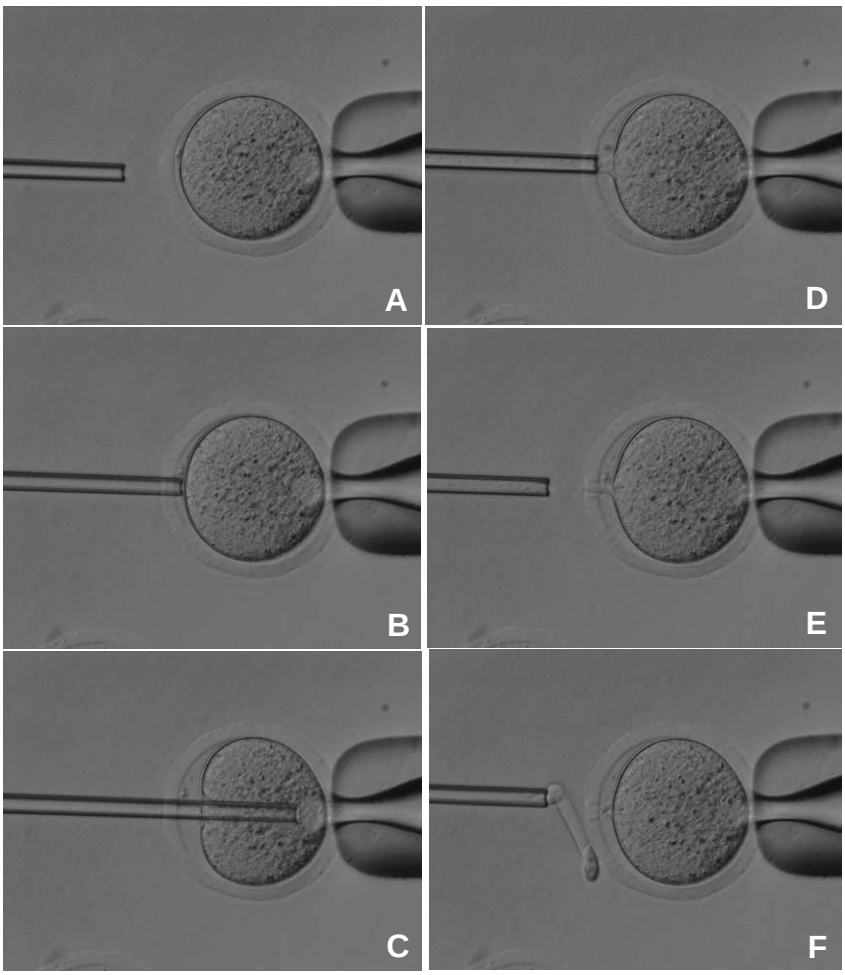

FIGURE 4 Oocyte enucleation. (A) Rotate and find the metaphase II spindle and place it in the 8 to 10 o'clock position. Then hold this oocyte on the holding pipette. (B) Cut the zona pellucida using an enucleation pipette with piezo pulses. (C) Insert enucleation pipette until it reaches the spindle. (D) Remove the spindle by suction without breaking the plasma membrane and gently pull away the pipette from oocytes. (E) The stretched cytoplasmic bridge from oocytes to pipette was pinched off. (F) Push out the spindle in order to check enucleation, which is harder than cytoplasm.

3. Find the metaphase II spindle inside the oocyte. Without any staining, the spindle can be recognized under Nomarski or Hoffman optics. Locate the spindle between the 2 and 4 o'clock positions and then hold on the holding pipette (Fig. 4A).

4. Using a few piezo pulses, cut the zona pellucida (Fig. 4B). To avoid damaging the oocyte by piezo pulses, make a large space between the zona pellucida and the oolemma.

5. Insert the enucleation pipette into the oocyte without breaking the oolemma (Fig. 4C) and remove the metaphase II spindle by aspirating with a minimal volume of oocyte cytoplasm. Oocyte membrane and spindle must be pinched off slowly, do not apply piezo pulses to cut the membrane (Figs. 4D and 4E).

6. Wash the enucleated oocytes several times to remove cytochalasin B completely and keep in KSOM medium in the incubator until used for donor cell injection.

D. Donor Cell Preparation

1. Choose the cell type: Cumulus cell (Wakayama *et al.*, 1998; Wakayama and Yanagimachi, 2001a), tail tip cell (probably fibroblast; Wakayama and Yanagimachi, 1999b; Ogura *et al.*, 2000a), Sertoli cell (Ogura *et al.*, 2000b), fetus cell (Wakayama and Yanagimachi, 2001b; Ono *et al.*, 2001), and ES cell (Wakayama *et al.*, 1999) have been successful in producing cloned mice. The methods are slightly different among those cell types, as shown in Table II. Cumulus cells are easy to prepare as donors. However, tail tip cells must be prepared at least 1 week before nuclear transfer, and then single cell treatment is required.

TABLE II Type of Donor Cell and Preparation Method of Single Cells

Donor cell type	Culture period	Single cell treatment
Cumulus cell	Fresh	No need
Sertoli cell	Fresh	Collagenase and washing
Tail tip cell	1–2 weeks	Tripsin and washing
Fetus cell	Fresh or 1–2 weeks	Tripsin and washing
ES cell	Any time	Tripsin and washing

2. To make single cells, remove cells from culture flask or dish by trypsin treatment. Because trypsin is very toxic at the time of nuclear injection, donor cells must be centrifuged at least three times to remove trypsin completely. However, cumulus cells can be used immediately without any treatment.

3. For diffusing donor cells, pick up 1–3 µl donor cell suspension and introduce into a CZB–PVP drop on the micromanipulation chamber (Fig. 3). Mix the donor cells and PVP medium gently using sharp tweezers. If there is not enough mixture, donor cells stick to each other and it becomes difficult to pick up a single cell (Fig. 5A). Do not scratch the bottom of the chamber.

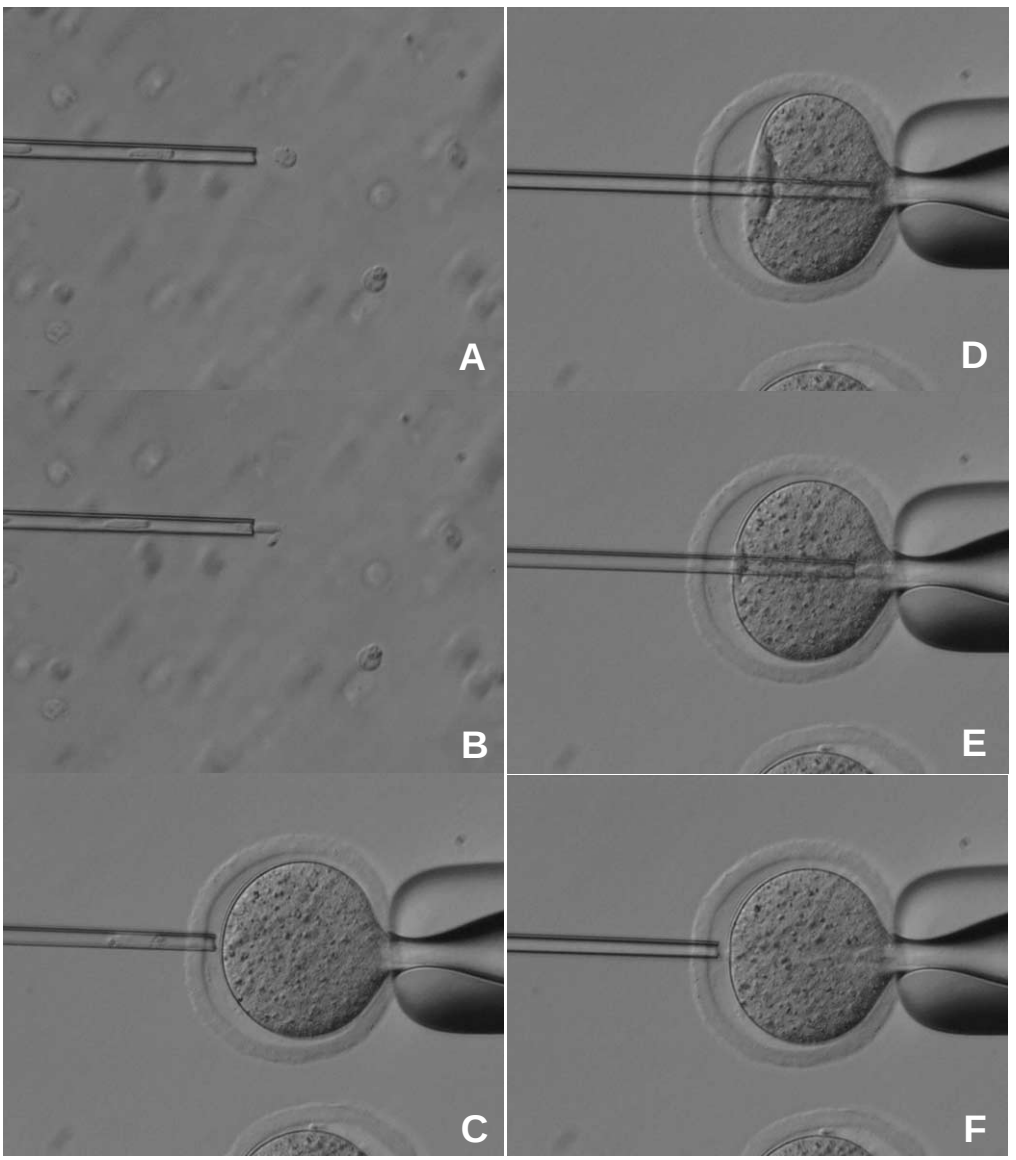

FIGURE 5 Donor nucleus injection. (A and B) Donor nuclei are aspirated in and out of the injection pipette gently until their nuclei are largely devoid of visible cytoplasmic material. (C) Hold the enucleated oocyte and cut the zona pellucida using piezo pulses. (D) Insert the injection pipette into enucleated oocyte. (E) Apply a single piezo pulse to break the membrane and immediately inject the donor nucleus. (F) Pull the pipette away gently.

E. Donor Cell Nucleus Injection

1. Place about 20 enucleated oocytes into CZB–HEPES (injection medium, Fig. 3).

2. Remove donor nuclei from cells and gently aspirate in and out of the injection pipette until the nucleus is devoid of visible cytoplasmic material (Figs. 5A and 5B). Put a few nuclei within the injection pipette.

3. Hold an enucleated oocyte using the holding pipette.

4. Cut the zona pellucida using a few piezo pulses as described in the enucleation method (Fig. 5C).

5. Push one nucleus forward until it is near the tip of the pipette and then advance the pipette through the enucleated oocyte until it almost reaches the opposite side of the oocyte cortex (Fig. 5D).

6. Apply one piezo pulse to puncture the oolemma at the pipette tip, which is indicated by a rapid relaxation of the oocyte membrane (Fig. 5E). Expel a donor nucleus into the enucleated oocyte cytoplasm immediately with a minimal amount of PVP medium. Gently withdraw the injection pipette from the oocyte (Fig. 5F).

7. After injection, leave the injected oocyte for at least 10 min at room temperature. Then transfer the oocytes into KSOM medium and store in the incubator until they are activated with strontium.

F. Oocyte Activation and Culture

1. Nuclear transferred oocytes should be cultured in KSOM medium for at least 30 min before activation. During this time, donor nuclei may be reprogrammed under oocyte cytoplasm (Wakayama *et al.*, 1998, 2000b).

2. Activate the oocytes in CZB-Sr medium for 6 h with medium containing 2–10 mM strontium chloride and 5 µg/ml cytochalasin B (Fig. 6). Strontium activates oocytes, and cytochalasin B prevents extrusion of the donor chromosomes as a polar body (Wakayama *et al.*, 1998).

3. Following activation, transfer all embryos and wash several times in KSOM medium to remove cytochalasin B completely (Wakayama and Yanagimachi, 2001b). Then culture until cloned embryos develop to the blastocyst stage. "Rarely, cytochalasin B seeps from activation drops and prevents cloned embryo development. In this case, it is better to culture all cloned embryo in another dish." These embryos may develop to full term when transferred into a pseudo-pregnant mother with about a 1–2% success rate (Wakayama and Yanagimachi, 2001a).

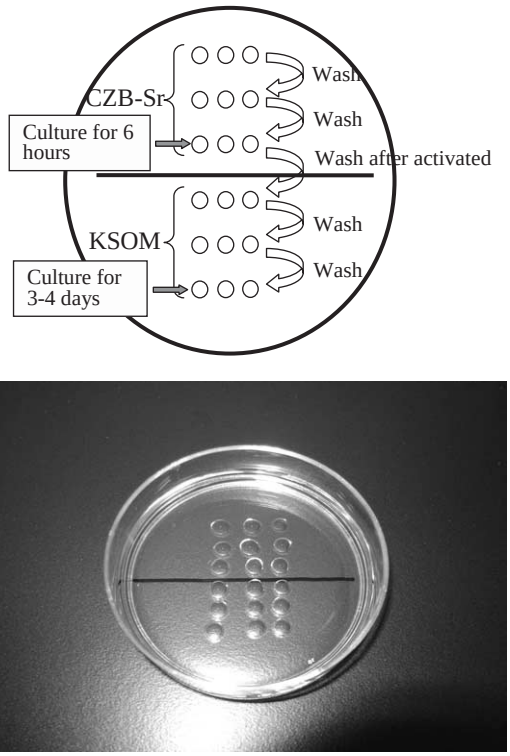

FIGURE 6 Reconstructed oocyte activation medium. Above the line is CZB–Sr medium, which activate the oocytes. The top two drops are used for washing oocytes to remove calcium from medium. Under the line is KSOM medium. The top two drops are used for washing activated oocytes and to remove A strontium and cytochalasin B.

G. Establishment of ntES Cell Line from Cloned Blastocysts

1. To make an embryonic feeder cell collect day 12.5 to 13.5 dpc fetuses from pregnant mother and then remove the head and internal organs on a 10-cm petri dish containing PBS. Place the embryos into a new 10-cm dish and mince the embryos into very small pieces with sterile scissors. Add 25 ml DMEM medium and plate into a larger size (175-cm^2) tissue culture flask. One or 2 days later, split the cells 1 : 5 by trypsinization and allow them to grow to confluence.

2. Mitomycin C treatment. When the cells become confluent, treat with 10 µg/ml mitomycin C for 2 h in an incubator. Wash the flask several times with PBS to remove mitomycin C and then collect the cells by trypsinization. Pellet the cells by centrifugation (1000 rpm for 10 min). Aspirate the supernatant and gently resuspend the cell pellet in freezing medium (final concentration about 1×10^6 cells/ml) and divide into cryovials. Place the vials in a –80°C freezer overnight; the next day, vials can be transferred to liquid nitrogen for long-term storage.

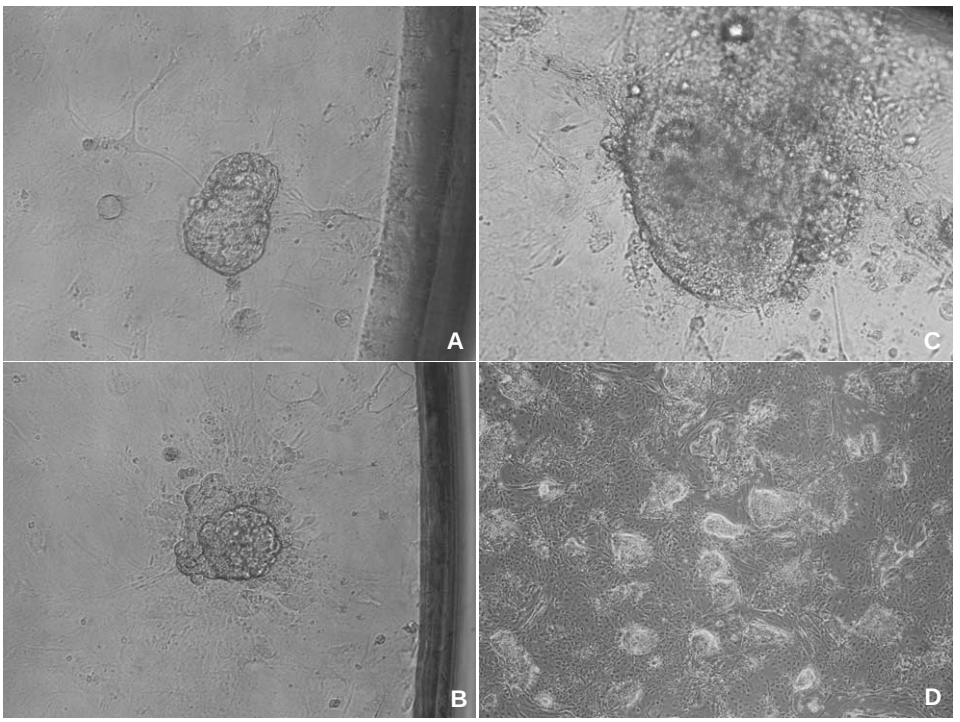

FIGURE 7 Establishment of ntES cell line. (A) A cloned blastocyst was attached to the feeder cell in the 96-well dish. (B) Spreading the trophoblast cells and an inner cell mass (ICM) appearing. (C) ICM grew up almost 5 to 10 times as large. (D) After trypsinization, some wells show a nearly established ntES cell line.

3. Thaw the vial quickly and transfer cells into a 15-ml tube filled with ES medium. Pellet the cells by centrifuging at 1000 rpm for 10 min and then aspirate the supernatant and resuspend with fresh ES medium. Plate on a 96-well multidish and culture in an incubator until use. This feeder cell preparation should be done at least 1 day before plating the cloned blastocysts.

4. Remove the zona pellucida from the cloned blastocysts using acidic tyrode solution. The zona pellucida dissolves quickly within 30 s.

5. Wash the cloned blastocysts several times in KSOM medium and then plate them into a 96-well multidish containing a performed feeder layer. Culture the multidish about 10 days. During this period, cloned blastocysts attach to the surface of the feeder layer and the inner cell mass (ICM) can be seen to grow (Figs. 7A and 7B).

6. Some wells of the multidish may have clumps of large ICM (Fig. 7C). If these clumps appear, treat with trypsin and disaggregate the clump using a 200 µl pipettor (Nagy *et al.*, 2003). Then replate the suspension into another well of the same multidish. Several days later, if ICM-like clumps appear on the dish, replate again the same as before.

7. When ES-like cell colonies dominate the well (Fig. 7D), the cells should be expanded gradually into 48-, 24-, and 12-wells and then into 12.5-, 25-, and 75-cm^2 flasks. After the cell number has increased greatly, freeze and store the cells the same as feeder cells.

IV. COMMENTS

1. So far many types of somatic cell have been used as donors, but only a few cell types have demonstrated the capacity of full-term developments.

2. For nuclear transfer, only 100 to 150 cells were used as donors. However, to pick up better cells, donor cells must be prepared with high concentrations (more than 10^5 cells) on the manipulation chamber.

3. When using cumulus cells, these cells can be picked up immediately after collection without washing, as hyaluronidase is not toxic for oocyte injection.

4. Nuclear injection by piezo is a very new method and very difficult. However, this is almost the same method as sperm injection into oocytes. You should begin with the sperm injection experiment before starting the nuclear transfer experiment. Sperm injection will help you understand the mechanisms of the piezo system.

V. PITFALLS

1. Washing the pipette by PVP is very important. This process affects not only the survival rate, but also development after nuclear transfer.

2. During strontium treatment, some eggs die and the medium becames dirty. This is a normal process and surviving oocytes suffer no damage by strontium treatment.

3. It will probably take a few months to generate data due to incomplete technical skills (Perry *et al*., 2002). Without hard practice, the establishment of a ntES cell line is impossible.

References

Chatot, C. L., Lewis, J. L., Torres, I., and Ziomek, C. A. (1990). Development of 1-cell embryos from different strains of mice in CZB medium. *Biol. Reprod.* **42**, 432–440.

Munsie, M. J., Michalska, A. E., O'Brien, C. M., Trounson, A. O., Pera, M. F., and Mountford, P. S. (2000). Isolation of pluripotent embryonic stem cells from reprogrammed adult mouse somatic cell nuclei. *Curr. Biol.* **10**, 989–992.

Nagy, A., Gertsenstein, M., Vintersten, K., and Behringer, R. (2003). Manipulating the Mouse Embryo, 3rd Ed. Cold Spring Harbor Laboratory Press, Cold Spring Harbor, NY.

Ogura, A., Inoue, K., Ogonuki, N., Noguchi, A., Takano, K., Nagano, R., Suzuki, O., Lee, J., Ishino, F., and Matsuda, J. (2000a). Production of male cloned mice from fresh, cultured, and cryopreserved immature sertoli cells. *Biol. Reprod.* **62**, 1579–1584.

Ogura, A., Inoue, K., Takano, K., Wakayama, T., and Yanagimachi, R. (2000b). Birth of mice after nuclear transfer by electrofusion using tail tip cells. *Mol. Reprod. Dev.* **57**, 55–59.

Ono, Y., Shimozawa, N., Ito, M., and Kono, T. (2001). Cloned mice from fetal fibroblast cells arrested at metaphase by a serial nuclear transfer. *Biol. Reprod.* **64**, 44–50.

Perry, A. C., and Wakayama, T. (2002). Untimely ends and new beginnings in mouse cloning. *Nature Genet.* **30**, 243–244.

Rideout, W. M., III, Hochedlinger, K., Kyba, M., Daley, G. Q., and Jaenisch, R. (2002). Correction of a genetic defect by nuclear transplantation and combined cell and gene therapy. *Cell* **109**, 17–27.

Wakayama, S., Kishigami, S., Van, Thuan, N., Ohta, H., Hikichi, T., Mizutani, E., Yanagimachi, R. and Wakayama, T. (2005) Propagation of an Infertile Hermaphrodite Mouse Lacking Germ Cells, Using Nuclear Transfer and Embryonic Stem Cell Technology. *Proc. Natl. Acad. Sci. USA* **102**, 29–33.

Wakayama, S., Ohta, H., Kishigami, S., Van, Thuan, N., Hikichi, T., Mizutani, E., Miyake, M. and Wakayama, T. (2005) Establishment of Male and Female Nuclear Transfer Embryonic Stem Cell Lines from Different Mouse Strains and Tissues. *Biol. Reprod*. In press.

Wakayama, T., and Perry, A. C. F. (2002). Cloning mice: Perspective and prospective. *In* "Principles of Cloning" (J. Cibelli, R. P. Lanza, K. H. S. Campbell, and M. D. West, eds.), pp. 301–341. Academic Press, San Diego.

Wakayama, T., Perry, A. C. F., Zuccotti, M., and Yanagimachi, R. (1998). Full term development of mice from enucleated oocytes injected with cumulus cell nuclei. *Nature* **394**, 369–374.

Wakayama, T., Rodriguez, I., Perry, A. C. F., Yanagimachi, R., and Mombaerts, P. (1999). Mice cloned from embryonic stem cells. *Proc. Natl. Acad. Sci. USA* **26**, 14984–14989.

Wakayama, T., Shinkai, Y., Tamashiro, K. L. K., Niida, H., Blanchard, D. C., Blanchard, R. J., Ogura, A., Tanemura, K., Tachibana, M., Perry, A. C. F., Colgan, D. F., Mombaerts, P., and Yanagimachi, R. (2000a). Cloning of mice to six generations. *Nature* **407**, 318–319.

Wakayama, T., Tabar, V., Rodriguez, I., Perry, A. C. F., Studer, L., and Mombaerts, P. (2001). Differentiation of embryonic stem cell lines generated from adult somatic cells by nuclear transfer. *Science* **292**, 740–743.

Wakayama, T., Tateno, H., Mombaerts, P., and Yanagimachi, R. (2000b). Nuclear transfer into mouse zygotes. *Nature Genet.* **24**, 108–109.

Wakayama, T., and Yanagimachi, R. (1999). Cloning of male mice from adult tail-tip cells. *Nature Genet.* **22**, 127–128.

Wakayama, T., and Yanagimachi, R. (2001a). Mouse cloning with nucleus donor cells of different age and type. *Mol. Reprod. Dev.* **58**, 376–383.

Wakayama, T., and Yanagimachi, R. (2001b). Effect of cytokinesis inhibitor, DMSO and the timing of oocyte activation on mouse cloning using cumulus cell nuclei. *Reproduction* **122**, 49–60.

CHAPTER

11

T-Cell Isolation and Propagation *in vitro*

Mads Hald Andersen and Per thor Straten

I. INTRODUCTION

Cellular immunity is largely based on T-lymphocytes. Like B cells, T cells also arise from the bone marrow. However, unlike B cells, they migrate to the thymus for maturation. A T-cell expresses a unique antigen-binding molecule called the T-cell receptor (TCR) on the cell surface. In contrast to membrane-bound antibodies on B cells, which can recognize the antigen alone, the majority of TCR recognizes a complex ligand, comprising an antigenic peptide bound to a protein called the major histocompatibility complex (MHC) [known in humans as human leukocyte antigen (HLA)] molecule (Moss *et al*., 1992). When a T-cell encounters an antigen in the context of an HLA molecule, it undergoes clonal expansion and differentiates into memory and various effector T-cells: $CD4^+$ T-helper cells and $CD8^+$ cytotoxic T-lymphocytes (CTL). Activation of both humoral and cell-mediated parts of the immune response requires cytokines produced by T-helper cells. The activation of T-helper cells is carefully regulated, and naïve cells only become activated when they recognize an antigen presented by class II HLA molecules in context with the appropriate costimulatory molecules on the surface of professional antigen-presenting cells (macrophages, B cells, and dendritic cells) (Stockwin *et al*., 2000).

Although antigen-presenting cells encounter and incorporate an antigen in many different compartments, the interaction with T-helper cells is largely confined to secondary lymphoid organs (Fu *et al*., 1999). While the T-helper cells provide help to activate B-cells, antigen-presenting cells, and CTL, only the latter has a vital function in monitoring the cells of the body and in eliminating cells that display antigen, primarily virus-infected cells. However, in addition to providing protection against infectious agents, CTL are thought to provide some degree of protection against spontaneous tumors by virtue of their ability to detect quantitative and qualitative antigenic differences in transformed cells (Castelli *et al*., 2000). Tumorigenic alterations result in an altered protein repertoire inside the cell. Class I MHC molecules sample peptides from protein degradation inside the cell and present these at the cell surface to CTL. Hence, this enables CTL to scan for cellular alterations.

Until recently, measurements of the levels of cellular immune responses, i.e., those mediated by $CD4^+$ and $CD8^+$ T-lymphocytes, have depended largely on culture *in vitro* and the subsequent measurement of specific functions (such as cytolysis). More recently, new technologies based around tetrameric class I peptide complexes (tetramers) have allowed immunologists to isolate and measure $CD8^+$ T-lymphocyte levels directly *ex vivo*. This article describes measures used to generate and clone specific T-cells in culture as well as measures to isolate specific T-cells by means of recombinant HLA/peptide complexes. Finally, it describes the conventional chrome release assay and the ELISPOT assay for the measurement of specific T-cell immunity. It should be noted, however, that T-cells behave very differently and that a T-cell protocol should not be considered as the definitive receipt but rather as a guideline that can be altered depending on the target or the donor. Finally, the making of dendritic cells has been described in detail elsewhere in this volume. However, this is an important first step of making primary T-cells and is consequently mentioned shortly here.

Copyright 2006, Elsevier Science (USA).
All rights reserved.

II. MATERIALS AND INSTRUMENTATION

A. Tissue Culture Medium

X-vivo medium (Cambrex Bio Science, Cat. No. 04-418Q). Store at 4°C.
Human serum (Sigma, Cat. No. H1513). Store at –20°C.
Standard medium: X-vivo, 5% human serum. Store at 4°C.
RPMI 1640 medium (GIBCO, Cat. No. 61870-010). Store at 4°C.
Fetal calf serum (FCS) (Sigma, Cat. No. F7524). Store at 4°C.
R10 medium: RPMI 1640 + 10% FCS. Store at 4°C.

B. Cytokines

Interleukin (IL)-2 [Apodan, Cat. No. 004184]. Store at –80°C. Aliquot 20 units/µl.
IL-4 [Peprotech (trichem), Cat. No. 200-04]. Store at –20°C. Aliquot 10 units/µl.
IL-7 [Peprotech (trichem), Cat. No. 200-07]. Store at –20°C. Aliquot 5 ng/µl.
IL-12 [Peprotech (trichem), Cat. No. 200-12]. Store at –20°C. Aliquot 20 units/µl.
GM-CSF [Peprotech (trichem), Cat. No. 300-03]. Store at –20°C. Aliquot 800 units/µl.
TNF-α [Peprotech (trichem), Cat. No. 300-01A]. Store at –20°C. Aliquot 10 ng/µl.
PHA (Sigma, Cat. No.). Store at –20°C. Aliquot 0.9 mg/µl.

C. Antibodies

Anti-CD28 (eBioscience, Clone 28.8, Cat. No. 16-0288-81). Store at 4°C.
Anti-CD3 (eBioscience, Clone OKT3, Cat. No. 14-0037-82). Store at 4°C.
Tricolor-anti-CD8 (Caltag, Burlingame, CA, Cat. No.). Store at 4°C.

D. Sterile Plastic Plates

96-well plates [Boule (Corning Costar), Cat. No. 3799]
48-well plates [Boule (Corning Costar), Cat. No. 3548]
24-well plates [Boule (Corning Costar), Cat. No. 3526]
6-well plates [Boule (Corning Costar), Cat. No. 3516]

E. Additional Materials

Lymphoprep/Ficoll (Medinor, Cat. No. 30066.03). Store in the dark at 4°C.
^{51}Crom (Amersham, Cat. No. CJS1) 5 mCi/1 ml. Store at –20°C. Dilute 1:5 in phosphate-buffered saline (PBS) before use.
Biotinylated monomers or PE-labeled tetramer (Proimmune, Oxford, UK). Store at 4°C.
Streptavin-coated magnetic beads (Dynabeads M-280, Dynal A/S, Cat. No. M-280). Store at 4°C.

F. Materials for ELISPOT

Nitrocellulose plates (Millipore MAIPN 4550)
Coating antibody: Mab anti-hIFN γ clone 1-D1K, 1 mg/ml, MABTECH 3420-3. Store at 4°C. Dilute to 7.5 µg/ml in PBS before use.
Secondary antibody: Biotinylated Mab anti-hIFN-γ, 7-b6-1, 1 mg/ml, MABTECH 3420-6. Store at 4°C. Dilute to 0.75 µg/ml in diluting buffer before use.
Streptavidin AP: Calbiochem CAL 189732, 2 ml. Add 2 ml H_2O and 2 ml glycerol (85%). Store at 4°C. Dilute 1:1000 in diluting buffer before use.
NBT/BCIP substrate system. DAKO, Cat. No. K 0598. Store at 4°C. Dilute 1:5 in substrate buffer before use.

In addition to standard cell culture instruments:

Gamma counter (Cobra 5005, Packard Instruments, Meriden, CT)
ELISPOT counter [ImmunoSpot Series 2.0 analyzer (CTL Analyzers, LLC, Cleveland, OH]
Magnetic isolator (Dynal A/S, Oslo, Norway)
FACSVantage (Becton-Dickinson, Mountain View, CA)

III. PROCEDURES

A. Induction of Specific T Cells as Primary Responses

The following is a description on how to grow antigen-specific T-cells using peptide-loaded dendritic cells as stimulator cells (Pawelec, 2000). This protocol can also be used to grow tumor-specific T cells if tumor lysate-loaded dendritic cells are used as stimulator cells as described.

1. Stimulator Cell (Dendritic Cell) Culture

Day –7

Dilute 50 ml blood 1:1 with RPMI medium and separate on lymphoprep by centrifugation for 30 min at 1200 rpm. Harvest mononuclear cells, mix with an equal volume of RPMI, and centrifuge at 1500 rpm for 10 min, followed by two washes in R10 (1200 rpm, 5 min). Resuspend cells to 20×10^6 cells/ml and plate

out at 3 ml/well in 6-well plates. Incubate the cells for 2 h at 37°C. Remove nonadherent cells (lymphocytes) by gentle suction. If necessary, the lymphocytes may be frozen. Add 2.5 ml standard medium containing 800 units/ml GM-CSF and 500 units/ml IL-4 to each well.

Day –5

Add 2.5 ml standard medium containing 1600 units/ml GM-CSF and 1000 units/ml IL-4.

Day –3

Remove 2.5 ml of medium from each well and replace with 2.5 ml of fresh medium containing 1600 units/ml GM-CSF and 1000 units/ml IL-4.

Day –1

Remove 1 ml of medium from each well and replace with 1 ml of fresh medium containing 10 ng/ml of TNF-α.

Day 0

Harvest the cultured DC and wash twice in RPMI medium. Resuspend in 1 ml RPMI medium containing 50 µg/ml peptide and 3 µg/ml β_2m. Incubate the cells for 4 h at 37°C; gently resuspend every hour. Irradiate at 25 Gy, wash twice with RPMI medum, and resupend cells (stimulator cells) at 3×10^5/ml in standard medum.

2. *Initiation of Primary T-Cell Culture*

Mix 3×10^6 freshly isolated lymphocytes and 3×10^5 peptide-pulsed stimulator cells in a 24-well plate at 2 ml/well.

Day 1

Add IL-7 to a final concentration of 5 ng/ml and 100 pg/ml IL-12.

Day 7

Remove 1 ml of medium and replace with 1 ml of standard medium containing 20 ng/ml of IL-7.

Day 12

Harvest responder cells, separate over Ficoll, wash once, and count viable cells. Resuspend at 1.5×10^6/ml in standard medium and keep tube at 37°C. Thaw 2×10^6 autologous peripheral blood mononuclear cells (PBMC) per 1.5×10^6 responder cells. Wash the PBMC once in RPMI medium and irradiate at 60 Gy. Wash again in RPMI and incubate 2 h at 37°C with 20 µg/ml peptide and 2 µg/ml β_2m. Remove medium and gently wash once in RPMI. Mix 1.5×10^6/ml and 2×10^6 peptide-pulsed autologous PBMC in 2 ml of standard medium. Alternatively, instead of peptide-pulsed PBMC, use peptide-pulsed DC prepared as on Day 0.

Day 14

Remove 1 ml of medium and replace with 1 ml of fresh medium containing 40 units/ml IL-2 to each well.

Day 19

Restimulate as on day 12. Add IL-2 to the culture as on day 14. Restimulation is needed four or five times before a primary response is measurable.

B. Cloning of T Cells by Limiting Dilution

Day 0

Wash autologous PBMC once in RPMI medium and irradiate at 30 Gy. Wash again in RPMI and incubate 2 h at 37°C with 20 µg/ml peptide and 2 µg/ml β_2m. Plate T-cells at limiting dilution (featuring 10; 3; 1; 0.3 cells/well) in 96-well round-bottom microtiter plates containing 10^5 irradiated, autologous peptide-pulsed PBL, 10 units/ml IL-4, and 40 units/ml IL-2 in 100 µl standard medium.

Day 4

Add 50 µl standard medium containing IL-2 and IL-4 to a final concentration of 10 and 40 units/ml, respectively.

Day 8

Add 50 µl standard medium containing IL-2 and IL-4 to a final concentration of 10 and 40 units/ml, respectively.

Day 12

Inspect cells for growing cells microscopically. Transfer growing cells to 48-well plates containing peptide-pulsed autologous feeder cells and antigen. At the same time, test clones for antigen specificity by the chrome release assay or ELISPOT. Incubate plates 7 days at 37°C in a 5% CO_2 incubator adding IL-2 and IL-4 every third day and transfer antigen-specific T-cells to 24-well plates.

An Alternative Cloning Protocol Using Anti-CD3 and Anti-CD28 Antibodies

This procedure is modified from Oelke *et al*. (2000).

Day –1

Coat a 96-well plate with 100 ng/ml of anti-CD3 and anti-CD28 antibodies in PBS for 24 h at room temperature.

Day 0

Plate T cells at limiting dilution in precoated 96-well plates containing 10^5 irradiated, autologous PBL, 10 units/ml IL-4, and 40 units/ml IL-2 in 100 µl standard medium. Continue as described in previously.

C. Expansion of T-Cell Clones

This is a protocol for the expansion of already established clones modified from Dunbar *et al*. (1998). The cloning mix described in the following can, however, also be used as stimulators to clone T-cells instead of autologous PBL as described previously.

Day 1

For *preparing the cloning mix* isolate fresh lymphocytes from at least three individuals, resuspend them in standard medium, and irradiate (20 Gy). Count the lymphocytes and mix them together to give a final total concentration of 1×10^6/ml. Add PHA to a final concentration of 1 µg/ml and leave in the incubator while the clone is thawed and counted. Thaw the clone, count, and resuspend in prewarmed cloning mix at between 10^5 and 5×10^5 cellsml. Plate out into a U-bottomed, 96-well plate at 100 µl/well.

Day 3

Add 100 ml medium and 40 units/ml IL-2 to each well.

Day 7

Prepare fresh cloning mix, plate 1 ml per well into 24-well plates and prewarm in an incubator.

Transfer 1 well of the 96-well plate into 1 well of the prewarmed 24-well plate.

Day 10

Add 1 ml of medium and 40 units/ml IL-2 to each well.

Day 14

Pool the wells for each individual clone, count, and remove the required amount of cells for a chrome release assay to check if the clones have maintained antigen specificity. Freeze the remaining cells in aliquots of 2 to 7 million per vial.

D. Isolation of Peptide-Specific T Cells

Momomeric or tetrameric MHC/peptide complexes can be bought commercially, e.g., proimmune (Oxford, UK). They can, however, also be made as described by Pedersen *et al*. (2001). However, these rather complex procedures are not the scope of this review.

1. Isolation of Specific T-Cells Using MHC Class I/Peptide Complexes Coupled to Magnetic Beads

This procedure is performed according to Andersen *et al*. (2001; Schrama *et al*., 2001). Incubate 2.5 µg biotinylated monomer of a given HLA/peptide complex with 5×10^6 streptavin-coated magnetic beads in 40 µl PBS for 20 min at room temperature. Wash the magnetic complexes three times in PBS using a magnetic field.

Add 10^7 PBL or lymphocytes in 100 µl PBS with 5% bovine serum albumin (BSA) and rotate very gently for 1 h. Wash the antigen-specific T-cells associating with the magnetic complexes gently three times in PBL. Incubate for 2 h at 37°C and resuspend several times in standard medium to release the cells from the magnetic beads.

Assay the antigen specificity of isolated antigen-specific $CD8^+$ T-cells in an ELISPOT or chrome release assay after at least 5 days in culture.

2. Isolation of Specific T-Cells by FACS

This protocol is modified from Dunbar *et al*. (1999). Culture PBL overnight in standard medium before sorting. Alternatively, pulse PBL with 10 µ*M* peptide in standard medium, plus 10 U/ml IL-7 and culture for 10 days before sorting. Stain cells with PE-labeled tetrameric HLA/peptide complex for 15 min at 37°C before the addition of tricolor-anti-CD8 for 15 min on ice. Wash the cells six times in PBS before analysis on FACS.

Gate specific T-cells according to tetramer/CD8 double staining by forward and side scatter profile. Sort single cells directly into U-bottom, 96-well plates and stimulate these as described in Section III,B.

E. Examination of Antigen Specificity

1. Crome Release Assay

Conventional ^{51}Cr release assays for CTL-mediated cytotoxicity can be used to test the specificity of CTL lines against relevant target cells, e.g., autologous EBV-transformed B-cell lines or cancer cell lines. This procedure is performed according to Brunner *et al*. (1968).

Label 10^6 target cells in 50 µl R10 medium with [^{51}Cr] (100 µCi) in a round-bottomed well of a 96-well plate at 37°C for 60 min. If necessary, add 4 µg of peptide. Wash the target cells four times and plate out in 96-well plates in 100 µl R10 medium. Add T-cells at various effector:target ratios in another 100 µl R10 and incubate at 37°C for 4 h. Aspirate 100 µl of medium and

count [^{51}Cr] release in a gamma counter. Determine the maximum [^{51}Cr] release in separate wells by the addition of 100 µl 10% Triton X-100 and the spontaneous release by the addition of 100 µl R10 only to target cells.

Calculate the specific lysis using the following formula:

[(experimental release – spontaneous release)/ (maximium release – spoontaneous release)] × 100.

2. *ELISPOT*

For the measurement of specific T-cell immunity, ELISPOT analysis, involving the incubation of primary PBMC with one or more peptide epitopes, is probably the most sensitive and reliable assay (Pittet *et al.*, 1999). ELISPOT is based on the detection of the peptide-induced release of cytokines such as interferon (IFN)-γ by single T-cells upon stimulation with a peptide antigen (Scheibenbogen *et al.*, 1997).

Single T-cells can be detected and quantified as cytokine spots on special nitrocellulose filter plates. Cytokine-specific antibodies are coated to the filters to capture the secreted cytokine; peptide-pulsed target cells are added together with cells containing the precursor T-cells. If a T-cell recognizes the peptide epitope examined, the cell releases cytokine. This can be detected as a spot by a colorimetric reaction with secondary antibodies, which represents the cytokine after secretion by a single activated cell. The principle of ELISPOT is illustrated in Fig. 1. If case responses are weak, a single round of *in vitro* stimulation can be used. For cytotoxic T-cells, IFN-γ, or granzyme B, ELISPOT can be performed; for T-helper cells, IFN-γ, or IL-4 (for T-helper 1-type and T-helper 2-type immunity, respectively) can be performed.

Solutions

PBS

Washing buffer: PBS and 0.05% Tween 20; store at room temperature

Diluting buffer: PBS, 1% BSA, and 0.02% NaN_3; store at room temperature

Substrate buffer: 0.1 *M* NaCl, 50 m*M* $MgCl_2$, and 0.1 *M* Tris–HCl, pH 9.50; store at room temperature

Coating of Plates

Add 75 µl 7.5 ug/ml coating antibody. The antibody concentration may change depending on the cytokine target. Leave overnight at room temperature (if coating

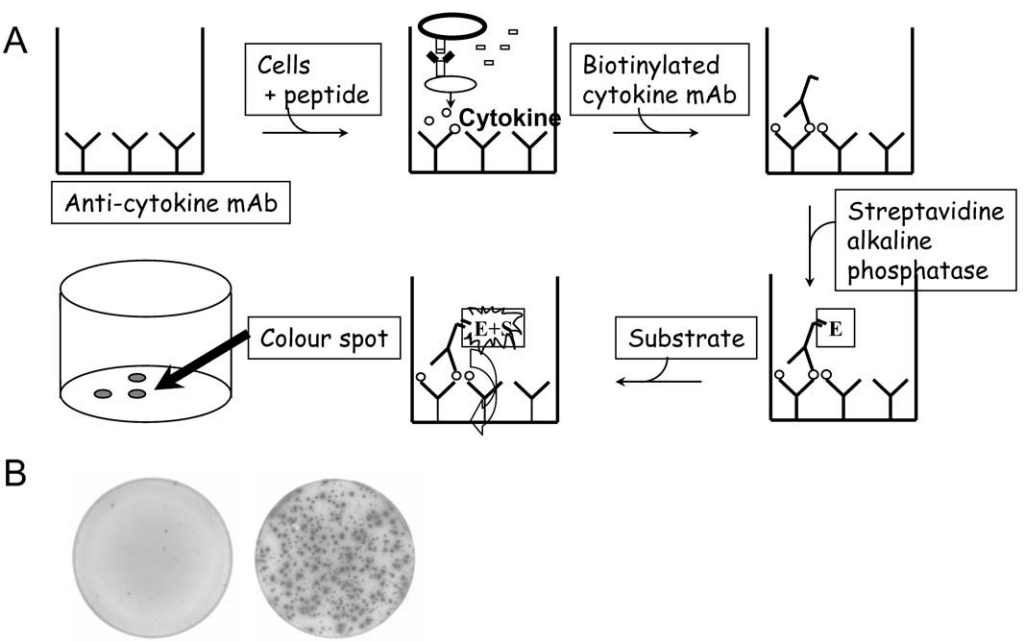

FIGURE 1 (A) Schematic illustration of the ELISPOT assay. Cytokine-specific antibodies are coated onto nitrocellulose filter plates to capture the secreted cytokine; a peptide-pulsed target cell is added together with cells containing the precursor T-cells. If a T-cell recognizes the peptide epitope examined, the cell releases cytokine. This can be detected as a spot by a colorimetric reaction with secondary antibodies. Thus, the spot represents the cytokine after secretion by a single activated cell. (B) ELISPOT wells after incubation with T-cells that were either nonreactive (*left*) or reactive (*right*) against the antigen examined.

3–5 days in advance, leave at 4°C). Wash the plate with 6 × 200 µl PBS. Block the plate with 200 µl media. Leave in incubator for 2 h.

Setting up the ELISPOT

Prepare the serial dilutions of the cells (sterile) at relevant concentrations in order to add the cells to each well in 200 µl media. Poor off the blocking media, and add 200 µl cells and 0.5 µl peptide (2 m*M*) to each well.

Leave overnight in incubator. (The plate must not shake during incubation.) Wash the plate with 6 × 200 µl washing buffer. Add 75 µl of the secondary antibody (1 µg/ml) to each well. The antibody concentration may change depending on the cytokine target. Incubate for 2 h at room temperature. Wash the plate with 6 × 200 µl washing buffer.

Add 75 µl streptavidin (diluted 1 : 1000) to each well.

Incubate for 1 h at room temperature.

Wash the plate with 6 × 200 µl washing buffer and 1 × 200 µl substrate buffer. Mix the substrate: 10 ml substrate buffer + 44 µl NBT + 33 µl BCIP.

Add 75 µl fresh substrate to each well.

Leave at room temperature for 2–20 min.

Stop the reaction with tap water when spot development is satisfactory.

Count the spots using the ImmunoSpot Series 2.0 analyzer and calculate the peptide-specific T-cell frequency from the number of spot-forming cells.

IV. COMMENTS AND PITFALLS

It is always optimal to prepare T-cell cultures from fresh material. T-cells behave very differently, and it is always important to carefully inspect T-cell cultures daily in a microscope. Thus, it is always possible to alter the T-cell protocol depending on the target or the donor, e.g., the concentration of cytokines, the addition of new cytokines, the amount of antigen-presenting cells, the day of restimulation, and the addition of antibodies such as anti-CD28 anti-CD3, or other costimulatory factors. Additionally, T-cells should never be kept at too low cell densities, as cell-to-cell contact is very important. This is also why round-bottom wells are used instead of flat-bottom wells during the cloning of T-cells. Furthermore, when T-cells are transferred from small to larger wells, it is important to carefully inspect the cells microscopically to ensure that the cells are in good condition. In this regard, feeder cells (e.g., irradiated, autologous PBL) may be added if needed.

References

Andersen, M. H., Pedersen, L. O., Capeller, B., Brocker, E. B., Becker, J. C., and thor, S. P. (2001). Spontaneous cytotoxic T-cell responses against survivin-derived MHC class I-restricted T-cell epitopes in situ as well as ex vivo in cancer patients. *Cancer Res.* **61**, 5964–5968.

Brunner, K. T., Mauel, J., Cerottini, J. C., and Chapuis, B. (1968). Quantitative assay of the lytic action of immune lymphoid cells on 51-Cr-labelled allogeneic target cells *in vitro*; inhibition by isoantibody and by drugs. *Immunology* **14**, 181–196.

Castelli, C., Rivoltini, L., Andreola, G., Carrabba, M., Renkvist, N., and Parmiani, G. (2000). T-cell recognition of melanoma-associated antigens. *J. Cell Physiol.* **182**, 323–331.

Dunbar, P. R., Chen, J. L., Chao, D., Rust, N., Teisserenc, H., Ogg, G. S., Romero, P., Weynants, P., and Cerundolo, V. (1999). Cutting edge: Rapid cloning of tumor-specific CTL suitable for adoptive immunotherapy of melanoma. *J. Immunol.* **162**, 6959–6962.

Dunbar, P. R., Ogg, G. S., Chen, J., Rust, N., van der Bruggen, P., and Cerundolo, V. (1998). Direct isolation, phenotyping and cloning of low-frequency antigen-specific cytotoxic T-lymphocytes from peripheral blood. *Curr. Biol.* **8**, 413–416.

Fu, Y. X., and Chaplin, D. D. (1999). Development and maturation of secondary lymphoid tissues. *Annu. Rev. Immunol.* **17**, 399–433.

Moss, P. A., Rosenberg, W. M., and Bell, J. I. (1992). The human T-cell receptor in health and disease. *Annu. Rev. Immunol.* **10**, 71–96.

Oelke, M., Moehrle, U., Chen, J. L., Behringer, D., Cerundolo, V., Lindemann, A., and Mackensen, A. (2000). Generation and purification of $CD8^+$ melan-A-specific cytotoxic T-lymphocytes for adoptive transfer in tumor immunotherapy. *Clin. Cancer Res.* **6**, 1997–2005.

Pawelec, G. (2000). New methods to approach immunotherapy of cancer–and strategies of tumours to avoid elimination. Conference report, on behalf of EUCAPS. European Cancer Research Consortium. *Cancer Immunol. Immunother.* **49**, 276–280.

Pedersen, L. O., Nissen, M. H., Nielsen, L. L., Lauemøller, S. L., Hansen, N. J. V., Blicher, T., Hansen, A., Hviid, C. S., Thomsen, A. R., and Buus, S. (2001). Efficient assembly of recombinant major histocompatibility complex class I molecules with preformed disulfide bonds. *Eur. J. Immunol.* **31**, 2986–2996.

Pittet, M. J., Valmori, D., Dunbar, P. R., Speiser, D. E., Lienard, D., Lejeune, F., Fleischhauer, K., Cerundolo, V., Cerottini, J. C., and Romero, P. (1999). High frequencies of naive Melan-A/MART-1-specific $CD8^{(+)}$ T-cells in a large proportion of human histocompatibility leukocyte antigen (HLA)-A2 individuals. *J. Exp. Med.* **190**, 705–715.

Scheibenbogen, C., Lee, K. H., Mayer, S., Stevanovic, S., Moebius, U., Herr, W., Rammensee, H. G., and Keilholz, U. (1997). A sensitive ELISPOT assay for detection of $CD8^+$ T-lymphocytes specific for HLA class I-binding peptide epitopes derived from influenza proteins in the blood of healthy donors and melanoma patients. *Clin. Cancer Res.* **3**, 221–226.

Schrama, D., Andersen, M. H., Terheyden, P., Schroder, L., Pedersen, L. O., thor Straten, P., and Becker, J. C. (2001). Oligoclonal T-cell receptor usage of melanocyte differentiation antigen-reactive T-Cells in stage IV melanoma patients. *Cancer Res.* **61**, 493–496.

Stockwin, L. H., McGonagle, D., Martin, I. G., and Blair, G. E. (2000). Dendritic cells: Immunological sentinels with a central role in health and disease. *Immunol. Cell Biol.* **78**, 91–102.

CHAPTER

12

Generation of Human and Murine Dendritic Cells

Andreas A.O. Eggert, Kerstin Otto, Alexander D. McLellan, Patrick Terheyden, Christian Linden, Eckhart Kämpgen, and Jürgen C. Becker

I. INTRODUCTION

Dendritic cells (DC) are professional antigen-presenting cells (APC) that serve as sentinels for the induction and regulation of immune responses. Because they are potent stimulators for B and T lymphocytes and activate natural killer cells, they link the innate and the acquired immune system (Fernandez *et al.*, 1999). Dendritic cells are migratory leucocytes originating from the bone marrow, specialized for the uptake, processing, and presentation of antigens. In peripheral tissues, they are found in an immature stage. After contact with antigenic material in the context of danger signals, they mature and upregulate major histocompatibility complexes and costimulatory molecules required for effective interaction with T cells. They are considered a powerful tool to manipulate the immune system (Banchereau and Steinman, 1998).

In humans, by virtue of several *in vitro* techniques, monocyte-derived DC, stem cell-derived DC, and DC isolated directly from peripheral blood can be distinguished depending on the origin of progenitor cells. Directly isolated peripheral blood DC can be subdivided into myeloid and plasmacytoid DC (Cella *et al.*, 2000). The physiological counterpart or *in vivo* relevance of each DC type is not entirely clear. This article focuses on protocols that allow the reliable and reproducible generation of the respective cell types.

In mice, DC subsets in different tissues can be distinguished (Shortman and Liu, 2002), e.g., Langerhans cells in skin, three subsets of spleen DC characterized by their CD8 and CD4 expression (Vremec *et al.*, 2000; McLellan and Kämpgen, 2000), and at least three subsets of lymph node DC (Ruedl *et al.*, 2000; Vremec *et al.*, 1997). In addition, dendritic cells can be generated from precursors in bone marrow or from peripheral blood monocytes (Inaba *et al.*, 1992; Schreurs *et al.*, 1999).

II. MATERIALS AND INSTRUMENTATION

A. Human Dendritic Cells

Acid citrate dextrose (ACD-A, Prod. No. 70010035) can be obtained from Fresenius, Bad Homburg, Germany, and Lymphoprep. (Cat. No. 1053980) from Axis-Shield PoC AS, Oslo, Norway. Phosphate-buffered saline (PBS) (Cat. No. BE17-512F); EDTA, 0.2 mg/ml (Cat. No. 17-711E), RPMI 1640 (Prod. No. BE12-167F); Hanks' balanced salt solution (HBSS) (Cat. No. BE10-547F); and L-glutamine, 200 m*M* (Cat. No. BE17-605E), are available from Bio Whittaker, Cambrex Company, Verviers, Belgium, 20% human serum albumin (HSA) from Aventis Behring, Marburg, Germany, glucose 40% (Prod. No. 2357542) from Braun, Melsungen, Germany, and dimethyl sulfoxide (DMSO) (Prod. No. D-2650), as well as bovine serum albumin (5% stock solution, Prod. No. A-4128), are from Sigma-Aldrich Chemie, Taufkirchen, Germany. For cytokine use, GM-CSF (Leucomax 400) from Essex Pharma, München, Germany, interleukin (IL)-4 (Cat. No. 9511231), TNF-α (Cat. No. 9511512), IL-1β (Cat. No. 9511180), and IL-6 (Cat. No. 9511260) from Strathmann, Hamburg, Germany, can be used. PGE_2 (Minprostin E2 10 mg/ml) is produced by Pharmacia, Erlangen, Germany. Refobacin 10 mg is provided by Merck, Darmstadt, Germany, penicillin/streptomycin

Copyright 2006, Elsevier Science (USA).
All rights reserved.

(PenStrep, Cat. No. 15140-122) by Invitrogen Corporation, Karlsruhe, Germany, and Liquemin N 10000 by Hoffmann-La Roche AG, Grenzach-Wyhlen, Germany. Fetal calf serum (FCS, Cat. No. 14-801E) can be obtained from Bio Whittaker. Syringes, 10 ml (Prod. No. 4606108) and 20 ml (Prod. No. 4606205), can be obtained from Braun. Culture flasks, 80 cm^3 (Prod. No. 201045) and 175 cm^3 (Prod. No. 200573), as well as cryotubes, 1.8 ml (Prod. No. 363401) and 3.6 ml (Prod. No. 366524), are available from Nunc GmbH & Co. KG, Wiesbaden, Germany. Tubes, 15 ml (Prod. No. 25315-15) and 50 ml (Cat. No. 430829), are from Corning GmbH, Bodenheim, Germany. Disposable filter units (red rim, Ref. No. 10462200) are from Schleicher & Schuell, Dassel, Germany. Pipettes, 2 ml (Cat. No. 4486), 5 ml (Cat. No. 4487), 10 ml (Cat. No. 4488), and 25 ml (Cat. No. 4489), are from Corning GmbH. Pipette tips, 10 µl (Cat. No. 790011), are available from Biozym, Hessisch-Oldendorf, Germany; 100 µl (Cat. No. 0030 010.035) and 1000 µl (Cat. No. 0030 010.051) are from Eppendorf. Tissue culture dishes (Prod. No. 35-3003) are from Falcon, Becton-Dickinson, New Jersey, syringe needles, 0.9 × 40 mm (Prod. No. 4657519), are from Braun, trypan blue (Cat. No. S11-004) is from PAA Laboratories, Linz, Austria, and antibodies for FCM analysis are from Becton-Dickinson. Antibodies, antibody-conjugated diamagnetic beads, separation columns, and magnets for the isolation of peripheral blood dendritic cells can be obtained from Miltenyi Biotech GmbH, Bergisch-Gladbach, Germany (blood dendritic cell isolation kit, Cat. No. 130-046-801). For further reference, we recommend the frequently updated online protocols of Miltenyi (http://www.miltenyibiotech.com).

B. Murine Dendritic Cells

Bovine serum albumin (BSA) (Cat. No. B 4287), β-mercapthoethanol (Cat. No. M 6250), and EDTA (Cat. No. 6511) are from Sigma-Aldrich, Deisenhofen, Germany. Cytokines are from Strathmann Biotech, Hamburg, Germany: rmGM-CSF (Cat. No. mGMCSF-10) and rmIL-4 (Cat. No. mIL4-10). Collagenase type II (Cat. No. LS04176) or type III (Cat. No. LS04182) is from Cell Systems Biotech GmbH, St. Katharinen, Germany. DNase I is from Roche Diagnostics GmbH, Mannheim, Germany (20 mg/ml, Cat. No. 92566700). Fetal calf serum (FCS) (Cat. No. 14-801E) was tested before usage and obtained as IMDM (Cat. No. 12-726F) from Cambrex/Bio Witthaker Europe, Verviers, Belgium. Hank's (Cat. No. 14175-053), HBSS (Cat. No. 14175-053), L-glutamine (Cat. No. 25030-024), penicillin/streptomycin (Cat. No. 15140-122), PBS (Cat. No. 14190094), and RPMI 1640 (Cat. No. 31870-025) are from Invitrogen, Karlsruhe, Germany. Heparin (Cat. No. L6510) and HEPES are from Biochrom AG Seromed, Berlin, Germany (Cat. No. L 1603). KCl (Cat. No. 104933) and NaCl (Cat. No. 106404) are from Merck, Darmstadt, Germany. Trypsin (Cat. No. 59227) is from JRH Biosciences, Shawnee Mission, Kansas. Nycodenz powder (Nycoprep) is from Nycomed Pharma AS, Asker, Norway. Plastic materials are obtained from Becton-Dickinson, Heidelberg, Germany: cell culture dish (Cat. No. 353003), petri dish (Cat. No. 351001), 70-µm cell stainer (Cat. No. 352350), 6-well plate (Cat. No. 353224), 24-well plate (Cat. No. 353226), syringe needle (Cat. No. 300400), and 50-ml tube (Cat. No. 352070). Instruments are from NeoLab, Heidelberg, Germany: sieve (diameter 70 mm, Cat. No. 2-7530) and tweezers (Cat. No. 2-1034). Cy5-PE-conjugated anti-CD4 monoclonal antibody (mab) (clone H129.19; Cat. No. 553654) is from Becton-Dickinson. Multiple species Ig-absorbed, fluorescein isothiocyanate (FITC)-conjugated antihamster Ig (Cat. No. 127-096-160) and PE antirat Ig (Cat. No. 112-116-143) are both from Dianova, Hamburg, Germany.

III. PROCEDURES

Solutions for the Generation of Human Dendritic Cells

1. *PBS/0.1 M EDTA buffer:* 2.5 ml 2*M* EDTA and 497.5 ml PBS. Store at 4°C and use within 1 week.
2. *Freezing medium:* 20% HSA, 20% DMSO, and 6% glucose. To prepare 200-ml, pipette 130 ml HSA 20% into a sterile 200-ml flask and add 40 ml DMSO and 30 ml 40% glucose. Store at 4°C and use within 1 week.
3. *R0 culture medium (R0):* To one bottle of 500 ml RPMI 1640, add 5 ml glutamine and 2 ml 10 mg Refobacin. Store at 4°C and use within 1 week.
4. *Complete medium (CM):* To one bottle of 500 ml RPMI 1640, add 5 ml glutamine, 2 ml 10 mg Refobacin, and 5 ml sterile-filtered autologous heat-inactivated plasma. Store at 4°C and use within 1 week.
5. *PBS/ACD buffer:* Add 50 ml ACD-A to one bottle (500 ml) PBS and use within 1 day.
6. *PBS/heparin solution:* Add 500 µl Liquemin N 10000 (5000 IE sodium heparin) to 500 ml PBS buffer. Store at 4°C.
7. *R10 culture medium (R10):* 1% glutamine, 1% PenStrep, and 10% FCS in RPMI 1640. To one bottle of 500 ml RPMI 1640, add 5 ml glutamine, 5 ml PenStrep, and 50 ml heat-inactivated FCS. Store at 4°C.

8. *Adherence medium (AM):* To one bottle of 500 ml RPMI 1640, add 5 ml PenStrep, 5 ml glutamine, 15 ml sterile-filtered plasma surrogate, and 20,000 U GM-CSF. Store at 4°C and use within 1 day.

9. *BSA/EDTA buffer (BEB)*: 0.5% bovine serum albumin and 2 m*M* EDTA. For preparation of 100 ml buffer, add 10 ml of 5% bovine serum albumin stock solution and 3.2 ml 2% EDTA to 86.8 ml PBS. *Note*: it is necessary to degas buffer prior to use. Store and use at 4°C.

A. Generation of Mature Dendritic Cells from Precursor Cells Obtained from Leukapheresis Products and Whole Blood

The development of techniques to generate large numbers of homogeneous DC populations *in vitro* from human progenitors allowed their use for research purposes as well as for clinical applications. Protocols established by several different groups describe the generation of DC either from rare, proliferating $CD34^+$ cells or from more frequent, but nonproliferating CD 14^+ monocytic cells, which can be both isolated from peripheral blood. Currently, monocyte-derived DC are used more frequently, as no special pretreatment (e.g., systemic application of G-CSF) of the donor is required; moreover, DC yielded from this progenitor population still seem to be more homogeneous and easier to generate with reproducible characteristics; hence we will restrict the provided protocol to this population.

Monocyte-derived DC from $CD14^+$ precursors are generated by use of GM-CSF and IL-4 as key cytokines, whereas the generation of DC from $CD34^+$ progenitors requires GM-CSF and TNF-α. The following protocols are adapted from procedures reported by Feuerstein *et al*. (2000) and Thurner *et al*. (1999) for the generation of mature DC from $CD14^+$ precursors isolated from leukapheresis products and buffy coats/whole blood. It should be noted that not only the used progenitor cell population but also the method of their isolation influence the subsequent generation process, e.g., upon culture in the presence of GM-CSF and IL-4, $CD14^+$ monocytes differentiate within 5–6 (leukapheresis cells) or 7 (buffy coat/whole blood cells) days to immature DC, which are characterized phenotypically as large adherent cells with irregular outlines possessing only rarely longer processes or veils. The Addition of cytokine mix at the respective day, consisting of TNF-α, PGE2, IL-1β, and IL-6, however, results in fully mature DC, which are nonadherent and veiled. Flow cytometry using antibodies recognizing typical DC surface molecules additionally allows quality control of generated cells (Fig. 1).

1. Protocol to Start from Leukapheresis Products

Day 0

1. Fill leukapheresis product (200–250 ml) into a 1000-ml culture flask and add warm (room temperature) PBS-ACD buffer to a final volume of 480 ml.
2. Fill 15 ml Lymphoprep. into each of sixteen 50-ml tubes.
3. Overlay Lymphoprep. carefully with 30 ml of the cell suspension.
4. Spin in a warm centrifuge for 30 min (22°C, 300 *g*). Make sure that the centrifuge runs off without brake.
5. While the cells are spinning, fill autologous plasma in 50-ml tubes and incubate for 30 min in a 56°C hot water bath. Thereafter, spin tubes for 10 min (22°C, 600 *g*), aliquot supernatants into 15-ml tubes, and freeze at –20°C.
6. Take leukapheresis product-containing tubes carefully out of the centrifuge and harvest the interphase into 50-ml tubes containing 15 ml of cold PBS/EDTA. Add cold PBS/EDTA buffer to a final volume of 45 ml.
7. Spin tubes for 10 min (4°C, 200 *g*).
8. Remove supernatant, resuspend pellet with cold PBS/EDTA buffer by observing a 2:1 transfer, and spin tubes for 5 min (4°C, 300 *g*).
9. Repeat step 8.
10. Remove supernatant and resuspend with 40 ml cold R0.
11. Take an aliquot of all four tubes and dilute each 1:50 for cell counting using a Neubauer chamber. While counting cells, put 50-ml tubes containing cells on wet ice.
12. After calculating the amount of cells, devide cells in fractions for immediate replating and for freezing. Spin cells in cold centrifuge for 5 min (4°C, 300 *g*).
13. Cells that are not used for immediate generation of DC should be frozen in 20% HSA at 120×10^6 cells per 1.8 ml and freezing medium (1:1) in cold 3.6-ml vials using a freezing device on wet ice before they are transferred to a nitrogen-freezing machine to cool down to –150°C. Store frozen cells in liquid nitrogen.
14. For immediate generation of DC, spin cells in a cold centrifuge for 5 min (4°C, 300 *g*), remove supernatant, and resuspend at $15–25 \times 10^6$ cells/ml of CM.
15. Preload dishes with 8 ml CM. Add 2 ml of cell suspension per dish, swing slightly, and transfer dishes into the incubator for at least 30 min.
16. Subsequently, control adherence. If sufficient (close layer of adherent cells), wash away the nonad-

herent fraction with warm PBS (room temperature) twice. Add 10 ml of warm CM per dish and retransfer into an incubator overnight.

Day 1

1. Take dishes out of the incubator and control cell adherence under a microscope.
2. Remove CM from dishes by pipetting carefully.
3. Add 9 ml of warm CM (room temperature).
4. Fill 1 ml CM per dish into a 50-ml tube and add 8000 U GM-CSF and 10,000 U IL-4 per dish.
5. Add diluted cytokine mix to dishes, swing slightly, and transfer dishes into an incubator.

Day 5

1. Take dishes out of the incubator and control cell adherence under a microscope.
2. Carefully collect 5 ml of culture supernatant from each dish into a 50-ml tube.
3. Add 4 ml of room-temperatured CM to each dish.
4. Spin 50 ml tubes for 5 min (room temperature 300 *g*).
5. Remove supernatant, add 1 ml CM, 8000 U GM-CSF, and 10,000 U IL-4 per dish and resuspend.
6. Redistribute 1 ml of this suspension to each dish, swing slightly, and transfer dishes into an incubator.

Day 6

1. Take dishes out of incubator and control cell morphology under a microscope.

2. Remove 1 ml from all dishes by pipetting into a 50-ml tube.

3. Add TNF-α (10 ng/ml cell culture volume), PGE_2 (1 μg/ml), IL-1β (2 ng/ml), and IL-6 (5 ng/ml), resuspend, and add equal amounts into each dish. Swing slightly and retransfer dishes to an incubator. Incubate for at least 24 h.

Day 7

1. Take dishes out of incubator and control cell morphology under a microscope. Mature DC appear veiled and nonadherent.
2. Harvest cells into 50-ml tubes, spin for 5 min (room temperature 300 *g*), remove supernatant, and resuspend cells in CM. Remove an aliquot to count cells.
3. Determine the phenotype of the cells by FCM analysis (Fig. 1).

2. Protocol to Start from Frozen PBMC Isolated from Leukapheresis Products

Day 0

1. Fill 5 ml of cold HBSS in 15-ml tubes.
2. Thaw vials with frozen cells in warm water to an extent that a frozen core of cells remains in each tube.
3. Dump frozen cells into the 15-ml tubes preloaded with 5 ml HBSS. Use one vial of frozen cells per 15-ml tube.
4. Rinse the storage tube once with cold HBSS, pipette suspension into the 15–ml tubes, and fill up with HBSS to a final volume of 13–14 ml.
5. Spin in a cold centrifuge for 10 min (4°C, 240 *g*).
6. Remove supernatants, resuspend pellets with a small amount of cold R0, and pool pellets into one 50-ml tube.
7. Spin in a cold centrifuge for 5 min (4°C, 300 *g*).
8. Remove supernatant and resuspend pellet with 40 ml of cold R0.
9. Take an aliquot and count cells.
10. Follow steps 14–16 of the protocol described in the previous protocol.

For day 1 to day 7 proceed as described in the previous protocol.

3. Protocol to Start from Buffy Coats or Whole Blood

Day 0

1. Transfer buffy coat or whole blood into a culture flask and dilute 1:3 with PBS/heparin solution.
2. Fill 15 ml Lymphoprep. into 50-ml tubes.
3. Overlay Lymphoprep. carefully with 30 ml of the cell suspension.
4. Spin in a warm centrifuge for 30 min (22°C, 300 *g*). Make sure that the centrifuge runs off without brake.
5. Collect supernatant, further called plasma surrogate, into a 50-ml tube and incubate for 30 min in a 56°C hot water bath. Thereafter, centrifuge for 10 min (room temperature 600 *g*). Save supernatant in a 50-ml tube for preparing AM.
6. Harvest interphase carefully to a tube containing 15 ml cold PBS/EDTA buffer. Fill up to a final volume of 40 ml using PBS/EDTA buffer.
7. Centrifuge for 10 min (4°C, 200 *g*).
8. Remove supernatant and resuspend pellet in a small volume of PBS/EDTA buffer. Pool pellets (2:1 transfer) and add cold PBS/EDTA buffer to a final volume of 40 ml per tube.
9. Centrifuge for 5 min (4°C, 300 *g*).
10. Repeat steps 8 and 9.
11. Remove supernatant, resuspend pellets in a small volume of AM, and pool cells into one 50-ml tube.
12. Remove an aliquot and count cells.
13. Load dishes with AM and cell suspension by observing 30–50 × 10^6 cells per dish. Swing slightly

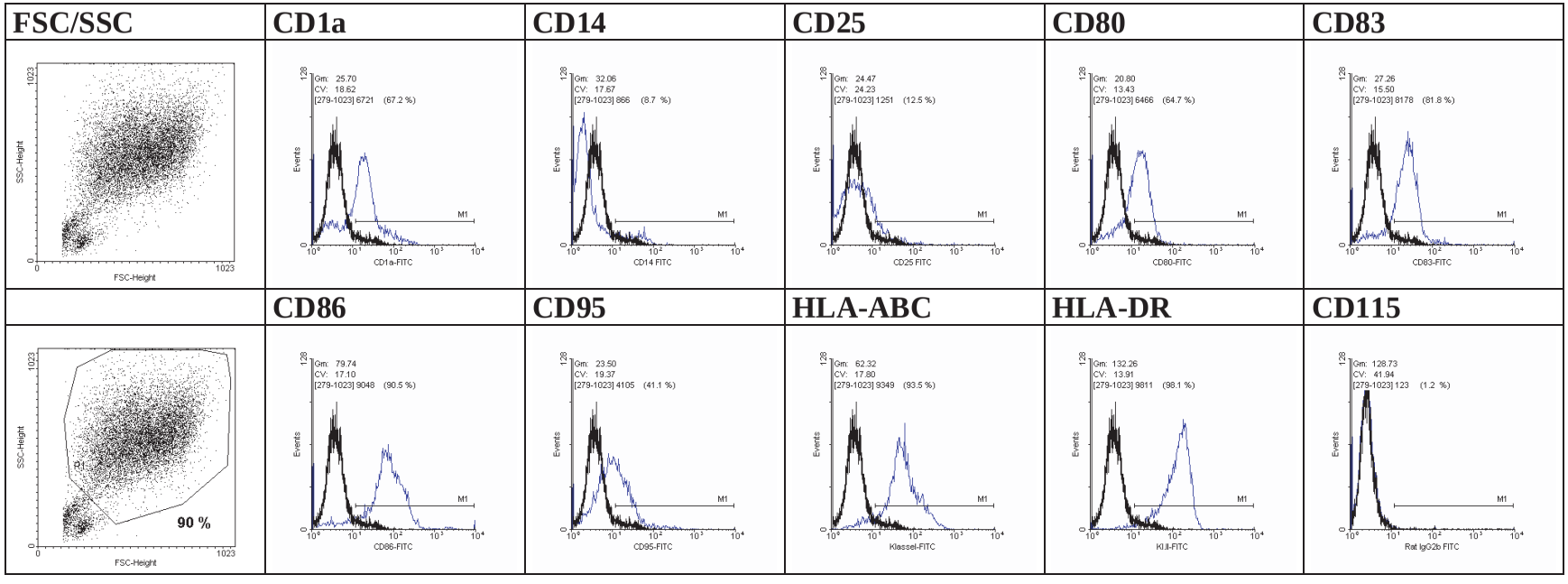

FIGURE 1 Phenotypic characterization of day 7 cells generated by FCM analysis.

and transfer dishes into the incubator for 60 min.

14. If cells adhere sufficiently, gently wash away nonadherent cells with warm PBS (room temperature). Repeat once. Add 10 ml warm R10 supplemented with 10,000 U IL-4 and 8000 U GM-CSF per dish and put into an incubator overnight.

Day 3

1. Take dishes out of the incubator and control cell adherence under a microscope.
2. Remove 5 ml R10 from dishes by pipetting carefully.
3. Add 4 ml of warm R10 (room temperature) to each dish.
4. Add 4000 U GM-CSF and 5000 IL-4 diluted in 1 ml of R10 to each dish.
5. Swing slightly and transfer dishes into the incubator.

Day 5

1. Follow steps 1–5 as described for day 3.

Day 7

1. Take dishes out of incubator and control cell morphology under a microscope.

2. Harvest cells into 50-ml tubes, spin for 5 min (4°C, 300 *g*), and collect supernatant. Resuspend cells in R10. Remove an aliquot to count cells.

3. Replate 5–7 $\times$ 10^6 cells into each culture dish containing 10 ml final volume (1 : 1 saved supernatant and R10). Add 4000 U GM-CSF and 5000 IL-4 per dish, as well as TNF-α (10 ng/ml cell culture volume), PGE_2 (1 μg/ml), IL-1β (2 ng/ml), and IL-6 (5 ng/ml), and pipette equal portions into the dishes.

4. Swing dishes slightly and transfer them into the incubator.

Day 10

1. Take dishes out of the incubator and control cell morphology under a microscope. Mature dendritic cells look veiled and nonadherent.
2. Harvest cells into 50-ml tubes, spin for 5 min (4°C, 300 *g*), remove supernatant, and resuspend cells in R10.
3. Determine the phenotype of cells by FCM analysis.

B. Direct Isolation of Myeloid and Plasmacytoid DC from Peripheral Blood

In principle, peripheral blood DC are obtained by isolation of lineage marker negative, $CD4^+$ cells (O'Doherty *et al.*, 1994). This basic procedure is described in the following text. However, advanced procedures were developed for the isolation of DC subtypes based on blood DC antigen (BDCA) expression; therefore, myeloid DC can be isolated by depletion of B cells from PBMC and positive selection of BDCA-1+ cells; plasmacytoid cells are isolated directly by the selection of BDCA-4 expressing cells. Techniques for the isolation of peripheral blood DC are based on positive and/or negative selection of primary and secondary antibody-conjugated magnetic bead-binding subpopulations in PBMC.

Steps

1. Isolate PBMC from heparinized whole blood by standard gradient centrifugation with Lymphoprep; about 2 $\times$ 10^8 cells are usually needed. *Note*: Due to large cell need, i.e., about 1% cell yield at the end of the procedure, we recommend buffy coats.

2. Resuspend cells in 300 μl of buffer per 1 $\times$ 10^8 cells. Add 100 μl human IgG (FcR blocking reagent) and label cells with 100 μl haptenized murine anti-CD3, anti-CD11b, and anti-CD16 antibodies (Hapten-Antibody cocktail) per 10^8 cells. Incubate at 4°C for 10 min.

3. Wash cells twice with 20-fold labeling volume with buffer and centrifuge at 300 *g* for 10 min. Finally, resuspend the pellet in 900 μl buffer/10^8 cells.

4. Add 100 μl cells antihapten antibodies attached to diamagnetic beads (antihapten microbeads), per 10^8 mix well, and incubate for 15 min at 4°C.

5. Separate magnetic (T cells, monocytes, and natural killer cells) cells from the nonmagnetic fraction using a magnetic separation column. To do this, a depletion column must be placed into a magnet (we usually use VarioMACS) and must be assembled with a flow resistor (an injection needle of 20–22 gauge is appropriate; follow the manufacturer's instructions) together with a side syringe and a three-way stopcock. Fill the column with degassed cool buffer and rinse. Cool the magnet until use; the procedure itself can be performed at room temperature.

6. Apply the cell suspension on top of the depletion column and allowed it to enter for 5 min. Wash the column six times and collect the flow through, which contains the desired cells.

7. Wash cells at 300 *g* for 10 min. Remove the supernatant and resuspend the cell pellet in 100 μl buffer.

8. To separate B cells from the DC, which are enriched in the resulting cell fraction, label cells with 100 μl anti-CD4-conjugated magnetic beads (MACS CD4 MicroBeads) and incubate for 30 min at 4°C.

9. Wash cells once by adding 4 ml of buffer and centrifuge at 300 *g* for 10 min. Resuspend in 500 μl of buffer.

10. For the next depletion step, a column must be prepared, again following the manufacturer's instruc-

tion (we use a MS+ column and a miniMACS magnet). Prepare the column by washing with 500 µl buffer.

11. Apply and allow cells to penetrate the column.

12. Rinse the column with 3 × 500 µl buffer (flow through contains nondendritic cells).

13. Remove the column from the magnet, place it on a 15-ml plastic tube, and elute cells by rinsing with 1 ml buffer. Use an appropriate plunger to press fluid through the column. Fill the eluate into a fresh column and repeat the procedure.

14. Assess DC purity by flow cytometry, with DC defined as HLA-DR$^+$ cells lacking expression of CD3, CD4, CD14 , CD16, and CD19.

C. Preparation of Murine Langerhans Cells

This method was published by Kämpgen *et al.* (1994) and is described here with some important modifications to improve LC yield and purity.

Solutions

1. *Nycodenz gradient (Vremec and Shortman, 1997)*

Solution A (Shortman buffer) (500 ml of 308 mOsm (EDTA-SS)): 0.154 *M* NaCl (4.5 g), 4 m*M* KCl (0.1491 g), 14.8 m*M* HEPES (2.96 ml of 2.5 *M* stock, pH 7.2), and 5 m*M* EDTA (5 ml of 0.5 *M*) and make up to 500 ml volumetrically with dH_2O (Osm = 308 mOs*M*)

Solution B (230.78 ml of 30.55% Nycodenz (d = 1.16)): 70.5 g Nycodenz powder; make up to 230.78 ml volumetrically with dH_2O (Osm = 308 mOsM)

For 14.1% Nycoprep (d~1.077, 308 mOsm): Add 269.22 ml of solution A to 230.78 ml of solution B to a final volume of 500 ml. Both solutions and the remaining EDTA-SS should be sterile filtered.

2. *Langerhans cell culture medium (I10)*: IMDM, 10% FCS, 50 µ*M* β-mercapthoethanol, 200 µ*M* L-glutamine, 100 µg/ml penicillin, and 50 µg/ml streptomycin

Steps

1. Kill 15–30 mice by CO_2 inhalation, cut off both ears right above the ring cartilage, and place them in a petri dish (Falcon 1001) filled with 10 ml 70% alcohol for 3 min. Hold ears under alcohol and strike out blood and air with a round side of a bent tweezers. Place ears on a sterile 10 × 10-cm swab and dry them for 20 min at room temperature under a hood.

2. Prepare one petri dish containing 6 ml HDSS for the inner ear (ventral side with cartilage) and a dish with 9 ml HBSS for the soft outer dorsal half of the ear. Split ears by using two Edson forceps and place the corresponding side on top of the HBSS and add 9 ml 2.5% trypsin into the dish with the ventral side of the ears and 3.5 ml 2.5% trypsin for the outer halves of the ears. Incubate ventral ear halves for 90 min and the dorsal ear halves for 45 min at 37°C in 5% CO_2.

3. Place a metal sieve in a petri dish containing 15 ml of cold I10. Peel off the epidermis using two bent curved watchmaker's forceps and lay the epidermal sheets onto the medium. The sheets will tend to spread out upon reaching the surface of the medium. Knock against the sieve for 3 min. Wash cells once prior to an incubation at a density of 1–2 × 10^7 per 10-ml cell culture dish or 1–2 × 10^6/ml in a 6-well plate in I10 and 10 ng/ml rmGM-CSF at 37°C, 5% CO_2 in humidified air for 2–3 days.

4. After 2–3 days, cells are harvested and resuspended in 10 ml 14.1% Nycodenz gradient (p = 1.077) before transfer to two 15-ml tubes. This suspension is overlayed with 2 ml of Shortman buffer and spun at 4°C at 600 *g* for 20 min without the brake. Harvest low-density cells and wash once with medium prior to use.

D. Preperation of Murine Spleen Dendritic Cells

This procedure is performed according to McLellan *et al.*, (2002) with minor modifications.

Solutions

1. *Nycodenz gradient*: See Section A
2. *Würzburger wash buffer*: PBS, 1% BSA, 5 m*M* EDTA, and 20 µg/ml DNase
3. *FACS buffer*: PBS and 0.2% BSA
4. *Dendritic cell culture medium (R10)*: RPMI 1640, 10% FCS, 50 µ*M* β-mercapthoethanol, 200 µ*M* L-glutamine, 100 µg/ml penicillin, and 50 µg/ml streptomycin

Steps

1. Kill five to six mice by CO_2 inhalation, disinfect skin with 70% alcohol for 1 min, cut abdominal skin using sterile siccors below left ribs, and tear away the skin. Cut the peritoneum directly above the spleen, which is isolated by removal of all other tissues. Under laminar air flow, place spleens into 5 ml Hanks buffered salt solution in a petri dish. Add 120 µg/ml DNase I, pierce splenic capsule at both ends, and with curved watchmaker's forceps squeeze out all cellular contents. Tear the splenic capsule into small pieces, add 400 µl FCS to the dish, and transfer the cell suspension and fragments to a 50-ml polypropylene tube and add collagenase to a concentration of 1 mg/ml. Wash plate once with 5 ml Hanks'. Store petri dish after adding another 5–10 ml of Hanks' on ice. In a 50-ml tube, pipette cells up and down ten times with a 10-ml pipette to break up loose aggregates. Subsequently,

incubate the tube with constant but gentle swirling for 25 min at 37°C.

2. After this incubation, add 200 µl 0.5 *M* EDTA (pH 7.2) and incubate for an additional 5 min. Gently press remaining fragments through a coarse metal sieve with a rubber syringe plunger and collect into the original petri dish.

3. Rinse sieve and petri dish with Hanks' and add this to the cell suspension. Filter the cell suspension through a 70-µm cell stainer into a 50-ml tube. Top up to 50 ml with cold washing buffer. Wash once.

4. Keep tube in ice and gently add to the cell pellet 10 ml 14.1% Nycodenz (308 mOsm; ρ = 1.077) for six spleens and slowly resuspend until all clumps are resolved. Transfer the suspension to two 15-ml polypropylene tubes, overlay with 2 ml 308 mOsm Shortman buffer, and spin at 4°C at 600 *g* for 20 min without any brake.

5. Harvest low-density cells from all layers without touching the cell pellet and wash once in ice-cold washing buffer. A normal yield should be around 5–10 × 10^6 $CD11c^+$ DC/spleen at 30–50% purity.

6A. **Isolation of spleen DC subsets ($CD11c^+/CD4^-/CD8\alpha^-$, $CD11c^+/CD4^-/CD8\alpha^-$, $CD11c^+/CD4^-/CD8\alpha^+$) by FACS.** Block nonspecific Ig-binding sites on low-density spleen cells by incubation for 10 min in 25 µl 10% goat and mouse serum before labeling with 500 µl N418 culture supernatant (hamster antimouse CD11c mab) and 500 µl 53-6.7 culture supernatant (rat antimouse CD8α mab) for 30 min and ice. After one wash with Würzburger buffer, incubate spleen cells with multiple species Ig-absorbed, FITC-conjugated antihamster Ig and PE antirat Ig for 30 min on ice in the dark. After an additional washing step, add 400 µl 10% rat serum and Cy5-PE-conjugated anti-CD4 mab (clone H129.19); incubate for 30 min, subsequently wash cells once, and resuspend at 5 × 10^7 cells/ml in PBS/1 m*M* EDTA. Stained cells can now be sorted into $CD11c^+/CD4^-/CD8\alpha^-$, $CD11c^+/CD4^{+/}CD8\alpha^-$, and $CD11c^+/CD4^-/CD8\alpha^+$ subsets by FACS (e.g., FACS Vantage, Becton-Dickinson, Heidelberg, Germany).

6B. **Enrichment of spleen DC by adherence.** Incubate up to 50 × 10^6 Nycodenz-enriched, low-density cells per each Falcon 3003 dish in R10 supplemented with 10 ng/ml mGM-CSF for 2 h. For 3003 plates, wash gently against the wall of the dish with warm (37°C) R10 about five times. For 24-well plates, wash gently (5 ×) by removal of media with a R10 Pasteur pipette under vacuum and immediately refill each well with R10. Washes must be performed with extreme care to avoid dislodging too many DC. For the final wash, refill wells with 0.5 ml R10 with 10 ng/ml mGM-CSF (for 24-well plate). The next day, harvest nonadherent DC prior to use in experiments.

For serum-free culture conditions, substitute 0.5–1% mouse serum for BSA or FCS, including wash buffers.

E. Preperation of Murine Bone Marrow-Derived Dendritic Cells (BMDC)

This procedure is performed according to Inaba *et al*. (1992) with minor modifications.

Solution

BMDC culture medium: IMDM, 10% FCS, 50 µ*M* β-mercapthoethanol, 200 µ*M* L-glutamine, 100 µg/ml penicillin, and 50 µg/ml streptomycin

Steps

1. Kill needed number of mice by cervical dislocation or CO_2 inhalation, disinfect skin of the legs and lower abdomen with 70% alcohol for 1 min, cut the skin with a scissors at the inside of the leg upward, tear the skin away, and remove the muscle tissue. Disconnect the complete leg by cutting the ligaments holding the femur in the joint. Scrape the residual tissue with a scalpel from the bone, break it at the distal diaphysis, and transfer the femur and tibia to a tube with PBS.

2. Place bones in 70% alcohol for 1 min, wash them with PBS, and place them in a 2-cm petri dish. Cut off both ends of the bones with the scalpel with gently sawing movements; while placing the bone over a 50-ml tube with tweezers, flush the bone marrow with 1 ml of medium using a 10-ml syringe armed with a 0.5 × 24-mm cannula, turn the bone upside down, and repeat flushing.

3. Resuspend flushed bone marrow vigorously with a 10-ml pipette for 1 min to dislodge clusters. Transfer the cell suspension into a new 50-ml tube through a 70-µm filter to remove pieces of bone, pellet at 1500 rpm for 4 min, and resuspend cells. Incubate cells in one 6-well plate/mouse in 3 ml medium/well for overnight adherence.

4. The following day, harvest and count nonadherent cells. Up to 50% are lost upon adherence. Seed 0.8–1 × 10^6 cells/well/6-well plate in 4 ml BMDC culture medium supplemented with 15 ng/ml rmGM-CSF and 15 ng/ml rmIL-4.

5. On day 3 of culture, add 1 ml medium containing 50 ng/ml rmGM-CSF and 50 ng/ml rmIL-4 to each well.

6. On day 6, after resuspending cells three times with a 5-ml pipette to dislodge DC clusters (adherent and nonadherent), harvest, pellet at 1500 rpm for 5 min, and replate cells in 6-well plates with new BMDC culture medium-supplemented cytokines as described earlier.

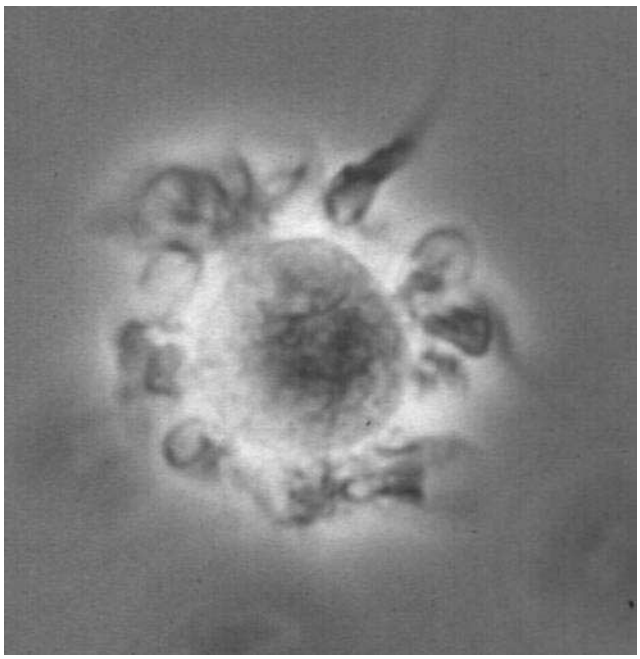

FIGURE 2 Murine bone marrow-derived dendritic cell in culture (400×) showing veils and dendrites spread homogeneously over the cell surface.

7. On day 8, swirl the plates gently, harvest nonadherent cells (Fig. 2) by gently washing the bottom of the well once, and count cells. The expected yield of BMDC is 10×10^6 cells per mouse, depending on the age of the animal.

F. Preperation of Murine Monocyte-Derived Dendritic Cells (MoDC)

This procedure is performed according to Schreurs *et al*. (1999) with little modification.

Solutions

1. *Transport medium*: ice-cold HBSS (without Ca, Mg) supplemented with 100 U/ml heparin
2. *Stock solution for mouse monocyte gradient*: Nine parts Percoll and one part 10× PBS. Do not use longer than 2 days.
3. *Working solution for mouse monocyte gradient*: Take 18.3 ml of the gradient stock solution and add 11.7 ml HBSS; mix well and store at 12°C.
4. *MoDC culture medium*: IMDM, 10% FCS, 50 µ*M* β-mercapthoethanol, 200 µ*M* L-glutamine, 100 µg/ml penicillin, and 50 µg/ml streptomycin
5. *MoDC adherence medium*: IMDM, 3% FCS, 50 µ*M* β-mercapthoethanol, 200 µ*M* L-glutamine, 100 µg/ml penicillin, and 50 µg/ml streptomycin

Steps

1. Anesthetize mice one by one, disinfect skin of the upper abdomen with 70% alcohol for 1-min, puncture heart with a 1-ml syringe harnessed with a 0.5 × 24-mm cannula containing 50 U heparin, and aspirate blood slowly. Expect 0.7–1 ml blood per mouse. Transfer blood to the tube containing transport medium. Immediately afterward kill the mouse by cervical dislocation. In general, 30 mice are needed to obtain sufficient numbers of MoDC precursors. In the following steps, all measures are described for this number of mice.

2. Dilute blood to 100 ml in HBSS and overlay carefully in four fractions on a 7-ml mouse monocyte gradient in four 50-ml tubes. Spin for 30 min at 2850 rpm, 12°C, without any brake. Pool two interphases, wash twice with ice-cold HBSS, pool the remaining pellets, and wash five times with ice-cold HBSS to remove all thrombocytes. Finally wash once with MoDC adherence medium and count cells.

3. Resuspend cells in 12 ml MoDC adherence medium and incubate for 90 min at 37°C in a 6-well plate at 2 ml per well for adherence. Discharge nonadherent cells, wash each well four times, and subsequently check the purity of the adherent cells using a microscope at 100× magnification. If satisfactory, add 3 ml DC medium/well supplemented with 20 ng/ml rmGM-CSF and 20 ng/ml rmIL-4.

4. After 3 days of culture, add 1 ml medium containing 50 ng/ml rmGM-CSF and 50 ng/ml rmIL-4 to each well.

5. On days 7–9 of culture, swirl the plates gently and harvest nonadherent cells. Gentle washing of the well, which should avoid the detachment of macrophages, improves the yield of cells. Expect 1.5×10^6 MoDC per 30 mice.

References

Banchereau, J., and Steinman, R. M. (1998). Dendritic cells and the control of immunity. *Nature* **392**, 245–252.

Cella, M., Facchetti, F., Lanzavecchia, A., and Colonna, M. (2000). Plasmacytoid dendritic cells activated by influenza virus and CD40L drive a potent TH1 polarization. *Nature Immunol.* **1**, 305–310.

Fernandez, N. C., Lozier, A., Flament, C., Ricciardi-Castagnoli, P., Bellet, D., Suter, M., Perricaudet, M., Tursz, T., Maraskovsky, E., and Zitvogel, L. (1999). Dendritic cells directly trigger NK cell functions: Cross-talk relevant in innate anti-tumor immune responses *in vivo*. *Nature Med.* **5**, 405–411.

Feuerstein, B., Berger, T. G., Maczek, C., Roder, C., Schreiner, D., Hirsch, U., Haendle, I., Leisgang, W., Glaser, A., Kuss, O., Diepgen, T. L., Schuler, G., and Schuler-Thurner, B. (2000). A method for the production of cryopreserved aliquots of antigen-preloaded, mature dendritic cells ready for clinical use. *J. Immunol. Methods* **245**, 15–29.

Inaba, K., Inaba, M., Romani, N., Aya, H., Deguchi, M., Ikehara, S., Muramatsu, S., and Steinman, R. M. (1992). Generation of large

numbers of dendritic cells from mouse bone marrow cultures supplemented with granulocyte/macrophage colony-stimulating factor. *J. Exp. Med.* **176**, 693–1702.

Kämpgen, E., Koch, F., Heufler, C., Eggert, A., Gill, L. L., Gillis, S., Dower, S. K., Romani, N., and Schuler, G. (1994). Understanding the dendritic cell lineage through a study of cytokine receptors. *J. Exp. Med.* **179**, 1767–1776.

McLellan, A. D., and Kämpgen, E. (2000). Functions of myeloid and lymphoid dendritic cells. *Immunol. Lett.* **72**, 101–105.

McLellan, A. D., Kapp, M., Eggert, A., Linden, C., Bommhardt, U., Brocker, E. B., Kammerer, U., and Kampgen, E. (2002). Anatomic location and T-cell stimulatory functions of mouse dendritic cell subsets defined by CD4 and CD8 expression. *Blood* **99**, 2084–2093.

O'Doherty, U., Peng, M., Gezelter, S., Swiggard, W. J., Betjes, M., Bhardwaj, N., and Steinman, R. M. (1994). Human blood contains two subsets of dendritic cells, one immunologically mature and the other immature. *Immunology* **82**, 487–493.

Ruedl, C., Koebel, P., Bachmann, M., Hess, M., and Karjalainen, K. (2000). Anatomical origin of dendritic cells determines their life span in peripheral lymph nodes. *J. Immunol.* **165**, 4910–4916.

Schreurs, M. W., Eggert, A. A., de Boer, A. J., Figdor, C. G., and Adema, G. J. (1999). Generation and functional characterization of mouse monocyte-derived dendritic cells. *Eur. J. Immunol.* **29**, 2835–2841.

Shortman, K., and Liu, Y. J. (2002). Mouse and human dendritic cell subtypes. *Nature Rev. Immunol.* **2**, 151–161.

Steinman, R. M., and Pope, M. (2002). Exploiting dendritic cells to improve vaccine efficacy. *J. Clin. Invest.* **109**, 1519–1526.

Thurner, B., Roder, C., Dieckmann, D., Heuer, M., Kruse, M., Glaser, A., Keikavoussi, P., Kaempgen, E., Bender, A., and Schuler, G. (1999). Generation of large numbers of fully mature and stable dendritic cells from leukapheresis products for clinical application. *J. Immunol. Methods* **1**, 1–15.

Vremec, D., Pooley, J., Hochrein, H., Wu, L., and Shortman, K. (2000). CD4 and CD8 expression by dendritic cell subtypes in mouse thymus and spleen. *J. Immunol.* **164**, 2978–2986.

Vremec, D., and Shortman, K. (1997). Dendritic cell subtypes in mouse lymphoid organs: Cross-correlation of surface markers, changes with incubation, and differences among thymus, spleen, and lymph nodes. *J. Immunol.* **159**, 565–573.

SECTION

3

Culture of Specific Cell Types: Haemopoietic, Mesenchymal, and Epithelial

CHAPTER

13

Clonal Cultures *in vitro* for Haemopoietic Cells Using Semisolid Agar Medium

Chung Leung Li, Andreas Hüttmann, and Eugene Ngo-Lung Lau

I. INTRODUCTION

An exponential increase in knowledge of the regulation of haemopoiesis has been witnessed since the mid-1980s. Over 20 cytokines (colony-stimulating factors, erythropoietin, thrombopoietin, and interleukins) have now been identified, molecularly cloned, and expressed. Many of these recombinant haemopoietic growth factors are now being used in clinical situations where they have been found to be useful in correcting anaemia and white cell deficiencies either in chronic-inherited disease or following acute treatment (e.g., chemotherapy, bone marrow transplantation) (Atkinson, 1993; Clark and Kamen, 1987; Mertelsmann *et al*., 1990; Sheridan *et al*., 1989).

The discovery of haemopoietic growth factors was facilitated greatly by the ability to grow haemopoietic cells *in vitro*. These culture systems enable the undifferentiated haemopoietic precursors to proliferate and differentiate into various haemopoietic cell lineages. Especially valuable has been the development of clonal cultures using semisolid agar or methylcellulose culture medium for haemopoietic precursor cells. In the presence of appropriate growth factors, these precursor cells proliferate and produce a clonal colony of differentiated cells. This will allow biological, viral, biochemical, or molecular studies to be performed on individual cell clones. In addition, by counting colonies, it is also possible to infer the number of precursor cells in the starting cell population. This is possible because a linear relationship exists between the number of colonies formed and the number of cells cultured. By comparison, liquid suspension cultures of primary haemopoietic cells do not allow enumeration of precursor cell numbers as the progeny are intermingled in the culture dish. The second feature of clonal cultures is the dose–response relationship that exists between the amount of growth factor and the number of colonies stimulated. This dose–response relationship is sigmoid, having a linear phase and a plateau phase. The linear portion of the curve can be used to determine the amount of growth factor activity; in cultures described here, 50 units of growth factor activity correspond to the amount of activity stimulating 50% of maximal colony numbers. More detailed information on haemopoietic colony formation and cytokines can be found in Metcalf (1984, 1985, 1986, 1991) and Nicola (1991).

II. MATERIALS AND INSTRUMENTATION

A. Semisolid Agar Medium Cultures

Iscove's modified Dulbecco's medium powder, with 4 m*M* L-glutamine and 25 m*M* HEPES buffer (IMDM, Cat. No. 12200-085 for a 5-litre batch), is from GIBCO-Invitrogen. DEAE-dextran hydrochloride (Cat. No. D9885), L-asparagine monohydrate (Cat. No. A4284), 2-mercaptoethanol (Cat. No. M7522), penicillin G (Cat. No. P7794), and streptomycin (Cat. No. S9137) are from Sigma-Aldrich. Bacto agar is from Bacto Laboratories (Cat. No. 0140-17). Recombinant haemopoietic growth factors and cytokines can be purchased from a

Copyright 2006, Elsevier Science (USA).
All rights reserved.

number of commercial suppliers (e.g., PeproTech EC Ltd, R&D Systems). For routine cultures, conditioned medium can be prepared from a number of tissues (see later). Foetal calf serum (FCS) can be obtained from a number of suppliers, but requires pretesting (see later). Bacteriological graded petri dishes (35–36 and 100 mm diameter) can be obtained from a number of suppliers as a tissue culture grade dish is not required. For viable cell count, eosin Y from Sigma-Aldrich (Cat. No. E4009) is required. Distilled Milli-Q endotoxin-free water (H_2O) is routinely used.

B. Conditioned Medium

IMDM (Cat. No. 12200-085) and pokeweed mitogen (PWM, Cat. No. 15360-019) are from GIBCO-Invitrogen. 2-Mercaptoethanol (2ME, Cat. No. M7522), sodium bicarbonate ($NaHCO_3$, Cat. No. S6014), penicillin G (Cat. No. P7794), and streptomycin (Cat. No. S9137) are from Sigma-Aldrich. FCS can be obtained from various suppliers, and batches can only be selected by prior testing. If a batch is available that is known to support good colony formation, then this can be used to prepare conditioned media. A variety of flasks can be used to prepare PWM-stimulated spleen cell-conditioned media (PWM-SCM) for murine cultures, although we routinely use 1- to 2-litre glass flasks fitted with a cotton plug to allow gas diffusion. For preparation of human placental conditioned media, a variety of flasks can also be used, but we routinely use disposable 75-cm^2 tissue culture flasks (Cat. No. 25110-75, Corning).

C. *In Situ* Colony Staining

Glutaraldehyde solution (grade II, 25% in water, Cat. No. G6257), ethanol (Cat. No. 02862), urea (Cat. No. U6504), acetylthiocholine iodide (Cat. No. A5751), sodium phosphate dibasic (Na_2HPO_4, Cat. No. 71629), sodium phosphate monobasic (NaH_2PO_4, Cat. No. 71492), sodium citrate (Cat. No. S1804), copper(II) sulphate ($CuSO_4$, Cat. No. C1297), potassium ferricyanide [$K_3Fe(CN)_6$, Cat. No. 60310], and Mayer's haematoxylin staining solution (Cat. No. MHS-16) are from Sigma-Aldrich. Luxol fast blue MBS (Code Pack No. 10732) is from NBS Biologicals. Hardened ashless 541 filter paper of 5.5-cm diameter (Cat. No. 1541 055) is from Whatman, and DePex (D.P.X) neutral mounting medium (Cat. No. 3197) is from Bacto Laboratories. Plain 2 × 2-in. microscope slides (Cat. No. 5075) and 45 × 50-mm cover glasses (Cat. No. 4550-1) can be obtained from Brain Research Laboratories.

D. Instrumentation

For colony examination and counting, a zoom stereomicroscope (Model SZ4045) fitted with a clear stage plate and a base illuminator from Olympus is used routinely. Many brands of CO_2 incubators are available and it is recommended that one with stainless-steel water jackets be obtained. In addition, to minimize the desiccation of cultures, an incubator without an inbuilt fan is preferred. A standard light microscope equipped with 10 and 40× objectives will be sufficient for routine cell counting and *in situ* colony typing. Graduated, glass blow-out pipettes in volumes of 1, 5, 10, and 25 ml are routinely used, although they can be replaced by disposable pipettes. For the concentration of conditioned media, we use an Amicon hollow-fibre concentrator (Model DC2A) fitted with a HIP10 membrane.

III. PROCEDURES

A. Method for Establishing and Scoring Agar-Medium Cultures

The fundamental steps in establishing agar-medium cultures are fourfold: (1) mix equal volumes of double-strength medium and double-strength agar solution, (2) add the cells to be cultured and mix, (3) pipette the cell suspension onto the culture dishes, and (4) after gelling the culture dishes are put in an incubator for colony formation.

Solutions

1. *IMDM for agar cultures (AIMDM)*: 88.3 g IMDM, 0.6 g penicillin G, 0.375 g streptomycin, 7.5 ml DEAE-dextran (50 mg/ml solution), 1.0 g L-asparagine, 24.5 g $NaHCO_3$, and 29.5 µl 2-mercaptoethanol. Dissolve the contents of a 5-litre package IMDM (88.3 g) in 1 litre of H_2O using a magnetic stirrer for mixing. Rinse the inside of the package to remove all traces of powder. Add afore-listed reagents while stirring continuously. Add H_2O to a final volume of 1.95 litres and gas medium with 100% CO_2 until it is a yellow–orange colour. The prepared endotoxin-free medium should then be filter sterilized and distributed in 100- or 250-ml aliquots, which are then tightly capped, stored at 4°C, and protected from light. Each preparation of AIMDM should be batch tested against one that is currently in use if applicable.

2. *Agar*: 0.6 g Bacto-agar and 100 ml H_2O. Weigh agar into a 100-ml flask, add 100 ml H_2O, and plug flask loosely. Bring to boiling for 2 min over a gas flame. Prepare immediately before setting up cultures

and maintain at 45°C in a water bath. Each new lot of Bacto-agar should be batch tested against one that is currently in use if applicable.

3. *Foetal calf serum*: FCS is used as a source of nutrients in cell cultures. Batches of FCS should be tested extensively prior to purchase, for optimal colony formation in colony number and colony size, in semisolid cultures. They should also be titrated to determine the optimal concentration (final concentration is usually 5–20%). The storage/shelf life of FCS at –20°C is at least 2 years and at –70°C it as long as 10 years. Centrifugation may be necessary to remove any sediment that forms after thawing. It is otherwise ready for use. Heat inactivation is optional but not necessary.

4. *Eosin for viable cell counts*: Prepare stock solution [10% eosin-yellow powder (w/v)] in normal saline and keep at 4°C. Mix 0.2 ml of stock eosin solution with 8.6 ml normal saline and 1.5 ml FCS to prepare working solution. Aliquots of the working solution should be store frozen.

5. *Hemopoietic growth factors*: If purchased commercially, they should be pretested to determine the amount required for optimal colony formation. If conditioned media are prepared (see later), they also require titration to determine the optimal concentration for maximal colony formation without evidence of high-dose inhibition. Stimuli should be divided into aliquots at a concentration at least 10-fold higher than that to be used finally in the culture dish. They can be stored frozen, but once thawed, they should not be frozen again as this can result in a loss of activity.

6. *Single-strength Iscove's modified Dulbecco's medium*: Dissolve the entire contents of a 5-litre package IMDM (88.3 g) with 4.8 litres of H_2O and mix with gentle stirring. Rinse the inside of the package to remove all traces of powder. Add 15.12 g $NaHCO_3$, 29.5 µl 2-mercaptoethanol, 150 mg penicillin G, and 100 mg streptomycin while stirring continuously. Add H_2O to a final volume of 5 litres and gas medium with 100% CO_2 until it is a yellow–orange colour. The prepared endotoxin-free medium should then be filter sterilized and distributed in 100- or 500-ml aliquots, which are then capped tightly, stored at 4°C, and protected from light.

7. *Pokeweed mitogen*: This should be prepared immediately prior to use. Any material not used should be discarded. Make up powder with 5 ml of double-distilled, deionized water. Remove from the vial and dilute 1:15 (v/v) with H_2O.

Steps

1. Warm AIMDM to room temperature.
2. Prepare agar solution.
3. Count viable cells using a haemocytometer and eosin as dye.
4. Draw culture layout, in a book, showing culture number, stimuli for each culture dish, and the number of cells for each culture dish.
5. Place required number of culture dishes on incubator trays and number lids individually according to the culture book.
6. Add required stimuli to appropriate culture dishes as described in the culture book. For each culture, the required amount of stimulus is usually added in 0.1 ml per culture dish. This amount can be less but should not exceed 0.2 ml as the agar may not gel properly.
7. For agar cultures with 20% FCS final concentration, mix AIMDM (three parts) and foetal calf serum (two parts) first and then add an equal volume of agar (five parts). Cells are added last to this single-strength agar medium, which should be now roughly at 36–37°C before plating. For each group of cultures, allow 1 ml of agar medium each per culture plus at least 1 ml extra for wastage in pipetting. If by pretesting, a lower concentration of FCS is sufficient for optimal colony formation, replace the leftover volume with H_2O so that the amount of AIMDM and FCS equals 0.5 ml for each 1 ml of culture.
8. Aliquot 1-ml volumes into petri dishes and swirl to mix stimuli and agar medium-containing cells.
9. Allow mixture to gel and place in a fully humidified containing 5–10% CO_2 in air.
10. After the required incubation period (normally 7 days for murine progenitor cells and 14 days for human progenitors and murine high-proliferative stem/progenitor cells), remove cultures from incubator and count colonies using an Olympus SZ stereomicroscope at 30–35× magnification. Murine haematopoietic colonies are defined routinely as clones greater than 50 cells and human colonies greater than 40 cells (some investigators count human colonies as having greater than 20 cells). Place the microscope on top of a black platform and adjust the concave side of the mirror until cells appear white against a black background (Fig. 1). To aid in the enumeration of colonies, we routinely put the 35-mm agar culture dishes on top of an inverted 60-mm culture dish marked with 6-mm^2 grids.

B. Preparation of Conditioned Media

Although specific stimuli may be required for many situations, and always for use as a positive control, a variety of conditioned media containing mixtures of haemopoietic growth factors can be prepared. The following examples provide descriptions for the preparation of two conditioned media: one suitable for human cultures and the other for murine cultures.

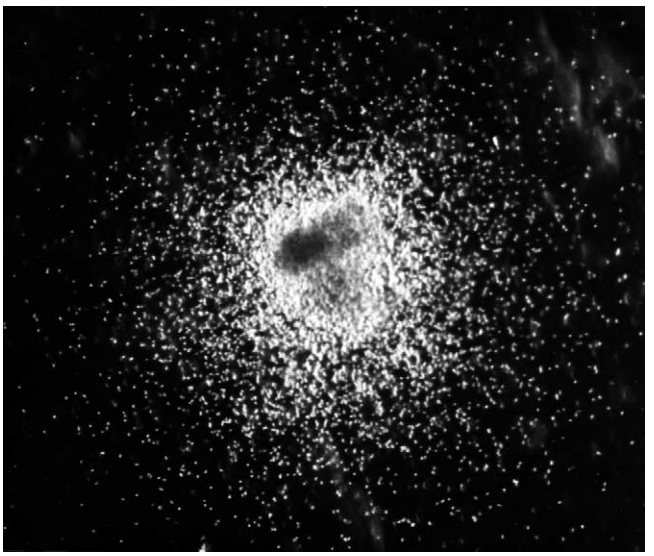

FIGURE 1 Photomicrograph of a dispersed granulocyte–macrophage colony (×100).

1. Preparation of Human Placenta-Conditioned Medium

Steps

1. Placenta should be obtained within 9 h of birth. Place it on a large sterile tray in a biological safety cabinet.
2. Using sterile instruments, remove outer layer of placenta. Assume that this portion is not sterile. Instruments can be kept sterile by periodically returning them to boiling water.
3. Cut a portion (1 cm^3) of exposed placenta and place in a 100-mm petri dish containing 10 ml IMDM. Limit each petri dish to 8–10 pieces.
4. Having removed sufficient pieces of placenta, rinse each piece through three changes of IMDM in 100-mm petri dishes to remove most of the blood.
5. Place 18–20 pieces of placenta into tissue culture flasks (75 cm^2, Cat. No. 25110-75, Corning) in 60 ml IMDM with 5% (v/v) FCS.
6. Place the placenta cultures, with the caps sealed loosely, in a 37°C fully humidified incubator containing 5–10% CO_2 in air.
7. After 5–7 days of incubation, harvest the medium free of placenta by pouring the contents of each flask through cotton gauze into a collection flask. Centrifuge the medium at 3000 *g* and store the supernatant at –20°C until 4–5 litres has accumulated.
8. Concentrate the placenta-conditioned medium approximately 10-fold using a hollow fibre concentrator (this type of concentrator is preferred because of the relatively large volumes involved).
9. Filter sterilize the concentrate and test by titration using human bone marrow semisolid agar cultures. Select the batches of conditioned media that display a sigmoid dose–response relationship with the number of colonies formed and without evidence of a high-dose inhibition.

2. Preparation of Murine Pokeweed Mitogen-Stimulated Spleen Cell-Conditioned Medium

Steps

1. Prepare a single-cell suspension of murine spleen cells, either by teasing the spleen tissue with needle or by forcing it through a fine stainless steel mesh.
2. Place the spleen cells in a tube and allow them to stand for 5 min to allow larger tissue fragments to sediment. Remove the supernatant and determine viable cell numbers.
3. Make up the cells to 2×10^6/ml in IMDM containing 10% FCS. (The concentration of FCS should be as low as possible and can be determined only by preliminary testing.) Add pokeweed mitogen (0.05 ml of a 1:15 dilution of freshly prepared stock is added for each millilitre of culture medium).
4. Incubate the cells in medium for 7 days at 37°C in a fully humidified incubator containing 5–10% CO_2 in air. The cells can be incubated in a variety of containers. We routinely use 2-litre flasks, with cotton plugs, containing 250 ml of medium.
5. After incubation, harvest the conditioned medium and centrifuge at 3000 *g* to remove cellular debris. Concentrate the medium 10-fold as described earlier for human placenta-conditioned medium.
6. Titrate the concentrated PWM-SCM using cultures of murine bone marrow cells to determine the concentration required to give plateau numbers of colonies.
7. The conditioned medium can then be diluted to a concentration 10 times that is required for maximal colony formation, divided into 20-ml aliquots, and stored at –20°C until required. Once thawed the PWM-SCM should be stored at 4°C.

III. COLONY TYPING

Colonies grown in agar cultures can be typed using an *in situ* whole plate staining sequentially with Luxol Fast Blue to detect eosinophil granules (Johnson & Metcalf, 1980), acetylcholinesterase to detect megakaryocytes (von Melchner and Lieschke, 1981) and Mayer's haematoxylin for nuclear morphology to detect neutrophils and monocyte/macrophages.

Preparation of Fixative and Staining Solutions

A 2.5% (v/v) glutaraldehyde in PBS is prepared by mixing 1 part of 25% glutaraldehyde with 9 parts of PBS. The luxol fast blue staining solution is prepared by dissolving 0.1 g powdered luxol fast blue MBS dye (NBS Biologicals Ltd., Hungtingdon, Cambs, England) in 100 ml of 70% ethanol saturated with urea. The substrate solution for acetylcholinesterase staining should be prepared fresh each time by dissolving 10 mg acetylthiocholine iodide (Sigma-Aldrich) in 15 ml of 100 m*M* sodium phosphate buffer, pH 6.0. One millilitre of 100 m*M* sodium citrate, 2 ml of 30 m*M* copper sulphate, and 2 ml of potassium ferricyanide solutions are then added sequentially with constant stirring.

Steps

1. Add 2 ml 2.5% glutaraldehyde into individual culture dishes and leave at room temperature overnight.
2. Transfer the gel onto a 3 × 2-in. glass slide with the aid of a water bath and then cover the gel with a wet 5.5-cm Whatman 541 filter paper and allow drying at room temperature in a fume hood.
3. Remove the filter paper, leaving a thin film of gel containing compressed colonies on the glass slides.
4. Slides are first stained for acetylcholinesterase by incubating the slides in the dark with the substrate solution at room temperature for 3 h.
5. After washing under running tap water for 10–15 min, transfer slides into the luxol fast blue staining solution and stain for 30 min at room temperature.
6. After another washing under running tap water for 30 min, counterstain slides with Mayer's haematoxylin for 1 min, wash, and "blue" in running tap water.
7. Dry slides at room temperature, mount with DePex, and examine under a light microscope after drying.

IV. PITFALLS

1. Numerous pitfalls are associated with these procedures. A major problem involves selection of a suitable batch of FCS. If possible, a known positive sample should be obtained from a colleague or a commercial source (e.g., StemCell Technologies) for use as a control when testing new batches.
2. The agar needs to be boiled to ensure that it is dissolved properly. For this reason, it is recommended to use a gas flame. The agar will initially bubble up when boiliing, and care must be taken to prevent it from overflowing. Once the bubbling has subsided, the agar should be boiled for another minute. An autoclave should not be used to prepare the agar solution.
3. It is imperative that the incubator being used is fully humidified, as desiccation of the cultures will prevent colony growth. With satisfactory cultures, a small volume of liquid will be evident at the edge of the agar medium when the cultures are tilted. If desiccation has occurred, the surface of the agar medium will display irregularities instead of being smooth and shiny. To prevent desiccation, the incubator should contain one or more large open trays containing H_2O. Humidity can be improved by pumping the air–gas mixture into the incubator via a tube immersed in one of the trays of water. Many incubators are fitted with a fan to produce a uniform atmosphere with the closed incubator. This can also cause the desiccation of cultures and the fan may have to be disconnected.
4. The possibility of cultures drying out is increased by extending the incubation time. For cultures in excess of 7 days it is a good policy to place culture dishes in a 100-cm petri dish (two cultures per dish) containing a third open-lid, 35-mm culture dish with H_2O. It is also a good policy to minimize the number of openings of the incubator.
5. When establishing the cultures, problems can arise due to the temperature of the agar–medium mixture. If too cold, it will gel prematurely and the cells will not be immobilized properly. If too hot, it will kill the cells. It is recommended that the agar be maintained at 45°C and that the AIMDM and FCS be allowed to warm to room temperature (18–20°C). When agar, medium, and FCS are mixed, the temperature of the solution will be about 37°C, which will not kill the cells but will still be above the gelling temperature of the agar. Once cells have been added to the agar medium mixture and mixed, it should be dispensed to culture dishes as soon as possible. As 0.1 ml of stimulus is usually present in the culture dish, the mixture should be swirled gently to allow homogeneous mixing. All these actions should be executed before gelling starts to occur.

References

Atkinson, K. (1993). Cytokines in bone marrow transplantation. *Today's Life Sci.* **5**, 28–38.

Clark, S. C., and Kamen, R. (1987). The human hematopoietic colony-stimulating factors. *Science* **236**, 1229–1237.

Johnson, G. R., and Metcalf, D. (1980). Detection of a new type of mouse eosinophil colony by Luxol-Fast-Blue staining. *Exp. Hematol.* **8**, 549–561.

Mertelsmann, R., Herrman, F., Hecht, T., and Schulz, G. (1990). Hematopoietic growth factors in bone marrow transplantation. *Bone Marrow Transplant.* **6**, 73–77.

Metcalf, D. (1984). "The Hemopoietic Colony Stimulating Factors." Elsevier, Amsterdam.

Metcalf, D. (1985). The granulocyte-macrophage colony-stimulating factors. *Science* **229**, 16–22.

Metcalf, D. (1986) How reliable are *in vitro* clonal cultures? Some comments based on hemopoietic cultures. *Int. J. Cell Cloning* **4**, 287–294.

Metcalf, D. (1991). Control of granulocytes and macrophages: Molecular, cellular, and clinical aspects. *Science* **254**, 529–533.

Nicola, N. A. (1991). Receptors for colony stimulating factors. *Br. J. Haematol.* **77**, 133–138.

Sheridan, W. P., Morstyn, G., Wolf, M., Lusk, J., *et al*. (1989). Granulocyte colony-stimulating factor and neutrophil recovery after high dose chemotherapy and autologous bone marrow transplantation. *Lancet* **2**, 891–895.

von Melchner, H., and Lieschke, G. J. (1981). Regeneration of hemopoietic precursor cells in spleen organ cultures from irradiated mice: Influence of genotype of cells injected and of the spleen microenvironment. *Blood* **57**, 906–912.

CHAPTER

14

Human Skeletal Myocytes

Robert R. Henry, Theodore Ciaraldi, and Sandeep Chaudhary

I. INTRODUCTION

Human muscle tissue consists of many cell types, including adipocytes, fibroblasts, nerve cells, and stromal-vascular components. In the past, biochemical studies of human muscle used organ culture or dissociated monolayers of primary cells. By the nature of theses techniques, both methods would result in contamination of the muscle cells with other cell types. In 1981, Blau and Webster developed a method to maximize proliferation and differentiation of muscle satellite cells to produce *cultures of pure human muscle cells*. Subsequently, serum-free media were developed to optimize the growth of human myocytes without differentiation (Ham *et al*., 1988). It then became feasible to use a sequential two-media approach to grow and differentiate human myocytes. With these techniques, and more recent modifications, it is now possible to study human muscle myocytes without the confounding complication of contamination by other cellular components of muscle tissue.

There are many reasons why it is valuable to be able to study myocytes in isolation. Some investigators have considered the potential of human myoblasts in gene therapy. This exploits the important characteristic of muscle cells; the progeny of a single cell can be taken full circle from the animal to the culture dish and then back to the animal where they fuse into mature myofibers of the host (Blau *et al*., 1993). In fact, this quality of myoblasts affords itself as a way to develop gene- and cell-based therapies for many genetic disorders, including Duchenne muscular dystrophy (Gussoni *et al*., 1997). A number of investigators have been studying the effects of insulin on multiple aspects of metabolism in human muscle cells as it relates to type 2 diabetes mellitus and other insulin-resistant states (Borthwick *et al*., 1995; Park *et al*., 1998; Gaster *et al*., 2002). Maintenance of muscle cells under controlled conditions permits evaluation of the contribution of the components of the type 2 diabetic environment, such as hyperglycemia, hyperinsulinemia, and hyperlipidemia, to the metabolic behaviors of muscle as compared to the intrinsic or genetic properties of muscle. The culture conditions can also be manipulated to reproduce acquired behaviors. As a final example of how human myoblast cultures can be employed, investigators have also looked at the development of factors during the maturation of human myocytes to myotubes (Gunning *et al*., 1987). Therefore, the ability to investigate human muscle cells *in vitro* has a great importance in discovering clinically significant *in vivo* pathophysiology.

Investigators have discovered that the differentiation of myoblasts to myotubes while in culture involves changes in gene expression (Gunning *et al*., 1987). Using the technique illustrated in this article, *characterization of the muscle cells* in terms of the biochemical markers they express during the fusion process has been described previously. Some of the changes in gene expression in major markers that are expressed include increases in sarcomeric specific α-actin protein (3.5-fold), the muscle-specific isoform of creatinine phosphokinase (CPK-M) mRNA (2-fold), and CPK-M enzyme activity (6-fold). The process of myoblast fusion into myotubes can also be observed structurally through fluorescent micrographs of cells stained for nuclei, as seen in Fig. 1 (Henry *et al*., 1995). A more complete list of changes in biochemical and histologic markers following differentiation of myocytes into myotubules is presented in Table I. It is important to monitor a number of these markers when manipulating conditions or comparing cells from different individuals.

Copyright 2006, Elsevier Science (USA).
All rights reserved.

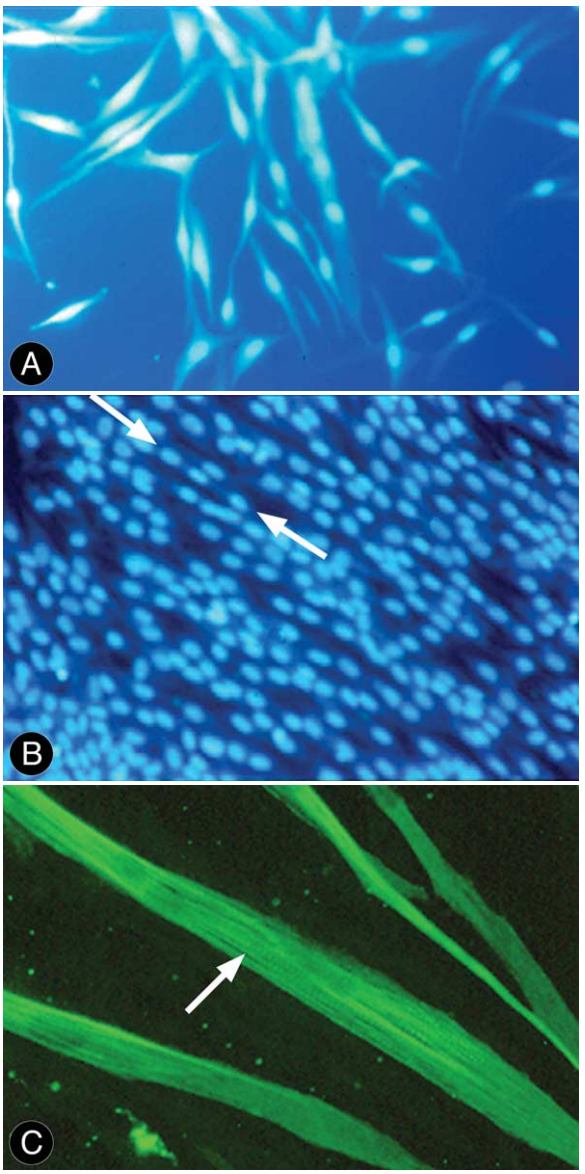

FIGURE 1 Myocytes and myotubules in various stages of differentiation. (A) Individual myocytes prior to differentiation. (B) Myotubules showing the classic "peas in a pod" appearance of multiple nuclei within single cells. Note that there are several mononucleated as well as multinucleated cells in the culture. (C) Striations in differentiated myotubules.

II. MATERIALS AND INSTRUMENTATION

Hams F10 media (Cat. No. 9056), custom ATV (Cat. No. 9920), α-MEM (Cat. No. 9142), Fungibact (Cat. No. 9350), penicillin/streptomycin (pen/strep) (Cat. No. 9366), and glutamine (Cat. No. 9317) are from Irvine Scientific (Santa Ana, CA). The SKBM and bullet kit (Cat. No. 3160) are from BioWhittaker (Walkersville, MD). To make SKGM, the components of the bullet kit are added to one bottle of SKBM, along with 10 ml Fungibact and 5 ml glutamine. The insulin bullet can be added or omitted depending on the final purpose for which the cells will be utilized (see later).

Fetal bovine serum (FBS) is from Gemini (Calabasas, CA) (Cat. No. 100–106). The Hams F10 media, SKGM, and α-MEM should all be stored at 4°C. Stocks of custom ATV, fetal bovine serum, glutamine, Fungibact, and pen/strep should be stored at –20°C. To make fusion media, add fetal bovine serum to a final concentration of 2%, 10 ml of pen/strep, and 5 ml of glutamine to 500 ml of α-MEM.

The following were all obtained from Fisher Scientific: 6-well tissue culture plates (Cat. No. 08772-1G), 12-well tissue culture plates (Cat. No. 08772-3A), 24-well tissue culture plates (Cat. No. 07200-84), 100-mm culture dishes (Cat. No. 08772-E), sterile scalpel (Cat. No. 08927-5A), sterile pasteur pipettes (Cat. No. 13678-20B), sterile flasks (Cat. No. 100429-A), 15-ml conical polypropylene tubes (Cat. No. 145970C), 50-ml conical tubes (Cat. No. 1495949-A), 5-cc pipettes (Cat. No. 13675-22), 10-cc pipettes (Cat. No. 13675-20), 25-cc pipettes (Cat. No. 13655-30), p200 pipette tips (Cat. No. 02681422), and p100 pipette tips (Cat. No. 02681422). No special treatment or substrate is needed for the cells to attach to the plastic. Cells are grown and maintained in a humidified, 37°C incubator under 5% CO_2.

III. PROCEDURE

The following techniques for the growth of human skeletal muscle cultures were established through modifications of previously described methods (Blau and Webster, 1981; Sarabia *et al*., 1990).

A. Cell Isolation

All steps are to be performed under sterile conditions.

1. Collect muscle tissue in a 50-ml conical tube in 20 ml cold (4°C) Hams F10 media: approximately 100–200 mg of tissue is needed.
2. Aspirate media. Wash tissue three times with chilled (on ice) Hams F10 to remove blood.
3. Transfer tissue in a small volume (~5 ml) of Hams F10 to a 100-mm culture dish.
4. Mince tissue with sterile scalpels. Make pieces as small as possible.
5. Transfer tissue and media back to centrifuge tube and aspirate media with a sterile Pasteur pipette.

TABLE I Markers of Differentiation of Human Myocytes to Myotubues

	Change during differentiation	Reference
Biochemical marker		
Sarcomeric-specific α-actin protein	Increase from 20 to 40% of actin produced	Blau and Webster (1981)
CPK gene expression as measured by mRNA	Increase 2-fold	Henry *et al.* (1995)
Acetylcholine receptor as measured by α-bungarotoxin staining	Increase 33-fold	Blau and Webster (1981)
CPK enzyme activity	Increase 6- to 18-fold	Blau and Webster (1981); Henry *et al.* (1995)
Sarcomeric myosin heavy Chain mRNA	Increase from 7 to 42% of maximum concentration during first day of differentiation and then increase slowly over 14 days	Gunning *et al.* (1987)
α- and β-tubulin mRNA	Peak at day 5 to 10 with a change in β:α ratio from 3 to greater than 8	Gunning *et al.* (1987)
Desimin protein	Increases	van der Ven *et al.* (1992)
Human myoglobin protein	Increases	Caviedes *et al.* (1992)
Total myosin	Increases	Caviedes *et al.* (1992)
Morphologic markers		
Multinucleation contained within myotubules	Rapid increase to 40% of nuclei in myotubes in the first 24 h, with a progressive doubling of multinucleation over the next 14 days	Gunning *et al.* (1987)
Striation	Appears	Blau and Webster (1981)
Myosin light chain staining	Increases	Blau and Webster (1981)

Because the tissue will settle out on its own, the sample does not need to be centrifuged.

6. Add 20 ml of trypsin/EDTA (custom ATV) and transfer to a small flask (e.g., 50-ml Erlenmeyer flask) containing a stir bar.
7. Stir 20–30 min at room temperature in a sterile hood. Collect supernatant and place on ice.
8. Add 20 ml ATV to flask and repeat step 7 two more times. Pool the supernatants together on ice.
9. To the pooled supernatants add FBS to a final concentration of 10%.
10. Centrifuge cells for 5 min at 1600 rpm (550 *g*) at room temperature.
11. Aspirate supernatant and add 20 ml of SKGM [SKBM + bullet kit (with or without insulin) + 10 ml Fungibact + 5 ml glutamine] to cell pellet. Pipette up and down gently to resuspend cells.
12. Transfer media with cells into two 100-mm dishes. Mark plates with subject identifier and place in incubator at 37°C, 5% CO_2.
13. Change SKGM media approximately every 3 days. Continue for 2–3 weeks.
14. During the next 2–3 weeks, the muscle cells will grow attached to the surface of the culture dish. Eventually, the cells will form a confluent layer on the bottom of the dish.

B. Cell Culture

1. When the cells are 60–70% confluent, aspirate media and rinse the cells once with 5 ml of custom ATV and aspirate.
2. Place another 5 ml custom ATV on plates, aspirate after 30 s, and then incubate for 5 min at 37°C.
3. Check cells under a microscope to see if they are detached (cells will look rounded).
4. If cells are detached, add 5 ml SKGM to rinse plate, collect cells, and transfer to a 15-ml centrifuge tube. If they are only partially detached, remove the attached cells by pipetting up and down gently.
5. Add 5 ml SKGM media to trypsinized cells and centrifuge at room temperature for 5 min at 1600 rpm (550 *g*).
6. Aspirate supernatant and resuspend cells in up to 5 ml SKGM media (not more than 6 ml, depending on volume needed) by pipetting up and down gently.
7. Count cells in a hemocytometer chamber.

8. Plate cells:
   100-mm dishes: 60,000 cells per plate (approximately 60 µl cell suspension)
   6-well dishes: 20,000 cells per well (approximately 30 µl)
   12-well dishes: 6000 cells/well (approximately 20 µl)
   24-well dishes: 3000 cells/well (approximately 10 µl per well)
9. Cover wells with SKGM: 10 ml per 100-mm dish, 2 ml for each well per 6-well plate, and 1 ml for each well per 12-well and 24-well plates.
10. Change the SKGM every 2–3 days.

C. Cell Fusion/Differentiation

1. When cell cultures are 80–90% confluent, aspirate media and rinse two times with α-MEM/pen–strep/5 m*M* glutamine/2% FCS (fusion media).
2. Add fusion media to wells: 10 ml per 100-mm dish, 2 ml /well per 6-well plate, and 1 ml/well per 12-well and 24-well plates.
3. Culture at 37°C, 5% CO_2.
4. Change media every 48 h.
5. Fusion/differentiation is complete by 96 h.

IV. COMMENTS

The technique just described has been modified primarily to investigate the metabolic characteristics of human muscle cells. The system has been employed to study insulin action on glucose uptake and glycogen synthesis, fatty acid uptake and oxidation, insulin signaling, and regulation of gene expression. Other investigators have employed different techniques for the culture of human muscle cells; however, the focuses of those investigations were not on hormone action or metabolic activities (Rando and Blau, 1994; Webster and Blau, 1981), which is why the types of media employed differ from those described in this article. The major differences from the procedure described here are that growth media include Hams F-10 with 0.5% chick embryo extract and 20% fetal calf or horse serum. Furthermore, fusion media contain Dulbecco's modified Eagle's media with 2% horse serum. It is uncertain how the constituents of these other media would differ in their impact on human skeletal muscle metabolism when compared to the defined SKGM and fusion media described in this article.

In the system described here, cells are passed only a single time before terminal differentiation and are not maintained over multiple passages. Our experience is that both the extent of differentiation (percentage multinucleated cells) and the insulin responsiveness for metabolic events are diminished in a passage-dependent manner. Other investigators have maintained cultures from a single subject for a greater number of passages (as high as 15) (Halse *et al*., 1998).

V. PITFALLS/CAUTIONS

1. It is critical to use sterile technique to avoid cell contamination. Bacteria or fungal contamination can lead to altered metabolic activity of the muscle cells.
2. Omit insulin from the SKBM if planning to investigate the effect of insulin on muscle cultures. If the insulin bullet is added, the final concentration (~30 µ*M*) is high enough to produce a state of insulin resistance.
3. To avoid excessive cell damage from the trypsin, do not overincubate with ATV.
4. Change media every 48 h to avoid exhaustion of growth factors and glucose. This can alter the metabolic activity of the muscle culture.
5. Treatment of cells can be performed either during the fusion/differentiation period or at completion. If treatment is done during differentiation, then the extent of differentiation must be monitored for each new manipulation. This can be done with careful checking of differentiation by following muscle markers mentioned in Table I.
6. It is important to pass the cells at 60–70% confluency. Beyond that point spontaneous fusion may begin in adjacent cells, reducing subsequent proliferation.
7. If the fusion media and SKBM are used more than 10 days after assembly, it will be necessary to supplement media with additional glutamine.

References

Blau, H., Jyotsna, D., and Grace, P. (1993). Myoblasts in pattern formation and gene therapy. *TIG* **9**(8), 269–274.

Blau, H., and Webster, C. (1981). Isolation and characterization of human muscle cells. *Proc. Natl. Acad. Sci.* USA **78**(9), 5623–5627.

Borthwick, A., Wells, A., Rochford, J., Hurel, S., Turnbull, D., and Yeaman, S. (1995). Inhibition of glycogen synthase kinase-3 by insulin in cultured human skeletal muscle myoblasts. *Biochem. Biophys. Commun.* **210**(3), 738–745.

Caviedes, R., Liberona, J., Hidalgo, J., Tascon, S., Salas, K., and Jaimovich, E. (1992). A human skeletal muscle cell line obtained from an adult donor. *Biochem. Biophys. Acta* **1134**(3), 247–255.

Gaster, M., Petersen, I., Hojlund, K., Poulsen, P., and Beck-Nielsen, H. (2002). The diabetic phenotype is conserved in myotubules established from diabetic subjects: Evidence for primary defects in glucose transport and glycogen synthase activity. *Diabetes* **51**(4), 921–927.

Gunning, P., Hardeman, E., Wade, R., Ponte, P., Bains, W., Blau, H., and Kedes, L. (1987). Differential patterns of transcript accumulation during human myogenesis. *Mol. Cell. Biol.* **7**(11), 4100–4114.

Gussoni, E., Blau, H., and Kunkel, L. (1997). The fate of individual myoblasts after transplantation into muscles of DMD patients. *Nature Med*. **3**(9), 970.

Halse, R., Rochford, J., McCormack, J., Vandenheede, J., Hemmings, B., and Yeaman, S. (1998). Control of glycogen synthesis in cultured human muscle cells. *J. Biochem. Chem.* **274**(2), 776–780.

Ham, R., St. Clair, J., Webster, C., and Blau, H. (1988). Improved media for normal human muscle satellite cells: Serum-free clonal growth and enhanced growth with low serum. *In Vitro Cell. Dev. Biol.* **24**(8), 833–844.

Henry, R., Abrams, L., Nikoulina, S., and Ciaraldi, T. (1995). Insulin action and glucose metabolism in nondiabetic control and NIDDM subjects. *Diabetes* **44**, 936–946.

Park, K., Ciaraldi, T., Lindgren, K., Abrams-Carter, L., Mudaliar, S., Nikoulina, S., Tufari, S., Veerkamp, J., Vidal-Puig, A., and Henry, R. (1998). Troglitazone effects on gene expression in human skeletal myocytes of type II diabetes involve upregulation of peroxisome proliferator-activated receptor-γ. *J. Clin. Endrocrinol. Metab.* **83**(8), 2830–2835.

Rando, T., and Blau, H. (1994). Primary mouse myoblast purification, characterization and transplantation for cell-mediated gene therapy. *J. Cell Biol.* **125**(6), 1275–1287.

Sarabia, V., Lam, L., Burdett, E., Leiter, L.A., and Klip, A. (1990). Glucose uptake in human and animal muscle cells in culture. *Biochem. Cell Biol.* **68**, 536–542.

Van der Ven, P.F., Schaart, G., Jap, P.H., Sengers, R.C., Stadhounders, A.M., and Ramaekers, F.C. (1992). Differentiation of human skeletal muscle cells in culture: Maturation as indicated by titin and desmin striation. *Cell Tissue Res.* **270**(1), 189–198.

CHAPTER

15

Growing Madin–Darby Canine Kidney Cells for Studying Epithelial Cell Biology

Kai Simons and Hilkka Virta

I. INTRODUCTION

Epithelial cells display a structural and functional polar organization (Simons and Fuller, 1985). In these cells, the plasma membrane can be divided into two distinct domains, the apical membrane and the basolateral membrane, each containing different sets of proteins. The apical membrane facing a secretory or an absorptive lumen is delimited by a junctional complex from the basolateral membrane. The tight junction (zonula occludens) is the most apical member of the complex. It is found at the intersection between the apical and the lateral plasma membranes and joins each cell to its neighbors, thus limiting the diffusion of molecules between the luminal and the serosal compartments (Gumbiner, 1987). This junction also prevents the lateral diffusion of membrane proteins from one domain to another, thus maintaining their unique composition. Immediately basal to the tight junctions is the intermediate junction (zonula adherens or belt desmosomes). The other more basal junctional elements are desmosomes (maculae adherentes) and gap junctions, which attach the lateral membranes of adjacent cells to each other. The junctional complex is involved in sealing the epithelium; it prevents molecules from diffusing between adjacent cells. The basolateral membrane faces the bloodstream and is involved in cell–cell contact and cell adhesion to the basement membrane.

For most studies on epithelial cell polarity, cultured cells have been used. These cells are superior to cells obtained from tissues because they can be grown under carefully controlled conditions and are easily manipulated. The cell population is homogeneous. Biosynthetic experiments using pulse–chase techniques with radioactive precursors can be accomplished at an analytical level with a short time resolution. Endocytosis and transcytosis can also be studied.

The most well-studied epithelial cell is the Madin–Darby canine kidney (MDCK) cell. This cell line is derived from normal dog kidney (McRoberts *et al*., 1981). An unusual feature of these cells is that while in culture they retain many differentiated properties characteristic of kidney epithelial cells. Among these are an asymmetric distribution of enzymes and vectorial transport of sodium and water from the apical to the basolateral faces. The latter gives rise to "domes" or "blisters" in confluent cultures, which are transient areas where collected fluid has forced the monolayer to separate from the substratum. Morphologically, the cells resemble a typical cuboidal epithelium with microvilli on the apical side of the cells. Two different strains of the MDCK cell are known (Richardson *et al*., 1981; Balcarova-Ständer *et al*., 1984). Strain I cells are derived from a low-passage MDCK cell stock and these cells form a tight epithelium with transepithelial resistance above $2000\,\Omega\cdot cm^2$. Strain II cells form a monolayer of lower resistance of $100–200\,\Omega\cdot cm^2$. MDCK strain II cells have been used primarily for studies of the cell biology of epithelial cells. Transcytosis is, however, studied more conveniently in MDCK strain I cells because of their high electrical resistance.

Copyright 2006, Elsevier Science (USA).
All rights reserved.

Several factors are important for optimal expression of the epithelial phenotype *in vitro* (Simons and Fuller, 1985). A primary consideration is the polarity of nutrient uptake. *In vivo*, many nutrients reach the epithelial sheet from the basolateral side, which faces the blood supply; however, when epithelial cells are cultured on glass or plastic, they are forced to feed from the apical surface, which faces the culture medium. Hence, the basolateral surface becomes isolated from the growth medium as the monolayer is sealed by the formation of tight junctions. To grow properly, the epithelial sheet must remain somewhat leaky or expose basolateral proteins responsible for the uptake of nutrients and binding of growth factors on the apical side.

These problems can be overcome simply by growing the epithelial cells on permeable supports, such as polycarbonate and nitrocellulose filters. Epithelial cells form monolayers with a higher degree of differentiation when the basolateral surface is directly accessible to the growth medium. This is evident from the morphology of the cells, their increased responsiveness to hormones, and the exclusion of basolateral proteins from their apical surfaces.

II. MATERIALS AND INSTRUMENTATION

Minimal essential medium with Earle's salt (MEM) is purchased as a powder (Cat. No. 11700-077) from Biochrom, mixed with Milli-Q-filtered H_2O, and sterile filtered. Glutamine (200 m*M*, Cat. No. 25030-024), penicillin (10,000 IU/ml)–streptomycin (10,000 mg/ml) (Cat. No. 15140-122), trypsin (0.05%)–EDTA (0.02%) (Cat. No. 25300-054), and phosphate-buffered saline (PBS, Cat. No. 041-04040H) are from GIBCO-BRL. The Transwell polycarbonate filters (2.45 cm, Cat. No. 3412, and 10 cm, Cat. No. 3419) are from Costar. Tissue culture flasks (75 cm^2, Cat. No. 156499) are from Nunc. The glass petri dishes (140 mm diameter and 30 mm high) for holding six 2.4-cm Transwell filters are from Schott Glasware. The laminar flow hood (Steril-Gard Hood Model VMB-600) is from Baker. The CO_2 incubator (Model 3330) is from Forma Scientific. The inverted Diavert microscope is from Leitz. The electrical resistance measuring device (EVOM) is from World Precision Instruments. The centrifuge (Type 440) is from Hereaus-Christ.

III. PROCEDURES

A. Growing Madin–Darby Canine Kidney Cells on Plastic

MDCK I and II cells are passaged every 3–4 days up to 25 passages. One flask is usually split into five new flasks. MDCK II cells usually form domes within 2 days of splitting, whereas MDCK I cells do not blister.

Solutions

1. *MEM growth medium*:

	Stock	Volume/liter
5% fetal calf serum (MDCK II)	100%	50 ml
10% fetal calf serum (MDCK I)	100%	100 ml
2 m*M* glutamine	200 m*M*	10 ml
100 IU/ml penicillin 100/µg/ml streptomycin	100X	10 ml

2. *Phosphate-buffered saline*
3. *0.05% trypsin/0.02% EDTA*

Steps

1. Wash hands and wipe laminar flow hood with 70% ethanol. Warm all solutions to 37°C. All manipulations are done in the laminar flow hood. When splitting the cells, remove the growth medium from the 75-cm^2 flasks containing the confluent layer of MDCK cells and add 10 ml PBS. Rinse and discard wash solution.

2. Add 5 ml trypsin–EDTA solution, seal flask, and incubate for 10–15 min at room temperature (until small patches of cells are rounded up but not yet detached from the flask).

3. Remove the trypsin–EDTA solution and add 1.5 ml of fresh trypsin–EDTA. Reseal the flask and incubate at 37°C for 10–15 min (MDCK II) or 25–30 min (MDCK I). At this point the cells should flow down to the bottom of the flask when the flask is turned up. Hit the flask hard against the palm of your hand.

4. Add 10 ml prewarmed MEM growth medium and resuspend the cells with a sterile 10-ml pipette (at least five times up and down). Using the inverted microscope, check that the cells are not sticking to each other.

5. Plate 2 ml of the cell suspension in a new 75-cm^2 flask containing 20 ml of MEM growth medium.

B. Seeding MDCK Cells on Polycarbonate Filters

Solutions

1. *MEM growth medium containing 10% fetal calf serum, penicillin-streptomycin, and 2 mM glutamine* (see solution A1).
2. *Phosphate-buffered saline*
3. *0.05% trypsin/0.02% EDTA*

Steps

1. Seed the cells on the filters at high density, higher than that achieved by confluent cells on plastic. The cells form tight junctions within 24 h and reach maximum tightness on the filters in 4 days. During this time cell density increases to more than five times that achieved on plastic. We place the filters in the petri dishes containing growth medium. For seeding we use one 75-ml flask, containing a confluent layer of MDCK I and II cells, for 2.4-cm-diameter filters (Transwell 3412). If you use large 10-cm-diameter filters (Transwell 3419), seed one 75-cm^2 culture flask of MDCK cells into each large filter.

2. Pour off medium from the culture flask and rinse cells with 10 ml of warm PBS. Pour off PBS.

3. Add 5 ml of warm trypsin–EDTA to cells. Leave in laminar flow hood.

4. After 15 min remove the trypsin–EDTA with a pipette, add 1.5 ml of trypsin–EDTA, and put the flask into a CO_2 incubator (37°C) for 10–15 min (MDCK II) or 25–30 min (MDCK I).

5. Remove flask (cells should be loose). Hit the flask hard against your palm. Add 10 ml of warm growth medium and suspend cells by pipetting up and down with a 10-ml pipette. Put suspension into a 50-ml Falcon tube and centrifuge for 5 min at 1000 rpm in a Hereaus-Christ centrifuge.

6. Remove supernatant and suspend cells in 9.5 ml of growth medium.

7. Pour 90 ml medium into glass petri dish containing six Transwell 3412 filters. Use 140 ml for one Transwell 3419 filter. The petri dishes contain filter holders specially made to fit either 3412 or 3419 filters (Fig. 1). Autoclave these units before use. Place filters into filter holders and allow filters to get wet from the bottom with medium. This should be done while the cells are in the centrifuge.

8. Add 1.5 ml of cell suspension to each filter in its holder. Use six Transwell 3412 filters or one Transwell 3419 filter per petri dish. Be careful not to spill cells over the edge of the filter holder.

9. Swirl petri dish gently to remove any trapped air from beneath filters.

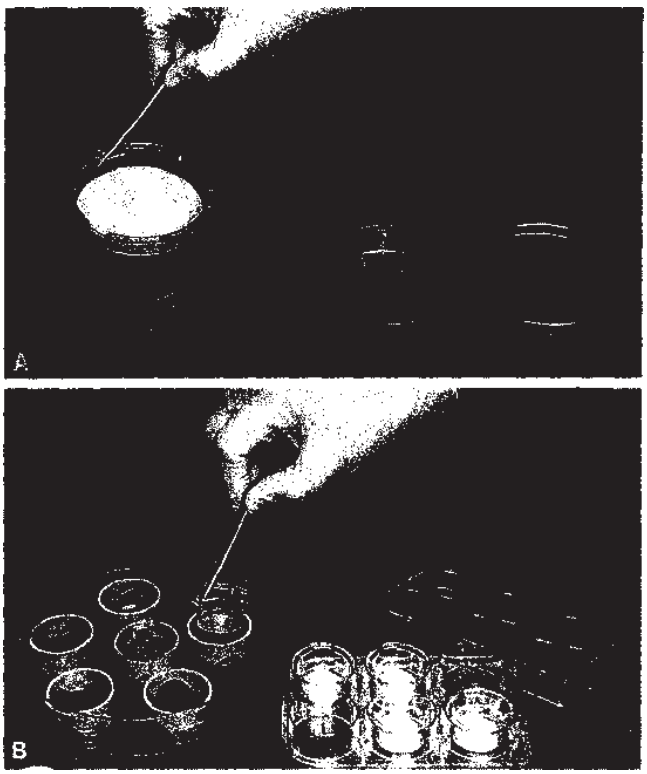

FIGURE 1 (A) The glass petri dish contains one filter holder for one Transwell 2419 filter. (B) The glass petri dish contains six filter holders for Transwell 3412 filters.

10. Place the petri dish with the filters in the CO_2 incubator.

11. Leave for 3–4 days in the incubator. No medium change is required during this time.

C. Transepithelial Resistance Measurement

Steps

1. Transepithelial resistance of filter-grown MDCK cells is measured with EVOM "chop-stick" electrodes. Each leaf has an outer and an inner electrode. The outside electrodes are small silver pads for passing current through the membrane sample. Inside the electrodes are small Ag/AgCl voltage sensors.

2. To test the instrument, switch the mode switch to R and turn the power on. Push the test R button. With the range switch in the 2000-V position, the meter will read 1000 (±1 digit). In the 20-k range, the meter will read 1.00. The meter is now ready for use.

3. To test the electrodes, insert the small telephone-type plug at the end of the chopsticks electrode cable into the jack on the front panel of the EVOM. Place the

tips of the electrodes into 0.1 *M* KCl. Switch the mode switch to Volts. Turn the power switch on. The digital panel meter may read 1 or 2 mV due to the asymmetry of the voltage sensor pair. After 15 min, adjust this voltage to 0 mV with the screwdriver adjustment labeled "Zero V."

4. Measure resistance. The electrode set is designed to facilitate measurements of membrane voltage and resistance of cultured epithelia in culture cups by dipping one stick electrode inside the cup on top of the cell layer and the second stick electrode in the external bathing solution. To measure resistance, immerse the electrode pair again into the electrolyte and set the mode switch to "Ohm." The display should read zero; if not, adjust the display to zero with the Ohms Zero screwdriver adjustment. Push the measure R button. A steady ohm reading of the resistance should result.[1]

Example

a. Measure resistance R from solution + sample membrane support	109
b. Measure resistance R from solution + membrane support + tissue	189
c. Subtract (a) from (b)	$189 - 109 = 80$, R (tissue) = 80 V
d. Calculate resistance × area product	resistance × area $= 1.2\,\text{cm} \times p \times r^2$ $= 80\,\text{V} \times 3.14 \times (1.2\,\text{cm})^2$ $= 361.9\,\text{V cm}^2$

5. When moving the electrodes from one dish to another it is best not to rinse the electrodes with distilled water. If it is necessary to wash the electrodes between measurements, they should be rinsed with the membrane perfusate (e.g., PBS). Do not touch the cell layer with the internal electrode when making a measurement. Small differences in the apparent fluid resistance may occur if the depth to which the electrodes' tips are immersed varies. If the tips are unusually dirty, a light and very brief sanding with a fine nonmetallic abrasive paper will clean the sensor tip. For sterilization the electrodes may be soaked in alcohol or bactericides. After sterilization, the electrodes should be rinsed extensively with sterile perfusing solution or 1 *M* KCl.

[1] If the electrode asymmetry potential difference exceeds the zero adjustment range, the central electrodes may be dirty or contaminated.

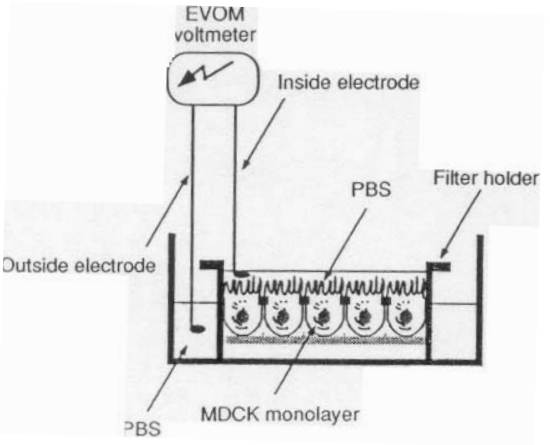

FIGURE 2 Scheme illustrating the setup for measuring electrical resistance. The stick designated for external use is slightly longer than its companion.

IV. COMMENTS

The cell layer on the filter cannot be observed in the inverted microscope because the filters are not transparent. Transparent filters are also available commercially' but they are more expensive than the polycarbonate ones; however, either the cells in one filter can be stained or the transepithelial resistance can be measured to ensure that the layer is intact. Our experience is that when one filter in the petri dish checks out, the other filters will also be fine.

It is recommended that MDCK cells not be used for more than 20–25 passages. New stock cells should then be thawed from liquid nitrogen storage.

We use filter holders for growing MDCK cells on either 2.4- or 10-cm polycarbonate filters. It is possible to grow cells in either the six-well plate for the Transwell 3412 filter or in the petri dish supplied with the Transwell 3419 filters. Under these latter culture conditions, growth media have to be changed every day, as the cells do not get enough nutrients and do not grow to optimal density. The problems with changing the medium every day are (1) the extra work involved and (2) the considerably increased risk of contamination. Therefore, we prefer to place filter holders in petri dishes into which one can add enough growth medium to last 4 days.

References

Balcarova-Stander, J., Pfeiffer, S. E., Fuller, S. D., and Simons, K. (1984). Development of cell surface polarity in the epithelial Madin-Darby canine kidney (MDCK) cell line. *EMBO J.* **3**, 2687–2694.

Gumbiner, B. (1987). Structure, biochemistry and assembly of epithelial tight junctions. *Am. J. Physiol.* **253**, C749–C758.

McRoberts, J. A., Taub, M., and Saier, M. H., Jr. (1981). The Madin-Darby canine kidney (MDCK) cell line. *In* "*Functionally Differentiated Cell Lines*" (G. Sato, ed.), pp. 117–139. A. R. Liss, New York.

Richardson, J. C. W., Scalera, V., and Simmons, N. L. (1981). Identification of two strains of MDCK cells which resemble separate nephron tubule segments. *Biochim. Biophys. Acta* **673**, 26–36.

Simons, K., and Fuller, S. D. (1985). Cell surface polarity in epithelia. *Annu. Rev. Cell. Biol.* **1**, 243–288.

CHAPTER

16

Cultivation and Retroviral Infection of Human Epidermal Keratinocytes

Fiona M Watt, Simon Broad, and David M Prowse

I. INTRODUCTION

There are many techniques for culturing human epidermal keratinocytes, but the method described here is the one devised by Rheinwald and Green (1975). With this method, keratinocytes grow as multilayered sheets in which proliferation is confined to the basal layer and terminal differentiation takes place in the suprabasal layers, thus mimicking the spatial organization of normal interfollicular epidermis. These cultures have a range of applications in basic research and in the clinic. They are used to study the factors that regulate stem cell proliferation, terminal differentiation, and tissue assembly, as well as the events that take place during neoplastic transformation (Jones and Watt, 1993; Zhu and Watt, 1996; Levy *et al*., 2000; Dajee *et al*., 2003). Practical applications include the treatment of burns victims with cultured autografts (Compton *et al*., 1989; Ronfard *et al*., 2000) and the use of transduced keratinocytes as vehicles for gene therapy (Gerrard *et al*., 1993; Dellambra *et al*., 2001; Ortiz-Urda *et al*., 2002).

What follows is a description of the procedures our laboratory uses to initiate and maintain cultures of keratinocytes from neonatal foreskins; it is based on the original Rheinwald and Green method, improved over the years as described by Rheinwald (1989). The key component of the culture system is the presence of a feeder layer of 3T3 cells that supports the growth of keratinocytes from clonal seeding densities (see Fig. 1). In the laboratory, our preferred method for manipulating gene expression in keratinocytes is by retroviral infection (Zhu and Watt, 1996; Levy *et al*., 1998; Zhu and Watt, 1999) and we have therefore included our current protocol.

II. MATERIALS AND INSTRUMENTATION

FAD powder [three parts Dulbecco's modified Eagle's medium (DMEM) and one part Ham's F12 medium (F12) supplemented with $1.8 \times 10^{-4} M$ adenine] is custom made by Bio Whittaker. Alternatively, F12 (liquid, Cat. No. 41966-029) and DMEM (liquid, Cat. No. 21765-029) can be bought separately from Invitrogen, and adenine can be purchased from Sigma Aldrich Co. Ltd (Cat. No. A3159). Penicillin and streptomycin can be purchased from Invitrogen (Cat. No.15070-063). A suitable supplier of foetal calf serum (FCS) and bovine serum (BS) is Invitrogen. Hydrocortisone (Cat. No. 386698) and cholera enterotoxin (Cat. No. 227036) are purchased from Merck Biosciences Ltd. Cholera enterotoxin is from ICN Biomedicals Ltd. (Cat. No. 190329). Epidermal growth factor (EGF) is purchased from Peprotech EC Ltd. (Cat. No. 100 15). Insulin is from Sigma Aldrich Co. Ltd. (Cat. No. I5500). Mitomycin C is also obtained from Sigma Aldrich Co. Ltd (Cat. No. M0503). Trypsin (0.25%) (Cat. No. M0503) and 0.02% EDTA (Cat. No. 15040-033) can be obtained from Invitrogen. Mikrozid is purchased from Schulke & Mayer UK Ltd. Dimethyl sulfoxide (DMSO, Cat. No. 10323) is obtained from VWR International Ltd. CelStirs are made by Wheaton, USA (Cat. No. 356873; Wheaton products are available through Jencons Scientific Ltd.). Cryotubes are purchased from Alpha Laboratories Ltd. UK (Cat. No. LW 3435). Puromycin (Cat. No. P8833), chloroquine (Cat. No. C6628), polybrene (Cat. No. H9268), HEPES (Cat. No. H7006), and calcium chloride (Cat. No. C5080) are from Sigma-Aldrich Co. Ltd. Collagen-coated dishes are purchased from BD Biosciences. Hygromycin B

Copyright 2006, Elsevier Science (USA).
All rights reserved.

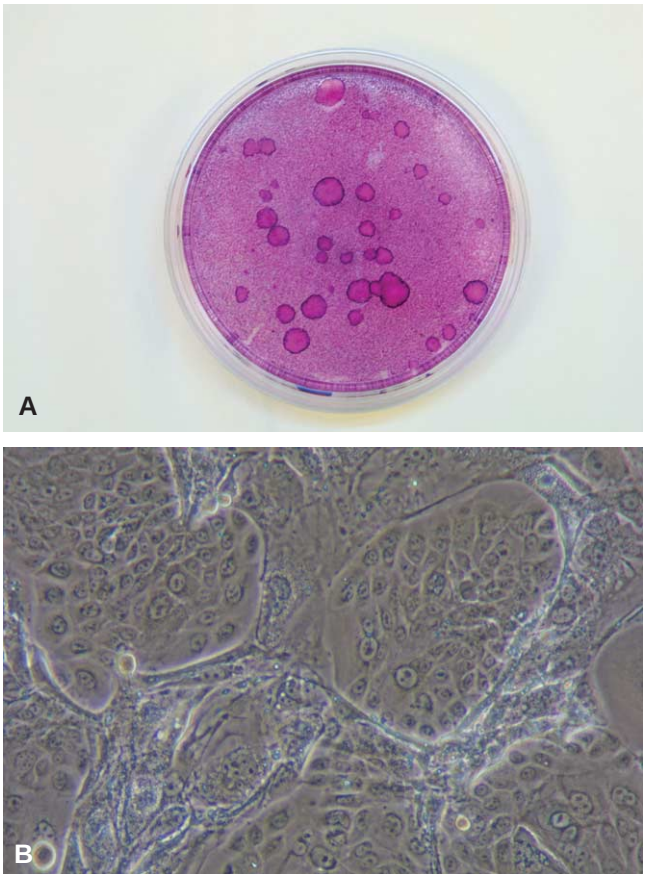

FIGURE 1 (A) Dish of cultured human keratinocytes plated on a feeder layer of 3T3 J2 cells and stained with rhodanile B. Individual clones of keratinocytes are seen as large round plaques. (B) Phase-contrast view of clones of cultured human keratinocytes on a feeder layer of 3T3 J2 cells.

(Cat. No. 10687 010) is from Invitrogen and diphtheria toxin (Cat. No. 322326) can be purchased from Merck Biosciences Ltd.

III. PROCEDURES

A. Feeder Layer

1. Solutions

1. *Culture medium for 3T3 J2 cells*: This consists of DMEM supplemented with 100 IU/ml penicillin, 100 µg/ml streptomycin, and 10% bovine serum. It is essential to batch test the serum for optimal growth of 3T3 J2.

2. *Trypsin–EDTA*: Mix one part 0.25% trypsin and four parts 0.02% EDTA. The same solution is used to harvest keratinocytes.

3. *Phosphate-buffered saline*: To make 1 litre, dissolve 0.2 g KCl, 0.2 g KH_2PO_4, 8.0 g NaCl, and 2.16 g $Na_2HPO_4 \cdot 7H_2O$ in 900 ml distilled water. Adjust pH to 7.4, add distilled water to 1-litre final volume, autoclave, and store at room temperature.

4. *Mitomycin C in PBS*: Prepare a stock solution of 0.4 mg/ml in PBS. Filter sterilize and store in aliquots at –20°C.

1. Cells

The J2 clone of random-bred Swiss mouse 3T3 cells was selected to provide optimal feeder support of keratinocytes (Rheinwald, 1989). The cells are maintained by weekly passaging at 1:10 to 1:20 dilution. Fresh cells are thawed every 3 months, as with prolonged passaging the cells start to senesce or undergo spontaneous transformation.

2. Preparing the Feeder Layer

Steps

1. To irreversibly inhibit proliferation, add mitomycin C (final concentration, 4 µg/ml) to confluent flasks of 3T3 J2 and incubate for 2 h at 37°C.

2. Remove the medium, rinse the cells once with 0.02% EDTA, and then harvest in trypsin–EDTA. The optimal density of the feeder layer is one-third confluent (Rheinwald and Green, 1975; Rheinwald, 1989); hence each mitomycin C-treated flask is split 1:3.

3. The feeders can be used immediately (i.e., plated at the same time as the keratinocytes) or prepared 1–2 days before they are required; if prepared in advance, maintain in DMEM + 10% BS. The feeder layer should not be prepared more than 2 days before use because the feeder cells will start to degenerate.

B. Keratinocyte Culture Medium

Solutions

1. *Hydrocortisone*: Prepare a 5 mg/ml stock in absolute ethanol. Store at –20°C.
2. *Cholera enterotoxin*: Prepare a 10^{-5} *M* stock in distilled water. Store at 4°C.
3. *EGF*: Prepare at 100 µg/ml stock in FAD + FCS. Store at –20°C.
4. *Insulin*: Prepare a 5 mg/ml solution in 5 m*M* hydrochloric acid. Store at –20°C.

Steps

1. The basic medium consists of three parts DMEM and one part F12 supplemented with 1.8×10^{-4} *M* adenine (FAD), 100 IU/ml penicillin, and 100 µg/ml streptomycin. Store at 4°C.

2. Supplement FAD with 10% FCS. It is essential to batch test the serum for its ability to support high colony-forming efficiency, rapid growth, and serial passage of keratinocytes. Serum batches optimal for keratinocytes tend to be completely unsuitable for

fibroblastic cells or hybridomas. Store FCS at –20°C before use.

3. Supplement FAD + FCS further with a HICE cocktail consisting of hydrocortisone (0.5 µg/ml), insulin (5 µg/ml), cholera enterotoxin (10^{-10} *M*), and EGF (10 ng/ml) (all final concentrations).

4. Store complete medium (FAD + FCS + HICE) at 4°C and use within 1 week.

C. Source of Keratinocytes

The usual source of keratinocytes is neonatal foreskin obtained, with ethical approval, from routine circumcisions. When handling any human tissue it is essential to take appropriate precautions against the transmission of infectious agents. Obtain the foreskin as soon as possible after circumcision and transfer to the laboratory dry in a sterile Bijou. If it cannot be used immediately, store overnight at 4°C.

D. Isolation of Keratinocytes

Solutions

1. *PBS containing 100 IU/ml penicillin and 100 µg/ml streptomycin.* Other solutions are as described in Sections III,A and III,B.

Steps

1. Rinse the foreskin thoroughly in PBS containing 100 IU/ml penicillin and 100 µg/ml streptomycin.
2. Transfer the tissue to a 100-mm-diameter petri dish, epidermis down. Remove as much connective tissue (muscle and dermis) as possible using sterile curved scissors.
3. Transfer the epidermis and remaining connective tissue to a fresh dish and chop into fine pieces (1–3 mm^2) using scalpels.
4. Flood the dish with 10 ml trypsin–EDTA and transfer the solution containing pieces of skin with a wide-bore pipette to a sterile CelStir. A CelStir is an autoclavable glass vessel containing a magnet suspended by a rod from the lid. Solutions are introduced and removed via a side arm in the vessel.
5. Incubate the CelStir at 37°C for 30 min on a magnetic stirrer; allow the lumps of tissue to settle out and remove the supernatant.
6. Add fresh trypsin–EDTA and repeat the procedure.
7. Determine the number of cells in the supernatant with a haemocytometer. Collect the cells by centrifugation and resuspend in FAD + FCS + HICE. There are usually no cells from the first incubation and then 1–5 $\times 10^6$ cells per subsequent incubation.
8. After four or five incubations the cell yield starts to decline; discard any remaining lumps of tissue.
9. Pool cells from each incubation and seed onto the feeder layer at a density of 5×10^5 per 75-cm^2 flask. The average yield per foreskin is approximately $5 \times 10^6 - 10^7$ cells.
10. After 2–3 days, small colonies of keratinocytes are visible, surrounded by 3T3 J2 feeder cells. Over the following weeks, individual colonies expand, displacing the feeder layer and merging with one another. At confluence, virtually no feeder cells remain. Feed the cells with fresh medium three times per week.

E. Passaging Keratinocytes

Solutions are as described in Sections III,A and III,B.

Steps

1. Passage keratinocytes prior to confluence (approximately 7–10 days after plating). Remove the medium and rinse the cultures once with 0.02% EDTA.
2. Add fresh EDTA and incubate the cultures at 37°C for about 5 min. Then selectively detach the feeders by gentle aspiration with a pipette (Rheinwald, 1989).
3. To detach the keratinocytes, add tryspin–EDTA (see Section III,A, solution 2) to the flasks and incubate at 37°C for about 10 min.
4. Transfer the cells to a centrifuge tube; use a small volume of culture medium to rinse the flask and then add it to the tube, inactivating the trypsin.
5. Recover the cells by centrifugation, count in a haemocytometer, and resuspend in complete medium.
6. Cells can be passaged at a density of 1–2 $\times 10^5$ per 75-cm^2 flask containing 3T3 J2 feeders.

F. Frozen Stocks of Keratinocytes and 3T3 J2 Cells

Solution

1. *10% DMSO/90% fetal calf serum*

Steps

1. Most of the primary keratinocyte cultures are used to prepare frozen stocks; most experiments are carried out on second and subsequent passages.
2. For freezing, harvest the keratinocytes as described earlier, but resuspend at 10^6/ml in 10% DMSO/90% foetal calf serum.
3. Place 1 ml of cell suspension in each 1.8-ml CryoTube.

4. Place the tubes in a rubber rack wrapped in cotton wool overnight at –70°C and then transfer to liquid nitrogen
5. Freeze the 3T3 J2 cells in the same way.

G. Preparation of Stable Packaging Lines for Retroviral Vectors

Solutions

1. *Culture medium for packaging lines*: This consists of DMEM supplemented with 100 IU/ml penicillin, 100 µg/ml streptomycin, and 10% heat-inactivated foetal calf serum. The serum is heat inactivated in a water bath at 56°C for 45 min and can then be stored frozen in aliquots. Heat inactivation of FCS improves retroviral titres.

2. *Transfection solutions*: 50 m*M* chloroquine (2000×) in dH_2O, 2 *M* $CaCl_2$ in dH_2O, and 2xHBS, pH 7.0. Filter sterilise each solution, aliquot, and store at –20°C.

3. *2xHBS*: This is made up with 8.0 g NaCl, 6.5 g HEPES, and 10 ml Na_2HPO_4 stock solution (5.25 g in 500 ml of water). Adjust the pH to 7.0 using NaOH or HCl, bring the volume up to 500 ml, and check the pH again.

4. *Polybrene*: Prepare a 5 mg/ml stock solution in PBS. Filter sterilise, aliquot, and store at –20°C.

5. *Puromycin*: Prepare a 2 mg/ml stock solution in PBS. Filter sterilise, aliquot, and store at –20°C.

Cells

Phoenix E (ecotropic) packaging cells (Swift *et al*., 1999) are obtained from ATCC with prior approval of G. Nolan (Stanford University, USA). The AM12 amphotropic packaging line was generated by Markowitz *et al*. (1988). Packaging cells are maintained by passage at 1:5 (Phoenix E) or 1:10 (AM12) dilution. For optimal virus production, Phoenix cells should initially be reselected sequentially for 4 weeks, 2 weeks in 1 µg/ml diphtheria toxin, and then two weeks in 500 µg/ml hygromycin to increase Envelope and Gag-Pol expression (http://www.stanford.edu/group/nolan/index.html). Packaging cells are frozen at 10^6/ml in 10% DMSO/90% foetal calf serum as described (in Section III, F,) and fresh cells are thawed every 3 months. J2 puro are 3T3 J2 cells that have been transfected with pBabe puro to render them resistant to puromycin (Levy *et al*., 1998).

Generation of Stably Transduced AM12 Cells

Packaging lines that are generated by retroviral infection tend to have higher viral titres than those generated by transfection (Levy *et al*., 1998). Therefore, we use a two-step procedure in which Phoenix E cells are transiently transfected with retroviral vector, and packaged virus released by Phoenix E cells is used to infect AM12 cells.

Steps

1. Twenty-four hours prior to transfection, plate 5×10^6 Phoenix E cells into one 10-cm-diameter petri dish in 10 ml medium.

2. Add chloroquine (final concentration 25 µ*M*) to each plate 5 min before transfection. Add 20 µg retroviral vector DNA (we routinely use pBabe puro; Morgenstern and Land, 1990; Levy *et al*., 1998) to 61 µl 2 *M* $CaC1_2$ and make up to a 500 µl total volume with ddH_2O. Add 500 µ1 2xHBS quickly and then bubble vigorously with an automatic pipettor for 15 s. Add the HBS/DNA solution dropwise into the Phoenix E culture dish and then rock the plate gently a few times to distribute DNA/$CaPO_4$ particles evenly. Transfer the plate to a 37°C incubator.

3. Twenty-four hours posttransfection, change the culture medium. Gently add 6 ml of fresh medium per 10 cm plate. Leave cells overnight in a 32°C incubator; retroviruses are more stable at 32°C than at 37°C. In addition, seed 2×10^5 AM12 cells per 10 cm plate in 10 ml medium and incubate overnight at 37°C.

4. The next day (i.e., 48 h posttransfection) harvest virus by collecting the medium from Phoenix E cultures. Gently add fresh medium to cells and harvest virus again 8 h later. Add fresh medium for a third time, incubate the cells overnight at 32°C, and collect the medium. All three supernatants contain active virus. Each viral supernatant should be filtered using a 0.45-µm filter on collection and either used immediately (i.e., added to AM12 cells) or stored at –80°C (titre will halve on each freeze/thaw cycle).

5. Virus harvested from Phoenix E cells is used to infect AM12 cells. Remove 8 ml medium from the AM12 culture. Add 5 µl polybrene (5 mg/ml) and 3 ml viral supernatant to each plate (5 ml total volume), shake gently, and place in a 32°C incubator for 24 h.

6. Twenty-four to 48 h postinfection the AM12 cells are 60–80% confluent and are ready to be selected by adding 2 µg/ml puromycin to the medium. Change medium every 2–3 days. Once the cells are confluent, passage them, prepare frozen cell stocks, and use the rest to infect keratinocytes.

7. For some applications, AM12 are subjected to further selection to achieve maximal viral titres. This can be achieved by either cloning at limiting dilution or, if there is a suitable surface marker, FACS sorting of bulk populations. Both methods have been described previously (Levy *et al*., 1998).

H. Retroviral Infection of Cultured Human Keratinocytes Using Viral Supernatant

J2 puro are 3T3 J2 cells that have been stably transfected with pBabe puro to render them resistant to puromycin (Levy *et al*., 1998). They are handled in the same way as 3T3 J2 cells, except that the medium is supplemented with 2 µg/ml puromycin.

Steps

1. Grow infected AM12 packaging cells to 95% confluence and transfer to keratinocyte culture medium. Collect virus over a 24- to 48-h period at 32°C, harvesting virus every 8–12 h and replacing with fresh medium. The virus should be filtered through a 0.45-µm filter on collection and either used immediately or stored at –80°C (titre will halve on each freeze/thaw cycle).
2. Keratinocytes with the greatest proliferative potential (putative stem cells) can be enriched by rapid adhesion to collagen (Jones and Watt, 1993). Selection of keratinocytes on collagen prior to infection increases the retroviral infection efficiency to 60–80%. Harvest subconfluent keratinocytes, first removing the 3T3 J2 feeders. Plate 2×10^6 keratinocytes per 10-cm collagen-coated plate (or equivalent plating density if smaller dishes are used). Allow cells to adhere for 15–20 min. Wash gently with PBS and add fresh keratinocyte medium and mitomycin C-treated J2 puro cells. The final volume of medium should be 10 ml per 10-cm dish. Incubate cells overnight at 37°C.
3. The next day, remove 8 ml of medium and add 3 ml of retrovirus supernatant and 5 µl polybrene (5 mg/ml).
4. Incubate cells overnight at 32°C. The next day remove virus containing medium and add fresh keratinocyte medium.
5. Infected keratinocytes are ready to use or can be transferred to puromycin containing medium and passaged 24 h later.

Retroviral Infection of Cultured Human Keratinocytes by Coculture with Packaging Line

Steps

1. Prepare AM12 by treatment with mitomycin C in the same way as for 3T3 J2 cells (Section III,A).
2. Plate keratinocytes in the same way as when plating on 3T3 J2 cells (Section III,E). Use complete keratinocyte medium.
3. After 2–3 days remove AM12, with EDTA treament, as for 3T3 J2 cells (Section III,E). Add mitomycin C-treated J2 puro and supplement the culture medium with puromycin.

IV. COMMENTS

It is possible to obtain up to 100 population doublings of neonatal foreskin keratinocytes prior to senescence (Rheinwald, 1989). The number of passages prior to senescence varies between cell strains: 5 is the minimum, 10 is the average, and greater than 20 is the maximum.

The same basic culture procedure can be used to grow keratinocytes from adult epidermis (although the number of population doublings obtained will be somewhat reduced) and from other stratified squamous epithelia, such as the lining of the mouth and the exocervix (Rheinwald, 1989).

Methods for transfecting Phoenix cells and retrovirally infecting AM12 cells are based on those of Swift *et al*. (1999; http://www.stanford.edu/group/nolan/index.html). We routinely use the pBabe puro retroviral vector (Morgenstern and Land, 1990). Puromycin is the optimal drug for selection, as it is not toxic to transduced keratinocytes and kills nontransduced cells within 2–4 days (Levy *et al*., 1998). Following culture and selection, the proportion of stably transduced cells obtained with the supernatant and coculture methods are equal (>90%). The advantage of the supernatant method is that large numbers of cells are infected simultaneously; however, with the coculture method, fewer keratinocytes are required initially.

V. PITFALLS

1. Under the conditions described, fibroblast contamination of keratinocytes is very rarely a problem because the feeder layer and culture medium suppress the growth of any human fibroblasts isolated from the skin at the same time as the keratinocytes (Rheinwald, 1975). We have noted that some strains of keratinocytes contain ndk-like (for nondifferentiating keratinocyte; see Adams and Watt, 1988) epithelial cells, but these cells are not abundant and can usually be removed with EDTA.
2. When keratinocytes are plated in culture there is selective attachment of the basal cells, but within 1 day the cultures consist of a mixture of basal and terminally differentiating keratinocytes (e.g., Jones and Watt, 1993). Seeding keratinocytes at high density appears, in our experience, to promote terminal differentiation and is not, therefore, the answer if you are in a hurry to obtain more cells.
3. Because keratinocytes are maintained in culture for long periods it is essential to be scrupulous in sterile technique and laboratory cleanliness to avoid

fungal or bacterial contamination. We spray our incubators three times a week with Mikrozid.

4. It is essential to be well organised and to plan your experiments in advance. It takes about 10 days from plating for keratinocytes to be ready for use and sufficient feeders must be available on the days when keratinocytes are ready for passaging.

5. Use of an amphotropic retrovirus is potentially hazardous because the virus can infect human cells. Special care should therefore be taken and appropriate local safety guidelines followed.

References

Adams, J. C., and Watt, F. M. (1988). An unusual strain of human keratinocytes which do not stratify or undergo terminal differentiation in culture. *J. Cell Biol.* **107**, 1927–1938.

Compton, C. C., Gill, J. M., Bradford, D. A., Regauer, S., Gallico, G. G., and O'Connor, N. E. (1989). Skin regenerated from cultured epithelial autografts on full-thickness burn wounds from 6 days to 5 years after grafting: A light, electron microscopic and immunohistochemical study. *Lab. Invest.* **60**, 600–612.

Dajee, M., Lazarov, M., Zhang, J. Y., Cai, T., Green, C. L., Russell, A. J., Marinkovich, M. P., Tao, S., Lin, Q., Kubo, Y., and Khavari, P. A. (2003). NF-KB blockade and oncogenic Ras trigger invasive human epidermal neoplasia. *Nature* **421**, 639–643.

Dellambra E., Prislei, S., Salvati, A. L., Madeddu, M. L., Golisano, O., Siviero, E., Bondanza, S., Cicuzza, S., Orecchia, A., Giancotti, F. G., Zambruno, G., and De Luca, M. (2001). Gene correction of integrin β4-dependent pyloric atresia-junctional epidermolysis bullosa keratinocytes establishes a role for β4 tyrosines 1422 and 1440 in hemidesmosome assembly. *J Biol Chem*. **276**, 41336–41342.

Gerrard, A. J., Hudson, D. L., Brownlee, G. G., and Watt, F. M. (1993). Towards gene therapy for haemophilia B using primary human keratinocytes. *Nature Genet.* **3**, 180–183.

Jones, P. H., and Watt, F. M. (1993). Separation of human epidermal stem cells from transit amplifying cells on the basis of differences in integrin function and expression. *Cell* **73**, 713–724.

Levy, L., Broad, S., Diekmann, D., Evans, R. D., and Watt, F. M. (2000). β1 integrins regulate keratinocyte adhesion and differentiation by distinct mechanisms. *Mol. Biol. Cell*. **11**, 453–466.

Levy, L., Broad, S., Zhu, A. J., Carroll, J. M., Khazaal, I., Péault, B, and Watt, F. M. (1998). Optimised retroviral infection of human epidermal keratinocytes: Long-term expression of transduced integrin gene following grafting on to SCID mice. *Gene Ther.* **5**, 913–922.

Markowitz, D., Goff, S., and Bank, A. (1988). Construction and use of a safe and efficient amphotropic packaging cell line. *Virology*. **167**, 400–406.

Morgenstern, J. P., and Land, H. (1990). Advanced mammalian gene transfer: High titre retroviral vectors with multiple drug selection markers and a complementary helper-free packaging cell line. *Nucleic Acids Res*. **18**, 3587–3596.

Ortiz-Urda, S., Thyagarajan, B., Keene, D. R., Lin, Q., Fang, M., Calos, M. P., and Khavari, P. A. (2002). Stable nonviral genetic correction of inherited human skin disease. *Nature Med*. **8**, 1166–1170.

Rheinwald, J. G. (1989). Methods for clonal growth and serial cultivation of normal human epidermal keratinocytes and mesothelial cells. *In "Cell Growth and Division: A Practical Approach"* (R. Baserga, ed.) pp. 81–94. IRL Press, Oxford.

Rheinwald, J. G., and Green, H. (1975). Serial cultivation of strains of human epidermal keratinocytes: The formation of keratinizing colonies from single cells. *Cell* **6**, 331–343.

Ronfard, V., Rives, J. M., Neveux, Y., Carsin, H., and Barrandon, Y. (2000). Long-term regeneration of human epidermis on third degree burns transplanted with autologous cultured epithelium grown on a fibrin matrix. *Transplantation* **15**, 1588–1598.

Swift, S. E., Lorens, J. B., Achacoso, P., and Nolan, G. P. (1999). Rapid production of retrovirus for efficient gene delivery to mammalian cells using 293T cell-based systems. *In "Current Protocols in Immunology"* (J. E. Coligan, A. M. Kruisbeek, D. H. Margulies, E. M. Shevach, and W. Strober, eds.), Vol 1. 17C, pp: 1–17. *Wiley, New York*.

Zhu, A. J., and Watt, F. M. (1996). Expression of a dominant negative cadherin mutant inhibits proliferation and stimulates terminal differentiation of human epidermal keratinocytes. *J. Cell Sci*. **109**, 3013–3023.

Zhu, A. J., and Watt, F. M. (1999). β-Catenin signalling modulates proliferative potential of human epidermal keratinocytes independently of intercellular adhesion. *Development* **126**, 2285–2298.

CHAPTER

17

Three-Dimensional Cultures of Normal and Malignant Human Breast Epithelial Cells to Achieve *in vivo*-like Architecture and Function

Connie Myers, Hong Liu, Eva Lee, and Mina J. Bissell

I. INTRODUCTION

Apicobasal polarity, properly positioned cell–cell contacts, and attachment to basement membrane are fundamental characteristics of simple glandular epithelia, such as the mammary gland. The development and maintenance of this polarized structure are essential for the formation of tissue architecture, control of proliferation, and the differentiated function of epithelial cells (Roskelley *et al.*, 1995). Loss of architectural intactness and polarity is one of the pathological hallmarks of epithelial carcinoma (Bissell and Radisky, 2001). Although traditional studies of epithelial cells grown as a monolayer on tissue culture plastic remain a powerful tool to dissect and understand the molecular events of signaling machineries, tissue culture plastic does not recapitulate the microenvironment or morphology of glandular epithelium *in vivo*. Animal models have provided us with invaluable insights, which have led to a greater understanding of the events involved in mammary morphogenesis and tumorigensis *in vivo*, and aid in the translation from basic cellular research into clinical application. However, the complexity of animal model systems prevents us from precisely pinning down the specific biochemical and cell biological pathways involved in mammary morphogenesis and tumor formation. Therefore an *in vitro* cell-based model system that provides epithelial cells with an *in vivo*-like microenvironment, recapitulates both the three-dimensional (3D) organization and multicellular complexity, and is conducive to systematic experimental pertubation is optimal to bridge the gaps between epithelial monolayer cultures and animal models.

We have developed an assay in which primary or phenotypically normal human breast epithelial cells cultured in a laminin-rich basement membrane (lrBM) undergo a three-dimensional reorganization to form structures that mimic *in vivo* acinar structures in culture (Petersen *et al.*, 1992). LrBM, available commercially as Matrigel, is a mixture of basement membrane proteins that include ~80% laminin, ~10% type IV collagen, entactin, and ~10% heparin sulfate proteoglycan, derived from Engelbreth–Holm–Swarm mouse tumor (Orkin *et al.*, 1977; Kleinman *et al.*, 1986, 1987). The malleability of this specialized gel and its ability to signal through integrins, as well as other ECM receptors, induce changes in the cells, which allow them to withdraw from the cell cycle, organize, and form a central lumen. The entire acinar structures achieve apical basal polarity, and cells within the acini express tissue-specific genes, processes that are not easily accomplished by the same cells cultured on conventional tissue-culture plastic. We refer to the assay as 3D BM assay. The following are advantages of 3D BM assays in studying normal and malignant cells. (1) Because the cells are able to form tissue-like structures, mechanisms of tissue specificity can be studied *ex vivo*. These cultures are amenable to a variety of perturbations and manipulations that can be used to understand how cells may signal *in vivo*. (2) The assay allows

Copyright 2006, Elsevier Science (USA).
All rights reserved.

breast tumor cells to be distinguished easily from their nonmalignant counterparts because the tumor cells fail to stop proliferating and do not become organized into tissue-like structures (Petersen *et al*., 1992; Weaver *et al*., 1996). (3) Addition of specific signaling inhibitors or blocking antibodies or delivery of genes to the tumorgenic cells can be used to analyze signaling pathways involved in the acquisition of the nontumorgenic phenotype (Weaver *et al*., 1997; Wang *et al*., 1998, 2002). (4) The 3D BM cultures can be used to understand the novel roles of oncogenes and tumor supressors genes (Howlett *et al*., 1994; Spancake *et al*., 1999; Muthuswamy *et al*., 2001; Debnath *et al*., 2002). (5) These assays can assess the response of tumorigenic vs nontumorigenic cells to potential therapeutics and unravel novel mechanisms (Weaver *et al*., 2002). (6) The assays (3–10 days) can be performed rapidly and in a high throughput manner relative to costly animal studies. (7) Last but not least, these assays allow us to study and manipulate human cellular responses in physiological context. For a brief review of the results obtained with these models and studies in rodents cells in 3D cultures and *in vivo*, see Bissell *et al*. (1999). For a history of development of 3D cultures in general see Schmeichel and Bissell (2003). For a review of more complex organotypic cultures, see Gudjonsson *et al*. (2003).

II. MATERIALS AND INSTRUMENTATION

Primary breast luminal cells from human reduction mammoplasty (Petersen *et al*., 1992) as well as human mammary epithelial cell lines have been successfully cultured utilizing the 3D BM assay. These include the following.

The HMT3522 progression series (Briand *et al*., 1987) consists of immortal human mammary epithelial cells originally isolated from fibrocystic breast tissue and includes the phenotypically normal S1 cells, as well as their tumorigenic derivative T4-2 cells, which were selected for their ability to grow in the absence of EGF (Briand *et al*., 1996; Weaver *et al*., 1996).

This article focuses mainly on the HMT3522 series but provides examples of the morphology of a few other nonmalignant cell lines, such as 184B5 (Walen and Stampfer, 1989); for a description of these series, see http://www.lbl.gov/~mrgs/review.html and MCF10A (Soule *et al*., 1990). For further information and culture conditions, see http://www.atcc.org /ATCC Number: CRL-10317.

TABLE I Growth Medium for HMT3522 Cells

Components	Growth medium
DMEM/F12	10 ml
Insulin (100 µg/ml stock)	25 µl (250 ng/ml final)
Transferrin (20 mg/ml stock)	5 µl (10 µg/ml final)
Sodium selenite (2.6 µg/ml stock)	10 µl (2.6 ng/ml)
Estradiol (10^{-7} *M* stock)	10 µl (10^{10} *M* final)
Hydrocortisone (1.4×10^{-3} *M* stock)	10 µl (1.4×10^{-6} *M* final)
Prolactin (1 mg/ml stock)	50 µl (5 µg/ml final)
EGF[a] (20 µg/ml stock)	5 µl (10 ng/ml final)

[a] S1 cells only.

A. Culture Media Composition

Media for the HMT3522 progression series of human mammary epithelial cells are composed of DMEM/F12 media (GibcoBRL Cat. No. 12400-024) supplemented with insulin (Sigma Cat. No. I-6634), human transferrin (Sigma Cat. No. T-2252), sodium selenite (Collaborative Research Cat. No. 40201), estradiol (Sigma Cat. No. E-2758), hydrocortisone (Sigma Cat. No. H-0888), prolactin (Sigma Cat. No. L-6520), and epidermal growth factor (EGF) (Roche Cat. No. 855731) as described in Briand *et al*. (1987) and Blaschke *et al*. (1994). Concentrations and stability are outlined in Table I.

B. Additional Reagents Required for Culture and Manipulation in Three-Dimensional Culture

Vitrogen (collagen I, Cohesion Technologies) can be made from rat tail collagen, phosphate-buffered saline (PBS) (any vendor), 0.25% trypsin–EDTA (any vendor), soybean trypsin inhibitor (Sigma Cat. No. T6522), trypan blue (Sigma Cat. No. T8154), growth factor reduced Matrigel (Becton-Dickenson-Collaborative Research Cat. No. 354230), AIIB2, blocking antibody against β1 integrin (Sierra BioSource Inc. Cat. No. SB959), LY294002 (Cell Signaling Technologies Cat. No. 9901), Mab225 (Oncogene Research Cat. No. GR13L), PP2 (Calbiochem Cat. No. 529573), PD98059 (Calbiochem Cat. No. 513000) and tyrphostin AG1478 (Calbiochem Cat. No. 658552). All other equipment and supplies can be purchased from a variety of vendors.

C. Minimal Equipment Required for Cell Culture

Hemacytometer, low-speed centrifuge, inverted light microscope equipped with 4, 10, 20, and 40×

objectives, pipetman p20, p200, p1000, pipette aid, biological safety cabinet, 37°C, 5% CO_2 humidified culture incubator, air-tight plastic container, 37°C water bath.

D. General Tissue Culture Supplies

Tissue culture plasticware including T75 flasks, 4-, 6-, 24-, 48-, and 96-well dishes, 5-, 10-, and 25-ml individually wrapped sterile pipettes, 15- and 50-ml sterile conical centrifuge tubes, sterile 1- to 200- and 500- to 1000-µl pipette tips, and sterile 9-in. Pasteur pipettes and cell lifters.

III. PROCEDURES

Successful growth of these cells requires special attention to the media, confluency, trypsinization, and feeding regime in order to maintain healthy cells capable of undergoing differentiation. Insufficient attention to any of the aforementioned parameters will quickly result in cells acquiring a fibroblast-like morphology and concomitant failure to undergo 3D organization when cultured in IrBM.

A. Cell Maintenance

1. Preparation of Collagen-Coated Tissue Culture Flasks

1. Make a working solution of collagen I [~65 µg/ml] by the addition of 1 ml Vitrogen (collagen I) to 44 ml of cold 1× PBS.
2. Add 3 ml of collagen solution for every 25-cm^2 surface area of flask; tilt flask to make sure entire surface is coated.
3. Store in an air-tight container, on even surface at 4°C, a minimum of overnight and a maximum of 3 weeks.
4. Before use, aspirate liquid in the flask, wash once with 2 ml DMEM/F12 per 25 cm^2 and add prewarmed growth media.

2. Passage of HMT3522 Cells

Change media every 2–3 days; it is important to ensure that fresh media be added 1 day before splitting. HMT3522 S1 cells should be passaged once the 2D colonies form rounded islands with the flask being approximately 75% confluent, as shown in Fig. 1A. This is usually occurs 8 to 10 days after the initial plating.

Passage HMT3522 T4-2 cells when the flask reaches 75% confluency, as shown in Fig. 1B. This usually occurs 3 to 5 days after initial plating. Maintain T4-2 cells on Vitrogen (collagen I) or rat tail collagen-coated flasks.

Perform the following steps in a tissue culture hood.

1. Aspirate medium.
2. Rinse cells in 0.5 to 1 ml of prewarmed 0.25% trypsin–EDTA for every 25 cm^2 of surface area.
3. Add 0.35 ml of 0.25% trypsin for every 25 cm^2 of surface area and cover cells by rotating the flask gently.
4. Place flask in 37°C incubator for 3 min.
5. Remove flask from incubator and check under the microscope to see if the cells have detached.

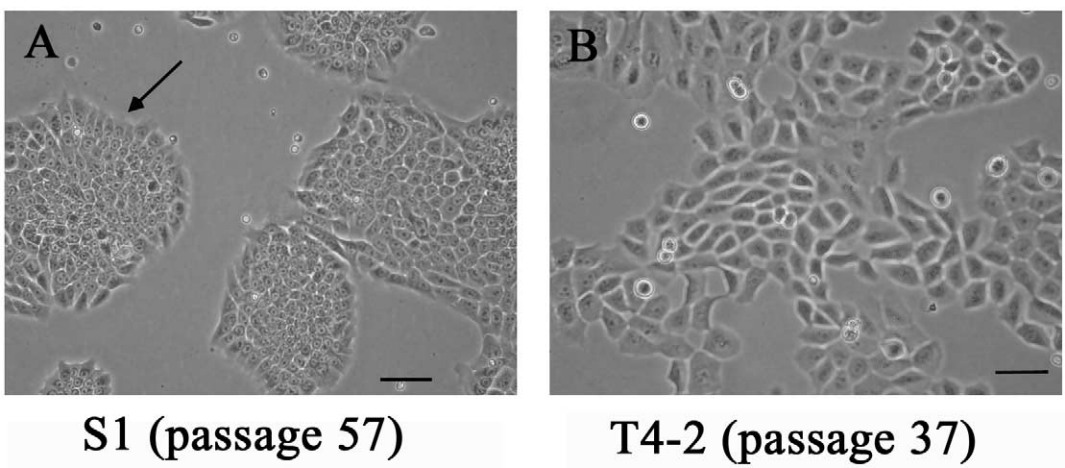

FIGURE 1 The morphology of S1 and T4-2 cultured on tissue culture plastic. (A) S1 cells, passage 57, at day 10 after plating. The colonies are essentially round with smooth edges and with the inner cells somewhat compacted. Cells at the edge should take on a polar-like appearance indicated by the arrows. (B) T4-2, passage 37, at day 5 after plating. Cells are larger than S1, the colonies are irregular, and cells at the edges rarely show any organization. Bar: 25 µm.

a. If cells are still adherent, redistribute the trypsin and return the flask to the 37°C incubator for 1 min. Repeat until cells are detached.
b. Once the majority of the cells are detached, knock the side of the flask gently; add ~3 ml of prewarmed DMEM/F12 and 30 µl of soybean trypsin inhibitor per 25 cm^2.

6. Gently pipette cells up and down three to five times to dissociate cell aggregates and transfer to a 15-ml conical centrifuge tube.
7. Pellet the cells by spinning at ~115 *g* for 5 min.
8. Aspirate media and resuspend the cell pellets in their appropriate growth media (~3.25 ml per 25 cm^2 of surface area of their original flask).
9. Determine the cell concentration by removing a 95-µl aliquot and placing into a 1.5-ml Eppendorf tube, add 5 µl of 0.4% trypan blue, mix gently with a pipetman, load onto a hemacytometer, count on an inverted microscope, and determine the number of viable (nonblue) cells per milliliter.
10. Plate
a. HMT 3522 S1 cells at a density of 2×10^4 cells/cm^2 on tissue culture plastic.
b. HMT 3522 T4-2 cells at a density of 1×10^4 cells/cm^2 on collagen I-coated flasks.

3. Three-Dimensional BM Assay Embedded in lrBM/EHS/(Matrigel)

Single phenotypically normal mammary epithelial cells embedded into lrBM will undergo several rounds of cell division, withdraw from cell cycle between 6 and 8 days (depending on the cell type), organize into polarized structures, and form acini-like structures, including a central lumen. Malignant cells, however, continue to proliferate and form disorganized, tumor-like structures (Fig. 2). Starting on day 4 but clearly by day 10, one can distinguish nonmalignant from malignant cells. Immunohistochemistry analysis for the Ki67 antigen on day 10 shows that ~60% of the malignant cells are still proliferating, whereas only <10% of the nonmalignant remain in the cell cycle.

Procedure

The following volumes and concentrations given are appropriate for a 35-mm tissue culture dish (9.6-cm^2 surface area). The volumes and concentrations must be adjusted to correct for the area of the plate used in the analysis. IrBM should be stored at –80°C. Thaw ***immersed in ice*** at 4°C overnight before use. Once thawed it should ***not be refrozen*** but can be kept ***in ice*** at 4°C for more than 1 month. Matrigel lots are tested before use and batches are purchased for experimental use. Alternatively, the basement membrane mixture (EHS) can be made from the Engelbreth–Holm–Swarm mouse tumor described in Kleinman *et al*. (1982); see Section III,B details.

Note: EHS or Matrigel should always be kept on ice as it will polymerize quickly at room temperature.

1. Chill plates on ice inside a tissue culture hood.
2. Add 120 µl of EHS per 35-mm dish spread in the center of the dish without introducing bubbles, spread EHS evenly across the surface of the dish using a sterile cell lifter or the back of a sterile pipette tip (make sure the entire surface is covered, including the edges), and place in a 37°C incubator for a minimum of 15 min to allow the EHS to polymerize. (Do not let sit more than 1 h in incubator as it will begin to dry out.)
3. While the EHS is polymerizing, trypinsize and count the cells as described earlier.
4. Place an aliquot containing the appropriate number of cells into a sterile centrifuge tube: 1.0×10^6 cells S1 (and other *non*tumorgenic cell lines) and 0.7×10^6 cells T4-2 (and other tumorgenic cell lines).
5. Centrifuge for 5 min at ~115 *g* to pellet the cells, aspirate media, and resuspend the pellet by flicking the tube.
6. Place the cell pellet on ice, add 1.2 ml EHS, and carefully pipette mixture up and down to distribute cells evenly but not introduce bubbles into the EHS.
7. Transfer to a precoated 35-mm dish.
8. Place in 37°C incubator for ~30 min until the EHS is polymerized.
9. Once a gel is formed, add 1.5 to 2.0 ml of the appropriate media to the dish.
10. Culture the cells for 10 days, changing media every 2 to 3 days.

Figures 3A–3D show cells cultured in Matrigel for 10 days.

4. Three-Dimensional BM Assay on Top of EHS/Matrigel

The culture of mammary epithelial cells, developed previously in our laboratory for functional studies of mouse cells (Barcellos-Hoff *et al*., 1989; Roskelley *et al*., 1994), has now been adopted to human cells as well. Making 3D BM cultures on top of EHS as opposed to inside the gel has some advantages and a few drawbacks. The proliferation and morphological differences between nonmalignant and malignant cells can be distinguished by 4 days in culture as opposed to the 8–10 days required for embedded cultures. The cell colonies can readily be imaged utilizing a live cell imager, allowing one to follow a single cell to an acini-like structure. Furthermore, cell colonies can be harvested easily by scraping the culture gently with a pipette tip and depositing the isolate on a glass slide for analysis

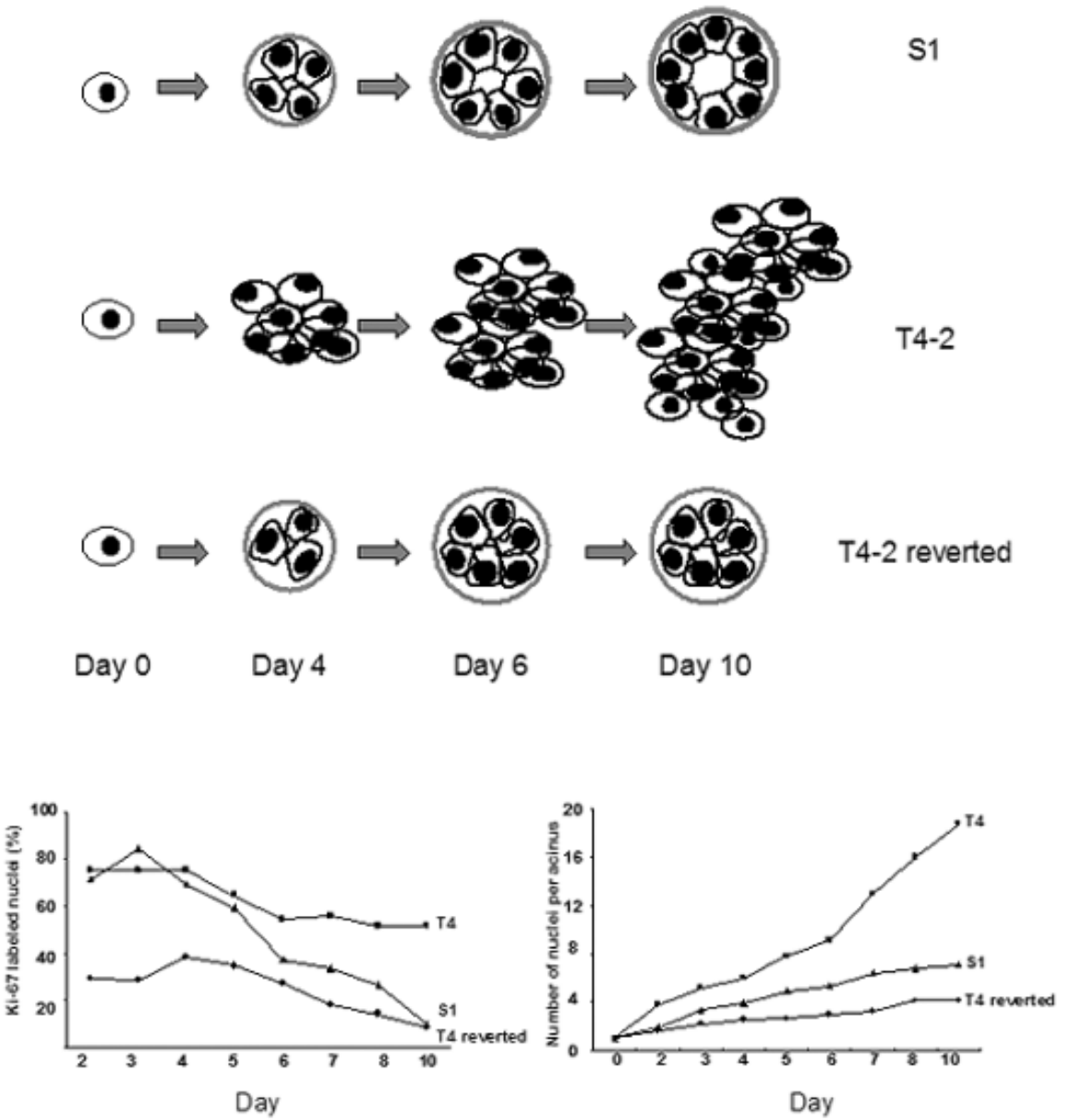

FIGURE 2 Morphology, size, and proliferation rate of S1 and T4-2 and T4-2 reverted cells embedded in 3D BM. (A) Schematic representations of the morphology of S1, T4-2, and T4-2 cells treated with signaling inhibitors as a function of time. (B) The percentage of Ki67 positive cells for S1, T4-2, and T4-2 cells treated with tyrophostin AG1478 from days 2 to 10. (C) The number of cells/acini for S1, T4-2, and T4-2 cells treated with tyrophostin AG1478 from days 2 to 10.

by immunohistochemistry. The advantage of this method of harvest is that the remaining culture can be harvested for DNA, RNA, or protein. However, neither the morphology nor the growth rate of the acini is as tightly controlled as the embedded cultures. An additional disadvantage of the *on-top* culture is that the amount of material collected per plate is less than the embedded cultures, as plating of the cells is restricted to one plane. Therefore, there are significantly less cells per millimeter dish to be harvested compared to the embedded assay.

The following volumes and concentrations are appropriate for a 35-mm tissue culture dish (9.6-cm^2 surface area). The volumes and concentrations must be adjusted to correct for the area of the plate used in the analysis.

Before splitting the cells, prepare the EHS-coated plates.

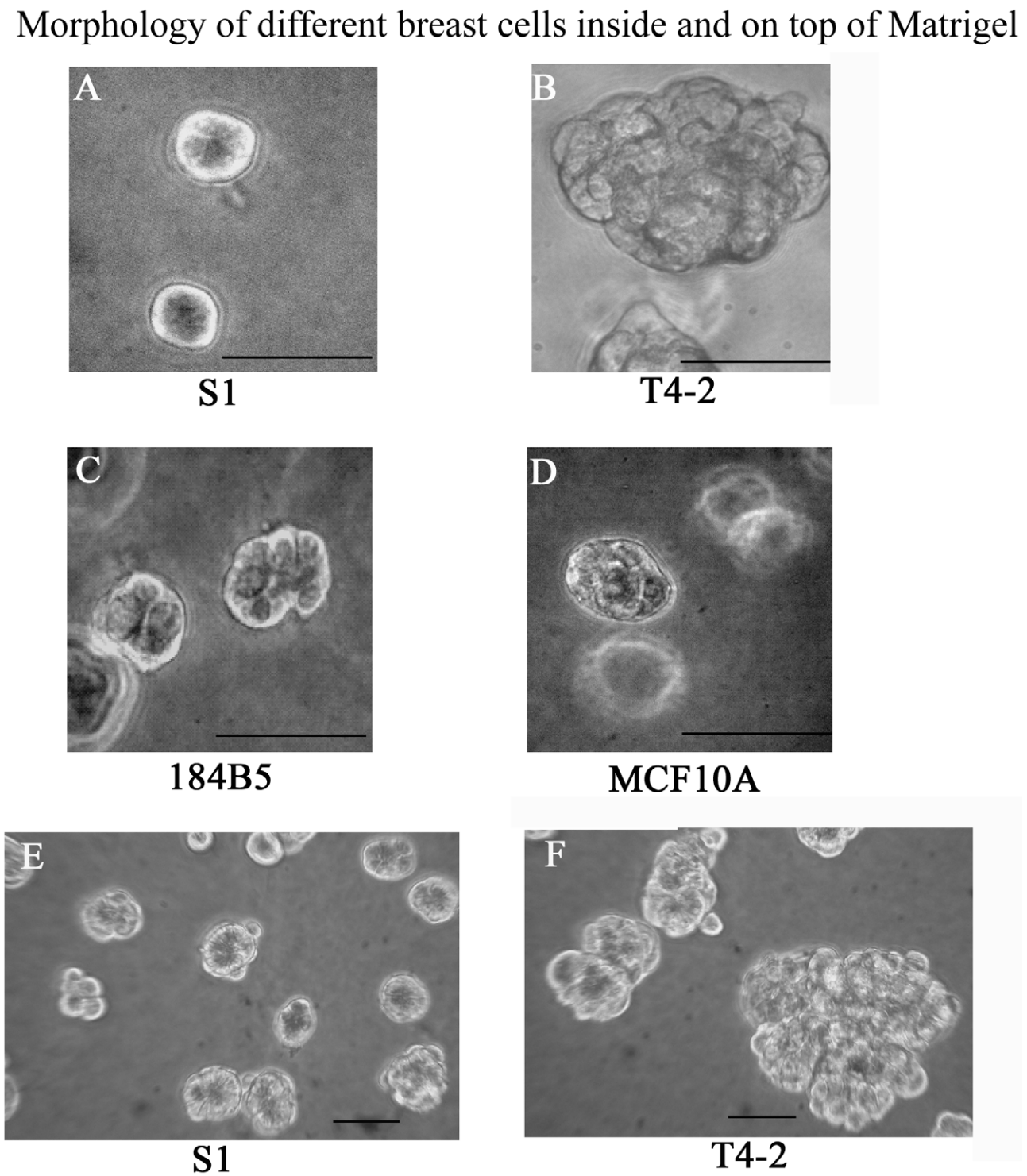

FIGURE 3 Morphologies of S1 (A), T4-2 (B), 184B5 (C), and MCF10 (D) cells embedded in 3D BM (all cells were cultured in Matrigel for 10 days) and S1 (E) and T4-2 (F) cells cultured on top (cells were cultured on top of Matrigel for 4 days). Photographs were taken using a phase-contrast microscope. Bar: 25 μm.

1. Chill plates on ice in a tissue culture hood.
2. Add 0.5 ml to the center of the dish and spread EHS evenly without creating bubbles as described earlier.
3. Place in 37°C incubator for ~30 min until the EHS is polymerized.
4. Trypsinize cells as described previously.
5. Place an aliquot containing the appropriate

number of cells into a sterile centrifuge tube: 0.3×10^6 cells S1 (and other *non*tumorgenic cell lines) and 0.2×10^6 cells T4-2 (and other tumorgenic cell lines).

6. Centrifuge for 5 min at ~115 *g* to pellet the cells, aspirate media, and resuspend the pellet by flicking the tube.

7. Resuspend the cells in half of the total volume of the appropriate media for the cells (1 ml for 35 mm) according to the size of the plate (see later).

8. Plate the cells on top of the polymerized EHS-coated dishes, let sit in hood for 5 min, and then check under a microscope to see if cells are distributed evenly. If not, move plate on a flat surface, back to front and then side to side, to distribute and let sit for 5 min.

9. Return plates to the incubator for ~30 min until the cells have adhered.

10. Prepare media plus 10% EHS on ice.

11. Add the appropriate amount of media with 10% EHS to the cells to achieve a final concentration of 5% EHS.

12. Culture the cells for 4–6 days, changing media every 2–3 days.

Figures 3E and 3F show cells cultured on top of EHS for 4 days,

5. *Reversion Assay*

The reversion assay can determine the ability of tumor cells to become phenotypically normal or to undergo apoptosis as a function of treatments. In addition, the differential response of tumorigenic and nonmalignant cells to a wide variety of perturbations can be analyzed. Analyses can be performed both on cells cultured embedded in or on top of EHS. This assay can be used as a screen for potential therapeutics by manipulating various genes, signaling pathways, and/or protein modifications and for determining their role in the establishment or maintenance of the tumorigenic phenotype. Cancer cells, cultured as described earlier, can be treated with a wide variety of agents, including inhibitory or stimulatory antibodies to integrins or growth factor receptors, small molecule inhibitors to different signaling pathways, gene delivery via transfection with expression vectors or transduction with virus overexpressing genes of interest, and RNAi for specific gene silencing.

Quantitative end points include morphology, proliferation index, degree of polarity, and level of expression of genes of interest using RT-PCR, Northern, or Western analysis, as well as immunofluorescence. Table II details a variety of molecules that have been shown to revert T4-2 cells. A typical reversion morphology of T4-2 cells is illustrated in Fig. 4.

TABLE II Reversion Agents in Three-Dimensional Assay

Reversion agent	Final concentration	Activity
AIIBII (6–10 mg/ml stock in PBS)	In Matrigel (0.16 mg/ml final)[a]	β1 integrin inhibitory antibody
Mab225 (200 μg/ml stock in PBS)	In Matrigel (6–9 μg/ml final)[b]	EGF receptor inhibitory antibody
LY294002 (10 m*M* stock in DMSO)	In growth medium (10 μ*M* final)	PI3 kinase inhibitor
Tyrophostin AG1478 (100 μ*M* stock in DMSO)	In growth medium (100 n*M* final)	EGF receptor inhibitor
PD98059 (10 m*M* stock in DMSO)	In growth medium (10 μ*M* final)	MEK1 inhibitor

[a] Antibodies may need slight adjustment in concentration from lot to lot.

[b] Add to IrBM/cell mix as well as to media.

6. *Release of Cellular Structures from 3D BM*

For molecular analysis of cell extracts, it is important to remove them from the gel. Apart from scraping the colonies as described earlier, which will still have minor EHS contamination, intact cellular structures can be released from EHS utilizing chelating agents, a procedure described in Weaver *et al*. (1997). A modified version is described here. Note that the solutions must be cold and the cells kept on ice for the entire harvest period. The maximum harvest should be 1 h as the cell–cell junctions will begin to come apart if left in these solutions for too long.

Perform the following steps on the day of harvest.

1. Wash cultures twice with cold PBS without Ca^{2+} or Mg^{2+} plus 0.005 *M* EDTA.

2. Scrape cultures into 3 ml cold PBS without Ca^{2+} or Mg^{2+} plus 0.005 *M* EDTA/25-cm^2 surface area, transfer into an appropriate size centrifuge tube, wash the plates twice with 3 ml each cold PBS, and bring final volume to 10 ml.

3. Incubate cells on ice for ~45 min, gently inverting the tube two or three times every 10 min.

4. Cell release from 3D BM is complete when the cellular structures begin to settle at the bottom of the centrifuge tube and the supernatant does not contain floating gel or flocculent substances.

5. Centrifuge gently for 2–4 min at 115 *g* until a loose pellet is obtained (the cells are very fragile at this point; therefore, centrifuging too hard or long will result in cell lysis).

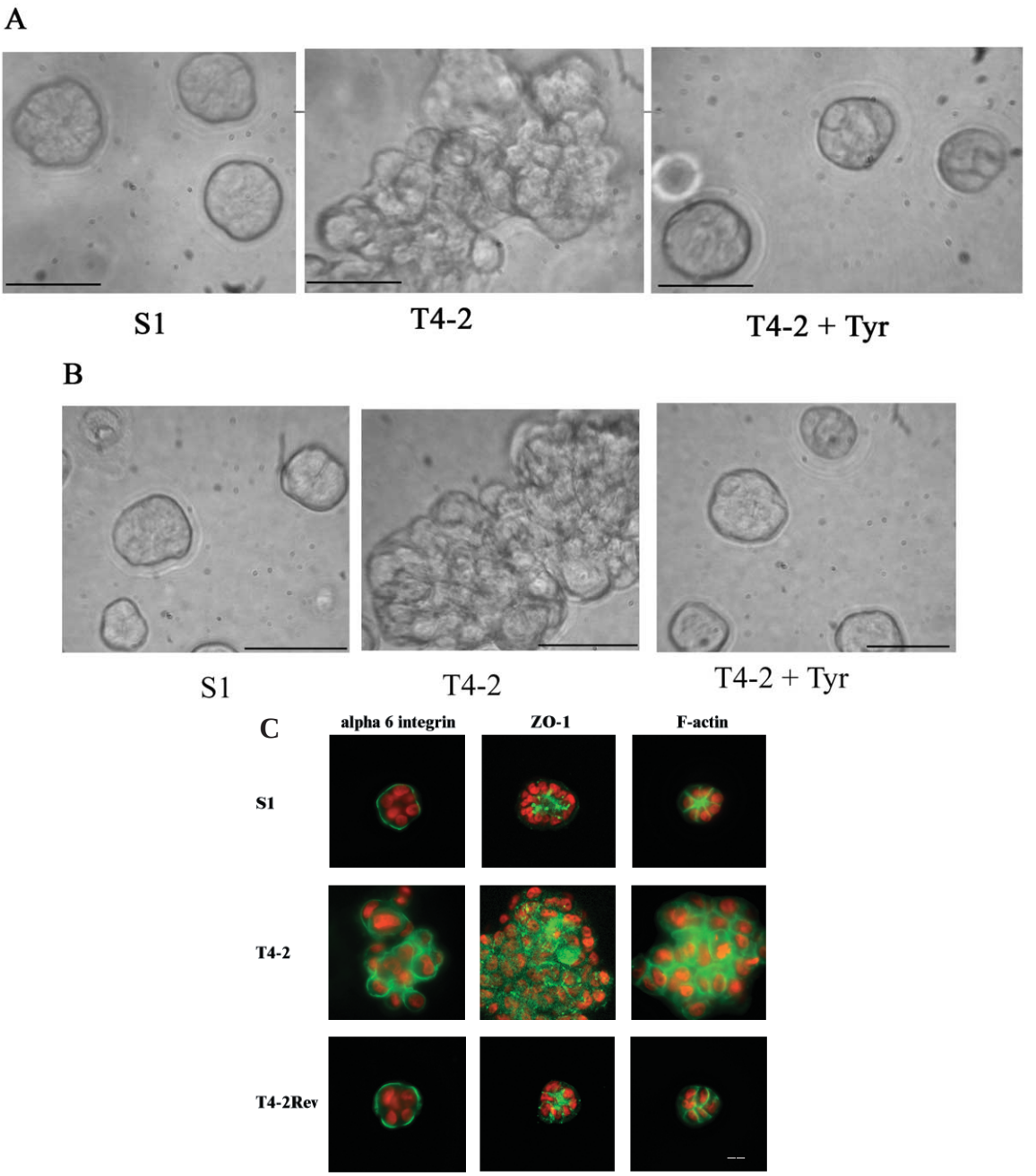

FIGURE 4 Morphological and immunofluorescence analyses of S1, T4-2, and T4-2 treated with LY 294002 or tyrphostin AG1478. (A) Cells were embedded in Matrigel and cultured for 10 days. (B) Cells were cultured for 4 days on top of Matrigel. S1, T4-2, and T4-2Rev cells were treated with 0.1 m*M* AG1478 tyrphostin. Photographs were taken using a phase-contrast microscope. A & B Bars: 25 mm. (C) Structures isolated from 3D BM after 10 days in culture were stained with the basal marker α_6 integrin, the apical marker ZO-1, and the cytoplasmic marker F-actin. S1, T4-2, and T4-2Rev cells were treated with 10 m*M* LY 294002. Photographs were taken using a fluorescence microscope. Bars: 10 mm.

6. Aspirate the supernatant, leaving a very small amount of liquid above the pellet.
   a. For immunohistochemistry or immunofluorescence, smear a small aliquot gently across a small area of a glass slide and fix, using the appropriate fixative for antibody of interest and store at –20°C until use.
   b. For RNA isolation, lyse an aliquot in lysis buffer of choice and store at –80°C.
   c. For Western or immunoprecipitation analyses, lyse aliquots in appropriate buffer and store at –80°C.

Note: Trizol or Tripure can be used to isolate RNA and DNA directly from the cultures without release of the cells from the gel.

B. Additional Procedures

1. Criteria for Purchase of Appropriate Matrigel Lots

Test lots of Matrigel and choose those that are low in epidermal growth factor (EGF), low endotoxin, which have a protein concentration close to 10 mg/ml.

Test the cells of interest by always comparing old and new lots side by side using the 3D BM-embedded and *on top* culture conditions as described earlier. Also test the ability of malignant cells of interest to revert in the presence of tyrphostin AG1478 or known reverting agents.

1. On the final day of culture measure the colony sizes using an inverted microscope equipped with an eyepiece reticule. Eighty percent or greater of the colonies should be within the following diameters: 24 μm S1, >74 μm T4-2, and 25–32 μm T4rev.
2. Isolate colonies from the 3D BM as described previously to determine:
   a. by immunofluorescence
      i. cell proliferation index by determining the percentage of positive Ki67 cells
      ii. degree of polarity by localization of molecules such as α_6-integrin, E-cadherin, and cortical actin.
   b. by Western blot (for S1 and T4-2)
      i. relative levels of β1 integrin
      ii. relative levels of EGF receptor

2. Preparation of EHS Matrix from EHS Tumors

The EHS tumor is grown in C57 black mice. Typical propagation of the tumor starts with one-third of a fresh tumor, which is enough to inject 10 mice. The tumor sample is minced with a scalpel blade suspended into 2 ml PBS and is then further disassociated by pushing it through an 18-gauge needle followed by a 20-gauge needle. This tumor slurry is then injected intramuscularly (IM) into the hind limb (0.2 ml/limb) of mice. Tumors are allowed to grow for 4 weeks. For the last 2 weeks of tumor growth, 0.1% β-aminopropionitrile fumarate (BAPN) is added to the drinking water to prevent the collagen from cross-linking. The tumors should be harvested, weighed, frozen in liquid nitrogen, and stored at –80°C until use. For further information, see Kleinman *et al*. (1986).

The following buffers are needed for isolation.

Buffer 1: 3.4 *M* NaCl, 50 m*M* Tris–Cl, pH 7.4, 4 m*M* EDTA, and 2 m*M* *N*-ethylmalenmide (NEM) (make up 100× stock in H_2O fresh for each other preparation)

Buffer 2: 0.2 *M* NaCl, 50 m*M* Tris–Cl, pH 7.4, 4 m*M* EDTA, 2 m*M* NEM (make up 100× stock in H_2O fresh for each preparation), and 2 *M* urea, ultrapure or deionized

Buffer 3: 0.15 *M* NaCl, 50 m*M* Tris–Cl, pH 7.4, 4 m*M* EDTA, and 2 m*M* NEM (make up 100× stock in H_2O fresh for each preparation). Sterilize

All solutions should be at 4°C and kept on ice

1. Distribute 10–15 g of frozen tumor tissue (stored previously at –80°C) into two 50-ml tubes.
2. Add approximately 2 ml buffer 1 for each gram of tissue and homogenize (add more buffer as needed until all tissue is homogenized evenly).
3. Transfer homogenate to an appropriate ultracentrifuge tubes, balance tubes using buffer 1, and spin for 20 min at 4°C at 83472 RCF (ave) (corresponds to 26,000 rpm when using a SW 41 rotor).
4. Decant supernantant, add 1–2 ml fresh buffer 1, rehomogenize, transfer to fresh ultracentrifuge tubes, balance with buffer 1, and spin again as just described; repeat these steps so that the tissue has been homogenized and spun for a total of three times.
5. Resuspend the pellet in buffer 2 as follows: add 1 ml/tube, homogenize briefly to get pellet into suspension, add buffer 2 until equivalent to 1.8 ml/g of original tumor weight, transfer suspension into a beaker with a stir bar, cover well, and stir overnight in a cold room.
6. Transfer liquid to ultracentrifuge tubes and spin as described earlier (try to add the minimum amount of additional buffer to balance). *Save the supernantant*.
7. Load supernatant into medium-sized dialysis tubing. Dialyze in cold room against 1 liter of buffer 3 for 1.5 to 2 days with three changes of buffer.

8. Dialyze in cold room against the media of choice for 3 h.

9. Store on ice in thermos at 4°C if used within 2 months. Otherwise, freeze aliquots at –80°C and thaw on ice before use.

IV. COMMENTS

Using this assay system, one can screen a wide variety of breast tumor cell lines and assess their ability to revert or die when treated with various signaling inhibitors and/or potential therapeutics, as outlined in Wang *et al*. (2002).

V. PITFALLS

1. Use healthy cells that are no more than 75% confluent.
2. Make sure the cells have been dispersed into single cells and that you do not introduce bubbles into the lrBM for 3D BM-embedded cultures. Cell clumps will make it hard to interpret morphological characteristics at the end of the assay.
3. Feed cells every 2–3 days with fresh media when appropriate, include test compound.

Always include a cell line with a known positive response when performing the reversion assay.

Acknowledgments

Work from the authors' laboratory was supported by the United States Department of Energy, Office of Biological and Environmental Research (DE-AC03 SF0098 to M.J.B.). Additional funding was contributed by the Department of Defense Breast Cancer Research Program (#DAMD17-02-1-0438 to M.J.B.) and the National Cancer Institute (CA64786-02 to M.J.B., and CA57621 to Zena Werb and M.J.B). The authors thank Paraic Kenny for editorial comments.

References

Barcellos-Hoff, M. H., Aggeler, J., Ram, T. G., and Bissell, M. J. (1989). Functional differentiation and alveolar morphogenesis of primary mammary cultures on reconstituted basement membrane. *Development* **105**, 223–235.

Bissell, M. J., and Radisky, D. (2001). Putting tumours in context. *Nature Rev. Cancer* **1**, 46–54.

Bissell, M. J., Weaver, V. M., Lelievre, S. A., Wang, F., Petersen, O. W., and Schmeichel, K. L. (1999). Tissue structure, nuclear organization, and gene expression in normal and malignant breast. *Cancer Res.* **59**, 1757–1763s; discussion 1763s–1764s.

Blaschke, R. J., Howlett, A. R., Desprez, P. Y., Petersen, O. W., and Bissell, M. J. (1994). Cell differentiation by extracellular matrix components. *Methods Enzymol.* **245**, 535–556.

Briand, P., Nielsen, K. V., Madsen, M. W., and Petersen, O. W. (1996). Trisomy 7p and malignant transformation of human breast epithelial cells following epidermal growth factor withdrawal. *Cancer Res.* **56**, 2039–2044.

Briand, P., Petersen, O. W., and Van Deurs, B. (1987). A new diploid nontumorigenic human breast epithelial cell line isolated and propagated in chemically defined medium. *In Vitro Cell Dev. Biol.* **23**, 181–188.

Debnath, J., Mills, K. R., Collins, N. L., Reginato, M. J., Muthuswamy, S. K., and Brugge, J. S. (2002). The role of apoptosis in creating and maintaining luminal space within normal and oncogene-expressing mammary acini. *Cell* **111**, 29–40.

Gudjonsson, T., Ronnov-Jessen, L., Villadsen, R., Bissell, M. J., and Petersen, O. W. (2003). To create the correct microenvironment: Three-dimensional heterotypic collagen assays for human breast epithelial morphogenesis and neoplasia. *Methods* **30**, 247–255.

Howlett, A. R., Petersen, O. W., Steeg, P. S., and Bissell, M. J. (1994). A novel function for the nm23-H1 gene: Overexpression in human breast carcinoma cells leads to the formation of basement membrane and growth arrest. *J. Natl. Cancer Inst.* **86**, 1838–1844.

Kleinman, H. K., Graf, J., Iwamoto, Y., Kitten, G. T., Ogle, R. C., Sasaki, M., Yamada, Y., Martin, G. R., and Luckenbill-Edds, L. (1987). Role of basement membranes in cell differentiation. *Ann. N. Y. Acad. Sci.* **513**, 134–145.

Kleinman, H. K., McGarvey, M. L., Hassell, J. R., Star, V. L., Cannon, F. B., Laurie, G. W., and Martin, G. R. (1986). Basement membrane complexes with biological activity. *Biochemistry* **25**, 312–318.

Kleinman, H. K., McGarvey, M. L., Liotta, L. A., Robey, P. G., Tryggvason, K., and Martin, G. R. (1982). Isolation and characterization of type IV procollagen, laminin, and heparan sulfate proteoglycan from the EHS sarcoma. *Biochemistry* **21**, 6188–6193.

Muthuswamy, S. K., Li, D., Lelievre, S., Bissell, M. J., and Brugge, J. S. (2001). ErbB2, but not ErbB1, reinitiates proliferation and induces luminal repopulation in epithelial acini. *Nature Cell Biol.* **3**, 785–792.

Orkin, R. W., Gehron, P., McGoodwin, E. B., Martin, G. R., Valentine, T., and Swarm, R. (1977). A murine tumor producing a matrix of basement membrane. *J. Exp. Med.* **145**, 204–220.

Petersen, O. W., Ronnov-Jessen, L., Howlett, A. R., and Bissell, M. J. (1992). Interaction with basement membrane serves to rapidly distinguish growth and differentiation pattern of normal and malignant human breast epithelial cells. *Proc. Natl. Acad. Sci. USA* **89**, 9064–9068.

Roskelley, C. D., Desprez, P. Y., and Bissell, M. J. (1994). Extracellular matrix-dependent tissue-specific gene expression in mammary epithelial cells requires both physical and biochemical signal transduction. *Proc. Natl. Acad. Sci. USA* **91**, 12378–12382.

Roskelley, C. D., Srebrow, A., and Bissell, M. J. (1995). A hierarchy of ECM-mediated signalling regulates tissue-specific gene expression. *Curr. Opin. Cell Biol.* **7**, 736–747.

Schmeichel, K. L., and Bissell, M. J. (2003). Modeling tissue-specific signaling and organ function in three dimensions. *J. Cell Sci.* **116**, 2377–2388.

Soule, H. D., Maloney, T. M., Wolman, S. R., Peterson, W. D., Jr.,

Brenz, R., McGrath, C. M., Russo, J., Pauley, R. J., Jones, R. F., and Brooks, S. C. (1990). Isolation and characterization of a spontaneously immortalized human breast epithelial cell line, MCF-10. *Cancer Res.* **50**, 6075–6086.

Spancake, K. M., Anderson, C. B., Weaver, V. M., Matsunami, N., Bissell, M. J., and White, R. L. (1999). E7-transduced human breast epithelial cells show partial differentiation in three-dimensional culture. *Cancer Res.* **59**, 6042–6045.

Walen, K. H., and Stampfer, M. R. (1989). Chromosome analyses of human mammary epithelial cells at stages of chemical-induced transformation progression to immortality. *Cancer Genet. Cytogenet*. **37**, 249–261.

Wang, F., Hansen, R. K., Radisky, D., Yoneda, T., Barcellos-Hoff, M. H., Petersen, O. W., Turley, E. A., and Bissell, M. J. (2002). Phenotypic reversion or death of cancer cells by altering signaling pathways in three-dimensional contexts. *J. Natl. Cancer Inst.* **94**, 1494–1503.

Wang, F., Weaver, V. M., Petersen, O. W., Larabell, C. A., Dedhar, S., Briand, P., Lupu, R., and Bissell, M. J. (1998). Reciprocal interactions between beta1-integrin and epidermal growth factor receptor in three-dimensional basement membrane breast cultures: A different perspective in epithelial biology. *Proc. Natl. Acad. Sci. USA* **95**, 14821–14826.

Weaver, V. M., Fischer, A. H., Peterson, O. W., and Bissell, M. J. (1996). The importance of the microenvironment in breast cancer progression: Recapitulation of mammary tumorigenesis using a unique human mammary epithelial cell model and a three-dimensional culture assay. *Biochem. Cell Biol.* **74**, 833–851.

Weaver, V. M., Lelievre, S., Lakins, J. N., Chrenek, M. A., Jones, J. C., Giancotti, F., Werb, Z., and Bissell, M. J. (2002). beta4 integrin-dependent formation of polarized three-dimensional architecture confers resistance to apoptosis in normal and malignant mammary epithelium. *Cancer Cell* **2**, 205–216.

Weaver, V. M., Petersen, O. W., Wang, F., Larabell, C. A., Briand, P., Damsky, C., and Bissell, M. J. (1997). Reversion of the malignant phenotype of human breast cells in three-dimensional culture and in vivo by integrin blocking antibodies. *J. Cell Biol.* **137**, 231–245.

CHAPTER

18

Primary Culture of *Drosophila* Embryo Cells

Paul M. Salvaterra, Izumi Hayashi, Martha Perez-Magallanes, and Kazuo Ikeda

I. INTRODUCTION

Primary cultures of *Drosophila* embryonic cells offer a unique system to study the transitions of undifferentiated cells into a variety of cell types. Coupled with the power of *Drosophila* classical and molecular genetics, the analyses that are possible *in vitro* using differentiating embryo cells will continue to contribute to a deeper understanding of development. Preparation of primary embryo cell cultures was developed independently in the laboratories of Seecof and colleagues (Seecof and Unanue, 1968) and Shields and Sang (1970). The procedures for preparing cultures are technically undemanding and can be adapted to solve a wide range of biological problems. Important variations include the culture of single embryos (Cross and Sang, 1978), as well as the development of techniques for isolating the precursors of different cell types such as neurons and muscle cells (Furst and Mahowald, 1985; Hayashi and Perez-Magallanes, 1994). Figure 1 shows a convenient way to collect embryos from large populations of egg-laying adults, and Fig. 2 illustrates a typical setup used for preparing primary embryo cultures.

Cultures are initiated from embryos in the early gastrula stage, making it possible to observe cell development from committed precursor to final differentiated cell type. The types of cells that differentiate in culture are primarily neurons (Seecof *et al.*, 1973a) and multinucleate myotubes (Seecof *et al.*, 1973b), but other epidermal and mesodermal derivatives are also present (Shields *et al.*, 1975). Cultures form a variety of neurons with highly differentiated phenotypes, including neurotransmitter systems (Salvaterra *et al.*, 1987), ion channels (Byerly and Leung, 1988; Germeraad *et al.*, 1992), axonal specializations, and even functional neuromuscular junctions (Seecof *et al.*, 1972) and synaptic activity (Lee and O'Dowd, 1999). Medium conditioned by embryo cells has also been shown to contain a variety of activities that can modulate the growth and differentiation properties of neurons (Salvaterra *et al.*, 1987; Hayashi *et al.*, 1992). Figure 3 shows some of the cell types observed in a differentiated *Drosophila* primary embryo culture and neurons marked with a fluorescent transgenes specific for different neurotransmitter phenotypes. Remarkably, cultured *Drosophila* embryo cells have also been shown to express a temporally specific transcriptional factor cascade thought to be important for establishing the developmental potential of subsequent cell lineages from primary neuroblasts (Brody and Odenwald, 2000, 2002).

II. MATERIALS AND INSTRUMENTATION

Penicillin and streptomycin are from GIBCO/BRL (Cat. No. 15140-122). Insulin is from Sigma (Cat. No. I-5500). 1X Schneider's *Drosophila* medium with glutamine is from GIBCO (Cat. No. 11720-034). Fetal bovine serum is from GIBCO (Cat. No. 10082-139).

Cells are usually cultured in 35-mm plastic dishes from Corning (Cat. No. 430165). For finer morphological observations, cells are plated directly onto round

Copyright 2006, Elsevier Science (USA).
All rights reserved.

FIGURE 1 Large plastic jars used for embryo collections. The jar on the left is empty and the one on the right has a grape juice agar embryo collection plate taped to the bottom and is stocked with about 3000 adult flies as described. Holes have been cut into the sides of the jars and are covered with nylon mesh to allow efficient air circulation.

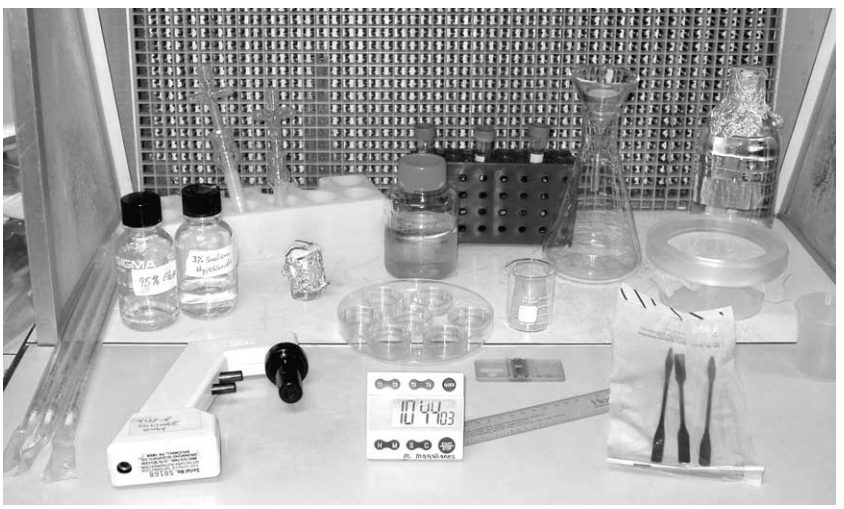

FIGURE 2 Typical items used to prepare *Drosophila* gastrula stage embryo cultures are arranged in a small laminar flow hood.

glass coverslips placed in the bottom of a 35-mm plate (five per culture dish, Fisher Scientific, Cat. No. 12-545-801-1THK). Coverslips are presterilized using standard gas or autoclave procedures.

Dechorionated embryos are dissociated in 15-ml Dounce glass–glass homogenizers from Baxter Diagnostics (Cat. No. T4018-15). Nylon mesh (25–100 µm pour size) can be obtained from most fabric stores. All other equipment and reagents are commonly used for general laboratory work or tissue culture and can be obtained from any scientific supply company.

III. PROCEDURES

A. Egg Collection and Aging to Early Gastrula Stage

Solution and Egg Collection Plates

Yeast–proprionic acid paste: Dissolve dry yeast in 2% proprionic acid

Grape–juice–agar egg collection plates: 160 ml water, 160 ml grape juice (we use Welch's), 6.4 g Bacto-agar

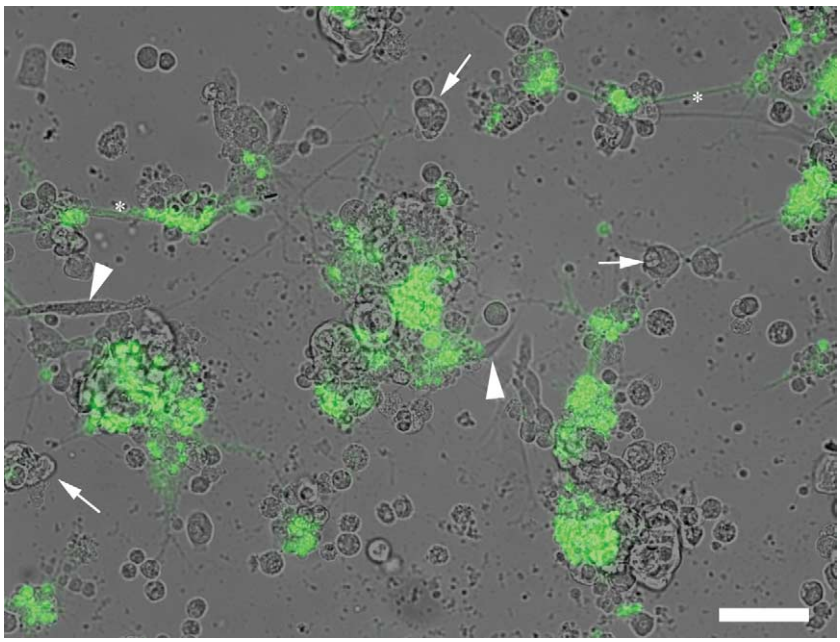

FIGURE 3 A *Drosophila* gastrula stage embryo cell culture after about 2 days of *in vitro* differentiation. The majority of cells differentiate into neurons organized in clusters. This image is a composite of a bright-field image overlaid with a false-colored fluorescent image of the same field. Green cells are neurons expressing a cholinergic-specific fluorescent transgene and are indicative of cells with a cholinergic neurotransmitter phenotype. White arrowheads show some multinuicleate myotubes, white and the asterisk indicates axonal-like processes emanating from neurons or neural clusters and are often connected to neurons in adjacent clusters. Scale bar: 50 µm.

(Becton, Dickinson, Cat. No. 214010), 0.8 g Nipagin [*p*-hydroxybenzoic acid methyl ester (methylpraben)] (Sigma, Cat. No. H-5501). Combine water, grape juice, and Bacto-agar in a 1-liter flask. Microwave to dissolve agar, being careful not to let the solution boil over. Remove from the microwave, add Nipagin, mix, and pour into 12 large (14 cm) culture plates.

Steps

1. Prepare large egg-laying population by transferring 1.5-week-old adult flies from 8 to 12 ordinary culture bottles to fresh culture bottles supplemented with dry yeast sprinkled over the food. Allow the population to adapt for 1–2 days in a 25°C humidified room and transfer the adults to an embryo collection bottle on the day cultures will be prepared. Figure 1 shows an example of a homemade collection bottle or a similar one can be obtained commercially (Doc Frugal Scientific, Cat. No. 55-100). We generally stock each egg-laying population with about 3000 adult flies. For convenience, maintain the room on a reverse light–dark cycle so collections can be done in the investigators' morning (i.e., the flies' dusk).
2. Apply a small amount of yeast–proprionic acid paste on a small piece of filter paper and place in the center of a large (14-cm) grape juice–agar egg collection plate to attract females to lay eggs.
3. Invert the embryo collection bottles onto the food plate and collect eggs for 1 or 2 h.
4. If better developmental timing (synchronization) is desired, do a 30-min to 1-h precollection and discard plates. This may be necessary to induce females to lay eggs they have been storing for longer times.
5. Remove egg collection plates from the embryo collection bottles, cover, and allow embryos to develop to early gastrula stage at 25°C for 3.5 h.

B. Harvesting of Embryos

Solution

Deionized water: Prepare 2 to 3 liters of deionized water.

Steps

1. Embryos should be harvested 5–10 min before the 3.5-h aging period so the cultures can be initiated immediately at 3.5 h.

2. Discard filter papers with yeast mixture.

3. Transfer plates to sink and rinse extensively and gently with deionized water to remove adult flies and other debris.

4. Pour water on the plates and gently loosen embryos with a camels' hair paint brush.

5. Pour suspended embryos into a nylon mesh filter to allow further washing and collection from other food plates.

6. Continue washing and remove large food particles and other debris with forceps if necessary.

7. Transfer nylon mesh with embryos to a sterile tissue culture hood.

C. Preparation of Embryonic Cultures

Solutions

Penicillin–streptomycin stock solution: Penicillin–streptomycin solution (10,000 U/ml) is obtained from GIBCO/BRL (Cat. No. 15140-122). Use 10 ml per liter of medium (i.e., final concentration of 100 U/ml penicillin, 100 µg/ml streptomycin).

Insulin stock solution: Dissolve insulin in 0.05 *N* HCl at a final concentration of 2 mg/ml. Filter sterilize (0.2 µm) and store at 4°C (stock is stable for 1 year). Use at a final concentration of 0.2 µg/ml of medium.

Schneider's Drosophila medium with glutamine, insulin, and 5% fetal bovine serum: Add 10 ml of sterile penicillin/streptomycin stock solution, 0.1 ml of insulin stock solution, and 50 ml of fetal bovine serum (final serum concentration = 5%) to 1 liter of Schneider's *Drosophila* medium with glutamine. The medium supports good differentiation when stored at 4°C for up to 1 month.

Sodium hypochlorite–ethanol: In a small beaker mix 10 ml of 95% EtOH and 10 ml of 3% sodium hypochlorite. This solution will dechorionate the embryos and sterilize them.

Deionized water: Prepare about 1 liter of sterile deionized water.

Steps

1. Preclean the laminar flow hood with ethanol using normal tissue culture procedures. All further operations are carried out under sterile conditions in the hood.

2. Transfer embryos to the beaker of sodium hypochlorite–ethanol using a sterile spatula and swirl gently for 1 to 2 min. The time may vary slightly but do not exceed 3 min. Timing depends on the freshness of the hypochlorite and the compromises you are willing to make with respect to yield and sterility. Shorter times tend toward better yields and longer times are necessary if you wish to totally eliminate yeast contamination.

3. Pour dechorionated embryos onto a small nylon mesh filter funnel and wash extensively with about 500 ml sterile distilled water.

4. Transfer to a 15-ml Dounce homogenizer that contains about 6 ml of culture medium and dissociate cells by gently homogenizing with three rotary up and down strokes.

5. Filter dissociated cells through a 25- to 100-µm nylon mesh filter (the mesh is taped loosely over a 5-cm-diameter glass funnel or fitted into a 3.5-cm metal ring that is placed into the funnel) to remove undissociated clumps and other large debris.

6. Collect filtrate in a 15-ml centrifuge tube and pellet cells by centrifugation at 1400 rpm for 4 min. Wash cells one time in 6 ml of culture medium and centrifuge as described earlier, followed by a final suspension in 10 ml of culture medium.

7. Place a small aliquot in a hemocytometer and count the round, intact, medium-sized cells and cell clusters to determine cell number.

8. Calculate the concentration of cells, add sufficient medium to obtain a final density of 8×10^5 cells/ml, and plate approximately 1.6×10^6 cells in a 35-mm culture dish (i.e., 2 ml of cell suspension per dish).

9. Culture cells in a humidified 25°C incubator (CO_2 is not necessary). Cells begin to differentiate in a few hours and are substantially developed after about 24 h. Cells can be cultured for several days before replacing the medium. It is possible to keep cultures for more than 1 year.

IV. COMMENTS

Cells are usually grown in 35-mm dishes but it is also possible to plate directly onto coverslips (see earlier) and even to grow cells in the raised condensation rings found on the lids of many 96-well microtiter plates. This is especially convenient when screening monoclonal antibodies, as each embryo culture can be isolated and matched with the corresponding position for a hybridoma clone growing in a 96-well culture dish. A proceedure has been described for treating the lids of culture plates with H_2SO_4 that results in a significant improvement in the attachment and differentiation of *Drosophila* embryo cells (Furst and Mahowald, 1984).

The yield of cells depends on how vigorously the cells are dissociated and how long the embryos are exposed to the ethanol–hypochlorite mixture. Using

the previously described procedures, we can routinely obtain ~10^6 cells for plating from a single embryo collection bottle stocked with about 3000 adult flies. This is sufficient for preparing five 35-mm culture dishes. The procedure can be scaled up or down easily using additional embryo collection bottles or using a smaller egg-laying population.

V. PITFALLS

In the past we have used up to 20% fetal calf serum; however, such high concentrations are not necessary to support optimal growth and differentiation. It is especially important to use prescreened lots of fetal calf serum that are suitable for *Drosophila* embryo cultures. Some lots of fetal calf serum do not support differentiation and even appear to be toxic to *Drosophila* embryonic cells. We have had good success with serum from GIBCO and Gemini Products. A chemically defined medium for preparing embryo cultures has also been described (O'Dowd, 1995).

The surface coating of tissue culture plasticware varies from different manufacturers. We have found that some types of 35-mm plastic dishes, such as those from Falcon, are not optimal for *Drosophila* cultures.

Acknowledgments

Work in the authors' laboratories has been supported by grants from NIH-NINDS. We thank our past and current laboratory colleagues for many helpful suggestions and ideas about *Drosophila* primary embryo cultures, especially Drs. N. Bournias-Vardiabasis and S. Song.

References

Brody, T., and Odenwald, W. F. (2000). Programmed transformations in neuroblast gene expression during *Drosophila* CNS lineage development. *Dev. Biol.* **226**, 34–44.

Brody, T., and Odenwald, W. F. (2002). Cellular diversity in the developing nervous system: A temporal view from *Drosophila*. *Development* **129**, 3763–3770.

Byerly, L., and Leung, H. T. (1988). Ionic currents of *Drosophila* neurons in embryonic cultures. *J. Neurosci.* **8**, 4379–4393.

Cross, D. P., and Sang, J. H. (1978). Cell culture of individual *Drosophila* embryos. I. Development of wild-type cultures. *J. Embryol. Exp. Morphol.* **45**, 161–172.

Furst, A., and Mahowald, A. P. (1984). Rapid immunofluorescent screening procedure using primary cell cultures or tissue sections. *J. Immunol. Methods* **70**, 101–109.

Furst, A., and Mahowald, A. P. (1985). Differentiation of primary embryonic neuroblasts in purified neural cell cultures from *Drosophila*. *Dev. Biol.* **109**, 184–192.

Germeraad, S., O'Dowd, D., and Aldrich, R. W. (1992). Functional assay of a putative *Drosophila* sodium channel gene in homozygous deficiency neurons. *J. Neurogenet.* **8**, 1–16.

Hayashi, I., and Perez-Magallanes, M. (1994). Establishment of pure neuronal and muscle precursor cell cultures from *Drosophila* early gastrula stage embryos. *In Vitro Cell Dev. Biol. Anim.* **30A**, 202–208.

Hayashi, I., Perez-Magallanes, M., and Rossi, J. M. (1992). Neurotrophic factor-like activity in *Drosophila*. *Biochem. Biophys. Res. Commun.* **184**, 73–79.

Lee, D., and O'Dowd, D. K. (1999). Fast excitatory synaptic transmission mediated by nicotinic acetylcholine receptors in *Drosophila* neurons. *J. Neurosci.* **19**, 5311–5321.

O'Dowd, D. K. (1995). Voltage-gated currents and firing properties of embryonic *Drosophila* neurons grown in a chemically defined medium. *J. Neurobiol.* **27**, 113–126.

Salvaterra, P. M., Bournias-Vardiabasis, N., Nair, T., Hou, G., and Lieu, C. (1987). *In vitro* neuronal differentiation of *Drosophila* embryo cells. *J. Neurosci.* **7**, 10–22.

Seecof, R. L., Donady, J. J., and Teplitz, R. L. (1973a). Differentiation of *Drosophila* neuroblasts to form ganglion-like clusters of neurons *in vitro*. *Cell Differ.* **2**, 143–149.

Seecof, R. L., Gerson, I., Donady, J. J., and Teplitz, R. L. (1973b). *Drosophilia* myogenesis *in vitro*: The genesis of "small" myocytes and myotubes. *Dev. Biol.* **35**, 250–261.

Seecof, R. L., Teplitz, R. L., Gerson, I., Ikeda, K., and Donady, J. (1972). Differentiation of neuromuscular junctions in cultures of embryonic *Drosophila* cells. *Proc. Natl. Acad. Sci. USA* **69**, 566–570.

Seecof, R. L., and Unanue, R. L. (1968). Differentiation of embryonic *Drosophila* cells *in vitro*. *Exp. Cell Res.* **50**, 654–660.

Shields, G., Dubendorfer, A., and Sang, J. H. (1975). Differentiation *in vitro* of larval cell types from early embryonic cells of *Drosophila melanogaster*. *J. Embryol. Exp. Morphol.* **33**, 159–175.

Shields, G., and Sang, J. H. (1970). Characteristics of five cell types appearing during *in vitro* culture of embryonic material from *Drosophila melanogaster*. *J. Embryol. Exp. Morphol.* **23**, 53–69.

CHAPTER

19

Laboratory Cultivation of *Caenorhabditis elegans* and Other Free-Living Nematodes

Ian M. Caldicott, Pamela L. Larsen, and Donald L. Riddle

I. INTRODUCTION

Nematodes have been cultured continuously in the laboratory since 1944 when Margaret Briggs Gochnauer isolated and cultured the free-living hermaphroditic species *Caenorhabditis briggsae*. Work with *C. briggsae* and other rhabditid nematodes, *C. elegans*, *Rhabditis anomala*, and *R. pellio*, demonstrated the relative ease with which they could be cultured (Dougherty, 1960; Vanfleteren, 1980). The culturing techniques described here were developed for *C. elegans*, but are generally suitable (to varying degrees) for other free-living nematodes. Whereas much of the early work involved axenic culturing, most of these techniques are no longer in common use and are not included here.

In the 1970s, *C. elegans* became the predominant research model due to work by Brenner and coworkers on the genetics and development of this species (Brenner, 1974). An adult *C. elegans* is about 1.5 mm long and, under optimal laboratory conditions, has a life cycle of approximately 3 days. There are two sexes, males and self-fertile hermaphrodites (Fig. 1), that are readily distinguishable as adults. The animals are transparent throughout the life cycle, permitting the observation of cell divisions in living animals using differential interference microscopy. The complete cell lineage and neural circuitry have been determined, and a large collection of behavioral and anatomical mutants has been isolated (Wood, 1988). *C. elegans* has six developmental stages: egg, four larval stages (L1–L4), and adult. Under starvation conditions or specific manipulations of the culture conditions, a developmentally arrested dispersal stage, the dauer larva, can be formed as an alternative third larval stage (Golden and Riddle, 1984).

Many of the protocols included here and other experimental protocols have been summarized in Wood (1988). We also include a previously unpublished method for long-term chemostat cultures of *C. elegans*. General laboratory culture conditions for nematode parasites of animals have been described (Hansen and Hansen, 1978), but none of these nematodes can be cultured in the laboratory through more than one life cycle. Marine nematodes and some plant parasites have been cultured xenically or with fungi (Nicholas, 1975). Laboratory cultivation of several plant parasites on *Arabidopsis thaliana* seedlings in agar petri plates has also been reported (Sijmons *et al*., 1991).

II. MATERIALS AND INSTRUMENTATION

Caenorhabditis elegans strains, as well as strains of other free-living nematodes, and bacterial food sources for them are available from the Caenorhabditis Genetics Center (250 Biological Sciences Center, University of Minnesota, 1445 Gourtner Ave., St. Paul, MN 55108). Most chemicals are obtained from general laboratory supply companies such as Fisher Scientific and Sigma; catalog numbers are for Fisher except where noted. Three sizes of polystyrene petri dishes are used in culturing nematodes: 35 × 10 mm (Cat. No. 8-757-100-A), 60 × 15 mm (Cat. No. 8-757-13-A), and 100 × 15 mm

Copyright 2006, Elsevier Science (USA).
All rights reserved.

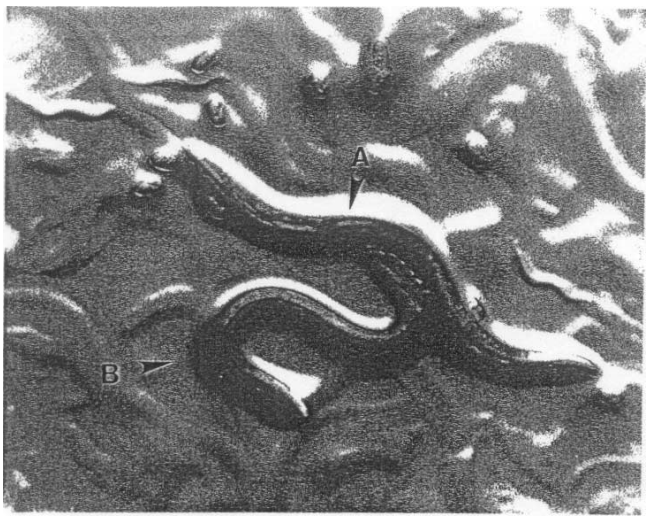

FIGURE 1 *Caenorhabditis elegans* hermaphrodite (A) and male (B) copulating. Several eggs and young larvae are also visible.

(Cat. No. 8-757-13). Triple-baffled Fernbach flasks (250 ml, 1 liter, and 2.8 liter, Cat. No. 2554) for liquid culture are from Bellco. The programmable dispensing pump (Model DP-200) used when making plates and the chemostat (Bioflo I) are from New Brunswick Scientific Company. An IEC clinical centrifuge (Cat. No. 05-101-5) with rotor 221 and metal shields 303 at setting 4 (RCF approximately 750) for 30 s is used for pelleting nematodes.

Tools for manipulating individual nematodes on plates are made by anchoring a 1.5-cm piece of 32-gauge platinum wire (Cat. No. 13-766-10-B) in a 6-in. inoculating loop holder or in a Pasteur pipette (by breaking off the pipette at the point where it narrows and holding in a flame with the wire to seal the end). For best results the end of the wire used for manipulation should be flattened and, if necessary, rounded to remove sharp edges. Observation of nematodes on plates is performed through a dissecting microscope with a magnification range of approximately 6 to 50×, fitted with a variable-angle transmitted light source. The microscopes in most common use for research are the Wild M3, M5, and M8 (Leica Inc.).

III. PROCEDURES

A. Preparation of Plates

The procedure for preparation of plates is modified from that of Brenner (1974).

Solutions

1. *Cholesterol stock* (*5 mg/ml*): Dissolve 0.5 g cholesterol (Cat. No. C314) in a final volume of 100 ml of 95% ethanol.
2. *1 M* $CaCl_2$: Dissolve 14.7 g of $CaCl_2 \cdot 2H_2O$ (Cat. No. C79) in a final volume of 100 ml of distilled water and autoclave.
3. *1 M* $MgSO_4$: Dissolve 24.65 g of $MgSO_4 \cdot 7H_2O$ (Cat. No. M63) in a final volume of 100 ml of distilled water and autoclave.
4. KH_2PO_4 *stock* (*1 M*): Dissolve 68.04 g of KH_2PO_4 (Cat. No. P285) in approximately 425 ml of distilled water. Add KOH (Cat. No. P250) pellets while monitoring the pH until pH is 6.0. Bring the volume to 500 ml; autoclave in 100-ml aliquots.
5. *B broth*: Add 1.0 g of tryptone and 0.5 g of NaCl (Cat. No. S640) to 100 ml of distilled water in a 250-ml screw-cap flask and autoclave.
6. *OP50 stock*: Inoculate 100 ml of B broth (in screw-cap flask) with *Escherichia coli* strain OP50, a uracil auxotroph, and shake overnight at 37°C. Store the stationary-phase culture at 4°C for up to 60 days.
7. *NG agar*: Add 3 g of NaCl, 17 g of Difco agar (Cat. No. DF0140-01-0), 2.5 g of peptone (Cat. No. DF0118-15-2), and 975 ml of distilled water to a 2-liter Erlenmeyer flask. Autoclave. Place the flask in a 50°C water bath to prevent solidification while dispensing medium into plates. Allow the flask to cool to approximately 65°C and add the following, using sterile technique and swirling the flask after adding each ingredient: 1 ml cholesterol stock, 1 ml 1 *M* $CaCl_2$, 1 ml 1 *M* $MgSO_4$, and 25 ml KH_2PO_4 stock.

Steps

1. Accurate dispensing of medium is accomplished most easily with the aid of a programmable dispensing pump. Fill 60 × 15-mm plates with 13 ml of agar, 100 × 15-mm plates with 30 ml, and 35 × 10-mm plates with 4 ml. The plates should be bubble free; flame the surface to remove bubbles.
2. Allow the plates to cool overnight; then put plates at 37°C for 24 h. Allow the plates to return to room temperature; store at 4°C.
3. Seed the plates (Fig. 2) with OP50 stock by spreading approximately 0.05 ml on the surface using a 1-ml pipette, and incubate overnight at 37°C or for 24–48 h at room temperature. Plates should be at room temperature before placing worms on them.

B. Liquid Culture

The procedure is modified from that of Sulston and Brenner (1974).

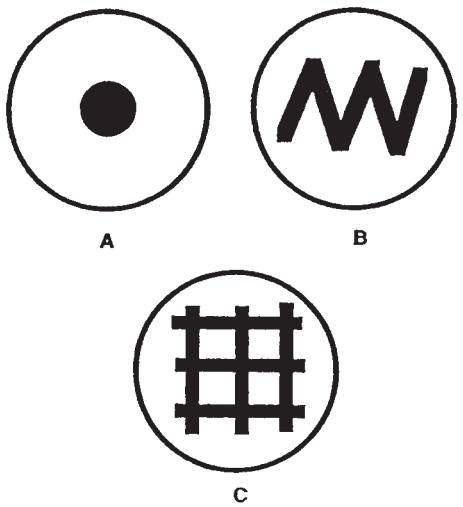

FIGURE 2 Examples of seeded plates. (A) Spot plate used for matings with single males or with mutant animals that do not mate well. (B) Zig-zag plate used for routine strain maintenance and crosses. (C) Grid plate used for mutant screens, strain maintenance, or crosses in which progeny are counted.

Solutions

1. *M9 buffer*: Dissolve 3 g of KH_2PO_4, 6 g of Na_2HPO_4 (Cat. No. S393), and 5 g of NaCl in distilled water; then add 1 ml of 1 *M* $MgSO_4$. Bring the volume to 1 liter with distilled water and autoclave in 100-ml aliquots.
2. *S basal*: Add 5.84 g of NaCl, 50 ml KH_2PO_4 stock, and 1 ml cholesterol stock to 950 ml of distilled water; autoclave in 100-ml aliquots.
3. *Potassium citrate stock* (*1 M*): Add 105.07 g of citric acid monohydrate (Cat. No. A104) to 250 ml of distilled water. Add KOH pellets while monitoring the pH until pH is 6.0. Bring the volume to 500 ml and autoclave in 100-ml aliquots.
4. *100× trace metals*: Dissolve 0.69 g of $FeSO_4{\cdot}H_2O$ (Cat. No. 1467), 1.86 g of Na_2EDTA (Cat. No. O2793), 0.197 g of $MnCl_2{\cdot}4H_2O$ (Sigma, Cat. No. M-3634), 0.287 g of $ZnSO_4{\cdot}7H_2O$ (Cat. No. Z76), and 0.025 g of $CuSO_4{\cdot}5H_2O$ (Cat. No. C493) in 1 liter of distilled water. Autoclave in 100-ml aliquots; store in foil-wrapped bottles.
5. *50% glucose*: Add 50 g of glucose (Cat. No. D16) to 50 ml of distilled water and autoclave.
6. *60% sucrose*: Add 120 g of sucrose (Cat. No. S5) to 80 ml distilled water and autoclave. Store at 4°C.
7. *S medium*: Add in the order indicated, using sterile technique, 1 ml potassium citrate stock, 1 ml 100× trace metals, 0.3 ml 1 *M* $CaCl_2$, and 0.3 ml 1 *M* $MgSO_4$ to 100 ml of S basal.
8. *XI666 medium*: Add 20 g of $Na_2HPO_4{\cdot}7H_2O$ (Cat. No. S373), 4.5 g of KH_2PO_4, 1.2 g of NH_4C1 (Cat. No. A661), 16 g of tryptone (Cat. No. DF0123-15-5), and 4 g of yeast extract (Cat. No. DF0127-15-1) to 980 ml distilled water in a 2.8-liter baffled flask. Mix, autoclave, allow to cool, and add 20 ml of 50% glucose and 8 ml of 1 *M* $MgSO_4$.
9. XI666 *stock*: Inoculate X1666 medium with X1666, a nalidixic acid-resistant, prototrophic, plasmid-free strain of *E. coli*. Shake at 37°C overnight. Transfer to preweighed sterile centrifuge bottles/tubes and centrifuge at 4000 RCF for 10 min. Remove supernatant and determine weight of bacteria. Resuspend in S medium to 5% (w/w). Store at 4°C.

Steps

1. With 2 ml of M9 buffer per plate, wash worms off five 60 × 15-mm plates that have just cleared of bacteria. Pellet nematodes. Remove supernatant and wash twice with fresh M9.
2. Add the washed worms to 250 ml X1666 stock in a 1-liter sterile baffled flask and place on shaker at 20°C. When the medium is cleared of bacteria, centrifuge at 750 RCF for 5 min.
3. Remove supernatant and resuspend in 15 ml of M9 buffer, divide between two 15-ml tubes, and place on ice. When cold, add 7.5 ml of cold 60% sucrose to each tube. Mix by inversion and centrifuge immediately at 1500 RCF for 5 min.
4. Remove nematodes from top of tube immediately and wash twice with 15 ml of M9 buffer. Place at 20°C on shaker for 30 min to allow digestion of bacteria in nematode intestines.
5. Wash twice with M9 buffer and use immediately or freeze at –70°C.

C. Chemostat Culture

Solution

OP50 concentrate: Make in same manner as X1666 stock except use *E. coli* strain OP50 and resuspend the pellet in M9 buffer (1/20th volume, or less, of the overnight culture).

Steps

Figure 3 is a diagram of the chemostat assembly.

1. Fill nutrient reservoir with 10 liters of 1/5 × S basal [substitute polyoxyethanyl-cholesteryl sebacate (Sigma, Cat. No. C-1145) for cholesterol] and add large stir bar.
2. Fill culture vessel with 0.2 vol water. Attach autoclavable 0.2-jiim filters to the vents and air entry tubing. Autoclave connected nutrient reservoir, culture vessel, and effluent tank.

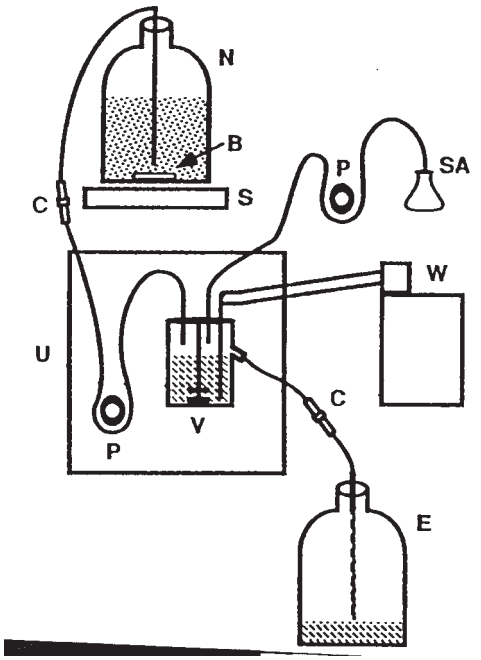

FIGURE 3 Chemostat assembly. N, nutrient reservoir; V, culture vessel; E, effluent tank; S, large stir plate; B, large stir bar (in reservoir to keep bacteria evenly suspended); W, refrigerated circulating water bath (set at 12°C) connected to cold finger of chemostat culture vessel; U, Bioflo I control unit; P, peristaltic pump; SA, selective agent; C, compression fitting (Swagelok Co.) used in the line for easy reservoir replacement (see Section III,C, step 12). Sterility is critical for the maintenance of long-term cultures.

3. When cool, add the other stock solutions, as to complete 1/5 × S medium (see Section B), to the nutrient reservoir.

4. Add the concentrate from 12 liters of overnight OP50 cultures to the nutrient reservoir (final $OD_{600\,nm}$ = ~3.7).

5. Install culture vessel in chemostat control unit and make connections.

6. Start air flow and stir the culture vessel impeller at 220 rpm. Set the heat regulator to 20°C.

7. Run the feeding pump until culture vessel is full; then turn it off.

8. Inoculate culture vessel with sterile LI larvae prepared as described in Section III,E, steps 10 and 11.

9. Add OP50 concentrate from a 1-liter overnight culture to culture vessel. Add approximately 1 ml sterile antifoam A (Sigma, Cat. No. A-5758) as necessary to minimize foam.

10. Monitor the culture every 2 days by removing a sample and counting replicate aliquots spotted on plates (see Section III,A). Continue to add sterile antifoam A to culture vessel as needed. When the culture reaches ~50 animals per 100/*A*, turn on the feeding pump (setting 9).

11. Monitor population density and adjust the speed of the feeding pump as necessary to maintain a reproducing culture. A dense population (~125 animals/10//I) that is mostly LI and L2 larvae and roughly one-fourth dauer larvae can be maintained.

12. Prepare a replacement nutrient reservoir for use when the first one is depleted. The effluent tank should be changed at the same time.

D. Freezing Strains for Long-Term Storage

The procedure is modified from that of Brenner (1974).

Solutions

1. *1M NaCl*: Dissolve 29.22 g of NaCl in a final volume of 500 ml distilled water and autoclave.

2. *S + glycerol*: Add 20 ml of 1*M* NaCl, 10 ml of KH_2PO_4 stock, and 60 ml of glycerol (Cat. No. G33) to 110 ml distilled water and autoclave.

Steps

1. Take three contaminant-free 60 × 15-mm plates 1 day after food is depleted and wash worms off plates with 2 ml M9 buffer.

2. Add equal volume of S + glycerol and mix by brief vortexing. Transfer in 0.5-ml aliquots to 2-ml cryovials (Vangard International, Cat. No. MS4502). Place vials in a styrofoam freezing box (a styrofoam block with holes the size of cryovials and a styrofoam lid) and immediately put at –70°C (cool at approximately 1°C/min).

3. After 6 h the vials can be transferred to liquid nitrogen or to standard –70°C freezer boxes.

4. One vial should be thawed to check for viability, strain accuracy, and microbial contamination. Thaw vial by warming between hands until liquid; then pour contents onto seeded plate. Transfer young healthy worms to fresh plates the next day.

E. Isolation of Staged Animals

Solutions

1. *Dauer-inducing pheromone stock* (*modified from Golden and Riddle, 1984*): Take 1 liter of starved liquid culture. Reduce volume 75% by evaporation under a stream of air at 100°C. Centrifuge at 10,000 RCF for 10 min. Dry the supernatant completely at 60°C. Extract four to six times with 50 ml of 95% ethanol until the extract is only slightly colored. Combine the extracts and dry under a stream of air at 60°C. Back-extract the resulting oily residue with 10 ml distilled water. Filter through Whatman 3 MM paper and store at 4°C.

2. *OP50 strep*: Transfer OP50 stock (see Section III, A) to preweighed sterile centrifuge bottles/tubes and centrifuge at 4000 RCF for 10 min. Remove supernatant and determine weight of bacteria. Resuspend in S medium to 5% (w/w). Add streptomycin (Sigma, Cat. No. S-6501) to 50/μg/ml final concentration. Store at 4°C for a maximum of 2 days.

Steps

1. Wash the worms off approximately five 60 × 15-mm plates containing a large number of gravid adults with approximately 2 ml M9 buffer per plate.
2. Combine in a 15-ml Corning polystyrene conical centrifuge tube and pellet nematodes. Remove all but 8 ml of the liquid.
3. Mix together 0.5 ml 5 *N* KOH and 1.2 ml 20% NaOCl (Cat. No. SS290) in a separate tube; combine with M9 and worms and vortex briefly.
4. Remove a small aliquot and monitor under a dissecting scope while agitating the remaining sample gently. When 50 to 75% of the adults in the sample have broken open, pellet nematodes.
5. Remove the supernatant, add 8 ml of fresh M9 buffer, and pellet. Repeat two more times leaving 0.5-ml volume after the last wash.
6. Resuspend the eggs and pipette onto plates. This method will generally leave some carcass parts.

Dauer Larvae

This procedure should give greater than 80% dauers.

1. Make NG agar without peptone (see Section III,A). Add approximately 25 ∧1/ml dauer-inducing pheromone stock just before pouring (make only as much as will be used immediately). Pour 2 ml per 35 × 10-mm plate.
2. After plates solidify, spot with 10 μl OP50 strep solution and allow to dry.
3. Add approximately 100 eggs or allow adults to lay 100 eggs; then remove the adults and incubate at 25°C for 48–60 h.

Other Stages

1. Follow the egg isolation procedure through step 5.
2. Bring volume to 10 ml with fresh M9 buffer; incubate on a rocker for 12 h or overnight.
3. Feed synchronized L1 larvae from the previous step. At 20°C mid-L1 larvae can be harvested after approximately 8 h, mid-L2 larvae at 18 h, mid-L3 larvae at 25 h, and L4 larvae at 37 h (Byerly *et al*., 1976).

IV. COMMENTS

For genetic analysis and maintenance of strains in active use, the nematodes should be grown on 60 × 15-mm petri plates. When large numbers of worms are needed, 100 × 15-mm plates are used. When special additives are being used that are expensive or in limited supply, 35 × 10-mm plates are used. Long-term storage of all strains and those not in active use is best accomplished by freezing in liquid nitrogen. For biochemical purposes the nematodes should be grown in liquid culture. Chemostat culturing enables selection on a continuously reproducing population whose density is held constant (Dykhuizen and Haiti, 1983). Most commonly, selection is for an altered growth rate, whether due to induced or spontaneous mutations. Liquid or gaseous selective agents are compatible with the system described.

More precise synchronization for L4 larvae and adults can be accomplished by synchronizing through the dauer stage. If large numbers of dauers are needed, they can be obtained by slightly modifying the liquid culturing procedure. The culture should be allowed to continue for 2–3 days after clearing. After sucrose flotation, treat with a sterile solution of 1% sodium dodecyl sulfate (SDS) for 1 hr [resuspend in 22.5 ml of M9 and add 2.5 ml of 10% SDS (dissolve 10 g of SDS, Cat. No. S529, in a final volume of 100 ml distilled water)]. Wash twice with M9 buffer and then repeat liquid culture protocol starting with step 3.

References

Brenner, S. (1974). The genetics *of Caenorhabditis elegans*. *Genetics* **77**, 71–94.

Byerly, L., Cassada, R. C., and Russell, R. L. (1976). The life cycle of the nematode *Caenorhabditis elegans*. I. Wild type growth and reproduction. *Dev. Biol*. **51**, 23–33.

Dougherty, E. C. (1960). Cultivation of Aschelminths, especially Rhabditid nematodes. *In* "*Nematology*" (J. N. Sasser and W. R. Jenkins, eds.), pp. 297–318. Univ. of North Carolina Press, Chapel Hill.

Dykhuizen, D. E., and Haiti, D. L. (1983). Selection in chemostats. *Microbiol. Rev.* **47**(2), 150–168.

Golden, J. W., and Riddle, D. L. (1984). The *Caenorhabditis elegans* dauer larva: Developmental effects of pheromone, food, and temperature. *Dev. Biol*. **102**, 368–378.

Hansen, E. L., and Hansen, J. W. (1978). *In vitro* cultivation of nematodes parasitic on animals and plants. *In* "*Methods of Cultivating Parasites in Vitro*" (A. E. R. Taylor and J. R. Baker, eds.), pp. 227–278. Academic Press, London.

Nicholas, W. L. (1975). "The Biology of Free-Living Nematodes," pp. 74–91. Clarendon Press, Oxford.

Sijmons, P. C., Grundler, F. M. W., von Mende, N., Burrows, P. R., and Wyss, U. (1991). *Arabidopsis thaliana* as a new model host for plant-parasitic nematodes. *Plant J*. **1**, 245–254.

Sulston, J. E., and Brenner, S. (1974). The DNA of *Caenorhabditis elegans*. *Genetics* **77**, 95–104.

Vanfleteren, J. R. (1980). Nematodes as nutritional models. *In* "*Nematodes as Biological Models*" (B. M. Zuckerman, ed.). Vol. 2, pp. 47–79. Academic Press, New York.

Wood, W. B. (1988). "The Nematode *Caenorhabditis elegans*" (W. B. Wood, ed.), pp. 1–16. Cold Spring Harbor Laboratory Press, Cold Spring Harbor, NY.

SECTION

4

Differentiation and Reprogramming of Somatic Cells

CHAPTER

20

Induction of Differentiation and Cellular Manipulation of Human Myeloid HL-60 Leukemia Cells

David A. Glesne and Eliezer Huberman

I. INTRODUCTION

The human myeloid HL-60 leukemia cell line has enjoyed widespread use in studies of the molecular mechanisms involved in the control of cell growth, differentiation, and apoptosis. Following stimulation with specific agents, these cells acquire a granulocytic (Collins *et al*., 1980), monocytic, or macrophage-like phenotype (Murao *et al*., 1983). The maturation of these precursor cells into their mature progeny occurs at a high percentage and with some degree of predictable temporal uniformity. The acquisition of mature phenotypes can be demonstrated by a variety of differentiation markers. These include enzymatic markers such as an increase in the activities of nonspecific esterase or lysozyme; morphological changes such as the appearance of segmented nuclei, which are characteristic of a granulocyte-like phenotype (Collins *et al*., 1980); or other markers such as cell attachment and spreading on culture dishes or increased phagocytosis, which are indicators of a macrophage phenotype (Tonetti *et al*., 1994). Additionally, there are a variety of well-characterized immunological markers, some of which are lineage and/or stage specific. The use of these markers and forceful expression of specific cDNAs or inhibition of a particular gene's expression by pertinent antisense oligonucleotides has allowed for the identification of the temporal order of many components involved in the signal transduction processes that lead to HL-60 cell differentiation (Semizarov *et al*., 1998; Laouar *et al*., 1999; Xie *et al*., 1998ab).

II. MATERIALS AND INSTRUMENTATION

HL-60 cells (Cat. No. CCL-240) are available from the American Type Culture Collection (ATCC). Culture medium RPMI 1640 (Cat. No. 11875-093), penicillin–streptomycin–glutamine (Cat. No. 10378-016), geneticin (Cat. No. 10131-035), and trypsin–EDTA (Cat. No. 15400-054) are from Invitrogen Life Technologies. Phorbol 12-myristate 13-acetate (PMA; Cat. No. P-1680) is from L.C. Laboratories, Inc. All-*trans* retinoic acid (ATRA; Cat. No. R-2625), L-α-lysophosphatidylcholine (Cat. No. L-4129), paraformaldehyde (Cat. No. P-1648), bovine serum albumin (BSA) fraction V (Cat. No. A-7906), anti-cd11b (Cat. No. C-0051), transferrin (Cat. No. T-2036), and insulin (Cat. No. I-6634) are available from Sigma Chemical Co. 1α,25-Dihydroxy-vitamin D_3 [1,25-$(OH)_2$vitD3; Cat. No. 679101] and hygromycin B (Cat. No. 400050) are from CalBiochem. PolyMount solution (Cat. No. 16866), 1.72-μm fluoresbrite beads (Cat. No. 17687), and hydroethidine (Cat. No. 17084) are from Polysciences Inc. 4′,6-Diamidine-2′-phenylindole dihydrochloride (DAPI; Cat. No. 236276) is available from Boehringer Manneheim Biochemicals. Lab-Tek chamber slides (eight-well, Cat. No. 178599) are from Nunc, Inc. Fetal bovine serum (FBS; Cat. No. SH30071) is from HyClone. Dimethyl sulfoxide (DMSO) molecular biology grade (Cat. No. BP231-100) is from Fisher. Antibodies against CD14 (Cat. No. 30541A) and HLA-DR (Cat. No. 555562) are available from BD Pharmingen. Antibody against human glyceraldehde-

Copyright 2006, Elsevier Science (USA).
All rights reserved.

3-phosphate dehydrogenase (GAPDH, Cat. No. CR1093SP) is from Cortex Biochem. Antibody against actin (Cat. No. sc-1615) is from Santa Cruz Biotech. Vector pRL-null (Cat. No. E227A) is from Promega, and pIRES2-EGFP (Cat. No. 6029-1) is from BD Clontech.

III. PROCEDURES

A. Cell Growth and Differentiation Induction

Materials

1. *Culture medium*: Supplement RPMI 1640 culture medium with penicillin–streptomycin (100 µg/ml), L-glutamine (200 m*M*), and 10% FBS. If cells are to be used for viable immunostaining, inactivate serum complement by heat inactivation (65°C for 15 min followed by slow cooling to room temperature). Culture medium can be stored at 4°C for several months.

2. *Differentiation inducer stock solutions*: Dissolve PMA, 1,25-$(OH)_2$vitD3, and ATRA in DMSO at a concentration of 1 mg/ml. Store small aliquots in sterile microcentrifuge tubes at –70°C and avoid repeated freezing/thawing.

3. *Differentiation inducer working solutions*: The most effective concentration for the induction of differentiation depends on the potency of individual lots of the inducer and the endogenous sensitivity of the HL-60 cells being used. Examples of appropriate concentrations for some common inducers of HL-60 differentiation are shown in Table I. For new chemical inducers, a series of concentrations of the inducer should be tested, and conditions that impart an inhibition of cell multiplication and the appearance of one or more myelomonocytic differentiation markers should be tested further. For many differentiation inducers, cells will exhibit maturation markers at inducer concentrations that inhibit about 50% or greater of cell multiplication rates.

4. *Cell culture*: The HL-60 cell line has a population doubling time of 20–24 h. Cell density should be maintained between 2×10^4 and 1×10^6 cells/ml with replacement of medium at high densities by pelleting of the cells by centrifugation if medium becomes acidified. Cultures should be maintained in either petri dishes or tissue culture plates at 37°C in an 8% CO_2, 95% water-humidified atmosphere.

Steps

1. Collect the cells and obtain cell density by hemocytometer chamber counting. Pellet the cells by gentle (250 *g*) centrifugation. Resuspend in fresh growth medium and plate the cells at 2–10 $\times 10^4$ cells/ml in culture dishes. Allow the cells to recover for several hours prior to addition of the inducing agent.

2. Dilute the differentiation-inducing agent in a minimal volume of culture medium and add to the experimental plates. Be sure to include a control culture to which the solution vehicle alone is added.

3. Culture cells at 37°C in an 8% CO_2 humidified atmosphere.

4. The appearance of differentiation markers occurs as early as 12 h and up to 6 days after treatment, depending on the concentration of the inducing agent and the marker to be assessed. To evaluate the phenotypic changes associated with cell differentiation, a series of morphological, biochemical, and immunological assays are performed (see Table II). We recom-

TABLE I Recommended Concentrations for Known Inducers of Differentiation in HL-60 Cells

Inducer	Concentration	End point	Reference
PMA	1–10 n*M*	Macrophage	Murao *et al.* (1983)
1,25-$(OH)_2$vitamin D_3	10–100 n*M*	Monocytic	Murao *et al.* (1983)
ATRA	100–1000 n*M*	Granulocytic	Breitman *et al.* (1980)
Mycophenolic acid	3–10 µ*M*	Granulocytic	Collart and Huberman (1990)
DMSO	1–2%	Granulocytic	Collins *et al.* (1980)

TABLE II Examples of Markers Used to Characterize Differentiation in HL-60 Cells

Marker	Gran[a]	Mono[b]	Mac[c]	Reference
OKMl MAb (CDllb)	+++	+++	++	Foon *et al.* (1982)
Banded and segmented nuclei	+++	–	–	Breitman *et al.* (1980)
Nonspecific esterase staining	Weak	+++	++	Yam *et al.* (1971)
Lysozyme activity	Weak	+++	+++	Murao *et al.* (1983)
Attachment and spreading	–	+	+++	Tonetti *et al.* (1994)
Phagocytosis	Weak	+	+++	Tonetti *et al.* (1994)
NM-6 MoAb	+++	+++	–	Murao *et al.* (1989)

[a] Granulocytic cells; treated with 1.2% DMSO.
[b] Monocytic cells; treated with 100 n*M* 1,25-$(OH)_2$vitamin D_3.
[c] Macrophage-like cells; treated with 3 n*M* PMA.

mend that two to three different assays be used to determine whether the cells acquire a granulocytic, monocytic, or macrophage-like phenotype. Many of the biochemical or histochemical markers can be assessed using commercially available kits.

B. Cell Adhesion and Spreading Assay

Material

Phosphate-buffered saline (PBS): To make 1 liter of stock solution (10×), dissolve 80.0 g of NaCl, 2.0 g of KCl, 2.0 g of KH_2PO_4, and 11.4 g of Na_2HPO_4 in high-quality (Milli-Q) water and sterilize by autoclaving. Dilute to 1× in water.

Steps

1. Treat HL-60 cells cultured in bacteriological petri dishes (see Section IV) with PMA and incubate at 37°C in an 8% CO_2, humidified atmosphere for 2 days.
2. Collect unattached cells by gentle pipetting and wash petri dishes twice with PBS, combining the washes with the initially collected cells.
3. Recover the remaining attached cells by treatment for 10 min with PBS supplemented with 0.05% trypsin–EDTA followed by forceful pipetting and/or use of a rubber policeman.
4. Count the number of attached and unattached cells using a hemocytometer chamber and calculate the percentage of attached cells as a function of the total recovered cell number.
5. In parallel, determine the number of spread cells by counting flattened cells (Fig. 1) in several microscopic fields of view. Count at least 200 cells/data point; the percentage cell spreading = (number of spread cells/total number of adherent cells) × 100.

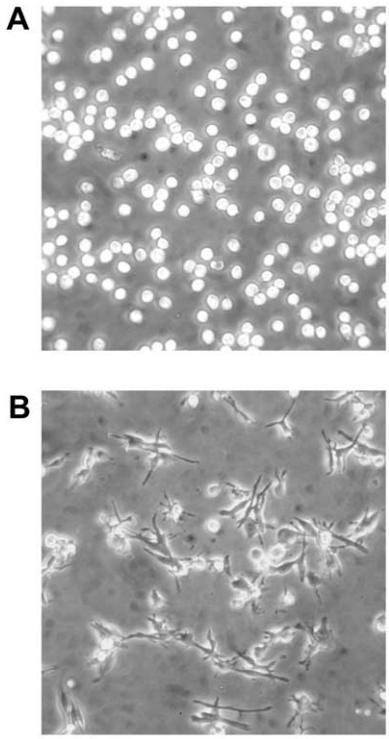

FIGURE 1 Bright-field microscopy images representing an example of HL-60 cells either untreated in suspension (A) or attached and spread following a 3-day treatment with 10 n*M* PMA (B).

C. Phagocytosis Assay

Materials

1. *Fluorescent beads*: Sterilize and opsonize fluorespbrite beads by first adding three drops of beads to 10 ml of 70% ethanol. Mix and agitate at room temperature for 20 min. Recover the beads by centrifugation (400 *g*) and wash twice with PBS. After the second wash, add 5 ml of RPMI 1640 supplemented with 1 ml FBS (not heat inactivated). Mix and incubate overnight at 37°C with slow agitation. Pellet the beads at 1000 *g* and resuspend in 1 ml of culture medium at a concentration of 4×10^8 beads/ml.
2. *Working solutions*: Prepare the following solutions using PBS as solvent: 4% paraformaldehyde, 10 µg/ml L-α-lysophosphatidylcholine, 0.1 µg/ml DAPI, and 10 µg/ml hydroethidine.

Steps

1. Plate 1.2×10^4 cells in 400 µl of growth medium into each well of an eight-well Lab-Tek chamber slide. Treat the cells with PMA or other inducer as described previously.
2. After 30 h, add 100 µl of the bead suspension to each well.
3. Incubate for an additional 18 h, gently remove the growth medium, and air dry the cells for 30 s using a heated slide dryer.
4. Fix the cells by adding 100 µl of 4% paraformaldehyde to each well for 20 min and then washing each well several times with PBS.
5. Add 100 µl of L-α-lysophosphatidylcholine solution to each well for 20 min to permeabilize the cells, followed by several washes with PBS.
6. Cell nuclei are stained by incubation with DAPI for 5 min. Remove excess stain by washing with PBS and then counterstain the cytoplasm by incubating with hydroethidine for 10 min.
7. After three washes in PBS, remove the well partitions and mount the slide with Poly-Mount or other mounting medium and a coverslip.

8. Examine the cells using a fluorescent microscope equipped with a DAPI/UV-range filter set. DAPI-stained nuclei should appear blue, the stained cytoplasm red, and the fluoresbrite beads as small blue dots. A cell is considered positive for phagocytosis activity if it has engulfed more than 20 beads. Count >200 cells per point.

D. Immunofluorescence

Materials

1. *PBSA*: dissolve BSA (Cohn fraction V) to 1% in PBS.

2. *Primary antibodies*: Numerous monoclonal and polyclonal antibodies are available to characterize the phenotype of mature myeloid cells. These include but are not limited to the Mac-1/antiCDllb, CD14, or class II HLA-DR antigens. A more categorical listing is available online (http://www.bdbiosciences.com/pdfs/other/01-81024-3.pdf). These are available from many commercial sources (e.g., Immunotech, Coulter Immunology, Santa Cruz, Sigma, Pharmingen) and should be prepared and used according to the manufacturer's recommendations. For a new antibody, it is often prudent to perform a dilution series with both positive and negative controls to select an antibody concentration that provides a positive signal with a low background. For semiquantitative ratio imaging, useful standard antibodies are against GAPDH (sheep polyclonal, Cortex Biochem.) or actin (goat polyclonal, Santa Cruz). All antibody stock solutions are created by dilution in PBSA.

3. *Secondary antibodies*: There are numerous sources of labeled secondary antibodies. If one is to perform multiantigen imaging, it is critical that the secondary antibodies have been cross-absorbed against the other host organisms antibody repertoire. Such cross-absorbed antibodies are available tagged to a variety of fluorophores from both Jackson Immunoresearch and Molecular Probes. Stock solutions of these secondary antibodies are prepared at 1 mg/ml in 50% glycerol/50% PBS. Store aliquots of the stock solution at –70°C. Prepare a working solution of the secondary antibody by diluting from 1:50 to 1:500 in PBSA using the furthest dilution that still provides significant signal.

4. *Microscopy*: A microscope equipped with multiple filter sets and/or cubes is required to visualize the fluorescence signal from multiple fluorophores. If one is to perform semiquantitative ratio imaging using multiple fluorescent signals, it is useful to have either an automated cube turret or automated excitation and emission filter wheels and a multipass dichroic cube. Both this hardware and SlideBook software for processing such images are available from Intelligent Imaging Innovations (Denver, CO).

5. *Flow cytometery*: For the assessment of marker induction in granulocytic differentiation, flow cytometry has many advantages, particularly regarding the stastical significance attainable by scanning larger cell populations. However, in the case of monocytic and macrophage differentiation, significant clumping of cells is unavoidable and may lead to artifactual results. We therefore recommend fluorescence microscopy for such experiments and the examination of at least 200 cells per data point.

Steps

Reactions are performed on ice using either microcentrifuge tubes or, to facilitate the handling of numerous samples simultaneously, V-bottom 96-well plates.

1. Recover the cells by centrifugation and resuspend in PBS at 2×10^6/ml; add 200 µl of the cells for each collection of antibodies to a well of the microtiter plate.

2. Centrifuge the plate (400 *g*), remove the supernatant gently by inversion, and fix the cells by incubation with 100 µl of 4% paraformaldehyde for 15 min. Wash twice with PBS.

3. If the antigen to be visualized is not on the outside of the cell membrane, permeabilize the cells by the addition of either L-α-lysophosphatidylcholine solution or 0.1% Triton X-100 in PBS for 5 min. Wash the cells three times with PBS.

4. Resuspend the cells in 100 µl of PBSA and allow for blocking of nonspecific sites by incubation for 15 min. Recover cells by centrifugation and mix the cells with 100 µl of diluted primary antibody or mixture of antibodies (or a dilution series may be used) and incubate for 45 min at room temperature.

5. After washing the cells twice with PBS, add 100 µl of diluted secondary antibodies and continue incubating for 30 min.

6. Wash the cells three times with PBS and then mount onto microscope slides using a small volume of a mounting solution. Overlay with a cover glass and seal with nail polish. Examine by fluorescence microscopy.

E. Transfection and Establishment of Stable Cell Lines

Materials

1. Most chemical approaches (e.g., charged lipids) for the transfection of HL-60 cells produce very poor results. Better transfection is achieved using electro-

poration, particularly with a square-wave device, and to a lesser degree by an exponential-decay device. We use a BTX T820 square-wave electroporator and achieve maximally 10–20% transfection rates.

2. For analysis of promoter activities, either CAT assays or luciferase activities can be monitored in HL-60 cells. However, standard firefly luciferase is unstable or degrades rapidly and the *Renilla* luciferase should be employed instead (pRL vectors, Promega).

3. Due to the low transfection efficiency of HL-60 cells, transient transfection assays should include a readily visualizable marker of transfection such as cotransfection with an EGFP plasmid, or preferably using a vector that expresses both your gene of interest and EGFP from the same plasmid (pIRES2-EGFP, Clontech).

Steps

1. If transient assays are to be performed, use 15 µg of supercoiled plasmid per transfection. If stable transfectants are to be isolated, linearize each plasmid with a restriction endonuclease that cleaves the vector but leaves your gene of interest, the selectable marker, and any regulatory elements intact. Solve either preparation in a small volume of PBS.

2. Collect HL-60 cells by centrifugation and resuspend at 1.0×10^6 in growth medium. Combine 400 µl of cells with DNA in a 0.4-cm-gap electroporation cuvette. Allow to stand for 5 min at room temperature.

3. Mix the cuvette by gentle tapping and insert into a square-wave electroporation device. Electroporate with three pulses of 1500 V each and 90 µs duration.

4. Allow the cells to recover for 5 min and then plate into 10 ml of growth medium and incubate at 37°C in 8% CO_2 in a humidified atmosphere.

5. For transient assays, recover the cells the next day and perform CAT or luciferase assays by standard protocols. For monitoring of fluorescence from EGFP expression, prepare the cells as in steps 1 and 2 of the immunofluorescence protocol, mount the cells, and examine for EGFP expression using a FITC filter set.

6. For stable transfectant recovery, wait 24 h and then add appropriate selective agent. Geneticin and hygromycin B are effective at 500 and 150 µg/ml, respectively, in HL-60 cells.

7. Allow for selection of stable transfectants by growth for 7–10 days. Cells can either be maintained at this stage as a pooled group of transfectants or individual clones can be isolated by single-cell dilution and expansion in 96-well plates.

8. Successful transfection in pools or individual clones should be monitored either by immunofluorescence or by Western blotting using either an antibody against the protein or an epitope tag if present.

F. Inhibition of Gene Expression Using Synthetic Oligonucleotides

Materials

1. Synthetic oligonucleotides should be synthesized as 15-mers using standard base chemistry. The exact concentration at which an oligonucleotide effectively disrupts translation or targets a given mRNA for RNase-mediated decay is a function of intracel-lular concentration, expression level of the target, and ability of the oligonucleotide to hybridize, i.e., secondary structure limitations. Therefore, several oligonucleotides and a range of oligonucleotide concentrations with a suitable scrambled control oligonucleotide need to be empirically tested. Initial experiments with siRNA indicate that effective gene knockdown by this approach can be performed transiently, but long-term expression of dsRNA may induce an interferon response (Bridge *et al*., 2003) in HL-60 cells.

2. Prepare solutions of 5 mg/ml transferrin and 5 mg/ml insulin in unsupplemented RPMI 1640 medium. Prepare serum-free growth medium by supplementing RPMI 1640 with standard concentrations of penicillin–streptomycin (100 µg/ml) and L-glutamine (200 m*M*).

Steps

1. Collect HL-60 cells by centrifugation and wash three times in serum-free growth medium. Count the cells by hemocytometer chamber counting and plate the cells at 1×10^5 cells/ml in serum-free growth medium.

2. Supplement the cells with 5 µg/ml transferrin and 5 µg/ml insulin. Add a series of dilutions of your test and control oligonucleotides spanning a concentration range from 100 n*M* to 100 µ*M*.

3. Allow uptake of the oligonucleotide to occur over a period of 6 h incubation at 37°C in an 8% CO_2 in a humidified atmosphere.

4. Restore FBS levels to 10% and allow overnight growth.

5. Monitor toxicity to the cells by trypan blue dye exclusion assays. Determine the effect of your test and control oligonucleotides on the expression of your gene of interest by either immunofluorescence or reverse transcriptase polymerase chain reaction (rtPCR) approaches.

6. Subsequent effects on differentiation induction and specific marker appearance can then be determined by following steps 1–4 and then adding the specific chemical inducer.

IV. COMMENTS AND PITFALLS

1. When thawing materials (antibodies, antigen, or samples), mix thoroughly before dilution or processing. Avoid multiple freeze–thaw cycles by aliquoting small volumes of reagents into multiple microcentrifuge tubes for storage.

2. When using all-*trans* retinoic acid, avoid exposure to light.

3. Fluorescent-activated cell sorting quantitation is not recommended when the differentiation inducer causes cell clumping, as is the case with PMA and related chemicals.

4. For some inducers that cause attachment, trypsin–EDTA treatment may not remove all cells from the surface of tissue culture dishes. Therefore, bacteriological grade petri dishes are utilized for procedures that require removal of the attached cells.

5. Use multiple differentiation markers when testing the effect of a new inducer.

6. In preparing cells for immunological analysis, use heat-inactivated serum to eliminate cell killing due to active complement.

Acknowledgments

This work was supported by the U. S. Department of Energy, Office of Health and Environmental Research, under Contract W-31-109-ENG-38, and the National Institutes of Health under Grant CA80826.

References

Breitman, T. R., Selonick, S. E., and Collins, S. I. (1980). Induction of differentiation of the human promyelocytic leukemia cell line (HL-60) by retinoic acid. *Proc. Natl. Acad. Sci. USA* **77**, 2936–2940.

Bridge, A. J., Pebernard, S., Ducraux, A., Nicoulaz, A. L., and Iggo, R. (2003). Induction of an interferon response by RNAi vectors in mammalian cells. *Nature Genet.* **34**, 263–264.

Collart, F., and Huberman, E. (1990). Expression of IMP dehydrogenase in differentiating HL-60 cells. *Blood* **75**, 570–576.

Collins, S. I., Bonder, A., Ting, R., and Gallo, R. C. (1980). Induction of morphological and functional differentiation of human promyelocytic leukemia cells (HL-60) by compounds which induce differentiation of murine leukemia cells. *Int. J. Cancer* **25**, 213–218.

Foon, K. A., Schroff, R. W., and Gale, R. P. (1982). Surface markers on leukemia and,lymphoma: Recent advances. *Blood* **60**, 1–19.

Laouar, A., Collart, F. R., Chubb, C. B., Xie, B., and Huberman, E. (1999). Interaction between alpha 5 beta 1 integrin and secreted fibronectin is involved in macrophage differentiation of human HL-60 myeloid leukemia cells. *J. Immunol.* **162**, 407–414.

Murao, S., Collart, F. R., and Huberman, E. (1989). A protein containing the cystic fibrosis antigens is an inhibitor of protein kinases. *J. Biol. Chem.* **264**, 8356–8360.

Murao, S., Gemmell, M. A., Callal1am, M. F., Anderson, N. L., and Huberman, E. (1983). Control of macrophage cell differentiation in human promyelocytic HL-60 leukemia cells by 1,25-dihydroxyvitamin D3 and phorbol-12-myristate-13-acetate. *Cancer Res.* **43**, 4989–4996.

Semizarov, D., Glesne, D., Laouar, A., Schiebel, K., and Huberman, E. (1998). A lineage-specific protein kinase crucial for myeloid maturation. *Proc. Natl. Acad. Sci. USA.* **95**, 15412–15417.

Tonetti, D. A., Henning-Chubb, C., Yamanishi, D. T., and Huberman, E. (1994). Protein kinase C-β is required for macrophage differentiation of human HL-60 leukemia cells. *J. Biol. Chem.* **269**, 23230–23235.

Xie, B., Laouar, A., and Huberman, E. (1998a). Autocrine regulation of macrophage differentiation and 92-kDa gelatinase production by tumor necrosis factor-alpha via alpha5 beta1 integrin in HL-60 cells. *J. Biol. Chem.* **273**, 11583–11588.

Xie, B., Laouar, A., and Huberman, E. (1998b). Fibronectin-mediated cell adhesion is required for induction of 92-kDa type IV collagenase/gelatinase (MMP-9) gene expression during macrophage differentiation: The signaling role of protein kinase C-beta. *J. Biol. Chem.* **273**, 11576–11582.

Yam, L., Li, C. Y., and Crosby, W. H. (1971). Cytochemical identification of monocytes and granulocytes. *Am. J. Clin. Pathol.* **55**, 283–290.

CHAPTER

21

Cultured PC12 Cells: A Model for Neuronal Function, Differentiation, and Survival

Kenneth K. Teng, James M. Angelastro, Matthew E. Cunningham, and Lloyd A. Greene

I. INTRODUCTION

Since its initial description and characterization in 1976 (Greene and Tischler, 1976), the rat pheochromocytoma PC12 cell line has become a commonly employed model system for studies of neuronal development and function. In particular, PC12 cells have been a convenient alternative to cultured neurons for studying the trophic and differentiative actions of nerve growth factor (NGF; reviewed by Levi-Montalcini and Angeletti, 1968; Levi and Alemá, 1991). When cultured in serum-containing medium, PC12 cells adopt a round and phase-bright morphology and proliferate to high density. Under these conditions, PC12 cells display many of the properties associated with immature adrenal chromaffin cells and sympathicoblasts. When challenged with physiological levels of NGF, these cells cease division, become electrically excitable, extend long branching neurites, and gradually acquire many characteristics of mature sympathetic neurons. Under serum-free conditions, NGF promotes not only neuronal differentiation of PC12 cells, but also their survival (Greene, 1978; Rukenstein *et al.*, 1991).

Several attributes of PC12 cells have led to their widespread popularity in neurobiological research. These include their relatively high degree of differentiation before and after NGF treatment, homogeneous response to stimuli, availability in large numbers for biochemical studies, and suitability for genetic manipulations. This article details experience gained with this cell line in terms of tissue culture requirements and treatment with NGF, as well as quantitative assessment of NGF actions. In addition, we describe some of the potential difficulties that one may encounter when culturing PC12 cells and suggest possible means to avoid or ameliorate these problems. The reader is referred to several prior articles (Greene and Tischler, 1982; Greene *et al.*, 1987, 1991) for a more in-depth discussion of the properties and experimental exploitation of the PC12 cell line.

II. MATERIALS AND INSTRUMENTATION

Rosewell Park Memorial Institute 1640 (RPMI 1640) medium is purchased from Invitrogen (Carlsbad, CA; Cat. No. 23400062) in powder form. Donor horse serum (Cat. No. 12-44977P), fetal bovine serum (Cat. No. 12-10377P), and penicillin/streptomycin (Cat. No. 59-60277P) are obtained from JRH Biosciences (Lenexa, KA). It is recommended that sera be prescreened for their capacities to promote PC12 cell growth and maintenance The horse serum should be heat inactivated in a 56°C water bath for 30 min before use.

Tissue culture plasticwares are obtained from Falcon, Becton Dickson and Company (Lincoln Park, NJ). Freezing vials are purchased from Nunc, Denmark (Cat. No. 377267). Millipak-60 filters (0.22 µm, Cat. No. MPGL06SH2) are from Millipore (Bedford, MA). Filter units (0.45 µm, Cat. No. 245-0045) are obtained from Nalgene Company (Rochester, NY). Ethylhexadecyldimethylammonium bromide (Cat.

Copyright 2006, Elsevier Science (USA).
All rights reserved.

No. 117 9712) is purchased from Eastman Kodak Company (Rochester, NY).

NGF is prepared from adult male mouse submaxillary glands as described by Mobley *et al*. (1976). The glands can be purchased from Harlan Bioproducts for Science (Indianapolis, IN; Cat. No. 516) and stored at –80°C until use. NGF stocks (>100 µg/ml; in pH 5.0 acetate buffer, 0.4 M NaCl) are stored at –80°C and, once thawed, can be kept at 4°C for at least 1 month without significant loss of activity. Recombinant or purified NGF may also be purchased from a variety of commercial suppliers, including Harlan Bioproducts for Science, Roche Molecular, and Upstate Biotechnology, Inc.

Rat tail collagen is prepared in 0.1% acetic acid as described previously (Greene *et al*., 1991) from the tendons of rat tails [see Fig. 14.2 of Kleitman *et al*. (1991) for a photographic illustration of the procedure for exposing and removing rat tail tendons]. Each large tail furnishes approximately 200 ml of stock collagen. Aliquots of collagen stock are stored at –20°C. Once thawed, the stock can be stored for up to several months at 4°C. Sterile technique should be employed throughout the preparation.

III. PROCEDURES

A. Routine Tissue Culture Techniques

Solutions

1. *Complete growth medium*: Prepare RPMI 1640 medium according to the supplier's protocol in reverse osmosis/Milli-Q or double-distilled water. After the addition of sodium bicarbonate (2 g/liter), penicillin (final concentration 25 U/ml), and streptomycin (final concentration 25 µg/ml), sterilize the medium by pressure filtration (driven by 90% air, 10% CO_2 mixture) through a Millipak-60 filter unit, dispense into 500-ml autoclaved bottles, and store in the dark at 4°C. The bottles should be dedicated to tissue culture only and should be cleaned by thorough rinsing without soap or detergent. To make up complete growth medium, add 50 ml of heat-inactivated horse serum and 25 ml of fetal bovine serum to 500 ml of RPMI 1640 medium. Store complete growth medium at 4°C.

2. *Medium for freezing of cells*: Mix 1 volume of dimethyl sulfoxide (DMSO) with 9 volumes of complete growth medium. This medium should be freshly prepared for immediate use only.

Steps

1. PC12 cells show optimal adherence to collagen-coated culture dishes. Before applying to dishes, freshly dilute the stock collagen solution with autoclaved reverse osmosis/Milli-Q water as noted later. The optimal final dilution of the collagen should be determined empirically by testing various concentrations for their capacities to foster cell attachment and NGF-promoted neurite outgrowth (Greene *et al*., 1991). At too low a dilution, adhesion to substrate is poor, whereas at too high a concentration, neurite outgrowth is impeded and cells are difficult to dislodge for subculture. For application to plates without the necessity of spreading a thin layer, add the diluted collagen solution (typically a 1:50 dilution of the stock is optimal) to plastic tissue cultureware (10 ml/150-mm dish; 5 ml/100-mm dish; 1 ml/35-mm dish; 0.5 ml/well of 24-well culture plates). Leave dishes uncovered to air dry overnight in a tissue culture hood. Alternatively, for quicker drying, dilute the collagen by a factor of five less and add to cultureware in one-fifth the aforementioned volumes. Spread the collagen evenly over the surface of the culture dish with the use of an L-shaped glass rod. Dry collagen by leaving the plates uncovered for 1–2 h in a tissue culture hood. Store collagen-coated dishes at room temperature and use within 1 week after preparation.

2. Feed PC 12 cells three times a week with complete growth medium. Remove approximately two-thirds of the culture1 medium from each plate and replace with fresh complete growth medium (10 ml for 150-mm dishes; 5 ml for 100-mm dishes; 1.5 ml for 35-mm dishes). The medium should be added gently and from the side of the tissue culture dish. The feeding schedule should be kept rigid for maximum cell viability. Maintain PC12 cells in a 37°C incubator with a water-saturated, 7.5% COs atmosphere.

3. Passage PC12 cells (subcultured) when the cultures are 80–90% confluent. Dislodge the cells from the surface of the dish by repeated and forceful discharge of the culture medium directly onto the cells with a disposable glass Pasteur pipette. Forceful trituration of the cell suspension within the Pasteur pipette also decreases cell clumping. Mix the culture medium containing detached PC12 cells with fresh complete medium in a 1:3 or 1:4 ratio. Plate the PC12 cells onto collagen-coated dishes, and increase the passage number of the newly plated PC12 cells by one. As the cell doubling time is 3–4 days, subculture every 7–10 days. To avoid the potential accumulation of variants within the cultures, experiments should be carried out with cells that have undergone no greater than 50 passages.

4. Stock cultures of PC12 cells are frozen at high density (>5 × 10^6 cells/ml; see later for cell counting procedure) as follows. Dislodge cells from tissue culture dish as described earlier, pellet by centrifuga-

tion at room temperature for 10 min at 500 *g*, and remove the medium. Add the appropriate volume of freezing medium (described earlier) and resuspend the cell pellet. Aliquot into a Nunc freezing vial (1 ml/vial) and transfer to a –80°C freezer for at least 1 day. For high-viability, long-term storage, the vials should be maintained in liquid nitrogen. The vials should not be permitted to warm up during the transfer to liquid nitrogen (e.g., transfer on dry ice).

5. Thaw frozen PC12 cell stocks (in freezing vials) rapidly in a 37°C water bath (2–3 min). Immediately transfer the cells into 9 volumes of complete growth medium. Pellet the cells by centrifugation at room temperature for 10 min at 500 *g*. Discard the supernatant. Resuspend the cell pellet in fresh, complete growth medium and plate cells on collagen-coated dishes.

B. Promotion and Assessment of NGF-Dependent Neurite Outgrowth

Solution

Low serum medium: Mix 1 ml of heat-inactivated horse serum per 100 ml of RPMI 1640 medium. Store at 4°C.

Steps

1. Dislodge PC12 cells from stock culture dishes and triturate well using a glass Pasteur pipette to break up cell clumps. Then plate cells at low densities (5×10^6 cells per 150-mm dish; $1–2 \times 10^6$ cells per 100-mm dish; $2–5 \times 10^5$ cells per 35-mm dish; see cell-counting procedure described later) on collagen-coated dishes in medium supplemented with NGF (50–100 ng NGF final concentration/ml of medium). Dilute NGF from the stock into the medium just before use. Because NGF binds to glass surfaces, use plasticware. Diluted solutions of NGF are not stable. Although neurite outgrowth is satisfactory in complete growth medium, low serum medium is recommended instead in order to economize on serum as well as to reduce cell clumping. Once plated, the cultures should be maintained in a 37°C incubator with a water-saturated, 7.5% CO_2 atmosphere and exchange the medium three times per week as described earlier. Neurite-bearing cells should be noticeable within 1–3 days of NGF treatment, and the number of PC12 cells with neurites should increase progressively with time of NGF exposure. By 7–10 days of treatment, at least 90% of the cells should generate neurites.

2. To determine the proportions of neurite-bearing PC12 cells after NGF treatment, observe cultures with a phase-contrast microscope under high magnification (e.g., 200×). Within random fields, score the proportions of cells that possess at least one neurite greater than 20 µm (about two cell body diameters) in length. Continue counting until the total number of cells assessed exceeds 100. For consistent results, count only discernible and/or single cells, but not cell clumps. To determine mean neurite lengths and rates of neurite elongation, observe cultures using an eyepiece equipped with a calibrated micrometer. The latter is used to measure the entire length of randomly chosen neurites. At least 20–25 neurites are measured per culture.

3. Neurite regeneration experiments are carried out with NGF-pretreated PC12 cell cultures. This permits study of rapid neurite growth as well as a quantitative bioassav for NGF. Treat the cells first with NGF for 7–10 days as described in step 1. Then rinse the cultures five times with medium (without NGF) while the cells are still attached to the substrate. Mechanically dislodge the cells from the dish by trituration through a Pasteur pipette and wash them an additional five times in medium (without NGF) by repeated centrifugation at 500 *g* for 10 min at room temperature. Plate the washed cells at low density (about 10^5 cells/35-mm dish) in medium (complete or low serum) in the presence or absence of NGF (see step 1). Examine the cultures 24 h later and score for percentage of neurite-bearing cells or cell clumps. Because NGF-treated PC12 cells tend to aggregate, it is often necessary to score clumps rather than single cells. The ability of NGF to induce neurite regeneration from PC12 cells is determined by subtracting the number of neurite-bearing cells in culture medium without NGF from the number of neurite-bearing cells in NGF-containing culture medium. For well-washed cultures, 80–100% of the cells or cell clumps should regenerate neurites with NGF, whereas no more than 10–20% should regenerate neurites in the absence of NGF. The regeneration protocol can be used as a quantitative bioassay for NGF (Greene *et al*., 1987).

C. Assessment of Survival-Promoting Actions of NGF and Other Substances

Solutions

1. *Nuclei counting solution stock (Soto and Sonnenschein, 1985):* Dissolve 5 g ethylhexadecyldimethylammonium bromide and 0.165 g NaCl in 80 ml of reverse osmosis/Milli-Q water. Add 2.8 ml glacial acetic acid and 1 drop bromphenol blue. Bring final volume to 100 ml and filter through a 0.45-µm filter unit. Store the solution at room temperature.

2. *Working nuclei counting solution (Soto and Sonnenschein, 1985):* Mix phosphate-buffered saline (10 ml),

10% Triton X-100 (5 ml), 1 *M* $MgCl_2$ (200 µl), and nuclei-counting solution stock (10 ml) with enough reverse osmosis/Milli-Q water so that the final volume is 100 ml. Pass through a 0.45 µm filter unit. Store the working nuclei-counting solution at room temperature.

Steps

1. To determine the numbers of PC12 cells suspended in culture or other medium, pellet the cells by centrifugation, aspirate to remove the medium, and resuspend the cells in a known volume of the working nuclei-counting solution. This solution provides a homogeneous suspension of intact nuclei, which are quantified using a hemocytometer. To count cells attached to a substrate, remove the medium and replace with a known volume of working nucleus-counting solution. Resuspend nuclei by trituration and quantify with a hemocytometer.

2. Wash PC12 cells (either naïve cells growing with serum or neuronally differentiated cells growing with serum and NGF) with serum-free RPMI medium five times while still attached to culture dishes and then, after detachment by trituration, wash another five times in serum-free RPMI medium by centrifugation/resuspension. Resuspend the cells in RPMI 1640 medium with or without NGF or other potential trophic agents. Plate the cells in collagen-coated, 24-well culture plates in 0.5 ml of medium ($0.5–2 \times 10^5$ cells/well). Exchange the serum-free culture medium three times per week. Carry out cell counts by removing the medium, adding working nuclei-counting solution, and counting intact nuclei. Typically, without trophic substances such as NGF, 50% of the cell die by 24 h of serum deprivation and 90% by 3–4 days.

D. Cationic Lipid-Based Transfection Protocol for PC12 Cells

Solutions

OptiMEM-I and Lipofectamine2000: Both reagents are purchased from Invitrogen. OptiMEM-I is used for transfection without antibiotics.

Steps

1. As noted in Section I, an advantage of PC12 cells is that they can be subjected to genetic manipulation. A relatively high transient transfection efficiency (at least 20–30%) of PC12 cells is attainable by the use of lipid-based transfection reagents (Fig. 1). Following transfection, stable lines of PC12 transfectants can also be obtained by applying the appropriate selection pressure (e.g., G418 for mammalian expression plasmid carrying the neomycin resistance gene). The day before transfection, seed PC12 cells at high density (at least 90–95% confluency) on collagen-coated tissue culture plates and maintain in complete growth medium.

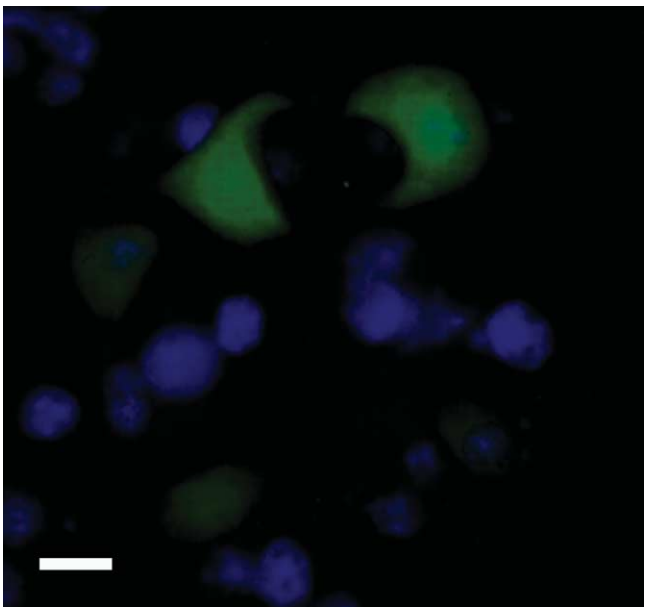

FIGURE 1 PC12 cells expressing green fluorescent protein (GFP). Photomicrograph of non-NGF-treated (naive) PC12 cells transfected with plasmid expressing GFP (green), followed by DAPI staining (blue). Bar: 50 µm.

2. For PC12 cells plated on a 100-mm dish, add 8 µg DNA to 500 µl OptiMEM-I in one tube (tube 1) and add 20 µl Lipofectamine2000 to 500 µl OptiMEM-I in another (tube 2). The contents of tube 2 should be incubated at room temperature for at least 5 min before dropwise addition to tube 1. After which, incubat the mixture further at room temperature for 20 min.

3. During this time, remove complete growth medium from PC12 cells and replace with 4 ml of OptiMEM-I.

4. Add the Lipofectamine2000/DNA mixture to the PC12 cells and return the culture to the incubator. After 4–6 h, aspirate the Lipofectamine2000/DNA mixture (in OptiMEM-I) off completely and replace with complete growth medium. Expression of the transgene can be monitored 24–48 h afterward.

5. Note that the amount of DNA and Lipofectamine2000, as well as the volume of OptiMEM-I, can be adjusted proportionally to accommodate PC12 cells that are plated on smaller/larger size tissue culture plates. The aforementioned procedure can also been used to transfect PC12 cells that were already differentiated by NGF treatment. However, the transfection efficiency is significantly lower (1–2%) due to the need

to culture neuronally differentiated PC12 cells at lower density.

IV. COMMENTS

By adhering to the aforementioned protocols, our laboratory has been able to maintain (since 1977) PC12 cell stocks that are consistently responsive to NGF and that present a stable phenotype. However, a survey of the literature concerning the use of PC12 cells occasionally reveals conflicting or inconsistent results between laboratories. One possible cause for this may be the generation of variant "PC12 cell" lines. Like other continuous cell lines, PC12 cells are subjected to spontaneous mutations, and clonal PC12 cell variants have been identified from past studies. The introduction of nonstandard culture methods (e.g., changing sera, medium, substrate) can favor the selection of such variants over the wild-type population. Although the use of "variant" PC12 cell lines does not necessarily undermine the validity of data generated with them, it can give rise to uncertainty or confusion when one attempts to integrate/reproduce the finding from various reports. It is therefore our suggestion that a uniform standard of culturing PC12 cells be adopted for studies with this cell line.

Another cautionary note on the use of the PC12 cell line is that although it is a convenient model system for studying neuronal development and function, it is not a full substitute for "bona fide" nerve cells. Therefore, whenever feasible, experimental results obtained with PC12 cells should be verified or compared with representative neurons.

V. PITFALLS

1. Poor survival or growth of stock cultures has three probable causes: (i) the initial plating density is too low, (ii) the horse serum is not properly heat inactivated or is of insufficient quality (the latter is the usual cause for failure to thrive), and (iii) the culture medium is outdated (the glutamine has degraded).

2. The most probable cause of poor cell adherence is an insufficient level of collagen as the substrate.

3. A poor NGF response is indicated by the continuous proliferation of PC12 cells in NGF-containing medium and by the lack of neurite-bearing cells even after long-term NGF treatment. A possible cause is that the initial plating density is too high. Another is that the NGF may be inactive. Alternatively, the collagen concentration on the dishes is too high or too low or the collagen has deteriorated. Finally, the cultures may contain a high proportion of nonresponsive variants (in this case, start with a new cell stock of lower passage number).

4. Spontaneously arising PC12 cell variants are indicated by the presence of flat (phase-dark), rapidly dividing, non-NGF responsive cells. Alternatively, contaminating variants may appear spiky in morphology even in the absence of NGF. The best solution to this is to replace the entire stock with PC12 cells from an earlier passage and to adopt culture conditions that do not favor selection of variants.

5. More than 50% of PC12 cells in serum-free medium without NGF should die within 24 h after plating. However, PC12 cells at high density are capable of conditioning the culture medium, retarding death. Therefore, if cultures exhibit a delay in serum-free cell death, the experiment should be repeated with a lower density of cells. Alternatively, a delay of cell death could be due to an insufficient washout of serum or, for neuronally differentiated cultures, of NGF. In this case, a more stringent washing procedure should be instituted.

6. Generally, it is prudent to discard contaminated cultures and replace with fresh PC12 cell stock. However, if it is necessary to rescue a nonreplaceable culture (such as cell line established from transfection experiments), the following treatments may be effective in removing common sources of contamination. (i) Yeast: treat the culture with 1% fungizone (final concentration) in complete medium. (ii) Mold: remove the contaminant by aspiration. Alternatively, use a Pasteur pipette to remove some of the PC12 cells from a small unaffected area of the dish and replate the cells onto a new dish. Treat the cells with 1% fungizone in complete medium. (iii) Bacteria: a combination of antibiotics and bacterial static agents [see Sambrook *et al*. (1989) for appropriate doses] may be added to the culture. PC12 cells can tolerate ampicillin, kanamycin, spectinomycin, tetracycline, and chloramphenicol.

References

Greene, L. A., Aletta, J. M., Rukenstein, A., and Green, S. H. (1987). PC12 pheochromocytoma cells: Culture, nerve growth factor treatment, and experimental exploitation. *Methods Enzymol.* **147B**, 207–216.

Greene, L. A., Sobeih, M. M., and Teng, K. K. (1991). Methodologies for the culture and experimental use of the PC12 rat pheochromocytoma cell line. *In* "*Culturing Nerve Cells*" (G. Banker and K. Goslin, eds.), pp. 207–226. *MIT Press*, Cambridge, MA.

Greene, L. A., and Tischler, A. S. (1976). Establishment of a noradrenergic clonal line of rat adrenal pheochromocytoma cells which respond to nerve growth factor. *Proc. Natl. Acad. Sci. USA* **73**, 2424–2428.

Greene, L. A., and Tischler, A. S. (1982). PC12 pheochromocytoma cultures in neurobiological research. *Adv. Cell. Neurobiol.* **3**, 373–414.

Kleitman, N., Wood, P. M., and Bunge, R. P. (1991). Tissue culture methods for the study of myelination. *In* "*Culturing Nerve Cells*" (G. Banker and K. Goslin, eds.), pp 337–377. *MIT Press*, Cambridge, MA.

Levi, A., and Alemá, S. (1991). The mechanism of action of nerve growth factor. *Annu. Rev. Pharmacol. Toxicol.* **31**, 205–228.

Levi-Montalcini, R., and Angeletti, P. U. (1968). Nerve growth factor. *Physiol. Rev.* **48**, 534–569.

Mobley, W. C., Schenker, A., and Shooter, E. M. (1976). Characterization and isolation of proteolytically modified nerve growth factor. *Biochemistry* **15**, 5543–5552.

Sambrook, J., Fritsch, E. F., and Maniatis, T. (1989). "Molecular Cloning: A Laboratory Manual," 2nd Ed. *Cold Spring Harbor Laboratory*, Cold Spring Harbor, NY.

Soto, A. M., and Sonnenschein, C. (1985). The role of estrogen on the proliferation of human breast tumor cells (MCF-7). *J. Steroid Biochem.* **23**, 87–94.

CHAPTER

22

Differentiation of Pancreatic Cells into Hepatocytes

David Tosh

I. INTRODUCTION

The phenomenon of transdifferentiation is defined as the conversion of one differentiated cell type to another (Tosh and Slack, 2002). Generally, cells that have the potential to transdifferentiate arise from adjacent regions in the developing embryo. Therefore, transdifferentiation between adult cells probably reflects their close developmental relationship. Numerous examples of transdifferentiation have been described in literature (Eguchi and Kodama, 1993). Two examples are the transdifferentiation of pancreas to liver (reviewed in Tosh and Slack, 2002; Shen *et al*., 2003) and the reverse, liver to pancreas conversion (Horb *et al*., 2003). The liver and pancreas exhibit a close developmental relationship, as they arise from the same region of the endoderm (Wells and Melton, 1999). We have developed two different *in vitro* approaches for inducing the transdifferentiation of pancreatic cells to hepatocytes. The conversion of pancreatic cells to hepatocytes can be induced by culture of either the pancreatic cell line AR42J (Longnecker *et al*., 1979; Christophe, 1994) or the mouse embryonic pancreas (Percival and Slack, 1999). The first system, AR42J cells, is a cell line originally isolated from a carcinoma of an azaserine-treated rat (Longnecker *et al*., 1979); although a single cell type, they are considered to be amphicrine in nature, i.e., they possess both exocrine and neuroendocrine properties (Christophe, 1994). The expression of the exocrine enzyme amylase can be enhanced by short-term culture with 10 n*M* dexamethasone (Logsdon *et al*., 1985). The advantage of the second system for studying transdifferentiation, the cultured embryonic pancreas system, is that it is more physiological than the AR42J cell line, which has been around for more than 20 years (Shen *et al*., 2000). In addition, as the dorsal pancreatic organ grows as a flattened, branched structure, it is suitable for whole mount immunostaining. As well as being of interest to individuals who plan to investigate the transdifferentiation of pancreas to liver, the system is also relevant to those working on normal pancreas development. This article describes the use of AR42J cells and mouse embryonic pancreas as models for the transdifferentiation of pancreas to liver.

A. Models for Differentiation of Pancreatic Cells to Hepatocytes

Several protocols have been produced for inducing the *in vivo* appearance of hepatocytes in the pancreas. For example, administration of a methionine-deficient diet and exposure to a carcinogen (Scarpelli and Rao, 1981) can induce hepatocytes in the pancreas of hamsters. However, one of the most efficient means of converting pancreas to liver is to feed rats a copper-deficient diet in combination with a copper chelator, Trien (Rao *et al*., 1988). After 7–9 weeks of copper deficiency, the animals are returned to their normal diet and hepatocytes begin to appear soon afterwards. Hepatocytes in the pancreas express a range of liver-specific proteins, e.g., albumin, and are able to respond to xenobiotics (Rao *et al*., 1982, 1988).

One drawback to *in vivo* studies is that it is difficult to study individual changes at the cellular or molecular levels. An alternative approach is to use *in vitro* models, e.g., AR42J cells. The hepatocytes that are induced to differentiate from pancreatic AR42J cells express many of the proteins that are found in normal liver, e.g., albumin, glucose-6-phosphatase, transferrin, transthyretin, and proteins involved in

Copyright 2006, Elsevier Science (USA).
All rights reserved.

detoxification (e.g., UDP-glucuronosyltransferases, CYP family) (Shen *et al*., 2000; Tosh *et al*., 2002). This system offers the ability to generate hepatocytes that express a whole range of liver proteins while at the same time avoiding the necessity to isolate hepatocytes from *in vivo*. It also permits the opportunity to study factors for inducing the conversion of one cell type to another. The *in vitro* culture of mouse embryonic pancreas is particularly suitable for whole mount immunostaining. This in turn provides a three-dimensional visualisation of the cell arrangements (Percival and Slack, 1999; Horb and Slack, 2000). The current system offers a relatively simple approach and depends on the presence of a substrate (in this case fibronectin), orientation of the cut pancreas, and a serum-rich medium.

B. Induction of Transdifferentiation

Both AR42J cells and embryonic pancreas can be induced to transdifferentiate to hepatocytes by exposure to the glucocorticoid dexamethasone. We find 1 μ*M* dexamethasone to be sufficient. To unambiguously demonstrate the conversion of pancreatic cells to hepatocytes, a number of criteria have to be fulfilled. These include (1) the phenotypic characterisation of the parent cells (i.e., pancreatic cells) and the descendants (the liver cells) and (2) the lineage relationship between the ancestor and the descendant. Characterization of the phenotypes can be morphological and biochemical and/or molecular. In the case of AR42J cells, they exhibit an exocrine phenotype. Therefore the cells can be characterised with markers of digestive enzymes, e.g., amylase. Because the embryonic pancreas contains both exocrine and endocrine cell types, it is possible, with the correct combination of antibodies, to immunostain for at least three cell types (exocrine cells, glucagon-secreting α cells, and insulin-secreting β cells). In contrast, hepatocytes exhibit a vast array of proteins, including albumin, transferrin, and transthyretin so it is easy to determine the expression of the descendant. The second criterion (to demonstrate the ancestor–descendant relationship) can be satisfied by using the Cre-lox system *in vivo* (Herrera, 2000) or by lineage labelling *in vitro*, e.g., using green fluorescent protein (GFP) (Shen *et al*., 2000).

Dexamethasone can be replaced by the naturally occurring glucocorticoid cortisol to induce the conversion of AR42J cells to hepatocytes. To determine whether the effect of the glucocorticoid is specific, the cells can be exposed to RU486, the glucocorticoid receptor antagonist, prior to the addition of dexamethasone or cortisol. Furthermore, the number of AR42J cells that will transdifferentiate can be enhanced by the culture of dexamethasone in combination with oncostatin M. Oncostatin M is a member of the IL-6 family of interleukins and has been shown to enhance the maturation of embryonic liver (Kamiya *et al*., 1999).

II. MATERIALS AND INSTRUMENTATION

Dexamethasone (D1756) and cortisol are from Sigma Chemical Co (St. Louis, MO). RU-486 (Mifepristone) is from Biomol Research Laboratories, Inc. (Plymouth, PA). Recombinant human oncostatin M is from R&D System Inc. (Minneapolis, MN). Dulbecco's minimum essential medium (DMEM; D5546), basal medium Eagle (BME, B1522), minimum essential medium Eagle (MEM Eagle, M5775), penicillin–streptomycin solution (10,000 U/ml/10-mg/ml stock, P4333), and L-glutamine (G7153) are from Sigma (Poole, Dorset, UK). Trypsin–EDTA solution (25300-054), gentamycin (15710-049), and fetal bovine serum (FBS) (10106-169) are all from Invitrogen (Paisley, UK). Tissue culture 35-mm plastic dishes are from Fischer and 22 × 22-mm (MIC 3114) glass coverslips are from Scientific Laboratory Supplies (Nottingham, UK). Blocking reagent (1 096 176) is from Roche (Welwyn Garden City, UK).

Phosphate-buffered saline (PBS) tablets are supplied by Oxoid Ltd. (Basingstoke, UK). MilliQ-filtered H_2O is sterilised by autoclaving. Dissecting instruments, including small scissors, large scissors, tungsten wire needle (Goodfellow Metals, Cambridge, UK) in a glass capillary tube, and two pairs of forceps (Dumont No. 5, Sigma F6521), are required.

III. PROCEDURES

A. Cell Lines and Culture Conditions

Transdifferentiation of AR42J Cells to Hepatocytes

AR42J cells can be obtained as a frozen aliquot or growing culture from the ECACC (93100618) or ATCC (CRL-1492). AR42J-B13 cells (kindly provided by Dr. Itaru Kojima, Japan) are a subclone of the parent line AR42J. The subclone was isolated on the basis of an increased tendency to convert to β cells (Mashima *et al*., 1996). Either cell type can be induced to transdifferentiate to hepatocytes, the difference being that the AR42J-B13 subclone transdifferentiates more readily than the parent cell line (Shen *et al*., 2000). Cells are maintained in Dulbecco's modified Eagle's medium containing penicillin, streptomycin, and 10% fetal

bovine serum. Dex (1 μ*M*) is added as a solution in ethanol, and medium is changed every 1–2 days. RU486 is added at a concentration of 2.5 μ*M*, with the treatment commencing 1 h before addition of the Dex. Oncostatin M is added as a solution in phosphate-buffered saline containing 0.1% bovine serum albumin at a final concentration of 10 ng/ml together with 1 μ*M* Dex.

B. Other Procedures

Immunofluorescence Analysis and Antisera

1. For immunofluorescent staining, culture AR42J-B13 cells on noncoated glass coverslips, rinse with PBS, and fix with 4% paraformaldehyde in PBS for 30 min. Immunostain the cells on a coverslip as described later and mount on a microscope slide in a suitable mounting media such as gelvatol.

2. Permeabilise with 0.1% (v/v) Triton X-100 in PBS for 30 min.

3. Incubate the coverslips in 2% blocking buffer (Roche) and 0.1% (v/v) Triton X-100, and then incubate sequentially with primary and secondary antibodies. Dilute and obtain the antibodies as follows: rabbit polyclonal antiamylase (A8273; 1/300) and rabbit polyclonal antialbumin (1/500; A0433), both from Sigma Chemical Co., and rabbit polyclonal anti-transferrin (A0061; 1/200) and rabbit polyclonal anti-transthyretin (A0062; 1/100), both from DAKO (Ely, Cambridge). The goat polyclonal antirabbit IgG FITC conjugate (FI-1000; 1/150) is from Vector Laboratories (Fig. 1).

Gelvatol Medium

1. Produce gelvatol medium by dissolving 20 g of polyvinyl alcohol in 80 ml of 10 m*M* Tris, pH 8.6, along with 0.2% NaN_3.
2. In a separate tube, mix 3 g of *n*-propyl gallate and 50 ml glycerol until clear. This will take 2–3 days at room temperature with rotating.
3. When both solutions are dissolved, mix the two. Occasionally lumps are present, which can be removed by centrifugation at 2500 rpm for 15 min.
4. Pour off the supernatant into a new tube, leaving the lumps at the bottom of the old tube.
5. This tube can now be wrapped in foil and stored at 4°C.

C. Isolation of Mouse Embryonic Pancreas

This procedure is modified from Percival and Slack (1999) and from Horb and Slack (2000).

Embryonic Culture of Mouse Pancreatic Buds

Isolate dorsal pancreatic buds from 11.5-day mouse embryos as described later. Following isolation, dissect the pancreatic buds out in minimum essential medium with Hank's salts (Hank's medium) containing 10% FBS, 2 m*M* glutamine, and 50 μg/ml gentamycin. Culture the buds on fibronectin-coated coverslips in medium containing basal medium Eagle with Earle's salts (Earle's medium), 2 m*M* glutamine, 50 μg/ml gentamycin, and 20% FBS. Change the medium daily for up to 6 days.

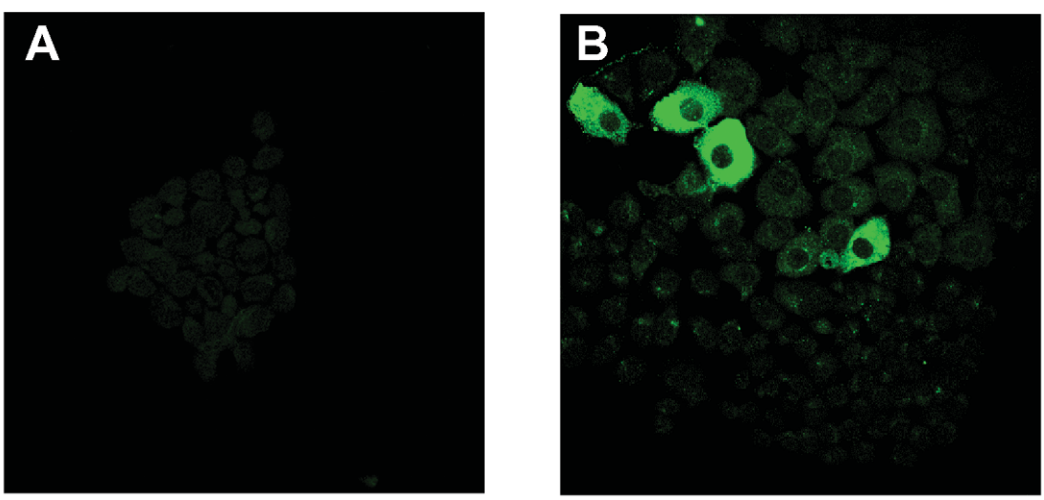

FIGURE 1 Immunostaining for albumin in control (A) and dexamethasone-treated AR42J-B13 cells (B).

Preparation of Fibronectin-Coated Coverslips

Fibronectin comes as a lyophilised powder (Invitrogen, Cat. No. 33010-018).

1. Add 1 ml of sterilised water to a 1-mg vial of fibronectin and dissolve (1 mg/ml final concentration).
2. Aliquot 50 µl into 1-ml Eppendorfs and freeze at –20°C.
3. Prepare glass coverslips by baking for at least 3 h at 180°C.
4. Prior to adding fibronectin, coat the coverslips with 2% 3-aminoporpyltriethoxysilane (APTS) to enhance attachment of the bud to the coverslip.
5. To coat the coverslip with fibronectin, take one tube of the frozen 50 µl fibronectin and add 950 µl of sterilised water (make sure it is well dissolved).
6. In the tissue culture hood, pipette 50 µl of solution onto a sterilised coverslip that has been placed in a 35-mm culture dish. The final concentration of fibronectin is 50 µg/ml.
7. Allow the fibronectin to dry on the coverslips. This takes 2–3 h.

Preparation of Embryos

Mouse embryos are generated by timed matings. The day of the vaginal plug is taken as 0.5. For the purpose of the present study, we use 11.5-day embryos.

Mouse Embryonic Dissection and Culture

1. Kill mouse by cervical dislocation.

2. Test reflexes generally by gripping the paw. If reflexes are absent, then proceed.

3. Soak the fur in 70% ethanol. This is generally a source of infection.

4. Using blunt forceps and scissors, cut open the abdomen (first layer) by a small incision and then tear this back with the fingers and expose the peritoneal sack.

5. Cut the layer with the sharp scissors and forceps and expose one of the uterine horns by displacing the abdominal contents and fatty tissue to the side.

6. Find the furthest embryo from the base of the uterus in either horn and remove the whole string of embryos into a 90-mm petri dish containing ice-cold PBS.

7. Separate the embryos from each other using blunt forceps and scissors; alternatively, simply hold the embryo and uterus with blunt forceps in one hand and squeeze gently until the embryo pops out of the uterus. Place embryos in a clean petri dish of PBS.

8. Dissect the embryos from the sacs and remove their heads. Place in a new petri dish containing Hank's medium.

9. Dissect open the embryo and locate the stomach. At the lower end, just as the stomach empties into the intestine, there is a tissue lying over the surface of the organ. This is the dorsal embryonic bud. Separate the stomach (along with the dorsal pancreas) from the intestine and liver using the needle as a knife. Always remember to cut away from the tissue that you require to avoid damaging the delicate tissue. Finally, with the needle, prise the pancreas away from the stomach and place in a fresh dish of Hank's medium.

10. To culture the pancreatic bud, first place a cloning ring on top of the fibronectin-coated region of the coverslip. Fibronectin is visible as a dried "ring" on the coverslip so it is easy to locate. Add 2.5 ml of Earle's culture medium. Initially add some medium dropwise to the cloning ring but avoid bubbles, as this makes it difficult for the pancreas to settle and attach to the substratum.

11. For each pancreas culture, suck up tissue into a pipette and lower onto medium in the cloning ring. Although two to three pancreatic buds can be cultured within a single cloning ring, they sometimes grow and overlap so it is best to culture only one per dish.

12. Centre the pancreas with the tungsten needle and make sure that the cut surface of the pancreas bud is face down. It is important that the culture is placed in the centre, as occasionally the cloning ring can move slightly and could crush the bud, especially if it is too close to the edge of the cloning ring. Also, ensuring that the bud is placed cut surface down will increase the chances of the bud sticking to the fibronectin matrix.

13. Place the dish in the incubator at 37°C and culture overnight.

14. The following day, check the cultures under an inverted microscope. Generally, allow 24 h before changing the medium. Remove the cloning rings from the coverslips with forceps and then change the medium to fresh medium. Repeat medium changes every 1–2 days (Fig. 2).

The cultured pancreatic buds generally flatten out onto the substratum over the first 1–2 days, and mesenchymal cells spread rapidly out of the explant to form a monolayer of cells surrounding the epithelia in the centre. On the second or third day, branches begin to appear in the epithelium. Scattered cells expressing insulin or glucagon become evident during the first 3 days in culture. Over the next 3 days, the epithelium becomes an extended branched structure radiating from the original centre, and the development of exocrine cells can be recognized. Insulin cells become more numerous and strongly stained, and some islet-like architecture can be seen from day 6. These time

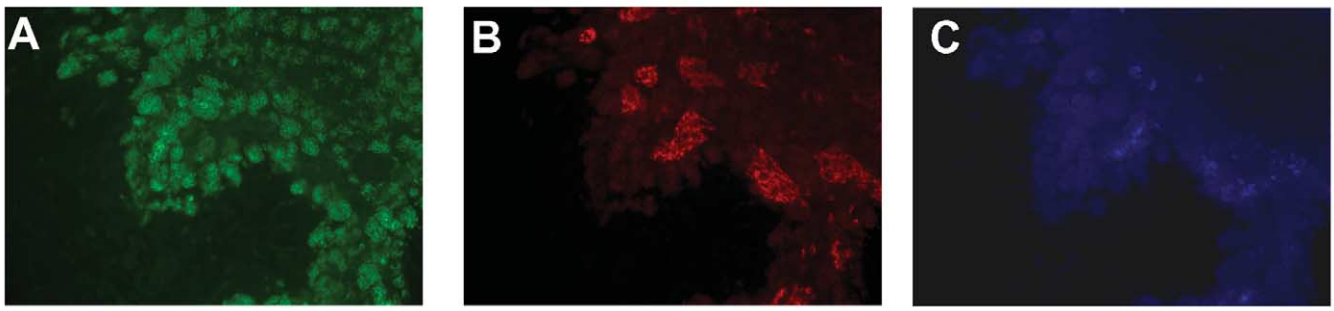

FIGURE 2 Immunostaining for amylase, insulin, and glucagon in normal pancreatic buds. Pancreatic buds were cultured for 7 days and then immunostained for amylase (A), insulin, (B), and glucagon (C).

courses show that the cell differentiation in the cultures resembles quite closely what occurs *in vivo*, although it is delayed about 1 day over a 4-day culture period.

Induction of Transdifferentiation

To induce transdifferentiation of pancreatic cells to hepatocytes, add 1 μ*M* dexamethasone. This should be added at 1- to 2-day intervals from the 1 m*M* stock that is kept at –20°C. Dexamethasone can be added to the medium prior to pipetting onto the dishes or directly to the dish. Add an equivalent volume of ethanol to control dishes.

The embryonic buds can be analysed by immunofluorescent analysis, but the fixation and permeabilisation conditions are different from those for AR42J cells.

D. Immunofluorescence Analysis of Embryonic Pancreas

1. For immunofluorescent staining, fix the pancreata in MEMFA (10% formaldehyde, 0.1 *M* Mops, pH 7.4, 2 m*M*, EGTA, 1 m*M* $MgSO_4$) for 30–45 min at room temperature.
2. Wash in PBS; they can be stored in PBS at 4°C for up to a few days.
3. Prior to immunostaining, treat the cultures with 1% Triton X-100 in PBS to permeabilise and then block in 2% blocking buffer (Roche), which contains 0.1% Triton X-100.
4. The buds can then be incubated sequentially with primary and secondary antibodies. We can perform triple labelling for the detection of amylase (FITC), insulin (TRITC), and glucagon (AMCA). Dilute the primary antibodies in blocking buffer and apply to the coverslip overnight at 4°C. Dilute and obtain the antibodies as follows: rabbit polyclonal antiamylase (1/300, Sigma A8273), guinea pig polyclonal antiinsulin (1/300, Sigma, I6163), mouse monoclonal antiglucagon (1:100, Sigma G2654), goat polyclonal antirabbit IgG FITC conjugate (1/100; Vector Laboratories FI-1000), rabbit polyclonal antiguinea pig IgG TRITC conjugate (1/300; Sigma T7153), and horse antimouse IgG AMCA conjugate (1/100; Vector Laboratories CI-2000). The following day, wash the coverslips three times (15 min each) and apply the secondary antibody and leave on for 3 h. On the last day (day 4), wash the coverslip again (three times 15 min each) and mount the coverslip in an appropriate medium, e.g., gelvatol or mobiol. View specimens under a fluorescent microscope. After induction of transdifferentiation with dexamethasone, the hepatocytes can be detected in buds by using the liver antibodies described in Section III,B.

E. Imaging

For confocal imaging, we use a Zeiss LSM 510 confocal system on an inverted Zeiss fluorescent microscope fitted with a ×40/NA 1.30 or ×63/NA 1.40 oil immersion objective (Zeiss, Welwyn Garden City, UK). Alternatively, we use a Leica DMRB microscope fitted with a digital camera. Generally, when two or more antibodies are visualized through different fluorescent channels in the same specimen, the initial black-and-white CCD images are coloured and then recombined to form a single multicoloured image.

IV. COMMENTS

The differentiation of pancreatic AR42J cells to hepatocytes results in a marked morphological change. The cells become flattened and enlarged. These changes occur with 5 days of dexamethasone treatment. It is therefore possible to check the differentiation by noting the number and degree of flattening of cells.

V. PITFALLS

1. For the best results with the embryonic pancreatic cultures, ensure that the bud is placed cut surface down and in the centre of the cloning ring. If not, there is a chance that the cloning ring will move when the incubator door is closed, squashing the bud.

2. When immunostaining for liver proteins, do not be tempted to use serum as a blocking agent. Although good for conventional immunostaining, it is not suitable for some of the liver markers, which are serum proteins normally secreted from the organ, e.g., albumin.

3. Prior to inducing transdifferentiation, inoculate the AR42J cells at low density (e.g., we routinely inoculate at 10–15%). These cells have a high rate of cell division and although dexamethasone inhibits cell division, you may end up with too confluent a dish for optimal immunofluorescence.

Acknowledgment

This work was supported by the Medical Research Council.

References

Christophe, J. (1994). Pancreatic tumoral cell-line AR42J. An amphicrine model. *Am. J. Physiol.* **266**, G963–G971.

Eguchi, G., and Kodama, R. (1993). Transdifferentiation. *Curr. Opin. Cell Biol.* **5**, 1023–1028.

Herrera, P. L. (2000). Adult insulin and glucagon cells differentiate from two independent cell lineages. *Development* **127**, 2317–2322.

Horb, L. D., and Slack, J. M. W. (2000). Role of cell division in branching morphogenesis and differentiation of the embryonic pancreas. *Int. J. Dev. Biol.* **44**, 791–796.

Horb, M. E., Shen, C.-N., Tosh, D., and Slack, J. M. W. (2003). Experimental conversion of liver to pancreas. *Curr. Biol.* **13**, 105–115.

Logsdon, C. D., Moessner, J., William, J. A., and Goldfine, I. D. (1985). Glucocorticoids increase amylase mRNA levels, secretory organelles, and secretion in pancreatic acinar AR42J cells. *J. Cell Biol.* **100**, 1200–1208.

Longnecker, D. S., Lilja, H. S., French, J. I., Kuhlmann, E., and Noll, W. (1979). Transplantation of azeserine-induced carcinomas of pancreas in rats. *Cancer Lett.* **7**, 197–202.

Kamiya, A., *et al*. (1999). Fetal liver development requires a paracrine action of oncostatin M through gp130 signal transducer. *EMBO J.* **18**, 2127–2136.

Mashima, H., Shibata, H., Mine, T., and Kojima, I. (1996). Formation of insulin-producing cells from pancreatic acinar AR42J cells by hepatocyte growth factor. *Endocrinology* **137**, 3969–3976.

Percival, A. C., and Slack, J. M. W. (1999). Analysis of pancreatic development using a cell lineage label. *Exp. Cell Res.* **247**, 123–132.

Rao, M. S., Reddy, M. K., Reddy, J. K., and Scarpelli, D. G. (1982). Response of chemically induced hepatocyte-like cells in hamster pancreas to methyl clofenapate, a peroxisomal proliferator. *J. Cell Biol.* **95**, 50–56.

Rao, M. S., *et al*. (1988). Almost total conversion of pancreas to liver in the adult rat: A reliable model to study transdifferentiation. *Biochem. Biophys. Res. Commun.* **156**, 131–136.

Scarpelli, D. G., and Rao, M. S. (1981). Differentiation of regenerating pancreatic cells into hepatocyte-like cells. *Proc. Natl. Acad. Sci. USA* **78**, 2577–2581.

Shen, C.-N., Horb, M. E., Slack, J. M. W., and Tosh, D. (2003). Transdifferentiation of pancreas to liver. *Mech. Dev.* **120**, 107–116.

Shen, C.-N., Slack, J. M. W., and Tosh, D. (2000). Molecular basis of transdifferentiation of pancreas to liver. *Nature Cell Biol.* **2**, 879–887.

Tosh, D., Shen, C.-N., and Slack, J. M. W. (2002). Differentiated properties of hepatocytes induced from pancreatic cells. *Hepatology* **36**, 534–543.

Tosh, D., and Slack, J. M. W. (2002). How cells change their phenotype. *Nature Rev. Mol. Cell Biol.* **3**, 187–194.

Wells, J. M., and Melton, D. A. (1999). Vertebrate endoderm development. *Annu. Rev. Cell Dev. Biol.* **15**, 393–410.

CHAPTER

23

TERA2 and Its NTERA2 Subline: Pluripotent Human Embryonal Carcinoma Cells

Peter W. Andrews

I. ORIGINS OF NTERA2

TERA2 is one of the oldest extant cell lines established from a human teratocarcinoma. It was derived from a lung metastasis of a testicular germ cell tumour and reported by Fogh and Tremp in 1975. However, its pluripotent embryonal carcinoma (EC) properties were not immediately obvious, in part because maintenance of its undifferentiated EC phenotype requires that cultures of these cells are passaged by scraping in order to retain small clumps of cells instead of using trypsinisation, which results in single cell suspensions. In an early study of human teratocarcinoma-derived cell lines we ourselves dismissed TERA2 as a potential EC cell line (Andrews *et al*., 1980).

Initially, we failed to derive xenograft tumours from TERA2 (Andrews *et al*., 1980). Nevertheless, after a number of attempts we did succeed in obtaining a single xenograft tumour after injecting a nude, athymic (*nu/nu*) mouse with TERA2 cells. Fortunately, we explanted some of this tumour back into culture, as well as fixing part for histology. To our surprise, histological examination then revealed that the tumour contained a variety of differentiated elements, as well as embryonal carcinoma components; indeed it was a teratocarcinoma. Meanwhile, it was evident that the cells in culture, now named NTERA2 to designate their passage through a nude mouse, did not resemble morphologically the cells that predominated in the culture of TERA2 that had been used to inoculate the host mouse (Andrews *et al*., 1980). Indeed, the NTERA2 cells closely resembled other cells that we believed to represent human EC cells (Andrews *et al*., 1982, 1984b).

From NTERA2 a number of cloned lines were obtained by isolating single cells and culturing clones from them. Detailed cytogenetic study and genetic analyses using isozyme markers demonstrated clearly that NTERA2 and its clones did indeed originate from TERA2 (Andrews *et al*., 1984b). Subsequently, clones were also derived directly from earlier passages of TERA2 itself and these also exhibited EC cell properties (Thompson *et al*., 1984; Andrews *et al*., 1985). It was clear that the TERA2 line does contain EC cells but that these can be lost by differentiation and overgrowth if the cultures are maintained under suboptimal conditions. Nevertheless, remaining subpopulations of EC cells can be rescued from such cultures by cloning or by growing of xenograft tumours in immunosuppressed animals; evidently only undifferentiated EC cells are tumourigenic.

Several single cell clones of NTERA2 were initially studied, in particular NTERA2 clone B9, clone D3, and clone D1. However, there was no obvious difference among these and most subsequent studies have utilised the clone NTERA2 cl. D1, which has also been abbreviated NT2/D1 or sometimes simply NT2. The different clones do exhibit slightly different karyotypes, and it is certain that a small amount of genetic drift occurs upon prolonged culture. Nevertheless, the modal chromosome numbers of the NTERA2 clones, and of TERA2 itself, are very similar, about 61 chromosomes, including a variety of rearrangements. Many of these rearrangements are common to all clones, but new rearrangements continue to appear

Copyright 2006, Elsevier Science (USA).
All rights reserved.

and characterise the individual clones (Andrews *et al*., 1984b, 1985).

II. UNDIFFERENTIATED NTERA2 EC CELLS

The features of undifferentiated human EC cells are best exemplified by another cell line, derived from a testicular germ cell tumour, 2102Ep (Andrews *et al*., 1982). 2102Ep cells, and indeed a number of other "nullipotent" human EC cell lines (Andrews *et al*., 1980; Andrews and Damjanov, 1994), tend to grow in tightly packed colonies of small cells with little cytoplasm and few prominent nucleoli within a nucleus that comprises most of the cell. They exhibit doubling times of about 20–24 h, and eventually form monolayers from which domes may form and floating vesicles bud off. The cells of these vesicles do not seem to be significantly different from cells that remain attached to the substrate. However, high-density cultures are required to retain these features—typically we seed cultures at densities of at least 5×10^6 cells per 75-cm^2 flask. At lower densities, the cells begin to flatten out and evidently some differentiate into trophectoderms (Andrews *et al*., 1982; Andrews, 1982; Damjanov and Andrews, 1983).

NTERA2 EC cells behave similarly, although there are differences. Maintenance at high cell densities is essential but, in this case, for passaging, cultures should be dispersed by scraping instead of using trypsin and EDTA—cell:cell contact seems to be required for the long-term retention of an undifferentiated phenotype. Like 2102Ep, NTERA2 cells at low density also flatten out and appear to differentiate, e.g., inducing expression of fibronectin, but they do not seem to produce trophectoderm (Andrews, 1982; Andrews *et al*., 1984b). Extraembryonic endoderm, evidenced by the production of laminin, may be formed (Andrews *et al*., 1983).

NTERA2 EC cells also share with other human EC, and indeed embryonic stem (ES) cell lines, the expression of characteristic marker genes, e.g., *Oct4*. However, of particular utility is their expression of surface antigens characteristic of undifferentiated human EC cells (Andrews *et al*., 1983, 1984a,b,c, 1996) (**Table I**). These include the glycolipid antigens stage-specific embryonic antigen (SSEA) -3 and SSEA4, but not SSEA1, the proteoglycan antigens TRA-1-60, TRA-1-81, and GCTM-2, the liver/bone/kidney alkaline phosphatase (L-ALP) associated antigens, TRA-2-49 and TRA-2-54, and also human Thy-1. This same surface antigen phenotype is also expressed by human ES cells (Thomson *et al*., 1998; Reubinoff *et al*., 2000; Draper *et al*., 2002), and several of the same antigens (SSEA3, SSEA4, TRA-1-60, and TRA-1-81) are expressed by the inner cell mass of human blastocysts (Henderson *et al*., 2002).

In these respects, human EC cells differ from their murine counterparts, which do not express SSEA3 or SSEA4, or murine Thy-1 (Shevinsky *et al*., 1982; Kannagi *et al*., 1983; Martin and Evans, 1974), but do express SSEA1 (Solter and Knowles, 1978). Murine EC cells do express high levels of alkaline phosphatase (Bernstine *et al*., 1973), but that is not recognised by the antibodies TRA-2-49 and TRA-2-54. The antibodies TRA-1-60, TRA-1-81, and GCTM2 also do not appear to recognise epitopes expressed by mouse cells. A further difference between mouse and human EC cells is the expression of class 1 major histocompatibility complex (MHC) antigens, of which HLA is commonly expressed by human EC cells (Andrews *et al*., 1981), whereas H-2 is not expressed by mouse EC cells. In fact, undifferentiated NTERA2 cells only express low and variable levels of HLA-A,B,C, in contrast to other human EC cells (Andrews *et al*., 1984b), but these levels are increased markedly by exposure to interferon-γ (Andrews *et al*., 1987).

III. DIFFERENTIATION OF NTERA2 EC CELLS

NTERA2 EC cells differ from many other human EC cells by their susceptibility to differentiation induced by retinoic acid (Andrews, 1984) and to other inducing agents such as hexamethylene bisacetamide (HMBA) (Andrews *et al*., 1986, 1990) and the bone morphogenetic proteins (Andrews *et al*., 1994). These agents induce differentiation in distinct directions, although the best studied is retinoic acid-induced differentiation, which results in the formation of neurons as well as other cell types (Andrews, 1984). By contrast, many other human EC cells do not respond to retinoic acid (Matthaei *et al*., 1983).

Within 24–48 h after exposure to 10^{-5} *M* all-*trans* retinoic acid, NTERA2 cells commit to differentiate. During the following 2 weeks, expression of the key surface markers SSEA3, SSEA4, TRA-1-60, and TRA-1-81 is eliminated in most cells, while they lose the characteristic EC morphology, and begin expressing a range of new markers. Prominent among these induced markers are surface antigens SSEA1, A2B5, and ME311 (**Table I**), which appear to segregate to discrete subsets of cells (Fenderson *et al*., 1987). At the same time, expression of members of *HOX* gene clus-

ters is induced (Mavilio *et al*., 1988). This induction of *HOX* gene expression is dose dependent in a way that relates to the position of the genes in the *HOX* cluster (Simeone *et al*., 1990; Bottero *et al*., 1991). Thus, genes located at the 5′ end of the clusters tend to require higher concentrations of retinoic acid for maximal induction than genes located at the 3′ end of the clusters. This pattern appeared to relate to the expression pattern of the *HOX* genes along the anterior–posterior axis of the developing embryo and the postulated role for retinoic acid in establishing that axis. However, differentiation induced by HMBA, which causes a similar elimination of the EC surface marker antigens, was not accompanied by a comparable induction of the surface antigens, or the *HOX* genes, induced by retinoic acid (Andrews *et al*., 1990).

Differentiation of NTERA2 cells induced by retinoic acid, and also HMBA, results in the appearance of susceptibility of the cells to replication of both human cytomegalovirus (HCMV) (Gönczöl *et al*., 1984) and human immunodeficiency virus (HIV) (Hirka *et al*., 1991). Neither virus is able to replicate in undifferentiated cells, although they can gain entry. In the case of HCMV, the block appears to lie directly in the inability of the cells to support transcription from the major immediate early promoter of the virus (LaFemina *et al*., 1986; Nelson *et al*., 1987). The nature of the block in the case of HIV is less certain. However, both viruses replicate readily in the differentiated derivatives of NTERA2 cells, yielding fully infectious virions. In the case of HIV, the entry of the virus into the cells does not involve CD4 as the receptor (Hirka *et al*., 1991).

Among cells arising from the differentiation of NTERA2, the neurons that appear after retinoic acid induction are the most well defined and studied. These appear only rarely after induction with HMBA or BMPs (Andrews *et al*., 1986, 1990, 1994). A variety of other cell types do appear in cultures induced with each of these agents. These are poorly defined and are not identified readily with specific cell types, although they may include mesenchymal cell types, including smooth muscle, fibroblasts, and chondrocytes (Duran *et al*., 1992).

Neurons were initially identified in retinoic acid-induced cultures by their expression of neurofilaments and toxin receptors (Andrews, 1984). Subsequently, a detailed analysis of neurofilament expression confirmed their neural identity (Lee and Andrews, 1986), and electrophysiological studies indicated that they expressed ion channels appropriate to embryonic neurons (Rendt *et al*., 1989). The neurons formed by the differentiation of NTERA2 cells can be purified readily and have been widely used in a variety of studies of human neural behaviour (Pleasure *et al*., 1992; Pleasure and Lee, 1993). Neural differentiation of NTERA2 cells appears to follow a sequence of events that parallel neural differentiation in the developing neural tube. Thus an early marker induced following initial exposure to retinoic acid is nestin, which is followed sequentially by the expression of neuroD1, a HLH transcription factor characteristic of postmitotic neuroblasts, and finally by markers of mature neurons such as synaptophysin (Pryzborski *et al*., 2000). The appearance of the cell surface antigen A2B5 in differentiating cells appears to be related to the neural lineage and it seems that A2B5 expression is activated shortly before cells leave the cell cycle. A2B5 is expressed by the terminally differentiated NTERA2 neurons (Fenderson *et al*., 1987).

IV. REAGENTS, SOLUTIONS, AND MATERIALS

Medium

All cells are cultured in Dulbecco's modified Eagle's medium (DMEM) (high glucose formulation), supplemented with 10% fetal calf serum (FCS). DMEM may be purchased from any reputable supplier of tissue culture reagents. Samples of FCS should be obtained from a number of suppliers and tested to identify a batch that supports optimal growth of NTERA2 cells and maintenance of an undifferentiated state, assayed by the expression of appropriate markers (see later). A batch of FCS that provides for good maintenance of undifferentiated NTERS2 cells is not necessarily the best for supporting differentiation. FCS should be batch tested separately for both purposes.

Dulbecco's Phosphate-Buffered Saline (PBS)

For the following procedures, PBS without Ca^{2+} and Mg^{2+} is used and may be purchased from any reputable supplier of tissue culture reagents.

Retinoic Acid

all-*trans* Retinoic acid can be purchased from Sigma-Aldrich or from Eastman-Kodak. It should be stored in the dark at –70°C, preferably under nitrogen. A stock solution of 10^{-2} *M* retinoic acid (3 mg/ml) in dimethyl sulphoxide (DMSO) should be prepared and also stored at –70°C. If prepared carefully under asceptic conditions, this stock solution may be assumed to be sterile.

Hexamethylene Bisacetamide (HMBA)

A 0.3 *M* stock solution of HMBA should be prepared in PBS and may be stored at 4°C. It may be sterilised by passage through a 0.2-μm filter.

Glass Beads

Purchase 3-mm flint glass beads from a reputable laboratory supplier. These should be washed in 10 *N* HCl and rinsed thoroughly with water. After drying, about 20 should be placed in a Wasserman tube and sterilised by autoclaving.

Trypsin:EDTA

A solution of 0.25% trypsin in 1 m*M* EDTA and PBS (Ca^{2+}/Mg^{2+} free) may be purchased from any reputable tissue culture supplier.

Mitotic Inhibitors

1. ***Cytosine arabinoside:*** Prepare a fresh 1 m*M* stock solution every 2 weeks and store at 4°C.
2. ***Fluorodeoxyuridine:*** Store a 1 m*M* stock solution in water at –20°C.
3. ***Uridine:*** Store a 1 m*M* stock solution in water at –20°C.

Matrigel

Matrigel is a proprietary product of Invitrogen and consists of a mixture of extracellular matrix components produced by an established tumour cell line. It gels spontaneously at 37°C, but remains as a liquid at 4°C. It should be stored at –20°C on receipt. To use, thaw a vial by standing on ice overnight. The thawed Matrigel may be distributed into convenient aliquots and refrozen once for further storage. To coat tissue culture surfaces, the thawed Matrigel should be diluted 1:30 in cold medium and enough to cover the surface should be pipetted into the desired tissue culture vessel (e.g., 1.5 ml per 25-cm^2 tissue culture flask), which should then be incubated at 37°C for 2 h. The Matrigel may then be aspirated and the flask is ready for plating cells.

V. PROCEDURES

A. Maintenance of NTERA2 Stock Cultures

NTERA2 cells should be maintained at high cell densities in DMEM plus 10% FCS at 37°C under a humidified atmosphere of 10% CO_2 in air. The FCS should be batch tested to ensure that it is suitable for supporting optimal growth of the cells (population doubling times of approximately 20 h) in an undifferentiated state, as assessed by morphology and expression of surface markers (SSEA3, SSEA4, TRA-1-60, and TRA-1-81).

The cells should be harvested for subcultivation by scraping, which can be achieved most easily with the use of 3-mm-diameter glass beads, stored in Wasserman tubes. The contents of the tube may then be tipped directly into a flask of cells to affect the detachment of adherent cells as described.

Steps

1. Choose a 75-cm^2 flask of a well-grown, subconfluent culture of NTERA2 cells (if harvested as a single cell suspension, such a culture would yield about 20×10^6 cells).
2. Aspirate some of the medium, leaving about 10 ml behind (alternatively, remove all the medium and add 10 ml fresh medium).
3. Tip about 20–30 sterile, acid-washed 3-mm glass beads into the flask and roll them over the surface of the flask. Rolling should be just vigorous enough that the adherent cells detach in clumps.
4. Gently triturate the detached cell clumps to reduce their size to the order of 10–50 cells and transfer approximately one-third of these to a new flask, to which 20 ml fresh medium should be added.
5. The resulting culture should be maintained at 37°C under a humidified atmosphere of 10% CO_2 in air; it should be subcultivated as just described after about 3–4 days.

B. Cryopreservation and Recovery of NTERA2 Cells

NTERA2 cells may be frozen in a freezing mixture consisting of 10% DMSO and 90% FCS.

Steps

1. Harvest a well-grown, healthy culture of NTERA2 by scraping as described earlier.
2. Centrifuge the cell suspension at 1000 rpm for 5 min.
3. Remove the supernatant and resuspend the cells in freezing mixture: use about 0.6 ml for cells harvested from a 75-cm^2 flask.
4. Distribute about 0.2 ml of cell suspension in freezing mixture to screw-cap cryovials and transfer, in a cardboard box, to a –70°C freezer overnight.
5. The next day, transfer the frozen vials of cells to a liquid nitrogen freezer.

To Recover the Cells

6. Thaw the cell suspension rapidly in a water bath at 37°C.
7. Dilute the cell suspension in 5 ml medium and centrifuge at 1000 rpm for 5 min.
8. Resuspend the cell pellet in fresh medium and transfer to a new 75-cm^2 flask; culture at 37°C as before.

C. Differentiation of NTERA2

NTERA2 may be induced to differentiate by a variety of agents. However, the most widely used agents are all-*trans* retinoic acid and HMBA. The following protocol is used for the preparation of purified neural cells from retinoic acid-induced cultures of NTERA2 and is based upon the procedures of Andrews (1984) and Pleasure *et al*. (1992).

Steps

1. Harvest cells from a stock culture using trypsin:EDTA and reseed at 1×10^6 cells per 75-cm^2 tissue culture flask in 15 ml DMEM (high glucose formulation) with 10% FCS and 10^{-5} *M* all-*trans* retinoic acid diluted from the stock solution (10^{-2} *M*) in DMSO. [*Note: 10^{-5} M retinoic acid is a relatively high concentration; lower concentrations may be used but certainly these have different effects, for example, with respect to induction of Hox genes (Simeone et al., 1990); also serum acts to buffer the concentration of free retinoic acid, and lower concentrations are necessary if used in conjunction with serum-free conditions*.]

2. Maintain the cultures at 37°C and refeed with fresh medium containing 10^{-5} *M* retinoic acid every 7 days. [*Note: Our standard protocol is to maintain the differentiating cells continuously in retinoic acid. However, it is possible to remove the retinoic acid after 2–3 days and achieve full differentiation of the cells with the formation of neurons, but there may be differences in the properties of the derivative cells*.]

3. After 3 weeks harvest the cells with trypsin:EDTA and reseed in a fresh flask at a split ratio of 1:2 in DMEM with 10% FCS but no retinoic acid. This is called "**replate 1**.'

4. After 2–3 days add trypsin:EDTA (1 ml per 75-cm^2 flask) and observe under the microscope. As the cells on the surface begin to detach (about 1 min), hit the side of the flask sharply with the flat of your hand to dislodge the loosely adhering, neural precursor cells. Dilute the detached cells in fresh medium. [*Note: The object is to begin to purify the neural precursors from the other differentiated derivatives, which adhere to the substrate more strongly. Therefore, do not leave the trypsin:EDTA on the cells long enough to cause all the cells to detach, i.e., less than 3min*.]

5. Combine the harvested cells from several flasks and reseed at $6–8 \times 10^6$ cells per 25-cm^2 flask in DMEM with 10% FCS and inhibitors (10^{-6} *M* cytosine arabinoside, 10^{-5} *M* fluorodeoxyuridine, 10^{-5} *M* uridine). This is called "**replate 2**.' Feed these cultures with fresh medium including inhibitors every 3–4 days).

6. After 1–2 weeks, treat the cultures with trypsin:EDTA (1 ml per 25-cm^2 flask). Monitor the cultures under a microscope and preferentially remove the neurons that detach first (as in step 4). Dilute the suspended detached neurons in 10 ml fresh medium and replate onto surfaces coated with Matrigel (see later) at a density of about 10^5 cells/cm^2, as required for further experiments. The resulting neuronal cultures (called "**replate 3**")can be maintained for several weeks with refeeding every 4–7 days.

D. Immunofluorescence and Flow Cytometry

Monoclonal antibodies that are often used to assess surface antigens on undifferentiated NTERA2 cells and during their differentiation are shown in Table I. These antibodies are generally available as culture supernatants, purified antibodies, or ascites. They may be used in a variety of immunoassays, but indirect immunofluorescence, detected by flow cytometry, is especially useful. The latter can be readily adapted for sorting viable populations of cells for further functional or developmental studies (e.g., Ackerman *et al*., 1994; Pryzborski *et al*., 2000). Whichever preparation that is available should be pretitred on cells known to express the relevant antigen. As a negative control, we use the antibody from the original parent myeloma of most hybridomas, namely P3X63Ag8 (Kohler and Milstein, 1975). However, others may prefer a class-matched nonreactive antibody if one is available or else no first antibody at all.

Steps

1. Prepare a single cell suspension by harvesting cells with trypsin:EDTA. After pelleting, resuspend the cells in HEPES-buffered medium or wash buffer (PBS plus 4% FCS and 0.1% sodium azide) at 2×10^6/ml.

2. Choose antibodies and dilute as appropriate in wash buffer.

3. Distribute the diluted antibodies at 50 µl per well of a round-bottom 96-well plate.

4. Add 50 µl of cell suspension (i.e. 10^5 cells) to each 50 µl of antibody.

5. Seal the plate by covering with a sticky plastic cover, ensuring that each well is sealed, and incubate at 4°C, with gentle shaking, for 30–60 min.

6. Spin the plate at 280 *g* for 3 min using microtitre plate carriers in a tissue culture centrifuge. Check that the cells are pelleted and remove the plastic seal using a sharp motion but holding the plate firmly to avoid disturbing the cell pellet. Dump the supernatant by inverting the plate with a rapid downward movement; blot the surface and turn the plate over. Provided that this is done in a single movement without hesitation, the cells remain as pellets at the bottom of the wells. If there are any concerns about pathogens contaminating

TABLE I Common Antibodies[a] Used to Detect Antigens Expressed by Human EC and ES Cells

Antibody	Antigen	Antibody species and Isotype	Reference
Surface Antigens of undifferentiated NTERA2 cells			
Globoseries glycolipids			
MC631	SSEA3	Rat IgM	Shevinsky *et al.* (1982); Kannagi *et al.* (1983)
MC813-70	SSEA4	Mouse IgG	Kannagi *et al.* (1983)
Keratan sulphate proteoglycans			
TRA-1-60	TRA-1-60	Mouse IgM	Andrews *et al.* (1984a); Badcock *et al.* (1999)
TRA-1-81	TRA-1-81	Mouse IgM	Andrews *et al.* (1984a); Badcock *et al.* (1999)
GCTM2	GCTM2	Mouse IgM	Pera *et al.* (1988); Cooper *et al.* (2002)
Liver/bone/kidney alkaline phosphatase			
TRA-2-49	L-ALP	Mouse IgG	Andrews *et al.* (1984c)
TRA-2-54	L-ALP	Mouse IgG	Andrews *et al.* (1984c)
Surface Antigens marking differentiated NTERA2 cells			
Lactoseries glycolipids			
MC480	SSEA1 [Le^x]	Mouse IgM	Solter and Knowles (1978); (Gooi *et al.* (1981); Kannagi *et al.* (1982)
Ganglioseries glycolipids			
A2B5	GT3	Mouse IgM	Eisenbarth *et al.* (1979)
ME311	9-*O*-AcetylGD3	Mouse IgG	Thurin *et al.* (1985)
VINIS56	GD3	Mouse IgM	Andrews *et al.* (1990)
VIN2PB22	GD2	Mouse IgM	Andrews *et al.* (1990)

[a] MC631, MC813-70, MC480, TRA-2-54, TRA-2-49, VNIS56, and VIN2PB22 are available from Chemicon Inc., Santa Cruz Inc., and the Developmental Studies Hybridoma Bank (University of Iowa). TRA-1-60 and TRA-1-81 are available from Chemicon Inc and Santa Cruz Inc. GCTM2 is available from ES Cell International, A2B5 from the American Type Culture Collection, and ME311 from the Wistar Institute of Anatomy (Philadelphia, PA).

a culture, supernatants can be removed by aspiration rather than dumping.

7. Wash the cells by adding 100 µl wash buffer to each well, seal, and agitate to resuspend the cells. Spin down as described earlier. After removing the supernatant, repeat with two further washes.

8. After the third wash, remove the supernatant and add 50 µl fluorescent-tagged antibody, previously titred and diluted in wash buffer to each well. FITC-tagged goat antimouse IgM or antimouse IgG, as appropriate to the first antibody, may be used. Antimouse IgM, but not antimouse IgG, usually works satisfactorily with MC631 (a rat IgM). Affinity-purified and/or $F(ab)_2$ second antibodies may be used if required to eliminate background.

9. Seal the plate as described earlier and repeat the incubation and washings as before.

10. Resuspend the cells at about 5×10^5/ml in wash buffer and analyze in the flow cytometer. The precise final cell concentration will depend upon local operating conditions and protocols.

Fluorescent-Activated Cell Sorting (FACS)

1. Harvest the hES cells using trypsin:EDTA as for analysis.
2. Pellet the cells and resuspend in primary antibody, diluted in medium without added azide, as determined by prior titration (100 µl per 10^7 cells). The primary and secondary antibodies should be sterilized using a 0.2-µm cellulose acetate filter.
3. Incubate the cells with occasional shaking at 4°C for 20–30 min.
4. Wash the cells by adding 10 ml medium and pellet by centrifugation at 200 *g* for 5 min; repeat this wash step once more.
5. Remove supernatant and flick gently to disperse the pellet. Add 100 µl of diluted secondary antibody per 10^7 cells and incubate, with occasional shaking, at 4°C for 20 min.
6. Wash the cells two times as just described. After the final wash, resuspend the cells in medium at 10^7 cells/ml. Sort cells using the flow cytometer according to local protocols.

Acknowledgments

This work was supported in part by grants from the Wellcome Trust, Yorkshire Cancer Research, and the BBSRC.

References

Ackerman, S. L., Knowles, B. B., and Andrews, P. W. (1994). Gene regulation during neuronal and non-neuronal differentiation of

NTERA2 human teratocarcinoma-derived stem cells. *Mol. Brain Res.* **25**, 157–162.

Andrews, P. W. (1982). Human embryonal carcinoma cells in culture do not synthesize fibronectin until they differentiate. *Int. J. Cancer* **30**, 567–571.

Andrews, P. W. (1984). Retinoic acid induces neuronal differentiation of a cloned human embryonal carcinoma cell line in vitro. *Dev. Biol.* **103**, 285–293.

Andrews, P. W., Banting, G., Damjanov, I., Arnaud, D., and Avner, P. (1984a). Three monoclonal antibodies defining distinct differentiation antigens associated with different high molecular weight polypeptides on the surface of human embryonal carcinoma cells. *Hybridoma* **3**: 347–361.

Andrews, P. W., Bronson, D. L., Benham, F., Strickland, S., and Knowles, B. B. (1980). A comparative study of eight cell lines derived from human testicular teratocarcinoma. *Int. J. Cancer* **26**, 269–280.

Andrews, P. W., Bronson, D. L., Wiles, M. V., and Goodfellow, P. N. (1981). The expression of major histocompatibility antigens by human teratocarcinoma derived cells lines. *Tissue Antigens* **17**, 493–500.

Andrews, P. W., Casper, J., Damjanov, I., Duggan-Keen, M., Giwercman, A., Hata, J. I., von Keitz, A., Looijenga, L. H. J., Millán, J. L., Oosterhuis, J. W., Pera, M., Sawada, M., Schmoll, H. J., Skakkebaek, N. E., van Putten, W., and Stern, P. (1996). Comparative analysis of cell surface antigens expressed by cell lines derived from human germ cell tumors. *Int. J. Cancer* **66**, 806–816.

Andrews, P. W., and Damjanov, I. (1994). Cell lines from human germ cell tumours. *In* "*Atlas of Human Tumor Cell Lines*" (R. J. Hay, J.-G. Park, and A. Gazdar, eds.), pp. 443–476. Academic Press, San Diego.

Andrews, P. W., Damjanov, I., Berends, J., Kumpf, S., Zappavingna, V., Mavilio, F., and Sampath, K. (1994). Inhibition of proliferation and induction of differentiation of pluripotent human embryonal carcinoma cells by osteogenic protein-1 (or bone morphogenetic protein-7). *Lab. Invest.* **71**, 243–251.

Andrews, P. W., Damjanov, I., Simon, D., Banting, G., Carlin, C., Dracopoli, N. C., and Fogh, J. (1984b). Pluripotent embryonal carcinoma clones derived from the human teratocarcinoma cell line Tera-2: Differentiation *in vivo* and *in vitro*. *Lab. Invest.* **50**, 147–162.

Andrews, P. W., Damjanov, I., Simon, D., and Dignazio, M. (1985). A pluripotent human stem cell clone isolated from the TERA-2 teratocarcinoma line lacks antigens SSEA-3 and SSEA-4 *in vitro* but expresses these antigens when grown as a xenograft tumor. *Differentiation* **29**, 127–135.

Andrews, P. W., Gönczöl, E., Plotkin, S. A., Dignazio, M., and Oosterhuis, J. W. (1986). Differentiation of TERA-2 human embryonal carcinoma cells into neurons and HCMV permissive cells: Induction by agents other than retinoic acid. *Differentiation* **31**, 119–126.

Andrews, P. W., Goodfellow, P. N., and Bronson, D. L. (1983). Cell-surface characteristics and other markers of differentiation of human teratocarcinoma cells in culture. *In* "*Teratocarcinoma Stem Cells*" (Silver, Martin, and Strickland, eds.), pp. 579–590. Cold Spring Harbor Press, Cold Spring Harbor, NY.

Andrews, P. W., Goodfellow, P. N., Shevinsky, L. H., Bronson, D. L., and Knowles, B. B. (1982). Cell-surface antigens of a clonal human embryonal carcinoma cell line: Morphological and antigenic differentiation in culture. *Int. J. Cancer* **29**, 523–531.

Andrews, P. W., Meyer, L. J., Bednarz, K. L., and Harris, H. (1984c). Two monoclonal antibodies recognizing determinants on human embryonal carcinoma cells react specifically with the liver isozyme of human alkaline phosphatase. *Hybridoma* **3**, 33–39.

Andrews, P. W., Nudelman, E., Hakomori, S., and Fenderson, B. A. (1990). Different patterns of glycolipid antigens are expressed following differentiation of TERA-2 human embryonal carcinoma cells induced by retinoic acid, hexamethylene bisacetamide HMBA or bromodeoxyuridine BUdR. *Differentiation* **43**, 131–138.

Andrews, P. W., Trinchieri, G., Perussia, B., and Baglioni, C. (1987). Induction of class 1 major histocompatibility complex antigens in human teratocarcinoma cells by interferon without induction of differentiation, growth inhibition or resistance to viral infection. *Cancer Res.* **47**, 740–746.

Badcock, G., Pigott, C., Goepel, J., and Andrews, P. W. (1999). The human embryonal carcinoma marker antigen TRA-1-60 is a sialylated keratan sulfate proteoglycan. *Cancer Res.* **59**, 4715–4719.

Bernstine, E. G., Hooper, M. L., Grandchamp, S., and Ephrussi, B. (1973). Alkaline phosphatase activity in mouse teratoma. *Proc. Natl. Acad. Sci. USA.* **70**, 3899–3903.

Bottero, L., Simeone, A., Arcioni, L., Acampora, D., Andrews, P. W., Boncinelli, E., and Mavilio, F. (1991). Differential activation of homeobox genes by retinoic acid in human embryonal carcinoma cells. *In* "*Recent Results in Cancer Research*" (J. W. Oosterhuis, H. Walt, and I. Damjanov, eds.), Vol. 123, pp. 133–143. Springer-Verlag, New York.

Cooper, S., Bennett, W., Andrade, J., Reubinoff, B. E., Thomson, J., and Pera, M. F. (2002). Biochemical properties of a keratan sulphate/chondroitin sulphate proteoglycan expressed in primate pluripotent stem cells. *J. Anat.* **200**, 259–265.

Damjanov, I., and Andrews, P. W. (1983). Ultrastructural differentiation of a clonal human embryonal carcinoma cell line *in vitro*. *Cancer Res.* **43**, 2190–2198.

Draper, J. S., Pigott, C., Thomson, J. A., and Andrews, P. W. (2002). Surface antigens of human embryonic stem cells: Changes upon differentiation in culture. *J. Anat.* **200**, 249–258.

Duran, C., Talley, P. J., Walsh, J., Pigott, C., Morton, I., and Andrews, P. W. (2001). Hybrids of pluripotent and nullipotent human embryonal carcinoma cells: Partial retention of a pluripotent phenotype. *Int. J. Cancer* **93**, 324–332.

Eisenbarth, G. S., Walsh, F. S., and Nirenberg, M. (1979). Monoclonal antibody to a plasma membrane antigen of neurons. *Proc. Natl. Acad. Sci. USA* **76**, 4913–4917.

Fenderson, B. A., Andrews, P. W., Nudelman, E., Clausen, H., and Hakomori, S. (1987). Glycolipid core structure switching from globo- to lacto- and ganglio-series during retinoic acid-induced differentiation of TERA-2-derived human embryonal carcinoma cells. *Dev. Biol.* **122**, 21–34.

Fogh, J., and Trempe, G. (1975). New human tumor cell lines. *In* "*Human Tumor Cells in Vitro*" (J. Fogh, ed.), pp. 115–159. Plenum Press, New York.

Gönczöl, E., Andrews, P. W., and Plotkin, S. A. (1984). Cytomegalovirus replicates in differentiated but not undifferentiated human embryonal carcinoma cells. *Science* **224**, 159–161.

Gooi, H. C., Feizi, T., Kapadia, A., Knowles, B. B., Solter, D., and Evans, M. J. (1981). Stage specific embryonic antigen involves α1 $\rightarrow$ 3 fucosylated type 2 blood group chains. *Nature* **292**, 156–158.

Henderson, J. K., Draper, J. S., Baillie, H. S., Fishel, S., Thomson, J. A., Moore, H., and Andrews, P. W. (2002). Preimplantation human embryos and embryonic stem cells show comparable expression of stage-specific embryonic antigens. *Stem Cells* **20**, 329–337.

Hirka, G., Prakesh, K., Kawashima, H., Plotkin, S. A., Andrews, P. W., and Gönczöl, E. (1991). Differentiation of human embryonal carcinoma cells induces human immunodeficiency virus permissiveness which is stimulated by human cytomegalovirus coinfection. *J. Virol.* **65**, 2732–2735.

Kannagi, R., Cochran, N. A., Ishigami, F., Hakomori, S.-I., Andrews, P. W., Knowles, B. B., and Solter, D. (1983). Stage-specific embryonic antigens SSEA3 and -4 are epitopes of a unique globo-series ganglioside isolated from human teratocarcinoma cells. *EMBO J.* **2**, 2355–2361.

Kannagi, R., Nudelman, E., Levery, S. B., and Hakomori, S. (1982). A series of human erythrocyte glycosphingolipids reacting to the monoclonal antibody directed to a developmentally regulated antigen, SSEA1. *J. Biol. Chem.* **257**, 14865–14874.

Kohler, G., and Milstein, C. (1975). Continuous cultures of fused cells secreting antibody of predefined specificity. *Nature* **256**, 495–497.

LaFemina, R., and Hayward, G. S., (1986). Constitutive and retinoic acid-inducible expression of cytomegalovirus immediate-early genes in human teratocarcinoma cells. *J. Virol.* **58**, 434–440.

Lee, V. M-Y., and Andrews, P. W. (1986). Differentiation of NTERA-2 clonal human embryonal carcinoma cells into neurons involves the induction of all three neurofilament proteins. *J. Neurosci.* **6**, 514–521.

Martin, G. R., and Evans, M. J. (1974). The morphology and growth of a pluripotent teratocarcinomas cell line and its derivatives in tissue culture. *Cell* **2**, 163–172.

Matthaei, K., Andrews, P. W., and Bronson, D. L. (1983). Retinoic acid fails to induce differentiation in human teratocarcinoma cell lines that express high levels of cellular receptor protein. *Exp. Cell Res.* **143**, 471–474.

Mavilio, F., Simeone, A., Boncinelli, E., and Andrews, P. W. (1988). Activation of four homeobox gene clusters in human embryonal carcinoma cells induced to differentiate by retinoic acid. *Differentiation* **37**, 73–79.

Nelson, J. A., Reynolds-Kohler, C., and Smith, B. A., (1987). Negative and positive regulation by a short segment in the 5′-flanking region of the human cytomegalovirus major immediate-early gene. *Mol. Cell. Biol.* **7**, 4125–4129.

Pera, M. F., Blasco-Lafita, M. J., Cooper, S., Mason, M., Mills, J., and Monaghan, P. (1988). Analysis of cell-differentiation lineage in human teratomas using new monoclonal antibodies to cytostructural antigens of embryonal carcinoma cells. *Differentiation* **39**, 139–149.

Pleasure, S. J., and Lee, V. M. Y. (1993). NTERA-2 cells a human cell line which displays characteristics expected of a human committed neuronal progenitor cell. *J. Neurosci. Res.* **35**, 585–602.

Pleasure, S. J., Page, C., and Lee, V. M.-Y. (1992). Pure, post-mitotic, polarized human neurons derived from Ntera2 cells provide a system for expressing exogenous proteins in terminally differentiated neurons. *J. Neurosci.* **12,** 1802–1815.

Przyborski, S. A., Morton, I. E., Wood, A., and Andrews, P. W. (2000). Developmental regulation of neurogenesis in the pluripotent human embryonal carcinoma cell line NTERA-2. *Eur. J. Neurosci.* **12**, 3521–3528.

Rendt, J., Erulkar, S., and Andrews, P. W. (1989). Presumptive neurons derived by differentiation of a human embryonal carcinoma cell line exhibit tetrodotoxin-sensitive sodium currents and the capacity for regenerative responses. *Exp. Cell Res.* **180**, 580–584.

Reubinoff, B. E., Pera, M. F., Fong, C. Y., Trounson, A., and Bongso, A. (2000). Embryonic stem cell lines from human blastocysts: somatic differentiation *in vitro*. *Nature Biotechnol* **18**, 399–404.

Shevinsky, L. H., Knowles, B. B., Damjanov, I., and Solter, D. (1982). Monoclonal antibody to murine embryos defines a stage-specific embryonic antigen expressed on mouse embryos and human teratocarcinoma cells. *Cell* **30**, 697–705.

Simeone, A., Acampora, D., Arcioni, L., Andrews, P. W., Boncinelli, E., and Mavilio, F. (1990). Sequential activation of human HOX2 homeobox genes by retinoic acid in human embryonal carcinoma cells. *Nature* **346**, 763–766.

Solter, D., and Knowles, B. B. (1978). Monoclonal antibody defining a stage-specific mouse embryonic antigen SSEA1. *Proc. Natl. Acad. Sci. USA* **75**, 5565–5569.

Thompson, S., Stern, P. L., Webb., M., Walsh, F. S., Engström, W., Evans, E. P., Shi, W. K., Hopkins, B., and Graham, C. F. (1984). Cloned human teratoma cells differentiate into neuron-like cells and other cell types in retinoic acid. *J. Cell Sci.* **72**, 37–64.

Thomson, J. A., Itskovitz-Eldor, J., Shapiro, S. S., Waknitz, M. A., Swiergiel, J. J., Marshall, V. S., and Jones, J. M. (1998). Embryonic stem cell lines derived from human blastocysts. *Science* **282**, 1145–1147.

Thurin, J., Herlyn, M., Hindsgaul, O., Stromberg, N., Karlsson, K. A., Elder, D., Steplewski, Z., and Koprowski, H. (1985). Proton NMR and fast-atom bombardment mass spectrometry analysis of the melanoma-associated ganglioside 9-O-acetyl-GD3. *J. Biol. Chem.* **260**, 14556–14563.

CHAPTER

24

Embryonic Explants from *Xenopus laevis* as an Assay System to Study Differentiation of Multipotent Precursor Cells

Thomas Hollemann, Yonglong Chen, Marion Sölter, Michael Kühl, and Thomas Pieler

I. INTRODUCTION

A mayor question in developmental biology is how cells or groups of cells are committed to their distinct fate during the elaboration of the body plan. An experimental system, which has been used to investigate the nature of inductive signals and therefore has led to the identification of components and interactions of various signal transduction pathways, is the so-called animal cap explant system of amphibian embryos. The animal cap consists of the ectodermal roof of a blastula stage embryo that can be kept in culture under the simplest conditions. An early use of this explant system was described by Johannes Holtfreter in an attempt to investigate the nature of inductive signals. In 1933, he established experimental tissue combination systems, referred to as "Umhüllungsversuch" (coating test) and "Auflagerungsversuch" (bedding test), to study the influence of factors emanating from mortified tissues on explanted ectoderm (Fig. 1) (Holtfreter, 1933).

Holtfreter showed that the mortified dorsal lip of a gastrula stage amphibian embryo led to the induction of neural tissue (neurale Blasen) in conjugated ectodermal explants (Fig. 1b). In 1971, Sudarwati and Nieuwkoop demonstrated that vegetal tissue is capable of inducing mesoderm in combined animal cap explants using the South African clawed frog *Xenopus laevis* as a source for animal cap explants (mesoderm induction assay). More recently, the animal cap system has been utilized to tackle a broad variety of developmental problems, including the specification of all germ layers, organ formation, and expression screenings for secreted proteins (Sudarwati and Nieuwkoop, 1971; Gurdon *et al*., 1985; Slack, 1990; Smith *et al*., 1990; Green *et al*., 1992; Moriya *et al*., 2000).

II. MATERIALS AND INSTRUMENTATION

Adult *X. laevis* frogs are from NASCO (Wisconsin). The reagents used are agarose (Cat. No. 15510-027, GibcoBRL); albumin bovine (BSA, Cat. No. A-8806, Sigma); chorionic gonadotropin (HCG, Cat. No. CG-10, Sigma); L-15 (Leibovitz, GibcoBRL); L-cysteine hydrochloride monohydrate (Cat. No. 30129, Fluka); HEPES (Cat. No. H-3375, Sigma); and penicillin/streptomycin solution (with 10,000 units penicillin and 10 mg streptomycin/ml, Cat. No. P-0781, Sigma). All other chemicals used are from Merck.

The gastromaster and replacement microsurgery tips are from XENOTEK Engineering (Belleville, IL). The microinjector for RNA injection is from Eppendorf (Microinjector 5242, Eppendorf).

III. BASIC PROCEDURES

The basic principles of the procedure have been described previously (Grunz and Tacke, 1989;

Copyright 2006, Elsevier Science (USA).
All rights reserved.

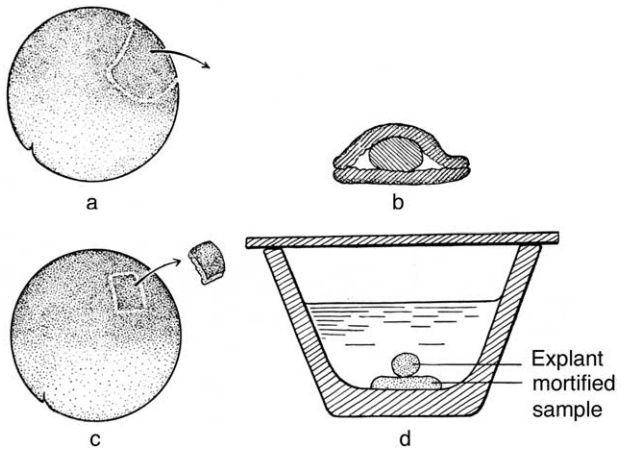

FIGURE 1 Schematic representation of the "Umhüllungsversuch" (coating test) and "Auflagerungsversuch" (bedding test) by Johannes Holtfreter, 1933. (a) Two pieces of ectoderm were isolated using a self-made cutting tool (eyebrow). (b) The mortified implant was placed between ectodermal tissues. (c) A small piece of animal ectoderm of a gastrula stage embryo was excised (c) and placed on the mortified sample (d). Adapted from Spemann, 1936.

Hollemann *et al.*, 1998). In addition to an update of the basic protocol, this article describes several readout systems that can be applied.

Solutions

Modified Barth's solution (MBS): 88 m*M* NaCl, 2.4 m*M* $NaHCO_3$, 1.0 m*M* KCl, 10 m*M* HEPES, 0.82 m*M* $MgSO_4$, 0.41 m*M* $CaCl_2$, and 0.33 m*M* $Ca(NO_3)_2$, pH 7.4

Ca^{2+}/Mg^{2+}-free MBS: 88 m*M* NaCl, 2.4 m*M* $NaHCO_3$, 1.0 m*M* KCl, and 10 m*M* HEPES, pH 7.4

L-15/BSA solution: 65% L-15 and 0.1% BSA, pH 7.4

PCR mix *(one reaction; 25 µl)*: 2.5 µl 10× polymerase chain reaction (PCR) buffer containing 15 m*M* $MgCl_2$ (Roche), 0.2 µl 25 m*M* dNTPs (Biomol), 0.375 µl 10 µ*M* forward primer, 0.375 µl 10 µ*M* reverse primer, 21.425 µl PCR grade H_2O and 0.125 µl Ampli *Taq* DNA polymerase (5 U/µl) (Roche)

Histone H4 primer: H4-F: 5′-CGGGATAACATTC AGGGTATCACT-3′ and H4-R: 5′-ATCCATGGCG GTAACTGTCTTCCT-3′

RT mix *(one reaction; 5 µl)*: 1 µl 25 m*M* $MgCl_2$ solution, 0.5 µl 10× PCR buffer II, 2 µl 2.5 m*M* dNTPs, 0.25 µl RNase inhibitor (20 U/µl), 0.25 µl MuLV reverse transcriptase (RT) (50 U/µl), 0.25 µl 50 µ*M* random hexamers, and 0.75 µl (35 ng) RNA sample

PCR(RT) mix *(one reaction; 20 ml)*: 0.5 ml 25 m*M* $MgCl_2$ solution, 2 ml 10× PCR buffer II, 16.625 ml RNase-free H_2O, 0.375 ml 10 m*M* forward primer, 0.375 ml 10 m*M* reverse primer, and 0.125 ml Ampli *Taq* DNA polymerase (5 U/ml)

A. Preparation of Animal Cap Explants

At the late blastula stage (stage 8.5–9), *Xenopus* embryos show a relatively defined segregation of presumptive ectoderm (animal pole), mesoderm (equatorial area), and endoderm (vegetal pole); the blastocoel has attained its full size, and the inner surface of the blastocoel becomes smooth. The roof of the blastocoel, the animal cap (very top of the animal pole), consists of a single outer layer and two inner layers of cells. The pigmentation pattern and the cell size differences make it possible to roughly distinguish the presumptive ectoderm, mesoderm, and endoderm from outside of the embryo. However, the easiest way to identify the animal pole (animal cap) is to look at the embryos directly. What you see from the top is the animal pole, as the embryos are naturally floating inside the vitelline membrane with the animal pole up and the vegetal pole down due to gravity.

Preparation of Xenopus Embryos

Eggs from adult *Xenopus* are obtained from females 6–8 h after injection with human chorionic gonadotropin (500–1000 U/frog) and fertilized with minced testis in 0.1× MBS. Forty minutes after fertilization, dejelly the embryos in 2% cysteine (pH 8.0) and wash extensively in 0.1× MBS.

Isolation (Cutting) of Animal Cap Explants

As there is no marker to clearly delineate the boundary of presumptive ectoderm and mesoderm in a living embryo, it is difficult to isolate animal caps without presumptive mesodermal cell contamination. Many tools, including forceps, hair loops, fine glass needles, and tungsten needles, have been developed for cutting animal caps. The most advanced tool is the gastromaster. No matter which tool is used, the first step is to manually remove the vitelline membrane of stage 8.5–9 embryos (the best stage for capping) with a pair of watchmaker's forceps in a petri dish coated with 1% agarose. Although the manufacturer of the gastromaster demonstrates that it is possible to directly isolate animal caps without removing the vitelline membrane (see video clips at http://www.gastromaster.com/), we strongly recommend removing the membrane manually. The forceps do not have to be very sharp, but the two tips should be well matching. Digging a small pit into the surface of the coated agarose is helpful for fixing the embryo during manipulation. It is recommended to hold and remove the vitelline membrane with forceps from the equatorial area or from the vegetal pole, thus avoiding damage to the animal pole cells. Once the embryos are released from the vitelline membrane, they can no

longer rotate freely according to gravity. Therefore, in order to isolate a clean animal cap from the right animal pole region, it is extremely important to properly orientate the nude embryo animal pole up and vegetal pole down (Fig. 2a). Dissect the animal cap (very top region of the animal pole, illustrated by the dashed circle in Fig. 2a) in 0.5× MBS using a gastromaster equipped with a yellow microsurgery tip of 400–500 mm in width (Figs. 2b–2e). This step is quite easy compared to the removal of vitelline membrane. We encourage visiting the gastromaster manufacturer's website for video clips that nicely demonstrate the dissecting process. Culture animal caps in 0.5× MBS containing penicillin (100 U/ml) and streptomycin (100 µg/ml) and harvest until control siblings have reached desired developmental stages for further analyses.

B. Manipulation of Animal Cap Cells

RNA Injection Techniques

One approach to investigate the activity of individual proteins is to introduce the corresponding mRNAs into the animal pole of early cleavage stage embryos followed by the isolation of animal caps for further analysis. Depending on the gene of interest, 5–2000 pg, e.g., FGF or XCYP26 (Isaacs *et al.*, 1992; Hollemann *et al.*, 1998), of *in vitro*-synthesized capped mRNA (Mega Message Machine, Ambion, USA) in 10 nl RNase-free water can be microinjected into the animal pole of both blastomeres of two-cell stage embryos, which are transferred into 1× MBS and kept at 13°C to slow down development during injection. Two hours after injection, culture embryos again in 0.1× MBS.

Application of Growth Factors

An alternative approach to monitoring the inductive activities of growth factors is to directly apply the active form of a given growth factor protein to the isolated animal caps with or without dissociation. The advantage of dissociation is that each cell is exposed to a uniform factor concentration.

Dissect animal caps from uninjected embryos as described earlier and keep in 1× Ca^{2+}/Mg^{2+}-free MBS in petri dishes coated with 0.7% agarose (about 50 caps per 60-mm petri dish). All the solutions used during disaggregation and reaggregation include penicillin (100 U/ml) and streptomycin (100 µg/ml). After approximately 15 min, cells start to dissociate. Mechanical sucking and blowing of the caps with a yellow pipette tip facilitates the disaggregation process. Caution should be taken to avoid damaging the cells. When the caps are completely disaggregated, replace the Ca^{2+}/Mg^{2+}-free MBS first with 1× MBS and

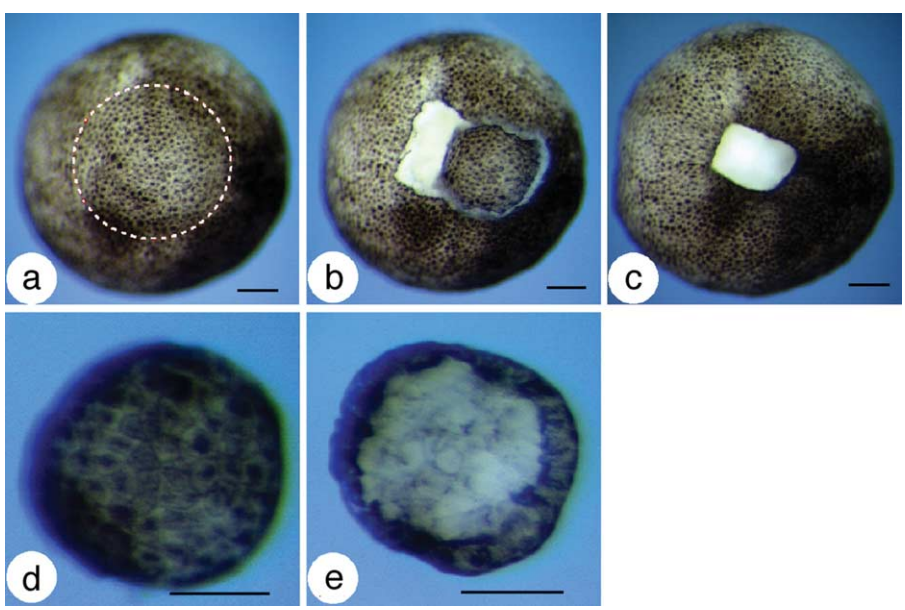

FIGURE 2 Cutting an animal cap with the gastromaster. (a) Animal pole view of a demembranated stage 9 *Xenopus* embryo. The dashed circle demarcates the very top region of the animal pole (the animal cap or presumptive ectoderm). (b) An animal cap freshly dissected with the gastromaster, still sitting on the mother embryo. (c) Wound after the isolation of the animal cap. (d) Outer layer view of an isolated animal cap. (e) Inner layer view of an isolated animal cap. Bars: 100 µm.

then with the L-15/BSA solution. After the treatment, wash and reaggregate cells in 1× MBS by gentle shaking of the petri dish. To reaggregate the cells, remove most of the solution from the petri dish with a vacuum pump and then swirl the cells together to the center of the dish by applying 1× MBS from one edge of the dish with the special apparatus invented by Horst Grunz that can supply continuous flow over a regulated tube connected to a glass bottle (for details of the apparatus, please visit Horst Grunz's website at http://www.uni-essen.de/zoophysiologie). Alternatively, aggregation can be done by shaking the petri dish gently. After one hour, cut the reaggregated cell mass (cake-like) into several pieces with a glass needle and transfer to sterilized larger glass culture bottles (100 ml) coated with 0.7% agarose. Freeze the tissues with liquid nitrogen when control siblings have developed to the desired stage of development.

C. Analysis (Readout Systems)

Effects on gene transcription can be analyzed by RT-PCR and whole mount *in situ* hybridization.

RT-PCR Analysis

The animal cap system can be used to elucidate which factors and signal transduction pathways regulate genes of interest or, vice-versa, which genes are downstream targets. Effects on gene transcription in explants can be analysed either by RNase protection or RT-PCR. We use a nonradioactive RT-PCR assay. It is normally sufficient to use this simple, semiquantitative approach to analyse strong effects on gene expression. A variety of other RT-PCR methods have also been described for *Xenopus*: quantitative, radioactive RT-PCR (Rupp and Weintraub, 1991) and quantitative, competitive RT-PCR (Onate *et al*., 1992). The most sensitive and most reproducible technique based on fluorescence kinetics is quantitative real-time RT-PCR (Xanthos *et al*., 2002), but it requires a special thermocycler.

RNA Isolation from Animal Cap Explants

We use the RNeasy minikit (Qiagen) to isolate RNA from animal caps and whole embryos for RT-PCR analysis following the RNeasy miniprotocol for the isolation of total RNA from animal tissues (see manufacturer's instructions with modifications detailed later). Digest genomic DNA using DNase I (Qiagen) for on column treatment according to the manufacturer's protocol.

Collect 10–12 animal cap explants (or 5 embryos) per sample at the appropriate time in a microcentrifuge tube, remove excess buffer, and freeze animal cap explants (embryos) with liquid nitrogen for storage at –80°C. For RNA isolation, add 350 µl (600 µl) buffer RLT/βME to each tube directly on the frozen sample. Carry out all further steps at room temperature. Homogenize animal cap explants (embryos) immediately by passing the lysate five times through a 24-gauge needle fitted to an RNase-free syringe. Elute RNA by 30 µl (70 µl) RNase-free water (60°C) and place on ice. After measuring the RNA concentration, adjust all samples to the same concentration with RNase-free water and store at –80°C. Control RNA integrity by use of a 1.5% TBE agarose gel; 75–100 ng of total RNA is normally obtained from a single animal cap explant.

Analysis of Genomic DNA Contamination

The exon–intron structure of most *Xenopus* genes is unknown. Therefore, primers used for the analysis that can target the same exon and genomic DNA contamination of isolated RNA would thus result in false-positive signals. In order to control for genomic DNA contamination, a regular PCR reaction for histone H4 genomic DNA is performed. Add 1 µl RNA (50 ng/µl) to 25 µl PCR mix containing the histone H4-specific primer. Use genomic DNA (5 ng) as a positive control and H_2O as a negative control, with the following cycling parameters: 94°C 2 min (94°C 45 s, 58°C 45 s, 72°C 30 s) × 35, 72°C 5 min. Analyze one-half of the PCR on a 2% TBE agarose gel.

RT-PCR

Carry out the reverse transcriptase reaction in 5-µl reactions (or a corresponding multiple of 5 µl) using the Gene Amp RNA PCR core kit (Roche) according to the manufacturer's instructions in a TRIO Thermoblock (Biometra). Use total RNA isolated from whole embryos collected at corresponding developmental stages and diluted to the same concentration as the animal cap explant RNA preparations as a positive control. As a negative control, perform the same reaction without adding reverse transcriptase (H_2O). Conditions for the RT reaction are 22°C 10 min, 42°C 30 min, 99°C 5 min, 5°C 5 min. Mix a 5-µl aliquot of the RT reaction with 20 µl PCR(RT) mix. We use the following cycling parameters: 94°C 2 min (94°C 45 s, X°C 45 s, 72°C 45 s) × *Y* cycles, 72°C 1 min. Analyze 10 µl of each RT-PCR on a 2% TBE agarose gel. The annealing temperature (*X*) and cycle number (*Y*) have to be optimized empirically for each primer pair. For that purpose, remove aliquots from a RT-PCR reaction using cDNA made from whole embryo RNA every second cycle over a 12-cycle range, usually starting at

20 cycles. The optimal cycle number is within the linear range of product accumulation. To control RNA quality, we perform histone H4-specific PCR; $X = 58°C$, $Y = 24$ cycles . Control contamination of animal cap explants by mesodermal tissue with primers for brachyury (early ACs) and muscle actin (later ACs). Sequences for these and other primers are available under http://www.xenbase.org.

Whole Mount in Situ Hybridization

Gene expression on the RNA level in animal cap explants can also be analyzed by whole mount *in situ* hybridization, originally adapted for *Xenopus* embryos by Harland (1991). The advantage of this method in comparison to RT-PCR is that individual explants can be controlled for homogeneity of gene expression on the level of individual cells. The disadvantage is that substantial numbers of explants are required if several genes are to be analyzed in parallel. We use the basic protocol for whole mount *in situ* hybridization described previously (Hollemann *et al*., 1999) with the following minor modifications. In case of several samples, a transfer of fixed animal caps from glass vials to 24-well tissue culture plates before rehydration facilitates handling. Proteinase K treatment should be shortened to 5–8 min at room temperature.

D. Examples

RT-PCR Analysis of Animal Cap Explants

Many different genes are involved in the activation of the neuronal differentiation program, which drives naive ectodermal cells to become postmitotic neurons. In animal cap explants, X-ngnr-1 can also promote neurogenesis, as monitored by the activation of the neural determination marker N-tubulin. The density of cells expressing endogenous X-ngnr-1 is controlled by lateral inhibition mediated through Notch signalling (Ma *et al*., 1996). In response to misexpression of the intracellular domain of Notch (ICD) that mimics active Notch signalling, the expression of target genes, such as Esr7, is induced (Fig. 3).

Whole Mount in Situ Hybridization in Animal Cap Explants

In addition to neural and mesodermal tissue, animal cap explants can also be converted into endoderm. For instance, VegT can synergize with β-catenin to induce a number of liver- and intestine-specific genes in animal cap explants. Figure 4 shows an example of whole mount *in situ* hybridization analysis for the induction of an endoderm marker gene in an animal cap upon VegT/β-catenin injection.

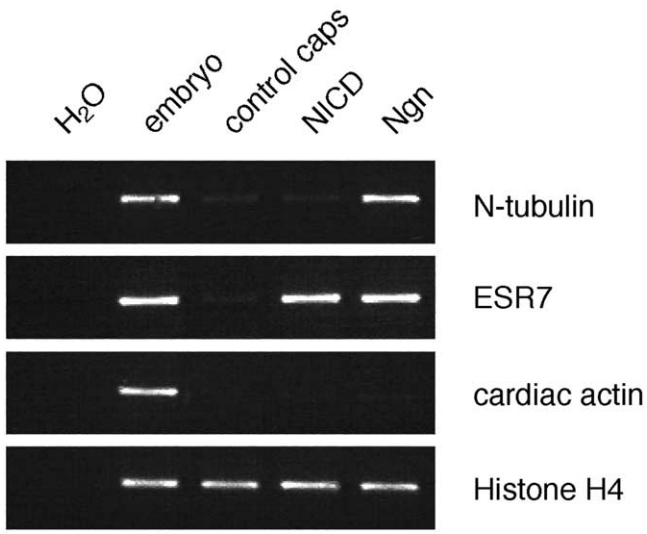

FIGURE 3 Induction of neuronal gene expression in animal caps as analyzed by RT-PCR. One hundred picograms X-Ngnr-1 mRNA (Ngn) or 300 pg Notch ICD mRNA (NICD) was injected in both cells of two-cell stage embryos, animal caps were dissected at early stage 9, cultured to stage 15, and then analyzed by RT-PCR. RNA isolated from uninjected total embryos of stage 15 was used as a positive control. X-Ngnr-1 induces the neuronal differentiation marker N-tubulin, as well as the Notch target gene ESR7 in animal caps. Histone H4-specific primers were used to control RNA input and quality. As shown by the absence of transcripts for cardiac actin, the isolated explants were not contaminated by mesodermal tissue (Sölter, *et al*., unpublished results).

The Animal Cap to Study Cell Migration

Upon treatment with activin or FGF, the animal cap is not only induced to become mesoderm (see above), but as a consequence of mesoderm induction, the animal cap also changes its form (Fig. 5). Whereas untreated animal caps round up and look like spherical balls, induced animal caps elongate as a consequence of cell movements within the animal cap (Kuhl *et al*., 2001). It is widely accepted that this kind of cell movement within the cap mimics mesodermal cell movements normally occurring during gastrulation of the *Xenopus* embryo. During gastrulation, cells from a more ventral position migrate towards the dorsal midline. The forces generated by this process *in vitro* not only push cells during gastrulation over the dorsal lip, but also lead to an elongation of the embryo along its anterior–posterior axis (for a review on cell movements during gastrulation, see Keller, 1986). With respect to gastrulation movements, the animal cap thus serves as an excellent system to study the molecular basis of cell migration. The elongation behaviour of injected or growth factor-treated caps can be studied and conclusions can be drawn on the function of a

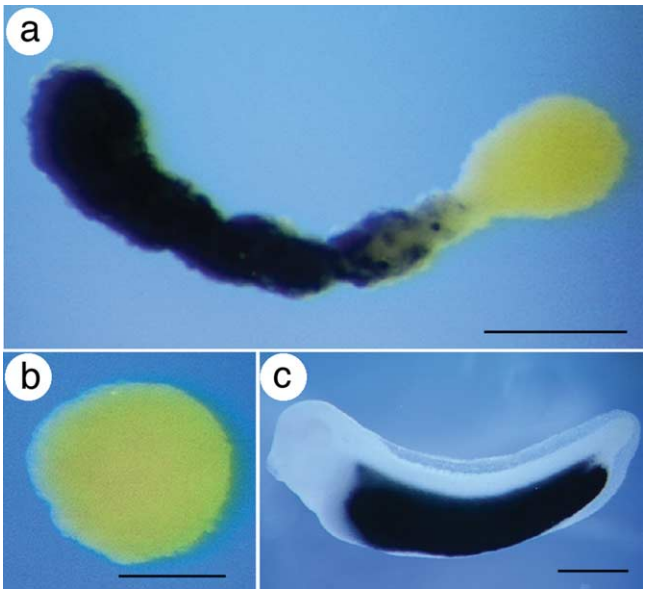

FIGURE 4 Induction of endodermal gene expression in animal cap explants as analysed by whole mount *in situ* hybridisation. Expression analysis of the activation of an endoderm-specific gene in VegT/β-catenin-injected animal cap explants. Cyl18 encodes a novel putative peptidase that demarcates the developing embryonic intestine. VegT (500 pg/embryo) and β-catenin (200 pg/embryo) mRNAs were injected into the animal pole of both blastomeres of two-cell stage embryos. Animal caps were isolated from stage 9 control uninjected and VegT/β-catenin-injected embryos and collected when control siblings had reached stage 34. (a) Cyl18 expression is activated in a subset of cells of an elongated animal cap injected with VegT/β-catenin. (b) Cyl18 is not expressed in the control cap. (b) Cyl18 is expressed exclusively in the presumptive intestine of stage 34 embryos (Chen *et al.*, 2003).

gene of interest with respect to cell migration. As an example, we show the effect of activin on animal caps (Fig. 5).

Recapitulation of Organ Formation in Animal Caps

a. Cement Gland Formation in Whole Animal Cap Explants. The homeobox-containing transcription factor PITX1 is expressed during all stages of cement gland formation (Hollemann and Pieler, 1999). The cement gland of young amphibian tadpoles is a specialised transient organ, which arises from the outer ectodermal layer (Fig. 6a). The function of the gland is to secrete sticky mucus that helps larvae adhere to solid surfaces, preventing larvae from being carried along by the water flow. To investigate the question if *Xpitx1* alone is able to induce cement gland formation, 100 pg of the corresponding synthetic messenger RNA was injected into one cell of a two-cell stage embryo. At the equivalent of embryonic stage 8, the animal cap was excised with the help of a gastromaster (yellow tip with 400 µm) and cultured in 0.5× MBS+P/S until nontreated siblings had reached stage 40. Whereas noninjected animal caps formed so-called artificial epidermis, a high number of animal caps injected with Xpitx1 developed groups of cells, which could be identified easily as typical cement gland cells based on their morphology (Fig. 6b).

b. Notochord from Dispersed Animal Cap Explant Cells. In response to different concentrations of activin, dispersed animal cap cells have been shown to exhibit sharp thresholds in respect to target gene activation. Activin A is added to the cells at a final concentration of 4 ng/ml for notochord differentiation and

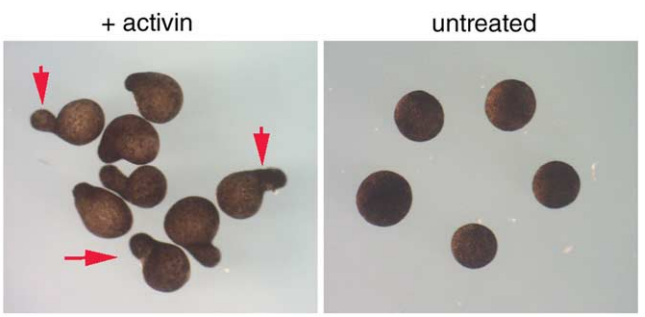

FIGURE 5 Elongation of animal caps mimics gastrulation movements. Animal cap explants of *Xenopus laevis* were isolated at stage 8 and treated with activin for 2 h. Treated caps elongate until stage 18 (left). Arrows indicate examples for elongation of the caps. In this example, all animal caps shown have indications of elongation. Untreated control caps remain spherical (right).

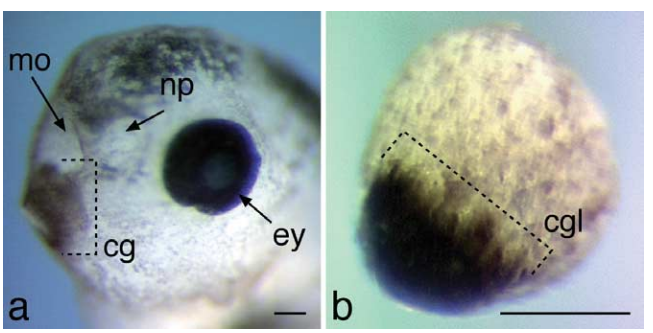

FIGURE 6 Cement gland formation in animal cap explants. (a) Anterior to the left, sloped lateral view of a head of a noninjected *Xenopus* larvae at NF stage 40. The cement gland is positioned ventrally immediately adjacent to the mouth opening. (b) Example of an animal cap explant that had been injected with Xpitx1 into one cell at the two-cell stage and cultured equivalent to stage 40. Bar: 50 µm. cg, cement gland; cgl, cement gland like; ey; eye; mo, mouth opening; np, nasal pit.

8 ng/ml for endoderm differentiation and incubated at room temperature for 1 h. In most cases, more than 90% of the reaggregated tissue mass from each batch of preparation differentiated into notochords. Some neural cells were formed concomitantly.

c. Inductive Processes: A Proteomics Approach. The animal cap assay has widely been used to study the inductive properties of growth factors such as activin or FGF. Molecular analysis of inductive events in general was on the level of mRNA expression. Changes in gene expression were analyzed by Northern blot or RT-PCR studies. This procedure resulted in the identification of a plethora of early and late response genes in the course of mesoderm or neural induction. However, posttranscriptional and posttranslational aspects of cellular regulation in this context (like protein translation, protein phosphorylation, and differential splicing events) were neglected. Two-dimensional (2D) protein analysis in conjunction with MALDI-TOF-based identification of proteins will be a useful tool to explore these processes (Shevchenko *et al.*, 1996). Figure 8 provides a 2D protein gel example of activin-treated animal caps in comparison to untreated animal cap explants, indicating that this rationale can be applied on the animal cap system in *Xenopus*. Thus, it can be expected that embryonic inductive processes will also be analyzed on the level of the proteome in the near future.

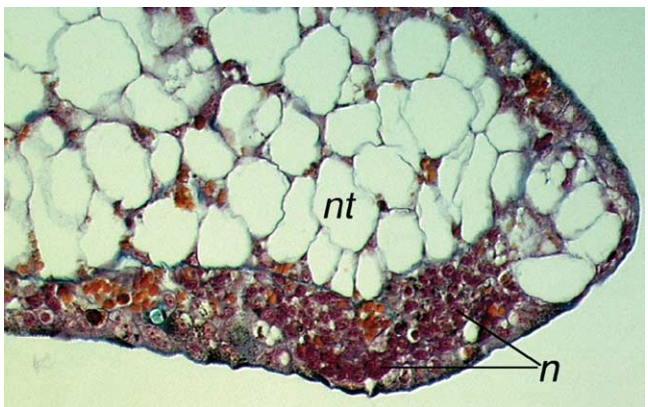

FIGURE 7 Histological staining of notochord tissues generated from animal cap cells treated with activin. In order to judge the inductive activities, one piece of the tissues from each batch of experiments was cultured further and finally fixed in Bouin's solution when control embryos reached stage 42. Differentiation of the tissues is assayed by histological analysis. nt, notochord cells; n, neural cells.

References

Chen, Y., Jurgens, K., Hollemann, T., Claussen, M., Ramadori, G., and Pieler, T. (2003). Cell-autonomous and signal-dependent expression of liver and intestine marker genes in pluripotent precursor cells from Xenopus embryos. *Mech. Dev.* **120**, 277–288.

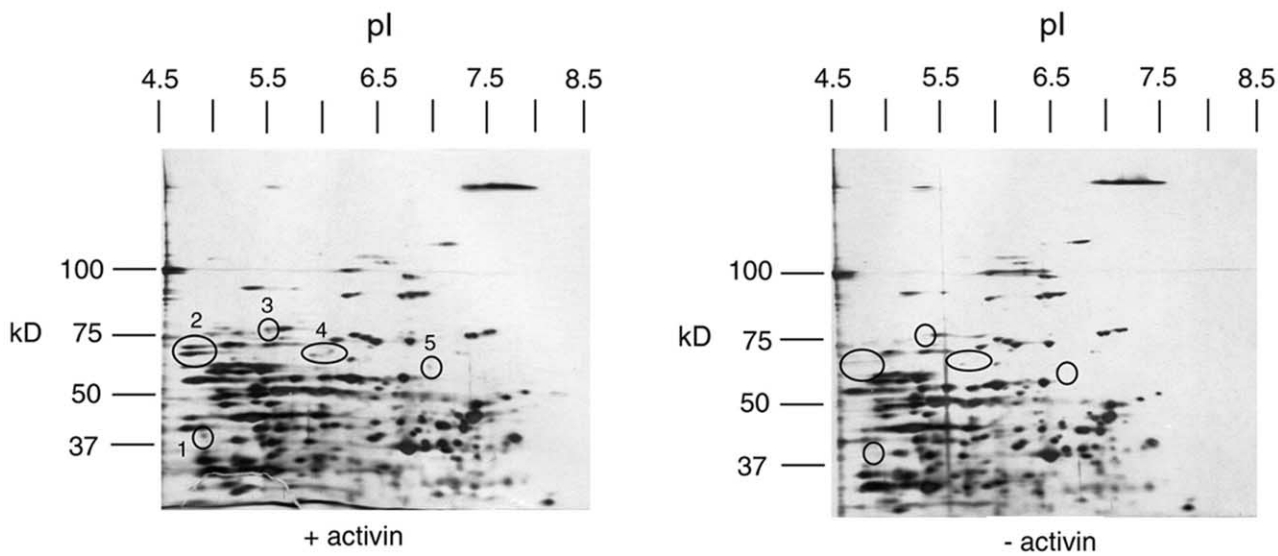

FIGURE 8 Two-dimensional gel analysis of proteins expressed in untreated and activin-treated animal caps. Embryos were injected at the two-cell stage with activin mRNA. Animal caps were isolated at stage 8 and cultured until stage 19. Equivalents of four animal caps were used for 2D protein gels. Circles indicate spots of different intensity upon treatment. Whereas spots 1 to 3 most likely represent proteins that are upregulated through activin treatment, spots 4 and 5 indicate two spots that are weakly affected and might also represent artefacts. Two-dimensional gels with a broad IP range were used. For a more detailed analysis of inductive processes, small range IP gels are required to increase the resolution. See detailed literature on 2D gel analysis for methods and detailed interpretation of the 2D gel. (Shevchenko *et al.*, 1996).

Green, J. B., New, H. V., and Smith, J. C. (1992). Responses of embryonic Xenopus cells to activin and FGF are separated by multiple dose thresholds and correspond to distinct axes of the mesoderm. *Cell* **71**, 731–739.

Grunz, H., and Tacke, L. (1989). Neural differentiation of Xenopus laevis ectoderm takes place after disaggregation and delayed reaggregation without inducer. *Cell Differ. Dev.* **28**, 211–217.

Gurdon, J. B., Fairman, S., Mohun, T. J., and Brennan, S. (1985). Activation of muscle-specific actin genes in Xenopus development by an induction between animal and vegetal cells of a blastula. *Cell* **41**, 913–922.

Harland, R. M. (1991). In situ hybridization: An improved whole-mount method for Xenopus embryos. *Methods Cell Biol.* **36,** 685–695.

Hollemann, T., Chen, Y., Grunz, H., and Pieler, T. (1998). Regionalized metabolic activity establishes boundaries of retinoic acid signalling. *EMBO J.* **17**, 7361–7372.

Hollemann, T., Panitz, F., and Pieler, T. (1999). In situ hybridization techniques with Xenopus embryos. *In* "*A Comparative Methods Approach to the Study of Oocytes and Embryos*" (J. D. Richter, ed.), pp. 279–290. Oxford Univ. Press, New York.

Hollemann, T., and Pieler, T. (1999). Xpitx-1: A homeobox gene expressed during pituitary and cement gland formation of Xenopus embryos. *Mech. Dev.* **88**, 249–252.

Holtfreter, J. (1933). Nachweis der Induktionsfähigkeit abgetöteter Keimteile. Isolations- und Transplantationsversuche. *Roux' Arch.* **128**, 585–633.

Isaacs, H. V., Tannahill, D., and Slack, J. M. (1992). Expression of a novel FGF in the Xenopus embryo: A new candidate inducing factor for mesoderm formation and anteroposterior specification. *Development* **114**, 711-720.

Keller, R. E. (1986). The cellular basis of amphibian gastrulation. *Dev. Biol.* **2**, 241–327.

Kuhl, M., Geis, K., Sheldahl, L. C., Pukrop, T., Moon, R. T., and Wedlich, D. (2001). Antagonistic regulation of convergent extension movements in Xenopus by Wnt/beta-catenin and Wnt/Ca2+ signaling. *Mech. Dev.* **106**, 61–76.

Ma, Q., Kintner, C., and Anderson, D. J. (1996). Identification of neurogenin, a vertebrate neuronal determination gene. *Cell* **87**, 43–52.

Moriya, N., Komazaki, S., Takahashi, S., Yokota, C., and Asashima, M. (2000). *In vitro* pancreas formation from Xenopus ectoderm treated with activin and retinoic acid. *Dev. Growth Differ.* **42**, 593–602.

Onate, A., Herrera, L., Antonelli, M., Birnbaumer, L., and Olate, J. (1992). *Xenopus laevis* oocyte G alpha subunits mRNAs: Detection and quantitation during oogenesis and early embryogenesis by competitive reverse PCR. *FEBS Lett.* **313**, 213–219.

Rupp, R. A., and Weintraub, H. (1991). Ubiquitous MyoD transcription at the midblastula transition precedes induction-dependent MyoD expression in presumptive mesoderm of *X. laevis*. *Cell* **65**, 927–937.

Shevchenko, A., Jensen, O. N., Podtelejnikov, A. V., Sagliocco, F., Wilm, M., Vorm, O., Mortensen, P., Boucherie, H., and Mann, M. (1996). Linking genome and proteome by mass spectrometry: Large-scale identification of yeast proteins from two dimensional gels. *Proc. Natl. Acad. Sci. USA* **93**, 14440–14445.

Slack, J. M. (1990). Growth factors as inducing agents in early Xenopus development. *J. Cell Sci. Suppl.* **13**, 119–130.

Smith, J. C., Price, B. M., Van Nimmen, K., and Huylebroeck, D. (1990). Identification of a potent Xenopus mesoderm-inducing factor as a homologue of activin A. *Nature* **345**, 729–731.

Spemann, H. (1936). "Experimentelle Beiträge zu einer Theorie der Entwicklung." *Verlag von Julius Springer, Berlin.*

Sudarwati, S., and Nieuwkoop, P. D. (1971). Mesoderm formation in the anuran *Xenopus laevis* (Daudin). *Roux' Arch.* **166**, 189–204.

Xanthos, J. B., Kofron, M., Tao, Q., Schaible, K., Wylie, C., and Heasman, J. (2002). The roles of three signaling pathways in the formation and function of the Spemann organizer. *Development* **129**, 4027–4043.

CHAPTER

25

Electrofusion: Nuclear Reprogramming of Somatic Cells by Cell Hybridization with Pluripotential Stem Cells

Masako Tada and Takashi Tada

I. INTRODUCTION

The technique of cell fusion, which was pioneered by Henry Harris (1965), has proved to be a powerful procedure with applications in cell biology, genetics, and developmental biology and in fields of practical concern such as medicine and agriculture. The spontaneous or induced cell fusion of two different types of cells (heterokaryons) generates intraspecific or interspecific hybrid cells. Genetically programmed spontaneous cell fusion is known to occur in the formation of polykaryons such as myotubes, osteoclasts, and syntrophoblasts *in vivo*. Under *in vitro* culture conditions, spontaneous cell fusion has been found to occur occasionally in some cell lines and malignant cells. Cell fusion due to membrane integrity between two different cells is induced by treatment with chemical agents such as calcium ions, lysolecithin, and polyethylene glycol; by mediation by viruses such as paramyxoviruses, including Sendai virus (HVJ), oncornavirus, coronavirus, herpesvirus and poxvirus; and by electrofusion.

In 1997, the successful production of the cloned sheep named Dolly demonstrated that committed animal somatic cell nuclei are able to reacquire totipotency as a result of nuclear transplantation into enucleated unfertilized oocytes and the subsequent embryonic development (Wilmut *et al.*, 1997). This nuclear reprogramming results from the resetting of the somatic cell-specific epigenetic program by *trans*-acting factors present in unfertilized oocytes. Nearly 20 years ago, genomic plasticity had already been examined by cell fusion experiments between differentiated cell types (Blau *et al.*, 1985; Baron and Maniatis, 1986; Blau and Baltimore, 1991). More recently, this approach has been used to study genomic reprogramming that occurs in X chromosome reactivation (Takagi *et al.*, 1983; Tada *et al.*, 2001; Kimura *et al.*, 2003) and switching of parental origin-specific marks of imprinted genes (Tada *et al.*, 1997).

An important finding is that pluripotential embryonic stem (ES) cells have an intrinsic capacity for epigenetic reprogramming of somatic genomes following cell fusion (Tada *et al.*, 2001, 2003; Kimura *et al.*, 2003). In hybrid cells between ES cells and adult thymocytes, nuclear reprogramming of the somatic genome has been demonstrated by (1) the contribution of ES hybrid cells to normal embryogenesis of chimeras, (2) reactivation of the silenced X chromosome derived from female somatic cells, (3) reactivation of pluripotential cell-specific genes, *Oct4*, *Xist*, and *Tsix*, which were derived from the somatic cell, (4) redifferentiation into a variety of cell types in teratomas, (5) tissue-specific gene expression from the reprogrammed somatic genome in addition to the ES genome in *in vivo*-differentiated teratomas and *in vitro*-differentiated neuronal cells, and (6) acquisition by reprogrammed somatic genomes of pluripotential cell-specific histone tail modifications. More interestingly, cell fusion experiments between somatic cells and embryonic germ (EG) cells derived from the gonadal primordial germ cells of mouse 11.5–12.5 dpc embryos have demonstrated that EG cells possess an additional potential for inducing the reprogramming of somatic cell-derived parental imprints accompanied by the

Copyright 2006, Elsevier Science (USA).
All rights reserved.

disruption of parental origin-specific DNA methylation of imprinted genes (Tada *et al*., 1997, 1998). Therefore, cell fusion with pluripotential stem cells is now recognized as a powerful approach for elucidating mechanisms of epigenetic reprogramming involving DNA and chromatin modifications.

More recent evidence has shown that neurosphere and bone marrow cells undergo nuclear reprogramming following spontaneous cell fusion with cocultured ES cells *in vitro* (Terada *et al*., 2002; Ying *et al*., 2002). Furthermore, experiments involving the *in vivo* transplantation of bone marrow cells have demonstrated that regenerated hepatocytes are derived from donor hematopoietic cells that undergo fusion with host hepatocytes, not from the transdifferentiation of hematopoietic stem cells or hepatic stem cells present in bone marrow (Vassilopoulos *et al*., 2003; Wang *et al*., 2003). Thus, the nuclear reprogramming of somatic cells by *in vivo* cell fusion is thought to play an important role in maintaining the homeostasis of some tissues by regeneration during defined self-renewal and following tissue damage.

This article describes a practical procedure for electrofusion to produce hybrid cells between pluripotential stem cells and committed somatic cells (mouse ES cells and lymphocytes isolated from the adult thymus) without the use of virus or chemicals to mediate the fusion. ES cells are adherent cells that undergo self-renewal by rapid cell division, whereas thymocytes are nondividing and nonadherent cells. In order to select the hybrid cells effectively, either thymocytes carrying the *neo* transgene or male ES cells deficient for the X-linked *Hprt* (*hyoxanthine phosphoribosyl transferase*) gene are used as the partner cells in the cell fusion. Consequently, only hybrid cell colonies are capable of surviving and growing in culture in the presence of antibiotic G418 or HAT (hypoxanthine, aminopterin, and thymidine).

II. MATERIALS AND INSTRUMENTATION

Cells: Adult mice, ES cells, and *neo*^{r} feeder cells (see Section II,A)

Instruments: ECM 2001 AC/DC pulse generator (BTX), 1-mm gap microslide chambers (BTX P/N450-10WG), inverted microscope with 10 and 20× objectives, humidified incubator at 37°C, 5% CO_2, 95% air, 60-mm plastic tissue culture dishes, 60- and 100-mm bacterial dishes, 10- and 30-mm well plastic tissue culture plates, 15- and 50-ml conical tubes, 0.2-µm microfilters, 200- and 1000-µl capacity adjustable pipetters with autoclaved tips, forceps, scissors, 2.5-ml syringes, 18-gauge needles

Compounds: Dulbecco's modified Eagle's medium/nutrient mixture F12 Ham (DMEM/F12) (Sigma D6421), Dulbecco's modified Eagle's medium (DMEM) (Sigma D5796), fetal bovine serum (FBS) (JRH Biosciences 12003-78P), recombinant leukemia inhibitory factor (LIF) (Chemicon ESG1107), 200 m*M* glutamine (GIBCO 320-5030AG), 2-mercaptoethanol (Sigma M7520), 10,000 IU/ml penicillin and 10 mg/ml streptomycin (penicillin–streptomycin 100×) (Sigma P-0781), 100 m*M* sodium pyruvate (Sigma S8636), 7.5% sodium bicarbonate (Sigma S8761), Ca^{2+}/Mg^{2+}-free phosphate-buffered saline (PBS) (GIBCO 10010-023), 0.25% trypsin/1 m*M* EDTA·4Na (GIBCO 25200-056), mytomycin C (Sigma M0503), gelatin from porcine skin, type A (Sigma G-1890), D-mannitol (Sigma M-9546), G418 (geneticin) (Sigma G-9516), HAT media supplement 50× (HAT) (Sigma H0262)

III. PROCEDURES

A. Mouse ES Cell and Feeder Cell Culture

One of the most important variables for cell fusion experiments is how stably ES cells ($2n = 40$) and hybrid cells ($2n = 80$) can be cultured without loss of the pluripotential competence and the full set of chromosomes derived from mouse ES cells and somatic cells through numerous cell divisions. The culture conditions are basically those described previously (Abbondanzo *et al*., 1993). A crucial point is quality control of the FBS, which is added to make the ES cell culture medium cocktail. FBS certified for ES cell culturing has become available commercially. We strongly recommend the use of a suitable production lot of FBS that can support effective cell growth without inducing differentiation equivalently to the ES cell-certified FBS.

Solutions

1. *ES medium*: Mix 500 ml of DMEM/F12, 75 ml of FBS, 5 ml of 200 m*M* glutamine, 5 ml of penicillin–streptomycin (100×), 5 ml of 100 m*M* sodium pyruvate, 8 ml of 7.5% sodium bicarbonate, 4 µl of 10^{-4} *M* 2-mercaptoethanol, and 0.05 ml of 10^7 U/ml LIF (final 1000 U/ml). Store at 4°C.
2. *PEF medium*: Mix 500 ml of DMEM, 50 ml of FBS, 5 ml of 200 m*M* glutamine, 5 ml of 10,000 IU/ml penicillin, and 10 mg/ml streptomycin. Store at 4°C.
3. *0.25% trypsin/1 mM EDTA·4Na*: Dispense into aliquots and store at –20°C.

4. *Ca^{2+}/Mg^{2+}-free phosphate-buffered saline (PBS)*
5. *10 μg/ml mytomycin C*: 0.2 mg/ml in PBS, dispense into aliquots, and store at –20°C.
6. *0.1% gelatin*: 0.1% gelatin in distilled water. Sterilize by autoclaving and store at 4°C.

Steps

1. Coat 60-mm culture dishes with 0.1% gelatin for at least 30 min at room temperature.
2. Prepare mouse primary embryonic fibroblasts (PEFs) produced from day 13 embryos of ROSA26 transgenic mice carrying the ubiquitously expressed *neo*/*lacZ* gene (Friedrich and Soriano 1991). Treat *neo*^{r} PEFs with 10 μg/ml mitomycin C (MMC) and incubate at 37°C in a CO_2 incubator for 2 h to produce mitotically inactivated feeder cells. Prepare frozen stocks of the MMC-treated PEFs at a concentration of 5×10^6 cells/ml and store in a cryotube in liquid nitrogen. The inactivated *neo*^{r} PEFs are routinely used as feeder cells (1×10^6 cells/60-mm culture dish and 2.5×10^6 cells/100-mm culture dish) for culture of ES and hybrid cells, and also for selection of hybrid cell colonies with G418. For establishment of PEFs, see Abbondanzo *et al*. (1993).
3. Culture exponentially growing ES cells on the inactivated PEFs with changes of culture medium once or twice a day. Carry out subculturing of the ES cells every 2 days by a 1:4 split. ES cells at early passages are used for experiments. Before cell fusion, it should be verified that the karyotype of the ES cells is normal.
4. Prepare gelatin-coated 30-mm culture dishes (6-well-culture plates) containing the inactivated PEFs (4×10^5 cells/well) in 3 ml of ES medium 1 day before cell fusion experiments.

B. Pretreatment of ES and Somatic Cells for Cell Fusion

Solution

Fresh nonelectrolyte solution; 0.3 M mannitol buffer: To make 50 ml, dissolve 2.74 g of mannitol in distilled water. Filter through a 0.2-μm filter. Store at 4°C.

Steps

1. Trypsinize ES cells and remove excess trypsin quickly. Add 3 ml of ES medium to inactivate the trypsin and dissociate the cells into a single-cell suspension by gentle pipetting. Plate them on a new gelatin-coated 60-mm culture dish. Incubate the ES cells in a CO_2 incubator for 30 min to separate feeder cells from ES cells.
2. Collect unattached ES cells and harvest them by centrifugation at 1500 rpm for 5 min. Resuspend the cell pellet in 10 ml of DMEM, transfer them into a 15-ml conical tube, and place at room temperature.
3. Sacrifice a 6- to 8-week-old adult mouse humanely and dissect out the thymus in a clean room if a clean bench is not available. All of the dissection instruments should be sterilized by immersion in 70% ethanol, followed by flaming.
4. Wash the tissues with sterilized PBS twice in 60-mm petri dishes and place one lobe of the thymus in the barrel of a sterile 2.5-ml syringe with a sterile 18-gauge needle.
5. To dissociate the thymus into a single-cell suspension, gently expel the thymus through the tip of the needle into 2 ml of DMEM in a 50-ml conical tube. Draw up and expel the suspension several times. Allow to stand for several minutes at room temperature.
6. Transfer the supernatant excluding cell clumps to a 15-ml conical tube and add 10 ml of DMEM.
7. Spin down the ES cells and thymocytes separately in 15-ml conical tubes at 1500 rpm for 5 min.
8. Wash them with 10 ml of DMEM and spin down at 1500 rpm for 5 min and repeat again to remove FBS completely.
9. Add 5–10 ml of DMEM and adjust the density of ES cells and thymocytes each to 1×10^6 cells/ml.
10. Pellet a 1:5 mixture of ES cells and thymocytes (1 ml of the ES cell suspension and 5 ml of the thymocyte suspension made in step 9). Keep the remaining cells for control experiments.
11. Spin down and resuspend the cell pellet in 0.3 *M* mannitol buffer at 6×10^6 cells/ml. Usually, 1 ml of the mixture of ES cells and thymocytes is sufficient for the following fusion experiment. Use the cells immediately for electrofusion (Fig. 1).

C. Operation of ECM 2001 Pulse Generator and Electrofusion Protocol

Solution

70% ethanol

Steps

1. Sterilize the microslides by immersion in 70% ethanol, followed by flaming.
2. Set a microslide in a 100-mm plastic dish chamber.
3. For each electrofusion, apply 40 μl of cell mixture between the electrodes with a 1-mm gap on the microslide.

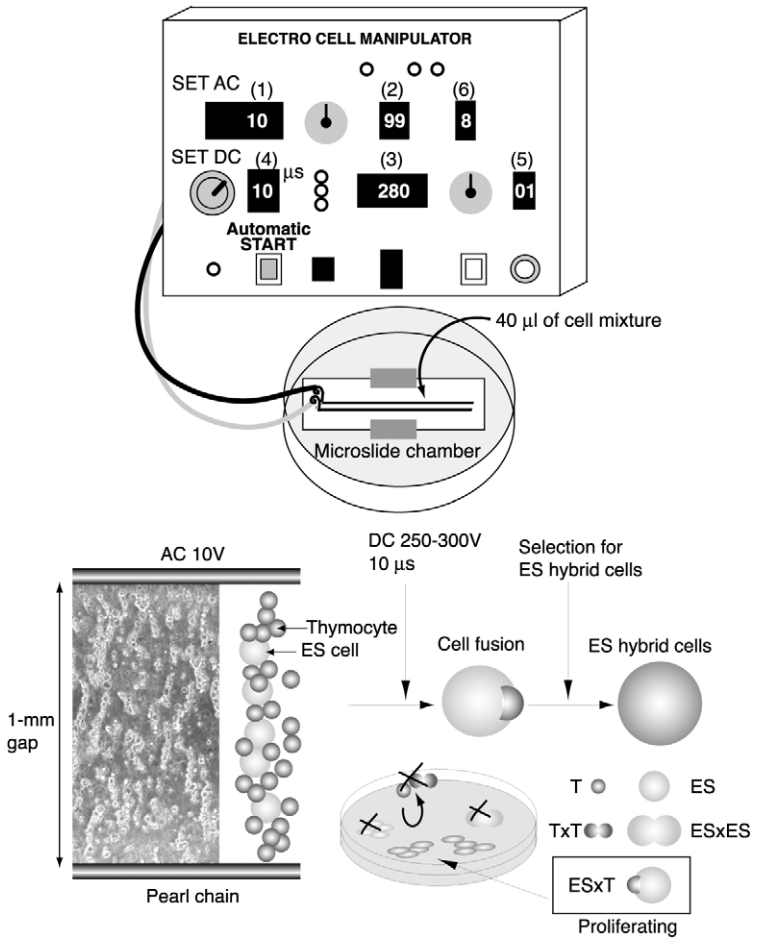

FIGURE 1 Schematic representation of the electrofusion system. A mixture of ES cells and somatic cells suspended in nonelectrolytic mannitol solution is placed in a 1-mm gap between electrodes on a microslide. Set parameters (1–6) of the AC/DC pulse generator and press the automatic start button. AC electric pulses induce pearl chain formation, and the subsequent DC electric pulse induces cell fusion. ES cells (ES) and ESxES hybrid cells are nonviable in the selection medium, whereas thymocytes (T) and TxT hybrid cells are nonadherent. ES hybrid cells (ESxT) rescued by the thymocyte genome are capable of surviving and proliferating in the selection medium.

4. Connect the microslide in the 100-mm plastic dish chamber with the ECM 2001 AC/DC pulse generator by electric cables. Set the chamber on an inverted microscope to allow for observation of cell alignment and the fusion processes. It is important to monitor the fusion process microscopically each time. The electrofusion may proceed somewhat differently depending on the density of cell preparations and on the cell type (cell size).

5. Set the optimized electrical parameters to fuse ES cells and thymocytes (Fig. 1): 10 V alternating current (AC), 99 s AC duration, and 250–300 V direct current (DC). Adjust the DC voltage according to the size of the gap between the electrodes. The appropriate electric field strength is 2.5–3.0 kV/cm. When microslides with a 2-mm gap are used, the DC voltage should be almost 600 V.

DC pulse length: 10 µs
Number of DC pulses: 1
Postfusion AC duration: 8 s

6. Use the automatic operation switch to initiate AC followed by DC. AC is utilized to induce an inhomogeneous, or divergent electric field, resulting in cell alignment and pearl chain formation. DC is utilized to produce reversible temporary pores in the cytoplasmic membranes. When juxtaposed pores in the physically associated cells reseal, cells have a chance to be hybridized via cytoplasmic membrane fusion. AC application after the DC pulse induces compression of

the cells, which helps the process of fusion between the cell membranes.

7. Add 40 µl of DMEM to the fusion mixture between the electrodes to induce the recovery of membrane formation.

8. Place the cell mixture at room temperature for 10 min and transfer the cells to a 30-mm culture dish containing inactivated PEFs with 3 ml of the ES medium.

9. Repeat the cell fusion procedure sequentially using several microslides. Usually, cells recovered from three microslides (40 µl × 3) are plated into one 30-mm culture dish.

10. As a control, plate the untreated cell mixture and culture under the same conditions.

11. Change the medium to ES medium with appropriate supplements for selecting ES hybrid cells 24 h after cell fusion. The selection medium should be changed once a day (see Section III,D). During the 7-day selection treatment, unfused ES cells and hybrid cells between ES cells are killed and hybrid cells between thymocytes are nonadherent. Thus, only the hybrid cells between ES cells and somatic cells survive, proliferate, and form colonies. Several colonies of hybrid cells per 10^4 host ES cells are obtained under appropriate cell fusion and culture conditions.

12. Pick up the colonies with a micropipette and transfer each colony into a 10-mm well of a 24-well culture plate containing 1×10^5 inactivated PEFs per well and 0.8 ml of the ES medium with supplements for selection.

13. Subculture the cells every 2 or 3 days and gradually expand the number of cells in 30- and then 60-mm culture dishes with the inactivated PEFs and ES medium with supplements for selection. When the cells become nearly confluent in a 60-mm culture dish, it is considered that a hybrid cell line of passage 1 has been established.

14. Change the ES medium without selection supplements once or twice a day and subculture the hybrid cell line every 2 days under optimal culture conditions by splitting 1:4.

15. Subject hybrid cells to chromosome analysis soon after they are established.

D. Fusion Examples: Selection System for Hybrid Cells

This section describes one independent chemical selection system that can be used to select for hybrid cells between ES cells and somatic cells.

1. Normal ES cells are hybridized with thymocytes containing the bacterial neomycin resistance (*neo*^{r}) gene (Tada *et al*., 1997, 2001). Thymocytes are derived from ROSA26 transgenic mice, which carry the ubiquitously expressed *neo/lacZ* transgene (Friedrich and Soriano, 1991). Only ES hybrid cells with the thymocytes can survive and grow in the ES medium supplemented with the antibiotic G418, a protein synthesis inhibitor. In this case, the ES hybrid cells and their derivatives are identified visually by their positive reaction with X-gal due to β-galactosidase activity, allowing one to analyze their contribution to the development of chimeric embryos and tissues (Tada *et al*., 1997, 2001, 2003). Male ES cells deficient for the *Hprt* gene on the X chromosome are a powerful tool for producing hybrid cells with wild-type somatic cells. Electrofusion-treated cells are cultured in ES medium with the HAT supplement. In DNA synthesis, purine nucleotides can be synthesized by the *de novo* pathway and recycled by the salvage pathway. *Hprt* is a purine salvage enzyme, responsible for converting the purine degradation product hypoxanthine to inosine monophosphate, a precursor of ATP and GTP. In the presence of aminopterin, the *de novo* pathway is inhibited and only the salvage pathway functions. Consequently, dysfunction of *Hprt* induces cell death in cultures grown in HAT medium. Thus, the HAT medium proves fatal to *Hprt*-deficient ES cells, whereas ES hybrid cells, which are rescued by the thymocytes-derived wild-type *Hprt* gene, are able to survive and proliferate (Tada *et al*., 2003; Kimura *et al*., 2003).

Solutions

1. *ES medium with G418*: Reconstitute G418 with water (50 mg/ml). Sterilize through a 0.2-µm filter and store at 4°C. Add 50 µl of the G418 solution to 10 ml of ES medium, yielding a final concentration of 250 µg/ml.

2. *ES medium with HAT*: Reconstitute the HAT media supplement obtained from the supplier in a vial with 10 ml of DMEM (50× solution) and store at –20°C. Each vial contains $5 \times 10^{-3} M$ hypoxanthine, $2 \times 10^{-5} M$ aminopterin, and $8 \times 10^{-4} M$ thymidine. Add 200 µl of 50× solution to 10 ml of ES medium.

Steps

Selection with G418

1. Perform electrofusion between normal ES cells and thymocytes collected from the 6- to 8-week-old ROSA26 transgenic mice carrying the *neo/lacZ* transgene according to the procedure described earlier.
2. Culture the electrofusion-treated cells in ES medium for 24 h.
3. Change to ES medium supplemented with G418. ES hybrid cell colonies can be detected by 7–10 days.

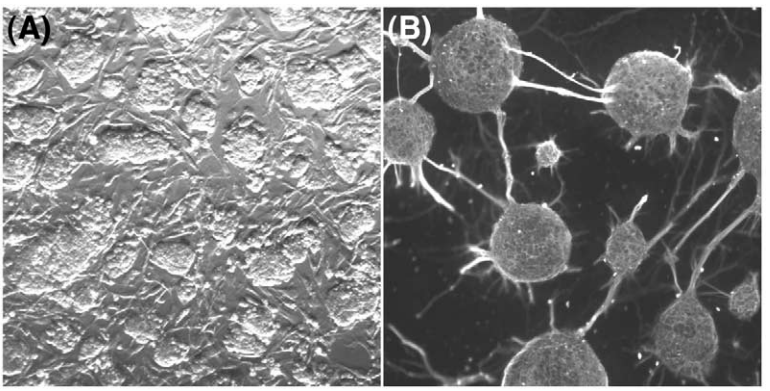

FIGURE 2 Pluripotential competence of ES hybrid cells with somatic cells. (A) Undifferentiated ES somatic hybrid cell colonies in culture on mitotically inactivated PEFs. (B) Neuronal cells differentiated *in vitro* from ES somatic hybrid cells on PA6 stromal feeder cells.

4. ES thymocyte hybrid cells are positive for X-gal staining and immunoreactive with the anti-β-galactosidase antibody.

Selection with HAT

1. Carry out electrofusion between ES cells (XY) deficient for *Hprt* and thymocytes collected from 6- to 8-week-old female mice (XX) according to the procedure described earlier.
2. Culture electrofusion-treated cells in ES medium for 24 h.
3. Change to ES medium containing the HAT supplement. ES hybrid cell colonies can be detected by 7–10 days.
4. ES thymocyte hybrid cells possess a karyotype of $4n = 80$ with an XXXY sex chromosome constitution.

Figure 2A shows representative ES hybrid cells in culture on feeder cells in the ES medium. Figure 2B shows representative neuronal cells differentiated from ES hybrid cells. The ES hybrid cells are pluripotential and can differentiate into a variety of tissues *in vivo* and *in vitro*. Tissue-specific transcripts derived from the reprogrammed somatic genomes can be identified based on genetic polymorphisms found in intersubspecific ES hybrid cells (*Mus musculus domesticus* × *M. m. molossinus*). The reprogrammed somatic cell genomes function similarly to the ES cell genomes in undifferentiated ES hybrid cells and also in ES hybrid cell derivatives differentiated *in vivo* and *in vitro* (Kimura *et al*., 2003; Tada *et al*., 2003).

IV. COMMENTS

ES hybrid cells can also be produced by 50% polyethylene glycol (PEG) treatment. Hybrid cells between embryonic carcinoma (EC) cells deficient for the *Hprt* gene and lymphocytes from the thymus or spleen are produced by cell fusion induced chemically by PEG (Takagi *et al*., 1983). To produce ES hybrid cells using PEG, wash a mixture of ES cells and thymocytes with DMEM and pellet the cells by centrifugation. Prewarm 1 ml of a 50% PEG mixture (PEG4000/DMEM = 1:1) at 37°C and then add the PEG mixture to the cell pellet gradually using the tip of a pipette. Add 9 ml of DMEM gradually. Collect the cells by centrifugation, resuspend the cells in ES medium, and transfer them to a culture dish. Selection of hybrid cells is begun 1 day after the PEG-induced fusion treatment. Electrofusion has the following advantages over the PEG-induced cell fusion: (1) electrofusion is appropriate for *in vivo* applications of the hybrid cells, whereas PEG-induced fusion is not because PEG is toxic to cells; (2) electrofusion is more efficient and reproducible than PEG-induced cell fusion for producing ES hybrid cells; and (3) it is easier to produce hybrid cells by electrofusion than by PEG-induced fusion.

V. PITFALLS

If there are problems with the AC procedure, you may be able to solve the problems as follows. Pellet the mixed cells by centrifugation and resuspend the cells in a suitable amount of fresh mannitol buffer.

1. Adjust the cell density according to the size of the cells used as the fusion partner. Remove cell debris from the mixture of ES cells and somatic cells. Cell debris, which is irregular in size, sometimes makes the formation of pearl chains difficult.
2. Increase the cell density if the pearl chains form poorly.

3. Decrease the cell density if the cell movement is disturbed.

References

Abbondanzo, S. J., Gadi, I., and Stewart, C. L. (1993). Derivation of embryonic stem cell lines. *In "Methods in Enzymology; Guide to Techniques in Mouse Development"* (P. M. Wassarman and M. L. DePamphilis, eds.), pp. 803–823. Academic Press, San Diego.

Baron, M. H., and Maniatis, T. (1986). Rapid reprogramming of globin gene expression in transient heterokaryons. *Cell* **46**, 591–602.

Blau, H. M., and Baltimore, D. (1991). Differentiation requires continuous regulation. *J. Cell Biol*. **112**, 781–783.

Blau, H. M., Pavlath, G. K., Hardeman, E. C., Chiu, C. P., Silberstein, L., Webster, S. G., Miller, S. C., and Webster, C. (1985). Plasticity of the differentiated state. *Science* **230**, 758–766.

Friedrich, G., and Soriano, P. (1991). Promoter traps in embryonic stem cells: A genetic screen to identify and mutate developmental genes in mice. *Genes Dev.* **5**, 1513–1523.

Harris, H. (1965). Behaviour of differentiated nuclei in heterokaryons of animal cells from different species. *Nature* **206**, 583–588.

Kimura, H., Tada, M., Hatano, S., Yamazaki, M., Nakatsuji, N., and Tada, T. (2003). Chromatin reprogramming of male somatic cell-derived *Xist* and *Tsix* in ES hybrid cells. *Cytogenet. Genome Res.* **99**.

Tada, M., Morizane, A., Kimura, H., Kawasaki, H., Ainscough, J. F.-X., Sasai, Y., Nakatsuji, N., and Tada, T. (2003). Pluripotency of reprogrammed somatic genomes in ES hybrid cells. *Dev. Dyn*.

Tada, M., Tada, T., Lefebvre, L., Barton, S. C., and Surani, M. A. (1997). Embryonic germ cells induce epigenetic reprogramming of somatic nucleus in hybrid cells. *EMBO J*. **16**, 6510–6520.

Tada, M., Takahama, Y., Abe, K., Nakatsuji, N., and Tada, T. (2001). Nuclear reprogramming of somatic cells by *in vitro* hybridization with ES cells. *Curr. Biol*. **11**, 1553–1558.

Tada, T., Tada, M., Hilton, K., Barton, S. C., Sado, T., Takagi, N., and Surani, M. A. (1998). Epigenotype switching of imprintable loci in embryonic germ cells. *Dev. Gene Evol*. **207**, 551–561.

Takagi, N., Yoshida, M. A., Sugawara, O., and Sasaki, M. (1983). Reversal of X-inactivation in female mouse somatic cells hybridized with murine teratocarcinoma stem cells *in vitro*. *Cell* **34**, 1053–1062.

Terada, N., Hamazaki, T., Oka, M., Hoki, M., Mastalerz, D. M., Nakano, Y., Meyer, E. M., Morel, L., Petersen, B. E., and Scott, E. W. (2002). Bone marrow cells adopt the phenotype of other cells by spontaneous cell fusion. *Nature* **416**, 542–545.

Vassilopoulos, G., Wang, P. R., and Russell, D. W. (2003). Transplanted bone marrow regenerates liver by cell fusion. *Nature* **422**, 901–904.

Wang, X., Willenbring, H., Akkari, Y., Torimaru, Y., Foster, M., Al-Dhalimy, M., Lagasse, E., Finegold, M., Olson, S., and Grompe, M. (2003). Cell fusion is the principal source of bone-marrow-derived hepatocytes. *Nature* **422**, 897–901.

Wilmut, I., Schnieke, A. E., McWhir, J., Kind, A. J., and Campbell, K. H. S. (1997). Viable offspring derived from fetal and adult mammalian cells. *Nature* **385**, 810–813.

Ying, Q. L., Nichols, J., Evans, E. P., and Smith, A. G. (2002). Changing potency by spontaneous fusion. *Nature* **416**, 545–548.

CHAPTER

26

Reprogramming Somatic Nuclei and Cells with Cell Extracts

Anne-Mari Håkelien, Helga B. Landsverk, Thomas Küntziger, Kristine G. Gaustad, and Philippe Collas

I. INTRODUCTION

Genomic plasticity has generated considerable interest in the past two decades; nevertheless the mechanisms underlying nuclear programming remain poorly understood. We report a method that allows the processes of nuclear reprogramming to be investigated *in vitro*.

Nuclear reprogramming occurs in a variety of natural and experimental contexts. After fertilization, epigenetic alterations of the embryonic genome take place during successive stages of development. Epigenetic changes and alterations in gene expression also occur after the fusion of somatic cells with less differentiated cell types (Blau and Blakely, 1999; Tada *et al.*, 2001). The birth of clones and the production of embryonic stem cells by transplantation of nuclei into oocytes also provide evidence of complete reprogramming of somatic nuclei (Cibelli *et al.*, 1998; Gurdon *et al.*, 1979; Munsie *et al.*, 2000; Wilmut *et al.*, 1997). Based on these examples, reprogramming can be defined as an alteration of a differentiated nucleus into a totipotent or mutipotent state. Additional studies have shown that a somatic cell type could be, at least partially, turned into another somatic cell type. This was achieved in coculture conditions (Morrison, 2001) and, more recently, by exposing somatic nuclei or cells to an extract derived from another somatic cell type (Håkelien *et al.*, 2002; Landsverk *et al.*, 2002). These observations have led to the proposal of a simple definition of nuclear reprogramming. Reprogramming may not necessarily involve dedifferentiation or return to a more pluripotent state, but may refer to the dominance of the program of one cell type over another, resulting in "the transformation of the pliant nucleus [in]to the dominant type" (Western and Surani, 2002).

We describe a procedure to redirect the nuclear program of a transformed human fibroblast cell line toward a T-cell program. The approach is outlined in **Fig. 1** and may, in principle, be applied to multiple cell types. The procedure involves the use of a nuclear and cytoplasmic extract derived from Jurkat T-cells in which reversibly permeabilized fibroblasts are incubated. At the end of incubation, the fibroblasts are resealed and cultured to assess the expression of T-cell-specific markers and the establishment of T-cell-specific functions. As large numbers of cells or nuclei can be processed simultaneously, and considering the ability of cell extracts to be manipulated biochemically, *in vitro* manipulation of nuclei and cells provides a potentially powerful system for analyzing the mechanisms of nuclear reprogramming.

II. MATERIALS AND INSTRUMENTATION

A. Materials

1. 293T human fibroblasts cultured on glass coverslips
2. Round, 12-mm glass coverslips, autoclaved
3. Poly-L-lysine (Cat. No. P8920, Sigma-Aldrich Co., St. Louis, MO)
4. Propidium iodide (Cat. No. P4170, Sigma). Make a 1-mg/ml stock solution in H_2O and store at –20°C in the dark.
5. RPMI 1640 medium (Cat. No. R0883, Sigma) supplemented with 10% fetal calf serum

Copyright 2006, Elsevier Science (USA).
All rights reserved.

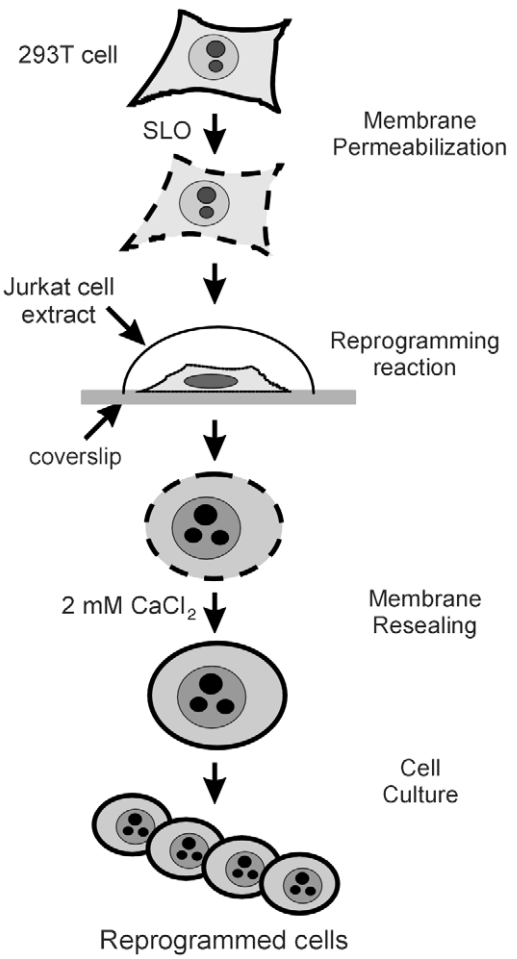

FIGURE 1 Strategy of *in vitro* cell reprogramming. 293T cells grown on coverslips are reversibly permeabilised with SLO. The permeabilised cells are incubated in a nuclear and cytoplasmic extract derived from Jurkat TAg cells for 1 h. The cells are resealed for 2 h in culture medium containing 2 m*M* $CaCl_2$. The $CaCl_2$-containing medium is replaced by regular complete culture medium, and the resealed, reprogrammed cells are cultured for assessment of reprogramming.

6. Hanks balanced salt solution (HBSS; Cat. No. 14170-088, Gibco-BRL; Paisley, UK)
7. Protease inhibitor cocktail (Cat. No. P2714, Sigma). This is a 100× stock solution.
8. Cell lysis buffer (50 m*M* NaCl, 5 m*M* $MgCl_2$, 20 m*M* HEPES, pH 8.2, 1 m*M* dithiothreitol, 0.1 m*M* phenylmethylsulphonyl fluoride and the protease inhibitor cocktail) at 4°C
9. Streptolysin O (SLO) (Cat. No. S5265, Sigma) at 100 µg/ml in H_2O, aliquoted, and stored at –20°C
10. 1 *M* $CaCl_2$ (Cat. No. C4901, Sigma) in sterile H_2O
11. ATP (Cat. No. A3377, Sigma) at 200 m*M* in H_2O, aliquoted, and stored at –20°C
12. Creatine kinase (Cat. No. C3755, Sigma) at 5 mg/ml in H_2O, aliquoted, and stored at –20°C
13. Phosphocreatine (Cat. No. P7936, Sigma) at 2 *M* in H_2O, aliquoted, and stored at –20°C
14. GTP (Cat. No. G8752, Sigma) at 10 m*M* in H_2O, aliquoted, and stored at –20°C
15. Nucleotide triphosphate (NTP) set (Cat. No. 1277057, Roche; Basel, Switzerland). Prepare a stock solution by mixing 20 µl of each NTP provided in the set at a 1:1:1:1 ratio on ice. Aliquot in 10 µl and store at –20°C. This makes an NTP mix at 25 m*M* of each NTP. Prepare more stock solution as needed.

B. Instrumentation

1. Sonicator fitted with a 2-mm-diameter probe (Model Labsonic M, B. Braun Biotech International; Melsungen, Germany)
2. Regular atmosphere incubator set at 37°C (for human cells)
3. 5% CO_2 incubator set at 37°C
4. 50- and 15-ml conical tubes (Corning; Corning, NY)
5. 1.5-ml centrifuge tubes
6. 24-well cell culture plates (Costar Cat. No. 3524, Corning)
7. Refrigerated centrifuge with swinging buckets suited for 15- and 50-ml conical tubes

III. PROCEDURES

The methods describe (1) the preparation of "donor" cells to be reprogrammed, (2) the preparation of the reprogramming extract, (3) the permeabilisation of the donor cells, (4) the reprogramming reaction, (5) the resealing of the reprogrammed cells, and (6) examples of assessments of nuclear and cell reprogramming. The procedures described are based on the reprogramming of a human fibroblast cell line (293T) in an extract derived from the human Jurkat TAg cell line (Håkelien *et al.*, 2002).

A. Seeding 293T Cells

On the day prior to reprogramming reaction, plate 293T cells onto 12-mm round, sterile, poly-L-lysine-coated glass coverslips at a density of 50,000 cells per coverslip. Each coverslip is placed in individual wells of a 24-well culture plate. Overlay coverslips with 500 µl of complete RPMI 1640 medium and place in a 5% CO_2 incubator at 37°C.

B. Preparation of the Reprogramming Extract

1. Cell Harvest

1. Transfer the Jurkat TAg cell suspension culture into 50-ml conical tubes and sediment the cells at 800 *g* for 10 min at 4°C.
2. Wash the cells twice in ice-cold phosphate-buffered saline (PBS) by suspension and sedimentation at 800 *g* for 10 min at 4°C. Cells can be pooled into a single tube after the first wash.

2. Cell Swelling

1. Resuspend the cells in 10 ml ice-cold cell lysis buffer (CLB). It is preferable to use a graduated 15-ml conical tube to estimate the cell volume after sedimentation.
2. Centrifuge at 800 *g* for 10 min at 4°C.
3. Estimate the volume of the cell pellet. Resuspend the pellet into 2 volumes of ice-cold CLB.
4. Hold the cells on ice for 45 min to allow swelling. This makes it easier to lyse the cells during sonication. Keep the cells well suspended by occasional tapping of the tube during swelling. Note that the cells can be allowed to swell for longer than 45 min. This swelling step can be omitted for Jurkat TAg or primary T-cells as these cell types lyse promptly during sonication.

3. Extract Preparation

1. Aliquot the cell suspension into 200 µl in 1.5-ml centrifuge tubes previously chilled on ice. Sonicate each tube one by one (on ice) until all cells and nuclei are lysed. Lysis is assessed by complete disruption of the cells and nuclei, as judged by the sole appearance of cell "debris" by phase-contrast microscopy examination of 3-µl samples. Once lysis is achieved in a tube, keep the tube on ice and proceed with all other tubes. Power and duration of sonication varies with each cell type. For Jurkat TAg cells, sonication of each tube at 25% power and 0.5-s pulse cycle over 1 min 40 sec is recommended.

2. Pool all the lysates into one (or multiple, if needed) chilled 1.5-ml centrifuge tube. Sediment the lysate at 15,000 *g* for 15 min at 4°C in a fixed-angled rotor. Note that a swing-out rotor can also be used.

3. Carefully collect the supernatant with a 200-µl pipette and transfer it into a new 1.5-ml tube chilled on ice. This is the reprogramming extract.

4. It is possible to aliquot the extract into 200-µl tubes such as those used for polymerase chain reaction, with 100 µl extract per tube. Snap-freeze each tube in liquid N_2 and store at –80°C. However, we recommend carrying out reprogramming with freshly made extract as the stability of the extract at –80°C may vary with cell types and batches.

5. Following sedimentation in step 3, remove 20 µl of extract to determine protein concentration and pH. The protein concentration should be between 20 and 25 mg/ml. The pH should be between 6.7 and 7.0 (see Comment 2).

4. Extract Toxicity Assay

Each new batch of Jurkat TAg cell extract requires a cell toxicity test.

1. Add 50,000 293T cells (or, in principle, HeLa cells or any other epithelial of fibroblast cell line growing in the laboratory) to 35 µl of extract on ice in a 1.5-ml centrifuge tube. The extract does not need to contain any additives (unlike for a reprogramming reaction; see Section III,E,1).

2. Incubate for 1 h at 37°C in a water bath.

3. Remove a 3-µl aliquot and assess cell morphology by phase-contrast microscopy. **Fig. 2** illustrates primary rat fetal fibroblasts after a 30-min exposure to reprogramming extracts. In our hands, the morphology of the cells after a 30-min incubation in the extract reflects their survival in culture as judged 24 h after the toxicity assay. Cells shown in **Fig. 2A** survive the extract exposure, whereas cells in **Fig. 2B** have been damaged by the extract and do not survive in culture. Extract batches producing such cells should be discarded.

4. If so wished, replate the cells directly from the extract in complete RPMI 1640 for an overnight culture to assess survival further. There is no need to remove the extract prior to replating.

C. Permeabilisation of 293T Cells

In order for components from the reprogramming extract to enter 293T cells, the cells must be reversibly permeabilised. Permeabilisation is accomplished with the *Streptococcus pyogenes* toxin, streptolysin O. SLO is a cholesterol-binding toxin that forms large pores in the plasma membrane of mammalian cells (Walev *et al.*, 2002).

1. Preparation of SLO Stock Solution

1. Dissolve SLO powder in sterile-filtered MilliQ H_2O to 100 µg/ml. Keep on ice while dissolving the SLO.
2. Aliquot 10 µl in 200-µl tubes and store at –20°C.
3. Discard all tubes after 1 month of storage at –20°C and prepare a new stock. Stock aliquots should be thawed only once. Note that because commercial batches of SLO vary in specific activity, a range of SLO concentrations (200, 500, 1000, 2000, and

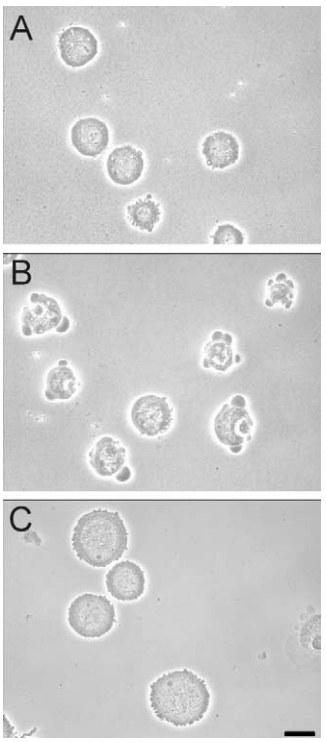

FIGURE 2 Results from toxicity assay. Rat embryo fibroblasts were exposed to a reprogramming extract for 1 h as described in the text. Cells were examined by phase-contrast microscopy. (A) Viable cells. (B) Nonviable cells. Reprogramming extracts producing such cells are discarded. (C) Control cells exposed for 30 min to the cell lysis buffer used to prepare the extract. Bar: 20 µm.

4000 ng/ml SLO) should be tested on the cell type to be reprogrammed after a new stock is prepared.

2. Cell Permeabilisation

1. Dilute the SLO stock in ice-cold HBSS to 230 ng/ml. This is the working solution. Note that this concentration is valid for 293T cells and should be adjusted for other cell types using a cell permeabilisation assay described in Section III,D.
2. Keep the SLO on ice until addition to 293T cells.
3. Remove the RPMI 1640 medium from wells containing 293T cells grown on coverslips and wash the cells four times with PBS at room temperature to remove all Ca^{2+} from the culture medium. This step is essential as Ca^{2+} inhibits SLO activity.
4. Add 250 µl SLO working solution to each well.
5. Incubate at 37°C in regular atmosphere for 50 min. Proceed to Section III,E,1.

D. Cell Permeabilisation Assay

This assay allows evaluation of the efficiency of the SLO treatment. It is recommended to carry out this assay using four additional coverslips supporting 293T cells as described in Section III,A, in addition to those used for the reprogramming reaction. This assay is based on the uptake of the fluorescent DNA stain, propidium iodide, by permeabilised cells, but not by intact cells.

1. Permeabilise cells on two coverslips with SLO as described under Section III,C,2. However, in the first step, add propidium iodide to 0.1 µg/ml to the SLO dilution in HBSS on one of the coverslips. Propidium iodide will be taken up as cells are being permeabilised. The other coverslip receives 250 µl SLO dilution in HBSS without propidium iodide.
2. Two additional coverslips should also be used as controls for the absence of SLO. Add 250 µl HBSS containing propidium iodide to one of the control coverslips as in step 1. The other coverslip receives 250 µl HBSS without propidium iodide.
3. Incubate at 37°C in regular atmosphere for 50 min.
4. For SLO-treated and control coverslips *not* containing propidium iodide, remove HBSS and immediately add 1.5 ml of preheated (37°C) complete RPMI 1640 containing 2 m*M* Ca^{2+} added from a 1 *M* stock (see Section II,A). Incubate at 37°C for 2 h to allow resealing of the plasma membranes.
5. For SLO-treated and control coverslips labelled with propidium iodide, remove HBSS, rinse with PBS, and add 250 µl PBS.
6. Assess propidium iodide labelling of the nuclei by epifluorescence microscopy.
7. After the 2-h membrane resealing step described in step 4, remove the culture medium, rinse with PBS, and add 250 µl PBS containing 0.1 µg/ml propidium iodide; incubate for 10 min.
8. Assess propidium iodide uptake, or lack thereof, in the resealed cells as in step 6.

E. Reprogramming Reaction

1. Extract Preparation

During SLO treatment, the extract should be prepared for reprogramming.

1. Prepare the ATP-regenerating system: mix on ice ATP : GTP : creatine kinase : phosphocreatine in a 1 : 1 : 1 : 1 ratio from each separate stock (described in Section II,A) and keep on ice.
2. Add 5 µl of the ATP-regenerating system mix to 100 µl of extract on ice.
3. Add 4 µl of the 25 m*M* NTP mix (see Section II,A) to 100 µl of extract on ice.
4. Vortex briefly and replace the extract on ice.

2. *Reprogramming Reaction*

1. Remove SLO from the cells by careful aspiration.
2. Quickly add PBS to prevent drying.
3. Immediately transfer each coverslip into a new dry well of a 24-well plate and carefully lay 65 µl of extract (prepared as described in Section III,B,3) onto each coverslip. Be careful that cells do not dry out upon transfer of the coverslip(s) to the new wells and prior to addition of the extract. It is important that the coverslip be covered by the extract during the entire incubation time. Should the extract spread out of the coverslip, transfer the coverslip into a new well and pipette the extract back onto the cells.
4. Incubate at 37°C for 1 h in regular atmosphere. Note that reprogramming has also proven to be successful upon incubation in a 5% CO_2 incubator at 37°C.

F. Resealing Reprogrammed Cells

1. At the end of incubation, directly add to each well 1.5 ml of preheated (37°C) complete RPMI 1640 containing 2 m*M* Ca^{2+} added from the 1 *M* stock (see Section II,A). Do not remove the extract before adding the Ca^{2+}-containing medium.
2. Incubate for 2 h in a 5% CO_2 incubator at 37°C.
3. Remove the Ca^{2+}-containing medium by gentle aspiration and replace with 250 µl of complete RPMI 1640 (Jurkat TAg cell culture medium).
4. Place the cells back into the 5% CO_2 incubator and culture until reprogramming assessments are performed.

G. Assessment of Nuclear Reprogramming

Various assessments of nuclear and cell reprogramming can be performed, depending on the purpose of the experiment. Using the method described here, we have reported changes in the gene expression profile of the reprogrammed 293T cells using cDNA macroarrays from R&D Systems (Abington, UK) (Håkelien *et al.*, 2002). Expression of new proteins can also be monitored at regular intervals after the reprogramming reaction by immunofluorescence or flow cytometry using standard protocols. We have shown the expression of several antigens on the surface of the reprogrammed cells, which are specific for hematopoietic cells. These include CD3, CD4, CD8, CD45, and components of the T-cell receptor (TCR) complex (Håkelien *et al.*, 2002). A variety of functional assays can also be carried out, such as cytokine secretion in response to stimulation of the T-cell receptor/CD3 complex in the reprogrammed cells, or expression of additional cytokine receptors on the cell surface

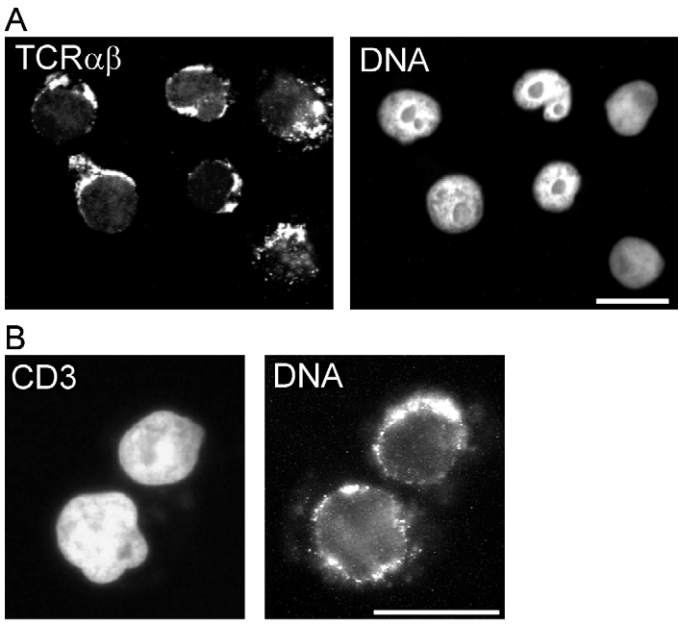

FIGURE 3 Immunofluorescence detection of (A) T-cell receptor (TCR) α and β chain expression and (B) CD3 expression on the surface of 293T cells reprogrammed in a Jurkat TAg cell extract. DNA is labelled with 0.1 µg/ml propidium iodide. Analysis was performed ~14 days after the reprogramming reaction. Bars: 20 µm.

(Håkelien *et al.*, 2002). **Fig. 3** illustrates the expression of the TCR α and β chains and of CD3 molecules on the surface of 293T cells reprogrammed in a Jurkat TAg cell extract.

IV. COMMENTS

1. Commercially available SLO batches vary greatly in activity. Thus, it is recommended to test a range of SLO concentration on the cell type to be reprogrammed prior to initiating reprogramming reactions. The efficiency of SLO-mediated permeabilisation also varies for various cell types.
2. pH of the extract. We usually observe a drop of 1-1.5 pH unit upon extract preparation, which explains the pH 8.2 of the CLB. Notably, raising the pH of CLB to 8.7 with a HEPES buffer does not increase the pH of the final extract. Other buffers with greater buffering capacity have not been tested.
3. The method described here can be used easily with either purified cell nuclei (Landsverk *et al.*, 2002) or permeabilised cells (Håkelien *et al.*, 2002). Procedures for purifying intact (membrane-enclosed) nuclei from interphase cultured cells have been reported earlier (Collas *et al.*, 1999; Landsverk *et al.*, 2002; Martins *et al.*, 2000; Steen *et al.*, 2000).

V. PITFALLS

1. It is currently difficult to objectively assess the extent of sonication of Jurkat TAg cells or any other cell type. It is important to sonicate until all cells and nuclei are completely lysed. Whether extended sonication after cell lysis is complete is detrimental or beneficial is at present unknown.

2. Variability in batches of reprogramming extracts is seen, even among extracts that have been rated as "nontoxic" in the toxicity assay described in Section III,B,4. Variability is evident by the absence of markers of cell reprogramming approximately 1 week after the reprogramming reaction.

3. Currently, the duration of expression of a reprogrammed phenotype is limited to at least 2 months for 293T cells reprogramming in Jurkat TAg extract (Håkelien *et al*., 2002). The reprogrammed phenotype may also last for shorter periods depending on the marker analyzed.

Acknowledgments

Our work was supported by Nucleotech, LLC and grants from the Research Council of Norway, the Norwegian Cancer Society, and the Human Frontiers Science Program.

References

Blau, H. M., and Blakely, B. T. (1999). Plasticity of cell fate: Insights from heterokaryons. *Semin. Cell D* **10**, 267–272.

Cibelli, J. B., Stice, S. L., Golueke, P. J., Kane, J. J., Jerry, J., Blackwell, C., Ponce, D. L. F., and Robl, J. M. (1998). Cloned transgenic calves produced from nonquiescent fetal fibroblasts. *Science* **280**, 1256–1258.

Collas, P., Le Guellec, K., and Tasken, K. (1999). The A-kinase anchoring protein, AKAP95, is a multivalent protein with a key role in chromatin condensation at mitosis. *J. Cell Biol.* **147**, 1167–1180.

Gurdon, J. B., Laskey, R. A., De Robertis, E. M., and Partington, G. A. (1979). Reprogramming of transplanted nuclei in amphibia. *Int. Rev. Cytol. Suppl.* 161–178.

Håkelien, A. M., Landsverk, H. B., Robl, J. M., Skålhegg, B. S., and Collas, P. (2002). Reprogramming fibroblasts to express T-cell functions using cell extracts. *Nature Biotechnol.* **20**, 460–466.

Landsverk, H. B., Håkelien, A. M., Küntziger, T., Robl, J. M., Skålhegg, B. S., and Collas, P. (2002). Reprogrammed gene expression in a somatic cell-free extract. *EMBO Rep.* **3**, 384–389.

Martins, S. B., Eide, T., Steen, R. L., Jahnsen, T., Skålhegg, B. S., and Collas, P. (2000). HA95 is a protein of the chromatin and nuclear matrix regulating nuclear envelope dynamics. *J. Cell Sci.* **113**, 3703–3713.

Morrison, S. J. (2001). Stem cell potential: Can anything make anything? *Curr. Biol.* **11**, R7-R9.

Munsie, M. J., Michalska, A. E., O'Brien, C. M., Trounson, A. O., Pera, M. F., and Mountford, P. S. (2000). Isolation of pluripotent embryonic stem cells from reprogrammed adult mouse somatic cell nuclei. *Curr. Biol.* **10**, 989–992.

Steen, R. L., Martins, S. B., Tasken, K., and Collas, P. (2000). Recruitment of protein phosphatase 1 to the nuclear envelope by A-kinase anchoring protein AKAP149 is a prerequisite for nuclear lamina assembly. *J. Cell Biol.* **150**, 1251–1262.

Tada, M., Takahama, Y., Abe, K., Nakastuji, N., and Tada, T. (2001). Nuclear reprogramming of somatic cells by *in vitro* hybridization with ES cells. *Curr. Biol.* **11**, 1553–1558.

Walev, I., Hombach, M., Bobkiewicz, W., Fenske, D., Bhakdi, S., and Husmann, M. (2002). Resealing of large transmembrane pores produced by streptolysin O in nucleated cells is accompanied by NF-kappaB activation and downstream events. *FASEB J.* **16**, 237–239.

Western, P. S., and Surani, M. A. (2002). Nuclear reprogramming. Alchemy or analysis? *Nature Biotechnol.* **20**, 445–446.

Wilmut, I., Schnieke, A. E., McWhir, J., Kind, A. J., and Campbell, K. H. S. (1997). Viable offspring derived from fetal and adult mammalian cells. *Nature* **385**, 810–813.

SECTION

5

Immortalization

CHAPTER

27

Immortalization of Primary Human Cells with Telomerase

Kwangmoon Lee, Robert L. Kortum, and Michel M. Ouellette

I. INTRODUCTION

One major obstacle to the immortalization of primary human cells is telomere-controlled senescence. Telomere-controlled senescence is caused by the shortening of the telomeres that occurs each time somatic human cells divide. The enzyme telomerase can prevent the erosion of telomeres and block the onset of telomere-controlled senescence, but its expression is restricted to the human embryo and, in the adult, to rare cells of the blood, skin, and digestive track. However, we and others have shown that the transfer of an exogenous hTERT cDNA, encoding the catalytic subunit of human telomerase, can be used to prevent telomere shortening, overcome telomere-controlled senescence, and immortalize primary human cells (Bodnar *et al.*, 1998). Most importantly, hTERT alone can immortalize primary human cells without causing cancer-associated changes or altering phenotypic properties (Jiang *et al.*, 1999; Morales *et al.*, 1999; Ouellette *et al.*, 2000). Primary human cells that have been immortalized successfully with hTERT alone include fibroblasts, retinal pigmented epithelial cells, endothelial cells, myometrial cells, esophageal squamous cells, mammary epithelial cells, keratinocytes, osteoblasts, and Nestin-positive cells of the pancreas (Bodnar *et al.*, 1998; Yang *et al.*, 1999; Ramirez *et al.*, 2001; Yudoh *et al.*, 2001; Condon *et al.*, 2002; Lee *et al.*, 2003; Morales *et al.*, 2003). This article describes the use of hTERT for the purpose of immortalizing primary human cells using the primary human fibroblast as an example.

II. MATERIALS AND INSTRUMENTATION

Packaging cell line Phoenix-ampho (ϕNX-A) for the production of amphotropic viruses is available from Dr. Gary Nolan (Stanford University, Stanford, CA; http://www.stanford.edu/group/nolan/). Retroviral vectors pBabePuro and pBabePuro-hTERT are from Geron Corp. (Menlo Park, CA; Ouellette *et al.*, 1999). Dulbecco's modified Eagle's medium (DMEM; Cat. No. 11995), medium 199 (Cat. No. 11150), gentamicin (Cat. No. 15710), and trypsin–EDTA (0.05% trypsin, 0.53 m*M* EDTA; Cat. No. 25300) are from Invitrogen Corp. (Carlsbad, CA). Electrophoresis apparatus (Cat. Series 21070), including glass plates, spacers, and combs, are from Life Technologies (Rockville, MD). Cosmic calf serum (Cat. No. SH30087) and fetal bovine serum (Cat. No. SH30070) are from HyClone (Logan, UT). The polysulfone filter (0.45 μm, Cat. No. DD50402550) is from Life Science Products Inc. (Frederick, CO). Dimethyl sulfoxide (DMSO; Cat. No. D 2650), polybrene (Cat. No. H 9268), puromycin (Cat. No. P 7255), and bovine serum albumin (BSA; Cat. No. A 2153) are from Sigma-Aldrich (St. Louis, MO). The MBS mammalian $CaPO_4$ transfection kit is from Stratagene (Cat. No. 200388; La Jolla, CA). The TrapEZE kit is from Serologicals Corp. (Cat. No. S7700; Norcross, GA). *N*,*N*,*N*′,*N*′-Tetramethylenediamine (TEMED; Cat. No. 161–0800) and 40% acrylamide:bisacrylamide [19:1] solution (Cat. No. 161-0146) are from Bio-Rad (Hercules, CA). The PhosphorImager is from Molecular Dynamics (Model No. 810; Sunnyvale, CA). Nalgene

Copyright 2006, Elsevier Science (USA).
All rights reserved.

Cryo 1°C freezing containers are from Nalge Nunc International (Cat. No. 5100-0001; Rochester, NY). T4 polynucleotide kinase is from New-England BioLabs (Cat. No. M0201S; Beverly, MA). [γ-^{32}P]ATP is from New England Nuclear (Cat. No. 502A12070; Boston, MA). The polymerase chain reaction (PCR) is performed using a PCRExpress thermocycler from Hybaid (Ashford, Middlesex, UK). All other chemicals are from Fisher Biotechnology (Fait Lawn, NJ), Fisher Scientific Co. (Pittsburgh, PA), or Sigma-Aldrich (St. Louis, MO).

III. PROCEDURES

A. Production of Replication-Defective Retroviruses Carrying the hTERT cDNA

Primary human cells tend to transfect very poorly. Consequently, the preferred method of transferring exogenous telomerase to such cells is their transduction with replication-defective retroviruses carrying an hTERT cDNA. The following procedure, modified from Pear *et al.* (1993), yields high-titer viruses following the transient transfection of ϕNX-A cells, a retroviral packaging cell line.

Solutions

1. *293T medium*: To 500 ml of DMEM, add 50 ml of fetal bovine serum and 500 µl of 10 mg/ml gentamicin. Store at 4°C and protect from light.
2. *Complete medium X*: To a clean sterile 500-ml bottle, combine 400 ml of DMEM, 100 ml of medium 199, 50 ml of cosmic calf serum, and 500 µl of 10 mg/ml gentamicin. Store at 4°C and protect from light.

Steps

1. In a 37°C water bath, thaw a vial of ϕNX-A cells and transfer cells to a culture dish containing 293T medium. Incubate cells at 37°C under 5% CO_2. The next day, replace medium with fresh medium.

2. Expand ϕNX-A cells in 293T medium using split ratios of 1 : 4 to 1 : 6. Avoid letting the cells grow beyond 90% confluence. To split cells, remove medium by aspiration, gently wash cells once with PBS. Take extra care not to dislodge the cells, as ϕNX-A cells tend to detach very easily. Add 2 ml of trypsin–EDTA per 100-mm dish and let cells detach at 37°C for 1–2 min. Tap dish to help dislodge cells, add 5 ml of 293T medium, and pipette up and down to break cell clusters. Transfer suspension to a sterile tube and pellet cells by low-speed centrifugation (2000 *g* for 5 min at room temperature). Remove supernatant and resuspend cells in 5 ml of 293T medium.

3. Following the manufacturer's instructions, count cells using a Coulter counter or hemacytometer. In two 100-mm plates containing 293T medium, seed 5.0×10^6 cells/dish. Freeze remaining cells to replenish archival stocks, if needed (refer to Section III,C).

4. On the following day, ϕNX-A cells should be ~80% confluent and ready to be transfected with the retroviral vectors. Transfect each dish with 10–20 µg of plasmid; one with vector pBabePuro-hTERT and the other with the empty vector, pBabePuro. ϕNX-A cells are transfected most easily using the $CaPO_4$ method, but other methods can be used as well. To $CaPO_4$ transfect the ϕNX-A cells, we have used the Stratagene's MBS mammalian transfection kit following the manufacturer's instructions. In a 5-ml Falcon 2054 polystyrene tube, prepare a calcium–DNA precipitate by mixing plasmid DNA (10–20 µg in 450 µl of sterile water) with 50 µl of solution I (2.5 *M* $CaCl_2$) and then adding 500 µl of solution II [*N*,*N*-bis(2-hydroxyethyl)-2-aminoethanesulfonic acid in buffered saline].

5. Incubate the calcium–DNA mixtures at room temperature for 10–20 min. In the meantime, prepare the cells by washing cells once with PBS and feeding them with 10 ml/dish of 293T medium, in which 6% modified bovine serum (provided by the kit) is used in place of the fetal bovine serum.

6. Resuspend the DNA precipitate gently and then apply dropwise in a circular motion to the dishes, as to distribute the DNA evenly. Swirl dishes once.

7. Incubate cells at 37°C under 5% CO_2 for 3 h.

8. Remove medium by aspiration.

9. Wash cells once with sterile PBS and feed with 293T medium. Return cells to 37°C under 5% CO_2. Cells have now been transfected and should start producing retroviruses within the next 24 h.

10. Viruses can be collected in three consecutive harvests over the next 24–72 h posttransfection. To collect viruses, replace the 293T medium with 4–5 ml of the target cells culture medium, in which the viruses will now be allowed to accumulate. For primary human fibroblasts, collect viruses in complete medium X. Return cells to 37°C under 5% CO_2 with the dishes spread on a leveled shelf to ensure good coverage of all surfaces.

11. After 8–16 h of exposure to the cells, harvest supernatants and then force through a 0.45-µm polysulfone filter so that all remaining cells are removed. Bleach and discard the transfected cells once the last batch of viral supernatant has been collected.

12. Keep viral supernatants either on ice and use within the hour or else aliquot, freeze, and store at

–80°C, where they can last for approximately 6 months. Label each aliquot with name of retroviral vector, harvest medium, date, and harvest number (1st, 2nd, etc . . .). Freezing does not appear to cause substantial drops in titer, but cycles of freeze/thaw do.

B. Transduction of Human Primary Cells with Retroviruses Carrying hTERT

Solutions

1. *400 µg/ml polybrene:* Dissolve 8 mg of polybrene in 20 ml of deionized double-distilled water. Sterilize by filtration through a 0.45-µm polysulfone filter. Store at 4°C.
2. *500 µg/ml puromycin:* Dissolve 10 mg of puromycin in 20 ml of deionized double-distilled water. Sterilize by filtration through a 0.45-µm polysulfone filter. Store aliquots at –20°C.

Steps

1. Thaw primary human fibroblasts in complete medium X. Incubate cells at 37°C under 5% CO_2. The next day, replace medium with fresh medium.

2. Expand cells in complete medium X using split ratios of 1:2, 1:4, and 1:8 for late, mid, and early passage cells, respectively. Avoid leaving monolayers at full confluence for extensive periods of time, as cells may then resist trypsinization. To split cells, remove medium and wash cells twice with 2 ml of trypsin–EDTA per 100-mm dish. Incubate dishes at 37°C until cells have detached (1–3 min). Tap dishes to help dislodge cells, add 5 ml of complete medium X, and pipette up and down to dissociate clumps. Transfer suspension to a sterile tube and pellet cells by low-speed centrifugation (2000 *g* for 5 min at room temperature). Remove supernatant and resuspend cells in 5 ml of complete medium X. While keeping track of population doublings (see later), expand fibroblasts until sufficient cells are available.

3. Seed four wells of a 6-well plate with target cells so that the cells are in log-phase growth on the next day. For primary human fibroblasts, seed cells in complete medium X at 2×10^5 cells per well. Take note of the population doubling of the seeded cells as the initial PD (or PD_i). Freeze remaining cells to replenish archival stocks, if needed. Label frozen vials with name of strain, date, population doubling, and approximate number of cells per vial (refer to Section III,C).

4. Incubate dishes overnight at 37°C under 5% CO_2.

5. Remove the medium from all dishes. Infect one dish with viruses carrying hTERT (sample A; infected with pBabePuro-hTERT) and a second dish with control viruses carrying no insert (sample B; infected with pBabePuro). Feed the remaining two dishes with virus-free medium (samples C and D; uninfected). Perform infections at 37°C under 5% CO_2 for 8–16 h using 1–2 ml of a mixture containing 1 volume of viral supernatant, 1 volume of the target cells culture medium, and 4 µg/ml polybrene. Within 24–48 h, cells can be infected sequentially with all of the different harvests of the same virus.

6. Remove the last viral supernatants and replenish all four dishes with the target cell culture medium, using complete medium X for primary human fibroblasts. Return cells at 37°C under 5% CO_2.

7. Let cells divide once or twice over the next 24–48 h to allow integration of the viral genomes.

8. Select cells for viral integrations using puromycin. The exact dose of puromycin to use should be determined in a preliminary experiment, in which uninfected cells are exposed to increasing doses of puromycin (e.g., 0, 250, 500, 750, 1000 ng/ml) for 7–10 days; use the lowest dose that kills all cells. For primary human fibroblasts, 500–750 ng/ml is a good starting point. Add puromycin to sample A, B, and C. Leave sample D puromycin free.

9. Maintain cells in continuous log-phase growth. Samples that reach confluence should be trypsinized and expanded to a larger dish; do not discard any excess cells yet. Replace puromycin-containing media as needed or twice a week until selection is complete. Selection is complete when all of the uninfected cells of control sample C have died, after typically 7–10 days of selection.

10. Expand cells until samples A and B have reached the size of a 100-mm dish. Count total number of cells in samples A, B, and D. Evaluate the number of population doublings done during the infection/selection phases of the experiment ($\Delta PD_{i/s}$). For this purpose, the simplest approximation is to assume that samples A, B, and D have done an equivalent number of doublings during this same period of time. Using sample D as a reference, calculate $\Delta PD_{i/s}$ knowing that $\Delta PD_{i/s}$ = log[(final number of cells in sample D) ÷ (initial number of cells plated in step 3)] / log[2]. Discard sample D and set PD of samples A and B to $PD_{time0} = PD_i + \Delta PD_{i/s}$.

11. Cells are now ready to be tested for telomerase activity and assessed for life span extension. Put aside 5×10^4 cells of each sample for a telomerase assay (see Section III,C). Start a growth curve by seeding 2×10^5 cells of each sample in a 100-mm dish (see Section III,C). Freeze remaining cells and label vial with name of strain, vector transduced, population doubling (PD_{time0}), and approximate number of cells.

C. Other Procedures Related to the Immortalization of Human Primary Fibroblasts

1. Freezing ϕNX-A Cells and Primary Human Cells

Solution

Freeze medium: Mix 10 ml of DMSO with 90 ml of fetal bovine serum. Store aliquots at –20°C and keep working solution at 4°C.

Steps

1. Trypsinize cells as described earlier, resuspend in culture medium, and recover by low-speed centrifugation (2000 *g* for 5 min at room temperature).
2. Remove supernatant by aspiration, and resuspend pellet in freeze medium so that each milliliter contains the cell equivalent of 25–150 cm^2 of confluent dish surface.
3. Aliquot suspension in 2-ml cryogenic vials, at 1 ml per vial.
4. Label vials with name of sample, population doublings, date, and approximate number of cells.
5. Place vials into a Nalgene Cryo 1°C freezing container filled with fresh isopropanol. Transfer container to –80°C.
6. On the next day, transfer the frozen vials to either a liquid nitrogen tank or a –135°C freezer.

2. Measuring Cellular life Span

To verify that exogenous telomerase has an extended cellular life span, a growth curve is generated to measure and compare the life span of the vector- and hTERT-transduced cells.

Steps

1. Maintain the vector- and hTERT-transduced cells in continuous log-phase growth as cells are counted once a week. For this purpose, seed cells at a density that requires a week for early passage cells to reach confluence. For most primary human fibroblasts, a density of 2×10^5 cells per 100-mm dish is adequate. Take note of the population doublings of the two samples, using the value of PD_{time0} for cells that have just been transduced and then selected.
2. Let cells grow for a week at 37°C under 5% CO_2.
3. Trypsinize, wash, recover in culture media, and then count cells using either a Coulter counter or a hematocytometer.
4. Calculate the number of population doublings done by the cells since they were last seeded (or ΔPD), where ΔPD = log[(number of cells recovered) ÷ (number of cell seeded)] / log[2].
5. Calculate the current PD of each of the two cell populations by adding the value of their ΔPD to that of their previous PD (at which cells were when they had been plated a week earlier). If ΔPD is negative, set the value of ΔPD to zero.
6. Replate cells at the exact same density as in step 1 and freeze all remaining cells. Label frozen vials with name of strain, vector transduced, population doubling (current PD), and approximate number of cells.
7. Repeat steps 2 though 6 until all of the vector-transduced cells have become senescent. For both samples, each cycle of growth will yield a ΔPD that is then added to the previous PD to increase the current PD to its present value.
8. For each sample, plot PD_{n+1} as a function of time. Cells transduced with the empty vector should eventually reach a plateau corresponding to telomere-controlled senescence, at which point cells will cease to divide. Pursue the experiment until the vector-transduced cells have reached senescence. Cells can be considered senescent once they perform less than a doubling over a 2-week period. Most strains of primary human cells reach senescence after 15–90 doublings. A complete bypass of senescence by the hTERT-transduced cells would then confirm that the cellular life span has been extended by exogenous telomerase. In this eventuality, grow the hTERT-transduced cells until the life span has been extended by a factor of at least 3, at which point the cells can be considered functionally immortal.

3. Measuring the Activity of Telomerase Using the Telomere Repeat Amplification Protocol (TRAP) Assay

The TRAP assay is based on an improved version of the original method described by Kim *et al*. (1994). It is typically performed using a commercial kit, the TRAPeze telomerase detection kit (Serologicals Corp., Norcross, GA).

Solutions

1. *50 mg/ml BSA:* Dissolve 0.5 g of BSA in 10 ml of deionized water. Aliquot and store at –20°C.
2. *0.5 M EDTA:* To make 500 ml, add 93.1 g of EDTA (disodium salt) to 400 ml of deionized water. Adjust pH to 8.0 using sodium hydroxyde. Complete to 500 ml with deionized water.
3. *6X loading dye:* To make 10 ml, combine 6.4 ml of deionized water, 3 ml of glycerol, 600 µl of 0.5 *M* EDTA, 25 mg of bromphenol blue, and 25 mg of xylene cyanol.
4. *12.5% acrylamide gel solution:* To make 50 ml, combine 15.6 ml of a 40% acrylamide : bisacrylamide [19 : 1] solution with 5 ml of 5X TBE. Complete to 50 ml

with deionized water. Just before casting the gel, add 50 µl of TEMED and 500 µl of 10% ammonium persulfate. Mix well and cast immediately.

5. *5X TBE:* To make 1 liter, add 54 g of Tris base, 27.5 g of boric acid, and 20 ml of 0.5 *M* EDTA, pH 8.0, to 800 ml of deionized water. Mix until solute has dissolved. If needed, readjust pH to 8.1–8.5. Complete to 1 liter with deionized water.

Steps

1. Prepare the following samples for analysis: uninfected cells, hTERT-transduced cells, vector-transduced cells, and a positive control (telomerase-positive cancer cell line, such as 293, H1299, or HeLa cells). Trypsinize and count cells; for each sample, transfer 5×10^4 cells to an Eppendorf tube.

2. Pelet cells by low-speed centrifugation (2000 *g* for 5 min) and remove supernatant. Spin sample once more for just a few seconds so that the very last drop of remaining medium can be removed with the use of a micropipette. Freeze pellets at –80°C.

3. Thaw cell pellets on ice. To each sample, add 100 µl of ice-cold TRAPeze kit CHAPS lysis buffer (10 m*M* Tris–HCl, pH 7.5, 1 m*M* $MgCl_2$, 1 m*M* EGTA, 0.1 m*M* benzamidine, 5 m*M* β-mercaptoethanol, 0.5% CHAPS, 10% glycerol). Disperse cells by forcing the pellets 5–10 times through the tip of a P200.

4. Incubate cell lysates on ice for 30 min.

5. Spin samples in a microcentrifuge at 12,000 *g* for 20 min at 4°C.

6. Transfer 80 µl of the supernatant into a fresh Eppendorf tube. Cell extracts should now contain 500 cell equivalents per microliter. Keep on ice and use within the hour or else freeze and store at –80°C.

7. End label the Telomerase Substrate (TS) primer (5′-AATCCGTCGAGCAGAGTT-3′). To prepare a sufficient amount of TS primer for six telomerase reactions, combine 6 µl of TS primer, 1.2 µl of 10X kinase buffer (provided with the enzyme), 3 µl water, 1.5 µl of [γ-32P]ATP (3000 Ci/mmol, 10 mCi/ml), and 0.3 µl of T4 polynucleotide kinase (10 units/µl). Incubate at 37°C for 20 min. Kill the enzyme at 85°C for 5 min.

8. Prepare a master mix containing all components of the telomerase assay, minus the extracts to be tested. To prepare sufficient master mix for six assays, combine 30 µl of 10X TRAP reaction buffer (200 m*M* Tris–HCl, pH 8.3, 15 m*M* $MgCl_2$, 630 m*M* KCl, 0.5% Tween-20, 10 m*M* EGTA), 3 µl of 50 mg/ml BSA, 6 µl of dNTP mix (2.5 m*M* each dATP, dTTP, dCTP, and dGTP), 6 µl of TRAP primer mix (contains the PCR primers needed for amplifying the telomerase products), 234.6 µl of water, 12 µl of ^{32}P-labeled TS primer (from the previous step), and 2.4 µl of *Taq* DNA polymerase (5 units/µl). Mix well. Aliquot the master mix in four RNase-free PCR tubes at 49 µl/tube.

9. On ice, thaw all of the cell extracts to assay. Samples should include the uninfected cells, vector-transduced cells, hTERT-transduced cells, a negative control (TRAPeze kit 1X CHAPS lysis buffer), and a positive control (telomerase-positive cancer cell line).

10. Add 1 µl of sample per tube (500 cell equivalents), mix, and place in the thermocycler.

11. Incubate at 30°C for 30 min.

12. Perform the following two-step PCR for 27–30 cycles: 94°C for 30 s, followed by 59°C for 30 s. While these conditions work on most thermocyclers, optimization of the annealing temperature and addition of a 72°C extension step may be necessary on certain machines.

13. Add 10 µl of 6X loading dye to all samples. Store at –20°C in a β blocker.

14. Prepare a vertical 12.5% polyacrylamide gel. Choose glass plates, spacers, and comb so that the gel will be 1.5 mm in thickness and 10–12 cm in length. Once the mold is ready, add TEMED and ammonium persulfate to the 12.5% acrylamide gel solution and pour the gel immediately.

15. Once the gel has polymerized, load 30 µl of each sample per lane. Run at 400 V for 90 min or until the xylene cyanol has run 70–75% of the gel length.

16. Dispose of the electrophoresis buffer as liquid radioactive waste. Wrap gel in saran wrap.

17. Expose gel to an X-ray film or PhosphoImager cassette.

18. The presence of an active telomerase should yield a ladder of products with 6-bp increments, starting at 50 nucleotides. For the TRAP assay to be valid, the following conditions should first be met: (1) the negative control corresponding to the lysis buffer should display no such ladder; (2) the positive control (e.g., 293, H1299, or HeLa cells) should yield an intense ladder; and (3) all samples should display a 36-bp band corresponding to the internal TRAP assay standard (ITAS), a control template included in the TRAP primer mix whose amplification serves to document the efficiency the PCR step of the protocol. The lack of ITAS amplification would suggest that inhibitors of *Taq* DNA polymerase may have been present in some of the samples. If the assay has met these conditions, analysis of the experimental samples can now proceed. A successful reconstitution of telomerase activity by exogenous hTERT should produce a telomerase ladder similar in intensity to that of the positive control, with no such activity detected in either vector-transduced cells or uninfected cells.

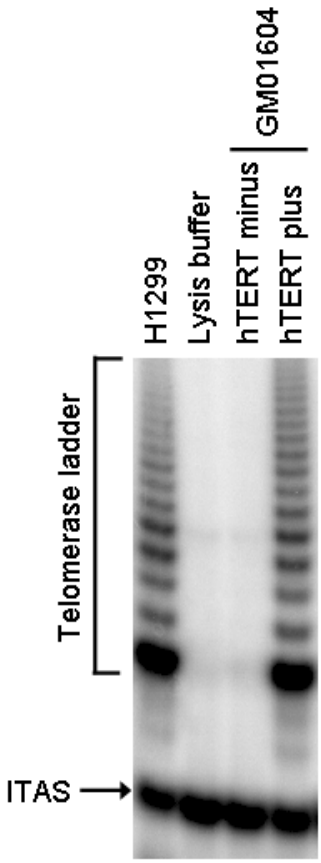

FIGURE 1 Telomerase activity in hTERT-transduced fibroblasts. GM01604 fibroblasts engineered to express exogenous hTERT or no hTERT were assayed for telomerase activity using the TRAPeze telomerase detection kit. H1299 and lysis buffer, respectively, serve as positive and negative controls. ITAS, internal TRAP assay standard.

D. Example of the Use of hTERT to Extend Cellular Life Span

1. Primary Human Fibroblasts

Primary human fibroblasts (GM01604; Coriell Institute, Camden, NJ) were infected with pBabePuro-hTERT retroviruses under the conditions described in this article. Infected cells were selected for 2 weeks with 750 ng/ml puromycin and were then tested for telomerase activity using the TRAPeze telomerase detection kit. Figure 1 shows a strong telomerase ladder in both hTERT-transduced cells and positive control H1299. The 36-bp ITAS is visible in all lanes, indicating that inhibitors of *Taq* DNA polymerase, which could have resulted in false negatives, were absent. The life span of hTERT-transduced cells was then compared to that of uninfected cells. Cells were maintained in continuous log-phase growth and counted once a week. Figure 2 is a graphic representation of the cumulative number of PD executed by the cells as a function of time. Note that hTERT minus cells ceased dividing at PD 60 whereas hTERT-transduced cells grew beyond PD 180, at which point these cells were considered functionally immortal.

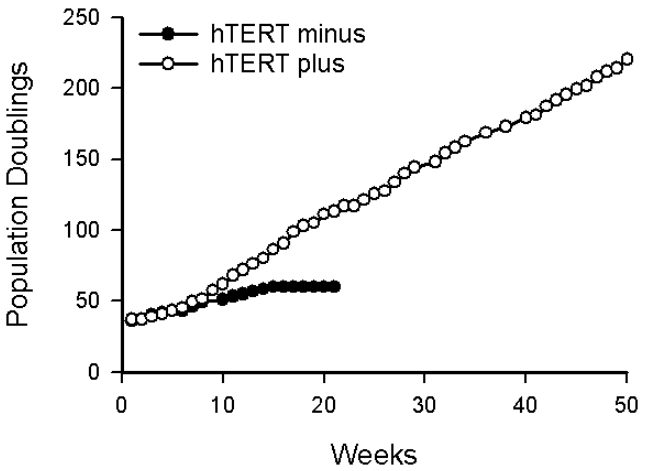

FIGURE 2 Extension of cellular life span by exogenous hTERT. GM01604 fibroblasts engineered to express exogenous hTERT or no hTERT were maintained in continuous log-phase growth and counted once a week. Population doublings executed expressed as a function of time.

IV. COMMENTS

1. Other retroviral vectors carrying hTERT are available from Dr. Robert A. Weinberg. (Whitehead Institute for Biomedical Research, Cambridge, MA). These additional vectors include an alternate version of vector pBabePuro-hTERT, as well as plasmid pCIneo-hTERT, a retroviral construct that confers resistance to G418. Be sure to use a vector carrying an hTERT cDNA that has not been epitope tagged at the C terminus, as these modifications can block the access of telomerase to the telomeres (Ouellette *et al*., 1999).

2. To adapt the protocol described for other primary human cells, replace complete medium X with a culture medium that is compatible with the long-term growth and survival of your target cells. Transfected ϕNX-A cells can be made to produce viruses in a large variety of culture media.

3. It should be noted that hTERT alone may not be sufficient to immortalize all types of primary human cells. First, the enzyme telomerase does not appear to alter the phenotypic properties, such that postmitotic terminally differentiated cells are unlikely to be rescued by the enzyme. Second, certain primary

human cells experience additional forms of senescence that are independent of telomere size (Kiyono *et al*., 1998). It has been suggested that these extra barriers represent a stress response to inadequate culture conditions, in some cases elicited by the loss of mesenchymal–epithelial interactions (Ramirez *et al*., 2001; Shay and Wright, 2001). In addition to exogenous hTERT, the immortalization of such primary cells might also require a reoptimization of the culture conditions for long-term growth, the cultivation of the cells over feeder layers, or, alternatively, the use of oncogenes that can block pRB function, such as the SV40 large T antigen, HPV type 16 E7, or adenovirus type 5 E1A.

V. PITFALLS

1. When working with amphotropic retroviruses, due caution must be exercised in the production, use, and storage of recombinant viruses. Transfected ϕNX-A cells, viral supernatants, and all plasticwares that have been in contact with these reagents should be bleached and treated as biohazard.

2. When using ^{32}P, appropriate measures must be taken to ensure that the user remains shielded from radiation and that radioactive by-products and wastes are being contained appropriately. Working areas should also be monitored for radioactive contamination.

3. When performing the TRAP assay, precautions should be taken to limit PCR contamination. To limit such contamination, electrophoresis analysis of the samples should be run in a separate area away from the bench where samples are prepared and TRAP reactions performed.

References

Bodnar, A. G., Ouellette, M., Frolkis, M., Holt, S. E., Chiu, C. P., Morin, G. B., Harley, C. B., Shay, J. W., Lichtsteiner, S., and Wright, W. E. (1998). Extension of life-span by introduction of telomerase into normal human cells. *Science* **279**, 349–352.

Condon, J., Yin, S., Mayhew, B., Word, R. A., Wright, W. E., Shay, J. W., and Rainey, W. E. (2002). Telomerase immortalization of human myometrial cells. *Biol. Reprod.* **67**, 506–514.

Jiang, X. R., Jimenez, G., Chang, E., Frolkis, M., Kusler, B., Sage, M., Beeche, M., Bodnar, A. G., Wahl, G. M., Tlsty, T. D., and Chiu, C. P. (1999). Telomerase expression in human somatic cells does not induce changes associated with a transformed phenotype. *Nature Genet.* **21**, 111–114.

Kim, N. W., Piatyszek, M. A., Prowse, K. R., Harley, C. B., West, M. D., Ho, P. L., Coviello, G. M., Wright, W. E., Weinrich, S. L., and Shay, J. W. (1994). Specific association of human telomerase activity with immortal cells and cancer. *Science* **266**, 2011–2015.

Kiyono, T., Foster, S. A., Koop, J. I., McDougall, J. K., Galloway, D. A., and Klingelhutz, A. J. (1998). Both Rb/p16INK4a inactivation and telomerase activity are required to immortalize human epithelial cells. *Nature* **396**, 84–88.

Morales, C. P., Gandia, K. G., Ramirez, R. D., Wright, W. E., Shay, J. W., and Spechler, S. J. (2003). Characterization of telomerase immortalized normal human oesophageal squamous cells. *Gut* **52**, 327–333.

Morales, C. P., Holt, S. E., Ouellette, M., Kaur, K. J., Yan, Y., Wilson, K. S., White, M. A., Wright, W. E., and Shay, J. W. (1999). Absence of cancer-associated changes in human fibroblasts immortalized with telomerase. *Nature Genet.* **21**, 115–118.

Ouellette, M. M., Aisner, D. L., Savre-Train, I., Wright, W. E., and Shay, J. W. (1999). Telomerase activity does not always imply telomere maintenance. *Biochem. Biophys. Res. Commun.* **254**, 795–803.

Ouellette, M. M., McDaniel, L. D., Wright, W. E., Shay, J.W., and Schultz, R. A. (2000). The establishment of telomerase-immortalized cell lines representing human chromosome instability syndromes. *Hum. Mol. Genet.* **9**, 403–411.

Pear, W. S., Nolan, G. P., Scott, M. L., and Baltimore, D. (1993). Production of high-titer helper-free retroviruses by transient transfection. *Proc. Natl. Acad. Sci. USA* **90**, 8392–8396.

Ramirez, R. D., Morales, C. P., Herbert, B. S., Rohde, J. M., Passons, C., Shay, J. W., and Wright, W. E. (2001). Putative telomere-independent mechanisms of replicative aging reflect inadequate growth conditions. *Genes Dev.* **15**, 398–403.

Shay, J. W., and Wright, W. E. (2001). Aging. When do telomeres matter? *Science* **291**, 839–840.

Yang, J., Chang, E., Cherry, A. M., Bangs, C. D., Oei, Y., Bodnar, A., Bronstein, A., Chiu, C. P., and Herron, G. S. (1999). Human endothelial cell life extension by telomerase expression. *J. Biol. Chem.* **274**, 26141–26148.

Yudoh, K., Matsuno, H., Nakazawa, F., Katayama, R., and Kimura, T. (2001). Reconstituting telomerase activity using the telomerase catalytic subunit prevents the telomere shortening and replicative senescence in human osteoblasts. *J. Bone Miner Res.* **16**, 1453–1464.

CHAPTER

28

Preparation and Immortalization of Primary Murine Cells

Norman E. Sharpless

I. INTRODUCTION

The generation of immortal cell lines from genetically defined mice has proven useful in the understanding of molecular pathways in mammalian biology. This article describes the preparation and immortalization of murine embryo fibroblasts (MEFs), the workhorse cell type of genetically defined mice. These cells are used most frequently because of their ease of preparation, relative homogeneity, and high frequency of immortalization with serial passage in culture. These techniques can be used, with modification, to immortalize rat embryo fibroblasts as well. Furthermore, variations of these techniques can be applied to other murine cell types (e.g., astrocytes or keratinocytes) for the study of cell-type specific pathways (see Section V).

The genetics of immortalization in murine cells are now largely understood [Fig. 1, reviewed in Sharpless and DePinho (1999)]. As opposed to human cells, the spontaneous immortalization of cultured rodent cells occurs with high frequency resulting from a stochastic genetic event. This difference in frequency is attributable to the additional requirement in human cells for telomerase expression as detailed in the previous article. In murine cells, the act of cell culture, with a few exceptions, potently induces both antiproliferative products ($p16^{INK4a}$ and $p19^{ARF}$) of the *Ink4a/Arf* locus, which regulate the Rb and p53 pathways, respectively (Fig. 1). Immortalization of murine cells requires circumventing at least $p19^{ARF}$–p53 or, in some cell types, both of the pathways regulated by the products of the *Ink4a/Arf* locus (for examples, see Bachoo *et al.*, 2002; Kamijo *et al.*, 1997; Randle *et al.*, 2001). This can be done in one of three ways: spontaneous, stochastic genetic deletion through serial culture; the use of immortalizing oncogenes; or the use of genetically defined mice. This article deals predominantly with the former method, the latter two are described in Section V.

II. MATERIALS

Sterile 10-cm dishes (Falcon Cat. No. **353003**)
Sterile 6-cm dishes (Falcon Cat. No. **353002**)
Sterile phosphate-buffered saline (PBS, GIBCO Cat. No. **14190-144**)
100 and 70% ethanol
0.25% trypsin–EDTA (GIBCO Cat. No. **25200-056**).
DMEM (with glucose and L-glutamine, GIBCO Cat. No. **11995-065**)
Heat-inactivated fetal calf serum (FCS, Sigma Cat. No. **F-2442**; to heat inactivate, thaw and then place in water bath at 56°C for 30 min)
100× penicillin/streptomycin (P/S 10,000 units/ml, GIBCO Cat. No. **15140-122**)
Optional: β-mercapoethanol (β-ME, Sigma Cat. No. **M-7522**)
Liquid nitrogen-safe cryotybes (Corning Cat. No. **2028**)
Dimethyl Sulfoxide (DMSO, Mallinkrodt AR Cat. No. **4948**)

III. INSTRUMENTATION (ALL STERILE)

6 3/4 in. Mayo scissors (Fisher Cat. No. **13-804-8**)
Large forceps (Fisher Cat. No. **13-812-36**)
Curved fine scissors (Fisher Cat. No. **08-951-10**)

Copyright 2006, Elsevier Science (USA).
All rights reserved.

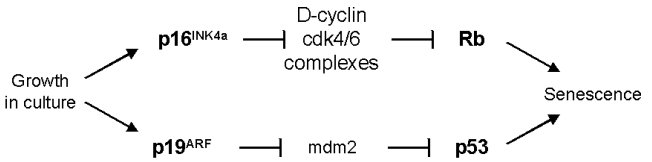

FIGURE 1 The genetics of senescence. In murine cells, the act of culture [("culture shock" (Sherr and DePinho, 2000)] induces both products of the *Ink4a/Arf* locus. $p16^{INK4a}$ inhibits cyclin-dependent kinases 4 and 6, leading to Rb hyphophorylation and growth arrest. $p19^{ARF}$ stabilizes p53 by inhibiting its mdm2-mediated degradation; p53 also induces growth arrest. In MEFs, the $p19^{ARF}$–p53 axis dominates the growth phenotype (Kamijo *et al.*, 1997; Sharpless *et al.*, 2001), although both $p16^{INK4a}$ and $p19^{ARF}$ contribute to senescence in other cell types (Bachoo *et al.*, 2002; Randle *et al.*, 2001).

Two curved small forceps (Fisher Cat. No. **08-953D**)
Two 5 1/2 in. Kelly clamps (Fisher Cat. No. **08-907**)
9-in. cotton-plugged Pasteur pipettes (Fisher Cat. No. **13-678-8B**).
Razor blades (place in 100% ethanol in 15-m dish prior to use)

IV. PROCEDURES

A. Murine Embryo Fibroblast Production

Day 1

1. The embryo dissection need not be performed in the hood but rather can be done on a clean bench covered with a diaper. Use sterile reagents (e.g., autoclave or flame dissecting equipment).

2. Sacrifice the pregnant mother at approximately noon on postcoital day 13.5 (see Section VI) through CO_2 inhalation. If the embryos are of potentially different genotypes (e.g., the progeny of a heterozygous intercross), regenotype the mother at this stage.

3. Place the mother on a dissection stand and clean by spraying generously with 70% ethanol.

4. Using Mayo scissors and large forceps, carefully open the abdomen, locate the embryos, and remove the bicornuate uterus with embryos. The embryos will appear as ~1-cm "beads on a string," in general there will be 6–12 embryos in a normal litter. If a mating produces an embryo with a genotype associated with developmental lethality, it is often possible to see partially resorbed embryos at this time.

5. Place uterus plus embryos in sterile PBS in 10-cm dish. Using fine forceps and/or scissors, gently dissect each balloon-like embryo with fetal membranes from the thicker uterus and place individually into a 6-cm dish with sterile PBS. If there are a large (>12) number of embryos, place the 6-cm dishes on ice. If the fetal membranes rupture during dissection, separate the embryos from the placenta and membranes and put in a 6-cm dish in PBS. Some investigators use a dissecting microscope for this step, although we do not find this necessary.

6. Perform the rest of the dissection in a tissue culture hood.

7. Dissect away placenta and fetal membranes. Of note, the placenta is partly of maternal origin and can therefore contaminate genotyping if the mother's genotype differs from those of the embryos. To remove placenta, use a pair of fine forceps. Grasp umbilical vessels from the placenta to the embryo with one set of forceps and grasp the placenta with the other and pull in opposite directions. Pulling the placenta directly can cause the abdominal viscera to herniate and detach. The fetal membranes may still be wrapped around the embryo after placental removal, but these can be gently pulled away from the embryo after placental detachment. The fetal membranes are of embryonic origin and can be used for genotyping, although we prefer to use nonadherent cells obtained on day 2 (see later).

8. Place the entire embryo without membranes or placenta in a 10-cm dish with 1 ml 0.25% trypsin–EDTA (this is preferable to the 0.05% trypsin–EDTA commonly used to passage cells).

9. Hold a razor blade in each of two Kelly clamps and flame after dipping in 100% ethanol. Briefly cool razor blades in sterile PBS in a 10-cm dish and then use to mince the embryos. The pieces of tissue need not be too fine; chopping approximately 30 times per embryo is generally adequate. Change razor blades between embryos if the embryos are of differing genotypes.

10. Allow minced tissue to sit in trypsin–EDTA for 10 min at 37°C, 5% CO_2.

11. Add 2 ml of growth media (DMEM + 10% FCS + pen/strep with 50 μM β-ME; the β-ME is optional) and disaggregate by repeated pipetting: 10 times with a 5-ml pipette and 10 times with a plugged Pasteur pipette. After disaggregation, there should be no large (<1 mm in largest dimension) chunks of tissue remaining.

12. Add 8 ml of growth media and swirl plates for even seeding. We grow cells at this stage in an incubator dedicated for primary cells in the rare event of bacterial contamination.

Day 2

1. The 10-cm dish should be 100% confluent after attachment of MEFs overnight. If subconfluent, this generally indicates poor disaggregation of the embryo,

improper media, or bacterial contamination (see Section VI).

2. Gently remove the media and save nonadherent cells for genotyping (see later). Take care as the cells are poorly adherent at this stage and large chunks of the monolayer can detach with poor handling.

3. Add 10 ml of fresh growth media.

4. If genotyping is necessary (i.e., the embryos are of different genetic composition), this can be done on DNA prepared from nonadherent cells collected on day 2. This is done by pelleting these cells in 15-cm conical tubes (1000 rpm × 5 min), detergent lysis, and precipitation of DNA. The exact method used depends on the manner of genotyping (e.g., polymerase chain reaction vs Southern blot). One can easily obtain >100 µg of good-quality DNA from these pellets if needed. We prepare using a commercially available DNA extraction kit (Promega #A1125).

Day 3

1. The culture should be superconfluent on day 3 and ready to freeze down or passage for further experiments. If cells are less than 100% confluent by day 3, freeze down on day 4.

2. To freeze, wash cells once with sterile PBS and add 1 ml of 0.25% trypsin–EDTA. Cells will detach in 5–10 min and then add to a 15-ml conical tube with 10 ml of growth media.

3. Spin cells at 1000 rpm for 5 min.

4. Resuspend cell pellet in 3 ml of ice-cold freezing media (90% FCS + 10% DMSO) and put in three well-labeled, chilled cryovials. We label with date prepared, the line number, and the passage number upon thawing. The lines are numbered as the mother's number first, followed by the embryo number (e.g., 115-7 would be the seventh embryo of mother 115). The cells will be passage 2 upon thawing if not passaged further before freezing.

5. Keep cells on ice for 10–15 minutes and then put in a –80°C freezer in a sealed styrofoam block overnight. Alternatively, the cells can be placed in a cryo-freezing container (Nalgene Cat. No. **5100-001**) and then placed in a –80°C freezer overnight.

6. The day after freezing, cells should be moved to a liquid nitrogen tank for long-term storage.

B. Thawing MEFs

1. Keep cells on dry ice until absolutely ready to thaw.

2. Place the vial of cells in a 37°C water bath and watch carefully. As soon as the cells begin to thaw, pour the entire pellet into a 15-ml conical tube.

3. Add 10 ml of growth media dropwise over about 30 s with gentle mixing while adding. Mix well after all 10 ml of media is added.

4. Spin cells down (1000 rpm for 5 min), resuspend in 3 ml media, and plate in a 10-cm dish. One vial of frozen cells can go into one 10-cm dish; add another 7 ml media.

5. The cells should be 90–100% confluent the day after thawing. If confluence is less with large numbers of floating (dead) cells noted, this suggests improper freezing, improper storage (e.g., freezer malfunction), or improper thawing (see Section VI).

C. Immortalizing MEFs

This can be done using a rigorously defined passaging protocol (e.g., 3T3 or 3T9 assay) or, more simply, by serial replating of cells. The advantage of the passaging protocol is that one learns about the growth kinetics and immortalization frequency of the cell (see Section V). The immortalization of wild-type MEFs requires a stochastic genetic event: generally *p53* loss or, less frequently, loss of $p19^{ARF}$ (Kamijo *et al*., 1997). Other immortalizing events, such as *mdm2* amplification (Olson *et al*., 1993), have also been noted, but these are considerably rarer. In our experience, this genetic event is most likely to be loss of p53 (~60–70% of immortalized lines) or $p19^{ARF}$ (~20–30%) regardless of growth conditions (passage at high or low density). Therefore, serial passaging without counting cells at every passage is an appropriate way to derive immortalized cells. In fact, the "3T3 cell" has become a nondescript term referring to immortal murine embryo fibroblasts obtained through serial passaging, but few laboratories except those interested in growth and senescence do rigorous 3T3 assays to obtain them.

D. Immortalization by Serial Passage

1. Split MEFs 1:3 twice per week during the rapid growth phase of the culture (the first 6–10 passages).

2. As cells enter senescence, split 1:2 or merely replate (aim to keep cells near 100% confluency on the day of passaging). If the cultures are seeded too sparsely, this will decrease the immortalization frequency.

3. Between passages 10 and 20 (4 to 9 weeks in culture), immortalized lines will begin to overgrow the culture. These cells are smaller and spindle shaped, initially appearing as small nests of cells obvious on the day of passaging. These cells can be subcloned, but are used more frequently as pooled immortalized cells.

E. 3T9 Assay

This assay was originally described by Todaro and Green (1963). The "3" refers to passaging every 3 days, and the "9" refers to 9×10^5 cells plated per passage. 3T3 (3×10^5 cells) and 3T12 (1.2×10^6 cells) assays can also be done to study growth and immortalization at varying densities. In our experience, immortalization frequency is highest for the 3T3 assay (and therefore this assay has lent its name to all immortalized lines of murine fibroblasts), whereas 3T9 is more useful for measuring immortalization frequency (Sharpless *et al*., 2001). As stated earlier, serial replating of murine fibroblasts at almost any density will eventually yield immortalized lines as long as the cells are not seeded too sparsely.

1. For the first passage, wash cells growing in a 10-cm dish (usually passage 2 at this stage) with PBS, trypsinize (0.05% trypsin–EDTA is adequate for this purpose), dilute into 10 ml of growth media, and count.
2. Spin down and resuspend cells at a concentration of 9×10^5 cells/ml. Seed 1 ml of cells (9×10^5 cells) into a 6-cm dish and add 2.5 ml of media. Swirl the cells to ensure uniform seeding. Label the dish with the MEF line number and the passage number.
3. For subsequent passages, trypsinize and recount cells every 3 days in a manner identical to steps 1 and 2. Record the number of cells counted before each passage. Growth curves and immortalization frequencies can be determined from analysis of these data as described in Section V.
4. Immortalized lines will emerge between passages 10 and 20; virtually all lines proliferating after 20 passages will be immortal. If necessary, these lines can be subcloned by limiting dilution, but this is not generally done. The majority of immortalized lines will have lost either p53 or $p19^{ARF}$ function (Kamijo *et al*., 1997), although various other genetic events can increase or decrease the frequency of immortalization (Frank *et al*., 2000; Jacobs *et al*., 1999; Kamijo *et al*., 1999; Sharpless *et al*., 2001).

V. COMMENTS

A. Immortalization through the Use of Oncogenes or Genetic Background

A problem with immortalization by serial passage is that the nature of the immortalizing genetic event is not known, although predominantly p53 or $p19^{ARF}$ is inactivated as MEFs escape senescence. As the behavior of $p19^{ARF}$-deficient cells may be quite different from p53-deficient cells, however, the stochastic inactivation of these pathways may produce significant line-to-line variability and therefore be undesirable. For example, *p53* null MEFs are more aneuploid and more resistant to DNA damage than *$p19^{ARF}$* null MEFs (Kamijo *et al*., 1997; Pomerantz *et al*., 1998; Serrano *et al*., 1996; Stott *et al*., 1998). To assure that all lines will evade senescence via a similar mechanism, cells can either be immortalized through the use of an immortalizing oncogene or by using cells derived from animals of a genetic background that resists senescence.

Classically, the most commonly used oncoprotein to immortalize cells is the SV40 large T antigen (Colby and Shenk, 1982; Jat and Sharp, 1986; Todaro and Green, 1966). This molecule inactivates the p53 and Rb pathway, and the majority of murine cell types can be immortalized by transfection or retroviral transduction of T Ag. A disadvantage of T Ag, however, is that cells expressing this molecule are unstable and are prone to clonal *in vitro* evolution. Furthermore, as Rb pocket proteins are required for the differentiation of many cells types (Dannenberg *et al*., 2000), T Ag generally impairs or precludes the study of differentiation. Alternatively, MEFs and several other murine cell types can be immortalized with a dominant-negative form of p53 [e.g., p53-DD (Bowman *et al*., 1996)], which preserves the Rb pathway, although these cells are still more prone to aneuploidy than $p19^{ARF}$-deficient lines.

The most elegant method of obtaining immortal cell lines is by deriving cells from animals resistant to senescence. The most commonly used strains for this purpose are *Ink4a/Arf*-deficient (Serrano *et al*., 1996), *$p19^{ARF}$*-deficient (Kamijo *et al*., 1997), or *p53*-deficient (Donehower *et al*., 1992) mice. These strains are widely available and can be obtained from the mouse models of the human cancer consortium (MMHCC http://web.ncifcrf.gov/researchresources/mmhcc/). For studies of genetically defined animals, the genetic background of interest can be crossed two generations to mice of these backgrounds and then MEFs (or other cell types) derived as described earlier, which will be immortal in most cases if derived from p53- or $p19^{ARF}$-deficient embryos. This method can be employed to derive immortal cells from difficult genetic backgrounds that undergo premature senescence in culture (Frank *et al*., 2000; Jacobs *et al*., 1999). This strategy can also be employed to obtain cells of nonfibroblast lineages. For example, immortal melanocytes (Chin *et al*., 1997), skin keratinocytes (unpublished observations), glia (Bachoo *et al*., 2002), lymphocytes (unpublished observations; Randle *et al*., 2001), and macrophages (Randle *et al*., 2001) have been derived successfully from *$p19^{ARF}$*- or *Ink4a/Arf*-deficient mice using standard

culture methods for these cell types. To immortalize with high efficiency, cells must be homozygous null for p53, $p19^{ARF}$, or *Ink4a/Arf*; therefore, the principal disadvantage of this approach is the extra time needed to backcross to these defined genetic backgrounds.

B. Data Analysis of 3T9 or 3T3 Assay

These data can be plotted as cell number per passage or population doublings (PDs) per passage (Fig. 2). PDs for any given passage = $\log_2(N_f/N_0) = 1.44 * \ln(N_f/N_0)$, where N_f = number of cells counted at the end of the passage and N_0 = number of cells seeded at the beginning of the passage (i.e., 9×10^5 for a 3T9 assay). For the purpose of immortalization frequency, "senescence" occurs if less than 9×10^5 cells are recovered for two consecutive passages. The immortalization frequency = 1-number of senescent lines/total number of lines analyzed. Measured in this way, the immortalization frequency of wild-type MEFs can vary significantly depending on culture conditions, method of embryo preparation, and so on and therefore is only meaningful when compared to proper littermate control embryos analyzed concurrently.

VI. PITFALLS

1. *Embryo dates*. By convention, the day a coital plug is detected is day 0.5 for timed matings, and embryos should be made at midday 13 days later. While it is difficult to be sure of correct plugging dates at the time of dissection, in general day 13.5 embryos have paddle-like front paws, whereas day 14.5 embryos have more fully formed individual digits. Embryos that are too large and well developed or too small suggest an incorrect date of plugging. Cells of different embryonic ages do differ in several *in vitro* growth properties; therefore, littermate controls are always preferable in MEF experiments. In our experience, MEFs from embryos older than 13.5 grow less well and immortalize less frequently than 13.5 embryos.

2. *MEFs are not confluent the day after dissection*. In general, cells from a single embryo should cover a 10-cm plate fully the morning after plating. Poor coverage of the dish can result from inadequate embryo disaggregation, tissue mincing with razor blades that were not cooled properly after flaming, improper media, or bacterial contamination. In particular, one should be vigilant for bacterial contamination as this can be difficult to note given that there is copious debris in the culture 1 day after plating.

3. *MEFs are not confluent the day after thawing*. This results most often from freezer or liquid nitrogen tank malfunction, but can also be due to improper technique when the cells were frozen, malfunction of the cryo-freezing container, or improper thawing. DMSO is toxic to these primary cells so it is important to resuspend the frozen cell pellet well in growth media, spin the cells down, and then respsund in fresh growth media prior to plating. Thawed vials of cells should

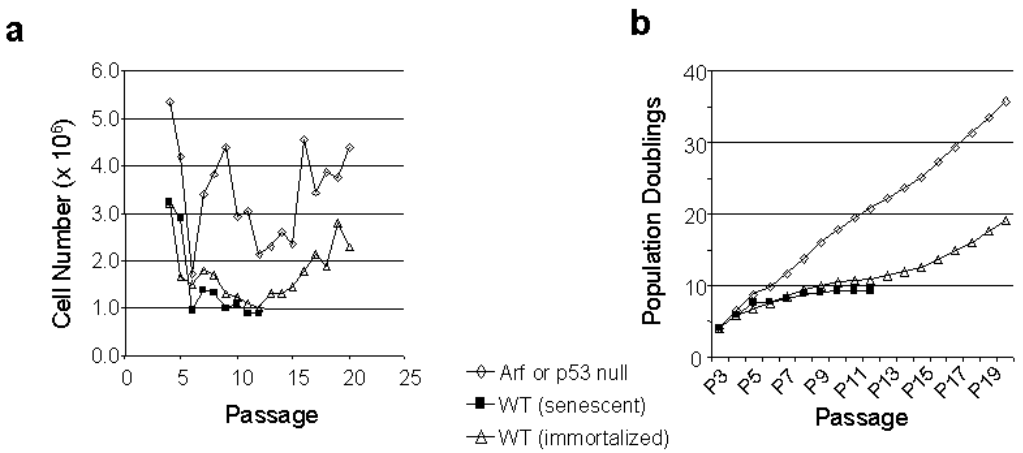

FIGURE 2 The 3T9 assay can be used to quantify both growth and immortalization frequency. Data from a 3T9 (or 3T3) assay can be graphed in either of two ways: (a) as cell number per passage or (b) as population doublings (PDs) per passage (PDs defined in text). The same data are graphed by either method showing a senescent line, an immortalized line, or a line lacking *Ink4a/Arf*. The $p19^{ARF}$–dependent slow growth period seen in wild-type MEFs between passages 5–15 is called "senescence," although in actuality it represents a culture-induced phenomena.

not be left in freezing media for a significant period of time prior to replating.

4. *Cells grow poorly and/or fail to immortalize*. This can result from poor growth media (e.g., the fetal calf serum is too old), the use of embryos significantly later than E13.5, or occult pathogen contamination. Embryos of certain genetic backgrounds grow poorly in culture ("premature senescence"), which can sometimes be obviated by backcrossing to *Ink4a/Arf-*, $p19^{ARF}$-, or *p53*-deficient animals (Frank *et al*., 2000; Jacobs *et al*., 1999; Kamijo *et al*., 1999).

References

Bachoo, R. M., Maher, E. A., Ligon, K. L., Sharpless, N. E., Chan, S. S., You, M. J., Tang, Y., DeFrances, J., Stover, E., Weissleder, R., *et al*. (2002). Epidermal growth factor receptor and Ink4a/Arf: Convergent mechanisms governing terminal differentiation and transformation along the neural stem cell to astrocyte axis. *Cancer Cell* **1**, 269–277.

Bowman, T., Symonds, H., Gu, L., Yin, C., Oren, M., and Van Dyke, T. (1996). Tissue-specific inactivation of p53 tumor suppression in the mouse. *Genes Dev.* **10**, 826–835.

Chin, L., Pomerantz, J., Polsky, D., Jacobson, M., Cohen, C., Cordon-Cardo, C., Horner, J. W., II, and DePinho, R. A. (1997). Cooperative effects of INK4a and ras in melanoma susceptibility *in vivo*. *Genes Dev.* **11**, 2822–2834.

Colby, W. W., and Shenk, T. (1982). Fragments of the simian virus 40 transforming gene facilitate transformation of rat embryo cells. *Proc. Natl. Acad. Sci. USA* **79**, 5189–5193.

Dannenberg, J. H., van Rossum, A., Schuijff, L., and te Riele, H. (2000). Ablation of the retinoblastoma gene family deregulates G(1) control causing immortalization and increased cell turnover under growth- restricting conditions. *Genes Dev.* **14**, 3051–3064.

Donehower, L. A., Harvey, M., Slagle, B. L., McArthur, M. J., Montgomery, C. A., Jr., Butel, J. S., and Bradley, A. (1992). Mice deficient for p53 are developmentally normal but susceptible to spontaneous tumours. *Nature* **356**, 215–221.

Frank, K. M., Sharpless, N. E., Gao, Y., Sekiguchi, J. M., Ferguson, D. O., Zhu, C., Manis, J. P., Horner, J., DePinho, R. A., and Alt, F. W. (2000). DNA ligase IV deficiency in mice leads to defective neurogenesis and embryonic lethality via the p53 pathway. *Mol. Cell* **5**, 993–1002.

Jacobs, J. J., Kieboom, K., Marino, S., DePinho, R. A., and van Lohuizen, M. (1999). The oncogene and Polycomb-group gene bmi-1 regulates cell proliferation and senescence through the ink4a locus. *Nature* **397**, 164–168.

Jat, P. S., and Sharp, P. A. (1986). Large T antigens of simian virus 40 and polyomavirus efficiently establish primary fibroblasts. *J. Virol.* **59**, 746–750.

Kamijo, T., van de Kamp, E., Chong, M. J., Zindy, F., Diehl, J. A., Sherr, C. J., and McKinnon, P. J. (1999). Loss of the ARF tumor suppressor reverses premature replicative arrest but not radiation hypersensitivity arising from disabled atm function. *Cancer Res.* **59**, 2464–2469.

Kamijo, T., Zindy, F., Roussel, M. F., Quelle, D. E., Downing, J. R., Ashmun, R. A., Grosveld, G., and Sherr, C. J. (1997). Tumor suppression at the mouse INK4a locus mediated by the alternative reading frame product p19ARF. *Cell* **91**, 649–659.

Olson, D. C., Marechal, V., Momand, J., Chen, J., Romocki, C., and Levine, A. J. (1993). Identification and characterization of multiple mdm-2 proteins and mdm-2-p53 protein complexes. *Oncogene* **8**, 2353–2360.

Pomerantz, J., Schreiber-Agus, N., Liegeois, N. J., Silverman, A., Alland, L., Chin, L., Potes, J., Chen, K., Orlow, I., Lee, H. W., *et al*. (1998). The Ink4a tumor suppressor gene product, p19Arf, interacts with MDM2 and neutralizes MDM2's inhibition of p53. *Cell* **92**, 713–723.

Randle, D. H., Zindy, F., Sherr, C. J., and Roussel, M. F. (2001). Differential effects of p19(Arf) and p16(Ink4a) loss on senescence of murine bone marrow-derived preB cells and macrophages. *Proc. Natl. Acad. Sci. USA* **98**, 9654–9659.

Serrano, M., Lee, H., Chin, L., Cordon-Cardo, C., Beach, D., and DePinho, R. A. (1996). Role of the INK4a locus in tumor suppression and cell mortality. *Cell* **85**, 27–37.

Sharpless, N. E., Bardeesy, N., Lee, K. H., Carrasco, D., Castrillon, D. H., Aguirre, A. J., Wu, E. A., Horner, J. W., and DePinho, R. A. (2001). Loss of p16Ink4a with retention of p19Arf predisposes mice to tumorigenesis. *Nature* **413**, 86–91.

Sharpless, N. E., and DePinho, R. A. (1999). The INK4A/ARF locus and its two gene products. *Curr. Opin. Genet. Dev.* **9**, 22–30.

Sherr, C. J., and DePinho, R. A. (2000). Cellular senescence: Mitotic clock or culture shock? *Cell* **102**, 407–410.

Stott, F. J., Bates, S., James, M. C., McConnell, B. B., Starborg, M., Brookes, S., Palmero, I., Ryan, K., Hara, E., Vousden, K. H., and Peters, G. (1998). The alternative product from the human CDKN2A locus, p14(ARF), participates in a regulatory feedback loop with p53 and MDM2. *EMBO J.* **17**, 5001–5014.

Todaro, G. J., and Green, H. (1963). Quantitative Studies of mouse embyo cells in cutture and their development into established linos. *J. Cell Biol.* **17**, 299–313.

Todaro, G. J., and Green, H. (1966). High frequency of SV40 transformation of mouse cell line 3T3. *Virology* **28**, 756–759.

SECTION

6

Somatic Cell Hybrids

CHAPTER

29

Viable Hybrids between Adherent Cells: Generation, Yield Improvement, and Analysis

Doris Cassio

I. INTRODUCTION

Somatic cell hybridization was discovered and introduced by Barski *et al*. (1960) and Sorieul and Ephrussi (1961). This technique allows one to examine the result of introducing various genomes in different functional states and from different species into the *same* cell. Hybrid cells have been widely used in various fields (genetics, cell biology, tumour biology, virology) and the most famous hybrids are hybridomas.

One important application of somatic cell hybridization is chromosomal gene assignment. Breeding analysis, which is effective for this purpose in lower animals and plants, is too slow in mammals (even in mice the generation time is about 3 months) and is impossible in humans. Gene mapping techniques based on somatic cell genetics have been central to the study of human genetics. In 1968, only two genes had been mapped to specific autosomes, and a decade later this number had risen to 300, mostly using human–rodent somatic cell hybrids. Such hybrids present the advantage to retain only a few human chromosomes and they are now currently used as donor cells in irradiation and fusion gene transfer (IFGT) experiments for constructing detailed genetic maps (Walter and Goodfellow, 1993).

Cell fusion was also used to analyse how specialized cells acquire and maintain their differentiation. The activities of somatic cells can be divided into two main categories: essential or ubiquitous functions that are indispensable for cell survival and growth and "luxury" or differentiated functions. Essential functions continue to be expressed in hybrids, whereas differentiated functions are subject to different regulations (expression, extinction, activation) depending on the histogenetic nature of the parental cells that have been fused (see examples in Cassio and Weiss, 1979; Hamon-Benais *et al*., 1994; Killary and Fournier, 1984; Mevel-Ninio and Weiss, 1981). Cell determination is, however, not modified in hybrids, as extinction or activation requires retention of the chromosomes coding for the appropriate regulatory factors.

Somatic cell hybridization has not only shown that tissue-specific genes are regulated by *trans*-acting factors, but has provided strong evidence for the existence of tumour suppressor genes (Anderson and Stanbridge, 1993). Cell fusion experiments have also demonstrated that cellular senescence is a dominant active process and that several genes or genes pathways are implicated in the senescence program (Goletz *et al*., 1994).

Spontaneous fusion of cells in culture occurs at a very low frequency. To obtain hybrid cells, inactivated Sendai virus or, more commonly, polyethylene glycol (PEG), which was introduced by Pontecorvo (1976), is used as the fusogen. Cell hybridization has also been performed by electrofusion on filters (Ramos *et al*., 2002). The inital products of fusion contain within a common cytoplasm two or more distinct nuclei from one single parent (homokaryons) or from both (heterokaryons). Only a very small proportion of these polykaryons will progress to nuclear fusion and then through mitosis. Moreover, the first divisions of the

Copyright 2006, Elsevier Science (USA).
All rights reserved.

heterokaryons and of their daughter cells often fail because of abnormalities of the mitotic spindle and abnormal chromosome movements. The formation of viable hybrids from heterokaryons is thus a rare event, and the use of selective methods that favour the survival of the hybrids at the expense of the parental cells is often a requisite. These selective methods are also necessary because hybrid cells often grow more slowly than parental cells and are rapidly overgrown by parental cells.

A. Selective Methods

The best known of such methods is the application of hypoxanthine + aminopterin + thymidine (HAT) selection (Littlefield, 1964) for the fusion of cells deficient in hypoxanthine guanosine phosphoryl transferase ($HGPRT^-$) with cells deficient in thymidine kinase (TK^-), but different combinations of selectable markers can be used (Hooper, 1985), provided that the two selective systems do not interfere. If the lines that are fused have no selective markers, a good strategy is to select sequentially for HGPRT deficiency (thioguanine resistance) and ouabain resistance in one parental cell line. Then this marked cell line may be fused with any unmarked cell line and hybrids selected in HAT + ouabain (Jha and Ozer, 1976). Other couples of selective markers, such as TK deficiency (5–bromo-2'deoxyuridine resistance) and neomycine resistance, can also be used. For producing primate–rodent hybrids, the selection of an $HGPRT^-$ rodent parent is sufficient because rodent cells are more resistant to ouabain than primate cells. Moreover, hybrid cells can also be isolated on the basis of their size, morphology, growth parameters, and DNA content.

B. Yield of Viable Hybrids

Whatever the method used to isolate hybrids, the most important is to optimize the fusion conditions in order to obtain a number of viable hybrids as high as possible. In the best cases the fusion of several millions of parental cells leads to the formation of only a few hundred hybrids and often the yield of viable hybrids is much lower, as illustrated in Table I for hepatoma-derived hybrids. The protocol described here has been used routinely to produce large amounts of hybrid clones between differentiated rat hepatoma cells and various cells of different histogenetic origin and of different species, particularly mouse and human fibroblasts (Mevel-Ninio and Weiss, 1981; Sellem *et al*., 1981). Moreover, some of the hybrids obtained have been used themselves as partners of fusion and new hybrids were generated successfully using exactly the same method (Bender *et al*., 1999; Hamon-Benais *et al*., 1994). The most important parameters in fusion experiments are the yield of viable and growing hybrids and their stability. Thus it is recommended to define optimal fusion conditions and to vary different parameters, particularly the ratio of parental cells, for improving the yield. It is also recommended to analyze regularly hybrid clones for their phenotype and chromosomal content.

II. MATERIALS

PEG 1000 ultrapure (Merck, Cat. No. 9729)
Trypsin (pig pancreas; United States Bioch. Corp., Cleveland, OH, Cat. No. 22715)

TABLE I Production of Rat Hepatoma-Derived Hybrids[a]

Partner of fusion	Hybrid yield (10^{-6})	Reference
Normal diploid human fibroblast	<1	Sellem *et al*. (1981)
Normal diploid mouse fibroblast	5–8	Mevel-Ninio and Weiss (1981) Killary and Fournier (1984)
Normal rat hepatocytes	6	Polokoff and Everson (1986)
Mouse fibroblastic line cl1-D	1000	Mevel-Ninio and Weiss 1981
Mouse hepatoma BW1-J	100	Cassio and Weiss (1979)
Rat hepatoma–mouse fibroblast hybrid	400	Hamon-Benais *et al*. (1994)
Rat hepatoma–mouse fibroblast monochromosomal hybrid	100	Hamon-Benais *et al*. (1994)
Rat hepatoma–human fibroblast segregated hybrid	30–300	Bender *et al*. (1999)

[a] In all cases, parental cells were fused at pH 7.2 in a ratio 1:1, except for the fusion with hepatocytes (hepatoma:hepatocytes = 1:2). The same rat hepatoma parental cells were used in all experiments.

Complete growth medium (available from local suppliers)
Serum-free growth medium (available from local suppliers)
Selective complete growth medium (available from local suppliers)
35- and 50-mm tissue culture dishes (Falcon, Cat. No. 3001, 3002)
15-ml tube (Falcon, Cat. No. 352099)
22 × 22-mm sterile glass coverslips

III. PROCEDURES

A. Before Fusion

Solutions

1. *50% PEG (for fusion)*: Autoclave PEG 1000. This both liquifies and sterilizes the PEG. Cool it to 50°C and mix with an equal volume of sterile serum-free medium prewarmed for a short period at 50°C. Adjust, if necessary, to the desired pH with 1.0 *M* NaOH (range of pH generally used is 7.2–7.9). This solution can be stored at 4°C for up to 2 weeks.

2. *0.25 and 0.05% trypsin (to detach fusion products)*: To make 100 ml of solution, solubilize 0.8 g of NaCl, 0.04 g of KCl, 0.058 g of $NaHCO_3$, 0.1 g dextrose, and 0.25 g (0.25%) or 0.05 g (0.05%) of trypsin. Complete to 100 ml distilled water. Incubate at 37°C for 1–2 h. Sterilize by filtration and store at 4°C (rapid use) or –20°C.

Step

Grow parental cells in *nonselective medium* for a short period.

B. Fusion

Steps

1. Inoculate the mixture of parental cells to be fused into several 50-mm tissue culture dishes containing complete (nonselective) growth medium. The total number of cells has to be adjusted to occupy all the dish surface, such that the fusion will be done on cells that are in close contact. For 50-mm petri dishes, the total cell number could vary from 5×10^5 to 4×10^6 depending on the density at confluence of the cell lines used. Although equal numbers of parental cells are generally recommended, use different ratios of parental cells (see Table II and Section IV).
2. Incubate the mixed cultures a few hours (4 h to overnight). This allows the cells to adhere to the support and to establish contacts with neighbors.
3. Warm the serum-free medium and the 50% PEG solution to 37°C.
4. Remove the medium thoroughly from the culture and wash once with 5 ml of serum-free medium.
5. Add gently 3.0 ml of PEG 50% all over the cell layer.
6. After 45 s aspirate the PEG.
7. Exactly 1 min after PEG treatment, add 5 ml of serum-free medium.
8. Aspirate half the medium and add 2.5 ml of serum-free medium.
9. Repeat step 8 four times.
10. Aspirate all the medium.
11. Add 5 ml of complete growth medium and let the cells recover for at least 2 h and no more than 12 h.

Notes: Steps 4 to 11 must be done *dish per dish*. Some control dishes must be included. They will be treated

TABLE II Production of Rat Hepatoma × Human Fibroblast Hybrids[a]

Ratio of parental cells[b] (hepatoma:fibroblast)	Fusion conditions	Selection conditions	Hybrid yield[c] (10^{-6})
1:1	PEG, pH 7.2	HAT, ouabain, pH 7.2	<1
4:1			5
10:1			20
1:1	PEG, pH 7.8	HAT, ouabain, pH 7.8[d]	15
4:1			30
10:1			150
10:1	Sendai virus, pH 7.8	HAT, ouabain, pH 7.8[d]	100
1:1	No fusogen, pH 7.8	HAT, ouabain, pH 7.8[d]	<1
	No fusogen, pH 7.2	HAT, ouabain, pH 7.2	<0.5

[a] For details of the parental cell lines, see Sellem *et al*. (1981).
[b] 2×10^6 cells were plated per 50-mm petri dish.
[c] Total number of hybrid clones/total cell number of minority parent.
[d] Cells were maintained at pH 7.8 for 6 days after fusion and then cultured at pH 7.2, as usual.

as the others except that the PEG solution will be replaced by serum-free medium.

C. After Fusion

Steps

1. Aspirate the medium and add 3 ml of 0.25% trypsin per dish.
2. As soon as the cell layer begins to detach, add 3 ml of 0.05% trypsin and detach the cells by repeated pipetting.
3. Add the cell suspension in a 15-ml tube containing 2 ml of complete growth medium (to arrest the trypsin action). If necessary, rinse the dish with 2 ml medium and add this medium to the tube containing the cells.
4. Centrifuge the cells at 500 *g* (1500 rpm) for 5 min at room temperature.
5. Resuspend thoroughly the cell pellet in complete growth medium and count the cell number in a hemacytometer. Using the described protocol, generally at least 80% of the cells are recovered after fusion.
6. Pool, if necessary, cells recovered from identical dishes and inoculate different numbers of cells (10^3–10^6) in either culture dishes or on 22-mm glass coverslips (in 35-mm dishes).
7. Incubate the cells at least overnight (eventually a few days) in complete growth medium before adding selective medium that will kill the parental cells and let the hybrid cells survive.
8. At regular intervals, watch for the appearance of growing hybrid colonies. Count their number in dishes or coverslips that contain well-isolated colonies. From this number the yield of growing hybrids can be calculated. For one fusion, this yield is equal to the total number of hybrid clones obtained divided by the total cell number of the minority parent engaged in the fusion.
9. Use dishes that contain a small number of colonies to isolate independent hybrid clones (one per dish will be scraped, subcultured, characterized, as soon as possible, frozen, and recharacterized). From dishes that contain a lot of colonies, if this situation arises, hybrid cell populations can be obtained in mass and studied rapidly.
10. Use glass coverslips to control by cytogenetic methods the hybrid nature of the clones and to test if their chromosomal content is stable with time in culture. The karyotyping *in situ* method, described by Worton and Duff (1979), is highly recommended. This method is easy, of general application for adherent cells, and can be performed on small colonies even a few generations after fusion (Fig. 1). Glass coverslips can also be used for phenotypic characterization of hybrid clones.

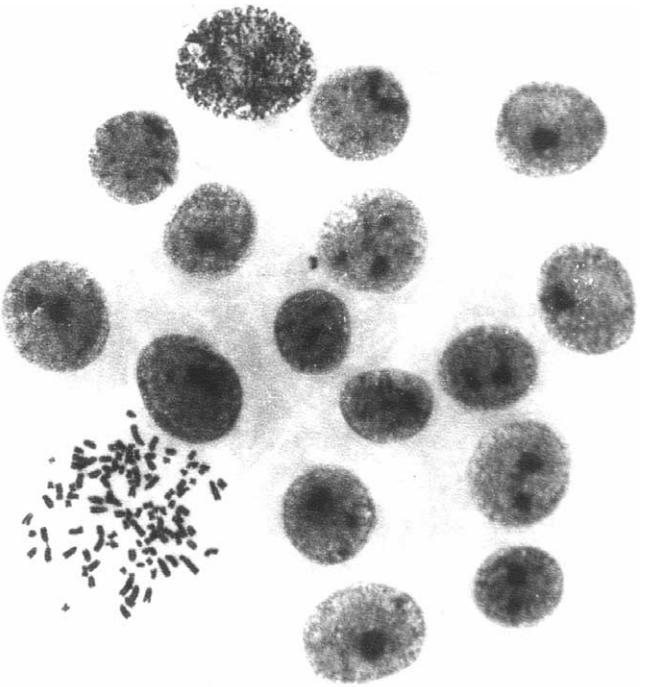

FIGURE 1 Karyotypic analysis of emerging hybrids. The *in situ* karyotyping method (Worton and Duff, 1979) was performed on rat hepatoma-derived hybrid colonies 8 days after fusion. The colony shown was composed of 17 cells, 1 of which was in metaphase. This metaphase contains 100 chromosomes, corresponding to the expected sum of the mean chromosome number of each parent (46 and 52, respectively).

IV. COMMENTS

The production of hybrid clones in large amounts depends greatly on the parental cells (cell type and growth capacity) and on the fusion conditions. These two points are illustrated in Tables I and II for rat hepatoma-derived hybrids. The frequency of occurrence of hybrids between rat hepatoma and normal fibroblast was particularly low compared to other hepatoma-derived hybrids (Table I). Consequently, various fusion conditions were tested. The use of unbalanced ratios of parental cells is one of the most important parameters to improve the hybrid yield (Table II). Therefore, to save time and to obtain the highest number of hybrid cells, it is recommended to fuse parental cells in different ratios.

Mixed parental cell populations that have not been treated by PEG can give rise to colonies that grow in

selective medium at low frequency. These colonies could be either spontaneous hybrids or revertants from parental cells. The isolation of revertants is one of the most common difficulties that may arise in selecting hybrids. Therefore the hybrid nature of the cells selected has to be verified by checking their chromosomal content.

V. PITFALLS

1. Some PEG preparations produce enormous lethality, whereas ultrapure PEG from Merck results in acceptable levels of lethality (generally below 20%).

2. Detach and dissociate very carefully cells after fusion (avoid aggregates).

3. Because it is impossible to predict if hybrid clones will be produced with a high yield or not, once fusion has been performed and the products of fusion detached, inoculate them at different concentrations (that could cover a 1000× range) such that well-isolated hybrids could be obtained even if the yield varies from 10^{-6} to 10^{-3}.

4. A lower number of hybrid clones is obtained if the cells are not detached after fusion.

5. A lower number of hybrid clones is obtained if the mixture of parental cells is fused in suspension. This result is due to the fact that the relative proportion of binucleate heterokaryons is higher in monolayer fusion, whereas suspension fusion favours the formation of giant heterokaryons that die soon after fusion. Hence, there is no reason and no advantage to fuse adherent cells in suspension as often recommended (except if one of the parent grows in suspension).

Acknowledgments

I thank M. C. Weiss for training in cell culture and C. H. Sellem and C. Hamon-Benais for the illustrations.

References

Anderson, M. J., and Stanbridge, E. J. (1993). Tumor suppressor genes studied by cell hybridization and chromosome transfer. *FASEB J.* **7**, 826–833.

Barski, G., Sorieul, S., and Cornefert, F. (1960). Production dans des cultures *in vitro* de deux souches cellulaires en association, de cellules de caractère "hybride". *C. R. Acad. Sci. Paris* **251**, 1825–1827.

Bender, V., Bravo, P., Decaens, C., and Cassio, D. (1999). The structural and functional polarity of the hepatic human-rat hybrid WIF-B is a stable and dominant trait. *Hepatology* **30**, 1002–1010.

Cassio, D., and Weiss, M. C. (1979). Expression of fetal and neonatal hepatic functions by mouse hepatoma-rat hepatoma hybrids. *Som. Cell Genet.* **5**, 719–738.

Goletz, T. J., Smith, J. R., and Pereira-Smith, O. M. (1994). Molecular genetic approaches to the study of cellular senescence. *Cold Spring Harb. Symp. Quant. Biol.* **LIX**, 59–66.

Hamon-Benais, C., Delagebeaudeuf, C., Jeremiah, S., Lecoq, O., and Cassio, D. (1994). Efficiency of a specific albumin extinguisher locus in monochromosomal hepatoma hybrids. *Exp. Cell Res.* **213**, 295–304.

Hooper, M. (1985). In "*Mammalian Cell Genetics*" (E. Bittar, ed.), pp. 77–81. Wiley-InterScience, New York.

Jha, K. K., and Ozer, H. L. (1976). Expression of transformation in cell hybrids. I. Isolation and application of density-inhibited Balb/3T3 cells deficient in hypoxanthine phosphoribosyl transferase and resistant to ouabain. *Som. Cell Genet.* **2**, 215–233.

Killary, A. M., and Fournier, R. E. K. (1984). A genetic analysis of extinction: Trans-dominant loci regulate expression of liver-specific traits in hepatoma-hybrid cells. *Cell* **38**, 523–534.

Littlefield, J. W. (1964). Selection of hybrid from matings of fibroblasts *in vitro* and their presumed recombinants. *Science* **145**, 709–710.

Mevel-Ninio, M., and Weiss, M. C. (1981). Immunofluorescence analysis of the time-course of extinction, reexpression and activation of albumin production in rat hepatoma-mouse fibroblast heterokaryons and hybrids. *J. Cell Biol.* **90**, 339–350.

Polokoff, M. A., and Everson, G. T. (1986). Hepatocyte-hepatoma cell hybrids: Characterization and demonstration of bile acid synthesis. *J. Biol. Chem.* **261**, 4085–4089.

Pontecorvo, G. (1976). Production of indefinitely multiplying mammalian somatic cell hybrids by polyethylene glycol (PEG) treatment. *Somat. Cell Genet.* **1**, 397–400.

Ramos, C., Bonenfant, D., and Teissie, J. (2002). Cell hybridization by electrofusion on filters. *Anal. Biochem.* **302**, 213–219.

Sellem, C. H., Cassio, D., and Weiss, M. C. (1981). No extinction of tyrosine aminotransferase inducibility in rat hepatoma-human fibroblast hybrids containing the human × chromosome. *Cytogenet. Cell Genet.* **30**, 47–49.

Sorieul, S., and Ephrussi, B. (1961). Karyological demonstration of hybridization of mammalian cells *in vitro*. *Nature (Lond.)* **190**, 653–654.

Walter, M. A., and Goodfellow, P. N. (1993). Radiation hybrids: Irradiation and fusion gene transfer. *Trends Genet.* **9**, 352–356.

Worton, R. G., and Duff, C. (1979). Karyotyping. *Methods Enzymol.* **58**, 322–344.

Suggested Reading

Harris, H. (1995). "The Cells of the Body: A History of Somatic Cell Genetics." Cold Spring Harbor Laboratory Press, Cold Spring Harbor, NY.

Ringertz, N. R., and Savage, R. E., (1976). "Cell Hybrids." Academic Press, London.

Zallen, D. T., and Burian, R. M. (1992). On the beginnings of somatic cell hybridization: Boris EPHRUSSI and chromosome transplantation. *Genetics* **132**, 1–8.

SECTION

7

Cell Separation Techniques

CHAPTER

30

Separation and Expansion of Human T Cells

Axl Alois Neurauter, Tanja Aarvak, Lars Norderhaug, Øystein Åmellem, and Anne-Marie Rasmussen

I. INTRODUCTION

For the characterization of specific cell types and the investigation of their functions, it is essential that the cells can be purified. Cell separation techniques based on the use of antibody-coated magnetic beads, e.g., Dynabeads (Ugelstad *et al*., 1980, 1994), are now widely used in research and clinical laboratories. Specific cells can, after binding to the magnetic beads, be selected by the use of a magnet and, following brief washing, high cell purity can be achieved. This technique continues to encompass new fields for the selective isolation of eukaryotic cells (Funderud *et al*., 1987; Luxembourg *et al*., 1998; Marquez *et al*., 1998; Soltys *et al*., 1999; Chang *et al*., 2002). The use of pure cell populations has also reached the field of therapy. *Ex vivo* expansion and manipulation of isolated cells have given promising possibilities in therapy, especially in immunotherapy. Dynabeads, having approximately the same size as eukaryotic cells, have proven to be very efficient in the *ex vivo* activation of T cells, the prime effectors of the acquired immune system (Garlie *et al*., 1999; Lum *et al*., 2001). An *ex vivo*-expanded population of T cells may be administrated to the patient, thereby helping to fight diseases such as cancer, HIV, and autoimmune disorders (Liebowitz *et al*., 1998; Levine *et al*., 1998, 2002; Thomas and June, 2001).

There are two main strategies for isolating a specific cell type: a "positive selection" of cells of interest or a "negative selection" where unwanted cells are depleted (Fig. 1). By positive selection, a specific cellular subset is isolated directly from a complex mixture of cells based on the expression of a distinct surface antigen. The resulting immune complexes of beads and target cells are collected using a magnet. By negative selection, all unwanted cell types are removed from the sample by the magnetic beads. Cells isolated by negative selection have not been bound to antibodies at any time. Surface antigen-bound antibodies may elicit the transmission of signals across the cell membrane. However, in general the purity obtained by negative selection is lower than for positive selection.

It is important to note that Dynabeads can be used directly in complex samples such as whole blood, which offers rapid and direct access to the maximum number of target cells that have undergone the minimum amount of interference. Usually, Dynabeads are precoated with target-specific antibodies (direct technique). Alternatively, antibodies are first added to the cell suspension and thereafter the labeled cells are immobilized to Dynabeads through secondary antibodies, e.g., pan antimouse IgG (indirect technique).

The particular properties of the magnetic beads make it possible to use positively selected cells directly for cell stimulation or molecular studies, such as PCR or RT-PCR, without the necessity of removing the beads. However, in functional studies the beads should be removed. For several cell types, Dynabeads can be detached from the cells after isolation using a polyclonal antibody (DETACHaBEAD) that binds to the Fab-region of the cell-specific monoclonal antibody (Rasmussen *et al*., 1992). No antibodies remain on the isolated cells after detachment when using DETACHaBEAD (Fig. 2). CELLection is another system for the removal of beads from isolated cells. DNase is used to cut a DNA linker between the beads and the antibodies, removing the beads and leaving only the

Copyright 2006, Elsevier Science (USA).
All rights reserved.

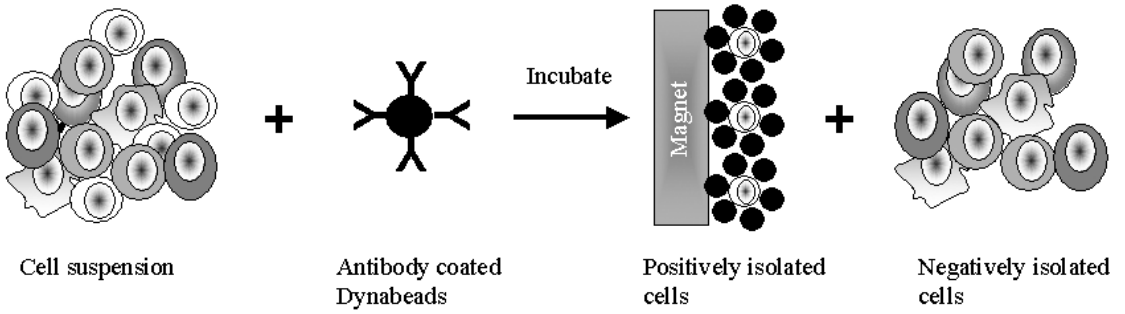

FIGURE 1 Positive and negative isolation of cells using antibody-coated Dynabeads. By positive selection, a specific cellular subset is isolated directly from a complex mixture of cells based on the expression of a distinct surface antigen. The resulting immune complexes of beads and target cells are collected using a magnet. By negative selection, all unwanted cell types are removed from the sample by the magnetic beads.

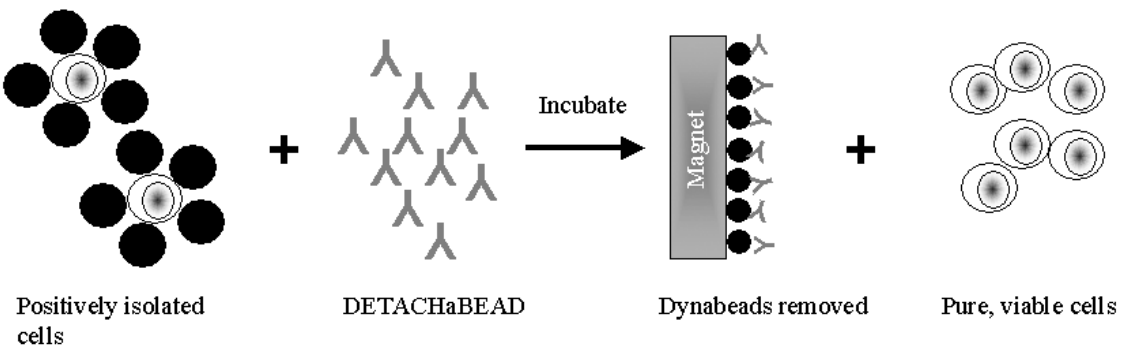

FIGURE 2 Detachment of cells from Dynabeads using DETACHaBEAD. Cells are detached from the beads by a polyclonal antibody (DETACHaBEAD) that binds the Fab-region of the cell-specific monoclonal antibody, thereby altering its affinity for the antigen. The cells are left without antibody on their surface.

antibodies on the cell surface (Soltys *et al*., 1999; Werther *et al*., 2000).

Factors such as incubation time, temperature, and concentration of reactants have a measurable effect on the efficiency of cell isolation using magnetic beads. Furthermore, the process is also affected by specific key parameters, such as the nature and state of the target cell, characteristics of the antigen/antibody binding, sample type, concentration, and ratio of beads and cells. Successful cell isolation with Dynabeads, which implies high yield and purity, is dependent on the concentration of the magnetic beads, the ratio of beads to target cells, and the choice of antibody. Monoclonal antibodies are generally recommended due to their high specificity toward the target antigen.

II. MATERIALS AND INSTRUMENTATION

Lymphoprep 6 × 500 ml (Prod. No.1114547), density 1.077 ± 0.001 g/ml, osmolality 290 ± 15 mOsm from Axis-Shield Poc is stable for 3 years if stored at room temperature in the dark. Human serum, AB 100 ml (Part Code US14–490E) from BioWhittaker is stable for 3 years if stored at –20°C. Human serum, AB should be heat inactivated (56°C, 30 min) before use. All human blood-based products should be handled in accordance with currently acceptable biosafety practices and guidelines for the prevention of blood-borne viral infections. Fetal bovine serum, premium, US origin 500 ml (Part Code US14-501F) from BioWhittaker is stable for 3 years if stored at –20°C. Fetal bovine serum should be heat inactivated (56°C, 30 min) before use. Bovine serum albumin (BSA) >96% by electrophoresis, 500 g (Prod. No. A-4503) is from Sigma. DPBS, without Ca^{2+} or Mg^{2+} 500 ml (Part Code BE17-512F) from BioWhittaker is stable for 2 years if stored at 15–30°C. RPMI 1640, with L-glutamine 500 ml (Part Code BE12-702F) from BioWhittaker is stable for 2 years if stored at 15–30°C. Proleukin interleukin-2 (recombinant IL-2) 22 × 10^6 IU from Chiron B.V. was reconstituted in sterile H_2O at 6 × 10^5 IU/ml and stored at –20°C for up to 1 year. CD4-FITC 100 tests/2 ml

(Prod. No. 3021) from Diatec is a mouse monoclonal IgG2a/κ, clone EDU-2 recommended for flow cytometry. CD4-FITC should be stored at 2–8°C (short term) or –20°C (long term). CD25-PE 100 tests (Cat. No. 341010) from BD Biosciences Pharmingen is a mouse monoclonal IgG1, clone 2A3 recommended for flow cytometry. CD25-PE should be stored at 2–8°C. CD8-PC5 100 tests/2 ml (Part No. IM2638) from Beckman Coulter is a mouse monoclonal IgG1, clone B9.11 recommended for flow cytometry. CD8-PC5 should be stored at 2–8°C. Dynal CD4 positive isolation kit, 2 ml (Prod. No. 113.03), Dynabeads CD25, 2 ml (Prod. No. 111.33), DETACHaBEAD CD4/CD8, 5 ml (Prod. No. 125.04), Dynal CD4 negative isolation kit, 5 ml (Prod. No. 113.17), Dynal CD8 negative isolation kit, 5 ml (Prod. No. 113.19), Dynabeads Tcap™ EBV/BMLF-1 (Prod. No. 103.01), and Dynabeads CD3/CD28 T-cell expander, 2 ml (Prod. No. 111.31) are from Dynal Biotech. These products, which contain magnetic beads (2.8–4.5 µm) and/or antibody cocktails (mouse monoclonal antibodies) and/or release agents (polyclonal sheep antimouse antibodies), are stable for 12–36 months when stored at 2–8°C. Magnets: Dynal MPC (Prod. No. 120.01, 120.20, and 120.21) and from Dynal Biotech. Sodium citrate dihydrate pro analysis, >99% pure, 1 kg (Cat. No. 1.06448.1000) is produced by Merck and sold by VWR International. rHLA-A2/GLC-PE MHC tetramers 50 tests (code T2A-G) from ProImmune are stable for >6 months when stored at 2–8°C. Centrifuge: Rotanta 460 R from Hettich was delivered by Nerliens. Sample mixer: Dynal MX1 (Prod. No. 159.07) with 12-tube mixing wheel (Prod. No. 159.03) is from Dynal Biotech ASA. Flow cytometer: BD LSR II with 488- and 633-nm lasers from BD Biosciences was delivered by Laborel. Laminar flow bench: Biowizard Kojair KR 200 from Kojair Tech Oy was delivered by Houm AS. 37°C CO_2 incubator: Forma Scientific Model 3548 (water-jacked incubator) was delivered by Houm AS. Pipettes: Finnpipette 0.5–10 µl, 5–50 µl, 20–200 µl, and 200–1000 µl from Thermo Labsystem were delivered by VWR International.

III. PROCEDURES

This article covers procedures for some basic principles of cell isolation and cell stimulation using Dynabeads.

The isolation of $CD4^+CD25^+$ regulatory T cells (Shevach, 2002) demonstrates the different isolation techniques. The isolation is performed in two steps; the first step involves isolation of $CD4^+$ cells by positive selection (protocol A) or negative selection (protocol B). The second step involves isolation of $CD25^+$ cells from the $CD4^+$ cell population (protocol C).

Isolation of antigen-specific $CD8^+$ T cells using recombinant HLA molecules on Dynabeads demonstrates enrichment of rare cells from a complex cell sample (protocol D). Expansion of these antigen-specific $CD8^+$ T cells demonstrates *ex vivo* cell stimulation and manipulation (protocol E). For further questions, contact the supplier at: techcentre@dynalbiotech.com.

A. Positive Selection of $CD4^+$ T Cells (Direct Technique)

$CD4^+$ T cells are isolated from buffy coat by positive selection using the Dynal CD4 positive isolation kit. The isolated $CD4^+$ cells are then ready for further studies, e.g., isolation of the $CD4^+CD25^+$ regulatory T-cell subpopulation (protocol C).

Solutions

1. *Phosphate-buffered saline (PBS) pH 7.4*: Dulbecco's PBS without Ca^{2+} and Mg^{2+}
2. *PBS/citrate*: PBS with 0.6% (w/v) sodium citrate (to prevent microcoagulation)
3. *Heat-inactivated fetal calf serum (FCS)*
4. *PBS/BSA or PBS/FCS*: PBS with 0.1% (w/v) bovine serum albumin or PBS with 2% (v/v) FCS.
5. *Culture medium*: RPMI 1640 with 1% (v/v) FCS.

Steps for Cell Isolation

1. Dynabeads required: 2×10^7 beads/ml × 40 ml = 8×10^8 beads (2.0 ml).
2. Wash Dynabeads; mix vial, transfer beads to a 50-ml tube, add 10 ml PBS/BSA, collect beads on a magnet for 1 min, remove supernatant, and replace with 2 ml PBS/BSA; cool to 2–8°C.
3. Dilute 15 ml buffy coat in 25 ml PBS/citrate; cool to 2–8°C.
4. Add 40 ml of cell suspension to the Dynabeads (2 ml) directly into the 50-ml tube. Mix *gently* by tilting and rotation for 30 min at 2–8°C.
5. Isolate the cells that are attached to beads (rosetted cells) by placing the tube in the magnet for 2 min. Discard the supernatant while the rosetted cells are held at the tube wall by the magnet.
6. Wash cells; remove the tube from the magnet and resuspend the rosetted cells gently in 10 ml PBS/citrate. Repeat steps 5 and 6 four to five times.
7. Resuspend the rosetted cells in 1 ml of culture medium in a 5-ml tube. The cells are now ready for the removal of beads.

Steps for Removal of Dynabeads from Cells (DETACHaBEAD)

1. Add 10 µl DETACHaBEAD per 10^7–10^8 beads used for cell capture.
2. Mix *gently* by tilting and rotation for 45–60 min at room temperature.
3. Pipette gently five to six times to resuspend the cell/beads suspension and place the tube in a magnet for 2 min.
4. Collect the supernatant while the beads are held at the tube wall by the magnet.
5. To obtain residual cells, resuspend the beads in culture medium and repeat steps 3 and 4 twice.
6. Combine the supernatants, and wash the cells twice with PBS/BSA to remove DETACHaBEAD.
7. The cells are now ready for further analysis or isolation of subpopulations (protocol C).

B. Negative Selection of $CD4^+$ T Cells (Indirect Technique)

$CD4^+$ T cells are isolated from peripheral blood mononuclear cell (PBMC) by negative selection using the Dynal CD4 negative isolation kit. Unwanted cells are removed, and the $CD4^+$ T cells are then ready for further studies, e.g., isolation of the $CD4^+CD25^+$ regulatory T-cell subpopulation (protocol C).

Solution

PBS/citrate, PBS/BSA, FCS, and culture medium are prepared as in protocol A.

Steps for Cell Isolation

1. Dynabeads required: 4 beads/PBMC × 10^8 PBMC = 4×10^8 beads (1.0 ml).
2. Wash Dynabeads as described in protocol A, resuspend in 1 ml.
3. Isolate PBMC with low platelet content; add 35 ml solution (10 ml buffy coat +25 ml of PBS/citrate) on top of 15 ml of Lymphoprep at room temperature. Centrifuge for 20 min at 160 *g* at 20°C. Remove 20 ml of supernatant by suction to eliminate platelets. Centrifuge for 20 min at 350 *g* at 20°C. Recover PBMC from the plasma/Lymphoprep interface. Wash PBMC three times in PBS/BSA (centrifuge for 8 min at 500 *g* the first time and then at 225 *g*) and resuspend the PBMC at 10^7 cells per 100–200 µl in PBS/BSA. Keep cells at 2–8°C.
4. Incubate 10^8 PBMC with the 200-µl antibody mix and 200 µl FCS for 10 min at 2–8°C.
5. Wash cells; add 5–10 ml PBS/BSA and centrifuge for 8 min at 500 *g* at 2–8°C. Resuspend cells in 9 ml PBS/BSA at room temperature.
6. Add 9 ml of PBMC to the depletion Dynabeads (1 ml) directly into the 50-ml tube. Mix *gently* by tilting and rotation for 15 min at room temperature.
7. Pipette gently five to six times to resuspend the rosetted cells and double the sample volume with PBS/BSA. Place the tube in a magnet for 2 min. Collect the supernatant containing $CD4^+$ T cells. The cells are now ready for further analysis or isolation of subpopulations (protocol C).

C. Positive Selection of $CD4^+CD25^+$ Regulatory T Cells (Fig. 3)

$CD4^+$ T cells have been isolated by either positive (protocol A) or negative (protocol B) selection. From these cells the $CD4^+CD25^+$ regulatory T-cell subpopulation can be isolated using Dynabeads CD25, and the beads are removed with DETACHaBEAD.

Solutions

1. PBS, PBS/BSA, FCS, and culture medium are prepared as in protocol A
2. *PBS/10% FCS*: PBS with 10% (v/v) FCS

Steps for Cell Isolation

1. Dynabeads required: 4 beads/$CD4^+$ cell × 5 × 10^7 $CD4^+$ cells = 2×10^8 beads (500 µl).
2. Wash Dynabeads as described in protocol A, but in a 15-ml tube, resuspend in 500 µl.
3. Prepare cells by protocol A or B, resuspend at 10^7 cells/ml in PBS/BSA, and cool to 2–8°C.
4. Add 5 ml of cells to the Dynabeads (500 µl) directly into the 15-ml tube. Mix *gently* by tilting and rotation for 20 min at 2–8°C.

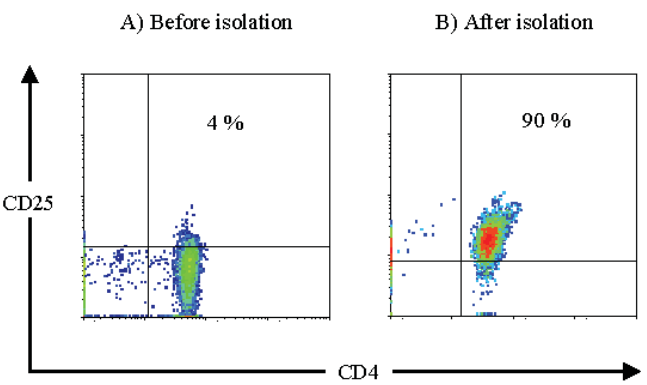

FIGURE 3 Isolation of $CD4^+CD25^+$ regulatory T cells. $CD4^+CD25^+$ regulatory T cells were isolated according to protocol C. Diatec CD4-FITC and Pharmingen CD25-PE (clone 2A3) were used for cell staining. (A) Staining of $CD25^+$ T-cells in the $CD4^+$ T-cell population. (B) Staining of $CD25^+$ T-cells after positive isolation from the $CD4^+$ T-cell population.

5. Isolate and wash the rosetted cells as described in protocol A (steps 5 and 6), but use 2 ml PBS/BSA for washing.
6. *Use precoated tubes* (10 min at room temperature using PBS/10% FCS) from this step to avoid cell loss. Resuspend the rosetted cells in 200 µl of culture medium in a 1.5-ml tube. The cells are now ready for removal of beads.

Steps for Removal of Dynabeads from cells (DETACHaBEAD)

1. Add 10 µl DETACHaBEAD per 10^7 beads used for cell capture.
2. Incubate, resuspend, collect, and wash cells as described in protocol A; use precoated tubes. The cells are now ready for further analysis and functional studies.

D. Isolation of Antigen-Specific $CD8^+$ T Cells (Fig. 4)

Dynabeads coupled with recombinant HLA (rHLA) class I molecules loaded with the relevant peptide can be used to enrich antigen-specific $CD8^+$ T cells (Garboczi *et al*., 1992; Luxembourg *et al*., 1998; Ostergaard Pedersen *et al*., 2001). The starting material is PBMC or preferably negatively isolated $CD8^+$ T cells (protocol B, using Dynal CD8 negative isolation kit). Antigen-specific $CD8^+$ T cells are isolated using Dynabeads Tcap™ EBV/BMLF-1.

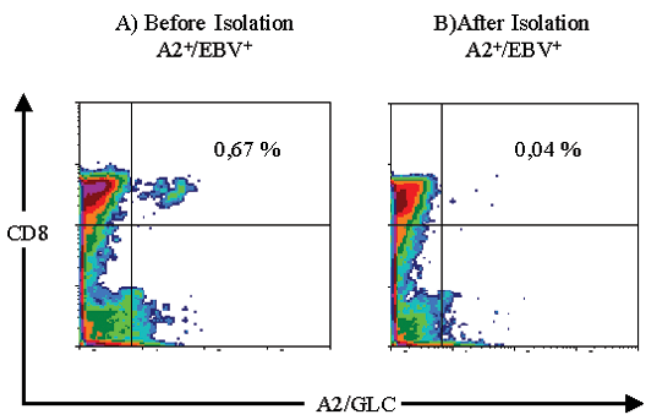

FIGURE 4 Isolation of rHLA-A2/GLC positive T cells from PBMC. (A) PBMC from a HLA-A2/GLC positive donor stained with rHLA-A2/GLC tetramers. (B) PBMC after removal of rHLA-A2/GLC tetramer positive T cells by rHLA-A2/GLC coated Dynabeads, i.e., Dynabeads HLA-A2 EBV/BMLF-1 (see protocol D). The rHLA-A2 was produced and loaded with the peptide GLCTLVAML according to Ostergaard Pedersen *et al*. (2001).

Solutions

1. PBS/BSA and FCS are prepared as in protocol A.
2. *Culture medium*: RPMI 1640 with 5% (v/v) FCS or 5% (v/v) AB serum.

Steps for Cell Isolation

1. Dynabeads required: 10^7 beads/ml × 1 ml = 10^7 beads (25 µl).
2. Wash Dynabeads; mix vial, transfer beads to a 1.5-ml tube, add 0.5 ml PBS/BSA, collect beads on a magnet for 1 min, remove supernatant, and replace with 100 µl PBS/BSA; cool to 2–8°C.
3. Prepare cells by protocol B (preferably negatively isolated $CD8^+$ T cells), resuspend at 5×10^7 cells/ml in PBS/BSA, and cool at 2–8°C.
4. Add 1 ml of cells to the Dynabeads directly into the 1.5-ml tube. Mix *gently* by tilting and rotation for 30 min at 2–8°C.
5. Isolate and wash the rosetted cells at 2–8°C as described in protocol A (steps 5 and 6), but use 1 ml PBS/BSA for washing. Resuspend the rosetted cells in 100 µl of culture medium (2–8°C). The cells are now ready for further analysis or expansion (protocol E).

E. Activation and Expansion of T Cells Using Dynabeads

T-cell activation *in vivo* is initiated by the binding of T-cell receptors on its surface to appropriate peptide-HLA molecules on the surface of antigen-presenting cells (APC). However, activation of highly pure T cells *in vitro* is difficult to perform without the presence of APC. The Dynabeads CD3/CD28 T-cell expander can mimic the APC and therefore be used to activate pure T cells. Some T cells are CD28 negative and will require other costimulatory signals than through CD28, e.g., through CD137 (Maus *et al*., 2002).

Solutions

1. FCS is prepared as in protocol A.
2. *Culture medium*: RPMI 1640 with 5% (v/v) FCS or 5% (v/v) AB serum
3. *Culture medium/rIL-2*: culture medium with 20–100 IU/ml recombinant IL-2

Steps for in Vitro *Cell Expansion*

1. Dynabeads required: 4 beads/T cell × 10^7 cells = 4×10^7 beads (1.0 ml).
2. Starting material may be monocyte-depleted PBMC, pure $CD3^+$, $CD4^+$, or $CD8^+$ T cells (e.g., prepared according to protocol A or B). Resuspend at 10^6 cells/ml in culture medium and add 1 ml of this cell

suspension to each well in a 24-well culture plate. If rare cells are isolated and beads are still attached to the cells (e.g., protocol D), each well should contain a maximum of 10^6 beads (used for isolation), regardless of the number of cells isolated.

3. Add the Dynabeads CD3/CD28 T-cell expander directly to the cells at a ratio of four beads per cell. Mix *gently* by pipetting.

4. Incubate cells for 3 days at 37°C, resuspend, and count the cells. Dilute to 0.5×10^6 cells/ml with culture medium/rIL-2. Split cells every second to third day with culture medium/rIL-2 to keep the cell concentration at $0.5–1 \times 10^6$ cells/ml.

5. Cells can be expanded for 14 days without adding extra beads, and cell expansion rates are usually between 100- and 1000-fold, depending on the donor.

IV. COMMENTS

Immunomagnetic cell isolation offers rapid and direct access to target cells from whole blood and bone marrow without cell loss or damage. If necessary, unwanted elements such as erythrocytes, free DNA, fat, or serum proteins may be removed before cell isolation to improve the performance of the beads. Buffy coat, a concentrate of white blood cells, has the advantage of high target cell concentration. However, the quality of buffy coat preparations may vary considerably. Density gradient isolation of cells provides removal of possible interfering elements and the ability to manipulate target cell concentration to perform cost-efficient cell isolation. Drawbacks include cell losses during centrifugations and negative effects on the cells due to contact with the density gradient medium. Generally the concentration of nucleated cells should be 10^8 cells/ml when performing immunomagnetic cell isolation.

By positive selection the cells of interest are isolated for analysis. General isolation parameters are $\geq 1 \times 10^7$ beads/ml, bead : cell ratio 4 : 1–10 : 1, and 10–30 min of incubation. Typically, 95–100% purity and viability are achieved with 60–95% yield. For some downstream applications the beads can remain attached to the cells (e.g., mRNA or DNA isolation). By negative selection (= *depletion*), unwanted cells are removed prior to analysis of the remaining population. General isolation parameters are $\geq 2 \times 10^7$ beads/ml, bead : cell ratio ≥4 : 1, and 20–60 min of incubation. Typically, 95–99% depletion of unwanted cells is achieved. Two successive depletion cycles may result in higher purity for small cell populations. The direct technique offers fast cell isolation with antibody-coated beads. Cell handling is minimized, reducing the risk for cell damage and loss. The indirect technique is especially useful when the affinity/avidity of the primary antibody is low or when the epitope density on the target cell is limited. The disadvantage of the indirect technique is cell handling (centrifugation).

Cross-reactivity and Fc binding can be blocked by the addition of free proteins (e.g., Fc receptor blocking with γ-globulin). Nonspecific binding of "sticky" cells to beads can be avoided by predepletion of these cells with protein-coated beads (e.g., secondary coated or BSA-coated beads). Free DNA will contribute to binding of unwanted cells to the beads. Freezing/thawing may damage cells and release free DNA. DNase treatment prior to cell selection will abolish this problem. Platelets may also induce nonspecific binding of cells to Dynabeads. Preparation of PBMC with a low platelet content (see protocol B) will reduce this problem.

Primary-coated Dynabeads are ready-to-use products for a wide variety of cell surface markers. In addition, secondary-coated Dynabeads offer an excellent possibility to make beads with the reactivity of choice using mouse, rat, or rabbit antibodies directly from culture supernatant, ascites, or polyclonal sera (without the need of purification). This is especially useful when only small amounts of nonpurified antibody are available. However, affinity-purified antibodies are preferred.

V. PITFALLS

1. Prolonged incubation (>60 min) and increased bead concentration ($>1 \times 10^8$ beads/ml) will rarely improve the cell selection efficiency. However, nonspecific binding may increase, damage of cells from sheer forces of the beads may occur, and risk of cell trapping increases.

2. A soluble form of cell surface antigens or other serum components can reduce the efficiency of immunomagnetic cell isolation. One or two washing steps will overcome this problem.

3. Nonspecific binding. Genomic DNA from lysed cells (e.g., present in buffy coat, PBMC, or after freezing/thawing of cells) will induce non-specific binding of cells to beads. DNase treatment of the cell suspension prior to cell selection will prevent this problem without harming intact cells. Some sample tubes (e.g., glass or polystyrene) tend to bind cells nonspecifically, which can be a major problem when working with minor cell populations (e.g., rare, circulating tumour

cells). Precoating of sample tubes with a protein solution before use or the use of low-binding plastic tubes is recommended.

4. Phagocyte cells (e.g., monocytes) will bind and engulf beads if incubation is performed at temperatures above 2–8°C.

References

Chang, C. C., Ciubotariu, R., Manavalan, J. S., Yuan, J., Colovai, A. I., Piazza, F., Lederman, S., Colonna, M., Cortesini, R., Dalla-Favera, R., and Suciu-Foca, N. (2002). Tolerization of dendritic cells by T(S) cells: The crucial role of inhibitory receptors ILT3 and ILT4. *Nature Immunol*. **3**, 237–243.

Funderud, S., Nustad, K., Lea, T., Vartdal, F., Gaudernack, G., Stenstad, P., and Ugelstad, J. (1987). Fractionation of lymphocytes by immunomagnetic beads. *In "Lymphocytes: A Practical Approach"* (G. G. B. Klaus, ed.), pp. 55–65. IRL Press, Oxford.

Garboczi, D. N., Hung, D. T., and Wiley, D. C. (1992). HLA-A2-peptide complexes: Refolding and crystallization of molecules expressed in *Escherichia coli* and complexed with single antigenic peptides. *Proc. Natl. Acad. Sci. USA* **89**, 3429–3433.

Garlie, N. K., LeFever, A. V., Siebenlist, R. E., Levine, B. L., June, C. H., and Lum, L. G. (1999). T cells coactivated with immobilized anti-CD3 and anti-CD28 as potential immunotherapy for cancer. *J. Immunother*. **22**, 336–345.

Levine, B. L., Bernstein, W. B., Aronson, N. E., Schlienger, K., Cotte, J., Perfetto, S., Humphries, M. J., Ratto-Kim, S., Birx, D. L., Steffens, C., Landay, A., Carroll, R. G., and June, C. H. (2002). Adoptive transfer of costimulated $CD4^+$ T cells induces expansion of peripheral T cells and decreased CCR5 expression in HIV infection. *Nature Med*. **8**, 47–53.

Levine, B. L., Cotte, J., Small, C. C., Carroll, R. G., Riley, J. L., Bernstein, W. B., Van Epps, D. E., Hardwick, R. A., and June, C. H. (1998). Large-scale production of CD4+ T cells from HIV-1-infected donors after CD3/CD28 costimulation. *J. Hematother*. **7**, 437–448.

Liebowitz, D. N., Lee, K. P., and June, C. H. (1998). Costimulatory approaches to adoptive immunotherapy. *Curr. Opin. Oncol*. **10**, 533–541.

Lum, L. G., LeFever, A. V., Treisman, J. S., Garlie, N. K., and Hanson, J. P. Jr. (2001). Immune modulation in cancer patients after adoptive transfer of anti-CD3/anti-CD28-costimulated T cells-phase I clinical trial. *J. Immunother*. **24**, 408–419.

Luxembourg, A. T., Borrow, P., Teyton, L., Brunmark, A. B., Peterson, P. A., and Jackson, M. R. (1998). Biomagnetic isolation of antigen-specific CD8+ T cells usable in immunotherapy. *Nature Biotech*. **16**, 281–285.

Marquez, C., Trigueros, C., Franco, J. M., Ramiro, A. R., Carrasco, Y. R., Lopez-Botet, M., and Toribio, M. L. (1998). Identification of a common developmental pathway for thymic natural killer cells and dendritic cells. *Blood* **91**, 2760–2771.

Maus, M. V., Thomas, A. K., Leonard, D. G., Allman, D., Addya, K., Schlienger, K., Riley, J. L., and June, C. H. (2002). Ex vivo expansion of polyclonal and antigen-specific cytotoxic T lymphocytes by artificial APCs expressing ligands for the T-cell receptor, CD28 and 4-1BB. *Nature Biotechnol*. **20**, 143–148.

Ostergaard Pedersen, L., Nissen, M. H., Hansen, N. J., Nielsen, L. L., Lauenmoller, S. L., Blicher, T., Nansen, A., Sylvester-Hvid, C., Thromsen, A. R., and Buus, S. (2001). Efficient assembly of recombinant major histocompatibility complex class I molecules with preformed disulfide bonds. *Eur. J. Immunol*. **31**, 2986–2996.

Rasmussen, A.-M., Smeland, E., Eriksten, B. K., Calgnault, L., and Funderud, S. (1992). A new method for detachment of Dynabeads from positively selected B lymphocytes. *J. Immunol. Methods* **146**, 195–202.

Shevach, E. M. (2002). $CD4^+CD25^+$ suppressor T cells: More questions than answers. *Nature Rev*. **2**, 389–400.

Soltys, J., Swain, S. D., Sipes, K. M., Nelson, L. K., Hanson, A. J., Kantele, J. M., Jutila M. A., and Quinn, M. T. (1999). Isolation of bovine neutrophils with biomagnetic beads: Comparison with standard Percoll density gradient isolation methods. *J. Immunol. Methods* **226**, 71–84.

Thomas, A. K., and June, C. H. (2001). The promise of T-lymphocyte immunotherapy for the treatment of malignant disease. *Cancer J*. **7**, S67–S75.

Ugelstad, J., Kilaas, L., Aune, O., Bjørgum, J., Herje, R., Schmid, R., Stenstad, P., and Berge, A. (1994). Monodisperse polymer particles. *In "Advances of Biomagnetic Separation"* (M. Uhlén, E. Hornes, and Ø. Olsvik, eds.), pp 1–20, Eaton Publ. Comp., Natick, MA.

Ugelstad, J., Mørk, P. C., Herder Kaggerud, K., Ellingsen, T., and Berge, A. (1980). Swelling of oligomer particles: New methods of preparation of emulsions and polymer dispersions. *Adv. Colloid Interface Sci*. **13**, 101.

Werther, K., Normark, M., Hansen, B. F., Brunner, N., and Nielsen H. J. (2000). The use of the CELLection kit in the isolation of carcinoma cells from mononuclear cell suspensions. *J. Immunol. Methods* **238**, 133–141.

CHAPTER

31

Separation of Cell Populations Synchronized in Cell Cycle Phase by Centrifugal Elutriation

R. Curtis Bird

I. INTRODUCTION

Centrifugal elutriation is the only method whereby large numbers of cells can be separated rapidly on the basis of size (Diamond, 1991; Merrill, 1998; Davis *et al.*, 2001). The capability of discriminating between very small differences in cell size provides the ability to separate cells into sequential cell cycle phase populations of relatively high purity without the use of drugs or inhibitors (Bludau *et al.*, 1986; Braunstein *et al.*, 1982; Hann *et al.*, 1985; Iqbal *et al.*, 1984; Wu *et al.*, 1993; Brown and Schildkraut, 1979; Bialkowski and Kasprzak, 2000; Datta and Long, 2002; Deacon *et al.*, 2002; Hengstschlager *et al.*, 1999; Houser *et al.*, 2001; Karas *et al.*, 1999; Rehak *et al.*, 2000; Sugikawa *et al.*, 1999; Syljuasen and McBride, 1999; Van Leeuwen-Stok *et al.*, 1998). It has been used successfully to separate a wide variety of cell types from suspension and substrate-dependent cultures and to separate mixed cell populations liberated directly from tissues or body fluids (Boerma *et al.*, 2002; Dagher *et al.*, 2002; Wong *et al.*, 2001, 2002). The purity of the samples is relatively high and the cells proceed to grow, following separation, without a detectable lag period. Thus, centrifugal elutriation combines speed of separation of large numbers of cells with little or no perturbation of the cell growth cycle and avoids the use of agents that might induce artifact. As additional advantages, centrifugal elutriation overcomes the limits on cell number imposed by fluorescence-activated cell sorting and the long separation times required for unit gravity sedimentation, as well as problems associated with osmotic stress in centrifugation media. The only real compromise is that the purity of the samples is somewhat lower than commonly achieved with alternative methods. The developmental history and theory of centrifugal elutriation are reviewed elsewhere (Conkie, 1985; Beckman Instruments, 1990).

Centrifugal elutriation was developed by Lindahl (1948) for the separation of cells and particulate fractions of cells (Lindahl and Nyberg, 1955; Lindahl, 1986) based on the original work of Lindbergh (1932). Counterstreaming centrifugation was used by these investigators to separate a variety of cell types but was not generally available to other laboratories until the introduction of a commercial centrifugal elutriator by Beckman Instruments in 1973 (reviewed in Beckman Instruments, 1990). Once available commercially, centrifugal elutriation was applied to the separation of many kinds of cells, including bacteria, yeast, and mammalian cells, grown in culture or liberated directly from tissues and solid tumors (reviewed in Beckman Instruments, 1990). In addition, elutriation has been used to separate cells in different phases of the cell cycle based on the small differences in size as cells gradually grow between divisions (Bird *et al.*, 1996a,b). In all cases, successful separation is dependent on complete dissociation of the cells to a single cell suspension. Failure to accomplish this affects the quality of separation as well as cell yield and thus cell clumps must be removed or dissociated prior to elutriation.

Centrifugal elutriation imposes two opposing forces on mixed cell populations to facilitate their fractionation into subpopulations (Fig. 1 and see Section IV).

Copyright 2006, Elsevier Science (USA).
All rights reserved.

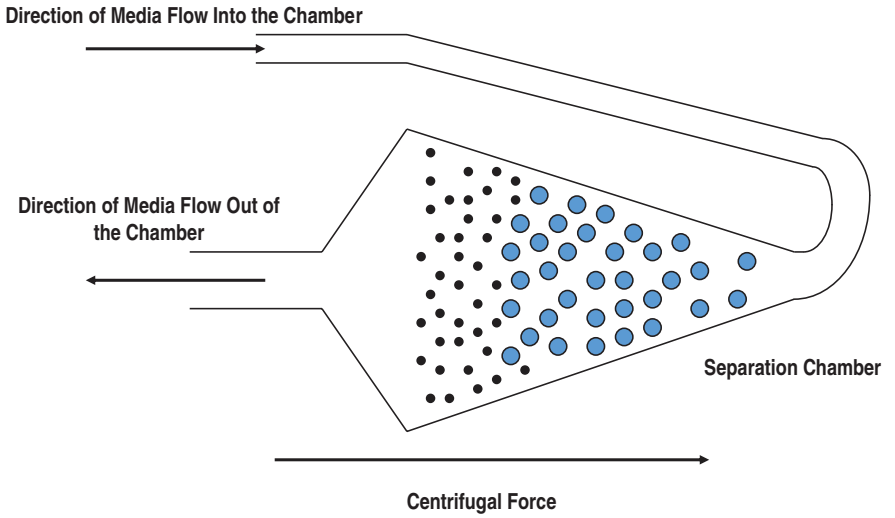

FIGURE 1 Cell separation dynamics and opposing forces in the elutriation chamber. The flow of media is opposed by centrifugal force in a balance that holds particles in equilibrium in the separation chamber. Due to different levels of force applied proportional to surface area presented, smallest particles sort to the inside of the chamber relative to larger particles. Separation is achieved by increasing the flow rate incrementally to push the smallest population of particles past the widest part of the chamber and into the inner narrowing section where media flow accelerates affecting elutriation of the population.

This technology has proven to be effective in fractionating cells, based on very small differences in cell size, with nominal cross contamination, and in numbers unmatched by other methods of cell separation. In addition, centrifugal elutriation can be performed rapidly, requiring only a few minutes (usually 20–120 min) to affect separation and this occurs in media containing no special additives that might affect the osmolarity or viscosity of the medium. Thus, with very little physiological change perceived by the cells, separation can be affected rapidly. Some shear force is exerted on the cells during separation, but this is not sufficient to appreciably affect viability or behavior of the cells in most cases. Compared to other methods of separation, such as fluorescence-activated cell sorting or unit gravity separation, centrifugal elutriation is by far the most gentle and the most rapid in manipulation and separation of the cell populations.

In this example application, synchronous fractions of HeLa S3 cells were analyzed, following centrifugal elutriation, by flow cytometry and [^{3}H]thymidine incorporation into acid-precipitable materials (Wu *et al.*, 1993; Pai and Bird, 1994). Both means of analysis demonstrated that sequential fractions of elutriated cells represent sequential cell cycle phases as determined by the analysis of cell volume, DNA content, and ability to incorporate thymidine during five sequential 1-h periods following return to culture. From this analysis, cells collected at flow rates of 21–25 ml/min were designated the G_1-phase population, cells collected at flow rates of 29–35 ml/min were designated the S-phase population, and cells collected at flow rates of 43 ml/min were designated the G_2/M-phase population. Flow cytometric analysis, based on measurements of DNA content and cell volume, were also used to determine the level of contamination of S-phase cells in the G_1-phase fractions (approximately 3%) and G_1-phase cells in the S-phase cell population (approximately 10%) (Hann *et al.*, 1985). Thus, large populations of cells were separated rapidly into seven to eight synchronous fractions without the use of drugs, with little evidence of perturbation, and with low levels of contaminating cells.

II. MATERIALS AND INSTRUMENTATION

The centrifugal elutriator is from Beckman Instruments (elutriator rotor assembly Cat. No. JE-6B was run in a Model J2-21 elutriation centrifuge). Accessories are used as specified by the manufacturer throughout, and the rotor is equipped with a standard separation chamber. A Masterflex digital peristaltic pump (0–100 rpm Model 07523-70 fitted with a model 7014-21 pump head, Cole-Parmer) is used to pump cells and media through the rotor.

Materials for cell culture include α-modification of Eagle's minimal essential growth medium (α-MEM,

Invitrogen, Cat. No. 11900-073), fetal bovine serum (FBS, Hyclone, Cat. No. SH30070.03), donor horse serum (DHS, ICN Biomedicals, Inc., Cat. No. 29-211-49), 100× antibiotic/antimycotic solution (Invitrogen, Cat. No. 15240-062), 10× trypsin solution (Invitrogen, Cat. No. 15090-046), and Hanks' balanced salt solution (Sigma, Cat. No. H9394). All plasticware is tissue culture grade (Corning Plasticware, Fisher Scientific). All other reagents are standard reagent grade and available from numerous sources. The water used throughout this procedure is ultrapure in quality and is prepared by ion-exchange chromatography (Barnstead Nanopure) to 18-MΩ resistance and then glass distilled to remove residual endotoxin and RNase activity. Solutions are sterilized by autoclaving or ultrafiltration (0.2 μm).

III. PROCEDURES

A. Cell Culture

Growth medium and elutriation medium are used per standard protocols for the growth of HeLa cells (Pai and Bird, 1992). If different cell lines are to be elutriated, appropriate media should be substituted (see Section V).

Solutions

1. *Growth and elutriation media*: Dissolve powdered α-MEM (10-liter pack) in ultrapure water containing a final concentration of 1× antibiotics and 22.2 g $NaHCO_3$ and make up to a total volume of 10 liters. Place the medium in a pressurizable vessel (Millipore), filter through a 0.2-μm filter (Corning) by positive pressure into sterile 0.5-liter bottles, and store at 4°C. Prior to use, add FBS (10%, v/v) to make growth medium or add DHS (5%, v/v) to make elutriation medium. Use of DHS reduces the cost of elutriation greatly without detectable effects on cell growth or quality of the fractionation (see Section V).

2. *0.5 M HEPES*: Dissolve 14.17 g HEPES buffer (Fisher, Cat. No. BP310-100) in ~80 ml water and adjust pH to 7.2. Adjust volume to 100 ml, filter sterilize, and store in the cold at 4°C.

3. *0.5 M Na_2EDTA*: Begin to dissolve 14.61 g EDTA-free acid (Fisher, Cat. No. BP118-500) in ~40 ml water with a magnetic stir bar. Monitor pH of the solution continuously while slowly adding 1 *M* NaOH (40 g/liter for 1 *M* stock) dropwise. Continue to adjust the pH up to ~8.0. As the EDTA dissolves, the pH will continue to fall. Carefully adjust the final pH to 8.0 without exceeding this value. Adjust volume to 100 ml, filter sterilize, and store at 4°C.

4. *Trypsin solution*: Add 8 ml of 2.5% trypsin stock solution (10 ×), 2 ml 0.5 *M* HEPES, pH 7.2, and 2 ml 0.5 *M* Na_2EDTA, pH 8.0, to 100 ml of Hanks' salt solution. Make additions from sterile stock solutions, maintaining sterility of the final solution. Store at 4°C.

5. *70% ethanol*: Combine 700 ml absolute (not denatured) ethanol with 300 ml water. Store in 0.5-liter bottles at room temperature.

Steps

1. Grow cultured HeLa S3 cells in 20 ml of modified Eagle's α-MEM medium (Invitrogen/Gibco) with 10% FBS and antibiotics in a 15-cm diameter culture plates at 37°C with 5% CO_2 and 100% humidity (Pai and Bird, 1992).

2. Collect cells at 60–70% confluence by trypsin digestion. Harvest just before the rotor is filled with medium.

3. Concentrate cells by low-speed centrifugation (3000 *g* for 5 min) at 4°C and resuspend in 5 ml of ice cold α-MEM with 5% DHS for every three plates (15 cm). Use this medium throughout the elutriation procedure. Maintain the cells on ice until they are loaded into the elutriator.

B. Elutriation

Steps

1. Arrange the elutriation system as described in the schematic diagram (Fig. 2A). Assemble the elutriator rotor according to the manufacturer's directions (Fig. 2B). Lightly lubricate each O ring, which seals the rotating assembly on top of the rotor, with silicone grease, taking care to wipe off any excess. Place the lower washer and spring on top of the rotor followed by the outer ring and rotating seal. Note that the screw threads on the top assembly are reversed. Lightly tighten the top and check that the outer ring spins freely. Tighten the side set screw and repeat the check for a freely spinning assembly. Loosen the lower washer inside the outer ring half a turn. Check that the assembly spins freely, retighten the lower washer, and check that it spins freely again. Care should be taken to ensure that the rotating seal connecting the rotor to the fluid lines is freshly cleaned and polished with the scintered glass plate and polishing paper provided. Only a lint-free tissue with an appropriate solvent (e.g., $CHCl_3$) should be used as even a small speck of lint can cause leakage. A *very thin* layer of silicone grease can be applied to the upper edge of the rotating seal to help create and maintain a good seal but all excess silicone must be removed. Stick the seal to the polypropylene disk on the bottom surface of the top of

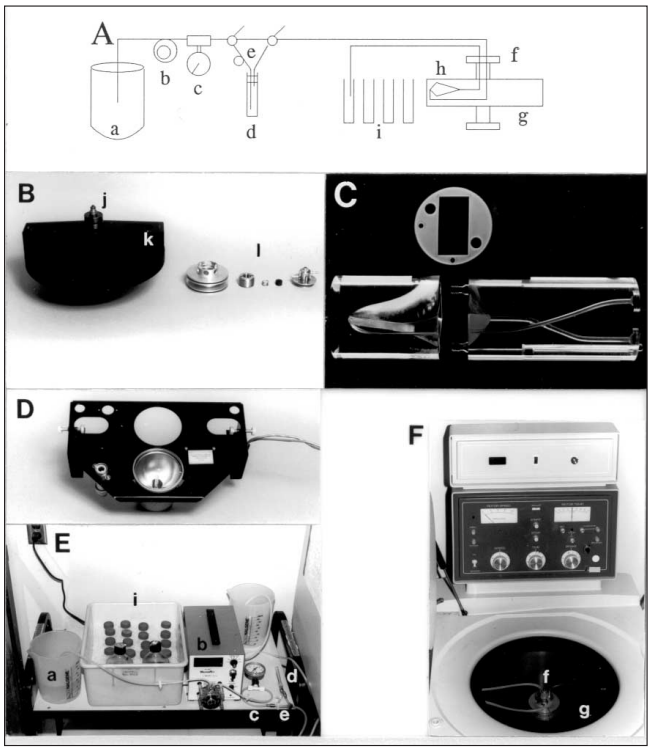

FIGURE 2 Assembly and setup of centrifugal elutriator. (A) Schematic of the centrifugal elutriator. Elutriation medium is pumped from the reservoir beaker (a) by the peristaltic pump (b) through the pressure gauge (c) and the sample tube (d) or the bypass harness (e) through the rotating seal (f) and into the rotor (g). The sample is separated in the elutriation chamber (h) and is pumped back to the sample collection tubes on ice (i). (B) Rotor and rotating seal assembly, including O rings on top of the rotor (j), which seal the rotating assembly to the rotor, the elutriation chamber (k), and, from left to right, the outer ring, lower washer, the spring that is placed inside the lower washer, rotating seal, and top of the seal assembly (l). (C) Elutriation chamber showing left (outer) and right (inner) halves separated by the gasket (above). Note the actual separation chamber within the left side and the set screws and alignment pins extending beyond both edges of the right side of the chamber. (D) Strobe assembly located below the rotor. (E) Elutriation setup showing the reservoir beaker (a), the peristaltic pump (b), pressure gauge (c), sample tube (d), bypass harness (e), and sample collection tubes (i). Note the positions of beakers to supply/accept media. (F) Elutriation centrifuge showing the complete rotating seal assembly (f), elutriation rotor (g), with strobe wires/waste tubing extending through the right centrifuge wall, and the inlet/outlet tubing extending through the left centrifuge wall.

the seal assembly by gently seating the silicone on the seal with a half turn. Carefully screw the top of the seal assembly onto the outer ring (note reverse threads) and hand tighten. This connection should not leak more than 1–3 ml during a normal elutriation run of <1 h. Even very small leaks encountered at low initial flow rates can result in significant loss of fluid and cells toward the end of the run as the flow rate rises. If persistent leaks are encountered, reexamine the seal and check for a perfectly clean and even surface on both edges. Repolish the rotating seal if necessary and then repeat the assembly procedure. If none of these measures seals the rotor connections adequately, the seal should be replaced.

2. Assemble the elutriator chamber according to the manufacturer's directions (Fig. 2B). Ensure that both halves of the chamber are perfectly clean and that the polypropylene gasket is positioned to allow alignment of the sample tube (see Section V). Tighten the screws to assemble but do not overtighten. Lightly lubricate both O rings, on the base of the chamber assembly, with silicone grease, taking care to wipe off any excess. Insert the chamber and align the base pin and sample tube connections. Secure it in place with the metal plug. The screw threads on the plug should be lubricated with Spincoat (Beckman) provided with the elutriator. Tighten with the tool provided but do not overtighten as the O rings can be crushed.

3. Assemble the elutriator centrifuge according to the manufacturers directions (Fig. 2C). Remove the high-speed rotor (if present) from the centrifuge and wipe out any moisture in the centrifuge chamber. Install the strobe assembly in the centrifuge chamber and secure with thumb screws while ensuring that it is centered over the rotor spindle in the center (Fig. 2D). Feed both wire connections through the ports on the right side of the centrifuge chamber and secure them with the metal plate. Carefully place the rotor on the spindle in the center of the centrifuge and ensure that it spins freely. Connect the three pieces of silicone tubing to the rotor (inlet, outlet, and overflow) and feed them through the appropriate port (inlet and outlet to the left, overflow to the right with the wires). Ensure that all are pulled tight enough so that none have any slack in them but not so tight as to pinch or pull off any of the connections (Fig. 2F). The overflow tube should wrap around the top of the seal assembly and pass under the inlet port (the upper of the two ports on the sides of the top of the seal assembly). Seal each of the ports around each tube and wire with a slit stopper (provided with the centrifuge), where they pass through the centrifuge chamber wall, to ensure a good vacuum.

4. Prepare a large ice bucket containing two 0.5-liter bottles of elutriation medium, 30 sterile-capped tubes (50 ml), and the cell suspension (Fig. 2E). Place the bucket on a cart or table next to the centrifuge with the pump and three 2-liter beakers. One beaker contains 1 liter of sterile water. Include a 20-ml syringe with an 18-gauge needle and the sample injection harness with a pressure gauge (Cole-Parmer, Cat. No. EW-07380-75). If sterile samples are to be collected, an additional

beaker of 70% ethanol and a bottle of sterile water must also be included. If elutriated cells are to be cultured for more than a few hours after separation, a sterile hood must be positioned next to the centrifuge to allow both reservoir beakers and samples to be collected under sterile conditions.

5. Clean the exterior of the silicone tubing with ethanol and place the inlet in the beaker containing the sterile water and the outlet in an empty beaker. The inlet tubing should also be installed into the pump head and attached to the sample application and bypass harness, with an inline pressure gauge, so that they are between the pump and the rotor (Fig. 2E). Begin pumping water through the rotor (which is stationary and the centrifuge is off, see Section V) at 45 ml/min (>200 ml). Carefully observe the water as it fills the equipment (~100 ml) and dislodge any bubbles with gentle pressure on the tubing or tapping of other components. Release the air from dead spaces within the pressure gauge by pinching the tubing just after the gauge and releasing it rapidly. Do not let the pressure rise above 15 psi or the tubing may burst. Adjust the stopcocks on the sample/bypass harness to allow the harness, stopcocks, and sample tube to fill completely. Continue to pump water through the equipment until all the bubbles have been cleared. Observe all connections, particularly at the rotor, for leakage.

6. Close the centrifuge door and start the rotor. Allow the speed to gradually rise and stabilize at 2000 rpm (±1 rpm is acceptable) at 4°C. Be sure to increase the speed slowly as the fine speed control can easily overshoot the set point on acceleration. Check each of the stoppers to ensure that the seals are adequate to allow development of a vacuum in the centrifuge. Observe the chamber through the periscope assembly in the door and adjust the strobe firing timer to center the image. If the chamber appears to have a rod running along the center rather than two screws running near each edge, then the strobe is 180° out of phase with the rotor and is allowing visualization of the balance chamber, not the elutriation chamber. Continue to adjust the strobe until the elutriation chamber is visible. Check for bubbles at the outlet using the squeeze-and-release technique described earlier. Turn off the pump and observe the outlet tubing as you raise it out of the beaker and suspend it free in the air. If a slow leak occurs, the fluid and air will be drawn back up into the tube as the fluid leaks out of the system. The system is sealed if the fluid level in the outlet tube does not change.

7. If sterile collection is required, switch to 70% ethanol and pump 200 ml through the rotor followed by 200 ml of sterile water from a bottle in the laminar flow hood. Switch to elutriation medium (without DHS) on ice and pump 200 ml (if sterile collection is not required, omit ethanol rinse). Be sure to include all sections of the sample injection harness, including the sample tube and the stopcocks, during the rinse with each of these solutions. Turn off the pump before switching the stopcocks. Turn the pump off and change to elutriation medium with 5% DHS to prevent the cells from sticking. Pump 100 ml at 45 ml/min through the sample tube. At this point, two people are required to operate the system: one collects samples and one monitors rotor and pump speeds as well as managing sample injection.

8. Disperse the trypsinized cells (~$1–2 \times 10^8$), which have been held on ice in 5 ml of elutriation medium (containing 5% DHS), with seven *very gentle* passes through an 18-gauge needle on a 20-ml syringe. Be careful not to introduce bubbles. Turn off the pump. Gently inject the cells into the sample tube (positioned with the stopper up), allowing the cells to settle to the bottom of the tube. Carefully turn the tube over (stopper down) and *gently* inject about 2 ml of air into the sample tube to act as a shock absorber against the pulsing peristaltic action of the pump. Adjust the pump, which is still off, to zero and then turn the pump on. Gradually adjust the pump up to 10 ml/min, being careful not to overshoot this value. Observe the sample tube and watch the cells enter the system. Take care to avoid pulsing of the medium or leaving a residual pools of cells in the sample tube. Collect three tubes of 50 ml each in the sample collection tubes on ice. Once the cells are loaded, the harness can be set on the bench in a stable position that maintains the inverted orientation of the sample tube (stopper down). Continue to monitor the entry of the cells into the elutriation chamber through the periscope. Carefully increase the pump speed to 15 ml/min. Do not overshoot. We collect G_1-phase cells between 21 and 25 ml/min, S-phase cells at 29–35 ml/min, and G_2/M-phase cells at 43 ml/min. Be prepared to work quickly at the end of an elutriation run as the flow rate becomes very fast and tubes containing elutriated cells fill at the rate of approximately one every minute. Following elutriation, pellet the cells by centrifugation (3000 *g* 5 min) and resuspend in growth medium. Adjust cell density with additional growth medium, after determination of cell concentration in each sample by counting in a hemacytometer, and transfer to tissue culture dishes.

C. Cell Cycle Analysis

Part of the synchronous cell fractions are fixed and analyzed by flow cytometry and the remainder of the cells are immediately prepared for RNA isolation or

placed back into culture for further manipulation (Fig. 3). Cultured cells are analyzed for their ability to synchronously enter S phase by determining the kinetics of [^{3}H]thymidine incorporation (Fig. 4).

Solutions

1. *Phosphate-buffered saline (PBS)*: Dissolve 0.71 g of Na_2HPO_4 (0.01 *M* final, Sigma, Cat. No. S-1934) and 4.5 g NaCl (0.9%, w/v final) in ~400 ml water and adjust pH to 7.6. Adjust volume to 500 ml, filter sterilize, and store at 4°C.

2. *Staining solution*: Make 50 µg/ml propidium iodide (PI) and 40 µg/ml RNase A by dilution of stock solute/ons. Add 111 µl PI stock (4.5 mg/ml, Sigma, Cat. No. P-1764) and 20 µl RNase A stock (20 mg/ml, Sigma, Cat. No. R-1859) to 10 ml water. Do not attempt to weigh RNase as any contamination will make future isolation of RNA very difficult. Open a 250-mg bottle in the fume hood and add 12.5 ml water. Cap, dissolve, and boil for 15 min to inactivate DNase (Sambrook *et al.*, 1989). Aliquot with a plugged disposable pipette (tissue culture type) in 1-ml lots in microcentrifuge tubes. Store at approximately –20°C. Use only disposable tubes and pipettes with RNase solutions and avoid any contamination or aerosols. Dissolve 100 mg of PI in 22.22 ml of water directly in the bottle. Do not weigh out. PI is extremely toxic and is a carcinogen as well as a potential mutagen and should be handled with care, including the use of gloves. Be careful not to create aerosols or liberate dust from the granular reagent. Dispose of all PI solutions and contaminated materials as hazardous waste. Use only disposable tubes and pipettes. Store PI at –20°C in the dark as it is light sensitive.

3. *100% trichloroacetic acid*: To a 500 g bottle of trichloroacetic acid (TCA, Sigma, Cat. No. T-2069), add sufficient water to bring the volume in the bottle to approximately the shoulder. Add a stir bar, cap the bottle, and stir to dissolve the contents. Carefully adjust the volume to 500 ml. TCA is extremely caustic. Do not attempt to measure or weigh TCA granules. Use caution when pipetting the solution. TCA 100% solution is very stable when stored at approximately ~4°C. Dilutions should be freshly prepared from the stock daily. Store dilutions on ice while in use and dispose of unused portions.

4. *[^{3}H]Thymidine growth medium*: Add 10 µCi/ml [^{3}H]thymidine (1 µCi/µl stock, PerkinElmer Life and Analytical Sciences, Inc., Cat. No. NET-027Z) directly to growth medium under sterile conditions at the rate of 10 µl/ml of medium. Prepare fresh on a daily basis.

5. *1.0 M Tris buffer*: Dissolve 60.55 g Tris buffer (Fisher, Cat. No. BP152-1) in ~400 ml water and adjust pH to 7.6. Adjust volume to 500 ml, filter sterilize, and store at 4°C.

6. 20% *sodium dodecyl sulfate* (*SDS*): Dissolve 20 g SDS (Sigma, Cat. No. L-1926) in sterile water using a sterile beaker and a stir bar rinsed in ethanol. Adjust

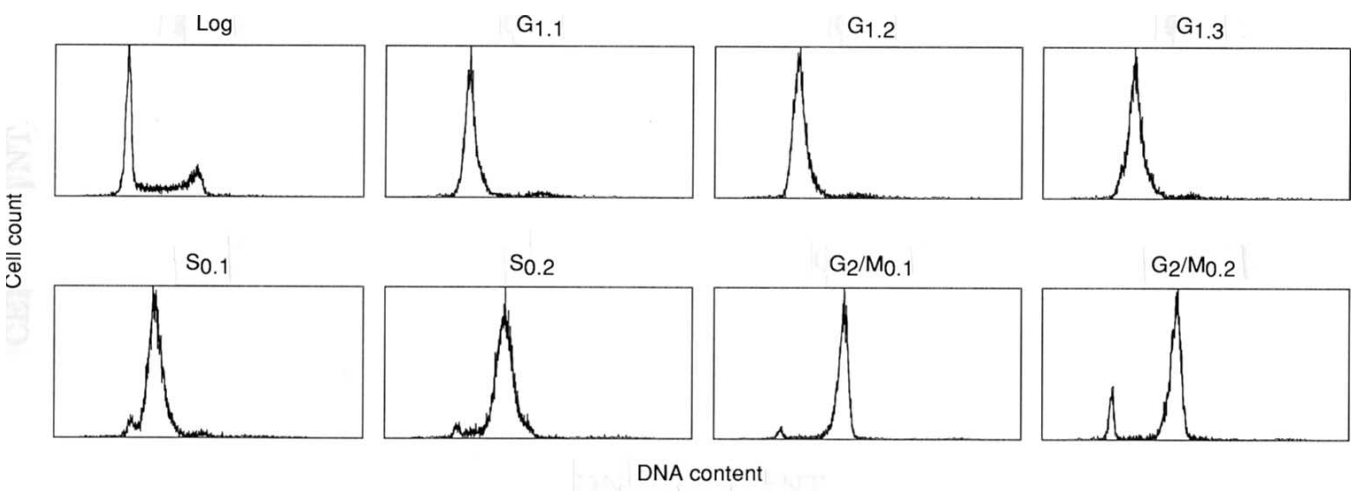

FIGURE 3 Flow cytometric analysis of cell cycle synchrony in sequential centrifugal elutriator fractions of HeLa S3 cells. Synchronous populations of HeLa S3 cells were selected by centrifugal elutriation of exponential cultures (log), and the degree of synchrony was analyzed by flow cytometry. Cell number was plotted against DNA content based on propidium iodide fluorescence for each cell cycle fraction. Flow cytometric analysis of sequential G_1-phase fractions collected at flow rates of 21 ml/min ($G_{1.1}$), 23 ml/min ($G_{1.2}$), and 25 ml/min ($G_{1.3}$). S-phase cells were selected by centrifugal elutriation at flow rates of 29 ml/min ($S_{0.1}$) and 35 ml/min ($S_{0.2}$), and G_2/M-phase cells were collected at 43 ml/min.

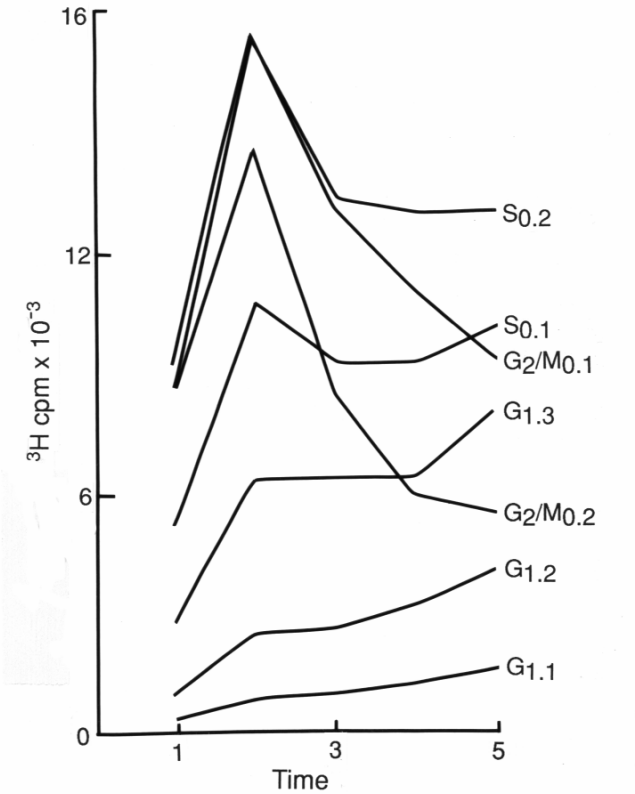

FIGURE 4 Analysis of synchrony of entry into DNA synthesis in centrifugal elutriation fractions of HeLa S3 cells. HeLa cells were separated into synchronous fractions by centrifugal elutriation, and kinetics of entry into DNA synthesis phase (S phase) was determined by measuring mean acid-precipitable [^{3}H]thymidine incorporation (10 µCi/ml in growth medium) for five sequential 1-h incubations, in duplicate, for each cell cycle fraction identified in Fig. 3. Note that each cell fraction reaches S phase at sequentially later times after return to culture.

final volume to 100 ml. SDS cannot be autoclaved or filtered. Store at room temperature.

7. *TES buffer*: Add 10 m*M* Tris–HCl, pH 7.6 (1 ml of 1 *M* stock), 1 m*M* EDTA, pH 8.0 (0.5 ml of 0.5 *M* stock), and 1% SDS (5 ml of 20% stock) to 93.5 ml water, filter, and store at room temperature.

8. *4% paraformaldehyde*: Dissolve 4 g paraformaldehyde (Electron Microscopy Sciences, Cat. No. 15710) in 100 ml water and stir to dissolve by heating gently to 60–65°C in a fume hood. This can take an extended period and the solution will still appear cloudy. Clarify by the addition of a few drops of 1 *M* NaOH (up to ~20 drops). Cool before use and store at 4°C. Fixative fumes are extremely toxic. Always use in a fume hood and avoid any contact.

Steps

1. Analyze cell cycle fractions by flow cytometric analysis (Fig. 3). Wash approximately 5×10^5 cells by centrifugation and resuspend in ice-cold Hanks' balanced salt solution. Fix cells by addition of an equal volume of ice-cold 4% paraformaldehyde. After a 24-h incubation at 4°C, collect the cells by centrifugation and resuspend in 2 ml of ice-cold PBS. Alternatively, fix cells by slow dropwise addition of 3 volumes of 70% ethanol (–20°C) while applying continuous gentle agitation with a vortex mixer. Allow cells to fix for at least 1 h at 4°C and then wash as described earlier. Approximately 30 min prior to flow cytometric analysis, add 3 ml of staining solution to each aliquot of 300 µl of cell suspension and incubate at room temperature. Analyze fluorescence on a flow cytometer (Elite Flow Cytometer, Coulter Electronics).

2. Analyze acid precipitable [^{3}H]thymidine incorporation by synchronous cell populations by pulse labeling each separated fraction of cells with 10 µCi/ml [^{3}H]thymidine in complete growth medium (Fig. 4) for 1 h at hourly intervals after return of the cells to culture (Wu *et al.*, 1993; Bird *et al.*, 1988). Place cells in 96-well plates (2×10^4/well) in 100 µl growth medium and incubate under normal growth conditions. Add 1 µCi [^{3}H]thymidine to each well at the appropriate time and incubate for 1 h at 37°C. Wash each cell fraction twice with Hanks' balanced salt solution, drain fluid, lyse in 100 µl TES, load 100 µl of lysate onto a 2.4-cm filter paper circle (Whatman 540, Cat. No. 1540-324) labeled with a No. 2 pencil, and allow to air dry. Precipitate samples with excess solutions of 200 ml for up to 50 filters for 20 min (do not exceed this time or the filters may be damaged): 20% TCA, 10% TCA, absolute ethanol, ether, absolute ethanol. Then, air dry and determine the radioactivity in each sample by liquid scintillation counting in a 5-ml ScintiSafe Econ 1 scintillation fluor (Fisher, Cat. No. SX20-5) as described previously (Wu *et al.*, 1993; Bird *et al.*, 1988).

IV. COMMENTS

A. Theoretical Basis of Separation

Cells are separated in the centrifugal elutriator by a process that was originally called counterstream centrifugation. This process is based on the opposition of two forces: media flow and angular acceleration due to an applied centripetal force. All of the cells in the suspension to be separated by centrifugal elutriation are pumped under gentle pressure into the separation chamber, entering at the extreme outside end of the chamber where the radius of rotation is maximal (r_{max}) to begin accumulating in the chamber (Fig. 1). As the cells fill the chamber, they change direction (as the

loading tube turns) from flowing out to the perimeter of the rotor to flowing toward the center of the rotor. As they do, the particles enter a chamber that is designed with a conical profile. As the particles enter the chamber, the cross-sectional area increases rapidly, dramatically decreasing inward movement of the cells under a constant flow rate. Thus, the cells begin to decelerate as the cross-sectional area of the chamber increases. At some point, determined by cell size, media flow rate and viscosity, and centripetal force, the cells cease to move inward and become suspended in the chamber at a position where cell movement inward due to flow rate is balanced by apparent centrifugal force outward. At this point, medium is flowing by the cells but inward movement of the cells is offset by the apparent outward centrifugal force applied due to the angular momentum of the rotor. The population of cells has thus reached equilibrium and their position remains unchanged, although the cells tend to sort themselves under this combination of opposing forces with the smallest particles sorting closest to the center of the rotor.

There are now two choices for the operator with respect to fractionation of the cells: rotor speed can be decreased incrementally or the flow rate can be increased incrementally. In practice, the latter choice is the more practical due to the ease and precision with which the pump can be adjusted compared to the centrifuge. In either case, adjustments are made such that the equilibrium position of the smallest population of cells can move inward into the chamber until it reaches the constriction in the chamber where flow rate accelerates due to a rapid decrease in cross-sectional area. Thus, by adjusting the flow rate up in small increments (size of the increments must be determined empirically), cells can be fractionally separated from the population.

The actual elutriation characteristics depend on the shape and size of the cells in the population. For trypsinized cells, whose specific gravity is not much greater than the buffer in which they are suspended, shape generally approaches spherical unless cell processes or applied forces alter this. Thus, separation is usually the product of apparent cell diameter. Centrifugal elutriation has been shown to be unusually subtle in its ability to discriminate subfractions based on very small differences in cell size. For example, in separation of cells in different phases of the cell cycle, cells approximately double in volume as they pass through the cell cycle from G_1 phase to mitosis (Mitchison, 1971). This translates into an increase of only about 26% in the radius of an average premitotic cell compared to an average freshly divided G_1 phase cell. This relationship can be demonstrated by the following equations where V is cell volume and r is cell radius, assuming a spherical shape. The G_1 phase cell is represented by a volume of V_{G1} and an apparent radius of r_{G1}, the premitotic cell is represented by a volume of V_M and an apparent radius of r_M, and the assumption is made that cell volume exactly doubles on average during the intervening period.

Thus

$$4/3\ \pi\ (r_{G1})^3 = V_{G1}$$

1 (volume of a spherical G_1 phase cell) (1)

$$4/3\ \pi\ (r_{G1})^3 = V_M$$

2 (volume of a spherical premitotic cell) (2)

$$2\ V_{G1} = V_M$$

3 (volume doubles during the cell cycle) (3)

Substituting Eqs. (1) and (2) into Eq. (3) for each volume and then simplifying,

$$2[4/3\ \pi\ (r_{G1})^3] = [4/3\ \pi\ (r_M)^3]$$

$$2\ (r_{G1})^3 = (r_M)^3$$

Taking the cube root of each side,

$$1.26\ r_{G1} = r_M$$

Thus, the radius of the largest cell in the cell cycle, on average, has an apparent radius (and diameter) only 26% larger than the smallest cell on average. We have successfully separated cells in this narrow continuum of cell sizes into seven distinct fractions with little overlap. This demonstrates that the subtle differences in cell size that occur as cells proceed through the cell cycle can be detected and efficiently separated using this technique. Successful separation was based on only about a 3–5% difference in radius (or diameter) between succeeding fractions that could be discriminated clearly by centrifugal elutriation.

The theoretical basis on which centrifugal elutriation is capable of separating cells, by balancing changes in medium flow balanced against angular momentum, has revealed that sequential fractions were frequently differentiated by as little as a 3% difference in cell diameter. In most cases, apart from the expense of purchase of the elutriation centrifuge, the only compromise consists of a somewhat lower level of purity in some samples, although purities approaching 100% have been reported. To balance this drawback, great improvements in yield, speed, and gentleness of handling of the cells have been achieved. Due to these obvious benefits, centrifugal elutriation has been applied to a wide variety of cells and cell types to successfully affect separation based on cell size.

The theoretical considerations described earlier have been applied to allow separation of a great

variety of cell types and separation of cultured cells based on cell cycle phase (reviewed extensively in Conkie, 1985; Beckman Instruments, 1990). Using this protocol, it is possible to separate approximately 1×10^8 to 1×10^9 cells into up to eight sequential cell cycle phase fractions in about 40–60 min (sequential fractions designated: $G_{1.1}$, $G_{1.2}$, $G_{1.3}$, $S_{0.1}$, $S_{0.2}$, $G_2/M_{0.1}$, $G_2/M_{0.2}$, see Figs. 3 and 4). Later cell cycle fractions contained increasing numbers of contaminating cells from the phase preceding it. The first fractions were of the highest purity (approximately 97%, see Fig. 3) while the purity of the fractions dropped (to approximately 90%) in samples representing later times during the cell cycle. In G_2/M fractions, significant numbers of cells synthesizing DNA are recovered, although this activity declines rapidly once the cells are placed back in culture (Fig. 4). Only centrifugal elutriation can produce so many fractions of relatively high purity and of such large size so quickly with little detectable lag in cell growth and without drug/inhibitor-induced artifacts.

V. PITFALLS

1. In the time since we acquired our centrifugal elutriator, Beckman Instruments has released newer models designed to separate, among other qualities, larger numbers of cells. While the principles governing separation remain the same, details of procedures necessary in setting up the rotor and the seals may differ, depending on the model, and thus the manufacturer's directions should be adhered to carefully to ensure correct assembly and operation.

2. It is critical that separations be attempted only with single cell populations. Steps should be taken to ensure complete dissociation of cells liberated from tissues or culture vessels. When in doubt, dispersion of samples should be monitored microscopically.

3. Only Beckman neutral pH rotor detergent should be used to clean the rotor and separation chamber. It is particularly important to ensure that the sample tube at the outer edge of the separation chamber is soaked in detergent overnight to remove any cell debris that has accumulated as this will affect flow rate greatly as well as the fluid dynamics of sample loading in the chamber. This aperture is too small to be cleaned with a tool, and no instrument should be applied that could scratch the interior surface of the chamber. The operator must be extremely careful with the separation chamber, as overtightening of the screws or scratches to the surface will damage the chamber, affecting performance significantly.

4. If alterations to the growth medium or elutriation medium are contemplated, the new medium must be tested to empirically determine at what flow rate cell cycle fractions elute. Even very small changes in media formulation (e.g., as little as 0.5% change in DHS concentration) will change the fluid dynamics of the elutriation system dramatically. Changes in cell-loading density and temperature can also create detectable effects on elutriation profiles. A simple pilot experiment is usually sufficient to determine what effects such alterations have on elution flow rate if it is followed by flow cytometric analysis.

5. All O rings and gaskets should be inspected before each run to ensure that they are in good condition. All worn seals should be replaced.

6. Failure to secure the wires and tubing connecting the rotor and strobe light to the exterior of the centrifuge will result in them becoming wrapped around the rotor, resulting in serious damage to the equipment.

7. We have replaced the Oakridge-style sample application tube supplied by the manufacturer with a straight glass test tube (13×100 mm) with the same size aperture at the top as the tube supplied. This eliminates the shoulder at the top of the Oakridge tube, which can trap cells, resulting in a continuous residual loading of cells throughout the elutriation procedure. The tube should be siliconized to within approximately 2 cm from the top with Gel Slick (FMC BioProducts). Gel Slick should not be allowed to contact the glass surface above this point as the stopper will no longer hold securely under pressure.

8. Rotor speed should be monitored frequently during the run as fluctuations of only a small amount can affect purity of the samples greatly. It is particularly important to check rotor speed each time that the refrigeration system in the centrifuge cycles on.

9. If sterilization of the assembly is required, be sure that the centrifuge is *turned off* while the ethanol is in the system. Failure to observe this safety measure could result in a fire hazard. Alternatively, the system can be sterilized with 6% hydrogen peroxide while the centrifuge is running (Conkie, 1985).

Acknowledgments

The author thanks Dr. Gin Wu, Dr. Suresh Pai, and Dr. Shiawhwa Su for consultation on this protocol and Patricia DeInnocentes and Randy Young-White for valuable technical support. The author also thanks Dr. Lauren G. Wolfe for critical reading of the manuscript.

References

Beckman Instruments (1990). Centrifugal Elutriation of Living Cells: An Annotated Bibliography. In Applications Data, Number DS-534, pp. 1–41, Beckman Instruments Inc., Palo Alto, CA.

Bialkowski, K., and Kasprzak, K. S. (2000). Activity of the anti-mutagenic enzyme 8-oxo-2′-deoxyguanosine 5′-triphosphate pyrophosphohydrolase (8-oxo-dGTPase) in cultured chinese hamster ovary cells: Effects of cell cycle, proliferation rate, and population density. *Free Radic. Biol. Med.* **28**, 337–344.

Bird, R. C. (1996a). Cell separation by centrifugal elutriation. *In "Cell Biology: A Laboratory Handbook"* (J. E. Celis, ed.), 2nd Ed., pp. 205–208. Academic Press, New York.

Bird, R. C. (1996b). Synchronous populations of cells in specific phases of the cell cycle prepared by centrifugal elutriation. *In "Cell Biology: A Laboratory Handbook"* (J. E. Celis, ed.), 2nd Ed., pp. 209–217. Academic Press, New York.

Bird, R. C., Bartol, F. F., Daron, H., Stringfellow, D. A., and Ridell, G. M. (1988). Mitogenic activity in ovine uterine fluids: Characterization of a growth factor which specifically stimulates myoblast proliferation. *Biochem. Biophys. Res. Commun.* **156**, 108–115.

Bludau, M., Kopun, M., and Werner, D. (1986). Cell cycle-dependent expression of nuclear matrix proteins of Ehrlich ascites cells studied by *in vitro* translation. *Exp. Cell Res.* **165**, 269–282.

Boerma, M., van der Wees, C. G., Wondergem, J., van der Laarse, A., Persoon, M., van Zeeland, A. A., and Mullenders, L. H. (2002). Separation of neonatal rat ventricular myocytes and non-myocytes by centrifugal elutriation. *Pflug. Arch.* **444**, 452–456.

Braunstein, J. D., Schulze, D., DelGiudice, T., Furst, A., and Schildkraut, C. L. (1982). The temporal order of replication of murine immunoglobulin heavy chain constant region sequences corresponds to their linear order in the genome. *Nucleic. Acids Res.* **10**, 6887–6902.

Brown, E. H., and Schildkraut, C. L. (1979). Perturbation of growth and differentiation of Friend murine erythroleukemia cells by 5-bromodeoxyuridine incorporation in early S phase. *J. Cell. Physiol.* **99**, 261–277.

Conkie, D. (1985). Separation of viable cells by centrifugal elutriation. *In "Animal Cell Culture: A Practical Approach"* (R. I. Freshney, ed.), pp. 113–124. IRL Press, Oxford.

Dagher, R., Long, L. M., Read, E. J., Leitman, S. F., Carter, C. S., Tsokos, M., Goletz, T. J., Avila, N., Berzofsky, J. A., Helman, L. J., and Mackall, C. L. (2002). Pilot trial of tumor-specific peptide vaccination and continuous infusion interleukin-2 in patients with recurrent Ewing sarcoma and alveolar rhabdomyosarcoma: An inter-institute NIH study. *Med. Pediatr. Oncol.* **38**, 158–164.

Datta, N. S., and Long, M. W. (2002). Modulation of MDM2/p53 and cyclin-activating kinase during the megakaryocyte differentiation of human erythroleukemia cells. *Exp. Hematol.* **2**, 158–165.

Davis, P. K., Ho, A., and Dowdy, S. F. (2001). Biological methods for cell-cycle synchronization of mammalian cells. *Biotechniques* **30**, 1322–1331.

Deacon, E. M., Pettitt, T. R., Webb, P., Cross, T., Chahal, H., Wakelam, M. J., and Lord, J. M. (2002). Generation of diacylglycerol molecular species through the cell cycle: A role for 1-stearoyl, 2-arachidonyl glycerol in the activation of nuclear protein kinase C-betaII at G2/M. *J. Cell Sci.* **115**, 983–989.

Diamond, R. A. (1991) Separation and enrichment of cell populations by centrifugal elutriation. *Methods* **2**, 173–182.

Hann, S. R., Thompson, C. B., and Eisenman, R. N. (1985) c-*myc* oncogene protein synthesis is independent of the cell cycle in human and avian cells. *Nature* **314**, 366–369.

Hengstschlager, M., Holzl, G., and Hengstschlager-Ottnad, E. (1999). Different regulation of c-Myc- and E2F-1-induced apoptosis during the ongoing cell cycle. *Oncogene* **18**, 843–848.

Houser, S., Koshlatyi, S., Lu, T., Gopen, T., and Bargonetti, J. (2001). Camptothecin and zeocin can increase p53 levels during all cell cycle stages. *Biochem. Biophys. Res. Commun.* **289**, 998–1009.

Iqbal, M. A., Plumb, M., Stein, J., Stein, G., and Schildkraut, C. L. (1984). Coordinate replication of members of the multigene family of core and H1 human histone genes. *Proc. Natl. Acad. Sci. USA* **81**, 7723–7727.

Karas, M., Zaks, T. Z., Liu, J. L., and LeRoith, D. (1999). T cell receptor-induced activation and apoptosis in cycling human T cells occur throughout the cell cycle. *Mol. Biol. Cell* **10**, 4441–4450.

Lindahl, P. E. (1948). Principle of counterstreaming centrifuge for the separation of particles of different sizes. *Nature* **161**, 648–649.

Lindahl, P. E. (1986). On counterstreaming centrifugation in the separation of cells and cell fragments. *Biochim. Biophys. Acta* **21**, 411–415.

Lindahl, P. E., and Nyberg, E. (1955). Counterstreaming centrifuge for the separation of cells and cell fragments. *IVA* **26**, 309–318.

Lindberg, C. A. (1932). A method for washing corpuscles in suspension. *Science* **75**, 415–416.

Merrill, G. F. (1998). Cell synchronization. *Methods Cell Biol.* **57**, 229–249.

Mitchison, J. M. (1971). *"The Biology of the Cell Cycle."* Cambridge Univ. Press, Cambridge.

Pai, S. R., and Bird, R. C. (1992). Growth of HeLa S3 cells cotransfected with plasmids containing a c-fos gene under the control of the SV40 promoter complex, pRSVcat, and G418 resistance. *Biochem. Cell Biol.* **70**, 316–323.

Pai, S. R., and Bird, R. C. (1994). Overexpression of c-*fos* induces expression of the retinoblastoma tumor suppressor gene in transfected cells. *Anticancer Res.* **14**, 2501–2508.

Rehak, M., Csuka, I., Szepessy, E., and Banfalvi. G. (2000). Subphases of DNA replication in Drosophila cells. *DNA Cell Biol.* **19**, 607–612.

Sambrook, J., Fritsch, E. F., and Maniatis, T. (1989). *"Molecular Cloning: A Laboratory Manual"* (J. Sambrook, E. F. Fritsch, and T. Maniatis, eds.), 2nd Ed., p B.17. Cold Spring Harbor Laboratory Press, Cold Spring Harbor, NY.

Sugikawa, E., Hosoi, T., Yazaki, N., Gamanuma, M., Nakanishi, N., and Ohashi, M. (1999). Mutant p53 mediated induction of cell cycle arrest and apoptosis at G1 phase by 9-hydroxyellipticine. *Anticancer Res.* **19**, 3099–3108.

Syljuasen, R. G., and McBride, W. H. (1999). Radiation-induced apoptosis and cell cycle progression in Jurkat T cells. *Radiat. Res.* **152**, 328–331.

Van Leeuwen-Stok, E. A., Jonkhoff, A. R., Visser-Platier, A. W., Drager, L. M., Teule, G. J., Huijgens, P. C., and Schuurhuis, G. J. (1998). Cell cycle dependency of 67gallium uptake and cytotoxicity in human cell lines of hematological malignancies. *Leuk. Lymphoma* **31**, 533–544.

Wong, E. C., Lee, S. M., Hines, K., Lee, J., Carter, C. S., Kopp, W., Bender, J., and Read, E. J. (2002). Development of a closed-system process for clinical-scale generation of DCs: Evaluation of two monocyte-enrichment methods and two culture containers. *Cytotherapy* **4**, 65–76.

Wong, E. C., Maher, V. E., Hines, K., Lee, J., Carter, C. S., Goletz, T., Kopp, W., Mackall, C. L., Berzofsky, J., and Read, E. J. (2001). Development of a clinical-scale method for generation of dendritic cells from PBMC for use in cancer immunotherapy. *Cytotherapy* **3**, 19–29.

Wu, G., Su, S., Kung, T.-Y. T., and Bird, R.C. (1993). Molecular cloning of G_1-phase mRNAs from a subtractive G_1-phase cDNA library. *Biochem. Cell Biol.* **71**, 372–380.

CHAPTER

32

Polychromatic Flow Cytometry[1]

Stephen P. Perfetto, Stephen C. De Rosa, and Mario Roederer

I. INTRODUCTION

The flow cytometer has proven to be one of the most powerful scientific techniques for the analysis of immunobiology in the past 35 years. Recent advances allowing the detection of 14 distinct cell parameters on each cell have revealed the immense heterogeneity of the immune system; e.g., the identification of more than 100 functionally distinct cell phenotypes in the peripheral blood of humans. In addition, the evolution in computer technology brings to bear the ability to analyze very large sample sets using sophisticated algorithms, increasing the power of analysis of low-frequency cell populations.

Current state-of-the-art cytometric evaluation allows for distinct cell population delineation using two physical parameters—side scattered light (SSC) and forward scattered light (FS)—and 12 separate fluorescent parameters. Each fluorescence parameter can be used to independently measure the expression of a protein or function; combined, these measurements may predict disease progression, vaccine responses, or other immunological parameters.

Still, the use of high-end multicolor flow cytometry is in its infancy; many challenges must still be overcome before this technology will become routinely available in research laboratories. The most difficult obstacle at this time is reagent availability; many laboratories are forced to conjugate fluorochromes not yet available commercially. Many dyes are now available that can be conjugated easily to antibodies for use in polychromatic flow cytometry (PFC) to supplement the commercially available conjugates. With regard to instrument development, by far the most important requirement is automation. Instrument setup and calibration are still far more complex with the use of multiple lasers and detectors for PFC; computer-aided validation of instrument performance is necessary. In addition, automated compensation (fluorescence spillover) is necessary; however, this is adequately handled by most contemporary software packages.

Data analysis is by far the most time-consuming aspect of PFC experiments. The complexity of data is such that, with current software tools, analysis of individual samples requires inordinate amounts of time. There is a considerable demand for tools that can organize the analyses into databases, as well as assist in the exploration of the complex data sets. To help researchers analyze such data, automated multivariate techniques have been developed by this laboratory. These algorithms are designed to compare multidimensional distributions to identify and quantify the degree of difference between data sets (De Rosa *et al.*, 2001; Roederer and Hardy, 2001). In addition, these algorithms can rapidly identify regions of multivariate distributions that differ, thereby providing a mechanism for identifying those cells that are different between two samples. Tools such as these help researchers explore the complex data sets and identify interesting aspects that no combination of two-dimensional graphs could have revealed. The probability binning (PB) algorithm can be used to quantify the degree of similarity or disparity of highly complex distributions for the purposes of ranking these distributions (Roederer *et al.*, 2001a,b). This may be useful for quantifying the number of cells that respond to a particular stimulus (perhaps having responded in complex multivariate patterns) or for identifying variations in immunophenotyping patterns that correlate

[1] The National Institutes of Health does not endorse or recommend any commercial products, processes, or services. The views and opinions of authors expressed in this manuscript do not necessarily state or reflect those of the U.S. Government and may not be used for advertising or product endorsement purposes. The U.S. Government does not warrant or assume any legal liability or responsibility for the accuracy, completeness, or usefulness of any information, apparatus, product, or process disclosed.

Copyright 2006, Elsevier Science (USA).
All rights reserved.

with pathogenic states (Baggerly, 2001). These strategies allow for the most useful and comprehensive display of complex data in the field of flow cytometry today.

This article presents some of the latest techniques used in our implementation of our 12-color flow cytometric technology. It discusses the reagents, calibration and setup, and analysis of the resulting data, including some of the hurdles and pitfalls encountered. This guide will aid research laboratories wishing to implement flow cytometric technology capable of more than 5 or 6 colors.

II. MATERIALS AND INSTRUMENTATION

A. Monoclonal Antibodies

Purified monoclonal antibodies are available from manufacturers as bulk concentrated protein in the absence of any exogenous protein. All conjugations are performed as detailed (http://www.drmr.com/abcon/). Large quantities of reactive fluorochromes are prepared and stored (and are stable for many months at 4C); the conjugation to antibodies is a fairly rapid procedure that can then be accomplished in 2–3 h.

Figure 1 shows the common fluorochromes currently used in our laboratory, which can all be directly conjugated to monoclonal antibodies. Also shown are the excitation and emission spectra and suggested bandpass filters for each fluorochrome. Ideally, each fluorochrome should be conjugated to a wide variety of monoclonal specificities in order to provide a wide range of possible panels; of course, this requires a fairly substantial investment of both fluorochromes and monoclonal antibodies. New fluorochromes are becoming available that are more photo stable and easier to conjugate, such as the Alexa family of fluorochomes (i.e., Alexa, 488, 532, 660, 633, 647, and 680). Commercial manufacturers currently offer only a limited range of fluorochromes conjugated to specific

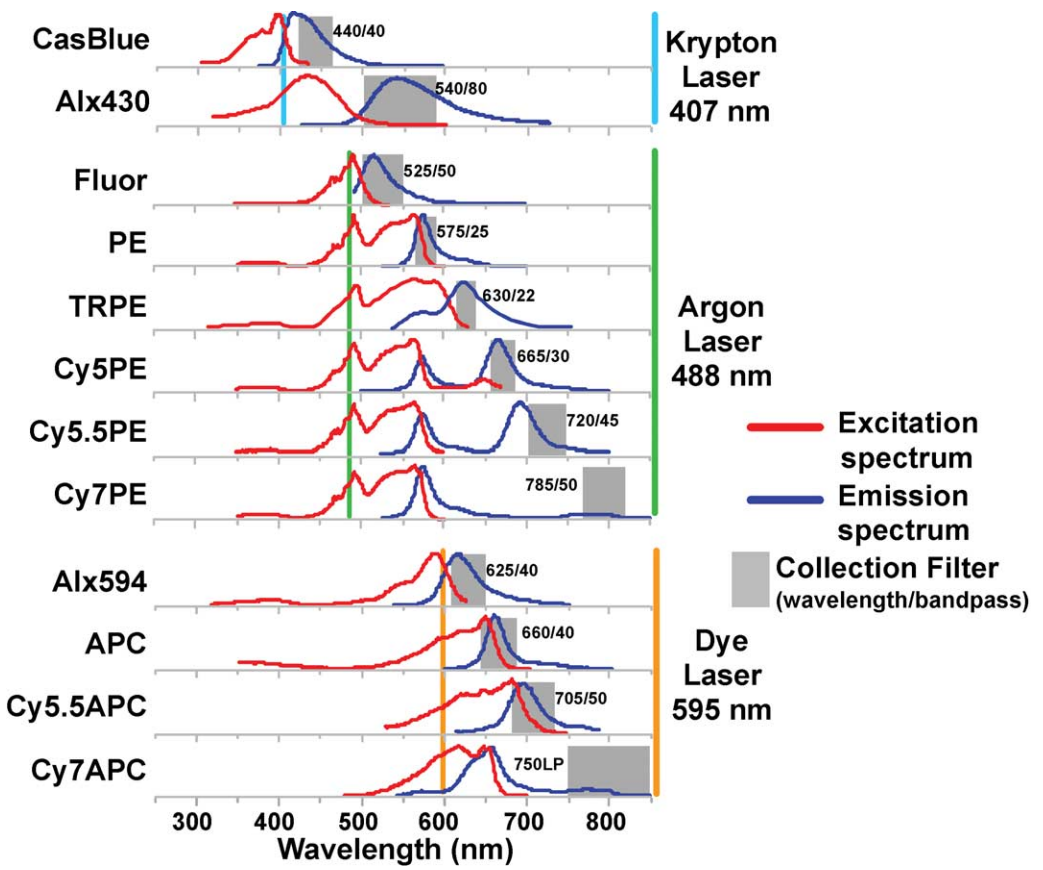

FIGURE 1 Conjugate spectrum chart of excitation and emission curves for common fluorochomes used in PFC. Laser lines show which conjugates are excited by the individual laser lines and the selected bandpass filters used to measure the specific emission.

monoclonal antibodies. Table I shows that only 7 of the 12 fluorochromes used in our laboratory are available commercially; this range is currently increasing but is still a limiting factor. In addition, newer conjugates have far more limited reagent combinations available until manufacturers can build up a significant inventory. Hence, it is likely that researchers who wish to perform more than 6-color flow cytometry will likely need to invest in the ability to manufacture reagents in-house. In general, this is incorporated most efficiently into a core facility that can supply reagents to multiple research laboratories.

B. Qualification of Fluorescently Conjugated Monoclonal Antibodies (mAbs)

Regardless of the conjugate used (i.e., commercial or in-house), all mAbs require titration against a target cell population to determine the optimal concentration for staining. Note that staining conditions (temperature, time, and volume) impact the titration; thus, qualification should be performed under the same conditions as experimental staining. By plotting the median of the positive cell population against the serial dilution of the mAb as illustrated in Fig. 2, the lowest concentration at which the maximum separation can be discerned; in general, this is the optimal concentration to use (in this example, 10μg/ml). Lower concentrations of mAb result in loss of resolution (note, however, that for some mAbs the separation is still highly adequate at very low concentrations, allowing the use of the reagent at a more economical rate). It cannot be overemphasized that proper titration and selection of mAb concentration are paramount for successful multicolor analysis. Adding too much antibody conjugate can have as much effect on sample analysis as the addition of too little antibody conjugate. In this situation, backgrounds increase due to nonspecific binding of the antibody conjugate, thus reducing the signal-to-background ratio dramatically.

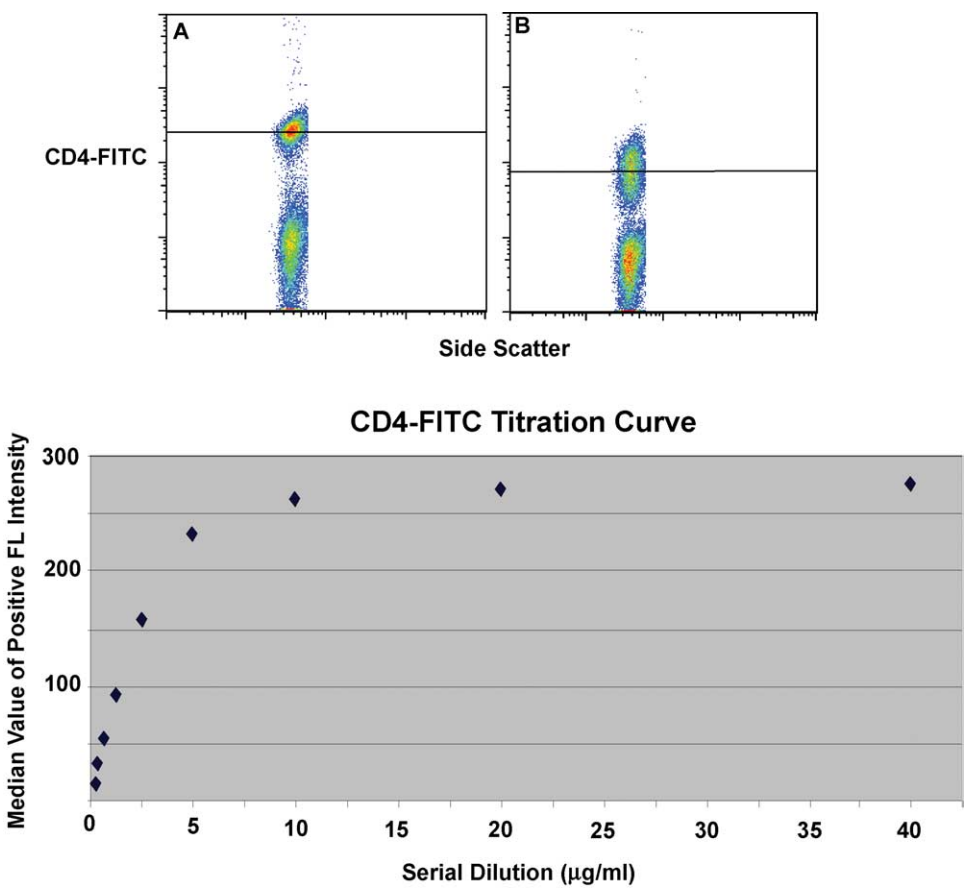

FIGURE 2 Serial dilution of anti-CD4-FITC-labeled PBMCs and the median value of the positive signal (black line). (A) The point on the titration curve (10μg/ml) yielding the greatest separation (highest median value with the lower auto fluorescence) as compared to poor separation (B) at a lower titer (<2μg/ml).

TABLE I Current Breadth of Availability of Antibody Conjugates[a]

Fluorochrome	VRC	Caltag	Coulter	BDIS
FITC	>100	>100	>100	>100
PE	>100	>100	>100	>100
TRPE	26	5	20	1
Cy5PE	96	38	30	76
Cy55PE	43	—	—	—
Cy7PE	54	6	15	18
Ax594	66	—	—	—
APC	>100	28	15	137
Cy55APC	46	—	—	—
Cy7APC	44	7	—	14
CasBlue	58	—	—	—
Ax430	12	—	—	—

[a] The approximate number of distinct specificities available from three major manufacturers compared to what we have conjugated in our laboratory ("VRC") is shown. A wide range of conjugates is necessary to have the greatest flexibility in creating multicolor antibody staining panels.

C. Instrumentation

Samples are acquired on a modified FACSDiVa flow cytometer (BDIS, San Jose, CA), which measures 12 fluorescent parameters and 2 physical parameters (FS and SSC). Figure 3 illustrates the optical configuration and filter selection of this instrument. The geometry of this instrument is based on the traditional collection optics and is far more complex than more recent instrumentation using optical fibers such as the LSR II (BDIS). In these instruments, photons of light from the laser-excited conjugates are transmitted through optical fibers and measured in unique optical arrays. Figure 4 shows an example of an argon laser array containing eight detectors called an Octagon. The advantage of these systems includes increased efficiency of photon transfer, thus lower-energy lasers can be used with good signal reproducibility as compared to higher-end systems equipped with powerful lasers. Figure 5 shows the laser configuration of older traditional high-end systems as compared to newer instruments using low-powered diode lasers (5–10 mW). Clearly another advantage of lower-power lasers and optical fibers is the smaller footprint, yielding a more compact system with the measurement capability of a high-end research instrument.

D. Alignment and Calibration Beads

Alignment beads containing a single peak bead (single peak Rainbow beads) are from Spherotech Inc. (Rainbow beads, Cat. No. RFP-30-5A). Calibration beads containing eight separate peaks (eight peak Rainbow beads) are from Spherotech Inc. (Rainbow beads, Cat. No. RFP-30-5A) and Blank Beads are from Becton Dickinson Immunocytometry Systems (Cat. No. RFP-30-5A). All beads are diluted by the addition of one drop (approximately 20 µl) per milliliter of phosphate-buffered saline (PBS) containing 1% HIFCS (Quality Biological—PAA labs, Cat. No. 110-001-101) and 1 mg/ml of sodium azide (Sigma Chemical, Cat. No. S202).

E. Monoclonal Antibody Selection and Combinations

A laboratory Web-based database containing all of the antibody conjugate reagents is used to select the antibody conjugate combinations. This database lists the correct mAb concentration (determined from a titration curve; see the titration procedure in Section III) and displays the concentration, specificity, lot number, and location on a laboratory worksheet. Such databases become necessary—laboratories doing 6–12 color flow cytometry will inevitably have a very large storehouse of reagents; it is necessary to have a centralized repository of the qualification and validation data for each reagent in an easily accessible location. Researchers planning experiments need access to this information in order to know how much of each reagent to use, as well as some idea of the quality of the staining that can be expected with that reagent.

F. Compensation Beads

Latex beads coated with anti-mouse κ antibody are from Becton Dickinson Immunocytometry Systems (Cat. No. 557640). After incubating with mAb conjugate, beads are fixed in a final concentration of 0.5% paraformaldehyde (PFA). These "capture" beads are used with each antibody conjugate tested to set up the compensation matrix.

III. PROCEDURES

A. Alignment and Instrument Calibration

All flow cytometers, regardless of engineered advances in alignment techniques, require alignment and calibration quality control to determine reproducibility and sensitivity. For this purpose, alignment beads and calibration standards must be stable and reproducible from day to day. It is important to point out that such quality control measurements are not a substitute for proper cell controls as outlined in this

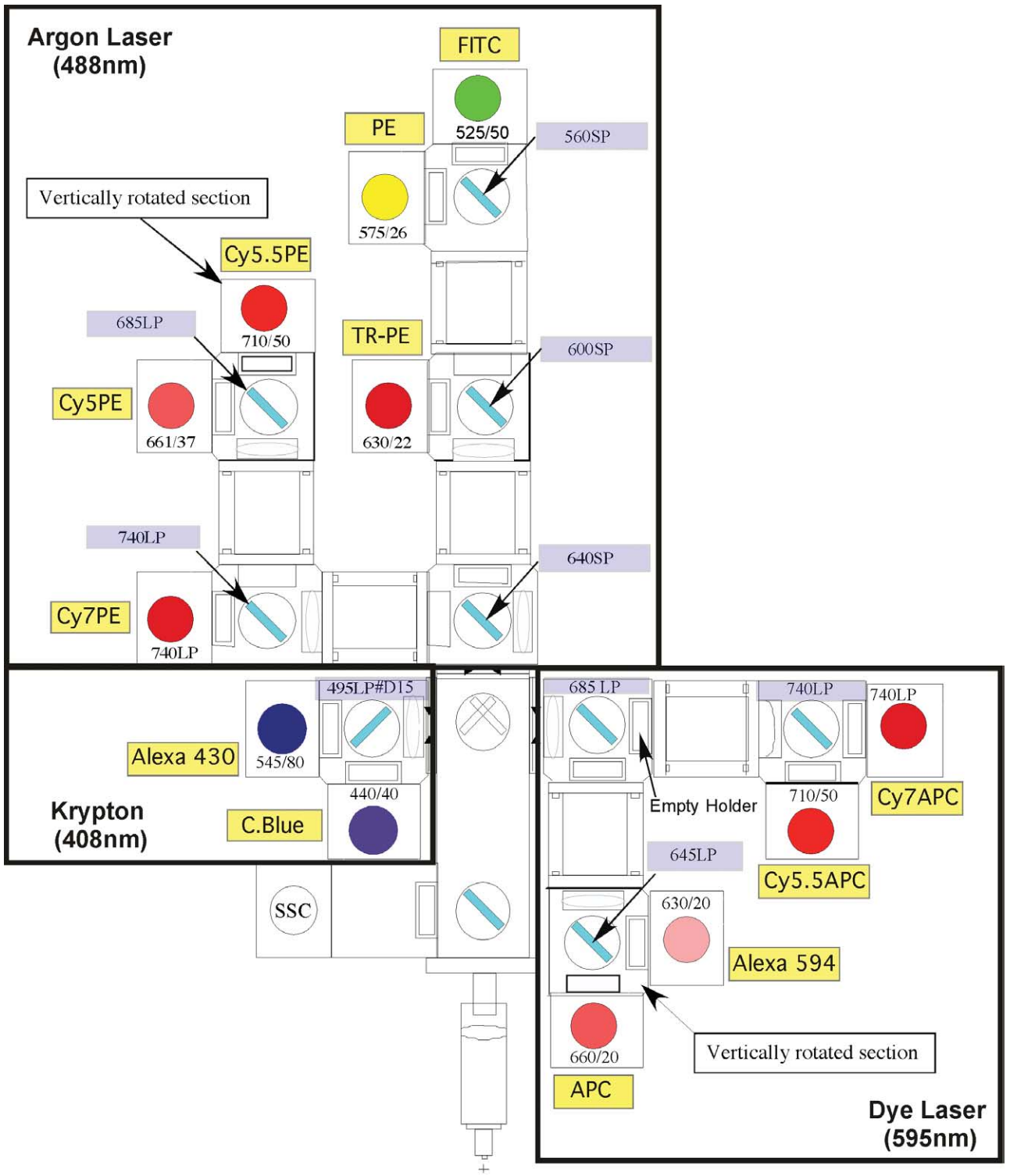

FIGURE 3 Digital Vantage optical configuration used to detect 12 colors using three lasers: 488-nm argon, 408-nm krypton, and 595-nm dye lasers. Each section of detectors is outlined (black boxes) to indicate the laser associated with the emission. Also illustrated are the dichroic mirrors and bandpass filter combinations for each PMT.

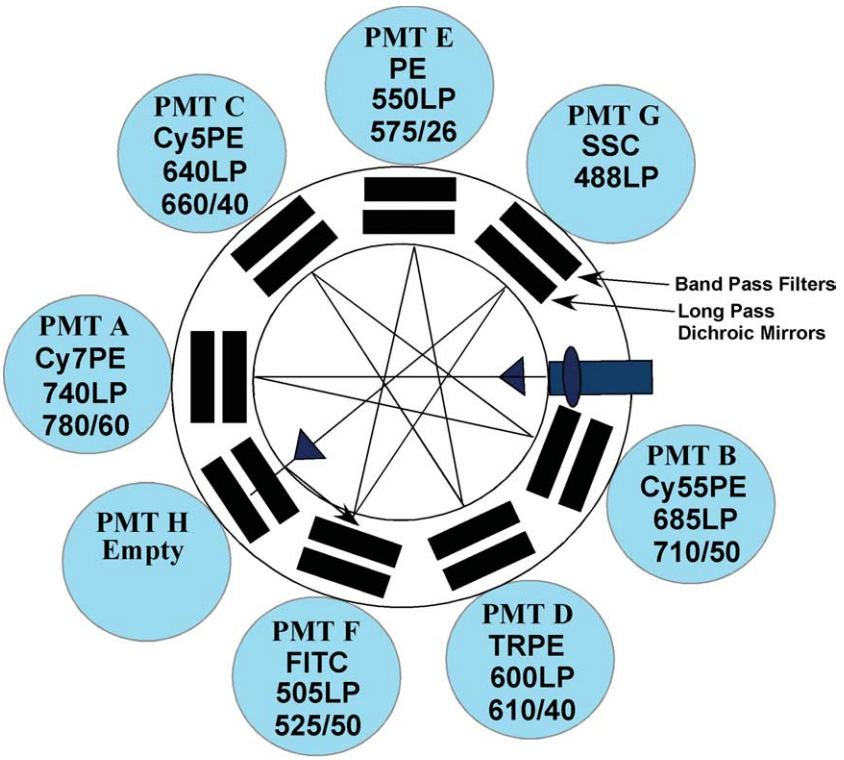

FIGURE 4 LSR II optical configuration of detectors for only the 488-nm diode laser. This configuration shows the light path with the typical dichroic mirrors and bandpass filters used to detect six different conjugates excited by this laser plus side scattered light.

article to assure testing quality. Alignment beads are used to determine good instrument performance and, if successful, should determine proper light collection in all detectors as measured by fluorescence intensity and fluorescence CV at a consistent voltage. Once the instrument lasers are aligned properly, calibration beads can be used to determine the correct tolerance range of fluorescent intensity by adjusting the detector sensitivity (e.g., photomultiplier voltage). These tolerance ranges are determined by unstained cell analysis set to a predetermined value. In addition, calibration standards determine the signal-to-background ratio, which must remain consistent within at most a 5% variation.

Steps

1. Place diluted single peak Rainbow beads onto the sample insertion tube and adjust the sample pressure to approximately 600 beads per second.

2. While observing dual-parameter histograms of FS vs SSC and all other fluorescence parameter combinations, adjust instrument to achieve the narrowest CV and highest intensity possible according to the manufacturer's instructions. Figure 6 shows the incorrect (A) and the correct (B) display for two fluorescence parameters. It is important to note that while slight misalignments may have only a small impact on the measurement of any given single parameter, they can have a serious impact on the visualization of data after compensation (Roederer, 2001a,b). This is because the spread in compensated data is directly related to the efficiency of light collection; larger CVs, as illustrated in Fig. 6, result from decreased light efficiency and result in much poorer data quality after compensation.

3. Adjust the voltages for each PMT to result in predetermined intensity levels for the bead population. Such levels are defined previously as optimal for the particular types of samples that are being analyzed; this calibration procedure ensures that the instrument sensitivity is comparable across experiments, allowing for the best comparison of data. As an example, for the analysis of lymphocytes, we typically analyze completely unstained lymphocytes and adjust the PMT voltages such that the upper end of the unstained cells is at the top of the first (of four) decades of fluorescence. Then the beads are reanalyzed at those voltages

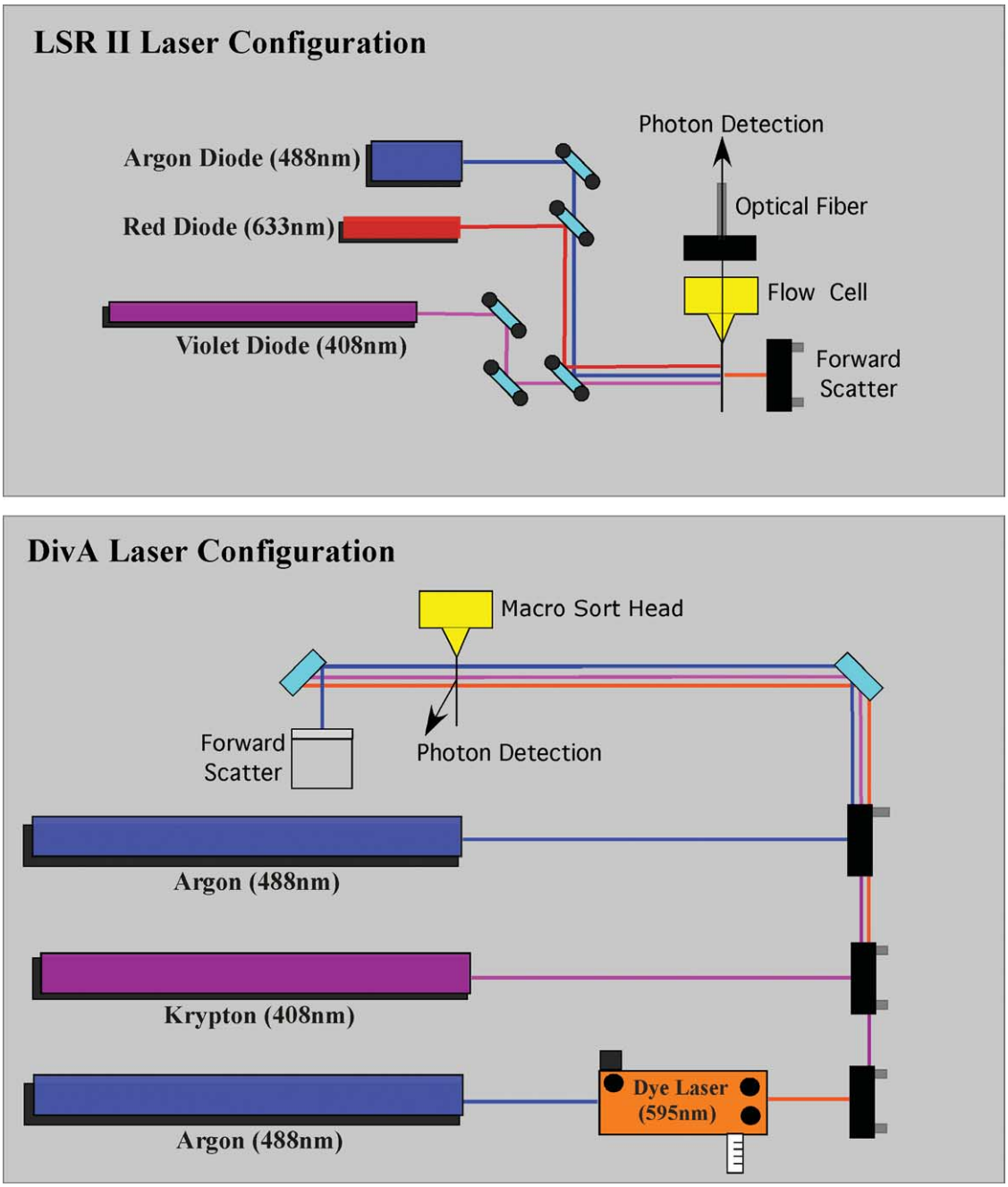

FIGURE 5 Comparison between the Digital Vantage and the LSR II laser configuration system. Due to the use of the low-powered diode laser in the LSR II system, this instrument can be very compact and inexpensive to operate.

and the intensities are recorded for future target settings. These same voltage settings are used for sample acquisition and instrument calibration.

4. Place diluted eight peak Rainbow beads onto the sample insertion tube and adjust the sample pressure to approximately 600 beads per second.

5. Collect and save all single parameter histograms for future analysis.

6. Place diluted Blank beads onto the sample insertion tube and adjust the sample pressure to approximately 600 beads per second.

7. Collect and save all single parameter histograms for future analysis.

8. From data collected on the single peak beads, chart voltage versus time. Correct tolerances for each PMT should be ±5% variance.

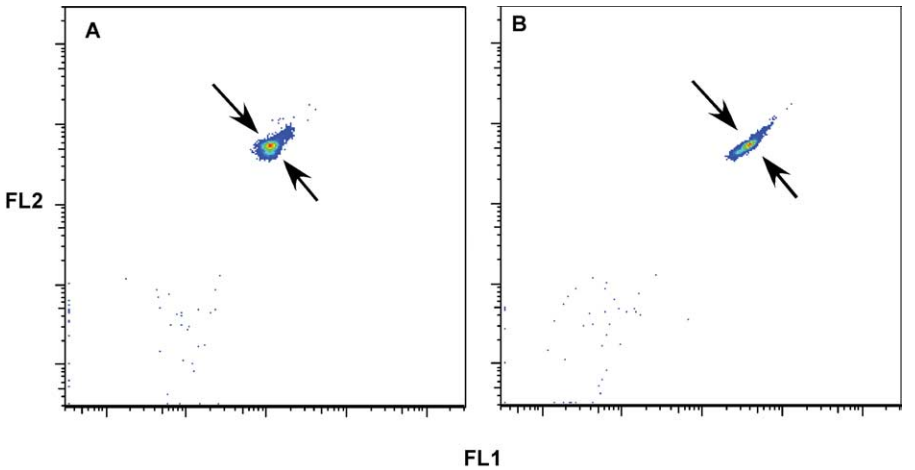

FIGURE 6 Rainbow beads with incorrect (A) and correct (B) alignment of two fluorescent parameters. Tolerance ranges for the coefficient of variance and fluorescent intensity are established for all instrument parameters. Setting quality control of all parameters within these tolerance ranges can avoid incorrect alignment and compensation error.

9. Data collected on the eight peak beads (median channel of the eight peak) divided by the median channel of the blank bead yield the signal-to-background ratio (see Fig. 7). Each PMT will have a characteristic S/B ratio; however, the correct tolerance plotted against time should produce a range of ±10%.

B. Compensation

Compensation and analysis of samples can be done either online or after data collection with appropriate software. In general, if cell samples are sorted, the user must perform compensation online; however, in most cases, sample compensation and analysis are performed off-line. Regardless of when compensation is performed, the same rules apply to correctly compensate the sample. It is important to note that each experiment must have matching compensation controls. These controls must produce signals, which are of as high or higher fluorescence intensity than the test sample. In many cases the use of compensation beads will satisfy this condition; however, if any of the experimental samples are more than severalfold brighter than the beads, then single-stained cells of the appropriate reagents must be used as compensation controls. In addition to matched compensation controls, a negative (unstained beads) must be collected. This control and individually labeled compensation tubes are used in the compensation algorithm to calculate compensation. Finally, to verify cell autofluoresence relative to the unstained bead location, an unstained cell sample control must be collected. Online compensation for the FACSDiVa is described later. Figure 8 shows an example of compensation beads labeled with anti-CD8 APC. Figure 8A shows the location of unstained beads as compared to the stained beads in Fig. 8B. As expected, the degree of spillover for the excitation of APC from the argon into the Cy5PE

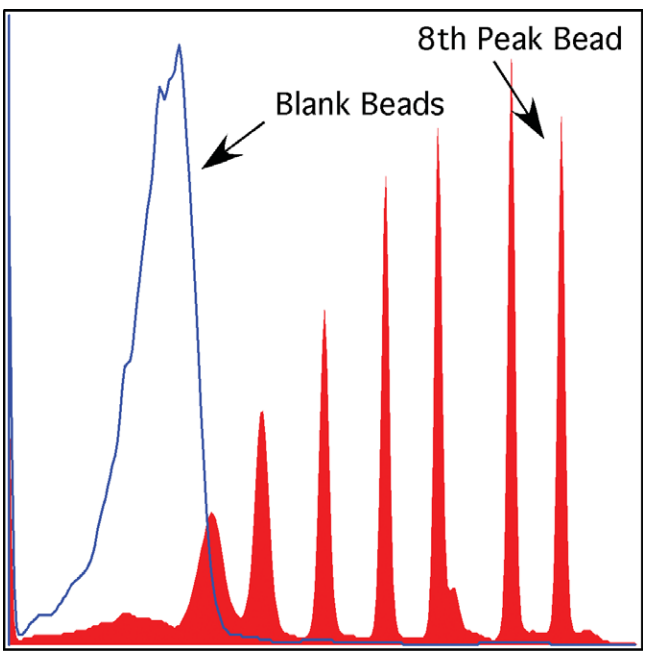

FIGURE 7 An overlay of eight peak rainbow beads with blank beads of 1 of the 12 parameters. The signal/background ratio is calculated using the median channel of the eighth peak bead and dividing by the median channel of the blank bead.

channel is negligible (Fig. 8C). However, the dye laser (595 nm) excites APC and the spillover is seen in the Cy55APC channel. This will require compensation correction of the Cy55APC channels due to the spillover of APC (Fig. 8D). As shown in Fig. 9, the degree of compensation (percentage of spillover) or light contamination can be considerable, and the complexity of this issue is only magnified by the addition of multiple parameters. A detailed explanation of compensation and controls is beyond the scope of this article; however, additional information can be found at http://www.drmr.com/compensation/index.html.

Steps

1. Into a 12 × 75 test tube add 40 µl of compensation beads (mouse anti-κ beads) and the volume of a previously tittered antibody conjugate. Dilute volume to 100 µl with PBS containing 1 mg/ml of sodium azide and 1% fetal calf serum (FCS). Note that each antibody conjugate tested will have a single stained tube for the compensation control used in the experiment. Each compensation control tube will be used to set the compensation matrix.
2. Incubate in the dark for 15 min at room temperature.
3. Wash once in PBS containing 1 mg/ml of sodium azide and 1% FCS.
4. Remove supernatant and resuspend in 250 µl of PBS containing 1 mg/ml of sodium azide and 1% FCS.
5. Vortex and add 250 µl of 0.5% PFA.
6. Acquire each compensation control tube and the unstained bead control on the flow cytometer using previously defined voltage settings.

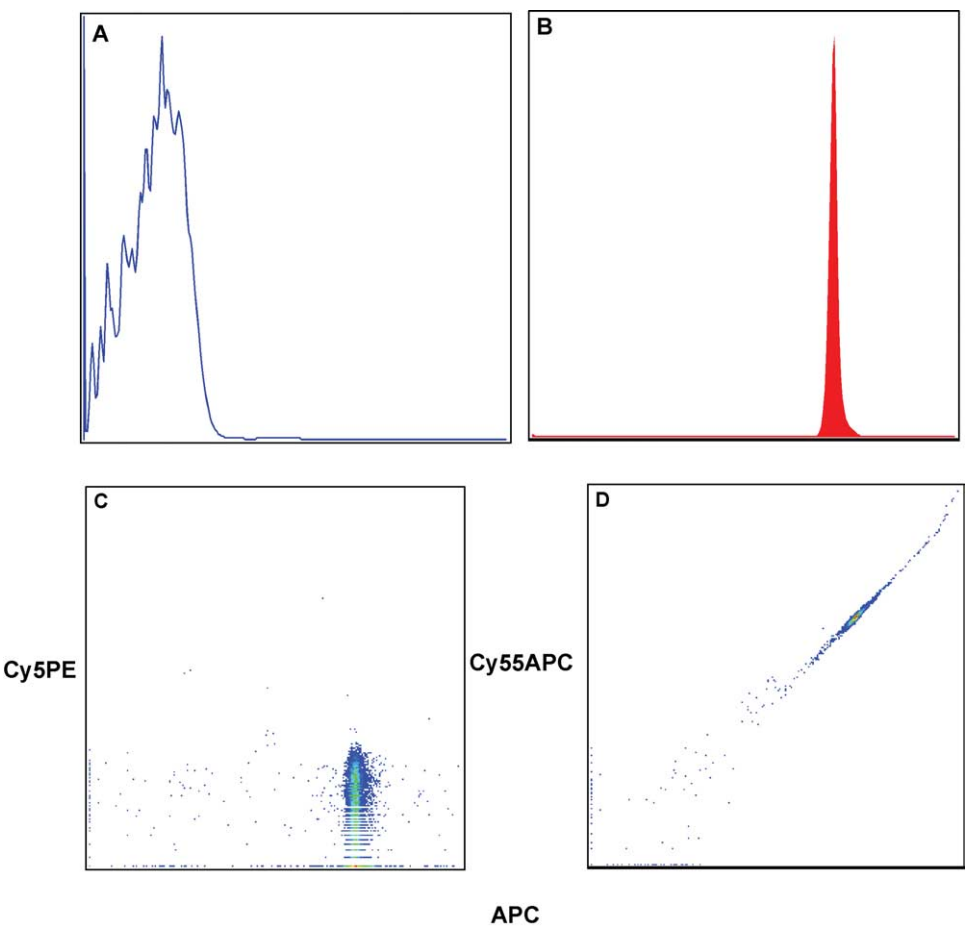

FIGURE 8 Fluorescent intensity of unstained (A) compensation beads (anti-mouse κ) and stained beads with anti-CD8 APC (B). (C and D) The effect of contaminated light from the excitation of CD8-APC. In C, no compensation is required because no contaminating light or spillover occurs into the Cy5PE channel. However, D shows that compensation correction is required because of the large spillover of contaminating light into the Cy55APC channel. After applying compensation correction, D will appear like C.

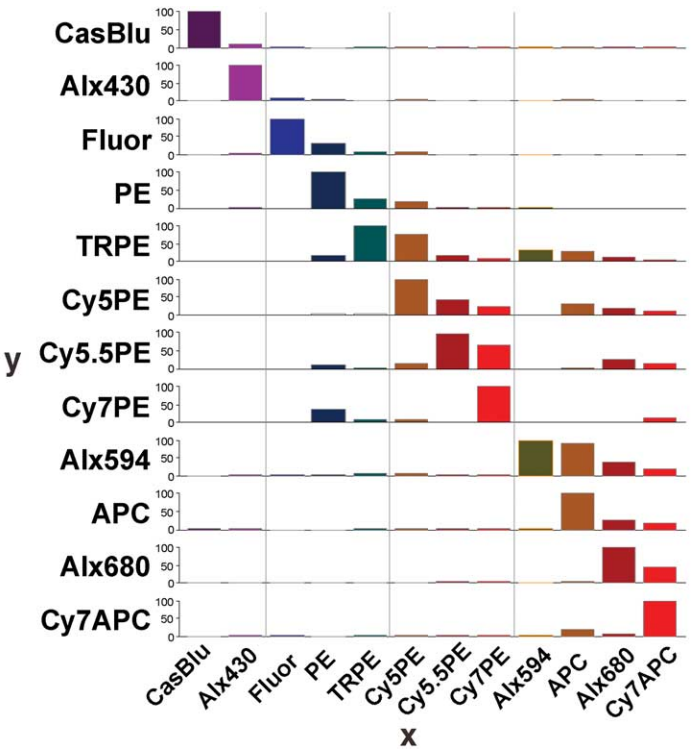

FIGURE 9 Compensation percentage of contaminated light, which must be subtracted from all of the other detectors for accurate analysis. The *x* axis shows the signal, and the *y* axis indicates the percentage of contaminated light removed from the signal. In general the largest contamination occurs within the same laser excitation group.

7. Set automated compensation matrix either on the instrument or by off-line software. Once completed, the test sample is correctly compensated and is ready for acquisition.

8. Compensation should be checked frequently by acquiring cell samples stained with combinations of antibody conjugates. After applying the compensation matrix, median values of the unstained cells should match the median values of the positive cells.

C. Sample Acquisition for Immunophenotyping

Steps and Considerations

1. Altering sample pressure and sheath velocity should be avoided. When possible, cells should be analyzed at low sheath pressure to ensure greatest sensitivity; increasing sample pressure increases the CV of the measurement, thus affecting alignment and compensation negatively. Therefore, it is recommended to maintain the lowest useful sample pressure and sheath velocity.

2. Collecting enough events for statistical analysis is key. However, the number of events needed for 12-color analysis is no different than for 2-color analysis. What is important is the size of the population of cells of interest. For example, if the subset of interest represents 0.1% of the input population, then collecting 1 million events yields 1000 events of the subset of interest. In general, 1000 events is more than enough for phenotypic analysis; for quantitative enumeration, a count of 1000 has an associated precision of 3% (i.e., the square root of 1000 divided by 1000). If a 1% precision was required, then 10 million events of the original sample need to be acquired.

3. Particle size and cell aggregates should be considered before sample collection. In addition to sample clogging the macro-sort tip, small changes in alignment can alter fluorescent intensity, compensation, and forward scatter detection. In general, if the particle size is greater than one-fourth the size of the macro-sort tip, the user should consider a larger macro-sort tip. Alternatively, cell aggregates can be avoided by prefiltering samples through a 100-µm filter cap tube prior to sample acquisition.

D. Sample Analysis

Steps and Considerations

1. Fluorescence minus one (FMO) control refers to a staining strategy, which uses all mAbs in the staining mix as in the test sample except for one mAb. This method allows for the correct determination of gate selection and verification of cell percentages. Figure 10 shows an example of the FMO strategy. In this example, cells were stained with four colors: anti-CD3-FITC, anti-CD4-PE, anti-CD8-Cy5PE, and anti-CD45RO-Cy7PE. The FMO control lacked anti-CD4-PE. In Fig. 10A, the sample is compensated correctly and shows that the FMO control is a better indicator of negative cell control cursor position than the unstained control sample (compare line 1 and line 2). Figure 10B demonstrates that even poorly compensated samples can benefit from the FMO control sample (compare line 1 and line 2). After setting the positive gate cutoff the test sample percentages can be determined more accurately. Thus this control reduces false negatives (best specificity) and better identifies positive cell populations (lower sensitivity). In addition, the FMO control can help identify compensation issues within the test sample. Therefore, FMO controls should be used whenever accurate discrimination is essential or when antigen expression is relatively low. While theoretically there could be as many FMO controls for each staining combination as

	Unstained Control	FMO Control	Test Stain
FITC	–	CD3	CD3
PE	–	–	CD4
Cy5PE	–	CD8	CD8
Cy7PE	–	CD45RO	CD45RO

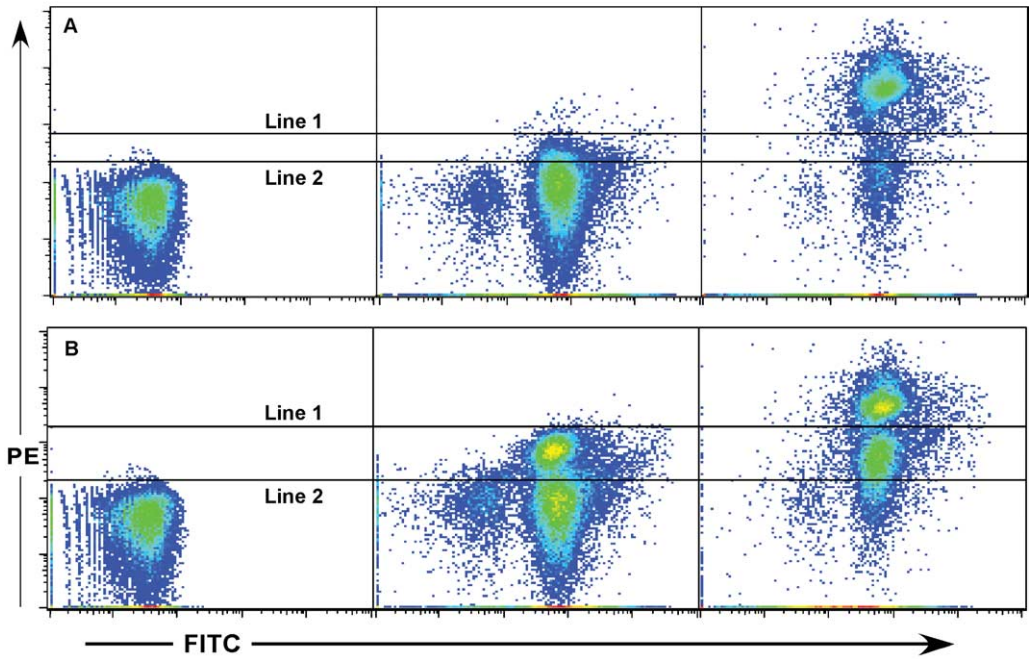

FIGURE 10 Use of the FMO control (fluorescence minus one) stained with all mAbs except for anti-CD4-PE. (A and B) The unstained control, the FMO control, and the fully stained cell sample (anti-CD3-FITC, anti-CD4-PE, anti-CD8-Cy5PE, and anti-CD45RO-Cy7PE) are compared. (A) The sample is compensated correctly and shows that the FMO control is a better indicator of negative cell control cursor position than the unstained control sample (compare line 1 and line 2). (B) Even samples that are poorly compensated can benefit from the FMO control sample (compare line 1 and line 2).

there are colors, in reality most of these are not necessary. For example, in many cases (e.g., CD3 or CD8 staining), the distinction of positive and negative cells is made easily enough based on visual inspection. In no case, however, is a completely unstained (or completely isotype-stained) sample the appropriate control for setting discriminatory gates.

2. Use only titered antibody conjugates prior to use in combinations as described earlier.

IV. COMMENTS

A. Sample Viability

Dead cells will bind many antibody conjugates nonspecifically and erroneously count these as a positively labeled cell. Therefore, gating strategies must be employed to properly gate out these cells. Intercalating dyes such as ethidium monoazide (EMA) or propidium iodide (PI) can be useful in gating out these nonspecifically labeled cells. One advantage of the use of PI over EMA is the ability to use the same channel (Cy5PE channel) for both PI and another mAb stained with Cy5PE. This can be done due to the high intensity of PI over most mAbs sharing this channel. Figure 11 shows an example of EMA used as a dead cell discriminator. In this example, unfixed cells were stained with 0.5 µg/ml of EMA (Molecular Probes Inc, Cat. No. E1374) for 10 min on ice covered with aluminum foil followed by 15 min under a bright fluorescent light. Samples can be fixed with 2% PFA and run within the same day. Dead cells are labeled positive with EMA, as seen in Fig. 11B, and can be removed from the gated live cells (live cell gate, B). Without the use of EMA, Fig. 11A shows the total number of dead cells and live cells combined. Cells within a standard

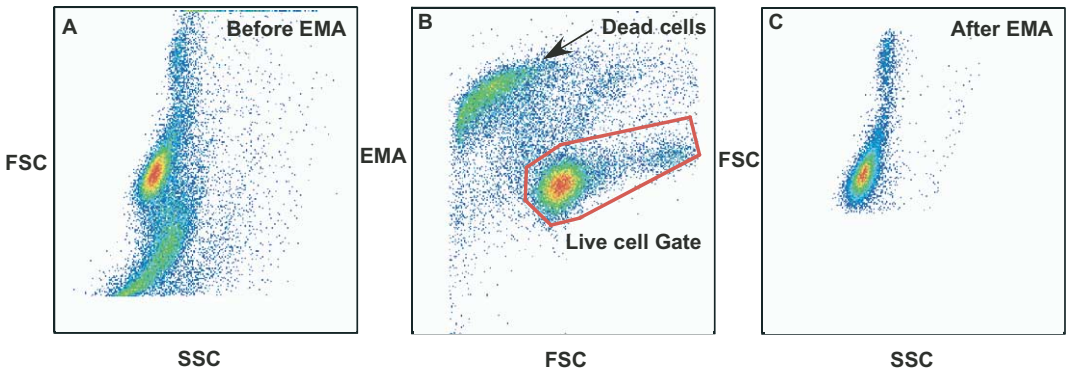

FIGURE 11 Use of ethidium monazide (EMA) as a method to discriminate live cells from dead cells. Dead cells are labeled positive with EMA as seen in B and can be removed from gated live cells (live cell gate). Without the use of EMA, A shows the total number of dead cells and live cells combined. Cells within a standard light scatter gate could contain dead cells as shown in A; however, after the dead cells were gated out using the live cell gate in B, dead cells were removed from the analysis (C).

light scatter gate could contain dead cells as shown in Fig. 11A; however, after the dead cells were gated out using the live cell gate in Fig. 11B, the dead cells were removed from the analysis (Fig. 11C).

B. Antibody Aggregation

Cyanine conjugates can potentially form immune complexes or aggregates during storage. Typically, cyanine tandem dyes form these aggregates and must be removed before using in the staining procedure. Ultracentrifugation of the antibody conjugate mixture at 13,000 *g* for 3 min will remove these aggregates.

V. CONCLUSION

Routine polychromatic flow cytometry is now closer to reality than ever before. Recent advances in instrumentation, computer technology, and biochemistry will prove to be the ingredients necessary to successfully understand the human immune system (Eckstein *et al*., 2001; Roederer *et al*., 1997). As engineering goals meet science objectives, the last frontier to cross will be analysis and comprehension of data never seen before or not very well understood. It will be this area where intense effort is needed to understand the massive amount of information collected and interpreted. Nonetheless, significant hurdles remain to be crossed by all laboratories wishing to implement this technology, and significant education of all immunologists regarding the interpretation of data generated by this technology is crucial to the understanding of its vagaries.

References

Baggerly, K. A. (2001). Probability binning and testing agreement between multivariate immunofluorescence histograms: Extending the chi-squared test. *Cytometry* **45**, 141–150.

De Rosa, S. C., Herzenberg, L. A., and Roederer, M. (2001). 11-color, 13-parameter flow cytometry: Identification of human naive T cells by phenotype, function, and T-cell receptor diversity. *Nature Med*. **7**, 245–248.

Eckstein, D. A., Penn, M. L., Korin, Y. D., Scripture-Adams, D. D., Zack, J. A., Kreisberg, J. F., Roederer, M., Sherman, M. P., Chin, P. S., and Goldsmith, M. A. (2001). HIV-1 actively replicates in naive CD4(+) T cells residing within human lymphoid tissues. *Immunity* **15**, 671–682.

Roederer, M. (2001a). Compensation is not dependent on signal intensity or on number of parameters. *Cytometry* **46**, 357–359.

Roederer, M. (2001b). Spectral compensation for flow cytometry: Visualization artifacts, limitations, and caveats. *Cytometry* **45**, 194–205.

Roederer, M., De Rosa, S., Gerstein, R., Anderson, M., Bigos, M., Stovel, R., Nozaki, T., Parks, D., and Herzenberg, L. (1997). 8 color, 10-parameter flow cytometry to elucidate complex leukocyte heterogeneity. *Cytometry* **29**, 328–339.

Roederer, M., and Hardy, R. R. (2001). Frequency difference gating: A multivariate method for identifying subsets that differ between samples. *Cytometry* **45**, 56–64.

Roederer, M., Moore, W., Treister, A., Hardy, R. R., and Herzenberg, L. A. (2001a). Probability binning comparison: A metric for quantitating multivariate distribution differences. *Cytometry* **45**, 47–55.

Roederer, M., Treister, A., Moore, W., and Herzenberg, L. A. (2001b). Probability binning comparison: A metric for quantitating univariate distribution differences. *Cytometry* **45**, 37–46.

CHAPTER

33

High-Speed Cell Sorting

Sherrif F. Ibrahim, Timothy W. Petersen, Juno Choe, and Ger van den Engh

I. INTRODUCTION

Flow cytometric sorting is an extremely versatile technology that has established itself as a cornerstone in biological research for the foreseeable future. The strength and long-term success of this approach to cell purification can be attributed to its highly quantitative, rapid, and serial nature of analysis. Each passing particle is individually interrogated for the presence or absence of potentially limitless combinations of light scattering and fluorescence parameters. If user-defined threshold values are met, desired cells are then isolated from a heterogeneous sample. As such, the cell sorter becomes a launching point for many downstream cellular and molecular investigations, as well as a powerful tool for the analysis of complex mixtures.

The modern age of discovery-based, system-wide approaches to research is contingent upon high throughput analysis, and cell sorters have had to evolve accordingly to keep pace with these changes. Aptly, the most significant improvements in sorting technology were catalyzed by large-scale DNA sequencing efforts such as the Human Genome Project (Van Dilla and Deaven, 1990). It was obvious that by providing chromosome-specific DNA libraries, cell sorters could accelerate as well as improve sequencing results. The problem, however, was that literally days of sorting would be necessary to isolate sufficient genetic material for sequencing [modern polymerase chain reaction (PCR) techniques had not yet been reported]. Ensuing advances in the fluidics, illumination, optics, computers, and electronics of sorters led to the development of several experimental instruments that could sort at rates nearly two orders of magnitude above existing machines, and eventually laid the groundwork for modern, high-end, high-speed sorters (Peters *et al*., 1985; Gray *et al*., 1987).

It is important to stress that the term "high speed" does not refer to simply speeding up the sort process, but is the product of careful engineering of each individual component in order to optimize overall performance. Coupled with these developments, the newest instruments have also become modular, with openly accessible and changeable parts, resulting in greater flexibility and sophistication with simpler and more stable operation.

The continuing evolution of high-speed cell sorters illustrates how advances in scientific knowledge and laboratory techniques allow for novel applications of existing methodologies, whereas improvements in instrument design facilitate previously unapproachable experiments. Accordingly, we have divided this article into two main parts. The first presents ideas that will yield better results in any experimental setting, with focus geared toward cytometer setup and general instrumentation. The following sections discuss biological aspects of study design, particularly pertaining to newer applications that rely on the added features and throughput of high-speed machines. The latter protocols do not include the traditional bulk separation of biological material, but instead take advantage of the capacity to screen rapidly through extremely complex cell and molecular populations for the isolation of highly defined, rare events. Specifically, fluorescent reporter proteins have provided the cytometrist with a real-time window into gene expression and have become the focus of many of these experimental approaches. It is these newest applications of high-speed cell sorting coupled with our increasing ability to study fewer, more characterized

Copyright 2006, Elsevier Science (USA).
All rights reserved.

cells that will have the greatest impact on basic science research and our knowledge of human biology.

II. HIGH-SPEED CELL SORTERS: TECHNIQUES FOR RELIABLE SORTING

High-speed cell sorters are currently available from a handful of manufacturers with varying specifications, capabilities, facility requirements, and user interfaces. The purchase of any one particular instrument will depend on the desires of individual laboratories and should come after careful consideration of these differences. Although there are a number of mechanisms for sorting cells into discrete populations, the most widely used method for high-speed cell sorting involves using a jet in air, where cells contained in charged droplets are deflected using a static electric field. While the discussion that follows is most relevant to these sorters, the majority of protocols will have broader application. This section outlines some suggestions for consistent, reliable cell sorting that can be instituted at any sorting laboratory.

A. Cell Sorter Maintenance

Successful high-speed cell sorting requires both careful preparation of the sample to be studied and maintenance of the instrument being used. In most cases, the upkeep of electronics, lasers, deflection plates, software, and other hardware is left to service professionals, while alignment of optics and maintenance of fluidics and associated systems remain the purview of the user. In practice, however, basic knowledge of all aspects of the sort process is needed to ensure optimal and consistent operation.

In cell sorters, the fluidics layout is composed of two subsystems: the sample injection system and the sheath fluid system that surrounds the sample core. Together, these two subsystems contain several feet of tubing, and it is into the interstices and cracks of the tubing and valves that contaminants collect and can affect sort purity. As a result, the tubing material should be chosen to be as inert as possible and changed on a regular basis. Likewise, valves and corners should be kept to a minimum. Typically, the sheath tubing, sample tubing, and associated in-line filters should be changed at least monthly. New tubing should be washed and flushed for at least 10 min prior to use with a 2% bleach solution, followed by sterile sheath fluid. For cell sorting where even slight contamination can skew results greatly, such as cases in which the sorted fraction will be used for quantitative PCR, it is not farfetched for the sample tubing to be replaced at the start of each sort. For its combination of inertness and cost, materials such as FEP (Teflon) are a good choice for the sheath tubing. FEP is chemically inert to a wide range of materials, holds up well to both acids and alkalis, and is autoclavable. An alternative to FEP that has better mechanical properties, particularly with respect to plastic deformation, is Tygon S-50-HL surgical grade tubing. Like FEP, this material can be sterilized by autoclaving (30 min, 15 psi, 250 F). Unfortunately, sterilization does not always free tubing of inert inorganic contaminants, and thorough flushing prior to each use is recommended. For sample injection tubing, an ideal choice is PEEK tubing. Like FEP, it is chemically inert and has good mechanical properties necessary for rigidity of the smaller diameter tubing.

At the start of each day, the sorter should be flushed for 10 min with a 2% bleach solution through both the sample and sheath lines, again followed by sterile sheath fluid to remove the bleach. In a similar manner, the sample injection should be flushed between samples when cross contamination is an issue. Finally, at the end of each day of sorting, it is recommended to flush the sheath and sample lines with a 2% bleach solution for 10 min followed by deionized water to reduce salt crystal accumulation and then air-dried. Attaching an empty sample tube and sheath container to the sorter and pressurizing each for a brief period can accomplish air drying of the sample and sheath lines. The tubing and the sheath containers should be stored dry in a clean place.

B. Sheath Fluid

It is often overlooked that cell samples can be sensitive to even minor changes in the composition of the sheath fluid. One may erroneously assume that the sample does not interact significantly with the sheath, as there is no mixing between the two (the flow at the sample injection is laminar) and ions and solutes can move only by diffusion. This is not always the case, and the sample often interacts significantly with the sheath fluid, as shown in Fig. 1. In Fig. 1, zymosan particles have been labeled with FITC, a fluorophore whose absorption cross section is pH sensitive at 488 nm, but not at 458 nm. In Fig. 1a, fluorescence efficiency at 488 nm (normalized by the fluorescence at 458 nm) changes when the pH of the sample is altered, causing an apparent change in measured fluorescence and potentially altering experimental results. However, these changes are observed only when the pH of the sheath is altered in the same manner as the

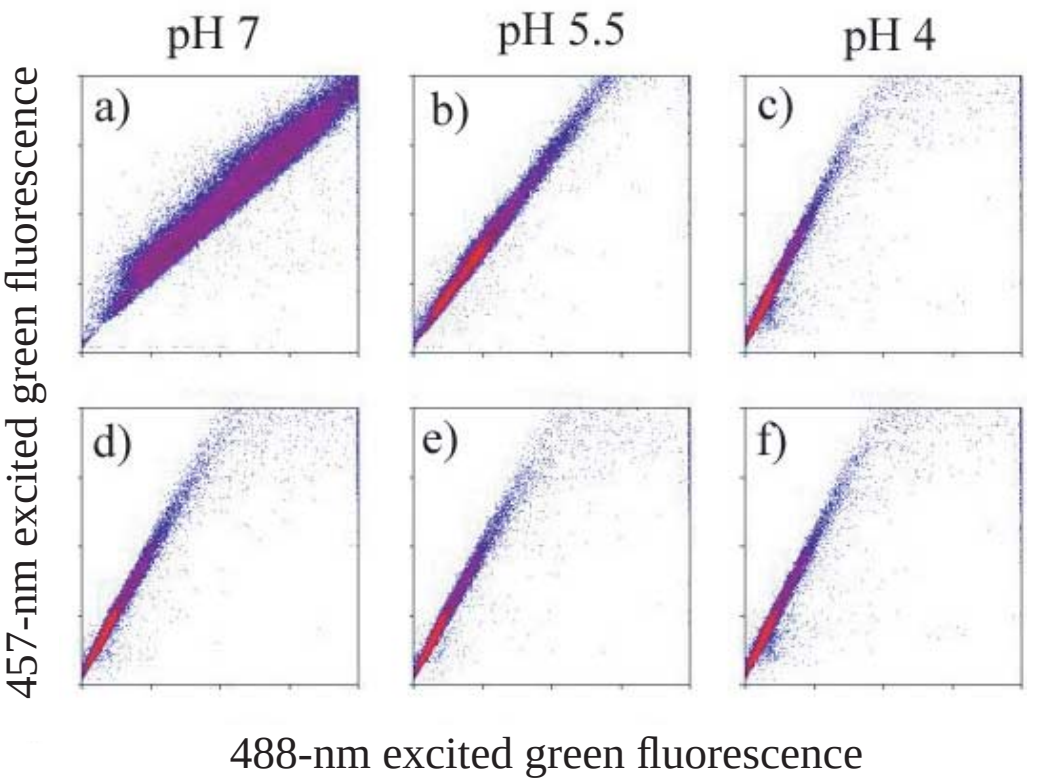

FIGURE 1 FITC-labeled zymosan particles excited at two wavelengths. When excited with 488-nm light, FITC shows a pH-dependent fluorescence emission that is not seen when 457-nm light is used. Columns show the pH of the *sample*. In the top row, the pH of the sheath was adjusted to match that of the sample, but in the bottom row, it was maintained at pH 4. One can see that the pH of the sheath is a determinant for fluorescence efficiency.

sample fluid and are no longer apparent without changes in sheath fluid pH (Fig. 1b). Commercial sheath fluid can be obtained with various chemical properties and constituents that can potentially affect the characteristics of the sample being studied. It is necessary to be familiar with the exact makeup of any sheath selection and to determine its likelihood of either chemical or biological interaction with the experiment. A simpler and less expensive alternative is to prepare a 0.9% NaCl solution and filter sterilize it or to filter the solution and then sterilize by autoclaving. Filtration of self-prepared sheath will reduce the number of nozzle clogs dramatically.

C. Sample Preparation and Determination of Sort Rate

High-speed cell sorters separate complex cell mixtures into constituent fractions so they can be studied in isolation. In the sorter, a jet of sheath fluid emanating from a nozzle surrounds the cell suspension coaxially. In order to separate events from one another, an acoustic vibration is coupled to the tip of the nozzle, and the vibrating nozzle leaves a trail of cyclical imprints onto the surface of the liquid. Because of surface tension energy, the cylinder of fluid is inherently less stable than a sphere of fluid, and soon the jet separates into regularly spaced droplets. Therefore, the cells, first carried by a cylinder of liquid, soon find themselves distributed randomly among the droplets. To separate the desired fraction of cells, an electrical charge may be applied to the droplets containing cells of interest as they separate from the main jet. In this manner, droplets with different cell types are directed toward collection vials by a static electrical field. On average, there are several empty droplets between each passing cell. As a result, the event rate (number of cells analyzed per second) should not be greater than the droplet formation rate. A typical droplet formation rate for a high-speed machine will be on the order of 50,000 drops/s, and the maximal throughput will be obtained if, on average, there is one cell per droplet. For this situation, however, statistics regarding the distribution of the cells among the droplets

dictate that only 37% of the droplets will have one cell. The remainder of the droplets will be empty or contain more than one cell. Thus, the maximal sort rate becomes roughly 37% of the droplet formation rate; higher rates will cause too many cells to be lost due to coincident drop occupation (and hence, equivocal signal measurement), and lower rates will result in unnecessarily slow sorts. Without this information, standard coincidence rejection protocols require a 1.5 droplet interval between sortable events. As a result, we recommend limiting sort rates to roughly one-third of the droplet formation rate. Again, each sorting facility will have to perform a series of basic experiments to determine what is most appropriate for a given application. A more thorough derivation of the physics of drop formation and determinants of sort rate can be found in van den Engh (2000).

As a consequence of the desire to sort cells with maximal throughput, one must also determine the density of cells in the sample suspension. This consideration arises from needing to control the droplet occupancy rate (as described earlier) independent of the droplet formation rate and the sheath fluid pressure. Control of the sample injection rate is achieved by independently pressurizing the sample and the sheath fluid and altering the differential pressure between the two fluidic systems. There is a limit, however, to the degree one can increase the sample injection rate by increasing the sample pressure. Jet velocity is proportional to the square root of jet pressure, so large increases in pressure will result in relatively smaller changes in jet velocity. Furthermore, as the sample pressure continues to increase, a critical point will be reached that will disrupt the laminar injection of the sample into the core of sheath fluid. In this situation, the cells will not be hydrodynamically focused by the sheath fluid and will disperse throughout the fluid column. Cells would then encounter different laser light intensity as a function of their position in the sheath fluid, compromising measurements of fluorescence and scattered light from particles and resulting in decreased sort purity. To preserve fluidics integrity, the sample injection pressure should be within 1–3 psi of the sheath pressure. Additionally, it is difficult to control the event rate of a sample that has far too many cells per unit volume, as small changes in the differential pressure will result in uncontrollably large changes in the event rate. Although the desired density of the sample depends critically on the diameter of the sample injection tube (most are of the order of 125 μm), the majority of situations dictate sample densities of roughly $1–10 \times 10^6\,ml^{-1}$ with higher densities appropriate for smaller diameter sample injection tubes. Other factors to consider will depend on the inherent biological characteristics of the sample itself. For instance, certain cell lines are adhesive and may clump easier, making control of the sort rate difficult.

III. TROUBLESHOOTING

Cell sorters are complex machines and, as such, seemingly minor alterations or inconsistencies in set up and/or calibration can have an additive effect on sort purity. This section lists some common problems and suggested solutions.

A. Droplet Formation

Poor droplet formation, as evidenced by movement of the break-off point (the point at which the stream becomes discrete drops) with respect to the laser, will result in both poor yield and contamination. If the break-off point is not well stabilized, check to ensure that the nozzle is free of trapped air or debris and that the sheath fluid has equilibrated to the temperature of the room in which sorting is conducted. Other causes of poor droplet formation can be the presence of detergent in the system (which changes the surface tension energy of the fluid column) or a piezoelectric element that is poorly coupled to the nozzle.

B. High Background Event Rates

High background count rates (triggering of sort electronics without sample injection and/or event rates disproportionately above expected rates for a given sample) are generally the result of poorly maintained tubing or improperly prepared sheath fluid. These considerations are of particular importance when sorting or analyzing samples that are relatively dilute. We have found that a well-maintained sorter should have a background count of less than three particles per second. A good way to measure this is by using 1-μm beads and adjusting the forward and perpendicular scatter detector gains to one-fourth of their full range. After the sample injection valve is closed, one should then be able to differentiate background count rates from particles that are larger than 0.5 μm. Should the background be unacceptably high, filtering of sheath fluid through a 0.22-μm filter or changing the sample and/or sheath fluid lines may be necessary.

C. Nozzle Clogs

Frequent nozzle clogs are usually the result of poor cleanup from a prior sort, suboptimal sample prepa-

ration, or inappropriate injection rate. Most commonly, sheath fluid left throughout the fluidics system from a previous sort dries and salt crystals are formed that clog the nozzle at the start of the following sort. Following the suggestions for flushing at the conclusion of each sort will remedy this issue. Additionally, one should examine the nozzle tip with a microscope to ensure that it is free of contamination and is uniformly smooth and patent. Certain samples will be more prone to causing clogs and, as such, the maximum injection pressure that will avoid clogs will have to be determined for each case.

The preceding points of discussion will vary to some degree among individual machines, laboratory settings, and instrument operators. In practice, machine start up, shut down, maintenance, sample manipulation, and so on, will all have an impact on overall, effective sort rate and general practice habits, being somewhat unique to each application. With consistent and thorough protocols for maintaining the sorting machinery, familiarization with the components of the sort process, and a systematic, skilled approach to troubleshooting, one can focus on the more exciting and challenging experimental aspects of high-speed cell sorting.

IV. STRATEGIES FOR EXPERIMENTAL DESIGN

While the original applications of high-speed cell sorting focused on the bulk purification of cellular and molecular material, modern biology has become increasingly focused on the minor nuances that distinguish one cell type from another. Although many biological experiments can still be approached through the analysis of cell populations, there is a growing need and improving ability to attain information from highly specified phenotypes, or even single cells. High-speed cell sorters are ideally suited for these applications because, by definition, a more highly classified cell will be present in less numbers, and it is often necessary to serially screen millions of individual events in a relatively short time period to find those particles of interest. Recent examples in the literature include the analysis of B cells from multiple myeloma patients to isolate subpopulations of cells with specific mutations in pathogenic genes (Kalakonda *et al*., 2001) or the haplotyping of individual sperm cells to look for trinucleotide repeat expansion in the Huntington's disease locus (Chong *et al*., 1997).

Beyond the study of naturally occurring variations and mutations, cell sorters have emerged as tools to screen engineered cell-based or solid support molecular libraries to select genetic clones and/or molecules of interest. Ingenious fluorescent-labeling schemes are employed to screen immensely complex libraries of particles to detect rare yet significant molecular processes such as enzyme activity or antibody binding and to monitor gene expression (Boder *et al*., 2000; Olsen *et al*., 2000). A revolution in molecular biology that is ideally suited to flow cytometry is the cloning of fluorescent reporter genes such as green fluorescent protein (GFP), *discosoma* Red (dsRed), and their variants (Chalfie *et al*., 1994; Matz *et al*., 1999). When fused to coding sequences of interest, these proteins generate fluorescent molecules from cells that express the cloned sequences in a dose-dependent fashion. Simple excitation of fluorescent proteins with a laser of appropriate wavelength results in the emission of a highly quantitative signal easily detectable by a flow cytometer. Combinations of these proteins allow for the design of gene expression studies under a variety of experimental conditions. Cells expressing the desired proteins (and hence cloned sequences) can be separated in a cell sorter and interrogated in further studies.

V. PROCEDURES

A. Library Construction and Clone Selection

The ability to isolate useful DNA fragments from larger complex mixtures is critical for all of molecular biology. Because single molecules of DNA cannot be readily seen or handled, target DNA is ligated into a larger vector that can be manipulated and propagated in a host bacterial strain, most commonly *E. scherichia coli*. This construct usually consists of a plasmid or phage, but can be larger, such as with bacterial artificial chromosomes (BACs), or the entire bacterial chromosome. Well-described molecular biology techniques can be applied in this fashion to create highly diverse libraries rapidly with complexities greater than 10^9 and lie outside the scope of this article. With traditional methods, *E. coli* cells are grown on agar plates under antibiotic selection, with each colony representing a construct that has entered a bacterial cell successfully. Colonies with the desired genotype are then selected based on a colormetric phenotype and transferred to liquid media or streaked out on another agar plate for growth. Selected species can then be isolated efficiently with commercially available plasmid prep kits (Qiagen, Inc.) or by other established DNA extraction and amplification methods.

B. Cell Sorters as a Tool for Clone Selection and Genetic Screening

While the aforementioned approach is accurate and has been successfully employed for decades, cell sorters are ideally equipped to perform the same tasks in less time with added flexibility. At the most basic level, markers can be devised to simply indicate the presence or absence of a cloned insert. With more sophisticated study design and genetic manipulation, sorters become tools to potentially screen genomes of entire organisms in rapid fashion, providing a window into genetic regulation. Libraries can be screened and clones displaying a desired phenotype can be isolated, their DNA amplified, and eventually sequenced. As an example, an experiment could be fashioned to screen the entire *Saccharomyces cerevisiae* genome (~14 Mbp) by generating 100-bp fragments placed strategically in relation to a reporter construct. High-end sorters would be capable of scanning the genome to 10X coverage for specific expression events in a matter of minutes. A similar approach was reported in a study by Barker *et al*. (1998) that generated a library of 200- to 1000-bp fragments of the *Mycobacterium marinum* genome fused to a promoterless copy of GFP. Like its counterpart *Mycobacterium tuberculosis*, this bacterium is able to avert the normal function of the immune system and survive within macrophages. By isolating phagosomes emitting green fluorescence and sequencing the regions of DNA upstream of GFP, they were able to determine which regions of the genome may be responsible for circumventing normal bacterial killing.

C. Fluorescence Encoding Strategies

The major challenge in experimental design is then to devise a strategy for expressing some characteristic of the cloned and/or expressed DNA as fluorescence. Because fluorescent proteins such as GFP and its variants can be coupled to genetic sequences and produced endogenously within bacteria without the need for added substrates, they become the obvious starting point. Basic approaches to clone selection indicate the presence of foreign DNA with the loss of a fluorescent signal. Inouye *et al*. (1997) developed a plasmid vector that directs the production of GFP under a constitutive promoter. When an insert is cloned into the vector, stop codons within the insert prevent the successful translation of GFP. Therefore, nonfluorescent colonies can be picked to obtain individual clones. In our experience, negative selection (based on the absence of fluorescence) can be a poor criterion for the analysis of individual cells in a cell sorter. Background particles are usually weakly fluorescent and, as such, it becomes difficult to segregate them from nonfluorescent (i.e., insert containing) bacteria. Additionally, a large degree of cell-to-cell variability exists that is widely determined by different sizes of bacterial cells and varying levels of protein expression. The combination of these factors makes it difficult to be certain that a nonfluorescent cell is not simply expressing a fluorescent marker at low levels and will result in sort contamination.

More complex schemes can be derived to represent unique characteristics of individual clones as positive fluorescence signals that result in sorts of higher purity. For instance, Olsen *et al*. (2000) created a scheme in which protease variants from a mutant library were expressed on the surface of *E. coli*. Functional enzyme mutants successfully cut a synthetic substrate bound to the *E. coli* membrane containing BODIPY and tetramethylrhodamine fluorophores connected by a linker with a specific target site. The tetramethylrhodamine acts as a quencher for the BODIPY dye by fluorescence resonance energy transfer. If the OmpT mutant on a particular cell cleaved the substrate, then the tetramethylrhodamine diffused away and BODIPY was no longer quenched. Sorting the fluorescent particles resulted in a 5000-fold enrichment for clones containing active variants of the protease.

As an additional example of immense potential for such techniques, Koo *et al*. (2004) devised a means to encode the activity of mRNA processing in *E. coli* as a fluorescent signal. A GFP construct was created as a fusion to a mRNA processing region. If functional mRNA processing was present, many of the GFP transcripts were degraded, leading to a low level of GFP fluorescence. If the ability to perform mRNA processing was disrupted, cells had high levels of GFP and were isolated. Using this method, over 60% of bacteria were highly fluorescent after four rounds of sorting.

VI. PRACTICAL CONSIDERATIONS

Once an algorithm for encoding biological function as a fluorescent signal has been conceived, it is vital to test the system under a variety of culture and cellular conditions. Often times, fluorescence from GFP and other fluorescent proteins is not visible in actively growing *E. coli* cultures. Because the rate of replication of *E. coli* is so high, any fluorescent protein that is produced is diluted continuously and, as such, fluorescence will not usually begin to appear until late log phase or stationary phase. To obtain higher cell-to-cell consistency of fluorescence, it is often helpful to grow

the cells under conditions that repress fluorescent protein production during active growth. This can be achieved by cloning the fluorescent protein downstream from a tightly regulated promoter. If a *lac* promoter is used, growth in 0.5% glucose results in almost complete repression. In late log or stationary phase, cells can be resuspended in an equal volume of culture medium that does not repress protein production. With this approach, all cells begin producing fluorescent protein at approximately the same time and the rate of division has slowed, resulting in more consistent levels of fluorescent protein expression.

During testing, it is often convenient to use a fluorescence microscope with appropriate excitation and emission filters, as well as high-power objectives to image individual bacterial cells. Direct observation of cultured cells can be a quick method for assessing the levels of various fluorescent markers, as well as looking for undue elongation of cells that can indicate unhealthy cellular states. Only after thorough testing should bacterial cultures be inspected by flow cytometry. Typically, forward scatter is not an informative measurement to record but is an excellent parameter to trigger on as it can easily detect bacterial cells in a flow stream regardless of their orientation. This is a better method than triggering on fluorescence to prevent nonfluorescent cells from altering sort outcome.

A. Optical Setup and Instrument Settings

Fluorescence measurements can be performed with a variety of optical configurations. If a 488-nm laser is used to detect forward scatter, it is convenient to use this same laser for GFP measurements. Additionally, some variants of YFP (yellow mutant of GFP) and DsRed can be excited readily with a 488-nm beam. Other laser lines such as multiline UV or 514.5 nm can be used as needed. If multiple fluorescent proteins or markers are being utilized it is often efficient to use a dichroic beam splitter to efficiently separate fluorescence into short and long wavelength pathways. Further filtering with long-pass, band-pass, or short-pass filters can fine tune wavelength ranges to increase the number of measured parameters and to minimize cross talk between signals.

Bacterial cultures should be diluted approximately 200:1 in saline before injection into the flow cytometer. This can be variable depending on densities of cultures and cytometer configuration. The sample injection pressure on the flow cytometer should be adjusted for optimal event rate on each individual sorter as discussed previously. Test sorts should be performed using control cells first until the researcher attains some level of confidence that desired cell populations can be isolated successfully. In addition, these initial tests can often provide some estimate as to the enrichment that can be achieved with a particular fluorescence-encoding scheme. Tests should also be performed to assess the viability of bacteria after culturing and sorting. This can be achieved easily by sorting a particular number of cells into LB medium or saline and then serial dilutions of these sorted cells can be plated. After overnight growth, colony counts will provide a measure of viability. Optimally, 50–70% of injected cells should be viable. However, viability can drop below 1% depending on factors such as cell strain and culture conditions.

When initial testing has been completed, the actual experiment can proceed. Cells can be batch sorted with hundreds to thousands of cells per tube or individual cells can be sorted into 96-well plates for clone isolation. If an inadequate level of enrichment is achieved after the first round of sorting, cells can be cultured and then resorted. This process can be repeated until the desired level of enrichment is achieved, and final processing of the cells will be highly dependent on experimental design. Cells can be further cultured for DNA isolation, or PCR amplification of genetic elements can be performed from bacterial cultures and/or single cells. Other protocols may culture sorted cells before isolating proteins for various *in vitro* assays.

VII. CONCLUSIONS

The sections presented herein serve to provide the sorter with a foundation in appropriate sorting techniques, as well as to provoke thought toward elegant experimental design. These approaches take advantage of the latest advances in molecular biology as well as the full range of capabilities inherent to high-end cell sorters. As sorting technology has improved, these instruments have become more stable, easier to operate, and amenable to almost any laboratory setting as opposed to dedicated, core-sorting facilities. The high-speed cell sorter has become a tool for discovery —diversity of heterogeneous populations can be assessed, entire genomes and molecular libraries can be screened in short periods of time, pure populations can be purified, and their constituents can be amplified and studied further with minimal confounding variables. No other technology has the ability to purify cells based on so many parameters with such high speed and accuracy as the high-speed cell sorter. The tight interplay between biology and

technology has resulted in an improved ability to highlight increasingly specified nuances between cells. In combination with the latest tools, such as mass spectrometry and expression arrays, these differences will unravel the earliest molecular underpinnings in processes such as disease pathogenesis and developmental biology.

References

Barker, L. P., Brooks, D. M., and Small, P. L. (1998). The identification of Mycobacterium marinum genes differentially expressed in macrophage phagosomes using promoter fusions to green fluorescent protein. *Mol. Microbiol.* **5**, 1167–1177.

Boder, E. T., Midelfort, K. S., and Wittrup, K. D. (2000). Directed evolution of antibody fragments with monovalent femtomolar antigen-binding affinity. *Proc. Natl. Acad. Sci. USA* **97**(20), 10701–10705.

Chalfie, M., Tu, Y., Euskirchen, G., Ward, W. W., and Prasher, D. C. (1994). Green fluorescent protein as a marker for gene expression. *Science* **263**(5148), 802–805.

Chong, S. S., Almqvist, E., *et al*. (1997). Contribution of DNA sequence and CAG size to mutation frequencies of intermediate alleles for Huntington disease: Evidence from single sperm analyses. *Hum. Mol. Gene.* **6**, 301–309.

Gray, J. W., Dean, P. N., Fuscoe, J. C., Peters, D. C., Trask, B. J., van den Engh, G. J., and Van Dilla, M. A. (1987). High-speed chromosome sorting. *Science* **238**(4825), 323–329.

Inouye, S., Ogawa, H., *et al*. (1997). A bacterial cloning vector using a mutated Aequorea green fluorescent protein as an indicator. *Gene* **189**, 159–162.

Kalakonda, N., Rothwell, D. G., *et al*. (2001). Detection of N-Ras codon 61 mutations in subpopulations of tumor cells in multiple myeloma at presentation. *Blood* **98**, 1555–1560.

Koo, J. T., Choe, J., and Moseley, S. L. (2004). HrpA, a DEAH-box RNA helicase, is involved in mRNA processing of a fimbrial operon in *Escherichia coli*. *Mol. Microbio.*

Matz, M. V., Fradkov, A. F., Labas, Y. A., Savitsky, A. P., Zaraisky, A. G., Markelov, M. L., and Lukyanov, S. A. (1999). Fluorescent proteins from nonbioluminescent Anthozoa species. *Nature Biotechnol.* **10**, 969–973.

Olsen, M. J., Stephens, D., Griffiths, *et al*. (2000). Function-based isolation of novel enzymes from a large library. *Nature Biotechnol.* **18**, 1071–1074.

Peters, D., Branscomb, E., Dean, P., Merrill, T., Pinkel, D., Van Dilla, M., and Gray, J. W. (1985). The LLNL high-speed sorter: Design features, operational characteristics, and biological utility. *Cytometry* **6**(4), 290–301.

van den Engh, G. (2000). High speed cell sorting. *In "Emerging Tools for Single Cell Analysis: Advances in Optical Measurement Technologies"* (G. Durack, and J. P. Robinson, eds.). Wiley-Liss, New York.

Van Dilla, M. A., and Deaven, L. L. (1990). Construction of gene libraries for each human chromosome. *Cytometry* **11**(1), 208–218.

SECTION

8

Cell Cycle Analysis

CHAPTER

34

Cell Cycle Analysis by Flow and Laser-Scanning Cytometry

Zbigniew Darzynkiewicz, Piotr Pozarowski, and Gloria Juan

I. INTRODUCTION

The cytometric methods for cell cycle analysis can be grouped into three categories. The first comprises methods that rely on a single time point ("snapshot") measurement of the cell population. This analysis may be either univariate, based on the measurement of cellular DNA content alone (Crissman and Hirons, 1994), or multivariate (multiparameter), when in addition to DNA content another cell attribute is measured (Darzynkiewicz *et al*., 1996; Endl *et al*., 2001; Larsen *et al*., 2001). The measured attribute is expected to provide information about a particular metabolic or molecular feature(s) of the cell that correlates with a rate of cell progression through the cycle or is a marker the cell proliferative potential or quiescence. While the single time measurement reveals the proportions of cells in G_1 *vs* S *vs* G_2/M, it provides no direct information on cell cycle kinetics. However, if duration of the cell cycle (or time of doubling of cells in the culture) is known, the length of G_1, S, or G_2/M phase can be estimated from the percentage of cells in the respective phase.

In the second category are methods that combine time-lapse measurements of populations of cells synchronized in the cycle or whose progression through the cycle was perturbed, e.g., halted by the agent arresting them at a specific point of the cycle. These methods reveal kinetics of cell progression through the cycle. A classical example of this group is the stathmokinetic approach where cells are arrested in mitosis, e.g., by vinblastine or colcemide, and the rate of cell entrance to mitosis ("cell birth" rate) is estimated from the slope representing a cumulative increase in the percentage of mitotic cells as a function of time of the arrest (Darzynkiewicz *et al*., 1987).

Methods of the third category rely on analysis of DNA replication concurrent with measurement of DNA content. They may be either single time point measurements or use the time-lapse strategy to measure cell cycle kinetics. Incorporation of the thymidine analogue and the S phase marker 5′-bromo-2′-deoxyuridine (BrdUrd) is detected either cytochemically, based on the use of DNA dyes such as Hoechst 33258, whose fluorescence is quenched by BrdUrd (Poot *et al*., 2002), or immunocytochemically using fluoresceinated BrdUrd antibodies (Dolbeare and Selden, 1994). Still another method of this category detects incorporated BrdUrd by the increased sensitivity of DNA to photolysis: utilizing terminal deoxynucleotidyl transferase, the photolytically generated strand breaks are then labeled with fluorochrome-tagged deoxynucleotides (Li *et al*., 1996). Because the latter method escapes the harsh conditions used to induce DNA denaturation (heat or acid), it is applicable in conjunction with immunocytochemical detection of intracellular proteins. The time-lapse measurements of the cohort of BrdUrd-labeled cells allows one to estimate their rate of progression through different points of the cell cycle (Terry and White, 2001).

The methods described in this article, representative of each of the three categories, can be applied both to cells measured by flow cytometry and to cells mounted on slides. The latter can be analyzed by laser-scanning cytometer (LSC), the microscope-based cytofluorimeter that measures the fluorescence of individual cells deposited on slides rapidly, with sensitivity and accuracy comparable to that of flow cytom-

Copyright 2006, Elsevier Science (USA).
All rights reserved.

etry (Kamentsky, 2001). One advantage of LSC is that the cells are stained and measured while attached to microscope slides. This eliminates cell loss that inevitably occurs due to repeated centrifugations during sample preparation for flow cytometry. Another advantage stems from the possibility of relocation of particular cells on slides for their visual inspection or morphometry, following the initial measurement of a large cell population and electronic selection (gating) of cells of interest. The instrument thus combines advantages of both flow and image cytometry.

Only a few selected methods are presented in this article. More detailed descriptions of these and other methods, their applicability to different cell systems, and advantages and limitations are provided elsewhere in books devoted specifically to the cell cycle (Gray and Darzynkiewicz, 1987; Fantes and Brooks, 1993; Studzinski, 1995, 1999) or flow cytometry (Darzynkiewicz *et al*., 1994, 2001; Gray *et al*., 1990).

II. MATERIALS AND INSTRUMENTATION

The materials listed for each of the different procedures can be purchased from the following sources: Triton X-100 (Cat. No. T 9284), Pipes (Cat. No. P 3768), RNase A (Cat. No. R 5000), and 5′-bromo-2′-deoxyuridine (Cat. No. B 5002) are from Sigma Chemical Co.; DAPI (4′,6′-diamidino-2-phenylindole; Cat. No. D 1306), propidium iodide (PI, Cat. No. P-1304), and high-purity acridine orange (AO, Cat. No. A-1301) are from Molecular Probes; and methanol-free formaldehyde (Cat. No. 4018) is from Polysciences Inc.

The greatest selection of monoclonal and polyclonal antibodies applicable to cell cycle analysis is offered by DACO Corporation, Sigma Chemical Co., Upstate Biotechnology Incorporated, B.D. Biosciences PharMingen, and Santa Cruz Biotechnology, Inc.

A variety of models of flow cytometers of different makers can be used to measure cell fluorescence following staining according to the procedures listed in this article. The manufacturers of the most common flow cytometers are Becton Dickinson Immunocytometry Systems, Beckman/Coulter Inc., DACO/Cytomation, and PARTEC GmbH. The multiparameter laser-scanning cytometer is manufactured by CompuCyte Corp.

The software used to deconvolute DNA content frequency histograms, to estimate the proportions of cells in the respective phases of the cycle, is available from Phoenix Flow Systems and Verity Software House.

III. PROCEDURES

A. Univariate Analysis of Cellular DNA Content

Progression through S phase and completion of mitosis (cytokinesis) result in changes in cellular DNA content. The cells position in the major phases ($G_{0/1}$ *vs* S *vs* G_2/M) of the cycle, therefore, can be estimated based on DNA content measurement. A variety of fluorochromes and numerous methods are used for DNA content analysis. A simple protocol, which can be modified to accommodate different dyes, has been developed and applied to numerous cell types.

1. Cell Staining with DAPI

Solution

Staining solution: Phosphate-buffered saline (PBS) containing 0.1% (v/v) Triton X-100 and 1 µg/ml DAPI (final concentrations)

Steps

1. Suspend approximately 10^6 cells in 0.5 ml of PBS. Vortex gently (~3 s) or gently aspirate several times with a Pasteur pipette to obtain a mono-dispersed cell suspension, with minimal cell aggregation.
2. Fix cells by transferring this suspension, with a Pasteur pipette, into 12 × 75-mm centrifuge tubes containing 4.5 ml of 70% ethanol on ice. Keep cells in ethanol for at least 2 h at 4°C (cells may be stored in 70% ethanol at 4°C for weeks).
3. Centrifuge the ethanol-suspended cells 3 min at 200 *g*. Decant thoroughly ethanol.
4. Suspend the cell pellet in 5 ml of PBS, wait ~30 s, and centrifuge at 300 *g* for 3 min.
5. Suspend the cell pellet in 1 ml of DAPI staining solution. Keep in the dark, at room temperature, for 10 min.
6. Transfer sample to the flow cytometer and measure cell fluorescence. Maximum excitation of DAPI, bound to DNA, is at 359 nm and emission is at 461 nm. For fluorescence excitation, use the available ultraviolet (UV) light laser line at the wavelength nearest to 359 nm. When a mercury arc lamp serves as the excitation source, use a UG1 excitation filter. A combination of appropriate dichroic mirrors and emission filters should be used to measure cell fluorescence at wavelengths between 450 and 500 nm.
7. The data acquisition software of most flow cytometers/sorters allows one to record the fluorescence intensities (the integrated area of the electronic pulse signal) of 10^4 or more cells per sample. Data are presented as cellular DNA content frequency his-

tograms (Fig. 1). The data analysis software packages (e.g., Rabinovitch, 1994) that deconvolute the frequency histograms to obtain percentage of cells in $G_{0/1}$, S, and G_2 + M are either included with the purchase of the flow cytometer or are available commercially from other vendors, as listed under Section II. For details of the methods of deconvolution of DNA content frequency histograms, see Rabinovitch (1994).

2. *Staining with Propidium Iodide*

If excitation with UV light is not possible, the procedure given earlier for DAPI can be modified to apply PI as the DNA fluorochrome. Thus, instead of DAPI, PI is included into the staining solution at a concentration of 10 µg/ml. Because PI also stains double-stranded RNA, RNA is removed enzymatically during the staining reaction. This is accomplished by the addition of RNase A into the staining solution.

Solution

Staining solution: PBS containing 0.1% (v/v) Triton X-100, 10 µg/ml of PI, and 100 µg/ml of DNase-free RNase A.

Steps

1–4. Follow steps 1 to 4 as described earlier for cell staining with DAPI.

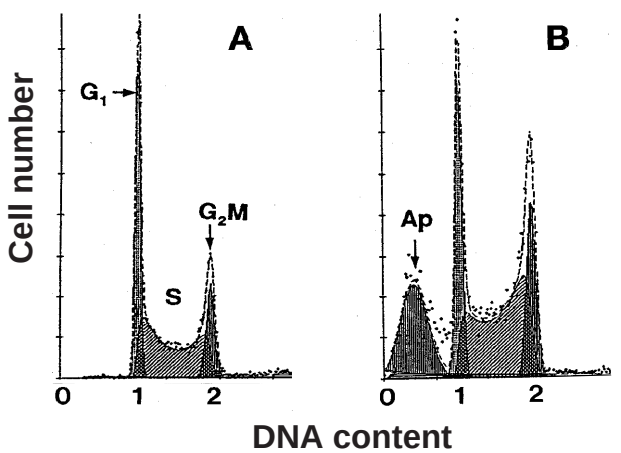

FIGURE 1 Frequency distribution DNA content histograms of human leukemic HL-60 cells untreated (A) or treated with DNA topoisomerase II inhibitor fostriecin (B) and stained with PI as described in the text. The "multicycle" deconvolution program (Phoenix Flow Systems) has been used to identify and calculate percentage of cells with fractional DNA content (apoptotic cells; Ap) and cells in G_1, S, and G_2/M phases of the cycle content, as shown. The drug treatment caused an increase in the proportion of S and G_2M cells and induced apoptosis.

5. Suspend the cell pellet in 1 ml of PI staining solution. Keep in the dark, at room temperature, for 30 min or at 37°C for 10 min.

6. Transfer sample to the flow cytometer and measure cell fluorescence. Maximum excitation of PI, bound to DNA, is at 536 nm and emission is at 617 nm. Blue (488 nm) or green light lines of lasers are optimal for excitation of PI fluorescence. Emission is measured using the long-pass 600- or 610-nm filter. Data acquisition and analysis are as described earlier for DAPI-stained cells.

Comments

All cells in G_1 have a uniform DNA content, as do cells in G_2 and M; the latter have twice as much DNA as G_1 cells. Under ideal conditions of DNA staining, the fluorescence intensities of all G_1 or G_2/M cells are expected to be uniform and, after analog to digital conversion of the electronic signal from the photomultiplier (representing their fluorescence intensity), to have uniform numerical values, respectively. In practice, however, G_1 and G_2 cell populations are represented on frequency histograms by peaks of various width. The coefficient of variation (*cv*) of the mean value of DNA-associated fluorescence of the G_1 population (width of the peak) is a reflection of an accuracy of DNA content measurement and should not exceed 8%. Improper staining conditions, instrument missadjustment, and the presence of a large number of dead or broken cells all result in high *cv* of the G_1 cell populations.

Apoptotic cells often have fractional DNA content due to the fact that the fragmented (low MW) DNA undergoes extraction during the staining procedure. Some cells may also lose DNA (chromatin) by shedding apoptotic bodies. Only a fraction of DNA thus remains within apoptotic cells. They are represented then on the DNA content frequency histograms by the "sub-G_1" peak (Fig.1). Commercially available software packages to deconvolute DNA histograms are able to identify and quantity the "sub-G_1" cell population.

If the length of the cell cycle (or cell doubling time) is known, the duration of each of the phases can be estimated from the percentage (fraction) of cells in that phase. For example, during the exponential phase of cell growth, the duration of G_1 (T_{G1}) can be calculated from

$$T_{G1} = \frac{T_C \times \ln(f_{G1}+1)}{\ln 2}$$

where T_C is duration of the cell cycle and f_{G1} is a fraction of cells residing in G_1. T_C, with generally

acceptable approximation, equals the cell doubling time in cultures. The latter can be estimated from the growth curve.

B. Multiparameter Analysis

Multiparameter analysis of other attributes of the cell, in addition to DNA content, allows one not only to distinguish cells in G_1 *vs* S *vs* G_2/M, but also to identify quiescent (G_0) or mitotic cells. Thus, bivariate analysis of cell population with respect to their cellular DNA and RNA content discriminates between G_0 and G_1 cells. Bivariate analysis of DNA content and proliferation-associated proteins, particularly cyclins, provides another means to distinguish between proliferating and quiescent cells and yields additional information about the proliferative potential of cell populations (Darzynkiewicz *et al*., 1996). Immunocytochemical detection of histone H3 phosphorylation combined with DNA content analysis offers a convenient approach to distinguish M from G_2 cells and to quantify the mitotic index in the cell population (Juan *et al*., 2001). This section presents examples of these methods.

1. Differential Staining of Cellular DNA and RNA

Quiescent (G_0) cells are characterized by a manyfold lower RNA content compared to their cycling G_1 counterparts (Darzynkiewicz *et al*.,1976). Simultaneous staining of RNA and DNA, therefore, allows one to distinguish G_0 from G_1 cells (based on differences in RNA content), as well as to identify cells in S and G_2/M. Differential staining of cellular DNA and RNA can be accomplished with the metachromatic fluorochrome acridine orange (AO). At appropriate concentrations and ionic conditions AO intercalates into dsDNA and fluoresces green, while its interactions with RNA result in red fluorescence (Darzynkiewicz *et al*., 1994). Prior to staining with AO the cells are permeabilized with Triton X-100 in the presence of 0.08 *M* HCl and serum proteins. Such treatment makes cells permeable to AO, yet they are not lysed and their DNA and RNA content is preserved. Alternatively, the cells may be prefixed in 70% ethanol, as described previously for univariate DNA content analysis. Apoptotic cells stained under these conditions are characterized by markedly diminished DNA associated (green) AO fluorescence.

Solutions

1–4. *AO stock solution*: Dissolve 1 mg AO in 1 ml of distilled water. This solution of AO is stable for several months when kept at 4°C in the dark (foil wrapped).

2. *First-step solution (solution A)*: Dissolve 0.1 ml of Triton X-100 and 0.87 g of NaCl in 92 ml of distilled water. Add 8 ml of 1 *M* HCl solution.

3. *Second-step solution (solution B)*: Prepare 100 ml of the phosphate – citric acid buffer at pH 6.0 by combining 37 ml of 0.1 *M* citric acid with 63 ml of Na_2HPO_4. Add 0.87 g of NaCl and 34 mg EDTA, dissodium salt. Stir until dissolved. Add 0.6 ml of AO stock solution. This solution is stable for several months when kept at 4°C in the dark.

Steps

1. Transfer a 0.2-ml aliquot of the cell suspension ($<5 \times 10^5$ cells) directly from tissue culture to a 2- or 5-ml tube.
2. *Gently* add 0.4 ml of ice-cold solution A. Wait 15 s, keeping sample on ice.
3. *Gently* add 1.2 ml of ice-cold solution B. Keep sample on ice prior the measurement.

NOTE 1 *Vortexing, syringing, and vigorous mixing of cells when suspended in solution A or B break down the cells and should be avoided.*

NOTE 2 *As an alternative to detergent (Triton X -100) treatment, cells may be fixed in 70% ethanol as described for staining with DAPI (Section III, A,1). Carry out steps 1–4 of the DAPI staining protocol, suspend $<10^5$ cells in 0.2 ml of PBS, and follow with steps 2 and 3 as just described.*

4. Measure cell fluorescence during the next 2–10 min after the addition of solution B. Excite AO fluorescence with blue light (use 488- or 457-nm laser lines or BG12 excitation filter in the case of mercury lamp illumination). Measure the green fluorescence of AO bound to DNA at 530 ± 20 nm and red fluorescence of AO bound to RNA at >640 nm (long-pass filter).

Comments

A characteristic distribution of G_0, G_1, S, G_2/M, and apoptotic cells, differing in RNA and DNA content, is shown in Fig. 2. The differences in RNA content enable G_0 cells to be discriminated from G_1 cells. However, the differences in DNA content provide the basis to identify apoptotic and nonapoptotic cells and, among the latter, to distinguish $G_{0/1}$, S, and G_2/M cell subpopulations.

The major advantages of this assay are its simplicity, applicability to different instruments that use either laser or mercury lamp as a light source for fluorescence excitation, and the possibility it offers to distinguish G_0 from G_1 cells. Differential stainability of DNA *vs* RNA, however, requires very stringent conditions of cell staining in terms of dye concentration and

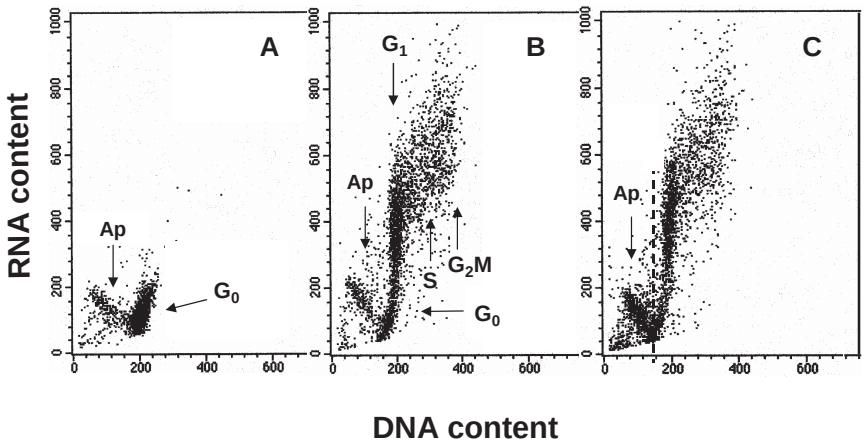

FIGURE 2 Bivariate distributions (scatter plots) demonstrating differential staining of DNA and RNA with acridine orange (AO). Nonstimulated (A) and stimulated mitogenically with phytohemagglutinin (PHA) (B and C) lymphocytes were cultured for 48 h and then stained with AO according to the presented protocol. Nonstimulated G_0 cells have minimal RNA content and uniform DNA content. During stimulation, a subset of lymphocytes undergoes apoptosis (Ap; activation-induced apoptosis), another subset enters cell cycle, while some cells remain in G_0. All these subpopulations can be identified after differential staining of DNA and RNA: cells in G_1 *vs* S *vs* G_2/M differ in DNA content, whereas G_0 cells are distinct from G_1 cells due to differences in RNA content. The antitumor drug onconase was included in one of the PHA-treated cultures (C) to enhance "activation-induced apoptosis." The dashed line in C separates apoptotic from nonapoptotic cells.

ionic composition of the medium. AO also has a propensity to attach to sample flow lines of flow cytometers and therefore requires careful rinsing of the instrument with a bleaching solution (~15 min) to lower the background fluorescence for the subsequent analysis of weakly fluorescent samples. Further details of the AO methodology are presented elsewhere (Darzynkiewicz *et al*., 1994).

2. *Cellular DNA Content and Expression of Proliferation-Associated Proteins*

The expression of proliferation-associated proteins often varies during the cell cycle, as well as is different in cycling and quiescent cells. Their immunocytochemical detection, therefore, provides information on the proliferative status of the cell. The most common markers of proliferating cells are the proliferating cell nuclear antigen (PCNA) (Larsen *et al*., 2001), the antigen detected by the Ki-67 antibody (Endl *et al*., 2001) and certain cyclins (Darzynkiewicz *et al*., 1996).

Methods for detection of the proliferation associated proteins, particularly the choice of optimal fixative, may vary depending on the particular antigen (Jacobberger, 2001). The following method is applicable not only to cyclins (Darzynkiewicz *et al*., 1994, 1996), but also other intracellular antigens.

Solutions

1. Fixatives: Methanol (see Comments)
2. *Cell permeabilizing solution*: 0.25% Triton X-100, 0.1% sodium azide in PBS
3. *Rinsing solution*: 1% bovine serum albumin (BSA), 0.1% sodium azide in PBS

Steps

1. Prepare the fixative by filling 5-ml polypropylene tubes with 4.5 ml of methanol (or 70% ethanol; see Comments). Keep tubes on ice.
2. Suspend 1–2 × 10^6 cells in 0.5 ml of PBS. Fix the cells by transferring this suspension with a Pasteur pipette into an ice-cold methanol tube. Keep cells in the fixative at –20°C at least overnight (cells can be stored in the fixative at –20°C for days).
3. Centrifuge at 300 g for 3 min. Resuspend the cell pellet in 5 ml PBS. Keep at room temperature for 5 min. Spin at 200 g for 5 min.
4. Resuspend cells in 0.5 ml of the permeabilizing solution. Keep at room temperature for 5 min. Centrifuge as in step 3.
5. Resuspend cell pellet in 100 µl of the rinsing solution that contains the primary Ab. Follow instructions supplied by the vendor regarding the final titer of the

supplied antibody (0.5–1.0 µg of the Ab per 10^6 cells suspended in 100 µl is generally optimal). Incubate for 60 min at room temperature with gentle agitation or overnight at 4°C.

6. Add 5 ml of the rinsing solution. Centrifuge at 300 g for 5 min.

7. *Use the isotype immunoglobulin as a negative control. Process as in steps 5 and 6.*

8. Resuspend cells in 100 µl of rinsing solution that contains the fluoresceinated secondary Ab, generally at a final 1 : 20 to 1 : 40 dilution. Incubate at room temperature for 30–60 min, agitating gently.

9. Add 5 ml of the rinsing solution and centrifuge at 300 *g* for 5 min.

10. Suspend the cell pellet in 1 ml PBS containing 5 µg/ml of PI and 100 µg of DNase-free RNase A. Keep in the dark at room temperature for 1 h.

11. Transfer cells to flow cytometer. Use blue light (488-nm laser line) for fluorescence excitation. Measure cell fluorescence in green (FITC, 530 ± 20 nm) and red (PI, >620 nm) light wavelengths.

NOTE If the primary Ab is fluorochrome tagged, skip step 8.

Comments

The critical steps for immunocytochemical detection of intracellular proteins are cell fixation and permeabilization. The fixative is expected to stabilize the antigen *in situ* and preserve its epitope in a state where it remains reactive with the Ab. The cells have to be permeable to allow the access of the Ab to the epitope. The choice of optimal fixative and permeabilizing agent varies, primarily depending on the intracellular antigen, less on the cell type. General strategies of cell fixation, permeabilization, and stoichiometry of antigen detection are discussed by Jacobberger (2001). Cold methanol appears to be optimal for the detection of D-type cyclins. For cyclins E, A, and B1, 70% cold ethanol is equally good.

Also critical is choice of a proper Ab. Often, the Ab applicable to immunoblotting fails in immunocytochemical application, and *vice versa*. This may be due to differences in the *in situ* accessibility of the epitope or differences in degree of denaturation of the antigen on the immunoblots compared to that within the cell. Some epitopes may not be accessible *in situ* at all, whereas the accessibility of others may vary depending on their functional state, e.g., due to phosphorylation or steric hindrance. Because there is strong homology between different cyclin types, cross-reactivity may also be a problem. Because commercially available Abs may differ in specificity, degree of cross-reactivity, and so on, it is essential to provide detailed information (vendor and the hybridoma clone number) of the reagent used in the study.

Cyclins are key components of the cell cycle progression machinery (Sheer, 2000). During unperturbed growth of normal cells the timing of expression of several cyclins, particularly cyclins D, E, A, and B, is discontinuous, occurring as discrete and well-defined periods of the cell cycle (Fig. 3). This periodicity in cyclins expression provides new cell cycle landmarks that can be used to subdivide the cell cycle into several

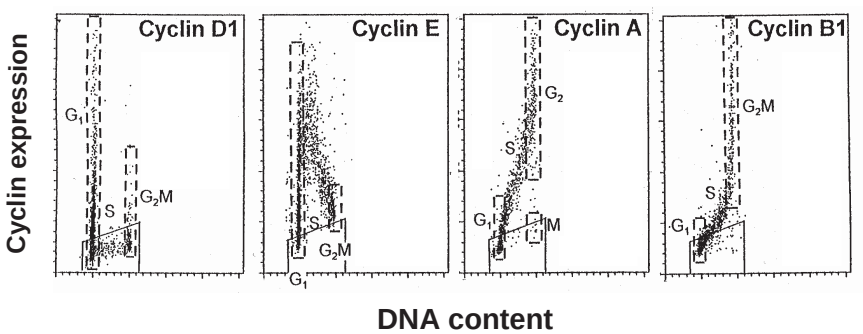

FIGURE 3 Typical expression of cyclins D1, E, A, and B1 *vs.* DNA content as seen in normal, nontumor cells, processed as described in the text. Expression of cyclin D1 is shown in exponentially growing human normal fibroblasts. Expression of cyclins E, A, and B1 in PHA-stimulated human lymphocytes 48 h after administration of PHA. Boundaries of G_1 and G_2/M populations are marked by dashed lines. Trapezoid windows show the level of the unspecific, background, fluorescence measured separately using the isotypic irrelevant Ab. It is evident that cyclin D1 is expressed by a fraction of G_1 cells; cells entering and progressing through S and most in G_2/M cells are cyclin D1 negative. Cyclin E is maximally expressed by cells entering S phase and its level drops during progression through S. Cyclin A is expressed by S phase and maximally by G_2 cells; mitotic cells (postprometaphase) are cyclin A negative. Cyclin B1 is expressed by late S cells, maximally in G_2 and M.

subcompartments, additional to the subdivision of into four major phases (Darzynkiewicz *et al*., 1996). Furthermore, bivariate analysis of cyclins expression *vs* DNA content makes it possible to discriminate between cells having the same DNA content but residing in different phases of the cycle, such as between G_2 and M cells (based on differences in cyclin A content), or between G_2 diploid and G_1 tetraploid cells (based on differences in expression of cyclins E and/or B1). Likewise, G_0 cells lacking expression of D-type cyclins or cyclin E can be distinguished from cells that entered cell cycle and become cyclins D, and subsequently cyclin E, positive. Strategies for the use of cyclins as additional markers of the cell cycle position are discussed elsewhere (Darzynkiewicz *et al*., 1996). It should be noted, however, that some tumor cell lines, or normal cells when their cell cycle progression is perturbed, show unscheduled expression of cyclins D, E, and B1; namely G_1 cyclins (e.g., cyclin E) are expressed during G_2/M and the G_2/M cyclins (cyclin B1) during G_1 (Darzynkiewicz *et al*., 1996).

3. *Identification of Mitotic Cells by Cytometry*

There is often a need to estimate mitotic index, e.g., to assess effectiveness of the drugs that disrupt microtubules or in stathmokinetic experiment (Darzynkiewicz *et al*., 1987) to reveal the rate of cell entrance to mitosis. The cytometric methods used to identify mitotic cells are reviewed by Juan *et al*. (2001). The most convenient immunocytochemical method appears to be the one that utilizes Ab that is specific to histone H3 phosphorylated on *Ser*-10 (H3-P), the event that occurs during mitosis (Juan *et al*., 2001). Because histone H3 is phosphorylated during prophase and is dephosphorylated late in telophase, the "time window" of detection of mitosis by this Ab spans these two mitotic stages. Histone H3-P-specific Abs are offered by Sigma Chemical Co. (monoclonal) and Upstate Biotechnology, Inc. (polyclonal). The methodology of cell staining and fluorescence measurement is similar to that described earlier for analysis of DNA content and proliferation-associated proteins. Optimal cell fixation, however, requires a brief (15 min) pretreatment with 1% formaldehyde (in PBS, on ice) followed by postfixation in 70% ethanol. The results of fluorescence measurement are shown in Fig. 4.

C. Analysis of DNA Replication and Cell Cycle Kinetics

1. *Stathmokinetic Approach*

In a classical stathmokinetic experiment, the agent arresting cells in mitosis (e.g., colcemide or vinblastine) is added into the culture during the exponential phase of cell growth and the proportion of cells in mitosis is estimated as a function of the time of arrest. The slope of the plot representing an increase in the percentage of M cells during stathmokinesis reveals the *rate* of cell entry to M ("mitotic rate"; "cell birth rate").

Flow cytometric analysis of the stathmokinetic experiment can be based either on quantification of the increased proportions of cells in G_2 + M, represented by the G_2/M peak on the DNA content frequency histograms (by DNA content measurement followed by univariate data analysis), or by enumeration of cells in M (by selective staining of M cells, e.g., as shown in Fig. 4, followed by multivariate analysis of such data). Depletion of cells from the G_1 compartment (G_1 exit rate), as well as the rate of cell progression through S

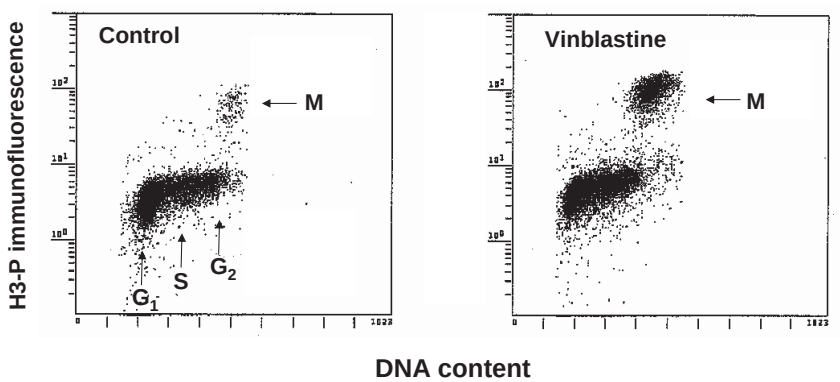

FIGURE 4 Immunocytochemical identification of mitotic cells (M) using Ab that reacts with histone H3 phosphorylated on *Ser*-10. To increase the proportion of mitotic cells, the culture shown at the right was treated for 4 h with the metaphase-arresting agent vinblastine.

phase can also be measured during stathmokinesis (Darzynkiewicz *et al*., 1987). This section describes the scheme of a simple stathmokinetic *in vitro* experiment.

Solutions

Depending on the method used to stain DNA (Fig. 1) or detect mitotic cells (Fig. 4), appropriate solutions, as described earlier in the article, should be applied.

Steps

1. To the exponentially and asynchronously growing cell culture add the stathmokinetic agent (e.g., colcemid, vinblastine, or nocodazole) at the concentration that arrests all cells entering mitosis and yet does not perturb the progression through other phases. Different cell types show different sensitivities to particular agents and pilot experiments testing various concentrations of the agents are often needed to estimate efficiency of the cell arrest. Vinblastine, at a final concentration of 50 ng/ml, is quite effective in arresting most cell types of hematopoietic lineage in mitosis.
2. Collect cells hourly, during a time interval equivalent to approximately one-third of the cell doubling time, and fix them in suspension.
3. Use the flow cytometric staining techniques that allow either identification of cells in G_1, S, and G_2 + M (e.g., as in Fig. 1) or multiparameter analysis, which allows one to distinguish M cells (e.g., as in Fig. 4).
4. Analyze data to obtain the percentage of cells in the respective phases of the cycle per each sample.
5. Plot data as in Fig. 5. From the graphic display estimate the kinetic parameters, as shown in Fig. 5 and described in the legend. A more detailed analysis of the stathmokinetic experiment was presented elsewhere (Darzynkiewicz *et al*., 1987).

Comments

A major drawback of the methods based on single time point measurement is lack of kinetic information. These methods, thus, cannot distinguish whether cell cycle progression is accelerated, slowed down, or even halted, e.g., during drug treatment, if G_1, S, and G_2/M phases are affected proportionally to each other. The stathmokinetic approach can be used in such instances to reveal cell kinetics. The alternative method, namely cell synchronization followed by observation of the cycle progression of the synchronized cells cohort, is more complex and time-consuming.

2. *BrdUrd Incorporation*

Incubation of cells in medium containing BrdUrd results in its incorporation during DNA replication (S phase). The incorporated BrdUrd can be detected either cytochemically, by virtue of its propensity to quench the fluorescence of several DNA fluorochromes such as Hoechst 33358 or AO, or immunocytochemically using poly- or monoclonal Abs against this precursor.

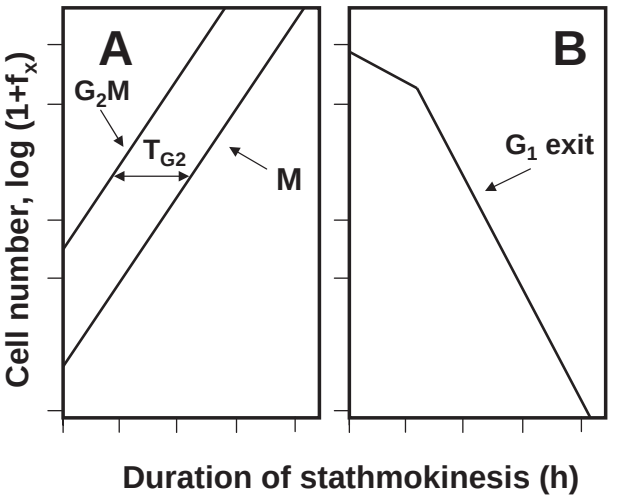

FIGURE 5 The scheme of analysis of the stathmokinetic experiment. Asynchronously and exponentially growing cell cultures were treated with the metaphase-arresting stathmokinetic agent and subsequently sampled to obtain percentage of cells in M or G_2/M and in G_1 (e.g., as in Fig. 1 or 4). The percentage of cells in these phases (expressed as fraction of total; f_x) at a given time point of mitotic arrest is then plotted as log (1 + f_x). The slope representing the rate of entrance to M (or G_2 + M) reveals duration of the cell cycle (T_c). The duration of G_2 (T_{G2}) is estimated as the time–distance of the G_2 + M *vs* M slopes (A). Because of block of the cell cycle progression in M, the rates of emptying the G_1 (G_1 exit) can also be estimated (B). The stochastic component of the rate of cell exit from G_1 manifests as the straight-line slope that reveals the half-time of cell residence in G_1 (Darzynkiewicz *et al*., 1987).

Continuous or pulse-chase cell labeling with BrdUrd, followed by detection of BrdUrd simultaneously with measurement of cellular DNA content and bivariate data analysis (Dolbeare *et al*., 1983; Terry and White, 2001), allows one to estimate a variety of cell cycle parameters. The protocol of Dolbeare *et al*., (1983), with more recent modifications (Gray *et al*., 1990), is given here. DNA denaturation by acid (HCl) gives more satisfactory results in some cell types.

a. Thermal Denaturation of DNA

Solutions

1. DNA denaturation buffer: 0.1 m*M* Na–EDTA in 1 m*M* Na–cacodylate; final pH 6.0
2. *Diluting buffer*: PBS containing 0.1% Triton X-100 and 0.5% bovine serum albumin (BSA)

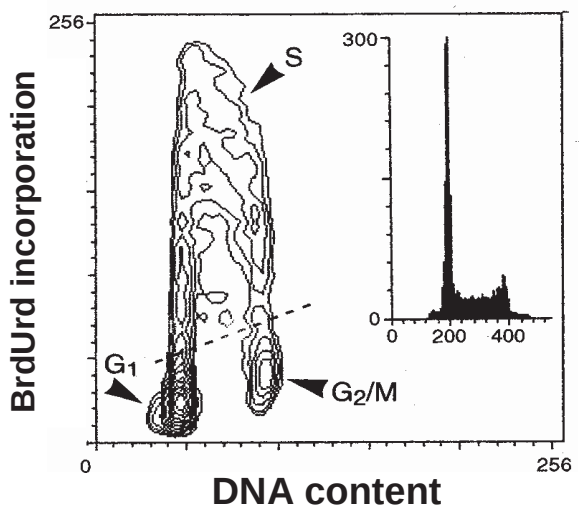

FIGURE 6 Bivariate distribution of cellular DNA content and BrdUrd incorporation. HL-60 cells were incubated with BrdUrd for 30 min, fixed, DNA was denatured by 2*M* HCl, the incorporated BrdUrd was detected by the monoclonal antibody, and DNA was counterstained with PI, as described in the text.

Steps

1. Incubate cells with 10–30 µg/ml of BrdUrd under light-proof conditions.
2. Fix cells in suspension in 70% ethanol.
3. Centrifuge cells (1–2 × 10^6) at 200 g for 3 min, resuspend cell pellet in 1 ml of diluting buffer containing 100 µg/ml of RNase A, and incubate at 37°C for 30 min.
4. Centrifuge cells (300 g, 3 min) and suspend cell pellet in 1 ml of ice-cold 0.1*M* HCl containing 0.1% Triton X-100. After 1 min, centrifuge cells again. Drain thoroughly and resuspend in 5 ml of DNA denaturation buffer.
5. Centrifuge cells again and resuspend cell pellet in 1 ml of DNA denaturation buffer.
6. Heat cells at 90 or 95°C for 5 min and then place on ice for 5 min.
7. Add 5 ml of diluting buffer. Centrifuge (300 g).
8. Drain well and suspend cells in 100 µl of BrdUrd Ab, dissolved in diluting buffer, for 30 min at room temperature (follow the instructions provided by the supplier regarding the dilution, time, and temperature of incubation with anti-BrdUrd).
9. Add 5 ml of dilution buffer and centrifuge.
10. Suspend cells in 100 µl of FITC-labeled goat antimouse IgG (dissolved in diluting buffer) and incubate for 30 min at room temperature.
11. Add 5 ml of diluting buffer, centrifuge, drain, and resuspend in 1 ml of this buffer containing 5 µg/ml of PI.
12. Measure the BrdUrd-associated green fluorescence and DNA-associated red fluorescence as described earlier in procedure B2.

NOTE: If the primary Ab is fluorochrome-tagged, skip step 10.

b. Denaturation of DNA by HCl

Solution

Diluting buffer: same as for thermal denaturation of DNA

Steps

1. Follow steps 1–4 as described earlier for thermal denaturation of DNA.
2. Centrifuge cells (300 g, 3 min) and resuspend cell pellet in 1 ml of 2*M* HCl. After 20 min at room temperature, add 5 ml of HBSS, centrifuge, and drain well. Resuspend cells in 5 ml of 0.2*M* phosphate buffer at pH 7.4 to neutralize traces of the remaining HCl.
3. Centrifuge cells at 300 *g*
4. Follow steps 8–12 as described earlier for thermal denaturation of DNA.

Comments

The critical step in this procedure is induction of partial DNA denaturation. This step often results in cell damage and leads to significant cell loss. Use of silinized tubes during centrifugations may decrease cell loss. Also, there are differences in sensitivity of DNA to denaturation between cell types, depending on their chromatin structure. Thus, while induction of DNA denaturation by acid may prove to be satisfactory with one cell type, it may fail with another. Some cell types require higher acid concentration (4*M*) for optimal results.

The alternative approach is based on selective photolysis of DNA that contains the incorporated BrdUrd followed by DNA strand break labeling (Li *et al.*, 1996). Because no heat or acid treatment is required, the latter procedure is applicable in combination with immunocytochemical analysis.

The scope of this article makes it impossible to describe all possibilities of analysis of the cell cycle based on BrdUrd incorporation, either after the pulse-chase or continuous cell labeling. Readers are advised to consult Dolbeare and Selden (1994) and Terry and White (2001) for a more detailed description of these methods.

IV. CELL ANALYSIS BY LASER-SCANNING CYTOMETER

All the methods described earlier can be adapted to stain cells mounted on microscope slides, to be analyzed by the multiparameter (three-laser excitation, four-color fluorescence detection) LSC (Darzynkiewicz *et al*., 1999; Kamentsky, 2001). To be analyzed by LSC the cells are attached to the slides electrostatically or by cytospinning, fixed, rinsed and then subjected to the procedures as presented earlier. To attach cells by cytospinning, 300 µl of cell suspension in tissue culture medium (with serum) containing approximately 20,000 is added to a cytospin chamber. The cells are then cytocentrifuged at 1000 rpm for 6 min and are submerged in the respective fixative in Coplin jars.

Small volumes of the respective buffers, rinses, or staining solutions as described for each of the methods in this article, are carefully layered on the cytospin area of the horizontally placed slides. At appropriate times these solutions are removed with a Pasteur pipette (or vacuum suction pipette). Small pieces (1 × 1 cm) of thin polyethylene or Parafilm foil may be layered on slides atop of the drops of the solutions used for cell incubations, over the cytospins, to prevent drying. The incubations should be carried out in a moist atmosphere.

At the final step of each particular staining procedure the cells are mounted in a drop of the respective staining solution, made identical as for flow cytometry, under the coverslip. The coverslips may be sealed with melted paraffin or a gelatin-based sealer. The cell fluorescence is measured by LSC, and the choice of the fluorescence excitation wavelength and emission filters is the same as described earlier for flow cytometers.

V. LIMITATIONS AND PITFALLS

1. Each approach has different type of limitations and possible pitfalls. The most frequent pitfall in univariate cell cycle analysis is lack in accuracy of DNA content measurement. As noted earlier, the accuracy is expressed as cv of the mean DNA content of G_1 cells. The results are unacceptable if the cv is larger than 8%; optimally, cv should be below 2%. Inappropriate adjustment of optics and fluidics of the flow cytometer are the most common causes of inaccuracy of DNA content analysis.

2. Common pitfalls in analysis of proliferation-associated antigens are due to inappropriate cell fixation and inappropriate choice of the antibody. Pilot experiments, testing different fixatives, different means of cell permeabilization, and different titer of the antibody, should be performed in the case of each new antigen. Many monoclonal antibodies that are available commercially have been developed to denatured proteins may not be applicable for immunocytochemistry. Although the isotypic IgG is commonly used as a negative control, some IgG preparations may show reactivity to various cell constituents. The optimal negative control is the same cell line having gene coding for the studied protein deleted, if available.

3. In the case of BrdUrd techniques, the unpredictable variable that affects cell stainability is variation in chromatin structure between different cell types. Hence, the methods should often be optimalized for a particular cell type by testing different temperatures of DNA denaturation (80–100°C) or different strength of HCl used to induce DNA denaturation (1–4 *M*).

Acknowledgment

Supported by NCI RO1 96 704. Dr. Gloria Juan is currently at the Sloan-Kettering Cancer Institute, New York. Dr. P. Pozarowski is on leave from the Department of Immunology, School of Medicine, Lublin, Poland.

References

Bauer, K. D., and Jacobberger, J. (1994). Analysis of intracellular proteins. *Methods Cell Biol*. **41**, 352–376.

Crissman, H. A., and Hirons, G. T. (1994). Staining of DNA in live and fixed cells. *Methods Cell Biol*. **41**, 196–209.

Darzynkiewicz, Z., Crissman, H. A., and Robinson, J. P. (eds.) (2001). *Methods Cell Biol*. **63** and **64**.

Darzynkiewicz, Z., Gong, J., Juan, G., Ardelt, B., and Traganos, F. (1996). Cytometry of cyclin proteins. *Cytometry* **25**, 1–13.

Darzynkiewicz, Z., Gong, J., and Traganos, F. (1994). Analysis of DNA content and cyclin protein expression in studies of DNA ploidy, growth fraction, lymphocyte stimulation and cell cycle. *Methods Cell Biol*. **41**, 422–436.

Darzynkiewicz, Z., Robinson, J. P., and Crissman, H. A. (eds.) (1994). *Methods Cell Biol*. **41** and **42**.

Darzynkiewicz, Z., Traganos, F., and Kimmel, M. (1987). Assay of cell cycle kinetics by multivariate flow cytometry using the principle of stathmokinesis. *In* "*Techniques in Cell Cycle Analysis*" (J. W. Gray and Z. Darzynkiewicz, eds.), pp. 291–336. Humana Press, Clifton, NJ.

Darzynkiewicz, Z., Traganos, F., Sharpless, T., and Melamed, M. R. (1976). Lymphocyte stimulation: A rapid multiparameter analysis. *Proc. Natl. Acad. Sci. USA* **73**, 2881–2884.

Dolbeare, F., and Selden, J. L. (1994). Immunochemical quantitation of bromodeoxyuridine: Application to cell kinetics. *Methods Cell Biol*. **41**, 298–316.

Endl, E., Hollmann, C., and Gerdes, J. (2001). Antibodies against the Ki-67 protein: Assessment of the growth fraction and tools for cell cycle analysis. *Methods Cell Biol*. **63**, 399–418.

Fantes, P., and Brooks, R. (eds.) (1993). "*The Cell Cycle: A Practical Approach*." Oxford Univ. Press, Oxford.

Gray, J. W., and Darzynkiewicz, Z. (eds.) (1987). "*Techniques in Cell Cycle Analysis*." Humana Press, Clifton, NJ.

Gray, J. W., Dolbeare, F., and Pallavicini, M. G. (1990). Quantitative cell cycle analysis. *In* "*Flow Cytometry and Sorting*" (M. R. Melamed., T. Lindmo, and M. L. Mendelsohn, eds.), pp. 445–467. Wiley-Liss, New York.

Jacobberger, J. M. (2001). Stoichiometry of immunocytochemical staining reactions. *Methods Cell Biol.* **63**, 271–298.

Juan, G., Traganos, F., and Darzynkiewicz, Z. (2001). Methods to identify mitotic cells by flow cytometry. *Methods Cell Biol.* **63**, 343–354.

Kamentsky, L. A. (2001). Laser scanning cytometry. *Methods Cell Biol.* **41**, 51–88.

Larsen , J. K., Landberg, G., and Roos, G. (2001). Detection of proliferating cell nuclear antigen. *Methods Cell Biol.* **63**, 419–431.

Li, X., Melamed, M. R., and Darzynkiewicz, Z. (1996). Detection of apoptosis and DNA replication by differential labeling of DNA strand breaks with fluorochromes of different color. *Exp. Cell Res.* **222**, 28–37.

Poot, M., Silber, J. R., and Rabinovitch, P. S. (2002). A novel flow cytometric technique for drug cytotoxicity gives results comparable to colony-forming assays. *Cytometry* **48**, 1–5.

Rabinovitch, P. S. (1994). DNA content histogram and cell cycle analysis. *Methods Cell Biol.* **41**, 364–387.

Sheer, C. J. (2001). The Pezcoller lecture: Cancer cell cycles revisited. *Cancer Res.* **60**, 3689–3695.

Studzinski, G. P. (1995). "Cell Growth and Apoptosis: A Practical Approach." Oxford Univ. Press, Oxford.

Studzinski, G. P. (1999). "Cell Growth, Differentiation and Senescence: A Practical Approach." Oxford Univ. Press, Oxford.

Terry, N. H. A., and White, R. A. (2001). Cell cycle kinetics estimated by analysis of bromodeoxyuridine incorporation. *Methods Cell Biol.* **63**, 355–374.

CHAPTER

35

Detection of Cell Cycle Stages *in situ* in Growing Cell Populations

Irina Solovei, Lothar Schermelleh, Heiner Albiez, and Thomas Cremer

I. INTRODUCTION

Microscopic *in situ* detection of the cell cycle stages is based on immunocytochemical techniques and allows one to determine the stage of the cell cycle of individual cells. Of numerous antigenes specific for a certain cell cycle stage, the most often used one is nuclear protein Ki-67 (pKi-67). This protein is expressed only in cycling cells and is, therefore, used routinely in histopathological analyses to assess proliferating activity in suspected neoplastic tissues. Despite many investigations, its function remains not wholly clear (Endl and Gerdes, 2000). Importantly, pKi-67 changes its intranuclear distribution during progression of the cell cycle (Bridger *et al.*, 1998; Kill, 1996; Starborg *et al.*, 1996). **Figure 1** shows the distribution of pKi-67 at the main cell cycle stages of human primary fibroblasts. In early G1, pKi-67 accumulates in the assembling nucleoli and in sites enriched in heterochromatin; it forms numerous granules scattered over the nucleoplasm ("jaguar" pattern). Then—in late G1, during the entire S phase, and in G2—pKi-67 is localized predominantly in the nucleoli, mostly at their periphery. During late G2 and early prophase, when the nucleoli disassemble, the protein is diffusely distributed in the nucleoplasm. In later prophase, pKi-67 coats the surface of condensing chromosomes (forming "perichromosomal layer") and persists on the surface of mitotic chromosomes until late telophase. The protein especially strongly decorates heterochromatin regions of mitotic chromosomes (with exception to the centromeric heterochromatin), while NORs are free from pKi-67 (Traut *et al.*, 2002). Biochemical studies indicate that pKi-67 resides in the regions of the nucleus containing densely packed chromatin, most probably, heterochromatin (Kreitz *et al.*, 2000), and presumably, is involved in chromatin compaction. Indeed, the C-terminal domain of pKi-67 binds mammalian heterochromatin protein 1 (HP1) (Scholzen *et al.*, 2002) and sites where pKi-67 accumulates in early G1 become later HP1-binding foci (Kametaka *et al.*, 2002).

Based on pKi-67 immunostaining (see protocol **A**), one can distinguish between proliferating and quiescent cells and identify cells in early G1. Additional markers are still required to distinguish among late G1, S, and G2. Labeling with halogenated thymidine analogues (replication labeling) allows the recognition of S-phase cells (Aten *et al.*, 1992; Gratzner, 1982). The simple addition of bromdeoxyuridine (BrdU), chlorodeoxyuridine (CldU), or iododeoxyuridine (IdU) to growth medium leads to uptake and incorporation of these substances into nascent DNA. Halogenated nucleotides can be visualized by immunostaining after denaturation of DNA, which makes incorporated halogenated dUTPs accessible for antibodies. Denaturation is a critical step of detection because it can negatively affect preservation of cell morphology. In particular, incubation of cells in 2*N* HCl for 30–60 min (often used for denaturation) strongly impairs cell and nuclear morphology and, therefore, should be avoided in assays where the conservation of cell morphology is important. Heat denaturation in 70% formamide (**protocol B**) is a more protective method (Solovei *et al.*, 2002a,b), although it also damages cell morphology to a certain degree and can destroy useful antigenes. Noteworthy, this treatment causes significant losses in GFP fluorescence (Solovei *et al.*, 2002a). The recently developed protocol, based on enzymatic digestion of DNA (Tashiro *et al.*, 2000), combines good preservation of cell morphology

Copyright 2006, Elsevier Science (USA).
All rights reserved.

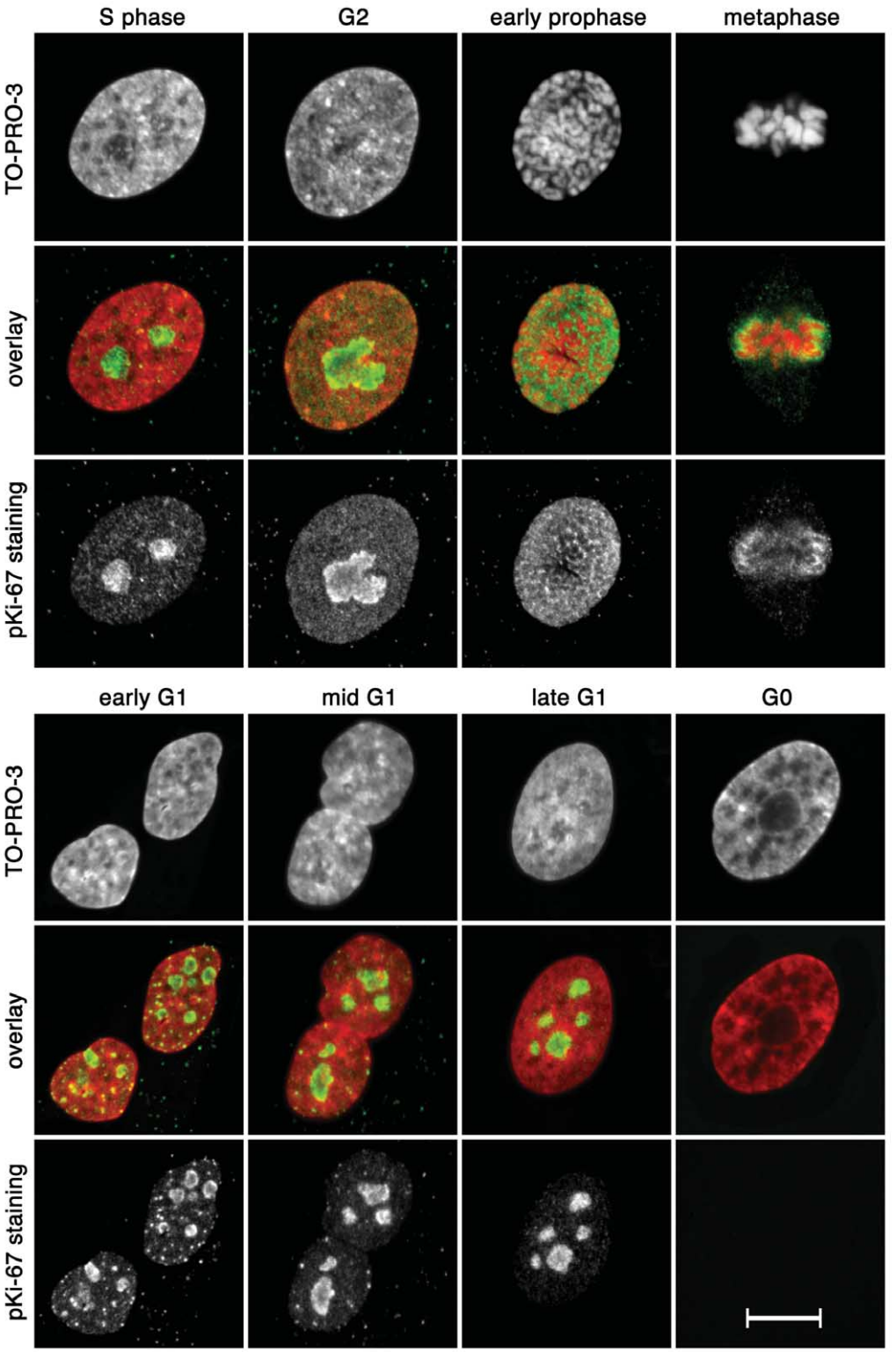
S phase
G2
early prophase
metaphase
TO-PRO-3
overlay
pKi-67 staining
early G1
mid G1
late G1
G0
TO-PRO-3
overlay
pKi-67 staining

◀ **FIGURE 1 Immunostaining of pKi-67 (protocol A).** The cells stained are human primary fibroblasts. For each stage of the cell cycle, three images represent DNA staining with TO-PRO-3 (top), pKi-67 immunostaining (bottom), and an overlay of the two with pseudocolors (mid): red for TO-PRO-3 and green for pKi-67. Each image is a maximum intensity projection of four midconfocal sections (1 µm) through a nucleus. **S phase** (S-phase cells were identified by BrdU labeling, data not shown)**:** only nucleoli are stained; a weak diffuse staining is observed in the nucleoplasm. **G2:** nucleoli often fuse, forming one huge nucleolus of a lobulated shape with an irregular edge; staining of the nucleoplasm is more intense than in S phase. **Early prophase:** pKi-67 is distributed over the entire nucleus and occupies all the space between condensing chromosomes. **Metaphase**: protein covers condensed chromosomes. The same distribution is observed in later prophase and in anaphase (not shown). **Early G1:** characteristic "jaguar" staining pattern; pKi-67 is located in reassembling nucleoli and in small multiple foci in the nucleoplasm. **Mid G1:** the number of foci in the nucleoplasm decreases. **Late G1:** staining is limited to the nucleoli. **G0:** in contrast to cycling cells, quiescent cells do not express pKi-67. Note that in cycling cells (but not in G0 cells), small foci of pKi-67 are also present in the cytoplasm; apparently, they are sites of pKi-67 synthesis. Scale bar: 10 µm.

and antigenes with effective disclosure of incorporated halogenated dUTPs (**protocol C**).

BrdU labeling also allows one to differentiate among early, mid, and late S-phase stages (**Fig. 2**). Pulse labeling with two halogenated nucleotides during two different time points results in differential staining of chromatin replicating at different periods of S phase in the same nuclei (Aten *et al*., 1992, 1993, 1994) (**protocol D**). Double replication labeling is an indispensable method used to establish the time sequence of replication events and is widely used in the studies of DNA replication in different cells and organisms (e.g., Ma *et al*., 1998; Visser *et al*., 1998; Zink *et al*., 1999; Habermann *et al*., 2001; Alexandrova *et al*., 2004). To exemplify the application of this method, **Fig. 3** shows different nuclear location of early (green) and mid (red) replicating chromatin in human fibroblast nucleus visualized by double replication labeling.

A combination of pKi-67 immunostaining and BrdU immunodetection (**protocol E**; **Fig. 4**) allows one to differentiate between all cell cycle stages with exception to late G1 and G2. It may be noted though that G2 nuclei have a more diffuse distribution of pKi-67 and fusing nucleoli; they are also noticeably larger than G1 nuclei. Though these characters are not clearly manifested in all cell types, with some experience they often help distinguish between G1 and G2 cells.

It is noteworthy, for a growing cell population with a known doubling time, that combined pKi-67 staining and BrdU labeling are sufficient to estimate duration of the main cell cycle stages. Duration of the cell cycle (or doubling time), T_d, is calculated from the formula:

$$T_d = \frac{\log 2 \times \Delta t}{\log N_2 - \log N_1}$$

where N_1 and N_2 are the number of counted cells per given area of a coverslip at time points 1 and 2, correspondingly, and Δt is the duration between two observations. The doubling time is equivalent to the cell cycle length when 100% of the cells proliferate, as can be estimated by immunodetection of pKi-67.

The proportion of quiescent (G0) cells, p_{G0}, is simply the proportion of pKi-67 negative cells. The length of S phase (T_S) is proportional to the proportion of S-phase (p_S, BrdU positive) cells:

$$T_S = T_d \cdot p_S / (1 - p_{G0}).$$

Similarly, the lengths of each substage of S phase can be estimated from proportions of cells showing early, mid, and late replication patterns, correspondingly. The proportion of early G1 cells, p_{G1e}, can be estimated by counting nuclei with specific "jaguar" pattern and duration of early G1:

$$T_{G1e} = T_d \cdot p_{G1e} / (1 - p_{G0}).$$

The length of mitosis and G2 do not vary significantly in mammalian cells and it is therefore assumed that they take about 1 and 2–3 h, respectively. On this basis, one can also assess the total duration of G1, T_{G1}, as difference between doubling time and duration of other cell cycle stages:

$$T_{G1} = T_d - (T_S + T_M + T_{G2}).$$

These calculations are simplified for immortalized cell lines in which there are no quiescent cells, i.e., essentially all cells are cycling, as, e.g., HeLa cells. Such populations indeed show a nearly 100% positive staining with pKi-67. In such cases,

$$T_S = T_d \cdot p_S \quad \text{and} \quad T_{G1e} = T_d \cdot p_{G1e}.$$

Table I exemplifies estimation of cell cycle stages lengths for two immortalized cell lines: neuroblastoma cells SH-EP N14 and HeLa.

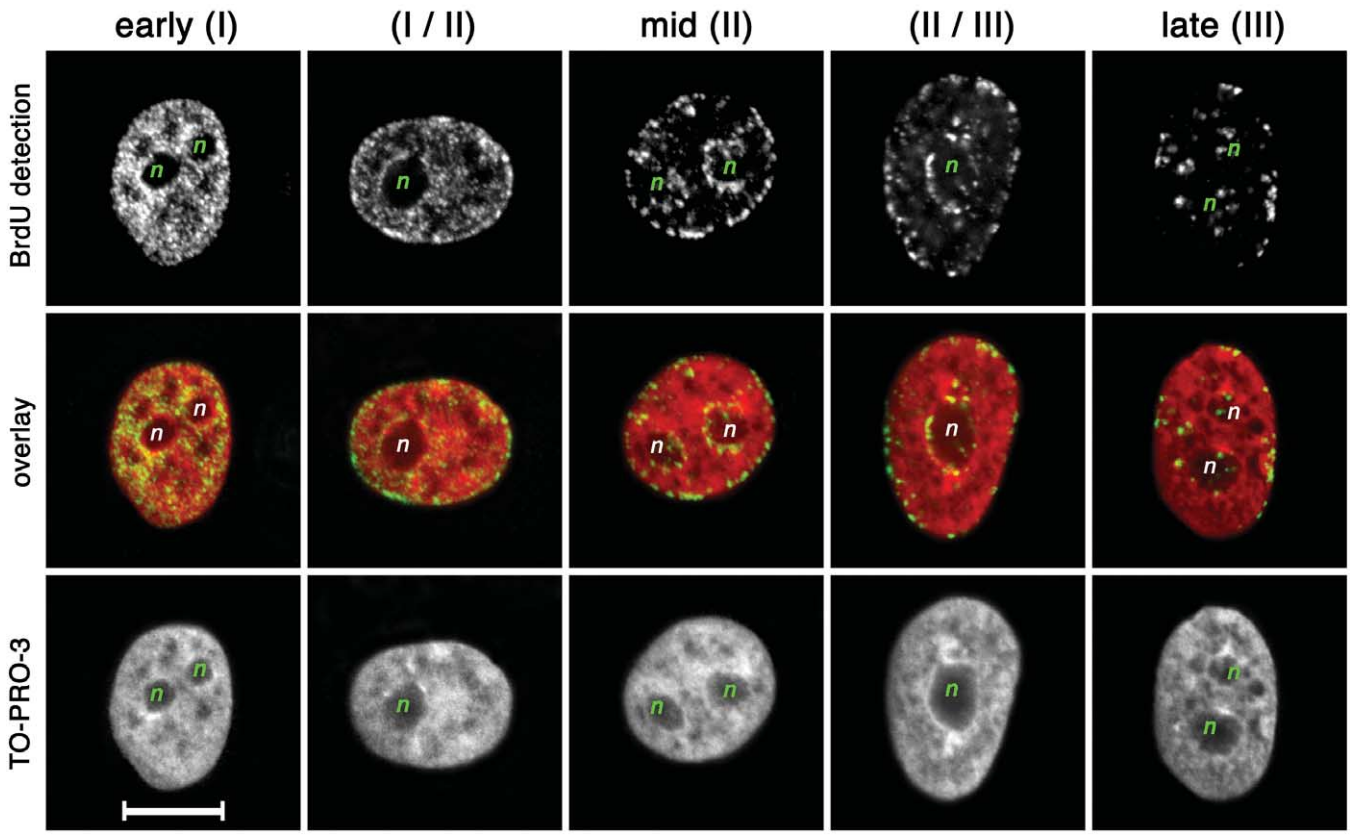

FIGURE 2 Replication labeling with BrdU (protocol C). Neuroblastoma SH-EP N14 cells were pulse labeled with BrdU for 40 min; BrdU immunodetection was performed using DNase digestion, counterstaining with TO-PRO-3. For each stage of the S phase, three images represent BrdU labeling (top), DNA staining with TO-PRO-3 (bottom), and overlay of the two with pseudocolors (mid): red for TO-PRO-3 and green for BrdU. Each image is a maximum intensity projection of four midconfocal sections (1 µm) through a nucleus. Three characteristic patterns change one another as the S phase proceeds. **Early S phase (pattern I):** all nucleoplasm is labeled with exception to the nucleoli (*n*) and speckles (dark areas in counterstaining). **Mid S phase (pattern II):** characteristic labeling is seen along the nuclear periphery and the border of the nucleolus (*n*); between these sites, signals are rare or lacking. **Late S phase (pattern III):** replication foci are significantly larger than in early and mid S phase; signals are observed at the periphery of the nucleus, at the border of nucleoli (*n*), and in nucleoplasm between them. Two transient patterns (I/II and II/III) are sometimes considered as separate S-phase stages (O'Keefe *et al.*, 1992). Scale bar: 10 µm.

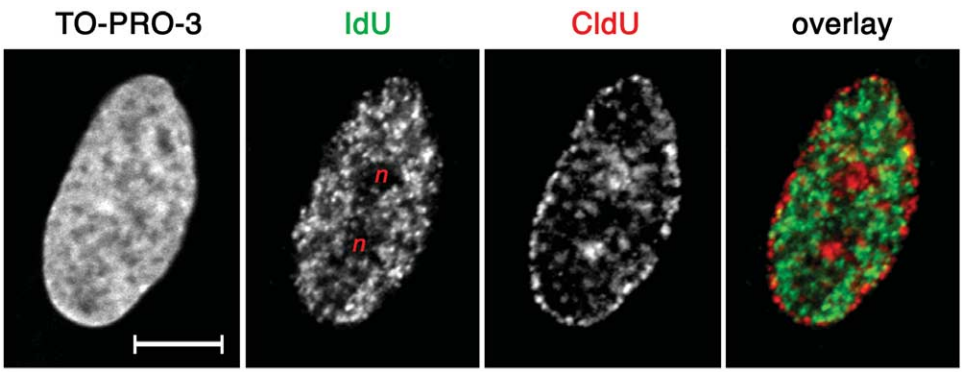

FIGURE 3 Double replication labeling with IdU and CldU (protocol D). Primary human fibroblasts were pulse labeled with IdU (green) in early S phase and with CldU (red) in mid S phase after a 4-h chase. Counterstaining with TO-PRO-3. Images represent the same midoptical section through the nucleus. Note that the midreplicating chromatin is mainly located at the very nuclear periphery and around nucleoli (*n*), whereas early replicating chromatin is distributed throughout the nuclear interior with exception of the nucleoli. Scale bar: 10 µm.

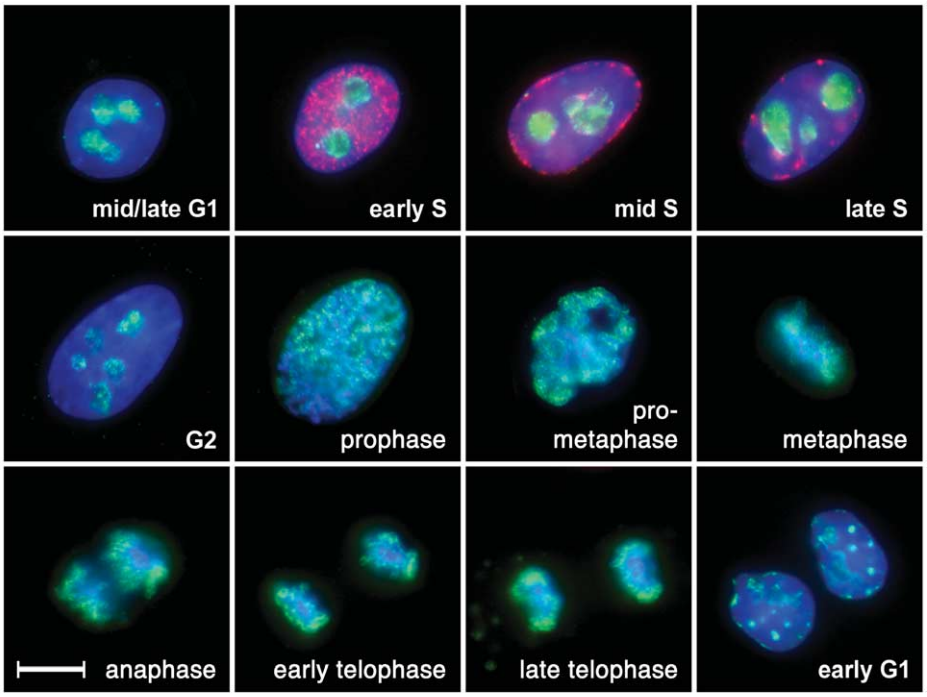

	S phase (early, mid, late)	G2	prophase metaphase anaphase telophase	early / mid G1	late G1	G0
BrdU	+	-	-	-	-	-
pKi-67	+ *nucleoli*	+ *nucleoli*	+ *chromosomes coating*	+ *nucleoli, heterochromatin granules*	+ *nucleoli*	-

FIGURE 4 Combined immunodetection of pKi-67 and BrdU (protocol E). Neuroblastoma cells SH-EP N14 were pulse labeled with BrdU for 30 min. After simultaneous detection of pKi-67 (green) and BrdU (red), nuclei were counterstained with DAPI (blue). Images are overlays of three gray scale pictures (one for each fluorochrome) collected using an epifluorescence microscope. Differences among stages of the cell cycle are summarized in Table I. Scale bar: 10 μm.

TABLE I Estimated Lengths of Main Cell Cycle Stages in Two Immortalised Nonsynchronized Cell Lines, Neuroblastoma Cells SH-EP N14, and HeLa Cells

	SH-EP N14		HeLa	
Doubling time = cell cycle length	**~13 h**		**~18 h**	
Proportion of cycling cells (pKi67 positive)	**100%**		**100%**	
Cell cycle stages	**% of cells**	**Length (h)**	**% of cells**	**Length (h)**
S phase (BrdU positive)	**47**	**~6.1**	**36**	**~6.5**
Early S	*25*	*~3.2*	*21.1*	*~3.8*
Mid	*17.5*	*~2.3*	*12.2*	*~2.2*
Late	*4.5*	*~0.6*	*2.7*	*~0.5*
G2 (constant)		**~2.5**		**~2.5**
Mitosis (constant)		**~1**		**~1**
Early G1 (specif. pKi67 pattern)	**15**	**~2**	**15**	**~2**
Mid–late G1 (remaining)		**~1.4**		**~6**

II. MATERIAL AND INSTRUMENTATION

1. Grow cell on coverslips of desirable size and thickness of 0.17 ± 0.01 mm. In case of cells growing in suspension, we recommend attaching living cells to coverslips coated with polylysine as described in detail elsewhere (Solovei *et al*., 2002b).

2. We recommend performing fixation and washings in 6-well plates; each well accommodates one coverslip of size ranging from 15 × 15 to 22 × 22.

3. To handle coverslips, use fine forceps (e.g., Dumont No. 4 or 5).

4. Special care must be taken not to dry cells at any steps of immunostaining. Make sure that when solutions are changed, coverslips always remain covered with liquid.

5. For incubation with antibody, use humid dark chambers with Parafilm on the bottom. Place drops of antibody solutions on Parafilm, and lay coverslips with cells on these drops with the cell side down. Carry out incubations at room temperature.

6. We recommend using Vectashield (Vector Laboratories; Cat. No. H-1000) as the antifade mounting medium. To mount cells, place a drop of Vectashield on a clean microscopic slide and quickly put coverslip with cells upside down on the antifade. Gently remove excess antifade medium with soft paper and seal with colourless nail polish (preferably, so called, base coat).

7. Mounted and sealed preparations can be stored in the dark at 4°C for months.

III. PROCEDURES

A. Immunostaining with Anti-Ki67 Antibodies

Solutions

1. Cell culture mediums used for respective cells

2. *Phosphate-buffered saline (1× PBS):* 140 m*M* NaCl, 2.7 m*M* KCl, 6.5 m*M* Na_2HPO4, 1.5 m*M* KH2PO4, pH 7.2

3. *Fixative:* 3.7% formaldehyde made before use from 37% stock solution (Sigma, Cat. No. F-1268) by dilution with 1× PBS

4. *PBST:* PBS with 0.05% Tween 20 (Calbiochem, Cat. No. 655204)

5. 1× PBS with 0.04% sodium azide (Merck, Cat. No. 106688)

6. 0.5% Triton X-100 (Sigma, Cat. No. T-8787) in 1× PBS

7. *Blocking solution:* 4% bovine serum albumin (BSA) in PBST. Store the stock solution of 12% BSA in PBS with 0.04% sodium azide at 4°C

8. Mouse anti-pKi-67 (DakoCytomation, Cat. No. M7240); working dilution = 1 : 100 in blocking solution

9. Any antimouse antibodies conjugated to a desirable fluorochrome. As two examples, we suggest goat antimouse-Cy3 (orange–red fluorescence, Jackson ImmunoResearch Laboratories, Cat. No. 115-165-072; working dilution = 1 : 200) or goat antimouse-Alexa 488 (green fluorescence; Molecular Probes, Cat. No. A-11017; working dilution = 1 : 500); antibodies are diluted in blocking solution

10. DNA-specific dye. The choice depends on the available microscopic filters or confocal laser lines and on fluorochrome chosen for secondary antibodies. The most popular counterstaining dyes are 4′,6-diamidino-2-phenylindole (DAPI, Sigma, Cat. No. D-9564) with blue fluorescence; propidium iodide (PI, Sigma, Cat. No. P-4170) with red fluoroscence; and TO-PRO-3 (Molecular Probes, Cat. No. T-3605) with emission in the far-red part of the spectrum. DAPI stock = 5 µg/ml in H_2O; working solution = 0.05 µg/ml. PI stock = 500 µg/ml in H_2O; working solution = 25 µg/ml. TO-PRO-3 stock = 1 m*M* in dimethyl sulfoxide (DMSO); working solution = 1 µ*M*. All stock solutions are kept frozen; working dilutions in PBST are done before use

11. RNase (Roche, Cat. No. 109169); stock solution = 20 mg/ml in 10 m*M* Tris–HCl + 15 m*M* NaCl; working solution = 0.2 mg/ml in PBS

Steps

1. Fix cells in 3.7% formaldehyde/PBS at room temperature for 10 min; wash in PBST, 3 × 5 min. If needed, fixed cells can be kept in PBS with 0.04% sodium azide at 4°C overnight or longer.

2. Permeabilize with 0.5% Triton X-100 in PBS for 5 min.

3. Incubate in blocking solution for 10 min.

4. Incubate with primary antibodies, mouse anti-pKi-67 for 30 min and wash with PBST 3 × 5 min.

5. Incubate with secondary antibodies, e.g., goat antimouse Alexa488 or goat antimouse-Cy3, for 30 min and wash with PBST 3 × 5 min.

6. Counterstain nuclei with DNA-specific dye (DAPI, PI, or TO-PRO-3) for 5 min and then rinse briefly in PBST. *Optional*: Because PI and TO-PRO-3 also stain RNA, slides can be preincubated in RNase working solution at 37°C for 30 min.

7. Mount cells in antifade medium and seal with nail polish.

B. Replication Labeling with BrdU and Detection with Heat Denaturation

Solutions

1. 5-bromo-2′-deoxyuridine (Sigma, Cat. No. B-9285). Make a 1 m*M* stock solution in H_2O, store aliquots at –20°C
2. 2 × SSC, pH 7.0; 1 × SSC is 0.15 *M* NaCl and 0.015 *M* sodium Na-citrate
3. 0.1 *N* HCl
4. 50% formamide (Merck, Cat. No. 1.09684) in 2 × SSC. Formamide is toxic, so all steps that involve the use of this reagent should be performed in a hood and gloves should be worn.
5. 70% formamide in 2 × SSC.
6. Mouse anti-BrdU (Roche, Cat. No. 7580), working dilution = 1 : 200 in blocking solution.
7. Any antimouse antibodies coupled to desirable fluorochrome. As two examples, we suggest the same secondary antibodies as for detection in protocol **A**.

The rest of the solutions are the same as for protocol **A**.

Steps

1. Grow cells to ≥50% confluency.
2. Add BrdU to the cell culture medium to a final concentration of 10–20 µ*M* and incubate for 15–60 min at 37°C in a CO_2 incubator.
3. Fix and permeabilize cells as described in protocol **A**.
4. Incubate in 0.1 *N* HCl for 10 min.
5. Wash with 2 × SSC for 5 min and equilibrate in 50% formamide/2 × SSC at room temperature for a minimum of 15 min. At this step, slides may be kept in 50% formamide at 4°C overnight or longer.
6. For cell DNA denaturation, warm up 70% formamide/2 × SSC to 70°C, immerse coverslips with cells for 2 min, and then immediately move them to ice-cold PBST and wash with PBST 3 × 5 min.
7. Incubate in blocking solution for 10 min.
8. Incubate with primary antibodies, mouse anti-BrdU for 30 min and wash with PBST 3 × 5 min.
9. Incubate with secondary antibodies, e.g., goat antimouse Alexa488 or sheep antimouse-Cy3, for 30 min and wash with PBST 3 × 5 min.
10. Mount cells in antifade medium and seal with nail polish.

Comments

BrdU pulse length can vary: only 5 min may be sufficient to detect the typical replication pattern. However, extended incubation time results in brighter signals, as more BrdU per replication focus is incorporated. At the same time, the replication pattern gradually becomes less distinct as pulse length exceeds 1 h.

C. Replication Labeling with BrdU and Detection with DNase Digestion

Roche Applied Science sells a kit for BrdU detection for immunofluorescence microscopy (Cat. No. 1296736), which is based on enzymatic digestion of DNA. The antibody to BrdU supplied with the kit contains nucleases generating single-stranded DNA fragments in the nucleus. As an alternative to the kit, this section describes a simple and inexpensive method that allows incorporated molecules of BrdU to be exposed to antibodies after DNase digestion.

Solutions

1. DNase I (Roche, Cat. No. 104 159); to make a stock solution, dilute to 1 mg/ml in 0.15 *M* NaCl in 50% glycerol, make aliquots, and store them at –20°C.
2. *DNase incubation buffer:* 0.5 × PBS, 30 m*M* Tris, 0.3 m*M* $MgCl_2$, 0.5 m*M* 2-mercaptoethanol, 0.5% bovine serum albumin, and 10 µg/ml DNase I.

The rest of the solutions are the same as for protocol **A**.

Steps

Steps 1–3 are the same as in protocol **A**.

4. Incubate in blocking solution for 10 min.
5. Dissolve primary antibodies against BrdU in the DNase incubation buffer and incubate as specified in protocol **B**.

The rest of the steps are the same as steps 9 and 10 in protocol **B**.

Pitfalls

The most probable cause for weak staining is bad DNase. In addition, an extra step with incubation in 0.1 *N* HCl for 5–10 min (see step 4 in protocol **B**) is recommended.

D. Double Labeling with IdU and CldU

Solutions

1. 5-Iodo-2′-deoxyuridine (IdU) (Sigma, Cat. No. I-7125). Make a 1 m*M* stock solution in 40% DMSO, store aliquots at –20°C

2. 5-Chloro-2′-deoxyuridine (CldU) (Sigma, Cat. No. C-6891). Make a 1 m*M* stock solution in H_2O, store aliquots at –20°C

3. Mouse anti-IdU and -BrdU [Becton Dickinson; Cat. No. 347580 (7580), clone B44], working dilution = 1:50

4. Goat antimouse-Alexa488 highly cross-adsorbed (Molecular Probes; Cat. No. A-11029), working dilution = 1:500

5. Rat anti-CldU and -BrdU [Harlan Sera-Labs, Cat. No. MAS 250, clone BU1/75 (ICR1)], working dilution = 1:200

6. Donkey antirat-Cy3 (Jackson ImmunoResearch, Cat. No. 712-165-153), working dilution = 1:200. All antibodies are diluted in blocking solution. Of course one can use a different pair of fluorochromes conjugated to secondary antibodies than Alexa488 and Cy3. Secondary antibodies themselves can also be changed without serious risk to spoil staining, whereas the choice of primary antibodies is crucial for successful staining.

7. *High stringency buffer*: 0.5 *M* NaCl, 36 m*M* Tris, 0.5% Tween 20, pH 8.0

The rest of the solutions are the same as for protocol **A.**

Steps

1. Grow cells to ≥50% confluency.

2. Add the required amount of IdU to the cell culture medium at a final concentration of 1–10 μ*M*; incubate for 30–45 min.

3. Remove incubation medium, rinse cells twice in PBS, and replace with fresh medium. Chase: incubate cells in fresh medium for the period equal to one-half to three-fourth of the S-phase duration. A chase time of 4–6 h is recommended for, e.g., human and mouse fibroblasts, HeLa cells, stimulated human lymphocytes, and lymphoblastoid cells.

4. Add the required amount of CldU to the cell culture at a final concentration of 1–10 μ*M*; incubate for 15 to 45 min.

5. Fix cells in 3.7% formaldehyde/PBS at room temperature for 10 min; wash in PBST, 3 × 5 min. If necessary, fixed cells could be kept in PBS with 0.04% sodium azide at 4°C overnight or longer.

6. Permeabilize cells with 0.5% Triton X-100 in PBS for 5 min.

7. The denaturation of DNA can be done either by heating in formamide (steps 5–7 in protocol **B**) or by DNase digestion (as described in protocol **C**). In the latter case, antibodies diluted in DNase incubation buffer should be rat anti-CldU/-BrdU (see later).

8. The recommended rat anti-BrdU antibodies detect both BrdU and CldU, but not IdU, and should be applied first. The recommended mouse anti-BrdU antibodies (Becton Dickinson), which are used for the detection of IdU, also have some affinity to CldU and must therefore be used after the detection of CldU. Apply antibodies against CldU (rat anti-CldU and -BrdU), incubate for 30 min, and wash in PBST 3 × 5 min.

9. Apply secondary antibodies for CldU detection, donkey antirat-Cy3; incubate for 30 min and wash in PBST 3 × 5 min.

10. Apply antibodies against IdU (mouse anti-IdU/-BrdU), incubate for 30 min, and wash in PBT 3 × 5 min.

11. Wash in the stringency buffer for 10 min to remove nonspecifically bound antibodies. This step is important, as some binding of mouse anti-IdU antibodies to CldU epitops still takes place, even after primary rat anti-CldU and secondary goat antirat antibodies were applied.

12. Apply secondary antibodies for IdU detection, goat antimouse-Alexa488, incubate in a dark humid chamber for 30 min, and wash in PBST 3 × 5 min.

13. Counterstain nuclei (with DAPI and/or TO-PRO-3), mount cells in antifade medium, and seal with nail polish.

Pitfalls

When the mouse anti-IdU/-BrdU antibody cross-reacts with CldU, the time of washing in the stringency buffer (step 11) should be increased.

E. Combination of Both Methods with Anti-Ki-67 Staining

Epitops of Ki-67 protein are stable and the protein can be detected after 0.1 *N* HCl and denaturation steps (with heat denaturation or DNase). Therefore, pKi-67 immunostaining can be performed either simultaneously or after detection of incorporated halogenated thymidine analogues. For simultaneous detection, primary antibodies against pKi-67 and BrdU are mixed; both secondary antibodies may also be applied as one solution.

Solutions

1. Mouse anti-BrdU (Roche, Cat. No. 7580); working dilution = 1:200
2. Rabbit anti-Ki-67 (DakoCytomation, Cat. No. A0047); working dilution = 1:50
3. Goat antimouse-Cy3 (Jackson ImmunoResearch Laboratories, Cat. No. 115-165-072); working dilution = 1:200
4. Goat antirabbit-FITC (BioSource, Cat. No. ALI 4408); working dilution = 1:200

All antibody dilutions are done in blocking solution.

Steps

Steps 1–7 are the same as in protocol **B**.

8. Incubate in mixture of mouse anti-BrdU and rabbit anti-Ki-67 antibodies at room temperature and wash with PBST 3 × 5 min.
9. Incubate in a mixture of goat antimouse-Cy3 and goat antirabbit-FITC and wash with PBST 3 × 5 min.
10. Counterstain nuclei, mount cells in antifade medium, and seal with nail polish.

Pitfalls

Special care should be taken to prevent cross-reaction of antibodies: use preadsorbed secondary antibodies and avoid using in the same experiment primary antibodies raised in closely related animals, e.g., mouse and rat or sheep and goat.

References

Alexandrova, O., Solovei, I., Cremer, T., and David, C. (2003). Replication labeling patterns and chromosome territories typical of mammalian nuclei are conserved in the early metazoan Hydra. *Chromosoma* **112**, 190–200.

Aten, J. A., Bakker, P. J., Stap, J., Boschman, G. A., and Veenhof, C. H. (1992). DNA double labelling with IdUrd and CldUrd for spatial and temporal analysis of cell proliferation and DNA replication. *Histochem. J.* **24**, 251–259.

Aten, J. A., Stap, J., Hoebe, R., and Bakker, P. J. (1994). Application and detection of IdUrd and CldUrd as two independent cell-cycle markers. *Methods Cell Biol.* **41**, 317–326.

Aten, J. A., Stap, J., Manders, E. M., and Bakker, P. J. (1993). Progression of DNA replication in cell nuclei and changes in cell proliferation investigated by DNA double-labelling with IdUrd and CldUrd. *Eur. J. Histochem.* **37**(Suppl. 4), 65–71.

Bridger, J. M., Kill, I. R., and Lichter, P. (1998). Association of pKi-67 with satellite DNA of the human genome in early G1 cells. *Chromosome Res.* **6**, 13–24.

Endl, E., and Gerdes, J. (2000). The Ki-67 protein: Fascinating forms and an unknown function. *Exp. Cell Res.* **257**, 231–237.

Gratzner, H. G. (1982). Monoclonal antibody to 5-bromo- and 5-iododeoxyuridine: A new reagent for detection of DNA replication. *Science* **218**, 474–475.

Habermann, F., Cremer, M., Walter, J., Hase, J., Bauer, K., Wienberg, J., Cremer, C., Cremer, T., and Solovei, I. (2001). Arrangements of macro- and microchromosomes in chicken cells. *Chromosome Res.* **9**, 569–584.

Kametaka, A., Takagi, M., Hayakawa, T., Haraguchi, T., Hiraoka, Y., and Yoneda, Y. (2002). Interaction of the chromatin compaction-inducing domain (LR domain) of Ki-67 antigen with HP1 proteins. *Genes Cells* **7**, 1231–1242.

Kill, I. R. (1996). Localisation of the Ki-67 antigen within the nucleolus: Evidence for a fibrillarin-deficient region of the dense fibrillar component. *J. Cell Sci.* **109**, 1253–1263.

Kreitz, S., Fackelmayer, F. O., Gerdes, J., and Knippers, R. (2000). The proliferation-specific human Ki-67 protein is a constituent of compact chromatin. *Exp. Cell Res.* **261**, 284–292.

Ma, H., Samarabandu, J., Devdhar, R. S., Acharya, R., Cheng, P. C., Meng, C., and Berezney, R. (1998). Spatial and temporal dynamics of DNA replication sites in mammalian cells. *J. Cell Biol.* **143**, 1415–1425.

O'Keefe, R. T., Henderson, S. C., and Spector, D. L. (1992). Dynamic organization of DNA replication in mammalian cell nuclei: Spatially and temporally defined replication of chromosome-specific alpha-satellite DNA sequences. *J Cell Biol.* **116**, 1095–1110.

Schmidt, M. H., Broll R., Bruch H. P., Bogler O., and Duchrow, M. (2003). The proliferation marker pKi-67 organizes the nucleolus during the cell cycle depending on Ran and cyclin B. *J. Pathol.* **199**, 18–27.

Schmidt, M. H., Broll, R., Bruch, H. P., and Duchrow, M. (2002). Proliferation marker pKi-67 affects the cell cycle in a self-regulated manner. *J. Cell Biochem.* **87**, 334–341.

Scholzen, T., Endl, E., Wohlenberg, C., van der Sar, S., Cowell, I. G., Gerdes, J., and Singh, P. B. (2002). The Ki-67 protein interacts with members of the heterochromatin protein 1 (HP1) family: A potential role in the regulation of higher-order chromatin structure. *J. Pathol.* **196**, 135–144.

Solovei, I., Cavallo, A., Schermelleh, L., Jaunin, F., Scasselati, C., Cmarko, D., Cremer, C., Fakan, S., and Cremer, T. (2002a). Spatial preservation of nuclear chromatin architecture during three-dimensional fluorescence in situ hybridization (3D-FISH). *Exp. Cell Res.* **276**, 10–23.

Solovei, I., Walter, J., Cremer, M., Habermann, F., Schermelleh, L., and Cremer, T. (2002b). FISH on three-dimensionally preserved nuclei. *In "FISH: A Practical Approach"* (B. Beatty, S. Mai, and J. Squire, eds.), pp. 119–157. Oxford Univ. Press, Oxford.

Starborg, M., Gell, K., Brundell, E., and Hoog, C. (1996). The murine Ki-67 cell proliferation antigen accumulates in the nucleolar and heterochromatic regions of interphase cells and at the periphery of the mitotic chromosomes in a process essential for cell cycle progression. *J. Cell Sci.* **109**, 143–153.

Tashiro, S., Walter, J., Shinohara, A., Kamada, N., and Cremer, T. (2000). Rad51 accumulation at sites of DNA damage and in postreplicative chromatin. *J. Cell Biol.* **150**, 283–291.

Traut, W., Endl, E., Garagna, S., Scholzen, T., Schwinger, E., Gerdes, J., and Winking, H. (2002). Chromatin preferences of the perichromosomal layer constituent pKi-67. *Chromosome Res.* **10**, 685–694.

Visser, A. E., Eils, R., Jauch, A., Little, G., Bakker, P. J., Cremer, T., and Aten, J. A. (1998). Spatial distributions of early and late replicating chromatin in interphase chromosome territories. *Exp. Cell Res.* **243**, 398–407.

Zink, D., Bornfleth, H., Visser, A., Cremer, C., and Cremer, T. (1999). Organization of early and late replicating DNA in human chromosome territories. *Exp. Cell Res.* **247**, 176–188.

CHAPTER

36

In vivo DNA Replication Labeling

Lothar Schermelleh

I. INTRODUCTION

DNA replication in higher eukaryotes takes place in a well-defined spatial and temporal manner. Large numbers of replication sites are simultaneously active, creating characteristic replication patterns during progression through S phase (Nakamura *et al.*, 1986; O'Keefe *et al.*, 1992). Each site is typically active for ~45 min, forming a replication focus of some 100 kb up to several Mb in size, consisting of a cluster of 1–10 simultanously firing replicons (Berezney *et al.*, 2000). Because the higher order chromatin structures revealed by replication foci persist through all stages of the cell cycle, they are referred to as ~1-Mb chromatin domains. Importantly, replication timing reflects important functional chromatin features, as the gene-rich, transcriptionally active euchromatin replicates during the first half of S phase, whereas gene-poor, heterochromatic sequences are later replicating (Cremer and Cremer, 2001).

In contrast to DNA labeling with halogenated thymidine analogues, which can be detected immunocytochemically after cell fixation and DNA denaturation, usage of fluorescent precursors allows the investigation of dynamic properties of ~1-Mb chromatin domains in living cells. Depending on the time period in S phase when the labeling is accomplished, early and mid to late replication foci can be specifically marked (Schermelleh *et al.*, 2001). Moreover, further proliferation of directly labeled cells results in the random distribution of sister chromatids with labeled and unlabeled chromatin domains during the second mitosis. Subsequent cell generations result in nuclei with few labeled chromosome territories (within a bulk of unlabeled chromatin). These cells are ideally suited to study chromatin domain/chromosome territory movements *in vivo* in relation to other nuclear components tagged, e.g., with green fluorescent protein (Walter *et al.*, 2003).

Several fluorochrome-coupled deoxynucleotides (dNTPs) are available commercially. The charged phosphate group and the attached fluorophore prevent the uptake of these nucleotides across the cell membrane. Hence, a procedure is required for dNTPs to pass the cell membrane barrier. A well-established and reliable method is microinjection of a nucleotide solution through a thin glass capillary directly into the cytoplasm or nuclei of adherently growing cells. (Ansorge and Pepperkok, 1988; Pepperkok and Ansorge, 1995; Zink *et al.*, 1998). However, this procedure is tedious, requires costly equipment, and allows only labeling of a rather small number of cells in each experiment.

A transient permeabilization that allows the uptake of macromolecules from the surrounding medium can be achieved by a number of methods (for review, see McNeil, 1989), yet not all of them are useful for *in vivo* replication labeling. Detergents (e.g., Triton X-100, saponin, or digitonin) permeabilize cells effectively, but have detrimental effects on cell viability, whereas more gentle "noninvasive" methods, such as lipofection and osmotic shift, are not efficient in our experience. More suitable regarding loading efficiency and viability are methods creating slight mechanical damage to the cell membrane in the presence of nucleotides. This can be achieved by shaking a labeling solution with small glass beads over a cell layer or by detaching a cell layer with a cell scraper.

Copyright 2006, Elsevier Science (USA).
All rights reserved.

The best results in terms of labeling efficiency, reproducibility, and amount of nucleotides needed were obtained by a modified scratch-loading protocol, termed scratch replication labeling. This protocol can be applied on any adherently growing cell line. It allows the labeling of a high number of cells within one experiment with little effort. Most importantly, it does not impair further growth of a large fraction of affected cells (Schermelleh *et al.*, 2001). This protocol has been applied for live cell studies of chromatin domains and chromosome territories (Walter *et al.*, 2003).

II. MATERIALS AND INSTRUMENTATION

Cy3-dUTP (Amersham Bioscience, Cat. No. PA53022), Cy5-dUTP (Amersham Bioscience, Cat. No PA55022), fluorescein-12-dUTP (Roche Cat. No. 1373242), disposable hypodermic needles (e.g., 0.45 mm × 25 mm), 15 × 15-mm square coverslips, 60/15-mm tissue culture dishes, phase-contrast microscope, appropriate cell culture medium (with HEPES), paper wipes (e.g., Kimwipes lite precision wipes, Kimberly-Clark), fine forceps, live cell chamber with fitting coverslips (e.g., Bioptechs FCS2).

III. PROCEDURE

Solutions

Appropriate cell culture medium (with 25 m*M* HEPES and supplemented with 10% fetal calf serum and antibiotics); labeling solution: 20 µ*M* (Cy3-dUTP) or 50 µ*M* (Cy5-dUTP, fluorescein-12-dUTP) in medium.

Steps

1. Seed cells on small coverslips (15 × 15 mm) and grow them until they reach near confluence.
2. Pick up the coverslip with fine forceps, drain excess medium, dry the bottom side of the coverslip briefly with a wipe, and place it into an empty tissue culture dish. This will prevent the coverslip from sliding during the subsequent scratching procedure.
3. Add 8–10 µl of the labeling solution onto the coverslip and distribute it evenly over the cells by gently tilting the dish. Surface tension will prevent the solution from running off the coverslip.
4. With the tip of a hypodermic needle, apply parallel scratches into the cell layer. For a high fraction of labeled cells, scratches should be performed a few cell diameters apart from each other and cover the complete coverslip (Fig. 1). For optimal coverage, the procedure can be performed under a low magnification phase-contrast microscope (e.g., 5× objective lens). The procedure should not take longer than a few minutes to avoid drying of the cells.
5. Add 5 ml prewarmed medium and incubate further. Exchange medium after 30–60 min to remove nonincorporated nucleotides.
6. To obtain nuclei with segregated labeled and unlabeled chromosome territories, the cells are harvested by trypsinization some hours later and cultivated further for two or more cell cycles prior to live cell observation. The day before live cell observations are carried out, seed cells on coverslips fitting the live cell chamber (Fig. 2).

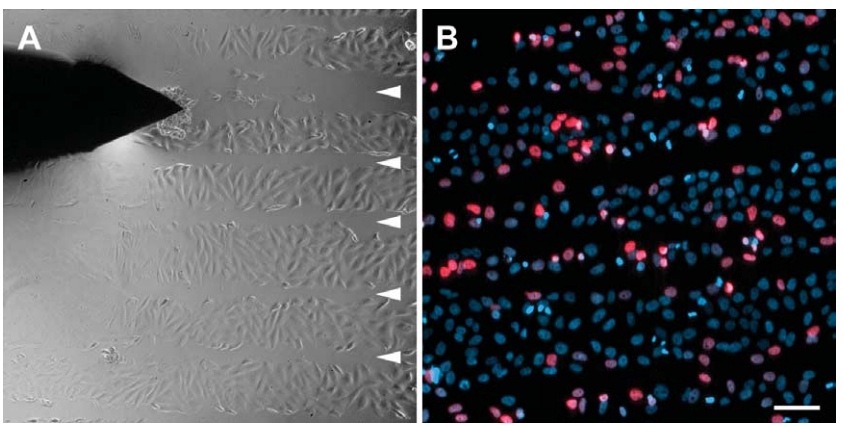

FIGURE 1 (A) Scratch replication labeling of human neuroblastoma cells. Arrowheads indicate scratches in the monolayer applied with the tip of a hypodermic needle (top left) in the presence of Cy3-dUTP. (B) Cells were fixed with 4% formaldehyde two hours after the scratching procedure and counterstained with 4', 6-diamidino-2-phenylindole (DAPI, blue). Numerous cells display Cy3-dUTP labeled nuclei (red) along the scratch lines. Bar: 100 µm.

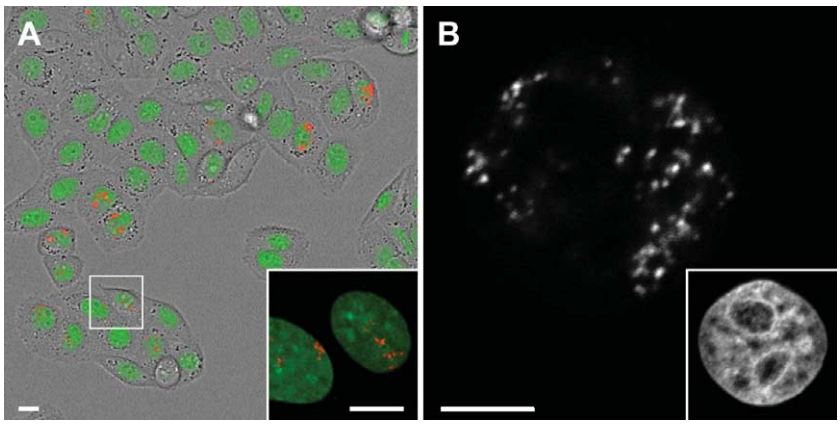

FIGURE 2 (A) Living HeLa cells with green fluorescent protein (GFP)-tagged histone H2B reveal green fluorescent nuclear chromatin. The cell culture was scratch labeled with Cy3-dUTP 5 days prior to observation in the live cell chamber. Numerous cells display nuclei with a few Cy3-labeled chromosome territories/~1-Mb chromatin domains. The framed cells are shown at higher resolution in the inset. Bars: 10 µm. (B) Confocal midsection of a HeLa cell expressing histone H2B-GFP fixed 3 days after labeling with Cy3-dUTP shows segregated chromosome territories/~1-Mb chromatin domains at high resolution. (Inset) GFP-labeled chromatin of the same nucleus. Bar: 5 µm.

IV. COMMENTS

The scratch procedure creates damage in the cell membrane that may last for only a few seconds ("transient holes"). This allows the uptake of charged macromolecules (such as fluorochrome-coupled dUTPs) from the surrounding medium, to which cells would normally be impermeable. Accordingly, most S-phase cells damaged alongside the scratch line or lifted off from the surface by the needle will incorporate the modified nucleotides.

The fraction of replication-labeled cells depends on the (1) density of scratches applied, i.e., how many cells are affected, and (2) number of cells that are in S phase. Synchronization of cells at the G1/S transition (e.g., by aphidicolin) is recommended to obtain a high yield of labeled cells.

A pool of fluorescent nucleotides is available for DNA replication over a time scale of roughly 1 h. The labeling pattern therefore resembles a BrdU-labeling experiment with ≤1-h pulse length.

Cy3-dUTP is significantly brighter and more photostable than Cy5- and fluorescein-dUTP and thus is best suited for *in vivo* observation. In cases where especially high fluorescence intensities are desirable (e.g., for long-term *in vivo* observations after segregation), a higher concentration of nucleotides (100 µ*M*) is advantageous. We did not note any improvement of label intensities when adding nonfluorescent dNTPs to the labeling solution or by using different labeling buffers (phosphate-buffered saline or Tris-buffered saline instead of medium).

For studies of nascent RNA formation, the scratch protocol can be applied accordingly using BrUTP (5 m*M* in medium) followed by immunofluorescent detection.

References

Ansorge, W., and Pepperkok, R. (1988). Performance of an automated system for capillary microinjection into living cells. *J. Biochem. Biophys. Methods* **16**, 283–292.

Berezney, R., Dubey, D. D., and Huberman, J. A. (2000). Heterogeneity of eukaryotic replicons, replicon clusters, and replication foci. *Chromosoma* **108**, 471–484.

Cremer, T., and Cremer, C. (2001). Chromosome territories, nuclear architecture and gene regulation in mammalian cells. *Nature Rev. Genet.* **2**, 292–301.

McNeil, P. L. (1989). Incorporation of macromolecules into living cells. *Methods Cell Biol.* **29**, 153–173.

Nakamura, H., Morita, T., and Sato, C. (1986). Structural organizations of replicon domains during DNA synthetic phase in the mammalian nucleus. *Exp. Cell Res.* **165**, 291–297.

O'Keefe, R. T., Henderson, S. C., and Spector, D. L. (1992). Dynamic organization of DNA replication in mammalian cell nuclei: Spatially and temporally defined replication of chromosome-specific alpha-satellite DNA sequences. *J. Cell Biol.* **116**, 1095–1110.

Pepperkok, R., and Ansorge, W. (1995). Direct visualization of DNA replication sites in living cells by microinjection of fluorescein-conjugated dUTPs. *Methods Mol. Cell Biol.* **5**, 112–117.

Schermelleh, L., Solovei, I., Zink, D., and Cremer, T. (2001). Two-color fluorescence labeling of early and mid-to-late replicating chromatin in living cells. *Chromosome Res.* **9**, 77–80.

Walter, J., Schermelleh, L., Cremer, M., Tashiro, S., and Cremer, T. (2003). Chromosome order in HeLa cells changes during mitosis and early G1, but is stably maintained during subsequent interphase stages. *J. Cell Biol.* **160**, 685–697.

Zink, D., Cremer, T., Saffrich, R., Fischer, R., Trendelenburg, M. F., Ansorge, W., and Stelzer, E. H. (1998). Structure and dynamics of human interphase chromosome territories *in vivo*. *Hum. Genet.* **102**, 241–251.

CHAPTER

37

Live Cell DNA Labeling and Multiphoton/Confocal Microscopy

Paul J. Smith and Rachel J. Errington

I. INTRODUCTION

Techniques for the discrimination and location of DNA, chromatin architecture, chromosomes, nuclear superstructures, and cell nuclei in their various forms through the cell cycle are of increasing interest in the biosciences and the generation of automated screening systems. The appropriate selection of a DNA-labeling dye may also be important for tracking events in microscale devices (e.g., lab on a chip). Here the critical issue is the transmittance advantage of longer wavelengths using external laser excitation or an incorporated source (e.g., a red laser diode within an optical biochip).

Advanced microscopy methods such as multi-photon excitation laser scanning (MPLSM) are now becoming more generally accessible, as they provide significant advantages in live cell studies. Although it is apparent that MPLSM technology will evolve, providing more convenient and adaptable systems, the principles discussed here will still apply. Currently, MPLSM instrumentation usually consists of a tuneable femtosecond pulsed infrared (IR) laser attached to a scanning microscope with IR-compatible optics to ensure efficient transfer of long wavelength light (690–1000 nm). Such a laser configuration provides virtually simultaneous delivery of two photons to a focal point of the microscope objective lens, achieving volume limited excitation by two or more photons of any fluorophor molecule with appropriate absorption characteristics. The advantages of this approach compared to confocal laser scanning microscopy (CLSM) are numerous. Because photons are only emitted from the "in focus" plane, all the photons can be collected via a nondescanning route, including those photons scattered by the sample and usually rejected at the confocal aperture. This provides a massively improved efficiency of emission light collection, an important consideration in photon-limited systems (White and Errington, 2002). Importantly, infrared light penetrates biological material further than shorter wavelengths and the potential damaging effects of ultraviolet (UV)-visible wavelengths are avoided. Reviews of the subject and information on two-photon fluorescence excitation cross sections are available (e.g., Denk *et al.*, 1995; Williams *et al.*, 2001; Albota *et al.*, 1998). However, a pragmatic outcome of the combined advantages of MPLSM is a resurgence of the use of UV-excited fluorescent probes, although these have pitfalls for use with GFP-based fluorophors (see later). Two-photon fluorescence absorption and emission spectra have been obtained for DNA probes relevant for live cell work. The technique of multi-photon excitation of a fluorophore, using a pulsed laser light source, provides solutions to several problems associated with continuous wave excitation via single photon absorption. Typically for multi-photon excitation the sample is illuminated with light of a wavelength which is approximately twice (or three times) the wavelenghth of the absorption peak of the fluorophore in use (Errington *et al.*, 2005) (Bestvater *et al.*, 2002; Smith *et al.*, 2000; van Zandvoort *et al.*, 2002) and a selection is shown in Table I.

DNA offers a highly attractive substrate for chemical and biophysical probe interactions and there are excellent references for the chemical descriptions and cytometric applications of a wide range of DNA dyes (Darzynkiewicz *et al.*, 1990; Latt and Langlois, 1990; Waggoner, 1990). The forms of interaction range from covalent binding, inter- and intrastrand cross-linking, adduct formation, to ternary complex formation with

Copyright 2006, Elsevier Science (USA).
All rights reserved.

TABLE I Cell-Permeant Nucleic Acid Probes Characterized for Both Single-Photon and Multiphoton Studies

Probe (product code)	SPE $Ex_{\lambda}max$[a] (nm)	MPE $Em_{\lambda}max$[b] (nm)	Em max (nm)	Reference for more MPE information
Acridine orange (A-3568)	500 (DNA) 460 (RNA)	837 > 882 >> 981	526 (DNA) 650 (RNA)	Bestvater *et al.* (2002)
DAPI (D-1036)	358	685 > 697 970[c]	461 (DNA) 500 (RNA)	Bestvater *et al.* (2002)
DRAQ5	647	1064	670	Smith *et al.* (2000)
Hoechst 33342 (H-3570)	350	660 > 715	461	Bestvater *et al.* (2002)
SYTO 13 (S-7575)	488	800	509	van Zandvoort *et al.* (2002)

[a] Single photon excitation wavelength maximum.
[b] Multiphoton excitation emission wavelength maximum.
[c] Three-photon excitation (Lakowicz *et al.*, 1997).

DNA-binding proteins. Additionally, major or minor groove residence are potentially stabilized through hydrogen bonding and van der Waals forces, phosphate group interactions, and various levels of intercalation between the base pairs. A restricted number of agents are now available for DNA labeling in live cell systems and MPLSM. The most frequently used are UV-excitable fluorochromes such as the bisbenzimidazole dyes Hoechst 33258 and Hoechst 33342, and the agent DAPI (4′, 6-diamidino-2-phenylindole). Cell-permeant, acridine orange displays metachromatic staining of nucleic acids that precludes its convenient use as an exclusively DNA-discriminating probe. The introduction of cell-permeant cyanine SYTO nucleic acid stains (Frey, 1995; Frey *et al.*, 1995) has provided many different reagents with a wide range of spectral characteristics. These agents passively diffuse through the membrane of most cells and can be excited by UV or visible light but stain RNA and DNA in both live and dead eukaryotic cells. Such dyes would be accessible to two-photon excitation (Table I). Their extremely low intrinsic fluorescence, with quantum yields typically less than 0.01 unbound (>0.4 when bound to nucleic acids), reduces the need to remove extracellular dye prior to imaging. It has been stressed that the highly versatile SYTO dyes do not act exclusively as nuclear stains in live cells and that they should not be equated in this regard with compounds such as DAPI or the Hoechst 33258 and Hoechst 33342 dyes.

At the other end of the fluorescence spectrum, DRAQ5, a DNA-binding anthraquinone derivative, can provide sufficient discrimination of cellular DNA content in multiparameter fluorescence studies. Anthraquinones are a group of synthetic DNA-intercalating agents (Lown *et al.*, 1985) but are only weakly fluorescence (Bell, 1988). DRAQ5 is a modified anthraquinone with enhanced DNA affinity and intracellular selectivity for nuclear DNA (Smith *et al.*, 1999, 2000). DRAQ5 appears to achieve its live cell nuclear discrimination by its high affinity for DNA. Excitation at the 647-nm wavelength, close to the $Ex_{\lambda max}$, produces a fluorescence spectrum extending from 665-nm out to beyond 780-nm wavelengths. Thus the emission spectrum is beyond that of fluorescein, phycoeryrthrin, Texas Red, Cy 3, and, perhaps most importantly, EGFP. (Waggoner, 1990) DRAQ5 enters cells and nuclei rapidly, the broad excitation spectrum of DRAQ5 means that flow cytometric applications can utilize excitation wavelengths down to 488 nm (Smith *et al.*, 2000); two-photon excitation is also permissible at wavelengths >1047 nm. The two-photon dark excitation region of DRAQ5 (720–860 nm) permits detection of low-intensity intracellular fluorescence of other probes by MPLSM and then definition of nuclear location by CLSM. This article provides simple procedures for two DNA-specific probes for living cells and their use in MPLSM studies. These dyes sit at either end of the excitation spectrum, Hoechst 33342 (UV excitable) and DRAQ5 (far red excitable), and therefore offer maximum flexibility in multiprobe analyses.

II. MATERIALS AND INSTRUMENTATION

Materials

DRAQ5 (molecular weight 412.54) dye is supplied as an aqueous stock solution of 5 m*M* (Biostatus Ltd) and can be diluted in aqueous buffers or added directly to full culture medium. DRAQ5 is stable at room temperature as a stock solution but can be stored routinely at 4°C, although freezing of the stock solution should be avoided. 33342 Hoechst (H-3570; termed here Hoechst 33342) has a molecular weight of 615.99 in the trihydrochloride/trihydrate form and is supplied by Molecular Probes Inc. as a 10-mg/ml stock solution in water in a light-excluding container. It is routinely stored at 4°C, without freezing. With both DNA dyes, appropriate safety information is available from the suppliers. Because both agents have the potential to damage DNA, they should be considered both cyto-

toxic and potentially mutagenic. Currently available information indicates that although they are not listed as carcinogens by the National Toxicology Program (NTP), the International Agency for Research on Cancer (IARC), or the Occupational Safety and Health Administration (OSHA), the dyes should be treated as such. Mitotracker Orange CMTMRos (M7510) is supplied by Molecular Probes in 20 × 50-μg aliquots, stored at –20°C. Before use a stock solution is made by the addition of 50 μl dry dimethyl sulfoticle, which can be subsequently frozen; however, repeated freeze–thawing is not recommended. Zinquin ethyl ester [Zinquin E, [2-methyl-8-(4-methylphenylsulfonylamino) quinolinyl] oxyacetic acid ethyl ester] (Alexis Corporation, Nottingham, UK) is stored as a 5 m*M* stock solution in ethanol at 4°C. The HEPES buffer (1 *M*) (Sigma; H-0887) filter-sterilized solution is stored at 4°C. Stock preparations of 8% paraformaldehyde (Sigma; P 6148) are made up in phosphate-buffered saline (PBS) lacking calcium and magnesium and are kept in aliquots of 20 ml at –20°C. All live cell work is conducted with cells seeded onto Nunc Lab-tek (#1 coverglass) chambered wells, appropriate for high-resolution imaging and recommended when handling cytotoxic agents.

Cytometry

The flow cytometry system is a FACS Vantage cell sorter (Becton Dickinson Inc., Cowley, UK) incorporating two lasers: (1) a Coherent Enterprise II laser simultaneously emitting at multiline UV (350- to 360-nm range) and 488-nm wavelengths and (2) a Spectra Physics 127–35 helium–neon laser (maximum 35-mW output) emitting at 633 nm with a temporal separation of about 25 μ from that of the primary 488-nm beam for the UV or red lines. Light scatter signals are collected as standard. The analysis optics are (i) primary beam-originating signals analyzed at FL3 (barrier filter of LP715 nm) after reflection at a SP610 dichroic and (ii) delayed beam-originating signals analyzed at FL4 (barrier filter of LP695 nm for DRAQ5 emission or DF660/20 nm for Hoechst 33342 emission) or at FL5 (barrier filter of DF424/44 nm for Hoechst 33342 emission). Forward and 90° light scatter are analyzed to exclude any cell debris. Optical filters are originally sourced from Becton Dickinson Inc. or Melles Griot Inc.). All parameters are analyzed using CellQuest software (Becton Dickinson Inc.).

Imaging

Multiphoton excitation at wavelengths between 720 and 980 nm uses a laser-scanning microscope comprising a 1024 MP scanning unit controlled by LaserSharp software (Bio-Rad Cell Science Division) attached to a Zeiss Axiovert 135 (Carl Zeiss Ltd.). MPLSM mode is achieved with a Verdi- Mira excitation source (Coherent UK Ltd.). The Mira Optima 900-F (Coherent UK Ltd.) is a simple, stable titanium:sapphire, KLM mode-locking system with X-wave optics, a broadband, single optics set tuning 700–1000 nm, and a purged enclosure. The continuous wave diode pump laser (Verdi) operates at 5 W at 532 nm. CLSM mode is achieved using the same scanning unit and 488-, 568-, and 647-nm lines of a krypton–argon laser. All images are collected with either a ×63, 1.4 NA oil immersion lens or a ×40 1.3 NA oil immersion lens. Typically, each optical slice consists of 512 × 512 (x,y resolution = 0.35 μm, z resolution is approximately 1 μm). Multiphoton excitation at 1047 nm uses a similar BioRad 1024 MP system incorporating an all solid-state excitation source Nd:YLF laser (Coherent UK Ltd.) and mode-locked femtosecond pulsed laser providing two-photon excitation of DRAQ5 at a 1047-nm wavelength at 15 mW with detection of fluorescence in the far red.

III. PROCEDURES

A. General Considerations

Hoechst 33342 is more lipophilic than Hoechst 33258 and is the form recommended for live cell studies showing high affinity for A-T base pairs through noncovalent binding in the minor groove of DNA. The ligand shows fluorescence enhancement upon binding. DRAQ5 is weakly fluorescent but has high DNA affinity and intracellular selectivity for nuclear DNA due to increased AT base pair preference but with no apparent fluorescence enhancement upon binding. When considering live cell labeling, the performance status of the cell is the most critical issue for achieving optimal staining. There is a subtle shift in the violet to red bias in the emission spectrum of Hoechst 33342 upon DNA binding. A small (approximately 10 nm) red shift in peak wavelength also occurs upon DRAQ5 binding. Nuclear staining is straightforward and most cultured cells label well in full culture medium (containing 10% fetal calf serum) supplemented with 10 m*M* HEPES, reaching equilibrium over some 5–60 min for concentrations in the 1–20 μ*M* range. Staining in phosphate buffers is less efficient. Staining rate is enhanced at 37°C. The following procedures are for generic uses of the dyes.

B. Two-Photon Excitation of Hoechst 33342

Steps

1. Seed cells onto a sterile glass coverslip in a culture dish (approximately 1×10^5 cells/25 cm^2) or

seed into a Nunc chamber coverslip. Incubate attached cultures under standard conditions until analysis is required. Add Hoechst 33342 directly to culture medium at a final concentration of 5 μ*M* (3.1 μg/ml).

2. For greater pH control conditions, especially when manipulating cells out of 5% CO_2 incubation, supplement the culture medium with HEPES buffer (final concentration 5–25 m*M*).

3. After a 60-min incubation (minimum of 15 min) at 37°C, wash coverslips gently in PBS to preserve mitotic cell attachment. Mount coverslips in an inverted position onto a microscope slide in PBS. To avoid cell crushing, the edges of the coverslip can be supported and sealed (e.g., using a piping of petroleum jelly). To clean the noncell side of the coverslip, the surface can be wiped (lens tissue).

4. Imaging conditions and typical results are shown in Fig. 1.

C. Two-Photon Coexcitation of Different Fluorophors

Steps

1. Generate cultures and label Hoechst 33342 as in Section III,B.

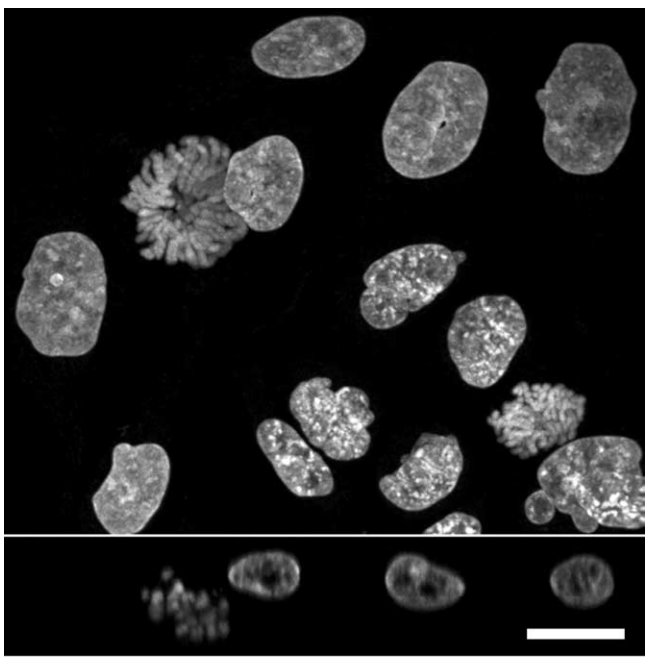

FIGURE 1 Two-photon excitation (Ex_λ 750 nm) of nuclear-located Hoechst 33342 in live HeLa cells (5 μ*M* × 60 min). (Top) Main image is a *z*-axis projection of a series of optical slices ($Em_\lambda > 460$ nm) revealing intranuclear chromatin architecture and a display of condensed metaphase chromosomes in a mitotic cell. (Bottom) The corresponding *z*-axis slice for an *x* axis intercepting the mitotic and three adjacent cells. Size bar: 10 μm.

2. A second cell-permeant probe may be introduced concurrently with Hoechst 33342 staining or after culture washing. Typically, Hoechst 33342-labeled cells will lose approximately 25% nuclear fluorescence over a 15- to 30-min postlabeling period in fresh medium. Here we exemplify the signal separation of Hoechst 33342 and the probe Mitotracker Orange CMTMRos, the latter introduced into the culture medium at 5 ng/ml for the final 5-min period of Hoechst 33342 labeling.

3. Sample preparation is as in Section III,B, whereas dual-imaging conditions and typical results are shown in Fig. 2.

D. Hoechst 33342 Staining Kinetics and Population Spectral Shift Analysis

Steps

1. Detach cultured cells by a standard trypsin/EDTA method and resuspend at 2×10^5 cell/ml full culture medium supplemented with 10 m*M* HEPES and allow to equilibrate at 37°C prior to Hoechst 33342 addition (see Section III,B).

2. Analyze single cell suspensions, in the presence of the dye, by one-photon UV excitation flow cytometry and acquire data for different dye uptake periods.

3. The change of spectral emission with dye uptake by mouse L cells is shown for populations of 10^4 cells in Fig. 3. Cells showing a rapid, essentially immediate, red shift are damaged and can be excluded by additional electronic gating using light scatter changes.

E. Two-Photon Excitation of Hoechst 33342 and Spectral Shift Analysis

Steps

1. Generate cultures and label Hoechst 33342 as in Section III,B.

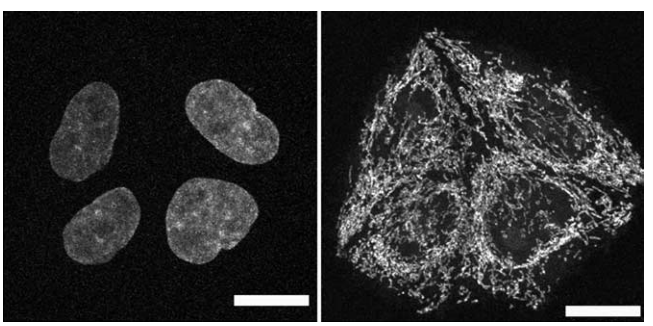

FIGURE 2 Dual images of four live HeLa cells using two-photon coexcitation (Ex_λ 800 nm) of nuclear-located Hoechst 33342 (5 μM × 60 min; left side Em_λ 455/25 nm) and cytoplasmic Mitotracker orange CMTMRos (5 ng/ml × 5 min; right side Em_λ 585/32 nm). Size bar: 10 μm.

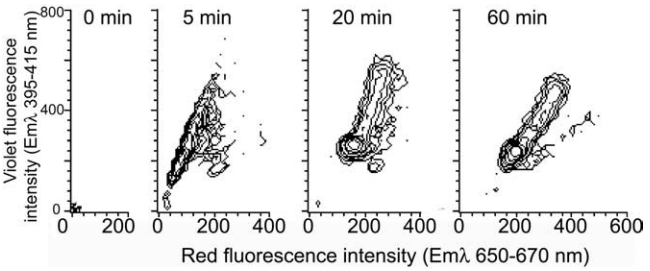

FIGURE 3 Flow cytometric contour plots of mouse L-cell populations undergoing a violet-to-red spectral shift in fluorescence during nuclear localization of Hoechst 33342 (10 μ*M*; 4 × 10^5 cells/ml) using one-photon excitation by multiline UV. The broad fluorescence emission spectrum was monitored simultaneously in the red region (Em_λ 660/20 nm) and the violet region (Em_λ 405/20 nm) for 10^4 cells at the specified time points. Data show the rapid development of violet fluorescence and the later red shift. Residual levels of damaged cells not excluded by light scatter gating are evident by their rapid red-shift pattern.

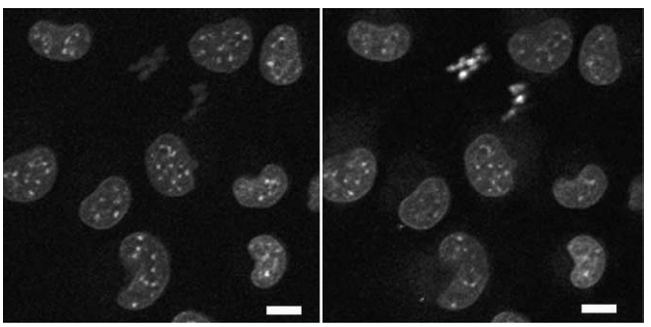

FIGURE 4 Dual images of live mouse L cells using two-photon excitation (Ex_λ 750 nm) of nuclear-located Hoechst 33342 (5 μ*M* × 60 min) showing a red-biased fluoresence emission in metaphase versus interphase cells (right side shows Em_λ 585/32 nm and the left side shows Em_λ 405/35 nm). Size bar: 10 μm.

2. Sample preparation is as in Section III,B with dual-imaging conditions and typical results shown in Fig. 4. The dual images of live mouse L cells show the differences in emission by condensed chromatin in metaphase cells lacking a nuclear envelope and interphase nuclei.

F. One-Photon Excitation of DRAQ5 for Live and Persistence in Fixed Cells

Steps

1. Generate cultures and mount coverslips as in Section III,B.

2. Cultures can be exposed to DRAQ5 by direct addition to full culture medium (10 μ*M* × 10 min) prior to coverslip washing (optional) and mounting.

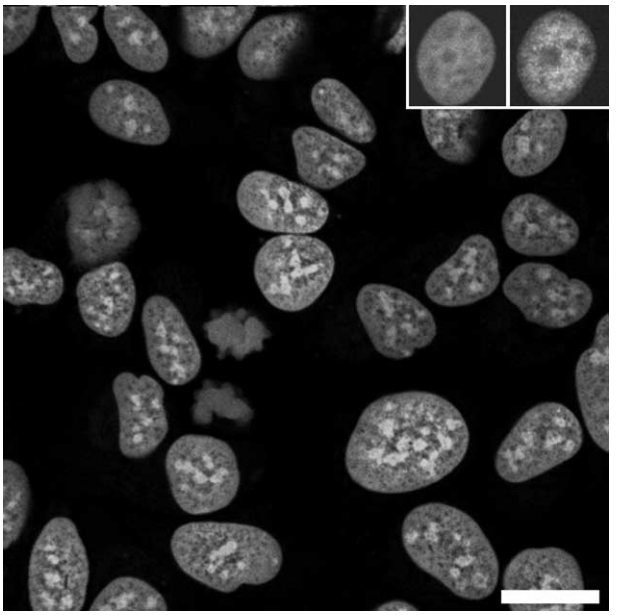

FIGURE 5 Confocal image of live MCF-7 breast tumor cells using one-photon excitation (Ex_λ 647 nm; Em_λ 680/32 nm) of nuclear-located DRAQ5 (10 μM × 10 min) revealing nuclear architecture and the presence of an anaphase cell. (Left insert) Nuclear retention of the dye following preparation washing and conventional paraformaldehyde fixation for the purposes of subsequent immunofluorescence colocalization analysis. (Right insert) An example of immunolocalization is shown for the expression of nuclear-located protein detected using a secondary antibody conjugated to Alexa488 (Ex_λ 488 nm; Em_λ 522/35 nm). Size bar: 10 μm.

However, the rapid staining kinetics of DRAQ5 (see Section III,G) permit direct introduction of the dye to already mounted samples and imaging immediately for nuclear tracing.

3. Figure 5 shows one-photon excitation images of nuclear-located DRAQ5 and dye persistence following standard 4% paraformaldehye fixation and the sample subsequently processed for immunofluorescence, which permits colocalization of an immunofluorescence signal (Alexa 488) with nuclear structures.

G. DRAQ5 Staining Kinetics and DNA Content Analysis

Steps

1. Prepare cells as in Section III,D and the conditions given in Fig. 6.

2. DRAQ5 far-red fluorescence is detectable within seconds of dye addition to cell suspensions and can be generated by both 488- and 633-nm wavelength one-photon excitation with similar outcomes. The optical configurations are shown in Fig. 6. The flow cytometry protocol acquires fluorescence emissions with time

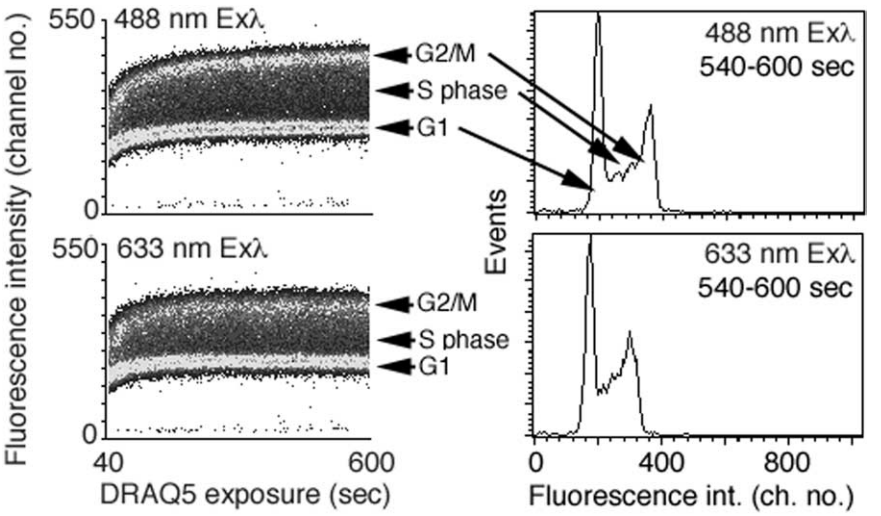

FIGURE 6 Flow cytometric analysis of the rapid cellular uptake of DRAQ5 demonstrating the ability to discriminate DNA content using one-photon excitation at either Ex_λ 488 nm ($Em_\lambda > 715$ nm) or Ex_λ 633 nm ($Em_\lambda > 695$ nm). Suspensions of live human B-cell lymphoma cells (4×10^5 cells/ml) were exposed to 20 μ*M* DRAQ5 in complete medium supplemented with 10 m*M* HEPES and incubated at 37°C for 600 s. (Left) Density dot plots for continuous event acquisition for sequential 488 nm then 633 nm excitation, monitoring far red fluorescence commencing 40 s after dye addition (total of approximately 1.2×10^6 cells acquired; background unlabeled cells located in channel ≤ 25). Data show rapid equilibration of DNA staining, the discrimination even at early staining times of relative DNA content, and the final equivalence of the content, distributions (right) irrespective of blue or red line excitation.

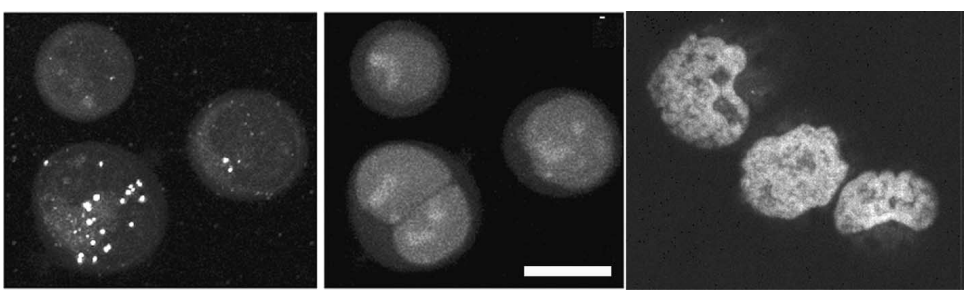

FIGURE 7 Sequential acquisition of a nuclear DNA signal (single-photon excitation of DRAQ5; Ex_λ 647 nm; Em_λ 680/32 nm; 10 μ*M* × 10 min; center) and the intracellular localization of a UV-excitable fluorophor (two-photon excitation of the intracellular Zn^{2+}-sensitive reporting probe Zinquin-E; Ex_λ 780 nm; $Em_\lambda >$ 460 nm; left) in live human B-cell lymphoma cells. Images are dual-channel projections revealing bright punctate Zinquin–Zn^{2+} complexes found to be exclusively cytoplasmic upon three-dimensional image reconstruction. (Right) Two-photon excitation of nuclear-located DRAQ5 using a YLF mode-locked femtosecond pulsed laser (Exλ 1047 nm and far-red fluorescence) in ethanol-fixed human lymphoma cell cytocentrifuge preparations mounted in 20 μ*M* DRAQ5 in phosphate-buffered saline. Size bar: 10 μm.

and shows the ability to discriminate cells of different DNA contents.

H. Discrimination of the Intracellular Location of Two-Photon Excited Fluorophors using DRAQ5

Steps

1. Generate cultures as in Section III,B and probe for the expression of a given characteristic using a cell-permeant reporter (e.g., here using the UV-excitable probe Zinquin-E for free zinc ions; Zalewski *et al.*, 1993). Following probe treatment, cells can be processed for nuclear tracing using one-photon excitation achieved rapidly by mounting of cells directly in PBS containing 20 μ*M* DRAQ5 (see Fig. 7).

2. If two-photon acquisition of a DRAQ5 image is sought, then wavelengths beyond 1 μm are required. Figure 7 shows such acquisition (Ex_λ 1047 nm) for ethanol-fixed human lymphoma cells mounted in

20 μ*M* DRAQ5 obtained using a 60× N.A. 1.4 oil objective, a zoom of 1.9, and a Kalman filtering average of 37 scans.

IV. COMMENTS

1. Probe selection issues include (i) excitation and emission spectral characteristics, including differential spectral shifts pertinent for multiparameter imaging; (ii) dye "brightness" dictated by molar absorptivity, quantum yield with fluorescent enhancement; and (iii) advanced properties for more complex studies, including lifetime signatures and molecular quenching capabilities.

2. Fluorescence lifetime microscopy (FLIM) provides an important avenue for investigating the binding of DNA probes to macromolecular structures. The image contrast is concentration insensitive, but is sensitive to the local environment. Multiphoton instruments can be adapted to capture fluorescence decay signals. Some dyes that cannot be used to differentiate DNA/RNA using steady-state fluorescence do have unique lifetime signatures when bound to these different sites. Hence this provides a mechanism for deriving the spatial map of RNA and DNA location sites within a cell (Lakowicz *et al*., 1997; van Zandvoort *et al*., 2002).

3. Investigators should always question both the timing and the purpose of the staining within the analysis procedures. The rapid staining of cells by DRAQ5 is a significant advantage when tracking events over short time frames and nuclear discrimination can be achieved within seconds.

V. PITFALLS

1. MPLSM requires careful selection of optical filters capable of efficient IR blocking.

2. MPLSM requires a fundamental shift in experimental design, as using a single (albeit well-chosen) wavelength will excite multiple probes, and so good separation of the emission wavelengths is absolutely required. Thus the UV-excitable dyes are limited when two-photon excitation of GFP-based fluorophors is undertaken due to coexcitation and overlap of the fluorescence spectra.

3. Live cell labeling is subject to micropharmacokinetic effects, which can vary with cell type. For example, the ability of bisbenzimiazoles dyes to access cellular DNA can be affected by dye efflux (e.g., via a membrane-located p-glycoprotein encoded by the mdr-1 gene; Morgan *et al*., 1989), nuclear ejection (Smith, 1988), and differences in chromatin compactness. DRAQ5 is less subject to drug resistance efflux, but at suboptimal concentrations, nuclear access may restrict binding potential.

4. Both dyes discussed can damage DNA. Benzimidazoles can cause DNA strand breaks by photolytic (UV) DNA strand cleavage or as a consequence of ternary complex formation with intranuclear DNA topoisomerases I and II. Anthraquinones can also trap DNA topoisomerases but may also cause DNA–protein cross-linking damage. Some cells appear to be resistant to Hoechst 33342 cytotoxicity (e.g., HeLa), whereas others will undergo apoptosis readily (e.g., p53 wild-type B-cell lymphoma). In the case of DRAQ5, toxicity is clearly dose dependent (20 n*M*–20 μ*M* range), and the persistence of the agent makes it unsuitable for long-term (>12 h) tracking experiments or viable cell sorting. The initial stress responses to dye binding may be occult but result in progressive cell cycle arrest or indeed modulation of sensitivity to other agents under investigation.

Acknowledgments

This work was funded by Research Councils (GR/s23483), BBSRC (75/E19292), AICR (00-292) and SBRI (19666).

References

Albota, M., Xu, C., and Webb, W. (1998). Two-photon fluorescence excitation cross sections of biomolecular probes from 690 to 960 nm. *Appl. Opt*. **37**, 7352–7356.

Bell, D. H. (1988). Characterization of the fluorescence of the antitumour agent, mitoxantrone. *Biochim. Biophys. Acta* **949**, 132–137.

Bestvater, F., Spiess, E., Strobrawa, G., Hacker, M., Fuerer, T., Porwol, T., Berchner-Pfannschmidt, U., Wotzlaw, C., and Acker, H. (2002). Two-photon fluorescence absorption and emission spectra of dyes relevant for cell imaging. *J. Microsc*. **208**, 108–115.

Darzynkiewicz, Z., and Kapuscinski, J. (1990). Acridine orange: A versatile probe of nucleic acids and other cellular constituents. *In* "*Flow Cytometry and Sorting*" (M. R. Melamed, T. Lindmo, M. L. Mendelsohn, eds.), pp. 291–314. Wiley-Liss, New York.

Denk, W., Piston, D. W., and Webb, W. W. (1995). Two-photon molecular excitation in laser scanning microscopy. *In* "*Handbook of Biological Confocal Microscopy*" (J. B. Pawley, ed.), pp. 445–458. Plenum Press, New York.

Errington, R. J., Ameer-Beg, S. M., Vojnovic, B., Patterson, L. H., Zloh, M., and Smith, P. J. (2005). Advanced microscopy solutions for monitoring the kinetics and dynamics of drug-DNA targeting in living cells. Adv. Drug Deliv. Rev. 51, 153–167.

Frey T., Yue S., and Haugland, R. P. (1995). Dyes providing increased sensitivity in flow-cytometric dye-efflux assays for multidrug resistance. *Cytometry* **20**, 218–227.

Frey, T. (1995). Nucleic acid dyes for detection of apoptosis in live cells. *Cytometry* **21**, 265–274.

Lakowicz, J., Gryczynski, I., Malak, H., Schrader, M., Engelhardt P., Kano, H., and Hell, S. (1997). Time-resolved spectroscopy and imaging of DNA labelled with DAPI and Hoechst 33342 using three-photon excitation. *Biophys. J*. **72**, 567–578.

Latt, S. A., and Langlois, R. G. (1990). Fluorescent probes of DNA microstructure and DNA synthesis. *In* "*Flow Cytometry and Sorting*" (M. R. Melamed, T. Lindmo, and M. L. Mendelsohn, eds.), pp. 249–290. Wiley-Liss, New York.

Lown, J. W., Morgan, A. R., Yen, S.-F., Wang, Y. H., and Wilson, W. D. (1985). Characteristics of the binding of the anticancer agents mitoxantrone and ametantrone and related structures to deoxyribonucleic acids. *Biochem. J.* **24**, 4028–4035.

Morgan, S. A., Watson, J. V., Twentyman, P. R., and Smith, P. J. (1990). Reduced nuclear binding of a DNA minor groove ligand (Hoechst 33342) and its impact on cytotoxicity in drug resistant murine cell lines. *Br. J. Cancer* **62**, 959–965.

Smith, P. J., Blunt, N., Wiltshire, M., Hoy, T., Teesdale-Spittle, P., Craven, M. R., Watson, J. V., Amos, W. B., Errington, R. J., and Patterson, L. H. (2000). Characteristics of a novel deep red/infrared fluorescent cell-permeant DNA probe, DRAQ5, in intact human cells analyzed by flow cytometry, confocal and multiphoton microscopy. *Cytometry* **40**, 280–291.

Smith, P. J., Lacy, M., Debenham, P. G., and Watson, J. V. (1988). A mammalian cell mutant with enhanced capacity to dissociate a bis-benzimidazole dye-DNA complex. *Carcinogenesis* **9**, 485–490.

Smith, P. J., Wiltshire, M., Davies, S., Patterson, L. H., and Hoy, T. (1999). A novel cell permeant and far red-fluorescing DNA probe, DRAQ5, for blood cell discrimination by flow cytometry. *J. Immunol. Methods* **229**, 131–139.

Van Zandvoort, M., de Grauw, C., Gerritsen, H., Broers, J., oude Egbrink, M., Ramaekers, F., and Slaaf, D. (2002). Discrimination of DNA and RNA in cells by a vital fluorescent probe: Lifetime imaging of SYTO13 in healthy and apoptotic cells. *Cytometry* **47**(4), 226–235.

Waggoner, A. S. (1990). Fluorescent probes for cytometry. *In* "*Flow Cytometry and Sorting*" (M. R. Melamed, T. Lindmo, M. L. Mendelsohn, eds.), pp. 209–225. Wiley-Liss, New York.

White, N. S., and Errington, R. J. (2002). Multi-photon microscopy: Seeing more by imaging less. *Biotechniques* **33**(2), 298–305.

Williams, R. M., Zipfel, W. R., and Watt, W. W. (2001). Multi-photon microscopy in biological research. *Curr. Opin. Chem. Biol.* **5**, 603–608.

Zalewski, P. D., Forbes, I. J., and Betts, W. H. (1993). Correlation of apoptosis with change in intracellular labile Zn(II) using zinquin [(2-methyl-8-p-toluenesulphonamido-6-quinolyloxy)acetic acid], a new specific fluorescent probe for Zn(II). *Biochem J.* **296**, 403–408.

SECTION

9

Cytotoxic and Cell Growth Assays

CHAPTER

38

Cytotoxicity and Cell Growth Assays

Giuseppe S. A. Longo-Sorbello, Guray Saydam, Debabrata Banerjee, and Joseph R. Bertino

I. INTRODUCTION

Various assays are in use to determine the effect of a drug (broadly defined chemical or other inhibitory substance) on cells propagated *in vitro*. They range from simple assays that measure cell viability after drug exposure, i.e., dye exclusion that measures membrane integrity and effect of the drug on cell growth (simply enumerating cells), to other assays that measure cell viability, indirectly, by assessing the ability of the cell to reduce compounds such as XTT, MTS, SRB, and alamarBlue or to generate ATP. The advantages of these assays are that they are performed easily and, with the use of 96-well plates, many dilutions or many compounds can be tested rapidly.

Other assays that measure the ability of a cell to incorporate radiolabeled thymidine into DNA come closer to measuring the effect of drugs on the proliferative potential of the cell population. The gold standard, but a more difficult and time-consuming assay that measures the proliferative potential of cells, is the clonogenic assay. This assay measures the percentage of cells in the population capable of giving rise to clones, thus measuring the effect the compound has on the proliferating fraction of the population.

II. CYTOTOXICITY ASSAYS

This section describes dye exclusion assays and other commonly used assays that measure cell viability: XTT, MTS, SRB, AlamarBlue, [^{3}H]-thymidine incorporation, and ATP formation.

A. Dye Exclusion Test Using Trypan Blue

The trypan blue exclusion test is a rapid method to assess cell viability in response to environmental insults. It is simple and inexpensive.

The dye exclusion test is based on the ability of viable cells to be impermeable to trypan blue, naphtalene black, erythrosine, and other dyes. When membrane integrity of the cells is compromised, there is uptake of the dye into the cells so that viable cells, which are unstained, appear clear with a refractile ring around them and nonviable cells appear dark blue colored with no refractile ring around them. The following method is for trypan blue, the dye used most commonly.

An automatic system, the Vi-Cell cell viability analizer (Beckman Coulter Inc., Fullerton, CA), has been introduced. As compared to the manually performed assay, this technique allows rapid analysis and quantitation. It performs the test with video imaging of the flow-through cell.

Materials and Instrumentation

Trypan blue solution (0.4%) (Cat. No. T 8154) is from Sigma-Aldrich (St. Louis, MO); hemocytometer (improved Neubauer) (Cat. No. 02-671-5), lab counter (Cat. No. 02-670-12), and Eppendorf tubes (Cat. No. 05-402-24A) are from Fisher Scientific (Agawam, MA). Micropipettes (Cat. No. P-3950-200) and pipette tips (Cat. No. P3020-CPS) are from Denville Scientific (Metuchen, NJ).

Steps

1. Prepare cells by trypsinization or resuspension. Make sure that the cells are well resuspended as aggregates make the counting inaccurate. Avoid

Copyright 2006, Elsevier Science (USA).
All rights reserved.

allowing the cells to settle or adhere to the flask before transfering to the improved Neubauer chamber.
2. Mix thoroughly 50 µl of cell suspension with 50 µl of trypan blue in a 500-µl Eppendorf tube. Leave the mixture no more than 1–2 min because longer incubation with the dye may be toxic to viable cells and will result in overestimating the number of dead cells.
3. Place a coverslip over the hemocytometer so that it covers the central 1 mm^2 of the semisilvered counting area.
4. With a micropipette, collect the mixture of 1 : 1 cell suspension and trypan blue and transfer it to the edge of the hemocytometer chamber.
5. Let the mixture flow under the coverslip by capillary action, being careful not to overfill or underfill the chamber, as it will affect the counting.
6. If any surplus fluid is present over the edges, use absorbing paper to remove it.
7. Place the Neubauer chamber under the microscope and select the 10× objective. Focus on the center of the semisilvered counting area where the grid lines are evident by contrast.
8. Triple parallel grid lines surround a 1-mm^2 area divided in 25 smaller squares further subdivided in 16 smaller squares that are used for counting.
9. Unstained cells with a refractile ring around them are the viable cells, whereas dark blue colored cells that do not have refractile ring around them are nonviable cells.
10. Count the total amount of cells, stained and unstained. The percentage of unstained cells gives you the percentage of viable cells with this method. For routine culture, count 100 cells/mm^2. Counting more cells makes the test more accurate.

B. Cell Viability Assays

1. XTT/PMS Assay

This procedure exploits the fact that the internal environment of proliferating cells is more reduced than one of nonviable cells. Tetrazolium salts are used to measure this reduced state. Among them, XTT is preferred to MTT because it is more soluble. However, there are some disadvantages with this method. XTT is generally cytotoxic and destroys the cells under investigation, allowing only a single evaluation. It requires the presence of phenazine methosulfate for efficient reduction.

Materials and Instrumentation

Falcon Microtest tissue culture plates (96 wells) (Cat. No. 35-3072) and Falcon polystirene pipette (Cat. No. 35-7551) are from Becton-Dickinson (Franklin Lakes, NJ); RPMI 1640 medium with L-glutamine (Cat. No. 11875-093), fetal bovine serum (FBS) (Cat. No. 10437-028), phosphate-buffered saline (PBS), 7.4 (Cat. No. 10010-023), and trypsin–EDTA (Cat. No. 25200-056) are from GIBCO BRL (Rockville, MD); multichannel pipette (50–300 µl) (Cat. No. P3970-18), micropipettes (200 µl) (Cat. No. P-3950-200), and pipette tips (Cat. No. P3020-CPS) are from Deville Scientific (Metuchen, NJ); XTT sodium salt [2,3-bis(2-methoxy-4-nitro-5-sulfophenyl)-2*H*-tetrazolium-5-carboxanilide inner salt] (Cat. No. X 4626) and phenazine methosulfate (*N*-methylphenazonium methyl sulfate salt) (Cat. No. P 9625) are from Sigma-Aldrich (St. Louis, MO); and microplate reader SpectraMax Plus is from Molecular Devices (Sunnyvale, CA).

Two 96-wells plates are required: one for cells and one for drug dilutions.

a. Preparation of Cells in Plate A

Steps

1. The method may be used on cells that are adherent or growing in suspension.
2. Culture cell lines in RPMI 1640 media with 10% FBS, 1% glutamine, and 1% pen/strep or other appropriate media.
3. For harvesting, the cells should be in log-phase growth (300–500 × 10^3 cells/ml) or, if dealing with adherent cells, trypsinization must be done before cells reach 80% confluence.
4. Harvest 100,000 cells per each 96-well plate and resuspend in a total volume of 10 ml/medium with 20% FBS, 1% glutamine, and 1% pen/strep.
5. From 100,000 cells in 10 ml medium, pipette 100 µl of medium+cells in each well to have 1000 cells/well.
6. Leave the first row for the blank. The second row is a control (cells without drug).
7. For adherent cells, allow 1 h for cells to reattach before adding the drug under study.

The amount of medium per well in each experiment may change depending on the amount of drug that is added after the cells are plated. The following example uses 100 µl of medium containing 1000 cells and 100 µl of drug, resulting in 200 µl of medium in each well.

b. Drug Preparation in Plate B

Steps

1. Pipette 125 µl of RPMI 1640 medium in each well of a 96-well plate.
2. Add 125 µl of the drug in each well in the first row. Then, after mixing, transfer 125 µl of the mix to

the following row and repeat the procedure up to the last row. In this way X concentration of the drug will be present in the first row, a $X/2$ concentration in the second row, and so on.

3. Pipette 100 µl from the 10th row of the plate (plate B) with the drug dilutions to the last row of the plate with the cells (plate A) so that the lower concentrations do not affect subsequent transfers.

4. When all the transfers are completed, add 100 µl of plain RPMI 1640 medium to the control row. You will have 200 µl of medium with 10% FBS in each well.

5. Add 200 µl of medium to the blank row. Start the incubation.

c. Assay Procedure

Steps

1. Warm 5 ml of plain RPMI 1640 medium at 50°C for each plate tested. This temperature allows the XTT salt to dissolve better.
2. Add 5 mg of XTT powder to the 5 ml of RPMI 1640 (it is important that no more than 1 mg of XTT/ml of medium is used).
3. Prepare a stock solution of 5 m*M* PMS. Add 326 µl of warm PBS to the vial containing the 0.5 mg of PMS (FW 306.3).
4. Add 25 µl of the stock 5 m*M* PMS to the solution containing 5 ml of medium + 5 mg of XTT.
5. Pour the solution in a reservoir and, with a multichannel pipette, transfer 50 µl of it per each well. The ratio of 0.25 ml of the XTT/PMS solution/ml of cell culture must be maintained. In the procedure described earlier there is 200 µl of medium/well × 96 wells, or a total of 1820 µl, and 50 µl of the XTT/PMS solution should be added to each well.
6. Incubate at 37°C for 2–4 h.
7. Measure absorbance with a microplate reader at the wavelength of 450 and 630 nm as a reference wavelength.

Pitfalls

Warming up the RPMI 1640 media is critical for total XTT solubilization. When dissolved incompletely, XTT salt will affect the results. The incubation time after XTT is added may vary and could be longer than the 2–4 h as suggested earlier.

2. MTS/PMS Assay

The tetrazolium compound [3-(4,5-dimethylthiazol-2-yl)-5-(3-carboxymethoxyphenyl)-2-(4-sulfophenyl)-2*H*-tetrazolium, inner salt MTS, in the presence of the electron coupling reagent phenazine methosulfate (PMS)] is bioreduced by viable cells into a formazan product that is soluble in culture media. The advantage of MTS over XTT is that it is more soluble and nontoxic, allowing the cells to be returned to culture for further evaluation. The disadvantage is that like XTT it requires the presence of PMS for efficient reduction.

Materials and Instrumentation

Falcon Microtest tissue culture plates (96 wells) (Cat. No. 35-3072) and Falcon polystirene pipette (Cat. No. 35-7551) are from Becton-Dickinson (Franklin Lakes, NJ); RPMI 1640 medium with L-glutamine (Cat. No. 11875-093), fetal bovine serum (Cat. No. 10437-028), Dulbecco's PBS (Cat. No. 14190-136), and trypsin–EDTA (Cat. No. 25200-056) are from Gibco BRL (Rockville, MD); multichannel pipette (50–300 µl) (Cat. No. P3970-18), micropipettes (200 µl) (Cat. No. P-3950-200), and pipette tips (Cat. No. P3020-CPS) are from Deville Scientific (Metuchen, NJ); phenazine methosulfate (*N*-methylphenazonium methyl sulfate salt) (Cat. No. P 9625) is from Sigma-Aldrich (St. Louis, MO); CellTiter 96 AQ_{ueous} MTS reagent powder (Cat. No. G1111) is from Promega Co. (Madison, WI); and microplate reader Spectra®Max Plus[384] is from Molecular Devices (Sunnyvale, CA).

The **preparation of cells and drug preparation** are similar to the XTT/PMS assay.

Assay Procedure

Steps

1. Add 2 mg of MTS powder to each 1 ml of Dulbecco's PBS. Per each 96-well plate add 4 mg of MTS to 2 ml of DPBS.
2. Prepare a stock solution of PMS at a concentration of 0.92 mg/ml.
3. Add 100 µl of PMS to the MTS solution immediately before addition to the cultured cells.
4. Pour the solution in a reservoir and, with a multichannel pipette, transfer 20 µl of it per each well.
5. Incubate the plate for 1–4 h at 37°C in a humidified, 5% CO_2 atmosphere.
6. Measure absorbance with a microplate reader at a wavelength of 490 and 630 nm as a reference wavelength.

Comments

The incubation time after MTS/PMS is added may vary and could be longer than the 1–4 h suggested earlier.

3. Sulforhodamine B Assay (SRB)

The SRB assay is based on binding of the dye to basic amino acids of cellular proteins, and colorimetric evaluation provides an estimate of total protein

mass, which is related to cell number. This assay has been widely used for the *in vitro* measurement of cellular protein content of both adherent and suspension cultures. The advantages of this test as compared to other tests include better linearity, higher sensitivity, a stable end point that does not require time-sensitive measurement, and lower cost. The disadvantage lies in the need for the addition of TCA for cell fixation. This step is critical because, if not added gently, TCA could dislodge cells before they become fixed, generating possible artifacts that will affect the results.

Materials and Instrumentation

Falcon microtest tissue culture plates (96 wells) (Cat. No. 35-3072) and Falcon polystirene pipette (Cat. No. 35-7551) are from Becton-Dickinson (Franklin Lakes, NJ); RPMI 1640 medium with L-glutamine (Cat. No. 11875-093), FBS (Cat. No. 10437-028), PBS, 7.4 (Cat. No. 10010-023), and trypsin–EDTA (Cat. No. 25200-056) are from GIBCO BRL (Rockville, MD); multichannel pipette (50–300 µl) (Cat. No. P3970-18), micropipettes (200 µl) (Cat. No. P-3950-200), and pipette tips (Cat. No. P3020-CPS) are from Deville Scientific (Metuchen, NJ); trichloroacetic acid (TCA) (Cat. No. T9159), Trizma base [tris (hydroximethyl)aminomethane] (Cat. No. 25-285-9), acetic acid (Cat. No. A6283), and sulforhodamine B sodium salt (Cat. No. S 9012) are from Sigma-Aldrich (St. Louis, MO). Microplate reader SpectraMax®Plus is from Molecular Devices (Sunnyvale, CA).

The **preparation of cells and drug preparation** are similar to the XTT/PMS assay.

Assay Procedure

Steps

1. Prepare a stock solution of 50% TCA and add 50 µl of this cold solution (4°C) to each well containing 200 µl of medium + cells so that a final concentration of 10% TCA is reached in each well.
2. Place the 96-well plate for 1 h at 4°C to allow cell fixation.
3. Prepare a 0.4% SRB (w/v) solution in 1% acetic acid and add 70 µl of this solution to each well and leave at room temperature for 30 min.
4. Wash the plate with 1% acetic acid five times in order to remove unbound SRB.
5. Prepare a stock solution of 10 m*M* Trizma base and add 200 µl of this solution to each well in order to solubilize bound SRB. Place the 96-well plate on a plate shaker for at least 10 min.
6. Read abosrbance with a microplate reader at 492 nm, subtracting the background measurement at 620 nm.

Pitfalls

The addition of TCA for fixation is critical and if it is not done with caution can cause dislodgement of the cells before fixation and subsequent alteration of the results.

4. Alamar BlueAssay

AlamarBlue is used to monitor the reducing enviroment of proliferating cells. Because it is not toxic, cells exposed to it can be returned to culture or used for other purposes. AlamarBlue takes advantage of mitochondrial reductase to convert nonfluorescent resazurin to fluorescent resorufin.

Proliferation measurements with alamarBlue may be monitored using a standard spectrophotometer, a standard spectrofluorometer, or a spectrophotometric microtiter well plate reader.

Materials and Instrumentation

AlamarBlue (Cat. No. DAL1100) is from Biosource (Camarillo, CA); Falcon microtest tissue culture plates (96 wells) (Cat. No. 35-3072) and Falcon polystirene pipettes (Cat. No. 35-7551) are from Becton-Dickinson (Franklin Lakes, NJ); RPMI 1640 medium with L-glutamine (Cat. No. 11875-093), FBS (Cat. No. 10437-028), PBS, 7.4 (Cat. No. 10010-023), and trypsin–EDTA (Cat. No. 25200-056) are from GIBCO BRL (Rockville, MD); multichannel pipettes (50–300 µl) (Cat. No. P3970-18), micropipettes (200 µl) (Cat. No. P-3950-200), and pipette tips (Cat. No. P3020-CPS) are from Deville Scientific (Metuchen, NJ); and microplate reader SpectraMax Plus^{384} is from Molecular Devices (Sunnyvale, CA).

The **preparation of cells** is similar to XTT/PMS assay, except for the following.

Steps

1. The assay can be performed on adherent cells or suspension culture.
2. Culture cells in RPMI 1640 medium with 10% FBS, 1% glutamine, and 1% pen/strep and amphotericin to avoid microbial contaminants that may reduce AlamarBlue.
3. For harvesting, the cells in suspension must be in log-phase growth (300–500 $\times$ 10^3 cells/ml) or, if dealing with adherent cells, trypsinization must be done before the cells reach 80% confluence.
4. Harvest 100,000 cells for each 96-well plate resuspended in a total volume of 10 ml/medium with 20% FBS, 1% glutamine, 1% pen/strep, and amphotericin.
5. Pipette 100 µl of medium+cells in each well to have 1000 cells/well.

Assay Procedure

Steps

1. Leave the first row for the blank. The second row is used as a control (cells without drug)
2. For adherent cells, allow 1 h for cells to reattach before adding the drug in study.
3. Add 25 µl of alamarBlue *is then added* to a resulting final volume of 250 µl of media+cells.
4. Measure viability after a 1-h incubation at 37°C in humidified 5% CO_2 when the medium in the control row turns from blue to pink. If the reduction observed is insufficient, you may allow the incubation to proceed for a longer period of time.
5. Place the 96-well plate in a automated plate-reading spectrofluorophotometer, with excitation at 530 nm and emission at 590 nm. Fluorescence is expressed as a percentage of control (cells with no drug) after reading the substraction of background fluorescence (blank without cells). AlamarBlue reduction can also be measured spectrophotometrically at two wavelengths, 570 and 600 nm, which are the wavelengths where the reduced and oxidized forms of AlamarBlue absorb maximally.

Pitfalls

The whole procedure has to be performed under aseptic conditions because proliferating bacterial and fungal cells are able to reduce AlamarBlue and may affect the results.

5. ATP Cell Viability Assay

ATP is the most important source of energy for the living cells and can be quantitated in a luminometer by measuring the light generated using the luciferase-luciferin reagent. Typically, apoptotic cells exhibit a significant decrease in ATP levels due to loss of cell integrity.

The ATP cell viability assay is based on two steps. In the first step, ADP is added as a substrate for adenylate kinase and, in the presence of this enzyme, ADP is converted to ATP. In the second step, the enzyme luciferase catalizes the formation of light from ATP and luciferin. The intensity of the light emitted is measured using a luminometer or a β counter. When the measurement is done on cells in culture using microtiter plates, it is necessary to perform this procedure using white-walled microtiter plates suitable for measuring luminescence.

Materials and Instrumentation

White-walled tissue culture plates (96 wells) (Cat. No. LT07-102) and ToxiLight nondestructive cytotoxicity assay (Cat. No. LT07-117) are from BioWhittaker-Cambrex (Rutherford, NJ); Falcon polystyrene pipette (Cat. No. 35-7551) is from Becton-Dickinson (Franklin Lakes, NJ); RPMI 1640 medium with L-glutamine (Cat. No. 11875-093), FBS (Cat. No. 10437-028); PBS, 7.4 (Cat. No. 10010-023), and trypsin–EDTA (Cat. No. 25200-056) were from GIBCO BRL (Rockville, MD); multichannel pipette (50–300 µl) (Cat. No. P3970-18), micropipettes (200 µl) (Cat. No. P-3950-200), and pipette tips (Cat. No. P3020-CPS) are from Deville Scientific (Metuchen, NJ); and the Reporter microplate luminometer (Cat. No. 9600-001) is from Turner BioSystem (Sunnyvale, CA).

The **preparation of cells** is similar to the XTT/PMS assay except that white-walled microtiter plates are used.

Drug Preparation

Steps

1. Pipette 75 µl of RPMI 1640 medium in each well of a 96-well plate.
2. Add 75 µl of the drug in each well in the first row. Then, after mixing, transfer 75 µl of the mix to the following row and repeat the procedure up to the last row. In this way you will have 1*X* concentration of the drug in the first row, a $X/2$ concentration in the second row, and so on.
3. Pipette 50 µl from the 10th row of the plate with the drug dilutions to the last row of the plate with the cells so that the lower concentrations will not affect the subsequent transfers.
4. When all the transfers are completed, add 50 µl of plain RPMI 1640 medium to the control row. Each well will contain 100 µl of medium with 10% FBS.
5. Add 100 µl of medium to the blank row. Start the incubation.

Assay Procedure

Steps

1. Reconstitute the AK detection reagent by adding 10 ml of Tris–AC buffer and, after mixing it, gently allow the reagent to equilibrate at room temperature for 15 min.
2. After the planned period of incubation for cells and drug in the white-walled microplates, remove the plate from the incubator and allow the plate to equilibrate to room temperature prior to measurement.
3. Add 100 µl of the AK detection reagent to all the wells with a multichannel pipette.
4. Wait 5 min before reading to allow for detectable ADP conversion to ATP. Measurement of the light emission should be performed within 30 min from the addition of the AK detection reagent.

5. Place the plate into a luminometer or a β counter. Measure the light emission. Results are expressed as relative light units (luminometer) or counts per second (β counter).

6. [^{3}H]-Thymidine Incorporation Assay

This assay is based on the ability of proliferating cells to incorporate [^{3}H]-thymidine into replicating DNA. Despite its precision to produce accurate data on DNA synthesis, this assay has some disadvantages. It uses radioactivity, requires extensive sample preparation, and the method is sample destructive as compared to a clonogenic assay. The assay described is for human cells grown on agar; the assay may also be used for cells grown in suspension or attached to glass or plastic.

Materials and Instrumentation

Falcon Microtest tissue culture plates (24 wells) (Cat. No. 35-3047), Falcon polystirene pipette (Cat. No. 35-7551), and BlueMax Falcon 15-ml tubes (Cat. No. 35-2097) are from Becton-Dickinson (Franklin Lakes, NJ); RPMI 1640 medium with L-glutamine (Cat. No. 11875-093), FBS (Cat. No. 10437-028), and PBS, 7.4 (Cat. No. 10010-023) are from GIBCO BRL (Rockville, MD); micropipettes (200 µl) (Cat. No. P-3950-200) and pipette tips (Cat. No. P3020-CPS) are from Deville Scientific (Metuchen, NJ); agar (Cat. No. A 7002), sodium azide (Cat. No. S 2002), and TCA (Cat. No. T 9159) are from Sigma-Aldrich (St. Louis, MO); KHO (Cat. No. SP208-500), 20-ml Wheaton glass liquid scintillation vials (Cat. No. 03-341-25G), and ScintiVerse scintillation liquid (Cat. No. SX18-4) are from Fisher Scientific Co. (Suwanee, GA); thymidine [6-^{3}H] specific activity 10 Ci (370 GBq/mmol) at a concentration of 1 m Ci/ml (Cat. No. 355001MC) is from Perkin Elmer Life Science (Boston, MA); and LS 6500 liquid scintillation counter is from Beckman Coulter Inc. (Fullerton, CA).

a. Preparation of Cells

Steps

1. Prepare 0.5% agar by mixing 3.5 ml of 3% Noble agar with 16.5 ml of RPMI 1640 containing 20% fetal bovine serum.
2. Add 500 µl of this agar mixture to each well of a 24-well plate. Then refrigerate the plate at 4°C for 10 min.
3. Resuspend cells in a mixture containing 0.4% agar in RPMI 1640 containing 20% fetal bovine serum at a final concentration of 10^4 cells/ml.
4. Add 1 ml of the cell suspension to each well containing the hardened underlayer.
5. Incubate the plate at 37°C in a 5% CO_2 atmosphere for 24 h.

Assay Procedure

Steps

1. Add sodium azide at a final concentration of 4×10^3 µg/ml to the contol wells (cells without drug).
2. Add the drug to all the remaining wells at the concentrations planned.
3. Incubate cells + drug for 72 h.
4. At the end of this incubation, layer 5 µ Ci of [^{3}H]-thymidine over each well.
5. Incubate the plate for an additional 24 h.
6. Transfer the agar layers from each well to 15-ml centrifuge tubes and bring the volume to 13 ml adding PBS to each tube.
7. Boil the tubes for 30 min and then centrifuge at 1000 rpm for 5 min.
8. Aspirate the supernatants and wash each pellet two times with cold PBS.
9. Centrifuge the tubes and collect the precipitates. Then wash each pellet with 5% TCA.
10. Dissolve each pellet by adding 0.3 ml of 0.075 *N* KOH and pipetting up and down to completely solubilize cells.
11. Transfer each solubilized cell solution into a scintillation vial containing 5 ml scintillation liquid.
12. Count the radioactivity of each vial in a LS 6500 Beckman liquid scintillation counter.

Comments

When used for cells in suspension the assay may be modified to obtain several time points, e.g., 5, 10, 20, 40, and 60 min, thus generating a rate of thymidine incorporation into DNA and more quantitative data.

III. CLONOGENIC ASSAYS

One of the most important methods for the assessment of survival is the measurement of the ability of a single cell to form colonies. This is usually done by simple dilution after generating a single cell suspension and counting the colonies that arise from single cells. For effective and correct counting, a lower threshold, such as five or six doublings (32 or 64 cells/colony), is quantitated, taking into account the doubling time. Thus the effect of a concentration of a drug on cell survival may be measured with this assay.

In addition to counting colonies, as some drugs may have a delayed effect on cell proliferation, it might be necessary to do colony size analysis. This can be done by counting the cells per colony, by measuring the diameter, or by measuring the absorbance of colonies stained with 1% crystal violet.

The clonogenic assay for tumor colony-forming cells has applicability to a broad spectrum of cell lines and fresh cells obtained from human tumors and has provided information on the biology, clinical course, and chemosensitivity of human cancers

A. Monolayer Cloning

In this method, adherent cells are plated onto a plastic or glass surface and colonies formed are stained and counted. The method is straightforward and useful for cell lines that grow on plastic if a reasonable percentage of cells generate colonies.

Materials and Instrumentation

25-cm^2 flasks (Corning, Cat. No. 430639)
Phosphate-buffered saline (GIBCO, Cat. No. 10010-023)
Trypsin (GIBCO, Cat. No. 25200-056)
Petri dishes (Falcon, Cat. No. 1007, 60 × 15 mm)
Methanol (J. T. Baker, Cat. No. 9069-03)
1% crystal violet
Hemocytometer (Reichert-Improved Neubauer, Cat. No. 132501)

Steps

1. Prepare replicate 25-cm^2 flasks, two for each concentration of drug and two for controls.
2. Add the drug to the test flask and solvent to the control flask when the cells reach the required growth phase (usually 24 h after plating) and incubate for 1 h at 37°C.
3. Remove the drug, rinse the monolayer with PBS, and prepare a single cell suspension by trypsinization (desirable).
4. Count the cells and dilute the cell concentration to give 100–200 colonies per 6-cm petri dish. The cell number used per dish depends on the efficiency of plating and the effect of the drug. Plate setup should contain at least two different cell concentrations: one for lower concentrations of the drug and one for higher drug concentrations.
5. Plate out the appropriate number of the cells and incubate at 37°C with 5% CO_2 until colonies grow. This time varies according to the doubling time of the cells, but generally ranges from 10 to 21 days. The colonies should grow to 1000 cells or more on average for the survival assays.
6. Rinse dishes with PBS, fix in 1% methanol or 0.5% glutaraldehyde, and stain with 1% crystal violet. Rinse in running tap water, distilled water, and dry. Count colonies above threshold and calculate as a fraction of control. Plot on a log scale against drug concentration.

Comments

Longer drug exposures can also be assessed by incubating cells with drug for different times, removing media and adding fresh media.

B. Cloning by Limiting Dilution

Puck and Marcus (1955) first established this method. It is more useful for suspension cultures. To improve plating efficacy, modifications for improving the yield of harvested cells, such as using a rich medium that has been optimized for the cell type in use, may be necessary. Cells in log phase should be selected for this method. Also, where serum is required, fetal bovine serum is generally better than calf or horse serum. Sometimes changing the conditions may be useful for obtaining high colony efficiency such as filtering the media or incubating cells for a further 48 h.

Materials and Instrumentation

DMEM, high glucose (Life Technologies, Inc., Cat. No. 10313-021 or equivalent)
Fetal bovine serum (Gibco-Invitrogen, Co. Cat. No. 10437-028 or equivalent)
L-Glutamine (Gibco-Invitrogen, Co. Cat. No. 25030-081 or equivalent)
Hybridoma cloning factor (Fisher, Cat. No. IG50-0615)
50-ml sterile centrifuge tubes (Falcon, Cat. No. 2070)
15-ml sterile centrifuge tubes (Falcon, Cat. No. 2099)
24- and 96-well culture plate (Falcon 353047-0413 and Falcon 353072-0664)
Hemocytometer (Reichert-Improved Neubauer, Cat. No. 132501)
Trypan blue, 0.4% (Sigma Chemicals, Co. Cat. No. 72K2328)
Multichannel pipetter (Thermo Labsystem, Cat. No. 4610050) and sterile tips (Denville Scientific, Cat. No. P-3950-200)
Reagent reservoir (Labcor, Inc., Cat. No. 730-004)
HT (Life Technologies, Inc., Cat. No. 11067-30)

Steps

1. Refeed cells in 24-well plates or flasks with fresh medium 24 h before cloning.

2. Prepare the cloning media by using 10% hybridoma cloning factor, 20% FBS, 4 m*M* L-glutamine, and DMEM.

3. Resuspend the cells to be cloned in 15-ml sterile tubes; use the trypan blue dye exclusion method to determine viability. Viability should be greater than 80%.

4. For each cell line calculate the dilutions to give 4, 2, and 1 cell/ml in cloning medium. Using 50-ml tubes, serially dilute to contain 4, 2, and 1 cell/ml. The final dilution tube should contain 50 ml of cloning medium at 1 cell/ml.

5. Pour each of the dilutions into a sterile reservoir. Plate 250 µl/well into 96-well plates (one plate with 4 cells/ml, one plate with 2 cells/ml, and two plates with 1 cell/ml). Complete dilutions and plating for each cell line.

6. Incubate all plates at 37°C with 8–10% CO_2 for 5–7 days. At the end of this time, examine all plates microscopically to ensure cloning and plating efficiency before refeeding the plates.

7. Count colonies

C. Soft Agar Clonogenic Assay

Another useful method for cytotoxicity studies is the soft agar technique. It is particularly useful for cells that grow in suspension, but may also be used for cells that attach to glass or plastic. The cells are treated with drug, washed, instead of creating a growth curve as in the outgrowth method, the cells are cloned in soft agar as described next. Agar solution, medium, and cell suspensions are the three basic components in the cloning technique.

Materials and Instrumentation

Noble agar (Agar-Noble Difco Lab)
Fetal bovine serum (Gibco-Invitrogen, Co. Cat. No. 10437-028 or equivalent)
RPMI 1640 medium (GIBCO, Cat. No. 11875-093)
Large culture tubes (Daigger, Cat. No. EF4003)
24-well plate (Falcon, Cat. No. 3487)

Use the following steps for preparing the agar.

Steps

1. Weigh 0.11 g Noble agar and put into a dry flat-bottom bottle that can hold 50 ml.
2. To the 0.11 g agar, add 5.2 ml distilled water. In adding the water, be sure that the water runs in gently so that the agar does not explode.
3. Autoclave 15 min, slow exhaust, and remove immediately upon completion of sterilization.

Use the following steps for preparing the medium.

Steps

1. Measure 50 ml of medium plus serum into a bottle and store at 37°C. (The medium should contain serum in excess of the normal amount used for liquid cultures, such as 15–20%.)
2. For each condition being tested, prepare a culture tube 125 × 20 mm containing 9.0 ml of medium.
3. Treat the cells with drug and resuspend in 15–20% serum-supplemented medium. Cells will need to be diluted so that no more than 1.0 ml (tube cloning) and 0.5 ml (double-layer cloning) of cell suspension will contain the desired number of cells.

   Example: For L5178Y cells, a mouse leukemia cell line, the cloning efficiency is 88%. In order to get a cloning tube with 20 clones per tube, 10 ml of cell suspension is made having 120 cells in 10 ml. This is done in the tube containing 9.0 ml of medium, as described previously.

   Example: Cell stock after centrifuging is 2×10^4 cells/ml. Dilute 1:100; take 0.6 ml of the 1:100 dilution, and add to the 9.0 ml of medium. Bring the volume to 10 ml by adding 0.3 ml of medium and 0.1 ml of appropriate drug solution. Each condition tested will require a separate cell suspension, i.e., each cell suspension tube supplies cells for a maximum of five cloning tubes. Only four are generally used.

For Tube Cloning Procedure

1. Add the previously measured 50 ml of medium to the bottle of liquified agar solution. It should be cooled enough so that it can be held by hand comfortably.
2. Distribute 3 ml of agar-medium mixture to each cloning tube.
3. Add 2 ml of cell suspension in the large culture tubes, being sure they are well suspended.
4. Tighten the cap, and mix in the following manner: Hold the tube horizontally and rotate. At the same time, rock the tube to mix. Do this gently to avoid bubbles.
5. Place the tube upright in ice for 2 min.
6. Remove from ice and place in culture tube rack.
7. Keep at room temperature for 15 min.
8. Incubate in an upright position at 37°C.
9. Clones of fast growing lines, such as L5178Y and L1210, are counted on the 10th day. Others take longer, depending on the generation of time of the cancer cell line.

Double-Layer Soft Agar Clonogenic Assay Procedure

This method has some additional benefits compared to the monolayer agar method (Runge *et al.*, 1985). It is very useful for cell cultures whose cloning capacity is low and for fresh cells obtained from tumor biopsy samples.

Materials and Instrumentation

The materials are the same used in other agar-clonogenic assays mentioned earlier.

Steps

Plate 1 ml of underlyer (feeder layer) consists of 15–20% serum-supplemented RPMI 1640 medium and 0.5% Noble agar in 24-well culture plates. The underlayers have to be gelled at least 1 h prior to plating the 1 ml cell and drug(s) (based on design) containing upper layer. For each condition, a suspension is prepared with 4 ml of 20% supplemented RPMI 1640 medium, 0.5 ml of 3% agar solution (final concentration 0.3%), and 0.5 ml of cell suspension containing 5000 cells and appropriate concentration(s) of drug(s). Plate 1 ml of such suspension in each well with a gelled underlayer. Each condition is in quadruplicate. Place all double-layered plates at room temperature for 20 min and then incubate for 10–14 days at 37°C in 100% humidity in 5% CO_2 of atmosphere. For continuous exposure, leave the drug(s) in culture for the entire period of incubation. For time point exposures, such as 4 h, 24 h, 48 h, and even 7 days, incubate cells with drug in suspension culture, wash cells twice with PBS, harvest, resuspend, and finally clone per the procedure described earlier. After 10–14 days of incubation, count clones greater than 50 cells in each well under an inverted microscope (×40). Results are expressed as the mean of 4 well as the percentage of untreated control colony counts.

D. Use of Image Analysis System to Count Colonies

The clonogenic assay for tumor colony-forming cells has applicability on a broad scope of human tumors and has proved valuable in studies of biology, clinical course, and chemosensitivity of human cancers. However, visual counting of colonies has several problems: it is time-consuming and therefore very expensive, the size of colonies changes very rapidly, and there is variability in counting from one researcher to another, partly because of differences in criteria for what constitutes a colony and fatigue.

Bausch and Lomb Omnicon FAS-II image analysis system provides sufficient reliability to be used for counting human tumor colonies grown *in vitro* (Kressner *et al*., 1980). In addition, the colony counter performed the petri dish counts 10 times faster than experienced technicians did and without associated operator fatigue (Salmon *et al*., 1984)

References

Cory, A. H., Owen, T. C., Barltrop, J. A., and Cory, J. G. (1991). Use of an aqueous tetrazolium/formazan assay for cell growth assays in culture. *Cancer Commun.* **3**, 207–212.

Denizot, F., and Lang, R. (1986). Rapid colorimetric assay for cell growth and survival: Modification to the tetrazolium dye procedure giving improved sensitivity and reliability. *J. Immunol. Method* **89**, 271–277.

Donacki, N. http://www.protocol-online.org/protocols/cloning_by_limiting_dilution.htm

Freshney, R. I. (1994). Cloning and selection of specific cell types. *In* "*Culture of Animal Cells*" (I. R. Freshney, ed.), pp. 161–178. Wiley-Liss, New York.

Garewal, H. S., Ahmann, F. R., Schifman, R. B., and Celniker, A. (1986). ATP assay: Ability to distinguish cytostatic from cytocidal anticancer drug effect. *J. Natl. Cancer Inst.* **77**, 1039–1045.

Goegan, P., Johnson, G., and Vincent, R. (1995). Effects of serum protein and colloid on the almarBlue assay in cultures. *Toxicol. in Vitro* **9**, 257–266.

Hamburger, A. W. (1987). The human tumor clonogenic assay as a model system in cell biology. *Int. J. Cell Cloning* **5**(2), 89–107.

H-Zanki, S. U., and Kern, D. H. (1987). *In vitro* assay for new drug screening: Comparison of a thymidine incorporation assay with the human tumor colony-forming assay. *Int. J. Cell Cloning* **5**, 421–431.

Kaltenbach, J. P., Kaltenbach, M. H., and Lyons, W. B. (1958). Nigrosin as a dye for differentiating live and dead ascites cells. *Exp. Cell Res.* **15**, 112–117.

Kangas, L., Gronroos, M., and Nieminen, A. L. (1984). Bioluminescence of cellular ATP: A new method for evaluating cytotoxicity agents *in vitro*. *Med. Biol.* **62**, 338–343.

Kressner, B. E., Morton, R. R. A., Martens, A. E., Salmon, S. E., Von Hoff, D. D., and Soehlen, B. (1980). Use of image analysis system to count colonies in stem cell assays of human tumors. *In* "*Cloning of Human Tumor Cells*," pp. 179–193. A. R. Liss, New York.

Mollgard, L., Tidefelt, U., Sundman-Engberg, B., Lofgren, C., and Paul, C. (2000). *In vitro* chemosensitivity testing in acute non lymphocytic leukemia using the bioluminescence ATP assay. *Leuk. Res.* **24**, 445–452.

Mosmann, T. (1983). Rapid colorimetric assay for cellular growth and survival: Application to proliferation and cytotoxicity assays. *J. Immunol. Methods* **65**, 55–63.

Papazisis, K. T., Geromichalos, G. D., Dimitriadis, K. A., and Kortsaris, A. H. (1997). Optimization of the sulforhodamine B colorimetric assay. *J. Immunol. Methods* **208**, 151–158.

Puck, T. T., and Marcus, P. I. (1955). A rapid method for viable cell titration and clone production with HeLa cells in tissue culture: The use of X-radiated cells to supply conditioning factors. *Proc. Natl. Acad. Sci. USA* **41**, 432–437.

Roehm, N. W., Rodgers, G. H., Hatfield, S. M., and Glasebrook, A. L. (1991). An improved colorimetric assay for cell proliferation and viability utilizing the tetrazolium salt XTT. *J. Immunol. Methods* **142**, 257–265.

Rynge, H. M., Neuman, H. A., Bucke, W., and Pfleiderer, A. (1985). Cloning ovarian carcinoma cells in an agar double layer versus a methylcellulose monolayer system: A comparison of two method. *J. Cancer Res. Clin. Oncol.* **110**(1), 51–55.

Salmon, S. E., Young, L., Lebowitz, J., Thompson, S., Einsphar, J., Tong, T., and Moon, T. E. (1984). Evaluation of an automated image analysis system for counting human tumor colonies. *Int. J. Cell Cloning* **2**, 142–160.

Scudiero, D. A., Shoemaker, R. H., Paull, K. D., Monks, A., Tierney, S., Nofziger, T. H., Currens, M. J., Seniff, D., and Boyd, M. R. (1988). Evaluation of a soluble tetarzolium/formazan assay for cell growth and drug sensitivity in culture using human and other tumor cell line. *Cancer Res.* **48**, 4827–4833.

Sevin, B. U., Peng, Z. L., Perras, J. P., Ganjei, P., Penalver, M., and Averette, H. E. (1988). Application of an ATP-bioluminescence assay in human tumor chemosensitivity testing. *Gynecol. Oncol.* **31**, 191–204.

Skehan, P., Storeng, R., Scudiero, D., Monks, A., McMahon, J., Vistica, D., Warren, J. T., Bokesh, H., Kenney, S., and Boyd, M. R. (1990). New colorimetric cytotoxicity assay for anticancer-drug screening. *J. Natl. Cancer Inst.* **82**, 1107–1112.

Soehneln, B., Young, L., and Liu, R. (1980). Cloning of human tumor stem cells. *In* "*Standard Laboratory Procedures for in Vitro Assay of Human Tumor Stem Cells*," pp. 331–338.

Westermark, B. (1974). The deficient density dependent growth control of human malignant glioma cells and virus-transformed glia-like cells in culture. *Int. J. Cancer* **12**, 438–451.

White, M. J., Di Caprio, M. J., and Greenberg, D. A. (1996) Assessment of neuronal viability with Alamar blue in cortical and granule cell cultures. *J. Neurosci. Methods* **70**, 195–200.

CHAPTER

39

Micronuclei and Comet Assay

Ilona Wolff and Peggy Müller

I. INTRODUCTION

To evaluate genotoxic effects of chemical substances *in vitro*, various methods are available differing in their sensitivity, their practicability, and, finally, the genetic end points considered. The micronucleus assay is one of the methods used to detect chromosomal aberrations in proliferating cell culture systems (Fenech and Morley, 1985). Its advantages are sensitivity as well as uncomplicated realisation and evaluation of results. Because of its relevance and applicability for human cell systems, the cytokinese-block Micronucleus assay with human lymphocytes is described in detail (Fenech, 2000). Micronuclei represent chromosome fragments or whole chromosomes which are not incorporated into the main nuclei at mitosis and they consequently appear only in dividing eukaryotic cells. In order to score micronuclei exclusively in cells that have completed one nuclear division only, the cytokinese-block method is applied in this test version, which prevents the cytoplasmic division after nuclear division by use of cytochalasin B.

The comet assay, or single cell gel electrophoresis, is another widely used assay for identifying genetic damage such as DNA strand breaks. The alkaline version of the assay introduced by Singh *et al*. (1988) allows the identification of DNA single strand breaks in a very sensitive manner. In addition, there are further advantages, such as the relatively low cell number (<10,000 cells per slide), its ease of application, the applicability of nearly all human and other eukaryotic cells proliferating *in vitro*, and its time- and cost-saving performance, which argue for the use of this assay. To summarize main test principles: agarose-embedded cells are lysed by the help of high salts and detergents; DNA unwinding is promoted by incubating in alkaline electrophoresis buffer (pH > 13); and single-stranded DNA is electrophoresed under alkaline conditions, allowing the DNA fragments to migrate to the anode. After neutralization of slides, the amount of DNA damage may be detected by use of a fluorescent dye such as ethidium bromide visualizing the migrated DNA as the so-called comet tail. The migration length (i.e., the tail length) depending on the DNA fragment size is the most commonly used parameter for quantifying DNA damage. Other metrics considered only by use of image analysis systems are the percentage of migrated DNA and the tail moment (Olive *et al*., 1990).

Exemplarily, three cell types are presented considering different species (human and rat cells), different culture types (suspension or monolayer culture), and diversity in metabolic activation capacity (normal human bronchial epithelial cells and human lymphocytes versus rat hepatocytes). Selected cell types are capable for genotoxicity testing of single substances and complex mixtures (Müller *et al*., 2002), and the presented test protocols may be transferred to any other eukaryotic cell type proliferating *in vitro*.

II. MATERIALS AND INSTRUMENTATION

RPMI 1640 instamed (T 121-01) is from Biochrom AG Seromed, as well as the trypan blue solution (L-6323), phosphate-buffered saline (PBS, L-182-01), collagenase CLS II (C 2-22), fibronectin from human plasma (L 7117), and gentamycine (A-271-23).

Epith-o-ser (FM-56-L) and Leibovitz's L-15 (PM-23-S) are from cc-pro, as well as fetal calf serum (FCS, S-10-L), trypsin–EDTA (Z-26-M), and

Copyright 2006, Elsevier Science (USA).
All rights reserved.

penicilline–streptomycine solution (Z-13-M). Minimum essential medium Eagle (MEM, M-1018) is from Sigma-Aldrich Chemie, as well as phytohaemagglutinine (PHA, L-9132), cytochalasine B (C-6762), $CaCl_2$ anhydride (C-1016), $MgSO_4 \times 7H_2O$ (M-1880), acridine orange (A-6014), phenol red (P 3532), insulin from bovine pancreas (I-6634), *N*-[tris(hydroxymethyl)methyl]-2-aminoetharesuforic acid (TES, T 5691), HEPES (H 4034), tricine (T 5816), $MgCl_2 \times 6H_2O$ (24,696-4), $Na_2HPO_4 \times 2H_2O$ (21,988-6), and $Na_2HPO_4 \times 7H_2O$ (22,199-6) and Na_2HPO_4 anhydride (S-9763). Normal melting temperative agarose (NMA, 11400) and collagen R (47254.02) are from Serva, as well as ethidium bromide (EtBr, 21251), glucose-6-phospate (22775.01), and Na-pyruvic acid (15220). Low melting temperature agarose (LMA, 35-2010) is from peqLab. Triton X-100 (6683.1), NaCl (3957.2), Na-EDTA (8043.1), Tris (4855.2), dimethyl sulfoxide (DMSO, 7029.1), ethanol (P.076.1), and isopropanole (6752.1) are from Roth. Lymphocyte separation medium (Ficoll-Paque, 17 1440-03) is from Amersham Biosciences. NADP (93208) and formic acid (33015) are from Fluka. Aroclor 1254 (RPC-1254) is provided by Ultra Scientific. All other chemicals are from VWR International: glucose anhydride (1.08337.1000), Na_2HCO_3 (1.063290.500), methanol (1.06009.1000), glacial acetic acid (1.00056.1000), NaOH (1.06462.1000), KH_2PO_4 (1.04873.0250), methoxymagresium–methylcarborate (MMC, 8.18156.0100), KCl (1.04933.0500), Na_2SO_4 (106647), H_2O_2 (1.08597.1000), 2-mercaptoethanol (1.15433.0050), and L-glutamine (1.00289.0100). Heparin sodium salt (101931) is from ICN Biomedicals Inc. Bovine serum albumin fraction V (11018-025) is from Invitrogen. Peanut oil is from the pharmacy of the clinic of Martin Luther University Halle-Wittenberg.

For preparation of lymphocytes, Leucosep vials (227.290) are used, which are from Greiner. For Aroclor treatment of rats, a gauge needle (Sterican, 4667123) from B. Braun Melsungen AG is used. Surgery instruments are from Sigma Chemie: curved microdissecting forceps (F 4142), dressing tissue forceps (F 4267), straight microdissecting forceps (F 4017), curved microdissecting scissors with a sharp point (S 3271), straight microdissecting scissors with a sharp point (S 3146), scalpel blade (S 2771), and handle (S 2896). Cell culture supplies are from TPP: culture dishes (60 cm^2, 93100), cell culture vials (20 cm^2, 91106), cryo vials (2.0 ml, 89020), 15-ml centrifuge vials (91015), 50-ml centrifuge vials (91050), serological pipettes (10 ml, 94010), and culture flasks (25 cm^2, 90026). Automatic pipettes (Eppendorf research variable: 0.5–10, 10–100, 20–200, 100–1000, and 500–5000 µl) are from Eppendorf. The pipette aid (Drummond pipette aid, 28081410) is from Heinemann Labortechnik.

Heating plate (453N1120), water bath (Memmert WB 7, 4623520), swap thermostat (MP 5, 4613411), membrane pump for liquids (ND 100 KT.18, 2245110), electrophoresis chamber (Phero-Sub 2, 344797), power supply (Consors E835, 5822150), and the gel carrier (5817129) are from VWR International. The cell counting chamber (Fuchs-Rosenthal, T731.1), minicentrifuge (X409.1), staining tanks (Hellendahl, H549.1), slides (76 × 26 × 1 mm, 0656.1), and coverslips (24 × 40 mm, 1870) are from Roth. For the comet assay, fully frosted slides (61224) from Menzel are used. The CO_2 incubation chamber CB 150 (9040-0001) is from wtb-Binder. Clean bench Uniflow (KR-125-GS) is from UniEquip. The table centrifuge (Megafuge, 75003060) is from Kendro. For microscopic analysis, a Nikon fluorescence microscope Eclipse E 600 (MBA 70400) is used. Data processing is performed with the Komet analysis system, including software Komet 4.0 from Kinetik Imaging Ltd., purchased by BFI Optials.

III. PROCEDURES

A. Preparation and Cultivation of Cells

All cell types are cultivated in a CO_2-incubation chamber under the same conditions: 37°C, 5% CO_2, and 95% relative humidity.

1. Human Lymphocytes

Solutions:

Heat-inactivated FCS: Fill the necessary volume of FCS in a centrifuge vial, deposit the vial in a water bath, and heat the water continuously up to a temperature of 56°C. Hold this temperature for 30 min.

RPMI 1640 cell culture medium: To prepare 1 litre of cell culture medium, add the specified volume of powdered RPMI 1640, 2 g $NaHCO_3$, and 750 ml dH_2O while stirring. Complete to 890 ml with dH_2O, adjust pH to 7.4, and store at 4°C. Before use, add 100 ml of heat-inactivated FCS and 10 ml of penicilline–streptomycine and proof the pH to be 7.4.

Phosphate-buffered saline (PBS): To make 1 litre of PBS, add the specified volume of powdered PBS (Ca^{2+}/Mg^{2+} free) and 750 ml dH_2O while stirring. Complete to 1 litre with dH_2O and store at 4°C.

Steps

Before starting cell preparation, warm up all media, buffer, and supplements in a water bath (37°C). Use certified buffy coat or other human blood preparation.

1. For setup of the vials, pour 15 ml Ficoll-Paque in 50 ml Leucosep tubes and centrifuge at 900 *g* for 2 min.
2. Mix cold buffy coat with warm PBS in 1:2 proportion.
3. Layer 30 ml of this buffy coat PBS mixture onto a separation ring of the centrifuged Leucosep tubes and centrifuge at 800 *g* for 25 min, not using the brake.
4. After centrifugation, remove the lymphocytes carefully from the white lymphocyte ring, deliver them in a new tube, wash with a double quantity of PBS, and then centrifuge again at 800 *g* for 10 min.
5. Perform a second washing with 40 ml PBS and repeat centrifugation (800 *g* for 10 min).
6. Finally, resuspend lymphocytes in warm RPMI 1640 culture medium and cultivate the cells overnight in cell culture vials to allow sedimentation of the mononuclear cells, B lymphocytes, and regeneration of lymphocytes from the isolation procedure.

2. *Hepatocytes of Rat*

Solutions

Presuspension buffer: To make 2 litres, add 1500 ml dH_2O, 16.6 g NaCl, 1 g KCl, and 4.8 g HEPES while stirring. After dissolving, complete to 2 litres with dH_2O and adjust pH to 7.4. Keep at 4°C.

Collagenase buffer: To make 1 litre of stock solution, add 750 ml dH_2O, 3.9 g NaCl, 0.5 g KCl, 0.7 g $CaCl_2 \times 2$ H_2O, and 2.4 g HEPES while stirring. After dissolving, complete to 1 litre with dH_2O and adjust pH to 7.6. Keep at 4°C. To make 200 ml of working solution, add 27,300 U of collagenase.

Suspension buffer: To make 1 litre, add 750 ml dH_2O, 4 g NaCl, 0.4 g KCl, 0.13 g $MgCl_2 \times 6$ H_2O, 0.15 g KH_2PO_4, 0.1 g Na_2SO4, 7.2 g HEPES, 6.9 g TES, and 6.5 g Tricine while stirring. After dissolving, adjust pH to 7.6. Furthermore, add 1 g glucose, 30 g BSA, and 5 mg phenol red and sterilize by filtration. Keep at 4°C.

Pentobarbital solution: To get 1 ml, weigh 50 mg of pentobarbital and complete to 1 ml with dH_2O.

Heparin solution: To make 2.5 ml, weigh 1 mg heparin sodium salt and complete to 2.5 ml with 0.9% NaCl.

MEM culture medium with Hank's salts, L-gluthamine, and nonessential amino acids: To prepare 1 litre, add the specified volume of powdered MEM, 320 mg $NaHCO_3$, and 750 ml dH_2O while stirring, complete to 1 litre, adjust pH to 7.6, and aliquot. Keep at 4°C. Before use, weigh 0.5 µg/ml insulin from bovine pancreas and 50 µg/ml gentamicin and add to medium.

Steps

Hepatocytes may be isolated from untreated young laboratory rats by the *in situ* perfusion method with collagenase buffer following the modified methods by Berry and Friend (1969) and Seglen (1976). *Note*: It needs a special authorisation and large experience to perform manipulations with laboratory animals. Therefore, the method described in the following is only a summary.

1. Sterilise all surgical instruments, several glass beakers, and tubes. Warm up presuspension buffer and collagenase buffer (water bath, 40°C).
2. Anaesthetize rat with ip injection of 5 mg/100 g body mass pentobarbital (0.1 ml/100 g body mass) and inject 1 ml heparin solution per 250 g body mass through the penis vein.
3. Open the rat, dissect vena portae, and induct a gauge needle for injection the buffer solutions. Fix the needle by ligature.
4. Open the thorax, cut the superior caval vein, and start perfusion with warm presuspension buffer for 15–20 min at a constant flow rate of 10 ml/min.
5. Continue perfusion with warm collagenase buffer for about 10–20 min until the liver loses its typical elasticity and colour and becomes soft and pale. (Among other things, perfusion time depends on the activity of collagenase, flow rate, and constitution of liver.)
6. Gently dissect liver lobes and transfer to a culture dish with cold suspension buffer.
7. Carefully remove liver capsule and mechanically disaggregate cells using two forceps. Filtrate the cell suspension through different layers of gauze, transfer suspension to centrifuge vials, and centrifuge at 50 *g* for 6 min (4°C).
8. Discard supernatant and resuspend pellet in MEM medium. Transfer cell suspension to culture vials. Adjust cell number to 1×10^7 cells/ml after counting and estimation of viability by the trypan blue method (see later).
9. Use freshly prepared hepatocytes in tests without cultivation.

3. *Normal Human Bronchial Epithelial Cells (NHBEC)*

NHBEC may be isolated from explants from the bronchial airways of patients after lob- or pneumectomia (i.e., the resection of one of the lobes or of the lung at a hemithorax because of bronchial carcinoma) following the method of Lechner and LaVeck (1989) modified by Stock (2002).

Solutions

Epith-o-ser culture medium with supplements (serum free): Thaw the frozen supplements delivered and add to 500 ml of basal medium. Prepare the medium before use.

L-15 medium: To make 1 litre, dissolve the specified volume of powdered L-15 in 750 ml dH_2O and complete to 1 litre with dH_2O.

Coating solution: To make 100 ml solution, dissolve 1 mg fibronectine, 3 mg collagen R, and 1 mg BSA in 90 ml L-15 medium while stirring. Complete to 100 ml with L-15 and filtrate. Keep at 4°C. *Trypsin–EDTA solution*: Aliquot the delivered solution (0.05% trypsin/0.02% EDTA in Ca^{2+}- and Mg^{2+}-free PBS).

Steps

1. Coat culture dishes: Transfer 0.2 ml/cm^2 coating solution into culture dishes (60 mm diameter) while working under a clean bench. Incubate at 37°C, 5% CO2, and 95% relative humidity for 24 h. Aspirate remaining solution and let the layer dry. Dishes may be stored enveloped in folio at 4°C for about 6 weeks.
2. Fragment the bronchial tissue into pieces of 5 to 10 mm^2 and wash in PBS tree times.
3. Place six to eight tissue pieces into a coated culture dish (see earlier discussion), close, and allow adhesion for 5 min.
4. Add 4 ml of epith-o-ser medium and cultivate cells while changing culture medium every 2–3 days until a subconfluent status (about 2 weeks).
5. Before use of cells in the comet assay, carefully remove culture medium from the well, add warm 1.5 ml trypsin–EDTA solution, and allow digestion for about 5 min (37°C).
6. To stop digestion of cells, add 4.5 ml cold PBS and gently move the well in order to get all cells free from the well surface.
7. Transfer cell suspension into a centrifuge vial, centrifuge at 125 *g* for 10 min, remove the supernatant, and resuspend the pellet in fresh medium.
8. Calculate cell number and test viability by the trypan blue method (see later).

Viability Test by Trypan Blue Method

Dilute 1 ml of cell suspension with 9 ml culture medium or buffer, mix gently, extract 1 ml of this mixture, and add 1 ml trypan blue solution. Identify living (pale) and nonliving (blue) cells.

B. Micronucleus Assay

Peripheral lymphocytes are one of the most applied cell types for the identification of micronuclei in human tissue. Therefore, the method of the cytokinese-block micronucleus assay with human lymphocytes is described (Fenech, 2000).

Solutions

RPMI 1640 cell culture medium: To prepare 1 litre of cell culture medium, add the specified volume of powdered RPMI 1640 as described in the catalogue to 750 ml dH_2O while stirring. Complete to 890 ml with dH_2O, adjust pH to 7.4, and store at 4°C. Before use, add 100 ml of FCS and 10 ml of penicilline–streptomycine and proof the pH to be 7.4.

Fixative: To make 100 ml, add 75 ml of methanol and 25 ml of glacial acetic acid and keep at 4°C.

Staining solution: To make 100 ml of stock solution (0.24 m*M*), take 100 µl acridine orange and complete to 100 ml with dH_2O. Store at 4°C. To make 100 ml of working solution, add 1 ml of stock solution and 15 ml of Soerensen buffer.

Soerensen buffer: 60 m*M* Na_2HPO_4:60 m*M* KH_2PO_4 = 1:1, pH 6.8.

Solution 1: To make 1 litre, weigh 11.876 g of Na_2HPO_4 and complete to 1 litre with dH_2O.

Solution 2: To make 1 litre, weigh 9.078 g of KH_2PO_4 and complete to 1 litre with dH_2O.

To get 100 ml of buffer with pH of 6.8, add 50 ml of Solution 1 and 50 ml of Solution 2.

Steps

Perform the micronucleus test following the modified methods of Fenech and Morley (1985) and Sgura *et al*. (1997).

1. Resuspend cultivated lymphocytes, centrifuge at 800 *g* for 5 min, and remove the medium above the pellet.

2. Resuspend the cells in fresh RPMI medium supplemented with 10% inactivated FCS and 1% penicilline–streptomycine-solution at a concentration of 1×10^6 cells ml, add PHA in a final concentration of 2 mg/ml, and cultivate for 20 h.

3. After this time, add the test substance in the selected test concentrations. Cultivate cells for 24 h.

4. Add cytochalasin B in the final concentration of 3 µg/ml and continue cultivation for another 24 h. (Cytochalasin B prevents cells from completing cytokinesis, resulting in the formation of multinucleated cells.)

5. Centrifuge this suspension at 425 *g* for 10 min, remove the supernatant, wash the pellet with 2 ml PBS, and centrifuge again at 425 *g* for 10 min.

6. After removing the supernatant, resuspend cells in 1 ml of fixative, centrifuge at 200 *g* for 5 min, aspirate

the supernatant, and dissolve the pellet in few drops of fixative.

7. Transfer the fixed cells to normal, precleaned air-dried slides. Stain the cells with acridine orange solution for 3 min, rinse three times with Sörensen buffer, and finally cover with coverslips.

8. Score the slides (two slides per concentration and control) for micronucleated lymphocytes: 1000 binucleate lymphocytes have to be scored for the number of micronuclei using a fluorescent microscope (400× magnification) fitted with a epifluorescent condensor and filter set (excitation filter 510–590 nm). Perform two replicate experiments for each test.

9. Statistical differences between controls and each treated sample may be identified with the one-tailed χ^2 test following Lovell *et al*. (1989).

C. Alkaline Single Cell Gel Electrophoresis (Comet Assay)

Solutions

Trypsin–EDTA solution

NMA in aqueous solution: To make 100 ml 1% agarose solution, add 1 g NMA to 100 ml distilled water, heat carefully until the agarose is dissolved, and store at 4°C.

NMA in PBS: To make 100 ml of a 0.6% solution, add 0.6 g NMA to 100 ml PBS (without Ca^{2+} and Mg^{2+}), heat carefully until agarose is dissolved completely, and store at 4°C.

LMA in PBS: To make 100 ml of a 0.5% solution, add 0.5 g LMA to 100 ml PBS (without Ca^{2+} and Mg^{2+}), heat carefully until agarose is dissolved completely, and store at 4°C.

Lysing solution: To make 1 litre, add 1.21 g Tris (10 m*M*), 146. 1 g NaCl (2.5 *M*), and 37 g Na–EDTA (100 m*M*) to about 700 ml dH_2O while stirring. After dissolving, complete to 890 ml with dH_2O, adjust pH to 10, and keep at room temperature. Immediately before use, add 1% Triton-X and 10% DMSO.

Electrophoresis buffer: To make 1 litre, add 0.37 g Na–EDTA (1 m*M*) and 12 g NaOH (300 m*M*) to about 700 ml dH_2O under stirring. After dissolving, complete to 1 litre with dH_2O and adjust pH to 13. Prepare fresh.

Neutralisation buffer: Per litre, add 48 g Tris to 750 ml dH_2O and complete to 1 litre with dH_2O (400 m*M*, pH 7.4).

Ethidium bromide solution: To get 10 ml, dissolve 200 µg EtBr in distilled water and complete to 10 ml. Aliquot in 1-ml portions and keep at 4°C.

Steps

1. Preparation and Treatment Schedule of Cells

1. *Human lymphocytes and rat hepatocytes (or other cells in suspension culture)*: Decant medium from lymphocyte overnight culture or from hepatocyte suspension, respectively. Centrifuge cells for 5 min at 200 *g*. Resuspend cells in fresh culture medium. Calculate cell number (Fuchs–Rosenthal counting chamber) and test viability by the trypan blue method (see earlier discussion).

2. *In case of culture treatment with test substance (*in vitro *experiments)*: Decant medium from deposited cells, add mixture of culture medium, test substance in the required test concentration, resuspend cells in this mixture, and cultivate while stirring vials gently.

3. After treatment, centrifuge cells for 5 min at 200 *g*, discard supernatant, resuspend pellet in fresh culture medium, decant medium from deposited cells, and resuspend cells gently in 85 µl melted LMA per slide.

NHBEC (or Other Monolayer Cultures)

Short-term Treatment (1–2 hs)

1. Carefully remove media from subconfluent cell culture, add 1.5 ml of warm trypsin–EDTA solution, and incubate for 5 min.
2. Follow steps 6–8 as described in Section III,A,3.
3. Centrifuge cells for 5 min at 200 *g*, discard supernatant, add mixture of culture medium and test substance in the required test concentration, resuspend cells in this mixture, and cultivate while stirring vials gently.
4. After treatment, centrifuge cells for 5 min at 200 *g*, discard supernatant, resuspend pellet in fresh culture medium, decant medium from deposited cells, and resuspend cells gently in 85 µl melted LMA per slide.

Long-term Treatment (>2 hs)

1. Carefully remove media from subconfluent cell culture, add mixture of culture medium, and test substance in the required test concentration. Cultivate cells over the required treatment period.
2. After treatment, remove the treatment solution carefully, rinse with fresh medium, remove it, and add 1.5 ml of warm trypsin–EDTA solution. Incubate for 5 min.
3. Follow steps 6–8 as described in Section III,A,3.
4. Centrifuge cells for 5 min at 200 *g*, discard supernatant, resuspend pellet in fresh culture medium, decant medium from deposited cells, and resuspend cells gently in 85 µl melted LMA per slide.

2. *Preparation of Cells from* in Vivo *Experiments*

Follow the procedures described earlier except for the treatment of cells.

Cells from Suspension Culture. Decant medium from cultured cells and resuspend cells gently in 85 µl melted LMA per slide.

Cells from Monolayer Culture

1. Carefully remove media from subconfluent cell culture, add 1.5 ml of warm trypsin–EDTA solution, and incubate for 5 min.
2. Follow steps 6–8 as described in Section III,A,3.
3. Centrifuge cells for 5 min at 200 *g*, discard supernatant, resuspend pellet in fresh culture medium, decant medium from deposited cells, and resuspend cells gently in 85 µl melted LMA per slide.

Note: For administration of LMA, do not exceed temperature of 37°C. Adjust cell number to 10,000 per slide. In human cell culture systems (lymphocytes and NHBEC), S9 mix as an external metabolising system should be involved (described in Section III,D) in parallel experiments. Do not treat cells longer than 3 h with S9 mix.

3. *Slide Preparation*

The slide preparation follows the basic method of Singh *et al*. (1988). All steps following step 3 are performed in a dark room under yellow light.

1. Melt NMA (1% in dH_2O) in a microwave (1 ml per slide). Cover a labelled fully frosted microscopic slide with 1 ml of NMA, spread it evenly, and remove the layer after drying by scratching.
2. Overload the slide with 300 µl of melted NMA (0.6% in PBS), cover with a large coverslip, and store at room temperature until the agarose is solidified.
3. Meanwhile, prepare cell suspension (see earlier discussion).
4. Remove coverslip gently and transfer the cell agarose suspension onto the prepared slide.
5. Cover with a fresh coverslip and incubate for 10 min on ice. After the agarose is solidified, slide off coverslip gently and apply a layer of 85 µl melted LMA.
6. Cover with a fresh coverslip and incubate for 10 min on ice.
7. Slide off coverslip gently and incubate slide in freshly prepared chilled lysing solution for 1 h at 4°C in the dark using a staining tank.

Note: Steps 5 and 6: For incubation of slides on ice, prepare an ice bath, cover it with a piece of blotting paper, and apply an appropriate pane of glass.

4. *Electrophoresis*

1. Remove slide from the lysing solution and wash gently with fresh electrophoresis buffer (pH > 13).
2. Apply slides side by side (without distances) on the horizontal gel box of the electrophoresis chamber, fill the chamber with freshly made electrophoresis buffer, avoiding bubbles, and incubate slides for 1 h in order to allow DNA unwinding. The buffer just has to cover the slides!
3. Switch on power supply: Conduct electrophoresis at 25 V and 300 mA (0.66 V/cm) for 30 min and cover the chamber with aluminium foil.
4. Switch off power supply, remove slides from the chamber gently, and rinse carefully with neutralisation buffer three times to remove alkali and detergents. It is possible to store slides in neutralisation buffer until examination in the dark at 4°C, but do not exceed 24 h.

5. *Examination*

1. Gently remove slides from neutralisation buffer, place on a slide drainer, and stain every slide after draining with 60 µl EtBr. Cover with a coverslip and allow staining for 10 min.
2. For DNA analysis, use an epifluorescence microscope with a 510- to 590-nm excitation filter and a short arc mercury lamp. Examine at 400-fold magnification. Per test concentration not less than 50 cells should be scored; two replicate experiments should be performed per test. It is possible to determine comet tail length as a result of DNA damage by use of a micrometer in the microscope eyepiece. However, this method is time-consuming and is subject to various mistakes. A better method of processing data is to use an imaging analysis system in connection with special software for the comet assay, such as described earlier. In this case, follow the manual.
3. To determine the lowest test concentration at which a significant increase in DNA damage (given as comet tail length or tail moment) has occurred, multiple pairwise comparisons have to be conducted between control data and each dose using the Student's *t* test.

Note: To avoid confusion of results by concomitant processes leading to apoptosis, do not observe highly damaged cells. To ensure reproducibility of data between various experiments, do not use short arc mercury lamps with different wattage.

D. Further Procedures

1. *Preparation of S9 Mix from S9 Fraction*

Most of the cell culture systems, apart from hepatocytes, should be exposed to test substance both in the

presence and in the absence of an external metabolising system, i.e., the postmitochondrial supernatant of the rat hepatocyte preparation of Aroclor 1254 pretreated male rats (S9 mix) as described by Czygan *et al*. (1973), Ames *et al*. (1975), and Natarajan *et al*. (1976), to consider the effectivity of test substance in dependency on its metabolisation. Usually, the final concentration of S9 mix ranges from 1 to 10%, depending on the classification of test substance.

2. Preparation of S9 Fraction

Solutions

1. *Aroclor 1254*: Suspend 200 mg Aroclor in 1 ml peanut oil.
2. *0.15 M KCl*: Dissolve 5.59 g KCl in destilled water and fill up to 500 ml; sterilize this solution by filtration. Store at 4°C.

Steps

1. Aroclor is administered to rat by ip injection using a final dose of 500 mg/kg. Because of the high viscosity of the Aroclor suspension, use a gauge needle not smaller than 18 gauge.
2. Five days after injection, anaesthetize the rat, open the abdomen, and bleed and remove the liver immediately while working under sterile conditions at 4°C.
3. Weigh the liver, cut it into small pieces, and mix with cold sterilized KCl (1 g per 3 ml KCl).
4. Homogenize this mixture and centrifuge at 6000 *g* at 4°C for 10 min using sterile centrifuge vials.
5. Aliquot the supernatant to sterile cryo vials and store frozen at –80°C.

3. Preparation of S9 Mix

Solutions

Stock phosphate solution: (a) Dissolve 4.804 g KH_2PO_4 in dH_2O and complete to 100 ml. (b) Dissolve 6.286 g Na_2HPO4 in dH_2O and complete to 100 ml. Mix 19.6 ml of solution a with 80.4 ml of solution b, adjust pH to 7.4, and sterilize by heat (20 min at 121°C in autoclave). Store at 4°C.

$MgCl_2$: Dissolve 406.51 mg $MgCl_2 \times 6\ H_2O$ in dH_2O and complete to 50 ml, aliquot, and sterilize by microfiltration. Store at 4°C.

KCl: Dissolve 615 mg KCl in dH_2O and complete to 50 ml and sterilize by microfiltration. Store at 4°C.

NADP: Dissolve 726 mg NADP in distilled water and complete to 20 ml and sterilize by microfiltration. Aliquot and store frozen at –30°C.

Glucose-6-phosphate: Dissolve 304 mg glucose-6-phosphate in dH_2O and complete to 20 ml, aliquot, and sterilize by microfiltration. Store at –30°C.

Steps

1. To thaw components slowly, put all vials and bottles in an ice bath.
2. To make 10 ml of S9 mix, take 3 ml of stock phosphate solution, add 2 ml of KCl solution, 2 ml of MgCl, and 1 ml (10%) of S9 fraction. Complete this mixture with 1 ml NADP solution and finally add 1 ml of glucose-6-phosphate solution. It is very important to follow this sequence exactly and to take care that all components are mixed completely before adding the next one.

IV. COMMENTS

In each experiment, in addition to the test concentrations, a negative control (culture medium) and a positive control should be included for validation of results [micronucleus test: 0.5 *M* MMC, following Surralés and Natarajan (1997), comet assay: 300 µ*M* H_2O_2]. If a test substance has to be dissolved or suspended in any vehicle, a vehicle control has to be included too.

It is important to determine the concentration range as well as the treatment period in prestudies for every test substance and for various cell systems. The number of different test concentrations should be three or more. For more detailed description of test parameters, see Tice *et al*. (2000).

V. PITFALLS

1. In the case of elevated room temperature (about 30°C or more) it is possible that LMP agarose will not solidify; therefore, keep the slides together with the ice bath into the refrigerator.
2. To assign the slides, use a pen capable for cryopreservation or a pen for scratching on glass.

References

Ames, B. N., McCann, J., and Yamasaki, E. (1975). Methods for detecting carcinogens and mutagens with Salmonella/mammalian microsome mutagenicity test. *Mutat. Res.* **31**, 347–364.

Berry, M. N., and Friend, D. S. (1969). High-yield preparation of isolated rat liver parenchymal cells. *J. Cell Biol.* **43**, 506–520.

Czygan, P., Greim, H., Garro, J., Hutterer, F., Schaffner, F., Popper, H., Rosenthal, P., and Cooper, D. Y. (1973). Microsomal metabolism of dimethylnitrosamine and the cytochrom P-450 dependency of its activition to a mutagen. *Cancer Res.* **33**, 2983–2986.

Fenech, M. (2000). The in vitro micronucleus technique. *Mutat. Res.* **455**, 81–95.

Fenech, M., and Morley, A. A. (1985). Measurement of micronuclei in lymphocytes. *Mutat. Res.* **147**, 29–36.

Lechner, J. F., LaVeck, M. A., Gerwin, B. I., and Matis, E. A. (1989). Differential responses to growth factors by normal human mesothelial cultures from individual donors. *J. Cell Physiol.* **139**(2), 295–300.

Lovell, D. P., Albanese, R., Clare, G., Richold, M., Savage, J. R. K., Anderson, D., Amphlett, G. E., Ferguson, R., and Papworth, D. G. (1989). Statistical analysis of *in vivo* cytogenetic assays. *In* "*Statistical Evaluation of Mutagenicity Test Data*" (D. J. Kirkland, ed.). Cambridge Univ. Press, Cambridge.

Müller, P., Stock, T., Bauer, S., and Wolff, I. (2002). Genotoxicological characterisation of complex mixtures: Genotoxic effects of a complex mixture of perhalogenated hydrocarbons. *Mutat. Res.* **515**, 99–109.

Natarajan, A. T., Tates, A. D., van Buul, P. P. W., Meijers, M., and de Vogel, N. (1976). Cytogenetic effects of mutagens / carcinogens after activation in a microsomal system *in vitro*. I. Induction of chromosome aberrations and sister chromatid exchanges by diethylnitrosamine (DEN) and dimethylnitrosamin (DMN) in CHO cells in the presence of rat-liver microsomes. *Mutat. Res.* **37**, 83–90.

Olive, P. L., Banath, J. P., and Durand, R. E. (1990). Heterogeneity in radiation-induced DNA damage and repair in tumor and normal cells using the "comet" assay. *Radiat. Res.* **122**, 86–94.

Seglen, P. O. (1976). Preparation of isolated rat liver cells. *Methods Cell Biol.* **XIII**, 29–83.

Sgura, A., Antoccia, A., Ramirez, M. J., Macros, R., Tanzerella, C., and Degrassi, F. (1997). Micronuclei, centromere-positive micronuclei and chromosome nondisjunction in cytogenesis blocked human lymphocytes following mitomycin C or vincristine treatment. *Mutat. Res.* **392**, 97–107.

Singh, N. P., McCoy, M. T., Tice, R. R., and Schneider, A. L. (1988). A simple technique for quantitation of low levels of DNA damage in individual cells. *Exp. Cell Res.* **175**, 184–191.

Stock, T. (2002). Culture of normal human bronchial epithelial cells and its test for toxicological application. Martin Luther University Halle-Wittenberg, medical thesis. (http://sundoc.bibliothek.uni-halle.de/diss-online/02/02H153/index.htm)

Surrallés, J., and Natarajan, A. T. (1997). Human lymphocytes micronucleus assay in Europe. An international survey. *Mutat. Res.* **392**, 165–174.

Tice, R. R., Agurell, E., Anderson, D., Burlinson, B., Hartmann, A., Kobayashi, H., Miyamae, Y., Rojas, E., Ryu, J.-C., and Sasaki, Y. F. (2000). Single cell gel/comet assay: Guidelines for *in vitro* and *in vivo* genetic toxicology testing. *Environ. Mol. Mutagen.* **35**, 206–221.

SECTION

10

Apoptosis

CHAPTER

40

Methods in Apoptosis

Lorraine O'Driscoll, Robert O'Connor, and Martin Clynes

I. INTRODUCTION

Apoptosis and necrosis are two mechanisms of cell death, each with its own distinguishing morphological and biochemical features. Necrosis, which occurs within seconds of cell insult (Majno and Joris, 1995), may be described as "cell murder" resulting from external damage to the cell membrane, loss of homeostasis, water and extracellular ion influx, intracellular organelle swelling, cell rupture (lysis), and so inflammatory cell attraction. Initially described by Kerr *et al.* (1972), apoptosis is a much slower process of events than necrosis, requiring from a few hours to several days (depending on the initiator) and resulting from molecular signals initiated within individual cells (see Nagata, 1997; Barinaga, 1998; Van Cruchten and Van Den Broeck, 2002). The initiators of apoptosis that instigate the cascade of events leading to activation of a series of cytoplasmic proteases, termed caspases (cysteinyl-asparatate-specific proteinases), are multiple. Two such pathways involve (i) activation of cell surface death receptors, resulting in direct activation of caspases, and (ii) cytochrome *c* release from the mitochondria into the cytoplasm following induction of leakiness in its membrane. The terminal caspases downstream from these initiator mechanisms lead to the morphological and biochemical events of apoptosis.

The mechanisms of apoptosis, which is analogous to "cell suicide," are essentially the same, whether induced by genetic signals or through external initiators. The events involved include cell membrane blebbing; chromatin aggregation; nuclear and cytoplasmic condensation leading to cell shrinkage; and partitioning of cytoplasm and nucleus into membrane-bound apoptotic bodies, which contain ribosomes, morphologically intact mitochondria, and nuclear material. As a result of the efficient mechanism for the removal of apoptotic cells by phagocytic cells *in vivo*, an inflammatory response is not stimulated. *In vitro* apoptotic bodies swell and finally lyse (Darzynkiewicz and Traganos, 1998; Kiechle and Zhang, 2002).

Apoptosis is key to many fundamental aspects of biology, including embryonic development and normal tissue homeostasis, as well as in many pathological events, such as loss of regulated cell death in cancer, response of cancer cells to chemo- and radiotherapy (Clynes *et al.*, 1998), and death of cells in diabetes (Sesti, 2002) and neurodegenerative diseases (Vila and Przedborski, 2003). Accurate detection of apoptosis is of great importance to increase our understanding of biological events that may allow us to understand and to manipulate these events as a form of therapy.

Major elements involved in the apoptotic pathway, which should be considered when selecting suitable methods for apoptosis detection, include the following.

a. Death receptor activation: Following receptor cross-linking by ligand (e.g., the Fas receptor by the CD95 (APO-1 Fas) or Tumor Necrosis Factor (TNF) receptor type 1 by TNF), signal transduction leads to caspase activation (see (f) below).

b. Changes in cellular morphology: As described earlier.

c. Membrane alterations: Translocation of phosphatidylserine (PS) from the cytoplasmic to the extracellular side of the cell membrane is an early event in apoptosis.

d. DNA fragmentation: Prior to the induction of cell membrane permeability, fragmentation of genomic DNA at sites located between nucleosomal units,

Copyright 2006, Elsevier Science (USA).
All rights reserved.

generating mono- and oligonucleosomal DNA fragments, irreversibly commits the cell to die.

e. Disruption of mitochondria: As described, disruption of the mitochondrial membrane results in cytochrome *c* (Apaf-2) release. This subsequently promotes caspase activation by binding to Apaf-1 and inducing activation of Apaf-3 (caspase-9). Similarly, release of apoptosis-inducing factor (AIF) induces apoptosis.

f. Activation of caspases: At least 11 different caspases have been identified in mammalian cells. Activation of this protease cascade *via* a range of stimuli is central to the execution of apoptosis.

The range of techniques and methods for analysis of apoptosis is extensive. Due to space limitations in this article, we do not propose to describe all methods comprehensively. Table I lists a number of techniques for analysis of the cellular events described earlier. A selection of techniques used for studying these events is described in further detail.

TABLE I Methods Used for Detecting Cellular Changes That Occur during Apoptosis

Cellular morphology
Cellular features by light microscopy and time-lapse video microscopy
Fluorescence microscopy and laser-scanning confocal microscopy, e.g., using DNA stains for nuclear morphology
Membrane alterations
Annexin V binding for phospholipid externalisation
Impermeable dyes (PI) and permeable DNA stains (DAPI, Hoechst) for membrane permeability
Biochemical activation events
Caspase cleavage products
Caspase activity
PARP activity
Transglutaminase activity
Nuclear events and DNA fragmentation
Gel electrophoresis for DNA ladder (internucleosomal cleavage) detection
in situ nick translation
Comet assay
Immunohistochemistry for single-stranded DNA
FACS analysis for cell cycle (pre-G1 peak) dissolution
TUNEL
Mitochondrial permeability
Metabolic activity
Accessibility of mitochondrial antigens
Permeability of vital dyes
Detection of cytochrome *c* release
Detection of apoptosis-related genes (e.g., bcl-2 family members, survivin, caspases) and death antigens
For gene transcript analysis
RT-PCR
Northern blotting
RNase protection assay
Microarrays
For protein analysis
Immunocytochemistry/immunofluorescence
Western blotting
ELISA
Two-dimensional gel electrophoresis surface enhanced laser desorption lonisation (SELDI)

II. MATERIALS AND INSTRUMENTATION

A. Light Microscopy (LM) and Fluorescence Microscopy (FM)

Frost-ended slides and coverslips (Chance Propper); ice-cold methanol; Coplin jars; forceps; micropipettes; grease pen (DAKO S2002); and mounting medium (Vectashield mounting solution with antifade additive [Vector Labs.; H-1000]) suitable for fluorescence slides and may also be used for LM slides. Alternatively, 20% glycerol prepared in H_2O is also suitable for mounting slides for LM.

If analysing suspension cells, a cytospin (e.g., Heraeus Labofuge 400) and cytospin cups are required.

For LM only: haematoxylin, aluminium potassium sulphate, citric acid, and chloral hydrate.

For FM only: Stains include 4′,6-diamidino-2-phenylindole (DAPI, Sigma D-9542), propidium iodide (PI, Sigma P-4170), Hoechst 33258 (Sigma B-2883), Hoechst 33342 (Sigma B-2261), and acridine orange (AO, Sigma A-6014) in phosphate-buffered saline (PBS), pH 7.4.

B. Gel Electrophoresis for DNA Ladder

Horizontal agarose gel electrophoresis chamber and combs (Bio-Rad); electric power supply; UV transilluminator or gel analyser (e.g., EpiChemi II Darkroom, UVP Laboratory Products); PBS (Oxoid BR14a); ethidium bromide (Sigma E-8751); agarose (Sigma A-9539); Tris (Sigma T-8524); EDTA (Tris E-5134); NaCl (Sigma S-9899); sodium dodecylsulfate (SDS) (BDH 442152V); RNase A (Sigma R-5250); proteinase K (Sigma P-2308); boric acid (Sigma B-7901); bromphenol blue (Sigma B-5525); glycerol (Sigma G-2025); molecular markers, e.g., Phi X174 DNA *Hae*III digest (Sigma D-0672); micropipettes.

C. Terminal Deoxynucleotidyl Transferase-Mediated Deoxyuridine Triphosphate Nick End-Labelling Assay (TUNEL)

Apoptosis detection system: (1) fluorescein-containing equilibrating buffer, (2) nucleotide mix, (3)

TdT enzyme, (4) 20X SSC solution, (5) proteinase K, (6) protocol (Promega; G3250); plastic coverslips, glass slides and coverslips (Chance Propper); propidium iodide (Sigma P-4170); Coplin jars; forceps; humidifying chamber; 37°C incubator; Triton X-100 (Sigma T-8787), PBS (Oxoid BR14a); 4% paraformaldehyde (Sigma P-6148) in PBS (pH 7.4) (*freshly prepared*); Vectashield mounting solution with antifade additive (Vector Labs.; H-1000); 70% ethanol [prepare from absolute ethanol (Sigma E-7037)]; and micropipettes.

Note: Items 1–6 are included in the apoptosis detection system available commercially from Promega (G3250). There are, however, other detection kits available commercially that may be equally suitable.

D. Reverse Transcriptase–Polymerase Chain Reaction

As all general laboratory glassware, spatulas, etc., are often contaminated by RNases, these items should be treated by baking at 180°C for a minimum of 8 h. Sterile, disposable plasticware is essentially free from RNases and so generally does not require pretreatment. All solutions/buffers used should be prepared in baked glassware using sterile ultrapure water treated by the addition of diethylpyrocarbonate (DEPC) [Sigma D-5758, (0.1%, v/v)] and autoclaved. As for all laboratory procedures described in this article, gloves should be worn at all times to protect both the operator and the experiment. This, too, prevents the introduction of RNases and foreign RNA or DNA in the reverse transcriptase (RT) and polymerase chain reaction (PCR).

1. For RNA Isolation and Quantification

TRI Reagent (Sigma T-9424), chloroform (Sigma C-2432), isopropanol (Sigma I-9516), ethanol [Sigma E-7037; prepare as 75% (v/v) in H_2O], DEPC, micropipettors, tips, Eppendorf tubes, etc., spectrophotometer (e.g., SpectraMax Plus plate reader, Molecular Devices), and quartz cuvettes or Nanodrop (ND-1000; Labtech Int. Ltd.)

2. For RT and PCR Reactions

DEPC-treated H_2O; oligo$(dT)_{12–18mer}$ (Oswel, Southampton, UK); MMLV-RT enzyme (200 U/µl) (Sigma M-1302); 5X buffer (Sigma B-0175); dithiothreitol (DTT, 100 m*M*) (Sigma D-6059); RNasin (40 U/ml) (Sigma R-2520); dNTPs (10 m*M* each of dATP, dCTP, dGTP, and dTTP for RT; 1.25 m*M* each for PCR) (Sigma DNTP-100); $MgCl_2$ (25 m*M*) (Sigma M-8787), *Taq* DNA polymerase enzyme (5 U/µl) (Sigma D-6677); 10X buffer (Sigma P-2317); target primers and internal control primer (see Table II) (for further details on primer selection criteria, see O'Driscoll *et al*., 1993); thermocycler.

3. Gel Electrophoresis

Amplified products are analysed by gel electrophoresis (see Section IIIB).

Note: Several of the stains and other reagents used (e.g., DEPC) should be handled with caution as they are known or thought to be toxic, carcinogenic, and/or mutagenic.

III. PROCEDURES

A. Light and Fluorescence Microscopy Detection of Apoptotic Cell Morphology

As described previously, a cell undergoing apoptosis proceeds through various stages of morphological change (Wilson and Potten, 1999). Light microscopy and fluorescence microscopy are probably the simplest and most basic techniques by which such apoptotic cell death can be investigated. A broad range of stains and dyes are available to assist in the assessment of nuclear morphology. For light microscopy, the nuclear stain haematoxylin is used frequently (often with eosin as a counterstain). The most commonly used DNA nucleic acid-reactive fluorochromes for UV light fluorescence microscopic analysis of fixed (porated using, e.g., methanol or ethanol) cells include DAPI, PI, Hoechst 33258 and 33342, and AO. (As mentioned previously, PI, DAPI, and Hoechst are also very useful for assessing the membrane permeability of cells).

Using LM, cells dying by apoptosis are identified by their reduced size, cell membrane "blebbing/budding," and loss of normal nuclear structural features—nuclear fragmentation and chromatin condensation. In contrast, characteristic features of necrotic cell death include cell and nuclear swelling, cytoplasmic vacuolisation, patchy chromatin condensation, and plasma membrane rupture.

If assessing adherent cell types, the cells may be grown directly on coverslips (plated in Petri dishes). For suspension cells, cytospins are generally prepared. For both monolayer and suspension cultures, it is important to consider cell concentration. Fifty to 70% confluency of the area being analysed is generally considered optimal—if the cells are more confluent, overlapping may occur, which may hinder analysis; if cells are too sparse, an accurate examination may not be achievable. Typically, 1–2 $\times$ 10^5 cells suspended in 100 µl PBS containing 1% (w/v) fetal calf serum (FCS) should be cytocentrifuged onto microscope slides

using a low-speed, short centrifugation (e.g., 600–1000 rpm for 2–4 min); however, this should be optimised as relevant for cells being analysed.

Solutions

For LM only. **0.1*M* haematoxylin:** In a fume hood, dissolve 1 g haematoxylin (BDH 34242) in 1 litre distilled water, boil for 5 min, remove from heat, and add 0.2 g sodium iodate (Sigma S-4007). After 10 min, in the order listed, add 50 g aluminium potassium sulphate (Sigma A-7167), 1 g citric acid (Sigma C-2404), and 50 g chloral hydrate (Sigma C-8383), allowing each to dissolve completely prior to adding the next. The complete solution is stable for approximately 3 months at room temperature.

For FM only. Fluorescent stains should be stored in light-proof containers to prevent quenching.

1. ***DAPI:*** Prepare stock at 5 mg/ml in methanol (store at –20°C for up to 3 months). Prior to use, dilute 1:10,000 in PBS, pH 7.4.
2. ***PI*:** Prepare stock at 2 mg/ml in PBS, pH 7.4 (store at –20°C for up to 3 months). Prior to use, dilute 1:1500 in PBS.
3. ***Hoechst 33258 and 33342***: Prepare stock at 100 µg/ml in PBS, pH 7.4 (store at –20°C for up to 3 months). Prior to use, dilute 1:10 in PBS.
4. ***AO***: Prepare stock at 2 mg/ml in PBS, pH 7.4 (store at –20°C for up to 3 months). Prior to use, dilute 1:400 in PBS.

Steps

Note: When working with fluorochromes, minimise exposure to light at all stages of preparation.

1. Fix cells in ice-cold methanol for 5–7 min.
2. Allow to air dry.
3. Using a grease pen, encircle area of cells for analysis. Typically a circle of 10 mm diameter or smaller is drawn (to contain solutions and to minimise volumes of solutions, antibodies, etc., required).
4. Stain cells with 0.1% hematoxylin (for LM) or DAPI, PI, Hoechst, or AO (for FM) for 3–5 min.
5. Wash in distilled H_2O (for LM) or PBS (for FM).
6. Mount coverslip on slide using an aqueous-based mountant medium and fix in place (clear nail varnish may be used to secure coverslip).
7. Immediately analyse and photograph samples by fluorescence microscopy. Slides cannot be stored long term as fluorescence quenches. However, storing at 4°C in the dark will prolong the life span of the signal. Haematoxylin-stained slides may be stored indefinitely.

B. Gel Electrophoresis for DNA Ladder

Activation of endogenous Ca^{2+}- and Mg^{2+}-dependent nuclear endonuclease(s) cleaves DNA into discrete fragments, initially into 300- to 50-kb fragments and subsequently into 180-bp fragments. In brief, for DNA fragment detection by gel electrophoresis, DNA is extracted from cells and loaded onto a 1.5% agarose gel containing ethidium bromide. The DNA fragments form a characteristic "ladder" pattern resulting from multiples of a 180-bp DNA subunit, representing DNA of the size of individual nucleosomes and oligonucleosomes. [Nuclear DNA damage resulting in death by necrosis, however, is random and results in smears on a gel (Ramachandra and Studzinski, 1995).]

Solutions

1. ***Lysis solution***: 50 m*M* Tris–HCl (pH 8.0), 20 m*M* EDTA, 10 m*M* NaCl, and 1% (w/v) SDS. A 50-ml aliquot stock may be prepared and aliquotted in 2-ml volumes (store at –20°C for up to 3 months).
2. ***TBE buffer***: 1X TBE consists of 10.8 g Tris base, 5.5 g boric acid, and 4 ml 0.5 *M* EDTA (pH 8.0) made up to 1 litre with ultrapure water. It is advisable to prepare as a 10X concentrate and store at room temperature for up to 3 months.
3. ***RNase A***: Prepare stock of 200 µg/ml and store at –20°C (for up to 3 months) to use at a final concentration of 20 µg/ml.
4. ***Proteinase K***: Prepare stock of 1 mg/ml and store at –20°C (for up to 3 months) to use at a final concentration of 100 µg/ml.
5. ***Ethidium bromide***: Prepare a 10 mg/ml stock of ethidium bromide by adding 1 g of ethidium bromide to 100 ml of H_2O. Stir on a magnetic stirrer for several hours to ensure that the dye has dissolved. Wrap the container in aluminium foil or keep in a dark bottle. Store at room temperature. *Note:* It is important to consider that ethidium bromide is a potential carcinogen. Due caution should be taken when preparing ethidium bromide stock, adding ethidium bromide to gel, disposing of exposed pipette tips and ethidium bromide-containing gels, etc.
6. ***DNA loading buffer***: DNA loading buffer may be prepared at a 6X concentrate by mixing 1 mg/ml bromphenol blue, 1 m*M* EDTA, and 50% glycerol (v/v) in ultrapure H_2O. Store at room temperature (should be stable for up to 12 months).

Steps

1. Harvest cells for analysis, wash with PBS, and pellet by centrifugating for 5 min at 1000 rpm.

2. Lyse cell pellet by adding a volume of lysis solution containing 50 m*M* Tris–HCl (pH 8.0), 20 m*M* EDTA, and 10 m*M* NaCl, 1% (w/v) SDS and incubating for 10 min at 37°C (the cell number used and the volume of lysis solution added must be optimised for each cell type being analysed because if the sample is too viscous the resulting gel resolution may be reduced). It is important to ensure at this stage that the pellet has broken up. This may be assisted by "flicking" the tube gently.

3. Add RNase A (final concentration of 20 µg/ml) to the lysate and incubate for 60 min at 37°C.

4. Add proteinase K (final concentration of 100 µg/ml) to the lysate and incubate for 4 h at 37°C. Lysates may then be loaded directly onto an agarose gel (as described later). If clear bands are not detected using whole cell lysates, DNA may be purified from cell lysates at this stage using standard phenol/chloroform/isoamyl alcohol procedures (see Sambrook and Russell, 2001).

5. During the incubation steps, dilute a stock of 10X TBE to 1X TBE to use in preparation of a 1.5% agarose gel. 1X TBE buffer is also prepared for use as running buffer.

6. Melt and pour 1.5% agarose gel in a horizontal gel support (taking safety pre cautions when working with molten agarose). Insert the comb and allow the gel to solidify.

7. Add loading buffer to lysates (to resulting in a final 1X concentration of loading buffer), "flick" tubes, and centrifuge briefly.

8. Load 10- to 50-µl samples to the gel wells and run the gel in 1X TBE at 75 V for approximately 1.5 h at room temperature. Molecular weight markers should be loaded to allow lysate band sizes to be estimated following electrophoresis.

9. Stain gel with 5 µg/ml ethidium bromide in 1X TBE for 30 min.

10. Place the gel on a UV transilluminator box to visualise (and photograph) resolved DNA fragments in a ladder pattern. (*Note*: Wear appropriate safety gear to ensure that eyes and skin are not exposed to UV radiation.)

C. TUNEL

TUNEL is a cytochemical method suitable for analysis of apoptotic DNA fragmentation in individual cells. This technique involves *in situ* enzymatic labelling of the 3′-OH ends of fragmented DNA in fixed, permeabilised cells with either enzyme (phosphatase or peroxidase) or fluorochrome-tagged deoxynucleotides using terminal deoxynucleotidyl transferase (TdT). (*Note*: If DNA polymerase I is used instead of TdT, the method is termed *in situ* nick translation.) If fluorescence labelling is chosen, the fluorescein-12-dUTP-labelled DNA can then be visualised directly by fluorescence microscopy to give qualitative results. If facilities are available and quantitative results are required, flow cytometric analysis may be used.

Solutions

1. ***Fixation solution***: 4% paraformaldehyde in PBS (pH 7.4) is prepared immediately before use. To help dissolve the paraformaldehyde, this solution may be placed on a magnetic stirring box and heated very gently. Paraformalydehyde should only be prepared and used in a fume hood.

2. ***Permeabilisation solution***: 0.1% Triton X-100 in PBS.

Steps

1. Grow cells for analysis as a monolayer on glass slides. Alternatively, cytospin preparations of cells may be used.

2. Remove culture medium, wash cells twice with PBS, and allow to air dry.

3. Fix cells by immersing slides in a Coplin jar containing fixation solution, i.e., freshly prepared 4% paraformaldehyde in PBS (pH 7.4), for 25 min at 4°C.

4. Rinse the slides by immersing in PBS for 5 min at room temperature (two times). It is very important that the slides are not allowed to dry out during the following steps.

5. Gently tap off excess PBS, cover cells with 100 µl of equilibration buffer, and incubate for 5–10 min at room temperature.

6. While incubating in equilibration buffer (step 5), prepare the TdT incubation buffer by adding 45 µl equilibration buffer + 5 µl nucleotide mix + 1 µl TdT enzyme per sample (prepare as a master mix, depending on the number of samples being analysed). As a negative control, TdT may be eliminated from some samples and replaced with an equal volume of ultrapure H_2O. It is important to keep the nucleotide mix and TdT incubation buffer on ice and to ensure that all steps from now on be protected from direct light.

7. Following equilibration, carefully blot off excess equilibration buffer and add 50 µl of TdT incubation buffer to the cells. Cover with plastic coverslips to ensure even distribution of the TdT incubation buffer and to prevent slides from drying out.

8. Place slides in a humidified chamber (a suitably sized flat-bottomed plastic box containing a layer of

paper towels soaked in water is ideal for this purpose). Cover with aluminium foil to protect from light and incubate for 60 min at 37°C to allow the "tailing" reaction to occur.

9. To terminate the reaction, 20X SCC buffer should be diluted to a 2X SCC solution with ultrapure water and placed in a Coplin jar, the coverslips removed from the slides, and the slides immersed for 15 min at room temperature.

10. To remove unincorporated fluorescein-12-dUTP, the slides should be washed by placing in PBS for 5 min at room temperature (repeat wash two times).

11. If desired, slides may be stained at this stage by immersing in Coplin jars containing freshly prepared PI solution (see preparation details given earlier) and incubating for 15 min at room temperature. Following this, wash slides in ultrapure water (3 × 5 min at room temperature).

12. Mount slides using Vectashield and glass coverslips.

13. Immediately analyse and photograph cells by fluorescence microscopy (520 mm filter for fluorescein and >620 mm filter if propidium iodide has been included. Slides cannot be stored long term as fluorescence quenches. However, storing at 4°C in the dark may prolong the life span of the signal.

D. RT-PCR

Expression of apoptosis-related mRNAs may be analysed using RT-PCR methods. This section describes the use of "basic" RT-PCR, but it is important to be aware that depending on the requirements of the study and the resources available, RT-PCR may be used to indicate the presence or absence of transcripts of interest or it may be developed as a semi-quantitative or a quantitative level using real-time PCR.

RNA may be isolated from cells using the procedure described by Chomczynski and Sacchi (1987). However, there are now a number of less laborious, commercially available methods, including the use of TRI reagent (Sigma), as described here. The RT procedure detailed involves use of the MMLV-RT (Sigma) enzyme for cDNA synthesis and the PCR uses *Taq* DNA polymerase (Sigma). Again, however, there are other reverse transcriptases and DNA polymerase enzymes available that may be equally suitable.

Primers suitable for the analysis of human bcl-2, bag-1, bax-α, mcl-1, galectin-3 (designed in our laboratory), and survivin are included in Table II, as examples of apoptosis-related gene transcripts that may be desirable to analyse by RT-PCR. There are, of course, many more mRNAs involved in apoptotic pathways

TABLE II Primers Used to Amplify Apoptosis-Related cDNAs Formed by Reverse Transcription of mRNA Templates[a]

cDNA	Primer sequence	Annealing temperature	Amplified product (bp)
Bcl-2	(F): 5′ TCATGTGTGTGGAGAGCGTCAA 3′ (R): 5′ CTACTGCTTTAGTGAACCTTTTGC 3′	50	306
Bag-1	(F): 5′ TCCAGCTGGTTAGCTATCTT 3′ (R): 5′ AGCAGTGAACCAGTTGTCCA 3′	52	251
Bax-α	(F): 5′ GACGAACTGGACAGTAACATG 3′ (R): 5′ AGGAAGTCCAATGTCCAGCC 3′	50	230
Mcl-1	(F): 5′ TCTCTCGGTACCTTCGGG 3′ (R): 5′ CTATCTTATTAGATATGC 3′	53	217
Survivin	(F): 5′ GCATGGGTGCCCCGACGTTG 3′ (R): 5′ GCTCCGGCCAGAGGCCTCAA 3′	62	431 (survivin) 500 (S-2B) 329 (S-ΔEx3)
Galectin-3	(F): 5′ GCTGGGCCACTGATTGTGCCTTAT 3′ (R): 5′ ACCAGTACTTGTATTTTGAATGGT 3′	54	281
β-Actin (S)[b]	(F): 5′ TGGACATCCGCAAAGACCTGTAC 3′ (R): 5′ TCAGGAGGAGCAATGATCTTGA 3′	AR	142
β-Actin (L)	(F): 5′GAAATCGTGCGTGACATTAAGGAGAAGC 3′ (R): 5′ TCAGGAGGAGCAATGATCTTGA 3′	AR	383

[a] As β-actin is coamplified with other cDNAs as an endogenous control, the annealing temperature used is relevant for the cDNA of interest.

All primers except for survivin were selected in our laboratory [O'Driscoll *et al.*, 1993, 1996, 2003, 2004; survivin primers were selected by Mahotka *et al.*, 1999]. (F) = Forward Primer; (R) = Reverse Primer.

[b] Short-amplified β-actin product.

[c] Long-amplified β-actin product.

that should be considered. The methods described here may be adapted by using relevant primers for the amplification of other apoptosis-related cDNAs [for information on primer design and selection criteria, see O'Driscoll *et al*. (1993)].

Table II also includes primer sequences for coamplification of cDNA derived from an endogenous "housekeeping" mRNA, β-actin, as control. Inclusion of such primers serves to indicate that the RT and PCR reactions have been performed successfully; if performing semiquantitative PCR, this allows the apoptosis-related gene transcript results to be normalised relative to a control that (generally) should be constant.

Steps

RNA Isolation and Quantitation

1. Pellet cells and wash with PBS (three times).
2. In a 0.5-ml Eppendorf tube, lyse cells in TRI reagent; 1 ml TRI reagent is suitable to lyse approximately 0.5–1 $\times 10^7$ cells.
3. RNA may be isolated immediately or lysates stored at –80°C for up to 1 month.
4. Incubate lysates at room temperature for 5 min.
5. Add 200 µl chloroform per 1 ml TRI reagent used, shake samples vigorously for 15 s, and incubate at room temperature for 15 min.
6. Centrifuge at 12,000 *g*, at 4°C, for 15 min. Following this, the RNA will be contained in the upper aqueous phase, below which are the DNA-containing interface and the protein-containing organic phase.
7. Transfer the RNA-containing aqueous phase to a clean 0.5-ml Eppendorf tube, add 0.5 ml isopropanol, mix, and incubate at room temperature for 10 min.
8. Centrifuge at 12,000 *g* at 4°C, for 10 min to pellet RNA.
9. Remove supernatant (carefully, to prevent disturbing RNA pellet), wash RNA with 1 ml 75% ethanol, vortex for 5 s, and centrifuge at 7500 *g* at 4°C for 5 min.
10. Remove ethanol, air dry pellet briefly, and resuspend in 25–50 µl DEPC-H_2O. (Ensure that the pellet does not dry completely, as this decreases its solubility greatly. The solubility of RNA can be improved by heating to 55–60°C with intermittent vortexing or by passing the RNA through a pipette tip, if necessary). Store RNA at –80°C.
11. Quantify RNA spectrophotometrically at 260 nm and 280 nm. The A_{260}/A_{280} ratio of RNA is approximately 2. [Partially solubilised RNA has a ratio <1.6 (Ausubel *et al*., 1991).]

Typical RT Reaction

1. To a 0.5-ml Eppendorf tube add 1 µl oligo(dT)$_{12–18mer}$ (1 µg/µl), 1 µl RNA (at 1 µg/µl), and 3 µl DEPC-H_2O. Mix gently, incubate at 70°C for 10 min, and chill on ice. [*Note*: For survivin analysis, to avoid coamplification of the homologous cDNA for effector protease receptor-1 (EPR-1), instead of including the oligo(dT) primer, use 250 ng of the survivin-specific RT primer 5′ AGGAACCTGCAGCTCAGA 3′.]
2. Add the following reagents: 4 µl 5X buffer, 2 µl (100 m*M*) DTT, 1 µl (40 U/µl) RNasin, 1 µl (10 m*M* each) dNTPs, and 6 µl (200 U/µl) MMLV-RT. Mix.
3. Incubate at 37°C for 1 h, followed by 95°C for 2 min.

Typical PCR Reaction

1. To a 0.5-ml Eppendorf tube add the following reagents: 24.5 µl H_2O, 5 µl 10X buffer, 3 µl (25 m*M*) $MgCl_2$, 8 µl (1.25 m*M*) dNTPs, 1 µl target forward primer (250 ng/µl) (see Table II), 1 µl target reverse primer (250 ng/µl), 1 µl control forward primer (250 ng/µl), 1 µl control reverse primer (250 ng/µl), and 0.5 µl (5 U/µl) *Taq* polymerase enzyme. Mix gently. Add 5 µl cDNA (from RT reaction). Mix gently and centrifuge very briefly to collect solution at bottom of tube. (*Note*: Primer concentrations used may need to be increased or decreased to optimise amplification.)
2. Amplify on a thermocycler using the following PCR cycle: 94°C for 2 min; 30 cycles of 94°C for 30 s, relevant annealing temperature (Table II) for 30 s, 72°C for 30 s; completion step of 72°C for 5 min. Cycle numbers may be reduced to prevent reaching the plateau phase of PCR amplification if semiquantitative analysis is required.
3. Analyse RT-PCR products by agarose gel electrophoresis (see Section III,B).

IV. SELECTION OF A SUITABLE METHOD FOR APOPTOSIS DETECTION

There are many factors to be considered when selecting a suitable method for investigating apoptosis. These factors include the cell type being analysed, the nature of the cell death inducer, the stage of cell death, the information required from the study (e.g., whether information on single cells or on the cell population, as a whole, is required), and the resources available (e.g., where or not access is available to a fluorescence microscope, flow cytometer, thermocycler, etc.). To assist with selection, Table III summarises the "advantages" and "disadvantages" of the procedures detailed in this article. To form a more extensive understanding of the events occurring within cells, it is advisable, whenever possible, to investigate cell death using more than one technique.

TABLE III Comparison of Methods of Apoptosis Detection[a]

Method	Advantages	Disadvantages
Light and fluorescence microscopy	Indication of apoptosis in individual cells Relatively few ($1–2 \times 10^5$) cells required compared to some techniques Relatively easy to perform Simultaneous immunofluorescence analysis of specific proteins (e.g., death receptors, caspases) possible	Subjective; requires a skilled analyst Not quantitative Undefined cells lost during fixation—may result in loss of specific (sensitive) population
Gel electrophoresis for DNA ladder	Very specific marker of apoptosis	Not suitable for all cell types, i.e., some cell lines, e.g., MCF-7 and DU145, show almost no DNA ladders, although they portray typical morphological changes of apoptosis Indication of apoptosis in cell population, not individual cells Not quantitative Minimum of 1×10^6 cells required generally
TUNEL	Indication of apoptosis in individual cells Relatively few ($1–2 \times 10^5$) cells required compared to some techniques Simultaneous assessment of morphology can be made	Relatively labour-intensive and time-consuming Subjective; requires a skilled analyst Not quantitative Undefined cells lost during fixation—may result in loss of specific (sensitive) population
RT-PCR	Very sensitive, so relatively few cells required compared to some techniques May be quantitative	Indication of apoptosis in cell population, not individual cells

[a] An ability to determine apoptosis in individual cells or in populations is not so much an "advantage" or "disadvantage" of a method, but a factor that should be considered when selecting a suitable method, based on the information required.

References

Ausubel, M. A., Brent, R., Kinston, R. E., Moore, D. D., Seidman, J. G., Smith, J. A., and Struhl, K. (eds.) (1991). *Current Protocols in Molecular Biology*, pp. 4.0.1–4.0.9. Greene Publishing Associates and Wiley Interscience, New York.

Barinaga, M. (1998). Death by dozens of cut. *Science* **280**, 32–34.

Chomczynski, P., and Sacchi, N. (1987). Single-step method of RNA isolation by acid guanidinium thiocyanate-phenol-chloroform extraction. *Anal. Biochem.* **162**, 156–159.

Clynes, M., Daly, C., NicAmhlaoibh, R., Cronin, D., Elliot, C., O'Connor, R., O'Doherty, T., Connolly, L., Howlett, A., and Scanlon, K. (1998). Recent developments in drug resistance and apoptosis research. *Crit. Rev. Oncol. Hematol.* **28**, 181–205.

Darzynkiewicz, Z., and Traganos, F. (1998). Measurement in apoptosis. *In* "*Apoptosis: Advances in Biochemical Engineering Biotechnology*" (T. Scheper, ed.), pp. 33–73. Springer, New York.

Kerr, J. F. R., Wyllie, A. H., and Currie, A. R. (1972). Apoptosis: A basic biological phenomenon with wide-ranging implications in tissue kinetics. *Br. J. Cancer* **26**, 239–257.

Kiechle, F. L., and Zhang, X. (2002). Apoptosis: Biochemical aspects and clinical implications. *Clin. Chim. Acta* **326**, 27–45.

Mahotka, C., Wenzel, M., Springer, E., Gabbert, H. E., and Gerharz, C. D. (1999). Survivin-ΔEx3 and survivin-2B: Two novel splice variants of the apoptosis inhibitor survivin with different antiapoptotic properties. *Cancer Res.* **59**, 6097–6102.

Majno, G., and Joris, I. (1995). Apoptosis, oncosis, and necrosis: An overview of cell death. *Am. J. Pathol.* **146**, 3–15.

Nagata, S. (1997). Apoptosis by death factor. *Cell* **88**, 355–365.

O'Driscoll, L., Daly, C., Saleh, M., and Clynes, M. (1993). The use of reverse transcriptase-polymerase chain reaction (RT-PCR) to investigate specific gene expression in multi-drug resistant cells. *Cytotechnology* **12**, 289–314.

O'Driscoll, L., Kennedy, S., Mc Dermott, E., Kelehelan, P., and Clynes, M. (1996). Multiple drug resistance-related messenger RNA expression in archival formalin-fixed paraffin-embedded human breast tumour tissue. *Eur. J. Cancer* **32**, 128–133.

O'Driscoll, L., Linehan, R., Kennedy, S. M., Cronin, D, Purcell, R., Glynn, S., McDermott, E. W., Hill, A. D., O'Higgins, N. J., Parkinson, M., and Clynes, M. (2003). *Cancer Lett.* **201**(2), 225–36.

O'Driscoll, L., Crowin, D., Kennedy, S. M., Purcell, R., Linehan, R., Glynn, S., Larkin, A., Scanlon, K., McDermott, E. W., Hill, A. D., O'Higgins, N. J., Parkinson, M., Clynes, M. (2004) *Anticancer Res.* **24**(2A):473–82.

Ramachandra, S., and Studzinski, G. P. (1995). Morphological and biochemical criteria of apoptosis. *In* "*Cell Growth and Apoptosis*" (G. P. Studzinski, eds.), pp. 119–142. IRL Press, Oxford.

Sambrook, J., and Russell, D.W. (2001). "*Molecular Cloning: A Laboratory Manual*," 3rd Ed. *Cold Spring Harbor Laboratory Press*, Cold Spring Harbor, New York.

Sesti, G. (2002). Apoptosis in the beta cells: Cause or consequence of insulin secretion defect in diabetes? *Ann. Med.* **34**, 444–450.

Van Cruchten, S., and Van Den Broeck, W. (2002). Morphological and biochemical aspects of apoptosis, oncosis and necrosis. *Anat. Histol. Embryol.* **31**, 214–223.

Vila, M., and Przedborski, S. (2003). Targeting programmed cell death in neurodegenerative diseases. *Nature Rev. Neurosci.* **4**, 365–375.

Wilson, J. W., and Potten, C. S. (1999). *In* "*Apoptosis. A Practical Approach*" (G. P. Studzinski, ed.), pp. 19–39. IRL Press, Oxford University Press.

SECTION

11

Assays of Cell Transformation, Tumorigenesis, Invasion, and Wound Healing

CHAPTER

41

Cellular Assays of Oncogene Transformation

Michelle A. Booden, Aylin S. Ulku, and Channing J. Der

I. INTRODUCTION

A critical step in the validation of the role of candidate oncogenes in oncogenesis involves a demonstration of their ability to endow nonneoplastic cells with growth properties characteristics of tumor cells. The most widely utilized model system for the analyses of oncogene function involves the use of NIH 3T3 mouse fibroblasts. NIH 3T3 mouse fibroblasts have been a useful model cell system to evaluate transformation caused by aberrant activation of many different functional classes of oncogenes, including serine/threonine (e.g., Raf) and tyrosine (e.g., Src) protein kinases, nuclear transcription factors (e.g., Fos), G-protein-coupled receptors (GPCRs; e.g., Mas, PAR1), and small (e.g., Ras) and large (e.g, $G\alpha_{12}$) GTPases. This article describes the application of various cellular assays for the study of growth transformation caused by GPCR oncogenes that promote the aberrant activation of Rho family small GTPases.

Mutationally activated and transforming forms of the three human Ras proteins (H-, K-, and N-Ras) are found in 30% of human cancers. In contrast, mutations in the Ras-related Rho GTPases are not found in human cancers (Sahai and Marshall, 2002). Instead, Rho GTPases are activated indirectly by alterations in expression or activity. In particular, Rho GTPases are activated by persistent upstream signaling, e.g., by Dbl family guanine nucleotide exchange factors (GEFs) or by activated GPCRs (Schmidt and Hall, 2002; Whitehead *et al.*, 2001). The first section of this article describes methods that assess the transforming capabilities of proteins that cause transformation, in part, by activation of Rho family proteins. The assays described provide both qualitative and quantitative information of transforming potential.

In addition to their abilities to induce tumorigenesis, Ras and Rho family proteins have attracted considerable research attention as important mediators of tumor cell invasion and metastasis. For example, previous studies from our laboratory determined that Rac1, Cdc42, and RhoA can promote breast cancer cell invasion (Keely *et al.*, 1997), while Hynes and colleagues showed that upregulation of RhoC promoted metastatic growth of melanoma cells (Clark *et al.*, 2000). Therefore, the second section of this article describes assays to examine human tumor cell invasion *in vitro* induced by the activation of Rho family proteins. The applications described can be used to implicate GPCRs, direct activators of Rho family members, and Rho proteins themselves as important for promoting cellular invasion.

II. NIH 3T3 MOUSE FIBROBLAST TRANSFORMATION ASSAYS

Three types of focus formation assays can be used to evaluate the transforming potential of oncoproteins that cause persistent activation of Rho family proteins (Clark *et al.*, 1995; Solski and Der, 2000). The most commonly used assay is the primary focus formation assay, which provides a straightforward method for quantitation of transforming potential. A second assay is a primary focus formation cooperation assay, where activated Raf is coexpressed along with the oncogene under evaluation. Our laboratory and others showed that Rho GTPase activators cooperate with activated

Copyright 2006, Elsevier Science (USA).
All rights reserved.

Raf and cause synergistic focus forming activity (Khosravi-Far *et al*., 1995; Qiu *et al*., 1995). A third type of assay involves the establishment of cells stably expressing an oncoprotein of interest, which can be used in secondary focus-formation assays, as well as in additional assays to examine other aspects of cellular transformation. These additional assays are used to evaluate the loss of density-dependent inhibition of growth, loss of anchorage-dependent growth, reduced requirement for growth factors, and tumorigenic growth potential in immunodeficient mice.

Materials and Reagents

NIH 3T3 mouse fibroblasts: There is considerable variation in the growth properties of different isolates of NIH 3T3 cells. Consequently, the assays described here apply specifically to the strain used in our assays and were obtained originally from Dr. Geoffrey M. Cooper (Boston University). We have described detailed protocols for the routine culture techniques for the maintenance and long-term storage of NIH 3T3 cells previously (Clark *et al*., 1995).

1.25 M *$CaCl_2$*: Autoclave to sterilize and store at room temperature.

HEPES-buffered saline (HBS), pH 7.05: To 900 ml of distilled H_2O, add 8.0 g of NaCl, 0.37 g KCl, 0.19 g $Na_2HPO \cdot 7H_2O$, 1.0 g glucose, and 5 *M* NaOH. Adjust the volume to 1 liter, autoclave to sterilize, and store at room temperature. The correct pH is critical to generating a good DNA precipitation.

45% glycerol/HBS: Mix autoclaved glycerol and HBS at 45:55 (v/v) and store at room temperature.

Carrier DNA: High molecular weight carrier DNA (e.g., calf thymus) is required to facilitate the formation of calcium phosphate precipitate of the transfected plasmid DNA. Prepare a 1-mg/ml stock in sterile H_2O and store at –20°C.

Transfection Protocol

This protocol describes a 20 dish transfection assay, where duplicate dishes are used for each experimental condition. This assay involves one set of dishes to control for the appearance of spontaneous transformed foci (empty vector control) and one set of dishes for a positive control. An expression plasmid encoding activated Ras [e.g., pZIP-H-*ras*(61L)] (20 ng per dish) is generally used as a positive control.

Plate stock NIH 3T3 cells the day before transfection at a density of 2.5×10^5 cells per 60-mm dish. Add 0.2 ml of the high molecular weight carrier DNA (e.g., calf thymus or salmon sperm DNA) stock solution (1 mg/ml) to 4.3 ml HBS, vortex vigorously to mix, and aliquot 0.9 ml into five 15-ml polystyrene conical tubes. Add the desired amount of plasmid DNA to each tube. For the positive control, add 20 ng of H-Ras(61L)-expressing plasmid DNA per dish. This results in approximately 20–50 transformed foci per dish. For experimental dishes, the amount of DNA depends on the expected potency. The equivalent amount of empty vector plasmid DNA should be used for the negative control dishes. Vortex to mix the plasmid and carrier DNAs and then add 0.1 ml 1.25 *M* $CaCl_2$ to each tube and vortex for 20 to 40 s. Allow precipitate to form for 20 min at room temperature. Add dropwise 0.5 ml per dish of the precipitated DNA solution directly onto the growth medium. Swirl gently to distribute the DNA and incubate for 3 to 4 h at 37°C in a humidified 10% CO_2 incubator.

To increase efficiency of DNA uptake, glycerol shock of the transfected cells is performed after the incubation with DNA. For a 20 dish transfection assay, prepare a 15% glycerol/HBS solution by mixing together 7 ml of the 45% glycerol/HBS stock with 14 ml HBS. Aspirate the DNA-containing growth medium and add 1 ml per dish of the 15% glycerol/HBS solution. The glycerol shock is somewhat toxic to the cells. Therefore, the total time of exposure to the glycerol solution should be no longer than 4 to 5 min, from time of addition to time of rinsing with the addition of 5 ml of growth medium. Incubate the transfected cells for 14 to 21 days at 37°C in a humidified 10% CO_2 incubator.

Ras-induced foci should be readily visible after 7 to 10 days, whereas various Dbl or Rho family protein-induced foci may not be visible until 14 to 21 days (Booden *et al*., 2002; Martin *et al*., 2001) (Fig. 1A). Rinse the cells once with phosphate buffered saline (PBS) and fix with 2 ml per dish of 10% (v/v) acetic acid and 10% (v/v) methanol in H_2O. Once the cells are fixed, they can be quantitated at a later time (on day 14 for Ras, day 21 for Rho). This fixation procedure does not alter the morphology of the foci. Another less accurate and sensitive method of counting involves staining the fixed cells with crystal violet (0.4% in ethanol) to visualize the foci.

A. Cooperation and Secondary Focus Formation Assays

Because GPCRs require agonist stimulation and generally display weak or no focus forming activity when assayed in primary transfection assays, two other focus formation assays that provide a more sensitive detection of transforming activity are used routinely in our laboratory. The first assay is a cooperation, primary focus-formation assay utilizing activated Raf. For these assays, we typically use the

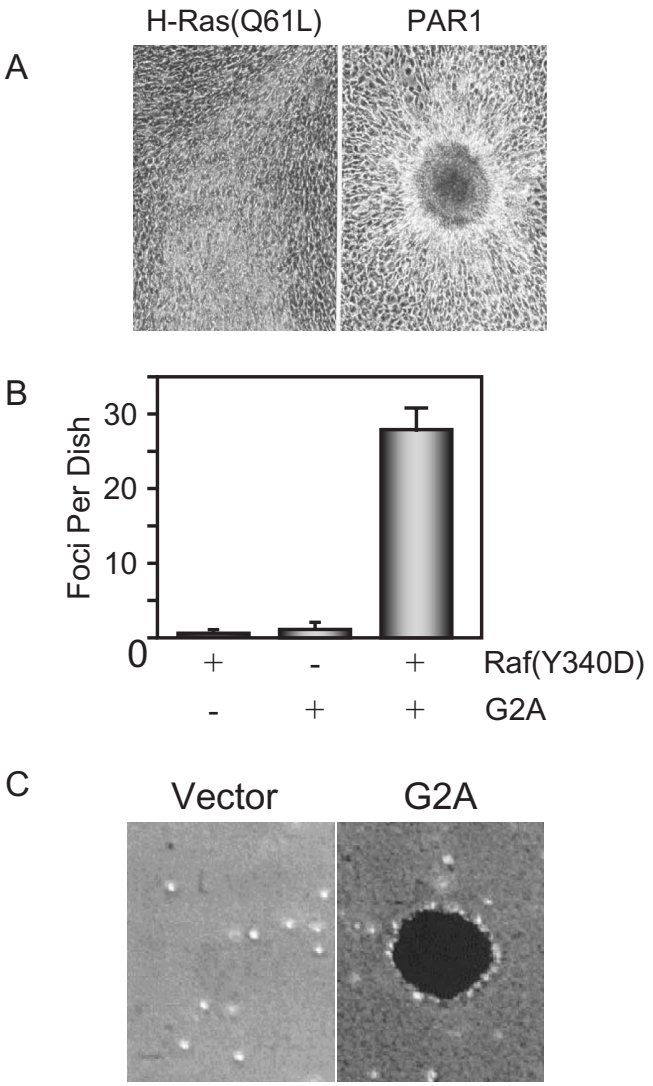

FIGURE 1 NIH 3T3 transformation assays. PAR1 and G2A are GPCRs that cause transformation by activation of RhoA. (A) NIH 3T3 focus formation assay. Appearance of foci of transformed cells caused by mutationally activated H-Ras(Q61L) and the PAR1 GPCR. PAR1 causes transformation, in part, by activation of the RhoA small GTPase. Ras causes the appearance of foci that contain highly refractile, spindle-shaped cells that form a well-spread focus of proliferating, multilayered cells. Like activated RhoA, PAR1 causes the appearance of foci that consist of nonrefractile cells that form a tight well-contained focus of proliferating, mutilayered cells. (B) NIH 3T3 focus cooperation assay. Coexpression of activated Raf(Y340D) together with G2A caused synergistic enhancement of focus formation. (C) NIH 3T3 soft agar assay. NIH 3T3 cells transfected stably with the empty vector or encoding G2A were suspended in soft agar to evaluate anchorage-independent growth potential.

weakly transforming Y340D mutant of human c-Raf-1 (Fabian *et al.*, 1993). When transfected alone, this mutant displays little or no focus-forming activity (Fig. 1B). However, coexpression of Raf(Y340D), together with ligand-activated GPCRs, activated Rho GTPases, or activators of Rho GTPases (at concentrations that alone result in no focus-forming activity), will cause focus-forming activities that range from severalfold to more than 10- to 50-fold above their additive activity. For these assays we combine 1 μg per dish of pZIP-*raf*(Y340D) along with 1 μg per dish of plasmid DNA encoding either the activated Rho GTPase or the Rho GTPase activator. Trial assays with different amounts of each plasmid should be performed to optimize the assay conditions to obtain the maximum level of cooperation. The appearance of transformed foci from these cooperation assays is distinct from those caused by Raf alone. However, foci arising from the specific activated GPCR, Rho family protein, or Rho family activator can range from typical Rho-like foci to those that exhibit a refractile appearance similar to that caused by activated Ras or Raf.

Other activated Raf-1 mutants have been used in this assay, such as membrane-targeted Raf (Raf-CAAX) or amino-terminally truncated (Raf-22W). However, these constitutively activated variants of c-Raf-1 possess potent focus-forming activities that are comparable to those of activated Ras mutants. Thus, small changes in transfection efficiency or DNA concentrations can cause the appearance of significant numbers of foci on cultures transfected with activated Raf alone. Therefore, use of the Raf(Y340D) is advantageous because it is easier to achieve Raf-transfected-only dishes that contain no transformed foci.

The second type of focus formation assay is a secondary focus formation assay, which employs NIH 3T3 cells stably expressing a weakly transforming oncoprotein. For the secondary assay, plate 10^6 untransfected NIH 3T3 cells onto 60-mm dishes and incubate overnight to form a monolayer. The next day, plate 10^3 NIH 3T3 cells stably transfected with an expression vector encoding the oncogene protein under evaluation on top of the monolayer and stimulate with ligand if the oncoprotein is a GPCR. The efficiency of the stably transfected cells to form colonies is reflected by the appearance of densely packed cells within the monolayer of untransfected NIH 3T3 cells. The cultures should be fed every 2 days with growth medium and ligand as indicated. The appearance of foci is quantitated after 7–10 days. A variation on this assay is to simply plate the stably transfected cell populations at 10^5 cells per dish and then maintain the cultures for 2 weeks. Cells stably transfected with the empty expression vector provide the negative control for this assay.

B. Growth in Soft Agar

The acquisition of anchorage-independent growth potential is an essential step for tumor cell progression

(Hanahan and Weinberg, 2000). Colony formation in soft agar is the most widely used assay to evaluate anchorage-independent growth *in vitro* and correlates strongly with *in vivo* tumorigenic growth potential. Untransformed NIH 3T3 cells need to adhere to a solid matrix in order to remain viable and proliferate. NIH 3T3 cells transformed by activated Ras and Rho GTPases lose this requirement, which results in their ability to form proliferating colonies of cells when suspended in a semisolid agar.

Briefly, transfect NIH 3T3 cells as described earlier for focus-formation assays. Three days after transfection, replate the transfected cells onto three individual 100-mm dishes containing growth medium supplemented with the appropriate drug for selection (400 µg/ml G418, 400 µg/ml hygromycin, or 1 mg/ml puromycin). After approximately 2 weeks, trypsinize and pool together the multiple drug-resistant colonies (>100) that have arisen to establish mass populations of stably transfected cells. Perform Western blot analysis to confirm ectopic overexpression of the introduced gene; these stably transfected cells are then used to assay for the oncoprotein-mediated acquisition of various transformation phenotypes described later.

Materials and Reagents

1.8% Bacto-Agar (Difco 214050): Prepare a 1.8% stock (w/v, in distilled water) by boiling the solution in a microwave to dissolve the agar. Place 50-ml aliquots in 100-ml bottles and autoclave to sterilize. Store at room temperature. Microwave to melt.

2× DMEM: 2× DMEM and other culture medium components can be purchased from GIBCO (Invitrogen Life Technologies).

C. Soft Agar Assay

This modified protocol is based on a similar protocol described previously (Clark *et al*., 1995). Aliquot a layer of bottom agar (0.6% in growth medium) and allow to solidify. Trypsinize the cell lines of interest to generate a single-cell suspension, count, and resuspend in a layer of top agar (0.4% in growth medium). For weakly transforming Dbl family proteins or GPCRs, it is best to resuspend 10^4 to 10^5 cells per plate in the top agar layer given that they cause a low efficiency of colony formation. Further, if these analyses require stimulation with a ligand or pharmacological inhibition of a specific signaling pathway, the ligand or drug should be added to both the top and the bottom layers of agar.

Compared to Ras-transformed cells that develop colonies within 10 days, Dbl and GPCR-induced colonies are only visible after 21 to 30 days (Fig. 1C). Therefore, it is important to include both a positive (Ras-transformed cells) and negative (empty vector-transfected) control cell population. These controls are also important given that it is very easy to kill the cells if the agar solution is too hot or is made incorrectly. The following section describes the procedure to prepare reagents for a 14 dish assay where duplicates are used for each condition; one set would be used for a negative control, one set for a positive control, and five sets for five cell lines or experimental conditions.

Melt the sterile 1.8% Bacto-agar stock solution in a microwave and place in a 55°C water bath to cool. Place the complete growth medium, 2× DMEM, and calf serum in a 37°C water bath to prewarm.

Preparation of the bottom agar layer (0.6% agar in medium) is as follows (Table I). For 14- to 60-mm dishes, add 33 ml of 2 × DMEM, 27 ml of regular growth medium, 7.3 ml serum, and 73 µl of 1000× penicillin/streptomycin to a sterile bottle and place in a 37°C water bath to prewarm. Add 33 ml of the melted agar that was cooled to 55°C. Mix the solution and quickly aliquot 5 ml onto 60-mm dishes, allow to solidify for 10 to 15 min at room temperature, and transfer to a 37°C incubator until you are ready to pour the top agar layer. Avoid introducing bubbles when pouring the bottom agar.

Trypsinize each set of cells and transfer to a sterile 15-ml conical tube. Spin the cells out of the trypsin and resuspend in complete growth medium. Count the cells and transfer anywhere from 5×10^3 to 10^5 cells per 0.5 ml to a 5-ml Falcon tube. The appropriate cell densities should be optimized for each cell line. Place the cell suspension in a 37°C water bath to prewarm while preparing the top agar layer.

TABLE I Preparation of Solutions for Soft Agar Assay

	Bottom layer (0.6% agar)		Top layer (0.4% agar)	
	Per dish	14 dish assay	Per dish	14 dish assay
1.8% Bacto-agar	1.65 ml	33 ml	0.33 ml	1.65 ml
2× DMEM	1.65 ml	33 ml	0.33 ml	1.65 ml
Complete growth medium[a]	1.35 ml	27 ml	0.27 ml	1.35 ml
Calf serum	365 µl	7.3 ml	73 µl	365 µl
1000× pen/strep	3.65 µl	73 µl	0.73 µl	3.65 µl
Cell suspension[b]	N/A	N/A	0.50 ml	N/A
Total volume	5.00 ml	100.3 ml	1.50 ml	5.0 ml

[a] DMEM supplemented with final concentrations of 10% calf serum and 1× penicillin/streptomycin.

[b] In complete growth medium.

To prepare 5 ml of the top agar layer, combine 1.65 ml of 2× DMEM, 1.35 ml growth medium, 365 µl serum, and 3.65 µl of 1000× penicillin/streptomycin in a 15-ml conical tube and place in a 37°C water bath to prewarm. If the experimental conditions require the addition of a ligand or inhibitor, those compounds should be added before the solution is prewarmed. Add 1.65 ml of the melted 1.8% Bacto-agar cooled to 55°C and mix. Quickly add 1 ml of the top agar-medium solution to the 0.5-ml cell suspension and gently pipette the cell agar/solution onto the solid bottom agar layer. Allow the top agar to solidify for 30 min at room temperature and then transfer to a 37°C humidified 10% CO_2 incubator. Feed each dish with 2 to 3 drops of complete growth medium every 2 to 3 days.

III. *IN VITRO* CELLULAR INVASION ASSAYS

Three general types of *in vitro* assays can be used to assess the invasive potential of oncogene proteins that cause activation of Rho GTPases. The first and most widely used assay is the Matrigel transwell invasion assay, which provides quantitation of invasive potential. A second set of assays involves qualitative assessment invasive capabilities. These assays evaluate basal cellular invasion and correlate with *in vivo* metastatic potential. This section describes the analyses of human tumor cells where invasion is mediated, in part, by the persistent activation of Rho GTPase function by upstream activation of the PAR1 GPCR.

Reagents for Invasion Assays

Human breast carcinoma cell lines: Obtain from ATCC and culture according to their recommended media. Maintain MDA-MB-231 cells in DMEM supplemented with 10% fetal bovine serum. Maintaine MCF-7 cells in α-MEM supplemented with 10% FBS and 10 µg/ml insulin.

Matrigel invasion chamber: Purchase BD BioCoat growth factor reduced (GFR) Matrigel invasion chambers with a 8-µm pore size PET membrane (Cat. No. 354483) from BD Biosciences.

G8 Myoblasts: Maintain mouse fetal G8 myoblasts (American Type Culture Collection, Rockville, MD) in DMEM supplemented with 10% fetal calf serum and 10% horse serum and grow at 37°C with 10% CO_2. Cells should be subcultured when they reach 70–80% confluency to avoid alterations in the growth properties of the cells.

Matrigel: Purchase Matrigel from Collaborative Biomedical Products (Cat. No. 356234)

Cell dissociation media: Enzyme-free cell dissociation solution PBS based (1× liquid) can be purchased from Specialty Media (Cat. No. S-014-B)

A. Transwell Matrigel Invasion Assay

This modified assay is based on a similar protocol described previously (Albini *et al*., 1987) and it should be emphasized that it is extremely important to optimize the starvation, cell density, and chemoattractant conditions for each cell line used in this assay. For example, we have determined that to assay the invasive potential of MDA-MB-231 cells, the cells must be starved in serum-free medium for a minimum of 24 h and no more than 5×10^3 cells per well should be added to the upper chamber of the Matrigel transwell chamber. If these conditions are not used, we have found that too many cells invade into the Matrigel to accurately quantitate. Therefore, we have described the procedures and amounts of MDA-MB-231 cells required for a 12 transwell chamber assay, where duplicate dishes are used for each experimental condition. This would involve one set of chambers for a positive control, one set for a negative control, and four sets for experimental conditions. We usually use MDA-MB-231 as a positive control and MCF-7 cells as a negative control (Booden *et al*., 2003) (Fig. 2A). For the negative control, we generally seed 2×10^5 cells per 0.5 ml in the upper chamber of each transwell.

Plate the cells of interest on 100-mm dishes 2 days before the invasion assay at a density of 10^6 cells per dish. After an overnight incubation, rinse the cells with PBS and replace the normal grown media with starvation media [base medium supplemented with 1% bovine serum albumin (BSA) and 10 m*M* HEPES]. Starve the cells for at least 24 h.

Matrigel is a solubilized basement membrane preparation extracted from the Engelbreth–Holm–Swarm (EHS) mouse sarcoma cell line, which gels quickly at room temperature to form a reconstituted basement membrane. The growth factor-reduced (GFR) Matrigel is a more defined and characterized reconstituted basement membrane than Matrigel. Remove GFR Matrigel invasion chambers from −20°C and gently add 0.5 ml of starvation medium to the inner chamber. Allow the Matrigel to rehydrate for 2 h at 37°C. Once the Matrigel is rehydrated, it is important not to let it dry out. Therefore, do not remove the rehydration medium until it is time to add the cell suspension to the upper chamber.

While the Matrigel is rehydrating, dissociate the serum-starved cells of interest with enzyme-free cell

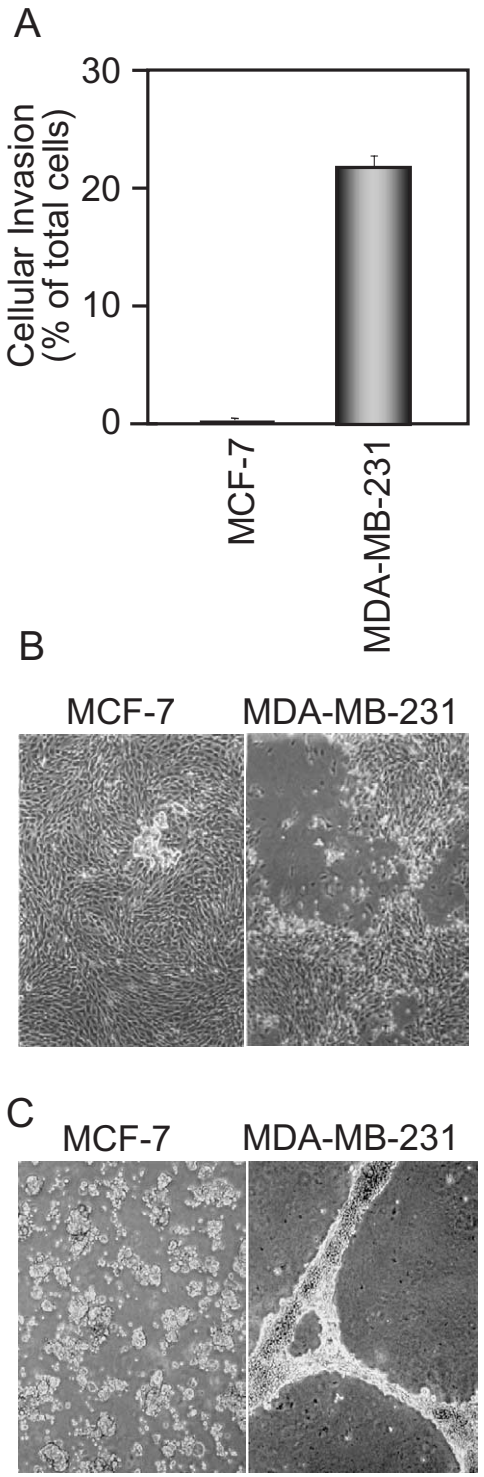

FIGURE 2 *In vitro* invasion assays. The behavior of noninvasive MCF-7 (low PAR1 expression) and highly invasive MDA-MB-231 (high PAR1 expression) human breast carcinoma cells was evaluated in the Matigel transwell invasion assay (A), the G8 myoblast invasion assay (B), or the two-dimensional Matrigel invasion assay (C).

dissociation media. We use the enzyme-free dissociation medium instead of trypsin, as trypsin can act as a mitogen that stimulates multiple signaling pathways, including GPCRs, that can cause Ras and Rho GTPase activation. Make sure to rinse the cells thoroughly with calcium-free PBS and, if need be, incubate them in calcium-free PBS for 5 to 10 min at 37°C before stimulating with enzyme-free dissociation medium. This incubation will facilitate a more rapid dissociation of the cells and will decrease the sheeting of epithelial cells, making them easier to count and plate. Spin the cells out of the dissociation medium and prepare cell suspensions in starvation medium containing 1% BSA and 10 m*M* HEPES at 10^4 cells/ml. For each transwell chamber, add 750 µl of medium to the bottom well of the 24-well companion plate. Remove the base medium from the inner chamber with a pipette, one chamber at a time, and immediately add 0.5 ml of cell suspension (5×10^3 cells) to the inner chamber. Transfer the Matrigel chambers to the wells containing the starvation medium. If these assays require receptor stimulation, allow the cells to incubate for 30 min and then stimulate with the ligand of interest. Be sure that no air bubbles are trapped beneath the membrane. Air bubbles will impede cells from invading through the Matrigel. Incubate the Matrigel transwell chambers for 24 h at 37°C and 5% CO_2.

After incubation, remove the noninvading cells by pipetting off the medium in the upper chamber of the transwell insert. Remove the Matrigel from the surface of the filter in the inner chamber by swabbing the insert with a cotton tip. These steps should be done quickly and just prior to fixing and staining the cells to avoid drying of the cells adhering to the bottom surface of the membrane.

Cells on the lower surface of the membrane should be fixed and stained. We use a Diff-Quick Kit (Dade Behring Inc.) to stain the cells on the lower surface of filter. With this kit, the cell nucleus stains purple and the cytoplasm stains pink. Alternative staining methods include fixation followed by hematoxylin and eosin or crystal violet. To fix and stain the cells using the Diff-Quick kit, add 750 ml of each Diff-Quick solution to three individual wells in a 24-well plate and add distilled water to two beakers. Immediately after removal of noninvading cells and Matrigel, sequentially transfer the transwell chambers, every 45 s, through each stain solution and the two beakers of water. Remove excess solution by gently swabbing the inner chamber with a cotton tip and allow the inserts to air dry for a minimum of 60 min.

Depending on the proportion of cells that invade, quantitation can be done by directly counting the stained cells by visual inspection using a phase-

contrast microscope. We generally place the chamber on a grid and count the stained cells on one-half of the filter of duplicate membranes at 10× magnification. It is also important to examine the bottom well for cells that have invaded through the Matrigel but did not adhere to the filter. This phenomenon is quite common for highly invasive breast carcinoma cell lines such as MDA-MB-231, BT549, and Hs578T. Quantitate these cells using a hemacytometer. We do not recommend removing the membrane from the insert housing as the filter generally tears.

B. G8 Myoblast Invasion Assay

G8 monolayer invasion provides a simple and highly reproducible assay to test the ability of tumor cells to invade a monolayer that is enriched in a variety of extracellular matrix components. This provides a qualitative assay that monitors activity that correlates well with *in vivo* metastasis. The G8 myoblast assay was determined to correlate with the invasive and metastatic ability of TA3/St mouse mammary carcinoma cells *in vivo* (Yu and Stamenkovic, 1999; Yu *et al*., 1997). While they cannot be employed to directly quantitate *in vitro* invasion mediated by a specific protein or signaling pathway, the G8 myoblast and two-dimensional Matrigel assays report the ability of cells to invade and degrade extracellular matrix, as well as the cell monolayer that has deposited the matrix proteins, and, more importantly, they report the ability of the cells to organize, move through an unnatural environment, and proliferate at a distant site (Fig. 2B).

The G8 invasion assay is relatively simple. Plate G8 myoblasts at a density of 2×10^5 cells per well in 6-well dishes 3 days before the assay begins. This time in culture allows the myoblasts to deposit extracellular matrix proteins on the cell surface. When the cells reach confluence, wash the monolayer once with PBS and fix with dimethyl sulfoxide for 2 h at room temperature, which results in a monolayer of both extracellular matrix protein and myoblast cells. After fixation, rinse the monolayer gently four times with PBS and incubate with 1 ml of culture medium.

Dissociate the cells to be evaluated with the enzyme-free dissociation medium as described earlier. Then collect the cell suspension by centrifugation to remove the dissociation medium, resuspend in growth medium, and count. Add a 1-ml suspension of the cells to the top of the G8 myoblast monolayer and observe daily. Invasion generally occurs within 1 to 3 days of seeding. The appropriate cell density and growth medium for each cell line used in this assay should be determined empirically. The percentage of fetal bovine serum used in the culture medium is a critical consideration; different cells require different amounts of FBS for the assay to be interpretable. In our experience with the MDA-MD-231, MCF-7, OVCA-420, -429, 432, 433, OVCAR-3, and -5 human tumor cell lines, a good starting point for the optimization of this assay is a cell density of 5×10^3 cells per well in growth medium supplemented with 1% FBS. The ability of cells to invade and degrade the myoblast monolayer and begin to proliferate can be visualized using an inverted phase-contrast microscope. A good positive control for this assay is the OVCA-432 cell line, and a good negative control is the NIH 3T3 cell line.

C. Two-Dimensional Matrigel Assay

The two-dimensional Matrigel assay provides a qualitative assay that correlates well with *in vivo* invasion and metatasis (Petersen *et al*., 1992) (Fig. 2C). Thaw Matrigel overnight on ice at 4°C. Matrigel will begin to solidify at temperatures above 4°C. Therefore, it is important to thaw the Matrigel slowly and not allow it to warm before it is aliquoted. Each 12-well dish should be placed on ice for 10 to 15 min in order to cool the dish to 4°C. After chilling each dish, add 700 µl of Martigel to each well. Transfer the Matrigel-coated dishes to 37°C and incubate for a minimum of 30 min. While the Matrigel is solidifying, dissociate the cells of interest with enzyme-free cell dissociation medium. Spin the cells out of the dissociation medium and plate 2×10^5 per well in 1 ml of growth media. The ability of the cells to invade the Matrigel and organize into honeycomb-like structures can be assessed 24 h after incubation using an inverted phase-contrast microscope. A good positive control for this assay is the highly invasive MDA-MB-468 cell line, and a good negative control is the noninvasive MCF-7 cell line (Eckert et al. 2004).

References

Albini, A., Iwamoto, Y., Kleinman, H. K., Martin, G. R., Aaronson, S. A., Kozlowski, J. M., and McEwan, R. N. (1987). A rapid *in vitro* assay for quantitating the invasive potential of tumor cells. *Cancer Res*. **47**, 3239–3245.

Booden, M. A., Campbell, S. L., and Der, C. J. (2002). Critical but distinct roles for the pleckstrin homology and cysteine-rich domains as positive modulators of Vav2 signaling and transformation. *Mol. Cell. Biol*. **22**, 2487–2497.

Booden, M. A., Eckert, L. B., Der, C. J., and Trejo, J. (2004). Persistent signaling by dysregulated thrombin receptor trafficking promotes breast carconoma cell invasion. *Mol. Cell. Biol*. **24**, 1990–1999.

Clark, E. A., Golub, T. R., Lander, E. S., and Hynes, R. O. (2000). Genomic analysis of metastasis reveals an essential role for RhoC. *Nature* **406**, 532–535.

Clark, G. J., Cox, A. D., Graham, S. M., and Der, C. J. (1995). Biological assays for Ras transformation. *Methods Enzymol*. **255**, 395–412.

Eckert, L. B., Repasky, G. A., Ülkü, A. S., McFall, A., Zhou, H., Sartor, C. I., and Der, C. J. (2004). Involvement of Ras activation in human breast cancer cell signaling, invasion, and anoikis. *Cancer Res*. **64**, 4585–4592.

Fabian, J. R., Daar, I. O., and Morrison, D. K. (1993). Critical tyrosine residues regulate the enzymatic and biological activity of Raf-1 kinase. *Mol. Cell. Biol*. **13**, 7170–7179.

Hanahan, D., and Weinberg, R. A. (2000). The hallmarks of cancer. *Cell* **100**, 57–70.

Keely, P. J., Westwick, J. K., Whitehead, I. P., Der, C. J., and Parise, L. V. (1997). Cdc42 and Rac1 induce integrin-mediated cell motility and invasiveness through PI(3)K. *Nature* **390**, 632–636.

Khosravi-Far, R., Solski, P. A., Kinch, M. S., Burridge, K., and Der, C. J. (1995). Activation of Rac and Rho, and mitogen activated protein kinases, are required for Ras transformation. *Mol. Cell. Biol*. **15**, 6443–6453.

Martin, C. B., Mahon, G. M., Klinger, M. B., Kay, R. J., Symons, M., Der, C. J., and Whitehead, I. P. (2001). The thrombin receptor, PAR-1, causes transformation by activation of Rho-mediated signaling pathways. *Oncogene* **20**, 1953–1963.

Petersen, O. W., Ronnov-Jessen, L., Howlett, A. R., and Bissell, M. J. (1992). Interaction with basement membrane serves to rapidly distinguish growth and differentiation pattern of normal and malignant human breast epithelial cells. *Proc. Natl. Acad. Sci. USA* **89**, 9064–9068.

Qiu, R.-G., Chen, J., Kirn, D., McCormick, F., and Symons, M. (1995). An essential role for Rac in Ras transformation. *Nature* **374**, 457–459.

Sahai, E., and Marshall, C. J. (2002). RHO-GTPases and cancer. *Nature Rev. Cancer* **2**, 133–142.

Schmidt, A., and Hall, A. (2002). Guanine nucleotide exchange factors for Rho GTPases: Turning on the switch. *Genes Dev*. **16**, 1587–1609.

Solski, P. A., and Der, C. J. (2000). Analyses of transforming activity of Rho family activators. *Methods Enzymol*. **325**, 425–441.

Whitehead, I. P., Zohn, I. E., and Der, C. J. (2001). Rho GTPase-dependent transformation by G protein-coupled receptors. *Oncogene* **20**, 1547–1555.

Yu, Q., and Stamenkovic, I. (1999). Localization of matrix metalloproteinase 9 to the cell surface provides a mechanism for CD44-mediated tumor invasion. *Genes Dev*. **13**, 35–48.

Yu, Q., Toole, B. P., and Stamenkovic, I. (1997). Induction of apoptosis of metastatic mammary carcinoma cells *in vivo* by disruption of tumor cell surface CD44 function. *J. Exp. Med*. **186**, 1985–1996.

CHAPTER

42

Assay of Tumorigenicity in Nude Mice

Anne-Marie Engel and Morten Schou

I. INTRODUCTION

Tumorigenicity is defined as the ability of viable cultured cells to give rise to progressively growing tumor nodules, showing viable and mitotically active cells, in immunologically nonresponsive animals over a limited observation period (WHO, 1987). It is, however, no absolute property in a cell line, but will always be defined by the assay in which it is tested. In order to ensure reproducibility, it is therefore very important that the cells tested are from the same batch and that the animals used are syngenic. The only way of testing whether a cell line has achieved all the characteristics needed for solid tumor growth is by testing its ability to form such tumors *in vivo*. In order to rule out the interference of the immune defense of the recipient, testing must take place in a host organism that will not reject the transplant. If the cells being tested are originally from mice or rats, syngenic animals can be used as recipients of cell inocula. Otherwise, immune-deficient animals that are incapable of recognizing and rejecting nonself tissue are used. The nude mouse is ideal in this respect in that its immune defect affects thymic development, resulting in a lack of functional T lymphocytes in the animals (Rygaard, 1973). Therefore, a large proportion of mammalian tumors can be transplanted to nude mice without being rejected. If a cell line will not produce tumors in nude mice, it will sometimes help to mix irradiated mouse or human fibroblasts 1:1 with the tumor cell inoculum (Wilson *et al*., 1984). The severe combined immune deficiency (SCID) mouse, in which both T and B lymphocyte maturation are impaired due to a deficiency in a gene coding for recombinase, which participates in the recombination of genes coding for T and B lymphocyte antigen receptors, can also be used in this kind of assay (Bosma *et al*., 1983). Some reports say that SCID mice will let some cell lines form tumors even though they are not tumorigenic in nude mice (Xie *et al*., 1992).

Testing the tumorigenicity of cells propagated and perhaps transformed *in vitro* is relevant in a number of different contexts, such as transfection with antisense DNA in order to decrease tumor formation (Cheng *et al*., 1996) or investigation of the role of specific genes in increased or decreased tumorigenicity after *in vitro* manipulation (Sun *et al*., 1996). In the production of vaccines, it is important to know that the cells used for propagating a virus are not tumorigenic *in vivo* (WHO, 1987). The potential tumorigenic effect of different genes can be tested by transfecting immortalized cell lines with oncogenes and subsequently inoculating them on nude mice (Chisholm and Symonds, 1992) or by assaying the baseline expression of a gene in a cell line and relating this to the tumorigenicity of the cells. Immortalized cell lines are also used for determining the carcinogenic effect of chemical compounds by *in vitro* treatment and subsequent *in vivo* tumorigenicity testing in nude mice (Iizasa *et al*., 1993). A number of phenotypical features are characteristic of malignantly transformed cells. As opposed to normal cells, they are immortalized, i.e., they can grow in culture for more than 100 population doublings. They lose contact inhibition, resulting in piling up of cultured cells, and they exhibit high plating efficiency (i.e., a high number of colonies obtained per 100 cells plated at 2–50 cells/cm^2). The growth rate of such cells is normally higher than for normal cells, and they can exhibit chromosomal abnormalities such as aneuploidy or heteroploidy (Shimizu *et al*., 1995). These are all characteristics that can be observed in *in vitro*

Copyright 2006, Elsevier Science (USA).
All rights reserved.

experimental setups. The ability to form colonies in soft agar is another characteristic closely connected to the malignant phenotype. During the multistep process of malignant transformation, cells become anchorage independent, probably as a result of cell surface modifications (Nicolson, 1976). This enables them to grow in suspension or in semisolid media such as soft agar. Testing for this characteristic is widely used to evaluate the possible tumorigenic effect of different manipulations performed on cells *in vitro* (Hamburger and Salmon, 1977).

Angiogenesis, the ability to induce blood vessel formation, is characteristic of cancer cells. The angiogenic potential of a cell line can be assayed by implanting tumor cells at the edge of rabbit cornea or by incubating it with tumor cell extracts and observing the formation of blood vessels. Implantation into the chorioallantroic membrane of chicken embryos followed by observation of the formation of blood vessels is also used for assaying angiogenesis (Folkman, 1985). Invasiveness is another characteristic of tumor cells, which can be assayed in *in vitro* setups.

The *in vivo* protocol suggested here is adapted from the guidelines of WHO given for tumorigenicity testing of tumor cells used for propagation of the poliomyelitis virus used in the manufacturing of polio vaccine (WHO, 1987).

II. MATERIALS AND INSTRUMENTATION

Mice used are 6- to 8-week-old Balb/cA nu/nu females. They are from Taconic M&B, Ry, Denmark, and are kept at our institute for 1 week before experiments are initiated. They are fed autoclaved water and sterilized food pellets and kept in Macrolon II cages under SPF conditions.

All plasticware used for tissue culture and harvest of cells is from Greiner GmbH. Tissue culture medium is RPMI 1640 with UltraGlutamin (BioWhittaker, Cat. No. 12-702F/U1). The trypsin–EDTA solution (Cat. No. 17-161E) and phosphate-buffered saline (PBS) without Ca^{2+} and Mg^{2+} (Cat. No. 17-516F) are also from BioWhittaker. Syringes for injection of tumor cells are 1-ml Luer tuberculin from Once (Cat. No. 1202) fitted with a 0.5 × 16 Terumo Neolus needle (Cat. No. NN-2516R).

For fixation of excised tissue, buffered formalin (Lillies fixative) is prepared: 163.1 g 24.5% formaldehyde solution, 4.5 g natriumdihydrogenphosphatdihydrate (Merck 6345), and 8.2 g dinatriumphosphatdihydrate (Merck 6580). Add sterile water until the volume reaches 1000 ml.

III. PROCEDURES

A positive and a negative control cell line should always be included in an assay of tumorigenicity in order to ensure that the procedure has been carried out correctly. HeLa cells (American Type Culture Collection CLL-2) can be used as positive controls, and MRC-5 cells (American Type Culture Collection CLL-171) can be used as negative controls.

A. Preparation of Cells

Solutions

1. *Tissue culture medium:* Prepare the same cell culture medium for each of the cell lines tested that you would normally use for propagation *in vitro.* For this experiment, we use RPMI 1640 with 50 ml/500 ml of heat-inactivated calf serum (heat inactivate in a water bath at 56°C for 30 min) and penicillin/streptomycin to a final concentration of 100 IU/ml penicillin and 10 mg/ml streptomycin.
2. *PBS without Ca^{2+} and Mg^{2+}*
3. *Trypsin–EDTA solution*

Steps

1. Expand the cell line(s) to be tested for tumorigenicity and the two control cell lines in culture until an appropriate number of cells has been obtained. At least 10 mice should be used for each cell line. Each mouse must receive 10^7 cells. Harvest the cells when they are subconfluent and thus still in the logarithmic growth phase (Fig. 1A).
2. The harvest of cells from culture flasks depends on whether they grow in suspension or adhere to the flask. If cells grow adherently, they can be removed either by scraping with a cell scraper or by trypsination for 5–10 min at 37°C (in an incubator). Prior to adding trypsin, remove culture medium and wash cells with 10 ml PBS without calcium and magnesium in order to remove any traces of serum that will otherwise inhibit the action of trypsin.
3. After removal from the flask, centrifuge the cells for 5 min at 200 *g*, discard the supernatant, and resuspend the cells in 10 ml PBS or culture medium without antibiotics and serum. Centrifuge again at 200 *g* for 5 min. Discard supernatant and resuspend cells in 10 ml PBS or medium as described earlier.
4. Dilute a small sample (e.g., 0.5 ml) of the cell suspension 1:10 in PBS or medium. Dilute this solution 1:1 with 0.4% trypan blue. Let the suspension stand for 2–5 min and then count cells in a hemocytometer. Keep the rest of the cells on ice while preparing and counting the sample. Calculate the number of viable

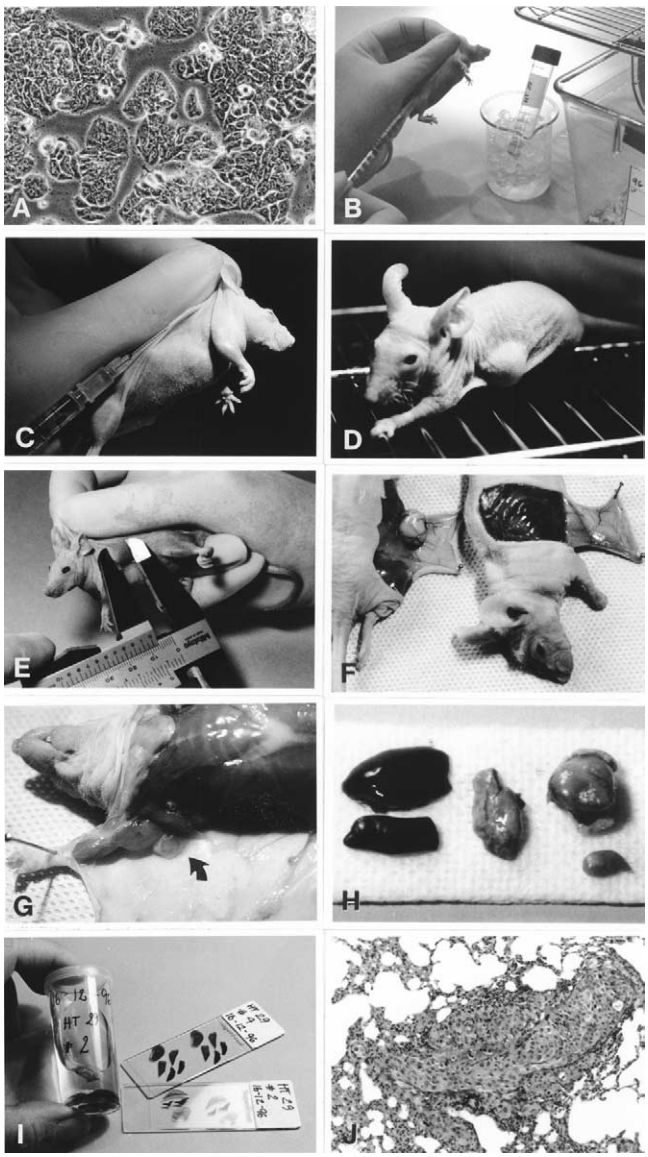

FIGURE 1 (A) Subconfluent cells (colon adenocarcinoma HT29) ready to be harvested. (B) Cells kept on ice, ready to be injected. (C) Subcutaneous injection of 0.2 ml cell suspension. (D) Mouse with tumor growth. (E) Measurement of tumor. (F) Autopsy after 21 days. Mouse with and without tumor growth. (G) Axillary lymph node (arrow). (H) Organs removed for fixation in formalin. (I) Fixed tissue and histological preparations. (J) Lung metastasis (objective x).

cells per milliliter of the original suspension as follows: viable cells in larges squares counted/number of large squares counted × dilution of cells × 10^4.

5. Adjust the concentration of the cell suspension to be inoculated to 5×10^7/ml viable cells in serum-free culture medium or PBS. This may include one more step of centrifugation and resuspension in a suitable volume. Always make sure to have an excess of cell suspension as some of it will be trapped in the syringe. An extra 0.5 ml for 10 mice to be injected is sufficient.

6. Keep cells on ice until use and be sure to inoculate as soon as possible after the adjustment of concentration (Fig. 1B).

B. Inoculation and Inspection

Steps

1. Inject 0.2 ml of the cell suspension subcutaneously in the right lateral aspect of the thoracic wall (Fig. 1C).
2. Mice should be observed daily and inspected for tumor growth at least three times a week (Fig. 1D).

C. Examination of Recipients and Tumors

Solution

Prepare Lillies fixative (see Section II) and store at room temperature.

Steps

1. Tumors are measured in two perpendicular dimensions (Fig. 1E). After 21 days of observation, sacrifice mice and autopsy immediately. Inspect the inoculation site from the deep aspect and excise (Fig. 1F). In order to describe the metastatic potential of the cell line tested, excise the ipsilateral axillary lymph node (Fig. 1G), part of the spleen, one-third of the liver, and the inferior lobe of the left lung for histological examination (Fig. 1H).

2. Fix tissues in buffered formalin (Lillies fixative), embed in paraffin, and section in 5-μm sections. Stain with hematoxylin and eosin and study under a light microscope (Fig. 1I). Histological examination enables the investigator to see if the tumor has retained the morphological characteristics of the primary tumor from which the cell line was established and whether it gives rise to metastases (Fig. 1J).

D. Reporting of Findings

Reports of macroscopic and microscopic findings should be given for each cell line. Macroscopic findings include the conditions of mice during the test period and macroscopic tumor growth, if any. The macroscopic appearance of the tumor-inoculation site at autopsy should also be reported. Microscopic findings should include a description of the tumor tissue or the inoculation site if no tumor appears. Metastases, location, and frequency should be reported.

An example of an observation table is given in Table I for HeLa cells used as a positive control in a tumorigenicity assay carried out in nude Balb/cA mice.

TABLE I HeLa Cells Used as Positive Controls in a Tumorigenicity Assay

Mouse No.	Site of inoculation/ no cells	Lymph node	Liver	Spleen	Lung
1	Subcutaneous in the right flank / 10^7 cells	0	0	0	0
2	Subcutaneous in the right flank / 10^7 cells	0	0	0	0
3	Subcutaneous in the right flank / 10^7 cells	0	0	0	0
4	Subcutaneous in the right flank / 10^7 cells	0	0	0	0
5	Subcutaneous in the right flank / 10^7 cells	0	0	0	0
6	Subcutaneous in the right flank / 10^7 cells	0	0	0	0
7	Subcutaneous in the right flank / 10^7 cells	0	0	0	0
8	Subcutaneous in the right flank / 10^7 cells	0	0	0	0
9	Subcutaneous in the right flank / 10^7 cells	0	0	0	0
10	Subcutaneous in the right flank / 10^7 cells	0	0	0	0

E. Conclusions

According to the World Health Organization, the positive control cell (HeLa) should give rise to progressively growing tumors in 9 out of 10 mice if the assay is carried out correctly. Furthermore, when a histopathological examination of tumor nodules is performed, mitotic activity must be detected in the tumor tissue.

For the cell line tested for tumorigenicity, at least 9 out of 10 mice should develop a tumor if the cell line is to be designated tumorigenic. If only some mice in a group develop tumors, the assay should be repeated with the same cell dose and with an increased cell dose, e.g., 5×10^7. As mentioned in Section I, it is a prerequisite that the cells used are from the same batch and that the recipient mice are syngenic. The cell line used as a negative control should not, of course, give rise to tumor growth in any of the 10 animals. Some authors use a more differentiated assay, administering cells in differentiated doses and categorizing cell lines as high, moderate, low, or nontumorigenic (Gurtsevitch and Lenoir, 1985).

IV. PITFALLS

It is of the utmost importance for the interpretation of results that the cell lines tested be free of mycoplasma infection, as mycoplasma can alter their ability to form tumors (Fogh, 1973). If there is not a routine of regular mycoplasma testing in the cell culture laboratory, a mycoplasma test should be performed and a negative outcome ensured before cell lines are used in a tumorigenicity assay.

References

Bosma, G. C., Custer, R. P., and Bosma, M. J. (1983). A severe combined immunodeficiency in the mouse. *Nature* **301**, 527–530.

Cheng, J. Q., Ruggeri, B., Klein, W. M., Sonoda, G., Altomare, D. A., Watson, D. K., and Testa, J. R. (1996). Amplification of AKT2 in human pancreatic cells and inhibition of AKT2 expression and tumorigenicity by antisense RNA. *Proc. Natl. Acad. Sci. USA S* **93**, 3636–3641.

Chisholm, O., and Symonds, G. (1992). An *in vitro* fibroblast model system to study myc-driven tumour progression. *Int. J. Cancer* **51**, 149–158.

Fogh, J. (ed.) (1973). "Contamination in Tissue Culture." Academic Press, New York.

Folkman, J. T. (1985). Tumor angiogenesis. *Adv. Cancer Res.* **43**, 175–203.

Gurtsevitch, V. E, and Lenoir, G. M. (1985). Tumorigenic potential of various Burkitt's lymphoma cell lines in nude mice. *In "Immune-Deficient Animals in Biomedical Research"* (J. Rygaard *et al.*, eds.), pp. 199–203. Karger, Basel.

Hamburger, A. W., and Salmon, S. E. (1977). Primary bioassay of human tumor stem cells. *Science* **197**, 461–463.

Iiaza, T., Momiki, S., Bauer, B., Caamano, J., Metcalf, R., Lechner, J., Harris, C. C., and Klein-Szanto, A. J. (1993). Invasive tumors derived from xenotransplanted, immortalized human cells after *in vivo* exposure to chemical carcinogens. *Carcinogenesis* **14**, 1789–1794.

Nicolson, G. L. (1976). Trans-membrane control of the receptors on normal and tumor cells. II. Surface changes associated with transformation and malignancy. *Biochim. Biophys. Acta* **458**, 1–72.

Rygaard, J. (1973). "Thymus and Self: *Immunobiology of the Mouse Mutant Nude*." Wiley, London.

Shimizu, T., Kato, M. V., Nikaido, O., and Suzuki, F. (1995). A specific chromosome change and distinctive transforming genes are necessary for malignant progression of spontantous transformation in cultured Chinese hamster embryo cells. *Jpn. J. Cancer Res.* **86**, 546–554.

Sun, Y., Kim, H., Parker, M., Stetler-Stevenson, W. G., and Colburn, N. H. (1996). Lack of suppression of tumor cell phenotype by

overexpression of TIMP-3 in mouse JB6 tumor cells: Identification of a transfectant with increased tumorigenicity and invasiveness. *Anticancer Res*. **16**, 1–17.

Wilson, E. L., Gärtner, M., Campbell, J. A. H., and Dowdle, E. B. (1984). Growth and behaviour of human melanomas in nude mice: Effect of fibroblasts. *In "Immune–Deficient Animals"* (B. Sordat, ed.), pp. 357–361. Karger, Basel.

World Health Organization (WHO) (1987). "Requirements for Continuous Cell Lines Used for Biologicals Production." *WHO Technical Report Series*, No. 745, Annex 3.

Xie, X., Brünner, N., Jensen, G., Albrectsen, J., Gotthardsen, B., and Rygaard, J. (1992). Comparative studies between nude and scid mice on the growth and metastatic behavior of xenografted human tumors. *Clin. Exp. Metast*. **10**, 201–210.

CHAPTER

43

Transfilter Cell Invasion Assays

Garth L. Nicolson

I. INTRODUCTION

The ability to invade surrounding extracellular matrices and tissues is an important phenotype of malignant tumor cells. To determine the invasive properties of malignant cells, several invasion assays have been developed. For example, organ fragments (Nicolson *et al.*, 1985), reconstituted tissue spheroids (Mareel *et al.*, 1988), membranous tissues (Nabeshima *et al.*, 1988; Yagel *et al.*, 1989), cultured cell monolayers (Kramer and Nicolson, 1979; Waller *et al.*, 1986), or extracellular matrices (Albini *et al.*, 1987; Schor *et al.*, 1980) have been used as tissue or matrix for cell invasion studies. Commercially available Matrigel, a mouse EHS tumor extract consisting of major basement membrane components polymerized into a gel, has been the most commonly used material to determine the invasiveness of various types of cells (Albini *et al.*, 1987). The apparatus of choice for measuring cell invasion has been a modified Boyden chamber or Transwell. Briefly, the apparatus contains two chambers (upper and lower) that are separated by a microporous polycarbonate filter, the upper surface of which is coated with a thin layer of Matrigel. Tumor cells are placed into the upper chamber where they settle by gravity onto the Matrigel layer. In the lower chamber a chemotactic agent can be placed to stimulate directional cell migration of cells that invade the Matrigel layer. The invasive ability of these cells can be expressed as the number of cells invading through the Matrigel layer and filter with time. For the most part, the invading cells are found on the lower surface of the filter and are not released into the fluid of the lower chamber. Although there are some exceptions to this (Simon *et al.*, 1992), the invasive abilities of tumor cells in the transfilter invasion assay are usually related to their *in vivo* invasion behavior (Albini *et al.*, 1987; Repesh, 1989; Hendrix *et al.*, 1987). This article describes the basic protocol of the Matrigel transfilter invasion assay.

II. MATERIALS AND INSTRUMENTATION

Culture medium DME/FI2 (Cat. No. 11330-032), fetal bovine serum (FBS), phosphate-buffered saline (PBS) (Cat. No. 14040-133), and trypsin (2.5%, Cat No. 15090-046) are from GIBCO-BRL. Matrigel (Cat. No. 40234) and fibronectin (Cat. No. 40008) are from Collaborative Biomedical Products. Bovine serum albumin (BSA) (Cat. No. 810661, fraction V) is from ICN. EDTA (Cat. No. 423-384) is from CMS. Hematoxylin (Cat. No. GHS-1-16), eosin (Cat. No. HTIIO-3-16), and 10% neutralized formaldehyde solution (Cat. No. HT50-1-128) are from Sigma.

Transwells (Cat. No. 3421, 6.5-mm diameter, 5-µm pore size) and 24-well culture plates (Cat. No. 25820) are from Corning Costar Corporation. Additional equipment includes general tissue culture supply and equipment, forceps, cotton swabs, a reticle (1/10-mm measurement), and a cell-counting device (Coulter counter, hemocytometer, or equivalent equipment).

III. PROCEDURES

A. Matrigel Coating on the Microporous Transwell Filter

Solutions

1:30 diluted Matrigel solution (sterile): To make 900 µl Matrigel solution for 12 Transwells (50 µl X the number

Copyright 2006, Elsevier Science (USA).
All rights reserved.

of Transwells), thaw Matrigel at 4°C overnight and mix 30 µl with 870 µl of ice-cold PBS. Keep ice cold until the solution is applied to the Transwell. Aliquot the remaining Matrigel (e.g., 1 ml each), freeze, and store at –80°C.

1:100 diluted Matrigel solution (sterile): To make 2 ml, mix 20 µl of Matrigel with 2 ml of ice-cold PBS. Keep solution ice-cold.

Steps

1. Place 500 µl of 1:100 diluted Matrigel solution in a small culture dish (i.e., 30 mm diameter) on an ice-cold plate.
2. Use a forceps for the handling of Transwells. The Transwell invasion chamber system is shown in Fig. 1. Soak the lower surface of the polycarbonate filter of each Transwell in the Matrigel solution. After briefly removing any excessive amount of the solution, place the Transwell into a 24-well culture plate and allow it to dry in a hood overnight at room temperature.
3. Pour 50 µl of the 1:30 diluted Matrigel solution into the upper chamber of the Transwell.
4. Carefully overlay 200 µl of sterilized, double-distilled H_2O to each filter and allow it to dry completely in a hood at room temperature under occasional ultraviolet light. This usually takes about 2 or 3 days.
5. Proceed to the next step or store the coated Transwell sets in a scaled 24-well culture plate at 4°C.

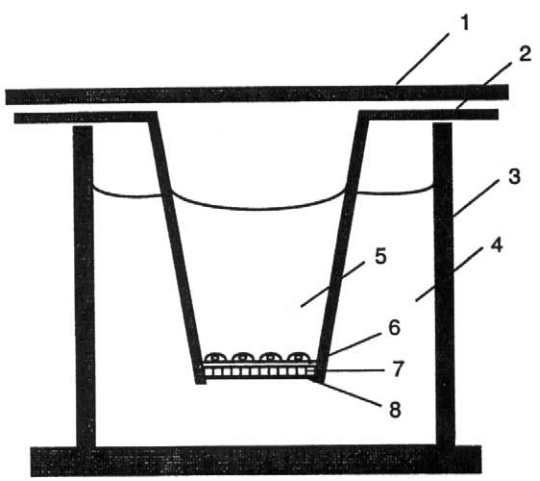

FIGURE 1 Transwell invasion chamber system: (1) lid, (2) Transwell, (3) 24-well culture plate, (4) lower chamber (800 µl of 10 µg/ml fibronectin in invasion buffer), (5) upper chamber (200 µl), (6) Matrigel layer, (7) microporous polycarbonate filter (5-µm pore size), and (8) lower surface of the filter coated with a thin layer of Matrigel.

B. Setting up the Invasion Assay

Solutions

2% BSA stock solution: To make 100 ml, slowly dissolve 2 g of BSA in ice-cold PBS for 20 min and sterilize by filtration through a 0.22-µm filter.

Invasion buffer, 0.1% BSA in DME/F12: To make 40 ml, mix 2ml of 2% BSA stock solution with 38 ml of DME/FI2 medium.

EDTA stock solution (200 mM): To make 100 ml, dissolve 7.44 g EDTA with double-distilled H_2O and adjust the pH to 7.4.

Trypsin–EDTA (0.25%): To make 100 ml, add 10 ml of 2.5% trypsin solution and 1 ml of EDTA stock solution into 89 ml of PBS.

10% FBS-DME: To make 20 ml, mix 2 ml of FBS with 18 ml of DME/FI2 medium.

Fibronectin solution (10 µg/ml): To make l0 ml, mix 100 µl of fibronectin stock solution (1 mg/ml) with 10 ml of invasion buffer. In the example here, fibronectin is used as a chemoattractant.

Steps

1. These procedures should be performed under sterile conditions. Culture (4 × 100-mm-diameter dishes) B16-F10 cells in DME/FI2 medium supplemented with 5% FBS at 37°C in an atmosphere of 5% CO_2–95% air and grow to about 80% confluency.
2. Prewarm the Matrigel-coated Transwells in the 24-well culture plate to room temperature, and rehydrate the Matrigel with 200 µl of invasion buffer for 1 h.
3. Wash the B16-F10 culture dishes with 10 ml of DME/FI2 medium and incubate with 3 ml each of trypsin–EDTA for 5 min. Place in a 50-ml tube and sediment cells by centifugation at 1000 rpm for 5 min.
4. Wash the cells with 10 ml of 10% FBS-DME medium by centrifugation at 1000 rpm for 5 min and resuspend the cells in 10 ml of 10% FBS-DME medium. Let the cells incubate for 15 min at room temperature.
5. Wash the cells with 40 ml of DME/FI2 medium twice by centrifugation at 1000 rpm for 10 min. Resuspend the cells in 5 ml of invasion buffer.
6. Prepare 2.5×10^5 cells/ml in invasion buffer by counting the cells with a Coulter counter, hemocytometer, or equivalent equipment.
7. Carefully discard the buffer in the upper chambers of the Transwells, wash the chambers again with 200 µl of invasion buffer, and carefully pour 800 µl of the fibronectin solution (chemoattractant solution) through the slit of the Transwell into the lower chamber.
8. Add 200 µl of the cell suspension into the upper chamber. Avoid making bubbles in the upper chamber

so that the cells can settle down evenly on the filter. Carefully put the Transwell invasion chamber system into an incubator and incubate for 48 h at 37°C in 5% CO_2–95% air.

C. Staining Invading Cells with Hematoxylin–Eosin

Steps

1. Prepare a 24-well culture plate with 400 µl of 10% formaldehyde, hematoxylin, or eosin in each well and fill four jars (about 500 ml each) with distilled water.
2. Place the Transwell in the 10% formadehyde solution for 10 min and then rinse the Transwell by submerging it in a jar containing distilled water.
3. Transfer the Transwell to the hematoxylin solution for 10 min and then rinse with water. Place the Transwell into the well with warm distilled water (about 40°C) for 10 min.
4. Transfer the Transwell to the eosin well for 5 min and then place it into a jar containing distilled water. Gently rub the cells off the upper side of the filter using a cotton swab and rinse the Transwell with distilled water.

D. Counting Invading Cells Using a Phase-Contrast Microscope (or Coulter Counter)

Steps

1. Place the Transwell into a 24-well culture place. Make sure that there is moisture on the inside of the culture plate. Count the cells in the 16 fields indicated in Fig. 2 at 200 × magnification.

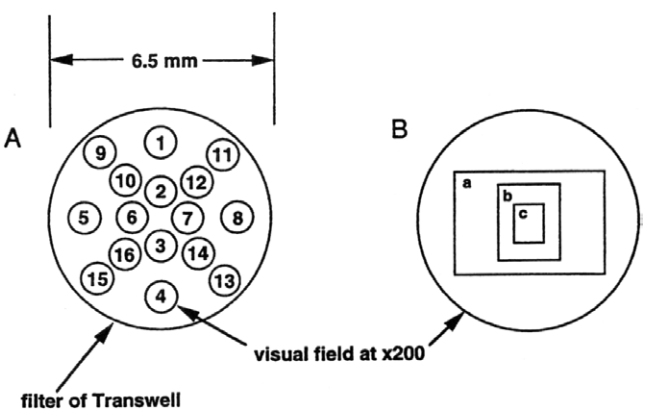

FIGURE 2 A Transwell filter in a microscopic field. (A) Spots used to count the cells on the filter are shown as numbered circles. The numbers of the spots are an example of the sequence recommended for cell counting. (B) Photo frames of the Diaphot (Nikon). Relative sizes of the frames to the field are 47 (a), 17 (b), and 4.3% (c).

2. Using a reticle with 1/10-mm guides (Bausch & Comb Inc.), place the cell suspension onto the stage of a phase-contrast microscope, and measure the diameter of the field (r; mm) with the magnification at 40×. The total number of invading cells (1) can be calculated with the formula

$$I = c \times (5 \times R/r)^2,$$

where c is the average number of invading cells per ×200 magnification field and R is the diameter of the filter (6.5 mm). For example, the value of r of a Diaphot (Nikon) is 4.45. Therefore, $(5 \times R/r)^2 = 53.3$. If the cells are too dense to count the entire field, a photo as shown in Fig. 2 can be used. Using a Diaphot (Nikon), the areas of a, b, and c in Fig. 2 are 47, 17, and 4.3% of the total area of the field, respectively.

E. Reusing Transwells

Steps

1. After counting invading cells, wipe the cells off the lower surface of the filter using a cotton swab and soak the Transwells in a detergent solution (e.g., 1% Contrad 70) for at least 1 day.
2. Wipe both surfaces of the filter gently and thoroughly using a cotton swab and place the Transwells into the 24-well culture plate.
3. Fill the entire Transwell plate with distilled water, cover the plate with a lid, shake it several times, and discard the water.
4. Repeat step 3 at least three times. After the final wash, let the Transwell plate sit for 1 h filled with distilled water.
5. Wash the plate with double-distilled water several times and rinse with 70% ethanol as in step 3. Dry the Transwells in a tissue culture hood overnight under ultraviolet light.

IV. COMMENTS

Although tumor cells *in vivo* usually invade connective or parenchymal tissue, a number of reports indicate that the invasive and metastatic phenotypes of cells correlate with their *in vitro* Matrigel invasion capacity (Albini *et al.*, 1987; Repesh, 1989; Hendrix *et al.*, 1987). This may be due to the fact that invasion *in vivo* into connective or parenchymal tissue is limited by the capability of tumor cells to undergo basement membrane invasion, a key event in malignant progression. The invasive process involves at least three events (adhesion, degradation, and migration) (Liotta,

1986); for tumor cells to be invasive, they must be at least somewhat proficient in each step (Nicolson, 1989).

V. PITFALLS

The incubation time for the invasion assay is usually 24 to 72 h. We feel that shorter incubation times are better as long as a significant number of cells invade the filter. Using longer incubation times, other parameters, such as the growth of the cells on the Matrigel, loss of cell viability, or the detachment of cells from the underside of the filter, must be taken into account. The incubation time can be varied by changing the amount of Matrigel used in coating the filter, usually in the range of 5 to 50 µg (or 10 µg in our case).

The very thin Matrigel coating on the lower surface of the filter should be completely dried before adding the 1:30 Matrigel solution in the upper chamber. This will avoid leaks in the filter.

The overlay of 200 µl of double-distilled H_2O on the Matrigel solution is necessary for an even coating of Matrigel on the filer.

The number of cells applied onto the filter of the Transwell should not exceed the number that will yield 100% confluency on the filter. Usually the cells are 50–80% confluent on the filter after settling.

The cell suspension volume in the upper chamber should be 200 µl instead of 100 µl to reduce the meniscus effect that can cause uneven settling of the cells onto the Matrigel layer. Thus the volume of the lower chamber should be increased to 800 µl (from the usual 600 µl).

The treatment with 10% FBS medium after harvesting the cells by trypsinization is necessary for the quantitative recovery of the cells.

Several other methods can be used to count the invading cells. For example, cells can contain fluorogenic substrates (Garrido *et al*., 1995), radioisotopes (Garrido *et al*., 1995; Muir *et al*., 1993), or dyes (Imamura *et al*., 1994). These labels are suitable when dealing with a large number of samples; however, visual cell counting is still necessary for optimizing the methods or for checking reproducibility of the methods. When the number of invading cells is large enough (>1000), the cells can be counted using a Coulter counter after collecting the invading cells by trypsinization of the filter.

Transwells are normally reusable four or five times or until their polycarbonate filters become cracked.

References

Albini, A., Iwamoto, Y., Kleinman, H. K., Martin, C. R., Aaronson, S. A., Kozlowski, J. M., and McEwan, R. N. (1987). A rapid *in vitro* assay for quantitating the invasive potential of tumor cells. *Cancer Res*. **47**, 3239–3245.

Garrido, T., Riese, H. H., Quesada, A. R., Barbacid, M. M., and Aracil, M. (1995). Quantitative assay for cell invasion using the fluorogenic substrate 2′. 7′-bis(2-carboxyethyl)-5(and-6)-carboxyfluorescein acetoxymethylester. *Anal. Biochem*. **235**, 234–236.

Hendrix, M. J. C., Seftor, E. A., Seftor, R. E. B., and Fidler, L. J. (1987). A simple quantitative assay for studying the invasive potential of high and low human metastatic variants. *Cancer Lett*. **38**, 137–147.

Imamura, H., Takao, S., and Aikou, T. (1994). A modified invasion 3-(4,5-dimethylthiazole-2-yl)-2,5-diphenyltetrazolium bromide assay for quantitating tumor cell invasion. *Cancer Res*. **54**, 3620–3624.

Kramer R. H., and Nicolson, C. L. (1979). Interactions of tumor cells with vascular endothelial cell monolayers: A model for metastatic invasion. *Proc. Natl. Acad. Sci. USA* **76**, 5704–5708.

Liotta, L A. (1986). Tumor invasion and metastatic-role of extracellular matrix: Rhoads memorial award lecture. *Cancer Res*. **46**, 1–7.

Mareel, M., Dragonetti, C., Travernier J., and Fiers, W. (1988). Tumor-selective cytotoxic effects of murine necrosis factor (TNF) and interferon-gamma in organ culture of BIG melanoma cells and heart tissue. *Int. J. Cancer* **42**, 470–473.

Muir, D., Sukhu, L., Johnson, J., Lahorra, M. A., and Maria, B. L. (1993). Quantitative methods for scoring cell migration and invasion in filter-based assays. *Anal. Biochem*. **215**, 104–199.

Nabeshirna, K., Kataoka, H., Koita, H., Murayama, T., and Koono, M. (1988). A new long-term *in vitro* invasion assay using fibrous connective tissue matrices maintaining architectural characteristics of connective tissue. *Invas. Metast*. **8**, 301–316.

Nicolson, G. L. (1989). Metastatic tumor cell interactions with endothelium, basement membrane and tissue. *Curr. Opin. Cell Biol*. **1**, 1009–1019.

Nicolson, G. L., Dulski, K., Basson, C., and Welch, D. R. (1985). Preferential organ attachment and invasion *in vitro* by B16 melanoma cells selected for differing metastatic colonization and invasive properties. *Invas. Metast*. **5**, 144–158.

Repesh, L. A. (1989). A new *in vitro* assay for quantitating tumor cell invasion. *Invas. Metast*. **9**, 192–208.

Schor, S. L., Allen, T. D., and Harrison, C. J. (1980). Cell migration through three-dimensional gels of native collagen fibres: Collagenolytic activity is not required for the migration of two permanent cell lines. *J. Cell Sci*. **46**, 171–186.

Simon, N., Nöel, A., and Foidart, J.-M. (1992). Evaluation of *in vitro* reconstituted basement membrane assay to assess the invasiveness of tumor cells. *Invas. Metast*. **12**, 156–167.

Waller, C. A., Braun, M., and Schirrrnacher, V. (1986). Quantitative analysis of cancer invasion *in vitro*: Comparison of two new assays and of tumour sublines with different metastatic capacity. *Clin. Exp. Metast*. **4**, 73–89.

Yagel, S., Khokha, R., Denhardt, D. T., Kerbel, R. S., Parhar, R. S., and Lala, P. K. (1989). Mechanisms of cellular invasiveness: A comparison of amnion invasion *in vitro* and metastatic behavior *in vivo*. *JNCI* **81**, 768–775.

CHAPTER

44

Endothelial Cell Invasion Assay

Noona Ambartsumian, Claus R. L. Christensen, and Eugene Lukanidin

I. INTRODUCTION

Angiogenesis is defined as the sprouting of new capillaries from preexisting blood vessels (Folkman and Shing, 1992). The formation of new blood vessels occurs in a variety of normal and pathologic conditions. During embryogenesis or wound healing, neovascularization is the result of a balance of stimulatory and inhibitory angiogenic factors. Normally this balance is strictly controlled. However, during the development of many diseases, including inflammation, retinopathies, and cancer metastasis, the angiogenesis controlling mechanisms may fail and result in formation of a pathologic capillary network (Folkman, 1992).

During vascular assembly, endothelial cells respond to a variety of extracellular growth factors and different molecules involved in cell–cell and cell–matrix interactions (Gale and Yancopoulos, 1999). Signaling molecules, more commonly associated with neuronal development, also play an important role in capillary formation during angiogenesis (Wang *et al.*, 1998; Soker *et al.*, 1998).

The angiogenic response is considered to be composed of a series of sequential steps, including degradation of the **basement membrane** surrounding the endothelial cells, migration of the endothelial cells into the surrounding tissues, proliferation and differentiation of the endothelial cells, and finally formation of new **capillary vessels** (Folkman, 1986). Most of these distinctive steps of the angiogenic process can be mimicked *in vitro*. *In vitro* assays classically rely on the use of two sources of endothelial cells: large vessel endothelial cells, such as bovine aortic endothelial cells (BAEC), or human umbilical vein endothelial cells (HUVEC) (Zetter, 1988; Springhorn *et al.*, 1995), and endothelial cells of microvascular origin (Kråling *et al.*, 1994; Lamszus *et al.*, 1999). *In vitro* assays are quantifiable and may specifically address each step of the angiogenic cascade such as basement membrane disruption (metalloproteinase assays), cell migration (*in vitro* wounding; phagokinetic track assay; modified Boyden chamber chemotaxis assay), proliferation (thymidine incorporation assay), and tube formation by endothelial cells in three-dimensional gels, such as collagen or **Matrigel**. Matrigel is a tumor basement membrane matrix extract enriched with laminin. During angiogenesis, the proliferating and migrating endothelial cells are eventually organized into newly formed capillary structures. **Endothelial cells** of all origins are able to form tube-like structures *in vitro* when growing in appropriate extracellular matrix components. Matrigel considerably enhances tube formation (Grant *et al.*, 1985; Madri *et al.*, 1988).

There are several aspects of cell culture assays involving endothelial cells that need to be taken into account for the accurate interpretation of the obtained results. Prolonged cultivation of endothelial cells may change their properties dramatically, including alterations in activation state, karyotype, expression of cell surface antigens, and growth properties. Another problem is that all endothelial cells are not alike. Microvascular endothelial cells differ in different organs or even are different within blood vessels of the same organ (Gumkowski *et al.*, 1991). Different endothelial cells produce different factors (cytokines, growth factors, and their inhibitors) that make the assay system even more complex for evaluation. From that point of view, organ culture assay systems including aortic ring assay (Nicosia and Ottinett, 1990) and chick aortic arch assay (Muthukkaruppan *et al.*, 2000) are even more complex. In these assays, entire aortic segments, including nonendothelial cells, are placed in

Copyright 2006, Elsevier Science (USA).
All rights reserved.

Matrigel. In 1–2 weeks the segments are monitored for the outgrowth of endothelial cells and for the formation of three-dimensional tube-like structures. The main drawback of this system is using adult aorta endothelial cells in the case of the aortic ring assay or microvascular endothelial cells obtained from embryonic arch, which are composed of cells dividing before exposure to angiogenic factors. Nevertheless the ability of endothelial cells to form tube-like structures in Matrigel makes this *in vitro* cell culture model the most faithful assay system.

This article describes the modification of a tube forming assay in Matrigel in which a dense clump of cultured endothelial cells is formed by cultivation of the cells in a hanging drop of growth media. During incubation, cells form dense "clump" at the bottom of the drop. The sediment of the cells is transferred onto a layer of Matrigel and is covered with a thin layer of Matrigel in which an interconnecting network of endothelial capillary tubes is formed rapidly. Tube formation occurs through an ordered sequence of events. Endothelial cells localized on the surface of the "cellular island" first develop large, dynamic cellular protrusions and then form small aggregates and cord-like structures. These early cord structures are dense and do not have lumens. Cells start to migrate to form a complex network of tube-like structures. The advantages of the assay are the ability to directly visualize the changes in cell morphology and the ability of endothelial cells to generate tube-like structures. Endothelial cells in the "clump" can survive for more than a few days, leaving adequate time for assessing angiogenic reactions. Introduction of angiogenesis-inducing factors or cells into Matrigel at some distance from the "island" allows one to test **chemotactic** activity. The assay is readily quantifiable but utilizes already mentioned problems characteristic of the *in vitro* angiogenesis assay.

Another advantage is that in this assay, cultivated endothelial cell lines can be used, which can give more standard results than the use of primary cultures, or organ cultures.

II. MATERIALS AND INSTRUMENTATION

Growth medium: Dulbecco's modified Eagle's medium (DMEM) with a high concentration of glucose (Cat. No. 31966-021,GIBCO) supplemented with fetal bovine serum (FBS, Cat. No. F 7524, Sigma) at 10%, 100× penicillin/streptomycinx (Cat. No. 15140-148, GIBCO).

PBS(-) Ca^{2+} and Mg^{2+}-free Dulbecco's phosphate-buffered saline (PBS, 2.7 m*M* KH_2PO_4, 8.1 m*M* Na_2HPO_4, 137 m*M* NaCl), sterile.

Trypsin–EDTA solution (Cat. No. 25200-056, GIBCO)

HEPES buffer solution 1 *M* (Cat. No. 15630-049, GIBCO)

Stock of Matrigel – basement membrane matrix (BD Biosciences, Cat. No. 354234). Matrigel is supplied frozen and is stored at –70°C.

25-cm^2 tissue culture flasks, 48-well tissue culture plates, Pasteur pipettes, 10-ml pipettes (sterile), and syringe needles (23 gauge).

III. PROCEDURES

1. For culture in 75-cm^2 flasks, suspend murine microvascular endothelial SVEC4-10 cells in culture medium at a concentration of 2×10^5 cells/ml and plate out 2–4 ml of cell suspension/flask. Place the flasks in a 37°C tissue culture incubator and incubate in an atmosphere of 5% CO_2 overnight.

2. The next day, examine cells under an inverted microscope fitted with phase-contrast objectives. Choose the flasks with the cell density >80% of confluence.

3. Remove media and wash the cells with 10 ml PBS(–).

4. Replace the PBS with 1 ml of trypsin–EDTA and incubate at 37°C for approximately 1 min. Cell rounding should be observed in the inverted microscope. When the cells are rounded, detach them by strong agitation. Add 10 ml of culture medium supplemented with 10% FBS to the flask, pipette the cells up and down five times, and transfer contents to a 15-ml centrifuge tube.

5. Centrifuge the cells at 800 *g* for 5 min at room temperature. Resuspend the cells in 10 ml DMEM/FBS. Count an aliquot of the cell suspension with the Coulter counter or in a hemocytometer.

6. Centrifuge the cells at 800 *g* for 5 min at room temperature.

7. Resuspend the cells in DMEM supplemented with 20% FBS, 1 *M* HEPES, pH 7.5, at a concentration of 3×10^6 cells/ml.

8. Dispense 1.0 ml of DMEM/FBS into each well of a 48-well tissue culture plate.

9. Turn the lid of the plate upside down. Plate out 0.02 ml of the cell suspension in the middle of the inner side of the lid. The cell suspension should form a drop (Fig. 1A).

10. Carefully turn over the lid and place it on the plate. The drops of the cell suspension will hang over the media in the wells (Fig. 1B).

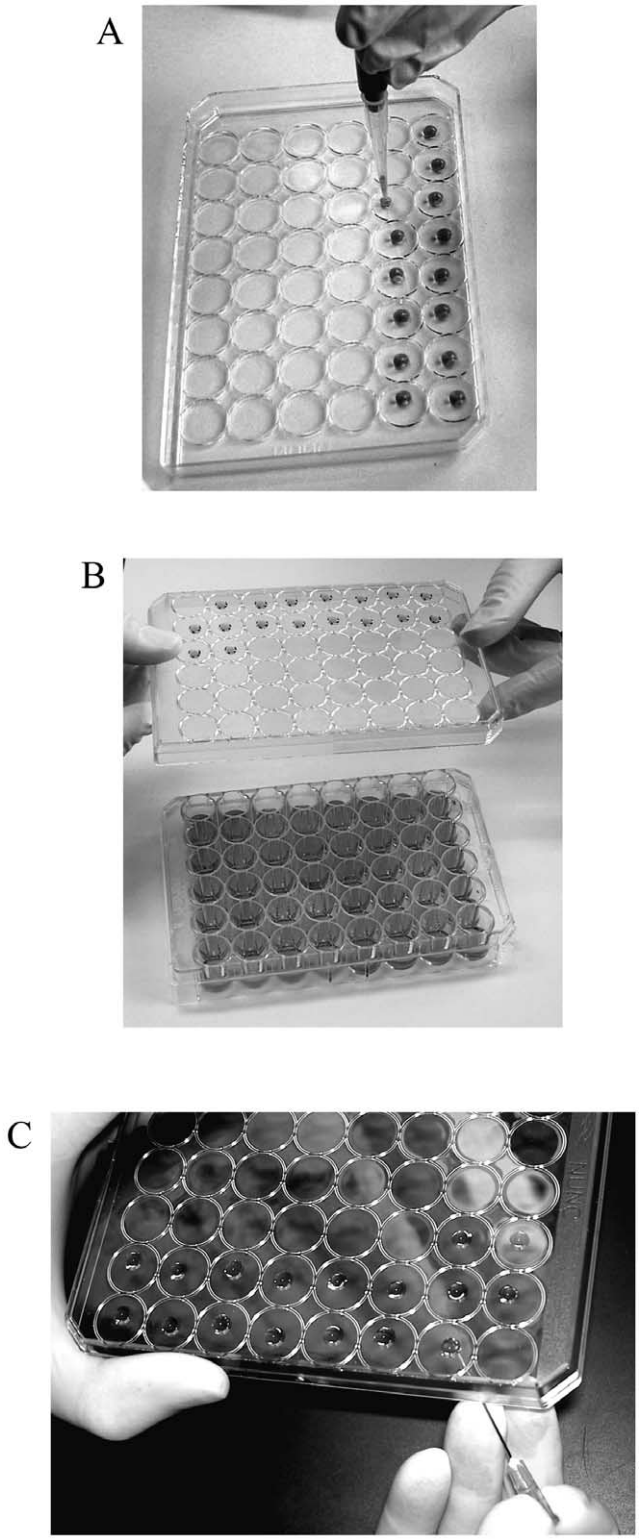

FIGURE 1 Culturing cells in the hanging drops. (A) Plating of the cell suspension in the middle of the inner side of the lid. (B) Turning over the lid with the hanging drops. (C) Transferring the cell "clump" with a syringe needle.

11. Incubate plates at 37°C in a tissue culture incubator. During overnight incubation, cells form a dense "clump" at the bottom of the drop.
12. Defreeze the necessary amount of Matrigel overnight at 4°C with rotation.
13. The next day, examine all the wells under a stereomicroscope and select those that have the most compact, well-formed "clump" of cells.
14. Place Matrigel on ice. Add 5 × DMEM and FBS to obtain a final concentration of 1× DMEM and 10% FBS. Keep the mixture on ice.
15. Place a fresh 48-well plate on ice. Dispense 0.15 ml/well of Matrigel/mix into the plate. Incubate the plate at 37°C in an incubator for 3–4 hours. The Matrigel should solidify.
16. Carefully lift the lid of the plate with hanging drops, stick the cell "clump" to the tip of a syringe needle, and transfer the "clump" on the surface of the solidified Matrigel in the 48-well tissue culture plate (Fig. 1C).
17. Cover the cell "clump" with 0.01 ml of Matrigel/mix and incubate the plate for 15 min at 37°C in an incubator.
18. Add 0.3 ml of DMEM/FBS in each well and return the plate to the incubator. The cells will remain viable for several days.

IV. COMMENTS

Using the protocol described in this assay, it is possible to demonstrate the effects of compounds on the ability of endothelial cell to form capillary-like tubes *in vitro*. We have also used this protocol to cocultivate endothelial cells with other cell types and to study the influence of the molecules produced by these cells on the ability of endothelial cells to form capillaries (Fig. 2D).

V. PITFALLS

1. To obtain maximum viability of cells growing in the hanging drops, avoid long exposure of the cells to trypsin during harvesting cells from the 75-cm^2 flasks.
2. Choose only well-formed, round-shaped, dense cellular "clumps."
3. When lifting the lid with the hanging drops, caution must be exercised to avoid disrupting the cell "clumps."

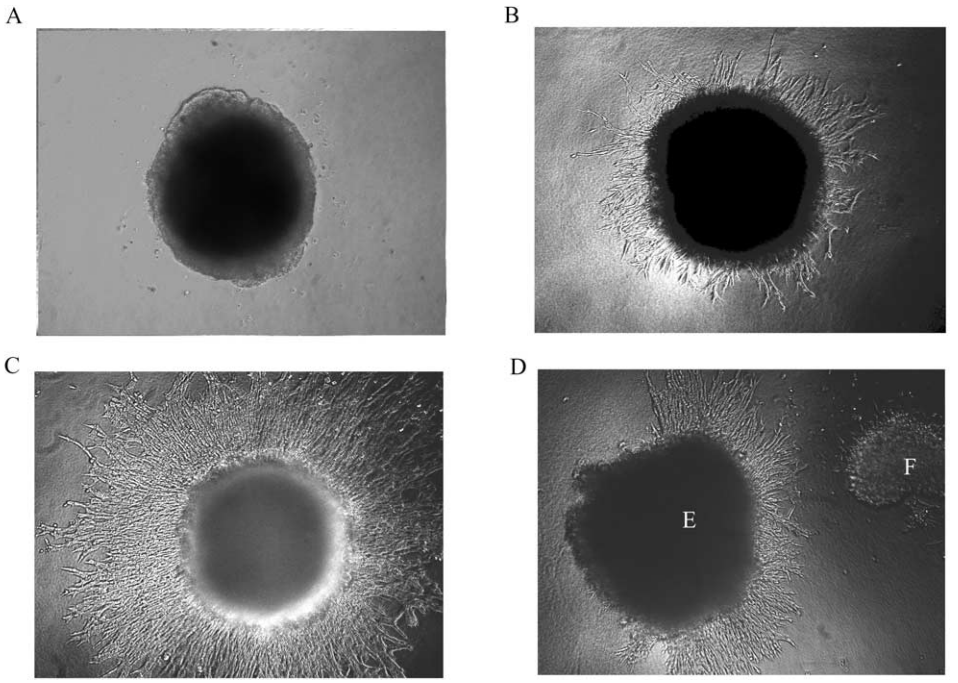

FIGURE 2 Mouse endothelial cells SVEC4-10 migrating from a dense "clump" of the cells into Matrigel containing an angiogenic compound: (A) 0 h of cultivation, (B) 24 h, (C) 48 h, and (D) chemotactic activity of an angiogenic compound. E, endothelial cells; F, tumor cells.

References

Folkman, J. (1986). How is blood vessel growth regulated in normal and neoplastic tissue? G.H.A. Clowes memorial award lecture. *Cancer Res.* **46**, 467–473.

Folkman, J. (1992). The role of angiogenesis in tumor growth. *Semin. Cancer Biol.* **3**, 65–71.

Folkman, J., and Shing (1992). Angiogenesis. *J.Biol.Chem.* **267**, 10931–1093.

Gale, N., and Yancopoulos, G. D. (1999). Growth factors acting via endothelial cell-specific receptor tyrosine kinases: VEGFs, angiopoietins and ephrins in vascular development. *Genes Dev.* **13**, 1055–1066.

Grant, D. S., Kleinman, H. K., Leblong, C. P., Inoue, S., Chung, A. E., and Martin, G. R. (1985). The basement-membrane-like matrix of the mouse EHS tumor. II. Immunochemical quantitation of six of its components. *Am.J.Anat.* **174**, 387–398.

Gumkowski, F., Kaminska, G., Kaminski, M., Morrissey, L. M., and Auerbach R. (1991). Heterogeneity of mouse vascular endothelium: *In vitro* studies of lymphatic, large blood vessels and microvascular endothelial cells. *Blood Vessels* **24**, 11–23.

Kråling, B. M., Jimenez, S. A., Sorger, T., and Maul, G. G. (1994). Isolation and characterization of microvascular endothelial cells from the adult human dermis and from skin biopsies of patients with systemic sclerosis. *Lab. Invest.* **71**, 745–754.

Lamszus, K., Schmidt, N. O., Ergun, S., and Westphal, M. (1999). Isolation and culture of human neuromicrovascular endothelial cells for the study of angiogenesis in vitro. *J. Nerosci. Res.* **55**, 370–381

Madri, J. A., Pratt, B. M., and Tucker, A. M. (1988). Phenotipic modulation of endothelial cells by transforming growth factor-β depends upon the composition and organization of the extracellular matrix. *J. Cell Biol.* **106**, 1375–1384.

Muthukkaruppan, V. R., Shinners, B. L., Lewis, R., Park, S-J., Baechler, B. J., and Auerbach, R. (2000). The chick embryo aortic arch assay: A new, rapid, quantifiable in vitro method for testing the efficacy of angiogenic and anti-angiogenic factors in a three-dimensional, serum-free organ culture system. *Proc. Am. Assoc. Cancer Res.* **41**, 65.

Nicosia, R. F., and Ottinett, A. (1990). Growth of microvessels in serum-free matrix culture of rat aorta. A quantitative assay of angiogenesis in vitro. *Lab Invest.* **63**, 115–122.

Soker, S., Takashima, S., Miao, H. Q., Neufeld, G., and Klagsbrun, M. (1998). Neuropilin1 is expressed by endothelial and tumor cells as an isoform-specific receptor for vascular endothelial growth factor. *Cell* **92**, 735–745.

Springhorn, J. P., Madri, J. A., and Squinto, S. P. (1995). Human capillary endothelial cells from abdominal wall adipose tissue: Isolation using an anti-PECAM antibody. *In Vitro Cell Dev. Biol* **31**, 473–481.

Wang, H. U., Chen, Z. F., and Anderson, D. J. (1998). Molecular distinction and angiogenic interaction between embryonic arteries and viens revealed by ephrin B2 and its receptor EphB4. *Cell* **93**, 741–753.

Zetter, B. R. (1988). Endothelial heterogeneity: Influence of vessel size, organ localization, and species specificity on the properties of cultured endothelial cells. *In "Endothelial Cells"* (U.S. Ryan, ed.), vol. 2, pp. 63–79. V. 2. CRC, Boca Raton, FL.

CHAPTER

45

Analysis of Tumor Cell Invasion in Organotypic Brain Slices Using Confocal Laser-Scanning Microscopy

Takanori Ohnishi and Hironobu Harada

I. INTRODUCTION

Organotypic cultures of nervous tissue, including those of the hippocampal and cortical regions, have been produced successfully with a simple method in which brain slices are maintained in a culture at the interface between air and culture medium (Yamamoto *et al*., 1989, 1992; Stoppini *et al*., 1991; Tanaka *et al*., 1994). In these organotypic brain slice cultures, not only is the normal cytoarchitecture such as cortical lamination and pyramidal cells preserved, but the biochemical and electrophysiological properties of neuronal cells are also maintained for 2 or 3 months. By modifying this organotypic culture of nervous tissues, we established a model for glial tumor cell invasion with conditions analogous to those of normal brains *in situ* (Ohnishi *et al*., 1998; Matsumura *et al*., 2000). This model enables not only to quantitatively analyze the tumor cell invasion in brain tissues, but also to investigate molecular events *in vitro* (events actually occur between transplanted cells and brains *in vivo*).

II. MATERIALS

Hanks' balanced salt solution (HBSS) (Cat. No. H9269), Eagle's minimum essential medium (MEM) with HEPES (Cat. No. M7278), D-glucose (Cat. No. G7021), penicillin–streptomycin solution (Cat. No. P0781), amphotericin B (Cat. No. A2942), propidium iodide (PI) (Cat. No. P4170), L-glutamine (Cat. No. G5763), *N*-methyl-D-aspartate (NMDA) (Cat. No. M3262), and agar (Cat. No. A5431) are from Sigma. Dulbecco's phosphate-buffered saline, calcium-magnesium free [PBS(-), pH 7.4] (Cat. No. 14190-250), horse serum (Cat. No. 16050-122), and fetal bovine serum (FBS) (Cat. No. 16000-044) are from Invitrogen Corp. Culture plate inserts with a 0.4-μm-pore membrane, 30 mm (Millicell-CM) (Cat. No. PICM 030 50) are from Millipore Corp. Six-well culture plates (Cat. No. 3506), 60-mm culture dishes (Cat. No. 430166), and 100-mm culture dishes (Cat. No. 430167) are from Corning. The PKH2 fluorescent cell staining kit is from ZYNAXIS Cell Science. C6 rat glioma cells and T98G human glioma cells are from American Type Culture Collection. For these cell cultures, Ham's F10 powder (Cat. No. N6635) and MEM (Cat. No. M4655) are from Sigma.

III. PROCEDURES

A. Preparation of Brain Slice and the Oraganotypic Culture

This procedure is modified from the method of Stoppini *et al*. (1991).

Solutions and Instruments

Scissors (large one for decapitation and small one for dissection of brains)
Microforceps with fine chips
10% povidone–iodine solution

Copyright 2006, Elsevier Science (USA).
All rights reserved.

Phoshate-buffered saline without calcium and magnesium (pH 7.4)
Microslicer with a sliding cut mode (possible to cut nonfrozen fresh brains with a range of 50 to 1000 μm thick)
Culture plate inserts with 0.4 μm-pore membranes (30 mm in diameter) (Millicell-CM)
Six-well culture plates (35 mm in diameter/well)
60-mm culture dishes
CO_2 incubator
Culture medium: 50% Eagle's MEM (Earle salt with L-glutamine, 25 μ*M* HEPES, and NaHCO3), 25% HBSS, 25% heat-inactivated horse serum, 6.5 mg/ml D-glucose, 100 U/ml penicillin, 100 μg/ml streptomycin, and 2.5 μg/ml amphotericin B. To make 200 ml, add 96 ml of a Eagle's MEM solution, 50 ml of HBSS, 50 ml of horse serum, 1.3 g of D-glucose, 2 ml of a penicillin (10,000 U/ml)–streptomycin (10 mg/ml) solution, and 2 ml of an amphotericin B solution (250 μ/ml). Keep at 4°C.

Steps

1. Anesthetize a 2-day-old neonatal rat with diethyl ether and plunge into a 10% povidone–iodine solution.
2. Cut off the head with large scissors, remove the skin and the skull with a small scissors, and take out the whole brain quickly and place in a 60-mm culture dish with HBSS.
3. Cut the brain vertically to the base, 1 mm inward from both rostral and caudal ends of the cerebrum with a blade, and mount on the stage of a microslicer, which is sterilized with 70% ethyl alcohol.
4. 300-μm-thick cut brain slices and transfer each slice onto a porous (0.4 μm pore size) membrane of a culture plate insert, which is placed in a well of a six-well culture plate filled with PBS.
5. After aspiration of PBS from the outer well of the six-well culture plate, add 1 ml of culture medium to the outer well but without covering the brain slice placed on the membrane.
6. Incubate the brain slice at 37°C under standard conditions of 100% humidity, 95% air, and 5% CO_2.
7. After 3 days of the culture, replace half of the medium with fresh medium twice a week. Reduce the volume of the medium after the second change to 0.8 ml so that the slices remain well exposed to the air. (This is critical for long-term survival of the neuronal cells.) (Fig. 1).

B. Assessment of Viability of Brain Slices

The viability of cultured brain slices can be assessed by morphological observation, neuronal activity, electrophysiological features, and production of bioactive substances such as γ-aminobutyric acid and neuropeptides. Normal cytoarchitecture such as cortical lamination and hippocampal structure is clearly

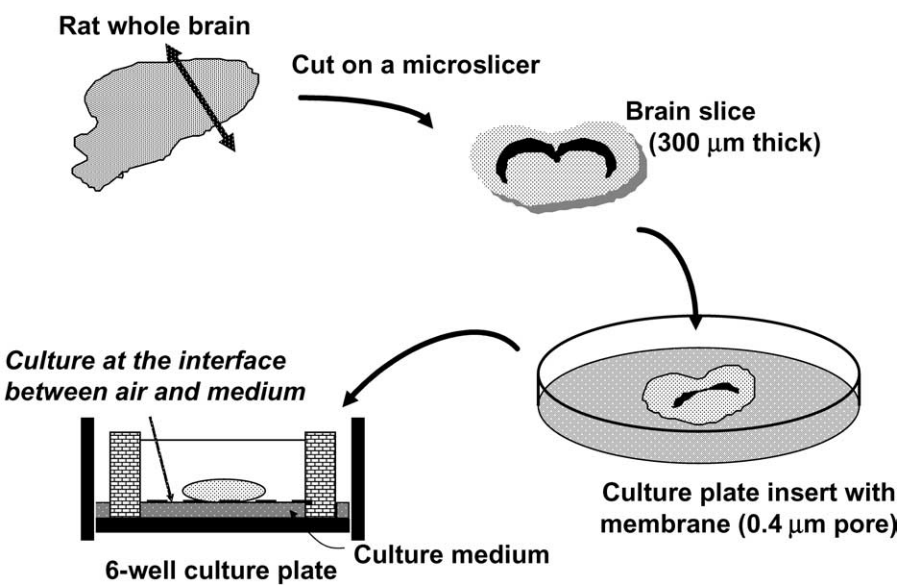

FIGURE 1 Illustrative procedures of brain slice culture. A rat whole brain slice 300 μm thick is placed on a porous membrane affixed to the culture plate insert and cultured at the interface between air and culture medium.

observed for about 2 months after the slice culture if the culture condition is kept properly (Fig. 2). This section describes the method used to assess the neuronal viability of brain slices by NMDA insult that can induce early and delayed neuronal cell death (Sakaguchi *et al*., 1996).

Solutions and Instruments

100 µM N-methyl-D-aspartate solution: Dissolve 1.47 mg of NMDA in 100 ml of artificial cerebrospinal fluid (CSF). Prepare artificial CSF from three stock solutions, A, B, and C, before use. Stock solution A consists of 18.12 g of NaCl, 0.488 g of $NaH_2PO_4 \cdot 2H_2O$, 0.932 g of KCl, and 1.232 g of $MgSO_4 \cdot 7H_2O$ in 100 ml of H_2O. Stock solution B contains 2.22 g of $CaCl_2$ in 100 ml of H_2O, and stock solution C contains 4.62 g of $NaHCO_3$ in 100 ml of H_2O. Store at 4°C. To make 100 ml of artificial CSF, add 4 ml of stock solution A, 4 ml of stock solution C, and 91 ml of H_2O and then place the mixed solution under the current of 95% air and 5% CO_2 to lower the pH of the solution. Then, add 1 ml of solution B and 0.18 g of D-glucose to the mixed solution (the final pH is 7.4).

4.6 µg/ml propidium iodide solution. Dissolve PI in a serum-free solution containing 75% MEM, 25% HBSS, 2 m*M* L-glutamine, and 6.5 mg/ml D-glucose to a final concentration of 4.6 µg/ml.

Fluorescence microscope with a tetramethylrhodamine isothiocyanate (TRITC) filter

Steps

1. Incubate brain slices in 1 ml of the artificial CSF solution containing 100 µ*M* NMDA, which is placed in the bathing well of a six-well culture plate for 15 min. Incubate the slices in PI solution for 1 h to measure early neuronal death or for 24 h to measure delayed neuronal cell death.
2. View PI signals under a fluorescence microscope with a TRITC filter.
3. As a control, incubate brain slices in PI solution for 1 h or 24 h following incubation in the CSF solution without NMDA for 15 min. (Fig. 3).

C. Preparation of Tumor Cell Spheroids

Tumor Cells, Solutions, and Instruments

Tumor cells in culture and their culture medium (Ham's F10 medium containing 10% FBS is used for C6 rat glioma cells, and MEM supplemented with 1% nonessential amino acid, 1% sodium pyruvate, and 10% FBS is used for T98G human glioma cells)
PKH2 fluorescent cell-staining kit
1.25% agar-coated culture dish (100 mm in diameter)
Place 5 ml of 1.25% agar solution on a culture dish and dry under air.
Reciprocating shaker (usable in a CO_2 incubator)
CO_2 incubator

Steps

1. Grow tumor cells as a monolayer culture under standard conditions.
2. Harvest the tumor cells by trypsinization, wash twice, and resuspend in labeling diluent "A" (provided with the PKH2 staining kit) at a concentration of 2 x 10^7 cells/ml (cell/diluent suspension).

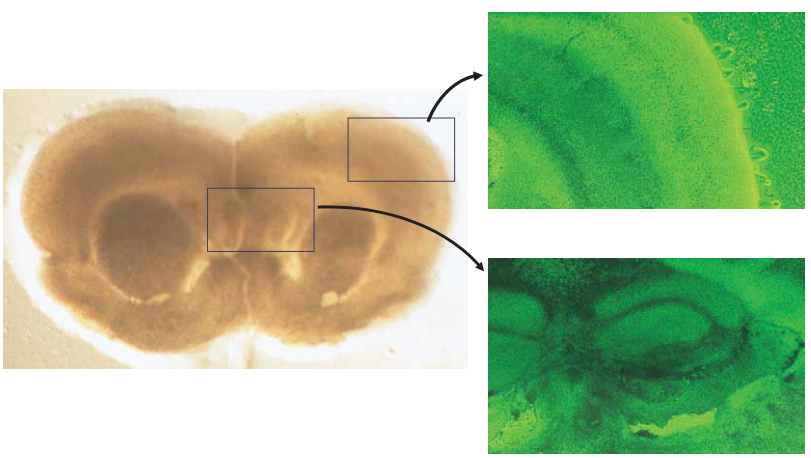

FIGURE 2 Morphological pictures of a rat brain slice after 8 days of culture. Normal cytoarchitecture, including cortical lamination and hippocampal structure, is clearly observed (left: macroscopic picture, ×0.5; right: phase contrast, ×40).

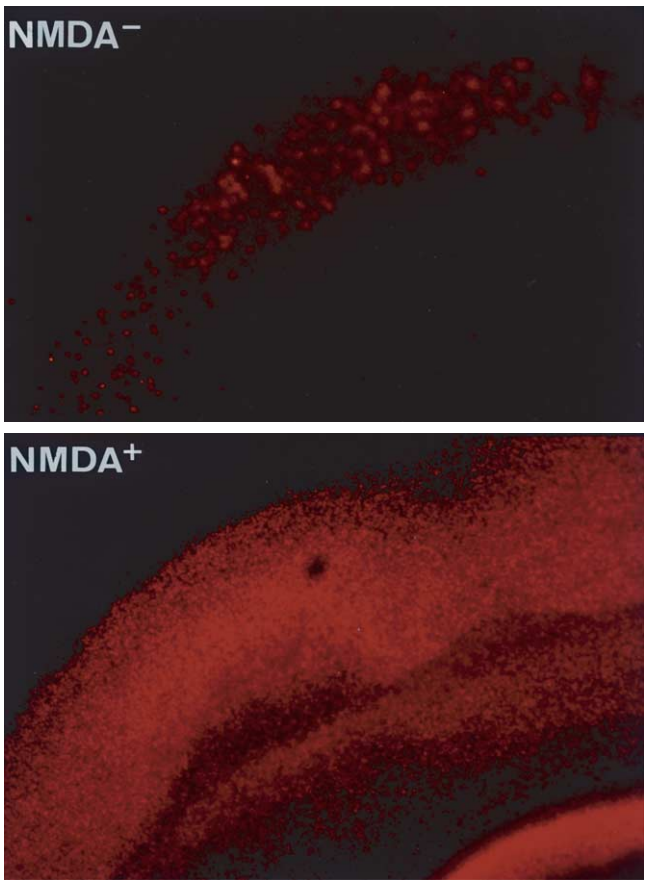

FIGURE 3 Neuronal viability of rat brain slices assessed by cellular uptake of propidium iodide (PI) without (upper) and with (lower) treatment of *N*-methyl-D-aspartate (NMDA). Normally functioned neurons can exclude PI and show early or delayed neuronal cell death by NMDA insult, thus permitting entry of the PI into the cells.

3. Add PKH2 dye to an equal volume of diluent "A" to make a 4 µ*M* solution. Add this solution to the cell/diluent suspension and mix by gentle agitation.

4. After incubating the cells at room temperature for 5 min, stop the labeling reaction by adding a double volume of the culture medium containing 10% FBS and four times the volume of FBS into the sample tubes.

5. Wash the cells and resuspend in the culture medium with 10% FBS.

6. Seed the labeled tumor cells (5×10^6) into a 1.25% agar-coated culture dish and incubate under continuous agitation at a speed of 40 rpm on a reciprocating shaker at 37°C in a humidified atmosphere of 5% CO_2 and 95% air for 2 to 3 days.

7. For the experiments, select cell aggregates with a size of 150 to 200 µm.

D. Migration Assay of Tumor Cells on Brain Slices (Fig. 4)

Instuments and Molecules

Barin slices after 7 days culture
Tumor cell spheroids
Micropipette with a volume of 10 µm
Molecules or agents affecting cell migration
Fluorescence microscope with a FITC filter
Color-chilled 3-CCD camera
Personal computer

Steps

1. Using a micropipette, take one spheroid of tumor cells place on the surface of brain slice, and coculture at 37°C under standard conditions.

2. Four hours later, apply 2 µl of molecules in investigation directly to the tumor spheroid. Carry out the application of the molecule once a day for 3 to 6 days.

3. To estimate the extent of cell migration, calculate the distance between the margin of the initially placed spheroids and the population of the migrating cells showing half of the density (area) of the maximum density of migrating cells from the tumor spheroid by using computer images for which the original fluorescent pictures of the slices are taken with a color-chilled 3-CCD camera.

4. For this calculation, draw concentric circles 10 µm apart around the margin of the spheroid and measure cell density (area of fluorescence-stained cells) within each ring by an NIH image. Then, do the summation of area of the cells contained in each ring and plot as a function of the distance from the margin of the tumor spheroid. Thus the distribution curve of migrating cells outside the spheroid is constructed for each brain slice (Fig. 5). The migratory strength of the cells on the slice is defined as the distance (µm) that shows half of the value of the maximum density (area) of migrating cells on the distribution curve.

E. Invasion Assay in Brain Slices (Fig. 4)

Instruments

Barin slices after 7 days culture
Tumor cell spheroids
Micropipette with a volume of 10µm
Inverted confocal laser-scanning microscope with FITC filter optics
Personal computer

Steps

1. With a micropipette, take one spheroid of tumor cells tagged with the PKH2-fluoresent dye, place on

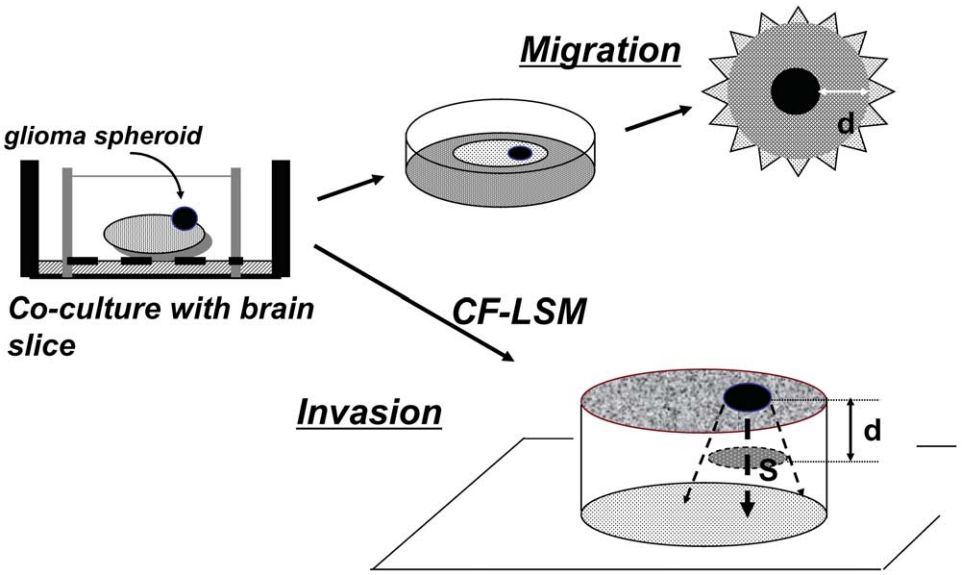

FIGURE 4 Illustrative procedures of tumor cell migration and invasion assay in cocultured brain slices. A tumor (glioma) spheroid is placed on the brain slice and is cocultured at the interface between air and culture medium. For tumor cell migration, the extent of the spread of fluorescent dye-stained tumor cells on the surface of the slice is measured. For tumor cell invasion, the spatial extent of the tumor cell infiltration in the slice is analyzed by confocal laser-scanning microscopy (CF-LSM). d, distance; S, area.

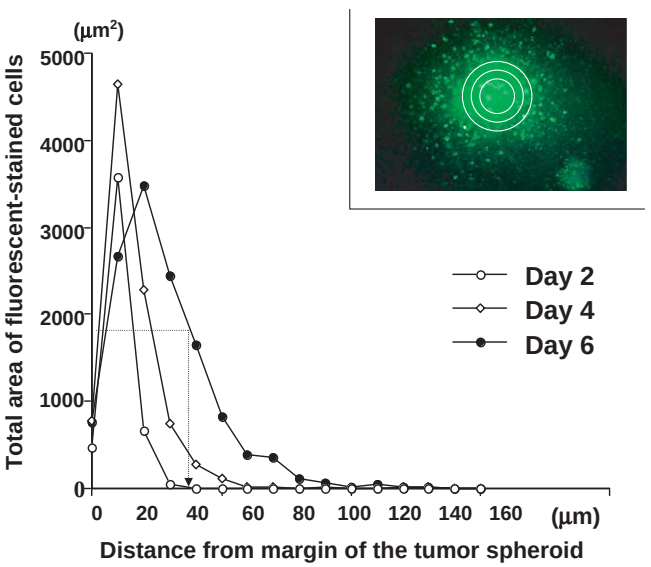

FIGURE 5 Construction of distribution curves of migrating cells for a quantitative analysis of tumor cell migration in brain slices. The total area of the labeled cells contained in each ring is plotted as a function of the distance from the margin of the tumor spheroid. (Inset) Concentric circles 10 μm apart are drawn around the margin of the tumor spheroid, and cell density (area of fluorescent-stained cells) within each ring is measured by an NIH image. Distribution curves represent L1-stimulated C6 glioma migration at day 2, day 4, and day 6 after the coculture with brain slices. The migratory strength of the cells is determined as the distance (μm) that shows half of the value of the maximum density (area) of migrating cells on the distribution curve (see the distribution curve on day 6).

the surface of brain slice, and coculture at 37°C under standard conditions.

2. To detect PKH2-stained tumor cells in brain slices, use an inverted confocal laser-scanning microscope with FITC (520 nm) filter optics.

3. At the first observation, determine the level of the basal plane (0 μm) in accordance with the upper surface of the brain slice.

4. Obtain serial sections every 20 μm downward from the basal plane to the bottom of the slice (Fig. 6).

F. Quantitative Analysis of Tumor Invasion

The total area of PKH2-stained cells in each section is calculated with NIH image software. The area is plotted as a function of the distance from the basal plane of the brain slice and the distribution curve is constructed for each experiment. The extent of tumor cell invasion in the slice is defined as the depth (μm) that shows half of the maximum density (area) of invasive cells on the distribution curve.

IV. COMMENTS

1. As a source of brain slices, brain tissues from mice and humans (obtained from epilepsy surgery) are also applicable. In the case of rats, 2- to 5-day-old

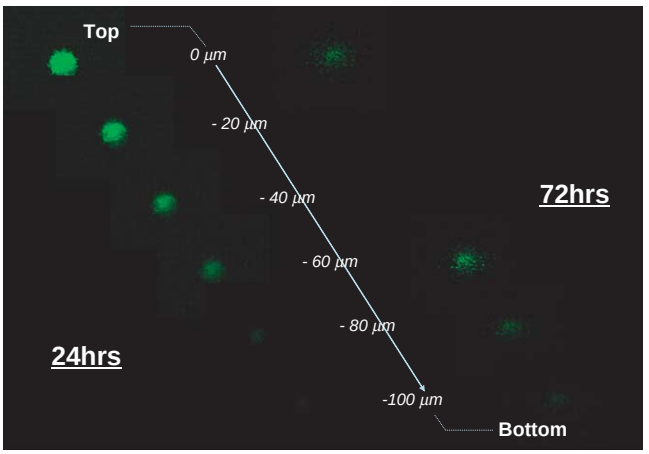

FIGURE 6 Confocal laser-scanning microscopic pictures of invading glioma cells in rat brain slices. At 24 h after coculture of T98G glioma spheroid and the brain slice, most glioma cells remain at the top of the slice (0 μm), while the glioma cells migrate extensively within the brain slice (show the maximum spread at –40 μm from the top of the slice) at 72 h after coculture.

neonatal brains are best. As brains from much younger rats are smaller and more soft, it is difficult to manuplate the whole brain as intact slices. Brains prepared from rats of an older age have a tendency to be resistant to tumor invasion into the slices.

2. For about 4–5 days after initiating the brain slice culture, several neuronal death and glial cell migration to the bottom of the slices occur. After 5 days in culture, the exposure of slices to PI alone without NMDA insult does not elicit a detectable fluorescence signal. Therefore, for tumor invasion experiments, brain slices after 5 days in culture should be used. Usually, brain slices after 7 days in culture are used for any kind of studies. At this time, the thickness of the brain slices is reduced to about 200 μm from the original thickness of 300 μm. Brain slices maintain their normal structures, such as cortical lamination, and are functionally viable for about 2 months after the culture, but it seems that the best time for experiments is from 7 to 30 days after culture.

3. To detect migrating tumor cells in the brain slice, a tumor-labeling method using green fluorescent protein (GFP) is also applicable. Once tumor cell clones with persistent expression of GFP are established, their use is of great advantage in analyzing the behavior of the tumor cells because the GFP is transmitted to the tumor cells after cell division. An EGFP vector (pEGFP-C1, obtained from Clonetics Corp., San Diego, CA) can be used to transfect and label malignant glioma cells.

References

Matsumura, H., Ohnishi, T., Kanemura, Y., Maruno, M., and Yoshimine, T. (2000). Quantitative analysis of glioma cell invasion by confocal laser scanning microscopy in a novel brain slice model. *Biochem. Biophys. Res. Commun*. **269**, 513–520.

Ohnishi, T., Matsumura, H., Izumoto, S., Hiraga, S., and Hayakawa, T. (1998). A novel model of glioma cell invasion using organotypic brain slice culture. *Cancer Res*. **58**, 2935–2940.

Sakaguchi, T., Okada, M., Kuno M., and Kawasaki, K. (1996). Dual mode of N-methyl-D-aspartate-induced neuronal death in hippocampal slice cultures in relation to N-methyl-D-aspartate receptor properties. *Neuroscience* **76**, 411–423.

Stoppini, L., Buchs, P.-A., and Muller, D. (1991). A simple method for organotypic cultures of nervous tissue. *J. Neurosci. Methods* **37**, 173–327.

Tanaka, M., Tomita, A., Yoshida, S., Yano, M., and Shimuzu, H. (1994). Observation of the highly organized development of granule cells in rat cerebellar organotypic cultures. *Brain Res*. **641**, 319–327.

Yamamoto, N., Kurotani, T., and Toyama, K. (1989). Neural connections between the lateral geniculate nucleus and visual cortex *in vitro*. *Science* **245**, 192–194.

Yamamoto, N., Yamada, K., Kurotani, T., and Toyama, K. (1992). Laminar specificity of extrinsic cortical connections studied in coculture preparations. *Neuron* **9**, 217–228.

CHAPTER

46

Angiogenesis Assays

Yihai Cao

I. INTRODUCTION

All healthy and pathological tissue growth requires the formation of functional blood vessels (Hanahan and Folkman, 1996). Angiogenesis, sprouting of new capillaries from the existing vessels, is the key process that contributes to both physiological and pathological neovascularization. Angiogenesis has paradoxical implications in the treatment of the most severe human diseases. In disorders such as atherosclerosis/infarction of the heart, stroke, and peripheral occlusive limb disease, the growth of new vessels in the affected tissue is obviously beneficial for the improvement of blood circulation (Cao *et al.*, 2003). In addition, organ transplantation and tissue regeneration need new blood vessels. However, inhibition of angiogenesis has become an important therapeutic approach for the treatment of diseases such as cancer, diabetic retinopathy, and arthritis in which angiogenesis plays an important role (Cao, 2001; Folkman, 1995). It has been reported that therapeutic angiogenesis or antiangiogenesis could delay the onset and progression of obesity (Rupnick *et al.*, 2002). Based on their broad therapeutic implications and potential economic values, discovery and development of novel angiogenic and antiangiogenic agents have become a competitive business for pharmaceutical companies. As a result, a novel angiogenesis regulator is identified almost every week. There are at present many assay systems to be used for testing the angiogenic or antiangiogenic activity of compounds (Jain *et al.*, 1997; Kenyon *et al.*, 1996). The process of angiogenesis includes several critical steps: endothelial cell morphological changes, endothelial migration, endothelial proliferation, endothelial cell reorganization, and lumen formation, formation of new branches, followed by reconstitution of the basement membrane and vascular remodeling. Each of these steps can be monitored using appropriate *in vitro* and *in vivo* assay systems. This article describes *in vivo* and *in vitro* assays that are reliable, reproducible, and convenient and that are important for the characterization of compounds for use in angiogenesis–related disorders. Migration assays are described elsewhere in this volume, while this article includes the capillary endothelial cell proliferation assay and functional vessel formation assays, including the shell-less *in vivo* chick chorioallantoic membrane (CAM) assay and the mouse corneal angiogenesis assay.

II. MATERIALS AND INSTRUMENTS

A. Endothelial Proliferation Assay

Primary bovine capillary endothelial (BCE) cells are from Dr. Judah Folkman's laboratory at the Children's Hospital, Boston. All tissue culture plastic bottles and discs are from Falcon, Becton Dickinson. DME (low glucose) medium is from JRH Biosciences Limited (Cat. No. 2D0113). Gelatin is from Difco (Becton Dickinson, Cat. No. 214340). Recombinant human fibroblast growth factor (FGF-2) is from Scios Nova (Mountain View, CA). Bovine calf serum (BCS) is from Boule Nordic AB (Cat. No. SH300072.03). Trypsin solution (0.05%) is from Sigma (Cat. No. T9906). The Isoton phosphate-buffered saline (PBS) solution is from KEBO (Stockholm, Sweden). The Coulter counter is by Coulter, KEBO, Sweden.

B. Chick Chorioallantoic Membrane Assay

Fertilized white leghorn eggs are from OVA Production, Sörgåden, Sweden. Epigallocatechin-3-gallate

Copyright 2006, Elsevier Science (USA).
All rights reserved.

is from Sigma (Cat. No. E4143). Methylcellulose is from Sigma (Cat. No.M-0262). Tissue culture plates (100 × 20 mm) are from Falcon, Becton Dickinson. The chick embryo incubator is made in Germany. The stereomicroscope is from Nikon, Japan.

C. Mouse Corneal Angiogenesis Assay

C57Bl6/J male and female mice are from the Microbiology and Tumor Biology Center, Karolinska Institute, Stockholm, Sweden. Vascular endothelial growth factor (VEGF) is from R&D System Inc. (Cat. No. 293-VE-050). FGF-2 is from Scios Nova. Sulcralfate is from Bukh Meditec, Vaerlose, Denmark. Hydron (type NCC) is from Interferon Sciences, Inc. (New Brunswick, NJ) (Cat. No. NCC-97001). Nylon mesh (15 × 15 mm) is from Tetko (Lancaster, NY). Methoxyflurane and proparacaine are from Ophthetic (Alcon, TX). The operation microscope is made by Zeiss, Oberkochen, Germany. Surgical blades are from Bard-Parker No. 15; Becton Dickinson (Franklin Lakes, NY). The eye examination microscope is from Nikon, Sf-2, Tokyo, Japan.

III. PROCEDURES

A. Endothelial Cell Proliferation Assay

For additional information, see Cao *et al*. (1996, 1997, 1999, 2001).

1. Stimulation of Endothelial Cell Proliferation

Steps

1. Set a CO_2 incubator to 10% CO_2.
2. Set up tissue culture hood for at least 15 min before use.
3. Coat 24-well tissue culture plates with 0.5 ml 1.5% gelatin in PBS solution (previously sterilized by autoclaving)/well for at least 1 h at 37°C or overnight at room temperature.
4. Prewarm the following solution to room temperature: 1x PBS, 0.05% trypsin solution, and 10% BCS-DMEM medium.
5. Thaw the FGF-2 solution in ice and dilute with sterile 10% BCS-DMEM to appropriate concentrations.
6. Add FGF-2 to 10% BCS-DMEM to a final concentration of 3 ng/ml.
7. Remove culture medium from BCE cells (cultured in 6-well plates) and wash cells with PBS twice.
8. Add 0.5 ml trypsin solution/well and expose cells to trypsin solution until they detach from the bottom.
9. Once cells are detached, add immediately 5 ml/well of 10% BCS-DMEM to cells.
10. Transfer cell solution into a centrifuge tube and centrifuge cells at 1500 rpm for 5 min.
11. Remove supernatant and resuspend cells in 10 ml 10% BCS-DMEM containing 3 ng/ml FGF-2.
12. Count cell numbers and seed cells at a density of 10,000 cells/well. Make sure that each sample is at least in triplicate.
13. Incubate cells at 37°C and 10% CO_2 for 72 h.
14. After 72 h, remove the culture medium and wash cells twice with PBS.
15. Add 0.5 ml of 0.05% trypsin solution to each well.
16. When cells are detached completely, resuspend cells into a single cell solution by tituration.
17. Transfer cell solution to a Coulter cup containing 10 ml Isoton solution and counter cell numbers.

2. Inhibition of Endothelial Cell Proliferation

1. Repeat steps 1–10 described in Section III,A,1.
2. Resuspend cells in 5% BCS-DMEM in an appropriate volume.
3. Seed BCE cells at a density of 10,000 cells/well in a volume of 0.5 ml of 5% BCS-DMEM.
4. Add tested angiogenesis inhibitors (e.g., angiostatin or EGCG) at various concentrations and incubate the cells for 1 h at 37°C with 10% CO_2.
5. Add FGF-2 to a final concentration of 1 ng/ml and incubate the cells for 72 h.
6. Repeat steps 14–17 described in Section III,A,1.

B. Chick Chorioallantoic Membrane Assay

For additional information, see Cao *et al*. (1998, 1999, 2001).

Steps

1. All procedures should be carried out in a 37°C warm room equipped with a sterile ventilation hood and a humidifier.
2. Set up the chick incubator at 37°C with 75% humidity.
3. Place freshly fertilized eggs onto the selves of the incubator and incubate the eggs for 72 h.
4. Switch on the humidifier to make sure that the room air has a similar humidity as that in the egg incubator.
5. Prewarm plastic tissue dishes (100 × 20 mm) at 37°C.

6. In the sterile hood, hold the egg in one hand and gently make a small crack using a metal or a glass stick. Open the egg using both thumbs placed on each side of the crack and gently place the contents into a prewarmed tissue culture dish. It is important that the yolk sac remains intact.
7. Immediately place the dish into a tissue culture incubator supplied with 3 or 4% CO_2 and 75% humidity at 37°C.
8. Incubate the embryos for 48 h in case of testing inhibitors of angiogenesis. Use 6 days for testing angiogenesis stimulators.
9. During the incubation, prepare 0.9% methylcellulose in H_2O as autoclaved sterile solution and tested angiogenic or antiangiogenic compounds at appropriate concentrations (e.g., 2 mg/ml) with H_2O.
10. Place a piece of nylon mesh onto a glass beaker in a sterile ventilation hood.
11. Mix 10 µl of 0.9% methylcellulose with 10 µl of tested compounds and carefully transfer the mixture onto the nylon mesh (the drop will hang on the mesh).
12. When the drop has dried out, carefully cut out the area as a square (about 3 × 3 mm).
13. For antiangiogenesis, after a 48-h incubation carefully place the nylon mesh containing the test compounds onto the newly formed chorioallantoic membrane.
14. Return the chick embryos to the incubator and incubate the embryos for 1–2 days.
15. Detect the antiangiogenic effect of the tested compound under a stereomicroscope.
16. For a typical potent angiogenesis inhibitor, the formation of avascular zones around the implant can be detected readily after 24–48 h of implantation.
17. Testing of angiogenesis stimulators takes place after 6 days of incubation. Carefully place the nylon mesh on the almost fully developed chorioallantoic membrane, preferably at a site with sparse vessel formation.
18. Return the chick embryos to the incubator and incubate the embryos for 3–5 days. For a typical potent angiogenic factor, the formation of new microvessel sprouts and branches can now be detected (see Fig. 1).

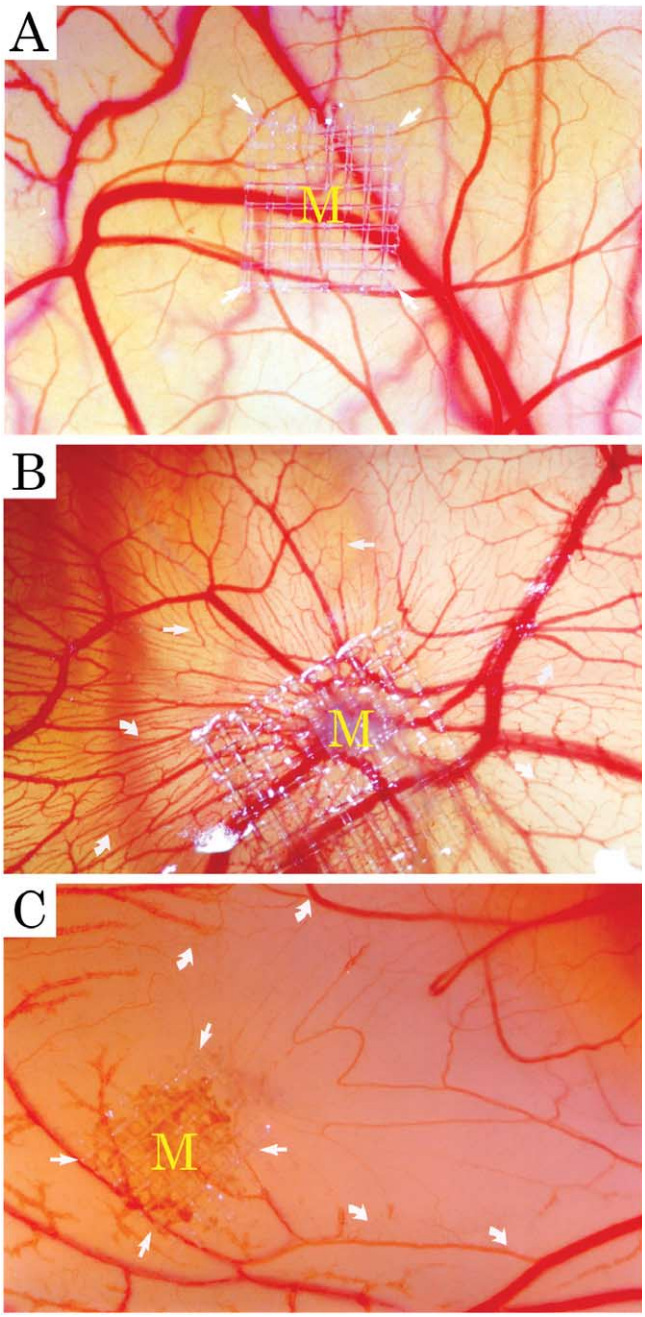

FIGURE 1 (A) Normal chick chorioallantoic membrane after 8-day incubation. (B) A typical example of the CAM stimulated by FGF-2. New vessel sprouting stimulated by 2.5 µg of FGF-2 after a 5-day implantation (arrows). (C) A typical example of inhibition of CAM angiogenesis by 50 µg of epigallocatechin-3-gallate. Formation of avascular zones is marked by arrows.

C. Mouse Corneal Angiogenesis Assay

For additional information, see Cao *et al.* (2003), Kenyon *et al.* (1996); and Cao and Cao (1999).

1. Stimulation of Angiogenesis

Steps

1. Order male or female mice at the age of between 6 and 9 weeks. For routine angiogenesis analysis, the C57Bl/6 strain is commonly used.
2. Suspensions of sterile H_2O containing the appropriate amount of angiogenic factors such as FGF-2 or VEGF and 10 mg of sucralfate.
3. Vacuum the mixture solution for 5 min in a speed centrifuge.
4. Add 10 µl of 12% hydron in ethanol.
5. Deposit the suspension onto a nylon mesh (pore size 0.4 × 0.4 mm) and embed between the fibers (the total grid area: 15 × 15 mm).
6. Cover both sides with a thin layer of hydron and allow the materials to dry at room temperature.
7. When the immobilized angiogenic factors are dried on the mesh, pull apart the grid fibers and uniformed pellets (0.4 × 0.4) are released.
8. Choose equal sized pellets; each pellet contains equal amounts of angiogenic factors.
9. Anesthetize mice with methoxyflurane and anesthetize topically with 0.5% proparacaine.
10. Proptose the eye globes with a jeweler's forceps.
11. Under an ophthalmological operation microscope, perform a central intrastromal linear keratotomy with a surgical blade.
12. Using a modified von Graefe knife (2 × 3 mm), dissect a lamellar micropocket toward the temporal limbus.
13. The micropocket is usually extended to 1.0–1.2 mm of the temporal limbus.
14. Place a single pellet on the corneal surface at the base of the pocket with jeweler's forceps.
15. Using one arm of the forceps, push the pellet to the end of the pocket.
16. Apply erythromycin ointment immediately to the operated eyes.
17. Examine the implanted eyes routinely under a slit lamp biomicroscope between days 4 and 7 after pellet implantation.
18. Anesthetize mice with methoxyflurane and position the eyes properly.
19. Measure the maximal vessel length of neovascularization zone from the limbal vascular plexus toward the pellet with a linear reticule through the microscope (equipped with the microscope).
20. Measure the contiguous circumferential zone of neovascularization as clock hours (if the eye is visualized as a clock).

2. Inhibition of Angiogenesis

Steps

1. Repeat steps 1–16 described in Section III,C,1.
2. Systemically inject potential angiogenesis inhibitors into mice with angiogenic factor-implanted eyes. The injection routes include intravenous, intraperitoneal, subcutaneous, and intramuscular injections. The injected volume usually should not exceed 0.1 ml/10 g mouse.
3. The duration and frequency of treatment are dependent on the potency and the half-lives of tested angiogenesis inhibitors.
4. In a control group of mice, inject the relevant buffer that is used to suspend the angiogenesis inhibitors.
5. The examination of corneal neovascularization is described in steps 17–20 in Section III,C,1 (see Fig. 2).

IV. COMMENTS

Endothelial cell division is an essential process for the growth of new blood vessels. Therefore, the endothelial cell proliferation assay is the most relevant and reliable assay system used to detect endothelial cell growth. As new blood vessels usually bud from microvessels, endothelial cells isolated from capillaries are most optimal for endothelial cell growth assay. This article described a method that employs BCE cells as primary endothelial cells for the *in vitro* proliferation assay. Among *in vivo* angiogenesis models, the mouse corneal angiogenesis model is the most rigorous and clear system to detect angiogenic responses. As the corneal organ is naturally avascular, corneal neovascularization indicates that all blood vessels are newly formed vessels. In contrast to the CAM assay, corneal angiogenesis is devoid of preexisting blood vessels. Thus, this system is convenient for studying new blood vessel formation, new blood vessel stability, and structures of newly formed vessels. For example, a recent study of blood vessel stability in the cornea has found that not all angiogenic factors can stabilize the newly formed vasculature (Cao *et al.*, 2003). As most transgenic or knockout animal models are performed in mice, the mouse corneal model is very valuable in detecting the impact of overproduction or loss of a particular gene on new blood vessel formation. With exceptional skills, the corneal angiogenic responses in knockout mice can be detected in newborns (Zhou *et al.*, 2000). Although the CAM assay is not an ideal quantitative angiogenesis assay, this assay is a fast screening system that allows the determination of angiogenic or antiangiogenic responses within

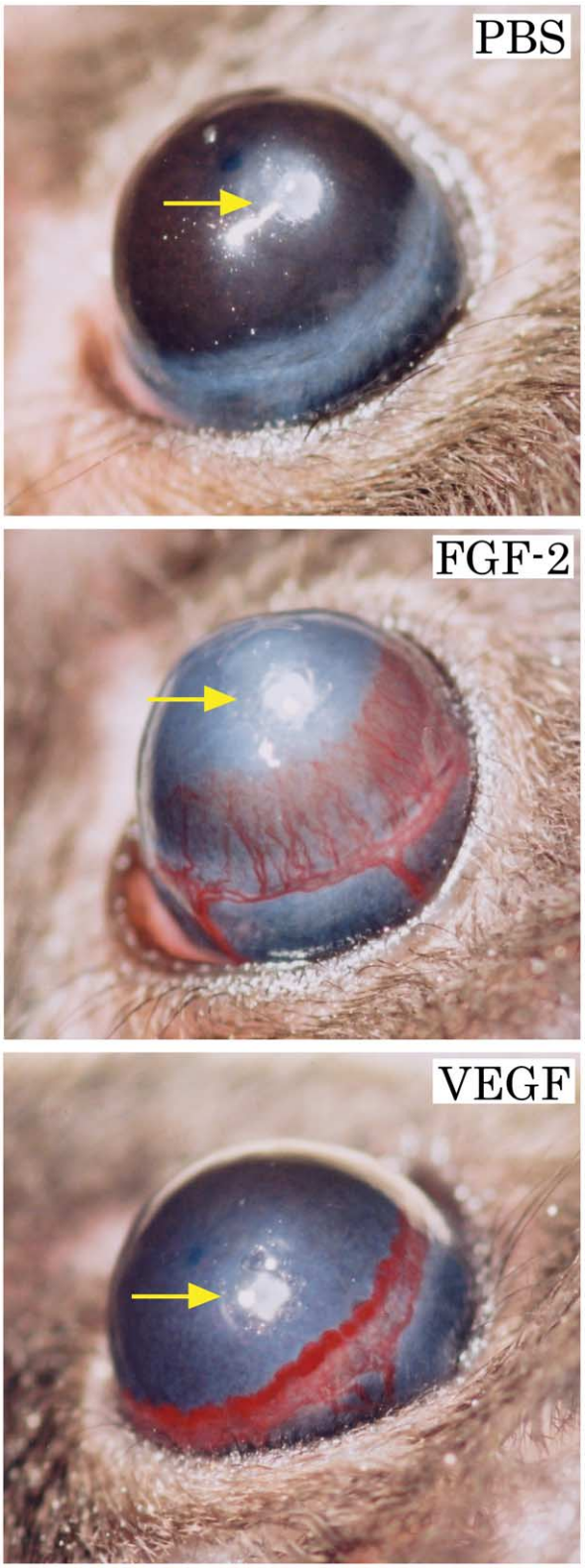

FIGURE 2 Typical examples of FGF-2- and VEGF-induced corneal neovascularization on day 5 after implantation. (Top). PBS buffer and sucralfalte polymer alone without angiogenic factors. (Center) FGF-2 at a 80-ng dose induces intense neovascularization originating from the limbal vessels toward the implanted pellet. (Bottom) VEGF at a 160-ng dose induces a robust neovascularization response.

a relatively short time. In addition, the CAM assay requires less sophisticated equipment and less cost.

V. PITFALLS

A. Endothelial Cell Proliferation Assay

1. The success of *in vitro* endothelial cell proliferation assay is entirely dependent on the number of population doublings (PDLs) of the BCE cells. In principle, low PDLs of BCE cells will increase successful rates. Primary BCE cells will stop their responses to angiogenic stimuli around the age of 40 PDLs. Ultimately, these cells enter into a senescent state at the average of 45 PDLs. Therefore, it is important to avoid using presenescent BCE cells in endothelial cell proliferation assay.

2. Primary endothelial cells isolated from different tissues or organs may react to different mitogens. Indeed, a tissue-specific endothelial growth factor has been identified (LeCouter *et al.*, 2001). Thus, it is important to determine the stimulatory/inhibitory activity of a compound using primary endothelial cells isolated from different tissues.

3. Not all angiogenic factors are able to induce endothelial cell proliferation or migration due to the diverse biological functions of various angiogenic factors. For example, FGF-2 is a potent angiogenic factor that preferentially stimulates endothelial cell proliferation but not cell migration. In contrast, VEGF is a potent endothelial chemotactic factor but a poor endothelial mitogen (Yoshida *et al.*, 1996). Thus, the stimulatory effect of an angiogenic factor should be tested in various endothelial cell assays.

4. In endothelial cell inhibition assays, it is critically important that low concentrations of angiogenic factors be used. For example, in the BCE cell assay, usually 1 ng/ml of FGF-2 is used to stimulate cell growth. If higher concentrations of FGF-2 were used, angiogenesis inhibitors would not be able to counteract the stimulatory effect.

B. CAM Assay

1. Make sure that the entire experimentation is performed with optimal temperature and humidity. The chick embryos are extremely vulnerable to pathogen infections. Thus, a strict sterile condition is required, including washing hands and wearing gloves when handing eggs and embryos.

2. Use fresh fertilized eggs, which should not be more than 3 days old, as the survival rate of embryos will be reduced dramatically.

3. Do not shake or crack eggs by hitting them against other solid objects.

4. Avoid cutting the embryonic vessels by the sharp edge of the egg shell.

5. Do not keep embryos with nonintact yolk.

6. Avoid hemorrhages of the CAM during the implantation of meshes.

7. The release half-life of small chemical compounds immobilized on the nylon mesh can be different. Thus, it is important to analyze the results at different time points.

C. Mouse Corneal Assay

1. Do not choose aged mice that usually produce delayed angiogenic responses.
2. Avoid using Balb/C or other white background mice. Their red-color eyes may disturb the quantification of corneal neovascularization.
3. Avoid accommodating many mice, especially male mice, in one case. Their unusual behaviors may interrupt corneal neovascularization.
4. Prepare corneal implants under sterile conditions, as corneal inflammation could cause neovascularization.

References

Cao, R., Brakenhielm, E., Pawliuk, R., Wariaro, D., Post, M. J., Wahlberg, E., Leboulch, P., and Cao, Y. (2003). Angiogenic synergism, vascular stability and improvement of hind-limb ischemia by a combination of PDGF-BB and FGF-2. *Nature Med.* **31**, 31.

Cao, R., Brakenhielm, E., Wahlestedt, C., Thyberg, J., and Cao, Y. (2001). Leptin induces vascular permeability and synergistically stimulates angiogenesis with FGF-2 and VEGF. *Proc. Natl. Acad. Sci. USA* **98**, 6390–6395.

Cao, R., Wu, H. L., Veitonmaki, N., Linden, P., Farnebo, J., Shi, G. Y., and Cao, Y. (1999). Suppression of angiogenesis and tumor growth by the inhibitor K1–5 generated by plasmin-mediated proteolysis. *Proc. Natl. Acad. Sci. USA* **96**, 5728–5733.

Cao, Y. (2001). Endogenous angiogenesis inhibitors and their therapeutic implications. *Int. J. Biochem. Cell. Biol.* **33**, 357–369.

Cao, Y., and Cao, R. (1999). Angiogenesis inhibited by drinking tea. *Nature* **398**, 381.

Cao, Y., Chen, A., An, S. S., Ji, R. W., Davidson, D., and Llinas, M. (1997). Kringle 5 of plasminogen is a novel inhibitor of endothelial cell growth. *J. Biol. Chem.* **272**, 22924–22928.

Cao, Y., Ji, R. W., Davidson, D., Schaller, J., Marti, D., Sohndel, S., McCance, S. G., O'Reilly, M. S., Llinas, M., and Folkman, J. (1996). Kringle domains of human angiostatin. Characterization of the anti-proliferative activity on endothelial cells. *J. Biol. Chem.* **271**, 29461–29467.

Cao, Y., Linden, P., Farnebo, J., Cao, R., Eriksson, A., Kumar, V., Qi, J. H., Claesson-Welsh, L., and Alitalo, K. (1998). Vascular endothelial growth factor C induces angiogenesis *in vivo*. *Proc. Natl. Acad. Sci. USA* **95**, 14389–14394.

Folkman, J. (1995). Angiogenesis in cancer, vascular, rheumatoid and other disease. *Nature Med.* **1**, 27–31.

Hanahan, D., and Folkman, J. (1996). Patterns and emerging mechanisms of the angiogenic switch during tumorigenesis. *Cell* **86**, 353–364.

Jain, R. K., Schlenger, K., Hockel, M., and Yuan, F. (1997). Quantitative angiogenesis assays: progress and problems. *Nature Med.* **3**, 1203–1208.

Kenyon, B. M., Voest, E. E., Chen, C. C., Flynn, E., Folkman, J., and D'Amato, R. J. (1996). A model of angiogenesis in the mouse cornea. *Invest. Ophthalmol. Vis. Sci.* **37**, 1625–1632.

LeCouter, J., Kowalski, J., Foster, J., Hass, P., Zhang, Z., Dillard-Telm, L., Frantz, G., Rangell, L., DeGuzman, L., Keller, G. A., Peale, F., Gurney, A., Hillan, K. J., and Ferrara, N. (2001). Identification of an angiogenic mitogen selective for endocrine gland endothelium. *Nature* **412**, 877–884.

Rupnick, M. A., Panigrahy, D., Zhang, C. Y., Dallabrida, S. M., Lowell, B. B., Langer, R., and Folkman, M. J. (2002). Adipose tissue mass can be regulated through the vasculature. *Proc. Natl. Acad. Sci. USA* **99**, 10730–10735.

Yoshida, A., Anand-Apte, B., and Zetter, B. R. (1996). Differential endothelial migration and proliferation to basic fibroblast growth factor and vascular endothelial growth factor. *Growth Factors* **13**, 57–64.

Zhou, Z., Apte, S. S., Soininen, R., Cao, R., Baaklini, G. Y., Rauser, R. W., Wang, J., Cao, Y., and Tryggvason, K. (2000). Impaired endochondral ossification and angiogenesis in mice deficient in membrane-type matrix metalloproteinase I. *Proc. Natl. Acad. Sci. USA* **97**, 4052–4057.

CHAPTER

47

Three-Dimensional, Quantitative *in vitro* Assays of Wound Healing Behavior

David I. Shreiber and Robert T. Tranquillo

I. INTRODUCTION

Wound healing *in vivo* is a dynamic process involving the coordinated regulation of cell proliferation, cell migration, cell traction, and apoptosis (Clark, 1996). For instance, during dermal wound healing, inflammatory cells are induced to infiltrate a wound site primarily by factors released from platelets. Fibroblasts are stimulated to migrate up a chemotactic gradient of soluble factors, and possibly a haptotactic gradient of matrix-bound factors, released by the inflammatory cells and platelets into a provisional matrix composed primarily of fibrin and fibronectin. These fibroblasts proliferate and secrete collagen and other extracellular matrix molecules to form granulation tissue. The cells often contract this granulation tissue while continuing to secrete collagen. Ultimately, the cells die through apoptosis and leave a dense, collagenous, acellular scar as a reparative patch. The progression of fibroblast behavior is dictated in part by cues from the wound healing environment, such as soluble growth factors, integrin binding to network proteins, and mechanical stress associated with wound contraction. Therefore, it becomes a great challenge to design and implement bioassays that capture quantitatively the key features of wound healing in a controlled, but physiologically relevant manner. This article describes several assays that allow quantitative evaluation of fundamental aspects of cell behavior involved in the wound healing response—cell migration, chemotaxis, cell traction, and cell proliferation—in controlled environments with improved physiological relevance. The relevance of the assays is improved by examining cellular phenomena within three-dimensional (3D) hydrogels of biopolymers involved in wound healing, namely type I collagen and fibrin. Many studies have demonstrated dramatic differences in tissue cell behavior when cultured in a 3D gel rather than on a 2D substrate (Bell *et al.*, 1979; Nusgens *et al.*, 1984).

II. MATERIALS

Trypsin (Product No. T6763), paraformaldehyde (Product No. 158127), ethylenediaminetetraacetic acid (EDTA) (Product No. E26282), $CaCl_2$ (Product No. 21075), NaOH (Product No. 72079), bovine fibrinogen (Product No. 46312), bovine thrombin (Product No. T4265), and agarose (Product No. A2790) are from Sigma Chemical Company (St. Louis, MO). Vitrogen 100 bovine type I collagen (Product No. FXP-019) is from Cohesion Technologies, Inc. (Palo Alto, CA). Tissue culture medium, penicillin/streptomycin (pen-strep; Cat. No. 15070063, fungizone (Cat. No. 15240062), HEPES buffer (Cat. No. 15630080), phosphate-buffered saline (PBS; Cat. No. 10010023), and L-glutamine (Cat. No. 21051024) are from GIBCO Laboratories (Grand Island, NY). Fetal bovine serum (FBS; Product No. SH30073.02) is from HyClone Laboratories (Logan, UT). Polystyrene beads (Product No. 64130) are from Polysciences, Inc. (Warrington, PA). Stock Teflon (Product No. B-ZRT-2), stock polycarbonate (Product No. B-211040), and stock hydrophilic

Copyright 2006, Elsevier Science (USA).
All rights reserved.

porous polyethylene disk (Product No. B-PEH-060/50) are from Small Parts (Miami Lakes, FL).

III. EQUIPMENT

Inverted microscope with computer-controlled stage and on-stage incubation system, biological hood, air or CO_2 incubator.

IV. METHODS

A. Biopolymer Gel Solution Preparations

Type I Collagen Gel (2.0 mg/ml)

Collagen gels are prepared by neutralizing stock type I collagen solution and raising the temperature to facilitate self-assembly of monomeric collagen into fibrils and forming an entangled network of fibrils with interstitial medium (Knapp *et al*., 1997).

Steps

1. To make 1 ml of collagen, add the following reagents to a 15-ml conical tube in order in a biological safety cabinet/laminar flow hood under sterile conditions: 20 µl 1 *M* HEPES buffer, 132 µl 0.1 *N* NaOH, 100 µl 10X MEM, 60 µl FBS, 1 µl pen/strep, 10 µl *L*-glutamine, and 677 µl Vitrogen 100.
2. Mix gently by pipetting.
3. Keep the solution on ice until ready to prepare the assay.

Note: The final solution should be a light pink color/red color indicating neutral pH.

B. Fibrin Gels (3.3 mg/ml)

Fibrin gels are prepared by enzymatically cleaving fibrinogen with thrombin in the presence of Ca^{2+} ions (Knapp *et al*., 1999).

Solutions

1. *Fibrinogen solution* A: Dissolve fibrinogen powder in a 20 m*M* HEPES-buffered saline solution to a concentration of 30 mg/ml. Pass the solution through a 0.20-µm filter. Store in 1-ml aliquots at –80°C.
2. *Thrombin solution* B: Dissolve thrombin (250 units) in 1 ml sterile water and 9 ml of PBS. Pass the solution through a 0.20-µm filter. Store in 100-µl aliquots at –80°C.

Gel Preparation

1. Add 1 aliquot of fibrinogen solution A to 5 ml 20 m*M* HEPES-buffered saline to make a 5-mg/ml fibrinogen solution.
2. In a separate vessel, add one aliquot of thrombin solution B to 1 ml unsupplemented M-199 no serum and 15 µl of 2 *M* $CaCl_2$ solution to make solution C.
3. Prepare cell suspension D in cell culture medium with the cell concentration six time the desired final concentration. Solution D will be diluted 1:6.
4. Keep the solutions separated and on ice until you are ready to prepare the assay.
5. To make the fibrin gel, mix one part of thrombin/Ca^{2+} solution C, one part of cell suspension D, and four parts of fibrinogen solution A. Mix gently by pipetting and fill the assay chamber quickly.

Pitfalls

Frequently, mixing of fibrin and collagen solutions generates many bubbles, which can affect the geometry and rheology of gels and blur microscopy images. To limit bubbles, apply a vacuum to conical tubes holding the solutions (for collagen, degas the solution after mixing but before gelation, for fibrin, degas the fibrinogen solution, thrombin solution, and cell culture medium before mixing) to draw dissolved air out of solution and into the vacuum. Make sure that the solution is not too close to the top of the conical tube (10 ml or less).

Because the fibrin gel can form quickly, add the fibrinogen solution last and pipette the mixed solution into the assay chamber quickly.

Disrupting forming gels can affect structural and rheological properties that are important for cell behavior assays. Take care when handling the gels during and after formation.

C. Cells

The following assays were developed to examine phenomena associated with dermal wound healing and therefore incorporate dermal fibroblasts as the cell of choice. However, the assays can be adapted easily for other cell types (e.g., smooth muscle cells or corneal fibroblasts.) The key is to maintain tight control over cell populations and the cell density used in the assays, as cell behavior can vary widely from passage to passage, and cell density dramatically affects the potential for cell–cell signaling, which, if not accounted for, can cloud results. Cell densities delineated below are recommended but should be optimized according to the cell type and the phenomena to be studied.

V. CHEMOTAXIS ASSAY

Chemotaxis experiments are performed in a conjoined 3D gel system (Knapp *et al.*, 1999; Moghe *et al.*, 1995). Manufacture of chemotaxis chambers and image analysis are involved. The experiments require machining of chemotaxis chambers (see later). The chambers allow the generation of a gradient of a protein/growth factor-sized diffusible species (Fig. 1). Briefly, one-half of the chamber is filled with collagen or fibrin solution and a defined concentration of chemotactic species, and the other, initially separated by a thin divider, is filled with an equal volume of biopolymer solution with a defined density of cells of interest. After removing the divider, a gradient of the species is formed in the gel with cells.

1. Have chemotaxis chambers (at least 6–10) machined according to Fig. 2.
   a. Chambers are designed to fit on top of a standard microscope slide (7.5 × 2.5 cm).
   b. Chambers have a groove at the midline for a thin, Teflon divider.
   c. Thoroughly clean chambers with soapy water and autoclave prior to each use

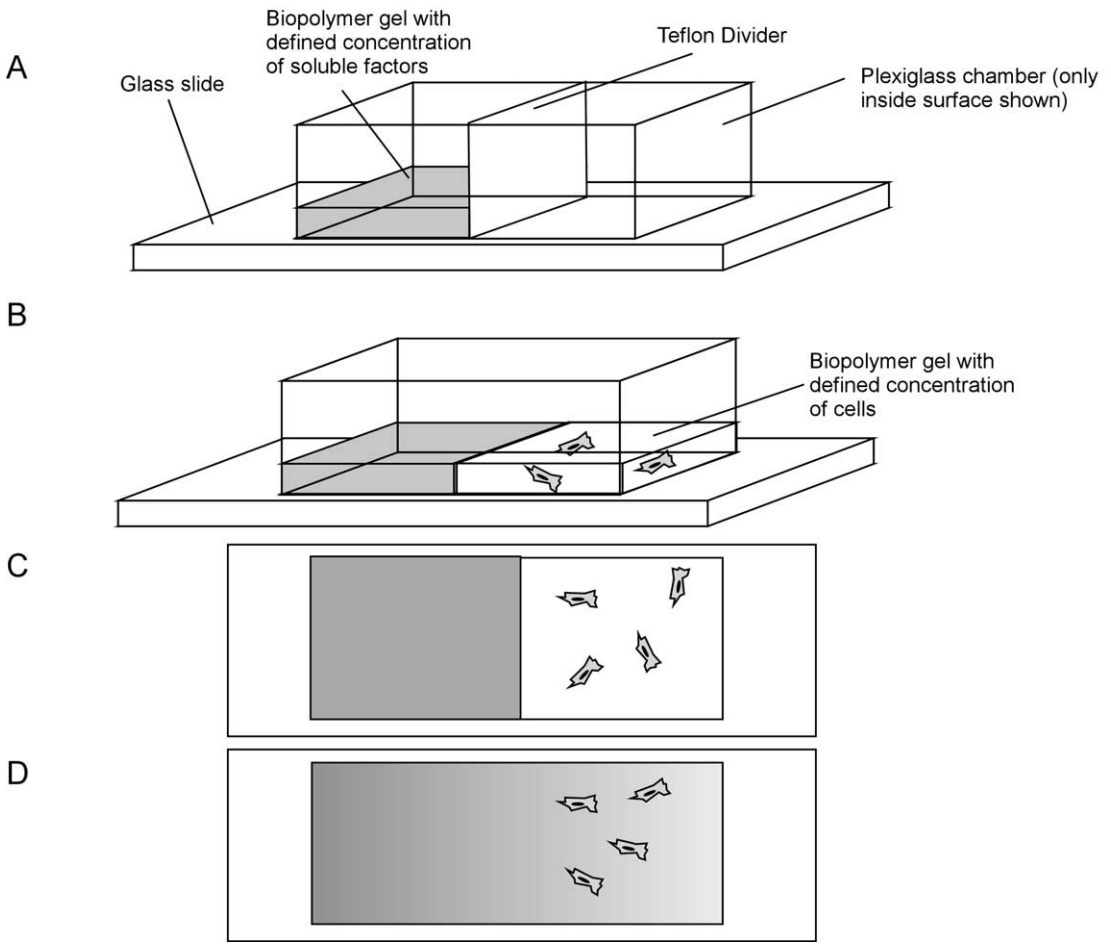

FIGURE 1 Schematic of linear chemotaxis chamber preparation. The chamber consists of a hollow, plexiglass box that is sealed to a standard glass slide with vacuum grease. A Teflon plate divides the chamber into two sections. (A) One side of the chamber is filled with biopolymer gel with a defined concentration of chemotactic factor. For collagen assays, the chamber is placed in the incubator, and the biopolymer solution is allowed to gel. (B) The Teflon divider is removed, and the other half of the chamber is filled with biopolymer solution with a defined cell concentration. The chamber is returned to the incubator to facilitate gelation. (C) Initially, all of the chemotactic factor is in the left half of the chamber, and the cells in the right half are oriented randomly. (D) Over time, the soluble factor diffuses into the right half, and the cells (if responsive to the soluble factor) reorient and migrate in the direction of the gradient.

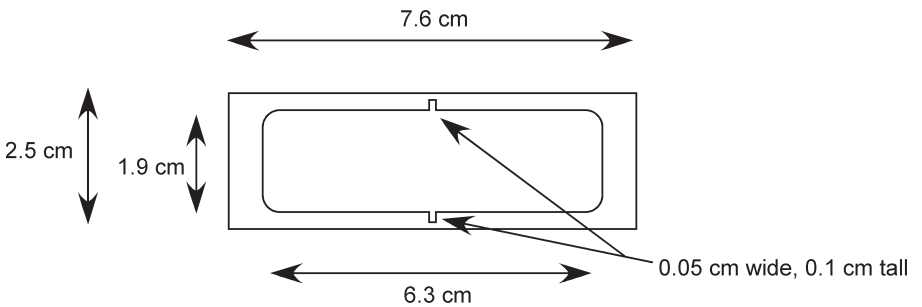

FIGURE 2 Mechanical drawing of linear chemotaxis chamber. The chamber is machined from plexiglass (polycarbonate) and is 1.3 cm high. A Teflon plate (1.2 × 0.05 × 2 cm) is also required to fit into the notched area and divide the chamber in half.

2. Sterilize all chambers and glass slides.
3. Under sterile conditions, secure bottom of chamber to glass slide with vacuum grease.
4. Place Teflon dividers into grooves.
5. Prepare solutions for assay (either fibrin or collagen).
   a. Each chamber requires ~3.5 ml biopolymer solution, which should be divided into two equal volumes of 1.75 ml/chamber.
   b. Add enough chemotactic factor to one of the volumes of the solution to generate the desired final concentration. Generally for growth factors, the working range is 0.1–100 ng/ml. This is now called "solution A."
   c. Add cells to the other half of the solution to a final concentration of 10,000 cells/ml. This is now called "solution B."
6. Add 1.75 ml of solution A to one-half of each chamber. This should fill the half approximately 3 mm.
7. Secure another glass slide to the top of each chamber and place the chambers in a humidified incubator until gelation/self-assembly is complete.
8. After gelation, remove chambers from the incubator and, again under sterile conditions, remove the Teflon divider.
9. Mix solution B by pipetting to ensure uniform distribution of cells and fill the empty half of the chamber with 1.75 ml of solution B.
10. Replace top glass slide, ensuring a good seal, and place back in humidified incubator for 24–36 h
11. At desired time points (typically 12–36 h after gelation), place chamber under microscope and capture images of all cells through the thickness of the gel. This should be done with sufficient objective power (4× or greater) to observe the orientation of cells. This is facilitated greatly using automated microscopy/confocal microscopy with a motorized stage to build a mosaic, but can be done by hand if necessary. With automation, a projection mosaic of the gel containing cells is generated incorporating all planes throughout the thickness of the gel.
12. For each cell, using standard image analysis packages (such as NIH Image), draw a line segment representing the prevailing orientation of the cell (Fig. 3) and calculate and record the angle, θ (from 0° to 90°), the line segment makes with the horizontal axis, which represents the direction of the chemotactic gradient.
13. For each cell, calculate $\sin^2(\theta)$
14. Determine the average value of $\sin^2(\theta)$ for all of the cells in a given chamber. In other words,

$$\Phi = \sum_{i=1}^{n} \frac{\sin^2 \theta_i}{i} \tag{1}$$

where n represents the number of cells (Fig. 3).

In the case of no chemotactic factor, cells should be oriented randomly. Therefore, the average angle should be 45° and $\Phi = 0.5$. For a pure chemotactic response, $\theta = 0°$ and $\Phi = 0$. Generally, values of $\Phi < 0.5$ signify a chemotactic response, but results should be analyzed statistically after measuring the response in multiple chambers.

Helpful Hints and Pitfalls

1. Control experiments should include no chemotactic factor, as well as uniform chemotactic factor (half-loading in both solution A and solution B).
2. If imaging requires a large block of time, gels can be fixed with 2–4% paraformaldehyde to ensure equal exposure times to chemotactic gradients across experiments.
3. To avoid settling of cells to the bottom of the gel due to gravity, prewarm solution B to ~28–30°C prior to filling the second half of the chamber. This is more crucial for experiments with collagen.
4. Alignment of cells in the direction of the gradient may indicate a negative chemotaxis response. If the

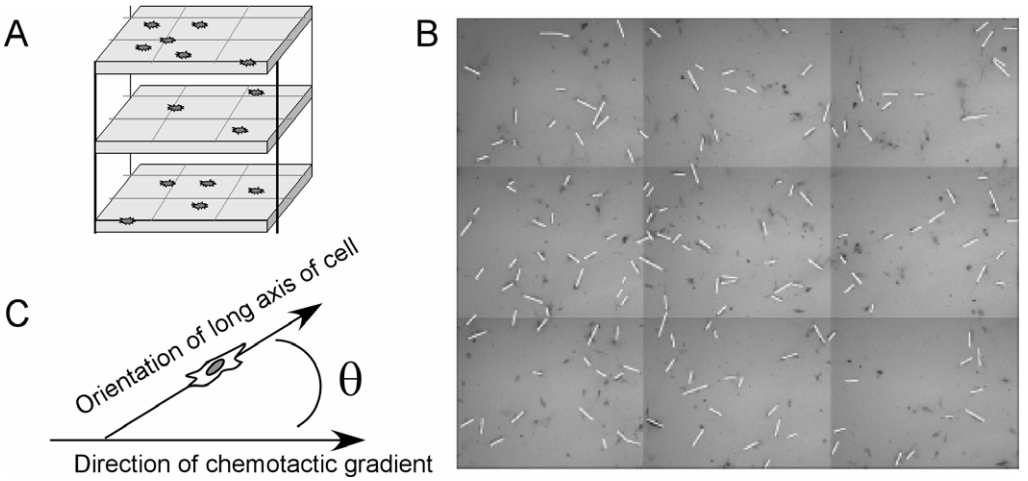

FIGURE 3 Chemotaxis analysis. (A) After a period of time (or at regular intervals, if desired), a composite, mosaic image of the cell-populated half of the chamber is captured and projected into one image. (B) The orientation of each cell is defined by tracing the long axis of the cell with a line. (C) The orientation of each line is compared to the orientation of the gradient via the angle θ. The response of the population is then evaluated using Eq. (1).

polarity of the cells cannot be determined easily, it is necessary to record the migration of the cells to confirm that they migrate toward the source of the factor (positive chemotaxis or chemoattraction) or away from the source (negative chemotaxis or chemorepulsion).

A similar assay can be developed to study chemotaxis toward peptide fragments much smaller than a growth factor (e.g., RGD) (Fig. 4) (Knapp *et al*., 1999). Because these species are much smaller, they diffuse more rapidly and would equilibrate in concentration if the linear chambers described earlier were used. By maintaining a divider between the two halves with a small notch in the divider, diffusion across the two halves is restricted and gradients can be maintained for at least 24 h.

1. Machine chambers identical to those described earlier, but add a small notch to the Teflon divider.
2. When preparing the chamber, include a glass coverslip alongside the Teflon divider.
3. Fill one-half of the chamber with biopolymer solution with a defined concentration of the peptide sequence and allow to gel.
4. Fill the other half with biopolymer solution with defined cell concentration and allow to gel.
5. Remove coverslip, but leave notched Teflon divider in place. This should create radial gradients (see Fig. 4).
6. Transfer to microscope and quantify as described previously, with the exception that the direction of the gradient is now radially outward from the notch.

VI. CELL TRACTION ASSAY

Simple cell traction assays can be performed with either mechanically constrained, stressed gels or unconstrained, unstressed gels in various geometries (Neidert *et al*., 2002; Ehrlich and Rajaratnam, 1990). This section describes the simplest one to implement—cylindrical disks (Neidert *et al*., 2002; Tuan *et al*., 1994). The geometry is a hemisphere initially, but evolves to a cylindrical disk shape as the cell traction proceeds.

1. With a sterile scribe, score a 1-cm-diameter circle in each well of a six-well plate.
2. Prepare collagen or fibrin solution with a final cell concentration between 10,000 and 500,000 cells/ml.
3. Carefully pipette 0.5 ml collagen or fibrin solution into the scored region. The scratch in the culture plate should force the solution to maintain shape.
4. Carefully place the plate in an incubator and allow solution to gel.
5. After gelation, fill each well with 2.5 ml of culture medium with defined concentrations of the desired soluble factors.
6. If the assay is for unstressed gels, with a sterile, flat spatula, gently pry the gels off of the bottom surface so that they are "free floating."
7. Transfer the plate to a microscope and measure the thickness of the gel. When using a microscope equipped with motorized focus, this is done most easily by focusing on the top of the gel, recording the motor position, and then focusing on the bottom of the

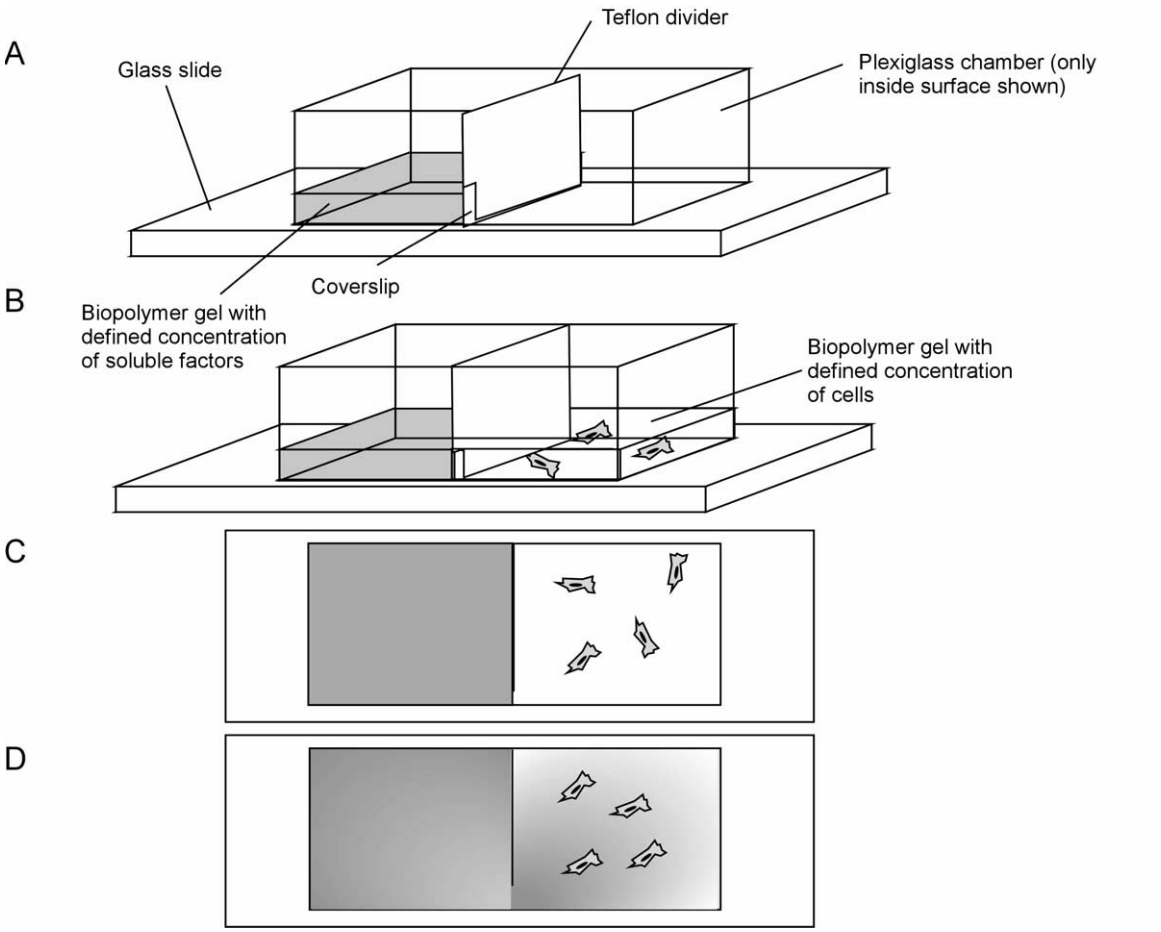

FIGURE 4 Schematic of radial chemotaxis assay for small chemotactic molecules. The assay is similar to the linear chambers, except that the Teflon divider remains in the chamber and has a small notch to restrict diffusion between the two halves. A glass coverslip prevents premature diffusion.

gel and determining the change in motor position, and therefore the thickness. For unstressed gels, also measure the diameter of the gel. (The diameter should remain unchanged for stressed gels.)

8. Return the gels to the incubator.

9. Repeat measurement performed in step 7 at regular intervals of your discretion. Once every 1–2 h is generally sufficient for a short duration (12–24 h experiment. Once every 4–6 h is sufficient for longer duration experiments. Return the samples to the incubator immediately after recording the thickness.

10. After completion, normalize results by the original dimension and plot percentage compaction vs time for the various conditions.

Remarks

1. Gel thickness measurements reflect the gel rheology (and possibly cell proliferation) as much as cell traction. An intrinsic measure of the latter can be obtained by analyzing data using a mechanical model for cell–matrix interactions (Barocas *et al*., 1995; Barocas and Tranquillo, 1997a,b).

2. If only measurements are desired for the constrained case, the sample can be attached to a force transducer (Eastwood *et al*., 1996; Kolodney and Wysolmerski, 1992).

3. Cell alignment that typically results during the contraction of mechanically constrained gels can complicate the interpretation of data (Barocas and Tranquillo, 1997a,b).

VII. CELL MIGRATION

Time-lapse cell migration assays in a 3D matrix can be performed to evaluate cell migration in two or three dimensions (Knapp *et al*., 2000; Shreiber *et al*., 2001,

2003). Both techniques require an automated image analysis system and an XY motorized stage. Motorized focus is advantageous for evaluation in 2D and is required for 3D.

Generally, it is advised to perform each experimental condition in triplicate. For instance, if the assay was to determine the effects of PDGF-BB on fibroblast migration and the experiment called for testing cells in the presence of 0, 10, 20, and 50 ng/ml, then 12 wells would be needed.

The migration assay can be performed in practically any assay chamber. It is written here for a 96-well plate arrangement.

In these assays, data are recorded to fit to the persistent random walk model of cell migration (Dunn and Brown, 1987). This model implies that cell migration is purely random over long periods of time, but can have persistent direction over short period of times. To assess cell migration, there are three parameters, two of which are independent: persistence time, P; cell speed, S; and cell motility, μ. These three parameters are related via calculation of the mean-squared displacement (MSD) of the cells:

$$\mathrm{MSD} = \langle d^2(t) \rangle = 2n_d\mu[t - P(1 - e^{-1/p})]$$
$$S = \sqrt{\mu n_d / P} \qquad (2)$$

where n_d = number of dimensions tracked (two for X–Y tracking, three for X–Y–Z tracking).

Assays can be designed to improve measurement accuracy of any of these three parameters (Dickinson and Tranquillo, 1993); it is left to the researcher to decide which is most appropriate and design accordingly. Briefly, in order to evaluate the persistence time accurately, cell positions must be recorded at a time lapse significantly less than the actual persistence time in order to observe the directed motion of the cell. For example, if the persistence time of a cell is estimated to be 30 min (on average it changes direction in its motion every half-hour), then to observe this phenomenon, cell position must be monitored at a minimum every 5–10 min, as the cell will appear to be moving randomly without any directional persistence. However, if the position of each cell needs to be recorded every 5 min, then the total number of cells that can be monitored is decreased. (More images of wells of a 96-well plate or individual cells can be captured in 10 min than in 5 min.) Thus, the amount of data that is averaged to determine S, P, and μ is decreased. The timing of the imaging sequence must be determined by the individual laboratories and can be influenced by the imaging hardware and software and the inherent motility of the cells. Generally, this timing issue is negligible for 2D analysis and only becomes a problem in 3D, where each cell is generally monitored individually with high magnification.

Both 2D and 3D analyses require complex image analysis codes that can perform object identification and/or correlation. Many software packages now include such algorithms, and they can also be programmed by the individual laboratories. The actual codes will differ according to the software packages, and presentation of a code is beyond the scope of this article. A brief outline for 2D and 3D is presented.

The general steps are the same for 2D and 3D analysis for preparing the assays.

1. Prepare collagen or fibrin solution with a final cell concentration between 7500 and 30,000 cells/ml and 5000–10,000 10-µm polystyrene after beads/ml. Beads serve as fiduciary markers to allow measurement of any drift in the stage or movement of the gel. They are especially crucial for 3D, high-magnification tracking and analysis.
2. Pipette 100 ml of collagen or fibrin solution into a well of the 96-well plate. Fill as many wells as warranted to complete the experimental test matrix.
3. Carefully place the plate in an incubator and allow solution to gel.
4. After gelation, fill each well with 100 ml of cell culture medium with twice the defined concentration of the desired soluble factor(s) to yield the correct final concentration.
5. Transfer the plate to an inverted microscope that includes an automated image analysis system and motorized stage, potentially motorized focus, and an environmental chamber to maintain proper humidity and CO_2 concentration. Air-buffered media can be used (e.g., M199) if on-stage CO_2 regulation is unavailable.

The followings steps are used for analysis of migration in 2D (without automated focus).

1. Using a 10x objective, select a focal plane that is consistent among all of the wells.
2. Move the stage from desired well to well and record images of each well. Build a mosaic image if necessary. Develop a numbering scheme to save the images (e.g., [date]_[condition]_[sample]_[image number]). Be sure to record the centroid position of each well so that the computer can move the microscope stage to those same positions at future time points.
3. Determine the total duration of an individual interval, and the total number of intervals, which define the overall length of the time-lapse experiment. Be certain that your system is capable of capturing the desired number of images required for one complete

interval in the time allocated. Generally, intervals should be as short as possible, so it frequently helps to work backward and determine how quickly the desired number of images can be captured. In this case, be sure to include a safety factor (usually a minute or two is sufficient to ensure that all required images are captured).

4. Instruct the computer to return to each position, in sequence, record an image(s) of the well, move to the next position, etc. After the last picture in one interval has been recorded, the computer should instruct the stage to wait until the beginning of the next time interval to return to the first well. For instance, if a time interval is 10 min and all pictures from an interval are captured in 8 min, the computer should wait 2 min to begin the next interval instead of immediately beginning the next time interval. Maintaining a consistent time interval simplifies data analysis greatly.

5. Object identification can be performed during an experiment or off-line. In either case, the general scheme is the same: (a) capture image and (b) filter image to accentuate "objects," i.e., cells and beads.

Filtering usually involves

i. Equalizing contrast.
ii. Low-pass filter.
iii. Edge detection filter (e.g., Sobel).
iv. Generating a binary image based on an appropriate gray-scale level.
v. Rejecting objects that are too big and/or too small.
vi. Recording the centroid position of objects, and correlating those positions, and possible shapes to the previous interval to track individual cells properly. Shape matching is not necessarily advised for tracking cells, as they change morphology during migration, but will certainly work for beads.
vii. Tabulate the cell/bead positions in a text file in a rational sequence. Include a flag to represent whether the object is a bead (1) or a cell (0). For instance.

Interval 1, Well 1, Object (cell or bead) 1, Type of object (Cell = 0, Bead = 1), Xposition 1, Yposition 1
Interval 1, Well 1, Object 2, Type, Xposition 1, Yposition 1 . . .
Interval 1, Well 2, Object 1, Type, X1, Y1
Interval 1, Well 2, Object 2, Type X1, Y1 . . .
Interval 2, Well 1, Object 1, Type X2, Y2
Interval 2, Well 1, Object 2, Type X2, Y2 . . .
Proceed to step 10.

Use the following steps for analysis of migration in 3D (must have automated focus).

6. Use the lowest power objective that generally allows you to focus on any object so that it is the only object in the volumetric field of view (FOV). To do this:
   a. Scan through the sample until you find an object.
   b. Maneuver the stage so that the object is in the center of the FOV and in focus.
   c. Make sure that the object is the only one in the volume immediately surrounding that object in all directions (including the focal plane, *Z*).
   d. Recenter and focus the object and record the position of the stage and focus on the computer

7. Select the cells and beads to track. Optimally, search for a bead with many (at least three to four; the more the better) cells within 200–400 µm of the bead, but not within the FOV. The motion of that bead would then represent the local absolute motion of the stage and gel to allow the subtraction of any convective effects that occur due to gel contraction.
   a. Find a bead that is the only object in its volumetric FOV.
   b. Scan the regions immediately outside that FOV for cells. Find beads with multiple cells in the immediately adjacent FOV.
   c. Return to the bead. Focus and center the bead and then record the *X*, *Y*, *Z* position with the computer
   d. Move to the cells in the adjacent volumes, focus and center each cell, and record the *X*, *Y*, *Z* position of each cell.
   e. Proceed to another bead and repeat

As with 2D tracking and analysis, there are opportunity costs that allow the optimization of the number of assay conditions, the number of beads/cells tracked per condition, and the duration of a single interval. This optimization is even more crucial for 3D tracking. Ideally, at least 20–30 cells are tracked for each condition.

8. When finished identifying the final object to be tracked, program the computer to return the stage to the first cell.
   a. Execute an autofocus routine to focus the object. If it has moved from the center, recenter.
   b. Run the object identification algorithm (see earlier discussion) to locate the centroid of the object.
   c. Record the position of the object and write the position of the object to a database. Include a flag to represent whether the object is a bead (1) or a cell (0). For instance: Interval #, Well #, Object #(cell or bead), Type (Cell = 0; Bead = 1), Xposition, Yposition, Zposition
   d. Automatically move to the next object and repeat until all objects are recentered.

9. Initiate the time-lapse loop. The time-lapse loop essentially performs the same procedures as step 8, but

the computer recenters the object. The main steps that need to be programmed are as follows.

a. Move to the recorded *XYZ* position of an object, $X_iY_iZ_i$.
b. Search in the *Z* direction for that object using an autofocus routine, returning the objective to the position of best focus. This is the new *Z* position of the cell, Z_{i+1}.
c. Identify the centroid of the object with the object identification algorithm.
d. Calculate the *X* and *Y* distance between the position of the centroid and the center of the FOV in pixels. Convert this to micrometers or stage position units and add this to the current stage position. This is the new *XY* position of the object, $X_{i+1}Y_{i+1}$.
e. Move the stage to the new *XY* position, $X_{i+1}Y_{i+1}$, which you just calculated.
f. Proceed to the next object and complete all objects for a given interval.
g. Wait until the duration of the interval is over before returning to the first object. See 2D tracking and analysis for an explanation.
h. Following completion of the time lapse, proceed to step 10.

The reasoning behind the high magnification cell-tracking algorithm is that in a given time interval, a cell cannot migrate fast enough to exit the FOV scanned during the autofocus. By recentering the object at each time interval, the likelihood of finding that object successfully in the next interval is maximized (see Fig. 5 for a schematic of the high magnification tracking algorithm).

10. Cell track analysis. Analysis requires three general steps: (A) correcting cell tracks for stage error and gel compaction (cell convection), (B) generating mean-squared displacement data, and (C) fitting data to the persistent random walk model.

A. Correcting cell tracks

a. Subtract initial position for each object from subsequent positions for that object. Each object should now begin at 0,0,0.
b. Subtract the *XYZ* position of the bead from *XYZ* colocalized cells for each time interval.
c. Write a new file of corrected object positions.

B. Calculating MSD

$$\mathrm{MSD} = \Delta x^2 + \Delta y^2 + \Delta z^2 \tag{3}$$

Mean-squared displacement data can be generated in two manners: overlapping intervals and nonoverlapping intervals (Fig. 6). Overlapping intervals generates more data but introduces covariance into the error. Analyses have been formulated to account for these (and other) complex errors (Dickinson and Tranquillo, 1993), but a full discussion is beyond the scope of this article. The two techniques are discussed briefly, and then we proceed assuming we are using overlapping intervals.

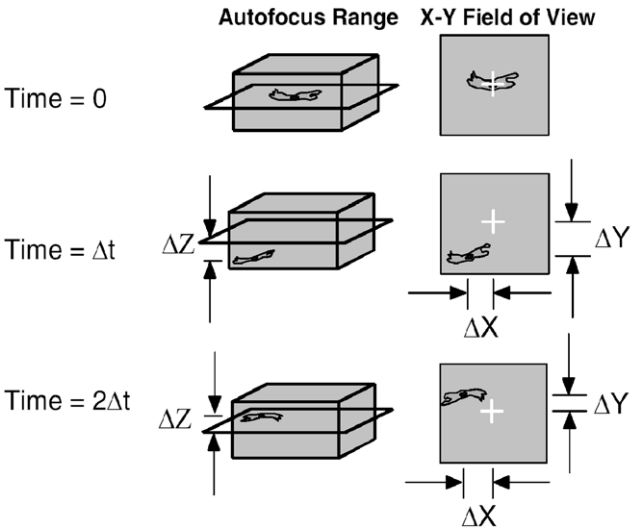

FIGURE 5 Schematic of autofocus and cell-tracking scheme for high magnification tracking in 3D. Initially, cells are focused and positioned in the center of the field of view. At the next time interval, the computer-controlled stage and focus move to the previously recorded position and execute an autofocus routine to locate the cell and determine the distance moved in the *Z* direction. A snapshot is taken, the centroid of the cell is located, and the *X* and *Y* distances moved by the cell are recorded. The process is repeated for the next and subsequent intervals, always returning the stage to the centroid recorded at the previous interval for each cell.

In an MSD calculation, we generate *X*-*Y* data that address the question: How far did an object, on average, migrate over a time interval of a given duration? In analyzing cell migration, we assume that cells have no inertia. That is, the fact that a cell is moving at a particular speed in a particular direction at time 1 has no assumed influence on the speed or direction at time 2, or any future time. Therefore, to determine the average distance traveled by a cell over one time interval, we average all displacements that occurred over 1 time interval. Thus, if the time lapse were four intervals long (five time points), we would calculate:

From $t = 1$ to $t = 2$: MSD1
From $t = 2$ to $t = 3$: MSD2
From $t = 3$ to $t = 4$: MSD3
From $t = 4$ to $t = 5$: MSD4

MSD for 1 time interval = average (MSD1–4)

We then average these over all of the cells in a given condition to arrive at the MSD value for that number of time intervals.

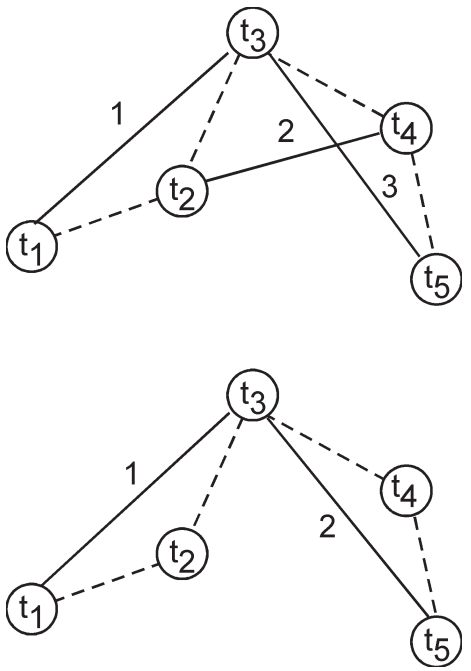

FIGURE 6 Overlapping vs nonoverlapping intervals for calculating mean-squared displacement (MSD). In this example, an object is imaged five times (t1–t5) over four time intervals. Suppose we are determining the MSD over two time intervals. With the overlapping interval procedure (top), the distance traveled by the object during two time intervals can be measured three times (solid lines), whereas with the nonoverlapping technique, the same measurement can only be made twice.

The use of overlapping vs nonoverlapping intervals arises when calculating the MSD over durations greater than 1 time interval (Fig. 6). For instance, in the example just given, if we want to calculate the MSD that occurs over 2 time intervals, we have two choices:

Option 1: Overlapping intervals
From $t = 1$ to $t = 3$: MSD1
From $t = 2$ to $t = 4$: MSD2
From $t = 3$ to $t = 5$: MSD3

Option 2: Nonoverlapping intervals
From $t = 1$ to $t = 3$: MSD1
From $t = 3$ to $t = 5$: MSD2

As can be seen, overlapping intervals result in 3 MSD measurements to average, while nonoverlapping results in only 2. However, the overlapping intervals are interdependent; any error that occurs from interval 2 to 3 will be included in the calculation from interval 1 to 3 and from interval 2 to 4. Generally, overlapping intervals are preferred as the improvement in signal-noise outweighs the cost of error covariance. Also, as mentioned, there are statistical means of accounting for this error in determining cell traction parameters.

The MSD should be calculated for all possible interval durations. Again, using our 5 time point, 4 interval example and assuming overlapping intervals we would have

Over 1 time interval: MSD1 = average of 4 MSD measurements (1–2, 2–3, 3–4, 4–5)
Over 2 time intervals: MSD2 = average of 3 MSD measurements (1–3, 2–4, 3–5)
Over 3 time intervals: MSD3 = average of 2 MSD measurements (1–4, 2–5)
Over 4 time intervals: MSD4 = 1 MSD measurement (1–5)

X-*Y* data are then generated as follows

***X* = duration**	***Y* = average MSD over that number of intervals**
1 Δt	MSD1
2 Δt	MSD2
3 Δt	MSD3
4 Δt	MSD4

A full time-lapse experiment would include many more intervals and therefore a much greater amount of data.

C. Fitting data to the random walk model. The easiest way to fit data is to use a program (or write one yourself) capable of nonlinear regression. Fit *X*–*Y* data to Eq. (2) to identify μ and *P* (or *S* and *P*). If a nonlinear regression package is not available, the parameters can be estimated by recognizing that the MSD vs duration plot can be separated into two distinct regions: at short durations, the curve goes as time^2, with slope $\sim n_d S^2$, and at long durations the curve goes as time, with slope $\sim 2n_d\mu$. An investigator can split MSD curves into these two regions and then use standard linear regression to identify cell traction parameters.

Finally, Shreiber *et al*. (2003) have detailed a technique to temporally resolve mean-squared displacement data.

Potential Pitfalls and Helpful Hints

1. Do not trust that all objects are tracked appropriately. Review time-lapse movies of each experiment and note which objects are lost or switched to a different object and disregard these cells in data analysis.

2. Equation (2) assumes that cells move randomly. If it appears that cells are not moving randomly, examine the cell tracks of individual cells (look at *all*, not just a few) to visually inspect for any directional bias. Also, mean-squared displacement data can be generated for one direction at a time and the MSD in

each direction independently fit to Eq. (2). If the migration is indeed random, then cell migration parameters should be (within error) the same for analysis of the X direction, the Y direction, and the Z direction.

3. Note that in calculating values for MSD, more measurements go into calculating the average MSD over one interval than over two intervals, more over two than over three intervals. Thus, there is generally more error in the calculation of MSD over long durations than short durations. This can be accounted for in the analysis by repeating data for a given duration to represent the number of samples that were included in the average calculation.

4. The increase in error in the MSD calculation over long durations can also produce aberrant behavior in the MSD plot. Specifically, the MSD plot may deviate from linear behavior as the error in the MSD calculation increases. These points can be ignored in processing data.

VIII. MIGRATION/TRACTION

The combined migration/traction assay allows assessment of the contractile ability of cells and their motility (Knapp *et al.*, 2000; Shreiber *et al.*, 2001, 2003). It is more technically challenging than either assay is individually and requires machining of special chambers. A schematic of the chamber is shown in Fig. 7, but the dimensions are somewhat arbitrary and can be tuned to the specific need of the investigator. Our assay chamber consists of a stainless-steel annulus (2.5 cm o.d., 1.5 cm i.d., 0.6 cm thick) with 3-mm holes located 1 mm from the bottom surface, bored through the side of the annulus. For stressed gel assays, two stainless-steel posts (3 mm diameter, 1.2 and 0.8 cm in length) with flared ends fit securely into opposing holes. On the inside ends of the two posts is glued a 3-mm-diameter, 1-mm-thick disk of porous polyethylene. A polycarbonate tube with an inner diameter matching the diameter of the posts/disks is supported by the two posts and serves as a mold for the assay. When the tube is filled with a collagen or fibrin solution, the solution penetrates the pores to form a fixed boundary condition upon gel formation. For unstressed, free-floating gels, the stainless-steel posts are replaced with polycarbonate posts that are each 1 mm longer to account for the lack of a porous polyethylene disk. In these cases, the gel forms without a rigid attachment, and the gel is free to compact uniformly in all directions.

All steps are performed under sterile conditions.

1. Prepare collagen or fibrin solution as described earlier. Be sure to degas the collagen/fibrin.

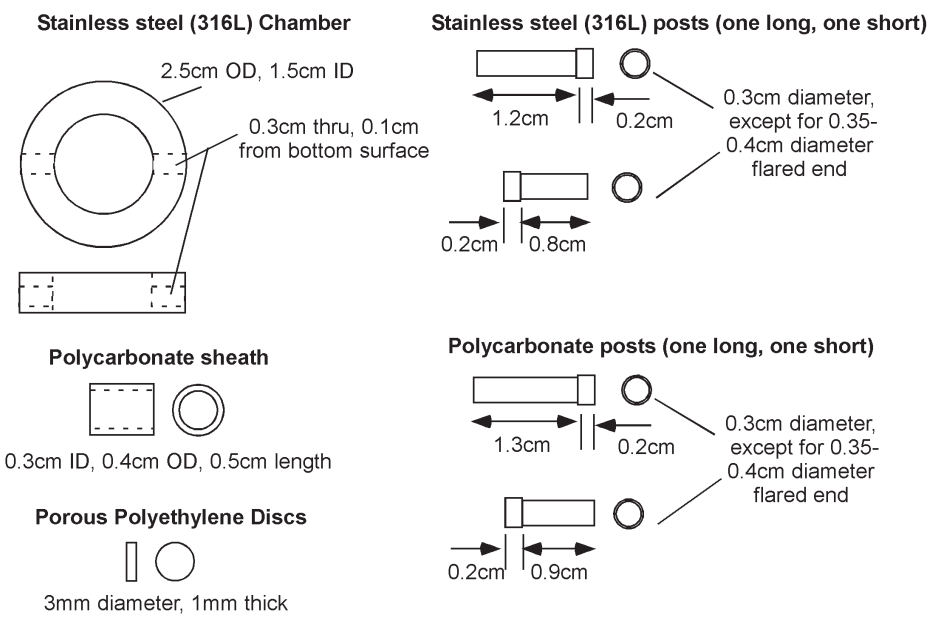

FIGURE 7 Individual components of a single traction/migration chamber. The stainless-steel posts and porous polyethylene discs are used in the stressed, constrained assay. The polycarbonate posts are used in the unstressed, free floating assay and are slightly longer to accommodate the length lost by not including the porous polyethylene.

2. Add cells to desired concentration (7500–30,000 cells/ml).
3. Add beads (7500–10,000 beads/ml).
4. Prepare culture medium with defined soluble factors of interest (e.g., 50 ng/ml PDGF).
5. Under sterile conditions, hold the assay chamber in one hand with the sheath supported by one post. Fill the sheath with the gel solution from steps 1–3.
6. Gently push the opposing post into the mold.
7. With vacuum grease, secure a coverslip to the top and bottom of the chamber and place in an incubator.
8. Gently flip the chamber every 5 min until the solution is gelled to prevent cells and beads from settling to the bottom.
9. Remove chamber from incubator, place right side up, and carefully remove the top coverslip.
10. Fill the chamber with medium from step 4.
11. With sterile tweezers, gently slide the sheath over the long post to expose gel to culture medium.
12. Replace the coverslip, again securing with vacuum grease.
13. Transfer chambers to microscope stage and prepare tracking algorithm (section VIII,A).

A schematic of the final steps is provided in Fig. 8.

A. Microscopy

The migration/traction assay requires at least an *XY* motorized stage. Automated focus is preferred and rotating objectives are ideal. The routines for tracking cell migration are identical to those described previously. To record cell traction, follow initial selection of cell/bead positions, move the stage to the center of each chamber, and instruct the computer to build a mosaic image of the gel at the midplane. This is done most easily with a low power objective; if available, use the motorized objective feature to switch objectives to 2 or 4X. This process should be repeated automatically at the end of each time interval. A typical time lapse is run for 12–48 h. Typical "before" and "after" images of the stressed and unstressed assays are shown in Fig. 9.

B. Analysis

Cell migration and traction analyses are performed as before. For traction, measure the diameter at the midplane of the gel at each time point. The fixed, stressed gel should form an hourglass during cell-mediated gel compaction, so the diameter measurement should essentially be the middle of the hourglass. The free floating, unstressed gels should compact uni-

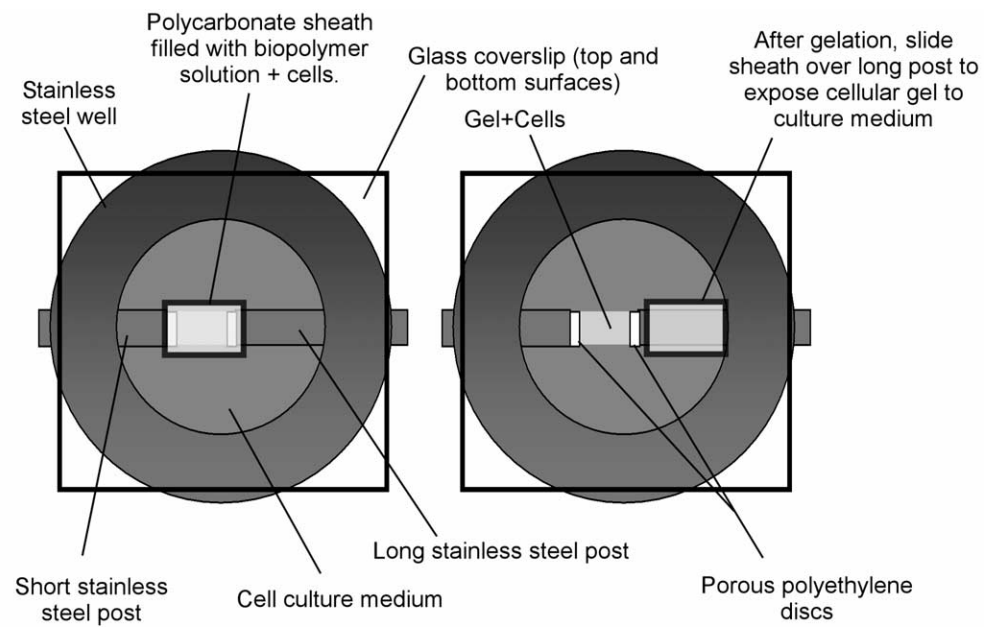

FIGURE 8 Schematic of cell traction/cell migration assay preparation. Fill the polycarbonate sheath with the biopolymer solution (+cells and beads) and support with stainless-steel posts, use vacuum grease to cover top and bottom surfaces with glass coverslips, and transfer to the incubator to facilitate gelation. After gelation, remove the top coverslip and fill the chamber with culture medium with defined concentrations of soluble factors of interest. Slide the sheath over the long post to expose the gel to the culture medium. Replace the top coverslip and transfer to the microscope stage for traction and migration tracking.

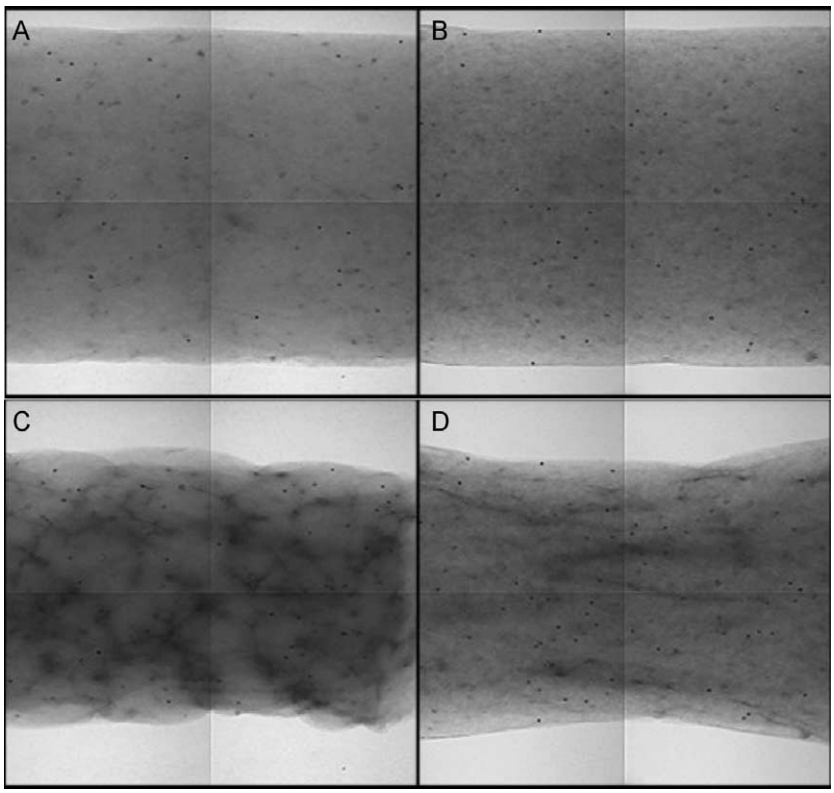

FIGURE 9 Examples of unstressed, free-floating assay (A,C) and stressed, constrained assay (B,D). Migration–traction assays are prepared as described and are nearly identical after initial preparation. (A) Free-floating cylindrical gel at time = 0. The gel was formed by supporting a sheath with smooth-ended polycarbonate posts. (B) Contstrained cylindrical gel at time = 0. The gel was prepared by filling an identical sheath that is supported by stainless-steel posts with porous polyethylene discs glued to the ends (outside field of view). The biopolymer solution penetrates the pores to form a fixed boundary condition upon gelation. Following incubation, cells that are entrapped in the gel exert traction and compact the gel. (C) Without physical constraints to compaction, the free-floating, cylindrical gel compacts (roughly) uniformly. (D) In contrast, the physical connection to the posts via the porous polyethylene prevents the constrained gel from compacting in the axial direction. The result is pure radial compaction and subsequent fiber and cell alignment. The characteristic "hourglass" shape results. In both cases, the degree of cell traction is related to the amount of gel compaction, measured as the decrease in radius at the midplane of the sample.

formly, so the diameter measurement can be taken from any cross-section. The result is X–Y data of percentage compaction vs time, which can be examined for temporal trends or quantified on the basis of final midplane compaction and compared to results of the migration analysis.

C. Pitfalls

1. Be careful not to introduce bubbles into the assay that can affect gel compaction and obscure imaging.
2. Similarly, do not smear vacuum grease over the coverslip in an area that will obscure imaging.
3. Use hydrophilic porous polyethylene (Small Parts, Miami Lakes, FL) to ensure good penetration of the gel-forming solution for the fixed case.
4. In the free-floating case, cell traction and/or convective motion of the culture medium may lead to rigid body motion of the cylindrical gel. Because cell migration may be tracked at high magnification, a small translocation of the gel can result in "losing" all of the cells during the traction algorithm, as it is only prepared to follow movements of 0.5 xFOV per interval. Use a low percentage, sterile, agarose solution (1%) to increase the viscosity of the culture medium and to reduce the ability for gel movement.
5. Similarly, under some conditions (high cell concentration, certain concentrations of soluble factors, etc.), gels may compact too quickly to monitor cell position. Some trial and error is likely necessary to converge on appropriate conditions.

6. Bubbles in the medium can also diminish imaging capabilities. Degas the culture medium and be careful when filling and sealing the chambers to avoid introducing air.

7. Strong compaction in the stressed case leads to fiber alignment in the axial direction, which can lead to anisotropic migration. It may be necessary to quantify migration in the individual directions (X,Y, and Z) for these cases.

8. Generally, because of the high variability in cell lines from culture to culture and passage to passage, it is recommended to run all experimental conditions in one set of experiments rather than running all controls one day, all at one condition the next, and so on.

References

Barocas, V. H., Moon, A. G., and Tranquillo, R. T. (1995). *The fibroblast-populated collagen microsphere assay of cell traction force 2. Measurement of the cell traction parameter. J. Biomech. Engin.* **117**(2), 161–170.

Barocas, V. H., and Tranquillo, R. T. (1997a). *A finite element solution for the anisotropic biphasic theory of tissue-equivalent mechanics: The effect of contact guidance on isometric cell traction measurement. J. Biomech. Engin.* **119**(3), 261–268.

Barocas, V. H., and Tranquillo, R. T. (1997b). *An anisotropic biphasic theory of tissue-equivalent mechanics: the interplay among cell traction, fibrillar network deformation, fibril alignment, and cell contact guidance. J. Biomech. Engin.* **119**(2), 137–145.

Bell, E., Ivarsson, B., and Merrill, C. (1979). *Production of a tissue-like structure by contraction of collagen lattices by human fibroblasts of different proliferative potential in vitro. Proc. Natl. Acad. Sci. USA* **76**(3), 1274–1278.

Clark, R. A. F. (ed.) (1996). "*The Molecular and Cellular Biology of Wound Repair*." Plenum Press, New York.

Dickinson, R. B., and Tranquillo, R. T. (1993). *Optimal estimation of cell movement indices from the statistical analysis of cell tracking data. AIChE J.* **39**(12), 1995–2010.

Dunn, G. A., and Brown, A. F. (1987). *A unified approach to analysing cell motility. J. Cell Sci. Suppl.* **8**, 81–102.

Eastwood, M., *et al*. (1996). *Quantitative analysis of collagen gel contractile forces generated by dermal fibroblasts and the relationship to cell morphology. J. Cell. Physiol.* **166**, 33–42.

Ehrlich, H. P., and Rajaratnam, J. B. (1990). *Cell locomotion forces versus cell contraction forces for collagen lattice contraction: An in vitro model of wound contraction. Tissue Cell* **22**(4), 407–417.

Knapp, D. M., *et al*. (1997). *Rheology of reconstituted type I collagen gel in confined compression. J. Rheol.* **41**(5), 971–993.

Knapp, D. M., Helou, E. F., and Tranquilllo, R. T. (1999). *A fibrin or collagen assay for tissue cell chemotaxis: Assessment of fibroblast chemotaxis to GRGDSP. Exp. Cell Res.* **247**, 543–553.

Knapp, D. M., *et al*. (2000). *Estimation of cell traction and migration in an isometric cell traction assay. AIChE J.* **45**(12), 2628–2640.

Kolodney, M. S., and Wysolmerski, R. B. (1992). *Isometric contraction by fibroblasts and endothelial cells in tissue culture: A quantitative study. J. Cell Biol.* **117**(1), 73–82.

Moghe, P. V., Nelson, R. D., and Tranquillo, R. T. (1995). *Cytokine-stimulated chemotaxis of human neutrophils in a 3-D conjoined fibrin gel assay. J. Immunol. Methods* **180**(2), 193–211.

Neidert, M. R., *et al*. (2002). *Enhanced fibrin remodeling in vitro with TGF-beta1, insulin and plasmin for improved tissue-equivalents. Biomaterials* **23**(17), 3717–3731.

Nusgens, B., *et al*. (1984). *Collagen biosynthesis by cells in a tissue equivalent matrix in vitro. Coll Relat Res.* **4**(5), 351–363.

Shreiber, D. I., Barocas, V. H., and Tranquillo, R. T. (2003). *Temporal variations in cell migration and traction during fibroblast-mediated gel compaction. Biophys J.* **84**(6), 4102–4114.

Shreiber, D. I., Enever, P. A., and Tranquillo, R. T. (2001). *Effects of pdgf-bb on rat dermal fibroblast behavior in mechanically stressed and unstressed collagen and fibrin gels. Exp. Cell Res.* **266**(1), 155–166.

Tuan, T. L., *et al*. (1996). *In vitro fibroplasia: Matrix contraction, cell growth, and collagen production of fibroblasts cultured in fibrin gels. Exp Cell Res.* **223**(1), 127–134.

SECTION

12

Electrophysiological Methods

CHAPTER

48

Patch Clamping

Beth Rycroft, Fiona C. Halliday, and Alasdair Gibb

I. INTRODUCTION

The patch-clamp technique was first utilized in 1976 with the exclusive intention of recording single channel currents from acetylcholine receptor ion channels in frog skeletal muscle fibres (Neher and Sakmann, 1976). The following 25 years have witnessed refinements of the technique such that it is now applicable to a diversity of biological preparations, including animal and plant cells, intracellular organelles, yeast, fungi, and bacteria. Furthermore, the versatility of the technique permits many questions to be addressed. Undoubtedly, the most common application of the patch-clamp technique is to manipulate the cell membrane voltage and measure the electrical currents that flow across the membrane through ionic channels. These channels include voltage-operated ion channels (e.g., Na^+, K^+, Ca^{2+}, and Cl^- channels), channels regulated by intracellular second messengers (cAMP, cGMP, Ca^{2+}, G-proteins as well as numerous kinases and phosphatases), and neurotransmitter-activated receptor-operated channels. Currents can be recorded either from individual channels or from an entire cellular population of channels. The patch pipette can be used in whole-cell mode to introduce Ca^{2+}, second messengers, or ion-sensitive dyes into the cell (Park *et al*., 2002). Combining patch clamp with optical imaging (Park *et al*., 2002) has become a very powerful two-dimensional technique used to investigate the concentration or movement of labeled cellular biomolecules and their effect on the cell (Voipio *et al*., 1994). Furthermore, the versatility of the patch-clamp technique extends beyond simply measuring ionic currents. It can be used to measure changes in cell membrane area caused by vesicular secretion. Using flash photolysis, rapid concentration jumps of caged intracellular messengers (e.g., Ca^{2+} or inositol trisphosphate) introduced through the patch pipette can be achieved (Gurney, 1990; 1994). This article provides a general introduction to the principles as well as an overview to the practical side of patch clamping. More detailed descriptions of patch clamping and other electrophysiological techniques can be found elsewhere (Ogden and Stanfield, 1994; Sakmann and Neher, 1995; Levis and Rae, 1998).

Although the choice of preparation used depends on the questions being asked, several limitations must be considered before embarking on an experiment. First, the technique relies on formation of a tight seal between the cell membrane and the patch pipette (see later). For this reason, cells with clean membranes must be used. Examples include tumour-derived cell lines and cells in primary culture, which tend to have a less extracellular matrix. Adult cells from complex tissues require enzymatic treatment to clean the membranes of connective tissue and extracellular matrix. Enzymes used most commonly include collagenase and proteases (Sigma-Aldrich). Enzymatic methods have the potential disadvantage that the enzyme treatment may damage or alter the properties of the channels or receptors of interest. However, a major drawback of cultured cells is that depending on the growth phase, different subpopulations of cells can be expressed that have properties different to freshly isolated cells.

In addition, some cell types are not an ideal shape for voltage clamping. If a cell has long processes, such as dendrites or axons, then the membrane voltage in these regions may not be controlled, leading to inaccuracies in current measurement.

Copyright 2006, Elsevier Science (USA).
All rights reserved.

II. MATERIALS AND INSTRUMENTATION

In addition to equipment required for fabricating patch pipettes (Section VIII), the following are required for a patch-clamp setup.

A. Microscope

A dissection microscope may be adequate in order to make patch-clamp recordings from *Xenopus* oocytes and other large cells. For anything smaller, i.e., cultured or freshly isolated cells, inverted microscopes (Narishige) are used commonly for visualizing the patch pipette and cell.

B. Micromanipulators

Precise movement of the patch pipette in three axes is required at the submicrometer level prior to giga seal formation. For very small cells, fine movement can be obtained using remotely controlled manipulators, such as piezoelectric (Newport, Burleigh intracell) or hydraulic (Narishige) manipulators. Once the giga seal has been formed, the pipette must not drift but should remain in a fixed position so that whole-cell and cell-attached recordings can be sustained.

C. Flotation Table

These are required to dampen out both horizontal and vertical vibrations from the surrounding environment down to a few hertz (Section VIIIB).

D. Faraday Cage

To shield the recording electronics from electromagnetic radiation, primarily line-frequency pick-up (50 Hz), the patch-clamp setup is enclosed in an earthed cage consisting of a metal framework with three of its sides and top covered with wire mesh. The fourth side is open for access to the microscope and recording electronics. Faraday cages are available commercially (Newport, Intracel). They can be made easily, however, and the parts for the cage can be obtained from most hardware shops.

E. Oscilloscope

Software packages are available (Axotape, Axon Instruments) that enable the computer to emulate the oscilloscope. This may be a less expensive alternative than buying both an oscilloscope and a computer, but should be avoided because the display on the computer monitor may be slow and it may also be difficult to scale appropriately. It is also common practice to tape record raw data (see later) as it is produced and store it on the tape for later "off-line" analysis on the computer.

F. Amplifiers

Commercially available patch-clamp amplifiers provide compensation for both pipette capacitance and cell capacitance associated with whole-cell recordings (Axon, Heka, Cairn). They also enable series resistance to be compensated for, thus eliminating voltage error that arises from the voltage drop across the access resistance of the electrode. Low-pass filters are incorporated in the amplifier so that the recording bandwidth can be adjusted in order to be compatible with the acquisition rate. Amplifiers also permit the membrane potential to be altered by the user. Several different types are available that can be used to record from a diversity of preparations, including oocytes and bilayers. For patch-clamp recordings, Axopatch-1D and Axopatch 200B amplifiers are available, which permit both whole-cell and single-channel recordings. The advantage of the latter model is that the internal circuitry within the amplifier headstage is cooled to –15°C in order to reduce thermal noise, and thus the contribution of noise from the amplifier is minimised.

G. Tape Recorder

It is often necessary to store patch-clamp recordings, particularly of single-channel openings, on tape for "off-line" analysis. This provides a permanent record of data, which can be replayed under different gain and filter settings. Digital audio tape recorders (e.g., Biologic DTR 1200 or DTR 1600) are probably the most commonly used.

H. Equipment for Online Data Acquisition, Data Storage, and Analysis

Computers are increasingly used "online" to generate voltage protocols and store data as it occurs. An interface (e.g., Axon Instruments Digidata 1200, Cambridge Electronic Design 1401) between the computer and the recording setup provides both analogue-to-digital (ADC) and digital-to-analogue (DAC) conversion. ADC conversion enables the analogue signal from the cell, which is a continuous time-varying voltage, to be converted into a digitized record. DAC conversion allows voltage signals generated by the computer in data form (binary digits) to be applied to

the cell via the amplifier voltage command input. Software used to generate voltage protocols and analyse acquired data can either be bought individually or along with the interface. pCLAMP (Axon) is a commonly used software package for PC users, which can be bought with the Digidata 1200 interface, as is Axograph for Macintosh users. Academic users can also use free packages such as the Strathclyde Electrophysiology Software (www.strath.ac.uk/Departments/PhysPharm).

I. Filters

Although most commercially available patch-clamp amplifiers have built-in filters, it is useful to have an additional filter/amplifier system with different characteristics from those of the patch-clamp amplifier. This provides a more finely tuned filtering system for single channel data or noise analysis. The most suitable type of filter for single-channel recordings is the Bessel filter, which does not produce an oscillation in response to a rectangular input. Because single-channel currents are essentially rectangular, filters lacking in this property will cause the currents to become distorted. Filter and digitizing frequencies must be chosen carefully in order to prevent aliasing. To prevent this from occurring, the sample rate should be at least five times the cutoff (–3 dB) frequency of the Bessel filter.

III. PRINCIPLES OF PATCH-CLAMP RECORDING

Electrical or chemical stimulation of the cell membrane causes a change in membrane potential. Normally the change is counteracted quickly by the activation of voltage-dependent ion channels, which helps restore the membrane potential back to resting levels. The flux of the different ionic species responsible for shaping the depolarization/repolarization is too brief to enable the experimenter to identify the ions involved or the change in membrane conductance. The voltage-clamp technique permits the experimenter to clamp the membrane voltage at a fixed level so that the ion channels responsible for the current at that particular voltage can be identified.

The key element in the patch clamp is the feedback amplifier in the headstage (Fig. 1). The feedback amplifier controls the membrane potential. Current flows from the output of the amplifier when the voltage of its two inputs is not equal. The amplifier receives two inputs: a positive input from a command potential

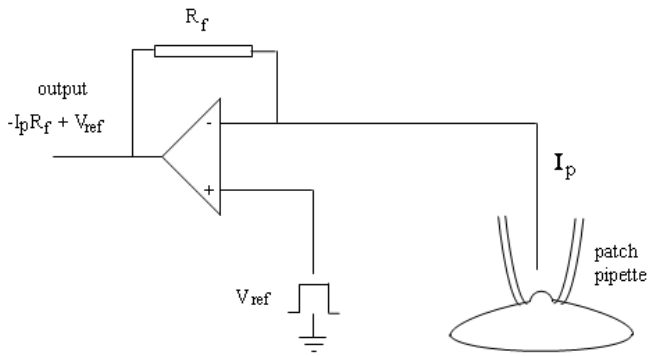

FIGURE 1 A headstage current/voltage amplifier.

source of variable setting (V_{ref}), which is determined by the user, and a negative input from the pipette potential (V_p). When both inputs are at the same potential, the output will be zero. When a discrepancy arises between the two inputs, the amplifier strives to null this discrepancy and force V_p to equal V_{ref}. This is achieved by the amplifier passing current across the feedback resistor, R_f, to drive the inside of the cell to the reference potential. This current supplied by the feedback amplifier is equal and opposite to the current carried by ions flowing across the membrane. The current flowing through the pipette (I_p) to clamp the cell membrane is proportional to the voltage drop ($V_{out} - V_p$) across the resistor, R_f, according to Ohm's law

$$I_p = V_{out} - V_p / R_f \quad (1)$$

Because the feedback amplifier clamps V_p at V_{ref}, then in addition,

$$i_p = V_{out} - V_{ref} / R_f \quad (2)$$

In practice, therefore, pipette current is monitored by a differential amplifier that constantly measures the difference between V_{ref} and V_{out}. From Eq. (2) it follows that the sensitivity of current measurement is inversely proportional to the size of the feedback resistor, with a large resistor enabling measurement of smaller current amplitudes. Because the gain of the amplifier is set by the resistor connecting V_o to the (–) input, the larger the value of R_f, the larger the gain and the more closely V_p approaches V_{ref}.

The feedback resistor also contributes thermal noise, which can contribute to noise in the current recording. The variance of the current noise (s_i^2) through the feedback resistor is related to Johnson noise due to the resistance (R_f), being given by

$$s_i^2 = 4kTf_c / R_f \quad (3)$$

where k is Boltzmann's constant (1.381×10^{-23} VCK^{-1}), T is the absolute temperature (° Kelvin), and f_c is the

bandwidth (Hz), i.e., the low-pass filter setting. It follows that for a high-resolution, low-noise recording, R_f should be high, and is usually around 50 GΩ. However, the amplifier cannot put out more voltage than is provided by its power supply, which is approximately ±12 V, indicating from Eq. (1) that the headstage output will be saturated if i_p exceeds 240 pA. For this reason, large whole cell currents are measured with a lower feedback resistor, and the value of R_f must be chosen to suit the experiment, typically 500 MΩ.

IV. PATCH-CLAMP CONFIGURATIONS

The principle of the technique is to electrically isolate a patch of membrane from the external solution and record current flowing into the patch. This is achieved by pressing the tip of a heat-polished pipette onto a clean membrane. The resulting seal between pipette tip and membrane is very tight, with a resistance greater than 10 GΩ, hence the term "giga seal." This is obtained using the following procedure.

1. After lowering the pipette into the solution in the recording chamber, zero the voltage output to subtract the junction potential (see later).
2. Apply a regular rectangular test voltage pulse of 1–10 mV for 5 ms every 20 ms to the pipette to measure its resistance. This should result in the appearance of a rectangular waveform on the current trace, which can be monitored on the oscilloscope. The pipette resistance can be worked out from Ohm's law by dividing the test voltage by the resulting current amplitude.
3. Position the pipette so that it is just above the cell. Apply positive pressure to prevent the pipette tip from becoming clogged with dirt and gently blowing away any debris near the cell. This procedure will also indicate when the pipette tip is very near the cell, as the positive pressure will cause a small dimple to appear on the cell surface.
4. When a small dimple is seen, a small decrease in the size of the test voltage current pulse should occur, indicating an increase in pipette resistance following contact between membrane and pipette. At this point, stop moving the pipette, release the positive pressure, and apply gentle suction, e.g., with a 1-ml syringe or by mouth. Progress of seal formation is indicated by the rectangular waveform on the current trace becoming smaller. Application of negative voltage (–50 to –60 mV) in the pipette at this stage encourages seal formation. When the pipette resistance is greater than 1 GΩ, a giga seal has been formed.

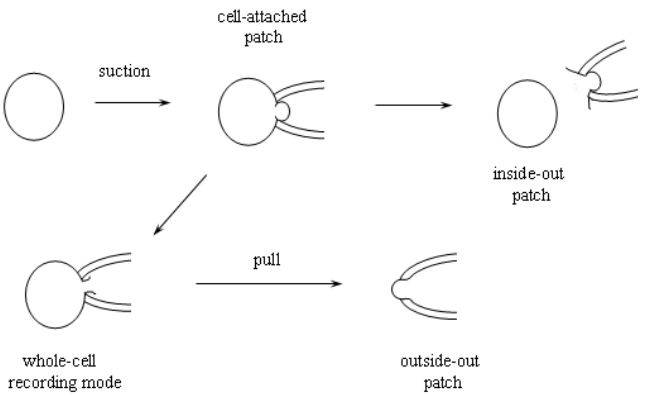

FIGURE 2 Giga-seal recording configurations.

After giga-seal formation, it is now possible to record either currents from the entire cell using the whole-cell recording mode or single channel activity with cell-attached, inside-out or outside-out modes (Fig. 2).

A. Cell-Attached Recording

This configuration is not only the simplest to achieve, as it is formed by obtaining a giga seal, but it is also the most physiological. The major disadvantage of this configuration is that the resting potential of the cell is unknown, which is added to the applied pipette potential.

B. Inside-out Recording

Upon formation of a giga seal, withdrawing the pipette from the cell usually results in an excised membrane patch with its cytoplasmic side exposed to the bath solution. Inside-out patches can be used to study the influence of cytoplasmic constituents or second messengers on channel activity. A disadvantage of this configuration is that cytoplasmic constituents are lost, which may be important in modulating the behavior of ion channel proteins.

C. Whole-Cell Recording

Instead of withdrawing the patch pipette from the membrane after seal formation, application of gentle suction will disrupt the membrane patch directly under the pipette, leading to the formation of a low resistance pathway between the cell interior and the solution in the pipette. Because the cell interior is being perfused with pipette solution, this configuration has the disadvantage that certain cytosolic factors important for cellular function may be washed out. Formation of the whole-cell configuration becomes

immediately apparent by the sudden appearance of large capacity transients at the leading and trailing ends of the test pulse, which reflect the charging and discharging of the capacitance of the cell membrane. These transients can be minimized using the whole-cell capacitance cancellation and series resistance (Section IXA) compensation dials on the patch-clamp amplifier. This allows a crude estimation of the cell capacitance (and hence cell size) to be made because cell membranes have a fairly constant specific capacitance of 1 μF/cm^2.

D. Outside-out Recording

Upon obtaining the whole-cell configuration, slow withdrawal of the pipette from the cell causes the membrane to stretch until it finally breaks. The membrane should reseal to form a patch with its intracellular face in contact with the pipette solution. This configuration can be used to study the effects of extracellular agents on single-channel activity.

E. Perforated Patch Recording

It is possible to prevent important cytosolic components from being washed out of the cell interior, whilst also allowing the electrical contact between cell interior and pipette to be sustained. Two polyene antibiotics are available, nystatin and amphotericin B, which, when present in the pipette solution, generate ionic channels within the cell membrane (Korn *et al*., 1991; Rae *et al*., 1991). These channels are small enough to permit the passage of monovalent cations and anions across the membrane, but will impede the passage of larger molecules (MW > 300). Thus, it is possible to control the concentrations of internal Na^+, K^+, and Cl^- (in contrast, gramicidin allows only positively charged ions to cross the cell membrane, hence avoiding disruption of the membrane chloride gradient) whilst ensuring that cytosolic constituents will remain trapped within the cell. It is important that the very tip of the pipette contains only nystatin-free solution because the antibiotic impedes the formation of giga seals. To fill the pipette, the tip must first be dipped into nystatin-free solution for a few seconds and then filled with nystatin-containing solution in the usual way. Once a giga seal has formed between pipette and cell, the development of ionic channels in the membrane can be monitored by applying a –10 mV hyperpolarising pulse. As more and more channels are formed, capacity transients at the leading and trailing ends of the pulse should get larger and faster, as the series resistance of the membrane patch decreases. This process can take between 5 and 30 min. The path that is eventually formed between pipette and cell interior should be of low enough resistance to permit recordings in the whole-cell configuration. Furthermore, channels formed by the antibiotics are virtually voltage independent, enabling studies on voltage-dependent channels to be performed.

F. Planar Electrode Array and Automated Patch-Clamp Recording

In addition to the conventional patch-clamp techniques described earlier, advancements have been made towards amplification and automation of this time-consuming process (Sigworth and Klemic, 2002). At present, these techniques can only be performed on cultured or dissociated cells and in the whole-cell configuration. One method employs a planar chip made from quartz in which a submicron aperture has been made (Fertig *et al*., 2002). The cell suspension solution is poured onto the chip and suction is applied to the apertures to secure a single cell to the aperture. Although giga-ohm resistance seals are hard to obtain with this material, advances have been made using hydrophilic-oxidised Sylgard [polydimethylsiloxane (PDMS)] instead of quartz. Advantages of the planar electrode include high-resolution, low-noise recordings due to the small diameter of the aperture; with the development of several apertures on the same chip, multiple parallel experiments can be performed simultaneously. Other automated methods, such as the PatchXpress 7000A (Axon), employ conventional glass micropipettes but use a new protocol that involves filling a glass pipette with the cell suspension solution and flushing it towards the pipette tip to create a seal with a cell (Lepple-Wienhues *et al*., 2003).

V. RECORDING SOLUTIONS FOR PATCH CLAMPING

The composition of solutions used to fill the pipette or bathe the cells will depend on the nature of the ion channels being investigated. A standard extracellular solution might have the following composition (m*M*): KCl 5, NaCl 140, $CaCl_2$ 1, $MgCl_2$ 1, and HEPES 10; while the pipette solution may be KCl 140, HEPES 10, and EGTA 10, with pH adjusted to 7.3 with NaOH in both cases. EGTA is used to buffer the intracellular calcium concentration to very low levels. Specific EGTA/Ca^{2+} mixtures can be used to buffer intracellular calcium at a particular value, e.g., 100 n*M*, and ATP, Mg^{2+}, kinases, or other intracellular enzymes may also be added.

VI. ELECTRICAL CONTINUITY BETWEEN MEMBRANE PATCH AND RECORDING CIRCUITRY

A problem that can arise at the interface between the metal recording electrode and the pipette solution is the development of a junction potential. This potential difference arises due to the diffusional flux of anions and cations between mediums of different ionic composition or concentration. In order to overcome this problem, connections made to the recording circuitry are via nonpolarisable reversible Ag/AgCl electrodes. These electrodes consist of a silver wire with a chlorided tip produced by dipping in bleach (20% sodium hypochlorite solution) for about 1 min to make a nonpolarisable electrode. The electrode will turn grey/black with the formation of AgCl on the surface. The AgCl coating is fairly robust, but needs to be renewed every few days. It is also good practice to heat polish the back end of the patch pipettes in the flame of a spirit burner (Merck) before pulling so that sliding the pipette onto the silver wire electrode prevents the AgCl from being scratched off. A second AgCl wire, the reference electrode, is present in the recording chamber, which is connected to the headstage ground socket. For either of these electrodes, a good indication of the AgCl coating beginning to deteriorate can be seen from the current trace on the oscilloscope, which may display erratic 50-Hz interference or develop a considerable offset potential (50–100 mV).

VII. PATCH PIPETTES

Many of the electrophysiological properties of patch pipettes depend on the type of glass and the size and shape of the pipette tip. Pipette glass (Harvard) has an outer diameter of 1.5–2 mm and is available with an internal filament running the whole length of the tube to ease filling of the pipette. The glass of choice for single-channel recording is thick-walled glass, such as borosilicate glass, as pipette capacitance and hence background noise levels are low. Noise can be reduced further by using quartz electrodes for single-channel recordings, although this incurs additional costs for materials and a specialized puller (Levis and Rae, 1998). Thin-walled borosilicate glasses are preferable for whole-cell recordings, as these provide a lower access resistance. The access resistance can also be minimized by producing pipettes with a steep angle of taper and a tip diameter of 1 µm after fire polishing to yield a low-resistance pipette (<5 MΩ). In general, for small cells, relatively high pipette resistances are necessary to prevent the patched cell from being sucked up the pipette during formation of the giga seal. Low-resistance, wide-bore pipettes tend to cover a greater surface area of membrane and hence a high number of channels, and so for this reason higher pipette resistances are preferable for single-channel recordings.

A. Making Patch Pipettes

There are three stages involved in making patch pipettes: pulling the pipette, coating it with Sylgard, and fire polishing the pipette tip.

Several types of pipette pullers are available commercially (Sutter, Narishige) that pull the glass either horizontally or vertically, by mechanical or gravitational force, respectively. The pipettes are pulled over two stages: during the first, the centre of the tubing is heated in a coil of nichrome wire until it stretches over a length of around 10 mm to form an hour-glass shape; at its thinnest part, the pipette should measure approximately 400–500 µm in diameter. The length of the first pull determines the taper of the pipette, with a higher heat causing a steeper taper, thus reducing electrode resistance and capacitance. Once the glass has cooled, the coil is recentred around the thinnest part of the tube, heated at a lower temperature, and the two ends pulled apart to form two similar pipettes. The temperature of the second pull determines the final tip diameter, with high temperatures producing pipettes with narrow tips.

B. Coating Pipettes with Sylgard

Coating the pipette shank with an inert, hydrophobic material such as Sylgard (Merck) resin or beeswax (Sigma-Aldrich, Merck) is necessary for two reasons: (1), the pipette wall is an insulator separating two electrolyte solutions, which means that it acts as a capacitor and is thus a source of noise. This may be of particular significance for single-channel recording, where currents as small as a fraction of a pA are being measured. Because capacitance is proportional to 1/thickness, the capacitance can be reduced by coating the pipette with a thick, nonconducting layer. The hydrophobic nature of either Sylgard or beeswax also prevents the bath solution from creeping up the sides of the pipette. This will decrease the area of electrical contact between pipette and bath solution and also therefore the pipette capacitance. Sylgard is available as a resin and a curing agent, which must be mixed together in a 10:1 ratio. A good idea is to mix 10 ml of resin with 1 ml of curing agent and dispense the resulting mixture into 1 ml Eppendorf tubes. The aliquots

can then be stored in the freezer until required, where the mixture remains in a fluid state. Because polymerization is temperature dependent, an aliquot will remain fluid for several hours at room temperature. Sylgard should be applied as near the pipette tip as possible without causing it to become blocked, i.e., ~100 µm, and extend along the pipette to just beyond the shoulder of the pipette. It is cured by placing the pipette tip in a heated wire coil for a few seconds.

Note: Sylgard residue on the pipette tip is a potential source of consistent failure to obtain giga-ohm seals. If this happens, it is worth trying to seal with a few pipettes that have not been coated.

Beeswax is almost as effective as Sylgard in reducing noise associated with pipette capacitance, but has the advantage that its application is simpler in that wax only requires gentle heating in order to melt and dries almost instantaneously at room temperature when applied to the pipette tip.

C. Fire Polishing

Fire polishing produces a clean and smooth pipette tip with which tight seals can be obtained. In general it is best to make patch pipettes on the day that they will be used. The basic fire-polishing apparatus consists of a micromanipulator to which the pipette is attached, which is brought into close proximity to a heated platinum wire. The wire is mounted onto the stage of a microscope and is bent into a V shape in order to focus the heat onto the pipette tip. A small blob of glass is positioned onto the tip by melting the end of a pipette onto the wire. The glass blob prevents tiny fragments of the heated platinum from sputtering onto the pipette tip and making it dirty. To polish the pipette tip, the wire is heated until it glows a dull red, and the pipette is advanced towards the wire until the tip is seen to darken slightly and shrink back (by ~2 µm).

VIII. PITFALLS

A. Series Resistance

Because the membrane possesses channels that have finite resistance, the cell membrane can be modeled by a circuit comprising a variable resistor, R_m, in series with a parallel plate capacitor, C_m (Fig. 3). The series resistance (R_s) is introduced into the model to represent the pipette and access resistance, which is in series with the cell and the pipette during whole-cell recordings of currents. The rate at which the membrane potential is changed is restricted by the charging of the membrane capacitance. This capacity current decays exponentially with a time constant (τ) equivalent to the product of the capacitance and resistance R, where

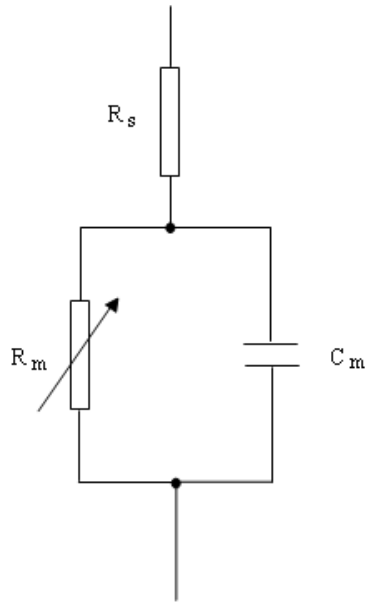

FIGURE 3 A simple electrical analog of the cell.

$$\tau = RC \tag{4}$$

where $R = R_m R_s/(R_m + R_s)$. This means that the cell capacitance can limit the speed of the voltage clamp and the ability to observe rapidly activating ionic currents. It is also clear that the membrane resistance and series resistance influence the speed of the membrane charging. Keeping R_s low by using large-tipped pipettes with low resistance is essential for rapid clamping of the membrane voltage. Minimising R_s is also important for reducing errors in the measurement of membrane voltage and current. Several resistances contribute to R_s, with the major one being the access resistance of the pipette, usually in the order of a few MΩ. When a current flows across the membrane, the presence of R_s leads to a discrepancy between the clamped pipette potential V and the true value of the cell membrane potential, V_m. The size of the error is $I \times R_s$ and is therefore large if the current being recorded is large. It is possible to compensate for R_s electronically by adding to the command voltage a voltage signal proportional to the membrane current. In commercial amplifiers this is achieved by multiplying the series resistance value from the whole-cell transient cancellation by I_p and adding a proportion, between 80 and 90%, to V_{ref}. Overcompensation of R_s causes the

clamp circuit to oscillate. Usually R_s can change over a short time scale during recording, causing R_s measurements to be imprecise. The most accurate compensation is obtained when the initial value of R_s is low and compensation is adjusted periodically during experiments. A reasonable value of R_s would be around 10 MΩ, which can often occur with pipette resistances of 4–5 MΩ. Occasionally R_s can be 50 MΩ or greater.

When using whole-cell recording, it is important to quantify the errors that may arise from parameters such as R_s and cell capacitance. These values may be estimated from the current transient that arises from small voltage steps (5 mV) in the voltage range where voltage-dependent currents are inactive. Provided that $R_s \ll R_m$, the area under the capacitive transient, which gives the charge on the cell membrane (Q), can be used to calculate cell capacitance, as $C = Q/V$. The time constant τ is obtained by measuring the single exponential rate of decay of the capacity transient, and thus from Eq. (4) provides a value for R_s.

B. Vibration

Sources of vibration can only successfully be dampened out by the use of a vibration isolation system. Electrical recordings from *Xenopus* oocytes, which measure up to 1 mm in diameter, can withstand mild mechanical disturbance and therefore it may be adequate to place the microscope, manipulators, and headstage on a heavy metal base plate positioned on an air-filled rubber support, such as bicycle tyre inner tubes or tennis balls. Cell-attached and whole-cell recordings may not withstand even the mildest wobbling of the pipette tip and so a more substantial vibration isolation system is required, such as a commercial air-damped flotation table (e.g., Newport, Melles Griot).

C. Removing Unwanted Signals

In order to minimise electrical interference, principally 50Hz signals, the experimental setup must be enclosed in an earthed Faraday cage. Within the cage, all metal components, including the manipulators, flotation tabletop, and microscope, must have good, low-resistance (<1 MΩ) connections to ground via a common earth point. This could be earth on the front of the oscilloscope, but most patch-clamp amplifiers also have a high-quality signal ground. The resistance between any two metal components on the setup should be measured using a multimeter and should be less than 1 Ω. All of the other instrumentation, including the oscilloscope, patch-clamp amplifier, microscope power source, computer interface, and filter, must be kept outside the cage, and it is also good practice to have shielded cables from these instruments to the main power supply as an added precaution.

IX. PATCH-CLAMP STUDIES IN CELL BIOLOGY

Perhaps the most common utilization of the patch-clamp technique is the measurement of ionic currents. These can be elicited in response to changes in membrane voltage, as well as to the application of synthetic or endogenous agonists such as neurotransmitters, growth factors, and hormones. Because the cell under analysis will contain a heterogeneous population of ionic channels, it is common practice to isolate the current of interest whilst blocking the remaining components of current. Voltage protocols can be developed such that the current of interest will be activated at a particular potential where the other ionic channels will be rendered inactive (Ogden and Stanfield, 1994). It is also possible to separate ionic currents pharmacologically.

Using the patch-clamp technique it is also possible to determine if agents stimulate membrane currents directly or via intracellular second messengers. For example, the atrial muscarinic K^+ channel is shown to be regulated by the βγ subunit of GTP-binding proteins using inside-out patches (Logothetis *et al.*, 1987), whereas activation of ligand-gated ion channel receptors, including NMDA receptors, P_{2X} receptors, GABA-A receptors, 5-HT_3 receptors, and nicotinic acetylcholine receptors, is directly related to agonist binding.

The patch-clamp technique can also be exploited to measure the secretion of vesicles from the cell, quantified by measuring stepwise changes in cell membrane capacitance, which occur upon fusion of the vesicles with the cell membrane (Neher and Marty, 1982). With newer sophisticated methods of noise reduction (Johnson *et al.*, 2002), cell capacitance measurements are now approaching resolution of the release of large synaptic vesicles into the synaptic cleft (Debus and Lindau, 2000).

Flash photolysis, which can be carried out in association with patch clamping, is a technique whereby a substance can be released rapidly inside or outside the cell from a photolabile "caged" compound present in the pipette or extracellular solution. An excellent review on the theory of flash photolysis is available (Park *et al.*, 2002). Flash photolysis of caged calcium has demonstrated the calcium dependence of vesicle

exocytosis in excitable cells (Heidelberger *et al*., 1994), allowing vesicle release kinetics and probability to be determined (Wolfel and Schneggenburger, 2003). Caged IP_3 has been used to map out calcium release sites within nonexcitable exocrine acinar cells (Hassoni and Gray, 1994), and caged ATP has been used to modulate the activity of ATP-sensitive K^+ currents (Clapp *et al*., 1994), as well as to determine the contribution these currents make to the resting membrane potential in pulmonary arterial myocytes (Clapp and Gurney, 1992).

References

Clapp, L. H., and Gurney, A. M. (1992). ATP-sensitive K^+ channels resting potential of pulmonary arterial smooth muscle cells. *Am. J. Physiol.* **262**, H916–H950.

Clapp, L. H., Gurney, A. M., Standen, N. B., and Langton, P. D. (1994). Properties of the ATP-sensitive K^+ current activated by levcromakalim in isolated pulmonary arterial myocytes. *J. Membr. Biol.* **140**, 205–213.

Debus, K., and Lindau, M. (2000). Resolution of patch capacitance recordings and of fusion pore conductances in small vesicles. *Biophys J.* **78**, 2983–2997.

Fertig, N., Blick, R. H., and Behrends, J. C. (2002). Whole cell patch clamp recording performed on a planar glass chip. *Biophys J.* **82**, 3056–3062.

Gurney, A. M. (1990). *In* "*Receptor-Effector Coupling: A Practical Approach*" (E. C. Hulme, ed.), p. 117. IRL Press.

Gurney, A. M. (1994). *In* "*Microelectrode Techniques: The Plymouth Workshop Handbook*" (D. Ogden, ed.), p. 389. Company of Biologists Ltd., Cambridge, UK.

Hassoni, A., and Gray, P. T. A. (1994). Flash photolysis studies of the localization of calcium release sites in rat parotid isolated acinar cells. *J. Physiol.* **478**, 461–467.

Heidelberger, R., Heinemann, C., Neher, E., and Matthews, G. (1994). Calcium dependence of the rate of exocytosis in a synaptic terminal. *Nature* **371**, 513–515.

Johnson, S. L., Thomas, M. V., and Kros, C. J. (2002). Membrane capacitance measurement using patch clamp with integrated self-balancing lock-in amplifier. *Pflug. Arch.* **443**, 653–663.

Korn, S. J., Marty, A., Connor, J. A., and Horn, R. (1991). Perforated patch recording. *Methods Neurosci.* **4**, 264–273.

Lepple-Wienhues, A., Ferlinz, K., Seeger, A., and Schafer, A. (2003). Flip the tip: An automated, high quality, cost-effective patch clamp screen. *Recept. Channels* **9**, 13–17.

Levis, R. A., and Rae, J. L. (1998). Low-noise patch-clamp techniques. *Methods Enzymol.* **293**, 218–266.

Logothetis, D. E., Kurachi, Y., Galper, J., Neer, E. J., and Clapham, D. E. (1987). The βγ subunits of GTP-binding proteins activate the muscarinic K^+ channel in heart. *Nature* **325**, 321–326.

Neher, E., and Marty, A. (1982). Discrete changes of cell membrane capacitance observed under conditions of enhanced secretion in bovine adrenal chromaffin cells. *Proc. Natl. Acad. Sci. USA* **79**, 6712–6716.

Neher, E., and Sakmann, B. (1976). Single channel currents recorded from membrane of denervated frog muscle fibres. *Nature* **260**, 799–802.

Ogden, D., and Stanfield, P. (1994). *In* "*Microelectrode Techniques: The Plymouth Workshop Handbook*" (D. Ogden, ed.), p. 53. Company of Biologists Ltd., Cambridge, UK.

Park, M. K., Tepikin, A. V., and Petersen, O. H. (2002). What can we learn about cell signalling by combining optical imaging and patch clamp techniques? *Pflug. Arch.* **444**, 305–316.

Rae, J., Cooper, K., Gates, G., and Watsky, M. (1991). Low access resistance perforated patch recordings using amphotericin B. *J. Neurosci. Methods* **37**, 15–26.

Sakmann, B., and Neher, E. (eds.) (1995). "*Single-Channel Recordings*" Plenum, New York.

Sigworth, F. J., and Klemic, K. G. (2002). Patch clamp on a chip. *Biophys J.* **82**, 2831–2832.

Voipio, J., Pasternack, M., and MacLeod, K. (1994). *In* "*Microelectrode Techniques: The Plymouth Workshop Handbook*" (D. Ogden, ed.), p. 275. Company of Biologists Ltd., Cambridge, UK.

Wolfel, M., and Schneggenburger, R. (2003). Presynaptic capacitance measurements and Ca^{2+} uncaging reveal submillisecond exocytosis kinetics and characterize the Ca^{2+} sensitivity of vesicle pool depletion at a fast CNS synapse. *J. Neurosci.* **23**, 7059–7068.

SECTION

13

Organ Cultures

CHAPTER

49

Preparation of Organotypic Hippocampal Slice Cultures

Scott M. Thompson and Susanne E. Mason

I. INTRODUCTION

Brain slice cultures are prepared by cutting thin sections of brain tissue from neonatal animals and culturing them as intact slices of tissue rather than as dissociated cells. Like all culture methods, these preparations offer the advantages of (1) long-term survival; (2) precise control of the experimental conditions; (3) excellent accessibility for viral vectors, biolistic transfection, and other means of gene transfection; (4) survival of tissue from neonatal-lethal transgenic animals; and (5) excellent visibility of cells and subcellular structures for morphological and electrophysiological studies. Unlike cell cultures, however, these tissue slices retain many features of their organotypic organization, as has been described extensively (e.g., Zimmer and Gähwiler, 1984; Gähwiler, 1984; Gähwiler *et al*., 1997). This permits the identification of defined cell groups, the stimulation or lesioning of specific axonal pathways, and the formation of relatively normally sized synaptic connections (Debanne *et al*., 1995). Other advantages of the slice culture technique include the ability to coculture slices from different brain regions, thus facilitating the experimental manipulation of long-distance connections *in vitro* (e.g., Gähwiler *et al*., 1987), and the ability to induce conventional long-term potentiation (e.g., Debanne *et al*., 1994).

There are two variations of the technique that are in use currently. In the roller tube technique, pioneered by Gähwiler (1981), the slices are attached to glass coverslips and placed in sealed test tubes on a roller drum in a dry air incubator. In the membrane or interface technique, pioneered by Stoppini *et al*. (1991), the slices are placed on semipermeable membranes and grown statically in CO_2 incubators. Primary differences between the two techniques are that the roller tube cultures generally become thinner than the membrane cultures, but may be slightly more demanding and time-consuming to prepare.

This article provides a concise description of the steps involved in preparing and maintaining hippocampal slice cultures. More details can be obtained in Gähwiler *et al*. (1998). Of course, many other brain structures can be cultured readily using these techniques. It is recommended that beginners start with the hippocampus, as it is large, easy to dissect, has a readily visible cell body layer, and has proven to be robust when cultured with these methods.

II. SOLUTIONS

Keep all solutions refrigerated until use. Maintain sterility.

1. *Roller tube culture medium*:

100 ml	basal medium Eagle (GIBCO, product # 21010)
50 ml	Hank's balanced salt solution (HBSS) with Earle's salts (GIBCO, product # 24020) or Hanks' balanced salt solution without phenol red for fluorescence applications (GIBCO product # 14025 or Cellgro, product # MT21-023-CV)
50 ml	horse serum (GIBCO, heat inactivated previously at 56°C for 30 min in a water bath, product # 16050)
4 ml	50% glucose solution, and
1 ml	200 m*M* glutamine (from frozen aliquots)

Copyright 2006, Elsevier Science (USA).
All rights reserved.

2. *Membrane culture medium*:

100 ml	MEM with Hank's salts and glutamine (GIBCO product # 11575)
50 ml	HBSS as described earlier
50 ml	horse serum as described earlier
1 ml	penicillin/streptomycin solution (Sigma product # P-4333)
1 g	HEPES
1 ml	50% glucose solution

3. *HBSS + glucose*:

500 ml	Hanks' balanced salt solution and
6 ml	50% glucose solution

4. *HBSS + glucose + kynurenate*:

50 ml	*HBSS + glucose* and
0.5 ml	300 µ*M* kynurenate stock solution

5. *Chicken plasma*: There is variability in the amount and type of anticoagulants contained in commercial plasmas. We recommend lyophilized chicken plasma from Cocalico Biologicals (product # 30-0390L). Reconstitute to appropriate volume with tissue culture water. Centrifuge for 18–20 min at 2500 rpm.

6. *Thrombin*: Prepare aliquots at 150 units/ml. Store frozen. Add 0.75 ml *HBSS + glucose* to 1 ml aliquot of thrombin. This dilution can be adjusted to modify the firmness of the plasma clot (see later).

7. *Antimitotics*: 3 mg each of cytosine-β-D-arabinofuranoside, uridine, and 5-fluoro-2'-deoxyuridine in 100 ml HBSS. Aliquot and freeze.

III. MATERIALS

A. Coverslips

Purchase 12 × 24-mm coverslips of 0/1 thickness. Place coverslips individually in the bottom of a large glass dish. Fill the dish with enough 95% ethanol to cover the coverslips. Soak them overnight. Replace the 95% ethanol with 100% ethanol and soak overnight. Let the coverslips dry overnight with the dish covered with a paper towel. Transfer the coverslips to a petri dish, wrap in aluminum foil, and bake at 200°C for 4–8 h.

B. Membrane Culture Dishes

Corning Costar Transwell polyester membrane inserts and multiwell dishes (product # 3460) (also available with various substrate coatings). Millipore Millicell membrane inserts can also be used.

C. Instruments

Small (ca. 3-cm blades) surgical scissors (1×)
Large (ca. 5-cm blade) surgical scissors (1×)
Scalpel or holder for razor blade shards (1×)
Small (ca. 3 × 20-mm) flat spatulas (6×)
Curved surgical forceps (1×)
Alcohol lamp (1×)

D. Plasticware

Aclar plastic (Ted Pella, Inc., product # 10501-25) (Cut into 4 × 4-cm squares.)
Culture tubes (Nunclon Flat sided TC tubes, 110 × 16 mm)
Petri dishes (60 × 15 and 35 × 10 mm)

E. Roller Drum and Drive Unit

Available from Bellco Glass (product # 7736-10164 and -20351). Set tilt angle to ca. 12° and rotation to ca. 10 rpm.

F. Tissue Chopper

McIlwain Mechanical Tissue Chopper (Brinkmann Instr., product # 023401002).

IV. PROCEDURES

A. Prior to Dissection

Day before Culturing

1. Using sterile forceps, place five coverslips in the upside down lid of a 60 × 15-mm petri dish.
2. Place 10 µl of poly-D-lysine (MW 30,000–70,000) on each coverslip and spread thoroughly with a small sterile spatula.
3. Allow to dry overnight before culturing.

Day of Culturing

1. Set out three 150-ml glass beakers with distilled water, 70% ethanol, and 95% ethanol. Turn on hood and light alcohol lamp.
2. Sterilize instruments by dunking in 70% ethanol and then in 95% ethanol. Large scissors and spatulas should be flamed in the alcohol lamp after removing from 95% ethanol.
3. Fill culture tubes with 750 µl of medium. Seal and store refrigerated.
4. Sterilize one aclar sheet for each animal by dunking in 70% ethanol and then in 95% ethanol. Allow to dry on sterile gauze pads in the hood.
5. Break a double-edged razor blade in half, wipe with 95% ethanol, and insert into the tissue chopper.

Swab the stage and mounted blade with 95% ethanol.

6. Set the micrometer on the chopper for the desired slice thickness (start with 400 µm). Set blade force (start at the "9 o'clock" position).
7. Thaw and prepare thrombin and chicken plasma.
8. Fill one 60 × 15-mm petri dish with *HBSS + glucose* solution to cover the bottom of the dish. These dishes are used for the dissected hippocampi. One dish is needed for each animal to be dissected. Store in a refrigerator.
9. Fill one 35 × 10-mm petri dish with *HBSS + glucose + kynurenate* to cover the bottom of the dish. These dishes are for the cut slices. One dish is needed for each animal to be dissected. Store in a refrigerator.

B. Tissue Dissection

1. Mount an aclar sheet on the chopper stage.

2. Place a 60 mm × 15-mm petri dish containing chilled *HBSS + glucose* in the hood.

3. It is recommended that you start with rat or mouse pups that are 5–7 days old. Younger animals can also be used, but the dissection will be more challenging. Animals older than 10 days rarely survive more than a few days *in vitro*.

4. Place one pup in a closed beaker with a small piece of dry ice for anesthesia.

5. When anesthetized, hold animal gently by head, rinse neck area with 70% ethanol, and decapitate with large scissors.

6. Hold head right side up with the nose pointing away. Insert tip of small scissors into the foramen magnum toward the nose with the flat of the blades in the horizontal plane. Cut by moving primarily the blade on the outside of the skull. Repeat on the other side. Discard bottom of head.

7. Hold top of head nose down over the petri dish. Using a spatula dipped in HBSS, push the brain stem, cerebellum, and midbrain down gently, leaving the cortex and hippocampus inside the dorsal skull. While sliding the wet spatula along the sides of the cortex, slide the cortex and hippocampus gently into the petri dish.

8. Under a dissecting microscope, position the brain dorsal side down. Use one spatula in your left hand to hold the brain in place by impaling the anterior brain. Use the razor blade chip to free one hippocampus at a time (Fig. 1). First, cut the lateral end of the hippocampus and then cut posterior to the hippocampal fissure, using the prominent blood vessel as a guide. Repeat for the other hippocampus, making one cut along the midline and another between septal nuclei and the hippocampus.

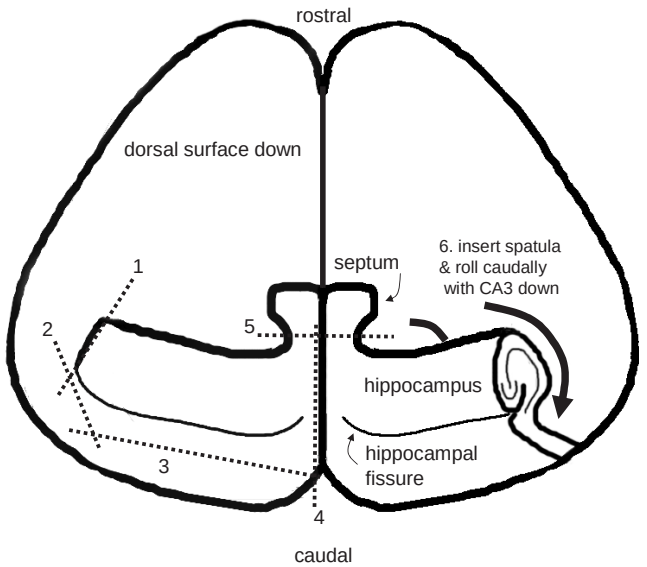

FIGURE 1 Dissection of the hippocampus. The diagram shows a view of the brain after peeling away the brain stem, midbrain, and thalamus and removing it from the skull as described in the text. It is pictured laying on its dorsal (i.e., cortical) surface and is viewed from the ventral aspect. The hippocampus is dissected free by making a series of sequential cuts with a razor blade shard as indicated by the numbered dashed lines. After cutting, a spatula is placed under the hippocampus and it is rolled caudally so that it becomes free of the cortex and rests on its CA3/DG surface.

9. Using a spatula dipped in HBSS, gently lift and roll the hippocampus away from the cortex in the rostral to caudal direction so that it rests with area CA1 up. **It is important that this be done without bending the hippocampus.**

10. Transfer the hippocampus to the aclar sheet on the chopper stage with CA1 up. The long axis of the hippocampus should be perpendicular to the length of the razor blade. Use a spatula to wipe any excess HBSS away from the hippocampus on the aclar. Failure to do so will result in the hippocampus being lifted by the blade while chopping. Repeat for the other hippocampus.

11. Chop slices.

12. Remove the aclar sheet from the chopper and, holding one corner, trim the aclar sheet into a "tongue" shape around the sliced hippocampi. Insert the aclar tongue into the small petri dish with *HBSS + glucose + kynurenate* and slide the slices off.

13. Under a dissecting microscope, separate the slices using two sterile spatulas. It is important that this be done gently, without bending the slices.

14. With proficiency, repeat steps 1–12 with a second animal.

15. If desired, X-irradiate the dishes containing the slices (1500 rad over ca. 1.5 min).

C. Mounting Slices for Roller Drum Cultures

1. Place one 20-µl drop of *chicken plasma* in the center of each coverslip in one 60-mm dish.
2. Under the dissecting scope, choose a healthy slice and transfer to the plasma droplet with a spatula. Healthy slices have a clear, well-defined continuous cell body layer and no obvious signs of damage. Repeat for all coverslips in dish.
3. Spread the plasma around and around the entire surface of the first coverslip around the slice (~3 s). Add a 20-µl drop of *thrombin* to the coverslip and mix thoroughly with the plasma over the entire coverslip (~3 s). Position the slice in the center of the coverslip and wipe excess plasma/thrombin off with a spatula. Repeat with the other coverslips and then for the second dish. After 5 min, the clot should have the consistency of a fairly liquid gelatin and should retain an indentation produced with a spatula.
4. Lift coverslips from dishes and slide into tissue culture tubes so that the bottom surface of the coverslip rests on the flat surface of the tube. Cap the tube tightly and gently tap the coverslip down to the bottom of the tube, if necessary. If slices fall off coverslips, increase the concentration of the thrombin to produce a firmer clot.
5. Place tubes in incubator.

D. Mounting Slices in Interface Culture Wells

The tissue dissection procedures are identical for the roller tube and membrane culture methods. Procedures for the latter preparations are different primarily in the substrate upon which the slices are placed. For membrane cultures, transfer slices with a wide-bore, fire-polished glass Pasteur pipette into the wells. To facilitate removal of slices from wells, small membrane pieces (e.g., Whatman Nucleopore membranes # 112107) can be cut and placed at the bottom of the insert before plating the slices.

E. Antimitotics

1. Add antimitotics after the first 4 or 5 days in culture.
2. Add 20 µl to each tube.
3. Exchange culture medium after 24 h.

F. Feeding the Cultures

1. Feed the cultures once per week.
2. Pour off medium into a beaker in the hood. About 250 µl will remain in tube.
3. Replace with 500 µl fresh medium.

G. Assessing the Health of the Cultures

1. Cultures should remain adhered firmly to the plasma and coverslip. If they fall off despite a firm clot at the time of culturing, suspect either insufficiently cleaned coverslips or a problem with the poly-L-lysine.
2. After 24–48 h *in vitro*, the slices will appear more opaque as the macrophages and other cells proliferate; remove damaged tissue. The cell body layer should remain relatively clear and visible. Glial cells migrating out of the edges of the slice should be apparent.
3. After 14 days *in vitro*, most of the macrophages should have disappeared and the cell body layer should be continuous and more transparent than the dendritic layers. Our studies indicate that the cultures are not completely mature before this time.
4. In our experience, unhealthy cultures can usually be attributed to mishandling of the tissue during dissection and mounting. If you have had good cultures previously and an entire batch goes bad, suspect a bad ingredient common to all of the cultures. If some cultures are good and some are bad, suspect a problem of dissection (it is helpful to note which slices came from which pups).

References

Debanne, D., Gähwiler, B. H., and Thompson, S. M. (1994). Asynchronous pre- and postsynaptic activity induces associative long-term depression in area CA1 of the rat hippocampus *in vitro*. *Proc. Natl. Acad. Sci. USA* **91**, 1148–1152.

Debanne, D., Guerineau, N. C., Gähwiler, B. H., and Thompson, S. M. (1995). Physiology and pharmacology of unitary synaptic connections between pairs of cells in areas CA3 and CA1 of rat hippocampal slice cultures. *J. Neurophysiol.* **3**, 1282–1294.

Gähwiler, B. H. (1981). Organotypic monolayer cultures of nervous tissue. *J. Neurosci. Methods.* **4**, 329–342.

Gähwiler, B. H. (1984). Development of the hippocampus *in vitro*: Cell types, synapses, and receptors. *Neuroscience* **11**, 751–760.

Gähwiler, B. H., Capogna, M., Debanne, D., McKinney, R. A., and Thompson, S. M. (1997). Organotypic slice cultures: A technique has come of age. *Trends Neurosci.* **20**, 471–477.

Gähwiler, B. H., Enz, A., and Hefti, F. (1987). Nerve growth factor promotes development of the rat septo-hippocampal cholinergic projection *in vitro*. *Neurosci. Lett.* **75**, 6–10.

Gähwiler, B. H., Thompson, S. M., McKinney, R. A., Debanne, D., and Robertson, R. T. (1998). Organotypic slice cultures of neural tissue. *In "Culturing Nerve Cells"* (G. Banker and K. Goslin, eds.), 2nd Ed., pp. 461–498. MIT Press, Cambridge, MA.

Stoppini, L., Buchs, P.-A., and Muller, D. (1991). A simple method for organotypic cultures of nervous tissue. *J. Neurosci. Methods* **37**, 173–182.

Zimmer, J., and Gähwiler, B. H. (1984). Cellular and connective organization of slice cultures of the rat hippocampus and fascia dentate. *J. Comp. Neurol.* **228**, 432–446.

CHAPTER

50

Thyroid Tissue-Organotypic Culture Using a New Approach for Overcoming the Disadvantages of Conventional Organ Culture

Shuji Toda, Akifumi Ootani, Shigehisa Aoki, and Hajime Sugihara

I. INTRODUCTION

The organ culture of thyroid tissue has been applied to the studies of thyroid biology (Bussolati *et al*., 1969; Cau *et al*., 1976; Young and Baker, 1982). However, the conventional organ culture system can not retain viable three-dimensional (3D) thyroid follicles containing both thyrocytes and C cells for a term long enough to investigate their biological behavior, as the tissue becomes necrotic progressively. Although the conventional method allows thyrocytes to grow out only in a monolayer from the tissue periphery placed on culture dishes, it cannot enable them to organize and maintain 3D follicles due to the lack of a 3D microenvironment of extracellular matrix (ECM) (Toda *et al*., 1996, 2001). Thyroid follicles *in vivo* are embedded in an interfollicular ECM, supported by a dense network of fenestrated capillaries (Fujita and Murakami, 1974). This suggests that both ECM and sufficient oxygen supply are important for the maintenance of follicular structure and function. By simulating this *in vivo* microenvironment of follicles, we have established a new organotypic culture using a 3D collagen gel culture of thyroid tissue fragments with improved oxygenation through air exposure (Toda *et al*., 2002). This system maintains very well the 3D follicle structures containing both thyrocytes and C cells for more than 1 month. Furthermore, the new follicle formation from preexisting follicles (mother follicle-derived folliculogenesis) takes place actively in the peripheral zones of each tissue fragments in our system (Toda *et al*., 2003). We herein describe a useful tool for the long-term organ culture of thyroid tissue. In relation to our method, we propose a new approach to cell type-specific culture systems on the basis of *in vivo* microenvironments of various cell types.

II. MATERIALS AND INSTRUMENTATION

Materials, reagents, and equipment are as follows: (1) 6-month-old porcine or human thyroid, (2) Eagle's MEM (EMEM, Cat. No. 05900, Nissui Pharmaceutical Co., Ltd., Tokyo, Japan), (3) dispase I solution (bacterial neutral protease, 1000 protease U/ml in EMEM, Cat. No. GD 81020, Goudoh-Shusei, Tokyo, Japan), (4) Ham's F12 (Cat. No. 05910, Nissui Pharmaceutical Co., Ltd.), (5) fetal bovine serum (FBS, Cat. No. F9423, Lot No. 92K2301, Sigma Chemical Co., MO), (6) gentamicin (Gentamicin, Shering-Plough Co., Ltd., Osaka, Japan), (7) complete medium (Ham's F-12 medium supplemented with 10% FBS and 50 μg/ml gentamicin), (8) acid-soluble type I collagen (Cellmatrix type I-A, Nitta Gelatin Co. Ltd., Osaka, Japan), (9) reconstructive buffer (2.2 g $NaHCO_3$ and 4.77 g HEPES in 100 ml 0.05 *M* NaOH), (10) a special culture dish of which the bottom is made with nitrocellulose membrane (30 mm diameter, Millicell-CM, Cat. No. PICAM 3050, Millipore, Bedford, MA), (11) 90-mm-diameter

Copyright 2006, Elsevier Science (USA).
All rights reserved.

bacterial dish (Cat. No. SH-2OS, Terumo Co., Ltd., Tokyo, Japan), and (12) stainless-steel mesh (840 µm, Cat. No. Testing Sieve 840, Ikemoto Rikakogyo Co., Ltd., Tokyo, Japan). All materials, reagents, and equipment used in culture must be sterile.

III. PROCEDURES

A. Initial Preparation of Tissue for the Organotypic Culture of the Thyroid

1. For porcine thyroid, tissues must be kept in ice-cold EMEM from the slaughterhouse to laboratory. Wash the tissue three times with ice-cold EMEM and remove connective and adipose tissues.
2. For human thyroid, obtain tissues from surgical materials with permission and follow the same procedures as in step 1.
3. For obtaining C cell-rich follicles, use tissue derived from only the middle to upper third of the lateral lobe of porcine and human thyroids, as C cells are mainly restricted to this area.

Steps

1. Mince thyroid tissue into small fragments (~2 mm) with sterile scissors.
2. Transfer the tissue fragments (5 g) into a 100-ml beaker containing 50 ml dispase I solution and incubate at 37°C for 1 h.
3. Remove the dispase I solution by filtrating the fluid through mesh (840 µm).
4. Further mince the tissue remaining on the mesh into smaller pieces (~0.5 mm) with sterile scissors.
5. Transfer the fragments into a 50 ml-test tube, wash the tissue fragments with ice-cold EMEM by pipetting, and then centrifuge the tissue suspension at 186 *g* for 5 min at room temperature. Repeat these procedures twice.
6. The thyroid tissue fragments obtained as a pellet after the final centrifugation are subjected to the following organotypic culture.

B. Preparation of Culture Assembly for Organotypic Culture

In comparison with the conventional organ culture, our culture system is characterized by the following items. (1) Minced tissues are placed in a 3D collagen gel. (2) They are supplied sufficient oxygen through air exposure. The two conditions result in allowing the tissue fragments to situate under a 3D air–liquid (A-L) interface, but not under a submerged state. In this system, the tissues are kept moist and fed with the culture medium that percolated by capillary action from the medium-containing outer dish, through the acellular layer, and into the cellular layer (Toda *et al.*, 2000, 2002, 2003). Likewise, the culture cells can be stimulated by various reagents added to the culture medium of the outer dish. In addition, exposing the cellular layer to various concentrations of oxygen permits the embedded cells to be supplied those of oxygen. Figure 1 illustrates our organotypic culture system.

Steps

1. Prepare the collagen gel solution as follows (Elsdale and Bard, 1972). First, mix 8 volumes of acid-soluble type I collagen with 1 volume of 10× concentrated Ham's F-12 medium by gently pipetting in a test tube. Second, add 1 volume of reconstructive buffer to the mixture and pipette it gently. Keep this mixture on ice.
2. Place 2 ml cold collagen gel solution in a special dish containing the nitrocellulose membrane and immediately warm the dish to 37°C for at least 30 min in a 5% CO_2 incubator for gel formation. The collagen gel layer is called the acellular layer. Preparation of this layer should be completed before the beginning the steps in Section III,A.
3. Pore 1 ml cold collagen solution into a test tube containing the tissue fragments obtained as a pellet. Then, gently and fully mix 1 ml cold collagen gel solution with the tissue fragments (a total of 0.5 g). The initial amount of 5 g tissue results in the preparation of 10 culture dishes.

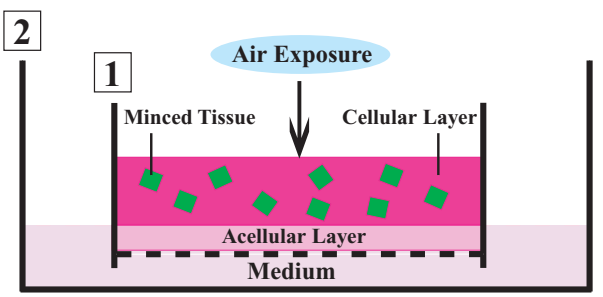

FIGURE 1 Scheme of thyroid tissue-organotypic culture system. Minced tissues embedded in type I collagen gel (cellular layer) are placed on the acellular gel (acellular layer) in the inner dish (1). The inner dish (1) is put in the outer dish (2) with culture medium. In this way, tissues in the cellular layer are localized under air exposure-induced oxygenation. Tissues are kept moist and are fed by culture medium that percolates by capillary action from the medium-containing outer dish through the acellular layer and into the cellular layer.

4. Place 1 ml collagen gel solution containing the fragments on the acellular layer and immediately warm the dish to 37°C for at least 30 min in a 5% CO_2 incubator to allow gel formation. The resultant overlayer is the cellular layer. The culture dish prepared in this way is referred to as the "inner" dish.

5. After at least 30 min, when the gel is fully firm, place the inner dish in a larger "outer" dish (90 mm in diameter) containing 10 ml complete medium.

6. Place this culture assembly in a conventional culture incubator, thereby exposing the cellular layer to a humidified air atmosphere supplemented with 5% CO_2 at 37°C. In this way, the tissue fragments are situated under a microenvironment that consists of both type I collagen and air exposure-induced oxygenation. We call this culture condition a 3D A-L interface.

C. Analyses of Organotypic Culture Cells

Culture cells can be observed by phase-contrast microscopy. The collagen gel layer containing viable cells is scraped easily from the culture assembly. The layer can be treated similar to the various tissues resected from the body and used for analyzing the cellular behavior as follows. (1) The cellular layer gels are fixed in 4% formalin, processed routinely, and embedded in paraffin. The deparaffinized and frozen sections are applied easily to histochemistry, immunohistochemistry, and *in situ* hybridization. (2) To examine the fine structure of the cells, transmission electron microscopy is carried out using cellular layer gels fixed in 2.5% glutaraldehyde and prepared by a standard method. (3) Biochemical and genetic analyses of the cells can be carried out by the various methods described in this volume.

D. Examples of Thyroid Tissue-Organotypic Cultures

In this system, viable 3D follicles within thyroid tissue fragments are maintained for more than 1 month. These follicle structures consist of thyrocytes and C cells with their specific differentiation (Fig. 2). In the tissue periphery, thyrocytes undergo actively growth and mother follicle-derived thyroid folliculogenesis. Likewise, isolated or clustered thyrocytes, which were localized in the tissue periphery at the starting time of the culture, reconstruct follicles. C cells show no proliferative ability and cannot grow even with the stimulation of various concentrations of free calcium. Most endothelial cells of capillaries disappear until 7 days in culture (for further details, see Toda *et al.*, 1990, 1992, 1993, 1997, 2002, 2003).

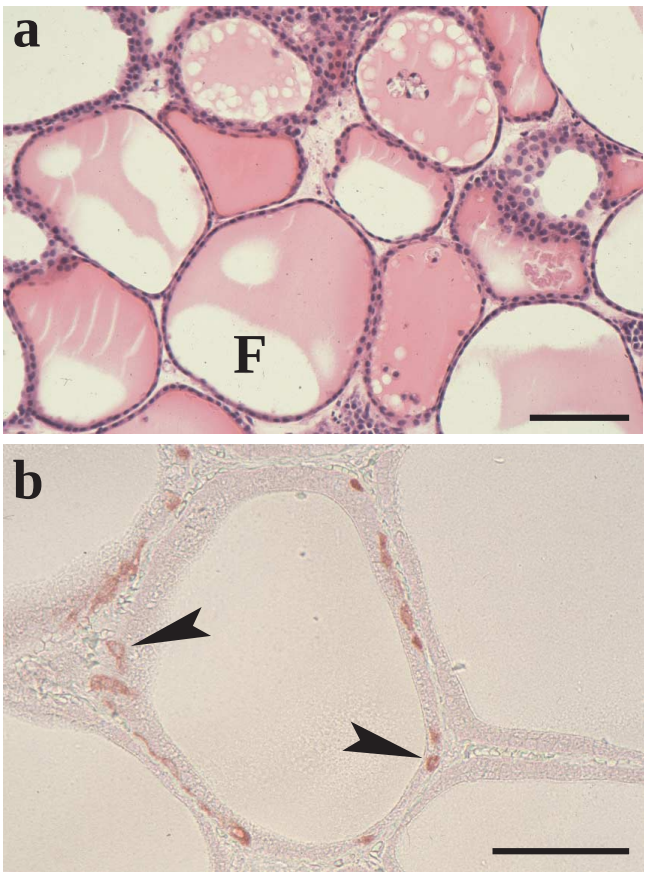

FIGURE 2 Histology of thyroid tissues (a) and immunohistochemistry for calcitonin (b) in the organotypic culture. (a) At 40 days in culture, viable thyroid follicles enclosed by thyrocytes contain colloid substance in their lumens (F). (b) At 30 days in culture, thyroid follicles consisting of both thyrocytes and C cells (arrowheads) are clearly maintained. Scale bar: 100 μm.

IV. COMMENTS

In relation to our culture system, it seems that the time has come to reconsider conventional culture methods in a cell type-specific way. The microenvironments of many cell types of the body are subdivided mainly into the following three types. The first is that of parenchymal and stromal cell types of solid organs, e.g., thyroid, adrenal, and liver. The second is that of surface-lining cell types on which sufficient liquid is not overlayed, e.g., those of the skin, cornea, respiratory, and digestive tracts. The third is the microenvironment of surface-lining cell types on which enough fluid is overlayed, e.g., those of the cardiovascular system and cerebral ventricle. With respect to the first microenvironment, the following is our notion regarding that of the *in vivo* extravascular stroma by which various cell types are supported. The

extravasucular space consists of ECM and tissue fluid percolated from blood vessels. The tissue fluid blended by nutrients and air molecules infiltrates into ECM and results in formation of the moist stroma. The moist microenvironment is different from the intravascular one, which has the sufficient liquid of blood. Our culture system seems to simulate simply the first microenvironment of extravascular stroma (Toda *et al*., 2001, 2002, 2003). Thus, our system is suitable for culturing various cell types other than surface-lining cell types.

On the basis of the *in vivo* microenvironment of various cell types, we propose the following three culture systems in a cell type-specific manner. (1) The usual monolayer culture under a submerged condition with enough medium is suitable for culturing the surface-lining cell types of endothelial cells, ependymocytes, and so on (Tokunaga *et al*., 1991). (2) The A-L interface culture is useful for culturing the surface-lining cell types of epidermis, cornea, respiratory, and digestive tracts (Nishimura *et al*., 1998; Yamada *et al*., 1999; Sugihara *et al*., 2001; Ootani *et al*., 2003). (3) A three-dimensional collagen gel culture with an A-L interface is suitable for culturing parenchymal and stromal cell types of solid organs (Toda *et al*., 2000, 2002, 2003).

V. PITFALLS

The organ culture method described in this article is very simple and it is reproduced easily by beginners. The only one pitfall regarding our method is as follows: the collagenase solution should not be used to loosen ECM of thyroid tissue because the collagen gel layer is often digested by the remaining collagenase, even after washing the tissue fragments three times. Thus, dispase I solution is recommended.

References

Bussolati, G., Navone, R., Gasparri, G., and Monga, G. (1969). *In vitro* study of C (parafollicular) cells of dog thyroid in organ culture. *Experimentia* **25**, 641–642.

Cau, P., Michel-Bechet, M., and Fayet, G. (1976). Morphogenesis of the thyroid follicles *in vitro*. *Adv. Anat. Embry. Cell Biol.* **52**, 5–65.

Elsdale, T., and Bard, J. (1972). Collagen substrata for studies on cell behavior. *J. Cell Biol.* **54**, 626–637.

Nishimura, T., Toda, S., Mitsumoto, T., Oono, S., and Sugihara, H. (1998). Effects of hepatocyte growth factor, transforming growth factor-beta1 and epidermal growth factor on bovine corneal epithelial cells under epithelial-keratocyte interaction in reconstruction culture. *Exp. Eye Res.* **66**, 105–116.

Ootani, A., Toda, S., Fujimoto, K., and Sugihara, H. (2003). Foveolar differentiation of mouse gastric mucosa *in vitro*. *Am. J. Pathol.* **162**, 1905–1912.

Sugihara, H., Toda, S., Yonemitsu, N., and Watanabe, K. (2001). Effects of fat cells on keratinocytes and fibroblasts in a reconstructed rat skin model using collagen gel matrix culture. *Br. J. Dermatol.* **144**, 244–253.

Toda, S., Aoki, S., Suzuki, K., Koike, E., Ootani, A., Watanabe, K., Koike, N., and Sugihara, H. (2003). Thyrocytes, but not C cells, actively undergo growth and folliculogenesis at the periphery of thyroid tissue fragments in three-dimensional collagen gel culture. *Cell Tissue Res.* **312**, 281–289.

Toda, S., Koike, N., and Sugihara, H. (2001). Thyrocyte integration, and thyroid folliculogenesis and tissue regeneration: Perspective for thyroid tissue engineering. *Pathol. Int.* **51**, 403–417.

Toda, S., Matsumura, S., Fujitani, N., Nishimura, T., Yonemitsu, N., and Sugihara, H. (1997). Transforming growth factor-β1 induces a mesenchyme-like cell shape without epithelial polarization in thyrocytes and inhibits thyroid folliculogenesis in collagen gel culture. *Endocrinology* **138**, 5561–5575.

Toda, S., and Sugihara, H. (1990). Reconstruction of thyroid follicles from isolated porcine follicle cells in three-dimensional collagen gel culture. *Endocrinology* **126**, 2027–2034.

Toda, S., and Sugihara, H. (1996). Primary culture of the thyroid: Three-dimensional culture using extracellular matrix. *In* "Cell and Tissue Culture: Laboratory Procedures" (J. B. Griffiths, A. Doyle, and D. G. Newell, eds.), pp. 17B:2.1–12. Wiley, Baffins Lane, England.

Toda, S., Watanabe, K., Yokoi, F., Matsumura, S., Suzuki, K., Ootani, A., Aoki, S., Koike, N., and Sugihara, H. (2002). A new organotypic culture of thyroid tissue maintains three-dimensional follicles with C cells for a long term. *Biochem. Biophys. Res. Commun.* **294**, 906–911.

Toda, S., Yokoi, F., Yamada, S., Yonemitsu, N., Nishimura, T., Watanabe, K., and Sugihara, H. (2000). Air exposure promotes fibroblast growth with increased expression of mitogen-activated protein kinase cascade. *Biochem. Biophys. Res. Commun.* **270**, 961–966.

Toda, S., Yonemitsu, N., Hikichi, Y., Koike, N., and Sugihara, H. (1992). Differentiation of human thyroid follicle cells from normal subjects and Basedow's disease in three-dimensional collagen gel culture. *Pathol. Res. Pract.* **188**, 874–882.

Toda, S., Yonemitsu, N., Minami, Y., and Sugihara, H. (1993). Plural cells organize thyroid follicles through aggregation and linkage in collagen gel culture of porcine follicle cells. *Endocrinology* **133**, 914–920.

Tokunaga, O., Yamada, T., Fan, J. L., and Watanabe, T. (1991). Age-related decline in prostacyclin synthesis by human aortic endothelial cells: Qualitative and quantitative analysis. *Am. J. Pathol.* **138**, 941–949.

Yamada, S., Toda, S., Shin, T., and Sugihara, H. (1999). Effects of stromal fibroblasts and fat cells and an environmental factor air exposure on invasion of laryngeal carcinoma (HEp-2) cells in a collagen gel invasion assay system. *Arch. Otolaryngol. Head Neck Surg.* **125**, 424–431.

Young, B. A., and Baker, T. G. (1982). The ultrastructure of rat thyroid glands under experimental conditions in organ culture. *J. Anat.* **135**, 407–412.

PART

B

VIRUSES

SECTION

14

Growth and Purification of Viruses

CHAPTER

51

Growth of Semliki Forest Virus

Mathilda Sjöberg and Henrik Garoff

I. INTRODUCTION

Semliki Forest virus (SFV) is an enveloped RNA virus, with a genome of positive polarity that belongs to the Alphavirus group of the family Togaviridae. It readily infects a variety of mammalian and insect cells and can be grown to high titres in tissue culture. Upon infection, host cell-specific synthesis of macromolecules is suppressed within a few hours, structural viral components are made, and new virus particles bud out from the plasma membrane of the infected cell. The SFV particle is spherical with a diameter of approximately 65 nm (molecular mass $\approx 42 \times 10^3$ kDa). It consists of a nucleocapsid (NC), a single copy of the RNA genome packed together with 240 copies of a capsid (C) protein (33 kDa), that is surrounded by a lipid membrane in which 80 glycoprotein complexes, the viral spikes, are anchored. The viral spikes are trimeric associations of a protein complex: two membrane-spanning proteins, E1 and E2 (49 and 52 kDa), and a peripheral protein, E3 (10 kDa) (Garoff *et al.*, 1982; Strauss and Strauss, 1994). This article provides protocols to grow SFV in intermediate scale (up to ≈1.5 mg; protocol A) and small scale (^{35}S-methionine labelled; protocol B).

II. MATERIALS AND INSTRUMENTATION

Culture medium Glasgow minimum essential medium (MEM) (BHK-21) (Cat. No. 21710), foetal bovine serum (FBS) (Cat. No. 10106), tryptose phosphate broth (Cat. No. 18050), 1 *M* HEPES (Cat. No. 15630), L-glutamine 200 m*M* (100X) (Cat. No. 25030), penicillin–streptomycin (Cat. No. 15140), MEM (Cat. No. 21090-022), bovine albumin fraction V solution 7.5% (BSA; Cat. No. 15260-037), and phosphate-buffered saline (PBS) Dulbecco's with Ca^{2+} and Mg^{2+} (Cat. No. 14040) are from GIBCO BRL. Sea-plaque agarose (Cat. No. 50100) is from FMC Bio Products. Redivue-[^{35}S]methionine (Cat. No. AG 1094) is from Amersham Biosciences. Sucrose (Cat. No. 0335) is from Amresco. Tris (Cat. No. 146861) is from Angus. Sodium chloride (NaCl) (Cat. No. 106404), HCl (Cat. No. M317), and Titriplex III (EDTA; Cat. No. 108418) are from Merck. NaOH (Cat. No. 05-400201) is from EKA Nobel AB (Tamro). Cholesterol (Cat. No. C3045), neutral red (Cat. No. N6634), and methionine-free MEM (Cat. No. 31900-012) are from Sigma-Aldrich. The density gradient fractionator (Model 185) is from Instrumentation Specialities Company (ISCO). Filter papers No. 1 (Cat. No. 1001 090) are from Whatman. The 75-cm^2 flasks (Cat. No. 3375) and 162-cm^2 flasks (Cat. No. 3150) are from Corning Life Sciences. Sixty-millimeter tissue culture plates (Cat. No. 50288) are from Nunc. BHK-21 cells C-13 (Cat. No. CRL-8544) are from American Type Culture Collection. Cotton-tipped applicators are from Solon manufacturing company. Fifty-milliliter Nalgene tubes (Cat. No. 3139-0050) are from Nalge Incorporated. SW 28 tubes (Cat. No. 344058), SW 40 tubes (Cat. No. 331374), and 6 ml-scintillation vials (Cat. No. 566831) are from Beckman. Eppendorf tubes, 1.5 ml (Cat. No. 0030 102.002) and 2.0 ml (Cat. No. 0030 120.094), are from Eppendorf-Netheler-Hinz GmbH. Emulsifier Safe is from Packard Instrument Co. Inc.

Copyright 2006, Elsevier Science (USA).
All rights reserved.

III. PROCEDURES

A. Growth of SFV

Solutions

1. *Complete BHK-21 medium*: To make 585 ml, add 50 ml of tryptose phosphate broth, 25 ml of FBS, 5 ml of 1 *M* HEPES, and 5 ml of 200 m*M* glutamine to 500 ml of Glasgow MEM (BHK-21). Store at 4°C.
2. *Complete BHK-21 medium + cholesterol* (optional): To make 250 ml, add 0.5 ml 10 mg/ml cholesterol stock solution (dissolve at 37°C prior to use) to 250 ml complete BHK medium.
3. *10 mg/ml cholesterol stock solution* (optional): Add 50 mg cholesterol to 5 ml 99.5% ethanol. Dissolve. Aliquot and store at –20°C.
4. *Supplemented MEM*: To make 529 ml, add 14 ml of 7.5% BSA, 5 ml of 1 *M* HEPES, 5 ml of 200 m*M* glutamine, 5 ml of 10,000 U/ml penicillin/10,000 µg/ml streptomycin to 500 ml of MEM. Store at 4°C.
5. *TN*: 50 m*M* Tris–HCl, pH 7.4, 100 m*M* NaCl. To make 500 ml, add 3.0 g of Tris and 2.9 g NaCl to distilled water, adjust pH to 7.4 by adding 1 *M* HCl, and complete the volume to 500 ml. Autoclave. Store at room temperature.
6. *0.25 M EDTA pH 8.0 stock solution*: To make 50 ml, add 4.65 g of Titriplex III to 30 ml of distilled water. Adjust the pH to 8.0 by adding 1 *M* NaOH and complete the volume to 50 ml. Autoclave. Store at room temperature.
7. *TNE*: 50 m*M* Tris–HCl, pH 7.4, 100 m*M* NaCl, 0.5 m*M* EDTA. To make 100 ml, add 200 µl 0.25 *M* EDTA, pH 8.0, stock solution to 100 ml TN. Store at room temperature.
8. *200 g/kg sucrose solution*: To make 100 g, weigh 20 g of sucrose and adjust to 100 g with TNE. Store at –20°C.

Steps

1. Grow BHK-21 cells to 100% confluency in a 162-cm^2 tissue culture bottle in complete BHK medium with or without cholesterol (≈2.2×10^7 cells/bottle).
2. Dilute the virus to a concentration of 1.1×10^6 pfu/ml in supplemented MEM.
3. Remove the medium and wash the cells with 10 ml of PBS (with Ca^{2+} and Mg^{2+}). Add 2.0 ml of the diluted virus to the cells. Incubate for 60 min at 37°C and 5% CO_2. Tilt the bottle every 20 minute to ensure even distribution of virus particles.
4. Remove virus solution and rinse with 10 ml PBS (with Ca^{2+} and Mg^{2+}). Add 30 ml complete BHK medium with or without cholesterol and incubate for 18 h at 37°C and 5% CO_2.
5. Transfer the virus containing medium to a 50-ml Nalgene tube (30 ml/tube) and centrifuge at 26,500 *g* and 4°C for 10 min in a J2-21 Beckman centrifuge equipped with a JS 13.1 rotor (13,000 rpm).
6. Pipette the medium to a fresh tube, without disturbing the pellet, and centrifuge as in step 5.
7. Repeat step 6.
8. Transfer 20 ml of the clarified medium to an SW 28-tube. Layer 4.0 ml 200 g/kg sucrose in TNE under the sample. Add the remaining 8–10 ml of clarified medium to the top of the tube and centrifuge at 112,000 *g* and 4°C for 90 min in a L8-M Beckman centrifuge equipped with a SW 28 rotor (25,000 rpm).
9. Aspirate off the supernatant. Pour the last 0.5 ml into the pipette by tilting the tube. Wipe off the last drops of supernatant from the inside of the tube with a sterile, cotton-tipped applicator.
10. Add 200 µl TNE, cover the tube with Parafilm, and leave on ice for 15 h.
11. Pass the virus suspension slowly up and down in a Gilson P-200 pipette to resuspend the virus. Transfer the suspension to a 1.5-ml Eppendorf tube, rinse the SW 28 tube with 100 µl TNE, and pool.
12. Mix 10 µl of the virus suspension with 90 µl TNE (dilution factor, $D = 10^{-1}$) and measure the optical density at 260 and 280 nm, e.g., in a Pharmacia Ultrospec plus spectrophotometer equipped with a 50-µl cuvette with a 10-mm path length. Calculate the ratio $R = A_{260}/A_{280}$ ($R = 1.4 \pm 0.1$ for pure SFV particles). Estimate the virus concentration (C_{SFV}) if the preparation is sufficiently pure; $C_{SFV} = A_{260}/(D \times 8)$ [mg/ml].
13. Analyse the virus preparation by SDS–PAGE under nonreducing conditions and visualise the bands by Coomassie brilliant blue staining.
14. Aliquot the virus suspension in smaller portions, quick freeze in dry ice/ethanol, and store at –70°C.

B. Growth of ^{35}S-Methionine-Labelled SFV

Solutions

1. *Starvation medium*: To make 103 ml, add 1 ml of 200 m*M* glutamine, 1 ml of 1 *M* HEPES, and 1 ml of 10,000 U/ml penicillin/10,000 µg/ml streptomycin to 100 ml of methionine-free MEM. Store at 4°C.
2. *Labelling medium*: To make 7.5 ml, add 50 µl Redivue [^{35}S]methionine (370 MBq/ml) to 7.5 ml starvation medium.
3. *550 g/kg sucrose*: To make 50 g, weigh 27.5 g sucrose and adjust to 50 g with TNE. Store at –20°C.
4. *Complete BHK medium, supplemented MEM, and 200 g/kg sucrose*: see Section III,A.

Steps

1. Grow BHK-21 cells to 100% confluency in a 75-cm^2 tissue culture bottle in complete BHK medium ($\approx 1 \times 10^7$ cells/bottle).
2. Dilute the virus to a concentration of 1×10^8 plaque-forming units (pfu)/ml in supplemented MEM.
3. Remove the medium and wash the cells with 10 ml of PBS (with Ca^{2+} and Mg^{2+}). Add 1.0 ml of the diluted virus to the cells. Incubate for 60 min at 37°C and 5% CO_2. Tilt the bottle every 20 min to ensure even distribution of virus particles.
4. Remove virus solution, add 15 ml complete BHK medium, and incubate for 3.5 h at 37°C and 5% CO_2.
5. Rinse the cells two times with 10 ml PBS (with Ca^{2+} and Mg^{2+}). Add 15 ml of starvation medium, and incubate for 30 min at 37°C and 5% CO_2.
6. Remove the starvation medium, add 7.5 ml of labelling medium, and continue incubation at 37°C and 5% CO_2 for 15–16 h.
7. Harvest the labelling medium and dispense in four 2-ml Eppendorf tubes.
8. Centrifuge at 12,400 *g* and 4°C for 5 min in an Eppendorf 5416 centrifuge equipped with a 16 F24-11 rotor (11,000 rpm).
9. Transfer the supernatants into new tubes, without disturbing the pellet, and repeat centrifugation as in step 8.
10. Repeat step 9.
11. Pool the clarified medium in an SW 40 tube. Layer 4.5 ml of 200 g/kg sucrose under the radioactive medium and 1 ml 550 g/kg sucrose under the lighter sucrose.
12. Centrifuge at 143,000 *g* and 4°C for 2 h in an L8-M Beckman centrifuge equipped with a SW 40 rotor (30,000 rpm).
13. Connect the ISCO density gradient fractionator to a peristaltic pump (Pharmacia Pump P1, inner diameter of tubing = 1.0 mm, speed setting = 2 × 10) and a Gilson FC 203B fraction collector. Clamp the SW 40 tube in the fraction collector, perforate the tube from the bottom, and collect 20 fractions of five drops each.
14. To measure the radioactivity in each fraction, pipette 50 µl H_2O followed by 2 µl of the fraction (delivered into the water droplet) and 3 ml Emulsifier-Safe into twenty 6-ml scintillation vials. Mix and count using the ^{35}S window in a liquid scintillation counter.
15. Pool the peak fractions (usually fractions 5–9) and analyse the virus preparation by SDS–PAGE under nonreducing conditions. Aliquot 25-µl portions in 1.5-ml Eppendorf tubes, quick freeze in dry ice/ethanol, and store at –70°C.

C. Quantitation of Infectious Virus Particles by Plaque Titration

Solutions

1. *Complete BHK medium and supplemented MEM*: see Section III,A.
2. *Agarose stock solution*: To make 100 ml, add 1.9 g of Seaplaque, low melting point agarose to 100 ml MEM. Autoclave and store at 4°C.
3. *BHK-medium + 2x additives*: To make 136 ml, add 20 ml of tryptose phosphate broth, 10 ml of FBS, 2 ml of 1 *M* HEPES, 2 ml of 200 m*M* glutamine, and 2 ml of 10,000 U/ml penicillin/10,000 µg/ml streptomycin to 100 ml of Glasgow-MEM (BHK-21). Store at 4°C.
4. *Neutral red (2% stock solution)*: To make 50 ml, add 1.0 g neutral red to 50 ml H_2O. Filter through a Whatman No. 1 paper and store at room temperature.
5. *Neutral red stain*: To make 100 ml, add 3 ml of neutral red, 2% stock solution to 99 ml of PBS (with Ca^{2+} and Mg^{2+}). Use fresh.

Steps

1. Grow BHK-21 cells to ≈90% confluency on 60-mm tissue culture plates in complete BHK medium ($\approx 3.4 \times 10^6$ cells per plate). Prepare 10 plates per virus preparation to be titrated and 2 extra plates to be used as negative and positive controls.

2. To make a serial dilution of the virus preparation, label ten 2.0-ml Eppendorf tubes (1–10) and pipette 445 µl supplemented MEM to the first tube and 1.35 ml supplemented MEM to the following nine tubes. Add 5 µl of the virus preparation to the first tube, mix thoroughly, and transfer 150 µl of the mixture to the second tube. Mix the contents of the second tube and transfer 150 µl to the third tube using a fresh pipette tip. Continue in the same fashion with the last seven tubes. Make two parallel dilution series for each virus preparation to be titrated.

3. Melt the agarose stock solution in a microwave oven. Mix 35 ml of the agarose stock solution and 35 ml of the BHK-medium + 2× additives to complete the overlay solution. Keep in a 37°C water bath until use.

4. Remove the medium from the cells and wash with 2 ml of PBS (with Ca^{2+} and Mg^{2+}).

5. Add 1.0 ml of diluted virus (use tubes 6–10 from the two dilution series; these correspond to dilution factors 10^{-7} through 10^{-11}). Use supplemented MEM

as a negative control and a suitable dilution of a known virus stock (if available) as a positive control.

6. Incubate for 60 min 37°C and 5% CO_2. Tilt the plates every 20 min to ensure even distribution of virus particles.

7. Remove the virus solution from the cells, rinse with 2 ml of PBS (with Ca^{2+} and Mg^{2+}), and add 4 ml of overlay solution (keep the bottle in a beaker filled with 37°C water). Leave the plates at room temperature until the agarose solidifies.

8. Incubate the plates for 48 h at 37°C and 5% CO_2.

9. Add 3 ml of neutral red stain and incubate for 3 h at 37°C (5% CO_2 is optional).

10. Score the number of plaques (diffuse, clear areas on a dark red background) on each plate. To calculate the virus titre as plaque-forming units per milliliter, divide the number of plaques per plate by the appropriate dilution factor.

IV. COMMENTS

Cells used for SFV infections in this protocol (old BHK cells) are BHK-21 cells that with time in culture have transformed further. In doing so, they have lost the extended form of normal BHK-21 cells (freshly obtained from ATCC) and appear more like penta- or hexagons. The SFV strain used [SFV4 (Liljeström *et al*., 1991)] had undergone an unknown number of passages in the old BHK cells (Glasgow *et al*., 1991) before it was cloned. At present the specific titre (i.e., the number of infectious virus particles divided by the total number of virus particles produced) is approximately 10 times higher when a virus preparation is titrated on old BHK cells as compared to normal BHK-21 cells. This is also the case when the virus is produced in normal BHK-21 cells and most likely reflects an adaptive change in SFV4 that facilitates entry into the old BHK cells.

The expected yield of SFV particles is approximately 1 µg/cm^2 of confluent BHK cells. When larger amounts (mg) of SFV are desirable, the amount of complete BHK medium used in the production step (Section III,A, step 4) can be reduced down to 20 ml per 162-cm^2 bottle.

An alternative method to estimate the amount of SFV in a preparation is to use CBB-stained SDS–PAGE gels and compare the intensity of the capsid protein band to that of known amounts of BSA ran under reducing conditions on the same gel (five wells with 0.15, 0.3, 0.6, 1.2, and 2.4 µg, respectively, is sufficient). The amount of C protein (m_C) in a band is half the amount of BSA in a band of equal intensity. The amount of SFV (m_{SFV}) is calculated as $m_{SFV} = (3 \times m_C)/2$.

The stability of the produced SFV is improved if the producer cells are supplied with cholesterol in the growth media. This procedure is indicated as optional in the protocol and is not necessary for the production of stock virus intended for infection of new cells.

The crude virus preparation obtained in Section III,A, step 11 can be purified by isopycnic tartrate gradient centrifugation as described by Haag and collegues (2002). To this end, cholesterol should be used during virus production and the TNE used in step 10 should be replaced by TNM (50 m*M* Tris–HCl, 50 m*M* NaCl, 10 m*M* $MgCl_2$, pH 7.4) for improved virus stability.

The E1 and E2 proteins of SFV comigrate upon SDS–PAGE under reducing conditions. Without reduction, E1 and E2 are separated readily, with E2 showing a higher apparent molecular mass than E1.

Intact SFV particles contains 88% (w/w) of protein and 12% (w/w) of RNA (Garoff *et al*., 1982). This is equivalent to an A_{260}/A_{280} ratio of 1.4, provided that A_{260}/A_{280} of pure RNA equals 2.0 (Glaser, 1995; Manchester, 1995). Deviations from this figure ($A_{260}/A_{280} = 1.4 \pm 0.1$) imply that the SFV preparation contains impurities and/or defective particles.

To maintain high virus quality in successive SFV preparations, it is important to use a low multiplicity of infection (MOI). The use of MOI = 0.1 (i.e., 0.1 infectious particle per cell) or less ensures that the initial infection is caused by a single virus particle. In this case, virus particles that carry deletions or other deleterious mutations in their genomes cannot be rescued by multiple infection with functional virus particles. If a high MOI is used in a series of successive infections, the number of so-called defective interfering (DI) particles will increase dramatically (Stark and Kennedy, 1978). The presence of high numbers of DI particles may express itself by low specific infectivity of the newly produced virus. In single round infections, such as radiolabelling experiments, a MOI of 5 to 10 can be advantageous as this will produce a synchronised burst of SFV production in the shortest possible time.

V. PITFALLS

Avoid repeated freeze/thaw cycles, as this will reduce virus infectivity.

If SFV infection is carried out in serum-containing medium, e.g., complete BHK medium, the infectivity of the particles is reduced dramatically. Without interference, at maximum 30% complete BHK medium may be present during infection.

Efficient clarification of the virus containing medium (Section III,A, steps 5–7) is important. Cell debris present during virus pelletation (step 8) will glue the virus particles together and make resuspension difficult.

To preserve the three-dimensional structure of the virus particles, it is important to allow sufficient time for resuspension. Do not decrease the time that the virus is left on ice (Section III,A, step 10).

When trace amounts of SFV proteins are separated on SDS–PAGE, the C protein tends to smear over the lane. This can be avoided if a small volume of BHK cell lysate is included in the sample buffer prior to heating (add 1 µl BHK cell lysate for every 10 µl of SDS–PAGE sample buffer). To make BHK cell lysate, grow BHK-21 cells to 100% confluency in a 35-mm tissue culture plate, lyse in 300 µl 1× lysis buffer, and remove cell nuclei by low-speed centrifugation. Store the BHK cell lysate at –20°C. The addition of cell lysate is not necessary when the amount of virus protein in the gel is sufficient for Coomassie brilliant blue staining. Silver staining is not recommended.

References

Garoff, H., Kondor-Koch, C., and Riedel, H. (1982). Structure and assembly of alphaviruses. *Curr. Top. Microbiol. Immunol.* **99**, 1–50.

Glaser, J. A. (1995). Validity of nucleic acid purities monitored by 260 nm/280 nm absorbance ratios. *Biotechniques* **18**, 62–63.

Glasgow, G. M., Sheahan, B. J., Atkins, G. J., Wahlberg, J. M., Salminen, A., and Liljeström, P. (1991). Two mutations in the envelope glycoprotein E2 of Semliki Forest virus affecting the maturation and entry patterns of the virus alter pathogenicity for mice. *Virology* **185**, 741–748.

Haag, L., Garoff, H., Xing, L., Hammar, L., Kan, S.-T., and Cheng, R. H. (2002). Acid-induced movements in the glycoprotein shell of an alphavirus turn the spikes into membrane fusion mode. *EMBO J.* **21**, 255–264.

Liljeström, P., Lusa, S., Huylebroeck, D., and Garoff, H. (1991). In vitro mutagenesis of a full-length cDNA clone of Semliki Forest virus: The 6000-molecular-weight membrane protein modulates virus release. *J. Virol.* **65**, 4107–4113.

Manchester, K. L. (1995). Value of A_{260}/A_{280} ratios for measurement of purity of nucleic acid. *Biotechniques* **19**, 208–210.

Stark, C., and Kennedy, S. I. T. (1978). The generation and propagation of defective-interfering particles of Semliki Forest virus in different cell types. *Virology* **89**, 285–299.

Strauss, J. H., and Strauss, E. G. (1994). The alpha viruses: Gene expression, replication and evolution. *Microbiol. Rev.* **58**, 491–562.

CHAPTER

52

Design and Production of Human Immunodeficiency Virus-Derived Vectors

Patrick Salmon and Didier Trono

I. INTRODUCTION

Lentiviral vectors (LV) can govern the efficient delivery and stable integration of transgenes both *in vitro* and *in vivo*, can transduce a wide range of targets, including stem cells, and can be used for generating transgenic animals from several species. Lentiviral vector-mediated gene transfer results in the ubiquitous, tissue-specific, and/or regulated expression of these transgenes, depending on the promoter contained in the vector. Finally, this gene delivery system can mediate the knockdown of endogenous genes by RNA interference via the polymerase III promoter-driven production of small hairpin RNAs.

II. DESIGN

The potential of lentiviral vectors was first revealed in 1996 through the demonstration that they could transduce neurons *in vivo* (Naldini *et al*., 1996). Since then, many improvements have been brought to achieve high levels of efficiency and biosafety. The principle, however, remains the same and consists of building replication-defective recombinant chimeric lentiviral particles from three different components: the genomic RNA, the internal structural and enzymatic proteins, and the envelope glycoprotein. A schematic diagram of the evolution of human immunodeficiency virus (HIV)-based vectors is represented in Fig. 1. The genomic RNA contains all *cis*-acting sequences, whereas packaging plasmids contain all the *trans*-acting proteins necessary for adequate transcription, packaging, reverse transcription, and integration.

A. Envelope

Although various envelope proteins can efficiently pseudotype LV particles (Sandrin *et al*., 2002), the G protein of the vesicular stomatitis virus (VSV) is the most widely used. The main reasons for this choice are that the VSV envelope (1) allows for high titers achieved in unconcentrated supernatants; (2) provides an extremely wide range for the transduction of target cells (virtually all mammalian cells of any tissue tested so far can be transduced by VSV-G pseudotyped LVs); (3) is very robust, allowing for concentration by ultracentrifugation; and (4) has a good resistance to freeze–thaw cycles.

B. Core and Enzymatic Components ("Packaging System")

The first-generation lentiviral vectors were manufactured using a packaging system that comprised all HIV genes but the envelope (Naldini *et al*., 1996). In a so-called second-generation system, five of the nine HIV-1 genes were eliminated, leaving the *gag* and *pol* reading frames, which encode for the structural and enzymatic components of the virion, respectively, and the *tat* and *rev* genes, fulfilling transcriptional and posttranscriptional functions (Zufferey *et al*., 1997). Sensitive tests have so far failed to detect replication-competent recombinants (RCRs) with this system. This

Copyright 2006, Elsevier Science (USA).
All rights reserved.

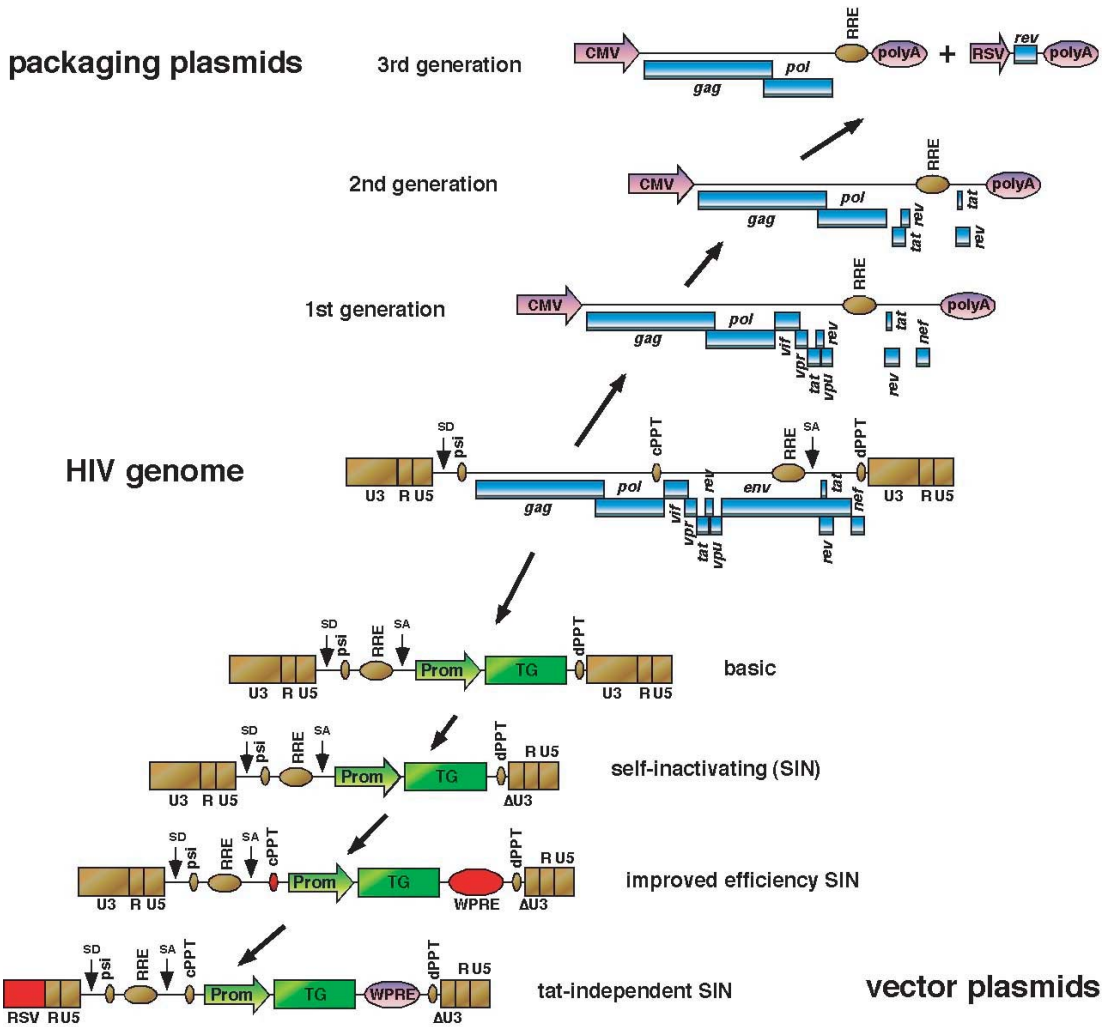

FIGURE 1 Evolution in the design of HIV-1-based LV vectors. HIV-1-based LV vectors are derived from wild-type HIV-1 by dissociation of the *trans*-acting components (blue boxes, above HIV genome) coding for structural and accessory proteins and the *cis*-acting sequences required for packaging and reverse transcription of the genomic RNA (golden boxes, below HIV genome). Sequences added between two vector versions are in red. CMV, human cytomegalovirus immediate-early promoter; RRE, rev-responsive element; RSV, Rous sarcoma promoter; polyA, polyadenylation site; U3-R-U5, HIV-1 LTR: SD, major splice donor; psi, HIV-1 packaging signal; cPPT, central polypurine tract; SA, splice acceptor; dPPT, distal (3′) polypurine tract; Prom, promoter of the internal expression cassette; TG, transgene of the internal expression cassette; ΔU3, self-inactivating deletion of the U3 part of the HIV-1 LTR; WPRE, woodchuck hepatitis virus posttranscriptional regulatory element.

good safety record, combined with its high efficiency and ease of use, explains why the second-generation lentiviral vector packaging system is utilized for most experimental purposes. In a third-generation system, geared toward clinical applications, only *gag*, *pol*, and *rev* genes are still present, using a chimeric 5′ long terminal repeat (LTR) to ensure transcription in the absence of Tat (see later).

C. Genomic Vector

The genetic information contained in the vector genome is the only one transferred to the target cells. Early genomic vectors were composed of the following components: the 5′ LTR, the major splice donor, the packaging signal (encompassing the 5′ part of the gag gene), the Rev-responsive element (RRE), the envelope

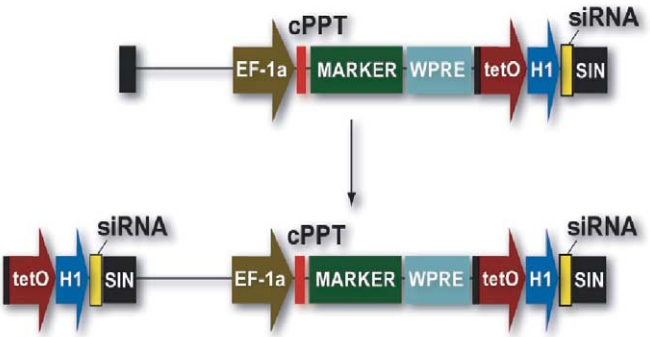

FIGURE 2 Vector for RNA interference. Small hairpin (interfering) RNAs (shRNA or siRNA) are expressed from a polymerase III promoter as described (Brummelkamp *et al.*, 2002). In this example, the expression cassette is placed in the U3 region of the 3′ LTR. Because of the modalities of reverse transcription, two copies of the siRNA inducing module will be present in the integrated provirus, facilitating high levels of production. For convenience, a transgene can be placed in the same vector, downstream of an internal promoter.

splice acceptor, the internal expression cassette containing the transgene, and the 3′ LTR. In the latest generations, several improvements have been introduced. The woodchuck hepatitis virus posttranscriptional regulatory element (WPRE) has been added to increase the overall levels of transcripts in both producer and target cells, hence increasing titers and transgene expression (Zufferey *et al.*, 1999). The central polypurine tract of HIV has also been added back in the central portion of the genome of the transgene RNA (Follenzi *et al.*, 2000; Zennou *et al.*, 2000). This increases titers in some targets. The 3′ LTR has been deleted in the U3 region to remove all transcriptionally active sequences, creating the so-called self-inactivating (SIN) LTR (Zufferey *et al.*, 1998). Finally, chimeric 5′ LTRs have been constructed in order to render the LV promoter Tat independent. This has been achieved by replacing the U3 region of the 5′ LTR with either the CMV enhancer (CCL LTR) or the corresponding Rous sarcoma virus (RSV) U3 sequence (RRL LTR) (Dull *et al.*, 1998). Vectors containing such promoters can be produced at high titers in the absence of the Tat HIV transactivator. However, the Rev dependence of these third-generation LV has been maintained in order to maximize the number of recombination events that would be necessary to generate an RCR (Fig. 2).

III. MATERIALS AND REAGENTS

293T and HeLa cell lines (ATCC) (www.atcc.org)
Chemicals (Sigma-Fluka) (www.sigmaaldrich.com)
Cell culture media and additives (GIBCO-BRL-Life Technologies) (www.gibcobrl.com) and CellGenix Technologie Transfer GmbH, Germany (www.cellgenix.com)
Plastics for tissue cultures, flow cytometer (BD Biosciences) (www.bdbiosciences.com)
DNA purification kits (Qiagen) (www1.qiagen.com) and Genomed (www.genomed-dna.com)
Centrifuges (Sorvall) (www.sorvall.com)
Filters (Millipore) (www.millipore.com)
Ultracenrifuge tubes (Beckman) (www.beckman.com)
Sequence detector ABI7700 plus ABI SDS software for analysis, optical reaction plates and caps for QPCR (Applied Biosystems) (http://www.appliedbiosystems.com)
QPCR reaction mixes and probes (Eurogentech) (www.eurogentec.com)
HIV-1 p24 antigen capture assay (AIDS Vaccine Program) (Frederick, MD. email: schadent@mail.ncifcrf.gov—http://web.ncifcrf.gov)

IV. PRODUCTION

The production of LV can be achieved by transient transfection of the plasmid set into 293T cells by the calcium phosphate method or from stable producer cell lines. Although proof of principle for the latter approach has been provided (Klages *et al.*, 2000), it still suffers from limitations, e.g., for the production of SIN vectors. Unless very large amounts of a same vector are needed on a regular basis, transient production is still the method of choice for research purposes.

A. Cells

Cells (293T/17 from ATCC Cat. No. SD-3515) are probably the most critical factor for good titers. They need to be passaged every 2–3 days, as they start to form clumps that cannot be dissociated with one round of trypsin.

B. Solutions

1. *0.5 M $CaCl_2$*: Dissolve 36.75 g of $CaCl_2$ and $2H_2O$ (MW 147) (*SigmaUltra* Cat. No. *C5080*) into 500 ml of H_2O (distilled or double distilled). Store at –70°C in 50-ml aliquots. Once thawed, the $CaCl_2$ solution can be kept at 4°C for several weeks without observing a significant change in the transfection efficiency.

2. *2x HeBS*: Dissolve 16.36 g of NaCl (MW 58.44) (*SigmaUltra* Cat. No. *S7653* (0.28 *M* final), 11.9 g of

HEPES (MW 238.3) (*SigmaUltra* Cat. No. *H7523*) (0.05 *M* final), and 0.213 g of Na_2HPO_4, anhydrous (MW 142) (*SigmaUltra* Cat. No. *S7907*) (1.5 m*M* final) into 800 ml of H_2O (distilled or double distilled). Adjust pH to 7.00 with 10 *M* NaOH. Be careful, as obtaining a proper pH is *very* important. Below pH 6.95, the precipitate will not form, above pH 7.05, the precipitate will be coarse and transfection efficiency low. Then add H_2O to 1000 ml and make the final pH adjustment. Store at –70°C in 50-ml aliquots. Once thawed, the HeBS solution can be kept at 4°C for several weeks without observing a significant change in the transfection efficiency.

3. *Solution for mixing with plasmids*: 50 ml H_2O distilled or double-distilled, 1 *M* HEPES, pH 7.3 (*GibcoBRL*, Cat. No. *15630-056*) 125 µl (2.5 m*M* final). We have observed that the aspect and quality of the precipitates can vary among batches of distilled water. To circumvent this problem, we advise buffering distilled water that is used to dilute the plasmids. A final concentration of 2.5 m*M* HEPES in the water will help maintain a proper pH and will not compete for the final pH with the HeBS, pH 7.00 (HEPES, pH 7.00, provided by HeBS is 25 m*M* final, whereas HEPES, pH 7.3, provided by water is 0.625 *M* final). Store at 4°C.

C. DNA

We use JetStar kits (Genomed GmbH, Germany) or Qiagen kits (Qiagen, GmbH, Germany) to prepare DNAs for transfection. In any case, the last step of the DNA prep should be an additional precipitation with ethanol (EtOH) and resuspension in 10 m*M* Tris (*SigmaUltra* Cat. No. *T6791*)/1 m*M* EDTA (*SigmaUltra* Cat. No. *E6758*) (TE 10/1). Do not treat DNA with phenol/chloroform as it may result in chemical alterations. Also, to avoid salt coprecipitation, we do not precipitate DNA below 20°C.

D. Transfection and Harvesting

The day before transfection, detach the 293T cells using trypsin/EDTA (Cat. No. 25300, GibcoBRL Life Technologies). Seed the 293T cells at 1 to 3 millions (cells must be approximately one-fourth to one-third confluent on the day of transfection) per 10-cm culture dishes (Cat. No. 353003, BD Biosciences) with 10 ml of D10 complete medium composed of DMEM (Cat. No. 41966, GibcoBRL Life Technologies) supplemented with 10% fetal calf serum (FCS, Cat. No. 10099, GibcoBRL Life Technologies), 1% penicillin–streptomycin (Cat. No. 15140, GibcoBRL Life Technologies), and 1% L-glutamine (Cat. No. 25030, GibcoBRL Life Technologies) (Fig. 3).

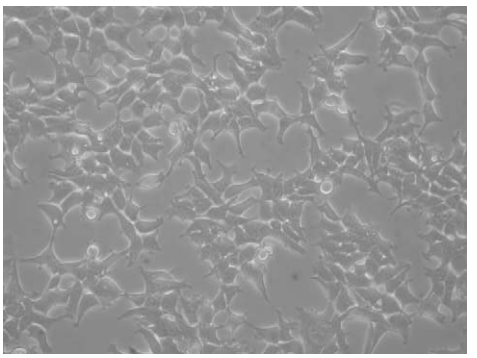

FIGURE 3 Phase-contrast photograph of 293T cells. 293T/17 cells are seeded the day before transfection at 1 to 3 million per 10-cm culture dish. At the time of transfection, cells must have the morphology and density as shown here.

On day 0, in the evening, make the precipitate according to the recipes[1] (cf Table I for one 10-cm plate).

Adjust to 250 µl with buffered water. Add 250 µl of 0.5 *M* $CaCl_2$. Mix well and add this mix, *dropwise, slowly* (one drop every other second), on 500 µl of HeBS 2×, while vortexing at maximum speed. Let stand still for 20 to 30 min minimum (40 min max) on the bench. This time is critical for optimal formation of the precipitate. Excessive incubation times may induce the formation of a coarse precipitate, which is detrimental to transfection efficiency. A too short incubation will not induce the formation of a significant amount of precipitate, which will have no chance to develop further once diluted in the 10 ml of culture medium. Also, it is advisory to incubate the solutions at room temperature or 37°C before mixing to standardize the precipitate characteristics. Add the precipitate slowly, dropwise on the cell monolayer. The plate should then be shaken gently but not stirred or all the precipitate will be in the center. At this point, the precipitate may not be visible, for it is too fine and will take several hours to sediment on the cells. If the precipitate is readily visible, it is too coarse and the transfection will most likely be less efficient.

On day 1 in the morning, check the cells. At this point, a very fine and sandy precipitate all over the plate should be seen, except on the cells and in their vicinity, possibly because cells absorb the $CaPO_4$/DNA precipitate. Discard the medium after gentle, but firm, stirring (to eliminate the maximal amount of precipitate) and replace it with 10–15 ml of fresh medium.

[1] These recipes are the result of long optimizations in our laboratory and in the laboratory of Luigi Naldini and discussions with Antonia Follenzi.

TABLE I Recipes

	Second generation		Third generation	
Recipe 1				
Envelope plasmid	pMD2G	5 µg	pMD2G	5 µg
Packaging plasmid	pCMVΔR8.74	15 µg	pMDLg/pRRE	10 µg
Rev-expression plasmid	pRSV-Rev		pRSV-Rev	5 µg
Transfer vector	pHR[a]	20 µg	pRRL[a]	20 µg
Recipe 2				
Envelope plasmid	pMD2G	3 µg	pMD2G	3 µg
Packaging plasmid	pCMVΔR8.74	6.5 µg	pMDLg/pRRE	5 µg
Rev-expression plasmid	pRSV-Rev	2 µg	pRSV-Rev	2.5 µg
Transfer vector	pHR[a]	10 µg	pRRL[a]	10 µg

[a] pHR refers to second-generation vectors with wild-type 5′ LTR, and pRRL refers to third-generation vectors with chimeric 5′ LTR.

Notes: The medium must be prewarmed at 37°C because the 293T are very sensitive to thermal shock and can shrink and detach. Also, the medium must be added very gently to the cells. Even so, it is difficult not to make a hole in the monolayer.

On day 2, harvest the supernatant and replace with 10–15 ml of medium as the day before. Spin the supernatant at 2500 rpm for 10 min at 4°C [in a tabletop centrifuge such as a Multifuge 3SR (Sorvall)], filter through a 0.45-µm PVDF filter (such as Millex-Durapore, Cat. No. SLHV 033, Millipore), and store at 4°C.

On day 3, harvest the supernatant, spin at 2500 rpm for 10 min at 4°C, filter through a 0.45-µm filter, and pool with the supernatant of day 2. At this point, the pool of supernatants must contain approximately 10^6 transducing units (TU) per milliliter (as titered on HeLa cells, see later).

V. CONCENTRATION AND STORAGE

If a more concentrated lentivector suspension is required, the vector preparation needs to be concentrated. For concentration, we use Beckman Conical tubes (*Cat. No. 358126, Beckman-Coulter*) in a Surespin 630 rotor and a Discovery 90SE ultracentrifuge (Sorvall). Put 4–5 ml of 20% sucrose (SigmaUltra, Cat. No. S7903) in water at the bottom of the tube and fill up to the top with filtered supernatant, spin at 2600 rpm for 90 min and discard gently the supernatant by inversion. Let the tube dry inverted and resuspend the pellet (not always visible) with complete medium or serum-free medium, such as CellGro stem cell growth medium (Cat. No. 2001, CellGenix Technologie Transfer GmbH, Germany) if the subsequent experiments require the absence of serum.

The use of protein-containing medium is preferable over PBS to resuspend the viral pellet for two reasons: (1) the presence of proteins will stabilize the viral particles and (2) the surfactant effect of proteins will help redissolve the pellet.

VI. TITRATION

Titers of viruses in general and lentivectors in particular critically depend on the method and cells used for titration. The quantification of vector particles capable of achieving every step from cell binding to expression of the transgene depends on both vector and cell characteristics. First, the cell used as the target must be readily permissive to all steps from viral entry to integration of the vector genetic cargo. Second, the expression of the foreign gene must be monitored easily and rapidly reach levels sufficient for reliable quantification. Early vectors had the LacZ bacterial gene as the reporter under the control of the CMV promoter (Naldini *et al*., 1996). Current vectors now have the green fluorescent protein (GFP) gene as a reporter under the control of promoters that are active in most primary cells (Salmon *et al*., 2000). Measured titers can also vary with the conditions used for titration, i.e., volume of sample during vector-cell incubation, time of vector-cell incubation, and number of cells used. For several years now, we have been using HeLa cells as target. These cells are stable, easy to grow, and 100% susceptible to transduction by VSV-G-pseudotyped LVs. There are also now used commonly by many laboratories, which helps in comparing titers between laboratories.

A. Titration of Vectors in HeLa Cells by FACS

This method can only be used to titer stocks of vectors that carry a transgene that is easily monitored by FACS (such as GFP, any living colors, or any membrane protein that can be detected by flow cytometry) and whose expression is governed by a promoter that is active in HeLa cells (tissue-specific promoter-containing vector must be functionally assayed in specific cells), and titered by quantitative polymerase chain reaction (QPCR) in HeLa cells (see later).

We describe here the titration of a PGK-GFP vector. On day 0, seed Hela cells (Cat. No. CCL-2, ATCC) at 100k cells per well in a MW6 plate (Cat. No. 353224, BD Biosciences) in D10 complete medium. On day 1, put 500, 50, or 5 µl of the vector suspension (either pure from unconcentrated supernatants or diluted if it comes from a concentrated stock) in three independent wells. On day 2, remove the supernatant and replace with 2 ml of fresh D10. On days 4 to 5, wash the cells with 2 ml of PBS without calcium–magnesium (Cat. No. 14190, Gibco-BRL Biosciences), detach them with 250 µl of trypsin/EDTA (Cat. No. 25300, Gibco-BRL Life Technologies) for 1 min at 37°C, add 250 µl of 2% (w/v) formaldehyde (Cat. No. F8775, Sigma) in PBS without calcium–magnesium (to fix the cells, inactivate the trypsin and the vector particles), resuspend thoroughly, and analyze them for GFP expression using a flow cytometer (FACScan, Becton-Dickinson).

A reliable measure of the fraction of GFP+ cells relies on the level of GFP expression. In the example shown in Fig. 4, GFP-positive and GFP-negative cells can be readily discriminated when GFP is expressed from a human PGK promoter and allowed to accumulate in cells for 4 days. A marker can then be set to measure the fraction of transduced versus total cells.

In a typical titration experiment, only dilutions yielding 1–20% GFP positive should be considered for titer calculations. Below 1%, the FACS may not be accurate enough to reliably determine the number of GFP-positive cells. Above 20%, the chance for each GFP-positive target cell to be transduced twice increases significantly, resulting in an underestimation of the number of transducing particles. Once the appropriate dilution is chosen, apply the following equation:

$$\text{titer (HeLa-transducing units/ml)} = 100{,}000 \text{ (target HeLa cells)} \times (\%\text{ of GFP-positive cells}/100)/\text{volume of supernatant (in milliliters)}.$$

B. Total Vector Concentration Using Anti-p24 Immunoassay

Determination of total particle concentration is important to monitor the efficiency of vector production and packaging. One must keep in mind, however, that a high concentration of pelletable p24 viral capsid antigen can be measured from vector particles not containing any genomic RNA and/or devoid of envelope protein. Such an assay can thus not replace a transduction assay as described earlier and later. We currently use the p24 antigen capture assay provided by the AIDS vaccine program (Frederick, MD; email: schadent@mail.ncifcrf.gov). The minimal p24 concentration detected by this assay is 150 pg/ml. HIV-1 or vector-containing supernatants are lysed by adding Triton X-100 (SigmaUltra Cat. No. T9284) to a final concentration of 1%. Lysed samples can be analyzed just after or stored at –20°C. Following the instructions provided by the manufacturer and using dilutions comprised between 1/10 and 1/10,000, we find that most of our vector preparations have a p24 concentra-

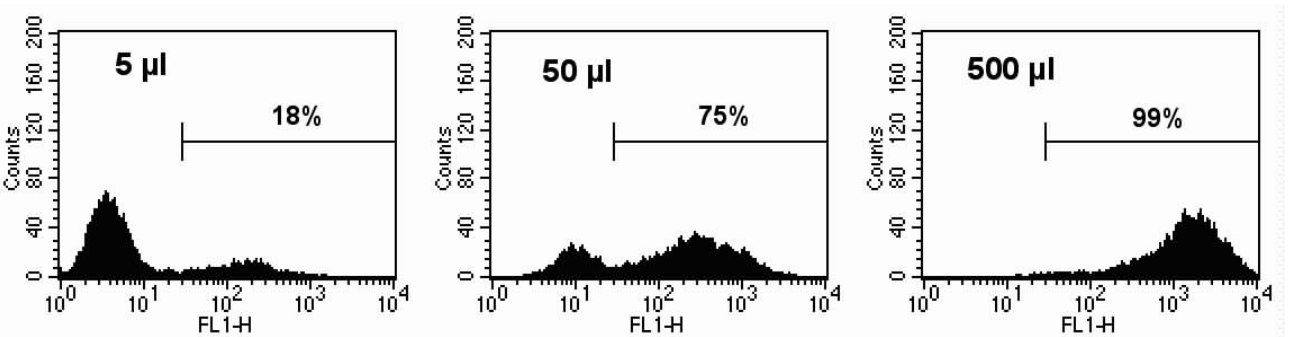

FIGURE 4 A representative FACS analysis of HeLa cells used for titration of GFP-coding LV. HeLa cells (10^5) were incubated with various volumes of a supernatant containing a LV expressing GFP under the control of the human PGK promoter [pRRLSIN.cPPT.PGK.GFP.WPRE (Follenzi *et al.*, 2000)] as described in the text. After 4 days, cells were detached, fixed, and analyzed by FACS for GFP fluorescence (*x* axis, four-decade log scale, FL1) versus number of cells (*y* axis, linear scale). The percentage of GFP-expressing cells was measured by placing a marker discriminating between GFP-negative (mean of fluorescence intensity 3–4) and GFP-positive (mean of fluorescence intensity 200) cells.

tion comprised between 100 ng/ml and 1 µg/ml. Given that most vector preparations have titers ranging from 5×10^5 to 10^7 Hela-TU/ml, this implies that the relative titer of our LV stocks is comprised between 1 and 20 Hela-TU/pg of p24. Of course, these results may vary depending on the packaging efficiency of a given transfer vector.

C. Titration of Vectors in HeLa Cells by Quantitative PCR

In the case of vectors coding for genes that cannot be detected readily by FACS or if the promoter is not active in HeLa cells, an alternative method is to measure the number of copies of LV stably integrated in HeLa target cells, after transduction as described earlier for GFP vectors. This assay, however, only measures the number of LV copies integrated in the target cell genome. The overall functionality of the vector must be tested at least once in cells in which the promoter is active and/or with appropriate techniques to detect the expression of the transgene product.

The QPCR assay proceeds as follows using a 7700 sequence detector (Applied Biosystems). HeLa cells are transduced as described earlier, but instead of being detached by trypsin, they are lysed with 200 µl of lysis buffer in the plate and DNA is extracted using a DNAeasy kit (Qiagen GmbH, Germany). Then, 1–2 µl of 200 µl total of DNA solution is analyzed for the copy number of HIV sequences using the following real-time PCR protocol.

1. Reaction

Always use filter tips. Mix for each sample and distribute in duplicate in a 96-well optical reaction plate (Cat. No. 4306737, Applied Biosystems): 12.5 µl 2× mix (Cat. No. RT-QP2X-03 Eurogentech, Belgium), 2.5 µl 10× oligonucleotide mix 1, 2.5 µl 10× oligonucleotide mix 2, 1–2 µl DNA sample, and up to 25 µl final with H_2O. Close with optical caps (Cat. No. N801-0935, Applied Biosystems). Run a program appropriate for the probes, depending on the fluochrome used (FAM, VIC, TET, etc).

Notes: 10× oligonucleotide mixes are 1 µ*M* probe and 3 µ*M* of each primer in water. Stocks of probes and primers usually come lyophilyzed and are stored at 10 µ*M* in water. DNA ideally comes from 2×10^6 HeLa cells extracted and resuspended in 100 µl (DNAeasy, Qiagen).

2. Oligonucleotides

Oligonucleotides can be ordered online from several companies such as Eurogentech or Sigma.

Oligonucleotides used to normalize for the amount of genomic DNA are specific for the β-actin (BAC) gene. The sequences are originally from a PE-Applied TAQMAN β-actin control reagent (Cat. No. 401846), which has been discontinued.

BAC-P (probe, sense) human β-actin
5′-(TET or VIC)- ATGCCCTCCCCCATGCCATCCT GCGT -(TAMRA)-3′
BAC-F (forward primer): TCACCCACACTGTGCC CATCTACGA
BAC-R (reverse primer): CAGCGGAACCGCTCAT TGCCAATGG

Oligonucleotides for the amplification of HIV-1-derived vectors are specific for the 5′ end of the gag gene (GAG). This sequence is present in all HIV-1 vectors for it is part of the extended packaging signal.

GAG-P (probe, antisense) HIV gag
5′-(FAM)-ACAGCCTTCTGATGTTTCTAA CAGGCCAGG-(TAMRA)-3′
GAG-F (forward primer): GGAGCTAGAACGATT CGCAGTTA
GAG-R (reverse primer): GGTTGTAGCTGT CCCAGT ATTTGTC

3. Analysis

An example of amplification profiles of HIV sequences in human DNA is given in Fig. 5 (as displayed by the ABI Prism program, Applied Biosystems). To analyze the amplification reaction, first set the threshold where the amplification curve is the steepest, both for the gene of interest (GAG-FAM, Fig. 5A) and for the internal control (BAC-VIC, Fig. 5B). Then, export the results as a Microsoft Excel sheet and draw a standard curve with standards of cells containing 1, 0.1, 0.01, and 0.001 copy of HIV per cell using the deltaCt values (Ct GAG minus Ct BAC). Ask Excel to display the formula (exponential). Apply the formula to unknown samples, it will give the HIV copy number of the corresponding sample. The titer of the supernatant can then be calculated as follows:

Titer (HeLa-transducing units/ml) = 100,000 (target HeLa cells) × number of copy per cell of the sample/volume of supernatant (in milliliters).

Notes: It is advisory to run a dual titration (FACS plus TAQMAN) using one GFP vector alongside the other vectors for each set of QPCR titration. This will help in comparing FACS titration with QPCR titration. A standard curve of HIV DNA in human DNA can also be made using a human cell line. In this case, keep in mind that the DNA content of these cell lines is different from the DNA content of normal primary human diploid cells. Small adjustments can be made using the table in Fig. 5D, which summarizes the chromosome counts of HeLa and CEM cells as provided in the

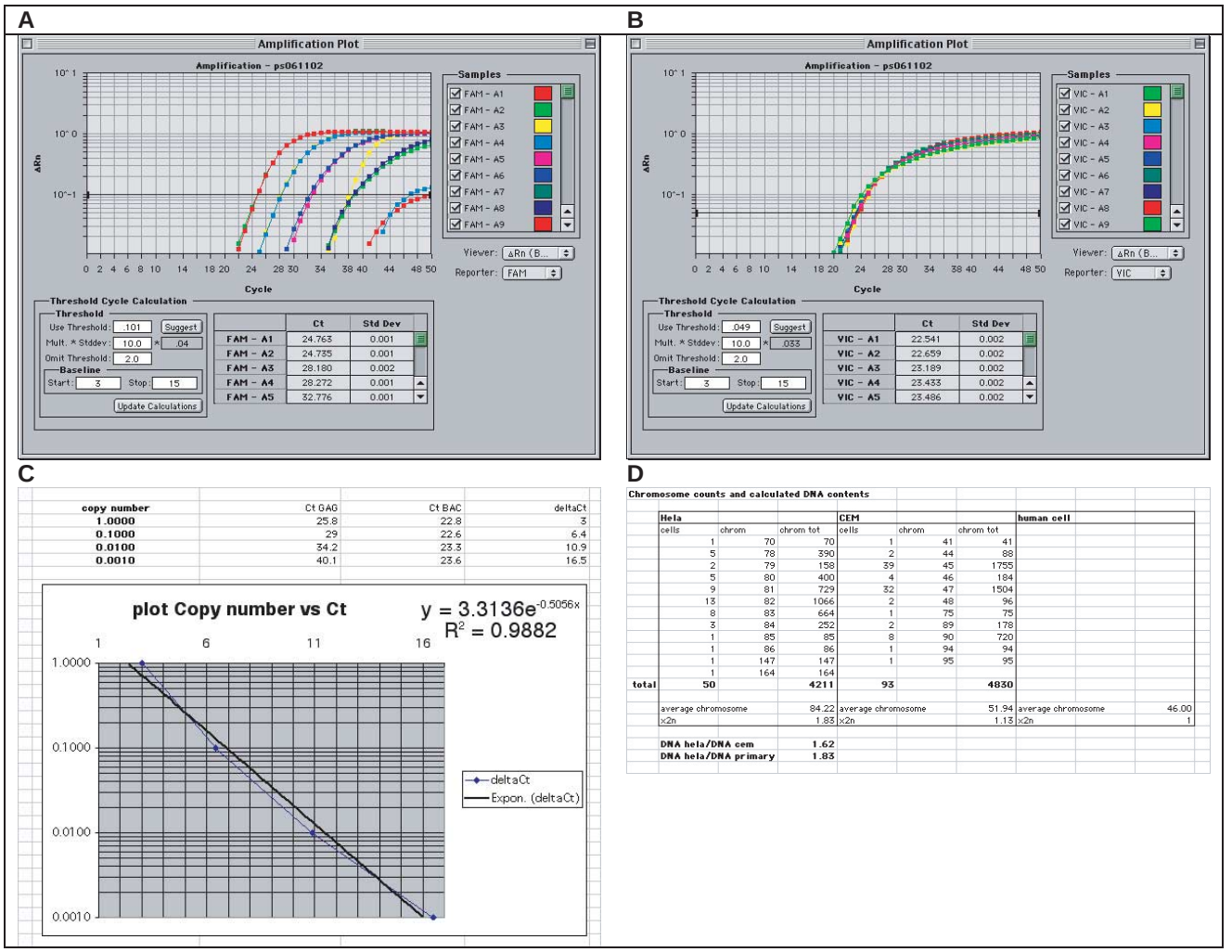

FIGURE 5 A representative QPCR analysis used for titration of HIV-1-based LVs. DNA from 8E5 cells, a CEM-derivative (Cat. No. CRL-8993, ATCC; which contains a single copy of a replication defective HIV-1 provirus), was diluted by ten-fold increments in DNA from CEM cells. A sample of each dilution was submitted to QPCR amplification and monitoring using a Perkin-Elmer 7700 (Applied Byosystems) and sets of primers and probes specific for HIV gag sequences (GAG-FAM, A) or β-actin sequences (BAC-VIC, B). Amplification plots were displayed, and cycle threshold values (Ct) were set as described in the text. Values of GAG Ct and BAC Ct were exported in an Excel worksheet to calculate ΔCt values (*x* axis, linear scale) and plot them against copy number values (*y* axis, log scale) (C). The regression curve can then be used to calculate GAG copy numbers (*Y* value) of unknown samples by applying the formula to ΔCt values (*X* values) of the sample. (D) Calculated DNA contents of primary human cells, CEM, cells and HeLa cells based on the chromosome contents (after ATCC catalog).

ATCC catalog and gives calculated DNA contents for each cell.

VII. TROUBLESHOOTING

In the case of lack of transduction of a specific cell type with a specific lentiviral vector, Fig. 6 helps in addressing most of the problems that could account for it.

VIII. CONCLUSION

Lentivector are vehicles of choice for the transduction of many primary cell targets, including neurons, retinal cells, pancreatic islet cells, lymphocytes, and hematopoietic stem cells. Although HIV-derived vectors have been best characterized, gene delivery systems have similarly been developed from other lentiviruses, such as simian (Negre *et al.*, 2000), feline

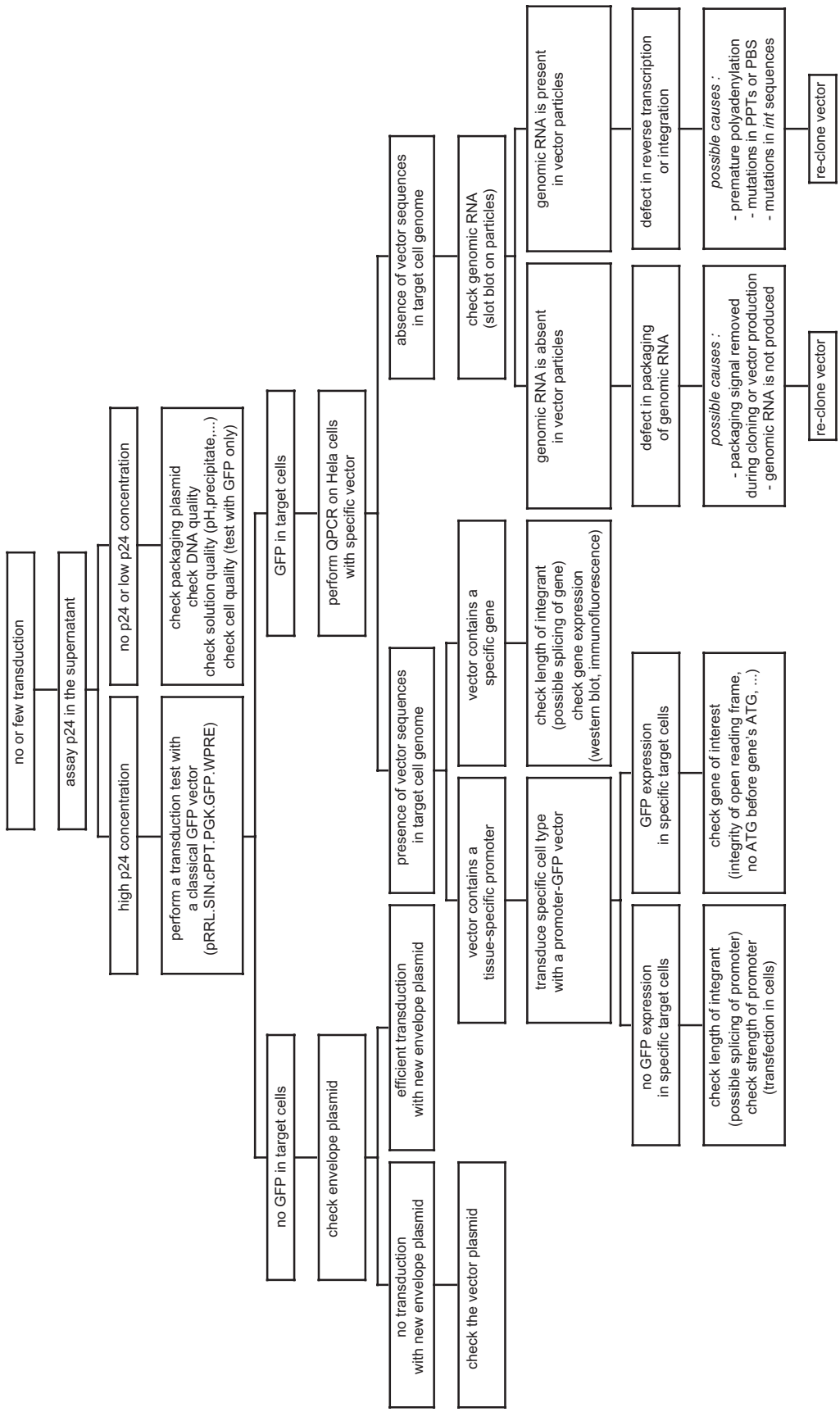

FIGURE 6 Troubleshooting diagram for lentiviral vector production and transduction.

(Curran *et al*., 2000), and bovine (Berkowitz *et al*., 2001) immunodeficiency viruses and the equine infectious anemia virus (Mitrophanous *et al*., 1999). These other systems seem to have the same general properties as their HIV counterpart, but in human cells, HIV-derived vectors appear to be more generally efficient, illustrating the fact that a virus adapts to its cognate target. From a biosafety standpoint, HIV-derived vectors may be safer than their nonhuman virus homologues. First, the genomic complexity of HIV is far greater than that of most other lentiviruses, including feline immunodeficiency virus and equine infectious anemia virus, which each have only six genes instead of the nine present in their human counterpart. Because in all cases a minimum of three genes, *gag*, *pol*, and *rev*, will likely be required for generating vector particles efficiently, the multiply attenuated HIV-based packaging system will be the farthest away from its parental virus. In addition, past experience with zoonoses teaches us that the pathogenicity of a given organism is largely unpredictable when it is transferred from its normal animal host into humans. Finally, millions of individuals worldwide have been screened for lentivirus-related diseases. No pathology has been associated with massively deleted forms of HIV-1; however, well-documented cases of long-term clinical nonprogression have occurred in patients infected with HIV-1 strains that carry genetic alterations far more subtle than those introduced in the third-generation HIV-1 packaging system.

Most recent developments of lentivector technology, such as its application for transgenesis (Lois *et al*., 2002) and RNA interference (Brummelkamp *et al*., 2002), indicate that the exploitation of this formidable tool is only beginning. Exciting times are ahead, in both experimental and therapeutic arenas.

Acknowledgments

We thank Antonia Follenzi for helpful discussions and Maciej Wiznerowicz for Fig. 2. Additional resources, such as vector sequences, are available at http://www.tronolab.unige.ch/. Downloading of QPCR oligonucleotide sequences and Excel QPCR calculation sheets can be made at http://www.medecine.unige.ch/~salmon/.

References

Berkowitz, R., Ilves, H., Lin, W. Y., Eckert, K., Coward, A., Tamaki, S., Veres, G., and Plavec, I. (2001). Construction and molecular analysis of gene transfer systems derived from bovine immunodeficiency virus. *J Virol.* **75**, 3371–3382.

Brummelkamp, T. R., Bernards, R., and Agami, R. (2002). A system for stable expression of short interfering RNAs in mammalian cells. *Science* **296**, 550–553.

Curran, M. A., Kaiser, S. M., Achaso, P. L., and Nolan, G. P. (2000). Efficient transduction of nondividing cells by optimized feline immunodeficiency virus vectors. *Mol. Ther.* **1**, 31–38.

Dull, T., Zufferey, R., Kelly, M., Mandel, R. J., Nguyen, M., Trono, D., and Naldini, L. (1998). A third-generation lentivirus vector with a conditional packaging system. *J Virol.* **72**, 8463–8471.

Follenzi, A., Ailles, L. E., Bakovic, S., Geuna, M., and Naldini, L. (2000). Gene transfer by lentiviral vectors is limited by nuclear translocation and rescued by HIV-1 pol sequences. *Nature Genet.* **25**, 217–222.

Klages, N., Zufferey, R., and Trono, D. (2000). A stable system for the high-titer production of multiply attenuated lentiviral vectors. *Mol. Ther.* **2**, 170–176.

Lois, C., Hong, E. J., Pease, S., Brown, E. J., and Baltimore, D. (2002). Germline transmission and tissue-specific expression of transgenes delivered by lentiviral vectors. *Science* **295**, 868–872.

Mitrophanous, K., Yoon, S., Rohll, J., Patil, D., Wilkes, F., Kim, V., Kingsman, S., Kingsman, A., and Mazarakis, N. (1999). Stable gene transfer to the nervous system using a non-primate lentiviral vector. *Gene Ther.* **6**, 1808–1818.

Naldini, L., Blomer, U., Gallay, P., Ory, D., Mulligan, R., Gage, F. H., Verma, I. M., and Trono, D. (1996). *In vivo* gene delivery and stable transduction of nondividing cells by a lentiviral vector. *Science* **272**, 263–267.

Negre, D., Mangeot, P. E., Duisit, G., Blanchard, S., Vidalain, P. O., Leissner, P., Winter, A. J., Rabourdin-Combe, C., Mehtali, M., Moullier, P., Darlix, J. L., and Cosset, F. L. (2000). Characterization of novel safe lentiviral vectors derived from simian immunodeficiency virus (SIVmac251) that efficiently transduce mature human dendritic cells. *Gene Ther.* **7**, 1613–1623.

Salmon, P., Kindler, V., Ducrey, O., Chapuis, B., Zubler, R. H., and Trono, D. (2000). High-level transgene expression in human hematopoietic progenitors and differentiated blood lineages after transduction with improved lentiviral vectors. *Blood* **96**, 3392–3398.

Sandrin, V., Boson, B., Salmon, P., Gay, W., Negre, D., Le Grand, R., Trono, D., and Cosset, F. L. (2002). Lentiviral vectors pseudotyped with a modified RD114 envelope glycoprotein show increased stability in sera and augmented transduction of primary lymphocytes and CD34+ cells derived from human and nonhuman primates. *Blood* **100**, 823–832.

Zennou, V., Petit, C., Guetard, D., Nerhbass, U., Montagnier, L., and Charneau, P. (2000). HIV-1 genome nuclear import is mediated by a central DNA flap. *Cell* **101**, 173–185.

Zufferey, R., Donello, J. E., Trono, D., and Hope, T. J. (1999). Woodchuck hepatitis virus posttranscriptional regulatory element enhances expression of transgenes delivered by retroviral vectors. *J. Virol.* **73**, 2886–2892.

Zufferey, R., Dull, T., Mandel, R. J., Bukovsky, A., Quiroz, D., Naldini, L., and Trono, D. (1998). Self-inactivating lentivirus vector for safe and efficient *in vivo* gene delivery. *J. Virol.* **72**, 9873–9880.

Zufferey, R., Nagy, D., Mandel, R. J., Naldini, L., and Trono, D. (1997). Multiply attenuated lentiviral vector achieves efficient gene delivery *in vivo*. *Nature Biotechnol.* **15**, 871–875.

CHAPTER

53

Construction and Propagation of Human Adenovirus Vectors

Mary M. Hitt, Phillip Ng, and Frank L. Graham

I. INTRODUCTION

Adenoviruses (Ads), which have been used extensively as a model system for molecular studies of mammalian cell DNA replication, transcription, and RNA processing, are now being increasingly investigated as potential mammalian expression vectors for gene therapy and for recombinant vaccines (Berkner, 1988; Graham and Prevec, 1992; Hitt *et al.*, 1999). There are many reasons for this renewed popularity of Ad vectors: the 36,000-bp double-stranded DNA genome of Ad is relatively easy to manipulate by recombinant DNA techniques; Ad infects a wide variety of mammalian cell types, both proliferating and quiescent, with high efficiency; the genome does not undergo rearrangement at a high rate; the viral particle is relatively stable; and the virus replicates to high titer in permissive cells, producing up to 10,000 plaque-forming units (PFU) per infected cell. Late in infection, most of the infected cell protein is virally encoded, potentiating the use of replication-proficient recombinant Ads as short-term high-level expression vectors. In nondividing, nonpermissive cells the viral genome may persist as an episome and continue to express for long periods *in vitro*. This holds true *in vivo* as well in the absence of an immune response against vector-infected cells. This article describes methods for inserting foreign genes into the Ad genome and for purifying, growing, and titrating the recombinant viruses. Our vectors are based on the human Ad5 genome, the structure of which is shown in Fig. 1. In a wild-type infection, early genes (E1a, E1b, E2, E3, and E4) are expressed prior to DNA replication, and late gene expression, driven predominantly by the major late promoter at 16 map units, occurs after the initiation of DNA replication. Deletion of the E1 region renders the virus replication defective, which is desirable for most gene therapy applications. However, such vectors must then be propagated in E1-complementing cells, such as the 293 cell line (Graham *et al.*, 1977). Deletion of E3, which is nonessential for virus growth *in vitro*, together with deletion of E1, allows insertion of foreign genes up to about 8 kb in length. Without deleting E3, the insertion capacity of Ad is about 5 kb.

The vector systems described here rely on site-specific recombination in 293 cells between a shuttle plasmid derived from the E1 region at the "left" end of Ad and a larger plasmid carrying nearly the entire Ad genome in a circular form (Fig. 2). In the Cre/loxP system (Ng *et al.*, 2000a), the genomic plasmid pBHGloxΔE1,E3Cre carries an expression cassette encoding the Cre recombinase in a region of the plasmid that is excluded from the final vector genome. Cre mediates recombination between a loxP site downstream of the E1 insertion site in the shuttle plasmid and a loxP site in the E1 region of the genomic plasmid. The FLP/frt system (Ng *et al.*, 2000b) is identical except that it uses the FLP recombinase to mediate recombination between frt sites in the shuttle and genomic plasmids. The Ad packaging signal has been deleted from both genomic plasmids, which virtually eliminates the generation of nonrecombinant infectious progeny following cotransfection with an E1 shuttle plasmid.

With either system, vectors can be generated with inserts in place of E1, E3, or both (Fig. 2). E1 replacement vectors, by far the most common, are constructed by insertion of a transgene expression cassette into the E1 shuttle plasmid and subsequent rescue by recombination with the genomic plasmid in 293 cells. Some

Copyright 2006, Elsevier Science (USA).
All rights reserved.

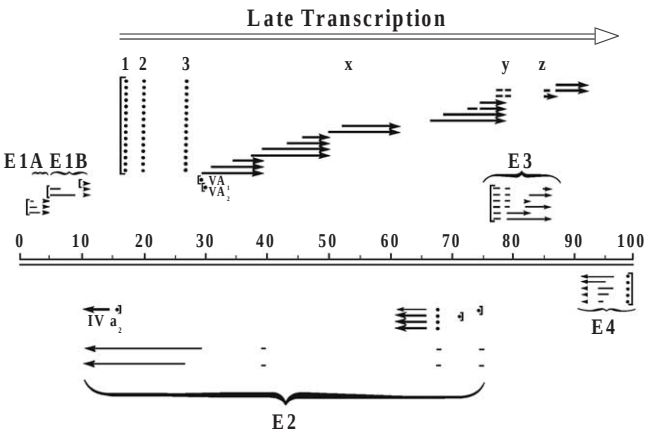

FIGURE 1 *Transcription map of the human adenovirus type 5.* The approximately 36-kb genome of Ad5 is divided here into 100 map units. Messages from the early regions are indicated as light lines and late messages are indicated in bold. Late transcription originating from the major late promoter at 16 map units and terminating near the right end of the genome is indicated by the open arrow. This transcript is processed into five families of late mRNAs spliced to a common tripartite leader (1, 2, and 3 at map units 16.5, 19.5, and 26.5, respectively), although some mRNA species contain additional leaders. (For more details, see Ginsberg, 1984.)

of the most commonly used shuttle plasmids for this system are illustrated in Fig. 3. E3 replacement vectors are constructed by inserting the transgene expression cassette directly into the genomic plasmid at the *Pac*I site engineered in place of E3 (Bett *et al.*, 1994). The genomic plasmid carrying an insert in E3 can be cotransfected with a shuttle plasmid carrying no insert (i.e., E1 deleted) to generate a replication-defective vector. Double recombinant Ad vectors can be produced by cotransfecting 293 cells with the E3 replacement genome-size plasmid together with an E1 shuttle plasmid encoding a second transgene. This latter strategy has been used successfully to rescue a recombinant Ad vector containing the p35 subunit of interleukin-12 (IL-12) in E1 and the IL-12 p40 subunit in E3 (Bramson *et al.*, 1996).

Foreign coding sequences, including their own or heterologous promoters, can be inserted into the shuttle plasmids or into the E3 region of the pBHG plasmids in an orientation either parallel or antiparallel to the E1 or E3 transcription unit. In general, higher expression levels have been obtained with inserts in the parallel orientation in either E1 or E3 (unpublished results); however, the sequence of the insert itself can affect expression levels, particularly for E3 insertions. Once the desired plasmids have been constructed, the following protocols are used to produce and purify the recombinant Ad viruses.

II. MATERIALS AND INSTRUMENTATION

The Cre/loxP and FLP/frt based AdMax vector rescue systems are available, as Kit D (Cat. No. PD-01-64) and Kit E (Cat. No. PD-01-65) respectively, from Microbix Biosystems, Incorporated. Minimal essential medium (MEM) F11 (Cat. No. 61100-087), L-glutamine (Cat. No. 25030-081), penicillin/streptomycin (Cat. No. 15140-122), horse serum (Cat. No. 16050-159), newborn calf serum (NCS) (Cat. No. 16010-159), agarose (Cat. No. 15510-027), and dithiothreitol (Cat. No. 15508-013) can be obtained from Invitrogen. Bovine serum albumin fraction V (Cat. No. A2153), fetal bovine serum (FBS) (Cat. No. F4135), Joklik's modified MEM (Cat. No. M0518), salmon sperm DNA (Cat. No. D1626), and orcein (Cat. No. O7380) are available from Sigma Chemical Company. All sera are inactivated prior to use by heating to 56°C for 30 min. Fungizone can be purchased from Bristol-Myers-Squibb (Cat. No. 043780). Nunc tissue culture dishes (Cat. No. 1-68381A) can be obtained from VWR. Sterile petri dishes (Cat. No. 08-757-12), Difco agar (Cat. No. 0145-17-0), Difco Bacto Lennox LB broth base (Cat. No. 0402-07-0), Becton Dickinson BBL trypticase peptone (Cat. No. B11921), and yeast extract (Cat. No. B11929) can be obtained from Fisher Scientific. Pronase (Cat. No. 1459643) and bovine pancreatic deoxyribonuclease I (Cat. No. 104-159) can be purchased from Roche Diagnostics. Analytical grade $CaCl_2{\cdot}2H_2O$ (Cat. No. B10070) can be obtained from BDH. All other chemicals can be purchased from standard chemical suppliers (e.g., BDH). Spinner flasks (1969 series) can be obtained from Bellco and Pierce Slide-A-Lyzer 10K dialysis cassettes (Cat. No. 66425) from Chromatographic Specialities. Beckman SW41 Ti and SW 50.1 rotors are also required. Reagents for plasmid DNA isolation, as well as restriction enzymes and reagents and apparatus for horizontal slab gel electrophoresis, are described in a number of cloning manuals (e.g., Sambrook and Russell, 2001).

III. PROCEDURES

A. Preparation of Plasmid DNA for Cotransfections

In order to minimize the generation of bacterial clones containing rearranged plasmid DNA, which is occasionally observed in preparations of very large plasmids such as pBHGloxΔE1,E3Cre and pBHGfrtΔE1,E3FLP, we have adopted the following

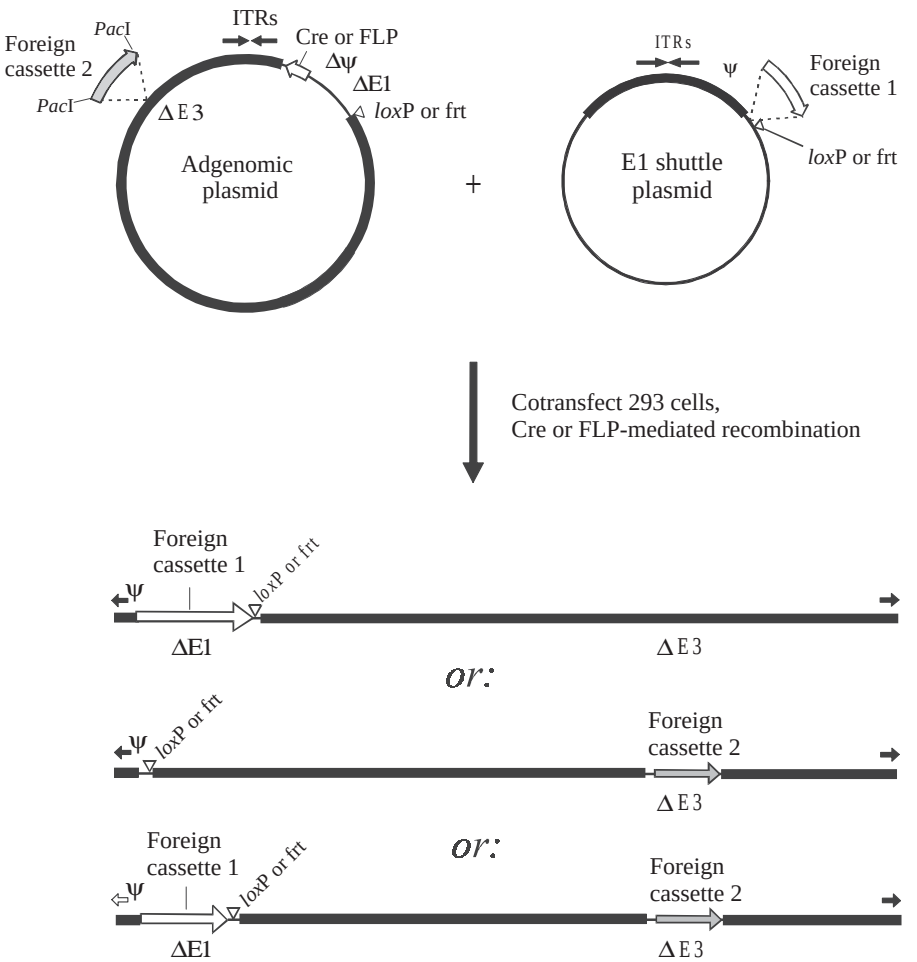

FIGURE 2 *Construction of Ad vectors by two-plasmid site-specific recombination in 293 cells.* The AdMax strategy used to introduce foreign DNA inserts into the E1 and/or E3 regions for rescue into virus is illustrated. Expression cassettes can be inserted in place of the E1 region (Ad5 nucleotides 455–3523) by cloning into E1 shuttle plasmids carrying the recognition site (e.g., *lox*P) for a site-specific recombinase. E1 shuttle plasmids are described further in Fig. 3. The 293 cells are then cotransfected with this shuttle plasmid and an Ad genomic plasmid carrying the appropriate recombinase (Cre for *lox*P-containing shuttles or FLP for frt-containing shuttles). Genomic plasmids are available with E3 deleted (Ad5 nucleotides 28138–30818; pBHGloxΔE1,E3Cre or pBHGfrtΔE1,E3FLP) as shown or with a wild-type E3 region (pBHGloxE3Cre and pBHGfrtE3FLP) (Ng and Graham, 2002). Expression of recombinase in 293 cells results in recombination between recognition sites in the shuttle and in the genomic plasmid, generating an E1 replacement Ad vector (top vector in illustration). E3 replacement Ad vectors are constructed by inserting the transgene expression cassette into a unique *Pac*I site that replaces the E3 region in the Ad genomic plasmid. The 293 cells cotransfected with this genomic construct and an "empty" (i.e., no transgene) E1 shuttle plasmid will produce a replication-defective E3 replacement Ad vector (middle vector in illustration). Note that it is also possible to cotransfect with a plasmid containing the intact left end of Ad5 to produce an E1+ nondefective vector by overlap recombination (Bett *et al.*, 1994). Double recombinant vectors are generated by recombination between an E1 shuttle plasmid carrying one expression cassette and a genomic plasmid carrying a second expression cassette (bottom vector in illustration). Ad and bacterial sequences are indicated by thick and thin black bars, respectively, *lox*P and frt sites by open triangles, inverted terminal repeats (ITRs) by black arrows, and the packaging signal by the symbol ψ.

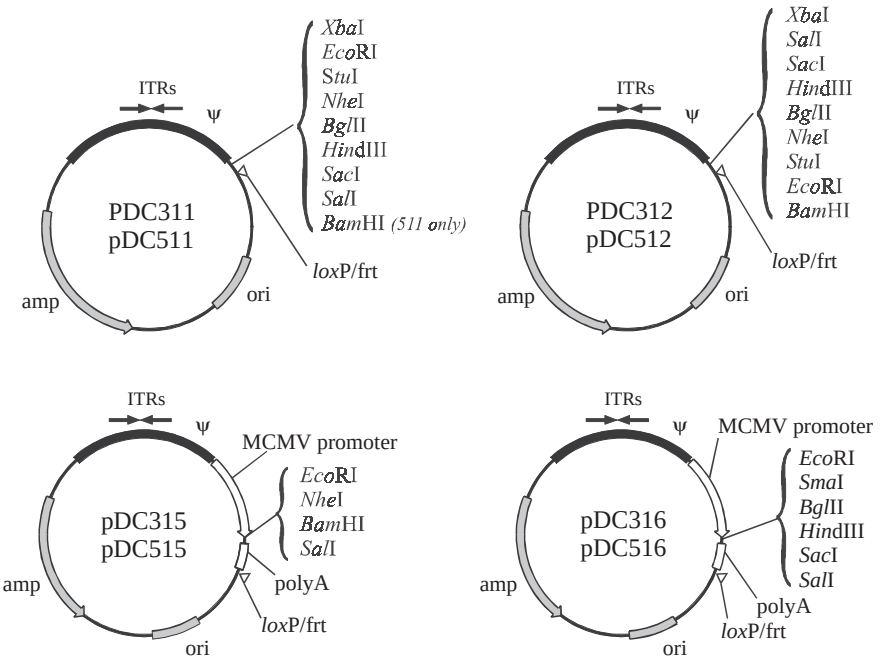

FIGURE 3 *Structure of E1 shuttle plasmids used for vector rescue by* in vivo *site-specific recombination.* The shuttle plasmids pDC311, pDC312, pDC315, and pDC316 are used to rescue vectors by Cre-mediated recombination. The shuttle plasmids pDC511, pDC512, pDC515, and pDC516 are used to rescue vectors by FLP-mediated recombination. Plasmids pDC311, pDC312, pDC511, and pDC512 are designed for insertion of a cassette consisting of a promoter, transgene, and polyadenylation signal sequence. The polycloning sites of plasmids pDC315, pDC316, pDC515, and pDC516 are flanked 5′ by the murine CMV promoter and 3′ by the SV40 polyadenylation signal sequence. Coding sequences cloned into the latter plasmids generate vectors with high levels of expression in both human and murine cells (Addison *et al.*, 1997).

protocol for bacterial growth prior to plasmid DNA isolation.

Solutions

1. *Super broth (SB)*: Dissolve 5 g NaCl, 32 g trypticase peptone, 20 g yeast extract, and 1 g glucose in 1 liter H_2O. Add 5 ml 1 *N* NaOH. Sterilize by autoclaving.
2. *LB-agar plates*: Dissolve 10 g BBL Lennox LB broth base in 500 ml H_2O. Add 7.5 g agar and sterilize by autoclaving. Cool LB-agar to about 50°C, add antibiotics as required, and pour 25 ml into each of 20 sterile petri dishes. Store at 4°C.
3. *Reagents for isolating plasmid DNA on CsCl gradients*: Not described here.

Steps

1. Streak plasmid-bearing bacteria on an LB-agar plate containing appropriate antibiotics and grow overnight at 37°C.

2. Pick two or more colonies off the plate, resuspend each in 5 ml SB plus antibiotics, and incubate at 37°C on a shaker for several hours.

3. Add each 5 ml culture to 500 ml SB plus antibiotics and continue incubating overnight.

4. Purify the plasmid DNA from each culture separately by alkaline lysis of the bacteria and CsCl banding as described in standard cloning manuals (e.g., Sambrook and Russell, 2001). Plasmid DNA that has not undergone any detectable rearrangement, as indicated from comparison between predicted and observed restriction enzyme cleavage pattens, is suitable for use in cotransfections.

B. DNA Transfection for Rescue of Recombinant Adenovirus Vectors: Calcium Phosphate Coprecipitation

Solutions

1. *Complete MEMF11 (or Joklik's modified MEM)*: Add 5 ml 0.2*M* L-glutamine, 5 ml penicillin/streptomycin (10,000 U/ml and 10 mg/ml, respectively), and 5 ml 0.25 mg/ml fungizone to 500 ml MEMF11 (or Joklik's modified MEM). Store at 4°C for up to 2 weeks. Add 55 ml heat-inactivated NBS, FBS or HS prior to use in cell culture.

2. *10X citric saline*: Dissolve 50 g KCl and 22 g trisodium citrate dihydrate ($Na_3C_6H_5O_7{\cdot}2H_2O$) in H_2O to

a final volume of 500 ml. Sterilize by autoclaving and store at 4°C. Dilute 1:10 in sterile H_2O to prepare 1X citric saline.

3. *HEPES-buffered saline (HEBS)*: Dissolve 5 g HEPES free acid, 8 g NaCl, 0.37 g KCl, 0.1 g Na_2HPO_4, and 1 g glucose in 900 ml H_2O. Adjust pH to 7.1. Adjust volume to 1 liter with H_2O. Aliquot into small glass bottles, sterilize by autoclaving, and store at 4°C.

4. *10X SSC*: Dissolve 8.7 g NaCl and 4.4 g tri-sodium citrate dihydrate in H_2O to a final volume of 100 ml. Adjust pH to 7.0. Autoclave. Prepare 0.1X SSC by diluting 10X SSC and then autoclaving.

5. *2 mg/ml carrier DNA*: Dissolve 100 mg salmon sperm DNA in 50 ml sterile 0.1X SSC by stirring overnight at room temperature. Determine concentration by reading the OD at 260 nm (one OD unit = 50 µg/ml). Store in small aliquots at –20°C.

6. *2.5 M $CaCl_2$*: Add H_2O to 36.8 g $CaCl_2 \cdot 2H_2O$ (analytical grade) to a final volume of 100 ml. Sterilize by filtration and store in small plastic tubes at 4°C.

7. *MEMF11-agarose overlay*: To make approximately 200 ml, add 10 ml horse serum (HS) and 2 ml each of L-glutamine, penicillin/streptomycin, fungizone (at concentrations given earlier), and autoclaved 5% yeast extract (w/v in H_2O) to 100 ml 2X MEMF11. Autoclave 1 g agarose in 100 ml H_2O. Bring the 2X medium and agarose to 44°C before mixing and use within an hour.

Steps

1. Grow monolayer cultures of 293 cells in 150-mm dishes in complete MEMF11 medium plus 10% FBS (or NBS). At 90% confluence, remove medium, wash each dish twice with 10 ml 1X citric saline, and then incubate for a maximum of 15 min at room temperature in 3 ml 1X citric saline to detach cells. Resuspend cells in medium and divide between two or three 150-mm dishes. 293 cells should be refed with fresh medium every 3 days if not ready to passage.

2. Set up low-passage (<p40) 293 cells in 60-mm dishes to be about 70–80% confluent at the time of use. As a rule of thumb, one 150-mm dish of nearly confluent 293 cells can be split into eight 60-mm dishes each containing 5 ml complete MEMF11 + 10% FBS, which will be ready for transfection the next day.

3. Add 0.005 volume 2 mg/ml carrier DNA to 1X HEBS and shear by vortexing for 1 min.

4. For each virus to be rescued, aliquot 2 ml HEBS + carrier DNA (enough for four dishes) into each of three sterile clear plastic tubes.

5. To these tubes add E1 shuttle plasmid DNA and the appropriate genomic plasmid (e.g., pBHGloxΔE1,E3Cre) in the following amounts: 20 µg of each plasmid, 8 µg of each plasmid, and 2 µg of each plasmid. If a negative control is desired, set up similar coprecipitations omitting the first plasmid. A useful positive control is 2 µg of the infectious plasmid pFG140.

6. Gently mix by shaking and then slowly add 0.1 ml 2.5 *M* $CaCl_2$ to each tube.

7. Gently mix and let stand at room temperature for 15–30 min. (A fine precipitate should form within a few minutes.) Without removing the growth medium, add 0.5 ml DNA suspension to each dish of cells (four dishes for each tube of coprecipitate) and then incubate at 37°C in a CO_2 incubator for at least 5 h, preferably overnight.

8. Remove the medium and add to each dish 10 ml MEMF11-agarose overlay previously equilibrated to 44°C. After the agarose solidifies, incubate at 37°C. Plaques should appear after about 5–14 days. When dishes are examined from below by eye, plaques appear turbid as a consequence of light scattering by dead cells in an otherwise smooth cell monolayer. Microscopic examination reveals plaques as zones of dead or lysed cells surrounded by rounded infected cells.

9. At about 10 days posttransfection, pick well-isolated plaques by punching out agar plugs from the cultures using a sterile Pasteur pipette. Transfer each agar plug to 1 ml sterile PBS^{++} + 10% glycerol in a sterile vial. Store at –70°C until use.

C. Screening Adenovirus Plaque Isolates

The following protocol describes the expansion of plaque isolates by growth in monolayer cultures of 293 cells. A portion of the infected cell material is stored for further purification; the remainder is harvested for analysis of viral DNA.

Solutions

1. *Phosphate-buffered saline^{++} (PBS^{++})*: To make solution A, dissolve 80 g NaCl, 2 g KCl, 11.5 g Na_2HPO_4, and 2 g KH_2PO_4 in H_2O to a final volume of 1 liter. To make solution B, add 1 g $CaCl_2 \cdot 2H_2O$ to 100 ml H_2O. To make solution C, add 1 g $MgCl_2 \cdot 6H_2O$ to 100 ml H_2O. Sterilize solutions separately by autoclaving. For 100 ml PBS^{++}, mix 88 ml sterile H_2O with 10 ml solution A and 1 ml each of solutions B and C.

2. *PBS^{++} + 10% glycerol*: Add 10 ml sterile glycerol to 90 ml PBS^{++}.

3. *Pronase stock solution*: Dissolve 0.5 g pronase in 100 ml 10 m*M* Tris–HCl, pH 7.5; heat at 56°C for 15 min and then incubate at 37°C for 1 h. Aliquot and store at –20°C. To prepare working solution, thaw stock solution just before use and add 0.1 volume to 10 m*M* Tris–HCl, pH 7.5, 10 m*M* EDTA, 0.5% (w/v) sodium dodecyl sulfate (SDS).

4. *Complete MEMF11 + 5% HS*: Add 25 ml HS to 475 ml complete MEMF11.

5. *0.1X SSC*: See Section III.B, solution 4.

6. *Reagents for restriction analysis of viral DNA*: Not described here.

Steps

1. Set up 60-mm dishes of 293 cells to be 80–90% confluent at time of infection. The denser and older the cell monolayer, the longer it takes for the cytopathic effect to reach completion.

2. Remove medium from 293 dishes and add 0.2 ml virus (agar plug suspension). Rock dishes once and adsorb at room temperature for 30 min. Add 5 ml complete MEMF11 + 5% HS and incubate at 37°C.

3. A cytopathic effect should be visible within 1–2 days. Harvest virus and extract infected cell DNA (steps 4 to 6) when all cells are rounded and most have detached from the dish (usually 3–4 days).

4. Release semiadherent cells from the dish by gentle pipetting. Transfer 3.5 ml of the cell suspension to a sterile vial containing 0.5 ml sterile glycerol. Store at –70°C until you wish to amplify the vector.

5. Transfer the remaining 1.5 ml to a microfuge tube and spin 2 min at 7000 rpm. Aspirate all but about 0.1 ml supernatant. Vortex well to suspend infected cells. To extract DNA, add 0.5 ml pronase working solution to the cells in the microfuge tube and incubate at 37°C for 4–18 h.

6. Add 1 ml cold 96% ethanol to precipitate the DNA. Mix well by inverting the tube several times—a fibrous precipitate should be easily visible and the solution should no longer be viscous. Spin 5 min at 14,000 rpm and then aspirate supernatant. Wash pellet twice with 70% ethanol and air dry.

7. Dissolve DNA pellet in 50 µl 0.1X SSC by heating at 65°C with occasional vortexing. Digest 5 µl with *Hind*III (1 unit overnight is usually sufficient for complete digestion).

8. Apply digested samples and appropriate markers (a *Hind*III digest of wild-type Ad5 being one convenient marker) to a 1% agarose gel containing ethidium bromide and subject to electrophoresis until the dye front has migrated at least 10 cm. If the cytopathic effect was complete, viral DNA bands should be easily visible (under ultraviolet light) above a background smear of cellular DNA. Note that in *Hind*III digests of human DNA there will be a band of cellular repetitive DNA at 1.8 kb.

9. Verify candidate recombinants using other diagnostic restriction enzymes. Although generally 100% of viral plaques obtained using AdMax are correct, it is good laboratory practice to carry out one round of plaque purification, as described later, and screening as described in this section prior to preparation of high-titer stocks.

D. Plaque Assays for Purification and Titration of Adenovirus

Solutions

PBS^{++} and MEMF11-agarose overlay (at 44°C): See Section III.C.

Steps

1. Set up 60-mm dishes of 293 cells to be confluent at time of infection.

2. Remove medium from dishes. Add 0.2 ml virus (dilution of agar plug suspension in PBS^{++} if you wish to plaque purify or dilution of stock for titration). We typically assay dilutions ranging from 10^{-3} to 10^{-6} for plaque purification or 10^{-4} to 10^{-10} for virus titration. Adsorb the virus for 30–60 min in an incubator, occasionally rocking the dishes. Add 10 ml MEMF11-agarose overlay, cool, and then continue incubation at 37°C.

3. Plaques should be visible within 4–5 days and should be counted for titration at 7 days and again at 10 days. For plaque purification, proceed as for isolation of plaques following transfections (Section III.C).

E. Preparation of High-Titer Viral Stocks (Crude Lysates) from Cells in Monolayer

Because most of the virus remains associated with the infected cells until very late in infection, high-titer stocks can be prepared easily by concentrating infected 293 cells as described here.

Solutions

PBS^{++}, PBS^{++} + 10% glycerol, and complete MEMF11 + 5% HS: See Section III.C.

Steps

1. Set up 150-mm dishes of 293 cells to be 80–90% confluent at time of infection. We generally use eight or more dishes for each virus.

2. To prepare high-titer stocks, remove medium from the 293 cells and infect at a multiplicity of infection (MOI) of 1–10 PFU per cell (1 ml diluted virus per 150-mm dish). For the initial stock preparation, we dilute virus (from the untitered 4-ml sample stored at –70°C after the last round of viral screening) 1:8 with PBS^{++}. To minimize generation and amplification of rearranged forms of the vector, always prepare high-titer stocks from viral screening samples, not from CsCl-banded stocks (Section III.F).

3. Adsorb for 30–60 min and then refeed with complete MEMF11 + 5% HS. Incubate at 37°C and examine daily for signs of a cytopathic effect.

4. When the cytopathic effect is nearly complete, i.e., most cells rounded but not yet detached, harvest by scraping the cells off the dish, combining the cells plus spent medium, and centrifuging at 800 *g* for 15 min. Aspirate the medium and resuspend the cell pellet in 2 ml PBS^{++} + 10% glycerol per 150-mm dish. Freeze (–70°C) and thaw (37°C) the crude virus stock two or three times prior to titration. Store aliquots at –70°C.

F. Preparation of High-Titer Viral Stocks (Purified) from Cells in Suspension

Recombinant Ads can be purified from crude lysates of either monolayer or suspension cultures. Due to the greater ease of handling suspension cultures, however, this source is preferable for the preparation of purified high-titer viral stocks as described here. Similar yields can be obtained from thirty to sixty 150-mm dishes of 293 cell monolayers.

Solutions

1. *Complete Joklik's modified MEM + 10% HS*: Add 50 ml HS to 450 ml complete Joklik's modified MEM (described in Section III.B). Store at 4°C.

2. *1% sodium citrate*: Dissolve 1 g trisodium citrate dihydrate in H_2O to a final volume of 100 ml.

3. *Carnoy's fixative*: Add 25 ml glacial acetic acid to 75 ml methanol.

4. *Orcein solution*: Add 1 g orcein dye to 25 ml glacial acetic acid plus 25 ml H_2O. Filter through Whatman No. 1 paper.

5. *0.1 M Tris–HCl, pH 8.0*: Add 1.2 g Tris base to 80 ml H_2O. Adjust pH to 8.0 with HCl. Adjust volume to 100 ml and autoclave.

6. *5% Na deoxycholate*: Add 5 g Na deoxycholate to 100 ml H_2O.

7. *2 M $MgCl_2$*: Add 40.6 g $MgCl_2 \cdot 6H_2O$ to 100 ml H_2O and sterile filter.

8. *DNase I solution*: Dissolve 100 mg bovine pancreatic deoxyribonuclease I (DNase I) in 10 ml of 10 m*M* Tris–HCl, pH 7.4, 50 m*M* NaCl, 1 m*M* dithiothreitol, 0.1 mg/ml bovine serum albumin, 50% glycerol. Store in small aliquots at –20°C.

9. *CsCl solutions for banding*: Transfer the indicated amounts of analytical grade CsCl into small beakers to give the desired final densities:

Solution	Density of final solution (g/ml)	Weight of CsCl (g)
1.5 d	1.5	83.1
1.35 d	1.35	54.3
1.25 d	1.25	37.0

Add 100 ml 10 m*M* Tris–HCl, pH 8, to each beaker and stir to dissolve. Verify density by weighing 1.0 ml of each solution (e.g., 1.0 ml of the 1.35 d solution should weigh 1.35 g). Sterile filter and store at room temperature.

10. *Sterile glycerol*: Prepare by autoclaving.

11. *TE/SDS*: Add 0.5 ml 20% SDS to 100 ml 10 m*M* Tris–HCl, 1 m*M* EDTA, pH 8.

Steps

1. Grow 293N3S cells in spinner culture to a density of 2–4 × 10^5 cells/ml in 3 liters of complete Joklik's modified MEM + 10% HS. Centrifuge cell suspension at 750 *g* for 20 min, saving half of the conditioned medium. Resuspend the cell pellet in 0.1 vol fresh medium and transfer to a sterile 500-ml bottle containing a sterile stir bar.

2. Add virus at an MOI of 10–20 PFU/cell and stir gently at 37°C. After 1 h, return culture to the spinner flask and bring to the original volume using 50% conditioned medium and 50% fresh medium. Continue stirring at 37°C.

3. Monitor infection daily by inclusion body staining as follows.

   a. Remove a 5-ml aliquot from the infected spinner culture. Spin for 10 min at 750 *g* and resuspend the cell pellet in 0.5 ml of 1% sodium citrate.

   b. Incubate at room temperature for 10 min, add 0.5 ml Carnoy's fixative, and fix for 10 min at room temperature.

   c. Add 2 ml Carnoy's fixative, spin for 10 min at 750 *g*, aspirate, and resuspend the pellet in a few drops of Carnoy's fixative. Add one drop of fixed cells to a slide, let air dry for about 10 min, add one drop orcein solution and a coverslip, and examine in the microscope. Inclusion bodies appear as densely staining nuclear structures resulting from the accumulation of large amounts of virus and viral products at late times in infection. A negative control should be included in initial tests.

4. When inclusion bodies are visible in 80–90% of the cells (1.5 to 3 days), harvest by centrifugation at 750 *g* for 20 min in sterile 1-liter bottles. Combine pellets in a small volume of medium and spin again. Resuspend pellet in 15 ml 0.1 *M* Tris–HCl, pH 8.0. Store at –70°C until use.

5. Thaw the frozen crude stock and add 1.5 ml 5% Na deoxycholate. Mix well and incubate at room temperature for 30 min. This disrupts cells without disrupting virions, resulting in a relatively clear, highly viscous suspension.

6. Add 0.15 ml 2 *M* $MgCl_2$ and 0.075 ml DNase I solution and then mix well. Incubate at 37°C for

60 min, mixing every 10 min. The viscosity should be reduced greatly.

7. Spin at 3000 *g* for 15 min at 4°C in a tabletop centrifuge.

8. Prepare three CsCl step gradients in SW41 Ti ultraclear tubes: Add 0.5 ml of 1.5 d CsCl solution to the bottom of each tube, carefully overlay with 3.0 ml of the 1.35 d solution, and then overlay with 3.0 ml of the 1.25 d solution. Mark the level of the interface between the 1.35 d and the 1.25 d layers.

9. Carefully add 5 ml of supernatant from step 6 to the top off each gradient. If necessary, top off tubes with 0.1 *M* Tris–HCl, pH 8.0.

10. Spin at 35,000 rpm in a Beckman SW41 Ti rotor at 10°C for 1 h.

11. Collect the virus band at the interface between the 1.35 d and the 1.25 d layers by piercing the side of the tube with an 18-gauge needle attached to a 5-ml syringe. Pool the virus from all three tubes into a Beckman SW50.1 ultraclear tube. If necessary, top off the tube with 1.35 d CsCl solution.

12. Centrifuge the pooled virus in a Beckman SW50.1 rotor at 35,000 rpm, 4°C, for 16–20 h.

13. Collect the virus band in the smallest volume possible, transfer to a Slide-A-Lyzer dialysis cassette, and dialyze at 4°C against three changes of 500 volumes 10 m*M* Tris–HCl, pH 8.0, for at least 24 h total.

14. After dialysis, add sterile glycerol to a final concentration of 10%. Store the purified virus at –70°C in small aliquots.

15. Determine titer of virus by plaque assay (Section III.D).

16. The concentration of virus particles, based on DNA content, can be determined spectrophotometrically as follows.

a. Dilute purified virus 20-fold with TE/SDS. Set up blank by diluting virus storage buffer (10 m*M* Tris, pH 8.0, supplemented with glycerol to 10%) 20-fold with TE/SDS.

b. Incubate for 10 min at 56°C. Vortex sample briefly. Measure OD_{260} with a spectrophotometer.

c. Calculate the number of particles per milliliter, based on the extinction coefficient of wild-type Ad as determined by Maizel *et al*. (1968) as follows:

$$\text{particles/ml} = (OD_{260})(20)(1.1 \times 10^{12})$$

IV. COMMENTS

Once the desired recombinant Ad virus is obtained, the ability to express the foreign gene must be tested. The most suitable procedure for detecting expression would depend on the particular properties of the foreign protein. If antibodies to the protein are available, then ELISA, Western blotting analysis, or immunoprecipitation of infected cell extracts may be the simplest method to quantitate protein expression. If possible, the biological activity of the recombinant protein should also be tested to ensure that the expressed protein is functional (for additional details, see Graham and Prevec, 1991).

It is important to use caution when handling recombinant Ads. Experimentation with these vectors should be carried out in accordance with relevant regulations. If exposed inadvertantly, individuals without previous immunity to Ad5 may seroconvert not only against Ad5, but also against the foreign gene product expressed. This should be avoided, especially if the development of antibody may confuse diagnosis of a particular disease. Finally, no toxic or oncogenic gene product should be expressed from replication-proficient Ad vectors without an appropriate increase in biocontainment.

V. PITFALLS

1. There can be a number of different causes for failure to obtain the proper recombinant virus following cotransfection. First, the transfection efficiency may be low (a suitable control would be transfection of wild-type viral DNA or infectious plasmid DNA such as pFG140). The 293 cells used in transfections must be at low passage, growing slowly, and slightly subconfluent. In addition, the plasmid DNA must be of high quality; we routinely use CsCl-banded DNA in cotransfections. Finally, although infrequently, the desired recombinant might not be obtained because the foreign gene insert is toxic to the cells or virus, in which case it may be necessary to use an alternate adenovirus rescue system (e.g., Hi-IQ AdMax from Microbix).

2. For many applications, particularly those involving *in vivo* studies or infection of human cells, it is important to confirm that preparations of E1 replacement Ad vectors are not contaminated with replication-competent Ad (RCA). Most often RCA are generated by recombination of the vector with E1 sequences in the 293 cell genome. The latter is most problematic when the wild-type Ad has a growth advantage over the desired recombinant virus. Several tests for RCA contamination have been described, including a functional assay for virus growth in non-complementing cell lines such as HeLa or A549, as well as protocols that detect contaminating wild-type viral

DNA sequences, such as Southern blot hybridization analysis and quantitative polymerase chain reaction amplification (Lochmuller *et al*., 1994). It is advisable to perform at least one of these tests in order to estimate the maximum possible RCA contamination in recombinant virus stocks before use.

3. The level of expression in E1 replacement vectors depends mainly on the strength of the promoter immediately upstream of the coding sequence for the foreign gene. In E3 insertion vectors, this is not necessarily true; even some promoterless constructs express relatively high levels of recombinant proteins. In these cases the major late or E3 promoter is presumably driving expression of the foreign gene insert. It is not, at this time, possible to predict which E3 constructs will utilize an inserted promoter; consequently, care must be taken in analyzing E3 insertion recombinants for appropriate expression, in particular, for example, when transcriptionally regulated expression is required.

Acknowledgments

We thank Uma Sankar, John Rudy, and Derek Cummings for excellent technical assistance. This work was supported by grants from the National Institutes of Health, the Canadian Breast Cancer Research Initiative, the Canadian Institutes of Health Research (CIHR), and the National Cancer Institute of Canada. P.N. was supported by a CIHR Postdoctoral Fellowship.

References

Addison, C. L., Hitt, M., Kunsken, D., and Graham, F. L. (1997). Comparison of the human versus murine cytomegalovirus immediate early gene promoters for transgene expression by adenoviral vectors. *J. Gen. Virol*. **78**, 1653–1661

Berkner, K. L. (1988). Development of adenovirus vectors for expression of heterologous genes. *Biotechniques* **6**, 616–629.

Bett, A. J., Haddara, W., Prevec, L., and Graham, F. L. (1994). An efficient and flexible system for construction of adenovirus vectors with insertions or deletions in early regions 1 and 3. *Proc. Natl. Acad. Sci. USA* **91**, 8802–8806.

Bramson, J., Hitt, M., Gallichan, W. S., Rosenthal, K. L., Gauldie, J., and Graham, F. L. (1996). Construction of a double recombinant adenovirus vector expressing a heterodimeric cytokine: *In vitro* and *in vivo* production of biologically active interleukin-12. *Hum. Gene Ther.* **7**, 333–342.

Ginsberg, H. S. (1984). "The Adenoviruses." Plenum, New York.

Graham, F. L., and Prevec, L. (1991). Manipulation of adenovirus vectors. *In* "*Methods in Molecular Biology*" (E. J. Murray, ed.), Vol. 7, pp. 109–128. Humana Press, Clifton, NJ.

Graham, F. L., and Prevec, L. (1992). Adenovirus-based expression vectors and recombinant vaccines. *In* "*Vaccines: New Approaches to Immunological Problems*" (R. W. Ellis, ed.), pp. 363–389. Butterworth-Heinemann, Boston, MA.

Graham, F. L., Smiley, J., Russell, W. C., and Nairn, R. (1977). Characteristics of a human cell line transformed by DNA from human adenovirus type 5. *J. Gen. Virol.* **36**, 59–72.

Hitt, M. M., Parks, R. J., and Graham, F. L. (1999). Structure and genetic organization of adenovirus vectors. *In* "*The Development of Human Gene Therapy*" (T. Friedmann, ed.), pp. 61–86. Cold Spring Harbor Laboratory Press, Cold Spring Harbor, NY.

Lochmuller, H., Jani, A., Huard, J., Prescott, S., Simoneau, P. M., Massie, B., Karpati, F., and Acsadi, G. (1994). Emergence of early region 1-containing replication-competent adenovirus in stocks of replication-defective adenovirus recombinants (ΔE1 + ΔE3) during multiple passages in 293 cells. *Hum. Gene Ther.* **5**, 1485–1491.

Maizel, J. V., White, D., and Scharff. M. D. (1968). The polypeptides of adenovirus. I. Evidence of multiple protein components in the virion and a comparison of types 2, 7a, and 12. *Virology* **36**,115–125.

Ng, P., Cummings, D. T., Evelegh, C. M., and Graham, F. L. (2000b). Yeast recombinase FLP functions effectively in human cells for construction of adenovirus vectors. *Biotechniques* **29**, 524–526, 528.

Ng, P., and Graham, F. L. (2002). Construction of first-generation adenoviral vectors. *Methods Mol. Med.* **69**, 389–414.

Ng, P., Parks, R. J., Cummings, D. T., Evelegh, C. M., and Graham, F. L. (2000a). An enhanced system for construction of adenoviral vectors by the two plasmid rescue method. *Hum. Gene Ther.* **11**, 693–699.

Sambrook, J., and Russell, D. (2001). "Molecular Cloning: A Laboratory Manual" 3rd Ed. Cold Spring Harbor Laboratory Press, Cold Spring Harbor, NY.

CHAPTER

54

Production and Quality Control of High-Capacity Adenoviral Vectors

Gudrun Schiedner, Florian Kreppel, and Stefan Kochanek

I. INTRODUCTION

High-capacity adenovirus (HC-Ad) vectors [also called pseudoadenovirus (PAV), helper-dependent (HD-Ad), gutted, or gutless adenovirus vectors] have been developed to address capacity, toxicity, and immunogenicity problems of first- and second-generation adenovirus vectors. As only viral elements this vector type contains the inverted terminal repeats (ITRs), which are essential for replication of the viral DNA, and the packaging signal close to the left terminus that is required for encapsidation of the DNA into the viral capsids. Since the size of the ITRs and the packaging signal together are less than 0.6 kb, up to 37 kb of foreign DNA can be transported.

For practical reasons, most HC-Ad vectors will carry genes or expression cassettes that are smaller than 37 kb. For stability reasons during amplification in most cases additional "stuffer" DNA has to be incorporated into the vector DNA to increase the genome size to at least around 27 kb.

HC-Ad vectors cannot be produced similar to helper-independent vectors, in which most viral functions are provided from the vector. Because adenovirus is a relatively large DNA virus that expresses many different protein and RNA functions, it is unlikely that complementing cell lines can be generated to provide appropriate levels of all viral functions in *trans*. Therefore, a helper virus is used for production that subsequently is eliminated from the end product.

The currently preferred production system is based on excision of the packaging signal of the helper virus by a recombinase expressed in the producer cell line. Most HC-Ad vectors so far have been produced using the Cre-loxP recombination system of the bacteriophage PI. In this system the packaging signal of the helper virus is flanked by two loxP sites (Hardy *et al.*, 1997; Parks *et al.*, 1996). The HC-Ad vector is produced in E1-complementing cells that express the recombinase constitutively. The Cre-mediated excision is surprisingly efficient and the contamination of vector by helper virus is reduced compared to the earlier production system.

The complete characterization of HC-Ad vector preparations comprises three parameters: (1) the number of infectious particles, (2) the number of total particles, and (3) the number helper virus particles remaining in the preparation after purification (Kreppel *et al.*, 2002). Due to the fact that HC-Ad vectors do not possess any viral coding sequences, the number of infectious particles cannot be determined by plaque assay or tissue culture infectivity dose $TCID_{50}$ because these methods rely on vector replication and viral protein expression in E1-transformed cell lines. The number of total particles can be determined by particle lysis and subsequent measuring light absorbance at 260 nm. However, the reliability of this method is usually low and strongly depends on the purity of the vector preparations. The DNA-based method described here allows for fast and reliable determination of all three parameters with standard laboratory equipment independent of viral or reporter gene expression. For quantifying the number of infectious particles, a reference cell line with defined susceptibility for Ad5 is transduced with the HC-Ad vector, cell lysates are prepared, and vector genomes that entered the cells are detected after immobilization on a nylon membran by hybridization with a radiolabeled vector-specific probe. Total particle numbers can easily be determined with the same probe on the

Copyright 2006, Elsevier Science (USA).
All rights reserved.

same membrane by preparing particle lysates and immobilizing the DNA. Finally, by choosing a probe specific for the helper virus genome the number of helper virus particles can be quantified in the particle lysates.

This article is divided in two parts: in the first part the production process includes serial amplification in producer cells and ends with CsCl density centrifugation for purification. In the second part a method for titration of purified vectors is described that is based on slot blot methods and that not only allows one to determine particle and infectious vector titers, but also the contamination with helper virus.

II. PRODUCTION OF HC-Ad VECTORS

Materials

Cells and Plasmids

E1-Expressing Cell Lines

Several cell lines have been described that express the adenovirus type 5 (Ad5) early region E1 (E1A and E1B) and thus support the growth of E1-deleted vectors and helper viruses (Fallaux *et al*., 1998; Gao *et al*., 2000; Graham *et al*., 1977; Schiedner *et al*., 2000). In contrast to HEK293 cells, PER.C6 and N52.E6 cells have been designed not to produce replication-competent adenovirus (RCA) and thus are a preferred cell type for the production of E1-deleted vectors and helper viruses.

Cre-Expressing Cell Lines

The production process of HC-Ad vectors builds on two viral components; vector and E1-deleted helper virus with packaging signal flanked by loxP sites and serial amplifications in producer cells expressing Cre-recombinase. Excision of the packaging signal from the helper virus in the producer cells results in preferential packaging of vector genomes and a reduction of helper virus contamination. Several HEK293-based Cre-expressing cell lines have been described (Hilgenberg *et al*., 2001; Parks *et al*., 1996). Similar to first-generation adenoviral vectors, the helper virus is prone to turn into RCA when HEK-293 based cells are used for HC-Ad vector production. Based on PER.C6, a Cre-expressing cell line has been described preventing the occurrence of RCA in HC-Ad vector preparations (Sakhuja *et al*., 2003). Similarly, a Cre-expressing cell line 73/29 has been generated (manuscript submitted) that is based on N52.E6 cells.

Helper Virus Plasmids

A preferred helper virus used for preparation of HC-Ad vectors contains loxP (Parks *et al*., 1996) or frt (Ng *et al*., 2001; Umana *et al*., 2001) sites flanking the packaging signal. Consequently, in Cre- or FLPe-recombinase expressing producer cells the packaging signal of the helper virus is excised and vector genomes are preferentially packaged. Most published helper viruses are E1 and E3 deleted and contain a reporter gene cassette in E3 in order to allow easy quantitation of helper virus contamination (Hartigan-O'Connor *et al*., 2002; Hilgenberg *et al*., 2001; Ng *et al*., 2001; Palmer and Ng, 2003; Parks *et al*., 1996; Sandig *et al*., 2000; Umana *et al*., 2001). However, this insertion may affect helper virus yield and can provoke an immune reaction against the reporter *in vivo*. Recombination events between helper and vector inverted terminal repeats (ITRs) occur frequently and can result in loss of a loxP site in the helper virus genomes and thus outgrowth of mutated helper virus. Figure 1 shows the schematic structure of helper virus plasmid pGS102#21, which contains Ad5 sequences from nucleotides 1–341 with a loxP site introduced at nucleotide 192, a second loxP site introduced at nucleotide 341 followed by 4.6 kb of λ DNA, and Ad5 sequence nucleotides 3523 to 35935. The adenoviral packaging signal consists of seven functional units called A repeats with the consensus sequence [ATTTGN$_8$GC] (Schmid and Hearing, 1998). In order to minimize sequence homologies between vector and helper virus genome, pGS102#21 contains only A repeats I to IV. In addition, sequences from phage λ were inserted in the helper virus genome in order to increase the size of the helper virus, thus improving separation of helper and vector particles in a CsCl-gradient. pGS102#21 is an infectious plasmid based on pBluescript with unique *Swa*I sites flanking both ITRs.

Plasmids for Cloning HC-Ad Vectors

Early observations using different sizes of HC-Ad vectors suggested that only vector genomes with sizes of at least 27 kb allowed efficient and stable vector amplification (Parks and Graham, 1997). The sizes of most expression cassettes used currently for gene transfer are smaller than this 27-kb minimal size for HC-Ad vectors. Therefore, additional DNA has to be incorporated into the vector genome as stuffer DNA. Since the source of the stuffer sequences may influence transgene expression (Parks *et al*., 1999), the use of non-coding DNA from human origin is preferred. Figure 2 shows different plasmids constructed for the incorporation of different sized transgenes. Most plasmids contain noncoding stuffer sequences derived either

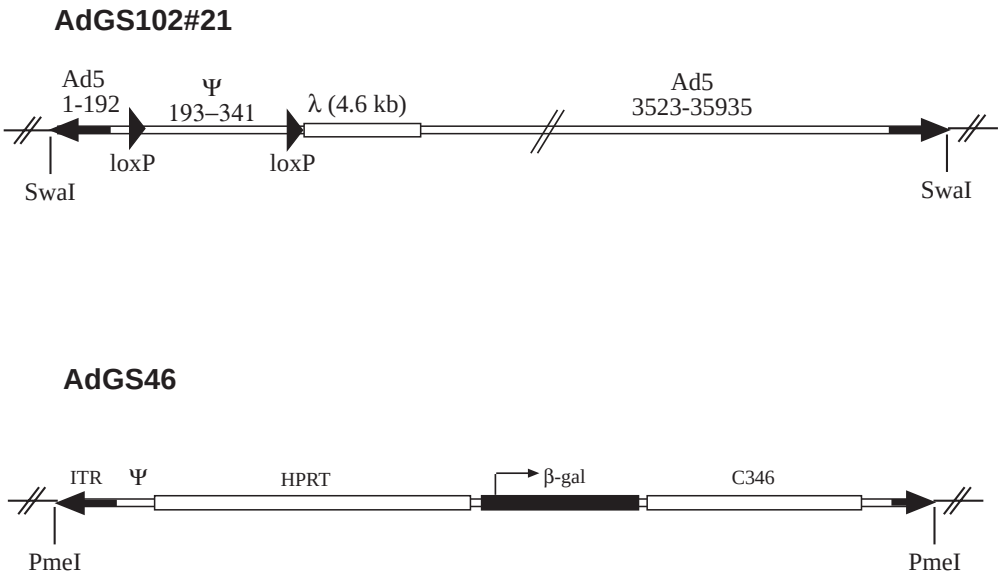

FIGURE 1 Structure of helper virus AdGS102#21 and HC-Ad vector AdGS46. Helper virus AdGS102#21 is E1 deleted and contains Ad5 sequences from nucleotides 1 to 341 with a loxP oligo nucleotide introduced at nucleotide 192, a second loxP oligo nucleotide introduced at nucleotide 341 followed by 4.6 kb of λ DNA, and Ad5 sequences from nucleotides 3523 to 35935. AdGS46 contains the Ad5 left terminus, 16 kb of HPRT stuffer, a β-galactosidase expression cassette, 9 kb of C346 stuffer DNA, and the Ad5 right terminus. Both AdGS102#21 and AdGS46 were constructed as plasmids based on pBluescript with unique *Swa*I (AdGS102#21) and *Pme*I (AdGS46) sites flanking both inverted terminals for easy release of the plasmid backbone.

from the human HPRT locus or from the human cosmid C346. In addition, all plasmids contain left (nucleotides 1–440) and right (nucleotides 35818–35935) termini of Ad5 DNA. Both left and right adenoviral termini are flanked by unique *Pme*I or *Sna*BI (pSTK142) restriction sites. The plasmid backbone in all constructs is pBluescript.

The HC-Ad vector AdGS46 has been described previously (Thomas *et al*., 2000) and is based on pSTK120. Plasmid pGS46 contains the Ad5 left terminus, 16 kb of HPRT stuffer, a β-Gal expression cassette containing the hCMV promoter and SV40 polyadenylation signal, a 9-kb stuffer from C346, and the Ad5 right terminus (Fig. 1).

Cell Culture Reagents

All tissue culture reagents, including α-modified Eagle's medium (αMEM, Cat. No. 12000-063), fetal calf serum (FBS, Cat. No. 10270-106), phosphate-buffered saline (PBS, Cat. No. 14190-169), trypsin solution (Cat. No. 25300-096), and antibiotics (Cat. No. 10378-016) are from Invitrogen. G418 for selection of neomycin expression is from Sigma (geneticin, Cat. No. G5013). Tissue culture dishes (6- and 15-cm dishes) are from Renner.

Additional Reagents and Solutions

Centrifuge tubes: SW41 ultraclear centrifuge tubes (Beckmann, Cat. No. 344059)

Desalting column: PD-10 column (Amersham Bioscience, Cat. No. 17-0851-01)

Chloroform/isoamyl alcohol: Mix 10 ml isoamyl alcohol with 230 ml chloroform

TE: 10 m*M* Tris, 1 m*M* EDTA, pH 7.5

0.5 *M* EDTA: Dissolve 186.1 g EDTA·2H_2O in 800 ml H_2O, adjust pH to 8.0 using NaOH pellets (approximately 20 g), fill up to 1 liter, and autoclave

MEM agarose overlay: Dissolve 1 g agarose (AppliChem, Cat. No. A2114,0500) in 100 ml H_2O, autoclave, and cool to 40°C. Add prewarmed (37°C) 90 ml 2× MEM (Gibco, Cat. No. 61100-087), 10 ml FBS, 1 ml antibiotics (Gibco, Cat. No. 10378-016), and 2 ml 5% yeast extract

Na-acetate (3 *M*): Dissolve 24.6 g Na-acetate in 100 ml H_2O, adjust pH to 5.2 using acetic acid, and autoclave

Phenol, buffer saturated: Gibco (Cat. No. 15513-039)

Proteinase K (Sigma, Cat. No. P6556): 5 mg/ml dissolved in sterile H_2O

QIAamp DNA Minikit: Qiagen (Cat. No. 51104)

RNase: DNase free (Roche, Cat. No. 1119915)

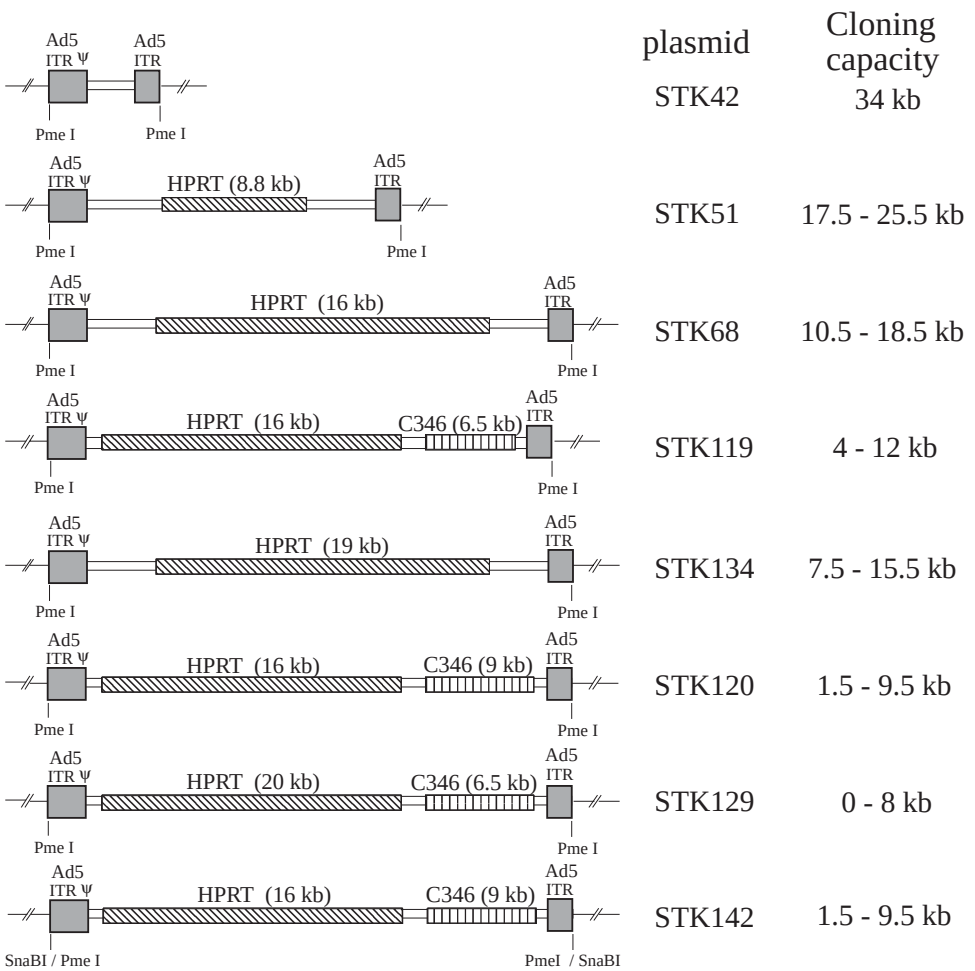

FIGURE 2 Plasmids for cloning HC-Ad vectors. Plasmids contain Ad5 left (Ad5 sequences nucleotides 1 to 440) and right (Ad5 sequences nucleotides 35818 to 35935) termini. In addition, cloning plasmids contain noncoding stuffer sequences from the HPRT gene locus or the C346 cosmid. Again, to release the pBluescript backbone, both inverted terminal repeats are flanked by *Pme*I sites (or *Sna*BI for pSTK42). In order to incorporate different sizes of transgenes, the plasmids contain several unique cloning sites.

10% SDS: Dissolve 10 g SDS in 100 ml sterile H_2O
Superfect transfection kit (Qiagen Cat. No. 301305)
Tris-buffered saline (TBS): 25 m*M* Tris, 137 m*M* NaCl, 2.7 m*M* KCl, pH 7.4, autoclave
TBS/10% glycerol: TBS containing 10% glycerol
TBS/CsCl: Dissolve 10 g CsCl (Roche, Cat. No. 757306) in 20 ml sterile TBS
Ultracentrifuge, SW41 rotor: e.g., Beckmann
Yeast extract (5%): Dissolve 2 g yeast extract (AppliChem, Cat. No. A1552,0100) in 40 ml H_2O, sterile filter

Production of Helper Virus

Preparation of DNA for Transfection

1. Digest 10 µg of plasmid pGS102#21 with 20–50 units of *Swa*I (New England Biolabs) at 25°C for 2 h.
2. Add TE buffer, pH 8.5, up to 200 µl, add 200 µl phenol, vortex gently, and precipitate for 5 min at 14,000 rpm.
3. Take upper phase, add 200 µl chloroform/Isoamyl alcohol, vortex gently, and centrifuge for 5 min at 14,000 rpm.
4. Take upper phase, add 20 µl 3 *M* Na-acetate, mix, add 400 µl ethanol, mix, and precipitate for 30 min at 14,000 rpm and 4°C.
5. Discard supernatant, add 400 µl 70% ethanol, centrifuge for 10 min at 14,000 rpm and 4°C, and discard supernatant.
6. Dissolve pellet in 20 µl TE, pH 7.5 (0.5 µg/µl).

Preparation of N52.E6 Cells for Transfection

N52.E6 cells are used for the production of helper virus and are cultivated in αMEM supplemented with

10% FBS and antibiotics in 5% CO_2 at 37°C. N52.E6 cells are usually passaged twice a week 1:4–5.

7. The day before transfection, wash cells in PBS, detach cells in trypsin, and resuspend in culture medium. Count cells and plate 2×10^6 cells on a 6-cm dish. The cells should be ready for transfection at 60–80% confluency the following day.

Transfection

8. Transfect N52.E6 cells in 6-cm dishes using 5 µg of the *Swa*I-linearized pGS102#21 and the Superfect transfection kit. Perform transfection according to the manufacturer.

Comments

DNA transfections can also be performed using the calcium–phosphate coprecipitation method as described in a number of different manuals. The commercially available Effectene transfection Kit (Qiagen) also shows very high efficiency in transfection but should not be used for large-sized linearized plasmids.

Plaque Isolation and Preparation of High-Titer Helper Virus Stocks

9. Six to 7 days posttransfection, harvest cells by scratching cells into medium, pellet cells for 10 min at 400 *g*, and resuspend in 2 ml Tris-buffered saline (TBS). Lyse cells by three cycles of freeze/thawing in dry ice/ethanol. Lysate can be stored at –80°C.

10. Split 2×10^6 N52.E6 cells into 6-cm dishes the day before. Infect cells by removing medium, adding 3 ml fresh medium plus 0.2 ml of the lysate. After 2 h add 2 ml medium. Five days after infection, harvest cells as described earlier and lyse by freeze/thawing.

11. Split six 6-cm dishes N52.E6 the day before with 2×10^6 cells per dish. Dilute the lysate 1:100 in TBS and infect each two dishes with 1, 5, and 25 µl of the lysate.

12. Three to 4 h later, overlay cells with agarose: remove medium from infected cells and carefully add 10 ml of prewarmed MEM-agarose solution. After the agarose solidifies, incubate at 37°C until plaques appear (usually 7–10 days).

13. Pick well-isolated single plaques by punching out agar using a sterile Pasteur pipette and transfer agar to 0.2 ml TBS/10% glycerol. Plaques can be stored at –80°C.

14. Infect 2×10^6 N52.E6 cells on 6-cm dishes with 100 µl of the plaque lysate. After complete cytopathic effect (CPE) has occurred, harvest cells in 2 ml TBS and lyse by freeze/thawing.

15. Amplify helper virus by first infecting 2×10^6 N52.E6 cells on a 6-cm dish with 1 ml of the lysate. Complete CPE should be visible 48 to 72 h after infection. Harvest cells and titer helper virus in the lysate by infecting N52.E6 cells on a 6-cm dish (2×10^6 cells per dish, split the day before) with 30, 10, 5, and 1 µl (lysate 1:10 diluted).

16. Infect ten 15-cm dishes N52.E6 cells (2×10^7 per dish) with the amount of lysate titered before and resulting in complete CPE after 48 h.

17. Harvest cells 48 h after infection and centrifuge cells 10 min at 400 *g*. Dissolve pellet in 5 ml TBS. Lyse by freeze/thawing. Centrifuge for 15 min at 400 *g* and 4°C.

Gradient Purification of Helper Virus

18. Take supernatant and add TBS up to exactly 10 ml. Add 5 g CsCl and mix gently. Be sure that CsCl is dissolved completely. Transfer lysate to SW41 centrifuge tube.

19. Spin in Beckmann SW41 for 16–22 h at 4°C and 32,000 rpm.

20. Collect the helper virus band by puncturing the tube with a needle and by drawing off the virus band in minimal volume.

21. Add TBS/CsCl solution up to 10 ml. Transfer to centrifuge tube and spin in a Beckmann SW41 as described earlier. Collect virus in minimal volume as before.

22. Desalt virus using the PD-10 desalting column according to the manufacturer.

Titration of Helper Virus

23. Determine particles and infectious units using the slot-blot protocol described later.

24. Alternatively, determine the approximate amount of helper virus resulting in complete cpe of N52.E6 cells after 48 h.

DNA Preparation from CsCl-Purified Helper Virus Particles

In order to exclude helper virus rearrangement, viral DNA should be isolated from CsCl-purified particles. Take 200 µl of gradient-purified and desalted vector. Isolate DNA using the QiaAmp DNA Minikit according to the manufacturer. Subsequent to ethanol precipitation, dissolve the pellet in 20 µl AE buffer. Digest 10 µl with the appropriate enzyme and run in an 0.8% agarose gel containing EtBr. As a positive control, double digest the corresponding helper virus plasmid with *Swa*I and the aforementioned enzyme.

Production of HC-Ad Vectors

Cloning of HC-Ad Vector Plasmids

General cloning reagents and equipment, as well as procedures, have been described in a number of

cloning manuals. Thus, only important steps, observations, and suggestions are discussed in this section.

i. The gene of interest including promoter and polyadenylation signal should be excisable in one piece.

ii. The fragment containing the gene of interest should be purified in an agarose gel using standard protocols (e.g., QIAEXII gel extraction kit, Qiagen Cat. No. 20021 for fragments <5 kb, electroelution for DNA fragments >5 kb). In order to improve the efficiency of cloning, it is important that the agarose gel does not contain EtBr. The DNA in the gel should never be exposed to a UV screen. Instead, the DNA fragments should be stained using Sybr-Gold (Molecular Probes Cat. No. S-11494) and visualized with a Dark Reader (e.g., Molecular Probes).

iii. For cloning, highly competent bacteria should be used (e.g., Stratagene XL2-Blue ultracompetent cells, Cat. No. 200150).

iv. Despite the size of 30–35 kb, the vector plasmid DNA can be isolated in a good amount and quality using standard plasmid DNA isolation protocols or kits.

v. Plasmids should never be stored as glycerol stock but as DNA in TE either at 4°C or in ethanol at –20°C. Repeated freezing and thawing should be avoided. In addition, plasmid colonies on agar plates containing antibiotics should not be stored for more than 3 days.

Preparation of Plasmid DNA for Transfection

In order to release the left and right adenoviral termini (ITR), HC-Ad vector plasmids usually contain restriction sites flanking both ITRs. ITRs in the HC-Ad vector plasmids depicted in Fig. 2 are flanked by unique *Pme*I sites (or *Sna*BI site in pSTK142). The HC-Ad vector plasmid is digested and further purified as described earlier for the helper virus plasmid.

Culture of 73/29 Cells

Cre-expressing 73/29 cells are used for the production of HC-Ad vectors and are cultivated in αMEM containing 10% FBS and antibiotics, supplemented with 200 µg/ml G418. 73/29 cells were usually passaged twice a week and diluted 1:4–5.

Amplification of HC-Ad Vectors

First Amplification/Transfection

1. Seed 2×10^6 73/29 cells in one 6-cm dish the day before transfection.
2. Transfect 5 µg of *Pme*I-digested phenol/chloroform-purified and ethanol-precipitated HC-Ad vector plasmid using the Qiagen Superfect transfection kit according to the manufacturer. Incubate at 37°C in a CO_2 incubator.
3. Four to 16 h after transfection, infect cells with 5 MOI of helper virus (multiplicity of infection).
4. Forty-eight hours later, centrifuge infected cells (complete cpe should have occurred) for 10 min at 400 *g*. Dissolve pellet in 2 ml TBS and lyse by freeze/thawing. Lysate can be stored at –80°C.

Second and Third Amplification

5. Seed 2×10^6 73/29 cells in one 6-cm dish the day before.
6. The next day infect cells with 1 ml of the lysate from the first amplification. At the same time, add 5 MOI of helper virus.
7. Harvest the cells 48 h later and centrifuge for 10 min at 400 *g*. Dissolve pellet in 2 ml TBS and lyse by freeze/thawing.
8. Infect 73/29 cells in one 6-cm dish (2×10^6 cells seeded the day before) with 1 ml of the lysate from the second amplification and coinfect with 5 MOI of helper virus.
9. Again harvest cells 48 h after infection when complete cpe is visible and spin for 10 min at 400 *g*. Dissolve the pellet in 2 ml TBS and lyse three times by freeze/thawing.

Fourth and Fifth Amplification

10. Seed $1–2 \times 10^7$ 73/29 cells in one 15-cm dish the day before.
11. Infect cells with half of the lysate from the third amplification and coinfect with 5 MOI of helper virus.
12. Forty-eight hours later harvest cells and pellet for 10 min at 400 *g*. Dissolve cells in 2 ml TBS and lyse three times by freeze/thawing.
13. Infect two 15-cm dishes of 73/29 cells (2×10^7 cells per dish seeded the day before) with 2 ml of the lysate from the fourth amplification and coinfect with 5 MOI of helper virus.
14. Fourty-eight hours later harvest cells and pellet for 10 min at 400 *g*. Dissolve cells in 2 ml TBS and lyse three times by freeze/thawing. Centrifuge for 15 min at 400 *g* and 4°C. Keep the supernatant for further amplifications. Keep the pellet for further testing (see later).

Titering Amplifications

After the fifth amplification it is important to titer the amount of vector present in the lysate. In case HC-Ad vectors express a reporter gene (e.g., β-gal, EGFP), the vector can be titered easily in a reporter gene assay.

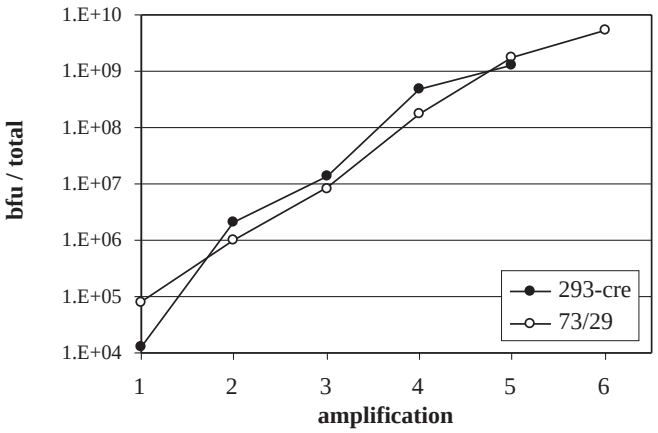

FIGURE 3 Amplification of HC-Ad vector AdGS46 using helper virus AdGS102#21 and a HEK293-based (293-cre) or N52.E6-based (73/29) Cre-expressing producer cell line. Both cell lines were transfected with *Pme*I-digested pGS46 and, at the same time, infected with helper virus (amplification 1). AdGS46 was serially amplified in both cell lines. Titers in each amplification were assayed by infecting N52.E6 cells with aliquots of the lysate followed by staining for β-galactosidase and quantitation as blue forming units (bfu).

Figure 3 shows blue forming unit (bfu) titers in amplifications of AdGS46 (see Fig. 1). However, most HC-Ad vectors do not contain a reporter gene and thus the ratio of helper and vector genomes and possible vector genome rearrangements should be tested using DNA isolated from infected cells.

15. Resuspend the pellet obtained in step 14 in 500 µl TBS.
16. Take 100 µl, add 50 µl TE, 20 µl 10% SDS, 20 µl proteinase K, 10 µl 0.5 *M* EDTA, vortex, and incubate for 2 h at 37°C.
17. Extract DNA by phenol/chloroform extraction and subsequent precipitation with ethanol.
18. Digest 1 µg DNA with an appropriate enzyme and add RNase to the digest. As a useful positive control, double digest 200 ng of the corresponding HC-Ad vector plasmid with *Pme*I and the aforementioned enzyme. Separate fragments in an 0.8% agarose gel containing EtBr (run gel at low voltage, preferably overnight).

Comments

At this stage of amplification the majority of DNA within the producer cell is vector DNA with only little helper virus contamination. Therefore, if the amplification was successful, only bands corresponding to the vector should be visible with a weak background of the helper virus bands and a faint smear of cellular DNA. In addition, rearranged vector genomes can be detected. If there are no or only weak vector bands visible, one or two additional amplifications can be performed. However, it is not recommended to carry out more than seven amplifications, as the risk of outgrowth of mutated helper virus and vector rearrangements increases significantly.

Preparation of Gradient-Purified HC-Ad Vector

19. Plate ten 15-cm dishes of 73/29 cells with 2×10^7 cells per dish.
20. The next day infect cells with the lysate from the last amplification (supernatant obtained in step 14) and 5 MOI of helper virus. Incubate for 48 h until complete cpe has occurred.
21. Harvest the cells by spinning for 15 min at 400 *g*. Resuspend cells in 5 ml TBS and lyse by freeze/thawing. Spin for 15 min at 400 *g*.
22. Split supernatant into two sterile 15-ml tubes, fill up to 10 ml with TBS, and add 5 g CsCl to each tube. Mix carefully until CsCl is dissolved. Transfer to two ultraclear centrifuge tubes.
23. Spin in a Beckmann SW41 for 16–22 h at 4°C and 32,000 rpm.
24. In optimal vector preparations, only one band containing vector particles should be visible. If helper virus contamination is high, a second helper virus particle band is visible in addition to the upper vector particle band separated by only a few millimeters. The upper vector band can be collected by puncturing the tube with a needle just below the vector band and drawing off the vector band in a small volume. Combine vector particles from both tubes. It is also possible to start vector purification by a CsCl step gradient followed by one or two continuous gradients.
25. Add TBS/CsCl solution up to 10 ml. Transfer to a new ultraclear centrifuge tube and spin in a Beckmann SW41 as described previously. Collect the vector in a small volume as described earlier.
26. Desalt vector particles using the PD-10 desalting column according to the manufacturer.

DNA Preparation from CsCl-Purified Vector Particles

In order to finally exclude vector rearrangement vector DNA should be isolated from CsCl-purified particles as described for extraction of helper virus DNA. The DNA should be digested with the appropriate enzyme and run on a 0.8% agarose gel containing EtBr. As a positive control, double digest the corresponding HC-Ad vector plasmid with *Pme*I and the aforementioned enzyme.

Troubleshooting

Problem	Comments and suggestions
Low helper virus titer	Helper virus might be impaired in DNA replication. Test for rearrangements in the helper virus genome. Alternatively, use an E3-containing helper virus
Instability of HC-Ad vector cloning plasmids	pBluescript containing large inserts tend to rearrange. DNA should be isolated from colonies that have been transformed the day before. Increasing the ampicillin concentration to 100 µg/ml is recommended
Poor transfection efficiency	Transfection efficiency should be tested and optimized using a linearized HC-Ad vector plasmid expressing a reporter gene (β-gal, EGFP). Transfection can be inhibited by traces of phenol present in the linearized DNA. Purify DNA by an additional ethanol precipitation
Adding 5 MOI of helper virus during amplification does not results in complete cpe after 48 h	Because the amount of vector increases during amplification, it might also be necessary to increase the amount of helper virus. Because amplification efficiency depends on the producer cell and the type of helper virus used, it is highly recommended to standardize amplification using a reporter gene expressing vector for each type of producer cell and helper virus
Vector rearranges during amplification	Make sure that the vector size ranges between 27 and 35 kb. Smaller vectors tend to rearrange
No vector obtained even after sever or eight rounds of amplification	Make sure your that the transgene is not toxic for producer cells and that the vector did not rearrange during amplifications. Another possible explanation for a failed vector amplification is helper virus outgrowth due to deletion of a loxP site
High helper virus content in CsCl-purified vector	There are several possible explanations for high helper virus contamination: (1) The producer cell expresses low or no Cre-recombinase. Grow cells for several passages in the selection medium (e.g., G418). (2) One loxP site in the helper virus is lost due to recombination with vector genomes. Test for the presence of both loxP sites using PCR and primers corresponding to sequences flanking both loxP sites. (3) The helper virus turned into RCA in case HEK293-based producer cells have been used. Test for presence of RCA using PCR
Helper and vector particle bands do not separate clearly	Especially if vector yield is low, the vector or helper virus band is hardly visible. Using a fiber-optic gooseneck lamp when drawing off the band from the CsCl gradient simplifies this procedure significantly

III. COMPLETE CHARACTERIZATION OF HC-Ad VECTOR PREPARATIONS

Materials

First Day: Seeding Cells

Cell lines: A549 (ATCC number: CCL-185) or, alternatively, HeLa cells (ATCC number: CCL-2)
Supplies: 24-well tissue culture plates

Second Day: Transduction of Cells with HC-Ad Vectors

Reagents and solutions: Tris-buffered saline (TBS, see Section II.)

Third Day: Slot Blotting of Cell and Vector Lysates; Hybridization

Equipment

Shaker (e.g., Scientific Industries: Vortex Genie Model G-560E)

Vacuum pump (e.g., Biometra: Typ PM12640-026.3)
Slot-blot apparatus (e.g., Amersham Biosciences: Hoefer PR648)
Hybridisation oven (e.g., Biometra: Duo-Thermo-Oven OV5)

Supplies

Positively charged nylon membrane (Pall: Biodyne B, 0.45 µm)
50 µCi [^{32}P] dCTP
RediPrime II DNA labeling kit (Amersham-Biosciences)

Reagents and Solutions

Phosphate-buffered saline (PBS): 6.46 m*M* Na_2HPO_4, 1.47 m*M* KH_2PO_4, 137 m*M* NaCl, 2.7 m*M* KCl, pH 7.4, autoclave
PBS/20 mM EDTA: Add EDTA from aqueous stock solution (0.5 *M*, pH 8, see Section II) to PBS
0.8 N NaOH: Dissolve 32 g NaOH pellets in 1 liter deionized H_2O, always prepare fresh
(Pre-)hybridisation solution: 2 × SSC (300 m*M* NaCl, 30 m*M* Na-citrate, pH 7.0) containing 10% dextran sulfate, 1% SDS, 0.5% milk powder (low fat), and 0.5 mg/ml salmon sperm DNA

DNA Templates for Generation of Probes

Template for generation of HC-Ad vector-specific probe: This should be a purified PCR fragment of 600–1200 bp length. Usually the PCR fragment is derived from the stuffer DNA or the transgene expression cassette of the HC-Ad vector plasmid. This probe is used for determination of both the number of infectious units and total particles. Alternatively, an Ad5-ITR probe can be used that is generated by PCR with the primers P1 (5′-CATCATCAATAATATACCTTATTTTG-3′) and P2 (5′-AACGCCAACTTTGACCCGGAACGCGG-3′) from a plasmid containing at least the left Ad5 ITR.
Template for generation of helper virus-specific probe: This is a PCR fragment comprising Ad5 nucleotides 31042–32390 (Ad5 fiber gene) obtained from a plasmid containing the fiber gene of Ad5 with the primers P3 (5′-ATGAAGCGCGCAAGACCGTCTG-3′) and P4 (5′-CCAGATATTGGAGCCAAACTGCC-3′).

Plasmids for Generating Standard Curves

Comment: It is recommended to prepare a large stock of standard plasmids at appropriate concentrations (1–3E+06 copies/µl) and keep it frozen (–20°C).

The plasmid used to generate the standard curve for determining infectious and total particle contents of HC-Ad vector preparations is usually the HC-Ad vector shuttle plasmid that was used to generate the vector and/or the PCR template for the probe. The concentration of this standard plasmid should be determined as accurately as possible.

The plasmid used to generate the standard curve for determining the helper virus content of HC-Ad vector preparations is usually a shuttle plasmid for the generation of E1-deleted vectors and should contain the Ad5 fiber gene. The concentration of this standard plasmid should be determined as accurately as possible.

Fourth Day: Exposition of PhosphorScreen and Signal Quantification

Equipment

PhosphorScreen (e.g., Amersham-Biosciences/Molecular Dynamics: Kodak Storage Phosphor Screen SO230)
PhosphorImager (e.g., Amersham-Biosciences/Molecular Dynamics: Storm 860)
Quantification Software (e.g., Amersham-Biosciences/Molecular Dynamics: ImageQuaNT)

Supplies

Saran wrap

Reagents and Solutions

Wash buffer I: 2 × SSC (300 m*M* NaCl, 30 m*M* Na-citrate, pH 7.0) containing 0.1% SDS
Wash buffer II: 0.1 × SSC (15 m*M* NaCl, 1.5 m*M* Na-citrate, pH 7.0) containing 0.1% SDS

Procedure

First Day: Seeding Cells

1. Calculate the amount of wells needed: [No. of vectors to be titered × 6] +10.
2. Seed 1–2E+05 A549 or HeLa cells per well.
3. Let cells attach overnight in 1 ml of medium (37°C).

Second Day: Transduction of Cells with HC-Ad Vectors

1. Dilute the vectors 1:20 with TBS.
2. Aspirate medium from the cells and replace with 300 µl fresh medium.
3. Transduce the cells with 2, 10, and 20 µl of the vector dilutions in duplicates (six wells per vector).
4. Leave 10 wells untransduced to generate a standard curve for infectious particles.
5. Incubate cells for 12–14 h at 37°C.

Third Day: Slot Blotting of Cell and Particle Lysates; Hybridization

Preparation of Cell Lysates from Transduced Cells for Determining the Number of Infectious Particles

1. Aspirate the medium from transduced cells.
2. Wash the cells once with 1 ml prewarmed PBS (37°C) per well.
3. Incubate the cells with 1 ml prewarmed PBS for 5 min at 37°C.
4. Aspirate PBS and add 200 µl of PBS/EDTA per well. Incubate for 10 min at 37°C.
5. Detach the cells by pipetting up and down several times and transfer them into 1.5-ml reaction tubes.
6. Add 200 µl 0.8 *N* NaOH per reaction tube, mix thoroughly, and incubate at room temperature for 30 min. During incubation mix thoroughly every 10 min.

Preparation of Cell Lysates for Generation of a Standard Curve for Infectious Particles

Comment: The debris in the cell lysate that is slot blotted onto the membrane will influence the signal intensity due to partial blocking of the membrane. Therefore, to obtain reliable standard curves for determining the number of infectious HC-Ad vector particles, it is absolutely required to mix the standard plasmid with untransduced cells and prepare lysates in the same way as for transduced cells before blotting.

7. Aspirate the medium from untransduced cells.
8. Wash the cells once with 1 ml prewarmed PBS (37°C) per well.
9. Incubate the cells with 1 ml prewarmed PBS for 5 min at 37°C.
10. Aspirate PBS and add 200 µl of PBS/EDTA per well. Incubate for 10 min at 37°C.
11. Detach the cells by pipetting up and down several times and transfer them into 1.5-ml reaction tubes.
12. Add 1E+06, 5E+06, 1E+07, 5E+07, and 1E+08 copies of the standard plasmid in duplicates to the cells in the reaction tubes. Do not to add more than 40 µl.
13. Add 200 µl 0.8 *N* NaOH per reaction tube, mix thoroughly, and incubate at room temperature for 30 min. During incubation mix thoroughly every 10 min.

Preparation of Particle Lysates for Determining the Number of Total Particles

Comment: Particle lysates for determining the number of total and helper virus particles do not contain any debris that blocks the membrane. Therefore, standard plasmids are prepared in PBS/EDTA and treated the same way as particle lysates.

14. Dilute the vectors 1:600 with TBS.
15. Transfer in duplicates 2, 10, and 20 µl of the vector dilutions into 1.5-ml reaction tubes and fill up to 200 µl with PBS/EDTA.
16. Add 200 µl 0.8 *N* NaOH per reaction tube, mix thoroughly, and incubate at room temperature for 30 min. During incubation mix thoroughly every 10 min.

Preparation of a Standard for Determining the Number of Total Particles

17. Prepare 1E+06, 5E+06, 1E+07, 5E+07, and 1E+08 copies of the standard plasmid in 200 µl PBS/EDTA in duplicates in 1.5-ml reaction tubes.
18. Add 200 µl 0.8 *N* NaOH per reaction tube, mix thoroughly, and incubate at room temperature for 30 min. During incubation mix thoroughly every 10 min.

Preparation of Particle Lysates for Determining the Number of Helper Virus Particles

19. Transfer 2, 10, and 20 µl of the undiluted vector stocks in duplicates into 1.5-ml reaction tubes and fill up to 200 µl with PBS/EDTA.
20. Add 200 µl 0.8 *N* NaOH per reaction tube, mix thoroughly, and incubate at room temperature for 30 min. During incubation mix thoroughly every 10 min.

Preparation of a Standard for Determining the Number of Helper Virus Particles

21. Prepare 1E+06, 5E+06, 1E+07, 5E+07, and 1E+08 copies of the standard plasmid in 200 µl PBS/EDTA in duplicates in 1.5-ml reaction tubes.
22. Add 200 µl 0.8 *N* NaOH per reaction tube, mix thoroughly, and incubate at room temperature for 30 min. During incubation mix thoroughly every 10 min.

Slot Blotting of Lysates and Standard onto Positively Charged Nylon Membranes

Comment: The cell lysates and particle lysates for determining the number of infectious and total HC-Ad-vector particles can be blotted onto the same membrane, as the same probe is used for hybridization. Particle lysates for determining the number of helper virus particles must be blotted onto a separate membrane and will be hybridized with a different probe.

23. Soak an appropriately sized membrane 2 min in 0.4 *N* NaOH.
24. Assemble the slotbot apparatus with the membrane in correct position.

25. Connect the slot blot apparatus to the vacuum pump and apply vacuum (max –400 mbar).
26. Check tightness by applying 200 µl deionized water to one slot.
27. Release vacuum.
28. Pipet two-thirds of each lysate into separate slots.
29. Apply vaccum starting with –400 mbar and slowly inrease up to –800 mbar until lysates pass the membrane completely.
30. Release vacuum and disassemble slot blot apparatus.
31. Rinse the membrane twice in 2 × SSC (5 min).
32. Bake the membrane at 80°C for 20 min.
33. Boil prehybridization buffer for 10–15 min in a water bath. Cool down to room temperature on ice. Use 20 ml of prehybridization buffer per membrane.
34. Prehybridize membrane at 68°C in 20 ml prehybridization buffer (1–2 h).
35. Label 100 ng of the DNA probe with [^{32}P]dCTP and add it to the prehybridization buffer.
36. Hybridize for 12–15 h.

Fourth Day: Exposition of PhosphorScreen and Signal Quantification

1. Prewarm wash buffers I and II to 68°C in a water bath.
2. Wash membrane twice with prewarmed wash buffer I for 10 min at 68°C.
3. Wash membrane with prewarmed wash buffer II for 10 min at 68°C.
4. Wash membrane with wash buffer II for 5 min at room temperature.
5. Air dry membrane.
6. Start exposition of the PhosphorScreen (usually 2–3 h).
7. Read the phosphor screen with PhosphorImager and quantify signals.
8. Calculate standard curve from signal intensities and use linear regression to quantify the signal intensities of the vector samples. The coefficient of correlation for the standard should be above 0.99.
9. Calculate the inverse bioactivity [No. of total particles/No. of infectious particles].

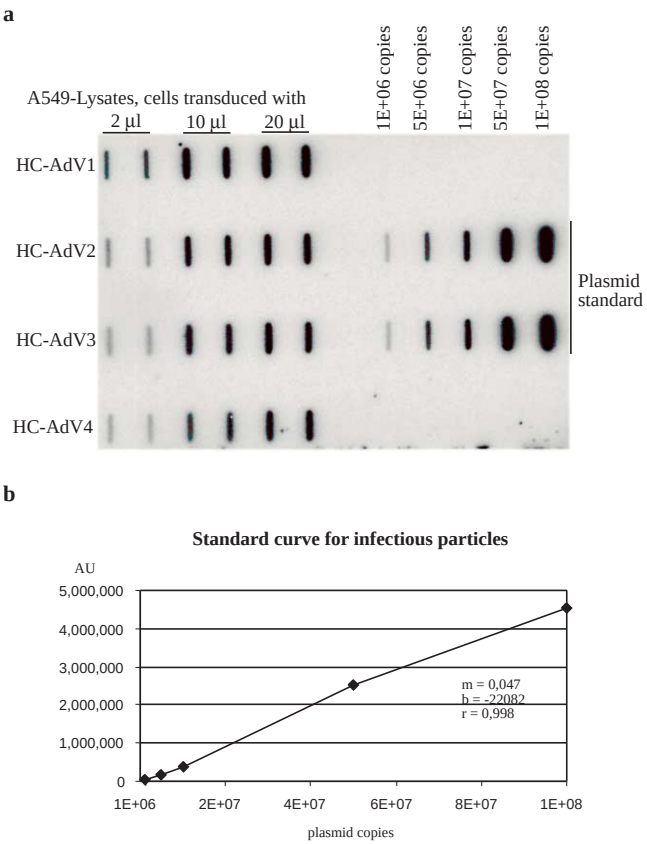

FIGURE 4 (**a**) Slot blot to determine the number of infectious units of different HC-Ad-vector preparations (HC-AdV1 to HC-AdV4). (**b**) The standard curve obtained from signal intensities of the standard plasmid. r, coefficient of correlation; b, intercept, and m, slope. These parameters were used to calculate the number of infectious particles for HC-AdV1 to HC-AdV4.

TABLE I Number for Infectious Units Calculated from Signal Intensities for HC-AdV1 to HC-AdV4 as Shown in Fig. 4

Vector	Titer
HC-AdV1	$1.4 \pm 0.2 \times 10^7$ ip/µl
HC-AdV2	$7.8 \pm 1.2 \times 10^6$ ip/µl
HC-AdV3	$6.6 \pm 0.4 \times 10^6$ ip/µl
HC-AdV4	$5.5 \pm 0.9 \times 10^6$ ip/µl

IV. RESULTS

Figure 4a shows a typical result for determination of the number of infectious particles of different HC-Ad vector preparations. Figure 4b shows the standard curve obtained from the signal intensities of the standard plasmid. The parameters of the standard curve (slope *m* and intercept *b*) were used to calculate the number of infectious particles of the vector preparations HC-AdV1 to HC-AdV4. These titers are given in Table I. Slot blots to determine the number of total particles and helper virus particles look similar and are omitted for brevity. The inverse bioactivity (number of total particles divided by number of infectious parti-

cles) usually is between 10 and 200, and the helper virus contamination is between 0.1 and 2%.

References

Fallaux, F. J., Bout, A., van der Velde, I., van den Wollenberg, D. J., Hehir, K. M., Keegan, J., Auger, C., Cramer, S. J., van Ormondt, H., van der Eb, A. J., Valerio, D., and Hoeben, R. C. (1998). New helper cells and matched early region 1-deleted adenovirus vectors prevent generation of replication-competent adenoviruses. *Hum. Gene Ther*. **9**, 1909–1917.

Gao, G. P., Engdahl, R. K., and Wilson, J. M. (2000). A cell line for high-yield production of E1-deleted adenovirus vectors without the emergence of replication-competent virus. *Hum. Gene Ther*. **11**, 213–219.

Graham, F. L., Smiley, J., Russel, W. C., and Nairn, R. (1977). Characteristics of a human cell line transformed by DNA from human adenovirus type 5. *J. Gen. Virol*. **36**, 59–74.

Hartigan-O'Connor, D., Barjot, C., Crawford, R., and Chamberlain, J. S. (2002). Efficient rescue of gutted adenovirus genomes allows rapid production of concentrated stocks without negative selection. *Hum. Gene Ther*. **13**, 519–531.

Hilgenberg, M., Schnieders, F., Löser, P., and Strauss, M. (2001). System for efficient helper-dependent minimal adenovirus construction and rescue. *Hum. Gene. Ther*. **12**, 643–657.

Kreppel, F., Biermann, V., Kochanek, S., and Schiedner, G. A DNA-based method to assay total and infectious particle contents and helper virus contamination in high-capacity adenoviral vector preparations. *Hum. Gene Ther*. **13**, 1151–1156.

Ng, P., Beauchamp, C., Evelegh, C., Parks, R., and Graham, F. L. (2001). Development of a FLP/frt system for generating helper-dependent adenoviral vectors. *Mol. Ther*. **3**, 809–815.

Palmer, D., and Ng, P. **(**2003). Improved system for helper-dependent adenoviral vector production. *Mol. Ther*. **11**, 504–511.

Parks, R. J., Bramson, J. L., Wan, Y., Addison, C. L., and Graham, F. L. (1999). Effects of stuffer DNA on transgene expression from helper-dependent adenovirus vectors. *J. Virol*. **73**, 8027–8034.

Parks, R. J., Chen, L., Anton, M., Sankar, U., Rudnicki, M. A., and Graham, F. L. (1996). A helper-dependent adenovirus vector system: Removal of helper virus by Cre-mediated excision of the viral packaging signal. *Proc. Natl. Acad. Sci. USA* **93**, 13,565–13,570.

Parks, R. J., and Graham, F. L. (1997). A helper-dependent system for adenovirus vector production helps define a lower limit for efficient DNA packaging. *J. Virol*. **7**, 3293–3298.

Sakhuja, K., Reddy, P. S., Ganesh, S., Cantaniag, F., Pattison, S., Limbach, P., Kayda, D. B., Kadan, M. J., Kaleko, M., and Connelly S. (2003). Optimization of the generation and propagation of gutless adenoviral vectors. *Hum. Gene Ther*. **14**, 243–254.

Sandig., V., Youil, R., Bett, A. J., Franlin, L. L., Oshima, M., Maione, D., Wang, F., Metzker, M. L., Savino, R., and Caskey, C. T. (2000). Optimization of the helper-dependent adenovirus system for production and potency *in vivo*. *Proc. Natl. Acad. Sci. USA* **97**, 1002–1007.

Schiedner, G., Hertel, S., and Kochanek, S. (2000). Efficient transformation of primary human amniocytes by E1 functions if Ad5: Generation of new cell lines for adenoviral vector production. *Hum. Gene Ther*. **11**, 2105–2116.

Schmid, S. I., and Hearing, P. (1998). Cellular components interact with adenovirus type 5 minimal DNA packaging domains. *J. Virol*. **72**, 6339–6347.

Thomas, C. E., Schiedner, G., Kochanek, S., Castro, M. G., and Löwenstein., P. R. (2000). Peripheral infection with adenovirus causes unexpected long-term brain inflammation in animals injected intracranially with first-generation, but not with high-capacity, adenovirus vectors: Toward realistic long-term neurological gene therapy for chronic diseases. *Proc. Natl. Acad. Sci. USA* **97**, 7482–7487.

Umana, P., Gerdes, C. A., Stone, D., Davis, J. R., Ward, D., Castro, M. G., and Löwenstein, P. R. (2001). Efficient FLPe recombinase enables scalable production of helper-dependent adenoviral vectors with negligible helper-virus contamination. *Nature Biotechnol*. **19**, 582–585.

CHAPTER

55

Novel Approaches for Production of Recombinant Adeno-Associated Virus

Angelique S. Camp, Scott McPhee, and R. Jude Samulski

I. INTRODUCTION

This article describes how to produce a recombinant adeno-associated virus (rAAV) stock of high purity. The adeno-associated virus (AAV) is a human parvovirus that was first engineered as a recombinant viral vector for gene delivery by Hermonat and Muzyczka in 1984. The unique biology and life cycle of rAAV make it a popular choice as a gene delivery system as it satisfies the main criteria for successful gene vectors. These criteria include but are not limited to (1) efficient transduction of the target cell; (2) stable and long-term expression of the transgene of interest, especially with the use of promoters and enhancers that are not inactivated in the transduced cell; and (3) a lack of stimulation of a cytotoxic immune response to the vector or transduced cell, resulting in a very good safety profile for clinical application. Wild-type AAV has not previously been associated with disease in healthy adult humans and is classified as a risk group 1 agent under the NIH's recombinant DNA guidelines (rev. 04/02). Recombinant AAV vectors retain only the inverted terminal repeat (ITRs) sequences from the wild-type AAV genome, with 96% of the DNA genome removed. This includes all viral coding genes. Normally recombinant AAV is considered nonpathogenic, noninfectious, and nonhazardous. However, the incorporation of oncogenes or toxin encoding genes into the vector genome may alter this status. Therefore, laboratory facilities used to produce rAAV may be required by local institutions to operate in accordance with biosafety level 2 guidelines, despite rAAV not being a risk group 2 agent in typical circumstances. Wild-type AAV requires helper functions provided in *trans* by a helper virus such as adenovirus or herpes virus for AAV replication. Early generation rAAV preparations were produced using a helper adenovirus that was then almost completely eliminated in the purification process. More recently, trace levels of helper virus in rAAV stocks have been shown to elicit a cellular immune response to the AAV-transduced tissue (Monohan *et al.*, 1998). Soon after this observation, efforts were made to improve the procedure for generating rAAV vectors, with our laboratory developing a packaging procedure that uses nonoverlapping plasmid constructs to produce rAAV vectors free of contamination by wild-type AAV or helper adenovirus (Xiao *et al.*, 1998). All AAV vectors utilize a plasmid substrate carrying the viral ITR sequences flanking the therapeutic gene of interest. For efficient packaging, the rAAV insert size must be ~4.6 kb or smaller, consistent with wild-type genome size ~4.7 kb. The AAV plasmid is then cotransfected into human embryonic kidney (HEK) 293 cells, along with a plasmid(s) that provides AAV and adenovirus helper functions. HEK 293 cells contain an adenovirus 5 E1A gene integrated into the genome that activates the AAV Rep and Cap, as well as other essential Ad genes required for productive AAV infection. In this setting, only the gene insert along with the flanking ITRs is then packaged into rAAV virions. Major advances in AAV production have been directly related to better understanding the unique biology of this virus. For example, Summerford and Samulski (1998) identified the primary receptor for AAV type 2 as heparin sulfate proteoglycan. As a result, a novel purification procedure using affinity chromatography was developed to generate virus stocks with a very high level of purity. In addition to the affinity chromatography step, this protocol also uses an iodixanol gradient in place of the cesium chloride step used in

Copyright 2006, Elsevier Science (USA).
All rights reserved.

earlier protocols to significantly shorten the high-speed centrifugation step and improve the quality of the vector preparations. The aim of this article is to discuss methods for quantifying the purified vectors using the most current approaches that are reproducible from laboratory to laboratory.

II. MATERIALS AND INSTRUMENTATION

A. Cell Culture

Human 293 cells are from American Type Culture Collection (ATCC, Rockville, MD; CRL 1573).
Phosphate–buffered saline (PBS)(No. D-5837; Sigma-Aldrich)
Dulbecco's modified Eagle's medium (DMEM) (No. D-6429; Sigma-Aldrich)
Penicillin–streptomycin (No. 15140-122) (Gibco-BRL Life Technologies)
Fetal bovine Serum (No. F-2442) (Sigma-Aldrich)
Trypsin–EDTA (No. T-4049) (Sigma-Aldrich)
Falcon integrid tissue culture dish (No. 08-772-6) (Fisher-Scientific)
Light microscope

B. Plasmids

Plasmid with transgene of interest
Plasmid pXX2, the AAV helper plasmid (Samulski laboratory); map and sequence are available on the internet at http://www.med.unc.edu/genether/
Plasmid pXX6, the adenoviral helper plasmid (Samulski laboratory); map and sequence are available at the just-listed web address

C. Production of Adenovirus-Free Recombinant Virus

Monolayers of 293 cells at approximately 80% confluency
Corning 50-ml concical centrifuge polystyrene tubes (No. 05-538-55A, Fisher)
2X HeBs (HEPES-buffered saline): Mix 16.4 g of NaCl, 11.9 g of HEPES, and 0.21 g of Na_2HPO_4 (pH 7.05). Adjust to 1 liter and filter sterilize.
Nalgene nitrocellulose filter sterilization unit (0.45 µm) (1000 ml, No. 09-761-40; Fisher)
2.5 *M* $CaCl_2$
Filter-sterilized ddH_2O
Restriction enzymes *Xba1* and *Hind*III.
Sure bacteria (Stratagene)

D. Purification of Recombinant Virus

Sorvall RT 6000B and Sorvall GS3 rotor
Beckman Ultracentrifuge and SW-41 and Ti-70
Ultrasonic processor (Cole-Palmer) with 1/8-in diameter probe (processor No. U-04711-30; microtip No. U-04710-46; Cole Palmer)
Pump Pro (Watson-Marlow) (No. 14-283-13; Fisher)
Ethanol/dry ice bath
Opti-seal tubes (No. 361625; Beckman)
Corning 50-ml conical centrifuge tubes
PBS-MK: Mix 50 ml of 10X PBS, 0.5 ml of 1 *M* $MgCl_2$, and 0.5 ml of 2.5 *M* KCl and adjust to a final volume of 0.5 liter with ddH_20.
Ultraclear tubes (12.5 and 32.4 ml) for SW-41 rotor (Beckman)
Heparin sepharose column (1 ml) Hi Trap No. 17-0407: Amersham Pharmacia Biotech
Optiprep (No. 103-0061) (Gibco-BRL Life Technologies)
Opti-mem 1 (No. 31985-013) (Gibco-BRL Life Technologies)
Sodium deoxycholate (No. D-5670; Sigma)
Benzonase (No. E-8263; Sigma)
AKTA FPLC (Amersham-Pharmacia Biotech)
15% iodixanol with 1 *M* NaCl: Mix 5 ml of 10X PBS, 0.05 ml of 1 *M* $MgCl_2$, 0.05 ml of 2.5 *M* KCl, 10 ml of 5 *M* NaCl, 0.075 ml 0.5% stock phenol red, and 12.5 ml of Optiprep. Adjust to a final volume of 50 ml with ddH_20 and filter sterilize.
25% iodixanol: Mix 5 ml of 10X PBS, 0.05 ml of 1 *M* $MgCl_2$, 0.05 ml of 2.5 *M* KCl, 0.1 ml of 0.5% stock phenol red, and 20 ml of Opti-prep. Adjust to a final volume of 50 ml with ddH_2O and filter sterilize.
40% iodixanol: Mix 5 ml of 10X PBS, 0.05 ml of 1 *M* $MgCl_2$, 0.05 ml of 2.5 *M* KCl, 33.3 ml of Opti-prep. Adjust to a final volume of 50 ml with ddH_20 and filter sterilize.
60% iodixanol: Mix 0.05 ml of 1 *M* $MgCl_2$, 0.05 ml of 2.5 *M* KCl, and 0.025 ml of 0.05% stock phenol red in 50 ml of Opti-prep. Filter sterilize.
Phenol red (Gibco-BRL Life Technologies)
Slide-A-Lyzer 10,000 MWCO (No. 66451; Pierce)
Syringes (5 ml)
Needles (18 gauge)
Rubber policeman wings (no. 14-110; Fisher)

E. Dot Blot Assay

DNase1 digestion mixture: 10 m*M* Tris–HCl, pH 7.5, 10 m*M* $MgCl_2$, 2 m*M* $CaCl_2$, 50 U/ml DNase 1
Proteinase K digestion mixture: 1 *M* NaCl, 1% (w/v) Sarkosyl, 200 µg/ml of proteinase K
Whatman 3MM paper

Dot blot apparatus
Gene-Screen Plus membrane (New England Nuclear)
Random primer labeling kit (Roche Biomedical)
^{32}P-dCTP (Amersham Pharmacia Biotech)
Church buffer: Mix 5 g of bovine serum albumin, 1 ml of 0.5 *M* EDTA, 33.5 g of $Na_2HPO_4 \cdot 7H_2O$, 1 ml of 85% H_3PO_4, 35 g of sodium dodecyl sulfate (SDS). Adjust to a final volume of 0.5 liter with ddH_2O. Heat at 65°C to dissolve. Store on the laboratory bench indefinitely.
Hybridization low-stringency wash solution: 2X saline sodium citrate (SSC), 2X 0.1% (w/v) SDS
Hybridization medium-stringency wash solution: 0.5X SSC, 1X 0.1% (w/v) SDS
Hybridization high-stringency wash solution: 0.1X SSC, 0.5X 0.1% (w/v) SDS
2X SSC: Mix 17.5 g of NaCl and 8.8 g of trisodium citrate $\cdot 2H_2O$. Adjust the final volume to 1 liter and adjust the pH to 7.0.
Hybridization bottles (Gibco-BRL Life Technologies)
Phosphoimager or scintillation counter

III. PROCEDURES

A. Ad-Free Production of Recombinant Virus

1. Construction of rAAV Plasmid Vector

a. Modify the plasmid psub201 by digestion with enzymes *Xba*I and *Hind*III to remove the *Rep* and *Cap* genes. This should produce a fragment less than 4.6 kb and should contain the AAV ITRs.
b. Insert the foreign gene cassette made of the transgene and its promoter between the *Xba*I sites.

2. Transfection of 293 cells

Note: Warm up 2X HeBS buffer, 2.5 *M* CaCl, and filtered distilled water to room temperature.

a. Seed 293 cells 24 h before transfection at 22×10^6 cells per 15-cm dish in complete DMEM. Generally a total of 20 dishes are transfected for the viral preparation procedure.

b. Three hours before the transfection, aspirate media and replace with 25 ml prewarmed complete 10% FBS/DMEM.

c. Prepare transfection mixture. Each 15-cm dish is transfected with 25 ml of preformed DNA–$CaPO_4$ precipitate. A total of 37.5 µg DNA per dish will give the optimal precipitate. This should include 7.5 µg vector plasmid, 7.5 µg helper plasmid (i.e., XX2), and 22.5 µg of Ad plasmid (i.e., XX6-80). The precipitates should be formed in reactions of 40-ml. A 40-ml reaction will transfect 20 × 15-cm dishes.

d. Aliquot DNA mixture into a sterile 50-ml Corning conical tube. Bring volume to 18 ml with sterile ddH_2O. Add 2 ml of 2.5 *M* $CaCl_2$. Aliquot 20 ml of 2X HeBS to a separate 50-ml Corning conical tube.

e. Add the DNA mixture by pipette dropwise to the tube containing the 2X HeBS. Gently mix by inversion. Allow 3–5 min for precipitate to form.

f. Once precipitate has formed, quickly but gently add 2 ml of transfection solution dropwise in a circular motion around the plate. Swirl gently to mix.

g. Sixteen hours posttransfection, aspirate the media of each plate and replace with 25 ml of complete 2% FBS/DMEM.

3. Cell Harvesting

Note: Harvesting should occur within 64 h but not less than 48 h of transfection.

a. Use a rubber policeman to detach cells from dishes using a scraping motion. Pipette the entire mixture into two sterile 500-ml centrifuge bottles (maximum 250 ml per bottle). Spin at 5000 rpm for 10 min. Pour off the supernatant. (***Note:*** Cell pellets may be frozen in a –20°C freezer overnight if necessary.)

4. Purification of Recombinant Virus

a. Resuspend the cell pellet in 1X PBS in a sterile 50-ml conical tube.
b. Add 0.35 ml of stock 10% DOC (sodium deoxycholate). Final concentration should be 0.5%.
c. Add 1.4 µl of stock 250 µg/µl benzonase. Final concentration should be 50 µg/µl.
d. Incubate at 37°C for 30 min.
e. Spin for 30 min at 6500 rpm (8400 *g*). Transfer the supernatant to a sterile 50-ml conical tube.
f. Freeze/thaw the cell suspension using a dry ice-ethanol bath and a 37°C H_2O bath.
g. Repeat the freeze/thaw step two more times.
h. Spin for 20 min at 6500 rpm. Decant the supernatant to a new tube. (**Note:** Sample may be stored in –80°C freezer at this point).

5. Purification Using an Iodixanol (Optiprep)Gradient

a. Dissolve the pellet into PBS-MK. Place half (7.5 ml) of the resuspended pellet into each of two Optiseal tubes. Using the Pump Pro, create a step gradient by underlying the sample with 6 ml of 15% iodixanol, 6 ml of 25% iodixanol, 7 ml of 40% iodixanol, and 5 ml of 60% iodixanol. Carefully remove the tubing without disturbing the gradient layers. (**Note:** A syringe and small diameter tubing may also be used to layer the gradients.)

b. Balance the tubes and fill them completely by slowly adding 1X PBS dropwise to the tube to the uppermost layer. Insert a plug and centrifuge at 4°C for 1 h using a Beckman Ti-70 rotor at 70,000 rpm (350,000 *g*).

c. Carefully remove the Optiseal tubes from the rotor. In a viral hood, remove the plug from the top of the tube. Use a 5-ml syringe with an 18-gauge needle to puncture the tube at the 40–60% iodixanol interface. Remove 75% of the 40% iodixanol layer.

6. Purification Using a Heparin Column

Note: A viral preparation made from twenty 15-cm dishes of 293 cells can be purified on a 1-ml column with a single injection.

a. Sterilize the lines of the AKTA FPLC with 0.5 *M* NaOH and 1X PBS.
b. Run the "pump wash" program.
c. Set up the heparin column and check it for leaks.
d. Inject the sample and autozero the UV.
e. Run the 1-ml heparin column program.
f. Collect 0.5-ml fractions.
g. Sterilize the lines again using 0.5 *M* NaOH and 1X PBS.
h. Discard the column.
i. Test the fractions for the presence of virus using the dot blot hybridization assay and combine the fractions with the highest concentration of virus.

7. Delivery of Recombinant Virus in Vitro

a. Determination of rAAV titer by Dot Blot Assay

1. Place 5 µl of each fraction collected from the heparin sulfate column into a well of a 96-well microtiter plate. Assay duplicate samples of each fraction.

2. Add 50 µl of DNase 1 digestion mixture and incubate for 1 h at 37°C. This treatment digests any viral DNA that has not been packaged into capsids.

3. After 1 h, stop the digestion by adding 10 µl of 0.1 *M* EDTA to each reaction. Mix well.

4. Add 60 µl of proteinase K digestion mixture to each sample to release the viral DNA from the capsid. Incubate for 30 min at 50°C.

5. To create a set of DNA hybridization standards, use plasmid DNA that was used for the transfection. Linearize the plasmid and do serial dilutions in 10 m*M* Tris–HCl (pH 8.0) and 1 m*M* EDTA. A volume of 25 µl is convenient for each standard in wells of a 96-well microtiter plate. A suitable standard working range is 500 ng to 10 fg.

6. Denature the samples and control DNA by adding 100 µl of 0.5 *M* NaOH to each.

7. Equilibrate a nylon membrane and one piece of Whatman blotting paper in 0.4 *M* Tris–HCl (pH 7.5) and place them between the upper and lower blocks of a dot blot manifold apparatus; membrane should be on top of the Whatman paper.

8. Add the denatured DNA from the 96-well microtiter plate to wells of the dot blot manifold apparatus in the absence of a vacuum. After all the DNA has been transferred into the manifold, apply a vacuum for 3–5 min.

9. Radiolabel a transgene cassette-specific probe. (**Note:** The probe should not contain plasmid backbone or ITR sequences.)

10. In a hybridization bottle, prehybridize the nylon membrane with 5 ml of Church buffer for 5 min at 65°C. Discard the prehybridization Church buffer and replace with 5 ml of fresh Church buffer. Place at 65°C.

11. Boil the ^{32}P-dCTP-radiolabeled probe for 5 min, place on ice, and add to the hybridization bottle containing the dot blot. Hybridize overnight at 65°C.

12. Remove the hybridization solution and add 10 ml of low-stringency wash solution. Wash for 10 min at 65°C. Repeat the wash with 10 ml of fresh solution.

13. Wash the dot blot for 10 min at 65°C with the medium-stringency wash solution and discard the wash solution.

14. Monitor the dot blot with a Geiger counter. Continue the washes if needed using the high-stringency wash solution. Do not let the membrane dry out or the probe will permanently adhere to the membrane.

15. To quantitate each spot on the dot blot, expose the filter to a Phosphoimager cassette. Alternatively, employ X-ray film to identify labeled regions on the nylon membrane, excise each sample, and quantitate using a scintillation counter.

16. Plot a standard curve of DNA concentration vs integrated intensity per counts per minute for the DNA standards and employ the curve to determine the concentration of DNA in fractions obtained from the heparin sulfate column. (**Note:** The replication center assay is also a useful method to calculate the rAAV titer. The rAAV particle number of each fraction can be calculated. Remember to take into consideration that plasmid standards are double stranded whereas rAAV virions harbor only a single strand.)

IV. NOTES

1. *Hind*III is used in the digest to cut the *rep* and *cap* fragment in half for easy isolation of the plasmid backbone.

2. DNA preparation should be pure. Purify your viral fragment by agarose gel separation and running onto Whatman DEAE-8 1 paper or a preparation of equivalent high quality.

3. Alternatively, blunt-end ligation may be used to construct the rAAV vector plasmid.

4. For efficient packaging into AAV capsids, the size of the rAAV construct (including the 190-bp ITRs) must be 4.6 kb or less.

5. Plasmids are grown in the Sure strain of *Escherichia coli*. The literature shows that AAV ITRs are unstable in bacteria. To avoid deletion, restrict bacterial growth in the stationary phase. If you still obtain deletions, grow the plasmids at 30°C for only 12 h. The integrity of the plasmids can be assayed by restriction enzyme digests.

6. Polypropylene and glass attract ionic strength-dependent aggregates more than polystyrene. For this reason, mixing containers made of polystyrene are preferred for transfections.

7. The total DNA is equal to 37.5 µg/plate, and the ratio of rAAV construct to the pXX2 and pXX6 is equal to a molecular ratio of about 1:1:1.

8. If a coarse precipitate forms, decrease the incubation time. If a precipitate forms too quickly (i.e., less than 1 min) check the pH of the 2X HeBS. The pH range of 2X HeBs should be between 7.05 and 7.12.

9. Only use sterile ddH_2O. Do *not* autoclave!

10. After 24 h, the 293 cells (when viewed through a microscope) should have a rounded appearance, indicating viral replication. If detached cells are noted, the incubation was too long.

11. Cell suspensions or cell precipitates may be stored at –20°C for up to 6 months.

12. The NaCl in the 15% iodixanol layer will separate viral aggregates that may form due to the high concentration of virus.

13. Collecting fractions from the flow-through and washing steps ensures that all the virus was bound to the column and eluted as the salt gradient increased.

14. Using a new heparin column for each purification ensures that you will not cross-contaminate viral preparations.

References

Amiss, T. J., and Samulski, R. J., (2000). Methods for adeno-associated virus-mediated gene transfer into muscle. *In "Methods in Molecular Biology"* (M. P. Starkey, R. Elaswarapu, ed.), Vol. 175, pp. 455–469. Humana Press, Totowa, NJ.

Berns, K. I., and Giraud, C. (1995). Adeno-associated virus (AAV) vectors in gene therapy. *Curr. Topics Microbiol. Immun.* **218**, 1–25.

Bartlett, J. S., and Samulski, R. J. (1996). Production of recombinant adeno-associated viral vectors. *In "Current Protocols in Human Genetics"*, pp. 12.1.1–12.1.24. Wiley, Philadelphia.

Daly, T. M., Okuyama, T., Vogler, C., Haskins, M. E., Muzyczka, N., and Sands, M. S. (1999). Neonatal intramuscular injection with recombinant adeno-associated virus results in prolonged beta-glucuronidase expression in situ and correction of liver pathology in mucopolysaccharidosis in type VII mice. *Hum.Gene Ther.* **10**, 85–94.

Ferrari, F. K., Xiao, X., McCarty, D., and Samulski, R. J. (1997). New developments in the generaion of Ad-free, high-titer rAAV gene therapy vectors. *Nature med.* **3**, 1295–1296.

Hermonat, P. L., Mendelson, E., and Carter, B. J. (1984). Use of adeno-associated virus as a mammalian DNA cloning vector: Transduction of neomycin resistance into mammalian tissue culture cells. *Proc. Natl. Acad. Sci. USA* **81**, 6466–6470.

Kotin, R. M., Siniscalco, M., Samulski, R. J., Zhu, X. D., Hunter, L., Laughlin, C. A., Mclaughlin, S., Muzyczka, N., Rocchi, M., and Berns, K. I. (1990). Site-specific integration by adeno-associated virus. *Proc. Natl. Acad. Sci. USA* **87**, 2211–2215.

Monahan, P. E., Samulski, R. J., Tazelaar, J., Xiao, X., Nichols, T. C., Bellinger, D. A., and Read, M. S. (1998). Direct intramuscular injection with recombinant AAV vectors results in sustained expression in a dog model of hemophilia. *Gene Ther.* **5**, 40–49.

Samulski, R. J. (1993). Adeno-associated virus: Integration at a specific chromosomal location. *Curr. Opin. Gen. Dev.* **3**, 74–80.

Samulski, R. J., Sally, M., and Muzycka, N. (1999). Adeno-associated viral vectors. *In "The Development of Human Gene Therapy"* (T. Friedmann, ed.), pp. 131–172. Cold Spring Harbor Laboratory, Cold Spring Harbor, NY.

Samulski, R. J., Zhu, X., Xiao, X., Brook, J. D., Housman, D. E., Epstein, N., and Hunter, L. A. (1991). Targeted integration of adeno-associated virus (AAV) into human chromosome 19 [published erratum appears in *EMBO J* **11**(3), 1228 (1992)]. EMBO J. **10**, 3941–3950.

Song, S., Morgan, M., Ellis, T., Poirier, A., Chesnut, K., Wang, J., Brantly, M., Muzyzcka, N., Byrne, B. J., Atkinson, M., and Flotte, T. R. (1998). Sustained secretion of human alpha-1-antitrypsin from murine muscle transduced with adeno-associated virus vectors. *Proc. Natl. Acad. Sci. USA* **95**, 14,384–14,388.

Summerford, C., and Samulski, R. J. (1998). Membrane-associated heparin sulfate proteoglycan is a receptor for adeno-associated virus type 2 virions. *J. Virol.* **72**, 1438–1445.

Summerford, C., and Samulski, R. J. (1999). Viral receptors and vector purification: New approaches for generating clinical-grade reagents. *Nature Med.* **5**, 587–588.

Xiao, X., Li, J., and Samulski, R. J. (1996). Efficient long-term gene transfer into muscle tissue of immunocompetent mice by adeno-associated virus vector. *J. Virol.* **11**, 8098–8108.

Xiao, X., Li, J., and Samulski, R. J. (1998). Production of high-titer recombinant adeno-associated virus vectors in the absence of helper adenovirus. *J. Virol.* **72**, 2224–2232.

Zolotukhin, S., Byrne, B. J., Mason, E., Zolotuknin, I., Potter, M., Chesnut, K., Summerford, C., Samulski, R. J., and Muzyczka, N. (1999). Recombinant adeno-associated virus purification using novel methods improves infectious titer and yield. *Gene Ther.* **6**, 973–985.

PART

C

ANTIBODIES

SECTION

15

Production and Purification of Antibodies

CHAPTER

56

Production of Peptide Antibodies in Rabbits and Purification of Immunoglobulin

Gottfried Proess

I. INTRODUCTION

As a consequence of the completion of human genome sequencing, a huge number of new putative proteins can be derived from the DNA sequence information. The new challenge is how to discover their function and cellular localization, as well as their interaction with other proteins. The characterization of proteins is facilitated greatly by the availability of specific antibodies. There are at least two commonly used strategies to obtain antigen needed for antibody production: (1) cloning of the gene in an expression vector followed by transfection in an expression system and subsequent protein purification, often with the help of a peptide tag to facilitate detection and purification, and (2) chemical synthesis of a peptide corresponding to a short portion of the protein against which antibodies are to be raised. The latter strategy has several big advantages over the cloning expression method: (1) it is less time-consuming; (2) many potential problems, such as difficult cloning, low expression level, or difficult purification of the protein, can be avoided; the peptide antigen is easily available in large quantities and can be used for subsequent affinity purification of the antiserum; and by correct choice of the peptide sequence, **antibodies** of extreme specificity can be obtained and be used to detect one specific member out of a protein family with strong homologies.

The cloning expression of the entire protein would of course display many epitopes shared by other members of the family and therefore give rise to cross-reacting antibodies (recognizing several members of the family or even unrelated proteins); the only solution here is to make monoclonal antibodies, which is more time-consuming and needs intense screening work. Other applications for which peptide antibodies are the better strategy include detection of one specific splice form, one specific mutation, or one specific phosphorylation site.

The only real disadvantage of antibody production using peptides as a general antibody production approach is the risk related to the choice of the region in the protein sequence. In fact, the correct choice of a suitable peptide sequence is the most crucial step in the production process and particular attention should be paid to this selection. For a given protein, it is always advised to use more than one synthetic peptide as antigen to increase the chances of getting antibodies recognizing the protein and, if possible, in its native form. As a detailed discussion of the many parameters influencing the selection of a well-suited peptide would be beyond the scope of this article, only a few hints can be given here.

Short synthetic peptides are not immunogenic by their own because of their low molecular mass (generally 1–3 kDa); in order to elicit an immune response in the animals, they must be either coupled covalently to a so-called carrier protein or synthesized on a special resin, called MAP (Tam, 1988). This article does not cover the synthesis of the peptides, as custom-made peptides can be easily obtained commercially. A second important issue to consider when selecting a peptide sequence is the choice of the conjugation strategy to allow for a proper display of the entire peptide

Copyright 2006, Elsevier Science (USA).
All rights reserved.

sequence for antibody production in the animals. The conjugated peptide (or MAP peptide) is then used as antigen in rabbits as described (Huet, 1998).

High-titered **antiserum** can be obtained within about 2–3 months and can be subsequently affinity purified using the synthetic peptide coupled to a suitable matrix. This process allows to get rid of all the unrelated antibodies present in the antiserum (endogenous antibodies from the rabbits and the antibodies produced against the carrier protein) that otherwise may give rise to background signals.

II. MATERIALS AND INSTRUMENTATION

15–25 mg of custom-made peptide (or MAP peptide) at >70% purity, stored lyophilized at 4°C under inert gas and protected from moisture

KLH (Sigma Cat. No. H7017), stored lyophilized at 4°C

Glutaraldehyde (Sigma Cat. No. G6257), 25% solution in water, stored at room temperature. Because this product is toxic, always work under a hood and wear gloves.

EDC (Pierce Cat. No. 22980)

MBS (Pierce Cat. No. 22311)

Dimethyl formamide (DMF) (Sigma Cat. No. D8654), stored at room temperature

Glycine (Sigma Cat. No. G7126), stored at room temperature

Boric acid (Vel Cat. No. 1021), phosphate-buffered saline (PBS) 10× (Sigma Cat. No. P7059), tromethamine (Tris) (Sigma Cat. No. T1503), sodium hydrogen carbonate trihydrate ($NaHCO_3 \cdot 3H_2O$) (Vel Cat. No. 7958), sodium chloride (NaCl) (Vel Cat. No. 1723), disodium hydrogen phosphate dodecahydrate ($Na_2HPO_4 \cdot 12H_2O$) (Vel Cat. No. 1773), glacial acetic acid (Vel Cat. No. 1005), 0.1 *M* hydrochloric acid (Sigma Cat. No. 210-4), sodium hydroxide (Sigma Cat. No. S5881), and guanidine hydrochloride (Sigma Cat. No. G4505), all stored at room temperature

PD10 column (Pharmacia Cat. No. 17-0851-01), activated CH-Sepharose 4B (Pharmacia Cat. No. 17-0490-01), EAH-Sepharose 4B (Pharmacia Cat. No. 17-0569-01), stored at room temperature

Dialysis membrane Spectra/Por (Spectrum Cat. No. 132678), molecular weight cutoff 12-14000

pH meter MP220 (Mettler-Toledo) or similar

Spectrophotometer Ultraspec 3300P20 (Pharmacia) or similar

FPLC Akta with UV detector (Pharmacia) or similar

III. PROCEDURES

A. Selection of Suitable Peptide Sequences and Definition of Coupling Strategy

1. Selection of Antigenic Peptides

Whenever possible, use a software for predicting the "antigenicity" of the **peptide**. We use the Lasergene software from DNASTAR, Inc., particularly the EditSeq (sequence edition), Protean (antigenicity prediction), MegAlign (sequence alignments), and GeneMan (homology searches) modules.

Other useful free software can be used on the Expasy Molecular Biology Server of the Swiss Institute of Bioinformatics (http://www.expasy.org/); e.g., the Protscale program can be used to assess hydrophilicity and other parameters. Links to software for predicting signal peptides, transmembrane domains, potential phosphorylation, and glycosylation sites can be found there too. Another good source is the protein analysis software contained in the GCG Wisconsin package from Accelrys (http://www.accelrys.com/products/gcg_wisconsin_package/program_list.html#Protein) and there may be many more available through the web. All these computer programs can be very helpful in selecting a well-suited peptide. A few hints are given here to facilitate the selections based on the most used algorithms.

Check in an international database if the protein has been described. There is often helpful information concerning different domains of known proteins in their description (e.g., transmembrane regions, signal peptides, potential glycosylation or phosphorylation sites, or even a link to the three-dimensional structure if this has been resolved). If the three-dimensional structure is known, use the structure information to define a surface-located region (e.g., using the Swiss Viewer software available at the Expasy server: http://www.expasy.org/spdbv/). After pasting the sequence in the EditSeq module, open it with the Protean program and check the following parameters over the whole length of the protein sequence: hydrophilicity (Hopp-Woods and Kyte-Doolittle), antigenic index (Jameson-Wolf), surface probability (Emini), flexibility (Karplus-Schulz), turn, α, β, and coil plot (Garnier-Robson), as well as positive and negative regions in terms of charge.

If the N or C terminus of the protein is hydrophilic, it is often a good choice. Some proteins contain signal sequences, which are cleaved in the mature proteins. Those signal peptides are very often hydrophobic parts of about 20–30 amino acids, which are not well suited. If doubt persists, use a software (e.g., SignalP

program available at http://www.cbs.dtu.dk/services/SignalP/) to predict its cleavage site.

If internal peptides have to be used, they should be hydrophilic, present a high surface probability, and should not be predicted as strongly α helical. Short synthetic peptides will hardly adopt the same α-helical structure and therefore the antibodies will not recognize such structured regions in the native protein. Good hydrophilicity and surface probability are essential if the antibodies have to recognize the native protein (e.g., immunohistochemistry experiments).

Choose a peptide in a flexible region whenever possible. Avoid potential phosphorylation (serine, threonine, and tyrosine) and glycosylation sites (not predicted by these algorithms, but can be predicted by other software if no better information is available). Antibodies made against a simple peptide will off course not fix at the corresponding region in the protein if this contains a large sugar moiety.

Avoid peptides containing several cysteines, as they may participate to disulfide bridges impossible to mimic with a short synthetic peptide. If the protein contains transmembrane regions, avoid loops between two transmembrane domains that are shorter than 30–35 amino acids. Short loops are not well mimicked by flexible and linear peptides.

Choose several well-suited peptides of about 12–15 amino acids length and rank them from best to less good based on the aforementioned parameters. Shorter peptides (9–11 amino acids) can be used if the antibodies have to recognize only a very small region, e.g., a phosphorylation site, which should then be placed about in the middle of the peptide.

2. *Homology Searches*

In order to avoid unspecific or background signals, it is important to check the chosen peptide sequences for possible homologies with known proteins other than the target one. Depending on the application, interspecies cross-reactivities may not be disturbing or may even be desired.

For every chosen peptide sequence, run a BLAST search (available at the NCBI: http://www.ncbi.nlm.nih.gov/BLAST/) using the Protein Blast and the "Search for short nearly exact matches" option. A standard BLAST with a short peptide will hardly return any result, while the option here above gives matches for short parts of proteins.

Discard those peptides for which stretches of more than five identical amino acids are found in another protein(s). Because one epitope generally contains more than five amino acids, specific antibodies can be expected if less or equal than five amino acids one following the other are present. The following example illustrates these issues:

```
peptide:        EHRTPRGKEDSSVP
                | | | | | | |   | ||
other protein:  EHRTPRGKYQSIVP
```

antibodies may cross-react (8 identical amino acids in a stretch)

```
peptide:        EHDTDRGMIDSSVP
                | |  |  | |     ||||
other protein:  EHRTPRGKYQSSVP
```

antibodies will be specific (no stretch >4 identical amino acids)

Care should also be taken with very similar amino acids, such as serine and cysteine, with the only difference being the functional group on the side chain (OH vs SH), which is only a very minor difference that may not be sufficient to avoid cross-reaction if the rest of the epitope is identical.

If specificity is the major goal (e.g., antibodies against one specific member out of a protein family), select those peptides with the lowest homologies as first choices. If the first goal is to obtain working antibodies, give a higher weight to antigenicity analysis than to the homology part.

3. *Coupling Strategy*

It is very important to consider the following rules for the coupling of peptides to the carrier protein. After coupling to the carrier, the peptide should mimic the original structure in the best possible way, which means that the peptide should be linked to the carrier protein at one end and not in the middle of the peptide. A **conjugation** in the middle of the sequence would only display two small parts useful for antibody production (considering that the antibodies containing the conjugation residue in their epitope will not recognize the protein of interest in which this conjugation reagent is not present of course).

If the chosen peptide corresponds to the real N terminus of the protein, coupling must be done on the C-terminal part of the peptide. If the peptide sequence contains lysine, aspartate, or glutamate, add a cysteine C-terminally for conjugation using MBS and synthesize the peptide as C-terminal amide (C terminus: —$CONH_2$), which better mimics the normal amide bond and does not introduce an unnatural negative charge. If it does not contain lysine, aspartate, or

glutamate, synthesize the peptide as free acid (C terminus: —COOH) and use this acid group for coupling with EDC (this reagent would also react with internal glutamates, aspartates, and, to a lesser extent, lysines and the conjugation would not be specific in that case).

If the chosen peptide corresponds to the real C terminus of the protein, coupling must be done on the N-terminal part of the peptide and the peptide must be synthesized as free acid (C terminus: COOH). If the peptide sequence contains lysine, add a cysteine at the N terminus of the peptide to allow for a specific conjugation using MBS. If no lysine is present, the peptide can be coupled specifically on the N-terminal amino group using glutaraldehyde (lysine would also cross-react with the glutaraldehyde and the conjugation would result in peptide multimers rather than specific conjugation to carrier). In that case, no additional cysteine is required.

If the chosen peptide corresponds to an internal peptide, coupling should be done on the less suited end of the peptide (the end showing the lowest hydrophilicity, surface probability, and antigenicity index). For N-terminal conjugation, a cysteine should be added in case the peptide sequence contains lysine. The peptide should be synthesized as C-terminal amide (C terminus: $CONH_2$). For C-terminal conjugation, a cysteine should be added C-terminally if the peptide sequence contains glutamate, aspartate, or lysine for the aforementioned reasons. The peptide should be acetylated on the N terminus to avoid introduction of an unnatural positive charge at that point. If no aspartate, glutamate, and lysine are present, the C-terminal acid function of the peptide can be used for specific coupling by EDC.

Once the coupling strategies are defined, synthesize the corresponding peptides using standard Fmoc or Boc chemistry on a peptide synthesizer. Synthetic peptides are routinely obtained from commercial sources and should be synthesized in quantities of at least 10–15 mg and in purities above 70%. There is no need for very high-purity peptides (which are much more expensive), as quite low amounts of impurities will not give rise to antibody production (the injected quantities of impurities are not high enough to elicit immune responses generally).

B. Conjugation of Peptides to Carrier Proteins

1. Coupling Using Glutaraldehyde (Coupling of N-Terminal Amine of Peptide to Lysine Residues of KLH)

Buffer preparation: Borate buffer, pH 10; dissolve 6.2 g of boric acid in 1 liter of distilled water.

1 *M* glycine: dissolve 751 mg glycine in 10 ml water

Dissolve 5 mg of peptide in 1 ml of borate buffer in a 10-ml glass tube.

Dissolve 5 mg carrier protein (KLH) in 1 ml of borate buffer and add this solution to the peptide solution.

Prepare a solution of 0.3% glutaraldehyde by mixing 120 µl glutaraldehyde solution (25%) in 9.88 ml of water.

Add dropwise 1 ml of this solution to the stirred peptide–KLH mix. Incubate 2 h at room temperature. The solution will turn yellow.

Add 0.25 ml of 1 *M* glycine solution to block unreacted glutaraldehyde. Stir 30 min at room temperature.

Dialyze twice for 4 h against 5 liters of PBS buffer. Measure the absorbance at 280 nm (nanometers if the peptide sequence contains tryptophan or tyrosine). The resulting solution is ready for antibody production. Measure the final volume and divide in injection aliquots considering a coupling yield of 50%. We inject generally 200 µg of coupled peptide (based on peptide content), which corresponds to 1/12.5 of the total volume. Dilute the aliquot with PBS to 0.5 ml and mix with adjuvant prior to injection as described (Huet, 1998).

2. Coupling Using EDC (Coupling of C-Terminal Acid to Lysine Residues of KLH)

Dissolve 5 mg of peptide in 1 ml of water in a 10-ml glass tube.

Add 20 mg EDC to the stirred peptide solution and adjust the pH to 4.5 using 0.1 *M* hydrochloric acid solution. Incubate for 10 min at room temperature.

Dissolve 5 mg carrier protein (KLH) in 1 ml of water and add this solution to the activated peptide solution.

Stir for 2 h at room temperature.

Dialyze twice for 4 h against 5 liters of PBS buffer. Measure the absorbance at 280 nm (nanometers if the peptide sequence contains tryptophan or tyrosine). The resulting solution is ready for antibody production. Measure the final volume and divide in injection aliquots considering a coupling yield of 50%. We inject generally 200 µg of coupled peptide (based on peptide content), which corresponds to 1/12.5 of the total volume. Dilute the aliquot with PBS to 0.5 ml and mix with adjuvant prior to injection as described (Huet, 1998).

3. Coupling Using MBS (Coupling of Thiol Group of Cysteine on the Peptide to Lysine Residues of KLH)

Buffer preparation: phosphate buffer 10 m*M*, pH 7.0; dissolve 3.6 g of disodium hydrogen phosphate dodecahydrate ($Na_2HPO_4{\cdot}12H_2O$) in 1 liter of water

Phosphate buffer 50 m*M*, pH 6.0; dissolve 17.9 g of disodium hydrogen phosphate dodecahydrate ($Na_2HPO_4 \cdot 12H_2O$) in 1 liter of water

Dissolve 5 mg of KLH in 2.5 ml of 10 m*M* phosphate buffer, pH 7. Dialyze or desalt against the same buffer.

Dissolve 15 mg MBS in 1 ml of DMF. Use this solution within 1 h!

Add 70 µl of the MBS solution to the solution of KLH. Stir for 30 min at room temperature.

Equilibrate a PD10 column by washing with 50 ml 50 m*M* phosphate buffer, pH 6.0, charge the KLH solution on the column, and add 3.5 ml of 50 m*M* phosphate buffer, pH 6.0. Recover 3.5 ml phosphate buffer containing the activated carrier.

Dissolve 5 mg of peptide in 1 ml of PBS buffer and add to the activated carrier solution. Stir for 3 h at room temperature.

Dialyze twice for 4 h against 5 liters of PBS buffer. Measure the absorbance at 280 nm (nanometers if the peptide sequence contains tryptophan or tyrosine). The resulting solution is ready for antibody production. Measure the final volume and divide in injection aliquots considering a coupling yield of 60%. We inject generally 200 µg of coupled peptide (based on peptide content), which corresponds to 1/15 of the total volume. Dilute the aliquot with PBS to 0.5 ml and mix with adjuvant prior to injection as described (Huet, 1998).

C. Affinity Purification

In many cases, crude peptide antiserum from the rabbits can be used in different techniques to probe the protein of interest. However, background signals may be a problem, either already in the preimmune serum or only in the serum from the hyperimmunized animal. Those antibodies may be very disturbing in techniques such as immunohistochemistry or even in Western blots. The best way to get rid of those background signals is to purify the antibodies by affinity against the peptide. The fact that the synthetic peptide is generally available in large amounts (in contrast to many protein antigens) makes the affinity purification of peptide antibodies very attractive in obtaining an improved signal-to-noise ratio or getting rid of cross-reacting antibodies. This technique is also best if the antibodies are to be labeled by biotin or a fluorescent compound if one wants to avoid the use of secondary antibodies.

It is important to link the peptide to the affinity matrix through the same residue used for coupling. Otherwise, the peptide is not displayed the same way and good antibodies may be lost because they would not bind to a changed environment. For this reason, we advise using different resins depending on the coupling strategy used for the conjugation to the carrier protein. We generally use 10 mg of the peptide for preparation of the affinity column; in most cases, this quantity is sufficient to deplete up to 50 ml antiserum and to get, depending on specific titer, 8–25 mg of pure antibodies.

1. Conjugation of Peptide to Activated CH-Sepharose 4B

This procedure is used for peptides that have undergone a glutaraldehyde coupling to a carrier protein.

Buffer preparation: 1 m*M* HCl; dilute 1 ml of 0.1 *M* hydrochloric acid by water to 100 ml Carbonate buffer, 0.5 *M* salt, pH 8.5; dissolve 6.89 g of sodium hydrogen carbonate trihydrate ($NaHCO_3 \cdot 3H_2O$) and 29.29 g of sodium chloride in 1 liter of water

Weigh 0.75 g of Activated CH-Sepharose in a 50-ml tube and swell the resin in 40 ml of 1 m*M* HCl for 30 min under stirring.

Dissolve 10 mg of peptide in 1 ml of carbonate buffer, 0.5 *M* salt, pH 8.5.

Centrifuge the gel and discard the supernatant. Wash the gel three times with 40 ml carbonate buffer, 0.5 *M* salt, pH 8.5. Centrifuge and discard the supernatant each time. Suspend the gel material in 1 ml carbonate buffer, 0.5 *M* salt, pH 8.5.

Add the peptide solution to the gel, add 1 ml carbonate buffer, 0.5 *M* salt, pH 8.5, and let it react for 2 h at room temperature under gentle stirring.

Centrifuge and discard the supernatant. Resuspend in 1 ml carbonate buffer, 0.5 *M* salt, pH 8.5, centrifuge, and discard the supernatant.

Suspend the gel in 1 ml PBS buffer and transfer the gel in the column adapted to the FPLC instrument.

2. Conjugation of Peptide to EAH-Sepharose 4B Using EDC

This procedure is used for peptides that have undergone a EDC coupling to a carrier protein.

Buffer preparation: 0.1 *M* acetate buffer, 0.5 *M* salt, pH 4.0; dilute 57.2 ml of glacial acetic acid by water to 1 liter and dissolve 29.29 g of NaCl

Phosphate buffer, 0.5 *M* salt, pH 7.4; dissolve 29.29 g of sodium chloride in 1 liter of PBS buffer

Water, pH 4.5: adjust pH of water by adding 0.1 *M* hydrochloric acid solution

0.1 *M* sodium hydroxide: dissolve 4 g of sodium hydroxide in 1 liter of water

Take 3 ml of EAH-Sepharose 4B suspension, centrifuge, and discard the supernatant. Wash the gel

three times by 2 ml water, pH 4.5. Resuspend the gel in 1 ml of water and adjust pH to 4.5 by adding some 0.1 *M* hydrochloric acid solution.

Dissolve 10 mg of peptide in 1 ml of water and adjust pH to 4.5 by adding some 0.1 *M* hydrochloric acid solution.

Add the peptide solution to the gel suspension. Add 70 mg EDC and adjust the pH again to 4.5 by adding some 0.1 *M* hydrochloric acid solution.

Incubate for 4 h at room temperature. During the first hour of reaction, the pH decreases and it is very important to readjust the pH to 4.5 regularly by adding small volumes of 0.1 *M* sodium hydroxide solution.

Centrifuge and wash the gel with 3 ml of 0.1 *M* acetate buffer, 0.5 *M* salt, pH 4.0 buffer and then 3 ml of phosphate buffer, 0.5 *M* salt, pH 7.4. Repeat this washing at least three times.

After the last centrifugation, discard the supernatant, resuspend the gel in 1 ml PBS, and transfer the gel in the column adapted to the FPLC instrument.

3. Conjugation of Peptide to EAH-Sepharose 4B Using MBS

This procedure is to be used for peptides that have undergone a MBS coupling to a carrier protein.

Buffer preparation: 50 m*M* phosphate buffer, pH 6.0; dissolve 17.9 g of disodium hydrogen phosphate dodecahydrate ($Na_2HPO_4{\cdot}12H_2O$) in 1 liter of water

Take 3 ml of EAH-Sepharose 4B suspension, centrifuge, and discard the supernatant. Wash the gel three times by 2 ml of 50 m*M* phosphate buffer, pH 6.0. Discard the supernatant each time.

Resuspend the gel in 1 ml of 50 m*M* phosphate buffer, pH 6.0

Dissolve 15 mg MBS in 1 ml of DMF. Use this solution within 1 h!

Add 140 µl of the MBS solution and 500 µl DMF to the gel suspension and let react for 30 min at room temperature under gentle stirring.

Centrifuge and discard the supernatant. Wash with 2 ml of PBS buffer, pH 7.4, centrifuge, and discard the supernatant. Repeat this washing three times and then resuspend in 1 ml of PBS buffer.

Dissolve 10 mg of peptide in 1 ml of PBS buffer, pH 7.4, and add this solution to the gel suspension. Incubate under gentle stirring for 3 h at room temperature.

Centrifuge, discard the supernatant, resuspend in 1 ml of PBS buffer, pH 7.4, and transfer the gel in the column adapted to the FPLC instrument.

4. Affinity Purification of Antiserum

Buffer preparation: PBS high salt; dissolve 20 g of sodium chloride in 1 liter of PBS buffer

100 m*M* glycine buffer, pH 2.5; dissolve 7.5 g of glycine in 1 liter of water

1 *M* Tris buffer, pH 9.0; dissolve 121.14 g of Tris in 1 liter of water

1.5 *M* guanidine hydrochloride: dissolve 143.30 g of guanidine hydrochloride in 1 liter of water

Thaw the serum to be purified (we use generally 50 ml serum in one run), place it in a graduated cylinder, and add 1 g of sodium chloride per milliliter of serum.

Mount the column on the FPLC instrument and wash the column with 10 ml of 1.5 *M* guanidine hydrochloride followed by 10 ml of PBS high salt.

Prepare a Falcon tube for antibody recovery and place 400 µl of 1 *M* Tris buffer in the tube.

Charge the serum slowly on the column (maximum flow rate should be 0.5 ml/min) and take care of the counterpressures that may arise (in case the counterpressure gets too high, decrease the flow rate). Recover the flow through of the column in the original serum tube. Never discard any liquids before making sure the affinity purification has worked correctly!

Once all the serum has been charged, wash the column with PBS high salt until the absorbance (measured at 280 nm) decreases to zero. Stop the recovery in the original serum tube as soon as the absorbance starts to decrease.

Elute the antibodies by passing the glycine buffer, pH 2.5, on the column and recover the antibodies (increase in absorbance) in a Falcon tube containing Tris buffer. Stop the recovery as soon as the absorbance gets back close to zero.

Measure immediately the pH in the Falcon and adjust to pH 7–7.5 if necessary (by Tris buffer or glycine buffer). Dialyze the antibody solution against 5 liters PBS buffer for 4 h at 4°C; repeat the dialysis with 5 fresh liters of PBS.

Divide the antibody solution in working aliquots and store the aliquots at –20°C. If the antibodies are to be stored a long time, it is best to add 0.1% sodium azide as a preservative (except if it is planned to label the antibodies afterward, in this case 0.1% thimerosal as a preservative is preferred).

Wash the affinity column for 5 min with guanidine hydrochloride solution, check the absorbance during this process, and recover eventual peaks in a Falcon tube. Dialyze immediately (see Section IV) against 5 liters PBS buffer (two times).

Wash the column for 10 min by PBS, recover the gel material, and store it at 4°C after the addition of one equivalent volume of ethanol.

Quantify the antibody solution by measuring the absorbance of an aliquot at 280 nm. One optical density unit corresponds to about 0.75 mg of pure antibody.

IV. PITFALLS

Depending on the sequence, peptides are sometimes difficult to get into aqueous solution. In case a peptide does not dissolve in water, dissolve a dry quantity in a minimum amount of dimethyl sulfoxide (DMSO); once it is dissolved completely, dilute by water to the appropriate concentration. The DMSO does not influence the coupling process.

Coupling may sometimes give rise to precipitates, depending on the peptide sequence. These precipitates should not be discarded for the antibody production; vortex the solution well before aliquoting the injection amounts to include the peptide–carrier aggregates. Some antigens are known to be phagocytosed even better than soluble material. In case the aggregates are too large, crush them first with a spatula to get them as fine as possible. Never freeze the affinity gels; these are best kept at 4°C in PBS buffer containing sodium azide or PBS/50% ethanol.

It may happen that the glycine buffer does not elute some high-affinity antibodies. These antibodies will come off the column during the guanidine hydrochloride wash. Dialyze *immediately* the recovered solution two times against PBS as described earlier, as the antibodies will generally still be active.

References

Huet, C. (1998). Production of polyclonal antibodies in rabbits. *In "Cell Biology: A Laboratory Handbook"* (J. Celis, ed.), 2rd Ed., Vol. 2, pp.381–391. Academic Press, New York.

Tam, J. P. (1988). Synthetic peptide vaccine design: Synthesis and properties of a high-density multiple antigen peptide system. *Proc. Natl. Acad. Sci. USA* 85, 5409–5413.

CHAPTER

57

Preparation of Monoclonal Antibodies

Peter J. Macardle and Sheree Bailey

I. INTRODUCTION

In 1975 Kohler and Milstein reported the outcome of fusing antibody-producing mouse spleen cells with a mouse myeloma cell line. The monoclonal antibodies produced were of the specificity dictated by the spleen cells but in the quantity characterized by the myeloma cell line. From this beginning the preparation of monoclonal antibodies has become an important tool in almost every scientific discipline. No longer restricted to the immunology laboratory, monoclonal antibodies are used in a variety of experimental techniques and diagnostic assays and now, with improvements in molecular engineering techniques, are realizing their potential in therapeutic applications (Grillo-Lopez, 2000).

When the need arises to produce monoclonal antibodies to a particular antigen, the decision to establish the technology, use commercial enterprises, or approach private groups to produce them has to be made.

For laboratories that decide to establish the technology, this article describes a method that has evolved in our laboratory since the mid-1980s. The method is robust, in routine use, and has produced hundreds of monoclonal antibodies to a wide variety of antigens. The method uses commercial high-quality reagents, including cloning supplements that replace the messy and wasteful use of *in vivo*-derived feeder cells. The reagents detailed are the ones used in our laboratory but other manufacturers make equivalent reagents.

The intention of this article is to describe the reagents, equipment, and techniques used to prepare monoclonal antibodies. Full reviews of monoclonal antibody production, including methods for characterization, purification, use of monoclonal antibodies, and antibody engineering applications, are available in a number of monographs, including Campbell (1991), Donohoe *et al*. (1994) and Goding (1986).

Sterile culture technique and accurate record keeping are essential for success in monoclonal antibody preparation. The sterile culture technique is not difficult to learn, with attention to detail paramount for success. There are many excellent texts on basic and advanced tissue culture techniques, including Freshney (2002) and Harrison and Rae (2003).

II. MATERIALS AND INSTRUMENTATION

A. Essential Equipment

Sterile laminar flow hood, benchtop centrifuge, liquid nitrogen storage or equivalent, 37°C water bath, and a 37°C, 5% CO_2 gassed tissue culture incubator. An inverted microscope to view cell growth is also useful.

B. Cell Culture Reagents

RPMI 1640 (10 × 500 ml) (Cat. No. 21870-092), penicillin (10,000 U)/streptomycin (10,000 µg), L-glutamine (29.2 mg) (PSG×100, Cat. No. 10378-016), 10 m*M* sodium hypoxanthine, 40 µ*M* aminopterin, 1.6 m*M* thymidine (HAT×100, Cat. No. 31062-011), 10 m*M* sodium hypoxanthine, and 1.6 m*M* thymidine (HTx100, Cat. No. 11067-030) are from GIBCO Invitrogen Corporation. Fetal bovine serum (FBS, Cat. No. 12003-500M) is from JRH Biosciences; select batches of FBS that have been screened for hybridoma produc-

Copyright 2006, Elsevier Science (USA).
All rights reserved.

tion. Complete Freund's adjuvant (CFA, Cat. No. 77140) and incomplete Freund's adjuvant (IFA, Cat. No. 77145) are from Pierce Biotechnology Inc. Hybridoma fusion cloning supplement (HFCS, Cat. No. 592247800) and polyethylene glycol 1500 in 75 m*M* HEPES, sterile and fusion tested (PEG, Cat. No. 783641), are from Roche Diagnostics. Red blood cell lysing buffer (8.3 g/liter NH_4Cl in 0.01 *M* Tris–HCl) (Cat. No. R-7757) and trypan blue solution (Cat. No. T-8154) are from Sigma. Dimethyl sulfoxide (DMSO, Cat. No. 102950) is from Merck. ELISA-based isotyping kits are available from a number of manufacturers, including Roche Diagnostics (Cat. No. 1183117) and Pierce Biotechnology Inc (Cat. No. 37502). Store all stock reagents as recommended by the manufacturer.

C. Cell Culture Materials

Tissue culture plates, 24-well (Cat. No. 143982) and 96-well (Cat. No. 167008) flat-bottom plates with lids, 25-cm^2 (Cat. No. 136196) and 80-cm^2 (Cat. No. 178891) tissue culture flasks, cryotubes (Cat. No. 375418), 10-ml disposable pipettes (Cat. No. 159633) and petri dishes (Cat. No. 150350) are from Nalge Nunc Int. V-bottom 30-ml tubes (Cat. No. 128A) and wide-bore graduated transfer pipettes (Cat. No. PP88SA) are from Bibby-Sterilin Ltd.

A container (Cat. No. 5100 Nalgene Nunc) or a foam box with walls of about 1 cm thick is required for the control rate freezing of cells.

In addition, we use Gilson Pipetman 5- to 20- and 20- to 200-µl pipettes and a Gilson Distriman repeating pipette for cloning, all with sterile tips. Hamilton 500-µl glass luer lock syringes are used for immunization (Cat. No. 1750 Hamilton, Reno. Nev). Sterile forceps and scissors are also required.

D. Myeloma Cell Line

Several myeloma cell lines are commonly used for fusion with murine spleen cells; most have been derived from the P3X63Ag8.653 murine myeloma line (Kearney *et al*., 1979). The myeloma clones SP2/0 (Shulman *et al*., 1978) and FO (de St Groth and Scheidegger, 1980), derived from P3X63Ag8.65, are commonly used. These cell lines are available from the American Type Culture Collection (ATCC) (http://www.atcc.org) as CRL1580, CRL1581, and CRL1646, respectively. We use P3X63Ag8.653 cells that have been maintained in our laboratory for many years, which are screened regularly for mycoplasma, and we select batches that have been previously successful in hybridoma production.

III. PROCEDURES

A. General

The preparation of monoclonal antibodies depends on a series of steps that require attention to detail and careful laboratory management. The major requirement is time; Table I gives an approximate time frame for monoclonal antibody preparation. Phase 1 is largely taken up by the immunization protocol, ensuring that the screening method is working, growing the myeloma cells, and finally performing the fusion. Phase 2 encompasses testing, cloning, and freezing and is more labor-intensive. However, the workload is variable and unless the screening method is cumbersome or many fusions are carried out, it is not a full-time occupation.

In our experience the secret to success in monoclonal antibody preparation is the screening method. Ideally the method should be in place before the animals are immunized. The method needs to be robust and reliable and, as there may be 30 to 50 samples to screen a day, reagents and equipment need to be readily available. The method should be appropriate to the intended use of the monoclonal antibod-

TABLE I Time Frame for Monoclonal Antibody Preparation

Phase One	
Light workload	
Prepare antigen and develop screening assay	
Immunize animals	4–8 weeks
Test bleed	Week 7
Thaw myeloma line	Fourth or 8th week
Fuse spleen and myeloma line HAT selection medium	Day 1
Feed with HT medium	Day 7
Feed with HT medium	Day 14
Colonies become visible, screening begins	Day 14 to about day 32
Phase Two	
Heavy workload	
Screen wells as required	
Clone, freeze, feed, test	About 21-day cycle
Reclone, freeze, feed, test	About 21-day cycle
Third clone cycle	About 21-day cycle
Keep extensive records	
Phase Three	
Variable workload	
Isotype and scale up	
Characterization.	
Antibody purification, labeling, etc.	
Maintenance of frozen stock	

ies. Although many antibodies do perform in alternative protocols, there is no guarantee unless they have been screened appropriately. Some suggestions for screening methods are included in Table II, but detailed descriptions are outside the scope of this article.

B. Antigen Preparation and Immunization

A number of protocols that we have used to immunize mice to a variety of antigens are shown in Table II. Animals can make antibodies to a wide range of molecular structures with two important general exceptions: animals will not usually make antibodies to self-antigen (see Section V) and will not usually recognize small molecules. Small molecules need to be conjugated to a carrier protein. Selection of the carrier protein appears to be largely personal, but the ease of and position of conjugation are important criteria. When linking peptides to carrier proteins, Landsteiner's principle (Landsteiner, 1945) should be taken into account, that antibody specificity tends to be directed to epitopes of the hapten furthest removed from the functional group linked to the carrier protein.

Commonly used carrier proteins include keyhole limpet hemocyanin (KLH) and bovine serum albumin (BSA). If you are going to screen for monoclonal antibodies by ELISA, make both peptide–KLH and peptide–BSA combinations; immunize with one and screen against the other. There are a number of methods for the conjugation of peptides to carrier proteins and the protocol selected will depend on the amino acid sequence of the peptide and the epitope of interest. However, if you are having a peptide synthesized, consider adding a biotin tag; a streptavidin-conjugated carrier protein can then make a convenient carrier.

If high-affinity IgG monoclonal antibodies are required, the immunization protocol needs to invoke T-cell help. Hence, adjuvant and several booster injections may be needed and test bleeds should be examined for the presence of antigen-specific IgG. If IgG isotype monoclonal antibodies are essential, they should be screened for specifically.

The protein antigen immunization schedule used in our laboratory is shown in Table III. Most protocols require antigen in adjuvant for immunization. Complete Freund's adjuvant (CFA) is highly effective but may cause toxic side effects. A number of new adjuvants are becoming available, including Hunter's TiterMax (http://www.titermax.com), Pierce's AdjuPrime Immune Modulator (http://www.piercenet.com), and RIBI adjuvant systems (http://www.corixa.com) among others. Advice from the Institutional Animal Ethics Committee should be taken on which adjuvants are recommended.

If CFA is used, it should only ever be used subcutaneously for the primary immunization and Freund's incomplete used for subsequent boosts.

Complete Freund's adjuvant causes inflammation and granuloma formation in mice and will cause severe injury in humans. Take suitable precautions to prevent self-injection and employ eye protection.

Six-week-old female BALB/c mice are preferred for immunization as the myeloma lines used for fusion were derived from that strain. Routinely, we immunize six animals, in batches of two, with a 2-week interval between immunizing the next two animals.

TABLE III Immunization Schedule for Protein Antigens

Primary immunization	Day 0
First boost	Day 14
Second boost	Day 28
Test bleed	Day 35
Third boost	Day 42
Fusion	Day 45

TABLE II Suggested Immunization and Screening Protocols

Immunogen	Concentration	Route of injection	Screening assay
Cells, bacteria, virus, nematodes	5×10^6–5×10^7	Intraperitoneal (200 µl saline)	Flow cytometry Dot blot, ELISA Immunohistochemistry
Plasmid DNA	50 µg plasmid	Intramuscular (50 µl/site, both rear legs)[a]	ELISA
Glycoprotein peptides/carrier Proteins	2–50 µg	Subcutaneous[b] (100 µl/site, CFA, IFA) or intraperitoneal (200 µl saline)	Western blot ELISA

[a] Anesthesia is essential or muscle contraction will eject the immunogen.
[b] Typically at the nape of the neck and at the base of the tail.

Steps

Wear eye protection.

1. Draw an equal volume of antigen in saline and CFA into two separate Hamilton 500-µl glass luer lock syringes.
2. Connect the syringes with a three-way stopcock and emulsify the mixture slowly by passing material from one syringe to the other.
3. Check that an emulsion has been formed by taking a drop of the mixture from the stopcock and placing on water, an emulsion will float and not dissipate.
4. Using the Hamilton syringe and a 21-gauge needle, immunize the animals with 100 µl of emulsion subcutaneously at the base of the tail and nape of the neck.

C. Test Bleeds

Analysis of a test bleed can allow the fusion to be postponed and the animals reimmunized if the antibody titer is low or nonexistent. Test bleeds should only be carried out by experienced personnel. Test bleeds should preferably be from the lateral tail vein using a 26-gauge needle and syringe. A maximum of 1% of the body weight of the animal should be collected, about 100–200 µl. Larger volumes of blood can be collected at the time of euthanasia and can provide a valuable positive control sample for the screening protocol.

D. Myeloma Cell Preparation

About 1 week before the fusion, thaw a vial of the myeloma cell line from the liquid nitrogen stock (see Section IV,B).

The myeloma cells should be of known pedigree; it is vital to maintain the myeloma line carefully. Mycoplasma-contaminated stock or stock that has been overgrown will result in poor production of hybridomas.

Steps

1. Transfer the cells into 24-well plates at about 2×10^5 per well, check cell numbers daily, and scale up as they double in number into 25-cm^2 flasks and then into 80-cm^2 flasks containing 50 ml of RF10.

2. Maintain vigorous growth rates during the scale-up period. The day prior to the fusion the myeloma cells should be given a one-to-one split so that the cells are in an exponential growth phase at the time of fusion.

3. The number of myeloma cells required depends on how many spleen cells are to be fused. Typically, we use a spleen to myeloma cell fusion ratio of 10:1. Normal BALB/c mice produce about 10^8 leukocytes per spleen, hence 10^7 myeloma cells are required for each spleen.

4. On the day of the fusion and before the animals are euthanized, examine the myeloma cells carefully to check that the culture is not contaminated.

IV. CELL FUSION PROCEDURE

Solutions

1. *RF10 medium:* To 500 ml of RPMI 1640 add 50 ml of FBS and 5 ml of PSGx100. Store at 4°C for up to 14 days; after 14 days replace the PSG. Warm to 37°C in a water bath before use.

2. *HAT selection medium:* Reconstitute 100× lyophilized HAT supplement with 10 ml of sterile distilled water and store 1-ml aliquots at 4°C protected from light. Add 1 ml HAT and 2 ml of HFCS to 100 ml of RF10 medium. Make only as much as required for the fusion. Warm to 37°C in a water bath before use.

3. *HT medium:* To 500 ml of RF10 medium add 5 ml of HT supplement. Warm to 37°C in a water bath before use.

4. *HT medium +2% HFCS:* Add 2 ml of HFCS to 100 ml HT medium. Warm to 37°C in a water bath before use.

A. Background Notes

HAT medium is used to selectively grow hybrids following fusion. Aminopterin selects against unfused myeloma cells and myeloma:myeloma-fused cells by blocking the main synthetic pathway for DNA. Unfused spleen cells do not have the capacity to survive for more than a few days. In hybridomas, hypoxanthine and thymidine supply purines and pyrimidines for DNA synthesis via HGPRTase salvage pathways derived from the spleen cells. The HT medium acts as a rescue medium while the aminopterin is being diluted out. Although the HT medium can be withdrawn once the nucleoside biosynthesis pathways are re-established, in our experience it is rarely worth the effort.

Cells under pressure often require "supplements" to maintain growth. In many monoclonal antibody preparation methods, these are supplied by feeder cells, usually mouse thymocytes or peritoneal washout cells. In the method described, feeder cells are replaced with hybridoma fusion cloning supplement HFCS, which in addition to being preferred for reasons of

animal ethics, is more convenient and, in our experience, more effective.

B. Fusion Protocol

Steps

1. For each spleen to be fused, place a 1-ml aliquot of PEG mixture and a 3- and a 7-ml aliquot of RF10 in a 37°C water bath.
2. After euthanasia, submerge the mouse in 70% alcohol for a few minutes; this prevents hair and bedding material from contaminating the laminar flow hood.
3. Place the animal on its right-hand side, grasp the skin posterior to the rib cage with sterile forceps, and make a small incision to cut the skin but not to penetrate the subcutaneous fascia. With two pairs of forceps, grasp the skin at either side of the incision and pull. The skin should peel away, revealing the subcutaneous fascia. Flush the area with 70% alcohol to remove any stray hair. Using forceps and scissors, cut through the subcutaneous fascia into the peritoneal cavity and locate the spleen and remove by cutting away the connective tissue.
4. Place the spleen into a petri dish containing about 15 ml of RF10. At this point, blood can be collected by opening the thoracic cavity, quickly puncturing the heart, and collecting blood; this can be useful as a positive control.
5. Half-fill two 10-ml syringes with RF10 from the petri dish and, using 21-gauge needles, gently disrupt the spleen by injecting the medium. Inject the media slowly, a little at a time; you should see clouds of cells going into the medium and the spleen turning lighter in color. Finally, when the spleen looks like a limp sack, gently tease apart the spleen with the needle and flat tweezers to remove any remaining cells. Discard the spleen connective tissue.
6. Gently pipette the cell suspension to break up clumps and transfer into a 30-ml V-bottom tube, ignoring large clumps and the remains of the spleen connective tissue; let the tube stand for about 5 min.
7. Remove cells from the tube and transfer into another 30-ml V-bottom tube, leaving behind the debris and connective tissue that has settled to the bottom.
8. Pellet the spleen cells at 400 *g* for 5 min.
9. Resuspend the cell pellet in 5 ml of red cell lysing solution, leave for 5 min, and then fill the tube with media and pellet at 400 *g* for 5 min.
10. Resuspend the spleen cells in 5 ml of media and perform a cell count. The number of leucocytes derived from a single spleen should be approximately 10^8 cells total.
11. Wash and count the myeloma cells; for 10^8 spleen cells, 10^7 myeloma cells will be required.
12. Add the myeloma cells to the spleen cell suspension to give a spleen/myeloma cell ratio of 10:1. *Note:* **This is the critical bit, for the next 20 min you will be committed to fusing the cells.**
13. Pellet the cells (400 *g* for 5 min) and remove *all* of the supernatant; this is best done with a Pasteur pipette attached to a vacuum line.
14. Tap the pellet to loosen the cells.
15. With a wide-bore transfer pipette, add 1 ml of PEG solution per spleen. Gently mix with the pipette for 10 s and then continue to mix the cells gently by tapping the tube for a further 50 s.
16. Retrieve the 3-ml RF10 sample and slowly add dropwise over a 10-min period continually mixing the cells gently by tapping the tube. This can be accomplished (for a right-handed person) by holding the tube in the left hand between thumb and forefinger, tapping the tube with the second or third finger, depending on comfort and reach, and adding the medium with a transfer pipette held in the right hand. With a little practice a steady rhythm can be produced.
17. After the first 3 ml, retrieve the 7-ml aliquot and add over the next 10-min period.
18. Pellet the cells at 400 *g* for 5 min and resuspend in about 10 ml of RF10; loosen the tube cap to allow for CO_2 transfer and place the cells in the tissue culture incubator for about 1 h.
19. Pellet the cells at 400 *g* for 5 min.
20. Gently resuspend the cell pellet in a small volume of the HAT selection medium.
21. Add this suspension back into HAT selection medium; 50 ml of HAT selection medium will be needed for every 10^7 myeloma cells used in the fusion.
22. Add about 1 ml of the cell suspension to each well of the 24-well plates. This is the equivalent of 2×10^5 myeloma cells per well. We prefer plating the fusion into 24-well plates, as evaporation is less of a problem. The larger volume also provides enough supernatant for any screening assay.
23. Label and place the plates in the tissue culture incubator.

With the exception of the 1-h incubation period, the entire fusion protocol should take no more then 2 to 3 h.

C. Maintaining Hybridomas

Examine the wells using the inverted microscope on days following the fusion. Do not keep the plates out of the incubator for more than about 10 min, as media

in the wells will cool and the pH may also change. Large numbers of dead cells may be seen, this is normal. You may also see some small moving particles; this is due to Brownian movement of debris and does not indicate bacterial infection.

After 7 days, media needs to be replenished, this is also the beginning of diluting out the aminopterin from the HAT selection medium. To each well add 1 ml of HT medium +2% HFCS. Add the medium slowly so as not to break up any colonies; this is not critical, but it is easier to judge when to test a well if you can see the size of intact colonies.

From now on it is a matter of observing colony growth and changes in the pH of the medium. Screen for antibody from wells in which the medium is yellow (acidic) and colonies are about 25% confluent. Keep feeding wells on a 7-day cycle for slow growers and as needed for fast growers. For the second and subsequent feeds we use HT medium +1% HFCS.

D. Testing and Cloning

When testing for antibody, ensure that appropriate negative controls are used. A positive control can be a dilution of the test bleed or of serum collected when the spleen was removed. If screening by ELISA, false-positive "antiplastic responses" can be a nuisance. The use of antigen-negative wells as a control can help screen these out. It is a waste of time cloning cells from wells that display an antiplastic response.

Cells from wells that are positive in the screening assay need to be cloned and stored in liquid nitrogen as soon as possible. Cloning is performed not only to produce a monoclonal population, but also to stabilize cell growth and eliminate antibody nonproducers. Nonproducers often grow faster than cells producing antibody and can quickly outgrow the antibody-producing population.

We routinely clone at 3 cells per well and observe about two-thirds of the wells with cell growth. This approximates to Poisson's distribution of a probable cell cloning number of 1 cell per well. If you find more wells with cell growth, clone at a lower cell number per well, 1 or even 0.5 cells per well.

E. Cloning

Solutions

1. *HT medium +2% HFCS*: Add 2 ml of HFCS to 100 ml of HT medium. Store at 4°C. Warm to 37°C in a water bath before use.
2. *Trypan blue solution* (Cat. No. T8154 Sigma)

Steps

1. Gently resuspend the cells in a positive well of the 24-well plate using a sterile transfer pipette; avoid creating air bubbles. Transfer the cells to a new 24-well plate.
2. Perform a viable cell count at a 1:2 dilution in trypan blue solution.

In this example we will work from a viable cell count of 6×10^5 cells/ml

3. To obtain 3 cells/well, perform a series of dilutions: 1/1000 dilution = 600 cells/ml; add 10 µl cells into 10 ml of HT medium. From this make a 1/20 dilution = 30 cells/ml or 3 cells/100 µl.
4. Conveniently make this dilution by taking 500 µl of cells from the 1/1000 dilution and place into 9.5 ml of HT medium +2% HFCS. This gives 10 ml of cells, which is sufficient for one cloning plate at 100 µl per well.
5. Using a Gilson Distriman, add 100 µl of cell suspension to each well of a flat-bottomed 96-well plate. Label the new plate with the date and code of the original well and plate that it came from, e.g., P1D3 means plate 1 row D well 3.
6. Examine the cloning plates regularly and replenish with HT medium +2% HFCS on at least day 7 but beforehand if noticeable evaporation of media occurs. Some methods suggest wrapping 96-well plates with plastic film to slow down evaporation. This can be successful but makes viewing the wells difficult and can also give a false sense of security, care also needs to be taken when removing the film so as not to contaminate the plate.
7. Test wells that display cell growth as required, reclone, and freeze cells from positive wells using the same procedure. We clone a minimum of three times in order to achieve monoclonality.

When storing positive wells in liquid nitrogen, we routinely store two vials from the initial positive 24-well plate. From subsequent 96-well cloning plates we keep no more than three or four positive wells and store about two cryotubes of each and the same at each subsequent cloning step.

F. Isotyping and Scaling up of Hybridomas

Isotyping of the monoclonal antibody can be performed with a commercial ELISA kit, this can help confirm monoclonality and determine the strategy for antibody purification from the culture supernatant.

Care should be taken in scaling up the cultures from wells to flasks, ensure that cell growth is stable, and split cells into a number of wells of the 24-well plate;

we establish confluent growth in at least four wells before transferring the cells to a 25-cm^2 flask.

V. LIQUID NITROGEN STORAGE PROCEDURE

The only means by which long-term survival of hybridomas can be achieved is by storing cells in liquid nitrogen. It is essential that an up-to-date catalogue of stocks is maintained. Valuable hybridoma stocks should be kept in more than one freezer, preferably at separate sites.

A. Cell Freezing Protocol

Solutions

1. *Solution A*: Gently mix 10 ml of RF10 and 10 ml FBS. This solution may be stored at 4°C indefinitely if kept sterile. Warm to 37°C in a water bath before use.
2. *Solution B*: Add 6 ml of DMSO to 14 ml of RF10. This mixture causes an exothermic reaction and may be stored at 4°C for several days if kept sterile. Warm to 37°C in a water bath before use.

Steps

1. Resuspend cells in solution A.
2. To this add an equal volume of solution B. Mix the suspension gently and dispense into labeled sterile cryotubes.
3. After sealing the tubes, place them into a Nunc freezing container or a foam box.
4. Put the container into a –80°C freezer for 24 h, after which the tubes should be transferred into a liquid nitrogen store. The location and contents of the tubes have to be catalogued carefully.

B. Cell Thawing Protocol

We strongly recommend that full-face protection be worn when retrieving cells from liquid nitrogen.

1. Remove vials using cryogloves and forceps.
2. Transfer vials ***immediately*** to a shatter-proof container.
3. Using a beaker, transfer warm water from the 37°C water bath into the container.
4. The lid of the container need only be partially removed to allow access with the beaker and replaced as soon as water is added. *The use of the shatter-proof container prevents injury from tubes that explode on contact with warm water. This is a comparatively rare event but has caused severe injury.*
5. After a few minutes when the contents have thawed, remove and wash the vials in alcohol.
6. Remove the cells with a transfer pipette and place in a sterile 30-ml tube.
7. Slowly add an equal volume of RF10 medium dropwise.
8. Let stand for 5 min.
9. Add 10 ml of RF10 and let stand for a further 5 min.
10. Centrifuge at 400 *g* for 5 min and resuspend in HT medium for hybridomas and in RF10 for myeloma.
11. We routinely start cells growing at about 2×10^5 cells/well in a 24-well plate. The addition of 1% HFCS will speed up cell growth. Do not let cells overgrow and scale up to other wells and flasks as required.
12. The first priority is to maintain frozen stock, so ensure that more tubes are stored in liquid nitrogen.

V. COMMENTS

We have overcome tolerance to self-antigen by linking the conserved peptide to a fusion protein and using the construct as the immunogen. Using this strategy, we have been successful in making antibodies to a human peptide with 95% homology to the murine protein (Cavill *et al*., 1999).

If purchasing a tissue culture incubator, ensure that it can be cleaned easily, has readily accessible filters that are changed easily, and does not have "hidden" tubing that cannot be cleaned and acts as a harbor for infections.

VI. PITFALLS

1. Make sure that the marker pen ink used to label the cryotubes tubes is resistant to alcohol.
2. We cannot overemphasize the importance of storing positive hybridomas in liquid nitrogen for subsequent retrieval.

References

Campbell, A. M. (1991). Monoclonal antibody and immunosensor technology. *In "Laboratory Techniques in Biochemistry and Molecular Biology"* (van der Vliet, P. C., ed.) Elsevier, Amsterdam.

Cavill, D., Macardle, P. J., Beroukas, D., Kinoshita, G., Stahl, J., McCluskey, J., and Gordon, T. P. (1999). Generation of a monoclonal antibody against human calreticulin by immunization with a recombinant calreticulin fusion protein: Application in

paraffin-embedded sections. *App. Immunohistochem. Mol. Morphol.* **7**, 150–155.

de St Groth, S. F., and Scheidegger, D. (1980). Production of monoclonal antibodies: Strategy and tactics. *J. Immunol. Methods* **35**, 1–21.

Donohoe, P. J., Macardle, P. J., and Zola, H. (1994). Making and using conventional mouse monoclonal antibodies. *In* "*Monoclonal Antibodies: The Second Generation*" (H. Zola, ed.), *Biological Sciences*, Coronet Books, Philadelphia, PA.

Freshney, R. I. (2002). "Culture of Animal Cells: A Manual of Basic Technique," 4th Ed. Wiley-Liss, New York.

Goding, J. W. (1986). "Monoclonal Antibodies: Principles and Practice," 2nd Ed. Academic Press, London.

Grillo-Lopez, A. J. (2000). Rituximab: An insider's historical perspective. *Semin. Oncol.* **27**(Suppl. 12), 9–16.

Harrison, M. A., and Rae, I. F. (2003). General Techniques of Cell Culture. *In Handbooks in Practical Animal Cell Biology* (M. Harrison, I. E. Roe, A. Harris, Series Eds.) Cambridge Univ. Press, Cambridge, U.K.

Kearney, J., Radbruch, A., Liesegang, B., and Rajewsky, K. (1979). A new mouse myeloma cell line that has lost immunoglobulin expression but permits the construction of antibody-secreting cell lines. *J. Immunol.* **123**, 1548–1550.

Kohler, G., and Milstein, C. (1975). Continuous cultures of fused cells secreting antibody of predefined specificity. *Nature* **256**, 495–497.

Landsteiner, K. (1945). "The Specificity of Serological Reactions." Harvard Univ. Press, Boston, MA.

Shulman, M., Wilde, C. D., and Kohler, G. (1978). A better cell line for making hybridomas secreting specific antibodies. *Nature* **276**, 269–270.

CHAPTER

58

Rapid Development of Monoclonal Antibodies Using Repetitive Immunizations, Multiple Sites

Eric P. Dixon, Stephen Simkins, and Katherine E. Kilpatrick

I. INTRODUCTION

An in-depth understanding of both the formation of germinal centers and the immunoregulatory processes involved in T-cell-dependent B-cell responses (Levy *et al.*, 1989; Berek *et al.*, 1991; Jacob *et al.*, 1991; Kroese *et al.*, 1990; Nossal, 1992; MacLennan, 1994; Kelsoe, 1996) led us to initially explore the feasibility of modifying immunization and fusion time lines used for developing monoclonal antibodies. Our studies demonstrated that monoclonal antibodies could be generated quickly using an immunization and somatic fusion strategy, which we refer to as repetitive immunizations, multiple sites (RIMMS) (Kilpatrick *et al.*, 1997). Immunizations, somatic fusion, screening, and isolation of affinity-matured IgG-secreting hybridoma cell lines can be achieved within 1 month. RIMMS capitalizes on somatic fusion of immune B cells undergoing germinal center maturation in draining lymph nodes (Kilpatrick *et al.*, 1997, 2003). The immunization sites used for RIMMS are proximal to easily accessible regional lymph nodes. RIMMS involves the use of P3X63/Ag8.653 murine myeloma cells stably transfected with human BCL-2 (Kilpatrick *et al.*, 1997). Fusions can be performed as early as 7 days (Bynum *et al.*, 1999) out to 14 days after the onset of immunization using recombinant protein, conjugated synthetic peptides, or drug haptens (Kilpatrick *et al.*, 1997; Ignar *et al.*, 1998; Kinch *et al.*, 1998; Wring *et al.*, 1999; Alligood *et al.*, 2000; Ellis *et al.*, 2000; Lindley *et al.*, 2000). RIMMS has also been used successfully to generate high-affinity antibodies using DNA-based immunizations in conjunction with the PowderJect gene gun (Kilpatrick *et al.*, 1997, 1998, 2000, 2002, 2003; Kinch *et al.*, 2002).

This article describes the RIMMS procedure, including the preparation of adjuvant, immunization, isolation of lymph nodes, and our high-efficiency polyethylene glycol (PEG)-induced somatic fusion process. We also provide the reader with protocols for developing a BCL-2-modified myeloma cell line.

II. MATERIALS AND INSTRUMENTATION

Fine curved forceps (Cat. No. 1-23-20) and microdissecting scissors (Cat No. 11-250) are from Biomedical Research Instruments. The following items are from Corning Costar: 0.2-µm vacuum filter/storage units (Cat. No. 431205), T 25-cm^2 tissue culture flasks (Cat. No. 3056), and 96-well tissue culture plates (Cat. No. 3595), as well as 24-well tissue culture plates (Cat. No. 3524). Items purchased from Sigma include Freund's complete adjuvant (FCA) (Cat. No. F-5881), Hybri-MAX azaserine hypoxanthine, 50× (Cat. No. A9666), Hybri-MAX dimethyl sulphoxide (DMSO) (Cat. No. D2650), deoxycholic acid sodium salt (Cat. No. D-6750), and Igepal CA 630 (Cat. No. I-3021, used in place of NP-40). The following products are from InVitrogen: 0.45-µm nitrocellulose (Cat. No. LC2001), RPMI 640 (Cat. No. 11875-119), 10 m*M*, 100× nonessential amino acids (Cat. No. 11140-050), L-glutamine, 29.2 mg/ml with 10,000 units penicillin, 10,000 µg/ml streptomycin

Copyright 2006, Elsevier Science (USA).
All rights reserved.

(Cat. No. 10378-016), gentamycin reagent, 50 mg/ml (Cat. No. 10131-035), 8–16% Tris–glycine gels (Cat. No. EC6045), and SeeBlue Plus2 markers (Cat. No. LC5925), as well as pcDNA3.1+ (Cat. No. V790-20), Topo TA cloning (Cat. No. K4500-01), imMedia Amp (Cat. No. Q600-20), imMedia Amp Agar (Cat. No. Q601-20), and ethidium bromide (Cat. No. 15582-018). NUNC 1.8-ml freezer vials (Cat. No. 66021-986), as well as 10× phosphate-buffered saline (PBS) (Cat. No. EX-6506), are from VWR. Defined fetal bovine serum (FBS) (Cat. No. SH30070.03) is from Hyclone, and Origen cloning factor (Cat. No. 210001) is from Igen. JRH EX-Cell 610 HSF medium (Cat. No. 14610-1000M) is from JRH Bioscience. The P3-X63Ag8.653 cells (ATCC CRL-1580) and PEG 1450, MW 1300–1600, 2-g bottle are from ATCC. The RIBI adjuvant (Cat. No. R-700) is from Corixa. The anti-human BCL-2 monoclonal antibody (Cat. No. M0887) is from Dako. The following items are from Becton Dickinson: 1-ml Leur Lok syringes (Cat. No. 309626), 5-ml Leur Lok syringes (Cat. No. 309603), and 26G1/2 (Cat. No. 305111) and 16G1 (Cat. No. 305197) needles. BCIP/NBT color development substrate (Cat. No. S3771) is from Promega.

A PTC-200 Peltier thermal cycler is from MJ Research, Inc. (Cat. No. ALD-1244). DNA encoding human bcl-2 is from Genecopoeia (Cat. No. GC-B0284). Enzymes and lipid transfection reagents, Asp718 (Cat. No. 814 245), *XbaI* (Cat. No. 674 257), T4 DNA ligase (Cat. No. 481 220), and FuGENE 6 (Cat. No. 1 815 091) are from Roche. Software to analyze chromatographs is from Gene Codes Corporation (Sequencer Cat. No. SWC4.0). DNA isolation and cleanup kits are from Qiagen, Inc. (QiaPrep spin DNA kit, Cat. No. 27106 and QiaQuick gel extraction kit, Cat. No. 28704). Oligonucleotides are generated by Integrated DNA Technologies, and Microspin S400 columns are from Amersham Bioscience (Cat. No. 27-5140-01) for buffer exchange.

Eight- to 12-week-old female SJL mice are from Jackson Laboratories, and BALB/c mice are from Charles Rivers. Isoflurane (Iso Flo, Cat. No. 06-8550-2/R1) is from Abbott Labs and is administered to mice using a Vapomatic (Model 2) from AM Bickford, Inc.

III. PROCEDURES

A. Preparation of Culturing Media

Solutions

1. *Fusion selection medium, 1 liter*: Combine 500 ml ExCell-610 HSF media, 260 ml RPMI 1640, 100 ml Origen hybridoma cloning factor, 100 ml FBS, 10 ml L-glutamine/pen-strep, 10 ml nonessential amino acids, 2 vials of azaserine hypoxanthine 50×, each reconstituted with 10 ml RPMI 1640. Sterile filter media in a Corning 0.2-µm vacuum filter storage unit and store at 4°C.

2. *Fusion selection medium without Origen cloning factor, 1 liter*: Follow the directions in solution 1, but eliminate the Origen cloning factor and increase FBS from 10 to 20%. This medium is used to eliminate background from unfused B cells following somatic fusion.

3. *Fusion cloning medium, 1 liter:* This medium is used for limit dilution cloning of hybridomas. Combine 500 ml ExCell-610 HSF media, 280 ml RPMI 1640, 100 ml Origen hybridoma cloning factor, 100 ml FBS, 10 ml L-glutamine/pen-strep, and 10 ml nonessential amino acids. Sterile filter medium in a Corning 0.2-µm vacuum filter storage unit and store at 4°C.

4. *Culturing medium for BCL-2-transfected P3-X63Ag8.653 (ATCC CRL-1580) cells, 1 liter*: Combine 890 ml RPMI 1640, 100 ml FBS, 10 ml L-glutamine/pen-strep solution, and 200 µg/ml geneticin (G418). Sterile filter medium in a Corning 0.2-µm vacuum filter storage unit and store at 4°C. One week before using the cells for fusion, pass the cells into the just-described medium without G418. The same medium without G418 is used to culture the parental P3-X63Ag8.653 myeloma cell line.

5. *Serum-free wash medium, 500 ml*: Add 5 ml L-glutamine/pen-strep solution to 495 ml RPMI 1640, sterile filter medium in a Corning 0.2-µm vacuum filter storage unit, and store at 4°C.

B. Preparation of Antigen in Adjuvant

Steps

1. *Dose per mouse*: In a 1.5-ml Eppendorf tube, add 100 µl of antigen diluted in sterile PBS to a final concentration of 15 µg for the primary immunization. Add 100 µl of RIBI adjuvant to the tube containing the antigen and then vortex. Using a 1-ml Leur Lok syringe outfitted with a 16G1 needle, remove 100 µl of Freund's complete adjuvant (vortex the vial of FCA right before use).

2. To make an emulsion for the primary immunization, place the bevel of the needle against the inner wall at the bottom of the Eppendorf tube containing the antigen/RIBI mixture. Expel the Freund's complete adjuvant from the syringe into the tube and then draw the solution back up into the syringe holding the bevel of the needle against the inner wall of the tube. Repeat the process until a milky, slightly thickened

emulsion is formed. Draw the emulsion back up into the syringe. Carefully remove the 16G needle and replace it with a 26G 1/2 needle. The 300-µl volume is then delivered to the six subcutaneous sites indicated in Fig. 1, 50µl per site, as detailed later.

3. The final concentration of antigen used for the secondary immunization is 5µg, and 2–5µg of the antigen is used for the tertiary immunization. For secondary and tertiary immunizations, dilute the antigen in a 100-µl volume of sterile PBS, increase the RIBI adjuvant volume to 200µl, and eliminate FCA.

C. Immunization of Mice

Steps

1. For each antigen, immunize two 8- to 12-week-old female SJL or two BALB/c mice (one mouse will serve as a backup) at the sites indicated in Fig. 1 on days 0, 7, and 10. Using this immunization time line, fusion can be performed on day 11, 12, or 13. Alternatively, mice can be immunized on days 0, 4, and 8, and fusions can be performed on day 11. Fusions can also be performed as early as day 7 by immunizing mice on days 0, 2, and 4 (Bynum *et al.*, 1999). The backup mouse can be boosted every 2–3 weeks using conventional protocols (see previous article).

2. Anesthetize the mice with isoflourane for all immunization time points.

3. Inject 50µl of the antigen/adjuvant emulsion into six sites proximal to axillary and brachial lymph nodes (thoracic region), superficial inguinal lymph nodes (abdominal region), and popliteal lymph nodes (located behind the knee) as indicated in Fig. 1.

D. Harvesting Lymph Nodes

Steps

1. Perform euthanasia of mice using carbon dioxide.

2. Wet down the fur of the mouse with 70% ethanol.

3. Lay the mouse on its back and lift up the skin in the lower groin using 70% ethanol forceps. Using 70% ethanol-rinsed microdissecting scissors, make a small incision to open up the skin (do not cut open the abdominal wall). To make a midsection incision, insert the scissors under the skin and then make an incision starting from the lower groin region up to the neck using forceps to lift up the skin. Make incisions across the top of the shoulders, down to the front feet on the left and right sides. Then make incisions from the lower groin area across to the top of the legs continuing down to the hind feet. To expose the lymph nodes, peel the skin back from the midsection incision, pull back the skin from the hind legs, and secure with pins as shown in Fig. 1.

4. Using curved forceps that have been rinsed in 70% ethanol, remove the lymph nodes by placing curved microforceps under each node and then pull up gently to separate lymph nodes from surrounding tissue.

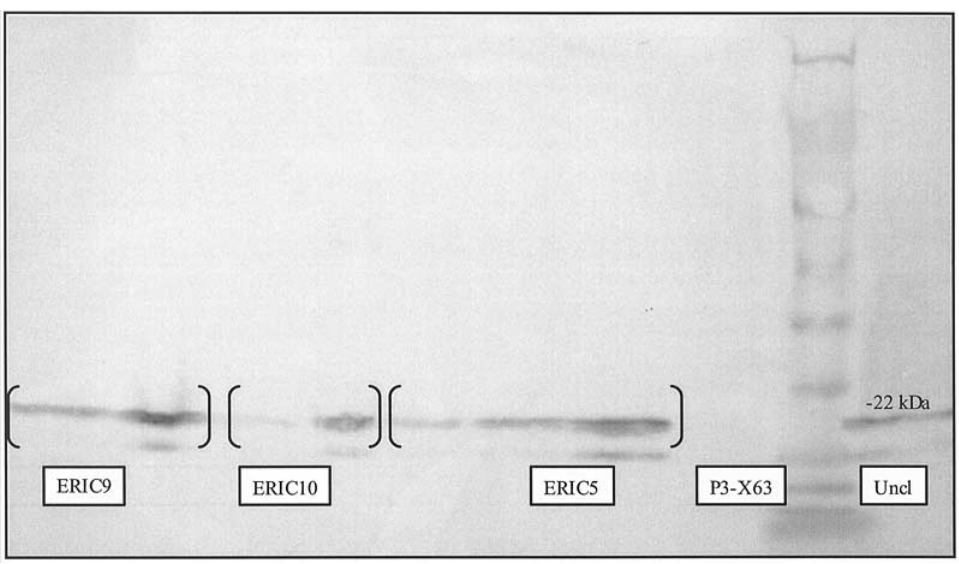

FIGURE 1 Immunization sites used for RIMMS are indicated by arrows. Following immunization, the axillary, brachial, superficial inguinal, and popliteal lymph nodes are exposed and then removed aseptically. Lymphocytes are isolated from the lymph nodes and are then used in a PEG-induced fusion.

5. Place the lymph nodes into a 60-mm sterile tissue culture dish containing 5 ml of serum-free wash medium.

E. Isolation of Lymphocytes from Lymph Nodes

Steps

1. In a laminar flow hood, remove the lymph nodes from the 60-mm tissue culture dish and transfer the nodes into a new 60-mm dish containing 5 ml of serum-free wash medium. Fill a 5-ml syringe with serum-free wash medium and add a 26G needle. Gently hold individual lymph nodes with 70% ethanol-rinsed curved microforceps. Insert the needle into the node and then profuse with medium in order to flush out the lymphocytes. Repeat process on each node. Using two curved microforceps, gently tease remaining cells from the capsules.
2. Pipette the lymphocyte cell suspension into a 15-ml conical tube and allow the debris from the capsules of the nodes to settle to the bottom of the tube (less than 1 min). Pipette the cells away from the debris and then transfer the cell suspension into a new 15-ml conical tube. Count the cells (see article by Hoffman). For each fusion, use 3×10^7 lymphocytes (see step 3 in Section IIIF).

Note: The number of lymphocytes isolated from pooled lymph nodes will range from $1–2 \times 10^7$ (weak immunogen) to 1×10^8 when one female SJL mouse is immunized using RIMMS. You can expect one-half of this range when one female BALB/c mouse is used.

3. Remaining immune lymphocyte cells not used for fusion can be frozen back by pelleting the cells by centrifugation at 400 *g* for 5 min. Resuspend the cells in 1 ml of 90% FCS, 10% DMSO freezing media. Place cells into 1×1.8-ml NUNC freezing vials labeled with the antigen designation and the date. Place the vial overnight at –80°C in a styrofoam container and then transfer the cells to liquid nitrogen storage the following day. These cells can be subsequently thawed and used for somatic fusion.

F. PEG-Induced Somatic Fusion

Steps

1. To affect a 1:1 lymphocyte-to-myeloma ratio, harvest 3×10^7 P3-X63Ag8.653 (ATCC CRL-1580) or P3X-BCL-2-transfected myeloma cells to be used for the fusion in a 50-ml conical tube (see protocols on how to generate a bcl-2-modified fusion partner in Section IIIH). Check the viability of the myeloma cells using trypan blue; ideally you want 90–98% viability. Wash the cells in serum-free wash medium by centrifuging at 400 *g* for 5 min. Resuspend the cells in 2 ml serum-free wash medium.
2. To prepare the PEG for fusion (ATCC PEG 1450, MW 1300–1600, 2-g bottle), very slowly heat the bottle on a hot plate on a low setting, just enough to melt the PEG. Do not boil the PEG. Using a 5-ml syringe outfitted with a 16G1 needle, immediately add 3 ml of serum-free wash medium that has been prewarned to 37°C to make a 40% stock solution. Keep the PEG solution in a 37°C incubator until you are ready to perform the fusion. Use the PEG solution within 1.5 h, as the efficiency of the fusion will drop off significantly if you use the PEG beyond 2 h after preparation.
3. In a 15-ml conical tube, mix 3×10^7 immune lymphocyte cells isolated from lymph nodes with 3×10^7 myeloma cells (from step 1). Centrifuge the cell mixture at 400 *g* for 5 min. Decant the media to leave a "dry pellet" by removing as much media as possible. Gently disrupt the pellet of mixed cells by tapping the bottom of the tube.
4. Using a 1-ml pipette, slowly add 300 µl of the PEG solution to the "dry pellet" of the myeloma and lymph node cell mixture in the bottom of the 15-cc tube. Mix gently and then allow the tube to incubate in the hood for 5 min. Gently mix the cell suspension again by tapping the tube and then allow the suspension to incubate in the hood for another 5 min.
5. Using a 5-ml pipette add 4 ml of the fusion selection media to the fusion, resuspend the cells gently, and then transfer the fusion suspension into a 250-ml sterile bottle containing 196 ml of fusion selection media. Swirl gently to mix cell suspension. Plate out the fusion in 10×96-well tissue culture plates by adding 200-µl per well.

G. Postfusion Care and Handling

Steps

1. Avoid removing the fusion plates from the incubator for microscopic observation during the first few days after the fusion.
2. Within 7 days, remove one-half of the hybridoma selection media and then replace with fresh hybridoma selection media (containing azaserine hypoxanthine). If you observe a high number of unfused lymphocytes still growing, change the media to hybridoma selection media containing 20% FBS, without Origen cloning factor. Antibody from unfused B cells will give misleading results in primary screening assays.
3. Within 5–10 days you will be able to observe the outgrowth of hybridomas in the fusion plates. Harvest supernatant for ELISA analysis. ELISA positives

are further tested in Western blot and immunoprecipitation.

4. For limit dilution cloning for the isolation and identification of monclonal antibody-producing cell lines, please refer to the previous article.

H. Generation of a P3X-BCL-2 Myeloma Cell Line

Cloning of Human BCL-2

Solutions

1. *10× TBE*: 108 g Tris base, 55 g boric acid, 40 ml 0.5 *M* EDTA (pH 8.0)
2. *Ethidium bromide*: 10 mg/ml in dH_2O

Steps

1. *PCR reaction mix*: Mix 20 pmol of primers (sense 5′ cgg ggt acc gcc acc atg gcg cac gct ggg aga ac 3′ and anti-sense 5′ ccg tct aga tca ctt gtg gcc cag ata ggc a 3′), human BCL-2 cDNA, 10× Advantage PCR buffer, 200 µ*M* dNTP mix, dH_2O, and Advantage HF polymerase.
2. Set parameters for human bcl-2 in a PTC-200 Peltier thermal cycler with the following conditions. Cycle steps: a denaturation step of 3 min at 95°C to generate a hot start, 30 cycles at 95°C for 15 s, 65°C for 15 s, and then 72°C for 1 min, followed by a soak step at 4°C.
3. After amplification of the cDNA, separate the PCR products and primers electrophoretically on a 1% agarose/TBE ethidium gel and purify the 642-bp band using the QiaQuick gel purification kit.
4. Perform buffer exchange over a Sephadex-400 column.
5. Insert the cloned cDNA into pCR2.1 using the TOPO TA cloning kit and transform into Top10 *Escherichia coli*.
6. Prepare 6–10 cultures with 2 ml LB-amp media in a 15-ml sterile culture tube. Pick a single isolated colony with a sterile loop and inoculate each miniculture with the isolated bacteria. Incubate and shake overnight at 37°C.
7. Isolate recombinants using the QiaPrep spin DNA kit and digest 1 µg of the plasmid DNA with the restriction endonucleases Asp718 and *Xba*I for 1 h at 37°C.
8. Isolate the human BCL-2 cDNA fragment by excising the 642-bp band and then subclone into a linear pcDNA3.1(+) vector (digested with Asp718 and *Xba*I) using T4 DNA ligase.
9. Transform 2.5 µl of the ligation reaction into chemically competent Top 10 *E. coli* and spread onto a LB-amp agar plate. Incubate overnight at 37°C.
10. Culture, isolate, and digest another 6–10 plasmid DNA recombinants. Determine correct recombinants by restriction endonuclease digests and electrophoresis.
11. Transfect pcDNA3.1(+) human BCL-2 plasmid DNA into the P3-X63Ag8.653 cell line.

I. Transfection, Isolation, and Identification of BCL-2-Transfected Myeloma Cells

Solutions

1. *RIPA buffer*: 150 m*M* NaCl, 50 m*M* Tris, 1% Igepal, 0.25% deoxycholate, pH 7.5. To make 1 liter, add 8.76 g of sodium chloride, 6.35 g Tris–HCl, 1.18 g Tris base, 10 ml Igepal, and 2.5 g deoxycholate to a total volume of 1 liter. Sterile filter in a Corning 0.2-µm vacuum filter storage unit and store at 4°C.
2. *Culturing medium for P3X63/Ag8.653 murine myeloma cells*: Combine 890 ml RPMI 1640, 100 ml FBS, and 10 ml L-glutamine/pen-strep solution. Sterile filter in a Corning 0.2-µm vacuum filter storage unit and store media at 4°C.
3. *G418 selection medium, 1 liter, used for selection of BCL-2- transfected P3-X63Ag8.653 cells (parental cells P3-X63Ag8.653, ATCC CRL-1580)*: Combine 890 ml RPMI 1640, 100 ml FBS, and 10 ml L-glutamine/pen-strep solution. Add geneticin (G418) from 50-mg/ml stock (potency is 600 µg/mg) to final concentrations of 1 mg/ml, 500 µg/ml, and 250 µg/ml. Sterile filter in a Corning 0.2-µm vacuum filter storage unit and store media at 4°C.
4. *Culturing medium for BCL-2-transfected P3-X63Ag8.653 cells, 1 liter*: Combine 890 ml RPMI 1640, 100 ml FBS, 10 ml L-glutamine/pen-strep solution, and a final concentration of G418 at 200 µg/ml. Sterile filter in a Corning 0.2-µm vacuum filter storage unit. One week before using the cells for fusion, pass the cells into the just-described media without G418.
5. *Phosphate-buffered saline*: 10× PBS from VWR (137 m*M* NaCl, 2.7 m*M* potassium chloride, 10 m*M* phosphate buffer). To 100 ml of 10× PBS stock, add 900 ml distilled water. Sterile filter in a Corning 0.2-µm vacuum filter storage unit.
6. *Hybridoma freezing medium:* 90 ml fetal bovine serum, 10 ml Hybri-Max DMSO, sterile filter, and store at 4°C.
7. *Alkaline phosphatase developing buffer, pH 9.5 (0.1 M Tris HCL, 0.1 M NaCl, 5 mM $MgCl_2$)*: 1.52 g Tris–HCl, 10.94 g Tris–OH, 5.85 g NaCl, 1.15 g $MgCl_2 \cdot 6H_2O$ dissolved in 1 liter of distilled water, pH to 9.5, sterile filter, and store at 4°C.
8. *5% PBST Blotto*: To 100 ml of 1× PBST (0.05% Tween-20), add 5 g powdered milk, mix well, and then store at 4°C.

Steps

1. The day before transfection, plate P3X63/Ag8.653 cells into 12 wells of a 24-well tissue culture plate at a density of 4×10^5 cells per well in 2 ml of culturing media. Six of the wells will be used for transfection, and 6 wells will be used for controls for the G418 selection (see step 5). Incubate the cells overnight in a 37°C, 5% CO_2 humidified incubator. The cells should be approximately 50% confluent.

2. The DNA ratio used for transfection is 3:1. For each well, use 0.5 ml of serum-free RPMI 1640 medium containing 0.6 µl of FuGENE 6 with 0.2 µg of DNA encoding human BCL-2.

3. The following steps are taken to prepare the FuGENE 6 reagent:DNA complex for transfection of P3X63/Ag8.653 murine myeloma with the human BCL-2 gene. Add 50 µl of serum-free RPMI 1640 media to a small sterile tube. Add 3 µl of FuGENE 6 transfection reagent directly to the serum-free medium. Mix by tapping the tube gently. Add 0.2 µg of the DNA in a volume of 1 µl to the tube. Mix the contents by tapping the tube gently (do not vortex). Incubate the reaction at room temperature for 15–30 min.

4. Remove the medium from six wells of the plated P3X63/Ag8.653 cells. Add 0.6 ml culture medium to each well. Using a sterile tip, add dropwise 53 µl of the complex mixture from step 3. Gently mix the cell suspension to disperse the reagent:DNA complex evenly. Return the cells to the incubator.

5. Within 24 h, carefully remove medium from wells that underwent transfection. To duplicate wells add 2 ml of the 1-mg/ml, 500-µg/ml, and 250-µg/ml G418 selection media. To the remaining six wells that were not transfected, add to duplicate wells 2 ml of the 1-mg/ml, 500-µg/ml, and 250-µg/ml G418 selection media. These cells will serve as controls for the G418 selection process (cells should die).

6. Within 4 days, remove selection media and replace wells with fresh selection media. As the selected cells grow, continue to maintain the cells in selection media. Change the media every 3 to 5 days.

7. Expand the selected cell lines into T25-cm^2 flasks in the respective G418 selection media. Grow the cells to 7–9 $\times 10^5$/ml. Spin down the cells at 400 *g* for 5 min. Decant the supernatant, resuspend the cells in hybridoma freezing medium, and aliquot 1 ml per 1.8-ml Nunc freezing vials. Place the cells into a styrofoam rack and then freeze overnight at –80°C. The next day, transfer the cells to LN_2. Freeze back stocks of the transfected cell lines at 1×10^6 cells per vial in freezing media. Continue to maintain the cells in culture in respective selection media in order to prepare RIPA extracts to determine the presence of the human BCL-2 protein (see later).

J. Western Blot Detection of Human BCL-2

Steps

1. Following the transfections and selection of P3-X63Ag8.653 cells with plasmid encoding human BCL-2, maintain the myeloma cells in G418 selection media containing final concentrations of 1 mg/ml, 500 µg/ml, and 250 µg/ml in T25-cm^2 flasks. Also maintain the parental P3-X63Ag8.653 cells, which will serve as negative controls.

2. Count the parental P3-X63Ag8.653 and the BCL-2 transfected cell lines using trypan blue (see article by Hoffman). For each cell line, centrifuge 1×10^6 cells in a 15-ml conical tube at 400 *g* for 5 min.

3. Remove all of the culture supernatant. To make cell extracts in order to determine the presence of human BCL-2 by Western blot, add 10 µl of chilled RIPA buffer to the cell pellet, resuspend the cells, and then transfer the respective cell suspensions to 1.5-ml Eppendorf tubes. Incubate tubes on ice for 15 min.

4. Microfuge the sample tubes in a microfuge set on high for 15 min at 4°C. Remove the supernatant (discard the pellet) and then mix the supernatant 1:1 with 2× sample buffer. Heat samples at 96°C for 5 min.

5. Load a 20-µl volume of the P3-X63Ag8.653 RIPA extract (parental cell line) and each P3XBCL-2-transfected cell extract onto individual lanes of a 1×10 well 8–16% Tris–glycine gel (InVitrogen) using one lane for SeeBlue Plus2 markers. Run the gel for 90 min at 125 V and then transfer the gel to nitrocellulose. Block the nitrocelluose in 5% PBST Blotto overnight at 4°C.

6. For detection of human BCL-2, add 10 ml of anti-human BCL-2 (Dako). Dilute 160 µl of the antibody per 10 ml in 5% PBST Blotto blocking buffer. Incubate the blot for 1 h at room temperature on a shaker or rocker platform.

7. Wash the blot four times for 5 min with PBST. Add 10 ml of a 1:1000 dilution of goat anti-mouse IgG-alkaline phosphatase-labeled conjugate diluted in 5% PBST Blotto blocking buffer to the blot. Incubate for 1 h on a rocker platform.

8. Wash the blot four times with PBST. Develop the blot using 10 ml alkaline phosphatase buffer containing 66 µl of NBT and 33 µl of BCIP. Immerse the blot into the developing substrate, place on a rocking platform, and incubate until a purple color develops. Stop the reaction by removing the developing substrate and rinsing the blot with ddH_2O.

9. Figure 2 demonstrates a Western blot indicating the presence of BCL-2 in RIPA extracts made from

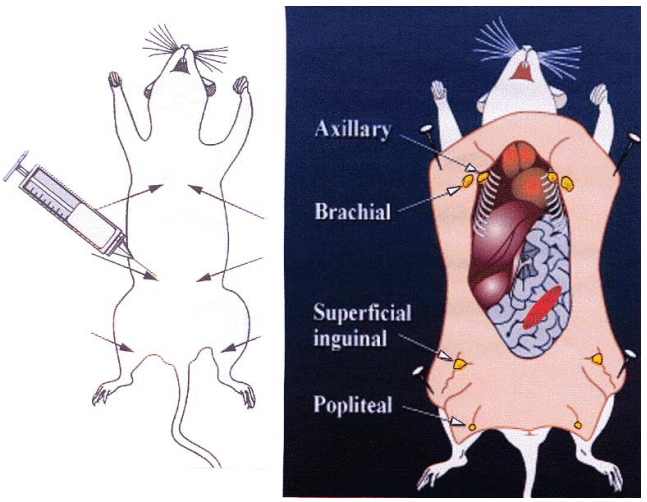

FIGURE 2 Titration of RIPA extracts of P3-X63Ag8.653 clones (ERIC5, ERIC9, and ERIC10) stably expressing human BCL-2, as well as uncloned parental BCL-2 transfected cells, indicates the presence of human BCL-2 by Western blot using an anti-human bcl-2-specific monoclonal antibody. Control untransfected P3-X63Ag8.653 cells serve as a negative control.

transfected, G418 selected P3-X63Ag8.653 myeloma cells.

10. Expand the uncloned cells from wells that demonstrate the presence of BCL-2 into a 75-cm^2 tissue culture flask containing 35 ml of media supplemented with 250 µg/ml G418. Grow the cells to 7–9 × 10^5/ml. Spin down the cells at 400 *g* for 5 min. Decant the supernatant, resuspend the cells in hybridoma freezing media, and aliquot 1 ml per 1.8-ml Nunc freezing vials. Place the cells into a styrofoam rack and then freeze overnight at –80°C. The next day, transfer the cells to LN_2.

K. Limit Dilution Cloning of P3Xbcl-2 Myeloma Cells

Steps

1. Count the P3XBCL-2 cells (see article by Hoffman) and then dilute the cells to 330 cells in a total of 200 ml of culturing media containing 250 µg/ml G418. To increase the limit dilution cloning efficiency, the Origen cloning factor can be added to the G418 selection medium.

2. Add 200 µl of the cell suspension per well to 10 × 96-well sterile tissue culture plates.

Incubate the cells at 37°C in a humidified incubator.

3. Microscopically scan the wells to identify one cell per well within 48 h of plating. Mark the wells that have clones derived from single cells.

4. Once the clones have grown to cover 50–75% of the well, expand the cells into 24-well plates containing 2 ml per well culturing media containing 200 µg/ml G418. Allow the cells to grow to 80–90% confluency in 6 wells. Remove cells from 3 wells and make RIPA lysates using the aforementioned procedure. Test for expression of BCL-2 using the Western blotting procedure. (Fig. 2).

5. Expand the cells that exhibit high BCL-2 expression levels to T25-cm^2 tissue culture flasks. Freeze back master stocks as detailed earlier.

6. Test the P3XBCL-2-transfected cells for their ability to negatively select (die) by placing the cells in fusion selection media containing HybriMax azaserine hypoxanthine. Due to the presence of BCL-2, the cells will take approximately 2–3 days longer to die as compared to the parental untransfected P3-X63Ag8.653 cell line.

IV. PITFALL

Unfused B cells producing antigen-specific immunoglobulin can contribute to background, which may indicate false positives in a primary ELISA screen. It is imperative to change the media on fusion plates one to two times before screening (see Section IIIG, step 2).

References

Alligood, K. J., Milla, M., Rhodes, N., Ellis, B., Kilpatrick, K. E., Lee, A., Gilmer, T. J., and Lansing, T. L. (2000). Monoclonal antibodies generated against recombinant ATM support kinase activity. *Hybridoma* **19**, 317–321.

Berek, C., Berger, A., and Apel, M. (1991). Maturation of the immune response in germinal centers. *Cell* **67**, 1121–1129.

Bynum, J., Andrews, J. L., Ellis, B., Kull, F. C., Austin, E. A., and Kilpatrick, K. E. (1999). Development of class-switched, affinity matured monoclonal antibodies following a 7 day immunization schedule. *Hybridoma* **18**, 407–411.

Ellis, J. H., Ashman, C. A., Burden, M. N., Kilpatrick, K. E., Morse, M. A., and Hamblin, P. A. (2000). GRID, a novel Grg-2-related adapter protein which interacts with the activated T cell costimulatory receptor CD28. *J. Immunol.* **164**, 5805–5814.

Ignar, D. M., Andrews, J. L., Witherspoon, S. M., Leray, J. D., Clay, W. C., Kilpatrick, K. E., Onori, J., Kost, T. A., and Emerson, D. L. (1998). Inhibition of establishment of primary and micrometastatic tumors by a urokinase plasminogen activator receptor antagonist. *Clin. Exp. Metast.* **16**, 9–20.

Jacob, J., Kelsoe, G., Rajewsky, K., and Weiss, U. (1991). Interclonal generation of antibody mutants in germinal centres. *Nature* **354**, 389–392.

Kelsoe, G. (1996) Life and death in germinal centers (Redux). *Immunity* **4**, 107–111.

Kilpatrick, K. E., Cutler, T., Whitehorn, E., Drape, R. J., Macklin, M. D., Witherspoon, S. M., Singer, S., and Hutchins, J. T. (1998). Gene

gun delivered DNA-based immunizations mediate rapid production of murine monoclonal antibodies to the Flt-3 receptor. *Hybridoma* **17**, 569–576.

Kilpatrick, K. E., Danger, D. P., Hull-Ryde, E. A., and Dallas, W. (2000). High affinity monoclonal antibodies generated in less than 30 days using 5μg of DNA. *Hybridoma* **19**, 297–302.

Kilpatrick, K. E., Kerner, S., Dixon, E. P., Hutchins, J. T., Parham, J. H., Condreay, J. P., and Pahel, G. (2002). *In vivo* expression of a GST-fusion protein mediates the rapid generation of affinity matured monoclonal antibodies using DNA-based immunizations. *Hybridoma Hybridomi.* **21**, 237–243.

Kilpatrick, K., Sarzotti, M., and Kelsoe, G. (2003). Induction of B cells by DNA vaccines. *In* "*DNA Vaccines*" (H. C. J. Ertl, ed.), pp 66–81. Eurekah Publ.

Kilpatrick, K. E., Wring, S. A., Walker, D. H., Macklin, M. D., Payne, J. A., Su, J.-L., Champion, B. R., Caterson, B., and McIntyre, G. D. (1997). Rapid development of affinity matured monoclonal antibodies using RIMMS. *Hybridoma* **16**, 381–389.

Kinch, K. C., Kilpatrick, K. E., Stewart, J. C., and Kinch, M. S. (2002). Antibody targeting of the EphA2 receptor tyrosine kinase on malignant carcinomas. *Cancer Res.* **62**, 2840–2847.

Kinch, M. S., Kilpatrick, K. E., and Zhong, C. (1998). Identification of tyrosine phosphorylated adhesion proteins in breast cancer. *Hybridoma* **17**, 227–235.

Kroese, F. G. M., Timens, W., and Nieuwenhuis, P. (1990). Germinal center reactions and B lymphocytes: Morphology and function. *Curr. Topics. Pathol.* **84**, 103–148.

Levy, N. S., Malipiero, U. V., Lebecque, S. G., and Gearhart, P. J. (1989). Early onset of somatic mutations in immunoglobulin V_H genes during the primary immune response. *J. Exp. Med.* **169**, 2007–2019.

Lindley, K. M., Su, J.-L., Hodges, P. K., Wisely, C. B., Bledsoe, R. K., Condreay, J. P., Wineager, D. A., Hutchins, J. T., and Kost, T. A. (2000). Production of monoclonal antibodies using recombinant baculovirus displaying gp64-fusion proteins. *J. Immunol. Methods* **234**, 123–135.

MacLennan, I. C. M. (1994). Germinal centers. *Annu. Rev. Immunol.* **12**, 117–139.

Nossal, G. J. V. (1992). The molecular and cellular basis of affinity maturation in the antibody response. *Cell* **68**, 1–2.

Wring, S. A., Kilpatrick, K. E., Hutchins, J. T., Witherspoon, S. M., Ellis, B., Jenner, W. N., and Serabjit-Singh, C. (1999). Shorter development of immunoassay for drugs: Application of the novel RIMMS technique enables rapid production of monoclonal antibodies to Ranitidine. *J. Pharma. Biomed. Anal.* **19**, 695–707.

CHAPTER

59

Phage-Displayed Antibody Libraries

Antonietta M. Lillo, Kathleen M. McKenzie, and Kim D. Janda

I. INTRODUCTION

Phage-displayed antibody libraries consist of large repertoires of Fab fragments (Barbas *et al.*, 1991), single chain variable regions (scFv) (McCafferty *et al.*, 1990), or diabodies (dimer scFv) (McGuinness *et al.*, 1996) cloned into genetically engineered phage or phagemid vectors (Smith, 1985; Smith and Petrenko, 1997), and expressed on the surface of a bacteriophage. This phenotype–genotype linkage enables phage-displayed antibodies to be selected by multiple rounds of antigen-based affinity purification and amplification. In addition, phage-displayed libraries can be constructed bypassing the immune system and therefore can be targeted to self-antigens (Zeidel *et al.*, 1995), as well as to nonimmunogenic and even toxic substances (Vaugham *et al.*, 1996). Furthermore, being an *in vitro* technique, phage display technology makes it easier to build fully human antibody libraries (Holt *et al.*, 2000). This article illustrates a general protocol for the generation of scFv libraries displayed on the surface of the pCGMT phage vector as part of either surface protein pIII (Gao *et al.*, 1997; Mao *et al.*, 1999; Gao *et al.*, 1999) or pIX (Gao *et al.*, 2002).

II. MATERIALS AND INSTRUMENTATION

First-strand cDNA synthesis kit is from Amersham Pharmacia (Cat. No. 27-9261-01). Carbenicillin, tetracycline, kanamycin, and IPTG are from Research Products International (Cat. No. C46000-1.0, T17000/1.0, K22000-1.0, and I56000-5.0). *Pfu* DNA polymerase, *Escherichia coli* XL-1 blue, VCSM13 interference-resistant helper phage, and total RNA purification kit are from Stratagene (Cat. No. 6000154, 200249, 200251, and 400790). Ultrapure agarose, electroporation cuvettes, 1-kb plus DNA ladder, T4 DNA ligase, bovine serum albumin (BSA), and 100 m*M* dNTP mix are from Invitrogen (Cat. No. 15510027, 15224017, P450-50, 10787018, 15561012, and 10216018). Dimethyl sulfoxide (DMSO) is from Aldrich (Cat. No. 27,043-1). *Sfi*I is from New England Biolabs (Cat. No. R0123S). QIAquick gel extraction kit is from Qiagen (Cat. No. 28704). Tryptone is from Becton Dickinson (Cat. No. 211043). Yeast extract is from obtained EM Science (Cat. No. 1.03753.5007). Nonfat dry milk is from Bio-Rad (Cat. No. 170-6404). All the salts, glycerol, polyethylene glycol, Tween 20, ethanol, and glucose are from Sigma (Cat. No. G5516, P2139, P1379, 27,074-1, G5767). Petri dishes and Nunc MaxiSorb Immunotubes are from Fisher (Cat. No. 08-757-1000, and 12-565-144). Polymerase chain reaction (PCR) tubes are from USA Scientific (Cat. No. 1402-4300). Nalgene 500-ml centrifuge bottles are from VWR (Cat. No. 21020-050). The thermocycler (Mastercycler Gradient) and benchtop centrifuge (5415C) are from Eppendorf. The electrophoresis chamber (Easy-Cast) is from Electrophoresis System. The electroporation apparatus (Gene Pulser II) is from Bio-Rad. The J2-H2 centrifuge is from Beckman.

III. PROCEDURES

A. Construction of a scFv Library

Solutions

1. *2xYT*: To make 1 liter, dissolve 16 g tryptone, 10 g yeast extract, and 5 g NaCl in 900 ml distilled

Copyright 2006, Elsevier Science (USA).
All rights reserved.

water. After adjusting the pH to 7.0 with NaOH, bring the volume to 1 liter. Sterilize by autoclaving.

2. *SB medium*: To make 1 liter, dissolve 30 g tryptone, 20 g yeast extract, and 10 g MOPS in 1 liter deionized water. Sterilize by autoclaving.
3. *LB-agar*: To make 1 liter, dissolve 10 g tryptone, 5 g yeast, and 10 g NaCl in 900 ml distilled water. Add 15 g agar and adjust the pH to 7.0 with NaOH. Fill to 1 liter and autoclave. Allow to cool to a reasonable temperature and supplement with 1 ml carbenicillin stock, 10 µg/ml tetracycline, and 2% glucose. Pour in petri dishes.
4. *SOC*: To make 1 liter, dissolve 20 g tryptone, 5 g yeast, and 0.5 g NaCl in 900 ml distilled water. Add 10 ml 250 m*M* KCl. Adjust the pH to 7.0, fill to 975 ml, and autoclave. Once cooled, add 5 ml 2 *M* $MgCl_2$ and 20 ml 1 *M* glucose
5. *Phosphate-buffered saline* (*PBS*): To make 1 liter, dissolve 1.44 g sodium phosphate, 0.24 g potassium phosphate, 0.2 g potassium chloride, and 8 g NaCl in 900 ml distilled water. Adjust the pH to 7.4. Fill to 1 liter and autoclave.
6. *Blotto*: To make 100 ml, dissolve 4 g nonfat dry milk in enough PBS to make 100 ml final volume.
7. *3 M NaOAc*: Dissolve 24.61 g NaOAc in 90 ml distilled water. Adjust the pH to 5.2. Fill to 100 ml and autoclave.
8. *250 mM KCl*: Dissolve 1.86 g KCl in 100 ml distilled water. Sterilize by autoclaving.
9. *2 M* $MgCl_2$: Dissolve 40.7 g magnesium chloride hexahydrate in 100 ml distilled water. Sterilize by autoclaving.
10. *1 M glucose*: Dissolve 90 g glucose in 500 ml distilled water. Sterile filter.
11. *Carbenicillin stock*: Dissolve 1 g carbenicillin in 10 ml deionized water. Sterile filter. Store at –20°C.
12. *Tetracycline stock*: Dissolve 50 mg tetracycline in 10 ml 70% ethanol. Store at –20°C
13. *Kanamycin stock*: Dissolve 500 mg kanamycin in 10 ml deionized water. Sterile filter. Store at –20°C.
14. *0.5 M IPTG stock*: Dissolve 5 g isopropyl-β-D-thiogalactopyranoside (IPTG) in 42 ml deionized water sterile filter. Store at –20°C.
15. *VCSM13 helper phage solution*: Prepare this solution according to the vendor's instructions.

Steps

1. *Preparation of mRNA.* Extract mRNA from either human peripheral blood lymphocytes (human library) or mouse spleen cells (murine library) using the RNA Purification Kit (Stratagene) according to the vendor's instructions. Prepare first-strand cDNA from the total RNA by using the First-strand cDNA Synthesis Kit (Pharmacia) and dT18 primer according to the manufacturer's recommendations.

2. *PCR amplification of antibody variable region genes* (*see* ***Fig. 1*** *and* ***Appendix***). In a 250-µl PCR tube, combine 2 µl of cDNA template, 2 µl of one forward primer (100 pmol/µl), 2 µl of an equimolar mixture of the respective reverse primers (100 pmol/µl), 200 µ*M* dNTPs, 5% DMSO, 10 µl 10× *Pfu* DNA polymerase buffer, and 5 units *Pfu* DNA polymerase (final volume: 100 µl). For example, for the human heavy chain, set up 12 PCR reactions total, in which each HVH forward primer is combined with a mixture of HJH reverse primers. Set the temperature program as follows: denaturation at 94°C for 5 min; 30 cycles of amplification, including denaturation, 1 min, 94°C; annealing, 1 min, 50°C; extension, 1 min, 72°C; and final extension at 72°C for 10 min. Run a 1% agarose gel and cut out the appropriate bands. Combine the heavy chain bands into one pool and the light chain bands (including V_λ and V_κ) into a separate pool. Purify using a Qiagen gel extraction kit.

3. *Construction of the scFv library* (*see* ***Fig. 1*** *and* ***Appendix***). Assemble the scFv library by overlap PCR. In a 250-µl PCR tube, combine ~20 ng of each scFv fragment pool, 200 µ*M* dNTPs, 2 µl 10× *Pfu* polymerase buffer, and 1 unit *Pfu* polymerase (final volume: 20 µl). Set the temperature program as follows: denaturation at 94°C for 5 min; 5 cycles of amplification, including denaturation, 1 min, 94°C; annealing, 1 min; 55°C; and extension, 1.5 min, 72°C. Add the outer primers HVH(Sfi) and HLJ(Sfi) [or MVH(Sfi) and MLJ(Sfi)] to a final concentration of 2 m*M* and bring the final volume to 50 µl. Set the thermocycler for 30 more cycles of denaturation, 30 s at 94°C; annealing, 30 s at 60°C; extension, 1.5 min at 72°C; and final extension at 72°C for 10 min. Gel purify the full-length scFv library on a 1% agarose gel using a Qiagen gel extraction kit.

4. *Digestion of the scFv library and vector*. Digest both the scFv library and either pCGMT (pIII library; Gao *et al*., 1997) or pCGMT9 (pIX library; Gao *et al*., 2002)

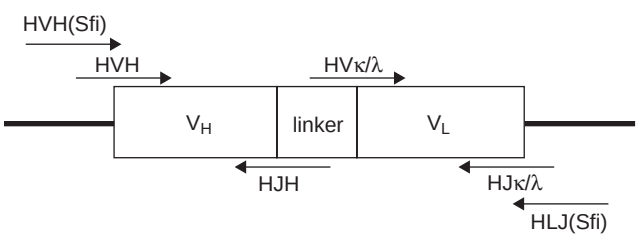

FIGURE 1 scFv diagram indicating design and primer overlap. HVH, human variable heavy chain; HJH, human constant heavy chain; HVκ/λ, human variable light chain; HJκ/λ, human constant light chain; HVH(Sfi), human forward *Sfi*I primer; HLJ(Sfi), human reverse *Sfi*I primer.

vector by combining 46 µl DNA, 6 µl 10× BSA, 6 µl 10× NE buffer 2, and 2 µl *Sfi*I. Incubate the mixture for 2 h or overnight at 50°C. Gel purify each digestion on a 1% agarose gel using a Qiagen gel extraction kit.

5. *Ligation into vector.* Combine 5 µl *Sfi*I digested vector, 10 µl scFv library, 4 µl 5X ligase buffer, and 1 µl T4 DNA ligase for a final volume of 20 µl. Incubate at 16°C for 2–10 h. Add 2 µl of 3 *M* NaOAc, pH 5.2, and mix well. Add 40 µl absolute ethanol and store at –20°C for >20 min. Centrifuge at ≥12,000 rpm for 10 min. Decant supernatant and wash the pellet with 1 ml 70% ethanol, mixing well. Spin at ≥12,000 rpm for 1–2 min and aspirate the solution. Air dry the pellet and resuspend in 10 µl distilled water.

6. *Transformation into electrocompetent E. coli XL-1 Blue.* Add 10 µl of the ligation mixture to 500 µl of a suspension of *E. coli* XL-1 Blue. Add 50-µl aliquots to 10 prechilled electroporation cuvettes. Electroporate at 2.5 kV per manufacture's instructions. Immediately add 200 µl SOC medium to the cuvette and incubate at 37°C for 30 min. Repeat as many times as necessary. Plate the cells on LB-agar plates supplemented with 2% glucose, 50 µg/ml carbenicillin, and 10 µg/ml tetracycline. Grow each plate overnight at 30°C.

7. *Library titer and storage*. Scrape the clones off each plate with 10 ml SB medium supplemented with 10% glycerol and store at -70°C. Determine the size of the library by counting the number of independent transformants. To titer the library, serially dilute the library (1 : 10) in SB out to 10^{-9}. Starting with the lowest dilution, add 100 µl onto a LB-carb plate and spread evenly. Incubate overnight at 37°C and count the colony-forming units for each dilution.

8. *Rescue of the scFv phage library*. Inoculate ~5×10^5 cells obtained from the previously described glycerol stock into 100 ml SB medium containing 2% glucose, 50 µg/ml carbenicillin, and 10 µg/ml tetracycline. Incubate the culture at 37°C on a reciprocal shaker until OD_{600} ~ 0.6 is reached. Add ~4×10^{13} plaque-forming units of VCSM13 helper phage and let incubate for 30 min at room temperature and then for 90 min on the shaker at 37°C. Add 200 µl of 0.5 *M* IPTG and 140 µl kanamycin and allow the culture to grow over-night at 30°C.

9. *Phage precipitation*. Pellet the cells by centrifuging at 7000 rpm for 20 min in a 400-ml centrifuge tube. Decant the supernatant into clean tubes. Dissolve 3 g NaCl and 4 g PEG-8000 in each tube and place on ice for 30 min. Centrifuge at 7000 rpm for 20 min to pellet phage. Resuspend in an appropriate volume of PBS.

10. *Panning*. Add 1 ml of ~5–50 µg/ml antigen/hapten to an immunotube and incubate overnight at 4°C. Remove the antigen solution and block the tube with 1 ml Blotto for 1 h at 37°C. Grow a culture of *E. coli* XL-1 Blue in 20 ml SB until the OD_{600} ~ 0.6. Save for phage titration and rescue. Remove the blocking solution and add 10^{12}–10^{13} colony-forming units of phage library in PBS containing 1% nonfat dry milk and 3% BSA. Incubate at 37°C for 2 h. Aspirate unbound phage solution and remove weakly bound phage by washing with 0.05% Tween 20 in PBS. Elute the tightly bound phage by either adding 1 ml of 0.1 *M* glycine, pH 2.5, or adding a solution of free antigen. Incubate at room temperature for 10 min. Remove the solution and neutralize with concentrated Tris base (usually 60 µl 2 *M* Tris, pH 8.0). Titrate the eluted phage by serially diluting (1:10) in SB out to 10^{-9}. Starting with the lowest dilution, add 10 µl diluted phage to 90 µl *E. coli* XL-1 Blue. Plate 50 µl onto a LB-carb plate and spread evenly. Incubate overnight at 37°C and count the colony-forming units for each dilution. Rescue the remaining eluted phage by adding to 20 ml *E. coli* XL-1 Blue, mixing gently, and letting sit for 10 minutes at room temperature. Centrifuge at 3000 rpm for 10 minutes and resuspend the pellet in approximately 500 µl of the SB medium. Spread evenly on a LB-carb plate and incubate overnight at 37°C. Rescue the library as outlined in step 7. This will be the input library for the next round of panning. Phage libraries are usually subjected to four to six rounds of panning. The number of rounds is dependent on enrichment as determined by library titer.

IV. COMMENTS

This procedure outlines the construction of a human or murine scFv library, including a list of suitable primers (see **Appendix**). The technique is also applicable to the formation of a Fab library with suitable primers (Barbas *et al.*, 1991).

The stringency of the phage selection can be increased at the end of each round of panning in several ways. The first is to decrease the amount of antigen immobilized on the immunotubes. Similarly, the incubation time of the library with the antigen can be decreased. Alternatively, one can increase the number of washing steps and/or the amount of detergent in the wash buffer. Finally, one can use a progressively lower concentration of free antigen during the elution step. Note that when selecting for interactions influenced by the ionic strength of the medium, buffers other than PBS might be used for panning.

The number of transformations needed to obtain an appropriate library size has to be determined experimentally. Upon titration of the first transformation mixture, 30–50 colonies must be picked and the corre-

sponding plasmids digested to determine the percentage of those containing inserts. Based on this number and the overall titer, one can determine the number of transformations needed to obtain ~10^9 independent transformants.

The quality of a library depends not only on the quantity of independent transformants, but also on diversity. In order to test such diversity, a set of 30–50 random clones should be sequenced so that the percentage of repeats can be determined. It is customary to define a library as satisfactory if it contains less than 10% repeated sequences.

V. PITFALLS

1. Take extreme care when working with RNA to prevent degradation by nucleases. This includes wearing gloves and using nuclease-free solutions.
2. Failure in the primary PCR reaction is typically due to a low concentration of cDNA. Repeat the first-strand synthesis if necessary. It may also be necessary to adjust the annealing temperature. Note that lowering the annealing temperature allows for less fidelity in primer overlap.
3. If overlap fails in step 3, check the concentrations of the various V_H, V_κ, and V_λ fragments by running a small amount on a gel and examining the intensity of the bands. Adjust the amounts accordingly to give approximately equimolar concentrations.
4. Scale the amount of phage preparation as necessary for library size.

References

Barbas, C. F., Kang, A. S., Lerner, R. A., and Benkovic, S. J. (1991). Assembly of combinatorial antibodies libraries on phage surfaces: the gene III site. *Proc. Natl. Acad. Sci. USA* **88**, 7978–7982.

De Haard, H. J., van Neer, N., Reurs, A., Hufton, S. E., Roovers, R. C., Henderikx, P., de Bruine, A. P., Arends, J. W., and Hoogemboom, H. R. (1999). A large non-immunized human Fab fragment phage library that permits rapid isolation and kinetic analysis of high affinity antibodies. *J. Biol. Chem.* **274**, 18218–18230.

Gao, C., Lin, C. H., Lo, C. H., Mao, S., Wirsching, P., Lerner, R. A., and Janda, K. D. (1997). Making chemistry selectable by linking it to infectivity. *Proc. Natl. Acad. Sci. USA* **94**, 11777–11782.

Gao, C. S., Brummer, O., Mao, S. L., and Janda, K. D. (1999). Selection of human metalloantibodies from a combinatorial phage single-chain antibody library. *J. Am. Chem. Soc.* **121**, 6517–6518.

Gao, C. S., Mao, S., Kaufmann, G., Wirsching, P., Lerner, R. A., and Janda, K. D. (2002). A method for the generation of combinatorial antibody libraries using pIX phage display. *Proc. Natl. Acad. Sci. USA* **99**, 12612–12616.

Haidaris, C. G., Malone, J., Sherrill, L. A., Bliss, J. M., Gaspari, A. A., Insel, R. A., and Sullivan, M. A. (1999). Recombinant human antibody single chain variable fragments reactive with *Candida albicans* surface antigens. *J. Immunol. Methods* **257**, 185–202.

Holt, L. J., Enever, C., de Wildt, R. M., and Tomlinson, I. M. (2000). The use of recombinant antibodies in proteomics. *Curr. Opin. Biotech.* **11,** 445–449.

Jahn, S., Grunow, R., Kiessig, S. T., Specht, U., Matthes, H., Hiepe, F., Heinak, A., and Von Baehr, R. (1988). Establishment of human Ig producing heterohybridomas by fusion of mouse myeloma cells with human lymphocytes derived form peripheral blood, bone marrow, spleen, lymph nodes and synovial fluids. *J. Immun. Methods* **107,** 59–66 and references therein.

Mao, S., Gao, C., Lo, C. H., Wirsching, P., Wong, C.-H., and Janda, K. D. (1999). Phage-display library selection of high-affinity human single-chain antibodies to tumor-associated carbohydrate antigens sialyl Lewis X and Lewis X. *Proc. Natl. Acad. Sci. USA* **96**, 6953–6958.

Marks, J. D., Tristem, M., Karpas, A., and Winter, G. (1991). Oligonucleotides primers for polymerase chain reaction amplification of human immunoglobulin variable genes and design of family-specific oligonucleotide probes. *Eur. J. Immunol.* **21**, 985–991.

McCafferty, J., Griffiths, A. D., Winter, G., and Chiswell, D. J. (1990). Phage antibodies: Filamentous phage displaying antibody variable domains. *Nature* **348**, 552–554.

McGuinness, B. T., Walter, G., FitzGerald, K., Schuler, P., Mahoney, W., Duncan, A. R., and Hoogenboom, H. R. (1996). Phage diabody repertoires for selection of large numbers of bispecific antibody fragments. *Nature Biotech.* **14**, 1149–1154.

Smith, G. P. (1985). Filamentous fusion phage: Novel expression vectors that display cloned antigens on the virion surface. *Science* **228**, 1315–1317.

Smith, G. P., and Petrenko, V. A. (1997). Phage display. *Chem. Rev.* **97**, 391–410.

Vaughan, T. J., Williams, A. J., Pritchard, K., Osbourn, J. K., Pope, A. R., Earnshaw, J. C., McCafferty, J., Hodits, R. A., Wilton, J., and Johnsons, K. S. (1996). Human antibodies with sub-nanomolar affinities isolated from a large non-immunized phage display library. *Nature Biotech.* 14, 309–314.

Welschof, M., Terness, P., Kolbinger, F., Zewe, M., Dubel, S., Dorsam, H, Hain, C., Finger, M., Jung, M., Moldenhauer, G., Hayashi, N., Little, M., and Opelz, G. (1995). Amino acid sequence based PCR primers for amplification of rearranged human heavy and light chain immunoglobulin variable region genes. *J. Immunol. Methods* **179**, 203–214.

Zeidel, M., Rey, E., Tami, J., Fischbach, M., and Sanz, I. (1995). Genetic and functional characterization of human autoantibodies using combinatorial phage display libraries. *Ann. N. Y. Acad. Sci.* **764**, 559–564.

APPENDIX

The following primers were designed based on those published previously and the most recent genes segments entered in the V-Base sequence directory (de Haard *et al*., 1999; Haidaris *et al*., 1999; Welschof *et al*., 1995; Marks *et al*., 1991; Jahn *et al*., 1988).

Primers for Human scFv Library

Primers for Amplification of Human V_H Genes

Forward primers

HVH(Sfi): TTGTTATTACTCGCGGCCCAGCCGGCC ATGGCACAGGT;

HVH-1: CAGCCGGCCATGGCACAGGTNCAGCTG GTRCAGTCTGG;
HVH-2: CAGCCGGCCATGGCACAGGTCCAGCTG GTRCAGTCTGGGG;
HVH-3: CAGCCGGCCATGGCACAGGTKCAGCTG GTGSAGTCTGGG;
HVH-4: CAGCCGGCCATGGCACAGGTCACCTTG ARGGAGTCTGGTCC;
HVH-5: CAGCCGGCCATGGCACAGGTGCAGCTG GTGGAGWCTGG;
HVH-6: CAGCCGGCCATGGCACAGGTGCAGCTG GTGSAGTCYGG;
HVH-7: CAGCCGGCCATGGCACAGGTGCAGCTG CAGGAGTCGG;
HVH-8: CAGCCGGCCATGGCACAGGTGCAGCTG TTGSAGTCTG;
HVH-9: CAGCCGGCCATGGCACAGGTGCAGCTG GTGCAATCTG;
HVH-10: CAGCCGGCCATGGCACAGGTGCAGCT GCAGGAGTCCGG;
HVH-11: CAGCCGGCCATGGCACAGGTGCAGCTA CAGCAGTGGG;
HVH-12: CAGCCGGCCATGGCACAGGTACAGCT GCAGCAGTCAG.

Reverse primer

HJH: GGAGCCGCCGCCGCCAGAACCACCACCAC CTGAGGAGACGGTGACCAKKGTBCC

Primers for Amplification of Human V_K Genes

Forward primers

HVκ-a: GGCGGCGGCGGCTCCGGTGGTGGTGGTT CTGACATCSWGATGACCCAGTCTCC
HVκ-b: GGCGGCGGCGGCTCCGGTGGTGGTGGTT CTGAAATTGTGYTGACKCAGTCTCC
HVκ-c: GGCGGCGGCGGCTCCGGTGGTGGTGGTT CTGATGTTGTGATGACTCAGTCTCC
HVκ-d: GGCGGCGGCGGCTCCGGTGGTGGTGGTT CTGAAACGACACTCACGCAGTCTCC

Reverse primers

HJκ-1: TGGAATTCGGCCCCCGAGGCCACGTTTG ATTTCCACCTTGGTCCC;
HJκ-2: TGGAATTCGGCCCCCGAGGCCACGTTTG ATCTCCAGCTTGGTCCC;
HJκ-3: TGGAATTCGGCCCCCGAGGCCACGTTTG ATATCCACTTTGGTCCC;
HJκ-4: TGGAATTCGGCCCCCGAGGCCACGTTTG ATCTCCACCTTGGTCCC;
HJκ-5: TGGAATTCGGCCCCCGAGGCCACGTTTAA TCTCCAGTCGTGTCCC.

Primers for Amplification of Human V_λ Genes

Forward primers

HVλ-a: GGCGGCGGCGGCTCCGGTGGTGGTGGTT CTCAGTCTGTGTTGACGCAGCCGCC
HVλ-b: GGCGGCGGCGGCTCCGGTGGTGGTGGTT CTCAGTCTGCCCTGACTCAGCCTGC
HVλ-c: GGCGGCGGCGGCTCCGGTGGTGGTGGTT CTTCCTATGTGCTGACTCAGCCACC
HVλ-d: GGCGGCGGCGGCTCCGGTGGTGGTGGTT CTTCTTCTGAGCTGACTCAGGACCC
HVλ-e: GGCGGCGGCGGCTCCGGTGGTGGTGGTT CTCACGTTATACTGACTCAACCGCC
HVλ-f: GGCGGCGGCGGCTCCGGTGGTGGTGGTT CTCAGGCTGTGCTCACTCAGCCGTC
HVλ-g: GGCGGCGGCGGCTCCGGTGGTGGTGGTT CTAATTTTATGCTGACTCAGCCCCA

Reverse primers

HLJ(Sfi): GTCCTCGTCGACTGGAATTCGGCCCCC GAGGCCAC;
HJλ-1: TGGAATTCGGCCCCCGAGGCCACCTAGGA CGGTGACCTTGGTCCC;
HJλ-2: TGGAATTCGGCCCCCGAGGCCACCTAGGA CGGTCAGCTTGGTCCC;
HJλ-3: TGGAATTCGGCCCCCGAGGCCACCTAAAA CGGTGAGCTGGGTCCC.

Primers for Mouse scFv Library

Primers for Amplification of Mouse V_H Gene

Forward primers

MVH(Sfi): TTGTTATTACTCGCGGCCCAGCCGGC CATGGCA
MVH-1: GCCCAGCCGGCCATGGCAGAGGTRMAG CTTCAGGAGTCAGGAC
MVH-2: GCCCAGCCGGCCATGGCAGAGGTSCAG CTKCAGCAGTCAGGAC
MVH-3: GCCCAGCCGGCCATGGCACAGGTGCAG CTGAAGSASTCAGG
MVH-4: GCCCAGCCGGCCATGGCAGAGGTGCAG CTTCAGGAGTCSGGAC
MVH-5: GCCCAGCCGGCCATGGCAGARGTCCAG CTGCAACAGTCYGGAC
MVH-6: GCCCAGCCGGCCATGGCACAGGTCCAG CTKCAGCAATCTGG
MVH-7: GCCCAGCCGGCCATGGCACAGSTBCAG CTGCAGCAGTCTGG
MVH-8: GCCCAGCCGGCCATGGCACAGGTYCAG CTGCAGCAGTCTGGRC
MVH-9: GCCCAGCCGGCCATGGCAGAGGTYCAG CTYCAGCAGTCTGG
MVH-10: GCCCAGCCGGCCATGGCAGAGGTCCA RCTGCAACAATCTGGACC
MVH-11: GCCCAGCCGGCCATGGCACAGGTCCA CGTGAAGCAGTCTGGG
MVH-12: GCCCAGCCGGCCATGGCAGAGGTGAA SSTGGTGGAATCTG
MVH-13: GCCCAGCCGGCCATGGCAGAVGTGAA GYTGGTGGAGTCTG

MVH-14: GCCCAGCCGGCCATGGCAGAGGTGC
AGSKGGTGGAGTCTGGGG
MVH-15: GCCCAGCCGGCCATGGCAGAKGTGCA
MCTGGTGGAGTCTGGG
MVH-16: GCCCAGCCGGCCATGGCAGAGGTGA
AGCTGATGGARTCTGG
MVH-17: GCCCAGCCGGCCATGGCAGAGGTGCA
RCTTGTTGAGTCTGGTG
MVH-18: GCCCAGCCGGCCATGGCAGARGTRAA
GCTTCTCGAGTCTGGA
MVH-19: GCCCAGCCGGCCATGGCAGAAGTGAA
RSTTGAGGAGTCTGG
MVH-20: GCCCAGCCGGCCATGGCAGAAGTGAT
GCTGGTGGAGTCTGGG
MVH-21: GCCCAGCCGGCCATGGCACAGGTTA
CTCTRAAAGWGTSTGGCC
MVH-22: GCCCAGCCGGCCATGGCACAGGTCCA
ACTVCAGCARCCTGG
MVH-23: GCCCAGCCGGCCATGGCACAGGTYCA
RCTGCAGCAGTCTG
MVH-24: GCCCAGCCGGCCATGGCAGATGTGAA
CTTGGAAGTGTCTGG
MVH-25: GCCCAGCCGGCCATGGCAGAGGTGAA
GGTCATCGAGTCTGG

Reverse primers

MJH-1: GGAGCCGCCGCCGCCAGAACCACCACC
ACCTGAGGAAACGGTGACCGTGGT
MJH-2: GGAGCCGCCGCCGCCAGAACCACCACC
ACCTGAGGAGACTGTGAGAGTGGT
MJH-3: GGAGCCGCCGCCGCCAGAACCACCACC
ACCTGCAGAGACAGTGACCAGAGT
MJH-4: GGAGCCGCCGCCGCCAGAACCACCACC
ACCTGAGGAGACGGTGACTGAGGT

Primers for Amplification V_κ and V_λ Gene

Forward primers

MVκ-1: GGCGGCGGCGGCTCCGGTGGTGGTGGTT
CTGACATTGTTCTCACCCAGTCTCC
MVκ-2: GGCGGCGGCGGCTCCGGTGGTGGTGGTT
CTGACATTGTGCTSACCCAGTCTCC
MVκ-3: GGCGGCGGCGGCTCCGGTGGTGGTGGTT
CTGACATTGTGATGACTCAGTCTCC
MVκ-4: GGCGGCGGCGGCTCCGGTGGTGGTGGTT
CTGACATTGTGCTMACTCAGTCTCC
MVκ-5: GGCGGCGGCGGCTCCGGTGGTGGTGGTT
CTGACATTGTGYTRACACAGTCTCC
MVκ-6: GGCGGCGGCGGCTCCGGTGGTGGTGGTT
CTGACATTGTRATGACACAGTCTCC
MVκ-7: GGCGGCGGCGGCTCCGGTGGTGGTGGTT
CTGACATTMAGATRACCCAGTCTCC
MVκ-8: GGCGGCGGCGGCTCCGGTGGTGGTGGTT
CTGACATTCAGATGAMCCAGTCTCC
MVκ-9: GGCGGCGGCGGCTCCGGTGGTGGTGGTT
CTGACATTCAGATGACDCAGTCTCC
MVκ-10: GGCGGCGGCGGCTCCGGTGGTGGTGGT
TCTGACATTCAGATGACACAGACTAC
MVκ-11: GGCGGCGGCGGCTCCGGTGGTGGTGGT
TCTGACATTCAGATGATTCAGTCTCC
MVκ-12: GGCGGCGGCGGCTCCGGTGGTGGTGGT
TCTGACATTGTTCTCAWCCAGTCTCC
MVκ-13: GGCGGCGGCGGCTCCGGTGGTGGTGGT
TCTGACATTGTTCTCTCCCAGTCTCC
MVκ-14: GGCGGCGGCGGCTCCGGTGGTGGTGGT
TCTGACATTGWGCTSACCCAATCTCC
MVκ-15: GGCGGCGGCGGCTCCGGTGGTGGTGGT
TCTGACATTSTGATGACCCARTCTC
MVκ-16: GGCGGCGGCGGCTCCGGTGGTGGTGGT
TCTGACATTKTGATGACCCARACTCC
MVκ-17: GGCGGCGGCGGCTCCGGTGGTGGTGGT
TCTGACATTGTGATGACTCAGGCTAC
MVκ-18: GGCGGCGGCGGCTCCGGTGGTGGTGGT
TCTGACATTGTGATGACBCAGGCTGC
MVκ-19: GGCGGCGGCGGCTCCGGTGGTGGTGGT
TCTGACATTGTGATAACYCAGGATG
MVκ-20: GGCGGCGGCGGCTCCGGTGGTGGTGGT
TCTGACATTGTGATGACCCAGTTTGC
MVκ-21: GGCGGCGGCGGCTCCGGTGGTGGTGGT
TCTGACATTGTGATGACACAACCTGC
MVκ-22: GGCGGCGGCGGCTCCGGTGGTGGTGGT
TCTGACATTGTGATGACCCAGATTCC
MVκ-23: GGCGGCGGCGGCTCCGGTGGTGGTGGT
TCTGACATTTTGCTGACTCAGTCTCC
MVκ-24: GGCGGCGGCGGCTCCGGTGGTGGTGGT
TCTGACATTGTAATGACCCAATCTCC
MVκ-25: GGCGGCGGCGGCTCCGGTGGTGGTGGT
TCTGACATTGTGATGACCCACACTCC
MVλ: GGCGGCGGCGGCTCCGGTGGTGGTGGT
TCTCAGGCTGTTGTGACTCAGGAATC

Reverse primers

MJκ-1: TGGAATTCGGCCCCCGAGGCCACGTTTG
ATTTCCAGCTTGG
MJκ-2: TGGAATTCGGCCCCCGAGGCCACGTTTT
ATTTCCAGCTTGG
MJκ-3: TGGAATTCGGCCCCCGAGGCCACGTTTT
ATTTCCAACTTTG
MJκ-4: TGGAATTCGGCCCCCGAGGCCACGTTTC
AGCTCCAGCTTGG
MJλ: TGGAATTCGGCCCCCGAGGCCACCTAGG
ACAGTCAGTTTGG
MLJ(Sfi): GTCCTCGTCGACTGGAATTCGGCCCCC-
GAGGCCAC

CHAPTER

60

Ribosome Display: *In Vitro* Selection of Protein–Protein Interactions

Patrick Amstutz, Hans Kaspar Binz, Christian Zahnd, and Andreas Plückthun

I. INTRODUCTION

Ribosome display is an *in vitro* technology to identify and evolve proteins or peptides binding to a given target (Fig. 1) (Hanes *et al.*, 2000a). While most selection technologies need living cells to achieve the essential coupling of genotype and phenotype, ribosome display uses the ribosomal complexes formed during *in vitro* translation to generate the physical coupling between polypeptide (phenotype) and mRNA (genotype) (Amstutz *et al.*, 2001). Hence, no transformation step limiting the size of the usable library is necessary, allowing the selection from very large combinatorial libraries. In addition, the rapid selection cycles require an integral polymerase chain reaction (PCR) step, which can be used for randomization, making this method ideal for directed evolution experiments. The fact that the ribosomal complex used for selection is not covalent allows an uncomplicated separation of the mRNA from the selected ribosomal complexes, even if the selected molecules bind the target with very high affinity or are even trapped covalently (Amstutz *et al.*, 2002; Jermutus *et al.*, 2001). All these benefits make ribosome display a good alternative to other selection techniques, such as phage display (Smith, 1985).

Ribosome display has been applied successfully for the selection of peptides (Matsuura and Plückthun, 2003; Mattheakis *et al.*, 1994), as well as folded proteins such as antibody fragments (Hanes and Plückthun, 1997; He and Taussig, 1997; Irving *et al.*, 2001). Ribosome display can also be considered for the screening of cDNA libraries for interaction partners. Ribosome display ultimately selects always for a specific binding event. However, by designing the selection pressure carefully, molecules can be selected for many other parameters, such as enzymatic turnover (by selection with a suicide inhibitor, or active site ligand) (Amstutz *et al.*, 2002; Takahashi *et al.*, 2002), protein stability (by selecting for binding under conditions where most library members will not fold) (Jermutus *et al.*, 2001), or protein biophysical properties (resistance to proteases and nonbinding to hydrophobic surfaces) (Matsuura and Plückthun, 2003). It is the combination of this array of selection pressures with the convenient PCR-based randomisation techniques that makes ribosome display a powerful and versatile technology.

II. MATERIALS AND INSTRUMENTATION

A. Reagents

The following chemicals and enzymes are necessary to prepare the extract and to perform ribosome-display selections: Luria broth base (GibcoBRL 12795-084); agarose (Invitrogen 30391-023); glucose (Fluka 49150); potassium dihydrogen phosphate (KH_2PO_4, Fluka 60230); dipotassium hydrogen phosphate ($K_2HPO_4{\cdot}3H_2O$, Merck 1.05099.1000); yeast extract (GibcoBRL 30393-037); thiamine (Sigma T-4625); Tris (Serva 37190); magnesium acetate (MgAc, Sigma M-0631); potassium acetate (KAc, Fluka 60034); L-glutamic acid monopotassium salt monohydrate (KGlu, Fluka 49601); 20 natural amino acids (Sigma LAA-21 kit); adenosinetriphosphate (ATP, Roche Diagnostics 519 987); phosphoenolpyruvate trisodium salt (PEP, Fluka 79435); pyruvate kinase (Fluka 83328);

Copyright 2006, Elsevier Science (USA).
All rights reserved.

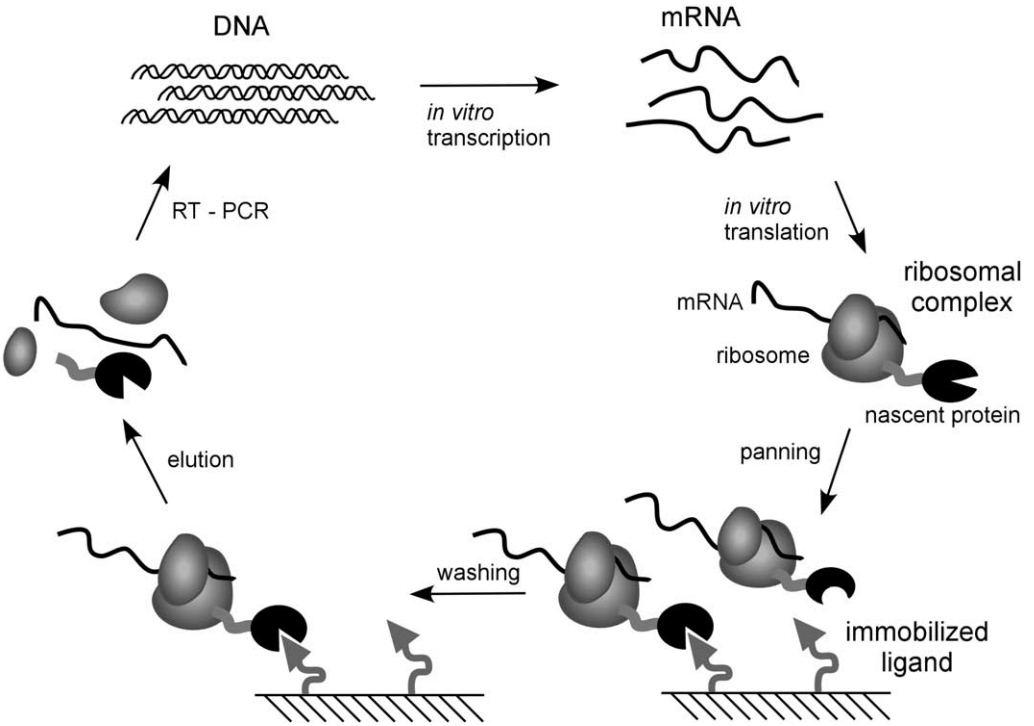

FIGURE 1 Ribosome-display selection cycle. The DNA of the library of interest, fused in frame to a spacer carrying no stop codon, is transcribed *in vitro*. The resulting mRNA is used for *in vitro* translation. After a short time of translation (a few minutes) the ribosomes have probably run to the end of the mRNA and synthesized the encoded protein, but because of the absence of the stop codon, the protein remains connected to the tRNA. Stopping the translation reaction in ice-cold buffer with a high Mg^{2+} concentration stabilizes this ternary complex, consisting of mRNA, ribosome, and nascent protein. The spacer, occupying the ribosomal tunnel, enables the domain of interest to fold on the ribosome. These ribosomal complexes are used for affinity selection. After washing, the mRNA of the selected complexes is released by complex dissociation. The genetic information of binders is rescued by RT-PCR, yielding a PCR product ready to go for the next selection cycle.

GTP (Sigma G-8877); cAMP (Sigma A-6885); acetylphosphate (Sigma A-0262); *Escherichia coli* tRNA (Sigma R-4251); folinic acid (Sigma 47612); PEG 8000 (Fluka 81268); 1,4-dithiothreitol (DTT, Promega V3155); sodium chloride (NaCl, Fluka 71376); Tween-20 (Sigma P-7949); neutravidin (Pierce 31000); bovine serum albumin (BSA, Fluka 05476), *Sacchoromyces cerevisiae* RNA (Fluka 83847); ribonuclease inhibitor RNasin (Promega N211B); reverse transcriptase Stratascript (50 U/µl, Stratagene 600085-51); 10× Stratascript buffer (Stratagene 600085-52); dNTPs (5 m*M* of each dNTP, Eurogentec NU-0010-50); DNA polymerase for PCR (e.g., Vent polymerase, NEB M0254L); PCR buffer (e.g., thermopol buffer, delivered with Vent polymerase), dimethyl sulfoxide (DMSO, Fluka 41640); NTPs (50 m*M*, Sigma); nitrocefin (Calbiochem 484400); HEPES (Sigma H-3375); spermidine (Sigma S-2501); T7 RNA polymerase (NEB M0251L); lithium chloride (LiCl, Fluka 62476); 100% ethanol (EtOH); sodium acetate (NaAc, Fluka 71180); heparin (Fluka 51550); disodium ethylenediaminetetraacetate (EDTA, Fluka 03680); T4 DNA ligase (MBI Fermentas EL0011); 4-morpholinopropanesulfonic acid (MOPS, Fluka 69949); boric acid (Fluka 15660); guanidine thiocyanate (Fluka 50990); *N,N*-dimethyl formamide (Sigma Aldrich 27.054-7); 37% formaldehyde (Fluka 47629); UHP water; if proteins are displayed that depend on the correct formation of disulfide bonds, protein disulfide isomerase should be used (PDI; Sigma P3818); [^{35}S]methionine (PerkinElmer NEG009H); triethylamine (Sigma-Aldrich 90335); OptiPhase2 scintillation liquid (PerkinElmer 1200-436).

B. Bacterial Strain and Plasmid

We use *E. coli* strain MRE600 for the preparation of the extract. This strain is RNase I deficient (Kushner, 2002) and does not contain any antibiotic resistance (Wade and Robinson, 1966).

Ribosome-display vector (pRDV), containing β-lactamase as insert (gene bank accession: AY327136).

C. Laboratory Equipment and Hardware

The following material is used in ribosome display: ART filter pipette tips (10 µl, 20 µl, 200 µl, 1000 µl, nucleic acid and nuclease-free tips, Molecular Bioproducts); QIAquick PCR purification and gel extraction kit (QIAgen 28104 and 28704); Maxisorp plate (Nunc-Immuno plate, Nunc 430341); step pipette (Eppendorf Multipipette Plus 4981 000.019) with 5- and 10-ml tips (Eppendorf 0030 069.250 and 0030 069.269); plastic seal (Corning Inc., Costar® 6524); RNase-free 1.5-ml reaction vials (MolecularBioProducts 3445); Roche high pure RNA isolation kit (Roche 1 828 655); 0.2-mm syringe filter (Millipore SLGPR25KS); dialysis tubing with a molecular weight cutoff of 6000–8000 Da (e.g., Spectrum Laboratories SpectraPor 132 650).

Furthermore, standard laboratory equipment is needed, such as Sorvall RC-5C Plus centrifuge with rotors SS-34 and GS-3 or equivalent; refrigerated table centrifuge; shaker incubator; 5-liter and 100-ml baffled shake flasks for *E. coli* culture; Emulsiflex (Avestin, Canada) or French Press (American Instrument Company, AMINCO); 4°C room; liquid nitrogen (N_2); ELISA plate shaker; UV/VIS spectrophotometer; agarose gel electrophoresis system; latex gloves, Speed-Vac (Savant Speed Vac Concentrator SVC100H); –20 and –80°C freezer; Scintillation counter.

III. PROCEDURES

A. Reagents

Preparation of S30 Extract

General considerations: 1 liter *E. coli* culture yields approximately 8 ml extract. If you plan to do ribosome display at a large scale, grow several cultures in parallel. It is important that the cells used for extract preparation are harvested in an early logarithmic phase. If the libraries used for selection contain disulfide bonds, one should omit DTT from the extract. If no disulfides need to be formed, 1 m*M* DTT can be added to the S30 buffer as it increases the translation efficiency slightly.

Preparation of the S30 extract is performed according to Lesley, Zubay, and Pratt, with minor modifications (Chen and Zubay, 1983; Lesley, 1995; Pratt, 1984; Zubay, 1973).

Buffers

The following buffers are used in standard ribosome-display selection rounds and we advise preparing stocks: Tris-buffered saline (TBS; 50 m*M* Tris–HCl, pH 7.4, at 4°C; 150 m*M* NaCl), TBS with Tween [TBST; TBS with 0.05% (500 µl/l) Tween-20], washing buffer with Tween (WBT; 50 m*M* Tris–acetate, pH 7.5, at 4°C; 150 m*M* NaCl; 50 m*M* MgAc; 0.05% Tween-20) and elution buffer (EB; 50 m*M* Tris–acetate, pH 7.5, at 4°C; 150 m*M* NaCl; 25 m*M* EDTA); 10× MOPS (0.2 *M* MOPS, pH 7, 50 m*M* sodium acetate, 10 m*M* EDTA); 10× TBE buffer (89 m*M* Tris-buffered saline, 89 m*M* boric acid, 10 m*M* EDTA).

Note: The washing buffer used for ribosome display can be adjusted to any particular requirements given by the target molecule. Different buffer salts and detergents are compatible, only the Mg^{2+} concentration should be held at around 50 m*M*. If a new buffer composition is applied, a ribosome-display test selection round with a known binder is recommended to determine compatibility.

Oligonucleotides

αssrA: (200 µ*M*, 5′-TTAAGCTGCTAAAGCGTAGTTTTCGTCGTTTGCGACTA-3′, standard quality)

T7B: Forward RD primer. Introduces T7 promotor and part of the 5′ loop (100 µ*M*, 5′-ATACGAAATTAATACGACTCACTATAGGGAGACCACAACGG-3′)

SDplus: Forward RD primer. Introduces the Shine–Dalgarno sequence and connects the T7 promoter with the FLAG tag: (100 µ*M*, 5′-AGACCACAACGGTTTCCCAATAATTTTGTTTAACTTTAAGAAGGAGATATATCCATGGCGGACTACAAAGATGACG-3′)

tolAk: Reverse primer for RD used with tolA as spacer introducing a stabilizing 3′ loop (100 µ*M* 5′-CCGCACACCAGTAAGGTGTGCGGTTTCAGTTGCCGCTTTCTTTCT-3′)

RDlinktolA: (100 µ*M*, 5′-GGGGAAAGCTTTATATGGCCTCGGGGGCCGAATTCGAATCTGGTGGCCAGAAGCAAGCTGAAGAGGCG-3′)

Primers (reverse and forward) specific for the library of interest, which must introduce appropriate restriction sites for ligation into the ribosome-display vector.

Solutions, Strain, and Hardware

Escherichia coli strain MRE600 (Wade and Robinson, 1966); Luria broth base; incomplete rich medium: 5.6 g/liter KH_2PO_4, 37.8 g/liter $K_2HPO_4{\cdot}3H_2O$, 10 g/liter yeast extract, 15 mg/liter thiamine—after autoclaving, add 50 ml 40% (w/v) glucose sterile filtered; 0.1 *M*

MgAc; 10× S30 buffer: 100 m*M* Tris–acetate, pH 7.5, at 4°C, 140 m*M* MgAc, 600 m*M* KAc—store at 4°C or chill buffer in ice bath before use; 10 ml preincubation mix—must be prepared immediately before use: 3.75 ml 2*M* Tris–acetate, pH 7.5 (at 4°C), 71 µl 3*M* MgAc, 75 µl amino acid mix (10 m*M* of each of the 20 natural amino acids), 0.3 ml 0.2*M* ATP, 0.2 g PEP, 50 U pyruvate kinase.

Material: 5-liter baffled flasks; shaker at 37°C for *E. coli* culture; refrigerated centrifuges (GS-3, SS-34); dialysis tubing MW cutoff 6000–8000 Da; emulsiflex or French press.

Steps

Day 1

1. Prepare an LB/glucose plate and streak out MRE600 on the plate. Grow it overnight at 37°C

2. Prepare all chemicals, media, and buffers for *E. coli* extract preparation: Autoclave 1 liter incomplete rich medium, 500 ml of LB/glucose medium, and one 100-ml and one 5-liter shake flask. Prepare 50 ml 40% glucose, 10 ml 0.1*M* MgAc, and 1 liter 10× S30 buffer (use it as 1× S30 buffer afterwards). All buffers should be stored at 4°C.

Day 2

3. Prepare an overnight preculture by inoculating 50 ml LB/glucose medium with a colony of MRE600, which is shaken overnight at 37°C.

Day 3

4. Add 1 liter incomplete rich medium into the 5-liter shake flask and add 50 ml 40% glucose and 10 ml 0.1*M* MgAc both by sterile filtration (0.2-µm syringe filter).

5. Inoculate the culture with 10 ml overnight culture (approximately 1%) and let it shake at 37°C to OD_{600} = 1.0–1.2. Then transfer the culture in an ice-water bath and quickly add 100 g ice (small shovel) to the culture. Shake the culture in the ice-water bath by hand for 5 min. Collect the cell pellet by centrifugation at 4°C (15 min, GS-3, 5000 rpm). Wash the pellet at least three times with 50–100 ml of S30 buffer.

6. Determine the weight of the pellets (typically 1–1.5 g/liter). The cell pellet can now be shock-frozen in liquid nitrogen and stored at –80°C until further processing. Do not store the pellets longer than 2 days.

Day 4

Do wear gloves during all following steps!

7. Thaw the pellets on ice and resuspend the cells in S30 buffer (50 ml). Centrifuge at 4°C, full speed, in an appropriate centrifuge to collect the cell pellet. Resuspend the cells in 4 ml/g (wet cell weight) S30 buffer.

8. Lyse the cells with one passage through an EmulsiFlex (approximately 17,000 psi) or a French press (at 1000 psi). Repeating passages will decrease translation activity. Centrifuge the lysate at 4°C for 30 min (SS-34, 20,000 *g*). Take the supernatant and repeat this centrifugation step.

9. Transfer the supernatant to a 50-ml Falcon tube. Add preincubation mix (1 ml/6.5 ml supernatant) and incubate at room temperature for 60 min by slowly shaking the tube. In this step most endogenous RNA and DNA will be degraded by nucleases and translation will run out.

10. Transfer the extract into a dialysis device (MW cutoff 6000–8000 Da) and dialyze the extract three times for at least 4 h each at 4°C against S30 buffer (500 ml).

Day 5

11. Transfer the extract into a single 50-ml tube. Aliquot the extract into RNase-free tubes immediately (e.g., 110- and 55-µl aliquots, use filter tips to avoid RNase contamination) and directly freeze the aliquots in liquid nitrogen. Store the aliquoted extract at –80°C (it will be fully active for months to years).

B. Premix Preparation and Extract Optimization

The premix provides the S30 extract with all amino acids (except for methionine, see later), tRNAs, the energy regeneration system, and salts, which are needed for translation. For optimal translation efficiency, every premix should be adjusted to fit the corresponding extract, especially with respect to the concentration of magnesium, potassium, PEG-8000, and amount of extract. The premix A recipe given later contains only minimal concentrations of KGlu, MgAc, and PEG-8000. By performing translations (compare Section III,F) using a test mRNA and by gradually adding increasing amounts of these components, the translation efficiency of the extract will be optimized to its maximal activity. The optimization of the premix to the S30 extract is optimally done by translating the mRNA encoding an enzyme, whose activity is determined easily, such as β-lactamase. We routinely use a cysteine-free version of the enzyme (Laminet and Plückthun, 1989) in a ribosome-display suitable format (described in Section III,C) for optimization.

Solutions

You will need approximately equivalent amounts of premix and extract. Premix A: 250 m*M* Tris–acetate, pH

7.5, at 4°C, 1.75 m*M* of each amino acid except methionine, 10 m*M* ATP, 2.5 m*M* GTP, 5 m*M* cAMP, 150 m*M* acetylphosphate, 2.5 mg/ml *E. coli* tRNA, 0.1 mg/ml folinic acid, and 4 μ*M* α-ssrA DNA. KGlu (180–220 m*M*), MgAc (5–15 m*M*), and PEG-8000 [0–15% (w/v)] have to be adjusted to the corresponding extract. β-Lactamase assay buffer: Dissolve 5.3 mg nitrocefin in 250 μl DMSO and add this to 50 ml 50 m*M* potassium phosphate buffer (pH 7) (Laminet and Plückthun, 1989).

Steps

To avoid RNase contamination, use filter tips and wear gloves for all of the following steps.

1. Mix all components to yield premix A.
2. Incubate the premix in a water bath at 37°C to solubilize all components.
3. Perform different *in vitro* translations in parallel of β-lactamase mRNA as described in (Section III,F). Add increasing concentrations of MgAc (5–15 m*M*), KGlu (180–220 m*M*), PEG-8000 [0–15% (w/v) of premix], and amount of extract (30–50 μl for a 110-μl translation reaction).
4. First optimize the MgAc concentration, then the KGlu concentration, and finally the PEG-8000 concentration. The translation time relevant for optimization should be around 10 min. Stop translation by diluting the reaction five times in WBT.
5. To detect β-lactamase activity, use a nitrocefin assay. Use 10–20 μl of the stopped translation per milliliter β-lactamase assay buffer and follow the reaction with a photospectrometer at 486 nm.
6. After determining the conditions giving the highest activity, add the chemicals at the optimal concentration to the premix A stock yielding premix Z, optimized for this very batch of extract.
7. Aliquot the premix Z in RNase-free tubes and shock freeze the samples in liquid nitrogen (e.g., 500-μl aliquots).

C. Preparation of the Ribosome-Display Construct

To perform ribosome display, one needs a high-quality library in the appropriate format. This section does not explain how to generate this library, as this depends entirely on the experimental goal, but rather how to convert an existing one into a format suitable for ribosome display.

A ribosome-display construct is composed of a T7 promoter, followed by a ribosomal-binding site and an open reading frame, which in turn consists of the library fused in frame to a C-terminal spacer polypeptide that has no stop codon (Figs. 2 and 3). The lack of a stop codon prevents the binding of the termination factors TF-1, TF-2, and TF-3. A high magnesium concentration "sinters" the ribosome, which consists largely of folded RNA with a protein coat. The low temperature presumably prevents the hydrolysis of the peptidyl-tRNA and minimizes mRNA degradation. All these measures together ensure that the ternary complex of mRNA (genotype), ribosome, and displayed protein (phenotype) remains stable. The C-terminal spacer (usually derived from tonB, tolA, M13 gpIII or pD), which will partially remain in the ribosomal tunnel, ensures that the library protein can fold and is displayed on the ribosome. The T7 promoter allows efficient *in vitro* transcription of the construct. A 5′ and a 3′ stem loop protect the mRNA against exonucleases.

Solutions, Plasmids and Strains

QIAquick PCR purification and gel extraction kit; pRDV; appropriate restriction enzymes; T4 DNA ligase.

1. Generation of the Ribosome-Display Construct via pRDV

To accelerate the procedure of bringing a library into the ribosome-display format, we generated a vector containing the necessary flanking regions (ribosome-display vector, pRDV; Fig. 2). The library is PCR amplified, cut with the appropriate restriction enzymes, and ligated into the vector such that it is in frame with the spacer (Fig. 3). A second PCR on this ligation product directly amplifies the library with all features necessary for ribosome display: the T7 promoter, the RBS, and the spacer without stop codon (Fig. 2). This PCR product is used directly for *in vitro* transcription to yield the library mRNA ready to go. The main advantages of the ribosome-display vector are that it can be generated in large amounts (mini to maxi prep), it is easy to handle, and always provides error-free library flanking regions. The use of the vector is not only interesting for the initial generation of the ribosome-display construct, but also for the first selection rounds. If one only amplifies the library gene of the selected clones after the panning procedure without all the flanking regions, one is able to even recover library members partly degraded by RNases in the flanking regions. The recovered genes are then religated into pRDV and one is again ready to go for another round of selection.

Steps

1. Amplify the library with primers carrying the appropriate restriction sites for cloning into pRDV (Fig. 3).

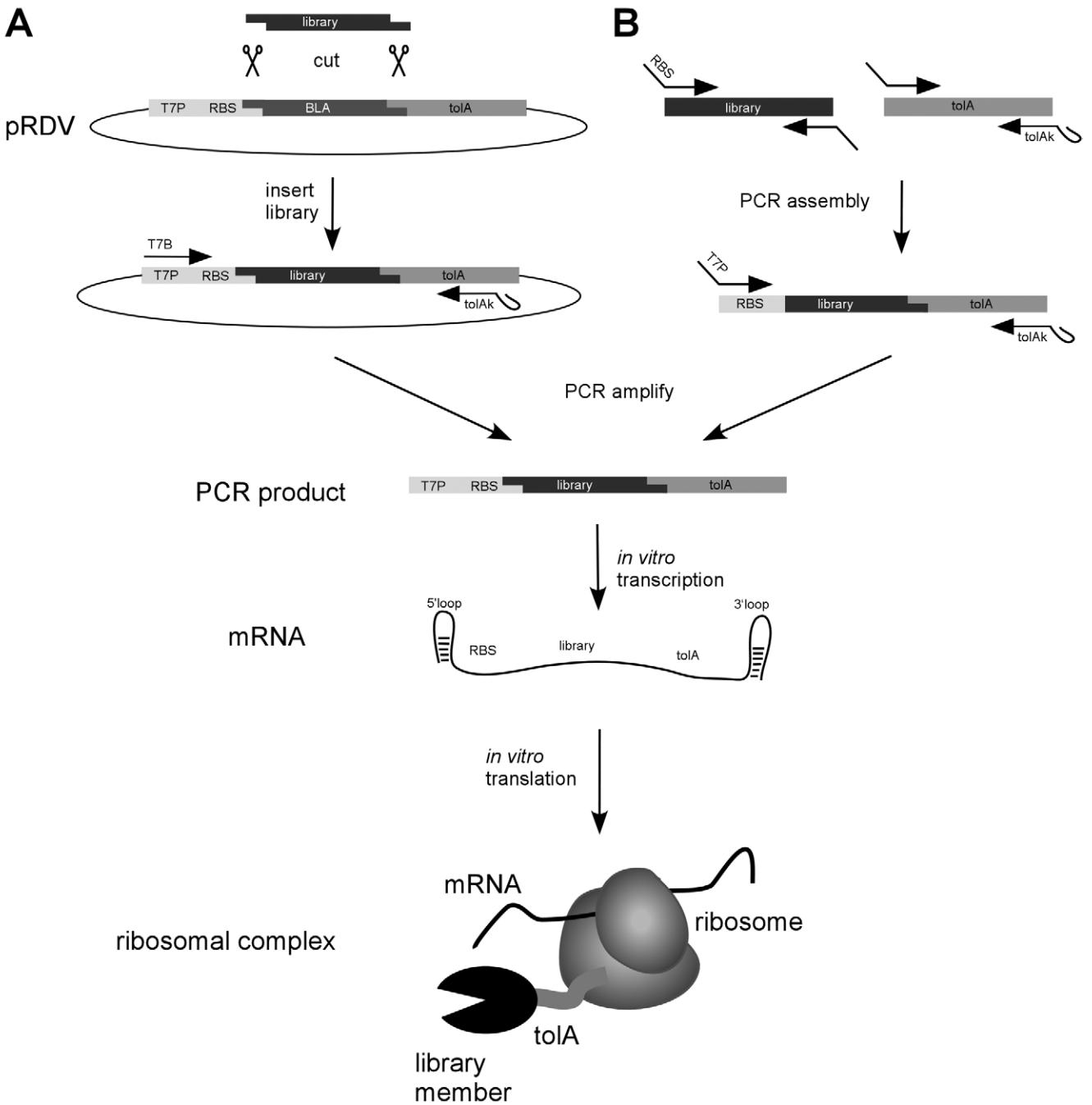

FIGURE 2 Generation of the ribosome-display construct. For ribosome display the library of interest has to be flanked by an upstream promoter region and a C-terminal spacer carrying no stop codon (Fig. 3). **(A)** The library is PCR amplified with primers carrying restriction sites suitable for ligation into the ribosome-display vector (pRDV), which carries the necessary library flanking regions. The PCR product of the library is digested and ligated into pRDV. A second PCR on this ligation reaction with the primers T7B and tolAk yields a PCR product ready for *in vitro* transcription. **(B)** Alternatively, the ribosome-display construct can be generated by assembly PCR. The library and the spacer are PCR amplified separately with primers so that the C-terminal part of the library and the N-terminal part of the spacer share overlapping sequences. An assembly PCR with the library and the spacer DNA, using appropriate primers, finally yields the ribosome-display construct. *In vitro* transcription of the PCR product of either **A** or **B** yields mRNA carrying 5′ and 3′ stem loops (which make the mRNA more stable toward exonuclease digestion), a ribosome-binding site (RBS), the library of interest, and a spacer carrying no stop codon. By stopping the *in vitro* translation in ice-cold buffer with high Mg^{2+} concentration, stable ternary complexes of mRNA, ribosome, and nascent protein are formed, ready for panning.

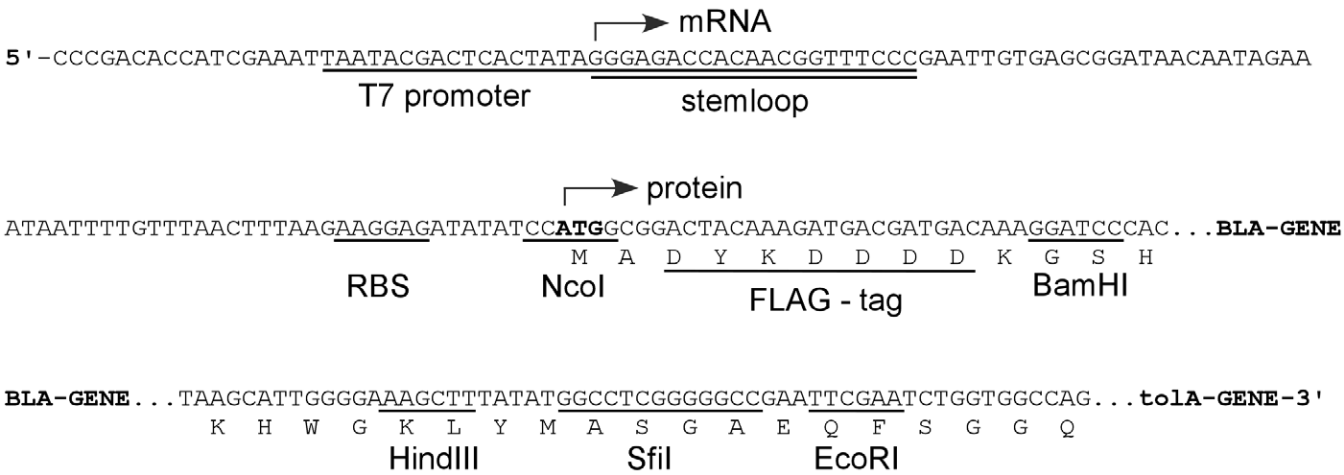

FIGURE 3 DNA sequence of the expression cassette of the ribosome-display vector (pRDV). mRNA is produced from a T7 promoter starting with a 5′ stem loop, with no additional overhang. The ribosome-binding site (RBS), also called Shine–Dalgarno sequence, is located upstream of the start codon. The open reading frame consists of a FLAG tag, the β-lactamase gene (serving as a dummy insert) in frame with a protein spacer, here *tolA*. Different restriction sites allow cloning of the library into pRDV to replace the β-lactamase gene.

2. Digest the PCR product and purify it using QIAquick columns (≥150 ng; amount depending on the library size). pRDV is digested, optionally dephosphorylated, and the backbone is agarose gel purified. The vector insert has to be removed, as it would also ligate to the library DNA, decreasing the final complexity.

3. Ligate the PCR product of the library into pRDV (molar ratio insert : vector = 7 : 1).

4. Perform a PCR reaction on the ligation mix with the forward primer T7B (annealing on the T7 promoter with a stabilizing 5′ loop) and the reverse primer tolAk (annealing on the C-terminal spacer carrying a stabilizing 3′ loop).

5. Analyze the DNA on an agarose gel, checking size, purity, and amount. If the band is sharp and indicates a concentration higher than 40 ng/μl, the PCR product is used directly (i.e., without purification) for *in vitro* transcription.

2. *Generation of the Ribosome-Display Construct via Assembly PCR*

In some cases, it may be preferable not to ligate the library into pRDV, but to use PCR assembly to generate the ribosome display construct (Fig. 2). In this case, both the library and the spacer (e.g., tolA) are PCR amplified so that the 3′ end of the library and the 5′ end of the spacer share overlapping sequences (Fig. 2). The PCR products of the library and the spacer are assembled and amplified with the primers SDplus (introducing the ribosome-binding site and the connection to the T7 promoter) and tolAk. A final PCR reaction with the primers T7B (introducing the T7 promoter) and tolAk completes the construct, ready for transcription (Fig. 2).

Steps

1. Amplify the library of interest with appropriate primers, introducing the FLAG tag at the 5′ end of the library, on which the primer SDplus can anneal in step 3. The reverse primer should anneal on the library and add an overlap corresponding to RDlinktolA. There is no need to introduce restriction sites; however, we strongly recommend the use of the same primers as for the cloning into the RDV to have the possibility of using pRDV and to reduce the number of different fragments.

2. Amplify the ribosome-display spacer using the primers RDlinktolA (forward) and tolAk (reverse). Thereby, the forward primer generates an overlap between the library and the spacer.

3. In an assembly PCR reaction, the spacer is fused to the library. Mix DNA of the library with an excess of spacer DNA and perform 7 cycles of PCR without the addition of primers. For this step, we use a lower annealing temperature as for the normal amplification. After 7 cycles, add primers tolAk and SDplus to the reaction and perform another 25 cycles of amplification.

4. Isolate the full-length band from an agarose gel and amplify the band using the primers T7B and tolAk.

5. Analyze the DNA on an agarose gel, checking

size, purity, and amount. If the band is sharp and indicates a concentration higher than 40 ng/µl, the PCR product is used directly (i.e., without purification) for *in vitro* transcription.

D. Transcription of PCR Products

Solutions and Hardware

5× T7 polymerase buffer: 1 *M* HEPES-KOH, pH 7.6, 150 m*M* MgAc, 10 m*M* spermidine, 200 m*M* DTT; NTPs (50 m*M* each); T7 RNA polymerase; RNasin; 6 *M* LiCl; 70% EtOH; 100% EtOH; 3 *M* NaAc; agarose; guanidine thiocyanate; formamide; 37% formaldehyde; MOPS; Speed-Vac; heating blocks; UV/VIS spectrophotometer.

Steps

To avoid RNase contamination, use filter tips and wear gloves for all of the following steps.

1. Mix the components for the following reaction using the PCR product from Section III,C. The PCR product should not be purified. Add 20.0 µl 5× T7 polymerase buffer, 14.0 µl NTPs (50 m*M* each), 4.0 µl T7 RNA polymerase, 2.0 µl RNasin, 22.5 µl PCR product (unpurified PCR reaction), and 37.5 µl UHP water. Let the transcription reaction run for 2–3 h at 37–38°C.
2. Add 100 µl UHP water and 200 µl 6 *M* LiCl, both ice cold, and place on ice for 30 min, before centrifugation at 20,000 *g* (4°C, 30 min). Discard supernatant and wash the pellet with 500 µl ice-cold 70% EtOH. Dry the pellet on the bench (5 min, open lid) and take it up in 200 µl ice-cold UHP water. Make sure it is dissolved completely before centrifuging at 20,000 *g* (4°C, 5 min).
3. Transfer 180 µl supernatant to a new tube and add 20 µl 3 *M* sodium acetate and 500 µl ice-cold 100% EtOH. Keep the solution on ice or at –20°C for 30 min before centrifuging it at 20,000 *g* (4°C, 30 min). Discard the supernatant and wash the pellet with 500 µl ice-cold 70% EtOH. Discard the supernatant and dry the pellet in a Speed-Vac apparatus.
4. Take up the mRNA pellet in 30 µl ice-cold UHP water and make sure it is dissolved completely. Take 2 µl of this solution and dilute to 500 µl with ice-cold UHP water for OD_{260} quantification and immediately N_2 freeze the rest of the RNA for further use.
5. Immediately (the RNA will be degraded and the signal will increase) measure the OD_{260}. For RNA, an OD_{260} of 1 corresponds to a concentration of 40 µg/ml.
6. Add UHP water to the RNA stock in order to reach a standard concentration of 2.5 µg/µl.
7. The RNA quality can optionally be checked by agarose gel electrophoresis. Cast an agarose gel (1.5%, depending on your RNA size) adding 2% (w/v) of 1 *M* guanidinium thiocyanate. Denature 5 µg (i.e., 2 µl) RNA for 10 min at 70°C in 15.5 µl sample buffer (10 µl formamide, 3.5 µl 37% formaldehyde, 2 µl 5× MOPS), place it on ice, add 2 µl DNA loading buffer (50% glycerol, 1 m*M* EDTA in H_2O), and run the gel.

E. Target Molecule Immobilization

To perform a selection, the target molecule must be immobilized in a conformation relevant for further applications. Typically, a protein will have to be in its native conformation. A very promising way to achieve this to biotinylate the target molecule and immobilize it via neutravidin or streptavidin. Biotinylation can be done chemically with commercially available reagents, either attaching the biotin to cysteine or lysine residues. The problem of this unspecific approach is that biotinylation might destroy epitopes. Alternatively, the target protein can be expressed in recombinant form with a biotinylation tag, i.e., a peptide sequence, which is recognized and biotinylated by the *E. coli* biotinylation enzyme BirA (Schatz, 1993). If for any reason biotinylation is not an option, one can either immobilize the target molecule directly on the hydrophobic surface of a microtiter plate well or use a specific antibody, which itself can be immobilized easily via protein A or G. Note that the buffers used here may have to be adapted to the needs of the target molecules.

Solutions and Hardware

TBS, TBST, WBT at 4°C
Maxisorp plate; plastic seal; step pipette; plate shaker; 20 µ*M* stock neutravidin; BSA; target molecule of choice

Steps

To avoid RNase contamination, use filter tips and wear gloves for all of the following steps. We also recommend carrying out the selection, RT and PCR in duplicate, to check the reproducibility of the selection. Therefore, one target molecule is routinely immobilized in two wells.

Day 1

1. Wash a Maxisorp plate three times with TBS and beat dry. Pipette (with a step pipette) 100 µl of a 66 n*M* neutravidin solution in TBS into the wells. Seal with plastic and store overnight at 4°C. If the target molecule is not biotinylated it can also be directly immobilized by the same procedure as neutravidin, but it might denature at least partly during this procedure.

Day 2 (Day of the Ribosome-Display Round)

2. Wash the plate incubated overnight with cold TBS three times. Add 300 µl 0.5% BSA in TBS to the wells (with a step pipette) to block all hydrophobic

surfaces with BSA. Seal the plate with plastic and incubate on a shaker for 1 h at room temperature. Alternatively, sensitive or fragile targets should be incubated for 2.5 h at 4°C. If the target molecule is immobilized directly, incubate the BSA solution for 2 h at 4°C and proceed directly to step 5.

3. Wash the plate three times with TBS, beat dry, and add 200 µl 0.5% BSA in TBS to each well (step pipette).

4. Add 5 µl of the target molecule (~10 µ*M*) to the respective well. Use a biotinylated target molecule void of free biotin. Seal with plastic and incubate on a shaker for 1 h at 4°C. To avoid binders to BSA or neutravidin, it is recommended to immobilize the target molecule only in every second well and use the alternate wells for prepanning.

5. Wash the plate four times with TBS to get rid of the unbound target molecule. Wash at least once with WBT (step pipette) to equilibrate the well with the ribosome-display buffer. Incubate wells that will not be used directly for panning with WBT (amount of liquid as will be used for panning). Keep the plate at 4°C.

F. *In Vitro* Translation

Solutions

UHP water; WBT; WBT with 0.5% BSA; heparin (200 mg/ml); methionine (200 m*M*); S30 extract; premix Z; the mRNA of the library; optionally PDI (4 mg/ml, reconstituted from lyophilized protein); all buffers should be kept on ice, the RNA in liquid nitrogen unless stated otherwise

Steps

We recommend carrying out the panning in duplicate to check the reproducibility of the selection. To avoid RNase contamination, use filter tips and wear gloves for all of the following steps.

1. Mix the following components (amounts given are for one reaction): 13.0 µl UHP water, 2.0 µl Met (200 m*M*), 41.0 µl premix Z (thaw on ice, vortex before pipetting), and 50.0 µl extract. Volumes might vary, depending on the batch of S30 extract. This mix can be kept on ice for a short period (few minutes). If disulfide bridges are to be formed, add 0.625 µl PDI (4 mg/ml).

2. Add 4 µl mRNA (2.5 µg/µl) into a fresh RNase-free tube and freeze it in liquid nitrogen.

3. Add the translation mix to the frozen mRNA, dissolve the pellet by flicking the tube, and translate for 6–12 min at 37°C.

4. In the meantime, prepare 440 µl stopping buffer [WBT with 0.5% BSA and 12.5 µl/ml heparin (200 mg/ml)] in RNase-free tubes and put them on ice.

5. After the 6- to 12-min translation, pipette 100 µl translation into the ice-cold stopping buffer to stop translation (always keep the ribosomal complexes on ice or at 4°C).

6. Centrifuge at 20,000 *g*, 4°C for 5 min and use the supernatant containing the ribosomal complexes for panning.

G. Panning

Solutions and Hardware

WBT; EB; yeast RNA (25 µg/µl); cold room; microtiter plate shaker; Roche High Pure RNA isolation kit

Steps

All the following steps should be performed in a cold room (at 4°C or slightly below). The low temperature guarantees complex and mRNA stability. Under such conditions ribosomal complexes have survived off-rate selection procedures of 10 days and longer. During all binding and elution steps, shake the microtiter plate gently. To avoid RNase contamination, use filter tips and wear gloves.

1. Add 100–200 µl stopped translation mix to the well, where no target molecule is immobilized and incubate for 1 h. In this prepanning step, all BSA-binding, neutravidin-binding, or simply sticky complexes are removed. If unspecific complexes are causing problems, more than one prepanning step should be done.

2. Transfer the solution to the well with the immobilized target molecule and incubate for 1 h.

3. Wash the well to remove nonbinding complexes. The time span of the washing step and the number of washing steps define the selection pressure. One usually starts with short washing times in the first rounds (only rinsing six times) and increases the washing periods for later rounds (up to 3–4 h). As washing is always a dilution, it is important to fill the wells to the top and exchange the buffer many times (at least six times, in all rounds!). If harsher selection pressure than simple washing is required, e.g., to select for affinities below nanomolar, one should consider immobilisation of low target molecule concentrations, competitive elution (with free target molecule in the solution), or off-rate selection procedures (see Section III,J).

4. Before the mRNA of the selected complexes is eluted, prepare three RNase-free tubes for each well to be eluted: one tube with 400 µl lysis buffer of the Roche RNA purification kit to purify the RNA, one tube to collect the purified mRNA, and one tube for reverse transcription. Also prepare one Roche-RNA

purification column for each well to be eluted. Label all tubes and columns appropriately.

5. Calculate and prepare the amount of elution buffer you need (200 µl/well) and add 50 µg/ml *S. cerevisiae* RNA (2 µl/ml of a 25-µg/µl stock) to it. Keep the buffer on ice.

6. Elution is done in the cold room. Wash your well one last time with WBT, remove the supernatant completely, and beat the plate dry. Add 100 µl elution buffer, shake for 10 min, transfer this eluate to the tube containing the lysis buffer, and mix well. Repeat this procedure with another 100 µl of elution buffer. In the lysis buffer, the RNA is stable and can be brought to room temperature.

H. RT-PCR

Solutions and Hardware

Roche High Pure RNA isolation kit; 100 m*M* DTT; RNasin; Stratascript (50 U/µl; Stratagene); dNTPs; DNA polymerase; oligonucleotides; 10x Stratascript buffer; polymerase buffer; DMSO; agarose

Steps

The RNA purification is done according to the Roche protocol, with slight modifications. All the centrifugation steps are carried out at 4°C.

mRNA Purification

1. Just before RNA purification, thaw the reagents for reverse transcription (DTT, 10x Superscript buffer, dNTPs, oligonucleotide for reverse transcription).

2. Set two heating blocks to 70°C and 50°C, respectively.

3. Apply the lysis buffer/eluate mixture on the column and spin for 1 min at 8000 *g*. Discard the flow-through and wash with 500 µl buffer 1 (black-capped bottle in the Roche kit; the DNase incubation step, described in the Roche protocol is not necessary). Discard the flow through and wash with 500 µl buffer 2 (blue-capped bottle in the Roche kit). Discard the flow through. Add 100 µl buffer 2 (blue cap) and spin for 2 min at 13000 *g*. Transfer the column to a tube to collect the RNA.

4. Elute with 30 µl Roche elution buffer (at 8000 *g* for 1 min) and directly put the RNA containing collection tube to 70°C for 10 min to denature the RNA. During this incubation time, pipette the reverse transcription (i.e., directly proceed with step 5).

Reverse Transcription.

5. In a master mix tube, add the following components (amounts given are for one reaction): 0.25 µl reverse primer (100 µ*M*), 0.5 µl dNTP (5 m*M* each), 0.5 µl RNasin, 0.5 µl Stratascript, 2.0 µl 10x Stratascript buffer, 2.0 µl DTT (100 m*M*), and 2.0 µl UHP water. Distribute the RT mix (7.75 µl) to the previously labelled tubes and keep them on ice.

6. Spin the denatured eluted RNA samples shortly and set them on ice. Add 12.25 µl of the eluted RNA to the RT-mix (N_2 freeze the rest of the RNA directly after adding it to the reaction).

7. Place the RT reaction on a 50°C heat block for 45 min.

PCR

8. Mix the following components (amounts given are for one reaction): 5.0 µl Thermopol buffer, 2.0 µl dNTPs, 2.5 µl DMSO, 1.0 µl forward primer (100 µ*M*), 1.0 µl reverse primer (100 µ*M*), 5.0 µl RT template, 0.5 µl polymerase, and 33.0 µl UHP water. PCR results can be improved if a hot start is performed (adding the polymerase in the 5-min preincubation step at 95°C).

9. Run the following PCR program (to be adapted according to primers and template): 5 min at 95°C, *X* times (30 s at 95°C, 30 s at 50°C, 1 min at 72°C), 5 min at 72°C, and 4°C infinitely. Adjust the number of cycles (*X* = 25–45) to the corresponding selection round.

10. Verify the PCR product quality by an appropriate agarose gel electrophoresis.

11. Usually the quality of the PCR product is not good enough to be used directly for *in vitro* transcription to generate mRNA for the next round. Gel purify the desired band and perform a second PCR on the purified first PCR to yield high-quality DNA.

12. If you wish to check the pool of selected clones for binders, ligate the selected library members after PCR amplification into a vector suitable for expression, transform *E. coli* to obtain individual clones, and test binding specificity, e.g., by crude extract ELISA. To assess the specificity of the binders, one can either compare binding of the selected molecules to the specific target molecule with the binding to an unrelated molecule or test that the specific binding can be inhibited by adding the purified unbiotinylated target molecule. The level of inhibition gives a first crude estimate of the affinity.

Troubleshooting

RT-PCR. If the RT-PCR with the forward (e.g., T7B) and reverse (e.g., tolAk) primers does not yield a high-quality product, one can amplify only the coding region of the selected library members. This usually improves the yield and the quality of the PCR product. This is most likely due to the fact that RNases degrade the mRNA from the ends. Amplifying only the central (library) stretch can rescue partly degraded clones. The

PCR product of the library stretch is subsequently religated into pRDV as described in Section III,C. As this procedure rescues more clones than the PCR of the whole construct, we would recommend it for the first rounds to guarantee that no binders are lost.

Panning Controls. Ribosome display has many error-sensitive steps. It is therefore recommended to do panning, RT, and PCR in duplicate to check the reproducibility of the selection. Specific binders should be enriched from round to round. This should correlate with the number of PCR cycles needed to amplify the DNA after RT, which should decrease from round to round. Usually, one can reduce the cycle number by around five per round. If the selection pressure is increased, the yield will drop. When enrichment is observed (for designed ankyrin repeat protein libraries, (Binz et al., 2004) e.g., after round two, while for antibody libraries after round three to four), one can test the specificity of the selected pool by comparing panning results against the correct and an unrelated target molecule. If the pool is specific, only the correct target molecule will give a PCR product after RT. If the pool also gives a signal with the unspecific target molecule, the majority of the clones are still unspecific. However, there may also be a population of specific binders in the pool. An additional panning round with increased prepanning can reduce the background. Alternatively, single clone analysis might directly yield specific binders.

I. Radioimmunoassay (RIA)

Radioimmunoassay is another fast and convenient method to check whether specific target-binding molecules have been enriched in a pool (Hanes *et al.*, 1998). It can be used for the evaluation of both selected pools and individual binders. RNA of a pool or single binder is translated in the presence of radioactively labelled [^{35}S]-methionine. Therefore, the radioactive protein that binds to the surface-immobilized target molecule can be quantified easily. The binding should be performed in the presence and absence of soluble competitor target molecules, and a control for unspecific binding should be included. In the competition assay, the minimal concentration of competitor still leading to half-inhibition of the maximal binding signal is a crude measure for the affinity. Therefore, RIA facilitates the ranking of the affinities of different clones isolated after affinity maturation.

Solutions and Hardware

The general handling is the same as for the *in vitro* translation. However, the radioactive material must be handled with the appropriate precautions. Do the radioactive work in a designated area of your laboratory. We recommend using filter tips and wearing gloves during the experiment. We recommend doing the RIA in duplicate.

UHP water; WBT; WBT with 0.5% BSA; milk powder; heparin (200 mg/ml); [^{35}S]-methionine (10 mCi/ml, 1175 Ci/mmol); S30 extract; premix Z; mRNA of a selected pool or single binders; pRDV; optionally PDI (4 mg/ml); 0.1 *M* triethylamine; liquid scintillation cocktail "OptiPhase2"

Scintillation counter, ELISA plate shaker

Steps

RNA Preparation

1a. The analysis of whole pools of potential binders can be performed similarly to a normal ribosome-display round. A PCR reaction is performed on the selected pool but with primers introducing a 3′ stop codon and the standard ribosome display 5′ end (including T7 promotor and ribosome-binding site). From this PCR product, RNA is produced as described in Section III,D.

1b. Alternatively, if you wish to analyze single binders, digest the PCR product from step 1a with the appropriate restriction enzymes and ligate into the ribosome-display vector (RDV). After transformation, isolate plasmids from single colonies. The transcription can be performed directly from the plasmid, which should be present at a concentration of at least 100 ng/µl.

RIA

2. Prepare a Maxisorp plate with immobilized target molecules as described in Section III,E.

3. Perform *in vitro* translations as described in Section III,F with the following modifications: instead of cold methionine use 2 µl of [^{35}S]-methionine (0.3 µ*M*, 50 µCi/ml final concentration) per 110-µl reaction and perform translation for 30–45 min at 37°C.

4. Stop the translation with 440 µl WBT and centrifuge the samples for 5 min at 14,000 rpm, 4°C.

5. Aliquot the supernatant and dilute the samples with 4% milk in WBT to a final concentration of 1% milk. For inhibition studies, different concentrations of competitor should be added to the different aliquots and the mixture should be equilibrated for 1 h at room temperature prior to step 6.

6. Split the samples to at least duplicates and apply them to the blocked plate. Let the protein bind to the target molecule by shaking slowly for maximally 30 min.

7. Wash the plate rigorously 5–10 times with WBT.
8. Elute bound protein with 100 µl of a 0.1 *M* solution of triethylamine (10 min at room temperature).
9. Transfer the eluates into scintillation tubes containing 5 ml scintillation solution "OptiPhase2."
10. Quantify the radioactivity in a scintillation counter.

IV. COMMENTS

This section states some observations we have made during the years of performing ribosome display and gives a summary of how ribosome display can be used for directed evolution experiments.

A. Selection from Naïve Libraries

Naïve libraries, in our hands synthetic antibody libraries or designed repeat protein libraries, are a difficult challenge for selection experiments. The task is to select the specific binders, which are few in numbers, out of a very large number of nonbinders. The outcome of such experiments is not only dependent on the presence of high-affinity binders in the library, but also on the behavior, or "stickiness," of the rest of the library population. In other words, selection must be directed toward specific binding, in contrast to nonspecific binding. This can be achieved with experimental tricks, such as introducing a prepanning step, or by trying to reduce the stickiness of the library population. For selection with naïve scFv libraries, it has turned out that six selection rounds were necessary to obtain specific binders (Hanes *et al*., 2000b). The designed ankyrin repeat protein libraries routinely yield binders after only three to four rounds (Binz et al., 2004). We suspect this might be due to the fact that these repeat proteins, which are extremely well expressed in *E. coli*, fold well, and are very stable, are also displayed better *in vitro* than scFv fragments, which are intrinsically somewhat more aggregation prone.

B. Affinity Maturation of Binders

In vitro evolution, the alternation of diversification and selection, is a powerful strategy used to improve proteins. Ribosome display is an ideal platform to perform such experiments. It allows very fast selection cycles and the PCR step is ideal to generate diversity in between the selection rounds. This diversification of the selected pools by random mutations increases the sampled sequence space. Error-prone PCR, e.g., using high Mn^{2+} concentrations (Leung *et al*., 1989), imbalanced dNTP concentrations (Cadwell and Joyce, 1994), or nucleotide analogues (Zaccolo and Gherardi, 1999; Zaccolo *et al*., 1996), is one strategy often applied to achieve diversification. Another powerful strategy to create diversity is DNA shuffling on the selected pools in between the rounds (Stemmer, 1994).

When compared to a selection experiment from a naïve library, the challenge in affinity maturation is different. The applied library will usually be created from a single clone or a pool of clones, which are already good binders. Since in affinity maturation we do not wish to select for binding as such but for better binding, we need an adjustable selection pressure (Jermutus *et al*., 2001). In principle, two strategies can be used to select tight binders out of a pool of binders.

The first affinity maturation strategy is to supply very little of the immobilized antigen. The concept is that the binders all compete with each other and, at equilibrium, the tight binders keep the binding spaces occupied. In practice, however, there are several complications to this concept. At extremely low target molecule concentrations, the relative proportion of unspecific binding sites gets very high (BSA, neutravidin) so that great care has to be taken to avoid unspecific binders. Also, if medium-affinity binders outnumber the tight binders, the enrichment will be very slow. Finally, if binding is very tight, the equilibrium is reached exceedingly slowly.

The second very successful strategy for affinity maturation is off-rate selection. The assumption fundamental to off-rate selection is that the on-rate of most protein–protein interactions is in the range of 10^5–$10^6\,M^{-1}\,s^{-1}$ (Wodak and Janin, 2002) and protein–ligand interactions in the range of 10^6–$10^7\,M^{-1}\,s^{-1}$, such that the affinity is largely governed by the off-rate. By first incubating the ribosome-displayed polypeptide with the biotinylated target molecule (typically for 1 h) followed by the addition of a large excess of nonbiotinylated target (1000-fold excess), the selection pressure is governed by the dissociation of the binders from the biotinylated target. While tight binders will remain bound to the biotinylated target, others will dissociate and then rebind to the excess of unbiotinylated target. The incubation time equals the selection pressure and should be adjusted to the expected off-rate. If the recovery is poor, it is often useful to include a nonselective round to enrich the binders.

C. Evolution of Properties Other Than High-Affinity Binding

The selection strategies for molecular properties other than high-affinity binding were summarised in Section I. A library can be evolved for these properties,

just as it can be for affinity. It exceeds the scope of this chapter to discuss each strategy in detail, and there are many more possibilities that have not been explored experimentally.

Acknowledgment

The authors thank all former and present members of the Plückthun laboratory involved in ribosome display who helped in developing the present protocol.

References

Amstutz, P., Forrer, P., Zahnd, C., and Plückthun, A. (2001). *In vitro* display technologies: Novel developments and applications. *Curr. Opin. Biotechnol.* **12**, 400–405.

Amstutz, P., Pelletier, J. N., Guggisberg, A., Jermutus, L., Cesaro-Tadic, S., Zahnd, C., and Plückthun, A. (2002). *In vitro* selection for catalytic activity with ribosome display. *J. Am. Chem. Soc.* **124**, 9396–9403.

Binz, H. K., Amstutz, P., Kohl, A., Stumpp, M. T., Briand, C., Forrer, P., Grütter, M. G., and Plückthun, A. (2004). High-affinity binders selected from designed ankyrin repeat protein libraries. *Nature Biotechnol.* **22**, 575–582.

Cadwell, R. C., and Joyce, G. F. (1994). Mutagenic PCR. *PCR Methods Appl.* **3**, 136–140.

Chen, H. Z., and Zubay, G. (1983). Prokaryotic coupled transcription-translation. *Methods Enzymol.* **101**, 674–690.

Hanes, J., Jermutus, L., and Plückthun, A. (2000a). Selecting and evolving functional proteins *in vitro* by ribosome display. *Methods Enzymol.* **328**, 404–430.

Hanes, J., Jermutus, L., Weber-Bornhauser, S., Bosshard, H. R., and Plückthun, A. (1998). Ribosome display efficiently selects and evolves high-affinity antibodies *in vitro* from immune libraries. *Proc. Natl Acad. Sci. USA* **95**, 14130–14135.

Hanes, J., and Plückthun, A. (1997). *In vitro* selection and evolution of functional proteins by using ribosome display. *Proc. Natl Acad. Sci. USA* **94**, 4937–4942.

Hanes, J., Schaffitzel, C., Knappik, A., and Plückthun, A. (2000b). Picomolar affinity antibodies from a fully synthetic naive library selected and evolved by ribosome display. *Nature Biotechnol.* **18**, 1287–1292.

He, M., and Taussig, M. J. (1997). Antibody-ribosome-mRNA (ARM) complexes as efficient selection particles for *in vitro* display and evolution of antibody combining sites. *Nucleic Acids Res.* **25**, 5132–5134.

Irving, R. A., Coia, G., Roberts, A., Nuttall, S. D., and Hudson, P. J. (2001). Ribosome display and affinity maturation: From antibodies to single V- domains and steps towards cancer therapeutics. *J. Immunol. Methods* **248**, 31–45.

Jermutus, L., Honegger, A., Schwesinger, F., Hanes, J., and Plückthun, A. (2001). Tailoring *in vitro* evolution for protein affinity or stability. *Proc. Natl Acad. Sci. USA* **98**, 75–80.

Kushner, S. R. (2002). mRNA decay in *Escherichia coli* comes of age. *J. Bacteriol.* **184**, 4658–4665.

Laminet, A. A., and Plückthun, A. (1989). The precursor of beta-lactamase: Purification, properties and folding kinetics. *EMBO J.* **8**, 1469–1477.

Lesley, S. A. (1995). Preparation and use of *E. coli* S-30 extracts. *Methods Mol. Biol.* **37**, 265–278.

Leung, D. W., Chen, E., and Goeddel, D. V. (1989). A method for random mutagenesis of a defined DNA segment using a modified polymerase chain reaction. *Technique* **1**, 11–15.

Matsuura, T., and Plückthun, A. (2003). Selection based on the folding properties of proteins with ribosome display. *FEBS Lett.* **539**, 24–28.

Mattheakis, L. C., Bhatt, R. R., and Dower, W. J. (1994). An *in vitro* polysome display system for identifying ligands from very large peptide libraries. *Proc. Natl Acad. Sci. USA* **91**, 9022–9026.

Pratt, J. M. (1984). Coupled transcription-translation in prokaryotic cell-free systems. *In "Current Protocols"* (B. D. Hemes, and S. J. Higgins, eds.), pp. 179–209. IRL Press, Oxford.

Schatz, P. J. (1993). Use of peptide libraries to map the substrate specificity of a peptide-modifying enzyme: A 13 residue consensus peptide specifies biotinylation in *Escherichia coli*. *Biotechnology* (*New York*) **11**, 1138–1143.

Smith, G. P. (1985). Filamentous fusion phage: Novel expression vectors that display cloned antigens on the virion surface. *Science* **228**, 1315–1317.

Stemmer, W. P. (1994). Rapid evolution of a protein *in vitro* by DNA shuffling. *Nature* **370**, 389–391.

Takahashi, F., Ebihara, T., Mie, M., Yanagida, Y., Endo, Y., Kobatake, E., and Aizawa, M. (2002). Ribosome display for selection of active dihydrofolate reductase mutants using immobilized methotrexate on agarose beads. *FEBS Lett.* **514**, 106–110.

Wade, H. E., and Robinson, H. K. (1966). Magnesium ion-independent ribonucleic acid depolymerases in bacteria. *Biochem. J.* **101**, 467–479.

Wodak, S. J., and Janin, J. (2002). Structural basis of macromolecular recognition. *Adv. Prot. Chem.* **61**, 9–73.

Zaccolo, M., and Gherardi, E. (1999). The effect of high-frequency random mutagenesis on *in vitro* protein evolution: A study on TEM-1 β-lactamase. *J. Mol. Biol.* **285**, 775–783.

Zaccolo, M., Williams, D. M., Brown, D. M., and Gherardi, E. (1996). An approach to random mutagenesis of DNA using mixtures of triphosphate derivatives of nucleoside analogues. *J. Mol. Biol.* **255**, 589–603.

Zubay, G. (1973). *In vitro* synthesis of protein in microbial systems. *Annu. Rev. Genet.* **7**, 267–287.

CHAPTER

61

Epitope Mapping by Mass Spectrometry

Christine Hager-Braun and Kenneth B. Tomer

I. INTRODUCTION

Antigenic determinants, or epitopes, are the specific chemical structures within an antigen molecule that are recognized by either B-cell or T-cell antibodies. Knowledge of the structure of the epitope recognized by an antibody is important for the development of vaccines, for understanding antibody–antigen interactions, for validating some diagnostic tests, and in the investigation of the pathogenesis of autoimmmune diseases. There are a number of approaches for determination of epitopes currently in use, including peptide reactivity, nuclear magnetic resonance (NMR), crystallography, mutation analysis, and phage display and limited proteolysis (Jemmerson and Paterson, 1986). There are various limitations to each of these techniques. For example, NMR can be limited by relatively high sample levels needed and the antibody–antigen mass. Crystallography requires high analyte levels and crystal formation. Mutation analysis can be misleading when a mutation distant from the epitope induces a change in the conformation of the epitope. Peptide scanning and phage displays can be used to determine linear epitopes but are less applicable to conformational epitopes or epitopes containing posttranslational modifications. Limited proteolysis involves the comparison of proteolytic products from the antigen with those arising from the antigen–antibody complex. Enzymatic cleavage sites that are part of the epitope will be protected from cleavage in the presence of the antibody but not in the free antigen. This approach requires a detection system that can provide structural information about the proteolytic fragments.

The high sensitivity and specificity provided by high-accuracy mass measurement have made mass spectrometry the detection method of choice for use with limited proteolysis experiments (Suckau *et al*., 1990; Zhao *et al*, 1996; Macht *et al*., 1996; Yu *et al*., 1998; Legros *et al*., 2000). Our approach involves the use of antibodies immobilized on Sepharose beads (Papac *et al*., 1994; Parker *et al*., 1996; Jeyarajah *et al*., 1998). After binding the antigen, the complex is treated sequentially with one or more proteolytic enzymes. The nonspecifically bound peptides are washed off the beads, and then an aliquot of the beads is placed on a matrix-assisted laser desorption/ionization mass spectrometry (MALDI/MS) target. The MALDI matrix is then applied to the beads, releasing the affinity-bound peptides, which are then analyzed. By using an endopeptidase such as trypsin or Lys-C followed by an exopeptidase such as aminopeptidase or carboxypeptidase, the fine structure of the epitope can be determined.

We have modified our procedure to incorporate the use of a secondary Fc-specific antibody to capture the primary antibody from crude biological preparations (Fig. 1) (Peter and Tomer, 2001; Parker *et al*., 2001). The two antibodies are then cross-linked. Incorporating this step has the advantage of significantly reducing the chemical background in MALDI spectra and increasing the antibody-binding capacity. Few ions are observed in the mass spectrum that can be attributed to proteolysis of the antibodies. This is due to a combination of factors: antibodies in general appear to be resistant to proteolysis, possibly due to resistance to denaturation and to extensive glycosylation shielding proteolytic sites; proteolytic cleavages do not always give rise to free peptides because of the presence of

Copyright 2006, Elsevier Science (USA).
All rights reserved.

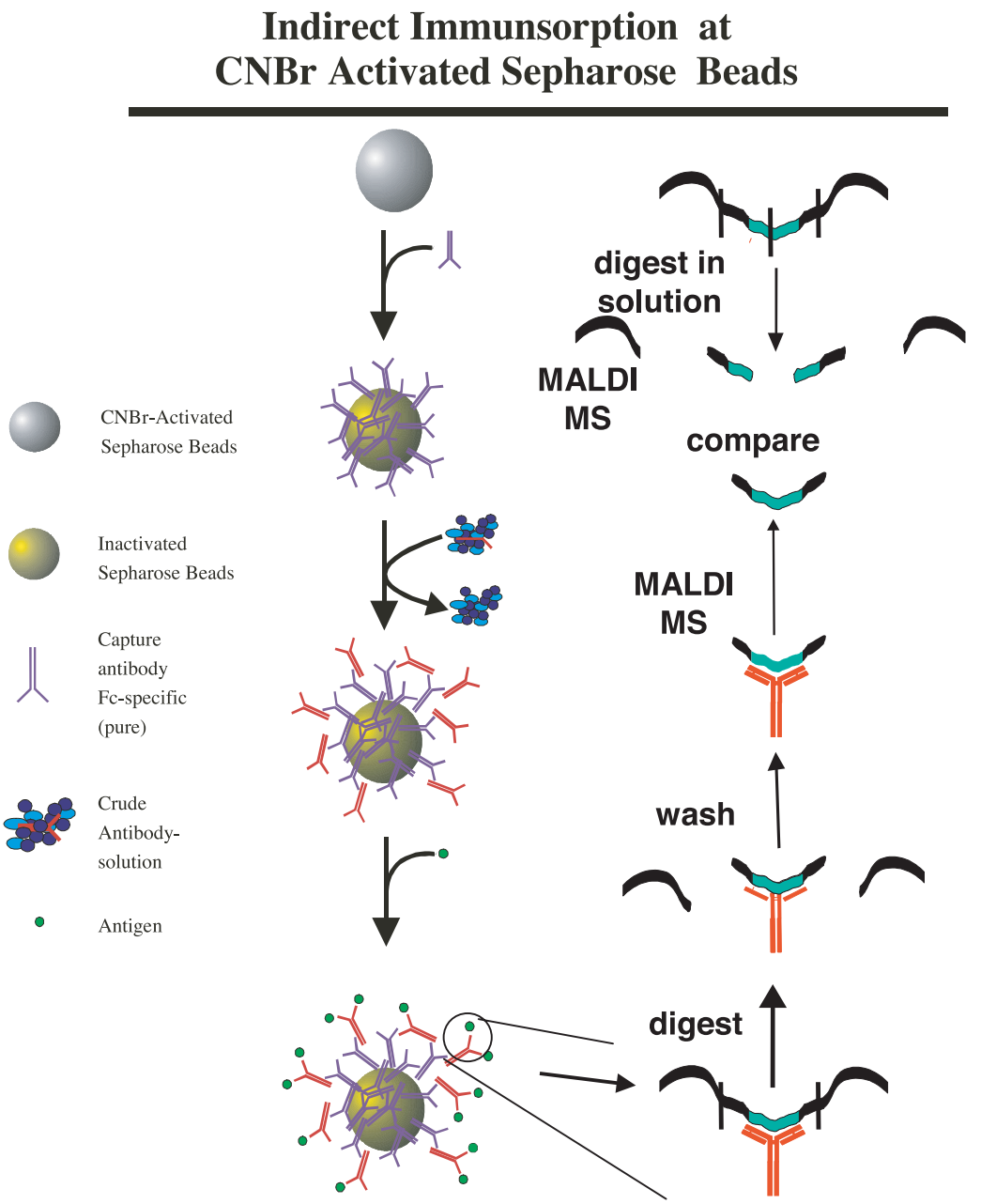

FIGURE 1 Scheme of proteolytic footprinting incorporating capture antibodies with cross-linking. [Adapted with permission from Peter and Tomer (2001). Copyright 2001 American Chemical Society.]

disulfide bonds; peptides originating from proteolysis at sites that do not disrupt antigen–antibody binding are washed off prior to analysis; and, when the primary and secondary antibodies are cross-linked, many potential proteolysis sites for the most commonly used enzymes are blocked. The capabilities of this approach are illustrated by mapping the epitope on adrenocorticotropin recognized by a mouse anti-ACTH IgG antibody (Peter and Tomer, 2001).

II. MATERIALS AND INSTRUMENTATION

Adrenocorticotropin is from Bachem, California (Cat. No. H1160). Monoclonal IgG1 anti-ACTH (clone 58) is from Biodesign International (Cat. No. E54008M). Polyclonal IgG goat antimouse Fc specific is from Sigma (Cat. No. M-4280), as are Trizma–HCl, (Cat. No. T-6666), Trizma–base (Cat. No. T-6791),

Tween 20 (Cat. No. P-8942, 10% in water), NaH_2PO_4-H_2O (Cat. No. S-9638), leucine aminopeptidase M (Cat. No. L-0632), and EDTA (Cat. No. E-5513). Endoproteinases are obtained from Roche Diagnostics (Lys-C Cat. No. 1 047 825; Glu-C Cat. No. 1 047 817; trypsin Cat. No. 1 418 025; and carboxypeptidase Y Cat. No. 1 111 914). Formic acid, 96% (Cat. No. 25,136-4), α-cyano-4-hydroxycinnamic acid (Cat. No. 47,687-0), and NH_4HCO_3 (Cat. No. 28,509-9) are from Aldrich Chemical Co. Bis(sulfosuccinimidyl) suberate, BS^3 (Cat. No. 21580), is from Pierce. Cyanogen bromide-activated Sepharose 4B beads are from Amersham Biosciences (Cat. No.17-0820-01). Compact reaction columns, CRC (Cat. No. 13928), and 35 µ*M* compact column filters (Cat. No. 13912) are from USB. HCl, 1 *M* (Cat. No. 920-1), and NaOH, 1 *M* (Cat. No. 930-65), are from Sigma Diagnostics. $CaCl_2{\cdot}2H_2O$ (Cat. No. 4160), $Na_2HPO_4{\cdot}3H_2O$ (Cat. No. 7914), $NaHCO_3$ (Cat. No. 7412), NH_4OAc (Cat. No. 3272), and NaOAc-$7H_2O$ (Cat. No. 7364) are from Mallinckrodt. NaCl is from Baker (Cat. No. 3624-05), and ethyl alcohol is from Pharmco Products. Becton Dickinson Falcon tubes, 15 ml, No. 352059, are from Fisher Scientific (Cat. No. 14-959-11B). The rotating incubator is a Lab Line hybridization incubator or similar. Deionized water is obtained from a Hydro Picopure 2 system (Hydro Systems, Research Triangle Park, NC).

MALDI mass spectra are obtained on a Voyager DE-STR mass spectrometer (Applied Biosystems). Similar results should be obtained from similar instrumentation.

III. PROCEDURES

A. Immobilization of Secondary Antibody to Cyanogen Bromide-Activated Sepharose Columns

Solutions

1. *Phosphate buffer, pH 7.2*: Prepare 100 ml 0.1 *M* Na_2HPO_4 by dissolving 2.68 g $Na_2HPO_4{\cdot}7H_2O$ in water and 100 ml 0.1 *M* NaH_2PO_4 by dissolving 1.38 g $NaH_2PO_4{\cdot}H_2O$ in water. Use 100 ml of the 0.1 *M* Na_2HPO_4 solution and titrate to pH 7.2 with the 0.1 *M* NaH_2PO_4 solution (approximately 37 ml necessary).
2. Phosphate-buffered Saline *(PBS), pH 7.2*: To make 100 ml of PBS, pH 7.2, containing 0.1 *M* phosphate buffer and 150 m*M* NaCl, dissolve 0.88 g NaCl in previously prepared 100 ml 0.1 *M* phosphate buffer.
3. *1 mM HCl*: To make 1 liter of 1 m*M* HCl, dilute 1 ml 1 *M* HCl to 1000 ml.
4. *Coupling buffer*: To prepare 50 ml of coupling buffer, add 0.42 g sodium bicarbonate to sufficient deionized water to make 50 ml of solution. The pH will be between 8.2 and 8.35 and does not need further adjustment.
5. *0.1 M NaHCO₃/0.15 M NaCl*: To make 50 ml of solution, add 0.42 g sodium bicarbonate and 0.44 g NaCl to sufficient deionized water to make 50 ml of solution. Again, the pH does not need to be adjusted any further.
6. *Antibody solution*: Mix 20 µl of goat anti-mouse Fc-specific IgG (supplied as a 2.0-mg/ml solution in 10 m*M* phosphate buffered saline, pH 7.4, containing 15 m*M* sodium azide) with 80 µl 0.1 *M* $NaHCO_3$/0.15 *M* NaCl.
7. *0.1 M Tris, pH 8.0*: To make 50 ml of solution, add 0.79 g Trizma–HCl to approximately 45 ml deionized water and adjust pH with 1 *M* NaOH. Add sufficient deionized water to yield 50 ml final volume.
8. *0.1 M NaOAc/0.5 M NaCl, pH 4.0*: To prepare 50 ml of solution, add 0.68 g NaOAc·$3H_2O$ and 1.46 g NaCl to approximately 45 ml deionized water and adjust pH with HCl. Add sufficient deionized water to make 50 ml final volume.

Steps

1. Place *ca.* 0.2 g of dry CNBr-Sepharose beads into a Falcon tube.
2. Add 10 ml of 1 m*M* HCl. Mix gently and equilibrate for 15 min.
3. Place *ca.* 20 µl of the wet beads in a CRC and then drain the column.
4. Wash the column six times with 0.8 ml 1 m*M* HCl and then six times with 0.4 ml coupling buffer (0.1 *M* $NaHCO_3$).
5. Add 100 µl of antibody solution with a final concentration of 400 µg/ml to the beads and incubate for 1 h at room temperature.
6. Remove the antibody solution and then, to block unreacted binding positions, add 200 µl of 0.1 *M* Tris, pH 8.0, and react for 2 h at room temperature with slow rotation.
7. Wash alternately three times with 0.1 *M* NaOAc/0.5 *M* NaCl, pH 4.0, 0.1 *M* Tris, pH 8.0, and PBS, pH 7.2.
8. Check immobilization of the secondary antibody by MALDI/MS using a 1-µl aliquot. Ions attributable to the antibody should be observed in low abundance only.

B. Binding of Primary Antibody to Immobilized Secondary Antibody

Solutions

1. *PBS/0.1% Tween 20*: To make 5 ml of solution, add 50 µl of 10% Tween 20 in water to 5 ml of previously prepared PBS, pH 7.2.

2. *10 mM BS^3 in PBS, pH 7.2*: For a 1-ml solution, dissolve 5.72 mg BS^3 in 1 ml previously prepared PBS, pH 7.2.
3. *0.1 M Tris, pH 8.0*: To make 50 ml of solution, add 0.79 g Trizma–HCl to approximately 45 ml deionized water and adjust pH with NaOH. Add sufficient deionized water to yield 50 ml final volume.
4. *Anti-ACTH IgG solution*: Prepare initial solution by dissolving 200 µg anti-ACTH IgG in 1 ml previously prepared PBS, pH 7.2.

Steps

1. Add 50 µl of mouse anti-ACTH IgG (200 µg/ml in PBS, pH 7.2) to the beads from step 7 and react for 1 h at room temperature.
2. Drain solution and wash the beads three times with 0.5 ml PBS/0.1% Tween 20 and three times with 0.5 ml PBS, pH 7.2.
3. Check that the primary antibody is bound to the immobilized secondary antibody by obtaining a MALDI/MS from a 1-µl aliquot. Ions arising from the antibody should be observed (Fig. 2A). If no ions are detected the procedure has not worked.
4. To cross-link the primary antibody to the secondary antibody, add a 10-µl aliquot of a 10 m*M* solution of BS^3 in PBS, pH 7.2, to the beads. Incubate the mixture at RT in the dark with rotation for 45 min.
5. Drain and then quench the cross-linker with 400 µl 0.1 *M* Tris, pH 8.0, for 15 min at room temperature.
6. Wash the beads twice with 100 µl of 0.1 *M* Tris, pH 8.0.
7. Wash three times with 400 µl PBS, pH 7.2.
8. Set aside one-fourth of the beads for use as a control. *Note*: All further experiments should be performed on the control except that no ACTH should be bound to the immunocomplex. This will provide information about chemical background for subsequent MALDI analyses.
9. Check that the primary antibody has been cross-linked to the secondary antibody by MALDI/MS using a 1-µl aliquot. Ions attributable to the antibody should be of low abundance. (Fig. 2B, cf. Fig. 2A).

C. Binding of Antigen (ACTH) to Secondary Antibody

Solutions

1. *Phosphate buffer, pH 7.2*: Prepare 100 ml 0.1 *M* Na_2HPO_4 by dissolving 2.68 g $Na_2HPO_4{\cdot}7H_2O$ in water and 100 ml 0.1 *M* NaH_2PO_4 by dissolving 1.38 g $NaH_2PO_4{\cdot}H_2O$ in water. Use 100 ml of the 0.1 *M* Na_2HPO_4 solution and titrate to pH 7.2 with the 0.1 *M* NaH_2PO_4 solution (approximately 37 ml necessary).
2. *PBS*: To make 100 ml of PBS, pH 7.2, containing 0.1 *M* phosphate buffer and 150 m*M* NaCl, dissolve 0.88 g NaCl in 100 ml previously prepared 0.1 *M* phosphate buffer.
3. *10 µg/ml ACTH in PBS*: Dissolve 10 µg ACTH in 1 ml PBS from solution 2.

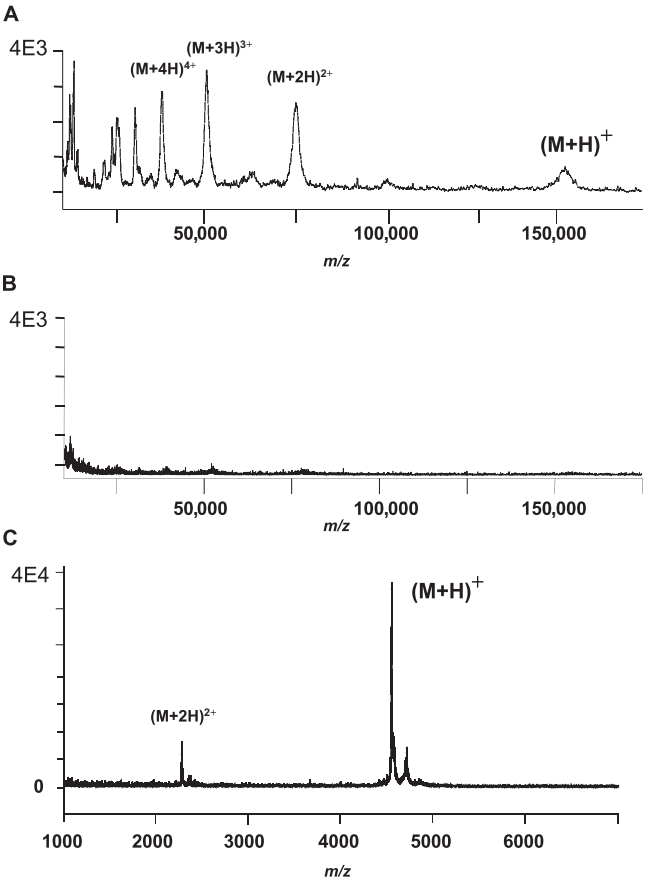

FIGURE 2. (A) Direct MALDI/MS of mouse anti-ACTH antibody from immunocomplex with Sepharose-bound antimouse Fc-specific IgG without cross-linking. (B) Direct MALDI/MS of mouse anti-ACTH antibody from immunocomplex with Sepharose-bound antimouse Fc-specific IgG with cross-linking. (C) Direct MALDI/MS of ACTH bound to cross-linked immunocomplex. [Adapted with permission from Peter and Tomer (2001). Copyright 2001 American Chemical Society.]

Steps

1. Drain the beads.
2. Add 100-µl aliquot of a 10-µg/ml solution of ACTH in PBS to the remainder of the beads from step 7. Allow reaction at room temperature for 1 h with slow rotation.
3. Incubate the control aliquot from step 8 in a CRC with 100 µl PBS, pH 7.2, for 1 h at room temperature with rotation.

4. Drain the two CRCs and wash the beads three times with 400 µl PBS and store in sufficient PBS to keep the beads moist.
5. Remove a 1-µl aliquot of the beads for MALDI/MS analysis (Fig. 2C).

D. Proteolytic Footprinting (Epitope Excision)

Successive enzymatic digestions can be performed. In this example, the immunocomplex is treated successively with Lys-C, Glu-C, trypsin, carboxypeptidase Y, and aminopeptidase M. Prepare all proteinase-containing solutions just prior to use to limit autolysis.

Solutions

1. *Lys-C solution*: To prepare 1 µg/µl Lys-C stock solution, dissolve 50 µg endoproteinase Lys-C in 50 µl deionized water. To make 50 ml stock buffer solution, dissolve 0.30 g Trizma–base and 18.6 mg EDTA disodium salt dihydrate in approximately 45 ml deionized water and adjust pH to 8.5 with HCl. Add sufficient deionized water to yield 50 ml final volume. To 90 µl of the buffer stock, add 10 µl of the Lys-C stock solution. Take 10 µl of this 0.1-µg/µl Lys-C solution and dilute it further with 990 µl of the buffer stock.

2. *Phosphate buffer, pH 7.2*: Prepare 100 ml 0.1 *M* Na_2HPO_4 by dissolving 2.68 g $Na_2HPO_4{\cdot}7H_2O$ in water and 100 ml 0.1 *M* NaH_2PO_4 by dissolving 1.38 g $NaH_2PO_4{\cdot}H_2O$ in water. Use 100 ml of the 0.1 *M* Na_2HPO_4 solution and titrate to pH 7.2 with the 0.1 *M* NaH_2PO_4 solution (approximately 37 ml necessary).

3. *PBS, pH 7.2*: To make 100 ml of PBS, pH 7.2, containing 0.1 *M* phosphate buffer and 150 m*M* NaCl, dissolve 0.88 g NaCl in 100 ml 0.1 *M* phosphate buffer.

4. *Glu-C solution*: To prepare 1 µg/µl Glu-C stock solution, dissolve 50 µg Glu-C in 50 µl deionized water. To make 50 ml stock buffer solution, dissolve 98.8 mg ammonium bicarbonate in 45 ml deionized water and adjust pH to 7.8 with NaOH. Add sufficient deionized water to yield 50 ml final volume. To 90 µl of the buffer stock, add 10 µl of the Glu-C stock solution. Take 10 µl of this 0.1-µg/µl Glu-C solution and dilute it further with 990 µl of the buffer stock.

5. *Trypsin solution*: To prepare 1 µg/µl trypsin stock solution, dissolve 25 µg trypsin in 25 µl deionized water. To make 50 ml stock buffer solution, add 0.30 g Trizma–base and 5.55 mg $CaCl_2$ to approximately 45 ml deionized water and adjust pH to 8.5 with HCl. Add sufficient deionized water to yield 50 ml final volume. To 90 µl of the buffer stock, add 10 µl of the trypsin stock solution. Take 10 µl of this 0.1-µg/µl trypsin solution and dilute it further with 990 µl of the buffer stock.

6. *Carboxypeptidase Y solution*: To prepare 0.4 µg/µl carboxypeptidase Y stock solution, dissolve 20 µg carboxypeptidase Y in 50 µl deionized water. Buffer stock solution, 50 ml, is prepared by adding 193 mg ammonium acetate to 45 ml deionized water. Adjust the pH to 4.5 with acetic acid and add sufficient deionized water to yield 50 ml final volume. Add 10 µl carboxypeptidase Y to 90 µl of the stock solution. Take 10 µl of this 0.04-µg/µl carboxypeptidase Y solution and dilute it further with 90 µl of the buffer stock.

7. *Phosphate buffer, pH 7.0*: Prepare 100 ml 0.1 *M* Na_2HPO_4 by dissolving 2.68 g $Na_2HPO_4{\cdot}7H_2O$ in water and 100 ml 0.1 *M* NaH_2PO_4 by dissolving 1.38 g $NaH_2PO_4{\cdot}H_2O$ in water. Use 100 ml of the 0.1 *M* Na_2HPO_4 solution and titrate to pH 7.0 with the 0.1 *M* NaH_2PO_4 solution (approximately 58 ml necessary).

8. *Leucine aminopeptidase solution*: To prepare 1 µg/µl aminopeptidase M stock solution, dissolve 50 µg aminopeptidase M in 50 µl deionized water. Dilute 10 µl of the aminopeptidase stock solution with 90 µl phosphate buffer, pH 7.0. Take 10 µl of this 0.1 µg/µl aminopeptidase M solution and dilute it further with 990 µl of the buffer stock.

Steps

1. Lys-C:
   a. Prepare a solution of Lys-C (1 ng/µl) in a solution of 50 m*M* Tris and 1 m*M* EDTA, pH 8.5. Add the enzyme solution (50 µl) (approximately 20:1 substrate-to-enzyme ratio) to the immunocomplex in the CRC.
   b. Incubate the beads overnight at 37°C with slow rotation.
   c. Remove the enzyme solution and wash the beads three times with 0.4 ml PBS, pH 7.2.
   d. Add sufficient buffer solution to keep beads moist.
   e. Remove a 1-µl aliquot for MALDI/MS analysis (Fig. 3A).
2. Glu-C:
   a. Prepare a solution of Glu-C (1 ng/µl) in a solution of 25 m*M* NH_4HCO_3, pH 7.8. Add the enzyme solution (50 µl) (approximately 20:1 substrate-to-enzyme ratio) to the immunocomplex in the CRC.
   b. Incubate the beads overnight at 37°C with slow rotation.
   c. Remove the enzyme solution and wash the beads three times with 0.4 ml PBS, pH 7.2.
   d. Add sufficient buffer solution to keep beads moist.
   e. Remove a 1-µl aliquot for MALDI/MS analysis (Fig. 3B).

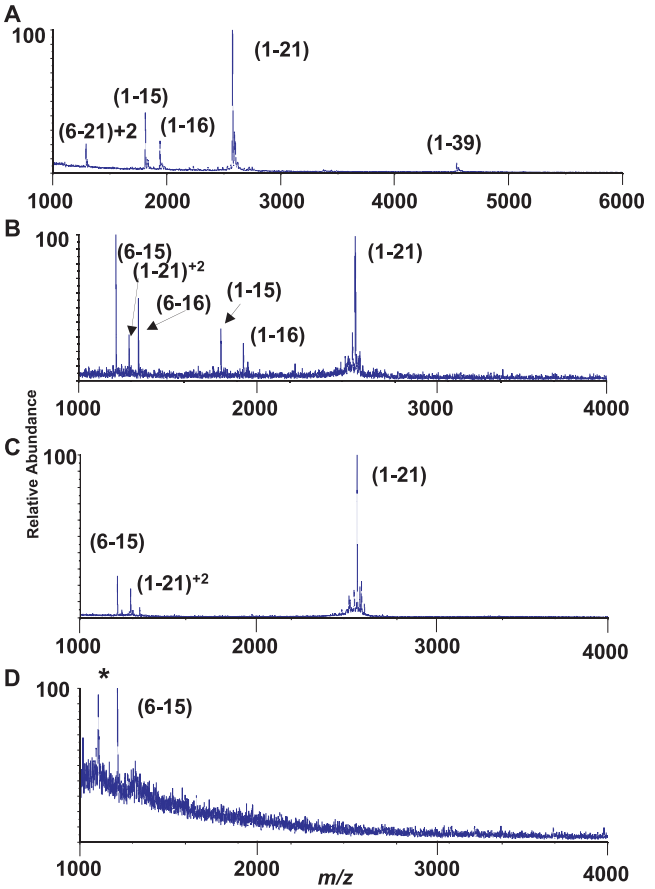

FIGURE 3. (A) Direct MALDI/MS of ACTH bound to the cross-linked immunocomplex after digestion with Lys-C. (B) Direct MALDI/MS of ACTH bound to the cross-linked immunocomplex after digestion with Lys-C followed by Glu-C. (C) Direct MALDI/MS of ACTH bound to the cross-linked immunocomplex after digestion with Lys-C followed by Glu-C and then trypsin. (D) Direct MALDI/MS of ACTH bound to the cross-linked immunocomplex after digestion with Lys-C followed by Glu-C, trypsin, and carboxypeptidase Y. Peak marked with an asterisk is background as observed in the control. [Adapted with permission from Peter and Tomer (2001). Copyright 2001 American Chemical Society.]

3. Trypsin:
   a. Prepare a solution of trypsin (1 ng/µl) in a solution of 50 m*M* Tris, 1 m*M* $CaCl_2$, pH 8.5. Add the enzyme solution (50 µl) (approximately 20:1 substrate-to-enzyme ratio) to the immunocomplex in the CRC.
   b. Incubate the beads overnight at 37°C with slow rotation.
   c. Remove the enzyme solution and wash the beads three times with 0.4 ml PBS, pH 7.2.
   d. Add sufficient buffer solution to keep beads moist.
   e. Remove a 1-µl aliquot for MALDI/MS analysis (Fig. 3C).
4. Carboxypeptidase Y:
   a. Prepare a solution of carboxypeptidase Y (4 ng/µl) in a 50 m*M* NH_4OAc, pH 4.5, solution. Add the enzyme solution to the immunocomplex in the CRC at a 3:1 substrate-to-enzyme ratio (83 µl).
   b. Incubate the beads overnight at 37°C with slow rotation.
   c. Remove the enzyme solution and wash the beads three times with 0.4 ml PBS, pH 7.2.
   d. Add sufficient buffer solution to keep beads moist.
   e. Remove a 1-µl aliquot for MALDI/MS analysis (Fig. 3D).
5. Leucine aminopeptidase:
   a. Prepare a solution of leucine aminopeptidase (1 ng/µl) in a 100 m*M* sodium phosphate, pH 7.0, solution. Add the enzyme solution to the immunocomplex in the CRC at a 20:1 substrate-to-enzyme ratio.
   b. Incubate the beads overnight at 37°C with slow rotation.
   c. Removed the enzyme solution and wash the beads three times with 0.4 ml PBS, pH 7.2.
   d. Add sufficient buffer solution to keep beads moist.
   e. Remove a 1-µl aliquot for MALDI/MS analysis. In this experiment, no additional cleavages are observed.

E. Preparation of Samples for MALDI/MS Analysis

1. Mix approximately 1 µl of the affinity beads on the MALDI target with 0.5–1.0 µl of saturated α-cyano-4-hydroxycinnamic acid in ethanol/water/formic acid (45/45/10 v/v/v).
2. Let the target air dry.
3. Obtain spectra as indicated by the instrument's user guide.

IV. COMMENTS

This procedure works well for linear epitopes and many continuous conformational epitopes. Problems can be encountered for conformational epitopes that are conformationally constrained by the presence of disulfide bonds when the disulfide bond is lost during proteolysis. For discontinuous epitopes, a combination of limited proteolysis and chemical modification of surface accessible amino acids may provide the required structural information (Hochleitner *et al.*, 2000).

[1]SYSMEHFRWGKPVGKKRRPVKVYPNGAEDESAEAFPLEF[39]

Lys-C peptides observed

1-15 SYSMEHFRWGKPVGK

1-16 SYSMEHFRWGKPVGKK

1-21 SYSMEHFRWGKPVGKKRRPVK

Lys-C/Glu-C peptides observed

6-15 HFRWGKPVGK

6-16 HFRWGKPVGKK

1-15 SYSMEHFRWGKPVGK

1-16 SYSMEHFRWGKPVGKK

1-21 SYSMEHFRWGKPVGKKRRPVK

Lys-C/Glu-C/Tryp peptides observed

6-15 HFRWGKPVGK

1-21 SYSMEHFRWGKPVGKKRRPVK

Lys-C/Glu-C/Tryp/CPY peptides observed

6-15 HFRWGKPVGK

FIGURE 4. Proteolytic peptides observed for the various digestion steps involved in obtaining spectra shown in Fig. 3.

The aforementioned order of proteolytic enzymes used was used to provide initially large proteolytic peptides, followed by enzymes that would cleave within the sequence of the smallest peptide observed (Fig. 4).

V. PITFALLS

Do not use dithiothreitol because it can denature the antibody as well as the antigen.

Do not use too high a concentration of Ca^{2+} as this can interfere with the MALDI/MS analysis.

Although we have been able to perform four consecutive proteolysis experiments on one aliquot of antigen–antibody beads, the levels of background ions increase significantly while the abundance of analyte ions decreases.

References

Hochleitner, E. O., Borchers, C., Parker, C., Bienstock, R. J., and Tomer, K. B. (2000). Characterization of a discontinuous epitope of the human immunodeficiency virus (HIV) core protein p24 by epitope excision and differential chemical modification followed by mass spectrometric peptide mapping analysis. *Protein Sci.* **9**, 487–496.

Jemmerson, R., and Paterson, Y. (1986). Mapping epitopes on a protein antigen by the proteolysis of antigen-antibody complexes. *Science* **232**, 1001–1004.

Jeyarajah, S., Parker, C. E., Sumner, M. T., and Tomer, K. B. (1998). MALDI/MS mapping of HIV-gp120 epitopes recognized by a limited polyclonal antibody. *J. Am. Soc. Mass Spectrom.* **9**, 157–165.

Legros, V., Jolivet-Reynaud, C., Battail-Poirot, N., Saint-Pierre, C., and Forest, E. (2000). Characterization of an anti-Borrelia burgdorferi OspA conformational epitope by limited proteolysis of monoclonal antibody-bound antigen and mass spectrometric peptide mapping. *Protein Sci.* **9**, 1002–1010.

Macht, M., Fiedler, W., Kuerzinger, K., and Przybylski, M. (1996). Mass spectrometric mapping of protein epitope structures of myocardial infarct markers myoglobin and troponin T. *Biochemistry* **35**, 15633–15639.

Papac, D. I., Hoyes, J., and Tomer, K. B. (1994). Epitope mapping of the gastrin releasing peptide/anti-bombesin monoclonal antibody complex by proteolysis followed by matrix-assisted laser desorption mass spectrometry. *Protein Sci* **3**, 1488–1492.

Parker, C. E., Deterding, L. J., Hager-Braun, C., Binley, J. M., Schülke, N., Katinger, H., Moore, J. P., and Tomer, K. B. (2001). Fine definition of the epitope on the gp41 glycoprotein of human immunodeficiency virus type 1 for the neutralizing monoclonal antibody 2F5. *J. Virol* **75**, 10906–10911.

Parker, C. E., Papac, D. I., Trojak, S. K., and Tomer, K. B. (1996). Epitope mapping by mass spectrometry: Determination of an epitope on HIV-1_{IIIB} p26 recognized by a monoclonal antibody. *J. Immunol.* **15**(1), 198–206.

Peter, J. F., and Tomer K. B. (2001). A general strategy for epitope mapping by direct MALDI-TOF mass spectrometry using secondary antibodies and crosslinking. *Anal. Chem.* **73**, 4012–4019.

Suckau, D., Kohl, J., Karwath, G., Schneider, K., Casaretto, M., Bitter-Suermann, D., and Przybylski, M. (1990). Molecular epitope identification by limited proteolysis of an immobilized antigen-antibody complex and mass-spectrometric peptide-mapping. *Proc. Natl. Acad. Sci. USA* **87**, 9848–9851.

Yu, L., Gaskell, S. J., and Brookman, J. L. (1998). Epitope mapping of monoclonal antibodies by mass spectrometry: Identification of protein antigens in complex biological systems. *J. Am. Soc. Mass Spectrom.* **9**, 208–215.

Zhao, Y., Muir, T. M., Kent, S. B. H., Tischer, E., Scardina, J. M., and Chait, B. T. (1996). Mapping protein-protein interactions by affinity-directed mass spectrometry. *Proc. Natl. Acad. Sci. USA* **93**, 4020–4024.

CHAPTER

62

Mapping and Characterization of Protein Epitopes Using the SPOT Method

Claude Granier, Sylvie Villard, and Daniel Laune

I. INTRODUCTION

Obtaining information on the epitope recognized by a given antibody can be achieved by a variety of techniques, including antibody recognition of truncated or mutated recombinant antigens, purified antigen fragments after enzymatic digestion, or synthetic peptides predicted as being antigenic from algorithms, and so on. Methods of parallel peptide synthesis (Geysen *et al.*, 1984) have been a breakthrough in deciphering protein–antibody interactions. By using a cleverly modified format of the standard solid-phase peptide synthesis procedure, it is possible to prepare a comprehensive set of peptides covering the entire sequence of a given protein and to probe the reactivity of the whole set of peptides in a single assay. The basic concept of parallel peptide synthesis is to divide the solid phase into discrete, addressable synthesis sites, where many different sequences can be synthesized concurrently. The initial technology made use of small polyethylene rods (called "pins"), the tips of which were chemically derivatized so as to allow peptide synthesis. Being physically separated, the pins could be used as individual chemical reactors on which peptides with defined sequences are synthesized. The pins are arrayed in a 8 × 12 format, compatible with standard ELISA plates, therefore making very practical the quantitative evaluation of peptide reactivity with a labeled antibody. The first applications of this approach were to map antibody epitopes (Geysen *et al.*, 1984, 1986). Due to its novelty, the method stimulated research aimed at developing new strategies for parallel peptide synthesis. In 1992, the use of cellulose membranes to perform the concurrent synthesis of peptides was reported: in this approach, dubbed the SPOT method (Frank, 1992), small circular areas on a cellulose membrane are used as discrete sites for peptide synthesis. Conveniently protected and activated amino acids are (manually or automatically) spotted on the membrane so as to achieve the stepwise construction of peptides. On each spot a different peptide can be synthesized so that arrays of peptides can be prepared easily (Fig. 1). The amount of peptide is in the order of 50 nmol per spot. In a typical application, some 200 peptides can be arrayed on a 8 × 12-cm paper sheet within a few working days. The method is robust, economical and susceptible to automation.

Peptides remain attached to the membrane once the synthesis is completed, making it possible to probe the reactivity of all the peptides with a labeled ligand just by dipping the membrane into a solution of the ligand. Should any peptide be recognized by the ligand, the binding is easily revealed by appropriate means, e.g., autoradiography and enzyme-labeled secondary antibody. Once used, the membrane can be regenerated and used several times, with excellent reproducibility. The method initially described by R. Frank has been modified and improved (Molina *et al.*, 1996; Reineke *et al.*, 1999a; Koch and Mahler, 2002).

One of the most familiar uses of this technique is to map sites on a protein that are recognized by antibodies (epitopes). The main advantage of this approach, as compared with predictive methods, is that all peptides enclosed within the amino acid sequence of the protein

Copyright 2006, Elsevier Science (USA).
All rights reserved.

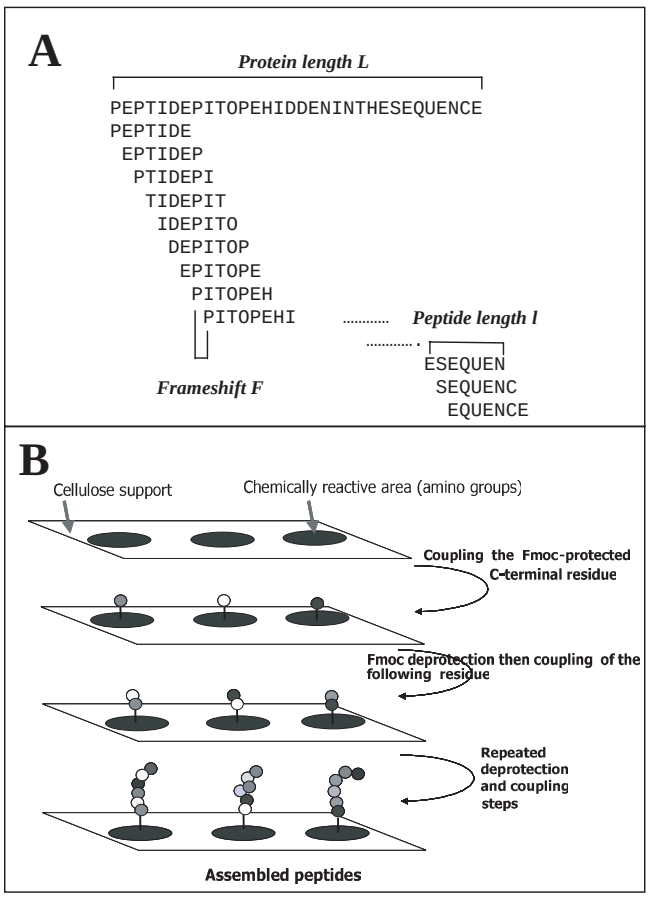

FIGURE 1 Principle of epitope identification using the SPOT method. (A) Design of overlapping peptides from a putative protein sequence. (B) Principle of the SPOT method.

antigen can be synthesized in the form of a series of overlapping peptides (Fig. 1) and further simultaneously probed for reactivity with antibody. The straightforward identification of peptides bound by the antibody has many advantages over methods using antigen modification or cleavage, mutagenesis, and so on to disclose the epitope. The identified peptide can be further prepared in large amounts and used as antigen, e.g., in diagnostic kits. Once the epitope of a monoclonal antibody has been mapped, the SPOT method can conveniently be used to determine key residues in the interaction by performing alanine scanning of the peptide. The reactivity of polyclonal antibodies with a set of immobilized peptides can also be assessed. In this case, however, it is only possible to identify antigenic regions and not precise epitopes. Nevertheless, the information derived from such an analysis is certainly more valuable than any epitope prediction method (Van Regenmortel and Pellequer, 1994) to design peptides suitable for raising antipeptide antibodies cross-reactive with the cognate protein.

However, as all methods relying on peptides, only continuous epitopes can be mapped by the SPOT approach. The identification of conformation-dependent epitopes using the SPOT technique has been reported but requires slightly more sophisticated methods for revealing low-affinity binding and discarding the background signal (Reineke *et al*., 1999b).

The techniques used to synthesize peptides on a cellulose membrane and to probe the membrane with an antibody are described in the following sections.

II. MATERIALS AND INSTRUMENTATION

A. Spotter

The ASP 222 robot from Intavis (http://www.intavis.com) is used. The protein sequence file is submitted to the specific software together with the requirements for peptide length and frameshift, and the software automatically generates the files for synthesis. The computer then drives the spotting of the activated Fmoc amino acid by the robot according to the sequence of the individual peptides. The reader is encouraged to read the instructions carefully for use of the ASP 222 robot for efficient setup of the robot. Verification of the correct functioning of the robot is recommended before starting the synthesis: a mock synthesis is initiated using a sheet of paper instead of the membrane and is then stopped once accurate spotting has occured.

B. Chemicals

Recommended most common Fmoc amino acids (from Novabiochem, http://www.merckbiosciences.de) are as follows.

Fmoc-L-Ala; Fmoc-L-Arg(Pbf); Fmoc-L-Asn(Trt); Fmoc-L-Asp(OtBu); Fmoc-L-Cys(Trt); Fmoc-L-Gln(Trt); Fmoc-L-Glu(OtBu); Fmoc-Gly; Fmoc-L-His(Trt); Fmoc-L-Ile; Fmoc-L-Leu; Fmoc-L-Lys(Boc); Fmoc-L-Met; Fmoc-L-Phe; Fmoc-L-Pro; Fmoc-L-Ser(tBu); Fmoc-L-Thr(tBu); Fmoc-L-Trp(Boc); Fmoc-L-Tyr(tBu); Fmoc-L-Val; Fmoc-L-Cys(Acm).

C. Solvents and Reagents

N, *N*′-Dimethylformamide (DMF), ref. 0343549 from SDS (http://www.sds.tm.fr/)
N-Methylpyrrolidone-2 (NMP), ref. 0873516 from SDS
Piperidine, ref. 0663516 from SDS
N, *N*′-Diisopropylcarbodiimide (DIPC), ref. 38370F from Sigma-Aldrich (www.sigma-aldrich.com)

N-Hydroxybenzotriazole (HOBT), ref. 02–62-0008 from Novabiochem
Methanol, ref. 20847320 from VWR (http://www.vwr.com)
Bromphenol blue, ref. B-8026 from Sigma-Aldrich
Acetic anhydride, ref. 0140216 from SDS
Trifluoroacetic acid, ref. 80203 from SDS
Dichloromethane, ref. 029337E21 from SDS
Acetic acid, ref. 20103295 from VWR
Triethylsilane, ref. 90550 from Sigma-Aldrich
Dimethyl sulfoxide (DMSO), ref. 41640 from Sigma-Aldrich

D. Membranes for Spot Synthesis

Cellulose membranes (ref. 30100) are available from Intavis (http://www.intavis.com). They can be stored for months at –20°C. They consist of cellulose paper derivatized with amino polyethylene glycol. SPOT synthesis membranes should be identified. At the end of the first synthesis cycle, when spots are colored, the first and last spot number of each row of peptides should be noted in pencil, out of the arrayed area.

III. PROCEDURES

A. Chemical Synthesis

Reagents

1. *Fmoc amino acid solutions:* Weigh out each Fmoc amino acid derivative and prepare the corresponding stock solution in NMP using Table I. Use polypropylene tubes. Be sure that each derivative is completely dissolved, as at 0.6*M*, most of the Fmoc-protected amino acids are at their solubility limit. Distribute, in 1.5 ml Eppendorf tubes, each stock solution into N 300 µl aliquots except for arginine (150 µl) (where N corresponds to twice the number of days the synthesis is planned to last. For example, four synthesis cycles can be performed in one working day. Supposing four membranes have to be prepared and if the peptides are 12 amino acids long, it will take 3 days to synthesize them. In this case therefore N = 8). The N series of amino acids are disposed on N tube racks and kept at –20°C.
2. *Bromphenol blue stock solution:* Prepare 10 ml of a 10 mg/ml solution of bromphenol blue in pure DMF
3. *Activators*: Prepare 1.2*M* HOBT (648 mg/4 ml NMP) and 1.2*M* DIPC (0.746 ml in 3.254 ml NMP) and store at –20°C
4. *Fmoc deprotection reagent:* Prepare daily 500 ml of a 20% piperidine solution in DMF

TABLE I Preparation of Fmoc Amino Acid Solutions[a]

One letter code	Amino acid	Molecular weight	Weight for a final volume of		
			1.6 ml	2.4 ml	3.2 ml
A	Fmoc-L-Ala	329	316	474	632
N	Fmoc-L-Asn(Trt)	597	574	861	1148
R	Fmoc-L-Arg(Pbf)	649	624	936	1248
D	Fmoc-L-Asp(OtBu)	412	396	594	792
C	Fmoc-L-Cys(Acm)	415	399	598.5	798
Q	Fmoc-L-Gln(Trt)	611	587	880.5	1174
E	Fmoc-L-Glu(OtBu)	444	427	640.5	854
G	Fmoc-Gly	297	286	429	572
H	Fmoc-L-His(Trt)	620	596	894	1192
I	Fmoc-L-Ile	354	340	510	680
L	Fmoc-L-Leu	354	340	510	680
K	Fmoc-L-Lys(Boc)	487	468	702	936
M	Fmoc-L-Met	372	358	537	716
F	Fmoc-L-Phe	388	373	559.5	746
P	Fmoc-L-Pro	338	325	487.5	650
S	Fmoc-L-Ser(tBu)	384	369	553.5	738
T	Fmoc-L-Thr(tBu)	398	383	574.5	766
W	Fmoc-L-Trp(Boc)	527	506	759	1012
Y	Fmoc-L-Tyr(tBu)	460	442	663	884
V	Fmoc-L-Val	340	327	490.5	654
O	Fmoc-L-Cys(Trt)	588	565	847.5	1130

[a] According to the desired final volume of solution, weigh out the indicated quantities, dissolve in the selected volume of NMP, and aliquot under 300 µl.
[b] Aliquot under 150 µl.

5. *Acetylation reagent:* Prepare daily 500 ml of 10% acetic anhydride in DMF
6. *Coloration reagent:* Add 5 ml bromphenol blue stock solution to 395 ml DMF preface translight.
7. *Side chain deprotection reagent:* Mix 15 ml trifluoroacetic acid, 15 ml dichloromethane, and 0.75 ml triethylsilane. *Warning*! Trifluoroacetic acid is extremely corrosive. Gloves and protective mask should be used when preparing and using this reagent.

Procedures

1. *Purity control for DMF and NMP:* Solvents used in Fmoc peptide synthesis should not contain contaminating free amines that could untimely deprotect Fmoc amino acid. To verify the absence of amines, pipette 10 µl of the bromphenol blue stock solution and add 990 µl of the solvent to be tested in a 1.5 ml Eppendorf tube. The solution should be light yellow. A greenish or blueish color indicates contamination with free amines, thus precluding the use of such a solvent.
2. *Synthesis:* Each synthesis cycle involves incorporation of a defined amino acid in the sequence of all peptides at the same time. There are two coupling

steps per cycle to allow the most efficient incorporation of each amino acid. For the first cycle, we recommend repeating the two coupling steps so as to ensure maximum incorporation of the C-terminal residue; it is also advisable to use a 0.2 µl spotting volume instead of 0.3 µl, which is used after.

Synthesis Steps

Thaw the membrane, activators (DIPC solution and HOBT solution), and Fmoc amino acid aliquots for 10 min before step 1.

1. Activate each Fmoc amino acid aliquot: To 300 µl Fmoc amino acid solution, add 150 µL of 1.2 *M* HOBT solution and 150 µl 1.2 *M* DIPC [exception: add 75 µl of each solution to Fmoc-Arg (Pbf), aliquoted under 150 µl. This is done because activated Fmoc-Arg (Pbf) is unstable and has to be renewed for each new cycle.]
2. Place the tubes on the robot tray and initiate the synthesis cycle through the computer interface.
3. Once the two coupling steps are performed, remove the membrane from the robot, place it in a polypropylene box, and then perform the following steps in a fume hood.
4. Wash the membrane with DMF (3 × 2 min).
5. Wash the membrane with methanol (3 × 2 min).
6. Dry the membrane using a hairdryer on the cold position.
7. Install the membrane again on the robot and initiate recoupling.
8. After couplings are performed, remove the membrane from the robot.
9. Wash the membrane with DMF (3 × 2 min).
10. Wash the membrane with acetic anhydride 10% DMF (3 × 10 min) or until the yellow color disappears.
11. Wash the membrane with DMF (3 × 2 min).
12. Wash the membrane with 20% piperidine in DMF (1 × 10 min).
13. Wash the membrane with DMF (5 × 2 min).
14. Wash the membrane (2 × 2 min) with the bromphenol blue working solution (0.5 ml stock solution/40 ml DMF).
15. Wash the membrane with methanol (3 × 2 min).
16. Cold air dry.
17. Before starting a new cycle, activate Fmoc-Arg (Pbf) as before.
18. Place the membrane on the robot and initiate next cycle.

Remarks: (a) steps 4–8 are performed only for cycle 1, i.e., for incorporation of the first residue. (b) After incorporation of the last Fmoc amino acid, the deprotection step is followed by acetylation of the N-terminal residue of each peptide. The protocol is modified as follows:

8. After spotting is performed, remove the membrane from the robot.
9. Wash the membrane with DMF (3 × 2 min).
10. Wash the membrane with 20% piperidine in DMF (1 × 10 min).
11. Wash the membrane with DMF (3 × 2 min).
12. Wash the membrane with acetic anhydride 10% DMF (3 × 10 min).
13. Wash the membrane with DMF (3 × 2 min).
14. Wash the membrane with methanol (3 × 2 min).
15. Cold air dry.

2. *Side chain deprotection:* Because Fmoc amino acids are introduced during synthesis with their side chain rendered chemically inert by protecting groups, a side chain deprotection step is required before using the membrane for immunoassay.

Steps

Warning: Operate under a fume hood. The operator must wear a protection mask and gloves.

1. Put the membrane into a polypropylene box.
2. Add 30 ml of the deprotection reagent.
3. Cover the box and gently agitate it for 1 h.
4. Discard the side chain deprotection reagent and wash the membrane as follows: Dichloromethane (3 × 2 min), DMF (3 × 2 min), 1% acetic acid in water (3 × 2 min), and Methanol (3 × 2 min).
5. Dry the membrane with cold air.
6. Place the membrane in between two pieces of filter paper and then in a sealed plastic bag and store at –20°C.

3. *Cysteine pairing:* Cystine-bridged peptides can be prepared on the membrane. Cysteine residues are introduced into the peptides as *S*-trityl derivatives. After TFA treatment, the cysteine residues are freed of their protecting group and can then be oxidized to cystine using the following procedure.

1. Place the membrane in a polypropylene box.
2. Add 50 ml 10% DMSO in TBS.
3. Cover the box and agitate it gently overnight.
4. Discard the solution and wash the membrane with TBS (5 × 2 min) and Methanol (3 × 2 min).
5. Dry the membrane with cold air.

Recommendations

The length of the peptides that can be prepared in this way has theoretically no limit. However, because side products or impurities cannot be eliminated at the end of the synthesis, it is recommended to keep

peptide length under 30 residues. Preparation of 12-to 15-mers is recommended for routine experiments.

If cysteine residues occur in the protein sequence, it is recommended to incorporate it into peptides as a *S*-acetamidomethyl cysteine derivative. This will keep the sulfhydyl groups definitively protected (to avoid unwanted reactions with the test antibodies, for example). Otherwise, substitution of Cys by Ser is also possible due to the structural similarity between both amino acids.

When preparing overlapping peptides, set the frameshift number to low values: 1 is the best, as all possible overlapping peptides are prepared, whereas a frameshift of two or three has the advantage of decreasing the total number of peptides to be prepared by a factor of two and three, respectively. The number n of overlapping peptides is related to the length of the protein L, the length of the peptides l, and the frameshift F through the formula: $n = 1+[(L\text{-}l)/F]$.

Because there is no easy way to assess the chemical integrity of synthesized peptides, it is recommended to include in the set of peptides to be synthesized one or more a control peptides whose reactivity with a control antibody could be validated. For example, the sequence EQKLISEEDL is the epitope of the commercially available 9E10 anti-myc antibody; therefore, this peptide can be assembled on a spot and tested further for reactivity with the anti-myc antibody.

The bromphenol blue coloration of free amino groups is a convenient but not absolute means to verify coupling efficiency. After Fmoc deprotection, the free amino group is colored by addition of the bromphenol blue solution and, during coupling, acylation of the amino group provokes a color change toward yellow–green. However, some residues (Gly, Pro, *S*-trityl Cys) do not turn blue and phosphorylated residues (Ser, Thr, Tyr) also fail to color because of side chain acidity.

B. Epitope Identification: Membrane Probing with an Antibody

Reagents

Alkaline phosphatase-labeled species-specific antibody (preferably anti-whole molecule antibody) (e.g., anti-mouse or anti-rabbit)
Western Blocking Rangoant, ref 1921 681 from Roche Diagnostics.
MTT, ref. M2128 from Sigma-Aldrich
BCIP, ref. B6149 from Sigma-Aldrich

Solutions

1. *Tris-buffered saline (TBS):* 8 g NaCl, 0.2 g KCl, 6.1 g Tris dissolved in 800 ml Milli-Q water. Adjust to pH 7.0 using HCl and then make up to 1 liter with Milli-Q water.
2. *Tween-TBS (T-TBS):* Add 1 ml Tween 20 to 1 liter TBS
3. *Blocking buffer:* 5 g saccharose plus 10 ml concentrated blocking buffer and 98 ml T-TBS
4. *Citrate-buffered saline (CBS)*: 8 g NaCl, and 0.2 g KCl, and 2.1 g citric acid monohydrate dissolved in about 800 ml Milli-Q water and adjusted to pH 7.0 using concentrated HCl. Then make the solution up to 1 liter.
5. *Alkaline phosphatase substrate:* 180 µl MTT, 150 µl BCIP, 120 µl 1 *M* $MgCl_2$, and 30 ml of CBS
6. *BCIP solution:* Dissolve 60 mg BCIP disodium salt (Sigma) in 1 ml water. Aliquot under 150 µl, keep at –20°C and in the dark.
7. *MTT solution:* Dissolve 50 mg MTT in 0.7 ml DMF plus 0.3 ml water. Aliquot under 200 µl, keep at –20°C and in the dark.
8. *Regeneration reagent A:* Dissolve in about 500 ml Milli-Q water 480 g urea and 10 g sodium dodecyl sulfate (stir and gently warm). When completely dissolved, make the solution up to 1000 ml. Add 0.1% 2-mercaptoethanol just before use.
9. *Regeneration reagent B:* Mix (in this order) 500 ml ethanol, 400 ml Milli-Q water, and 100 ml acetic acid.

Procedures

1. *Probing the membrane:* After synthesis and deprotection, the air-dried membranes should be stored in a sealed plastic bag at –20°C. Probing the reactivity of the membrane with a defined antibody takes 24 h and should be ideally started on the evening.

Steps

Prior to use, warm the membrane up to room temperature if it has been stored at –20°C and wash it three times with methanol.

1. Wash the membrane three times 10 min with TBS.
2. Incubate overnight with blocking buffer.
3. Wash with T-TBS (3 × 10 min).
4. Incubate with the antibody in blocking buffer (90 min, 37°C).
5. Wash with T-TBS (3 × 10 min).
6. Add the alkaline phosphatase-labeled secondary antibody in blocking buffer and incubate for 60 min at room temperature.
7. Wash with T-TBS (2 × 10 min).
8. Wash with CBS pH 7.0.[1]
9. Incubate with the alkaline phosphatase substrate (5–40 min, depending on the rapidity of apparition of the blue color on reactive spots).
10. Wash with Milli-Q water (3 × 2 min).

[1] In the case where the reactivity of spots is low, the signal can be enhanced by using 50 m*M* Tris buffer, pH 8.5, instead of CBS, pH 7.0.

The first experiment should consist of probing the reactivity of the alkaline phosphatase-conjugated antibody with the set of peptides in order to assign any further reactivity unambiguously to the antibody. The protocol is as described earlier except that steps 4 and 5 are omitted. Some recommendations concerning this protocol are given later.

1. Blocking nonspecific binding sites. The standard dilution of the concentrated blocking buffer is 1:50; however, if some background binding occurs, a more concentrated solution might be tested (e.g., 1:10).
2. Choosing the appropriate dilution of the antibody. Monoclonal antibodies are generally used at 1 µg/ml in a first attempt; depending on their affinities for peptides, concentrations ranging from 0.1 to 10 µg/ml can be used. We do not recommend the use of more concentrated antibody solutions, which would favor nonspecific binding. For polyclonal antibodies, a 1:1000 dilution can be tested as a first experiment.
3. Detecting antibody bound to peptides. The standard procedure involves secondary antibodies coupled to alkaline phosphatase and a precipitating substrate of the latter. Although other systems can be used, this one is appreciated because of its sensitivity, very low background, and reversibility of the coloration. Stop the coloration reaction by washing the membrane (step 10) before background coloration appears.

Quantification of the results: If necessary, semiquantitative estimates of the coloration can be obtained by scanning the membrane in a black-and-white mode and using freely available software such as Scion or NIH image to integrate the resulting pixel numbers.

Regeneration of the membrane: Stripping off the membrane is important to allow reuse of the membrane. This consists in incubation with DMF to dissolve the precipitated dye and with antigen–antibody dissociation reagents. Use the following protocol.

Steps

Place the membrane into a polypropylene box and perform the successive washings in the indicated order.

1. Milli-Q water (3 × 10 min).
2. DMF (3 × 10 min).
3. Milli-Q water (3 × 10 min).
4. Regeneration reagent A (3 × 10 min).
5. Regeneration reagent B (3 × 10 min).
6. Methanol (3 × 10 min).
7. Dry with cold air.
8. Either start a new experiment or store the membrane at –20°C in a sealed plastic bag.

Problems and Solutions

1. Lack of reactivity. There are many possible explanations for the lack of reactivity of an antibody with the membrane. The first to consider is the dependence of the antibody reactivity on protein conformation, which is often poorly mimicked by short peptides. It is nevertheless recommended to repeat the synthesis step by preparing peptides of a larger size, e.g, 25-mer peptides. This strategy has been very useful in characterizing the epitope of the antifactor VIII mouse antibody (Villard *et al.*, 2002). There are other reasons such as low affinity of the antibody for the peptides. It is recommended to try using a more sensitive revelation system such as chemiluminescence.
2. Background reactivity. The lack of cross-reactivity of the secondary antibody with peptides should be verified in a first experiment (experiment conducted in the absence of the primary antibody). Should any reactivity be observed, another secondary antibody should be tried. If many spots are colored either by the secondary antibody or by the primary plus secondary antibody, this might be due to inadequate saturation; therefore, use a more concentrated solution of blocking buffer.
3. Nonremovable signal. It may occur that the reactivity of the antibody is high and that the standard procedure is not able to clean off the membrane, resulting in a "memory" signal. In this case, stronger cleaning conditions should be used in the regeneration protocol. The number of DMF washes can be increased to six and washings with reagent A and reagent B performed at 37°C. Check the membrane for the absence of reactivity in a standard experiment in which the primary antibody has been omitted.

IV. CONCLUSION

The SPOT method of parallel peptide synthesis has proved over the years to be an excellent approach to decipher protein–protein interaction sites. Its application to the identification of epitopes recognized by monoclonal or polyclonal antibodies is one of the most direct and informative methods available. Hereafter, we briefly comment and illustrate several useful applications of the method.

Defining the main continuous antigenic regions of a protein. By using one or several polyclonal antibodies raised against the protein of interest, the SPOT method can disclose regions of the sequence that are antigenic. From the results, the corresponding antigenic peptide sequences could be made in the form of soluble synthetic peptides to be used either as an antigen to detect

the antibody (typical application for diagnostics) or as an immunogen to raise site-specific antipeptide antibodies that might cross-react with the parent protein with a high probability.

Mapping the epitope recognized by a monoclonal antibody. Due to the monospecificity of monoclonal antibodies, any reactivity of an mAb with one or several peptides from a set of overlapping sequences representing collectively the protein antigen will disclose its epitope with a high degree of precision. As an example, Fig. 2 shows the straightforward identification of the epitope recognized by an anti-human factor VIII antibody.

Deciphering the contribution of every amino acid from the peptide epitope. Once a peptide epitope has been disclosed by using the strategy described earlier, one can easily assess the contribution of each residue in the reactive sequence by preparing a series of alanine analogues of the epitope. Replacing in turn the naturally occurring amino acid by an alanine and comparing the reactivity of each peptide with the reactivity of the natural sequence will pinpoint which amino acid side chain cannot be changed to a simple methyl group (the side chain of Ala). It is currently admitted that the lack of reactivity with an alanine-mutated peptide indicates that this amino acid is critical for epitope recognition by the antibody.

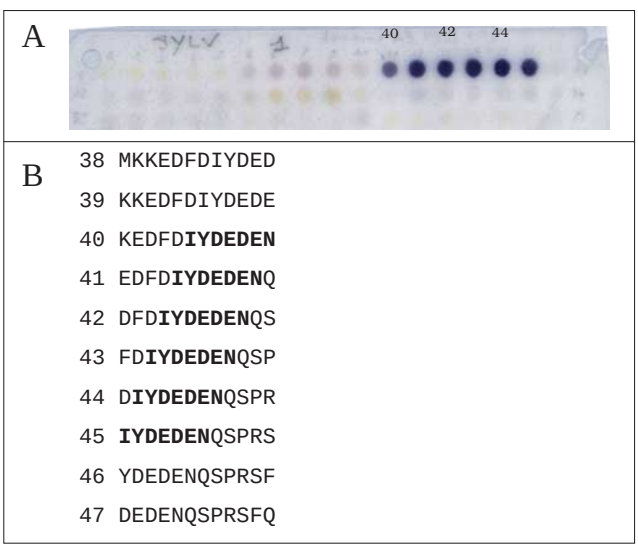

FIGURE 2 Mapping the epitope of a monoclonal anti-human factor VIII antibody. (A) Pattern of recognition of a set of overlapping docecapeptides (frameshift 1) corresponding to (part of) the amino acid sequence of human factor VIII with an anti-factor VIII monoclonal antibody. Peptides 40 to 45 are reactive. (B) Identification of the sequence of the epitope. Sequences of peptides are aligned, and the sequence common to all reactive spots (40–45) is indicated in bold.

It is well known that mAbs raised against globular proteins are mainly dependent on the appropriate conformation of the protein, and as such will not react with peptides. However, many other types of proteins (receptors, structural proteins, regulatory proteins) may behave differently than standard globular proteins when used as immunogens and generate peptide-reactive monoclonals.

Thanks to its versatility, the SPOT method is certainly a key technique to map peptides involved in protein interaction sites. Listing all applications of this approach is clearly beyond the scope of this article. The interested reader will find it useful to read a review on the application of methods of parallel peptide synthesis for deciphering molecular interactions in the immune system (Granier, 2002) or a more general technical book on peptide arrays (Koch and Mahler, 2002).

Acknowledgment

The authors thank Dr. Sharon Lynn Salhi for the editorial revision of the manuscript.

References

Frank, R. (1992). Spot-Synthesis: An easy technique for the positionally addressable, parallel chemical synthesis on a membrane support. *Tetrahedron* **48**, 9217–9232.

Geysen, H. M., Meloen, R. H., and Barteling, S. J. (1984). Use of peptide synthesis to probe viral antigens for epitopes to a resolution of a single amino acid. *Proc. Natl. Acad. Sci. USA* **81**, 3998–4002.

Geysen, H. M., Rodda, S. J., and Mason, T. J. (1986). A priori delineation of a peptide which mimics a discontinuous antigenic determinant. *Mol. Immunol.* **23**, 709–715.

Granier, C. (2002). Special issue on "Methods of parallel peptide synthesis and their contributions to deciphering molecular interactions in the immune system." *J. Immunol. Methods* **267**, 1–2.

Koch, J., and Mahler, M. (2002). *Peptide Arrays on Membrane Supports: Synthesis and Applications.* Springer-Verlag, Berlin.

Molina, F., Laune, D., Gougat, C., Pau, B., and Granier, C. (1996). Improved performances of Spot multiple peptide synthesis. *Pept. Res.* **9**, 151–155.

Reineke, U., Kramer, A., and Schneider-Mergener, J. (1999a). Antigen sequence- and library-based mapping of linear and discontinuous protein-protein-interaction sites by Spot synthesis. *Curr. Top. Microbiol. Immunol.* **243**, 23–36.

Reineke, U., Sabat, R., Misselwitz, R., Welfle, H., Volk, H. D., and Schneider-Mergener, J. (1999b). A synthetic mimic of a discontinuous binding site on interleukin-10. *Nature Biotechnol.* **17**, 271–275.

Van Regenmortel, M. H., and Pellequer, J. L. (1994). Predicting antigenic determinants in proteins: Looking for unidimensional solutions to a three-dimensional problem? *Pept. Res.* **7**, 224–228.

Villard, S., Piquer, D., Raut, S., Leonetti, J. P., Saint-Remy, J. M., and Granier, C. (2002). Low molecular weight peptides restore the procoagulant activity of factor VIII in the presence of the potent inhibitor antibody ESH8. *J. Biol. Chem.* **277**, 27232–27239.

CHAPTER

63

Determination of Antibody Specificity by Western Blotting

Julio E. Celis, José M. A. Moreira, and Pavel Gromov

I. INTRODUCTION

Recent advances in functional genomics, particularly in gene and protein expression profiling technologies (Figeys 2002; Panisko *et al*., 2002; Gerling and Solomon, 2003; Valle and Jendoubi, 2003), have underlined the importance of antibodies to rapidly validate the results in both cultured cells and tissues (see other articles in this volume). The utility of antibodies, however, depends very much on their specificity, and today immunoblotting (Towbin *et al*., 1979; Symington, 1984; Harlow and Lane, 1988; Otto and Lee, 1993), in combination with high-resolution two-dimensional electrophoresis (see articles by Celis *et al*. and by Görg and Weiss), provides the most efficient procedure to determine their specificity.

II. MATERIALS AND INSTRUMENTATION

Tris base (Cat. No. 648311) and Nonident P-40 (NP-40, Cat. No. 492015) are from Calbiochem. Glycine (Cat. No. 808822) is from ICN Biomedicals. Thirty percent hydrogen peroxide (Cat. No. 7209), dehydrated skim milk (Cat. No. 1.15363), and Tween 20 are from Merck. Peroxidase-conjugated antimouse immunoglobulins (Cat. No. P0447) and peroxidase-conjugated antirabbit immunoglobulins (Cat. No. P0217) are from DAKO. The monoclonal antibodies against MEK2, crk-1, NCK, and p27 are from Transduction Laboratories. The polyclonal antibodies against hnRNP K and stratifin are from our laboratory. The monoclonal antibody against hsp28 was kindly provided by A.-P. Arrigo. The HRP colour development reagent (Cat. No. 170-6534) is from Bio-Rad. Nitrocellulose Hybond-C (Cat. No. RPN 203C), the ECL kit (Cat. No. RPN 2106), Lumigen TMA-6 or ECL Advance Western blotting detection kit (Cat. No. RPN 2135), and ECL Advance Western blocking kit are from Amersham. Tissue culture media and supplements are as described elsewhere (Celis and Celis, 1998; see also article by Gromov and Celis). Plates (96 wells, Cat. No. 655180) are from Greiner. Rectangular (24 × 19 cm) dishes are from Corning (Cat. No. PX 38567), and X-ray films (X-Omat UV; 18 × 24 cm, Cat. No. 524 9792) are from Kodak. The Trans-Blot electrophoretic transfer cell is from Bio-Rad (Cat. No. 170-3910), the orbital shaker (Red Rotor PR75) is from Pharmacia, and the roller bottle-type blotter (Navigator, Cat. No. 128-10T1) is from Biocomp.

III. PROCEDURES

The procedure is illustrated using whole protein extracts obtained from noncultured human keratinocytes and the bladder TCC cell line RT4. Proteins are separated by two-dimensional (2D) gel electrophoresis (see article by Celis *et al*.) blotted to a nitrocellulose membrane (Towbin *et al*., 1979), and developed using the HRP colour development reagent and/or the ECL procedure.

A. Blotting

Solution

Tris, glycine, methanol (TGM): 25 m*M* Tris, 192 m*M* glycine, and 20% (v/v) methanol. To make 5 liters,

Copyright 2006, Elsevier Science (USA).
All rights reserved.

weigh 15.14 g of Tris base and 72.07 g of glycine. Add 1 liter of methanol and complete to 5 liters with distilled water.

Steps

1. Prepare the protein extracts and run 2D gels as described in the article by Celis *et al*. Mix the unlabeled cell extract in O'Farrel lysis solution with a small amount of [^{35}S]methionine-labeled proteins from the same source (about 500,000 cpm; for labelling of cells; see article by Celis *et al*.) in order to facilitate the immunodetection of the antigen(s). For 1D blots, resuspend the samples in Laemmli's buffer (Laemmli, 1970).

2. Place a piece of 3MM Whatmann paper, a bit larger than the size of the gel, in a rectangular glass pie dish (24 × 19 cm) containing about 100 ml of TGM. Place the gel on top of the paper.

3. Equilibrate for 5 min at room temperature**.**

4. Wet the fiber gel pads in TGM.

5. Open the gel holder (Fig. 1C) and place one fiber gel pad in each side.

6. Wet the nitrocellulose membrane (14 × 16 cm) in TGM by capillary action as shown in Fig. 1A. Use gloves to handle the membranes.

7. Place the wet nitrocellulose membrane on top of the gel (Fig. 1B). The operation should be done under the buffer. Rub the membrane from one end to the other to eliminate bubbles.

8. Place another wet 3MM Whatmann paper on top of the nitrocellulose membrane. Rub the paper carefully to avoid bubbles. Lift the "sandwich" (same side up) and place it on top of the fiber gel pad located on the black holder (Fig. 1C).

9. Close the gel holder and place it in the Trans-Blot tank containing about 750 ml of TBM. The black side of the holder should face the cathode side (indicated with black in the tank). Up to three holders can be inserted in the tank. If only one cassette is used, insert in the middle track.

10. Fill the tank with TGM, connect the electrodes, and run at room temperature for 24 h at 130 mA.

11. Following protein transfer, dry the membranes and expose to an X-ray film to assess the quality of the transfer (Fig. 3A). Dry sheets can be kept for extended periods of time without significant changes in the reactivity of the proteins. Blots that do not contain radioactivity can be stained with amido black.

B. Immunodetection

1. HRP Colour Development

Solutions

1. *Hank's buffered saline solution (HBSS) without Ca^{2+} and Mg^{2+}*: 10× stock solution. To make 1 liter, weigh 4 g of KCl, 0.6 g of KH_2PO_4, 80 g of NaCl, and 0.621 g of $Na_2HPO_4 \cdot 2H_2O$. Complete to 1 liter with distilled water.

2. *1× HBSS without Ca^{2+} and Mg^{2+}*: To make 1 liter of HBSS, use 100 ml of the 10× stock solution and complete to 1 liter with distilled water.

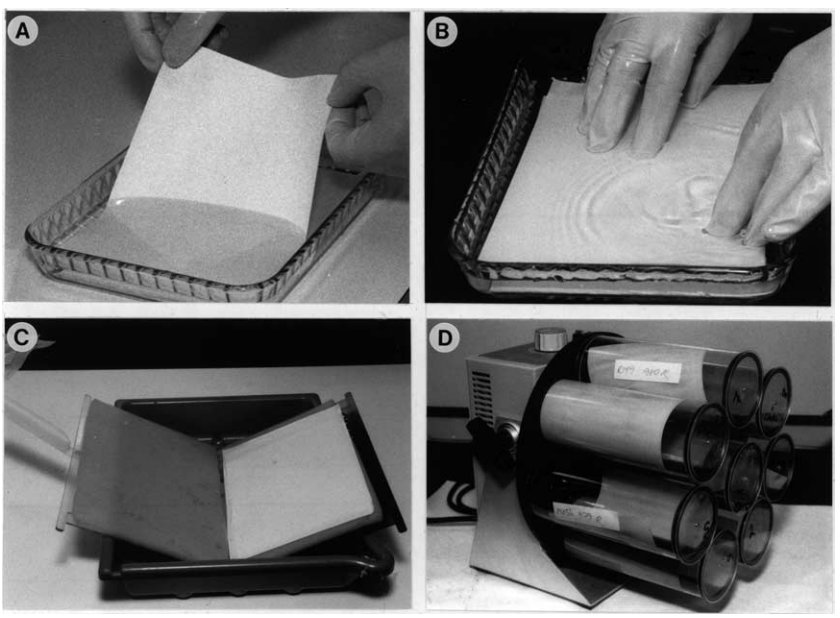

FIGURE 1 (A) Wetting the nitrocellulose membrane. (B) Placing the membrane on top of the gel. (C) Holder with fiber gel pads. (D) Rotating roller system (Navigator).

3. *2× TBS stock*: 0.04 *M* Tris and 0.274 *M* NaCl, pH 7.5. To make 1 liter, add 4.84 g of Tris base and 16 g of NaCl. Adjust to pH 7.5 with HCl and complete to 1 liter with distilled water. Store at 4°C.

4. *Dehydrated skim milk*: 50 mg/ml in HBSS

5. *Primary antibody*: Primary antibodies should be diluted to the a volume of 8 ml. The dilution (1:10 to 1:10,000) should be optimised in preliminary experiments for the best results in terms of high signal and low background.

6. *Horseradish peroxidase-conjugated immunoglobulins (HRP-labeled second antibodies)*: HRP-conjugated secondary antibodies should be diluted to a final volume of 8 ml. The dilution (1:1000 to 1:10,000) should be optimised in preliminary experiments for the best results in terms of high signal and low background

7. *HRP colour development solution*: To make 60 ml, dissolve 30 mg of HRP color development reagent in 10 ml of methanol (protect from light). Mix 30 ml of 2× TBS and 20 ml of distilled water. Just before use add 30 µl of ice-cold 30% H_2O_2 to the TBS and mix the two solutions.

Steps

1. Cut the appropriate area of the blot with a scalpel using the X-ray film as reference and wet by capillarity in the skim milk solution. Incubate with shaking for 1 h at room temperature (or overnight in the cold room) in the same solution. Incubation can be done in a roller bottle-type blotter (Navigator Model 128, Fig. 1D) or a rectangular plastic dish (15 × 18.7 cm; a minimum volume of 40 ml per dish is needed). In the former case, the volume needed is considerably less (8 ml). For 1D gel strips we use the chamber shown in Fig. 2 (Pierce). The following immunodetection procedure is illustrated using the roller bottle-type blotter.

FIGURE 2 Chamber for incubating one-dimensional gel strips with antibodies.

2. Wash the blots three times for 10 min each in HBSS.

3. Add 8 ml of primary antibody diluted in HBSS. Roll for 2 h at room temperature.

4. Wash three times for 10 min each with HBSS.

5. Add 8 ml of a 1:200 dilution of peroxidase-conjugated rabbit antimouse immunoglobulins in HBSS. Roll for 2 h at room temperature.

6. Transfer the blot to a rectangular plastic dish and wash three times for 10 min each in HBSS.

7. Prepare the HRP colour development solution just before use.

8. Aspirate the HBSS and add 30 ml of the HRP solution. Shake at room temperature until staining appears. Discard the HRP colour developer according to the safety regulations enforced in your laboratory.

9. Rinse well with demineralised or tap water and dry. Superimpose the dry blot and the X-ray film with the help of the radioactive marks.

2. ECL Detection

The procedure has been slightly modified from the ECL Western blotting protocol described by Amersham.

Solutions

1. 10× *TBS, pH 7.6, stock*: To make 2 liters, add 48.4 g Tris base (0.20 *M*) and 160 g NaCl (1.37 *M*). Adjust to pH 7.6 with HCl (37% fuming) and complete to 2 liters with distilled water. Store at 4°C.

2. *TBS–Tween 0.05%*: To make 1 liter, add 100 ml of 10× TBS, 0.5 ml of Tween 20, and complete to 1 liter with distilled water.

3. *Blocking solution*: 5% skim milk; 5 g per 100 ml of TBS–Tween.

4. *Primary antibody*: Primary antibodies should be diluted to a final volume of 8 ml. The dilution (1:10 to 1:10,000) should be optimised in preliminary experiments to achieve high signal and low background.

5. *Horseradish peroxidase-conjugated immunoglobulins (HRP-labeled second antibodies)*: HRP-conjugated secondary antibodies should be diluted to a final volume of 8 ml. The dilution (1:1000 to 1:10,000) should be optimised in preliminary experiments to achieve high signal and low background.

Steps

1. Wet the nitrocellulose blot with TBS–Tween in a rectangular plastic dish and transfer it to a bottle (fitting the Nagivator system, Fig. 1D) containing 8 ml of blocking solution.

2. Block for 1 h at room temperature or overnight in a cold room.

3. Rinse the membranes briefly two times in TBS–Tween and wash three times for 10 min each.
4. Add 8 ml of the primary antibody diluted in TBS–Tween and incubate for 1.5 h at room temperature.
5. Rinse the membranes briefly two times in TBS–Tween and wash three times for 10 min each.
6. Add 8 ml of HRP-labelled secondary antibody diluted in TBS–Tween for 1 h at room temperature.
7. Transfer the membrane blot to a plastic dish, rinse briefly two times in TBS–Tween, and wash three times for 10 min each. The next steps are carried out in a dark room.
8. Prepare the detection reagent by mixing 1 ml of detection solution 1 with 1 ml of detection solution 2. This amount is sufficient for one 13 × 15-cm blot.
9. Lift the blot carefully and dry it gently by touching a piece of paper towel. Place the blot on a piece of Saran wrap or on another transparent plastic sheet, protein side up. Add the detection reagent to the protein side of the blot, cover it quickly with another piece of Saran wrap, and smooth out air pockets gently.
10. Incubate for 1 min at room temperature.
11. Drain off excess detection reagent with a soft kitchen paper and place the sandwich in the film cassette. Try to work as quickly as possible. The next step is carried out in a dark room.
12. Turn off the light (red safety light is allowed). Place an X-ray film on top of the membrane and close the cassette. Expose for 5, 15, and 30 s and up to 15 min if necessary.

Figure 3 shows several IEF 2D gel blots of protein from noncultured human keratinocytes reacted with antibodies against crk-1, galectin 1, hnRNP K, NCK, hsp28, and p27 antibodies (Figs. 3B). The positions of the corresponding spots in the autoradiograms are indicated (Fig. 3A).

3. Ultrasensitive Chemiluminescent Detection on Blotting Membranes

While the ECL chemiluminescent detection system for assaying proteins yields rapid luminescence with a good signal-to-noise ratio, such luminescence is short lived and of modest intensity. This detection method is thus significantly limited in its ability to detect small amounts of the target analyte. Therefore, assays of longer duration and/or higher sensitivity are required in cases of limiting amounts of sample/antibody or proportionally minute amounts of target analyte in a sample. Several high-sensitivity substrates, such as the SuperSignal West substrates (Pierce Biotechnology, Inc.), Lumigen PS-3, and TMA-6 (Lumigen, Inc.), have been developed to address this need. The following protocol is based on an ultrasensitive HRP substrate,

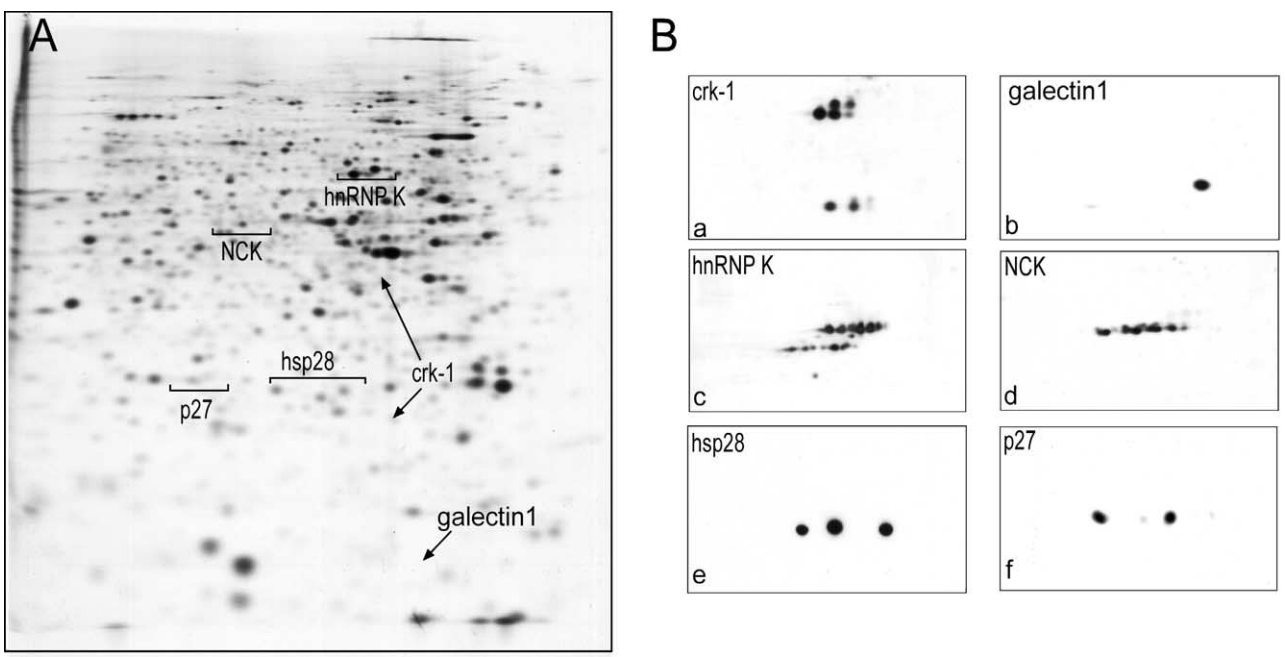

FIGURE 3 Two-dimensional ECL immunoblots of proteins from a bladder transitional cell carcinoma labelled with [^{35}S]methionine (A) and reacted with antibody (B) against crk-1 (a), galectin 1 (b), hnRNP K (c), NCK (d), hsp28 (e), and p27 (f).

Lumigen TMA-6 (commercialised by Amersham as ECL Advance western blotting detection kit), as an alternative to the standard ECL detection method. This procedure is particularly useful for low abundance proteins or limited availability of antibody.

Solutions

1. *10× TBS, pH 7.6, stock*: To make 2 liters, add 48.4 g Tris base (0.20 *M*) and 160 g NaCl (1.37 *M*). Adjust to pH 7.6 with HCl (37% fuming) and complete to 2 liters with distilled water. Store at 4°C.
2. *TBS–Tween 0.2%*: To make 1 liter, add 100 ml of 10× TBS, 2 ml of Tween 20, and complete to 1 liter with distilled water.
3. *Blocking solution*: 2% ECL Advance blocking agent; 2 g per 100 ml of TBS–Tween
4. *Rabbit polyclonal antistratifin* (14-3-3σ) *peptide antibody*

Steps

1. Wet the nitrocellulose blot with TBS–Tween in a rectangular plastic dish and transfer it to a bottle (fitting the Nagivator system, Fig. 1D) containing 10 ml of blocking solution.
2. Block for 1 h at room temperature or overnight in a cold room.
3. Wash twice for 1 min in TBS–Tween.
4. Add 10 ml of the primary antibody, in this case rabbit polyclonal antistratifin (14-3-3σ) diluted 1 : 15,000 in blocking solution, and incubate for 1 h at room temperature.
5. Wash three times for 5 min and once for 15 min in TBS–Tween.
6. Briefly rinse the membrane with two changes of TBS–Tween.
7. Add 10 ml of peroxidase-conjugated secondary antibody diluted 1 : 10,000 in blocking solution for 1 h at room temperature.
8. Transfer the membrane blot to a plastic dish and wash three times for 5 and once for 15 min in TBS–Tween.
9. Briefly rinse the membrane with two changes of TBS–Tween.
10. Mix 5 ml of detection solution A with 5 ml of detection solution B. This is sufficient for at least one 13 × 15 cm blot.
11. Lift the blot carefully with forceps and dry it gently by touching the edge against a piece of paper towel. Place the blot in a clean plastic dish and add the detection solution. Leave for 5 min. Do not shake.
12. Let the solution run off the blot as described earlier and put it on top of a piece of plastic in a film cassette (protein side up). Cover it quickly with Saran wrap and carefully smooth out air pockets with a piece of paper. The next steps are carried out in a dark room.
13. Turn off the light (red safety light is allowed). Place an X-ray film on top of the membrane and close the cassette. Expose for 5, 15, and 30 s and up to 1 h if necessary.

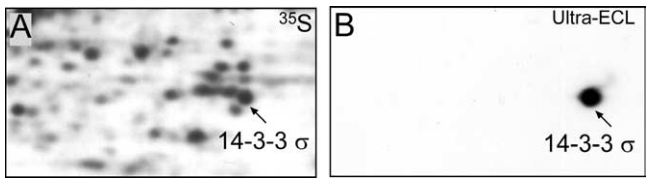

FIGURE 4 Two-dimensional immunoblot of proteins from the bladder cancer cell line RT4 labelled with [35]Smethionine (A) reacted with a peptide antibody against 14-3-3σ (B) and developed with Lumigen TMA-6.

Figure 4 shows an IEF 2D gel blot of [35S]methionine-labeled proteins from RT4 cells reacted with the anti-stratifin (14-3-3σ) peptide antibody.

IV. PITFALLS

A. Blotting

1. Remove excess vaseline floating in the buffer with a tissue.
2. Avoid air bubbles when making the "sandwich" and lifting it to the fiber gel pad.
3. For 2D gel blotting, it is important to run a range of concentrations of the protein mixture. Choose a protein concentration that does not give streaking. Never run more protein than is necessary.
4. Membrane proteins may streak and it may be necessary to use special detergents (Santoni *et al.*, 2000; Tastet *et al.*, 2003)

B. HRP Colouring Development

H_2O_2 is unstable. Check the expiration date on the bottle.

C. ECL Detection

1. It is essential to determine optimal antibody concentrations using dot blots. Be aware that some antibodies may require dilutions of up to 1 : 100,000 when using the ECL Advance Western blotting kit.
2. Use abundant volumes of buffer during the washing steps.

3. It is important to use an optimised the amount of blocking agent. We usually use the ECL Advance blocking agent, but other blocking agents (e.g., SuperBlock, Pierce Biotechnology Inc.) can be used and, in certain circumstances, perform better. As signal emission is stable for several hours, maximal reduction of background noise and nonspecific binding allows detection of even minute amounts of the target protein.

References

Celis, J. E., *et al.* (1991). The master two-dimensional gel database of human AMA cells proteins: Towards linking protein and genome sequence and mapping information. *Electrophoresis* **12**, 765–801.

Figeys, D. (2002). Functional proteomics: Mapping protein-protein interactions and pathways. *Curr. Opin. Mol. Ther*. **4**, 210–215.

Gerling, I. C., Solomon, S. S., and Bryer-Ash, M. (2003). Genomes, transcriptomes, and proteomes: Molecular medicine and its impact on medical practice. *Arch. Intern. Med*. **163**, 190–198.

Harlow, E., and Lane, D. (1988). "Antibodies: A Laboratory Manual." Cold Spring Harbor Laboratory, Cold Spring Harbor, NY.

Laemmli, U. K. (1970). Cleavage of structural proteins during the assembly of the head of bacteriophage T4. *Nature (London)* **227**, 680–685.

O'Farrell, P. H. (1975). High resolution two-dimensional electrophoresis of proteins. *J. Biol. Chem*. **250**, 4007–4021.

O'Farrell, P. Z., Goodman, H. M., and O'Farrell, P. H. (1977). High resolution two-dimensional electrophoresis of basic as well as acidic proteins. *Cell* **12**, 1133–1142.

Otto, J. J. (1993). Immunoblotting. *In* "Antibodies in Cell Biology" (D. J. Asai, ed.), pp 105–117. Academic Press, San Diego.

Panisko, E. A., Conrads, T. P., Goshe, M. B., and Veenstra, T. D. (2002). The postgenomic age: Characterization of proteomes. *Exp. Hematol*. **30**, 97–107.

Santoni, V., Molloy, M., and Rabilloud T. (2000). Membrane proteins and proteomics: un amour impossible? *Electrophoresis* **21**, 1054–1070.

Symington, J. (1984). *In* "Two-Dimensional Gel Electrophoresis of Proteins: Methods and Applications" (J. E. Celis, R. Bravo, eds.), pp. 126–168, Academic Press, New York.

Tastet, C., Charmount, S., Chevallet, M., Luche, S., and Rubilloud, T. (2003). Structure-efficiency relationships of zwitterionic detergents a protein solubilizers in two-dimensional electrophoresis. *Proteomics* **3**, 111–121.

Towbin, H., Staehelin, T., and Gordon, J. (1979). Electrophoretic transfer of proteins from polyacrylamide gels to nitrocellulose sheets: Procedure and some application. *Proc. Natl. Acad. Sci. USA* **76**, 4350–4354.

Valle, R. P., Jendoubi, M. (2003). Antibody-based technologies for target discovery. *Curr. Opin. Drug. Disco v. Dev*. **6**, 197–203.

CHAPTER

64

Enzyme-Linked Immunosorbent Assay

Staffan Paulie, Peter Perlmann, and Hedvig Perlmann

I. INTRODUCTION

The enzyme-linked immunosorbent assay (ELISA) (Engvall and Perlmann, 1971) is a highly versatile and sensitive technique that can be used for qualitative or quantitative determinations of practically any antigen or antibody (Berzofsky *et al*.,1999). Reagents are stable, nonradioactive, and, in most cases, available commercially. Its use ranges from testing of individual samples to fully automated systems for high throughput screening. In one of its simplest forms, the assay involves immobilization of one reagent (e.g., antigen) on a plastic surface, followed by the addition of test antibodies specific for the antigen and, after washing, enzyme-conjugated secondary antibodies against the test antibodies. The addition of substrate giving coloured, fluorescent, or luminescent reaction products makes it possible to determine the concentrations of the reactants at very low levels (Butler, 1994). Depending on the quality of the reagents used and the choice of substrate, sensitivities in the picogram or subpicogram per milliliter range can be obtained.

Of several enzymes suitable for ELISA, alkaline phosphatase (ALP) and horseradish peroxidase (HRP) are the most commonly used. Various methods of enhancing sensitivity may be employed, most of which, like the commonly used biotin–streptavidin system, are designed to amplify the signal by increasing the amount of enzyme bound (Ternynck and Avrameas, 1990).

This article provides three examples of ELISA protocols: an indirect ELISA to determine antibodies (the prototype for many serological assays) and two sandwich or catcher ELISAs designed for the detection of antigen and antibodies, respectively. For the many other variants and applications of ELISA, the literature should be consulted (e.g., see Butler, 1994; Maloy *et al*., 1991; Mark-Carter, 1994; Ravindranath *et al*., 1994; Zielen *et al*., 1996).

One important modification of the ELISA is the ELISpot, which instead of measuring an analyte in solution measures it at the site of a producing cell. This is made possible by using a precipitating rather than a soluble substrate, with the result being a visible imprint or spot, each representing an individual, producing cell. Enumeration of the spots gives the frequency of producing cells, which may be as low as 1 in 100,000 cells. Due to its very high sensitivity, the ELISpot is particularly well suited for measuring specific immune responses and it was originally developed for the detection of immunoglobulin production by specifically stimulated B cells (Czerkinsky *et al*., 1983; Sedgwick and Holt, 1983). However, today it is mainly used for the analysis of specific T-cell responses where the induced production of cytokines by antigen-triggered T-cells is exploited (Lalvani *et al*., 1997; Larsson *et al*., 2002). Depending on the cytokine analysed the test may, apart from the number of responding cells, also give information about the type of responding cell (e.g., CTL, Th-1, or Th-2).

II. MATERIALS AND INSTRUMENTATION

A. Elisa

Flat-bottomed microtiter plates: Maxisorp from Nunc A/S or High Binding from Costar (Cat. No. 3590)
Round-bottomed microtiter plates for preparation of dilutions

Copyright 2006, Elsevier Science (USA).
All rights reserved.

Micropipette, multichannel pipette (Cat. 4540-500), and disposable pipette tips (Finnpipette)
Microplate washer (Skatron Instruments)
V_{max} kinetic microplate reader with computer program SOFTmax (Cat. No. 79-200 105, 79-200 100)

B. ELISpot

96-well PVDF (polyvinylidene) filter membrane plates (Millipore Corporation)
Sterile plastic vials for the handling of cells and preparation of dilutions
Cell culture medium RPMI 1640 with 10% fetal calf serum (FCS, Invitrogen)
Cell incubator with 5% CO_2 atmosphere
Dissection microscope (40×) or ELISpot reader (AID, Autoimmun Diagnosticka GmbH)

III. PROCEDURES

A. Biotinylation of Immunoglobulin

See *Ternynck and Avrameas (1990).*

Solutions

1. *0.1 M $NaHCO_3$*: 84.01 g/1000 ml H_2O, pH 8.4
2. *Biotin*: Sulfo-NHS-LC-biotin [sulfosuccinimidyl-6-(biotinamido)hexanoate] (Cat. No. 2135) (Pierce)

Steps

1. Dialyze affinity-purified polyclonal antibodies or purified monoclonal antibodies against 0.1 *M* $NaHCO_3$ at 4°C overnight and adjust to 2 mg/ml.
2. Immediately prior to use, dissolve 1 mg of biotin in deionized water and add the biotin to the antibody solution at a molar ratio of 20:1. Incubate for 30–60 min.
3. Dialyze overnight at 4°C against phosphate-buffered saline (PBS) with 0.02% NaN_3.

B. Optimal Reagent Concentrations

1. *Concentration of coating reagent*: Most plates designed for ELISA have a protein-binding capacity of 300–600 ng protein per well (96-well plates). In practice, if using purified antigens, affinity-purified polyclonal antibodies, or monoclonal antibodies, coating with 1 µg/ml (100 µl/well) is normally sufficient. Most proteins coat well in PBS but, if there are indications of poor coating efficiency, buffers with different pH should be tried. This may be particularly important when using smaller peptides for coating.

2. *Concentration of test reagent*: If possible, use one known positive, one known negative, and, if available, a standard. Find the concentration where the known positive sample gives a good positive reading and responds to dilution.

3. *Concentration of developing reagent*: Choose the lowest concentration assuring excess; the only limiting factor in the setup should be the amount of test reagent. Typically, the detecting reagents (e.g., biotinylated or enzyme-conjugated secondary antibody) are used at concentrations around 1 µg/ml but should be determined by titration.

C. ELISA and ELISpot Protocols

Solutions

1. *Coating buffer*: PBS, pH 7.4: 100 ml PBS stock (10×), 200 mg NaN_3, and H_2O to 1000 ml or, alternatively, 0.1 *M* $NaHCO_3$ pH 9.6: 1.59 g Na_2CO_3, 2.93 g $NaHCO_3$, 200 mg NaN_3, and H_2O to 1000 ml
2. *Incubation (diluent) buffer*: 100 ml PBS stock (10×), 5 g bovine serum albumin (BSA), 0.5 ml Tween 20, 200 mg NaN_3, and H_2O to 1000 ml
3. *Washing buffer*: 45 g NaCl, 2.5 ml Tween 20 (0.05%), and H_2O to 5000 ml
4. *Streptavidin-ALP*: Sigma-Aldrich
5. *Enzyme substrate buffer*: 97 ml diethanolamine, 800 ml H_2O, 200 mg NaN_3, and 101 mg $MgCl_2 \cdot 6H_2O$ (should be added last). Adjust finally to pH 9.8 with 1 *M* HCl (~100 ml).
6. *Substrates for ALP*: *p*-nitrophenyl phosphate (NPP), 5-mg tablets (Sigma-Aldrich), 1 tablet/5 ml of enzyme substrate buffer (ELISA). BCIP/NBT-Plus (Moss, Inc.)

1. Indirect ELISA for Screening of Specific Antibodies in Serum or Hybridoma Supernatants

Reactants

1. *Antigen*
2. *Antibody specific for test antigen*
3. *Anti-immunoglobulin enzyme conjugate*
4. *Substrate*

Steps

1. Coat plate with 100 µl/well of antigen, diluted in PBS, pH 7.2, overnight at 4°C.
2. Block with 100 µl/well of incubation buffer for 1 h at room temperature (37°C). Wash four times with washing buffer.
3. Add 100 µl/well of immune serum, e.g., diluted 1/1000, or hybridoma supernatant, e.g., diluted 1/5, in incubation buffer and incubate for 2 h at room temperature. Wash four times with washing buffer.

4. Add 100 µl/well of ALP-conjugated anti-immunoglobulin (e.g., goat antihuman γ chains, rabbit antimouse Ig) diluted in incubation buffer. Incubate for 1 h at room temperature (37°C). Wash four times with washing buffer.
5. Develop with fresh NPP, 100 µl/well, and read absorbance at 405 nm.

2. *Sandwich ELISA for Detecting Antigens*

Reactants

1. *Capture antibody specific for test antigen*
2. *Antigen*
3. *Biotinylated antibody specific for test antigen*; See Section IV
4. *Streptavidin-ALP*
5. *Substrate*

Steps

1. Coat plate overnight at 4°C with 100 µl/well of antigen-specific monoclonal or polyclonal antibody diluted in PBS.
2. Block with 100 µl/well of incubation buffer for 1 h at room temperature. Wash four times with washing buffer.
3. Add 100 µl/well of test reagent (e.g., cell culture supernatant or diluted serum sample) and, if available, a standard antigen in serial dilutions. Incubate for 1 h at 37°C. Wash four times with washing buffer.
4. Add 100 µl/well of biotinylated monoclonal antibody specific for a different determinant of the antigen or biotinylated polyclonal antibody of the same antigen specificity as used for coating (see Section IV) diluted in incubation buffer. Incubate for 1 h at 37°C. Wash four times with washing buffer.
5. Add 100 µl/well of ALP-conjugated streptavidin in incubation buffer for 1 h at 37°C. Wash four times with washing buffer.
6. Develop with fresh NPP, 100 µl/well, and read absorbance at 405 nm.

3. *Sandwich ELISA for Detection of Specific Antibodies*

Several recently developed serological assays are similarly based on the sandwich ELISA principle but use antigen rather than antibodies for coating and detection. Exploiting the fact that antibodies, also after binding to an antigen immobilized on an ELISA plate, usually retain a free antigen-binding site (IgG) or sites (IgM), labeled antigen may be used as a detecting agent. Being less prone to background problems often encountered in conventional serological assays it is more reliable and, as it allows the testing of less diluted samples, also more sensitive.

Reactants

1. *Capture antigen to which antibody reactivity is to be tested*
2. *Biotinylated form of the same antigen*
3. *Streptavidin-ALP*
4. *Substrate*

Steps

1. Coat plate overnight at 4°C with 100 µl/well of relevant antigen in PBS.
2. Block with 100 µl/well of incubation buffer for 1 h at room temperature. Wash four times with washing buffer.
3. Add 100 µl/well of serum to be tested. Incubate for 1 h at 37°C. Wash four times with washing buffer.
4. Add 100 µl/well of the same antigen as used for coating in biotinylated form (see Section IV) diluted in incubation buffer. Incubate for 1 h at 37°C. Wash four times with washing buffer.
5. Add 100 µl/well of ALP-conjugated streptavidin in incubation buffer for 1 h at 37°C. Wash four times with washing buffer.
6. Develop with fresh NPP, 100 µl/well, and read absorbance at 405 nm.

4. *Cytokine ELISpot*

Different types of cells can be analysed in the ELISpot. Typically, for the analysis of specific T-cell responses in humans, peripheral blood mononuclear cells (PBMC) containing both T-cells and antigen presenting cells are used.

Reactants

1. *Antibody specific for the test cytokine*
2. *Biotinylated anticytokine antibody*: Of noncompeting specificity
3. *Streptavidin-ALP*
4. *Substrate*

Steps

1. Before coating with antibody, activate the PVDF membrane by adding 100 µl/well with 70% EtOH and incubate for 1–2 min. Wash plates with 4 × 200 µl sterile-filtered PBS and, without letting the membrane dry, add 100 µl of antibodies against test cytokine (15µg/ml in sterile PBS) and incubate overnight at 4°C.
2. Remove excess antibody by washing (4 × 200 µl/well) and block the membrane by adding 150 µl/well with serum containing (e.g., 10% FCS) tissue culture medium. Incubate for 1 h at room temperature.
3. Add PBMC together with the antigen to be tested in triplicate. Use cells without antigen as control for spontaneous cytokine production and a polyclonal

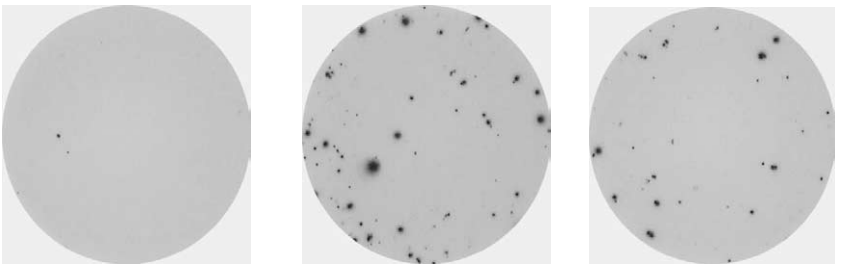

unstimulated (250,000 cells) | *PPD stimulation* (250,000 cells) | *TT stimulation* (250,000 cells)

FIGURE 1 PBMC from a vaccinated donor was exposed *in vitro* for 16 h to the antigens purified protein derivative (PPD) or tetanus toxoid (TT) and investigated for the presence of IFN-γ-producing cells.

activator (e.g., 1–10 µg/ml of phytohemagglutinin) as a positive control for activation. The suitable number of cells analysed should be determined for each situation but do not add more than 300,000 cells/well, as this will result in multiple cell layers leading to diffuse spots. Depending on the kinetics of the cytokine analysed, incubate for 12–48 h at 37°C in a cell incubator with a humid atmosphere and containing 5% CO_2. Do not move the plates during incubation.

4. Wash the plates with filtered PBS (4 × 200 µl/well).
5. Add 100 µl of biotinylated anticytokine antibody in filtered PBS. Incubate for 2 h at room temperature.
6. Wash as described earlier and add 100 µl streptavidin-ALP, diluted 1/1000 in filtered PBS. Incubate for 1 h at room temperature.
7. Wash as described previously, add substrate (BCIP/NBT-plus), and incubate at room temperature until dark spots emerge (10–30 min). Stop color development by washing with 4 × 200 µl/well of tap water.
8. Leave plates to dry and count spots in a dissection microscope or an ELISpot reader.
9. Store plates in the dark at room temperature (Fig. 1).

IV. COMMENTS

A. Blocking

1. ELISA

Aftercoating is required to block vacant protein-binding sites on the plastic surface. BSA, casein, milk powder, or gelatin is commonly used. To avoid cross-reactive antibody binding to the blocking protein, the same protein as used for dilution of the reagents should be included in the incubation (diluent) buffer.

2. ELISpot

Although the filter membranes used in ELISpot have a much higher binding capacity than ELISA plates (up to 100 times higher binding), aftercoating is not always required due to the blocking effect of serum components in the cell culture medium. However, to avoid possible triggering of cell surface receptors through interactions with the highly adsorptive membrane, blocking for 1 h in culture medium before the addition of cells is usually recommended.

B. Controls

1. ELISA

Wells containing substrate but no reagents serve as a general background to be subtracted from all measured values. All samples are set up in duplicates. Negative controls with incubation buffer replacing the reagents to be tested should always be included and should give readings well below OD 0.100. Particularly in the two-site sandwich applications, it is essential that the capture antibody does not bind to the second antibody and vice versa. For screening of unknown samples, and comparison between different runs, include a known positive sample as a reference. For estimation of background, include expected negatives, e.g., nonimmune sera, cell culture medium, or irrelevant antigen.

2. ELISpot

Controls usually comprise wells with unstimulated cells, giving the frequency of spontaneously producing cells. In the case of cytokine-producing cells, the levels of spontaneous production may differ significantly for different cytokines and are usually higher in individuals with acute infections. Positive controls in the form of polyclonally activating reagents (e.g., PHA

or anti-CD3) or specifically activating peptides from common infectious agents can be used (Currier *et al*., 2002).

C. Incubations

Coating the plates overnight is often practical and the coated plates can be stored for several weeks at 4°C, wrapped in plastic film. Coating for 3–4 h at room temperature or 1 h at 37°C may often be enough. The same holds true for the specific binding of the reagents. The signal may be increased significantly by longer incubations but shorter incubations at 37°C may suffice as well. Development of colour with the substrate varies in time but requires usually between 10 and 60 min depending on the enzyme system used.

D. Amplification

Amplification of the signal in ELISA may be obtained by various means. Using an extra layer such as enzyme-conjugated anti-immunoglobulin as developing reagent or biotinylated antibody followed by the streptavidin–enzyme conjugate can lead to increased sensitivity. Similarly, using fluorescent (Rodriguez *et al*., 1998) or chemiluminscent (Tatsumi *et al*., 1996; Fukuda *et al*., 1998) substrates instead of chromogenic substrates, sensitivity can be improved 10- to 100-fold. Due to the increased sensitivity, amplified assays are often more prone to variations and background problems and usually require more careful handling and extensive washings.

E. Sandwich ELISA

Antibody sandwich ELISAs are sensitive and very useful for the detection of antigen, e.g., cytokines in cell culture supernatants. To work, the analysed substance needs to have at least two separate binding sites for antibodies and is therefore not amenable to the analysis of small molecules. Both polyclonal and monoclonal antibodies may be used. As an example, for determining human interleukin (IL)-4 we use monoclonal antibodies of two different specificities against IL-4. For immunoglobulin isotype determinations in human serum or lymphocyte culture supernatants we use goat or rabbit antibodies made highly Fc specific by affinity purification. The same polyvalent antibody preparation can be used both as capture antibody and as enzyme-conjugated or biotinylated second antibody. For IgG subclass determinations, we use subclass-specific monoclonal antibodies as capture antibodies and Fc-specific, affinity-purified (depleted of antimouse Ig reactivity) goat antihuman IgG as the secondary antibody. For quantitation of isotypes or IgG subclasses, standard immunoglobulin preparations or myeloma protein solutions of known concentrations are available commercially.

F. Quantitation

For quantitation of specific antibodies, a standard curve with serial dilutions (e.g., 300, 100, 30, 10, 3, and 1 ng/ml) of a relevant standard immunoglobulin is prepared in wells coated with affinity-purified anti-immunoglobulin instead of the antigen. The linear range from a log/log curve is used for interpolation of the experimental values. Similarly, the amount of antigen can be determined in a sandwich ELISA with the help of a standard curve with known amounts of the antigen run in parallel. One standard curve can be used for several plates if care is taken that all plates are developed at the same time.

V. PITFALLS

A. Background

In both ELISA and ELISpot, a high purity and specificity of the reagents are basic requirements for reliable determinations. As much of the sensitivity of the assays depends on having a low background, low readings of the negative controls are absolutely essential. With appropriate controls it is usually possible to identify reagents giving rise to unwanted binding of the enzyme conjugate. However, this is not always the case as, when analyzing serum/plasma samples in sandwich ELISA, the presence of naturally occurring anti-immunoglobulin in some individuals may lead to cross-linking of the coating and detecting antibodies and thereby cause false-positive signals not easily discernible from a true positive signal. This effect can be prevented or minimized by the inclusion of irrelevant blocking antibodies in the incubation buffers.

Another phenomenon that may affect both ELISA and ELISpot is the so-called "edge effect," which refers to the often lower reproducibility obtained in the outer wells of a 96-well plate. Being at least partly due to a greater evaporation in these wells, it is essential that all incubations are performed in a way that evaporation is minimized.

A particular background problem that may occur in the ELISpot assay is the presence of artifactual spots or spot-like formations. Normally caused by debris from the cells or the buffers, the problem may be largely alleviated by careful washing of the plates and the filtration of the buffers and substrate used. As the

artifactual "spots" are usually smaller and lack the diffuse rim that is characteristic for true spots, they can usually be discriminated from real spots when evaluated in the microscope. Similarly, in most of the existing ELISpot readers a similar function to discriminate artifacts and true spots has been incorporated. In the ELISpot, it is also important that the plate is not moved or shaken during incubation in the cell incubator, as this may result in "blurry" spots and/or an uneven distribution of spots in the wells.

B. Adsorption-Induced Protein Denaturation

Lost functional activity of antibodies is not an uncommon problem and can seriously affect the sensitivity of an assay. As much as 90% of the activity of polyclonal antibodies and all for some monoclonal antibodies can be lost due to the absorption to a solid support (Butler, 2000). Similarly, a changed conformation of antigens at coating may lead to masking of native epitopes, as well as to exposure of "new" epitopes. Varying the binding conditions by using coating buffers of different pH, the addition of stabilizing agents, or the use of alternative binding strategies (e.g., binding biotinylated antibodies to immobilized streptavidin) may help solve this type of problem.

References

Berzofsky, J. A., Berkower, I. J., and Epstein, S. L. (1999). Antigen–antibody interactions and monoclonal antibodies. *In* "*Fundamental Immunology*" (W. E. Paul, ed.), 4th Ed., pp. 88–91, Lippincott-Raven, Philadelphia.

Butler, J. E. (1994). Enzyme linked immuno-sorbent assay. *In* "*Immunochemistry*" (Oss C. J. Van, Regenmortel Van, eds.), pp. 759–803. Dekker, New York.

Butler, J. E. (2000). Solid supports in enzyme-linked immunsorbent assay and other solid-phase immuno-assays. *Methods* **22**, 4–23.

Currier, J. R., Kuta, E. G., Turk, E., Earhart, L. B., Loomis-Price, L., Janetzki, S., Ferrari, G., Birx, D. L., and Cox, J. H. (2002). A panel of MHC class I restricted viral peptides for use as a quality control for vaccine trial ELISPOT assays. *J. Immunol. Methods* **260**, 157–172.

Czerkinsky, C. C., Nilsson, L. A., Nygren, H., Ouchterlony, Ö., and Tarkowski, A. (1983). A solid-phase enzyme linked immunospot (ELISPOT) assay for enumeration of specific antibody secreting cells. *J. Immunol. Methods* **65**, 109–121.

Engvall, K., and Perlmann, P. (1971). Enzyme-linked immunosorbent assay (ELISA): Quantitative assay of immunoglobulin G. *Immunochemistry* **18**, 871–874.

Fukuda, S., Tatsumi, H., and Maeda, M. (1998). Bioluminescent enzyme immunoassay with biotinylated firefly luciferase. *J. Clin. Ligand Assay* **21**, 358–362.

Lalvani, A., Brookes, R., Hambleton, S., Britton, W. J., Hill, A. V., and McMichael, A. J. (1997). Rapid effector function in CD8+ memory T-cells. *J. Exp. Med.* **186**, 859–865.

Larsson, M., Wilkens, D. T., Fonteneau, J. F., Beadle, T. J., Merritt, M. J., Kost, R. G., Haslett, P. A., Cu-Uvin, S., Bhardwaj, N., Nixon, D. F., and Shacklett, B. L. (2002). Amplification of low-frequency antiviral CD8 T cell responses using autologous dendritic cells. *AIDS* **25**, 171–180.

Maloy, W. L., Coligan, J. E., and Paterson, Y. (1991). Indirect ELISA to determine antipeptide antibody titer. *In* "*Current Protocols in Immunology*" (J. E. Coligan, A. M. Kruisbeek, D. H. Margulies, E. M. Shevach, W. Strober, eds.), pp. 9.4.8.–9.4.11. Greene and Wiley-Interscience, New York.

Mark-Carter, J. (1994). Epitope mapping of a protein using the Geysen (Pepscan) procedure. *In* "*Methods in Molecular Biology*" (B. M. Dunn, M. W. Pennington, eds.), Vol. 36, pp. 207–223.

Ravindranath, M. H., Ravindranath, R. M. H., Morton, D. L., and Graves, M. C. (1994). Factors affecting the fine specificity and sensitivity of serum antiganglioside antibodies in ELISA. *J. Immunol. Methods* **169**, 257–272.

Rodriguez, C. D., Fei, D. T., Keyt, B., and Baly, D. L. (1998). A sensitive fluorometric enzyme-linked immunosorbent assay that measures vasculare endothelial growth factor$_{165}$ in human plasma. *J. Immunol. Methods* **219**, 45–55.

Sedgwick, J. D., and Holt, P. G. (1983). A solid phase immuno enzymatic technique for the enumeration of specific antibody-secreting cells. *J. Immunol. Methods* **57**, 301.

Tatsumi, H., Fukuda, S., Kikuchi, M., and Koyama, Y. (1996). Construction of biotinylated firefly luciferases using biotin acceptor peptides. *Anal. Biochem.* **243**, 176–180.

Ternynck, T., and Avrameas, S. (1990). Avidin-biotin system in enzyme immunoassays. *In* "*Methods in Enzymology*" (M. Wilchek E. A. Bayer, eds.), Vol. 184, pp. 469–581. Academic Press, San Diego.

Zielen, S., Broker, M., Strnad, N., Schwenen, L., Schon, P., Gottvald, G., and Hofmann, D. (1996). Simple determination of polysaccharide specific antibodies by means of chemically modified ELISA plates. *J. Immunol. Methods* **193**, 1–7.

CHAPTER

65

Radioiodination of Antibodies

Stephen J. Mather

I. INTRODUCTION

Antibodies are usually radiolabelled in order to characterise the interaction of an antibody with its specific epitope. This characterisation may consist of the localisation of the interaction, e.g., on a Western blot or an immunoscintigraphic image, or alternatively the quantification of the interaction, e.g., in radioimmunoassay. The radionuclide employed and the technique used to incorporate it into the antibody depend on the application envisaged and the means of localisation and/or quantification. Both the *in vitro* and the *in vivo* uses of labelled antibodies span more than 50 years and, during this time, methods for labelling antibodies with at least 20 diffferent radionuclides have been developed. A detailed description of all the techniques used to incorporate all of these radioisotopes is not possible within the space limitations of this book and therefore this article is restricted to the techniques likely to be of interest to the majority of its readership, i.e., radioiodination of antibodies for *in vitro* applications. A more comprehensive review of methods for labelling antibodies with a wider range of radionuclides can be found in Mather (2000).

II. MATERIALS AND INSTRUMENTATION

The antibody to be labelled must be available in a purified form (any contaminating proteins will also be radiolabelled). The antibody concentration should be 100 µg–5 mg/ml in either 0.1 *M* phosphate buffer, pH 7.4, or borate, phosphate, or HEPES buffer, pH 8, as indicated in the procedures.

Radioisotopes are available from Amersham Biosciences: Radioiodine Na^{125}I (100 mCi/ml 3.7 GBq/ml) (IMS30 Amersham), *N*-Succimidyl-3-(4-hydroxy-3-[^{125}I]iodophenyl)propionate, Bolton and Hunter reagent (IM5861). Unless otherwise indicated, all reagents are from Sigma Aldrich Chemical Company, Poole, UK: chloramine-T (40,286-9), sodium metabisulphite (S9000), disodium hydrogen phosphate (21,988-6), sodium dihydrogen phosphate (S8282), Iodogen (Pierce Chemical Company, 28,600), dichloromethane (43,922-3), methanol (44,347-6), Sephadex-G50 fine grade (G-50-80), prepacked PD-10 column (Amersham Biosciences 17-0851-01), bovine serum albumin (BSA) (A7906), silica gel-coated plastic TLC sheets (Polygram 805013, Marchery-Hagel, Duren, Germany), silica gel-impregnated glass fibre (ITLC) sheets (61,885, Pall Corp., Ann Arbor, MI), and Whatman 3 MM Chr paper (Z27,085-7).

Many alternatives exist for the equipment used for these procedures. The following are the ones used in this laboratory: Gamma counter (LKB Ultragamma, Wallac, Finland), vortex mixer (MS2 minishaker, Staufen, Germany), microcentrifuge (MSE Microcentaur, Crawley, UK), rotamixer (Denley Spiramix, Thermo Life Sciences, Basingstoke, England), and Savant Speed-Vac (Westwood, MA).

All radiolabelling procedures must be performed with attention to good radiation safety practice. In particular, radioiodinations should be performed in a well-ventilated fume hood and all containers should be locally shielded by keeping them in small lead pots. A lead–glass L-shield should be used to reduce whole-body radiation doses.

Copyright 2006, Elsevier Science (USA).
All rights reserved.

III. PROCEDURES

A. Radioiodination with Iodine-125 Using Chloramine-T as Oxidant

This procedure is adapted from that originally published by Hunter and Greenwood (1962).

Solutions

1. *0.1 M phosphate buffer, pH 7.4*: Add 19 ml of 0.1 *M* sodium dihydrogen phosphate solution to 81 ml of 0.1 *M* disodium hydrogen phosphate solution. Check the pH and adjust with monobasic or dibasic solutions as required. Store at room temperature for 4 weeks.
2. *Chloramine-T*: 0.5 mg/ml in 0.1 *M* phosphate buffer, pH 7.4. Weigh 5 mg of chloramine-T in a universal container and add 10 ml of 0.1 *M* posphate buffer, pH 7.4. Swirl gently to dissolve. Keep cool until required. Prepare fresh.
3. *Sodium metabisulphite*: 0.5 g/ml weigh 5 mg of sodium metabisulphite in a universal container and add 10 ml of 0.1 *M* phosphate buffer, pH 7.4. Swirl gently to dissolve. Keep cool until required. Prepare fresh.
4. *0.5 M phosphate buffer, pH 7.4*: Add 19 ml of 0.5 *M* sodium dihydrogen phosphate solution to 81 ml of 0.15 disodium hydrogen phosphate solution. Check the pH and adjust with monobasic or dibasic solutions as required. Store at room temperature for 4 weeks.

Steps

1. Into a 1- to 2-ml polypropylene tube pipette 10–100 µg of the antibody and 50 µl of 0.5 *M* phosphate buffer, pH 7.4. Add the desired amount of iodine-125, typically 100 µCi–1 mCi, and mix by gently drawing the solution up and down in the pipette tip.
2. Add 20 µl of chloramine-T solution and mix again.
3. Cap the tube and leave for 5 min.
4. Add 40 µl of sodium metabisulphite solution and mix.
5. If desired, check labelling efficiency by ITLC (see Section III,E). This will typically range from 50 to 80%.
6. Separate labelled antibody from free iodine (see Section III,D).
7. If desired, determine the immunoreactive fraction of the radiolabelled antibody (see Section III,F).

B. Radioiodination with Iodine-125 Using Iodogen as Oxidant

This procedure is adapted from that originally published by Fraker and Speck (1978).

Solutions

1. *Iodogen tubes*: Dissolve 1 mg of Iodogen in 10 ml of dichloromethane in a glass or polypropylene container. Pipette 500 µl into as many 2-ml glass or polypropylene test tubes as required. Evaporate the solvent in a Speed-Vac, with a stream of nitrogen, or by leaving in a laminar flow hood for 2–4 h with the lights turned off. Cap the tubes and store in a closed container at –20°C for up to a year until required.
2. *0.1 M phosphate buffer, pH 7.4*: Add 19 ml of 0.1 *M* sodium dihydrogen phosphate solution to 81 ml of 0.1 *M* disodium hydrogen phosphate solution. Check the pH and adjust with monobasic or dibasic solutions as required. Store at room temperature for 4 weeks.
3. *0.5 M phosphate buffer, pH 7.4*: Add 19 ml of 0.5 *M* sodium dihydrogen phosphate solution to 81 ml of 0.15 *M* disodium hydrogen phosphate solution. Check the pH and adjust with monobasic or dibasic solutions as required. Store at room temperature for 4 weeks.

Steps

1. Into an Iodogen tube pipette 10–100 µg of the antibody and 50 µl of 0.5 *M* phosphate buffer, pH 7.4. Add the desired amount of iodine-125, typically 100 µCi–1 mCi, and mix by gently drawing the solution up and down in the pipette tip. Wait for 10 min mixing gently every 2–3 min.
2. Transfer the reaction mixture to a fresh test tube, wash the Iodogen tube with 0.5 ml of 0.1 *M* phosphate buffer, pH 7.4, and add to the mixture.
3. If desired, check labelling efficiency by ITLC (see Section III,E). This will typically range from 50 to 80%.
4. Separate labelled antibody from free iodine (see Section III,D).
5. If desired, determine the immunoreactive fraction of the radiolabelled antibody (see Section III,F).

C. Iodination of Antibody with "Bolton and Hunter" Reagent

This procedure is adapted from that originally published by Bolton and Hunter (1973).

Solutions

1. *Antibody solution*: 10–100 µg at a concentration of 2–5 mg/ml in 0.1 *M* HEPES, phosphate, or borate buffer, pH 8.0.
2. *Glycine solution*: 0.2 *M* in 0.1 *M* phosphate buffer, pH 8.0.
3. *N*-Succimidyl-3-(4-hydroxy-3-[^{125}I]iodophenyl) propionate. Bolton and Hunter reagent [IM5861, Amersham Pharmacia Biotech, or equivalent].

4. *0.1 M phosphate buffer, pH 7.4*: Add 19 ml of 0.1 *M* sodium dihydrogen phosphate solution to 81 ml of 0.1 *M* disodium hydrogen phosphate solution. Check the pH and adjust with monobasic or dibasic solutions as required. Store at room temperature for 4 weeks.
5. *0.1 M phosphate buffer, pH 7.4 containing 0.05% polysorbate 20 (PBS/Tween)*: Add 50 µl of Tween 20 to 100 ml of 0.1 *M* phosphate buffer, pH 7.4. Mix gently but thoroughly. Store at room temperature for 4 weeks.

Steps

1. Into a 1.5-ml microcentrifuge tube (e.g., Eppendorf) pipette the required radioactivity of Bolton and Hunter reagent. Evaporate the solvent, ideally with a Speed-vac or, alternatively, under a gentle stream of nitrogen.
2. Add the required amount of antibody to the vial. Mix briefly and incubate for 30 min at room temperature.
3. Add 0.5 ml of 0.2 *M* glycine solution. Mix and incubate for a further 10 min.
4. If desired, check labelling efficiency by ITLC (see Section III,E and use ITLC paper and 20% trichloracetic acid as mobile phase). This will typically range from 30 to 50%.
5. Separate labelled antibody from free iodine (see Section III,D).
6. If desired, determine the immunoreactive fraction of the radiolabelled antibody (see Section III,F).

D. Separation of Radiolabelled Antibody from Free Iodide

Solutions

1. *Sephadex gel*: Weigh out 1 g of Sephadex G-50 powder and add 15 ml of deionised water. Mix well and either leave overnight or heat in a boiling water bath for 1 h to allow the gel to swell. Keep at 4°C for 4 weeks.

2. *0.1 M phosphate buffer, pH 7.4*: Add 19 ml of 0.1 *M* sodium dihydrogen phosphate solution to 81 ml of 0.1 *M* disodium hydrogen phosphate solution. Check the pH and adjust with monobasic or dibasic solutions as required. Store at room temperature for 4 weeks.

3. *Bovine serum albumin solution*: 1% BSA in phosphate-buffered saline, pH 7.4 (1% BSA/PBS). Weigh out 1 g of BSA and dissolve by gentle continuous mixing in 100 ml of 0.1 *M* phosphate buffer, pH 7.4. Keep at 4°C for 4 weeks.

Steps

1. Use either a prepacked PD-10 gel-filtration column or, if not available, prepare one as follows: Remove the barrel from a 10-ml disposable syringe and cap the luer tip. Plug the end of the syringe with a small circle of filter paper or lint dressing. Clamp the syringe vertically in a retort stand. Swirl the swollen Sephadex gel and pour as much as possible into the syringe. Allow the gel to settle for a few minutes. Then remove the luer cap and allow the liquid supernatant to run through into a waste container. Gently layer 10 ml of deionised water on top of the gel and allow to run through to waste. Replace the luer cap and use the prepared column as soon as possible.

2. Clamp either a prepacked or the home-made column vertically in a retort stand and remove the luer cap.

3. Wash the column with 30 ml of cold 1% BSA/PBS.

4. Apply the labelled antibody reaction mixture to the surface of the column and allow it to run into the gel. Gently pipette 1 ml of cold 1% BSA/PBS onto the gel and collect the eluate in a test tube.

5. Repeatedly elute the column with ten 1-ml aliquots of 1% BSA/PBS and collect each 1 ml of eluate in a fresh, numbered test tube.

6. Pipette 10-µl samples from each of the eluate fractions into counting tubes and count them in a gamma counter in order to identify tubes containing the labelled antibody fractions (typically tubes 3–5). Use or store the contents as required.

E. Determination of Radiochemical Purity by TLC

Solution

85% methanol solution: Pour 85 ml of methanol into a measuring cylinder and make up to 100 ml with deionised water. Store in a tightly closed container at room temperature for up to 4 weeks.

Steps

1. Cut a piece of chromatographic support material: Whatman 3-mm chromatography paper, silica gel-coated plastic TLC sheets, or silica gel-impregnated glass fibre (ITLC) approximately 1 × 10 cm in size. Make a faint pencil mark 1.5 cm from one end.
2. Pour enough 85% methanol into a 10- to 15-cm-tall glass beaker or similar container until it is 0.5 cm deep. Cover the beaker with a petri dish lid, aluminium foil, or similar.
3. Place a 1-µl spot of the sample to be analysed onto the centre of the pencil mark on the chromatographic strip and allow it to dry.

4. Using forceps, gently place the strip upright in the beaker with the pencil mark at the lower end just above the solvent level. Cover the beaker and allow the solvent to run up the support material.
5. When the solvent is about 5 mm from the top of the strip, remove it from the beaker using forceps and lay it on a clean piece of tissue to dry.
6. Cut the strip into upper and lower halves, place each half into counting tubes, and count the tubes in a gamma counter.
7. Calculate the labelling efficiency as follows:

$$\%\ \text{Labelling efficiency} = \frac{\text{Radioactive counts on lower half of strip}}{\text{Counts on lower half counts on upper half}} \times 100\%$$

F. Measurement of the Immunoreactive Fraction of Radiolabelled Antibody

This assay has been adapted from a method published by Lindmo *et al*. (1984). Modifications include a number of simplifications that make the assay easier and quicker but which could correctly be criticised if used out of context. This modified assay is, therefore, only recommended as a "quality control check" rather than as a way of determining the real immunoreactive fraction of the antibody for which the original published method is recommended.

Solutions

1. *0.1 M phosphate buffer, pH 7.4*: Add 19 ml of 0.1 *M* sodium dihydrogen phosphate solution to 81 ml of 0.1 *M* disodium hydrogen phosphate solution. Check the pH and adjust with monobasic or dibasic solutions as required. Store at room temperature for 4 weeks.

2. *Bovine serum albumin solution*: 1% BSA in phosphate-buffered saline, pH 7.4 (1% BSA/PBS). Weigh out 1 g of BSA and dissolve by gentle continuous mixing in 100 ml of 0.1 *M* phosphate buffer, pH 7.4. Keep at 4°C for 4 weeks.

3. Cells expressing the appropriate antigen. Harvest at least 15×10^6 cells from a sufficient number of tissue culture flasks, using trypsin/EDTA or manual scraping to detach adherent cell lines. Wash the cells and resuspend them in cold 1% BSA/PBS. If required, break up small clumps of cells by repeatedly drawing them up and down in a pipette or by syringing them through a 23-gauge needle until a single-cell suspension is obtained. Measure the cell concentration with a haemocytometer or automated cell counter and dilute to a final concentration of 4×10^6 ml in cold 1% BSA/PBS.

4. Radiolabelled antibody at a concentration of 50 ng/ml in cold 1% BSA/PBS. Freshly prepare at least 4 ml.

5. *Unlabelled antibody*: 400 µg at a concentration of at least 0.5 mg/ml.

Steps

1. Place duplicate rows of 7 × 1.5-ml microcentrifuge tubes in a test tube rack. With a marker pen, label the tubes 1–7 and 8–14. Pipette 0.5 ml of cold 1% BSA/PBS into tubes 2–5 and 9–12.

2. Pipette 0.5 ml of the cell suspension into tubes 1, 2, 6, 8, 9, and 13.

3. Pipette 200 µg of unlabelled antibody into tubes 6 and 13. Mix well.

4. Briefly vortex tube 2 and transfer 0.5 ml of the contents to tube 3. Vortex tube 3 and transfer 0.5 ml to tube 4. Vortex tube 4 and transfer 0.5 ml to tube 5. Vortex tube 5 and discard 0.5 ml.

5. Repeat step 4 with tubes 9–12.

6. Pipette 250 µl of radiolabelled antibody into all tubes. Mix well.

7. Incubate the tubes for 2 h at a constant temperature (preferably 4°C but alternatively at room temperature or 37°C). Mix the tubes either constantly using a mechanical shaker or roller or about every 15 min by hand during the incubation.

8. After the incubation, leave the tubes on ice for 10 min to cool. Centrifuge tubes 1–6 and 8–13 at high speed (e.g., >1000 rpm) for 2 min. Carefully remove and discard the supernatant, taking care not to disturb the cell pellet. Pipette 0.5 ml of cold 1% BSA in PBS into each tube and quickly vortex each tube to resuspend the cell pellet. Recentrifuge and again discard the supernatant.

9. Count all tubes in a gamma counter on the appropriate isotope setting.

10. Analyse data as follows: Divide the counts in tubes 1–5 and 8–12 (bound counts) by an average of the counts in tubes 7 and 14 (total counts) in order to calculate the fraction of counts bound to the cells for each cell concentration. Average the values for duplicate tubes (1 and 8, 2 and 9, 3 and 10, 4 and 11, and 5 and 12).

11. Calculate the cell concentration in each tube (approximately 40, 20, 10, 5, and 2.5×10^5 ml).

12. Plot as y values the *reciprocal* of fraction bound (i.e., total/bound) against the *reciprocal* of cell concentrations as x values. A straight line plot should be obtained. Determine the intercept on the y axis and calculate the reciprocal. This is the immunoreactive fraction.

13. Calculate the contribution made by nonspecific binding (i.e., binding in the presence of a large excess

of unlabelled antibody) by dividing the average of the counts in tubes 6 and 13 by the average of the counts in tubes 7 and 14. This value is generally very low and the nonspecific binding contribution can therefore reasonably be excluded from the calculation of the immunoreactive fraction. If the nonspecific binding is greater that 5% of the total binding, then the causes should be identified and eliminated.

IV. COMMENTS

Many techniques have been developed in the last 50 years for labelling proteins with radioiodine but, for various reasons, most of these are now only of academic interest, at least so far as the routine labelling of antibodies is concerned. For the interested reader, a detailed review has been put together by Dewanjee (1992). The methods practised most widely are those in which the radioiodine is oxidised to a reactive intermediate positively charged species such as the hydrated iodinium ion H_2OI^+, which then reacts via electrophilic substitution for the activated protons on the phenolic ring of the tyrosine side chains. These iodinium species or related cations can be produced by reacting the radioiodide with a variety of oxidising agents, but two in particular have become the most popular: chloramine-T (*N*-chloro-*p*-toluenesulphonamide) and Iodogen (diphenylglycoluril). Methods for labelling antibodies with radioiodine using these two methods were described in Sections III,A and III,B. Both techniques have their own inherent advantages and drawbacks. The Iodogen method (Fraker and Speck, 1978) is extremely simple and largely invariable. The concentration of the oxidant is determined by its very poor solubility in aqueous solvents and therefore the only variables one can change in order to influence the reaction are incubation time and temperature. Even so, this method normally produces very acceptable labelling efficiencies of the order of 80–95%. In contrast, details of the chloramine-T method (Hunter and Greenwood, 1962) vary widely from laboratory to laboratory. Different researchers have their own favoured oxidant concentrations, incubation times, and choice of quenching reagents. This method has the (somewhat theoretical) advantage that it can be tailored for different proteins, but has the disadvantage that the reagents have to be freshly prepared prior to use and overenthusiastic attempts to improve labelling efficiencies with high concentrations of the oxidant can lead to antibody damage.

Only in rare circumstances will either labelling procedure result in labelling efficiencies approaching 100%. The consequence of this is that the reaction mixture will contain a significant proportion of unreacted "free iodide." It is normally desirable to remove this free iodine in order to provide a preparation with sufficiently high radiochemical purity. The most widely used method for the purification of labelled antibody preparations is size-exclusion chromatography on a short Sephadex column as described in Section III,D, but several alternatives, such as ion-exchange chromatography or the use of spin columns, exist, some of which are potentially more convenient. Before and after purification of the labelled antibody it is useful to measure the purity of the labelled antibody preparation, initially to check the efficiency of the labelling procedure and then later to determine the purity of your reagent. A very simple means of measuring this purity, based on ascending thin-layer chromatography, is described in Section III,E.

The main reason for labelling an antibody is to obtain a radioactive molecule that binds to a specific recognition site. It is therefore essential that the antibody retains the ability to bind to its epitope throughout the labelling procedure. The best tests to ensure that this is the case are radioligand binding assays, which measure directly the binding of the radiolabelled molecules rather than the whole population of antibody molecules in solution, most of which will not be labelled. These assays fall into two categories: those used to determine the binding affinity of the antibody and those intended to measure the proportion of labelled molecules that retain some ability to bind specifically to their epitope. For the purposes of a relatively simple check to see if the antibody remains functional after labelling, the latter type of assay is the more appropriate and a protocol describing such a test can be found in Section III,F.

Two main types of mechanism can compromise the immunoreactivity of a labelled antibody. The first is due to the effect of the steric hindrance of the large iodine atom when it is substituted into a critical tyrosine residue close to the binding site of the antibody. Although the radioiodine can potentially react with any of several tyrosine amino acids scattered throughout the antibody molecule, factors such as local charge distribution and accessibility mean that one or more residues will be labelled preferentially. If one of these sites happens to be in one of the critical CDRs, then a significant degree of antibody binding will be lost. If this happens, the number of possibilities for solving the problem are limited. It is possible that a change in pH during the labelling procedure may alter the local charge distribution and favour an alternative tyrosine residue, albeit at the risk of a lower labelling efficiency. If this does not work, then the only alternative is to

use an entirely different chemistry for radioiodination. The most well-established alternative is the Bolton and Hunter method described in Section III,C, which results in antibody labelling at the site of lysine residues.

The other type of mechanism responsible for loss of immunoreactivity is oxidation. In addition to its desired role in oxidising the radioiodide to a reactive species, the oxidant may potentially oxidise critical residues, particularly methionine, in the antibody molecule. A way to find out which of the two possible mechanisms may in fact be the cause of a loss in immunoreactivity is to perform the labelling procedure without the addition of the radioiodine and to perform an ELISA assay. If an oxidative mechanism is responsible, then immunoreactivity will still be lost, as all the antibody molecules will be affected, not only those substituted with radioiodine. If this is found to be the case then either a Bolton and Hunter approach can be pursued or an alternative electrophilic substitution method that does not subject the antibody to such strong oxidising conditions can be employed. Two approaches may work. The first is to use a milder oxidising agent, such as the lactoperoxidase system (Morrison and Bayse, 1970). The alternative is to use a modification of the Iodogen system in which the radioiodine is first oxidised in the iodogen tube but is then transferred from the oxidising environment to another tube containing the antibody (van der Laken *et al*., 1997). It is likely that both of these procedures will result in a lower labelling efficiency but either may solve the problem of oxidative damage to the antibody.

The shelf life of radioiodinated antibodies is limited by radiolysis, which causes a gradual loss in both purity and immunoreactivity. The rate of deterioration can be reduced by the addition of carrier proteins or antioxidants that scavenge the radiolytic free radicals (Chakrabarti *et al*., 1996). A concentration of 0.1–1% albumin or 0.5% ascorbic acid is commonly used and antibodies may be stored in these solutions at either 4 or –20°C for at least a month without a significant loss of quality. If stored below 0°C, then the preparation should be divided into aliquots to save repeated freezing and thawing, which tends to favour aggregation of the antibody. If stored above 0°C, provided it does not interfere with the ultimate application, sodium azide can be added to a final concentration of 0.05% to limit microbial growth.

V. PITFALLS

The most likely cause of failure of any of the labelling methods described here is the presence of impurities in the antibody solution. The best solution is to repurify the antibody by either dialysis or gel filtration into freshly prepared buffers.

The most common problem experienced with the immunoreactive fraction assay described in Section III,F is that a curve, rather than a straight line, is obtained when data are plotted. This is nearly always caused by inaccuracies in diluting and losses in washing the cells. With practice and care, the problem usually goes away.

References

Bolton, A. E., and Hunter, W. M. (1973). The labelling of proteins to high specific activities by conjugation to a 125-I-containing acylating agent. *Biochem. J.* **133**, 529–538.

Chakrabarti, M. C., Le, N., Paik, C. H., De Graff, W. G., and Carrasquillo, J. A. (1996). Prevention of radiolysis of monoclonal antibody during labeling. *J. Nuclear Med.* **37**(8), 1384–1388.

Dewanjee, M. K. (1992). Radioiodination: Theory, Practice and Biomedical Applications. Kluwer Academic, Dordrecht.

Fraker, P. J., and Speck, J. C. (1978). Protein and cell membrane iodinations with a sparingly soluble chloramide 1,3,4,6-tetrachloro 3a.6a diphenylglycoluril. *Biochem. Biophys. Res. Commun.* **80**, 849.

Hunter, W. M., and Greenwood, F. C. (1962). Preparation of iodine-131 labelled human growth hormone of high specific activity. *Nature* **194**, 495–496.

Lindmo, T., Boven, E., and Cuttita, F. (1984). Determination of the immunoreactive fraction of radiolabelled monoclonal antibody by linear extrapolation to binding at infinite antigen excess. *J. Immunol Methods* **27**, 77–89.

Mather, S. (2000). Radiolabelling of monoclonal antibodies. *In* "*Monoclonal Antibodies, a Practical Approach*" (P. Shepherd and C. Dean, eds.), pp. 207–236. Oxford Univ. Press, Oxford.

Morrison, M., and Bayse, G. S. (1970). Catalysis of iodination by lactoperoxidase. *Biochemistry* **9**, 2995–3000.

van der Laken, C. J., Boerman, O. C., Oyen, W. J., van de Ven, M. T., Chizzonite, R., Corstens, F. H., and van der Meer, J. (1997). Preferential localization of systemically administered radiolabeled interleukin1 alpha in experimental inflammation in mice by binding to the type II receptor. *J. Clin. Invest.* **100**(12), 2970–2976.

PART

D

IMMUNOCYTOCHEMISTRY

SECTION

16

Immunofluorescence

CHAPTER

66

Immunofluorescence Microscopy of Cultured Cells

Mary Osborn

I. INTRODUCTION

Immunocytochemistry is the method of choice for locating an antigen to a particular structure or subcellular compartment provided that an antibody specific for the protein under study is available. Immunofluorescence is a sensitive method requiring only one available antigenic site on the protein. Usually the indirect technique is used. In this technique the first antibody is unlabeled and can be made in any species. After it has bound to the antigen, a second antibody, made against IgGs of the species in which the first antibody is made and coupled to a fluorochrome such as fluoroscein isothiocyanate, is added. The distribution of the antigen can then be viewed in a microscope equipped with the appropriate filters.

Immunofluorescence as a method to study cytoarchitecture and subcellular localization gained prominence with the demonstration that antibodies can be produced to actin even though it is a ubiquitous component of cells and tissues (Lazarides and Weber, 1974). Cytoskeletal structures visualized in cells in immunofluorescence microscopy include the three filamentous systems: microfilaments, microtubules, and intermediate filaments (Figs. 1–4 and micrographs in the article by Prast *et al.*). In addition, proteins can be located to other cellular subcompartments and organelles, e.g., the plasma or nuclear membranes, the Golgi apparatus, or the endoplasmic reticulum, or to other cellular structures such as mitochondria and vesicles. Other proteins can also be localized to subcompartments of the nucleus or even of the nucleolus. In addition to its use in identifying cytoskeletal structures and organelles, immunocytochemistry has proved useful in building up a biochemical or protein chemical anatomy of a structure. Examples include the location of the microfilament-associated proteins to the stress fiber and the description of the biochemical anatomy of such structures as microvilli and stereo cilia. A third use of the technique has been to demonstrate heterogeneity in mixed cultures, e.g., of neuronal cultures (Raff *et al.*, 1978), or of other primary or secondary cell cultures (cf. Fig. 4). Immunofluorescence with selected antibodies has also been used to check the histological derivation of particular cell lines or indeed of whole cell culture collections (see Quentmeier *et al.*, 2001 and http://www.dsmz.de).

The micrographs that accompany this article show not only the beauty of some of the structures, but also some of the advantages of the technique. First, only the arrangement of the particular protein against which the antibody is made is visualized. Second, for those proteins that form part of a supramolecular structure, the arrangement of such structures throughout the cell is revealed. Third, numerous cells can be visualized at the same time, and therefore it is relatively easy to determine how the structures under study vary under particular conditions or during different phases of the cell cycle. Immunofluorescence microscopy is also a useful method to establish appropriate conditions to study a structure at higher resolution in the electron microscope.

A 1:1 correspondence has been shown for a parallel-processed or even the same specimen when studied by fluorescence microscopy and as a whole mount under the electron microscope (Osborn *et al.*, 1978b). Electron microscopic methods not only allow location of the antigen to a particular structure at higher resolution, but may also allow the determination of interactions between a structure that is immunolabeled and other unlabeled structures in the cell.

Copyright 2006, Elsevier Science (USA).
All rights reserved.

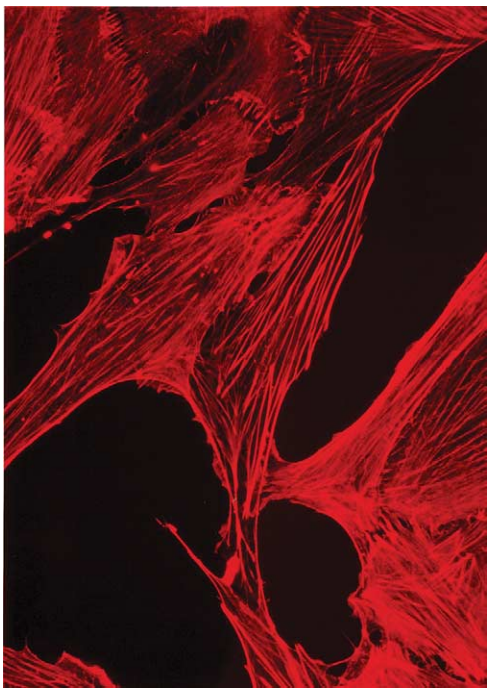

FIGURE 1 Actin stress fibers in the RMCD rat mammary cell line revealed by staining with rhodamine-labeled phalloidin (×400).

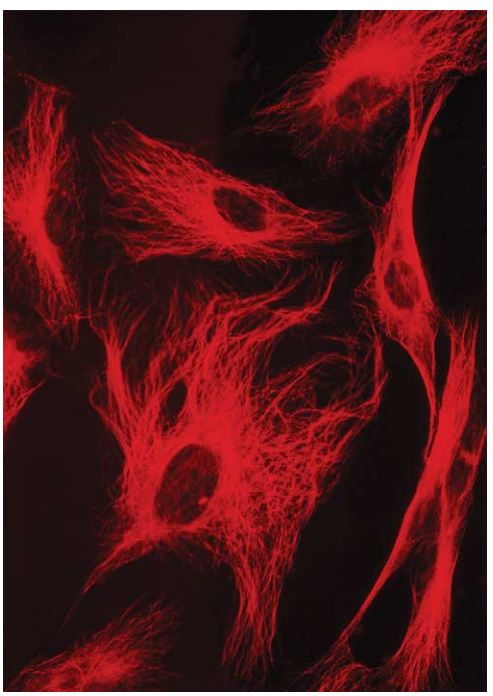

FIGURE 2 Microtubules in cells in culture revealed by staining with antibodies to tubulin followed by a rhodamine-labeled second antibody (×400).

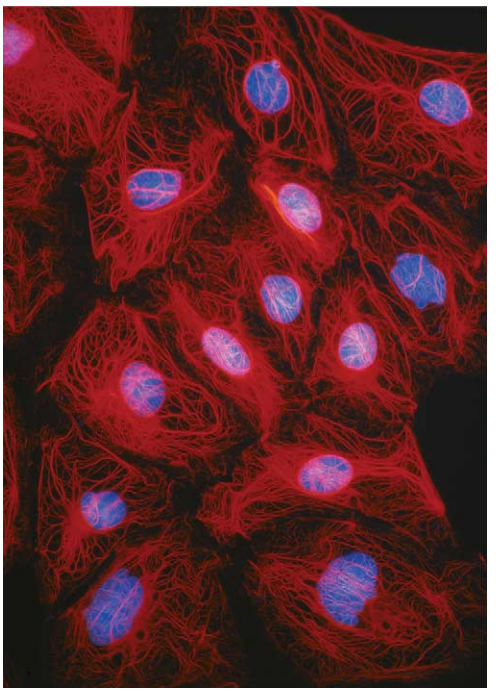

FIGURE 3 Keratin filaments in the rat kangaroo PtK2 cell line revealed by staining with antibodies to keratin and a rhodamine-labeled second antibody. DNA has been counterstained with Hoechst dye (×150).

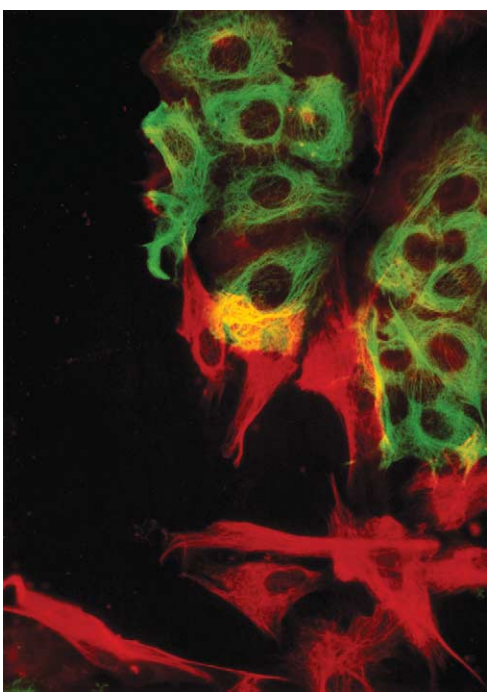

FIGURE 4 Artificial mixture of cells from the human breast carcinoma cell line MCF-7 and the human fibroblast cell line HS27 stained with an antibody to keratin (in green) and with the V9 antibody to vimentin (in red). Note that each cell type contains only a single type of intermediate filament. The yellow color results from MCF-7 and HS27 cells that lie over each other (×150).

Other reviews of immunofluorescence of cultured cells that concentrate on methods include those of Osborn (1981), Osborn and Weber (1981), and Wheatley and Wang (1981) and for live cells, Wang and Taylor (1989) and Prast *et al*. (2004). Alternatively, see Allan (2000). For an overview of the different cytoskeletal and motor proteins, see Kreis and Vale (1999). For interesting collections of color immunofluorescence micrographs from a wide variety of organisms, see Haugland *et al*. (2004) or the BioProbes newsletter (http://www.probes.com).

II. MATERIALS AND INSTRUMENTATION

A. Antibodies

Antibodies to many cellular proteins can be purchased commercially. Firms offering a variety of antibodies to cytoskeletal and other proteins include Amersham, Biomakor, Dako, Novocastra, Sigma-Aldrich, and Transduction Laboratories; other firms have specialized collections emphasizing narrower areas.

Primary antibodies today are usually monoclonal antibodies made in mice, although polyclonal antibodies made in species such as guinea pigs and rabbits are sometimes also available commercially. The appropriate dilution is established by a dilution series. Monoclonal antibodies supplied as hybridoma supernatants can often be diluted 1:1 to 1:20 for immunofluorescence or even more if other more sensitive immunocytochemical procedures are used (see also article by Osborn and Brandfass for additional information). Monoclonal antibodies supplied as ascites fluid can be diluted in the range of 1:100 to 1:1000. Use of ascites fluid at a dilution of less than 1:100 is not recommended as there are usually high titers of autoantibodies in such fluids. Polyclonal antibodies supplied as sera should be diluted in the range of 1:20 to 1:100. Note that many rabbits have relatively high levels of autoantibodies against keratins and/or other cellular proteins, so check presera. Affinity purification in which the antigen is coupled to a support and the polyclonal antibody is then put through the column usually results in a dramatic improvement in the quality of the staining patterns. Affinity-purified antibodies should work in the range of 5–20 µg/ml.

Secondary antibodies directed against IgGs of the species in which the first antibody is made are usually purchased already coupled to a fluorophore (e.g., from Jackson Laboratories http://jacksonimmuno.com, Molecular Probes http://www.probes.com and other companies listed earlier). Originally, only FITC and rhodamine-labeled antibodies were available commercially. Today there is a very wide choice of commercial antibodies coupled to different fluorophores, including AMCA, Cy2, FITC, Cy3, TRITC, phycoerythrin, RRX, Texas red, and Cy5 (see Haugland, 2004 and http://jacksonimmuno.com). Cy2 and Cy3 fluoresce in the green region of the visible spectrum, as does FITC. They are more photostable, less sensitive to pH, and are reported to give less background than many other fluorophores. Cy2 can be visualized with FITC filters and Cy3 with TRITC filters. Cy5 has an emission maximum at 670 nm and cannot be seen well by eye. Choice among the red fluorophores depends in part on the application. In addition, Molecular Probes has produced a series of Alexa Fluor dyes that cover the visible spectrum. Alexa Fluor 488 is claimed to be the best green fluoresent dye available. Alexa Fluor 555 spectra match those of Cy3, but are more fluorescent and more photostable. Alexa Fluor 647 spectra are very similar to those of Cy5. The working dilution for the secondary antibody is established by running a dilution series. Usually 1:50 to 1:150 dilutions of the commercial products are appropriate. An essential control is to check that the second antibody is negative when used alone. If nonspecific staining is present, it can sometimes be removed by absorbing the antibody on fixed monolayers of cells or on an acetone cell powder.

Antibodies other than IgMs should be stored in the freezer (–70°C for valuable primary antibodies and affinity-purified antibodies, –20°C for the rest). Antibodies should be stored in small aliquots and repeated freezing/thawing should be avoided. IgMs may be inactivated by freezing/thawing and are best kept in 50% glycerol in a freezer set at –20 to –25°C. If dilutions are made in a suitable buffer [e.g., phosphate-buffered saline (PBS), 0.5 mg/ml bovine serum albumin, 10^{-3} *M* sodium azide], diluted antibodies are stable for several months at 4°C.

B. Reagents and Other Useful Items

Methanol is of reagent grade. Formaldehyde can be diluted 1:10 from a concentrated 37% solution (e.g., Analar grade BDH Chemicals). As such solutions usually contain 11% methanol, it may be better to make the formaldehyde solution from paraformaldehyde. In this case, heat 18.5 g paraformaldehyde in 500 ml PBS on a magnetic stirrer to 60°C and filter through a 0.45-µm filter. Store at room temperature. PBS contains per liter 8 g NaCl, 0.2 g KCl, 0.2 g KH_2PO_4, and 1.15 g Na_2HPO_4, adjusted to pH 7.3 with NaOH.

Polyvinyl alcohol-based mounting media have the advantage in that although they are liquid when the sample is mounted, they solidify within hours of application. In addition, the fluorescence is stable if the sample is held in the dark and at 4°C. Samples can be reexamined and photographed after months or even years. Commonly used mounting media include Mowiol 4–88 (Calbiochem Cat. No. 475904). To make the mounting medium, place 6 g analytical grade glycerol in a 50-ml plastic conical centrifuge tube, add 2.4 g of Mowiol 4.88, and stir for 1 h to mix. Add 6 ml distilled water and stir for a further 2 h. Add 12 ml of 0.2 *M* Tris buffer (2.42 g Tris/100 ml water, pH adjusted to 8.5 with HC1 as FITC has maximal fluorescence emission at this pH) and incubate in a water bath at 50°C for 10 min, stirring occasionally to dissolve the Mowiol. Clarify by centrifugation at 1200 *g* for 15 min and aliquot. Store at –20°C; unfreeze as required. Once unfrozen, the solution will be stable for several months at room temperature. While some laboratories add antifade reagents to mounting media, we have never found this to be necessary for our applications.

Other useful items include round (12 mm) or square (12 × 12 mm) glass coverslips (thickness 1.5). Ten round coverslips fit in a petri dish of 5.5 cm diameter. For screening purposes or when a large number of samples is needed (e.g., for hybridoma screening), microtest slides that contain 10 numbered circles 7 mm in diameter (Flow Labs, Cat. No. 6041505) are useful. Tweezers (e.g., Dumont No. 7) are used to handle the coverslips. Ceramic racks into which coverslips fit (Thomas Scientific, Cat. No. 8542E40) and glass containers in which these racks fit are also needed. Glass beakers (30 ml) are used to wash the specimens. Cells growing in suspension can be firmly attached to microscope slides using a cytocentrifuge such as the Cytospin 2 (Shandon Instruments).

C. Equipment

The essential requirement is access to a microscope equipped with appropriate filters to visualize the fluorochromes in routine use. Microscopes with CCD or digital cameras so that results can be viewed directly on screen are available from several manufacturers, e.g., Zeiss. Epifluorescence, an appropriate high-pressure mercury lamp (HBO 50 or HBO 100) and appropriate filters (so that specimens doubly labeled with, e.g., fluorescein and rhodamine can be visualized) are basic requirements. Lenses should also be selected carefully. The depth of field of the lens will decrease as the magnification increases. Round cultured cells will be in focus only with a ×25 or ×40 lens, whereas flatter cells can be studied with a ×63 or ×100 lens. To enable phase and fluorescence to be studied on the same specimen, some lenses should have phase optics. Only certain lenses transmit the Hoechst DNA stain (e.g., Neofluar lenses), and this stain also requires a separate filter set.

Increased resolution particularly in the *z* direction can be obtained by confocal microscopy (see Mason, 1999). Other forms of microscopy allow a further increase in resolution, but are not widely available (see later). Some institutes are pooling their light microscopy facilities (e.g., the Advanced Light Microscope Facility at EMBL, http:/www.embl-heidelberg.de/ExternalInfo/EurALMF, which provides state-of-the-art light microscopy image analysis and support for internal groups as well as visitors to EMBL).

III. INDIRECT IMMUNOFLUORESCENCE PROCEDURE

Steps

1. Trypsinize cells 1–2 days prior to the experiment onto glass coverslips or on multitest slides that have been washed in 100% ethanol and oven sterilized. For most applications, choose coverslips or multitest slides on which cells are two-thirds or less confluent. Drain coverslip or touch to filter paper to remove excess medium, but do not allow it to dry.
2. Place coverslips in a ceramic rack and multitest slides in metal racks, and immerse in methanol precooled to –10 to –20°C. Leave for 6 min at room temperature.
3. Make a wet chamber by lining a 13-cm-diameter (for coverslips) or a 24 × 24-cm^2 petri dish (for slides) with two or three sheets of filter paper and add sufficient water to moisten the filter paper. Numbers identifying the samples can be written on the top sheet of filter paper prior to wetting it.
4. Wash the fixed specimens briefly in PBS, remove excess PBS by touching to dry filter paper, and place cell side up over the appropriate number in the wet chamber.
5. Add 5–10 µl of an appropriate dilution of the primary antibody with an Eppendorf pipette. Use the tip to spread the antibody over the coverslip without touching the cells. Replace the top of the wet chamber, transfer to a humidified incubator at 37°C, and incubate for 45 min.
6. Wash by dipping each coverslip individually three times into each of three 30-ml beakers containing PBS. Wash slides by replacing slides in metal rack and

transferring through three PBS washes (180 ml each, leave for 2 min in each). Remove excess PBS with filter paper.

7. Replace specimens in wet chamber. Add 5–10 µl of an appropriately diluted second antibody carrying a fluorescent tag. Return to 37°C incubator for a further 30–45 min.

8. Repeat step 6.

9. Identify microscope slides with small adhesive labels on which date, specimen number, antibody, or other information is written. Place slides in cardboard microslide folders (e.g., Thomas Scientific, Cat. No. 6708-M10). Mount two coverslips per slide by inverting each coverslip and placing cell side down on a drop of mounting medium placed on the slide, with a disposable ring micropipette. Cover with filter paper and press gently to remove excess mounting medium. For samples on multitest slides, use 6 × 2.5-cm glass coverslips on which a drop of mounting medium has been placed. Secure the coverslips with nail polish. Store samples in the dark in slide boxes at 4°C.

10. Documentation. Use a fast film (e.g., Kodak 35 mm Tri-X) and push the development, e.g., with Diafine (Acufine), or record the image digitally. Phase micrographs of specimens embedded in Mowiol should be made as soon as possible after mounting the specimens. The fluorescence decreases a little in the first few days, but is then stable for years if the samples are stored in the dark at 4°C.

IV. COMMENTS

Specimens should not be allowed to dry out at any stage in the procedure. If coverslips are dropped accidentally, the side on which the cells are can be identified by focusing on the cells under an upright microscope and scratching gently with tweezers.

A. Fixation

The procedure gives good results with many cytoskeletal and other antigens; however, the optimal fixation protocol depends on the specimen, the antigen, and the location of the antigen within the cell. Three requirements have to be met. First, the fixation procedure must retain the antigen within the cell. Second, the ultrastructure must be preserved as far as possible without destroying the antigenic determinants recognized by the antibody. Third, the antibody must be able to reach the antigen; i.e., the fixation and permeabilization steps must extract sufficient cytoplasmic components so that the antibodies can penetrate into the fixed cells. In the procedure just given, fixation and permeabilization are achieved in a single step, i.e., with methanol. Alternative fixation methods include the following:

1. Formaldehyde–methanol: 3.7% formaldehyde in PBS for 10 min (to fix the cells) and then methanol at –10°C for 6 min (to permeabilize the cells).

2. Formaldehyde–Triton: 3.7% formaldehyde in PBS for 10 min (to fix) and then PBS with 0.2% Triton X-100 for 1 min at room temperature (to permeabilize).

3. Glutaraldehyde: Fix in 1% glutaraldehyde (electron microscopic grade) in PBS for 15 min and then methanol at –10°C for 15 min. Immerse in sodium borohydride solution (0.5 mg/ml in PBS made minutes before use) for 3 × 4 min. Wash with PBS 2 × 3 min each. Note that the sodium borohydride step is necessary to reduce the unreacted aldehyde groups; without this step the background will be very high.

Note that formaldehyde treatment destroys the antigenicity of many antigens. Alternatively, in a very few cases, positive staining may be observed only after formaldehyde fixation. Very few antigens react after glutaraldehyde fixation.

B. Special Situations

1. Fluorescently labeled phalloidin (extremely poisonous), a phallotoxin that binds to filamentous actin, is available commercially and is usually used to reveal the distribution of filamentous actin in cells (Fig. 1). To obtain good staining patterns, fix cells for 10 min in 3.7% formaldehyde in PBS. Wash with PBS. Incubate for 1 min in 0.2% Triton X-100 in PBS and wash with PBS. Incubate with an appropriate dilution of rhodamine-labeled phalloidin (e.g., Sigma Cat. No. P-1951) for 30 min at 37°C, wash with PBS, and mount in Mowiol. Note that phalloidin staining will not work after methanol fixation (for further discussion, see article by Prast *et al.*, and Small *et al.*, 1999).

2. To stain endoplasmic reticulum, use either an antibody, e.g., ID3 against a sequence region of protein disulfide isomerase (Vaux *et al.*, 1990), or the lipophilic, cationic fluorescent dye $DiOC_6$ (3,3-dihexyloxacarbocyanine iodide, Kodak Cat. No. 14414) (Terasaki *et al.*, 1984). To stain with dye, fix for 5 min in 0.25% glutaraldehyde in 0.1 *M* cacodylate and 0.1 *M* sucrose buffer, pH 7.4. Wash. Stain for 80 s with dye, mount in buffer, and observe using a ×63 or ×100 lens and the fluorescein filter. Reticular structures should be apparent. Note that mitochondria will also be stained. To stain only mitochondria, use either an antibody, e.g., to cytochrome oxidase, or the dye rhodamine 123.

3. Special fixation procedures may also be needed for other membrane structures in cells. In addition, lectins can be used to stain carbohydrate-containing organelles, e.g., staining of Golgi apparatus with fluorescently labeled wheat germ or other agglutinins.

4. To stain DNA for fluorescent applications dyes that bind to the minor groove in DNA such as the Hoechst dyes and DAPI are usually used. To stain with Hoechst use either Hoechst 33242 (Sigma Cat. No. 2261) or Hoechst 33258 (Sigma Cat. No. B2883). Note that Hoechst 33242 can also be used to stain DNA in live cells. When bound to DNA, Hoechst dyes fluoresce bright blue (cf. Fig. 1C). To stain with Hoechst prepare a 1 m*M* stock solution in sterile water and store at 4°C. To stain cells dilute the stock solution 1:1000 in PBS to a final working concentration of 1 µ*M*. After step 8 in the immunofluorescence procedure, pipette 20–100 µl of the working solution onto each coverslip and leave for 4 min at room temperature. Wash twice with PBS, drain the coverslip, and mount in Mowiol. DNA can also be stained with DAPI, which shows a 20-fold fluorescence enhancement on binding to DNA and also gives blue fluorescence.

5. Some cellular structures, such as microtubules, are sensitive to calcium. In this case, add 2–5 m*M* EGTA to the 3.7% formaldehyde solution in Section IV,A and to the methanol in Section III, step 2.

6. Blocking steps are usually not necessary if antibodies are diluted in BSA containing buffers. If a blocking step is used it should be performed after fixation and prior to adding the first antibody. Blocking to reduce nonspecific staining is performed with 10% serum from the same host species as the labeled antibody.

7. Sometimes for cell surface components it may be advantageous to stain live cells. Expose such cells to antibody for 25 min and proceed with steps 6–8 in Section III. Then fix cells in 5% acetic acid/95% ethanol for 10 min at –10°C (Raff *et al*., 1978).

8. Another application of immunofluorescence microscopy is to monitor directly the distribution of fluorescently labeled proteins in live cells by video microscopy (e.g., Sammak and Borisy, 1988).

C. Double or Triple Immunofluorescence Mircroscopy

It is often advantageous to visualize two or three antigens in the same cell (Fig. 4). Here it is important to choose fluorophores that give good color separation, e.g., a Texas red/FITC combination will give a better separation than TRITC/FITC (see also article by Prast *et al*.). Most important is that the microscope is optimized for the fluorophores in use by the selection of the appropriate filters so that there is no overlap between the channels used to observe each of the fluorophores.

D. Stereomicroscopy

Fluorescence microscopy gives an overview of the whole cell. With practice, specimens can be seen in three dimensions when looking through a conventional microscope. Stereomicrographs can be made using a simple modification of commercially available parts (Osborn *et al*., 1978a). Today, however, confocal microscopy is the method of choice and is particularly useful for round cells, which are not in focus with the higher-power ×63 or ×100 lenses, or to document arrangements and obtain greater resolution at multiple levels in the same cell or organism (cf. Fox *et al*., 1991).

E. Limit of Resolution

Theoretically, this is ~200 nm when 515-nm wavelength light and a numerical aperture of 1.4 are used. Objects with dimensions above 200 nm will be seen at their real size. Objects with dimensions below 200 nm can be visualized provided they bind sufficient antibody, but will be seen with diameters equal to the resolution of the light microscope (cf. visualization of single microtubules in Osborn *et al*., 1978b). Objects closer together than 200–250 nm cannot be resolved by conventional fluorescence microscopy, e.g., microtubules in the mitotic spindle or ribosomes. However, some increase in the resolution of fluorescent images can be obtained using new forms of microscopy (see Hell, 2003).

F. New Developments

Immunofluorescence microscopy is an important technique not only for fixed cells (this article), but also because of the possibility of expressing GFP vectors coupled to particular constructs in living cells (see article by Prast *et al*.) and following changes in distribution by video microscopy. FRET imaging techniques (see this volume) and other novel techniques, such as the use of quantum dot ligands (e.g., Lidke *et al*., 2004), are also opening up new possibilities for more quantitative fluorescence measurements on live cells.

V. PITFALLS

Occasionally no specific structures are visualized, even though the cell is known to contain the antigen. This may be because:

1. Antibodies can be species specific. This can be a particular problem with monoclonal antibodies, which, for instance, may work with human but not with other species. If in doubt, check the species specificity with the supplier before purchase.

2. The fixation procedure may inactivate the antigen. For instance, many intermediate filament antibodies no longer react after fixation protocols such as those in Section IV,A.

3. The antigen may be present only at very low concentrations and therefore it may be necessary to use more sensitive methods to detect the antigen.

4. The antigen can be poorly fixed or extracted by the fixation procedure.

5. The antibody may not be able to gain access to the antigen, e.g., antibodies to tubulin often do not stain the midbody of the intracellular bridge.

6. The specimens may be generally fluorescent and it can be hard to decide whether this is due to specific or nonspecific staining.

References

Allan, V. J. (2000). Basic immunofluorescence. *In* "*Protein Localisation by Fluorescence Microscopy: A Practical Approach*," pp. 1–26. Oxford Univ. Press, New York.

Fox, M. H., Arndt-Jovin, D. J., Jovin, T. M., Baumann, P. H., and Robert-Nicoud, M. (1991). Spatial and temporal distribution of DNA replication sites localized by immunofluorescence and confocal microscopy in mouse fibroblasts. *J. Cell Sci.* **99**, 247–253.

Haugland, R. P. (2004). Molecular probes. *In* "*Handbook of Fluorescent Probes and Research Products*," 9th Ed.

Hell, S. W. (2003). Toward fluorescence nanoscopy. *Nature Biotechnol.* **21**, 1347–1355.

Kreis, T., and Vale, R. (1999). "Guidebook to the Cytoskeletal and Motor Proteins," 2nd Ed. Oxford Univ. Press, London.

Lazarides, E., and Weber, K. (1974). Actin antibody: The specific visualization of actin filaments in non-muscle cells. *Proc. Natl. Acad. Sci. USA* **71**, 2268–2272.

Lidke, D. S., Nagy, P., Heintzmann, R., Arndt-Jovin, D. J., Post, J. N., Grecco, H. E., Jares-Erijman, E. A., and Jovin, T. M. (2004). Quantum dot ligands provide new insights into erbB/HER receptor-mediated signal transduction. *Nature Biotechnol.* **22**, 198–203.

Mason, W. T. (1999). "Fluorescent and Luminescent Probes for Biological Activity." Academic Press, San Diego.

Osborn, M. (1981). Localization of proteins by immunofluorescence techniques. *Techniq. Cell. Physiol.* **P107**, 1–28.

Osborn, M., Born, T., Koitzsch, H. J., and Weber, K. (1978a). Stereo immunofluorescence microscopy. I. Three-dimensional arrangement of microfilaments, microtubules and tonofilaments. *Cell* **13**, 477–488.

Osborn, M., and Weber, K. (1981). Immunofluorescence and immunochemical procedures with affinity purified antibodies. *In* "Methods in Cell Biology," Vol. 23. Academic Press, New York.

Osborn, M., Webster, R. E., and Weber, K. (1978b). Individual microtubules viewed by immunofluorescence and electron microscopy in the same PtK2 cell. *J. Cell Biol.* **77**, R27–R34.

Pruss, R. M., Mirsky, R., Raff, M. C., Thorpe, R., Dowding, A. J., and Anderton, B. H. (1981). All classes of intermediate filaments share a common antigenic determinant defined by a monoclonal antibody. *Cell* **27**, 419–428.

Quentmeier, H., Osborn, M., Reinhardt, J., Zaborski, M., and Drexler, H. G. (2001). Immunocytochemical analysis of cell lines derived from solid tumors. *J. Histochem. Cytochem.* **49**, 1369–1378.

Raff, M. C., Mirsky, R., Fields, K. L., Lisak, R. P., Dorfman, S. H., Pilbenberg, D. H., Gregeon, N. A., Leibowitz, S., and Kennedy, M. C. (1978). Galactocereboside is a specific cell surface antigenic marker for oligodendrocytes in culture. *Nature* **274**, 813–816.

Sammak, P. J., and Borisy, G. G. (1988). Direct observation of microtubule dynamics in living cells. *Nature* **332**, 724–726.

Small, J. V., Rottner, K., Hahne, P., and Anderson, K. I. (1999). Visualising the actin cytoskeleton. *Microsc. Res. Tech.* **47**, 3–17.

Terasaki, M., Song, J., Wong, J. R., Weiss, M. J., and Chen, L. B. (1984). Localization of endoplasmic reticulum in living and glutaraldehyde fixed cells with fluorescent dyes. *Cell* **38**, 101–108.

Vaux, D., Tooze, J., and Fuller, S. (1990). Identification by anti-idiotype antibodies of an intracellular membrane protein that recognizes a mammalian endoplasmic reticulum retention signal. *Nature* **345**, 495–502.

Wang, Y. L., and Taylor, D. L. (1989). "Methods in Cell Biology," Vols. 29 and 30. Academic Press, New York.

Wheatley, S. P., and Wang, Y. L. (1998). Indirect immunofluorescence microscopy in cultured cells. *Methods Cell Biol.* **57**, 313–332.

CHAPTER

67

Immunofluorescence Microscopy of the Cytoskeleton: Combination with Green Fluorescent Protein Tags

Johanna Prast, Mario Gimona, and J. Victor Small

Immunofluorescence microscopy is now a standard procedure for the localisation of molecules in cells (for an introduction to the method, see article by Osborn). Nevertheless, the method has its pitfalls, not least in requiring the immobilisation of cells by chemical fixation and multiple manipulations during labelling. This can lead to the loss of antigen as well as to the distortion of cell structure. Unfortunately, published pictures still appear in which distortions in cell structure are overlooked and where the conclusions drawn are consequently tenuous. Advances in live cell imaging, combined with green fluorescent protein (GFP) tags (and analogues) now provide independent methods for assessing the localisation of molecules. Nevertheless, immunofluorescence microscopy remains an important technique when used with discretion. Indeed, when applied in combination with cells expressing fluorescently tagged probes, it adds a further dimension to characterise the relative localisation of multiple components. This article provides some recipes suitable for labeling the cytoskeleton and gives examples where GFP tags and immunofluorescence can be usefully combined.

II. MATERIALS AND REAGENTS

1. *Coverslips*: Round glass coverslips 12 or 15 mm in diameter, cleaned in 60% ethanol/40% HCl (10 min), rinsed with H_2O (2 × 5 min), drained, cleaned with lint-free paper, and sterilized for tissue culture by exposure to ultraviolet light in the culture dish.

2. *Humid chamber*: Large petri dish 14 cm in diameter, or similar container with lid, containing a glass plate (around 9 cm^2) coated with a layer of Parafilm and supported on a moistened piece of filter paper on the bottom of the dish. A few drops of water on the glass plate facilitate spreading and flattening of the Parafilm.

3. *Washing reservoir*: Two multiwell dishes, 24 wells each (e.g., Nunc).

4. *Filter paper*: Whatman No. 1, 9 cm in diameter.

5. *Forceps*: Dumont No. 4 or No. 5 or equivalent watchmaker forceps.

6. *Pipettes*: Set of automatic pipettes (0–20, 20–200, 50–1000 µl) or capillary pipettes for diluting and aliquoting antibodies. Pasteur pipettes.

7. *Phalloidin*: Alexa 568- and Alexa 488-coupled phalloidins from Molecular Probes and CPITC (coumarin) phalloidin from Sigma. Store as 0.1-mg/ml stocks in methanol at –20°C.

8. *Secondary antibodies*: Commercial secondary antibodies carrying Molecular Probes Alexa 488, 568, and 350 conjugates are, in our experience, of generally good quality.

9. *Gelvatol, Vinol*: The basic ingredient of the mounting medium is polyvinyl alcohol (MW 10.000, around 87% hydrolysed), which comes under various trade names: Elvanol, Mowiol, and Gelvatol. We use Vinol 203 from Air Products and Chemical Inc.

Copyright 2006, Elsevier Science (USA).
All rights reserved.

II. PROCEDURES

Solutions

1. *0.5 M EGTA stock solution*: For 500 ml stock, weigh out 95.1 g EGTA (Sigma E-4378) into 400 ml H_2O, adjust pH to 7.0 with 1 *N* NaOH, and make up to 500 ml with H_2O. Store at room temperature in a plastic bottle.

2. *1 M $MgCl_2$ stock solution*: For 500 ml stock, weigh out 101.6 g $MgCl_2$, add H_2O to 500 ml, dissolve, and store at 4°C.

3. *Cytoskeleton buffer (CB)*: 10 n*M* MES (Sigma M-8250), 150 m*M* NaCl, 5 m*M* EGTA, 5 m*M* $MgCl_2$, and 5 m*M* glucose. For 1 liter, add the following amounts to 800 ml H_2O: MES, 1.95 g; NaCL, 8.76 g; 0.5 *M* EGTA, 10 ml; 1 *M* $MgCl_2$, 5 ml; and glucose, 0.9 g. Adjust pH to 6.1 with 1 *N* NaOH and fill up to 1 liter. Store at 4°C. For extended storage, add 100 mg streptomycin sulfate (Sigma S-6501).

4. *Phosphate-buffered saline (PBS) working solution*: 137 m*M* NaCl, 2.7 m*M* KCl, 4.3 m*M* $Na_2HPO_4{\cdot}7H_2O$, and 1.4 m*M* KH_2PO_4, pH 7.4.

5. *Triton X-100*: Make up 10% aqueous stock and store at 4°C.

6. *Glutaraldehyde (GA) stock*: Make up 2.5% solution of glutaraldehyde by diluting 25% glutaraldehyde EM grade (Agar scientific Ltd., Cat. No. R 1020 or equivalent) in CB. Readjust pH to 6.1 and store at 4°C.

7. *Paraformaldehyde (PFA) stock*: Make up a stock 4% solution of paraformaldehyde in PBS or CB (see fixative mixtures) (analytical grade Merck Cat. No. 4005). To make 100 ml, heat 80 ml of CB (or PBS) to 60°C, add 3 g paraformaldehyde, and mix 30 min. Add a few drops of 10 *M* NaOH until the solution is clear, cool, adjust pH (see appropriate mixture), and make up to 100 ml. Store in aliquots at –20°C.

8. *Fixative mixtures*: Aldehyde fixative mixtures are made up using the stock solutions given earlier to give the combinations listed under step 2.

9. *Blocking solution*: 1% bovine serum albumin and 5% horse serum in PBS.

10. *Antibody mixtures*: These are made up in PBS or in the blocking solution without serum. To remove any unwanted particles, centrifuge (10,000 *g* for 10 min) the diluted mixture before use. The antibody combinations used for this article are listed in Table I.

11. *Mounting medium*: Mix 2.4 g of polyvinyl alcohol with 6 g glycerol (87%) and then with 6 ml H_2O. After at least 2 h at room temperature, add 0.2 ml 0.2 *M* Tris–HCl, pH 8.5, to the mixture and further incubate the solution for 10 min at 60°C. Remove any precipitate by centrifugation at 17,000 *g* for 30 min. Store in aliquots at –20°C. [Antibleach agents are available that considerably reduce bleaching and thus enable multiple pictures to be taken of the same cells. We use *n*-propyl gallate (Giloh and Sedat, 1982) at 5 mg/ml or phenylenediamine (Johnson *et al*., 1982) at 1–2 mg/ml in the mounting medium. After dissolving the additive, degas mounting medium before storage.]

Steps

1. Seed the cells onto coverslips in the petri dish and allow them to attach and spread for 4–48 h in an incubator at 37°C.

2. Aspirate growth medium and rinse dish gently with PBS (warmed 37°C PBS); avoid shifting of the coverslips over each other. Aspirate PBS and replace with one of the following fixative solutions.
   a. *Fix 1*: 4% PFA/0.1% Triton X-100 in PBS for 2 min. Rinse three times with PBS. 4% PFA in PBS for 20 min. Wash 2 × 10 min with PBS.
   b. *Fix 2*: 0.5% GA/0.25% Triton X-100 in CB for 1 min. Rinse 3× with CB. 4% PFA in CB for 20 min. Wash 2 × 10 min with CB.
   c. *Fix 3*: 0.25% GA/0.5% Triton X-100 in CB for 1 min. Rinse 3× with CB. 1% GA for 15 min. Wash 2 × 10 min with CB.
   d. *Fix 4*: 4% PFA/0.3% Triton X 100/0.1% GA in CB for 15 min. Wash 2 × 10 min with CB.

3. Block: Invert each PBS coverslip onto a 30-µl drop of blocking solution on Parafilm in the humid chamber. Before transfer to drop, dry the back side of the coverslip by holding it briefly on filter paper with a pair of forceps, taking care not to allow the cell side to dry. Drain any excess solution from the cell side by touching the edge of the coverslip to the filter paper. Incubate on blocking solution for 15 min or until first antibody mixtures are prepared. (Back side of coverslip should not be wet or else coverslip will sink during the washing step.)

4. Apply drops (20–50 µl) of first antibody mixture to unused part of Parafilm and transfer coverslips to appropriate drops after draining excess blocking solution on filter paper. Replace lid on petri dish and leave at room temperature for 45–60 min.

5. Wash: To ease removal of coverslips for washing, pipette 100 µl PBS under their edge to lift them up from the Parafilm. Using forceps, transfer coverslips to a multiwell dish in which the wells are filled to the brim with PBS so that the liquid surface is flat. The coverslips will float well, cell side down, as long as the back side remains dry. (For efficient washing, transfer dish gently to a tilting rotating table for 10 min.) Repeat washing steps after transfer of coverslips to a second dish containing fresh PBS two or three times.

6. Change Parafilm in humid chamber and apply drops of second antibody mixture. Transfer coverslips

to drops after briefly draining excess with filter paper and incubate for 45 min.

7. Wash as described in step 6.

8. Mount: Add a small drop of mounting medium to a cleaned glass slide using, for example, a plastic disposable pipette tip. Drain excess (PBS) from coverslip and gently invert onto drop. *Note*: The mounting medium dries quite fast so the drops should be applied singly and not in batches. If necessary, remove excess medium after mounting by applying small pieces of torn filter paper to the coverslip edge.

9. Observe directly in a fluorescence microscope with a dry lens. An oil immersion lens can be used the next day when the mounting medium has solidified. Alternatively, the drying time can be shortened by transfer of slides to a 27°C oven.

III. CHOICE OF FIXATION FOR MULTIPLE LABELLING

Different antibodies commonly require different fixation protocols to give optimal labelling. It is therefore important to test different fixation conditions for each antibody to determine the best compromise fixation for multiple labelling. Table I lists the characterics of the commercial antibodies used in this article in terms of the intensity of label obtained with each of the four fixation protocols described for cultured smooth muscle cells (A7r5, American Type Culture Collection). In general, you should establish the strongest fixation protocol that your antibodies can tolerate and draw your conclusions accordingly.

TABLE I Characteristics of Commercial Antibodies[a]

Staining	Fix 1	Fix 2	Fix 3	Fix 4
Mc. Anti-α-actinin mouse IgM (Sigma BM-75.2) 1:500	+++	++	++	++
Mc. Antiphosphotyrosine (Santa Cruz pY99) Mouse IgG 1:1000	+++	+	++	++
Mc. Anti-α-Tubulin mouse IgG (Sigma DM1A) 1:1000	–	+++	+++	+++
Mc. Antivimentin mouse IgG (Sigma V9) 1:200	+++	+++	+++	+++
Mc. Antivinculin mouse IgG (Sigma vVin-1) 1:400	+	++	+++	+++
Phalloidin CPITC (Sigma) 1:25	+	+	++	++
Phalloidin Alexa 488 (Molecular Probes) 1:300	++	+++	+++	+++
***Phalloindin Alexa* 568 (Molecular Probes)** 1:300	++	+++	+++	+++

[a] **Secondary antibodies** used in this screen were as follows: (1) Rhodamine Red-conjugated donkey anti-mouse **IgM** [Affini Pure $F(ab')_2$ Fragment-Immuno Research Laboratories, Inc.] and (2) Alexa Fluor 568- and 488-conjugated goat anti-mouse **IgG** (H+L) (Molecular Probes)

IV. COMBINING IMMUNOFLUORESCENCE AND GFP TAGS

The ability to express fluorescent proteins as tags to gene products in living cells represents an important advance in localisation methods. In addition to facilitating the visualisation of protein dynamics *in vivo* with sensitive imaging systems, these tagging methods can be usefully combined with the imunofluorescence procedure. Additional flexibility is offered by the fact that the tagged protein is already fluorescent so that restrictions with the use of secondary antibodies are reduced and triple labelling is relatively straightforward. With the cytoskeleton, phalloidin is a probe of choice for actin; when applying this probe, four labels in one cell would not be problematic, given a suitable choice of fluophores (including Cy-5 in the infrared, for example).

An interesting aspect of proteins that are washed away easily during fixation is that they are retained more readily when tagged with a GFP moiety (M. Gimona, unpublished observations). This property offers an unexpected advantage of GFP-tagged probes for localisation studies with fixed cells.

Figures 1–3 show examples of cells expressing GFP-tagged proteins and then fixed and labelled with phalloidin (for actin) and a single antibody. The fixation procedure was "fixation 1" in step 2.

V. COMMENTS

We have generally aimed for fixation protocols that best preserve the actin cytoskeleton. Although stress fibers are easily preserved with most fixative protocols, the delicate peripheral lamellipodia are normally

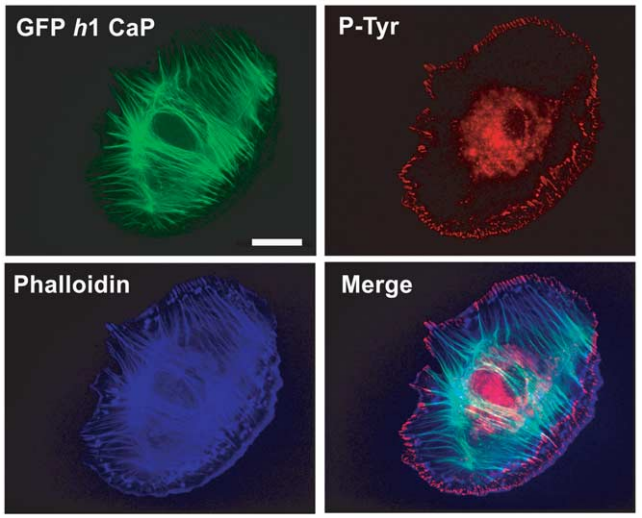

FIGURE 1 Flourescence images of an A7r5 smooth muscle cell transfected with GFP *h*1calponin (Gimona, 2003) and then counterstained with Alexa phalloidin 350 (dilution, 1:200) and mouse antiphosphotyrosine (PY99 Santa Cruz dilution 1:1000), followed by a GaM Alexa 568 as secondary antibody at a dilution of 1:750. Images were recorded on a Zeiss Axioskop fitted with an Zeiss Axiocam imaging system. All three images are combined in the merged image (bottom right). Bar: 20 µm.

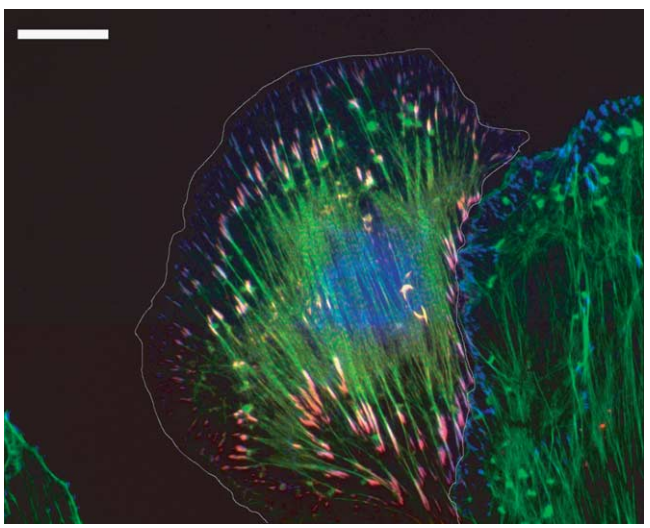

FIGURE 2 Merged fluorescence images (as Fig. 1) of an A7r5 smooth muscle cell transfected with Ds-Red zyxin (Bhatt *et al.*, 2002) to mark focal adhesions and then labelled with Alexa 488 phalloidin (dilution, 1:300) and antiphosphotyrosine (see Fig. 1) with GaM Alexa 350 at a dilution of 500 as secondary antibody. The boundary of the transfected cell is indicated by a white line. Bar: 20 µm.

distorted or lost after methanol or formaldehyde fixation. This is why glutaraldehyde is included in two of the present mixtures. A stronger glutaraldehyde fixation than what we have used here is best for lamellipodia (see, e.g., Small, 1988) but cannot be used with

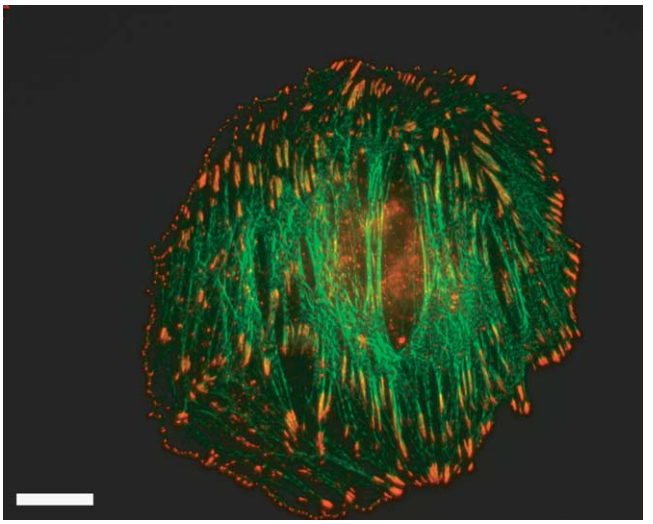

FIGURE 3 Merged fluorescence images (as Fig. 1) of an A7r5 smooth muscle cell transfected with GFP-α-actinin (Gimona *et al.*, 2003) and counterstained with mouse antiphosphotyrosine (as in Fig. 1). Bar: 20 µm.

several of the antibodies described. So again we have had to compromise. Weber and colleagues (1978) introduced the use of sodium borohydride to reduce free aldehyde groups after glutaraldehyde fixation and thereby the autofluorescence introduced by this fixative. If autofluorescence is observed, for example, in the region of the nucleus, this can be eliminated by a brief treatment (3 × 10 min) of the coverslips in ice-cold cytoskeleton buffer containing freshly dissolved sodium borohydride (0.5 mg/ml). The coverslips are rinsed three times prior to immunolabelling.

VI. PITFALLS

If problems arise from sinking of coverslips during washing, use another washing protocol, e.g., immersion of coverslips cell side up in separate petri dishes containing PBS. Damaged cells normally arise from inadvertently allowing the coverslip to dry at any stage of the procedure or by touching the cell side with filter paper. Labelling with phalloidin can be improved by including this probe also in the first antibody. Successful double or triple immunofluorescence labelling requires that the individual antibody combinations each produce intense staining with a clean background, when used alone.

References

Bhatt, A., Kaverina, I., Otey, C., and Huttenlocher, A. (2002). Regulation of focal complex composition and disassembly by the calcium-dependent protease calpain. *J. Cell Sci.* **115**, 3415–3425.

Giloh, H., and Sedat, J. W. (1982). Fluorescence microscopy: Reduced photobleaching of rhodamine and fluorescein protein conjugates by *n*-propyl gallate. *Science* **217**, 1252–1255.

Gimona, M., Kaverina, I., Resch, G. P., Vignal, E., and Burgstaller, G. (2003). Calponin repeats regulate actin filament stabilty and formation of podosomes in A7r5 smooth muscle cells. *Mol. Biol. Cell*.

Johnson, G. D., Davidson, R. S., McNamee, K. C., Russell, G., Goodwin, D., and Holborow, E. J. (1982). Fading of immunofluorescence during microscopy: A study of the phenomenon and its remedy. *J. Immunol. Methods*. **55**, 231–242.

Small, J. V. (1988). The actin cytoskeleton. *Electron Microsc. Rev*. **1**, 155–174.

Weber, K., Rathke, P. C., and Osborn, M. (1978). Cytoplasmic microtubular images in glutaraldehyde-fixed tissue culture cells by electron microscopy and by immunofluorescence microscopy. *Proc. Natl. Acad. Sci. USA* **75**, 1820–1824.

CHAPTER

68

Immunocytochemistry of Frozen and of Paraffin Tissue Sections

Mary Osborn and Susanne Brandfass

I. INTRODUCTION

Immunocytochemistry of tissue sections can yield valuable information as to the location of antigens. Thus it can determine whether the antigen is ubiquitous or is present only in certain tissues. It can further determine whether all cells in a given tissue are positive for a given antigen or whether the antigen is restricted to one or a few specialized cell types within the tissue. Its uses are not limited to normal tissues, and testing of tumor tissues in immunocytochemistry can yield information important for determination of tumor type. As stated in the articles on immunocytochemistry of cultured cells, choice of antibodies and of fixation method can be of critical importance. New antibodies should be tested on both frozen sections and paraffin sections of a variety of tissues in which the antigen is thought to be present. In general, more antibodies will react on frozen sections than on paraffin sections; however, morphology is better preserved in the paraffin sections.

For other reviews of methods, see Denk (1987) and Sternberger (1979), and for overviews of the use of these methods in histopathology, see Osborn and Weber (1983), Tubbs *et al.* (1986), Jennette (1989), and Osborn and Domagala (1997).

II. MATERIALS AND INSTRUMENTATION

A. Antibodies

See the article by Osborn in this volume. Establish working dilutions by running a dilution series. Usually monoclonal antibodies can be diluted 1:5 to 1:30, ascites fluid 1:100 to 1:1000, and polyclonal antibodies 1:20 to 1:40, but the dilutions depend critically on the detection technique that is employed. Dilute both primary and secondary antibodies as far as possible to save money and to avoid unspecific reactions.

B. Cryostat

Use a Leica CM1900 rapid sectioning cryostat (www.leica-microsystems.com). A useful accessory is a freezing head with variable temperature control. Use a C-knife and resharpen when necessary.

C. Tissue-tek

OCT 4583 compound from Miles Laboratories.

D. Paraffin Embedding

Automatic machines are useful only for laboratories that process a large number of samples. Check equipment for paraffin embedding in the local pathology department before purchasing.

E. Sliding Microtomes

These are relatively inexpensive and can be used with disposable knives.

F. Water Baths for Histology

These are thermostatically controlled and relatively shallow, e.g., 20 cm in diameter and 4 cm deep.

Copyright 2006, Elsevier Science (USA).
All rights reserved.

G. Microscopes

A microscope equipped with the appropriate filters to view immunofluorescence specimens is important. To view peroxidase- or streptavidin–biotin-stained specimens only a simple light microscope is required.

III. PROCEDURES

A. Cryostat Sections

1. Freezing of Tissue Blocks

Steps

1. Fill the inner beaker of the freezing apparatus with isopentane and the outer beaker with liquid nitrogen about 30 min before freezing tissues (Fig. 1). Use reagent-grade isopentane. Measure the temperature and wait until isopentane reaches –120 to –130°C. At –155°C the isopentane will freeze.
2. Dissect tissues. Cut into small blocks (~4–7 mm) using a scalpel. Place block on a prenumbered square of paper with the surface that will be sectioned furthest away from the paper. For small specimens, e.g., vessels, place a drop of Tissue-tek on the paper and then add the tissue.
3. Drop tissue blocks into iospentane. Leave for at least 30 s. Remove blocks with plastic tweezers and transfer directly to plastic vials (scintillation vials 6 × 2.5 cm work well) or metal cans (~3 × 3 cm) with screw tops that have been precooled on dry ice. Close vials and store in a –70°C freezer. Tissue blocks are stable for several years.

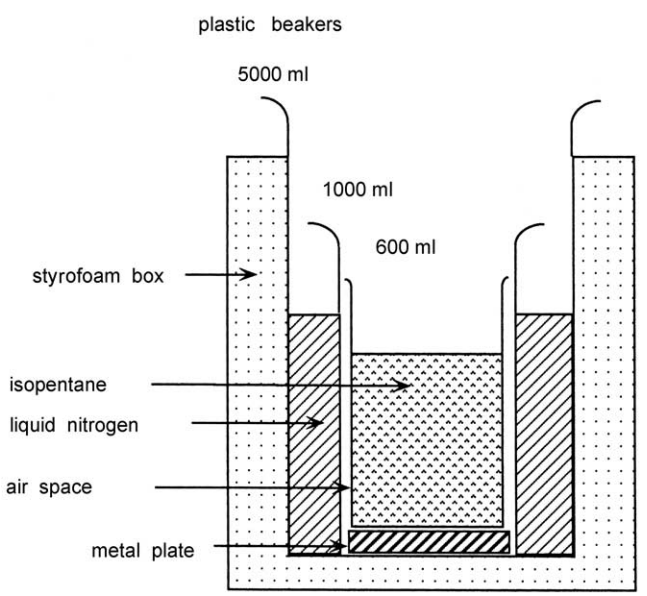

FIGURE 1 Apparatus used to freeze tissues.

2. Cutting Cryostat Sections

Stpes

1. Wash microscope slides by dipping in acetone, air dry, and store at room temperature. Store plastic tweezers and brush in the cryostat. Precool cryostat and freezing head.
2. Place Tissue-tek on precooled freezing head and mount block so that the larger side of the cut section is at 90° to the knife blade.
3. The optimal cutting temperature is different for different tissues. Most tissues cut well at –15 to –20°C. For liver, use –10°C. If the sections wrinkle as they are cut and look mushy, decrease the temperature. If the sections have cracks and look brittle, increase the temperature.
4. To cut sections use the C-knife. First trim the block to get a good cutting surface. Then adjust the section thickness to 5 µm and use the automatic advance. Now cut three or four sections so that the preset section thickness is achieved. Then bring the antiroll plate on the knife to stop the section from rolling up and to keep it flat on the knife. The antiroll plate must be parallel to the knife edge and should only protrude very slightly over the edge.
5. For optimal sections the knife and the antiroll plate must be kept clean (use a soft cloth dipped in acetone). Always clean the knife in the cutting direction and never the reverse so as not to damage the cutting edge of the knife.
6. Remove the antiroll plate and hold the microscope slide over but not touching the cut section. The section should now spring on to the slide because of the difference in temperature between knife and slide. The quality of the section can be checked using toluidine blue or hematoxylin–eosin staining (see later).
7. Dry the sections at room temperature for 30 min. Then either use directly or place in a slide box and put in a –70°C freezer. Cut sections are stable for months or years at –70°C.
8. Sections from a few tissues may not stick firmly enough to slides and may come off during subsequent processing. If this happens, try coating slides with 0.1% polylysine (e.g., Sigma Cat. No. 8920) in water.

B. Paraffin Sections

1. Embedding Tissues in Paraffin

Steps

Human material is often received from the clinic already embedded in paraffin. Protocols vary depend-

ing on the clinic, with time of fixation in formaldehyde being very variable (e.g., 4 h to over the weekend). To embed animal tissue in the laboratory, cut into 4 to 7-mm blocks and place it for 4–8 h in 3.7% formaldehyde in phosphate-buffered saline (PBS), 1 h in 50% ethanol, 2 × 1 h in 70% ethanol, 2 × 1 h in 96% ethanol, 2 × 1 h in 100% ethanol, 1 × 1 h in xylene, 1 × 2 h in xylene, and 2 × 2 h in Paraplast Plus (Shandon).

2. *Cutting Paraffin Sections*

Steps

1. To obtain very thin sections (1–2 µm), put the paraffin blocks in a freezer at –20°C for about 30 min. Mount the block in the holder of a sliding microtome. If the block cuts well do not use the automatic advance, but rely instead on the natural expansion of the block as it warms up to advance the block. If the block is not easy to cut, use the automatic advance set at a thickness of 1–2 µm. Correct adjustment of the knife and of the cutting angle is very important. Use an inclination angle (β) of 15° (Fig. 2). If the inclination angle is less than 10° the knife will not cut the block, and if it is greater than 15° the block will break.

2. Trim the block until the cutting surface is optimal. Then cut a section, using a paint brush to draw the section onto the knife so that it does not roll up.

3. Dip a second paint brush in water so that the section will adhere to it and move the section to a water bath held at 40–45°C. If the section is placed with the shiny smooth surface touching the water the warmth will smooth out the section and wrinkles will vanish!

4. Place a microscope slide under the section and, using a brush, position the section on the slide.

5. Dry the sections. For immunohistochemical methods, dry overnight at 37°C. For normal histological methods, set drying oven to 60°C so that the paraffin melts in part during the drying step and dry for 1–2 h.

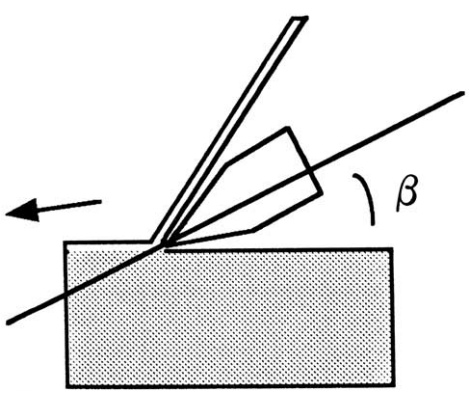

FIGURE 2 Correct adjustment of knife and of cutting angle to cut paraffin sections.

3. *Deparaffinization*

Immerse sections 2 × 10 min in xylene, 1 × 3 min in 100% ethanol, 1 × 3 min in 95% ethanol, and air dry.

4. *Trypsinization*

Some laboratories routinely use trypsinization or other proteolytic treatment of formalin-fixed, paraffin-embedded tissues prior to immunohistochemistry, e.g., 5 min in 0.1% trypsin (Sigma Cat. No. T-8128 or Dako Cat. No. S2012) in PBS at room temperature. As stressed by Ordonez *et al.* (1988), this can enhance the staining by certain antibodies but may also result in false negative staining with other antibodies. Thus, control trypsinization conditions carefully and recheck them each time a new antibody is used.

5. *Treating Sections in a Microwave Oven*

Cut sections onto Superfrost or similar slides. After deparaffinization, immerse slides in citrate buffer (2.1 g citric acid monohydrate/liter adjusted to pH 6.0 with NaOH). Microwave for two cycles of 5 min each at a setting of 650 or 700 W. Add more buffer between cycles so slides stay covered during the microwave step. Cool to room temperature (cf. Cattoretti *et al.*, 1992).

C. Histologic Staining of Sections

Stain frozen sections directly. Deparaffinize paraffin sections (see earlier), substituting a wash with distilled water for the air-drying step.

Solutions

1. *Toluidine blue:* Immerse sections in 1% toluidine blue for approximately 1 min. Wash with distilled water. Mount in water-soluble embedding medium, e.g., Glycergel (Dako Cat. No. C0563).

2. *Hemotoxylin–eosin:* Immerse sections for 10 min in Mayer's Hemalum solution (Merck). Wash for 10 min under running tap water, for 5 min in eosin (Merck), and twice with distilled water and then run through an alcohol series (e.g., 75%, 95% for 2 min each, then 100% for 5 min, then 2 × 5 min in xylol) and mount in Eukitt (Riedel de Haën Cat. No. 33949) or Entellan (Merck Cat. No. 107960).

D. Immunocytochemistry

Three methods are described in detail: immunofluorescence, the immunoperoxidase method, and the

more sensitive streptavidin–biotin method. The two latter methods have the advantage that nuclei can be counterstained with hemotoxylin and that only a simple light microscope is required to visualize the stain; however, fluorescence generally gives greater resolution.

As noted for cells, many antibodies that react well on cryostat sections may not react on the same tissue after it has been fixed in formaldehyde and embedded in paraffin. In such a case it may be advantageous to try fixing tissue, e.g., in B5, Bouin's, or Zenker's fixative or alcohol, prior to paraffin embedding. An interesting alternative is to use sections of formaldehyde-fixed, paraffin-embedded material that have been treated in a microwave oven.

For all methods mark the position of the section after fixation; either use a diamond pencil or circle the section with a water-repellent marker (Dako Cat. No. S2002). Remove excess buffer after rinsing steps with Q-tips. Use 10 µl of antibody per section. Apply with an Eppendorf pipette and use the pipette tip to spread the antibody over the section without touching the section. Several manufacturers (e.g., Dako) produce excellent protocol sheets for each immunocytochemical method.

1. Immunofluorescence

Steps

1. Fix cryostat sections or paraffin sections deparaffinized as described earlier for 10 min in acetone at –10°C. Air dry.
2. Use steps 2–9 of the protocol given in the article by Osborn in this volume for multitest slides. Nuclei can be counterstained with Hoechst dye (see Osborn's article). Positively stained cells will be green (see Fig. 3) if an FITC-labeled second antibody is used or red if a rhodamine-labeled second antibody is selected (see also the double label of a cytological sample in Fig. 4).

2. Peroxidase Staining

Steps

1. Fix cryostat sections for 10 min in acetone at –10°C, air dry, and wash in PBS.
2. Deparaffinize paraffin sections and incubate for 30 min at room temperature in 100 ml methanol containing 100 µl H_2O_2 to block endogenous peroxidase activity. Wash in PBS.
3. Incubate for 10 min at 37°C with normal rabbit serum. Drain, but do not wash after this step.
4. Incubate with primary antibody (e.g., mouse monoclonal) for 30 min at 37°C.
5. Wash three times in PBS.

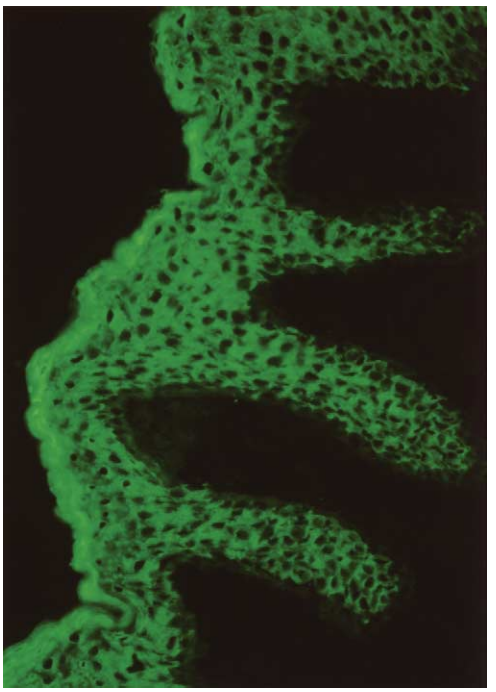

FIGURE 3 Frozen section of human skin stained with KL1 keratin antibody with FITC-labeled second antibody. Only the epidermis is stained (×150).

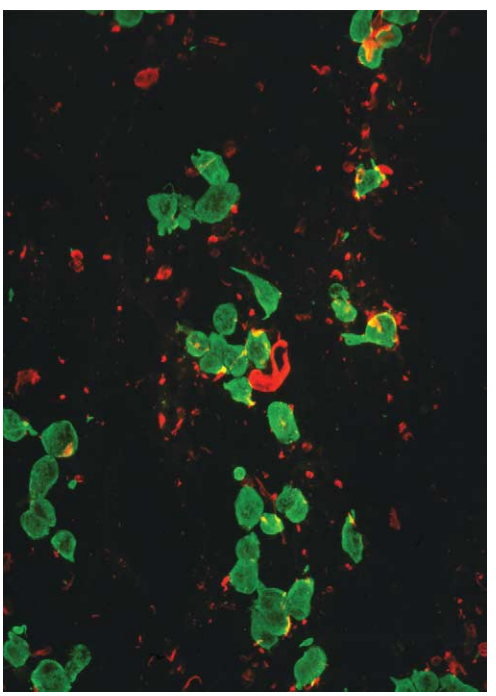

FIGURE 4 Cytological specimen from human breast carcinoma stained with a keratin antibody with FITC-labeled second antibody to show the tumor cells and with a vimentin antibody and a rhodamine-labeled second antibody to show the other cells in the specimen.

6. Incubate with second antibody coupled to peroxidase, e.g., rabbit antimouse for a monoclonal first antibody (Cat. No. P0260 from Dako diluted 1:10 to 1:20).
7. Wash three times in PBS and once in Tris buffer (6 g NaCI, 6 g Tris/liter, pH 7.4),
8. Develop for 10 min at room temperature using freshly made solutions (e.g., 0.06 g diaminobenzidine, Fluka Cat. No. 32750 in 100 ml Tris buffer, 0.03 ml H_2O_2). *Note:* Diaminobenzidine is a carcinogen; handle with care.
9. Wash in tap water.
10. Apply a light counterstain by immersing the slide in Hemalum for 1 to 10 s. Remove when staining reaches the required intensity.
11. Wash in tap water.
12. Mount in Glycergel (Dako Cat. No. C0563, http://www.dako.com).

Notes

1. Structures that are positively stained will be dark brown, whereas nuclei will be light blue (Figs. 5–7).
2. The method can be made more sensitive by using an additional step with a peroxidase–antiperoxidase complex (see Sternberger, 1979).
3. Blocking should be performed with a 5% solution of normal serum from the same host species as the labeled antibody, i.e., in this example the tissue is

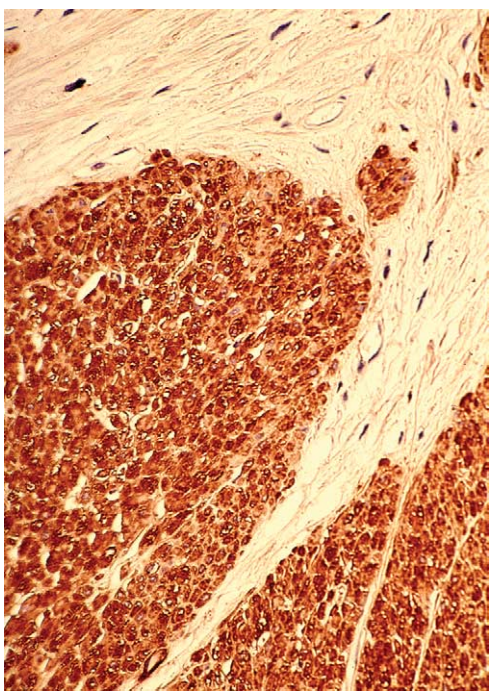

FIGURE 5 Paraffin section of human uterus stained with antibody after microwave fixation with the desmin DER 11 antibody in the peroxidase technique (×160).

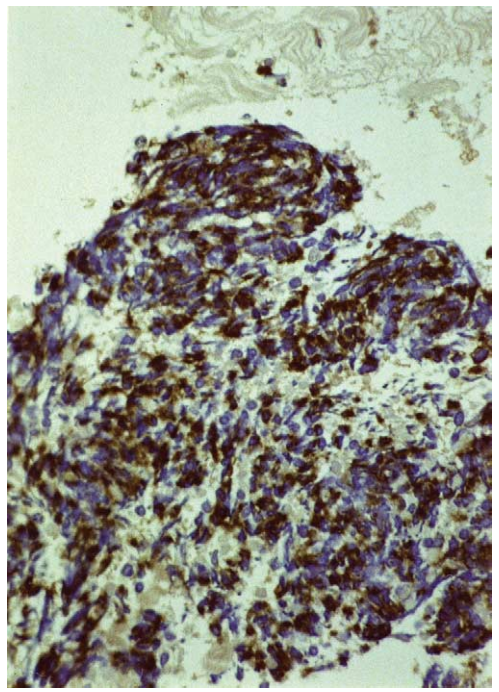

FIGURE 6 Frozen section of human rhabdomyosarcoma stained after microwave treatment with desmin antibody DEB5 and with peroxidase-labeled second antibody. Brown tumor cells are positive for desmin. Nuclei are counterstained blue (×160).

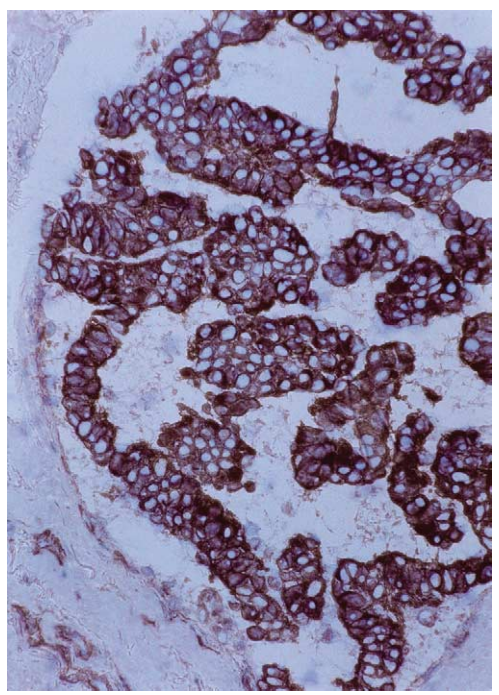

FIGURE 7 Frozen section of human breast carcinoma stained with the keratin KL1 antibody and with peroxidase-labeled second antibody. Brown tumor cells are positive for keratin. Nuclei are counterstained blue (×150).

blocked with normal rabbit serum because the labeled antibody is a rabbit antibody.
4. Bovine serum albumin (BSA) for diluting antibodies should be of high purity. Impure preparations can contain bovine IgGs that can cross-react with the labeled second antibodies.

3. *Streptavidin–Biotin Stain*

Buy the reagents separately or use the Histostain kit from Zymed Laboratories (http://www.zymed.com; Cat. No. 95-6543 for mouse primary antibody and Cat. No. 95-6143 for rabbit primary antibody). These kits are based on the strong binding between streptavidin, a 60,000-kDa protein isolated from *Streptomyces avidinii*, and biotin, a water-soluble vitamin (MW 244, $K_d = 10^{-15} M$). Instructions are given for the mouse kit.

Steps

1. Fix cryostat sections for 10 min in acetone at –10°C and air dry. Sections can be treated with 0.23% periodate for 45 s. Go to step 3.
2. Deparaffinize paraffin sections and air dry. Incubate 10 min in PBS at room temperature and then 10 min in H_2O_2 solution (nine parts methanol to one part 30% H_2O_2 in water). Wash 3 × 2 min in PBS.
3. Reduce nonspecific background staining by blocking for 10 min in 10% goat serum at room temperature (see Note 3 in Section III,D,2). Then drain but do not wash.
4. Incubate with primary antibody, e.g., mouse monoclonal antibody, in wet chamber for 30 min at 37°C.
5. Wash 3 × 2 min in PBS.
6. Add biotinylated second antibody, e.g., goat anti-mouse, for 10 min at room temperature and repeat step 5.
7. Add enzyme conjugate streptavidin–peroxidase diluted 1:20 for 5 min at room temperature. This binds to the biotin residues on the second antibody.
8. Develop by adding substrate–chromogen mixture for 5 min at 37°C or 15 min at room temperature. The enzyme peroxidase catalyzes the substrate hydrogen peroxide and converts the chromogen aminoethylcarbazole to a red, colored deposit.
9. Wash 3 × 2 min in distilled water.
10. Counterstain with Hemalum between 1 and 10 s.
11. Wash 7 min in tap water.
12. Mount in glycergel.

Notes

1. Structures that are positively stained will be red, whereas nuclei will be light blue (Figs. 8 and 9).

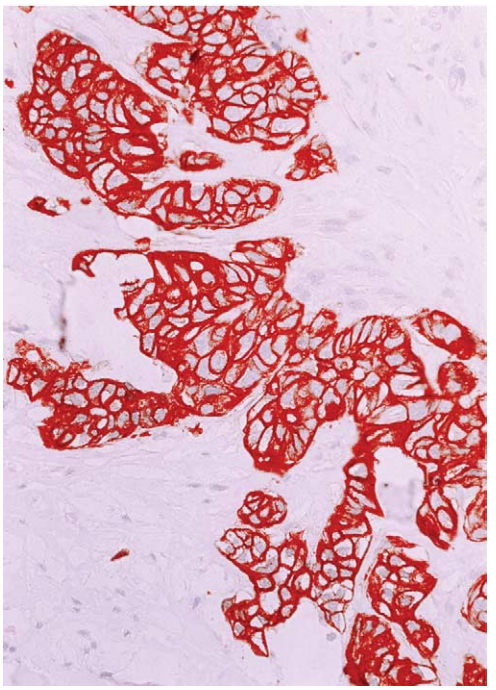

FIGURE 8 Paraffin section of human breast carcinoma stained after microwave treatment with keratin KL1 antibody in the streptavidin–biotin technique. Red tumor cells are keratin positive. Nuclei are counterstained blue (×150).

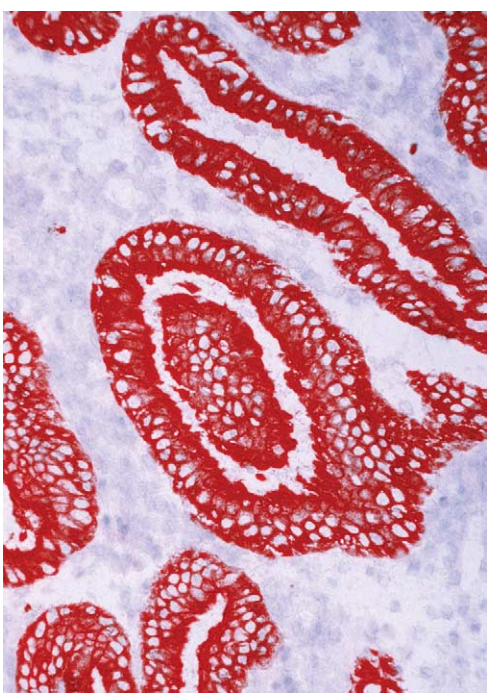

FIGURE 9 Frozen section of human uterus is stained with KL1 keratin antibody in the alkaline phosphatase–antialkaline phosphatase technique. Only epithelial cells are positive (×150).

2. The optimal dilution of primary antibody has to be determined for each antibody.
3. The streptavidin–peroxidase conjugate is the same for all species; the blocking serum and second antibody vary according to the species in which the first antibody is made.

Other Methods

1. The alkaline phosphatase–antialkaline phosphatase technique is also a very sensitive method (Fig. 8).

2. Both fluorescent and chromogenic signals can be enhanced up to 1000X with Tyramide Signal Amplification Technology (New England Nuclear). With this technique, primarily antibodies can be diluted in some instances more than 10,000-fold.

IV. COMMENTS

If possible, include (1) a positive control, i.e., a section of a tissue known to contain the antigen; (2) a negative control, i.e., a section known not to have the antigen; and (3) a reagent control, i.e., a section stained with nonimmune serum instead of the primary antibody. Ideally, the first control should be positive and the second and third controls negative. If high backgrounds are obtained, it may help to adjust the antibody concentrations by increasing the length of time for washing steps or by including 0.5*M* NaCl or 5% BSA in the antibody solutions.

References

Cattoretti, G., Backer, M. H. G., Key, G., Duchrow, M., Schlüter, C., Galle, J., and Gerdes, J. (1992). Monoclonal antibodies against recombinant parts of the Ki-67 antigen (MIB 1 and MIB 3) detect proliferating cells in microwave processed formalin-fixed paraffin sections. *J. Pathol.* **168**, 357–363.

Denk, H. (1987). Immunohistochemical methods for the demonstration of tumor markers. *In* "Morphological Tumor Markers" (G. Seifert, ed.), pp. 47–70. Springer-Verlag, Berlin.

Jenette, J. C. (1989). "Immunohistology in Diagnostic Pathology." CRC Press, Boca Raton, FL.

Ordonez, N. G., Manning, J. T., and Brooks, T. E. (1988). Effect of trypsinization on the immunostaining of formalin-fixed, paraffin-embedded tissues. *Am. J. Surg. Pathol.* **12**, 121–129.

Osborn, M., and Domagala, W. (1997). Immunocytochemistry. *In* "Comprehensive Cytopathology" (M. Bibbo, ed.), 2nd Ed., pp. 1033–1074. Saunders, Philadelphia.

Osborn, M., and Weber, K. (1983). Tumor diagnosis by intermediate filament typing: A novel tool for surgical pathology. *Lab. Invest.* **48**, 372–394.

Sternberger, L. A. (1979). "Immunohistochemistry," 2nd Ed. Wiley, New York.

Tubbs, R. R., Gephardt, G. N., and Petras, R. E. (1986). "Atlas of Immunohistology." American Society of Clinical Pathologists Press, Chicago.

PART

E

Appendix

CHAPTER

69

Representative Cultured Cell Lines and Their Characteristics

Robert J. Hay

Virtually thousands of different cell lines have been derived from human and other metazoan tissues. Many of these originate from normal tissues and exhibit a definable, limited doubling potential. Other cell lines may be propagated continuously, as they either have become immortalized from the normal by genetic changes or have been developed initially from tumor tissue. Finite lines of sufficient doubling potential and continuous lines can both be expanded to produce a large number of aliquots, frozen, and authenticated for widespread use in research.

Resources such as the American Type Culture Collection (ATCC) have been established to acquire, preserve, authenticate, and distribute reference cell lines and microorganisms for use by the academic and industrial scientific community (Hay *et al.*, 2000). The cell biology program at the ATCC performs these functions to include human and animal cell lines with over 4000 available in 2003.

The advantages of working with well-defined cell lines free from contaminating organisms may appear obvious. Unfortunately, however, the potential pitfalls associated with the use of cell lines casually obtained and processed still require emphasis (Stacey *et al.*, 2000). Numerous occasions where lines exchanged among cooperating laboratories have been contaminated with cells of other species have been recognized since the late 1960s (Nelson-Rees *et al.*, 1974, 1981; MacLeod *et al.*, 1999). The loss of time and research funds as a result of these problems is very extensive.

Although bacterial and fungal contaminations represent an added concern, in most instances they are overt and easily detected, and therefore have less serious consequences than the more insidious contaminations by mycoplasma. That the presence of these latter microorganisms in cultured cell lines often negates research findings entirely has been stated repeatedly over the years (Barile *et al.*, 1973; Hay *et al.*, 1989). However, the difficulties of detection and the prevalence of contaminated cultures in the research community suggest that the problem cannot be overemphasized. These and related difficulties associated with the use of cell lines obtained from different sources can be avoided if one acquires stocks from a centralized cell resource that applies appropriate quality control (Hay *et al.*, 2000).

Representative human cell lines from normal and tumor tissues available from the ATCC are listed in Table I with a selection of a few of the more important characteristics. Similar data on a variety of cell lines from other animals are included in Table II. More current information on these and other cell lines, their availability, and characteristics is available online via the ATCC website at www.atcc.org.

Copyright 2006, Elsevier Science (USA).
All rights reserved.

TABLE I Representative Human Cell Lines (January 2003)[a]

Tissue/tumor (number available)	Designation	ATCC No.	Age	Sex	Race	Diagnosis	Source	Medium[b]	Comments
Adrenal (4)	SW-13	CCL-105	55	F	W	SCC[c]	Cortex	L15/10	Grade IV adenocarcinoma; gap junctions
	NCI-H295	CRL-2218	48	F	B	Invasive CA	Cortex	DMEM/F12	Adherant variant selected
	NCI-H295	CRL-10296	48	F	B	Invasive CA	Cortex	R2+	Produce steroids; tumorigenic
	NCI-H51D	HTB-184	56	M	W	SCLC	—	F12K10	Metastasis to adrenal
Bladder (17)	J82	HTB-1	58	M	W	SCC	Bladder	MEM+	Tumorigenic in nude mice
	RT4	HTB-2	63	M	W	Transitional cell, papilloma	Primary	MC10	Tumorigenic; well-differentiated HLA-I and -II
	SCaBER	HTB-3	58	M	B	SCC	Urinary bladder	MEM+	Epidermoid CA inure mice
	T24	HTB-4	81	F	W	TCC	Urinary bladder	McCoy's 5A	H-Mas+; tumor in hamsters
	HT-1376	CRL-1472	58	F	W	Transitional cell, grade III, invasive	Primary	EM10	Tumorigenic, colonies in soft agar, not treated
	UM-UC-3	CRL-1749	?	M	?	Transitional cell	Primary	EM10	Tumorigenic
	SW780	CRL-2169	80	F	W	Grade I transitional CA	TCC	L15/10	Patient had chemotherapy tumors form in nude mice
	SW156	CRL-2175	75	M	W	Hypernephroma	Kidney	L15/10	Blood type O rh+
	Caki1	HTB-46	49	M	W	Clear cell CA	Kidney	McCoy's 5a	Fine structure revealed
Bone marrow (6)	K562	CCL-243	53	F	?	CML	Pleural effusion	Iscove's DMEM10	Used extensively in natural killer cell assays
	IM-9	CCL-159	?	F	W	Multiple myeloma	Bone marrow	R10	B lymphoblastic cell synthesizes IgG-k receptors for hGH, insulin, and calcitonin
	KG-1	CCL-246	59	M	W	Acute myelogenous leukemia	Bone marrow	IDM20	Responds to colony-stimulating factor, forming colonies in soft agar; differentiates to macrophages; near diploid
	R54;11	CRL-1873	32	F	W	Acute leukemia	Bone marrow	AMEM10	Has t(4;11)(q21;123) and isochromosome q7; lacks T/B cell markers; strong TdT
	HS-5	CRL-11882	30	M	W	HPV-16 E6/E7 Transformed bone marrow cells	Long-term Bone marrow	DMEM10	Produces G-CSF; M-CSF; KL; LIF; and other factors
Brain (12)	A-172	CRL-1620	53	M	?	Glioblastoma	Primary Tumor	DM10	Nontumorigenic; poor colony formation in soft agar; inversion (9)(p11q34); translocation (9:19)
	U-87MG	HTB-14	44	F	W	Glioblastoma, grade III	Primary tumor	EM10	Tumorigenic, hypodiploid
	H4	HTB-148	37	M	W	Neuroglioma	Primary tumor	DM10	Nontumoriginic
	HCN-1A	CRL-10442	18 mo.	F	?	Unilateral megalencephaly	Cortex	DM10	Positive for neuronal markers; responds to NGF
	HCN-2	CRL-10742	7	F	?	Rasmussen's encephalitis	Cortex	DM10	Positive for neuronal markers; responds to NGF. Stimulated by phorbol esters

TABLE I (*Continued*)

Tissue/tumor (number available)	Designation	ATCC No.	Age	Sex	Race	Diagnosis	Source	Medium[b]	Comments
	LNZTA-3WT4	CRL-11543	60	M	W	Astrocytoma grade 4	LN-Z308	DM10+	Clone with p53 gene controlled by tetracyclin
	DBTRG-05MG	CRL-2020	59	F	C	Glioblastoma multiforme	Primary tumor	RPMI	Positive for S100, vimentin, and neuron-specific enolase
Breast (54)	BT-20	HTB-19	74	F	W	Typical grade II adenocarcinoma	Primary tumor	EM10	Tumorigenic, hyperdiploid
	MCF-7	HTB-22	69	F	W	Adenocarcinoma	Pleural effusion	EM10+1	Estrogen receptors, bel-1 mRNA differentiated;
	SK-BR-3	HTB-30	43	F	W	Adenocarcinoma	Pleural effusion	MC10	Hypertriploid Tumorigenic, poorly differentiated microvilli, desmosomes
	MCF-12F	CRL-10783	60	F	W	Fibrocystic breast disease	Reduction mammo-plasty	DM/F12	One of a series. Not tumorigenic positive for mucin and fat globule antigen
	HCC-1187	CRL-2322	41	F	W	Invasive ductal CA TNM grade IIA	Primary	RPMI1640	One of a series of paired tumor/EBV-transformed lines
	HCC-1187BL	CRL-2323	41	F	W	Blymphoblastic	EBV trans-formed	RPMI1640	
	UACC-893	CRL-1902	57	F	W	Ductal CA stage II	Lumpec-tomy	L15/10	Amplified HER-2/neu
	MDA-MB-330	HTB-127	43	F	W	Lobular CA	Primary Pleural effusion	L15+/20	One of a series. Tubulin and actin positive. Nontumorigenic
	T-47D	HTB-133	54	F	?	Infiltrating ductal CA	Pleural effusion	R10+	Steroid receptor +'ve
Bronchus (11)	ChaGo K-1	HTB-168	45	M	W	Undifferentiated carcinoma	Subcu-taneous metastasis	R10	Secretes *a*-hCG, estradiol, and progesterone
	CCD-14	CCL-203	34	F	W	Cerebral aneurysm	Primary	EM10	Euploid fibroblast line; limited doubling potential
	HBE4-E6/E7	CRL-2078	60	M	W	Adeno CA T2(NO)	Normal bronchial tissue	Keratinocyte-serum free	E6/E7 immortalized undergo squamous differentiation
	NL20	CRL-2503	20	F	W	Apparently normal	Accident victim	F12 +/4	SV_{40} large T-transformed, nontumorigenic
	NCI-H727	CRL-5815	65	F	W	Bronchial CA	Primary	RPMI10	One of a series. Differentiated. Synthesizes neuromedin B and parathyroid-like hormone
	BEAS-2B	CRL-9609?	?	?	?	Normal bronchi	Autopsy normal	LHC-9+ serum-free	Immortalized with $Ad12SV_{40}$. Differentiate and stain for $SV_{40}T$. One of a series
Cervix (19)	HeLa	CCL-2	31	F	B	Adenocarcinoma	Primary	EM10	First human line; widely studied; G6PD A: 4 marker chromosomes, many derivatives
	CaSki	CRL-1550	40	F	W	Epidermoid carcinoma	Metastasis to mesentery	R10	Secretes ßhCG

TABLE I (*Continued*)

Tissue/tumor (number available)	Designation	ATCC No.	Age	Sex	Race	Diagnosis	Source	Medium[b]	Comments
	C-4I	CRL-1594	41	F	W	Cervical carcinoma	Primary tumor	Naymouth's MB752/ 1/10	Contains HPV-18 sequences and expresses HPV-18 RNA. Tumorigenic. One of a series
	ME-180	HTB-33	66	F	W	Invasive SCC	Metastasis to omentum	MC10	Tumorigenic; desmosomes hypotriploid, XXX
	Si Ha	HTB-35	55	F	Asian	Squamous cell CA	Primary tumor	MEM10	P53 and pRB + Integrated HPV-16
Colon (44)	SW480	CCL-228	50	M	W	Grade III–IV adenocarcinoma	Primary	L15/10	Tumorigenic; K-*ras* codon 12. One of an extensive series
	LoVo	CCL-229	56	M	W	Adenocarcinoma of colon	Metastasis to clevicula	F12/10	Tumorigenic; well characterized for growth kinetics and drug responses. Desmosomes shown. CEA produced
	T84	CCL-248	72	M	?	Colon carcinoma	Transplant tumor	F12DME/5	Desmosomes; receptor for peptide hormones and neurotransmitters; show vectorial transport
	NCI-H508	CCL-253	55	M	W	Cecum adenocarcinoma	Metastasis to abdo- minal wall	R10	High DOPA carboxylase; TAG-72, CA 19-9 and CEA antigens. One of a series
	FHC	RL 1831	Fetus 13 wk.	?	?	Normal	Colon	F12/DM10+	Epithelial-like; lacks keratin; limited doubling potential
	HT-29	HTB 38	44	F	W	Well-differentiated grade II adenocarcinoma	Primary	MC10	Tumorigenic; hypertriploid; 17 marker chromosomes
	Caco-2	HTB 37	72	M	W	Adenocarcinoma	Primary	EM20	Hypertetraploid; exhibits enterocyte differentiation; tumorigenic.
Duodenum (2)	FH 74	CCL-241	3- to 4-month fetus	F	?	Normal	Small intestine	DME10+	Epithelial-like; tonofibrils and microvilli; keratin –'ve
	HuTu80	HTB-40	53	M	W	Adenocarcinoma	Primary	EM10	Tumorigenic; forms well-differentiated papilloma; pseudodiploid
Embryonal carcinoma (5)	NTERA-2 cl-D1	CRL-1973	22	M	W	Testicular carcinoma	Metastasis to lung	DM10	Clone of Tera-2; pluripotent; differentiates on exposure to RA
	NCCIT	CRL-2073	Adult	M	J	Embryonal CA	Mediastinal mixed germ cell tumor	R10	Differentiates; -'ve for keratin; +'ve for vimentin and placental alkaline phosphatase
	Cates-1B	HTB-104	35	M	W	Testicular carcinoma	Metastasis to lymph node	MC15	Pseudodiploid; patient treated with cytoxan, vincristine, and actinomycin D

TABLE I (*Continued*)

Tissue/tumor (number available)	Designation	ATCC No.	Age	Sex	Race	Diagnosis	Source	Medium[b]	Comments
	Tera 1	HTB-105	47	M	W	Seminoma	Metastasis to lung	MC10	Not tumorigenic; bcl-1 mRNA
Endometrium (7)	AN3 CA	HTB-111	55	F	W	Adenocarcinoma	Metastasis to lymph node	EM10	Yields malignant, undifferentiated tumor
	HEC-1A	HTB-112	71	F	?	Adenocarcinoma stage IA	Primary tissue	MC10	Hyperdiploid; triploid variant available as HTC113
	SK-UT-1	HTB-114	75	F	W	Leiomyosarcoma grade III	Mixed Mesodermal tumor	MEM10+	Hypodiploid to hyperdiploid. Diploid line selected and available as HTB-115
	KLE	CRL-1622	64	F	W	Poorly differentiated adenocarcinoma	Primary	DM/F12–10	Tumorigenic; forms microvilli and junctional complexes
	RL95–2	CRL-1671	65	F	W	Moderately differentiated adenosquamous			Estrogen receptors; *a*-keratin; microvilli
Kidney (30)	293 [HEK293]	CRL-1573	Fetus	?	?	Normal kidney	Early passage cells exposed to sheared adenovirus 5 DNA	MEM10HS	Used extensively in virus propagation. Many variants and engineered derivatives available
	ACHN	CRL-1611	22	M	W	Adenocarcinoma	Pleural effusion	EM10	Tumorigenic; invasive
	769-P	CRL-1933	63	F	W	Clear cell adenocarcinoma	Primary	R10	Tumorigenic; colonies in soft agar; microvilli and desmosomes; hypodiploid
	HK-2	CRL-2190	Adult	M	?	Normal proximal tubular line	E6/E7 transformed	Keratinocyte serum-free medium + F12K/10	Positive for PT cell marker enzymes and other proteins
	CCD-1103 KIDTr	CRL-2304	Fetal	?	?	Normal kidney epithelia	E6/E7 transformed		Keratin and acid phosphatase positive; susceptible to coxsackie, measles, polio and syncytial virus infection
	SV7 tert	CRL-2461	63	F	?	Renal angiomyolipoma	Immortalized with SV40 large T and h-tert	DME10	For studies on tuberous sclerosis
	A-498	HTB-44	52	F	?	Kidney carcinoma	Primary tumor	MEM10	Hypertriploid line; used in virus and tumorigenicity studies
	Caki-1	HTB-46	49	M	W	Renal carcinoma	Metastasis to skin	MC10	Tumorigenic; hypertriploid
Leukemia/ lymphoma (55)	CCRF-CEM	CCL-119	4	F	W	ALL	Peripheral blood	R20	T lymphoblast; malignant in newborn hamsters; model chromosome number 45–47

TABLE I (*Continued*)

Tissue/tumor (number available)	Designation	ATCC No.	Age	Sex	Race	Diagnosis	Source	Medium[b]	Comments
	HL-60	CCL-240	36	F	W	ALL	Peripheral blood	L15/10	Neutrophilic promyelocytes differentiate when exposed to RA and others; surface receptors for Fc
	MOLT 4	CRL-1582	19	M	?	ALL	Peripheral blood	R10	Stable T cell; high Tdt; model chromosome number 95
	TUR	CRL-2367	37	M	W	Histiocytic lymphoma	Effusion	R10	Stable transfectant of U-937 resistant to both G418 and TPA
	NK-92	CRL-2407	50	M	W	Hodgkin's lymphoma	Peripheral blood	Alpha MEM/125 H/FBS	Natural killer cell line, IL-2-dependent surface markers defined series of lines available
	Loucy	CRL-2629	38	F	W	T-ALL	Peripheral blood	R10	Useful for defining role of t(16; 20) and genetic studies
	Hut 78	TIB-161	50	M	W	Sezary syndrome	Peripheral blood	R10	Mature T cell with inducer/helper phenotype; yields and responds to interleukin-2; parent to H9 cell line
Liver (13)	Hep- 3B	HB-8064	8	M	B	Hepatocellular carcinoma	Primary	EM10	Tumorigenic; produce haptoglobin; *a*-fetoprotein, albumin, a_2-macroglobulin; transferrin; fibrinogen, and other liver-specific proteins
	Hep-G2	HB-8065	15	M	W	Hepatocellular carcinoma	Primary	EM10	
	SNU-398	CRL-2233	42	M	A	Anaplastic hepatocellular carcinoma	Primary tumor	ACL4/5	Hyaline globules; HBV-DNA +'ve; HBV-RNA not expressed. One of a series of similar lines
	THLE-3	CRL-11233	Adult	?	?	Normal liver	Left lobe	BEGM	SV_{40} T antigen infected via PA317. Model for pharmacotoxicological studies
	SK-HEP-1	HTB-52	52	?	W	Adenocarcinoma	Ascites	EM10	Produces *a*-antitrypsin; has Weibel–Palade bodies and vimentin
Lung (203)	A-549	CCL-185	58	M	W	Carcinoma	Primary	F12K/15	Enzymes related to surfactant synthesis studied; lamellar inclusions but sparse.
	WI-38	CCL-75	Fetus	F	W	Normal	Primary	EM10	Euploid line, widely used in cell biology aging research, virology and vaccine manufacture. One of many normal fibroblast controls
	MRC-5	CCL-171	Fetus	M	W	Normal	Primary	EM10	Euploid line, widely used in cell biology aging research, virology and vaccine manufacture

TABLE I (*Continued*)

Tissue/tumor (number available)	Designation	ATCC No.	Age	Sex	Race	Diagnosis	Source	Medium[b]	Comments
	HLF-a	CCL-199	54	F	B	Normal	Primary	EM10	Diploid and stable; patient had epidermoid carcinoma of lung; tissue used was from site remote from cancer
	CCD-19Lu	CCL-210	20	F	W	Normal	Primary	EM10	Euploid; patient died of accidental head trauma
	NCI-H2126	CCL-256	65	M	W	Nonsmall cell lung CA	Plural effusion	HITES/5	One of an extremely large collection of human lung cancer lines and controls
	NCI-BL2126	CCL-256	65	M	W	Peripheral blood B lymphoblast line	EBV trans-formant	R10	Paired "control" for studies with NCI-H2126. Genomic DNA also available (ATCC# 45512 and 45513)
	NCI-H146	HTB-173	59	M	W	SCLC	Pleural fluid	R10	Tumorigenic; near triploid; high c-*myc* mRNA but no gene amplification; elevated biochemical markers for SCLC; keratin and vimentin positive
	NCI-H441	HTB-174	?	M	?	PapAC	Pericardial fluid	R10	Hyperdiploid; grows in soft agar; SP-A+' Clara and lamellar inclusions
	NCI-H82	HTB-175	40	M	W	SCLC	Pleural fluid	R10	Tumorigenic; near triploid, no Y, high c-*myc*; DNA and RNA, reduced amount and abnormal p53 mRNA (3.7 kb)
	NCI-H820	HTB-181	53	M	W	PapAC	Lymph node	A4	Near triploid; produces lamellar bodies and surfactants SP-A, -B and -C
	SK-LU-1	HTB-57	60	F	W	Adenocarcinoma	Primary	EM10	Tumorigenic in immunotolerant rats; hypotetraploid
Melanoma (32)	C32	CRL-1585	53	M	W	Amelanotic melanoma	Primary	EM10	Tumorigenic; hypodiploid with mode of 45
	Hs294T	HTB-140	56	M	W	Metastatic melanoma	Metastasis to lymph node	DM10	Nerve growth factor and interferon receptors; responsive to RA; tumorigenic and grows in soft agar
	MeWo	HTB-65	78	M	W	Malignant melanoma	Metastasis to lymph node	EMO	Well-studied line, XY karyottype, blood type A; HLA A2, A26, BW16, 18
	SK-MEL5	HTB-70	24	F	W	Metastatic melanoma	Metastasis to axillary node	EM10	Tumorigenic
	COLO 829	CRL-1974	45	M	W	Malignant melanoma	Subcuta-neous metastasis	R10	Prior to therapy; some melanin produced; B-cell counterpart available

TABLE I (*Continued*)

Tissue/tumor (number available)	Designation	ATCC No.	Age	Sex	Race	Diagnosis	Source	Medium[b]	Comments
	COLO 829BL	CRL-1980	45	M	W	Malignant melanoma	Peripheral blood EBV trans-formed	R10	"Control" B-cell line to CRL 1974; DNA fingerprinting confirms identity
Myeloma/ plasmacy-toma (18)	RPMI 8226	CCL-155	61	M	?	Multiple myeloma	Peripheral blood	R20	Produces λ light chains; no mature plasma cells
	U266B1	TIB-196	53	M	?	Myeloma	Perophiral	R15	IgE-A secreting
	HS-Sultan	CRL-1484	56	M	W	Plasmacytoma	Primary	R10	Produces IgG- *k*; hyperdiploid
	MC/CAR	CRL-8083	81	M	W	β-cell plasmacytoma	Peripheral blood	IDM20	Produce IgG1, have C3b complement receptors, and have normal diploid karyotype. Variant resistant to 8-aza-guanine available as CRL-8147
	NCI-H929	CRL-9068	62	F	W	Myeloma	Malignant effusion	R10+	Positive for PCA-1, transferrin receptor, and CD38. The 8q chromosomal anomaly is prevalent. Ras and C-myc RNA are expressed
Nasal septum (1)	RPMI 2650	CCL-30	52	M	?	Anaplastic SCC	Pleural effusion	EM10	Pseudodiploid with mode 46; keratin positive
Neuro-blastoma (13)	IMR-32	CCL-127	13 mo.	M	W	Neuroblastoma with organoid differentiation	Abdominal mass	EM10	Neuroblasts and large hyaline fibroblasts
	SK-N-MC	HTB-10	14	F	W	Neuroblastoma	Metastasis to supraorbital area	EM10 EM10	Pseudodiploid; dopamine hydroxlase positive
	SK-N-SH	HTB-11	4	F	?	Neuroblastoma	Metastasis to bone marrow		Hyperdiploid; dopamine hydroxylase
	BE(2)-M17	CRL-2267	2	M	?	Neuroblastoma	Metastasis to marrow	EM/F12 10	Grow in multilayer with long neuritic processes. Also as floating aggregates
	MC-IXC	CRL-2270	14	F	W	Neuroblastoma	Metastasis to supra-orbital area	EM/F12 10	High choline acetyltransferase clonal derivative of HTB-10
Ovary (11)	Caov-3	HTB-75	54	F	W	Adenocarcinoma	Primary	EM10	Extremely unusual chromosome morphology
	NIH: OVCAR-3	HTB-161	60	F	W	Progressive adenocarcinoma	Ascites	R20+	Tumorigenic; grows in soft agar; androgen and estrogen receptors
	PA-1	CRL1572	12	F	W	Teratocarcinoma	Ascites	EM10	Pseudodiploid, t(15q20q); highly malignant in nude mice
	TDV-112D	CRL-11731	42	F	W	Malignant adenocarcinoma	Primary ovary	MCDB104 and M199/15	Mutated p53, variants with deletions at 3p24 (CRL-11730 and 32)
Pancreas (19)	AsPC-1	CRL-1682	62	F	W	Metastatic carcinoma	Ascites	R20	Tumorigenic; CEA, PAA and PSA positive, hypotriploid

TABLE I (*Continued*)

Tissue/tumor (number available)	Designation	ATCC No.	Age	Sex	Race	Diagnosis	Source	Medium[b]	Comments
	SU86-86	CRL-1837	57	F	W	Pancreatic ductal adenocarcinoma	Liver metastasis	R10	Sensitivities in killer cell assays documented
	HPAF-11	CRL-1997	44	M	W	Pancreatic metastatic adenocarcinoma	Peritoneal fluid	EMIO	Highly metastatic
	MPanc-96	CRL-2380	67	M	W	Malignant adenocarcinoma	Lymph node	RI0	Transplantable to SCID mice. Recognized by autologous tumor-infiltrating leucocytes
	Capan-1	HTB-79	40	M	W	Metastatic carcinoma	Liver metastasis	R15	Tumorigenic; hypotriploid
	PANC-1	CRL-1469	56	M	W	Epitheloid ductal carcinoma	Primary	DM10	Hypertriploid
Pharynx (3)	Detroit 562	CCL-138	?	F	W	Metastatic carcinoma	Pleural fluid	EM10	Keratin positive
	FaDu	HTB-43	56	M	W	Squamous cell	Primary	EM10	Tumorigenic; desmosomes; 19 marker chromosomes
Placenta (5)	BeWo	CCL-98	Fetus	M	?	Malignant gestational choriocarcinoma	Hamster xenograft	F12-15	Secretes placental hormones, hCG, human placental lactogen, estrone, estradiol, progesterone
	JEG-3	HTB-36	Fetus	?	?	Choriocarcinoma, Edwin-Turner tumor	Hamster xenograft	EM10	Secretes hCG, human chorionic somatomammotropin, and progesterone; tumorigenic
	JAR	HTB-144	Fetus	?	?	Choriocarcinoma	Primary	R10	Secretes estrogen, progesterone, gonadotropin, and lactogen
	3A(tPA-30-1)	CRL-1583	Term	F	?	$TsA30SV_{40}$ + transformant	Normal term placenta	AMEM1O	Produce human chorionic gonadotrophin and are alkaline phosphatase positive at permissive (33) temperature. Postcrisis line available as CRL-1584
Prostate (10)	PC3	CRL-1435	60	M	W	Adenocarcinoma, grade IV	Primary	F12K-7	Tumorigenic and grows in soft agar; low acid phosphatase and steroid reductase
	LNCap.FGC	CRL-1740	50	M	W	Metastatic adenocarcinoma androgen-independent	Metastasis to supra-clavicular-lymph node	R10	Produces PSA, prostatic acid phosphatase; androgen receptors; tumorigenic
	PZ-HPV-7	CRL-2221	70	M	W	HPV-18 DNA transformed epithelium	Normal tissue peripheral prostate	KSFM	Keratins 5 and 8 positive. Not tumorigenic
	MDA Pca2b	CRL-2422	63	M	B	Prostatic adenocarcinoma	Bone	F12K/20	PSA and androgen receptor positive. Tumorigenic
	RWPE-1	CRL-11609	54	M	W	Transfected with plasmid carrying copy of HPV-18	Normal prostatic epithelia	KSFM	Nontumorigenic, positive for keratins 8 and 18. PSA develops on exposure to androgens. Transformed variants available as CRL-11610 and 11611

TABLE I (*Continued*)

Tissue/tumor (number available)	Designation	ATCC No.	Age	Sex	Race	Diagnosis	Source	Medium[b]	Comments
	DU145	HTB-81	69	M	W	Metastatic carcinoma	Metastasis to brain	EM10	Grows in soft agar; weak acid phosphatase; triploid; desmosomes
Rectum (5)	SW-837	CCL-235	53	M	W	Adenocarcinoma, grade IV	Primary	L15–10	Tumorigenic; hypodiploid
	SW-1463	CCL-234	66	F	W	Adenocarcinoma, grades II–III	Primary	L15–10	Tumorogenic; CEA positive; hypertriploid
Retinoblastoma (2)	WERI-Rb-1	HTB-169	1	F	W	Retinoblastoma	Primary	R10	Tumorigenic in rabbits; no colonies in soft agar; near diploid with 15 or 16 markers
	Y79	HTB-18	2.5	F	W	Retinoblastoma	Primary	R15	Reportedly reverse transcriptase positive
Rhabdomyosarcomas (5)	A204	HTB-82	1	F	?	Embryonal rhabdomyosarcoma	Primary	MC10	Tumorigenic; near diploid with abnormality on 22p
	HS729	HTB-153	74	M	W	Malignant rhabdomyosarcoma	Primary muscle	M5/10	Tumorigenic consistent with embryonal type
	RD	CCL-136	7	F	W	Malignant rhabdomyosarcoma	Pelvic tumor	DM10	No myofibrils but myoglobin and myosin ATPase activity; complex hyperdiploid karyology; also designated TE32 and 130T
Sarcoma (28 + genetic variants)	HT-1080	CCL-121	35	M	W	Fibrosarcoma	Acetabulum	EM10	Pseudodiploid tumorigenic. Susceptible to R0114 and FeLV. Contains activated N-ras
	HOS	CRL-1543	13	F	W	Osteogenic sarcoma	Primary	EM10	Flat morphology; sensitive to viral and chemical morphological transformation
	MES-SA	CRL-1976	56	F	W	Poorly differentiated sarcoma	Uterine tissue-hysterectomy	MCRO	Sensitive to chemotherapeutic agents. Resistant lines also available as CRL-1977 and CRL-2274
	MG-63	CRL-1427	14	M	W	Osteogenic sarcoma	Primary	EM10	Yields interferon on induction; hypotriploid with 18 or 19 markers
	SK-LMS-1	HTB-88	4	F	W	Leiomyosarcoma, grade II	Primary, vulva	EM10	Tumorigenic; hypertriploid with complex karyotype
	SW 1353	HTB-94	72	F	W	Chondrosarcoma	Primary, right humerus	L15/10	Hyperdiploid with trisomic N7 only
	U-205	HTB-96	15	F	W	Osteosarcoma	Tibia	MC15	Secretes osteosarcoma-derived growth factor similar to PDGFA chain
Skin (28)	Detroit-551	CCL-110	Fetus	F	W	Normal fibroblast	Skin	EM10	One of a series of lines from normal individuals and persons with genetic disorders

TABLE I (*Continued*)

Tissue/tumor (number available)	Designation	ATCC No.	Age	Sex	Race	Diagnosis	Source	Medium[b]	Comments
	A-431	CRL-1555	85	F	?	Epidermoid carcinoma	Primary	DM10	Tumorigenic and grows in soft agar; hypertriploid
	182-PFSK	CRL-1532	20	M	W	Normal	Skin	DM10	Apparently normal but carrying gene for hereditary adenomatosis of the colon
	MeKam	CRL-1279	10	M	W	Xeroderma pigmentosum	Skin	DM10	Xeroderma pigmentosum line from NIH. One of about 200 lines from humans with genetic disorders
	CCD 27Sk	CRL-1475	Fetus	M	B	Apparently normal fibroblasts	Skin	EM10	Established using skin from the chest area
	CD 977Sk	CRL-1900	20	F	W	Apparently normal fibroblasts	Skin	EM10	Established from skin of the breast
	CCD 966Sk	CRL-1881	78	F	B	Apparently normal fibroblasts	Skin	EM10	Established from skin of the breast
	CCD 1106 KERTr	CRL-2309	Fetus	19 wk.	W	E6/E7-transformed keratinocytes	Skin	KSFM	Epithelial specific and cytokeratin+; HLA not expressed, E6/E7 presence
	CCD 1102 KERTr	CRL-2310	Fetus	16 wk.	B	E6/E7-transformed keratinocytes	Skin	KSFM	Confirmed by PCR
Stomach (9)	AGS	CRL-1739	54	M	W	Adenocarcinoma	Primary	F12–10	No prior therapy; tumorigenic
	NCI-SNU-16	CRL-5974	33	F	A	Gastric carcinoma metastatic	Ascites	R10	DDC, CEA, and TAG-72 +'ve; muscarini and VIP receptors; c-myc amplified; one of a series of human cancer lines developed by J. Park and associates
	RF-48	CRL-1863	62	M	His-panic	Metastatic carcinoma	Primary metastasis	L15/10	Metastasis from CRL 1864 (RF-1); mucin and CEA negative
	RF-1	CRL-1864	62	M	His-panic	Metastatic carcinoma	Primary	L15/10	Stains for mucin; CEA positive Tuorigenic; hypertetraploid
	KATO-III	HTB-103	55	M	Mon-goloid		Pleural effusion	IDM10	
Submaxilla (1)	A-253	HTB-41	54	M	W	Epidermoid carcincoma	Primary	MC10	Hypotriploid; 14 marker chromosomes
Testes (3)	Cates-1B	HTB-104	34	M	W	Embryonal carcinoma	Metastasis to lymph node	MC10	Reportedly hypodiploid to diploid. See also HTB-105 and HTB-106
Thyroid (2)	SW579	HTB-107	59	M	W	SCC	Primary	L15/10	Tumorigenic
	TT	CRL-1803	77	F	W	Medullary thyroid carcinoma	Primary	F12K/10	Tumorigenic; neuropeptides produced
Tongue (4)	SCC—4	CRL-1624	55	M	?	SCC	Primary	F12/DM10	Tumorigenic; involucrin negative; hypopentaploid; positive for 40-kDa keratin. See CRL-1623 and 1629
	SCC-25	CRL-1628	70	M	?	SCC	Primary	F12/DM10	Tumorigenic, synthesizes low levels of involucrin; epidermal keratin; hypertriploid

TABLE I (*Continued*)

Tissue/tumor (number available)	Designation	ATCC No.	Age	Sex	Race	Diagnosis	Source	Medium[b]	Comments
	CAL27	CRL-2095	56	M	W	SCC	Primary	DME10	Tumorigenic; resistant to treatment with VDS, CDP, or ACTD. Cytokeratin+
Umbilicus (3)	HUV-EC-C	CRL-1730	Fetal-term			Apparently normal vascular endothelium	Umbilical vein	F12K/10+ECGS	Endothelial line; produces factor VIII; near diploid; limited life span.
	HUVE-12	CRL-2480	Fetal-term			Vascular endothelium apparently normal	Umbilical vein	F12K/10 + ECCS and heparin	Limited doubling potential. See "Wistar Special Collection" for more lines and detail
	HUVS-112D	CRL-2481	Fetal-term			Smooth muscle apparently normal	Umbilical vein	F12K/10 + ECCS and heparin	Limited doubling potential. See "Wistar Special Collection" for more lines and detail
Vulva (3)	SK-LMS-1	HTB-88	43	F	W	Leiomyosarcoma	Primary	EM10	Tumorigenic
	SW954	HTB-117	86	F	W	SCC	Primary	L15/10	Pseudodiploid
	SW962	HTB-118	64	F	W	SCC	Metastasis to lymph node	L15/10	Tumorigenic; hypertriploid with at least 15 marker chromosomes

[a] See Hay *et al*. (1992) for originators, references, and more details.

[b] Abbreviations for medium used (on the left-hand side) include (EM) Eagle's minimum essential medium; (R) RPMI 1640; (DM) Dulbecco's modification of Eagle's medium; (F12 and F12K) Ham's medium and Kaighn's modification, respectively; (IDM) Iscove's modification of Eagle's medium (L15) Leibovitz medium; (MC) McCoy's 5A medium; and (AMEM) α modification of Eagle's medium [see Hay *et al*. (1992) for formulas]. The number on the right-hand side indicates percentage of serum (usually fetal bovine) used. Additional recommended ingredients are indicated by a plus sign.

[c] SCC, squamous cell carcinoma; hGH, human growth hormone; Tdt, terminal deoxynucleotidyl transferase; hCG, human chorionic gonadotrpin; RA, retinoic acid; G6PD, glucose-6-phosphate dehydrogenase; ALL, acute lyphoblastic leukemia; SCLC, small cell lung cancer; CEA, carcinoembryonic antigen; PSA, pancreas-specific antigen; PAA, pancreas-associated antigen. See www.atcc.org for further details.

TABLE II Representative Cell Lines from Other Species (January 2003)

ATCC No.[a] (general category)	Designation	Species (No. of lines available)	Culture medium[b]	Comments
CCL-33	PK (15)	Pig (6)	MEM10	Adult kidney epithelial line. Used in virology. Keratin +. Produces plasminogen activator
CCL 34	MDCK	Canine (5)	EM10	Kidney epithelial line; model chromosomes number 78; forms domes in monolayer; used extensively in transport studies
CCL 70	CV1	African green monkey (14)	EM10	From male kidney; modal number 60; supports replication of SV40[c] and many other viruses
CCL-73	Ch1 Es (NBL-8)	Goat (3)	EM10	Continuous line from the esophagus of an adult animal. Used on studies of viruses affecting domestic animals
CCL 81	Vero	African green monkey	199-5	From adult kidney; hypodiploid (mode 58); used extensively in virus assay and production
CCL 92	3T3	Murine (129)	DM-CS10	From Swiss mouse embryo; hypertriploid (mode 68); contact sensitive; used for studies in oncogenic and viral transformation

TABLE II (*Continued*)

ATCC No.[a] (general category)	Designation	Species (No. of lines available)	Culture medium[b]	Comments
CCL-106	LLC-RK1	Rabbit (13)	199/10	Adult kidney, epithelial-like from New Zealand white animals. Viral susceptibility documented
CCL-208	4MBr-5	Rhesus monkey (8)	F12K/10	Normal, 2- to 3-year-old female animal. Bronchial epithelium. Required EGF, developed PAS-positive inclusions
CCL-209	CPAE	Bovine (101)	EM20	Enthothelial line from pulmonary artery; stable diploid karyotype; positive for angiotensin-converting activity
CRL-1476	A10	Rat (61)	DM20	Smooth muscle line from thoracic artery of a DB1X embryo; myokinase and creatine phosphokinase positive
CRL-1581	Sp2/0-Ag14	Murine	DM10	Myeloma used as fusion partner in hybridoma production; HAT sensitive; nonsecretor
CRL-1633	MDOK	Sheep (3)	EM10	From kidney of normal adult male. Epithelial-like cells support growth of several infectious viruses. Hypotetraploid
CRL-1651	COS-7	African green monkey	DM10	Transformed with origin-defective SV40; T antigen positive; suitable host in transfection studies
CRL-1711	Sf9	Fall armyworm (1)	G+10	Clonally derived from pupal ovarian tissue; susceptible to infection by baculovirus expression vectors
CRL-1721	PC12	Rat	R10HS-5	From pheochromocytoma; responsive to nerve growth factor; catecholamine; dopamine, and norepinephrine positive
CRL-1934	ES-B3	Murine	DME15 ± feeder	Stem cell line. Propagate on STO feeder layer or permit differentiation in its absence. Populations express Oct-3, SSEA-1, EMA-1, or TROMA-1 under appropriate conditions. See www.stemcells@atcc.org for more information
Patented				
CRL-8002	OKT4	Murine	IDM20	One of a series of patented hybridomas; produces monoclonal to human helper T subset
CRL-8305	FRTL-5	Rat	F12K-5+	Thyroid epithelial cell line; produces thyroglobulin; responsive to thyroid-stimulating hormone
CRL-8509	528	Murine	R10	One of a series of patented hybridomas; produces monoclonal to epidermal growth factor receptor
CRL-8873	FHCR	Murine	R12+	Hybridoma FHCR-1-2624/FH6/FHOT-1-3019; secretes monoclonal to Le^x ganglioside
CRL-10968	S4B6–1	Murine	R10	Produces monoclonal to murine interleukin-2
CRL-11422	MPRO clone 2–1	Murine	IDM + GMCSF/20	Infected with retroviral vector LRAR alpha 403SN. Neutrophil progenitor exhibits azurophilic granules, NSA7/4, chloroacetate esterase, and the RAR sequence
Hybridomas/tumor immunology Lines				
HB-55	L243	Murine	DM10	Secretes an IgG2a cytotoxic antibody to a nonpolymorphic determinant on human Ia
HB-95	WB/32	Murine	DM10	Secretes an IgG2a cytotoxic antibody that reacts with monomorphic determinants on HLA-A, -B, and -C
HB-170	R4–6A2	Murine/rat	DM10	Secretes IgG1 monoclonal to murine Interferon-γ

TABLE II (*Continued*)

ATCC No.[a] (general category)	Designation	Species (No. of lines available)	Culture medium[b]	Comments
HB-188	11B11	Murine/rat	R10	Secrets IgG1 monoclonal to murine B-cell stimulatory factor (BSF-1, interleukin-4)
HB-198 (215)	F4/80	Murine/rat	R5	Secretes rat IgG2b antibody to murine macrophages
TIB-63	$P388D_1$	Murine	R15	A phagocytic monocyte/macrophage line that produces interleukin-1 in response to PMA myelanonocyte LPS
TIB-68	WEHI-3	Murine	IDM10+	A myelomonocyte sensitive to LPS; produces colony-stimulating activity
TIB-71	RAW 264.7	Murine	DM10	A phagocytic monocyte/macrophage line; capable of antibody-dependent lysis of target cells
TIB-207	GK1.5	Murine	DM20	Secretes monoclonal to T-cell surface antigen L3T4 on a helper/inducer T-cell subset
TIB-214	CTLL-2	Murine	R10+	Clone of cytotoxic T cells dependent on interleukin-2 for proliferation

[a] Prefixes assigned to ATCC cell lines reflect the historical source of support for their addition to the collection and, to a certain extent, the degree of characterization applied. Representative certified cell lines (CCL); cell repository lines (CRL) in the general and patent collections; hybridomas in the collection supported by the National Institute for Allergy and Infectious Diseases (HB); and cells important for studies in tumor immunology (TIB) are listed. The CRL total does not include some 1900 additional cell lines in special collections. See www.atcc.org for names of originators, references, and more detail.

[b] Abbreviations for medium used (on the left-hand side) include (EM) Eagle's minimum essential medium; (R) RPMI 1640; (DM) Dulbecco's modification of Eagle's medium; (F12K) Kaighn's modification of Ham's F12; (IDM) Iscove's modification of Eagle's medium; (199) medium 199; and (G) Grace's insect medium [see Hay *et al.* (1992) for formulas]. The number on the right-hand side indicates percentage of serum used, usually fetal bovine, bovine calf (CS), or horse serum (HS). Additional recommended ingredients are indicated by a plus sign.

[c] SV40, simian virus 40; HAT, hypoxanthine aminopterin thymidine; PMA, phorbal myristic acetate; LPS, lipopolysaccharide. See www.atcc.org for further information.

References

Barile, M. F., Hopps, H. E., Grabowski, M. W., Riggs, D. B., and Del Giudice, R. A. (1973). The identification and sources of mycoplasmas isolated from contaminated cultures. *Ann. N.Y. Acad. Sci.* **225**, 252–264.

Hay, R. J., Cleland, M. M., Durkin, S., and Reid, Y. A. (2000). Cell line preservation and authentication. *In* "Animal Cell Culture: A Practical Approach" (J. R. W. Masters, ed.), 3rd Ed., pp. 69–103. Oxford Univ. Press, Oxford.

Hay, R. J., Caputo, J., Chen, T. R., Macy, M. L., McClintock, P., and Reid, Y. A. (1992). "Catalogue of Cell Lines and Hybridomas," 7th Ed. American Type Culture Collection, Rockville, MD.

Hay, R. J., Macy, M. L., and Chen, T. R. (1989). Mycoplasma infection of cultured cells. *Nature (London)* **339**, 487–488.

MacLeod, R. A. F., Dirks, W. G., Kaufmann M., Matsuo Y., Milch H., and Drexler H. G. (1999). Widespread intraspecies cross-contamination of human tumor cell line arising at source. *Int. J. Cancer* **83**, 555–563.

Nelson-Rees, W., Daniels, W. W., and Flandermeyer, R. R. (1981). Cross-contamination of cells in culture. *Science* **212**, 446–452.

Nelson-Rees, W. A., and Flandemeyer, R. R. (1977). Inter- and intraspecies contamination of human breast tumor cell lines HBC and BrCa5 and other cell cultures. *Science* **195**, 1343–1344.

Nelson-Rees, W. A., Flandermeyer, R. R., and Hawthorne, P. K. (1974) Banded marker chromosomes as indicators of intraspecies cellular contamination. *Science* **184**, 1093–1096.

Stacey, G. N., Masters, J. R. W., Hay, R. J., Drexler, H. G., MacLeod, R. A. F., and Freshney, R. I. (2000). Cell contamination leads to inaccurate data: We must take action now. *Nature* **403**, 356.

CELL BIOLOGY

A LABORATORY HANDBOOK

Third Edition
Volume 2

Editor-in-chief
Julio E. Celis, Institute of Cancer Biology, *Danish Cancer Society, Copenhagen, Denmark*

Associate Editors
Nigel P. Carter, *The Sanger Center, Wellcome Trust, Cambridge, UK*
Kai Simons, *Max-Planck Institute of Molecular Cell Biology and Genetics, Dresden, Germany*
J. Victor Small, *Austrian Academy of Sciences, Salzburg, Austria*
Tony Hunter, *The Salk Institute, La Jolla, California, USA*
David M. Shotten, *University of Oxford, UK*

CELL BIOLOGY

A LABORATORY HANDBOOK

Third Edition
Volume 2

Edited by

Julio E. Celis
Institute of Cancer Biology, Danish Cancer Society,
Copenhagen, Denmark

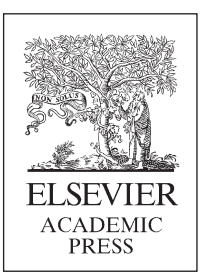

AMSTERDAM • BOSTON • HEIDELBERG • LONDON
NEW YORK • OXFORD • PARIS • SAN DIEGO
SAN FRANCISCO • SINGAPORE • SYDNEY • TOKYO

Elsevier Academic Press
30 Corporate Drive, Suite 400, Burlington, MA 01803, USA
525 B Street, Suite 1900, San Diego, California 92101-4495, USA
84 Theobald's Road, London WC1X 8RR, UK

This book is printed on acid-free paper.

Copyright © 2006, Elsevier Inc. All rights reserved.

No part of this publication may be reproduced or transmitted in any form or by any means, electronic or mechanical, including photocopy, recording, or any information storage and retrieval system, without permission in writing from the publisher.

Permissions may be sought directly from Elsevier's Science & Technology Rights Department in Oxford, UK: phone: (+44) 1865 843830, fax: (+44) 1865 853333, E-mail: permissions@elsevier.co.uk. You may also complete your request on-line via the Elsevier homepage (http://elsevier.com), by selecting "Customer Support" and then "Obtaining Permissions."

Library of Congress Cataloging-in-Publication Data
Application Submitted

British Library Cataloguing in Publication Data
A catalogue record for this book is available from the British Library

ISBN 13: 978-0-12-164732-2
ISBN 10: 0-12-164732-3
Set ISBN 13: 978-0-12-164730-8
Set ISBN 10: 0-12-164730-7

For all information on all Elsevier Academic Press publications
visit our Web site at www.books.elsevier.com

Printed in China
05 06 07 08 09 10 9 8 7 6 5 4 3 2 1

Working together to grow
libraries in developing countries
www.elsevier.com | www.bookaid.org | www.sabre.org
ELSEVIER BOOK AID International Sabre Foundation

Contents of Volume 2

Section 5. Membranes

Section 6. Mitochondria

Section 7. Nuclear Transport

Section 8. Chromatin Assembly

Section 9. Signal Transduction Assays

Contents of other Volumes

VOLUME 1

PART A. CELL AND TISSUE CULTURE: ASSOCIATED TECHNIQUES

Section 1. General Techniques

Section 2. Culture of Specific Cell Types: Stem Cells

Section 3. Culture of Specific Cell Types: Haemopoietic, Mesenchymal, and Epithelial

Section 15. In Situ Hybridisation

PART G. GENOMICS

Section 16. Genomics

PART H. TRANSGENIC, KNOCKOUTS, AND KNOCKDOWN METHODS

Section 17. Transgenic, Knockouts and Knockdown Methods

VOLUME 4

PART A. TRANSFER OF MACROMOLECULES

Section 1. Proteins

Section 2. Genes

Section 3. Somatic Cell Nuclear Transfer

PART B. EXPRESSION SYSTEMS

Section 4. Expression Systems

PART C. GENE EXPRESSION PROFILING

Section 5. Differential Gene Expression

Section 9. Detection of Proteins in Gels

Section 10. Gel Profiling of Posttranslationally Modified Proteins

Section 11. Protein/Protein and Protein/Small Molecule Interactions

Section 12. Functional Proteomics

Section 13. Protein/DNA Interactions

PART E. APPENDIX

Section 16. Appendix

Contributors

Numbers in parenthesis indicate the volume (bold face) and page on which the authors' contribution begins.

Mads Aaboe (**4**: 83) Clinical Biochemical Department, Molecular Diagnostic Laboratory, Aarhus University Hospital, Skejby, Brendstrupgaardvej, Aarhus N, DK-8200, DENMARK

Tanja Aarvak (**1**: 239) Dynal Biotech ASA, PO Box 114, Smestad, N-0309, NORWAY

Harindra R. Abeysinghe (**3**: 345) Department of Pathology and Laboratory Medicine, University of Rochester School of Medicine, 601 Elmwood Ave., Rm 1-6337, Rochester, NY 14642

Ruedi Aebersold (**4**: 437) The Institute for Systems Biology, 1441 North 34th Street, Seattle, WA 98103-8904

Ueli Aebi (**3**: 233, 241) ME Muller Institute for Microscopy, Biozentrum, University of Basel, Klingelbergstr. 50/70, Basel, CH-4056, SWITZERLAND

Cheol-Hee Ahn (**4**: 29) School of Materials Science and Engineering, Seoul National University, Seoul, 151-744, SOUTH KOREA

Natalie G. Ahn (**4**: 443) Department of Chemistry & Biochemistry, University of Colorado, 215 UCB, Boulder, CO 80309

Ramiro Alberio (**4**: 45) School of Biosciences, University of Nottingham, Sutton Bonington, Loughborough, Leics, LE12 5RD, UNITED KINGDOM

Donna G. Albertson (**3**: 445) Cancer Research Institute, Department of Laboratory Medicine, The University of California, San Francisco, Box 0808, San Francisco, CA 94143-0808

Heiner Albiez (**1**: 291) Department of Biology II, Ludwig-Maximilians University of Munich, Munich, GERMANY

Terence Allen (**3**: 325) CRC Structural Cell Biology Group, Paterson Institute for Cancer Research, Christie Hospital NHS Trust, Wilmslow Road, Withington, Manchester, M20 4BX, UNITED KINGDOM

Noona Ambartsumian (**1**: 363) Department of Molecular Cancer Biology, Danish Cancer Society, Institute of Cancer Biology, Strandboulevarden 49, Copenhagen, DK-2100, DENMARK

Øystein Åmellem (**1**: 239) Immunosystems, Dynal Biotech ASA, PO Box 114, Smestad, N-0309, NORWAY

Patrick Amstutz (**1**: 497) Department of Biochemistry, University of Zürich, Winterthurerstr. 190, Zurich, CH-8057, SWITZERLAND

Jens S. Andersen (**4**: 427) Protein Interaction Laboratory, University of Southern Denmark—Odense, Campusvej 55, Odense M, DK-5230, DENMARK

Mads Hald Andersen (**1**: 97) Tumor Immunology Group, Institute of Cancer Biology, Danish Cancer Society, Strandboulevarden 49, Copenhagen, DK-2100, DENMARK

Helena Andersson (**4**: 63) Bioscience at Novum, Karolinska Institutet, Halsovagen 7-9, Huddinge, SE-141 57, SWEDEN

Peter W. Andrews (**1**: 183) Department of Biomedical Science, The University of Sheffield, Rm B2 238, Sheffield, S10 2TN, UNITED KINGDOM

Elsa Anes (**2**: 57) Faculdade de Farmacia, Universidade de Lisboa, Av. Forcas Armadas, Lisboa, 1649-019, PORTUGAL

James M. Angelastro (**1**: 171) Department of Pathology and Center for Neurobiology and Behavior, Columbia University College of Physicians

and Surgeons, 630 West 168th Street, New York, NY 10032

Sergey V. Anisimov (**4**: 103) Molecular Cardiology Unit, National Institute on Aging, NIH, 5600 Nathan Shock Drive, Baltimore, MD 21224

Celia Antonio (**2**: 379) Department of Biochemistry & Molecular Biophysics, College of Physicians & Surgeons, Columbia University, 701 W 168ST HHSC 724, New York, NY 69117

Shigehisa Aoki (**1**: 411) Department of Pathology & Biodefence, Faculty of Medicine, Saga University, Nebeshima 5-1-1, Saga, 849-8501, JAPAN

Ron D. Appel (**4**: 207) Swiss Institute of Bioinformatics, CMU, Rue Michel Servet 1, Geneva 4, CH-1211, SWITZERLAND

Rolf Apweiler (**4**: 469) EMBL Outstation, European Bioinformatics Institute, Wellcome Trust Genome Campus, Hinxton, Cambridge, CB10 1SD, UNITED KINGDOM

Nobukazu Araki (**2**: 147) Department of Histology and Cell Biology, School of Medicine, Kagawa University, Mki, Kagawa, 761-0793, JAPAN

Christopher M. Armstrong (**4**: 295) Dana Faber Cancer Institute, Harvard University, 44 Binney Street, Boston, MA 02115

Anthony J. Ashford (**2**: 155) Antibody Facility, Max Planck Institute of Molecullar Cell Biology and Genetics, Pfotenhauerstrsse 108, Dresden, D-01307, GERMANY

Daniel Axelrod (**3**: 19) Dept of Physics & Biophysics Research Division, University of Michigan, Ann Arbor, MI 48109-1055

Sheree Bailey (**1**: 475) Dept of Immunology, Allergy and Arthritis, Flinders Medical Centre and Flinders University, Bedford Park, Adelaide, SA, 5051, SOUTH AUSTRALIA

Nathalie Q. Balaban (**2**: 419) Department of Physics, The Hebrew University-Givat Ram, Racah Institute, Jerusalem, 91904, ISRAEL

William E. Balch (**2**: 209) Department of Cell and Molecular Biology, The Scripps Research Institute, 10550 North Torrey Pines Road, La Jolla, CA 92037

Debabrata Banerjee (**1**: 315) Department of Medicine, Cancer Institute of New Jersey, 195 Little Albany Street, New Brunswick, NJ 08903

Jiri Bartek (**4**: 253) Department of Cell Cycle and Cancer, Danish Cancer Society, Strandboulevarden 49, Copenhagen, DK-2100, DENMARK

Werner Baschong (**3**: 5) ME Muller Institute for Microscopy, Biozentrum, University of Basel, Klingelbergstrasse 50/70, Basel, CH-4056, SWITZERLAND

Philippe I. H. Bastiaens (**3**: 153) Cell Biology and Cell Biophysics Program, European Molecular Biology Laboratory, Meyerhofstrasse 1, Heidelberg, 69117, GERMANY

Jürgen C. Becker (**1**: 103) Department of Dermatology, University of Würzburg, Sanderring 2, Würzburg, 97070, GERMANY

Martin Béhé (**4**: 149) Department of Nuclear Medicine, Philipp's-University of Marburg, Baldingerstraße, Marburg/Lahn, D-35043, GERMANY

Thomas M. Behr (**4**: 149) Department of Nuclear Medicine, Philipp's-University of Marburg, Baldingerstraße, Marburg, D-35043, GERMANY

Stefanie Benesch (**2**: 399) Department of Cell Biology, Gesellschaft fur Biotechnoogische Forschung, Mascheroder Weg 1, Braunschweig, D-38124, GERMANY

Aaron Bensimon (**3**: 429) Laboratoire de Biophysique de l'ADN, Departement des Biotechnologies, Institut Pasteur, 25 rue du Dr. Roux, Paris Cedex 15, F-75724, FRANCE

John J. M. Bergeron (**2**: 41) Department of Anatomy and Cell Biology, Faculty of Medicine, McGill University, STRATHCONA Anatomy & Dentistry Building, Montreal, QC, H3A 2B2, CANADA

Michael W. Berns (**3**: 351) Beckman Laser Institute, University of California, Irvine, 1002 Health Sciences Road E, Irvine, CA 92697-1475

Joseph R. Bertino (**1**: 315) The Cancer Institute of New Jersey, 195 Little Albany Street, New Brunswick, NJ 08901

Paulo Bianco (**1**: 79) Dipartimento di Medicina Sperimentale e Patologia, Universita 'La Sapienza', Viale Regina Elena 324, Roma, I-00161, ITALY

Hans Kaspar Binz (**1**: 497) Department of Biochemistry, University of Zürich, Winterthurerstr. 190, Zürich, CH-8057, SWITZERLAND

R. Curtis Bird (**1**: 247) Department of Pathobiology, Auburn University, Auburn, AL 36849

Mina J. Bissell (**1**: 139) Life Sciences Division, Lawrence Berkeley National Laboratory, 1 Cyclotron Road, Bldg 83-101, Berkeley, CA 94720

Stephanie Blackwood (**3**: 445) Cancer Research Institute, University of California San Francisco, PO Box 0808, San Francisco, CA 94143-0808

Blagoy Blagoev (**4**: 427) Protein Interaction Laboratory, University of Southern Denmark—Odense, Campusvej 55, Odense M, DK-5230, DENMARK

Kenneth R. Boheler (**4**: 103) Laboratory of Cardiovascular Science, National Institute on Aging, NIH, 5600 Nathan Shock Drive, Baltimore, MD 21224-6825

Michelle A. Booden (**1**: 345) Lineberger Comprehensive Cancer Center, University of North Carolina at Chapel Hill, Chapel Hill, NC 27599-7295

Gary G. Borisy (**3**: 277) Department of Cell and Molecular Biology, Northwestern University Medical School, Chicago, IL 6011-3072

Elliot Botvinick (**3**: 351) Beckman Laser Institute, University of California, Irvine, 1002 Health Sciences Road, East, Irvine, CA 92697-1475

Gérard Bouchet (**4**: 207) Swiss Institute of Bioinformatics (SIB), CMU, rue Michel-Servet 1, Genève 4, CH-1211, SWITZERLAND

Rosemary Boyle (**4**: 437) The Institute for Systems Biology, 1441 North 34th St., Seattle, WA 98109

Susanne Brandfass (**1**: 563) Department of Biochemistry and Cell Biology, Max Planck Institute of Biophysical Chemistry, Am Faßberg 11, Gottingen, D-37077, GERMANY

Pascal Braun (**4**: 73) Department of Chemistry and Chemical Biology, Harvard University, 12 Oxford Street, Cambridge, MA 02138

Steven A. Braut (**4**: 121) Department of Anatomy and Structural Biology, Golding # 601, Albert Einstein College of Medicine of Yeshiva University, 1300 Morris Park Avenue, Bronx, NY 10461

Alvis Brazma (**4**: 95) EMBL Outstation—Hinxton, European Bioinformatics Institute, Wellcome Trust Genome Campus, Hinxton, Cambridge, CB10 1SD, UNITED KINGDOM

J. David Briley (**3**: 471) Department of Genomic Sciences, Glaxo Wellcome Research and Development, 5 Moore Drive, Research Triangle Park, NC 27709-3398

Simon Broad (**1**: 133) Keratinocyte Laboratory, London Research Institute, 44 Lincoln's Inn Fields, London, WC2A 3PX, UNITED KINGDOM

Nicholas H. Brown (**3**: 77) Wellcome Trust/Cancer Research UK Institute and Departmentt of Anatomy, University of Cambridge, Tennis Court Road, Cambridge, CB2 1QR, UNITED KINGDOM

Heather L. Brownell (**2**: 329, 341) Office of Technology Licensing and Industry Sponsored Research, Harvard Medical School, 25 Shattuck Street, Gordon Hall of Medicine, Room 414, Boston, MA 02115

Damien Brunner (**3**: 69) Cell Biology and Cell Biophysics Programme, European Molecular Biology Laboratory, Meyerhofstrasse 1, Heidelberg, D-69117, GERMANY

Suzannah Bumpstead (**3**: 463) Genotyping / Chr 20, The Wellcome Trust Sanger Institute, The Wellcome Trust Genome Campus, Hinxton, Cambridge, CB10 1SA, UNITED KINGDOM

Deborah C. Burford (**3**: 403) Wellcome Trust, Sanger Institute, The Wellcome Trust Genome Campus, Hinxton, Cambridge, CB10 1SA, UNITED KINGDOM

Gerald Burgstaller (**2**: 161) Department of Cell Biology, Institute of Molecular Biology, Austrian Academy of Sciences, Billrothstrasse 11, Salzburg, A-5020, AUSTRIA

Ian M. Caldicott (**1**: 157)

Angelique S. Camp (**1**: 457) Gene Therapy Centre, University of North Carolina at Chapel Hill, 7119 Thurston-Bowles (G44 Wilson Hall), Chapel Hill, NC 27599-7352

Keith H. S. Campbell (**4**: 45) School of Biosciences, Sutton Bonington, Loughborough, Leics, LE12 5RD, UNITED KINGDOM

Yihai Cao (**1**: 373) Microbiology & Tumor Biology Center, Karolinska Institute, Room: Skrivrum (G415), Box 280, Stockholm, SE-171 77, SWEDEN

Maria Carmo-Fonseca (**2**: 277, **3**: 419) Institute of Molecular Medicine, Faculty of Medicine, University of Lisbon, Av. Prof. Egas Moniz, Lisbon, 1649-028, PORTUGAL

T. Carneiro (**3**: 419) Faculty of Medicine, Institute of Molecular Medicine, University of Lisbon, Av. Prof. Egas Moniz, Lisboa, 1649-028, PORTUGAL

Nigel P. Carter (**2**: 133) The Wellcome Trust, Sanger Institute, The Wellcome Trust, Genome Campus, Hinxton, Cambridge, CB10 1SA, UNITED KINGDOM

Célia Carvalho (**3**: 419) Faculty of Medicine, Institute of Molecular Medicine, University of Lisbon, Av. Prof. Egas Moniz, Lisboa, 1649-028, PORTUGAL

Lucy A. Carver (**2**: 11) Cellular and Molecular Biology Program, Sidney Kimmel Cancer Center, 10835 Altman Row, San Diego, CA 92121

Doris Cassio (**1**: 231, **3**: 387) INSERM U-442: Signalisation cellulaire et calcium, Bat 443, Universite Paris-Sud, Street George Clemenceau Pack, 444, Orsay, Cedex, F-91405, FRANCE

Chris Catton (**3**: 207) Department of Zoology, University of Oxford, South Parks Road, Oxford, OX1 3PS, UNITED KINGDOM

Julio E. Celis (**1**: 527, **4**: 69, 165, 219, 243, 289) Danish Cancer Society, Institute of Cancer Biology and Danish Centre for Translational Breast Cancer Research, Strandboulevarden 49, Copenhagen O, DK-2100, DENMARK

Pierre Chambon (**3**: 501) Institut de Génétique et de Biologie Moléculaire et Cellulaire, 1 rue Laurent Fries, B.P.10142, Illkirch CEDEX, F-67404, FRANCE

Francis Ka-Ming Chan (**2**: 355) Department of Pathology, University of Massachusetts Medical School, Room S2-125, 55 Lake Avenue North, Worcester, MA 01655

Ming-Shien Chang (**3**: 87) Department of Physics, Duke University, 107 Physics Bldg, Durham, NC 27708-1000

Samit Chatterjee (**2**: 241) Margaret M. Dyson Vision Research Institute, Department of Ophthalmology, Weill Medical College of Cornell University, 1300 York Avenue, New York, NY 10021

Sandeep Chaudhary (**1**: 121) Veterans Affairs Medical Center, San Diego (V111G), 3350 La Jolla Village Drive, San Diego, CA 92161

Jingwen Chen (**3**: 471) Department of Genomic Sciences, Glaxo Wellcome Research and Development, 5 Moore Drive, Research Triangle Park, NC 27709

Yonglong Chen (**1**: 191) Institute for Biochemistry and Molecular Cell Biology, University of Goettingen, Justus-von-Liebig-Weg 11, Göttingen, D-37077, GERMANY

Yong Woo Cho (**4**: 29) Akina, Inc., Business & Technology Center, 1291 Cumberland Ave., #E130, West Lafayette, IN 47906

Juno Choe (**1**: 269) Institute for Systems Biology, 1441 N. 34th St, Seattle, WA 98103

Claus R. L. Christensen (**1**: 363) Department of Molecular Cancer Biology, Danish Cancer Society, Institute of Cancer Biology, Strandboulevarden 49, Copenhagen, DK-2100, DENMARK

Theodore Ciaraldi (**1**: 121) Veterans Affairs Medical Center, University of California, San Diego, 9500 Gilman Drive, La Jolla, CA 92093-9111

Aaron Ciechanover (**4**: 351) Center for Tumor and Vascular Biology, The Rappaport Faculty of Medicine and Research Institute, Technion-Israel Institute of Technology, POB 9649, Efron Street, Bat Galim, Haifa, 31096, ISRAEL

Mark S. F. Clarke (**2**: 233, **4**: 5) Department of Health and Human Performance, University of Houston, 3855 Holman Street, Garrison—Rm 104D, Houston, TX 77204-6015

Martin Clynes (**1**: 335) National Institute for Cellular Biotechnology, Dublin City University, Glasnevin, Dublin, 9, IRELAND

Philippe Collas (**1**: 207) Institute of Medical Biochemistry, University of Oslo, PO Box 1112 Blindern, Oslo, 0317, NORWAY

Kristen Correia (**4**: 35) Krumlauf Lab, Stowers Institute for Medical Research, 1000 East 50th Street, Kansas City, MO 64110

Pascale Cossart (**2**: 407) Unite des Interactions Bacteries-Cellules/Unité INSERM 604, Institut Pasteur, 28, rue du Docteur Roux, Paris Cedex 15, F-75724, FRANCE

Thomas Cremer (**1**: 291) Department of Biology II, Ludwig-Maximilians University of Munich, Munich, 80333, GERMANY

Robert A. Cross (**2**: 371) Molecular Motors Group, Marie Curie Research Institute, The Chart, Oxted, Surrey, RH8 0TE, UNITED KINGDOM

Matthew E. Cunningham (**1**: 171) Hospital for Special Surgery, New York Hospital, 520 E. 70th Street, New York, NY 10021

Noélia Custódio (**3**: 419) Faculty of Medicine, Institute of Molecular Medicine, University of Lisbon, Av. Prof. Egas Moniz, Lisboa, 1649-028, PORTUGAL

Zbigniew Darzynkiewwicz (**1**: 279) The Cancer Research Institute, New York Medical College, 19 Bradhurst Avenue, Hawthorne, NY 10532

Ilan Davis (**3**: 187) Wellcome Trust Centre for Cell Biology, Institute of Cell and Molecular Biology, The University of Edinburgh, Michael Swann Building, The King's Buildings, Mayfield Road, Edinburgh, EH9 3JR, SCOTLAND

Stephen C. De Rosa (**1**: 257) Vaccine Research Center, National Institutes of Health, 40 Convent Dr., Room 5610, Bethesda, MD 20892-3015

Nicholas M. Dean (**3**: 523) Functional Genomics, GeneTrove, GeneTrove (a division of Isis Isis Pharmaceuticals, Inc.), 2292 Faraday Avenue, Carlsbad, CA 92008

Anne Dell (**4**: 415) Department of Biological Sciences, Biochemistry Building, Imperial College of Science, Technology & Medicine, Biochemistry Building, London, SW7 2AY, UNITED KINGDOM

Panos Deloukas (**3**: 463) The Wellcome Trust, Sanger Institute, Hinxton, Cambridge, CB10 1SA, UNITED KINGDOM

Nicolas Demaurex (**3**: 163) Department of Cell Physiology and Metabolism, University of Geneva Medical Center, 1 Michel-Servet, Geneva, CH-1211, SWITZERLAND

Chris Denning (**4**: 45) Division of Animal Physiology, School of Biosciences, Institute of Genetics Room C15, University of Nottingham, Queens Medical Centre, Nottingham, NG7 2UH, UNITED KINGDOM

Ami Deora (**2**: 241) Margaret M. Dyson Vision Research Institute, Department of Ophthalmology, Weill Medical College of Cornell University, 1300 York Avenue, New York, NY 10021

Julien Depollier (**4**: 13) Centre de Recherche en Biochimie Macromoléculaire (UPR 1086), Centre National de la Recherche Scientifique (CNRS), 1919 Route de Mende, Montpellier Cedex 5, F-34293, FRANCE

Channing J. Der (**1**: 345) Department of Pharmacology, University of North Carolina at Chapel Hill, Lineberger Comprehensive Cancer Center, Chapel Hill, NC 27599

Bart Devreese (**4**: 259) Department of Biochemistry, Physiology and Microbiology, University of Ghent, K.L. Ledeganckstraat 35, Ghent, B-9000, BELGIUM

Alberto Diaspro (**3**: 201) Department of Physics, University of Genoa, Via Dodecaneso 33, Genoa, I-16146, ITALY

James Fred Dice (**4**: 345) Department Physiology, Tufts University School of Medicine, 136 Harrison Ave, Boston, MA 02111

Thomas J. Diefenbach (**4**: 307) Department of Physiology, Tufts University School of Medicine, 136 Harrison Avenue, Boston, MA 02111

Chris Dinant (**2**: 121) Biomolecular Sciences, UMIST, PO Box 88, Manchester, M60 1QD, UNITED KINGDOM

Da-Qiao Ding (**3**: 171) Structural Biology Section and CREST Research Project, Kansai Advanced Research Center, Communications Research Laboratory, 588-2 Iwaoka, Iwaoka-cho, Nishi-ku, Kobe, 651-2492, JAPAN

Gilles Divita (**4**: 13) Centre de Recherche en Biochimie Macromoléculaire (UPR 1086), Centre National de la Recherche Scientifique (CNRS), 1919 Route de Mende, Montpellier Cedex 5, F-34293, FRANCE

Eric P. Dixon (**1**: 483) TriPath Oncology, 4025 Stirrup Creek Drive, Suite 400, Durham, NC 27703

Bernhard Dobberstein (**2**: 215) Zentrum fur Molekulare Biologie, Universitat Heidelberg, Im Neuenheimer Feld 282, Heidelberg, D-69120, GERMANY

Lynda J. Donald (**4**: 457) Department of Chemistry, University of Manitoba, Room 531 Parker Building, Winnipeg, MB, R3T 2N2, CANADA

Wolfgang R. G. Dostmann (**2**: 299) Department of Pharmacology, University of Vermont, Health Science Research Facility 330, Burlington, VT 05405-0068

Adam Douglass (**3**: 129) Department of Cellular and Molecular Pharmacology, The University of California, San Francisco, School of Medicine, Medical Sciences Building, Room S1210, 513 Parnassus Avenue, San Francisco, CA 94143-0450

Kate Downes (**3**: 463) Genotyping / Chr 20, The Wellcome Trust, Sanger Institute, The Wellcome Trust Genome Campus, Hinxton, Cambridge, CB10 1SA, UNITED KINGDOM

Harry W. Duckworth (**4**: 457) Department of Chemistry, University of Manitoba, Room 531 Parker Building, Winnipeg, MB, R3T 2N2, CANADA

Derek M. Dykxhoorn (**3**: 511) CBR Institute for Biomedical Research, Harvard Medical School, 200 Longwood Ave, Boston, MA 02115

Lars Dyrskjøt (**4**: 83) Clinical Biochemical Department, Molecular Diagnostic Laboratory, Aarhus University Hospital, Skejby, Brendstrupgaardvej, Aarhus N, DK-8200, DENMARK

Christoph Eckerskorn (**4**: 157) Protein Analytics, Max Planck Institute for Biochemistry, Klopferspitz 18, Martinsried, D-82152, GERMANY

Glenn S. Edwards (**3**: 87) Department of Physics, Duke University, 221 FEL Bldg, Box 90305, Durham, NC 27708-0305

Andreas A. O. Eggert (**1**: 103) Department of Dermatology, Julius-Maximillians University, Josef-Schneider-Str. 2, Würzburg, 97080, GERMANY

Maria Ekström (**4**: 63) Bioscience at Novum, Karolinska Institutet, Huddinge, SE-141 57, SWEDEN

Andreas Engel (**3**: 317) Maurice E. Müller Institute for Microscopy at the Biozentrum, University of Basel, Klingelbergstrasse 70, Basel, CH-4056, SWITZERLAND

Anne-Marie Engel (**1**: 353) Bartholin Institutte, Bartholinsgade 2, Copenhagen K, DK-1356, DENMARK

José A. Enríquez (**2**: 69) Department of Biochemistry and Molecular and Cellular Biology, Universidad de Zaragoza, Miguel Servet, 177, Zaragoza, E-50013, SPAIN

Rachel Errington (**1**: 305) Department of Medical Biochemistry and Immunology, University of Wales College of Medicine, Heath Park, Cardiff, CF14 4XN, UNITED KINGDOM

Virginia Espina (**3**: 339) Microdissection Core Facility, Laboratory of Pathology, National Cancer Institute, 9000 Rockville Pike, Building 10, Room B1B53, Bethesda, MD 20892

H. Dariush Fahimi (**2**: 63) Department of Anatomy and Cell Biology II, University of Heidelberg, Im Neuenheimer Feld 307, Heidelberg, D-69120, GERMANY

Federico Federici (**3**: 201) Department of Physics, University of Genoa, Via Dodecaneso 33, Genoa, I-16146, ITALY

Daniel L. Feeback (**2**: 233, **4**: 5) Space and Life Sciences Directorate, NASA-Johnson Space Center, 3600 Bay Area Blvd, Houston, TX 77058

Patricio Fernández-Silva (**2**: 69) Dept of Biochemistry and Molecular and Cellular Biology, Univeridad de Zaragoza, Miguel Servet 177, Zaragoza, E-50013, SPAIN

Erika Fernández-Vizarra (**2**: 69) Dept of Biochemistry and Molecular and Cellulary Biology, Universidad de Zaragoza, Miguel Servet, 177, Zaragoza, E-50013, SPAIN

Patrick F. Finn (**4**: 345) Department of Physiology, Tufts University School of Medicine, 136 Harrison Ave, Boston, MA 02111

Kevin L. Firth (**2**: 329, **2**: 341) ASK Science Products Inc., 487 Victoria St, Kingston, Ontario, K7L 3Z8, CANADA

Raluca Flükiger-Gagescu (**2**: 27) Unitec—Office of Technology Transfer, University of Geneva and University of Geneva Hospitals, 24, Rue Général-Dufour, Geneva 4, CH-1211, SWITZERLAND

Leonard J. Foster (**4**: 363, 427) Protein Interaction Laboratory, University of Southern Denmark, Odense, Campusvej 55, Odense M, DK-5230, DENMARK

Dimitrios Fotiadis (**3**: 317) M. E. Müller Institute for Microscopy at the Biozentrum, University of Basel, Klingelbergstrasse 70, Basel, CH-4056, SWITZERLAND

Patrick L. T. M. Frederix (**3**: 317) M. E. Müller Institute for Microscopy at the Biozentrum, University of Basel, Klingelbergstrasse 70, Basel, CH-4056, SWITZERLAND

Marcus Frohme (**4**: 113) Functional Genome Analysis, German Cancer Research Center, Deutsches Krebsforschungszentrum, Im Neuenheimer Feld 580, Heidelberg, D-69120, GERMANY

Masanori Fujimoto (**4**: 197) Department of Biochemistry and Biomolecular Recognition, Yamaguchi University School of Medicine, 1-1-1, Minami-kogushi, Ube, Yamaguchi, 755-8505, JAPAN

Margarida Gama-Carvalho (**2**: 277) Faculty of Medicine, Institute of Molecular Medicine, University of Lisbon, AV. Prof. Egas Moniz, Lisbon, 1649-028, PORTUGAL

Henrik Garoff (**1**: 419, **4**: 63) Unit for Cell Biology, Center for Biotechnology. Karolinska Institute, Huddinge, SE-141 57, SWEDEN

Susan M. Gasser (**2**: 359) Friedrich Miescher Institute fr Biomedical Research, Maulbeerstrasse 66, Basel, CH-1211, SWITZERLAND

Kristine G. Gaustad (**1**: 207) Institute of Medical Biochemistry, University of Oslo, PO Box 1112 Blindern, Oslo, 0317, NORWAY

Benjamin Geiger (**2**: 419) Dept. of Molecular Cell Biology, Weizman Institute of Science, Wolfson Building, Rm 617, Rehovot, 76100, ISRAEL

Kris Gevaert (**4**: 379, **4**: 457) Dept. Medical Protein Research, Flanders Interuniversity Institute for Biotechnology, Faculty of Medicine and Health Sciences, Ghent University, Instituut Rommelaere—Blok D, Albert Baertsoenkaai 3, Gent, B-9000, BELGIUM

Jilur Ghori (**3**: 463) Genotyping / Chr 20, The Wellcome Trust, Sanger Institute, The Wellcome Trust, Genome Campus, Hinxton, Cambridge, CB10 1SA, UNITED KINGDOM

Alasdair J. Gibb (**1**: 395) Department of Pharmacology, University College London, Gower Street, London, WC1E GBT, UNITED KINGDOM

Mario Gimona (**1**: 557, **2**: 161, **4**: 145) Department of Cell Biology, Institute of Molecular Biology, Austrian Academy of Sciences, Billrothstrasse 11, Salzburg, A-5020, AUSTRIA

David A. Glesne (**1**: 165) Biosciences Division, Argonne National Laboratory, 9700 South Cass Avenue, Argonne, IL 60439-4844

Martin Goldberg (**3**: 325) Science Laboratories, University of Durham, South Road, Durham, DH1 3LE, UNITED KINGDOM

Kenneth N. Goldie (**3**: 267) Structural and Computational Biology Programme, EMBL, Meyerhofstrasse 1, Heidelberg, D-69117, GERMANY

Jon W. Gordon (**3**: 487) Geriatrics and Adult Development, Mount Sinai School of Medicine, One Gustave L. Levy Place, New York, NY 10029

Angelika Görg (**4**: 175) Fachgebiet Proteomik, Technische Universität München, Am Forum 2, Freising Weihenstephan, D-85350, GERMANY

Martin Gotthardt (**4**: 149) Department of Nuclear Medicine, Philipp's-University of Marburg, Baldingerstraße, Marburg/Lahn, D-35043, GERMANY

Frank L. Graham (**1**: 435) Department of Biology, McMaster University, Life Sciences Building, Room 430, Hamilton, Ontario, L8S 4K1, CANADA

Claude Granier (**1**: 519) UMR 5160, Faculté de Pharmacie, 15 Av. Charles Flahault, Montpellier Cedex 5, BP 14491, 34093, FRANCE

Lloyd A. Greene (**1**: 171) Department of Pathology and Center for Neurobiology and Behavior, Columbia University, College of Physicians and Surgeons, 630 W. 168th Street, New York, NY 10032

Susan M. Gribble (**3**: 403) Sanger Institute, The Wellcome Trust, The Wellcome Trust Genome Campus, Hinxton, Cambridge, CB10 1SA, UNITED KINGDOM

Gareth Griffiths (**2**: 57, **3**: 299) Department of Cell Biology, EMBL, Postfach 102209, Heidelberg, D-69117, GERMANY

Sergio Grinstein (**3**: 163) Cell Biology Program, Hospital for Sick Children, 555 University Avenue, Toronto, Ontario, M5G 1X8, CANADA

Pavel Gromov (**1**: 527, **4**: 69, 165, 243, 289) Institute of Cancer Biology and Danish Centre for Translational Breast Cancer Research, Danish Cancer Society, Strandboulevarden 49, Copenhagen, DK-2100, DENMARK

Irina Gromova (**4**: 219) Department of Medical Biochemistry and Danish Centre for Translational Breast Cancer Research, Danish Cancer Society, Strandboulevarden 49, Copenhagen, DK-2100, DENMARK

Dale F. Gruber (**1**: 33) Cell Culture Research and Development, GIBCO/Invitrogen Corporation, 3175 Staley Road, Grand Island, NY 14072

Markus Grubinger (**4**: 145) Institute of Physics and Biophysics, University of Salzburg, Hellbrunnerstr. 34, Salzburg, A-5020, AUSTRIA

Jean Gruenberg (**2**: 27, 201) Department of Biochemistry, University of Geneva, 30, quai Ernest Ansermet, Geneva 4, CH-1211, SWITZERLAND

Stephanie L. Gupton (**3**: 137) 10550 North Torrey Pines Road, CB 163, La Jolla, CA 92037

Cemal Gurkan (**2**: 209) Department of Cell and Molecular Biology, The Scripps Research Institute, 10550 North Torrey Pines Road, La Jolla, CA 92037

Martin Guttenberger (**4**: 131) Zentrum für Molekulariologie der Pflanzen, Universitat Tübingen, Entwicklungsgenetik, Auf der Morgenstelle 3, Tübingen, D-72076, GERMANY

Thomas Haaf (**3**: 409) Institute for Human Genetics, Johannes Gutenberg-Universität Mainz, 55101, Mainz, D-55131, GERMANY

Christine M. Hager-Braun (**1**: 511) Health and Human Services, NIH National Institute of Environmental Health Sciences, MD F0-04, PO Box 12233, Research Triangle Park, NC 27709

Anne-Mari Håkelien (**1**: 207) Institute of Medical Biochemistry, Institute of Medical Biochemistry, University of Oslo, PO Box 1112 Blindern, Oslo, 0317, NORWAY

Fiona C. Halliday (**1**: 395) GlaxoSmithKline, Greenford, Middlesex, UB6 OHE, UNITED KINGDOM

Gerald Hammond (**2**: 223) Molecular Neuropathobiology Laboratory, Cancer Reasearch UK London Research Institute, 44 Lincoln's Inn Fields, London, WC2A 3PX, UNITED KINGDOM

Klaus Hansen (**4**: 253)

Hironobu Harada (**1**: 367) Department of Neurosurgery, Ehime University School of Medicine, Shitsukawa, Toon-shi, Ehime, 791-0295, JAPAN

Robert J. Hay (**1**: 43, 49, 573) Viitro Enterprises Incorporated, 1113 Marsh Road, PO Box 328, Bealeton, VA 22712

Izumi Hayashi (**1**: 151) National Medical Center and Beckman Research Institute, Division of Neurosciences, City of Hope, 1500 E. Duarte Rd, Duarte, CA 91010-3000

Timothy A. Haystead (**4**: 265) Department of Pharmacology and Cancer Biology, Duke University Medical Center, Box 3813 Med Ctr, Durham, NC 27710

Rebecca Heald (**2**: 379) Molecular and Cell Biology Department, University of California, Berkeley, Berkeley, CA 94720-3200

Florence Hediger (**2**: 359) Department of Molecular Biology, University of Geneva, 30, Quai Ernest Ansermet, Geneva, CH-1211, SWITZERLAND

Rainer Heintzmann (**3**: 29) Randall Division of Cell and Molecular Biophysics, King's College London, Guy's Campus, London, SE1 1UL, UNITED KINGDOM

Frederic Heitz (**4**: 13) Centre de Recherche en Biochimie Macromoléculaire (UPR 1086), Centre National de la Recherche Scientifique (CNRS), 1919 Route de Mende, Montpellier Cedex 5, F-34293, FRANCE

Johannes W. Hell (**2**: 85) Department of Pharmacology, University of Iowa, 2152 Bowen Science Building, Iowa City, IA 52242

Kai Hell (**4**: 269) Adolf-Butenandt-Institut fur Physiologische Chemie, Lehrstuhl: Physiologische Chemie, Universitat Munchen, Butenandtstr. 5, Gebäude B, Munchen, D-81377, GERMANY

Robert R. Henry (**1**: 121) Veterans Affairs Medical Center, San Diego (V111G), 3350 La Jolla Village Drive, San Diego, CA 92161

Johan Hiding (**2**: 45) Göteborg University, Institute of Medical Biochemistry, PO Box 440, Göteborg, SE-403-50, SWEDEN

Yasushi Hiraoka (**3**: 171) Structural Biology Section and CREST Research Project, Kansai Advanced Research Center, Communications Research Laboratory, 588-2 Iwaoka, Iwaoka-cho, Nishi-ku, Kobe, 651-2492, JAPAN

Mary M. Hitt (**1**: 435) Department of Pathology & Molecular Medicine, McMaster University, 1200 Main Street West, Hamilton, Ontario, L8N 3Z5, CANADA

Julie Hodgkinson (**3**: 307) School of Crystallography, Birkbeck College, Unversity of London, Malet Street, London, WC1E 7HX, UNITED KINGDOM

Klaus P. Hoeflich (**2**: 307) Division of Molecular and Structural Biology, Ontario Cancer Institute, Department of Medical Biophysics, University of Toronto, 610 University Avenue, 7-707A, Toronto, Ontario, M5G 2M9, CANADA

Tracy L. Hoffman (**1**: 21) ATCC, P.O. Box 1549, Manassas, VA 20108

Jörg D. Hoheisel (**4**: 113) Functional Genome Analysis, German Cancer Research Center, Deutsches Krebsforschungszentrum, Im Neuenheimer Feld 580, Heidelberg, D-69120, GERMANY

Thomas Hollemann (**1**: 191) Institute for Biochemistry and Molecular Cell Biology, University of Goettingen, Justus-von-Liebig-Weg 11, Göttingen, D-37077, GERMANY

Caterina Holz (**4**: 57) PSF biotech AG, Huebnerweg 6, Berlin, D-14059, GERMANY

Akira Honda (**2**: 299) Department of Pharmacology, University of Vermont, Health Science Research Facility 330, Burlington, VT 05405-0068

Masanori Honsho (**2**: 5) Max Planck Institute of Molecular Cell Biology and Genetics, Pfotenhauerstrasse 108, Dresden, D-01307, GERMANY

Andrew N. Hoofnagle (**4**: 443) School of Medicine, University of Colorado Health Sciences Center, Denver, CO 80262

Eliezer Huberman (**1**: 165) Gene Expression and Function Group, Argonne National Laboratory, 9700 South Cass Avenue, Argonne, IL 60439-4844

M. Shane Hutson (**3**: 87) Department of Physics, Duke University, 107 Physics Bldg, Durham, NC 27708-1000

Andreas Hüttmann (**1**: 115) Abteilung für Hämatologie, Universitäkrankenhaus Essn, Hufelandstr. 55, Essen, 45122, GERMANY

Anthony A. Hyman (**2**: 155) Max Planck Institute of Molecular Cell Biology and Gene Technology, Pfotenhauerstrasse 108, Dresden, D-01307, GERMANY

Sherrif F. Ibrahim (**1**: 269) Institute for Systems Biology, 1441 N. 34th St, Seattle, WA 98103

Kazuo Ikeda (**1**: 151) National Medical Center and Beckman Research Institute, Division of Neurosciences, City of Hope, 1500 East Duarte Road, Duarte, CA 91010-3000

Elina Ikonen (**2**: 181) The LIPID Cell Biology Group, Department of Biochemistry, The Finnish National Public Health Institute, Mannerheimintie 166, Helsinki, FIN-00300, FINLAND

Pranvera Ikonomi (**1**: 49) Director, Cell Biology, American Type Culture Collection (ATCC), 10801 University Blvd., Manassas, VA 20110-2209

Mitsuhiko Ikura (**2**: 307) Division of Molecular and Structural Biology, Ontario Cancer Institute, Department of Medical Biophysics, University of Toronto, 610 University Avenue 7-707A, Toronto, Ontario, M5G 2M9, CANADA

Arup Kumar Indra (**3**: 501) Institut de Génétique et de Biologie Moléculaire et Cellulaire (IGBMC), 1 rue Laurent Fries, B.P.10142, Illkirch CEDEX, F-67404, FRANCE

Takayoshi Inoue (**4**: 35) National Institute for Neuroscience, 4-1-1 Ogawahigashi, Kodaira, Tokyo, 187-8502, JAPAN

Kumiko Ishii (**2**: 139) Supra-Biomolecular System Research Group, RIKEN (Institute of Physical and Chemical Research), 2-1, Hirosawa, Wako-shi, Saitama, 351-0198, JAPAN

Dean A. Jackson (**2**: 121) Department of Biomolecular Sciences, UMIST, PO Box 88, Manchester, M60 1QD, UNITED KINGDOM

Reinhard Jahn (**2**: 85) Department of Neurobiology, Max-Planck-Institut for Biophysical Chemistry, Am Faßberg 11, Gottingen, D-37077, GERMANY

Kim D. Janda (**1**: 491) Department of Chemistry, BCC-582, The Scripps Research Institute, 10550 N. Torrey Pines Road, La Jolla, CA 92037

Harry W. Jarrett (**4**: 335) Department of Biochemistry, University of Tennessee Health Sciences Center, Memphis, TN 38163

Daniel G. Jay (**4**: 307) Dept. Physiology, Tufts University School of Medicine, 136 Harrison Avenue, Boston, MA 02111

David W. Jayme (**1**: 33) Cell Culture Research and Development, GIBCO/Invitrogen Corporation, 3175 Staley Road, Grand Island, NY 14072

Ole Nørregaard Jensen (**4**: 409) Protein Research Group, Department of Biochemistry and Molecular Biology, University of Southern Denmark, Campusvej 55, Odense M, DK-5230, DENMARK

Jae Hyun Jeong (**4**: 29) Department of Chemical & Biomolecular Engineering, Center for Ultramicrochemical Process Systems, Korea Advanced Institute of Science and Technology, Daejeon, 305-701, SOUTH KOREA

Jeff A. Jones (**2**: 233) Space and Life Sciences Directorate, NASA-Johnson Space Center, TX 77058

Gloria Juan (**1**: 279) Research Pathology Division, Room S-830, Memorial Sloan-Kettering Cancer Center, 1275 York Avenue, New York, NY 10021

Melissa S. Jurica (**2**: 109) Molecular, Cell & Developmental Biology, Center for Molecular Biology of RNA, UC Santa Cruz, 1156 High Street, Santa Cruz, CA 95064

Eckhart Kämpgen (**1**: 103) Department of Dermatology, Friedrich Alexander University, Hartmannstr. 14, Erlangen, D-91052, GERMANY

Roger Karlsson (**2**: 165) Department of Cell Biology, The Wenner-Gren Institute, Stockholm University, Stockholm, S-10691, SWEDEN

Fredrik Kartberg (**2**: 45) Göteborg University, Institute of Medical Biochemistry, PO Box 440, Gothenburg, SE, 403-50, SWEDEN

Irina N. Kaverina (**3**: 111) Institute of Molecular Biotechnology, Austrian Academy of Sciences, Dr. Bohrgasse 3-5, Vienna, A-1030, AUSTRIA

Ralph H. Kehlenbach (**2**: 267) Hygiene-Institut-Abteilung Virologie, Universitat Heidelberg, Im Neuenheimer Feld 324, Heidelberg, D-69120, GERAMNY

Daniel P. Kiehart (**3**: 87) Department of Biology, Duke University, B330g Levine Sci Bldg, Box 91000, Durham, NC 27708-1000

Katherine E. Kilpatrick (**1**: 483) Senior Research Investigator, TriPath Oncology, 4025 Stirrup Creek Drive, Suite 400, Durham, NC 27703

Jong-Duk Kim (**4**: 29) Department of Chemical & Biomolecular Engineering, Center for Ultramicrochemical Process Systems, Korea Advanced Institute of Science and Technology, Daejeon, 305-701, SOUTH KOREA

Maurice Kléber (**1**: 69) Institute of Cell Biology, Department of Biology, Swiss Federal Institute of Technology, ETH—Hönggerberg, Zurich, CH-8093, SWITZERLAND

Toshihide Kobayashi (**2**: 139) Supra-Biomolecular System Research Group, RIKEN (Institute of Physical and Chemical Research) Frontier Research System, 2-1, Hirosawa, Wako-shi, Saitama, 351-0198, JAPAN

Stefan Kochanek (**1**: 445) Division of Gene Therapy, University of Ulm, Helmholtz Str. 8/I, Ulm, D-89081, GERMANY

Anna Koffer (**2**: 223) Physiology Department, University College London, 21 University Street, London, WC1E 6JJ, UNITED KINGDOM

Antonius Koller (**4**: 383) Department of Cell Biology, Torrey Mesa Research Institute, 3115 Merryfield Row, San Diego, CA 92121

Erich Koller (**3**: 523) Functional Genomics, GeneTrove, Isis Pharmaceuticals, Inc., 2292 Faraday Ave., Carlsbad, CA 92008

Robert L. Kortum (**1**: 215) The Eppley Institute for Research in Cancer, The University of Nebraska Medical Center, 986805 Nebraska Medical Center, Omaha, NE 68198-6805

Irina Kratchmarova (**4**: 427) Protein Interaction Laboratory, University of Southern Denmark—Odense, Campusvej 55, Odense M, DK-5230, DENMARK

Geri E. Kreitzer (**2**: 189) Cell and Developmental Biology, Weill Medical College of Cornell University, LC-300, New York, NY 10021

Florian Kreppel (**1**: 445) Division of Gene Therapy, University of Ulm, Helmholtz Str. 8/I, Ulm, D-89081, GERMANY

Mogens Kruhøffer (**4**: 83) Molecular Diagnostic Laboratory, Clinical Biochemical Department, Aarhus University Hospital, Skejby, Brendstrupgaardvej, Aarhus N, DK-8200, DENMARK

Robb Krumlauf (**4**: 35) Stowers Institute for Medical Research, 1000 East 50th Street, Kansas City, MO 64110

Michael Kühl (**1**: 191) Development Biochemistry, University of Ulm, Albert-Einstein-Allee 11, Ulm, D-89081, GERMANY

Mark Kühnel (**2**: 57) Department of Cell Biology, EMBL, Postfach 102209, Heidelberg, D-69117, GERMANY

Anuj Kumar (**3**: 179) Dept. of Molecular, Cellular, and Developmental Biology and Life Sciences Institute, University of Michigan, 210 Washtenaw Avenue, Ann Arbor, MI 48109-2216

Thomas Küntziger (**1**: 207) Institute of Medical Biochemistry, Institute of Medical Biochemistry, University of Oslo, PO Box 1112 Blindern, Oslo, 0317, NORWAY

Yasuhiro Kuramitsu (**4**: 197) Department of Biochemistry and Biomolecular Recognition, Yamaguchi University School of Medicine, 1-1-1 Minami-kogushi, Ube, Yamaguchi, 755-8505, JAPAN

Sergei A. Kuznetsov (**1**: 79) Craniofacial and Skeletal Disease Branch, NIDCR, NIH, Department of Health and Human Services, 30 Convent Drive MSC 4320, Bethesda, MD 20892

Joshua Labaer (**4**: 73) Harvard Institute of Proteomics, 320 Charles Street, Boston, MA 02141-2023

Frank Lafont (**2**: 181) Department of Biochemistry, University of Geneva, 30, quai Ernest-Ansermet 1211, Geneva 4, CH-1211, SWITZERLAND

Yun Wah Lam (**2**: 103, 115) Wellcome Trust Biocentre, MSI/WTB Complex, University of Dundee, Dow Street, Dundee, DD1 5EH, UNITED KINGDOM

Angus I. Lamond (**2**: 103, 115) Wellcome Trust Biocentre, MSI/WTB Complex, University of Dundee, Dow Street, Dundee, DD1 5EH, UNITED KINGDOM

Lukas Landmann (**3**: 5) Institute for Anatomy (LL), Anatomisches Institut, University of Basel, Pestalozzistrasse 20, Basel, CH-4056, SWITZERLAND

Helga B. Landsverk (**1**: 207) Institute of Medical Biochemistry, Institute of Medical Biochemistry, University of Oslo, PO Box 1112 Blindern, Oslo, 0317, NORWAY

Christine Lang (**4**: 57) Department of Microbiology and Genetics, Berlin University of Technology, Gustav-Meyer-Allee 25, Berlin, D-13355, GERMANY

Paul LaPointe (**2**: 209) Department of Cell and Molecular Biology, The Scripps Research Institute, 10550 North Torrey Pines Road, La Jolla, CA 92037

Martin R. Larsen (**4**: 371) Department of Biochemistry and Molecular Biology, University of Southern Denmark, Campusvej 55, Odense M, DK-5230, DENMARK

Pamela L. Larsen (**1**: 157) Department of Cellular and Structural Biology, University of Texas Health Science Center at San Antonio, San Antonio, TX 78229-3900

Eugene Ngo-Lung Lau (**1**: 115) Leukaemia Foundation of Queensland Leukaemia Research Laboratories, Queensland Institute of Medical Research, Royal Brisbane Hospital Post Office, Brisbane, Queensland, Q4029, AUSTRALIA

Sabrina Laugesen (**4**: 371) Department of Biochemistry and Molecular Biology, University of Southern Denmark, Campusvej 55, Odense M, DK-5230, DENMARK

Daniel Laune (**1**: 519) Centre de Pharmacologie et Biotechnologie pour la Santé, CNRS UMR 5160, Faculté de Pharmacie, Avenue Charles Flahault, Montpellier Cedex 5, F-34093, FRANCE

Andre Le Bivic (**2**: 241) Groupe Morphogenese et Compartimentation Membranaire, UMR 6156, IBDM, Faculte des Sciences de Luminy, case 907, Marseille cedex 09, F-13288, FRANCE

Ronald Lebofsky (**3**: 429) Laboratoire de Biophysique de l'ADN, Departement des Biotechnologies, Institut Pasteur, 25 rue du Dr. Roux, Paris Cedex 15, F-75724, FRANCE

Chuan-PU Lee (**2**: 259) The Department of Biochemistry and Molecular Biology, Wayne State University School of Medicine, 4374 Scott Hall, 540 E. Canfield, Detroit, MI 48201

Eva Lee (**1**: 139) Life Sciences Division, Lawrence Berkeley National Laboratory, 1 Cyclotron Road, Bldg 83-101, Berkeley, CA 94720

Joon-Hee Lee (**4**: 45) School of Biosciences, University of Nottingham, Sutton Bonington, Loughborough, Leics, LE12 5RD, UNITED KINGDOM

Kwangmoon Lee (**1**: 215) The Eppley Institute for Research in Cancer, The University of Nebraska Medical Center, 986805 Nebraska Medical Center, Omaha, NE 68198-6805

Thomas Lee (**4**: 443) Dept of Chemistry and Biochemistry, Univ of Colorado, 215 UCB, Boulder, CO 80309-0215

Margaret Leversha (**3**: 395) Memorial Sloan Kettering Cancer Center, 1275 York Avenue, New York, NY 10021

Jeffrey M. Levsky (**4**: 121) Department of Anatomy and Structural Biology, Golding # 601, Albert Einstein College of Medicine of Yeshiva University, 1300 Morris Park Avenue, Bronx, NY 10461

Alexandre Lewalle (**3**: 37) Randall Centre, New Hunt's House, Guy's Campus, London, SE1 1UL, UNITED KINGDOM

Chung Leung Li (**1**: 115) Experimental Haematology Laboratory, Stem Cell Program, Institute of Zoology/Genomics Research Center, Academia Sinica, Nankang 115, Nankang, Taipei, 11529, R.O.C.

LiQiong Li (**3**: 345) Department of Pathology and Laboratory Medicine, University of Rochester School of Medicine, 601 Elmwood Ave., Rm 1-6337, Rochester, NY 14642

Mei Li (**3**: 501) Institut de Génétique et de Biologie Moléculaire et Cellulaire (IGBMC), 1 rue Laurent Fries, B.P.10142, Illkirch CEDEX, F-67404, FRANCE

Siming Li (**4**: 295) Dana Faber Cancer Institute, Harvard University, 44 Binney Street, Boston, MA 02115

Lih-huei Liaw (**3**: 351) Beckman Laser Institute, University of California, Irvine, 1002 Health Sciences Road E, Irvine, CA 92697-1475

Antonietta M. Lillo (**1**: 491) Department of Chemistry, BCC-582, The Scripps Research Institute, 10550 N. Torrey Pines Road, La Jolla, CA 92037

Uno Lindberg (**2**: 165) Department of Cell Biology, Stockholm University, The Wenner-Gren Institute, Stockhólm, S-10691, SWEDEN

Christian Linden (**1**: 103) Department of Virology, Julius-Maximillins University, Versbacher Str. 7, Würzburg, D-97080, GERMANY

Robert Lindner (**2**: 51) Department of Cell Biology in the Center of Anatomy, Hannover Medical School, Hannover, D-30625, GERMANY

Lance A. Liotta (**3**: 339) Chief, Laboratory of Pathology, National Cancer Institute Building 10, Room 2A33, 9000 Rockville Pike, Bethesda, MD 20892

Adam J. Liska (**4**: 399) Max Planck Institute of Molecular Cell Biology and Genetics, Pfotenhauerst 108, Dresden, D-01307, GERMANY

Hong Liu (**1**: 139) Life Sciences Division, Lawrence Berkeley National Laboratory, 1 Cyclotron Road, Bldg 83-101, Berkeley, CA 94720

Silvia Lommel (**2**: 399) Department of Cell Biology, German Research Center for Biotechnology (GBF), Mascheroder Weg 1, Braunschweig, D-38124, GERMANY

Giuseppe S. A. Longo-Sorbello (**1**: 315) Centro di Riferimento Oncologico, Ospedale "S. Vincenzo", Taormina, Contradra Sirinam, 08903, ITALY

Lovisa Lovmar (**3**: 455) Department of Medical Sciences, Uppsala University, Akademiska sjukhuset, Uppsala, SE-75185, SWEDEN

Eugene Lukanidin (**1**: 363) Department of Molecular Cancer Biology, Institute of Cancer Biology, Danish Cancer Society, Strandboulevarden 49, Copenhagen, DK-2100, DENMARK

Jiri Lukas (**4**: 253) Department of Cell Cycle and Cancer, Danish Cancer Society, Strandboulevarden 49, Copenhagen, DK-2100, DENMARK

Peter J. Macardle (**1**: 475) Department of Immunology, Allergy and Artritis, Flinders Medical Centre and Flinders University, Bedford Park, Adelaie, SA, 5051, SOUTH AUSTRALIA

Peder S. Madsen (**4**: 69) Institute of Medical Biochemistry, University of Aarhus, Ole Worms Alle, Building 170, Aarhus C, DK-8000, DENMARK

Nils E. Magnusson (**4**: 83) Clinical Biochemical Department, Molecular Diagnostic Laboratory, Aarhus University Hospital, Skejby, Brendstrupgaardvej, Aarhus N, DK-8200, DENMARK

Asami Makino (**2**: 139) Supra-Biomolecular System Research Group, RIKEN (Institute of Physical and Chemical Research) Frontier Research System, 2-1, Hirosawa, Wako-shi, Saitama, 351-0198, JAPAN

G. Mike Makrigiorgos (**3**: 477) Department of Radiation Oncology, Dana Farber-Brigham and Women's Cancer Center, 75 Francis Street, Level L2, Boston, MA 02215

Matthias Mann (**4**: 363, 427) Protein Interaction Laboratory, University of Southern Denmark, Odense, Campusvej 55, Odense M, DK-5230, DENMARK

Edward Manser (**4**: 285) Glaxo-IMCB Group, Institute of Molecular and Cell Biology, Singapore, 117609, SINGAPORE

Ahmed Mansouri (**3**: 491) Department of Molecular Cell Biology, Max-Planck-Institute of Biophysical Chemistry, Am Fassberg 11, Göttingen, D-37077, GERMANY

Alan D. Marmorstein (**2**: 241) Cole Eye Institute, Weill Medical College of Cornell Cleveland Clinic, 9500 Euclid Avenue, i31, Cleveland, OH 44195

Bruno Martoglio (**2**: 215) Institute of Biochemistry, ETH Zentrum, Building CHN, Room L32.3, Zurich, CH-8092, SWITZERLAND

Susanne E. Mason (**1**: 407) Department of Physiology, University of Maryland School of Medicine, 655 W. Baltimore St., Baltimore, MD 21201

Stephen J. Mather (**1**: 539) Dept of Nuclear Medicine, St Bartholomews Hospital, London, EC1A 7BE, UNITED KINGDOM

Arvid B. Maunsbach (**3**: 221, 289) Department of Cell Biology, Institute of Anatomy, Aarhus University, Aarhus, DK-8000, DENMARK

William Hayes McDonald (**4**: 391) Department of Cell Biology, The Scripps Research Institute, 10550 North Torrey Pines Rd, La Jolla, CA 92370

Kathleen M. McKenzie (**1**: 491) Department of Chemistry, BCC-582, The Scripps Research Institute, 10550 N. Torrey Pines Road, La Jolla, CA 92037

Alexander D. McLellan (**1**: 103) Department of Microbiology & Immunology, University of Otago, PO Box 56, 720 Cumberland St, Dunedin, NEW ZEALAND

Scott W. McPhee (**1**: 457) Department of Surgery, University of Medicine and Dentistry of New Jersey, Camden, NJ 08103

Jill Meisenhelder (**4**: 139) Molecular and Cell Biology Laboratory, The Salk Institute, 10010 North Torrey Pines Road, La Jolla, CA 92037

Paula Meleady (**1**: 13) National Institute for Cellular Biotechnology, Dublin City University, Glasnevin, Dublin, 9, IRELAND

Nicholas T. Mesires (**4**: 345) Department of Physiology, Tufts University School of Medicine, 136 Harrison Ave, Boston, MA 02111

Daniel Metzger (**3**: 501) Institut de Génétique et de Biologie Moléculaire et Cellulaire (IGBMC), Institut Clinique de la Souris (ICS), 1 rue Laurent Fries, B.P.10142, Illkirch CEDEX, F-67404, FRANCE

Martina Mirlacher (**3**: 369) Division of Molecular Pathology, Institue of Pathology, University of Basel, Schonbeinstrasse 40, Basel, CH-4031, SWITZERLAND

Suchareeta Mitra (**4**: 335) Department of Biochemistry, University of Tennessee Health Sciences Center, Memphis, TN 38163

Atsushi Miyawaki (**2**: 317) Laboratory for Cell Function and Dynamics, Advanced Technology Center, Brain Science Institute, Institute of Physical and Chemical Research (RIKEN), 2-1 Horosawa, Wako, Saitama, 351-0198, JAPAN

Dejana Mokranjac (**4**: 269) Adolf-Butenandt-Institut fur Physiologische Chemie, Lehrstuhl: Physiologische Chemie, Universitat Munchen, Butenandtstr. 5, Gebäude B, Munchen, D-81377, GERMANY

Peter L. Molloy (**4**: 325) CSIRO Molecular Science, PO Box 184, North Ryde, NSW, 1670, AUSTRALIA

Richard A. Moravec (**1**: 25) Promega Corporation, 2800 Woods Hollow Road, Madison, WI 53711-5399

José M. A. Moreira (**1**: 527) Institute of Cancer Biology and Danish Centre for Translational Breast Cancer Research, Danish Cancer Society, Strandboulevarden 49, Copenhagen O, DK-2100, DENMARK

May C. Morris (**4**: 13) Centre de Recherche en Biochimie Macromoléculaire (UPR 1086), Centre National de la Recherche Scientifique (CNRS), 1919 Route de Mende, Montpellier Cedex 5, F-34293, FRANCE

Robert A. Moxley (**4**: 335) Department of Biochemistry, University of Tennessee Health Sciences Center, Memphis, TN 38163

Anne Muesch (**2**: 189) Margaret M. Dyson Vision Research Institute, Department of Opthalmology, Weill Medical College of Cornell University, New York, NY 10021

Peggy Müller (**1**: 325) Zentrum für Angewandte Medizinische und Humanbiologische Forschung, Labor für Molekulare Hepatologie der Universitätsklinik und Polikinik für Innere Medizin I, Martin Luther University Halle-Wittenburg, Heinrich-Damerow-Street 1, Saale, Halle, D-06097, GERMANY

Steve Murray (**3**: 325) CRC Structural Cell Biology Group, Paterson Institute for Cancer Research, Christie Hospital NHS Trust, Wilmslow Road, Withington, Manchester, M20 4BX, UNITED KINGDOM

Connie Myers (**1**: 139) Life Sciences Division, Lawrence Berkeley National Laboratory, 1 Cyclotron Road, Bldg 83-101, Berkeley, CA 94720

Kazuyuki Nakamura (**4**: 197) Department of Biochemistry and Biomolecular Recognition, Yamaguchi University School of Medicine, 1-1-1 Minami-kogushi, Ube, Yamaguchi, 755-8505, JAPAN

Maithreyi Narasimha (**3**: 77) Wellcome Trust/Cancer Research UK Institute and Dept of Anatomyaraki, University of Cambridge, Tennis Court Road, Cambridge, CB2 1QR, UNITED KINGDOM

Dobrin Nedelkov (**4**: 279) Intrinsic Bioprobes, Inc., 625 S. Smith Road, Suite 22, Tempe, AZ 85281

Randall W. Nelson (**4**: 279) Intrinsic Bioprobes Inc., 625 S. Smith Road, Suite 22, Tempe, AZ 85281

Frank R. Neumann (**2**: 359) Department of Molecular Biology, University of Geneva, 30, Quai Ernest Ansermet, Geneva, CH-1211, SWITZERLAND

Walter Neupert (**4**: 269) Adolf-Butenandt-Institut fur Physiologische Chemie, Lehrstuhl: Physiologische Chemie, Universitat Munchen, Butenandtstr. 5, Gebäude B, Munchen, D-81377, GERMANY

Axl Alois Neurauter (**1**: 239) Immunosystem R & D, Dynal Biotech ASA, PO Box 114, Smestad, N-0309, NORWAY

Phillip Ng (**1**: 435) Dept of Molecular and Human Genetics, Baylor College of Medicine, One Baylor Plaza, Houston, TX 77030

Garth L. Nicolson (**1**: 359) The Institute for Molecular Medicine, 15162 Triton Lane, Huntington Beach, CA 92649-1041

Trine Nilsen (**4**: 275) Department of Biochemistry, Institute for Cancer Research, The Norwegian Radium Hospital, Montebello, Oslo, N-0310, NORWAY

Tommy Nilsson (**2**: 45) Göteborg University, Institute of Medical Biochemistry, PO Box, Göteborg, SE-403 50, SWEDEN

Lars Norderhaug (**1**: 239) Dynal Biotech ASA, PO Box 114, Smestad, N-0309, NORWAY

Robert O'Connor (**1**: 5, 13, 335) National Institute for Cellular Biotechnology, Dublin City University, Glasnevin, Dublin, 9, IRELAND

Lorraine O'Driscoll (**1**: 5, 335) National Institute for Cellular Biotechnology, Dublin City University, Glasnevin, Dublin, 9, IRELAND

Martin Offterdinger (**3**: 153) Cell Biology and Cell Biophysics Program, European Molecular Biology Laboratory, Meyerhofstrasse 1, Heidelberg, D-69117, GERMANY

Philip Oh (**2**: 11) Cellular and Molecular Biology Program, Sidney Kimmel Cancer Center, 10835 Altman Row, San Diego, CA 92121

Takanori Ohnishi (**1**: 367) Department of Neurosurgery, Ehime University School of Medicine, Shitsukawa, Toon-shi, Ehime, 791-0295, JAPAN

Sjur Olsnes (**4**: 19, 275) Department of Biochemistry, The Norwegian Radium Hospital, Montebello, Oslo, 0310, NORWAY

Shao-En Ong (**4**: 427) Protein Interaction Laboratory, University of Southern Denmark—Odense, Campusvej 55, Odense M, DK-5230, DENMARK

Akifumi Ootani (**1**: 411) Department of Internal Medicine, Faculty of Medicine, Saga University, Nebeshima 5-1-1, Saga, 849-8501, JAPAN

Valerio Orlando (**4**: 317) Dulbecco Telethon Institute, Institute of Genetics & Biophysics CNR, Via Pietro Castellino 111, Naples, I-80131, ITALY

Torben Faeck Ørntoft (**4**: 83) Clinical Biochemical Department, Molecular Diagnostic Laboratory, Aarhus University Hospital, Skejby, Brendstrupgaardvej 100, Aarhus N, DK-8200, DENMARK

Mary Osborn (**1**: 549, 563) Department of Biochemistry and Cell Biology, Max Planck Institute of Biophysical Chemistry, Am Faßberg 11, Gottingen, D-37077, GERMANY

Lawrence E. Ostrowski (**2**: 99) Cystic Fibrosis/Pulmonary Research and Treatment Centre, University of North Carolina at Chapel Hill, Thurston-Bowles Building, Chapel Hill, NC 27599-7248

Hendrik Otto (**2**: 253) Institut für Biochemie und Molekularbiologie, Universität Freiburg, Hermann-Herder-Str. 7, Freiburg, D-79104, GERMANY

Kerstin Otto (**1**: 103) Department of Dermatology, Julius-Maximillians University, Josef-Schneider-Str. 2, Würzburg, 97080, GERMANY

Michel M. Ouellette (**1**: 215) Department of Biochemistry and Molecular Biology, Eppley Institute for Research in Cancer, The University of Nebraska Medical Center, 986805 Nebraska Medical Center, Omaha, NE 68198-6805

Jacques Paiement (**2**: 41) Département de pathologie et biologie cellulaire, Université de Montréal, Case postale 6128, Succursale "Centre-Ville", Montreal, QC, H3C 3J7, CANADA

Patricia M. Palagi (**4**: 207) Swiss Institute of Bioinformatics, CMU, 1 Michel Servet, Geneva 4, CH-1211, SWITZERLAND

Kinam Park (**4**: 29) Department of Pharmaceutics and Biomedical Engineering, Purdue University School of Pharmacy, 575 Stadium Mall Drive, Room G22, West Lafayette, IN 47907-2091

Helen Parkinson (**4**: 95) EMBL Outstation—Hinxton, European Bioinformatics Institute, Wellcome Trust Genome Campus, Hinxton, Cambridge, CB10 1SD, UNITED KINGDOM

Richard M. Parton (**3**: 187) Wellcome Trust Centre for Cell Biology, Institute of Cell and Molecular Biology The University of Edinburgh, Michael Swann Building, The King's Buildings, Mayfield Road, Edinburgh, EH9 3JR, SCOTLAND

Bryce M. Paschal (**2**: 267) Center for Cell Signaling, University of Virginia, 1400 Jefferson Park Avenue, West Complex Room 7021, Charlottesville, VA 22908-0577

Wayne F. Patton (**4**: 225) Perkin-Elmer LAS, Building 100-1, 549 Albany Street, Boston, MA 02118

Staffan Paulie (**1**: 533) Mabtech AB, Box 1233, Nacha Strand, SE-131 28, SWEDEN

Rainer Pepperkok (**3**: 121) Cell Biology and Cell Biophysics Programme, European Molecular Biology Laboratory (EMBL), Meyerhofstrasse 1, Heidelberg, D-69117, GERMANY

Xomalin G. Peralta (**3**: 87) Department of Physics, Duke University, 107 Physics Bldg, Durham, NC 27708-1000

Martha Perez-Magallanes (**1**: 151) National Medical Center and Beckman Research Institute, Division of Neurosciences, City of Hope, 1500 E. Duarte Rd, Duarte, CA 91010

Stephen P. Perfetto (**1**: 257) Vaccine Research Center, National Institutes of Health, 40 Convent Dr., Room 5509, Bethesda, MD 20892-3015

Hedvig Perlmann (**1**: 533) Department of Immunology, Stockholm University, Biology Building F5, Top floor, Svante Arrhenius väg 16, Stockholm, SE-10691, SWEDEN

Peter Perlmann (**1**: 533) Department of Immunology, Stockholm University, Biology Building F5, Top floor, Svante Arrhenius väg 16, Stockholm, SE-10691, SWEDEN

Timothy W. Petersen (**1**: 269) Institute for Systems Biology, 1441 N. 34th St, Seattle, WA 98103

Patti Lynn Peterson (**2**: 259) Department of Neurology, Wayne State University School of Medicine, 5L26 Detroit Receiving Hospital, Detroit Medical Center, Detroit, MI 48201

Nisha Philip (**4**: 265) Department of Pharmacology and Cancer Biology, Duke University, Research Dr. LSRC Rm C115, Box 3813, Durham, NC 27710

Thomas Pieler (**1**: 191) Institute for Biochemistry and Molecular Cell Biology, University of Goettingen, Humboldtallee 23, Göttingen, D-37073, GERMANY

Daniel Pinkel (**3**: 445) Department of Laboratory Medicine, University of California San Francisco, Box 0808, San Francisco, CA 94143-0808

Javier Pizarro Cerdá (**2**: 407) Unite des Interactions Bacteries-Cellules/Unité INSERM 604, Institut Pasteur, 28, rue du Docteur Roux, Paris Cedex 15, F-75724, FRANCE

Andreas Plückthun (**1**: 497) Department of Biochemistry, University of Zürich, Winterthurerstrasse 190, Zürich, CH-8057, SWITZERLAND

Helen Plutner (**2**: 209) Department of Cell and Molecular Biology, The Scripps Research Institute, 10550 North Torrey Pines Road, La Jolla, CA 92037

Piotr Pozarowski (**1**: 279) Brander Cancer Research Institute, New York Medical College, Valhalla, NY 10595

Johanna Prast (**1**: 557) Institute of Molecular Biology, Austrian Academy of Sciences, Billrothstrasse 11, Salzburg, A-5020, AUSTRIA

Brendan D. Price (**3**: 477) Department of Radiation Oncology, Dana Farber-Brigham and Women's Cancer Center, 75 Francis Street, Level L2, Boston, MA 02215

Elena Prigmore (**3**: 403) Sanger Institute, The Wellcome Trust, The Wellcome Trust Genome Campus, Hinxton, Cambridge, CB10 1SA, UNITED KINGDOM

Gottfried Proess (**1**: 467) Eurogentec S.A., Liege Science Park, 4102 Seraing, B-, BELGIUM

David M. Prowse (**1**: 133) Centre for Cutaneous Research, Barts and The London Queen Mary's School of Medicine and Dentistry, Institute of Cell and Molecular Science, 2 Newark Street, Whitechapel London, WC2A 3PX, UNITED KINGDOM

Manuela Pruess (**4**: 469) EMBL outstation—Hinxton, European Bioinformatic Institute, Welcome Trust Genome Campus, Hinxton, Cambridge, CB10 1SD, UNITED KINGDOM

Eric Quéméneur (**4**: 235) Life Sciences Division, CEA Valrhô, BP 17171 Bagnols-sur-Cèze, F-30207, FRANCE

Leda Helen Raptis (**2**: 329, 341) Department of Microbiology and Immunology, Queen's University, Room 716 Botterell Hall, Kingston, Ontario, K7L3N6, CANADA

Anne-Marie Rasmussen (**1**: 239) Dynal Biotech ASA, PO Box 114, Smestad, N-0309, NORWAY

Andreas S. Reichert (**4**: 269) Department of Physiological Chemistry, University of Munich, Butenandtstr. 5, München, D-81377, GERMANY

Siegfreid Reipert (**3**: 325) Ordinariat II, Institute of Biochemistry and Molecular Biology, Vienna Biocenter, Dr. Bohr-Gasse 9, Vienna, A-1030, AUSTRIA

Guenter P. Resch (**3**: 267) Institute of Molecular Biology, Dr. Bohrgasse 3-5, Vienna, A-1030, AUSTRIA

Katheryn A. Resing (**4**: 443) Dept of Chemistry and Biochemistry, University of Colorado, 215 UCB, Boulder, CO 80309-0215

Donald L Riddle (**1**: 157) Division of Biological Sciences, University of Missouri, 311 Tucker Hall, Columbia, MO 65211

Mara Riminucci (**1**: 79) Department of Experimental Medicine, Universita' dell' Aquilla, Via Vetoio, Coppito II, L'Aquila, I-67100, ITALY

Terry L. Riss (**1**: 25) Promega Corporation, 2800 Woods Hollow Road, Madison, WI 53711-5399

Pamela Gehron Robey (**1**: 79) Craniofacial and Skeletal Disease Branch, NIDCR, NIH, Department of Health and Human Services 30 Convent Dr, MSC 4320, Bethesda, MD 20892-4320

Linda J. Robinson (**2**: 201)

Philippe Rocca-Serra (**4**: 95) EMBL Outstation—Hinxton, European Bioinformatics Institute, Wellcome Trust Genome Campus, Hinxton, Cambridge, CB10 1SD, UNITED KINGDOM

Alice Rodriguez (**3**: 87) Department of Biology, Duke University, Durham, NC 27708-1000

Enrique Rodriguez-Boulan (**2**: 189, 241) Margaret M Dyson Vision Research Institute, Department of Opthalmology, Weill Medical College of Cornell University, New York, NY 10021

Mario Roederer (**1**: 257) ImmunoTechnology Section and Flow Cytometry Core, Vaccine Research Center, National Institute for Allergy and Infectious Diseases, National Institutes of Health, 40 Convent Dr., Room 5509, Bethesda, MD 20892-3015

Peter Roepstorff (**4**: 371) Department of Biochemistry and Molecular Biology, University of Southern Denmark, Campusvej 55, Odense M, DK-5230, DENMARK

Manfred Rohde (**2**: 399) Department of Microbial Pathogenicity, Gesellschaft fur Biotechnoogische Forschung, Mascheroder Weg 1, Braunschweig, D-38124, GERMANY

Norbert Roos (**3**: 299) Electron Microscopical Unit for Biological Sciences, University of Oslo, Blindern, Oslo, 0316, NORWAY

Sabine Rospert (**2**: 253) Institut für Biochemie und Molekularbiologie, Universität Freiburg, Hermann-Herder-Str. 7, Freiburg, D-79104, GERMANY

Klemens Rottner (**3**: 111) Cytoskeleton Dynamics Group, German Research Centre for Biotechnology (GBF), Mascheroder Weg 1, Braunschweig, D-38124, GERMANY

Line Roy (**2**: 41) Department of Anatomy and Cell Biology, Faculty of Medicine, McGill University, STRATHCONA Anatomy & Dentistry Building, Montreal, QC, H3A 2B2, CANADA

Sandra Rutherford (**3**: 325) CRC Structural Cell Biology Group, Paterson Institute for Cancer Research, Christie Hospital NHS Trust, Wilmslow Road, Withington, Manchester, M20 4BX, UNITED KINGDOM

Beth Rycroft (**1**: 395) Department of Pharmacology, University College London, Gower Street, London, WC1E GBT, UNITED KINGDOM

Patrick Salmon (**1**: 425) Department of Genetics and Microbiology, Faculty of Medicine, University of Geneva, CMU-1 Rue Michel-Servet, Geneva 4, CH-1211, SWITZERLAND

Paul M. Salvaterra (**1**: 151) National Medical Center and Beckman Research Institute, Division of Neurosciences, City of Hope, 1500 E. Duarte Rd, Duarte, CA 91010-3000

R. Jude Samulski (**1**: 457) Gene Therapy Centre, Department of Pharmacology, University of North Carolina at Chapel Hill, 7119 Thurston Bowles, Chapel Hill, NC 27599-7352

Susanna-Assunta Sansone (**4**: 95) EMBL Outstation—Hinxton, European Bioinformatics Institute, Wellcome Trust Genome Campus, Hinxton, Cambridge, CB10 1SD, UNITED KINGDOM

Ugis Sarkan (**4**: 95) EMBL Outstation—Hinxton, European Bioinformatics Institute, Wellcome Trust Genome Campus, Hinxton, Cambridge, CB10 1SD, UNITED KINGDOM

Moritoshi Sato (**2**: 325) Department of Chemistry, School of Science, University of Tokyo, 7-3-1 Hongo, Bunkyo-Ku, Tokyo, 113-0033, JAPAN

Guido Sauter (**3**: 369) Institute of Pathology, University of Basel, Schonbeinstrasse 40, Basel, CH-4003, SWITZERLAND

Carolyn L. Sawyer (**2**: 299) Department of Pharmacology, University of Vermont, Health Science Research Facility 330, Burlington, VT 05405-0068

Guray Saydam (**1**: 315) Department of Medicine, Section of Hematology, Ege University Hospital, Bornova Izmir, 35100, TURKEY

Silvia Scaglione (**3**: 201) BIOLab, Department of Informatic, Systemistic and Telematic, University of Genoa, Viale Causa 13, Genoa, I-16145, ITALY

Lothar Schermelleh (**1**: 291, 301) Department of Biology II, Biocenter of the Ludwig-Maximilians University of Munich (LMU), Großhadernerstr. 2, Planegg-Martinsried, 82152, GERMANY

Gudrun Schiedner (**1**: 445) CEVEC Pharmaceuticals GmbH, Gottfried-Hagen-Straße 62, Köln, D-51105, GERMANY

David Schieltz (**4**: 383) Department of Cell Biology, Torrey Mesa Research Institute, 3115 Merryfield Row, San Diego, CA 92121

Jan E. Schnitzer (**2**: 11) Sidney Kimmel Cancer Center, 10835 Altman Row, San Diego, CA 92121

Morten Schou (**1**: 353) Bartholin Institute, Bartholinsgade 2, Copenhagen K, DK-1356, DENMARK

Sebastian Schuck (**2**: 5) Max Planck Institute of Molecular Cell Biology and Genetics, Pfotenhauerstrasse 108, Dresden, D-01307, GERMANY

Herwig Schüler (**2**: 165) Department of Cell Biology, The Wnner-Gren Institute, Stockholm University, Stockholm, S-10691, SWEDEN

Michael Schuler (**3**: 501) Institut de Génétique et de Biologie Moléculaire et Cellulaire (IGBMC), 1 rue Laurent Fries, B.P.10142, Illkirch CEDEX, F-67404, FRANCE

Ulrich S. Schwarz (**2**: 419) Theory Division, Max Planck Institute of Colloids and Interfaces, Potsdam, 14476, GERMANY

Antonio S. Sechi (**2**: 393) Institute for Biomedical Technology-Cell Biology, Universitaetsklinikum Aachen, RWTH, Pauwelsstrasse 30, Aachen, D-52057, GERMANY

Richard L. Segraves (**3**: 445) Comprehensive Cancer Center, University of California San Francisco, Box 0808, 2400 Sutter N-426, San Francisco, CA 94143-0808

James R. Sellers (**2**: 387) Cellular and Motility Section, Laboratory of Molecular Cardiology, National Heart, Lung and Blood Institute (NHLBI), National Institutes of Health, 10 Center Drive, MSC 1762, Bethesda, MD 20892-1762

Nicholas J. Severs (**3**: 249) Cardiac Medicine, National Heart and Lung Institute, Imperial College, Faculty of Medicine, Royal Brompton Hospital, Dovehouse Street, London, SW3 6LY, UNITED KINGDOM

Jagesh Shah (**3**: 351) Laboratory of Cell Biology, Ludwig Institute for Cancer Research, University of California, 9500 Gilman Drive, MC 0660, La Jolla, CA 92093-0660

Norman E. Sharpless (**1**: 223) The Lineberger Comprehensive Cancer Center, The University of North Carolina School of Medicine, Lineberger Cancer Center, CB# 7295, Chapel Hill, NC 27599-7295

Andrej Shevchenko (**4**: 399) Max Planck Institute for Molecular Cell Biology and Genetics, Pfotenhauerstrasse 108, Dresden, D-01307, GERMANY

David M. Shotton (**3**: 207, 249, 257) Department of Zoology, University of Oxford, South Parks Road, Oxford, OX1 3PS, UNITED KINGDOM

David I. Shreiber (**1**: 379) Department of Biomedical Engineering, Rutgers, the State University of New Jersey, 617 Bowser Road, Piscataway, NJ 08854-8014

Snaevar Sigurdsson (**3**: 455) Department of Medical Sciences, Uppsala University, Akademiska sjukhuset, Uppsala, SE-751 85, SWEDEN

Stephen Simkins (**1**: 483) TriPath Oncology, 4025 Stirrup Creek Drive, Suite 400, Durham, NC 27703

Ronald Simon (**3**: 369) Division of Molecular Pathology, Institute of Pathology, University of Basel, Schonbeinstrasse 40, Basel, CH-4031, SWITZERLAND

Kai Simons (**1**: 127, **2**: 5, 181) Max Planck Institute of Molecular Cell Biology and Genetics, Pfotenhauerstrasse 108, Dresden, D-01307, GERMANY

Jeremy C. Simpson (**3**: 121) Cell Biology and Cell Biophysics Programme, European Molecular Biology Laboratory (EMBL), Meyerhofstrasse 1, Heidelberg, D-69117, GERMANY

Robert H. Singer (**4**: 121) Department of Anatomy and Structural Biology, Golding # 601, Albert Einstein College of Medicine of Yeshiva University, 1300 Morris Park Avenue, Bronx, NY 10461

Mathilda Sjöberg (**1**: 419) Department of Biosciences at Novum, Karolinska Instituet, Huddinge, SE-141-57, SWEDEN

Camilla Skiple Skjerpen (**4**: 275) Department of Biochemistry, Institute for Cancer Research, The Norwegian Radium Hospital, Montebello, Oslo, N-0310, NORWAY

John Sleep (**3**: 37) Randall Division, Guy's Campus, New Hunt's House, London, SE1 1UL, UNITED KINGDOM

J. Victor Small (**1**: 557) Department of Cell Biology, Institute of Molecular Biology, Austrian Academy of Sciences, Billrothstrasse 11, Salzburg, A-5020, AUSTRIA

Joél Smet (**4**: 259) Department of Pediatrics and Medical Genetics, University Hospital, De Pintelaan 185, Ghent, B-9000, BELGIUM

Kim Smith (**3**: 381) Director of Cytogenetic Services, Oxford Radcliffe NHS Trust, Headington, Oxford, OX3 9DU, UNITED KINGDOM

Paul J. Smith (**1**: 305) Dept of Pathology, University of Wales College of Medicine, Heath Park, Cardiff, CF14 4XN, UNITED KINGDOM

Antoine M. Snijders (**3**: 445) Comprehensive Cancer Center, Cancer Research Institute, The University of California, San Francisco, Box 0808, 2340 Sutter Street N-, San Fransisco, CA 94143-0808

Michael Snyder (**3**: 179) Department of Molecular, Cellular and Developmental Biology, Yale University, P. O. Box 208103, Kline Biology Tower, 219 Prospect St., New Haven, CT 06520-8103

Irina Solovei (**1**: 291) Department of Biology II, Anthropology & Human Genetics, Ludwig-Maximilians University of Munich, Munich, GERMANY

Marion Sölter (**1**: 191) Institute for Biochemistry and Molecular Cell Biology, University of Goettingen, Justus-von-Liebig-Weg 11, Göttingen, D-37077, GERMANY

Lukas Sommer (**1**: 69) Institute of Cell Biology, Department of Biology, Swiss Federal Institute of Technology, ETH—Hönggerberg, Zurich, CH-8093, SWITZERLAND

Simon Sparks (**3**: 207) Department of Zoology, University of Oxford, South Parks Road, Oxford, OX1 3PS, UNITED KINGDOM

Kenneth G. Standing (**4**: 457) Department of Physics and Astronomy, University of Manitoba, 510 Allen Bldg, Winnipeg, MB, R3T 2N2, CANADA

Walter Steffen (**3**: 37, 307) Randall Division, Guy's Campus, New Hunt's House, London, SE1 1UL, UNITED KINGDOM

Theresia E. B. Stradal (**3**: 111) Department of Cell Biology, German Research Centre for Biotechnology (GBF), Mascheroder Weg 1, Braunschweig, D-38124, GERMANY

Per Thor Straten (**1**: 97) Tumor Immunology Group, Institute of Cancer Biology, Danish Cancer Society, Strandboulevarden 49, Copenhagen, DK-2100, DENMARK

Hajime Sugihara (**1**: 411) Department of Pathology & Biodefence, Faculty of Medicine, Saga University, Nebeshima 5-1-1, Saga, 849-8501, JAPAN

Chung-Ho Sun (**3**: 351) Beckman Laser Institute, University of California, Irvine, 1002 Health Sciences Road E, Irvine, CA 92697-1475

Mark Sutton-Smith (**4**: 415) Department of Biological Sciences, Imperial College of Science, Technology and Medicine, Biochemistry Building, London, SW7 2AY, UNITED KINGDOM

Tatyana M. Svitkina (**3**: 277) Department of Cell and Molecular Biology, Northwestern University Medical School, Chicago, IL 60611

Ann-Christine Syvänen (**3**: 455) Department of Medical Sciences, Uppsala University, Forskningsavd 2, ing 70, Uppsala, SE-751 85, SWEDEN

Masako Tada (**1**: 199) ReproCELL Incorporation, 1-1-1 Uchisaiwai-cho, Chiyoda-ku, Tokyo, 100-0011, JAPAN

Takashi Tada (**1**: 199) Stem Cell Engineering, Stem Cell Research Center, Institute for Frontier Medical Sciences, Kyoto University, 53 Kawahara-cho Shogoin, Sakyo-ku, Kyoto, 606-8507, JAPAN

Angela Taddei (**2**: 359) Department of Molecular Biology, University of Geneva, 30, Quai Ernest Ansermet, Geneva 4, CH-1211, SWITZERLAND

Tomohiko Taguchi (**2**: 33) Department of Cell Biology, Yale University School of Medicine, 333 Cedar Street, PO Box 208002, New Haven, CT 06520-8002

Kazusuke Takeo (**4**: 197) Department of Biochemistry and Biomolecular Recognition, Yamaguchi University School of Medicine, 1-1-1, Minami-kogushi, Ube, Yamaguchi, 755-8505, JAPAN

Nobuyuki Tanahashi (**2**: 91) Laboratory of Frontier Science, Core Technology and Research Center, The Tokyo Metropolitan Institute of Medical Sciences, 3-18-22 Honkomagome, Bunkyo-ku, Tokyo, 113-8613, JAPAN

Keiji Tanaka (**2**: 91) Laboratory of Frontier Science, Core Technology and Research Center, The Tokyo Metropolitan Institute of Medical Sciences, 3-18-22 Honkomagome, Bunkyo-ku, Tokyo, 133-8613, JAPAN

Chi Tang (**2**: 121) Dept of Biomolecular Sciences, UMIST, PO Box 88, Manchester, M60 1QD, UNITED KINGDOM

Kirill V. Tarasov (**4**: 103) Molecular Cardiology Unit, National Institute on Aging, NIH, 5600 Nathan Shock Drive, Baltimore, MD 21224

J. David Taylor (**3**: 471) Department of Genomic Sciences, Glaxo Wellcome Research and Development, 5 Moore Drive, Research Triangle Park, NC 27709-3398

Nancy Smyth Templeton (**4**: 25) Department of Molecular and Cellular Biology & the Center for Cell and Gene Therapy, Baylor College of Medicine, One Baylor Plaza, Alkek Bldg., Room N1010, Houston, TX 77030

Kenneth K. Teng (**1**: 171) Department of Medicine, Wiell Medical of Cornell University, 1300 York Ave., Rm-A663, New York, NY 10021

Patrick Terheyden (**1**: 103) Department of Dermatology, Julius-Maximillians University, Josef-Schneider-Str. 2, Würzburg, D-97080, GERMANY

Scott M. Thompson (**1**: 407) Department of Physiology, University of Maryland School of Medicine, 655 W. Baltimore St., Baltimore, MD 21201,

John F. Timms (**4**: 189) Department of Biochemistry and Molecular Biology, Ludwig Institute of Cancer Research, Cruciform Building 1.1.09, Gower Street, London, WC1E 6BT, UNITED KINGDOM

Shuji Toda (**1**: 411) Department of Pathology & Biodefence, Faculty of Medicine, Saga University, Nebeshima 5-1-1, Saga, 849-8501, JAPAN

Yoichiro Tokutake (**3**: 87) Department of Physics, Duke University, 107 Physics Bldg, Durham, NC 27708-1000

Evi Tomai (**2**: 329) Department of Microbiology and Immunology, Queen's University, Room 716 Botterell Hall, Kingston, Ontario, K7L3N6, CANADA

Kenneth B. Tomer (**1**: 511) Mass Spectrometry, Laboratory of Structural Biology, National Institute of Environmental Health Sciences NIEH/NIH, 111 Alexander Drive, PO Box 12233, Research Triangle Park, NC 27709

Derek Toomre (**3**: 19) Department of Cell Biology, Yale University School of Medicine, SHM-C227/229, PO Box 208002, 333 Cedar Street, New Haven, CT 06520-8002

Sharon A. Tooze (**2**: 79) Secretory Pathways Laboratory, Cancer Research UK London Research Institute, 44 Lincoln's Inn Fields, London, WC2A 3PX, UNITED KINGDOM

David Tosh (**1**: 177) Centre for Regenerative Medicine, Department of Biology and Biochemistry, University of Bath, Claverton Down, Bath, BA2 7AY, UNITED KINGDOM

Yusuke Toyama (**3**: 87) Department of Physics, Duke University, 107 Physics Bldg, Box 90305, Durham, NC 27708-0305

Robert T. Tranquillo (**1**: 379) Department of Biomedical Engineering and Department of Chemical Engineering and Materials Science, University of Minnesota, Biomedical Engineering, 7-112 BSBE. 312 Church St SE, Minneapolis, MN 55455

Signe Trentemølle (**4**: 165) Institute of Cancer Biology and Danish Centre for Translational Breast Cancer Research, Danish Cancer Society,

Strandboulevarden 49, Copenhagen, DK-2100, DENMARK

Didier Trono (**1**: 425) Department of Genetics and Microbiology, Faculty of Medicine, University of Geneva, CMU-1 Rue Michel-Servet, Geneva 4, CH-1211, SWITZERLAND

Kevin Truong (**2**: 307) Division of Molecular and Structural Biology, Ontario Cancer Institute, Department of Medical Biophysics, University of Toronto, 610 University Avenue, 7-707A, Toronto, Ontario, M5G 2M9, CANADA

Jessica K. Tyler (**2**: 287) Department of Biochemistry and Molecular Genetics, University of Colorado Health Sciences Center at Fitzsimons, PO Box 6511, Aurora, CO 80045

Aylin S. Ulku (**1**: 345) Department of Pharmacology, University of North Carolina at Chapel Hill, Lineberger Comprehensive Cancer Center, Chapel Hill, NC 27599-7295

Yoshio Umezawa (**2**: 325) Department of Chemistry, The School of Science, University of Tokyo, 7-3-1 Hongo, Bunkyo-ku, Tokyo, 113-0033, JAPAN

Ronald Vale (**3**: 129) Department of Cellular and Molecular Pharmacology, The Howard Hughes Medical Institute, The University of California, San Francisco, N316, Genentech Hall, 1600 16th Street, San Francisco, CA 94107

Jozef Van Beeumen (**4**: 259) Department of Biochemistry, Physiology and Microbiology, University of Ghent, K.L. Ledeganckstraat 35, Ghent, B-9000, BELGIUM

Rudy N. A. van Coster (**4**: 259) Department of Pediatrics and Medical Genetics, University Hospital, University of Ghent, De Pintelaan 185, Ghent, B-9000, BELGIUM

Ger van den Engh (**1**: 269) Institute for Systems Biology, 1441 North 34th Street, Seattle, WA 98103-8904

Peter van der Geer (**4**: 139) Department of Chemistry and Biochemistry, University of California, San Diego, 9500 Gilman Dr., La Jolla, CA 92093-0601

Joël Vandekerckhovr (**4**: 379, 457) Department of Medical Protein Research, Flanders Interuniversity Institute for Biotechnology, KL Ledeganckstraat 35, Gent, B-9000, BELGIUM

Charles R. Vanderburg (**4**: 5) Department of Neurology, Massachusetts General Hospital, 114 Sixteenth Street, Charlestown, MA 02129

John Venable (**4**: 383) Department of Cell Biology, Scripps Research Institute, 10550 North Torrey Pines Road, La Jolla, CA 92037

Isabelle Vernos (**2**: 379) Cell Biology and Cell Biophysics Programme, European Molecular Biology Laboratory, Meyerhofstrasse 1, Heidelberg, D-69117, GERMANY

Peter J. Verveer (**3**: 153) Cell Biology and Cell Biophysics Program, European Molecular Biology Laboratory, Meyerhofstrasse 1, Heidelberg, D-69117, GERMANY

Marc Vidal (**4**: 295) Cancer Biology Department, Dana-Farber Cancer Institute, 44 Binney Street, Boston, MA 02115

Emmanuel Vignal (**2**: 427) Department Genie, Austrian Academy of Sciences, Billrothstrasse 11, Salzbourg–Autriche, A-520, 5020, AUSTRIA

Sylvie Villard (**1**: 519) Centre de Pharmacologie et Biotechnologie pour la Santé, CNRS—UMR 5094, Faculté de Pharmacie, Avenue Charles Flahault, Montpellier Cedex 5, F-34093, FRANCE

Hikka Virta (**1**: 127) Department of Cell Biology, European Molecular Biology Laboratory, Cell Biology Programme, Heidelberg, D-69012, GERMANY

Alfred Völkl (**2**: 63) Department of Anatomy and Cell Biology II, University of Heidelberg, Im Neuenheimer Feld 307, Heidelberg, D-69120, GERMANY

Sonja Voordijk (**4**: 207) Geneva Bioinformatics SA, Avenue de Champel 25, Geneva, CH-1211, SWITZERLAND

Adina Vultur (**2**: 329, 341) Department of Microbiology and Immunology, Queen's University, Room 716 Botterell Hall, Kingston, Ontario, K7L3N6, CANADA

Teruhiko Wakayama (**1**: 87) Center for Developmental Biology, RIKEN, 2-2-3 Minatojima-minamimachi, Kobe, 650-0047, JAPAN

Daniel Walther (**4**: 207) Swiss Institute of Bioinformatics (SIB), CMU, rue Michel-Servet 1, Genève 4, 1211, SWITZERLAND

Gang Wang (**3**: 477) Department of Radiation Oncology, Dana Farber-Brigham and Women's Cancer Center, 75 Francis Street, Level L2, Boston, MA 02215

Nancy Wang (**3**: 345) Department of Pathology and Laboratory Medicine, University of Rochester School of Medicine, 601 Elmwood Ave., Rm 1-6337, Rochester, NY 14642

Xiaodong Wang (**2**: 209) Department of Cell and Molecular Biology, The Scripps Research Institute, 10550 North Torrey Pines Road, La Jolla, CA 92037

Yanzhuang Wang (**2**: 33) Department of Cell Biology, Yale University School of Medicine, 333 Cedar Street, PO BOX 208002, New Haven, CT 06520-8002

Yu-Li Wang (**3**: 107) Department of Physiology, University of Massachusetts Medical School, 377 Plantation St., Rm 327, Worcester, MA 01605

Graham Warren (**2**: 33) Department of Cell Biology, Yale University School of Medicine, 333 Cedar Street, PO Box 208002, New Haven, CT 06520-8002

Clare M. Waterman-Storer (**3**: 137) 10550 North Torrey Pines Road, CB 163, La Jolla, CA 92037

Jennifer C. Waters (**3**: 49) Department of Cell Biology, Department of Systems Biology, Harvard Medical School, 240 Longwood Ave, Boston, MA 02115

Fiona M. Watt (**1**: 133) Keratinocyte Laboratory, London Research Institute, 44 Lincoln's Inn Fields, London, WC2A 3PX, UNITED KINGDOM

Gerhard Weber (**4**: 157) Protein Analytics, Max Planck Institute for Biochemistry, Klopferspitz 18, Martinsried, D-82152, GERMANY

Peter J. A. Weber (**4**: 157) Proteomics Division, Tecan Munich GmbH, Feldkirchnerstr. 12a, Kirchheim, D-, 85551, GERMANY

Paul Webster (**3**: 299) Electron Microscopy Laboratory, House Ear Institute, 2100 West Third Street, Los Angeles, CA 90057

Jürgen Wehland (**2**: 399) Department of Cell Biology, Gesellschaft fur Biotechnoogische Forschung, Mascheroder Weg 1, Braunschweig, D-38124, GERMANY

Dieter G. Weiss (**3**: 57) Institute of Cell Biology and Biosystems Technology, Department of Biological Sciences, Universitat Rostock, Albert-Einstein-Str. 3, Rostock, D-18051, GERMANY

Walter Weiss (**4**: 175) Fachgebiet Proteomik, Technische Universität Muenchen, Am Forum 2, Freising Weihenstephan, D-85350, GERMANY

Adrienne R. Wells (**3**: 87) Department of Biology, Duke University, Durham, NC 27708-1000

Jørgen Wesche (**4**: 19) Department of Biochemistry, The Norwegian Radium Hospital, Montebello, Oslo, 0310, NORWAY

Pamela Whittaker (**3**: 463) Genotyping / Chr 20, The Wellcome Trust Sanger Institute, The Wellcome Trust Genome Campus, Hinxton, Cambridge, CB10 1SA, UNITED KINGDOM

John Wiemann (**3**: 87) Department of Biology, Duke University, B330g Levine Sci Bldg, Box 91000, Durham, NC 27708-1000

Sebastian Wiesner (**2**: 173) Dynamique du Cytosquelette, Laboratoire d'Enzymologie et Biochimie Structurales, UPR A 9063 CNRS, Building 34, Bat. 34, avenue de la Terrasse, Gif-sur-Yvette, F-91198, FRANCE

Ilona Wolff (**1**: 325) Prodekanat Forschung, Medizinnishce Fakultät, Martin Luther University Halle-Wittenburg, Magdeburger Str 8, Saale, Halle, D-06097, GERMANY

Ye Xiong (**2**: 259) The Department of Biochemistry and Molecular Biology, Wayne State University School of Medicine, 4374 Scott Hall, 540 E. Canfield, Detroit, MI 48201

David P. Yarnall (**3**: 471) Department of Metabolic Diseases, Glaxo Wellcome Inc, 5 Moore Drive, Research Triangle Park, NC 27709-3398

Hideki Yashirodas (**2**: 91) Laboratory of Frontier Science, Core Technology and Research Center, The Tokyo Metropolitan Institute of Medical Sciences, 3-18-22 Honkomagome, Bunkyo-ku, Tokyo, 133-8613, JAPAN

John R. Yates III (**4**: 383, 391) Department of Cell Biology, Scripps Research Institute, 10550 North Torrey Pines Road, La Jolla, CA 92037

Charles Yeaman (**2**: 189) Department of Cell and Developmental Biology, Weill Medical College of Cornell University, New York, NY 10021

Robin Young (**2**: 41) Département de pathologie et biologie cellulaire, Université de Montréal, Case postale 6128, Succursale "Centre-Ville", Montreal, QC, H3C 3J7, CANADA

Christian Zahnd (**1**: 497) Department of Biochemistry, Univerisity of Zürich, Winterthurerstr. 190, Zürich, CH-8057, SWITZERLAND

Zhuo-shen Zhao (**4**: 285) Glaxo-IMCB Group, Institute of Molecular and Cell Biology, Singapore, 117609, SINGAPORE

Huilin Zhou (**4**: 437) Department of Cellular and Molecular Medicine, Ludwig Institute for Cancer Research, University of California, San Diego, 9500 Gilman Drive, CMM-East, Rm 3050, La Jolla, CA 92093-0660

Timo Zimmermann (**3**: 69) Cell Biology and Cell Biophysics Programme, EMBL, Meyerhofstrasse 1, Heidelberg, D-69117, GERMANY

Chiara Zurzolo (**2**: 241) Department of Cell Biology and Infection, Pasteur Institute, 25,28 rue du Docteur Roux, Paris, 75015, FRANCE

Preface

Scientific progress often takes place when new technologies are developed, or when old procedures are improved. Today, more than ever, we are in need of complementary technology platforms to tackle complex biological problems, as we are rapidly moving from the analysis of single molecules to the study of multifaceted biological problems. The third edition of *Cell Biology: A Laboratory Handbook* brings together 236 articles covering novel techniques and procedures in cell and molecular biology, proteomics, genomics, and functional genomics. It contains 165 new articles, many of which were commissioned in response to the extraordinary feedback we received from the scientific community at large.

As in the case of the second edition, the *Handbook* has been divided in four volumes. The first volume covers tissue culture and associated techniques, viruses, antibodies, and immunohistochemistry. Volume 2 covers organelles and cellular structures as well as assays in cell biology. Volume 3 includes imaging techniques, electron microscopy, scanning probe and scanning electron microscopy, microdissection, tissue arrays, cytogenetics and in situ hybridization, genomics, transgenic, knockouts, and knockdown methods. The last volume includes transfer of macromolecules, expression systems, and gene expression profiling in addition to various proteomic technologies. Appendices include representative cultured cell lines and their characteristics, Internet resources in cell biology, and bioinformatic resources for in silico proteome analysis. The Handbook provides in a single source most of the classical and emerging technologies that are essential for research in the life sciences. Short of having an expert at your side, the protocols enable researchers at all stages of their career to embark on the study of biological problems using a variety of technologies and model systems. Techniques are presented in a friendly, step-by-step fashion, and gives useful tips as to potential pitfalls of the methodology.

I would like to extend my gratitude to the Associate Editors for their hard work, support, and vision in selecting new techniques. I would also like to thank the staff at Elsevier for their constant support and dedication to the project. Many people participated in the realization of the *Handbook* and I would like to thank in particular Lisa Tickner, Karen Dempsey, Angela Dooley, Carl Soares, and Tari Paschall for coordinating and organizing the preparation of the volumes. My gratitude is also extended to all the authors for the time and energy they dedicated to the project.

Julio E. Celis
Editor

PART

A

ORGANELLES AND CELLULAR STRUCTURES

SECTION

1

Isolation: Plasma Membrane, Organelles, and Cellular Structures

CHAPTER

1

Detergent-Resistant Membranes and the Use of Cholesterol Depletion

Sebastian Schuck, Masanori Honsho, and Kai Simons

I. INTRODUCTION

Lipid rafts have changed our view of membrane organization. Rafts are small platforms in cell membranes, composed of a specialized set of lipids (Ikonen and Simons, 1997). In the exoplasmic leaflet, rafts consist mainly of sphingolipids and cholesterol, which are connected to saturated glycerophospholipids and cholesterol in the cytoplasmic leaflet. Rafts are fluid assemblies, but they are more tightly packed and hence more ordered than the surrounding membrane. This difference is due to the more saturated hydrocarbon chains of sphingolipids and raft-associated glycerophospholipids as compared to the mostly unsaturated glycerophospholipids outside rafts. Cholesterol is thought to fill the spaces between the hydrocarbon chains of the sphingolipids, thus stabilizing rafts.

The raft concept transforms the classical membrane model (Singer and Nicolson, 1972) into a more complex system, in which proteins are embedded in a two-dimensional liquid that is itself a mosaic of lipid microdomains. Membrane proteins partition into raft and nonraft membranes according to their preferred lipid environment. Proteins with a high affinity for ordered membrane domains will mostly reside in rafts. Typical raft-associated proteins include glycosylphosphatidylinositol (GPI)-anchored proteins, doubly acylated proteins such as tyrosine kinases of the src family, and certain integral membrane proteins, especially palmitoylated ones such as caveolin and influenza virus hemagglutinin. Proteins with an intermediate affinity will move in and out of rafts, whereas proteins that do not pack well into ordered domains will be excluded from rafts.

Important for understanding the physiological functions of rafts, e.g., in signal transduction, is that their composition is dynamic and can be regulated (Simons and Toomre, 2000). Some receptors, such as the T- and the B-cell receptor (Janes *et al.*, 2000; Pierce, 2002), have a weak raft affinity in the unligated state. After ligand binding, they undergo a conformational change and/or become oligomerized, which increases their raft affinity and allows them to interact with proteins constitutively present in rafts. Other signalling molecules, such as the endothelial nitric oxide synthase, α subunits of heterotrimeric G proteins, and possibly ras, can undergo signal-induced depalmitoylation, leading to loss of raft association (Bijlmakers and Marsh, 2003; Hancock, 2003). Thus, rafts can serve to segregate signalling molecules at steady state and promote their interaction upon stimulation.

Isolation of detergent-resistant membranes (DRMs) is a simple and useful biochemical method for analyzing the possible raft association of proteins and lipids. Especially when used to monitor changes in DRM composition during processes such as exocytosis (Brown and Rose, 1992) immune cell activation and viral infection (Manes *et al.*, 2000), this technique can provide important clues about the mechanisms underlying protein sorting, signal transduation and pathogen entry into host cells (Ikonen, 2001; Simons and Toomre, 2000; van der Goot and Harder, 2001). Rafts largely resist solubilization with mild detergents due to their tight lipid packing, whereas less ordered membrane domains are disrupted. Raft proteins do not become solubilized, but remain associated with lipids. As a result, they have a lower apparent density than detergent-soluble membrane proteins and can be isolated by equilibrium density centrifugation (often referred to as "flotation"). Detergent lysates are

Copyright 2006, Elsevier Science (USA).
All rights reserved.

adjusted to high density, placed at the bottom of a density gradient, and centrifuged. Contrary to fully solubilized material, DRMs and DRM-associated proteins float up the gradient, allowing their recovery from low-density fractions. As the integrity of lipid rafts depends on cholesterol, its removal renders raft-associated proteins detergent soluble. Detergent solubility of an otherwise detergent-insoluble protein after cholesterol depletion with methyl-β-cyclodextrin (cyclodextrin) can therefore serve as an additional criterion for raft association.

However, the composition of DRMs may only imperfectly reflect the association of membrane components with lipid rafts in cell membranes (Shogomori and Brown, 2003). DRMs obtained with different detergents differ considerably in their protein and lipid content (Schuck *et al*., 2003). Different detergents clearly reflect the organization of membranes in different ways, with Triton X-100 and CHAPS seemingly being the most informative ones. In addition, the interpretation of experimental results obtained with cyclodextrin is complicated by the fact that severe cholesterol depletion may have pleiotropic effects on membrane functions. Cyclodextrin might be more effective on cell homogenate than on living cells, but the reasons for this are not completely clear (Schuck *et al*., 2003).

Finally, neither detergent insolubility nor loss of detergent insolubility after cyclodextrin treatment is a strict criterion. If a protein is detergent soluble, it may still have a weak affinity for rafts in native membranes, and persistent detergent insolubility after cholesterol depletion can be caused by the remaining cholesterol. Therefore, neither criterion allows excluding raft association.

II. MATERIALS AND INSTRUMENTATION

Standard chemicals are of the highest purity available. Minimal essential medium with Earle's salts (MEM, Cat. No. 21090-022), glutamine (Cat. No. 25030-024), and penicillin–streptomycin (Cat. No. 15140-122) are from Invitrogen. Fetal calf serum (FCS, Cat. No. A15-042) is from PAA Laboratories. One hundred-millimeter (Cat. No. 150350) and 35-mm (Cat. No. 153066) plastic tissue dishes are from Nunc. Chymostatin (Cat. No. C7268), leupeptin (Cat. No. L2884), antipain (Cat. No. A6191), pepstatin (Cat. No. P5318), DL-mevalonic acid lactone (Cat. No. M4667), and methyl-β-cyclodextrin (Cat. No. C4555) are from Sigma. Lovastatin (Cat. No. 438185) is from Merck Biosciences. Sixty percent (w/v) iodixanol (Optiprep, Cat. No. 1030061) is from Progen Biotechnik, sucrose (Cat. No. 21938) is from USB, and 10% (w/v) Triton X-100 (Surfact-Amps X-100, Cat. No. 28314) is from Perbio.

Ultraclear centrifuge tubes for an SW40 rotor (14 × 95 mm, Cat. No. 344060) and for a TLS55 rotor (11 × 34 mm, Cat. No. 347356), as well as SW 40 Ti and TLS55 rotors, are from Beckman. Ultracentrifugations are carried out using an Optima XL-100K or an Optima MAX ultracentrifuge from Beckman.

In addition, the following equipment is required: 1.5-ml microfuge tubes, cell scrapers, 15-ml plastic tubes, 25-gauge needles, and 1-ml plastic syringes.

III. PROCEDURES

A. Preparation of DRMs by Flotation on a Sucrose Step Gradient

Solutions

1. *Phosphate-buffered saline (PBS)*: 155 m*M* NaCl, 1.5 m*M* KH_2PO_4, 2.7 m*M* Na_2HPO_4, pH 7.2. To make 1 litre, dissolve 0.21 g KH_2PO_4, 0.73 g $Na_2HPO_4{\cdot}7H_2O$, and 9 g NaCl in double-distilled water and make up to 1 litre.

2. *1 M EDTA*: To make 1 litre, dissolve 372.2 g EDTA in double-distilled water by adjusting the pH to 8 with NaOH and make up to 1 litre.

3. *5× TNE:* 750 m*M* NaCl, 10 m*M* EDTA, 250 m*M* Tris–HCl, pH 7.4. To make 1 litre, dissolve 43.8 g NaCl and 30.3 g Tris in double-distilled water, add 10 ml 1 *M* EDTA, adjust pH to 7.4 with HCl, and make up to 1 litre.

4. *1000× CLAP*: To make 1 ml, dissolve 25 mg each of chymostatin, leupeptin, antipain, and pepstatin in 1 ml dimethyl sulfoxide and store at –20°C in small aliquots.

5. *TNE and TNE with protease inhibitors (TNE+)*: To make TNE, dilute 5× TNE 1:5 in double-distilled water. To make TNE+, dilute 1000× CLAP 1:1000 in TNE just before use. TNE+ has to be prepared freshly each time.

6. *56, 35, and 5% (w/w) sucrose*: To make 100 ml, dissolve 70.75, 40.29, or 5.1 g sucrose in 20 ml 5× TNE and bring to 100 ml with double-distilled water. Check refractive indices of the resulting solutions, which should be 1.266, 1.154, and 1.021, respectively. Store at 4°C.

7. *2% (w/v) Triton X-100*: To make 10 ml, dissolve 0.2 g Triton X-100 in 2 ml 5× TNE and bring to 10 ml with double-distilled water. For short-term storage, keep at 4°C and protect from light to prevent autoxidation. For long-term storage, store aliquots at –20°C.

Steps

1. Grow MDCK strain II cells in MEM with 5% FCS, 2 m*M* glutamine, and 100 U/ml penicillin and streptomycin on a 10-cm plastic tissue dish until confluent.
2. All subsequent steps are performed at 4°C unless stated otherwise. Remove culture medium and wash the cells once with PBS and once with TNE.
3. Collect the cells in 1 ml TNE with a cell scraper. Transfer suspension into a 1.5-ml microfuge tube and centrifuge for 5 min at 350×g.
4. Resuspend the cell pellet in 550 µl TNE+. Homogenize by 20 passages through a 25-gauge needle fitted on a 1-ml syringe. This treatment should break >90% of the cells without damaging nuclei (check microscopically).
5. Take 500 µl cell homogenate (about 1 mg total protein) and transfer into a new microfuge tube. Add 500 µl 2% Triton X-100. From now on, strictly avoid warming of the sample. Mix well by inverting the tube and place on ice for 30 min.
6. Transfer the sample into a 15-ml tube and bring to 40% (w/w) sucrose by adding 2 ml 56% sucrose. Mix well by inverting the tube.
7. Place the sample at the bottom of an SW40 centrifuge tube. Sequentially overlay with 8.5 ml 35% sucrose and 0.5 ml 5% sucrose.
8. Centrifuge for 18 h at 39,000 rpm (271,000×*g*) using an SW40 rotor. DRMs float to the top of the gradient during centrifugation. Carefully collect 2.5 ml from the top of the gradient with a smooth pipette.
9. To further concentrate DRMs, dilute 1:4 by adding 7.5 ml TNE and transfer into a new SW40 centrifuge tube. Following centrifugation for 2 h at 24,000 rpm (100,000×*g*) with an SW40 rotor, DRMs can be recovered from the pellet.

B. Analysis of DRMs by Flotation on a Linear Sucrose Gradient

Solutions

See Section III,A.

Steps

1–6. See Section III,A.

7. Using a gradient maker, prepare a linear 5–35% sucrose gradient in an SW40 centrifuge tube with 4.5 ml each of 35 and 5% sucrose. Cool to 4°C.
8. Place the sample under the gradient using a Pasteur pipette, disturbing the gradient as little as possible (alternatively, first transfer the sample into an SW40 centrifuge tube and then overlay with the gradient).
9. Centrifuge for 18 h at 39,000 rpm (271,000×*g*) using an SW40 rotor. Collect twelve 1-ml fractions from the top of the gradient and resuspend the pellet in 1 ml TNE. Fractions 9–12 contain the soluble material; DRMs are found in the lighter fractions.

C. Analysis of DRMs by Flotation on an Optiprep Step Gradient

Solutions

PBS, 5× TNE, TNE, and TNE+; see Section III,A.

1. *10% (w/v) Triton X-100*: To make 10 ml, dissolve 1 g of Triton X-100 in 2 ml of 5× TNE and make up to 10 ml with double-distilled water. Alternatively, use Surfact-Amps X-100.
2. *30% (w/v) iodixanol*: To make 5 ml, mix 2.5 ml Optiprep, 1 ml 5× TNE, and 1.5 ml double-distilled water.

Steps

1. Grow MDCK strain II cells to confluence on a 3.5-cm plastic tissue dish.
2. At 4°C, remove culture medium and wash the cells once each with PBS and TNE.
3. Collect and spin down the cells as in Section III,A.
4. Resuspend the cell pellet in 200 µl TNE+. Homogenize as in Section III,A.
5. Take 180 µl cell homogenate and transfer into a new microfuge tube. Add 20 µl 10% Triton X-100 solution, mix, and place on ice for 30 min.
6. Add 400 µl Optiprep to bring the sample to 40% (w/v) iodixanol and mix well by inverting the tube.
7. Place the sample at the bottom of a TLS55 centrifuge tube. Sequentially overlay with 1.2 ml 30% iodixanol and 0.2 ml TNE.
8. Centrifuge for 2 h at 55,000 rpm (259,000×*g*) with a TLS55 rotor. Collect two fractions of 1 ml each. The top fraction contains the DRMs.

D. Cholesterol Depletion of Live Cells

Solutions

PBS; see Section III,A.

1. *20* m*M lovastatin*: To make 2.5 ml, dissolve 20 mg lovastatin in 0.5 ml 100% ethanol and 0.75 ml 0.1 *M* NaOH. Incubate at 50°C for 2 h, cool briefly on ice, and adjust pH to 7.2 with HCl. Bring to 2.5 ml with double-distilled water and store aliquots at –20°C.
2. *500* m*M mevalonate*: To make 5 ml, dissolve 325 mg in 5 ml PBS. Store aliquots at –20°C.

3. *100* m*M methyl-β-cyclodextrin in MEM*: To make 1 ml, dissolve 150 mg methyl-β-cyclodextrin in MEM just before use and make up to 1 ml with MEM.

Steps

1. Grow MDCK strain II cells on a plastic tissue dish or on filter supports. For the last 48 h before the experiment, culture the cells in normal medium supplemented with 4 µ*M* lovastatin (dilute stock solution 1:5000) and 0.25 m*M* mevalonate (dilute stock solution 1:2000).
2. Wash the cells twice with PBS and add MEM containing 4 µ*M* lovastatin, 0.25 m*M* mevalonate, and 10 m*M* methyl-β-cyclodextrin. In the case of filter-grown cells, apply cyclodextrin to both the apical and the basolateral side.
3. Incubate the cells at 37°C for 30 min.

E. Cholesterol Depletion of Cell Homogenate

Solutions

PBS, TNE, TNE+, and 10% (w/v) Triton X-100; see Sections III,A and III,C.

1. *100* m*M methyl-β-cyclodextrin in TNE*: To make 100 µl, dissolve 15 mg methyl-β-cyclodextrin in TNE just before use and make up to 100 µl with TNE.

Steps

1–4. See Section III,C.
5. Take 180 µl cell homogenate and transfer into a new microfuge tube. Add 20 µl 100 m*M* methyl-β-cyclodextrin, mix, and incubate at 37°C for 30 min.
6. For subsequent DRM analysis, cool to 4°C, add 20 µl 10% Triton X-100, and incubate on ice for 30 min.
7. Add 440 µl Optiprep to bring to 40% (w/v) iodixanol. Mix and take 600 µl and continue as in Section III,C, step 7.

IV. COMMENTS

Separating DRMs from detergent-soluble material by flotation using equilibrium density centrifugation is usually preferable to pelleting. Pelleting of DRMs from detergent extracts leads to contamination with other sedimentable material, e.g., cytoskeletal components. In addition, a protein might be pelleted because of its association with the cytoskeleton rather than DRMs.

Which flotation gradient to use for DRM analysis depends on the purpose of the experiment. Continuous gradients give more information about the flotation behaviour of proteins and lipids, but to monitor changes in DRM composition after, e.g., cyclodextrin treatment, simple step gradients as in Section III,C are more convenient. Various density gradient media can be used, and the choice between sucrose and iodixanol is largely a question of personal preference. However, sucrose might be superior if lipids are to be analyzed by a very sensitive method such as mass spectrometry, as iodixanol seems to have a weak tendency to follow lipids during extraction from DRMs.

How to apply cyclodextrin strongly depends on the cell type used. Hippocampal neurons cannot be exposed to 5 m*M* cyclodextrin for longer than 20 min (Simons *et al*., 1998), whereas MDCK cells remain intact even when treated with 20 m*M* for 1 h. Hence, the conditions for cyclodextrin treatment have to be established in each case. In particular, it needs to be ensured that cholesterol is the only lipid extracted. Treating live cells will preferentially extract cholesterol from the plasma membrane and allows intracellular cholesterol transport to counteract the effects of cyclodextrin, whereas extracting cholesterol from cell homogenate will affect all cell membranes.

V. PITFALLS

Membrane solubilisation by detergent depends on the molar ratio of detergent to lipid. Therefore, this parameter, rather than detergent concentration alone, always needs to be taken into account. In the case of Triton X-100, a mass ratio of detergent to protein (taken as a measure for the molar detergent-to-lipid ratio) of greater than 5:1 seems to be necessary for maximum solubilization (Ostermeyer *et al*., 1999).

DRM-associated proteins are separated from soluble proteins by flotation gradients because of their low density; they float due to their detergent-resistant association with lipids. In contrast, the separation of DRMs from detergent micelles, which contain solubilized membrane lipids, is based largely on differences in size. Given enough time, detergent micelles will also float as a result of their low density. However, DRMs are larger than detergent micelles and therefore float up faster [the sedimentation or flotation velocity s is given by $s = V(\rho - \rho_m)/f$, where V is particle volume, ρ is particle density, ρ_m is density of the solvent, and f is friction coefficient. For a spherical particle, V is proportional to r^3, while f is proportional to r, so that s is proportional to r^2. Refer to biophysical textbooks for a more comprehensive treatment]. To avoid contamination of DRMs with detergent molecules and solubilized lipids, it is crucial to ensure that

detergent micelles are well separated from DRMs under the centrifugation conditions used. The distribution of Triton in the gradient can be measured by its absorption at 280 nm. For other detergents, their distribution can be determined semiquantitatively by thin-layer chromatography.

References

Bijlmakers, M. J., and Marsh, M. (2003). The on-off story of protein palmitoylation. *Trends Cell Biol.* **13**, 32–42.

Brown, D. A., and Rose, J. K. (1992). Sorting of GPI-anchored proteins to glycolipid-enriched membrane subdomains during transport to the apical cell surface. *Cell* **68**, 533–544.

Hancock, J. F. (2003). Ras proteins: Different signals from different locations. *Nature Rev. Mol. Cell Biol.* **4**, 373–384.

Ikonen, E. (2001). Roles of lipid rafts in membrane transport. *Curr. Opin. Cell Biol.* **13**, 470–477.

Ikonen, E., and Simons, K. (1997). Functional rafts in cell membranes. *Nature* **387**, 569–572.

Janes, P. W., Ley, S. C., Magee, A. I., and Kabouridis, P. S. (2000). The role of lipid rafts in T cell antigen receptor (TCR) signalling. *Semin. Immunol.* **12**, 23–34.

Manes, S., del Real, G., Lacalle, R. A., Lucas, P., Gomez-Mouton, C., Sanchez-Palomino, S., Delgado, R., Alcami, J., Mira, E., and Martinez-A, C. (2000). Membrane raft microdomains mediate lateral assemblies required for HIV-1 infection. *EMBO Rep.* **1**, 190–196.

Ostermeyer, A. G., Beckrich, B. T., Ivarson, K. A., Grove, K. E., and Brown, D. A. (1999). Glycosphingolipids are not essential for formation of detergent-resistant membrane rafts in melanoma cells: Methyl-beta-cyclodextrin does not affect cell surface transport of a GPI-anchored protein. *J. Biol. Chem.* **274**, 34459–34466.

Pierce, S. K. (2002). Lipid rafts and B-cell activation. *Nature Rev. Immunol.* **2**, 96–105.

Schuck, S., Honsho, M., Ekroos, K., Shevchenko, A., and Simons K. (2003). Resistance of cell membranes to different detergents. *Proc. Natl. Acad. Sci. USA* **100**, 5795–5800.

Shogomori, H., and Brown, D. A. (2003). Use of detergents to study membrane rafts: The good, the bad, and the ugly. *Biol. Chem.* **384**, 1259–1263.

Simons, K., and Toomre, D. (2000). Lipid rafts and signal transduction. *Nature Rev. Mol. Cell Biol.* **1**, 31–39.

Simons, M., Keller, P., De Strooper, B., Beyreuther, K., Dotti, C. G., and Simons, K. (1998). Cholesterol depletion inhibits the generation of beta-amyloid in hippocampal neurons. *Proc. Natl. Acad. Sci. USA* **95**, 6460–6464.

Singer, S. J., and Nicolson, G. L. (1972). The fluid mosaic model of the structure of cell membranes. *Science* **175**, 720–731.

van der Goot, F. G., and Harder, T. (2001). Raft membrane domains: From a liquid-ordered membrane phase to a site of pathogen attack. *Semin. Immunol.* **13**, 89–97.

CHAPTER

2

Isolation and Subfractionation of Plasma Membranes to Purify Caveolae Separately from Lipid Rafts

Phil Oh, Lucy A. Carver, and Jan E. Schnitzer

I. INTRODUCTION

Cellular membranes contain distinct microdomains with unique molecular topographies, including caveolae and lipid rafts (**Fig. 1**). Caveolae are specialized flask-shaped invaginated microdomains located on the cell surface membrane of many cell types that appear to form through the polymerization of caveolin (Monier *et al.*, 1995), have a dynamin collar around their necks for fission (Oh *et al.*, 1998), and contain other molecular machinery for vesicular budding, docking, and fusion, including VAMP-2, NSF, and SNAP (Schnitzer *et al.*, 1995a). In contrast, lipid rafts are flat domains without the characteristic omega-shaped form of caveolae that suggests possible trafficking function. Unlike caveolae, which form via protein–protein interactions, lipid rafts appear to form in the membrane when highly saturated sphingolipids self-assemble with cholesterol to pack into a highly ordered lipid phase (Brown and London, 2000). Caveolae and lipid rafts may share similar lipids but a detailed compositional analysis is lacking at this time.

Although easily distinguished morphologically by electron microscopy, caveolae and lipid rafts were considered equivalent for many years because similarities in detergent solubility and density profiles made their biochemical distinction quite difficult and confounded attempts to definitively characterize the two domains. Many of caveolar preparations in wide use were isolated using one-dimensional separation techniques that rely on detergent resistance and membrane density after cell lysis (Sargiacomo *et al.*, 1993; Smart *et al.*, 1995). These preparations were later found to be heavily contaminated not only with membranes derived from intracellular organellar structures, but also with lipid rafts enriched in glycosylphosphatidyl inositol-anchored proteins (GPI-AP) derived from both the plasma membrane and intracellular membranes (Oh and Schnitzer, 1999; Schnitzer *et al.*, 1995b). As a consequence, early reports demonstrating that these low-density detergent-resistant membrane fractions were rich in both GPI-AP and caveolin concluded that caveolae constituted the GPI-AP-enriched lipid rafts in the plasma membrane (Sargiacomo *et al.*, 1993; Smart *et al.*, 1995). These data were supported by the finding that antibodies to GPI-AP can be found in caveolae by immunocytochemistry (Rothberg *et al.*, 1990; Ying *et al.*, 1992). In contrast, other reports showed that similar detergent-resistant membranes rich in GPI-AP could be isolated from cells lacking caveolin or caveolae (Fra *et al.*, 1995; Gorodinsky and Harris, 1995). In addition, it was also shown that past localization of GPI-AP in caveolae had been induced artifactually by antibody sequestration resulting from cross-linking by secondary reporter antibodies (Fujimoto, 1996; Mayor *et al.*, 1994). Thus, these early conflicting data made clear that more sophisticated methods for isolating caveolae and lipid rafts were necessary to finally defining the molecular constituents and structure of these structures.

Since the mid-1990s, caveolae and lipid rafts have been increasingly recognized as separate domains due, in part, to the development of a multidimensional membrane isolation technique. The key to this technique is the use of positively charged colloidal silica particles to coat selectively the cell surface membrane

Copyright 2006, Elsevier Science (USA).
All rights reserved.

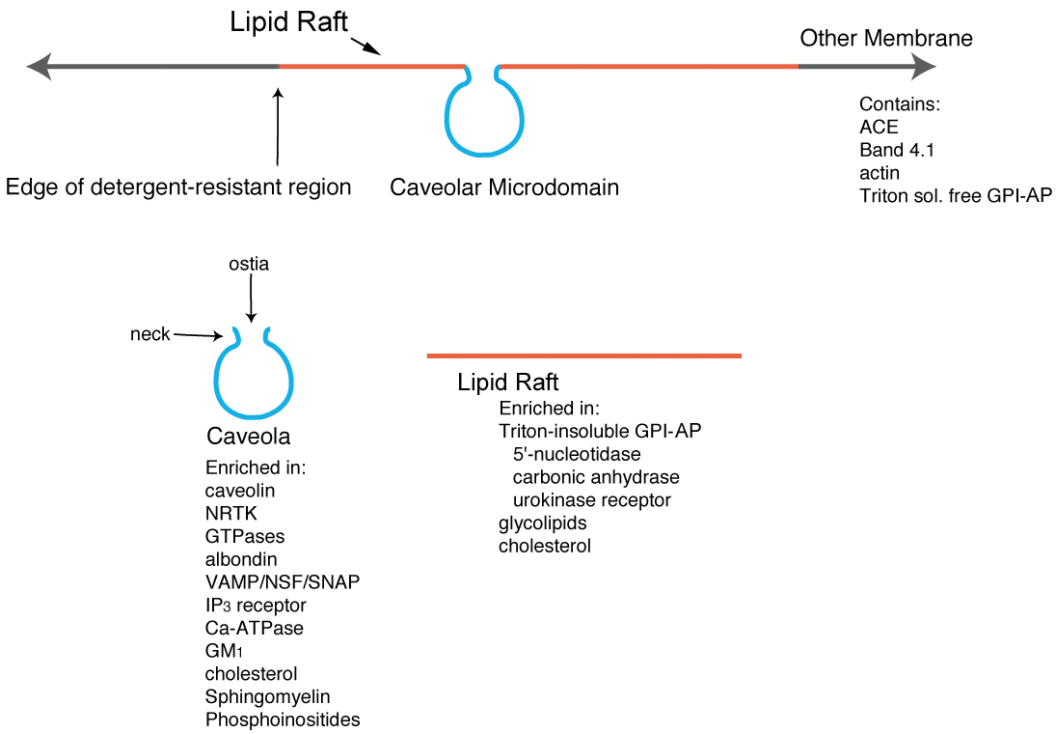

FIGURE 1 Microdomain structure of the plasma membrane. The plasma membrane contains various low-density microdomains, predominantly caveolae and lipid rafts rich in GPI-AP, that exist as distinct regions of the cell surface. Although caveolae and lipid rafts exhibit similar buoyant densities and detergent resistance, they each contain a distinct protein expression profile that differs from each other as well as from the rest of the plasma membrane proper. NRTK, nonreceptor tyrosine kinases; ACE, angiotensin-converting enzyme; VAMP, vesicle-associated membrane protein; NSF, *N*-ethylmaleimide-sensitive fusion protein; SNAP, soluble NSF attachment protein; IP3, inositol 1,4,5-trisphosphate.

before tissue/cell homogenization and centrifugation through a density gradient to yield the silica-coated plasma membranes as a membrane pellet. Intracellular membranes or membranes of other cell types (when processing tissue) are not silica coated, float on the gradient, and are thus eliminated from the pellet. This technique provides highly purified silica-coated plasma membranes largely free of other contaminating cellular membranes. Using these membranes as a starting material, it now becomes possible to isolate a nearly homogeneous preparation of caveolae (caveolin-coated small vesicles) either by physical homogenization or by physiological induction (i.e., budding) (Oh and Schnitzer, 1999; Schnitzer *et al*., 1995b, 1996). Once free of caveolae, the remaining silica-coated plasma membranes can subsequently be used to isolate detergent-resistant, caveolin-free lipid rafts (Schnitzer *et al*., 1995b).

These new preparations have revealed distinctions between the molecular constituents of caveolae and lipid rafts. Caveolae appear concentrated in caveolin but not several GPI-AP, which instead existed in lipid rafts isolated from the same plasma membranes and devoid of caveolin (Oh and Schnitzer, 1999; Schnitzer *et al*., 1995b). In addition, each microdomain contains a unique set of signaling molecules. For example, caveolae contain growth factor receptors (e.g., platelet-derived growth factor receptor), whereas lipid rafts contain immunoglobulin E receptors, T-cell receptors (TCR), and GPI-AP (Field *et al*., 1995; Gorodinsky and Harris, 1995; Liu *et al*., 1997; Montixi *et al*., 1998; Shenoy-Scaria *et al*., 1992; Stefanova *et al*., 1991; Xavier *et al*., 1998). In cells expressing caveolin and caveolae, the heterotrimeric G protein, G_q, concentrates in caveolae but not in lipid rafts, whereas G_i and G_s tend to concentrate in lipid rafts preferentially over caveolae (Oh and Schnitzer, 2001). The apparent ability of caveolin-1 to form a complex in the plasma membrane with G_q, but not G_i or G_s, appears to trap G_q effectively in caveolae and minimize its presence in lipid rafts. In cells without caveolae, G_q partitions into lipid rafts with other G proteins. These findings, discovered by tissue/cell subfractionation, were confirmed by immunofluorescence microscopy.

This article describes several protocols based primarily on a series of past studies (Brown and Rose, 1992; Oh and Schnitzer, 1999; Schnitzer *et al*., 1995b; Smart *et al*., 1995) using silica methodology to isolate first plasma membranes from tissue and cultured cells prior to further subfractionation to isolate their caveolae separately from lipid rafts rich in GPI-AP.

II. MATERIALS AND INSTRUMENTATION

A. Materials

Sodium chloride (Cat. No. BP358), potassium chloride (Cat. No. BP366), magnesium sulfate (Cat. No. BP213), glucose (Cat. No. BP350), EDTA disodium salt (Cat. No. BP120), sodium bicarbonate (Cat. No. BP328), sucrose (Cat. No. BP220), magnesium chloride (Cat. No. BP214), Tris (Cat. No. BP152), methanol (Cat. No. A412), hydrochloric acid (Cat. No. A144), sodium hydroxide (Cat. No. SS255), sodium carbonate (Cat. No. BP357), 2-mercaptoethanol (Cat. No. BP176), Tricine (Cat. No. BP315), Tween 20 (Cat. No. BP337), silver nitrate (Cat. No. S181), glacial acetic acid (Cat. No. A38), sodium phosphate dibasic (Cat. No. BP332), potassium phosphate monobasic (Cat. No. BP362), potassium phosphate dibasic (Cat. No. BP363), Tygon tubing (Cat. No. 14-169-1B), razor blades (Cat. No. 12-640), and 15-ml centrifuge tubes (Cat. No. 05-539-5) are from Fisher. HEPES (Cat. No. 737 151) and Pefabloc SC (Cat. No. 1 585 916) are from Roche Applied Science. 2-(*N*-Morpholine)ethanesulfonic acid (MES) (Cat. No. M2933), leupeptin (Cat. No. L 2884), *O*-phenanthroline (Cat. No. P9375), pepstatin A (Cat. No. P 4265), sodium nitroprusside (Cat. No. S 0501), E-64 (*trans*-epoxysuccinyl-L-leucylamido-[4-guanidino] butane) (Cat. No. E 3132), glycerol (Cat. No. G 5516), potassium acetate (Cat. No. p 3542), magnesium acetate (Cat. No. M 0631), and EGTA (Cat. No. E 4378) and from Sigma. Percoll (Cat. No. 17-0891-01) is from Amersham Biosciences. Protease inhibitor Cocktail I (2004) is from EMD Biosciences (Cat. No. 539131) Ten percent Triton X-100 (Cat. No. 28314) is from Pierce. Goat antimouse IgG–HRP conjugate (Cat. No. NA931) and goat antirabbit IgG–HRP conjugate (Cat. No. NA934) are from Amersham. Goat antimouse IgG–bodipy conjugate (Cat. No. B-2752), goat antimouse IgG–Texas red conjugate (Cat. No. T-862), goat antirabbit IgG–bodipy conjugate (Cat. No. B-2766), and goat antirabbit IgG–Texas red conjugate (Cat. No. T-2767) are from Molecular Probes. Polyacrylic acid (PAA) (Cat. No. 00627) is from Polysciences Inc. Nycodenz (Cat. No. AN-7050/BLK) is from Accurate Chemicals. Sprague Dawley rats (male) are from Charles River. SW28 tubes (Cat. No. 344058) and SW55 tubes (Cat. No. 344057) are from Beckman. Ketamine is from Fort Dodge Animal Health and xylazine is from Vedco Inc. Nitex filters 53 μm (Cat. No. 3-50/31) and 30 μm (Cat. No. 3-30/18) are from Sefar America Inc. Type "AA" homogenizer (Cat. No. 3431-E10), type "BB" homogenizer (Cat. No. 3431-E20), and type "C" homogenizer (Cat. No. 3431-E25) are from Thomas Scientific. Silk suture (3-0) is from Ethicon. Aluminum tubing (Cat. No. 89-78K101) is from McMaster-Carr. The three-way stopcock (Cat. No. 732-8103) is from Bio-Rad.

B. Instrumentation

Ultracentrifugation is carried out in a Beckman L8-80, Sorvall Pro 80, or Optima MaxE ultracentrifuge. Other centrifugation is carried out in a Brinkman Eppendorf 5415C or IEC Centra MP4R.

C. Perfusion Apparatus

On a ring stand, attach five 60-cc syringes attached to a series of five three-way stopcocks by way of Tygon tubing (0.0625 in. i.d.). The series of three-way stopcocks are attached to Tygon tubing with an stainless steel loop (0.046 in. i.d.) inserted in the middle of the tubing. The stainless-steel loop is used to regulate the temperature of the solutions perfused into the rat vasculature by emersion in temperature-controlled water. The pressure of flow is measured by a sphygmomanometer attached to the 60-cc syringes by Tygon tubing and a single hole rubber stopper. The flow for perfusion is normally 8 mm of Hg. The flow rate at 25°C is approximately 5 ml/min and at 10°C is 4 ml/min.

III. PROCEDURES

Unless otherwise specified in the protocol, all procedures should be performed at 4°C and all solutions must be kept and used ice cold.

Solutions

Buffer PM: 0.25 M sucrose, 1 m*M* EDTA, 20 m*M* Tricine in ddH_2O pH to 7.8 with NaOH (filter through 0.45-μm bottle top filter (can be stored at 4°C). For 500 ml: 42.79 g sucrose, 0.186 g EDTA (disodium salt), and 1.79 g Tricine.

Colloidal silica solution: From a 30% positively charged colloidal silica stock solution, dilute to 1% with MBS pH 6.0 [pH to 6.0 with NaOH if necessary and filter through 0.45-μm bottle top filter (can be

stored at 4°C]. For 300 ml: 10 ml stock silica in 490 ml MBS, pH 6.0, with pH strips (usually you do not have to adjust pH).

Cytosolic buffer: 25 m*M* potassium chloride, 2.5 m*M* magnesium acetate, 5 m*M* EGTA, 150 m*M* potassium acetate, 25 m*M* HEPES in ddH_2O pH to 7.4 with KOH and filter through 0.45-µm bottle top filter (can be stored at 4°C). For 500 ml: 0.93 g KCl, 0.27 g $Mg(C_2H_3O_2)_2 \cdot 4H_2O$, 0.95 g $C_{14}H_{24}N_2O_{10}$, 7.36 g $KC_2H_2O_2$, and 2.98 g HEPES.

250 mM HEPES, pH 7.4: 29.8 g in 450 ml ddH_2O, pH to 7.4 with NaOH, bring to 500 ml with ddH_2O

1M KCl: 7.46 g in 100 ml ddH_2O

20 mM KCl: 200 µl 1 *M* KCl, bring to 10 ml with ddH_2O

Mammalian Ringer's solution (without calcium): 114 m*M* sodium chloride, 4.5 m*M* potassium chloride, 1 m*M* magnesium sulfate, 11 m*M* glucose, 1.0 m*M* sodium phosphate (dibasic), 25 m*M* sodium bicarbonate in ddH_2O pH to 7.4 with HCl (filter through 0.45-µm bottle top filter (can be stored at 4°C). For 2 liters: 13.32 g NaCl, 0.67 g KCl, 0.492 g $MgSO_4 \cdot 7H_2O$, 3.96 g glucose, 0.28 g Na_2HPO_4, and 4.20 g $NaHCO_3$.

MES buffered saline (MBS): 20 m*M* MES, 135 m*M* NaCl in ddH_2O pH to 6.0 with NaOH [filter through 0.45-µm bottle top filter (can be stored at 4°C]. For 2 liters: 7.8 g MES and 14.6 g NaCl.

80% Nycodenz: 8 ml 100% Nycodenz, 200 µl 1 *M* KCl bring to 10 ml with ddH_2O

75% Nycodenz: 7.5 ml 100% Nycodenz, 200 µl 1 *M* KCl bring to 10 ml with ddH_2O

70% Nycodenz: 7 ml 100% Nycodenz, 200 µl 1 *M* KCl bring to 10 ml with ddH_2O

65% Nycodenz: 6.5 ml 100% Nycodenz, 200 µl 1 *M* KCl bring to 10 ml with ddH_2O

60% Nycodenz: 6 ml 100% Nycodenz, 200 µl 1 *M* KCl bring to 10 ml with ddH_2O

100% Nycodenz (v/w): 100 g Nycodenz in 100 ml of ddH_2O

70% Nycodenz/sucrose/HEPES: 7 ml 100% Nycodenz, 1 ml 60% sucrose, 1 ml 250 m*M* HEPES, pH 7.4, 200 µl 1 *M* KCl bring to 10 ml with ddH_2O

65% Nycodenz/sucrose/HEPES: 6.5 ml 100% Nycodenz, 1 ml 60% sucrose, 1 ml 250 m*M* HEPES, pH 7.4, 200 µl 1 *M* KCl bring to 10 ml with ddH_2O

60% Nycodenz/sucrose/HEPES: 6 ml 100% Nycodenz, 1 ml 60% sucrose, 1 ml 250 m*M* HEPES, pH 7.4, 200 µl 1 *M* KCl bring to 10 ml with ddH_2O

55% Nycodenz/sucrose/HEPES: 5.5 ml 100% Nycodenz, 1 ml 60% sucrose, 1 ml 250 m*M* HEPES, pH 7.4, 200 µl 1 *M* KCl bring to 10 ml with ddH_2O

30% Percoll in buffer PM: Mix 30 ml of stock Percoll with 70 ml of buffer PM

Phosphate-buffered saline (PBS): 137 m*M* sodium chloride, 2.7 m*M* potassium chloride, 4.3 m*M* sodium phosphate (dibasic), 1.4 m*M* potassium phosphate (monobasic) in ddH_2O pH to 7.4. For 1 liter: 8 g sodium chloride, 0.2 g potassium chloride, 0.61 g sodium phosphate (dibasic), 0.2 g potassium phosphate (monobasic).

Polyacrylic acid: From 25% stock solution, dilute to 0.1% with MBS, pH 6.0 [pH to 6.0 with NaOH and filter through 0.45-µm bottle top filter (can be stored at 4°C)]. For 500 ml: 2 ml stock 25% polyacrylic acid in 480 ml MBS, pH 6.0, pH to 6.0 and bring to 500 ml with MBS pH 6.0.

Potassium phosphate/polyacrylic acid: 4 M potassium phosphate (dibasic) 2% PAA in ddH_2O pH to 11 with NaOH. For 10 ml: 6.96 g potassium phosphate (dibasic) and 0.8 ml 25% stock polyacrylic acid.

60% sucrose (w/w): 385.95 g sucrose in 200 ml ddH_2O, add 10 ml 1 *M* KCl, after the sucrose has dissolve, bring to 50 ml with ddH_2O

Sucrose/HEPES: 250 m*M* sucrose, 25 m*M* HEPES, 20 m*M* potassium chloride in ddH_2O pH to 7.4 with NaOH and filter through 0.45-µm bottle top filter (can be stored at 4°C). For 2 liters: 171.16 g sucrose, 11.92 g HEPES and 2.98 g KCl.

60% sucrose (w/w)/20 mM KCl: 385.95 g sucrose in 200 ml ddH_2O, add 10 ml 1 *M* KCl, after the sucrose has dissolve, bring to 50 ml with ddH_2O

35% sucrose (w/w)/20 mM KCl: 5.2 ml 60% sucrose, 200 µl 1 *M* KCl, bring to 10 ml with ddH_2O

30% sucrose (w/w)/20 mM KCl: 4.4 ml 60% sucrose, 200 µl 1 *M* KCl, bring to 10 ml with ddH_2O

25% sucrose (w/w)/20 mM KCl: 3.8 ml 60% sucrose, 200 µl 1 *M* KCl, bring to 10 ml with ddH_2O

20% sucrose (w/w)/20 mM KCl: 2.8 ml 60% sucrose, 200 µl 1 *M* KCl, bring to 10 ml with ddH_2O

15% sucrose (w/w)/20 mM KCl: 2.1 ml 60% sucrose, 200 µl 1 *M* KCl, bring to 10 ml with ddH_2O

10% sucrose (w/w)/20 mM KCl: 1.3 ml 60% sucrose, 200 µl 1 *M* KCl, bring to 10 ml with ddH_2O

5% sucrose (w/w)/20 mM KCl: 0.7 ml 60% sucrose, 200 µl 1 *M* KCl, bring to 10 ml with ddH_2O

10% Triton X-100 *in PBS*

A. Purification of Silica-Coated Plasma Membranes (P)

1. Perfusion Procedure

1. Anesthetize rats with a cocktail of ketamine (60 mg/kg) and xylazine (1.6 mg/kg). Perform a tracheotomy to ventilate the lungs using a respirator.
2. Insert tubing from the perfusion apparatus into the pulmonary artery via the right ventricle and fasten

by tying a 3-0 silk suture around the artery. Cut the left atrium to allow the flow to exit.
3. Perfuse (4 ml/min) with Ringer's for 5 min starting at room temperature. After 1–1.5 min, begin lowering the temperature to ~10°C by placing the stainless-steel loop into an ice-cold bath. Gently drip ice-cold PBS over the lung to prevent drying. The remainder of the procedure should be performed at this cool temperature.
4. Perfuse MBS for 1.5 min.
5. Perfuse 1% colloidal silica solution for 1.5 min. At this point, keep the lungs inflated by replacing the tube attached to the respirator with a syringe and inflate with 3–5 ml of air.
6. Flush with MBS for 1.5 min.
7. Perfuse 0.1% PAA for 1.5 min.
8. Flush lungs with 8 ml of sucrose/HEPES with protease inhibitor Cocktail I (1×).
9. Excise lungs from the animal and keep cold by immersion in ice-cold sucrose/HEPES with protease inhibitor Cocktail I (1×).

2. Processing of the Lung

1. Finely mince the excised lung mince with a "new" razor blade on a cold aluminum block embedded in ice.
2. Add 20 ml of sucrose/HEPES with protease inhibitors and place into a type "C" homogenizer vessel.
3. Homogenize for 12 strokes at 1800 rpm in a cold (4°C) room.

3. Purification of Silica-Coated Luminal Endothelial Cell Plasma Membrane (P)

1. Filter the homogenate through a 53-µm Nytex filter, followed by a 30-µm Nytex filter.
2. Remove 200 µl from the filter solution, label "homogenate," and store at –20°C. Adjust the volume of the remaining solution to 20 ml with cold sucrose/HEPES with protease inhibitors.
3. Add an equal volume of 100% Nycodenz and mix (this is enough for two SW28 tubes). Layer onto a 70–55% continuous Nycodenz sucrose/HEPES gradient (form by placing 3 ml of 70, 65, 60, and 55 Nycodenz sucrose/HEPES and carefully swirling the solution, holding the tube at a 45° angle about 5–10 times).
4. Top with sucrose/HEPES with protease inhibitors. Spin at 15,000 rpm for 30 min at 4°C in a SW28 rotor. Aspirate off the supernatant. Resuspend the pellet in 1 ml MBS. Add equal volume of 100% Nycodenz and mix.
5. Layer onto a 80–60% continuous Nycodenz gradient (form by placing 350 µl of 80, 75, 70, 65, and 60% Nycodenz and twirling tube about 5–10 times). Top with 20 m*M* KCl. Spin at 30,000 rpm for 30 min at 4°C in a SW55 rotor. Aspirate and discard the supernatant. Resuspend the pellet in 1 ml MBS and label as "P." Store at –20°C.

4. Isolation of Silica-Coated Plasma Membranes from Cultured Cells (Monolayer)

This protocol is written for T75 flasks; alter proportionately for larger or smaller flasks. All parts of the procedure need to be performed on ice or in a 4°C room.

1. Wash cell monolayer three times with MBS.
2. Overlay with 1% ice-cold colloidal silica solution and incubate for 10 min. Wash cell monolayer three times with MBS.
3. Overlay with 0.1% PAA and incubate for 10 min. Wash cell monolayer three times with MBS.
4. Add 5 ml of sucrose/HEPES with protease inhibitors (1×). Scrape cells and place in 15-ml centrifuge tube. Centrifuge 1000 *g* for 5 min at 4°C.
5. Bring to 1 ml with cold sucrose/HEPES with protease inhibitors (1×) (you can use up to six T75 flasks per 1 ml of cold sucrose/HEPES with protease inhibitors).
6. Place in type "AA" homogenizer vessel. Homogenize with corresponding grinder for 20 strokes at 1800 rpm.
7. Remove 100 µl and label as "homogenate" and store at –20°C.
8. Add an equal volume of 100% Nycodenz and mix (SW55 tube). Layer onto a 70–55% continuous Nycodenz sucrose/HEPES gradient (form by placing 350 µl of 70, 65, 60, and 55% Nycodenz sucrose/HEPES and carefully twirling tube as described earlier).
9. Top with sucrose/HEPES with protease inhibitors. Spin at 30,000 rpm for 30 min at 4°C in a SW55 rotor. Aspirate off the supernatant. Resuspend the pellet in 1 ml MBS and label as "P." Store P at –20°C.

B. Isolation of Caveolae (V)

1. Isolation of Caveolae (V) (in the Presence of Detergent)

1. Take 900 µl "P" (as per step 5 of Section III,A,3 or step 6 of Section III,A,4), add 100 µl 10% Triton X-100, and mix. Save 100 µl "P." Mix on nutator for 10 min at 4°C. Place in type "AA" homogenizer vessel.

Homogenize with corresponding grinder for 20 strokes at 1800 rpm.

2. Bring to 40% sucrose (w/w) with 60% sucrose (w/w)/20 m*M* KCl (takes about 1.5 ml). Layer with discontinuous 35–0% sucrose (w/w)/20 m*M* KCl gradient (350 µl of 35, 30, 25, 20, 15, 10, and 5% sucrose/20 m*M* KCl and 20 m*M* KCl).

3. Spin at 50,000 rpm for 4 h at 4°C in a MLS-50 rotor.

4. Collect the band between 10 and 15% sucrose (w/w) density. Dilute the band material two to three times with MBS and spin at 15,000 rpm for 2 h at 4°C. Resuspend pellet in 100 µl MBS, pH 6.0, and label as "V."

5. Collect and resuspend membrane pellet from step 3 in 1 ml MBS and label as "P-V."

6. Store both fractions at –20°C.

2. Isolation of V′ (Detergent Free)

1. Process as in Section III,B,1 except omit the addition of Triton X-100 and homogenize for 60 strokes. Label floated caveolae as "V′" (V prime).
2. Collect and resuspend membrane pellet from step 3 in Section III,A,4 and label as "P-V.′"
3. Store V′ and P-V′ at –20°C.

C. Isolation of Budded Caveolae (V_b) (Caveolae Isolation without Physical Disruption)

1. Isolation of Rat Lung Cytosol

1. Perfuse rat lung as described in Section III,A using steps 1, 2, 3, 8, and 9 only.
2. Homogenize lung in cytosolic buffer (2–3×, v/w) for 10 strokes at 1800 rpm.
3. Spin at 35,000 rpm for 1 h at 4°C in a SW55 rotor. Place supernatant over PD-10 column and collect first peak. Aliquot (1 ml), label at "rat lung cytosol," and store at –80°C.

2. Isolation of "V_b"

1. Incubate "P" or "PM" (PM described later) (20–50 µg/ml) with rat lung cytosol (1–5 mg/ml) for 1 h at 37°C.
2. Bring to 40% sucrose (w/w) with 60% sucrose (w/w)/20 m*M* KCl solution. Layer with discontinuous 35–0% sucrose 20 m*M* KCl gradient (as described in Section III,B; 350 µl each layer).
3. Spin at 30,000 rpm overnight at 4°C in a SW55 rotor. Collect the band between 10 and 15% sucrose (w/w) density. Dilute the band material two to three times with MBS and spin at 15,000 rpm for 2 h at 4°C. Resuspend pellet in 100 µl MBS and label as "V_b."
4. Collect and resuspend membrane pellet from step 2 in 1 ml MBS and label as "P-V_b." Store at –20°C.

D. Isolation of Lipid Rafts (LR)

Isolation of LR

1. Resuspend membrane pellet (P-V) from Section III,B in 1 ml of ice-cold MBS, pH 6.0. Add equal volume of potassium phosphate/polyacrylic acid (pH should be greater than 9.5). Mix well.
2. Sonicate at maximum output for 10 bursts of 10 s each. Cool on ice between bursts. Mix using nutator at room temperature for 8 h and then sonicate as described earlier except use 5- to 10-s bursts.
3. Add Triton X-100 to a final concentration of 1%. Mix on nutator for 10 min at 4°C and then place in a type "AA" homogenizer vessel.
4. Homogenize with corresponding grinder for 30 strokes at 1800 rpm. Bring to 40% sucrose (w/w) using 60% sucrose (w/w)/20 m*M* KCl and layer with discontinuous 35–0% sucrose (w/w) with 20 m*M* KCl using 350 µl solution per layer as described Section III,A.
5. Centrifuge at 30,000 rpm overnight at 4°C in a SW55 rotor.
6. Collect band between 10 and 15% sucrose (w/w) density. Dilute the band material two to three times with MBS and centrifuge at 15,000 rpm for 2 h at 4°C. Resuspend pellet in MBS, label as "LR," and store at –20°C.
7. Collect the stripped membrane pellet from step 5 and resuspend in MBS. Label as "SP" and store at –20°C.

E. Isolation of Plasma Membrane-Enriched Fraction (PM)

Isolation of PM from Tissue

1. Perfuse rat lung as described in Section III,A using steps 1, 2, 3, 8, and 9 only.

2. Process rat lung as described in Section III,A except use 3 ml of buffer PM and type "BB" homogenizer vessel for step 2.

3. Filter the homogenate through a 53-µm Nytex filter and then through a 30-µM Nytex filter.

4. Remove 200 µl from the filter solution, label as "homogenate," and store at –20°C. Centrifuge the remaining supernatant at 1000 *g* for 10 min at 4°C. Save supernatant on ice. Resuspend the pellet in 3 ml buffer PM and repeat centrifugation. Pool the two supernatants.

5. Adjust the volume to 7 ml with buffer PM and then add 3 ml to make a 30% Percoll solution. Centrifuge at 84,000 *g* for 45 min at 4°C (no brakes) in MLS50 rotor. Collect the band around two-thirds to three-fourths from bottom of the tube. Dilute the band material two to three times with PBS and centrifuge at 15,000 rpm for 2 h at 4°C. Resuspend pellet in 100 µl PBS, label as "PM," and store at –20°C.

Isolation of PM from Cultured Cells

This protocol is written for T75 flasks, alter proportionately for larger or smaller flasks. All parts of the procedure need to be performed on ice or in a 4°C room.

1. Wash cell monolayer three times with cold buffer PM.
2. Add 5 ml of cold buffer PM with protease inhibitors (1×). Scrape cells and place in 15-ml centrifuge tube. Centrifuge at 1000 *g* for 5 min at 4°C.
3. Bring to 1 ml with cold buffer PM with protease inhibitors (1×) (you can use up to six T75 flasks per 1 ml of cold buffer PM with protease inhibitors).
4. Place in type "AA" homogenizer vessel. Homogenize with corresponding grinder for 20 strokes at 1800 rpm.
5. Remove 100 µl, label as "homogenate," and store at –20°C.
6. Centrifuge the remaining supernatant at 1000 *g* for 10 min at 4°C. Save supernatant on ice. Resuspend the pellet in 1 ml buffer PM and repeat centrifugation. Pool the two supernatants.
7. Adjust the volume to 3.5 ml with buffer PM and then add 1.5 ml to make a 30% Percoll solution. Centrifuge at 84,000 *g* for 45 min at 4°C (no brakes) in MLS50 rotor. Collect the band around two-thirds to three-fourths from bottom of the tube. Dilute the band material two to three times with PBS and centrifuge at 15,000 rpm for 2 h at 4°C. Resuspend pellet in 100 µl PBS, label as "PM," and store at –20°C.

F. Isolation of Triton-Resistant Membranes (TRM)

Isolation of TRM from Tissue

1. Perfuse rat lung as described in Section III,A using steps 1, 2, 3, 8, and 9 only.
2. Process rat lung as described in Section III,A except add 1% Triton X-100 to sucrose/HEPES solution in step 2.
3. Filter the homogenate through a 53-µM Nytex filter and then through a 30-µM Nytex filter.
4. Remove 200 µl from the filter solution, label as "homogenate," and store at –20°C. Bring the remaining supernatant to 40% sucrose (w/w)/20 m*M* KCl. Layer with discontinuous 35–0% sucrose (w/w)/20 m*M* KCl gradient (3 ml each of 35, 30, 25, 20, 15, 10, and 5% sucrose (w/w)/20 m*M* KCl and 20 m*M* KCl as described in Section III,B).
5. Centrifuge at 15,000 rpm overnight at 4°C in SW28 rotor. Collect the band between 10 and 15% sucrose (w/w) density. Dilute the band material two to three times with PBS and centrifuge at 15,000 rpm for 2 h at 4°C. Resuspend pellet in PBS, label as "TRM," and store at –20°C.

Isolation of TRM from Cells

This protocol is written for T75 flasks; alter proportionately for larger or smaller flasks. All parts of the procedure need to be performed on ice or in a 4°C room.

1. Wash cells three times with 1X PBS.
2. Scrape cells and place in 15-ml conical tube. Centrifuge at 1000 *g* for 5 min at 4°C.
3. Resuspend pellet in 1 ml of 1X PBS. Remove 100 µl, label this cellular homogenate as "H," and store at –20°C.
4. To the remaining H add Triton X-100 to 1% (100 µl of 10% Triton X-100) for a total volume of 1 ml.
5. Place in type "AA" homogenizer vessel. Homogenize with corresponding grinder for 20 strokes at 1800 rpm.
6. Bring to 40% sucrose (w/w)/20 m*M* KCl and layer with discontinuous 35–0% sucrose (w/w)/20 m*M* KCl and centrifuge as described in Section III,B.
7. Collect the band between 10 and 15% sucrose (w/w) density. Dilute the band material two to three with PBS and centrifuge at 15,000 rpm for 2 h at 4°C. Resuspend pellet in PBS, label as "TRM," and store at –20°C.

Isolation of TRM from PM

1. Isolate PM as described in Section III,E.
2. Bring pelleted PM to 1 ml with buffer PM.
3. Remove 100 µl, label as "PM," and store at –20°C.
4. To the remaining PM add Triton X-100 to 1% (100 µl of 10% Triton X-100) with a total volume of 1 ml. Mix on nutator for 10 min at 4°C.
5. Bring to 40% sucrose (w/w)/20 m*M* KCl, layer with discontinuous 35–0% sucrose (w/w)/20 m*M* KCl, and centrifuge as described in Section III,B.
6. Collect the band between 10 and 15% sucrose (w/w) density. Dilute the band material two to

three times with PBS and centrifuge at 15,000 rpm for 2 h at 4°C. Resuspend pellet in PBS, label as "TRM," and store at –20°C.

IV. POTENTIAL PITFALLS

1. When utilizing cellular membrane subfractions, a rigorous quality control protocol must be applied. It is very important that one first check the purity of the starting material to confirm that the preparation is enriched in markers of the desired membrane material and depleted in markers of other membrane-bound cellular organelles. At the very least, preparations should be checked for markers of the major microdomain components of the plasma membrane, such as caveolae, lipid rafts, adhesion complexes, and the plasma membrane proper, as well as for contaminating intracellular organellar membranes. A good plasma membrane preparation should be enriched 15- to 20-fold in cell surface marker proteins, such as caveolin-1, GPI-AP, integrins, and ion transporters. It should also be depleted by 15- to 20-fold in protein markers expressed in nuclei (ran, transportin), Golgi (p58, β-COP), lysosomes (lamp1), and mitochondria (cytochrome c). Likewise, caveolar preparations must be enriched in caveolar proteins, such as caveolin-1, Gq, and eNOS. LR should be enriched in GPI-AP but lack caveolin-1 expression. In addition, it is also very important to monitor the mass balance of all proteins. For plasma membrane preparations isolated by the silica method, this can be accomplished by examining by Western analysis the proteins left behind in the P-V fraction (containing LR and remaining plasmalemma proper) and comparing them to the protein expression in the P and V fractions to verify that the signal for all three fractions can be accounted for by the fractionation.

2. It is very important to maintain the recommended temperatures as presented in these protocols, especially when working with Triton X-100 solubilization. Any increases in temperature may solubilize a greater number of proteins, which may alter the final protein profile.

3. One needs to use the correct pH for the solutions, especially those associated with cationic silica particles, as alterations in pH will affect the binding of the silica to the luminal plasma membrane.

4. All solutions must be filtered with at least a 0.45-μm filter to ensure that they remain relatively free of contaminants and aggregates.

5. Do not mix phosphate solutions with solutions containing colloidal silica, as this will cause the silica to precipitate.

6. When perfusing rat organs, be careful to avoid getting air bubbles in the line of the perfusion apparatus, as this will interfere with the vessel lumen-coating procedure and decrease the amount of isolated material.

V. DISCUSSION

The overall goal of these procedures is to excise microdomains specifically from cellular membranes, in this case, from plasma membranes. To isolate any microdomain from a membrane, certain critical criteria are necessary to increase efficiency and purity. First, the microdomain excision must be highly selective. In most cases, however, this cannot be accomplished in one step. One must start with the appropriate highly purified membrane fraction containing the desired microdomain and then process this material to specifically excise and, if necessary, differentially isolate the desired microdomain away from other similarly excised domains.

If detergent-resistant microdomains were unique to the plasma membrane, then contamination with other organellar membranes would be rendered irrelevant. However, that seems quite unlikely given that newly synthesized GPI-AP also acquire resistance to detergent extraction upon entering the *trans*-Golgi compartment; in fact, TRM were first isolated from cultured MDCK cells as a tool for studying this maturation process (Brown and Rose, 1992). Hence, it is clearly advantageous to start with purified plasma membranes when trying to purify caveolae or other cell surface microdomains. The silica-coating method described here permits one to first isolate plasma membranes to high purity before further subfractionation to purify caveolae separately from other plasmalemmal microdomains (**Fig. 2**). To isolate the luminal endothelial cell plasma membrane directly from tissue, the tissue is first perfused with polycationic colloidal silica particles that selectively coat this luminal surface to increase the membrane density. Then, after electrostatic cross-linking and cation quenching, the tissue is homogenized and subjected to a series of centrifugations to sediment the higher density silica-coated membranes away from the other tissue components that are not silica coated and have much lower densities. Electron microscopy shows large silica-coated membrane sheets in these pellets.

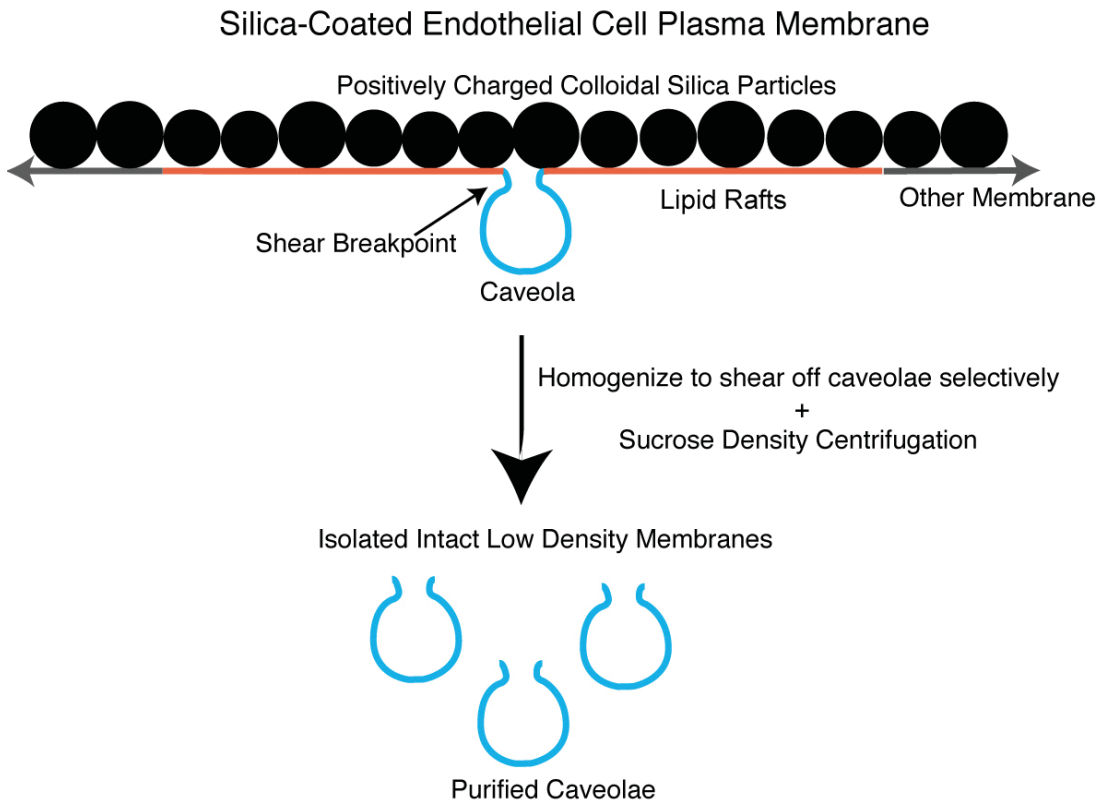

FIGURE 2 Two-step silica coating-based methodology for isolating plasma membrane caveolae. To purify endothelial plasmalemmal caveolae, the luminal endothelial cell membrane is first coated with positively charged colloidal silica particles to create a stable pellicle that specifically marks this membrane and facilitates its purification by density centrifugation of tissue homogenates. These pelleted membranes have many caveolae attached on the side of the membranes opposite to the silica coating that may be stripped from the endothelial membranes by shearing during homogenization at 4°C in the presence of Triton X-100. Further centrifugation through a sucrose density gradient yields a homogeneous population of distinct caveolar vesicles.

This procedure can also be performed on cultured cells (Schnitzer and Oh, 1996), even as a cell monolayer where the top membrane surface opposite to the plastic can be coated and purified. Using this method, the plasma membranes are enriched to levels exceeding standard subcellular fractionation techniques (e.g., Percoll) (Oh and Schnitzer, 1999) with minimal contamination from marker proteins of various intracellular organelles (nuclei, endoplasmic reticulum, Golgi, and mitochondria), as well as nonendothelial cells in the tissue (**Fig. 3B**; compare PM to P) (Schnitzer *et al*., 1995b) that are commonly present in other published preparations (Chang *et al*., 1994; Lisanti *et al*., 1994; Oh and Schnitzer, 1999; Smart *et al*., 1995).

Plasma membranes contain at least two types of microdomains, caveolae and lipid rafts, that although distinct in protein and possible lipid composition, share certain biochemical properties that often confound attempts at generating highly enriched isolates. Complicating matters further is the fact that caveolae and lipid rafts may be found on the cell surface not only as discrete entities, but also closely associated with each other, in some cases, with lipid rafts in close enough proximity to caveolae that they are essentially attached to a caveola at the annulus (**Fig. 1**) (Schnitzer *et al*., 1995b). Consequently, caveolae isolation methods that use as a starting material Triton-resistant membrane fractions (TRM) (either fractionated from whole cells or tissue) or Percoll gradient-isolated plasma membranes (PM) cannot distinguish between these very similar and sometimes associated membrane microdomains, resulting in a preparation that contains a mixture of caveolae, lipid rafts, and lipid rafts associated with caveolae (**Fig. 4**). When these preparations are examined by EM, they are revealed to contain individual caveolar vesicles in addition to

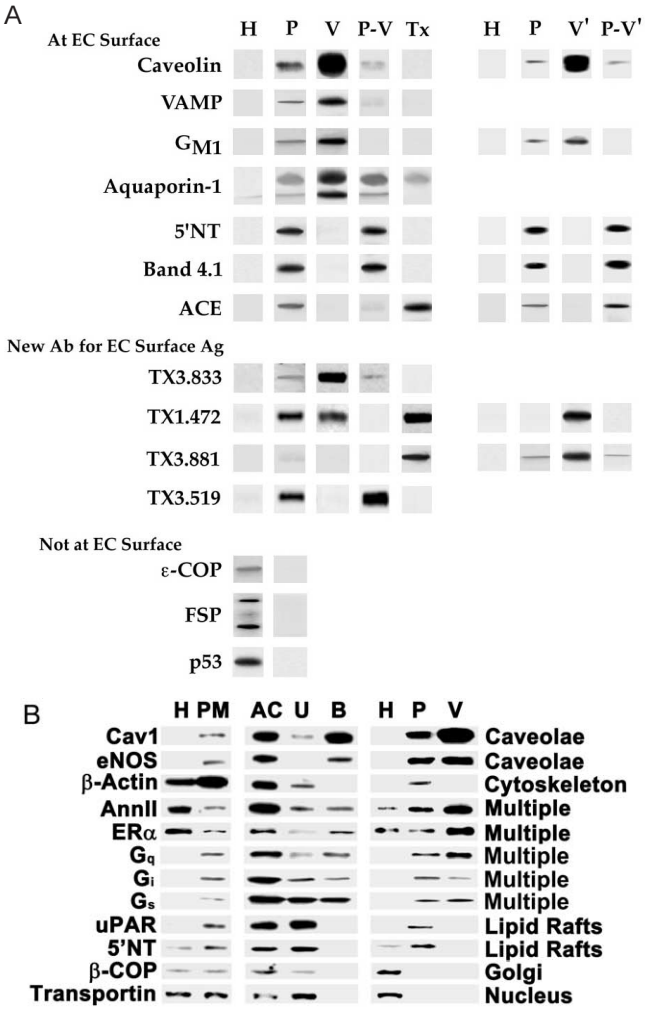

FIGURE 3 Molecular mapping of luminal plasma membrane subfractions. Proteins (5μg) from the indicated membrane fractions were subjected to SDS–PAGE followed by electrotransfer to filters for immunoblotting with antibodies to the indicated proteins. H, homogenate; P, silica-coated plasma membrane; PM, percoll-gradient isolated plasma membranes; V, caveolae [V (in the presence of Triton), V′ (in the absence of Triton)], P-V, silica-coated plasma membrane stripped of caveolae [P-V (in the presence of Triton), P-V′ (in the absence of Triton)]; Tx, Triton-soluble phase; AC, Optiprep-isolated, caveolin-enriched membranes; U, material not bound to caveolin antibody-coupled magnetic beads after immunoisolation; B, material bound to caveolin antibody-coupled magnetic beads after immunoisolation.

larger vesiculated lipid rafts (**Fig. 5A**) and even intact large vesicular lipid rafts with a caveolae attached (**Fig. 5B,C**) (Schnitzer *et al.*, 1995b). The attached caveola are usually found inside the larger vesicle, but can also be seen in an "inside-out" orientation outside the vesicle. Immunogold EM showed that the larger vesicles but not the attached caveolae could be labeled with gold-conjugated antibodies recognizing the GPI-AP carbonic anhydrase, indicating that these larger vesicles contain lipid rafts. Moreover, these preparations contain other detergent-resistant domains from other subcellular organelles and even the plasma membrane (**Fig. 3**) (Lisanti *et al.*, 1994; Oh and Schnitzer, 1999; Schnitzer *et al.*, 1995b). For instance, nuclear and Golgi marker proteins, such as transportin and β-COP, respectively, contaminate these preparations (Razandi *et al.*, 2002). Although caveolin-1 is an excellent marker for labeling caveolae selectively on the cell surface, it can also be present amply in exocytic vesicles of the trans-Golgi network. In cultured cells, such as Madin–Darby canine kidney cells, fibroblasts, or endothelial cells, it can even be found primarily in the Golgi. In addition, the membranes treated with cold Triton X-100 will also contain protein complexes resistant to detergent solubilization. For example, it is well known that plasma membrane proteins tethered to the cytoskeleton have increased resistance to detergent solubilization as do possibly other similar complexes, including focal adhesion sites and intercellular junctional complexes. Other detergent-resistant protein complexes may also float if they retain sufficient lipids. Even in cells that lack both caveolae and caveolin, TRM can readily be isolated as rich in GPI-AP. The TRM from cells with and without caveolae have very similar buoyant densities. It is apparent that the physical characteristic of vesicle buoyant density is unable to discriminate and thereby separate caveolae from LR, which clearly explains their coisolation in TRM, as well as other more recently developed detergent-free procedures (Smart *et al.*, 1995). Thus, isolation of detergent-resistant membrane microdomains yields a heterogeneous fraction consisting of a mixture of caveolar and noncaveolar components.

Caveolae can be isolated to near homogeneity using as a starting material plasma membranes prepared using the novel silica-coating procedure that bypasses the problems associated with other techniques. Examination of silica-coated plasma membranes by EM reveals that the positively charged colloidal silica particles form a strongly adherent layer over flat, noninvaginated portions of the cell surface plasma membrane (**Fig. 2**) and do not enter the caveolae, which appear amply present on the side of the endothelial cell membrane not coated with silica (**Fig. 6A**) (Oh and Schnitzer, 1998; Schnitzer *et al.*, 1995a,b). This coating serves to stabilize the flat plasma membrane, including the lipid raft domains, so that the caveolae can be selectively detached from the plasma membrane mechanically by homogenization, leaving behind the plasma membrane proper (including lipid rafts) still attached to the silica particles. The buoyant caveolae can then be floated away from the high-

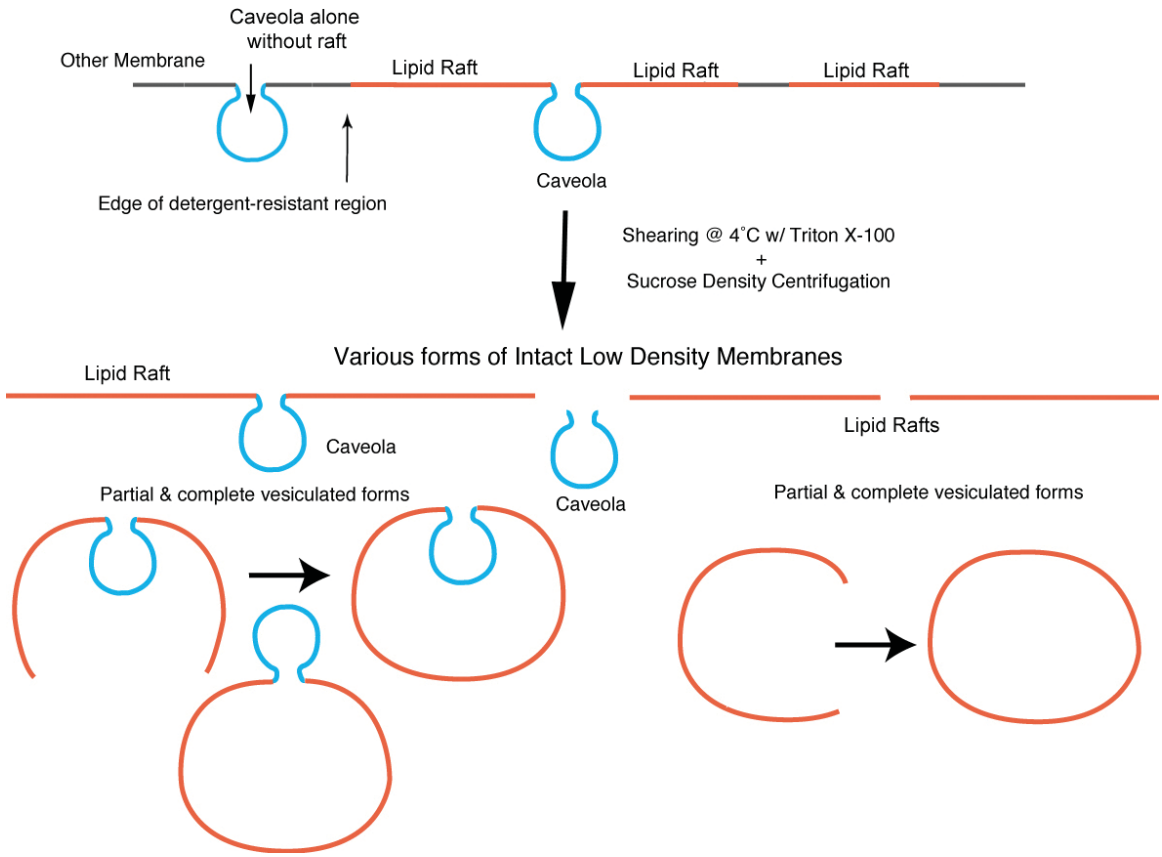

FIGURE 4 Isolation of detergent-resistant membranes without silica-coating procedure yields TRMs containing both caveolae and lipid rafts. Nonsilica-based methodologies that isolate detergent-resistant membranes by sucrose density centrifugation result in a heterogeneous preparation containing a mixture of low-density microdomains as sheets or as partial or fully vesiculated forms.

density lipid raft/silica membrane pellicle by sucrose gradient centrifugation. More than 95% of the caveolae on the silica-coated plasma membranes are removed and isolated in this manner as a rather uniform homogeneous population of distinct flask-shaped vesicles of approximately 80 nm in diameter (**Fig. 6B**) (Schnitzer *et al.*, 1995b). Biochemical analysis shows that the isolated caveolae represent specific microdomains of the cell surface with their own unique molecular topography (Schnitzer *et al.*, 1995a,b,c). They are enriched in seven caveolar markers established by immunogold EM: caveolin, Ca^{2+}-ATPase, the glycolipid GM_1, VAMP, eNOS, dynamin, and the IP_3 receptor (McIntosh and Schnitzer, 1999; Oh *et al.*, 1998; Rizzo *et al.*, 1998; Schnitzer *et al.*, 1995b,c). In contrast, 5′NT, Band 4.1, and β-actin are markedly depleted or absent from the caveolae, despite being amply present in the silica-coated plasma membrane starting material. More recent work in the laboratory has utilized these membranes successfully to generate and characterize monoclonal antibodies specific for the caveolae, as assessed by both subfractionation and immunomicroscopic analyses (McIntosh *et al.*, 2002). **Fig. 3A** shows representative immunoblots for various proteins of interest, including some of the markers discussed earlier and some of our new monoclonal antibodies.

As a test to confirm the hypothesized key role of silica coating in the isolation of caveolae separately from lipid rafts, we have performed the caveolar isolation on silica-isolated plasma membranes after removing the silica coating under high salt conditions (**Fig. 7**). The resulting caveolae preparation closely resembled the TRM fractions isolated without silica coating. GPI-linked proteins not normally associated with the highly purified V caveolar fraction, such as 5′-NT, were found in this isolate (data not shown). Furthermore, electron microscopy revealed that specimens, which appeared biochemically unpure by this criterion, contained caveolae mixed with larger vesicular structures very similar to those seen in **Fig. 5**. Thus, the uniform silica coating at the cell surface does indeed stabilize the plasma membrane by being firmly attached on one side of the membrane to most,

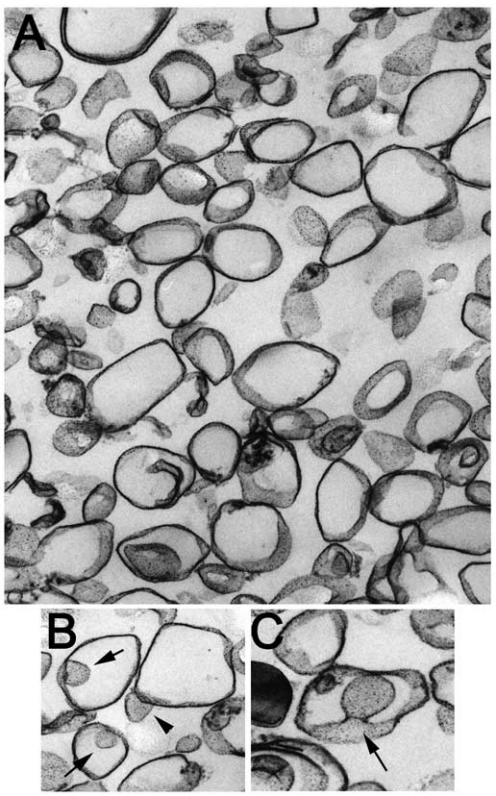

FIGURE 5 **Electron microscopy of nonsilica-isolated detergent-resistant membranes (TRMs)**. (**A**) Membranes isolated without silica consist of larger vesicles (150–700 nm diameter) interspersed with smaller caveolar vesicles (<100 nm) as well as nonvesiculated linear membrane sheets. (**B** and **C**) Caveolae were typically observed attached to a larger vesicle. Arrow: caveola within a larger vesicle. Arrowhead: "inside-out" caveola attached to a larger vesicle. Magnification: A,B = 10,000×; C = 20,000×.

if not all, nonvesiculated regions. The silica coat performs the essential function of preventing the interaction of the LR with various detergents, as well as the separation of noncaveolar detergent-resistant microdomains from the cell membranes during shearing to isolate caveolae. Without the silica coat, isolation of homogeneous preparations of caveolae is not possible.

In addition to allowing the isolation of highly purified preparations of caveolae, the stable attachment of silica particles to the detergent-resistant flat LR domains provides a means to isolate lipid rafts away from both caveolae and the plasmalemma proper (**Fig. 8**) (Schnitzer *et al.*, 1995b). Silica-coated membranes stripped of the caveolae are resedimented to form a membrane pellet (P-V) during the centrifugation and can be resuspended, treated with high salt to remove the silica coating, and used to isolate low-density, Triton-resistant lipid rafts by sucrose density centrifugation. **Figure 9** shows that each of our tissue subfractions has a distinct protein profile and that caveolae and LR differ considerably in this regard. Given that LR are difficult to follow biophysically, they currently require an operational definition based on their detergent resistance. With our strict definition and differentiation of caveolae and lipid rafts (see Section I), TRMs isolated from plasma membranes stripped of caveolae (P-V) should constitute lipid rafts. Because the starting preparation, i.e., silica-coated plasma membranes, appears minimally contaminated by intracellular membranes (Oh and Schnitzer, 1999; Razandi *et al.*, 2002), the resulting lipid raft preparation should be primarily, if not exclusively, from the cell surface. Of course, future experiments may provide further differentiation of detergent-resistant domains beyond just LR.

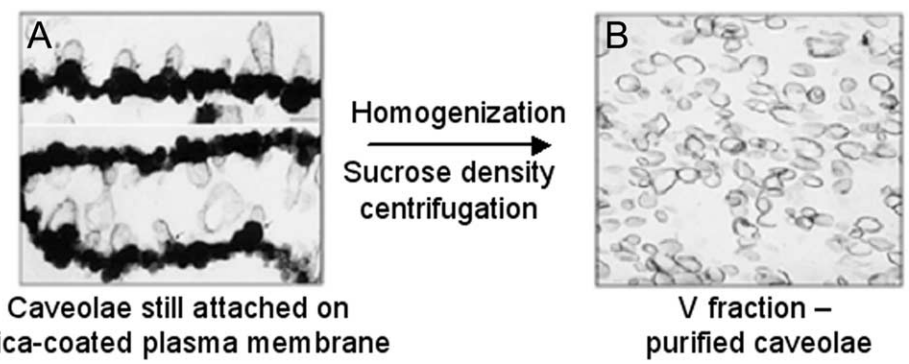

FIGURE 6 **Electron micrographs of P (A) and V (B) membrane fractions after isolation**. Electron microscopy demonstrates the presence of significant numbers of caveolae on the intracellular side of the plasma membrane not coated with silica (P fraction; A). Mechanical shearing of caveolae from the silica-coated plasma membrane yields a homogeneous population of morphologically distinct caveolae with diameters <90 nm (V fraction; B).

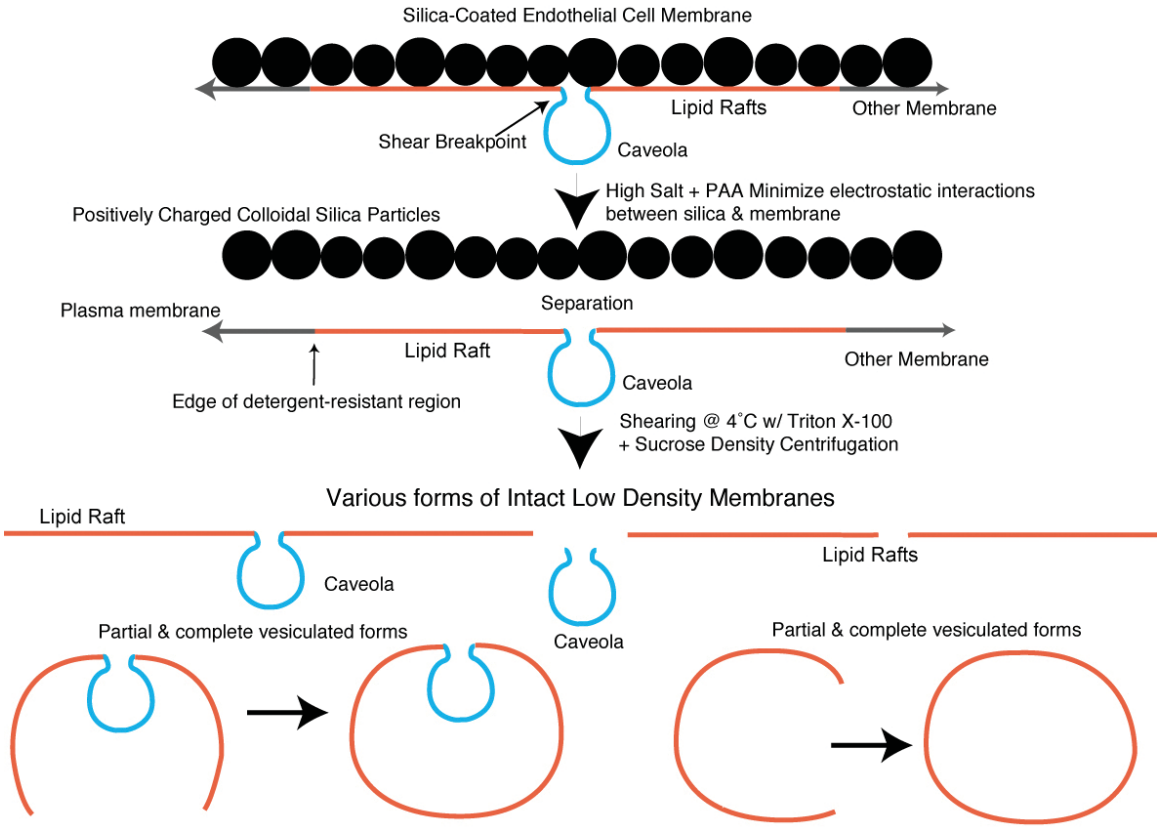

FIGURE 7 Silica coating prevents coisolation of caveolae and lipid rafts. Treatment of silica-coated plasma membranes with high salt prior to separation of caveolae by homogenization results in a heterogeneous mixture of membrane microdomains containing caveolae and lipid rafts alone or attached to each other in partial or fully vesiculated forms.

Using this methodology, we have shown that the heterotrimeric protein G_q specifically concentrates in caveolae, whereas G_s and G_i segregate preferentially to lipid rafts. These results were confirmed by dual immunofluorescence confocal microscopy to reveal that, in cultured endothelial cells, G_q but not G_i or G_s colocalized with caveolin-marked caveolae, whereas G_i and G_s, but not G_q, overlapped with folic acid receptor-marked lipid rafts (Oh and Schnitzer, 2001). In addition, we have shown that even in highly purified plasma membranes with minimal contamination from Golgi or other intracellular compartments, caveolae and GPI-anchored proteins exist distinctly at the cell surface and can actually be purified separately (Schnitzer *et al.*, 1995b). Thus, the extra dimension to the isolation process, namely the high-density silica coat, takes advantage of the distinct morphological characteristics of caveolae and lipid rafts (invaginated vs flat) and renders a new fractionation technique that is quite effective in separating two membrane microdomains of similar buoyant density.

A reconstituted cell-free system has also been developed to study further the dynamics and properties of caveolae (Schnitzer *et al.*, 1996). It shows that caveolae are dynamic structures that can be induced to bud from plasma membrane by GTP. Fission of caveolae from the plasmalemma without any physical disruption requires GTP hydrolysis and provides an alternative, and possibly more physiological, source to isolate caveolae. A comparison of GTP-induced budded caveolae with caveolae isolated via the silica-coating technique reveals that both isolates yield similar protein profiles (Schnitzer *et al.*, 1996).

Another widely used procedure leading to a similar isolate as TRM involves detergent-free sonication of plasma membranes isolated on a Percoll gradient before Optiprep gradient centrifugation to collect fractions over a wide range of densities (10–20%) (Smart *et al.*, 1995). This is then concentrated using a step gradient consisting of 5% layered over 23% to yield a caveolin-rich fraction (AC) that has been characterized as quite similar to TRM (Oh and Schnitzer, 1999). Further comparative investigation of the Optiprep-based caveolae isolate AC vs the silica-based isolate V by immunoisolation using caveolin-1 antibodies showed that ~50% vs 95%, respectively, of the material

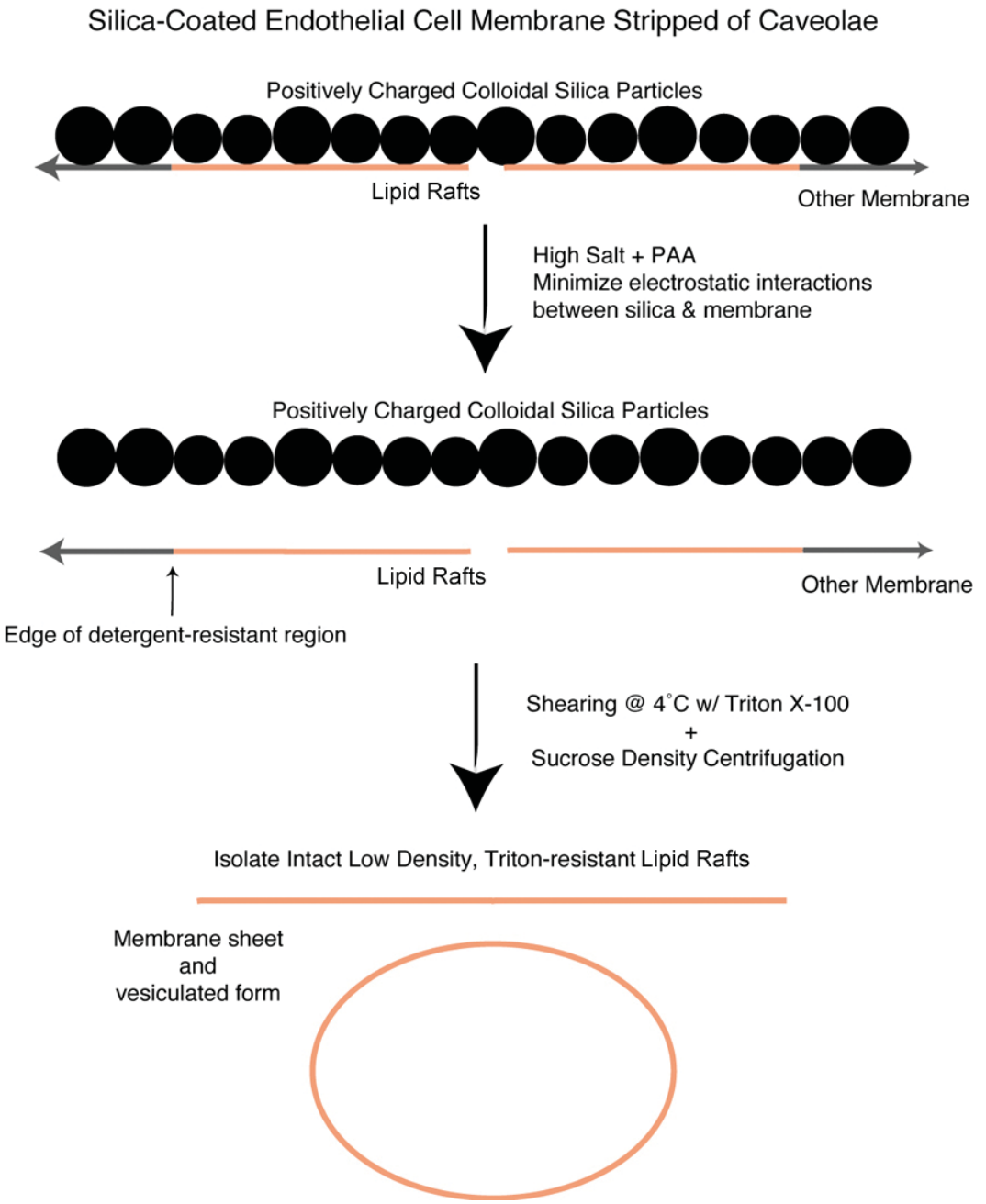

FIGURE 8 **Isolation of LR from silica-coated plasma membranes stripped of caveolae**. Because the silica coating prevents the release of detergent-resistant, GPI-anchored protein microdomains, it is possible to isolate these domains separately from caveolae. Incubation of silica-coated membranes stripped of caveolae in the presence of high salt and polyacrylic acid followed by homogenization in Triton X-100 and sucrose density centrifugation results in isolation of a membrane fraction containing membrane sheets as well as vesicles >200 nm in diameters. These membranes are enriched in GPI-AP, including 5′NT and carbonic anhydrase.

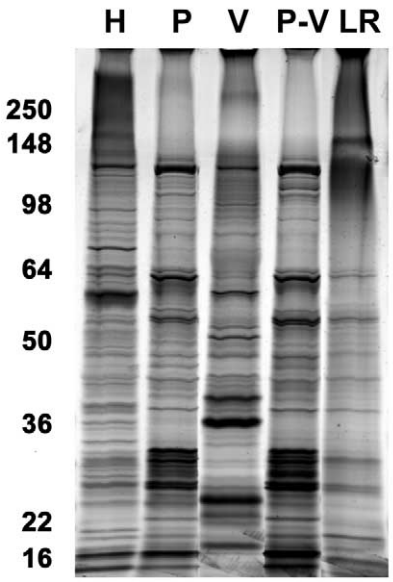

FIGURE 9 One-dimensional protein analysis of various membrane subfraction. Proteins (5μg) from the indicated membrane fractions were subjected to SDS–PAGE followed by silver staining. H, tissue homogenate; P, silica-coated plasma membrane; V, caveolae; P-V, silica-coated plasma membrane stripped of caveolae; LR, lipid rafts.

bound to the caveolin-1–antibody magnetic beads (Oh and Schnitzer, 1999). **Figure 3B** shows a comparative Western analysis for specific proteins in each fraction. AC clearly contains proteins of the cytoskeleton, lipid rafts, Golgi, and nucleus, but after immunoisolation, the protein profile is identical to that of silica-based caveolae isolate (**Fig. 3, compare fraction B to V**). Almost certainly the source of contamination in Optiprep-based caveolar isolates stems from the use of PM as a starting material. As discussed earlier, PM contains a mixture of cell membranes in addition to plasma membranes, such as Golgi, ER, nuclear, and mitochondrial, that are composed of multiple microdomains of different densities. Therefore, strategies that use flotation of membranes to isolate caveolae from this preparation naturally coisolate contaminating membrane fragments of similar low density to yield a caveolin-rich membrane fraction that also contains a significant amount of noncaveolar membranes. Immunoisolation should be used as a last step to validate more definitively the expression of a given protein in caveolae.

References

Brown, D. A., and London, E. (2000). Structure and function of sphingolipid- and cholesterol-rich membrane rafts. *J. Biol. Chem.* **275**, 17221–17224.

Brown, D. A., and Rose, J. K. (1992). Sorting of GPI-anchored proteins to glycolipid-enriched membrane subdomains during transport to the apical cell surface. *Cell* **68**, 533–544.

Chang, W. J., Ying, Y. S., Rothberg, K. G., Hooper, N. M., Turner, A. J., Gambliel, H. A., De Gunzburg, J., Mumby, S. M., Gilman, A. G., and Anderson, R. G. (1994). Purification and characterization of smooth muscle cell caveolae. *J Cell Biol.* **126**, 127–138.

Field, K. A., Holowka, D., and Baird, B. (1995). Fc epsilon RI-mediated recruitment of p53/56lyn to detergent-resistant membrane domains accompanies cellular signaling. *Proc. Natl. Acad. Sci. USA* **92**, 9201–9205.

Fra, A. M., Williamson, E., Simons, K., and Parton, R. G. (1995). De novo formation of caveolae in lymphocytes by expression of VIP21-caveolin. *Proc. Natl. Acad. Sci. USA* **92**, 8655–8659.

Fujimoto, T. (1996). GPI-anchored proteins, glycosphingolipids, and sphingomyelin are sequestered to caveolae only after crosslinking. *J. Histochem. Cytochem.* **44**, 929–941.

Gorodinsky, A., and Harris, D. A. (1995). Glycolipid-anchored proteins in neuroblastoma cells form detergent-resistant complexes without caveolin. *J. Cell Biol.* **129**, 619–627.

Lisanti, M. P., Scherer, P. E., Vidugiriene, J., Tang, Z., Hermanowski-Vosatka, A., Tu, Y. H., Cook, R. F., and Sargiacomo, M. (1994). Characterization of caveolin-rich membrane domains isolated from an endothelial-rich source: Implications for human disease. *J. Cell Biol.* **126**, 111–126.

Liu, J., Oh, P., Horner, T., Rogers, R. A., and Schnitzer, J. (1997). Organized cell surface signal transduction in caveolae distinct from GPI-anchored protein microdomains. *J. Biol. Chem.* **272**, 7211–7222.

Mayor, S., Rothberg, K. G., and Maxfield, F. R. (1994). Sequestration of GPI-anchored proteins in caveolae triggered by cross-linking. *Science* **264**, 1948–1951.

McIntosh, D. P., and Schnitzer, J. E. (1999). Caveolae require intact VAMP for targeted transport in vascular endothelium. *Am. J. Physiol.* **277**, H2222–2232.

McIntosh, D. P., Tan, X.-Y., Oh, P., and Schnitzer, J. E. (2002). Targeting endothelium and its dynamic caveolae for tissue-specific transcytosis *in vivo*: A pathway to overcome cell barriers to drug and gene delivery. *Proc. Natl. Acad. Sci. USA* **99**, 1996–2001.

Monier, S., Parton, R. G., Vogel, F., Behlke, J., Henske, A., and Kurzchalia, T. V. (1995). VIP21-caveolin, a membrane protein constituent of the caveolar coat, oligomerizes *in vivo* and *in vitro*. *Mol. Biol. Cell* **6**, 911–927.

Montixi, C., Langlet, C., Bernard, A. M., Thimonier, J., Dubois, C., Wurbel, M. A., Chauvin, J. P., Pierres, M., and He, H. T. (1998). Engagement of T cell receptor triggers its recruitment to low-density detergent-insoluble membrane domains. *EMBO J.* **17**, 5334–5348.

Oh, P., McIntosh, D. P., and Schnitzer, J. E. (1998). Dynamin at the neck of caveolae mediates their budding to form transport vesicles by GTP-driven fission from the plasma membrane of endothelium. *J. Cell Biol.* **141**, 101–114.

Oh, P., and Schnitzer, J. E. (1998). Isolation and subfractionation of plasma membranes to purify caveolae separately from glycosylphosphatidylinositol-anchored protein microdomain. *In Cell Biology: A Laboratory Handbook* (J. Celis, ed.), Vol. 2, pp. 34–36. Academic Press, Orlando.

Oh, P., and Schnitzer, J. E. (1999). Immunoisolation of caveolae with high affinity antibody binding to the oligomeric caveolin cage: Toward understanding the basis of purification [published erratum appears in *J. Biol. Chem.* **274**(41), 29582 (1999)]. *J. Biol. Chem.* **274**, 23144–23154.

Oh, P., and Schnitzer, J. E. (2001). Segregation of heterotrimeric G proteins in cell surface microdomains: Gq binds caveolin to

concentrate in caveolae whereas Gi and Gs target lipid rafts by default. *Mol. Biol. Cell* **12**, 685–698.

Razandi, M., Oh, P., Pedram, A., Schnitzer, J., and Levin, E. R. (2002). ERs associate with and regulate the production of caveolin: Implications for signaling and cellular actions. *Mol. Endocrinol.* **16**, 100–115.

Rizzo, V., McIntosh, D. P., Oh, P., and Schnitzer, J. E. (1998). In situ flow activates endothelial nitric oxide synthase in luminal caveolae of endothelium with rapid caveolin dissociation and calmodulin association. *J. Biol. Chem.* **273**, 34724–34729.

Rothberg, K. G., Ying, Y. S., Kolhouse, J. F., Kamen, B. A., and Anderson, R. G. (1990). The glycophospholipid-linked folate receptor internalizes folate without entering the clathrin-coated pit endocytic pathway. *J. Cell Biol.* **110**, 637–649.

Sargiacomo, M., Sudol, M., Tang, Z., and Lisanti, M. P. (1993). Signal transducing molecules and glycosyl-phosphatidylinositol-linked proteins form a caveolin-rich insoluble complex in MDCK cells. *J. Cell Biol.* **122**, 789–807.

Schnitzer, J. E., Liu, J., and Oh, P. (1995a). Endothelial caveolae have the molecular transport machinery for vesicle budding, docking and fusion including VAMP, NSF, SNAP, annexins and GTPases. *J. Biol. Chem.* **270**, 14399–14404.

Schnitzer, J. E., McIntosh, D. P., Dvorak, A. M., Liu, J., and Oh, P. (1995b). Separation of caveolae from associated microdomains of GPI-anchored proteins. *Science* **269**, 1435–1439.

Schnitzer, J. E., and Oh, P. (1996). Aquaporin-1 in plasma membrane and caveolae provides mercury-sensitive water channels across lung endothelium. *Am. J. Physiol.* **270**, H416–422.

Schnitzer, J. E., Oh, P., Jacobson, B. S., and Dvorak, A. M. (1995c). Caveolae from luminal plasmalemma for rat lung endothelium: Microdomains enriched in caveolin, Ca2+-ATPase and inositol trisphosphate receptor. *Proc. Natl. Acad. Sci. USA* **92**, 1759–1763.

Schnitzer, J. E., Oh, P., and McIntosh, D. P. (1996). Role of GTP hydrolysis in fission of caveolae directly from plasma membrane. *Science* **274**, 239–242.

Shenoy-Scaria, A. M., Kwong, J., Fujita, T., Olszowy, M. W., Shaw, A. S., and Lublin, D. M. (1992). Signal transduction through decay-accelerating factor: Interaction of glycosyl-phosphatidylinositol anchor and protein tyrosine kinases p56lck and p59fyn 1. *J. Immunol.* **149**, 3535–3541.

Smart, E. J., Ying, Y. S., Mineo, C., and Anderson, R. G. (1995). A detergent-free method for purifying caveolae membrane from tissue culture cells. *Proc. Natl. Acad. Sci. USA* **92**, 10104–10108.

Stefanova, I., Horejsi, V., Ansotegui, I. J., Knapp, W., and Stockinger, H. (1991). GPI-anchored cell-surface molecules complexed to protein tyrosine kinases. *Science* **254**, 1016–1019.

Xavier, R., Brennan, T., Li, Q., McCormack, C., and Seed, B. (1998). Membrane compartmentation is required for efficient T cell activation. *Immunity* **8**, 723–732.

Ying, Y. S., Anderson, R. G., and Rothberg, K. G. (1992). Each caveola contains multiple glycosyl-phosphatidylinositol-anchored membrane proteins. *Cold Spring Harb. Symp. Quant. Biol.* **57**, 593–604.

CHAPTER

3

Immunoisolation of Organelles Using Magnetic Solid Supports

Raluca Flükiger-Gagescu and Jean Gruenberg

I. INTRODUCTION

To study the molecular composition and functional properties of cellular organelles, these must first be purified. Classical *subcellular fractionation* methods are based on the physical properties of membrane-bound compartments, e.g., their density. However, many compartments have similar properties and cannot be separated from each other by such methods. *Immunoisolation*, however, allows you to affinity purify organelles using an antibody directed against a component of the compartment (Jones *et al*., 1998; Howell *et al*., 1989).

To set up an immunoisolation protocol, you first have to identify an appropriate antigen that is tightly associated with the membrane (or, even better, transmembrane) and localizes exclusively to the compartment that you wish to isolate. If the distribution of the antigen is broader, you might be able to remove unwanted organelles that contain this antigen by a prepurification step. Moreover, the antigen should be relatively abundant and its antigenic site should be well exposed on the cytoplasmic surface of the compartment.

In the absence of an ideal endogenous antigen, it is also possible to exogenously introduce a more convenient one, provided that you check thoroughly that it localizes to the correct compartment. We have transfected cells with a myc-tagged human transferrin receptor to provide a convenient marker for the *recycling endosome* (Gagescu *et al*., 2000; for a review on endocytic compartments, see Gruenberg, 2001). The myc tag allows us to use a well-characterized, high-affinity anti-myc antibody for immunoisolation, and it also provides us with an excellent means to control the specificity of the immunoisolation by carrying out all experiments in parallel with a second cell line that expresses the human transferrin receptor without the myc epitope.

Next, you need a high-affinity antibody that recognizes the native form of the chosen antigen. Because large amounts of the antibody may be needed to complete a set of experiments, it is better to use a monoclonal antibody whenever possible.

Finally, you have to choose a solid support. Of all the solid supports that we have tested, *magnetic beads* are the most convenient because of two key features: their smooth surface with low hydrophobidity ensures low nonspecific binding and they can be retrieved with a magnet, which minimizes membrane shearing when resuspending the beads.

It is possible to use either an indirect or a direct immunoisolation technique. In the first case, the antibody is bound to the organelle, and the complex is retrieved with a linker antibody that is bound to the solid support. In the second case, the antibody is first bound to a linker antibody that is bound to the solid support. The solid support with the two antibodies is then used to retrieve the organelle. Although it is slightly less convenient, the indirect immunoisolation method can, in some cases, give better results as it corresponds, to some extent, to an affinity purification of the antibody. Indeed, by incubating membranes with the antibody before adding the magnetic beads, you eliminate nonfunctional antibodies, thereby increasing the number of productive antibody–antigen interactions. Moreover, if the antigen is not well exposed, the indirect method is preferable, as it involves less steric hinderance.

Immunoisolated fractions can be analyzed by virtually any means, as the beads themselves are inert. A

Copyright 2006, Elsevier Science (USA).
All rights reserved.

small hinderance is caused by the high abundance of antibodies in the samples, which requires the use of metabolically labeled fractions to establish the general protein pattern. Most types of analysis, including Western blotting, bideminsional gel electrophoresis, lipid analysis, electron microscopy, or enzymatic assays, can be performed using standard protocols. The main limitation is that only small amounts of membranes can be isolated, so it is, for example, not possible to microsequence a protein directly from an immunoisolated fraction.

Importantly, cell-free assays can be performed with immunoisolated fractions by simply adding the reaction mix to the beads and removing it at the end of the incubation (Gruenberg and Howell, 1988). Successive steps can thus be performed more rapidly and with less damage to the membranes, as retrieval of the membranes is much simplified after each step.

II. MATERIALS AND INSTRUMENTATION

Cell scrapers (flexible rubber policemen) with a silicon rubber piece of about 2 cm, cut at a sharp angle, and attached to a metal bar can be made by your institute workshop. You need a standard low-speed cell centrifuge, Eppendorf centrifuge, and Beckman ultracentrifuges and rotors. Magnets can be purchased from Dynal Biotech (Cat. No. 120.20). A rotating wheel (e.g., Cat. No. 34526; Snijders) with a speed of about 2 rotations per minute should be used.

M450 sheep anti-mouse IgG Dynabeads (Cat. No. 110.01) and M450 goat anti-mouse IgG Dynabeads (Cat. No. 110.05) are manufactured by Dynal Biotech. It might be useful to buy Dynabeads in larger batches, as variation could occur between different lots. We find that M500 beads, which have been developed specifically for subcellular fractionation, work less well for our purposes than M450 beads, which are designed for cell isolation.

The anti-myc hybridoma cell line (Myc1-9E10.2; CRL1729) can be obtained from the American Type Culture Collection.

For the immunoisolation protocol described here, MDCK II cells were stably transfected with the pCB6 plasmid containing the human TfR with (mhTfR cells) or without (hTfR cells) a single myc tag (13 amino acids) at its cytoplasmic amino terminus. Transfection was carried out by the calcium phosphate method and was followed by selection with geneticin–sulphate (Invitrogen; Cat. No. 11811). Transfected cells should not be used for more than 8–10 passages to avoid loss of expression.

III. PROCEDURES

A. Postnuclear Supernatant

Any subcellular fractionation protocol starts with breaking the plasma membrane to release intact intracellular organelles (Howell *et al.*, 1989). This can be achieved through several methods, which are all compatible with immunoisolation. For MDCK cells, we use passage through a needle in a slightly hypotonic medium.

Steps

1. Briefly rinse the cells with ice-cold phosphate-buffered saline (PBS). Add 2.5 ml of ice-cold PBS to the dish. If MDCK cells grown on polycarbonate filters are used, add 2.5 ml of PBS to the apical side of the cells and transfer the filter to the inner side of the cool lid of the original filter support. Scrape the cells with a rubber policeman, taking care not to break them.
2. Transfer to a 15-ml Falcon tube and centrifuge at 900 rpm for 5 min.
3. Resuspend gently in 2.5 ml of HB (250 m*M* sucrose, 3 m*M* immidazole, pH 7.4) per tube and centrifuge at 2500 rpm for 10 min.
4. Add 150 µl of HB+ (HB, 1 m*M* EDTA, 1 µg/ml leupeptine, 1 µg/ml pepstatin, 1 µg/ml aprotinin, 100 µg/ml phenymethylsulfonyl fluoride) per filter and resuspend gently with a blue tip approximately eight times. Do not apply the tip to the bottom of the tube, but on the side, to minimize cell breakage while resuspending the cells. Homogenize with a 1-ml syringe and a 22-gauge needle one to three times, depending on the state of the nuclei as observed under a microscope. Nuclei should be clean of cellular material and intact (round and dark grey).
5. Dilute with 100 µl of HB+ per filter to facilitate pelleting of the nuclei and centrifuge at 2500 rpm for 10 min.
6. Preclear the postnuclear supernatant (PNS) 5 min at 13,000 rpm in an Eppendorf centrifuge.

B. Gradient Centrifugation

Before proceeding to immunoisolating the compartment of choice, a prepurification step can be useful. A simple method for partially purifying organelles is density centrifugation, e.g., on a sucrose gradient. Floatation gradients usually give purer frac-

tions, but sedimentation gradients also work well, in most cases. As our compartment of choice (the recycling endosome of MDCK cells) does not float well out of a high-density sucrose solution, we use a sedimentation gradient.

Steps

1. Form a step gradient in an SW60 ultraclear tube (Cat. No. 344062; Beckman Coulter, Inc.) by overlaying 1 ml of 20% sucrose (216.2 g/liter sucrose, 3 m*M* immidazole, pH 7.4) on top of 2.5 ml of 35% sucrose (403.0 g/liter sucrose, 3 m*M* immidazole, pH 7.4). Then add 500 µl of the precleared PNS on top of the gradient.
2. Centrifuge for 1 h at 35,000 rpm in an SW60 rotor.
3. Discard the upper band, which is often very faint. Use a 200-µl pipette to collect the lower band (usually well visible), which contains endosomes and many other membranes. Cut off about 0.5 cm of the yellow tip to avoid breaking the endosomes, which are fragile at this high sucrose density.

C. Immunoisolation

Steps

1. Preclear the antibody and the PNS for 5 min at 13,000 rpm in an Eppendorf centrifuge.
2. Add 15 µl of 9E10 culture supernatant (2 mg/ml) to 500 µl of PNS (4 mg/ml in HB+). Rotate in a cold room at 2 rpm for 45 min. Add 50 µl of 3 *M* KCl. Rotate for another 15 min.
3. Apply to a sucrose step gradient as described earlier, centrifuge, and retrieve the lower band.
4. Measure the protein concentration and use 25 µg per point for immunoisolation.
5. Use 50 µl bead slurry per point (2×10^7 beads) for the immunoisolation. Prepare the beads by washing three times with PBS/bovine serum albumin (BSA) (5 mg/ml, 0.45 µm filtered) in a 15-ml Falcon tube by centrifugation. Take the final bead pellet up in 100 µl PBS/BSA per point.
6. For each immunoisolation point, add 25 µg of membranes to an Eppendorf tube and complete to 900 µl with PBS/BSA. Keep enough endosomal fraction for Western blots (see step 3 of the protocol for sample analysis).
7. Preclear 5 min at 13,000 rpm and transfer the supernatants to new tubes.
8. Add 100 µl of bead slurry to each Eppendorf tube. Be very careful to distribute the beads equally.
9. Rotate for 2 h at 2 rpm in the cold room.
10. Retrieve the beads with a magnet. Keep the supernatants (see step 2 of the protocol for sample analysis).
11. Wash with 1 ml of PBS/BSA/0.3 *M* KCl, with 1 ml PBS/BSA, and finally with 1 ml PBS. For all washes, retrieve the beads with the magnet. Do not resuspend with a pipette as this could cause shearing of the endosomes. Instead, add the washing solution and resuspend by rotating (2 rpm) for 2 min on a wheel in the cold room. After the last wash, do not use the magnet, but pellet at 13,000 rpm. This allows one to remove the last drop of liquid so that the sample buffer is not diluted.
12. It is possible to include a carbonate wash: take up the initial bead pellet in 1 ml 0.1 *M* carbonate buffer, pH 11.0, and rotate for 15 min on the wheel. Then wash as just described.

D. Sample Analysis by Western Blotting

Steps

1. For analysis on minigels, resuspend the bead pellets in 30 µl of 1 × sample buffer. You can load the beads with the sample buffer into the wells as, unlike traces of salt or BSA, they do not perturb the migration.
2. Pellet the supernatants (unbound material) for 20 min at 200,000 *g* in a TLA100.2 rotor. Take up the pellets directly in sample buffer.
3. Dilute different amounts (e.g., 10, 25, 50%) of the starting material to 1 ml with PBS/BSA and pellet for 20 min at 200,000 *g* in a TLA100.2 rotor. Take up the pellets directly in sample buffer.
4. Load the pelleted starting material and the pelleted unbound material on the gel next to the immunoisolated fractions to calculate the yield by comparison (Fig. 1). Always include a negative control (see Section IV), as unspecific stickage may vary considerably from time to time depending on the state of

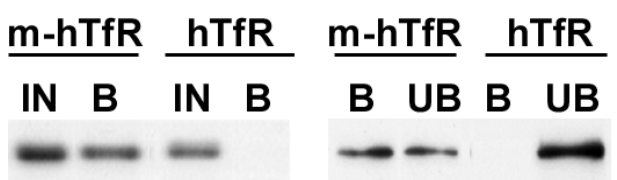

FIGURE 1 Immunoisolation of recycling endosomes. Transferrin receptor-positive endosomes were isolated as described, and fractions were analysed by Western blotting for the presence of the transferrin receptor. Yields were calculated by two means. (Left) The bound fraction (B) is compared with 50% of the starting material (IN). (Right) The bound fraction (B) is compared with the unbound fraction (UB). Both comparisons indicate a yield around 50%. In both types of analysis, a negative control is included consisting of fractions obtained in an identical manner from cells that do not contain the antigen for immunoisolation (a myc tag).

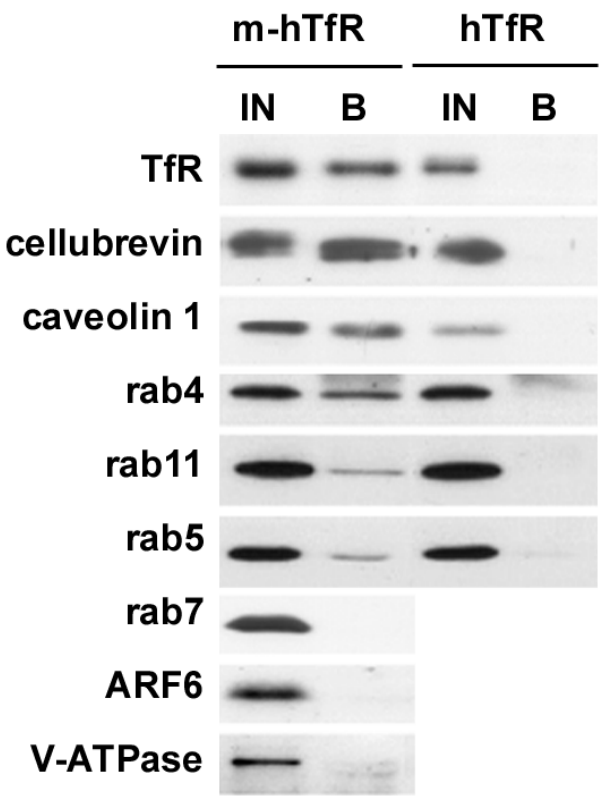

FIGURE 2 Immunoisolation of recycling endosomes. Transferrin receptor-positive endosomes were isolated as described, and fractions were analysed by Western blotting for the presence of various proteins. To estimate the yield of the immunoisolation and the degree of colocalization, bound fractions were compared with 50% of the starting material. Some markers, such as cellubrevin or caveolin 1, were isolated with similar yields as the transferrin receptor itself, indicating an excellent colocalization. Others, such as rab4, rab5, or rab11, were isolated to a lesser extent, indicating only partial colocalization. Finally, some proteins, including rab7, ARF6, and the 110-kDa subunit of the vacuolar ATPase, were absent, indicating that they do not localize to recycling endosomes.

aggregation of the starting material and on the quality of the antibody preparation.

5. Proteins that localize on the same compartment as the antigen used for immunoisolation will be isolated with a similar yield as the antigen itself, whereas proteins that only partially colocalize will be isolated with inferior yields (Fig. 2).

IV. COMMENTS

On the Importance of Negative Controls

Immunoisolation is a powerful technique for analyzing the molecular composition of organelles.

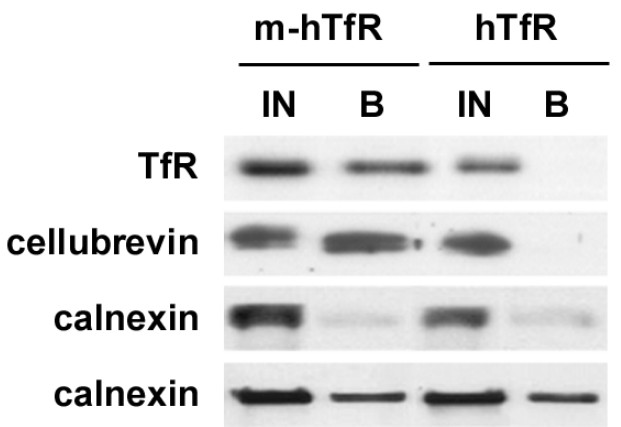

FIGURE 3 Immunoisolation of recycling endosomes. Transferrin receptor-positive endosomes were isolated as described, and fractions were analysed by Western blotting for the presence of contaminants. The ER marker calnexin is isolated with variable yields, but is always also present in the negative control (fractions from cells without the myc epitope). The transferrin receptor and cellubrevin, however, are isolated with a 50% yield in each experiment (only one experiment is shown here) and are not present in the negative control sample.

However, you can be easily misled by false positives if unspecific binding is not assessed accurately.

Whereas the components of the compartment of choice are isolated with similar yields in different experiments, contaminants are present in different proportions (Fig. 3). So to be confident that a given molecule is present in the isolated compartment, you should check that it is always isolated with similar efficiency with respect to the antigen used for immunoisolation.

In the absence of an appropriate negative control, you can use internal controls, provided that enough is known about the composition of the isolated compartment. Indeed, if several molecules that are known to be absent from the compartment are not isolated whereas several known components are isolated, you can be fairly confident that the immunoisolation is specific.

Due to its abundance in the cell, the endoplasmic reticulum is a frequent contaminant during subcellular fractionation so it may be useful to check that its known components, e.g., the transmembrane protein calnexin, are absent from your isolated fractions (Fig. 3).

As unspecific stickage varies considerably between different experiments, it is essential to always include a negative control. Frequently used negative controls consist of beads without antibodies or beads coated with irrelevant antibodies. Unfortunately, in our experience, both types of control are essentially useless. The

magnetic beads that we use never give any unspecific binding in any situation. Consequently, unspecific binding always originates from the use of suboptimal membrane or antibody preparations. Moreover, controls with irrelevant antibodies are unrepresentative, as the results are highly variable, ranging from no background stickage at all to very high stickage, depending strictly on the choice of control antibody.

We find that unspecific binding correlates best with the quality of the antibody preparation used for immunoisolation. Hence, a negative control should directly test the state of the antibody. In our experiments, this is achieved by performing all experiments in parallel with cells that express the myc-tagged human transferrin receptor and cells that express the untagged receptor. Thus, the negative control sample contains both cellular membranes and the antibody; it lacks only the 13 amino acid myc epitope.

V. PITFALLS

It is important to keep in mind that some antigen–antibody pairs just do not work for immunoisolation, either because the affinity is not high enough or because the antigen is not well exposed. If, after the first attempts, the yield is too low or the background is too high, you can try to optimize the conditions, e.g., by varying the amount of antibody, membranes, or beads. However, if you do not observe any improvement, it might be wise to simply drop this particular antigen–antibody combination and try another antibody or even another component of the compartment as the antigen for immunoisolation.

References

Gagescu, R., Demaurex, N., Parton, R. G., Hunziker, W., Huber, L. A., and Gruenberg, J. (2000). The recycling endosome of Madin-Darby canine kidney cells is a mildly acidic compartment rich in raft components. *Mol. Biol. Cell* **11**, 2775–2791.

Gruenberg, J. (2001). The endocytic pathway: A mosaic of domains. *Nature Rev. Mol. Cell Biol.* **2**, 721–730.

Gruenberg, J., and Howell, K. E. (1988). Fusion in the endocytic pathway reconstituted in a cell-free system using immunoisolated fractions. *Prog. Clin. Biol. Res.* **270**, 317–331.

Howell, K. E., Devaney, E., and Gruenberg, J. (1989). Subcellular fractionation of tissue culture cells. *Trends Biochem. Sci.* **14**, 44–47.

Howell, K. E., Schmid, R., Ugelstad, J., and Gruenberg, J. (1989). Immunoisolation using magnetic solid supports: Subcellular fractionation for cell-free functional studies. *In "Methods in Cell Biology"* (A. M. Taratakoff, ed.), pp. 265–292, Academic Press, New York.

Jones, S. M., Dahl, R. H., Ugelstad, J., and Howell, K. E. (1998). Immunoisolation of organelles using magnetic solid supports. *In "Cell Biology: A Laboratory Handbook"* (J. Celis, ed.), 2nd Ed., pp. 12–25. Academic Press, New York.

CHAPTER

4

Purification of Rat Liver Golgi Stacks

Yanzhuang Wang, Tomohiko Taguchi, and Graham Warren

I. INTRODUCTION

The study of intracellular organelles has been facilitated greatly by their purification from cellular homogenates. Such protocols yield an abundant source of material for both structural and functional studies. This article describes some simple protocols derived from several earlier methods (Leelavathi *et al*., 1970; Fleischer and Fleischer, 1970; Hino *et al*., 1978) for obtaining highly purified Golgi stacks from rat liver and for determining their relative purity over the homogenate.

II. MATERIAL AND INSTRUMENTATION

Centrifugation is carried out using an L8-70M or Optima LE-80K ultracentrifuge and either a SW-28 rotor (Cat. No. 342204) containing ultraclear tubes (Cat. No. 344058) or a SW-41 rotor (Cat. No. 331336) containing ultraclear tubes (Cat. No. 344059) from Beckman Coulter Inc. A 150-µm-mesh stainless-steel laboratory test sieve (Cat. No. 200SBW.150) and a stainless-steel receiver (Cat. No. 200BRASREC) are from Endecotts Ltd. A 0–50% Delta refractometer (Cat. No. 2–70) is from Bellingham and Stanley Ltd. Scintillation counter LS6500, spectrophotometer DU530 is from Beckman Coulter Inc.

Potassium phosphate dibasic (Cat. No. 3252), potassium phosphate (Cat. No. 3246), sucrose (Cat. No. 4072), magnesium chloride (Cat. No. 2444), concentrated hydrochloric acid (Cat. No. 9535), and dimethyl sulfoxide (DMSO, Cat. No. 9224) are from J. T. Baker. Tris (Cat. No. AB02000), SDS (Cat. No. AB01920), and β-mercaptoethanol (Cat. No. AB01340) from American Bioanalytical. The Bio-Rad protein assay (Cat. No. 500-0006) is from Bio-Rad. Manganese chloride (Cat. No. M-3634), Triton X-100 (Cat. No. T-9284), phosphotungstic acid (Cat. No. P-4006), ovomucoid (Cat. No. T-2011), ATP (Cat. No. A-7699), UDP-galactose (Cat. No. U-4500), pepstatin A (Cat. No. P-5318), and sodium cacodylate (Cat. No. C4945) are from Sigma. Complete EDTA-free tablet (protease inhibitor cocktail tablets, Cat. No. 1 873 580) is from Roche. [^{3}H]UDP-galactose with a specific activity of 30–50 Ci/mmol (Cat. No. NET758) is from NEN Research products. Ethyl alcohol (190 proof, ACS/USP grade) is from Pharmco products, Inc. Scintillation fluid (Opti-Fluor, Cat. No. 6013199) is from Packard BioScience. All reagents are of analytical grade or better. The water used is double distilled and filtered.

III. PROCEDURES

A. Purification of Rat Liver Golgi Stacks

Solutions

1. *0.5 M potassium phosphate buffer, pH 6.7:* Make up 500-ml solutions of 0.5 *M* anhydrous K_2HPO_4 (43.55 g) and 0.5 *M* anhydrous KH_2PO_4 (34.02 g). To 400 ml of the latter, gradually add the former until the pH reaches 6.7. Store at 4°C.
2. *2 M sucrose:* Dissolve 342.3 g in water prewarmed to 50°C. Make up to a final volume of 500 ml and store at 4°C.

Copyright 2006, Elsevier Science (USA).
All rights reserved.

TABLE I Buffers A–E

Buffer	A	B	C	D	E
Sucrose concentration (*M*)	0	0.25	0.5	0.86	1.3
0.5 *M* phosphate buffer, pH 6.7 (ml)	10	10	20	20	10
2 *M* sucrose (ml)	—	6.25	25	43	32.5
2 *M* $MgCl_2$	0.125	0.125	0.25	0.25	0.125
Water	39.9	33.6	54.8	36.8	7.4
Total volume (ml)	50	50	100	100	50
Sucrose % (w/w)	0	8.6	16.0	26.4	38.6
Refractive index	1.333	1.346	1.357	1.375	1.397

3. *2 M $MgCl_2$:* Dissolve 40.7 g of $MgCl_2 \cdot 6H_2O$ in water to a final volume of 100 ml. Store at room temperature.

4. *Protease inhibitors:* Directly dissolve one EDTA-free tablet in 50 ml solution and then add 50 µl pepstatin A (5 m*M* stock). To prepare the stock solution of pepstatin A, dissolve 3.43 mg of the powder in 1 ml DMSO and store at –20°C.

5. *Gradient buffers:* Make up buffers A–E from the preceding three stock solutions and cold water as shown in Table I. Fifty milliliters of each buffer A, B, and E and 100 ml of buffers C and D are needed for a medium-scale preparation. EDTA-free protease inhibitor tablet (1 tablet per 50 ml buffer) and pepstatin A (5 µM) are added to buffer C and D. We normally make 500 ml buffer C without protease inhibitors (which are expensive) for washing the liver. The water should be precooled to 4°C overnight to ensure that all the buffers are ice cold.

It is very important to be as accurate as possible when mixing various components and to check the refractive index of each buffer using a refractometer. The final refractive index should be adjusted to within ±0.5% sucrose (about 0.001 in refractive index) for buffers C and D in particular.

1. Standard Protocol (Medium-Scale Preparation)

This common protocol is used for general biochemical studies of Golgi membranes. It suffices for many electron microscopy studies as well.

Steps

1. Starve six female Sprague–Dawley rats (body weight 150–200 g) for 24 h.

2. After killing the rats with CO_2, rapidly remove the livers into large volume of ice-cold buffer C without protease inhibitors. This cools the liver and washes off the blood. Then transfer the livers into ice-cold buffer C with protease inhibitors. Mince into small pieces (approximately 4–5 mm in diameter) with a pair of scissors (Fig. 1A). Put the livers into a 50-ml Falcon tube.

3. Check the weight of livers, which is normally 40–45 g. A maximum of 50 g liver can be used for 12 gradients.

4. Homogenize the tissue by gently pressing through a 150-µm-mesh stainless-steel sieve with the bottom of a 250-ml conical flask using a rolling action (Fig. 1B). Adding a small amount of buffer C (with protease inhibitor) to the sieve will make it easier to press the liver through the mesh (Fig. 1C). Pool the homogenate (Fig. 1D) into a 50-ml Falcon tube; the final volume should be about 50 ml. Keep 200 µl on ice for enzyme assay.

5. Gradients (Fig. 2A):
   a. Place 6 ml of buffer D in each of the 12 SW-41 ultraclear tubes (size 14 × 89 mm).
   b. Overlay 4.5 ml of homogenate.
   c. Overlay 1.8 ml of buffer B and balance the tubes to within 0.01 g.

6. Centrifuge at 29,000 rpm in a SW-41 rotor for 60 min at 4°C.

7. Aspirate and discard the lipid at the top and the cytosol (colored red by hemoglobin) and collect Golgi fractions that accumulate at the 0.5/0.86 *M* interface (cloudy band) with a plastic Pasteur pipette (Fig. 2B).

8. Pool the fractions in a 50-ml Falcon tube. Typically, the total volume is about 15 ml with a refractive index of about 1.370 (0.77 *M* sucrose). Keep 200 µl on ice for enzyme assay. Adjust the Golgi sample to 0.25 *M* sucrose (refractive index 1.345) using buffer A. Make up to 50 ml with buffer B if necessary.

9. For the second gradient (Fig. 2C), put 1 ml of buffer E followed by 2 ml of buffer C into each tube and then overlay 8.0 ml of the diluted Golgi fractions.

10. Centrifuge at 8000 rpm in a SW-41 rotor for 30 min at 4°C.

11. Aspirate and discard the supernatant and collect the membranes (thin band) at the 0.5 *M*/1.3 *M*

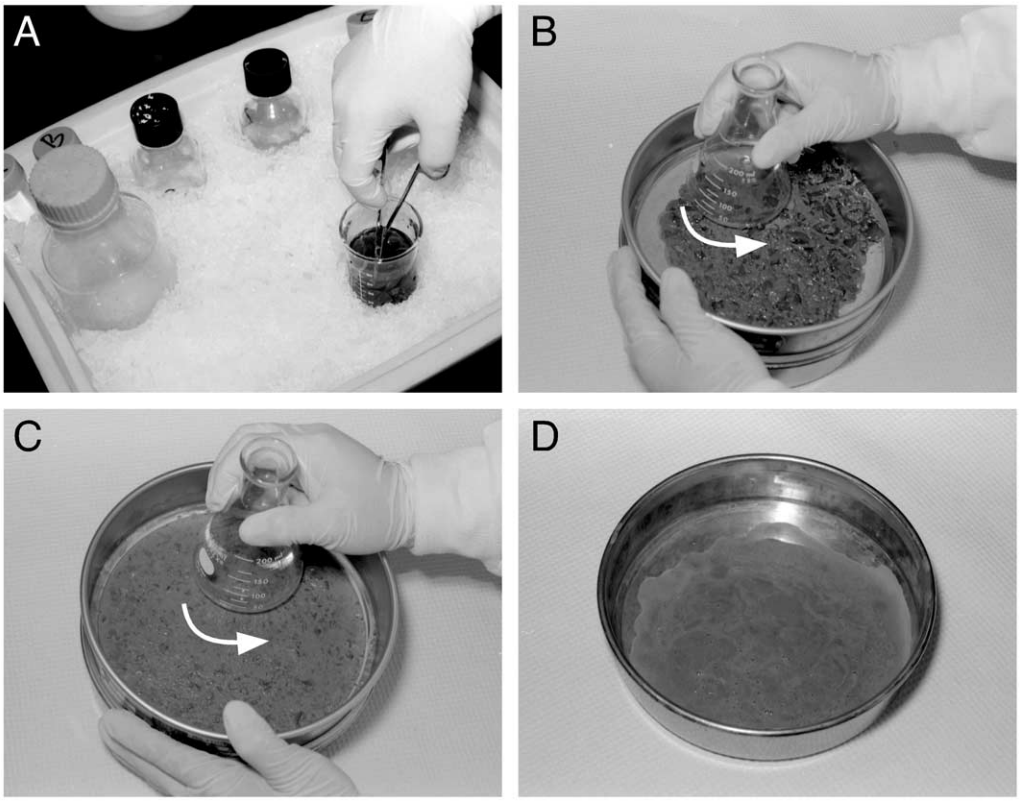

FIGURE 1 Steps in homogenizing rat liver. (A) Mince rat liver in ice-cold buffer C. (B and C) Gently press the liver through the metal mesh. (D) Homogenate in the sieve receiver.

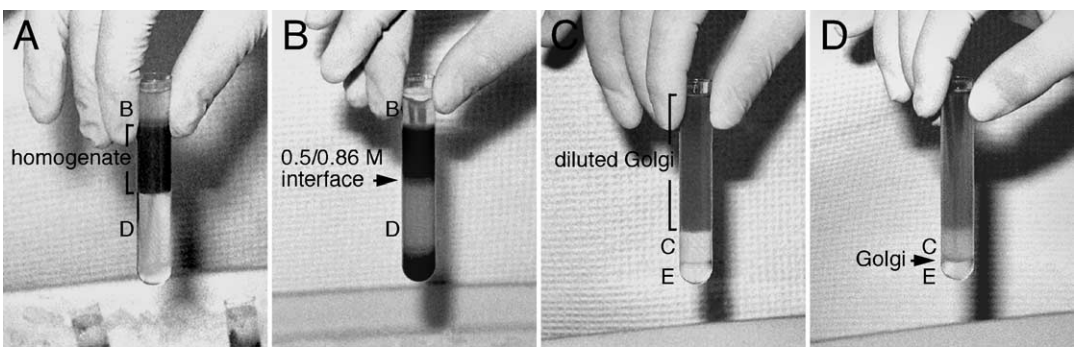

FIGURE 2 Sucrose gradients for Golgi purification from rat liver. (A) Liver homogenate was first loaded onto a 0.86*M* sucrose cushion (buffer D) and overlaid with 0.25*M* sucrose (buffer B). Letters on the left indicate sucrose buffers used to make the gradients. (B) After ultracentrifugation, Golgi stacks are enriched at the 0.5/0.86*M* interface. (C) Crude Golgi sample from the first gradient was loaded onto the second gradient. (D) After centrifugation, Golgi stacks form a thin band at the 0.5/1.3*M* interface and can be collected using a Pasteur pipette.

sucrose interface (Fig. 2D). Gently mix the Golgi membranes (about 1.5–2 ml) with 1 volume buffer A. Final volume is 3–4 ml. Check the protein concentration by the Bradford assay (Bio-Rad); typically this is 1–2 mg/ml.

12. Aliquot and freeze samples in liquid nitrogen and then store at –80°C. Samples can be thawed and frozen twice without significant loss of enzymatic activity or loss of morphology.

2. *Large-Scale Preparation*

This protocol ensures large amounts of Golgi membranes with minimal contamination by other membranes. However, stacked cisternal structures may be

less well preserved. The addition of protease inhibitors during the procedure is optional (see Section IV). Two consecutive spins at high speed are used to accommodate the large amount of homogenate used.

Steps

1. Use 8–12 female rats depending on size and requirement. Starve for 24 h. Kill the rats and ensure that all subsequent steps are performed as quickly as possible.
2. Rapidly remove the livers into 250 ml of ice-cold buffer C (without protease inhibitors) while swirling to speed cooling.
3. Weigh the livers, transfer to fresh buffer C, and mince the tissue into small pieces (about 5 mm in diameter) with a pair of scissors (Fig. 1A).
4. Homogenize the tissue by gently pressing through a 150-µm-mesh stainless-steel sieve using the base of a 250-ml conical flask (Figs. 1B and 1C). Take 100 µl of the homogenate for assay and record the total volume. The final volume for up to 100 g of liver should be about 120 ml, which is the maximum for six gradients.
5. Gradients:
   a. Place 16 ml buffer D in each of the six SW-28 ultraclear tubes.
   b. Overlay each gradient with 18–20 ml of the homogenate.
   c. Finally overlay with buffer B to top up and balance the tubes.
6. Centrifuge at 28,000 rpm in a SW-28 rotor for 60 min at 4°C.
7. Aspirate the lipid and collect Golgi fractions that accumulate at the 0.5/0.86 *M* interface between buffers C and D. About 3–4 ml should be collected from each gradient.
8. Pool the fractions and dilute to 0.5 *M* sucrose using buffer A. Check the refractive index: 0.5 *M* sucrose reads 1.357. Record the volume and keep 100 µl for enzyme assay. The total volume should be about 40 ml and should not exceed 60 ml.
9. For the second gradient, add 2 ml buffer E into SW-41 tubes and overlay 8–10 ml diluted Golgi sample. Spin at 8000 rpm for 30 min at 4°C.
10. Aspirate and discard supernatant as before. Collect membranes at the 0.5/1.3 *M* sucrose interface. Gently mix the Golgi sample (about 2.5 ml) with 1 volume buffer A. Final volume is about 5 ml. Check the protein concentration by the Bradford assay (Bio-Rad), which should typically be about 2 mg/ml.
11. Aliquot and freeze samples in liquid nitrogen and store at –80°C.

B. Determination of β-1,4-Galactosyltransferase Activity

The relative purification of the Golgi stacks can be assessed by measuring the increase in specific activity of the Golgi enzyme β-1,4-galactosyltransferase (GalT) over that of the whole liver homogenate. The enzyme assay used here is that of Bretz and Staubli (1977), which measures the addition of tritiated galactose onto the oligosaccharides of an acceptor protein, ovomucoid.

Solutions

1. *0.4 M sodium cacodylate, pH 6.6*: Dissolve 17.1 g in 150 ml of water and adjust the pH to 6.6 with HCl. Make up to 200 ml and store at room temperature.
2. *175 mg/ml ovomucoid*: Dissolve 1 g in water and make up to a final volume of 5.7 ml. Filter through a 0.45-µm nitrocellulose filter, aliquot, and store at –20°C.
3. *10 mM UDP-galactose*: Dissolve 25 mg in a final volume of 4.4 ml of water. Aliquot and store at –20°C.
4. *10% (w/v) Triton X-100*: Dissolve 10 g in 80 ml of water and make up to 100 ml. Store at 4°C.
5. *0.2 M ATP*: Dissolve 605 mg in 3 ml of water. Adjust the pH to 6.5–7.0 with 1 *M* NaOH and make up to a final volume of 5 ml with water. Aliquot and store at –20°C.
6. *2 M* $MnCl_2$: Dissolve 9.9 g of $MnCl_2 \cdot 4H_2O$ in 15 ml of water and make up to 25 ml. Store at 4°C.
7. *1% phosphotungstic acid/0.5 M HCl (PTA/HCl)*: Dissolve 5 g of phosphotungstic acid in 400 ml of water. Add 22 ml of concentrated HCl and make up to 500 ml with water. Store at 4°C.
8. *5% (w/v) SDS*: Dissolve 5 g of SDS in 80 ml of water and make up to 100 ml. Store at 4°C.
9. *2 M Tris*: Dissolve 24.2 g of Tris in 70 ml of water and make up to 100 ml. Store at room temperature.
10. *Assay mixture*: Make up a fresh batch of the assay mixture from the aforementioned stocks as follows: 200 µl sodium cacodylate, 6 µl β-mercaptoethanol, 200 µl ovomucoid, 40 µl UDP-galactose, 40 µl Triton X-100, 20 µl ATP, 40 µl $MnCl_2$, 10 µl [^{3}H]UDP-galactose, and 1040 µl of water. The concentration of UDP-galactose in the assay mixture is 0.25 m*M*.

Steps

1. Once the Golgi preparation has been completed, make 1:20 dilutions of the homogenate, intermediate, and Golgi fractions using water.

2. Add 80 µl of assay mixture (in duplicate) to screw-capped Eppendorf tubes containing 20 µl of the diluted samples or water (blanks). Vortex and incubate at 37°C for 30 min.
3. Stop the reaction by adding 1 ml of ice-cold PTA/HCl and spin at 13,000 rpm on a bench-top centrifuge for 10 s.
4. Aspirate and discard the supernatants. Add 1 ml of PTA/HCl. Resuspend the pellets by vortexing and spin as in step 3.
5. Aspirate and discard the supernatants. Add 1 ml of ice-cold 95% ethanol and resuspend the pellets as in step 4.
6. Spin as in step 3 and discard the supernatant. Resuspend the pellets in 50 µl of 2 *M* Tris followed by 200 µl of 5% SDS. Shake or vortex until dissolved.
7. Add 10 µl of assay mixture (containing 2.5 nmol of UDP-galactose), 40 µl of water, and 200 µl of 5% SDS to a fresh tube. This allows determination of the [^{3}H]UDP-galactose-specific activity in the mixture.
8. Add 1 ml of scintillation fluid to each sample. Vortex and count in a scintillation counter using the tritium channel.

C. Determination of Protein Concentration

Steps

1. While the GalT assays are incubating, make up the following dilutions of the three samples with water: 1:100 for the homogenate, 1:20 for the intermediate fraction, and 1:2 for the Golgi fraction.
2. Prepare a diluted Bio-Rad protein assay solution (fivefold dilution with water)
3. Aliquot 10 µl of each of the diluted samples in duplicate into 1-ml cuvettes using 10 µl water as a blank. Also aliquot 10 µl of 0.1, 0.2, 0.4, and 0.8 mg/ml of bovine serum albumin (BSA) for preparation of a standard curve.
4. Add 990 µl of the diluted Bio-Rad protein assay solution, mix well, and measure the absorbance at 595 nm.

D. Calculations of Purification Tables

Steps

1. Construct a protein standard curve by plotting the absorbance of each standard against the concentration of BSA. Calculate the slope (m) and the intercept at the ordinate axis (c).

$$\text{Protein concentration (mg/ml)} = \frac{(\text{sample absorbance} - c) \times \text{dilution}}{m}$$

$$\text{Total protein (mg)} = \text{Protein concentration (mg/ml)} \times \text{volume (ml)}$$

2. Calculate the specific activity (SA) of [^{3}H]UDP-galactose in the assay mixture as

$$\text{SA[}^3\text{H]UDP-galactose (dpm/nmol)} = \frac{\text{dpm of standard} - \text{blank}}{2.5\,\text{nmol}}$$

10 µl assay mixture contains 2.5 nmol of UDP-galactose (Section III,B, step 7).

3. Calculate the GalT activity in each sample as

$$\text{GalT activity concentration (nmol/h/ml)} = \frac{\text{average dpm} - \text{blank}}{\text{SA[}^3\text{H]UDP-galactose}} \times \frac{1}{0.02\,\text{ml}} \times \frac{1}{0.5\,\text{hr}} \times 20\ \text{(dilution factor)}$$

$$\text{Total GalT activity (nmol/h)} = \text{GalT activity concentration (nmol/h/ml)} \times \text{volume (ml)}$$

4. Calculate the SA of GalT by dividing its concentration by the protein concentration of the same sample to give SA in nanomoles per hour per milligram at 37°C.
5. The yields of Golgi membranes can be calculated from the ratio between the total GalT activity in the Golgi fractions and that of the homogenate.
6. The purification fold is the factor by which the SA of GalT increases in the Golgi fractions over the homogenate.

Table II was compiled using the results of 10 separate purifications, presented as the mean ± SEM for each parameter. As a consequence that the specific activity, yield and purification fold are only approximately related, arithmetically, to GalT and protein concentrations.

IV. COMMENTS

This protocol typically yields Golgi membranes that are purified 80- to 100-fold over the homogenate, as depicted in Table II. The Golgi preparations contain very little lysosomal or endoplasmic reticulum contamination as assessed by assay of β-*N*-acetylhexosaminidase (Landegren, 1984) and rotenone-insensitive NADH-cytochrome c reductase (Sottocasa *et al.*, 1967). The stacked nature of these Golgi membranes can be confirmed by examination of preparations by electron microscopy (Fig. 3). Samples

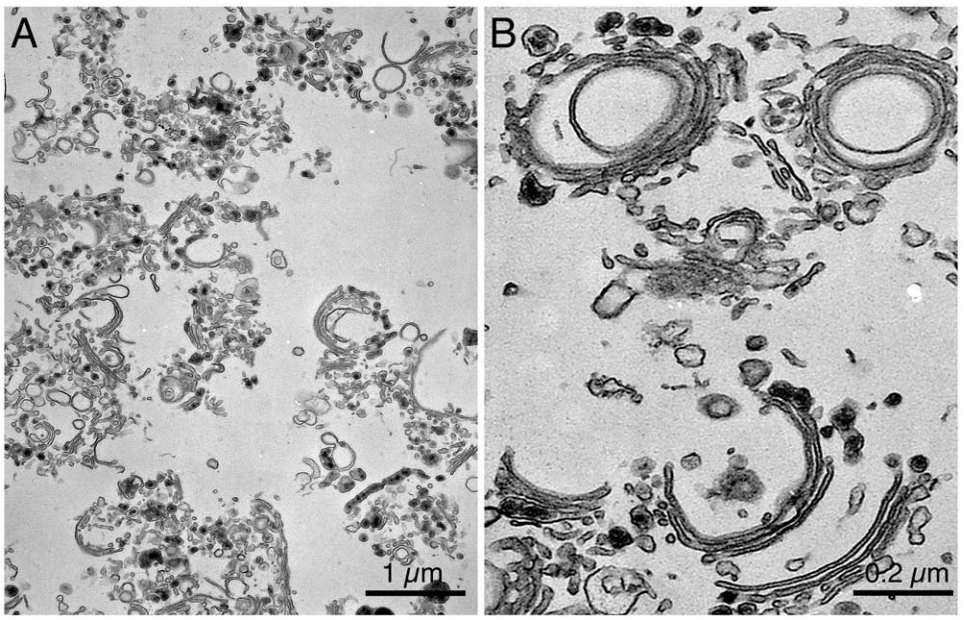

FIGURE 3 Representative micrographs of a typical rat liver Golgi preparation showing stacked membranes at low (A) and high (B) magnification. Bars: 1 μm (A) and 0.2 μm (B).

TABLE II Enrichment of the Golgi Marker β-1,4-Galactosyltransferase (GalT) over the Homogenate in Both the Intermediate Fraction (0.5/0.86 *M* Interphase) and the Golgi Preparation

Fraction	Volume (ml)	[Protein] (mg/ml)	Total GalT (nmol/h)	Specific activity (nmol/h/mg)	Yield of GalT (%)	Purification (-fold)
Homogenate	48.4 ± 2.7	103 ± 16	26,000 ± 700	5.3 ± 1.4	100.0	1.0
0.5/0.86 *M* interface	17.6 ± 2.1	12.9 ± 3.9	5350 ± 360	23.6 ± 1.6	20.2 ± 1.2	4.5 ± 0.4
Golgi	4.6 ± 0.6	1.5 ± 0.2	3560 ± 160	520 ± 22.8	13.7 ± 0.4	97.4 ± 4.2

are fixed in suspension by the method described by Pypaert *et al*. (1991).

The addition of protease inhibitors, although not essential, is recommended, especially when the Golgi protein of interest is known to be sensitive to proteases. The addition of protease inhibitors can reduce the apparent purification factor, although the reasons are not clear.

V. PITFALLS

1. As with many organelle purification procedures, it is vital to keep all solutions at 4°C during the whole protocol to prevent excessive protease digestion. If possible, steps 3–5 should be performed in a cold room. The addition of a protease inhibitors helps limit sample proteolysis.

2. All steps should be carried out as quickly as possible, and the entire procedure, from killing of the rats to freezing of the final samples, should take approximately 3–3.5 h.

3. Gradients should not be overloaded by increasing the concentration of the homogenate, as this increases the amount of mitochondrial contamination.

4. The final Golgi pellet should be white. A brown pellet indicates the presence of contaminating mitochondria. Lowering the concentration of the homogenate reduces such contamination.

5. The 150-μm sieve will become clogged with connective tissue after excessive use. This can be removed after each preparation by soaking the sieve in 4 *M* NaOH for 20–30 min followed by washing with

copious amounts of water and brushing. Prolonged soaking in 4 *M* NaOH attacks the glue used in binding the mesh to the wall of the sieves and should therefore be avoided.

Acknowledgments

The authors thank the former and current members of the Warren laboratory for contributions to the development of these methods, Henry Tan for providing the photographs in Fig. 1 and 2, and Matthew Beard for critical reading of the manuscript.

References

Bretz, R., and Staubli, W. (1997). Detergent influence on rat-liver galactosyltransferase activities towards different acceptors. *Eur. J. Biochem*. **77**, 181–192.

Fleischer, B., and Fleischer, S. (1970). Preparation and characterization of Golgi membranes from rat liver. *Biochem. Biophys. Acta* **219**, 301–319.

Hino, Y., Asano, A., Sato, R., and Shimizu, S. (1978). Biochemical studies of rat liver Golgi apparatus. I. Isolation and preliminary characterisation. *J. Biochem.* (*Tokyo*) **83**, 909–923.

Landegren, U. (1984). Measurement of cell numbers by means of the endogenous enzyme hexosaminidase: Applications to the detection of lymphokines and cell surface antigens. *J. Immunol. Methods* **67**, 379–388.

Leelavathi, D. E., Estes, L. W., Feingold, D. S., and Lombardi, B. (1970). Isolation of a Golgi-rich fraction from rat liver. *Biochim. Biophys. Acta* **211**, 124–138.

Pypaert, M., Mundy, D., Souter, E., Labbe, J.-C., and Warren, G. (1991). Mitotic cytosol inhibits invagination of coated pits in broken mitotic cells. *J. Cell Biol*. **214**, 1159–1166.

Sottocasa, G. L., Kuylenstierna, B., Ernster, L., and Bergstrand, A. (1967). An electron transport system associated with the outer membrane of liver mitochondrial. *J. Cell Biol*. **32**, 415–438.

CHAPTER

5

Isolation of Rough and Smooth Membrane Domains of the Endoplasmic Reticulum from Rat Liver

Jacques Paiement, Robin Young, Line Roy, and John J. M. Bergeron

I. INTRODUCTION

Subcellular fractionation from tissue homogenates have contributed extensively to our understanding of organelle structure and function. This article provides details of a tissue fractionation protocol evolved from several earlier methods (Paiement *et al.*, 1980; Paiement and Bergeron, 1983; Lavoie *et al.*, 1996), for the purification of rough microsomes, corresponding to derivatives of the rough endoplasmic reticulum, and for the purification of smooth microsomes, corresponding to derivatives of the smooth endoplasmic reticulum. The latter constitute a subcompartment of the transitional endoplasmic reticulum of hepatocytes (Lavoie *et al.*, 1996, 1999; Roy *et al.*, 2000).

II. MATERIALS AND INSTRUMENTATION

Sucrose solutions (0.25, 0.86, 1.0, 1.38, and 2.0 *M* solutions needed)[1]
Sucrose–Imidazole (0.25 m*M* sucrose, 3 m*M* imidazole, pH 7.4)
100-ml Beaker
Lint-free tissues (e.g., Kimwipes)
Surgical scissors
Potter–Elvehjem tissue grinder with ribbed Teflon pestle (50-ml capacity)
Nylon mesh (150 µm mesh, Thompson B & SH Co. Ltd., 8148 Devonshire, Montreal, Canada)
Glass funnel (60° funnel angle, 100 mm diameter)
100-ml graduated cylinder
Refrigerated low-speed centrifuge with fixed angle rotor (e.g., Beckman-Coulter Avanti J-20 with JA 25.50 rotor or equivalent)
Pasteur Pipettes
Loose-fitting Dounce homogenizer (7- and 15-ml capacity, with Wheaton type B piston, at least two of each)
Graduated conical tube
Parafilm
2.0-ml glass syringes with blunt-end syringe needles (10 cm long, 2 mm diameter)
Ultracentrifuge with swinging bucket and fixed-angle rotors (e.g., Beckman L-70 with SW60 and Ti50 rotors)

III. PROCEDURES

1. Rats must be fasting for 12 to 24 h prior to sacrifice.
2. Use two male rats of 300- to 400-g body weight (one liver weighs approximately 9 g).
3. Sacrifice rats via decapitation[2] and excise livers (free of connective tissue) and place in petri dish containing ice-cold 0.25 *M* sucrose.

[1] Densities of sucrose stock solutions should be checked for proper density with a refractometer.

[2] Animal sacrifice must be carried out according to the "*Guide to the Care and Use of Experimental Animals of the Canadian Council on Animal Care*" or equivalent protocol required by the country concerned.

Copyright 2006, Elsevier Science (USA).
All rights reserved.

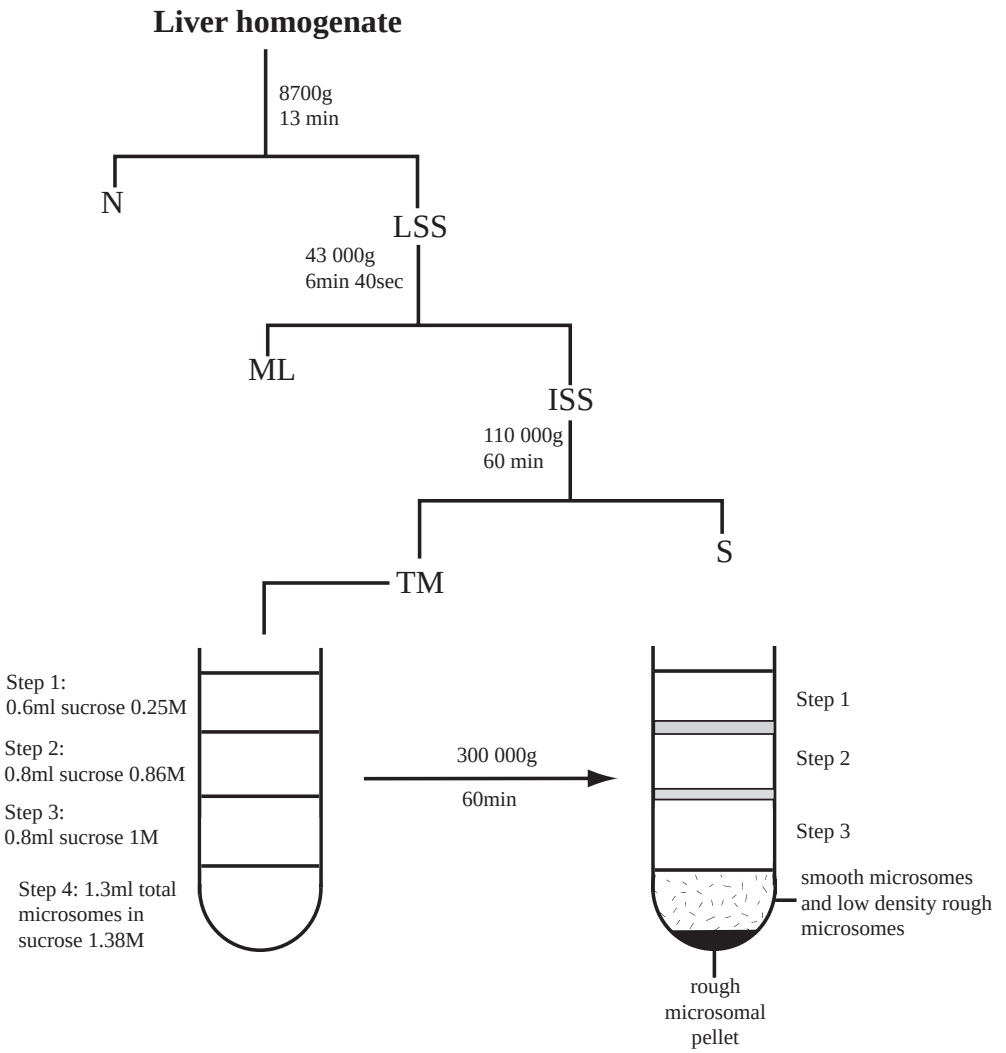

FIGURE 1

4. Blot the livers using lint-free tissues and transfer to a preweighed beaker containing ice-cold 0.25*M* sucrose and weigh (weight of two livers together should be a minimum of 18 g).

5. Blot the livers using lint-free tissues and chop them finely with scissors. Allow the pieces to fall into the mortar of the tissue grinder.[3]

6. Add a volume of ice-cold 0.25*M* sucrose, which is equivalent to 2.5 times the weight of the livers (e.g., 18.0 g × 2.5 = 45.0 ml).

7. Homogenize using the ribbed Teflon pestle for 20 strokes (down and up is one stroke) at 2850 rpm (mortar should be kept in plastic beaker filled with ice throughout homogenization process).

8. Filter the homogenate through the nylon mesh folded over four times in the glass funnel.[4]

9. The total homogenate at this point should be approximately 54 ml (45 ml sucrose plus about 9 ml liver tissue) and should be separated into 4 × 15 ml tubes.

10. Centrifuge in a Beckman-Coulter JA 25.50 fixed angle rotor that is precooled to 4°C at 8700 *g* for 13 min to sediment cellular debris and nuclei.

11. Transfer the supernatant [low-speed supernatant (LSS fraction), see Fig. 1] into three polycarbonate screw top tubes (10-ml capacity).

[3] Steps 5 to 8 are carried out in a cold room.

[4] The homogenate should not be squeezed through the nylon mesh, but instead stirred gently with a glass rod to facilitate the homogenate passing through the mesh.

12. Centrifuge in a Ti50 fixed angle rotor at 43,000 *g* for 6 min 40 s [press the stop button of the centrifuge at exactly 6 min 40 s. Complete stop (with brakes) should occur by about 10 min 20 s after the start of centrifugation].

13. With a Pasteur pipette, recover the supernatant [intermediate-speed supernatant (ISS fraction), see Fig. 1] and a portion of the flocculent layer that is covering the pellet (ML fraction, containing lysosomes and mitochondria).

14. Centrifuge the ISS fraction in a Ti50 rotor at 110,000 *g* for 60 min.

15. Discard supernatant (S fraction, see Fig. 1).

16. Resuspend the pellets in 1.38 *M* sucrose.[1] Recovery of total microsomes (TM) in the pellets is done as follows.

a. Add 0.5 ml of 2.0 *M* sucrose[1] to the first centrifuge tube and resuspend the microsomal pellet using a blunt-ended glass rod.
b. Transfer the suspension to subsequent tubes, resuspending the microsomal pellet with the glass rod in each one before transferring on to the next.
c. After resuspension is complete, rinse all centrifuge tubes with 2.0 *M* sucrose and transfer to a 7-ml Dounce.
d. Repeat rinsing as needed. However, do not exceed an accumulation of 5 ml in the Dounce.
e. Gently homogenize the resuspensions in the Dounce using the piston.

17. Measure volume using a graduated conical tube.

18. Rinse both the centrifugation tubes and the Dounce with 1 ml 2.0 *M* sucrose,[1] which is transferred to the conical tube and mixed in gently by covering the top of the tube with parafilm and inverting the tube two or three times. Repeat once.

19. Use a refractometer to adjust the density to 1.38 *M* by adding 0.25 or 2.0 *M* sucrose[1] to the TM resuspension as needed.

20. Bring the volume of the TM resuspension to 9.8 ml using the 1.38 *M* sucrose[1] stock.

21. Prepare six sucrose gradients using 4.0-ml tubes destined for the Beckman SW60 rotor as follows.

a. Carefully place 0.6 ml of 0.25 *M* sucrose[1] in the bottom of a Beckman SW60 tube with a glass syringe and blunt-ended needle.
b. Using a new syringe and needle, gently place the needle at the bottom of the tube and very gently inject 0.8 ml of 0.86 *M* sucrose[1] underneath previous layer.
c. Place a third syringe and needle carefully at the bottom of the tube and inject 0.8 ml of 1.0 *M* sucrose[1] very gently underneath the previous two layers.
d. Using a fourth new syringe and needle, very gently insert needle to the bottom of the tube again and very carefully inject 1.4 ml of TM fraction to produce the bottom layer of the gradient (see Fig. 1).
e. Repeat steps a–e for all six tubes.

22. Centrifuge gradients in a SW60 swinging-bucket rotor at 53,000 rpm (300,000 *g*) for 60 min.

23. For smooth microsomes (SM):

a. Carefully extract the top half of the bottom step (see step 4 in Fig. 1) using a Pasteur pipette and place in a Ti50 centrifuge tube.
b. Add 0.25 *M* sucrose–imidazole until tube is filled and mix gently.

24. For rough microsomes (RM):

a. Discard all gradient steps in all tubes.
b. Turn tubes upside down on a lint-free tissue for approximately 30 s to allow residual supernatant to drip out.
c. Wipe edges of tube (above pellet) using a lint-free tissue wrapped around a glass rod.
d. Resuspend pellets using a 15.0-ml Dounce and rinse tubes with sucrose–imidazole (using the same sequential rinsing method as described in Steps 16a to 16e). Transfer resuspended rough microsomes to a Ti50 tube.
e. Once sequential rinsing is done, add sucrose–imidazole to tube so that the final volume of sucrose–imidazole added is equivalent to approximately 11 ml.

25. Divide both SM and RM separately into two equal portions in Beckman Ti50 tubes and centrifuge at 140,000 *g* for 60 min.

26. Discard supernatants and resuspend as follow:

a. Resuspend the rough microsomal pellet in 2.0 ml sucrose–imidazole.
b. Resuspend the smooth microsomal pellet in 3.0 ml sucrose–imidazole.

27. Aliquot microsomal fractions into 60-, 110-, and 210-µl portions and store at –80°C in hermetically sealed tubes until needed.

IV. COMMENTS

The "rough" nature of the derivatives of the rough endoplasmic reticulum can be confirmed by examination of preparations by electron microscopy (Fig. 2). Samples were fixed in suspension and processed as

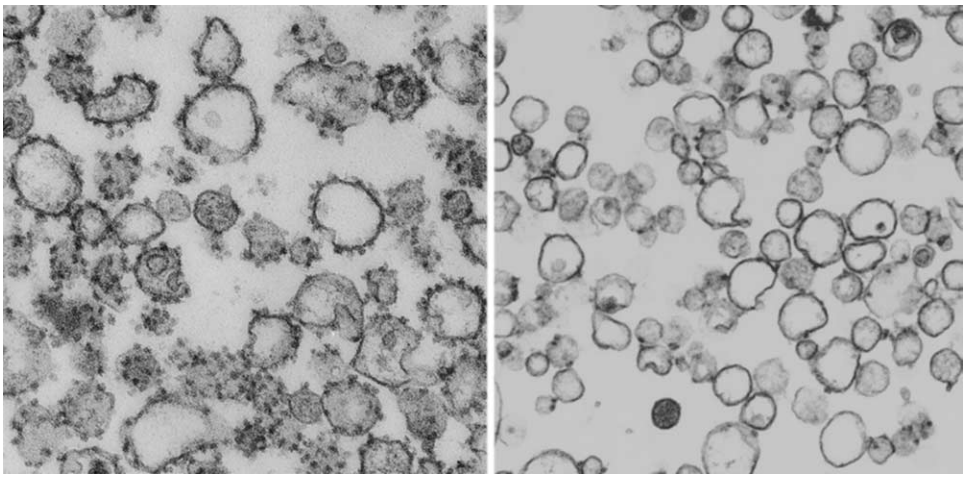

FIGURE 2

described previously (Paiement *et al*., 1980). Classical rough microsomes are shown in Fig. 2A and contain greater than 80% rough vesicles as determined by quantification of the number of vesicles with associated ribosomes. In Fig. 2B the microsomal fraction consists of approximately 60% smooth microsomal vesicles and 40% rough microsomal vesicles, which have few (one to four) ribosomes associated with their limiting membranes. Both microsomal fractions were shown previously to be enriched in enzyme markers for the endoplasmic reticulum and reduced in enzyme markers for Golgi and plasma membrane derivatives (Paiement *et al*., 1980; Paiement and Bergeron, 1983; Lavoie *et al*., 1996, 1999; Roy *et al*., 2000).

V. NOTES

This procedure takes approximately 12 h. All samples should be kept on ice at all times throughout this protocol. All centrifugations should take place at 4°C.

References

Lavoie, C., Lanoix, J., Kan, F. W. K., and Paiement, J. (1996). *J. Cell Sci.* **109**, 1415–1425.

Lavoie, C., Paiement, Dominguez, M. J., Roy, L., Dahan, S., Gushue, J. N., and Bergeron, J. J. M. (1999). *J. Cell Biol.* **146**, 285–299.

Paiement, J., and Bergeron, J. J. M. (1983). *J. Cell Biol.* **96**, 1791–1796.

Paiement, J., Beaufay, H., and Godelaine, D. (1980). *J. Cell Biol.* **86**, 29–37.

Roy, L., Bergeron, J. J. M., Lavoie, C., Hendriks, R., Gushue, J., Fazel, A., Pelletier, A., Morré, D. J., Subramaniam, V. N., Hong, W., and Paiement, J. (2000). *Mol. Biol. Cell.* **11**, 2529–2542.

CHAPTER

6

Purification of COPI Vesicles

Fredrik Kartberg, Johan Hiding and Tommy Nilsson

I. INTRODUCTION

This article describes the *in vitro* assay that was developed for the faithful formation, isolation, and characterisation of COPI-derived vesicles from highly purified rat liver Golgi membranes (Lanoix *et al*., 1999, 2001). These vesicles normally form from Golgi cisternae carrying material from cisterna to cisterna, as well as from the *cis* face of the Golgi stack to the endoplasmic reticulum. Although the exact mechanism for vesicle formation and cargo incorporation is still debated, the fundamental coat components, as well as the basic principles of vesicle formation, have been clear for some time. ADP-ribosylation factor 1 (Arf1), a small GTPase of the Ras family, is first loaded with GTP via its guanine exchange factor (GEF) at the cisternal membrane. This allows Arf1 to recruit coatomer (COPI) to the donor membrane. The functional cycling of coatomer on the Golgi membrane is thought to drive cargo incorporation into the forming vesicle, as well as membrane deformation and the subsequent budding of a COPI-coated vesicle. The hydrolysis of GTP by Arf1, stimulated by a GTPase-activating protein (GAP), is then thought to trigger vesicle uncoating, producing a transport intermediate capable of fusing with target membranes (Barlowe, 2000). By adding a nonhydrolysable analog of GTP to *in vitro* budding reactions, vesicles form but retain their coat, making them easier to isolate and analyse. The first *in vitro* COPI vesicle budding assays indeed relied on GTPγS for this purpose.

The following protocols are a modifications of the COPI-vesicle budding assay first described by Warren and co-workers (Sonnichsen *et al*., 1996). The main difference is that here we allow for GTP hydrolysis. This offers the possibilty to study vesicle formation in conditions that are more physiological by circumventing the previous need for GTPγS. Important observations have been made using this strategy. First, analysis of the protein content shows a preferential incorporation of resident proteins into COPI vesicles (Lanoix *et al*., 1999). Second, the mechanism of formation seems to depend on GTP hydrolysis by Arf1 and cargo incorporation is linked to GAP (Lanoix *et al*., 1999, 2001). The coupling between GAP and cargo incorporation effectively gives rise to a kinetic proofreading mechanism ensuring that vesicles only form when sufficient and correct cargo has been selected (Weiss and Nilsson, 2003).

To summarise: Golgi stacks are purifed from rat liver and are incubated together with rat liver cytosol at 37°C. By adding the recombinant α-SNAP^{dn} mutant to the reaction the heterotypic fusion between formed vesicles and acceptor compartments is blocked (Barnard *et al*., 1997). In this way only one round of vesicle formation is reconstituted. After terminating the reaction, slowly sedimenting vesicles are separated from heavier donor membranes by medium speed centrifugation. The COPI-derived vesicles are then recovered using high speed centrifugation onto a two-step sucrose cushion. Following resuspension, vesicles may then be used for a variety of biochemical or morphological purposes, such as analysis of protein or lipid content, processed for electron microscopy or used in other functional assays.

Copyright 2006, Elsevier Science (USA).
All rights reserved.

II. MATERIALS AND INSTRUMENTATION

Guanosine 5′-triphosphate lithium salt (GTP) (Cat. No. G-5884), guanosine 5′-[γ-thio]triphosphate tetralithium salt (GTPγS) (Cat. No. G-8634), benzamidine–HCl (Cat. No. B-6506), leupeptine (Cat. No. L-2884), and soybean trypsin inhibitor (Cat. No. T-9128) are from Sigma. KOAc (Cat. No. 104820), $MgCl_2$ (Cat. No. 105833), KCl (Cat. No. 104936), NaOH (Cat. No. 106469), and KOH (Cat. No. 105021) are from Merck. HEPES (Cat. No. 05288) and dithiothreitol (DTT, Cat. No. 4010-1) are from Biomol. ATP (Cat. No. 127523), creatine phosphate (Cat. No. 621714), and creatine kinase (Cat. No. 127566) are from Roche. Ultrapure sucrose (Cat. No. 21938) is from USB. The protein assay dye reagent (Cat. No. 500-0006) is from Bio-Rad. Bovine serum albumin (BSA, Cat. No. 23209) is from Pierce. The ECL Western blotting detection reagent (Cat. No. RPN2109) is from Amersham Biosciences. Water is of double-distilled grade (ddH_2O).

Ultracentrifugation is carried out using an Optima MAX-E tabletop ultracentrifuge using a TLA-100.2 rotor (Cat. No. 362046) with polycarbonate centrifugation tubes 11 × 34 mm with a 1-ml capacity (Cat. No. 343778), a TLA-55 rotor (Cat. No. 366752) with polyallomer tubes 9.5 × 38 mm with a 1.5-ml capacity (Cat. No. 357448), or a Optima XL-100K ultracentrifuge using a SW-60 rotor (Cat. No. 335649) with ultraclear centrifuge tubes 11 × 60 mm (Cat. No. 344062) from Beckman. Medium-speed centrifugation is carried out in a Biofuge (Cat. No. 75005510) from Heraeus using microcentrifuge tubes with a 1.5-ml capacity (Cat. No. 96.75114.9.01) from Treff lab. Round-bottom test tubes with a 14-ml capacity (Cat. No. 352006), needles 18G × 3 1/2 (Cat. No. 405184), thin needles 0.4 × 19 (Cat. No. 302200), 5-ml syringes (Cat. No. 309603), and 1-ml syringes (Cat. No. 309602) are from BD Biosciences. Glass micropipettes (Cat. No. 708757) are from BRAND. The rubber adaptor between micropipettes and syringes is homemade. A standard laboratory vortex and heating block or water bath are used for incubations at 37°C. P-10, P-20, P-100, P-500, and P-1000 pipettes are from Gilson.

III. PROCEDURES

Purification of Golgi membranes and cytosol from rat liver is described in the article by Wang *et al*. The concentration of the Golgi membrane aliquots should be at least 1 mg/ml and the concentration of rat liver cytosol aliquots at least 30 mg/ml to accommodate the final volume of the reaction. Purification of a 10-mg/ml (approximately) stock of the His_6-tagged α-$SNAP^{dn}$ mutant is performed as described (Barnard *et al*., 1997).

Protein concentration determination is performed using the Bio-Rad version of the Bradford protein assay reagent and BSA as a standard. One-dimensional SDS–polyacrylamide gel electrophforesis (SDS-PAGE) is carried out according to Laemmli (1970). Western blotting is carried out according to Towbin *et al*. (1979). Antibodies are revealed using chemiluminescence.

A. Small-Scale Purification

Solutions

1. *KOAc assay buffer*: 25 m*M* HEPES, 115 m*M* KOAc, and 2.5 m*M* $MgCl_2$, pH 7.0. To make 0.5 litre, dissolve 3.0 g of HEPES, 5.6 g of KOAc, and 0.1 g of $MgCl_2$ in 450 ml water. Adjust pH to 7.0 with 1 *M* KOH and bring to a total volume of 0.5 litre with water. Aliquot and store at –20°C.

2. *10× ATP-regenerating system*: 26 m*M* of ATP, 100 m*M* of creatine phosphate, and 116 U/ml of creatine kinase. (*A*) Dissolve 0.1 g of ATP in 370 µl of KOAc assay buffer. Adjust pH to 7.0 with 1 *M* NaOH and bring to a total volume of 700 µl with KOAc assay buffer. (*B*) Dissolve 223 mg of creatine phosphate in a total volume of 2.3 ml KOAc assay buffer. (*C*) Dissolve 1 mg of creatine kinase in 333 µl of KOAc assay buffer and 333 µl of glycerol. (D) Combine the solutions and add 3.3 ml of KOAc assay buffer. Aliquot, snap freeze in liquid nitrogen, and store at –80°C.

3. *GTP stock solution:* 40 m*M* GTP. Dissolve 24 mg of GTP in 1 ml of water. Aliquot and store at –20°C.

4. *GTPγS stock solution*: 2 m*M* GTPγS. Dissolve 5 mg of GTPγS in a final volume of 4 ml water. Aliquot and store at –20°C.

5. *100× protease inhibitor cocktail*: 50 m*M* benzamidine–HCl, 500 µg/ml leupeptine, and 200 µg/ml soybean trypsin inhibitor. Dissolve 39.2 mg of benzamidine–HCl, 2.5 mg of leupeptine, and 1 mg of soybean trypsin inhibitor in water to a final volume of 5 ml. Aliquot and store at –20°C.

6. *DTT stock solution*: 100 m*M* DTT. Dissolve 1.5 mg of DTT in 1 ml of water. Aliquot and store at –20°C.

7. *3 M KCl*: Dissolve 22.5 g KCl in 100 ml water. Filter sterilise with a 0.22-µm filter and store at 4°C.

8. *30% sucrose KOAc assay buffer*: 25 m*M* HEPES, 115 m*M* KOAc, 2.5 m*M* $MgCl_2$, and 30% (w/w) sucrose, pH 7.0. To make 50 ml, dissolve 0.3 g HEPES, 0.56 g KOAc, 10 mg $MgCl_2$, and 16.9 g sucrose in 45 ml of water. Adjust pH to 7.0 with 1 *M* KOH and bring to

a final volume of 50 ml with water. Aliquot and store at –20°C.

9. *50% sucrose KOAc assay buffer*: 25 m*M* HEPES, 115 m*M* KOAc, 2.5 m*M* $MgCl_2$, and 50% (w/w) sucrose, pH 7.0. To make 50 ml, dissolve 0.3 g HEPES, 0.56 g KOAc, 10 mg $MgCl_2$, and 30.7 g sucrose in 45 ml of water. Adjust pH to 7.0 with 1 *M* KOH and bring to a final volume of 50 ml with water. Aliquot and store at –20°C.

Order of operation

1. Thaw 500 µl of rat liver cytosol and dilute by adding 1 ml of KOAc assay buffer. Centrifuge the diluted cytosol for 1 h at 157,000 g_{max} at 4°C (60,000 rpm in a TLA 100.2 rotor).

2. Transfer the supernatant to microcentrifuge tubes with 1.5-ml capacity and centrifuge for 15 min at 16,000 *g* at 4°C (13,000 rpm in Biofuge) to further clear the cytosol.

3. Determine the protein concentration of the diluted cytosol and the Golgi membrane fraction used in the assay.

4. Just before mixing the assay mixture, dilute the His_6-tagged α-$SNAP^{dn}$ mutant to 1 mg/ml in KOAc assay buffer prewarmed to 37°C. Keep at 37°C until use.

5. Mix the assay mixture by adding the following reagents to a microcentrifuge tube with 1.5-ml capacity according to Table I.

6. Add KOAc assay buffer so that the final assay volume is 250 µl.

7. Vortex the tube *very briefly* (not more than 1 s) to mix the assay mixture.

8. Incubate for 30 min at 37°C.

9. Terminate the reaction by placing the tube on ice.

10. To detach vesicles from membranes, raise the salt concentration to 250 m*M* by adding 23 µl of a 3 *M* stock solution of KCl to the reaction.

TABLE I Standard Assay Mixture for the Small-Scale Purification Protocol

Reagent	Amount	Final concentration
10× ATP-regenerating system	25 µl	1×
GTP stock solution[a]	3.1 µl	0.5 m*M*
DTT stock solution	2.5 µl	1 m*M*
100× protease inhibitor cocktail	2.5 µl	1×
α-$SNAP^{dn}$ mutant (1 mg/ml)	4.5 µl	0.5 µ*M*
Diluted rat liver cytosol	1250 µg	5 mg/ml
Golgi membranes	40 µg	40 µg

[a] For blocking GTP hydrolysis, replace with 2.5 µl of GTPγS stock solution (20 µ*M* final concentration).

11. To separate donor membranes from slowly sedimenting vesicles, centrifuge for 15 min at 16,000 *g* at 4°C (13,000 rpm in a Biofuge).

12. Transfer the medium-spin supernatant to a polyallomer centrifugation tube with 1.5-ml capacity without disturbing the membrane pellet.

13. Create a two-step sucrose cushion by adding 50 µl of 30% (w/w) sucrose KOAc assay buffer very carefully to the side of the tube, just below the surface of the supernatant followed by 5 µl of 50% (w/w) sucrose KOAc assay buffer.

14. To collect vesicles, centrifuge for 45 min at 126,000 g_{max} at 4°C (45,000 rpm in a TLA-55 rotor).

15. Vesicles are found in the 30/50% sucrose interface. Carefully aspirate all but 20 µl of the contents in the tube with a thin needle connected to a vacuum.

16. For analysis of protein content by SDS–PAGE and Western blotting, add 20 µl of 2× sample buffer to the tube, vortex to mix, and resuspend vesicles thoroughly by pipetting up and down with a P-20 Gilson pipette for 1 min. To ensure that all vesicles are resuspended properly, place the tube in a thermomixer and shake at maxiumum speed for 15 min at 4°C. For analysis of vesicle fractions by other methods, use KOAc assay buffer instead of sample buffer.

17. For analysis of protein content by SDS–PAGE and Western blotting, boil sample for 5 min at 95°C and load the entire sample (40 µl) onto a 1.5-mm SDS–PAGE gel. On the same gel run 1, 2, 4, and 8 µg of Golgi membranes (corresponding to 2.5, 5, 10, and 20% of starting membranes used in assay) to create a standard of Golgi proteins for analytical purposes. Analyse the protein content in the vesicle fractions using specific antibodies.

B. Large-Scale Purification

Solutions (in Addition to Those Described in Section III.A)

1. *20% sucrose KOAc assay buffer 0.5 M KCl:* 25 m*M* HEPES, 115 m*M* KOAc, 2.5 m*M* $MgCl_2$, and 20% (w/w) sucrose, pH 7.0. To make 50 ml, dissolve 0.3 g HEPES, 0.56 g KOAc, 10 mg $MgCl_2$, 1.9 g KCl, and 10.8 g sucrose in 45 ml of water. Adjust pH to 7.0 with 1 *M* KOH and bring to a final volume of 50 ml with water. Aliquot and store at –20°C.

2. *50% sucrose KOAc assay buffer 0.5 M KCl:* 25 m*M* HEPES, 115 m*M* KOAc, 2.5 m*M* $MgCl_2$, and 55% (w/w) sucrose, pH 7.0. To make 50 ml, dissolve 0.3 g HEPES, 0.56 g KOAc, 10 mg $MgCl_2$, 1.9 g KCl, and 30.7 g sucrose in 45 ml of water. Adjust pH to 7.0 with 1 *M* KOH and bring to a final volume of 50 ml with water. Aliquot and store at –20°C.

3. *65% sucrose KOAc assay buffer 0.5 M KCl:* 25 m*M* HEPES, 115 m*M* KOAc, 2.5 m*M* $MgCl_2$, and 65% (w/w) sucrose, pH 7.0. To make 50 ml, dissolve 0.3 g HEPES, 0.56 g KOAc, 10 mg $MgCl_2$, 1.9 g KCl, and 42.8 g sucrose in 45 ml of water. Adjust pH to 7.0 with 1 *M* KOH and bring to a final volume of 50 ml with water. Aliquot and store at –20°C.

Order of operation

1. Thaw 2.5 ml of rat liver cytosol and dilute it by adding 5 ml of KOAc assay buffer. Centrifuge the diluted cytosol for 1 h at 157,000 g_{max} at 4°C (60,000 rpm in a TLA 100.2 rotor).
2. Transfer the supernatant to microcentrifuge tubes with 1.5-ml capacity and centrifuge for 15 min at 16,000 *g* at 4°C (13,000 rpm in Biofuge) to further clear the cytosol.
3. Pool supernatants and determine the protein concentration of the diluted cytosol and the Golgi membrane fractions used in the assay.
4. Just before mixing the assay mixture, dilute the His_6-tagged α-$SNAP^{dn}$ mutant to 1 mg/ml in KOAc assay buffer prewarmed to 37°C. Keep at 37°C until use.
5. Mix *five* standard assay mixtures by adding the following reagents to five round-bottom test tubes with 14-ml capacity according to Table II.
6. Add KOAc assay buffer up to 2.5 ml final reaction volume in each tube.
7. Vortex the tubes very briefly (not more than 1 s) to mix the assay mixture.
8. Incubate for 30 min at 37°C.
9. Terminate the reaction by placing tubes on ice.
10. To detach vesicles from membranes, raise the salt concentration to 250 m*M* by adding 230 µl of a 3 *M* stock solution of KCl to each of the five tubes.
11. To separate donor membranes from slowly sedimenting vesicles, divide the content of each tube into 0.3-ml fractions into several (around 40 in total) microcentrifuge tubes with 1.5-ml capacity and centrifuge for 15 min at 16,000 *g* at 4°C (13,000 rpm in Biofuge).
12. Pool the medium spin supernatants (around 12 ml in total volume) in a round-bottom test tube without disturbing the membrane pellets.
13. Prepare four two-step sucrose cushions by adding 800 µl of 20% (w/w) sucrose KOAc assay buffer 0.5 *M* KCl to an ultraclear SW-60 centrifuge tube and then underlay this with 150 µl of 50% (w/w) sucrose KOAc assay buffer 0.5 *M* KCl using a micropipette connected to a 1-ml syringe. Onto each gradient overlay 3 ml of the pooled supernatant using a 5-ml syringe connected to a needle.
14. To collect vesicles, centrifuge for 3 h at 407,000 g_{max} at 4°C (55,000 rpm in a SW-60 rotor).
15. Vesicles are found in the 20/50% sucrose interface. Carefully aspirate all but 500 µl of the contents in the tube with a thin needle connected to a vacuum.
16. Collect the vesicles by removing 300 µl from the bottom of each tube using a micropipette connected to a 1-ml syringe.
17. Pool these vesicle fractions into a new round-bottom test tube and adjust the sucrose concentration to approximately 55% sucrose (w/w) KOAc assay buffer 0.5 *M* KCl by adding 1550 µl 65% sucrose (w/w) KOAc assay buffer 0.5 *M* KCl.
18. To further purify vesicles by floatation, prepare a step sucrose gradient in an ultraclear SW-60 centrifuge tube. Start with the 20% sucrose (w/w) KOAc assay buffer 0.5 *M* KCl. This is underlaid with 50% sucrose (w/w) KOAc assay buffer, which is underlaid with the sample containing the vesicles in 55% sucrose using a micropipette connected to a syringe in the following order:
    i. 500 µl 20% sucrose (w/w) KOAc assay buffer 0.5 *M* KCl
    ii. 750 µl 50% sucrose (w/w) KOAc assay buffer 0.5 *M* KCl
    iii. 2750 µl 55% sucrose (w/w) KOAc assay buffer 0.5 *M* KCl sample from previous step.
19. To float vesicles, centrifuge for 16 h at 337,000 g_{max} at 4°C (50,000 rpm in a SW-60 rotor).
20. Collect vesicles by removing 100-µl fractions from the top of the gradient. The layer of vesicles at the interface is between 20/50% sucrose.

TABLE II Standard Assay Mixture for the Large-Scale Purification Protocol

Reagent	Amount	Final concentration
10× ATP-regenerating system	250 µl	1×
GTP stock solution[a]	31 µl	0.5 m*M*
DTT stock solution	25 µl	1 m*M*
100× protease inhibitor cocktail	25 µl	1×
α-$SNAP^{dn}$ mutant (1 mg/ml)	45 µl	0.5 µ*M*
Diluted rat liver cytosol	12.5 mg	5 mg/ml
Golgi membranes	400 µg	400 µg

[a] For blocking GTP hydrolysis, replace with 25 µl of GTPγS stock solution (20 µ*M* final concentration).

IV. Comments

The small-scale protocol is useful for comparing a variety of reaction conditions in one experiment. The recovery of various proteins in the vesicle fractions is

compared to the amount of protein in the protein standard on the gel. For any condition that is tested it is strongly recommended to always run controls containing GTP and GTPγS and one at 4°C. Comparing these three control conditions with the one tested usually gives a good indication of the effect that the particular condition has. The large-scale protocol gives a higher amount of vesicles and is more suitable when more material is needed, for example protein analysis through proteomics.

V. PITFALLS

1. Unless specified, all steps should be carried out on ice to minimise protein degradation. Aliquots for one-time use should be thawed and kept on ice until use.
2. Pipetting of Golgi membranes should be minimised to avoid shearing. Mix these aliquots by tapping carefully on the side of the tube.
3. Once the protein concentration of a certain batch of purifed Golgi membranes and cytosol has been established, it is not necessary to perform the protein concentration determination in step 3 of the protocols.
4. The sucrose content of the various buffers should be verified with a refractometer.
5. Aspiration steps may represent a source of variation. Take special care during these steps.

Acknowledgments

The authors thank Dr. Joel Lanoix for developing this assay and Nilsson group members for providing critical comments of the manuscript.

References

Barlowe, C. (2000). Traffic COPs of the early secretory pathway. *Traffic* **1**, 371–377.

Barnard, R. J., Morgan, A., and Burgoyne, R. D. (1997). Stimulation of NSF ATPase activity by alpha-SNAP is required for SNARE complex disassembly and exocytosis. *J. Cell Biol*. **139**, 875–883.

Laemmli, U. K. (1970). Cleavage of structural proteins during the assembly of the head of bacteriophage T4. *Nature* **227**, 680–685.

Lanoix, J., Ouwendijk, J., Lin, C. C., Stark, A., Love, H. D., Ostermann, J., and Nilsson, T. (1999). GTP hydrolysis by arf-1 mediates sorting and concentration of Golgi resident enzymes into functional COP I vesicles. *EMBO J.* **18**, 4935–4948.

Lanoix, J., Ouwendijk, J., Stark, A., Szafer, E., Cassel, D., Dejgaard, K., Weiss, M., and Nilsson, T. (2001). Sorting of Golgi resident proteins into different subpopulations of COPI vesicles: A role for ArfGAP1. *J. Cell Biol*. **155**, 1199–1212.

Sonnichsen, B., Watson, R., Clausen, H., Misteli, T., and Warren, G. (1996). Sorting by COP I-coated vesicles under interphase and mitotic conditions. *J. Cell Biol*. **134**, 1411–1425.

Towbin, H., Staehelin, T., and Gordon, J. (1979). Electrophoretic transfer of proteins from polyacrylamide gels to nitrocellulose sheets: Procedure and some applications. *Proc. Natl. Acad. Sci. USA* **76**, 4350–4354.

Weiss, M., and Nilsson, T. (2003). A kinetic proof-reading mechanism for protein sorting. *Traffic* **4**, 65–73.

CHAPTER

7

Purification of Clathrin-Coated Vesicles from Bovine Brain, Liver, and Adrenal Gland

Robert Lindner

I. INTRODUCTION

Clathrin-coated vesicles are intermediates in several selective membrane transport processes in eukaryotic cells (for review, see Bonifacino and Lippincott-Schwartz, 2003; Brodsky *et al*., 2001; Schmid, 1997). They are derived from clathrin-coated membrane regions on the plasma membrane, the TGN, endosomes (Stoorvogel *et al*., 1996), and possibly also lysosomes (Traub *et al*., 1996) by a process of invagination and fission. In addition to the main structural protein clathrin, a three-legged molecule composed of one heavy and one light chain per leg, a number of other proteins have been isolated from clathrin-coated vesicles: most prominent are the adaptor protein (AP) complexes, heterotetramers consisting of two heavy chains, an intermediate chain, and a light chain (for review, see Kirchhausen, 1999). AP-1 and AP-2 complexes link clathrin to specific membrane areas by binding to clathrin N-terminal domains and to cytosolic tails of transmembrane receptors. The recently discovered AP-3 and AP-4 complexes appear to function independently of clathrin and are not enriched in clathrin-coated vesicles. Furthermore, clathrin-coated vesicles contain monomeric adaptor proteins, such as AP 180 and members of the epsin family. These interact with coat components via their poorly structured C-terminal regions (Kalthoff *et al*., 2002) and with phosphoinositides of the membrane via their N-terminal ENTH domain (for review, see De Camilli *et al*., 2002). Also present are accessory proteins such as auxilins that provide a J-like domain for the recruitment of Hsc70 to clathrin, thereby serving to initiate the removal of the clathrin coat (Ungewickell *et al*., 1995). A novel bilayered clathrin coat without curvature has been described on multivesicular endosomes (Raiborg *et al*., 2002; Sachse *et al*., 2002). It contains the monomeric clathrin adaptor protein HRS and appears to be involved in the sorting of ubiquitinated membrane proteins to internal vesicles. This flat structure probably does not to give rise to coated vesicles.

Since the first report on the purification of clathrin-coated vesicles (Kanaseki and Kadota, 1969), a variety of protocols have been published. Most recent protocols are based on a purification procedure introduced by Campbell *et al*. (1984). This procedure rapidly provides crude clathrin-coated vesicles that are well suited for the preparation of various coat proteins (Ahle *et al*., 1988; Ahle and Ungewickell, 1990; Lindner and Ungewickell, 1991). This basic protocol has been further improved by the introduction of a centrifugation step involving a sucrose/D_2O cushion (Maycox *et al*., 1992). By this step, contaminations of smooth membrane vesicles are reduced further. A similar procedure has been used to purify rat brain clathrin-coated vesicles for proteomic characterization (Wasiak *et al*., 2002).

This article describes a purification protocol for bovine brain-coated vesicles that includes a sucrose/D_2O step gradient at the end. With appropriate volume adjustments, the protocol can also be used for the purification of coated vesicles from other species such as pigs or rats. For the preparation of clathrin-coated vesicles from other organs (adrenal gland, liver), some modifications in the protocol are suggested.

Copyright 2006, Elsevier Science (USA).
All rights reserved.

II. MATERIALS AND INSTRUMENTATION

Ficoll 400 (Cat. No. 17-0400-02) is from Pharmacia; sucrose (Cat. No. BP 220-1) is from Fisher Scientific; D_2O (Cat. No. 15,188-2) is from Aldrich; EGTA (Cat. No. E-3889), MES (Cat. No. M-3023), and phenylmethylsulfonyl fluoride (PMSF, Cat. No. P-7626) are from Sigma. All other reagents are from Sigma or Fisher in analytical grade.

Biological material is obtained from an local abattoir within 1 h of slaughter and is kept on ice until further processing (1–2 h). Fresh and cleaned material can be frozen in liquid nitrogen and stored at –80°C for several months. It is helpful to cut the tissue into small pieces before freezing. This supports a rapid drop of temperature in the tissue and minimizes ice crystal formation. The latter process reduces yield and purity of the following preparation, probably due to the destruction of membrane vesicles and liberation of proteolytic activities.

For homogenization of the tissue, a Waring commercial blender (VWR International, Cat. No. 58977-169) is used. Membrane pellets are resuspended with Potter–Elvehjem homogenizers of various sizes (10–55 ml) obtained from Fisher Scientific (Cat. No. 08414-14 A to D). The metal shaft of the larger homogenizers is attached to a variable-speed overhead drive so that the pestle can be rotated.

Low-speed centrifugations are done in a Sorvall RC-5B centrifuge using GS-3, GSA, or SS-34 heads. High-speed centrifugations are performed with Beckman Ti 45, Ti 35, and SW 28 rotors in conventional ultracentrifuges. For fixed angle ultracentrifugation rotors, Beckman polycarbonate bottles with screw caps (Cat. No. 355622) are used and for the SW 28 rotor open-top ultraclear tubes (Cat. No. 344058) are used.

III. PROCEDURES

A. Cleaning of Bovine Brain Cortices

Solutions

Phosphate-buffered saline (*PBS*): 137 m*M* NaCl, 2.7 m*M* KCl, 8.2 m*M* Na_2HPO_4, 1.9 m*M* KH_2PO_4, 0.02% NaN_3, pH 7.0. To make 1 liter of 10× PBS (stock solution), dissolve 80 g NaCl, 2 g KCl, 2.58 g KH_2PO_4, 11.64 g Na_2HPO_4, and 0.2 g NaN_3 in double-distilled water. Adjust the pH to 7.0 (if necessary) and bring the volume to 1 liter. Dilute this stock solution 1:10 with double-distilled water and chill to 4°C prior to use. Approximately 2–3 liters of 1× PBS are needed per kilogram tissue.

Steps

1. Separate the cerebellum and the lower part of the brain from the cortex.
2. Take a hemisphere of the cortex, place it in an ice bucket covered with plastic wrap, and remove the meninges along with blood vessels contained therein using forceps.
3. Collect the cleaned cortex hemispheres in a preweighed beaker on ice. Determine the weight of the tissue and estimate the volume of homogenization buffer needed in Section III,B (approximately 1 liter per kg of tissue).
4. Wash the cortex hemispheres with cold PBS several times to remove the remaining blood. To do this, fill the beaker containing the hemispheres with PBS, mix gently, and pour the liquid off. It is helpful to use a household sieve at this step. Repeat the washes until the blood is removed.
5. If you want to store the brain tissue for later processing, cut it into small pieces after the washing step and freeze it in liquid nitrogen. Store frozen material at –80°C. Otherwise continue with Section III,B.

B. Homogenization

Solutions

1. *Buffer A*: 0.1 *M* MES, 1.0 m*M* EGTA, 0.5 m*M* $MgCl_2$, 0.02% NaN_3, pH 6.5. To make 1 liter of 10× buffer A (stock solution), dissolve 195.2 g MES, 3.8 g EGTA, and 1.0 g $MgCl_2$ in double distilled water. Adjust the pH with 10 *N* NaOH to 6.5, add 2 g NaN_3, and bring the volume to 1 liter. Do not add NaN_3 prior to the adjustment of the pH because MES is acidic and may release HN_3. To prepare 1× buffer A for homogenization, dilute the stock solution 1:10 with double-distilled water, chill to 4°C, and supplement with 0.1 m*M* PMSF prior to use. Prepare about 3 liters buffer A per kilogram tissue.
2. *Protease inhibitor* (*PMSF stock solution, 1000× = 0.1 M*). To make 10 ml, dissolve 174 mg PMSF in 10 ml pure methanol, aliquot, and store at –20°C. Dilute 1:1000 to get a working concentration of 0.1 m*M*. Note that PMSF will hydrolyze in water and that it is not soluble in this solvent at high concentrations.

Steps

1. Fill the cup of a Waring commercial blender with 300–400 g of washed tissue and an equivalent amount of cold buffer A containing 0.1 m*M* freshly added

PMSF. Do not fill the cup up to the top, but leave space below the rim.

2. Homogenize the tissue by three to six bursts of 10–15 s duration with the setting on maximum speed. The number of bursts required to give a good homogenization varies: for brain, usually three bursts are sufficient, whereas other organs, especially adrenal glands, require more (see Section IV). Do not increase the length of the bursts but their number to prevent heating of the homogenate.

C. Differential Centrifugations

1. Preparation of Postmitochondrial Supernatants

Steps

1. Pour the homogenate into buckets of a Sorvall GS-3 or GSA rotor, balance the buckets, and centrifuge them in the precooled rotor at 7000 rpm (about 8000 *g* in both types of rotors) for 50 min at 4°C.

2. Pour the turbid supernatants through a funnel with several layers of gauze to separate floating lipids from the supernatant.

3. The bulky pellets (up to a third of the total volume) should be resuspended with an at least equivalent volume of cold homogenization buffer and recentrifuged under the aforementioned conditions.

4. Discard the pellets after the second centrifugation and keep the combined supernatants on ice.

2. Preparation of Microsomal Pellets

Steps

1. Fill the postmitochondrial supernatant into the tubes for a Beckman Ti 35 or Ti 45 rotor, balance the tubes, and ultracentrifuge them at 32,000 rpm at 4°C for 1.6 h (Ti 35) or at 40,000 rpm for 1 h (Ti 45) in precooled rotors.

2. After centrifugation, discard the clear supernatant and either refill the tubes with postmitochondrial supernatant for the next spin (leave the first pellet in the tube without resuspending it to save time) or remove the microsomal pellets when all the postmitochondrial supernatant has been centrifuged or pellets from three to four ultracentrifugations have been collected in one tube.

3. Resuspend the pellets with 1–2 volumes of buffer A supplemented with 0.1 m*M* PMSF using a 10-ml glass pipette in the reverse orientation (the wide top end down) and then homogenize thoroughly by 10–15 strokes in a Potter–Elvehjem device (overhead drive at slow rotation).

3. Preparation of Crude Clathrim-Coated Vesicles from Microsomal Pellets

Solution

12.5% Ficoll–sucrose: To make 1 liter, dissolve 125 g sucrose and 125 g Ficoll 400 in buffer A, pH 6.5, and stir overnight in the cold room. Ficoll 400 dissolves only slowly! Keep at 4°C.

Steps

1. Mix the well-homogenized microsomes with the same volume of Ficoll–sucrose solution and fill into open tubes suitable for an SS-34 Sorvall rotor. Centrifuge the tubes at 43,000 *g* (19,000 rpm) and 4°C for 40 min in a precooled rotor.

2. After centrifugation, pour the supernatants containing the clathrin-coated vesicles through a funnel with gauze to remove floating lipids. The compact sediment (about a fifth of the total volume) will stay in the tube and can be discarded.

3. Dilute the combined supernatants with 3–4 volumes of cold buffer A containing 0.1 m*M* PMSF.

4. Concentration of Crude Clathrim-Coated Vesicles by Pelleting

Steps

1. Ultracentrifuge the coated vesicles in the diluted Ficoll–sucrose solution as described in Section III,C,2. The pellets obtained in this step are considerably smaller than the microsomal pellets. The color usually varies from yellowish-white to brown and is most likely due to contaminating ferritin (Kedersha and Rome, 1986).

2. Pour off the supernatants and carefully remove the pellets from the tubes with a spatula. Use a small volume of buffer A + PMSF to wash off material still attached to the walls of the tube.

3. Homogenize the combined pellets in about 20 volumes of buffer A + PMSF per bovine brain using first a 10-ml glass pipette in the reverse orientation (the wide top end down) and then homogenize very thoroughly by 10–15 strokes in a Potter–Elvehjem device (overhead drive at slow rotation).

5. Removal of Aggregated Material

Steps

1. Fill the crude clathrin-coated vesicles into open tubes for an SS-34 Sorvall rotor. Centrifuge the tubes at 20,000 *g* (13,000 rpm) at 4°C for 10 min in a precooled rotor.
2. After centrifugation, retrieve, pool and place the supernatants on ice. Discard the pellets.

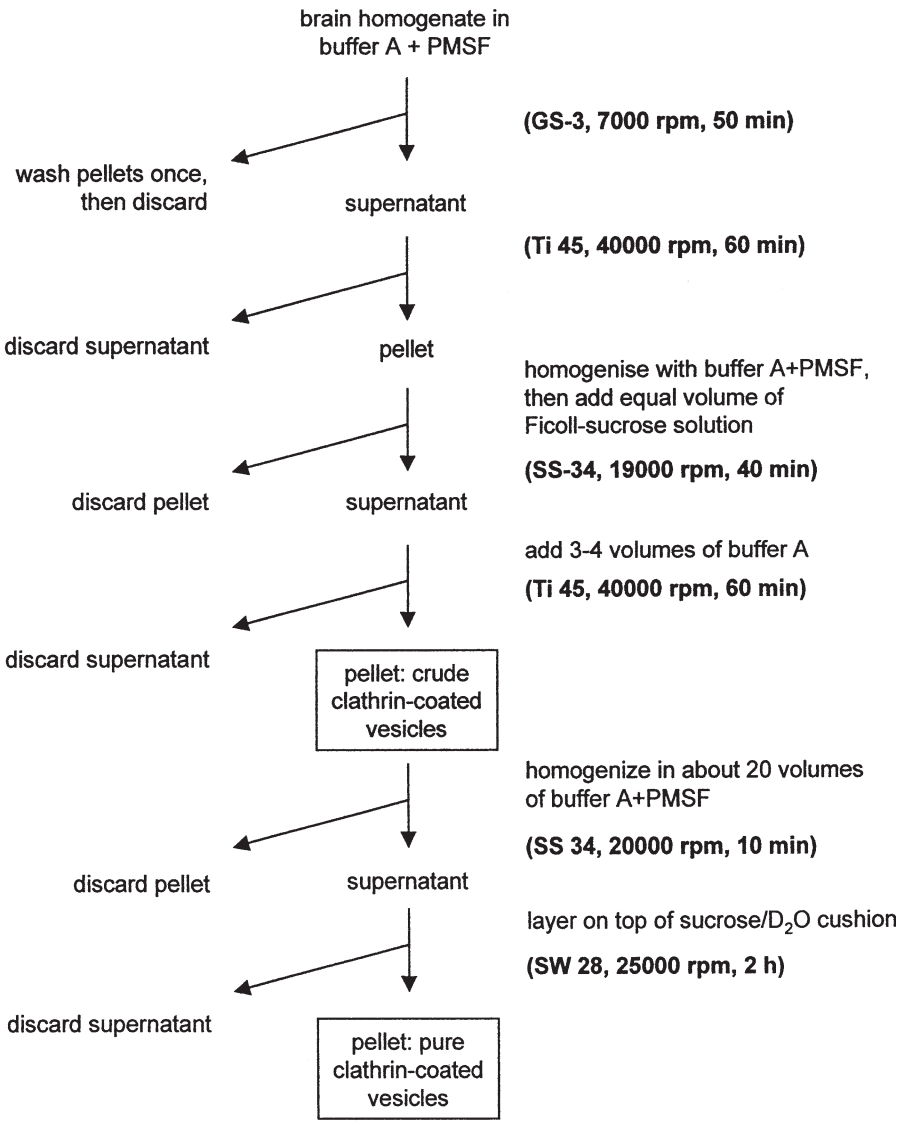

FIGURE 1 Purification scheme for clathrin-coated vesicles.

6. Removal of Smooth Membrane Contaminants

Solutions

1. *Buffer A/D_2O*: 0.1 *M* MES, 1.0 m*M* EGTA, 0.5 m*M* $MgCl_2$, 0.02% NaN_3, pH 6.5. To make 1 liter of 1× buffer A in D_2O, dissolve 19.5 g MES, 0.38 g EGTA, and 0.10 g $MgCl_2$ in D_2O. Adjust the pH with 5–10 *N* NaOH solution (prepared in D_2O as well) to 6.5, add 2 g NaN_3, and bring the volume to 1 liter using D_2O. Do not add NaN_3 prior to the adjustment of the pH because MES is acidic and may release HN_3. Chill to 4°C and supplement with 0.1 m*M* PMSF prior to use.
2. *Sucrose/D_2O solution*: 8% (w/v) sucrose in buffer A/D_2O. To make 200 ml, dissolve 16 g sucrose in buffer A/D_2O and adjust the volume with the same buffer. Keep on ice.

Steps

1. Precool an SW 28 rotor and the buckets.
2. Pour 30 ml of the sucrose/D_2O solution per SW 28 centrifugation tube (open top, ultraclear, Beckman #344058). Place the tubes on ice. Carefully overlay 5 ml of the coated vesicles from Section III,C,5 per tube.
3. Balance the tubes and assemble the buckets and the rotor. Spin the rotor in an ultracentrifuge at 110,000 *g* (25,000 rpm) at 4°C for 2 h.
4. Remove the supernatants and resuspend the pellets in 5–10 volumes of buffer A plus PMSF using a pipette and a suitable homogenizer.
5. Material obtained after this step can either be used directly or be frozen in liquid nitrogen and stored at –80°C.

IV. COMMENTS

Following this protocol (for summary, see Fig. 1), near homogeneous preparations of clathrin-coated vesicles are obtained from bovine brain. The yields usually are about 50–100 mg clathrin-coated vesicles/kg brain cortex.

For the preparation of various coat proteins, such as clathrin or the adaptor complexes, crude clathrin-coated vesicles obtained in Section III,C,4 are a good starting material of sufficient purity (80–90% pure, 100–120 mg/kg bovine brain). For a typical electrophoresis pattern of a Tris extract of crude bovine brain clathrin-coated vesicles as described in Section III,C,4, see Fig. 2.

This basic protocol can also be used with other organs rich in clathrin-coated membranes, such as adrenal glands, liver, or placenta. For adrenal glands, a more thorough homogenization (usually 6 or more 10-s bursts in a Waring commercial blender) is required to break up the very resistant capsule material.

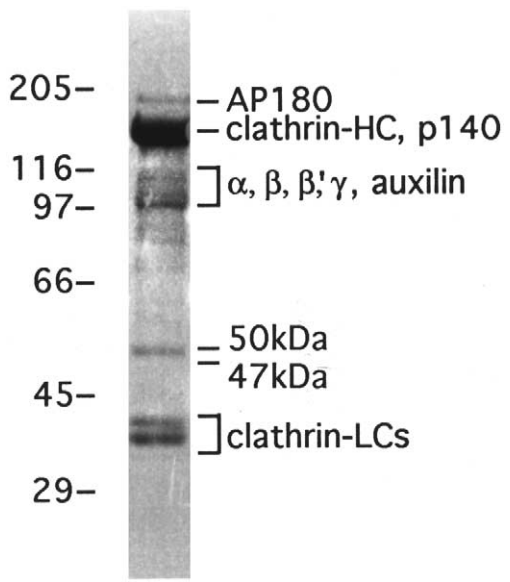

FIGURE 2 Coat proteins obtained by Tris extraction of a crude clathrin-coated vesicle preparation from bovine brain as described in the text. Coated vesicles were incubated in 0.5*M* Tris, pH 7.0, to release the peripheral membrane proteins and were then ultracentrifuged to remove the membranes. Approximately 12 µg Tris extract was electrophoresed in a low-Bis SDS–polyacrylamide gel (for details, see Lindner and Ungewickell, 1992). Note that in this gel system the brain-specific, clathrin-associated protein AP180 is well resolved from the clathrin heavy chain. Both AP180 and auxilin are only detectable in brain-derived, clathrin-coated vesicles. In nonneuronal tissues, homologues are expressed (CALM for AP180 and GAK/auxilin2 for auxilin).

Clathrin-coated vesicle preparations from liver usually contain a considerable amount of ribonucleoprotein complexes termed vaults. It is advisable to remove these structures by velocity centrifugation on 5–40% sucrose gradients as an additional step after the preparation described earlier (for details, see Kedersha and Rome, 1986). Vaults are at least partially dissociated by the conventional extraction methods for clathrin coat structures and thus contaminate coat protein extracts.

For the preparation of fusion-competent, clathrin-coated vesicle from cell culture cells, a more elaborate protocol has been described (Woodman and Warren, 1991)

V. PITFALLS

Do not mix the Ficoll–sucrose solution to microsomal pellets obtained in Section III,C,3 before thorough homogenization of the pellets. The high viscosity of the Ficoll–sucrose solution prevents proper homogenization.

In order to quantitatively pellet the clathrin-coated vesicles from the supernatant after centrifugation in Ficoll–sucrose, dilute with a *minimum* of 3 volumes of buffer A + PMSF to decrease both the density and the viscosity of the supernatant.

References

Ahle, S., Mann, A., Eichelsbacher, U., and Ungewickell, E. (1988). Structural relationships between clathrin assembly proteins from the Golgi and the plasma membrane. *EMBO J.* **7**, 919–929.

Ahle, S., and Ungewickell, E. (1990). Auxilin, a newly identified clathrin-associated protein in coated vesicles from bovine brain. *J. Cell Biol.* **111**, 19–29.

Bonifacino, J. S., and Lippincott-Schwartz, J. (2003). Coat proteins: Shaping membrane transport. *Nature Rev. Mol. Cell Biol.* **4**, 409–414.

Brodsky, F. M., Chen, C. Y., Knuehl, C., Towler, M. C., and Wakeham, D. E. (2001). Biological basket weaving: Formation and function of clathrin-coated vesicles. *Annu. Rev. Cell Dev. Biol.* **17**, 517–568.

Campbell, C., Squicciarini, J., Shia, M., Pilch, P. F., and Fine, R. E. (1984). Identification of a protein kinase as an intrinsic component of rat liver coated vesicles. *Biochemistry* **23**, 4420–4426.

De Camilli, P., Chen, H., Hyman, J., Panepucci, E., Bateman, A., and Brunger, A. T. (2002). The ENTH domain. *FEBS Lett.* **513**, 11–18.

Kanaseki, T., and Kadota, K. (1969). The "vesicle in a basket". A morphological study of the coated vesicle isolated from the nerve endings of the guinea pig brain, with special reference to the mechanism of membrane movements. *J. Cell Biol.* **42**, 202–220.

Kalthoff, C., Alves, J., Urbanke, C., Knorr, R., and Ungewickell, E. J. (2002). Unusual structural organization of the endocytic proteins AP180 and epsin 1. *J. Biol. Chem.* **277**, 8209–8216.

Kedersha, N. L., and Rome, L. H. (1986). Isolation and characterization of a novel ribonucleoprotein particle: Large structures contain a single species of small RNA. *J. Cell Biol.* **103**, 699–709.

Kirchhausen, T. (1999). Adaptors for clathrin-mediated traffic. *Annu. Rev. Cell Dev. Biol*. **15**, 705–732.

Lindner, R., and Ungewickell, E. (1991). Light-chain-independent binding of adaptors, AP180 and auxilin to clathrin. *Biochemistry* **30**, 9097–9101.

Lindner, R., and Ungewickell, E. (1992). Clathrin-associated proteins from bovine brain coated vesicles: An analysis of their number and assembly-promoting activity. *J. Biol. Chem*. **267**, 16567–16573.

Maycox, P. R., Link, E., Reetz, A., Morris, S. A., and Jahn, R. (1992). Clathrin-coated vesicles in nervous tissue are involved primarily in synaptic vesicle recycling. *J. Cell Biol.* **118**, 1379–1388.

Raiborg, C., Bache, K. G., Gillooly, D. J., Madshus, I. H., Stang, E., and Stenmark, H. (2002). Hrs sorts ubiquitinated proteins into clathrin-coated microdomains of early endosomes. *Nature Cell Biol*. **4**, 394–398.

Sachse, M., Urbe, S., Oorschot, V., Strous, G. J., and Klumperman, J. (2002). Bilayered clathrin coats on endosomal vacuoles are involved in protein sorting toward lysosomes. *Mol. Biol. Cell* **13**, 1313–1328.

Schmid, S. L. (1997). Clathrin-coated vesicle formation and protein sorting: An integrated process. *Annu. Rev. Biochem.* **66**, 511–548.

Stoorvogel, W., Oorschot, V., and Geuze, H. J. (1996). A novel class of clathrin-coated vesicles budding from endosomes. *J. Cell Biol.* **132**, 21–33.

Traub, L. M., Bannykh, S. I., Rodel, J. E., Aridor, M., Balch, W. E., and Kornfeld, S. (1996). AP-2-containing clathrin coats assemble on mature lysosomes. *J. Cell Biol.* **135**, 1801–1814.

Ungewickell, E., Ungewickell, H., Holstein, E. H., Lindner, R., Prasad, K., Barouch, W., Martin, B., Greene, L. E., and Eisenberg, E. (1995). Role of auxilin in uncoating clathrin-coated vesicles. *Nature* **378**, 632–635.

Wasiak, S., Legendre-Guillemin, V., Puertollano, R., Blondeau, F., Girard, M., de Heuvel, E., Boismenu, D., Bell, A. W., Bonifacino, J. S., and McPherson, P. S. (2002). Enthoprotin: A novel clathrin-associated protein identified through subcellular proteomics. *J. Cell Biol*. **158**, 855–862.

Woodman, P. G., and Warren, G. (1991). Isolation and characterization of functional clathrin-coated vesicles. *J. Cell Biol.* **112**, 1133–1141.

CHAPTER

8

Isolation of Latex Bead- and Mycobacteria-Containing Phagosomes

Mark Kühnel, Elsa Anes, and Gareth Griffiths

I. INTRODUCTION

Phagocytosis is a crucial mechanism by which specialized cells, especially macrophages, neutophils, and dendritic cells, remove ingested debris, dead cells, and pathogens from the body. Many pathogens are killed within the phagosome (phagolysosome) as a consequence of fusion between this organelle and lysosomes, which delivers hydrolases and the proton ATPase into the phagosome. An important technical advance has been the use of nondegradable latex beads as phagosome marker: these have facilitated studies both in cells and *in vitro* after phagosome isolation. This article describes how latex bead phagosomes are isolated for *in vitro* studies. It also summarizes recent approaches developed for the more difficult problem of isolating phagosomes containing live and killed mycobacteria.

II. BACKGROUND

In 1967 in Edward Korn's group a simple but crucial innovation for both phagosome analysis and the study of membrane organelles in general was introducted (Weisman and Korn, 1967a,b). They fed *Acanthamoeba* with latex beads and, following gentle homogenisation, could isolate a remarkably pure fraction of latex bead phagosomes (LBP) by a single centrifugation step using a discontinuous sucrose gradient. For efficient uptake of beads into (mostly) single bead phagosomes, the beads had to be between 0.13 and 0.26 µm (smaller and larger beads were taken in more ineffectively) (summarized by Desjardins and Griffiths, 2003). Although this system was used intermittently in subsequent years, the method was not used extensively until reintroduced by Desjardins *et al*. (1994a,b). Since that time we have mostly focused on the use of 1-µm latex beads conjugated with avidin or fish skin gelatin that are taken up by J774 macrophages. LBP functions can be monitored easily within macrophages, and *in vitro* assays are available to monitor the following phagosome functions: fusion with endocytic organelles (Jahraus *et al*., 1998, 2001), microtubule binding and motility (Blocker *et al*., 1996, 1997, 1998), binding to F-actin (Al Haddad *et al*., 2001), and *de novo* actin assembly (Dejardins *et al*., 1994; Defacque *et al*., 2000; Anes *et al*., 2003).

A recent proteomic analysis by Desjardins and collages has revealed that LBP from J774 cells have about 1000 proteins, of which ≈600 have already been identified (Garin *et al*., 2001; Desjardins and Griffiths, 2003). They also contain at least 100 different lipids (Kuehnel *et al*., 2004; Anes *et al*., 2003).

Since 1994 a large number of papers have appeared in which LBP have been analyzed in different cells or have been used after isolation. By October 2003, Medline listed 73 papers that involved LBP; the actual number is certain to be significantly larger, as LBP are often used as controls for pathogen-containing phagosomes and are often not mentioned in the titles or abstracts to these papers.

An enormous advantage of the use of latex beads is the ease by which thy can be conjugated to selected proteins, such as IgG, or complement. In an agreement with the "zipper hypothesis" originally put forward by Silverstein and colleges in the 1970s (see Greenberg and Silverstein, 1993), such beads form a phagosome in which the receptor for the bound ligand is concentrated. A large body of evidence argues that

Copyright 2006, Elsevier Science (USA).
All rights reserved.

phagosomes enriched in different receptors can show significant differences in their intracellular behaviour. Such differences are likely to become more clear in future studies.

This article summarizes the methods used to prepare different beads and to isolate the ensuing phagosomes. No other membrane organelle in the cell can be prepared with such ease and to such high purity after a single purification step. We subsequently discuss our recent efforts in isolating phagosomes enclosing mycobacteria, an approach first initiated by Chakraborty et al (1994).

III. PROCEDURES

A. Preparations of Latex Beads for Internalisation

Latex beads, either "naked" or coated with substances of interest, can be used for the generation of phagosomes. Our standard system uses avidin-coated latex beads. For coating beads with avidin, incubate 100 µl of latex beads (10%, w/v) with 100 µl 0.5 *M* MES buffer, pH 6.8, 722 µl of distilled water, and 50 µl of avidin (10 mg/ml in water) for 15 min on a rotating wheel. Add 14 µl of 10 mg/ml *N*-(3-dimethylaminopropyl)-*N*-ethylcarbodiimide hydrochloride (EDAC) and allow incubation for another 1.5 h. Subsequently, add another 14 µl EDAC to the reaction and incubate for a further 1.5 h. Stop the reaction by adding 1% Triton X-100 in 10 m*M* Tris pH 9.4. Pellet the beads by centrifugation in a desktop centrifuge at full speed (13,000×*g*) and then resuspend in Triton/tris buffer. Subsequently, wash the beads three times in phosphate-buffered saline (PBS) (each time followed by a centrifugation step) and store at 4°C in PBS containing a nonspecific protein; we use 0.03% fish skin gelatin (Sigma G7765) and 0.02% sodium azide. If determination of protein content on the beads is necessary, an aliquot of beads can be taken for protein measurement before adding the storage solution.

B. Internalisation of Latex Beads

For isolation of LBP, grow 20 × 20-cm petri dishes of macrophages (in our case J-774A.1 macrophages are used) in 50 ml of culture medium supplemented with 10% fetal calf serum (FCS) and 2 m*M* glutamine until the needed density of cells is reached. Use J774 macrophages at 50×10^6 cells per dish. For internalisation, dilute 1 ml of beads with 25 ml of Dulbecco's Modified Eagle's Medium (DMEM) per dish. Uptake is routinely allowed for 1 h on a shaker at 5% CO_2 at 37°C. Remove non internalised beads by intensive washing of the cells with PBS at 37°C. Thereafter, incubate cells with internalized beads until the desired phagosome age is reached in the presence of DMEM at 37°C and 5% CO_2.

C. Cell Lysis and Latex Bead Phagosome Isolation

Harvest cells by adding 20 ml PBS to the dish and scraping them with a suitable cell scraper. We use cell scrapers from Sarstedt (Nümbrecht, Germany). Collect cells in 50-ml tubes and centrifuge at 1000×g for 10 min, resuspend in 5 ml of homogenization buffer (HB: 0.25 *M* sucrose, 3 m*M* imidazole, pH 7.4) with protease inhibitors (Table I) and pellet again, as before. Resuspend pellets in a final volume of 1.5 ml of HB buffer and lyse using 15–20 stokes with a 1-ml syringe fitted to a 22-gauge needle. Monitor cell breakage by light microscopy. Remove nuclei and intact cells by gentle centrifugation at 800×*g* at 4°C, collect supernatants and mix gently with 62% sucrose. Prepare the gradient in ultraclear centrifugation tubes from Beckmann (Reorder NO. 344060) as follows. Overlay 3–4 ml of phagosome/62% sucrose mix with 5 ml of 25% sucrose containing protease inhibitors and overlay with 2 ml of HB buffer. Carry out centrifugation at 100,000 *g* for 60 min at 4°C. The visible band that forms between the HB buffer and 25% sucrose contains the LBP and can be collected in approximately 200 µl with a syringe by penetrating the tube wall with a 22-gauge needle (see Fig. 1). Aliquot phagosomes in 20 µl portions and store in liquid nitrogen until further use. For some purposes they can also be stored at –80°C; however, we have found that many activities are kept longer following liquid nitrogen storage.

D. Monitoring Phagosomal Integrity

If it is necessary to check the proportion of intact phagosomes, phagosomes containing avidin-coated

TABLE I Proteinase Inhibitors Used during Phagosome Isolation

Inhibitor (solvent used)	Final concentration
Pepstatin (methanol)	1 µg/ml
TLCK (methanol)	1 µg/ml
Aprotinin (water)	4 µg/ml
Leupeptin (water)	1 µg/ml
Dithiothreitol (water)	1 m*M*

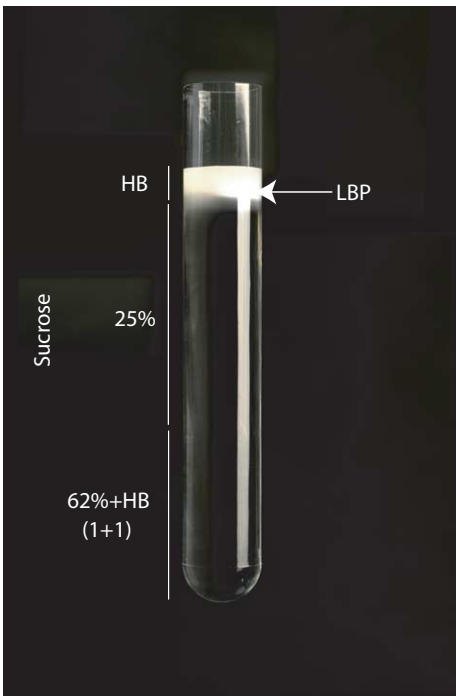

FIGURE 1

latex beads can be incubated conveniently with a suitable dye such as rhodamine–biotin 5 n*M* for 15 min at room temperature. The rationale here is that only broken phagosomes will be accessible to the label. Then the ratio of phagosomes labeled red (not intact) and nonlabelled phagosomes (intact) is determined by light microscopy. Routinely 70–80% of LBP are found to be intact in our experience.

E. Preparation of Mycobacterial Phagosomes

1. Preparation of Mycobacteria for Uptake

There are a wide range of growth characteristics among the genus *Mycobacterium*, from 3 h of generation time in *M. smegmatis*, 18–24 h of *M.tb*, and 3 to 6 days for *M. avium ssp. paratuberculosis* or *M. leprae*, which has never been cultured *in vitro*. Usually, Middlebrook 7H10 (solid agar medium, Difco) or 7H9 (liquid medium, Difco) is enough for fast-growing species such as *M. smegmatis* or *M. fortuitum*, but for slow-growing species such as *M. tuberculosis*, *M. avium*, or BCG, enrich the medium with bovine serum albumin (BSA) fraction V and glucose prepared by dissolving 5 g of albumin fraction V and 2 g glucose in distilled water that is brought to the final volume of 100 ml. Sterilise this by passing it through a 0.45-µm Nucleopore filter and store in aliquots of 10 ml at 4°C. When needed, for each 90 ml of Middlebrook (7H9 or 7H10), use 10 ml OADC (albumin, dextrose, catalase and oleic acid; Difco) to supplement the medium. For *M. avium ssp. paratuberculosis*, the medium has to be supplemented with 1 mg/liter Mycobactin J.

2. Preparation of a Suspension of Mycobacterium smegmatis

Grow bacterial cultures on petri dishes containing 4.7 g Middlebrook's 7H9 broth medium, 5 g of nutrient broth, supplemented with 0.5% glucose and 0.05% Tween 80 at 200 rpm on a shaker at 37°C until the exponential grown phase (OD_{600} = 0.2) is reached (~10^8 cells/ml).

Subsequently, pellet and wash cells twice in PBS, pH 7.4, and resuspend in PBS to a final concentration of 5–10 × 10^9 cells/ml. Treat the suspension for 2 min in a water bath sonicator (room temperature) using four 30-s pulses to disperse clumps. Subsequently, bacteria should be passed through a 23-gauge needle to disrupt remaining bacterial clumps. Before infection, remove residual bacterial aggregates by low-speed centrifugation (120 *g*) for 2 min. The absence of bacterial clumps can finally be verified by light microscopy. It should be noted that some investigations have been interested in differences in the biology of mycobacteria that are taken up as aggregates rather than as individual bacteria (Schuller *et al*., 2001).

3. Preparation of a Suspension of Slow-Growing Mycobacteria such as M. tuberculosis

Inoculate 20 ml of Middlebrook's 7H9 broth medium with OADC with colonies isolated from Loewenstein Jennsen agar plates. In order to prevent the loss of lipidic virulence components, detergents such as Tween 80 should not be added the medium. Incubate the cultures at 37°C. When they reach the exponential phase growth (approximately 10–15 days) stock solutions in 10% glycerol can be preserved at –20°C up to 3 months or at –70°C for at least 1 year.

F. Killing of Mycobacteria

For some experiments it is useful to compare the biology of phagosomes containing live versus killed pathogens. Mycobacteria can be killed either by using paraformaldyde or, more easily, by heat. Suspensions resuspended in PBS (pH 7.4) are heat inactivated for 15 min at 80°C. Such treatment completely blocks growth of bacteria as determined by colony-forming units, but keeps the appearance of the bacteria intact, as viewed by electron microscopy.

G. Labelling of Mycobaceria

For many experiments it is useful to fluorescently label bacteria before uptake. For this, wash freshly harvested bacteria twice (3000×*g*) in a Eppendorf centrifuge for 3 min in ice-cold PBS, pH 7,4 and resuspend in the same buffer. After harvesting, dilute mycobacteria using PBS to a OD_{600}: 1.0. Add sulpho-NHS-FITC to a final concentration of 5 µg/ml and allow labelling to continue for 20 min on a shaker at room temperature. Non-incorporated FITC can be removed by washing in PBS plus 100 m*M* glycine. Thereafter, wash bacteria three times with PBS and immediately freeze in 100 µl aliquots at –20°C. To avoid batch variability in experiments, bacteria can be stored after labelling at –20°C up to 3 months or at –70°C for 1 year. The use of bacteria expressing GFP has emerged as a more powerful alternative to the surface labelling approach, as can be seen in numerous publications (see, e.g., Dhandayuthapani *et al*., 1995; Kremer *et al*., 1995).

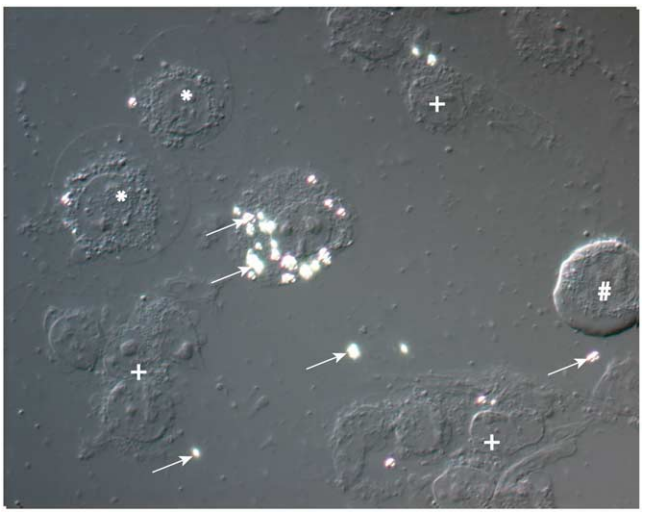

FIGURE 2 Nomarski interference microscopy image of *M. smegmatis*-infected J774 macrophages treated with a syringe equipped with a 22-gauge needle 10 times. *, cells in the process of breaking; +, nuclei with associated cell debris; #, intact cell; arrows indicate *M. smegmatis*-containing phagosomes that are phase refractile.

H. Cells Lysis and Isolation of Mycobacteria-Containing Phagosomes

The method we describe is a variation of that introduced by Chakraborty (1994). For preparing the mycobacteria-containing phagosome preparation, we usually infect macrophages of approximately 70% confluency in 245 × 245-mm dishes with mycobacteria. At desired times postinfection, wash cells in PBS. Harvest infected cells by scraping them in 20 ml of PBS and collecting them in one 50-ml tube per dish of cells and pellet by centrifugation at 800×*g* for 10 min at 4°C. Resuspend cells in 5 ml of HB with protease inhibitors and pellet again. In order to have a good lysis of the infected macrophages in the next step, cells have to be resuspended in an optimal volume of HB. As a rule of thumb, use an equal volume of HB (with inhibitors) to resuspend the pellet of cells. This should result in approximately 1 ml of suspension. Variations of this ratio can be applied to optimize breakage of cells. Lyse macrophages by approximately 30 strokes with a syringe fitted with 22-gauge needle and check the percentage of broken cells by light microscopy (Fig. 1). The process should continue until roughly 80% of the cells are broken, but with intact nuclei (Fig. 2). Subsequently, dilute the suspensions with an equal volume of HB plus inhibitors and centrifuge at 300 *g* for 10 min at 4°C and discard the pellet containing nuclei and intact cells. The postnuclear supernatant (PNS) contains the phagosomes, as well as endocytic and other organelles and cytoplasmic components. It is important to note that loss of phagosomes at this stage occurs mainly because of two reasons. First, cells are not broken properly and phagosomes are not set free in the supernatant. This can be a result of a too dilute suspension, which is more resistant to breakage, or from too gentle application or not enough strokes with the syringe. Second, phagosomes can be lost due to breakage of nuclei. This results in free DNA in the suspension that binds to phagosomes and keeps the phagosomes in the pellet together with nuclei and intact cells. As a result, cell lysis is one of the most critical stages of isolating bacterial phagosomes from macrophages.

A sucrose step gradient is then used to separate phagosomes from other organelles. For this, layer PNS on top of a discontinuous sucrose gradient in transparent centrifugation tubes consisting of 2 ml 62% sucrose, 4 ml 55%, and a 6-ml 37% (w/w) step cushion, prepared with protease inhibitors (Table I) and centrifuged at 100,000×*g* for 1 h at 4°C in Ultracentrifuge. Prepare one gradient per dish of cells. Dependent on the infection and age of the phagosomes, three different bands are found. One lies on the top of the 37% gradient, along with the majority of endocytic organelles, another in the interface between 55 and 37%, with the bacterial phagosomes, and, in the case of older (more mature) phagosomes, a third one is seen between 55 and 62% sucrose (Fig. 3). Phagosomes can be recovered using a syringe fitted to a 22-gauge needle by penetrating the tube wall from the side.

If a further concentration of the preparation is needed, a second step gradient can be done. The

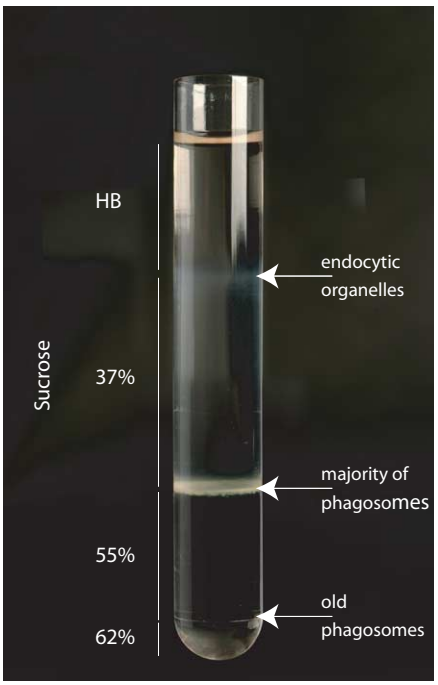

FIGURE 3

combined collected fractions (up to 2 ml) can be layered on the top of 2 ml 55% sucrose and centrifuged again at 100,000×*g* for 30 min at 4°C. The band on the top of the 55% sucrose contains the phagosomes and is collected as described earlier. Phagosomes can be used directly or stored in aliquots in liquid nitrogen until further use.

The successful isolation of intact phagosomes also depends on minimizing the interaction of phagosomes with tube surfaces. One must avoid pelleting the phagosomes until the final stage in the isolation.

IV. FINAL COMMENT

Latex bead phagosomes have emerged as a powerful model membrane organelle system that can be used to analyse many functions that are general properties of many intracellular membrane organelles, such as membrane fusion, their interaction with actin or microtubules, or acidification. The same particles can be used conveniently for *in vitro* analysis or for complementary studies in cells. In principle, any ligand that binds to cell surface receptors can be conjugated to beads in order to enrich for specific receptors in the phagosomes. It should be noted that the size of the particle is an important consideration; for phagocytosis, there is a minimum size (usually 0.2–0.3 µm in diameter) as well as a maximum size that depends on the cell type (for cultures macrophages, this is usually around 5 µm in diameter); for more details, see Desjardins and Griffiths (2003). A survey of the literature, as well as our own experience, convinces us that LBP are an excellent model system that behave similarly to phagosomes containing microorganisms that can be killed by macrophages (such as *M. smegmatis*; see Anes *et al*., 2003). LBP have also been used extensively as control phagosomes for analyses of pathogen-enclosing phagosomes; the latter usually modify the intracellular behaviour of the phagosome in a manner that facilitates the survival and growth of the pathogens. A key question that needs to be addressed individually for each intraphagosomal pathogen is how the pathogen manages to by-pass the normal phagosomal killing mechanisms. Also for this question the use of latex beads can be invaluable, as suspected pathogen surface "virulence" factors that bind to cell surface receptors can be conjugated to beads to see if and how the intracellular trafficking and molecular composition of the phagosome differ from control bead phagosomes.

For many questions there will be an increasing need to isolate pathogen-enclosing phagosomes. For no pathogen until now is it possible to enrich its phagosome to the same level of purity as is obtained routinely for the LBP. The method described here for isolating mycobacterial phagosomes can be taken as one of the current state-of-the-art methods in use. There is now a serious need to improve existing methods and to find new approaches that can provide more pure preparations of functionally intact pathogen phagosome preparations that will be important for protein and lipid analysis in the future.

References

Al-Haddad, A., Shonn, M. A., Redlich, B., Blocker, A., Burkhardt, J. K., Yu, H., Hammer, J. A., 3rd, Weiss, D. G., Steffen, W., Griffiths, G., and Kuznetsov, S. A. (2001). Myosin Va bound to phagosomes binds to F-actin and delays microtubule-dependent motility. *Mol. Biol. Cell* **12**, 2742–2755.

Anes, E., Kuhnel, M. P., Bos, E., Moniz-Pereira, J., Habermann, A., and Griffiths, G. (2003). Selected lipids activate phagosome actin assembly and maturation resulting in killing of pathogenic mycobacteria. *Nature Cell Biol.* **5**, 793–802.

Blocker, A., Griffiths, G., Olivo, J. C., Hyman, A. A., and Severin, F. F. (1998). A role for microtubule dynamics in phagosome movement. *J. Cell Sci.* **111**, 303–312.

Blocker, A., Severin, F. F., Burkhardt, J. K., Bingham, J. B., Yu, H., Olivo, J. C., Schroer, T. A., Hyman, A. A., and Griffiths, G. (1997). Molecular requirements for bi-directional movement of phagosomes along microtubules. *J. Cell Biol.* **137**, 113–129.

Blocker, A., Severin, F. F., Habermann, A., Hyman, A. A., Griffiths, G., and Burkhardt, J. K. (1996). Microtubule-associated protein-

dependent binding of phagosomes to microtubules. *J. Biol. Chem.* **271**, 3803.

Chakraborty, P., Sturgill-Koszycki, S., and Russell, D. G. (1994). Isolation and characterization of pathogen-containing phagosomes. *Methods Cell Biol.* **45**, 261–276.

Defacque, H., Egeberg, M., Antzberger, A., Ansorge, W., Way, M., and Griffiths, G. (2000). Actin assembly induced by polylysine beads or purified phagosomes: Quantitation by a new flow cytometry assay. *Cytometry* **41**, 46–54.

Desjardins, M., Celis, J. E., van Meer, G., Dieplinger, H., Jahraus, A., Griffiths, G., and Huber, L. A. (1994). Molecular characterization of phagosomes. *J. Biol. Chem.* **269**, 32194–32200.

Desjardins, M., and Griffiths, G. (2003). Phagocytosis: Latex leads the way. *Curr. Opin. Cell Biol.* **15**, 498–503.

Desjardins, M., Huber, L. A., Parton, R. G., and Griffiths, G. (1994). Biogenesis of phagolysosomes proceeds through a sequential series of interactions with the endocytic apparatus. *J. Cell Biol.* **124**, 677–688.

Dhandayuthapani, S., Via, L. E., Thomas, C. A., Horowitz, P. M., Deretic, D., and Deretic, V. (1995). Green fluorescent protein as a marker for gene expression and cell biology of mycobacterial interactions with macrophages. *Mol. Microbiol.* **17**, 901–912.

Garin, J., Diez, R., Kieffer, S., Dermine, J. F., Duclos, S., Gagnon, E., Sadoul, R., Rondeau, C., and Desjardins, M. (2001). The phagosome proteome: Insight into phagosome functions. *J. Cell Biol.* **152**, 165–180.

Greenberg, S., and Silverstein, S. C. (1993). Phagocytosis. *In "Fundamental Immunology"* Chap. 27, pp. 941–964.

Jahraus, A., Egeberg, M., Hinner, B., Habermann, A., Sackman, E., Pralle, A., Faulstich, H., Rybin, V., Defacque, H., and Griffiths, G. (2001). ATP-dependent membrane assembly of F-actin facilitates membrane fusion. *Mol. Biol. Cell.* **12**, 155–170.

Jahraus, A., Tjelle, T. E., Berg, T., Habermann, A., Storrie, B., Ullrich, O., and Griffiths, G. (1998). *In vitro* fusion of phagosomes with different endocytic organelles from J774 macrophages. *J. Biol. Chem.* **273**, 30379–30390.

Korn, E. D., and Weisman, R. A. (1967). Phagocytosis of latex beads by Acanthamoeba. II. Electron microscopic study of the initial events. *J. Cell Biol.* **34**, 219–227.

Kremer, L., Baulard, A., Estaquier, J., Poulain-Godefroy, O., and Locht, C. (1995). Green fluorescent protein as a new expression marker in mycobacteria. *Mol. Microbiol.* **17**, 913–922.

Schuller, S., Neefjes, J., Ottenhoff, T., Thole, J., and Young, D. (2001). Coronin is involved in uptake of *Mycobacterium bovis* BCG in human macrophages but not in phagosome maintenance. *Cell Microbiol.* **3**, 785–793.

Weisman, R. A., and Korn, E. D. (1967). Phagocytosis of latex beads by Acanthamoeba. I. Biochemical properties. *Biochemistry* **6**, 485–497.

CHAPTER

9

Isolation of Peroxisomes

Alfred Völkl and H. Dariush Fahimi

I. INTRODUCTION

The investigation of unique functional and structural aspects of peroxisomes (PO) requires the preparation of highly purified fractions of this organelle. This is, however, hampered by two serious problems: (1) the relative paucity of PO (2% of total liver protein) and (2) their considerable fragility. Thus, mild homogenization conditions minimizing mechanical, hydrostatic, and osmotic stress have to be sustained.

In general, the isolation of PO is accomplished in three steps: (a) homogenization of the tissue or disruption of the cells; (b) subfractionation of the homogenate by differential centrifugation usually according to the classical scheme of de Duve *et al*. (1955); and (c) isolation of purified peroxisomes by density gradient centrifugation of the so-called light mitochondrial (λ) fraction.

Homogenization is commonly carried out in an isotonic medium (e.g., see Section III,A,1) at low salt concentrations to avoid aggregation. Addition of a chelator (e.g., EDTA), however, is feasible, as it prevents the aggregation of microsomes that may contaminate PO. Moreover, the homogenization buffer (HB) should be supplemented with antioxidants (dithiothreitol, DTT), as well as protease inhibitors (phenylmethylsulfonyl fluoride, PMSF; ε-aminocaproic acid) to block oxidative and proteolytic activities in the course of the isolation procedure.

For the purification of PO by density gradient centrifugation, three approaches have been developed. In the classic procedure (Leighton *et al*., 1968), sucrose gradients and the specialized type Beaufay rotor were employed. A self-generating Percoll gradient in conjunction with a vertical rotor is used for the isolation of PO under isotonic conditions (Neat *et al*., 1980). The most straightforward approach to obtain highly purified PO makes use of iodinated gradient media such as metrizamide, nycodenz or Optiprep in combination with a vertical rotor (Völkl and Fahimi, 1985; Hartl *et al*., 1985; van Veldhoven *et al*., 1996). In the latter media, PO band at the quite high density of 1.24 g/cm^3 because of their permeability to low molecular weight compounds (van Veldhoven *et al*., 1983), well separated from lysosomes as well as from mitochondria and microsomes.

The method described in this article is a modification of the protocol established for the isolation of highly purified (>98%) PO from normal rat liver (Völkl and Fahimi, 1985). Meanwhile, it has been applied to livers and kidneys of several other mammalian species (Fahimi *et al*., 1993; Zaar *et al*., 1992), as well as for the isolation of PO from cell cultures (Schrader *et al*., 1994). With an additional differential centrifugation step, even peroxisomal subpopulations may be isolated according to this protocol, as has been demonstrated by Lüers *et al*. (1993).

II. INSTRUMENTATION AND MATERIALS

A. Instrumentation

1. Perfusion device (self-made)
2. A 30-ml Potter–Elvehjem tissue grinder (Cat. No. 1931 05145) with a loose-fitting Teflon pestle (Cat. No. 1931 05155; clearance 0.10–0.15 mm) and a motor-driven homogenizer (Cat. No. 5308 50001) are from Migge, 69123 Heidelberg, FRG.

Copyright 2006, Elsevier Science (USA).
All rights reserved.

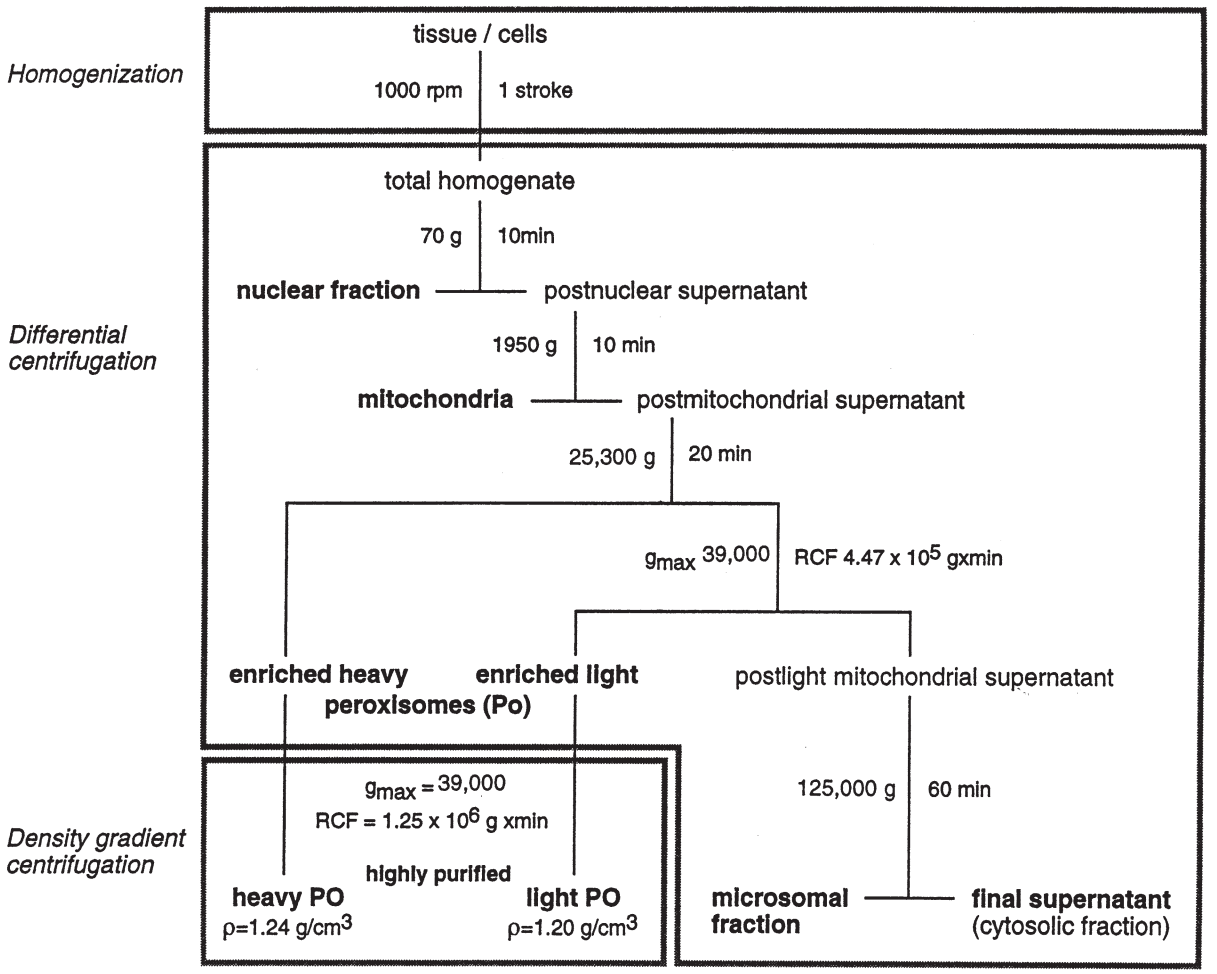

FIGURE 1 Flowchart for the isolation of highly purified (>98%) peroxisomes from rat liver.

3. Refrigerated low- and high-speed centrifuge (e.g., Beckman TJ-6 and J 2-21); ultracentrifuge (e.g., Beckman L90) with corresponding rotors (e.g., Beckman JA-20; VTi 50).
4. Refractometer

B. Chemicals

Morpholinopropane sulfonic acid (MOPS, Cat. No. 29 836), PMSF (Cat. No. 32 395), and DTT (Cat. No. 20 710) are from Serva (Heidelberg, FRG). Ethanol (Cat. No. 8006) and NaCl (Cat. No. 0277) are from J. T. Baker (Deventer, Netherlands). EDTA (Cat. No. E 2628-2) is from Max Keller (Mannheim, FRG), ε-aminocaproic acid (Cat. No. 62 075) is from Riedel-de Haen (Seelze, FRG), sucrose (Cat. No. 4621) is from Roth (Karlsruhe, FRG), and metrizamide (Cat. No. 10o 1983N) is from Life Technologies (76344 Eggenstein-Leopoldshafen).

C. Animals

Female rats of 220–250 g body weight, starved overnight

III. PROCEDURES (FIG. 1)

A. Perfusion and Homogenization

Solutions

1. *Homogenization buffer (HB)*: To make 1 liter, dissolve 85.56 g of sucrose (250 m*M*), 1.046 g of MOPS (5 m*M*), 0.372 g of EDTA–Na_2 (1 m*M*), and 1 ml of ethanol (0.1%) in distilled water, adjust pH to 7.2 with NaOH, and add water up to 1 liter. Store at 4°C. Prior to use add per 100 ml: 0.2 µl of 0.1 *M* PMSF, 0.1 ml of 1 *M* ε-aminocaproic acid, and 20 µl of 1 *M* DTT.

2. Saline (0.9%): To make 1 liter, dissolve 9 g of NaCl in distilled water and adjust to a total volume of 1 liter.

Steps

1. Anesthesize the animal (e.g., by ip injection of chloralhydrate).
2. Weigh the animal, open abdominal cavity, and perfuse liver with 0.9% saline via the portal vein until all blood is drained away.
3. Remove liver, dissect connective tissue, and weigh and cut liver into small pieces collected in a Potter tissue grinder held in an ice bath containing 3 ml/g (wet liver weight) of ice-cold HB.
4. Homogenize tissue with a loose-fitting pestle, applying a single down-and-up stroke at 1000 rpm.
5. Pour homogenate into a 50-ml centrifuge tube.

B. Subcellular Fractionation

Solution

HB as described in Section III,A.

Steps

1. To remove debris, unbroken hepatocytes, and blood cells, as well as most of nuclei, centrifuge the total homogenate at 70 *g* for 10 min in a refrigerated low-speed centrifuge.
2. Carefully pour off the supernatant (loose pellet !), resuspend pellet in 2 ml/g of ice-cold HB, rehomogenize, and spin again under the same conditions.
3. Pour off the second supernatant and combine it with the first one (postnuclear supernatant); discard the pellet.
4. Centrifuge postnuclear supernatant at 1950 *g* for 10 min in a refrigerated high-speed centrifuge.
5. Decant supernatant (firm pellet), resuspend pellet manually in 1 ml/g of ice-cold HB using a glass rod, and spin again at 1950 *g*. The final pellet (heavy mitochondrial fraction) contains the majority of ***mitochondria***, large microsomal sheets, and some remaining nuclei. The combined supernatants represent the postmitochondrial supernatant.
6. Subject the latter to 25,300 *g* for 20 min; remove supernatant, including the reddish fluffy layer by suction; resuspend pellet in about 10 ml of ice-cold HB using a glass rod; and recentrifuge at 25,300 *g* for 15 min. Resuspend the final pellet in 5 ml of ice-cold HB again by means of a glass rod, which comprises the ***enriched heavy peroxisomal*** = light mitochondrial (λ) fraction. The corresponding supernatant may be either used directly to prepare a microsomal fraction and a final supernatant (soluble proteins mostly of cytosolic origin) or processed further for the isolation of "light PO."
7. To this extent it is centrifuged at an integrated relative centrifugal force (RCF) of $4.47 \times 10^5\, g$ min (g_{max} = 39,000). Resuspend the pellet thus obtained in 5 ml of ice-cold HB using a glass rod; this pellet represents the ***enriched light peroxisomal fraction*** (Luers *et al.*, 1993).

C. Metrizamide Density Gradient Centrifugation

Solutions

1. *Gradient buffer (GB):* To make 1 liter, dissolve 1.046 g of MOPS (5 m*M*), 0.372 g of EDTA–Na_2 (1 m*M*), and 1 ml of ethanol (0.1%) in distilled H_2O, adjust with NaOH to pH 7.2, and add H_2O up to 1 liter. Store at 4°C. Prior to use add per 100 ml: 0.2 ml of 0.1 *M* PMSF, 0.1 ml of 1 *M* ε-aminocaproic acid, and 20 µl of 1 *M* DTT.
2. Metrizamide solutions (MS)
   a. *60% (w/v) stock solution*: Dissolve 60 g of metrizamide in GB by stirring. Add GB up to 100 ml. Store at 4°C.
   b. *Gradient solutions*: To prepare one gradient, take 3.78, 3.38, 3.53, 2.06, and 3.2 ml of the 60% stock solution. Add up GB to 10, 7, 6, 3, and 4 ml using a refractometer to definitely adjust densities to 1.12, 1.155, 1.19, 1.225, and 1.26 g/ml, respectively.

Steps

Preparation of a Metrizamide Gradient

1. Layer sequentially 4, 3, 6, 7, and 10 ml, respectively, of MS (1.26–1.12 g/ml) in a 40-ml centrifuge tube (e.g., Quick-seal polyallomer, Beckman) to form a discontiuous gradient.
2. Immediately freeze the gradient in liquid nitrogen and store it at –20°C.
3. Thaw the gradient quickly at room temperature using a metallic stand, thus transforming the step gradient into one with an exponential profile.

Gradient Centrifugation

1. Layer 5 ml of either the light or the heavy enriched peroxisomal fraction (corresponding to one liver of approximately 5–6 g) on top of the thawed gradient and seal the tube.
2. Centrifuge gradients in a vertical-type rotor (e.g., Beckman VTi50) at an integrated force of $1.256 \times 10^6\, g$ min (g_{max} = 39,000) using slow acceleration/deceleration modes. Under the conditions employed, ***highly purified heavy peroxisomes*** band at 1.23–1.24 g/ml and ***light peroxisomes*** band at 1.20–1.21 g/ml.

TABLE I Properties of Purified Heavy Peroxisomal Fractions from Normal Rat Liver[a]

Enzyme	mU/mg homogenate (mg/g liver)	Rate of recovery (%)	RSA
Protein	256.36 ± 82.94	0.28 ± 0.08	–
Catalase	203 ± 42.7	9.96 ± 1.92	37.67 ± 4.28
HA-oxidase	3.3 ± 0.7	9.46 ± 1.06	40.25 ± 5.83
FA β-oxidation	3.6 ± 0.96	11.18 ± 3.25	36.32 ± 5.09
β-Glucuronidase	38 ± 5.88	0.01 ± 0.01	0.07 ± 0.06
Acid phosphatase	31	0.15	0.07
Esterase	1229 ± 246.7	0.01 ± 0.01	0.09 ± 0.07
NADPH-CcR	18 ± 4.6	0.18	0.702
Cc-oxidase	127 ± 35.6	0.02 ± 0.02	0.09 ± 0.05
L-GlDH	57 ± 16.5	0.08 ± 0.02	0.679

[a] Values given are means ± SD. HA-oxidase, α-hydroxyacid oxidase; FA β-oxidation, fatty acid β-oxidation; NADPH-CcR, NADPH-cytochrome c reductase; Cc-oxidase, cytochrome c oxidase; L-GlDH, L-glutamate dehydrogenase; and RSA, relative specific activity.

3. Recover the peroxisomal fraction by means of a fraction collector; alternatively, the gradient tube can be punctured and the fraction aspirated by a syringe. Store fraction at –80°C.

4. To remove metrizamide, which interferes with the determination of some peroxisomal enzymes (e.g., urate oxidase) or of protein (Lowry method), dilute the peroxisome fraction about 10-fold with HB followed by centrifugation at 25,000 and 39,000 *g*, respectively, to pellet the organelles.

IV. OBSERVATIONS AND COMMENTS

The properties of the heavy peroxisomal fraction are listed in Table I. Estimated by the specific peroxisomal reference enzymes, it shows a purification rate of about 38-fold over the original homogenate. More than 95% of the total protein content of this fraction is contributed by peroxisomes (Völkl and Fahimi, 1985), with mitochondria and microsomes accounting for about 2% each and lysosomes for less than 1%. This is confirmed by electron microscopy, which shows that peroxisomes make up 98–99% of the fraction (Figs. 2 and 3). Many peroxisomes contain the typical inclusions of urate oxidase in the matrix (Fig. 2), but some extruded free cores are also found between the organelles. The electron-dense cytochemical reaction product of catalase after the incubation of filter preparations in the alkaline 3,3′-diaminobenzidine medium (Fahimi, 1969) is seen over the matrix of the majority of peroxisomes (Fig. 3), demonstrating their integrity and the absence of leakage of catalase.

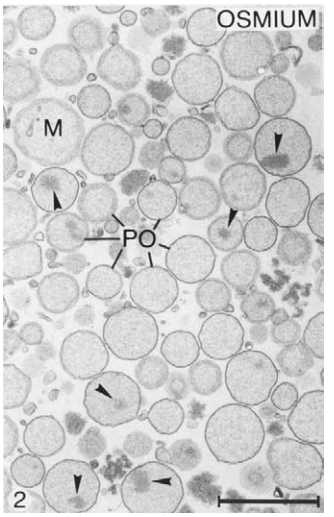

FIGURE 2 Electron microscopic appearance of isolated heavy peroxisomes after fixation in glutaraldehyde and osmium. The fraction consists almost exclusively of peroxisomes (PO) with only a rare mitochondrion (M). Many peroxisomes contain urate oxidase cores (arrowheads). Bar: 1 μm.

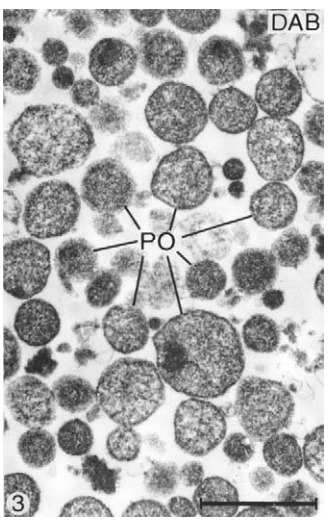

FIGURE 3 A preparation comparable to that in Fig. 2 but incubated with alkaline 3,3′-diaminobenzidine for localization of catalase (Fahimi, 1969). Note the electron-dense reaction product of catalase over the matrix of most peroxisomes. This illustrates the absence of catalase leakage, confirming their integrity. Bar: 1 μm.

The polypeptide pattern (SDS–PAGE) of rat liver heavy peroxisomes is shown in Fig. 4 (lane R) confirming their high degree of purity because of the absence of bands typical for mitochondria and microsomes. It also shows distinct differences in protein composition of hepatic peroxisomes between rat (R)

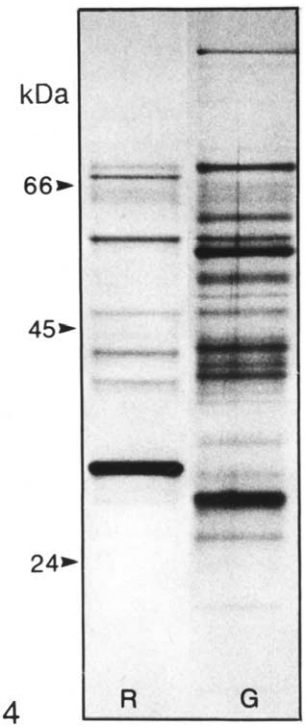

FIGURE 4 SDS–PAGE of highly purified heavy peroxisomes from rat (R) and guinea pig (G) liver. A 10–12.5% resolving gel was used, and the amounts of protein loaded per lane were (R) 2.4 µg and (G) 5.4 µg. Silver staining of polypeptide bands. M_r standards: BSA (66 kDa), ovalbumin (45 kDa), and trypsinogen (24 kDa). Note the distinct differences in the polypeptide patterns between rat and guinea pig peroxisomes.

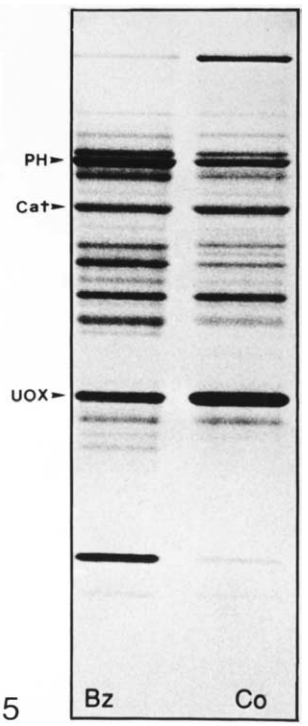

FIGURE 5 SDS–PAGE of highly purified peroxisomes from control (Co) and bezafibrate-treated (Bz) rat liver. A 10–15% resolving gel was used, and 5.0 µg of protein was loaded per each lane. Silver staining of bands. Peroxisomal polypeptides indicated by an arrowhead are PH, trifunctional protein; Cat, catalase; and UOX, urate oxidase. Note the induction of PH and the concomitant reduction of Cat and UOX in peroxisomes of Bz-treated rats. Also note that the control preparations, R in Fig. 4 and Co in Fig. 5, are not identical and that different resolving gels have been used.

and guinea pig (Fig. 4, lane G). The selective induction of specific peroxisomal proteins, such as the trifunctional protein (PH) in rats treated with hypolipidemic fibrates (lane Bz) with the concomitant reduction of catalase (Cat) and urate oxidase (UOx), is apparent in Fig. 5.

The extended procedure outlined here has been successfully employed to isolate heavy and light peroxisome subpopulations from normal and regenerating rat liver differing in density, size, shape, and enzymatic composition (Lüers *et al*., 1993). Moreover, peroxisome subsets as divergent as the former have been also obtained from the human heptoma cell line HepG2 (Schrader *et al*., 1994). However, further subpopulations, which are also present in those tissues, escape purification by conventional gradient centrifugation, most probably because their sedimentation properties are close to those of other subcellular organelles, particularly microsomes. Nevertheless, their purification has become an essential task in view of the functional significance of PO in humans in general (Wanders *et al*., 1995) and the putative importance of peroxisomal subpopulations in the biogenesis of this organelle in particular (Erdmann *et al*., 1997; Titorenko *et al*., 1997).

As an alternative to density gradient centrifugation, immune free flow electrophoresis (IFFE) has been introduced and applied successfully for the purification not only of regular PO (ρ = 1.22–1.24 g/cm^3) from a light mitochondrial fraction of rat liver, but also of PO from heavy and postmitochondrial fractions (Völkl *et al*., 1997, 1999). IFFE combines the advantages of eletrophoretic separation with the high selectivity of an immune reaction. It makes use of the fact that the electrophoretic mobility of a subcellular particle, complexed with an antibody directed against the cytoplasmic domain of one of its integral membrane proteins, is diminshed greatly, provided the pH of the electrophoresis buffer is adjusted to pH ~8.0, which is the pI of IgG molecules. The PO isolated by IFFE from the diverse hepatic subcellular fractions differed in their composition of matrix and membrane proteins as has been revealed by immunoblotting, thus supporting the view that IFFE is a valid method for the

purification of distinct subsets of the peroxisomal compartment.

Acknowledgments

The original work in the laboratory of the authors has been supported by grants of the Deutsche Forschungsgemeinschaft, Bonn, FRG (Fa 146/1-3; Vo 317/3-1; SFB 352 and Vo 317/4-1) and Landesforschungsschwerpunkt-Programm of the State of Baden-Württemberg, FRG.

References

De Duve, C., Pressman, B. C., Gianetto, R., Wattiaux, R., and Appelmans, F. (1955). Intracellular distribution patterns of enzymes in rat liver tissue. *Biochem. J.* **60**, 604–617.

Erdmann, R., Veenhuis, M., and Kunau, W. H. (1997). Peroxisomes: Organelles at the crossroads. *Trends Cell Biol.* **7**, 400–407.

Fahimi, H. D. (1969). Cytochemical localization of peroxidatic activity of catalase in rat hepatic microbodies (peroxisomes). *J. Cell Biol.* **43**, 275–288.

Fahimi, H. D., Baumgart, E., Beier, K., Pill, J., Hartig, F., and Völkl, A. (1993). Ultrastructural and biochemical aspects of peroxisome proliferation and biogenesis in different mammalian species. *In* "Peroxisomes: Biology and Importance in Toxicology and Medicine" (G. G. Gibson and B. Lake, eds.), pp. 395–424. Taylor and Francis, London.

Hartl, F. U., Just, W. W., Köster, A., and Schimassek, H. (1985). Improved isolation and purification of rat liver peroxisomes by combined rate zonal and equilibrium density centrifugation. *Arch. Biochem. Biophys.* **237**, 124–134.

Leighton, F., Poole, B., Beaufay, H., Baudhuin, P., Coffey, J. W., Fowler, S., and De Duve, C (1968). The large-scale preparation of peroxisomes, mitochondria and lysosomes from the livers of rats injected with Triton WR-1339. *J. Cell Biol.* **37**, 482–513.

Lüers, G., Hashimoto, T., Fahimi, H. D., and Völkl, A. (1993). Biogenesis of peroxisomes : Isolation and characterization of two distinct peroxisomal populations from normal and regenerating rat liver. *J. Cell Biol.* **121**, 1271–1280.

Neat, C. E., Thomassen, M. S., and Osmundsen, H. (1980). Induction of peroxisomal ß-oxidation in rat liver by high-fat diets. *Biochem. J.* **186**, 369–371.

Schrader, M., Baumgart, E., Völkl, A., and Fahimi, H. D. (1994). Heterogeneity of peroxisomes in human hepatoblastoma cell line HepG2: Evidence of distinct subpopulations. *Eur. Cell Biol.* **64**, 281–294.

Titorenko, V., Ogrydziak, D. M., and Rachubinski, R. A. (1997). Four distinct secretory pathways serve protein secretion, cell surface growth, and peroxisome biogenesis in the yeast *Yarrowia lipolytica*. *Mol. Cell Biol.* **17**, 5210–5226.

Van Veldhoven, P., Debeer, L. J., and Mannaerts, G. P. (1983). Water- and solute- accessible spaces of purified peroxisomes. *Biochem. J.* **210**, 685–693.

Van Veldhoven, P., Baumgart, E., and Mannaerts, G. P. (1996). Iodixanol (Optiprep), an improved density gradient medium for the isoosmotic isolation of rat liver peroxisomes. *Anal. Biochem.* **237**, 17–23.

Völkl, A., and Fahimi, H. D. (1985). Isolation and characterization of peroxisomes from the liver of normal untreated rats. *Eur. J. Biochem.* **149**, 257–265.

Völkl, A., Mohr, H., and Fahimi, H. D. (1999). Peroxisomal subpopulations of the rat liver: Isolation by immune free flow electrophoresis. *J. Histochem. Cytochem.* **47**, 1111–1117.

Völkl, A., Mohr, H., Weber, G., and Fahimi, H. D. (1997). Isolation of rat hepatic peroxisomes by means of free flow electrophoresis. *Electrophoresis* **18**, 774–780.

Wanders, R. J. A., Schutgens, R. B. H., and Barth, P. G. (1995). Peroxisomal disorders: A review. *J. Neuropathol. Exp. Neurol.* **54**, 726–739.

Zaar, K. (1992). Structure and function of peroxisomes in the mammalian kidney. *Eur. J. Cell Biol.* **59**, 233–254.

CHAPTER

10

Isolation of Mitochondria from Mammalian Tissues and Cultured Cells

Erika Fernández-Vizarra, Patricio Fernández-Silva, and José A. Enríquez

I. INTRODUCTION

Isolation of mitochondria can be a necessary procedure for many purposes: (1) as a primary step for further purification of mitochondrial subcomponents; (2) to perform metabolic assays, with respiration activity analysis the most common; and (3) to perform molecular analyses on the biogenetic activity of the organelle. The mitochondrial preparations obtained using the method described herein are perfectly suitable for biogenetical studies (mitochondrial DNA, RNA, protein synthesis, and as source for respiratory complex analysis by blue-native gel electrophoresis), as well as in a variety of different assays where isolated mitochondria are required, such as assessment of respiratory enzyme activities, protein import, aminoacylation, and *in organello* footprinting. The method consists of three basic steps: (1) cell rupture, (2) differential centrifugation: first at low speed to pellet mainly nuclei and unbroken cells and then at high speed to pellet mitochondria, and (3) washing of the mitochondrial pellet in order to reduce the presence of other subcellular contaminants. Mitochondria from different sources are obtained using basically the same methodology, although some modifications must be introduced depending on the tissue type or if mitochondria are to be isolated from cultured cells. When the purity of samples is considered, there is an elimination of a good part of the contaminants when mitochondrial preparations obtained by this procedure are compared with crude mitochondrial fractions. Because this purification protocol does not make use of gradient preparation or ultracentrifugation, further purification of the organelles is recommended when mitochondria are prepared for isolation of organelle subcomponents. In summary, the method described here produces reasonably pure mitochondria in a fairly short time and with a low cost. In addition, maintenance of integrity and functionality of the organelles are guaranteed.

II. MATERIALS AND INSTRUMENTATION

Sucrose (ACS for analysis) is from Carlo Erba Reagenti (Cat. No. 477183). Sodium chloride (ACS analytical reagent, Cat. No. 727 810) is from Prolabo. Potassium cyanide (KCN; BioChemika MicroSelect; Cat No. 60178) is from Fluka. Ethylenediaminetetraacetic acid disodium salt 2-hydrate (EDTA-Na_2; for analysis-ACS; Cat. No. 131669), potassium chloride (for analysis-ACS-ISO; Cat. No. 131494), magnesium chloride 6-hydrate (for analysis-ACS-ISO; Cat. No. 131396), sulphuric acid (96%; Cat. No. 251058), trichloroacetic acid [solution 20% (w/v); Cat. No. 252373], acetic acid glacial (chemically pure; Cat. No. 211008), sodium hydrogen sulphite [solution 40% (w/v); Cat. No. 211642], sodium sulphite (anhydrous purissimum; Cat. No. 141717); dipotassium hydrogen phosphate (anhydrous for analysis; Cat. No. 121512), potassium dihydrogen phosphate (for analysis, Cat. No. 121509) and orthophosphoric acid (85% for analysis-ACS-ISO; Cat. No. 131032) are from Panreac. D-Mannitol (ACS reagent; Cat. No. M-9647), ethylene glycol-bis(β-aminoethyl ether)-*N*,*N*,*N*′,*N*′-tetraacetic acid (EGTA; approximately 97%; Cat. No. E-4378), L-glutamic acid monosodium salt [glutamate; minimum 99% (TLC); Cat. No. G-1626], L-(-)-malic acid sodium salt [malate; 95–100% (enzymatic); Cat. No. M-1125], succinic acid disodium salt hexahydrate (succinate;

Copyright 2006, Elsevier Science (USA).
All rights reserved.

minimum 99%; Cat. No. S-2378), oxalacetic acid (approximately 98%; Cat. No. O-4126), acetyl coenzyme A trilithium salt (acetyl-CoA; approximately 95%, Cat. No. A-2181), 5-5′-ditio-bis(2-nitrobenzoic acid) or DTNB (Ellman's reagent; Cat. No. D-8130), glycerol 2-phosphate disodium salt hydrate (β-glycerophosphate; ≤ 0.1% α-isomer; Cat. No. G-6251), ammonium molybdate tetrahydrate (81–83% as MoO_3 ACS reagent; Cat. No. A-7302), β-D-glucose 6-phosphate sodium salt (crystalline, Sigma Grade; G-7879), imidazole [minimum 99% (titration), crystalline; Cat. No. I-0250], hydrogen peroxide (29–32% as H_2O_2 ACS reagent; Cat. No. H-0904), bovine serum albumin [BSA; fraction V; minimum 96% (electrophoresis); Cat. No. A-4503], and subtilisin (subtilisin A from *Bacillus* sp.; lyophilized powder, type VIII, 7–15 units/mg solid; Cat. No. P-5380) are from Sigma. Aldrich supplied the titanium (IV) oxysulfate [titanyl sulfate or $TiOSO_4$; 15% (w/v) solution in diluted H_2SO_4; Cat. No. 49,537-9] and the 4-amino-3-hydroxy-1-naphtelenesulphonic acid (aminonaphtosulphonic Acid; 98+% ACS reagent; Cat. No. 39,896-9). D-Sorbitol (high purity; Cat. No. SO0850) is from Scharlau. Tris (for analysis; Cat. No. 1.08382), hydrochloric acid fuming (37%; Cat. No. 1.00317) and 2-mercaptoethanol (for synthesis; Cat. No. 8.05740) are from Merck. BSA fraction V, fatty acid free (Cat. No. 775 827), adenosine-5′-diphosphate disodium salt (ADP; Cat. No. 127 507), cytochrome c (from horse heart, salt free, Cat. No. 103 888), and Triton X-100 (especially purified for membrane research; Cat. No. 789 704) are from Roche. For protein determination, the Bio-Rad protein assay dye reagent concentrate (450 ml; Cat. No. 500-0006) is used. Phosphate-buffered saline (PBS 1x, liquid, pH 7.4 ± 0.05; Cat. No. 10010) is from GIBCO (Invitrogen Corporation).

Elvejhem-type glass homogenisers with Teflon pestles, as well as the Dounce-type glass potter, are from local glassware providers (VidraFoc and Sumalsa). Fifty-milliliter polypropylene copolymer centrifuge tubes (Oak Ridge centrifuge tubes; Cat. No. 3119-0050) and the 0.2-µm syringe filters (Cat. No. 190-2520) are from Nalgene.

Centrifugations are performed in a Sorvall RC 5B Plus refrigerated centrifuge with the Sorvall HS-4 swinging rotor and the SS-34 fixed angle rotor. An Eppendorf 5415 C microfuge kept in the cold room is used to centrifuge the Eppendorf tubes.

Mitochondrial oxygen consumption measurements are obtained with a Hansatech CBID oxygen electrode and registered in a PC using software from Pico Technology Limited. The polytetrafluoroethylene (PTFE) membrane (ordering code: S4; thickness 0.0125 mm, width 25.4 mm, 30 m reel) is from Hansatech.

Spectrophotometric measurements are performed in a Unicam UV 500 spectrophotometer, where the temperature is kept constant by a DBS PCD 150 water peltier system. Data from these measurements are registered by a PC using the Vision 32 version 1.25 software from Unicam Limited.

III. PROCEDURES

A. Isolation of Mitochondria

1. Solutions

a. *Homogenisation medium A*: 0.32 *M* sucrose, 1 m*M* EDTA, and 10 m*M* Tris–HCl. For 1 liter, weigh 109.5 g of sucrose, dissolve in bidistilled water, and add 2 ml of 0.5 *M* disodium EDTA stock solution and 20 ml of 0.5 *M* Tris–HCl, pH 7.4. Check and adjust, if necessary, pH to 7.4 and autoclave at low pressure. Store at 4°C.

b. *Homogenisation medium AT*: 0.075 *M* sucrose, 0.225 *M* mannitol, 1 m*M* EGTA, and 0.01% BSA. For 500 ml, add 12.84 g of sucrose, 20.5 g of mannitol, and 5 ml of a stock solution of 100 m*M* EGTA. Adjust pH to 7.4 and autoclave at low pressure. Store at 4°C. Just before use add 500 µl of 10% (w/v) BSA. Once the BSA is added, the solution cannot be autoclaved again.

c. *Homogenisation medium IB 10×*: 0.35 *M* Tris–HCl, pH 7.8, 0.25 *M* NaCl, and 50 m*M* $MgCl_2$. To prepare 100 ml, add 70 ml of 0.5 *M* Tris–HCl, pH 7.8, 5 ml of 5 *M* NaCl, and 5 ml of 1 *M* $MgCl_2$. Complete to 100 ml with bidistilled water and sterilize by filtration. Store at 4°C.

d. *MAITE medium*: 25 m*M* sucrose, 75 m*M* sorbitol, 100 m*M* KCl, 0.05 m*M* EDTA, 5 m*M* $MgCl_2$, 10 m*M* Tris–HCl, pH 7.4, and 10 m*M* H_3PO_4 (pH 7.4). For 100 ml of solution weigh 0.86 g of sucrose, 1.37 g of sorbitol, and 0.74 g of KCl, dissolve, and then add 10 µl of 0.5 *M* EDTA, 500 µl of 1 *M* $MgCl_2$, 2 ml 0.5 *M* Tris–HCl, pH 7.4, and 68 µl of orthophosphoric acid. Adjust pH to 7.4 using Tris base 0.5 *M*. Sterilize by filtration through a 0.2-µm filter, make 10-ml aliquots, and store at 4°C.

e. *0.5 M EDTA*: Weigh 93.1 g of disodium EDTA, dissolve, adjust the pH to 8.0, and complete the volume to 500 ml with distilled water. Store at 4°C.

f. *0.5 M Tris–HCl pH 7.4 or pH 7.8*: For 500 ml, weigh 30.3 g of Tris and adjust pH to 7.4 or 7.8 with HCl. Store at 4°C.

g. *100* m*M EGTA*: Prepare 100 ml of this solution by weighing 3.8 g. In order to increase the solubility of EGTA, the pH has to be raised with NaOH when dissolving it. Once the EGTA is totally dissolved, complete to 100 ml with bidistilled water. Store at 4°C.

h. *1 M $MgCl_2$*: For 100 ml, weigh 2 g of magnesium chloride and dissolve. Store at 4°C.

i. *5 M NaCl*: Weigh 29.3 g of NaCl, dissolve, and adjust to 100 ml with bidistilled water.

j. *10% (w/v) or 100 mg/ml BSA*: Weigh 0.5 g of fatty acid-free BSA and dissolve in 5 ml of distilled water. Sterilize by filtration through a 0.2-µm filter and store at –20°C in 1-ml aliquots.

2. *Isolation of Mitochondria from Rat Tissues*

a. Mitochondria from Liver and Kidney

Use male Wistar rats weighing 200–300 g. It is recommended that glassware, scissors, and metal sieves be sterilized at 160°C overnight. Autoclave plastic tubes at 1 atm for 20 min.

1. Previous to the sacrifice of the animals, fill 100-ml glass beakers with enough homogenisation medium A to cover the organ to be utilised, weigh, and place them on ice.
2. Kill the animals, remove the organ of interest, and place it in a beaker with ice-cold homogenisation medium A (in this case liver or kidneys).
3. Weigh the beaker to know the amount of tissue that has been extracted.
4. Cut the tissue into small pieces with a pair of scissors.
5. Sift the tissues and wash them with more homogenisation medium in order to remove blood and connective tissue. Put them back in the beaker and repeat steps 4 and 5 three or four times until the tissue is well cleaned.
6. Add fresh homogenisation medium to the homogeniser in a proportion of 4 ml per gram of liver and 5 ml per gram of kidney.
7. Transfer the pieces of tissue to the homogeniser.
8. Homogenise with four up-and-down strokes in the Elvehjem–Potter with the motor-driven Teflon pestle at 600 rpm.
9. Transfer the homogenised tissue into the 50-ml sterile centrifuge tubes.
10. Centrifuge in the HS-4 swinging rotor at 1000 *g* (3000 rpm) for 5 min at 4°C in order to pellet unbroken tissue, cells, and nuclei.
11. Place eight Eppendorf tubes in a container with ice and fill them with supernatant from the previous step (this and the following steps are done in a cold room).
12. Centrifuge the Eppendorf tubes for 2 min at 13,000 rpm in a microfuge.
13. Using a sterile Pasteur pipette, remove the supernatant trying to draw out all the liquid and part of the light coloured fluffy layer on the top of the pellet without disturbing the darker part where mitochondria are.
14. To wash the mitochondrial fraction, add homogenisation medium A, up to 1.5 ml, to four of the eight Eppendorf tubes and resuspend. Transfer the resuspended pellet of one tube to one of the tubes without medium A and resuspend.
15. Centrifuge the four resulting tubes as described earlier.
16. Repeat steps 15, 16, and 17 so that now two tubes are centrifuged.
17. Repeat the same procedure once again until one tube, containing all the material, is left.
18. When the last tube is centrifuged and the supernatant is removed, wash the pellet by resuspending it with MAITE medium.
19. Centrifuge for 2 min at 13,000 rpm.
20. Resuspend the pellets with 1 ml of MAITE medium.

When a bigger amount of sample is needed, the procedure can be started using twice as much supernatant and then finishing with the mitochondrial preparation in two Eppendorf tubes.

b. Mitochondria from Heart

1. Follow the steps 1 to 7 described in Section III,A,2,a but instead of filling the beakers with homogenisation medium A, use homogenisation medium AT.
2. Fill the homogeniser with 10 ml of medium AT per gram of heart.
3. Homogenise with six strokes in the Elvehjem–Potter with the motor-driven Teflon pestle at 600 rpm.
4. Transfer the homogenised tissue to a sterile 50-ml centrifuge tube.
5. Centrifuge at 1000 *g* (3000 rpm) in the HS-4 swinging rotor for 5 min at 4°C.
6. Transfer the supernatant from the previous centrifugation step to a clean centrifuge tube.
7. Centrifuge at 12,000 *g* (9000 rpm) in the SS-34 fixed angle rotor for 10 min at 4°C to obtain the crude mitochondrial fraction.
8. Draw out and discard the supernatant.
9. Resuspend the pellet in 5.5 ml of homogenisation medium AT.
10. Transfer the mitochondrial suspension to four Eppendorf tubes for the washing steps in the cold room.
11. Proceed hereafter as described for liver and kidney mitochondria, but if the mitochondrial fraction is obtained from one rat heart, the final fraction has to be resuspended in a smaller volume than those from liver and kidney, usually with 0.5–0.75 ml.

An alternative isolation procedure for heart mitochondria has been described previously (McKee *et al*., 1990) where perfusion and homogenisation of the

hearts using subtilisin (0.4 mg/ml) are proposed to improve the yield, the respiratory performance, and the protein synthesis activity of the isolated organelles. In our hands, the addition of subtilisin to the homogenisation medium provides a higher yield in the preparations and increases the *in organello* transcription rate. However, no significant improvement in the rate of incorporation of a radioactive amino acid into the mitochondrial translation products could be observed. However, the electrophoretic pattern of *in organello* synthesized products reveals an abnormal accumulation of low molecular weight peptides when subtilisin is used, probably due to residual peptidase activity of the subtilisin after breaking the organelles.

c. Mitochondria from Brain

1. Again follow the same first five steps as for liver, kidney, and heart. Use homogenisation medium AT.
2. Add 5 ml of medium AT per gram of brain to the homogeniser.
3. Homogenise the pieces of brain with 10 to 15 strokes using a Dounce-type glass homogeniser with a manually driven glass pestle.
4. Transfer the homogenised tissue to a sterile 50-ml centrifuge tube.
5. Centrifuge at 1000 *g* in swinging rotor for 5 min at 4°C.
6. Transfer the supernatant from the previous centrifugation step to a clean sterile centrifuge tube.
7. Resuspend the pellet resulting from the previous centrifugation in another 5 ml of medium AT per gram of starting tissue.
8. Rehomogenise the nuclear pellet by repeating 10 to 15 strokes in the Dounce potter.
9. Transfer the homogenised nuclear pellet to the same 50-ml tube where the first centrifugation was done.
10. Centrifuge at 1000 *g* in the swinging rotor for 5 min at 4°C.
11. Remove this second supernatant and pour it into the tube with the first supernatant.
12. Centrifuge at 12,000 *g* (9000 rpm) in the fixed angle SS-34 rotor for 10 min at 4°C to obtain the crude mitochondrial fraction.
13. Wash and resuspend as described for heart mitochondria (steps 8–11).
14. Resuspended the final pellet in 0.9 ml of MAITE medium.

A great fraction of mitochondria is lost in the first nuclear pellet in whatever tissue is used; therefore, these steps (7–11) of rehomogenisation and a second centrifugation are especially necessary when isolating brain mitochondria because the homogenisation is much gentler than for the other tissues and the yield is too low when only one homogenisation step is done. The brain mitochondrial fraction obtained this way contains free as well as synaptic mitochondria. To separate free mitochondria from synaptosomes ("pinched off" synaptic ends with the synaptic mitochondria), several methods are available (reviewed in Whittaker, 1993). Partitioning in an aqueous two-phase system is recommended (Lopez-Perez, 1994).

3. Isolation of Mitochondria from Mammalian Cultured Cells

This procedure is the modified Gaines method (Enriquez and Attardi, 1996; Fernandez-Vizarra *et al.*, 2002; Gaines, 1996).

1. Harvest exponentially growing cells by trypsinization. Use the cells contained in ten to twelve 150-mm plates that are about 80–90% confluent.
2. Transfer the cells to a 50-ml Falcon tube.
3. Wash twice with cold PBS by centrifuging at 600 *g* in the clinical centrifuge for 8 min at 4°C. In the last wash, transfer the cells to a 15-ml Falcon tube and centrifuge as before.
4. Place the cells in ice. Measure the volume occupied by the packed cells.
5. Resuspend the cells in one-half of the packed cell volume of IB 0.1×. This is a hypotonic medium to facilitate the breakage of the cells.
6. Pipette the cell suspension into the homogeniser.
7. Wash the tube where the cells are with 0.1× IB using another half volume of the originally packed cells and pipette this into the homogeniser.
8. Perform four to five strokes in the homogeniser with the motor-driven Teflon pestle at 600 rpm.
9. Immediately add 1/10 of the initial volume of packed cells of 10× IB, to make the medium isotonic.
10. Transfer the homogenised cells to a 15-ml Falcon tube.
11. Centrifuge at 1600 *g* (3500 rpm) for 3 min at 4°C in the HS-4 swinging rotor to pellet unbroken cells, debris, and nuclei.
12. Draw out the supernatant and transfer it to a clean 15-ml Falcon tube.
13. Resuspend the nuclear pellet in one-half of its volume of 0.1× IB.
14. Repeat steps 6 to 11.
15. Collect the supernatant from this second round of homogenisation and centrifugation and add it to the first supernatant.
16. Centrifuge the supernatants at 1600 *g* (3500 rpm) for 3 min at 4°C in the HS-4 swinging rotor to remove remaining nuclei and unbroken cells.

17. Pipette the supernatant in (normally two) Eppendorf tubes placed in ice (this one and the following steps are performed in the cold room).
18. Centrifuge the Eppendorf tubes at 13,000 rpm in the microfuge for 1 min.
19. Wash the mitochondrial pellet with homogenisation medium 1× IB, until all the material is in one tube.
20. Remove supernatant and wash the pellet by resuspending it with homogenisation medium A.
21. Centrifuge the Eppendorf tube at 13,000 rpm in the microfuge for 1 min.
22. Remove supernatant and wash the pellet using MAITE medium.
23. Centrifuge the Eppendorf tubes at 13,000 rpm in the microfuge for 1 min.
24. Resuspend the mitochondrial pellet in the appropriate volume of MAITE medium, which is usually around 300 µl.

B. Assessment of Purity

Two different parameters have to be considered when assessing the purity of a mitochondrial fraction. One is the enrichment of the preparation in mitochondria and the other is the presence of contaminants. The enrichment in mitochondria is evaluated by measuring the activities of mitochondrial enzymes in the initial homogenate and in the final mitochondrial preparation. We usually measure two activities: the inner membrane-bound respiratory complex IV or cytochrome c oxidase (Wharton, 1967) and the mitochondrial matrix enzyme citrate synthase (Srere, 1969). Spectrophotometric measurement of individual respiratory complex activities has been reviewed previously (Birch-Machin and Turnbull, 2001; Trounce, 1996). However, to evaluate the presence and abundance of contaminants, different approaches can be proposed. The most common contaminants in a mitochondrial preparation are microsomes (mostly derived from endoplasmic reticulum), lysosomes, and peroxisomes, and their presence is monitored by the determination of specific enzyme activities present in each contaminant particle. Good examples of these activities that we have used to assess purity are glucose-6-phosphatase for endoplasmic reticulum (Morré, 1971), acid phosphatase for lysosomes (Trouet, 1974), and catalase for peroxisomes (Baudhuin, 1974). Electron microscopy morphometric analysis is good for estimating unidentified contaminants for which no enzymatic marker is available (Enriquez *et al*., 1990).

1. Treatment of Samples

Total homogenate samples that are used for spectrophotometric enzymatic activity measurements must undergo a freeze–thawing treatment in order to break the cells completely and liberate the enzymes from the subcellular particles. Crude mitochondrial fractions and mitochondrial preparations do not need such treatment, they are just divided in aliquots and kept at –70°C until they are used for the spectroscopic measurements. The single freezing and thawing step is sufficient to break them.

1. Use 1-ml aliquots of total homogenate that are in Eppendorf tubes.
2. Prepare a water bath at a temperature of 37°C.
3. Fill an appropriate container with liquid nitrogen.
4. Put the samples in the liquid nitrogen until they are completely frozen (2 min).
5. Immediately pass the samples to the water bath at 37°C and keep them there until they are thawed completely (5 min).
6. Repeat steps 4 and 5 four or five times.
7. Aliquot the homogenate in Eppendorf tubes, 50–100 µl in each tube, and keep them at –70°C.

2. Cytochrome c Oxidase Activity (EC 1.9.3.1)

Measurements of cytochrome c oxidase activity are performed spectrophotometrically using 5 µl of sample (nondiluted total homogenate or 1/10 diluted mitochondrial samples) in a final volume of 1 ml. The decrease of absorbance at 550 nm, due to the oxidation of cytochrome c, is measured for 90 s at 38°C (Wharton, 1967). Sensitivity to KCN is used to confirm that cytochrome c oxidase activity is measured.

3. Citrate Synthase Activity (EC 4.1.3.7)

To measure citrate synthase activity, use the same amount of sample as in the case of cytochrome c activity; the final reaction volume is also 1 ml. In the spectrophotometer, measure the increase of the absorbance at 412 nm due to the formation of a yellow complex of free CoA with DTNB, for 90 s at 30°C (Srere, 1969). The CoA is formed in the reaction of acetyl-CoA with oxalacetate to form citrate, catalysed by citrate synthase.

Mitochondrial enrichment assessed by these enzymatic activities in the indicated preparations is shown in Table I.

4. Glucose-6-phosphatase Activity (EC 3.1.3.9)

Glucose-6-phosphatase activity was measured according to (Morré, 1971), determining spectrophotometrically the inorganic phosphate (P_i) liberated by the enzyme from the substrate (glucose-6-phosphate). The amount of sample used is 0.1 ml, diluted 1/10 in the case of total homogenate and 1/20 for mitochon-

TABLE I Specific Activities Obtained for Two Mitochondrial Marker Enzymes: Cytochrome c Oxidase (Inner Membrane) and Citrate Synthase (Matrix)[a]

Enzyme	Source	Specific activity (units/g protein)			Purification (number of times)		Yield (%)	
		Homogenate	Crude	Mitochondria	Crude	Mitochondria	Crude	Mitochondria
COX	Liver	166 ± 51	537 ± 18	598 ± 51	3.4 ± 1.1	3.7 ± 0.8	22.2 ± 4.5	23.2 ± 0.6
	Kidney	387 ± 93	1162 ± 341	1397 ± 162	3.2 ± 1.7	3.8 ± 1.3	34.0 ± 7.5	19.1 ± 2.7
	Heart	477 ± 49	nd	2249 ± 92	nd	4.6 ± 0.6	nd	18.5 ± 0.9
	Brain	236 ± 11	nd	844 ± 47	nd	3.6 ± 0.1	nd	8.0 ± 4.0
CS	Liver	93 ± 10	345 ± 41	400 ± 33	3.8 ± 0.8	4.4 ± 0.8	24.7 ± 2.2	27.2 ± 0.2
	Kidney	259 ± 22	631 ± 97	689 ± 110	2.5 ± 0.6	2.7 ± 0.6	27.3 ± 2.1	13.7 ± 0.4
	Heart	1634 ± 48	nd	4669 ± 163	nd	2.9 ± 0.2	nd	11.2 ± 1.4
	Brain	623 ± 111	nd	2261 ± 263	nd	3.7 ± 0.2	nd	8.3 ± 4.6

[a] Homogenate, total homogenate; crude, crude mitochondrial fraction, which is obtained by differential centrifugation without the washing steps; mitochondria, final mitochondrial fraction obtained as described in the text; COX, cytochrome c oxidase (EC ***1.9.3.1***); CS, citrate synthase (EC ***4.1.3.7***); nd, not determined.

TABLE II Specific Activities of Marker Enzymes for Typical Contaminants in a Mitochondrial Preparation[a]

Enzyme	Source	Specific activity (units/g protein)			Purification (number of times)		Yield (%)	
		Homogenate	Crude	Mitochondria	Crude	Mitochondria	Crude	Mitochondria
G6Pase	Liver	32 ± 1	83 ± 17	36 ± 10	2.6 ± 0.7	1.1 ± 0.3	20.1 ± 6.1	7.9 ± 1.7
(microsomes)	Kidney	79 ± 7	106 ± 0.4	37 ± 13	1.4 ± 0.1	0.5 ± 0.2	11.6 ± 1.7	3.5 ± 0.8
Acid phosp	Liver	9 ± 1	28 ± 1	18 ± 2	3.2 ± 0.4	2.0 ± 0.4	24.5 ± 1.9	14.2 ± 2.6
(lisosomes)	Kidney	15 ± 6	24 ± 3	13 ± 3	1.7 ± 0.5	1.0 ± 0.6	14.5 ± 0.7	7.2 ± 2.9
Catalase	Liver	163 ± 27	276 ± 66	91 ± 17	1.8 ± 0.7	0.6 ± 0.2	13.5 ± 4.8	4.1 ± 1.3
(peroxisomes)	Kidney	81 ± 6	71 ± 17	32 ± 8	0.9 ± 0.1	0.4 ± 0.1	7.7 ± 3.0	3.1 ± 1.2

[a] Homogenate, total homogenate; crude, crude mitochondrial fraction, which is obtained by differential centrifugation without the washing steps; mitochondria, final mitochondrial fraction obtained as described in the text; G6pase, glucose-6-phosphatase (***EC 3.1.3.9***); acid phsp, acid phosphatase (***EC 3.1.3.2***).

dria and crude mitochondrial fractions. After a 15-min incubation at 37°C, there will be 0.1–1 µmol of P_i per milliliter. Protein is removed by TCA precipitation and centrifugation, and the amount of inorganic phosphate is measured in 1 ml of cleared supernatant.

5. *Acid Phosphatase Activity (EC 3.1.3.2)*

Incubate 1 ml of 1/10 diluted sample (total homogenate, mitochondria, or crude mitochondrial fractions) with 200 µl 0.5 *M* β-glycerophosphate, 100 µl of buffer, 100 µl of 2% (w/v) Triton X-100, and 600 µl of water for 30 min at 37°C (Trouet, 1974). Remove protein by TCA precipitation and centrifugation and measure the amount of inorganic phosphate in 1 ml of cleared supernatant.

The unit of activity is defined as the amount of enzyme liberating 1 µmol of phosphate per minute.

6. *Catalase Activity (EC 1.11.1.6)*

Catalase activity in the samples is measured using the method described in Baudhuin (1974), which is based on the formation of the yellow titanyl sulphate–H_2O_2 complex. Liver and kidney samples must be diluted (1/40 for liver and 1/10 for kidney), whereas heart and brain samples do not need to be diluted. After incubation for 10 min at 0°C and addition of the titanyl sulphate solution, measure the absorbance at 405 nm to evaluate how much of the initially added H_2O_2 is left. To calculate the activities, take into account that the reaction follows first-order kinetics and that one unit of enzyme is defined as the amount consuming 90% of the H_2O_2 present in a 50-ml reaction volume in 1 min.

Evaluation of the presence of contaminants is shown in Table II.

C. Yield of Mitochondria and Normalisation Criteria

The yield of mitochondria depends on the source of the organelles. Typically we obtain 6–9 mg of mitochondrial protein per gram of starting tissue for the liver samples, which is 5–6 mg/g for kidney, 2–3 mg/g for heart, and 3–4.5 mg of mitochondrial protein per gram of tissue in brain samples. The yield can also be calculated by the amount of mitochondrial activity (cytochrome c oxidase and citrate synthase) recovered in preparations from the total homogenate. Table I shows values obtained for the different mitochondrial preparations. The yield of mitochondria evaluated this way varies from 8% of recovery in brain to about 25% in liver.

Classically, the way of normalising mitochondrial parameters is using protein content in the sample. However, mitochondrial protein content in the different preparations is very variable. In each kind of sample, the nature and amount of contaminants vary, and even the protein composition of mitochondria is different depending on their source. In this way, specific mitochondrial enzyme activities are very different among organs; this is due to their intrinsic differences in activity and also to the different protein content in each preparation (Table I). More recently, citrate synthase activity is often taken to normalise mitochondrial parameters (Trounce, 1996), particularly respiratory chain enzyme activities, because it is considered a measurement of mitochondrial volume. However, the intertissue variation on citrate synthase specific activities is also too high and its use for normalization when comparing different sources of organelles is again questionable; i.e., when calculating the cytochrome c oxidase/citrate synthase ratio, there are significant differences between organs, with liver apparently the highest cytochrome c oxidase activity (these can easily be calculated from Table I values).

Taking all this into account, we propose that the best way to normalise mitochondrial parameters when comparing organelles from different sources is to extract mitochondrial DNA from the organelle preparations and total cell DNA from the homogenate of the same samples and quantify the amount of nuclear DNA and mitochondrial DNA. The quantification of DNA is performed easily by conventional slot blot or Southern blot and hybridisation using a specific probe for each genome (Diez-Sanchez *et al.*, 2003). Routinely we use 12S rRNA for mtDNA and 18S rRNA for nDNA using the following rat polymerase chain reaction-generated probes.

1. 12S rRNA 617-bp amplification product (12S1 forward: caccgcggtcatacgattaacc; 12S2 reverse: ctaatttgaggagggtgacggg).
2. 18S rRNA 429-bp amplification product (18S1 forward: cctcgatgctcttagctgagtg: 18S2 reverse: cagctttgcaaccatactcccc).

In this way, the parameter/nuclear DNA ratio would represent a "per cell" or "per genome" estimation and the parameter/mtDNA a "per mitochondria" or "per mitochondrial DNA" estimation. Although the mtDNA copy number per cell varies among cell types, tissues, and physiological condition, it can be monitored easily by following the mtDNA/nDNA ratio.

D. Assessment of Functionality

Mitochondria obtained using the purification protocols described here have intact membranes and are coupled. This means that electron transfer among the inner membrane complexes takes place when there is phosphorylation of ADP by the ATP synthetase; this is the main way to dissipate the proton gradient between the intermembrane space and the matrix. Mitochondrial electron transfer can be measured by oxygen consumption using an oxygen electrode (Trounce, 1996). The respiratory control ratio (RCR) is a way to determine how coupled mitochondria are The consumption of oxygen by mitochondria in the presence of electron donors (substrates) and ADP, called state 3 respiration, is measured and then compared with the respiration rate when all the ADP has been phosphorylated (state 4). When there is no difference between state 3 and state 4 respiration (RCR = 1), mitochondria are completely uncoupled, whereas RCRs higher than 4 are indicative of tightly coupled mitochondria. Another parameter to evaluate coupling using the same measurements in the oxygen electrode is the P/O ratio, which gives the moles of synthesized ATP per atom of oxygen transformed to water during oxidative phosphorylation. Coupled mitochondria usually exhibit P/O ratios higher than 2.5, approaching 3 with NAD-linked substrates, and ratios higher than 1.8, approaching 2 with succinate (Palloti and Lenaz, 2001). A detailed explanation on oxygen electrode functioning can be found in Rickwood (1987).

1. Perform measurements in the oxygen electrode using MAITE medium where mitochondria are resuspended. The final volume in the electrode chamber is 1 ml.

2. Add 10 µl of 100 mg/ml BSA and either 20 µl of 500 m*M* glutamate and 25 µl of 100 m*M* malate when measuring RCR with glutamate and malate (NAD-

TABLE III RCR and P/O Ratios in Different Mitochondrial Preparations

Source of mitochondria	Glutamate + malate		Succinate	
	RCR	P/O ratio	RCR	P/O ratio
Liver	4.0–5.7	2.0–2.6	2.8–3.4	1.3–1.7
Kidney	2.3–4.6	1.7–2.3	2.1–3.5	1.6–1.9
Heart	4.9–7.4	2.9–3.4[a]	1.3	1.4–1.8
Brain[b] (total)	1.7–2.5	1.7–2.3	1.4	1.0–1.1
Brain[c] (PH-PART)	3.4	2.4	3.4	1.8

[a] The observation with some substrates of P/O ratios higher than the theoretical value 3 is attributed to substrate-level phosphorylation (Palloti and Lenza, 2001).

[b] Low values in the coupling parameters are usually found in mitochondrial preparations from brain and can be due to the presence of synaptosomes.

[c] These parameters improve substantially after further purification by phase partition (PH-PART). Data from López-Pérez (1994).

linked substrates) or, as an alternative, 20 µl of 500 m*M* succinate.

3. Add 0.5 to 1 mg of mitochondrial protein from freshly isolated mitochondria. In the case of heart mitochondria, 0.2 mg of protein is enough to perform the assay.

4. When the chamber is closed, add 100 nmol of ADP (10 µl of ADP 10 m*M*) to stimulate mitochondria and start state 3 respiration. This addition is repeated after mitochondria return to state 4 respiration.

Values for RCR and P/O for different mitochondrial preparations are given in Table III.

IV. COMMENTS AND RECOMMENDATIONS

We would like to make a particular comment on the nature of the less commonly evaluated contaminants in the mitochondrial preparations, whose presence is variable depending on their source and that has been frequently underscored in classical preparative or metabolic assays. In addition to their utility in bioenergetic and metabolic studies, isolated organelles provide a unique tool to investigate the synthesis and expression of mtDNA in conditions that very much resemble the *in vivo* enzyme/substrate proportions, ionic composition, and integrated activity of the metabolic and biogenetic processes (Enríquez e*t al*., 1996, 1999; Enriquez and Attardi, 1996; Fernandez-Vizarra *et al*., 2002).

In this type of assay the presence of contaminants can be relevant or negligible depending on the type of investigations to be performed. For example, only brain crude mitochondria preparations contain large myelin membrane debris that can be estimated by monitoring the 2′, 3′-cyclic nucleotide 3′-phosphohydrolase (Enriquez *et al*., 1990; Olafson *et al*., 1969). They do not seem to interfere with biogenetic analyses, but can contribute to the overall protein content (see later). In addition, this crude preparation contains synaptosomes (also enclosing mitochondria). Crude mitochondrial preparations are suitable for *in organello* transcription and replication analysis when labeled UTP or dNTPs are used, as well as for protein import assays, as nucleotides or peptides do not cross the plasma membrane of synaptosomes. However, when analyzing protein synthesis and amino acylation using labeled amino acids, one should keep in mind that amino acids are also imported by synaptosomes and used by their mitochondria. Therefore, if trying to evaluate the influence of specific factors in the mitochondrial protein synthesis, one has to be aware that a relevant portion of mitochondria are protected by a plasma membrane.

Other relevant contaminants, not considered very often, are residual but partially active biogenetic components of the nucleocytoplasmic machinery, such as cytoplasmic ribosomes, transcriptionally or replicative partially active nuclear rests, or cytoplasmic aminoacyl tRNA synthetases. The use of additional purification steps using density gradient purification could reduce the presence of some of these contaminants, but it is expensive, not suitable for large-scale preparations, and, most important, can affect the functionality of the purified organelles. Protein synthesis due to contaminant cytoplasmic ribosomes is not very relevant (Fernandez-Vizarra *et al*., 2002) and it is possible to eliminate it completely using drugs that specifically inhibit cytoplasmic protein synthesis without affecting mitoribosomes such as cycloheximide or emetine. In our hands, no detectable aminoacylation of cytoplasmic tRNAs is observed when using purified organelles from cultured cells (Enríquez, 1996). The same is true for transcription in any source of mitochondria tested (Andreu *et al*., 1998; Enríquez, 1999; Enriquez *et al*., 1991, 1996; Fernandez-Vizarra *et al*., 2002; Micol *et al*., 1997), but a background of nonmitochondrial DNA is labeled when mitochondria are prepared from exponential growing cultured cells (unpublished results). To avoid this, it is recommended to add DNase (or micrococcal nuclease) during the mtDNA replication assay, as mtDNA and mtRNAs are protected by the mitochondrial double membrane. Then, as the standard DNA isolation procedure, after incubations, includes a strong step of proteinase K digestion, the DNase is fully removed before breaking

of the mitochondria. In that way only mitochondrial DNA is labeled.

V. Pitfalls

1. Always keep mitochondrial preparations on ice while they are being isolated and until they are used for biogenetical analyses or for measurements in the oxygen electrode.

2. Invert the tubes where the mitochondria are kept every once in a while in order to maintain mitochondria in suspension, avoiding sedimentation. During the incubation for activity determination, mixing is essential, as sedimentation of the organelles can make them become permanently impaired in their biogenetic activities due to a lack of oxygenation.

3. Irreversible uncoupling of mitochondria during purification can occur and is found more often when isolating brain or heart mitochondria. This is likely due to the well-known uncoupling activity of fatty acids and could be prevented by the inclusion of fatty acid-free BSA in the purification buffer.

Acknowledgments

We thank Drs. Julio Montoya, Acisclo Pérez-Martos, and Manuel, José López-Pérez for their valuable input in our work and Santiago Morales for his technical assistance. Our research was supported by the Spanish Ministry of Education PM-99-0082 grant to JAE, by the Ramón y Cajal 2001 grant to PF-S, and by a Diputación General de Aragón (CONSID B015/2001) fellowship to EF-V.

References

Andreu, A. L., Arbos, M. A., Perez-Martos, A., Lopez-Perez, M. J., Asin, J., Lopez, N., Montoya, J., and Schwartz, S. (1998). Reduced mitochondrial DNA transcription in senescent rat heart. *Biochem. Biophys. Res. Commun.* **252**, 577–581.

Baudhuin, P. (1974). Isolation of rat liver peroxisomes. *Methods Enzymol.* **31**, 356–368.

Birch-Machin, M. A., and Turnbull, D. M. (2001). Assaying mitochondrial respiratory complex activity in mitochondria isolated from human cells and tissues. *Methods Cell Biol.* **65**, 97–117.

Diez-Sanchez, C., Ruiz-Pesini, E., Lapena, A. C., Montoya, J., Perez-Martos, A., Enriquez, J. A., and Lopez-Perez, M. J. (2003). Mitochondrial DNA content of human spermatozoa. *Biol. Reprod.* **68**, 180–185.

Enríquez, J. A., and Attardi, G. (1996). Analysis of Aminoacylation of Human Mitochondrial tRNAs. *Methods Enzymol.* **264**, 183–196.

Enríquez, J. A., Fernández-Silva, P., Garrido-Pérez, N., López-Pérez, M. J., Pérez-Martos, A., and Montoya, J. (1999). Direct regulation of mitochondrial RNA synthesis by thyroid hormone. *Mol. Cell Biol.* **19**, 657–670.

Enriquez, J. A., Lopez-Perez, M. J., and Montoya, J. (1991). Saturation of the processing of newly synthesized rRNA in isolated brain mitochondria. *FEBS Lett.* **280**, 32–36.

Enriquez, J. A., Perez-Martos, A., Lopez-Perez, M. J., and Montoya, J. (1996). In organello RNA synthesis system from mammalian liver and brain. *Methods Enzymol.* **264**, 50–57.

Enriquez, J. A., Sanchez-Prieto, J., Muino Blanco, M. T., Hernandez-Yago, J., and Lopez-Perez, M. J. (1990). Rat brain synaptosomes prepared by phase partition. *J. Neurochem.* **55**, 1841–1849.

Fernandez-Vizarra, E., Lopez-Perez, M. J., and Enriquez, J. A. (2002). Isolation of biogenetically competent mitochondria from mammalian tissues and cultured cells. *Methods* **26**, 292–297.

Gaines, G. L., 3rd (1996). In organello RNA synthesis system from HeLa cells. *Methods Enzymol.* **264**, 43–49.

Lopez-Perez, M. J. (1994). Preparation of synaptosomes and mitochondria from mammalian brain. *Methods Enzymol.* **228**, 403–411.

McKee, E. E., Grier, B. L., Thompson, G. S., and McCourt, J. D. (1990). Isolation and incubation conditions to study heart mitochondrial protein synthesis. *Am. J. Physiol.* **258**, E492–E502.

Micol, V., Fernandez-Silva, P., and Attardi, G. (1997). Functional analysis of *in vivo* and in organello footprinting of HeLa cell mitochondrial DNA in relationship to ATP and ethidium bromide effects on transcription. *J. Biol. Chem.* **272**, 18896–18904.

Morré, D. J. (1971). Isolation of Golgi apparatus. *Methods Enzymol.* **31**, 130–148.

Olafson, R. W., Drummond, G. I., and Lee, J. F. (1969). Studies on 2',3'-cyclic nucleotide-3'-phosphohydrolase from brain. *Can. J. Biochem.* **47**, 961–966.

Palloti, F., and Lenaz, G. (2001). Isolation and subfractionation of mitochondria from animal cells and tissue culture lines. *Methods Cell Biol.* **65**, 1–35.

Rickwood, D., Wilson, M. T., and Darley-Usmar, V. M. (1987). Isolation and characteristics of intact mitochondria. *In* "*Mitochondria: A Practical Approach*" (V. M. Darley-Usmar, D. Rickwood, and M. T. Wilson, eds.) pp. 1–16. IRL Press, Oxford.

Srere, P. A. (1969). Citrate synthase. *Methods Enzymol.* **13**, 3–11.

Trouet, A. (1974). Isolation of modified liver lysosomes. *Methods Enzymol.* **31**, 323–329.

Trounce, I. A., Kim, Y. L., Jun, A. S., and Wallace, D. C. (1996). Assessment of mitochondrial oxidative phosphorylation in patient muscle biopsies, lymphoblasts, and transmitochondrial cell lines. *Methods Enzymol.* **264**, 484–509.

Wharton, D. C., and Tzagoloff, A. (1967). Cytochrome oxidase from beef heart mitochondria. *Methods Enzymol.* **10**, 245–250.

Whittaker, V. P. (1993). Thirty years of synaptosome research. *J. Neurocytol.* **22**, 735–742.

CHAPTER

11

Subcellular Fractionation Procedures and Metabolic Labeling Using [^{35}S]Sulfate to Isolate Dense Core Secretory Granules from Neuroendocrine Cell Lines

Sharon A. Tooze

I. INTRODUCTION

Subcellular fractionation techniques have been developed to allow isolation of a particular subcellular compartments. Typically subcellular fractionation is used as a starting point to characterize the composition of subcellular organelles, but has also been used frequently to provide membranes for cell-free assays that reconstitute a particular intracellular event or process.

Ideally, for both purposes (characterization and cell-free assays) the subcellular compartment should be purified to homogeneity. However, this is difficult to achieve, particularly when the starting material is from cell lines where amounts are limiting. Therefore, it is realistic to aim to achieve a highly enriched fraction (defined here as greater than 90% purity) with a good yield. In addition, it is important to carefully consider the purpose of the fractionation protocol as this will dictate how critical the purity is.

To study the formation of secretory granules in the PC12 cell line, a protocol was developed to identify nascent immature granules by optimizing their separation from the donor compartment, the Golgi complex (Tooze and Huttner, 1990). A combination of velocity-controlled differential and equilibrium density centrifugation achieved a separation of immature secretory granules and the *trans*-Golgi network (TGN). This protocol was also used to obtain a population highly enriched in immature secretory granules (ISG) and one highly enriched in mature secretory granules (MSG) (Tooze *et al.*, 1991). MSGs are easier to obtain in a more purified form as MSGs are denser than other subcellular compartments. This protocol has been used to characterise the ISG and MSG (Tooze *et al.*, 1991), study low pH-dependent prohormone processing (Urbé *et al.*, 1997), clathrin coat recruitment to ISGs (Dittié *et al.*, 1996), and the role of ADP-ribosylation factor (ARF) (Austin *et al.*, 2000), sorting of proteins in the ISG (Dittié *et al.*, 1999), cell-free homotypic fusion (Urbé *et al.*, 1998; Wendler *et al.*, 2001), and the recruitment of lipid kinases to ISGs (Panaretou and Tooze, 2002). This protocol has also been used by other researchers to investigate sorting sequences in regulated secretory proteins (Krömer *et al.*, 1996) and with, for example, the AtT20 cell line (Eaton *et al.*, 2000).

II. MATERIALS AND INSTRUMENTATION

PC12 cells are maintained in growth medium consisting of 10% horse serum, 5% fetal calf serum, and Dulbecco's modified Eagle's medium (DMEM) with 3.5 g/liter glucose, penicillin/streptomycin, and 4 m*M*

Copyright 2006, Elsevier Science (USA).
All rights reserved.

glutamine (note this is twice the standard concentration) under 10% CO_2. Reagents for cell culture are obtained from Sigma Aldrich and GIBCO.

PC12 cells are passaged once a week at a dilution of 1:6. For a standard granule preparation, nine, 245 × 245-mm confluent plates of PC12 cells are used. These plates are prepared from five, 175-cm^2 flasks harvested with trypsin, seeded, and grown for about 7 days or from nine, 175-cm^2 flasks harvested with trypsin, seeded, and grown for about 3 days.

All chemicals are available from Sigma-Aldrich, except sucrose (ultrapure grade Cat. 15503-02), which is from GIBCO.

A cell cracker (EMBL Workshop, EMBL Heidelberg, Germany) with a range of titanium balls. Assemble cell cracker with chosen ball, precool and wash cell cracker with 1 ml of homogenization buffer (HB)/protease inhibitor cocktail (pi) before use. For PC12 cells, use a 18-µm clearance.

Gradients are centrifuged in an SW40 rotor using Beckman ultraclear centrifuge tubes (Cat. No. 344060).

Velocity gradients are prepared using a BioComp gradient master (http://www.biocompinstruments.com), and equilibrium gradients are prepared using a Labconco Auto Densiflow gradient maker (http://www.labconco.com). Both velocity and equilibrium gradients are collected using the Auto Densiflow.

A cell scraper is made from a silicon rubber bung by cutting the bung with a single-sided razor blade first horizontally (across the widest part) and then vertically in half. The tip of a plastic 10-ml pipette is then inserted into the center of the cut bung.

III. PROCEDURES

A. Preparation of a Postnuclear Supernatant

Solutions

1. *Tris-buffered saline* (*TBS*): 137 m*M* NaCl, 4.5 m*M* KCl, 0.7 m*M* Na_2HPO_4, 25 m*M* Tris–HCl, pH 7.4
2. *Protease inhibitor (pi) cocktail*: 0.5 m*M* phenylmethylsulfonyl fluoride and 5-µg/ml leupeptin
3. *Homogenization buffer (HB)*: 0.25 *M* sucrose, 10 m*M* HEPES–KOH, pH 7.2, 1 m*M* EDTA, and 1 m*M* MgOAc

Steps

For preparation of sufficient postnuclear supernatant (PNS) to load six SW40 gradients, use nine 245 × 245-mm plates. All solutions must be at 4°C.

1. Place one 245 × 245-mm plate on ice.
2. Remove growth medium by decanting and wash gently twice with 40 ml TBS.
3. Wash each plate again with 40 ml TBS/pi.
4. Add 40 ml TBS/pi and remove PC12 cells from the plates by scraping with a cell scraper. Collect the suspension of cells from each plate into a 50-ml Falcon tube. Repeat for all nine plates.
5. Spin each tube for 7 min at 84 *g*. Remove supernatant and resuspend each pellet in 1 ml of HB/pi. Pool in a 50-ml Falcon tube containing 24 ml of HB/pi and divide into six 15-ml Falcon tubes.
6. Spin for 7 min at 500 *g*. Remove supernatant and resuspend each pellet in 700 µl HB/pi and pool all nine tubes of cell suspension into a 15-ml Falcon tube.
7. Using a 1-ml syringe with a 21- or 22-gauge needle, draw up 1 ml of cells and pass back and forth through the needle six to seven times. Check that cells are well dispersed by resuspending 5 µl of cells with 10 µl of trypan blue solution and monitoring by phase-contrast microscopy. Ensure that the cells are now dispersed uniformly and not still in clumps. A maximum of 20% of the cells should be permeable to trypan blue. Repeat until all the cells have been passed through the needle.
8. Using a 1-ml syringe and 21- or 22-gauge needle, draw up 1 ml of the cell suspension and place syringe on one port of the cell cracker. Place an empty syringe on the other port. Pass cells through chamber six to seven times. Check breakage with trypan blue as in step 7. Greater than 90% of the cells should be broken. Nuclei should be intact and spherical but free of subcellular membranes (see Tooze and Huttner, 1992).
9. Remove homogenate and repeat with remaining cell suspension. Rinse the cell cracker out with 1 ml of HB/pi. Pool all the homogenate into a 15-ml Falcon tube. Total volume will be between 9 and 10 ml.
10. Spin for 10 min at 1700 *g* to pellet nuclei. Remove postnuclear supernatant, avoiding the nuclear pellet. Because the interface between the supernatant and the pellet can be difficult to see, illuminate the tube from behind when removing the supernatant.
11. Respin the PNS for 5 min at 1700 *g* to ensure that all nuclear material is removed and collect the supernatant. Adjust volume if necessary to 9.0 ml.

B. Velocity Gradient Centrifugation

This method achieves separation of organelles by size rather than density. Thus, larger subcellular compartments will sediment faster during this centrifugation than smaller ones. This is the basis for the separation of ISGs and MSGs from the trans-Golgi

network (TGN). In particular, this step is essential for separation of ISGs from the TGN as these organelles have the same equilibrium density.

Solutions

Sucrose solutions: 0.3 *M* sucrose, 10 m*M* HEPES–KOH, pH 7.2, and 1.2 *M* sucrose, 10 m*M* HEPES–KOH, pH 7.2

Steps

1. Prepare the velocity gradients. Use 5.5 ml of 0.3 *M* sucrose and 6 ml of 1.2 *M* sucrose per gradient. Using the Biocomp gradient maker, perform two steps: step 1 for 10 min at a 50°C angle at 30 rpm and step 2 for 1 min at a 80°C angle at 12 rpm. If preparing the gradients manually, use a 15-ml gradient maker, gently mixing the heavy into the light. Using a narrow pipette, pump solution from the light chamber into the bottom of the tube and displace the solution upward with the heavier solutions.
2. Load 1.5 ml of PNS on top of each gradient. Spin at 25,000 rpm in a SW40 rotor at 4°C. Using maximum acceleration, allow centrifuge to reach 25,000 rpm and then spin for exactly 15 min with the brake applied at the end of the run.
3. Collect thirteen 1-ml fractions from the top. Fraction 1 will contain most of the soluble proteins from the PNS. Fractions 2–4 will contain the ISG and constitutive secretory vesicles (CSVs), fractions 5–7 will contain MSGs, and fractions 8–11 will contain TGN membranes. *Note*: There will be other subcellular membranes in these fractions so the ISGs, MSGs, and TGN fractions are only slightly enriched. Pool fractions 1–4 for preparation of ISGs and fractions 5–7 for preparation of MSGs.

C. Preparation of ISGs and MSGs by Equilibrium Gradient Centrifugation

This method achieves separation of organelles by density, allowing vesicles of the same size but different densities to be separated. ISG, which have an average diameter of 80 nm, can be separated Golgi-derived CSVs, which are reported to have a diameter of 50–200 nm (Salamero *et al*., 1990).

Solutions

Sucrose solutions: 0.8 *M* sucrose, 10 m*M* HEPES–KOH, pH 7.2; 1.0 *M* sucrose, 10 m*M* HEPES–KOH, pH 7.2; 1.2 *M* sucrose, 10 m*M* HEPES–KOH, pH 7.2; 1.4 *M* sucrose, 10 m*M* HEPES–KOH, pH 7.2; and 1.6 *M* sucrose, 10 m*M* HEPES–KOH, pH 7.2

Steps

1. Prepare equilibrium gradients. Pipette 1 ml of 1.6 *M* and then layer 2 ml of 1.4, 1.2, 1.0, and then 1.0 ml of 0.8 *M* sucrose into a SW40 tube, either by hand or using the Auto Densiflow, with probe moving upward.
2. Adjust pooled fractions from the velocity gradient to a final volume of 4 ml per gradient with 10 m*M* HEPES–KOH, pH 7.2. Load pooled fractions from velocity gradient onto prepared equilibrium gradients.
3. Spin gradients in a SW40 rotor at 25,000 rpm overnight or for at least 5.5 h at 4°C.
4. Collect twelve 1-ml fractions from the top of the gradient. If preparing ISGs, the ISGs will be found in fractions 7–9. If preparing MSGs, the MSGs will be found in fractions 10–12. These respective fractions can be pooled and aliquoted for storage for up to 6 months in liquid nitrogen.

D. Other Procedures

The centrifugation procedure can be checked by assaying for TGN, secretory granule, or other compartment-specific markers in each fraction from the velocity and equilibrium gradients. This can be done by Western blotting using antibodies to the marker proteins or by metabolic labelling. For the technique described earlier using PC12 cells, the most accurate method is posttranslational labelling of proteins with [^{35}S]sulfate on tyrosine residues (for a review, see Moore, 2003).

Protein tyrosine sulfation is a posttranslational modification found in some secretory proteins, including secretogranin II (SgII) and an unidentified constitutively secreted heparan sulphated proteoglycan (HSPG). The enzyme tyrosylprotein sulfotransferase responsible for sulfation is a resident TGN protein (Lee and Huttner, 1985). Thus, by incubating or pulsing the cells for a short period of time by the addition of [^{35}S]sulfate, proteins that contain the sulfation motif can be labelled in the TGN and can be used to identify TGN membranes. In addition, exit of sulphated proteins from the TGN into CSVs, which contain HSPG, and ISGs and MSGs, which contain SgII, can be followed accurately during the chase. Identification of CSV and ISGs by sulfate label of the specific markers, followed by subcellular fractionation, can be used to confirm that the cultured cells are correctly sorting regulated and constitutively secreted proteins into separate vesicles (Tooze and Huttner, 1990). Metabolic labelling with sulfate can also be applied more generally (Tooze, 1999). It is advisable to use a scaled down

version of the procedure described earlier to avoid having to use large amounts of radioactivity.

Solutions

1. *Labelling medium* (*sulfate-free DMEM*): DMEM is prepared by substituting $MgCl_2 \cdot 6H_2O$ for $MgSO_4 \cdot 7H_2O$ and reducing the normal concentration of cysteine and methionine to 1% of the original concentration; 0.1% dialysed horse serum; 0.05% dialysed fetal calf serum; and 2 m*M* glutamine. It is important not to include any sulphated antibiotics.
2. *[^{35}S]Sulfate* (*40–100 mCi/ml*): Amersham Biosciences (Cat. No. SJS.1).
3. *Chase medium*: growth medium supplemented with 1.6 m*M* $NaS0_4$.

Steps

To check the ability of PC12 cells to sort regulated proteins using the gradients described earlier, two 150-mm^2 dishes of PC12 cells should be prepared for each condition. Ideally the experiment should confirm the position of the TGN on the gradients, identified by a 5-min pulse of sulfate; the CSVs and ISGs, identified by a 5-min pulse followed by a 15-min chase; and the MSGs, identified by a 5-min pulse and 90-min chase. Alternatively, MSGs can be labelled using one-tenth the amount of [^{35}S]sulfate for 6 h and chased overnight.

1. Wash each 150-mm^2 dish once with labelling medium at 37°C. Replace with 20 ml labelling medium. Incubate for 20 min at 37°C to deplete endogenous sulfate.
2. Remove medium and replace with fresh medium at 37°C containing 1 mCi/ml [^{35}S]sulfate, or 0.1 mCi/ml for long-term MSG labelling. Incubate at 37°C for precisely 5 min. Dishes can be rocked gently to reduce the amount of labelling medium required. Five to 7 ml is sufficient when dishes are being rocked.
3. Remove labelling medium. To identify the TGN, transfer the dishes immediately to 4°C and add 10 ml of TBS at 4°C. To identify ISGs, add 20 ml chase medium at 37°C and return cells to incubator for 15 min. To label MSGs, add 20 ml chase medium at 37°C and return cells to incubator for 90 min. Alternatively, use the longer label-and-chase protocol for MSGs.
4. At the end of the chase period, transfer remaining dishes to 4°C, remove the chase medium, and add 10 ml TBS at 4°C.
5. Wash and harvest dishes as described previously. Pool the two dishes from each condition. Prepare a PNS as described earlier and load the PNS from both labelled 150-mm^2 dishes on one velocity gradient.
6. Collect thirteen 1-ml fractions from each gradient. Remove 30 µl from each fraction and analyse the [^{35}S]sulfate-labelled proteins by SDS–PAGE. For optimal resolution of SgII and HSPG, use a 7.5% gel.
7. Save the remaining material for equilibrium gradient centrifugation. Pool fractions 1–4 from the ISG gradient, and pool fractions 5–7 from the MSG gradient. Load each pool onto on an equilibrium gradient and continue as described in Section III.C.

IV. COMMENTS

1. It is possible to perform a cell-free budding assay to reconstitute the formation of ISGs from the TGN using this protocol and protocols described in Sections III.A and III.B.
2. The purity of ISGs and MSGs, while greater than 95% as judged by thin section electron microscopy, may allow assessment of the composition of these organelles by techniques such as two-dimensional gels or mass spectroscopy analysis using MUDPIT (Wu *et al*., 2003), for example. However, to acheive a purity approaching 100% and to confirm your results, additional techniques such as immunoisolation (Howell *et al*., 1989) with a compartment-specific marker are strongly advised.

V. PITFALLS

1. The PC12 cells are not passaged correctly and thus do not achieve maximum confluency, resulting in a very low yield of cells. The cells must be plated as single cell suspensions. This is best achieved by tituration using a flamed narrowed disposable glass pipette.
2. The cells are not completely homogenized, resulting in fewer broken cells as judged by trypan blue. This will result in a reduced yield.
3. The homogenate is very viscous. This is most likely a result of nuclei lysis during homogenization. A clean postnuclear supernatant cannot be obtained from this homogenate, and the experiment should be stopped as the subcellular organelles will not be separated properly on the gradients.

References

Austin, C., Hinners, I., and Tooze, S. A. (2000). Direct and GTP-dependent interaction of ADP-ribosylation factor 1 with clathrin adaptor protein AP-1 on immature secretory granules. *J. Biol. Chem.* **275**, 21862–21869.

Dittié, A. S., Hajibagheri, N., and Tooze, S. A. (1996). The AP-1 adaptor complex binds to immature secretory granules from

PC12 cells, and is regulated by ADP-ribosylation factor. *J. Cell Biol.* **132**, 523–536.

Dittié, A. S., Klumperman, J., and Tooze, S. A. (1999). Differential distribution of mannose-6-phosphate receptors and furin in immature secretory granules. *J. Cell Sci.* **112**, 3955–3966.

Eaton, B. A., Haugwitz, M., Lau, D., and Moore, H. P. (2000). Biogenesis of regulated exocytotic carriers in neuroendocrine cells. *J. Neurosci.* **20**, 7334–7344.

Howell, K. E., Schmid, R., Ugelstad, J., and Gruenberg, J. (1989). "Immunoisolation using Magnetic Solid Supports: Subcellular Fractionation for Cell Free Functional Studies," pp. 265–292. Academic Press, New York.

Krömer, A., Samenfeld, P., Loef, I., Huttner, W. B., and Gerdes, H.-H. (1996). Essential role of the granin-loop for sorting to secretory granules is revealed by expression of chromogranin B in the absence of endogenous protein synthesis. *J. Cell Biol.* **140**, 1059–1070.

Lee, R. W. H., and Huttner, W. B. (1985). (Glu62, Ala30, Tyr8)n serves as high-affinity substrate for tyrolsylprotein sulfotransferase; a Golgi enzyme. *Proc. Natl. Acad. Sci. USA* **82**, 6143–6147.

Moore, K. L. (2003). The biology and enzymology of protein tyrosine O-sulfation. *J. Biol. Chem.* **278**, 24243–24246.

Panaretou, C., and Tooze, S. A. (2002). Regulation and recruitment of phosphatidylinositol 4-kinase on immature secretory granules is independent of ADP-ribosylation Factor 1. *Biochem. J.* **363**, 289–295.

Salamero, J., Sztul, E., and Howell, K. (1990). Exocytic transport vesicles generated in vitro from the trans-Golgi network carry secretory and plasma membrane proteins. *Proc. Natl. Acad. Sci. USA* **87**, 7717–7721.

Tooze, S. A. (1999). Metabolic labeling with sulfate. *In "Current Protocols in Cell Biology"* (J. S. Bonifacino, M. Dasso, J. B. Harford, J. Lippincott-Schwartz, and K. M. Yamada, eds.), Vol. 1, pp. 7.3.1–7.3.7, Wiley, New York.

Tooze, S. A., Flatmark, T., Tooze, J., and Huttner, W. B. (1991). Characterization of the immature secretory granule, an intermediate in granule biogenesis. *J. Cell Biol.* **115**, 1491–1503.

Tooze, S. A., and Huttner, W. B. (1990). Cell-free protein sorting to the regulated and constitutive secretory pathways. *Cell* **60**, 837–847.

Tooze, S. A., and Huttner, W. B. (1992). Cell-free formation of immature secretory granules and constitutive secretory vesicles from trans-Golgi Network. *Methods Enzymol.* **219**, 81–93.

Urbé, S., Dittié, A., and Tooze, S. A. (1997). pH-dependent processing of secretogranin II by the endopeptidase PC2 in isolated immature secretory granules. *Biochem. J.* **321**, 65–74.

Urbé, S., Page, L. J., and Tooze, S. A. (1998). Homotypic fusion of immature secretory granules during maturation in a cell-free assay. *J. Cell Biol.* **143**, 1831–1844.

Wendler, F., Page, L., Urbé, S., and Tooze, S. A. (2001). Homotypic fusion of immature secretory granules during maturation requires syntaxin 6. *Mol. Biol. Cell* **12**, 1699–1709.

Wu, C. C., MacCoss, M. J., Howell, K. E., and Yates, J. R. III. (2003). A method for the comprehensive proteomic analysis of membrane proteins. *Nature Biotechnol.* **21**, 532–538.

CHAPTER

12

Preparation of Synaptic Vesicles from Mammalian Brain

Johannes W. Hell and Reinhard Jahn

I. INTRODUCTION

Synaptic vesicles are secretory organelles that store neurotransmitters in presynaptic nerve endings. When an action potential arrives in the nerve terminal, the plasma membrane is depolarized, leading to the opening of voltage-gated Ca^{2+} channels. The rise in intracellular Ca^{2+} concentration leads to exocytosis of synaptic vesicles within a time interval that can be as short as 200 µs (reviewed by Südhof, 1995).

Synaptic vesicles possess several remarkable properties that distinguish them from most other organelles involved in membrane traffic. First, they are very abundant in brain tissue. Model calculations show that an average neuron contains approximately 10^6 synaptic vesicles, with a total of around 10^{17} in the human central nervous system (Jahn and Südhof, 1993). Approximately 5% of the protein in the brain is contributed by synaptic vesicles; thus, about a 20-fold enrichment from homogenate is sufficient to obtain a pure preparation. Second, synaptic vesicles are highly homogeneous in size and shape and, in addition, are smaller than most other organelles, with an average diameter of only 50 nm. Therefore, size-fractionation techniques can be applied for the isolation of synaptic vesicles. Third, synaptic vesicles do not contain a matrix of soluble proteins (Jahn and Südhof, 1993), as they recycle many times in the nerve terminal and thus can only be reloaded with nonpeptide transmitters by means of specific transport systems.

The study of synaptic vesicles has been facilitated by recent advances in understanding their protein composition. To date, more than half a dozen protein families have been shown to be localized specifically on the membrane of synaptic vesicles. With the exception of some variation due to isoforms, most of these proteins are residents of all synaptic vesicles irrespective of their neurotransmitter content or of the location of the neuron. These include synapsins, synaptophysins, synaptotagmins, SV2s, synaptobrevins/VAMPs, rabs, cysteine string proteins, synaptogyrin, and the subunits of the vacuolar proton pump (for a review, see Südhof, 1995). Rapid progress during the last few years has clarified the function of many of these proteins in membrane traffic. Synaptic vesicles are thus presently regarded as the best-characterized "model" trafficking organelle of eukaryotic cells (Südhof, 1995). Antibodies against synaptophysin and synaptobrevin/VAMP are available commercially from several sources and may be used as probes to assess synaptic vesicle purity. In addition, synaptic vesicles contain neurotransmitter transporters that are specific for neurons exhibiting the corresponding neurotransmitter phenotype. Transporters for the main neurotransmitters have been cloned and sequenced (Reimer *et al*., 2001).

Purification protocols for synaptic vesicles can be divided into three groups. The first group involves the preparation of isolated nerve terminals (synaptosomes) by differential centrifugation. The synaptosomes are subsequently lysed in order to release the synaptic vesicles. An advantage of this procedure is that small membrane fragments generated during homogenization are removed prior to vesicle extraction as synaptosomes sediment at lower *g* forces than these fragments. The first protocol described here belongs in this category. These protocols are laborious and result in relatively low yields, but the resulting synaptic vesicles preparations are of high purity. In the second group of protocols, synaptic vesicles are purified directly from homogenate, without prior isolation of synaptosomes.

Copyright 2006, Elsevier Science (USA).
All rights reserved.

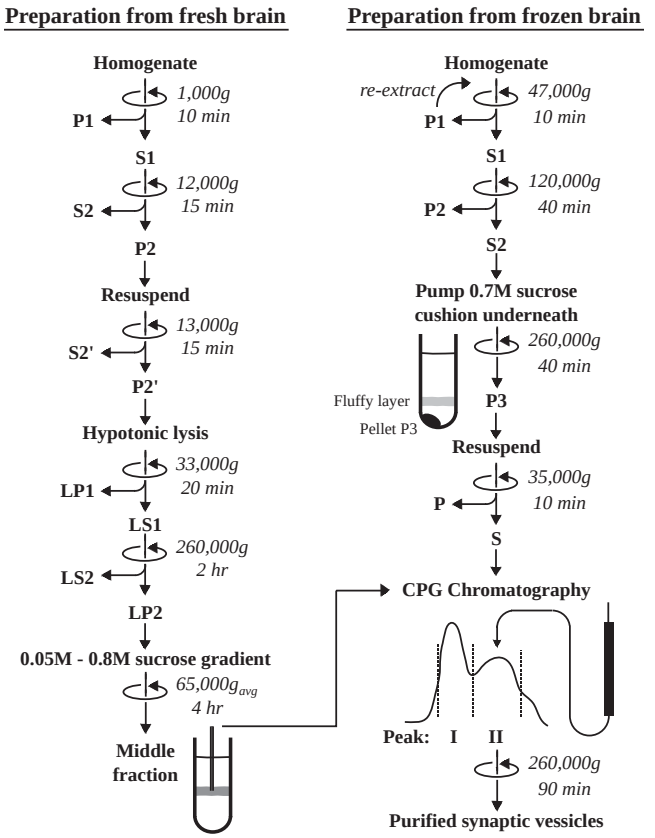

FIGURE 1 Flowchart depicting the main steps of the two preparation methods for synaptic vesicles described in the text. The final step for both methods is CPG chromatography.

In order to obtain high yields, initial homogenization is harsh in order to break up as many nerve terminals as possible, e.g., by freeze-powder homogenization, as described in the second procedure. In both cases, a combination of differential centrifugation, rate-zonal density gradient centrifugation or isopycnic density gradient centrifugation, and size-exclusion chromatography is employed for purification (Fig. 1). The third group involves immunoisolation using antibodies specific for synaptic vesicle proteins (see, e.g., Burger *et al*., 1989, Walch-Solimena *et al*., 1993). These procedures allow for the rapid isolation of small quantities of highly pure organelles from brain homogenates. However, they require access to large amounts of specific antibodies (preferably monoclonal antibodies) and are therefore not further discussed here.

II. MATERIALS AND INSTRUMENTATION

The following chemicals are used: HEPES (Research Products International, #H75030), sucrose (Sigma, # S-9378), glycine (Bio-Rad, 161-0718), phenylmethylsulfonyl fluoride (PMSF; ICN, #195381), pepstatin A (ICN, #195368), dimethyl sulfoxide (DMSO, Sigma, #D-8779), and controlled pore glass beads (CPG Inc., see Appendix). Note that the standard reagents can also be obtained from other sources.

The following instrumentation is required: loose-fitting, motor-driven glass–Teflon homogenizer (Braun, Melsungen, Germany), cooled centrifuge [Sorvall RC5 (DuPont) or comparable, SS34 rotor], ultracentrifuge with fixed angle and swing-out rotors [Beckman L80 (Beckman Instruments) or comparable, Ti70 or Ti50.2 rotor, SW-28 rotor, Ti 45 rotor] and corresponding tubes, equipment for column chromatography (peristaltic pump, UV monitor, fraction collector), gradient mixer for forming continuous sucrose gradients, filtration device for the filtration of buffers using 0.45-μ membranes (Millipore), and glass columns (see Appendix).

III. PROCEDURES

A. Preparation of Synaptic Vesicles from Synaptosomes

In this protocol (Nagy *et al*., 1976; Huttner *et al*., 1983), a crude synaptosomal fraction (P2) is first isolated by differential centrifugation. The synaptosomes are then lysed by osmotic shock and synaptic vesicles are released into the medium. After removal of synaptosomal fragments and large membranes, synaptic vesicles are sedimented by high-speed centrifugation. The resulting pellet, already five- to sixfold enriched in synaptic vesicles, is then purified further by sucrose velocity-density gradient centrifugation and size-exclusion chromatography on controlled pore glass beads (CPG). This procedure is the standard method for obtaining synaptic vesicles of the highest purity, with less than 5% contamination as judged by electron microscopy and biochemical analysis. This preparation does contain, however, endosomes derived from nerve terminals and decoated coated vesicles that lost their clathrin but retained adaptors. The degree of this contamination is probably minor but cannot be quantified easily.

Solutions

1. *Homogenization buffer*: 320 m*M* sucrose, 4 m*M* HEPES–NaOH, pH 7.3 (HEPES is optional; we found no difference when the buffer is omitted. Other buffers such as MES and slightly lower pH are also acceptable).

2. *1 M HEPES-NaOH, pH 7.4*
3. *40 mM sucrose*
4. *50 mM sucrose*
5. *800 mM sucrose*
6. *Glycine buffer*: 300 m*M* glycine, 5 m*M* HEPES–KOH, pH 7.4, degassed and filtered through a 0.45-µm filter
7. *Protease inhibitors*: 1 mg/ml pepstatin A in DMSO and 200 m*M* PMSF in dry ethanol. Keep stocks at room temperature. Add 1/1000 volume where indicated. Note that PMSF is unstable in aqueous solutions and should not be added to buffers prior to use. The PMSF stock solution should be prepared fresh every day.

Steps

After collecting the brains, all steps are carried out on ice or at 4°C.

1. Decapitate 20 rats (about 2 months old; 180–200 g body weight), remove the brains, avoiding myelin-rich areas such as corpus callosum or medulla oblongata, place into 180 ml ice-cold homogenization buffer, and homogenize in several aliquots with a loose-fitting glass Teflon homogenizer (nine strokes, 900 rpm). Add protease inhibitors.
2. Centrifuge the homogenate for 10 min at 1000 *g*max (2700 rpm, Sorval SS34 rotor), discard the resulting pellet (P1) containing large cell fragments and nuclei, and collect the supernatant (S1).
3. Centrifuge S1 for 15 min at 12,000 *g*max (10,000 rpm; SS34 rotor); remove the supernatant (S2) containing small cell fragments such as microsomes or small myelin fragments and soluble proteins. Wash the pellet (P2) by carefully resuspending in 120 ml homogenization buffer (pipette, avoiding the dark brown bottom part of the pellet that consists mainly of mitochondria) and recentrifuging at 13,000 *g*max (11,000 rpm, SS34 rotor); discard the supernatant (S2′). The resulting pellet (P2′) represents a crude synaptosomal fraction.
4. To release synaptic vesicles from the synaptosomes, resuspend P2′ in homogenization buffer to yield a final volume of 12 ml. Transfer this fraction into a glass–Teflon homogenizer, add 9 volumes (108 ml) ice-cold water and perform three up-and-down strokes at 2000 rpm. Add 1 ml of 1 *M* HEPES–NaOH, pH 7.4, and protease inhibitors.
5. Centrifuge the suspension for 20 min at 33,000 *g*max (16,500 rpm, SS34 rotor) to yield the lysate pellet (LP1) and the lysate supernatant (LS1). Using an electric pipetter, carefully remove LS1 immediately after the end of the run without disturbing LP1. It is crucial that LS1 does not get contaminated even with traces of membrane fragments from LP1 (rather, leave 1–2 ml behind in the tube). Contaminating LS1 with LP1 is the most common problem, which significantly reduces the purity of the final vesicle fraction.
6. Centrifuge LS1 for 2 h at 260,000 *g*max (50,000 rpm, Beckman 60Ti or comparable rotor). Discard the supernatant (LS2) and resuspend the pellet (LP2) in 6 ml of 40 m*M* sucrose utilizing a small, tight-fitting glass–Teflon homogenizer. Extrude the resuspended sample consecutively through a 23- and a 27-gauge hypodermic needle attached to a 10-ml syringe (avoid air bubbles).
7. Layer the suspension (3-ml aliquots) on top of a linear sucrose gradient formed from 18.5 ml of 800 m*M* sucrose and 18.5 ml of 50 m*M* sucrose (prepare two tubes containing identical gradients in advance) and centrifuge for 4 h at 65,000 *g*av (25,000 rpm, Beckman SW 28 rotor). After the run, a turbid (white-opaque) zone is visible in the middle of the gradient (in the range of 200 to 400 m*M* sucrose, best seen when viewed against a black background with light from the top). Collect these bands with the aid of a glass capillary connected to a peristaltic pump, yielding a combined volume of 25–30 ml. This fraction represents synaptic vesicles that are 8- to 10-fold enriched over the homogenate (Jahn *et al*., 1985). Note that synaptic vesicles do not reach isopycnic equilibrium during this velocity gradient-type centrifugation. Changes of angular velocity or of the run time will therefore affect the result.
8. Equilibrate a CPG-3000 column (180 × 2 cm, see Appendix) with 10 column volumes of glycine buffer (optimally done overnight before the preparation). Load the sample on top of the resin and overlay it carefully with glycine buffer without diluting the sample. Elute the column with glycine buffer at a flow rate of 40 ml/h, collecting 6- to 8-ml fractions. Monitor protein efflux at 280 nm. The first peak contains plasma membranes and some microsomes and is usually smaller than the second peak containing synaptic vesicles. If no separation into two clearly distinguishable peaks is obtained, the column may need to be repacked. Fractions of the second peak are pooled and centrifuged for 90 min at 260,000 *g*max (50,000 rpm, Beckman 60Ti rotor). The synaptic vesicle pellet should have a glassy appearance, being completely transparent and colorless. Resuspend it in the desired buffer as in step 6. The suspension is frozen rapidly (e.g., in liquid nitrogen) and stored at –70°C. Yields are typically between 2 and 3 mg of protein, based on one of the commercially available Coomassie blue protein determination kits.

Note: Size-exclusion chromatography on glyceryl-coated CPG beads or on Sephacryl S-1000 is omitted in

many protocols and, if applied, is the last step of the procedure. Both resins have a relatively low capacity, do not tolerate overloading, and require some experience in their use. Sephacryl S-1000 has higher separation capacity than CPG per gel volume, but the columns have low flow rates, do not tolerate increased pressure, and have a tendency to adsorb proteins and membrane particles, particularly during the first few separation runs in the life of the column. CPG columns are more difficult to set up and tolerate less material. However, glass beads are noncompressible and allow high flow rates, shortening separation times substantially. The experimenter who does not shy away from the effort to set up a large CPG column is rewarded with highly reliable results for many runs and exceptionally clean synaptic vesicle preparations. We utilized a CPG-3000 column (3 × 180 cm) continuously for 10 years for more than 200 synaptic vesicles preparations, with only a few repackings required, usually caused by experimental error (running dry). Column profiles and synaptic vesicle purity were highly reproducible.

B. Preparation of Synaptic Vesicles from Frozen Brain

This procedure starts with a harsh homogenization of frozen brains to efficiently break up the nerve terminals, thus releasing synaptic vesicles. Frozen brains are ground in a precooled mortar to yield a fine powder. This treatment does not affect the function or integrity of the small synaptic vesicles, but larger membrane structures are ruptured. After resuspending the tissue powder in sucrose solution, most of the cell fragments are removed by centrifugation with low and intermediate angular velocities, leaving synaptic vesicles in the supernatant. Synaptic vesicles are then sedimented at high speed through a cushion of 0.7 *M* sucrose, removing soluble proteins and membrane contaminants of lower buoyant density (mostly myelin). Synaptic vesicles are five- to sixfold enriched in the pellet and can be purified further by CPG chromatography.

The final enrichment factor for synaptic vesicles purified by this protocol is 15–20 (Hell *et al*., 1988), somewhat lower than in the previous method. However, there are several advantages. First, the tissue can be collected before the experiment and can be stored in liquid nitrogen for more than 1 year, allowing more efficient use of experimental animals. Second, the yield is severalfold higher under optimal conditions than the yield of the preparation from synaptosomes. Third, the procedure is faster, requiring only 12 h for completion, thereby allowing for higher activity of various synaptic vesicle functions such as neurotransmitter uptake.

Solutions

1. *Homogenization buffer:* 320 m*M* sucrose, degassed
2. *700 mM sucrose:* 700 m*M* sucrose and 10 m*M* HEPES–KOH, pH 7.3
3. *Resuspension buffer:* 320 m*M* sucrose and 10 m*M* HEPES–KOH, pH 7.3
4. *Glycine buffer:* 300 m*M* glycine and 5 m*M* HEPES–KOH, pH 7.3, degassed
5. *Protease inhibitors:* 1 mg/ml pepstatin A dissolved in DMSO and 200 m*M* PMSF in dry ethanol; add 1/1000 volume where indicated

Steps

After powdering the frozen brains, all steps are carried out on ice or at 4°C.

1. Decapitate 40 rats (2 months old, 180–200 g body weight); remove the brains, avoiding myelin-rich areas such as corpus callosum or medulla oblongata, and freeze immediately in liquid nitrogen. Immediate shock freezing is essential. In our experience, frozen brains available from commercial sources are usually not satisfactory for this reason.

2. To create a tissue powder, place the frozen brains into a porcelain mortar precooled with liquid nitrogen. Cover them with cheesecloth and break them carefully using a porcelain pestle. Grind to a fine powder. This step is crucial for obtaining high yields. After evaporation of the liquid N_2, suspend the powder in 320 ml ice-cold homogenization buffer (magnetic stirrer) and homogenize with a glass–Teflon homogenizer (eight strokes, 1000 rpm).

3. Centrifuge the homogenate for 10 min at 47,000 *g*max (20,000 rpm, Sorval SS-34 rotor). Collect the supernatant (S1). The pellet (P1) contains large cell fragments and nuclei, but also some entrapped synaptic vesicles. To increase the yield, reextract the pellet with 160 ml homogenization buffer by means of one slow stroke in the glass–Teflon homogenizer followed by centrifugation as described earlier. The resulting supernatant (S1′) is combined with S1.

4. Centrifuge S1 for 40 min at 120,000 *g*max (32,000 rpm, Beckman 45Ti rotor). Using an electric pipetter, collect the supernatant (S2) carefully without disturbing the pellet (P2). It is crucial that S2 is not contaminated with membrane fragments from the soft pellet P2. S2 should be clear with a reddish color. If it is turbid, it should be recentrifuged using the same conditions to remove contaminating membrane fragments.

5. To sediment synaptic vesicles through a sucrose cushion, fill 25-ml centrifuge tubes appropriate for a Beckman 60Ti rotor with 20 ml S2. Form the sucrose cushion by pumping 5.5 ml of 700 m*M* sucrose underneath S2 using a peristaltic pump and a glass capillary. Centrifuge for 2 h at 260,000 *g*max (50,000 rpm, Beckman 60Ti rotor). Remove the supernatant S3 and resuspend the pellet P3 in 6–10 ml resuspension buffer with a small, tight-fitting glass–Teflon homogenizer. Extrude the resuspended sample consecutively through a 23- and a 27-gauge hypodermic needle attached to a 10-ml syringe (avoid air bubbles). This sample represents a crude synaptic vesicles fraction. Clear the suspension by a short spin (10 min) at 35,000 *g*max (17,000 rpm, SS34) before loading onto the CPG-column.

6. Equilibrate a CPG column (see Appendix) with 10 column volumes of glycine buffer. Load the sample on top of the resin and overlay carefully with glycine buffer without disturbing the sample. A column of size 85 × 1.6 cm has a maximal capacity of 15 mg of protein, requiring several consecutive runs if all material is to be chromatographed. Elute the column with glycine buffer at a flow rate of 80 ml/h, collecting 2-ml fractions. Follow the elution of protein with a UV detector at 280 nm. The first peak, containing plasma membranes and microsomes, is usually larger than the second peak, containing synaptic vesicles. The two peaks are typically not completely separated in this protocol. The shoulder frequently observed at the end of the second peak represents soluble protein. Pool the fractions of the second peak and centrifuge for 2 h at 260,000 *g*max (50,000 rpm; 60Ti rotor). Resuspend the synaptic vesicle pellet in the desired buffer as described in step 5.

IV. COMMENTS

Scaling up or down is feasible but it should be kept in mind that changing rotors or using half-filled centrifuge tubes may affect yield and purity significantly and adversely. Contamination by other subcellular fractions (e.g., plasma membranes, mitochondria, endoplasmic reticulum) can be monitored conveniently by assaying for marker enzymes (Hell *et al*., 1988). In parallel to a decrease of these marker enzymes, proteins specific for synaptic vesicles, namely synaptophysin (p38), for which antibodies are available commercially (e.g., from Boehringer, Mannheim, Germany), should be enriched about 20- to 25-fold over homogenate (Jahn *et al*., 1985), best quantitated by immunoblotting.

Synaptobrevin is less reliable for quantification by SDS–PAGE/immunoblotting as histones present in the homogenate migrate alongside synaptobrevin/VAMP in nuclei-containing fractions (homogenate) and interfere with the signal, resulting in overestimation of the enrichment factor. The protein profile of the synaptic vesicles preparation as observed after SDS–PAGE exhibits a characteristic pattern (Huttner *et al*., 1983; Hell *et al*., 1988), with the prominent membrane proteins synaptobrevin/VAMP, synaptophysin (p38), synaptotagmin (p65), and synapsin I being clearly visible. Synaptic vesicle preparations contain various amounts of soluble proteins with affinity for membranes such as glyceraldehyde phosphate dehydrogenase, aldolase, actin, and tubulin. These proteins may be partially removed by a salt wash (resuspend synaptic vesicles in 160 m*M* KCl, 10 m*M* HEPES–KOH, pH 7.4, and centrifuge for 2 h at 50,000 rpm, 260,000 *g*max). However, this treatment also removes synaptic vesicle protein synapsin I.

The morphology of the synaptic vesicles fraction can be studied using electron microscopy (Fig. 2). Membranes can be visualized easily, e.g., by negative staining (Hell *et al*., 1988). Synaptic vesicle membranes are identified by their very uniform appearance (small vesicular profiles of approximately 50 nm diameter). Confirmation can also be obtained by immunogold labeling for the vesicle protein synaptophysin, which can be carried out conveniently on a single day when combined with negative staining (Jahn and Maycox, 1988).

APPENDIX: PREPARATION AND MAINTENANCE OF CPG COLUMNS

Controlled pore glass beads (CPG 3000, glycerol coated) are obtained from CPG Inc. Column dimensions may vary, but the diameter-to-length ratio should be at least 1 : 20–1 : 50. Use a sturdy, tension-free glass column that withstands mechanical stress during packing.

Steps

1. Resuspend CPG beads in distilled water and degas thoroughly.

2. Connect the column to a vibration device (e.g., an immobilized vortex apparatus) using a stiff, nonbreakable connection (e.g., a plastic cylinder). Attach the column with several clamps to a strong support such as a heavy stand or wall-mounted rack, with uneven spacing between the clamps to avoid the generation of waves with large amplitudes.

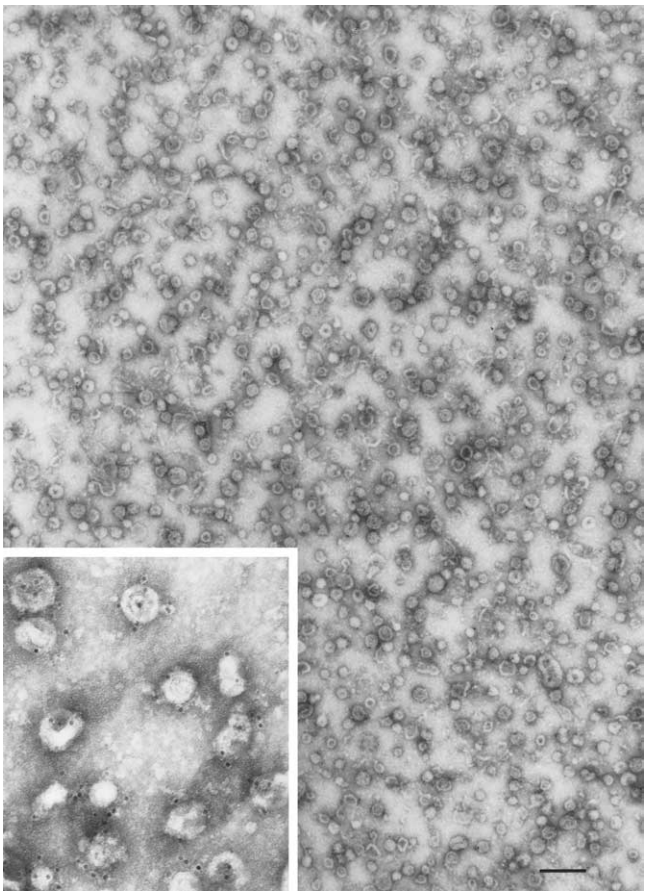

FIGURE 2 Electron micrograph showing a synaptic vesicle fraction purified by the procedure described in Section IIIB (negative staining). (Inset) Magnification of a field following immunogold labeling for the synaptic vesicle protein synaptophysin. For methods, see Jahn and Maycox (1988). Bar: 200 nm. Electron micrographs courtesy of Dr. Peter R. Maycox (London, UK).

3. Fill the column with the CPG bead slurry. Vibrate the column at a high-speed setting of the vortex apparatus and continue to add slurry. Avoid the generation of settled zones between additions. After filling, keep vibrating until the resin does not settle for at least 30 min. Packing of a small column (85 × 1.6 cm) and a large column (180 × 2 cm) requires approximately 4 and 10 h, respectively.

4. Equilibrate the column with 10 column volumes of column buffer.

5. For maintenance the column should be stored in buffer containing 0.02% sodium azide to prevent microbial growth. To avoid accumulation of debris, all samples should be cleared by a short centrifugation before loading and all buffers filtered by ultrafiltration. The column should not be allowed to run dry. If this occurs, the air may be removed by pumping large amounts of extensively degassed and temperature-equilibrated column buffer from the bottom through the column. However, if air bubbles remain, repacking is unavoidable. If contaminants accumulate (after 10–20 runs), the column can be cleaned by washing with 1–2 bed volumes of 4 *M* urea, buffered to pH 7.0, followed by extensive washing. The first run after urea cleaning results in lower yields.

Acknowledgment

The authors thank Dr. Duane D. Hall for preparation of Fig. 1.

References

Burger, P. M., Mehl, E., Cameron, P., Maycox, P. R., Baumert, M., Lottspeich, F., De Camilli, P., and Jahn, R. (1989). Synaptic vesicles immunoisolated from rat cerebral cortex contain high levels of glutamate. *Neuron* **3**, 715–720.

Hell, J. W., Maycox, P. R., Stadler, H., and Jahn, R. (1988). Uptake of GABA by rat brain synaptic vesicles isolated by a new procedure. *EMBO J.* **7**, 3023–3029.

Huttner, W. B., Schiebler, W., Greengard, P., and De Camilli, P. (1983). Synapsin I (protein I), a nerve terminal-specific phosphoprotein. III. Its association with synaptic vesicles studied in a highly purified synaptic vesicle preparation. *J. Cell Biol.* **96**, 1374–1388.

Jahn, R., and Maycox, P. R. (1988). Protein components and neurotransmitter uptake in brain synaptic vesicles. *In* "*Molecular Mechanisms in Secretion*" (N. A. Thorn, M. Treiman, and O. H. Peterson, eds.), pp. 411–424. Munksgaard, Copenhagen.

Jahn, R., Schiebler, W., Ouimet, C., and Greengard, P. (1985). A 38,000 dalton membrane protein (p38) present in synaptic vesicles. *Proc. Natl. Acad. Sci. USA* **82**, 4137–4141.

Jahn, R., and Südhof, T. C. (1993). Synaptic vesicle traffic: Rush hour in the nerve terminal. *J. Neurochem.* **61**, 12–21.

Nagy, A., Baker, R. R., Morris, S. J., and Whittaker, V. P. (1976). The preparation and characterization of synaptic vesicles of high purity. *Brain Res.* **109**, 285–309.

Reimer, R. J., Fremeau, R. T., Jr., Bellocchio, E. E., and Edwards, R. H. (2001). The essence of excitation. *Curr. Opin. Biol.* **105**, 273–281.

Südhof, T. C. (1995). The synaptic vesicle cycle: A cascade or protein-protein interactions. *Nature* **375**, 645–653.

Walch-Solimena, C., Takei, K., Marek, K., Midyett, K., Südhof, T. C., De Camilli, P., and Jahn, R. (1993). Synaptotagmin: A membrane constituent of neuropeptide-containing large dense-core vesicles. *J. Neurosci.* **13**, 3895–3903.

CHAPTER

13

Preparation of Proteasomes

Keiji Tanaka, Hideki Yashiroda, and Nobuyuki Tanahashi

I. INTRODUCTION

The proteasome is a protein-destroying machine capable of degrading a variety of proteins involved in the regulation of diverse processes, such as the cell cycle, immune response, signaling cascades, and developmental programs in various eukaryotes (Hershko and Ciechanover, 1998; Kloetzel, 2001; Rock *et al*., 2002). Early studies identified the proteasome as a latent protease complex with a sedimentation coefficient of 20S, and it was accordingly named the 20S proteasome (Coux *et al*., 1996). The 20S proteasome is a barrel-like particle formed by the axial stacking of four rings made up of two outer α rings and two inner β rings, being associated in the order of αββα. The active sites reside in a chamber formed by the centers of the abutting β rings (Bochtler *et al*., 1999; Unno *et al*., 2002). The latency of the proteasome may be explained by the tertiary structure, as the center of the α ring is almost closed, preventing penetration of proteins into the inner aspect of the β ring on which the proteolytically active sites are located (Fig. 1). The 20S proteasome possesses a variety of catalytic centers that presumably contribute to the hydrolysis of multiple peptide bonds in single polypeptide substrates by a coordinated mechanism.

Subsequently, the latent 20S proteasome was demonstrated to act as a catalytic core of a large multisubunit proteolytic complex. To date, three protein factors that can stimulate 20S proteasome activity have been described. One is PA700 (also known as the 19S regulatory particle), which can be divided into lid and base complexes. The lid consists of multiple Rpn (non-ATPase) subunits, while the base consists of six proteasomal ATPases, Rpt1–Rpt6, and a few additional Rpn subunits (Finley *et al*., 1998). PA700 can associate with the 20S proteasome in an ATP-dependent manner to form the 26S proteasome with a molecular mass of ~2500 kDa, a eukaryotic ATP-dependent protease (Fig. 2), capable of degrading mainly proteins tagged with a polyubiquitin (Ub) chain, which functions as a degradation signal (Baumeister *et al*., 1998; Pickart, 2001).

Another activator of the 20S proteasome is PA28 (equivalent to the 11S regulator) (DeMartino and Slaughter, 1993; Rechsteiner *et al*., 2000). PA28 is attached independently to both ends of the central 20S proteasome ATP to form a football-like proteasome and markedly stimulates the activities of various peptidase of the 20S proteasome *in vitro*. However, unlike the 26S proteasome, PA28 fails to enhance the hydrolysis of large protein substrates with native or denatured structures, even when they are polyubiquitinated. PA28 is composed of three related proteins, named PA28α, PA28β, and PA28γ, with an overall identity of approximately 50% (Tanaka, 1998). Of these, PA28α and PA28β are induced greatly by a major immunomodulatory cytokine, interferon-γ (Tanaka and Kasahara, 1998). Intriguingly, further studies identified that the "hybrid proteasome," which comprises the 20S proteasome flanked by PA28 on one side and PA700 on the other, functions as a new ATP-dependent protease (Tanahashi *et al*., 2000).

The third proteasome activator is PA200, which is localized in the nucleus and is involved in DNA repair (Ustrell *et al*., 2002).

Copyright 2006, Elsevier Science (USA).
All rights reserved.

II. MATERIALS AND INSTRUMENTATION

Q-Sepharose (Cat. No. 17-1014-03), Q-Sepharose fast flow (Cat. No. 17-0510-10), Superdex 200 pg (Cat. No. 17-1043-01), Mono Q (Cat. No. 17-5166-01), and heparin–Sepharose CL-6B (Cat. No. 17-0467-09) can be purchased from Amersham. Bio-Gel A-1.5m (Cat. No. 151-0440) and hydroxylapatite Bio-Gel HTP (Cat. No. 130-0420) are from Bio-Rad. Polyethylene glycol 6000 (Cat. No. P-2139), ubiquitin (Ub, Cat. No. U-6253), succinyl-Leu-Leu-Val-Tyr-4-methyl-courmaryl-7-amide (Suc-LLVY-MCA, Cat. No. S-6510), and Supelco TSK-DEAE 650M is from Sigma. Amicon PM-10 and PM-30 membranes (Cat. No. 13132 and 13232) can be obtained from Millipore. Complete protease inhibitor (Cat. No. 1 697 498) is from Roche.

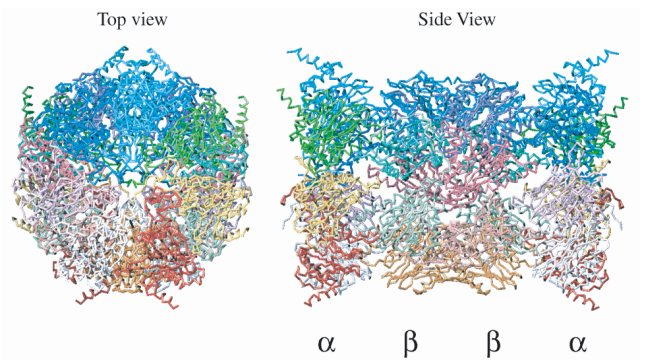

FIGURE 1 Crystal structure of the 20S proteasome from the bovine liver. For details, see Unno *et al*. (2002).

III. PROCEDURES

Solutions

1. *Buffer A:* 25 m*M* Tris–HCl (pH 7.5) containing 1 m*M* dithiothreitol (DTT) (or 10 m*M* 2-mercaptoethanol) and 20% glycerol

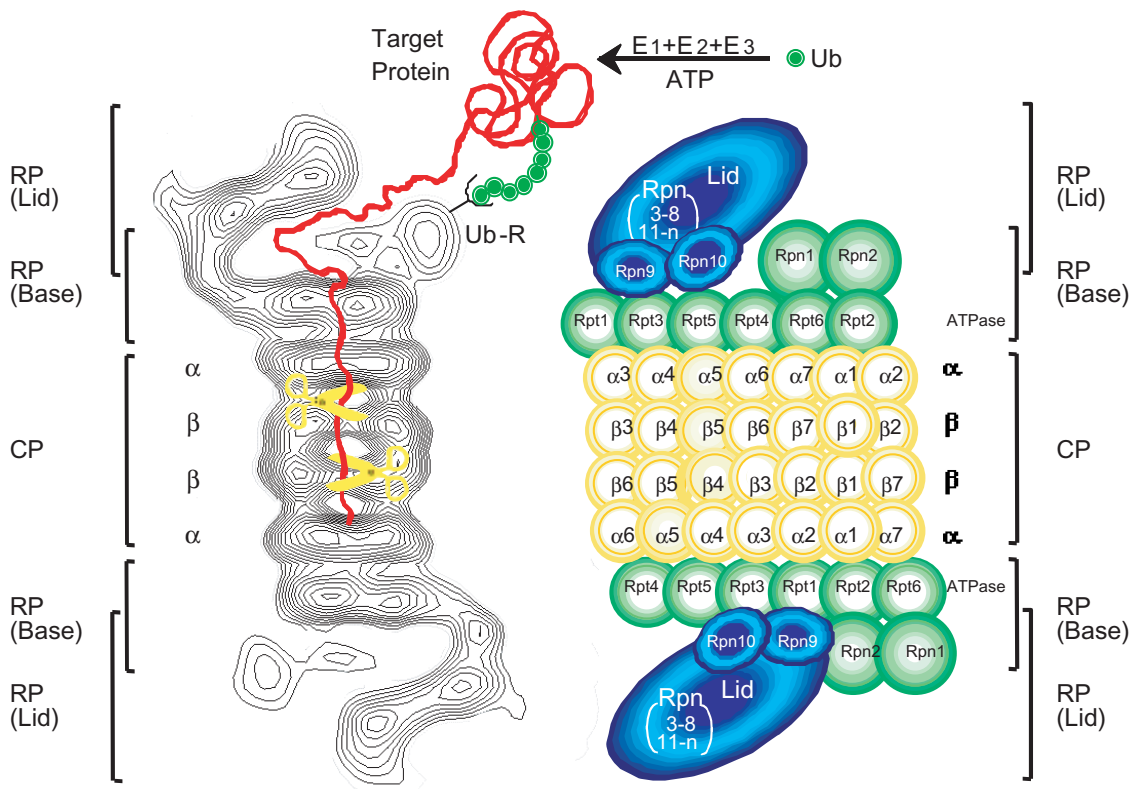

FIGURE 2 Molecular organization of the 26S proteasome. (Left): Averaged image based on electron micrographs of the complex of the 26S proteasome from rat. The α and β rings of the 20S proteasome are indicated. Photograph kindly provided by W. Baumeister. (Right): Schematic drawing of the subunit structure. Ub, ubiquitin; E1 (Ub-activating), E2 (Un-conjugating), and E3 (Ub-ligating) enzymes; CP, core particle; RP, regulatory particle; Rpn, RP non-ATPase; Rpt, RP triple ATPase; Ub-R, Ub receptor (poly-Ub binding subunit).

2. *Buffer B:* 10 m*M* phosphate buffer (pH 6.8) containing 1 m*M* DTT and 20% glycerol
3. *Buffer C:* Buffer A containing 0.5 m*M* ATP
4. *Buffer D:* Buffer B containing 5 m*M* ATP
5. *Buffer E:* 10 m*M* Tris–HCl (pH 7.0), 25 m*M* KCl, 10 m*M* NaCl, 1.1 m*M* $MgCl_2$, 0.1 m*M* EDTA, 1 m*M* DTT, and 10% glycerol
6. *Buffer F:* 10 m*M* Tris–HCl (pH 8.5), 25 m*M* KCl, 10 m*M* NaCl, 1.1 m*M* $MgCl_2$, 0.1 m*M* EDTA, 1 m*M* DTT, and 10% glycerol

A. Preparation of 20S Proteasomes

Procedures

1. Homogenize 200- to 400-g samples of animal tissues in 3 volumes of 25 m*M* Tris–HCl buffer (pH 7.5) containing 1 m*M* DTT and 0.25 *M* sucrose in a Potter–Elvehjem homogenizer. Centrifuge the homogenate for 1 h at 70,100 *g* and use the resulting supernatant as the crude extract.

2. Add glycerol at a final concentration of 20% to the crude extract. Then mix the extract with 500 g of Q-Sepharose that has been equilibrated with buffer A. Wash the Q-Sepharose with the same buffer on a Büchner funnel and transfer to a column (5 × 60 cm). Wash the column with buffer A, elute the material with 2 liters of a linear gradient of 0–0.8 *M* NaCl in the same buffer, and measure the activity of proteasomes using Suc-LLVY-MCA as a substrate (for details, see Section IV).

3. Pool fractions containing 20S proteasomes from the Q-Sepharose column and add 50% polyethylene glycol 6000 (adjust to pH 7.4) at a final concentration of 15% with gentle stirring. After 15 min, centrifuge the mixture at 10,000 *g* for 20 min, dissolve the resulting precipitate in a minimum volume (approximately 50 ml) of buffer A, and centrifuge at 20,000 *g* for 10 min to remove insoluble material.

4. Fractionate the material precipitated with polyethylene glycol on a Bio-Gel A-1.5m column (5 × 90 cm) in buffer A. Collect fractions of 10 ml and assay their proteasome activity. Pool fractions of 20S proteasomes.

5. Apply the active fractions from the Bio-Gel A-1.5m column directly to a column of hydroxylapatite equilibrated with buffer B. Wash the column with the same buffer and elute the material with 400 ml of a linear gradient of 10–300 m*M* phosphate. Collect fractions of 4 ml. Elute the 20S proteasomes with about 150 m*M* phosphate.

6. Combine the active fractions from the hydroxylapatite, dialyze against buffer A, and apply to a column of heparin–Sepharose CL-6B equilibrated with buffer A. Wash the column with the same buffer until the absorbance of the eluate at 280 nm returns to baseline. Then eluate with 200 ml of a linear gradient of 0–0.4 *M* NaCl in the same buffer and collect fractions of 2 ml. Eluate the 20S proteasomes with approximately 75 m*M* NaCl.

7. Pool the fractions with high proteasomal activity, dialyze against buffer A, and concentrate to about 5 mg/ml protein by ultrafiltration in an Amicon cell with a PM-10 membrane. The enzyme can be stored at –80°C for at least 2 to 3 years.

B. Preparation of 26S Proteasomes

Procedures

1. Homogenize 200- to 400-g samples of animal tissues in 3 volumes of 25 m*M* Tris–HCl buffer (pH 7.5) containing 1 m*M* DTT, 2 m*M* ATP, and 0.25 *M* sucrose in a Potter–Elvehjem homogenizer. Centrifuge the homogenate for 1 h at 70,100 *g* and use the resulting supernatant as the starting material.

2. Recentrifuge the crude supernatant for 5 h at 70,100 *g* to obtain 26S proteasomes, which precipitate almost completely. Dissolve the precipitate in a suitable volume (40–50 ml) of buffer C and centrifuge at 20,000 *g* for 30 min to remove insoluble material.

3. Apply samples of the preparation from step 2 to a Bio-Gel A-1.5m column (5 × 90 cm) in buffer C. Collect fractions of 10 ml and assay the 26S proteasome activity in the fractions (for the assay, see Section IV). Pool fractions of 26S proteasomes.

4. Add ATP at a final concentration of 5 m*M* to the pooled fractions of 26S proteasomes from the Bio-Gel A-1.5m column. Apply a sample directly to a hydroxylapatite column with a 50-ml bed volume that has been equilibrated with buffer D. Recover the 26S proteasomes in the flow-through fraction because they do not associate with this column in the presence of 5 m*M* ATP. Approximately 70% of the proteins, including free 20S proteasomes, bind to the hydroxylapatite resin.

5. Apply the flow-through fraction from the hydroxylapatite column to a Q-Sepharose column that has been equilibrated with buffer C without ATP and washed with 1 bed volume of buffer C. Wash the column with 5 bed volumes of buffer C and elute the adsorbed materials with 300 ml of a linear gradient of 0–0.8 *M* NaCl in the same buffer. Collect fractions of 3.0 ml of eluate. Proteins with the ability to degrade Suc-LLVY-MCA with or without 0.05% SDS are eluted with about 0.4 *M* NaCl as a single symmetrical peak. ATPase activity and the ATP-dependent activity necessary to degrade ^{125}I-labeled lysozyme–Ub conjugates are observed at the same position as the peptidase

activity and are eluted as superimposable symmetrical peaks, which suggests a specific association of ATPase with the 26S proteasome complex. Collect the protein in fractions exhibiting high activity.

6. Concentrate the 26S proteasome fraction obtained by Q-Sepharose chromatography to 2.0 mg/ml by ultrafiltration with an Amicon PM-30 membrane and subject samples of 2.0 mg of protein to 10–40% glycerol density gradient centrifugation (30 ml in buffer C containing 2 m*M* ATP). Centrifuge for 22 h at 82,200 *g* in a SW rotor and collect 1-ml fractions from the bottom of the centrifuge tube. A single major peak of peptidase activity, obtained in the absence of SDS, is eluted around fraction 15, but when the activity is assayed with 0.05% SDS, another small peak is observed around fraction 20. The latter peak corresponds to the elution position of 20S proteasomes. ATPase activity is observed at the same position as peptidase activity. Activity for ATP-dependent degradation of ^{125}I-labeled lysozyme–Ub conjugates is also observed as a single symmetrical peak, coinciding in position with the ATPase and peptidase activities in the absence of SDS. No significant ^{125}I-labeled lysozyme–Ub conjugate-degrading activity is detected in fractions of 20S proteasomes. Pool fractions 12–16 and store at –80°C.

Preparation of PA700

Steps for homogenization, ultracentrifugation, and Bio-Gel A-1.5m gel filtration are similar to those used for the preparation of 26S proteasomes. Apply the pooled fractions of the 26S proteasome from the Bio-Gel A-1.5m column directly to a hydroxylapatite column with a 50-ml bed volume that has been equilibrated with buffer C. Wash the column with the same buffer and elute the adsorbed materials with 300 ml of a linear gradient of 10–300 m*M* phosphate. Collect 3.0-ml fractions of eluate. Note that the 26S proteasome can be adsorbed in the hydroxylapatite column under a low concentration of ATP and that the 20S proteasome and PA700 regulatory complex can be eluted separately at different phosphate concentrations of approximately 150 and 50 m*M*, respectively. The 20S proteasome is detected by measuring the Suc-LLVY-MCA-degrading activity with 0.05% SDS as described earlier, whereas the PA700 complex is monitored by immunoblotting with antibodies against their subunits. Collect protein in fractions containing the PA700 complex from hydroxylapatite chromatography, concentrate it to 2.0 mg/ml by ultrafiltration with an Amicon PM-30 membrane, and subject samples of 1.0–2.0 mg of protein to 10–30% glycerol density gradient centrifugation, similar to step 6 used in preparation of the 26S proteasome. Collect 1-ml fractions from the bottom of the centrifuge tube. The PA700 complex can be monitored by ATPase activity and/or the aforementioned immunoblotting analysis. Pool fractions 14–18 containing PA700 complex and store at –80°C.

C. Preparation of Football Proteasomes

Procedures

1. Perfuse animal tissues with 25 m*M* Tris–HCl buffer (pH 7.5) containing 1 m*M* DTT, 1 m*M* pheryhrethylsulforyl fluoride (PMSF), 20 µg/ml E64, and 0.25 *M* sucrose and then homogenize in 3 volumes of the same buffer in a Potter–Elvehjem homogenizer. Centrifuge the homogenate for 1 h at 70,100 *g* and use the resulting supernatant as the crude extract.

2. Apply the crude extract directly to a Q-Sepharose column that has been equilibrated with buffer A. Wash the column with 5 bed volumes of buffer A and elute the adsorbed materials with a linear gradient of 0–0.8 *M* NaCl in the same buffer. For detection of PA28, the activator of 20S proteasome, the hydrolysis of Suc-LLVY-MCA is assayed after preincubation for 10 min at 4°C with approximately 0.5 µg of the latent 20S proteasome purified as described in Section IIIA. Eluate the PA28 activator with about 0.3 *M* NaCl. The endogenous activities of 20S and 26S proteasomes are monitored by assaying Suc-LLVY-MCA degradation with or without 0.05% SDS, respectively, which are coeluted at approximately 0.45 *M* NaCl.

3. Combine the PA28 fractions from the Q-Sepharose column, dialyze against buffer A, and apply it to a heparin–Sepharose CL-6B column that has been equilibrated in the same buffer. Recover PA28 in the flow-through fraction, as it does not bind to this resin.

4. Apply the flow-through fraction from the heparin–Sepharose CL-6B column directly to the hydroxylapatite column that has been equilibrated with buffer B. Wash the column with 5 bed volumes of the same buffer and elute the adsorbed material with a linear gradient of 10–200 m*M* phosphate. Pool fractions of PA28.

5. Concentrate the PA28 activator from the hydroxylapatite column to 2.0 mg/ml by ultrafiltration with an Amicon PM-10 membrane. Incubate the PA28 with the purified 20S proteasome (about 0.5 mg) for 30 min at 4°C to form the PA28–20S proteasome complex and subject 2.0-mg samples of protein to 10–40% glycerol density gradient centrifugation in a manner similar to step 6 used in preparation of the 26S proteasome. Note that excess PA28 should be used for association with the 20S proteasome because the PA28–20S proteasome complex is hardly separated from the 20S proteasome,

unlike the PA28 complex, by density gradient centrifugation analysis. Collect 1-ml fractions from the bottom of the centrifuge tube. The PA28–20S proteasome complex is monitored by assaying Suc-LLVY-MCA degrading activity. Pool fractions 14–18 and store at –80°C.

Preparation of PA28

Apply the PA28–20S proteasome complex from the glycerol density gradient centrifugation, the final material for preparation of football proteasomes, directly to a Q-Sepharose column that has been equilibrated in buffer A and wash extensively with the same buffer. Elute the adsorbed material with a linear gradient of 0–0.8 *M* NaCl in the same buffer because the 20S proteasome and PA28 are separated by this column operation. Eluate the PA28 activator with about 0.3 *M* NaCl (for details, see step 2). Pool fractions containing PA28 and store at –80°C.

Preparation of Hybrid Proteasomes

Hybrid proteasomes can be reconstituted by purified PA28 (or recombinant PA28α) and 26S proteasomes. Incubate 26S proteasomes (single- and double-capped PA700–20S proteasome complexes) with PA28 or PA28α at 37°C for 15–30 min in 20 m*M* Tris–HCl (pH 7.5) buffer containing 2 m*M* ATP, 5 m*M* $MgCl_2$, and 1 m*M* EDTA (Kopp *et al.*, 2001; Cascio *et al.*, 2001).

D. Preparation of PA200

Procedures

1. Homogenize a 125-g sample of animal tissues in 2.4 volumes (300 ml) of 10 m*M* Tris–HCl buffer (pH 7.5) containing 1 m*M* DTT, 0.25% Triton X-100, and three Complete protease inhibitor tablets in a Waring blender. Centrifuge the homogenate for 1 h at 100,000 *g* and use the resulting supernatant as the crude extract.

2. Apply the crude extract (400 ml) directly to TSK-DEAE (1.6 × 50 cm) that has been equilibrated with buffer E. Wash the column with buffer E and elute the material with a 1 liter linear gradient from 35 to 300 m*M* KCl in the same buffer. The proteasome activity is detected by measuring the Suc-LLVY-MCA-degrading activity. Monitor PA200 by immunoblotting with antibody PA200.

3. Dilute pool fractions containing PA200 from the DEAE column by twofold with buffer F and apply to 5 ml of Q-Sepharose fast flow resin equilibrated with buffer F. Elute bound proteins with 10 ml of 0.5 *M* KCl in the same buffer.

4. Apply the elution fractions from Q-Sepharose resin to a Superdex 200-pg (2.6 × 60 cm) column that has been equilibrated with buffer E containing 250 m*M* KCl and 5% glycerol. Pool fractions containing PA200.

5. Dilute fractions from the size column threefold with 5% glycerol in buffer F and apply to a Mono Q column (0.5 × 5 cm). Wash the column with the same buffer and resolve in 12 column volumes at 30 m*M*/ml from 35 to 200 m*M* KCl and then reduce the gradient to 20 m*M*/ml from 200–400 m*M* KCl and increase to 30 m*M*/ml from 400–500 m*M* KCl.

6. Subject samples of the Mono Q pools to 5–20% glycerol density gradient centrifugation (30 ml in buffer E containing Complete protease inhibitor tablets). Centrifuge for 19 h at 85,500 g in a SW28 rotor and collect 1-ml fractions from the bottom of the centrifuge tube. Monitor PA200 by measuring Suc-LLVY-MCA degradation for incubation of indicated fractions with 200 ng of purified proteasome and/or an immunoblotting analysis. Pool fractions containing PA200 and store at –80°C.

IV. COMMENTS

Various fluorogenic peptides are suitable for the measurement of 20S proteasomal activity because proteasomes show broad substrate specificity. However, Suc-LLVY-MCA is recommended as a sensitive substrate. Latent 20S proteasomes can be activated in various ways (Coux *et al.*, 1996). We recommend the use of SDS at low concentrations of 0.02–0.08% for the activation of Suc-LLVY-MCA breakdown; the optimal concentration depends on the enzyme source and the protein concentration used. The fluorogenic peptide (Suc-LLVY-MCA) can be used for assay of PA700–, PA28–, PA200–20S proteasome complexes, but these are active without any treatment, unlike latent 20S proteasomes. For a specific assay, ATP-dependent degradation of polyubiquitinated ^{125}I-labeled lysozyme should be measured, although such an assay is not easy because three kinds of enzymes, E1 (Ub-activating), E2 (Ub-conjugating), and E3 (Ub-ligating) must be purified for the *in vitro* preparation of ubiquitinated substrate (for the procedures, see Tamura *et al.*, 1991). There are various E2 and E3 enzymes. Most of them have not yet been characterized for use in *in vitro*-reconstituted proteolytic systems, so it is difficult to prepare large amounts of ubiquitinated proteins for use as substrates for 26S proteasomes. Therefore, for quantitative and sensitive measurement of ATP-dependent proteolysis

activity *in vitro* in mammalian cells, ornithine decarboxylase (ODC) is a useful substrate. ODC is the only known natural substrate independent of ubiquitination for recognition and degradation by 26S proteasomes and hybrid proteasomes. Antizyme (AZ), an ODC inhibitory protein, however, is needed for the process instead of Ub, but both ODC and AZ, required for this *in vitro* degradation assay, are available as recombinant proteins (Murakami *et al*., 1999; Tanahashi *et al*., 2000). Note that AZ is not present in lower organisms, such as yeasts, and thus this assay is not fit for these cells. It is also possible that their purification is monitored by measuring ATPase activity at later steps of their purification, since the 26S proteasome and PA700 regulator complex have intrinsic ATPase activity.

Proteasomes have been purified from a variety of eukaryotic cells by many investigators. Many purification methods have been reported, but no special techniques are necessary because 20S proteasomes are very stable and abundant in cells, constituting 0.5–1.0% of the total cellular proteins. The procedures used for the purification of 20S proteasomes obviously differ, depending on whether they are small or large operations. For their isolation from small amounts of biological materials, such as cultured cells, 10–40% glycerol density gradient centrifugation analysis is very effective. 20S proteasomes are present in a latent form in cells and can be isolated in this form in the presence of 20% glycerol. For their isolation in high yield, a key point is to keep them in their latent form because their activation results in autolytic loss of a certain subunit(s) and marked reduction of enzymatic activities, particularly their hydrolyses of various proteins. Accordingly, all buffers used contain 10–20% glycerol as a stabilizer. Furthermore, a reducing agent is required because 20S proteasomes precipitate in its absence. All purification procedures are performed at 4°C, but operations in a high-performance liquid chromatography (HPLC) apparatus can be carried out within a few hours at room temperature.

For purification of the 26S proteasome, ATP (0.5 or 2 m*M*), together with 20% glycerol and 1 m*M* DTT, should be added to all solutions used because they strongly stabilize the 26S proteasome complex; the purified enzyme is stable during storage at –70°C for at least 6 months in the presence of 2 m*M* ATP and 20% glycerol. Other drastic chromatographs should be avoided because these operations may result in dissociation of the 26S complex into its constituents. Alternative methods of purification of the PA28 and PA700 regulatory complexes have been reviewed by DeMartino and Slaughter (1993).

It should be noted that the hybrid proteasome is prepared by an *in vitro* reconstitution system using purified 26S proteasomes and PA28 (Kopp *et al*., 2001; Cascio *et al*., 2001) because it is hardly separated from 26S proteasomes by conventional chromatographic techniques (Tanahashi *et al*., 2000). In addition, PA200 is found both in complexes of the homologous type PA200–20S proteasome-PA200 and in complexes that also contain PA700, as PA700-20S proteasome-PA200 (Ustrell *et al*., 2002). To date, the procedures to separate the diverse forms of active proteasomes individually from cells and tissues have not yet been established.

References

Baumeister, W., Walz, J., Zuhl, F., and Seemuler, E. (1998). The proteasome: Paradigm of a self-compartmentalizing protease. *Cell* **92**, 367–380.

Bochtler, M., Ditzel, L., Groll, M., Hartmann, C., and Huber, R. (1999). The proteasome. *Annu. Rev. Biophys. Biomol. Struct.* **28**, 295–317.

Cascio, P., Call, M., Petre, B. M., Walz, T., and Goldberg, A. L. (2002). Properties of the hybrid form of the 26S proteasome containing both 19S and PA28 complexes. *EMBO J.* **21**, 2636–2645.

Coux, O., Tanaka, K., and Goldberg, A. L. (1996). Structure and functions of the 20S and 26S proteasomes. *Annu. Rev. Biochem.* **65**, 801–847.

DeMartino, G. N., and Slaughter, C. A. (1999). Regulatory proteins of the proteasome. *J. Biol. Chem.* **274**, 22123–22126.

Finley, D., Tanaka, K., Mann, C., Feldmann, H., Hochstrasser, M., Vierstra, R., Johnston, S., Hampton, R., Haber, J., McCusker, J., Silver, P., Frontali, L., Thorsness, P., Varshavsky, A., Byers, B., Madura, K., Reed, S. I., Wolf, D., Jentsch, S., Sommer, T., Baumeister, W., Goldberg, A., Fried, V., Rubin, D. M., Glickman, M. H. and Toh-e, A. (1998). Unified nomenclature for subunits of the *Saccharomyces cerevisiae* proteasome regulatory particle. *Trends Biochem. Sci.* **23**, 244–245.

Hershko, A., and Ciechanover, A. (1998). The ubiquitin system. *Annu. Rev. Biochem.* **67**, 425–479.

Kloetzel, P. M. (2001). Antigen processing by the proteasome. *Nature Rev. Mol. Cell. Biol.* **2**, 179–187.

Kopp, F., Dahlmann, B., and Kuehn, L. (2001). Reconstitution of hybrid proteasomes from purified PA700–20 S complexes and PA28αβ activator: Ultrastructure and peptidase activities. *J. Mol. Biol.* **13**, 465–471.

Murakami, Y., Matsufuji, S., Hayashi, S., Tanahashi, N., and Tanaka, K. (1999). ATP-dependent sequestration of ornithine decarboxylase by the 26S proteasome, a process coupled to unfolding, is a prerequisite for the degradation. *Mol. Cell. Biol.* **19**, 7216–7227.

Pickart, C. M. (2001). Mechanisms underlying ubiquitination. *Annu. Rev. Biochem.* **70**, 503–533.

Rechsteiner, M., Realini, C., and Ustrell, V. (2000). The proteasome activator 11 S REG (PA28) and class I antigen presentation. *Biochem. J.* **345**(Pt. 1), 1–15.

Rock, K. L., York, I. A., Saric, T., and Goldberg, A. L. (2002). Protein degradation and the generation of MHC class I-presented peptides. *Adv. Immunol.* **80**, 1–70.

Tanahashi, N., Murakami, Y., Minami, Y., Shimbara, N., Hendil, K. B., and Tanaka, K. (2000). Hybrid proteasomes: Induction by interferon-γ and contribution to ATP-dependent proteolysis. *J. Biol. Chem.* **275**, 14336–14345.

Tamura, T., Tanaka, K., Tanahashi, N., and Ichihara, A. (1991). Improved method for preparation of ubiquitin-ligated lysozyme as substrates of ATP-dependent proteolysis. *FEBS Lett.* **292**, 154–158.

Tanaka, K. (1998). Molecular biology of the proteasome. *Biochem. Biophys. Res. Commun.* **247**, 537–541.

Tanaka, K., and Kasahara, M. (1998). The MHC class I ligand-generating system: Roles of immunoproteasomes and the interferon-γ-inducible proteasome activator PA28. *Immunol. Rev.* **163**, 161–176.

Unno, M., Mizushima, T., Morimoto, Y., Tomisugi, Y., Tanaka, K., Yasuoka, N., and Tsukihara, T. (2002). The structure of the mammalian 20S proteasome at 2.75 A*P26 resolution. *Structure* **10**, 609–618.

Ustrell, V., Hoffman, L., Pratt, G., and Rechsteiner, M. (2002). PA200, a nuclear proteasome activator involved in DNA repair. *EMBO J.* **21**, 3516–3525.

CHAPTER

14

Preparation of Cilia from Human Airway Epithelial Cells

Lawrence E. Ostrowski

I. INTRODUCTION

For many years, the biochemical analysis of cilia, and flagella has focused primarily on organisms that are easy to grow and maintain in the laboratory and from which axonemal structures can be isolated in large quantities with a high degree of purity. For example, the isolation of flagella from *Chlamydomonas* in response to pH shock was described as early as 1972 (Witman *et al*., 1972) and cilia were isolated from *Tetrahymena* using dibucaine in 1974 (Thompson *et al*., 1974). While studies of these and other organisms have provided a wealth of valuable information concerning the structure and function of these fascinating axonemal structures, it is clearly important to also investigate the structure, function, and regulation of mammalian, especially human, cilia and flagella. While the axoneme of mammalian sperm has been isolated by a number of techniques (e.g., San Agustin and Witman, 1995), only a few reports detail isolations of mammalian cilia from the airway. This probably reflects in part the difficulty of obtaining sufficient quantities of suitable starting material and the inherent difficulties encountered when working with whole tissues.

In the last several years, the techniques used for culturing airway epithelial cells from both animal and human tissue have improved significantly. When cultured at an air/liquid interface on a collagen matrix and provided with suitable media, these cells have been shown to undergo ciliogenesis *in vitro*. In addition, human cells can be expanded for one or two passages and maintain their ability to differentiate, thus increasing the number of ciliated cells obtained. By culturing human airway epithelial cells under these conditions and modifying a technique originally described by Hastie *et al*.(1986) for isolating cilia from porcine trachea, it is possible to routinely produce highly enriched preparations of human ciliary axonemes. Although these preparations are not completely free of contamination by other cellular structures, they are suitable for many biochemical studies (Zhang *et al*., 2002; Reed *et al*., 2000; Ostrowski *et al*., 2002; Kultgen *et al*., 2002). Because this procedure utilizes a detergent, most of the ciliary membranes and soluble proteins are removed during the isolation, and the recovered material consists primarily of ciliary axonemes and their attached structures (dynein arms, radial spokes, etc.). Modifications of the procedure have been described that allow for at least partial recovery of ciliary membranes (Hastie *et al*., 1990; Salathe *et al*., 1993) from *in vivo* samples; these have not yet been tested extensively in the *in vitro* model. It should also be emphasized that the starting material for this procedure is well-differentiated, heavily ciliated airway cultures (Fig. 1A) grown under the conditions described in detail by Bernacki *et al*. (1999) and Randell *et al*. (2001) (and references therein). If the cultures are not completely confluent and heavily ciliated, the resulting preparation often contains a significant amount of cellular debris. The use of a nonionic detergent in the presence of calcium causes the cilia to be removed from the cell at a point just above the apical membrane, leaving the basal bodies intact (Figs. 1B and 1C).

II. REAGENTS AND SOLUTIONS

Protease inhibitor cocktail (P8340), dithiothreitol (DTT, D-9779), and Triton X-100 (T-8787) are from

Copyright 2006, Elsevier Science (USA).
All rights reserved.

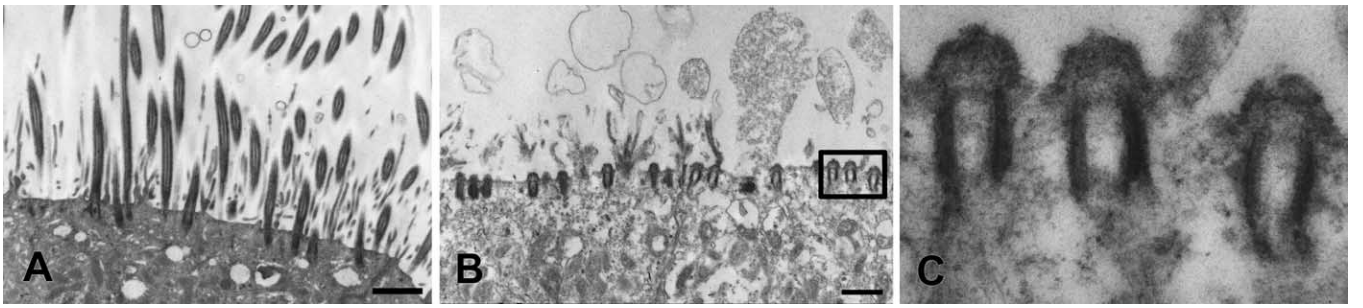

FIGURE 1 Electron micrographs of ciliated cultures of human airway epithelial cells before (A) and after (B and C) isolation of cilia. (A) A heavily ciliated culture after 6 weeks of culture. (B) A parallel culture fixed immediately after removal of cilia. Note the intact basal bodies, which are shown at higher magnification in C. Scale bar in A and B: 2.5 µm.

Sigma. β-Mercaptoethanol (0482) is from Amresco. The protease inhibitor cocktail is thawed upon arrival and frozen in small aliquots (100–200 µl). A 10% solution of Triton X-100 is made in sterile distilled water and stored in the refrigerator for no longer than 1 month. DTT is conveniently frozen in small aliquots at 100 m*M*. All other chemicals are standard laboratory reagents and can be obtained from most laboratory suppliers.

1. *Deciliation buffer (DB)*: 10 m*M* Tris–HCl (pH 7.5), 50 m*M* NaCl, 10 m*M* $CaCl_2$, 1 m*M* EDTA, 0.1% Triton X-100, 7 m*M* β-mercaptoethanol, and 1% protease inhibitor cocktail. Prepare a stock solution *without* protease inhibitor, β-mercaptoethanol, or Triton X-100. Sterile filter and store in the refrigerator. Before starting the procedure, add to 4.9 ml of the stock solution 50 µl of freshly thawed protease inhibitor cocktail, 50 µl of 10% Triton X-100, and 2.45 µl of β-mercaptoethanol.

2. *Resuspension buffer (RB)*: 30 m*M* HEPES (pH 7.3), 25 m*M* NaCl, 5 m*M* $MgSO_4$, 1 m*M* EGTA, 0.1 m*M* EDTA, 1 m*M* DTT, and 1% protease inhibitor cocktail. Prepare a 10× stock solution *without* protease inhibitor and DTT (300 m*M* HEPES, 250 m*M* NaCl, 50 m*M* $MgSO_4$,10 m*M* EGTA, 1 m*M* EDTA), sterile filter, and store in the refrigerator. Before starting the isolation procedure, dilute an aliquot to 1X with sterile water. To 4.9 ml of diluted stock, add 50 µl of freshly thawed protease inhibitor cocktail and 50 µl of freshly thawed 100 m*M* DTT.

III. PROCEDURE

As noted earlier, this procedure starts with heavily ciliated cultures of human airway epithelial cells. Cilia can be isolated from four 30-mm Millicell-CM culture inserts (PICM03050; Millipore) at one time. The inserts are first transferred to a six-well plate for ease of manipulation. Once started, the procedure should be carried out quickly.

1. Gently wash the mucus from the apical surface of the culture with at least two rinses of 2 ml of chilled phosphate-buffered saline (PBS). Add the PBS to the surface of the culture, swirl gently, and aspirate. If the cultures are producing large amounts of mucus, perform additional washes until the visible mucus is removed. After the last wash, carefully aspirate as much fluid as possible from both apical and basolateral sides of the insert.
2. Add 300 µl of cold DB to each insert.
3. Cover the six-well plate and rock vigorously for 1 min. Tilt the plate from side to side so the solution flows back and forth. Occasionally swirling the plate so the solution washes around the edges helps remove cilia from this area of the insert. Tilt the plate slightly so that the solution collects on one edge and remove with a pipetter. Pool the solution containing the cilia from two inserts into one tube. Keep isolated cilia on ice.
4. Repeat steps 2 and 3. Pool the second collection of cilia with the first. There should be 1.2 ml per microcentrifuge tube.
5. Pellet any cellular debris by centrifuging at 1000 RCF for 1 min at 4°C. Carry out the remaining steps in a cold room.
6. Collect the cilia containing supernatant into a new tube. When starting with heavily ciliated cultures that are washed well, there will be only a very small pellet of debris, with some stringy material along the sides of the tube. Try to remove the supernatant without disturbing the pellet. We have found that spinning at higher speeds or for longer times pellets cilia

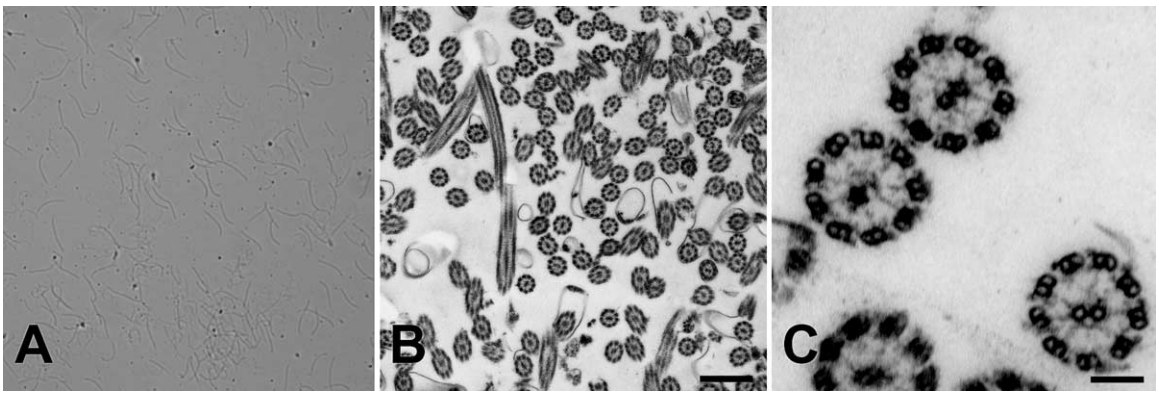

FIGURE 2 (A) Phase-contrast light micrograph of isolated cilia showing the appearance of the preparation after step 10 (original magnification, 400×). (B) Electron micrograph showing many intact ciliary axonemes after step 12. (C) Higher magnification of the same preparation as in B showing details of the isolated axonemes. Note the presence of radial spokes and dynein arms. Scale bars: 1.1 µm (B) and 0.15 µm (C).

as well as debris. Depending on the goal of the experiment (high purity or greatest recovery), the time of this centrifugation may be adjusted.

7. Pellet the ciliary axonemes by centrifugation at 12,000 RCF for 5 min at 4°C. After this centrifugation, a compact white pellet should be obtained. Carefully remove the supernatant and discard.

8. Resuspend the ciliary axonemes in 0.5 ml of RB buffer/insert (1.0 ml per tube). The pellet does not go into solution readily and must be pipetted gently to disrupt. While a homogeneous solution is desired, small clumps of material do not seem to affect the results.

9. Optional: To remove ciliary membranes, add 50 µl of 10% Triton-X 100 (final concentration of 0.5%) and incubate the solution on ice for 15 min. Repeat steps 7 and 8.

10. Withdraw and spot 5 µl of the solution onto a slide, coverslip, and examine by phase-contrast microscopy at 40× magnification. The axonemes should be readily visible as individual strands, with little cellular debris present (Fig. 2A).

11. If a protein determination is desired, remove an aliquot to a separate tube (typically 10%, or 100 µl). Pellet the cilia in both the sample and the protein determination tube by centrifugation at 12,000 RCF for 5 min at 4°C.

12. Remove as much of the supernatant as possible and freeze the pellets at –80°C until needed.

IV. NOTES

1. Protein concentration is determined using the BCA protein assay kit (Pierce, Rockford, IL). To solublize the axonemes, the pellet is dissolved in 0.5% SDS before performing the assay. The protein values obtained provide estimates of how much protein is in the cilia pellet. Although the amount of ciliary axonemes recovered varies with the degree of ciliated cell differentiation, each insert typically yields about 50 µg of protein.

2. The microscopic examination of the preparation in step 10 provides a simple and rapid qualitative estimate of the purity of the axonemes recovered.

3. Cilia isolated by this procedure can be reactivated by the addition of ATP to the cilia suspension obtained after step 10. ATP is added to an aliquot of the cilia and the reactivation is observed by phase-contrast microscopy (Hastie *et al*., 1986).

4. For detailed analysis, the pelleted axonemes can be fixed in 2% formaldehyde/2% glutaraldehyde with 0.5% tannic acid (Hayat, 1989) and examined by transmission electron microscopy. An example of a routine preparation of isolated axonemes examined by electron microscopy is shown in Figs. 2B and 2C.

5. A problem sometimes encountered has been the fragmentation of the axoneme into individual microtubules. While the cause of this phenomena has not been identified, proteolytic degradation or the use of old or improperly made solutions seems to be a likely cause. When this is observed, fresh solutions should be prepared and the procedure repeated to verify that intact axonemes are obtained.

Acknowledgments

This work was funded in part by NIH Grant HL63103 from the National Heart, Lung, and Blood Institute. The author thanks Dr. Scott Randell and the

members of the Cell and Tissue Core Facility for helpful discussions and providing the human airway epithelial cells, Kim Burns and the members of the Histology Core Facility for providing electron microscopy services, Kerri Kendrick for preparing the illustrations, and Dr. William Reed for helpful suggestions concerning the cilia isolation protocol.

References

Witman, G. B., Carlson, K., Berliner, J., and Rosenbaum, J. L. (1972). Chlamydomonas flagella. I. Isolation and electrophoretic analysis of microtubules, matrix, membranes, and mastigonemes. *J. Cell Biol*. **54**, 507–539.

Thompson, G. A., Jr., Baugh, L. C., and Walker, L. F. (1974). Nonlethal deciliation of Tetrahymena by a local anesthetic and its utility as a tool for studying cilia regeneration. *J. Cell Biol*. **61**, 253–257.

San Agustin, J. T., and Witman, G. B. (1995). Isolation of ram sperm flagella. *Methods Cell Biol*. **47**, 31–36.

Hastie, A. T., Dicker, D. T., Hingley, S. T., Kueppers, F., Higgins, M. L., and Weinbaum, G. (1986). Isolation of cilia from porcine tracheal epithelium and extraction of dynein arms. *Cell Motil. Cytoskel*. **6**, 25–34.

Zhang, Y. J., O'Neal, W. K., Randell, S. H., Blackburn, K., Moyer, M. B., Boucher, R. C., and Ostrowski, L. E. (2002). Identification of dynein heavy chain 7 as an inner arm component of human cilia that is synthesized but not assembled in a case of primary ciliary dyskinesia. *J. Biol Chem*. **277**, 17906–17915.

Reed, W., Carson, J. L., Moats-Staats, B. M., Lucier, T., Hu, P., Brighton, L., Gambling, T. M., Huang, C. H., Leigh, M. W., and Collier, A. M. (2000). Characterization of an axonemal dynein heavy chain expressed early in airway epithelial ciliogenesis. *Am. J. Respir. Cell Mol. Biol*. **23**, 734–741.

Ostrowski, L. E., Blackburn, K., Radde, K. M., Moyer, M. B., Schlatzer, D. M., Moseley, A., and Boucher, R. C. (2002). A proteomic analysis of human cilia: Identification of novel components. *Mol. Cell Prot*. **1**, 451–465.

Kultgen, P. L., Byrd, S. K., Ostrowski, L. E., and Milgram, S. L. (2002). Characterization of an a-kinase anchoring protein in human ciliary axonemes. *Mol. Biol. Cell*. **13**, 4156–4166.

Hastie, A. T., Krantz, M. J., and Colizzo, F. P. (1990). Identification of surface components of mammalian respiratory tract cilia. *Cell Motil. Cytoskel*. **17**, 317–328.

Salathe, M., Pratt, M. M., and Wanner, A. (1993). Cyclic AMP-dependent phosphorylation of a 26 kD axonemal protein in ovine cilia isolated from small tissue pieces. *Am. J. Respir. Cell Mol. Biol*. **9**, 306–314.

Bernacki, S. H., Nelson, A. L., Abdullah, L., Sheehan, J. K., Harris, A., William Davis, C., and Randell, S. H. (1999). Mucin gene expression during differentiation of human airway epithelia *in vitro*: Muc4 and muc5b are strongly induced. *Am. J. Respir. Cell Mol. Biol*. **20**, 595–604.

Randell, S. H., Walstad, L., Schwab, U. E., Grubb, B. R., and Yankaskas, J. R. (2001). Isolation and culture of airway epithelial cells from chronically infected human lungs. *In vitro Cell Dev. Biol. Anim*. **37**, 480–489.

Hayat, M. (1989). "*Principles and Techniques of Electron Microscopy*," 3rd Edn. CRC Press, Boca Raton, FL.

CHAPTER

15

Isolation of Nucleoli

Yun Wah Lam and Angus I. Lamond

I. INTRODUCTION

The human nucleolus is a prominent nuclear substructure assembled around tandemly repeated ribosomal genes (rDNA genes) on chromosomes 13, 14, 15, 21, and 22 and is the site of rDNA transcription and ribosome subunit synthesis (reviewed by Shaw and Jordan, 1995). Visualised under electron microscopy, the nucleolus is separated morphologically into three distinct substructures: fibrillar centres (FC), which are surrounded by dense fibrillar components (DFCs), and granular components (GC) (Shaw and Jordan, 1995). Its high density and structural stability allow effective purification using a straightforward procedure. Following the initial successful attempts to purify nucleoli from human tumour cells and rodent liver cells in the early 1960s (e.g., Muramatsu *et al*., 1963), numerous studies have reported on the characterization of isolated nucleoli. Nucleoli have been purified from a large variety of mammalian tissues, including liver, brain (Banks and Johnson, 1973), and thyroid (Voets *et al*., 1979), and from cells of nonmammalian species such as Xenopus (Saiga and Higashinakagawa, 1979) and Tetrahymena (e.g., Matsuura and Higashinakagawa, 1992). The ability to isolate nucleoli in large scale provides an excellent starting material for identifying, purifying, and studying nucleoli and has contributed significantly to the understanding of this nuclear structure.

The following protocol is based on one of the earliest published procedures for isolating nucleoli from cultured human cells (Muramatsu *et al*., 1963). This is a very robust procedure in which isolated nuclei are subjected to sonication whose power is adjusted so that nucleoli remain intact while the rest of nuclei are fragmented. Then nucleoli are isolated by spinning through a density gradient, exploiting their high density compared with other nuclear components. Detailed analysis using highly sensitive mass spectrometric techniques (Andersen *et al*., 2002) indicated that this method was a reproducible and efficient way to produce highly purified nucleoli.

II. PROCEDURES

Solutions

All solutions are supplemented with Complete protease inhibitor tablet (Roche, Cat. No. 1-873-580) at the final concentration of 1 tablet/50 ml).

Phosphate-buffered Saline (PBS)
Buffer A: 10 m*M* HEPES, pH 7.9, 10 m*M* KCl, 1.5 m*M* $MgCl_2$, 0.5 m*M* dithiothreitol (DTT)
S1 solution: 0.25 *M* sucrose and 10 m*M* $MgCl_2$
S2 solution: 0.35 *M* sucrose, 0.5 mM $MgCl_2$
S3 solution: 0.88 M Sucrose, 0.5 mM $MgCl_2$

See "Notes" on making stock sucrose solution.

Steps

1. Seed HeLa cells (ATCC number: CCL-2) onto 10 × 14-cm petri dishes and culture at 37°C in 5% CO_2 in Dulbecco's modified Eagle medium (DMEM) containing 4 m*M* L-glutamate, 4.5 mg/ml glucose, and 0.11 mg/ml sodium pyruvate (Invitrogen UK, Cat. No: 41966-029), supplemented with 100 U/ml penicillin and 100 µg/ml streptomycin [1% (v/v) penicillin/streptomycin solution, Invitrogen UK, Cat. No: 15140-122] until >90% confluence (approximately 10^7 cells per

Copyright 2006, Elsevier Science (USA).
All rights reserved.

dish). This number of HeLa cells consistently provides nucleoli with excellent yield and purity. It is possible to scale down the preparation, although the purity of isolated nucleoli may suffer. Make sure you monitor every step using a phase-contrast microscope (see later). One hour before nucleolar isolation, replace with fresh, prewarmed medium.

2. Harvest cells by trpysinization. Rinse each dish three times with prewarmed PBS and, on removal of the last rinse, add 2 ml of trypsin–EDTA solution (Invitrogen UK, Cat. No: 25300-054) per dish. Swirl the dishes to make sure the trypsin–EDTA is distributed evenly and return the dishes to the incubator for about 5 min. Check under a phase-contrast microscope that all the cells are detached. Prolong incubation if needed. Into each dish add 8 ml of prewarmed medium and pipette up and down so that all the cells are collected as a single-cell suspension. Pool all the harvested cells into 2 × 50-ml Falcon tubes. For some strains of HeLa cells, it is also possible to harvest the cells by scraping them in 5 ml ice-cooled PBS per dish. Because scraping may lead to an impure nucleolar preparation in some HeLa strains, it is not recommended as the method of first choice.

3. Wash three times with ice-cold PBS at 218 *g* (1000 rpm, Beckman GS-6 centrifuge, GH-3.8 rotor) at 4°C.

4. After the final PBS wash, resuspend the cells in 5 ml of buffer A and incubate the cells on ice for 5 min. Put a small drop of the cell suspension on a glass slide and check under a phase-contrast microscope, such as a Zeiss Axiovert 25, using a 20× objective. The cells should be swollen, but not burst (Fig. 1). Nucleoli of cultured mammalian cells disassemble at 37°C in hypotonic conditions (Zatsepina *et al*., 1997). It is therefore imperative to keep the cell suspension on ice during this step.

5. Transfer the cell suspension to a precooled 7-ml Dounce tissue homogenizer (Wheaton Scientific Product Cat. No: 357542). Homogenize 10 times using a tight pestle ("A" specification: 0.0010–0.0030-in. clearance) while keeping the homogenizer on ice. The number of strokes needed depends on the cell type used (see Section III). It is therefore necessary to check the homogenized cells under a phase-contrast microscope after every 10 strokes. Stop when >90% of the cells are burst, leaving intact nuclei, with various amounts of cytoplasmic material attached. In most cases, the presence of this cytoplasmic contamination does not affect the final purity of the isolated nucleoli (Fig. 2). Centrifuge the homogenized cells at 218 *g* (1000 rpm, Beckman GS-6 centrifuge, GH-3.8 rotor) for 5 min at 4°C. The pellet contains enriched, but not highly pure, nuclei.

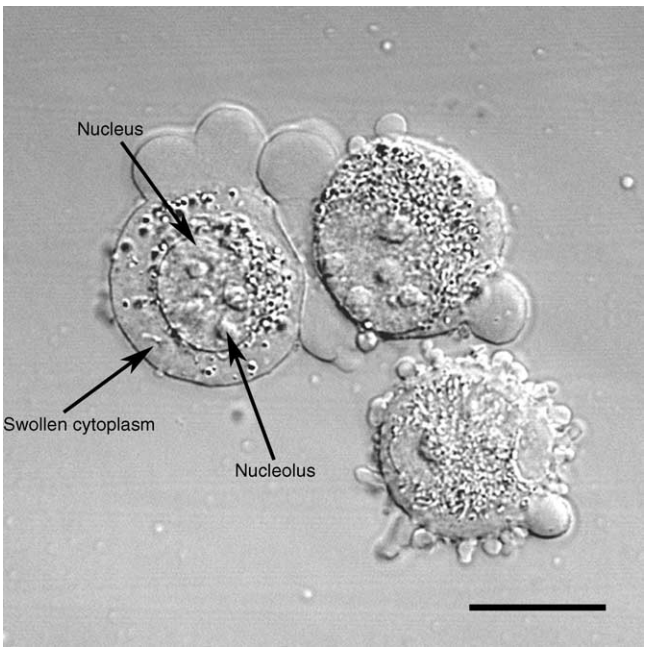

FIGURE 1 HeLa cells after step 4. Note the swollen cytoplasm and prominent nucleoli. Bar: 10 µm.

6. Resuspend the pellet with 3 ml S1 solution (Fig. 3). The pellet should be resuspended readily by pipetting up and down. A pellet that cannot be resuspended contains lysed nuclei and should be discarded. Layer the resuspended pellet over 3 ml of the S2 solution. Take care to keep the two layers cleanly separated. Centrifuge at 1430 *g* (2500 rpm, Beckman GS-6 centrifuge, GH-3.8 rotor) for 5 min at 4°C. This step results in a cleaner nuclear pellet (Fig. 3). Resuspend the pellet with 3 ml of the S2 solution by pipetting up and down.

7. Sonicate the nuclear suspension with six 10-s bursts (with 10-s intervals between each burst) using a Misonix XL 2020 sonicator fitted with a microtip probe and set at power setting 5 (Fig. 4A). Check the sonicated nuclei under a phase-contrast microscope. There should be virtually no intact cells and nucleoli should be readily observed as dense, refractile bodies (Fig. 4B). The optimal sonication time depends on the cell type used. If you attempt to isolate nucleoli from a cell type from the first time, it is necessary to check the sonicated material under a microscope after every 10 sec of sonication. Oversonication leads to destruction of nucleoli.

8. Layer the sonicated sample over 3 ml of the S3 solution and centrifuge at 3000 *g* (3500 rpm, Beckman GS-6 centrifuge, GH-3.8 rotor) for 10 min at 4°C (Fig. 5). The pellet contains nucleoli, whereas the supernatant can be retained as the "nucleoplasmic fraction" (Fig. 5).

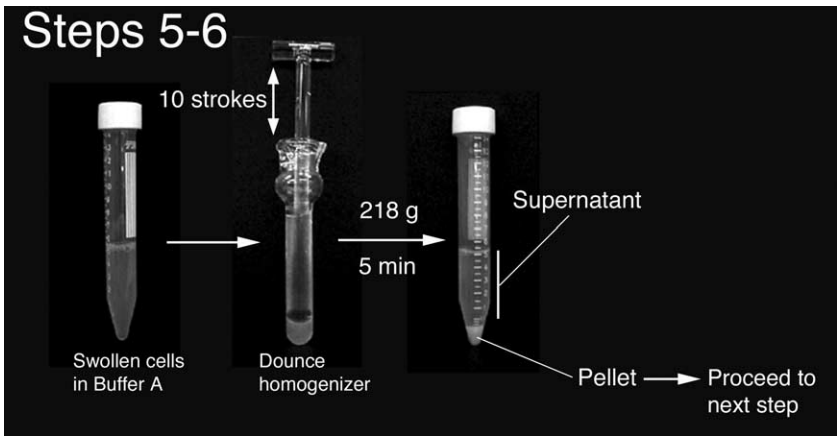

FIGURE 2 Steps 5 and 6 of the procedure.

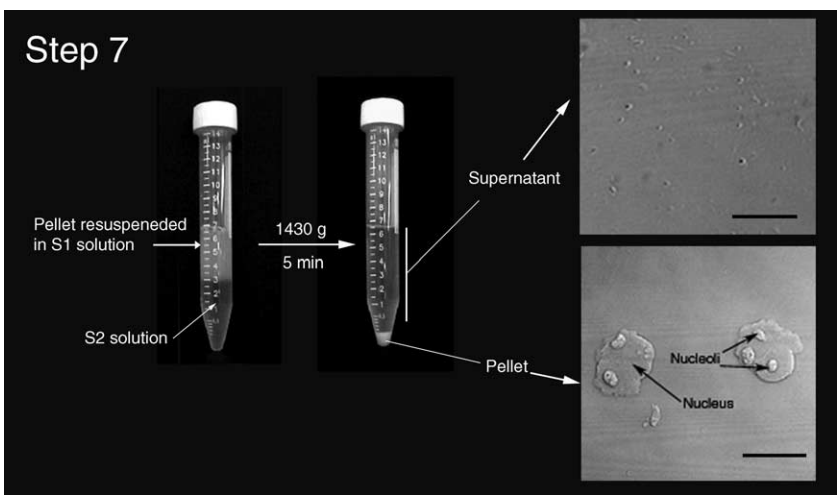

FIGURE 3 Step 7 of the procedure. Note the clear boundary between S1 and S2 layers before centrifugation. (Insets) DIC images of the supernatant and pellet. Note prominent nucleoli inside nuclei in the pellet. Bars: 10 μm.

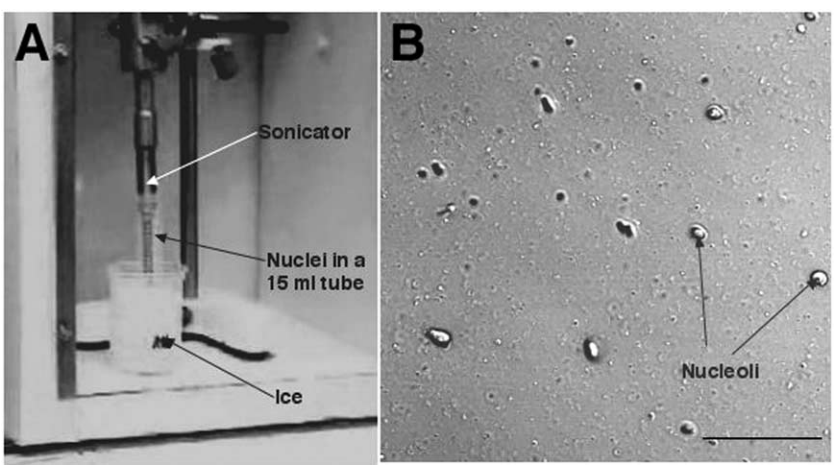

FIGURE 4 (A) Setup for sonication. (B) DIC image of sonicated nuclei. Note the presence of prominent nucleoli. Bar: 10 μm.

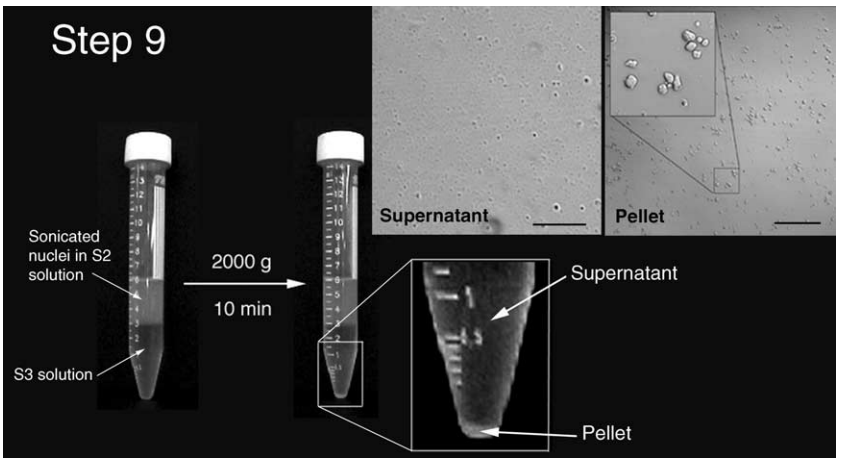

FIGURE 5 Step 9 of the procedure. Note the clear jboundary between S2 and S3 layers before and after centrifugation. The pellet should be small but visible. (Insets) DIC images of the supernatant and pellet. The pellet should contain purified nucleoli. Bars: 10 µm (left inset) and 20 µm (right inset).

9. Resuspend the nucleoli with 0.5 ml of the S2 solution, followed by centrifugation at 1430 *g* (2500 rpm, Beckman GS-6 centrifuge, GH-3.8 rotor) for 5 min at 4°C. The pellet contains highly purified nucleoli. Check under a phase-contrast microscope to ensure that this preparation contains only highly purified nucleoli without any other material (Fig. 5). Nucleoli can be resuspended in 0.5 ml of the S2 solution and stored at –80°C.

III. NOTES

1. Making 2.55 M Sucrose Stock

Here is a protocol for preparing a sucrose stock solution (Cline and Ryel, 1971) suitable for the nucleolar isolation protocol. The resulting solution is 2.55 *M*, or 66% by weight. Its density is 1.3224 g/cm^3 at 20°C, and its refractive index is 1.4558. The stock solution is stable indefinitely at 4°C. This procedure can be carried out at room temperature. There is no need to heat up the solution to help dissolve the sucrose. Heating up an incompletely dissolved sucrose solution can lead to charring of sucrose and affect the quality of the sucrose solution.

1. Weigh out 1710 g sucrose (BDH). Keep it aside in a clean container.
2. Put exactly 900 ml water and a magnetic bar in a 5 litre beaker. Put the beaker on a stirrer and start stirring.
3. Add one-third of the sucrose into the beaker. Make sure the magnetic bar is rotating freely. Stir for 1 h.
4. Add another one-third of the sucrose into the solution. Again make sure the rotation of the stir bar is not impaired. Stir for another 1 h.
5. Add the remaining sucrose. Stir for another 1 h or until all the sucrose has gone into solution. The final volume should be exactly 2 litres.

2. Sonication

We use a Misonix 2020 sonicator fitted with a microtip at power setting 5. To ensure reproducible soncation, the following points should be followed.

i. It is necessary to tune the sonicator every time after you change the probe. Follow the manufacturer's manual for the tuning procedure.

ii. Sonication produces intense and localized heat in your solution. If you are concerned about the heating, the correct way to reduce heating is to shorten the sonication time and to increase the intermission between bursts. Keeping the tube on ice or performing the sonication in the cold room is helpful, but is not the most effective way of heat control.

iii. If the probe is too close to the liquid surface, it produces a foam and reduces the efficiency of sonication. Make sure the probe is well submerged in the solution, about 5 mm above the bottom of the tube. Do not, however, touch the bottom or the wall of the tube with the probe.

iv. A sonicator probe that has been used repeatedly develops pits on its end. The sonication efficiency gradually decreases as time goes on. Therefore, the sonication time recommended here can only be used as a guideline. Always monitor the outcome of sonication using a phase-contrast microscope. You may

need to adjust the sonication time to maintain the efficiency, especially if the probe is getting old. Change the probe when the efficiency is noticeably down.

3. Analysis of Isolated Nucleoli

i. To immunolabel purified nucleoli, spot about 5 µl of the nucleolar suspension onto a polylysine-coated slide (BDH Cat. No: 406/0178/00) and air dry the spot. Rehydrate the slide in PBS for 5 min before carrying out a standard immunostaining procedure.

ii. To separate nucleolar proteins on a gel, resuspend directly either in Laemmli SDS sample buffer or in your preferred buffer. The high concentration of nucleic acid in isolated nucleoli makes the lysed sample very viscous. The sample can be clarified by passing through a QIAshredder spin column (Qiagen Cat. No: 79654). Nucleoli can also be extracted with RIPA buffer (150 m*M* NaCl, 1% NP40, 0.5% deoxycholate, 0.1% SDS, 50 m*M* Tris, pH 8.0, Complete protease inhibitor cocktail). Immunoprecipitations can be performed from nucleolar lysates prepared in RIPA buffer.

4. Adapting Nucleolar Isolation Protocol to Use with Other Cell Types

The aforementioned protocol can be adapted readily to other cell types. Apart from HeLa cells, we have used this protocol, with minor modifications, to isolated nucleoli from MCF-7 (human breast epithelium), WI-38 (human fibroblast), IMR-32 (human neuroblastoma), HL60 (human promyelocytic leukemia), and plant *Arabidopsis thalina* cells. When adapting the protocol to a different cell type, make sure that you control each step by carefully checking the products after each step under a phase-contrast microscope. For example, different cell types may require a different homogenization (step 4) and/or sonication strength (step 7). The concentration of $MgCl_2$ also appears crucial to the purity of the isolated nucleoli. If the isolated nucleoli are not pure enough, try lowering the concentration of $MgCl_2$ in the S2 and S3 solutions. If the yield is poor or if nucleoli look fragmented, use more $MgCl_2$.

References

Andersen, J. S., Lyon, C. E., Fox, A. H., *et al*. (2002). Directed proteomic analysis of the human nucleolus. *Curr. Biol*. **12,** 1–11.

Banks, S. P., and Johnson, T. C. (1973). Developmental alterations in RNA synthesis in isolated mouse brain nucleoli. *Biochim. Biophys. Acta* **294**, 450–460.

Cline, G. B., and Ryel, R. B. (1971). *Methods Enzymol.* **22**, 168–204.

Matsuura, T., and Higashinakagawa, T. (1992). *In vitro* transcription in isolated nucleoli of *Tetrahymena pyriformis*. *Dev. Genet*. **13,** 143–150.

Muramatsu, M., Smetana, K., and Busch, H. (1963). Quantitative aspects of isolation of nucleoli of the Walker carcinosarcoma and liver of the rat. *Cancer Res*. **25**, 693–697.

Saiga, H., and Higashinakagawa, T. (1979). Properties of *in vitro* transcription by isolated Xenopus oocyte nucleoli. *Nucleic Acids Res*. **6**, 1929–1940.

Shaw, P. J., and Jordan, E. G. (1995). The nucleolus. *Annu. Rev. Cell Dev. Biol*. **11**, 93–121.

Voets, R., Lagrou, A., Hilderson, H., *et al*. (1979). RNA synthesis in isolated bovine thyroid nuclei and nucleoli: alpha-amanitin effect, a hint to the existence of a specific regulatory system. *Hoppe Seylers Z Physiol. Chem*. **360**, 1271–1283.

Zatsepina, O. V., Dudnic, O. A., Chentsov, Y. S., Thiry, M., Spring, H., and Trendelenburg, M. F. (1997). Reassembly of functional nucleoli following in situ unraveling by low-ionic-strength treatment of cultured mammalian cells. *Exp. Cell. Res*. **233**(1), 155–168.

CHAPTER

16

Purification of Intermediate-Containing Spliceosomes

Melissa S. Jurica

I. INTRODUCTION

The spliceosome is the dynamic macromolecular machine responsible for removing intervening sequences (introns) from pre-mRNA transcripts. *In vitro* studies have been used to define a pathway of a spliceosome assembly consisting of several intermediate subcomplexes (Moore *et al.*, 1993). Isolating any one of these splicing complexes for subsequent characterization, and structural analysis requires a means to accumulate that specific complex (Jurica and Moore, 2002). A number of methods for purifying complexes along the spliceosome assembly pathway have been described (Das *et al.*, 2000; Hartmuth *et al.*, 2002; Jurica *et al.*, 2002; Makarov *et al.*, 2002; Zhou *et al.*, 2002). These protocols use similar approaches of combining size fractionation and affinity purification to isolate *in vitro*-assembled splicing complexes under native conditions. Presented here is a procedure developed for isolating intact splicing complexes arrested between the first and the second chemical steps of splicing (Jurica *et al.*, 2002).

Spliceosomes are assembled on an *in vitro*-transcribed splicing substrate from components present in the nuclear extract of HeLa cells. Using a substrate with a mutation at the 3′ splice site, complex assembly is arrested by a block at the second step of splicing. The substrate also contains binding sites for an RNA-binding protein that serves as an affinity tag. Purification of arrested spliceosomes is carried out in three steps: (1) RNase H digestion of excess pre-mRNA substrate, (2) size-exclusion chromatography, and (3) affinity selection via the RNA-binding adapter protein (Fig. 1). Digestion serves to improve the ratio of fully assembled complexes to earlier species by targeting substrate molecules not fully assembled into spliceosomes. Cleavage is mediated by endogenous RNase H present in nuclear extracts and DNA oligonucleotides targeted to the last 30 nucleotides of the 5′ exon in the pre-mRNA substrate, a region protected from digestion in arrested complexes, but accessible in earlier ones (Reichert *et al.*, 2002). Size exclusion employs a small sizing column to quickly separate a splicing reaction into basically two fractions: larger molecules, including the spliceosomes, that are excluded by the sizing resin and elute in the void volume, and smaller molecules that can enter the pores of the resin and are retained on the column, such as the bulk of nuclear extract proteins, degraded RNA, and unbound affinity adapter protein. Affinity selection is mediated by binding sites for the bateriophage MS2 coat protein in the pre-mRNA substrate. The substrate can then be bound to a fusion of MS2 and maltose-binding protein (MBP). The MS2:MBP serves as an affinity adapter so that spliceosomes assembled on the tagged substrate can be captured by amylose resin and eluted under native conditions with maltose. The main objectives in developing this protocol were to isolate homogeneous splicing complexes in the quantities (~100 µl) and concentrations (5–50 n*M*) useful for both biochemical characterization and electron microscopy analysis.

II. MATERIALS AND INSTRUMENTATION

HEPES (Cat. No. H-3375), EDTA (Cat. No. E-5134), isopropyl-β-D-thiogalactoside (IPTG, Cat. No. I-5502), maltose (Cat. No. M-5895), phenylmethylsulfonyl flouoride (PMSF, Cat. No. P-7626), L-glutamic acid,

Copyright 2006, Elsevier Science (USA).
All rights reserved.

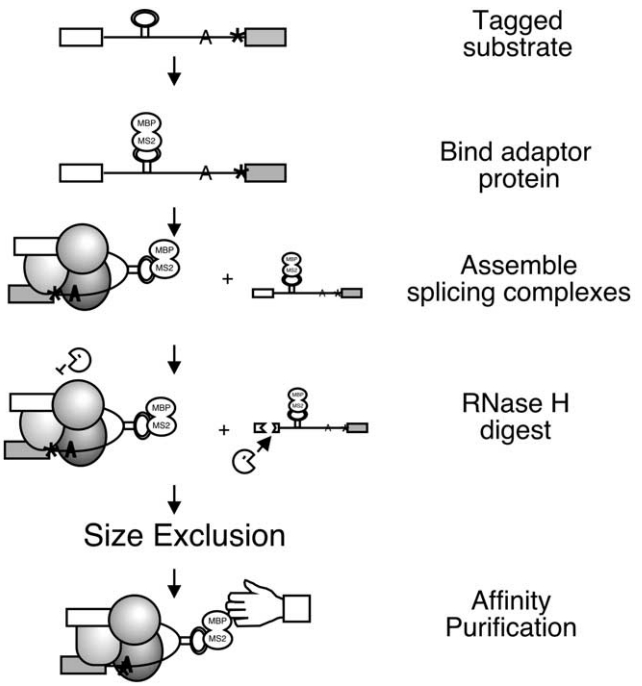

FIGURE 1 Purification scheme.

monopotassium salt (Cat. No. G-1501), Nonidet P-40 (Cat. No. N-6507), heparin (Cat. No. H-3900), phosphocreatine (Cat. No. P-7936), yeast tRNA (Cat. No. R-9001), Trizma base (Cat. No. T-1503), and formamide (Cat. No. 47671) are from Sigma. Tris–HCl (Cat. No. BP153), glycerol (Cat. No. G33), magnesium acetate (Cat. No. M13), and potassium chloride (Cat. No. P217) are from Fisher. Adenosine triphosphate (Cat. No. 27-2056-01), HiTrap heparin column (Cat. No. 17-0407-01), and S-400 Sephacryl (Cat. No. 217-0609-10) are from Amersham Biosciences. RNasin (Cat. No. N2515) is from Promega, and amylose resin (Cat. No. E8021) is from New England Biolabs. Acrylamide (Cat. No. EC-852) is from National Diagnostics, and urea (Cat. No. 821527) is from ICN. The splicing substrate is generated by *in vitro* runoff transcription under standard conditions (Moore and Query, 1998) from construct MJM273. MJM273 is derived from an AdML gene construct containing a single intron with an extended polypyrimidine tract, an AG->GG 3′ splice site mutation (Anderson and Moore, 1997; Gozani *et al*., 1994), and contains a tag of three MS2-binding sites located in the intron between the 5′ splice site and the branch point (Jurica *et al*., 2002). The substrate is transcribed with T7 RNA polymerase, radiolabeled uniformly using [α-^{32}P]UTP and capped with G(5′)ppp(5′)G. The RNA should be gel purified and quantified by comparison with the specific activity of the transcription reaction. Nuclear extract is derived from HeLa cells as outlined in Dignam *et al*. (1983) and stored in 400-µl aliquots at –80°C. DNA oligonucleotides for RNase H-mediated digestion were synthesized with the following sequences: oligo1 (5′-AGCTGGCCCTCG-3′), oligo2 (5′-CAGACAGCGATG-3′) and stored in 100 µ*M* aliquots of 100 µl at –20°C.

The FPLC (Cat. No. 18-1118-67) is from Amersham Biosciences, and the Centricon-10 (Cat. No. 4205) and Kontes Flex-column (Cat. No. K420401-1010) are from Fisher. Mobicols (Cat. No. M1002) and filter (Cat. No. M2135) are obtained from Mo Bi Tec, LLC, and low-adhesion microcentrifuge tubes (Cat. No. 1415-2600) are from USA Scientific. Gel plates, combs, spacers, and electrophoresis rigs are homemade. Power supplies are from Thermo EC (EC3000) or similar, and the phosphorimager is from Molecular Dynamics.

III. PROCEDURES

A. Purification of Spliceosomes

Solutions

1. *Potassium glutamate:* 1 *M*, pH 7.5. To make 50 ml, dissolve 9.26 g of L-glutamic acid, monopotassium salt in 35 ml of H_2O, and adjust the pH to 7.5 with 10 *N* potassium hydroxide. Complete to 50 ml with H_2O and filter sterilize. Store at 4°C.
2. *Magnesium acetate:* 1 *M* pH 7.5. To make 50 ml, dissolve 10.72 g of magnesium acetate in 35 ml of H_2O and adjust pH to 7.5 with sodium hydroxide. Complete to 50 ml with H_2O and filter sterilize. Store at room temperature.
3. *Creatine phosphate:* 250 m*M*. To make 5 ml, dissolve 319 mg phosphocreatine disodium salt in 5 ml of H_2O. Store at –20°C in 1-ml aliquots. Keep a 100-µl working aliquot at –20°C.
4. *Yeast tRNA:* 5 mg/ml. Add 5 ml of H_2O to a 500 unit bottle of Sigma yeast tRNA and store at –20°C. Keep a 100-µl working aliquot at –20°C.
5. *Heparin:* 10 mg/ml. Make a 1-ml stock by dissolving 10 mg heparin in 1 ml H_2O and filter sterilize. Store at 4°C.
6. *Maltose:* 0.5 M. To make 50 ml, dissolve 9 g of maltose in 40 ml of H_2O and complete to 50 ml. Filter sterilize and store at room temperature.
7. *5x SB:* 0.75 *M* KCl, 25 m*M* EDTA, 100 m*M* Tris, pH 7.9. Make 50 ml with 18.75 ml of 2 *M* KCl stock solution, 2.5 ml of 0.5 *M* of EDTA stock solution, 5 ml of 1 *M* Tris, pH 7.9, stock solution, and 23.75 ml of H_2O. Store at room temperature.
8. *SB-N:* 150 m*M* KCl, 20 m*M* Tris, pH 7.9, 5 m*M* EDTA, 1 m*M* dithiothreitol (DTT), and 0.5% NP-40.

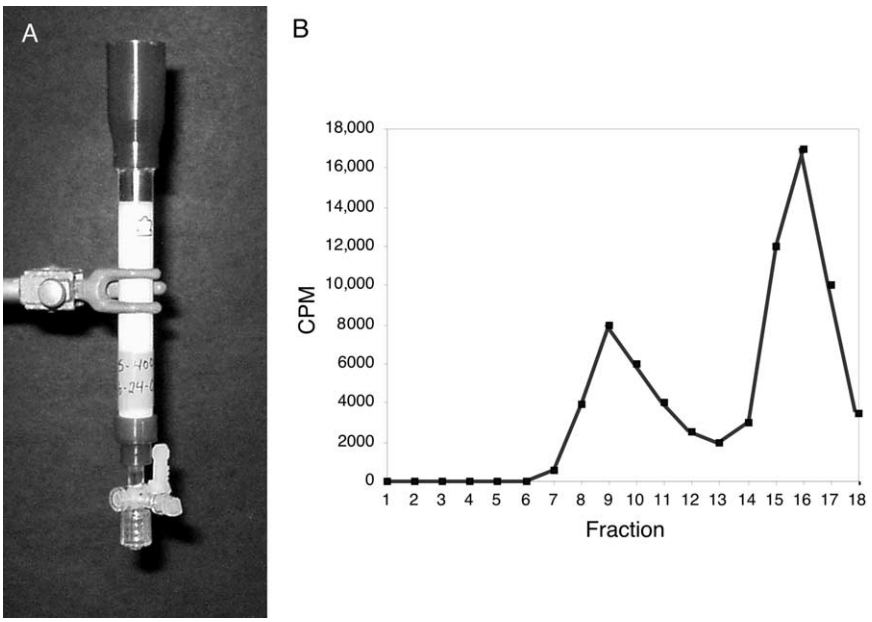

FIGURE 2 (A) Size-exclusion column. (B) Elution profile of size-exclusion column measured with a Gieger counter.

Make 50 ml fresh for each preparation with 10 ml of 5 × SB, 50 µl of 1 *M* DTT stock solution, 250 µl of 10% NP-40 stock solution, and 39.7 ml of H_2O. Keep at room temperature.

9. *SB:* 150 m*M* KCl, 20 m*M* Tris, pH 7.9, 5 m*M* EDTA, and 1 m*M* DTT. Make 15 ml fresh for each preparation with 3 ml of 5 × SB, 15 µl of 1 *M* DTT stock solution, and 12 ml of H_2O. Keep on ice.

10. *SB-M:* 150 m*M* KCl, 20 m*M* Tris, pH 7.9, 5 m*M* EDTA, 1 m*M* DTT, and 10 m*M* maltose. Make 1 ml fresh for each preparation with 200 µl of 5 × SB, 1 µl of 1 *M* DTT stock solution, 20 µl of 0.5 *M* maltose, and 779 µl of H_2O. Keep on ice.

Steps

1. At room temperature, pour 5 ml of S-400 resin equilibrated and resuspended in an equal volume of SB-N into a 1.0 × 10-cm glass column. Allow the resin to settle by gravity flow until the buffer is near the top of the column bed. This sizing column can be used multiple times by washing with 10 ml of SB-N before each use (Fig. 2A).

2. Set up a 1-ml splicing reaction as described in steps 3 and 4 to contain final concentrations of the following: 10 n*M* splicing substrate (MJM273), 500 n*M* MS2-MBP, 80 m*M* potassium glutamate, pH 7.5, 2 m*M* magnesium acetate, pH 7.5, 2 m*M* ATP, 5 m*M* creatine phosphate, 0.05 mg/ml yeast tRNA, 1% RNasin, and 40% nuclear extract.

3. First, place 50 µl substrate (0.2 pmol/µl) in a low-adhesion microcentrifuge tube. Heat at 95°C for 1 min and then place on ice to cool. Add 10 µl MS2-MBP (50 µ*M*) and mix by flicking. Incubate on ice for 5 min.

4. In a second tube, add the following in order: 381 µl H_2O, 80 µl potassium glutamate (1 *M*, pH 7.5), 2 µl magnesium acetate (1 *M*, pH 7.5), 20 µl ATP (100 m*M*), 20 µl creatine phosphate (250 m*M*), 10 µl tRNA (5 mg/ml, yeast), 10 µl RNasin, contents of the first tube (substrate plus MS2-MBP), and 400 µl nuclear extract. Mix by flicking the tube gently. (Place a 5-µl aliquot of the reaction on ice as a 0′ time point for RNA denaturing gel analysis.)

5. Aliquot 200 µl into five tubes. Incubate tubes at 30°C for 60 min to assemble spliceosomes. (Place a 5-µl aliquot of the reaction on ice as a 60′ time point for RNA denaturing gel analysis.)

6. During this incubation, assemble the MoBiCol column by placing a small filter in the bottom of the column. The column can be supported in a microcentrifuge tube on ice. Add 200 µl of amylose resin equilibrated and resuspended in an equal volume of SB-N. Allow the buffer to drain by gravity flow (Fig. 3A).

7. After the 60′ incubation add 2 µl each of oligo 1 and oligo 2 (100 µ*M*) to each tube of the splicing reaction. Mix by flicking the tube gently. Incubate tubes at 30°C for 20 min to induce RNase H digestion. (Place a 5-µl aliquot of the reaction on ice as an 80′ time point for RNA denaturing gel analysis.)

8. Add 10 µl of heparin (10 mg/ml) to each tube. Mix by flicking the tubes gently. Incubate tubes at 30°C for 5 min.

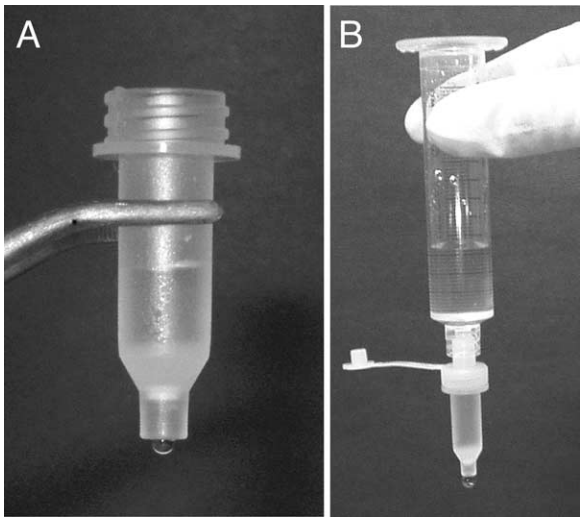

FIGURE 3 (A) Amylose affinity resin in a small MoBiCol column. (B) Setup for washing the amylose column.

9. Run the sizing column by gravity flow until the buffer head just reaches the top of the resin bed. Pool the splicing reactions from the five tubes and carefully load onto the sizing column. Run the column until the resin bed is exposed and load 500 µl SB-N to wash the column wall. Again run the column until the resin bed is exposed.

10. Run 10 ml of SB-N through the column, taking 500-µl fractions in tubes on ice. Gravity flow should be about ~0.4 ml/min. Collect 18–20 fractions total.

11. Count the fractions for the radioactively labeled the splicing substrate with a Geiger counter. There should be two peaks of radioactivity, with the first smaller peak (usually within the first 11 fractions) containing splicing intermediates (spliceosomes) and the larger second peak containing degraded splicing substrate (Fig. 2B). (This can be checked by taking 10-µl aliquots of the fractions for RNA denaturing gel analysis.)

12. Pool the first peak (usually ~2 ml) and flow this through the amylose column by gravity. Collect the column flow-through in tubes on ice and reapply to the amylose column. To wash the column, attach a 10-ml syringe barrel to the top of the column using a luer adaptor cap and place in a 15-ml Falcon tube. Fill the syringe with 10 ml of cold SB to wash the column by gravity flow at 4°C (Fig. 3B).

13. Elute the splicing complexes by pipetting 50-µl aliquots of SB-M onto the amylose resin and taking fractions dropwise into tubes on ice. Count the fractions for the radioactively labeled splicing substrate with a Geiger counter. The complexes should be contained within the first 100 µl of elution.

B. Purifying Affinity-Tag Adapter Protein, MS2-MBP

The affinity-tag adapter protein is a recombinant MS2-MBP fusion expressed in *Escherichia coli* (construct a gift from Josep Vilardell). This fusion places MBP N-terminal to MS2. The MS2 portion carries a double mutation (V75Q and A81G) that prevents oligomerization (LeCuyer *et al.*, 1995). Single-step purification of MS2-MBP over an amylose column yields a single band on a Coomassie-stained gel, but the A_{280}/A_{260} ratio (<1) reveals that a significant amount of bound nucleic acid remains as a contaminant. Heparin chromatography as a second purification step eliminates this contaminant.

Solutions

1. *AB1*: 20 m*M* HEPES, pH 7.9, 200 m*M* KCl, and 1 m*M* EDTA. Make 500 ml by combining 10 ml of 1 *M* HEPES, pH 7.9, stock solution, 50 ml of 2 *M* KCl stock solution, 1 ml of 0.5 *M* EDTA stock solution, and 439 ml of H_2O.
2. *AB2*: 20 m*M* HEPES, pH 7.9, 5 m*M* KCl, and 1 m*M* EDTA. Make 500 ml by combining 10 ml of 1 *M* HEPES, pH 7.9, stock solution, 1.25 ml of 2 *M* KCl stock solution, 1 ml of 0.5 *M* EDTA stock solution, and 487.75 ml of H_2O.
3. *ABE*: 20 m*M* HEPES, pH 7.9, 5 m*M* KCl, 1 m*M* EDTA, and 10 m*M* maltose. Make 100 ml by combining 2 ml of 1 *M* HEPES, pH 7.9, stock solution, 0.25 ml of 2 *M* KCl stock solution, 200 µl of 0.5 *M* EDTA stock solution, 2 ml of 0.5 *M* maltose, and 474.75 ml of H_2O.
4. *PMSF*: 100 m*M*. To make 5 ml, dissolve 87.1 mg PMSF in 5 ml of ethanol. Store at 4°C.
5. *IPTG*: 1 *M*. To make 10 ml, dissolve 1.19 g of IPTG in 5 ml of H_2O. Store in 1-ml aliquots at –20°C.
6. *HB1*: 20 m*M* HEPES, pH 7.9, and 1 m*M* EDTA. Make 500 ml by combining 10 ml of 1 *M* HEPES, pH 7.9, stock solution, 1 ml of 0.5 *M* EDTA stock solution, and 489 ml of H_2O.
7. *HB2*: 20 m*M* HEPES, pH 7.9, 1 *M* KCl, and 1 m*M* EDTA. Make 500 ml by combining 10 ml of 1 *M* HEPES, pH 7.9, stock solution, 250 ml of 2 *M* KCl stock solution, 1 ml of 0.5 *M* EDTA stock solution, and 239 ml of H_2O.

Steps

1. Inoculate a 5-ml culture of Luria broth (LB) with single bacterial colony of DH5α cells transformed with a plasmid expressing MS2-MBP and grow overnight to saturation at 37°C with shaking. The next morning, inoculate 1 liter of LB plus 2% glucose with the 5-ml culture. Grow the cells at 37°C with shaking to an OD_{600} of ~0.5 and then induce expression of the protein

by adding 1 ml of 1 *M* IPTG. Continue to grow the cells for 2–3 h and harvest by centrifugation at 6000 rpm for 10 min. Pour off the supernatant, freeze the cell pellet, and store at –20°C.

2. Thaw and resuspend ~1 g cells in 10 ml cold AB1 plus 200 µl PMSF. Break open the cells by sonication on ice. Centrifuge for 30 min at 15,000 rpm at 4°C.

3. Perform all the following steps of purification at 4°C. Load the supernatant on a –5-ml amylose column equilibrated with AB1, running the column at 0.3 ml/min. Wash the column with 40 ml of AB1, followed by 10 ml of AB2 to lower the salt concentration in preparation for heparin chromatography.

4. Elute the protein with 20 ml of ABE, taking 1-ml fractions. Check the OD_{280} of the fractions and pool the peak fractions. (The column can be cleaned with 5 ml of 0.1% SDS and reequilibrated with AB1 for future use.)

5. Concentrate the pooled peak fraction to ~1 ml in a Centricon-30.

6. On an FPLC, equilibrate a 1-ml heparin column with a mixture of HB1 and HB2 to 5 m*M* KCl. Load the concentrate on the column and wash with 5 ml at 5 m*M* KCl.

7. Run a gradient from 5 to 400 m*M* KCl over 10 column volumes. The MS2-MBP protein elutes at ~60 m*M* KCl. Pool peak fractions and concentrate to ~500 µl in a Centricon-30. Add glycerol to 10% and freeze at –20°C in 100-µl aliquots.

8. Determine the protein concentration for MS2-MBP. An OD_{280} of 1 corresponds to 16.5 µ*M* or 0.89 mg/ml.

C. Denaturing Gel Analysis and Quantification

Solutions

1. *Splicing dilution buffer*: 100 m*M* Tris, pH 7.5, 10 m*M* EDTA, 1% SDS, 150 m*M* NaCl, and 0.3 M NaAc, pH 5.2. To make 50 ml, combine stock solutions of 5 ml of 1 *M* Tris, pH 7.5, 1 ml of 0.5 *M* EDTA, 5 ml of 10% SDS, 3.75 ml of 2 *M* NaCl, 5 ml of 3 *M* NaAc, pH 5.2, and 30.25 ml of H_2O. Store at room temperature.

2. *Acrylamide solution*: 15% acrylamide (29:1 acrylamide:bis-acrylamide), 8 *M* urea, and 1 × TBE. To make 500 ml, dissolve 240.24 g of urea in 100 ml of stock solution of 5 × TBE and 187.5 ml of 40% acrylamide solution with stirring over low heat. Complete to 500 ml with H_2O and filter. Store in the dark at room temperature.

3. *FEB*: 94% formamide, 20 m*M* EDTA, 0.01% cyan blue, and 0.01% bromphenol blue. To make 10 ml, combine 9.4 ml of formamide, 0.4 ml of 0.5 *M* EDTA, 0.1 ml of 1% cyan blue, and 0.1 ml of 1% bromphenol blue stock solutions. Store 1-ml aliquots at –20°C.

Steps

1. To prepare the time point aliquots taken during the spliceosome purification for electrophoresis, remove the tubes from ice and add 95 µl of splicing dilution buffer. Then add 100 µl of phenol:chloroform:isoamyl alcohol (25:24:1, pH 4.5) stock solution. Vortex well and spin at 14,000 rpm in a microcentrifuge for 10 min at room temperature. (If taken, aliquots from the sizing column elution should be treated similarly.)

2. Take the top 90 µl, avoiding the interface, and place in a new tube. To this add 3 volumes ethanol and invert to mix. Place at –70°C for 30 min. Discard the lower layer.

3. Spin tubes in a microcentrifuge at 14,000 rpm for 30 min at 4°C. Remove the ethanol with a pipettor and wash the pellet with 100 µl of 70% ethanol. Dry the pellet.

4. Resuspend the pellet in 5 µl of FEB. Load 2.5 µl on the denaturing acrylamide gel.

5. To prepare elution samples, add 4 µl of FEB to 1 µl of elution aliquots. Load 2.5 µl on the gel.

6. To prepare standard, add 39 µl of FEB to 1 µl of 10 n*M* splicing substrate used during the purification. Load 1 µl on the gel.

7. Assemble a gel mold using 20 × 25-cm glass plates with 0.1-mm spacers and comb. Pour the gel using 25 ml acrylamide solution and polymerize with 75 µl of 20% APS and 25 µl of TEMED stock solutions. Allow the gel to set for at least 30 min.

8. Assemble the gel on a gel rig with TBE buffer stock. Prerun at 30 W for 30 min.

9. Prior to loading on the gel, incubate the samples at 95°C for 1 min and then place on ice.

10. After rinsing out the wells, load samples and standard. Run the gel at 30 W for 2 h. The cyan blue should migrate to near the bottom of the gel.

11. Take down the gel onto a piece of exposed X-ray film and cover with plastic wrap. Expose to a phosphorimager plate overnight.

12. To quantify the concentrations of the purified spliceosomes, the specific activity of the labeled splicing intermediates should be compared to the standard. (Figure 4)

IV. PITFALLS

1. Starting with 10 pmol of pre-mRNA substrate, this protocol generally yields 0.3–0.5 pmol of purified

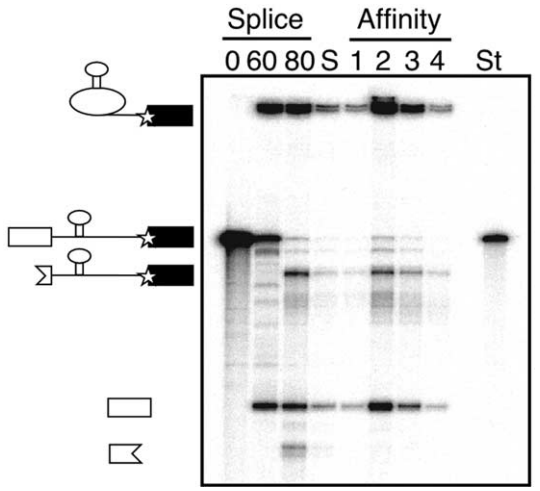

FIGURE 4 Example of denaturing gel (15% polyacrylamide) analysis of substrate RNA during purification. Time points taken during the splicing reaction (0 and 60 min) and after RNase H digestion (80 min), size-exclusion peak fraction (S), affinity column elutions (1–4), and standard used for quantification (St) are shown. The positions of MS2-tagged pre-mRNA, lariat intermediate, 5′ exon, and RNase H digestions products are indicated.

complexes. The yield is highly dependent on the efficiency of the first step of splicing in the reactions. Nuclear extracts can differ in their splicing efficiencies, and therefore titrations of potassium glutamate and magnesium acetate concentrations should be performed to maximize splicing efficiency for a given nuclear extract preparation.

2. The final buffer conditions for the purification were chosen with electron microscopy studies in mind. We found that the splicing complexes tended to aggregate when 2 m*M* $MgCl_2$ was present in the buffer instead of the 5 m*M* EDTA. Although some spliceosome proteins are disassociated in the presence of EDTA, the core splicing components remain intact (Jurica *et al.*, 2002).

3. We have yet to find a method to concentrate spliceosomes after purification, as the complexes adhere to the membranes of all concentration devices tested. By using the very small amount of affinity resin with a column geometry, the spliceosomes can be eluted at a high enough concentration for structural and biochemical analyses without further concentration. Typically peak elution fractions of 15–50 µl containing 5 to 15 n*M* splicing intermediates are obtained.

4. Contamination of reagents, tubes, and so on by RNases is always a concern when handling RNA. Care should be taken to wear clean gloves during the purification and, if possible, to designate reagents, tips, tubes, and so on as being for RNA use only.

References

Anderson, K., and Moore, M. J. (1997). Bimolecular exon ligation by the human spliceosome. *Science* **276**, 1712–1716.

Das, R., Zhou, Z., and Reed, R. (2000). Functional association of U2 snRNP with the ATP-independent spliceosomal complex E. *Mol. Cell* **5**, 779–787.

Dignam, J. D., Lebovitz, R. M., and Roeder, R. D. (1983). Accurate transcription initiation by RNA polymerase II in a soluble extract from isolated mammalian nuclei. *Nucleic Acids Res.* **11**, 1475–1489.

Gozani, O., Patton, J. G., and Reed, R. (1994). A novel set of spliceosome-associated proteins and the essential splicing factor PSF bind stably to pre-mRNA prior to catalytic step II of the splicing reaction. *EMBO J.* **13**, 3356–3367.

Hartmuth, K., Urlaub, H., Vornlocher, H. P., Will, C. L., Gentzel, M., Wilm, M., and Luhrmann, R. (2002). Protein composition of human prespliceosomes isolated by a tobramycin affinity-selection method. *Proc. Natl. Acad. Sci. USA* **99**, 16719–16724.

Jurica, M., Licklider, L., Gygi, S., Grigorieff, N., and Moore, M. (2002). Purification and characterization of native spliceosomes suitable for three-dimensional structural analysis. *RNA* **8**, 426–439.

Jurica, M. S., and Moore, M. J. (2002). Capturing splicing complexes to study structure and mechanism. *Methods* **28**, 336–345.

LeCuyer, K. A., Gehlen, L. S., and Uhlenbeck, O. C. (1995). Mutants of the bacteriophage MS2 coat protein that alter its cooperative binding to RNA. *Biochemistry* **34**, 10600–10606.

Makarov, E. M., Makarova, O. V., Urlaub, H., Gentzel, M., Will, C. L., Wilm, M., and Luhrmann, R. (2002). Small nuclear ribonucleoprotein remodeling during catalytic activation of the spliceosome. *Science* **298**, 2205–2208.

Moore, M. J., and Query, C. C. (1998). Uses of site-specifically modified RNAs constructed by RNA ligation. *In "RNA-Protein Interactions: A Practical Approach"* (C. W. J. Smith, ed.), pp. 75–108. IRL Press, Oxford.

Moore, M. J., Query, C. C., and Sharp, P. A. (1993). Splicing of precursors to mRNA by the spliceosome. *In "The RNA World"* (R. Gesteland and J. Atkins, eds.), pp. 303–357. Cold Spring Harbor Laboratory Press, Cold Spring Harbor,NY.

Reichert, V., Le Hir, H., Jurica, M. S., and Moore, M. J. (2002). 5′ exon interactions within the human spliceosome establish a framework for exon junction complex structure and assembly. *Genes Dev.* **16**, 2778–2791.

Zhou, Z., Sim, J., Griffith, J., and Reed, R. (2002). Purification and electron microscopic visualization of functional human spliceosomes. *Proc. Natl. Acad. Sci. USA* **99**, 12203–12207.

CHAPTER

17

Isolation of Cajal Bodies

Yun Wah Lam and Angus I. Lamond

I. INTRODUCTION

The Cajal body (CB) is a subnuclear organelle involved in the biogenesis of snRNPs and snoRNPs. It was first described by Ramon-y-Cajal as the "nucleolar-accessory body" in silver nitrate-stained neuronal cells (Cajal, 1903). Later, electron microscopy studies on neuronal cells showed that this nuclear domain sometimes resembled a ball of coiled threads 0.15 to 1.5 μm in diameter. The identification of CBs in the fluorescence microscope was facilitated by the discovery of p80 coilin, a human autoantigen that is enriched in the CB (Andrade *et al.*, 1991). Antibodies against human p80 coilin label CB-like nuclear foci in a wide spectrum of organisms, showing that the CB is a highly conserved structure. While various lines of experiment suggest a role of the CB in snRNA and snoRNA maturation (reviewed by Gall, 2000), CBs also contain proteins involved in other pathways, such as nucleolar functions, tumourigenesis, and cell cycle regulation (Sleeman and Lamond, 1999; Jacobs *et al.*, 1999; Liu *et al.*, 2000, Ma *et al.*, 2000). Therefore, CBs may also have other cellular functions that remain to be characterized.

This article describes an effective procedure for the large-scale isolation of CBs from mammalian somatic cell nuclei (Lam *et al.*, 2002). The procedure involves disrupting HeLa cell nuclei by sonication, treatment with detergent, nuclease, and polyanion, and subsequent density gradient fractionation. Density separation is carried out using Percoll, a silica sol coated with polyvinylpyrolidone, which generates a density gradient on ultracentrifugation. It results in the enrichment of particles containing known CB factors that are comparable in size, morphology, and composition to CBs detected *in situ*. These particles, therefore, correspond to isolated CBs. Judging by both immunofluorescence and immunoblotting analyses, we estimate that this protocol provides an enrichment factor of at least 750-fold for isolated CBs, as compared to intact nuclei. The protocol is reproducible and can be carried out on a sufficiently large scale to generate sufficient material for biochemical analysis.

II. BUFFERS AND SOLUTIONS

All solutions are supplemented with Complete protease inhibitor tablet (Roche, Cat. No. 1-873-580) at a final concentration of 1 tablet/50 ml).

S1 solution: 0.25 *M* sucrose and 10 m*M* $MgCl_2$
S2 solution: 0.35 *M* sucrose and 0.5 m*M* $MgCl_2$
S3 solution: 0.5 *M* sucrose and 25 m*M* Tris–HCl, pH 9.0
SP1 buffer: 1 *M* sucrose, 34.2% Percoll, 22.2 m*M* Tris–HCl, pH 7.4, and 1.11 m*M* $MgCl_2$
SP2 buffer: 20% Percoll, 10 m*M* Tris–HCl, pH 7.4, 1% Triton X-100, and 0.5 mg/ml heparin
HT buffer: 10 m*M* Tris–HCl, pH7.4, 1% Triton ×100, and 0.5 mg/ml heparin

See Section IV on making sucrose stock solution.

III. PROCEDURES

All procedures should be performed either on ice or at 4°C.

Copyright 2006, Elsevier Science (USA).
All rights reserved.

A. Sonication

1. Prepare the starting material of 2.5×10^9 HeLa nuclei. Suitable HeLa nuclei can be purchased from CIL Biotech (Mons, Belgium; Cat. No. CC-01-30-25). Add S1 solution to thawed nuclei to a final volume of 30 ml. Mix thoroughly but avoid vigorous vortexing.

2. Divide the diluted nuclei into 2×15 ml portions. Overlay each portion onto 15 ml of the S2 solution in a 50-ml Falcon tube. Make sure the interface of the two layers is sharp (Fig. 1).

3. Centrifuge at 1430 g (2500 rpm, Beckman GS-6 centrifuge, GH-3.8 rotor) for 5 min at 4°C.

4. Carefully decant the supernatant. The pellets should be solid and firm (Fig. 1). Resuspend each pellet with the S2 solution so that the final volume is 30 ml. The pellets should resuspend easily. A pellet that cannot be resuspended completely indicates the presence of lysed nuclei and should be discarded.

5. Divide resuspended nuclei into 10×3-ml portions, each in a 15-ml Falcon tube. In our experience, sonication is more effective with this sample size.

6. Sonicate each aliquot using a tuned sonicator (Misonix XL 2020) for 3×6 s, with a 6-s intermission between each burst. See Section IV on sonication.

7. Examine the sonicated nuclei under a phase-contrast microscope. The majority of nuclei should have been lysed, while nucleoli should be clearly visible. If the percentage of unlysed nuclei is too high (over 5%), sonicate again for 2–3 s and then reexamine under the microscope. Stop at the point when most nuclei are lysed. Over sonication disrupts CBs. The conditions used to sonicate HeLa nuclei not only maintain the structure of CBs, but also that of nucleoli (see Chapter 15, this volume). PML bodies, and splicing speckles. This indicates that, under suitable conditions, many nuclear domains remain intact even after the overall nuclear structure is destroyed.

B. Removal of Nucleoli

8. Pool the 10 aliquots back together. Measure the volume. Add 0.42× volume of 2.55 *M* sucrose to sonicated nuclei so that the final sucrose concentration is now 1 *M*. Mix thoroughly but do not vortex. Divide the mixture into two portions, approximately 20 ml each, in two 50-ml Falcon tubes (Fig. 2).

9. Centrifuge at 3000 g (3500 rpm, Beckman GS-6 centrifuge, GH-3.8 rotor) for 10 min at 4°C.

10. A small pellet should be visible in each tube (Fig. 2). This pellet contains nucleoli and unlysed nuclei, while the supernatant is nucleoplasm containing CBs. Using a pipette, collect the supernatant carefully. Do not decant, as the pellets are not firm. Stop when you are about 5 mm above the pellet. This is the region where the distinction between the pellet and the supernatent is blurred. This part of the supernatant should not be included in subsequent steps.

11. To collect nucleoli for other experiments, resuspend the pellet with 3 ml S2. Sonicate the mixture for 3×10 s. Proceed from step 7 of the nucleolar isolation protocol (see article by Lam and Lamond).

C. Gradient One

12. Measure the volume of the supernatant. Add 0.82× volume of SP1. For example, in a typical experiment, mix 37 ml of the supernatant with 30.27 ml SP1. Add 0.05× volume of 20% Triton X-100 (3.36 ml in the aforementioned example). Mix thoroughly but do not vortex.

13. Divide the mixture into precooled SW41 ultracentrifuge tubes (Fig. 3). The volume of the sample should fit six tubes perfectly. Balance the tubes carefully. Load the tubes into a precooled SW41 rotor. Transfer the rotor to a precooled ultracentrifuge.

14. Ultracentrifuge at 37,000 rpm for 2 h.

15. A loose pellet can be seen resting on the Percoll precipitate at the bottom of each tube (Fig. 3). This pellet contains most of the Cajal bodies. Carefully pipette away the turbid supernatant. Do not decant. Stop when you are 5–6 mm above the pellet. Keep the supernatant labeled as fraction 1S. Use a P1000 pipette and resuspend the pellets in the remaining supernant. Transfer the resuspended pellets to a 15-ml Falcon tube. This is fraction 1P. Measure the final volume of fraction 1P. In a typical experiment, the final volume is about 5 ml. In fraction 1P, the CBs present are mostly entangled with large pieces of chromatin, as revealed by DAPI staining. Nucleoli that have not been removed in the first step are also a significant contaminant.

D. Gradient Two

16. Add 600 units of DNase1 (Sigma Cat. No. D4527; 20,000 units/ml) to fraction 1P. Mix with a rotating wheel for 1 h at room temperature.

17. Add 0.05× volume of heparin (10 mg/ml). The mixture should become more transparent on mixing.

18. Add 1× volume of SP2. Mix gently with a rotating wheel for 1 min.

19. Load the mixture in precooled tubes suitable for SW55 rotor (Fig. 4). In a typical experiment, the mixture fits two tubes perfectly. Ultracentrifuge at 45,000 rpm for 1 h.

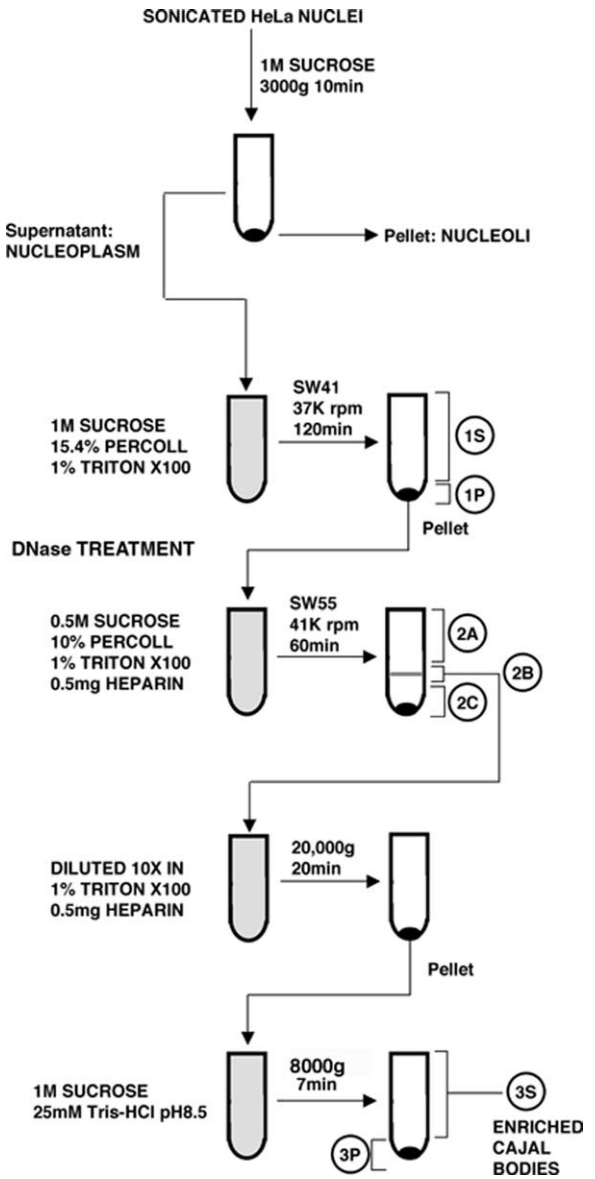

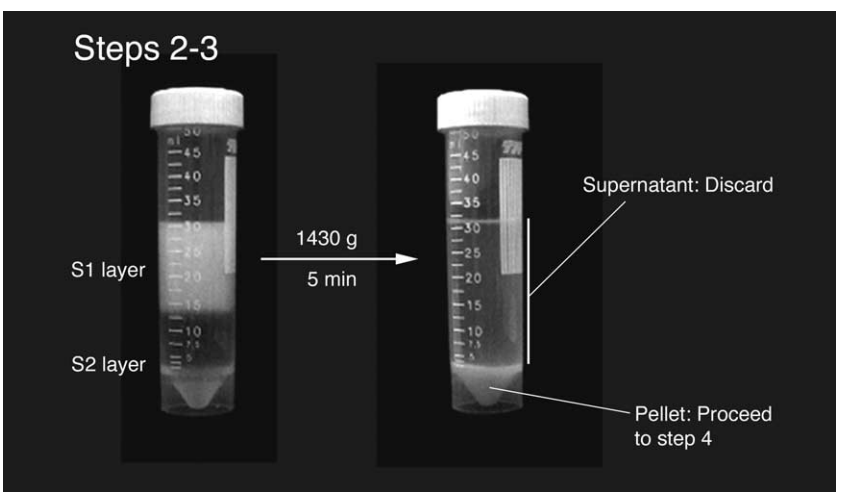

FIGURE 1 Steps 2–3 of the procedure. Note the clear boundary between S1 and S2 layers before centrifugation.

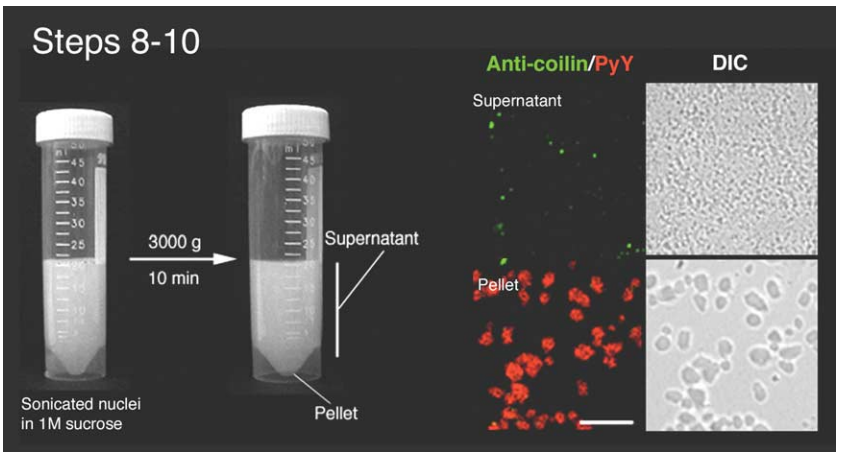

FIGURE 2 Steps 8–10 of the procedure. Note the small pellet after centrifugation. (Right) Microscope images of the supernatant and pellet. Anticoilin antibodies (5P10, green) and pyronin Y (red) were used to label CBs and nucleoli, respectively. Bar: 10 µm.

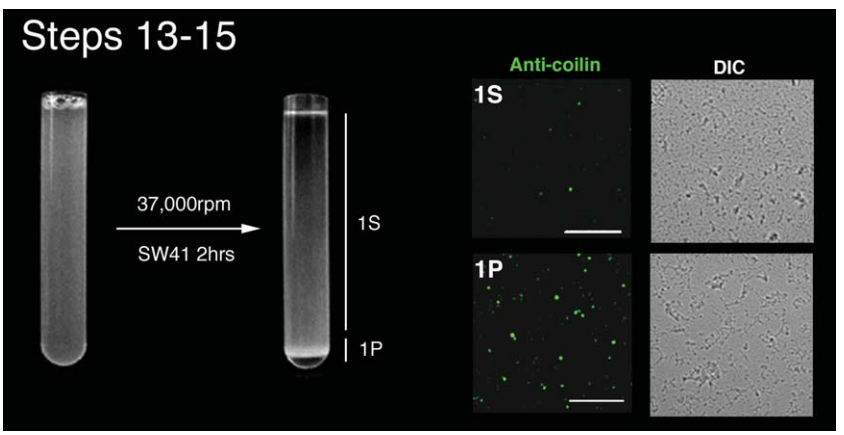

FIGURE 3 Steps 13–15 of the procedure. Note the loose pellet (1P) after centrifugation. Immunofluorescence (right) shows that most CBs are in 1P. Bar: 10 µm.

20. Three bands should be visible (Fig. 4). A broad white band floats on the top, a thin white band at the middle, and a pellet resting on the Percoll precipitate at the bottom. Using a P1000 pipette, very carefully unload the gradient from the top. Take the top band and go on until you are 2–3 mm above the middle band. This is fraction 2.1. Using a new pipette tip, take the middle band (fraction 2.2). Finally, resuspend the pellet using the remaining part of the gradient. This is fraction 2.3. For each 5-ml gradient, typical volumes of the three fractions are fraction 2.1, 2.5 ml; fraction 2.2, 1 ml; and fraction 2.3, 1.5 ml. Most of the CBs are contained in fraction 2.2 in the middle of the gradient, where the resolution is the greatest.

E. Concentration and Final Enrichment of Cajal Bodies

21. Add 10× volume of HT buffer into fraction 2.2. Mix well using a rotating wheel.

22. **Either** load the diluted fraction into 2 × SW41 tubes and ultracentrifuge at 12,000 rpm for 15 min **or** divide the mixture into 20 × 1.5-ml Eppendorf tubes and centrifuge at 14,000 rpm for 15 min in an Eppendorf centrifuge (Fig. 5).

23. Remove the supernatant carefully. Resuspend the pellet in 0.5 ml HT buffer. Pool all the resuspended pellets into a single tube and centrifuge again as described earlier. The final pellet should be visible, but very small. Remove the supernatant carefully .

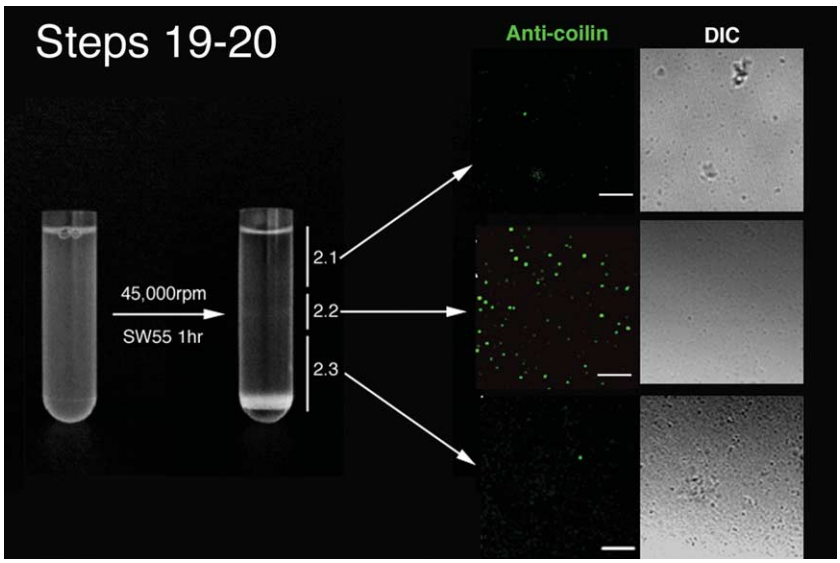

FIGURE 4 Steps 19 and 20 of the procedure. Note the thin band (2.2) in the middle of the gradient after centrifugation. Bar: 10 µm.

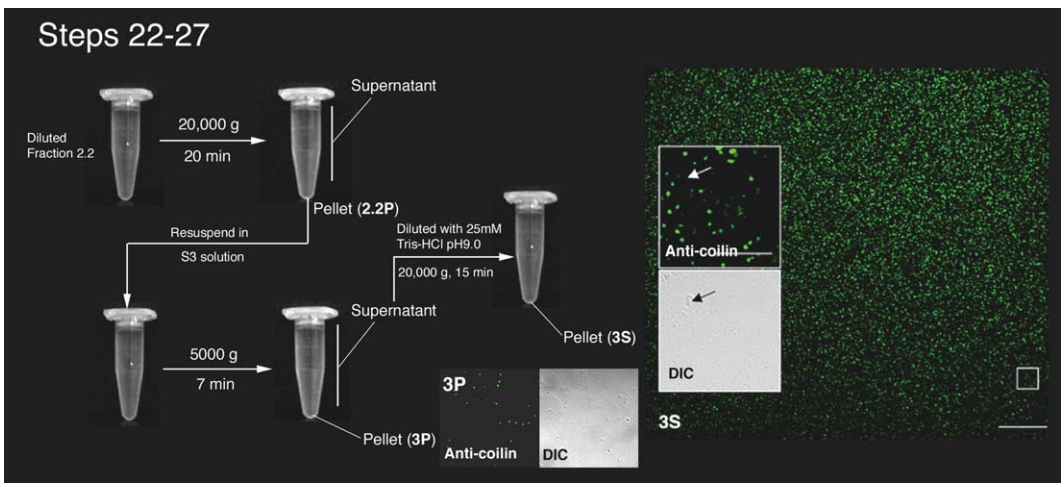

FIGURE 5 Steps 22–27 of the procedure. Most CBs are found in fraction 3S. (Inset) Arrows indicate the presence of a small amount of coilin-negative material in 3S. Bars: 25 µm (large inset) and 10 µm (small insets).

24. Resuspend the pellet with 0.5 ml S3 solution. The pellet detaches from the bottom of the tube and is resuspended on pipetting up and down.

25. Spin down the resuspended pellet in an Eppendorf centrifuge at 8000 rpm for 5 min. A visible pellet should be seen. Carefully take the supernatant and transfer it to a new Eppendorf tube. Repeat spinning the supernatant at 8000 rpm for 5 min. Carefully take the supernatant and transfer it to a new Eppendorf tube.

26. Combine the pellets. Label this fraction 3P.

27. Dilute the supernatant with 10× volumes of 25 m*M* Tris–HCl, pH 9.0. Divide the diluted supernatant into 3 × 1.5-ml Eppendorf tubes. Centrifuge at 14,000 rpm for 15 min. Remove the supernatants carefully, leaving about 0.1 ml at the bottom of each tube. Pipette the remaining supernatants up and down, resuspending the small pellet. Mix the contents of the three tubes together. Fill up the tube with 25 m*M* Tris–HCl, pH 9.0, and centrifuge again at 14,000 rpm for 15 min. Remove the supernatant carefully, leaving about 20 µl in the tube. Pipette the remaining super-

natants up and down to resuspend the small pellet. Label this fraction 3S. This fraction contains enriched CBs.

IV. NOTES

1. Making 2.55 M Sucrose Stock

Here is a protocol for preparing a sucrose stock solution (Cline and Ryel, 1971) suitable for the nucleolar isolation protocol. The resulting solution is 2.55 *M*, or 66% by weight. Its density is 1.3224 g/cm^3 at 20°C, and the refractive index is 1.4558. The stock solution is stable indefinitely at 4°C. This procedure can be carried out at room temperature. There is no need to heat up the solution to help dissolve the sucrose. Heating up an incompletely dissolved sucrose solution can lead to charring of sucrose and affect the quality of the sucrose solution.

1. Weigh out 1710 g sucrose (BDH). Keep it aside in a clean container.
2. Put exactly 900 ml water and a magnetic bar in a 5-litre beaker. Put the beaker on a stirrer and start stirring.
3. Add one-third of the sucrose into the beaker. Make sure the magnetic bar is rotating freely. Stir for 1 h.
4. Add another one-third of the sucrose into the solution. Again make sure the rotation of the stir bar is not impaired. Stir for another 1 h.
5. Add the remaining sucrose. Stir for another 1 h or until all the sucrose has gone into solution. The final volume should be exactly 2 litres.

2. Sonication

We use a Misonix 2020 sonicator fitted with a microtip at power setting 5. To ensure reproducible soncation, the following points should be followed.

i. It is necessary to tune the sonicator every time after you change the probe. Follow the manufacturer's manual for the tuning procedure.

ii. Sonication produces intense and localized heat in the solution. If you are concerned about the heating, the correct way to reduce heating is to shorten the sonication time and to increase the intermission between bursts. Keeping the tube on ice or performing the sonication in the cold room is helpful, but is not the most effective way of heat control.

iii. If the probe is too close to the liquid surface, it produces a foam and reduces the efficiency of sonication. Make sure the probe is well submerged in the solution, about 5 mm above the bottom of the tube. Do not, however, touch the bottom or the wall of the tube with the probe.

iv. A sonicator probe that has been used repeatedly develops pits on its end. The sonication efficiency gradually decreases as time goes on. Therefore, the sonication time recommended here can only be used as a guideline. Always monitor the outcome of sonication using a phase-contrast microscope. You may need to adjust the sonication time to maintain the efficiency, especially if the probe is getting old. Change the probe when the efficiency is noticeably down.

3. Analysis of the Enriched Cajal Body Fraction

i. To immunolabel the isolated CBs, spot about 5 µl of fraction 3S onto a polylysine-coated slide (BDH Cat. No. 406/0178/00) and air dry the spot. Rehydrate the slide in PBS for 5 min before using the standard immunostaining procedure.

ii. To separate and analyse the proteins by SDS–PAGE, resuspend directly either in Laemmli SDS sample buffer or in your preferred buffer.

References

Andrade, L. E., Chan, E. K., Raska, I., Peebles, C. L., Roos, G., and Tan, E. M. (1991). Human autoantibody to a novel protein of the nuclear coiled body: Immunological characterization and cDNA cloning of p80-coilin. *J. Exp. Med*. **173**(6), 1407–1419.

Cajal, S. (1903). Un sencillo metodo de coloracion seletiva del reticulo protoplasmatico y sus efectos en los diversos organos nerviosos de vertebrados e invertebrados Trab. *Lab. Invest. Biol*. **2**, 129–221

Cline, G. B., and Ryel, R. B. (1971). *Methods Enzymolo*., **22**, 168–204.

Gall, J. (2000). Cajal bodies: The first 100 years. *Annu. Rev. Cell Dev. Biol*. **16**, 273–300.

Jacobs, E. Y., Frey, M. R., Wu, W., Ingledue, T. C., Gebuhr, T. C., Gao, L., Marzluff, W. F., and Matera, A. G. (1999). Coiled bodies preferentially associate with U4, U11, and U12 small nuclear RNA genes in interphase HeLa cells but not with U6 and U7 genes. *Mol. Biol. Cell* **10**(5), 1653–1663.

Lam, Y. W., Lyon, C. E., and Lamond, A. I. (2002). Large scale isolation of Cajal bodies from HeLa cells. *Mol. Biol. Cell*. **13**, 2461–2473.

Liu, J., Hebert, M. D., Ye, Y., Templeton, D. J., Kung, H., and Matera, A. G. (2000) Cell cycle-dependent localization of the CDK2-cyclin E complex in Cajal (coiled) bodies. *J. Cell Sci*. **113**(Pt. 9), 1543–1552.

Ma, T., Van Tine, B. A., Wei, Y., Garrett, M. D., Nelson, D., Adams, P. D., Wang, J., Qin, J., Chow, L. T., and Harper, J. W. (2000). Cell cycle-regulated phosphorylation of p220(NPAT) by cyclin E/Cdk2 in Cajal bodies promotes histone gene transcription. *Genes Dev*. **14**(18), 2298–2313.

Sleeman, J., and Lamond, A. (1999). Nuclear organization of pre-mRNA splicing factors. *Curr. Opin. Cell Biol*. **11**(3), 372–377

CHAPTER

18

Replicon Clusters: Labeling Strategies for the Analysis of Chromosome Architecture and Chromatin Dynamics

Dean A. Jackson, Chi Tang, and Chris Dinant

I. INTRODUCTION

In all eukaryotes, the maintenance of genetic integrity requires that DNA replication is controlled precisely to ensure that a perfect set of chromosomes passes to each of the daughter cells during cell division. Mammalian chromosomes are so long that DNA synthesis must initiate at many positions on each in order to complete S phase in the observed time frame—typically 8–10 h. Direct observation of sites of DNA synthesis on spread DNA fibres shows that initiation events are spaced roughly 150 kb apart, giving ~1000 on a typical human chromosome. However, the initiation events are not performed simultaneously at all sites at the onset of S phase. Instead, small groups of origins within replicon clusters are activated at the onset of the replication programme such that only about 10% of possible origins operate at this time. Replication proceeds from these early origins until some unknown switch—probably related to changes in chromatin structure that arise during this first phase of synthesis—allows new sets of replicons to be activated. Different banks of replicons are activated in this progressive fashion until the replication process is complete.

During each phase of synthesis small clusters of replicons are activated together (Fig. 1). These clusters typically contain two to five adjacent replicons and appear to form stable units of **chromosome structure**, with ~0.5–1 Mbp DNA (Jackson and Pombo, 1998; Ma *et al*., 1998; Zink *et al*., 1998; Cremer and Cremer, 2001). The ability to label replicon clusters in mammalian cells to reveal DNA or replication foci provides an outstanding opportunity to analyse many aspects of chromosome architecture and chromatin function. The basic principle behind the approach is facile and relies on the use of modified DNA precursor analogues that can be incorporated into DNA in place of the natural precursor and subsequently detected to reveal sites of incorporation. **Bromodeoxyuridine** (BrdU) was the first compound to find common use in this approach (Dolbeare, 1995). BrdU can be added to culture medium—or indeed introduced by injection into whole animals—and is incorporated into DNA in place of thymidine. Patterns of incorporation can subsequently be visualised. Initially, low resolution techniques were used that relied on the variable biochemical properties of the BrdU-containing chromatin. The subsequent use of immunostaining techniques using antibromo antibodies (Gratzner, 1982) and fluorescence-based detection systems revolutionised the analysis of replicon clusters labelled in this way. In the seminal experiment, Nakamura *et al*. (1986) used BrdU incorporation **and indirect immunofluorescence** to show that early replication in rat embryonic fibroblasts occurred at some 130 sites that were each estimated to contain at least 10 active replicons. Further studies have defined a replication programme (Fig. 2), with characteristic patterns of synthesis correlating with the duplication of specific regions of the genome at different times during S phase (Nakayasu and Berezney, 1989; Humbert and Usson, 1992; O'Keefe *et al*., 1992; Hozák *et al*., 1994). The activation of specific groups of replicons also correlates with the structured assembly of active replication centres—also

Copyright 2006, Elsevier Science (USA).
All rights reserved.

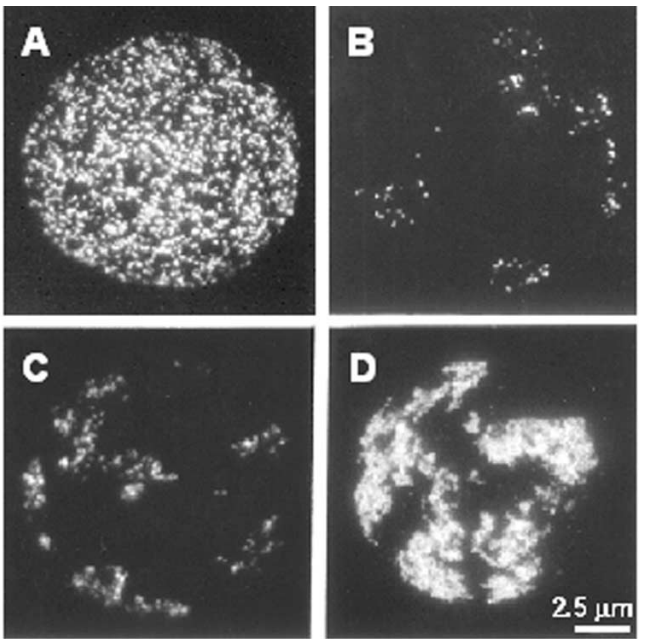

FIGURE 1 Chromosome territories in mammalian cells. HeLa cells were labelled with BrdU at the onset of S phase for 20 min (A and B), 3 h (C), and 10 h (D). Cells were attached to glass slides using the standard chromosome spreading technique, and BrdU-containing sites were visualised by immunofluorescence immediately after labelling (A) or 5 days later (B–D). Note the structure of individual replication foci and their organisation in individual chromosome territories (B–D). (D) Individual territories are labelled throughout S phase so that the boundary of each territory is seen. Bar: 2.5 μm. For details, see Jackson and Pombo (1998).

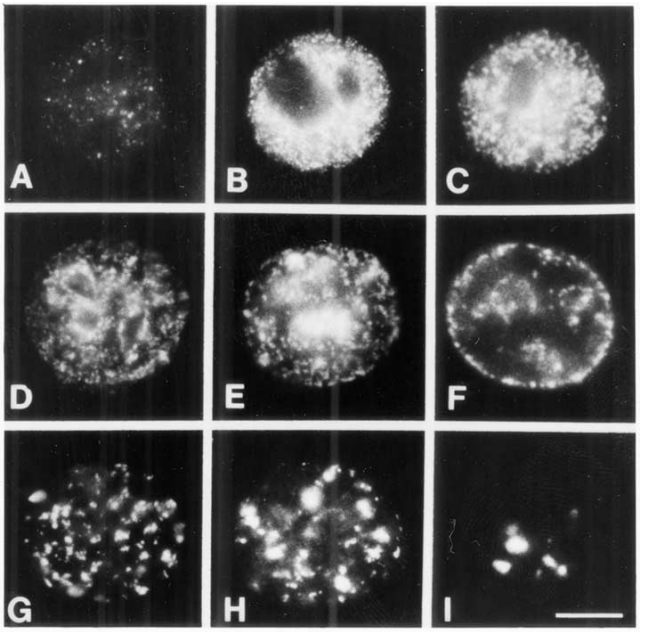

FIGURE 2 The S-phase programme. During S phase, different classes of DNA elements are replicated at specific times. Chromatin with the majority of transcribed genes is replicated over the first ~4 h of the S phase. During this period, active sites of DNA synthesis are in discrete foci dispersed throughout the nuclear interior (A–C). These are designated early or type 1 replication patterns. During mid-S phase (D–F) replication switches to peripheral inactive chromatin. These mid-S phase patterns are also referred to as type 2 (D and E) and type 3 (F) patterns. During late S phase (G–I) the replication of extended blocks of constitutive heterochromatin occurs throughout the nuclear interior. These late S phase patterns are also referred to as type 4 (G–H) and type 5 (I) patterns. Encapsulated HeLa cells were synchronised at the onset of S phase, and replication sites were labelled at 1-h intervals for 10 h. Images shown are replication sites labelled in permeabilised cells using biotin-dUTP. For details, see Hozak *et al*. (1994) and O'Keefe *et al*. (1992). Bar: 5 μm.

called replication "factories" (Hozák *et al*., 1993)—in the vicinity of active foci. These replication factories are assembled transiently at the appropriate sites in response to factors that determine the progress of S phase. The distribution of active sites appears to be influenced by fundamental features of nuclear structure. Many proteins involved in the replication machinery have targeting signals that direct their association with the active sites. The sites are dynamic, however, and can be shown using green fluorescent protein (GFP)-tagged replication proteins, such as proliferating cell nuclear antigen (PCNA) (Leonhardt *et al*., 2000), to assemble shortly before synthesis begins and disassemble as replication within a particular factory is complete.

Chromosome Structure and Dynamics

Mammalian chromosomes are highly structured. This is evident from the fact that their condensation during mitosis occurs in such a way that specific chromosomes from different cell types can be readily recognised if they are stained in specific ways. The banded chromosomal patterns revealed by stains such as Giemsa correlate with differences in gene density (transcriptionally active R bands have roughly fourfold the gene density of G bands), slight differences in base composition (R bands are commonly 3–5% more GC rich), and variations in chromatin structure (antibodies that recognize histone modification associated with gene activity stain R bands). Fundamental features of this organization persist during interphase when individual chromosomes maintain spatially discrete nuclear "territories" (Cremer and Cremer, 2001).

In mammalian nuclei, chromatin is locally dynamic but only over short distances, typically <100 nm. Long-range movement is constrained, and the best models for the corresponding organisation predict randomly arrayed structural subunits of roughly 1 Mbp DNA

(Cremer and Cremer, 2001), the typical size of DNA foci. The possibility that clusters of replicons act as stable cohorts that determine chromosome architecture and drive critical aspects of chromatin function, such as the replication programme, is an exciting insight that emphasises the importance of structure–function relationships.

In order to study this in living cells, strategies have been developed to label DNA foci with fluorescent precursor analogues so that it is now possible to perform detailed studies of the dynamic relationships between different foci and explore if these structures dictate fundamental features of chromosome structure and function.

II. MATERIALS AND INSTRUMENTATION

Solutions are prepared in molecular biology grade water from BDH Laboratory Supplies (Cat. No. 443847D). Cell culture media from Sigma-Aldrich are modified as required by the cells under study. For many purposes it is convenient to use HeLa cells grown in Dulbecco's MEM (Cat. No. D 5546) supplemented with penicillin and streptomycin (Cat. No. P 0781), sodium pyruvate (Cat. No. S 8636), glutamine (Cat. No. G 7513), and 5% foetal bovine serum (Cat. No. F 7524). Reagents for *in vitro* labelling are from Sigma-Aldrich: potassium acetate (Cat. No. P 5708), potassium chloride (Cat. No. P 9333), disodium hydrogen phosphate (Cat. No. S 7907), potassium hydrogen phosphate (Cat. No. P 9791), magnesium chloride (Cat. No. M 1028), adenosine triphosphate (Cat. No. A 7699), dithiotheritol (Cat. No. D 5545), phenylmethylulfonyl fluoride (PMSF; Cat. No. P 7626), deoxynecleoside triphosphate set (Cat. No. DNTP-100), nucleoside triphosphates (Cat. Nos. A 6559; C 8552; G 3776; U 1006), phosphate-buffered saline (PBS; Cat. No. P 4417), Triton X-100 (Cat. No. T 9284), saponin (Cat. No. S 7900), digitonin (Cat. No. D 1407), lysolecithin (Cat. No. L 4129), DNase I (Cat. No. D 7291), hydrocholric acid (Cat. No. H 1758), sodium borate (Cat. No. B 0127), acetic acid (Cat. No. A 0808), methanol (Cat. No. M 3641), low melting agarose (type VII-A; Cat. No. A 0701), poly-L-lysine (Cat. No. P 4707), bovine serum albumin (fraction V; Cat. No. A 4503), Tween 20 (Cat. No. P 7949), trypan blue (Cat. No T 8154), Hanks' balanced salt solution (HBSS; Cat. No. H 9269), and 4′,6-diamidine-2-phenylindole dihydrochloride (DAPI; Cat. No. D 8417). Inhibitors used for cell cycle studies are from Sigma-Aldrich: thymidine (Cat. No. T 1895), aphidicolin (Cat. No. A 0781), nocodazole (Cat. No. M 1404), and colcemid (Cat. No. D 7385). The protease inhibitor set (Cat. No. 1 206 893) and FuGene 6 (Cat. No. 1 815 091) are from Roche Applied Science. Liquid paraffin (Cat. No. 29436) is from BDH. The electron microscopy grade 16% paraformaldehyde solution is from Electron Microscopy Sciences (Cat. 15710-S). Vectashield is from Vector Laboratories (Cat. H 1000). TOTO III iodide is from Molecular Probes (Cat. T-3604). Different DNA precursor analogues that may be used to label DNA foci are indicated in Table I, and antibodies used for indirect immunolabelling are detailed in Table II. Plastics for cell culture are from Nunc, and prewashed glass slides and coverslips are from BDH. Culture dishes for live cell imaging are from IWAKI (Cat. 3911-035) or MatTek Corporation (Cat. P35GC-0-14-C), and coverslips with location grids are from MatTek Corporation (Cat. P35G-1.5-7-C-grid). Radioactive nucleotides are from Amersham Biosciences.

The routine procedures described later are commonly used to analyse **replication foci** at the single cell level. Accordingly the output will be recorded using light microscopy with epifluorescence capabilities. Many commercially available light microscopes are capable of generating the necessary output; the particular choice will depend both on the instrumentation that is readily available and on the specific aims of the analysis. For high-resolution work, an advanced machine such as the Zeiss LSM 510 or equivalent from other manufacturers should be used. For many applications it will be adequate to use a much simpler microscope equipped with a CCD camera. Certain labelling strategies can be adapted to study cell cycle parameters using flow cytometry techniques. Finally, if specific emphasis needs to be placed on the extent of DNA synthesis, it is often necessary to perform a single cell analysis in conjunction with radiolabelling. The incorporation of (^{32}P)dNTPs into DNA is measured using a scintillation counter.

III. PROCEDURES

A. Labeling Replication Foci in Cells Growing in Culture

5-Bromo-2′-deoxyuridine is phosphorylated by cells to give BrdUTP and this precursor is incorporated into DNA in place of dTTP.

Solutions

1. Prepare appropriate culture medium—as required by cells under investigation.

TABLE I DNA Precursor Analogues Used to Label DNA Foci[a]

Modified analogue	Supplier (Cat. No.)	Detection	Comments
5-Bromo-2′-deoxyuridine	Sigma (B 9285)	Indirect IF	Excellent
5-Fluoro-2′-deoxyuridine	Sigma (F 8791)	Indirect IF	Moderate detection
5-Chloro-2′-deoxyuridine	Sigma (C 6891)	Indirect IF	Used in double labelling
5-Iodo-2′-deoxyuridine	Sigma (I 7125)	Indirect IF	Used in double labelling
5-Bromo-2′-deoxyuridine 5′-triphosphate	Sigma (B 2506)	Indirect IF	Excellent in permeabilised cells
Biotin-16-dUTP	Roche (1 093 070)	Indirect IF	Excellent in permeabilised cells
Digoxigenin-11-dUTP	Roche (1 093 088)	Indirect IF	Excellent in permeabilised cells
Fluorescein-11-dUTP	Amersham (RPN2121)	Direct by lm[b]	Excellent
Rhodamine-4-dUTP	Amersham (RPN2122)	Direct by lm	Excellent
Cy3-dUTP	Amersham (PA53022)	Direct by lm	Excellent
Cy5-dUTP	Amersham (PA55022)	Direct by lm	Good
Cy3.5-dUTP	Amersham (PA53521)	Direct by lm	Some cytoplasmic binding
Fluorescein-12-dUTP	Roche (1 373 242)	Direct by lm	Excellent
Alexa 488-5-dUTP	Mol. Probes (C-11397)	Direct by lm	Excellent—as fluorescein
Alexa 532-5-dUTP	Mol. Probes (C-11398)	Direct by lm	Strong binding in cytoplasm
Alexa 546-14-dUTP	Mol. Probes (C-11401)	Direct by lm	Excellent—very similar to Cy3
Alexa 568-5-dUTP	Mol. Probes (C-11399)	Direct by lm	Good
Alexa 594-5-dUTP	Mol. Probes (C-11400)	Direct by lm	Good

[a] A selection of precursors used to visualise DNA foci either in living cells or *in vitro* after cell permeabilisation. Note that fluorescent analogues can be used to label foci in permeabilised cells, when they can be visualised directly by lm without further processing, or *in vivo*, providing they can be delivered into the cells.

[b] Light microscopy.

2. Prepare stock solution of desired replication precursor analogue (Table I; e.g., BrdU) in medium. For most purposes, it is convenient to prepare a 100× stock. Labelling is usually performed at 10–50 µ*M* BrdU, depending on the duration of labelling. Higher concentrations may be used for very short pulses, although concentrations in excess of 50 µ*M* may lengthen the cell cycle. IdU is much less soluble than BrdU and should be made as a 10× stock.

1. Adherent Cells

Steps

1. Place clean, sterile 13-mm glass coverslips in a 60-mm petri dish and coat with poly-L-lysine by applying a drop of sterile 0.01% solution for 1 h.
2. Rinse coverslips with medium and seed ~2×10^5 cells in 2 ml fresh medium and grow for 16–24 h or until cells reach ~50% confluency.
3. Replace medium with fresh medium containing 10–50 µ*M* BrdU and incubate for 1–10 h. The concentration should be modified according to the labelling time required—use lower concentrations for longer labelling periods. For very short pulse labels, concentrations in the range of 50–200 µ*M* BrdU can be used.
4. Rinse samples in PBS at room temperature and prepare for immunolabelling.

2. Nonadherent Cells

Nonadherent cells can be labelled directly in suspension in medium. However, for many *in vivo* and *in vitro* applications it is convenient to use cells encapsulated in **agarose microbeads** (Jackson and Cook, 1985). For some applications, particularly high-resolution analyses using electron microscopy (e.g., Hozak *et al.*, 1993), it is also convenient to perform experiments on adherent cells that are encapsulated after removing from the surface on which they normally grow. Use the following steps to encapsulate cells.

Steps

1. Warm 10 ml liquid paraffin to 37°C.
2. Heat 0.25 g low-gelling agarose in 10 ml PBS at ~95°C until dissolved and cool to 37°C.
3. Resuspend ~10^7 cells (a final cell density of 2×10^6 cells/ml beads is ideal for this application, although a wide range can be used) in 4 ml PBS at 37°C in a 100-ml round-bottomed flask.
4. Add 1 ml agarose solution at 37°C to 4 ml cell suspension at 37°C and mix thoroughly.
5. Add 10 ml paraffin at 37°C, seal flask with plastic film, and immediately shake (by hand or at 800 cycles/min using a flask shaker) until a creamy emulsion forms (~15 s).

6. Cool flask by periodic rotation in ice-cold water for 10 min; this allows spherical droplets of molten agarose suspended in the paraffin to gel.
7. Add 35 ml ice-cold PBS, mix, and transfer to a 50-ml plastic centrifuge tube.
8. Pellet microbeads by spinning at 1000 rpm on a bench centrifuge at 20°C.
9. Aspirate the supernatant and wash pelleted microbeads once in PBS. If some beads remain at the water/paraffin interface, remove most paraffin, mix thoroughly, and respin.
10. Encapsulated cells can now be regrown in medium or permeabilised directly.

Incorporate BrdU or alternative precursor analogue into encapsulated cells as follows.

Steps

1. Use cells adapted for suspension culture or cells encapsulated in agarose microbeads at a density of ~2 $\times 10^6$/ml and grow in fresh medium for at least 1 h.

2. Add 10–50 µ*M* BrdU for 1–10 h; use a higher concentration if shorter pulse times are required (see earlier discussion).

3. As an optional step, double labelling can be performed using iododeoxyuridine (IdU) and chlorodeoxyuridine (Aten *et al.*, 1992) or IdU and BrdU (Jackson and Pombo, 1998). After the first pulse, e.g., 20 µ*M* BrdU for 1 h, wash samples once in fresh medium by centrifugation (1000 rpm) and resuspension and add medium with a second precursor for a second pulse, e.g., 20 µ*M* IdU for 1 h.

4. Wash in PBS at room temperature and prepare for immunolabelling. The routine procedure for washing agarose microbeads is facile. Beads pellet readily during centrifugation at ~1000 rpm in a benchtop centrifuge for 1–2 min. The supernatant can then be aspirated (with care no beads should be lost) and the bead pellet resuspended in any solution of choice.

3. *Labeling* in Vitro

For many applications, labelling *in vitro* using **permeabilised cells** provides an appealing versatility. A major advantage of this option is that replication elongation rates can be manipulated precisely by adjusting the concentration of the precursor pools, incubation time, and temperature. It is also convenient to use a much wider variety of modified precursors (Table I), as permeabilised cells do not restrict access of the dNTPs to the nucleus. The chromatin structure is especially sensitive to changes in its ionic environment, and the choice of the buffer to use with permeabilised cells is particularly important. Many buffers are in common use, but the following "physiological buffer" (PB) is useful for preserving critical features of nuclear structure and function.

Solutions

1. Prepare PB containing 100 m*M* KCH_3COOH, 30 m*M* KCl, 10 m*M* Na_2PO_4, 1 m*M* $MgCl_2$, 1 m*M* Na_2ATP, 1 m*M* dithiothreitol, and 1 m*M* PMSF and add 100 m*M* KH_2PO_4 as required to give pH 7.4. Protease and nuclease inhibitors should be added to suit the demands of particular experiments.

2. In PB, prepare 10× concentrated initiation mix to give the following final concentrations: 250 µ*M* dATP, 250 µ*M* dCTP, 250 µ*M* dGTP, 100 µ*M* CTP, 100 µ*M* GTP, 100 µ*M* UTP, and 10–100 µ*M* TTP analogue (Table I), plus $MgCl_2$ at a molarity equal to that of the triphosphates.

Comments and Pitfalls

Various combinations of monovalent anion can be used. Different chloride/acetate/glutamate (or polyglutamate) combinations support similar rates of replication. However, acetate/glutamate is preferred to the smaller Cl^-, which is more damaging to the tertiary protein structure. The concentration of divalent cations must be controlled carefully. As little as 0.5 m*M* free Mg^{2+} causes the visible (by EM) collapse or aggregation of chromatin. The equimolar Mg/ATP combination used here preserves the chromatin structure and supports the action of Mg-dependent enzymes. Dithiothreitol, protease inhibitors, and ribonuclease inhibitors protect the sample and preserve cell morphology.

Steps

1. Prepare cells on coverslips or encapsulated in agarose microbeads as described earlier.
2. Wash samples in ice-cold PB to remove medium and permeabilise for ~2 min using 0.01–0.1% of a suitable detergent.
3. Wash cells three times in ice-cold PB to remove the detergent.
4. Incubate coverslips or microbeads in PB at 33°C for 5 min.
5. Add one-tenth volume of 10× IM, mix, and incubate at 33°C for 2–60 min.
6. Wash three times in >10 volumes ice-cold PB and proceed to fix and label.

Comments and Pitfalls

The choice of detergent will depend on the requirements of a particular experiment. We commonly use

saponin at 0.01%, as this preserves nuclear structure and supports endogenous levels of DNA or RNA synthesis. The extent of lysis is critical. To define conditions, use a twofold dilution series of detergent in PB and assess the level of permeabilisation using trypan blue exclusion (add 50 µl 1% trypan blue in PB to a coverslip or 50 µl packed microbeads; after 2 min, inspect by light microscopy; score percentage permeabilised, dark-blue cells). Choose the detergent concentration that permeabilises ~95% cells. If cells detach from coverslips during washing, use a lower concentration of detergent. The following (and related) detergents can be used (guideline concentrations are indicated): 0.02–0.05% Triton X-100; 0.01–0.02% saponin; 0.01–0.02% digitonin; and 0.02–0.05% lysolecithin.

The concentration of modified precursor and duration of labelling can be adjusted to suit individual requirements. The following provides some guidelines. Fifteen-minute incubations with 20 µ*M* biotin- or digoxigenin-coupled precursors give good indirect immunofluorescence signals, and longer incubations give correspondingly stronger signals. Five- and 2-min incubations with 100 µ*M* biotin-16-dUTP allow detection by light and electron microscopy, respectively, using standard detection protocols. Incorporated labels can be detected after ~30-min incubations with 20 µ*M* fluorescent precursors. Overall levels of incorporation can be quantitated by incorporating a radioactive trace—typically [P^{32}]dCTP—into the reaction; use ~50 µCi/ml [P^{32}]dCTP and reduce dCTP pool to ~10 µ*M*.

If inhibitors are to be used, incubate them for 15 min at 0°C prior to the addition of 10× IM.

B. Chromosome and Nuclear Spreads

Samples labelled in suspension can be fixed onto a glass surface using a standard **chromosome spreading** technique (Fig. 1).

Solutions

1. Hanks balanced salt solution (HBSS).
2. Prepare 0.075 *M* KCl in distilled water.
3. Prepare 3:1 (v/v) methanol:acetic acid fixative.

Steps

1. In a 10-ml plastic tube, wash cells labelled with DNA precursor analogue once in HBSS at room temperature. Resuspend the cell pellet in 0.075 *M* KCl (0.5–1 × 10^6 cells/ml) and incubate at 37°C for 15 min to swell the cells.

2. Using 2–5 ml of swollen cell suspension in a 10-ml plastic centrifuge tube, prefix cells by adding 3 drops/ml of methanol/acetic acid (3:1)—add the fixative dropwise from a Pasteur pipette while agitating the cell suspension gently. Leave the mix at room temperature for 15 min.

3. Pellet cells at 1000 rpm, aspirate the supernatant gently, and resuspend the pellet (by gentle agitation of the tube) in methanol/acetic acid (3:1). Stand at room temperature for 1 h.

4. Pellet the sample once more and resuspend cells in fresh methanol/acetic acid at 2 × 10^6 cells/ml. Spread immediately.

5. Glass slides should be rinsed in detergent (e.g., Decon 90), washed extensively in double-distilled water, and chilled to 4°C in water. Take a chilled slide, drain off excess water, and hold the slide at a ~30° angle against a work surface. Immediately drop 2–3 drops of the cell suspension from a Pasteur pipette onto the centre of the slide. The organic solvent and fixed cells will spread in the water film to cover most of the slide.

6. Place the slide on paper towels soaked in iced water and allow to dry. The dried slides can be stored in a fridge for many days before immunolabelling.

Comments and Pitfalls

If the analysis requires significant numbers of mitotic cells, it is usual to begin by growing cells for 30–60 min in medium supplemented with colcemid (50 ng/ml). This drug disrupts microtubule function and blocks cells in metaphase.

Hydrodynamic properties of the drying spread have a significant impact on the quality of mitotic spreads. Reproducibly high-quality spreads are usually obtained if the speed of drying is controlled by placing slides on cold, damp paper towels.

C. DNA Fibre Spreads

Many important aspects of the biology of replication clusters, as well as fundamental features of the replication process, can be studied using appropriately labelled **DNA fibre spreads** (Jackson and Pombo, 1998; Takebayashi *et al*., 2001).

Solutions

1. Prepare PBS in distilled water.
2. Prepare lysis mix with 0.5% (w/v) SDS, 200 m*M* Tris–HCl (pH 7.4), and 50 m*M* EDTA in distilled water.
3. Prepare 3:1 (v/v) methanol:acetic acid fixative.

Steps

1. Harvest cells labelled with the appropriate DNA precursor analogue (or analogues for multiple labelling) and resuspend in PBS at 10^6 cells/ml.

2. Take a clean glass slide and place 2 µl of the cell suspension on the slide, about 2 cm from one end. Leave the sample to stand for about 10 min so that the cells settle on to the glass surface; do not allow the sample to dry completely.
3. Add 5 µl of lysis mix to the cell sample and let stand for 5 min at room temperature to lyse the cells.
4. Tilt the slide to a ~20° angle so that the cell lysate flows as a uniform smear to the bottom of the slide (the smear will be about 4 cm).
5. Lie the slide on a flat surface and allow the spread sample to dry.
6. Fix the sample by immersing the slide in methanol/acetic acid (3:1) for 5 min.
7. Remove slides from the fixative and allow them to dry. The dried slides can be stored in a fridge for many days before immunolabelling.

D. Immunolabeling Procedures

Cell structures with incorporated DNA precursor analogues must be stabilised by fixation prior to immunolabeling. For light microscopy techniques, paraformaldehyde is the fixative of choice. Samples treated with methanol/acetic acid can be stained directly, although for some applications it is also advantageous to postfix samples with paraformaldehye. Fixation and immunolabeling procedures used for electron microscopy are specialised and beyond the scope of this article. For details of these techniques, see Hozák *et al*. (1993, 1994).

Solutions

1. Prepare PBS or physiological buffer (PB; see earlier discussion) in distilled water.
2. Prepare 4% paraformaldehyde in PBS or PB.
3. Prepare 0.25% Triton X-100 in PBS or PB.

1. Cells on Glass

Steps

1. After rinsing in PBS, place coverslips or slides in 4% paraformaldehyde for 10 min at room temperature. Permeabilised cells labelled *in vitro* should also be fixed in this way but must be first washed in buffer to remove unincorporated precursors.

2. Wash samples twice with PBS.

3. Permeabilise cells by incubation in 0.25% Triton X-100 in PBS for 2 min at room temperature—this improves subsequent access of the antibodies.

4. Wash gently in PBS (three changes over 5 min). Samples can now be labeled with antibodies.

2. Encapsulated Cells

Steps

1. After labelling *in vitro*, remove unincorporated precursors by washing beads three times in 10 volumes ice-cold PB for 15 min.
2. Permeabilise by incubating in 0.25% Triton X-100 in PB for 10 min at 0°C.
3. Wash three times in 10 volumes ice-cold PB.
4. Fix in ice-cold 4% paraformaldehyde in PB for 10 min.
5. Wash three times in 10 volumes ice-cold PBS. Samples can now be labelled with antibodies as described later.

3. Antibody Binding

Commercial anti-BrdU antibodies (Table II) react poorly with BrdUMP in native DNA. Binding is increased 10- to 20-fold if DNA is first denatured.

i. Acid Denaturation

Solutions

1. Prepare 2 *M* HCl by diluting concentrated acid in distilled water.
2. Prepare 0.1 *M* $Na_2B_4O_7$ dissolved in distilled water.
3. PBS/BSA/Tween is PBS containing 0.5% BSA and 0.1% Tween 20.

Steps

1. Rinse slides or coverslips in distilled water.

2. Denature DNA in 2 *M* HCl for 1 h at room temperature.

3. Rinse five times in 0.1 *M* $Na_2B_4O_7$ to remove acid.

4. Rinse twice in PBS/BSA/Tween and incubate samples with PBS/BSA/Tween for 1–2 h in a humid atmosphere at room temperature to block nonspecific-binding sites.

5. Add first antibody, cover sample with a few drops of PBS/BSA/Tween and 1/50 to 1/500 dilution (determine empirically) anti-BrdU antibody, and incubate 1–2 h in a humid atmosphere at room temperature.

6. Wash five times in PBS/BSA/Tween at room temperature for 1 h.

7. Add second antibody. Cover the sample with a few drops of PBS/BSA/Tween and 1/500 to 1/1000 dilution of the labelled second antibody (Table II) and incubate 1–2 h in a humid atmosphere at room temperature. The second antibody should be selected to react with antibodies from the species in which the first antibody was developed (Table II).

TABLE II Antibodies Commonly Used to Label DNA Foci and Sites of DNA Synthesis[a]

Antibody—clone	Supplier (Cat. No.)	Reactivity/crossreactivity	Comments
M anti-Br—mab—IU-4	Caltag (MD5100)	+++ BrdU+/IdU+/F/ClduU+	Used in double labelling
M anti-Br—mab—BR-3	Caltag (MD5200)	++ BrdU+/IdU$^-$	
M anti-Br—mab BMC9318	Roche (1 170 376)	++ BrdU+/IdU+	
M anti-Br—mab—B44	Becton Dickinson (347580)	+ BrdU+/IdU+	
M anti-Br—mab—BU-33	Sigma (B 2531)	+ BrdU+/IdU+	
R anti-Br—mab—BU1/75	Sera-Labs (MAS 250p)	+ BrdU+/IdU–	Used in double labelling
S anti-Br—polyclonal	Biodesign (M20105S)	+++ BrdU +F/Cl/IdU	Useful with other M antibodies
G antibiotin—polyclonal	Sigma (B 3640)	+++ Biotin	Excellent *in vitro*
M antibiotin—c33	Roche (1 297 597)	+++ Biotin	Excellent *in vitro*
M antidigoxigenin—mab—1.71.256	Roche (1 333 062)	+++ Digoxigenin	Excellent *in vitro*
S antidigoxigenin—polyclonal	Roche (1 333 089)	+++Digoxigenin	Excellent *in vitro*
M anti-PCNA—PC10	Sigma (P 8825)	+++PCNA	After methanol fixation
H anti-PCNA—autoimmune	Alpha Labs (6006)	+++PCNA	After paraformaldehyde fixation
Fluorochrome-conjugated secondary antibodies	Jackson Labs (see catalogue)	+++M/R/G/S/H determined by first antibody	

[a] A selection of reagents used commonly to visualise DNA foci and sites of DNA synthesis. Antibodies that bind to BrdU in DNA are available from many commercial sources. A selection of commonly used antibodies is given. The species are M, mouse; R, rat; S, sheep; G, goat; and H, human. Secondary antibodies that are labelled with a wide range of fluorochromes are available from many commercial sources. Appropriate reagents should be chosen as determined by the primary antibody or antibodies—if multiple labelling is required. Jackson Laboratories have an excellent range of reagents and supply absorbed ML antibodies that should be used for multiple labelling.

8. Wash five times in PBS/BSA/Tween at room temperature for 1 h.
9. Prepare samples for microscopy using an appropriate mountant (e.g., Vectashield) and seal coverslips with nail varnish.
10. Inspect samples using a suitable microscope.

Comments and Pitfalls

Fluorochrome-coupled second antibodies give high resolution and can be analyzed using confocal-scanning light microscopes and sensitive charge-coupled device (CCD) cameras. Fluorescence-based detection systems also allow convenient multiple labelling (e.g., Aten *et al*., 1992; Jackson and Pombo, 1998; Schermelleh *et al*., 2001). As an alternative, it is also possible to detect the location of the incorporated precursor using enzyme-coupled second antibodies (such as alkaline phosphatase). This approach is used in routine histology of tissue sections but generally offers lower resolution.

ii. Nuclease-Dependent Denaturation. Acid denaturation is accompanied by some loss of morphology. If morphological considerations are critical, nuclease-dependent detection systems are preferred.

Solution

PBS/BSA/Tween is PBS containing 0.5% BSA and 0.1% Tween 20.

Steps

1. Rinse slides or coverslips once in PBS, twice in PBS/BSA/Tween, and incubate in PBS/BSA/Tween for 1 h at room temperature.
2. Add first antibody, cover samples with a few drops of PBS/BSA/Tween, 1/50 to 1/500 dilution anti-BrdU antibody, and 50 µg/ml DNase I (Sigma), and incubate 1–2 h in a humid atmosphere at 37°C.
3. Perform steps 6–11 as following acid denaturation described earlier.

iii. Encapsulated Cells

Solutions

1. PBS/BSA/Tween is PBS containing 0.5% BSA and 0.1% Tween 20.
2. 0.02 mg/ml DAPI in sterile distilled water—this is a 1000× stock.

Steps

1. Wash beads containing fixed cells twice in ice-cold PBS/BSA/Tween and incubate in PBS/BSA/Tween for 1 h at 0°C.
2. Add first antibody, mix 100 µl beads with 400 µl PBS/BSA/Tween containing 1/50 to 1/500 dilution of appropriate first antibody, and incubate at 0°C for 2 h with periodic mixing.

3. Wash three times in 10 volumes ice-cold PBS/BSA/Tween for 30 min.

4. Add second antibody, mix the bead pellet with 400 µl PBS/BSA/Tween containing 1/500 dilution of appropriate fluorochrome-coupled second antibody (Table II), and incubate at 0°C for 2 h with periodic mixing.

5. Wash three times in 10 volumes ice-cold PBS/BSA/Tween for 30 min.

6. Wash three times in 10 volumes PBS at room temperature with 5 min between washes; add 0.02 µg/ml DAPI or 1/250 dilution TOTO III iodide (fluorescence in the far red spectrum) to second wash.

7. Mount by mixing 5 µl beads with an equal volume of mounting medium (Vectashield), apply coverslip with gentle pressure to eliminate excess fluid, and seal with nail varnish.

8. Inspect samples using a suitable microscope.

E. Patterns of DNA Synthesis

The techniques detailed earlier allow visualisation of labeled DNA foci. These foci can be analysed by indirect immunolabeling either immediately after incorporation or many hours later. If the precursor analogue (e.g., BrdU) is added to cells for <30 min and indirect immunolabeling is performed immediately, most labeled sites will correspond with sites of ongoing DNA synthesis. This can be confirmed by labeling DNA foci (as described earlier) in conjunction with a marker for the replication factory. Antibodies to PCNA are generally used for this purpose. Cells labeled either *in vivo* (Nakamura *et al*., 1986) or *in vitro* (Nakayasu and Berezney, 1989) to reveal the sites of nascent DNA synthesis display a few hundred discrete nuclear sites, with patterns that are characteristic of different stages of S phase (O'Keefe *et al*., 1992; Humbert and Usson, 1992). Foci labeled after very short incubations are associated with massive protein complexes (Hozák *et al*., 1993) where many replicons are duplicated together.

1. Labeling Sites of Ongoing DNA Synthesis

While nascent sites of DNA synthesis can be labeled in living cells using short pulse labels of appropriate analogues (e.g., BrdU), for technical reasons it is preferable to label nascent sites *in vivo* using permeabilised cells. The major advantages of *in vitro* labeling are that precursors dNTP (e.g., biotin-dUTP) can be used directly and that soluble pools of unassembled replication proteins are lost during cell lysis.

Solutions

1. Physiological buffer as detailed earlier.
2. 0.2% (w/v) saponin in PB—this is a 20× stock lysis solution.
3. 10× IM mix as indicated earlier supplemented with 20 µ*M* biotin-dUTP.
4. 4% paraformaldehyde in PB.

Steps

1. Permeabilise cells growing on coverslips or encapsulated in agarose microbeads and label for 15–30 min with a suitable labelled precursor analogue as described earlier. Biotin-dUTP is recommended for this application, although it may be convenient to label the nascent DNA directly using a fluorescent precursor analogue (Table I).

2. If biotin-dUTP is used, wash samples three times in PB to remove the unincorporated precursor and fix the samples in 4% paraformaldehyde in PB as described earlier.

3. Visualise sites of incorporation as described earlier, using an antibody to biotin (Table II).

4. The engaged replication machinery can be visualised in the same samples using an antibody to a protein component such as PCNA using the standard indirect immunolabelling technique: in PBS/BSA/Tween add 1/500 dilution of the first anti-PCNA antibody for 1–2 h, wash with PBS/BSA/Tween, and then apply appropriate fluorescently labelled second antibodies in PBS/BSA/Tween as described earlier. Wash the samples and mount as described earlier.

Comments and Pitfalls

PCNA antibodies can be used to visualise assembled replication proteins. The antibody from Alpha Laboratories is a human autoimmune serum and can be applied to samples directly. PC10, a mouse monoclonal antibody, reacts poorly with PCNA at replication sites fixed in paraformaldehyde. To use this reagent, samples should be fixed by incubating for 10 min in methanol at –20°C.

F. Chromosome Dynamics and Live Cell Techniques

Many directly labeled fluorescent analogues of DNA synthesis precursors can be used to visualise **replication foci in living cells** (Pepperkok and Ansorge, 1995; Zink *et al*., 1998; Manders *et al*., 1999). However, one limitation of this approach arises from the inability of these charged molecules to cross the cell membrane. Many techniques have been evaluated to address this problem. Microinjection (Pepperkok and

Ansorge, 1995; Zink *et al*., 1998) is an obvious possibility but this is technically tedious and only ideally suitable for labelling small numbers of cells. Other alternatives include bead loading (Manders *et al*., 1999) scratch loading (Schermelleh *et al*., 2001) and the use of synthetic carrier complexes.

1. Scratch Loading

Solutions

1. Culture medium—as required for the specific cell type under study.
2. Culture medium supplemented with 10–20 µ*M* dNTP analogue (Table I).

Steps

1. Cells should be 50–75% confluent and growing on glass coverslips or culture dishes with glass inserts.
2. Remove the medium and apply medium with fluorescent analogue—use 10 µl for each 13 mm diameter and proportionally more if larger samples are used.
3. Use the tip of a fine hypodermic needle to scratch a series of parallel lines across the coverslip surface —it is convenient to use lines separated by about 0.5–1 mm.
4. After 1 min, add 0.5 ml of prewarmed medium and let stand in incubator for 30 min.
5. Finally, wash in medium to remove any unincorporated precursors, add medium to normal growth conditions, and return culture dish to a humidified incubator until use.

2. Carriers

Carrier-mediated delivery of fluorescent nucleotides (Table I) can be performed as follows.

Solutions

1. For each coverslip, prepare 3 µl of the transfection reagent FuGENE 6 mixed with 12 µl PBS and incubate at 4°C for 5 min.
2. Add 1.5 µl of the desired fluorescent nucleotide analogue, mix, and incubate at 4°C for 20 min.

Steps

1. Grow cells on 13-mm coverslips coated with poly-L-lysine as described earlier.

2. Pipette the fluorescent nucleotide carrier complex (16.5 µl) onto a piece of parafilm and place the coverslip (cell face down) on the droplet for 15 min at 4°C.

3. Rinse the cells in full medium, replace with fresh medium, and return samples to an incubator prior to analysis or further labelling treatments.

4. If further analogues are to be used, simply repeat the procedure at the desired time interval. Note, however, that repeated applications do influence cell viability, which is particularly pronounced if two or more analogues are added consecutively without allowing cells time to recover. Good results are obtained if the separation between applications is at least 2 h.

5. Samples can be inspected directly following incorporation; using this technique, fluorescent nucleotides introduced into an S-phase cell are consumed in ~30 min. For live cell experiments, transfer the labelled cells into culture dishes with poly-L-lysine-coated glass coverslip inserts. Culture dishes with gridded coverslips are also of use for relocating individual cells during long-term analysis.

6. Inspect samples using a convenient microscope adapted for live cell imaging.

In living cells, studies of the dynamics of DNA foci and their association with replication machinery can be performed by labelling DNA foci in cells that have a component of the replication machinery, such as PCNA, tagged with GFP (Leonhardt *et al*., 2000).

G. Cell Cycle Analysis

In vertebrates, important features of the replication process have been revealed using cell populations that have been synchronised at critical points of the cell cycle. Two points in the cycle are generally amenable to **cell synchronisation**. First, reagents that disrupt microtuble function (e.g., nocodazole or colcemid) allow cells to accumulate in mitosis. Cells that generally grow as adherent monolayers can be purified in mitosis using simple shake-off techniques that dislodge only mitotic cells. Many compounds can be used to accumulate cells at or close to the beginning of S phase. Aphidicolin is the reagent of choice, as inhibition is readily reversible and low concentrations added to medium specifically inhibit the elongation phase of DNA synthesis. The following protocol was used to demonstrate the efficiency with which human replicons are activated in different cell cycles (Jackson and Pombo, 1998).

Solutions

1. Full medium, as required by cells under study—serum should be added to support optimal growth.
2. 250 m*M* thymidine in sterile distilled water—this is a 100× stock solution.
3. 50 µg/ml nocodazole in sterile distilled water—this is a 1000× stock solution.
4. 5 mg/ml aphidicolin in DMSO—this is a 1000× stock solution.

5. 10–100× stock solution of required DNA synthesis precursor analogue (Table I) in medium.

Steps

1. Synchronise cells in mitosis by incubating sequentially in medium supplemented with (i) 2.5 m*M* thymidine for 24 h; (ii) no additive for 12 h; (iii) 2.5 m*M* thymidine for 12 h; (iv) no additive for 10 h; and (v) 50 ng/ml nocodazole for 4 h. To remove inhibitors, remove medium, wash cells once in fresh medium for 5 min, and replace with fresh medium.

2. Wash cells to remove nocodazole and incubate in fresh medium for 4–7 h.

3. Add 5 µg/ml aphidicolin for 2–3 h.

4. Wash cells in fresh medium supplemented with a suitable precursor analogue (e.g., BrdU) and incubate for 15–30 minutes as described previously. This will pulse-label DNA foci in cells accumulated at the onset of S phase.

5. Return cells to fresh full medium.

6. After a specified time, typically 1–5 h, samples can be pulse labelled further in medium supplemented with a second precursor analogue (e.g., IdU).

7. Alternatively, from 12 h to many days later, steps 1–5 can be repeated using a second precursor analogue (e.g., IdU).

8. Indirect immunodetection of the two incorporated analogues can now be performed on fixed cells or spread DNA fibres as detailed earlier.

Comments and Pitfalls

Timings must be determined empirically, as different cell lines each have characteristic cell cycle parameters. Trial experiments should be performed to establish the time interval between releasing cells from mitosis and the onset of S phase. For most mammalian cell lines, cells synchronised in mitosis enter S phase after 5–10 h. Because G1 is the most variable period of the cell cycle, additional aphidicolin treatment is required to accumulate cells at the very beginning of S phase. Conditions should be used that give 20–50% cells undergoing replication.

The same approach can be applied using directly labelled analogues for live cell imaging.

Using a combination of pulse labelling and fluorescent *in situ* hybridisation (FISH) on DNA fibres, it is also possible to analyse where DNA synthesis initiates at specific chromosomal loci (Takebayashi *et al*., 2001).

H. Reconstituting Replication Sites

The protocols detailed earlier have been developed to visualise DNA foci and sites of nascent DNA synthesis in intact or permeabilised cells. For some applications it is convenient to extend our knowledge of the replication process using systems that are amenable to manipulation *in vitro*. While it is beyond the scope of this article to cover these applications in detail, the authors would like to comment on their potential merits. The best system in vertebrates takes advantage of the ability of *Xenopus laevis* egg extracts to assemble nuclei when incubated with a suitable DNA (commonly from sperm). Reconstituted nuclei are formed that perform a single but complete round of DNA synthesis, which begins about 30 min after mixing. Importantly, as the extracts can be manipulated by the removal or addition of replication or cell cycle components, this provides an excellent opportunity to study pathways of activation and assembly of the replication machinery. Mammalian nuclei cannot be assembled from basic components in the same way, although it is possible to manipulate assembly of the replication machinery using permeabilised cells from the late G1 phase of the cell cycle mixed with extracts derived from S-phase cells.

References

Aten, J. A., Bakker, P. J., Stap, J., Boschman, G. A., and Veenhof, C. H. (1992). DNA double labelling with IdUrd and CldUrd for spatial and temporal analysis of cell proliferation and DNA replication. *Histochem. J.* **24**, 251–259.

Chong, J. P. J., Thömmes, P., Rowles, A., Mahbubani, H. M., and Blow, J. J. (1997). Characterisation of the Xenopus replication licensing system. *Methods Enzymol*. **283**, 549–564.

Cremer, T., and Cremer, C. (2001). Chromosome territories, nuclear architecture and gene regulation in mammalian cells. *Nature Rev. Genet*. **2**, 292–301.

Dolbeare, F. (1995). Bromodeoxyuridine: A diagnostic tool in biology and medicine. 1. Historical perspectives, histochemical methods and cell kinetics. *Histochem. J*. **27**, 339–369.

Gratzner, H. G. (1982). Monoclonal antibody to 5-bromo and 5-iododeoxyuridine: A new reagent for detection of DNA replication. *Science* **218**, 474–475.

Hozák, P., Hassan, A. B., Jackson, D. A., and Cook, P. R. (1993). Visualization of replication factories attached to a nucleoskeleton. *Cell* **73**, 361–373.

Hozák, P., Jackson, D. A., and Cook, P. R. (1994). Replication factories and nuclear bodies: The ultrastructural characterization of replication sites during the cell cycle. *J. Cell Sci*. **107**, 2191–2202.

Humbert, C., and Usson, Y. (1992). Eukaryotic DNA replication is a topographically ordered process. *Cytometry* **13**, 603–614.

Jackson, D. A., and Cook, P. R. (1985). A general method for preparing chromatin containing intact DNA. *EMBO J*. **4**, 913–918.

Jackson, D. A., and Pombo, A. (1998). Replicon clusters are stable units of chromosome structure: Evidence that nuclear organization contributes to the efficient activation and propagation of S-phase in human cells. *J. Cell Biol*. **140**, 1285–1295.

Krude, T., Jackman, M., Pines, J., and Laskey, R. A. (1997). Cyclin/Cdk-dependent initiation of DNA replication in a human cell-free system. *Cell* **88**, 109–119.

Leonhardt, H., Rahn, H. P., Weinzierl, P., Sporbert, A., Cremer, T., Zink, D., and Cardoso, M. C. (2000). Dynamics of DNA replication factories in living cells. *J. Cell Biol*. **149**, 271–279.

Ma, H., Samarabandu, J., Devdhar, R. S., Acharya, R., Cheng, P. C., Meng, C. L., and Berezney, R. (1998). Spatial and temporal dynamics of DNA replication sites in mammalian cells. *J. Cell Biol*. **143**, 1415–1425.

Manders, E. M. M., Kimura, H., and Cook, P. R. (1999). Direct imaging of DNA in living cells reveals the dynamics of chromosome formation. *J. Cell Biol*. **144**, 813–821.

Nakamura, H., Morita, T., and Sato, C. (1986). Structural organisation of replicon domains during DNA synthesis phase in the mammalian nucleus. *Exp. Cell Res*. **165**, 291–297.

Nakayasu, H., and Berezney, R. (1989). Mapping replication sites in the eukaryotic cell nucleus. *J. Cell Biol*. **108**, 1–11.

O'Keefe, R. T., Henderson, S. C., and Spector, D. L. (1992). Dynamic organization of DNA replication in mammalian cell nuclei: Spatially and temporally defined replication of chromosome-specific ?-satellite sequences. *J. Cell Biol*. **116**, 1095–1110.

Pepperkok, R., and Ansorge, W. (1995). Direct visualization of DNA-replication sites in living cells by microinjection of fluorescein-conjugated dUTPs. *Methods Mol. Cell. Biol*. **5**, 112–117.

Schermelleh, L., Solovei, I., Zink, D., and Cremer, T. (2001). Two-color fluorescence labeling of early and mid-to-late replicating chromatin in living cells. *Chromosome Res*. **9**, 77–80.

Takebayashi, S. I., Manders, E. M. M., Kimura, H., Taguchi, H., and Okumura, K. (2001). Mapping sites where replication initiates in mammalian cells using DNA fibers. *Exp. Cell Res*. **271**, 263–268.

Zink, D., Cremer, T., Saffrich, R., Fischer, R., Trendelenburg, M. F., Ansorge, W., and Stelzer, E.H.K. (1998). Structure and dynamics of human interphase chromosome territories *in vivo*. *Hum. Genet*. **102**, 241–251.

CHAPTER

19

Isolation of Chromosomes for Flow Analysis and Sorting

Nigel P. Carter

I. INTRODUCTION

The bivariate analysis of mammalian chromosomes using the flow cytometer was first described by Gray and colleagues in 1979. In this method, metaphase chromosomes are released into a stabilising buffer and stained with two dyes, Hoechst 33258 (with specificity for AT-rich regions of DNA) and chromomycin A3 (specificity for GC-rich DNA) and then analysed or sorted using the flow cytometer. However, the technique has remained a somewhat specialist application limited to a relatively small number of laboratories. One reason for this is the requirement for the flow cytometer to be equipped with two large water-cooled and expensive lasers in order to excite the two dyes. However, arguably the most critical factor is the isolation of intact metaphase chromosomes from actively dividing cells. Several chromosome isolation procedures have been described (Sillar and Young 1981; van den Engh *et al*., 1984, 1985, 1988; general reference, Gray, 1989). Of these procedures, methods based on the stabilisation of chromosomes with polyamines (Sillar and Young, 1981) have proved to be most reliable for not only flow karyotype resolution, but also for the generation of high molecular weight DNA from sorted chromosomes. This article describes the procedure for isolating chromosomes from human lymphoblastoid cell lines using a polyamine buffer.

II. MATERIALS

Spermine tetrahydrochloride (Cat. No. S2876), spermidine trihydrochloride (Cat. No. S2501), Hoechst 33258 (Cat. No. B2883), chromomycin A3 (Cat. No. C2659), gentian violet (Cat. No. G2039), propidium iodide (Cat. No. P4170), Triton X-100 (Cat. No. X100), Trizma base (Tris-base, Cat. No. T6791), EGTA (Cat. No. E3889), EDTA (Cat. No. E5134), potassium chloride (Cat. No. P9541), sodium chloride (Cat. No. S3014), sodium sulphite (Cat. No. S8018), trisodium citrate (Cat. No. C3434), RPMI1640 medium (Cat. No. R8758), L-glutamine/penicillin/streptomycin solution (Cat. No. G6784), dithiothreitol (Cat. No. D9779), and magnesium sulphate (Cat. No. M2773) are obtained from Sigma. Foetal bovine serum (Cat. No. 16000-044) is obtained from Gibco. Invitrogen Corp.

III. PROCEDURES

A. Tissue Culture and Chromosome Preparation

Solutions

1. *Culture medium*: To 500 ml of RPMI 1640 medium add 100 ml of foetal bovine serum and 5 ml of L-glutamine/penicillin/streptomycin additive.
2. *Polyamine buffer and stain stock solutions*
   a. Dissolve 1.18 g of Tris-base and 832 mg of EDTA in sterile distilled water, adjust pH to 8.0, and bring final volume to 100 ml.
   b. Dissolve 1.18 g of Tris-base and 190 mg of EGTA in sterile distilled water, adjust pH to 8.0, and bring final volume to 100 ml.
   c. Dissolve 5.96 g of potassium chloride in sterile distilled water and bring final volume to 100 ml.

Copyright 2006, Elsevier Science (USA).
All rights reserved.

d. Dissolve 1.17 g of sodium chloride in sterile distilled water and bring final volume to 100 ml.

Solutions should be sterile filtered and stored at 4–10°C for up to 1 month.

e. Dissolve 1.39 g of spermine tetrahydrochloride in sterile distilled water and bring final volume to 10 ml. Aliquot and store at –20°C.
f. Dissolve 2.55 g of spermidine trihydrochloride in sterile distilled water and bring final volume to 10 ml. Aliquot and store at –20°C.
g. Dissolve 1 g of dithiothreitol in sterile distilled water and bring final volume to 21.6 ml. Sterile filter and store at 4–10°C.
h. Dissolve 3.15 g of sodium sulphite in sterile distilled water and bring final volume to 100 ml. Do not store.
i. Dissolve 2.94 g of trisodium citrate in sterile distilled water and bring final volume to 100 ml. Do not store.
j. Dissolve 10 mg of Hoechst 33258 in sterile distilled water and bring final volume to 10 ml. Sterile filter and store in the dark at 4–10°C.
k. Dissolve 5 mg of chromomycin A3 in ethanol and bring final volume to 2.5 ml. Aliquot and store at –20°C.
l. Dissolve 1 mg of propidium iodide in sterile distilled water and bring the final volume to 10 ml.
m. Dissolve 1.2 g of magnesium sulphate in sterile distilled water and bring final volume to 100 ml. Sterile filter and store at 4–10°C.
n. Add 1 ml of glacial acetic acid and 10 mg of gentian violet to sterile distilled water and bring the final volume to 100 ml (Turck's stain). Store at 4–10°C.

Steps

1. Grow 20 ml of the lymphoblastoid cell line to near confluence and add a further 30 ml of medium to the flask, gently breaking up any cell clumps. Incubate for 24 h.

2. Add 0.5 ml of colcemid and mix gently. Incubate for 6 h.

3. Transfer the cell suspension to a 50-ml centrifuge tube and centrifuge at 200 *g* for 10 min. Decant the supernatant and place the tube, inverted, on an absorbent paper tissue.

4. Dilute 4.7 ml of stock 800 m*M* potassium chloride solution to 50 ml with sterile distilled water and filter through a sterile 0.2-µm filter. Add 10 ml to the cell pellet and resuspend gently. Incubate at room temperature for 15 min.

5. Monitor swelling by staining 10 µl of the cell suspension with an equal volume of Turck's stain and viewing in a haemocytometer using phase-contract microscopy. Monitor cell bursting by staining 20 µl of the cell suspension with 1 µl of propidium iodide solution and viewing in a haemocytometer using fluorescence microscopy.

6. To make the polyamine buffer, mix together 10 ml of each of the four stock solutions (a–d), 50 µl of spermine tetrahydrochloride, 50 µl spermidine trihydrochloride, 250 µl of Triton X-100, 500 µl of dithiothreitol, and 50 ml of sterile distilled water, adjust pH to 7.2 with hydrochloric acid, and bring the final volume to 100 ml. Pass through a sterile 0.2-µm filter.

7. Centrifuge cell suspension at 400 *g* for 10 min, decant supernatant, and invert the tube on a paper tissue. Add 3 ml of the polyamine buffer, resuspend gently, and incubate on ice for 10 min.

8. Vortex the cell suspension for 10 s at a speed that produces a swirling film of suspension around the wall of the tube.

9. Monitor the chromosome release by staining 20 µl of the cell suspension with 1 µl of propidium iodide solution and viewing in a haemocytometer using fluorescence microscopy. Check that the majority of chromosomes are free in solution and not clumped. If clumps are apparent, vortex for periods of 5 s until few clumps are present. Too vigorous or too long vortexing will increase the number of broken chromosomes and debris.

10. Centrifuge 850 µl of the chromosome suspension at 100 *g* for 1 min. Transfer 740 µl of the supernatant to a tube suitable for use on the flow cytometer and add 20 µl of chromomycin A3, mixing immediately.

11. Add 20 µl of magnesium sulphate. Dilute 5 µl of Hoechst with 45 µl of sterile distilled water and add 20 µl to the chromosome suspension and mix well. Incubate for at least 2 h on ice.

12. Add 100 µl of trisodium citrate and 100 µl of sodium sulphite to the stained chromosome preparation 15 min prior to analysis.

IV. COMMENTS

The procedure detailed in this article is directly applicable, with minor modification, to any actively dividing preparation of cells. Care should be taken to block the cells at a time during cell culture when the

maximum number of cells are actively dividing and the time of incubation in colcemid should be adjusted to be approximately three-fourths of the time that the cells spend in the S phase of the cell cycle. Some cell types are resistant to disruption by vortexing (e.g., fibroblasts) and require gently syringing to release chromosomes into solution. The flow cytometer should be aligned according to the manufacturer's procedures such that the chromosomes first pass through the multiline ultraviolet beam required for Hoechst excitation and then, after the appropriate spatial separation, through the deep blue beam (457.9 nm) required for excitation of chromomycin. A nozzle orifice diameter of 50–70 µm is recommended.

V. PITFALLS

Poor preparations that generate flow karyotypes without good separation of peaks are invariably produced when a low mitotic index is produced. Attention must be paid to culture conditions and the timing of subculturing and colcemid blocking to generate the highest mitotic index possible.

References

Gray, J. W., ed. (1989). "*Flow Cytogenetics*." Academic Press.

Sillar, R., and Young, B. D. (1981). A new method for the preparation of metaphase chromosomes for flow analysis. *J. Histochem. Cytochem.* **29**, 74–78.

van den Engh, G., Trask, B., Cram, S., and Bartholdi, M. (1984). Preparation of chromosome suspensions for flow cytometry. *Cytometry* **5**, 108–117.

van den Engh, G., Trask, B., Lansdorp, P., and Gray, J. (1988). Improved resolution of flow cytometric measurements of Hoechst- and chromomycin-A3-stained human chromosomes after addition of citrate and sulfite. *Cytometry* **9**, 266–270.

van den Engh, G. J., Trask, B. J., Gray, J. W., Langlois, R. G., and Yu, L. C. (1985). Preparation and bivariate analysis of suspensions of human chromosomes. *Cytometry* **6**, 92–100.

SECTION

2

Vital Staining of Cells/Organelles

CHAPTER

20

Vital Staining of Cells with Fluorescent Lipids

Toshihide Kobayashi, Asami Makino, and Kumiko Ishii

I. INTRODUCTION

Although a number of fluorescent lipid analogs are now available, only a limited set of the molecules are frequently employed for cell biology. Because most of these molecules are less hydrophobic than naturally occurring counterparts, they are easily partitioned to cell membranes when added to the medium. This property and bulk fluorophore alter both physical and biological properties of the lipids. Therefore, the intracellular behavior of fluorescent lipids is not always the same as that of endogenous lipids. In this context, the results need to be evaluated carefully. However, together with appropriate control, fluorescent lipids are very useful tools to follow dynamics of membrane lipids.

II. MATERIALS AND INSTRUMENTATIONS

6-((*N*-(7-nitrobenz-2-oxa-1,3-diazol-4-yl)amino) hexanoyl)sphingosylphosphorylcholine (C6-NBD-SM, MW 740.88, Cat. No. N3524), 6-((*N*-(7-nitrobenz-2-oxa-1,3-diazol-4-yl)amino)hexanoyl)sphingosine (C6-NBD-Cer, MW 575.75, Cat. No. N1154) and *N*-(4,4-difluoro-5,7-dimethyl-4-bora-3a,4a-diaza-*s*-indacene-3-pentanoyl)sphingosine (C5-BODIPY-Cer, MW 601.63, Cat. No. D3521) are from Molecular Probes. 12-((*N*-(7-nitrobenz-2-oxa-1,3-diazol-4-yl)amino)dodecanoyl)sphingosine (C12-NBD-Cer, MW 659.90, Cat. No. N9158) is from Sigma. 1-Palmitoyl-2-(6-((7-nitro-2-1,3-benzoxadiazol-4-yl)amino)hexanoyl)-*sn*-glycero-3-phospho-L-serine (ammonium salt) (C6-NBD-PS, MW 790.85, Cat. No. 810192) is obtained from Avanti. Structures of fluorescent lipids are summarized in Fig. 1.

Dulbecco's modified Eagle's medium (DMEM, Cat. No. 11885-084) is obtained from Invitrogen. Dulbecco's modified Eagle's medium/nutrient mixture F-12 Ham, without phenol red (DMEM F-12, Cat. No. 6434), is from Sigma. Thirty-five-millimeter glass-bottom culture dishes are from Matsunami Glass (noncoat, Cat. No. 111100) or from IWAKI (Asahi Technoglass Scitech Division IWAKI brand, Cat. No. 3911-035) and 60-mm culture dishes are from Nunc. Dulbecco's phosphate-buffered saline (-) (PBS, Cat. No. 14249-95) and sodium dithionite (sodium hydrosulfite, Cat. No. 31509-55) are from Nacalai Tesque. Brefeldin A (Cat. No. G-405) is from BIOMOL. The stained cells are examined under a Zeiss LSM 510 confocal microscope equipped with C-Apochromat 63XW Korr (1.2 n.a.) objective.

III. PROCEDURES

A. Fate of Different NBD-Labeled Lipids Introduced into Plasma Membranes of Cultured Fibroblasts

This procedure describes the methods used to follow the fate of fluorescent lipids inserted into the outer leaflet of the plasma membranes. The fate of fluorescent lipids is different depending on the hydrophilic head group of the lipids.

Copyright 2006, Elsevier Science (USA).
All rights reserved.

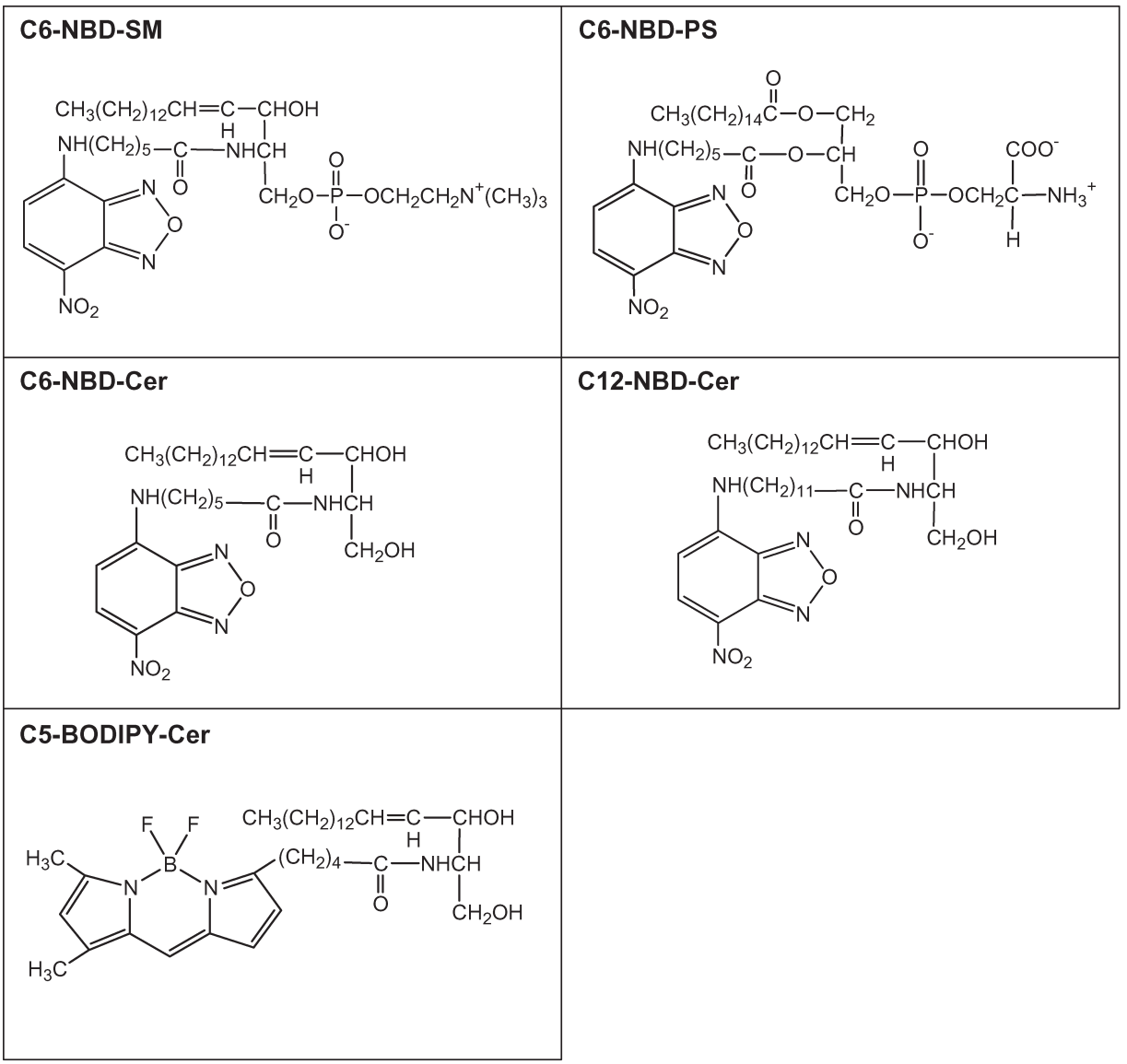

FIGURE 1 Structures of fluorescent lipids described in the text.

Solutions of Fluorescent Lipids

Stock solutions (1 mg/ml) of fluorescent lipids are prepared by dissolving C6-NBD-PS in chloroform and C6-NBD-SM in ethanol. The chloroform stock solution should be kept in screw-capped (Teflon-lined) glass tubes. The ethanol solution can be stored in either glass or plastic tubes. Stock solutions are stored at –20°C. An aliquot of a stock lipid solution is dried, first under a stream of nitrogen and then *in vacuo*. The dried lipid is then dissolved in DMEM to give final concentration 4 μ*M*. The solution is vortexed and kept at 4°C before use.

Steps

1. Grow HeLa cells in duplicate on 35-mm glass-bottom culture dishes for 1–2 days to reach 50–80% confluency.
2. Wash cells twice with ice-cold DMEM.

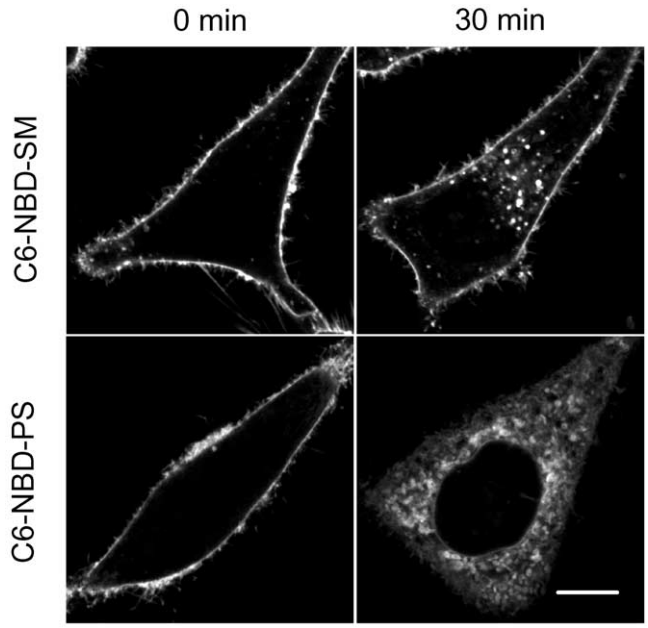

FIGURE 2 HeLa cells labeled with C6-NBD-SM or C6-NBD-PS for 30 min at 4°C (0 min) or 4°C treatment followed by a 30-min incubation at 37°C (30 min). Bar: 10 μm.

3. Incubate cells for 30 min at 4°C with 1 ml DMEM containing 4 μ*M* C6-NBD-SM or C6-NBD-PS.
4. Wash one dish twice with ice-cold DMEM F-12 and then add 1 ml ice-cold DMEM F-12. Record fluorescence images under a confocal microscope (Fig. 2, "0 min").
5. Wash the other dish twice with ice-cold DMEM and then add 1 ml prewarmed (37°C) DMEM.
6. Incubate cells for 30 min at 37°C in a CO_2 incubator.
7. Wash cells twice with DMEM F-12 at room temperature.
8. Add 1 ml DMEM F-12 and observe cells under a microscope (Fig. 2, "30 min").

Comments

C6-NBD-SM (Koval and Pagano, 1989) and C6-NBD-PS (Martin and Pagano, 1987) were first introduced by Pagano and co-workers. At low temperature (2 or 4°C), both fluorescent lipids are transported from the medium to the outer leaflet of the plasma membranes of cultured cells via spontaneous transfer of the lipids. Warming up of cells induces ATP-dependent transbilayer movement (flip-flop) of C6-NBD-PS (Martin and Pagano, 1987). In mammalian cells, the energy-dependent transbilayer movement of lipids is observed only with amino phospholipids such as phosphatidylserine and phosphatidylethanolamine (Devaux *et al.*, 2002). Flip-flop is observed as low as 7°C. Once internalized, C6-NBD-PS is transported spontaneously to intracellular membranes. Unlike C6-NBD-PS, C6-NBD-SM stays on the outer leaflet of the plasma membrane and is internalized by endocytosis. It is postulated that C6-NBD-SM is a marker for the bulk flow of membranes after endocytosis (Mayor *et al.*, 1993). C6-NBD-SM is also used together with C6-NBD-labeled glycolipids to study polarized lipid transport in hepatoma cells (Maier *et al.*, 2002). Because DMEM F-12 contains HEPES, the pH keeps constant during incubation outside the CO_2 incubator. We use phenol red-free DMEM F-12 when we take images under a microscope. BODIPY-labeled lipids (Pagano and Chen, 1998) and pyrene-labeled lipids (Somerharju, 2002) are also used for the similar purpose. The fluorescent cholesterol analog dihydroergosterol is introduced to follow the fate of cell surface cholesterol (Mukherjee *et al.*, 1998).

B. Measurement of Recycling of NBD-Labeled Sphingomyelin Using Dithionite

The dithionite method is a simple procedure used to bleach NBD located outside cells. With this procedure, it is possible to quantitate the appearance of NBD-lipid to the plasma membrane.

1. Cellular Distribution of Fluorescent Lipids

Solutions

The fluorescent lipid solution is prepared as described in Section III,A. Sodium dithionite solution is prepared by diluting a freshly made 1 *M* aqueous stock solution with DMEM (final concentration: 50 m*M*).

Steps

1. Grow HeLa cells in triplicate on 35-mm glass-bottom culture dishes for 1–2 days to reach 50–80% confluency.
2. Wash cells twice with ice-cold DMEM.
3. Incubate cells for 30 min at 4°C with 1 ml DMEM containing 4 μ*M* C6-NBD-SM.
4. Wash cells twice with ice-cold DMEM and then add 1 ml prewarmed (37°C) DMEM.
5. Incubate cells for 30 min at 37°C in a CO_2 incubator.
6. Wash one dish twice with DMEM F-12 at room temperature and then add 1 ml DMEM F-12 and observe under a microscope (Fig. 3, "before quench").
7. Wash the other two dishes twice with DMEM at room temperature.
8. Add 1 ml DMEM containing 50 m*M* sodium dithionite. Incubate for 1 min at room temperature.

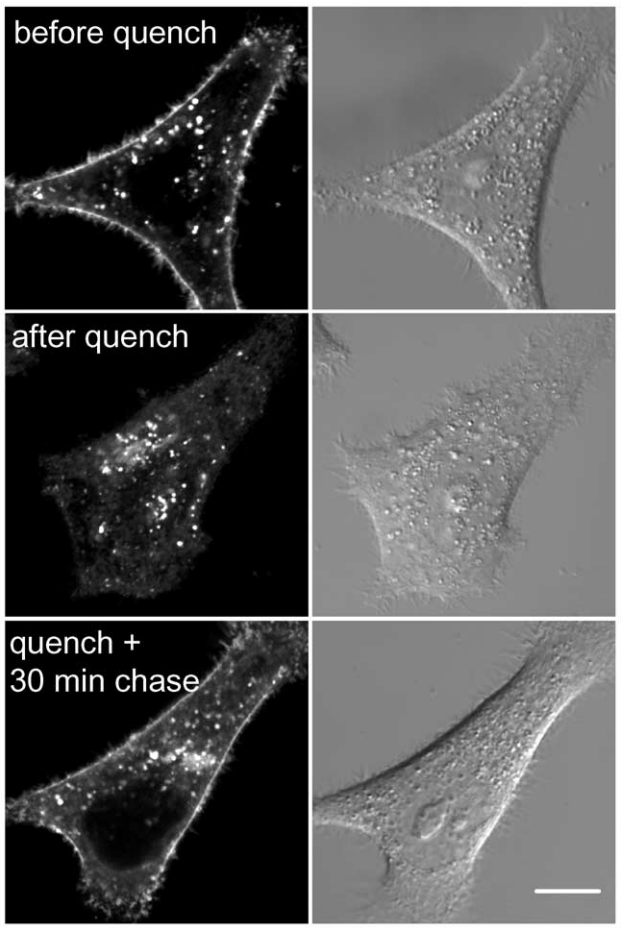

FIGURE 3 HeLa cells labeled with C6-NBD-SM for 30 min at 37°C (before quench). Cell surface fluorescent lipids are then quenched by sodium dithionite (after quench). Cells are further incubated for 30 min at 37°C (quench + 30 min chase). Bar: 10 µm.

9. Wash one dish twice with DMEM F-12 at room temperature and then add 1 ml DMEM F-12 and observe under a microscope (Fig. 3, "after quench").
10. Wash the last dish twice with DMEM at room temperature.
11. Incubate cells in 1 ml DMEM for 30 min at 37°C in a CO_2 incubator.
12. Wash cells twice with DMEM F-12 at room temperature.
13. Add 1 ml DMEM F-12 and observe under a microscope (Fig. 3, "quench + 30 min chase").

2. *Quantitation of Recycling of C6-NBD-SM*

Steps

1. Grow HeLa cells in duplicate on 60-mm culture dishes for 1–2 days to reach 50–80% confluency.
2. Wash cells twice with ice-cold DMEM.

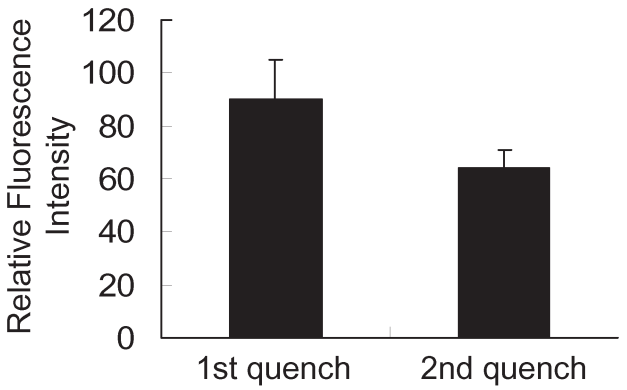

FIGURE 4 HeLa cells labeled with C6-NBD-SM for 30 min at 37°C and treated immediately with sodium dithionite (first quench) or incubated further for 30 min at 37°C in DMEM after the first dithionite treatment. Cells are then again treated with dithionite (second quench). Cells are scraped in PBS containing 1% Triton X-100. Fluorescence intensity/dish is shown. Results are mean ± SD of three experiments. The difference between the two histograms represents the NBD-lipid recycled back to the plasma membrane.

3. Incubate cells for 30 min at 4°C with 2 ml DMEM containing 4 µ*M* C6-NBD-SM.
4. Wash cells twice with ice-cold DMEM and then add 2 ml prewarmed (37°C) DMEM.
5. Incubate cells for 30 min at 37°C in a CO_2 incubator.
6. Wash cells twice with DMEM at room temperature.
7. Add 2 ml DMEM containing 50 m*M* sodium dithionite. Incubate for 1 min at room temperature.
8. Wash one dish twice with PBS at room temperature and then add 1 ml PBS containing 1% Triton X-100. Scrape cells and measure fluorescence at 535 nm with excitation at 475 nm using the Jasco FP-6500 spectrofluorometer (Fig. 4, "1st quench").
9. Wash the other dish twice with DMEM at room temperature.
10. Incubate cells in 2 ml DMEM for 30 min at 37°C in a CO_2 incubator.
11. Add 2 ml DMEM containing 50 m*M* sodium dithionite. Incubate for 1 min at room temperature.
12. Wash cells twice with PBS at room temperature and then add 1 ml PBS containing 1% Triton X-100.
13. Scrape cells and measure fluorescence at 535 nm with excitation at 475 nm using the Jasco FP-6500 spectrofluorometer (Fig. 4, "2nd quench").

Comments

Selective removal of fluorescent lipid present on the outer leaflet of the plasma membrane allows the quantitative analysis of the kinetics of lipid transport to the plasma membrane. This is achieved by extracting C6-

NBD- and C5-BODIPY-labeled phospho- and sphingolipids with BSA (Sleight and Pagano, 1984). Alternatively, one can selectively destroy NBD-labeled lipids on the outer monolayer with the water-soluble quencher dithionite (McIntyre and Sleight, 1991). The dithionite method is widely used to monitor transbilayer distribution (Nolan *et al*., 1995; Williamson *et al*., 1995) and vesicular traffic (Babia *et al*., 2001), as well as lateral mobility (Kobayashi *et al*., 1992), of NBD-labeled lipids. However, because dithionite can leak through the membrane in some cells, proper conditions have to be adapted to each specific case (Pomorski *et al*., 1994). Recycling of C6-NBD-SM is very rapid (Hao and Maxfield, 2000). The distribution of C6-NBD-SM shown here is the result of several recycling rounds of the fluorescent lipid. Internalized C6-NBD-SM is also transported to lysosomes and metabolized to C6-NBD-Cer. Transport to the degradative compartments is estimated to be 18- to 19-fold slower than the rate of C6-NBD-SM recycling (Koval and Pagano, 1990). In some cells, degradation of C6-NBD-SM occurs on the plasma membrane in a differentiation-dependent manner (Kok *et al*., 1995). Such degradation products are separated from C6-NBD-SM by thin-layer chromatography (Kobayashi and Pagano, 1989; Koval and Pagano, 1990).

C. Vital Stain of Golgi Apparatus by Fluorescent Ceramide Analogs

Fluorescent ceramide is widely used for vital staining of the Golgi apparatus (Pagano, 1989; Pagano *et al*., 1991). Dynamics of the Golgi membranes could be followed by using fluorescent ceramide.

1. Vital Stain of Golgi Apparatus by Fluorescent Ceramides

Solutions

Stock solutions (1 mg/ml) of fluorescent lipids are prepared by dissolving C6-NBD-Cer, C12-NBD-Cer, and C5-BODIPY-Cer in ethanol. An aliquot of a stock lipid solution is dried, first under a stream of nitrogen and then *in vacuo*. The dried lipid is dissolved in DMEM to give a final concentration 0.5 μ*M* (C6-NBD-Cer and C5-BODIPY-Cer) or 5 μ*M* (C12-NBD-Cer). The solutions are vortexed and kept at 4°C before use.

Steps

1. Grow HeLa cells on 35-mm glass-bottom culture dishes for 1–2 days to reach 50–80% confluency.
2. Wash cells twice with DMEM at room temperature.

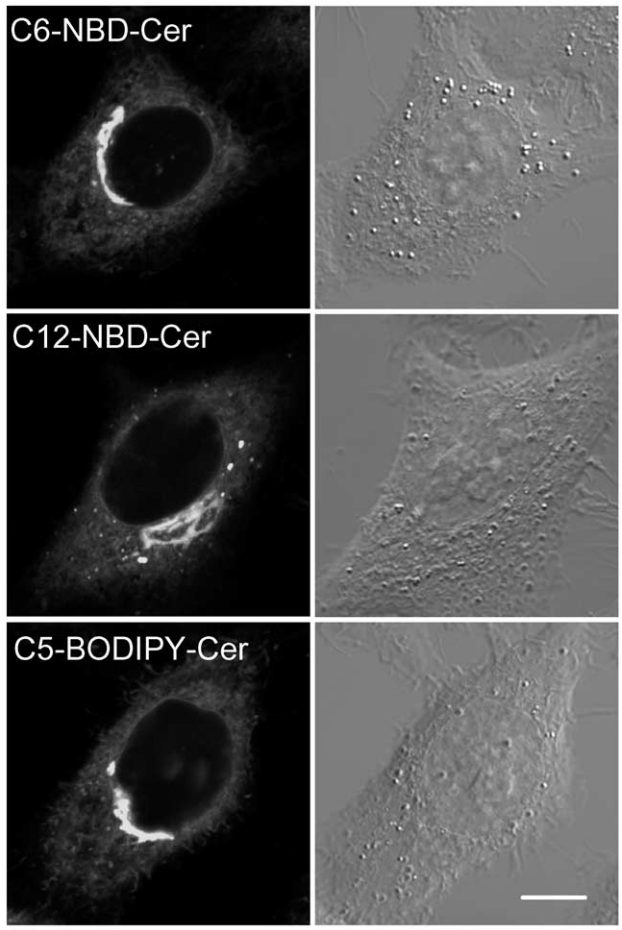

FIGURE 5 HeLa cells labeled with fluorescent ceramide analogs. Bar: 10 μm.

3. Incubate cells for 30 min at 37°C with 1 ml DMEM containing 0.5 μ*M* C6-NBD-Cer or C5-BODIPY-Cer or 5 μ*M* C12-NBD-Cer in a CO_2 incubator.
4. Wash cells twice with DMEM F-12 at room temperature.
5. Add 1 ml DMEM F-12 and observe under a microscope (Fig. 5.).

2. Alteration of Morphology of Golgi Apparatus Monitored by C5-BODIPY-Cer

Solutions

Lipid solutions are prepared as described in Section III,C,1. 5-mg/ml stock solution of brefeldin A is diluted with DMEM F-12 to give a final concentration 5 μg/ml.

Steps

1. Grow HeLa cells on 35-mm glass-bottom culture dishes for 1–2 days to reach 50–80% confluency.

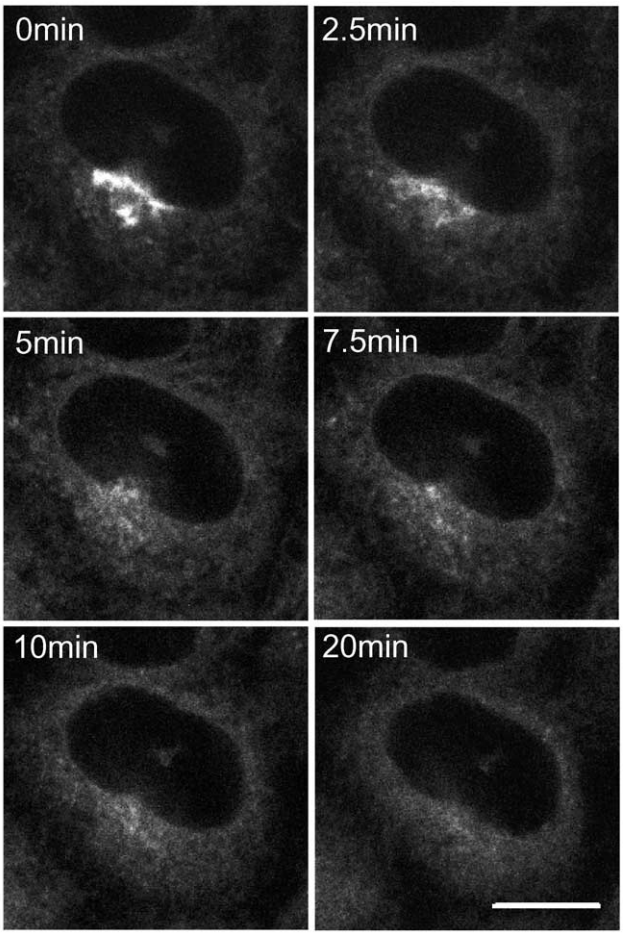

FIGURE 6 C5-BODIPY-Cer-labeled HeLa cells treated with brefeldin A for various times. Bar: 10 μm.

2. Wash cells twice with DMEM at room temperature.
3. Incubate cells for 30 min at 37°C with 1 ml DMEM containing 0.5 μ*M* C5-BODIPY-Cer in a CO_2 incubator.
4. Wash cells twice with DMEM F-12 at room temperature.
5. Add 1 ml DMEM F-12 containing 5 μg/ml brefeldin A.
6. Acquire images at appropriate intervals under a confocal microscope at room temperature (Fig. 6.).

Comments

Three different fluorescent ceramides are now available commercially. All three give similar Golgi labeling, although their working concentrations are different. Mechanisms of the accumulation of NBD-labeled ceramide and BODIPY-labeled ceramide are apparently different (Martin *et al*., 1993). Fluorescent ceramide makes it possible to follow the fate of Golgi lipids in living cells under various conditions such as brefeldin A treatment (Lippincott-Schwartz *et al*., 1991). Brefeldin A treatment induces redistribution of the Golgi apparatus into the endoplasmic reticulum (Chardin and McCormick, 1999). In Fig. 6, we adjusted the laser power of the confocal microscope to prevent bleaching of the fluorescence during observation. Spectral properties of BODIPY-labeled ceramides also allow us to differentiate membranes containing high concentrations of the fluorescent lipid and its metabolites from other regions of the cell where smaller amounts of the probe are present with a specific filter setup (Pagano *et al*., 1991).

IV. PITFALLS

1. Because of the evaporation of solvent, the stock lipid solution is gradually concentrated during storage. Concentrations of NBD- and BODIPY-lipid solution are adjusted by measuring absorbance at 475 nm and comparing the OD with that of the solution of a known concentration.
2. Degradation of lipids often occurs during storage. The purity of the lipid stock is checked periodically by thin-layer chromatography. Lipids are repurified or a new lot of fluorescent lipid is purchased when degradation compounds are detected.

References

Babia, T., Ledesma, M. D., Saffrich, R., Kok, J. W., Dotti, C. G., and Egea, G. (2001). Endocytosis of NBD-sphingolipids in neurons: exclusion from degradative compartments and transport to the Golgi complex. *Traffic* **2**, 395–405.

Chardin, P., and McCormick, F. (1999). Brefeldin A: The advantage of being uncompetitive. *Cell* **97**, 153–155.

Devaux, P. F., Fellmann, P., and Herve, P. (2002). Investigation on lipid asymmetry using lipid probes: Comparison between spin-labeled lipids and fluorescent lipids. *Chem. Phys. Lipids* **116**, 115–134.

Hao, M., and Maxfield, F. R. (2000). Characterization of rapid membrane internalization and recycling. *J. Biol. Chem.* **275**, 15279–15286.

Kobayashi, T., and Pagano, R. E. (1989). Lipid transport during mitosis: Alternative pathways for delivery of newly synthesized lipids to the cell surface. *J. Biol. Chem* **264**, 5966–5973.

Kobayashi, T., Storrie, B., Simons, K., and Dotti, C. G. (1992). A functional barrier to movement of lipids in polarized neurons. *Nature* **359**, 647–650.

Kok, J. W., Babia, T., Klappe, K., and Hoekstra, D. (1995). Fluorescent, short-chain C6-NBD-sphingomyelin, but not C6-NBD-glucosylceramide, is subject to extensive degradation in the plasma membrane: Implications for signal transduction related to cell differentiation. *Biochem. J.* **309**, 905–912.

Koval, M., and Pagano, R. E. (1989). Lipid recycling between the plasma membrane and intracellular compartments: Transport and metabolism of fluorescent sphingomyelin analogues in cultured fibroblasts. *J. Cell Biol.* **108**, 2169–2181.

Koval, M., and Pagano, R. E. (1990). Sorting of an internalized plasma membrane lipid between recycling and degradative pathways in normal and Niemann-Pick, type A fibroblasts. *J. Cell Biol.* **111**, 429–442.

Lippincott-Schwartz, J., Glickman, J., Donaldson, J. G., Robbins, J., Kreis, T. E., Seamon, K. B., Sheetz, M. P., and Klausner, R. D. (1991). Forskolin inhibits and reverses the effects of brefeldin A on Golgi morphology by a cAMP-independent mechanism. *J. Cell Biol.* **112**, 567–577.

Maier, O., Oberle, V., and Hoekstra, D. (2002). Fluorescent lipid probes: Some properties and applications. *Chem. Phys. Lipids* **116**, 3–18.

Martin, O. C., Comly, M. E., Blanchette-Mackie, E. J., Pentchev, P. G., and Pagano, R. E. (1993). Cholesterol deprivation affects the fluorescence properties of a ceramide analog at the Golgi apparatus of living cells. *Proc. Natl. Acad. Sci. USA* **90**, 2661–2665.

Martin, O. C., and Pagano, R. E. (1987). Transbilayer movement of fluorescent analogs of phosphatidylserine and phosphatidylethanolamine at the plasma membrane of cultured cells: Evidence for a protein-mediated and ATP-dependent process(es). *J. Biol. Chem.* **262**, 5890–5898.

Mayor, S., Presley, J. F., and Maxfield, F. R. (1993). Sorting of membrane components from endosomes and subsequent recycling to the cell surface occurs by a bulk flow process. *J. Cell Biol.* **121**, 1257–1269.

McIntyre, J. C., and Sleight, R. G. (1991). Fluorescence assay for phospholipid membrane asymmetry. *Biochemistry* **30**, 11819–11827.

Mukherjee, S., Zha, X., Tabas, I., and Maxfield, F. R. (1998). Cholesterol distribution in living cells: Fluorescence imaging using dehydroergosterol as a fluorescent cholesterol analog. *Biophys. J.* **75**, 1915–1925.

Nolan, J. P., Magargee, S. F., Posner, R. G., and Hammerstedt, R. H. (1995). Flow cytometric analysis of transmembrane phospholipid movement in bull sperm. *Biochemistry* **34**, 3907–3915.

Pagano, R. E. (1989). A fluorescent derivative of ceramide: Physical properties and use in studying the Golgi apparatus of animal cells. *Method Cell Biol.* **29**, 75–85.

Pagano, R. E., and Chen, C. S. (1998). Use of BODIPY-labeled sphingolipids to study membrane traffic along the endocytic pathway. *Ann. N. Y. Acad. Sci.* **845**, 152–160.

Pagano, R. E., Martin, O. C., Kang, H. C., and Haugland, R. P. (1991). A novel fluorescent ceramide analogue for studying membrane traffic in animal cells: Accumulation at the Golgi apparatus results in altered spectral properties of the sphingolipid precursor. *J. Cell Biol.* **113**, 1267–1279.

Pomorski, T., Herrmann, A., Zachowski, A., Devaux, P. F., and Muller, P. (1994). Rapid determination of the transbilayer distribution of NBD-phospholipids in erythrocyte membranes with dithionite. *Mol. Membr. Biol.* **11**, 39–44.

Sleight, R. G., and Pagano, R. E. (1984). Transport of a fluorescent phosphatidylcholine analog from the plasma membrane to the Golgi apparatus. *J. Cell Biol.* **99**, 742–751.

Somerharju, P. (2002). Pyrene-labeled lipids as tools in membrane biophysics and cell biology. *Chem. Phys. Lipids* **116**, 57–74.

Williamson, P., Bevers, E. M., Smeets, E. F., Comfurius, P., Schlegel, R. A., and Zwaal, R. F. (1995). Continuous analysis of the mechanism of activated transbilayer lipid movement in platelets. *Biochemistry* **34**, 10448–10455.

CHAPTER

21

Labeling of Endocytic Vesicles Using Fluorescent Probes for Fluid-Phase Endocytosis

Nobukazu Araki

I. INTRODUCTION

Endocytosis occurs by the invagination of plasma membrane to form an intracellular vesicle. Endocytic vesicles, and the intracellular organelles they communicate with, can be labeled by inclusion of fluorescent, membrane-impermeant molecules in the extracellular medium. Such probes are enclosed in the vesicles as they form and remain contained in endocytic compartments. Ultimately, these fluid-phase endocytic probes either accumulate in lysosomes, where they may be degraded, or are returned to the extracellular medium by recycling vesicles. Fluid-phase endocytosis is also called pinocytosis, which is sometimes subdivided into macropinocytosis and micropinocytosis, the formation of large and small pinosomes, respectively (Maniak, 2001; Swanson, 1989a; Swanson and Watts, 1995). Macropinocytosis is specialized for fluid-phase uptake, whereas micropinocytosis involves both receptor-mediated (membrane adsorptive) and fluid-phase uptake. Receptor-mediated endocytosis via clathrin-coated vesicles can be distinguished from fluid-phase endocytosis by using fluorescent specific ligands for the receptor, e.g., FITC-labeled transferrin for the transferrin receptor. Compared with receptor-mediated endocytosis, the biological function of macropinocytosis has been less investigated so far. However, attention has been increasingly paid to this fluid-phase endocytic pathway (Araki *et al.*, 2000, 2003; Maniak, 2001) because it has been known that macropinocytosis is utilized for antigen presentation in dendritic cells and macrophages (Norbury *et al.*, 1995; Sallusto *et al.*, 1995; Nobes and Marsh, 2000).

A variety of fluorescent probes can be used to label endocytic organelles in living cells. Vital staining techniques using such probes are useful not only for marking endocytic organelles, but also for exploring the kinetics of soluble molecules and the dynamics of endocytic organelles in the cell. This article describes methods for labeling and observing these compartments in living cells and for immunofluorescence microscopy of similarly labeled cells. In addition, it describes a method for the quantitative measurement of fluid-phase pinocytosis using fluorescent probes. These methods are optimized for the study of macrophages, which are actively endocytic cells. It should be kept in mind that most other kinds of cells exhibit lower rates of endocytosis and different kinetics of delivery from endosomes to lysosomes. One may therefore have to extend incubation times or increase probe concentrations to obtain strong fluorescent signals in the microscope or fluorometer. For any new cell type, compartment identities should be determined empirically by comparing fluorescent probe distributions in cells fixed after various pulse–chase intervals with the immunofluorescent localization of known markers for endocytic compartments (e.g., Racoosin and Swanson, 1993).

II. MATERIALS AND INSTRUMENTATION

The fluorescent fluid-phase probes, fluorescein dextran, MW 3000 (FDx3, Cat. No. D-3305), MW 10,000 (FDx10, Cat. No. D-1821), lysine fixable fluorescein

Copyright 2006, Elsevier Science (USA).
All rights reserved.

dextran, MW 10,000 (Cat. No. D-1820), and Texas red dextran, MW 10,000 (TRDx10, Cat. No. D-1828), are from Molecular Probes. Lucifer yellow CH (Cat. No. 86150-2) is from Aldrich. Fluorescein dextran, MW 150,000 (FDx150 Cat. No. FD-150), paraformaldehyde (Cat. No. P-6148), bovine serum albumin (BSA, fraction V., Cat. No. A-9647), Triton X-100 (Cat. No. T-9284), saponin (Cat. No. S-4521), HEPES (Cat. No. H-3375), and Trizma base (Cat. No. T-1503) are from Sigma Chemical. The 25% glutaraldehyde solution (EM grade, Cat. No. SP-17003-92) is from Nacalai Tesque. A primary antibody, rabbit anti-cathepsin D serum, was a gift from Dr. S. Yokota, Yamanashi Medical School. Monoclonal antibodies recognizing some marker proteins for endocytic compartments are available from the Developmental Studies Hybridoma Bank or commercial sources. Texas red-labeled anti-rabbit IgG (goat) (Cat. No. TI-1000) is from Vector Lab. Dulbecco's modified essential medium (DMEM, Cat. No. 31600-034), fetal bovine serum (FBS, Cat. No. 16000), and goat serum (Cat. No. 16210) are from GIBCO BRL. Circular glass coverslips 12 and 25 mm in diameter (No. 1 thickness, Cat. No. 12-545-102) and silicon oil (Cat. No. 5159-500) are from Fisher Scientific. Twenty-four-well (Cat. No. 430262) and 6-well (Cat. No. 430343) plates are from Corning Costar. A water aspirator with a Pasteur pipette and a digital micropipette (Nichipet EX1000) are used for quickly replacing media in cell culture wells. The Attofluor cell chamber (Cat. No. A7816) is from Molecular Probes. PermaFluor aqueous mounting medium (Cat. No. 434980) is from Lipshaw/Immunon.

An epifluorescence microscope (Axiophot, Carl Zeiss) is used for observation of both living and fixed cells. A Lucifer yellow filter set is from Omega Optical (Set No. XF-14), in addition to a conventional fluorescein filter set. For high-resolution observation, a 100× PlanApo lens, numerical aperture (NA) 1.4 or a 100× Plan-Neofluar lens, NA 1.3 is used. An inverted-type fluorescence microscope (Nikon TE300) equipped with a cooled CCD camera (Retiga EXi F-M-12-C, QImaging), light path shutter (Uniblitz VMMD1, Vincent Associates), and a thermo-controlled stage (Model TC-102, Harvard Apparatus) are used for longer observations of living cells. A personal computer (Precision 360, Dell) installed with MetaMorph version 4.6 imaging system software (Universal Imaging Co.) is used for collecting images from the CCD camera and for making time-lapse movies. For quantitation of fluorescent probes, a spectrofluorometer (Hitachi 650-40) is used.

III. PROCEDURES

A. Fluorescence Microscopy of Endocytic Compartments Labeled with Fluorescent Probes

Solutions

1. *Ringer's buffer + bovine serum albumin (BSA) (RB):* 155 m*M* NaCl, 5 m*M* KCl, 2 m*M* $CaCl_2$, 1 m*M* $MgCl_2$, 2 m*M* NaH_2PO_4, 10 m*M* HEPES, 10 m*M* D-glucose, pH 7.2, plus 0.05% BSA. To make 1 liter, add 9.1 g of NaCl, 0.37 g of KCl, 0.275 g of $NaH_2PO_4 \cdot H_2O$, 2.38 g of HEPES, 1.8 g of D-glucose, 0.22 g of $CaCl_2$, 0.2 g of $MgCl_2 \cdot 6H_2O$, and 0.5 g BSA to 950 ml distilled water, adjust to pH 7.2 with 1 *N* NaOH, and bring the volume to 1 liter. Sterilize with a 0.22-µm filter and store at 4°C.

2. *Fluorescent probe stock solutions:* Dissolve 10 mg of fluorescent probes such as Lucifer yellow, FDx3, FDx10, FDx150, and TRDx10 in 1 ml PBS. Lysine fixable dextran probes can be used to increase fluorescent signals in aldehyde-fixed cells. Divide in 200-µl aliquots in tubes and store at –20°C.

3. *Labeling medium:* Dilute fluorescent probe solutions to a final concentration at 1.0 mg/ml in RB. A volume of 0.4 ml labeling medium is required for each well of a 24-well dish. The concentrations of probes may be changed depending on cell types. One can differentially label macropinosomes and micropinosomes using different sized probes (Fig. 1). To label both macropinosomes and micropinosomes, use low molecular weight probes such as Lucifer yellow and FDx3. To label primarily macropinosomes, use larger probes, such as FDx150 (Araki *et al.*, 1996). Warm to 37°C before adding to cells.

4. *8% paraformaldehyde stock solution:* To make 50 ml, add 4 g paraformaldehyde to 30 ml distilled water and heat to 70°C while stirring. Add a few drops of 1 *N* NaOH so that the mixture becomes clear. Bring the final volume to 50 ml with distilled water and filtrate with paper filter. This solution may be kept in aliquots at –20°C. To make up a fixative, thaw an aliquot in a hot water bath (~50°C) until the solution becomes clear.

5. *80 mM HEPES stock solution, pH 7.2:* To make 100 ml, add 1.91 g of HEPES to 70 ml of distilled water. Adjust pH to 7.2 with 1 *N* NaOH while stirring. Bring the final volume to 100 ml with distilled water. Store at 4°C.

6. *Fixative*: 4% paraformaldehyde and 0.1% glutaraldehyde in 40 m*M* HEPES buffer, pH 7.2, containing 6.8% sucrose. To make 10 ml, add 5 ml of 8% paraformaldehyde solution, 40 µl of 25% glutaraldehyde solution, and 0.68 g of sucrose to 5 ml of 80 m*M* HEPES, pH 7.2.

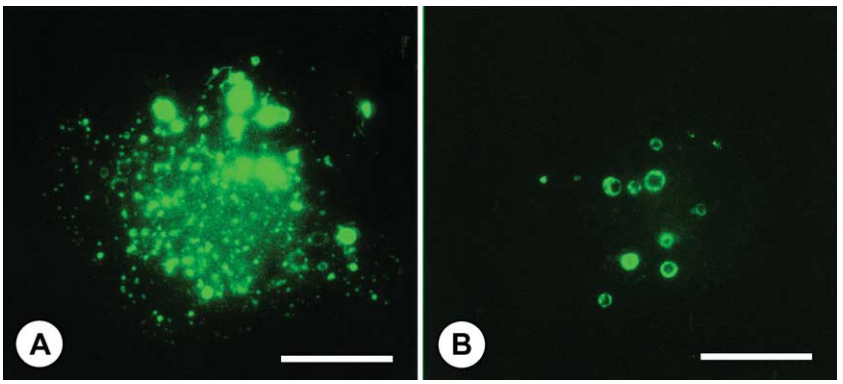

FIGURE 1 Differential labeling of macropinosomes and micropinosomes with Lucifer yellow (A) and FDx150 (B). Macrophages were incubated for 5 min in labeling medium containing Lucifer yellow or FDx150, washed briefly, and fixed immediately. A low molecular weight probe, Lucifer yellow (MW 457), labels both macropinosomes and micropinosomes (A). A larger probe, FDx150 (MW 150,000), labels predominantly macropinosomes (B). Bars: 10 µm.

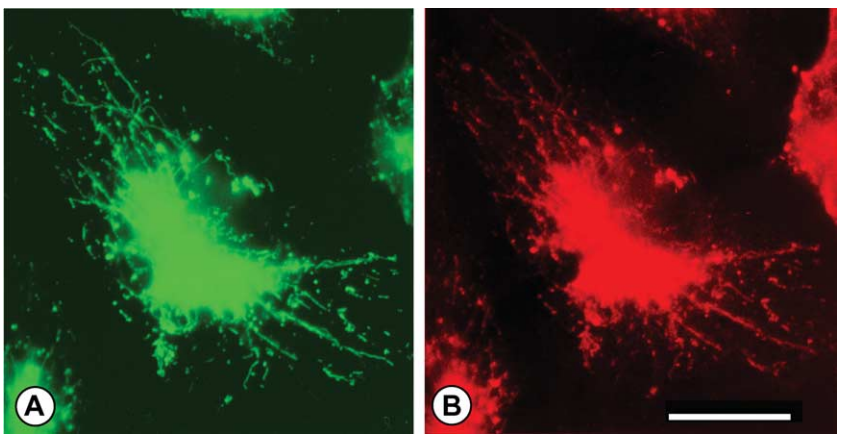

FIGURE 2 Immunofluorescence of cathepsin D in endocytic compartments labeled with endocytic probes. Macrophages were incubated for 30 min in labeling medium containing 0.5 mg/ml lysine-fixable FDx10 and were chased for 30 min. Cells were then fixed and processed for immunofluorescence using a primary antibody against cathepsin D and the Texas red-conjugated secondary antibody. (A) Fluorescein image shows that FDx10 labels tubular lysosomes. (B) Texas red image shows that tubular lysosomes, which are labeled with FDx10, are positive for cathepsin D. Bar: 10 µm.

7. *Phosphate-buffered saline (PBS):* To make 5 liters, dissolve 40 g of NaCl, 1 g of KCl, 7.1 g of Na_2HPO_4, and 1 g of KH_2PO_4 in 4 liters of distilled water. Bring the final volume to 5 liters with distilled water. The solution should be pH 7.2.

Steps

1. Culture cells on 12-mm, circular, No. 1 thickness coverslips in 24-well culture dishes in DMEM with 10% heat-inactivated FBS.

2. Aspirate the culture medium from the cell culture well and add prewarmed labeling medium. Swirl the dishes and incubate cells in labeling medium for various times at 37°C. Then rinse quickly by changing warm RB to remove fluorescent probe and chase in RB as necessary. For mouse macrophages, a 2- to 5-min labeling incubation without chase will label early endosomes, including micro- and macropinosomes (Fig. 1). A subsequent chase in the absence of the probe for 5 to 15 min should label late endosomes. A 30- to 60-min labeling incubation labels all endocytic compartments, including early and late endosomes and lysosomes, and a 30-min labeling followed by a chase longer than 60 min should label primarily lysosomes (Fig. 2).

3. Fix the cells in 4% paraformaldehyde and 0.1% glutaraldehyde in 40 m*M* HEPES, pH 7.2, containing 6.8% sucrose for 30 to 60 min at 37°C.

4. Rinse 3 × 5 min with PBS.

5. Mount the coverslip, cell side down, on a slide using mounting medium. Seal with nail polish between the coverslip and the slide.

6. Observe the slide with an epifluorescence microscope. We can observe living cells without fixation for short periods using a simple microscope culture chamber. This method has been described in detail previously (Swanson, 1989b; Raccosin and Swanson, 1994). Briefly, assemble a chamber on a slide using small coverslip fragments to support the coverslip. RB should be added to fill the space between the slide and the coverslip. Seal the coverslip to the slide using a heat-melted paraffin-based compound (Swanson, 1989b). The method for longer observations of living cells is described next.

B. Observation of Endocytic Compartments in Living Cells

Step

1. Plate cells on 25-mm No. 1 coverslips in a 6-well culture dish containing tissue culture medium.

2. Replace the culture medium with labeling medium. Incubate in labeling medium for various times at 37°C, as described earlier, to label the endocytic compartments.

3. Wash away fluorescent probe from the coverslip with RB.

4. Assemble the coverslip in an Attofluor chamber and fill with 1 ml of RB. You may slowly add a small amount of silicon oil to cover the surface of RB in the chamber. The thin layer of silicon oil protects evaporation of RB during long observations.

5. Put one drop of immersion oil on the objective lens of an inverted microscope and settle the Attofluor chamber in the Leiden chamber thermocontrolled at 37°C on the microscope stage.

6. Observe the coverslip and acquire images using a high sensitive cooled CCD camera under the lowest light exposure as possible, as intense excitation light may cause not only photobleaching, but also photochemical damage to living cells. Under optimal conditions of labeling, we can observe cells for several minutes under conditions of low-intensity illumination. This can be extended to an hour by inserting a shutter into the light path to control exposures.

7. Collect time-lapse images using MetaMorph imaging software, which controls the CCD camera and the light path shutter. These collected images can be saved as a stack file in electronic storage media such as CD-R or DVD-RAM for later processing into movies of living cells. For further information of imaging techniques, see also the sections on digital video microscopy and fluorescent microscopy of living cells in Volume 3.

C. Immunocytochemical Characterization of Endocytic Compartments Labeled with a Fluorescent Probe

Solutions

1. *Fixative:* Prepare 10 ml of 4% paraformaldehyde in 40 m*M* HEPES buffer, pH 7.2, containing 6.8% sucrose
2. *0.25% NH_4Cl in PBS (NH_4Cl/PBS):* To make 100 ml, dissolve 0.25 g of NH_4Cl in 100 ml PBS
3. *0.25% saponin or Triton X-100, 2% BSA in PBS (permeabilizing/blocking buffer):* To make 50 ml, dissolve 1 g BSA and 125 mg saponin or Triton X-100 in 50 ml of PBS
4. *Primary antibody:* Dilute serum or antibody with permeabilizing/blocking buffer. In the example shown, we diluted rabbit anti-cathepsin D serum at 1:500
5. *Secondary antibody:* Dilute Texas red-labeled anti-rabbit IgG with PBS at 1:250–500

Steps

1. Incubate the cells with labeling medium as described earlier. Lysine-fixable FDx or Lucifer yellow should be used when the other markers are to be localized by immunofluorescence. Nonfixable FDx would be lost during permeabilization of the cell.

2. Rinse in PBS to remove excess fluorescent probe, unless the cells were chased in RB without fluorescent probe.

3. Fix in 4% paraformaldehyde in 40 m*M* HEPES buffer, pH 7.2, containing 6.8% sucrose for 30–60 min at 37°C. Glutaraldehyde may be added to the fixative (0.1%), providing that antigenicity is resistant to glutaraldehyde.

4. Rinse with PBS 3 × 5 min and further immerse in NH_4Cl/PBS for 10 min to quench free aldehyde.

5. Treat cells with permeabilizing/blocking buffer for 2 × 5 min.

6. Put parafilm in a container with a moist paper. Place one 40-µl drop of primary antibody on the parafilm for each coverslip.

7. Wipe the cell-free side of the coverslip with Kimwipe paper. Place the coverslip cell side down on a drop of primary antibody. Incubate with the primary antibody for 1 h at room temperature in the moisture chamber. You may prolong the incubation time to overnight at 4°C.

8. After incubation, put the coverslip back into the well and wash three times for 5 min each with PBS.

9. Using the same method as for the primary antibody, incubate with secondary antibody, e.g., Texas red-conjugated anti-rabbit IgG diluted in PBS at a concentration 1:500, for 1 h at room temperature.

10. Wash the coverslip with PBS three times for 5 min each.

11. Mount the coverslip on a slide using the mounting medium. Seal the coverslip with nail polish. Observe the specimens with an epifluorescence microscope using fluorescein and Texas red filter sets.

D. Quantitative Fluorometric Analysis of Endocytic Compartments Labeled with Fluorescent Probes

Solutions

1. *Lysis buffer:* 0.1% Triton X-100 in 50 m*M* Tris, pH 8.5. To make 100 ml, dissolve 0.6 g of Trizma base and 0.1 g of Triton X-100 in 80 ml of distilled water. Adjust pH to 8.5 with 1 *N* NaOH. Bring the volume to 100 ml.

2. *PBS:* Make 3 liters of PBS as described earlier. Refrigerate before use.

3. *0.1% BSA/PBS:* To make 2 liters, dissolve 2 g of BSA in 2 liters of PBS.

4. *Standard solutions of fluorescent probes:* Dilute the labeling medium to concentrations of 0, 1, 5, 10, and 20 ng probe/ml in lysis buffer. Each solution should be more than 2 ml.

Steps

1. Plate the cells at a high density (e.g., 2×10^5 cells/well) in a 24-well culture dish. Triplicate experiments are desirable.

2. Replace the culture medium with labeling medium containing fluorescent probes. Dual labeling with FDx and Lucifer yellow is possible (Berthiaume *et al.*, 1995). Incubate at 37°C for various times. A 0-min incubation should be done as a control to determine the background level.

3. Discard the labeling medium and rinse the culture dish twice by dipping into a 1-liter beaker filled with ice-cold 0.1% BSA/PBS for 5 min each. Repeat with another beaker filled with cold PBS for 5 min.

4. Drain PBS and aspirate remaining PBS completely.

5. Put 0.5 ml of lysis buffer into each well and leave it at least 30 min to complete cell lysis.

6. Fill disposable 1-cm plastic cuvettes with 0.75 ml of lysis buffer. Add 0.4 ml of cell lysate into the plastic cuvette and dilute it with another 0.75 ml of lysis buffer so that the final volume is 1.9 ml.

7. Measure the fluorescence of lysate in a spectrofluorometer. Fluorescein can be measured at excitation (exc.) 495 nm and emission (em.) 514 nm. Lucifer yellow is exc. 430 nm and em. 580 nm. These wavelengths allow selective measurement of FDx and Lucifer yellow when the cells are labeled with both probes. Lucifer yellow alone is best measured at exc. 430 nm and em. 540 nm.

8. Measure the protein concentration of lysates remaining in wells using a BCA protein assay kit (Pierce Chemical Co.).

9. Prepare the standard solutions of 0, 1, 5, 10, and 20 ng probe/ml in lysis buffer and measure in a spectrofluorometer to obtain a standard curve.

10. Calculate the amount of probes from the standard curve and express the value as nanogram probe per milligram protein.

IV. PITFALLS

1. A prolonged exposure to intense excitation light may cause a release of fluorescent probes from endocytic vesicles into cytoplasm, especially in living cells. To avoid this, reduce the intensity of the excitation light or the exposure time as much as possible (Video 1 and 2 in the online version).

2. Lucifer yellow can be seen using some fluorescein filter sets with a wide band pass (e.g., Olympus BP490), but not some others (e.g., Zeiss No. 09). Choose an appropriate filter set for Lucifer yellow (e.g., Omega Optical Set No. XF-14, Zeiss No. 05).

3. Many kinds of fluorescent-conjugated probes are available commercially; however, some are not suitable for fluid-phase probes. Texas red albumin is taken up very efficiently by adsorptive endocytosis, although it is sometimes used as a fluid-phase probe. Lysine-fixable Texas red dextran may bind nonspecifically to coverslips and create a high background fluorescence.

4. In the combination of fluorescent fluid-phase probe labeling with immunocytochemistry, we are often faced with a problem that fluid-phase probes release from macropinosomes during membrane permeabilization that is necessary for antibody impregnation. In such a case, the author recommends using a mild detergent such as saponin rather than Triton X-100. The addition of 2% BSA to permeabilizing buffer considerably protects the fluid-phase probe release. The addition of 0.1% glutaraldehyde to the fixative also effectively fixes fluorescent probes in macropinosomes; however, because some antigens lose their

antigenicity, you have to examine the resistance of the antigen to glutaraldehyde.

5. For quantitative analysis using a less sensitive fluorescence plate reader, plate the cells at a higher density to increase the sensitivity for fluorescence.

References

Araki, N., Hatae, T., Furukawa, A., and Swanson, J. A. (2003). Phosphoinositide-3-kinase-independent contractile activities associated with Fc γ-receptor-mediated phagocytosis and macropinocytosis in macrophages. *J. Cell Sci.* **116**, 247–347.

Araki, N., Hatae, T., Yamada, T., and Hirohashi, S. (2000). Actinin-4 is preferentially involved in circular ruffling and macropinocytosis in mouse macrophages: Analysis by fluorescence ratio imaging. *J. Cell Sci.* **113**, 3329–3340.

Araki, N., Johnson, M. T., and Swanson, J. A. (1996). A role for phosphoinositide 3-kinase in the completion of macropinocytosis and phagocytosis by macrophages. *J. Cell Biol.* **135**, 1249–1260.

Berthiaume, E. P., Mediana, C., and Swanson, J. A. (1995). Molecular size-fractionation during endocytosis in macrophages. *J. Cell Biol.* **129**, 989–998.

Maniak, M. (2001). Macropinocytosis. *In* "*Endocytosis*" (M. Marsh, ed.), pp. 78–93. Oxford Univ. Press, Oxford.

Nobes, C., and Marsh, M. (2000). Dendritic cells: New roles for Cdc42 and Rac in antigen uptake? *Curr. Biol.* **10**, R739–R741.

Norbury, C. C., Hewlett, L. J., Prescott, A. R., Shastri, N., and Watts, C. (1995). Class I MHC presentation of exogenous soluble antigen via macropinocytosis in bone marrow macrophages. *Immunity* **3**, 783–791.

Racoosin, E. L., and Swanson J. A. (1993). Macropinosome maturation and fusion with tubular lysosomes in macrophages. *J. Cell Biol.* **121**, 1011–1020.

Racoosin, E. L., and Swanson, J. A. (1994). Labeling of endocytic vesicles using fluorescent probes for fluid-phase endocytosis. *In* "*Cell Biology: A Laboratory Handbook*" (J. E. Celis, ed.), pp. 375–380. Academic Press, San Diego.

Sallusto, F., Cella, M., Danieli, C., and Lanzavecchia, A. (1995). Dendritic cells use macropinocytosis and the mannose receptor to concentrate macromolecules in the major histocompatibility complex class II compartment: Downregulation by cytokines and bacterial products. *J. Exp. Med.* **182**, 389–400.

Swanson, J. A. (1989a). Phorbol esters stimulate macropinocytosis and solute flow through macrophages. *J. Cell Sci.* **94**, 135–142.

Swanson, J. A. (1989b). Fluorescent labeling of endocytic compartments. *In* "*Methods in Cell Biology*" (Y.-l. Wang and D. L. Taylor, eds.), Vol. 29, pp. 137–151. Academic Press, New York.

Swanson, J. A., and Watts, C. (1995). Macropinocytosis. *Trends Cell Biol.* **5**, 424–428.

For the online version

Video 1. Time-lapse video microscopy of a living macrophage labeled with Lucifer yellow. Cells were incubated with 1 mg/ml Lucifer yellow for 30 min, rinsed in RB, and observed with an inverted fluorescence microscope under the appropriate light exposure controlled by the light path shutter and ND filters. Images were acquired at 5-s intervals for 10 min and assembled into a QuickTime movie. Lucifer yellow labels macropinosomes, micropinosomes, and tubular lysosomes. A phase-contrast image was superimposed on the initial frame.

Video 2. Time-lapse video microscopy of a living macrophage exposed to intense excitation light without ND filters. Cells were labeled and observed similarly to Video 1, but ND filters were removed from the excitation light path. It is notable that an intense excitation induces rapid photobleaching and photodamage on Lucifer yellow-labeled organelles.

SECTION

3

Protein Purification

CHAPTER

22

Preparation of Tubulin from Porcine Brain

Anthony J. Ashford and Anthony A. Hyman

INTRODUCTORY COMMENT

In the previous edition to this series (2nd Ed., Vol. 2, pp. 205–212, 1998), we described a method to purify tubulin from bovine brains. Since that time there have been concerns in many countries over the risks of handling bovine nervous tissue relating to bovine spongioform encephalitis and its possible connection with human varient Creuzfeldt–Jakob disease. As a result, abattoirs have been reluctant or have even refused to handle these tissues. Consequently we have changed the species source from which we make the tubulin and have amended the title accordingly. However the protocols described are applicable in their entirety to the bovine source. The bovine and porcine equivalents are indicated in the protocol.

I. INTRODUCTION

Recent research on microtubules has given much insight into many fundamental problems in cell biology, such as cell structure and polarity, vesicular transport, cell division, and chromosomal segregation.

Furthermore, the ability to prepare polarity marked microtubules (Howard and Hyman, (1993) has contributed much to our understanding in the behavior of microtubule motors.

Microtubules are polymers of the heterodimeric protein tubulin. Because these heterodimers have the same orientation in the microtubule lattice and the dimers themselves are not symmetric, it follows that the microtubule itself must have an inherent polarity. Polymerization can take place from either end of the growing microtubule, although at different rates, having a slow growing (–) and more rapidly growing (+) end. The tubulin heterodimer has binding sites for two GTP molecules in its unpolymerized state, only one of which (that GTP that is bound to the E site of the tubulin β subunit) is hydrolyzable. While it is not within the scope of this article to examine all the properties of microtubules and tubulin, some of these are of direct relevance to their isolation. The current model first proposed by Mitchison and Kirschner (1984a) and developed further since then (reviewed by Hyman and Karsenti [1996]) suggests that GTP-unpolymerized tubulin is incorporated at the + growing end of the microtubule and that after a delay, during which time more GTP-bound tubulin is bound at the growing end, the GTP on the β subunit is then hydrolysed to GDP, possibly destabilizing the microtubule lattice. Because GTP-bound tubulin dissociates from the microtubules slowly and the dissociation rate of exposed bound GDP tubulin is two or three orders of magnitude higher, it follows that the presence of a so-called GTP–tubulin "cap" will protect the polymerized microtubule from depolymerization. Alternatively, the GTP "cap" structure may be inherently more stable, effectively preventing the GDP (destabilized) polymerized tubulin from dissociating from the lattice. Thus the "GTP cap" hypothesis states that if the microtubule loses this GTP "cap" structure because of slow growth (e.g., due to lack of free tubulin, cold temperature, presence of Ca^{2+}), the GDP–tubulin dissociates from the lattice. Microtubules growing more slowly are more likely to have GDP–tubulin exposed and thus dissociate rapidly, causing microtubule shrinkage.

The preparation of tubulin described here utilizes these phenomena by a series of alternate depolymerizing and polymerizing steps (see Fig. 1) to obtain

Copyright 2006, Elsevier Science (USA).
All rights reserved.

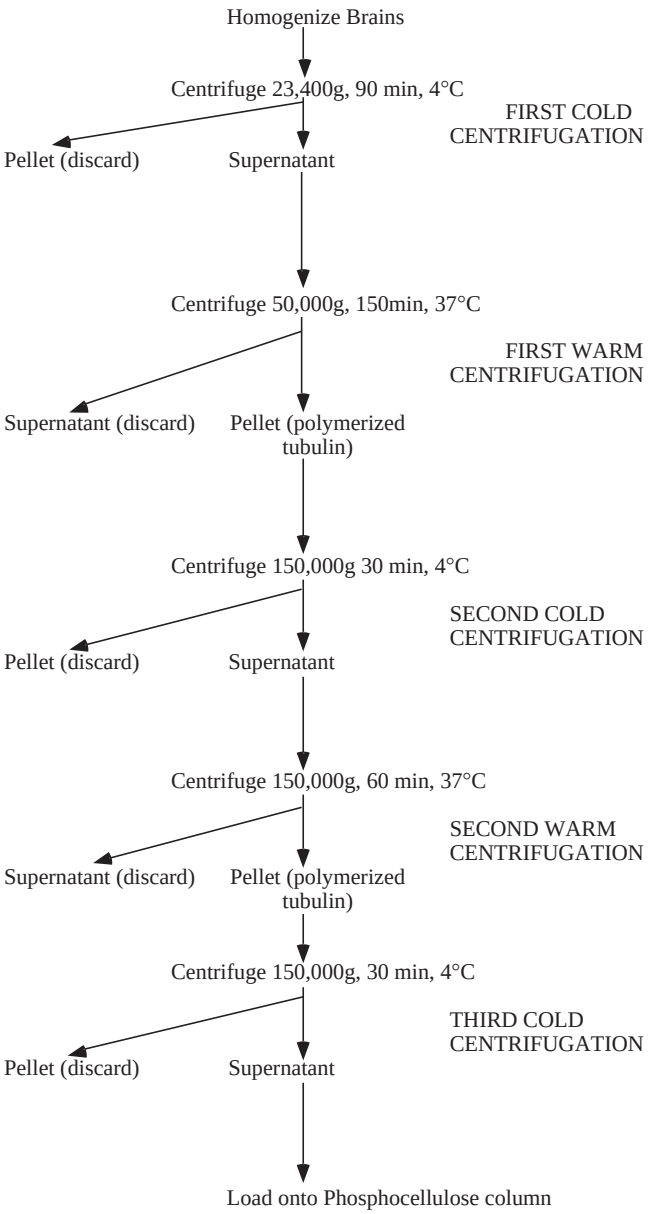

FIGURE 1 Summary of tubulin preparation.

tubulin and microtubule-associated proteins (MAPs), followed by ion-exchange chromatography to separate the tubulin from MAPs. This protocol is based on that originally described by Shelanski *et al.* (1973) and modified by Weingarten *et al.* (1974) and subsequently by Mitchison and Kirschner (1984b). Tubulin can be modified further for other uses (Hyman *et al.*, 1991).

This article describes how to make pure tubulin with emphasis on large-scale (gram quantities) purifications. This, as will be made clear in later sections, is quite an exercise in both organization and logistics. However, the method can easily be scaled downwards if large amounts of tubulin are not required.

Because the principle of tubulin preparation relies on successive rounds of polymerisation and depolymerisation steps based on temperature shifts, delays and not having the right equipment at the right temperature will reduce the yield drastically. Consequently, after one centrifuge run is completed, it is good practice to reset the temperature for the next spin and switch on the vacuum, checking the centrifuge regularly for faults. This also applies to the rotors, and it is a good idea to have some large water baths set at 37°C and some ice troughs in which to either raise or lower the rotor temperature accordingly. For the polymerization of tubulin, a good supply of hot running water is essential, as slow polymerization will reduce the overall yield.

II. MATERIALS AND INSTRUMENTATION

The protocol, as stated earlier, is suitable for preparation of large (2 to 3 gram) quantities of pure tubulin. To obtain this quantity, it will be necessary to obtain approximately 30 porcine (or 12 bovine) brains. It follows from this that the volumes involved in processing this number of brains, at least in the initial stages of preparation, will be quite large and many centrifuges will be necessary.

A. Centrifuges, Rotors, and Bottles

It is desirable, although not absolutely necessary, to have a centrifuge capable of spinning, at low speed, up to 10 litres of homogenate.

At least six Sorval RC5s, evolutions, or equivalent centrifuge series with SuperLite SLA 1500 are needed together with 36 GSA rotor bottles (250-ml capacity) and their adaptors. The Beckman equivalent to this is the Beckman Avanti using the JLA-16.250 rotor.

Four ultracentrifuges with three Beckman type 19 rotors and 24 corresponding bottles are needed along with four Beckman type 45Ti rotors and 24 (70-ml capacity) polycarbonate bottles.

As can be seen from this list, the rotors required are quite large and heavy and it is therefore important to check the vacuum and refrigeration efficiency of all the centrifuges beforehand using these rotors. Regarding the rotors themselves, these should be inspected beforehand, and any seals and "O" rings should be checked for signs of perishing, replacing where necessary. It is also important that these "O" rings are greased lightly with vacuum grease and that the screw threads for the rotor lids are smeared lightly with

Beckman "Spinkote" to ensure that the samples are sealed and that the vacuum is maintained during the run. Finally, the centrifuge rotors should be checked for the condition of the overspeed decals to prevent premature termination of the run. This is particularly true of the Beckman type 19 rotors, which seem especially sensitive on this point.

The centrifuge bottles too should be inspected for cracks and warping (particularly true of the polycarbonate Beckman type 45 bottles), and the lids and caps should be checked for condition and integrity of the "O" ring.

B. Other Equipment

A tissue blender, such as that made by Waring, along with a 4.5-litre capacity homogenizing beaker and a (motor-driven) continuous flow homogenizer, such as the Yamato LH-22 model for resuspending the tubulin pellets (or a very large Dounce hand homogenizer), as well as a 1-Litre capacity phosphocellulose (PC) column, are needed. Details of how to prepare such a column are described in detail later.

C. Chemicals

All chemicals should be of analytical grade and can be obtained from a variety of suppliers. Chemicals for the following solutions are obtained from the following suppliers.

MES (M-5057), PIPES (P-6757), EGTA (E-4378), $MgCl_2$ (104-20), GTP (G-8877), ATP (A-7699), and β-mercaptoethanol (M-6250) are from Sigma-Aldrich.

EDTA (1.08418.1000), anhydrous glycerol (1.04093. 2500), NaCl (1.06404.1000), NaOH (1.06498.1000), HCl (1.00319.2500), KH_2PO_4 (4873.1000), and K_2HPO_4 (5099. 1000) are from Merck.

III. PROCEDURES

A. Preparation of Tubulin

The buffer systems of choice for the preparation of tubulin are 2-[*N*-MES for the blending buffer (BB) and PIPES for the remainder. When making up K.PIPES buffer solutions, it is first necessary to raise the pH of the solution to about pH 6.0 using KOH in order to get the PIPES to go into solution. This initial pH adjustment must be done *without the use of a pH meter* (i.e., using pH indicator paper), as any undissolved PIPES can damage the electrode.

Approximately 6 litres of BB is needed. Blending buffer is 0.1 M MES, pH 6.5, 0.1 m*M* EDTA, 2 m*M* EGTA, and 0.5 $MgCl_2$. For 1 litre, use 21.7 g MES, 4 ml 0.5 *M* EDTA stock solution, 0.1 ml 0.5 *M* EGTA stock solution, and 0.5 ml 1 *M* $MgCl_2$ stock solution.

About six litres of polymerization buffer (PB) is needed for a large tubulin preparation; if preferred, it can be made as a 5× stock solution and then diluted with water at 4°C before use. Polymerization buffer is 0.1 *M* PIPES, pH 6.8, 0.5 m*M* $MgCl_2$, 2.0 m*M* EGTA, and 0.5 m*M* EDTA.

Approximately five litres of *Column buffer* (CB) is needed for such a preparation, which is made up as a 10× solution and diluted with water at 4°C prior to use. Column buffer is 50 m*M* PIPES, pH 6.8, 1 m*M* EGTA, and 0.2 m*M* $MgCl_2$. To make 1 litre of 10× column buffer, weigh out 151.2 g of PIPES, 3.8 g of EGTA, and 2 ms of a 1 *M* stock solution of magnesium chloride and add 45.6 g potassium hydroxide. This will adjust the pH to about pH 6.7 and further adjustments can be made using a 10 *M* solution of potassium hydroxide.

The BRB80 conversion buffer is added to the purified tubulin that has been eluted from the phosphocellulose column to convert the buffer from column buffer composition to BRB80 prior to storage of the tubulin. The BRB80 conversion buffer is added in a ratio of 1 part conversion buffer to 20 parts tubulin in column buffer.

To make up 150 mls of BRB80 conversion buffer combine 47.6 g PIPES, 4.2 ml $MgCl_2$ (1 *M*), and 1.25 ml EGTA (0.2 *M*). This should then be brought to pH 6.8 with potassium hydroxide. Having the correct pH is very important.

Nucleotides are made as stock solutions as 100 m*M* ATP and 200 m*M* GTP. It is important that the pH of these nucleotides does not become acidic, as hydrolysis will result. Consequently, they are made up in water and adjusted to pH 7.5 with sodium hydroxide. The ATP solution is made 200 m*M* with respect to $MgCl_2$. This is *not* the case with the GTP solution, as this will cause precipitation. These solutions should be stored at −80°C until needed.

Protein concentration determinations are made using the Bio-Rad version of the Bradford protein assay, reading the absorption at 595 nm using bovine serum albumin as a reference standard.

Steps

Note: All *g* forces quoted are R_{max} values.

Because brain tissue has a high density of microtubules in the dendrites and axons of its nerve cells, this is the tissue of choice for a tubulin preparation. Porcine brain is readily available from slaughterhouses. It is essential, however, to get the brains as

fresh as possible, as protein degradation will begin to take place soon after death. The brains should be warm when they are received and should be plunged immediately into a mixture of ice and saline solution for transport back to the laboratory. Do not use cold brains.

1. Preparation of Brain Tissue for the First Cold Spin

Cautionary note: As alluded to earlier, possible contact with pathogens associated with nervous tissue should be minimized by always handling the brains with gloves. Waste tissue should be disposed of by incineration.

At the laboratory cold room the brains should be stripped of brain stems, blood clots, and meninges (kitchen paper tissue is very good for this purpose). The brains are then weighed, transferred to the Waring blender, and cold BB containing 0.1% β-mercaptoethanol and 1 m*M* ATP, but without any protease inhibitors, is added in the ratio of 1 litre of buffer per kilogram of brain tissue. The brains are then homogenized twice for approximately 30 s each. Typically it can be expected to need approximately 5 litres of BB for 30 porcine (approximately 12 bovine) brains giving about 10 litres of total homogenate. If a large capacity rotor is available, this homogenate can be poured directly into the 1 litre centrifuge bottles and then centrifuged at 12,000 g for 15 min. Using this option has the advantage that any unhomogenized tissue and air (from the blending procedure) are removed rapidly. The homogenate is centrifuged further at 34,200 *g* for 60 min (SLA1500) at 4°C.

2. First Warm Centrifugation

1. Pool and pour the supernatants (approximately 5 litres for a 30 porcine brain preparation) into two 5-litre Ehrlenmeyer flasks.

2. Add a half volume of anhydrous glycerol that has been prewarmed to 37°C and then adjust the GTP, ATP, and $MgCl_2$ concentrations to 0.5, 1.5, and 3 m*M*, respectively. It is essential to bring the tubulin solution above 30°C as quickly as possible.

3. Warm the tubulin to 30°C under a continuously flowing hot tap while swirling the flask. At some point after the tubulin has reached 30°C it will be noticed that the solution becomes noticeably more viscous, indicating that polymerization is beginning to take place.

4. Incubate the tubulin for a further 60 min at 37°C in a water bath before recovery by centrifugation at 50,000 g for 150 min at 37°C in Beckman type 19 rotors.

3. Second Cold Centrifugation

1. Resuspend the pellets in approximately 700 ml of PB (with 0.1% β-mercaptoethanol) at 4°C using either a Dounce or a continuous flow homogenizer. At this point, determine the protein concentration of the resuspended pellet solution and lower the concentration to 25 mg/ml by the addition of cold PB.

2. Leave the solution on ice for 40 min to allow for complete depolymerization before centrifuging at 150,000 *g* for 30 min in Beckman type 45Ti rotors at 4°C.

4. Second Warm Centrifugation

1. Pool the supernatants from this centrifugation and adjust the concentrations of ATP, GTP, and $MgCl_2$ to 1, 0.5, and 4 m*M*, respectively.

2. As before, add a half volume of anhydrous glycerol prewarmed to 37°C and warm the entire mixture to 37°C. Allow the tubulin to polymerize at this temperature for a further 40 min prior to centrifugation at 150,000 *g* at 37°C for 1 h in Beckman type 45Ti rotors. If time is short, the polymerized tubulin pellets can be frozen in liquid nitrogen and stored at −80°C.

5. Third Cold Centrifugation

1. Collect and resuspend the polymerized tubulin pellets in a total volume of 200 ml of PB with 0.1% β-mercaptoethanol using either the continuous flow or the Dounce homogenizer.

2. Determine the protein concentration and dilute the solution with PB as necessary to a final concentration of 35 mg/ml.

3. Allow the tubulin to depolymerize on ice for a further 40 min and then centrifuge at 150,000 *g* for 30 min in the Beckman type 45Ti rotor.

4. The supernatant is now ready for loading onto the phosphocellulose column to separate the tubulin from microtubule-associated proteins.

6. Purification of Tubulin over a Phosphocellulose Column

1. Load the depolymerised tubulin onto a 1-litre-sized column (at 4°C) that has been equilibrated previously in CB. Tubulin should be loaded onto the column at a flow rate of approximately 1.5 ml/min. Once loaded, however, the flow rate can be increased to 6 ml/min or even faster if the phosphocellulose shows little sign of compressing, although some compression is inevitable.

2. The purified tubulin elutes in the flow through. Pool the protein peak and determine the protein concentration. The purified tubulin in CB can then be snap-frozen in liquid nitrogen or converted to tubulin in BRB80 using BRB80 conversion buffer prior to freez-

ing and subsequent storage at –80°C. When run on a 12% polyacrylamide gel, the purified tubulin, when stained with Coomassie, should appear as a single band free of any trace of contaminating proteins. The MAPs are retained on the column and these proteins can be eluted using CB containing 1 *M* NaCl.

B. Cycling Tubulin

It is inevitable that some tubulin will become inactivated or denatured during passage through the phosphocellulose column, as tubulin is an unstable entity. It is therefore recommended to "cycle" the tubulin after it passes through the column. To cycle tubulin means that it is polymerised at 37°C, reisolated by centrifugation through a glycerol cushion, and depolymerised at 4°C prior to freezing. This can be performed either immediately after elution from the column or after it has been stored at –80°C in CB. In both cases the tubulin buffer should be converted to BRB80 as described earlier. There are several advantages to cycling the tubulin: it enriches for active tubulin dimers, removes free nucleotides, removes denatured tubulin and other impurities, and concentrates the tubulin to approximately 10–20 mg/ml (cf. 5–10 mg/ml as it comes through the column.). The resulting cycled tubulin is suitable for use in *in vitro* assays such as video microscopy (e.g., Andersen *et al*., 1994). It is also recommended to use cycled tubulin for biochemical studies (e.g., purification of MAPs) because it is much easier to control the amount of microtubules formed when this highly active tubulin is used compared to that obtained directly from the phosphocellulose column.

Steps

To obtain a large stock of identical cycled tubulin, it is recommended to cycle approximately 30 ml of tubulin obtained directly from the phosphocellulose column.

1. Prewarm the rotor (a Beckman Ti50, TLA100, or MLA 80 rotor is suitable) in a water bath at 37°C. Fill the rotor tubes to half their volume with a glycerol cushion consisting of 60% glycerol in BRB80 (no GTP), place these in the rotor, and allow them to equilibrate to 37°C. While this is happening, proceed with polymerisation of the tubulin.
2. Thaw the tubulin rapidly using a water bath set at 37°C until the tube is half full of ice and then continue to thaw the remainder on ice. Adjust the solutes to glycerol PB using anhydrous (100%) glycerol. Allow polymerisation to occur for 40 min at 37°C.
3. Layer the polymerised tubulin onto the prewarmed cushions using tips with large openings to avoid depolymerising the microtubules. Centrifuge at 226,240 *g* (50,000 rpm in the Beckman Ti50 rotor) for 60 min or, alternatively, at 70,000 rpm for 30 min in the TLA100 rotor at 37°C.
4. Aspirate away the supernatant above the cushion. Rinse the cushion interface twice with water. Aspirate away the cushion. Resuspend the pellet in 0.25× BRB80 + 0.1% β-mercaptoethanol on ice using an homogeniser to depolymerise the microtubules. The volume of buffer used for the resuspension is chosen so that the final tubulin concentration is between 10 and 20 mg/ml (based on the assumption that approximately half the tubulin from the phosphocellulose column will polymerise). Incubate on ice for 15 min and then add 5× BRB80 to adjust the buffer to 1× BRB80. (*Note*: The volume of 5× BRB80 to add is 3/16ths of the volume of 0.25× BRB80–tubulin.)
5. Sediment the undepolymerised microtubules by centrifuging the sample at 213,483 *g* (70,000 rpm in the Beckman TLA100.2 rotor) for 15 min at 4°C.
6. Aliquots (10–200 µl) of the concentrated tubulin can be made, which should then be snap frozen in liquid nitrogen. The tubulin can then be stored either in liquid nitrogen (indefinitely) or at –80°C (for at least 12 months).

C. Preparation of Phosphocellulose Column

For large-scale preparations of tubulin (finally giving 1 g or more of purified tubulin) a phosphocellulose column of approximately 1 litre volume will be necessary. For successful preparation of PC, it has to be equilibrated *for short periods* first in base and then in acid, interspersed with water washes. This is normally achieved by suspension of the PC in either the acid or the base solution and then rapid filtration over a sintered glass funnel where the PC can be washed with large volumes of water. Large volumes of PC are, however, quite cumbersome to handle and the importance of setting up an efficient filtration system *before* commencing the PC preparation cannot be overemphasised. With volumes as large as 1 litre it may be unwise to rely on running water aspirators, as the vacuum produced may be insufficient (but for small volumes of PC these may be suitable). It is better to use a membrane-type pump and if, possible, to connect this to a wide, sintered glass funnel over which Whatmann 3 MM filter paper has been placed. Alternatively, and we have used this quite successfully, use some nylon or polypropylene meshing (available from SpectraMesh), as this allows rapid filtration rates with almost no risk of tear as there is when using Whatmann filter paper.

When considering what volume of phosphocellulose is needed, our laboratory uses 200 ml phosphocellulose to obtain 300–600 mg of purified tubulin. When equilibrated in buffer, 1 g of PC powder will give between 5 and 6 ml of PC column matrix (depending on the salt concentration), but do allow for some loss due to the removal of fines when calculating the amount of PC to prepare.

Phosphocellulose is obtained from Whatmann Scientific Ltd. and the column and adaptors can be obtained from Kontes, but any column with similar dimensions ($10 \times 30 \times 4.8$ cm) should be suitable.

Steps

Note: All stages should be performed at 4°C.

1. Having determined the amount of phosphocellulose that is needed using the information just given, slowly hydrate the dry powder by washing twice in 95% ethanol, once in 50% ethanol, and finally once in pure water.

2. Resuspend the hydrated phosphocellulose in 25 volumes (liquid volume per original dry weight of phosphocellulose) of 0.5 *M* NaOH and stir *gently* (stirring too fast produces fines, which will result in slow column flow rates if not removed later) for 5 min. Filter the phosphocellulose rapidly to remove the NaOH solution and continue to rinse with water until the pH of the washings is lower than 10 (usually at least three times the volume of the NaOH solution used).

3. As soon as the pH is sufficiently low, resuspend the phosphocellulose in 25 volumes of 0.5 *M* HCl (i.e., the same volume as the NaOH solution as used earlier) and again stir gently for 5 min and filter quickly. Continue to wash with water until no longer acid—usually around 10 times the volume of the HCl solution used.

4. If the column is not to be poured at this stage, the phosphocellulose should be resuspended and stirred for 5 min in a 2 *M* solution of potassium phosphate, pH 7.0. The PC can then be resuspended and stored in a solution of 0.5 *M* potassium phosphate, pH 7.0, containing 20 m*M* sodium azide as preservative. When the phosphocellulose is removed from storage, it should be resuspended and washed in at least 3 volumes of water.

5. At this stage, whether the column material was stored or not, the phosphocellulose should be resuspended in at least 3 volumes of water and transferred to a large measuring cylinder. The phosphocellulose should be stirred and then allowed to settle naturally. After the bulk of the phoshocellulose has settled, it will be noticed that there is a cloudy layer just above it. These are the fines and should be removed by aspiration to ensure fast column flow rates. This cycle of resuspension, stirring, and aspiration of the fines should be repeated until no more fines are visible.

6. Resuspend the phosphocellulose in column buffer solution and then degas for 30 min prior to pouring the column.

7. After use, wash the phosphocellulose column extensively and replace the buffer with a 50 m*M* potassium phosphate buffer containing 20 m*M* sodium azide.

References

Andersen, S., Buendia, B., Domínguez, J., Sawyer, A., and Karsenti, E. (1994). Effect on microtubule dynamics of XMAP230, a microtubule-associated protein present in *Xenopus laevis* eggs and dividing cells. *J. Cell Biol.* **127**, 1289–1299.

Howard, J., and Hyman, A. (1993). Preparation of marked microtubules for the assay of microtubule-based motors by fluorescence microscopy. *Methods Cell Biol.* **39**, 105–113.

Hyman, A., Drechsel, D., Kellogg, D., Salser, S., Sawin, K., Steffen, P., Wordeman, L., and Mitchison, T. (1991). Preparation of modified tubulins. *Methods Enzymol.* **196**, 478–485.

Hyman, A., and Karsenti, E. (1996). Morphogenetic properties of microtubules and mitotic spindle assembly. *Cell* **84**, 401–410.

Mitchison, T., and Kirschner, M. (1984a). Dynamic instability of microtubule growth. *Nature* **312**, 237–242.

Mitchison, T., and Kirschner, M. (1984b). Microtubule assembly nucleated by isolated centrosomes. *Nature* **312**, 232–237.

Shelanski, M., Gaskin, F., and Cantor, C. (1973). Microtubule assembly in the absence of added nucleotides. *Proc. Natl. Acad. Sci. USA* **70**(3), 765–768.

Weingarten, M., Suter, M., Littman, D., and Kirschner, M. (1974). Properties of the depolymerisation products of microtubules from mammalian brain. *Biochemistry* **13**, 5529–5537.

CHAPTER

23

Purification of Smooth Muscle Actin

Gerald Burgstaller and Mario Gimona

I. INTRODUCTION

Actin purified from mammalian or avian skeletal muscle is a readily available probe to study the potential interaction of a putative actin-binding protein or recombinant fragment *in vitro*. Yet, the use of a specific actin isotype for the determination of binding affinities or the tissue-specific regulatory potential of actin-associated proteins is often required.

Purification of actin from smooth muscle is much less straightforward than from skeletal muscle tissue. The major difficulty resides in the large number of actin-binding proteins, which populate the actin filaments in this tissue type. These proteins interfere with polymerization even at levels undetectable on conventional Coomassie blue-stained SDS–PAGE gels. A primary source of contamination is the copurification of tropomyosin. Moreover, because the total amount of actin present in smooth muscle is reduced compared to that in skeletal muscle, the yield is lower. However, despite the aforementioned potential pitfalls, smooth muscle actin can be purified in large quantities and high purity by the use of larger extraction volumes in the initial steps.

This article describes the method used for purifying polymerization-competent actin from mammalian or avian visceral smooth muscle (porcine stomach or turkey gizzard) and suggests some useful methods to test the functionality of the preparation prior to its use in analytical assays. The purification scheme follows the original modification of Sobieszek and Bremel (1975). The modified extraction buffer (containing 10 m*M* imidazole, 10 m*M* bis–Tris, 40 m*M* KCl, 2 m*M* $MgCl_2$, 1 m*M* cysteine, and 5 m*M* EGTA at pH 6.5) introduced by Fürst (1986) significantly improved the solubilization and removal of actin-binding/modulating proteins.

II. MATERIALS

Chemicals

ATP (Sigma, M_r 551.10, Cat. No. A-3377); bis–Tris (Fluka, M_r 209.24, Cat. No. 14880); cysteine (Sigma, M_r 175.60, Cat. No. C-7880); $CaCl_2$ (Merck, M_r 147.02, Cat. No. 2382); DTE (Serva, M_r 154.30, Cat. No. 20697); EGTA (Sigma, M_r 380.40, Cat. No. E-3889); imidazole (Merck, M_r 68.08, Cat. No. 1.04716); KCl (Merck, M_r 74.56, Cat. No. 1.04936); $MgCl_2$ (Merck, M_r 203.30, Cat. No. 5833); NaCl (Merck, M_r 58.40, Cat. No. 1.06404); sucrose (Fluka, M_r 342.39, Cat. No. 84–100); Tris (ICN, M_r 121.14, Cat. No. 819 623); and ammonium sulphate (Fluka, M_r 132.14, Cat. No. 09982)

Gel Filtration Media

Sephadex G-150 or Sephacryl S100HR (*Amersham Biosciences*)

III. SOLUTIONS

1. *G-actin buffer*: 2 m*M* Tris–HCl, pH 8.0, 0.1 m*M* $CaCl_2$, 0.2 m*M* ATP, and 0.1 m*M* DTE
2. *F-actin buffer*: 2 m*M* Tris–HCl, pH 7.4, 150 m*M* KCl, 2 m*M* $MgCl_2$, and 2 m*M* EGTA
3. *10x polymerization stock*: 1.5 *M* KCl, 20 m*M* $MgCl_2$, and 20 m*M* EGTA

Copyright 2006, Elsevier Science (USA).
All rights reserved.

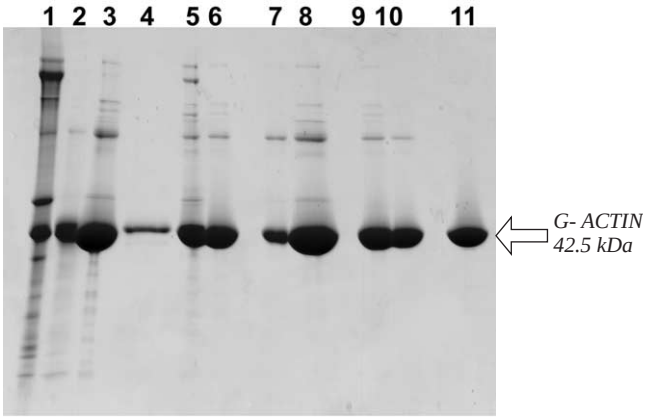

FIGURE 1 Commassie blue-stained 8–23% gradient SDS–PAGE gel showing the individual steps of the purification procedure. *Lane 1*, acetone powder extract; *lane 2*, supernatant after centrifugation; *lane 3*, 25% ammonium sulphate pellet; *lane 4*, supernatant after 25% ammonium sulphate; *lane 5*, precipitate after dialysis against G-actin buffer; *lane 6*, G-actin after dialysis and centrifugation; *lane 7*, supernatant after polymerization; *lane 8*, polymerized F-actin; *lane 9*, pellet after 48 h of dialysis against G-actin buffer; *lane 10*, G-actin after dialysis, applied to column; and *lane 11*, peak fraction from Sephacryl S-100 HR column (pure smooth muscle actin).

IV. PROCEDURE

The most convenient source of actin for relatively large yields is the powder remaining after the extensive drying of muscle homogenates in acetone. For this procedure, prepare the acetone powder from chicken gizzard smooth muscle according to Strzelecka-Golaszewska *et al*. (1980).

Starting with 15 g of dry acetone powder, the extraction in a final volume of 1.3 liters of G-actin buffer is let to proceed for 20–25 min at 4°C under constant agitation (using a magnetic stir bar). Centrifuge the resulting extract at 15,000 *g* for 60 min (*Sorvall GS-A rotor or equivalent*).

From the supernatant, precipitate actin by the slow addition of solid ammonium sulphate to reach 25% saturation. Let the precipitation proceed for 90 minutes at 4°C. Collect the precipitate by centrifugation at 15,000 *g* for 30 min (*Sorvall GS-A rotor or equivalent*).

Resuspend the pellet in about 50 ml G-actin buffer and dialyze against 2 liters of G-actin buffer overnight with two to three changes of buffer. Centrifuge the dialyzed actin solution to remove polymerized or aggregated actin at 32,000 *g* for 60 min (*Sorvall SS-34 rotor or equivalent*).

From this clarified solution, polymerize F-actin by the addition of 150 m*M* KCl, 2 m*M* $MgCl_2$, and 2 m*M* EGTA (final concentrations) by adding 1/10 volume of 10× polymerization solution. Allow polymerization to proceed for 90 min at 25°C.

Separate polymerized F-actin from "*dead*" (non-polymerizing) actin by centrifugating at 100,000 *g* for 30 min. Resuspend the pellets in 10–20 ml G-actin buffer and homogenize in a glass–glass homogenizer on ice.

Dialyze against 2 liters of G-actin buffer for 48 h with four to six changes of dialysis solution to thoroughly depolymerize the F-actin. Remove precipitated or polymerized material by centrifugation at 32,000 *g* as described earlier.

Apply the clarified supernatant onto a Sephadex G-150 or Sephacryl S-100 HR column, equilibrated in G-actin buffer, to remove the remaining, contaminating G-actin-binding proteins. Fractions should be analyzed by SDS–PAGE before storage.

Measure the final concentration of the G-actin solution using the absorption coefficient $A^{1\%}/_{290}$ of 6.5. Aliquots can be stored at –70°C after adding 2 mg sucrose/mg of G-actin from a 600-mg/ml stock solution.

V. TESTS

There are several possibilities to test the functionality of the actin solution before using it in *in vitro* assays.

A. General Polymerization

Polymerize the G-actin solution as described earlier (by adding 1/10 volume of the *10× polymerization stock solution*) and centrifuge the polymerized actin at 100,000 *g* for 30 min. Analyze the supernatant and pellet on a Coomassie blue-stained SDS–PAGE gel. The supernatant should essentially be devoid of actin, indicating 100% polymerization competence of the G-actin solution.

B. Cosedimentation Assays

Polymerize the G-actin solution as described earlier, but in the presence of actin-binding proteins such as α-actinin and/or tropomyosin, and analyze supernatants and pellets by SDS–PAGE. The presence of the actin-binding protein in the pellet indicates a "*functional surface*" and intact binding sites on the actin filament.

VI. COMMENTS

We found that dry acetone powder can be stored for at least 20 years at –20°C without a significant loss of quality of the purified actin. It thus may pay to stock up on acetone powder.

Initial extraction beyond the recommended 25 min results in the increased extraction of tropomyosin, which is difficult to remove at later stages. Accepting a lower yield is rewarded with higher purity!

The two tests described earlier are also recommended to evaluate the quality and functionality of fluorescently labeled actin.

The choice of buffer for the assays appears critical. F-actin reacts with structural alterations to different ionic strengths and the presence or absence of divalent or monovalent cations. The illuminating work by the Egelman group is a rewarding read.

References

Belmont, L. D., Orlova, A., Drubin, D. G., and Egelman, E. H. (1999). A change in actin conformation associated with filament instability after Pi release. *Proc. Natl. Acad. Sci. USA.* **96**, 29–34.

Fürst, D. O. (1986). Ph.D. Thesis, University of Salzburg.

Galkin, V. E., Orlova, A., Lukoyanova, N., Wriggers, W., and Egelman, E. H. (2001). Actin depolymerizing factor stabilizes an existing state of F-actin and can change the tilt of F-actin subunits. *J. Cell Biol.* **153**, 75–86.

Galkin, V. E., Orlova, A., VanLoock, M. S., Rybakova, I. N., Ervasti, J. M., and Egelman, E. H. (2002). The utrophin actin-binding domain binds F-actin in two different modes: Implications for the spectrin superfamily of proteins. *J. Cell Biol.* **157**, 243–251.

Orlova, A., and Egelman, E. H. (1993). A conformational change in the actin subunit can change the flexibility of the actin filament. *J. Mol. Biol.* **232**, 334–341.

Sobieszek, A., and Bremel, R. D. (1975). Preparation and properties of vertebrate smooth-muscle myofibrils and actomyosin. *Eur. J. Biochem.* **55**, 49–60.

Strzelecka-Golaszeska, H., Prochniewicz, E., Nowakl, E., Zmorsynski, S., and Drabikowski, W. (1980). Chicken gizzard actin: Polymerization and stability. *Eur. J. Biochem.* **104**, 41.

CHAPTER

24

Purification of Nonmuscle Actin

Herwig Schüler, Roger Karlsson, and Uno Lindberg

I. INTRODUCTION

In the past decade or so, a number of new actin regulatory proteins and their functions in the motility of nonmuscle cells have been unveiled. We now understand in some detail how extracellular stimuli are transmitted to the microfilament system *via* activation of the phosphatidylinositol cycle, rho-family of GTPases, causing polymerization of actin through the recruitment of WASp, WAVE, ARP2/3, or formin proteins. The polymerization of actin requires constant supply of actin kept in an unpolymerized form by proteins such as thymosin, cofilin, and profilin. Filament-capping, cross-linking, destabilising, and sequestering proteins cooperate with monomeric (G)-actin to contribute to the dynamics of the system. Thus, complex machineries for the controlled polymerisation of actin are now being revealed (see Ridley *et al*., 2003; Innocenti *et al*., 2004).

Isoforms of actin differ in their affinities for their ligands, their functioning, and subcellular locations. Therefore, to understand the function of actin in nonmuscle cells, it is important to work with nonmuscle actin when studying actin-binding proteins (ABPs) from nonmuscle tissues. Unfortunately, this is often neglected because of the ready access to α-actin from rabbit skeletal muscle (Pardee and Spudich, 1982). A further complication is the covalent modification introduced in α-actin during the commonly used purification protocol involving acetone extraction of muscle tissue (Selden *et al*., 2000). This modification leads to the formation of stable dimers, explaining fast polymerisation kinetics and other properties thought to be characteristic for α-actin. However, i- and -actin are prepared easily from various nonmuscle tissues using the method described in this article.

Here, the isolation of β- and γ-actin isoforms from profilin:actin obtained by affinity chromatography on poly-(L-proline) Sepharose is described. It also describes the purification of yeast and recombinant β-actin using a yeast expression system and DNase I affinity chromatography, enabling the production of large amounts of mutant actins.

II. MATERIALS AND INSTRUMENTATION

All chemicals (reagent grade) are from ICN or Sigma. Hydroxyl apatite is hypatite C of *even* lot number from Clarkson Chemical Co. (Williamsport, PA). This is the only hydroxyl apatite material we have used successfully to separate actin isoforms. DNase I is from ICN (Cat. No. 100579) and poly-(L-proline) is from Sigma (Cat. No. P-2129). CNBr-activated Sepharose 4B is from Amersham Biosciences (Cat. No. 17-0430). Empty columns are XK-16/20, XK-26/20, and XK-50/20 from Amersham Biosciences. All other chromatography equipments and matrices are from Amersham Biosciences.

Yeast nitrogen base without amino acids is from Difco (Cat. No. 291940), adenine sulfate is from ICN (Cat. No. 100195), and the casamino acid vitamin assay is from Difco (Cat. No. 228820). All other media components are from Difco. Lysis of yeast cells is achieved with a purpose-designed bead mill (Innomed Konsult) using glass beads 0.25–0.5 mm in diameter (Mahlkörper MK2GX, Willy Bachofen). However, alternative procedures to break up yeast cells have been described

Copyright 2006, Elsevier Science (USA).
All rights reserved.

(Jazwinski, 1990). Low-speed centrifugations are carried out in a Beckman-Coulter Avanti J-20XP with polypropylene tubes (50 ml; Beckman Cat. No. 357007) in a Beckman JA-25.0 rotor. Large-volume centrifugations are performed with polycarbonate centrifuge bottles (500 ml; Beckman no. 335605) in a Beckman JLA-16.250 rotor. Preparative ultracentrifugations are done in a Beckman-Coulter L-series centrifuge with polycarbonate bottles (70 ml; Beckman No. 355622) in Rotor Beckman 45Ti.

III. PROCEDURES

A. Preparation of Profilin:Actin Complexes from Bovine Thymus or Spleen

This protocol is used for the purification of profilin in complex with a mixture of the cytoplasmic β- and γ-actin isoforms. The isolation procedure involves affinity binding to poly-(L-proline) and chromatography on hydroxyl apatite to separate actin isoforms, either alone or in complex with profilin (Segura and Lindberg, 1984; Lindberg, 1988). The yield of profilin:actin complex is approximately 400 mg/kg of tissue. The following section describes a preparation starting with 700 g of calf thymus. All buffer volumes and column sizes refer to that preparation size. If calf thymus cannot be obtained, calf spleen can be used instead. Actin isoform distribution is approximately 60% β-actin and 40% γ-actin in thymus, whereas spleen contains slightly more β-actin. Spleen is easier to handle, but contains more proteolytic enzymes, which are difficult to control.

1. Affinity Purification of Profilin:Actin Complexes

Solutions and Columns

1. *Homogenisation buffer (2 liters)*: 10 m*M* Tris–HCl, pH 7.6, 0.1 *M* KCl, 0.1 *M* glycine, 1% Triton X-100, and 0.5 m*M*, dithiothreitol (DTT)
2. *2× PLP buffer (3 liters)*: 20 m*M* Tris–HCl, pH 7.6, 0.2 *M* KCl, and 0.2 *M* glycine
3. *PLP elution buffer (500 ml)*: make immediately before use. Mix 250 ml of 2× PLP buffer with 150 ml of dimethyl sulfoxide (DMSO) and 100 ml distilled H_2O. Mixing DMSO with water is an exothermic reaction, thus the buffer needs to be cooled on ice before being applied to the column (no DTT).
4. *HA buffer (5 liters)*: 5 m*M* KPO_4, pH 7.6
5. *HB buffer (0.5 liter)*: 40 m*M* KPO_4 pH 7.6, 1.5 *M* glycine, and 0.5 m*M* DTT
6. *Saturated ammonium sulfate (4 liters)*: Add about 1600 g of $(NH_4)_2SO_4$ to 2 liters of water to make a saturated solution. Adjust to pH 7.6 with ammonia.
7. *Poly-L-proline (PLP) affinity matrix*: For the preparation size described here, mix 0.5 g of poly-(L-proline) to 30 g of CNBr-activated Sepharose 4B for 2 h at room temperature or overnight at 4°C according to the supplier's recommendations. Avoid extensive stirring, as this will have deleterious effects on the matrix. Monitor the coupling reaction photometrically at 234 nm in supernatants of small samples of the incubation mixture, removed at intervals. After each use, wash the matrix immediately with 1 liter of water, followed by 1 liter of 1% *N*-lauryl sarcosine, followed with 1 liter of water. Reequilibrate with PLP buffer containing 0.01% sodium azide. Stored at 4°C, this matrix should be good for 10–15 preparations and last for 1–2 years.
8. *Hydroxyl apatite column*: Degas 100 ml of settled hypatite-C in 500 ml buffer HA. Pack an XK-26/20 column with hydroxyl apatite at a flow rate of 10 ml/min. Attach a top adaptor, but allow some buffer to be present on top of the matrix and equilibrate the hydroxyl apatite column with 1 liter of buffer HA at a flow rate of 10 ml/min.

Note: Wear gloves and take extra care when working with DMSO. Do not use DTT in DMSO-containing solutions due to the formation of toxic dimethyl sulfide. All buffers should be freshly degassed when used. Add DTT only after degassing. All steps are carried out at 4°C, and all solutions should be at 4°C, unless stated otherwise. Note that Tris buffers are temperature sensitive.

Steps

1. Make 5 liters (1×) PLP buffer using the (2×) buffer stock. Degas all buffers.
2. Partially thaw 700 g thymus and remove fat and connective tissue. Cut the organ into small pieces and homogenise in a blender using approximately 2 volumes of homogenisation buffer.
3. Transfer the tissue extraxt to 500-ml polycarbonate bottles and centrifuge at 20,000 *g* (12,000 rpm with the JLA-16.250 rotor) for 30 min.
4. Filter the supernatant through glass wool, transfer to 70-ml polycarbonate bottles, and centrifuge at 100,000 *g* (30,000 rpm with the 45TI rotor) for 30 min.
5. Prepare the PLP column in a laminar flow hood: Pack an XK-50/20 column with the affinity matrix described in step 6 of the previous section and equilibrate it with PLP buffer at a flow rate of 5–10 ml/min.
6. Filter the supernatant from step 4 through glass wool and load it onto the PLP column.
7. After all the protein has been loaded, wash the matrix with PLP buffer until the color is removed from the matrix.

8. Elute bound proteins with ice-cold PLP elution buffer into a 500-ml measuring cylinder on ice. After this step the preparation already contains mainly profilin and profilin:actin complexes.

9. Dilute the PLP eluate with 2 volumes of buffer HA and load the solution onto the hydroxyl apatite column at a rate of 10 ml/min, monitoring the UV absorbance at 280 nm. The DMSO accounts for a small increase in absorbance at 280 nm. A tough layer may form on top of the matrix bed, restricting buffer flow. If necessary, stop the pump, disconnect the top adaptor, and resuspend the top centimeter of matrix bed by careful stirring with a glass pipette. Allow the matrix to resettle, replace the top adaptor, and continue loading.

10. After the protein has entered the column, wash with buffer HA to remove DMSO. Finish washing when a low baseline is reestablished. Carefully press the top adaptor onto the gel matrix.

2. *Separation of Profilin-Bound β- and γ-Actin Isoforms*

11. For separation of profilin:β-actin from profilin:γ-actin complexes, elute the hydroxyl apatite-bound material with a linear gradient of 5 m*M* potassium phosphate to 40 m*M* phosphate/1.5 *M* glycine. Employ a gradient mixer containing 350 ml HA in the start buffer compartment and 350 ml HB in the finishing buffer compartment. (If a different column dimension is used, the gradient length should be approximately 12 column volumes.) Elute the protein at a flow rate of 0.3 ml/min. Collect 10-min fractions.

12. Identify the fractions containing profilin:γ-actin and profilin:β-actin and pool the appropriate fractions (see Fig. 1). Continue as described in step 14.

3. *Elution of Total PA*

13. If isoform separation is not aspired, elute the hydroxyl apatite-adsorbed protein using HB buffer. The eluate consists of mixed actin isoforms in complex with profilin, plus a slight excess of profilin.

4. *Ammonium Sulfate Precipitation of PA*

14. Precipitate the protein by dialysis against 2 liters of saturated ammonium sulfate using dialysis tubing with a molecular mass cutoff under 12 kDa. The resulting protein is suitably stored as a precipitate in ammonium sulfate. Stored in this form at 4°C the PA is stable for 6–12 months. Estimate the concentration of protein by diluting 25–50 µl of the well-suspended solution into 1 ml of water and determine the absorbance at 280 and 310 nm (280–310 roughly corresponds to milligram per milliliter).

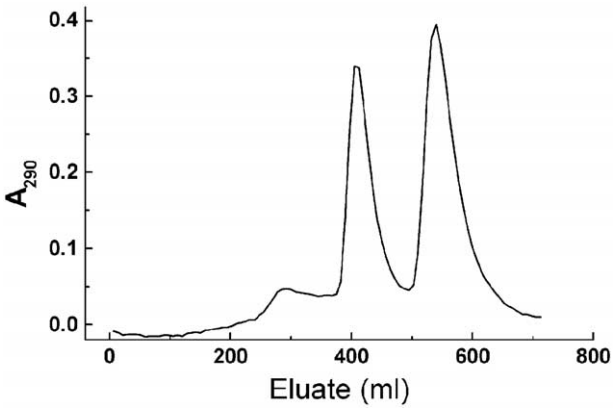

FIGURE 1 Separation of profilin, profilin:β-actin, and profilin:γ-actin using hydroxyl apatite chromatography (see Section III,A). The slightly more basic γ-actin:profilin complex elutes at lower ionic strength, followed by the β-actin:profilin complex at higher phosphate/glycine concentration. The small initial peak contains excess profilin.

The dialysis against saturated ammonium sulfate results in a reduction of the sample volume, ensuring effective protein precipitation. It is important to use enough saturated ammonium sulfate to avoid dilution of the salt below 40–50% saturation, which is the concentration precipitating the profilin:actin.

Pitfalls

For efficient extraction of the tissue, it may be helpful to pass the organ through a meat grinder before homogenisation in a blendor. The buffer over tissue ratio should not be lower than 2:1. Continue homogenisation until no chunks are visible, which should take about 2 to 3 min. Do not continue homogenisation over prolonged periods of time. Avoid excessive foaming.

5. *Isolation of Profilin and Actin from Precipitated P:A Complex*

Solutions and Columns

1. *G buffer (2 liters)*: 5 m*M* Tris–HCl, pH 7.6, 0.5 m*M* ATP, 0.1 m*M* $CaCl_2$, and 0.5 m*M* DTT
2. *Resuspension buffer (0.1 liter)*: G buffer, add DTT to 5 m*M*
3. *F buffer (0.1 liter)*: 5 m*M* Tris–HCl, pH 7.6, 0.5 m*M* ATP, 2 m*M* $MgCl_2$, 50 m*M* KCl, and 0.5 m*M* DTT
4. *2 M KPO_4 pH 7.6 (make 50 ml)*
5. *P buffer (1 liter)*: 10 m*M* KPO_4 pH 7.6, and 0.5 m*M* DTT
6. Prepare an XK-26/70 Sephacryl-300 gel filtration column equilibrated with G buffer
7. Prepare an XK-26/50 Sephadex G-25 gel filtration column equilibrated with P buffer

8. Prepare an XK-16/10 DEAE-Sephadex anion-exchange column equilibrated with P buffer

Steps

6. Purification of Actin

1. Collect 30–50 mg of ammonium sulfate-precipitated profilin:actin (either isoform; previous section, step 14) by centrifugation in a JLA-16.250 rotor at 10,000 rpm for 10 min. Discard the supernatant, leave the tubes upside down for a few minutes, and then wipe the inside of the tubes with Kleenex to remove residual ammonium sulfate.

2. Dissolve pellets in a small volume of resuspension buffer, stir, and add buffer until the solution becomes clear. Protein concentration should be 10–20 mg/ml. Centrifuge the solution again (as in step 1) to remove undissolved residues. Save the supernatant.

3. Measure the volume of the protein solution and add $MgCl_2$ to 5 m*M* and EGTA to 0.5 m*M*. Allow actin to polymerise at room temperature for 30 min.

4. Induce paracrystal formation by the addition of 1 volume of 2 *M* KPO_4. Mix carefully; avoid extensive pipetting. Leave for 1 h at room temperature or overnight at 4°C.

5. Collect the actin paracrystals by centrifugation at 10,000 *g* for 20 min at 15°C. The supernatant contains profilin and small amounts of remaining profilin:actin; save supernatant on ice for the profilin purification described later. The pellet contains actin paracrystals.

6. Resuspend the paracrystals in F buffer to dissolve the actin filaments. Mix by careful pipetting until all lumps have dissolved.

7. Sediment filaments by ultracentrifugation at 100,000 *g* for 3 h at 15°C. Remove the supernatant and add a small amount of G buffer to the F-actin pellet and leave it for 10–20 min. Seal the tip of a Pasteur pipette and use it to scrape the pellet off the walls of the tube. Carefully transfer the pieces of F-actin gel to a Dounce-type glass homogeniser and homogenise without introducing air. Measure the protein concentration using an extinction coefficient at $A_{290–310}$ of 0.63 ml/mg × cm. Dilute the F-actin to 5 mg/ml to get efficient depolymerisation.

8. Dialyze the actin sample against 10 volumes of G buffer in 12- to 14-kDa cutoff tubing with three buffer changes and homogenisations. Four to 6 h of dialysis is sufficient for every buffer change.

9. Subject the dialyzed actin to ultracentrifugation at 100,000 *g* for 3 h at 4°C in order to remove undissolved material. Load the supernatant onto the Sephacryl S-300 column. The sample volume should not exceed 4% of the column volume. Elute with G buffer at a flow rate of 30 ml/h. Collect 4- to 6-ml fractions. Measure protein concentration in the fractions and pool the protein peak. Analyze by SDS–PAGE, drop freeze (20 µl droplets) the actin in liquid N_2, and store in a nitrogen tank.

7. Purification of Profilin

10. Desalt the profilin solution from step 5 by gel filtration over Sephadex G-25. The volume of the protein solution may be up to approximately 30% of the column bed volume. Collect 2- to 3-ml fractions.

11. Determine protein concentrations across the chromatogram. Measure conductivity in the last fractions to make sure the solution will not be contaminated by salts and pool the protein-containing fractions.

12. Run the G-25 pool over the small DEAE-Sephadex column. Contaminating actin will stay on the ion exchanger. The column flow through contains pure profilin. Quick-freeze aliquots in liquid N_2 and store at –80°C.

Pitfalls

Before inducing paracrystal formation (step 4), check on the progress of the polymerisation reaction by rocking the tube carefully; the protein solution should have a gel-like consistence. If necessary, stimulate polymer formation by a few short bursts in an ultrasonicator.

Polymers of cytoplasmic actin are more cold sensitive than polymers of α-actin. Therefore, the ultracentrifugation step that aims at collecting actin filaments is carried out at 15°C.

B. Purification of Recombinant β-Actin from Baker's Yeast

This protocol is used for the large-scale preparation of recombinant actin expressed in *Saccharomyces cerevisiae* strain K923 using the temperature-inducible expression system described by Karlsson (1988). The heterologous actin cDNA is placed under the combined control of the PGK promoter and the negative transcription factor α2 and is introduced into strain K923 containing a temperature-sensitive mutation in the mating type switch (Walton and Yarranton, 1989; see also Sledziewski *et al*., 1988). This results in temperature-inducible expression of the heterologous actin. At 34°C, the cells are MATα and produce the α2 protein, which blocks transcription of the cloned cDNA. By lowering the temperature to 23°C, the cells switch mating type and cease to produce α2, leading to expression of the recombinant actin. Total actin is

isolated from yeast extracts by DNase I affinity chromatography (Zechel, 1980), and the recombinant isoform is separated from the endogenous actin by hydroxyl apatite chromatography (Karlsson, 1988). Ten liters of flask culture produces 120–150 g of yeast cells (the amount needed for a preparation as described later), yielding in the range of 10–15 mg each of yeast and recombinant actin. Usually, a fermentor culture in 10-liter fermentors is used, producing 700–800 g of yeast, which is material for five to six standard preparations of recombinant actin. The fermentation process has successfully been scaled to 50–100 liters. It should be noted that the yeast does not modify the N terminus of actin and does not methylate residue His73 (for discussion, see Nyman *et al*., 2001).

This method has been adapted for the production of human profilin (Aspenström *et al*., 1991) and should also work for other proteins.

1. Fermentor Culture of Yeast Expressing Recombinant Actin

Solutions

1. *S. cerevisiae strain K923*: HMLα, *mat::LEU2*$^+$, *hmr::TRP1*$^+$, *ura3*, *ade2*, *sir3ts*; MATa at 23°C, MATα at 34°C. This strain is grown on standard YPD medium (Sambrook and Russell, 2001) at 34°C.

2. *UYM media for transformed yeast strain K923*: Bottle 1: 8 g yeast nitrogen base without amino acids, 55 mg adenine sulfate, 55 mg L-Tyr; add H_2O to 580 ml. Bottle 2: 11 g casamino acid vitamin assay; add H_2O to 300 ml. Autoclave, allow to cool. Combine contents of bottles 1 and 2 and add 100 ml 20% glucose, 10 ml 0.5% L-Trp, and 10 ml 1% L-Leu. Grow the transformed strain on min-ura plates at 34°C.

Steps

1. Culture K923 transformed with pY-β-actin to single colonies on a min-ura plate at 34°C. Inoculate into 10 ml UYM and culture for 24 h under vigorous shaking at 34°C, transfer into 1 liter of UYM, and continue culturing for another 24 h at 34°C.

2. Transfer the inoculum into the fermenter, which has been prepared with 9 liters modified YPD [220 g peptone, 220 g yeast extract, 2.2 g adenine sulfate, 2.5 g glucose (0.25%), and PPG to avoid foaming]. Glucose is added continuously from a 50% stock, adjusting the concentration with the density of the culture (measured by OD_{640}) to keep it at approximately 0.5%. Approximately 12 h after inoculation, add 220 g of yeast extract in 500 ml water. Keep the culture at 34°C until OD_{640} is between 1 and 2 (this takes 6–8 h). At this stage, lower the temperature to 23°C to initiate the mating-type switch, which induces production of the recombinant protein. If larger scale (50–100 liters) fermenations are required, prepare the inoculum in the fermentor at a volume of 5–10 liters in UYM medium before transferring into a bigger fermentor with medium as described earlier.

3. Harvest the culture when OD_{640} no longer increases (ca. 24–26 h after inocculation). Rapidly cool the culture to below 10°C, start collecting it into ice-cold 1-liter centrifuge flasks, and centrifuge at 5000 rpm for 20 min (Sorvall RC-3 or equivalent). Collect all material into one or two flasks, centrifuge at 5000 rpm for 30 min, aliquot into suitable portions (150 g) for preparation of the protein, and store at –70°C.

2. Purification of Recombinant Actin from Yeast

Solutions and Columns

1. *2× G buffer (3 liters)*: 10 m*M* Tris–HCl, pH 7.6, 0.2 m*M* $CaCl_2$, and 1 m*M* ATP

2. *G buffer*: use 2.5 liters of the 2×G buffer to make 5 liters (5 m*M* Tris–HCl, pH 7.6, at 4°C, 0.1 m*M* $CaCl_2$, and 0.5 m*M* ATP)

3. *Na-acetate buffer (0.5 liter)*: 0.5 *M* sodium acetate, 0.5 m*M* ATP, pH 7.6, 0.1 m*M* $CaCl_2$, 10% glycerol, and 0.5 m*M* DTT

4. *DNase wash buffer Elu-I*: use the 2×G buffer to make 0.5 liter Elu-I: 5 m*M* Tris–HCl, pH 7.6, at 4°C, 0.1 m*M* $CaCl_2$, 0.5 m*M* ATP, 10% formamide, 10% glycerol, and 0.5 mM DTT

5. *DNase elution buffer Elu-II*: Use the 2×G buffer to make 0.3 liter Elu-II: 5 m*M* Tris–HCl, pH 7.6, at 4°C, 0.1 m*M* $CaCl_2$, 0.5 m*M* ATP, 40% formamide, 10% glycerol, and 0.5 m*M* DTT

6. *HA buffer (0.5 liter)*: 5 m*M* KPO_4, pH 7.6, and 0.5 m*M* DTT

7. *HB buffer (100 ml)*: 40 m*M* KPO_4, pH 7.6, 1.5 *M* glycine, and 0.5 m*M* DTT

8. *Water-diluted protease inhibitor mix (1000 × stock)*: 0.5 mg/ml each of antipain, leupeptin, pepstatin A, chymostatin, and aprotinin. Store 0.5-ml aliquots at –20°C

9. *Ethanol-diluted protease inhibitor mix (100 × stock)*: 0.1 *M* phenylmethyl-sulfonyl fluoride (PMSF) 1 m*M* benzamidine–HCl, and 0.1 mg/ml phenanthroline. Store 5-ml aliquots at –20°C

10. *RNase A (500 × stock)*: 10 mg/ml in 0.1 *M* sodium acetate, pH 5.0. Boil in a water bath for 20 min. Store 1-ml aliquots at –20°C

11. *ATP for Hypa fractions*: 10 m*M* ATP in 40 m*M* K_2HPO_4; gives a pH of approximately 7.0

12. *D buffer (1 liter)*: 10 m*M* Tris–HCl, pH 7.6, 150 m*M* NaCl, 0.5 m*M* $CaCl_2$, and 0.01% sodium azide

13. *DNase I affinity matrix*: Couple 0.3 g of DNase I to 15 g of CNBr-activated Sepharose 4B overnight at

4°C according to the supplier's recommendations. Include 1 m*M* $CaCl_2$ in all buffers. Monitor the coupling reaction photometrically at 280 nm (see step 6 of Section III,A). According to our experience, this matrix will have a capacity of approximately 40 mg actin and will allow purification of actin from up to 150 g (wet weight) of yeast coexpressing recombinant actin. Store the matrix in D buffer containing 0.01% sodium azide. If column capacity decreases after several preparations, wash off bound contaminants with 4 *M* guanidine hydrochloride, 0.5 *M* sodium acetate, and 30% glycerol. Kept at 4°C, this matrix should be good for 10–15 preparations and last for 1–2 years. Also note that long-term exposure of DNase I to reducing agents inactivates the enzyme.

14. *Hydroxyl apatite column*: Degas 20 ml of settled hypatite C. Pack an XK-16/20 column with the matrix and equilibrate with HA buffer at 120 ml/h.

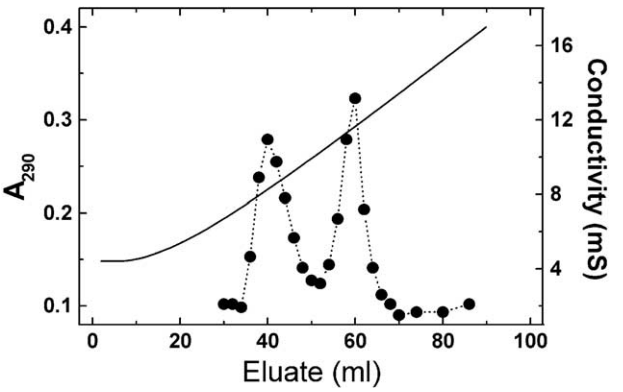

FIGURE 2 Separation of yeast actin and recombinant nonmuscle β-actin using hydroxyl apatite chromatography (Section III,B). The more acidic β-actin elutes at the higher phosphate/glycine concentration. Solid line represents the conductivity.

Steps

1. Use up to 150 g (wet weight) of yeast cells (corresponding to 10–12 liters of flask culture). Make 500 ml lysis buffer by adding water-diluted and ethanol-diluted protease inhibitors and 50 µl polypropylene glycol. Thaw the pelleted yeast in 100 ml lysis buffer. Lyse the yeast cells by passage through the bead mill and wash out the lysate using the remaining lysis buffer.

2. Add RNase A. Centrifuge the collected yeast lysate in a large-volume rotor at 12,000 rpm for 40 min at 4°C. Carefully decant the supernatant and filter it through glass wool.

3. Pour an XK-50/20 column using the DNase affinity matrix (step 13 of the previous section). Equilibrate the DNase column with G buffer. Pump the yeast lysate onto the DNase column. Wash with G buffer until a stable baseline is established as judged by OD_{290}. Wash consecutively with 5 column volumes of Na-acetate buffer, wash buffer Elu-I, and G buffer.

4. Prepare 200 ml of dilution buffer (G buffer containing 10% glycerol). Arrange a measuring cylinder with 100 ml dilution buffer on a magnetic stirrer. Blank a spectrophotometer with buffer Elu-II. Reduce the pump flow rate and start elution with buffer Elu-II. Follow the A_{290}; at 0.05–0.1, start collecting into the dilution buffer. The volume of dilution buffer should be at least 50%. Add more dilution buffer if necessary. Stop collecting when the A_{290} of the eluate is below 0.1.

5. Apply the diluted actin eluate onto the hydroxyl apatite column at a flow rate of max 100 ml/h, i.e., somewhat slower than the packing flow rate, to avoid further packing of the matrix with the more viscous actin eluate.

6. Prepare a fraction collector with 3-ml tubes containing 100-µl aliquots of buffered 10 m*M* ATP (for a final ATP concentration of 0.5 m*M*). Start collecting 2-ml fractions. Elute the actin isoforms using a gradient of 60 ml each of buffers HA and HB at a flow rate of 10 ml/h.

7. Identify actin-containing fractions by measuring the absorbance at 290 nm (Fig. 2), DNase I inhibition activity, SDS–PAGE, or dot blotting. Pool the fractions and dialyse against G buffer; alternatively, the pools may be concentrated and subjected to gel filtration.

Pitfalls

The protease inhibitor PMSF is counteracted by reducing agents. Therefore, DTT should be excluded from the lysis buffer and added to buffers only after the yeast extract has passed over the DNase column.

Failure to wash the DNase affinity column with high ionic strength (sodium acetate) buffer will result in contamination by a number of actin-binding proteins, with the most prominent one being yeast cofilin.

Prolonged exposure to 20% formamide will lead to actin denaturation. Therefore, it is important to collect the actin eluate into at least an equal volume of dilution buffer and apply it to the next column as quickly as possible. Attempts to store quick-frozen actin in this buffer have been unsuccessful.

The most probable reason for poor isoform separation is too high a flow rate during elution.

The aforementioned conditions for the separation of recombinant β-actin from yeast actin are not necessarily applicable to mutants of β-actin or other recombinant actins (e.g., Aspenström and Karlsson, 1991). Therefore, it may be necessary to alter conditions.

References

Aspenström, P., and Karlsson, R. (1991). Interference with myosin subfragment-1 binding by site-directed mutagenesis of actin. *Eur. J. Biochem.* **200**, 35–41.

Aspenström, P., Lassing, I., and Karlsson, R. (1991). Production, isolation and characterization of human profilin from *Saccharomyces cerevisiae*. *J. Muscle Res. Cell Motil.* **12**(2), 201–207.

De La Cruz, E. M., Mandinova, A., Steinmetz, M. O., Stoffler, D., Aebi, U., and Pollard, T. D. (2000). Polymerization and structure of nucleotide-free actin filaments. *J. Mol. Biol.* **295**(3), 517–526.

Gorbunoff, M. J. (1990). Protein chromatography on hydroxyapatite columns. *Methods Enzymol.* **182**, 329–339.

Innocenti, M., Zucconi, A., Disanza, A., Frittoli, E., Areces, L. B., Steffen, A., Stradal, T. E., Di Fiore, P. P., Carlier, M. F., and Scita, G. (2004). Abi1 is essential for the formation and activation of a WAVE2 signalling complex. *Nature Cell Biol.* **6**, 319–327.

Jazwinski, S. M. (1990). Preparation of extracts from yeast. *Methods Enzymol.* **182**, 154–174.

Karlsson, R. (1988). Expression of chicken beta-actin in *Saccharomyces cerevisiae*. *Gene* **68**, 249–257.

Lindberg, U., Schutt, C. E., Hellsten, E., Tjäder, A. C., and Hult, T. (1988). The use of poly(L-proline)-Sepharose in the isolation of profilin and profilactin complexes. *BBA* **967**, 391–400.

Nyman, T., Schüler, H., Korenbaum, E., Schutt, C. E., Karlsson, R. and Lindberg, U. (2002). The role of MeH73 in actin polymerization and ATP hydrolysis. *J. Mol. Biol.* **317**(4), 577–589.

Pardee, J. D., and Spudich, J. A. (1982). Purification of muscle actin. *Methods Enzymol* **85**, 164–181.

Ridley, A. J., Schwartz, M. A., Burridge, K., Firtel, R. A., Ginsberg, M. H., Borisy, G., Parsons, J. T., and Horwitz, A. R. (2003). Cell migration: Integrating signals from front to back. *Science* **302**, 1704–1709.

Sambrook, J., and Russell, D. (2001). "Molecular Cloning: A Laboratory Manual." 3rd Ed. Cold Spring Harbor Laboratory Press, Cold Spring Harbor, NY.

Segura, M., and Lindberg, U. (1984). Separation of non-muscle isoactins in the free form or as profilactin complexes. *JBC* **259**(6), 3949–3954.

Selden, L. A., Kinosian, H. J., Estes, J. E., and Gershman, L. C. (2000). Cross-linked dimers with nucleating activity in actin prepared from muscle acetone powder. *Biochemistry* **39**, 64–74.

Sledziewski, A. Z., Bell, A., Kelsay, K., and MacKay, V. L. (1988). Construction of temperature-regulated yeast promoters using the MATα2 repression system. *Bio/Technology* **6**, 411–416.

Walton, E. F., and Yarranton, G. T. (1989). Negative regulation of gene expression by mating-type. *In* "The Molecular and Cell Biology of Yeasts" (E. F. Walton and G. T. Yarranton eds.), pp. 43–69. Blackie, Glasgow, UK.

Zechel, K. (1980). Isolation of polymerization-competent cytoplasmic actin by affinity chromatography on immobilized DNase I using formamide as eluant. *Eur. J. Biochem.* **110**, 343–348.

CHAPTER

25

Purification of Skeletal Muscle Actin

Sebastian Wiesner

I. INTRODUCTION

Skeletal muscle is the most important preparative source for actin since the discovery of the protein in the 1940s. The original purification procedure developed by Feuer *et al*. (1948) is still the basis of modern protocols. In a first step, fresh skeletal muscle tissue is ground and most of the myosin is extracted by 0.5 *M* KCl. The tissue is then washed several times with distilled water and is dehydrated with acetone at –15°C to yield acetone powder, which can be stored conveniently. The second step, the actual actin preparation from this acetone powder, is based on cycles of actin extraction/depolymerization in low salt buffer, actin polymerization by the addition of salt, and sedimentation of the polymerized actin. Important methodical improvements were reached by the development of additional purification steps aimed at removing major protein contaminants. In particular, α-actinin (Ebashi and Maruyama, 1965) is eliminated by low-speed sedimentation of a thick gel formed with actin at 3 *M* KCl, and tropomyosin (Spudich and Watt, 1971) is dissociated from F-actin at high ionic strength. The procedure presented here is based on the widely used protocol of Spudich and Watt (1971; reviewed in Pardee and Spudich, 1982) followed by a gel filtration step at low ionic strength to isolate monomeric ATP-G-actin (MacLean-Fletcher and Pollard, 1980). It yields very high purity actin suitable for all common biochemical applications, such as actin binding and polymerization assays or chemical labelling. To store and handle actin efficiently, it is paramount to have an understanding of its biochemistry, especially of its interaction with Ca^{2+} and Mg^{2+} (for a review, see Carlier *et al*., 1994). At slightly alkaline pH, Ca-G-actin can be stored on ice at 2–3 mg/ml (50–75 μ*M*) without detectable self-assembly for weeks. This is not the case with Mg-actin, the prevalent species *in vivo*. The following protocol includes a procedure to convert Ca-actin to Mg-actin (Gershman *et al*., 1984).

II. MATERIALS AND INSTRUMENTATION

If not stated otherwise, chemicals are p.a. grade and are purchased from Merck. Na_2ATP is from Roche Molecular Diagnostics (0519987). Water is MilliQ grade. Acetone should be pure (99.5%). Sephadex G-200 is from Amersham Biosciences.

III. LABORATORY EQUIPMENT

Acetone powder preparation: sharp knife, large glassware (4-liter beaker, 4-liter Büchner flask), inox beaker, meat grinder, kitchen blender, gauze, and centrifuge. Actin purification: tissue grinder, thermometer, preparative ultracentrifuge, glass wool, dialysis tubes, and low-pressure chromatography system.

IV. PROCEDURES

A. Preparation of Acetone Powder from Rabbit Skeletal Muscle

Note that acetone powder is also available commercially (Sigma M-0637). To prevent protease

Copyright 2006, Elsevier Science (USA).
All rights reserved.

activity/contamination, the material should not be allowed to warm above 4°C and gloves should be worn throughout the preparation.

Solutions

1. *Extraction solution*: For 8 liters, add 298.2 g KCl and 40 g KHO_3 to 8 liters H_2O
2. *Acetone*: Chill to –20°C (acetone denatures proteins above 0°C)
3. *H_2O*: Chill to 4°C

Steps

1. **Mince preparation.** If possible, work in a group of two or three. Sacrifice two male rabbits (New Zealand white or equivalent). Skin and place in a large flat ice box. With a sharp knife, quickly excise the large muscles on both sides of the spine and from both hind legs. Chop muscles coarsely with scissors, removing as much connective tissue as possible. Grind. You should obtain about 600 g mince.

2. **Myosin extractions.** Place the mince in a large beaker and add 3 liters chilled extraction solution. Stir for 10 min and then centrifuge for 10 min at 2500 *g*. Discard supernatant and repeat this step once.

3. **Water extractions.** Discard supernatant and add pellet to 3 liters distilled water. Stir for 10 min and centrifuge as in step 3. Repeat this step three more times or until pellet begins to swell visibly; in this case, discontinue water extraction.

4. **Acetone washes.** Discard supernatant and mix washed tissue with cold acetone. Homogenize briefly with a kitchen blender. Centrifuge at 1200 *g* for 5 min. Repeat this step two more times.

5. **Drying.** After last acetone wash, pool all pellets in a large inox beaker and add 2 liters cold acetone. Stir vigorously for 20 min. Lay out a large Büchner funnel with several layers of gauze and place on a 4-liter Büchner flask. Apply suction and filter the acetone suspension. Squeeze out residual acetone by gathering the ends of the gauze and wringing. Spread the dehydrated material on filter paper and let dry overnight. Store dry acetone powder at –20°C.

B. Preparation of Ca-G-Actin from Acetone Powder

Gloves should be worn throughout the purification to avoid protease contamination.

Solutions

To prepare ATP-containing buffers, it is convenient to use a stock solution of ATP in H_2O buffered to pH 7.0. Store this stock solution at –20°C.

1. *X buffer*: 2 m*M* Tris–HCl, 0.5 m*M* ATP, 0.1 m*M* $CaCl_2$, 1 m*M* dithiothreitol (DTT), 0.01% (w/v) NaN_3, pH 7.8. Store at 4°C.
2. *Xb buffer*: 2 m*M* Tris–HCl, 1 m*M* $MgCl_2$, 1 m*M* DTT, pH 7.8. Store at 4°C.
3. *G buffer*: 5 m*M* Tris–HCl, 0.2 m*M* ATP, 0.1 m*M* $CaCl_2$, 1 m*M* DTT, 0.01% (w/v) NaN_3, pH 7.8. Store at 4°C.
4. *4 M KCl*: Store at room temperature
5. *1 M $MgCl_2$*: Store at 4°C

Steps

1. **G-actin extraction.** Add 270 ml of cold X buffer to 9 g acetone powder in a beaker on ice. Stir gently with a glass rod to completely moisten the acetone powder; excessive stirring will lead to increased α-actinin extraction. Leave on ice for 30 min, repeat stirring every 10 min.

2. **Clarification.** Centrifuge for 45 min at 25,000 *g* 4°C. Filter the supernatant through glass wool and determine the volume after filtration.

3. **Polymerization/α-actinin elimination.** Add solid KCl to a final concentration of 3.3 *M*, taking into account a volume increase of about 10%. Stir at room temperature until the solution has reached a temperature of 15°C to allow complete solubilization of the salt. Subsequently, chill the solution on ice without stirring until its temperature has fallen back to 5°C. Centrifuge for 30 min at 25,000 *g* / 4°C. Discard the F-actin/α-actinin pellet and filter the supernatant through glass wool.

4. **Dialysis.** Dialyse at 4°C overnight against 32 volumes of buffer Xb to bring $[K^+]$ to 0.1 *M*.

5. **Tropomyosin elimination.** Add 0.22 volumes of 4 *M* KCl to bring $[K^+]$ to 0.8 *M*. Stir for 90 min at 4°C. Centrifuge for 3 h 30 min at 70,000 *g*/4°C. Remove tropomyosin-containing supernatant. Collect the transparent F-actin pellets with a clean spatula and pool into a small glass tissue grinder. To collect residual actin, rinse centrifuge tubes with buffer X and add to pool. Homogenize the F-actin solution on ice, avoiding excessive foaming. Transfer to a 50-ml measuring cylinder. Add 75 µl 1 *M* $MgCl_2$ and 375 µl 4 *M* KCl and adjust volume to 38.6 ml with buffer X. (If necessary, the protocol can be interrupted at this point and the solution left to sit overnight at 4°C.) Repeat step 5 to remove tropomyosin completely, i.e., add 9 ml 4 *M* KCl, make up to 50 ml with buffer X, stir for 90 min at 4°C, centrifuge for 3 h 30 min at 85,000 g/4°C, and remove tromomyosin-containing supernatant.

6. **Depolymerization.** Resuspend and homogenize the F-actin pellets as in step 5 in a total volume of 20–30 ml buffer X. Dialyse overnight against 1 liter buffer G.

7. **Sonication.** Sonicate 2 × 10 s in the dialysis bag. Change dialysis buffer and continue dialysis for another 24 h.

8. **Clarification and gel filtration.** Centrifuge the actin for 2 h at 250,000 *g* / 4°C. Run the supernatant over a Sephadex G-200 gel filtration column equilibrated in buffer G at 15–20 ml/h. Collect 5-ml fractions. You should observe a first small and a second large peak by following the A_{290}; the second one is the actin peak. Avoid collecting the peak front because of possible CapZ contamination.

9. **Concentration determination.** Pool actin fractions and determine the concentration by spectrophotometry (ε_{290nm} = 26,600 $M^{-1}cm^{-1}$) using the G buffer as blank. Typically this will be 40–50 µ*M*. Ca-G-actin can be stored on ice for several weeks.

C. Conversion of Ca-Actin to Mg-Actin

Solutions

1. *10 mM $MgCl_2$*
2. *25 mM EGTA, pH 9.0*

Steps

1. Dilute Ca-G-actin to a concentration not higher than 10 µ*M* with G buffer.
2. Add $MgCl_2$ to a final concentration of (x + 10) µ*M*, where x is the actin concentration in µ*M*.
3. Add EGTA to a final concentration of 200 µ*M*. Mix gently by pipetting. The cation exchange will be complete in about 3 min.

V. COMMENTS

Actin can also be stored frozen or lyophilized, and lyophilized actin is available commercially (Sigma A-2522). However, these techniques lead to partial denaturation of the protein. If actin is frozen or lyophilized, sucrose should be added (2 mg/ml per mg/ml actin), and thawed or rehydrated actin should be dialysed against buffer G and recycled by a cycle of polymerization, high-speed sedimentation, and depolymerization. The protein concentration should be redetermined after this procedure.

References

Carlier, M.-F., Valentin-Ranc, C., Combeau, C., Fievez, S., and Pantaloni, D. (1994). Actin polymerization: Regulation by divalent metal ion and nucleotide binding, ATP hydrolysis and binding of myosin. *Adv. Exp. Med. Biol.* **358**, 71–81.

Ebashi, S., and Maruyama, K. (1965). Preparation and some properties of alpha-actinin-free actin. *J. Biochem. (Tokyo)* **58**, 20–26.

Feuer, G., Molnar, F., Pettko, E., and Straub, F. (1948). Studies on the composition and polymerization of actin. *Hung. Acta Physiol* **1**, 150–163.

Gershman, L., Newman, J., Selden, L., and Estes, J. (1984). Bound-cation exchange affects the lag phase in actin polymerization. *Biochemistry* **23**, 2199–2203.

MacLean-Fletcher, S., and Pollard, T. (1980). Identification of a factor in conventional muscle actin preparations which inhibits actin filament self-association. *Biophys. Res. Commun.* **96**, 18–27.

Pardee, J., and Spudich, J. (1982). Purification of muscle actin. *Methods Enzymol.* **85**, 164–181.

Spudich, J., and Watt, S. (1971). The regulation of rabbit skeletal muscle contraction. I. Biochemical studies of the interaction of the tropomyosin-troponin complex with actin and the proteolytic fragments of myosin. *J. Biol. Chem.* **246**, 4866–4871.

PART

B

ASSAYS

SECTION

4

Endocytic and Exocytic Pathways

CHAPTER

26

Permeabilized Epithelial Cells to Study Exocytic Membrane Transport

Frank Lafont, Elina Ikonen, and Kai Simons

I. INTRODUCTION

Polarized exocytic transport in epithelial cells can be measured by performing *in vitro* assays on filter-grown Madin–Darby canine kidney cells (MDCK strain II cells). Techniques have been developed to establish conditions where cytosol-dependent transfer of a viral marker protein is monitored in MDCK cells permeabilized with the cholesterol-binding and pore-forming toxin *Streptococcus* streptolysin-O (SLO). The transport is assayed either early in the biosynthetic pathway, from the endoplasmic reticulum (ER) to the Golgi complex, or from the *trans*-Golgi network (TGN) to the apical or from the TGN to the basolateral plasma membrane (for a detailed characterization of the assays and their properties, see Lafont *et al*., 1998).

The assays provide the possibility to analyze the effects of exogeneous molecules added to the cytosol. Cytosolic molecules can be inactivated prior to their addition to permeabilized cells or depleted using antibodies. Membrane-impermeable molecules can gain access to lipids or membrane proteins facing the cytosol. We have successfully used fluorescent lipid analogues, chemicals, antibodies, peptides, purified proteins, and toxins. The specificity of the inhibition of transport after depleting cells for a selected cytosolic molecule may be tested by rescuing transport when the purified molecule is added back to the transport reaction. Efficiency of the transport steps can also be tested after cells have been treated with drugs affecting biosynthetic pathways, e.g., after cholesterol biosynthesis inhibition using methyl-β-cyclodextrin.

II. MATERIALS AND INSTRUMENTATION

The recombinant SLO fused to a maltose-binding protein is obtained from Dr. S. Bhakdi (University of Mainz, Mainz, Germany). PhosphorImager and ImageQuant software are purchased from Molecular Dynamics. Sonifier cell disruptor B 15 is purchased from Branson. Media and reagents for cell culture are purchased from Gibco Biocult and Biochrom.; chemicals are from Merck; ATP (Cat. No. A-6033), antipain (Cat. No. A-6271), $CaCO_3$ (Cat. No. C-5273), chymostatin (Cat. No. C-7268), cytochalasin D (Cat. No. C-5394), leupeptin (Cat. No. L-2884), pepstatin (Cat. No. P-4265), and pyruvate (Cat. No. P2256) are from Sigma; creatine kinase (Cat, No. 127566), creatine phosphate (Cat. No. 621714), dimathyl sulfoxide (DMSO) (Cat. No. D-5879), endoglycosidase H (Cat. No. 1088734), and NADH (Cat No. 107727) are from Boehringer Mannheim; trypsin and soybean trypsin inhibitor are from Worthington Biochemical Corporation; protein A–Sepharose (Cat. No. 17-0780-01) is from Pharmacia; and cell filters (0.4-μm pore size; No. 3401, 12-mm-diameter Transwell polycarbonate filters) are from Costar.

Copyright 2006, Elsevier Science (USA).
All rights reserved.

III. PROCEDURES

A. SLO Standardization

Each batch of toxin is standardized for the amount of lactate dehydrogenase (LDH) released from the filter-grown MDCK cells, and the amount of LDH released is determined according to a previously described protocol. Alternatively, it is possible to use antibody cytosol accessibility to monitor SLO permeabilization.

Solutions

1. *Growth medium (GM)*: Eagle's minimal essential medium with Earle's salts (E-MEM) supplemented with 10 m*M* HEPES, pH 7.3, 10% (v/v) fetal calf serum, 2 m*M* glutamine, 100 U/ml penicillin, and 100 µg/ml streptomycin.
2. Either purified SLO or recombinant SLO fused to a maltose-binding protein is obtained from Dr. S. Bhakdi (University of Mainz, Mainz, Germany). The recombinant SLO preparation is strored as lyophilisate at –80°C.
3. *10X KOAc transport buffer*: To prepare 1 liter, dissolve 250 m*M* HEPES (59.6 g); 1150 m*M* KOAc (112.9 g), and 50 m*M* $MgCl_2$ (25 ml from 1 *M* stock) in 800 ml water. Adjust the pH to 7.4 with ~50 ml 1 *M* KOH and make it 1 liter with water.
4. *KOAc+ buffer*: KOAC buffer containing 0.9 m*M* $CaCO_3$ (90 mg/liter) and 0.5 m*M* $MgCl_2$ (0.5 ml/liter from 1 *M* stock)
5. *Assay buffer:* KOAc plus 0.011% Triton X-100 for media and KOAc for filter
6. NADH 14 mg/ml KOAc
7. 60 m*M* pyruvate: 30 mg in 50 ml water

Steps

1. Grow MDCK cells strain II on 1.2-mm-diameter filters for 3.5 days *in vitro* and change the medium every 24 h.
2. Wash cells by dipping in KOAc.
3. Prepare a range of SLO, e.g., from 0.5 to 10 µg of recombinant SLO per filter. Activate the SLO for 30 min at 37°C in 50 µl KOAc plus 10 m*M* dithiothreitol (DTT) per filter. Place the filters on a Parafilm sheet put on a metal plate on an ice bucket.
4. Add 50 µl of activated SLO on the apical side for 15 min at 4°C.
5. Wash excess SLO by dipping the filters twice in KOAc+.
6. Transfer the filters to a 12-well dish containing 0.75 ml TM at 19.5°C. Add 0.75 ml TM to the apical side and incubate at 19.5°C for exactly 30 min in a water bath.
7. Collect apical and basolateral media, cut the filters, and shake the filters with 1 ml KOAc containing 0.1% Triton X-100.
8. Mix in a disposable cuvette:
   a. 800 µl of assay buffer (KOAc or KOAc/Triton X-100)
   b. 200 µl of sample
   c. 10 µl of NADH
   d. 10 µl of pyruvate.

   Turn the cuvette upside down twice using Parafilm to close it.
9. Read immediately the OD at 340 nm for 60 s (the OD should be around 1.5).
10. Calculate the LDH activity as the change in OD in 10 s, taking the average of the first 30 s.
11. Dissolve the recombinant SLO in KOAc buffer and store in aliquots at –80°C with the amount necessary for one set of assays per aliquot.

B. Preparation of Cytosols

Solutions

1. *Growth medium*: For HeLa cells, use Joklik's medium supplemented with 50 ml/liter newborn calf serum (heat inactivated for 30 min at 56°C), 2 m*M* glutamine, 100 U/ml penicillin, 100 µg/ml streptomycin, and 150 µl 10 *M* NaOH. For MDCK cells, use Eagle's minimal essential medium with Earle's salts (E-MEM) supplemented with 10 m*M* HEPES, pH 7.3, 10% (v/v) fetal calf serum, 2 m*M* glutamine, 100 U/ml penicillin, and 100 µg/ml streptomycin.
2. *10X KOAc transport buffer*: To prepare 1 liter, dissolve 250 m*M* HEPES (59.6 g); 1150 m*M* KOAc (112.9 g), and 50 m*M* $MgCl_2$ (25 ml from 1 *M* stock) in 800 ml water. Adjust the pH to 7.4 with ~50 ml 1 *M* KOH and make it 1 liter with water.
3. *PBS+*: PBS containing 0.9 m*M* $CaCl_2$ and 0.5 m*M* $MgCl_2$.
4. *Swelling buffer (SB)*: For 100 ml, prepare 1 m*M* EGTA 0.5 *M* (200 µl), 1 m*M* $MgCl_2$ 1 *M* (100 µl), 1 m*M* DTT 1 *M* (100 µl), and 1 µ*M* cytochalasin D 1 m*M* (100 µl).
5. *Protease inhibitor cocktail (CLAP)*: To prepare a 1000X stock, dissolve antipain, chymostatin, leupeptin, and pepstatin each at 25 µg/ml DMSO and combine.

Steps

HeLa Cytosol

1. To grow 20 liters of HeLa cells in suspension to a density of 6×10^5 cells/ml:

a. Inoculate 250 ml cell suspension (6×10^5 cells/ml) in 1 liter medium and leave stirring in a 37°C room.
b. On the third day, split 1:4 by adding 250 ml to 750 ml of fresh medium. Leave stirring in the 37°C room. This will give 4 liters of cell suspension.
c. On the fifth day, again split 1:4 by adding 1 liter of the cell suspension to 3 liters of fresh medium in a 6-liter round-bottom flask. If the cells seem overgrown, add some fresh medium. Thus, between 16 and 20 liters of cell suspension are obtained.

2. Concentrate the cell suspension to 2 liters either by centrifugation or with any cell-concentrating system.

3. Centrifuge cells at 5000 rpm in a Sorvall GS-3 rotor (400-ml buckets) at 4°C for 20 min.

4. Discard the supernatant and wash cells by resuspending the pellet with 10 ml of ice-cold PBS with a sterile 10-ml pipette (10 ml PBS/bucket). Pool the suspension in 250-ml Falcon tubes.

5. Spin at 3000 rpm for 10 min at 4°C in a minifuge. The pellet will be loose. Discard the supernatant.

6. Fill the tube with cold SB (about 35 ml). Resuspend the cells carefully with a sterile 10-ml pipette in SB. Let the pellet swell for 5 min on ice.

7. Spin in the minifuge at 2000 rpm at 4°C for 10 min. Remove as much as possible of the supernatant. The pellet should be loose.

8. Transfer the pellet to a 30-ml Dounce homogenizer (use a spatula) and, after adding SB, perform five strokes. Add 0.1 volume of 10× KOAc and homogenize further by 15–20 strokes.

9. Spin the homogenate at 4°C at 10,000 rpm for 25 min in SS-34 tubes (Sorvall). Collect the supernatant.

10. Spin at 50,000 rpm in Ti70 tubes (Beckmann) for 90 min at 4°C. Aliquot the supernatant in screw-top 1.5-ml tubes. Avoid including lipids that might be on the top of the supernatant. Freeze the aliquots in liquid N_2 and store at −70°C.

11. Measure the protein concentration; it should be around 5 mg/ml. Lower concentrations do not work.

12. When needed, thaw the aliquots quickly and keep them on ice (up to 6 h) until use. Aliquots can be refrozen at least twice.

MDCK Cytosol

1. Trypsinize thirty 24 × 24-cm dishes of confluent MDCK cells. Resuspend trypsinized cells in cold growth medium (containing 5% FCS to inactivate trypsin) and leave on ice until all dishes are trypsinized and cells are pooled. After this, all handling should be done on ice using ice-cold solutions.

2. Centrifugate at 4°C for 10 min at 2000 rpm in a RF Heraeus centrifuge. Wash medium away with PBS.

3. Wash in PBS containing 2 mg/ml STI. Wash out STI with PBS and resuspend the cell pellet in the SB (cf. see earlier discussion) and keep 10 min on ice.

4. Centrifugate at 2000 rpm for 10 min at 4°C in a RF Heraus centrifuge.

5. Sonicate the loose cell pellet (~10 ml) (power 6, 0.5-s pulse, sonifier cell disruptor B 15, Branson) until cells are broken as judged by light microscopy. Add 0.1 volume of 10X KOAc to the sample and spin it for 20 min at 3000 rpm.

6. Spin the supernatant again at 75,000 rpm for 1 h in a TLA 100.2 rotor.

The procedure routinely yields ~6 ml of cytosol at 14 mg/ml. Other cell types, e.g., NIH 3T3 fibroblasts, can also be used as starting material for cytosol preparation using the protocol just described. We have not observed significant differences between the efficiencies of the different cytosols to support transport. However, HeLa cytosol is used routinely because of the ease of preparing large quantities.

C. Transport Assays

Solutions

All solutions are sterilized and kept at 4°C unless indicated.

1. *Growth medium*: E-MEM supplemented with 10 m*M* HEPES (10 ml/liter), pH 7.3, 10% (v/v) fetal calf serum, 2 m*M* glutamine 200 m*M* (10 ml/liter), 100 U/ml penicillin 10^4 U/ml (10 ml/liter), and 100 µg/ml streptomycin 10^4 µg/ml (10 ml/liter).

2. *Infection medium (IM)*: E-MEM supplemented with 10 m*M* HEPES, pH 7.3, 0.2% (w/v) BSA, 100 U/ml penicillin, and 100 µg/ml streptomycin.

3. *Labelling medium (LM)*: Methionine-free E-MEM containing 0.35 g/liter sodium bicarbonate instead of the usual 2.2 g/liter 10 m*M* HEPES, pH 7.3, 0.2% (w/v) BSA supplemented with 16.5 µCi of [^{35}S]methionine/filter.

4. *Chase medium (CM)*: Labelling medium without [^{35}S]methionine and containing 20 µg/ml cycloheximide and 150 µg/ml cold methionine.

5. *10X KOAc transport buffer*: To prepare 1 liter, dissolve 59.6 g HEPES (250 m*M*); 112.9 g KOAc (1150 m*M*), and add 25 ml from 1 *M* stock $MgCl_2$ (50 mM) in 800 ml water. Adjust the pH to 7.4 with ~50 ml 1 *M* KOH and make it 1 liter with water.

6. *KOAc+ buffer*: KOAC buffer containing 0.9 m*M* $CaCO_3$ (90 mg/liter) and 0.5 m*M* $MgCl_2$ (0.5 ml/liter from 1 *M* stock).

7. *PBS+*: PBS containing 0.9 m*M* $CaCl_2$ (0.13 g/liter $CaCl_2 \cdot 2H_2O$) and 0.5 mM $MgCl_2$ (0.5 ml/liter from 1 *M* stock).

8. *0.5 M EGTA*: To prepare 100 ml, dissolve 19 g in 60 ml water. The solution should be turbid (pH 3.5). Add slowly ~10 ml 10 *M* KOH. When the pH of the solution starts to clear, adjust to 7.4. Make it 100 ml with water.

9. *0.1 M Ca and 0.5 M EGTA*: To prepare 100 ml, stir 1 g $CaCO_3$ and 3.8 g EGTA in ~70 ml water for at least 45 min (degas). After adding 2 ml of 10 *M* KOH, the pH is about 6. Finally, make the pH 7.4 adding few drops of 1 *M* KOH. Make it 1 liter with water.

10. *Transport medium (TM)*: To prepare 50 ml, combine 50 µl 1 *M* DTT, 200 µl 0.5 *M* EGTA, and 1 ml 0.5 *M* EGTA/0.1 *M* $CaCO_3$ in 1X KOAc.

11. *ATP-regenerating system (ARS)*: 100X stock, prepare three solutions (10 ml each):

   a. 100 m*M* ATP (disodium salt, pH 6–7, neutralized with 2 *M* NaOH; 0.605 g/10 ml)
   b. 800 m*M* creatine phosphate (disodium salt, 2.620 g/10 ml)
   c. 800 U/mg (at 37°C) creatine kinase (0.5 mg/10 ml in 50% glycerol).

   Store stocks in aliquots at –20°C. Mix solutions a–c 1:1:1 just before use.

12. *Lysis buffer (LB)*: PBS+ containing 2% NP-40 and 0.2% SDS.

13. *CLAP*: To prepare a 1000X stock, combine 25 µg/ml DMSO of antipain, chymostatin, leupeptin, and pepstatin.

Steps

The basic steps of the assays can be summarized as follows. Grow MDCK cells on a permeable filter support until a tight monolayer is formed. Grow cells on 12-mm-diameter filters and use when they display a transmonolayer electrical resistance of at least 50 Ω× cm^2. Infect cells layers with either vesicular stomatitis (VSV) or influenza virus using the G glycoprotein of VSV (VSV G) or the hemagglutinin (HA) of influenza virus N as basolateral or apical markers, respectively. After a short pulse of radioactive methionine, block the newly synthesized viral proteins either in the ER at 4°C or in the TGN after a 20°C incubation. At this stage, one cell surface is permeabilized with SLO, which allows leakage of cytosolic proteins, whereas membrane constituents, including transport vesicles, are retained inside the cells. After removal of the endogenous cytosol by washing, add cytosol and ATP and raise the temperature to 37°C. Transport of the viral proteins from the ER to the Golgi complex or from the TGN to the apical or the basolateral plasma membrane is reconstituted in a cytosol-, energy-, and temperature-dependent manner. Measure the amount of viral proteins reaching the acceptor compartment by endoglycosidase H treatment (ER to Golgi transport), trypsinization of HA on the apical surface (TGN to apical transport), or immunoprecipitation of the VSV G at the basolateral surface (TGN to basolateral transport). Obtain quantitations of viral polypeptides resolved on SDS–PAGE by PhosphorImager analysis.

Due to the handling and the various steps, the entire procedure for running one assay requires about 9 h for the apical assay and 11 h for the basolateral assay. Carry out immunoprecipitation for the basolateral assay the following day (takes 5 h). The ER-to-Golgi transport takes about 6 h before an overnight enzymatic treatment step. Samples can be frozen at –20°C before running SDS–PAGEs (routinely performed the following day). It is worth noting that for the reproducibility of the results the assays should be performed strictly, obeying the schedule indicated in the protocol.

Grow the N strain influenza virus (A/chick/Germany/49/Hav2Neq1) in 11-day embryonated chick eggs as described. Prepare a stock of phenotypically mixed VSV (Indiana strain) grown in Chinese hamster ovary C15.CF1 cells, which express HA on their plasma membrane as described. Prepare the affinity-purified antibody raised against the luminal domain of the VSV G as described.

Apical Transport Assay

1. *Cell culture*: Seed 1:72 of the MDCK cells from one confluent 75-cm^2 flask per filter (6×10^4 cells/filter) with 0.75 ml of growth medium apically and 2 ml basolaterally. Change the growth medium every 24 h and use cells 3.5 days after plating.

2. *Infection*: Prior to viral infection, wash the monolayers in warm PBS+ and then IM and infect with the influenza virus in 50 µl IM (20 pfu/cell; enough to obtain 100% infection as judged by immunofluorescence) on the apical side. After allowing adsorption of the virus to the cells for 1 h at 37°C, remove the inoculum and continue the infection for an additional 3 h after adding 0.75 ml IM on the apical side and 2 ml IM on the basolateral side of the filter.

3. *Metabolic labeling*: Rinse the cell monolayers by dipping in beakers containing warm PBS+ and LM at 37°C. Place a drop of 25 µl of the LM containing 12.5 µCi of [^{35}S]methionine on a Parafilm sheet in a wet chamber at 37°C in a water bath. Add 100 µl of only LM to the apical side of the filters and place them basal side down on the drop. Incubate for 6 min at 37°C.

4. *TGN block*: Terminate all the pulse by moving the filters to a new 12-well plate containing 1.5 ml CM already at 20°C. Add 0.75 ml of CM (20°C) on the

apical side and incubate for 75 min in a 19.5°C water bath.

5. *SLO permeabilization*: Activate the SLO in KOAc buffer containing 10 m*M* DTT at 37°C for 30 min and keep at 4°C until used for permeabilization. Use the toxin within 1 h of activation. Wash the filters twice in ice-cold KOAc+ by dipping. Carefully remove excess buffer from the apical side and blot the basolateral side with a Kleenex. Place 25-µl drops of the activated SLO (enough to release 60% LDH in 30 min, about 20 mg/ml) on a Parafilm sheet placed on a metal plate on an ice bucket. Leave the apical side without buffer. Place the filters on the drop for 15 min. Wash the basolateral surface twice by dipping in ice-cold KOAc+ buffer. Transfer the filters to a 12-well dish containing 0.75 ml TM at 19.5°C. Add 0.75 ml TM to the apical side and incubate at 19.5°C for exactly 30 min in a water bath.

6. *Transport*: Remove the filters from the water bath, rinse them once with cold TM, blot the basolateral side, and place on a 35-µl drop on either TM (control) or HeLa cytosol (±treatment or molecule to be tested) supplemented each with ARS (3 µl/100 µl TM or HeLa cytosol). Add the ARS to TM or cytosol immediately before dispensing the drops onto which the filters are placed. Layer 100 µl of TM on the apical side and incubate at 4°C for 15 min in a moist chamber. Transfer the chamber to a warm water bath for 60 min at 37°C. Terminate the transport by transferring on ice and washing the filters with cold PBS+ three times.

7. *Trypsinization*: Add to the apical surface 250 µl of 100 µg/ml trypsin freshly prepared in PBS+ and then add 2 ml of PBS+ to the basolateral chamber. Keep on ice for 30 min and stop the reaction by adding 3 µl of soybean trypsin inhibitor (STI; 10 mg/ml) to the apical side and then wash the apical surface three times with PBS+ containing 100 µg/ml STI.

8. *Cell lysis*: Solubilize the monolayers in 100 µl LB containing freshly added CLAP. Scrape the cells and spin for 5 min in a microfuge; discard the pellet. Analyze 20 µl per sample by SDS–PAGE on a 10% acrylamide gel, fix, and dry the gel.

9. *Quantitation*: Scan the gels with a PhophorImager and measure the band intensities using ImageQuant software. Calculate the amount of HA transported as the percentage of HA (68 kDa) transported to the cell surface = [2 × HA2/(HA + 2 × HA2) × 100] with HA2 (32 kDA) being the small trypsin cleavage product of HA.

Basolateral Transport Assay

1. *Cell culture*: Seed 1:72 of MDCK cells from one confluent 75-cm^2 flask per filter (6×10^4 cells/filter) with 0.75 ml of growth medium apically and 2 ml basolaterally. Change the growth medium every 24 h and use cells 3.5 days after plating.

2. *Infection*: Prior to viral infection, wash the monolayers in warm PBS+ and then in IM and infect with the vesicular stomatitis virus in 50 µl IM (20 pfu/cell; enough to obtain 100% infection as judged by immunofluorescence) on the apical side. After allowing adsorption of the virus to the cells for 1 h at 37°C, remove the inoculum and continue the infection for an additional 3 h after adding 0.75 ml IM on the apical side and 2 ml IM on the basolateral side of the filter.

3. *Metabolic labeling and chase*: Rinse the cell monolayers by dipping in beakers containing warm PBS+ and then LM at 37°C. Place a drop of 25 µl of the LM containing 12.5 µCi of [^{35}S]methionine on a Parafilm sheet in a wet chamber at 37°C in a water bath. Add 100 µl of LM to the apical side of the filter and place the filter on the drop. Incubate for 6 min at 37°C and incubate for an additional 6 min at 37°C in CM with 0.75 ml on the apical side and 2 ml on the basolateral side before the 19.5°C block.

4. *TGN block*: Terminate the pulse by moving the filters to a new 12-well plate containing 1.5 ml CM already at 20°C. Add 0.75 ml of CM (20°C) on the apical side and incubate for 60 min in a 19.5°C water bath.

5. *SLO permeabilization*: Activate the SLO in KOAc buffer containing 10 m*M* DTT at 37°C for 30 min and keep at 4°C until used for permeabilization. Use the toxin within 1 h of activation. Wash the filters twice in ice-cold KOAc+ by dipping. Carefully remove excess buffer from the apical side and blot the basolateral side with a Kleenex. Add 50-µl drops of the activated SLO (enough to release 60% LDH in 30 min, about 40 mg/ml) on a Parafilm sheet placed on a metal plate layered on an ice bucket. Leave the basolateral side without buffer. Incubate for 15 min. Wash the apical surface twice with 0.75 ml of ice-cold KOAc+ buffer. Transfer the filters to a 12-well dish containing 0.75 ml TM at 19.5°C. Add 0.75 ml TM to the apical side and incubate at 19.5°C for exactly 30 min in a water bath.

6. *Transport*: Remove the filters from the water bath, rinse them once with cold TM, blot the basolateral side, and add 100 µl of either TM (control) or HeLa cytosol (±treatment or molecule to be tested) supplemented with ARS each (3 µl/100 µl TM or HeLa cytosol) on the apical side. Add the ARS to TM or cytosol prior to dispension onto drops. Incubate at 4°C for 15 min. Put the filters on already dispensed 35-µl drops of TM supplemented with ARS on a Parafilm in a moist chamber in a water bath at 37°C. Incubate for 60 min. Terminate the transport by transferring on ice and washing the filters with cold PBS+ three times.

7. *Anti-VSV G binding*: Wash twice (2–5 min) with 2 ml of CM containing 10% FCS (CM-FCS) on the basolateral side and once with 0.75 ml on the apical side. Dilute anti-VSV-G antibodies in CM-FCS (1:18, i.e., 50 µg/ml; 300 µl) and place the filters on 25-µl drops of PBS+/ab (1.5 µl ab/filter). Add nothing on the apical side and incubate in a cold room on a metal plate placed onto an ice bucket for 90 min. Remove the filters and wash (three times) on the basolateral side with CM-FCS (2 ml with constant rocking) and once on the apical side. Shake the filters gently for efficient removal of unbound antibodies. Wash the filters once with PBS+ and place each on a 25-µl drop of PBS+ supplemented with cold virus (1:25; 300 µl). Incubate for 10 min in the cold.

8. *Cell lysis*: Solubilize the monolayers in 200 µl LB containing freshly added CLAP and cold virus (1:166). Scrape the cells, spin for 5 min, and discard the pellet. Remove a 10-µl aliquot from each sample (total).

9. *Immunoprecipitation*: Wash protein A–Sepharose powder with PBS (3×), let it swell 10 min in PBS, wash it with LB, and store as 1:1 slurry in LB at 4°C for 3 weeks maximum. Add 30 µl of the 1:1 slurry of protein A–Sepharose to the lysate. Rotate in a cold room for 60 min. Spin the resin down and wash (3×) with 500 µl LB, elute the bound sample with 35 µl 2X Laemmli buffer, and boil for 5 min at 95°C. Load 20 µl of bound material and 10 µl of total (after boiling with 10 µl of 2X Laemmli buffer) on SDS–PAGE gels (10%). Run SDS–PAGE on 10% acrylamide gels, fix, and dry the gels.

10. *Quantitation*: Scan the gels with a PhophorImager and measure band intensities using ImageQuant software. Calculate the amount of VSV G (67 kDa) transported as follows: percentage of VSV G on the cell surface = (surface immunoprecipitated VSV G / total VSV G) × 100.

ER-to-Golgi Transport Assay

In the ER-to-Golgi transport assay, influenza N- or VSV- infected MDCK monolayers can be used. An infection with the influenza virus is used here as an example.

1. *Cell culture*: Seed 1:72 of the MDCK cells from one confluent 75-cm^2 flask per filter with 0.75 ml of growth medium apically and 2 ml basolaterally. Change the growth medium every 24 h and use cells 3.5 days after plating.

2. *Infection*: Prior to viral infection, wash the monolayers in warm IM and then infect with the influenza virus in 50 µl IM (20 pfu/cell; enough to obtain 100% infection as judged by immunofluorescence) on the apical side. After allowing adsorption of the virus to the cells for 1 h at 37°C, remove the inoculum and continue the infection for an additional 3 h after adding 0.75 ml IM on the apical side and 2 ml IM on the basolateral side of the filter.

3. *Metabolic labeling*: Rinse the cell monolayers by dipping in beakers containing warm PBS+ and then LM at 37°C. Place a drop of 25 µl of the LM containing 12.5 µCi of [^{35}S]methionine on a Parafilm sheet in a wet chamber at 37°C in a water bath. Add 100 µl of LM to the apical side of the filter and place the filter on the drop. Incubate for 6 min at 37°C.

4. Terminate the pulse by moving the filters to a new 12-well plate containing 1.5 ml CM already at 4°C. Add 0.75 ml of CM (4°C) on the apical side and incubate for 30 min at 4°C.

5. *SLO permeabilization*: Activate the SLO in KOAc buffer containing 10 m*M* DTT at 37°C for 30 min and keep at 4°C until used for permeabilization. Use the toxin within 1 h of activation. Wash the filters twice in ice-cold KOAc+ by dipping. Carefully remove excess buffer from the apical side and blot the basolateral side with a Kleenex. Place 25-µl drops of the activated SLO (enough to release 60% LDH in 30 min, about 20 mg/ml) on a Parafilm sheet placed on a metal plate layered on an ice bucket. Leave the apical side without buffer. Place the filters on the drops for 15 min. Wash the basolateral surface twice by dipping in ice-cold KOAc+ buffer. Transfer the filters to a 12-well dish containing 0.75 ml TM at 4°C. Add 0.75 ml TM to the apical side and incubate at 37°C for 3 min and 1.5 ml on the basolateral side of the filter (formation of pores), followed by an incubation at 4°C for 20 min in fresh TM on both sides (cytosol depletion).

6. *Transport*: Rinse the filters once with cold TM, blot on the basolateral side, and put on a 35-µl drop of either TM (control) or HeLa cytosol (±treatment or molecule to be tested) supplemented with ARS each (3 µl/100 µl TM or HeLa cytosol). Add the ARS to TM or cytosol prior to dispension onto drops. Layer the apical side with 100 µl of TM and incubate at 4°C for 15 min in a moist chamber. Transfer the chamber to a water bath at 37°C for 45 min. Terminate the transport by transferring on ice and washing the filters with cold PBS+ three times.

7. *Cell lysis*: Solubilize the monolayers in 100 µl LB containing freshly added CLAP. Scrape the cells and spin for 5 min in microfuge; discard the pellet.

8. *Endoglycosidase H treatment*: Remove a 75-µl aliquot and add to 25 µl of 0.2 *M* sodium citrate buffer, pH of 5.0. The resulting 100 µl mixture has a pH of 5.3. Divide it in two 50-µl aliquots. One receives 5 µl of 1 U/ml endoglycosidase H and the other receives only the citrate buffer. After 20 h at 37°C, terminate the reaction by boiling in Laemmli buffer. Analyze the samples

by running SDS–PAGE on a 10% acrylamide gel, fix, and dry the gel.

9. *Quantitation*: Scan the gels with a PhophorImager and measure band intensities using ImageQuant software. Calculate the amount of HA transported as the percentage of HA acquiring endoglycosidase H resistance with the following formula: percentage of HA reaching the Golgi complex = (endo H-resistant HA / total HA) × 100.

IV. COMMENTS AND PITFALLS

In all cases the values are expressed as control cytosol-dependent transport being 100% (transport in the presence of cytosol minus transport in the absence of added cytosol). For each manipulation a matched control is used (e.g., antibody or peptide tested vs. control antibody or peptide, respectively). Assays are carried out routinely on duplicate filters and quantifications represent the mean ± SEM obtained in several experiments.

A critical parameter for the successful performance of these transport assays is the quality of SLO. MDCK cells are difficult to permeabilize compared to several other cell types (e.g., BHK, CHO, and L cells), and with the available commercial sources of SLO, the degree of permeabilization, as measured by LDH release, has not been satisfactory. The wild-type toxin purified from *Streptococci* and the recombinant toxin produced in *Escherichia coli* have both worked equally well.

The available amount of reagent often determines whether the preincubation during cytosol depletion is possible, as cytosol depletion must be carried out in an excess volume of buffer. The routinely used volume (750 µl per filter) can be, however, somewhat reduced. By using 500 µl per filter there is not yet a significant effect on transport efficiency, and by using 200 µl per filter cytosol depletion is compromised moderately, which increases the background, cytosol-independent transport, and results in a transport efficiency of about three-fourths of normal.

Because the transport is carried out in a leaky cellular microenvironment with diluted cytosolic components, the increase in transport obtained with exogenous cytosol is usually two- to threefold (three- to fourfold in the ER-to-Golgi assay). This is the window in which the differences in cytosol dependent transport are measured. In assays measuring transport in the late secretory pathway, part of the efficiency is lost due to retention of some viral marker early in the exocytic route. However, because both markers, HA and VSV G, are glycoproteins whose mobility on SDS–PAGE shifts according to the degree of glycosylation, careful examination of their mobilities will reveal, in apical and basolateral assays, if the test condition retarded significantly the processing of the marker to the terminally glycosylated form. This may therefore serve as an internal control for the specificity of inhibition. A more accurate way to test the effect of a reagent in the early secretory pathway is to assay the ER-to-Golgi transport. The real advantage of having established similar procedures for three different transport assays is the possibility of using them as internal controls for each other. This enables the identification of molecules that are specifically involved in either apical or basolateral transport routes and allows the discrimination between compounds that are needed only in the polarized routes versus those that are common to all three transport processes.

Reference

Lafont, F., Verkade, P., and Simons, K. (1998). Annexin XIIIb associates with lipid microdomains to function in apical delivery. *J. Cell Biol.* **142**, 1413.

CHAPTER

27

Studying Exit and Surface Delivery of Post-Golgi Transport Intermediates Using *in vitro* and Live-Cell Microscopy-Based Approaches

Geri E. Kreitzer, Anne Muesch, Charles Yeaman, and Enrique Rodriguez-Boulan

I. INTRODUCTION

Study of the mechanisms of polarized protein sorting in epithelial cells has been facilitated greatly by the use of enveloped RNA viruses, such as vesicular stomatitis virus (VSV) and influenza virus, which bud from the basolateral and apical plasma membranes, respectively (Rodriguez-Boulan and Sabatini, 1978). Following infection, a rapid onset of viral protein synthesis occurs, leading to the vectorial transport of envelope glycoproteins to either the apical or the basolateral surface. This model continues to provide information on the mechanisms of protein sorting (Musch *et al*., 1996) and the basic protocols are included here. However, because cells cannot be coinfected efficiently with both types of viruses due to reciprocal inhibition of protein synthesis, a major drawback of this paradigm is the inability to study the segregation of apical and basolateral proteins from one another in the same cell.

Two alternative approaches have been developed that improve upon and greatly facilitate studying the molecular effectors of protein sorting in the *trans*-Golgi network (TGN) and polarized transport routes to the plasma membrane in epithelial cells. These approaches utilize either recombinant adenovirus vectors or intranuclear microinjection of cDNAs to introduce exogenous biosynthetic markers into cells. Both methodologies advance previous techniques in numerous ways: (i) they allow for high-level, simultaneous expression of two markers (Marmorstein *et al*., 2000); (ii) they are amenable to the use of temperature blocks, which allow for accumulation in and synchronous release of newly synthesized proteins from the TGN; (iii) neither method interferes with the ability of cells to synthesize and transport endogenous proteins, permitting the study of marker proteins in a normal cellular environment; (iv) adenoviral infection generally results in transduction of all cells in the culture and is thus ideal for metabolic labeling studies and biochemical analysis of biosynthetic events; (v) microinjection results in the rapid expression of cDNAs, providing a means by which to study anterograde membrane trafficking events selectively and dynamically in individual cells; and (vi) cDNAs or adenoviral particles can be introduced easily into a wide variety of cultured cells, making it relatively simple to compare secretory sorting pathways in different multiple cell types.

The most important advance provided by cDNA microinjection and adenoviral-mediated gene transfer in studying protein-sorting events is the ability to cointroduce two or more genes into cells and express simultaneously multiple secretory cargoes that follow divergent routes out of the TGN. This allows one to evaluate the role(s) of potential molecular effectors of protein sorting and targeting to different cellular domains. Furthermore, the level of expression of exogenous genes can be manipulated [by changing the amount of DNA introduced and the expression time allowed in microinjection-based assays or by varying

Copyright 2006, Elsevier Science (USA).
All rights reserved.

either the multiplicity of infection (moi) or the time in culture following adenoviral infection] to allow study of the ability to saturate the various sorting pathways available to the cell (Marmorstein *et al*., 2000). Adenoviral infection also results in high-level expression of reporter proteins in large cell populations, a factor essential in obtaining sufficient incorporation of radioactive amino acids for pulse–chase studies, as well as for immunoisolation of transport vesicles. (Once the adenovirus has been titrated and the infection conditions optimized, 100% of the cells express the desired proteins and remarkably consistent pools of cells are produced from experiment to experiment.) Procedures for adenoviral infection can be modified and adapted easily to a variety of different cell lines.

While cDNA microinjection is limited with respect to the number of cells that can be evaluated, it is exquisitely suited to live cell imaging studies aimed at evaluating highly dynamic membrane trafficking events occurring at specific points throughout the biosynthetic pathway (e.g., ER-to-Golgi events and Golgi-to-plasma membrane events, such as budding of Golgi membranes, transport of post-Golgi carriers, and exocytosis of post-Golgi carriers). Momentum in this area is due primarily to the advent of fluorescent tags, such as green fluorescent protein [GFP(Chalfie, 1994)] from the jellyfish *Aequorea* and dsRed from the coral *Discosoma* (Matz *et al*., 1999; Baird *et al*., 2000), which can be genetically appended to any DNA of choice. These tags serve as vital fluorescent indicators that facilitate direct observation and analysis of membrane-trafficking events in living cells.

This article describes an assay that monitors post-Golgi vesicle budding from semi-intact MDCK cells following infection either with enveloped RNA viruses or with recombinant adenovirus vectors. The adenoviruses we have found most useful for these applications encode receptors for neurotrophins ($p75^{NTR}$) and low-density lipoprotein (LDLR), which were shown previously to be sorted to the apical and basolateral surfaces of polarized MDCK cells, respectively (Le Bivic *et al*., 1991; Hunziker *et al*., 1991; Gridstaff *et al*., 1998). Each of these proteins, when expressed in MDCK cells, incorporates radiosulfate into carbohydrate moieties during posttranslational processing late in the secretory pathway, providing a convenient method to label markers in the sorting compartment.

In addition, this article describes methods we have developed pertaining to the use of time-lapse fluorescence imaging to study the transport of plasma membrane proteins through the biosynthetic pathway in living cells. While we only discuss this technique specifically with respect to MDCK epithelial cells, with slight modifications we have also successfully employed this approach for similar studies in several different cell lines. Additionally, we have found that these studies can be used with numerous reporter proteins of interest. Thus while we focus on reporters marking the apical or basolateral plasma membrane, the system is not limited to the study of membrane-associated proteins. Finally, this article discusses some quantitative measurements that can be made from this type of data related to protein-trafficking events occurring *in vivo*.

II. MATERIALS AND INSTRUMENTS

Dulbecco's modified Eagle's medium (DMEM, Cat. No. 10-013-CV), MEM nonessential amino acids (Cat. No. 25-025-CI), Hank's balanced salt solution (HBSS, Cat. No.21-023-CV), and L-glutamine (Cat. No. 25-005-CI) are from Cellgro. MEM SelectAmine kits (Cat. No. 19050), MEM vitamins (Cat. No. 11120), penicillin-streptomycin (Cat. No. 15140), 7.5% bovine serum albumin (BSA, Cat. No. 15260), and donor horse serum (Cat. No. 16050) can be purchased from Gibco-BRL (Grand Island, NY). Heat-inactivated fetal bovine serum (FBS, Cat. No. 100-106) is from Gemini Bioproducts. HEPES (Cat. No. H-4034), D-glucose (Cat. No. G-8270), and cycloheximide (Cat. No. C-7698) are from Sigma Chemicals. Polycarbonate filters (Transwells; 0.4 mm pore size, Cat. No. 3412 for 24-mm filters) can be purchased from Corning Costar Corp. (Cambridge, MA). Tissue culture grade plasticware is from Corning Plasticware. Tran^{35}S-label (Cat. No. 51006), [^{35}S]cysteine (Cat. No. 51002), and $H_2{}^{35}SO_4$ (Cat. No. 64040) can be purchased from ICN (Costa Mesa, CA). Reagents for the production of viruses are described elsewhere (Rodriguez-Boulan and Sabatini, 1978; see article by Hitt *et al*.) All other reagents are standard reagent grade and available from several sources. Sterile solutions are autoclaved or sterilized by ultrafiltration (0.2 mm).

There are numerous manufacturers of microscope heating and cooling chambers. We use the Harvard apparatus recording chamber (PDMI-2) and temperature controller (TC-202A). A variety of microinjection apparatuses are available from Narishige Inc. or from Eppendorf. Cooled charged-couple device (CCDs) cameras are also available from several manufacturers. For high-resolution time-lapse imaging, we recommend a camera capable of 12- to 16-bit digitization (4095–65,000 gray levels) with a 5- to 10-MHz controller for rapid acquisition rates. The Flaming Brown Micropipet puller (Model P-97) is from Sutter Instru-

ments. Glass capillaries for pulling microinjection needles are available from World Precision Instruments (Cat. No. 1B100F-6). The Sykes-Moore culture chamber, consisting of a 32 × 7-mm chamber (Cat. No. 1943-11111), silicone gaskets (Cat. No. 1943-33315), and the wrench assembly (Cat. No. 1943-44444) can be purchased from Bellco. Number 1 thickness, 25-mm glass coverslips for the chamber (Cat. No. 483800-80) are from VWR.

III. PROCEDURES

A. Adenovirus Transduction

1. Coinfection of MDCK Cells with Recombinant Adenovirus Vectors

Solutions

1. *Dulbecco's modified Eagle's medium (DMEM)*: Dissolve DMEM powder in 1 liter H_2O. Sterilize by filtering through a 0.2-μm pore filter.

2. *Complete DMEM (cDMEM)*: Add 50 ml heat-inactivated fetal bovine serum (FBS), 10 ml 0.2 *M* L-glutamine, 5 ml penicillin–streptomycin (10,000 U/ml and 10 mg/ml, respectively), and 5 ml MEM nonessential amino acids to 430 ml DMEM. Store at 4°C for up to 2 weeks.

Steps

1. For infection with replication-defective viruses, grow cells on semipermeable polycarbonate filter supports. Seed cells at confluency on day 1 and culture for 4 days with medium changed daily. MDCK strain II cells are confluent at a density of ca. 7×10^5 cells/cm^2, so approximately 3.3×10^6 cells should be seeded on each 24-mm filter.

2. Before applying adenovirus vectors, rinse cultures twice with serum-free DMEM (2 ml for the apical chamber and 2.5 ml for the basolateral chamber). Removal of serum proteins from the culture medium results in enhanced adsorption of adenovirus particles to the cell surface and improves infection efficiency. MDCK cells do not appear to be affected adversely by serum deprivation during the infection period, but this should be checked with other cell types before attempting infection.

3. Add recombinant adenoviruses, diluted in serum-free DMEM, at moi ranging from 1 to 1000 pfu/cell. Incubate at 37° for 1 h, gently tilting the plates every 15 min to mix. Two or more adenovirus vectors can be mixed together and applied simultaneously to cells. It is recommended that serial three-fold dilutions of viruses be tested in order to determine the optimal moi required for the quantitative expression of the marker proteins.

4. Vectors must be applied to the *apical* domain of epithelial cells, as infection is markedly more efficient from this surface. The reason for this is unclear, but a preference for adenovirus entry through the apical surface has been observed in every polarized epithelial cell type we have examined, including canine (MDCK), bovine (MDBK), and porcine (LLC-PK_1) kidney; rat thyroid (FRT) and retinal pigment epithelia (RPE-J); and human intestine (Caco-2). Serum-free DMEM, without virus, should be applied to the basolateral chamber. Infection should be performed in a minimum volume of DMEM required to keep the filter submerged. A recommended volume is 0.25 ml apical/0.5 ml basolateral for a 24-mm filter.

5. Following the infection period, add 2 ml cDMEM to both apical and basolateral chambers. It is not necessary to aspirate the virus because the addition of serum effectively terminates the infection. Culture the cells at 37°C for the desired incubation time. Expression of adenovirus-encoded proteins should be detectable by 4–6 h following infection, will rise gradually over the next 18 h and should reach a plateau by 24 h. This level of expression will be maintained for at least 1 week, provided the cells are fed daily. We routinely use cultures of polarized MDCK cells between 20 and 24 h postinfection.

6. Monitor infection after 24 h as follows:
   a. *Use indirect immunofluorescent staining* to determine (i) the percentage of cells in the culture expressing the transfected gene products and (ii) the intracellular distribution of the gene products. Under optimum infection conditions, at least 95% of the cells will express each adenovirus-encoded protein. If the ultimate goal of the experiment is the study of the molecular trafficking of two or more proteins in the same cell, it is essential that all of the cells that express one marker also express the second marker. Methods for fixation, permeabilization, and staining of epithelial cells grown on polycarbonate filters are described elsewhere in this manual.
   b. *Use immunoprecipitation or Western blotting* to determine (i) the molecular weight of the adenovirus-encoded proteins and (ii) the level of expression of the proteins in the culture. Ideally, both adenovirus-encoded proteins will be expressed at comparable levels.

Pitfalls

Each batch of adenovirus virus vector must be tested for optimum transduction. We find a batch-to-

batch variability in the correspondence of pfu obtained from plaque assays to the moi needed.

B. Infection of MDCK Cells with Enveloped RNA Viruses

Solutions

1. *DEAE-dextran (100X stock)*: Dissolve 100 mg DEAE-dextran (Sigma Cat. No. D1162) in 10 ml H_2O. Filter, sterilize, and store 1-ml aliquots at –20°C.

2. *Infection medium*: Add 13 ml 7.5% bovine serum albumin and 5 ml 1*M* HEPES, pH 7.4, to 482 ml DMEM. Filter, sterilize, and store at 4°C. Immediately before use, add 0.1 ml DEAE-dextran stock to 10 ml medium. DEAE-dextran is only necessary for infection with VSV.

3. *Virus stocks*: Vesicular stomatitis virus, Indiana strain (VSV), and influenza virus A (WSN strain) are grown in MDCK strain II cells, harvested, and plaque assayed as described by Rodriguez-Boulan and Sabatini (1978).

Steps

1. Set up 10-cm dishes of MDCK strain II cells, passages 6–20, and allow them to reach confluency. Cultures are infected with VSV or influenza virus 3 days after becoming confluent.

2. Before infecting cells, rinse cultures twice with infection medium. For viral infection, inoculate MDCK cells with 50 pfu/cell VSV or influenza WSN in 3.5 ml infection medium containing 0.1 mg/ml DEAE-dextran.

3. Incubate cultures for 1 h at 37°C.

4. Aspirate viral medium and rinse cultures twice with fresh infection medium.

5. Return VSV-infected cultures to 37°C and incubate a further 3.5 h before metabolic radiolabeling (see later). Incubate influenza WSN-infected cultures for 4.5 h at 37°C before labeling. Cultures should be examined hourly to monitor cytopathic effects.

C. Metabolic Radiolabeling and Accumulation of Marker Proteins in the Trans-Golgi Network

1. Radiosulfate Labeling of Glycoproteins at 20°C

Both $p75^{NTR}$ and LDLR are sulfated when expressed in MDCK cells. Sulfation occurs largely on asparagine-linked carbohydrate moieties on both proteins. Because this posttranslational modification occurs late in the secretory pathway, likely in the *trans*-Golgi or TGN, it provides a convenient method to label markers in the sorting compartment. When labeling is performed at the reduced temperature of 20°C, the labeled markers accumulate in the TGN because post-Golgi vesicular transport is inhibited.

Solutions

1. *Sulfate-free labeling medium*: Essentially, labeling medium is DMEM in which the $MgSO_4$ is replaced by $MgCl_2$. Combine 100 ml 10× DME salts (Ca^{2+}, Mg^{2+}-free), 10 ml 100× Ca^{2+}, Mg^{2+} stock, 10 ml MEM Vitamins, 10 ml of 100× stock MEM amino acid solutions (arginine, glutamine, histidine, isoleucine, leucine, lysine, phenylalanine, threonine, tryptophan, tyrosine, glycine, serine, and valine), 1 ml of 100× stock MEM solutions of methionine and cysteine, 10 ml MEM nonessential amino acid solution, 20 ml 1*M* HEPES, pH 7.4, 27 ml 7.5% BSA stock, and H_2O to a final volume of 1000 ml. Filter, sterilize, and store at 4°C.

2. *10× DME salts (Ca^{2+}, Mg^{2+}-free)*: Combine 50 ml 100 × $Fe(NO_3)_3$, 50 ml 100× NaH_2PO_4, 50 ml 100 × KCl, 22.5 g dextrose, 32 g NaCl, and 15 ml phenol red solution. Adjust volume to 500 ml with H_2O. Filter, sterilize, and store at 4°C.

3. *$Fe(NO_3)_3$ stocks*: Add 0.05 g $Fe(NO_3)_3$ to 50 ml H_2O to prepare a 100,000× stock solution. Dilute 100 µl into 100 ml H_2O to prepare 100× stock solution. Filter, sterilize, and store at 4°C.

4. *100× $Na\ H_2PO_4$*: Add 1.25 g NaH_2PO_4 to 100 ml H_2O. Filter, sterilize, and store at 4°C.

5. *100× KCl*: Add 4.0 g KCl to 100 ml H_2O. Filter, sterilize, and store at 4°C.

6. *100× Ca^{2+}, Mg^{2+}*: Add 2.96 g $CaCl_2{\cdot}2H_2O$ and 3.02 g $MgCl_2{\cdot}6H_2O$ to 100 ml H_2O. Filter, sterilize, and store at 4°C.

Steps

1. Twenty-four to 48 h following adenovirus infection, aspirate culture medium and rinse filters three times with sulfate-free labeling medium. Sulfate starve cells for 30 min at 37°C in this medium.

2. Label cells for 1 h at 20°C in sulfate-free labeling medium containing $H_2{}^{35}SO_4$. To label cells on one 75 mm Transwell filter, we use 0.5 mCi $H_2{}^{35}SO_4$ in 500 µl sulfate-free labeling medium. Place medium, preequilibrated at 20°C, on a sheet of Parafilm in a humid chamber and place the Transwell filter upon this so that label is exposed to the basolateral surface. Apply 2.5 ml sulfate-free labeling medium, without label, to the apical chamber to prevent drying.

2. Pulse–Chase Labeling with [^{35}S]Methionine/Cysteine

Solutions

1. *Methionine/cysteine-free labeling medium*: Prepare 1000 ml of medium following the product specification insert (Gibco SelectAmine kit, Cat. No. 19050), exclud-

ing the methionine and cysteine in the kit. Add 10 ml 1 *M* HEPES and 27 ml 7.5% BSA stock solution. Filter, sterilize, and store at 4°C.

For PC12 cells, replace the BSA will 20 ml dialyzed serum. To prepare the dialyzed serum, under sterile conditions, dialyze a mixture of two-thirds fetal bovine serum and one-third horse serum against PBS in 12,000 molecular weight cutoff dialysis tubing for 12–20 h. Dialyze serum to remove small molecules, which may be used to scavenge sulfate.

2. *Chase medium*: Add 5 ml of 100× MEM methionine and cysteine (left over from the Selectamine kit) solutions to 40 ml complete DMEM (or PC12 growth medium for PC12 cells). Immediately before use, add cyclohexamide to a concentration of 20 µg/ml.

Steps

1. Rinse MDCK cultures three times in methionine/cysteine-free labeling medium before incubation at 37°C for the final 30 min of incubation following viral infection. For PC12 cells, extensive rinsing may not be possible, so rinse once before the 30-min incubation.

2. Label VSV-infected MDCK cells with [^{35}S]methionine/cysteine (Tran^{35}S-label, ICN Cat. No. 51006). Label influenza WSN-infected cells with [^{35}S]cysteine (ICN Cat. No. 51002). Use 0.5 mCi, in a total volume of 3.5 ml labeling medium, to label each 10-cm plate. Pulse–label cells for 10 min at 37°C. Medium can be recycled twice if multiple dishes are to be labeled. Label LDLR- and p75-infected PC12 cells with [^{35}S]cysteine, due to the fact that these proteins are not sulfated as they are in MDCK cells. Use 0.5 mCi, in a total volume of 1 ml labeling medium, to label each 10-cm plate. Pulse–label cells for 15 min at 37°C, with gentle rocking every 5 min.

3. For MDCK cells, aspirate labeling medium and rinse plates three times with chase medium. For PC12 cultures, just aspirate medium.

4. Chase cultures at 20°C for 2 h in chase medium. During the chase at 20°C, roughly 60% of the labeled VSV G/influenza HA proteins are accumulated in the TGN (Muesch *et al*., 1996).

D. Vesicle Budding from the TGN in Semi-intact Cells

Semi-intact MDCK cells are prepared after accumulating marker proteins in the TGN (Muesch *et al*., 1996). Cells are first swollen in a low salt buffer and are subsequently scraped from the substratum, which produces large tears in the plasma membrane. Endogenous cytosol and peripheral membrane proteins are removed by washing with a high salt buffer. Addition of an exogenous source of cytosol, an energy-regenerating system, and incubation at 37°C typically result in the release of 25–65% of the total marker accumulated in the TGN into sealed vesicles. Budded vesicles are separated from the material that remains by a brief, low-speed centrifugation step.

Solutions

1. *Swelling buffer*: Add 7.5 ml 1 *M* HEPES/KOH, pH 7.2, and 7.5 ml 1 *M* KCl to 485 ml H_2O. Store at 4°C.

2. *10× transport buffer*: Add 20 ml 1 *M* HEPES/KOH, pH 7.2, 2 ml 1 *M* $Mg(OAc)_2$, and 18 ml 5 *M* KOAc to 60 ml H_2O. Store at 4°C.

3. *1× transport buffer*: Add 1 ml 10× transport buffer to 9 ml H_2O. Immediately before use, bring to 1 m*M* DTT and add protease inhibitors to 1× concentration.

4. *High salt buffer*: Add 10 ml 1 *M* HEPES/KOH, pH 7.2, 50 ml 5 *M* KOAc, and 1 ml 1 *M* $Mg(OAc)_2$ to 4391 ml H_2O. Store at 4°C. Immediately before use, bring to 1 m*M* DTT and add protease inhibitors to 1X concentration.

5. *1 M dithiothreitol stock*

6. *500× protease inhibitor stock*: Dissolve 5 mg of each of the following inhibitors individually in 330 µl dimethyl sulfoxide (DMSO) and combine the three solutions.
   a. *Pepstatin A*: (Sigma Cat. No. P-4265)
   b. *Leupeptin*: (Sigma Cat. No. L-8511)
   c. *Antipain*: (Sigma Cat. No. A-6191)

7. *100 mM PMSF stock*

8. *Energy mix*: Pipette in the following order: 3 µl ATP, 2 µl GTP, 4 µl creatine phosphate, and 3 µl creatine kinase.
   a. *0.1 M ATP* (Boehringer Mannheim Cat. No. 519 987)
   b. *0.2 M GTP* (Boehringer Mannheim Cat. No. 106 399)
   c. *0.6 M creatine phosphate* (Boehringer Mannheim Cat. No. 621 722)
   d. *8 mg/ml creatine kinase* (Boehringer Mannheim Cat. No. 127 566)

9. *Bovine brain cytosol*: Prepare gel-filtered bovine brain cytosol in batches exactly as described previously (Malhotra *et al*., 1989). The protein concentration should be 10–20 mg/ml. Snap freeze 50-µl aliquots in liquid nitrogen and store at –80°C.

Steps

All steps are performed on ice, unless otherwise specified.

1. Following the 20°C incubation, wash the monolayer twice briefly with ice-cold swelling buffer and incubate in the same for 15 min.

2. Scrape cells from the filter (or plastic dish) with a rubber policeman into 2.5 ml transport buffer. DiSPo scrapers (Baxter Scientific, McGaw Park, IL) work well for this purpose. The best way to scrape cells from the Transwell filter is to place the filter inside the lid of the dish so that the bottom lies flat against the plastic. This prevents the scraper from poking through the filter, but care must be exercised to prevent tearing the filter. Scraping does not have to be vigorous, but should be done with long, gentle strokes. Transfer cells to 1.5-ml microfuge tubes and rinse the filter (or dish) with 2.5 ml fresh transport buffer. Combine with cells from first scraping. Discard the filter as radioactive waste.

3. Pellet cells by centrifugation at 800 *g* for 5 min in a refrigerated microfuge.

4. Pool semi-intact cells into one tube and wash with 1.5 ml high salt buffer on ice for 10 min. Pellet cells by centrifugation at 800 *g* for 5 min in a refrigerated microfuge.

5. Resuspend cells in transport buffer. A volume of 250 µl is used to resuspend cells from one filter (or dish).

6. Set up vesicle budding assay.
   a. In standard assays, suspend semi-intact cells (ca. 10 µl = 20–25 µg protein) in an assay volume of 50 µl transport buffer supplemented with 50 µg gel-filtered bovine brain cytosol and an energy-regenerating system (1 m*M* ATP, 1 m*M* GTP, 5 m*M* creatine phosphate, and 0.2 IU creatine kinase). Combine components in the following order: mix 26 µl H_2O, 1 µl 100 m*M* PMSF, 4 µl 10× transport buffer, 4 µl energy mix, 5 µl cytosol (final concentration = 1 mg/ml), and 10 µl semi-intact cells.
   b. Important controls include assays in which either the cytosol or the energy mix or both components are omitted. For the complete depletion of energy from the system, cytosol and semi-intact cells must be preincubated for 10 min on ice with 0.6 U/ml apyrase before assembling the assay. In the absence of either cytosol or energy, vesicular release from semi-intact cells should be negligible. We suggest that serial dilutions of cytosol (i.e., 0.1–10 mg/ml) be tested in order to determine the optimal range of cytosol-dependent vesicle budding in the assay.

7. Incubate assays at 37°C for desired time. In standard assays, we incubate for 30–45 min. However, we suggest that a time course of vesicle budding be performed to optimize the assay for different marker proteins. As additional controls, two complete assays should be assembled and incubated at 0 and 20°C. At these reduced temperatures, vesicular release from semi-intact cells should be insignificant.

8. Pellet semi-intact cells by centrifugation at 800 *g* for 5 min in a refrigerated microfuge. Transfer supernatant fractions to clean microfuge tubes. The pellets (containing nonbudded material remaining in the TGN) and supernatants (containing the vesicles released during the 37°C incubation) can be analyzed further.
   a. To quantify the efficiency of vesicular release of each marker under different conditions, samples can be lysed in SDS–PAGE sample buffer and analyzed directly by PAGE. In cells infected with VSV or influenza WSN, the viral proteins should be the only labeled proteins in the lysates. Alternatively, following adenovirus-mediated transfer of cDNAs encoding $p75^{NTR}$ and LDLR into MDCK cells, these proteins are by far the most heavily labeled proteins when radiosulfate is used as a precursor.
   b. To confirm that markers are present inside sealed vesicles, the supernatant fraction should be treated with either proteinase K or trypsin. In the absence of Triton X-100, only the cytoplasmic domains of the proteins will be cleaved and this can be detected as a relatively small mobility increase during SDS–PAGE. In contrast, protease treatment in the presence of 1% Triton X-100 will result in complete digestion of markers. Use three 50-µl assay samples for this analysis. To tube 1, add nothing. To tube 2, add 2.5 µl protease (10 mg/ml stock → 0.5 mg/ml final). To tube 3, add 2.5 µl protease and 2.5 µl 20% Triton X-100. Incubate on ice for 30 min. Inactivate protease with 1 mM PMSF or 1 mg/ml soybean trypsin inhibitor before lysing samples in SDS–PAGE sample buffer. Analyze products by SDS–PAGE.
   c. Immunoisolation of specific classes of transport vesicles is performed using antibodies against the cytoplasmic portions of cargo proteins as well as appropriate negative controls. (i) Use 5 mg protein A-Sepharose (Pharmacia, Piscataway, NJ; Cat. No. 17-0780-01) for each immunoisolation. Swell in transport buffer for 10 min. (ii) If using a murine monoclonal primary antibody, use a bridge. Incubate 5 mg protein A–Sepharose with 50 µg rabbit anti-mouse IgG (Rockland Labs, supplied by VWR, New York, Cat. No. 610-4102) in 1 ml transport buffer for 60 min at room temperature. Wash twice with transport buffer. (iii) Block nonspecific binding sites in 1 ml trans-

port buffer containing 0.2% BSA for 60 min at room temperature. (iv) Couple primary antibody for 2 h at room temperature in transport buffer. Wash twice with transport buffer. Titrate each antibody to determine amount needed for quantitative recovery of vesicles. (v) Incubate immunoadsorbant with the supernatant fraction from the vesicle budding assay in a total volume of 1 ml transport buffer for 2–18 h at 4°C with end-over-end rotation. In some cases, vesicle coat proteins may mask epitopes on the cytoplasmic tails of cargo. Therefore, it may be necessary to wash the vesicles in high salt buffer prior to immunoisolation to strip coat proteins. Add 33 µl of 1 *M* KOAc to 50-µl vesicles. Incubate on ice for 10 min. Add 333 µl salt-free transport buffer [20 m*M* HEPES/KOH, 2 mM $Mg(OAc)_2$]. (vi) Wash immunoprecipitates six times with transport buffer. Elute bound markers by boiling 5 min in SDS–PAGE sample buffer. Analyze by SDS–PAGE.

E. Vesicle Budding from TGN-Enriched Membranes

A TGN-enriched membrane fraction is prepared from metabolically labeled PC12 cells after marker proteins have been accumulated in the TGN. Initially, a postnuclear supernatant is prepared following the method of Tooze and Huttner (1992). From the postnuclear supernatant a TGN-enriched membrane fraction is prepared (Xu *et al.*, 1995). As with semi-intact MDCK cells, addition of an exogenous source of cytosol and an energy-regenerating system leads to the release of accumulated marker protein from the TGN in sealed vesicles. All steps for the vesicle budding assay are identical to those for intact MDCK cells except that 50-µg aliquots of TGN-enriched membranes are used for each individual assay condition.

F. Expression of cDNA Using Microinjection

Solutions

1. *Preparation of cDNA stocks for microinjection*: Prepare DNA using either a midi or maxi preparation, making sure to suspend the DNA pellet (final concentration of at least 0.2 mg/ml) in sterile water rather than Tris–EDTA. DNA stocks can be stored at either 4 or –20°C.

2. *HEPEs:KCl microinjection buffer*: 10 m*M* HEPES, 140 m*M* KCl, pH 7.4

3. *cDNA for microinjection*: Dilute cDNA stock in HKCl to a final concentration of 5–20 µg/ml (see later for how to choose a concentration)

4. *MDCK cell culture medium*: DMEM prepared as per manufacturer's instructions. Add 50 ml FBS (10% FBS final concentration) and 10 ml of 1 *M* HEPES, pH 7.4 (20 m*M* final concentration), and 5 ml of MEM nonessential amino acids to 435 ml DMEM.

Steps

For microinjection, cells must be cultured on sterilized glass coverslips.

1. Sterilize coverslips using either of the following methods.
   a. ***Autoclaving:*** Place coverslips in a glass petri dish and autoclave on the dry cycle for 20 min. If cells adhere well to the glass, this method is most convenient, as many coverslips can be sterilized at once.
   b. ***Acid washing:*** Place coverslips in histology staining racks. Wash coverslips in a beaker of 2 *N* hydrochloric acid (2× 5-min washes), rinse in distilled water (2 × 5-min rinses), and wash in 100% ethanol (3 × 2 min). After the final ethanol wash, place the staining racks containing the cleaned coverslips into a dry beaker, cover with heavy-duty foil, and bake at 250°C for 1 h. Acid treatment "etches" the glass, creating a somewhat rough surface that is useful if cells are not sufficiently adherent on the coverslips.
2. Place the sterilized coverslips into a 10-cm tissue culture dish. Seven 25-mm coverslips can be placed in one 10-cm dish.
3. Trypsinize cells and seed onto coverslips placed previously in the 10-cm culture dish(es).
   a. ***For experiments in nonpolarized cells:*** Seed 5×10^5 cells onto coverslips. Use a cell stock that is actively dividing (i.e., sparse cells). Cells should be used between 36 and 48 h after they are seeded onto the coverslips. Do not use the cells prior to 36 h postplating.
   b. ***For experiments in polarized cells:*** Seed cells at confluency onto coverslips. Change the medium 24 h after plating and culture the cells another 2–4 days prior to use. Do not change the culture medium again as this can result in changes in cell morphology.
4. On the day of the experiment, transfer coverslips to 3.5-cm culture dishes. Add fresh medium and microinject the cDNA into cell nuclei. As one goal of these experiments is to achieve synchronized exogenous protein expression in a population of cells it is

important that you only inject cells on the same coverslip for ~5 min. If a sufficient number of cells was not injected in that time, take another coverslip from the incubator and repeat.

5. After injection, place cells into the incubator and wait for protein to be expressed.

6. Monitor and identify the minimum expression time.[1] We routinely find that 1 h is sufficient for the expression of many different cDNAs in both nonpolarized and polarized MDCK cells. However, we have also found that there is heterogeneity in expression time depending on the cDNA being injected, as well as on the cell types being used. Minimum expression time can be determined by merely looking at the injected cells at a series of time points (e.g., 1-h intervals) after microinjection. Fluorescently tagged reporter proteins can be visualized directly without fixation. If your reporter is not fluorescently tagged, then fix the cells at 1-h intervals after microinjection and immunostain with antibodies against the exogenous protein.

G. Synchronizing Transport through the Biosynthetic Pathway

Solutions

1. *Bicarbonate-free MDCK cell culture medium*: DMEM without bicarbonate prepared as per manufacturer instructions. Add 25 ml FBS (5% FBS final concentration), 10 ml of 1 *M* HEPES, pH 7.4 (20 m*M* final concentration), and cycloheximide (final concentration 100 µg/ml) to 475 ml DMEM.

2. *Recording medium*: Hank's balanced salt solution with calcium and magnesium (HBSS-CM). Add 5 ml FBS (1% FBS final concentration; serum does autofluoresce so it is important to keep the concentration low), 25 ml of 9% D-glucose (4.5 g/liter glucose final concentration), 5 ml HEPES, pH 7.4 (10 m*M* HEPES final concentration), and cycloheximide (final concentration 100 µg/ml) to 465 ml HBSS-CM.

Steps

Synchronization of protein trafficking can be achieved through the use of a series of temperature shifts. Cycloheximide added during the temperature shifts will effectively create a pulse of newly synthesized protein that can be chased synchronously from ER to Golgi and from the Golgi to the plasma membrane. Newly synthesized protein can be accumulated in the ER or the Golgi when cells are incubated at 15 or 20°C, respectively. These proteins will leave the Golgi when cells are shifted to the permissive temperature for secretion, (30–37°C). Because most laboratories do not maintain a tissue culture incubator set to 15 or 20°C (our laboratory uses a small refrigerator set to the desired temperature), you will need to use a bicarbonate-free medium during these incubation periods. Check that this medium remains between pH 7.2 and 7.4 during the course of the temperature blocks.

One hour after microinjection (or the minimum expression time for your protein of interest, see earlier discussion), place cells into bicarbonate-free medium with cycloheximide.

1. To study ER to Golgi events, place cells into recording medium and incubate at 15°C in the thermally regulated recording chamber mounted on a microscope for time-lapse imaging. (For a more extensive discussion on equipping an imaging work station, see Mikhailov).
   a. Monitor the total cellular fluorescence by acquiring images of your cells at 10-min intervals. When total cellular fluorescence stabilizes for ~10 min, acquire and save both transmitted light and fluorescent images of the cells you will be studying.
   b. Increase the temperature of the recording chamber to 20°C. Wait 5 min for the temperature and focus to stabilize.
   c. Acquire time-lapse images to evaluate ER to Golgi transport events. ER to Golgi transport can be studied at either low or high spatial and temporal resolution depending on the questions being addressed.

2. To study Golgi to plasma membrane events, place cells into bicarbonate-free medium and incubate at 20°C.
   a. Determine the time required to accumulate newly synthesized protein in the Golgi. We routinely find that 1–3 h is sufficient, but this time varies from protein to protein. The extent to which new protein has accumulated in the Golgi can be determined by assessing the degree of colocalization with Golgi markers at a series of time points (e.g., 30-min intervals) after shifting to 20°C.
   b. After accumulating protein in the Golgi in a 20°C incubator, place cells into recording medium and incubate at 20°C in the recording chamber mounted on a microscope for time-

[1] The minimum expression time is the time at which exogenous, newly expressed protein is present in the endoplasmic reticulum, but is not yet found at the plasma membrane. It is critical that no exogenous protein is at the cell surface for studies of Golgi to plasma membrane trafficking.

lapse imaging. Acquire and save both transmitted light and fluorescent images of the cells you will be studying.

c. Increase the temperature of the recording chamber to 32°C. Wait 5 min for the temperature and focus to stabilize.

d. Acquire time-lapse images to evaluate post-Golgi transport events. Post-Golgi transport can be studied at either low or high spatial and temporal resolution depending on the questions being addressed.

e. At the end of every time-lapse recording, save a transmitted light image of the cells from which you recorded data.

H. Kinetics of Protein Transport through the Secretory Pathway

Steps

To determine the rates at which a fluorescent protein moves from the ER to the Golgi and then to the plasma membrane using time-lapse fluorescence microscopy, it is necessary to introduce a pulse of fluorescence into individual cells. We find that microinjection of cDNA is best for this purpose, as the expression of injected cDNA is generally rapid and can be controlled temporally. The kinetics of ER-to-Golgi and Golgi-to-plasma membrane cargo transport can be determined by measuring the ratio of Golgi-associated fluorescence/total fluorescence over time. It is imperative to be able to distinguish Golgi-associated from non-Golgi-associated fluorescent signals. This can be done in two ways. First, you can coexpress a fluorescently tagged Golgi resident protein to use as a reference during time-lapse recordings. Alternatively, you can make an educated deduction as to whether your reporter is in the Golgi based on its localization and the intensity of its fluorescent signal (supplemental data in Kreitzer *et al.*, 2000). Using this differential in position and intensity, you can define a threshold above, which includes Golgi-associated fluorescence, and below, which includes all other cellular fluorescence. Given that you are trying to account for fluorescence present in the entire cell, these assays are best executed using low-magnification objectives capable of imaging an entire cell in a single focal plane.

One hour after microinjection (or the minimum expression time for your protein of interest, see earlier discussion), place cells into bicarbonate-free medium with cycloheximide and incubate at 20°C to accumulate newly synthesized protein in the Golgi.

1. To evaluate ER to Golgi transport kinetics, mount the coverslip into the precooled (20°C) recording chamber on the microscope in recording medium with cycloheximide.

   a. Acquire time-lapse images at 5- to 30-min intervals until the fluorescently tagged reporter has accumulated in the Golgi.

   b. Determine the minimum time required for maximal transport of protein from the ER to the Golgi by measuring the ratio of Golgi-associated fluorescence/total fluorescence over time.

2. To evaluate kinetics of Golgi emptying, place cells into bicarbonate-free DMEM with cycloheximide and incubate at 20°C. The duration of the 20°C temperature block depends on the time it takes to accumulate maximally your protein of interest in the Golgi (see earlier discussion).

   a. Acquire time-lapse images at 5- to 30-min intervals.

   b. Determine the rate at which fluorescently tagged cargo empties from the Golgi by measuring the ratio of Golgi-associated fluorescence/total fluorescence over time in individual cells.

I. Measuring Delivery of Post-Golgi Carriers to the Plasma Membrane

Solutions and Materials

1. Phosphate-buffered saline with calcium and magnesium (PBS-CM)

2. 2% paraformaldehyde prepared freshly in PBS-CM

3. Antibodies reactive with an extracellular epitope contained in the plasma membrane reporter protein. Surface immunolabeling is dependent on having an antibody that recognizes an extracellular epitope on the plasma membrane protein being studied. If this is not available, it may be desirable to create a cDNA probe that contains an epitope tag (e.g., HA, myc or FLAG tag) that can be immunostained.

Steps

Delivery of newly synthesized proteins to the plasma membrane can be evaluated using single cell assays or by biochemical methods. Evaluation of protein delivery to the plasma membrane in single cells can be analyzed from either fixed or living samples. Analysis in fixed samples involves cell surface selective immunolabeling of the expressed reporter protein. Analysis in living samples requires a relatively robust expression of the GFP-tagged reporter protein and acquisition of time-lapse images at relatively high frame rates using either total inter-

nal reflection fluorescence microscopy or spinning disk confocal microscopy. In TIR-FM, membrane-bound transport intermediates containing GFP-tagged fusion proteins are detected only when they move into an evanescent field, which in our experiments was within ~120 nm of the plasma membrane domain in contact with the substratum, i.e., the basal membrane. Schmoranzer and colleagues (2000) have established a quantitative method for detecting *bona fide* fusion of post-Golgi transport intermediates with the plasma membrane. Briefly, exocytic events are defined by a simultaneous rise in both the carrier's total fluorescence intensity and the area occupied by carrier fluorescence as it flattens into the plasma membrane and the cargo diffuses laterally. (For a more extensive description of TIR-FM in studying exocytosis, see Mikhailov). Exocytic events occurring in the lateral membrane of polarized epithelial cells can be identified using similar criteria when time-lapse images are acquired by high-speed confocal microscopy (for a complete description of lateral membrane fusion analysis, see Kreitzer *et al.*, 2003). Biochemical methods for studying delivery to the plasma membrane in a large population of cells, such as pulse–chase, cell surface biotinylation assays, have been described in detail previously (see article by Rodriguez–Boulan *et al.*).

1. Measuring the rate of protein delivery to the cell surface in fixed cell, "time-lapse" experiments. If cells are grown on glass (as would be the case if exogenous proteins are expressed by cDNA microinjection), this method is useful in evaluating the delivery of proteins to the apical membrane only. For surface-labeling analysis of delivery to the basolateral membrane, cells must be grown on semipermeable filter supports and exogenous proteins must be introduced by transfection or viral infection methods.
    a. Microinject GFP-tagged cDNA into the cell nuclei.
    b. Accumulate newly synthesized protein in the Golgi at 20°C.
    c. Shift to the permissive temperature for transport out of the Golgi (37°C).
    d. At 15- to 30-min intervals after releasing the Golgi block, fix cells in paraformaldehyde for 5 min at room temperature. Do not permeabilize with detergent. Fixation in a nonpermeabilizing fixative, such as paraformaldehyde, enables selective immunolabeling of surface-associated proteins.
    e. Label, by indirect immunofluorescence, the surface-associated reporter protein. Make sure to use a fluorescently conjugated secondary antibody other than fluorescein (or any dye excitable at 488 nm).
    f. Acquire images of both the surface-associated (immunostained) and the total (GFP) protein expressed at each time point after release of the Golgi block. It is imperative to use identical acquisition settings for the individual fluorophores in each time-lapse sample as this is all that allows you to quantitatively (ratiometrically) evaluate the relative amount of reporter protein delivered to the cell surface.
    g. Calculate the integrated fluorescence intensity of both surface-associated and total fluorescence in each cell expressing the reporter protein. The ratio of surface fluorescence (immunostained) to total fluorescence (GFP) of your reporter reflects the relative amount of protein that has been delivered to the plasma membrane at each time point. Over time, this ratio should increase and will directly reflect the rate of protein delivery from the Golgi to the plasma membrane.
2. Analysis of exocytosis using time-lapse total internal reflection fluorescence microscopy (TIR-FM).
    a. Microinject GFP-tagged cDNA into the cell nuclei.
    b. Accumulate newly synthesized protein in the Golgi at 20°C.
    c. Mount coverslip in the recording chamber on a microscope equipped for TIR-FM. Acquire and save both bright-field and epifluorescent images of the cells you will be studying.
    d. Shift to the permissive temperature for transport out of the Golgi and wait 5 min for the temperature and focus to stabilize.
    e. Acquire time-lapse images (aim for at least four to five frames per second) to visualize exocytic events occurring in the basal plasma membrane. The typical duration of our recordings is 1–2 min.
    f. Analyze images for exocytic events as described in Schmoranzer *et al.* (2000).
3. Analysis of exocytosis using time-lapse, spinning-disk confocal microscopy.
    a. Microinject GFP-tagged cDNA into the cell nuclei.
    b. Accumulate newly synthesized protein in the Golgi at 20°C.
    c. Mount coverslip in the recording chamber on a microscope equipped with a spinning disk confocal head. Acquire and save both bright-field and epifluorescent images of the cells you will be studying.

d. Shift to the permissive temperature for transport out of the Golgi and wait 5 min for the temperature and focus to stabilize.
e. Acquire time-lapse images (aim for four to five frames per second) to visualize exocytic events occurring along the lateral membrane. Photobleaching that occurs during confocal image acquisition typically limits the duration of time-lapse sequences to ~1–2 min.
f. To evaluate the spatial positioning of cargo delivery events, acquire time-lapse sequences as described in **step e** at multiple Z-axis positions throughout individual cells.
g. Analyze images for exocytic events as described in Kreitzer *et al.* (2003).

References

Baird, G. S., Zacharias, D. A., *et al.* (2000). Biochemistry, mutagenesis, and oligomerization of DsRed, a red fluorescent protein from coral. *Proc. Natl. Acad. Sci. USA* **97**(22), 11984–11989.

Chalfie, M., Tu, Y., Euskirchen, G., Ward, W. W., and Prasher, D. C. (1994). Green fluorescent protein as a marker for gene expression. *Science* **263**, 802–805.

Grindstaff, K., Yeaman, C., Anandasabapathy, N, Hsu, S.-C., Rodriguez-Boulan, E., Scheller, R., and Nelson, W. J. (1998). Sec 6/8 complex is recruited to cadherin-medicated cell-cell contacts and specifies transport vesicle delivery to the basal-lateral membrane in polarized epithelial cells. *Cell* **93**, 71–74.

Hunziker, W., Harter, C., *et al.* (1991). Basolateral sorting in MDCK cells requires a distinct cytoplasmic domain determinant. *Cell* **66**, 907–920.

Kreitzer, G., Marmorstein, A., *et al.* (2000). Kinesin and dynamin are required for post-Golgi transport of a plasma-membrane protein. *Nature Cell Biol.* **2**(2), 125–127.

Kreitzer, G., Schmoranzer, J., *et al.* (2003). Three-dimensional analysis of post-Golgi carrier exocytosis in epithelial cells. *Nature Cell Biol.* **5**(2), 126–136.

Le Bivic, A., Sambuy, Y., *et al.* (1991). An internal deletion in the cytoplasmic tail reverses the apical localization of human NGF receptor in transfected MDCK cells. *J. Cell Biol.* **115**, 607–618.

Marmorstein, A. D., Csaky, K. G., Baffi, J., Lam, L., Rahaal, F., and Rodriguez-Boulan, E. (2000). Saturation of, and competition for entry into, the apical secretory pathway. *Proc. Natl. Acad. Sci. USA* **97**, 3248–3253

Matz, M. V., Fradkov, A. F., *et al.* (1999). Fluorescent proteins from nonbioluminescent Anthozoa species. *Nature Biotechnol.* **17**(10), 969–973.

Mikhailov, A. (ed.) "Practical Fluorescence Microscopy: Protein Localization and Function in Mammalian Cells." Humana Press, Clifton, NJ.

Musch, A., Xu, H., *et al.* (1996). Transport of vesicular stomatitis virus G protein to the cell surface is signal mediated in polarized and nonpolarized cells. *J. Cell Biol.* **133**(3), 543–558.

Rodriguez-Boulan, E., and Sabatini, D. D. (1978). Asymmetric budding of viruses in epithelial monlayers: A model system for study of epithelial polarity. *Proc. Natl. Acad. Sci. USA* **75**, 5071–5075.

Schmoranzer, J., Goulian, M., *et al.* (2000). Imaging constitutive exocytosis with total internal reflection fluorescence microscopy. *J. Cell Biol.* **149**(1), 23–32.

CHAPTER

28

Assays Measuring Membrane Transport in the Endocytic Pathway

Linda J. Robinson and Jean Gruenberg

I. INTRODUCTION

Significant progress has been made in understanding mechanisms regulating endocytic membrane traffic using cell-free assays (Braell, 1987; Davey *et al*., 1985; Diaz *et al*., 1988; Gruenberg and Howell, 1986; Woodman and Warren, 1988) (see Fig. 1). Both early and late endosomes exhibit homotypic fusion properties *in vitro*, as *in vivo*, yet they do not fuse with each other (Aniento *et al*., 1993). Transport from early to late endosomes is achieved by multivesicular intermediates termed endosomal carrier vesicles (ECV/MVB), which are presumably translocated on microtubules between the two compartments (Aniento *et al*., 1996; Bomsel *et al*., 1990; Gruenberg *et al*., 1989). The vectorial or heterotypic interactions of ECV/MVBs with late endosomes have also been reconstituted *in vitro*, as has the involvement of microtubules and motor proteins in this process (Aniento *et al*., 1993; Bomsel *et al*., 1990). By reducing the components in these *in vitro* assays to a cytosol source, an ATP-regenerating system, salts, and the purified endosomal membranes, the specificity of endosomal fusion events has been addressed, and the molecules and mechanisms involved have been studied. In fact, a number of conserved molecules, as well as molecules specific for different steps of the endocytic pathway, have been identified and/or characterized using cell-free assays such as those described in this protocol (for review, see Gruenberg and Maxfield, 1995).

This assay for endocytic vesicle fusion is based on the formation of a complex resulting from a reaction between two products present in separate populations of endosomes: avidin and biotinylated horseradish peroxidase (bHRP). These reaction products can be internalized into endosomes by fluid phase or receptor-mediated endocytosis *in vivo*. Avidin and a biotinylated compound are used to provide a fusion-specific reaction because of the high binding affinity and low dissociation constant of avidin for biotin. Following internalization, cells are homogenized and purified endosomal fractions are prepared, which are combined in the assay together with cytosol and ATP. If fusion occurs, a complex is formed between avidin and bHRP. At the end of the assay, the reaction mixture is extracted in detergents in the presence of excess biotinylated insulin as a quenching agent. The avidin–bHRP complex is then detected by immunoprecipitation with antiavidin antibodies, and the enzymatic activity of the bHRP associated with the immunoprecipitate is quantified. This article describes techniques for the preparation and partial purification of three different loaded endosomal fractions from BHK cells: early endosomes, endosomal carrier vesicles, and late endosomes. In addition, this article describes the preparation of the cytosol source used, as well as the techniques for the fusion assays themselves.

II. MATERIAL AND INSTRUMENTATION

Standard laboratory rockers for washing cells and a large 37°C water bath, which can fit a metal plate of dimensions of 20 × 33 cm, are used. Large rectangular ice buckets (Cat. No. 1-6030), from NeoLab GmbH, can also accommodate metal plates of the same dimensions. Cell scrapers (flexible rubber policemen) with a silicone rubber piece of about 2 cm, cut at a sharp

Copyright 2006, Elsevier Science (USA).
All rights reserved.

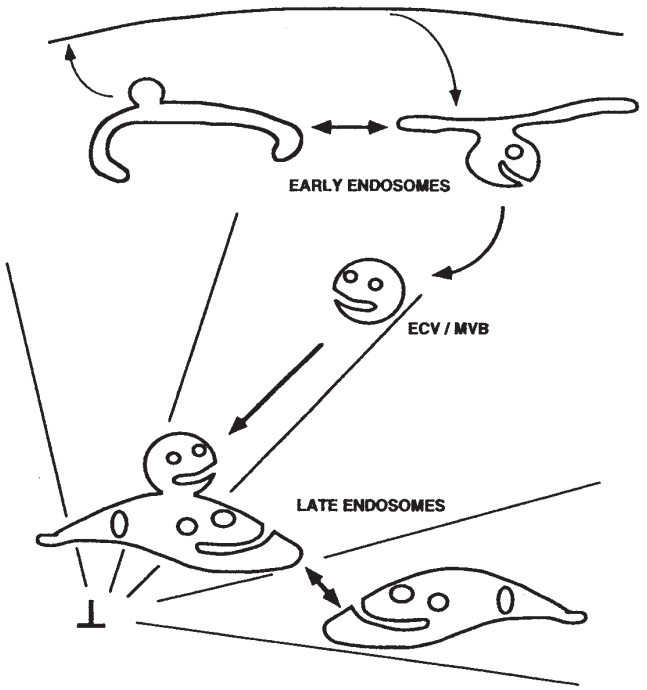

FIGURE 1 Membrane trafficking in the endocytic pathway. The reconstituted steps of the endocytic pathway described in this protocol are the (a) fusion of early endosomes with each other, (b) fusion of ECV/MVBs with late endosomes, and (c) fusion of late endosomes with each other. An *in vitro* budding assay for the formation of ECV/MVBs from early endosomes, which are competent to fuse with late endosomes, is described in Aniento *et al.* (1996). As shown, ECV/MVBs are transported along microtubules from early to late endosomes. If microtubules are depolymerized *in vivo*, prior to the loading of cells with an endocytic tracer, this tracer will accumulate in ECW/MVBs. These vesicles will then fuse with late endosomes, loaded with a different marker, *in vitro*.

angle, and attached to a metal bar, are made. A standard low-speed cell centrifuge and Beckman ultracentrifuges and rotors are used. The refractometer (Cat. No. 79729) is from Carl Zeiss Inc., and the pump for collecting sucrose gradients (peristaltic pump P-l) is from Pharmacia Fine Chemicals. A rotating wheel (such as Snijders Model 34528) with a speed of about 10 rotations per minute should be used. All tissue culture reagents, including modified Eagle's medium (MEM), are from either Sigma Chemical Company or GIBCO-BRL/Life Technologies. Peroxidase from horseradish (HRP) (Cat. No. P-8250), ATP (disodium salt, Cat. No. A-5394), and deuterium oxide (D_2O, Cat. No. D-4501) are from Sigma Chemical Company, Ltd. Biotinyl-ε-aminocaproic acid *N*-hydroxysuccinimide ester (biotin-X-NHS, Cat. No. 203188) is from Calbiochem. Avidin (egg white, Cat. No. A-887) is from Molecular Probes. Creatine phosphate (Cat. No. 621714), creatine phosphokinase (Cat. No. 127566), and hexokinase [$(NH_4)_2SO_4$ precipitate of yeast hexokinase, 1400 U/ml, Cat. No. 1426362] are from Boehringer-Mannheim GmbH. Protein A–Sepharose beads (Cat. No. CL-4B) are from Pharmacia. Antiavidin antibodies are generated by injecting purified avidin into rabbits and are affinity purified prior to use. Antiavidin antibodies are also available commercially from several companies. BCA protein assay reagents (Cat. No. 23223) are from Pierce, and Bio-Rad protein assay reagents (Cat. No. 500-0006) are from Bio-Rad Laboratories GmbH.

III. PROCEDURES

A. Internalization of Endocytic Markers into Early Endosomes (EE) from BHK Cells

Solutions

1. *Internalization media (IM)*: MEM containing 10 *mM* HEPES and 5 m*M* D-glucose, pH 7.4. Filter sterilize and store at 4°C.
2. *Phosphate-buffered saline (PBS)*: 137 m*M* NaCI, 2.7 m*M* KCL, 1.5 m*M* KH_2PO_4, and 6.5 m*M* Na_2HPO_4; should be pH 7.4. Filter sterilize and store at 4°C.
3. *Biotinylated horseradish peroxidase*: Dissolve 20 mg of HRP in 9.5 ml of 0.1 *M* NaHCO3/Na_2CO_3, pH 9.0, buffer (make fresh and check pH carefully) in a small glass Erlenmeyer flask. Dissolve 20 mg of biotin-X-NHS in 0.5 ml dirnethylformamide. Mix by adding the biotin dropwise to the HRP mixture while gently stirring or shaking the Erlenmeyer and incubate at room temperature with gentle stirring for at least 45 min (a 50:1 molar excess of biotin is important). Quench unreacted active groups with 1 ml of 0.2 *M* glycine, pH 8.0 (use KOH to pH), by adding dropwise while mixing, and mix for an additional 15 min at room temperature. Transfer to 4°C. Dialyze the mixture extensively against PBS—or IM at 4°C (at least four changes of 200 ml each time). The final dialysis should be in IM. Measure protein concentration (should be about 2 ml/ml) and HRP enzymatic activity (should be unchanged). Aliquot in sterile tubes, freeze in liquid N_2, and store at –20°C until use. Immediately before use, thaw quickly and warm to 37°C.
4. *Avidin*: Avidin powder dissolved in IM at 3 mg/ml. Make fresh immediately before use and warm to 37°C.
5. *PBS/BSA*: 5 mg/ml BSA in PBS-. Make fresh before use and cool to 4°C.

Steps

1. *Cell culture*: Maintain monolayers of baby hamster kidney (BHK-21) cells as described in Gruenberg *et al.*

(1989). For a fusion assay of 5–10 points, eight petri dishes (10 cm diameter) should be prepared 16 h before the experiment: four for preparing bHRP-labeled EEs and four for preparing avidin-labeled EEs.

2. *Fluid-phase internalization*: Wash each 10-cm dish of cells twice with 5 ml ice-cold PBS—on ice. This and other washes on ice to follow are performed most easily by placing four dishes onto a metal plate in a large ice bucket on a rocker. After the last wash, remove PBS and place the dish on a metal plate in a 37°C water bath. Add at least 3 ml/dish bHRP or avidin solution prewarmed to 37°C. Incubate for 5 min.

3. *Washes*: From now on, all work should be done at 4°C or on ice. Return the dishes to the metal plate in the ice bucket. Remove the avidin or bHRP solution and wash dishes three times for 5 min with 5 ml ice-cold PBS/BSA followed by 2 × 5 min with 5 ml ice-cold PBS.

4. *Homogenization and fractionation*: Go directly to Section IIIC.

B. Internalization of Endocytic Markers into Endosomal Carrier Vesicles (ECV) and Late Endosomes (LE)

Solutions

1. *Nocodazole stock*: 10 m*M* in dimethyl sulfoxide (DMSO), aliquoted, and stored at –20°C.
2. *IM/BSA*: IM containing 2 mg/ml BSA. Make fresh before use and warm to 37°C.
3. All solutions listed in Section III,A.

Steps

1. *Cell culture*: For a fusion assay of 5–10 points, 10 dishes (10 cm) of BHK cells should be prepared as described in Section III,A, step 1. For ECV–LE fusion assays, use 5 dishes for bHRP-labeled ECVs and 5 dishes for avidin-labeled LEs, For LE–LE fusion assays, use 5 dishes for bHRP-labeled LEs and 5 dishes for avidin-labeled LEs.

2. *Nocodazole pretreatment for ECV preparation*: Intact microtubules are required for the delivery of endocytosed markers to the LE. Therefore, markers accumulate in transport intermediates (ECVs) in the absence of microtubules. Whereas stable microtubules are cold sensitive, dynamic microtubules are depolymerized easily in the presence of nocodazole (Aniento *et al*., 1993; Bomsel *et al*., 1990). In BHK cells, microtubules can be depolymerized efficiently in the presence of nocodazole, whereas cold treatment is without effect. For ECV preparation, depolymerize the microtubules immediately before the experiment with 10 μ*M* nocodazole at 37°C for 1–2 h in media used to grow cells in a 5% CO_2 incubator. Following this step, nocodazole (10 μ*M)* should remain present in all solutions up to the homogenization step. For LE preparation, do not treat with nocodazole or include nocodazole in any solutions.

3. *Fluid-phase internalization*: Wash each 10-cm dish of cells twice with 5 ml ice-cold PBS+/– 10 μ*M* nocodazole on ice, as in Section III,A, step 2. After the last wash, remove the PBS and place the dish on a metal plate in a 37°C water bath. Add at least 3 ml bHRP or avidin solution for making LEs or bHRP + 10 μ*M* nocodazole for making ECVs. Incubate for 10 min.

4. *Chase*: Remove bHRP or avidin and wash twice quickly at 37°C with 10 ml PBS/BSA+/– 10 μM nocodazole, prewarmed to 37°C. Remove last wash, and add 8 ml IM/BSA+/– 10 μM nocodazole, prewarmed to 37°C. Incubate at 37°C (in water bath or in a 37°C incubator without CO_2) for 45 min.

5. *Washes*: Remove IM/BSA, move dishes to ice bucket, and wash 2 × 5 min with 5 ml cold PBS/BSA followed by 5 min with 5 ml cold PBS on ice.

C. Homogenization and Fractionation of Cells

Solutions

1. *PBS*: See Section IIIA.
2. *300 mM imidazole stock*: Dissolve imidazole in H_2O and adjust pH to 7.4 with NaOH, filter sterilize, and store at 4°C
3. *Homogenization buffer (HB)*: Add imidazole from 300 m*M* stock to H_2O and dissolve sucrose such that the final concentrations are 250 m*M* sucrose and 3 m*M* imidazole. Filter sterilize and store at 4°C.
4. *62% sucrose solution*: For 100 ml, add 1 ml of imidazole from 300 m*M* stock to 15 *ml* H_2O. Add 80.4 g sucrose and dissolve by stirring at 37°C. Add H_2O and mix until the refractive index is 1.4464.
5. *10 and 16% sucrose solutions in D_2O*: For 100 ml, add 1 ml imidazole from 300 m*M* stock to 50 ml D_2O. For 10% solution, add 10.4 g sucrose, and for 16% solution, add 17.0 g sucrose. Dissolve sucrose, add D_2O, and mix until the refractive index is 1.3479 for the 10% solution and 1.3573 for the 16% solution.

Steps

1. *Cell scraping*: All of the following steps should be performed on ice or at 4°C. After the last wash, remove all PBS. Add 2 ml/dish PBS and rock the dish so that cells do not dry. Using a flexible rubber policeman, scrape round 10-cm dishes by first scraping in a circular motion around the outside of the dish, followed by a downward motion in the middle of the dish. Scrape

gently in order to obtain "sheets" of cells. Using a plastic Pasteur pipette, gently transfer the scraped "sheets" of cells from four or five dishes into a 15-ml tube on ice.

2. Centrifuge at 1200 rpm for 5 min at 4°C. Gently remove supernatant.

3. Add 1 ml HB to pellet, using a plastic Pasteur pipette, gently pipette up and down one time and add an excess of HB (4–5 ml) to change buffer. Centrifuge again at 2500 rpm for 10 min at 4°C. Remove supernatant.

4. *Homogenization*: It is important that cells are homogenized under conditions where endosomes are released from cells, yet where latency is high so that the endosomes are not broken and retain their internalized marker. First add 0.5 ml HB to the cell pellet. Using a 1-ml pipetman, gently pipette up and down until the pellet is resuspended and particles can no longer be seen by eye. Do not introduce air bubbles. Using a 22-gauge needle connected to a narrow 1-ml Tubercutine syringe, prewet the needle and syringe with HB so that no air is introduced. Insert the needle into the cell homogenate, slowly pull up on the syringe until most of the cell homogenate is in the syringe, and gently expel without bubbles. Repeat this procedure until plasma membranes are broken, yet nuclear membranes are not. Monitor homogenization as follows. Take 3 µ*l* of homogenate and place in a 50-µ*l* drop of HB on a glass slide. Mix and cover with a glass coverslip. Observe by phase-contrast microscopy, using a 20× objective. Homogenize until unbroken cells are no longer observed, yet nuclei, which appear as dark round or oblong structures, are not broken. Usually between 3 and 10 up-and-down strokes through the needle are necessary. Centrifuge homogenate at 2000 rpm for 10 min at 4°C, and carefully collect the postnuclear supernatant (PNS) and nuclear pellet.

5. Save a 50-µ*l* aliquot of each PNS fraction for measuring latency and for calculating the balance sheet as described in Section III,D. Adjust the sucrose concentration of the remaining PNS to 40.6% by adding about 1.1 volume of 62% sucrose solution per volume of PNS. Mix gently but thoroughly, without bubbles. Check sucrose concentration using a refractometer.

6. Place adjusted PNS in the bottom of a SW60 centrifuge tube. On top of the PNS, layer 1.5 ml of 16% sucrose solution in D_2O, followed by 1 ml of 10% sucrose solution in D_2O, and fill tube with HB. Steps should be layered so that interfaces are clearly seen and not disturbed. See Gruenberg and Gorvel (1992) for diagram of gradients.

7. Centrifuge gradients in SW60 rotor at 35,000 rpm for 1 h at 4°C.

8. Carefully remove the interfaces from the gradients after centrifugation by first placing gradients in a test tube rack with a black backdrop. The interfaces should appear white. The layer of white lipids on top of the gradient should be removed carefully. Collect fractions at 4°C using a peristaltic pump at speed 2, with capillary tubes connected to each end. Place the outgoing end into a collection tube and collect the top interface carefully (10%/HB interface = LE + ECV fraction) first. Collect by holding the capillary tube directly in the middle of the wide interface and slowly move in a circular motion until most of the white interface is collected into the smallest possible volume. Wash the pump tubing with water and then collect the EE (16/10%) interface into another tube. Fractions can be frozen and stored in liquid N_2 until use in fusion assays if they are carefully frozen quickly in liquid N_2 and thawed quickly at 37°C immediately before use.

D. Measurement of Latency and Balance Sheet for Gradients

Solutions

1. *HRP stocks*: 1–10 ng HRP in 0.1 ml HB, for standards.

2. *HB*: See Section IIIC.

3. *HRP reagent*: 0.342 m*M* *o*-dianisidine and 0.003% H_2O_2 in 0.05 *M* Na-phosphate buffer, pH 5.0, containing 0.3% Triton X-100. To prepare, use very clean glassware or plasticware (as in for tissue culture) and mix 12 ml of 0.5 *M* Na-phosphate buffer, pH 5.0 (filter sterilized), and 6 ml of 2% Triton X-100 (filter sterilized) with 111 ml sterile H_2O. Add 13 mg *o*-dianisidine, dissolve gently, and add 1.2 ml 0.3% H_2O_2 (filter sterilized). Avoid magnetic stirring. Solution should be clear. Store at 4°C in the dark.

4. *1 mM KCN in H_2O*

5. Protein assay system (such as the BCA protein assay reagent or the Bio-Rad protein assay system)

Steps

1. Load a 20-µ*l* aliquot of bHRP PNS into an airfuge tube or a small tabletop ultracentrifuge tube of the Beckman TL-100 type and fill the tube with a known volme of HB. Mix thoroughly by pipetting without air bubbles. Centrifuge at 4°C for 20 min at 20 psi in an airfuge or at 200,000 *g* for 20 min in a tabletop ultracentrifuge rotor (such as Beckman TLA-100.1). Transfer the supernatant to another tube. Resuspend the pellet in 50 µl HB.

2. To measure the latency, adjust samples, blanks, and standards with HB so that the final volume of each is 0.1 ml. Assay both the pellet and the supernatant of

the latency measurement. If the supernatant volume is over 0.1 ml, assay only 0.1 ml. Add 0.9 ml of HRP reagent to each tube, mix quickly, and record the time with a stop clock. Allow color to develop in the dark, as this reagent is light sensitive. When a brown color has begun to develop, read the absorbance at 455 nm and record the time (results expressed as OD units/min or ng HRP/min). Stop the reaction with 10 µ*l* of 1.0 m*M* KCN if necessary.

3. Calculate latency by first adding the value (OD/min) for HRP in the pellet to that of HRP in the supernatant (OD/min after correcting for total supernatant volume). The value for the pellet divided by the total value is the percentage latency. Latency should be over 70% in order to measure endosome fusion.

4. The amount of HRP in each gradient fraction collected from the bHRP gradient can be measured by assaying an aliquot (about 50 µ*l*) of each fraction as described in step 2.

5. Measure the amount of protein in each gradient fraction using a standard protein assay system, as described in the manual.

6. Calculate percentage yield (percentage of HRP in each fraction compared to total amount of HRP in PNS), specific activity (SA) (HRP activity per unit protein), and relative specific activity (RSA) (divide specific activity of each fraction by the specific activity of the PNS). See Gruenberg and Gorvel (1992) for an example of a typical balance sheet.

E. Preparation of BHK Cell Cytosol

Solutions

1. *PBS-*: See Section IIIA.
2. *HB*: See Section IIIC.
3. *HB + protease inhibitors*: HB with the following protease inhibitors added immediately before use: 10 µ*M* leupeptin, 1 µ*M* pepstatin A, 10 ng/ml aprotinin, and, if needed, 1 µ*m* phenylmethylsulfonyl fluoride.

Steps

Two possible cytosol sources for all of the assays described are BHK and rat liver cytosol. For rat liver cytosol preparation, refer to Aniento *et al.* (1993).

1. BHK cells, maintained as described in Section IIIA, should be plated approximately 16 h before the experiment. Large (245 × 245 × 25 mm) square dishes are convenient for large cytosol preparations.

2. All steps should be performed on ice or at 4°C. Wash dishes four times with excess PBS (50 ml per dish for large square dishes).

3. Remove PBS from the last wash, add 12 ml PBS per dish, and rock the dish so that cells do not dry. Scrape cells with a rubber policeman using firm, downward motions, going from top to bottom while holding the plate at an angle, as described in Section IIIC, step 1.

4. Collect scraped cells into 15-ml tubes (one tube per dish). Centrifuge at 1200 rpm for 5 min at 4°C.

5. Remove supernatant and gently add 5 ml HB with a plastic Pasteur pipette and pipette up and down one time.

6. Centrifuge at 2500 rpm for 10 min at 4°C. Remove supernatant and resuspend pellet in 1.2 ml HB + protease inhibitors. Separate into two tubes (about 0.7 ml/tube) for homogenization and homogenize as described in step 4 of Section IIIC.

7. Centrifuge at 2500 rpm for 15 min at 4°C. Add supernatant (PNS) to a centrifuge tube for the TLS-55 rotor (for the Beckman TL-100 tabletop ultracentrifuge) and centrifuge in TLS-55 for 45 min at 55,000 rpm at 4°C. Remove fat from the top using an aspirator. Transfer supernatant (cytosol fraction) to a new tube without disturbing the pellet. Determine the protein concentration of supernatant. Cytosol should be at least 15 mg/ml to give a good signal for fusion assays. Aliquot on ice, freeze quickly, and store in liquid N_2 until use.

F. Preparation of Antiavidin Beads for the *in Vitro* Fusion Assay Described in Section IIIG

Solutions

1. *PBS/BSA*: Dissolve 5 mg/ml BSA in PBS. Filter sterilize and store at 4°C.
2. *Sterile PBS*: PBS as described in Section III,A, filter sterilize or autoclave, and store at 4°C.
3. *Antiavidin antibody*: Affinity purify and store aliquoted in 50% glycerol/PBS at –20°C.

Steps

To determine how many antiavidin beads to prepare, first determine the number of fusion assay points. From a typical gradient (see Gruenberg and Gorvel, 1992) about 150 µg of EE and 70 µg of ECV or LE are obtained. Optimal amounts of endosomes to use for fusion assays are 20 µg of each EE fraction and 10 µg of each ECV or LE fraction. Therefore, a typical experiment (one gradient each of avidin and bHRP-labeled fractions) will provide enough endosomes for about seven fusion assay points.

1. Swell 1.5 g of protein A–Sepharose beads in 10 ml sterile H_2O at room temperature overnight.

2. Wash beads three times in 10 ml sterile PBS by centrifuging beads in 15-ml tubes at 3000 rpm for 2 min, resuspending in PBS each time.

3. After the final wash, resuspend beads in an equal volume of sterile PBS per volume of packed beads. Store beads this way up to several months at 4°C.

4. One hundred microliters of this 1:1 slurry is required per fusion assay point. Therefore, for 10 assay points, block 1 ml of beads by washing 3× in 10 ml PBS/BSA, as described in step 2.

5. After final wash, resuspend beads in 10 ml PBS/BSA. For 10 assay points, add 50 µg of antiavidin antibody (5 µg per 100-µ*l* beads). Rotate tube for at least 5 h at 4°C.

6. Wash beads four times in PBS/BSA. After the last wash, for 10 assay points, resuspend beads in 10 ml PBS/BSA.

7. Aliquot 1 ml to each of 10 labeled Eppendorf tubes. Centrifuge in Eppendorf centrifuge at maximum speed for 2 min. Remove supernatant. Beads are now ready for the immunoprecipitation step of the fusion assay (Section III,G, step 10).

G. In Vitro Assay of Endocytic Vesicle Fusion

Solutions

1. *50× salts*: 0.625 *M* HEPES, 75 m*M* Mg-acetate, 50 m*M* dithiothreitol, pH 7, with KOH. Filter sterilize, aliquot, and store at –20°C.

2. *K-acetate (KOAc stock)*: 1 *M* in H_2O. Filter sterilize, aliquot, and store at –20°C. *Note:* Depending on the counterion requirement of the experiment, KOAc must be replaced by KCl (see Aniento *et al*., 1993).

3. *Biotinylated insulin*: 1 mg/ml in H_2O. Store at 4°C.

4. *AT?-regenerating system (ATP-RS)*: Mix 1:1:1 volumes of the following immediately before use.

   a. *100 mM* ATT: Dissolve in ice-cold H_2O, titrate to pH 7.0 with 1 *M* NaOH, filter sterilize, aliquot on ice, and store at –20°C.

   b. *800 mM creatine phosphate*: Dissolve in ice-cold H_2O, filter sterilize, aliquot on ice, and store at –20°C.

   c. 4 *mg/ml creatine phosphokinase*: To make 4 ml, add 80 *p*\ of 0.5 *M* $NaHPO_4$ buffer, pH 7.0, to 1.6 ml H_2O on ice. When cool, add 16 mg creatine phosphokinase. Vortex until dissolved. Add 2.3 ml ice-cold 87% glycerol. Vortex until well mixed. Aliquot on ice and store at –20°C.

5. *Hexokinase*: Vortex the suspension, pipette the desired amount (e.g., 10 µg–0.1 mg for one assay point), centrifuge for 2 min in Eppendorf at maximum speed, and aspirate supernatant. Dissolve pellet in the same volume of 0.25 *M* D-glucose. Prepare immediately before use.

6. *TxlOO stock*: 10% stock of Triton X-100 in H_2O

7. *PBS/BSA and sterile PBS*: See Section IIIF.

8. *HEP reagent*: See Section IIID.

9. *PBS/BSA/TxlOO*: PBS/BSA containing 0.2% Triton X-100, make immediately before use

Steps

1. For each fusion assay, at least three points should be included:—ATP, +ATP, and the total. To determine fusion efficiency, determine the total (maximal possible fusion value) by mixing 50 //I of each endosomal fraction in an Eppendorf tube on ice. Add 25 µ*l* Tx100 stock and vortex well. Leave on ice at least 30 min and add PBS/BSA and continue as described in step 9.

2. For all other fusion assay points, 3 µl of 50× salts, 8 µ*l* of biotinylated insulin, and 11 µ*l* of KOAc stock are needed for each point. Make a mixture of these three components by multiplying the number of assay points by 3, 8, and 11 and mix the respective amounts of each component together in one tube. Number Eppendorf tubes for the appropriate number of assay points and put them on ice. Add 22 µ*l* of the aforementioned mixture to each tube.

3. Add 50 µl (750 µ*g*–1 mg) of cytosol to each tube and mix.

4. Add either 5 µl of ATP-RS or 10 µl of hexokinase to each tube, as appropriate.

5. Add 50 µl (7–25 µg) of bHRP-labeled endosomes and 50 µ*l* (7–25 µg) of avidin-labeled endosomes to each tube. Endosomal fractions from the gradients can be diluted in HB prior to this step, if desired. Mix gently; avoid introducing air bubbles. Leave tubes on ice for 3 min.

6. Transfer tubes to 37°C for 45 min. Avoid agitation during this time.

7. Return tubes to ice. Add 5 µl of biotinylated insulin to each tube and mix.

8. Add 25 µl of Tx100 stock and vortex well. Leave tubes on ice for 30 min.

9. Add 1 ml of sterile PBS/BSA to each tube and mix well.

10. Centrifuge for 2 min at maximum speed in an Eppendorf centrifuge. Transfer supernatants to numbered tubes containing antiavidin beads, prepared as in Section IIIF.

11. Rotate beads for at least 5 h at 4°C.

12. Centrifuge in Eppendorf centrifuge at maximum speed for 2 min. Remove supernatant and wash four times with PBS/BSA/Tx100. Wash once with sterile PBS.

13. Remove final supernatant and add 900 //I of HRP reagent to each tube. Allow color to develop in

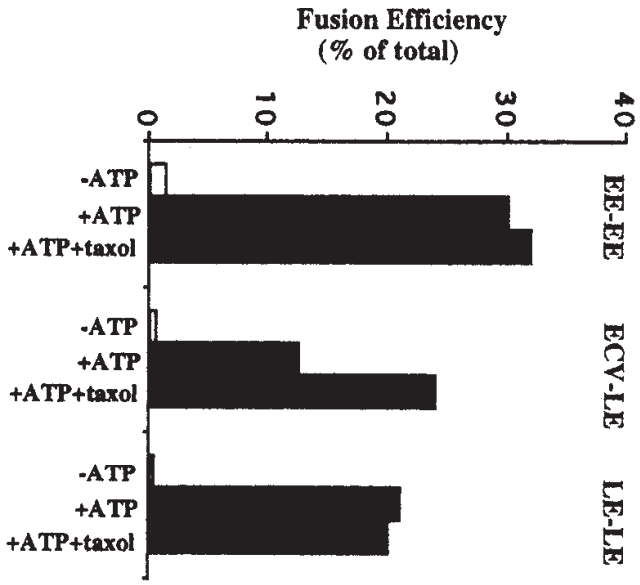

FIGURE 2 Typical fusion assay results. Fusion efficiency is expressed as a percentage of total fusion between each set of endosomal membranes. Total, or maximal, endosome fusion is measured by mixing bHRP and avidin-containing endosomal fractions together in the presence of detergent, followed by immunoprecipitation with antiavidin antibodies and HRP determination. Typical "total" values (measured as absorbance at 455 nm) are in the range of 0.6–1.0 ∧455 units for EE fusion assays and 0.3–0.7 ∧455 units for ECV and LE fusion assays. As a control for nonspecific reactions, the assay is typically carried out without ATP (—ATP). As shown, the polymerization of endogenous tubulin present in the cytosol in the presence of taxol is sufficient to facilitate interactions between ECVs and LEs (see Aniento *et al*., 1993).

the dark at room temperature. Vortex periodically for 2–3 h or put tubes on rotating wheel in the dark at room temperature while color develops.

14. Centrifuge tubes for 2 min in Eppendorf centrifuge. Measure the absorbance of the supernatants at 455 nm.

IV. COMMENTS

Refer to Gruenberg and Gorvel (1992) for an example of a typical balance sheet for the sucrose gradient fractionation step. Typical results for fusion assays are shown in Fig. 2.

Highly purified loaded endosomes can be prepared by immunoisolation as described in Howell *et al.* (1989). Immunoisolated endosomes can then be used in the fusion assays described in Section IIIG. See Gruenberg and Gorvel (1992) and Howell *et al.* (1989) for details.

ECV–LE fusion is stimulated by the addition of polymerized microtubules to the fusion assay. Endogenous microtubules can be polymerized by adding 20 μ*M* taxol to the fusion assay. The preparation of microtubules is described in the article by Ashford and Hyman. See Fig. 2 and Aniento *et al*. (1993) for more details on the effects of microtubules and MAPs on ECV–LE fusion.

V. PITFALLS

For ECV and LE preparations, cells should be homogenized until vesicles are no longer seen around the periphery of nuclei. If nuclei begin to aggregate during homogenization, however, this is a sign that some are broken as free DNA causes aggregation. Freezing and thawing of endosomes may cause a partial loss in latency. Use very clean plasticware or glassware for all fusion assay manipulations as HRP contamination can occur easily. Nocodazole, *o*-dianisidine, and KCN are very toxic.

References

Aniento, F., Emans, N., Griffiths, G., and Gruenberg, J. (1993). Cytoplasmic dynein-dependent vesicular transport from early to late endosomes. *J. Cell Biol.* **123**, 1373–1387.

Aniento, F., Gu, F., Parton, R. G., and Gruenberg, J. (1996). An endosomal /3COP is implicated in the pH-dependent formation of transport vesicles destined for late endosomes. *J. Cell Biol.* **133**, 29–41.

Aniento, F., Roche, E., Cuervo, A., and Knecht, E. (1993). Uptake and degradation of glyceraldehyde-3-phosphate dehydrogenase by rat liver lysosomes. *J. Biol Chem.* **268**, 10463–10470.

Bomsel, M., Parton, R., Kuznetsov, S. A., Schroer, T. A., and Gruenberg J. (1990). Microtubule- and motor-dependent fusion *in vitro* between apical and basolateral endocytic vesicles from MDCK cells. *Cell* **62**, 719–731.

Braell, W. A. (1987). Fusion between endocytic vesicles in a cell-free system. *Proc. Natl. Acad. Sci. USA* **84**, 1137–1141.

Davey, J. S., Hurtley, S. M., and Warren, G. (1985). Reconstitution of an endocytic fusion event in a cell-free system. *Cell* **43**, 643–652.

Diaz, R., Mayorga, L., and Stahl, P. D. (1988). *In vitro* fusion of endosomes following receptor-mediated endocytosis. *J. Biol. Chem.* **263**, 6093–6100.

Gruenberg, J., and Gorvel, J.-P. (1992). *In vitro* reconstitution of endocytic vesicle fusion. *In "Protein Targetting, a Practical Approach"* (A. I. Magee and T. Wileman, eds.), pp. 187–216. University Press, Oxford.

Gruenberg, J., Griffiths, G., and Howell, K. E. (1989). Characterization of the early endosome and putative endocytic carrier vesicles *in vivo* with an assay of vesicle fusion *in vitro*. *J. Cell Biol.* **108**, 1301–1316.

Gruenberg, J., and Howell, K. E. (1986). Reconstitution of vesicle fusions occurring in endocytosis with a cell-free system. *EMBO J.* **5**, 3091–3101.

Gruenberg, J., and Maxfield, F. R. (1995). Membrane transport in the endocytic pathway. *Curr. Opin. Cell Biol.* **7**, 552–563.

Howell, K. E., Schmid, R., Ugelstad, J., and Gruenberg J. (1989). Immuno-isolation using magnetic solid supports: Subcellular fractionation for cell-free functional studies. *Methods Cell Biol* **31A**, 264–292.

Woodman, P. G., and Warren, G. (1988). Fusion between vesicles from the pathway of receptor-mediated endocytosis in a cell-free system. *Eur. J. Biochem.* **173**, 101–108.

CHAPTER

29

Microsome-Based Assay for Analysis of Endoplasmic Reticulum to Golgi Transport in Mammalian Cells

Helen Plutner, Cemal Gurkan, Xiaodong Wang, Paul LaPointe, and William E. Balch

The trafficking of proteins along the first stage of the secretory pathway is mediated by small vesicles that bud from the endoplasmic reticulum (ER) and subsequently fuse with the *cis*-Golgi compartment. This article describes a biochemical assay using mammalian microsomes that can be used to measure these events independently. The microsomes are prepared from cells infected at the restrictive temperature (39.5°C) with the ts045 strain of vesicular stomatitis virus (VSV) (Lafay, 1974). As a reporter molecule the assay utilizes ts045 VSV-glycoprotein (VSV-G), which is retained in the ER during infection due to a thermoreversible folding defect; incubation *in vitro* at the permissive temperature (32°C) results in the synchronous folding and transport of VSV-G to the Golgi complex. To follow vesicle formation, a differential centrifugation procedure is employed to separate the more rapidly sedimenting ER and Golgi membranes from the slowly sedimenting vesicles. Consumption is analyzed using a two-stage assay in which vesicles isolated by differential centrifugation during stage 1 are subsequently added to stage 2 (fusion) reactions containing acceptor Golgi membranes. Transport to the Golgi is measured by following the oligosaccharide processing of VSV-G from the high mannose ER form, which is sensitive to endoglycosidase H (endo H), to the *cis/medial-Golgi* form, which is endo H resistant (Schwaninger *et al.*, 1992). The biochemical characteristics of the overall ER to Golgi transport reaction and the vesicle formation and consumption assays are described elsewhere (Aridor *et al.*, 1995, 1996b, 1998, 1999a,b, 2000, 2001; Rowe *et al.*, 1996a).

II. MATERIALS AND INSTRUMENTATION

Culture medium (α-MEM; Cat. No. 11900-099) is from Life Technologies. The medium is supplemented with penicillin/streptomycin from a 100× stock solution (Cat. No P0781; Sigma). Fetal bovine serum (FBS; Cat. No FB-01) is from Omega Scientific. D-Sorbitol (Cat. No. S-1876), leupeptin (Cat. No L-2884), chymostatin (Cat. No C-7268), pepstatin (Cat. No P-4265), phenylmethylsulfonyl fluoride (PMSF; Cat. No P-7626), actinomycin D (Cat. No A-1410), uridine 5′-diphospho-*N*-acetylglucosamine (UDP-GlcNAc; Cat. No. U-4375), and dimethyl sulfoxide (DMSO; Cat. No. D-2650), are from Sigma. The nitrocellulose membrane (Cat. No. 68260) is from Schleicher & Schuell. Horseradish peroxidase-conjugated goat anti-rabbit IgG (Cat. No. 31460) is from Pierce. Chemiluminescence reagent (Cat. No. NEL-101) and autoradiography film ("Reflection") are from NEN. Polyallomer microfuge tubes (Cat. No. 357448) are supplied by Beckman Instruments Inc. A polyclonal antibody to VSV-G is generated in rabbits immunized with the C-terminal 16 amino acids of VSV-G (Indiana serotype) coupled to KLH (Plutner *et al.*, 1991). Centrifugation at 20,000 or 100,000 *g* is performed using an Optima TL ultracentrifuge (Beckman) equipped with a TLA 100.3 rotor. A laser-scanning densitometer (personal densitometer; Molecular Dynamics) is used to quantitate data.

Copyright 2006, Elsevier Science (USA).
All rights reserved.

III. PROCEDURES

The following procedures are performed on ice unless otherwise stated.

A. Preparation of Cytosol

The following procedure for the preparation of rat liver cytosol is based on that described by Davidson *et al*. (1992).

Solutions

1. *Phosphate-buffered saline (PBS) (10× stock)*: 90 m*M* phosphate and 1.5 *M* NaCl (pH 7.4). To make 1 liter, add 80 g NaCl, 2 g KCl, 2 g KH_2PO_4, and 21.6 g $Na_2HPO_4{\cdot}7H_2O$ to distilled water. Store at room temperature.
2. *25/125*: 0.125 *M* KOAc, 25 m*M* HEPES (pH 7.4). To make 100 ml, add 3.125 ml of 4 *M* KOAc stock and 2.5 ml of 1 *M* HEPES–KOH (pH 7.4) stock to distilled water. Store at 4°C.
3. *Protease inhibitor cocktail (PIC)*: 10 µg/ml leupeptin, 10 µg/ml chymostatin, 0.5 µg/ml pepstatin A, and 1.0 m*M* PMSF. To supplement 50 ml of buffer (e.g., 25/125) with PIC, add 50 µl of 10 mg/ml leupeptin stock (in H_2O), 50 µl of 10 mg/ml chymostatin stock (in DMSO), 5 µl of 5 mg/ml pepstatin A stock (in DMSO), and 500 µl of 0.1 *M* PMSF stock (in ethanol). Use PIC buffer immediately or store at –20°C.

Steps

1. Decapitate two anesthetized adult Sprague–Dawley rats (~250 g), remove the livers, and place the tissue in a 250-ml glass beaker. Determine the weight of the tissue (typically ~20 g) and then wash two times with –50 ml of Ix PBS and once with ~50 ml of Ix PBS and once with ~50 ml of 25/125.
2. Finely mince the tissue using a pair of scissors and then homogenize in 2–3 volumes (ml/g of tissue) of 25/125 (PIC) with 20 strokes using a 40-ml Dounce (Wheaton). Use a "loose-fitting" Dounce for the first 10 strokes followed by a "tight-fitting" one for the second 10 strokes.
3. Pour the homogenate into a 38-ml polycarbonate tube (Nalgene; Cat. No. 3117-0380) and centrifuge for 10 min at 12,000 *g* (10,000 rpm) in a Beckman JA20 rotor (Beckman Instruments Inc.). Using a pipette, transfer ~13 ml of the supernatant into each of two 14 × 89-mm ultraclear centrifuge tubes (Beckman Cat. No. 344059) and centrifuge at 150,000 *g* (35,000 rpm) for 90 min in a Beckman SW41 rotor.
4. After centrifugation, remove the overlying lipid layer by aspiration and then withdraw the remaining supernatants (cytosol) from each tube using a pipette.
5. Divide the cytosol into 250-µl aliquots in 0.5-ml microfuge tubes, freeze in liquid N_2, and store at –80°C. The protein concentration of the cytosol is ~25 mg/ml.

B. Preparation of Microsomes

Solutions

1. *Actinomycin D (200× stock)*: Add 10 mg actinomycin D to 10 ml of ethanol. Store at –20°C.
2. *Homogenization buffer*: 0.375 *M* sorbitol and 20 *mM* HEPES (pH 7.4). To make 500 ml, add 34.2 g sorbitol and 10 ml of 1 *M* HEPES–KOH (pH 7.4) stock to distilled water. Store at 4°C.
3. *0.21 M KOAc buffer*: 0.21 *M* KOAc, 3 m*M* $Mg(OAc)_2$, and 20 m*M* HEPES (pH 7.4). To make 100 ml, add 5.25 ml of 4 *M* KOAc stock, 0.3 ml of 1 *M* $Mg(OAc)_2$ stock, and 2 ml of 1 *M* HEPES–KOH (pH 7.4) stock to distilled water. Store at 4°C.
4. *Transport buffer*: 0.25 *M* sorbitol, 70 *mM* KOAc, 1 *mM* $Mg(OAc)_2$, and 20 *mM* HEPES (pH 7.4). To make 100 ml, add 10 ml of 2.5 *M* sorbitol stock, 1.75 ml of 4 *M* KOAc stock, 0.1 ml of 1 *M* $Mg(OAc)_2$ stock, and 2 ml of 1 *M* HEPES–KOH (pH 7.4) stock to distilled water. Store at –20°C.

Steps

1. Prepare vesicular stomatitis virus (VSV; Indiana serotype) strain ts045 according to Schwaninger *et al.* (1992). Store the virus in 1-ml aliquots in screw-capped tubes at –80°C.
2. Grow normal rat kidney (NRK) cells on 150-mm tissue culture dishes (Cat. No. 3025; Falcon) in α-MEM medium supplemented with 5% FBS at 37°C and 5% CO_2. At confluency, infect the cells with a 5-ml cocktail (per dish) containing 0.1–0.25 ml (2–10 pfu/cell) of ts045 VSV (thawed at 32°C) and 25 µg of actinomycin D in serum-free α-MEM as described by Schwaninger *et al*. (1992). Rock the dishes for 45 min to ensure an even spread of the infection cocktail. After infection, add 20 ml of α-MEM medium supplemented with 5% FBS to each dish and incubate in the presence of 5% CO_2 for 3 h and 40 min to 4 h at the restrictive temperature (39.5°C) (see Comment 1). The method detailed later is based on a typical 12-dish microsome preparation.
3. Following incubation at 39.5°C, transfer each dish to ice, aspirate the medium immediately, and add 12 ml of ice-cold Ix PBS to cool the cells as quickly as possible.
4. Remove the PBS by aspiration, add 5 ml of homogenization buffer, and scrape the cells from the

dishes using a rubber policeman. Use a pipette to transfer the cells to 50-ml plastic tubes (Cat. No. 25325-50: Corning Inc.) and then repeat the scraping procedure to ensure that all the cells are collected. Centrifuge at 720 *g* for 3 min and remove the supernatant by aspiration.

5. Resuspend each cell pellet (from four dishes) in 0.9 ml of homogenization buffer supplemented with PIC and homogenize by three complete passes (three downward strokes with both plungers) through a 1-ml ball-bearing homogenizer (Balch and Rothman, 1985).

6. Combine the cell homogenates and dilute with an equal volume (~3 ml) of homogenization buffer + PIC. Divide the diluted homogenate into six 1.0-ml aliquots in 1.5-ml microfuge tubes and centrifuge at 720 *g* for 5 min.

7. Carefully remove the postnuclear supernatant (PNS) fractions and combine in a plastic 15-ml tube (Cat. No. 25319-15: Corning Inc.). Add 0.5 volume (~2.5 ml) of 0.21 *M* KOAc buffer to the PNS and mix. Divide the mixture into 0.8- to 1.0-ml aliquots in 1.5-ml microfuge tubes and centrifuge at 12,000 *g* (12,200 rpm) for 2 min in an Eppendorf Model 5402 refrigerated microfuge using the soft spin function.

8. Remove the supernatants by aspiration and resuspend the pellets (including any membranes on the sides of the tubes) using a P1000 Gilson tip in a total volume of 1.0 ml of transport buffer + PIC. Dispense 0.5-ml aliquots into two 1.5-ml microfuge tubes and recentrifuge the microsomes at 12,000 *g* for 2 min as described earlier.

9. Resuspend the membrane pellets by repeated trituration using a P1000 Gilson tip in 6–8 volumes (~1 ml per 75-µl membrane pellet) of transport buffer containing PIC. In a typical 12-dish preparation, 1.0–1.5 ml of resuspended microsomes (at a protein concentration of 3–4 mg/ml) is obtained depending on the starting cell density. Pool the membranes, divide into 50- or 100-µl aliquots in 0.5-ml microfuge tubes, freeze in liquid N_2, and store at –80°C. The microsomes can be stored for several months with no loss of transport activity.

C. Preparation of Acceptor Golgi Membranes

The following procedure for the preparation of Golgi membranes by flotation on a sucrose density gradient is a modification of that originally described by Balch *et al.* (1984).

Solution

57.5 mM KOAc buffer: 87.5 m*M* KOAc, 1.25 m*M* $Mg(OAc)_2$, and 20 m*M* HEPES (pH 7.4). To make 100 ml, add 2.18 ml of 4 *M* KOAc stock, 0.125 ml of 1 *M* $Mg(OAc)_2$ stock, and 2 ml of 1 *M* HEPES–KOH (pH 7.4) stock to distilled water. Store at 4°C.

Steps

1. Prepare an enriched Golgi membrane fraction from noninfected wild-type Chinese hamster ovary cells by flotation in sucrose density gradients as described by Beckers and Rothman (1992). Recover the membranes at the 29–35% sucrose interface, mix thoroughly with 4 volumes of 87.5 m*M* KOAc buffer, and divide into 0.5- to 1.0-ml aliquots in microfuge tubes. Centrifuge at 16,000 *g* (soft spin) for 10 min.

2. Remove the supernatants by aspiration, wash the pellets with 2 ml (final volume) of transport buffer, and combine the membranes into two 1.5-ml microfuge tubes. Centrifuge at 16,000 *g* (soft spin) for 10 min.

3. Resuspend the membranes using a P1000 Gilson tip in transport buffer (total volume of 1.0 ml per 1×10^6 cells). Divide the Golgi membrane fraction into 50- to 100-µl aliquots in 0.5-ml microfuge tubes, freeze in liquid N_2, and store at –80°C.

D. Reconstitution of ER to Golgi Transport

Steps

1. Set up 40-µl transport reactions containing the components indicated in Table I in 1.5-ml microfuge tubes (see Comment 2). A reaction cocktail consisting of the salts, ATP-regenerating system, and water is added first, followed by the cytosol and finally the microsomes. Mix by pipetting up and down four times using a P20 Gilson tip.

2. Transfer the reactions to a 32°C water bath and incubate for 75–90 min.

3. Terminate the reactions on ice, harvest the membranes by centrifugation at 20,000 *g* (27,000 rpm) in a Beckman TLA 100.3 rotor, and remove the supernatant by aspiration (see Comment 3).

4. Solubilize the membranes in one-third volume of 0.3% SDS in 1 *M* Na acetate, pH5.6, and freshly added 30 m*M* BME. Boil 5 min, cool, and two-third volume 1 *M* Na acetate containing 3 mU of endo H. Incubate overnight, then terminate the reactions by adding Laemmli sample buffer as described by Schwaninger *et al.* (1992).

5. Separate the endo H-sensitive and -resistant forms of VSV-G on 6.75% (w/v) SDS–polyacrylamide gels as described by Schwaninger *et al.* (1992).

6. Transfer the proteins to a nitrocellulose membrane and perform Western blotting using anti-VSV-G polyclonal primary antibody (1:10,000) and peroxidase-conjugated anti-rabbit IgG secondary antibody (1:10,000) according to Rowe *et al.* (1996).

TABLE I Reaction Cocktail for Standard ER to Golgi Transport Assay

Solution	Volume (µl)	Final concentration
Microsomes	5	~0.5 mg/ml protein [31.25 m*M* sorbitol, 8.75 m*M* KOAc, 0.125 m*M* $Mg(OAc)_2$, 2.5 m*M* HEPES (pH 7.4)]
Cytosol	8	5 mg/ml protein [25 m*M* KOAc, 5 m*M* HEPES (pH 7.4)]
20× ATP-regenerating system	2	1 m*M* ATP, 5 m*M* creatine phosphate, and 0.2 IU creatine phosphate kinase
40 m*M* UDP-GlcNAc	1	1 m*M*
10× Ca^{2+}/EGTA buffer	4	5 m*M* EGTA, 1.8 m*M* $Ca(Cl)_2$ (100 n*M* free Ca^{2+}), 2 m*M* HEPES (pH 7.4)
0.1 *M* $Mg(OAc)_2$	1	2.5 m*M*
1 *M* KOAc	1	40 m*M*
2.5 *M* sorbitol	3.5	218.75 m*M*
1 *M* HEPES (pH 7.4)	1.1	27.5 m*M*
H_2O	To 40 µl (final)	

7. Develop the blots using enhanced chemiluminescence and expose to autoradiography film. Quantitate the relative band intensities of the endo H-sensitive and -resistant forms of VSV-G in each lane by densitometry (see Comments 4 and 5).

E. Vesicle Formation Assay

Solution

Resuspension buffer: 0.25 *M* sucrose and 20 m*M* HEPES (pH 7.4). To make 100 ml, add 8.55 g of sucrose and 2 ml of 1 *M* HEPES–KOH (pH 7.4) stock to distilled water. Store at 4°C.

Steps

1. Set up 40-µl reactions as described in Section III,D, step 1, containing 5–10 µl of microsomes, 5–12 µl of cytosol, salts, and an ATP-regenerating system (see Comment 6).

2. Incubate at 32°C for 0–60 min and harvest the membranes as described in Section III,D, step 3. The membrane pellets can be stored for several hours at this stage prior to the differential centrifugation procedure described later.

3. Add 40 µl of resuspension buffer and disperse the membrane pellets by pipetting up and down 10 times using a P200 Gilson tip (see Comments 3 and 7). Incubate the membranes for 10 min on ice and repeat the trituration procedure to resuspend the membranes completely. Add 8.5 µl of a salt mix [7.3 µl of 1 *M* KOAc + 1.2 µl of 0.1 *M* $Mg(OAc)_2$] to the resupended membranes and mix by pipetting up and down 5 times with a P20 Gilson tip. Perform the differential centrifugation step at 16,000 *g* (14,000 rpm) for 3 min in an Eppendorf Model 5402 refrigerated microfuge using the soft spin function.

4. Using a P200 Gilson tip, carefully take the top 34-µ1 supernatant fraction from the side of the tube opposite the pellet. Transfer to a 1.5-ml polyallomer microfuge tube and centrifuge at 100,000 *g* (60,000 rpm) for 20 min. Carefully aspirate the remaining supernatant fraction from the 16,000-*g* (medium speed) pellet and the entire supernatant from the 100,000-*g* (high speed) pellet (see Comment 8).

5. Add 50 and 35 µl of IX Laemmli sample buffer (Laemmli, 1970) to the medium-speed pellet (MSP) and high-speed pellet (HSP) fractions, respectively, and boil at 95°C for 5 min. Determine the relative amounts of VSV-G in the MSP and HSP from each reaction by SDS–PAGE and quantitative immunoblotting as described by Rowe *et al*. (1996).

6. *A quicker alternative method to step 2 is as follows*: After incubation put the tubes on ice and spin at 16,000 *g* (14,000 rpm) for 3 min. Carefully remove the top 32 µl as described in step 4 and transfer to 1.5-ml polyallomer tubes. Spin at 100,000 *g* (60,000 rpm) for 20 min. Aspirate supernatant as in step 4 and add 40 and 32 µl 1× Laemmli sample buffer to the medium-speed pellet (MSP) and high-speed pellet (HSP) fractions, respectively. Vortex carefully and boil at 95°C for 5 min.

F. Two-Stage Fusion Assay

Solution

0.25 M sorbitol buffer: 0.25 *M* sorbitol and 20 m*M* HEPES (pH 7.4). To make 100 ml, add 10 ml of 2.5 *M* sorbitol stock and 2 ml of 1 *M* HEPES–KOH (pH 7.4) stock to distilled water. Store at 4°C.

Steps

1. For stage 1 incubations, prepare scaled-up (100 µl) vesicle formation reactions containing 25 µl of microsomes and 30 µl of cytosol as described in Section IIIE, step 1. Incubate for 10 min at 32°C.

2. Terminate the reactions by transfer to ice and sediment the membranes as described in Section IIID, step 3.

3. Resuspend the membranes in 90 µl of resuspension buffer, add 9.8 µl of salt mix [7.3 µl of 2 *M* KOAc + 2.5 µl of 0.1 *M* $Mg(OAc)_2$], and perform the differential centrifugation step as described in Section IIIE, step 3.

4. Withdraw the top 75-ml medium-speed supernatant fraction and recover the vesicles by centrifugation at high speed as described in Section IIIE, step 4.

5. Resuspend the HSPs in 25 µl of 0.25 *M* sorbitol buffer by pipetting up and down 10 times with a P200 Gilson tip and then add 1.9 µl of 1 *M* KOAc (70 m*M* KOAc final concentration) (see Comment 9).

6. Set up *40*-µl stage 2 reactions containing 10 µl of resuspended HSP fraction, 4 µl of Golgi membranes, 8 µl of cytosol, and an ATP-regenerating system and salts at the final concentrations indicated in Table I (see Comment 6).

7. Incubate for 60 min at 32°C and terminate the reactions on ice. Harvest the membranes and quantitate the conversion of VSV-G to the endo H-resistant form as described in Section IIID, steps 3–7.

IV. COMMENTS

1. To reproduce the temperature-sensitive phenotype of ts045 VSV-G transport *in vitro*, it is necessary to supplement the postinfection medium and homogenization buffer with dithiothreitol as described by Aridor *et al*. (1996).

2. Preparations of the ATP-regenerating system and Ca^{2+}/EGTA buffer are described by Schwaninger *et al*. (1992). Transport inhibitors such as antibodies are dialyzed against 25/125 prior to addition to the assay, and the volumes of the salts in the reaction cocktail are adjusted to achieve the final concentrations described in Table I. The reactions can be preincubated on ice for up to 45 min with no loss of transport activity.

3. All of the membrane-bound VSV-G is sedimented at 20,000 *g* following the 32°C incubation. In the vesicle formation assay, membranes are resuspended in sucrose buffer prior to differential centrifugation.

4. The detection system is linear over the range of VSV-G concentrations tested.

5. As an alternative to densitometry, VSV-G bands can be detected by direct fluorescence imaging (e.g., using a Bio-Rad GS-363 molecular imaging system).

6. In the vesicle formation and two-stage assays, the volumes of salts (see Table I) added to the reaction cocktail are adjusted to account for the salts present in the cytosol and membrane preparations in the assay. UDP-GlcNAc is omitted from the vesicle formation assay and from stage 1 of the two-stage assay.

7. Although in the original description of the assay (Rowe *et al*., 1996) a 0.25 *M* sorbitol buffer was used to resuspend the membranes prior to differential centrifugation, we have subsequently found that resuspension in 0.25 *M* sucrose buffer gives higher yields of vesicles at this step.

8. Because the HSP is small and translucent, care should be taken to avoid losing it during aspiration of the high-speed supernatant.

9. In a typical experiment, multiple stage 1 reactions are performed and the HSPs are resuspended successively in the desired final volume of sorbitol buffer and are then adjusted to 70 m*M* KOAc.

Acknowledgments

This work was supported by postdoctoral fellowships from the Cystic Fibrosis Foundation to XW and grants from the National Institutes of Health (GM 42336; GM33301) to WEB.

References

Aridor, M., and Balch, W. E. (1996). Membrane fusion: Timing is everything. *Nature* **383**, 220–221.

Aridor, M., and Balch, W. E. (1999). Integration of endoplasmic reticulum signaling in health and disease. *Nature Med*. **5**, 745–751.

Aridor, M., and Balch, W. E. (2000). Kinase signaling initiates coat complex II (COPII) recruitment and export from the mammalian endoplasmic reticulum. *J. Biol Chem*. **275**, 35673–35676.

Aridor, M., Bannykh, S. I., Rowe, T., and Balch, W. E. (1995). Sequential coupling between COPII and COPI vesicle coats in endoplasmic reticulum to Golgi transport. *J. Cell Biol*. **131**, 875–893.

Aridor, M., Bannykh, S. I., Rowe, T., and Balch, W. E. (1999). Cargo can modulate COPII vesicle formation from the endoplasmic reticulum. *J. Biol Chem*. **274**, 4389–4399.

Aridor, M., Fish, K. N., Bannykh, G. I., Weissman, J., Roberts, H. R., Lippincott-Schwartz, J., and Balch, W. E. (2001). The Sar1 GTPase coordinates biosynthetic cargo selection with endoplasmic reticulum export site assembly. *J. Cell Biol*. **152**, 213–229.

Aridor, M., Weissman, J., Bannykh, S., Nuoffer, C., and Balch, W. E. (1998). Cargo selection by the COPII budding machinery during export from the ER. *J. Cell Biol*. **141**, 61–70.

Balch, W. E., Dunphy, W. G., Braell, W. A., and Rothman, W. E. (1984). Reconstitution of the transport of protein between successive compartments of the Golgi measured by the coupled incorporation of N-acetylglucosamine. *Cell* **39**, 405–416.

Balch, W. E., and Rothman, J. E. (1985). Characterization of protein transport between successive compartments of the Golgi apparatus: Asymmetric properties of donor and acceptor activities in a cell-free system. *Arch. Biochem. Biophys*. **240**, 413–425.

Beckers, C. J. M., and Rothman, J. E. (1992). Transport between Golgi cisternae. *Methods Enzymology* **219**, 5–12.

Davidson, H. W., McGowan, C. H., and Balch, W. E. (1992). Evidence for the regulation of exocytic transport by protein phosphorylation. *J. Cell Biol*. **116**, 1343–1355.

Laemmli, U. K. (1970). Cleavage of structural proteins during the assembly of the head of bacteriophage T4. *Nature* **227**, 680–685.

Lafay, F. (1974). Envelope viruses of vesicular stomatitis virus: Effect of temperature-sensitive mutations in complementation groups III and V. *J. Virol*. **14**, 1220–1228.

Plutner, H., Cox, A. D., Find, S., Khosravi-Far, R., Bourne, J. R, Schwaninger, R., Der, C. J., and Balch, W. E. (1991). Rab 1b regulates vesicular transport between the endoplasmic reticulum and successive Golgi compartments. *J. Cell Biol* **115**, 31–43.

Rowe, T., Aridor, M., McCaffery, J. M., Plutner, H., Nuoffer, C., and Balch, W. E. (1996). COPH vesicles derived from mammalian ER microsomes recruit COPI. *J. Cell Biol*. **135**, 895–911.

Schwaninger, R., Beckers, C. J. M., and Balch, W. E. (1991). Sequential transport of protein between the endoplasmic reticulum and successive Golgi compartments in semi-intact cells. *J. Biol. Chem*. **266**, 13055–13063.

Schwaninger, R., Plutner, H., Davidson, H. W., Find, S., and Balch, W. E. (1992). Transport of protein between the endoplasmic reticulum and Golgi compartments in semi-intact cells. *Methods Enzymology* **219**, 110–124.

CHAPTER

30

Cotranslational Translocation of Proteins into Microsomes Derived from the Rough Endoplasmic Reticulum of Mammalian Cells

Bruno Martoglio and Bernhard Dobberstein

I. INTRODUCTION

In mammalian cells, secretory proteins and membrane proteins of the organelles of the secretory pathway are initially transported across and integrated into the membrane of the rough endoplasmic reticulum (ER), respectively (for reviews, see Rapoport *et al*., 1996; Johnson and van Weas, 1999). This process can be studied in a cell-free translation/translocation system in which a protein of interest is synthesized and imported into microsomal membranes derived from the rough ER. Components used in such a system are rough microsomes (RM) usually prepared from dog pancreas, a cytosolic extract supporting protein synthesis, mRNA coding for a secretory or a membrane protein, and a radio-labeled amino acid, e.g., [^{35}S]methionine, for detection of the newly synthesized protein.

Upon translocation across the ER membrane, proteins become processed and modified, fold with the help of lumenal chaperones, and can assemble into oligomeric complexes (Lemberg and Martoglio, 2002; Daniels *et al*., 2003). These functions are maintained in rough microsomes and can be studied. This article describes the basic cell-free *in vitro* translocation system and provides methods to analyze the translocation of proteins across the microsomal membrane and integration into the lipid bilayer.

II. MATERIALS AND INSTRUMENTATION

Ambion: RNase inhibitor (Cat. No. 2684). Amersham Pharmacia: DEAE–Sepharose (Cat. No. 17-0709-01), [^{35}S]methionine (Cat. No. AG 1594), and Sephacryl S-200 (Cat. No. 17-0584-10). Roche Applied Science: ATP (Cat. No. 1140965), CTP (Cat. No. 1140922), GTP (Cat. No. 1140957), UTP (Cat. No. 1140949), creatin kinase (Cat. No. 736988), creatin phosphate (Cat. No. 621714), and SP6 RNA polymerase (Cat. No. 810274). Fluka: EDTA (Cat. No. 03610), octaethylene glycol monododecyl ether (Cat. No. 74680), and SDS (Cat. No. 71725). Merck: Acetic acid (Cat. No. 100063), acetone (Cat. No. 100014), calcium chloride (Cat. No. 102389), HCl (Cat. No. 100317), isopropanol (Cat. No. 109634), magnesium acetate (Cat. No. 105819), magnesium chloride (Cat. No. 105833), 2-mercaptoethanol (Cat. No. 805740), potassium acetate (Cat. No. 104820), proteinase K (Cat. No. 124568), sodium acetate (Cat. No. 106268), sodium carbonate (Cat. No. 106392), sodium citrate (Cat. No. 106448), sucrose (Cat. No. 107654), and trichloroacetic acid (Cat. No. 100810). New England Biolabs: ^{7}mG(5′)ppp(5′)G (Cat. No. 1404) and endoglycosidase H (Cat. No. 0702). Promega: Amino acid mixture minus methionine (Cat. No. L9961). Sigma: Dithiothreitol (DTT, Cat. No. D 0632), HEPES (Cat. No. H 3375), phenylmethylsulfonyl

Copyright 2006, Elsevier Science (USA).
All rights reserved.

fluoride (PMSF, Cat. No. P 7626), Sephadex G-25 (Cat. No. G-25-150), Tris base (Cat. No. T 1503), and Triton X-100 (Cat. No. T 9284). Amersham Pharmacia: ÄKTAprime chromatography system (Cat. No. 18-2237-18). Braun Biotech Int.: Potter S homogenizer. Qiagen: Plasmid Maxi Kit (Cat. No. 12162). Millipore: Amicon ultrafiltration unit 8050 (Cat. No. 5122) and YM100 ultrafiltration discs (Cat. No. 14422AM).

III. PROCEDURES

A. Preparation of Components Required for Cell-Free in Vitro Protein Translocation across ER-Derived Rough Microsomes

1. Preparation of Rough Microsomes from Dog Pancreas

RMs can be prepared from most tissues or cells in culture. Dog pancreas, however, is the most convenient source for functional RMs because this tissue is specialized in secretion and contains an extended rough ER. Most importantly, pancreas from dog, in contrast to other animals, contains very little ribonuclease that would degrade the mRNA required for the translation reaction. Dogs may be obtained from an experimental surgery department or a pharmaceutical company. Ideally, the dogs are healthy and not operated or treated with drugs, and the pancreas is excised immediately after death.

Solutions

Glass and plasticware are autoclaved, and stock solutions and distilled water are either autoclaved or filtered through 0.45-µm-pore-sized filters.

1. *Stock solutions*:

2 M sucrose: To make 500 ml of the solution, dissolve 342.25 g sucrose in water and complete to 500 ml. Sucrose stock solution may be stored in aliquots at –20°C.

1 M HEPES–KOH pH 7.6: To make 200 ml of the buffer, dissolve 47.7 g HEPES in water, adjust pH to 7.6 with KOH solution, and complete to 200 ml.

4 M KOAc: To make 200 ml of the solution, dissolve 78.5 g KOAc in water, neutralize to pH 7 with diluted acetic acid, and complete to 100 ml.

1 M $Mg(OAc)_2$: To make 100 ml of the solution, dissolve 21.5 g $Mg(OAc)_2 \cdot 4\ H_2O$ in water, neutralize to pH 7 with diluted acetic acid, and complete to 100 ml.

500 mM EDTA: To make 100 ml of the solution, dissolve 14.7 g EDTA in water, adjust to pH 8.0 with NaOH solution and complete to 100 ml.

1 M DTT: To make 10 ml of the solution, dissolve 1.54 g DTT in water and complete to 10 ml. Store in aliquots at –20°C.

20 mg/ml PMSF: To make 2 ml of the solution, dissolve 40 mg PMSF in 2 ml isopropanol. Prepare just before use.

2. *Homogenization buffer*: 250 m*M* sucrose, 50 m*M* HEPES–KOH, pH 7.6, 50 m*M* KOAc, 6 m*M* $Mg(OAc)_2$, 1 m*M* EDTA, 1 m*M* DTT, and 30 µg/ml PMSF. To make 1 liter of the buffer, add 125 ml 2 *M* sucrose, 50 ml 1 *M* HEPES–KOH, pH 7.6, 12.5 ml 4 *M* KOAc, 6 ml 1 *M* $Mg(OAc)_2$, 2 ml 500 m*M* EDTA, and complete to 1 liter with water. Add 1 ml 1 *M* DTT and 1.5 ml 20 mg/ml PMSF to the cold buffer just before use.

3. *Sucrose cushion*: 1.3 *M* sucrose, 50 m*M* HEPES–KOH, pH 7.6, 50 m*M* KOAc, 6 m*M* $Mg(OAc)_2$, 1 m*M* EDTA, 1 m*M* DTT, and 10 µg/ml PMSF. To make 200 ml of the solution, add 130 ml 2 *M* sucrose, 10 ml 1 *M* HEPES–KOH, pH 7.6, 2.5 ml 4 *M* KOAc, 1.2 ml 1 *M* $Mg(OAc)_2$, 0.4 ml 500 m*M* EDTA, and complete to 200 ml with water. Add 0.2 ml 1 *M* DTT and 0.1 ml 20 mg/ml PMSF to the cold solution just before use.

4. *RM buffer*: 250 m*M* sucrose, 50 m*M* HEPES–KOH, pH 7.6, 50 m*M* KOAc, 2 m*M* $Mg(OAc)_2$, 1 m*M* DTT, and 10 µg/ml PMSF. To make 100 ml of the buffer, add 12.5 ml 2 *M* sucrose, 5 ml 1 *M* HEPES–KOH, pH 7.6, 1.25 ml 4 *M* KOAc, 0.2 ml 1 *M* $Mg(OAc)_2$, and complete to 100 ml with water. Add 0.1 ml 1 *M* DTT and 50 µl 20 mg/ml PMSF to the cold solution just before use.

Steps

This procedure is performed in the cold room. Samples and buffers should be kept on ice.

1. Excise the pancreas (10–15 g) from a dog (e.g., beagle) and rinse in ~500 ml ice-cold homogenization buffer.
2. Remove connective tissue and fat, and cut the pancreas into small pieces. (*Optional*: Shock-freeze the pieces in liquid nitrogen and store the tissue at –80°C.)
3. Place the pieces into ~120 ml homogenization buffer and pass the tissue through a tissue press with a 1-mm mesh steel sieve.
4. Homogenize the pancreas in a 30-ml glass/Teflon potter with eight strokes at full speed (1500 rpm).
5. Transfer homogenate into 30-ml polypropylene tubes. Centrifuge at 3000 rpm (1000 *g*) for 10 min at 4°C in a Sorvall SS34 rotor.
6. Collect the supernatant, avoiding the floating lipid. Extract the pellet once more in 50 ml homogenization buffer as described in step 4 and centrifuge again (see step 5).

7. Transfer the two 1000-*g* supernatants to 30-ml polypropylene tubes. Centrifuge at 9500 rpm (10,000 *g*) for 10 min at 4°C in a Sorvall SS34 rotor.
8. Collect the supernatant, avoiding the floating lipid and repeat step 7 (centrifugation at 10,000 *g*) twice.
9. In the meantime, prepare four 70-ml polycarbonate tubes for a Ti45 rotor and add 25 ml sucrose cushion per tube.
10. After the third 10,000 *g* centrifugation (step 8), collect the supernatant and apply carefully, without mixing, onto the 25-ml sucrose cushions (see step 9).
11. Centrifuge at 35,000 rpm (142,000 *g*) for 1 h at 4°C in a Beckman Ti45 rotor.
12. Discard the supernatant and resuspend the membrane pellet, the rough microsomes (RM), in 20 ml RM buffer using a Dounce homogenizer.
13. Measure the absorption at 260 and 280 nm of a 1 : 1000 dilution of the RM suspension in 0.5% (w/v) SDS. Usually an absorption of 0.05–0.1 A_{280}/ml and a ratio A_{260}/A_{280} of ~1.7 are obtained. When the pancreas is frozen (see step 2), the A_{260}/A_{280} is 1.5–1.6.
14. Freeze 500-µl aliquots in liquid nitrogen and store at –80°C until use.

Note: RMs prepared by this procedure largely retain SRP on the membrane.

2. *Preparation of Signal Recognition Particle (SRP)*

Purification of components involved in protein translocation revealed that a cytosolic component, the signal recognition particle, is required for targeting nascent polypeptide chains to the ER membrane (Walter and Johnson, 1994). SRP is present in cytosolic extracts, but is also associated with RMs to a variable degree. In order to improve the efficiency of the translocation system, purified SRP may be added to the translation/translocation system. This is particularly useful when wheat germ extract is used for cell-free *in vitro* translation because this extract contains low amounts of functional SRP. SRP is isolated most conveniently from RMs by treatment with high salt. Released SRP is then purified by gel filtration and anion-exchange chromatography.

Solutions

Glass and plasticware are autoclaved, and stock solutions and distilled water are either autoclaved or filtered through 0.45-µm-pore-sized filters.

1. *Stock solutions* (see also preparation of RMs, Section III,A,1)

1 M Tris-OAc, pH 7.5: To make 1 liter of the buffer, dissolve 121.1 g Tris base in water, adjust to pH 7.5 with acetic acid, and complete to 1 liter.

10% (w/v) octaethylene glycol monododecyl ether: To make 10 ml of the solution, dissolve 1 g of octaethylene glycol monododecyl ether in water and complete to 10 ml.

2. *RM buffer*: As in solution 4 of Section III,A,1 (preparation of RMs).

3. *High salt solution*: 1.5 *M* KOAc and 15 m*M* $Mg(OAc)_2$. To make 50 ml of the solution, add 18.75 ml 4 *M* KOAc, 0.75 ml 1 *M* $Mg(OAc)_2$, and complete to 50 ml with water.

4. *Sucrose cushion*: 500 m*M* sucrose, 50 m*M* Tris–OAc, pH 7.5, 500 m*M* KOAc, 5 m*M* $Mg(OAc)_2$, and 1 m*M* DTT. To make 100 ml of the solution, add 25 ml 2 *M* sucrose, 5 ml 1 *M* Tris–OAc, pH 7.5, 12.5 ml 4 *M* KOAc, 0.5 ml 1 *M* $Mg(OAc)_2$, and complete to 100 ml with water. Add 0.1 ml 1 *M* DTT to the cold solution just before use.

5. *Gel filtration buffer*: 50 m*M* Tris–OAc, pH 7.5, 250 m*M* KOAc, 2.5 m*M* $Mg(OAc)_2$, 1 m*M* DTT, and 0.01% octaethylene glycol monododecyl ether. To make 1 liter of the buffer, add 50 ml 1 *M* Tris–OAc, pH 7.5, 62.5 ml 4 *M* KOAc, 2.5 ml 1 *M* $Mg(OAc)_2$, 1 ml 10% octaethylene glycol monododecyl ether, and complete to 1 liter with water. Add 1 ml 1 *M* DTT to the cold solution just before use.

6. *Washing buffer*: 50 m*M* Tris–OAc, pH 7.5, 350 m*M* KOAc, 3.5 m*M* $Mg(OAc)_2$, 1 m*M* DTT, and 0.01% octaethylene glycol monododecyl ether. To make 100 ml of the buffer, add 5 ml 1 *M* Tris–OAc, pH 7.5, 8.75 ml 4 *M* KOAc, 0.35 ml 1 *M* $Mg(OAc)_2$, 0.1 ml 10% octaethylene glycol monododecyl ether, and complete to 100 ml with water. Add 0.1 ml 1 *M* DTT to the cold solution just before use.

7. *SRP buffer*: 50 m*M* Tris–OAc, pH 7.5, 650 m*M* KOAc, 6 m*M* $Mg(OAc)_2$, 1 m*M* DTT, and 0.01% octaethylene glycol monododecyl ether. To make 100 ml of the buffer, add 5 ml 1 *M* Tris–OAc, pH 7.5, 16.25 ml 4 *M* KOAc, 0.6 ml 1 *M* $Mg(OAc)_2$, 0.1 ml 10% octaethylene glycol monododecyl ether, and complete to 100 ml with water. Add 0.1 ml 1 *M* DTT to the cold solution just before use.

Steps

This procedure is performed in the cold room and samples and buffers should be kept on ice.

1. Prepare ER-derived rough microsomes from two dog pancreas as described previously and resuspend the final RM pellet (see step 8 in Section III,A,1) in 50 ml RM buffer using a Dounce homogenizer.

2. Add 25 ml high salt solution and incubate for 15 min at 4°C on a turning wheel.

3. Distribute the membrane suspension equally to two 70-ml polycarbonate tubes for a Ti45 rotor onto 25 ml sucrose cushion per tube, avoid mixing.

4. Centrifuge at 32,000 rpm (120,000 *g*) for 1 h at 4°C in a Beckman Ti45 rotor.

5. In the meantime, prepare ten 10.4-ml polycarbonate tubes for a Ti70.1 rotor and add 1 ml sucrose cushion per tube.

6. After centrifugation (step 4), collect the supernatant and apply carefully, without mixing, onto the 1-ml sucrose cushions (see step 5).

7. Centrifuge at 65,000 rpm (388,000 *g*) for 1 h at 4°C in a Beckman Ti70.1 rotor.

8. Collect again the supernatant.

9. Concentrate the supernatant to approximately 10 ml in a 50-ml Amicon ultrafiltration unit equiped with a YM100 membrane.

10. Load concentrated sample onto a Sephacryl S-200 (2.6 × 20 cm) equilibrated with gel filtration buffer and elute with gel filtration buffer. The flow rate is 1 ml/min. Follow elution with a UV monitor (l = 280 nm) by using, e.g., the ÄKTAprime chromatography system from Amersham Pharmacia.

11. Collect flow through (20–25 ml) and load immediately onto a DEAE–Sepharose column (1 × 3 cm) equilibrated with gel filtration buffer. The flow rate is again 1 ml/min.

12. Wash column with 20 ml gel filtration buffer and 20 ml washing buffer.

13. Elute SRP with SRP buffer and collect peak fraction (2–3 ml). The SRP eluate has an absorption of 1–4 A_{260}/ml and a ratio A_{260}/A_{280} of approximately 1.4. Freeze 100-µl aliquots in liquid nitrogen and store at –80°C until use.

B. *In Vitro* Translation and Translocation Assay

Solutions

1. *Wheat germ extract*: Wheat germ extract for cell-free *in vitro* translation is prepared as described by Erickson and Blobel (1983) except that we use a gel filtration buffer with lower potassium and magnesium concentrations [40 m*M* HEPES–KOH, pH 7.6, 50 m*M* KOAc, 1 m*M* $Mg(OAc)_2$, 0.1% 2-mercaptoethanol]. Fresh wheat germ may be purchased from a local mill or from General Mills California. Store wheat germ in a desiccator over silica gel beads at 4°C. Considerable differences in translation efficiency may yield from different batches. Store wheat germ extract in 110-µl aliquots at –80°C and thaw only once.

2. *Capped mRNA*: To obtain mRNA coding for a secretory or a membrane protein, clone a cDNA encoding the protein of interest into a suitable expression vector downstream of a T7 or a SP6 promotor (e.g., pGEM from Promega Biotech). We generally prefer the SP6 promotor as the respective transcripts yield more efficient translation. Prepare plasmid DNA from *Escherichia coli* cultures using the Plasmid Maxi kit from Qiagen. For transcription, linearize the purified plasmid DNA with a suitable restriction enzyme that cuts downstream of the coding sequence. Alternatively, a template for transcription may be generated by polymerase chain reaction. Amplify the coding region of interest using *Pfu* DNA polymerase (Stratagene), an appropriate plasmid DNA as template, a forward primer containing the SP6 promotor, a Kozak sequence (Kozak, 1983) and a ATG for the initiation methionine, and a reverse primer starting with 5'-NNNNNNNNNCTA- to introduce a TAG stop codon at the desired position. Perform runoff *in vitro* transcription according to a standard protocol (e.g., in Sambrook *et al*., 1989) or by using a commercially available transcription kit (e.g., mMESSAGAmMACHINE kits from Ambion Cat. No. 1340 and 1344). Dissolve the resulting capped messenger RNA in water after extraction with phenol and chloroform and precipitation with sodium acetate and ethanol. Store mRNA at –80°C.

3. *Energy mix*: 50 m*M* HEPES–KOH, pH 7.6, 12.5 m*M* ATP, 0.25 m*M* GTP, 110 m*M* creatine phosphate, 10 mg/ml creatine kinase, and 0.25 m*M* of each amino acid *except* methionine. To make 1 ml of the solution, dissolve 41 mg creatin phosphate (disodium salt · $4H_2O$) and 10 mg creatin kinase in 590 µl water and add 50 µl 1 *M* HEPES–KOH, pH 7.6, 125 µl 100 m*M* ATP solution (Roche Applied Science), 2.5 µl 100 m*M* GTP solution (Roche Applied Science), and 250 µl 19 amino acids mix without methionine (Promega, 1 m*M* of each amino acid). Store the energy mix in 22 µl aliquots at –80°C. Do not refreeze!

4. *Salt mix*: 500 m*M* HEPES–KOH, pH 7.6, 1 *M* KOAc, and 50 m*M* $Mg(OAc)_2$. To make 1 ml of the solution, mix 500 µl 1 *M* HEPES–KOH, pH 7.6, 250 µl 4 *M* KOAc, 70 µl 1 *M* $Mg(OAc)_2$, and 180 µl water.

5. *SRP buffer*: As in solution 7 of Section III,A,2. (preparation of SRP).

6. *20% ($^w/_v$) trichloroacetic acid*: To make 100 ml of the solution, dissolve 20 g trichloroacetic acid in water and complete to 100 ml.

Steps

1. Per assay (25 µl), mix on ice 6 µl water, 1 µl salt mix, 2 µl energy mix, 10 µl wheat germ extract, 2 µl SRP buffer or SRP solution (see Section III,A,2, step 12),

2 µl RM suspension (see Section III,A,1, step 8), 1 µl [^{35}S]methionine (>1000 Ci/mmol), and 1 µl capped mRNA.
2. Incubate for 60 min at 25°C.
3. Add 25 µl (1 volume) 20% trichloroacetic acid to precipitate proteins and centrifuge at 14,000 rpm for 3 min at room temperature in an Eppendorf centrifuge.
4. Discard supernatant. Wash pellet with 150 µl cold acetone, and centrifuge as in step 3.
5. Discard supernatant and repeat step 4.
6. Discard supernatant, centrifuge tube shortly, and remove residual acetone completely with a pipette.
7. Add 20–30 µl sample buffer for SDS–polyacrylamide gel electrophoresis and heat for 10 min at 65°C.
8. Load 5–10 µl onto a SDS–polyacrylamide gel and analyze the sample by electrophoresis. Radiolabelled proteins can be visualized by autoradiography, fluorography, or on a phosphorimager.

Controls: Translation without mRNA (add water instead); translation without membranes (add RM buffer instead, see solution 4 in Section III,A,1).

Note: Translation and translocation assays have to be optimized for each mRNA with respect to magnesium and potassium concentrations as well as to the amount of mRNA, SRP, and membranes. Optimal salt concentrations vary from 1 to 3.5 m*M* magnesium and from 70 to 150 m*M* potassium and are adjusted by using adapted salt mixes. The amount of SRP and membranes may be varied by diluting SRP and RM solutions with the respective buffers.

C. Assays to Characterize the Translocation Products

1. Protease Protection Assay

Proteinase K is used to test the translocation of proteins or parts of proteins across microsomal membranes (Blobel and Dobberstein, 1975). Membranes are impermeable to the protease and therefore only proteins or protein domains exposed on the cytoplasmic side of the microsomes are digested. To demonstrate that only intact microsomal vesicles protect lumenal proteins or protein domains, nonionic detergent (e.g., Triton X-100) is added to open the membrane.

Protease treatment is also used to characterize the topology of membrane proteins. In this case, protease treatment is often followed by immunoprecipitations with antibodies directed against defined regions of the protein investigated. Successful immunoprecipitations indicate that the respective domains are exposed on the lumenal side of the microsomes and are protected from the protease.

Solutions

1. *Sucrose cushion*: 500 m*M* sucrose, 50 m*M* HEPES–KOH, pH 7.6, 50 m*M* KOAc, 2 m*M* $Mg(OAc)_2$, and 1 m*M* DTT. To make 10 ml of the buffer, add 1.25 ml 2 *M* sucrose, 0.5 ml 1 *M* HEPES–KOH, pH 7.6, 125 µl 4 *M* KOAc, 20 µl 1 *M* $Mg(OAc)_2$, 10 µl 1 *M* DTT, and complete to 10 ml with water.
2. *3 mg/ml proteinase K*: To make 1 ml of the solution, dissolve 3 mg proteinase K in 1 ml water.
3. *20 mg/ml PMSF solution*: As is solution 1 of Section III,A,1 (preparation of RMs).
4. *10% ($^{w}/_{v}$) Triton X-100*: To make 10 ml of the solution, dissolve 10 g Triton X-100 in water and complete to 10 ml.
5. *20% ($^{w}/_{v}$) trichloroacetic acid*: As in solution 6 of Section III,B.

Steps

1. Perform a translation/translocation assay (25 µl) as described in Section III,B (steps 1 and 2).
2. In the meantime, prepare a 200-µl thick-wall polycarbonate tube for a TLA100 rotor and add 100-µl sucrose cushion.
3. After translation/translocation, apply the reaction mixture carefully onto the 100-µl sucrose cushion.
4. Wash microsomes by centrifugation through the sucrose cushion at 48,000 rpm (~100,000 *g*) for 3 min at 4°C in a Beckman TLA100 rotor.
5. Remove the supernatant with a pipette.
6. Resuspend the microsome pellet in 25 µl RM buffer (see solution 4 in Section III,A,1) and split the sample in three 8-µl aliquots.

7a. To the first aliquot (mock treatment) add 2 µl water.

7b. To the second aliquot add 1 µl proteinase K solution (3 mg/ml) and 1 µl water.

7c. To the third aliquot add 1 µl proteinase K solution (3 mg/ml) and 1 µl 10% Triton X-100.

8. Incubate the samples for 10 min at 25°C.
9. Stop proteolysis by adding 1 µl 10 mg/ml PMSF per sample.
10. Add 40 µl water and 50 µl 20% trichloroacetic acid to each sample to precipitate protein.
11. Centrifuge samples, wash protein pellets with acetone, and analyze samples by SDS–polyacrylamide gel electrophoresis as described in Section III,B, steps 3–8.

2. Sodium Carbonate Extraction

By alkaline treatment with sodium carbonate at pH 11, microsomal membranes are opened and release their content and peripherally associated proteins. The

method is used to separate these proteins from proteins integrated into the lipid bilayer (Fujiki *et al*., 1982).

Solutions

1. *0.1 M Na_2CO_3*: To make 10 ml of the solution, dissolve 106 mg Na_2CO_3 in water and complete to 10 ml. Prepare just prior to use.
2. *Alkaline sucrose cushion*: 0.1 *M* Na_2CO_3 and 250 m*M* sucrose. To make 10 ml of the solution, dissolve 106 mg Na_2CO_3 in water, add 1.25 ml 2 *M* sucrose (see solutions 1 of Section III,A,1), and complete to 10 ml with water.
3. *20% ($^w/_v$) trichloroacetic acid*: As in solution 6 of Section III,B.

Steps

1. Perform a translation/translocation assay (25 µl) as described in Section III,B (steps 1 and 2).
2. Wash microsomes by centrifugation through a sucrose cushion as described in Section III,C,1, steps 2–5.
3. Resuspend microsome pellet in 25 µl carbonate solution and incubate for 15 min on ice.
4. In the meantime, prepare a 200-µl thick-wall polycarbonate tube for a TLA 100 rotor and add 100-µl alkaline sucrose cushion.
5. For centrifugation, apply the sample (step 3) carefully onto a sucrose cushion in the polycarbonate tube.
6. Centrifuge at 55,000 rpm (130,000 *g*) for 10 min at 4°C in a Beckman TLA 100 rotor.
7. Recover the supernatant and pellet.

8a. To the supernatant add 150 µl 20% trichloroacetic acid to precipitate proteins. Centrifuge the sample, wash the protein pellet with acetone, and prepare the sample for SDS–polyacrylamide gel electrophoresis as described in Section III,B, steps 3–8.

8b. To the pellet add directly 20–30 µl sample buffer for SDS–polyacrylamide gel electrophoresis (see Section III,B, steps 7 and 8).

9. Analyze samples by SDS–polyacrylamide gel electrophoresis and autoradiography or phosphorimaging.

3. Inhibition of N-Glycosylation with Glycosylation Acceptor Tripeptide

The recognition sites for N-glycosylation in the ER are Asn-X-Ser and Asn-X-Thr. In the cell-free *in vitro* translation/translocation system described herein, the tripeptide *N*-benzoyl-Asn-Leu-Thr-methylamide efficiently competes with newly synthesized proteins for N-glycosylation (Lau *et al*., 1983). The translocated protein is therefore not glycosylated in the presence of acceptor tripeptide, and the effects of oligosaccharides, e.g., on protein folding and assembly, may be investigated.

Solution

Acceptor tripeptide solution: Synthesize *N*-Benzoyl-Asn-Leu-Thr-methylamide on a peptide synthesizer. Dissolve the tripeptide in methanol at a concentration of 0.5 m*M* (0.23 mg/ml) and store the stock solution at –80°C.

Steps

1. Evaporate per translation/translocation assay (25 µl) 1.5 µl acceptor tripeptide solution in a test tube using a Speed-Vac centrifuge.
2. Add the components for the translation/translocation assay to the tripeptide, vortex gently, and perform the assay as described in Section III,B (steps 1 and 2).
3. Precipitate the sample with trichloroacetic acid and analyze by SDS–polyacrylamide gel electrophoresis and autoradiography (see Section III,B, steps 3–8).

4. Endoglycosidase H Treatment

Treatment with endoglycosidase H is used to test N-glycosylation of proteins translocated into microsomal membranes. The glycosidase cleaves oligosaccharides of the high mannose type from glycoproteins, leaving an *N*-acetylglucosamine residue attached to the polypeptide (Tarentino *et al*., 1974).

Solutions

1. *Denaturing solution*: 0.5% (w/v) SDS and 1% (v/v) 2-mercaptoethanol. To make 10 ml of the solution, dissolve 50 mg SDS in water, add 100 µl 2-mercaptoethanol, and complete to 10 ml with water.
2. *0.5 M Na-citrate, pH 5.5*: To make 10 ml of the buffer, dissolve 1.47 g Na_3-citrate · 2 H_2O in water, adjust to pH 5.5 with HCl solution, and complete to 10 ml.

Steps

1. Perform a translation/translocation assay (25 µl) as described in Section III,B (steps 1 and 2).
2. Wash microsomes by centrifugation through a sucrose cushion as described in Section III,C,1, steps 2–5.
3. Resuspend microsome pellet in 25 µl denaturing solution and incubate for 10 min at 95°C.
4. Add 2.8 µl reaction buffer and 1 µl endoglycosidase H (1000 U/µl). Incubate for 1 h at 37°C.
5. Precipitate the sample with trichloroacetic acid and analyze by SDS–polyacrylamide gel electrophoresis and autoradiography or phorphorimaging (see Section III,B, steps 3–8).

IV. COMMENTS

As an alternative to wheat germ extract, commercially available rabbit reticulocyte lysate (e.g., from Promega) may be used for cell-free *in vitro* translation. Reticulocyte lysate contains sufficient SRP and therefore no additional SRP is usually required for optimization of translocation. When reticulocyte lysate is used, however, RMs should be treated with micrococcal nuclease to digest endogenous mRNA (Garoff *et al*., 1978). The reticulocyte translation machinery will otherwise promote completion of nascent pancreatic secretory proteins.

References

Blobel, G., and Dobberstein, B. (1975). Transfer of proteins across membranes. II. Reconstitution of functional rough microsomes from heterologous components. *J. Cell Biol*. **67**, 852–862.

Daniels, R., Kurowski, B., Johnson, A. E., and Hebert, D. N. (2003). N-linked glycans direct the cotranslational folding pathway of influenza hemagglutinin. *Mol. Cell* **11**, 79–90.

Erickson, A. H., and Blobel, G. (1983). Cell-free translation of messenger RNA in a wheat germ system. *Methods Enzymol*. **96**, 38–50.

Fujiki, Y., Hubbard, A. L., Fowler, S., and Lazarow, P. B. (1982). Isolation of intracellular membranes by means of sodium carbonate treatment: Application to endoplasmic reticulum. *J. Cell Biol*. **93**, 97–102.

Garoff, H., Simons, K., and Dobberstein, B. (1978). Assembly of the semliki forest virus membrane glycoproteins in the membrane of the endoplasmic reticulum *in vitro*. *J. Mol. Biol*. **124**, 587–600.

Johnson, A. E., and van Waes, M. A. (1999). The translocon: A dynamic gateway at the ER membrane. *Annu. Rev. Cell Dev. Biol*. **15**, 799–842.

Kozak, M. (1983). Comparison of initiation of protein synthesis in procaryotes, eukaryotes and organelles. *Microbiol. Rev*. **47**, 1–45.

Lau, J. T. Y., Welply, J. K., Shenbagamurthi, P., Naider, F., and Lennarz, W. J. (1983). Substrate recognition by oligosaccharyl transferase: Inhibition of translational glycosylation by acceptor peptides. *J. Biol. Chem*. **258**, 15255–15260.

Lemberg, M. K., and Martoglio, B. (2002). Requirements for signal peptide peptidase-catalyzed intramembrane proteolysis. *Mol. Cell* **10**, 735–744.

Rapoport, T. A., Jungnickel, B., and Kutay, U. (1996). Protein transport across the eukaryotic endoplasmic reticulum and bacterial inner membranes. *Annu. Rev. Biochem*. **65**, 271–303.

Sambrook, J., Fritsch, E. F., and Maniatis, T. (1989). Molecular Cloning: A Laboratory Manual. Cold Spring Harbor, NY.

Tarentino, A. L., Trimble, R. B., and Maley, F. (1978). Endo-β-*N*-acetylglucosaminidase from *Streptomyces plicatus*. *Methods Enzymol*. **50**, 574–580.

Walter, P., and Johnson, A. E. (1994). Signal sequence recognition and protein targeting to the endoplasmic reticulum membrane. *Annu. Rev. Cell Biol*. **10**, 87–119.

CHAPTER

31

Use of Permeabilised Mast Cells to Analyze Regulated Exocytosis

Gerald Hammond and Anna Koffer

I. INTRODUCTION

Cell permeabilisation allows manipulation of experimental conditions that is typical for *in vitro* assays while maintaining the integrity of cellular architecture. Permeabilised mast cells, both primary and cultured cell lines, such as rat basophilic leukemia (RBL-2H3) or human mast cells (HMC-1), have been used to investigate the mechanism of exocytosis, endocytosis, phospholipid metabolism, and cytoskeletal responses. After permeabilisation with a bacterial exotoxin, streptolysin-O (SL-O), cells lose their cytosolic components but retain intact and functional secretory vesicles. These cells provide a well-controlled system, ideal for reconstitution type experiments. Permeabilisation by SL-O is usually irreversible. Reversible permeabilisation of rat peritoneal mast cells can be achieved by exposure to the tetrabasic anion of ATP (ATP^{4-}). This creates lesions (Cockcroft and Gomperts, 1979) due to interaction with a specific cell surface receptor (Tatham *et al*., 1988), the dimensions of which vary with increasing ATP^{4-} concentration (Tatham and Lindau, 1990). The pores created by ATP^{4-} are, however, always smaller than those due to SL-O. Combination of the two methods allows control of the extent of leakage of cytosolic factors (Koffer and Gomperts, 1989).

The SL-O monomer binds to membrane cholesterol and then oligomerises to form large pores, up to 30 nm in diameter (Bhakdi *et al*., 1993; Buckingham and Duncan, 1983; Palmer *et al*., 1998). The concentration of SL-O and the time of exposure needed for the permeabilisation vary for different cells. Appropriate conditions can be found using nonpermeant fluorescent dyes, such as ethidium bromide or rhodamine phalloidin. Adherent cells usually require higher concentrations of SL-O and/or longer exposure times than suspended cells.

Holt and Koffer (2000) described the use of various recombinant mutants of small Rho GTPases in permeabilised mast cells. Other reviews of permeabilisation techniques have been published previously (Gomperts and Tatham, 1992; Larbi and Gomperts, 1996; Tatham and Gomperts, 1990). This article describes a "SL-O prebind" method for permeabilising glass-attached primary rat peritoneal mast cells. This method is based on the temperature-independent binding of SL-O to the plasma membrane and the temperature-dependent polymerisation of bound SL-O molecules required to form pores (Sekiya *et al*., 1996).

Hexosaminidase, released from stimulated permeabilised cells into the supernatant, is assayed biochemically, while the remaining cells are processed for imaging. Thus, functional and morphological studies can be done in parallel. Immunostaining of mast cells poses specific problems due to the presence of highly charged secretory granules. Cell permeabilisation allows introduction of antibodies into cells before fixation. This is advantageous, as antibodies come into contact with granules still intact rather than with those permeabilised by fixatives. Staining before fixation is also recommended for membranous structures (e.g., staining with anti-PIP_2), as these are often disrupted by fixatives. Moreover, pretreatment of permeabilised cells with antibodies is useful for functional studies investigating the effects of the activity of the blocking antigen on cellular responses. We describe pretreatment of permeabilised cells before triggering, the assay of released hexosaminidase, and subsequent immunostaining either before or after fixation, with steps taken to avoid unspecific staining. The former

Copyright 2006, Elsevier Science (USA).
All rights reserved.

method is an adaptation of a previously described procedure (Guo *et al*., 1998).

II. MATERIALS AND INSTRUMENTATION

Percoll (1.13 ± 0.005 g/ml stock) is from Amersham Biosciences (1 liter, Cat. No. 17-0891-01). 10× calcium/magnesium-free phosphate-buffered saline (PBS) with defined salt densities is from Gibco RBL (500 ml, Cat. No. 14200-067). Streptolysin-O (SL-O, Cat. No. 302) and sodium dithionite (Cat. No. 303, needed for reduction of SL-O) are from iTEST plus, Ltd. (Czech Republic). Other preparations of SL-O can be obtained from Sigma (e.g., Cat. No. S 5265), and SL-O can also be obtained from VWR Scientific, US (Cat. No. DF 0482-60, manufactured by Difco), but in our hands, the just-described reagent has given the most reproducible results. Sigma provides EGTA (Cat. No. E-4378), HEPES (Cat. No. H-4034), PIPES (Cat. No. P-1851), Tris (Cat. No. T-1503), glutamic acid, monopotassium salt (Cat. No. G-1501), 4-methylumbelliferyl-*N*-acetyl-β-D-glucosaminide (Cat. No. M2133), dimethyl sulphoxide (DMSO, Cat. No. D-8779), Triton X-100 (Cat. X-100), goat serum (Cat. No. G9023), unconjugated succinyl-concanavalin A (SCA, Cat. No. L 3885), lysophosphatidylcholine (LPC, Cat. No. L-4129), paraformaldehyde (Cat. No. P-6148), and polyethylene glycol (molecular weight 3550, Cat. No. P-4338). Na_2ATP (trihydrate, Cat. No. 519979), 100 m*M* GTPγS solution (Cat. No. 1110 349), and digitonin (1 g, Cat. No. 1500 643) are from Boehringer. Citric acid (Cat. No. 100813M), glycine (Cat. No. 101196X), solutions of 1 *M* $MgCl_2$ (Cat. No. 22093 3M) and 1 *M* $CaCl_2$ (Cat. No. 190464 K), and 18-mm^2 coverslips, thickness 1 (Cat. No. 406/0187/23), are from BDH. Mowiol 4–88 is from Harco (Harlow Chemical Company Ltd.).

Pointed bottom tubes (10 ml, Cat. No. B99 783) are from Philip Harris. "Multitest" 8-well slides (Cat. No. 6040805) are from ICN Biomedicals, Inc. Ninety-six V-well clear plates (Cat. No. 651 101) and 96-well flat-bottom black plates (Cat. No. 655 076) are from Greiner Bio-One Ltd. The eight channel pipettes are Transferepettes-8, 20–100 µl, from Brand, Germany. The refrigerated centrifuge, Omnifuge 2.ORS, is from Heraeus. The plate reader, Polarstar Galaxy, is from BMG Labtechnologies.

A moisture box is a small plastic box with a well-fitting lid lined with wet tissue paper. A plastic tray that can take up to five 8-well slides is placed inside the box. Nylon mesh is from net curtain material obtained from John Lewis Department Store (London).

III. PROCEDURES

A. Preparation of Rat Peritoneal Mast Cells

This procedure has been described in detail previously (Gomperts and Tatham, 1992) and only a brief version is given here.

Solutions

1. *Percoll at a final density of 1.114 g/ml*: Prepare using the following formula:

$$\rho_{\text{Final}} \cdot V_{\text{Final}} = \rho_{\text{Percoll stock}} \cdot V_{\text{Percoll stock}} + \rho_{10\times\ \text{PBS}} \cdot \left(\frac{V_{\text{Final}}}{10}\right) + \rho_{H_2O^{\infty}} \cdot \left(V_{\text{Final}} - V_{\text{Percoll stock}} - \frac{V_{\text{Final}}}{10}\right)$$

ρ is density (g/ml) and V is volume (ml). Use 10× PBS stock with defined density and highly purified sterile water so that the density may be taken as 1.000 g/ml. Prepare 50–100 ml of Percoll solution in a sterile environment and store in 2-ml aliquots at –20°C (may be stored several years). Warm at room temperature, mix thoroughly, and transfer into a pointed bottom tube just before use.

2. *Chloride buffer (CB)*: Final concentrations 20 m*M* HEPES, 137 m*M* NaCl, 2.7 m*M* KCl, 2 m*M* $MgCl_2$, 1.8 m*M* $CaCl_2$, 5.6 m*M* glucose, and 1 mg/ml bovine serum albumin (BSA), pH 7.2. Prepare 10× concentrated stock solution without BSA. To make 500 ml of 10× CB, dissolve 40 g NaCl, 1 g KCl, 23.83 g HEPES, 5 g glucose, 10 ml of 1 *M* $MgCl_2$, and 9 ml of 1 *M* $CaCl_2$ in distilled water, adjust pH to 7.2 with NaOH, and complete to 500 ml. Store in 50-ml aliquots at –20°C. Thaw, mix, dilute, add BSA, and readjust pH to 7.2 before use.

Steps

1. Use Sprague–Dawley rats. "Retired breeders" of either sex were used but other strains of various ages are also suitable; older rats provide more cells.
2. After peritoneal lavage of rats, pellet the cells present in the washings by centrifugation (5 min at 250 *g*).
3. Resuspend cells in ~7 ml of CB and filter the suspension through a nylon mesh.
4. Overlay the filtered suspension onto a 2-ml cushion of Percoll solution placed in a 10-ml pointed bottom tube.
5. Centrifuge (10 min at 250 *g*, room temperature, slow acceleration). Dense mast cells pellet through the Percoll cushion while contaminating cells (neutrophils, macrophages, red blood cells) remain at the buffer–Percoll interface.

6. Remove the buffer, interface cells, and Percoll, resuspend the pellet in ~1 ml CB, and transfer into a clean tube (avoid touching the tube wall where some of the contaminating cells may still adhere).
7. Add further ~10 ml CB, centrifuge (5 min at 250 *g*), and resuspend pellet in 1.5 ml CB. About 1×10^6 cells (>95% purity) are obtained from one rat. This is sufficient for at least five 8-well slides.

B. Permeabilisation

SL-O binds to the cells on ice, excess SL-O (and any other additives) is removed by washing with a cold buffer, and cells are then permeabilised by the addition of warm buffer. Permeabilised cells are finally washed to remove freely soluble ions, nucleotides, and proteins before the addition of triggering solutions. A small loss of responsiveness occurs due to the "run-down" during the washing (10–20%) but the advantage is that nucleotides, ions, and proteins leaking out from cells do not come into contact with those applied exogenously. If this is of no concern (e.g., when ATP levels have been depleted by metabolic inhibition), triggers can be added at the time of permeabilisation.

Solutions

1. *Glutamate buffer (GB)*: Final concentrations 137 m*M* Kglutamate, 20 m*M* PIPES, 2 m*M* $MgCl_2$, and 1 mg/ml BSA, pH 6.8. Prepare 10× concentrated stock solution without BSA. To make 250 ml of 10× GB, dissolve 63.43 g glutamic acid, 15.12 g PIPES, and 5 ml 1 *M* $MgCl_2$ in distilled water, adjust pH to 6.8 with glacial acetic acid, and complete to 250 ml. Store 50-ml aliquots at –20°C. Thaw, mix, dilute, add BSA, and readjust pH to 6.8 before use.

2. *100 mM EGTA stock solution*: Store in 5- to 10-ml aliquots at –20°C. To make 100 ml of 100 m*M* EGTA, dissolve 3.804 g EGTA in 100 ml distilled water.

3. *Glutamate buffer–3 mM EGTA (GBE)*: Add 300 µl of 100 m*M* EGTA to 10 ml GB.

4. *Streptolysin-O (SL-O)*: Streptolysin-O from iTEST is supplied as a lyophilized powder in vials of 22 IU and must be reduced before use with sodium dithionite. To prepare a working stock at 20 IU/ml, dissolve one vial of SL-O in 550 µl PBS containing 0.1% BSA and one vial of 20 mg sodium dithionite in 550 µl PBS containing 0.1% BSA. Mix these two solutions and incubate at 37°C for 1 h. SL-O is now reduced and the solution is ready for use. For storing, divide the reduced SL-O solution into 100-µl aliquots, freeze under liquid nitrogen, and store at –80°C. Just before use, warm and mix and use on the same day. For the "prebind" method, use SL-O at the final concentration of 1.6 IU/ml: Add 1.15 ml of GBE to 100 µl of 20 IU SL-O/ml. Thus, one aliquot will provide 1.25 ml of working solution, enough for one experiment.

Steps

1. Clean 8-well slides with distilled water and then ethanol. Leave to dry. Label the slides.
2. Pipette 30 µl cell suspension in CB per well (i.e., ~20,000 cells per well). Allow 2–4 wells for each condition. Keep 150 µl of the cell suspension aside for secretion assay (see solution D3 and step D2).
3. Let cells attach for 1 h at room temperature on a plastic tray in a moisture box[1].
4. Place the slides on a metal plate on ice.
5. Wash the cells once with 30 µl ice-cold GBE.
6. Add 30 µl ice-cold SL-O (1.6 IU/ml GBE) to each well and incubate on ice for 8 min to allow SL-O to bind to the plasma membranes.
7. Wash the cells once with 30 µl ice-cold GBE to remove unbound SL-O and additives.
8. Permeabilise the cells by adding 30 µl warm (37°C) GBE and transferring to a prewarmed moisture box at 37°C for 90 s.
9. Chill the cells by placing the slide back on ice.
10. Wash once with 30 µl GB (without EGTA) to remove freely soluble components.

C. Pretreatment and Triggering

Solutions

1. *GB–30 µM EGTA*: Add 3 µl of 100 m*M* EGTA to 10 ml GB.

2. *Agent to be tested, dissolved in GB–30 µM EGTA*. These can include an antibody directed against a specific antigen whose activity is being tested. Dilution of the antibody is 10–20× less than that used for immunostaining.

3. *100 mM MgATP*: To make 16.5 ml of 100 m*M* MgATP, add 6.61 ml of 0.5 *M* Tris and 1.65 ml of 1 *M* $MgCl_2$ to 1 g Na_2ATP and add H_20 to a final volume of 16.5 ml. Store in 100-µl aliquots at –20°C.

4. *10 mM GTPγS*: Dilute the 100 m*M* stock solution with GB just before use.

5. *Ca^{2+} /EGTA buffers system*: These are obtained as described previously (Gomperts and Tatham, 1992; Tatham and Gomperts, 1990) by mixing solutions of Ca:EGTA and EGTA, both at ~100 m*M* and pH 6.8 at specified ratios. Keep 10-ml aliquots of 100 m*M* stock

[1] In some experiments, it is desirable to deplete endogenous ATP from intact cells with metabolic inhibitors. In this case, after step 2, incubate attached intact cells with CB where glucose has been omitted and 10 µ*M* antimycin A with 6 m*M* 2-deoxyglucose included. More than 90% depletion of ATP is achieved in 20 min at 30°C (Koffer and Churcher, 1993).

TABLE I Assembling 1 ml Each of the Four Typical Triggering Solutions

Stock	EA	EGA	CA	CGA
EGTA (100 m*M*)	30 µl	30 µl	0	0
ATP (100 m*M*)	30 µl	30 µl	30 µl	30 µl
GTPγS (10 m*M*)	0	5 µl	0	5 µl
Ca:EGTA (pCa5) (100 m*M*[a])	0[a]	0[a]	30 µl[a]	30 µl[a]
GB[a]	940 µl	935 µl	940 µl	935 µl

[a] Note that 100 m*M* is an ideal stock concentration of Ca:EGTA buffer, although the final concentration of stock is calculated empirically when preparing the buffers (Tatham and Gomperts, 1990). Therefore, the volume required to give the final 3 m*M* concentration of Ca:EGTA final from stock will need to be adjusted.

solutions at –20°C. Free Ca^{2+} concentration is controlled by adding the appropriate Ca^{2+}/EGTA buffer to a final concentration of 3 m*M*.

6. *Triggering solutions*: Various combinations of calcium, MgATP, and GTPγS (or GTP) in GB are used for cell stimulation. The following four conditions (final concentrations) are used most frequently: EA (basal condition, 3 m*M* EGTA–3 m*M* ATP); EGA (as EA with 50 µ*M* GTPγS); CA (3 m*M* Ca:EGTA /to maintain [Ca^{2+}] at pCa5)–3 m*M* ATP; and CGA (as CA with 50 µ*M* GTPγS). Table I gives volumes for making triggering solutions using the aforementioned stock solutions.

Steps

1. Immediately after step B9 (permeabilised cells are still on the cold plate), add 15 µl of a solution containing the protein or reagent to be tested in GB–30 µ*M* EGTA.
2. Incubate on ice (in a moisture box) for 5–30 min. The time of incubation depends on the size of the protein/reagent to be introduced into the cells. For example, small proteins such as Rho GTPases require 5–10 min but antibodies may require up to 30 min to penetrate the SL-O lesions. The time and temperature for action of the agents should be considered.
3. Add 15 µl of 2× concentrated triggering solutions containing combinations of calcium/EGTA, MgATP, and GTPγS. (If no pretreatment was required, omit steps 1 and 2 and add 30 µl of 1× triggering solutions.)
4. Stimulate by transferring to a prewarmed moisture box and incubate for 30 min at 37°C. Note that a shorter time (10–15 min) may be sufficient when GTPγS is included in the triggering solution.
5. Stop reaction by transferring slides back onto the ice-cold metal plate.

D. Secretion Assay

Solutions

1. *Fluorogenic hexosaminidase substrate*: Final concentrations 1 m*M* 4-methylumbelliferyl-*N*-acetyl-β-D-glucosaminide, 0.1% DMSO, 0.01% Triton X-100, and 200 m*M* citrate, pH 4.5. To make 500 ml, mix 189.7 mg of the reagent with 0.5 ml DMSO and then add 500 ml of 0.2 *M* citrate–0.01% Triton X-100. To make citrate solution, dissolve 21 g of citric acid and 0.5 g of Triton X-100 in H_2O, adjust pH to 4.5 using NaOH, and make volume up to 500 ml. Using Whatman filter paper No. 1, filter and store in 20- to 50-ml aliquots at –20°C. Hexosaminidase, released from mast cells, hydrolyses the substrate, producing fluorescent 4-methylumbelliferone. Triton reduces surface tension and thus artifacts.
2. *0.5 M Tris*: Dissolve 60.55 g of Tris in water, total volume 1 liter.
3. *GB*
4. *Solution for assaying total hexosaminidase content*: To 150 µl of the original cell suspension (saved at step B2), add 1 ml of 0.2% Triton X-100 in GB and mix to lyse the cells.

Steps

1. After step C5, remove 15 µl (i.e., one-half) of the triggering solutions and transfer into cold transparent 96 V-well plates (on ice).
2. Add 100 µl of cold GB to each V well using a multichannel pipette.
3. Pipette 115 µl of the solution for assaying the total hexosaminidase content into one column of V wells (i.e., 8 × 115 µl).
4. Pipette 115 µl of GB into one column of V wells (i.e., 8 × 115 µl, to be used for blanks).
5. Balance with another 96 V-well plate.
6. Centrifuge for 5 min at 250 *g* at 4°C to remove any detached cells.
7. Using a multichannel pipette, remove 50 µl of the supernatant from each V well and transfer into a black flat-bottom 96-well plate.
8. Add 50 µl of the fluorogenic hexosaminidase substrate to each well to assay for the release of hexosaminidase.
9. Cover with lid and wrap in aluminium foil.
10. Incubate 1–2 h at 37°C or overnight at room temperature.
11. Quench with 100 µl of 0.5 *M* Tris.
12. Read fluorescence using a fluorescence plate reader (excitation and emission filter at 360 and 405 nm, respectively).
13. Calculate percentage secretion as follows: % secretion = 100 × (*X*-*B*)/(*T*-*B*), where *X*, *B*, and *T* are

fluorescence values of the sample, average blank, and average total hexosaminidase, respectively.

E. Immunostaining before Fixation

Cells remaining on eight-well slides after removal of the trigger solutions for secretion assays can be stained by fluorescent phalloidin to evaluate the morphology of F-actin (Holt and Koffer, 2000) or be immunostained. Processing of the cells should be done immediately after step D1 and the secretion assay delayed until the cells are in a blocking solution or fixed.

Solutions

1. *Stock solution of succinyl-Con A, SCA, 5 mg/ml*: Dissolve 25 mg in 5 ml GB without BSA. Store 100-µl aliquots at –20°C.
2. *Glutamate buffer–3 mM EGTA (GBE)*: Add 300 µl of 100 m*M* EGTA to 10 ml GB.
3. *Blocking solution*: 32% goat serum–250 µg/ml succinyl-Con A (SCA)–GBE. To make 1 ml, add 320 µl goat serum and 50 µl SCA (5 mg/ml stock) to 630 µl GBE.
4. *Antibody solution*: 16% goat serum in GBE. To make 1 ml, add 160 µl goat serum to 840 µl GBE. Higher concentrations of antibodies are usually required if these are introduced into permeabilised cells before fixation than those used for after-fixation staining. *Note*: After dilution, centrifuge all antibodies for 1 min at ~15,000 *g* to remove any aggregates.
5. *Fixative*: 3% paraformaldehyde in GBE (without BSA)–4% polyethylene glycol (PEG, MW 3200). To make 100 ml of fixative, first prepare GB (without BSA)–3 m*M* EGTA–4% (w/v) PEG. Add 3 g of paraformaldehyde to ~80 ml of GBE-PEG and gently heat and stir in a fume cupboard, adding 10 *M* NaOH in small doses until paraformaldehyde is dissolved and colourless. Adjust pH to 6.8. Filter (in a fume cupboard) using Whatman filter paper No. 1 and store 10-ml aliquots at –20°C.
6. *Mounting solution*: Add 12 ml of water to 12 g glycerol and 4.8 g Mowiol 4-88 in a conical flask and mix for 2 h or overnight at room temperature. Add 24 ml 0.2 *M* Tris, pH 8.5, and 400 µl of 100 m*M* EGTA and stir further at 50°C (~10 min). Centrifuge for 30 min at ~5000 *g*. Discard pellets, stir the supernatants again, and store in 1-ml aliquots at –20°C.

Steps

1. After step C5 and D1 (i.e., after triggering and removal of aliquots for secretion assay), remove the remaining triggering solutions.
2. Wash once in 30 µl GBE to remove residual calcium/GTPγS.
3. Add 30 µl of blocking solution to block unspecific binding.
4. Incubate in a moisture box for 30 min at room temperature.
5. Remove blocking solution and add 30 µl of the primary antibody diluted in antibody solution.
6. Incubate in a moisture box for 30–60 min at room temperature.
7. Wash the cells 4× with 30 µl GBE.
8. Add 30 µl of secondary antibody, conjugated to a fluorescent probe and diluted in antibody solution.
9. Incubate in a moisture box for 30 min at room temperature.
10. Wash the cells 4× with 30 µl GBE
11. Fix the cells by adding 30 µl fixative for 20 min at room temperature in a moisture box.
12. Wash the cells 4× with 30 µl GBE.
13. Aspirate wells until dry and add 4 µl mounting solution and remove any bubbles.
14. Cover eight wells with 18-mm^2 coverslips.

F. Immunostaining after Fixation

To improve access of antibodies into fixed cells, permeabilisation with either lysophosphatidyl choline or digitonin is required. Blocking can be done with a lower concentration of serum when cells are fixed, but succinyl–concanavalin A should still be included because fixation exposes granule matrices that may bind antibody nonspecifically. Including a 5-min wash step with 0.4 *M* NaCl before blocking also reduces nonspecific binding of antibodies to the granule matrices without affecting cellular morphology in fixed cells.

Solutions

1. *Fixative and mounting solutions as described earlier.*
2. *GBE*: Add 300 µl of 100 m*M* EGTA to 10 ml GB.
3. *LPC-GBE, 80 µg/ml of LPC in GBE*: Used for permeabilisation of fixed cells. Stock solution is 40 mg of LPC/ml ethanol. Store at –20°C. Warm to ~40°C and mix before use. Dilute 500×, i.e., 2 µl into 1 ml of GBE to obtain the final concentration.
4. *0.2 µM digitonin–GBE*. Used as an alternative solution for permeabilisation of fixed cells. Digitonin is stored as a 1 m*M* stock solution in DMSO at room temperature. Stock is prepared by dissolving 1.23 mg digitonin/ml in DMSO. Dilute 10 µl of stock digitonin in 990 µl GBE and then add 50 µl of this 10 µ*M* solution to 950 µl GBE to prepare the 0.2 µ*M* solution.
5. *50 mM glycine–GBE*: Make 10 ml of stock 1 *M* glycine solution by adding 0.75 g glycine to 10 ml GB (without BSA). Store in 1-ml aliquots at –20°C. Add 50 µl of 1 *M* glycine stock to 950 µl GBE.

6. *Blocking solution*: 5% goat serum–250 µg/ml succinyl-Con A (SCA)–GBE. To make 1 ml, add 50 µl goat serum and 50 µl stock SCA (5 mg SCA /ml GB without BSA) to 900 µl GBE.

7. *0.4 M NaCl*: For 1 ml, add 100 µl 4 *M* NaCl to 900 µl GBE.

8. *Antibody solution*: 5% goat serum in GBE. To make 1 ml, add 50 µl goat serum to 950 µl GBE. After dilution, centrifuge all antibodies for 1 min at ~15,000 *g* to remove any aggregates.

Steps

1. After step C5 and D1 (i.e., after triggering and removal of aliquots for secretion assay), remove the remaining triggers.
2. Fix the cells by adding 30 µl fixative for 20 min at room temperature in a moisture box.
3. Wash the cells 4× with 30 µl 50 m*M* glycine–GBE.
4. Add 30 µl of LPC-GBE (or digitonin-GBE).
5. Permeabilise fixed cells for 20 min with LPC-GBE or for 5 min with digitonin–GBE, both at room temperature.
6. Wash the cells 4× with 30 µl GBE.
7. Remove GBE and add 30 µl of 0.4 *M* NaCl in GBE to each well.
8. Incubate in a moisture box for 5 min at room temperature.
9. Wash the cells 4× with 30 µl GBE.
10. Add 30 µl of blocking solution.
11. Incubate in a moisture box for 30 min at room temperature.
12. Remove blocking solution and add 30 µl of the primary antibody diluted in antibody solution.
13. Incubate in a moisture box for 30–60 min at room temperature.
14. Wash the cells 4× with 30 µl GBE.
15. Add 30 µl of secondary antibody, conjugated to a fluorescent probe, diluted in antibody solution.
16. Incubate in a moisture box for 30 min at room temperature.
17. Wash the cells 4× with 30 µl GBE.
18. Aspirate wells until dry and add 4 µl mounting solution; remove any bubbles.
19. Cover eight wells with 18-mm^2 coverslips.

IV. COMMENTS

We have described a method that allows assessment of mast cell secretory function in parallel with studies of cell morphology. An example is shown in Fig. 1. Permeabilised mast cells were stained with anti-β-actin antibody after exposure to the combinations of calcium, ATP, and GTγS described in Table I. Confocal images of equatorial slices are shown together with typical secretory responses shown in parentheses (percentage of released hexosaminidase). The method provides a large potential for investigating the significance of rearrangements of specific molecules to exocytotic function.

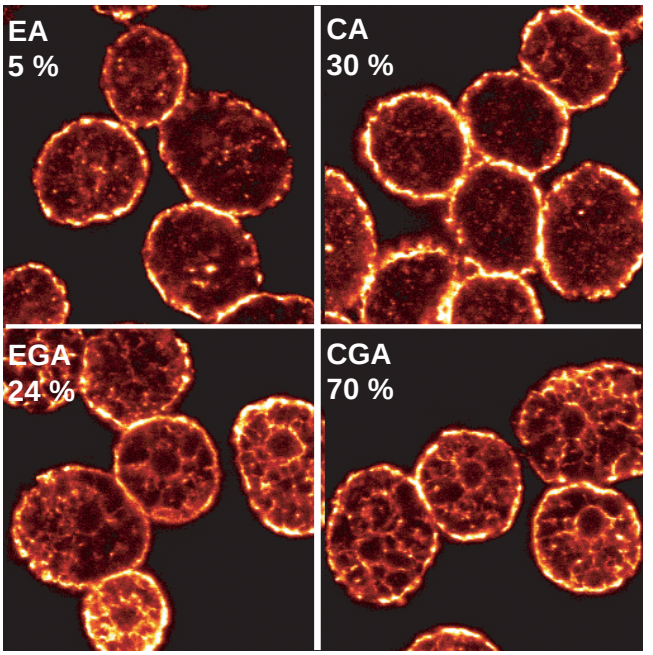

FIGURE 1 Glass-attached mast cells were permeabilised and exposed to the triggers described in Table I: EGTA/ATP (EA), calcium (pCa5)/ATP (CA), EGTA/GTP-γ-S/ATP (EGA), or calcium (pCa 5)/ GTPγS/ATP (CGA). After 20 min at 37°C, cells were fixed and stained with anti-β-actin monoclonal antibody (clone AC-15) from Sigma (used at 1/200 dilution). The secondary antibody (at 1/50 dilution in GBE) was goat antimouse IgG biotin from Sigma. Cy2 streptavidin (1/50, from Amersham Biosciences, UK) was the tertiary layer. Confocal micrographs of equatorial slices are shown. Numbers indicate the percentages of released hexosaminidase.

V. PITFALLS

Keep cells in the moisture box as much as possible to avoid evaporation. Maintain permeabilised mast cells at low (25–50 µ*M*) concentrations of EGTA before exposure to triggers to avoid spontaneous degranulation. When comparing activities of cells after various pretreatments, keep the time between permeabilisation and triggering standard; the length of the "run-down" period affects secretion. Keep 96-well plates clean, washing them with detergent and plenty of water immediately after use.

Note that when staining is performed before fixation, the nature of the endogenous antigen should be taken into account. Because Soluble proteins will leak out of the permeabilized cells, use this method for molecules known or expected to be tethered either to the membrane or to the actin cytoskeleton. Determination of the extent of leakage of the antigen under various conditions (by immunoblotting of the supernatants) is always helpful.

References

Bhakdi, S., Weller, U., Walev, I., Martin, E., Jonas, D., and Palmer, M. (1993). A guide to the use of pore-forming toxins for controlled permeabilization of cell membranes. *Med. Microbiol. Immunol. Berl*. **182**, 167–175.

Buckingham, L., and Duncan, J. L. (1983). Approximate dimensions of membrane lesions produced by streptolysin S and streptolysin O. *Biochim. Biophys. Acta* **729**, 115–122.

Cockcroft, S., and Gomperts, B. D. (1979). ATP induces nucleotide permeability in rat mast cells. *Nature* **279**, 541–542.

Gomperts, B. D., and Tatham, P. E. R. (1992). Regulated exocytotic secretion from permeabilized cells. *Methods Enzymol*. **219**, 178–189.

Guo, Z., Turner, C., and Castle, D. (1998). Relocation of the t-SNARE SNAP-23 from lamellipodia-like cell surface projections regulates compound exocytosis in mast cells. *Cell* **94**, 537–548.

Holt, M., and Koffer, A. (2000). Rho GTPases, secretion and actin dynamics in permeabilised mast cells. *Methods Enzymol*. **325**, 356–369.

Koffer, A., and Churcher, Y. (1993). Calcium and GTP-gamma-S as single effectors of secretion from permeabilised rat mast cells: Requirements for ATP. *Biochim. Biophys. Acta* **1176**, 222–230.

Koffer, A., and Gomperts, B. D. (1989). Soluble proteins as modulators of the exocytotic reaction of permeabilised rat mast cells. *J. Cell Sci*. **94**, 585–591.

Larbi, K. Y., and Gomperts, B. D. (1996). Practical considerations regarding the use of streptolysin-O as a permeabilising agent for cells in the investigation of exocytosis. *Biosci. Rep*. **16**, 11–21.

Palmer, M., Harris. R., Freytag, C., Kehoe, M., Tranum Jensen, J., and Bhakdi, S. (1998). Assembly mechanism of the oligomeric streptolysin O pore: The early membrane lesion is lined by a free edge of the lipid membrane and is extended gradually during oligomerization. *EMBO J*. **17**, 1598–1605.

Sekiya, K., Danbara, H., Yase, K., and Futaesaku, Y. (1996). Electron microscopic evaluation of a two-step theory of pore formation by streptolysin O. *J. Bacteriol*. **178**, 6998–7002.

Tatham, P. E. R., Cusack, N. J., and Gomperts, B. D. (1988). Characterisation of the ATP^{4-} receptor that mediates permeabilisation of rat mast cells. *Eur. J. Pharmacol*. **147**, 13–21.

Tatham, P. E. R., and Gomperts, B. D. (1990). Cell permeabilisation. *In "Peptide Hormones: A Practical Approach"* (K. Siddle and J. C. Hutton, eds.), pp. 257–269. IRL Press, Oxford.

Tatham, P. E. R., and Lindau, M. (1990). ATP-induced pore formation in the plasma membrane of rat peritoneal mast cells. *J. Gen. Physiol*. **95**, 459–476.

SECTION

5

Membranes

CHAPTER

32

Syringe Loading: A Method for Assessing Plasma Membrane Function as a Reflection of Mechanically Induced Cell Loading

Mark S. F. Clarke, Jeff A. Jones, and Daniel L. Feeback

I. INTRODUCTION

In the past, we have described a method for loading large macromolecules into the cytoplasm of cultured cells via the production of transient plasma membrane wounds inflicted by defined amounts of fluid shear stress (Clarke and McNeil, 1992, 1994). This technique is referred to as "syringe loading" and has been utilized to load a variety of macromolecules (i.e., fluorescent dextrans, proteins, immunoglobulins, calcium indicator dyes, plasmid DNA, and antisense oligonucleotides) into various different cell types (i.e., endothelial cells, fibroblasts, epithelial cells, lymphocytes, and amoeba). This technique is very simple and straightforward, relying on the capacity of the plasma membrane to reseal after the infliction of a *transient* plasma membrane disruption. During the syringe loading procedure, the mechanical force applied to the cells to produce plasma membrane wounding is fluid shear stress generated as a consequence of the cell suspension being forced through a narrow orifice in the form of a 30-gauge hypodermic needle. The macromolecule to be loaded is dissolved in the suspension medium and enters the cell cytoplasm across a diffusion gradient during the time the plasma membrane wound is open. As such, this technique for macromolecular loading of cells in suspension is simple, reproducible, and inexpensive.

The series of highly coordinated, multicomponent responses that occur both within the cell cytoplasm and at the plasma membrane in response to mechanical perturbation/rupture of the external plasma membrane is known collectively as the membrane wound response (McNeil and Steinhardt, 1997). Apart from its use as a simple cell loading technique, syringe loading has also been used to investigate the underlying cellular mechanisms involved in this phenomenon (Miyake and McNeil, 1995; Clarke *et al*., 1995b). It is increasingly evident that the wound response is a fundamental, highly conserved, and normal response to mechanical loading in a wide variety of cell types (McNeil and Terasaki, 2001). In addition, inappropriate levels of membrane wounding may be important in the etiology of a number of pathological conditions, such as atherosclerosis (Reidy and Lindner, 1991; Yu and McNeil, 1992; Clarke *et al*., 1995b), unloading induced muscle atrophy (Clarke *et al*., 1998), and left ventricular hypertrophy (Clarke *et al*., 1995a). The susceptibility of the plasma membrane to mechanically induced membrane disruption and the ability of the membrane to reseal itself after disruption has occurred (*disruption followed by resealing being the definition of membrane wounding*) are both dependent on the biophysical properties of the membrane, including fluidity, elasticity, compressibility, and overall membrane order. These factors have been used to enhance macromolecular loading efficiency by the inclusion of membrane active agents, such as pluronic F68, during the syringe loading procedure in order to enhance the cell membrane resealing process (Clarke and McNeil, 1992).

Copyright 2006, Elsevier Science (USA).
All rights reserved.

To date, the mechanical properties of biological membranes have been tested by various means, including the direct measurement of membrane mechanical properties (i.e., elastic area compressibility, tensile strength, membrane toughness), using micropipette aspiration techniques (Needham and Nunn, 1990; Song and Waugh, 1993; Zhelev and Needham, 1993). In addition, indirect measurement of membrane fluidity using steady-state fluorescent anisotropic measurements, nuclear magnetic resonance, and fluorescent probe diffusion techniques have proven useful in determining changes in the physical properties of biological membranes (Tanii *et al*., 1994; Kuroda *et al*., 1996; Gimpl *et al*., 1997) associated with such physiologically relevant alterations as membrane cholesterol content (Pritchard *et al*., 1991; Clarke *et al*., 1995b; Whiting *et al*., 2000). However, all of these techniques have the disadvantage of describing the physical properties of the cell membrane in purely mechanical terms without taking into consideration the complex "biological" nature of the cell membrane system being examined.

Although complex in nature, the membrane wound response *in toto* can be quantified using direct end point measures that describe the final outcome of the process. Such measures include cell survival at a given level of mechanical perturbation, the number of wounded cells present in the surviving cell population, the amount of membrane wound marker that enters the wounded cell, and the relative size of the membrane wound created based on membrane wound marker size. If membrane wounds are produced in a defined and reproducible manner, the effects of various environmental conditions on plasma membrane function, as reflected by alterations in the membrane wound response, can be quantified by the end point measures described earlier. We have used this approach to probe the effects of different gravitational conditions on the biophysical properties of the plasma membrane in cultured ***adherent*** cells using a technique known as impact mediated loading (Clarke *et al*., 2001). This article describes the use of syringe loading as a means of investigating the effects of environmental conditions on the plasma membrane wound response in ***suspension*** cells.

Syringe loading in its simplest configuration can be carried out utilizing a manual protocol, a single 1-ml hypodermic syringe and a 30-gauge hypodermic needle (Clarke and McNeil, 1992). The second-generation approach utilized a mechanized syringe pump apparatus that produced a defined expulsion pressure for a predetermined period of time (Clarke and McNeil, 1994). This article describes the development of a third-generation syringe loader device that is capable of processing a total of 10 separate samples in an identical fashion at the same time (Fig. 1). The multisample syringe loading technology essentially performs syringe loading under the same conditions as described previously except that many replicate samples can be loaded simultaneously. This device was designed to take into consideration the effects of temperature on membrane resealing dynamics, an experimental parameter that has not been fully controlled in previous syringe loading protocols. In the new configuration, individual sample vials containing identical cell suspensions are housed in a heating block maintained at 37°C throughout the syringe loading protocol (Fig. 1). As such, the technology produces a greater total yield of loaded cells with less variability between individual samples than using either the manual or the second-generation mechanized protocol. However, it does not exhibit a significant increase in cell loading efficiency relative to earlier syringe loading protocols. Rather, the goal for this technology was to develop a simple and rapid means of testing the biophysical properties of the plasma membrane of cells (as reflected by alterations in the membrane wounding response) exposed to different environmental conditions.

With this concept in mind and utilizing the multisample syringe loader detailed in Fig. 1, this article describes a series of experiments that illustrate the utility of the syringe loading technology as an experimental tool to probe the effects of environmental conditions on membrane function. In the following example, the effects of radiation exposure on cell membrane function as it impacts the membrane wounding response are investigated. The experiment described here was designed to determine whether gamma irradiation resulted in acute (i.e., within 2 h of radiation exposure) membrane modification that resulted in an increase in susceptibility to mechanical shear force-induced membrane wounding. Membrane wounding is defined as a survivable disruption of the plasma membrane and is detected experimentally using a normally plasma membrane-impermeant fluorescent tracer such as FDx (M_r 10 kDa). Wounded cells trap the wound marker in their cytoplasm by virtue of resealing the plasma membrane disruption. However, immediately after syringe loading there are cells in the loaded sample that are positive for the wound marker but will die within a matter of hours due to irreparable membrane damage. In the case of adherent cells, these cells detach from the culture substratum and hence can be washed away after a minimum period of culture (i.e., 4 h) and are not included in any further analysis. Unfortunately, this approach cannot be employed when using suspension cells. However, if

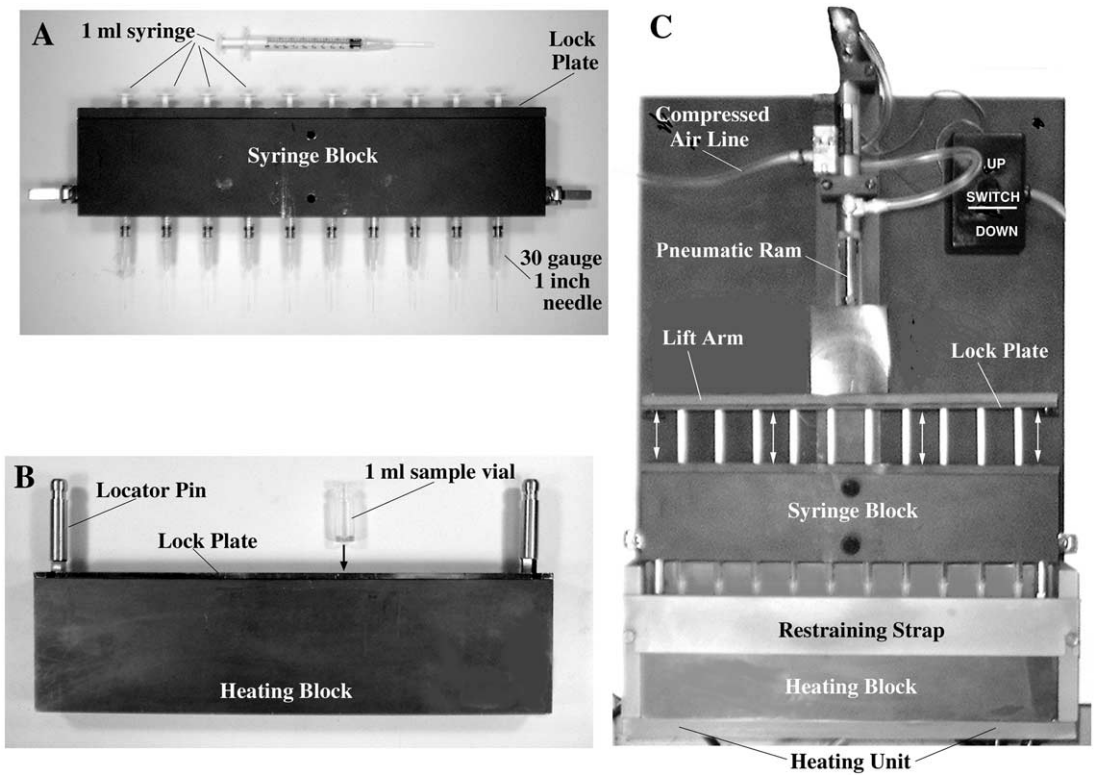

FIGURE 1 Multisample syringe loader. Ten, sterile, 1-ml disposable syringes are secured in the syringe block using a lock plate. A sterile, 30-gauge, 1-in. hypodermic needle is affixed to the tip of each syringe, making sure that the needle is seated firmly (Pl A). The syringe block is then attached to the pneumatic ram assembly of the main body of the device with the syringe plungers being secured directly to the lift arm using a lock plate (Pl C). Ten 1-ml sample vials, loaded with 0.5 ml of cells suspended in FDx loading solution, are loaded into a heating block (preequilibrated to 37°C) and secured in place using a lock plate (Pl B). The heating block containing the sample vials is then returned to its heating unit (set at 37°C) in the main body of the device and is secured in place with its restraining strap (Pl C). The pneumatic ram is placed in the "down" position so that the syringes are closed, and the whole syringe block is lowered and locked in place via the locator pins present on the top of the heating block. This arrangement ensures accurate registering of the each hypodermic needle into the center of its corresponding sample vial. The cell suspension in loading solution is pulled up into the syringe barrel by activating the pneumatic ram in the "up" direction and is expelled from the syringe by activating the pneumatic ram in the "down" direction. Expulsion pressure is controlled by a pressure valve attached to the compressed air line that feeds the ram assembly (Pl C).

the fluorescent cell viability marker, propidium iodide (PI), is introduced to the sample immediately after syringe loading, those cells that are dead or dying are positive for PI regardless if they are also positive for the membrane wound marker. As such, this approach allows rapid discrimination between those cells that are truly membrane wounded (i.e., FDx positive, PI negative) from those cells that are dead and dying (i.e., PI positive, FDx negative or positive) (Fig. 2). By utilizing our multisample syringe loading device and protocol, coupled with subsequent analysis by two-channel fluorescent flow cytometry, the experiment described here provides an example of how the syringe loading technique can be used to quantify the effects of radiation exposure on membrane function in suspension cells. We chose the lymphoblastic cell line Jurkat, as it is a widely used *in vitro* model for studying immune function, an area of specific concern with regard to radiation exposure.

II. MATERIALS AND INSTRUMENTATION

Dulbecco's modified Eagle's medium (X1 concentration) (DMEM, Cat. No. 320-1885AG), bovine calf serum (CS) (Cat. No. 200-6170AG), and penicillin–streptomycin solution (Cat. No. 600-5140AG) are obtained ready to use from Gibco BRL

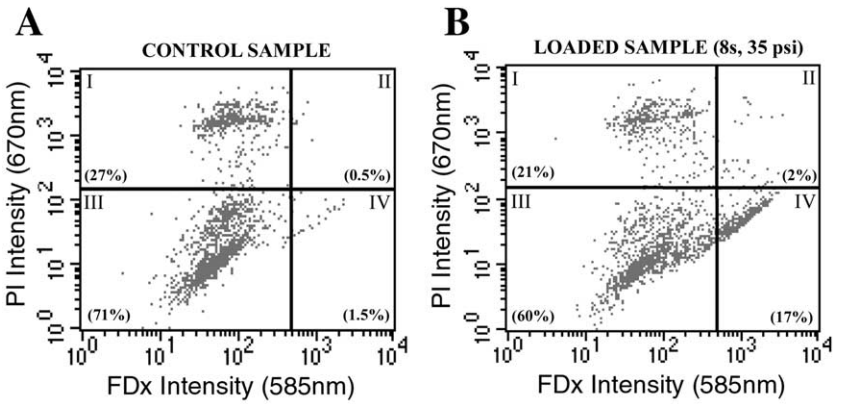

FIGURE 2 Dual-channel fluorescent flow cytometry analysis for the simultaneous determination of membrane wounding and irreparable membrane damage in suspension cells. Control samples, consisting of cell suspensions processed in an identical fashion to experimental samples other than they are not syringe loaded, are used to determine quadrant analysis parameters. Dead or dying cells, present even in the control, non-syringe loaded sample, stain positively for PI (i.e., quadrants I and II) (Pl A). After syringe loading at 35 psi expulsion for a total of eight strokes (Pl B), loaded cells stain positively for FDx (i.e., quadrants II and IV). Truly wounded cells (i.e., FDx positive and PI negative), which have completely resealed their plasma membrane disruptions before the addition of PI to the suspension, are positive only for FDx (i.e., quadrant IV). Numbers in parentheses are values (%) for the cells falling in each quadrant.

(Grand Island, NY). Fluorescein isothocyanate-labeled dextran (M_r 10 kDa) (FDx) (Cat. No. D-1821) and propidium iodide (Cat. No. P21493) are obtained from Molecular Probes (Eugene, OR). Tissue culture flasks (T75 and T25) (Cat. Nos. 10-126-41 and 10-126-26) and sterile polypropylene conical centrifuge tubes (50-ml capacity) (Cat. No. 05-538-55A) are obtained from Fisher Scientific (Pittsburgh, PA). Sterile polypropylene conical sample vials (1-ml capacity) (Cat. No. 05-538-55A) are obtained from National Scientific Company (Quakertown, PA). Disposable 1-ml syringes (Cat. No. 9602) and 30-gauge hypodermic needles (Cat. No. 305128) are from Becton-Dickinson (Rutherford, NJ). The multisample syringe loader described in Fig. 1 was built by a local machine shop to specifications provided by the authors. As such, sample vial dimensions can be varied depending on experiment requirements, including the use of sterile, septum-sealed sample vials.

III. PROCEDURES

A. Preparation of Tissue-Cultured Cells for Syringe Loading

Stock Solutions and Media Preparation

1. *Stock FDx solution*: Add 200 mg of dry FDx powder to 1 ml of serum-free DMEM and vortex periodically over a period of 30 min to achieve complete solubilization. Centrifuge this solution at 10,000 *g* for 10 min at room temperature to remove any undissolved FDx and sterilize, if desired, by ultrafiltration. Stock FDx (200 mg/ml) can be stored at 4°C in the dark for up to a month or aliquoted and frozen in the dark at –80°C for storage up to a year.

2. *Stock propidium iodide solution*: Add 100 mg of dry PI powder to 1 ml of serum-free DMEM and vortex periodically over a period of 30 min to achieve complete solubilization. Centrifuge this solution at 10,000 *g* for 10 min at room temperature to remove any undissolved PI and collect the supernatant as a stock solution. Stock PI (100 mg/ml) can be stored at 4°C in the dark for up to a month or aliquoted and frozen in the dark at –80°C for storage up to a year.

3. *FDx loading solution*: Add 250 µl of stock FDx solution to 4.75 ml of serum-free DMEM to obtain final concentrations of 10 mg/ml FDx. Use the solution immediately.

4. *5% CS.DMEM*: Add 5 ml of sterile penicillin/streptomycin solution and 50 ml of sterile CS to 445 ml of sterile (X1) DMEM solution to obtain DMEM culture medium containing 5% CS, 100 IU/ml penicillin, and 100 µg/ml streptomycin (5% CS.DMEM). Store at 4°C for up to 21 days.

Steps

1. Grow Jurkat cells to confluence in T75 (75 cm^2) culture flasks using 15 ml of 5% CS.DMEM maintained at 37°C in a 5% CO_2 humidified atmosphere with subculture every third day. Carry out subculture by

removing the cell suspension from the T75 flask and placing it in a sterile 50-ml centrifuge tube followed by centrifugation at 100 *g* (~550 rpm) for 5 min at room temperature. Decant the spent medium, resuspend the cell pellet gently in 30 ml of fresh 5% CS.DMEM, and dispense equal volumes into two fresh T75 flasks.

2. On the day of the experiment, collect cells by centrifugation as in step 1. Gently resuspend cells in 10 ml of 5% CS.DMEM and determine cell number using a hemacytometer or electronic cell counting device (i.e., a Coulter particle counter) and adjust the cell density to 2×10^6 cells/ml. Aliquot 5 ml of this cell suspension into T25 flasks in preparation for radiation exposure.

3. Expose cells to different doses of gamma irradiation using a Gammacell 1000 (Cs^{137} source). Our experiments were performed at Baylor College of Medicine (Houston, Texas).

4. Incubate cells at 37°C in a 5% CO_2 humidified atmosphere for a period of 2 h.

5. Remove cells from T25 flasks and collect each sample by centrifugation in sterile 50-ml centrifuge tubes at 100 *g* (~550 rpm) for 5 min at room temperature.

6. Carefully remove medium from the cells and filter through a 0.2-μm cellulose acetate filter to remove any remaining cell debris from the supernatant. Aliquot the medium in 1-ml aliquots and store at –80°C in the dark for subsequent biochemical testing, such as determination of lipid peroxidation marker production.

7. Resuspend each cell pellet in 2 ml of warm serum-free DMEM and determine the cell number by counting in a hemacytometer/Coulter counter.

8. Adjust the cell density of the cell suspension to 1×10^6 cells/ml by the addition of an appropriate amount of warm serum–free DMEM.

9. Dispense 0.5-ml samples of this cell suspension into a minimum of 13 sterile conical polypropylene 1-ml sample vials.

10. Add 25 μl of prewarmed stock FDx solution to all sample vials, mix by gentle vortexing, and load 10 of the 13 sample vials into the heating block (prewarmed to 37°C) of the multisample syringe loader (Fig. 1B).

11. Immediately perform syringe loading on the samples from **step 10** while the remaining three vials are incubated at 37°C in ambient air as control samples for FDx uptake by pinocytosis and cell loss due to processing.

B. Syringe Loading Protocol

1. Place heating block containing 10 sample vials containing identical aliquots of the cell suspension into the multisample syringe loader heating unit and attach the restraint strap as shown (Fig. 1C).

2. Insert the 10 separate 1-ml syringes with attached 1-in.-long, 30-gauge needles (which have been loaded previously into the syringe block, Fig. 1A) into the vials and lock in place using the guide posts (Fig. 1C).

3. Draw the cell suspension up into the barrel of the sterile syringes through the 30-gauge hypodermic needles by activating the pneumatic ram attached to the syringe plungers using the "up" switch (Fig. 1C). Set the pneumatic ram so that the syringe plungers do not move any further up than the 0.5-ml mark on the syringe barrels.

4. Once the barrels of the syringes are filled (which takes approximately 2 s), expel the cell suspensions through the 30-gauge needles back into their respective sample vials at a constant pressure of 35 psi by reversing the direction of the pneumatic ram using the "down" switch. This procedure is defined as two strokes.

5. Repeat this procedure three more times so that each cell suspension has been subjected to eight strokes under identical expulsion pressure conditions.

6. Remove the test sample vials from the multisample syringe loader.

7. Take all the samples (including the control samples, which have been incubated in FDx loading solution at 37°C but not syringe loaded), add 0.5 ml of 5% CS.DMEM to each vial, collect the cells by centrifugation at 100 *g* for 5 min at room temperature, and remove the supernatant (i.e., FDx loading solution).

8. Add 0.5 ml of warm 5% CS.DMEM to each cell pellet and resuspend the cells by gently vortexing the sample and store at 37°C in a 5% CO_2 humidified atmosphere in preparation for analysis. Analysis should be started as soon as possible.

C. Dual-Label Fluorescent Flow Cytometry Analysis

1. Immediately prior to fluorescent flow cytometry analysis, add a 10-μl aliquot of stock PI solution (final PI concentration of 1 mg/ml) to each sample and mix by gentle vortexing. Add PI to each individual sample immediately before analysis.

2. Analyze control samples first by dual-channel fluorescent flow cytometry using a Becton-Dickinson FACSCalibur system (or similar fluorescent flow cytometer) and plot a two-axis scatter plot of cell fluorescent intensity at 585 nm (FDx signal) and 670 nm (PI signal) using the associated software. These control samples are used to define "quadrant" gating

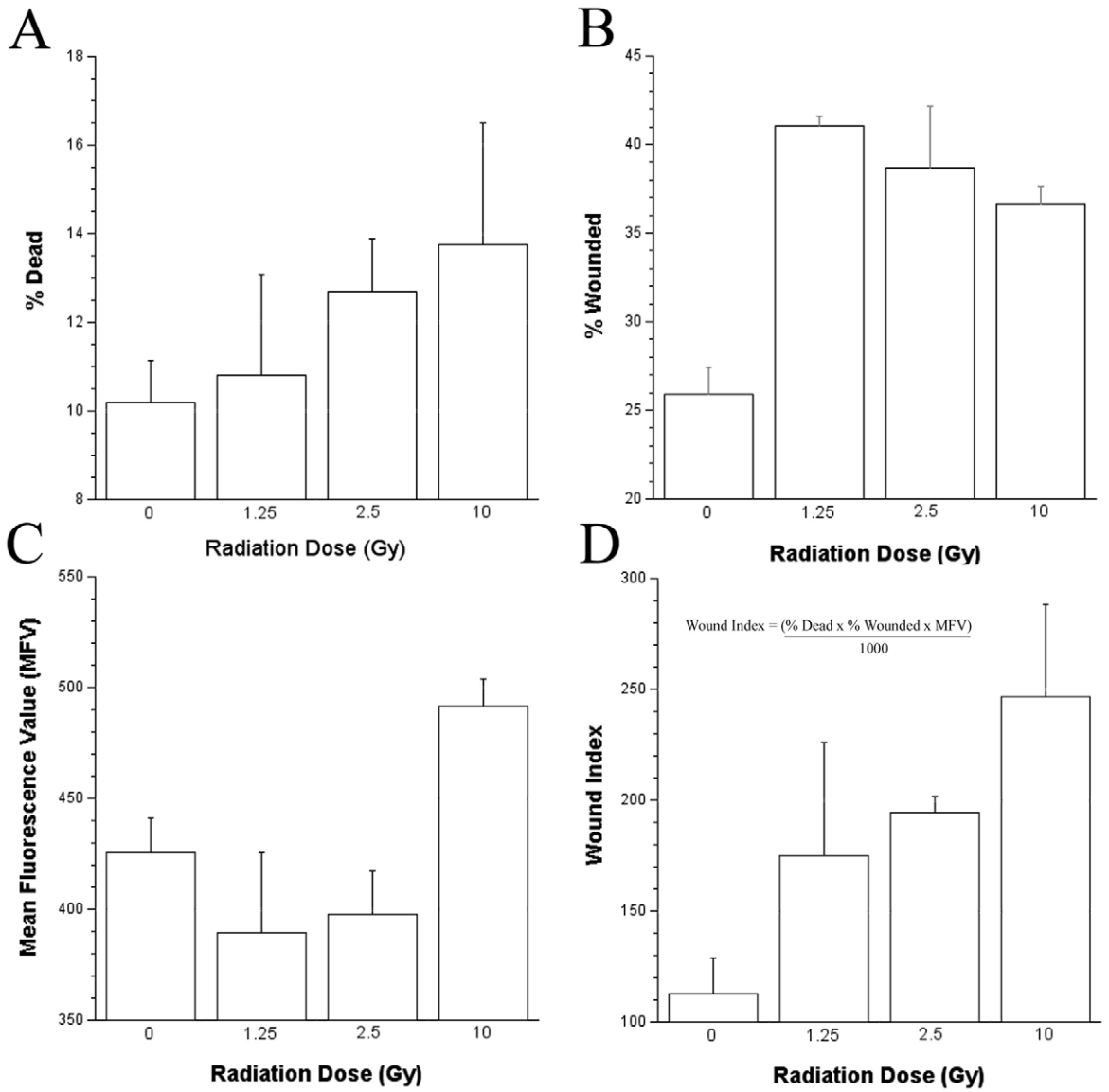

FIGURE 3 Dose-dependent effects of gamma irradiation on the syringe loading-induced membrane wounding response of the lymphoblastic cell line Jurkat.

thresholds for the control cell population with regard to FDx and PI background signals (Fig. 2). Collect a total of 10,000 events for analysis of each sample.

3. Analyze syringe loaded samples by dual-channel fluorescent flow cytometry using the quadrant gates defined earlier (Fig. 2). Collect a total of 10,000 events for analysis of each sample.

4. Calculate the number of dead or dying cells in each sample (expressed as a percentage of the total cells analyzed, Fig. 3A) by counting the number of cells in the sample that are positive for PI staining, including those cells that are also positive for FDx (i.e., Fig. 2, quadrants I and II, respectively).

5. Calculate the number of wounded cells (expressed as a percentage of the total cells analyzed, Fig. 3B) and the mean fluorescent value (MFV; Fig. 3C) of the wounded population by determining the number and staining intensity of cells that are positive for FDx staining only (i.e., Fig. 2, quadrant IV).

6. Calculate a wound index (which reflects cell survival of mechanically induced plasma membrane damage, the number, and the MFV of the wounded cells) as described previously (Clarke and McNeil, 1992) for each radiation dose (Fig. 3D), where the wound index = % dead cells × % wounded cells × mean fluorecent value/1000.

IV. COMMENTS

The technology described herein allows the effects of a wide range of environmental conditions and their potential countermeasures (e.g., radiation exposure and radio-protectants) to be assessed in a variety of cell suspension models, including peripheral blood lymphocytes from human subjects. A less refined version of this approach has been used previously to study the effects of increasing membrane cholesterol content on plasma membrane susceptibility to mechanical shear-induced membrane wounding (Clarke *et al*., 1995a). The apparatus and protocol described earlier have taken what was essentially a macromolecular loading technique and adapted it for use as a means of assessing the effects of radiation exposure on the membrane function of lymphoblastic cells in suspension. The technique also has the advantage of being able to immediately discriminate between dead and dying cells and truly wounded cells in suspension after the application of mechanical shear force using two-channel fluorescent flow cytometry (Fig. 2).

The apparent dose response in membrane wound susceptibility observed relative to radiation exposure in our model indicates that gamma irradiation induces alterations in the plasma membrane components of Jurkat cells, if not immediately, then most certainly within 2 h of exposure (Fig. 3). This time course of events suggests that these effects are not associated with genomic damage. The effects of radiation exposure on membrane wounding observed in this study are similar to that described previously after an increase in plasma membrane order. One possible reason for such an increase in membrane order after radiation exposure is the production of reactive oxygen species (ROS), such as superoxide, hydrogen peroxide, hydroxyl, peroxyl, and alkoxyl radicals, which may lead to membrane damage and consequent cross-linking of membrane components (Clarke *et al*., 2003). This concept is supported by the experimental observation that Jurkat cells exposed to gamma irradiation not only exhibit an increase in susceptibility to membrane wounding within 2 h, but also produce significant amounts of lipid peroxidation markers (data not shown).

We have observed previously that in order to obtain optimal levels of membrane wounding experimentally (i.e., maximizing cell loading while minimizing cell death caused by irreparable membrane disruption), a mechanical shear dose–response curve must be constructed. In general, most mammalian cells appear to wound best at expulsion pressures between 30 and 45 psi. However, this parameter varies with each individual cell type. Expulsion of the cell suspension under the conditions used in the example given earlier (i.e., 0.5 ml volume of cell suspension passing through a 1-in.-long, 30-gauge needle at a constant 35 psi expulsion pressure in 1.5 s) results in a theoretical average fluid shear stress of approximately 7340 dynes/cm^2. This value is derived from the equation wall shear rate $= 8 \times V_{mean}/D = 32Q/\pi D^3$, where D is the luminal diameter of the hypodermic needle (cm) and Q is the flow rate in cm^3/s, assuming that the viscosity of the loading solution is one centipoise (Clarke *et al*. 1995b). Due to the non-Newtonian fluid physics of the cell suspension, this calculated value for the shear stress inflicted on the cells syringe loading under these conditions could be artificially low. However, regardless of the actual shear stress value inflicted on the cells while passing through the needle, the multisample syringe loader induces a constant and reproducible level of mechanical shear stress from sample to sample. This translates into the infliction of well-defined and reproducible amounts of membrane wounding in cells subjected to syringe loading. The incorporation of a heating block into the device in order to maintain a constant temperature during the syringe loading procedure has also removed a potential confounding variable from the experimental protocol.

V. PITFALLS

1. Jurkat cells are relatively fragile in tissue culture. Cells should be handled gently with a minimum of agitation, being especially careful when performing manipulations that require pipetting or vortexing. This fragility is evidenced by the relatively large number of PI-positive cells (i.e., dead or dying cells) present in control samples that have not been subjected to syringe loading (see Fig. 2A).

2. Jurkat cells should be used for syringe loading experiments 1 day after subculture to ensure the optimal number of healthy cells in the culture.

3. When calculating the theoretical shear stress imposed during syringe loading, it is important to determine the flow rate through the needle experimentally. This will change primarily depending on the expulsion pressure and the number of cells in the suspension; both parameters are under the control of the investigator. These wounding parameters need to be optimized for each particular cell type.

4. It is important to prevent excessive pH changes caused by exposure of the bicarbonate-buffered

culture medium to atmospheric air during the procedure as these are potentially harmful to the cells.

References

Clarke, C. H., Weinberger, S. R., and Clarke, M. S. F. (2003). Application of ProteinChip array technology for detection of protein biomarkers of oxidative stress. *Crit. Rev. Oxid. Stress Aging* **1**, 366–379.

Clarke, M. S., Bamman, M. M., and Feeback, D. L. (1998). Bed rest decreases mechanically induced myofiber wounding and consequent wound-mediated FGF release. *J. Appl. Physiol* **85**(2), 593–600.

Clarke, M. S., Caldwell, R. W., Chiao, H., Miyake, K., and McNeil, P. L. (1995a). Contraction-induced cell wounding and release of fibroblast growth factor in heart. *Circ. Res.* **76**(6), 927–934.

Clarke, M. S., and McNeil, P. L. (1992). Syringe loading introduces macromolecules into living mammalian cell cytosol. *J. Cell Sci.* **102**(Pt. 3), 533–541.

Clarke, M. S. F., and McNeil, P. L. (1994). Syringe loading: a method for inserting macromolecules into cells in suspension. *In "Cell Biology: A Laboratory Handbook"* (J. E. Celis, ed.), pp. 30–36, Academic Press, San Diego.

Clarke, M. S. F., Pritchard, K. A., Medows, M. S., and McNeil, P. L. (1995b). An atherogenic level of native LDL increases endothelial cell vulnerability to shear-induced plasma membrane wounding and consequent FGF release. *Endothelium* **4,** 127–139.

Clarke, M. S. F., Vanderburg, C. R., and Feeback, D. L. (2001). The effect of acute microgravity on mechanically-induced membrane damage and membrane-membrane fusion events. *J. Grav. Physiol.* **8**, 37–47.

Gimpl, G., Burger, K., and Fahrenholz, F. (1997). Cholesterol as modulator of receptor function. *Biochemistry* **36**(36), 10959–10974.

Kuroda, Y., Ogawa, M., Nasu, H., Terashima, M., Kasahara, M., Kiyama, Y., Wakita, M., Fujiwara, Y., Fujii, N., and Nakagawa, T. (1996). Locations of local anesthetic dibucaine in model membranes and the interaction between dibucaine and a Na+ channel inactivation gate peptide as studied by 2H- and 1H-NMR spectroscopies. *Biophys. J.* **71**(3), 1191–1207.

McNeil, P., and Terasaki, M. (2001). Coping with the inevitable: How cells repair a torn surface membrane. *Nature Cell Biol.* **3**, E124–E129.

McNeil, P. L., and Steinhardt, R. A. (1997). Loss, restoration, and maintenance of plasma membrane integrity. *J. Cell Biol.* **137**(1), 1–4.

Miyake, K., and McNeil, P. L. (1995). Vesicle accumulation and exocytosis at sites of plasma membrane disruption. *J. Cell Biol.* **131**(6 Pt 2), 1737–1745.

Needham, D., and Nunn, R. S. (1990). Elastic deformation and failure of lipid bilayer membranes containing cholesterol. *Biophys. J.* **58**, 997–1009.

Pritchard, K. A., Schwarz, S. M., Medow, M. S. and Stemerman, M. B. (1991). Effect of low-density lipoprotein on endothelial cell membrane fluidity and mononuclear cell attachment. *Am. J. Physiol.* **260**, C43–C49.

Reidy, M. A., and Lindner, V. (1991). Basic FGF and growth of arterial cells. *Ann. N. Y. Acad. Sci.* **638,** 290–299.

Song, J., and Waugh, R. E. (1993). Bending rigidity of SOPC membranes containing cholesterol. *Biophys. J.* **64**(6), 1967–1970.

Tanii, H., Huang, J., Ohyashiki, T., and Hashimoto, K. (1994). Physical-chemical-activity relationship of organic solvents: Effects on Na(+)-K(+)-ATPase activity and membrane fluidity in mouse synaptosomes. *Neurotoxicol. Teratol.* **16**(6), 575–582.

Whiting, K. P., Restall, C. J., and Brain, P. F. (2000). Steroid hormone-induced effects on membrane fluidity and their potential roles in non-genomic mechanisms. *Life Sci.* **67**(7), 743–757.

Yu, Q. C., and McNeil, P. L. (1992). Transient disruptions of endothelial cells of the rat aorta. *Am. J. Pathol.* **141**, 1349–1360.

Zhelev, D. V., and Needham, D. (1993). Tension-stabilized pores in giant vesicles: Determination of pore size and pore line tension. *Biochim. Biophys. Acta* **1147**(1), 89–104.

CHAPTER

33

Cell Surface Biotinylation and Other Techniques for Determination of Surface Polarity of Epithelial Monolayers

Ami Deora, Samit Chatterjee, Alan D. Marmorstein, Chiara Zurzolo, Andre Le Bivic, and Enrique Rodriguez-Boulan

I. INTRODUCTION

A fundamental property of epithelial cells is the polarized distribution of proteins and lipids in the apical and basolateral domains of the plasma membrane. These two domains are physically separated from each other by the tight junction. Many studies have been done over the past 20 years to understand the mechanisms that lead to the establishment and maintenance of the polarized distribution of proteins and lipids in the plasma membrane of epithelial cells (Rodriguez-Boulan *et al.*, 2005; Yeaman *et al.*, 1999; Keller and Simons, 1997).

A major advance in the study of epithelial cell polarity was achieved with the introduction of porous filter supports for the growth of epithelial cell cultures (reviewed in Rodriguez-Boulan *et al.*, 2005). This method differs from classical cell culture in that it allows direct access to the basolateral surface of cultured cells. Epithelial cells and cell lines grown on such filter supports (either nitrocellulose or polycarbonate) attain a more differentiated appearance and become polarized after relatively short times in culture. While most studies on epithelial polarity and trafficking of plasma membrane proteins have been performed using a limited number of cell lines (MDCK, FRT, Caco-2), this culture technique has been gaining in popularity and has been used now for primary cultures as well. The confluency of cells grown on permeable supports can be determined by the measurement of transepithelial electrical resistance or transepithelial [^{3}H]inulin flux (Hanzel *et al.*, 1991).

One of the biggest advantages of this culture system is the accessibility of either the apical or the basolateral surface to any reagent added to the medium and the ability to add different reagents to contact either surface. This is the basis of the biotinylation techniques that have been developed to selectively label proteins present on the apical or basolateral domains of the plasma membrane of filter-grown epithelial cells.

The proteins present on the surface of filter-grown monolayers can be selectively modified by the water-soluble cell-impermeable biotin analog sulfo-NHS-biotin. Taking advantage of the access afforded by the filter support, the addition of sulfo-NHS-biotin to only one surface of the cell results in the selective labeling of only the apical or basolateral surface proteins. The biotinylated proteins can then be detected by blotting with [^{125}I]streptavidin or streptavidin conjugated to any number of enzymatic reporters. Furthermore, the cells can be metabolically pulse labeled and the proteins of interest can then be studied using biotinylation, immunoprecipitation and subsequent streptavidin–agarose precipitation. This technique is very versatile and is applicable to the study of diverse aspects of epithelial cell polarity, such as the steady-

Copyright 2006, Elsevier Science (USA).
All rights reserved.

state distribution of specific antigens, or dynamic processes, such as targeting to the cell surface and transcytosis of membrane proteins. Several biotin analogs are available, including one that contains a disulfide bond. By differentially labeling the surfaces of epithelia *in situ* with the cleavable NHS-S-S-biotin and a noncleavable biotin, we have been able to study the polarity of a native epithelium *in situ* (Marmorstein *et al*., 1996).

The first edition of this article described a basic protocol for selective cell surface biotinylation, plus some modifications of the assay to study protein targeting and endocytosis. The second edition included a basic protocol for *in situ* domain-specific biotinylation. In this edition, we have added a protocol of surface immunolabeling as an alternative to biotin labeling for determination of polarity. This technique is critical in cell lines that may exhibit leakiness to biotin. Additionally, we have also included two sections determining the polarity of a protein by means of intranuclear microinjection of its cDNA and quantitative microscopic analysis to determine distribution of the protein relative to known polarized markers.

II. MATERIALS

Sulfo-NHS-biotin (sulfosuccinimidobiotin, Cat. No. 21217); NHS-LC-biotin (sulfosuccinimidyl-6-(biotinamido)-hexanoate, Cat. No. 21335); NHS-SS-biotin (sulfosuccinimidyl-2-(biotinamido)-ethyl-1,3-dithioproprionate, Cat. No. 21331); and immunopure-immobilized streptavidin (Cat. No. 20347) are from Pierce (Rockville, IL). Protein A–Sepharose Cl-4B (Cat. No. 17-0780-01) is from Pharmacia/LKB (Piscataway, NJ). Glutathione (Cat. No. G-6529) and cycloheximide (Cat. No. C-7698) are from Sigma Chemical Co. (St. Louis, MO). *Staphylococcus aureus* cells (Pansorbin, Cat. No. 507858) are from Calbiochem (La Jolla, CA). Cells are grown on polycarbonate filters (Transwell, 12 mm diameter, Cat. No. 3401; 24 mm diameter, Cat. No. 3412) from Corning-Costar (Cambridge, MA); MEM-Select-Amine kits (Cat. No. 19050-012) are from GIBCO BRL Life Technologies (Grand Island, NY); [^{35}S]EXPRE^{35}S ^{35}S (methionine/cysteine) and [^{35}S]cysteine are from Dupont NEN (Boston, MA) (Cat. No. NEG 072 for Express and Cat. No. NEG 022T for [^{35}S]cysteine); [^{125}I]streptavidin can be obtained from Amersham (Arlington Heights, IL) (Cat. No. IM236); streptavidin conjugated to horseradish peroxidase can be obtained from Sigma (Cat. No. S-5512).

III. PROCEDURES

A. Cell Surface Biotinylation

This procedure is used to determine the relative percentage of a plasma membrane protein(s) in the apical versus basolateral plasma membrane of epithelial cells grown on permeable filter supports (modified from Sargiacomo *et al*., 1989).

Solutions

1. *PBS-CM*: Phosphate-buffered saline containing 1.0 m*M* $MgCl_2$, and 1.3 m*M* $CaCl_2$
2. *Sulfo-NHS-biotin or sulfo-NHS-LC-biotin*: Stock solution is 200 mg/ml in dimethyl sulfoxide (DMSO), which can be stored for up to 2 months at –20°C. Thaw just prior to use and dilute to a final concentration of 0.5 mg/ml in PBS-CM. Use immediately.
3. *50 mM NH_4Cl in PBS-CM or Dulbecco's modified Eagle's medium (DMEM)*: Use to quench the excess biotin at the end of the labeling reaction

Steps

All steps are carried out on ice and with ice-cold reagents.

1. For all experiments, use confluent monolayers of cells plated at confluency (for most cell lines, $2.5–3.5 \times 10^5$ cells/cm^2 of filter) 4–5 days prior to biotinylation. Measure transepithelial electrical resistance (TER) and discard monolayers that do not exhibit acceptable resistances (different cell lines exhibit different TER values ranging from tens to thousands of $\Omega \cdot cm^2$; monolayers should be used that exhibit TER values in the normal range for your cell line. We have successfully performed this assay on cells with TERs as low as $50\,\Omega \cdot cm^2$).
2. Wash filters on both sides three times with ice-cold PBS-CM.
3. Add a fresh solution of sulfo-NHS-biotin (0.5 mg/ml in PBS-CM) to the apical or basolateral chamber. Add PBS-CM to the other chamber. We use 0.7 ml apical and 1.4 ml basolateral for 24-mm-diameter filters and 0.4 and 0.8 ml for 12-mm-diameter filters. Incubate with gentle shaking for 20 min at 4°C and then repeat this step.
4. Quench the reaction by removing the solutions from both chambers and replacing with 1 ml of 50 m*M* NH_4Cl in PBS-CM. Incubate with gentle shaking for 10 min at 4°C.
5. Rinse twice with PBS-CM.
6. Excise filters and either freeze at –80°C (the freeze thaw involved with storage at –80°C appears to

inactivate some proteases) or immediately proceed with the extraction of biotinylated proteins as outlined in Section III,F.

Analysis of Results

The amount of protein present on the apical or basolateral surface is determined by a densitometric analysis of the autoradiographs. Multiple exposures are necessary if using the film to ensure that the values obtained are in the linear range of the film. Polarity is expressed as the percentage of total surface protein present on one surface of the monolayer.

B. Biotin Targeting Assay

This procedure is used to determine if proteins are delivered directly, indirectly (transcytotically), or nonpolarly to the apical and/or basolateral surface of an epithelial cell (modified from Le Bivic *et al*., 1990).

Solutions

1. *Starvation medium*: DMEM without methionine or cysteine. This solution is prepared using a MEM Select-Amine kit by not adding the methionine and cysteine.

2. *[^{35}S]EXPRESS (methionine/cysteine:) or [^{35}S]cysteine*: 1 mCi per multiwell plate (12 × 1.2-cm or 6 × 2.4-cm-diameter filters). In some cases, proteins are effectively labeled with [^{35}S]SO_4, an advantage for studies of post-Golgi sorting, because the addition of sulfate occurs in the *trans*-Golgi network (see chapter by Kreitzer *et al*.).

3. *Chase medium*: DMEM containing a 10× concentration of methionine and cysteine (made by addition of methionine and cysteine to starving medium) or the normal medium in which the cells grow.

4. *HCO_3-free DMEM containing 20 mM HEPES and 0.2% bovine serum albumin (BSA)*

5. *Sulfo-NHS-biotin (NHS-LC-biotin or NHS-SS-biotin)*: 0.5 mg/ml in PBS-CM + all of the reagents used in the cell surface biotinylation protocol.

6. *Lysis buffer*: 1% Triton X-100 in 20 m*M* Tris, 150 m*M* NaCl, 5 m*M* EDTA, 0.2% BSA, pH 8.0, and protease inhibitors

7. *Immunopure-immobilized streptavidin on agarose beads*

8. *10% SDS*: sodium dodecyl sulfate

Steps

1. Wash cells on filters three times with starvation medium and incubate for 20–40 min in starvation medium. The starving period will depend on your cell type. MDCK cells work well with a 20-min starvation; RPE-J require longer times.

2. Pulse for 20–30 min (again depends on cell line) in starving medium containing [^{35}S]EXPRESS of [^{35}S]cysteine at 37°C. The pulse solution is starving medium plus the ^{35}S label. Minimal volumes are recommended. For MDCK cells we pulse with 20–40 µl from the basolateral surface. A drop of pulse medium is placed on a strip of Parafilm in a humidified chamber (we use a plastic box lined with wet towels), and the insert containing the filter and MDCK monolayer is removed from the multiwell and dropped on top of the pulse medium. Some cell lines (i.e., RPE-J) are better labeled from the apical surface. For apical pulse, starvation medium is removed from both chambers and pulse medium is applied only to the apical chamber. For 1.2-cm-diameter filters we use a 100-µl volume; for 2.4-cm-diameter filters we use a 350-µl volume of pulse medium.

3. The pulse is terminated by washing with chase medium three times.

4. At different chase times, aspirate chase medium and replace with ice-cold $NaHCO_3$-free DMEM containing 20 m*M* HEPES and 0.2% BSA and store on ice until all chase points have been collected.

5. Proceed to apical or basolateral biotinylation following the protocol described earlier for cell surface biotinylation.

6. Excise filters and either freeze at –80°C or immediately lyse cells and immunoprecipitate specific proteins as described in the section extraction of biotinylated proteins.

7. Remove immunoprecipitated proteins from beads by adding 40 µl of 10% SDS and heating for 5 min at 95°C. Immediately dilute with 460 µl of lysis buffer and pellet for 1 min in a microfuge. Remove 450 µl and place in a new tube. Dilute the remaining 50 µl with 50 µl of 2× Laemmli sample buffer. This sample is used to normalize for differential incorporation of radiolabel from filter to filter. The remaining 450 µl is diluted with a further 1 ml of lysis buffer to which is added an additional 50 µl of streptavidin agarose that has been preblocked for 1–12 h with lysis buffer.

8. Streptavidin precipitation is allowed to proceed for 1 h to overnight at 4°C. Then the beads are washed successively in TPII, TPIII, and TPIV as described in Section III,F. After the final wash the beads are resuspended in Laemmli sample buffer and heated to 95°C for 5 min.

9. Both the sample representing total and surface protein are resolved on SDS–PAGE gels. The gels are dried and exposed for autoradiography.

C. Targeting Assay by Surface Immunolabeling

Epithelial cells such as LLC-PK1 may not form a tight monolayer and hence could be leaky to biotin analogs (MW~ 400–600). To overcome this problem, we have used antibody labeling against the protein of interest (Gan *et al*., 2002). Antibodies are less likely to traverse through leaky monolayers. Leakiness of antibodies should be directly determined before using this method.

Solutions

1. *PBS-CM*: See Section III,A
2. *DMEM containing 0.2% BSA*

Steps

1. The initial steps are similar to Section III,B (steps 1–4). Label the ice-cold filters from different chase time points with antibody added to either apical or basolateral domains for 1 h on ice in a cold room kept at 4°C. Dilute the antibody in DMEM containing 0.2% BSA at an approximate concentration of 1 µg/ml. After 1 h, wash filters four times in ice-cold PBS-CM containing 0.2% BSA.
2. Excise filters and either freeze at –80°C or immediately lyse cells in lysis buffer.
3. Pull down the antigen–antibody complex with protein A or G beads from nine-tenths of the postnuclear supernatants. Subject one-tenth of the supernatant again to immunoprecipitation to measure total labeled protein.
4. Wash immunoprecipitates on the beads successively in TPII, TPIII, and TPIV as described in Section III,F.
5. After the final wash, resuspend the beads in Laemmli sample buffer and heat to 95°C for 5 min.
6. Resolve both the sample representing total and surface proteins on SDS–PAGE gels. Dry and expose the gels for autoradiography.

Analysis of Results

The polarity of the protein is determined at each time point by densitometric analysis of the autoradiographic data. The values obtained for the surface protein should be normalized against the values obtained form the totals (including precursor forms). This controls for differences in the incorporation of label (specific activity) between monolayers. If the protein is highly polarized from the first time point at which it is detected on the cell surface, then it is delivered directly to that surface. If it is polarized on one surface early in the chase and then switches polarity later in the chase, then it is delivered indirectly. If the protein is nonpolar early in the chase and acquires polarity only after longer chase times, then it is not sorted in the TGN, but its final polarity is acquired by differential stability on the apical and basolateral surfaces.

D. Biotin Assay for Endocytosis

This assay examines the internalization of plasma membrane proteins (from Graeve *et al*., 1989)

Solutions

1. *PBS-CM*
2. *Cleavable biotin reagent*: NHS-SS-biotin
3. *DMEM containing 0.2% BSA*
4. *Reducing solution*: 310 mg glutathione (free acid) dissolved in 17 ml H_2O (50 m*M*). Add 1 ml of 1.5 *M* NaCl, 0.12 ml of 50% NaOH, and 2 ml of serum just before use.
5. *Quenching solution*: 5 mg/ml iodoacetamide in PBS-CM containing 1% BSA

Steps

1. Wash cells on filters four times, 15 min each time with ice-cold PBS-CM.
2. Add 1 ml of NHS-SS-biotin (0.5 mg/ml in ice-cold PBS-CM) to the chamber being labeled and PBS-CM to the other chamber. Incubate for 20 min at 4°C and repeat with fresh solutions.
3. Wash filters twice with DMEM/0.2% BSA. Keep two filters on ice (one of these will represent the total amount of proteins at the surface before internalization and the other will be treated with the reducing solution and represents your control of efficiency of reduction) and transfer the other filters to 37°C for various times to allow the biotinylated proteins to be internalized.
4. Stop incubation by transferring filters back to 4°C.
5. Wash twice in PBS-CM + 10% serum.
6. Incubate filters for 20 min in reducing solution. Repeat. (Mock treat one filter.)
7. After washing, quench free SH groups in 5 mg/ml iodoacetamide in PBS-CM + 1% BSA for 15 min.
8. Lyse cells and immunoprecipitate as described in the section extraction of biotinylated proteins.
9. Run the samples on SDS–PAGE gels, transfer to nitrocellulose or PVDF, blot with [^{125}I]streptavidin, and expose for autoradiography.

Analysis of Results

Endocytosis of the protein of interest is indicated by protection of the NHS-SS-biotin-labeled surface

protein from reduction by glutathione. By chasing the cells for various lengths of time, a rate of endocytosis can be calculated by comparing the percentage of protein protected at each time point. Obviously if none of the protein is protected from reduction, it is 100% at the surface; conversely, if all of the protein is protected, 100% has been internalized.

E. *In Situ* Domain Selective Biotinylation of Retinal Pigment Epithelial Cells

The retinal pigment epithelium is uniquely suited for biochemical studies of polarity *in situ*. The RPE exists as a natural monolayer with a broad apical surface that is easily exposed after gentle enzymatic treatment to remove the adjacent neural retina. The apical surface of the tissue is labeled with a noncleavable biotin analog such as NHS-LC-biotin for the identification of apical proteins. For identification of basolateral proteins the biotinylatable sites on the apical surface are labeled with the cleavable NHS-SS-biotin. After isolation of RPE cells, the nonlabeled basolateral proteins are labeled in suspension with the noncleavable form. Removal of the cleavable NHS-SS-biotin by reduction with 2-mercaptoethanol results in the presence of biotin only in the population of proteins present on the basolateral surface of the RPE (Marmorstein *et al*., 1996)

Solutions

1. *Sulfo-NHS-biotin, or NHS-LC-biotin, and NHS-SS-biotin stock solutions in DMSO*
2. *HBSS*: 10 m*M* HEPES buffered Hank's balanced salt solution
3. *PBS-CM*
4. *DMEM containing 10 mM HEPES*
5. *Bovine testicular hyaluronidase*
6. *CMF-PBS*: PBS calcium and magnesium free
7. *PBS-EDTA*: CMF-PBS + 1 m*M* EDTA

Steps

All steps are carried out on ice unless otherwise indicated.

1. Rats are euthanized by CO_2 asphyxiation, and the eyes are enucleated and stored for 3 h to overnight in the dark on ice in HBSS.
2. A circumferential incision is made above the ora serrata, and the cornea, iris, lens, and vitreous are removed.
3. The eyecups are incubated for 10–30 min at 37°C in HBSS containing 290 units/ml bovine testicular hyaluronidase.
4. The ora serrata is removed, and the neural retina is peeled carefully away from the RPE. The optic nerve head is severed and the neural retina is removed. The RPE is inspected under the dissecting microscope. Black spots on the outer surface of the retina or tracts of smooth reflective surface in the eyecup indicate damage. Damaged eyecups are discarded.
5. Soluble components of the interphotoreceptor matrix are removed by incubation in 2-ml microcentrifuge tubes (one eye per tube) on a rotator in ice-cold HBSS for 20 min. This is repeated three times.
6. The apical surface of the RPE in one eyecup is biotinylated with 1 ml of PBS-CM containing 2 mg of sulfo-NHS-biotin. The other eyecup is biotinylated with 1 ml of PBS-CM containing 2 mg of NHS-SS-biotin. This procedure is repeated three times.
7. The reaction is quenched with 1 ml of 10 m*M* HEPES buffered DMEM for 10 min at 4°C.
8. The eyecups are rinsed once in ice-cold CMF-PBS and are then incubated in PBS-EDTA on ice for 30 min.
9. The RPE is gently teased from the inner surface of the eyecup using a 22-gauge needle. The RPE layer is collected in a 1.5-ml microcentrifuge tube and pelleted for 10 s in a microfuge. Cells labeled apically with noncleavable sulfo-NHS-biotin or NHS-LC-biotin at this stage are held on ice until the basolateral samples are ready.
10. For cells labeled with cleavable NHS-SS-biotin, the pellet is resuspended in 1 ml of PBS-CM containing 2 mg/ml sulfo-NHS-biotin or NHS-LC biotin and incubated on a rotator at 4°C. After 20 min the cells are pelleted for 10 s in a microfuge and this step is repeated.
11. The reaction is quenched with 50 m*M* NH_4Cl in PBS-CM for 10 min. The cells are then pelleted in the microfuge for 10 s.
12. At this point, both apical and basolaterally labeled pellets are frozen dry at –80°C or immediately lysed and specific proteins immunoprecipitated as described in the section extraction of biotinylated proteins.
13. Immunoprecipitated proteins are resuspended in Laemmli sample buffer containing 5% 2-mercaptoethanol or 50 m*M* dithiothreitol to release the NHS-SS-biotin from the apical proteins in basolateral samples. After heating to 95°C for 5 min, samples are resolved by SDS–PAGE, transferred to nitrocellulose or PVDF membranes, and blotted with streptavidin.

Analysis of Results

Analysis of the results proceeds as in the section on cell surface biotinylation.

F. Extraction and Immunoprecipitation of Biotinylated Proteins

Solutions

1. *TPI*: 1% Triton X-100, 20 m*M* Tris, 150 m*M* NaCl, 5 m*M* EDTA, pH 8.0, containing 0.2% BSA, and protease inhibitors
2. *TPII*: 0.1% SDS, 20 m*M* Tris, 150 m*M* NaCl, 5 m*M* EDTA, pH 8.0, containing 0.2% BSA
3. *TPIII*: 20 m*M* Tris, 500 m*M* NaCl, 5 m*M* EDTA, pH 8.0, containing 0.2% BSA
4. *TPIV*: 50 m*M* Tris, pH 8.0
5. *Laemmli sample buffer*
6. *Protein A–Sepharose*
7. *Staphlycoccus A cells*: Pansorbin

Steps

1. Excise filters from inserts using a #11 scalpel blade or razor blade. Lyse in 1 ml of TPI at 4°C. In some cases it may be necessary to use more stringent conditions for lysis (i.e., RIPA buffer, which contains 0.5% deoxycholate and 0.1% SDS in addition to 1% Triton X-100).
2. Wash 100 µl/sample of Pansorbin three times with TPI. *Do not omit protease inhibitors.*
3. Centrifuge lysate in a microfuge at 4°C at 13,000 *g* for 10 min. Collect the supernatant and discard the pellet.
4. Add 100 µl of washed Pansorbin to each supernatant. Preclear for 1 h at 4°C.
5. Resuspend 5–10 mg of protein A-Sepharose/lysate in 1 ml TPI /lysate. If you are immunoprecipitating with a mouse IgG, after 10 min, when the Sepharose beads are swollen, add 2 mg of rabbit anti-mouse IgG. After 1 h wash the beads three times with TPI. On the last wash, pellet the beads in microcentrifuge tubes.
6. Pellet the Pansorbin by centrifugation at 13,000 *g* for 10 min. Collect the supernatant, add an appropriate volume of antibody, and incubate at 4°C for 1 h to overnight.
7. Transfer the immunoprecipitates to the tubes containing the protein A–Sepharose and incubate for 1 h at 4°C.
8. Centrifuge the immunoprecipitates in a microfuge at 13,000 *g* for 30 s. Remove the supernatant and resuspend the beads in 1 ml of TPI. Repeat this step three times with TPII, three times with TPIII, and once with TPIV.
9. Resuspend with an appropriate volume of Laemmli sample buffer, heat to 95°C for 5 min, and resolve by SDS–PAGE. For streptavidin blotting, transfer the gel to nitrocellulose or PVDF.

G. Streptavidin Blotting

Solutions

1. *Blocking buffer*: 5% Carnation instant milk, 0.3% BSA, in PBS-CM
2. *Rinse buffer*: 1% BSA, 0.2% Triton X-100 in PBS-CM
3. *[^{125}I]Streptavidin or streptavidin conjugated to horseradish peroxidase or alkaline phosphatase (streptavidin-HRP)*
4. A phosphorimager, Kodak X-OMAT AR film and a cassette with an intensifying screen, or an enhanced chemiluminescence reagent kit (such as those supplied by Amersham) and appropriate film.

Steps

1. After transfer to nitrocellulose or PVDF (PVDF is superior for chemiluminescent detection systems and is used in our laboratory for most streptavidin blots), block the blot for 1 h in blocking buffer.
2. Rinse once with rinse buffer.
3. Incubate for 1 h in 40 ml rinse buffer containing 1–2 × 10^6 cpm/ml of [^{125}I] streptavidin or 0.5–1.0 mg/ml streptavidin-HRP.
4. Wash three to five times for 5–10 min each with rinse buffer.
5. Dry the blot and expose to a phosphorimager screen, autoradiograph it with Kodak X-OMAT AR film, or use any of the many enhanced chemiluminescent kits that are available.

H. Quantitation of Polarized Distribution by Confocal Microscopy Imaging Technique

Modern quantitative optical microscopy offers an alternative method to quantify the relative polarity of fluorescently labeled cell surface proteins in cells developing polarity in settings such as the calcium switch assay (Rajasekaran *et al*., 1996). This quantitation is based on the relative fluorescent pixel intensities in serial horizontal confocal sections of the target protein to a known polarized marker.

Requirements

1. Confocal laser-scanning microscope
2. Software to measure fluorescence intensity, e.g., Metamorph, Image Space Software.

Steps

1. Samples subjected to immunofluorescence technique (not discussed here) are imaged on a laser confocal microscopic system. Samples are subjected to

optical sectioning (*xy*) of the entire thickness (*z*) of the monolayer. We select an interval between sections for optimized collection of fluorescence from a given plane without contribution from the neighboring *z* planes. Choice of interval depends on pinhole dimension, which in turn depends on characteristics of the excitation wavelength. [Refer to a handbook on confocal microscopy, e.g., Pawley (1995), or a confocal microscope manufacturer's manual for optimizing microscopic parameters.]

2. For each optical section, quantify the average per-pixel fluorescence intensity of the labeled proteins using the imaging software. Determine the ratio of intensity obtained for the protein of interest to that of a known marker.

Analysis of Results

The ratio of fluorescent intensity obtained represents the relative distribution of the target protein and is interpreted as follows.

a. A constant pixel intensity ratio for all optical sections of a given monolayer suggests overlapping distribution of the target protein with the known marker.

b. Decreasing pixel intensity ratio in from basolateral to apical domain of the target protein and the apical or tight junction marker would mean that the protein is localized in the basolateral domain.

c. Increasing intensity ratio with a basolateral marker would mean that the target protein is apically targeted (see Rajasekaran *et al*., 1996).

I. Determination of Plasma Membrane Protein Polarity after Intranuclear Microinjection of Its cDNA

This procedure is used for rapid qualitative determination of the steady-state polarity of a newly synthesized protein in polarized cells. Analysis is performed using either a fluorescence wide-field or a confocal microscope. We have utilized this technique to study the regulation of polarity of basolateral and apical membrane markers by GTPases and their downstream effectors. Normal polarization of the monolayer needs to be confirmed by studying the localization of known apical or basolateral markers.

Solutions

1. *Microinjection buffer*: H-KCl buffer containing 10 m*M* HEPES, pH 7.4, 140 m*M* KCl. Dissolve 1.04 g of KCl in 99 ml deionized H_2O and then add 1.0 ml HEPES from a 1 *M* stock (pH 7.4). Sterilize the buffer by passing through a 0.22-µm filter and store at 4°C (Müsch *et al*., 2001).

2. *PBS/CM*: See Section III,A

3. *H-DMEM*: DMEM containing HEPES. Dissolve bicarbonate-free powdered DMEM in 900 ml deionized H_2O. Add 20 ml HEPES from a 1 *M* stock and adjust the pH to 7.4. Sterilize the medium through a 0.22-µm filter and store at 4°C.

4. *B–DMEM*: DMEM containing sodium bicarbonate

Steps

1. Plate MDCK II cells on sterile glass coverslips at a concentration of 1.6×10^6 cells/ml or at an approximate plating density of 2×10^5 cells per cm^2 in B-DMEM and 10% fetal bovine serum (FBS). Allow the cells to polarize for 4–5 days and change the medium only once on day 2 postplating. Growth conditions required to attain polarity for different cell lines vary and require optimization.

2. Dilute the stock of cDNA (stock prepared in deionized H_2O at a concentration of 0.5 mg/ml) in microinjection buffer to a concentration of around 10 µg/ml. It is highly recommended that cDNA constructs also contain a tag sequence, such as Myc, HA, GFP, and its variants, in-frame with the gene of interest so as to distinguish the newly synthesized proteins from endogenous proteins. For experiments involving more than one cDNA construct, cDNAs can be coinjected. However, the efficiency of expression of a construct may vary in the presence of another. Therefore, proper conditions should be established for good expression of each coinjected construct. A range of concentrations between 1 and 20 µg/ml of DNA should be tested to optimize their expression levels.

3. Prepare microinjection needles by pulling 1-mm-diameter and 6-in.-long borosilicate glass capillaries (1B100F-6, World Precision Instruments, Inc, Sarasota, FL) using a micropipette puller (e.g., Flaming/Brown Micropipette Puller Model P-97, Sutter Instrument Co., Novato, CA).

4. Load the cDNA diluted in microinjection buffer through the blunt end of the needle into the needle holder of the micromanipulator (Narishige Company, Ltd., SE-TAGAYA-KU, Tokyo, Japan) attached to the inverted microscope (Zeiss-Axiovert 25, Germany).

5. Transfer coverslip into 35-mm-diameter tissue culture dishes. Add 4 ml of H-DMEM containing 5% FBS to each dish and place the dish on the dish holder of the micromanipulator-microscope described earlier. Microinject the nucleus of cells. Avoid microinjecting cells that are right next to each other. This simplifies

the analysis of distribution of apical and basolateral markers. In order to avoid unsynchronized protein synthesis, preferably microinject within 10–15 min of transferring the dish to the microscope stage.

6. Incubate the microinjected cells with B-DMEM–10% FBS medium at 37°C. Most of the proteins accumulate in the ER within 60 × 90 min at 37°C post-microinjection. Different levels of expression should be tested to ensure that the sorting pathways are not saturated. For coinjections, it is necessary to standardize the conditions for sufficient expression of each protein. Adjustment of DNA concentrations (as described in step 2) and time of incubation at 37°C postmicroinjection are two steps that need to be tuned for expression of multiple constructs.

7. After appropriate incubation at 37°C, replace medium with B-DMEM–10% FBS containing 100 µg/ml cycloheximide (concentration may be lowered down to 20 µg/ml if cells detach from coverslip) to inhibit new protein synthesis. the chase time for plasma membrane delivery of protein is initiated at 37°C for 3–4 h.

8. After an appropriate chase period, fix cells with either –20°C chilled methanol for 10 min or 2% paraformaldehyde at room temperature for 15 min. Methanol fixation should be followed by a blocking step at room temperature with 1% BSA prepared in PBS-CM for 30 min. Paraformaldehyde fixation of cells is followed by permeabilization at room temperature for 30 min with either 0.2% Triton-X 100 or 0.075% saponin prepared in PBS-CM containing 1% BSA. Cells can now be processed for immunofluorescence with the appropriate primary and secondary antibodies.

Analysis of Results

Cells processed for immunofluorescence are imaged on either a confocal or a wide-field microscope. The correct orientation of the cells is determined by analyzing the staining of known polarized markers. In case of a wide-field microscope, the entire monolayer is subjected to *z* sectioning at least at 0.5-µm intervals with a 60× 1.4 NA objective, and standard deconvolution software is used to enhance the resolution. Alternatively, we use a confocal microscope in frame-scan mode and collect *xyz* stacks of the entire monolayer and display the *xyz* stack in the orthogonal plane. The cells can be displayed directly as a *xz* cross section by doing a line scan, i.e., scanning in the *xzy* mode. Localization of the protein is determined depending on the staining pattern, e.g., relative to a tight junctional marker such as ZO-1.

IV. COMMENTS

The methods described here represent examples of applications of the biotinylation technique; other examples of possible applications are (1) a transcytotic assay using a combination of the targeting and endocytosis protocols (Le Bivic *et al*., 1989; Zurzolo *et al*., 1992) and (2) detection of GPI-anchored proteins at the cell surface using Triton X-114 phase separation and PI-PLC digestion in place of the standard lysis procedure (Lisanti and Rodriguez-Boulan, 1990). Another analog of biotin, biotin hydrazide, can be used to label oligosaccharides of surface glycoproteins following periodate oxidation (Lisanti *et al*., 1989).

V. PITFALLS/RECOMMENDATIONS

1. It has been suggested that the use of pH 9.0 buffer to dilute sulfo-NHS-biotin would enhance the efficiency of labeling of surface proteins (Gottardi and Caplan, 1993). In our experience this is not always true and depends on different proteins and cell lines.

2. Always cut the filters out of the plastic holder before lysis. We have found that the cells can grow along the inside of the plastic ring supporting the filter. Lysis of these cells can result in erroneous results (Zurzolo and Rodriguez-Boulan, 1993).

3. Occasionally, in targeting experiments, intracellular nonbiotinylated forms are recovered on streptavidin beads. Using NHS-LC-biotin and keeping the SDS concentration at 0.4% helps reduce this. Another approach is to use NHS-SS-biotin and remove it from the streptavidin beads by incubation in 50 m*M* dithiothreitol of 5–10% 2-mercaptoethanol in 62.5 m*M* Tris, pH 8.0. Then spin the beads out and dilute the supernatant 1:1 with 2× Laemmli sample buffer.

4. The *in situ* biotinylation assay works best for proteins that are restricted to the RPE cell (i.e., RET-PE2 antigen). Quantification of proteins present in adjacent tissues (particularly the choroid) can contaminate the basolaterally labeled material and yield an incorrectly high level of basolateral labeling.

5. Determination of polarity by confocal microscopy can provide visual validation of the biochemical assay. It is useful for measuring the polarity of steady-state protein and dynamic changes involved in tight junction assembly in the Ca^{2+} switch assay. A thorough analysis with known markers of different domains is recommended before determining polarity of the target protein.

6. For determination of polarity by means of intranuclear microinjection of cDNA, thorough optimization regarding the protein expression level and the incubation time is necessary. Moreover, it is critical to avoid saturating the sorting pathway. Hence, coinjecting and monitoring a known apical or basolateral marker are critical for final evaluation. Because the basolateral domain of the polarized monolayer on the coverslip is not accessible to the antibody without permeabilization, it is difficult to distinguish the pool of basolateral protein that is associated with submembrane structures closely juxtaposed to the cytoplasmic side of plasma membrane and the pool present in the external leaflet of the plasma membrane.

References

Gan, Y., McGraw, T.E., and Rodriguez-Boulan, E. (2002). The epithelial-specific adaptor AP1B mediates post-endocytic recycling to the basolateral membrane. *Nature Cell Biol.* **4**, 605–609.

Gottardi, C., and Caplan, M. (1993). Cell surface biotinylation in the determination of epithelial membrane polarity. *J. Tissue Culture Methods* **14**, 173–180.

Graeve, L., Drickamer, K., and Rodriguez-Boulan, E. (1989). Functional expression of the chicken liver asialoglycoprotein receptor in the basolateral surface of MDCK cells. *J. Cell Biol.* **109**, 2909–2816.

Hanzel, D., Nabi, I. R., Zurolo, C., Powell, S. K., and Rodriguez-Boulan, E. (1991) New techniques lead to advances in epithelial cell polarity. *Semin. Cell Biol.* **2**, 341–353.

Keller P. Simons K. (1997). Post-golgi biosynthetic trafficking. *J. Cell Sci.* 1103001–1103009.

Laemmli, U. K. (1970). Cleavage of structural proteins during the assembly of the head of bacteriophage T4. *Nature* **227**, 680–685.

Le Bivic, A., Real, F. X., and Rodriguez-Boulan, E. (1989). Vectorial targeting of apical and basolateral plasma membrane proteins in a human adenocarcinoma cell line. *Proc. Natl. Acad. Sci. USA* **86**, 9313–9317.

Le Bivic, A., Sambuy, Y., Mostov, K., and Rodriguez-Boulan, E. (1990). Vectorial targeting of an endogenous apical membrane sialoglycoprotein and uvomorulin in MDCK cells. *J. Cell Biol.* **110**, 1533–1539.

Le Gall, A., Yeaman, C., Muesch, A., and Rodriguez-Boulan, E. (1995). Epithelial cell polarity: New perspectives. *Semin. Nephrol.* **15**(4), 272–284.

Lisanti, M., Le Bivic, A., Sargiacomo, M., and Rodriguez-Boulan, E. (1989). Steady state distribution and biogenesis of endogenous MDCK glycoproteins: Evidence for intracellular sorting and polarized surface delivery. *J. Cell Biol.* **109**, 2117–2128.

Lisanti, M., and Rodriguez-Boulan, E. (1990). Glycosphingolipid membrane anchoring provides clues to the mecanism of protein sorting in polarized epiothelial cells. *Trends Biochem. Sci.* 113–118.

Marmorstein, A. D., Bonilha, V. L., Chiflet, S., Neill, J. M., and Rodriguez-Boulan E. (1996). The polarity of the plasma membrane protein RET-PE2 in retinal pigment epithelium is developmentally regulated. *J. Cell. Sci.* **109**, 3025–3034.

Müsch A., Cohen D., Kreitzer G., and Rodriguez-Boulan E. (2001). cdc42 regulates the exit of apical and basolateral proteins from the trans-Golgi network. *EMBO J.* **20**, 2171–2179.

Pawley J. B. (ed.) (1995). "Handbook of Biological Confocal Microscopy." Plenum Press, New York.

Rajasekaran, A.K., Hojo, M., Huima, T., and Rodriguez-Boulan, E. (1996). Catenins and zonula occudens-1 form a complex during early stages in the assembly of tight junctions. *J. Cell Biol.* **132**, 451–463.

Rodriguez-Boulan, E., Kreitzer, G., and Muesch, A. (2005). Organization of vesicular trafficking in epithelia. *Nature Rev. Mol. Cell Biol.* **6**, 233–247.

Rodriguez-Boulan, E., and Powell, S. K. (1992). Polarity of epithelial and neuronal cells. *Annu. Rev. Cell Biol.* **8**, 395–427.

Sargiacomo, M., Lisanti, M., Graeve, L., Le Bivic, A., and Rodriguez-Boulan, E. (1989). Integral and peripheral protein compositions of the apical and basolateral plasma membrane domains of MDCK cells. *J. Membr. Biol.* **107**, 277–286.

Yeaman, C., Grindstaff, K.K., and Nelson, W.J. (1999). New perspectives on mechanisms involved in generating epithelial cell polarity. *Physiol. Rev.* **79**,73–98.

Zurzolo, C., Le Bivic, A., Quaroni, A., Nitsch, L., and Rodriguez-Boulan, E. (1992). Modulation of transcytotic and direct targeting pathways in a polarized thyroid cell line. *EMBO J.* **11**, 2337–2344.

Zurzolo, C., and Rodriguez-Boulan, E. (1993). Delivery of Na,K-ATPase in polarized epithelial cells. *Science* **260**, 550–552.

SECTION

6

Mitochondria

CHAPTER

34

Protein Translocation into Mitochondria

Sabine Rospert and Hendrik Otto

I. INTRODUCTION

Mitochondria from different sources such as rat liver, rabbit brain, or yeast can be isolated as intact organelles. Isolated mitochondria are able to respire, maintain a membrane potential across their inner membrane, possess an active ATP synthase, and shuttle nucleotides across their membranes. In addition, even a process as complicated as import of mitochondrial precursor proteins can be studied outside the living cell. For this purpose, radiolabeled precursor proteins, synthesized in an *in vitro* transcription/translation system, are mixed with isolated mitochondria (Glick, 1991; Melton *et al*., 1984). In the presence of ATP, precursor proteins will cross the mitochondrial membranes, become processed to their mature form, and fold to their native state. Building on this basic "import assay," sophisticated experiments have been developed and the results of these experiments provide most of what we know about mitochondrial import today (Neupert, 1997; Pfanner and Geissler, 2001).

This article describes a standard protocol for the *in vitro* synthesis of a radiolabeled precursor protein and the subsequent import of this precursor into isolated yeast mitochondria. As an example, we have selected the precursor protein yeast malate dehydrogenase (Dubaquié *et al*., 1998). The N-terminal presequence of the yeast malate dehydrogenase precursor, as is of most mitochondrial precursor proteins, is removed by a protease localized in the mitochondrial matrix (Jensen and Yaffe, 1988). The mRNA of the precursor protein is transcribed with SP6 RNA polymerase (Melton *et al*., 1984).

II. MATERIALS AND INSTRUMENTATION

SP6 RNA polymerase (Cat. No. 810 274); RNase inhibitor from human placenta (Cat. No. 799 017); set of ATP, CTP, GTP, UTP, lithium salts, 100 m*M* solutions (Cat. No. 1 277 057); creatine kinase from rabbit muscle (Cat. No. 127 566); creatine phosphate, disodium salt (Cat. No. 127 574); and proteinase K (Cat. No. 1092766) are from Roche. Tris (Cat. No. 108382); KCl (Cat. No. 104936); KOH (Cat. No. 105021); $MgCl_2$ (Cat. No. 105833); NaN_3 (Cat. No. 822335); 25% NH_3 solution (Cat. No. 105432); ethanol (Cat. No. 100983); and sodium salicylate (Cat. No. 106602) are from Merck. Spermidine (Cat. No. S 0266); bovine serum albumin, essentially fatty acid free (BSA) (Cat. No. A-7511); dithiothreitol (DTT) (Cat. No. D 5545); HEPES (Cat. No. H 7523); trypsin (Cat. No. T 1426); trypsin inhibitor, from soybean (Cat. No. T 9003); α-nicotinamide adenine dinucleotide disodium salt, reduced form (NADH) (Cat. No. N 6879); EDTA (Cat. No. E 9884); $(NH_4)_2SO_4$ (Cat. No. A 2939); $CaCl_2$, dihydrate (Cat. No. C 5080); magnesium acetate tetrahydrate (Cat. No. M 2545); valinomycin (Cat. No. V 0627); ATP, disodium salt (Cat. No. A 7699); glycerol (Cat. No. G 6279); potassium acetate (Cat. No. P 5708); KH_2PO_4 (Cat. No. P 5379); L-methionine (Cat. No. M 9625); urea (Cat. No. U 5128); phenylmethylsulfonyl fluoride (PMSF) (Cat. No. P 7626); tRNA, from bovine liver (Cat. No. R 4752); and Triton X-100 (Cat. No. T 9284) are from Sigma. Rabbit reticulocyte lysate (Cat. No. L 4960) and amino acid mixture, minus methionine (Cat. No. L 4960), are from Promega. NaCl (Cat. No. 9265.1) and trichloroacetic acid (TCA) (Cat. No. 8789.1) are

Copyright 2006, Elsevier Science (USA).
All rights reserved.

from Roth. Sorbitol (Cat. No. 2039) is from Baker. L-[^{35}S]methionine, >1000 Ci/mmol (Cat. No. SJ 235), m^{7}G(5Ç)ppp(5Ç)G (G-cap) (Cat. No. 27 4635 02), and Kodak X-OMAT X-ray film (Cat. No. V1651496) are from Amersham Biosciences. Sorvall centrifuge RC M120 GX, Kendro. Sorvall Rotor S100 AT3-204, Kendro. Eppendorf centrifuge 5417 R, "microfuge" Eppendorf. Greiner PP-tubes 15 ml (Cat. No. 188261), Greiner. X-ray cassettes (Cat. No Rö 13), GLW. Plasmid is pSP65mdh1 (Dubaquié *et al*., 1998). Highly purified mitochondria (25 mg/ml) are prepared after Glick and Pon (1995).

III. PROCEDURES

Solutions used directly as obtained from the supplier are only listed in Section II. Protocols for the preparation of solutions used throughout the procedure are only given once.

A. Transcription Using SP6 Polymerase

Solutions

1. *1 M Tris–HCl stock solution, pH 7.5*: Dissolve 12.1 g Tris in 80 ml H_2O and adjust pH to 7.5 with 5 *M* HCl. Add H_2O to 100 ml. Autoclave and store at room temperature.
2. *1 M HEPES–KOH, pH 7.4*: Dissolve 23.8 g HEPES in 80 ml H_2O and adjust pH to 7.4 using 4 *M* KOH. Add H_2O to 100 ml. Autoclave and store at room temperature.
3. *1 M spermidine*: Dissolve 145 mg spermidine in 1 ml H_2O. Store at –20°C.
4. *100 mg/ml BSA*: Dissolve 500 mg BSA in 5 ml H_2O. Store at –20°C.
5. *2.5 M $MgCl_2$*: Dissolve 50.8 g $MgCl_2$ in 100 ml H_2O. Autoclave and store at 4°C.
6. *2.5 M KCl*: Dissolve 18.6 g KCl in 100 ml H_2O. Autoclave and store at 4°C.
7. *100 mM DTT*: Dissolve 15.4 mg DTT in 1 ml H_2O. Store at –20°C. Make a fresh solution about every 4 weeks.
8. *5× SP6 reaction buffer*: 200 m*M* Tris–HCl, pH 7.5, 30 m*M* $MgCl_2$, 10 mM spermidine, and 0.5 mg/ml BSA. To obtain 10 ml of a 5x reaction buffer, mix 2 ml 1 *M* Tris–HCl, pH 7.5, 120 µl 2.5 *M* $MgCl_2$, 100 µl 1 *M* spermidine and 50 µl 100 mg/ml BSA. If necessary, readjust the pH to 7.5. Store in 1-ml aliquots at –20°C.
9. *G-cap (m^{7}G(5′)ppp(5′)G)*: Dissolve 25 A_{250} units in 242 µl H_2O. Freeze 10-µl aliquots in liquid nitrogen. Store at –70°C.
10. *5 mM* NTP–GTP: To make a 500 µl stock, add 25 µl 100 m*M* ATP, 25 µl 100 m*M* UTP, and 25 µl 100 m*M* CTP to 425 µl 20 m*M* HEPES–KOH, pH 7.4. Store in 100-µl aliquots at –70°C.
11. *5 mM GTP*: Mix 475 µl 20 m*M* HEPES–KOH, pH 7.4, with 25 µl 100 m*M* GTP solution.
12. *RNase inhibitor buffer*: 20 m*M* HEPES–KOH, pH 7.4, 50 m*M* KCl, 10 m*M* DTT, and 50% glycerol. Make 10 ml of the buffer by mixing 200 µl 1 *M* HEPES–KOH, pH 7.4, 200 µl 2.5 *M* KCl, 1 ml 100 m*M* DTT, and 5 ml glycerol. Add H_2O to 10 ml and store at –20°C.
13. *4 units/µl RNase inhibitor*: Add 500 µl RNase inhibitor buffer to 2000 units of RNase inhibitor. Store at –20°C for up to 6 months.
14. *1 µg/µl linearized plasmid DNA*: Prepare the linearized plasmid (pSP65mdh1) according to standard molecular biology procedures.

Steps

1. Mix the following solutions carefully, avoiding the formation of air bubbles. Follow the indicated order of addition because the DNA might precipitate in 5× SP6 buffer. Precipitation of DNA can also occur if the mixture is placed on ice. Incubate the mixture at 40°C for 15 min.

H_2O	12 µl
4 units/µl RNase inhibitor	1 µl
1 µg/µl linear plasmid (pSP65mdh1)	5 µl
5 m*M* rNTPs minus GTP	5 µl
5 m*M* G-cap	5 µl
100 m*M* DTT	5 µl
5× SP6 buffer	10 µl
SP6 polymerase	2 µl

2. Start transcription by adding 5 µl 5 m*M* GTP solution and incubate for 90 min at 40°C.
3. Extract the mRNA with phenol/chloroform and then with chloroform/isoamylalcohol, precipitate with 100% ethanol, and wash with 70% ethanol. Resuspend the dried pellet in 125 µl H_2O.
4. The mRNA obtained by this procedure is used directly in the translation protocol. mRNA can be stored in 10-µl aliquots at –70°C. If frozen mRNA is used for translation, thaw rapidly and keep at room temperature before adding the mRNA to the translation reaction.

B. Translation Using Reticulocyte Lysate

Solutions

1. *1 M DTT*: Dissolve 154 mg DTT in 1 ml H_2O. Store at –20°C. Make a fresh solution about every 4 weeks.

2. *8 mg/ml creatine kinase*: Dissolve 8 mg creatine kinase in 475 µl H_2O. Add 20 µl 1 *M* HEPES–KOH, pH 7.4, 5 µl 1 *M* DTT, and 500 µl glycerol. Freeze in 10-µl aliquots in liquid nitrogen and store at –70°C.
3. *5 mg/ml tRNA*: Dissolve 10 mg tRNA from bovine liver in 2 ml H_2O. Store in 100-µl aliquots at –20°C.
4. *400 mM HEPES–KOH, pH 7.4*: Mix 6 ml H_2O with 4 ml 1 *M* HEPES–KOH, pH 7.4. If necessary, readjust pH.
5. *10 mM GTP*: Mix 450 µl 20 m*M* HEPES–KOH, pH 7.4, with 50 µl 100 m*M* GTP. Store at –20°C.
6. *100 mM ATP*: Dissolve 55.1 mg ATP in 900 µl H_2O. Adjust to pH ~7 using 4 *M* NaOH and pH indicator paper. Adjust volume to 1 ml and store at –20°C.
7. *600 mM creatine phosphate*: Dissolve 153.06 mg creatine phosphate in 1 ml H_2O. Store at –20°C.
8. *4 M potassium acetate*: Dissolve 3.92 g potassium acetate in 10 ml H_2O. Do not adjust the pH. Store at –20°C.
9. *50 mM magnesium acetate*: Dissolve 10.7 mg magnesium acetate tetrahydrate in 1 ml H_2O. Store at –20°C.

Steps

1. Prepare the reticulocyte lysate mix and the tRNA mix fresh. To obtain a 100-µl translation reaction, mix the following solutions.

Reticulocyte lysate mix		tRNA mix	
0.4 *M* HEPES–KOH	5 µl	5 mg/ml tRNA	6 µl
10 m*M* GTP	0.6 µl	4 units/µl RNase inhibitor	6 µl
100 m*M* ATP	0.5 µl	4 *M* potassium acetate	3 µl
1 m*M* amino acid mix	3.75 µl		
0.6 *M* creatine phosphate	2 µl		
reticulocyte lysate	50 µl		
8 mg/ml creatine kinase	2 µl		

2. Use the mRNA obtained in Section III,A. It is possible to use mRNA produced in a different transcription system, e.g., with T7 RNA polymerase. Mix 60 µl reticulocyte lysate mix, 10 µl tRNA mix, 2 µl 50 m*M* magnesium acetate, 18 µl mRNA, 10 µl [^{35}S]methionine, and 2 µl 1 *M* DTT.

3. Incubate this mixture for 60 min at 30°C. Shield it from light to prevent heme-induced photooxidation of the precursor proteins. Remove ribosomes after the translation reaction by centrifugation for 15 min at 150,000 *g* (65,000 rpm with S100 AT3-204 rotor in Sorvall centrifuge). Remove the supernatants, being careful not to disturb the ribosomal pellet.

C. Denaturation of Radiolabeled Precursor Protein

Solutions

1. *Saturated $(NH_4)_2SO_4$ solution*: Weigh 100 g $(NH_4)_2SO_4$ and add H_2O to a final volume of 100 ml. Stir for 30 min at room temperature. The $(NH_4)_2SO_4$ will not dissolve entirely. Remove the supernatant and keep at room temperature.
2. *8 M urea*: Dissolve 4.85 g urea in a final volume of 10 ml 25 m*M* Tris–HCl, pH 7.5, containing 25 m*M* DTT.

Steps

1. Proteins synthesized in reticulocyte lysate are either folded or bound to chaperone proteins present in the lysate (Wachter *et al*., 1994). In order to unfold the protein prior to import, it can be precipitated by high concentrations of ammonium sulfate and subsequently denatured in 8 *M* urea.

2. Add 200 µl of the $(NH_4)_2SO_4$ solution to the 100-µl translation reaction. Mix well and allow precipitation of the protein for 30 min on ice. Collect precipitate by centrifugation in an Eppendorf centrifuge at 20,000 *g* for 10 min.

3. Discard the supernatant and dissolve the pellet in 100 µl of 8 *M* urea solution. Keep the denatured precursor at room temperature for 10–30 min. This precursor solution is used for the import reaction (Section III,D) and preparation of the precursor standard (Section III,G).

D. Import of Denatured Radiolabeled Precursor Proteins

Solutions

For additional solutions required, see Sections III,A and III,B.

1. *2.4 M sorbitol*: Dissolve 43.7 g of sorbitol in a final volume of 100 ml H_2O. Autoclave and store at 4°C.
2. *1 M KH_2PO_4*: Dissolve 1.36 g KH_2PO_4 in 10 ml H_2O. Filter sterilize and keep at room temperature.
3. *1 M HEPES–KOH, pH 7.0*: Dissolve 23.8 g HEPES in 80 ml H_2O and adjust pH to 7.0 with 4 *M* KOH. Add H_2O to a final volume of 100 ml. Filter sterilize and store at room temperature.
4. *250 mM EDTA, pH 7.0*: Resuspend 7.3 g of EDTA in 70 ml H_2O. Adjust pH to 7.0 using 5 *M* NaOH. Add H_2O to a final volume of 100 ml. Filter sterilize and keep at room temperature.
5. 2× *import buffer*: 1.2 *M* sorbitol, 100 m*M* HEPES–KOH, pH 7.0, 100 m*M* KCl, 20 m*M* $MgCl_2$,

5 m*M* EDTA, pH 7.0, 4 m*M* KH_2PO_4, 2 mg/ml BSA, and 1.5 mg/ml methionine. To make 100 ml of 2× import buffer, mix 50 ml 2.4 *M* sorbitol, 400 µl 1 *M* KH_2PO_4 solution, 4 ml 2.5 *M* KCl, 10 ml 1 *M* HEPES–KOH, pH 7.0, 0.8 ml 2.5 *M* $MgCl_2$, 2 ml 250 m*M* EDTA, pH 7.0, 150 mg methionine, and 200 mg BSA. Adjust pH to 7.0 and add H_2O to 100 ml. Store at –20°C.

6. *1× import buffer minus BSA*: Prepare 2× import buffer, but without BSA. To obtain 1× import buffer minus BSA, mix 2 ml 2× import buffer with 2 ml H_2O.

7. *500 mM NADH*: Dissolve 35.5 mg of NADH in a final volume of 100 µl 20 mM HEPES–KOH, pH 7.0. Store at –20°C.

8. *1 mg/ml valinomycin*: Dissolve 2 mg valinomycin in 2 ml ethanol. Store at –20°C.

9. *Purified yeast mitochondria*: 25 mg mitochondrial protein/ml. Store at –70°C in 0.6 *M* sorbitol, 20 m*M* HEPES–KOH, pH 7.4, and 10 mg/ml BSA. Thaw rapidly at 25°C immediately before the experiment. Do not refreeze. A detailed protocol of the purification procedure is given in Glick and Pon, (1995).

Steps

1. Import into the matrix of mitochondria requires a membrane potential across the inner mitochondrial membrane. Therefore, the most thorough control for the specificity of an import reaction is to determine its dependence on a membrane potential. Adding ATP and the respiratory substrate NADH generates this potential. (Note that mammalian mitochondria cannot oxidize added NADH.)

2. Perform two import reactions, one in the absence and one in the presence of valinomycin. Preincubate the import reaction in a 15-ml Greiner tube at 25°C for 1–2 min.

Reaction 1 (+ membrane potential)		**Reaction 2 (no membrane potential)**	
2× import buffer	500 µl	2× import buffer	500 µl
100 m*M* ATP	20 µl	100 m*M* ATP	20 µl
500 m*M* NADH	4 µl	500 m*M* NADH	4 µl
Yeast mitochondria	20 µl	Yeast mitochondria	20 µl
H_2O	406 µl	H_2O	405 µl
		1 mg/ml valinomycin	1 µl

3. Add 50 µl of the denatured precursor protein solution (see Section III,C) containing denatured malate dehydrogenase to each reaction (reactions 1 and 2). Intact mitochondria should be handled gently. However, it is essential to mix the denatured precursor protein into the import reaction rapidly. Agitate the import reaction gently on a vortex mixer while adding the denatured precursor mixture dropwise. If mixing is performed only after addition, the precursor protein tends to aggregate and becomes import incompetent.

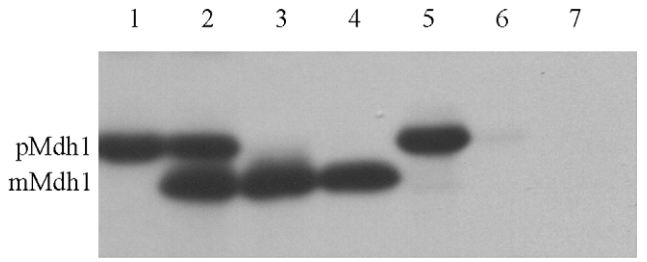

FIGURE 1 Import of radiolabeled yeast malate dehydrogenase into isolated yeast mitochondria. Lane 1, 10% of the material added to each import reaction; lanes 2–4, import in the presence of ATP and a membrane potential across the inner mitochondrial membrane; and lanes 5–7, import in the absence of ATP and a membrane potential across the inner mitochondrial membrane. Lanes 2 and 5: total; material isolated together with the mitochondrial pellet. Lanes 3 and 6: import; material protease protected in intact mitochondria. Lanes 4 and 7: folded; material protease resistant even after solubilization of the mitochondria with Triton X-100. pMdh1, precursor form of Mdh1; mMdh1, mature form of Mdh1. For experimental details, see text.

4. Incubate at 25°C for 10 min. Agitate gently every other minute to facilitate gas exchange. Stop the import reaction by transferring the tubes onto ice. Add 1 µl of 1 mg/ml valinomycin to reaction 1.

5. Remove 200 µl each from reactions 1 and 2 and put the samples on ice. Spin down mitochondria in an Eppendorf centrifuge and remove the supernatant (be careful, the pellet will be very small). Resuspend the mitochondrial pellets of reactions 1 and 2 in each 200 µl of 1× import buffer. These samples represent the **total** of the two import reactions (Fig. 1, lanes 2 and 5). Add 22 µl 50% TCA to each. Keep on ice and process further after all samples have been acid denatured (for the method of TCA precipitation, see Section III,G).

E. Protease Treatment of Intact Mitochondria

Solutions

1. *10 mg/ml trypsin*: Dissolve 3 mg of trypsin in 300 µl H_2O. Make fresh.
2. *20 mg/ml trypsin inhibitor*: Dissolve 6 mg of trypsin inhibitor in 300 µl H_2O. Make fresh.

Steps

Perform the following steps in parallel with both import reactions.

1. To digest precursor proteins that stick to the surface of the mitochondria, add 8 µl 10 mg/ml trypsin (final concentration 100 µg/ml). Incubate for 30 min on ice.

2. Add 8 µl 20 mg/ml trypsin inhibitor (final concentration 200 µg/ml) and incubate on ice for 5 min.
3. Transfer the sample into a new Eppendorf tube.
4. Spin for 3 min in an Eppendorf microfuge at 10,000 *g*. Remove the supernatant carefully by aspiration.
5. Carefully resuspend the mitochondrial pellet in 800 µl 1× import buffer minus BSA. As it is extremely important to resuspend the pellet completely, it should be done as follows. First add 100 µl of 1× import buffer minus BSA and resuspend mitochondria by pipetting up and down. Then add another 700 µl of 1× import buffer minus BSA to yield 800 µl final volume.
6. Remove 200 µl of each sample and add 22 µl 50% TCA. Keep on ice. These samples represent the material that has crossed the outer membrane completely (**import**, Fig. 1, lanes 3 and 6).

F. Inherent Protease Resistance of the Imported Protein

Solutions

1. *1 M Tris–HCl stock solution, pH 8.0*: Dissolve 12.1 g Tris in 80 ml H_2O and adjust pH to 8.0 using 5 *M* HCl. Add H_2O to a final volume of 100 ml. Autoclave and store at room temperature.
2. *2 M $CaCl_2$*: Dissolve 14.7 g $CaCl_2$ in 50 ml H_2O. Autoclave and store at room temperature.
3. *10% Triton X-100 (w/v)*: Dissolve 10 g of Triton X-100 in a final volume of 100 ml H_2O. Store at room temperature in the dark.
4. *10% NaN_3*: Dissolve 1 g NaN_3 in a final volume of 10 ml H_2O. Store at room temperature.
5. *Proteinase K buffer*: 50 m*M* Tris–HCl, pH 8.0, 1 m*M* $CaCl_2$, and 0.02 % NaN_3. To make 10 ml of proteinase K buffer, mix 500 µl 1 *M* Tris–HCl, pH 8.0, 5 µl 2 *M* $CaCl_2$, and 20 µl 10% NaN_3. Add H_2O to a final volume of 10 ml. Store at room temperature.
6. *10 mg/ml proteinase K stock*: Dissolve 5 mg of proteinase K in 500 µl proteinase K buffer. Store at 4°C for up to 1 week without loss of activity.
7. *200 µg/ml proteinase K solution*: Mix 10 µl of 10 mg/ml proteinase K stock with 390 µl H_2O. Add 100 µl 10% Triton X-100. Make fresh.
8. *200 mM PMSF*: Make a fresh solution of PMSF by dissolving 34.85 mg of PMSF in 1 ml of ethanol.

Steps

1. Transfer 200 µl from the remainder of the import reaction into a fresh Eppendorf tube. Add 200 µl of the 200-µg/ml proteinase K solution and mix rapidly. Leave the tube on ice for 15 min.

2. Add 2 µl 200 mM PMSF while agitating on a vortex mixer. Keep on ice for 5 min. Add 44 µl 50% TCA. Add 300 µl of acetone to dissolve the Triton X-100 that precipitates in the presence of TCA. These samples measure the fraction of the precursor protein that has completely crossed the outer membrane and has reached the folded state (**folded**, Fig. 1, lanes 4 and 7).

G. Final Processing of Samples and Preparation of a Precursor Standard

Steps

1. To inactivate proteases, incubate the TCA-precipitated samples (total, import, folded) at 65°C for 5 min. Place on ice for 5 min and subsequently collect the TCA precipitate by spinning for 10 min at 20,000 *g*.
2. Remove supernatant by aspiration and dissolve the pellets in 30 µl 1× sample buffer. If the sample buffer turns yellow, overlay the sample with NH_3 gas taken from above a 25% NH_3 solution. Agitate to mix the gaseous NH_3 gas into the sample buffer until the color turns blue again.
3. Incubate the samples for 5 min at 95°C.
4. To estimate the efficiency of the import reaction, the amount of precursor protein added to the import reaction has to be determined. The efficiency of import for most precursor proteins is between 5 and 30%. Here we use a 10% standard (Fig. 1, lane 1).
5. To obtain a 10% standard, mix 4µl of purified yeast mitochondria (see Section III,D) with 30 µl 1× sample buffer. Incubate at 95°C for 3 min.
6. Add 1 µl of the precursor protein solution (Section III,C) and incubate for 5 min at 95°C.

H. SDS–Gel Electrophoresis and Processing of the Gel

Solutions

1. *5% TCA*: To make 5 liter, add 250 g of TCA to 5 liter H_2O.
2. *1 M Tris base*: Dissolve 121 g of Tris in 1 liter H_2O.
3. *1 M sodium salicylate*: Dissolve 160 g of sodium salicylate in 1 liter H_2O.

Steps

1. Run samples on a 10% Tris–tricine gel (Schägger and von Jagow, 1987) stabilized by the addition of 0.26% linear polyacrylamide prior to polymerization.
2. To reduce radioactive background, boil 5% TCA in a beaker under the hood. Add the gel to the boiling TCA and incubate for 5 min.

3. Recover the gel and place it into a tray. Wash briefly with water. Neutralize by incubation in 1 *M* Tris-base for 5 min on a shaker.
4. Wash briefly with water. Add 1 *M* sodium salicylate and incubate for 20 min on a shaker.
5. Dry gel on a Whatman filter paper and expose to a Kodak X-OMAT X-ray film for the desired time. Exposure time for the experiment shown in Fig. 1 was 12 h.

IV. COMMENTS

The method describes a standard experiment to test a precursor protein that has not been used in mitochondrial import before. Most importantly, as demonstrated here for malate dehydrogenase, the protocol will reveal if import is dependent on a membrane potential (compare Fig. 1 lanes 3 and 6). This is essential, as sometimes protease-resistant precursor proteins tend to stick to the outside of mitochondria, thereby "mimicking" import.

The efficiency of import can be deduced by a comparison of the amount of imported material with a precursor standard (compare Fig. 1 lanes 1 and 3). In addition, the experiment reveals if a precursor protein folds to a protease-resistant conformation after its import into the mitochondrial matrix. Under the conditions chosen here, complete protease resistance was obtained for malate dehydrogenase (Fig. 1, lanes 3 and 4).

V. Pitfalls

The quality of the DNA used for transcription is essential for efficiency. Use a clean, RNA- and RNase-free plasmid preparation (e.g., purified with a Qiagen plasmid kit, Qiagen). Linearize plasmid by cutting with a restriction enzyme behind the coding region of the gene of interest. Extract with phenol/chloroform and then with chloroform/isoamylalcohol, precipitate with 100% ethanol, and wash with 70% ethanol. Resuspend the dried pellet in H_2O at a concentration of 1 µg/µl and store at 4°C. Never freeze DNA templates used for transcription.

To avoid RNase contamination, solutions used for transcription and translation have to be prepared with special caution. Always wear gloves even when loading pipette tips into boxes. If initiation at downstream AUG codons is a problem, try diluting the reticulocyte lysate up to fourfold.

It is important to establish that import is linear with time. To establish those conditions it is necessary to perform time course experiments of the import reaction and to try import at different temperatures.

Methods for determining the intramitochondrial localization of an imported precursor protein (Glick, 1991), investigating the energy requirements of mitochondrial import (Glick, 1995), and detecting interaction between imported precursor proteins and matrix chaperones (Rospert and Hallberg, 1995) have been published elsewhere.

References

Dubaquié, Y., Looser, R., Fünfschilling, U., Jenö, P., and Rospert, S. (1998). Identification of *in vivo* substrates of the yeast mitochondrial chaperonins reveals overlapping but non-identical requirement for hsp60 and hsp10. *EMBO J.* **17**, 5868–5876.

Glick, B. S. (1991). Protein import into isolated yeast mitochondria. *Methods Cell Biol.* **34**, 389–399.

Glick, B. S. (1995). Pathways and energetics of mitochondrial protein import in *Saccharomyces cerevisiae*. *Methods Enzymol.* **260**, 224–231.

Glick, B. S., and Pon, L. A. (1995). Isolation of highly purified mitochondria from *Saccharomyces cerevisiae*. *Methods Enzymol.* **260**, 213–223.

Jensen, R. E., and Yaffe, M. P. (1988). Import of proteins into yeast mitochondria: The nuclear MAS2 gene encodes a component of the processing protease that is homologous to the MAS1-encoded subunit. *EMBO J.* **7**, 3863–3871.

Melton, D. A., Krieg, P. A., Rebagliati, M. R., Maniatis, T., Zinn, K., and Green, M. R. (1984). Efficient *in vitro* synthesis of biologically active RNA and RNA hybridization probes from plasmids containing a bacteriophage SP6 promoter. *Nucleic Acids Res.* **12**, 7035–7056.

Neupert, W. (1997). Protein import into mitochondria. *Annu. Rev. Biochem.* **66**, 863–917.

Pfanner, N., and Geissler, A. (2001). Versatility of the mitochondrial protein import machinery. *Nature Rev. Mol. Cell. Biol.* **2**, 339–349.

Rospert, S., and Hallberg, R. (1995). Interaction of HSP 60 with proteins imported into the mitochondrial matrix. *Methods Enzymol.* **260**, 287–292.

Schägger, H., and von Jagow, G. (1987). Tricine-sodium dodecyl sulfate-polyacrylamide gel elektrophoresis for the separation of proteins in the range from 1 to 100 kDa. *Anal. Biochemi.* **166**, 368–379.

Wachter, C., Schatz, G., and Glick, B. S. (1994). Protein import into mitochondria: The requirement for external ATP is precursor-specific whereas intramitochondrial ATP is universally needed for translocation into the matrix. *Mol. Biol. Cell.* **5**, 465–474.

CHAPTER

35

Polarographic Assays of Mitochondrial Functions

Ye Xiong, Patti L. Peterson, and Chuan-pu Lee

I. INTRODUCTION

Mitochondrial metabolic functions are primarily concerned with the conservation of energy liberated by the aerobic oxidation of respiring substrates. Energy is conserved in the form that can subsequently be used to drive various cell functions. In recent years, it has been found that mitochondria also play critical roles in various cellular functions, including electrolyte balance, signal transduction, calcium homeostasis, oxidative stress, immunologic defense, and natural aging and/or apoptosis (cf. Lee, 1994).

Application of the oxygen electrode technique to study mitochondrial respiration and oxidative phosphorylation was first introduced by Chance and Williams in 1955. The kinetic dependence of mitochondrial respiration on the availability of inorganic phosphate and ADP had been earlier reported by Lardy and Wellman (1952). Together, these studies provided the basis of the concept of respiratory control. The polarographic technique for measuring rapid changes in the rate of oxygen utilization by cellular and subcellular systems is now widely used by many laboratories because of its simplicity and ease of performance. Concurrent monitoring of the metabolic changes induced kinetically by various substrates and reagent(s) can provide invaluable information.

This article describes a typical protocol employed in the authors' laboratory for the measurement of respiratory rates and its accompanied oxidative phosphorylation, which are catalyzed by isolated mitochondria. As an example, isolated intact mitochondria were chosen for presentation and discussion. The technique for preparation of isolated intact mitochondria has been described previously (Lee *et al.*, 1993a, b).

II. INSTRUMENTATION AND MATERIALS

The polarographic technique for measuring mitochondrial oxidative changes requires the following four basic components: an oxygen electrode, a closed reaction vessel, a constant voltage source, and a recorder. The Clark-type oxygen electrode is used most commonly (Yellow Springs Instrument Co., Yellow Springs, Ohio, 45387) and consists of a platinum cathode and a Ag/AgCl anode, which is bathed in a half-saturated KCl solution. The tip of the electrode is covered by a polyethylene membrane, which is held firmly over the end of the electrode by a rubber "O" ring. The reaction vessel can be constructed of glass, Plexiglas, or polycarbonate, and the design and the size of the vessel vary, depending on the requirements of the system under investigation. A number of vessels are available commercially. The reaction vessel used routinely in the authors' laboratory was made of polycarbonate and is composed of two parts: a cylindrical open top reaction chamber and a plug that fits in the top of the chamber. The temperature of the reaction chamber is constantly maintained with a water jacket. Constant stirring of the contents of the reaction chamber is accomplished by a disk-shaped, plastic-encased magnet located at the bottom of the reaction chamber. The polycarbonate plug, which is secured with a screw, fits tightly in the top of the reaction chamber. The plug has two vertical openings: the

Copyright 2006, Elsevier Science (USA).
All rights reserved.

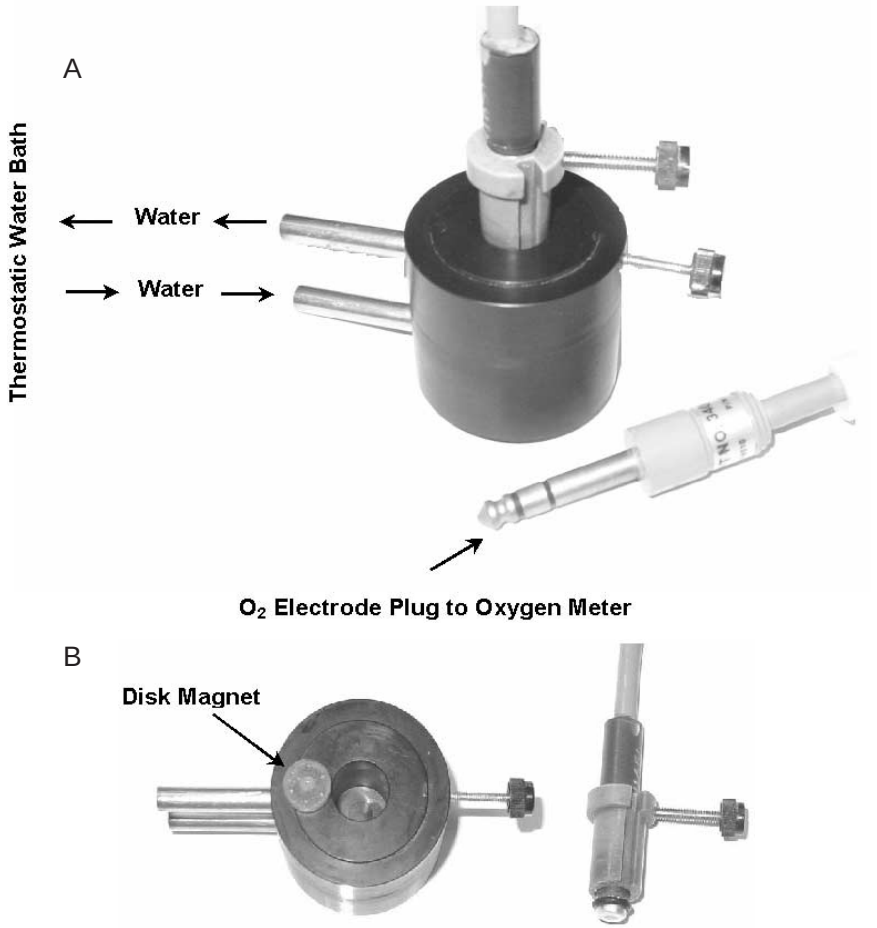

FIGURE 1 Reaction vessel for measurement of oxygen utilization with the oxygen electrode. Oxygen electrode and the reaction chamber are displayed in assembled form (A) and in disassembled form (B).

larger is fitted with a screw that holds the Clark electrode securely and the smaller one is used for the delivery of substrate(s) and reagent(s) into the reaction mixture. The physical arrangement of the reaction chamber and the oxygen electrode in the assembled form are shown in Fig. 1A. The disassembled form, which shows the details of each individual component, is shown in Fig. 1B.

It is imperative that closed reaction vessels are utilized so that air bubbles are not trapped and back diffusion of oxygen is reduced to a minimum. To facilitate this, the bottom of the plug is uneven to ensure that no air bubbles are trapped (cf. Fig. 1B). This aids the exit of air bubbles (if any) from the chamber and allows the mixing of added reagents without introducing air bubbles into the reaction mixture. Use of the magnetic stirrer permits continued steady mixing, at a constant temperature, of the reaction mixture. This facilitates the establishment of equilibrium between the oxygen dissolved in solution and the gas diffusing through the polyethylene membrane of the oxygen electrode. The electrode equilibrates with the air-saturated reaction mixture. Reactants and substrates are added through the small narrow opening at the top of the reaction chamber.

At the conclusion of each experiment the reaction chamber is cleaned by first disassembling the plug from the reaction chamber, aspirating the reaction mixture, and washing the plug, oxygen electrode, and the interior of the reaction chamber thoroughly with water. When a water-insoluble reagent is used, initial cleaning is accomplished with ethanol and is then followed with water rinsing. It is essential that no traces of ethanol are left behind as adverse effects may be induced. The reaction vessel is then reassembled and is ready for the next experiment.

When a voltage is imposed across the two electrodes immersed in an oxygen-containing solution, with the platinum electrode negative relative to the reference electrode, oxygen undergoes an electrolytic reduction. When current is plotted as a function of polarizing voltage, a plateau region is observed

between 0.5 and 0.8 V. With a polarization voltage of –0.6 V, the current is directly proportional to the oxygen concentration of the solution (Davies and Brink, 1942). The current is generally measured with a suitable amplifier and recorder combination. An oxygen meter (SOM-1, University of Pennsylvania Biomedical Instrumentation Group) and a Varian XY recorder (Model 9176) are used in our laboratory.

Reagents

From Sigma Chemicals Co.: Sucrose (Cat. No. S-978), bovine serum albumin (BSA, Cat. No. A-4378), EGTA (Cat. No. E-4378), EDTA (Cat. No. ED2SS), adenosine 5'-diphosphate (ADP, Cat. No. A-6646), L-malic acid (Cat. No. M-1000), pyruvic acid (Cat. No. P-2256), β-NADH (Cat. No. 340-110), HEPES (Cat. No. H-3375), carbonyl cyanide 4-trifluoromethoxyphenyl-hyddrazone (FCCP, Cat. No. C22920), antimycin A (Cat. No. A 8674), oligomycin (Cat. No. O-4876), Tris (Cat. No. T-1503), crystalline *Bacillus subtilis* protease (Nagarse) from Teikoku Chemical Company, Osaka, Japan, or Sigma P-4789, protease type XXVII (7.6 units/mg solid), phospho(enol)pyruvic acid (PEP, Cat. No. P-0564), pyruvate kinase (Cat. No. P-9136), β-hydroxybutyric acid (Cat. No. H 6501), and lactic dehydrogenase (LDH, Cat. No. L-2375).

From other sources: $MgCl_2 \cdot 6H_2O$ (M-33, Fisher Scientific), KH_2PO_4 (P-285, Fisher Scientific), HCl [UN1789, 36.5% (w/w), Fisher Scientific], K_2HPO_4 (3252-2, T. J. Baker), and KCl (No-3040, T. J. Baker), KOH (UN1813, Fisher Scientific), KCN (Lot 6878KBPH, Mallinckrodt, Inc., KT 40361).

III. PROCEDURES

A. Preparation of Solutions

1. *0.25 M sucrose*: Dissolve 171.15 g of sucrose in 1000 ml distilled water, filter through a layer of glass wool, add distilled water to 2 liters in a volumetric flask, mix well, and store at 4°C.

2. *0.5 M Tris–HCl, pH 7.4*: Dissolve 30.28 g Tris into 400 ml distilled water, adjust pH to 7.4 with 4 *N* HCl, add distilled water to 500 ml in a volumetric flask, mix well, adjust the pH if necessary, and store at 4°C.

3. *0. 5 M* $MgCl_2$: Dissolve 10.17 g of $MgCl_2 \cdot 6H_2O$ in 100 ml distilled water.

4. *0.1 M phosphate buffer, pH 7.4*: To 800 ml distilled water, dissolve 11.83 g of Na_2HPO4 and 2.245 g of KH_2PO4 with the aid of magnetic stirrer. Check the pH and adjust with 0.1 *M* HCl or 0.1 *M* NaOH if necessary. Add distilled water to 1000 ml in a volumetric flask, mix well, and store at 4°C.

5. *0.2 M EDTA, pH 7.4*: Dissolve 3.72 g EDTA in 35 ml of 1 *N* NaOH. Stir until it dissolves completely; adjust pH to 7.4 with 1 *N* HCl. Add distilled water to 50 ml. Divide into 10 × 5.0 ml and store at –20°C.

6. *0.1 M HEPES, pH 7.4*: Dissolve 23.83 g HEPES in 800 ml distilled water. Adjust with 1 *M* NaOH to pH 7.4. Add distilled water to 1000 ml in a volumetric flask. Mix well and store at 4°C.

7. *Sucrose/Tris–Cl (S/T) reaction medium*: 60 ml 0.25 *M* sucrose, 5 ml 0.5 *M* Tris–HCl (pH 7.4), and 35 ml distilled water to a final volume of 100 ml. Make the S/T medium fresh every day.

8. *1.0 M pyruvate, pH 7.4*: Dissolve 5.5 g pyruvic acid in 20 ml of 1 *N* NaOH; adjust with 5 *N* NaOH to pH 7.4. Add distilled water to 50 ml in a volumetric flask. Mix well, transfer into 10 test tubes with each containing 5 ml, and store at –20°C.

9. *0.5 M malate, pH 7.4*: Dissolve 3.35 g of DL-malic acid in 20 ml of 1 *N* NaOH; adjust with 5 *N* NaOH to pH 7.4. Add distilled water to 50 ml in a volumetric flask. Mix well and transfer into 10 test tubes and store at –20°C.

10. *0.1 M ADP, pH 6.8–7.4*: Dissolve 0.48 g ADP in 5 ml distilled water, adjust with 1 *N* NaOH to pH to 6.8–7.4, and add distilled water to 10 ml in a volumetric flask. Mix well, transfer into five test tubes (≈ 2 ml/tube), and store at –20°C. The concentration of ADP will be determined spectrophotometrically with the pyruvate kinase coupled with lactate dehydrogenase system (see later).

11. *0.1 M phosphoenolpyruvate (PEP), pH. 7.4*: Dissolve 20.8 mg PEP into 0.6 ml 1 *N* KOH, adjust pH to 7.4 with 5 *N* KOH, and add distilled water to 1.0 ml. Mix well, transfer into five vials (0.2 ml/vial), and store at –20°C.

12. *1.0 mg/ml oligomycin*: Dissolve 10 mg oligomycin in 10 ml absolute ethanol. Store at –20°C.

13. *FCCP 1 mM*: Dissolve 5.03 mg FCCP into 20 ml absolute ethanol in a glass tube (either dark glass or covered with aluminum foil to protect against light) and store at –20°C.

B. Enzymatic Assay of ADP Concentration (Jaworek et al., 1974)

This assay is based on a pair of coupled reactions. ADP in the presence of an excess amount of (PEP) and pyruvate kinase will be completely converted into ATP and an equal concentration of pyruvate. The pyruvate will then be converted to lactate in the presence of

lactate dehydrogenase and an excess amount of NADH. The NAD^+ formed is equal to the concentration of lactate. The stoichiometry of ADP to NADH bears a 1:1 relationship. The concentration of ADP is therefore equal to that of NADH oxidized. See the following reaction mixture: 2.8 ml S/T medium, 50 µl pyruvate kinase (3 IU), 10 µl lactic dehydrogenase (1 IU), 15 µl NADH (30 m*M*), 20 µl PEP (0.1 *M*), 80 µl $MgCl_2$ (0.25 *M*), and 20 µl KCl (1.0 *M*). The total volume equals 3.0 ml.

Calibrate the spectrophotometer and the settings of the recorder according to the instruction manuals of the instrument and set the wavelength at 340 nm.

1. Place the sample cuvette in the sample chamber with 150 µ*M* NADH (15 µl, 30 m*M*) present; an absorbance in the vicinity of 0.9 is indicated on the instrument and the recorder.
2. Turn on the recorder, let it proceed to a constant reading (a minute or two), add 3 µl of 0.1 *M* ADP, and stir the solution well with a glass or plastic stirrer; the absorbance at 340 nm will decline quickly (when sufficient pyruvate kinase and lactate dehydrogenase are present) followed by a sharp transition to a constant level where there are no more changes in 340 nm absorbance. The decline of 340 nm absorbance reflects the oxidation of NADH. The extent of absorbance change (i.e., $\Delta A = 0.63$) is dependent on the amount of ADP added into the cuvette.
3. The concentration of ADP can therefore be calculated from the absorbance changes at 340 nm. The millimolar absorbance coefficient for NADH is 6.22 $mM^{-1}\,cm^{-1}$. The ADP concentration = [0.63 / 6.22] × [3.0 / 0.003] = 101 m*M*.

C. Calibration of Oxygen Concentration

A simple and rapid method of determining the oxygen content of the reaction medium accurately is by using submitochondrial particles (SMP) with a limiting amount of NADH. The high affinity of SMP for NADH permits a stoichiometric titration of oxygen content. NADH concentration can be determined accurately spectrophotometrically (as shown in the previous section). When limiting concentrations of NADH are added, the change in current, which occurs with complete oxidation of the NADH, can be determined directly. A direct calibration can therefore be obtained. For example, add 0.98 ml of air-saturated S/T medium first followed by 10 µl SMP (0.2 mg protein) to the reaction chamber. Allow the reaction mixture to thermo equilibrate; no air bubbles should be trapped in the reaction vessel. Add 5 µl NADH (150 µ*M*) to the chamber. Immediately initiated oxygen uptake with a linear kinetics, followed by a sharp transition to a straight line (i.e., oxygen uptake ceases) when all the added NADH is oxidized. This assay can also be used to estimate of back diffusion of oxygen into the reaction mixture. For instance, if there is a back diffusion of oxygen, an increase in oxygen concentration in the reaction mixture will be noted on the left deflection (a negative slop) of the recorder tracing.

D. Determination of Rate of Oxygen Consumption and ADP/O Ratio of Intact Mitochondria

Figure 2A shows a recording tracing from a typical experiment utilizing the oxygen electrode apparatus of the type shown in Fig. 1 to determine the respiratory control index (RCI) and P/O ratio of a tightly coupled mitochondrial preparation. Suspend freshly prepared mouse skeletal muscle mitochondria (30–50 µl) in an air-saturated P_i-containing isotonic sucrose medium (0.9 ml); the addition of substrates [5 µl pyruvate (1 *M*) + 5 µl malate (0.5 *M*)] causes a slow rate of oxygen uptake (state 4). Subsequent addition of 3 µl ADP (100 m*M*) increases the rate (state 3) by 11-fold. Upon the expenditure of the added ADP, as indicated by the sharp transition in the polarographic tracing, the rate of oxygen uptake declines to that observed before the addition of ADP. The duration of the increased rate of oxygen uptake is proportional to the amount of ADP added to the reaction mixture. The concentration of oxygen consumed is proportional to the amount of ADP phosphorylated to ATP. These cycles of

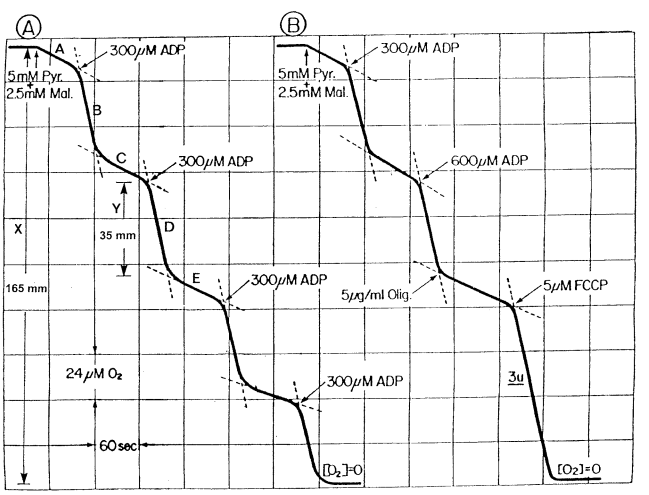

FIGURE 2 Polarographic tracing of mouse skeletal muscle mitochondria oxidizing pyruvate plus malate. The reaction mixture consists of 150 m*M* sucrose, 25 m*M* Tri–HCl, and 10 m*M* phosphate, pH 7.5. Additions are as indicated. Volume, 1.0 ml; temperature, 30°C.

stimulation of respiration by the addition of ADP could be repeated several times in a single experiment until all the oxygen in the reaction mixture is consumed (Fig. 2A). The ADP/O [P/O] ratio and RCI can be calculated directly from the oxygen electrode tracing. The dependence of substrate oxidation on the presence of ADP indicates that electron transfer of the respiratory chain and ATP synthesis are coupled to each other. Unless the energy generated during electron transfer is utilized for ATP synthesis or other energy-requiring processes, the oxidation of respiring substrate is restrained.

The recorder deflection "*X*" (165 mm) represents the total oxygen content of the reaction medium (e.g., 240 μ*M* O_2 at 30°C). Distance "*Y*" is determined by extending the slops of lines A, B, and C and measuring the length of the tracing from the intersects of lines A and B and lines B and C. "*Y*" (34 mm) represents the amount of O_2 utilized by the externally added ADP (300 μ*M*). The ADP/O ratio can therefore be calculated by dividing the amount of ADP by the amount of oxygen utilized. The amount of oxygen utilized can be calculated as follows: Total oxygen content {[240 μ*M*] ÷ "*X*" [165 mm]} × "*Y*" [34 mm] × volume of the reaction mixture [1.0 ml] × 2 = 99 mμatoms oxygen utilized. The amount of ADP was added at the point indicated, e.g., 300 μ*M* ADP or 300 mμmol ADP. The ADP/O ratio is therefore = 300 / 99 = 3.01.

The respiratory control index is defined as the ratio of respiratory rate in the presence of added ADP (state 3) to the rate either before ADP addition or the rate following ADP expenditure (state 4). State 3 and state 4 respiratory rates are 79 and 7 mm/min, respectively. Therefore, the RCI is 79/7 = 11.4. For tightly coupled intact mitochondria as shown in Fig. 2A, the respiratory rates before the addition of ADP and then following the expenditure of ADP are virtually identical. However, if mitochondria are loosely coupled and/or contaminated with ATPase, the respiratory rate following the expenditure of ADP is considerable faster than that with substrate alone before the addition of ADP. The quality of the mitochondrial preparation is readily reflected from the polarographic tracing.

Tightly coupled intact mitochondria exhibit a very low (if any) ATPase activity (basal ATPase) that can be stimulated by Mg^{2+} and/or uncouplers. Figure 2B illustrates the effects of energy transfer inhibitors and uncoupler on the respiratory rates of intact mitochondria. The best-known energy transfer inhibitors are oligomycin and aurovertin, which primarily inhibit the phosphorylation reaction (e.g., synthesis and hydrolysis of ATP). Electron transfer is inhibited secondarily because of the tight link between oxidation and phosphorylation. Uncoupling agents also prevent the synthesis of ATP, but differ from energy transfer inhibitors in that they do not inhibit phosphorylation directly but rather uncouple phosphorylation from respiration by dissipating the energy generated by substrate oxidation as waste. Thus no energy is available for the synthesis of ATP from ADP and P_i, or any other energy utilizing processes. Uncouplers do not inhibit ATP hydrolysis. In the presence of an uncoupler, respiration proceeds at its maximal rate even in the absence of ADP and P_i. The most commonly used uncouplers are dinitrophenol (DNP) and carbonyl cyanide *p*-trifluoromethoxyphenylhydrazone (FCCP).

As shown in Fig. 2B, The ADP-induced state 3 respiratory rate declined to the level comparable to state 4 upon the addition of oligomycin. The oligomycin-induced inhibition was released by the addition of FCCP. The FCCP-induced rate (usually referred to as state 3U) is virtually identical to that at state 3.

IV. COMMENTS, PITFALL, AND RECOMMENDATIONS

1. It is imperative that glass redistilled water be used throughout all the experiments.
2. A closed reaction vessel free of air bubbles and back diffusion of oxygen are essential for the success of polarographic assay of mitochondrial function.
3. It is imperative that the excessive part of the polyethylene membrane, which covers the electrode after secured by a rubber O ring, be removed with a sharp blade, as the presence of excessive polyethylene membrane may trap materials and make cleaning difficult.
4. All aqueous solutions of medium and reagent should be at neutral pH (i.e., 7.2–7.4). During the assays the temperature of the reaction mixture has to be maintained constant.
5. When water-insoluble reagents are used, at the completion of the experiment, the reaction chamber needs to be cleaned thoroughly first with ethanol followed by distilled water. Contamination of either reagent and/or ethanol of the chamber will result in obscure data, which cannot be interpreted.
6. Tarnish of the Ag/AgCl electrode can be removed by cleaning with a cotton-tipped swab dipped in 4*N* NH_4OH aqueous solution followed by rinsing thoroughly with distilled water.
7. The polarographic oxygen electrode technique is a convenient method for the determination of P/O ratio and RCI. However, its suitability is dependent on the quality of the mitochondrial preparations. Meaningful results can only be derived from tightly coupled

mitochondrial preparations that are free from contamination by other cellular constituents. Consideration of the tissue constituents, i.e., lipid content, and properties will aid in the design of isolation and purification procedures. For instance, as compared to liver and heart, only a small portion of the total mass of skeletal muscle consists of mitochondria, with the bulk of the tissue being myofibrils. Additionally, skeletal muscle contains a relatively high content of Ca^{2+}, which is capable of damaging mitochondria during the isolation process. Because of the high content of myofibril, the separation of mitochondria from other components is very difficult in nonelectrolyte medium (e.g., the isotonic sucrose used to isolate mitochondria from liver and heart). A similar difficulty results when attempts are made to isolate mitochondria from brain. Because of its high lipid content and high rate of aerobic metabolism, improper isolation may result in data fraught with artifact. In recent years, the polarographic technique has been widely used to evaluate the lesions of mitochondrial functions of skeletal muscle derived from patients suffering from mitochondrial myopathy. A reproducible technique that isolates tightly coupled, intact mitochondria is essential before statements regarding etiology can be made. Impairments in mitochondrial function may actually result from an artifact generated during the isolation procedure rather than a genuine impairment of mitochondrial function caused by the disease.

After many years of experience in our laboratory we have designed a simple method for the isolation and purification of intact skeletal muscle mitochondria (Lee *et al*., 1993a). This method allows preparation of isolated, intact mitochondria from a small amount (1–3 g, wet weight) of muscle biopsy specimens. Additionally, we have designed a simple and fast procedure to isolate intact brain mitochondria from one hemisphere of rat brain (approximately 0.6 g wet weight) (Lee *et al*., 1993b; Xiong *et al*., 1997a) with excellent yield and stability. This technique has been applied successfully on studies of the impairment of mitochondrial functions induced by head trauma (Xiong *et al*., 1997a,b, 1998, 1999) and ischemia (Sciamanna *et al*., 1992; Sciamanna and Lee, 1993).

References

Chance, B., and Williams, G. R. (1955). Respiratory enzymes in oxidative phosphorylation I: Kinetics of oxygen utilization. *J. Biol. Chem*. **217**, 383–393.

Davies, P. W., and Brink, F. J. (1942). Microelectrodes for measuring local oxygen tension in animal tissues. *Rev. Sci. Instr*. **13**, 524–533.

Jaworek, D., Gruber, W., and Bergmeyer, H. U. (1974). Adenosine-5′-diphosphate and adenosine-5′-monophosphate. *In "Methods of Enzymatic Analysis,"* 2nd ed., Vol. 4, pp. 2027–2029.

Lardy, H. A., and Wellman, H. (1952). Oxidative phosphorylations: Role of inorganic phosphate and acceptor systems in control of metabolic rates. *J. Biol. Chem*. **195**, 215–224.

Lee, C. P. (ed.) (1994). Molecular basis of mitochondrial pathology. *Curr. Top. Bioenerg*. **17**, 254.

Lee, C. P., Martens, M. E., and Tsang, S. H. (1993a). Small scale preparation of skeletal muscle mitochondria and its application in the study of human disease. *Methods Toxicol*. **2**, 70–83.

Lee, C. P., Sciamanna, M. A., and Peterson, P. L. (1993b). Intact brain mitochondria from a single animal: Preparation and properties. *Methods Toxicol*. **2**, 41–50.

Sciamanna, M. A., and Lee, C. P. (1993). Ischemia/reperfusion-induced injury of forebrain mitochondria and prevention by ascorbate. *Arch. Biochem. Biophys*. **305**, 215–224.

Sciamanna, M. A., Zinkel, J., Fabi, A. Y., and Lee, C. P. (1992). Ischemia injury to rat forebrain mitochondria and cellular calcium homeostasis. *Biochim. Biophys. Acta* **1134**, 223–232.

Xiong, Y., Gu, Q., Peterson, P. L., Muizelaar J. P., and Lee C. P. (1997a). Mitochondrial dysfunction and calcium perturbation induced by traumatic brain injury. *J. Neurotrauma* **14**, 23–34.

Xiong, Y., Peterson, P. L., and Lee, C. P. (1999). Effect of N-acetylcysteine on mitochondrial function following traumatic brain injury in rats. *J. Neurotrauma* **16**, 1067–1082.

Xiong, Y., Peterson, P. L., Muzelaar, J. P., and Lee, C. P. (1997b). Amelioration of mitochondrial dysfunction by a novel antioxidant U-101033E following traumatic brain injury. *J. Neurotrauma* **14**, 907–917.

Xiong, Y., Peterson, P. L., Verweij, B. H., Vinas, F. C., Muzelaar, J. P., and Lee, C. P. (1998). Mitochondrial dysfunction after experimental traumatic brain injury: Combined efficacy of SNX-111 and U-101033E. *J. Neurotrauma* **15**, 531–544.

SECTION

7

Nuclear Transport

CHAPTER

36

Analysis of Nuclear Protein Import and Export in Digitonin-Permeabilized Cells

Ralph H. Kehlenbach and Bryce M. Paschal

I. INTRODUCTION

Transport between the nucleus and the cytoplasm is mediated by nuclear pore complexes (NPCs), specialized channels that are embedded in the nuclear envelope membrane. Proteins that undergo nuclear import or nuclear export usually encode a nuclear localization signal (NLS) or a nuclear export signal (NES). These signals are recognized by import or export receptors that, in turn, facilitate targeting of the protein to the NPC and translocation through the central channel of the NPC. Both import and export pathways are regulated by the Ras-related GTPase Ran. Nuclear Ran in its GTP-bound form promotes the release of NLS-proteins from import receptors after the NLS-protein/import receptor has reached the nuclear side of the NPC. In contrast, nuclear Ran in its GTP-bound form promotes the assembly of NES-containing proteins with export receptors by forming an NES-protein/export receptor/RanGTP. Export complexes are then disassembled on the cytoplasmic side of the NPC through the action of a Ran GTPase-activating protein that stimulates GTP hydrolysis by Ran. More specific information regarding import and export complex assembly, models for translocation, and additional aspects of nuclear transport regulation are described elsewhere (Steggerda and Paschal, 2002; Weis, 2003 and references therein).

Digitonin-permeabilized cells have become one of the most widely used experimental systems for studying nuclear transport (Adam *et al*., 1990). They have been used to analyze nuclear import and export signals (Pollard *et al*., 1996), to purify nuclear transport factors from cell extracts (Görlich, 1994; Paschal and Gerace, 1995; Kehlenbach *et al*., 1998), and to measure nuclear transport kinetics (Görlich and Ribbeck, 2003). In all of these applications, the principle is that treating mammalian cells with a defined concentration of digitonin results in selective perforation of the plasma membrane, leaving the nuclear membrane intact. Thus, soluble transport factors are released from the cytoplasmic compartment and low molecular weight transport factors such as Ran (24 kDa) and NTF2 (28 kDa) are released from the nuclear compartment by diffusion through the NPC. Nuclear import and export can subsequently be reconstituted in digitonin-permeabilized cells by the addition of transport factors, an energy-regenerating system, and inclusion of a fluorescent NLS or NES reporter protein to monitor transport (Adam *et al*., 1990). Transport factors can be supplied as unfractionated cytosol from HeLa cells or as commercially available rabbit reticulocyte lysate. The level of import is then measured by following the accumulation of an NLS reporter in the nucleus or, in the case of export, by the loss of an NES reporter from the nucleus.

This article describes assays for both nuclear import and export (Fig. 1). The nuclear import assay can be performed with various cell lines and analyzed by fluorescence microscopy. The nuclear export assay is described for HeLa cells expressing a GFP-tagged reporter protein, the nuclear factor of activated T cells (GFP-NFAT). NFAT is a transcription factor that contains defined nuclear localization and nuclear export signals and that shuttles between the cytoplasm and the nucleus in a phosphorylation-dependent manner (for review, see Crabtree and Olsen, 2002). We take advantage of the tight regulation of nucleocytoplasmic transport of GFP-NFAT to induce nuclear import in intact cells, followed by export under controlled conditions from nuclei of permeabilized cells (Kehlenbach

Copyright 2006, Elsevier Science (USA).
All rights reserved.

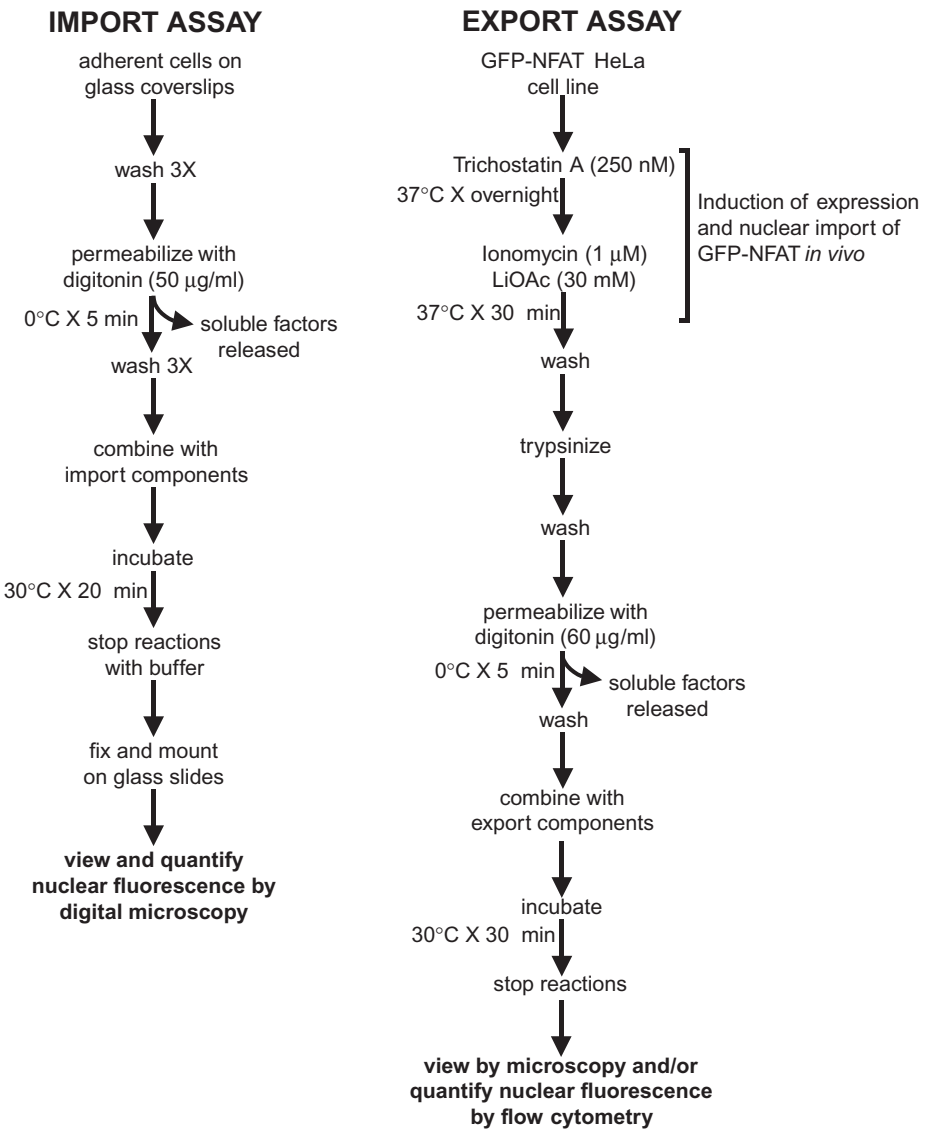

FIGURE 1 Overview of assays for measuring nuclear import and export in digitonin-permeabilized cells. See text for details.

et al., 1998). The efficiency of nuclear export can be analyzed either qualitatively by fluorescence microscopy (see Fig. 3) or quantitatively by flow cytometry (see Fig. 4). In the latter case, nuclear import of a fluorescently labeled reporter protein can be analyzed in parallel.

II. MATERIALS AND INSTRUMENTATION

Rabbit recticulocyte lysate (L4151) is from Promega. HeLa S3 cells (CCL-2.2) and NIH 3T3 cells are from the American Type Culture Collection. Joklik's modified minimum essential medium for suspension cell culture (JMEM; Cat. No. M0518) is from Sigma. Newborn calf serum (Cat. No. 16010-159), penicillin–streptomycin (Cat. No. 15140-122), and trypsin EDTA (Cat. No. 25200-056) are from GIBCO/Invitrogen. ATP (Cat. No. A-2383), creatine phosphate (Cat. No. P-7936), creatine phosphokinase (Cat. No. C-7886), sodium bicarbonate (Cat. No. S-4019), HEPES (Cat. No. H-7523), potassium acetate (Cat. No. P-5708), magnesium acetate (Cat. No. M-2545), EGTA (Cat. No. E-4378), dithiothreitol (DTT, Cat. No. D-5545), NaCl (Cat. No. S-9763), potassium phosphate, monobasic (Cat. No. P-0662), phenyl-

methylsulfonyl fluoride (PMSF, Cat. No. P-7626), dimethyl sulfoxide (DMSO, Cat. No. D-8779), sodium carbonate (Cat. No. S-7795), trypan blue (Cat. No. T-8154), ionomycin (Cat. No. I-0634), LiOAc (Cat. No. L-4158), Hoechst 33258 (Cat. No. B-2883), 4',6-diamidino-2-phenyindole, dilactate (DAPI; Cat. No. 9564), and trichostatin A (Cat. No. T-8552) are from Sigma. High-purity bovine serum albumin (BSA, Cat. No. 238031), aprotinin (Cat. No. 236624), leupeptin (Cat. No. 1017101), and pepstatin (Cat. No. 253286) are from Roche. The FITC isomer I (Cat. No. F-1906) and sulfo-SMCC (Cat. No. 22322) are from Molecular Probes and Pierce, respectively. PD-10 columns (Cat. No. 17-0851-01), Cy2 (Cat. No. PA-22000), and Cy5 (Cat. No. PA-25001) are from Amersham Pharmacia Biosciences. Centricon filters (30-kDa cutoff, Cat. No. 4208) are from Amicon. High-purity digitonin (Cat. No. 300410) is from Calbiochem. Vectashield mounting medium (Cat. No. H-1000) is from Vector Laboratories. Six-well dishes (Cat. No. 3516) are from Corning. Glass coverslips (#1 thickness; Cat. No. 12-548A) and the polystyrene tubes used for the transport assays (Cat. No. 2058) are from Fisher. The microscope used for measuring nuclear import in adherent cells is a Nikon E800 equipped with a charge-coupled device camera. The system is linked to a MacIntosh computer running OpenLab software for image acquisition. An Olympus IX70 inverted fluorescence microscope is used for analysis of nuclear export. Images from import and export assays are processed using Adobe Photoshop. The flow cytometric analysis system is the FACScan unit from Beckton-Dickinson.

The following equipment required for growing and harvesting HeLa cells is from Bellco Glass. The 250-ml spinner flask (Cat. No. 1965-00250) and stir plate (Cat. No. 7760-0600) are used for the continuous culture of HeLa cells. Additional spinner flasks are required to scale up the preparation to 15 liters. These include 100 ml (Cat. No. 1965-01000), 3000 ml (Cat. No. 1965-03000), and 15 liter (Cat. No. 7764-00110), cap assembly (Cat. No. 7764-10100), and Teflon paddle assembly (Cat. No. 1964-30015).

Equipment for centrifugation includes the JS5.2 swinging bucket rotor and J6B centrifuge, the JA-20 fixed angle rotor and J2 centrifuge, and the type 60Ti fixed angle rotor and L7 centrifuge, all from Beckman. Cytosol dialysis is carried out using the collodion vacuum dialysis apparatus (Cat. No. 253310), and 10,000-Da cutoff membranes (Cat. No. 27110) are from Schleicher and Schuell. The homogenizer used for cell disruption is a 0.02-mm-clearance stainless-steel unit (Cat. No. 885310-0015) from Kontes.

III. PROCEDURES

A. Preparation of Cytosol

The rabbit reticulocyte lysate contains all the soluble factors necessary to reconstitute import and export in digitonin-permeabilized cells (Adam *et al*., 1990). The only preparation involved is dialysis against 1× transport buffer containing 2 m*M* DTT and 1 µg/ml each of aprotinin, leupeptin, and pepstatin (two buffer changes). Reticulocyte lysate is used at 50% (by volume) of transport reactions. This results in a relatively high total protein concentration (~25–40 mg/ml) in transport assays because the reticulocyte lysate contains a high concentration of hemoglobin. A more economical approach, especially if larger quantities of cytosol are needed for protein purification, is to prepare cytosol from suspension culture HeLa cells. In this case, only 1–2 mg/ml (final assay concentration) of HeLa cell cytosol is required to obtain a maximum level of protein import or protein export in digitonin-permeabilized cells.

Solutions

1. *10× transport buffer*: 200 m*M* HEPES, pH 7.4, 1.1 *M* potassium acetate, 20 m*M* magnesium acetate, and 5 m*M* EGTA. To make 1 liter, dissolve 47.6 g HEPES, 107.9 g potassium acetate, 4.3 g magnesium acetate, and 1.9 g EGTA in 800 ml distilled water. Adjust the pH to 7.4 with 10 *N* NaOH and bring the final volume to 1 liter. Sterile filter and store at 4°C.
2. *1× transport buffer*: 20 m*M* HEPES, pH 7.4, 110 *M* potassium acetate, 2 m*M* magnesium acetate, and 0.5 m*M* EGTA. To make 1 liter, add 100 ml of 10× transport buffer to 900 ml distilled water.
3. *1 M HEPES stock, pH 7.4*: To make 500 ml, dissolve 119.1 g HEPES (free acid) in 400 ml distilled water. Adjust the pH to 7.4 with 10 *N* NaOH and bring the final volume to 500 ml. Sterile filter and store at 4°C.
4. *1 M potassium acetate stock*: To make 500 ml, dissolve 49 g potassium acetate in 400 ml distilled water. Bring the final volume to 500 ml, sterile filter, and store at 4°C.
5. *1 M magnesium acetate stock:* To make 500 ml, dissolve 107.2 g magnesium acetate (tetrahydrate) in 400 ml distilled water. Bring the final volume to 500 ml, sterile filter, and store at 4°C.
6. *0.2 M EGTA stock*: To make 500 ml, dissolve 38 g EGTA (free acid) in 400 ml distilled water. Adjust the pH to ~7.0 with 10 *N* NaOH and bring the final volume to 500 ml. Store at 4°C.
7. *Cell lysis buffer*: 5 m*M* HEPES, pH 7.4, 10 m*M* potassium acetate, 2 m*M* magnesium acetate, and

1 m*M* EGTA. To make 500 ml, combine 2.5 ml 1 *M* HEPES, pH 7.4, 5 ml 1 *M* potassium acetate, 1 ml 1 *M* magnesium acetate, 2.5 ml 0.2 *M* EGTA, and 489 ml distilled water. Store at 4°C.

8. *Phosphate-buffered saline (PBS)*: To make 1 liter, dissolve 8 g sodium chloride, 0.2 g potassium chloride, 1.44 g sodium phosphate (dibasic), and 0.24 g potassium phosphate (monobasic) in 900 ml distilled water. Adjust the pH to 7.4 and bring the final volume to 1 liter. Store at 4°C.

Steps

1. Grow HeLa cells at a density of 2–7 × 10^5 cells per milliliter in a spinner flask (30–50 rpm) in a 37°C incubator (CO_2 is not required). The medium is JMEM containing 2.0 g sodium bicarbonate and 2.38 g HEPES per liter. Adjust the pH to 7.3, sterile filter, and store at 4°C. Before use, supplement the medium with 10% newborn calf serum and 1% penicillin–streptomycin. The cells should have a doubling time of approximately 18 h, making it necessary to dilute the culture with fresh, prewarmed medium every 1–2 days.

2. HeLa cells from a 250-ml culture provide the starting point for scaling up the preparation to 15 liters. This is carried out by sequential dilution of the culture into larger spinner flasks. The culture should not be diluted to a density below 2 × 10^5 cells/ml. The spinner flasks used for scaling up preparation are 250 ml (1 each), 1 liter (1 each), 3 liters (2 each), and 15 liters (1 each). This process generally takes 5 days.

3. Perform the cell harvest and subsequent steps at 0–4°C. Collect the cells by centrifugation (300 *g* for 15 min) in 780-ml conical glass bottles in a Beckman J6B refrigerated centrifuge equipped with a JS5.2 swinging bucket rotor. The cell harvest takes about 1 h.

4. Wash the cells by sequential resuspension and centrifugation. Two washes are carried out in ice-cold PBS (1 liter each) and one wash is carried out in 1× transport buffer containing 2 m*M* DTT. The yield from a 15-liter culture should be approximately 40 ml of packed cells.

5. Resuspend the cell pellet using 1.5 volume of lysis buffer, supplemented with 3 µg/ml each aprotinin, leupeptin, pepstatin, 0.5 m*M* PMSF, and 5 m*M* DTT. Allow the cells to swell on ice for 10 min.

6. Disrupt the cells by two to three passes in a stainless-steel homogenizer. Monitor the progress of homogenization by trypan blue staining and phase-contrast microscopy. The goal is to obtain ~95% cell disruption. Excessive homogenization should be avoided because it results in nuclear fragmentation and the release of nuclear contents into the soluble fraction of the preparation.

7. Dilute the homogenate with 0.1 volume of 10× transport buffer and centrifuge in a fixed angle rotor such as the Beckman JA-20 (40,000 *g* for 30 min).

8. Filter the resulting low-speed supernatant fraction through four layers of cheesecloth. Subject the filtered low-speed supernatant to ultracentrifugation using a fixed angle rotor such as the Beckman type 60 Ti (150,000 *g* for 60 min).

9. Dispense the resulting high-speed supernatant fraction (~50 ml, protein concentration ~5 mg/ml) into 1- and 4-ml aliquots, flash freeze in liquid N_2, and store at –80°C indefinitely.

10. HeLa cell cytosol is generally subjected to a rapid dialysis step before use in transport reactions. Thaw a 4-ml aliquot of cytosol at 0–4°C and dialyze for 3 h in 1× transport buffer containing 2 m*M* DTT and 1 µg/ml each of aprotinin, leupeptin, and pepstatin (two buffer changes). We use a vacuum apparatus and a collodion membrane to achieve a twofold concentration of the sample (10 mg/ml). Dispense the dialyzed, concentrated cytosol into 100-µl aliquots, flash freeze in liquid N_2, and store at –80°C.

B. Preparation of FITC-BSA-NLS Import Substrate

Synthetic peptides containing an NLS can be used to direct the nuclear import of a variety of fluorescent reporter proteins. FITC- or Cy2-BSA-NLS and Cy5-BSA-NLS are all suitable for measuring import in the fluorescence microscope or in the flow cytometer. Because excitation and emission spectra of Cy5 are distinct from GFP, Cy5-BSA-NLS is ideal for measuring import and GFP-NFAT export in the same cells. Importantly, the average size of the protein conjugate (>70 kDa) is too large to allow diffusion through the NPC and it displays low nonspecific binding to the permeabilized cell. Preparation of fluorescent import ligands is carried out in three steps: fluorescent labeling of BSA, modification of the fluorescent BSA with the heterobifunctional cross-linker sulfo-SMCC, and attachment of NLS peptides. Sulfo-SMCC provides a covalent linkage between primary amines on BSA and cysteine present on the N terminus of the NLS peptide.

Solutions

1. *PBS*: To make 1 liter, dissolve 8 g sodium chloride, 0.2 g potassium chloride, 1.44 g sodium phosphate (dibasic), and 0.24 g potassium phosphate (monobasic) in 900 ml distilled water. Adjust the pH to 7.4 and bring the final volume to 1 liter. Store at 4°C.

2. *0.1 M* sodium carbonate: To prepare 250 ml, dissolve 3.1 g sodium carbonate in 200 ml distilled water, adjust the pH to 9.0, and bring the final volume to 250 ml. Store at 4°C.

3. *1.5 M* hydroxylamine: To prepare 100 ml, dissolve 10.4 g in a total volume of 100 ml distilled water. Store at room temperature.

4. *10 mg/ml FITC*: Add 1 ml DMSO to 10 mg FITC in an amber vial and vortex to dissolve.

5. *20 mM sulfo-SMCC*: Prepare a 20 m*M* stock of sulfo-SMCC in the following manner. Preweigh a microfuge tube on a fine balance and use a small spatula to add approximately 1–2 mg of sulfo-SMCC to the microfuge tube. Reweigh the tube containing the sulfo-SMCC and add DMSO for a final concentration of 8.7 mg/ml.

Steps

1. Dissolve 10 mg high-purity BSA in 1 ml sodium carbonate buffer, pH 9.0.
2. Stir the BSA solution in a glass test tube with a microstir bar and add 0.1 ml of 10 mg/ml FITC. Cover with foil and stir for 60 min at room temperature.
3. Stop the reaction by adding 0.1 ml 1.5 *M* hydroxylamine.
4. Separate FITC-labeled BSA from unincorporated FITC by desalting on a PD-10 column equilibrated in PBS, collecting 0.5-ml fractions. The bright yellow FITC-BSA will elute in the void volume of this column.
5. Pool the four or five most concentrated fractions, dispense into 1-mg aliquots, and freeze in foil-wrapped microfuge tubes at –20°C.
6. Combine 1 mg of FITC-BSA with 50 µl of freshly prepared 20 m*M* sulfo-SMCC and mix end over end for 45 min at room temperature.
7. Separate the sulfo-SMCC-activated FITC–BSA from unincorporated sulfo-SMCC by desalting on a PD-10 column equilibrated in PBS. After loading the sample, fill the buffer reservoir of the column with PBS and collect 0.5-ml fractions. The bright yellow FITC–BSA will elute in the void volume as before.
8. Pool the three most concentrated fractions of sulfo-SMCC-activated FITC–BSA and combine with 0.3 mg of NLS peptide (CGGGPKKKRKVED). Mix end over end in a foil-wrapped microfuge tube overnight at 4°C.
9. Remove unincorporated NLS peptide by subjecting the sample to four cycles of centrifugation and resuspension in 1× transport buffer using a 2-ml 30-kDa cutoff Centricon filter. Follow the manufacturer's recommendations for centrifugation conditions.
10. Adjust the FITC–BSA–NLS conjugate to a final concentration of 2 mg/ml, dispense into 50-µl aliquots, flash freeze in liquid N_2, and store at –80°C.

C. Preparation of Cy2- or Cy5-BSA-NLS Import Substrate

The preparation of Cy2- and Cy5-labeled import substrate is very similar to the method described earlier for the FITC-labeled substrate.

Steps

1. Dissolve 2.5 mg BSA in 1 ml 0.1 *M* sodium carbonate. Use one vial-activated Cy2 or Cy5 for coupling. Incubate for 40 min at room temperature.
2. Separate the CyDye-BSA conjugate from the free dye by chromatography on a PD-10 column equilibrated with PBS.
3. To activate CyDye-BSA, add sulfo-SMCC to a final concentration of 2 m*M*. Incubate for 30 min at room temperature. Remove free cross-linker using a PD-10 column as described earlier.
4. Dissolve 1 mg of NLS-peptide (CGGGP-KKKRKVED) with activated CyDye-BSA and incubate the solution overnight at 4°C. Remove free peptide and adjust protein concentration as described previously.
5. Freeze aliquots in liquid nitrogen and store at –80°C. After thawing, the import substrate can be kept at 4°C in the dark for a few weeks.

D. Nuclear Protein Import Assay

Solutions

1. *10× and 1× transport buffer*: See Section III,A.
2. *Complete transport buffer*: 1× transport buffer containing 1 µg/ml each aprotinin, leupeptin, pepstatin, and 2 m*M* DTT.
3. *10% digitonin*: To make 2 ml, add 0.2 g high-purity digitonin to 1.7 ml DMSO and dissolve by vigorous vortexing, Dispense into 20-µl aliquots and freeze at –20°C.
4. *100 mM MgATP*: To make 5 ml, add 0.5 ml 1 *M* magnesium acetate and 0.1 ml 1 *M* HEPES, pH 7.4, to 4 ml distilled water. Add 275.1 mg ATP, dissolve by vortexing, and bring the final volume to 5 ml. Dispense into 20-µl aliquots and freeze at –80°C.
5. *250 mM creatine phosphate*: To make 5 ml, add 0.32 g creatine phosphate to 4 ml distilled water, dissolve by vortexing, and bring the final volume to 5 ml. Dispense into 20-µl aliquots and freeze at –20°C.

6. *2000 U/ml creatine phosphokinase*: To make 5 ml, dissolve 10,000 U creatine phosphokinase in 20 m*M* HEPES, pH 7.4, containing 50% glycerol. Dispense into 1-ml aliquots and store at –20°C.

Steps

1. Plate NIH 3T3 cells onto glass coverslips in six-well dishes at a density of ~5×10^4 cells/well and grow overnight.
2. Place the six-well dishes on ice. Aspirate media and gently replace with 2 ml ice-cold, complete transport buffer. Aspirate the transport buffer and replace with fresh transport buffer twice, taking care not to disturb the cells. Complete transport buffer in this and subsequent steps refers to ice-cold, 1× transport buffer supplemented with DTT and protease inhibitors.
3. To permeabilize the cells, aspirate the transport buffer from each well and immediately add 0.05% digitonin diluted into complete transport buffer. Incubate for 5 min on ice.
4. Stop the permeabilization reaction by aspirating the digitonin solution and replacing with complete transport buffer. Wash the cells twice by alternate steps of aspiration and buffer addition.
5. Assemble the import reactions in 0.6-ml microfuge tubes on ice. Each reaction contains (final concentration given) unlabeled BSA (5 mg/ml), FITC-BSA-NLS (25 µg/ml), MgATP (1 m*M*), MgGTP (1 m*M*), creatine phosphate (5 m*M*), creatine phosphpkinase (20 U/ml), rabbit reticulocyte lysate (25 µl), and complete transport buffer in a total volume of 50 µl.
6. Create an incubation chamber by lining a flat-bottomed, air-tight box with parafilm and include a moistened paper towel in the chamber as a source of humidity. Place the chamber on ice.
7. Using fine forceps, remove each coverslip, wick excess buffer using filter paper, and place cells side up on the parafilm. Pipette the import reaction onto the coverslip surface without introducing bubbles.
8. Float the incubation chamber on a 30°C water bath for 20 min.
9. Using fine forceps, remove each coverslip, wick most of the import reaction using filter paper, and immediately place back into the wells of the six-well dish.
10. Wash the coverslips twice by alternate steps of aspiration and complete transport buffer addition.
11. Fix the coverslips by aspirating the complete transport buffer, adding formaldehyde (3.7%) diluted into PBS, and incubating for 15 min at room temperature.
12. Remove each coverslip, submerge in distilled water briefly, wick excess water, and mount on glass slides using Vectashield. Seal the edges with clear nail polish.
13. View the cells by fluorescence microscopy, and quantify the nuclear fluorescence in 50–100 cells per condition using image analysis software such as OpenLab.

E. Nuclear Protein Export Assay

Solutions and Reagents

1. The HeLa cell line stably expressing GFP-NFAT, which is used for the export assay, has been described in detail (Kehlenbach *et al*., 1998) and is available upon request.
2. *1 mM trichostatin A*: Dissolve 1 mg trichostatin A in 3.3 ml ethanol. Store in aliquots at –20°C. Trichostatin A is an inhibitor of histone deacetylases and promotes the expression of GFP-NFAT.
3. *1 mM ionomycin*: Dissolve 1 mg ionomycin in 1.34 ml DMSO. Store in aliquots at –20°C. Nuclear accumulation of the reporter protein is induced by the calcium ionophore ionomycin.
4. *Double-stranded oligonucleotides*: Dissolve oligonucleotides (5'AGAGGAAAATTTGTTTCATA and 5'TATGAAACAAATTTTCCTCT), each at 200 µ*M*, in 40 m*M* Tris, pH 7.4, 20 m*M* $MgCl_2$, and 50 m*M* NaCl. Anneal by heating to 65°C for 5 min and slow cooling to room temperature. Freeze in aliquots and store at –20°C. The oligonucleotide sequence corresponds to a DNA-binding site of NFAT. It stimulates export of GFP-NFAT about twofold, probably by releasing the protein from chromatin.
5. *1× transport buffer with LiOAc*: 20 m*M* HEPES, pH 7.4, 80 m*M* potassium acetate, 2 m*M* magnesium acetate, and 0.5 m*M* EGTA. To make 1 liter, dissolve 4.76 g HEPES, 7.85 g potassium acetate, 3.06 g lithium acetate dihydrate, 0.43 g magnesium acetate tetrahydrate, and 0.19 g EGTA in 800 ml distilled water. Adjust the pH to 7.4 with 1 *N* KOH and bring the final volume to 1 liter. Before use, add 1 µg/ml each of aprotinin, leupeptin, pepstatin, and 2 m*M* DTT.
6. *Complete transport buffer*: See Section III,D.

Steps

1. To stimulate expression of GFP-NFAT, add 250 n*M* trichostatin A to stably transfected HeLa cells and incubate overnight. One 15-cm dish containing ~10^6 cells is sufficient for 30 reactions.
2. Induce nuclear import of GFP-NFAT by adding 1 µ*M* ionomycin and 30 m*M* LiOAc directly to the culture media and return the cells to the 37°C incubator for 30 min. Lithium inhibits one of the kinases

involved in nuclear phosphorylation of NFAT, a step that is required for efficient export *in vivo*.

3. Rinse cells with PBS and remove from dish by adding trypsin EDTA containing 1 μ*M* ionomycin and 30 m*M* LiOAc. Transfer the cells to 50 ml of cold transport buffer with 5% newborn calf serum. Centrifuge for 5 min at 300 *g* at 4°C and wash once in 50 ml transport buffer.

4. Resuspend cells in complete transport buffer at 10^7/ml. Add digitonin to 100 μg/ml (1 μl of a 10% stock per 10^7 cells). Leave on ice for 3 min and check permeabilization with trypan blue. Dilute the cells to 50 ml with transport buffer to release soluble transport factors and collect by centrifugation as described previously.

5. Preincubation (optional): Resuspend cells in transport buffer containing 30 m*M* LiOAc at 10^7/ml and add MgATP (1 m*M*), creatine phosphate (5 m*M*) and creatine phosphokinase (20 U/ml). Incubate for 15 min in a 30°C water bath. Wash cells with transport buffer. This step results in the depletion of additional transport factors such as CRM1, rendering them rate limiting in the subsequent reaction. The reporter protein largely remains in the nucleus under these conditions.

6. Resuspend cells in transport buffer at 3×10^7/ml. Assemble 40-μl transport reactions in FACS tubes: 300,000 permeabilized cells (10 μl), ATP-regenerating system (1 m*M* MgATP, 5 m*M* creatine phosphate, 20 U/ml creatine phosphokinase), Cy5-BSA-NLS (25–50 μg/ml), 1 μ*M* annealed oligonucleotide, and HeLa cytosol (2 mg/ml).

7. Incubate tubes in a 30°C water bath for 30 min. Control reactions contain the same components but are kept on ice, as nuclear import and export are temperature dependent.

8. Stop the reaction by adding 4 ml of cold transport buffer. Centrifuge for 5 min at 400 *g* and 4°C. Remove most of supernatant by aspiration and resuspend cells in residual buffer. Proceed to step 9 or fix cells for microscopic analysis by the addition of 2 ml of formaldehyde (3.7% in PBS). Incubate cells for 15 min at room temperature, add 1 μl Hoechst 33258 (10 mg/ml in H_2O), and incubate for 5 more minutes. Collect cells by centrifugation (300 *g* for 5 min), wash twice with 1 ml PBS, and resuspend the final cell pellet in 15 μl PBS. Apply the cell suspension to a glass slide, cover with a coverslip, and seal with nail polish.

9. Measure the fluorescence of 10,000 cells by flow cytometry. In Becton-Dickinson instruments, GFP-NFAT (or BSA-NLS, labeled with FITC or Cy2, if only import is analyzed) is detected in FL1 and Cy5-BSA-NLS in FL4.

10. Normalize the mean fluorescence values with respect to a reaction kept on ice.

IV. COMMENTS

Several of the basic controls for assaying nuclear import in digitonin-permeabilized cells are shown (Fig. 2). Nuclear import in digitonin-permeabilized

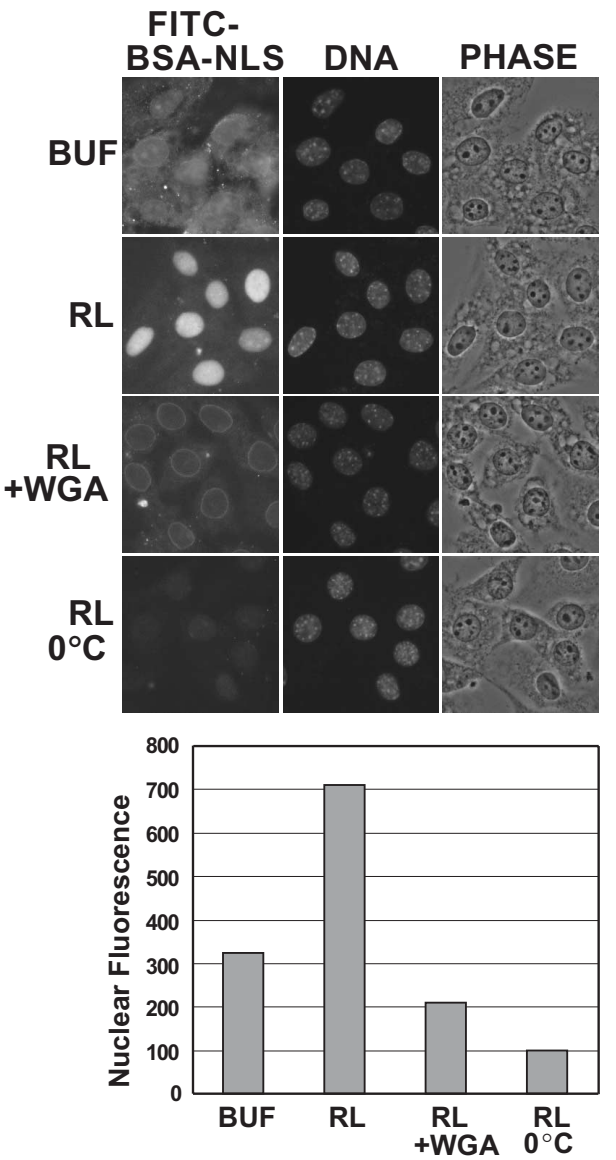

FIGURE 2 Nuclear import of FITC-BSA-NLS analyzed by fluorescence microscopy. (Top) NIH 3T3 cells were digitonin permeabilized and incubated with the indicated components (BUF, buffer; RL, reticulocyte lysate; WGA, wheat germ agglutinin). DAPI staining of DNA and phase-contrast (PHASE) images are also shown. Note that FITC-BSA-NLS binds nonspecifically to cells in the absence of cytosol. The rim fluorescence in the presence of WGA reflects the arrest of FITC-BSA-NLS in import complexes at the NPC. (Bottom) The level of nuclear import observed under each condition was quantified from 12-bit images. Values reflect the average fluorescence intensity per pixel from at least 100 nuclei per condition. Data courtesy of Leonard Shank (University of Virginia).

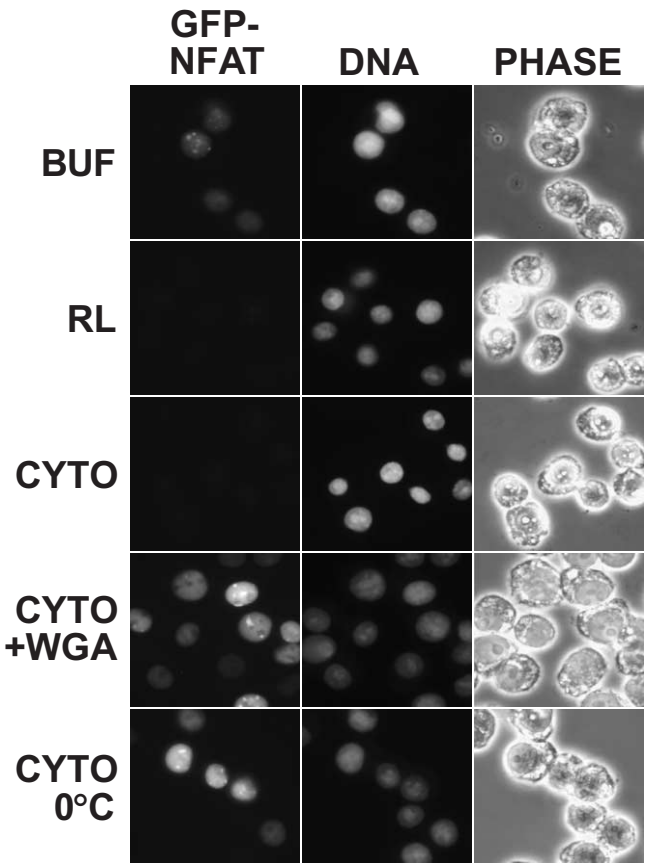

FIGURE 3 Nuclear export of GFP-NFAT was analyzed by fluorescence microscopy. GFP-NFAT cells were treated with trichostatin A and ionomycin to induce expression and nuclear import of GFP-NFAT. After digitonin permeabilization, the cells were incubated with the indicated components (BUF, buffer; RL, reticulocyte lysate; CYTO, HeLa cytosol; WGA, wheat germ agglutinin). Hoechst staining of DNA and phase-contrast (PHASE) images are also shown.

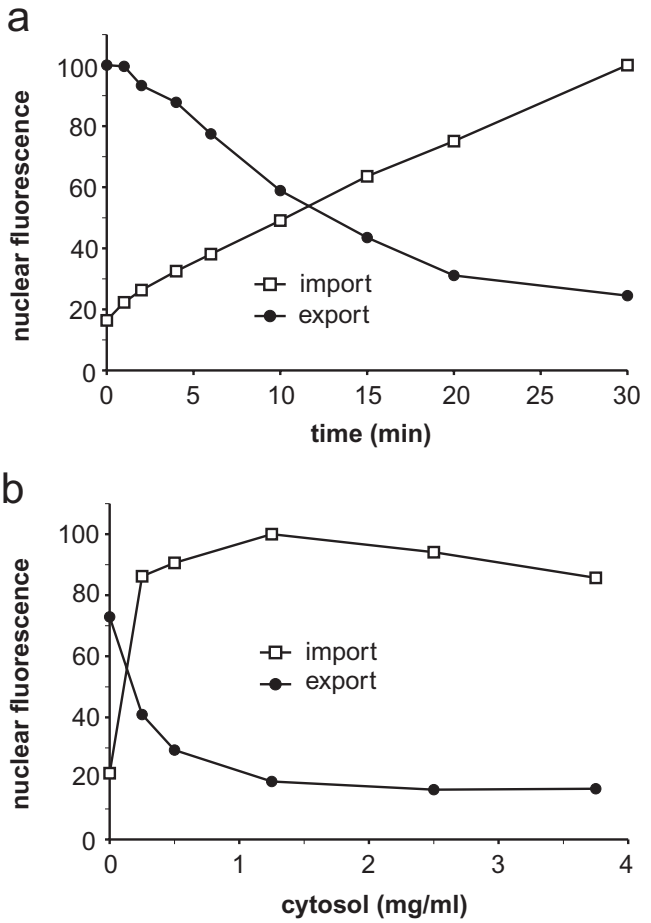

FIGURE 4 Nuclear export of GFP-NFAT and nuclear import of Cy5-BSA-NLS were analyzed in parallel by flow cytometry. (a) Time course of nuclear transport. All reactions contained 2 mg/ml of cytosol and 25 µg/ml of recombinant Ran. (b) Cytosol dependence of nuclear transport. Reactions contained 50 µg/ml of recombinant Ran and the indicated amounts of cytosol. All reactions were performed using preincubated cells (see step 5 in Section III,E) to enhance the cytosol dependence of transport. Portions of this figure were reprinted by permission from the *J. Cell Biol.*, Rockefeller University Press.

cells is stimulated by the addition of HeLa cytosol or reticulocyte lysate, which provides a source of factors, including import receptors and Ran. A low level of cytosol-independent import is usually observed because digitonin permeabilization does not result in the quantitative release of transport factors. Nuclear import is inhibited at low temperature or by incubation with wheat germ agglutinin (0.2–0.5 mg/ml), a lectin that binds to NPC proteins and blocks translocation through the pore. The level of nuclear import is quantified by measuring the nuclear fluorescence in 50–100 cells per condition using a commercially available program such as OpenLab or using a public domain program such as ImageJ (http://rsb.info.nih.gov/ij/).

The same controls that apply to nuclear import are also used to validate nuclear export reactions (Fig. 3). Export of GFP-NFAT is stimulated by the addition of cytosol or reticulocyte lysate and is inhibited at low temperature or by the addition of wheat germ agglutinin. Note that the preexport level of GFP-NFAT fluorescence, measured in cells that have been kept on ice, will vary depending on the cellular expression level. Therefore, a reliable quantification of nuclear export requires analysis of a large number of cells in order to obtain statistically meaningful results. To this end, we use flow cytometry to measure the residual fluorescence in 10,000 cells (Fig. 4). This approach allows rapid analysis of a large number of samples, e.g., for determination of the transport kinetics (Fig. 4a) or the cytosol dependence of transport (Fig. 4b). Nuclear import of a fluorescently labeled import substrate can

be analyzed simultaneously, allowing a direct comparison between different transport pathways. Nuclear import and nuclear export can be reconstituted using recombinant factors instead of cytosol, an approach that allows the contributions of individual transport factors to be analyzed (Görlich *et al*., 1996; Black *et al*., 2001; Kehlenbach and Gerace, 2002).

V. PITFALLS

Any compromise in the integrity of the nuclear envelope renders permeabilized cell assays uninterpretable. This could occur if cells are overpermeabilized with digitonin. Under such a condition, NLS-containing reporters can appear to undergo nuclear import when they are, in fact, simply binding to DNA after leakage through a permeabilized nuclear envelope. Likewise, NES-containing reporters can appear to undergo export due to simple leakage from the nucleus. The easiest way to establish that nuclear import or export is mediated by the NPC is to test for inhibition by WGA. Alternatively, the intactness of the nuclear envelope can be demonstrated by showing that a fluorescently labeled dextran (≥70 kDa) is excluded from the nucleus. Thus, it is helpful to test a range of digitonin concentrations (25–100 μg/ml) and stain with trypan blue to optimize permeabilization of the plasma membrane.

The assays described in this article feature NIH 3T3 and HeLa cells; however, these methods should be applicable to virtually any mammalian cell line. Digitonin permeabilization on adherent cells works best when the cells are 40–70% confluent and poorly if the cells are approaching confluence. Cells that are not well adhered may detach during the permeabilization and wash steps, a problem that usually can be overcome by coating coverslips with poly-D-lysine or by plating the cells 2 days before permeabilization. Also, because cells near the edge of the coverslip may be subject to evaporation artifacts even in a humid chamber, it is best to restrict analysis to the central region of the coverslip.

References

Adam, S. A., Sterne-Marr, R. E., and Gerace, L. (1990). Nuclear import in permeabilized mammalian cells requires soluble factors. *J. Cell Biol.* **111**, 807–816.

Black, B. E., Holaska, J. M., Lévesque, L., Ossareh-Nazari, B., Gwizdek, C., Dargemont, C., and Paschal, B. M. (2001). NXT1 is necessary for the terminal step of Crm1-mediated nuclear export. *J. Cell Biol.* **152**, 141–155.

Crabtree, G. R., and Olson, E. N. (2002). NFAT signaling: Choreographing the social lives of cells. *Cell* **109**, 67–79.

Görlich, D., Panté, N., Kutay, U., Aebi, U., and Bischoff, F. R. (1996). Identification of different roles for RanGDP and RanGTP in nuclear protein import. *EMBO J.* **15**, 5584–5594.

Görlich, D., Prehn, S., Laskey, R. A., and Hartmann, E. (1994). Isolation of a protein that is essential for the first step of nuclear protein import. *Cell* **79**, 767–778.

Kehlenbach, R. H., Dickmanns, A., and Gerace, L. (1998). Nucleocytoplasmic shuttling factors including Ran and CRM1 mediate nuclear export of NFAT *in vitro*. *J. Cell Biol.* **141**, 863–874.

Kehlenbach, R. H., and Gerace, L. (2002). Analysis of nuclear protein import and export *in vitro* using fluorescent cargoes. *Methods Mol. Biol.* **189**, 231–245.

Paschal, B. M., and Gerace, L. (1995). Identification of NTF2, a cytosolic factor for nuclear import that interacts with nuclear pore complex protein p62. *J. Cell Biol.* **129**, 925–937.

Pollard, V. W., Michael, W. M., Nakielny, S., Siomi, M. C., Wang, F., and Dreyfuss, G. (1996). A novel receptor-mediated nuclear import pathway. *Cell* **86**, 985–994.

Ribbeck, K., and Görlich, D. (2001). Kinetic analysis of translocation through nuclear pore complexes. *EMBO J.* **20**, 1320–1330.

Steggerda, S. M., and Paschal, B. M. (2002). Regulation of nuclear import and export by the GTPase Ran. *Int. Rev. Cytol.* **217**, 41–91.

Weis, K. (2003). Regulating access to the genome: Nucleocytoplasmic transport throughout the cell cycle. *Cell* **112**, 441–451.

CHAPTER

37

Heterokaryons: An Assay for Nucleocytoplasmic Shuttling

Margarida Gama-Carvalho and Maria Carmo-Fonseca

I. INTRODUCTION

Interspecies heterokaryon assays are used to analyse the shuttling properties of proteins that localise predominantly in the nucleus at steady state. Conventional localisation methods do not allow the detection of small amounts of protein transiently present in a cellular compartment. Thus, demonstration of a predominantly nuclear (or cytoplasmic) localisation for a given protein frequently obscures the existence of a constant shuttling activity between the two major cell compartments. Indeed, the number of proteins shown to possess nucleocytoplasmic shuttling activity has increased enormously in the past few years, highlighting the importance of shuttling in the regulation of many cellular processes (reviewed by Gama-Carvalho and Carmo-Fonseca, 2001).

Identification of shuttling cytoplasmic proteins can be achieved through analysis of the localisation pattern of deletion mutants affecting export signals or by analysing the effect of inhibition of the major protein export pathway by the drug leptomycin B. In either case, the observation of a shift in the steady-state localisation of the protein from the cytoplasm to the nucleus suggests that the protein under study shuttles continuously between both compartments and that the mutation or drug treatment has interfered with its export pathway.

Identification of nuclear shuttling proteins can be achieved by a number of assays. Using yeast cells, identification of nuclear proteins that shuttle to the cytoplasm can be performed with temperature-sensitive nuclear import mutant strains. In this case, cytoplasmic accumulation of the protein of interest at the restrictive temperature indicates shuttling activity (Lee *et al.*, 1996). In higher eukaryotes, the original demonstration that nuclear proteins shuttle between the nucleus and the cytoplasm was based on nuclear transfer experiments whereby the nucleus from a [^{35}S] methionine-labelled cell was transferred to an unlabelled cell and the appearance of radioactivity in the unlabelled nucleus was monitored (Goldstein, 1958). However, the identification of specific shuttling proteins had to await the development of antibody microinjection or interspecies heterokaryon assays (Borer *et al.*, 1989).

In the microinjection assay, antibodies against the protein of interest are introduced in the cytoplasm of the cell and their appearance in the nucleus is monitored in the presence of protein synthesis inhibitors. As immunoglobulins do not cross the nuclear envelope unless they are bound to a protein that is targeted to the nucleus via a receptor-mediated import pathway, the detection of the antibody in the nucleus in the absence of protein synthesis indicates that the target protein has the ability to shuttle between the nucleus and the cytoplasm. Although virtually any cultured cell type may be used, microinjection assays are often performed in *Xenopus laevis* oocytes, a widely used model system to study transport across the nuclear envelope. A major advantage of this model, in addition to the ease of microinjection, is the possibility to dissect and analyse the contents of the cytoplasm and germinal vesicle (i.e., the nucleus) of a single oocyte, allowing for quantitative biochemical assays. However, it is noteworthy that shuttling assays using *X. laevis* oocytes have provided contradictory results to microinjection or heterokaryon assays performed with human HeLa cells (e.g., Bellini and Gall, 1999; Almeida *et al.*, 1998; Calado *et al.*, 2000). One possibility is that the same protein may have different shuttling proper-

Copyright 2006, Elsevier Science (USA).
All rights reserved.

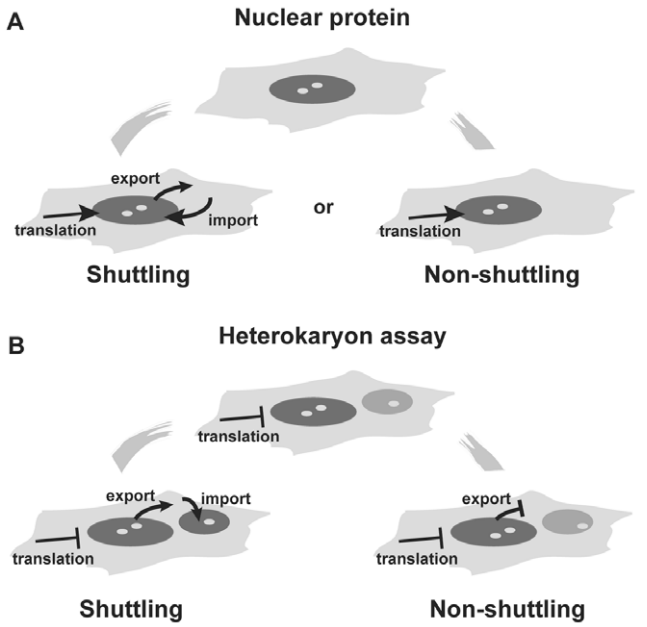

FIGURE 1 **The heterokaryon assay.** (**A**) Proteins may accumulate in the nucleus as the result of a unidirectional import pathway (nonshuttling nuclear proteins). Alternatively, proteins may be targeted simultaneously by import and export pathways, resulting in a dynamic cycling (shuttling) between the nucleus and the cytoplasm. (**B**) Heterokaryon assays distinguish between shuttling and nonshuttling nuclear proteins. If a protein originally present in the donor (large) nucleus shuttles, then it will appear in the receptor (small) nucleus. Nonshuttling proteins are not exported from the donor nucleus and are never detected in the receptor nucleus. Assays have to be performed in the presence of protein synthesis inhibitors in order to prevent the import of newly synthesised protein into the receptor nucleus.

ties in *X. laevis* oocytes and human somatic cells. Alternatively, oocytes may contain a surplus of nuclear proteins stored in the cytoplasm that are not normally present in somatic cells.

Interspecies heterokaryons, which constitute the most widely used shuttling assay, involve the formation of hybrid cells containing at least two nuclei from different species. In an interspecies heterokaryon, a cell line containing the protein of interest—donor cell—is fused with a cell line from a distinct species that does not contain the same protein—receptor cell. The appearance in the "receptor" nucleus of the protein of interest that was originally found exclusively in the "donor" nucleus is monitored by fluorescence microscopy. The assay is performed in the presence of translation inhibitors to ensure that the imported protein has not been newly synthesised in the cytoplasm but rather has been exported from the donor cell nucleus (Fig. 1).

Two different approaches may be taken to label the protein of interest present in donor nuclei. If a species-specific antibody is available, the endogenous protein can be identified by immunostaining of the heterokaryons. For example, when a monoclonal antibody directed against a human protein does not recognise its homologue in *Drosophila melanogaster*, heterokaryons can be made by fusion of human HeLa and *D. melanogaster* SL2 cell lines. These heterokaryons have the advantage that human and fly nuclei are easily distinguished by their different sizes. However, the small size of SL2 nuclei may limit the use of a *D. melanogaster*-specific antibody in a reverse assay, where the larger mammalian nuclei serve as receptors. In this case, the concentration of the target protein in the receptor nucleus may be below the detection limit of the fluorescence microscope. Depending on the specificity of the antibody available, other donor/receptor nuclei combinations are possible, namely human × mouse heterokaryons. An alternative approach to identify the protein of interest involves transfection of a vector encoding a tagged form of the protein into the donor cell line, followed by fusion with a nontransfected receptor cell line. Both green fluorescent protein or amino acid epitope tags have proven to work successfully in these assays. In this case, heterokaryon assays are usually performed with human HeLa and murine NIH 3T3 cell lines. Murine nuclei are easily distinguished by their typical heterochromatin staining pattern.

When a shuttling protein is identified, heterokaryon assays may be further employed to dissect the signals and pathways involved in the transport. More recently, heterokaryon assays have been used to characterise the intranuclear pathway of newly imported proteins (Leung and Lamond, 2002). In this case, a donor cell line transfected with a nucleolar shuttling protein was used as a source of labelled protein, whose entry into the receptor nuclei could be followed in a time course assay from the moment of cell fusion. As receptor nuclei do not contain this protein, the intranuclear pathway followed after import until it accumulated in the nucleolus could be determined.

To perform heterokaryons assays, knowledge of basic tissue culture, transient transfection, and immunofluorescence microscopy techniques is required and will not be addressed here.

II. MATERIALS AND INSTRUMENTATION

Human HeLa cells
Murine NIH 3T3 and/or *D. melanogaster* SL2 cells
Minimum essential medium (MEM) with Glutamax-I

(Cat. No. 41090-028) and MEM nonessential amino acids (Cat. No. 11140-035) (Gibco BRL)
Dulbeco's modified Eagle Medium (D-MEM) (Cat. No. 41966-029) or *D. melanogaster* Schneiders medium (Cat. No. 21720-024) and 200 m*M* L-glutamine (Cat. No. 25030-032) (Gibco BRL)
Fetal bovine serum (FBS, Cat. No. 10270-1064, Gibco BRL)
Basic tissue culture facility with a 37°C, 5% CO_2 incubator and a 29°C, 5% CO_2 incubator (required only for HeLa × SL2 heterokaryons)
35 × 10-mm (P35) tissue culture dishes and general tissue culture material required for cell line maintenance
10 × 10-mm glass coverslips
Curved tweezer
Transfection reagents: Lipofectin (Cat. No. 18292-037, Invitrogen) or Fugene (Cat. No. 1814443, Roche Applied Science)
Protein synthesis inhibitors: anisomycin (Cat. No. A9789), cycloheximide (Cat. No. L9535) or emetine dihydrochloride hydrate (Cat. No. E 2375) (all from Sigma-Aldrich)
Polyethylene glycol (PEG) 1500 (Cat. No. 783 641, Roche Applied Science)
Primary antibody specific for the human–target protein or protein–fusion construct in eukaryotic expression vector with GFP or amino acid epitope tags (e.g., Ha, FLAG, His) and anti-tag primary antibody
Anti-hnRNP C mAb 4F4 (Choi and Dreyfuss, 1984) and anti-hnRNP A1 9H10 mAb (Pinol-Roma *et al*., 1988)
DAPI, dilactate (Cat. No. D 9564, Sigma-Aldrich)
Fluorochrome-conjugated secondary antibodies (Jackson Laboratories)
Fluorescence microscope

III. PROCEDURES

A. HeLa × SL2 Heterokaryons

Cell Culture

1. Maintain HeLa cells routinely in MEM supplemented with nonessential amino acids and 10% FBS and grow in a 37°C, 5% CO_2 incubator. Cells should be split the day before the heterokaryon assay is performed.

2. Grow SL2 *D. melanogaster* cells in Schneider's medium supplemented with 12% FBS and 2 m*M* glutamine at 25°C without CO_2 (a clean laboratory drawer will provide a convenient "incubator"). This is a suspension cell line that can be induced to adhere to the coverslips in the absence of serum.

3. Heterokaryon medium: HeLa × SL2 heterokaryons should be maintained in MEM supplemented with nonessential amino acids and 12% FBS in a 29°C, 5% CO_2 incubator.

Solutions

1. *Protein synthesis inhibitors*: Prepare a stock solution at 10 mg/ml in 50% ethanol and store at –20°C. Final use concentrations should be established for the cell lines used; most widely used concentrations range between 20 and 100 µg/ml for cicloheximide or anisomycin and 0.5 and 20 µg/ml for emetine.

2. *Phosphate-buffered saline PBS*: 137 m*M* NaCl, 2.68 m*M* KCl, 8.06 m*M* Na_2HPO_4, and 1.47 m*M* KH_2PO_4. Prepare by weighing 8 g NaCl, 0.2 g KCl, 1.14 g Na_2HPO_4, and 0.2 g KH_2PO_4 for 1 liter of solution. Sterilise by autoclaving.

Steps

1. All the steps of the procedure should be performed in a laminar flow hood using sterile cell culture material and solutions. The procedure is adapted for cells grown on 10 × 10-mm coverslips placed in P35 dishes.

2. HeLa cells should be grown to subconfluent density on 10 × 10-mm coverslips. A 35 × 10-mm tissue culture petri dish can accommodate four of these coverslips.

3. Resuspend exponentially growing *D. melanogaster* SL2 cells in serum-free HeLa culture medium to a concentration of 3–4 × 10^7 cells/ml.

4. Remove the medium from the HeLa cell culture and overlay coverslips with 500 µl of the SL2 suspension. Incubate for 20 min in a 29°C, 5% CO_2 incubator to induce adherence of SL2 cells.

5. Replace medium with 1.5 ml heterokaryon medium and add the protein synthesis inhibitor. Place cells in the 29°C, 5% CO_2 incubator for at least 3 h to inhibit protein synthesis. A control experiment replacing the protein synthesis inhibitor with a similar volume of 50% ethanol should be performed.

6. For the fusion procedure, place a 50-µl drop of PEG 1500 prewarmed to 29°C in a sterile petri dish.

7. Remove the HeLa/SL2 coculture from the incubator and wash twice with PBS prewarmed to 29°C.

8. With a sterile forceps, remove a coverslip and invert it over the PEG drop for 2 min (cell side down). Then, place the coverslip (cell side up) in a new P35 dish and rinse twice with PBS prewarmed to 29°C. Replace the PBS with 1.5 ml of prewarmed heterokaryon medium with a protein synthesis inhibitor and place the heterokaryons in the incubator for the

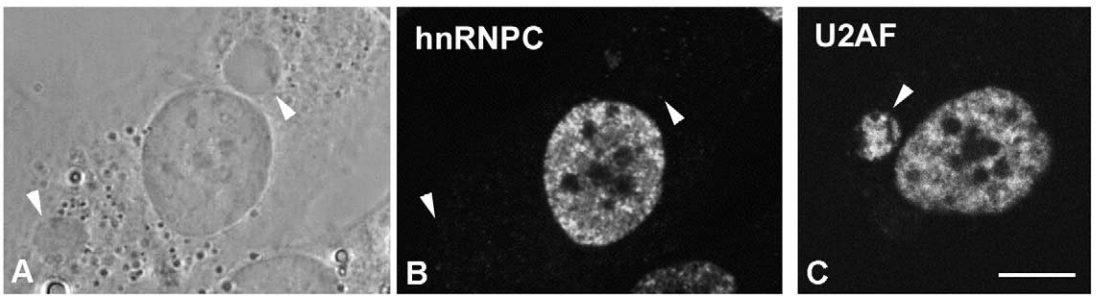

FIGURE 2 HeLa × SL2 heterokaryons. Monoclonal antibodies directed against a human protein often do not cross-react with its *Drosophila melanogaster* homologue. In this case, shuttling of the endogenous human protein can be analysed in a HeLa × SL2 heterokaryon. (**A**) Phase-contrast image of a HeLa × SL2 heterokaryon. Arrowheads label small SL2 nuclei from cells that have fused with the HeLa cytoplasm. (**B**) The heterokaryon shown in A has been immunostained with a monoclonal antibody specific for the human non-shuttling protein hnRNPC (mAb 4F4; Choi and Dreyfuss, 1989), showing it to be restricted to the HeLa nucleus in the presence of protein synthesis inhibitors (20 µg/ml emetine). Arrowheads point to the position of SL2 nuclei. (**C**) Immunostaining of a HeLa × SL2 heterokaryon with a monoclonal antibody specific for human $U2AF^{65}$ (mAb MC3; Gama-Carvalho *et al.*, 1997) shows that the human protein is present in the SL2 nucleus (arrowhead) in the presence of protein synthesis inhibitors, demonstrating the shuttling activity of this protein (Gama-Carvalho *et al.*, 2001).

duration of the shuttling assay (usually 6 h or more).

9. Fix and immunostain cells using standard procedures, following a time course with 1-h intervals. Positive and negative control experiments should be performed using monoclonal antibodies directed against human hnRNPA 1 (a protein that shuttles between the nucleus and the cytoplasm; Pinol-Roma *et al.*, 1988) and human hnRNPC (a protein that does not shuttle; Choi and Dreyfuss, 1984) (Fig. 2).

B. HeLa × 3T3 Heterokaryons

Cell Culture

1. Maintain HeLa cells routinely in MEM supplemented with nonessential amino acids and 10% FBS and grow in a 37°C, 5% CO_2 incubator. Cells should be split to petri dishes 2 days before the heterokaryon assay is performed and transfected on the following day.

2. Grow mouse 3T3 cells in D-MEM supplemented with 10% FBS at 37°C, 5% CO_2.

3. Heterokaryon medium: HeLa × 3T3 heterokaryons should be maintained as 3T3 cells.

Solutions

1. *PBS*: 137 m*M* NaCl, 2.68 m*M* KCl, 8.06 m*M* Na_2HPO_4, and 1.47 m*M* KH_2PO_4. Prepare by weighing 8 g NaCl, 0.2 g KCl, 1.14 g Na_2HPO_4, and 0.2 g KH_2PO_4 for 1 liter of solution. Sterilise by autoclaving.

2. *DAPI*: Prepare a stock solution at 1 mg/ml and store at –20°C protected from light; staining solution: dilute stock to 1 µg/ml in PBS and store at +4°C protected from light for several weeks.

3. *Protein synthesis inhibitors*: Prepare a stock solution at 10 mg/ml in 50% ethanol and store at –20°C. Final use concentrations should be established for the cell lines used; most widely used concentrations range between 20 and 100 µg/ml for cicloheximide or anisomycin and 0.5 and 20 µg/ml for emetine.

Steps

1. All the steps of the procedure should be performed in a laminar flow hood using sterile cell culture material and solutions. The procedure is adapted for cells grown on 10 × 10 mm coverslips placed in P35 dishes.

2. The evening before the assay, HeLa cells should be transfected with the desired construct and left to grow to subconfluent density on 10 × 10-mm coverslips. A 35 × 10-mm tissue culture petri dish can accommodate four of these coverslips. Common transfection reagents such as Lipofectin or Fugene work well with this procedure and can be used according to the instructions of the manufacturer. The number of hours between transfection and the heterokaryon assay should be determined for each construct to avoid overexpression of the exogenous protein.

3. Tripsinise and count 3T3 cells. For each P35 HeLa culture, prepare 1.5 ml of a 3T3 suspension with 1×10^6 cells/ml in DMEM with 10% FBS and protein synthesis inhibitor.

4. Remove the medium from the HeLa cell culture and overlay coverslips with the 3T3 suspension.

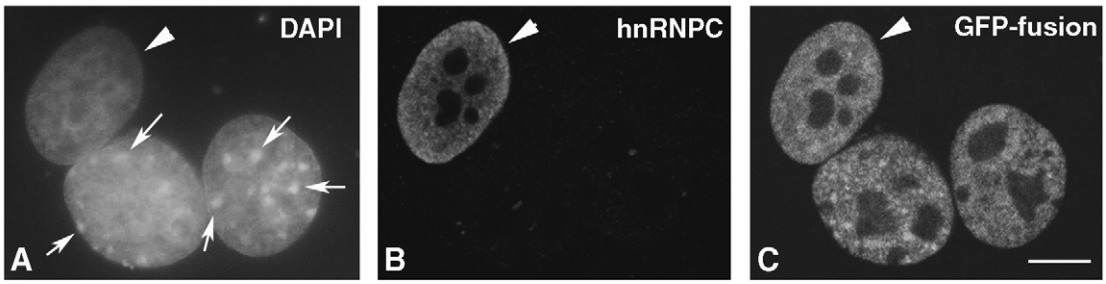

FIGURE 3 HeLa × 3T3 heterokaryons. HeLa cells were transiently transfected with a vector encoding GFP-U2AF^{65} (Gama-Carvalho *et al.*, 2001) and fused with murine NIH 3T3 cells in the presence of 20 µg/ml emetine. A single heterokaryon labelled with DAPI (A), anti-hnRNPC mAb (B), and GFP (C) is shown. (**A**) DAPI staining of the HeLa × 3T3 heterokaryon. Murine cells are easily distinguished by the presence of brightly stained blocks or pericentric heterochromatin (arrows). (**B**) The heterokaryon shown in A was stained with an antibody specific for the nonshuttling human hnRNP C protein (mAb 4F4; Choi and Dreyfuss, 1989). hnRNP C is restricted to the HeLa cell nucleus (arrowhead), confirming that there is an efficient inhibition of protein synthesis. (**C**) Detection of GFP in the HeLa × 3T3 heterokaryon reveals that the fusion protein originally present in HeLa cells shuttles between the nucleus and the cytoplasm. Bar: 10 µm.

Incubate for 3 h in a 37°C, 5% CO_2 incubator to allow 3T3 cells to adhere and inhibit protein synthesis.

5. For the fusion procedure, place a 50-µl drop of prewarmed PEG 2000 in a sterile petri dish per coverslip.

6. Remove the HeLa/3T3 coculture from the incubator and wash twice with prewarmed PBS.

7. With a sterile forceps, remove a coverslip and invert it over the PEG drop for 2 min. Then place the coverslip (cell side up) in a new P35 dish and rinse twice with prewarmed PBS. Replace the PBS with 1.5 ml of prewarmed heterokaryon medium with protein synthesis inhibitor and place the heterokaryons in the incubator for the duration of the shuttling assay (usually from 1 to 5 h).

8. Fix and stain cells using standard procedures, following a time course with 1-h intervals. In addition to the procedure (if any) necessary for detection of the exogenous protein, cells should be stained with DAPI to allow identification of heyterokaryon nuclei. Positive and negative control experiments should be performed using monoclonal antibodies directed against human hnRNPA 1 (a protein that shuttles between the nucleus and the cytoplasm; Pinol-Roma *et al.*, 1988) and human hnRNPC (a protein that does not shuttle; Choi and Dreyfuss, 1984) (Fig. 3).

IV. COMMENTS

Shuttling rates vary significantly from protein to protein, with some being extremely slow (e.g., nucleolin takes up to 16 h to be detected in the receptor nuclei) and others very fast (e.g., transport receptors are detected in receptor nuclei within minutes after the fusion). The ideal time period for a shuttling assay should thus be determined for each case by performing a time course analysis. As a general rule, detection of the protein in receptor nuclei in HeLa × 3T3 heterokaryon assays involving transient expression of exogenous protein is significantly faster than HeLa × SL2 assays with the endogenous protein. For example, for the same protein, equilibrium between donor and receptor nuclei may be achieved in 90 min in the first case and take up to 7 h in the second.

Proper interpretation of results from a heterokaryon assay requires the use of adequate controls. Whenever possible, shuttling activity should be demonstrated for both endogenous and exogenously expressed proteins, as amino acid tags and protein overexpression may modify the results. When assaying for shuttling of the endogenous protein, the specificity of the antibody has to be demonstrated carefully. The efficiency of protein synthesis inhibition must be controlled properly as different cell strains may show a wide variation in the sensitivity to protein synthesis inhibitors. Demonstration of efficient translation inhibition can be performed by staining the heterokaryons with a monoclonal antibody specific for a human nuclear nonshuttling protein, such as the hnRNP C protein (mAb 4F4, Choi and Dreyfuss, 1984). If cytoplasmic protein synthesis is going on, this protein will be detected in the nucleus of the receptor cell. Whenever possible, heterokaryons should be double stained for the protein of interest and hnRNPC. Alternatively, when the protein of interest is also detected with a mAb, a parallel assay should be performed in which the heterokaryons are labelled with the anti-hnRNP C antibody.

If a shuttling protein is identified, it is convenient to determine whether it is diffusing through the nuclear pores passively or being exported from the nucleus through a receptor-mediated pathway. For this purpose, donor cells should be placed at 4°C for the same period of time as used for the heterokaryon assay in culture medium supplemented with the protein synthesis inhibitor and 20 m*M* HEPES. Immunostaining for the protein of interest should then be performed. At low temperature, receptor-mediated nuclear import and export processes do not occur. Thus, if the protein is exported via a receptor-mediated pathway, it should be retained in the nucleus. In contrast, if the protein can leak through the nuclear pores passively, it will accumulate in the cytoplasm. If translation is not inhibited, newly synthesised proteins will also accumulate in the cytoplasm, invalidating the assay. When performing shuttling analysis based on transient transfection, it is important to note that accumulation of exogenous protein in the cytoplasm and passive leakage from the nucleus are common events in cells expressing the protein at high levels. Thus, analysis of exogenous proteins should always be centred on cells with low expression levels. A control experiment to determine the degree of exogenous protein leakage to the cytoplasm should also be performed (e.g., a low temperature shift experiment).

The use of interspecies heterokaryons in association with transient transfection opens the possibility to analyse the protein domains involved in the export pathway by the use of mutant forms of the protein. However, this analysis can only be performed with mutants that retain full nuclear localisation. Moreover, leakage of small deletion mutants to the cytoplasm should be monitored carefully.

V. PITFALLS

The confluence of HeLa cells is critical for the procedure. If the density of the culture is too low, few heterokaryons will form. If cells have reached confluence, there will be no space left for the SL2 or 3T3 cells to adhere and often their nuclei will be above HeLa nuclei, making analysis of the results impossible. HeLa coverslips should be checked one by one to choose those with an appropriate subconfluent density.

Often during the fusion procedure there is a significant loss of cells. This may result from the mechanical stress generated when the coverslips that were turned over the PEG droplet are picked. To avoid this, simply pipette PBS beneath the coverslip to make it float and then pick it up with a forceps. In addition, it is possible that the protein synthesis inhibitor is inducing apoptosis of a high percentage of cells in culture. Indeed, some cell strains are highly sensitive to these inhibitors at concentrations that have no negative effects for other cells. Thus, the choice of inhibitor and concentration should be assayed carefully for the particular cell strain used in the assay. Cycloheximide is the most widely used inhibitor, although some cell lines may be more sensitive to emetine. In some cases, efficient protein synthesis inhibition may be hard to achieve, with a significant proportion of cells in the culture showing significant levels of newly translated protein. To prevent this from influencing the interpretation of the assay, perform double labelling of heterokaryons with the anti-hnRNP C 4F4 mAb whenever possible and consider only heterokaryons in which this protein is restricted to the human nuclei.

Finding HeLa × 3T3 heterokaryons in the preparation may present some difficulty, as the observation in phase contrast does not always allow a clear visualisation of the cytoplasm. The best approach is to look for two nuclei that are very close together, which is done most easily when visualising DAPI staining. The identification of murine nuclei by staining with DAPI also requires some training. Staining with the 4F4 mAb can serve as an aid, as it will only label human cells when translation is inhibited.

As discussed earlier, when analysing the shuttling ability of transiently transfected proteins, it is crucial to consider only low expressing cells. A good fluorescence microscope is essential for detecting low levels of expression. Often, multinucleated heterokaryons form. These should not be considered in the shuttling assay, as it is hard to identify the donor nucleus and access the original expression level of the protein (as it has spread out to many nuclei).

References

Almeida, F., Saffrich, R., Ansorge, W., and Carmo-Fonseca, M. (1998). Microinjection of anti-coilin antibodies affects the structure of coiled bodies. *J. Cell Biol.* **142**, 899–912.

Bellini, M., and Gall, J. G. (1999). Coilin shuttles between the nucleus and cytoplasm in *Xenopus laevis* oocytes. *Mol. Biol. Cell* **10**, 3425–3434.

Borer, R. A., Lehner, C. F., Eppenberger, H. M., and Nigg, E. A. (1989). Major nucleolar proteins shuttle between nucleus and cytoplasm. *Cell* **56**, 379–390.

Calado, A., Kutay, U., Kuhn, U., Wahle, E., and Carmo-Fonseca, M. (2000). Deciphering the cellular pathway for transport of poly(A)-binding protein II. *RNA* **6**, 245–256.

Choi, Y. D., and Dreyfuss, G. (1984). Monoclonal antibody characterization of the C proteins of heterogeneous nuclear ribonucleoprotein complexes in vertebrate cells. *J. Cell Biol.* **99**, 1997–2204.

Gama-Carvalho, M., and Carmo-Fonseca, M. (2001). The rules and roles of nucleocytoplasmic shuttling proteins. *FEBS Lett.* **498**, 157–163.

Gama-Carvalho, M., Carvalho, M. P., Kehlenbach, A., Valcarcel, J., and Carmo-Fonseca, M. (2001). Nucleocytoplasmic shuttling of heterodimeric splicing factor U2AF. *J. Biol. Chem.* **276**, 13104–13112.

Gama-Carvalho, M., Krauss, R. D., Chiang, L., Valcarcel, J., Green, M. R., and Carmo-Fonseca, M. (1997). Targeting of U2AF65 to sites of active splicing in the nucleus. *J. Cell Biol.* **137**, 975–987.

Goldstein, L. (1958). Localization of nucleus-specific protein as shown by transplantation experiments in *Amoeba proteus*. *Exp. Cell Res.* **15**, 635–637.

Lee, M. S., Henry, M., and Silver, P. A. (1996). A protein that shuttles between the nucleus and the cytoplasm is an important mediator of RNA export. *Genes Dev.* **10**, 1233–1246.

Leung, A. K., and Lamond, A. I. (2002). *In vivo* analysis of NHPX reveals a novel nucleolar localization pathway involving a transient accumulation in splicing speckles. *J. Cell Biol.* **157**, 615–629.

Pinol-Roma, S., Choi, Y. D., Matunis, M. J., and Dreyfuss, G. (1988). Immunopurification of heterogeneous nuclear ribonucleoprotein particles reveals an assortment of RNA-binding proteins. *Genes Dev.* **2**, 215–227.

SECTION

8

Chromatin Assembly

CHAPTER

38

DNA Replication-Dependent Chromatin Assembly System

Jessica K. Tyler

I. INTRODUCTION

Chromatin is a periodic structure made up of repeating, regularly spaced subunits, the nucleosomes. Each nucleosome includes a core octamer of two molecules each of histone proteins H3, H4, H2A, and H2B, around which the DNA is wrapped almost twice. The assembly and structure of chromatin modulate the accessibility of proteins to the genome and hence regulate all processes that utilize the DNA. Analyses of transcription, DNA replication, and repair from *in vitro*-assembled chromatin templates reveal a wealth of information not provided by studies on naked DNA templates, as the chromatinized template more accurately reflects the state of the genome in the cell. This article outlines and compares systems for the assembly of recombinant DNA templates into arrays of nucleosomes *in vitro* to enable the reader to select the appropriate chromatin assembly system for their experimental question and resources. In addition, this article describes the DNA replication-coupled chromatin assembly system used in our laboratory and directs the reader to recent method chapters providing excellent descriptions of the other chromatin assembly systems. Chromatin assembly systems fall into two classes: "defined" systems where all the components are purified or recombinant and "cell-free" systems where the components required for assembly are supplied by a crude extract. The cell-free chromatin assembly systems can be further subcategorized into replication-independent systems and DNA synthesis-coupled systems. Defined chromatin assembly systems should be used if the experiment requires that any component of the chromatin assembly reaction or the resulting chromatin be manipulated, such as the nature of the histone proteins. Defined chromatin assembly systems fall into two classes: histone transfer systems and ATP-dependent chromatin assembly systems.

A. Defined Chromatin Assembly Systems for Histone Transfer

The core of the chromatin assembly reaction is the transfer of histone proteins to DNA, as mediated by a histone transfer vehicle or histone chaperone. If DNA and histones are combined in the absence of a histone transfer vehicle at physiological salt conditions, an undefined insoluble aggregate is obtained due to the intrinsic electrostatic attraction between the DNA and the highly basic histone proteins. A histone transfer vehicle binds to the histones and facilitates the ordered formation of nucleosomes from histones and DNA by reducing their inherent affinity for each other.

A variety of histone transfer vehicles can be used *in vitro* to assemble chromatin, including polyanions such as polyglutamate and counterions such as sodium chloride. The observation that high salt concentrations (>1.2 *M* NaCl) dissociate nucleosomes led to the discovery that this process was reversible by the progressive dialysis of mixtures of DNA and histones from high to low salt (Fig. 1A) (Lee and Narlikar, 2002). Chromatin assembly by salt dialysis is the simplest and cleanest way to form nucleosomes and has been invaluable for structural analyses of single nucleosomes (mononucleosomes; Luger *et al.*, 1999). However, arrays of nucleosomes made by salt dialysis are very close packed, with a nucleosome repeat length of around 150–160 bp as compared to that of 180–190 bp for nucleosomes *in vivo* (nucleosome repeat

Copyright 2006, Elsevier Science (USA).
All rights reserved.

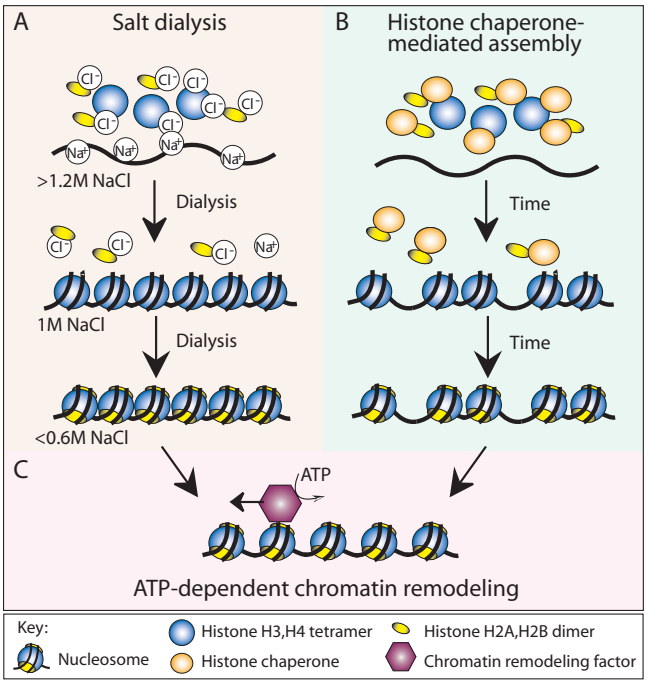

FIGURE 1 Overview of chromatin assembly systems. Histones can be deposited onto DNA to form nucleosomes *in vitro* via (A) the sequential reduction in the salt (NaCl) concentration via dialysis, resulting in regular, but close packed arrays of nucleosomes, or (B) histone chaperone-mediated histone deposition onto DNA, resulting in irregular arrays of nucleosomes. (C) The presence of an ATP-dependent chromatin remodeling activity, either during or after histone deposition, will result in regular, physiological spacing of the nucleosomes.

length is the center-to-center distance between adjacent nucleosomes; Fig. 1). This unphysiological close-packed characteristic of the salt dialysed chromatin can be overcome by incubation with an ATP-dependent chromatin remodeling factor (see later; Fig. 1C). Salt dialysis can yield nucleosomal arrays with more physiological spacing when DNA templates that comprise tandem arrays of nucleosome positioning sequences derived from the sea urchin 5S RNA gene are used (Carruthers *et al.*, 1999). However, the use of nucleosome positioning sequences places a sequence limitation on the DNA template and does not reflect the situation *in vivo* where nucleosomes are generally not positioned by the underlying DNA sequence.

Histone transfer *in vitro* can also be achieved by physiologically relevant histone chaperones, such as nucleosome assembly protein 1 (NAP-1), chromatin assembly factor 1 (CAF-1), and antisilencing function 1 (ASF1) or by histone storage proteins such as nucleoplasmin and N1/N2. Histone chaperone-mediated chromatin assembly (in the absence of an ATP-dependent chromatin remodeling factor) generally results in the unphysiological random spacing of nucleosomes along the DNA (Fig. 1B). The major applications for nucleosomal arrays assembled by histone transfer are for protein interaction analyses and for testing the ability of chromatin remodeling factors to convert irregularly spaced or close-packed nucleosomes into physiologically spaced, regular nucleosomal arrays.

B. Defined ATP-Dependent Chromatin Assembly Systems

In order to generate regularly spaced arrays of nucleosomes that resemble chromatin *in vivo*, an ATP-dependent chromatin remodeling factor is required in addition to a histone chaperone (Fig. 1C). Chromatin remodeling factors, e.g., ATP-utilizing chromatin assembly and remodeling factor (ACF) and chromatin accessibility complex (CHRAC), are multisubunit protein complexes that use the energy from ATP hydrolysis to space nucleosomes along the DNA template (Fig. 1C). These ATP-dependent chromatin assembly factors were identified by fractionation of *Drosophila* embryo chromatin assembly extracts and function together with histone chaperones, such as NAP-1 or CAF-1 (Fyodorov and Levenstein, 2002). A human ATP-dependent chromatin assembly factor, termed remodeling and spacing factor (RSF), appears to act as both the histone chaperone and the ATP-dependent chromatin remodeling factor during chromatin assembly *in vitro* (Loyola *et al.*, 2001). These defined ATP-dependent chromatin assembly systems provide powerful approaches to generate regular nucleosomal arrays with physiological nucleosomal spacing, albeit at the expense of time-consuming purification of the chromatin assembly factors and histones.

C. Generation of Reagents for Defined Chromatin Assembly Systems

In order to use defined chromatin assembly systems, it is necessary to use purified or recombinant chromatin assembly factors and histones. Recombinant histone chaperones and ATP-dependent chromatin remodeling factors are generated by affinity purification following baculovirus-mediated expression in Sf9 cells (Fyodorov and Levenstein, 2002). Core histones (H3, H4, H2A, and H2B) can be purified from a range of organisms using established protocols (Schnitzler, 2002). In addition, recombinant *Xenopus*, *Drosophila*, and yeast core histones can be expressed and purified from *Escherichia coli*, allowing assembly of chromatin lacking posttranslational modifications

or with specific histone mutations (Lee and Narlikar, 2002; Levenstein and Kadonaga, 2002; Luger *et al*., 1999; White *et al*., 2001). For those with time constraints, individual recombinant *Xenopus* core histones can be purchased from Upstate Biologicals and individual purified core histones from calf thymus can be purchased from Roche Applied Science. Due to the highly conserved nature of chromatin assembly factors and nucleosome structure across eukaryotes, it is not generally necessary to adhere to species specificity within the chromatin assembly machinery, histones, and the subsequent application of the chromatin templates. For example, there is no gross functional or structural difference in the chromatin assembled from yeast, human, or *Drosophila* core histones using human, *Drosophila*, or yeast chromatin assembly factors.

D. Cell-Free Replication-Independent Chromatin Assembly Systems

Cell-free chromatin assembly systems were developed prior to the defined ATP-dependent chromatin assembly systems, but are still the system of choice for many researchers. Technically, chromatin assembly in cell-free systems requires less empirical optimization than defined ATP-dependent chromatin assembly systems, while still generating high-quality regular arrays of nucleosomes with physiological spacing in an ATP-dependent manner. Extracts remain a requirement for the analysis of processes coupled to chromatin assembly, such as the assembly of chromatin during ongoing DNA synthesis *in vitro*. Limitations of cell-free chromatin assembly systems include the inability to fully control the nature of histones and nonhistone proteins incorporated into the chromatin or the chromatin assembly factors used for assembly, as these are contained within the cell-free extract. Conversely, the crude nature of these extracts can be an advantage if, for example, unknown factors are required to facilitate subsequent transcriptional activation from the chromatin template.

Cell-free extracts for generating physiologically spaced, regular arrays of nucleosomes have been derived from *Xenopus laevis* eggs and oocytes, *Drosophila melanogaster* embryos, and human tissue culture cells by high-speed (HS) centrifugation (Table I) (Bonte and Becker, 1999; Fyodorov and Levenstein, 2002; Gruss, 1999; Tremethick, 1999). The realization that the early developmental stages of *Xenopus* and *Drosophila* contain stockpiles of the components necessary to assemble the rapidly dividing DNA into chromatin was key to the development of highly active chromatin assembly extracts. For transcription analy-

TABLE I Comparison of Chromatin Assembly Systems

Organism/method	ATP dependent	Nucleosomal spacing[a]	Histone source[b]	Replication or repair-coupled chromatin assembly possible?[c]
Defined chromatin assembly systems				
Salt dialysis mediated	No	Close packed	Added	No
Histone chaperone mediated	No	Irregular	Added	No
NAP-1 + CHRAC/ACF mediated	Yes	Regular	Added	No
RSF mediated	Yes	Regular	Added	No
Cell-free chromatin assembly systems				
Budding yeast mitotic extract	Yes	Irregular	Endogenous	No
Drosophila embryo extract	Yes	Regular	Supplement[d]	SSS,[e] NER[f]
Xenopus egg extract	Yes	Regular	Endogenous	SSS,[e] NER[f]
Xenopus oocyte extract	Yes	Regular	Endogenous	No
Human HeLa cell extract	Yes	Regular	Supplement	SV40 DNA replication, SSS[e], NER[f]
Human 293 cell extract[g]	ND[h]	Irregular	Endogenous	SV40 DNA replication, NER[f]

[a] Nucleosomal spacing is interpreted as irregular if limited ladders were obtained from micrococcal digestion analyses.
[b] This column indicates whether histones are supplied by the extract "endogenous" or are only partially supplied by the extract and have to be supplemented ("supplement") or whether all the histones have to be added ("added").
[c] Refers to whether it is possible to perform replication or repair-coupled chromatin assembly in each system upon addition of single strand, damaged, or SV40-origin bearing templates (together with SV40 large T-antigen).
[d] The Kadonaga S190 extract requires supplementation with histones, whereas the Becker/Wu S150 extract does not.
[e] Refers to second-strand synthesis of M13 templates.
[f] Refers to nucleotide excision repair of damaged templates.
[g] Note that this extract requires supplementation with a source of CAF-1 to obtain replication-dependent chromatin assembly.
[h] Not determined.

ses, the DNA template is usually assembled into chromatin using these extracts, followed by the addition of transcription factors or a transcription extract. Chromatin templates generated from the *Xenopus* egg HS extract are inherently flawed for subsequent transcriptional analyses due to the abundance of variant linker histone B4 and transcription factors in the extract. In fact, assembly of transcription complexes competes with chromatin assembly in the *Xenopus* egg HS extract. In general, the *Xenopus* egg HS extract is used for DNA synthesis-coupled chromatin assembly, whereas the *Xenopus* oocyte extract (S150; where S refers to the sedimentation coefficient) is used for assembling templates into chromatin for their subsequent transcriptional analyses (Gaillard *et al*., 1999; Tremethick, 1999). The *Drosophila* S150 and S190 embryo extracts (Bonte and Becker, 1999; Fyodorov and Levenstein, 2002) have been widely used to assemble chromatin templates for subsequent analyses of transcriptional regulation, recreating many of the features of transcriptional regulation *in vivo* (Robinson and Kadonaga, 1998). These extracts also contain factors that can modify subsequent transcription reactions, such as chromatin remodeling activities, and therefore it may be desirable to purify the chromatin templates by sedimentation centrifugation or size exclusion prior to transcription analysis. Removal of nonhistone proteins from the chromatin may be achieved by treatment with Sarkosyl prior to purification of the chromatin template (Mizuguchi and Wu, 1999). However, defined chromatin assembly systems are the ideal method for complete control of the subsequent transcription reaction on chromatin templates.

A chromatin assembly extract has been developed from *Saccharomyces cerevisiae* that enables the powerful combination of genetics and biochemistry (Table I). This yeast extract also supports transcriptional activation and can be isolated from any yeast strain that has been altered by genetic manipulations. This enables investigation of the effect of specific mutations on chromatin assembly and transcriptional regulation of the *in vitro*-assembled chromatin templates (Schultz, 1999). However, this extract is limited by its inability to generate extensive regular arrays of nucleosomes (Table I).

E. DNA Synthesis-Coupled Chromatin Assembly Systems

In the cell, the majority of chromatin assembly is coupled to ongoing DNA replication and repair. The process of chromatin assembly coupled to double-strand DNA replication has been recreated *in vitro* using extracts from human tissue culture cells (Table I). In addition, *Drosophila*, human cell, and *Xenopus* egg HS extracts can mediate nucleotide excision repair-coupled chromatin assembly on damaged templates and second-strand synthesis-coupled chromatin assembly on M13 templates (Bonte and Becker, 1999; Gaillard *et al*., 1999). The human 293 cell extract has been widely used to study the process of DNA replication coupled-chromatin assembly using an SV40 origin to initiate replication via the method described in this article (Fig. 2). In this system, DNA replication occurs on only a portion of the total DNA templates, allowing comparison of chromatin assembly on the newly replicated DNA (labelled with a radioactive nucleotide) to chromatin assembly on the total DNA (Fig. 2). As such, this system has led to the identification and characterization of histone chaperones that mediate chromatin assembly onto newly synthesized DNA, such as CAF-1 and ASF1 (Smith and Stillman, 1989; Tyler *et al*., 1999). Furthermore, the SV40 DNA template can be preassembled into chromatin using *Drosophila* and *Xenopus* chromatin assembly extracts and then replicated using human DNA replication extracts (Gruss, 1999). Refinement of this approach may recreate epigenetic inheritance of chromatin structures *in vitro*.

F. Evaluation of *in Vitro*-Assembled Chromatin

Once assembled, it is important to check the extent of nucleosome assembly and the regularity of nucleosomal spacing. The extent of chromatin assembly can be measured by DNA supercoiling analysis, as the formation of each nucleosome introduces one negative supercoil into covalently closed circular DNA. The number of negative supercoils therefore corresponds to the number of nucleosomes assembled and is measured after deproteinization by agarose gel electrophoresis. Plasmid supercoiling by an extract cannot always be attributed to chromatin assembly, as these extracts potentially contain unrelated DNA supercoiling activities. Therefore, it is necessary to confirm that the supercoiling is due to chromatin assembly, usually by the micrococcal nuclease digestion assay. In this assay, the chromatin is partially digested by micrococcal nuclease, which cleaves both strands of DNA between the nucleosomal cores. The resulting chromatin fragments are deproteinized and the DNA is resolved by agarose gel electrophoresis. A DNA ladder derived from the chromatin fragments is observed if the assembly was efficient and the nucleosomes were regularly spaced, and the size of the DNA

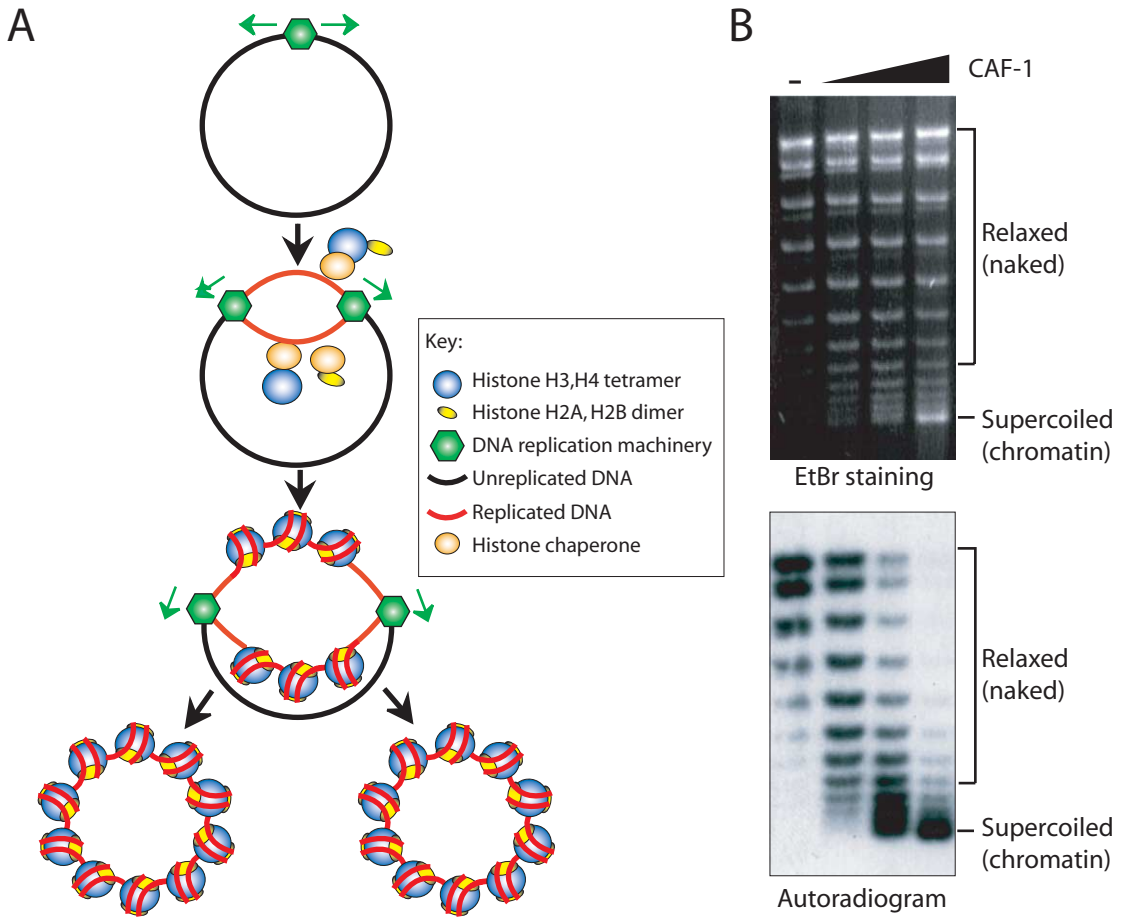

FIGURE 2 DNA replication-coupled chromatin assembly. (A) Overview of the SV40 T-antigen-driven replication assay in a human cell-free extract coupled to chromatin assembly. The newly replicated DNA (red) becomes labelled by the incorporation of a radioactive nucleotide. (B) Example of supercoiling analysis of the products of DNA replication-coupled chromatin assembly. By comparison of EtBr staining and autoradiogram of the same agarose gel, preferential assembly (supercoiling) of the replicated DNA into chromatin is apparent upon addition of CAF-1.

fragments allows the nucleosome repeat length to be estimated.

II. MATERIALS AND INSTRUMENTATION

Plasmid template carrying SV40 origin of DNA replication [we use pSV011 (Stillman, 1986)]. SV40-T antigen, affinity purified (Simanis and Lane, 1985) or purchased (Cat. No. 5800-01) from CHIMERx. Spinner-adapted version of HEK293 cells (Cat. No. CRL1573) is from ATTC. Joklik's modification of MEM (Cat. No. 1032324) and sodium butyrate (Cat. No. 218453) are from ICN. Fetal bovine serum (Cat. No. 16000-044) is from Life Technologies Inc. Ribonucleotides (ATP, CTP, GTP, UTP, Cat. Nos. E6011, E6021, E6031, E6041) and deoxyribonucleotides (dATP, dCTP, dGTP, dTTP, Cat. No. U1330) are from Promega. Filters (0.22 µm) (Cat. No. GSWP04700) are from Millipore. A 40-ml Wheaton dounce homogenizer with B pestle (Cat. No. 06-435-C), Corex 8445 tubes (Cat. No. 05-566-55), agarose (Cat. No. BP1356), chloroform (Cat. No. C298), EDTA (Cat. No. S311), dithiothreitol (DTT, Cat. No. BP172-25), glycerol (Cat. No. G3320), HEPES (Cat. No. BP310), magnesium chloride ($MgCl_2$, Cat. No. M33), phenol:chloroform:isoamylalcohol 25:24:1 (Cat. No. BP17521), potassium chloride (KCl, Cat. No. P217), potassium hydroxide pellets (KOH, Cat. No. P250), potassium phospate monobasic (KH_2PO_4 Cat. No. P285), proteinase K (Cat. No. BP1700), sodium acetate trihydrate (NaOAc, Cat. No. S209), sodium chloride (NaCl, Cat. No. S271), sodium phosphate dibasic ($Na_2HPO_4{\cdot}7H_2O$ Cat. No. S373), sodium phosphate monobasic (NaH_2PO_4 Cat. No. S369), Tris base

(Cat. No. BP152), xylene cyanol FF (XC, Cat. No. BP565), and X-ray film (Cat. No. 05-728-24) are from Fisher. Boric acid (Cat. No. B0252), bromphenol blue (BPB, Cat. No. B-6131), creatine phosphate (Cat. No. P7936), creatine phosphokinase (CPK, Cat. No. C3755), ethidium bromide (EtBr, Cat. No. E-8751), glycogen (Cat. No. G0885), IGEPAL (NP40, Cat. No. I3021), RNase A (Cat. No. R6513), and sodium hydroxide pellets (NaOH, Cat. No. S-0899) are from Sigma. Sodium dodecyl sulphate (SDS, Cat. No. 161-0302) is from Bio-Rad. [α-^{32}P]dATP 3000 Ci/mmol, 10 µCi/µl (Cat. No. BLU512H) is from Dupont NEN. Complete protease inhibitor cocktail (Cat. No. 1836153) is from Roche.

A 37°C tissue culture incubator (CO_2 not required) and a magnetic stir plate for spinner flasks (Thermodyne Cat. No. 45700) are from Fisher. The 6-liter spinner flask (Cat. No. 1965-06000) is from Bellco. Refrigerated centrifuge Sorvall RC-5B with SS34, HB6, and GSA rotors (or equivalent). Beckman ultracentrifuge with Ti70 rotor. Rotary Speed-Vac, gel dryer, and –80°C freezer are from Thermo Savant (or similar). Agarose gel electrophoresis equipment, Gibco H5 system (or similar). Liquid nitrogen tank. Eppendorf Model 5415D microcentrifuge (or similar).

III. PROCEDURES

A. Preparation of DNA Replication-Dependent Chromatin Assembly Extract

These procedures are modified from those of Stillman (1986).

Solutions

1. *Phosphate-buffered saline (PBS)*: 136 m*M* NaCl, 2.7 m*M* KCl, 3.4 m*M* Na_2HPO_4, and 1.47 m*M* KH_2PO_4. For 100 ml of 1X PBS, combine 90 ml MilliQ or double-distilled water (ddH_2O) and 10 ml 10X PBS, use within days. For 1 liter of 10X PBS, to 900 ml ddH_2O add 80 g NaCl, 2 g KCl, 9.2 g $Na_2HPO_4{\cdot}7H_2O$, and 2 g KH_2PO_4. Stir until dissolved and then add ddH_2O to 1-liter final volume. Autoclave and store 10X PBS at 4°C.

2. *1 M HEPES–KOH, pH 8.0*: For 1 liter, to 600 ml ddH_2O add 238.3 g HEPES. Once dissolved, adjust pH to 8.0 using KOH pellets and add ddH_2O to 1-liter final volume. Pass through 0.22-µm filters. Store in a sterile bottle at 4°C.

3. *3 M KCl*: For 1 liter, to 700 ml ddH_2O add 223.68 g KCl. Once dissolved, add ddH_2O to 1-liter final volume. Autoclave and store at room temperature.

4. *1 M $MgCl_2$*: For 1 liter, to 700 ml ddH_2O add 203.3 g $MgCl_2$. Once dissolved, add ddH_2O to 1-liter volume. Autoclave and store at room temperature.

5. *0.5 M DTT*: For 50 ml, dissolve 3.85 g DTT in 50 ml ddH_2O and store at –20°C.

6. *1 M sodium phosphate, pH 7.2*: Dissolve 26.807 g NaH_2PO_4 in 70 ml ddH_2O and adjust volume to 100 ml once dissolved. Dissolve 13.8 g $Na_2HPO_4{\cdot}7H_2O$ in 80 ml ddH_2O and adjust volume to 100 ml once dissolved. Combine the two solutions together (approximately 68 ml : 31 ml, respectively) until pH 7.2 is reached. Store at room temperature.

7. *1 M Na butyrate*: 1 *M* Na butyrate and 20 m*M* sodium phosphate, pH 7.2. For 100 ml, dissolve 11 g butyric acid (sodium salt) in 80 ml ddH_2O and then pH to 7.2 with NaOH. Next, add 2 ml 1 *M* sodium phosphate, pH 7.2. Add ddH_2O to 100-ml final volume. Store at 4°C. This solution has an unpleasant odour.

8. *Hypotonic buffer*: 20 m*M* HEPES–KOH, pH 8.0, 5 m*M* KCl, 1.5 m*M* $MgCl_2$, and 0.1 m*M* DTT. For 100 ml, add 2 ml 1 *M* HEPES–KOH stock, 0.16 ml 3 *M* KCl, 150 µl 1 *M* $MgCl_2$, and 20 µl 0.5 *M* DTT (stored at –20°C). Bring to volume with ddH_2O. Prepare fresh and chill on ice.

9. *5 M NaCl*: For 1 liter, to 700 ml ddH_2O add 292.2 g NaCl. Once dissolved, add ddH_2O to 1-liter final volume. Autoclave and store at room temperature.

Steps

1. Grow 4 liters of 293 cells in Joklik's modification of MEM plus 5% bovine calf serum in a 6-liter spinner flask to 6×10^5 cells/ml at 37°C. Note that because this medium is not buffered by sodium bicarbonate, you can use a sealed spinner in a 37°C room if necessary.
2. Spin down 293 cells in six GSA bottles at 2500 rpm at 4°C for 10 min with brakes off. Pour off and discard the supernatant.
3. Repeat step 2 using the same GSA bottles until all cells are pelleted. Keep the bottles on ice whenever possible. Perform all the following procedures in a 4°C room.
4. Resuspend cells in the liquid remaining in the GSA bottles and transfer to an SS34 tube on ice. Wash the remaining cells out of the GSA bottles with chilled PBS and pool into the SS34 tube.
5. Centrifuge at 2500 rpm at 4°C for 3 min and then slowly pour off and discard the supernatant.
6. Add 20 ml of chilled PBS to the cell pellet and resuspend by gentle pipetting with a plastic 25-ml pipette.
7. Centrifuge cells again for 3 min and slowly pour off and discard the supernatant.

8. Estimate the volume of packed cells in each tube in order to determine the volume of hypotonic buffer to be added later (by pipetting water into another SS34 tube and estimating the pellet volume by comparison, usually approximately 7–8 ml).
9. To 100 ml hypotonic buffer, add 0.5 ml of 1 *M* Na butyrate (to 5 m*M* final) and protease inhibitor cocktail tablets.
10. Add 20 ml of hypotonic buffer (with additives) to cells and resuspend by gentle pipetting.
11. Centrifuge at 2500 rpm at 4°C for 5 min and remove and discard the supernatant using a pipette.
12. Resuspend cells in 1 ml of hypotonic buffer for each milliliter of packed cell volume estimated in step 8. Resuspend cells by gentle pipetting. Incubate cells on ice for 10 min.
13. Transfer cell suspension to a 40-ml dounce homogenizer. Rinse SS34 tube with a small amount of hypotonic buffer and pour the rinse into the dounce homogenizer. Remove 10 µl of cell suspension for step 14.
14. Dounce cells on ice for 25–30 passages with a "B" pestle. Remove 10 µl of cell suspension, and compare cells before and after douncing using an optical microscope to estimate extent of lysis. If there are significant numbers of intact cells after douncing, dounce for a few more passages.
15. Pour lysed cells into two prechilled 30-ml Corex tubes. Incubate on ice for 30 min.
16. Centrifuge in an HB6 rotor at 10,000 rpm at 4°C for 10 min. Pour the supernatant into a 15-ml conical tube to estimate volume. Add NaCl to 0.1 *M* final concentration (a 1/50 dilution of 5 *M* NaCl) into the supernatant and mix gently.
17. Divide solution between two ultracentrifuge tubes (Beckman Ti70) and centrifuge in a prechilled Ti70 rotor at 31,000 rpm at 4°C for 60 min.
18. Transfer the supernatant to a new tube (it is okay if some lipids transfer over). Divide into 0.5-ml aliquots, freeze in liquid N_2, and store at –80°C.

B. DNA Replication-Dependent Chromatin Assembly and Supercoiling Assay

Solutions

1. *1 M creatine phosphate*: Add 1 g of creatine phosphate to 80 µl 1 *M* HEPES–KOH, pH 8.0, and 3.92 ml ddH_2O. Store at –80°C.

2. *5X RM*: 200 m*M* HEPES–KOH, pH 8.0, 15 m*M* ATP, 1 m*M* CTP, 1 m*M* GTP, 1 m*M* UTP, 0.125 m*M* dATP, 0.5 m*M* dCTP, 0.5 m*M* dGTP, 0.5 m*M* dTTP, 200 m*M* creatine phosphate, 40 m*M* $MgCl_2$, and 2.5 m*M* DTT. To make 1.2 ml 5X RM, combine, in order, 426.5 µl ddH_2O, 240 µl 1 *M* HEPES–KOH, pH 8.0, 180 µl 100 m*M* ATP, 12 µl 100 m*M* CTP, 12 µl 100 m*M* GTP, 12 µl 100 m*M* UTP, 1.5 µl 100 m*M* dATP, 6 µl 100 m*M* dCTP, 6 µl 100 m*M* dGTP, 6 µl 100 m*M* of dTTP, 240 µl 1 *M* creatine phosphate, 28 µl 1 *M* Mg_2Cl, and 6 µl 0.5 *M* DTT. Freeze in liquid N_2 and store at –80°C.

3. *2 M Tris–HCl, pH 7.5*: to make 2 liters, add 484.4 g Tris base to 1.5 liters of ddH_2O. Adjust pH to 7.5 with HCl. Pass through a 0.22-µm filter and store in in sterile bottle at room temperature.

4. *CPK*: 5 mg/ml CPK, 50% glycerol, 25 m*M* Tris–HCl, pH 7.5, 1 m*M* EDTA, 25 m*M* NaCl, and 1 m*M* DTT. To make 10 ml CPK, add 50 mg creatine phosphokinase to 4.785 ml ddH_2O, 5 ml glycerol, 125 µl 2 *M* Tris–HCl, pH 7.5, 20 µl 0.5 *M* EDTA, 50 µl 5 *M* NaCl, and 20 µl 0.5 *M* DTT. Make 10-µl aliquots, freeze in liquid N_2, and store at –80°C.

5. *Master mix*: For each of x reactions ($x = n + 1$, where n is the number of reactions being performed), combine on ice in the following order: 5 µl 5X RM, 0.1 µl CPK, 1 µl template DNA (at 50 ng/µl), 1 µl SV40 T-antigen, and 0.1 µl [α-^{32}P]dATP. Use immediately.

6. *0.5 M EDTA, pH 8.0*: For 1 liter, to 700 ml ddH_2O add 186.12 g EDTA. Add NaOH pellets until white emulsion begins to clear. Adjust pH to 8.0 with NaOH pellets. Add ddH_2O to 1-liter final volume. Autoclave and store at room temperature.

7. *25 mM buffer A*: 18.75 m*M* Tris–HCl, pH 7.5, 2.5% glycerol, 1 m*M* EDTA, and 0.125% NP-40. For 4 ml, combine 3.45 ml ddH_2O, 37.5 µl 2 *M* Tris–HCl, pH 7.5, 500 µl glycerol, 10 µl 0.5 *M* EDTA, and 4 µl NP-40. Store at 4°C.

8. *10 mg/ml RNase A*: Dissolve 1 g RNase A in 100 ml ddH_2O. Make aliquots and store at –20°C.

9. *EDTA/RNase buffer*: For 1 ml, combine 935 µl ddH_2O, 50 µl 0.5 *M* EDTA, pH 8.0, and 15 µl 10 mg/ml RNase A. Use immediately.

10. *Glycogen stop buffer*: 20 m*M* EDTA, 1% (w/v) SDS, 0.2 *M* NaCl, and 250 µg/ml glycogen. For 50 ml, combine 45.5 ml ddH_2O, 2 ml 0.5 *M* EDTA, 500 mg SDS, 2 ml 5 *M* NaCl, and 12.5 mg glycogen. Store at room temperature.

11. *Proteinase K*: 2.5 mg/ml proteinase K, 10 m*M* Tris–HCl, pH 7.5, and 1 m*M* EDTA. To make 10 ml, dissolve 25 mg proteinase K in 9.9 ml ddH_2O, 50 µl 2 *M* Tris–HCl, pH 7.5, and 20 µl 0.5 *M* EDTA. Make aliquots and store at –20°C.

12. *3 M NaOAc*: For 1 liter, to 500 ml ddH_2O add 408.24 g sodium acetate trihydrate. Once dissolved, add ddH_2O to 1-liter final volume. Autoclave and store at room temperature.

13. *1X TBE*: 89 m*M* Tris, 89 m*M* boric acid, and 2.5 m*M* EDTA. For 1 liter of 1X TBE, combine 900 ml

ddH_2O and 100 ml of 10X TBE, For 1 liter 10X TBE, to 600 ml ddH_2O add 108 g Tris base, 55 g boric acid, and 7.49 g EDTA. Stir until dissolved and then add ddH_2O to 1-liter final volume. Store at room temperature. Discard solution when white particles appear.

14. *1X TBE gel-loading buffer*: 89 m*M* Tris, 89 m*M* boric acid, 2.5 m*M* EDTA, 6% glycerol, 0.05% BPB, and 0.05% XC. For 50 ml of 1X TBE gel loading buffer, combine 15 ml ddH_2O, 15 ml glycerol, 25 ml 10X TBE, 0.125 g BPB, and 0.125 g XC. Store at 4°C.

15. *10 mg/ml EtBr*: Add 0.5 g EtBr (weighed in a fume hood) to 50 ml ddH_2O. Store in the dark at 4°C.

Steps

1. Thaw T-antigen, CPK, 293 extract, and samples being tested in a room temperature water bath and place on ice once thawed. Assemble master mix on ice. Set up replication reactions on ice by adding in order 7.8 µl 25 m*M* buffer A, 7.2 µl master mix, and 10 µl 293 replication extract. Mix by pipetting up and down. If samples are being tested for their effect on DNA replication and/or chromatin assembly, add the samples first and adjust the volume of 25 m*M* buffer A so that the reaction has a final volume of 25 µl. Discard remainder of CPK aliquot and master mix. Freeze all unused reaction components in liquid N_2 and store at –80°C.
2. Incubate replication reactions at 30°C for 90 min.
3. Stop reactions by the addition of 6.25 µl EDTA/RNase buffer. Incubate at room temperature for 15 min.
4. Add 95 µl glycogen stop buffer and 5 µl proteinase K. Incubate at 37°C for 15 min.
5. Extract samples with 1 volume of phenol:chloroform:isoamyl alcohol (25:24:1) and then with 1 volume of chloroform:isoamyl alcohol (24:1).
6. Precipitate DNA by addition of 1/10 volume of 3 *M* NaOAc and 3 volumes of 100% EtOH. Invert to mix and microcentrifuge at full speed for 15 min.
7. Remove and discard supernatant and wash pellets with 75% EtOH. Dry pellets in a Speed-Vac.
8. Resuspend pellets in 8 µl of 1X TBE gel loading buffer. Load into wells of 1% agarose gel in 1X TBE and run until BPB runs off the gel (35 V for 14 h).
9. Stain gel in 500 ml ddH_2O + 30 µl 10 mg/ml EtBr for 30 min. Destain in ddH_2O for 30–60 min and photograph.
10. Dry gel on two layers of Whatman 3 MM paper overlaid with Saran wrap on a gel drier for 2 h with heater set to 65°C. Expose gel to film.

Figure 2B shows the products of the DNA replication-coupled chromatin assembly reactions, where the top shows total DNA and the bottom shows the newly replicated DNA.

IV. COMMENTS

1. For each batch of T-antigen, the optimal amount needs to be determined empirically by determining the lowest amount that gives the maximum amount of replication. Occasionally, the volume of each extract for chromatin assembly may need to be determined in a similar manner.
2. The amount of sample to use in a typical reaction needs to be determined empirically, as addition of too much chromatin assembly factor (i.e., CAF-1, ASF1) will inhibit DNA replication. Because too much salt in the samples can interfere with replication efficiency, in general it is advisable to dialyze samples into 25 m*M* buffer A before replication analysis.
3. Controls for replication dependence, as opposed to nucleotide excision repair of the nicked plasmid, include omission of T-antigen or use of a plasmid lacking the SV40 origin of DNA replication.

V. PITFALLS

In our hands, there is significant variation between different 293 extracts in terms of the amount of active CAF-1 and ASF1 that they contain, for unknown reasons. For example, we have generated extracts that do not require the addition of CAF-1 for chromatin assembly, only require the addition of CAF-1, or require the addition of both CAF-1 and ASF1, and we have even generated extracts that fail to replicate DNA! Therefore, each extract needs to be assessed by performing the replication reaction and supercoiling analysis with and without complementation by CAF-1, ASF1, or crude extracts. This extract variability is not an issue if a crude extract (such as the cell-free chromatin assembly extracts described in Section I,C) are being used to supply chromatin assembly factors. In fact, the variability in the extracts has allowed the original biochemical identification of CAF-1 and ASF1 by complementation of the 293 extracts (Smith and Stillman, 1989; Tyler *et al*., 1999).

References

Bonte, E., and Becker, P. (1999). Preparation of chromatin assembly extracts from preblastoderm drosophila embryos. *In "Methods in Molecular Biology"* (P. B. Becker, ed.), pp. 187–194. Humana Press, Totowa.

Carruthers, L. M., Tse, C., Walter, K. P., and Hansen, J. C. (1999). Assembly of defined nucleosomal and chromatin arrays from pure components. *Methods Enzymol.* 19–34.

Fyodorov, D., and Levenstein, M. E. (2002). Chromatin assembly using Drosophila systems. *In* "*Current Protocols in Molecular Biology*" (F. Ausubel, R. Brent, R. E. Kingston, D. D. Moore, J. G. Seidman, J. A. Smith, K. Struhl, eds.), Unit 21.7. Wiley, New York.

Gaillard, P. H., Roche, D., and Almouzni, G. (1999). Nucleotide excision repair coupled to chromatin assembly. *In* "*Methods in Molecular Biology*" (P. B. Becker, ed.), pp. 231–243. Humana Press, Totowa.

Gruss, C. (1999). *In vitro* replication of chromatin templates. *In* "*Methods in Molecular Biology*" (P. B. Becker, ed.), pp. 291–302. Humana Press, Totowa.

Lee, K., and Narlikar, G. J. (2002). Assembly of nucleosomal templates by salt dialysis. *In* "*Current Protocols in Molecular Biology*" (F. Ausubel, R. Brent, R. E. Kingston, D. D. Moore, J. G. Seidman, J. A. Smith, K. Struhl, eds.), Unit 21.6. Wiley, New York.

Levenstein, M. E., and Kadonaga, J. T. (2002). Biochemical analysis of chromatin containing recombinant Drosophila core histones. *J. Biol. Chem.* **277**, 8749–8754.

Loyola, A., LeRoy, G., Wang, Y. H., and Reinberg, D. (2001). Reconstitution of recombinant chromatin establishes a requirement for histone-tail modifications during chromatin assembly and transcription. *Genes Dev.* **15**, 2837–2851.

Luger, K., Rechsteiner, T. J., and Richmond, T. J. (1999). Expression and purification of recombinant histones and nucleosome reconstitution. *Methods Mol. Biol.* **119**, 1–16.

Mizuguchi, G., and Wu, C. (1999). Nucleosome remodeling factor NURF and *in vitro* transcription of chromatin. *In* "*Methods in Molecular Biology*" (P. Becker, ed.), pp. 333–342. Humana Press, Totowa.

Robinson, K. M., and Kadonaga, J. T. (1998). The use of chromatin templates to recreate transcriptional regulatory phenomena *in vitro*. *Biochim. Biophys. Acta.* **1378**, M1–6.

Schnitzler, G. (2002). Isolation of histones and nucleosome cores from mammalian cells. *In* "*Current Protocols in Molecular Biology*" (F. Ausubel, R. Brent, R. E. Kingston, D. D. Moore, J. G. Seidman, J. A. Smith, K. Struhl, eds.), Unit 21.5. Wiley, New York.

Schultz, M. C. (1999). Chromatin assembly in yeast cell-free extracts. *Methods* **17**, 161–172.

Simanis, V., and Lane, D. P. (1985). An immunoaffinity purification procedure for SV40 large T antigen. *Virology* **144**, 88–100.

Smith, S., and Stillman, B. (1989). Purification and characterization of CAF-I, a human cell factor required for chromatin assembly during DNA replication *in vitro*. *Cell* **58**, 15–25.

Stillman, B. (1986). Chromatin assembly during SV40 DNA replication *in vitro*. *Cell* **45**, 555–565.

Tremethick, D. J. (1999). Preparation of chromatin assembly extracts from Xenopus oocytes. *In* "*Methods in Molecular Biology*" (P. B. Becker, ed.), pp. 175–186. Humana Press, Totowa.

Tyler, J. K., Adams, C. R., Chen, S. R., Kobayashi, R., Kamakaka, R. T., and Kadonaga, J. T. (1999). The RCAF complex mediates chromatin assembly during DNA replication and repair. *Nature* **402**, 555–560.

White, C. L., Suto, R. K., and Luger, K. (2001). Structure of the yeast nucleosome core particle reveals fundamental changes in internucleosome interactions. *EMBO J.* **20**, 5207–5218.

SECTION

9

Signal Transduction Assays

CHAPTER

39

Cygnets: Intracellular Guanosine 3′,5′-Cyclic Monophosphate Sensing in Primary Cells Using Fluorescence Energy Transfer

Carolyn L. Sawyer, Akira Honda, and Wolfgang R.G. Dostmann

I. INTRODUCTION

Guanosine 3′,5′-cyclic monophosphate (cGMP) is a key player in the regulation of various physiological processes, including smooth muscle tone, neuronal excitability, epithelial electrolyte transport, phototransduction in the retina, and cell adhesion (Eigenthaler *et al*., 1999; Kaupp and Seifert, 2002; Lincoln *et al*., 2001; Schlossmann *et al*., 2003). Although the cGMP second messenger pathway has been steadily gaining recognition for its role in intracellular signaling, cGMP remains the least well understood member of the cyclic nucleotide family due to the following peculiarities of the cGMP signal transduction system. (1) The control of cGMP levels is complex, with formation of cGMP occurring through two different forms of guanylyl cyclases (Russwurm and Koesling, 2002; Wedel and Garbers, 2001) and degradation by a number of cGMP-specific phosphodiesterases (PDEs) (Rybalkin *et al*., 2003). (2) The intracellular actions of cGMP are mediated by cGMP-dependent protein kinases (PKGs) (Hofmann *et al*., 2000) and by several types of cyclic nucleotide-activated ion channels (Kaupp and Seifert, 2002). (3) The enzymes modulating cGMP levels are expressed differentially throughout mammalian tissues. Furthermore, a tightly controlled equilibrium of synthesis and breakdown generates highly flexible intracellular cGMP transients, contributing to the experimental and conceptual obstacles posed by the multiplicity in mechanisms of cGMP signaling and the difficulty of studying cGMP in broken cell preparations.

Genetically encoded indicators based on the insertion of conformationally sensitive domains between two mutants of green fluorescent protein (GFP) that participate in fluorescence resonance energy transfer (FRET) have proved to be powerful tools for observing the dynamics of intracellular signaling molecules noninvasively. Examples of such indicators include those that detect the second messengers Ca^{2+} (Miyawaki *et al*., 1997) and cAMP (Zaccolo and Pozzan, 2002). For the construction of our cGMP indicators, which we have named cygnets (cyclic GMP indicators using energy transfer), we chose PKG as the central cGMP sensor because it binds cGMP with high affinity, undergoes a conformational change in response to cGMP, and is not restricted to membranes (Pfeifer *et al*., 1999; Ruth *et al*., 1991; Zhao *et al*., 1997). We have demonstrated the validity of this intramolecular FRET approach and could show that cygnets (i) are exclusively selective for cGMP, (ii) allow detection of intracellular cGMP in single living cells, (iii) are fully reversible to monitor fast spatial and temporal cGMP changes, and (iv) are minimally invasive when analyzing intracellular cGMP signaling events (Honda *et al*., 2001; Sawyer *et al*., 2003). This article provides a detailed methodology for the use of our latest cGMP indicator version, Cygnet-2.1, in primary cell culture.

Copyright 2006, Elsevier Science (USA).
All rights reserved.

II. MATERIALS AND INSTRUMENTATION

The RFL-6 (CCL-192) established cell line is from American Type Culture Collection. The FuGENE 6 transfection reagent is from Roche (1814443). Cygnet-2.1 DNA (pcDNA3.1(-)-Cygnet-2.1) is constructed as described previously (Honda *et al*., 2001).

Dulbecco's modification of Eagle's medium (DMEM, with 4.5 g/liter glucose and L-glutamine, with sodium pyruvate; MT 10-013-CM), Ham's F-12 medium (MT 10-080-CM), fetal bovine serum (FBS, MT 35-010-CV), trypsin EDTA (MT 25-052-CI), amphotericin B (MT 30-003-CI), and gentamycin sulfate (30-005-CR) are from cellgro by Mediatech, Inc. Bovine serum albumin (BSA, A7638) and potassium phosphate [dibasic (K_2HPO_4, P-3786) and monobasic (KH_2PO_4, P-0662)] are from Sigma-Aldrich. Elastase (100617) is from ICN Biomedicals. Collagenase (199152) is from Worthington Biochemical Corporation. Penicillin/streptomycin/neomycin (15640-055) is from Gibco-BRL/Invitrogen. Collagen (354231), BD Falcon polystyrene 35 × 10-mm (353001) and 60 × 15-mm (353004) cell culture dishes are from BD Biosciences. Benzamidine hydrochloride (105240250) and EDTA (118430010) are from Fisher Scientific. The extracellular solution used for microscopic imaging consists of Hank's balanced salt solution (HBSS; cellgro by Mediatech, MT 21-020-CV) with 20 m*M* HEPES (cellgro by Mediatech, MT 25-060-CI) and 2 g/liter glucose (Sigma-Aldrich, G-7021).

cGMP (40732-48-7; reconstituted in distilled H_2O) and fluorescence grade 8-(4-chlorophenylthio)guanosine-3′, 5′-cyclic monophosphate [8-pCPT-cGMP; 51239-26-0; reconstituted in dimethyl sulfoxide (DMSO)] are from BIOLOG Life Science Institute.

The following chemicals have been used to modulate intracellular cGMP levels: Nitric oxide donors *S*-nitrosoglutathione (GSNO; Calbiochem 487920, protect from light and reconstitute in cold distilled H_2O free of divalent cations other than Ca^{2+}; stock solution is stable for 2 h at 4°C), *N*-(2-aminoethyl)-*N*-(2-hydroxy-2-nitrosohydrazino)-1,2-ethylenediamine [NOC-22, spermine NONOate; Calbiochem 567703; reconstitute in 0.1 *N* NaOH, ≥pH 10; $t_{1/2}$ of NO release = 230 min in phosphate-buffered saline (PBS), pH 7.4, 22°C] diethylamine NONOate (DEA NONOate; Calbiochem 292500, reconstitute in distilled H_2O; $t_{1/2}$ of NO release = 16 min in PBS, pH 7.4, 22°C), and (±)-*S*-nitroso-*N*-acetylpenicillamine (SNAP; Calbiochem 487910; protect from light and reconstitute in DMSO; $t_{1/2}$ of NO release = 10 h) are reconstituted to 100× the final concentration of 100 μ*M* prior to use and stored on ice until needed.

Atrial [ANP (3-28), rat; 14-5-44A] and brain [BNP (1-32), Rat; 14-5-11A] natriuretic peptides are from American Peptide Company. The C-type natriuretic peptide [CNP (6-22), human and porcine; 05-23-0310] is from Calbiochem. Peptides are reconstituted in distilled H_2O to 100 μ*M* stock solutions and stored at –20°C for several months until their use at a final concentration of 0.1–1 μ*M*.

The phosphodiesterase inhibitors 3-isobutyl-1-methylxanthine (IBMX; 410957; nonspecific inhibitor of cAMP and cGMP phosphodiesterases, final concentration 0.6 m*M*), vinpocetine (677500; PDE I inhibitor; final concentration 0.2 m*M*), 8-methoxymethyl-3-isobutyl-1-methylxanthine (MM-IBMX; 454202; PDE I inhibitor; final concentration 40 μ*M*), erythro-9-(2-hydroxy-3-nonyl)adenine, HCl (EHNA; 324630; PDE II inhibitor; final concentration 8 μ*M*; reconstitute in distilled H_2O), 1,6-dihydro-2-methyl-6-oxo-(3,4′-bipyridine)-5-carbonitrile (Milrinone; 475840; PDE III inhibitor; final concentration 3 μ*M*), 4-[3-(cyclopentyloxy)-4-methoxyphenyl]-2-pyrrolidinone (Rolipram; 557330; PDE IV inhibitor; final concentration 8 μ*M*), and 1,4-dihydro-5-(2-propoxyphenyl)-7H-1,2,3-triazolo[4,5-d]pyrimidine-7-one (Zaprinast; 684500; PDE V inhibitor; final concentration 4.5 μ*M*) are from Calbiochem. After reconstitution in DMSO (unless otherwise noted), stock solutions are stored at –20°C and used within 2 months. Sildenafil is a generous gift from Pfizer.

The fluorescence spectrometer F-4500 is from Hitachi. Quartz fluorescence cells (14-385-918A) for spectrophotometers and Dithiothreitol (DTT, 16568-0050) are from Fisher Scientific. Dithiothreitol (DTT, 16568-0050),

A light-duty portable punch size XX (130010001) outfitted with a 0.5-in. round dye (Type O) is from Roper Whitney of Rockford, Inc. A Sylgard 184 silicone elastomer kit is from Dow Corning Corporation. Coverslips (22 × 22 mm, 1 thickness; 12-544-10) are acquired from Fisher Scientific.

An inverted Nikon Diaphot 200 microscope equipped with a Nikon Fluor 40/1.30 oil Ph4DL objective (Part 140010) is outfitted with an ORCA ER cooled charge-coupled device camera (Hamamatsu). Three filter wheels, one each for excitation, emission, and neutral density filters, and a shutter at the excitation filter wheel are controlled by Lambda 10-2 optical filter changers from Sutter Instruments. A lambda LS xenon arc lamp and power supply are also obtained from Sutter Instruments. The Cameleons 2 filter set (71007a) purchased from Chroma Technologies for dual emis-

sion consists of a D440/20x excitation filter, a 455DCLP dichroic, and two emission filters (D485/40m and D535/30m). Neutral density filters (0.1, 0.3, 0.5, 1, 2, 3) are also obtained from Chroma. Image acquisition is controlled by a computer loaded with Metamorph and Metafluor 4.64 software from Universal Imaging (Media, PA). A stage adaptor to hold 35-mm imaging dishes was constructed at the Instrumentation and Model Facility at the University of Vermont.

III. PROCEDURES

A. Cygnet Expression and Purification

Express recombinant Cygnet-2.1 protein in *Spodoptera frugiperda* (Sf9) cells using the Bac-to-Bac baculovirus system (GIBCO/BRL) and purify using cAMP-agarose as described earlier (Honda *et al*., 2001).

B. *In Vitro* cGMP Titration

Perform cGMP titrations of Cygnet-2.1 by adding 50 n*M* of protein to a quartz fluorescence cell with buffer (50 m*M* KPO_4, pH 6.8, 10 m*M* DTT, 10 m*M* benzamidine, and 5 m*M* EDTA) for a final volume of 500 µl. Excite samples in a fluorescence spectrometer at 432 nm and monitor emission intensities from 450 to 550 nm. Plat the ratios of the 475 to 525 emission intensities against the concentration of cGMP added to the sample to generate a titration curve.

C. Cell Culture

The following cell types have been used successfully to express cygnets and monitor intracellular cGMP levels. Details on their preparation and handling are as follow.

1. Rat Fetal Lung Fibroblast Cells (RFL-6)

Cells should be cultured according to the supplier. Briefly, grow RFL-6 cells in Ham's F12 medium supplemented with 20% fetal bovine serum at 37°C, 5% CO_2. Subculture every 5–6 days with 0.25% trypsin at a ratio of 1:4 and plate on glass-bottom dishes for imaging. RFL-6 cells should not used beyond passage number eight. Routinely verify cGMP responses with cygnet-transfected RFL-6 cells, an established cell line known to respond with high cGMP levels upon stimulation (Ishii *et al*., 1991).

2. Rat Aortic Smooth Muscle Cells (RASMC)

Preparation and Culture of RASMC

1. Euthanize mature female or male Sprague–Dawley rat (250–350 g) by a lethal dose of pentobarbital sodium and exsanguination and remove thoracic aorta.
2. Clean aorta of fat and connective tissue and slice into 1- to 2-mm rings with a sterile scalpel.
3. With a scalpel, score a 60-mm cell culture dish to create a grid of three horizontal and three vertical lines, and embed each ring where two grooves intersect.
4. To prevent rings from detaching from the bottom of the dish, carefully add DMEM containing 10% FBS, 50 µg/ml gentamicin, and 2.5 µg/ml amphoteracin B and incubate at 37°C in humidified 5% CO_2. Replenish media every 2–3 days and smooth muscle cells will proliferate from the aortic explants within 1 week.
5. When cells reach confluency between gridlines, remove artery sections and rinse plate with trypsin. Add 1 ml fresh trypsin and aspirate off, leaving only a small amount in the dish. Incubate at 37°C until cells have detached, less than 5 min.
6. Resuspend cells in 2–3 ml supplemented media and transfer approximately 300 µl of cell suspension to glass portion only of glass-bottom imaging dishes.
7. When cells have adhered to the coverslip, aspirate media and replace with 2 ml fresh media in entire dish. These cells are henceforth referred to as passage one (P1) cells. Use only P1 cells in imaging experiments.

Alternatively, RASMC can be dissociated from the aorta using an isolation protocol adapted from Cornwell and Lincoln (1989) and Smith and Brock (1983).

1. After extracting aorta, place in isolation media consisting of DMEM, 20 m*M* HEPES, 1 mg/ml BSA, 5 µg/ml amphoteracin B, and 50 µg/ml gentamicin.
2. Clean aorta of fat and connective tissue and incubate in isolation media supplemented with 1 mg/ml elastase and 130 units/ml collagenase for 8 min at 37°C.
3. Rinse aorta to remove endothelial and other nonadherent cells, and remove tunicae adventitia as an everted tube.
4. Mince the medial layer of the aorta and digest pieces in isolation media supplemented with 200 units/ml collagenase for 1 to 2 h or until single cells are attained.
5. Wash cells twice in isolation media and culture in DMEM, 10% FCS, and 50 µg/ml gentamicin.

D. Preparation of Imaging Dishes

1. Prepare glass-bottomed dishes for fluorescence imaging by punching 0.5-in. holes in the bottoms of 35-mm cell culture dishes with an industrial punch.
2. Mix 1 part Sylgard 184 curing agent with 10 parts Sylgard 184 silicone elastomer (w/w) carefully to avoid introducing air bubbles.
3. Pipette a thin line of Sylgard around the hole on the bottom of the dish. Place a coverslip over the ring of Sylgard and tamp down with a cotton-tipped applicator to seal.
4. Allow Sylgard to cure overnight.
5. Sterilize dishes in a sterile hood under ultraviolet light for at least 30 min.
6. Dishes may be treated with 0.1 mg/ml collagen to promote cell adherence to coverslips.

E. Transfection of Cygnet-2.1

1. Grow primary RASMC to 50–60% confluency on 35-mm glass-bottomed dishes.
2. For each 35-mm dish, pipette 3 µl FuGENE 6 directly into 200 µL serum-free DMEM in a plastic 1.5-ml microfuge tube, minimizing the contact that FuGENE 6 has with the wall of the tube.
3. Add 1 µg highly purified pcDNA3.1(-)-Cygnet-2.1 to the DMEM–FuGENE 6. Close the tube and mix by inversion.
4. Allow DNA/lipid complexes to form at room temperature for 15 min.
5. Without removing media from 35-mm dishes, add transfection mixture dropwise using a pipette. Distribute transfection mixture around dish by gently shaking dish side to side.
6. Incubate RASMC at 37°C for 24 h and RFL-6 cells 48 h before imaging. Culture media may be replaced after 6 h of transfection, if desired. However, leaving cells in FuGENE until the time of imaging does not cause toxicity.

F. Data Acquisition and Analysis

Dual-Emission Imaging Protocol Using Metafluor

1. Open Metafluor software from Universal Imaging Corporation and select "New" on the toolbar to begin a new experiment.

2. Select configure/configure acquisition and define wavelengths 1 and 2 as ECFP and EYFP, respectively, and the excitation wavelength for both as 440 nm. The emission wavelengths for ECFP and EYFP must be defined as 480 and 535 nm, respectively. Chose file/save protocol file to save these parameters. When starting Metafluor from now on, begin by selecting "Protocol" and then open a new experiment.

3. Check the "Save Images" box in the control panel. As long as the box remains checked, every image acquired from now on will be saved as part of the file you are now prompted to name. *Note*: Each experiment is saved as an .inf file, which is composed of a .tif file of every image acquired during the experiment.

4. To locate transfected cells, manually select the 440-nm excitation filter and open the shutter (if applicable) in the illumination control box found in the configure menu.

5. Focus the transfected cell(s) of interest through the camera by selecting "Focus" on the control panel and the focusing screen will appear. Choose "Start Focusing" and your image will appear. Bring the image displayed on the monitor into focus and then click on "Stop Focusing." Selecting "Close" will bring you back to the experimental menu.

6. Select "Acquire One" on the toolbar to get an idea of what your image will look like. Cygnet-transfected cells should be visible in both 475 and 535 emission channels (Figs. 1A and 1B). Cells can be pseudocolored during at a later period during data analysis to correlate color hue with 475/535 emission ratio (Figs. 1C and 1D). If the cell is too bright (saturated pixels appear black) or too dim, the exposure time may need to be altered in the configure acquisition menu.

7. To start the experiment, press "Acquire" on the control panel menu and images will be captured at intervals until "Pause" is pressed.

8. To set the time lapse between image acquisitions to 10 s, select "Timelapse" on the control panel menu and enter the desired time.

9. Define regions on your image in which to monitor intensity values by selecting "Regions" on the toolbar. Select the circle tool and place a circle on a dark area of the image for background measurements. Then trace several regions (shape and number depending on cell) on the cell(s) of which you would like to monitor the fluorescence. Select "Close" to return to the experimental menu.

Note: The defined regions appear on one of the images, but fluorescence intensity data are collected from both wavelength channels in the same exact position defined on the cell. Graph 1 and Graph 2 plot the wavelength intensity value and ratio of (wavelength 1)/(wavelength 2) intensity values, respectively, against time.

10. As the program acquires images and plots data collected from the regions that you have defined, monitor the trace in Graph 2, the plot of the ECFP/EYFP ratio. Once you have established a stable baseline, pharmacological agents can be added and the

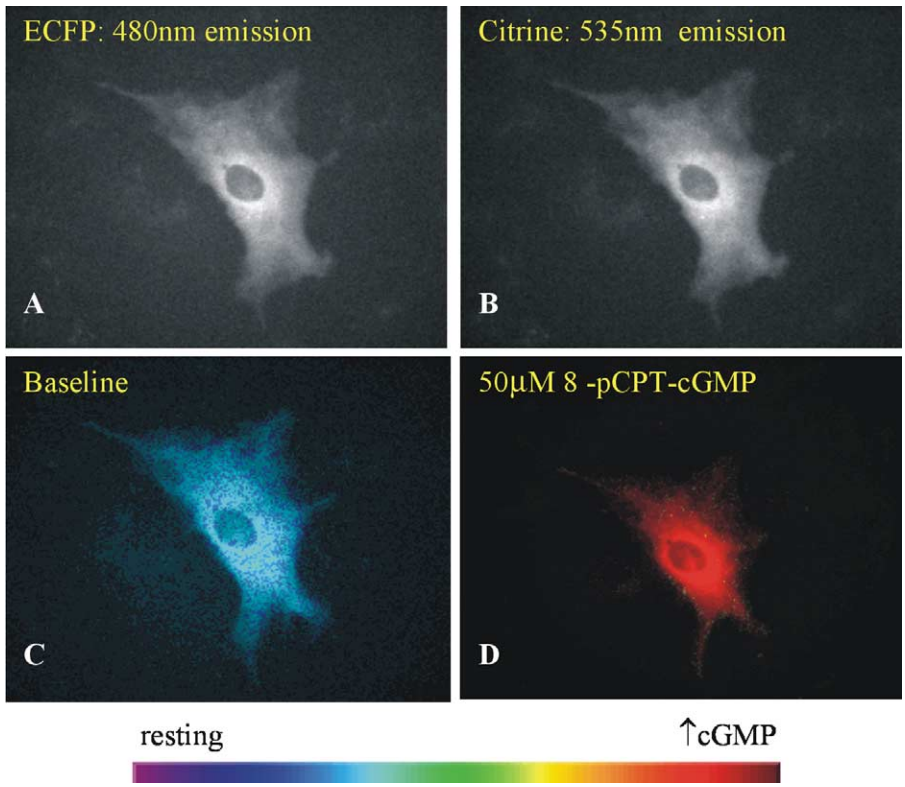

FIGURE 1 Cygnet-2.1 expression indicates cytosolic localization and nuclear exclusion in cultured rat aortic smooth muscle cells (top) as shown by the fluorescence images of (A) ECFP (480 nm emission) and (B) EYFPcitrine (535 nm emission). Pseudocolor representations of the 480- to 535-nm FRET ratio at resting (C) and elevated (D) cGMP levels were elicited with 50 µ*M* 8-pCPT-cGMP.

event markers used to note when things were added (select "Events" on the toolbar to define and mark events). At the end of an experiment, a cell-permeable cGMP analog can be applied to verify indicator fidelity (Fig. 2A).

11. To end the experiment, select "Close" on the control panel.

Data Collection

1. To collect data, select "Open" from the toolbar and select an experiment.
2. Define regions for background and on the cell(s) as before.
3. To subtract the background (i.e., make the intensity of background equal to zero), select run experiment/reference images. In the pull-down menu, choose to subtract the average intensity of a region and indicate which number refers to the region defining the background. Check the box on the lower left-hand corner to "Subtract Background" and close the menu.
4. Check "Log Data" on the control panel to save the intensity and ratio values of the wavelengths associated with each region.
5. Press "Forward" on the control panel to run through the experiment. As each image appears, the intensity and ratio values for each region on each wavelength channel (ECFP and EYFP) are saved. To make certain that the regions stay in the approximate same place on the cell, their placement may need adjustment. The log file that has been generated can be opened in a spreadsheet program and time plotted against the ECFP/EYFP intensity ratio.
6. To save individual images, select the desired image by playing through the experiment using the "Forward" button or the slider bar and then click on the image so that the window is highlighted. Under utilities/save as an 8-bit image, select to save the image as a .TIF file.

Making a Movie of a Pseudocolored Cell

1. To create a movie of a pseudocolored cell, define regions on the background and cell(s) and subtract background as described previously.
2. Play through the experiment and determine the minimum and maximum ratio values the cell displays by referencing Graph 2.

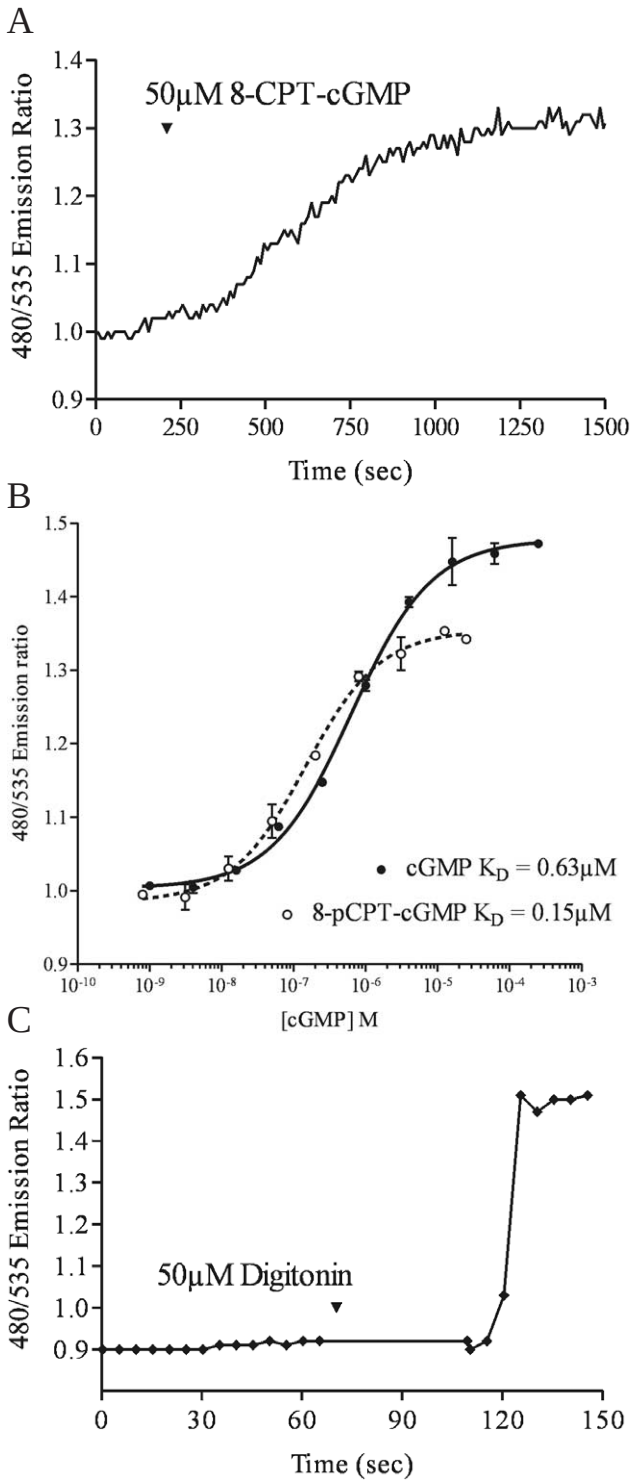

FIGURE 2 (A) Cygnet-2.1 expressed in an individual RASM cell exhibits a 30% EYFP/citrine ratio change in response to a saturating dose of the membrane-permeable cGMP analog 8-CPT-cGMP. (B) *In vitro* Cygnet-2.1 titration with cGMP reveals a maximum FRET ratio change of 45%. Saturating concentrations of the analog 8-CPT-cGMP can only generate a 30% change. (C) A RASM cell expressing Cygnet-2.1 was permeabilized with 50 μ*M* digitonin in an extracellular solution containing 8 μ*M* cGMP. The indicator responded to the cGMP influx with a FRET ratio change of 47%.

3. Select configure/image display control and choose Ratio 1 (ECFP/EYFP) from the top pull-down menu. From the lower pull-down menus choose intensity modulated display (IMD). In the "Minimum" and "Maximum" boxes, enter the approximate minimum and maximum ratio values determined from Graph 2. Setting the ratio values slightly inside the actual minimum and maximum values often enhances the visual effect as seen in the Ratio 1 box.

4. After optimizing the color changes the cell undergoes throughout the experiment, check the "Save Ratio" box on the control panel and forward through the entire experiment. The images displayed in the Ratio 1 box have now been saved as .TIF files.

5. Exit Metafluor and open Metamorph.

6. Select file/build stack/numbered names and select the first image. When prompted, select the last image. A "stack" of .TIF files has now been created.

7. Select stack/make movie, and a movie is generated from the compiled stack, which can be saved as an .AVI file under the stack menu.

8. A representative movie corresponding to the trace shown in Fig. 3 is published as supplemental data on the *Cell Biology* website.

Note: .AVI files generated with Metamorph are very large (40–100 MB) but can be compressed down to a few megabytes (50× or more) using a program such as VideoFramer.

G. Example of cGMP Sensing in Primary Rat Aortic Smooth Muscle Cells

At approximately 50–60% confluency, passage one cells were transfected with FuGENE 6 using a 3:1 ratio of FuGENE reagent to pcDNA3.1–Cygnet-2.1 DNA. Cells were imaged 24 h posttransfection at 25°C using Hank's balanced salt solution with 20 m*M* HEPES (pH 7.35) and glucose (2 g/liter) as the extracellular solution and 500-ms exposures at 10-s intervals.

Cygnet-2.1 expressed in both rat aortic smooth muscle cells (Figs. 1A and 1B) and RFL-6 cells (Honda *et al.*, 2001) demonstrated cytosolic localization and nuclear exclusion when ECFP and citrine emissions were viewed individually. Pseudocoloring of the cell (Figs. 2C and 2D) correlates the ratio of the ECFP/citrine emissions to a color scale, with lower and higher ratios and cGMP levels represented by blue and red, respectively. A saturating dose of the cell membrane-permeable cGMP analog 8-pCPT-cGMP changed the pseudocoloring from blue to red (Fig. 1D) and correlates to a 30% increase in FRET ratio (Fig. 2A). However, *in vitro* results with purified Cygnet-2.1 showed that cGMP consistently causes a 40–50% ratio

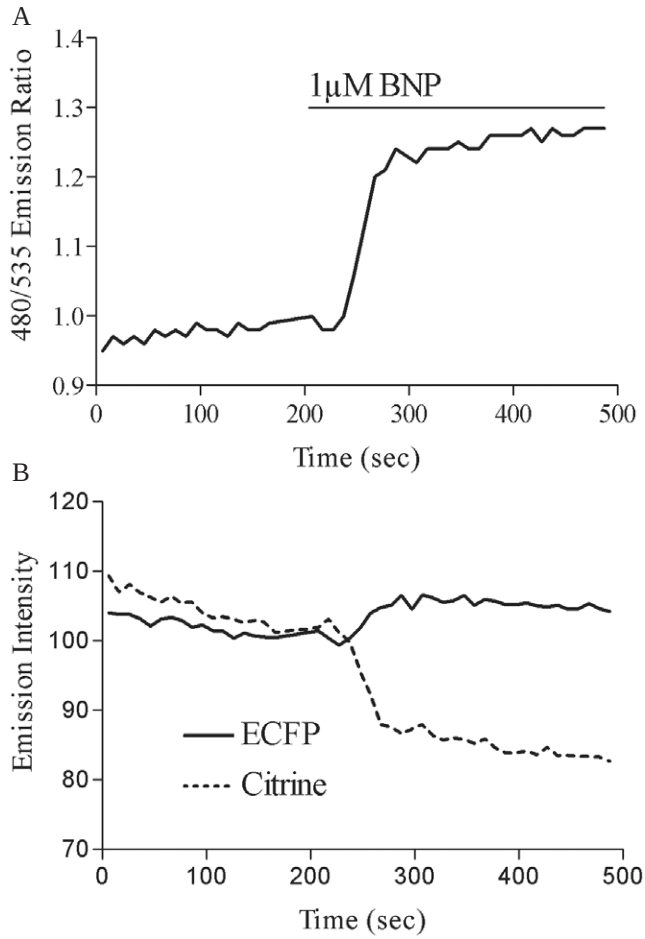

FIGURE 3 (A) Stimulation of the particulate guanylate cyclase (pGC) NPR-A with the natriuretic peptide BNP produces a FRET ratio change of approximately 28%. (B) Analysis of the individual emission intensities of ECFP and citrine during pGC activation demonstrates an increase in ECFP and a decrease in citrine emissions.

change. To analyze this apparent discrepancy, Cygnet-2.1 purified from Sf9 cells was titrated with cGMP and 8-CPT-cGMP (Fig. 2B). The purified indicator's maximum ratio change attained with cGMP was approximately 45%, while the analog still only elicited a maximal ratio change of 30%. In fact, in cells permeabilized with 50 μ*M* digitonin in the presence of saturating concentrations of cGMP, cygnets demonstrated a 47% FRET ratio change as expected from the *in vitro* results (Fig. 2C).

Activating the particulate guanylate cyclase with 1 μ*M* brain natriuretic peptide produced a FRET ratio change of 28% (Fig. 3A). Atrial natriuretic peptide produced a similar response, and both ANP- and BNP-induced cGMP accumulation could be washed out to near baseline (data not shown). Analysis of the individual emission intensities of ECFP and citrine demonstrates the mechanism of our cGMP indicator: cGMP generated in response to the activation of guanylate cyclase binds to the indicator and triggers a conformational change in the receptor. Subsequent alterations in the relative spatial arrangement of the two fluorophores result in a loss of energy transfer from ECFP to citrine and an increase in ECFP emission and a decrease in that of citrine (Fig. 3B).

IV. COMMENTS

Experiments acquiring images at 10-s intervals can run for greater than 30 min. We have accumulated as many as 200 exposures before applying a stimulus and have observed no significant loss in indicator sensitivity. It should be noted that cells have the tendency to react quite differently to the same stimulus.

V. PITFALLS

1. Transfection efficiency and cygnet expression may be low in some cells, particularly in primary cultures. Optimal expression may require alternative transfection reagents and optimization of transfection conditions, depending on the cell type.
2. Because intracellular cGMP fluctuations can potentially be buffered by the expression of the indicator, it is important to compare the total cGMP-binding capacity of untransfected and cygnet-transfected cells. This can be accomplished by the use of antibodies to PKG to determine if total PKG immunoreactivity, and therefore cGMP-binding capacity, is elevated by the expression of cygnets.
3. Because excessive illumination of cygnets may result in photobleaching of GFP mutants, fluorophore excitation should occur at the minimum intensity, frequency, and duration possible. The emission profiles of ECFP and citrine should be monitored to ascertain that changes in FRET are not due to aberrant behavior of the individual fluorophores due to photobleaching or other phenomena such as pH-induced alterations.

Acknowledgments

This work was supported by NSF Grant MCB-9983097 (WRGD) and the Totman Medical Research Trust.

References

Cornwell, T. L., and Lincoln, T. M. (1989). Regulation of intracellular Ca^{2+} levels in cultured vascular smooth muscle cells: Reduction of Ca^{2+} by atriopeptin and 8-bromo-cyclic GMP is mediated by cyclic GMP-dependent protein kinase. *J. Biol. Chem.* **264**, 1146–1155.

Eigenthaler, M., Lohmann, S. M., Walter, U., and Pilz, R. B. (1999). Signal transduction by cGMP-dependent protein kinases and their emerging roles in the regulation of cell adhesion and gene expression. *Rev. Physiol. Biochem. Pharmacol.* **135**, 173–209.

Hofmann, F., Ammendola, A., and Schlossmann, J. (2000). Rising behind NO: cGMP-dependent protein kinases. *J. Cell Sci.* **113**, 1671–1676.

Honda, A., Adams, S. R., Sawyer, C. L., Lev-Ram, V., Tsien, R. Y., and Dostmann, W. R. (2001). Spatiotemporal dynamics of guanosine 3',5'-cyclic monophosphate revealed by a genetically encoded, fluorescent indicator. *Proc. Natl. Acad. Sci. USA* **98**, 2437–2442.

Ishii, K., Sheng, H., Warner, T. D., Forstermann, U., and Murad, F. (1991). A simple and sensitive bioassay method for detection of EDRF with RFL-6 rat lung fibroblasts. *Am. J. Physiol.* **261**, H598–H603.

Kaupp, U. B., and Seifert, R. (2002). Cyclic nucleotide-gated ion channels. *Physiol. Rev.* **82**, 769–824.

Lincoln, T. M., Dey, N., and Sellak, H. (2001). cGMP-dependent protein kinase signaling mechanisms in smooth muscle: From the regulation of tone to gene expression. *J. Appl. Physiol.* **91**,1421–1430.

Miyawaki, A., Llopis, J., Heim, R., McCaffery, J. M., Adams, J. A., Ikura, M., and Tsien, R. Y. (1997). Fluorescent indicators for Ca^{2+} based on green fluorescent proteins and calmodulin. *Nature* **388**, 882–887.

Pfeifer, A., Ruth, P., Dostmann, W., Sausbier, M., Klatt, P., and Hofmann, F. (1999). Structure and function of cGMP-dependent protein kinases. *Rev. Physiol. Biochem. Pharmacol.* **135**, 105–149.

Russwurm, M., and Koesling, D. (2002). Isoforms of NO-sensitive guanylyl cyclase. *Mol. Cell. Biochem.* **230**, 159–164.

Ruth, P., Landgraf, W., Keilbach, A., May, B., Egleme, C., and Hofmann, F. (1991). The activation of expressed cGMP-dependent protein kinase isozymes Iα and Iβ is determined by the different amino-termini. *Eur. J. Biochem.* **202**, 1339–1344.

Rybalkin, S. D., Yan, C., Bornfeldt, K. E., and Beavo, J. A. (2003). Cyclic GMP phosphodiesterases and regulation of smooth muscle function. *Circ. Res.* **93**, 280–291.

Sawyer, C. L., and Dostmann, W. R. G. (2003). Cygnets: Spatial and temporal analysis of intracellular cGMP. *Proc Western Pharmacol Soc*.

Schlossmann, J., Feil, R., and Hofmann, F. (2003). Signaling through NO and cGMP-dependent protein kinases. *Ann. Med.* **35**, 21–27.

Smith, J. B., and Brock, T. A. (1983). Analysis of angiotensin stimulated sodium transport in cultured smooth muscle cells from rat aorta. *J. Cell Physiol.* **114**, 284–290.

Wedel, B., and Garbers, D. (2001). The guanylyl cyclase family at Y2K. *Annu. Rev. Physiol.* **63**, 215–233.

Zaccolo, M., and Pozzan, T. (2002). Discrete microdomains with high concentration of cAMP in stimulated rat neonatal cardiac myocytes. *Science* **295**, 1711–1715.

Zhao, J., Trewhella, J., Corbin, J., Francis, S., Mitchell, R., Brushia, R., and Walsh, D. (1997). Progressive cyclic nucleotide-induced conformational changes in the cGMP-dependent protein kinase studied by small angle X-ray scattering in solution. *J. Biol. Chem.* **272**, 31929–31936.

CHAPTER

40

Ca^{2+} as a Second Messenger: New Reporters for Calcium (Cameleons and Camgaroos)

Klaus P. Hoeflich, Kevin Truong, and Mitsuhiko Ikura

I. INTRODUCTION

The intracellular Ca^{2+} ion concentration has been found to be associated with a wide variety of cellular processes (Carafoli, 2003). These include diverse events such as secretion, fertilization, cleavage, nuclear envelope breakdown, and apoptosis. Several diseases, including types of muscular dystrophy, diabetes, and leukemia, involve proteins that directly respond to or control Ca^{2+}. Indeed, it may be more difficult to find cellular processes that do not involve Ca^{2+} than ones that do. From decades of research we have learned that the process of Ca^{2+} signaling consists, in general terms, of molecules for Ca^{2+} signal production, spatial and temporal shaping, sensors, and targets that elicit changes in biological function. Hence, this has prompted the development of sensitive signaling techniques to measure and image submicromolar levels of $[Ca^{2+}]$ and decode the dynamic Ca^{2+} messages throughout the propagation of the signal.

Ca^{2+} transients have traditionally been measured using synthetic fluorescent chelators (such as Fura-2 and Quin2) or recombinant aequorin (Grynkiewicz *et al.*, 1985: Montero *et al.*, 1995). Synthetic molecules provide a bright fluorescent signal, but these dyes are not easy to load and gradually leak out of cells at physiological temperatures. Cellular targeting is also not specific and some chemical indicators have been shown not to accumulate well in certain organelles. Aequorin is targeted easily but it requires incorporation of the cofactor coelenterazine, is irreversibly consumed by Ca^{2+}, and is very difficult to image due to low bioluminescence. By comparison, green fluorescent protein (GFP) and calmodulin (CaM)-based "cameleon" probes have been developed and retain several of the benefits of the aforementioned indicators, yet also provide significant improvements for *in vivo* imaging (Miyawaki, 2003; Zhang *et al.*, 2002; Truong and Ikura, 2001).

The use of cameleon indicators is gradually becoming more common within the Ca^{2+} signaling community and the literature is rich with examples of various applications. For instance, fusion of cameleons to specific signal sequences has successfully sorted them to nuclei, endoplasmic reticulum, caveolae, and secretory granule membranes (Isshiki *et al.*, 2002; Demaurex and Frieden, 2003; Emmanouilidou *et al.*, 1999). In addition to their use in detecting rapid stimulus-induced $[Ca^{2+}]$ transients, genetic studies in which cameleons were stably expressed in *Arabidopsis* stomatal guard cells (Allen *et al.*, 1999), nematode pharyngeal muscle (Kerr *et al.*, 2000), or larval thermoresponsive neurons of *Drosophila* (Liu *et al.*, 2003) show that the sensors are also applicable to long-term monitoring of Ca^{2+} concentration. This has been demonstrated further for murine cells where the circadian rhythm of cytosolic but not nuclear Ca^{2+} in hypothalmic suprachiasmatic neurons was demonstrated (Ikeda *et al.*, 2003).

It is hoped that this article provides some explicit and practical information relevant to the laboratory use of cameleon fluorescence resonance energy transfer (FRET) indicators. Our aim is that it will benefit and be of interest to colleagues both unfamiliar or experienced in using fluorescent Ca^{2+} indicators.

Copyright 2006, Elsevier Science (USA).
All rights reserved.

II. MATERIALS AND INSTRUMENTATION

A. Expression and Purification of Cameleons

Enhanced cyan fluorescent protein (ECFP) and enhanced yellow fluorescent protein (EYFP) expression constructus (Clontech Cat. No. 6075-1 and 6004-1, respectively); calmodulin cDNA (M. Ikura); pRSETB prokaryotic expression vector (Invitrogen Cat. No. V351-20); Luria broth (LB) media; isopropyl-β-D-thiogalactopyranoside (IPTG, Fermentas Cat. No. R0391); complete protease inhibitor cocktail tablets (Roche Cat. No. 1697498); Ni-NTA agarose (Qiagen Cat. No. 1018240); *Escherichia coli* BL21 (DE3) strain (Stratagene Cat. No. 200133); sonicator; EGTA buffer: 100 m*M* KCl, 50 m*M* HEPES (pH 7.4), and 10 m*M* EGTA; $CaC1_2$ buffer: 100 m*M* KCl, 50 m*M* HEPES (pH 7.4), 10 m*M* EGTA, and 10 m*M* $CaCl_2$.

B. *In Vitro* Fluorescence Quantitation

Shimadzu spectrofluorometer RF5301; 10-mm pathlength quartz cuvette.

C. *In Vitro* Imaging of Cameleons

pcDNA3 eukaryotic transient expression vector (Invitrogen Cat. No. V790-20); uncoated; γ-irradiated, 35-mm tissue culture dishes with glass bottom No. 0 (MatTek Cat. No. P35G-0-10-C); Dulbecco's modified Eagle medium (DMEM) supplemented with 10% dialyzed fetal bovine serum (FBS, Invitrogen Cat. No. 26400044), Hanks' balanced salts solution (HBSS) with Ca^{2+} (Invitrogen Cat. No. 14170120); 37°C CO_2 incubator; HeLa cells or appropriate eukaryotic strain; Lipofectamine (Invitrogen Cat. No. 18324012) and PLUS (Invitrogen Cat. No. 11514015) reagents; histamine, ionomycin, ethylene glycol-bis(2-aminoethylether)-*N*,*N*,*N*′,*N*′-tetraacetic acid (EGTA) and 1,2-bis(2-aminophenoxy)ethane-*N*,*N*,*N*′,*N*′-tetraacetic acid tetrakis(acetoxymethyl ester) (BAPTA-AM) (Sigma Cat. No. H7125, I0634, E0396, and A1076, respectively); Olympus IX70 inverted epifluorescence microscope; Olympus Xenon lamp; MicroMax 1300YHS CCD camera and Sutter Lambda 10-2 filter changers controlled by Metafluor 4.5r2 software (Universal Imaging); ECFP-EYFP FRET filter set (Omega Optical); 440AF21 excitation filter (ECFP excitation), 455DRLP dichroic mirror, 480AF30 emission filter (ECFP emission), and 535AF26 emission filter (EYFP emission); neutral density (ND) filter set (Omega Optical); UApo 40xOil Iris/340 objective (Olympus); U-MNIBA bandpass mirror cube unit (Olympus).

III. PROCEDURES

A. Engineering Cameleon Constructs

The history of cameleon engineering is reflected in its nomenclature (Table I). Optimization of Ca^{2+} affinities, pH dependency, maturation time, and other parameters is by no means complete. However, we present construction of a general cameleon designed in our laboratory, YC6.1, to serve as a reference point for future work (Truong *et al*., 2001). Molecular biology techniques for manipulating recombinant DNA are not given as they can be obtained from common reference books.

In these constructs, ECFP and EYFP function as a donor–acceptor pair for nonradiative, intramolecular FRET. During FRET, excitation of the donor (cyan) leads to emission from the acceptor (yellow), provided that the molecules are close enough (within 80 Å) and in a parallel orientation. In this way, on binding Ca^{2+} the CaM wraps around its adjacent CKKp target peptide and ECFP and EYFP are brought closer to each other and FRET increases (Fig. 1).

TABLE I Properties of Commonly Used Cameleon Indicators

Name	pK_a	[Ca^{2+}] range (μM)	Comments	Reference
Cameleon-1	6.9	0.1–10	BFP/GFP hybrid with CaM-M13 tandem	Miyawaki *et al*. (1997)
YC2	6.9	0.1–10	Use of ECFP/EYFP for donor/acceptor	Miyawaki *et al*. (1997)
YC2.1	6.1	0.1–10	V68L/Q69K for increased pH resistance	Miyawaki *et al*. (1999)
YC2.12	6.0	0.1–10	"Venus" quick-maturation derivative	Nagai *et al*. (2002)
YC3	6.9	0.5–1000	E104Q low-affinity indicator	Miyawaki *et al*. (1997)
YC3.3	5.7	0.5–1000	Q69M "citrine" for added pH resistance	Griesbeck *et al*. (2001)
YC4	6.9	10–1000	E31Q low-affinity indicator	Miyawaki *et al*. (1997)
YC6.1	6.1	0.1–1	Internal CKKp CaM recognition peptide	Truong *et al*. (2001)
SapRC2	5.5	0.2–0.4	Sapphire/DsRed cameleon	Mizuno *et al*. (2001)

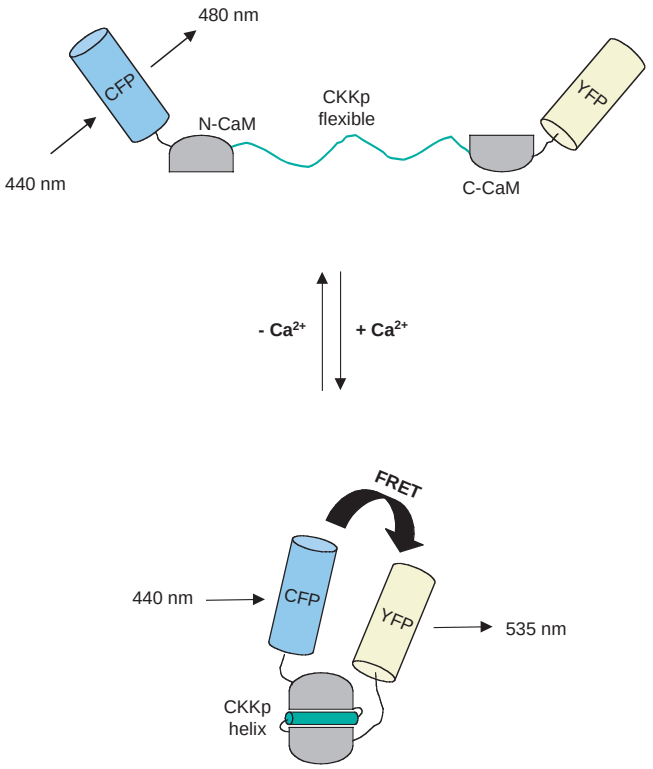

FIGURE 1 Schematic depiction of YC6.1 FRET in response to [Ca^{2+}]. See text for details.

1. A successful construction of GFP-fused protein indicators is facilitated greatly by careful inspection of available three-dimensional structure information of the protein or protein domain used for sensing functions. Typically, such structural analysis can be done using SwissPDBviewer (Windows) and MODELLER (Unix), which allow the measurement of atomic distances and the molecular modeling of fusion proteins, respectively. This was also the case for designing YC6.1. We found that by virtue of the hairpin-like complex structure of CKKp, the peptide can be inserted into the domain linker region (residues 78–81) of CaM.

2. Insert a CaM-binding peptide derived from CaM-dependent protein kinase kinase (CKKp; residues 438–463) between the terminal EF hand Ca^{2+}-binding domains (N-CaM and C-CaM) within the CaM linker domain (between CaM residues 79 and 80) and connect via two Gly-Gly linkers.

3. Add ECFP- and EYFP-encoding open reading frames to termini of the (N-CaM)-GG-CKKp-GG-(C-CaM) module by recombinant DNA methods. Expression vectors for many GFP family members are available through Clontech. Cameleon constructs can benefit from truncation of the last 11 C-terminal amino acids of ECFP (the minimal region to form GFP) to reduce the relative tumbling of the fluorophores. Additionally, linkers introduced between CaM domains and the target peptide can be optimized for complex formation.

4. Sequence construct to ensure polymerase chain reaction errors are not present. Note that oligonucleotides designed to the 5′ or 3′ end of ECFP open reading frames will also recognize the counterpart sequences in EYFP due to high sequence identity.

5. Subclone this cameleon domain into either pRSETB plasmid, for prokaryotic protein expression sufficient for biochemical and biophysical characterization, or pcDNA3.1 for mammalian expression and *in vivo* Ca^{2+}-imaging experiments. If optimal expression is not crucial, we also found that the pTriEx3 (Novagen) vector is convenient for expression in both prokaryotic and eukaryotic systems.

6. In addition to this cytoplasmic version of cameleon YC6.1, nucleus- and endoplasmic reticulum-targeted versions (YC6.1nu and YC6.2er, respectively) can be constructed by the addition of appropriate signal sequences to termini.

B. Overexpression and Purification of Cameleons

1. From a single colony of newly transformed *E. coli* strain BL21(DE3), grow liquid cultures at 37°C in LB medium containing 100 µg/ml ampicillin.
2. At OD_{600}, induce cultures with 0.5 m*M* IPTG at 15°C overnight.
3. Harvest cells by centrifugation at 6500 rpm for 20 min at 4°C.
4. Resuspend cell pellets in 1/20 culture volume of lysis buffer [50 m*M* HEPES (pH 7.4), 10% glycerol, 100 m*M* KCl, 1 m*M* $CaCl_2$, and 1 m*M* phenylmethyl sulfonyl fluoride (PMSF)], sonicate, and centrifuge at 15,000 rpm for 30 min to remove debris.
5. Incubate the supernatant with nickel chelate agarose for 1 h at 4°C and wash with of 50 m*M* HEPES (pH 7.4), 100 m*M* KCl, and 5 m*M* imidazole.
6. Elute YC6.1 with 300 m*M* imidazole in the aforementioned buffer. Proteolytic cleavage to remove the $(His)_6$ tag is not necessary as it does not interfere with YC6.1 fluorescent properties.
7. *Optional*: The eluant can be then purified further on a Superdex 75 HR 10/30 FPLC column using 20 m*M* HEPES, pH 7.5, 150 m*M* KCl, 5% glycerol, 5 m*M* dithiothreitol, and 1 m*M* PMSF.
8. Use the fraction that has the highest FRET ratio for fluorescence experiments.
9. Dialyze the sample against 2 liter of 50 m*M* HEPES (pH 7.4), 100 m*M* KCl at 4°C.

10. *Optional*: Glycerol can be added to the sample at a final concentration of 20%, and aliquot, flash freeze in liquid N_2, and store the YC6.1 at –70°C.

If necessary, it is possible to perform the characterization using a mammalian cell lysate. For harvesting, cells should be transfected in several 100-mm-diameter culture dishes, washed thoroughly to remove traces of phenol red and serum, and lysed in a hypotonic lysis buffer [50 m*M* HEPES (pH 7.4) 100 m*M* KCl, 5 m*M* $MgCl_2$, and 0.5% Triton X-100]. Following removal of cellular debris by centrifugation, dialyze the supernatant in 2 liter of buffer [50 m*M* HEPES (pH 7.4) and 100 m*M* KCl]. Finally, the sample can be used for characterization as described.

C. *In Vitro* Cameleon Fluorescence Spectroscopy

1. Record fluorescence spectra on a Shimadzu spectrofluorometer RF5301 using a 10-mm path-length quartz cuvette at room temperature.
2. Dilute cameleon chimeric proteins in 50 m*M* HEPES (pH 7.4), 100 m*M* KCl, and 20 μ*M* EGTA to a final concentration of 60 nM. Although many dilution factors are acceptable, intermolecular ECFP-EYFP FRET will occur at higher concentrations, thereby inflating the emission signal falsely.
3. Excitate at 433 nm and monitor the fluorescence emission between 450 and 570 nm with excitation and emission slit widths of 5 nm (Table II).
4. Record the fluorescence emission spectra of buffer (background) and cameleon protein solutions.
5. Subtract the background spectrum for buffer alone from the cameleon sample to find spectra of the cameleon in the absence of Ca^{2+}.
6. Determine the fluorescence emission ratio (R) by dividing the integration of fluorescence intensities of the FRET acceptor (for EYFP, between 520 and 536 nm) by that of the FRET donor (for ECP, between 470 and 485 nm).

TABLE II Fluorescent Properties of Fluorescent Protein Pairs Used for FRET Studies

Donor	Acceptor	Donor excitation wavelength (nm)	Donor emission wavelength (nm)	Acceptor emission wavelength (nm)
EBFP	EGFP	370	440	510
ECFP	EYFP	440	480	535
EYFP	mRFP1	510	535	607
Sapphire	DsRed	400	510	580

7. Determine R_{min} from this spectrum. A key parameter for a Ca^{2+} indicator is its dynamic range in response to $[Ca^{2+}]$. The dynamic range of a cameleon is defined as the division of the maximum ratio, R_{max}, by the minimum ratio, R_{min}.
8. In the presence of 1 m*M* $CaCl_2$, repeat to find spectra of the cameleon in the presence of saturating amounts of Ca^{2+}. Determine R_{max} from this spectrum.

The Ca^{2+}-binding curve is used to assess the effective range of $[Ca^{2+}]$ measurement. Ca^{2+}/EDTA and Ca^{2+}/EGTA buffers are used as standards because even trace Ca^{2+} contaminants can significantly distort $[Ca^{2+}]_{free}$ values at low $[Ca^{2+}]$ (Bers *et al*., 1994; Miyawaki *et al*., 1997).

1. Prepare EGTA buffer [100 m*M* KCl, 50 m*M* HEPES (pH 7.4), 10 m*M* EGTA] and $CaC1_2$ buffer [100 m*M* KCl, 50 m*M* HEPES (pH 7.4), 10 m*M* EGTA, 10 m*M* $CaCl_2$]. pH should be held constant.
2. Use a 1-ml cuvette and dilute the sample in the EGTA buffer. Record the fluorescence emission spectrum from 450 to 570 nm at 433-nm excitation. Determine the emission ratio.
3. To obtain the Ca^{2+}-binding curve, add successive fractions of the $CaC1_2$ solution to the sample and determine the emission ratio. Given that the experiment is performed in 20°C with these EGTA and $CaCl_2$ buffers, the free calcium can be calculated by solving the quadratic equation: $[Ca^{2+}]_{free}^2 + (10{,}000{,}060.5 - [Ca^{2+}]_{total}) * [Ca^{2+}]_{free} - 60.5 * [Ca^{2+}]_{total} = 0$.
4. To produce the Ca^{2+}-binding curve, plot the $[Ca^{2+}]_{free}$ versus emission ratio change (percentage of maximum). Initial cameleons show biphasic Ca^{2+} dependency, whereas YC6.1 has a monophasic response.
5. Extract the apparent dissociation constant (K'_d) and Hill coefficient (n) from the fitted curves.
6. The emission ratio can then be transformed to $[Ca^{2+}]$ according to

$$[Ca^{2+}] = K'_d[(R - R_{min})/(R_{max} - R)]^{1/n}$$

D. Live Cell Cameleon Fluorescence Imaging

This section describes a Ca^{2+}-imaging experiment using HeLa cells; however, with minor modifications the method can be applied to other cellular and physiological contexts.

1. Plate HeLa cells on 35-mm-diameter glass-bottom dishes with DMEM–10% FBS media.
2. Incubate the cells at 37°C (5% CO_2) until cells are 50–80% confluent.
3. Transfect cells with the mammalian expression plasmid containing your cameleon using Lipofecta-

mine and PLUS reagents (Invitrogen) according to the manufacturer's instructions.

4. Remove the transfection mixture after 5–18 h and replace with fresh 1.5 ml of DMEM–10% FBS media.

5. Incubate the cells at 37°C (5% CO_2) for 24 h. The cells are ready to perform the Ca^{2+}-imaging experiment.

6. All data acquisition should be performed in a dark room to reduce background light.

7. Wash with 1 ml of HBSS (+$CaCl_2$) and add 1 ml of fresh HBSS (+$CaCl_2$).

8. Put the cells on the stage of the microscope. Cells are viable and healthy for at least 60 minutes at ambient conditions. A CO_2 box and temperature controller are required for long-term/extended time course experiments.

9. The MetaFluor software controls the shutters, filter exchangers, and camera during data acquisition.

10. Screen for EYFP fluorescence (which is brighter and distinguished more easily than ECFP fluorescence) using the eyepiece to find transfected cells expressing the cameleon construct. Turn the filter turret to the U-WNIBA band-pass mirror cube and use ND filter in the range of 0.1–10% to reduce photobleaching depending on the intensity of fluorescence emission (Table III).

11. Using the 40× oil objective, center the microscope viewing area on a cell that has a healthy morphology and displays a strong cytosolic fluorescence.

12. Acquire single images on the computer screen using MetaFluor while adjusting the focus until you have the sharpest screen image. Focus through the eyepiece and the CCD usually vary slightly.

13. Turn the filter turret to the cube with the 455DRLP dichroic mirror. This allows visible light shorter and longer than ~455 nm to be reflected as excitation to the sample and collected as emission from the sample, respectively. Consult spectra from Omega Optical for relatively wavelength transmission efficiencies.

14. To monitor the peak emissions of ECFP and EYFP as a result of ECFP peak excitation over time, set the data acquisition conditions as follows: time interval to every 10 s and exposure time to 200 ms for ECFP and EYFP. Longer exposures improve resolution at the expense of bleaching the fluorescent signal. MetaFluor will display the emission ratio over time.

15. Draw a region of interest on the field of view of the CCD. Usually, this region will outline the whole cell, but one can specify only a portion of a cell if desired (e.g., the nucleus). It is important that the stage or the cell does not move during the observation period as the region initially drawn may drift from the region of interest. Additionally, the intensity in the region (the signal) should be at least five times the intensity of the background.

16. The emission intensities of both ECFP and EYFP will decrease over the course of the experiment due to some unavoidable photobleaching; however, the effect on the emission ratio should be negligible. To reduce photobleaching, decrease exposure time and excitation light intensity. Also, binning can sum the signal from multiple pixels on the CCD camera so that less light is required while keeping a good signal-to-noise ratio.

17. MetaFluor will record the fluorescence emission intensities of the ECFP and EYFP, together with their emission ratios in the regions over time.

18. When the emission ratio reaches a steady state, add 50 µl of 2 m*M* histamine to the culture dish for a final concentration of 100 µ*M*. Be careful not to move the culture dish in this process. The histamine binds to cell receptors on the plasma membrane that set off a signaling cascade, resulting in the release of Ca^{2+} from the endoplasmic reticulum through the inositol-1,4,5-triphosphate receptor. This should cause a conformational change in the cameleon that can be observed by

TABLE III Recommended Optical Components[a]

	FRET system			
	BFP/GFP	**ECFP/EYFP**	**ECFP/EYFP/RFP**	**Sap/DsRed**
Excitation filter	365WB50	440AF21	440DF21 (ECFP) 510DF23 (EYFP)	400DF15
Dichroic mirror	400DCLP	455DRLP	450-520-590TBDR	455DRLP
Emission filter, donor	450DF65	480AF30	480AF30 (ECFP) 535AF26 (EYFP)	480DF30
Emission filter, acceptor	535AF45	535AF26	535AF26 (EYFP) 600ALP (RFP)	535DF25

[a] The components are from Omega Optical but can be substituted with several equivalent products from other companies.

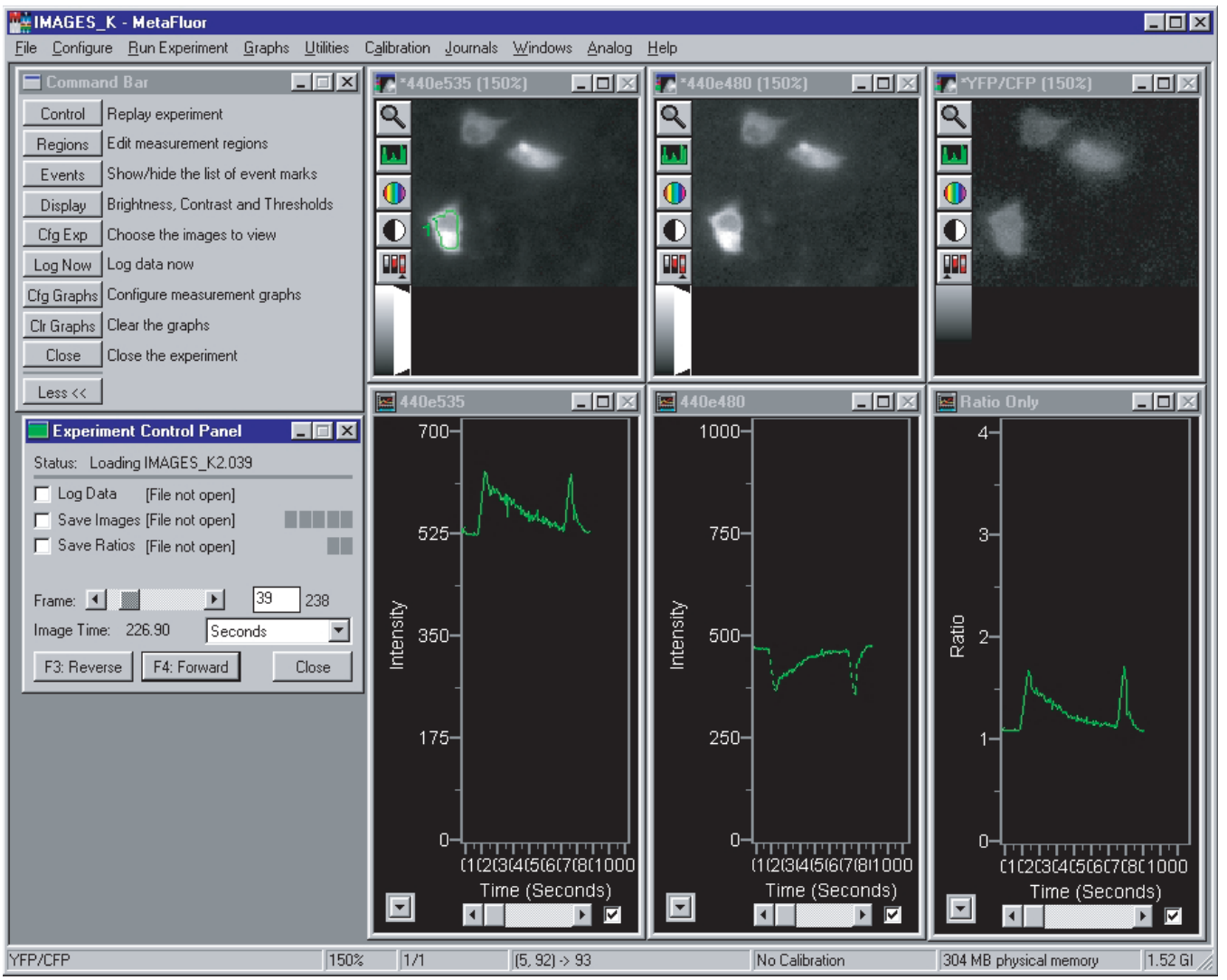

FIGURE 2 Example of Ca^{2+} imaging experiment using MetaFluor software. The region of observation is highlighted green in the 440e535 panel. The 440e535 panel and graph plot the change in EYFP fluorescence as a result of ECFP excitation; the 440e480 panel and graph plot the change in ECFP fluorescence as a result of ECFP excitation; the EYFP/ECFP panel and graph are the ratio of 440e535 and 440e480 panels and graphs. In this experiment, the graphs display a sharp rise in $[Ca^{2+}]_c$ from the initial stimulation with histamine followed by a slow decline in $[Ca^{2+}]_c$ to baseline levels. The second stimulation with histamine causes a significantly more rapid return to baseline levels.

a rise in emission intensity of EYFP and a decline in ECFP intensity. Therefore, the emission ratio should increase. The EYFP/ECFP emission ratio should return to steady-state levels when the effect of the histamine wanes. Figure 2 shows a representative example of MetaFluor software as it is collecting data.

19. In order to correlate the emission ratio to $[Ca^{2+}]_{cytosolic}$, it is necessary to determine R_{min} and R_{max} so that emission ratios can be mapped to the Ca^{2+}-binding curve. Add 50 µl of 20 µ*M* ionomycin for a final concentration of 1 µ*M*. Ionomycin open pores on the plasma membrane to allow permeability to Ca^{2+} ions. Because the medium is saturated with $CaCl_2$, the ratio will rise to R_{max}. To determine R_{min}, add 50 µl of 100 m*M* EGTA and 600 µ*M* BAPTA-AM for a final concentration of 5 m*M* and 30 µ*M*, respectively. The emission ratio should drop to R_{min}.

IV. OTHER APPROACHES

Several other Ca^{2+} probes are also being developed, including the so-called "camgaroos" and "pericams."

Camgaroos take an alternative approach to designing fluorescent Ca^{2+} sensors based on CaM and GFP family members (Baird *et al*., 1999). While ECFP and EYFP in cameleons are appended to the amino and carboxyl termini of CaM and Ca^{2+} binding is detected by FRET, camgaroo indicator proteins take advantage of the robust structure and profound fluorescence sensitivity of GFP to altered pK_a values and chromophore orientation. Circular permutations and insertion of whole CaM in place of Tyr-145 within EEYFP thereby render this indicator responsive to Ca^{2+} binding. As a result, both excitation and emission spectra of camgaroo simply increase in amplitude by up to seven-fold upon saturation with Ca^{2+}, without any significant shift in peak wavelength. This Ca^{2+}-dependent fluorescence enhancement is substantially larger than other published genetically encoded fluorescent indicators. However, camgaroos are limited by pH sensitivity inherent in the current mechanism of modulating fluorescence via changes in pK_a of the chromophore and have to date only been preliminarily subjected to systematic mutational improvement.

Pericams, in which EYFP is circularly fused to CaM and the M13 myosin light chain kinase peptide, improve approximately 10-fold upon the low affinity of camgaroo for Ca^{2+} ($K_d = 7\,\mu M$) and are thereby better capable of sensing low physiological changes in intracellular [Ca^{2+}] (Nagai *et al*., 2001). Taken together, these strategies offer alternatives complementary to cameleons for creating genetically encoded, physiological Ca^{2+} indicators.

V. OTHER CONSIDERATIONS AND PITFALLS

A. Ca^{2+} Ion Sensitivity

Although cameleon probes vary in their Ca^{2+} affinities, most are suitable for monitoring [Ca^{2+}] between 0.5 and 100 μM. This poses a problem for examining the relatively high [Ca^{2+}] found in the endoplasmic reticulum of resting cells (approximately 500 μM). However, CaM mutagenesis studies have shown that substitution of a conserved glutamic acid residue at the 12th position of each Ca^{2+}-binding loop abolishes its Ca^{2+}-binding ability (Zhu *et al*., 1998). The effect of combinations of these mutations on cameleon Ca^{2+} range is currently being examined further in our laboratory.

B. Maturation

GFP variants have been developed in which chromophore oxidative maturation (and thereby become fluorescent) occurs more quickly and efficiently at 37°C. It would be advantageous to utilize efficiently folding versions, such as the recently developed "Venus" form of EYFP (F46L/F64L/M153T/V163A/S175G). These EYFP mutations confer an eight-fold increase of fluorescence intensity when expressed in mammalian cells (Nagai *et al*., 2002; Rekas *et al*., 2002). This will enable assay of cells 24 h postrecovery transfection, if so desired.

C. pH Sensitivity

The hydrogen bond network within the β barrel of the chromophore is sensitive to external pH. Hence, in order to analyze Ca^{2+} levels in acidic organelles (such as secretory vesicles), the FRET donor/acceptor pair must be engineered so that it is pH resistant. Two mutations within EEYFP (V68L and Q69K) have been shown to decrease its pK_a to 6.1 (Miyawaki *et al*., 1999). The pH sensitivity was improved further via a Q69M or "citrine" mutation (pK_a 5.7; Griesbeck *et al*., 2001). Another approach would be to change the donor/acceptor pair to the pH-insensitive sapphire-red cameleon probe (SapRC2). Although this construct has a tendency to aggregate and form homotetramers, the recent engineering of a monomeric mRFP1 offers an interesting alternative (Campbell *et al*., 2002).

D. Oligomerization

GFP family proteins have been observed to form obligate dimers and may thereby generate false-positive FRET signals. However, this aggregation problem need not preclude their use in biological systems, even when present in higher local concentrations. Nonoligomerizing mutants of EYFP have been suggested from its crystal structure (Wachter *et al*., 1998; Rekas *et al*., 2002), but these have yet to be validated experimentally. Alternatively, using a monomeric version of the evolutionary distinct RFP (mRFP1) in tandem with a EYFP donor would also serve to eliminate this issue (Campbell *et al*., 2002).

E. Influences on Biological Systems

It is very important to consider potential competition of the FRET indicator for native CaM or CaM-dependent enzymes. Previous comparisons of the effect of recombinant CaM and cameleon chimeras on prototypical CaM-dependent enzymes have revealed that the primary effect of cameleons is on buffering [Ca^{2+}] and not interfering with CaM-mediated signaling (Miyawaki *et al*., 1999). This could be due to the CaM component of the cameleon being inhibited by

the adjoining CKKp efficiently occupying its substrate-binding site. Also, as the YC6.1 CKKp is embedded within the cameleon polypeptide, it is not likely to interact with endogenous CaM proteins.

F. Interpretation of Live Cell FRET Data

There are two commonly used simple and practical approaches. The first, measurement of donor emission quenching and acceptor emission enhancement by using three filter sets and then mathematical processing to determine emission/FRET ratios, is described in Section III. The alternative approach is by detection of donor dequenching following acceptor bleaching. We find bleaching with a minimum of 200 ms, compared to 1 ms for control excitation, is sufficient.

G. Additional Ways to Do Ratio Imaging

FRET requires rapid intensity measurements at different wavelengths. Switching time (in the millisecond range) may be an important parameter for some applications. New imaging systems have become available in the marketplace, notably TILLvisION (T.I.L.L. Photonics) and AquaCosmos (Hamamatsu), which allow for excellent time resolution for fluorescence–intensity ratio imaging.

H. FRET Using Red Fluorescence Protein

For YC6.1 applications, the ECFP-EYFP FRET filter set is sufficient. However, if you are using RFP for FRET, the following dichoric mirrors and filters from Omega Optical (or equivalents) will be needed: 450-520-590TBDR for the dichoric mirror; 440DF21 for ECFP excitation; 510DF23 for EYFP excitation; 575DF26 for RFP excitation; 480AF30 for ECFP emission; 535AF26 for EYFP emission; and 600ALP for RFP emission. This filter set allows you to excite or acquire emission from ECFP, EYFP, and RFP individually, albeit with a tradeoff in efficiency.

I. Imaging Systems

Using a confocal microscope is the best way to increase spatial resolution for FRET experiments. Confocal YC6.1 measurements can be performed with single-photon excitation using the 458-nm line of an argon laser, but much more efficient excitation of ECFP is attained with the 442-nm line of a HeCd laser. Two-photon excitation microscopy, in addition to providing optical sections of a specimen as with confocal microscopy, offers certain advantages. Its applicability to cameleons has been demonstrated using video-rate scanning instrumentation (Fan *et al*., 1999). This latter imaging approach may not be readily available to most laboratories, however.

J. Preparation of Ca^{2+}/EGTA Buffers

The accuracy of the Ca^{2+}-binding curve depends on accurate preparation of the Ca^{2+}/EGTA and Ca^{2+}/HEEDTA systems below 10^{-5} M free Ca^{2+} and unbuffered Ca^{2+} above (Bers *et al*., 1994). The purity of EGTA, temperature, and pH are all practical issues.

Acknowledgments

We are grateful to Atsushi Miyawaki for his help in setting up a FRET microscope system in our laboratory, as well as for much advice on the use of GFP variants. This work was supported by grants from the Cancer Research Society Inc. and the Institute for Cancer Research of the Canadian Institutes of Health Research (CIHR). K.P.H. is a recipient of a NCIC Research Fellowship, K.T. holds a CIHR scholarship, and M.I. is a CIHR senior investigator.

References

Allen, G. J., Kwak, J. M., Chu, S. P., Llopis, J., and Tsien, R. Y. (1999). Cameleon calcium indicator reports cytoplasmic calcium dynamics in Arabidopsis guard cells. *Plant J*. **19**, 735–747.

Baird, G. S., Zacharias, D. A., and Tsien, R. Y. (1999). Circular permutation and receptor insertion within green fluorescent proteins. *Proc. Natl. Acad. Sci. USA* **96**, 11241–11246.

Bers, D. M., Patton, C. W., and Nuccitelli, R. (1994). A practical guide to the preparation of Ca2+ buffers. *Methods Cell Biol*. **40**, 3–29.

Campbell, R. E., Tour, O., Palmer, A. E., Steinbach, P. A., Baird, G. S., Zacharias, D. A., and Tsien, R. Y. (2002). A monomeric red fluorescent protein: *Proc. Natl. Acad. Sci. USA* **99**, 7877–7882.

Carafoli, E. (2003). The calcium-signalling saga: Tap water and protein crystals. *Nature Rev. Mol. Cell Biol*. **4**, 326–332.

Demaurex, N., and Frieden, M. (2003). Measurements of the free luminal ER Ca(2+) concentration with targeted "cameleon" fluorescent proteins. *Cell Calcium* **34**, 109–119.

Emmanouilidou, E., Teschemacher, A. G., Pouli, A. E., Nicholls, L. I., Seward, E. P., and Rutter, G. A. (1999). Imaging Ca2+ concentration changes at the secretory vesicle surface with a recombinant targeted cameleon. *Curr. Biol*. **9**, 915–918.

Fan, G. Y., Fujisaki, H., Miyawaki, A., Tsay, R. K., Tsien, R. Y., and Ellisman, M. H. (1999). Video-rate scanning two-photon excitation fluorescence microscopy and ratio imaging with cameleons. *Biophys. J*. **76**, 2412–2420.

Griesbeck, O., Baird, G. S., Campbell, R. E., Zacharias, D. A., and Tsien, R. Y. (2001). Reducing the environmental sensitivity of yellow fluorescent protein: Mechanism and applications. *J. Biol. Chem*. **276**, 29188–29194.

Grynkiewicz, G., Poenie, M., and Tsien, R. Y. (1985). A new generation of Ca2+ indicators with greatly improved fluorescence properties. *J. Biol. Chem*. **260**, 3440–3450.

Ikeda, M., Sugiyama, T., Wallace, C. S., Gompf, H. S., Yoshioka, T., Miyawaki, A., and Allen, C. N. (2003). Circadian dynamics of

cytosolic and nuclear Ca2+ in single suprachiasmatic nucleus neurons. *Neuron* **38**, 253–263.

Isshiki, M., Ying, Y. S., Fujita, T., and Anderson, R. G. (2002). A molecular sensor detects signal transduction from caveolae in living cells. *J. Biol. Chem*. **277**, 43389–43398.

Kerr, R., Lev-Ram, V., Baird, G., Vincent, P., Tsien, R. Y., and Schafer, W. R. (2000). Optical imaging of calcium transients in neurons and pharyngeal muscle of *C. elegans*. *Neuron* **26**, 583–594.

Liu, L., Yermolaieva, O., Johnson, W. A., Abboud, F. M., and Welsh, M. J. (2003). Identification and function of thermosensory neurons in Drosophila larvae. *Nature Neurosci*. **6**, 267–273.

Miyawaki, A. (2003). Visualization of the spatial and temporal dynamics of intracellular signaling. *Dev. Cell* **4**, 295–305.

Miyawaki, A., Griesbeck, O., Heim, R., and Tsien, R. Y. (1999). Dynamic and quantitative Ca2+ measurements using improved cameleons. *Proc. Natl. Acad. Sci. USA* **96**, 2135–2140.

Miyawaki, A., Llopis, J., Heim, R., McCaffery, J. M., Adams, J. A., Ikura, M., and Tsien, R. Y. (1997). Fluorescent indicators for Ca2+ based on green fluorescent proteins and calmodulin. *Nature* **388**, 882–887.

Mizuno, H., Sawano, A., Eli, P., Hama, H., and Miyawaki, A. (2001). Red fluorescent protein from Discosoma as a fusion tag and a partner for fluorescence resonance energy transfer. *Biochemistry* **40**, 2502–2510.

Montero, M., Brini, M., Marsault, R., Alvarez, J., Sitia, R., Pozzan, T., and Rizzuto, R. (1995). Monitoring dynamic changes in free Ca2+ concentration in the endoplasmic reticulum of intact cells. *EMBO J*. **14**, 5467–5475.

Nagai, T., Ibata, K., Park, E. S., Kubota, M., Mikoshiba, K., and Miyawaki, A. (2002). A variant of yellow fluorescent protein with fast and efficient maturation for cell-biological applications. *Nature Biotechnol*. **20**, 87–90.

Nagai, T., Sawano, A., Park, E. S., and Miyawaki, A. (2001). Circularly permuted green fluorescent proteins engineered to sense Ca2+. *Proc. Natl. Acad. Sci. USA* **98**, 3197–31202.

Rekas, A., Alattia, J. R., Nagai, T., Miyawaki, A., and Ikura, M. (2002). Crystal structure of venus, a yellow fluorescent protein with improved maturation and reduced environmental sensitivity. *J. Biol. Chem*. **277**, 50573–50578.

Truong, K., and Ikura, M. (2001). The use of FRET imaging microscopy to detect protein-protein interactions and protein conformational changes in vivo. *Curr. Opin. Struct. Biol*. **11**, 573–578.

Truong, K., Sawano, A., Mizuno, H., Hama, H., Tong, K. I., Mal, T. K., Miyawaki, A., and Ikura, M. (2001). FRET-based *in vivo* Ca2+ imaging by a new calmodulin-GFP fusion molecule. *Nature Struct. Biol*. **8**, 1069–1073.

Wachter, R. M., Elsliger, M. A., Kallio, K., Hanson, G. T., and Remington, S. J. (1998). Structural basis of spectral shifts in the yellow-emission variants of green fluorescent protein. *Structure* **6**, 1267–1277.

Zhang, J., Campbell, R. E., Ting, A. Y., and Tsien, R. Y. (2002). Creating new fluorescent probes for cell biology. *Nature Rev. Mol. Cell. Biol*. **3**, 906–918.

Zhu, T., Beckingham, K., and Ikebe, M. (1998). High affinity Ca2+ binding sites of calmodulin are critical for the regulation of myosin Ibeta motor function. *J. Biol. Chem*. **273**, 20481–20486.

CHAPTER

41

Ratiometric Pericam

Atsushi Miyawaki

I. INTRODUCTION

Our understanding of the structure–photochemistry relationships of green fluorescent protein (GFP) (Tsien, 1998) has enabled the development of genetic calcium probes based on a circularly permuted GFP (cpGFP) in which the amino and carboxyl portions have been interchanged and reconnected by a short spacer between the original termini (Baird *et al*., 1999). The resulting new amino and carboxyl termini of the cpGFP have been fused to calmodulin and its target peptide M13, generating a chimeric protein named pericam (Nagai *et al*., 2001). This new protein was fluorescent, and its spectral properties changed reversibly with Ca^{2+} concentration, probably due to the interaction between calmodulin and M13, which alters the environment surrounding the chromophore. Three types of pericam have been obtained by mutating several amino acids adjacent to the chromophore. Of these, "flash pericam" becomes fluorescent with increasing Ca^{2+}, whereas "inverse pericam" dims. However, "ratiometric pericam" has an excitation wavelength that changes in a Ca^{2+}-dependent manner, thereby enabling dual-excitation ratiometric Ca^{2+} imaging. Ratiometric dyes permit quantitative Ca^{2+} measurements by minimizing the effects of several artifacts that are unrelated to changes in the concentration of free Ca^{2+} ($[Ca^{2+}]$), such as uneven loading or partitioning of dye within the cell or varying cell thickness. This article presents an outline of an imaging experiment using HeLa cells expressing ratiometric pericam to measure receptor-stimulated changes in intracellular $[Ca^{2+}]$ ($[Ca^{2+}]_i$) (Protocol 1).

In contrast to cameleons (Miyawaki *et al*., 1997), which are fluorescence resonance energy transfer-based Ca^{2+} indicators, pericams can be easily targeted into the mitochondria matrix using an upstream targeting sequence encoding subunit IV of cytochrome *c* oxidase. Ratiometric pericam has been used successfully to monitor changes in $[Ca^{2+}]$ in mitochondria ($[Ca^{2+}]_m$) (Nagai *et al*., 2001). In most dual-excitation imaging experiments, the excitation wavelength is alternated using a rotating wheel containing two bandpass filters. However, it is also possible to use a high-speed grating monochromator to increase the rate at which the ratio measurement is conducted to approximately 10 Hz. The latter instrumentation enables the measurement in spontaneously contracting cardiac myocytes of beat-to-beat changes in $[Ca^{2+}]_m$, contributing to the demonstration that $[Ca^{2+}]_m$ oscillates synchronously with cytosolic $[Ca^{2+}]$ during beating (Robert *et al*., 2001). This article discusses factors to be considered when using such a monochromator with ratiometric pericam.

Although the aforementioned measurements are typically performed using conventional microscopy, the monitoring of changes in $[Ca^{2+}]$ is often severely limited by the poor spatiotemporal resolution of such wide-field techniques. To obtain a more reliable representation of changes in subcellular $[Ca^{2+}]$, it is necessary to increase the *z*-axis resolution and the speed of production and collection of the ratios of the excitation peaks. This article provides a detailed protocol describing a modified laser-scanning confocal microscopic (LSCM) system for ratiometric pericam (Protocol 2). In our experiment (Shimozono *et al*., 2002), fast exchange between two laser beams was achieved

Copyright 2006, Elsevier Science (USA).
All rights reserved.

using acousto-optic tunable filters (AOTFs). Samples were scanned on each line sequentially by a violet laser diode (408 nm) and a diode-pumped solid-state laser (488 nm). In this way, the ratios of the excitation peaks can be obtained at a frequency of up to 200 Hz.

II. MATERIALS

HeLa cells (ATCC # CCL-2.2)
Culture medium: Add fetal bovine serum (Gibco BRL, Life Technologies) to Dulbecco's modified Eagle's medium (DMEM) (Sigma Aldrich) to a final concentration of 10% (v/v)
Hank's balanced salt solution (HBSS): Dissolve $CaCl_2$ (0.14 g), KCl (0.40 g), KH_2PO_4 (0.06 g), $MgCl_2{\cdot}6H_2O$ (0.10 g), $MgSO_2{\cdot}7H_2O$ (0.10 g), NaCl (8.00 g), $NaHCO_3$ (0.35 g), Na_2HPO_4 (0.048 g), and D-glucose (1.00 g) in 800 ml of distilled H_2O, adjust the pH to 7.4, and then adjust the volume to 1 liter.
Histamine solution: Dissolve 1.841 mg of histamine dihydrochloride (Sigma Aldrich, H7125) in 1 ml of HBSS to make a 10 m*M* stock solution.
Ratiometric pericam cDNA
Ratiometric pericam mitochondrial cDNA
35-mm glass-bottom cell culture plates (Matsunami-glass, Osaka, Japan)

Interference Filters

400DF15, XF1006, Omega
485DF15, XF1042, Omega
535AF45, XF3084, Omega
505DRLP, XF2010, Omega
505DRLP-XR, XF2031, Omega
500ALP, XF3092, Omega
DM420SP, Olympus
FV5-DM442, Olympus
BA505-525, Omega

III. INSTRUMENTATION

A. Conventional Microscopy for Time-Lapse $[Ca^{2+}]_i$ Imaging

Dual-excitation imaging with ratiometric pericam uses two excitation filters (485DF15 and 400DF15), which are alternated by a filter changer (Lambda 10-2, Sutter Instruments, Novato, CA), a 505DRLP-XR dichroic mirror, and a 535AF45 emission filter. The excitation and emission spectra of ratiometric pericam

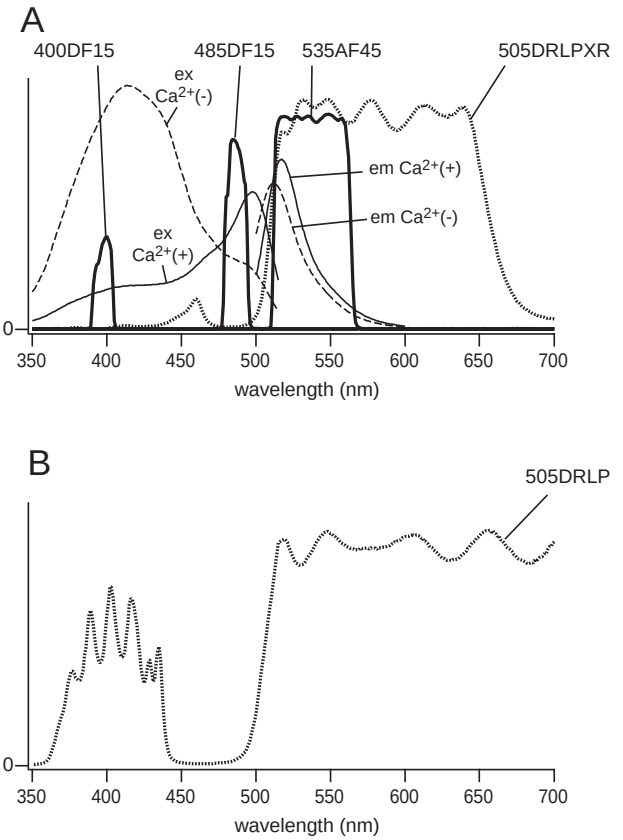

FIGURE 1 (A) Fluorescence excitation and emission spectra of ratiometric pericam in the presence (solid line) and absence (broken line) of Ca^{2+}. Transmittance spectra for filters (400DF15, 485DF15, and 535AF45) and the dichroic mirror (505DRLPXR) are shown with solid and dotted lines, respectively. (B) The transmittance spectrum for a 505DRLP dichroic mirror.

in the presence and absence of Ca^{2+} with passbands of the emission filter and two excitation filters are shown in Fig. 1A. Also, the transmittance of the dichroic mirror (505DRLP-XR) is superimposed. The dichroic mirror has an eXtended Reflection region below 505 nm; it was designed originally for the measurement of Ca^{2+} (fura-2) and pH (BCECF). In this situation, the broad reflection of a dichroic mirror is imperative. A more common long-pass dichroic mirror (505DRLP) cannot be used; superimposition of its transmission spectrum (Fig. 1B) makes one notice a complex transmission band at short wavelengths, which prevents reflection of the 400-nm light. The author strongly recommends that researchers make graphs of spectra plotted as percentage transmittance for the interference filters (excitation filters, emission filters, and dichroic mirrors) that are actually used, together with excitation and emission spectra of the relevant fluorescent dyes. The transmittance curves for the filters (normal incidence) and dichroic mirrors (45°

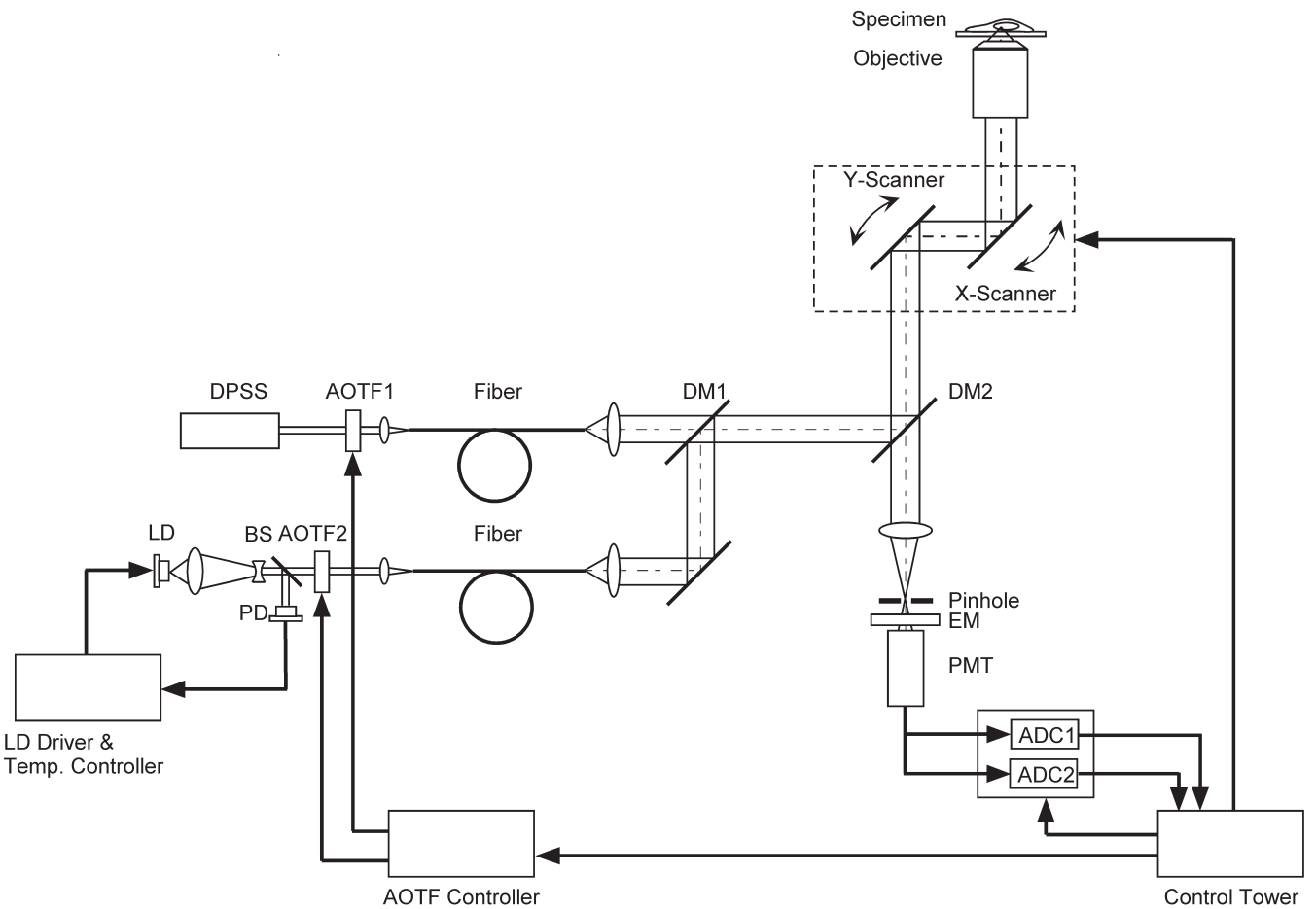

FIGURE 2 Schematic diagram of the laser-scanning confocal microscopy system for fast dual-excitation ratiometric imaging. DPSS, diode pumped solid-state laser; LD, laser diode; PD, photodiode; BS, beam splitter; DM, dichroic mirror; EM, emission filter; PMT, photomultiplier tube; ADC, analog-to-digital converter.

incidence) can be measured easily using a conventional spectrophotometer. This measurement also provides a chance for researchers to check the quality of their interference filters, which may deteriorate with time.

B. A Modified LSCM System for Ratiometric Pericam

Although the following procedure assumes familiarity with LSCM, and with the Olympus LSCM in particular, the procedure can be adapted easily to other LSCM types. The microscope and lasers we use are described in Fig. 2. The beam from a diode-pumped solid-state laser (Sapphire 488-20, COHERENT) directly enters an AOTF (AOTF1; AOTF.8C, AA Opto-Electronic). The light is relayed through an optical fiber (FV5-FUR, Olympus) to a confocal microscope scan head and passes through a dichroic mirror (DM1; DM420SP, Olympus). A laser diode (NLHV3000E, NICHIA) is mounted on a heat sink with temperature control, which consists of an LD mount and heat sink [F125-4A (Suruga Seiki)], LD current driver [LDX-3525 (ILX Lightwave)], and LD temperature controller [LDT5525 (ILX Lightwave)]. The output of the laser diode is collimated (made parallel) using multiple lenses, and its power is stabilized by a feedback-regulated device. The beam is directed into another AOTF (AOTF2; AOTF.4C UV, AA Opto-Electronic). The diffracted light is sent through another fiber-optic line (FV5-FUR-UV, Olympus) to the scan head and is then reflected on DM1. The two AOTFs are controlled electronically, allowing the reciprocal choice of one of the two laser lines. The chosen laser beam is reflected on a second dichroic mirror (DM2; FV5-DM442, Olympus). The scan head is coupled to an inverted microscope (IX70, Olympus) through its right-side port. The objective lens used is a PlanApo 60× N.A.

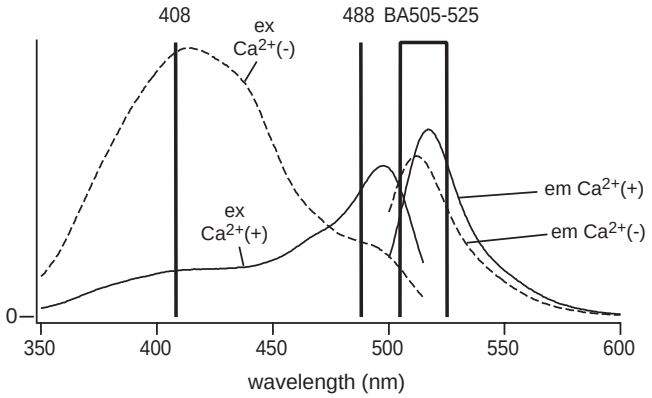

FIGURE 3 Fluorescence excitation and emission spectra of ratiometric pericam in the presence (solid line) and absence (broken line) of Ca^{2+}. The wavelengths of the two laser lines, 408 nm (laser diode) and 488 nm (diode-pumped solid state), are indicated by vertical lines. The wavelengths that pass through the emission filter BA505–525 are shown by a box. Modified with permission from T. Nagai, A. Sawano, E. S. Park, and A. Miyawaki, Proc. Natl. Acad. Sci. U.S.A. 98, 3197 (2001). Copyright (2001) National Academy of Sciences, U.S.A.

1.00 WLSM (Olympus). The fluorescent light is descanned, passed through DM2, a pinhole, and an emission filter (BA505-525 (Omega)), and detected by a photomultiplier. Fluorescence signals with excitation wavelengths of 408 and 488 nm are distributed into two channels during analog-to-digital conversion. The pair of galvanometer mirrors, the digitized detector output, and the AOTF controller are orchestrated. The excitation and emission spectra of ratiometric pericam in the presence and absence of Ca^{2+} , together with the passband of the emission filter (BA505-525) and the two laser lines, are shown in Fig. 3.

IV. PROCEDURES

Protocol 1

The procedure for time-lapse $[Ca^{2+}]_i$ imaging in HeLa cells is as follows.

1. Plate HeLa cells or cells of interest onto a 35-mm glass-bottom dish with culture medium.
2. Transfect the cells with 1 µg per dish of cDNA encoding ratiometric pericam mitochondria using Lipofectin according to the manufacturer's instructions.
3. Between 2 and 10 days after cDNA transfection, image HeLa cells on an inverted microscope (IX7) with a cooled CCD camera (MicroMax or Cool Snap HQ, Roper Scientific, Tucson, AZ). Expose cells to reagents in HBSS containing 1.26 m*M* $CaCl_2$. Image acquisition and processing are controlled by a personal computer connected to a camera and a filter wheel (Lambda 10-2, Sutter Instruments, San Rafael, CA) using the program MetaFluor (Universal Imaging, West Chester, PA). The excitation filter wheel in front of the xenon lamp (Lambda 10-2, Sutter Instruments, San Rafael, CA) is also under computer control. Excitation light from a 75-W xenon lamp is passed through a 400DF15 (400 ± 7.5) or 485DF15 (485 ± 7.5) excitation filter. The light is reflected onto the sample using a 505-nm long-pass (505DRLP-XR) dichroic mirror with an extended reflection. The emitted light is collected with a 40X (numerical aperture: 1.35) objective and passed through a 535 ± 22.5-nm band-pass filter (535AF45). Interference filters are from Omega Optical or Chroma Technologies (Brattleboro, VT).
4. Define several factors for image acquisition, including (i) excitation power, which depends on the type of light source and neutral density filter, (ii) numerical aperture of the objective, (iii) time of exposure to the light, (iv) image acquisition interval, and (v) binning. The last three factors should be considered in terms of whether temporal or spatial resolution is pursued.
5. Choose moderately bright cells. Select regions of interest so that pixel intensities are averaged spatially.
6. At the end of an experiment, convert fluorescence signals into values of $[Ca^{2+}]$. R_{max} and R_{min} can be obtained as follows. To saturate the intracellular indicator with Ca^{2+}, increase the extracellular $[Ca^{2+}]$ to 10–20 m*M* in the presence of 1–5 µ*M* ionomycin. Wait until the fluorescence intensity reaches a plateau. Then, to deplete the Ca^{2+} indicator, wash the cells with Ca^{2+}-free medium (1 µ*M* ionomycin, 1 m*M* EGTA, and 5 m*M* $MgCl_2$ in nominally Ca^{2+}-free HBSS). The *in situ* calibration for $[Ca^{2+}]$ uses the equation $[Ca^{2+}] = K'_d[(R - R_{min})/(R_{max} - R)]^{(1/n)}$, where K'_d is the apparent dissociation constant corresponding to the Ca^{2+} concentration at which R is midway between R_{max} and R_{min} and n is the Hill coefficient. The Ca^{2+} titration

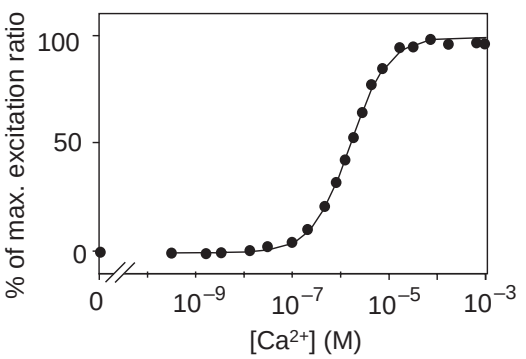

FIGURE 4 The Ca^{2+} titration curve of ratiometric pericam. Modified with permission from T. Nagai, A. Sawano, E. S. Park, and A. Miyawaki, Proc. Natl. Acad. Sci. U.S.A. 98, 3197 (2001). Copyright (2001) National Academy of Sciences, U.S.A.

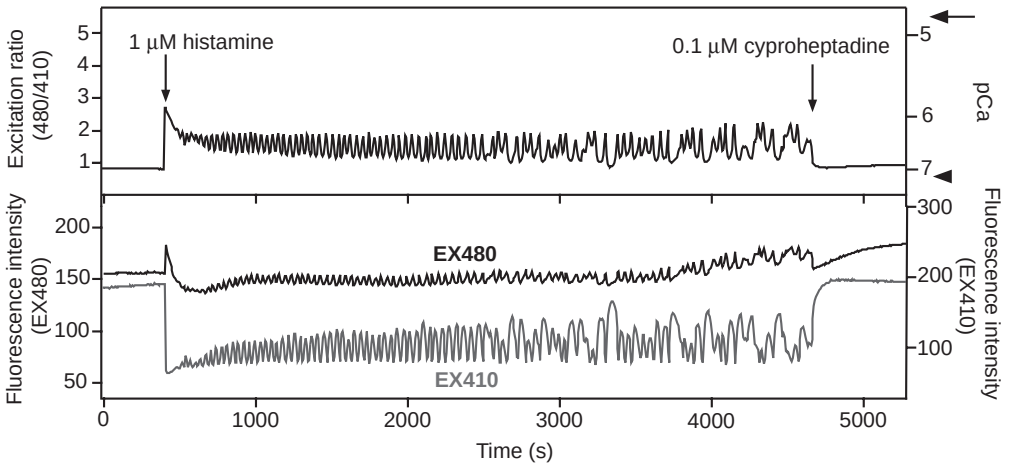

FIGURE 5 Typical $[Ca^{2+}]_i$ transients and oscillations induced by receptor stimulation in HeLa cells expressing ratiometric pericam. The sampling interval was 3–5 s. (Top) Excitation ratios of 480 and 410 nm. The right-hand ordinate indicates $[Ca^{2+}]_i$ in μM with R_{max} and R_{min} indicated by an arrow and arrowhead, respectively. (Bottom) Excitations of 480 nm (black line, left-hand scale) and 410 nm (gray line, right-hand scale). Modified with permission from T. Nagai, A. Sawano, E. S. Park, and A. Miyawaki, Proc. Natl. Acad. Sci. U.S.A. 98, 3197 (2001). Copyright (2001) National Academy of Sciences, U.S.A.

curve of ratiometric pericam can be fitted using a single K'_d of 1.7 μM and a single Hill coefficient of 1.1 (Fig. 4). A typical time course of $[Ca^{2+}]_i$ reported by ratiometric pericam is shown in Fig. 5.

Protocol 2

The following is a procedure for confocal imaging of $[Ca^{2+}]_m$ in HeLa cells using the modified LSCM system.

1. Plate HeLa cells or cells of interest onto a 35-mm glass-bottom dish with culture medium.
2. Transfect the cells with 1 μg per dish of cDNA encoding ratiometric pericam mitochondria using Lipofectin according to the manufacturer's instructions.
3. Incubate the cells in a humidified atmosphere at 37°C under 5% CO_2 for 1 to 3 days.
4. Replace the culture medium with HBSS.
5. Observe the cells on an inverted microscope (IX70, Olympus) for green fluorescence of the indicator (ratiometric pericam-mt) using a 490-nm excitation light generated using 490DF10.
6. Choose moderately bright cells in which the fluorescence is well distributed in the mitochondria.
7. Switch on the lasers, AOTF controller, scanning head, and the computer. The lasers need 30 min to warm up and stabilize.
8. Start the scanning process with only excitation from the 408-nm laser diode. Set the scan mode to "Normal (unidirectional)" and scan speed to "Fast." While looking at the acquired fluorescence images, adjust the laser intensity to the minimum level that allows easy identification of individual cells, adjust the sensitivity of the photomultiplier tube (PMT) for an optimal signal-to-noise ratio, and adjust the size of the pinhole for acceptable depth of the image. There is a trade-off between the scan speed and the pixel size: faster scanning speeds decrease resolution because fewer pixels of information are collected.
9. Adjust the intensity of the 488-nm laser by setting the microscope to "Normal (unidirectional)" scan mode and "Fast" scan speed. While looking at the acquired fluorescence images, adjust the laser intensity to a minimum level that allows easy identification of individual cells and adjust the sensitivity of the PMT for an optimal signal-to-noise ratio and the size of the pinhole for acceptable depth of the image. Establishing the microscope settings described in steps 8 and 9 is a process that must be iterated to produce adequate ratio images.
10. Start the control software for line-sequential dual-excitation ratio analysis. The "Normal" scan mode and "Fast" scan speed, with adequate pixel size, enable rapid exchange between the two lasers on a line every 5 to 20 ms.
11. Determine the desired scanning field (image size) and reduce the height of the image so that 5 to 10 frames can be obtained per second.
12. Start to acquire images every 100 to 200 ms for 1 to 5 min.
13. During image acquisition, add histamine solution to a final concentration of 10 μM for receptor stimulation.
14. Determine the image ratio by dividing the images acquired with excitation at 488 nm by those acquired at 408 nm.

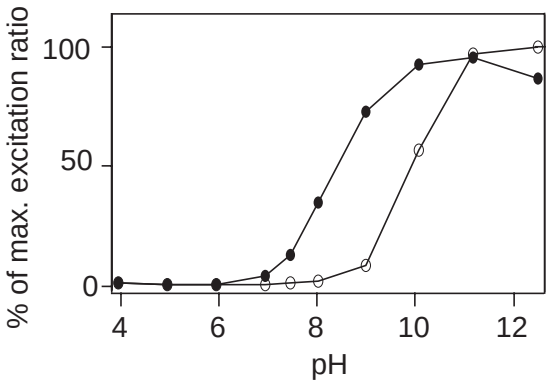

FIGURE 6 pH dependency of the 495/410-nm excitation ratio in the presence (●) and absence (○) of Ca^{2+}. Modified with permission from T. Nagai, A. Sawano, E. S. Park, and A. Miyawaki, Proc. Natl. Acad. Sci. U.S.A. 98, 3197 (2001). Copyright (2001) National Academy of Sciences, U.S.A.

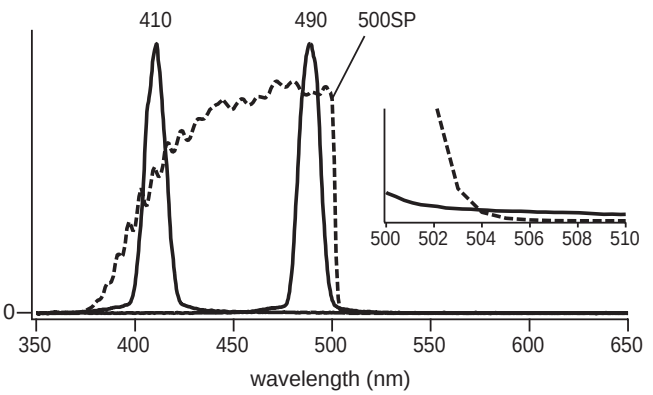

FIGURE 7 Spectrum of the 410- or 490-nm light selected by the monochromator (U7773-XX and U7794-16, Hamamatsu Photonics) (solid line) and transmittance of a 500SP short-pass filter (Omega, 3rd Milenium) (broken line). (*Inset*) The crossing of the two curves for 490-nm light and 500SP on an expanded scale.

V. COMMENTS

A. pH and Photochromism as Practical Considerations

Ratiometric pericam is sensitive to changes in pH in both the presence and the absence of Ca^{2+} (Fig. 6). pH-related artifacts were not an issue in experiments that used HeLa cells because agonist-induced $[Ca^{2+}]_c$ mobilization did not induce any intracellular pH changes detectable by the pH indicator, BCECF (data not shown). However, ratiometric pericam expressed in dissociated hippocampal neurons was perturbed by acidification following depolarization or glutamate stimulation (data not shown).

Pericams are derived from yellow fluorescent protein (YFP). If YFP is excited too strongly, its fluorescence will be reduced. This apparent bleaching is actually photochromism because the fluorescence recovers to some extent spontaneously and can be restored further by UV illumination (Dickson *et al.*, 1997). Intense excitation of ratiometric pericam also causes photochromism, which results in a decrease in the 490/410-nm excitation ratio independent of Ca^{2+} change. The extent of photochromism is dependent on excitation power, numerical aperture of the objective, and exposure time. Therefore, it is necessary to optimize these factors for each cell sample in order to minimize photochromism while preserving a high signal-to-noise ratio. A good solution is to bin pixels at the cost of spatial resolution. The increased signal-to-noise ratio permits a decrease in intensity of the excitation light with a neutral-density filter and the observation of $[Ca^{2+}]_i$ oscillations without significant photochromism of the indicators.

B. Use of a High-Speed Grating Monochromator

Instead of a filter wheel containing 400DF15 and 485DF15 excitation filters, a fast wavelength exchanger based on a grating monochromator (U7773-XX and U7794-16, Hamamatsu Photonics) can be used with a fast-acquisition CCD camera (HiSCA, C6790-81, Hamamatsu Photonics). The spectrum of the excitation light when the wavelength was set at 410 or 490 nm is shown in Fig. 7. Because light acquired with the setting at 490 nm spills over into the observing optical path, it is preferable to eliminate the unwanted light by putting a short-pass filter like 500SP (Fig. 7, broken line) in front of the microscope.

C. Calcium Transients in Motile Mitochondria

When changes in $[Ca^{2+}]_m$ are monitored by alternating the excitation wavelength automatically with wide-field conventional microscopy, the rate of acquisition of the excitation ratio is about 10 Hz, which is identical to the frame rate. Despite this rapid rate of data collection, the $[Ca^{2+}]_m$ measurements are often affected adversely by the active motion of mitochondria, especially at warmer temperatures. Using our LSCM technique, we attempted to increase the speed of the alternation of excitation wavelengths so that it was faster than the movement of mitochondria. With this method, the frame rate was 5 Hz and the rate of ratio acquisition was 200 Hz. Although the frame rate did not allow us to fully follow the rapid movement

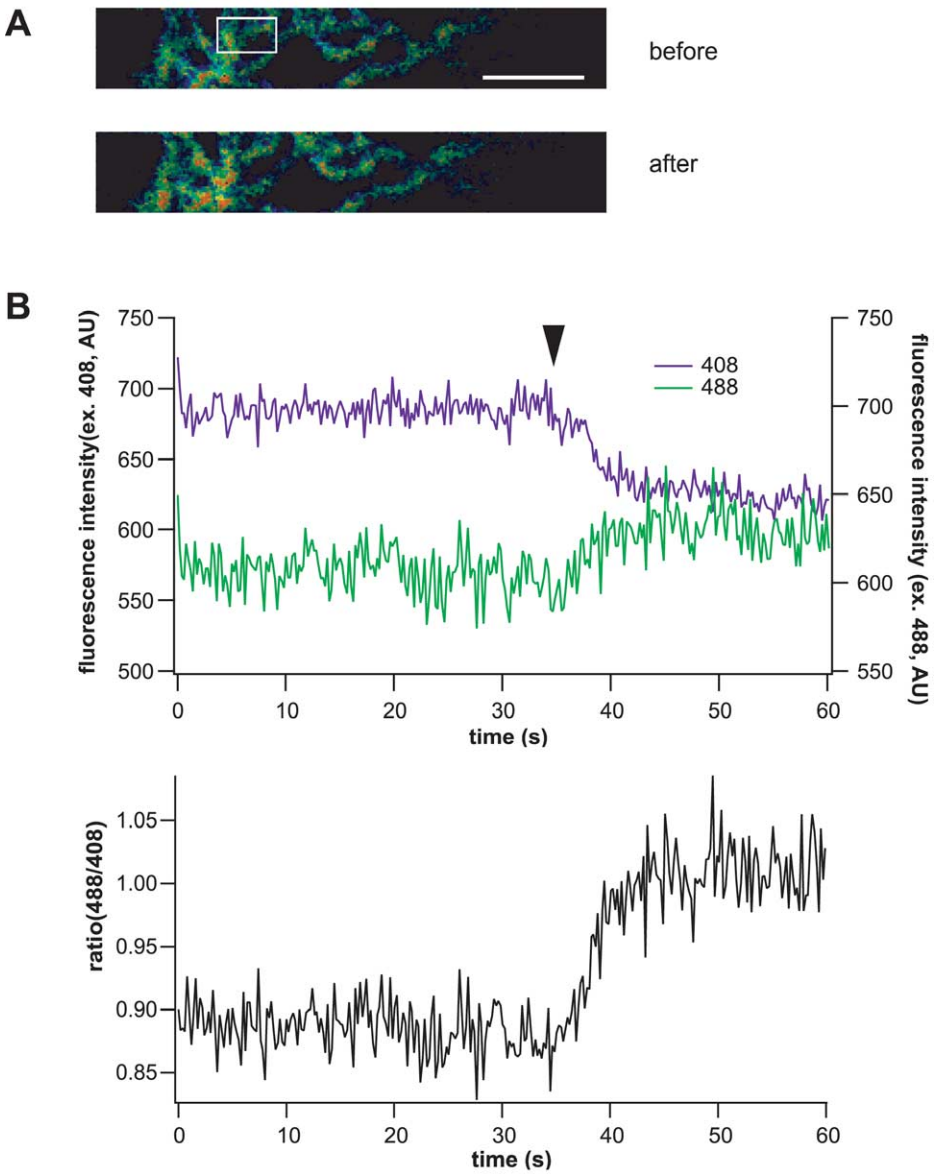

FIGURE 8 Confocal and dual-excitation imaging of $[Ca^{2+}]_m$ using ratiometric pericam mitochondia. (A) Ratio images before and after application of 10 μM histamine. Scale bar: 5 μm. (B) Time course of averaged fluorescence signals from the white box in A with excitation at 488 (green) and 408 nm (violet) (top) and their ratio (bottom). The arrowhead indicates the time when histamine was applied.

of mitochondria, the fast rate of ratio acquisition minimized the time lag between the two measurements used to calculate the ratiometric signal. We feel that this method of imaging $[Ca^{2+}]_m$ effectively corrects for mitochondrial movement in all three possible both laterally and into and out of the optical section. After the application of histamine, spots of $[Ca^{2+}]_m$ increase within a single mitochondrion were identifiable (Fig. 8A) and the global increase in $[Ca^{2+}]_m$ was found to occur relatively slowly (Fig. 8B).

References

Baird, G. S., Zacharias, D. A., and Tsien, R. Y. (1999). Circular permutation and receptor insertion within green fluorescent proteins. *Proc. Natl. Acad. Sci. USA* **96**, 11241–11246.

Dickson, R. M., Cubitt, A. B., Tsien, R. Y., and Moerner, W. E. (1997). On/off blinking and switching behaviour of single molecules of green fluorescent protein. *Nature* **388**, 355–358.

Miyawaki, A., Llopis, J., Heim, R., McCaffery, J. M., Adams, J. A., Ikura, M., and Tsien, R. Y. (1997). Fluorescent indicators for Ca^{2+} based on green fluorescent proteins and calmodulin. *Nature* **388**, 882–887.

Nagai, T., Sawano, A., Park, E. S., and Miyawaki, A. (2001). Circularly permuted green fluorescent proteins engineered to sense Ca^{2+}. *Proc. Natl. Acad. Sci. USA* **98**, 3197–3202.

Robert, V., Gurlini, P., Tosello, V., Nagai, T., Miyawaki, A., Di Lisa, F., and Pozzan, T. (2001). Beat-to-beat oscillations of mitochondrial $[Ca^{2+}]$ in cardiac cells. *EMBO J.* **20**, 4998–5007.

Shimozono, S., Fukano, T., Nagai, T., Kirino, Y., Mizuno, H., and Miyawaki, A. (2002). Confocal imaging of subcellular Ca^{2+} concentrations using a dual-excitation ratiometric indicator based on green fluorescent protein. *Sci. STKE* http://www.stke.org/cgi/content/full/OC_sigtrans;2002/125/pl4.

Tsien, R. Y. (1998). The green fluorescent protein. *Annu. Rev. Biochem.* **67**, 509–544.

CHAPTER

42

Fluorescent Indicators for Imaging Protein Phosphorylation in Single Living Cells

Moritoshi Sato and Yoshio Umezawa

I. INTRODUCTION

To study protein phosphorylation, investigators have used electrophoresis, immunocytochemistry, and *in vitro* kinase assays. However, these methods do not provide enough information about spatial and temporal dynamics of protein phosphorylation in each living cell. To overcome this limitation, we have developed genetically encoded novel fluorescent indicators and visualized signal transduction based on protein phosphorylation in living cells (Sato *et al*., 2002) (Fig. 1). Within the fluorescent indicator, a substrate domain for a protein kinase of interest is fused with a phosphorylation recognition domain via a flexible linker sequence. The tandem fusion unit consisting of the substrate domain, linker sequence, and phosphorylation recognition domain is sandwiched with two different color fluorescent proteins, cyan fluorescent protein (CFP) and yellow fluorescent protein (YFP), which serve as the donor and acceptor fluorophores for fluorescence resonance energy transfer (FRET). As a result of phosphorylation of the substrate domain and subsequent binding of the phosphorylated substrate domain with the adjacent phosphorylation recognition domain, FRET is induced from CFP to YFP when CFP is excited at 440 ± 10 nm. Upon activation of phosphatases, the phosphorylated substrate domain is dephosphorylated and the FRET signal is decreased. This FRET change is represented by the change in the fluorescence emission ratio of CFP at 480 ± 15 nm and YFP at 535 ± 12.5 nm, both of which were monitored continuously by a dual-emission fluorescence microscope. We named this indicator "phocus" (a fluorescent indicator for protein phosphorylation that can be custom-made). Until now, by using suitable substrates and phosphorylation recognition domains, we have developed a large number of phocus variants for several key protein kinases, such as a receptor tyrosine kinase, insulin receptor, and a serine/threonine protein kinase, Akt/PKB (Table I). In addition, these phocus variants were further tailored to visualize subcellular local activity of the respective protein kinases in living cells (Table I). For example, the phocus variant for Akt protein kinase was tethered to the cytoplasmic surface of mitochondria or Golgi membranes by connecting each appropriate sequence/domain. This membrane tethering prevented the free diffusion of the indicator and avoided the resulting loss of spatial information as to phosphorylation by the activated Akt. We thus found that the activated Akt is not in the cytosol but is localized at subcellular membranes, including Golgi and mitochondria membranes, when the cells were stimulated.

II. MATERIALS AND INSTRUMENTATION

ECFP (Cat. No. 6900-1) and EYFP (Cat. No. 6006-1) expression vectors are from Clonthech. Ham's F-12 medium (Cat. No. 21700), fetal bovine serum (Cat. No. 10099-141), and LipofectAMINE 2000 (Cat. No. 11668-019) reagent are from Invitrogen. Other chemicals used are all of analytical reagent grade. Glass-bottom dishes are from Asahi Techno Glass (Cat. No. 3911-035).

Copyright 2006, Elsevier Science (USA).
All rights reserved.

Cells are observed with a 40× oil-immersion objective (Carl Zeiss) on a Axiovert 135 microscope (Carl Zeiss) with a cooled CCD camera MicroMAX (Roper Scientific Inc.) controlled by MetaFluor (Universal Imaging). An excitation filter (440AF21), a dichroic mirror (455DRLP), and emission filters for CFP (480AF30) and YFP (535AF26) are from Omega Optical.

III. PROCEDURES

Solutions

1. *Culture medium*: Add fetal bovine serum to Ham's F-12 medium to give a final concentration of 10%.
2. *Serum starvation medium*: Add bovine serum albumin to Ham's F-12 medium to give a final concentration of 0.2%.
3. *Hank's balanced salt solution (HBSS)*: Dissolve 0.35 g of $NaHCO_3$, 0.06 g of KH_2PO_4, 0.048 g of Na_2HPO_4, 0.14 g of $CaCl_2$, 0.40 g of KCl, 0.10 g of $MgCl_2{\cdot}6H_2O$, 0.10 g of $MgSO_4{\cdot}7H_2O$, 8.00 g of NaCl, and 1.00 g of D-glucose in 800 ml of Milli-Q water, adjust the pH to 7.4, and then adjust the volume to 1 liter.

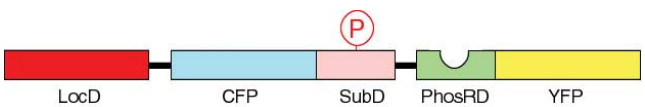

FIGURE 1 Schematic representation of the present fluorescence indicator for protein phosphorylation, which was named phocus. Upon phosphorylation of the substrate domain within phocus by the protein kinase, the adjacent phosphorylation recognition domain binds with the phosphorylated substrate domain, which changes the efficiency of FRET between the GFP mutants within phocus. By tethering a localization domain with phocus, the phocus can be localized in the specific intracellular locus of interest to visualize the local phosphorylation event there. LocD, localization domain; CFP, cyan fluorescent protein; SubD, substrate domain; PhosRD, phosphorylation recognition domain; YFP, yellow fluorescent protein; P in an open circle, the phosphorylated residue.

Steps

1. Plate CHO-IR cells that express human insulin receptor onto a glass-bottom dish with culture medium and incubate the cells at 37°C under 5% CO_2 for 1 day.
2. Transfect the cells with 0.8 μg of cDNA (phocus-2 or phocus-2pp) using Lippofecetamine 2000 reagent according to the manufacturer's instructions.
3. Incubate the cells at 37°C under 5% CO_2 for 1 to 2 days.
4. Replace the culture medium with serum starvation medium and incubate the cells at 37°C under 5% CO_2 for 2 to 4 h.
5. Replace the serum starvation medium with HBSS.
6. Set the glass-bottom dish onto the 40× oil immersion objective equipped on the fluorescence microscope.
7. Observe the cells with a 440-nm excitation filter (440AF21), 455-nm dichroic mirror (455DRLP), and 535-nm emission filter (535AF26).
8. By browsing the cells on the dish, choose moderately bright cells in which the fluorescence is well distributed in the cytosol.
9. Determine the desired observation field in which only the cells of interest are covered.
10. Select several regions of interest within the cells to examine time courses of CFP/YFP emission ratio during the following image acquisition.
11. Start to acquire images every 5 to 10 s for 10 to 30 min with the 440-nm excitation filter (CFP), 455-nm dichroic mirror, 480-nm emission filter (CFP), and 535-nm emission filter (YFP).

TABLE I Detailed Information on Composition of Each Fluorescent Indicator for Protein Phosphorylation and on Each Location Directed in Single Living Cells

Kinase	Indicator	Localization domain	Localization	Substrate domain	Phosphorylation recognition domain
Insulin receptor (tyrosine kinase)	phocus-2pp[a]	PH-PTB domain from IRS-1	Cytosol, nucleus, and membrane ruffles, including insulin receptor	ETGTEEYMKMDLG	$p85\alpha_{330–429}$
Akt/PKB (serine/threonine kinase)	Aktus[b]	—	Cytosol	RGRSRSAP	$14\text{-}3\text{-}3\eta_{82–235}$
	eNOS-Aktus[b]	$eNOS_{1–35}$	Golgi	RGRSRSAP	$14\text{-}3\text{-}3\eta_{82–235}$
	Bad-Aktus[b]	$Tom20_{1–33}$	Mitochondria	RGRSRSAP	$14\text{-}3\text{-}\eta_{82–235}$

[a] From Sato *et al*. (2002).
[b] From Sasaki *et al*. (2003).

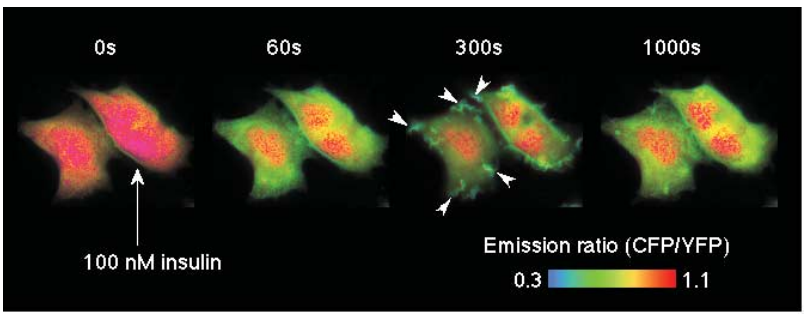

FIGURE 2 Fluorescence imaging with phocus-2pp upon insulin stimulation. Pseudocolor images of the CFP/YFP emission ratio are shown before (time 0 s) and 60, 300, and 1000 s after the addition of 100 n*M* insulin at 25°C, obtained from CHO-IR cells expressing phocus-2pp. Insulin-induced accumulation of phocus-2pp at the membrane ruffles is indicated by white arrows in the image at 300 s.

12. During image acquisition, add insulin to give a final concentration of 100 n*M*.
13. After finishing all the experiments, wipe the residual immersion oil out of the objective.

IV. EXAMPLES

Substrates for protein kinases and phosphatases often exhibit each unique localization, including mitochondria, Golgi, nucleus, and plasma membrane in living cells, which is thought to be critical for specific signal transduction in the respective intracellular loci (Hunter, 2000). Thus, we further tailored our phocuses to analyze the phosphorylation events in such particular locations in single living cells. Here we exemplify phocus for insulin receptor and that for Akt/PKB; the latter was named Aktus.

A. Phocus for Imaging Phosphorylation by Insulin Receptor

IRS-1 is one of the major substrates of insulin receptor. It contains a peckstrin-homology (PH) domain and a phosphotyrosine-binding (PTB) domain in its N-terminal end. The PH and PTB domains bind, respectively, with the phosphoinositides at the plasma membrane and with the juxtamembrane domain of insulin receptor, which is immediately tyrosine phosphorylated by insulin stimulation (Paganon *et al.*, 1999). Thus, the concentration of IRS-1 is thought to be increased around the insulin receptor at the plasma membrane upon insulin stimulation. These PH and PTB domains were fused with phocus, named phocus-2pp, to locate the phocus around the insulin receptor like the IRS-1 and to measure the local phosphorylation event there. When phocus-2pp was expressed in CHO-IR cells, fluorescence was observed throughout the cells (Fig. 2, time 0 s). Upon insulin stimulation, the CFP/YFP emission ratio, which is expressed with pseudocolor, was decreased in the cytosol due to phosphorylation-induced FRET from CFP to YFP within phocus-2pp. Three hundred seconds after insulin stimulation, membrane ruffles, in which a large extent of phocus-2pp were accumulated, appeared around the plasma and disappeared in 1000 s (Fig. 2). In these membrane ruffles, phocus-2pp has been found to colocalize with the insulin receptor accumulated there by insulin stimulation. Interestingly, in these membrane ruffles, the extent of phocus-2pp phosphorylation was visualized to be ~2-fold greater than that in the cytosol. This difference in phosphorylation levels between intracellular loci could be due to a different balance of kinase and phosphatase activities between intracellular loci. Phocus-2pp should contribute to reveal the biological significance of such a characteristic domain for tyrosine kinase signaling in the membrane ruffles, which were formed upon insulin stimulation, with high spatial and temporal resolution.

B. Aktus for Imaging Phosphorylation by Akt/PKB

Akt/PKB is a serine/threonine kinase that regulates a variety of cellular responses, such as cell proliferation, cell survival, and angiogenesis (Marte and Downward, 1997). To provide information on the spatial and temporal dynamics of the Akt activity in single living cells, we have developed a genetically encoded fluorescent indicator for Akt, named Aktus (Sasaki *et al.*, 2003). Almost all Akt substrates are localized to subcellular regions. For example, eNOS (Fulton *et al.*, 2001), which mediates a vasodilatory effect by nitric oxide production, is localized predominantly to

TABLE II Differential Subsellular Localization of Activated Akt between Cellular Stimuli

	Cytosol[a]	Golgi[b]	Mitochondria[c]
Insulin	–	+	–
17β-Estradiol	–	+	+

[a] Measured with Aktus.
[b] Measured with eNOS-Aktus.
[c] Measured with Bad-Aktus.

the Golgi apparatus, whereas Bad (Chao and Korsmeyer, 1998), which is related to apoptosis promotion, is present in mitochondrial outer membranes. By fusing the Aktus with the respectively subcellular localization domains within the eNOS and Bad, eNOS-Aktus and Bad-Aktus, which are respectively localized to the Golgi apparatus and mitochondrial outer membrane, were developed as shown in Table I and compared with the cytosolic diffusible indicator Aktus. We have shown that in vascular endothelial cells, the Golgi-localized indicator, eNOS-Aktus, was phosphorylated upon stimulation with insulin and with 17β-estradiol, whereas the mitochondria-localized Bad-Aktus was phosphorylated by 17β-estradiol but not by insulin (Table II). However, the diffusible indicator Aktus was not phosphorylated efficiently upon both insulin or 17β-estradiol stimulation (Table II). From these results, it is suggested that the activated Akt is localized to subcellular compartments, including the Golgi apparatus and/or mitochondria, rather than diffusing in the cytosol, thereby efficiently phosphorylating its substrate proteins. Different observation with the mitochondria-localized indicator indicates that localization of the activated Akt to mitochondria is directed differently between insulin and 17β-estradiol via distinct mechanisms. The present indicators and their applications are thus expected to contribute to the studies of a whole range of dynamics of the activated Akt in living cells.

V. PITFALLS

1. Avoid too bright cells to reproducibly obtain quantitative FRET signals. Also avoid too dim cells because they often exhibit noisy images.
2. Our measurement conditions do not significantly affect the stability of phocus, but if photobleaching of fluorescent proteins, particularly YFP, is still observed, we recommend using ND filters and/or to irradiate the cells less. We usually irradiate the cell for 50 to 100 ms.

References

Chao, D. T., and Korsmeyer, S. J. (1998). Bcl-2 family: Regulators of cell death. *Annu. Rev. Immunol.* **16**, 395–419.

Fulton, D., Gratton, J. P., and Sessa, W. C. (2001). Post-translational control of endothelial nitric oxide synthase: Why isn't calcium/calmodulin enough? *J. Pharmacol. Exp. Ther.* **299**, 818–824.

Hunter, T. (2000). Signaling-2000 and beyond. **100**, 113–127.

Marte, B. M., and Downward, J. (1997). PKB/Akt:connecting phosphoinositide 3-kinase to cell survival and beyond. *Trends Biochem. Sci.* **22**, 355–358.

Paganon, S. D., Ottinger, E. D., Nolte, R. T., Eck, M. J., and Shoelson, S. E. (1999). Crystal structure of the pleckstrin homology-phosphotyrosine binding (PH-PTB) targeting region of insulin receptor substrate 1. *Proc. Natl. Acad. Sci. USA* **96**, 8378–8383.

Sasaki, K., Sato, M., and Umezawa, Y. (2003). Fluorescent indicators for Akt/protein kinase B and dynamics of Akt activity visualized in living cells. *J. Biol. Chem.* **278**, 30945–30951.

Sato, M., Ozawa, T., Inukai, K., Asano, T., and Umezawa, Y. (2002). Fluorescent indicators for imaging protein phosphorylation in single living cells. *Nature Biotechnol.* **20**, 287–294.

CHAPTER

43

In Situ Electroporation of Radioactive Nucleotides: Assessment of Ras Activity or ^{32}P Labeling of Cellular Proteins

Leda Raptis, Adina Vultur, Evi Tomai, Heather L. Brownell, and Kevin L. Firth

I. INTRODUCTION

Binding to nucleotide(s) can determine a state of activation of a protein; a number of GTP-binding proteins such as Ras exist in two distinct, guanine nucleotide-bound conformations, the active Ras.GTP state and the inactive Ras.GDP form, so that the fraction of Ras bound to GTP (percentage Ras.GTP/GTP + GDP) can determine its state of activation (Lowy and Willumsen, 1993). Several indirect assays are in existence for measurement of Ras activity (Scheele *et al*., 1995; Taylor *et al*., 2001). However, in a number of instances, a direct measurement of Ras.GTP binding is necessary (Egawa *et al*., 1999) and is commonly performed through the addition of [^{32}P]orthophosphate to the growth medium followed by Ras immunoprecipitation and guanine nucleotide elution (Downward, 1995). This approach is relatively inefficient due to the fact that the isotope is incorporated into all phosphate-containing cellular components. To circumvent this problem, [α^{32}P]GTP has been introduced into the cell and its breakdown into [α^{32}P]GDP after Ras binding monitored as described earlier (Downward, 1995). Because, contrary to free bases or nucleosides, most nucleotides do not cross the cell membrane, [α^{32}P]GTP has to be introduced into intact cells after cell membrane permeabilization.

Protein phosphorylation is a ubiquitous regulator of a large variety of cellular functions. The *in vivo* radiolabelling and detection of phosphoproteins is usually conducted through the addition of [^{32}P]orthophosphate to the culture medium, followed by immunoprecipitation and electrophoretic separation of precipitated proteins. Just as in the case of Ras activity measurement, this method is relatively inefficient, hence ATP, the common immediate phosphate donor nucleotide, may be used for *in vivo* protein labelling, which must be introduced into intact cells through membrane permeabilization.

This article describes a technique where the introduction of nucleotides into adherent cells is performed through *in situ* electroporation. Cells are grown on a glass surface coated with electrically conductive, optically transparent indium-tin oxide at the time of pulse delivery, a coating that promotes excellent cell adhesion and growth. Unlike other techniques of cell membrane permeabilization, such as streptolysin-O (SLO) treatment, *in situ* electroporation does not detectably affect cellular metabolism, presumably because the pores reseal rapidly so that the cellular interior is restored to its original state; under the appropriate conditions there is no increase in the activity of the extracellular signal-regulated kinase (Erk1/2) or two stress-activated kinases, JNK/SAPK or p38^{hog} (Brownell *et al*., 1998). Results show that Ras activity measurement through electroporation of [α^{32}P]GTP could be performed using approximately 50–100 times lower amounts of radioactivity; although the ^{32}P is in the form of [α^{32}P]GTP exclusively, this technique offers higher specificity compared to labelling through the addition of [^{32}P]orthophosphate to the culture medium. In addition, labelling of two viral phosphoproteins, the large tumor antigen of simian virus 40 and adenovirus E1A, by *in situ* electroporation of [γ^{32}P]ATP requires a fraction of the amount of radioactive phosphorus, while offering enhanced specificity.

Copyright 2006, Elsevier Science (USA).
All rights reserved.

II. MATERIALS AND INSTRUMENTATION

Dulbecco's modification of Eagle's medium (DMEM) is from ICN (Cat. No. 10-331-22). Phosphate-free DMEM (Cat. No. D-3916) is from Sigma. Fetal calf serum (Cat. No. 2406000AJ) is from Life Technologies Inc. Calf serum is from ICN (Cat. No. 29-131-54). The following reagents are from Sigma: insulin (Cat. No. I-6643), NaCl (Cat. No. S-7653), HEPES (Cat. No. H-9136), Lucifer yellow CH dilithium salt (Cat. No. L-0259), trypsin (Cat. No. T-0646), $MgCl_2$ (Cat. No. M-8266), Triton X-100 (Cat. No. T-6878), deoxycholate (Cat. No. D-5760), EDTA (Cat. No. E-5134), EGTA (Cat. No. E-3889), phenylmethylsulfonyl fluoride (PMSF, P-7626), aprotinin (Cat. No. A-6279), leupeptin (Cat. No. L-2023), benzamidine (Cat. No. B-6506), dithiothreitol (DTT, Cat. No. D-9779), $CaCl_2$ (Cat. No. C-4901), Tris-base (Cat. No. T-6791), sodium orthovanadate (S-6508), and LiCl (Cat. No. L-4408). The following reagents are from BDH: Extran-300 detergent (Cat. No. S6036 39), SDS (Cat. No. 44244), TLC silica gel plates containing a fluorescence indicator (Cat. No. M05735-01), isopropanol (Cat. No. ACS720), concentrated ammonia solution (Cat. No. ACS033-74), Nonidet P-40 (Cat. No. 56009), and glycerol (Cat. No. B10118). GTP (Cat. No. 106 372) and GDP (Cat. No. 106 208) are from Boehringer Mannheim. The monoclonal anti-Ras antibody is from Oncogene Science (Pan-Ras Ab2, Cat. No. OP22), the monoclonal antibody to simian virus 40 large tumor antigen is from Pharmingen (p108, Cat. No. 14121A), and the monoclonal antibody to adenovirus E1A is from Calbiochem (M73, Cat. No. DP11). Staph. A Sepharose beads (17-0780-03) for immunoprecipitation are from Pharmacia. X-ray film is from Kodak (X-OMAT AR, Cat. No. 165 1454). CelTak™ (Cat. No. 354240) is from BD Biosciences. Tissue culture petri dishes (6 cm diameter) are from Corning or Sarstedt.

The purity of the material to be electroporated is of paramount importance. [α^{32}P]GTP (Cat. No. NEG 006H) and [γ^{32}P]ATP (Cat. No. NEG 002A) are from Dupont NEN Research Products (HPLC purified).

The apparatus for electroporation *in situ* (Epizap model EZ-16) is available from Ask Science Products Inc. (487 Victoria St. Kingston, Ontario Canada). The inverted, phase-contrast and fluorescence microscope, equipped with a filter for Lucifer yellow (excitation: 435, emission: 530), is from Olympus (Model IX70).

The technique can be applied to a large variety of adherent cell types. We have used a number of lines, such as the Fisher rat fibroblast F111 and its polyoma or simian virus 40 virus-transformed derivatives, mouse fibroblast NIH 3T3, mouse Balb/c 3T3, mouse NIH 3T6, mouse C3H10T½ fibroblast derivatives expressing a *ras*-antimessage [e.g., lines R14 and 25B8 (Raptis *et al*., 1997)], Ras^{leu61}-transformed 10T½, and rat liver epithelial T51B, as well as a variety of differentiated adipocytes (Brownell *et al*., 1996). All cells can be grown in plastic petri dishes in DMEM supplemented with 5% calf serum in a humidified 5% CO_2 incubator with the exception of R14 and 25B8, which are grown in DMEM supplemented with 10% fetal calf serum. Cells that do not adhere can be grown and electroporated on the same conductive slides coated with CelTak™, poly-L-lysine or collagen.

III. PROCEDURE

The apparatus for *in situ* electroporation is described in Fig. 1. Cells are grown on conductive and transparent glass slides, which are placed in a petri dish to maintain sterility. The cell growth area is defined by a "window" formed with an electrically insulating frame made of Teflon. The pulse is transmitted through a stainless-steel negative electrode, which is slightly larger than the cell growth area and is placed on top of the cells, resting on the Teflon frame. Another stainless-steel block is used as a positive contact bar. A complete circuit is formed by placing the electrode set on top of the slide as shown in Figs. 1A and 1B. The frame creates a gap between the conductive coating and the negative electrode so that current can only flow through the electroporation fluid and cells growing in the window. In order to obtain a uniform electric field strength over the entire area below the negative electrode, despite the fact that the conductive coating exhibits a significant amount of electrical resistance, the bottom surface of the negative electrode must be inclined relative to the glass surface, rising in the direction of the positive contact bar, in a manner proportional to the resistance of the coating (Raptis and Firth, 1990); glass with a surface resistivity of 2 Ω/sq requires an angle of 1.5°, whereas glass of 20 Ω/sq requires an angle of 4.4°. The procedure described is for glass with a surface resistivity of 20 Ω/sq, which is readily available and relatively inexpensive, hence it can be discarded after use to limit exposure to radioactivity (see *Comment* 1). Similarly, the electrode can be made out of inexpensive aluminum for a single use.

Upscaling

A large number of signal transducers are present in small amounts in the cell so that a large number of cells

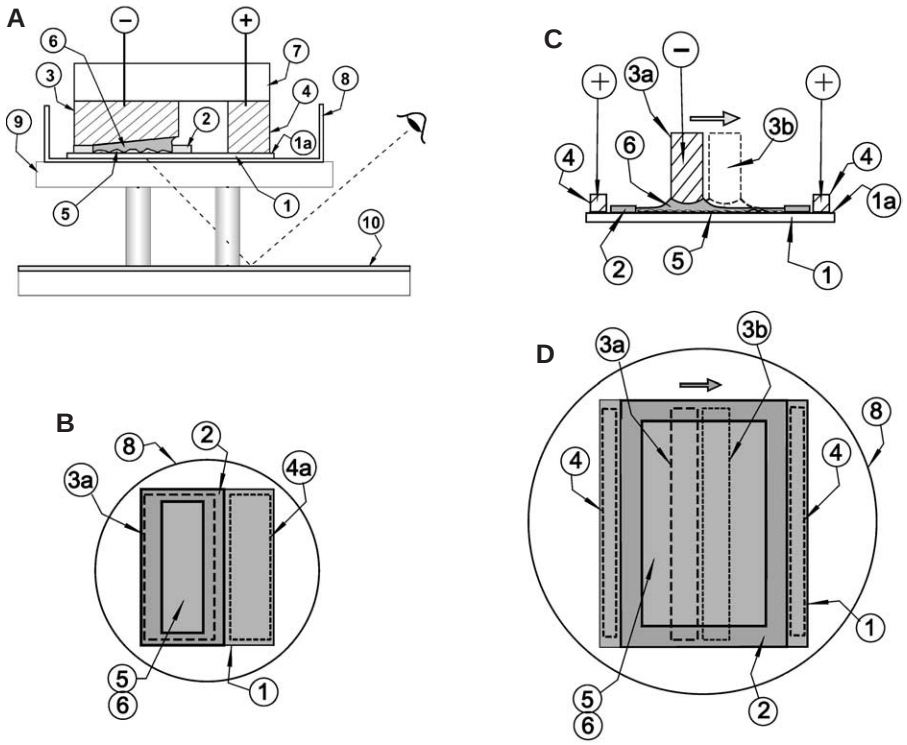

FIGURE 1 **Electroporation electrode assembly. (A) Side view.** A Delrin carrier (7) holds the negative electrode (3) and the positive contact bar (4) so that they form one unit, which can be placed on top of the slide (1) with its frame (2) and cells (5) in place. Negative (–) and positive (+) signs indicate the electrical connecting points via which the pulse of electricity is delivered to the electrodes from the pulse generator. The underside of the negative electrode (3) is machined to a slight angle, which compensates for the surface resistivity of the conductive slide to provide uniform electroporation of the whole cell growth area. The negative electrode rests on a Teflon frame (2), which insulates it from the conductive surface. The fluid containing the material to be electroporated just fills the cavity below the negative electrode. When a capacitor is discharged, current passes through the electroporation fluid (6) and cells (5) attached to the conductive glass slide (1) to the positive contact bar (4) and back to the pulse source. Note that the angle of the negative electrode has been exaggerated to better illustrate the meniscus of the radioactive electroporation solution (6). The slide and electrode fit in a 6 cm petri dish (8) that is locked in place on a stand (9). The top plate supports the petri dish and is made of transparent acrylic so that the operator can look in the mirror (10) to ensure that the liquid (6) is properly filling the cavity without air bubbles. **(B) Top view.** The outline of the conductive slide (1) with a Teflon frame (2) in place to define the area of cell growth and electroporation are indicated [from Brownell *et al*. (1997), reprinted with permission]. **Upscaling. (C) Side view.** Cells to be electroporated (5) are grown on a glass slide (1), coated with ITO (1a). The negative electrode (3a and 3b) is a narrow steel bar mounted across the width of the slide, resting on the Teflon frame (2), which is moved across the surface of the slide as shown by the arrow, by an insulated carrier. The underside of the negative electrode is curved in both directions, such as to optimise the uniformity of electrical field. Note that only the area of cells immediately below the electrode is electroporated by a given pulse. The curvature of the negative electrode has been exaggerated to better illustrate its contour. Note that due to the narrow shape of the electrode, air bubbles do not get trapped easily under it, hence a stand with a mirror may not be necessary. **(D) Top view.** The outline of the conductive slide with a Teflon frame (2) in place to define the area of cell growth and electroporation and the counterelectrodes (4) are indicated. The assembly is placed in a 10 cm petri dish (8) [from Raptis *et al*. (2003) and Tomai *et al*. (2003), reprinted with permission].

may be required to obtain a strong signal. Uniform electroporation of a cell growth area of 32 × 10 mm using 20 Ω/sq glass (i.e., an angle of 4.4°) and a Teflon frame with a thickness of 0.279 mm using the assembly in Figs. 1A and 1B requires a volume of ~280 µl. Simple scale-up of this assembly, e.g., to a cell growth area of 50 × 30 mm, which can be accommodated in a standard, 10 cm petri dish, is faced with the problem of burning the ITO coating that occurs at the higher voltage and capacitance settings required to electroporate this larger area because of the resistance generated by the greater distance the current has to travel. In addition, the volume required, ~1.7 ml, cannot be held in place by surface tension, while the cost of purchase and disposal of the

isotope can be prohibitive for certain experiments. These problems can be solved by using an assembly with a narrow, moveable electrode that electroporates a "strip" of cells at a time (Figs. 1C and 1D); in this configuration, only cells immediately below the negative electrode are electroporated by a given pulse of electricity. After electroporation of the first strip of cells, the electrode is translocated laterally, dragging the solution under it by surface tension so that a new strip of cells is electroporated using mostly the same solution (Figs. 1C and 1D). The electric circuit formed during pulse delivery starts at the negative electrode, passes through the electroporation fluid, the cells and the conductive slide surface, to the two positive contact bars, one on each side of the slide. The two positive contact bars form parallel circuit paths, both carrying current from the conductive surface. To compensate for the resistance of the coating, the bottom surface of the negative electrode must be inclined toward each of the positive contact bars; a 25 mm radius on the bottom of the electrode produces successive strips of even electroporation over the entire cell growth area. Using this assembly, an area of 32 × 10 mm can be electroporated using less than 50 µl of solution with a 2.5 mm-wide electrode, whereas an area of 50 × 30 mm can be electroporated effectively in four, 8 mm-wide strips, with a total of 200 µl of solution.

A. Electroporation of [α^{32}P]GTP for Measurement of Ras Activity

Solutions

1. ***Lucifer yellow solution, 5 mg/ml***: To make 1 ml, add 5 mg Lucifer yellow to 1 ml phosphate-free DMEM.

3. ***[α^{32}P]GTP***: Prepare a solution of 500–2000 µCi/ml in phosphate-free DMEM (*see Comment* 2).

4. ***Ras extraction buffer***: 50 m*M* HEPES, pH 7.4, 150 m*M* NaCl, 5 m*M* $MgCl_2$, 1% Triton, 0.5% deoxycholate, 0.05% SDS, 1 m*M* EGTA, 1 m*M* PMSF, 10 µg/ml aprotinin, 10 µg/ml leupeptin, 10 m*M* benzamidine, and 1 m*M* vanadate. The stock solutions can be made ahead of time. To make 50 ml, add 2.5 ml of HEPES stock, 1.5 ml of NaCl stock, 0.25 ml of $MgCl_2$ stock, 0.5 ml Triton, 0.05 g deoxycholate, 0.25 ml of SDS stock, and 0.5 ml of EGTA stock and then the protease inhibitors, 0.5 ml of PMSF stock solution, 0.05 ml of aprotinin stock, 0.05 ml of leupeptin stock, 0.5 ml of benzamidine stock, and 0.05 ml of vanadate stock and bring the volume to 50 ml with distilled H_2O on the day of the experiment.

10% sodium dodecyl sulfate stock solution: Dissolve 100 g in 1 liter H_2O. Store at room temperature. Stable for more than a year.

5 M NaCl stock solution: Dissolve 292.2 g NaCl in 1 liter distilled H_2O. Autoclave and store at room temperature. Stable for more than a year.

1 M $MgCl_2$ stock solution: Dissolve 203.3 g $MgCl_2 \cdot 6H_2O$ in 1 liter H_2O. Autoclave and store at room temperature. Stable for more than a year.

100 mM EGTA stock solution: Dissolve 38.04 g in 800 ml distilled H_2O. Adjust pH to 8.0 with NaOH and complete volume to 1 liter with distilled H_2O. Stable for more than a year at room temperature.

100 mM PMSF stock solution: Dissolve 17.4 mg PMSF in 10 ml isopropanol and store in aliquots at –20°C. Stable for several months.

10 mg/ml aprotinin stock solution: Dissolve 100 mg in 10 ml of 0.01 *M* HEPES, pH 8.0. Aliquot and store at –20°C. Stable for several months.

10 mg/ml leupeptin stock solution: Dissolve 100 mg in 10 ml distilled H_2O. Aliquot and store at –20°C. Stable for several months.

1 M benzamidine stock solution: Dissolve 1.56 g in 10 ml distilled H_2O. Aliquot and store at –20°C. Stable for several months.

1 M vanadate stock solution: Dissolve 1.84 g in 10 ml distilled H_2O. Aliquot and store at –20°C. Stable for several months.

5. ***Guanine nucleotide elution buffer***: 2 m*M* EDTA, 2 m*M* DTT, 0.2% SDS, 0.5 m*M* GTP, and 0.5 m*M* GDP.

1 M dithiothreitol stock solution: Dissolve 3.09 g DTT in 20 ml of 0.01 sodium acetate (pH 5.2). Store in 1 ml aliquots at –20°C. Stable for more than a year.

0.5 M EDTA, pH 8.0 stock solution: Add 186.1 g disodium ethylenediaminetetraacetate · $2H_2O$ to 800 ml distilled H_2O. To dissolve, adjust the pH to 8.0 with NaOH pellets while stirring. Bring volume to 1 liter. Stable for more than a year at room temperature.

10 mM GTP stock solution: Dissolve 52.3 mg in 10 ml distilled H_2O and store at –20°C. Stable for a month.

10 mM GDP stock solution: Dissolve 44.3 mg in 10 ml distilled H_2O and store at –20°C. Stable for a month.

See earlier list for other required stock solutions: To make 500 µl of elution buffer, add 10 µl of 10% SDS stock solution, 2 µl of EDTA stock solution, 1 µl of DTT stock solution, 25 µl each of GTP and GDP stock solutions, and bring volume up to 500 µl with H_2O.

6. ***Thin-layer chromatography (TLC) running buffer***: 66% isopropanol and 1% concentrated ammonia. To make 100 ml, mix 66 ml isopropanol, 1 ml concentrated ammonia solution, and 33 ml distilled H_2O in a fume hood. Make fresh the day of the experiment. Depending on the size of the chromatography tank, this volume may need to be increased.

Steps

The appropriate institutional regulations for isotope use must be followed for all experiments.

1. **Choice of slides.** Cell growth areas of 32 × 12 mm are sufficient for most cases. However, for some lines with low Ras levels, a larger number of cells may be required to obtain an adequate signal. In this case, the assembly in Figs. 1C and 1D (cell growth area, 50 × 30 mm) may be used. Make sure the glass is clean and free of fingerprints (see *Comment* 5).

2. **Plate the cells.** Uniform spreading of the cells is very important, as the optimal voltage depends in part on the degree of cell contact with the conductive surface (*see Comment* 3). Place the sterile glass slide inside a 6 cm (for 32 × 10 mm) or 10 cm (for 50 × 30 mm) petri dish. Add a sufficient amount of medium to cover the slide (approximately 9 ml for a 6 cm dish). Pipette the cell suspension in the window (Fig. 1) and place the petris in a tissue-culture incubator.

3. **Starve the cells from phosphates** by placing them in phosphate-free DMEM and the required amounts of dialysed serum for 2–3 h or overnight, depending on the experiment.

4. Prior to pulse application, **remove the growth medium** and wash the cells gently with phosphate-free DMEM.

5. Carefully **wipe** the Teflon frame with a folded Kleenex tissue to create a dry area on which a meniscus can form (see *Pitfall* 1).

6. **Add the [α^{32}P]GTP solution.** The volume of the solution under the electrode varies with the electroporation assembly and cell growth area. For the setup in Fig. 1A and a cell growth area of 32 × 10 mm, the volume is ~280 µl, whereas the assembly in Fig. 1C requires ~200 µl for a cell growth area of 50 × 30 mm. Depending on the exact concentration, this volume will contain ~200 µCi [α^{32}P]GTP in phosphate-free DMEM.

7. Carefully **place the electrode** on top of the cells. Make sure there is a sufficient amount of electroporation buffer under the positive contact bar to ensure electrical contact. Make sure there are no air bubbles between the negative electrode and the cells by looking in the mirror. If necessary, the electrode can be sterilized with 70% ethanol before the pulse, and the procedure carried out in a laminar-flow hood, using sterile solutions.

8. Apply three to six **pulses** of the appropriate strength (40–200 V, see *Comment* 3) from a 10- or 20-µF capacitor, depending on the apparatus used (Fig. 1A vs Fig. 1C).

9. **Remove the electrode set.** Because usually only a small fraction of the material penetrates into the cells, the [α^{32}P]GTP solution can be carefully aspirated and used again.

10. **Add phosphate-free medium** containing dialysed serum if permitted by the experimental protocol and incubate the cells for the desired length of time (see *Comment* 4).

11. **Remove the unincorporated material**: wash the cells twice with phosphate-free medium lacking serum.

12. **Extract the proteins.** Add 1 ml of extraction buffer to the window area of the slide. Scrape the cells using a rubber policeman into a 15 ml tube and rock the tubes on ice for 20 min. Centrifuge for 30 min at 1,000 rpm in a Beckman J-6 centrifuge to clarify. Preclear the lysates by adding 100 µl packed Staph. A–Sepharose beads, incubating on ice for 1 h, and centrifuging for 5 min at 1,000 rpm in a Beckman J-6 centrifuge.

13. **Immunoprecipitate Ras.** Incubate the precleared supernatant overnight with pan ras Ab2 antibody bound to Staph. A Sepharose beads while rocking on ice.

14. **Wash the immunoprecipitate** four times with 1 ml of extraction buffer lacking the inhibitors. Use a Hamilton syringe to completely remove all traces of wash solution.

16. **Elute** GTP and GDP off the beads by adding 10–20 µl elution buffer to the beads and incubating at 68°C for 20 min.

17. **Spot** the eluate containing the labelled nucleotides on a silica gel TLC plate containing a fluorescence indicator. Spot 1 µl each of the stock GTP and GDP solutions to serve as cold standards, easily visible under UV light. Develop the plate using a solution of 1% ammonia–66% isopropanol for about 3–4 h.

18. Dry the TLC plate, **expose** to Kodak X-OMAT AR film, and excise the spots for liquid scintillation counting or submit to phosphorimager analysis (see Fig. 2).

B. Electroporation of [γ^{32}P]ATP for Labeling of Cellular Proteins: Labeling of the Simian Virus 40 Large Tumor Antigen or Adenovirus E1A

Solutions

1. ***[γ^{32}P]ATP***: 600–1000 µCi/ml in phosphate-free DMEM.

2. ***Simian virus large tumor antigen (SVLT) or adenovirus E1A extraction buffer***: 122 m*M* NaCl, 18 m*M* Tris-base, pH 9.0, 0.8 m*M* $CaCl_2$, 0.43 m*M* $MgCl_2$, 10% glycerol, 1% NP-40, 10 µg/ml aprotinin, 10 µg/ml leupeptin, 1 m*M* PMSF, and 1 m*M* vanadate. Add 8.0 g

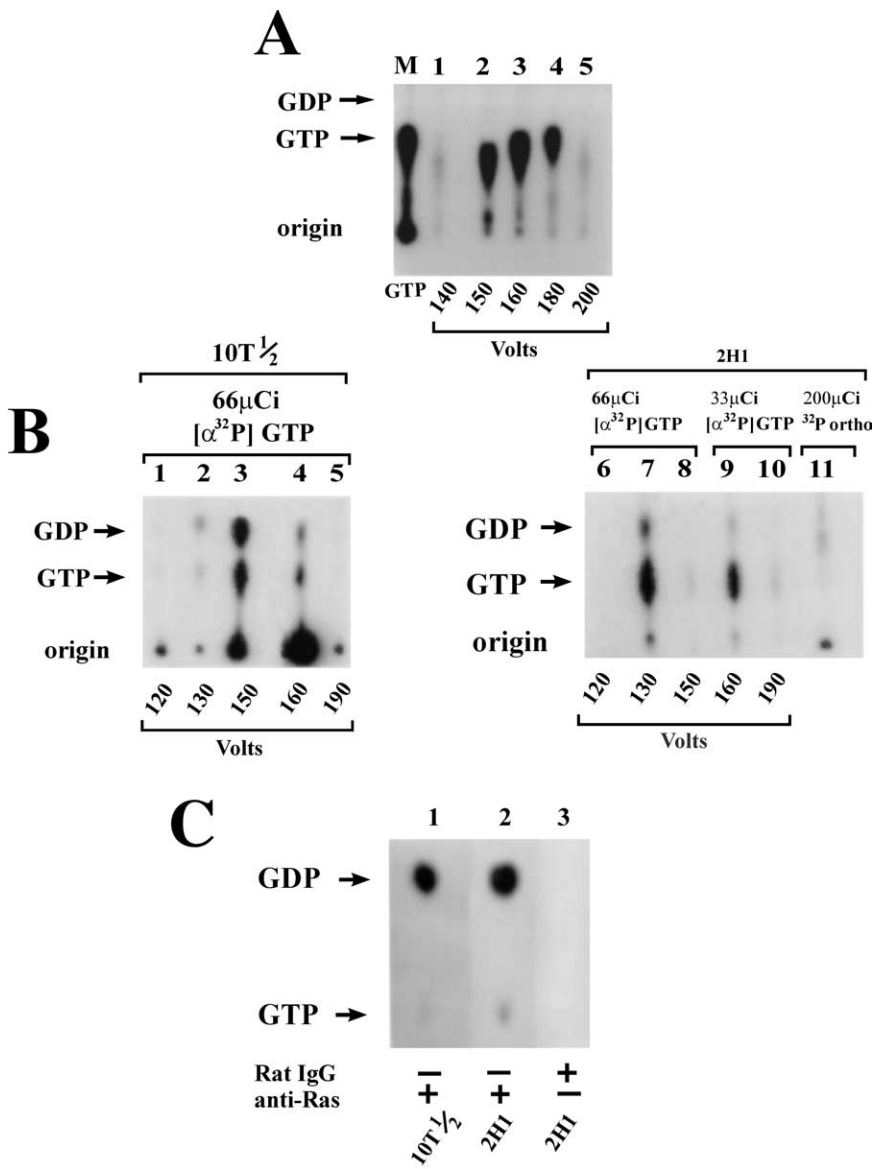

FIGURE 2 **Assessment of Ras activity through electroporation of [α[32]P]GTP.** Cells were grown on conductive glass (cell growth area, 32 × 10 mm, Figs. 1A and 1B) and starved from serum and phosphates. A solution containing [α[32]P]GTP was added to the cells and introduced with three pulses delivered from a 20 μF capacitor at different voltages as indicated. Cells were subsequently placed in a humidified 37°C, CO_2 incubator for 3 h. Ras was extracted and precipitated with the pan-ras Ab2 monoclonal antibody, the bound GTP and GDP eluted and separated by thin-layer chromatography (see text). The plate was exposed for 15 h to Kodak XAR-5 film with an intensifying screen. In all panels, arrows point to the positions of cold GTP and GDP standards, respectively. **(A) Electroporation does not induce a rapid breakdown of intracellular GTP.** Lanes 1–5: Mouse 10T½ fibroblasts were electroporated using voltages of 140–200 V as indicated in the presence of 5 μCi [α[32]P]GTP. Three hours later, nucleotides in a 2 μl aliquot of each clarified lysate were separated as described earlier without Ras immunoprecipitation. Lane M: As a marker, an aliquot of the [α[32]P]GTP used in this experiment was run in parallel. **(B) Assessment of Ras activity through electroporation of [α[32]P]GTP in normal 10T½ and their *ras*-transformed counterparts.** Lanes 1–10: 10T½ cells (lanes 1–5) or their *ras*^{val12}-transformed counterparts, 2H1 (lanes 6–10), were electroporated using voltages of 120–190 V as indicated in the presence of 66 or 33 μCi [α[32]P]GTP, respectively. Proteins were extracted, and the Ras-bound GTP and GDP were separated as described earlier. As a control (lane 11), 2H1 cells growing in a 3 cm petri to were metabolically labelled with 200 μCi [α[32]P]orthophosphate and processed as described previously. **(C) Assessment of Ras activity in normal 10T½ fibroblasts and their *ras*-transformed counterparts, 2H1, using the standard SLO permeabilization assay.** This assay was performed as described (Brownell *et al.*, 1997) and is shown here as a comparison. Lane 1, 10T½; lane 2, *ras*^{val12}-transformed, 10T½-derived line 2H1; and lane 3, 2H1 precipitated with control rat IgG instead of anti-Ras antibodies.

NaCl, 2.42 g Tris-base, 0.1 g $CaCl_2$, 0.04 g $MgCl_2$, 10 ml NP-40, and 100 ml glycerol to 800 ml H_2O. Adjust pH to 9.0 and store at –20°C. On the day of the experiment, add 0.1 ml aprotinin stock, 0.1 ml leupeptin stock, 1 ml PMSF stock, and 0.1 ml vanadate stock solutions to 100 ml of this solution.

3. ***Tris–LiCl solution for washing immunoprecipitates***: 0.1 *M* Tris-base and 0.5 *M* LiCl. Make a stock solution of 10X (4 litres). Add 484 g of Tris-base and 848 g of LiCl in 4 litres of H_2O. Adjust pH to 7.0 using concentrated HCl.

4. ***SDS gel-loading buffer***: 15 ml 10% SDS, 1.5 ml mercaptoethanol, 6 ml glycerol, 3 ml 1.25 *M* Tris, pH 6.8, 0.75 ml 0.3% bromphenol blue, and water to 30 ml.

5. *10% SDS stock solution*

6. *1.25 M Tris–HCl (pH 6.8) stock solution*: Add 151.3 g Tris-base to 800 ml distilled water. Adjust the pH to 6.8 using concentrated HCl and the volume to 1 liter with distilled water.

Steps

1. **Plate, starve from phosphates, and wash** the cells with phosphate-free DMEM as in Section III,A.

2. **Add the [γ^{32}P]ATP solution.**

3. Apply three to six **pulses** of the appropriate strength (40–200 V, see *Comment* 3) from a 10- or 20-μF capacitor, depending on the apparatus used (Fig. 1A vs Fig. 1C). If the setup in Fig. 1 A is employed, then the solution can be carefully aspirated and reused once more after the pulse.

4. **Add phosphate-free medium** and incubate the cells for 2–3 h in a tissue-culture incubator.

5. **Extract** the proteins by adding 1 ml SVLT extraction buffer to the window, scraping into a 15 ml tube, and rocking on ice. Clarify by spinning for 30 min at 1,000 rpm in a Beckman J-6 centrifuge (2,000 *g*).

6. **Precipitate** with the pAb108 (SVLT) or M73 (E1A) monoclonal antibody and wash three times with PBS, twice with the Tris–LiCl solution, and once with H_2O. Elute labelled proteins from the beads with SDS gel-loading buffer and resolve by acrylamide gel electrophoresis (Fig. 3).

IV. COMMENTS

The technique of *in situ* electroporation is very versatile. A large variety of molecules, such as peptides (Boccaccio *et al*., 1998; Raptis *et al*., 2000), nucleotides (Brownell *et al*., 1997), antibodies (Raptis and Firth, 1990), or drugs (Marais *et al*., 1997), can be introduced, alone or in combination, at the same or different times, in continuously growing or growth arrested cells or cells at different stages of thefir division cycle (see chapter 44 by Raptis *et al*.).

1. The slides can normally be washed with Extran-300 and reused a number of times. However, in the case of introduction of radioactive material, exposure of personnel to irradiation is an important consideration. The removal of ^{32}P-labelled nucleotides from the ITO-coated glass is difficult because the phosphate group is attracted to this coating (Tomai *et al*., 2000), hence the use of inexpensive slides and electrodes that can be discarded after use is highly desirable. Slides with a conductivity of 20 Ω/sq are sufficiently inexpensive that they can be discarded after use or stored for the ^{32}P to decay before washing. The use of less conductive ITO-coated glass (100 Ω/sq) would reduce the cost of the slides further. However, in our experience, the conductivity of this grade of glass is not sufficiently consistent for electroporation experiments due to problems related to uniformity of thickness encountered with the thinner coating of the less conductive, commercially available surface. On the other hand, the use of more conductive glass (2 Ω/sq) requires a smaller electrode angle, which reduces the cost of the material substantially. However, this glass is not a regular production item, hence it is more expensive.

2. The [α^{32}P]GTP must be of the highest purity. Because a number of lots were found to contain varying amounts of [α^{32}P]GDP, it is wise to test the preparation by thin-layer chromatography before use.

3. **Determination of the optimal voltage and capacitance.** Electrical field strength has been shown to be a critical parameter for cell permeation, as well as viability (Chang *et al*., 1992). It is generally easier to select a discrete capacitance value and then control the voltage precisely. The optimal voltage depends on the strain and metabolic state of the cells, as well as the degree of cell contact with the conductive surface, possibly due to the larger amounts of current passing through an extended cell (Yang *et al*., 1995; Raptis and Firth, 1990). Densely growing, transformed cells or cells in a clump require higher voltages for optimum permeation than sparse, subconfluent cells. Similarly, cells that have been detached from their growth surface by vigorous pipetting prior to electroporation require substantially higher voltages. In addition, cells growing and electroporated on collagen, poly-L-lysine, or CelTak™-coated slides require substantially higher voltages than cells growing directly on the slide.

The margins of voltage tolerance depend on the size and electrical charge of the molecules to be introduced. For the introduction of small, uncharged molecules such as Lucifer yellow or nucleotides, a wider range of field strengths permits effective permeation with

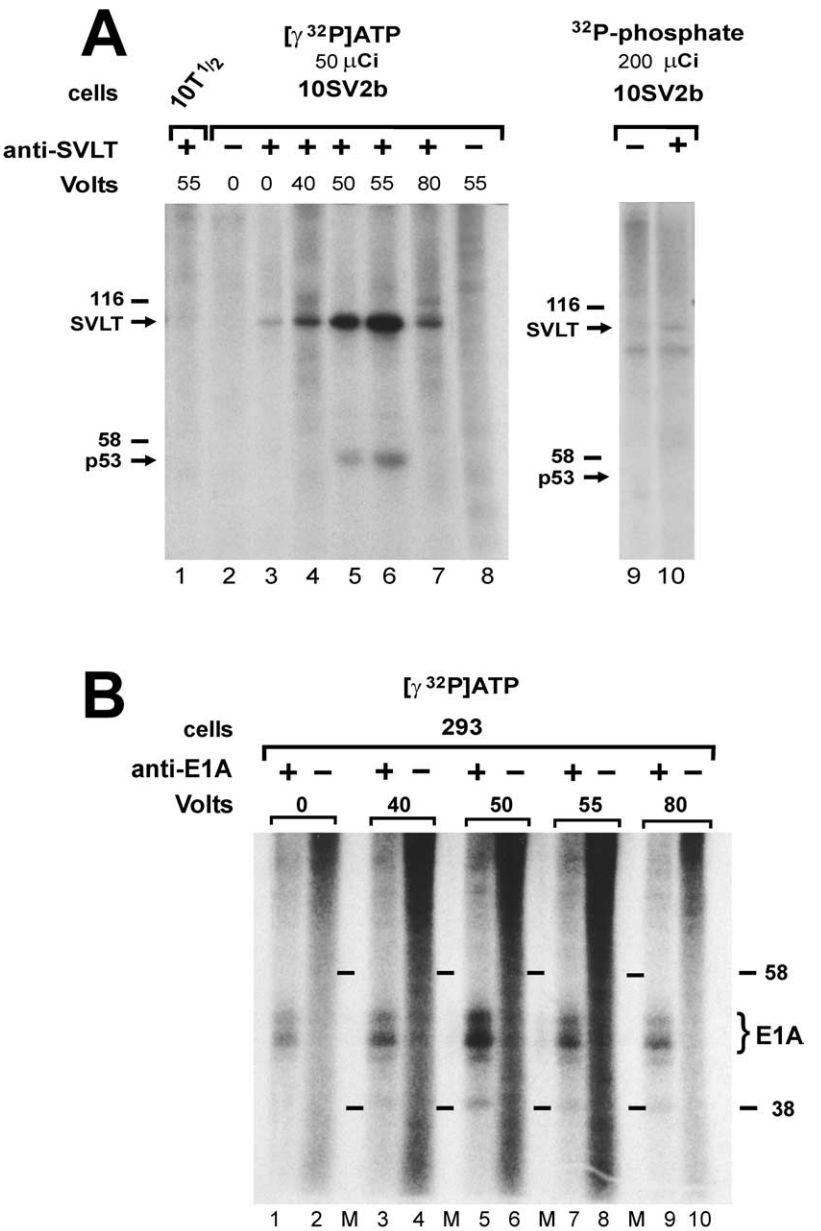

FIGURE 3 Labeling of the simian virus 40 large tumor antigen or adenovirus E1A through *in situ* electroporation of [γ^{32}P]ATP. (A) Mouse 10T½ cells (lane 1) or their SVLT-transformed derivatives (line 10SV2b, lanes 2–8) were grown on 50 × 30 mm conductive areas (Figs. 1C and 1D). A solution containing 50 μCi [γ^{32}P]ATP in phosphate-free DMEM was added to the cells, and six capacitor-discharge pulses of 10 μF, 40–80 V were applied as indicated. Cells were placed in a humidified incubator for 30 min. For a comparison (lanes 9 and 10), the same SVLT-transformed cells were labeled *in vivo* with the indicated amounts of [^{32}P]orthophosphate. SVLT was precipitated from detergent extracts with the pAb108, anti-SVLT antibody (lanes 1, 3–7, and 10), or normal mouse IgG (lanes 2, 8, and 9) and labeled proteins were resolved by acrylamide gel electrophoresis. Dried gels were exposed for 1 h to Kodak XAR-5 film with an intensifying screen. Note the intense and specific labeling of SVLT and the associated phosphoprotein, p53, by *in situ* electroporation (lanes 5 and 6) compared to cells labeled *in vivo* with 200 μCi [^{32}P]orthophosphate (lanes 9 and 10). **(B)** Human 293 cells transformed with adenovirus DNA were labeled as described earlier and extracts were preadsorbed with normal mouse IgG (lanes 2, 4, 6, 8, and 10) or immunoprecipitated using the M73, anti-E1A antibody (lanes 1, 3, 5, 7, and 9). Bracket points to the position of the phosphorylated E1A bands. M, molecular weight marker lanes.

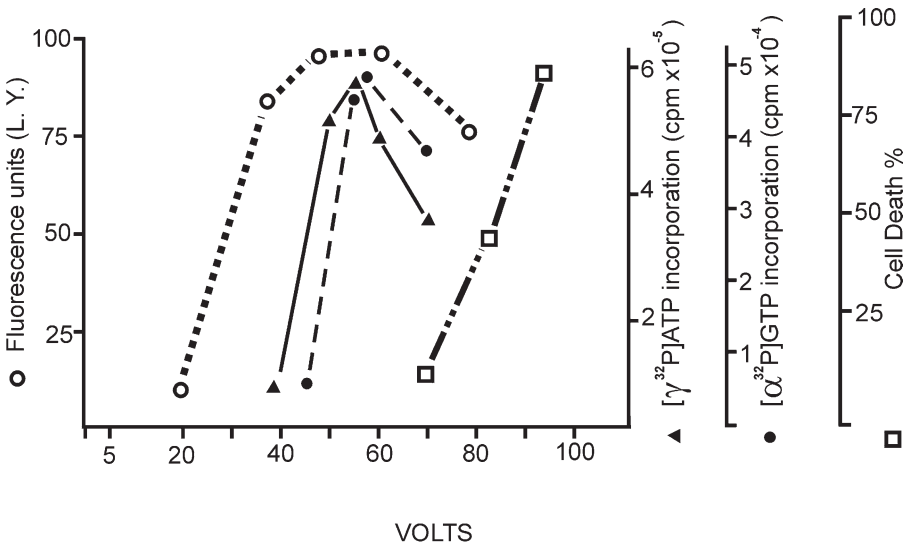

FIGURE 4 Effect of field strength on the introduction of nucleotides. Six pulses of increasing voltage were applied from a 10 µF capacitor to serum-starved $10T^{1}/_{2}$ cells growing on a conductive surface of 50 × 30 mm in the presence of 10 µCi [α^{32}P]GTP (●) or 10 µCi [γ^{32}P]ATP (▲). Total protein labelling was quantitated using a nitrocellulose filter-binding assay (Buday and Downward, 1993). Numbers refer to cpm per 100 µg of protein in clarified extracts. As a control, cells were electroporated with 5 mg/ml Lucifer yellow (○), and its introduction was assessed by fluorescence measurement of cell lysates using a Perkin–Elmer Model 204A fluorescence spectrophotometer. Cell killing (□) was calculated from the plating efficiency of the cells 2 h after the pulse [from Raptis *et al*. (2003) and Tomai *et al*. (2003), reprinted with permission].

minimal damage to the cells than the introduction of antibodies or DNA (Raptis and Firth, 1990; Brownell *et al*., 1997). For all cells tested, the application of multiple pulses at a lower voltage can achieve a better permeation and is better tolerated than a single pulse. This is especially important for the electroporation of serum-starved cells where the margins of voltage tolerance were found to be substantially narrower compared to their counterparts growing in 10% calf serum (Brownell *et al*., 1997). Results of a typical experiment are shown in Fig. 4. Rat F111 cells were grown on slides with a 50 × 30 mm cell growth area (Figs. 1C and 1D) and six pulses were delivered from a 10 µF capacitor. Following electroporation of the first strip of cells, the negative electrode was translocated laterally (Fig. 1C, arrow) so that the whole area was electroporated in four strips. The application of six exponentially decaying pulses of an initial strength of ~40–55 V resulted in essentially 100% of the cells containing the introduced dye, Lucifer yellow, whereas [α^{32}P]GTP required ~50 V for a maximum signal.

Cell damage is microscopically manifested by the appearance of dark nuclei under phase-contrast illumination. For most lines, this is most prominent 5–10 min after the pulse. Such cells do not retain Lucifer yellow and fluoresce very weakly, if at all (Fig. 5). It was also noted that the current flow along the corners of the window is slightly greater than the rest of the conductive area. For this reason, as the voltage is progressively increasing, damaged cells will appear on this area first. This slight irregularity has to be taken into account when determining the optimal voltage.

Example of determination of the optimal voltage. Prepare a series of slides with cells plated uniformly in a 32 × 10 mm window (Figs. 1A and 1B). Set the apparatus at 20 µF capacitance. Prepare a solution of 5 mg/ml Lucifer yellow in phosphate-free DMEM and a solution of [α^{32}P]GTP or [γ^{32}P]ATP containing 5 mg/ml Lucifer yellow in phosphate-free DMEM. Electroporate the Lucifer yellow solution at different voltages, 20 µF, three pulses, to determine the upper limits where a small fraction of the cells at the corners of the window (usually the more extended ones) are killed by the pulse, as determined by visual examination under phase-contrast and fluorescence illumination 5–10 min after the pulse (Fig. 5). Depending on the cells and growth conditions, this voltage can vary from 130 to 190 V. Repeat the electroporation using the radioactive nucleotide solution at different voltages starting at 20 V below the upper limit and at 5 V increments. The Lucifer yellow offers a convenient marker for cell permeation and it was found not to affect the results.

4. Serum was shown to facilitate pore closure (Bahnson and Boggs, 1990).

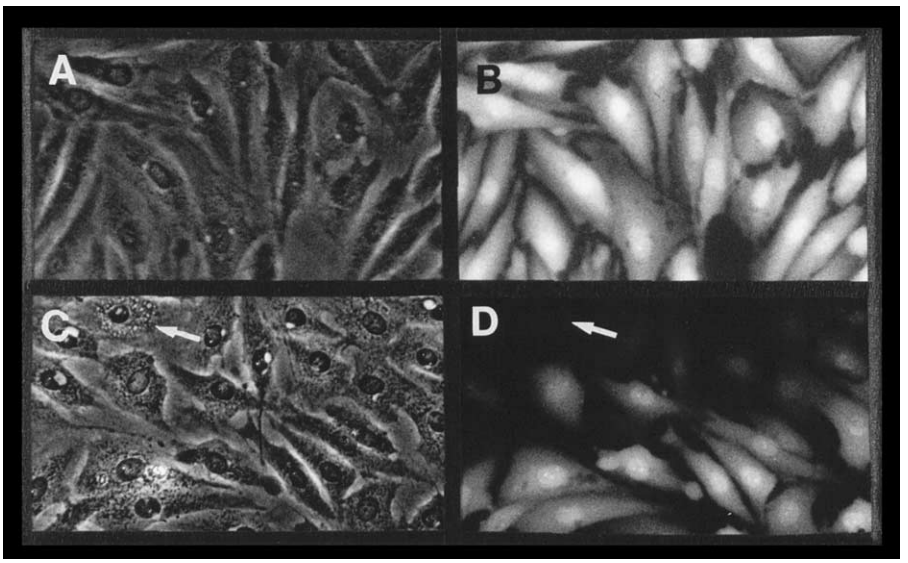

FIGURE 5 Determination of optimal voltage. Rat F111 fibroblasts growing on conductive slides (Figs. 1A and 1B, cell growth area, 32 × 10 mm) were electroporated in the presence of 5 mg/ml Lucifer yellow using three pulses of 155 (A and B) or 190 (C and D) volts delivered from a 20 μF capacitor. After washing of the unincorporated dye, cells were photographed under phase-contrast (A and C) or fluorescence (B and D) illumination. Arrows in C and D point to a cell that has been killed by the pulse. Note the dark, pycnotic and prominent nucleus under phase contrast and the flat, nonrefractile appearance. Such cells do not retain any electroporated material, as shown by the absence of fluorescence (C). It is especially striking that cells at the top of frames C and D, situated at the edge of the electroporated area, received a larger amount of current and have been killed by the pulse. Magnification: 240 times.

5. The slides come with the apparatus and are sterile. If sterility is compromised or if the slides have been washed to reuse, then place in petris and sterilize by adding 80% ethanol for 20 min and then removing the ethanol by rinsing with sterile distilled water.

Other characteristics of the technique. Under the appropriate conditions, *in situ* electroporation does not affect cell morphology or the length of the G1 phase of serum-stimulated cells and does not induce c-*fos* (Raptis and Firth, 1990; Brownell *et al*., 1997). In addition, it does not affect activity of the extracellular signal-regulated kinase (Erk1/2) or two kinases commonly activated by a number of stress-related stimuli, JNK/SAPK and $p38^{hog}$ (Robinson and Cobb, 1997), presumably because the pores reseal rapidly so that the cell interior is restored to its original state (Brownell *et al*., 1998).

Measurement of steady-state Ras activity is possible using this method because, contrary to other methods of cell permeabilization, such as streptolysin-O (Buday and Downward, 1993), the cells are not detectably affected by the procedure so that they can be incubated for long periods of time before extraction. In addition, electroporation does not appear to induce a rapid breakdown of intracellular GTP in any of the lines tested, even under conditions where a substantial fraction of the cells are killed by the pulse (Fig. 2). As a result, determination of the Ras-bound, GTP/GTP + GDP ratio is made easier by the fact that although the optimal voltage must be determined empirically as in all electroporation experiments, excessively high voltages, despite the fact that they may kill a substantial proportion of the cells, do not alter the ratios obtained (Fig. 2B), presumably because such cells rapidly lyse, without affecting the results.

V. PITFALLS

1. Care must be taken so that cells do not dry during the procedure, especially during wiping of the frame with a tightly folded Kleenex. It was found that serum-starved cells were especially susceptible. The morphology of cells that have been killed by drying is very similar to cells that have been killed by the pulse (Fig. 5).

2. Accurate determination of the optimal voltage is very important. For most nucleotide introduction applications, optimal labelling was observed in the range of 140–160 V, whereas these margins were found to be narrower for serum-starved cells. Nevertheless,

the Ras-bound GTP/GTP + GDP ratios or the profile of SVLT or E1A labelling obtained was found to be the same even when a substantial proportion of the cells were killed by the pulse, in which case merely ^{32}P incorporation is reduced.

Acknowledgments

The financial assistance of the Canadian Institutes of Health Research, the Natural Sciences and Engineering Research Council of Canada, and the Cancer Research Society Inc. to LR is gratefully acknowledged. AV is the recipient of NSERC and Ontario Graduate studentships, a Queen's University graduate award, and a Queen's University travel grant. ET is the recipient of a Queen's University graduate award, an NSERC studentship, and awards from the Thoracic Society and the Lemos foundation. HB was the recipient of a studentship from the Medical Research Council of Canada and Queen's University graduate school and Microbix Biosystems Inc. travel awards.

References

Bahnson, A. B., and Boggs, S. S. (1990). Addition of serum to electroporated cells enhances survival and transfection efficiency. *Biochem. Biophys. Res. Commun.* **171**, 752–757.

Boccaccio, C., Ando, M., Tamagnone, L., Bardelli, A., Michielli, P., Battistini, C., and Comoglio, P. M. (1998). Induction of epithelial tubules by growth factor HGF depends on the STAT pathway. *Nature* **391**, 285–288.

Brownell, H. L., Firth, K. L., Kawauchi, K., Delovitch, T. L., and Raptis, L. (1997). A novel technique for the study of Ras activation; electroporation of [α^{32}P]GTP. *DNA Cell Biol.* **16**, 103–110.

Brownell, H. L., Lydon, N., Schaefer, E., Roberts, T. M., and Raptis, L. (1998). Inhibition of epidermal growth factor-mediated ERK1/2 activation by *in situ* electroporation of nonpermeant [(alkylamino)methyl]acrylophenone derivatives. *DNA Cell Biol.* **17**, 265–274.

Brownell, H. L., Narsimhan, R., Corbley, M. J., Mann, V. M., Whitfield, J. F., and Raptis, L. (1996). Ras is involved in gap junction closure in mouse fibroblasts or preadipocytes but not in differentiated adipocytes. *DNA Cell Biol.* **15**, 443–451.

Buday, L., and Downward, J. (1993). Epidermal growth factor regulates the exchange rate of guanine nucleotides on p21ras in fibroblasts. *Mol. Cell. Biol.* **13**, 1903–1910.

Chang, D. C., Chassy, B. M., Saunders, J. A., and Sowers, A. E. (1992). Guide to Electroporation and Electrofusion. Academic Press, New York.

Downward, J. (1995). Measurement of nucleotide exchange and hydrolysis activities in immunoprecipitates. *Methods Enzymol.* **255**, 110–117.

Egawa, K., Sharma, P. M., Nakashima, M., Huang, Y., Huver, E., Boss, G. R., and Olefsky, J. M. (1999). Membrane-targeted phosphatidylinositol kinase mimics insulin actions and induces a state of cellular insulin resistance. *J. Biol. Chem.* **274**, 14306–14314.

Lowy, D. R., and Willumsen, B. M. (1993). Function and regulation of ras. *Annu. Rev. Biochem.* **62**, 851–891.

Marais, R., Spooner, R. A., Stribbling, S. M., Light, Y., Martin, J., and Springer, C. J. (1997). A cell surface tethered enzyme improves efficiency in gene-directed enzyme prodrug therapy. *Nature Biotechnol.* **15**, 1373–1377.

Raptis, L., Brownell, H. L., Vultur, A. M., Ross, G., Tremblay, E., and Elliott, B. E. (2000). Specific inhibition of growth factor-stimulated ERK1/2 activation in intact cells by electroporation of a Grb2-SH2 binding peptide. *Cell Growth Differ.* **11**, 293–303.

Raptis, L., Brownell, H. L., Wood, K., Corbley, M., Wang, D., and Haliotis, T. (1997). Cellular ras gene activity is required for full neoplastic transformation by simian virus 40. *Cell Growth Differ.* **8**, 891–901.

Raptis, L., and Firth, K. L. (1990). Electroporation of adherent cells *in situ*. *DNA Cell Biol.* **9**, 615–621.

Raptis, L., Vultur, A., Balboa, V., Hsu, T., Turkson, J., Jove, R., and Firth, K. L. (2003). *In situ* electroporation of large numbers of cells using minimal volumes of material. *Anal. Biochemi.*

Robinson, M. J., and Cobb, M. H. (1997). Mitogen-activated protein kinase pathways. *Curr. Opini. Cell Biol.* **9**, 180–186.

Scheele, J. S., Rhee, J. M., and Boss, G. R. (1995). Determination of absolute amounts of GDP and GTP bound to Ras in mammalian cells: Comparison of parental and Ras-overproducing NIH 3T3 fibroblasts. *Proc. Natl. Acad. Sci. USA* **92**, 1097–1100.

Taylor, S. J., Resnick, R. J., and Shalloway, D. (2001). Nonradioactive determination of Ras-GTP levels using activated ras interaction assay. *Methods Enzymol.* **333**, 333–342.

Tomai, E., Klein, S., Firth, K. L., and Raptis, L. (2000). Growth on indium-tin oxide-coated glass enhances ^{32}P-phosphate uptake and protein labelling of adherent cells. *Prep. Biochem. Biotechnol.* **30**, 313–320.

Tomai, E., Vultur, A., Balboa, V., Hsu, T., Brownell, H. L., Firth, K. L., and Raptis, L. (2003). *In situ* electroporation of radioactive compounds into adherent cells.

Yang, T. A., Heiser, W. C., and Sedivy, J. M. (1995). Efficient in situ electroporation of mammalian cells grown on microporous membranes. *Nucleic Acids. Res.* **23**, 2803–2810.

CHAPTER

44

Dissecting Pathways; *in Situ* Electroporation for the Study of Signal Transduction and Gap Junctional Communication

Leda Raptis, Adina Vultur, Heather L. Brownell, and Kevin L. Firth

I. INTRODUCTION

Electroporation has been used for the introduction of DNA and proteins, as well as various nonpermeant drugs and metabolites into cultured mammalian cells (reviewed in Neumann *et al*., 2000; Chang *et al*., 1992). Most electroporation techniques for adherent cells involve the delivery of the electrical pulse while the cells are in suspension. However, the detachment of these cells from their substratum by trypsin or EDTA can cause significant metabolic alterations (Matsumura *et al*., 1982), while the efficient incorporation of proteins, peptides, or drugs without cellular damage is an especially crucial requirement, since contrary to DNA, no convenient large-scale method exists for the selection of viable from damaged cells or cells where no introduction took place after electroporation, for most proteins or drugs of interest. For these reasons, a number of approaches have been taken to bypass this problem (Kwee *et al*., 1990; Yang *et al*., 1995).

This article describes a technique where cells are grown on a glass surface coated with electrically conductive, optically transparent indium-tin oxide (ITO) at the time of pulse delivery. This coating promotes excellent cell adhesion and growth, allows direct visualization of the electroporated cells, and offers the possibility of ready examination due to their extended morphology. The procedures described are applicable to a wide variety of nonpermeant molecules, such as peptides (Giorgetti-Peraldi *et al*., 1997; Boccaccio *et al*., 1998; Bardelli *et al*., 1998), oligonucleotides (Boccaccio *et al*., 1998; Gambarotta *et al*., 1996), radioactive nucleotides (Boussiotis *et al*., 1997), proteins (Nakashima *et al*., 1999), DNA (Raptis and Firth, 1990), or drugs (Marais *et al*., 1997). These compounds can be introduced alone or in combination, at the same or different times, in growth-arrested cells or cells at different stages of their division cycle. After introduction of the material, cells can be either extracted and biochemically analysed or their morphology and biochemical properties examined *in situ*. In a modified version, this assembly can be used for the study of intercellular, junctional communication. The instant introduction of the molecules into essentially 100% of the cells makes this technique especially suitable for kinetic studies of effector activation. Unlike other techniques of cell permeabilization, under the appropriate conditions, *in situ* electroporation does not affect cell morphology, the length of the G1 phase of serum-stimulated cells (Raptis and Firth, 1990), the activity of the extracellular signal regulated kinase (Erk1/2 or Erk), or two kinases commonly activated by a number of stress-related stimuli, JNK/SAPK and $p38^{hog}$ (Robinson and Cobb, 1997), presumably because the pores reseal rapidly so that the cell interior is restored to its original state (Brownell *et al*., 1998).

II. MATERIALS AND INSTRUMENTATION

The purity of the material to be electroporated is of paramount importance. Substances such as detergents,

Copyright 2006, Elsevier Science (USA).
All rights reserved.

preservatives, or antibiotics could kill the cells into which they are electroporated, even if they have no deleterious effects if added to the culture medium of nonelectroporated cells.

Dulbecco's modification of Eagle's medium (DMEM) is from ICN (Cat. No. 10-331-22). Fetal calf serum (Cat. No. 2406000AJ) and phosphate-buffered saline (PBS, Cat. No. 20012-027) are from Gibco Life Technologies. Calf serum is from ICN (Cat. No. 29-131-54). EGF is from Intergen (Cat. No. 4110-80). HEPES (Cat. No. H-9136), Lucifer yellow CH dilithium salt (Cat. No. L-0259), trypsin (Cat. No. T-0646), $MgCl_2$ (Cat. No. M-8266), Triton (Cat. No. T-6878), deoxycholate (Cat. No. D-5760), EDTA (Cat. No. E-5134), EGTA (Cat. No. E-3889), phenylmethylsulfonyl fluoride (PMSF, P-7626), aprotinin (Cat. No. A-6279), leupeptin (Cat. No. L-2023), benzamidine (Cat. No. B-6506), dithiothreitol (DTT, Cat. No. D-9779), $CaCl_2$ (Cat. No. C-4901), Tris (Cat. No. T-6791), paraformaldehyde (Cat. No. P-6148), bovine serum albumin (BSA, Cat. No. A-4503), SigmaFast DAB kit (Cat. No. D-9167 and Cat. No. U-5005), and sodium orthovanadate (Cat. No. S-6508) are from Sigma. Extran-300 detergent (Cat. No. B80002), SDS (Cat. No. 44244), NP-40 (Cat. No. 56009), glycerol (Cat. No. B10118), and peroxide (B 80017) are from BDH. CelTak™ is from BD Biosciences (Cat. No. 354240). The cell staining kit, including goat serum, secondary antibody, and avidin–biotin complex, was from Vector Labs (Vectastain kit Cat. No. PK-6101). Rabbit antipeptide antibodies against the double threonine and tyrosine phosphorylated (activated) Erk1/2 kinase are from Biosource International (Cat. No. 44-680). When stored frozen in aliquots, they are stable for more than 5 years. They are used at 1:500 for immunostaining and 1:10,000 for Western blotting. Three- and 6-cm tissue culture dishes are from Corning or Sarstedt. Please note that only these brands of plates fit the electroporation stand.

The Grb2-SH2 binding peptide is based on the sequence flanking the Y^{1068} of the EGF receptor (PVPE-Pmp-INQS, MW 1123). To enhance stability of the phosphate group, the phosphotyrosine analog, phosphono-methylphenylalanine (Pmp), which cannot be cleaved by phosphotyrosine phosphatases yet binds to SH2 domains with high affinity and specificity (Otaka *et al*., 1994), is incorporated at the position of phosphotyrosine. The Pmp monomer is custom synthesized by *Color your enzyme Inc*., (Kingston, Ontario, Canada). As control, we used the same peptide containing phenylalanine at the position of Pmp. Peptides are synthesized by the Queen's University Core Facility using standard Fmoc chemistry.

The system for electroporation *in situ* (Epizap Model EZ-16) can be purchased from Ask Science Products Inc. (Kingston, Ontario, Canada, phone: 613 545-3794). The inverted, phase-contrast and fluorescence microscope, equipped with filters for Lucifer yellow and fluorescein, was from Olympus (Model IX70).

III. PROCEDURES

The technique of *in situ* electroporation can be used equally effectively for large-scale biochemical experiments (Giorgetti-Peraldi *et al*., 1997; Boccaccio *et al*., 1998; Bardelli *et al*., 1998) or for the detection of biochemical or morphological changes *in situ* (Raptis *et al*., 2000a). Cells are grown on glass slides coated with conductive and transparent indium-tin oxide (ITO). The cell growth area is defined by a "window" formed with an electrically insulating frame made of Teflon as shown. A stainless-steel electrode is placed on top of the cells resting on the frame and an electrical pulse of the appropriate strength is applied, as illustrated in Fig. 1 (see also chapter 43 by Raptis *et al*.). The technique can be applied to a large variety of adherent cell types (Brownell *et al*., 1996). Cells that do not adhere well can be grown and electroporated on the same conductive slides coated with CelTak™ or poly-L-lysine used according to the manufacturer's instructions.

A. Electroporation of Peptides into Large Numbers of Cells for Large-Scale Biochemical Experiments. Use of Fully Conductive Slides

To study the effect of protein interactions *in vivo* on cellular functions, such complexes can be disrupted through the introduction of peptides corresponding to the proteins' point(s) of contact. An example of this approach is described here.

Growth factors such as the epidermal growth factor (EGF) stimulate cell proliferation by binding to, and activating, membrane receptors with cytoplasmic tyrosine kinase domains. *In vitro* binding and receptor mutagenesis studies have shown that ligand engagement induces receptor autophosphorylation at distinct tyrosine residues, which constitute docking sites for a number of effector molecules, such as the growth factor receptor-binding protein 2 (Grb2), which are recruited to specific receptors through modules termed Src-homology 2 (SH2) domains (reviewed in *Schlessinger*, 2000). Grb2 binds to the receptors for PDGF and EGF at a number of sites, an event activating the Sos/Ras/Raf/Erk pathway, which is central to the mitogenic response stimulated by many growth factors. Previous results indicated that a synthetic

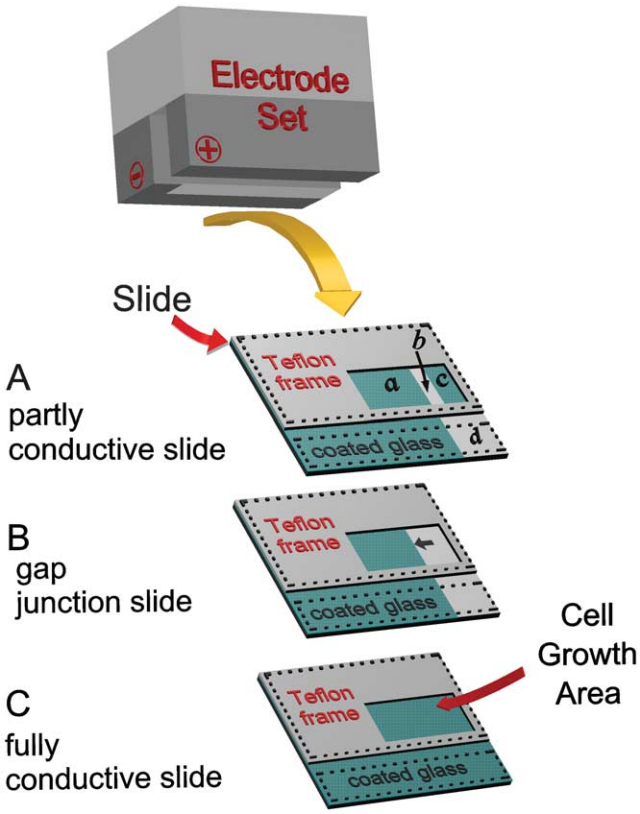

FIGURE 1 Electroporation electrode and slide assembly. Cells are grown on glass slides coated with conductive and transparent ITO within a "window" cut into a Teflon frame as shown. The window can be different sizes, depending on the cell growth area required. The peptide solution is added to the cells and introduced by an electrical pulse delivered through the electrode set, which is placed directly on the frame. Dotted lines point to the positions of negative and positive electrodes during the pulse. Three slide configurations are described. (A) Partly conductive slide assembly, with electroporated (*a*) and non-electroporated (*c*) cells growing on the same type of ITO-coated surface. (*b*) area where the conductive coating has been stripped, exposing the non-conductive glass underneath. Cells growing in areas *b* and *c* are not electroporated (Fig. 3). (B) Partly conductive slide assembly for use in the examination of gap junctional, intercellular communication. Arrow points to the transition line between conductive and non-conductive areas (Fig. 4). (C) Fully conductive slide assembly for use in biochemical experiments. In the setup shown, cell growth area can be up to 7 × 15 mm, but larger slides and electrodes offer larger areas, up to 32 × 10 mm (Fig. 2).

phosphopeptide corresponding to the Grb2-binding site of the EGF receptor (EGFR, flanking the EGFR tyr[1068], PVPE-pY-INQS), when made in tandem with peptides that allow for translocation across the cell membrane, could inhibit EGF-mediated mitogenesis and Erk activation in newt myoblasts induced by 1 ng/ml EGF, but was less effective at 10 ng/ml (Williams *et al.*, 1997). To better determine the functional consequences of disrupting the association of Grb2 *per se* with different receptors *in vivo* in mammalian cells, we delivered large quantities of this peptide into intact, living NIH3T3 fibroblasts by *in situ* electroporation.

Solutions

Spent medium: Grow cells to confluence in DMEM with 10% calf serum. Seven days postconfluence, collect the culture supernatant and dilute 1:1 with fresh DMEM. Growth-arrest cells by incubating in spent medium prepared from the same line.

Lucifer yellow solution, 5 mg/ml: To make 10 ml, dissolve 50 mg Lucifer yellow in 10 ml calcium-free DMEM. Stable at 4°C for at least a month.

Peptides: The peptide concentration required varies with the strength of the signal to be inhibited. For the inhibition of the EGF-mediated Erk activation, prepare a solution of 5–10 mg/ml (~5–10 m*M*) of the Grb2-SH2-blocking peptide (PVPE-pmp-INQS, MW 1123 Da) in calcium-free DMEM (see *Comment* 1).

Epidermal growth factor: To make a 10,000× stock solution, dissolve 100 µg of lyophilised EGF in 100 µl sterile water and freeze in 5 µl aliquots. Just prior to the experiment, add 1 µl stock solution to 10 ml calcium-free DMEM (final concentration, 100 ng/ml). The stock solution is stable at –20° or –70°C for up to 2 months.

Lysis buffer: 50 m*M* HEPES, pH 7.4, 150 m*M* NaCl, 10 m*M* EDTA, 10 m*M* $Na_4P_2O_7$, 100 m*M* NaF, 2 m*M* vanadate, 0.5 m*M* PMSF, 10 µg/ml aprotinin, 10 µg/ml leupeptin, 1% Triton X-100.

Steps

1. **Choice of slides**. For Western blotting experiments on cell extracts following electroporation, use fully conductive slides (Fig. 1C). Since the custom-made peptide is usually the most expensive reagent in this application, to avoid waste, choose the smallest possible cell growth area which provides a sufficient number of cells. Cell growth areas of 32 × 10 mm are generally sufficient to detect Erk1/2 activity inhibition by the Grb2-SH2 blocking peptide in EGF-stimulated, mouse NIH3T3 fibroblasts. In this case, the volume of the solution under the electrode is ~140 µl and will contain approximately 700–1,400 µg peptide in calcium-free DMEM. If fewer cells suffice, then slides with a cell growth area of 7 × 15 mm can be used, requiring ~40 µl of peptide solution. However, for the determination of [^{3}H]thymidine uptake, cell growth areas of 7 × 4 mm are preferred and they require only ~14 µl of solution (see *Comment* 2).

2. **Plate the cells**. Uniform spreading of the cells is very important, as the optimal voltage depends in part

on the degree of cell contact with the conductive surface (see *Comment* 3). Add a sufficient amount of medium (DMEM containing 10% calf serum) to cover the slide (approximately 9 ml for a 6 cm dish). Pipette the cell suspension in the window cut in the Teflon frame (Fig. 1) and place the petris in a tissue-culture incubator until confluent.

3. Prior to the experiment, **starve** the cells overnight in DMEM without serum. Alternatively, cells can be incubated in spent medium for 48 h; this treatment offers wider margins of voltage tolerance (see *Comment* 3).

4. Prior to pulse application, **remove the growth medium** and wash the cells gently once with calcium-free DMEM.

5. Carefully **wipe** the Teflon frame with a folded Kleenex tissue to create a dry area on which a meniscus can form (see *Pitfall* 1).

6. **Add the peptide** solution to the cells with a micropipettor in calcium-free DMEM.

7. Carefully **place the electrode** on top of the cells and clamp it in place. To ensure electrical contact, a sufficient amount of growth medium or PBS should be present under the positive contact bar. Make sure there are no air bubbles under the negative electrode. If necessary, the electrode can be sterilized with 80% ethanol before the pulse and the procedure carried out in a laminar flow hood, using sterile solutions.

8. Apply three to six **pulses** of the appropriate voltage and capacitance (see *Comment* 3).

9. **Remove the electrode set**. Since usually only a small fraction of the material enters the cells, the peptide solution may be carefully aspirated and used again. However, care must be exercised so that the cells do not dry (see *Pitfall* 1).

10. **Add serum-free growth medium** and incubate the cells for 2–5 min at 37°C to recover.

11. **Add EGF** to the medium to a final concentration of 100 ng/ml for 5 min. Controls receive the same volume of calcium-free DMEM.

12. **Extract** the cells with 50 µl extraction buffer for a cell growth area of 32 × 10 mm. For smaller cell growth areas, the voltage can be adjusted accordingly.

13. To **detect activated Erk1/2**, load 100 µg of total cell extract protein on an acrylamide–SDS gel and analyse by Western immunoblotting using the antibody directed against the dually phosphorylated, i.e., activated, form of Erk1/2.

14. For examination of the effect of the peptide upon [^{3}H]thymidine incorporation into DNA, serum-starve 50% confluent, NIH3T3 cells as described earlier and electroporate in the presence or absence of peptide. Incubate in medium with or without EGF for 12 h at 37°C, followed by a 2 h incubation with 50 µCi/ml [^{3}H]thymidine. Wash the cells with PBS and measure acid-precipitable counts. Growth areas of 4 × 7 mm are sufficient for this experiment, and [^{3}H]thymidine can be added to the window only, in a volume of ~50 µl which is held in place by surface tension.

As shown in Fig. 2A, electroporation of the Grb2-SH2 blocking peptide caused a dramatic reduction in EGF-mediated Erk activation in mouse NIH3T3 cells at growth factor concentrations permitting full receptor stimulation (compare lanes 2 and 3 with lane 4). In addition, electroporation of this peptide reduced EGF-mediated [^{3}H]thymidine uptake (Fig. 2B). In contrast, the same peptide had only limited or no effect on Erk activation triggered by HGF, although it could inhibit PDGF signalling (Raptis *et al.*, 2000a). These findings demonstrate that the *in situ* electroporation approach described can very effectively inhibit growth factor-stimulated mitogenesis and thereby detect the differential specificity in the coupling of activated receptor tyrosine kinases to the Erk cascade.

B. Electroporation for the Study of Morphological Effects or Biochemical Changes *in Situ*: Use of Partly Conductive Slides

Assessment of Erk activity by Western blotting following electroporation of the Grb2-SH2 blocking peptide can reveal the involvement of this domain in growth factor-mediated Erk activation. However, to ensure that the treatment itself does not cause cell stress, examination of cellular morphology, in conjunction with measurement of gene product activity by immunocytochemistry, offers a distinct advantage. This approach can demonstrate the specificity of action of the Grb2-SH2 binding peptide, as well as examine the distribution of signal inhibition across the cell layer. An added advantage is that it requires a small number of cells, hence a substantially smaller volume of the peptides (~14 µl in the setup shown in Fig. 1A), compared to Western blotting (~140 µl for a cell growth area of 32 × 10 mm), which could be a significant consideration given their production costs. To precisely assess small background changes in morphology or gene expression levels, the presence of non-electroporated cells side by side with electroporated ones can offer a valuable control and this can be achieved by growing the cells on a conductive slide where part of the coating has been stripped by etching with acids, thus exposing the non-conductive glass underneath. However, as shown in Fig. 3, area *a* vs *b*, the slight tinge of the glass combined with the more effective staining of cells growing on ITO (possibly due to a chemical attraction of different reagents to the coating) can

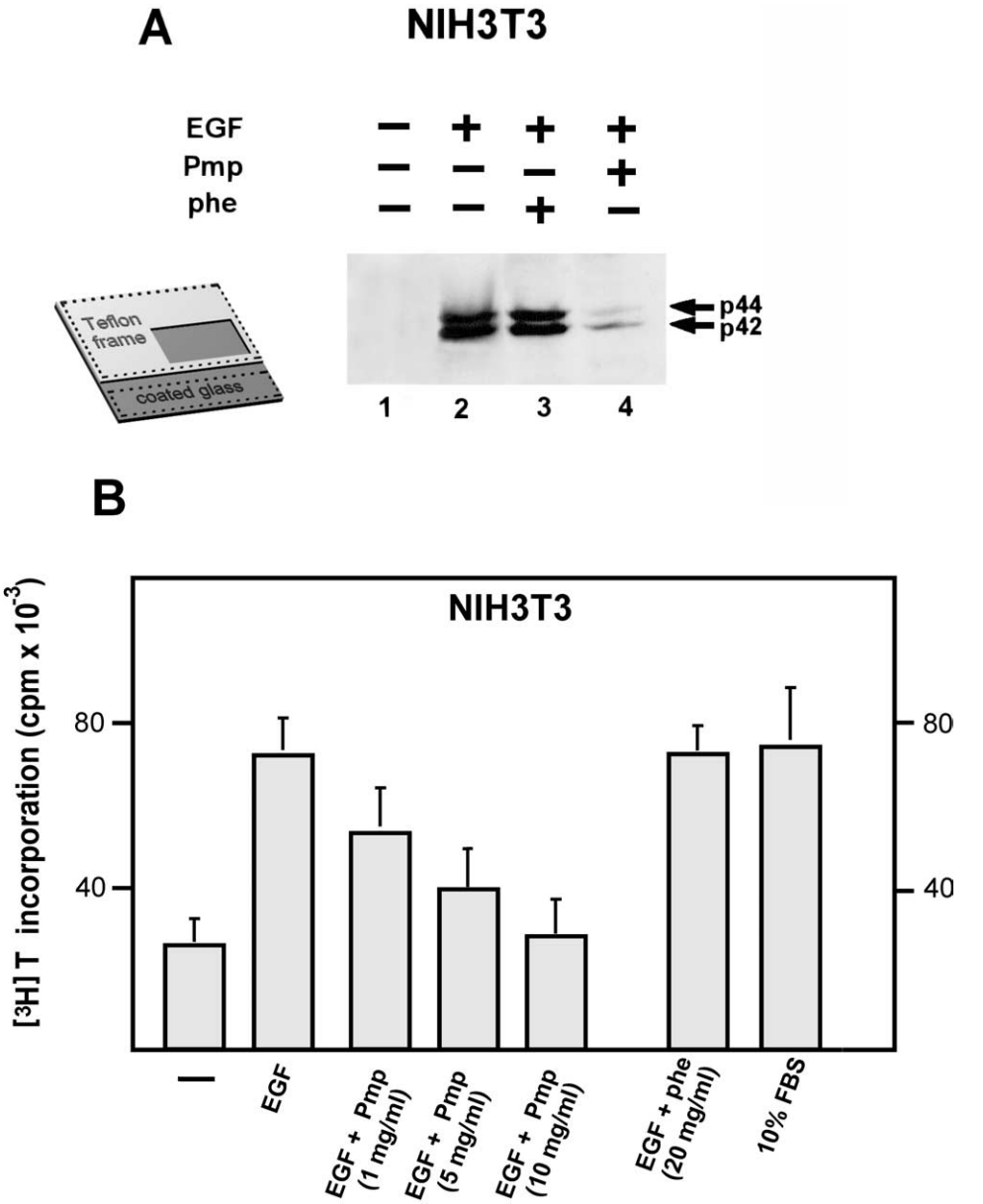

FIGURE 2 **(A) The Grb2-SH2 blocking peptide inhibits EGF-mediated Erk activation in living cells; detection by Western blotting.** The Grb2-SH2 blocking peptide was electroporated into NIH3T3 cells growing on fully conductive slides (inset, Fig. 1C, cell growth area 32 × 10 mm) and growth-arrested by serum starvation. After a 5 min incubation in DMEM, cells were stimulated with 100 ng/ml EGF (lanes 2–4) for 5 min. Proteins in detergent cell lysates were resolved by polyacrylamide gel electrophoresis and analysed by Western blotting using the antibody against the dually phosphorylated, active Erk enzymes. Lane 1, control, unstimulated cells; lane 2, control non-electroporated, EGF-treated cells; lane 3, cells electroporated with the control, phenylalanine-containing peptide and EGF stimulated; and lane 4, cells electroporated with the Grb2-SH2-binding peptide and EGF stimulated. From Raptis *et al.* (2000), reprinted with permission. **(B) The Grb2-SH2 blocking peptide inhibits EGF-mediated DNA synthesis.** The Grb2-SH2 blocking peptide (Pmp) or its phenylalaline-containing counterpart (phe) were electroporated at the indicated concentrations into NIH3T3 cells growing on fully conductive slides (Fig. 1C, cell growth area, 4 × 7 mm) and growth-arrested by serum starvation. Following incubation at 37°C and stimulation with EGF or 10% calf serum for 12 h, cells were labelled for 2 h with 50 μCi/ml [^{3}H]thymidine and acid-precipitable radioactivity was determined. Numbers represent the mean ± SE from three experiments. From Raptis *et al.*, (2000), reprinted with permission.

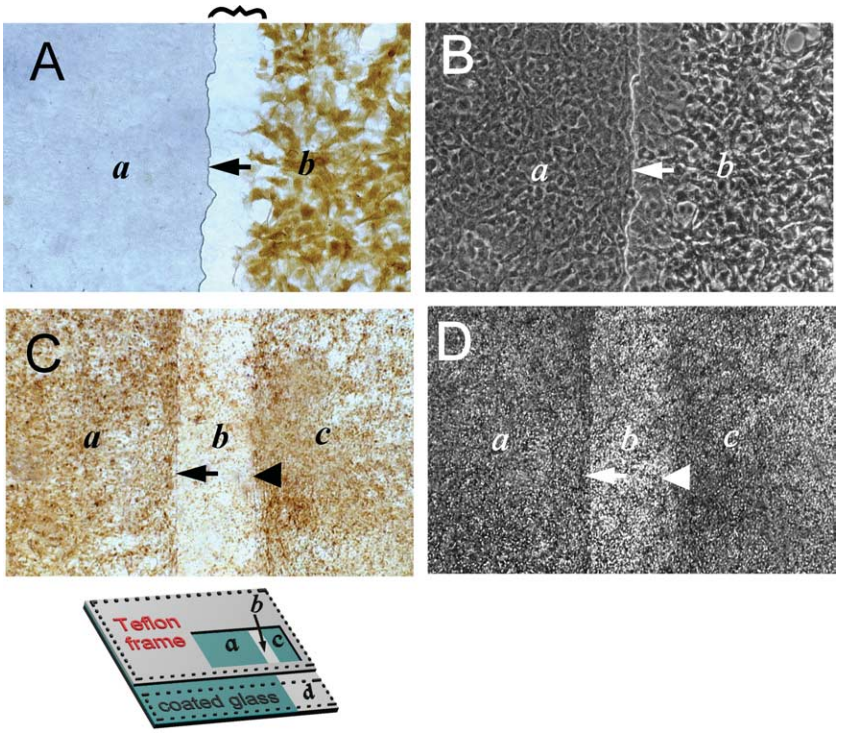

FIGURE 3 The Grb2-SH2 blocking peptide inhibits EGF-mediated Erk activation in living cells; detection by immunocytochemistry. The Grb2-SH2 blocking peptide (A and B) or its control, phenylalanine-containing counterpart (C and D) were introduced by *in situ* electroporation into NIH3T3 cells growing on partly conductive slides (inset, Fig. 1A) and growth arrested in spent medium. Five minutes after pulse application, cells were stimulated with EGF for 5 min, fixed, and probed for activated Erk1/2, and cells from the same field were photographed under bright-field (A and C) or phase-contrast (B and D) illumination. Magnification: A and B, 240×, C and D, 40×. Arrow points to the transition line between stripped (*b*) and electroporated (*a*) areas, while arrowhead points to the line between control ITO-coated (*c*) and stripped (*b*) areas (Fig. 1A). Cells growing on the left side (*a*) are electroporated, whereas cells on the stripped zone (*b*) or right side (*c*) of the slide do not receive any pulse. Note that the Grb2-SH2 blocking peptide dramatically reduced the EGF signal (A, *a*), whereas the degree of Erk activation is the same on both sides of the slide (*a* or *c*) for cells electroporated with the control, phenylalanine-containing peptide (C). In A, inhibition of the signal extends into approximatily three to four rows of adjacent cells in the non-electroporated area (squiggly bracket in *b*), probably due to movement of the peptide through gap junctions (Raptis *et al*., 1994). At the same time, there is no detectable effect on cell morphology as shown by phase contrast (B and D). From Raptis *et al*. (2000), reprinted with permission.

create problems in the interpretation of results. In addition, it was found that a number of cell lines grow slightly better on the conductive, ITO-coated glass than the nonconductive area, possibly due to the fact that the ITO-coated surface is not as smooth as glass, thus providing a better anchorage for the growth of adherent cells (Folkman and Moscona, 1978). As a result, cell density may be higher on the conductive than the etched side, which could have important implications if cell growth effects are being studied. It follows that, to assess the effect of the peptide, it is important to compare the staining and morphology of electroporated cells with non-electroporated ones while both are growing on the same type of surface. This was achieved by plating the cells on a slide where the conductive coating was removed in the pattern shown in Fig. 1A (Firth *et al*., 1997). A thin line of plain glass separates the electroporated and control areas while etching extends to area Fig. 1A,d so that there is no electrical contact between the positive contact bar and area Fig. 1A,c. Application of the pulse results in electroporation of the cells growing in area Fig. 1A,a exclusively, while cells growing in area Fig. 1A,b or c do not receive any pulse. In this configuration, electroporated cells are being compared to nonelectroporated ones, while both are growing on ITO-coated glass. Because the coating is only ~1,600 Å thick, this transition zone does not alter the growth of cells across it and is clearly visible microscopically, even under a cell monolayer (Figs. 3 and 4).

Solutions

Peptide solution: 5–10 mg/ml in calcium-free DMEM. See Section III,A and *Comment* 1

Lucifer yellow solution: 5 mg/ml in calcium-free DMEM. See Section III,A

Epidermal growth factor: 100 ng/ml in calcium-free DMEM. See Section III,A.

Steps

1. Choice of slides. Use partly conductive slides where the coating has been removed in a line as shown in Fig. 1A.
2. Plate the cells as described earlier and starve them from serum.
3. Aspirate the medium and wash the cells once with calcium-free DMEM.
4. Add the peptide solution as described previously.
5. Apply a pulse of the appropriate strength (see *Comment* 3).
6. Add serum-free growth medium and place the cells in a 37°C incubator for the pores to close (2–5 min).
7. Treat the cells with EGF for 5 min as in Section III,A.
8. Fix the cells with 4% paraformaldehyde and probe with the anti-active Erk antibody according to the manufacturer's instructions.

As shown in Fig. 3, electroporation of the Grb2-SH2 blocking peptide totally inhibited EGF-induced Erk activation (panel A, area "*a*"), while the control, phenylalanine-containing peptide had no effect (panel C, area "*a*"). This inhibition was uniform across the cell layer, in agreement with previous results indicating that *in situ* electroporation can introduce the material into essentially 100% of the treated cells. It is especially noteworthy that this inhibition ***extends into three to four rows of the adjacent, nonelectroporated cells*** growing on the nonconductive part of the slide (panel A, area "*b*", squiggly bracket), probably due to movement of the 1123 Da peptide through gap junctions (Raptis *et al*., 1994). This finding constitutes compelling evidence that the observed inhibition must be due to the peptide rather than an artifact of electroporation. At the same time, as shown by phase-contrast microscopy (panel B), there was no alteration in the morphology of the electroporated cells under these conditions, suggesting that the observed effect is a result of a specific inhibition rather than toxic action. EGF stimulation for up to 30 min after peptide electroporation did not result in lower levels of Erk signal inhibition, indicating that the binding of the peptide to Grb2 is stable during this period of time. As expected, the phenylalanine-containing, control peptide (panels C and D) had no effect on Erk activation. In contrast, the Grb2-SH2 binding peptide had little effect in inhibiting Erk activity triggered by the hepatocyte growth factor (HGF) in NIH3T3 cells expressing the HGF receptor through transfection or in human A549 cells that naturally express this receptor (Raptis *et al*., 2000a).

The introduction of peptides to interrupt signaling pathways using the modification of *in situ* electroporation described is a powerful approach for the *in vivo* assessment of the relevance of *in vitro* interactions. Results presented in Fig. 2 and 3 clearly demonstrate that an essentially complete and specific inhibition of EGF-dependent Erk activation can be achieved through peptide electroporation. The stepwise dissection of signaling cascades is essential for the understanding of normal proliferative pathways, which could lead to the development of drugs for the rational treatment of neoplasia.

C. Electroporation on a Partly Conductive Slide for the Assessment of Gap Junctional, Intercellular Communication

One of the targets of a variety of signals stemming from growth factors or oncogenes may be membrane channels, which serve as conduits for the passage of small molecules between the interiors of cells. Oncogene expression and neoplasia invariably result in a decrease in gap junctional, intercellular communication (GJIC) (Goodenough *et al*., 1996). The investigation of junctional permeability is often conducted through microinjection of a fluorescent dye such as Lucifer yellow, followed by observation of its migration into neighboring cells. This is a time-consuming approach, requiring expensive equipment, while the mechanical manipulation of the cells may disturb cell-to-cell contact areas, interrupt gap junctions, and cause artefactual uncoupling. These problems can be overcome using a setup where cells are grown on a glass slide, half of which is coated with electrically conductive, optically transparent, indium-tin oxide. An electric pulse is applied in the presence of Lucifer yellow, causing its penetration into cells growing on the conductive part of the slide, and migration of the dye to non-electroporated cells growing on the nonconductive area is observed microscopically under fluorescence illumination.

The technique can be applied to a large variety of adherent cell types, including primary human lung carcinoma cells (Tomai *et al*., 1998; Raptis *et al*., 1994; Brownell *et al*., 1996; Vultur *et al*., 2003).

Solutions

Lucifer yellow solution: 5 mg/ml in calcium-free DMEM or other growth medium. See Section III.A

Calcium-free growth medium with or without 5% dialysed serum

Steps

1. Plate the cells on partly conductive slides in 3 cm petris. Electroporated areas can be 4 × 4 mm and non-electroporated ones 4 × 3 mm (Fig. 1B). Other slide configurations are also available (Raptis *et al*., 2000b).
2. Aspirate the medium. Wash the cells with calcium-free DMEM.
3. Add the Lucifer yellow solution.
4. Apply a pulse of the appropriate strength so that cells growing on the conductive coating at the border with the non-conductive area are electroporated without being damaged. As described in *Comment* 3, this area receives slightly larger amounts of current than the rest of the conductive growth surface.
5. Add calcium-free DMEM containing 5% dialysed serum, remove the electrode, and incubate the cells for 3–5 min in a 37°C, CO_2 incubator. The inclusion of dialysed serum at this point helps pore closure.
6. Wash the unincorporated dye with calcium-free growth medium.
7. Microscopically examine under fluorescence and phase-contrast illumination (Fig. 4).
8. **Quantitate intercellular communication**. Photograph the cells with a 20× objective under fluorescence and phase contrast illumination (Figs. 4A and 4B). Identify and mark electroporated cells at the border with the non-conductive area (black stars) and fluo-

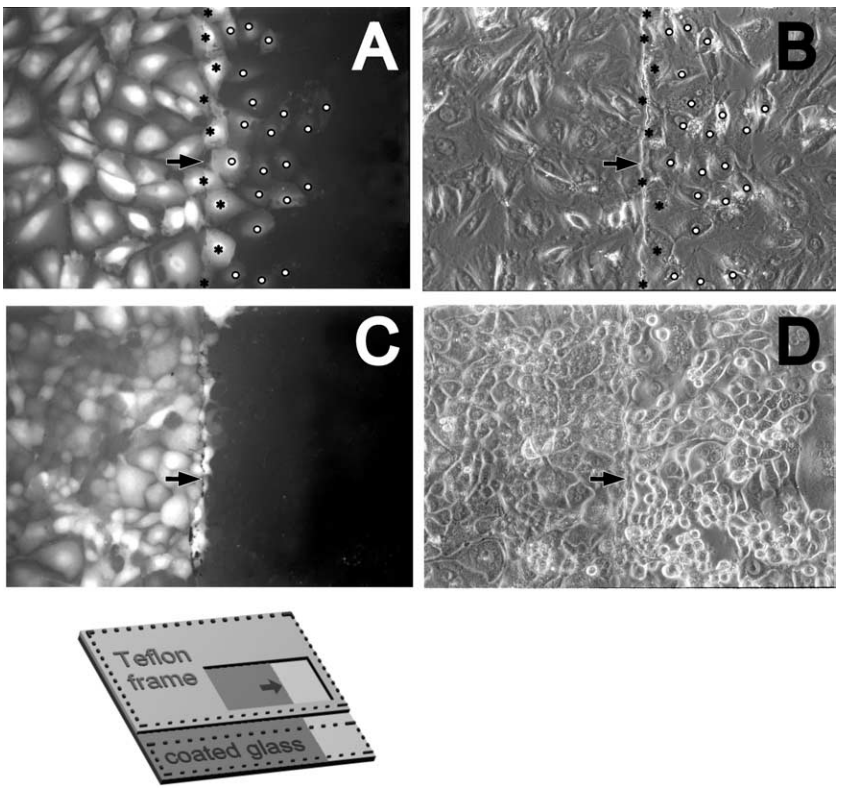

FIGURE 4 ***In situ*** **electroporation on a partly conductive slide for the measurement of intercellular, junctional communication.** (**A and B**) An established, mouse lung epithelial type II line (E10) was plated on partly conductive slides (inset, Fig. 1B) and at confluence was electroporated in the presence of 5 mg/ml Lucifer yellow. After washing away any unincorporated dye, cells from the same field were photographed under fluorescence (A) or phase-contrast (B) illumination (Raptis *et al*., 1994). Note the gradient of fluorescence indicating dye transfer through gap junctions. To quantitate intercellular communication, the number of cells into which the dye transferred through gap junctions per electroporated border cell was calculated by dividing the total number of fluorescing cells on the non-conductive side (white circles) by the number of cells growing at the border with the conductive coating (black stars). (**C and D**) A spontaneous transformant of the E10 line (line E9), was plated on partly conductive slides, electroporated, washed, and photographed as described earlier. Fluorescence (C) and phase-contrast (D) illumination photograph of the same field. Note the absence of dye transfer through gap junctions. In all photographs, the left side is conductive. Arrows on the conductive side point to the interphase between conductive and non-conductive areas. Magnification: 200×. From Vultur *et al*. (2003), reprinted with permission.

rescing cells on the nonconductive side (white circles) where the dye has transferred through gap junctions. Divide the total number of fluorescing cells on the non-conductive area by the number of electroporated cells along the border with the etched side. The transfer from at least 200 contiguous electroporated border cells is calculated for each experiment (Raptis *et al*., 1994). A careful kinetic analysis of dye transfer from 30 s to 2 h showed that the observed transfer is essentially complete by 5 min for all lines tested, while fluorescence is eliminated from the cells within approximately 60 min. After the transfer is complete, cells can be fixed with formaldehyde, in which case fluorescence is retained for approximately 2 h.

IV. COMMENTS

1. Peptides

The concentration of peptide required varies with the strength of the signal to be inhibited. For example, for the inhibition of the HGF-mediated Stat3 activation in MDCK cells, a concentration of 1 μg/ml of a peptide blocking the SH2 domain of Stat3 (^{P}YVNV) is sufficient (Boccaccio *et al*., 1998), whereas for the inhibition of the EGF-mediated Erk activation in a variety of fibroblasts or epithelial cells, a concentration of 5–10 mg/ml (~5–10 m*M*) of the Grb2-SH2 blocking peptide is necessary (Raptis *et al*., 2000a). The purity of the material is of utmost importance. Peptides must be HPLC-purified because impurities can cause cell death or give unexpected results. The pH of the peptide solution must be neutral, as indicated by the color of the DMEM medium where the peptide is dissolved. If it is too acidic, then it must be carefully neutralised with NaOH. In this case, the salt concentration of the no-peptide controls (DMEM without calcium) must be adjusted to the same level with NaCl because a change in conductivity may affect the optimal voltage required (see *Comment* 3).

Any peptide which is soluble in DMEM or other aqueous buffer can be very effectively electroporated. Good solubility is especially important because the concentration needed for effective signal inhibition can be as high as 10 mg/ml. It was nevertheless found that, at least for certain applications, the inclusion of DMSO in the electroporation solution at a concentration of up to 5%, which might aid peptide solubility, did not affect results significantly. However, a number of peptides, e.g., peptides made as fusions with the homeobox domain or other membrane translocation sequences, are usually not sufficiently soluble for this application.

2. Slides

As described in detail in Chapter 43 by Raptis *et al*., to obtain a uniform electrical field intensity over the entire area below the negative electrode, despite the fact that the conductive coating exhibits a significant amount of electrical resistance, the bottom surface of the negative electrode must be inclined relative to the glass surface in a manner proportional to the resistance of the coating. For electroporation of peptides, to minimise the volume of custom-made peptide used, slides with a conductivity of 2 Ω/sq, the most conductive commercial grade available, are used. The slides and electrodes come in different sizes, with the biggest cell growth area in this configuration being 32 × 10 mm. Depending on the experiment, if larger numbers of cells are required, extracts from two to three slides may be pooled. In this case, the peptide solution can be aspirated and used again. Alternatively, an electrode configuration with two positive contact bars can be employed, as described in Chapter 43 by Raptis *et al*.

The slides come with the apparatus, individually wrapped and sterile. However, they can be reused many times after washing with Extran-300 detergent while scrubbing with a toothbrush. In this case they must be sterilized with 80% ethanol for 20 min and the ethanol rinsed with sterile distilled water prior to plating the cells. Alternatively, the slides can be gas-sterilized. Do not autoclave. The glass can withstand high temperatures, but autoclaving would damage the Teflon frames.

3. Determination of the Optimal Voltage and Capacitance

Electrical field strength has been shown to be a critical parameter for cell permeation, as well as viability (Chang *et al*., 1992). It is generally easier to select a discrete capacitance value for a given electroporated area and space between the conductive coating and the negative electrode and then precisely control the voltage. Both parameters depend upon the size of the electroporated area; larger conductive growth areas necessitate higher voltages and/or higher capacitances for optimal permeation. For the 32 × 10 mm cell growth area, some damage to the coating may be noted at the higher voltages necessary if a single pulse is employed. However, using higher capacitance values and multiple pulses with lower voltage settings can yield efficient cell permeation with no damage to

the coating, and this treatment is also better tolerated by the cells. For greater growth areas, the dual positive contact bar design described in Chapter 43 by Raptis *et al.* can be employed.

The optimal pulse strength depends on the strain and metabolic state of the cells, as well as on the degree of cell contact with the conductive surface. Densely growing, transformed cells or cells in a clump require higher voltages for optimum permeation than sparse, subconfluent cells, possibly due to the larger amounts of current passing through an extended cell. Similarly, cells that have been detached from their growth surface by vigorous pipetting prior to electroporation require substantially higher voltages. It is especially striking that cells in mitosis remain intact under conditions where most cells in other phases of the cycle are permeated (Raptis and Firth, 1990). In addition, cells growing and electroporated on CelTak™-coated slides require substantially higher voltages than cells growing directly on the slide.

The margins of voltage tolerance depend on the size and electrical charge of the molecules to be introduced (Fig. 5). For the introduction of small, uncharged molecules such as Lucifer yellow or peptides, a wider range of field strengths permits effective permeation

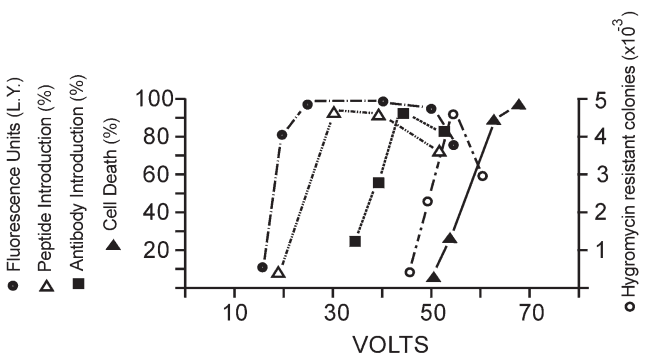

FIGURE 5 Effect of field strength on the introduction of different molecules. Three pulses of increasing voltage were applied to confluent rat F111 fibroblasts growing on a conductive surface of 32 × 10 mm from a 32 µF capacitor in the presence of 5 mg/ml Lucifer yellow (●), 5 mg/ml of the Grb2-SH2 blocking peptide (□), 5 mg/ml chicken IgG (■), or 100 µg/ml pY3 plasmid DNA, coding for resistance to hygromycin (Raptis and Firth, 1990) (○). Cells were lysed and Lucifer yellow fluorescence was measured using a Model 204A fluorescence spectrophotometer (●), probed with the anti-active Erk antibody (□), probed for incorporated IgG (■), or selected for hygromycin resistance (○) (Raptis and Firth, 1990). Introduction of chicken IgG was quantitated from the percentage of cells staining positive with their respective antibodies. Cell killing (▲) was assessed by calculating the plating efficiency of the cells after the pulse. Note that a wider range of voltages (20–50 V) permits efficient introduction of Lucifer yellow with no detectable loss in cell viability than the introduction of IgG or DNA. Points represent averages of at least three separate experiments. L.Y., Lucifer yellow.

with minimal damage to the cells than the introduction of antibodies or DNA (Raptis and Firth, 1990; Brownell *et al.*, 1997). For a number of experiments involving cell growth, it may be necessary to electroporate serum-arrested cells. Voltages required are lower, and especially the margins of voltage tolerance were found to be substantially narrower for serum-starved cells compared to their counterparts growing in 10% calf serum (Brownell *et al.*, 1997). Also, it is important to keep all solutions at 37°C, which facilitates pore closure and efficient electroporation. If the material is applied in a medium with a lower salt concentration than DMEM, then the voltages required are lower, presumably due to the hypotonic shock to the cells and to the longer duration of the pulse because of the lower conductivity of the medium. Conversely, electroporation in a hypertonic solution requires higher voltages for optimum permeation.

Cell damage is manifested microscopically by the appearance of dark nuclei under phase-contrast illumination. For most lines this is most pronounced 5–10 min after the pulse. Such cells do not retain Lucifer yellow and fluoresce very weakly, if at all (Fig. 6). Despite the fact that every effort is made to make the electric field uniform over the whole cell growth area, the current flow along the border with the etched side is greater than the rest of the conductive surface. For this reason, as the voltage is progressively increasing, damaged cells will appear on this edge first (Fig. 6). Another area receiving a slightly higher current is corners of the window. This slight irregularity has to be taken into account when determining the optimal voltage.

4. Example of the Determination of Optimal Voltage for the Introduction of Peptides

Prepare a series of slides with cells plated uniformly in a 4 × 7 mm window on a partly conductive slide (Figs. 1A or 1B). Set the apparatus at 0.5 µF capacitance. Prepare a solution of 5 mg/ml Lucifer yellow and electroporate at different voltages (0.5 µF, three pulses) to determine the upper limits where a small fraction of the cells at the border with the etched side (probably the more extended ones) are killed by the pulse, as determined by visual examination under phase-contrast and fluorescence illumination (Fig. 6). Depending on the cells, this voltage can vary from 20 to 40 V. Repeat the electroporation using the peptide solution at different voltages starting at 10 V below the upper limit and at 2 V increments. The Lucifer yellow dye offers an easy way to test for cell permeation.

Results of a typical experiment of electroporation of cells growing on a 32 × 10 mm surface are shown in

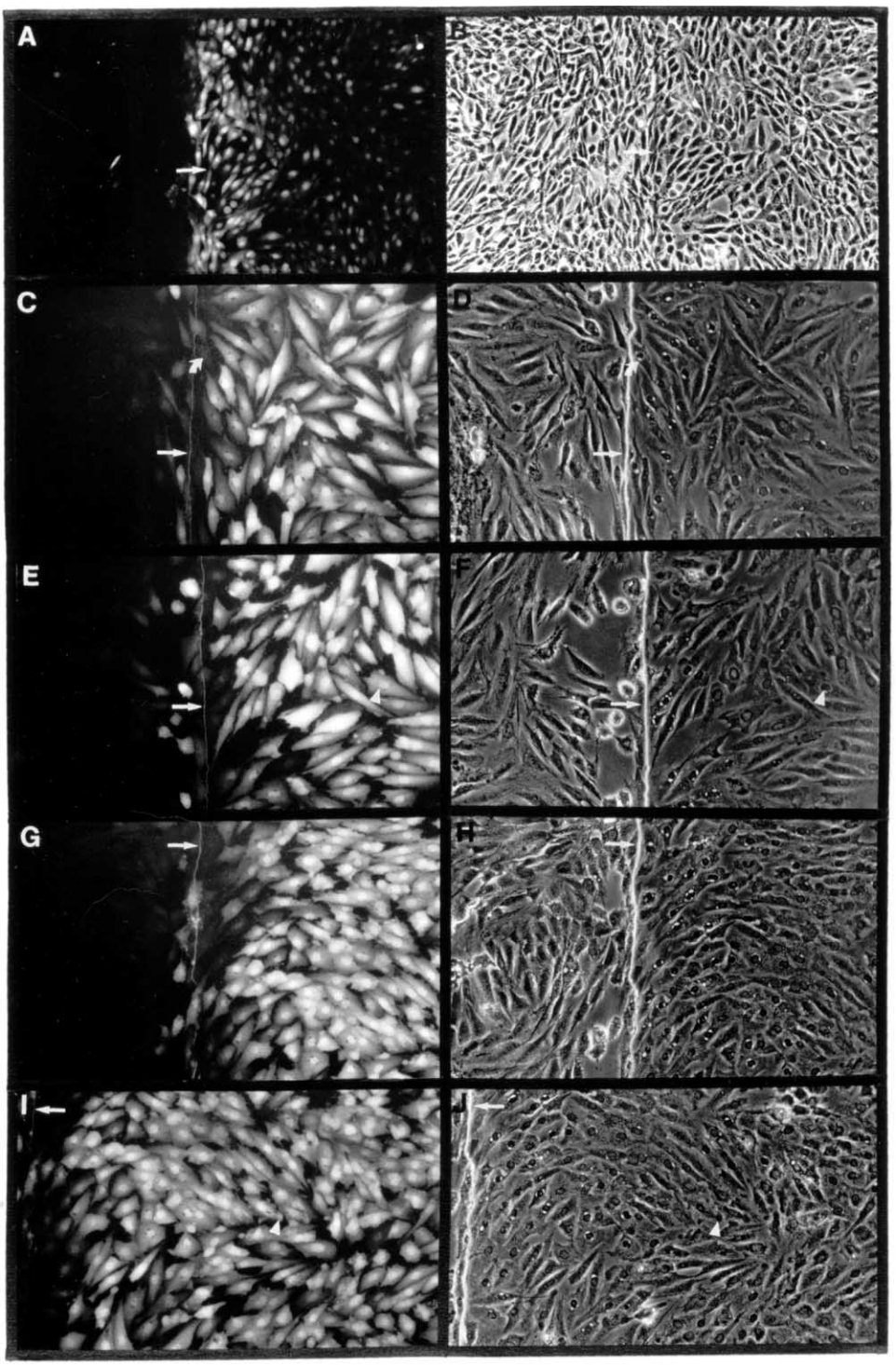

FIGURE 6 **Determination of the optimal voltage.** Rat F111 fibroblasts growing on partly conductive slides (Fig. 1B, conductive area, 4×4 mm) were electroporated in the presence of 5 mg/ml Lucifer yellow using three pulses of increasing voltage delivered from a 0.2 μF capacitor. (A and B) 18 V, (C and D) 26 V, (E and F) 28 V, (G and H) 32 V, and (I and J) 40 V. After washing of the unincorporated dye, cells were photographed under fluorescence (A, C, E, G, I) or phase-contrast (B, D, F, H and J) illumination. Straight arrow points to the interphase between conductive (right) and non-conductive (left) areas. Curved arrows in C and D point to a cell which has been killed by the pulse. Note the dark, pycnotic and prominent nucleus under phase contrast and the flat, nonrefractile appearance. Such cells do not retain any electroporated material as shown by the absence of fluorescence (C). Note that the number of such cells along the border with the non-conductive area increases with voltage. Arrowheads in E and F point to a cell that has a prominent nucleus under phase contrast (F) but has retained the dye (E). Such cells rapidly recover their normal morphology, indistinguishable from their non-electroporated counterparts. White arrowheads in I and J point to membrane blebs which tend to enclose Lucifer yellow and fluoresce strongly. Such membrane blebbing tends to be more prominent under higher voltages. Note that if the determination of intercellular communication is desired, then the voltage must be such that cells at the border with the non-conductive area are electroporated without being damaged (e.g., 18 V, A and B), whereas for all other applications, voltages of approximately 26–32 V would be preferred (C to H). Magnification: A and B, 120X; C–J, 240×.

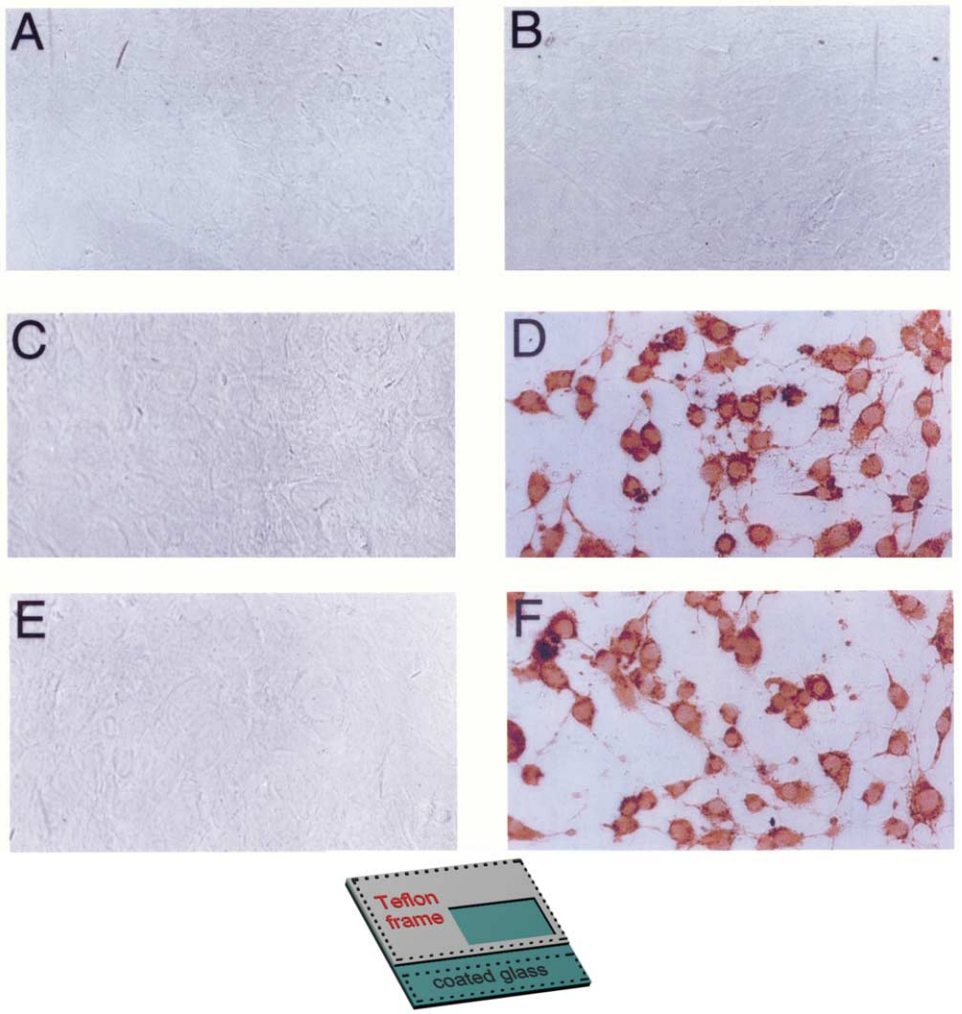

FIGURE 7 ***In situ*** **electroporation does not affect ERK activity or the stress pathway.** (**A, C, and E**) NIH3T3 cells were plated on fully conductive slides (inset, Fig. 1C, conductive growth area 4 × 8 mm), growth arrested in 50% spent medium, and electroporated in the presence of PBS containing 0.025% DMSO (0.2 µF, 70 V, four pulses). Ten minutes after the pulse, cells were fixed and stained for activated ERK (A), activated JNK/SAPK (C), or activated $p38^{hog}$ (E), respectively. Electroporated cells were photographed under bright-field illumination. (**B, D, and F**) NIH3T3 cells were plated on conductive slides, treated with UV light for 10 min, fixed, and stained for activated ERK (B), activated JNK/SAPK (D), or activated $p38^{hog}$ (F), respectively. From Brownell *et al.* (1998), reprinted with permission. Magnification: 240×.

Fig. 5. The Application of three exponentially decaying pulses of an initial strength of 25 V from a 32 µF capacitor to rat F111 cells growing on a conductive growth area of 32 × 10 mm, resulted in essentially 100% of the cells containing the introduced Lucifer yellow, whereas introduction of a nine amino acid peptide required 30 V and the stable expression of DNA 45 V, respectively, for maximum signal. If a 20 µF capacitor is used, the corresponding voltages are ~80–180. Electroporation on 7 × 15 mm slides requires a 2 µF capacitor and voltages of 25–50. For etched slides with a conductive area of 4 × 4 mm, if a 0.5 µF capacitor and three pulses are used, the voltages are 20–40. However, if a 0.1 µF capacitor and six pulses are used, the voltages will be ~30–50.

Under the appropriate conditions, electroporation was shown not to affect the activity of Erk1/2 or the stress-activated kinases JNK/SAPK and $p38^{hog}$. This was shown by probing with antibodies specific for the activated forms of these kinases (Fig. 7); no activation of JNK/SAPK or $p38^{hog}$ was found under conditions of up to 70 V (Figs. 7C and 7E). These kinases were,

however, slightly activated at voltages higher than 85 V, when more than 60% of the cells were killed by the pulse (not shown).

V. PITFALLS

1. Care must be taken so that cells do not dry during the procedure, especially during wiping of the frame with a tightly folded Kleenex. It was found that serum-starved cells were more susceptible than their counterparts grown in medium containing serum. The morphology of cells that have been killed by drying is very similar to cells that have been killed by the pulse (Fig. 6). Slightly dried cells may incorporate Lucifer yellow and appear almost normal under phase contrast, whereas cells that have dried to a great extent display dark nuclei and may not retain Lucifer yellow. It was also found that the combination of even slight drying with electroporation may have undesirable effects on gene expression (e.g., induction of *fos* by serum; unpublished observations). In the case of electroporation on a partly conductive slide (Figs. 1A or 1B), drying of the cells is immediately suspected if cells growing on the non-electroporated area exhibit Lucifer yellow fluorescence.

2. Accurate determination of the optimal voltage is very important. The limits of voltage tolerance are narrower for serum-starved cells (Brownell *et al*., 1997) or if the introduction of larger molecules is attempted.

3. For the determination of GJIC, it is important to wash the dye using a calcium-free solution (growth medium or PBS). If calcium-containing growth medium is used instead, the values obtained may be reduced, presumably because of the calcium influx, which was shown to interrupt junctional communication.

Acknowledgments

The financial assistance of the Canadian Institutes of Health Research, the Canadian Breast Cancer Research Initiative, the Natural Sciences and Engineering Research Council of Canada (NSERC), and the Cancer Research Society Inc. is gratefully acknowledged. AV is the recipient of NSERC and Ontario Graduate studentships, a Queen's University graduate award, and a Queen's University travel grant. HB was the recipient of a studentship from the Medical Research Council of Canada and a Microbix Inc. travel award. We are grateful to Dr. Erik Schaefer of Biosource Int. for numerous suggestions and valuable discussions.

References

Bardelli, A., Longati, P., Gramaglia, D., Basilico, C., Tamagnone, L., Giordano, S., Ballinari, D., Michieli, P., and Comoglio, P. M. (1998). Uncoupling signal transducers from oncogenic MET mutants abrogates cell transformation and inhibits invasive growth. *Proc. Natl. Acad. Sci. USA* **95**, 14379–14383.

Boccaccio, C., Ando, M., Tamagnone, L., Bardelli, A., Michielli, P., Battistini, C., and Comoglio, P. M. (1998). Induction of epithelial tubules by growth factor HGF depends on the STAT pathway. *Nature* **391**, 285–288.

Boussiotis, V. A., Freeman, G. J., Berezovskaya, A., Barber, D. L., and Nadler, L. M. (1997). Maintenance of human T cell anergy: Blocking of IL-2 gene transcription by activated Rap1. *Science* **278**, 124–128.

Brownell, H. L., Firth, K. L., Kawauchi, K., Delovitch, T. L., and Raptis, L. (1997). A novel technique for the study of Ras activation; electroporation of [α^{32}P]GTP. *DNA Cell Biol.* **16**, 103–110.

Brownell, H. L., Lydon, N., Schaefer, E., Roberts, T. M., and Raptis, L. (1998). Inhibition of epidermal growth factor-mediated ERK1/2 activation by *in situ* electroporation of nonpermeant [(alkylamino)methyl]acrylophenone derivatives. *DNA Cell Biol.* **17**, 265–274.

Brownell, H. L., Narsimhan, R., Corbley, M. J., Mann, V. M., Whitfield, J. F., and Raptis, L. (1996). Ras is involved in gap junction closure in mouse fibroblasts or preadipocytes but not in differentiated adipocytes. *DNA Cell Biol.* **15**, 443–451.

Chang, D. C., Chassy, B. M., Saunders, J. A., and Sowers, A. E. (1992). "Guide to Electroporation and Electrofusion." Academic Press, New York.

Firth, K. L., Brownell, H. L., and Raptis, L. (1997). Improved procedure for electroporation of peptides into adherent cells *in situ*. *Biotechniques* **23**, 644–645.

Folkman, J., and Moscona, A. (1978). Role of cell shape in growth control. *Nature* **273**, 345–349.

Gambarotta, G., Boccaccio, C., Giordano, S., Ando, M., Stella, M. C., and Comoglio, P. M. (1996). Ets up-regulates met transcription. *Oncogene* **13**, 1911–1917.

Giorgetti-Peraldi, S., Ottinger, E., Wolf, G., Ye, B., Burke, T. R., and Shoelson, S. E. (1997). Cellular effects of phosphotyrosine-binding domain inhibitors on insulin receptor signalling and trafficking. *Mol. Cell. Biol.* **17**, 1180–1188.

Goodenough, D. A., Goliger, J. A., and Paul, D. L. (1996). Connexins, connexons, and intercellular communication. *Annu. Rev. Biochem.* **65**, 475–502.

Kwee, S., Nielsen, H. V., and Celis, J. E. (1990). Electropermeabilization of human cultured cells grown in monolayers: Incorporation of monoclonal antibodies. *Bioelectrochem. Bioenerg.* **23**, 65–80.

Marais, R., Spooner, R. A., Stribbling, S. M., Light, Y., Martin, J., and Springer, C. J. (1997). A cell surface tethered enzyme improves efficiency in gene-directed enzyme prodrug therapy. *Nature Biotechnol.* **15**, 1373–1377.

Matsumura, T., Konishi, R., and Nagai, Y. (1982). Culture substrate dependence of mouse fibroblasts survival at 4°C. *In Vitro* **18**, 510–514.

Nakashima, N., Rose, D., Xiao, S., Egawa, K., Martin, S., Haruta, T., Saltiel, A. R., and Olefsky, J. M. (1999). The functional role of crk II in actin cytoskeleton organization and mitogenesis. *J. Biol. Chem.* **274**, 3001–3008.

Neumann, E., Kakorin, S., and Toensing, K. (2000). Principles of membrane electroporation and transport of macromolecules. *In "Electrochemotherapy, Electrogenetherapy and Transdermal Drug Delivery"* (M. J. Jaroszeski, R. Heller, and R. Gilbert, eds.), pp. 1–35. Humana Press, Clifton, NJ.

Otaka, A., Nomizu, M., Smyth, M. S., Shoelson, S. E., Case, R. D., Burke, T. R., and Roller, P. P. (1994). Synthesis and structure-activity studies of SH2-binding peptides containing hydrolytically stable analogs of O-phosphotyrosine. *In* "*Peptides; Chemistry, Structure and Biology*" (R. S. Hodges and J. A. Smith, eds.), pp. 631–633. Escom, Leiden.

Raptis, L., Brownell, H. L., Firth, K. L., and MacKenzie, L. W. (1994). A novel technique for the study of intercellular, junctional communication; electroporation of adherent cells on a partly conductive slide. *DNA Cell Biol.* **13**, 963–975.

Raptis, L., Brownell, H. L., Vultur, A. M., Ross, G., Tremblay, E., and Elliott, B. E. (2000a). Specific inhibition of growth factor-stimulated ERK1/2 activation in intact cells by electroporation of a Grb2-SH2 binding peptide. *Cell Growth Differ.* **11**, 293–303.

Raptis, L., and Firth, K. L. (1990). Electroporation of adherent cells *in situ*. *DNA Cell Biol.* **9**, 615–621.

Raptis, L., Tomai, E., and Firth, K. L. (2000b). Improved procedure for examination of gap junctional, intercellular communication by *in situ* electroporation on a partly conductive slide. *Biotechniques* **29**, 222–226.

Robinson, M. J., and Cobb, M. H. (1997). Mitogen-activated protein kinase pathways. *Curr. Opin. Cell Biol.* **9**, 180–186.

Schlessinger, J. (2000). Cell signaling by receptor tyrosine kinases. *Cell* **103**, 211–225.

Tomai, E., Brownell, H. L., Tufescu, T., Reid, K., Raptis, S., Campling, B. G., and Raptis, L. (1998). A functional assay for intercellular, junctional communication in cultured human lung carcinoma cells. *Lab. Invest.* **78**, 639–640.

Vultur, A., Tomai, E., Peebles, K., Malkinson, A. M., Grammatikakis, N., Forkert, P. G., and Raptis, L. (2003). Gap junctional, intercellular communication in cells from urethane-induced tumors in A/J mice. *DNA Cell Biol.* **22**, 33–40.

Williams, E. J., Dunican, D. J., Green, P. J., Howell, F. V., Derossi, D., Walsh, F. S., and Doherty, P. (1997). Selective inhibition of growth factor-stimulated mitogenesis by a cell-permeable Grb2-binding peptide. *J. Biol. Chem.* **272**, 22349–22354.

Yang, T. A., Heiser, W. C., and Sedivy, J. M. (1995). Efficient *in situ* electroporation of mammalian cells grown on microporous membranes. *Nucleic Acids. Res.* **23**, 2803–2810.

CHAPTER

45

Detection of Protein–Protein Interactions *in vivo* Using Cyan and Yellow Fluorescent Proteins

Francis Ka-Ming Chan

I. INTRODUCTION

The phenomenon of fluorescence resonance energy transfer (FRET) describes the transfer of energy from one fluorophore to another through dipole–dipole interaction (Forster, 1946, 1948). It is a sensitive "molecular ruler" that can detect molecular associations within a range of 100 Å (Stryer, 1978). Early work using FRET to measure biological associations relied on either fluorescent analogs of biomolecules or fluorescent antibodies as donors and acceptors. However, the utility of this technique in detecting biological associations was limited by the availability of monoclonal antibodies that recognize epitopes of the receptor where maximum energy transfer can occur without disrupting the interactions under examination. This limitation was overcome with the use of spectral variants of the green fluorescent protein (GFP) (Tsien, 1998). The use of GFP variants such as CFP (cyan) and YFP (yellow) in FRET analysis has the additional advantage of allowing detection of intracellular associations in living cells. While most of the applications of FRET have employed fluorescence microscopic imaging methods, it has recently become feasible to perform FRET analysis using flow cytometry. For example, it has been used successfully to determine the ligand-independent association between different Fas receptors (Siegel *et al*., 2000). More recently, flow cytometric FRET analysis has been used to study the interaction between histone acetylase PCAF and histone deacetylase HDAC1 and other chromatin-binding proteins (Kanno *et al*., 2004; Yamagoe *et al*., 2003), to detect the presence of *Bacillus anthracis* spores in a test biological sample (Zahavy *et al*., 2003) and to detect caspase activation during apoptosis induction (He *et al*., 2003). Flow cytometry-based FRET analysis permits the screening of a large number of interactions within a short time and will be a useful technique in the screening of molecular associations in the proteomics era. We will focus our discussion to flow cytometry-based FRET analysis. For a more detailed description of fluorescence microscopic FRET analysis, readers are referred to the following link: http://www.stke.org/cgi/content/full/OC_sitrans;2000/38/pl1.

II. MATERIALS AND INSTRUMENTATION

The FACS Vantage SE flow cytometer is from BD Bioscience (San Jose, CA). RPMI 1640 without phenol red (Cat. No. 11835055), penicillin and streptomycin (Cat. No. 10378016), L-glutamine (Cat. No. 25030081), phosphate-bultered saline (PBS, Cat. No. 14190250), and trypsin versene (Cat. No. 15040066) are from Invitrogen (Carlsbad, CA). Fetal calf serum (FCS) is from Biofluids (Cat. No. 200P-500). HEK 293T cells are from ATCC (Cat. No. CRL-11268). Fugene 6 (Cat. No. 1814443) and propidium iodide (Cat. No. 1348639) are from Roche. The CFP (Cat. No. 6900-1) and YFP (Cat. No. 6006-1) parental plasmids are from BD Clontech (CA). Flowjo software is from Treestar Inc. (San Carlos, CA). β-Mercaptoethanol (Cat. No. M-6250) and bovine serum albumin (BSA, Cat. No. A-7906) are from Sigma (MO).

Copyright 2006, Elsevier Science (USA).
All rights reserved.

III. PROCEDURES

A. Transfection of FRET Constructs

1. Split HEK 293T cells by washing the cell monolayer with 10 ml PBS and incubating cells at 37°C for 5–10 min in 1× trypsin versene (2–5 ml). Seed cells at 2.5×10^5 cells per well in 1 ml volume of phenol red-free RPMI 1640 (supplemented with 10% FCS, 100 units/ml of penicillin and streptomycin, 2 *mM* of L-glutamine, and 54 μ*M* β-mercaptoethanol) in a 12-well culture plate.

2. Incubate cells in a CO_2 incubator for 16–20 h. Cells should be 70–90% confluent at the time of transfection.

3. Prepare the DNA mixture by mixing an equal molar ratio of CFP to YFP plasmids in an Eppendorf tube. The optimal molar ratio of CFP to YFP plasmids may be different for different FRET pairs and should be determined empirically. The total amount of DNA should be 1 μg per 3 μl of Fugene 6 for transfection in 12-well plate.

4. Add 100 μl of serum-free Dulbecco's Modified Eagles Medium to an Eppendorf tube. Add 3 μl of Fugene 6 to the serum-free medium. Gently tap the tube to mix it. Incubate at room temperature for 5 min.

5. Add the diluted Fugene 6 solution from step 4 to the DNA mixture in step 3. Gently tap the tube to mix well. Incubate the mixture at room temperature for 15 min.

6. Add the DNA/Fugene 6 mixture from step 5 to the cells dropwise. Gently swirl the plate to distribute the mixture evenly.

7. Incubate the cells in a 37°C CO_2 incubator for 24–48 h. It is not necessary to change the medium after transfection.

8. After 24–48 h, aspirate the medium from the wells. Resuspend the cells in 1 ml PBS supplemented with 2% BSA. Spin the cells down at 1500 rpm in a Beckman tabletop centrifuge for 5 min at 4°C.

9. Decant the supernatant. Resuspend cells in 1 ml of PBS supplemented with 2% BSA. Keep cells on ice until they are ready for analysis. Alternatively, cells can be fixed in 4% paraformaldehyde until they are ready for analysis.

B. Collection of Data on FACS Vantage SE

1. Setup of Flow Cytometer

Analyze cells on a FACS Vantage SE flow cytometer (equipped with an ILT air-cooled argon laser and a Spectra Physics Model 2060 krypton laser). Tune the argon to 514 nm for direct excitation of YFP and the krypton laser to 413 nm for excitation of CFP. Replace the forward and side scatter filters with the 513/10 bandpass filter. Use a filter with 470/20-nm bandpass for CFP detection in the P6 channel and filters with 546/10-nm bandpass for YFP and FRET detection in P3 and P5 channels, respectively. Direct YFP fluorescence for detection in the P7 channel for interlaser compensation (see step 2). Use a 505LP dichroic mirror to separate the CFP and FRET signals in P5 and P6 channels. Adjust the fluidics pressure to 29–30 psi.

2. Compensations

Perform electronic compensation to remove CFP emission from the FRET channel (P5–P6). Perform interlaser compensation between CFP and YFP using Omnicomp circuitry to remove YFP excitation from the 413-nm laser. Alternatively, compensations can be performed "off-line" using softwares such as Flowjo during data analysis.

3. Run and Collect Samples

Collect 50,000 live events per sample. To facilitate distinction of live and dead cells, 1 μg/ml of propidium iodide can be added to cells prior to collection of events on the flow cytometer.

4. Analysis of Data

Analyze collected data using Flowjo software. Control samples transfected with noninteracting FRET pairs should be used as negative controls to determine the baseline FRET signal. An example of step-by-step analysis of the homotypic interaction of the ectodomain of p60 TNFR-1 using flow cytometric FRET analysis is given in Fig. 1. TNFR-1 forms ligand-independent complexes through a domain at the N terminus of the receptor called the preligand assembly domain (PLAD) (Chan *et al*., 2000). The cytoplasmic tail of TNFR-1 is replaced by CFP or YFP. The resulting fusions are expressed in HEK 293T cells. A positive interaction between the differentially tagged TNFR-1 ectodomains is observed as the FRET signal increases over cells expressing only the CFP-tagged receptor (Fig. 1a). Moreover, when TNF is added to the cells, a ligand-dependent rearrangement of the complex results in further increase of the FRET signal (Fig. 1a). The interaction between different TNFR-1 chains is specific, as replacing the fluorescence donor or acceptor with another TNFR-like receptor DR4 abolishes the FRET signal (Figs. 1b and 1d). However, cells expressing DR4-CFP and DR4-YFP exhibit a positive FRET signal (Fig. 1c), demonstrating that flow cytometric FRET analysis can accurately recapitulate the known biochemical interactions of these receptors (Chan *et al*., 2000).

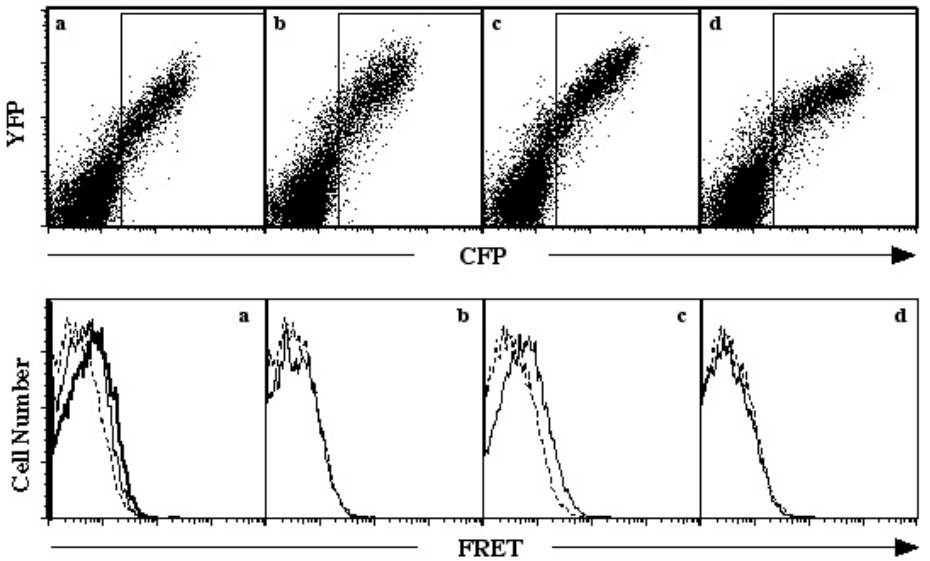

FIGURE 1 HEK 293T cells were transfected using Fugene 6 with (a) p60-CFP and p60-YFP, (b) p60-CFP and DR4-YFP, (c) DR4-CFP and DR-YFP, or (d) DR4-CFP and p60-YFP. (Top) Live cells were analyzed for their expression of CFP and YFP. Cells that express both CFP and YFP were gated (rectangular box) and analyzed for FRET. (Bottom) Histogram overlays of control cells expressing only CFP (dotted lines) or cells expressing CFP and YFP (solid lines) show that only (a) p60-CFP and p60-YFP or (c) DR4-CFP and DR4-YFP exhibited FRET. (a) The heavy line shows the increased FRET when the ligand TNF was added to the cells.

IV. COMMENTS

In addition to the FACS Vantage SE flow cytometer, other models of flow cytometers can be used for flow cytometric FRET analysis if the proper lasers are installed. For example, the LSRII flow cytometer from BD Bioscience can be adapted for FRET analysis if equipped with a violet laser for excitation at 405 nm. Other methods of detecting molecular interactions using the concept of FRET include fluorescence lifetime imaging microscopy and microscopic photobleaching (Bastiaens and Squire, 1999; Miyawaki and Tsien, 2000).

IV. PITFALLS

1. FRET is sensitive to the distance and orientation of the fluorescence donor and acceptor (Miyawaki and Tsien, 2000; Pollok and Heim, 1999; Truong and Ikura, 2001). Moreover, the spacer length between the CFP or YFP moieties and the protein of interest can also affect the efficiency of FRET (Chan *et al*., 2001). Therefore, it is sometimes necessary to test multiple fusion constructs to find the optimal fusions for FRET analysis.

2. Low transfection efficiency is detrimental in FRET analysis. For 293T cells, Fugene 6 is the transfection reagent of choice because of its consistency in yielding high protein expression. Cell culture conditions can also be significant in the success of transfections. Typically, seeding 2.5×10^5 cells on 12-well plates will yield a 70–80% confluent culture after a 16- to 20-h incubation, which is ideal for high transfection efficiency.

3. To optimize the FRET signal, it is necessary to have the fluorescence acceptor molecule in slight excess relative to the fluorescence donor molecule. Therefore, different ratios of CFP to YFP plasmids should be tested to determine the optimal ratio that will yield maximal FRET signals.

References

Bastiaens, P. I., and Squire, A. (1999). Fluorescence lifetime imaging microscopy: Spatial resolution of biochemical processes in the cell. *Trends Cell Biol.* **9**, 48–52.

Chan, F. K., Siegel, R. M., Zacharias, D., Swofford, R., Holmes, K. L., Tsien, R. Y., and Lenardo, M. J. (2001). Fluorescence resonance energy transfer analysis of cell surface receptor interactions and signaling using spectral variants of the green fluorescent protein. *Cytometry* **44**, 361–368.

Chan, F. K. M., Chun, H. J., Zheng, L., Siegel, R. M., Bui, K. L., and Lenardo, M. J. (2000). A domain in TNF receptors that mediates ligand-independent receptor assembly and signaling. *Science.*

Forster, T. (1946). Energiewanderung und fluoreszenz. *Naturwissenschaften* **6**, 166–175.

Forster, T. (1948). Zwischenmolekulare energiewanderung und fluoreszenz. *Ann. Phys. (Leipzig)* **2**, 55–75.

He, L., Olson, D. P., Wu, X., Karpova, T. S., McNally, J. G., and Lipsky, P. E. (2003). A flow cytometric method to detect protein-protein interaction in living cells by directly visualizing donor fluorophore quenching during CFP → YFP fluorescence resonance energy transfer (FRET). *Cytometry* **55A**, 71–85.

Kanno, T., Kanno, Y., Siegel, R. M., Jang, M. K., Lenardo, M. J., and Ozato, K. (2004). Selective recognition of acetylated histones by bromodomain proteins visualized in living cells. *Mol. Cell* **13**, 33–43.

Miyawaki, A., and Tsien, R. Y. (2000). Monitoring protein conformations and interactions by fluorescence resonance energy transfer between mutants of green fluorescent protein. *Methods Enzymol.* **327**, 472–500.

Pollok, B. A., and Heim, R. (1999). Using GFP in FRET-based applications. *Trends Cell Biol.* **9**, 57–60.

Siegel, R. M., Frederiksen, J. K., Zacharias, D. A., Chan, F. K. M., Johnson, M., Lynch, D., Tsien, R. Y., and Lenardo, M. J. (2000). Fast preassociation required for apoptosis signaling and dominant inhibition by pathogenic mutations. *Science.*

Stryer, L. (1978). Fluorescence energy transfer as a spectroscopic ruler. *Annu. Rev. Biochem.* **47**, 819–846.

Truong, K., and Ikura, M. (2001). The use of FRET imaging microscopy to detect protein-protein interactions and protein conformational changes *in vivo*. *Curr. Opin. Struct. Biol.* **11**, 573–578.

Tsien, R. Y. (1998). The green fluorescent protein. *Annu. Rev. Biochem.* **67**, 509–544.

Yamagoe, S., Kanno, T., Kanno, Y., Sasaki, S., Siegel, R. M., Lenardo, M. J., Humphrey, G., Wang, Y., Nakatani, Y., Howard, B. H., and Ozato, K. (2003). Interaction of histone acetylases and deacetylases *in vivo*. *Mol. Cell Biol.* **23**, 1025–1033.

Zahavy, E., Fisher, M., Bromberg, A., and Olshevsky, U. (2003). Detection of frequency resonance energy transfer pair on double-labeled microsphere and *Bacillus anthracis* spores by flow cytometry. *Appl. Environ. Microbiol.* **69**, 2330–2339.

CHAPTER

46

Tracking Individual Chromosomes with Integrated Arrays of *lac*^{op} Sites and GFP-*lac*^{i} Repressor: Analyzing Position and Dynamics of Chromosomal Loci in *Saccharomyces cerevisiae*

Frank R. Neumann, Florence Hediger, Angela Taddei, and Susan M. Gasser

I. INTRODUCTION

The visualisation of specific DNA sequences in living cells, achieved through the integration of *lac* operator arrays (*lac*^{op}) and expression of a GFP-lac repressor fusion, has provided new tools to examine how the nucleus is organised and how basic events such as sister chromatid separation occur (Straight *et al*., 1996; Belmont, 2001). In contrast to other methods, such as fluorescence *in situ* hybridisation, the *lac*^{op}/GFP-*lac* repressor (GFP-*lac*^{i}) technique is noninvasive and therefore interferes minimally with nuclear structure and function. In addition, it facilitates analysis of the rapid dynamics of specific DNA loci (Gasser, 2002). Although this technique has been adapted to organisms from bacteria to humans, the ease with which GFP fusions can be targeted to specific chromosomal sites depends on the ability of the organism to carry out homologous recombination. This process is very efficient in budding yeast, allowing pairs of chromosomal loci to be analysed at the same time through the use of two bacterial repressors (*lac*^{i} and *tetR*) fused to different GFP variants. Given the relatively advanced state of the art in budding yeast, this article presents protocols optimised for this organism. These provide a starting point for adapting multilocus tagging to other species. Moreover, the techniques described here for the quantitative analyses of locus dynamics are universally applicable.

II. MATERIALS AND INSTRUMENTATION

Yeast minimal and rich media (SD, YPD) are described in Guthrie *et al*. (1991). Cells can be mounted on a depression slide (Milian SA, Cat. No. CAV-1, Fig. 2A) upon 1.4% agarose (Eurobio Cat. No. 018645) containing SD medium with 4% glucose (Fluka). Aliquots of this can be kept at 4°C for several months. Alternatively, cells can be immobilised on a 18-mm coverslip treated with concanavalin A (Con A, Sigma, Cat. No. C-0412) in a cell observation chamber (Ludin chamber, Life Imaging Services, Fig. 2B). Con A dissolved to 1 mg/ml in H_2O is stable at –20°C for months. Widefield microscopy is performed on a Metamorph-driven Olympus IX 70 inverted microscope with Olympus Planapo 60×/NA = 1.4 or Zeiss Planapo 100×/NA = 1.4 objectives on a **piezoelectric translator** (**PIFOC;** Physik Instrumente), illuminating with a PolychromeII monochromator (T.I.L.L. Photonics). Also needed is a CoolSNAP-HQ digital camera (Roper Scientific) or equivalent, and both the FITC filter set for detecting

Copyright 2006, Elsevier Science (USA).
All rights reserved.

GFP (Chroma, Ref. 41001) and the CFP/YFP filter set (e.g., Chroma, Ref. 51017). Confocal microscopy can be performed on a Zeiss LSM510 Axiovert 200M, equipped with a Zeiss Plan-Apochromat 100×/NA = 1.4 oil immersion or a Plan-Fluar 100×/NA = 1.45 oil immersion objective. The stage is equipped with a hyperfine motor HRZ 200. Temperature is stabilised using a temperature-regulated box surrounding the microscope (The Box, Life Imaging Services). Software used for analysis is (a) Excel (Microsoft), (b) ImageJ public domain software (Rasband), (c) Imaris v 3.3 (Bitplane), (d) Mathematica 4.1 (Wolfram Research), and (e) Metamorph v 4.6r6 **(Universal Imaging Corp.)**.

III. PROCEDURES

A. Preparations

1. Plasmids and Strains

Yeast transformation and growth are as described (Guthrie *et al*., 1991). The *lac*^{op}/GFP-*lac*^{i} system for site recognition exploits the high affinity and specificity of the bacterial *lac* repressor for its recognition sequence (*lac*^{op}). All procedures are performed analogously for the *tetR*/*tet*^{op} system (Michaelis *et al*., 1997).

1. Plasmids or integrations of repetitive arrays are difficult to propagate in both bacteria and yeast due to recombination induced excision events. To avoid this, bacteria should be grown at 30°C in a recombination-deficient strain [STBL2 (Invitrogen Life Technologies) or SURE (Stratagene)].

2. Integrate a copy of *lac* repressor fused in frame to sequences encoding the S65T V163A, S175G derivative of GFP and a nuclear localisation signal, e.g., pAFS144 into the yeast strain. This red-shifted GFP derivative has a higher emission intensity and longer fluorescence time than natural GFP (Straight *et al*., 1998). The *lac*^{i} later helps to stabilise the *lac*^{op} array in yeast.

3. Insert a multimerised *lac*^{op} array (usually 256 copies or ~10kb) into the chromosome by standard transformation using a linearised construct that integrates by homologous recombination. Integration is directed to a genomic locus by a unique cleavage within a polymerase chain reaction (PCR)-generated genomic sequence >200bp inserted into the host plasmid (e.g., pAFS52 integration is selected by growth on SD-trp; Straight *et al*., 1996; Heun *et al*., 2001a; Hediger *et al*., 2002). In yeast as few as 24 contiguous *lac*^{op} sites can be detected readily.

4. Check the proper insertion by standard colony PCR and/or Southern blotting (Guthrie *et al*., 1991). Binding of *lac*^{i}-GFP to the *lac*^{op} array results in a bright focal spot, detected readily by fluorescence microscopy within the nucleoplasm. Confirmed transformants with bright signals should be frozen and stored immediately as individual colony isolates. When strains are recovered from frozen stocks, they should be grown on selective medium to avoid further excision events.

Note: Other GFP fusions, optimised forms of CFP or YFP (or ECFP and EYFP), have also been used successfully in yeast (Lisby *et al*., 2003). The lac repressor used is also modified to prevent tetramerisation, thus minimising artefactual higher order interactions between *lac*^{op} sites (Straight *et al*., 1996).

5. Double tagging. If the position or mobility of two genomic loci is to be compared, one should avoid tagging both with the same repeats. It has been shown that identical arrays can undergo a pairing event that, at least in the case of the *tet* system, depends on the expression of the repressor (*tetR;* Fuchs *et al*., 2002). By using *tet*^{op} for one site, and *lac*^{op} for the second, the risk of spurious pairing is eliminated. Useful pairs of GFP derivatives are CFP and YFP, or GFP and the new monomeric mRFP (Campbell *et al*., 2002).

6. In contrast to the *lac*^{i}–GFP fusion (Figs. 1A and 1B), the *tetR*–GFP gives a high and generally diffuse nucleoplasmic background in yeast, both in the presence and in the absence of *tet*^{op} repeats (Figs. 1C and 1D).

7. Dynamics. If movement analysis is to be pursued, it is important to differentiate the movement of the nucleus itself or that induced by mechanical vibrations from the dynamics of the chromosome. Nuclear movement must be determined and then subtracted from that of a specifically tagged site, using any of the following methods.

a. Visualisation of the nuclear envelope with Nup49–GFP (Belgareh *et al*., 1997; Heun *et al*., 2001a). In this case the nuclear centre can be interpolated from the oval or circular pore signal in an automated fashion by software such as ImageJ or Metamorph (Figs. 1A and 1B). The DNA locus position is then determined relative to the nuclear centre for each frame.
b. Diffuse nucleoplasmic signal of *tetR*–GFP (Figs. 1C and 1D). The centre of the nucleus is defined by interpolation frame by frame and locus movement is calculated relative to this.
c. By comparing the motion of two tagged loci, one can calculate average movement without concern for nuclear drift. The fact that both

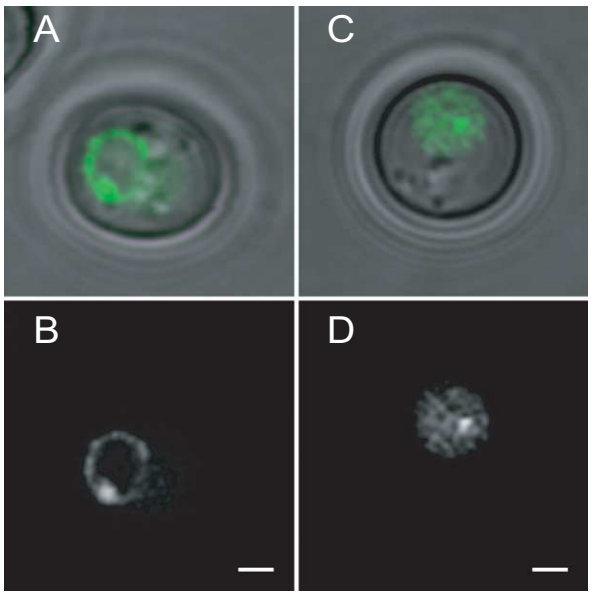

FIGURE 1 (**A** and **C**) An overlay of the phase image and the fluorescence image of a GFP-tagged yeast cell in G1 phase. (**B** and **D**) The corresponding fluorescence image. The *lac*^{op} array is integrated at the *LYS2* locus; the nucleus is visualised by the tagged nuclear pore component Nup49-GFP (**A,B**) or by using the diffuse staining of nucleoplasm by *tetR*-GFP (**C,D**). Bar: 1 µm.

loci are moving has to be taken into account for movement quantitation (see later).

2. *Growth and Cell Preparation*

1. All yeast strains to be analysed should be cultured identically and preferably to an early exponential phase of growth (<0.5×10^7 cells/ml) in synthetic or YPD medium, starting from a fresh overnight culture. Depletion of glucose or growth on alternative carbon sources can alter chronetin dynamics. Wash cells once before observation to avoid YPD autofluorescence. We recommend two mounting techniques for living cell visualisation.

2a. *SD–agarose-filled slides* (Fig. 2A): Immobilised cells between an agarose patch on a depression slide and a coverslip to avoid flattening or distortion of the yeast by coverslip pressure on a normal glass slide. Cells sealed in this way are in a closed environment in which the depletion of O_2 and production of CO_2 bubbles can influence growth and impair visualization. Optimally this technique is used for imaging periods limited to <60 min.

i. Melt an aliquot of SD/agarose at 95°C until the agarose has completely melted, but not longer.
ii. Vortex briefly and transfer 150 µl into the well of a depression slide that is preheated either by a heating block or by passage through the flame of a Bunsen burner.

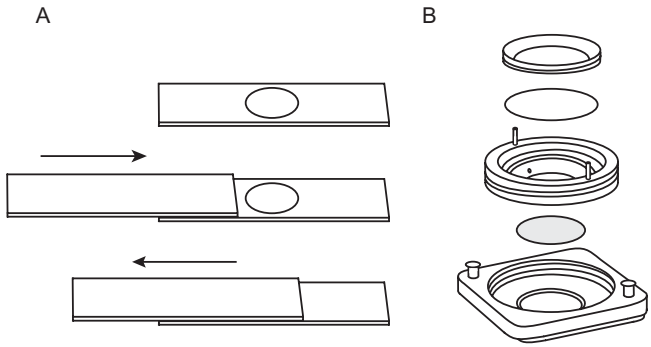

FIGURE 2 Yeast cells can be immobilised for imaging either using an agarose patch on a depression slide (**A**) or using a cell observation chamber (e.g., Ludin chamber; **B**).

iii. Immediately pass a normal microscope slide over the depression to remove excess agarose as depicted in Fig. 2A.
iv. While the agarose solidifies, recover the cells from 1 ml of culture by centrifugation for 1 min at <10,000 g.
v. Resuspend the cells in ~20 µl of appropriate medium.
vi. Once the agarose has solidified, remove the upper slide by sliding along the depression slide surface and place ~5 µl of concentrated cells on the agarose patch.
vii. Close with a coverslip, eliminate eventual air bubbles, and seal with nail polish.

Note: Monitor bud emergence and cell division carefully, as some brands of nail polish contain solvents that influence yeast cell physiology negatively.

2b. *Cell observation chamber* (Ludin chamber, Fig. 2B): The second technique uses a Ludin chamber in which cells are attached noncovalently to a coverslip by a lectin. The medium-filled chamber is assembled as shown in Fig. 2B. A flow of fresh medium can be applied.

i. Coat 18-mm coverslips with 10 µl Con A (1 mg/ml in H_2O) and let them air dry for >20 min. Coated slides can be kept for weeks at room temperature.
ii. Adhere cells to the Con A-coated coverslip by sedimenting 1 ml of the culture at 1 *g* for 3 min at room temperature.
iii. Remove excess culture and add ~1 ml fresh preheated medium before closing the chamber.

3. *Temperature Control*

In order to have a stable condition for microscopic observation, the temperature of the microscope and

room should be controlled carefully (±2°C). Two mechanisms are used standardly. The first is to enclose the entire imaging part of the microscope in a commercially available temperature-regulated box (e.g., Life Imaging Services or Zeiss). A second, less precise method is to regulate the temperature of the slide through a heated stage.

B. Image Acquisition

1. General

The choice of imaging technique depends on the question being asked. To derive quantitative information on the position of a given locus relative to a fixed structure (e.g., the spindle pole body, nucleolus, or nuclear envelope), three-dimensional (3D) stacks and detection of different wavelengths may be necessary. An analysis of fine movement and chromatin dynamics, however, requires the rapid and extended capture of one or more fluorochromes. Bleaching of the signal is often a major limiting factor in time-lapse imaging. One should note that chromatin movement is very fast [movements >0.5 µm in less than 10 s (Heun *et al.*, 2001a)], making it necessary to have rapid image acquisition with a minimal interval between sequential images. To optimise acquisition, parameters such as image resolution, the number of *z* frames, intervals between frames, light intensity, and exposure time can be varied. In all cases, it is of utmost importance to minimise and monitor laser- or light-induced damage to the organism during imaging, in part by comparing the time required for one division cycle in imaged and nonimaged cells.

Cell Cycle Determination

As position and mobility of a chromosomal locus can vary with stages of the cell cycle, it is crucial to determine precisely what stage each imaged cell is in. This is done by monitoring bud presence and bud size, as well as the shape and position of the nucleus, as visualised by the Nup49-GFP fusion and a transmission or phase image. Figure 3 summarises the morphologies that characterise each stage of the cell cycle.

2. Wide-Field Microscopy and Deconvolution

For the imaging of large fields of cells, best results are obtained with a wide-field microscope equipped with **a PIFOC**, Xenon light source, and monochromator that allows a broad and continuous range of incident light wavelengths, as well as rapid switching between these values. Images are acquired by a high-speed monochrome CCD camera run by a rapid imaging software, such as Metamorph. The limiting step is often the speed of signal transfer from the CCD chip to the RAM and/or hard disk of your computer.

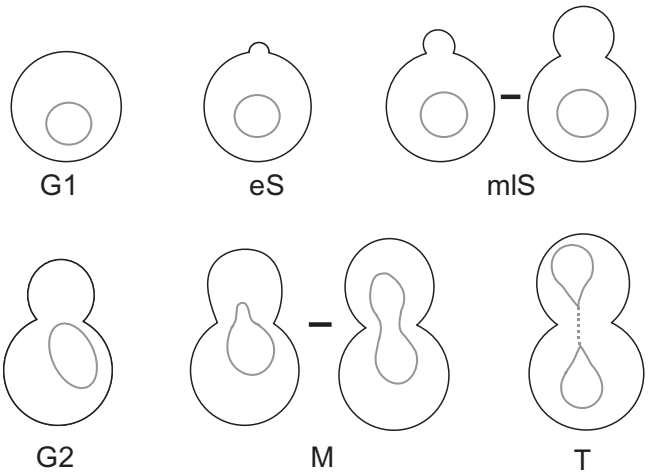

FIGURE 3 Diagrams of a budding yeast cell at different characteristic points in the cell division cycle. The following criteria are used to identify the indicated stage. *G1 phase*, unbudded cells with round nuclei or attached pairs of posttelophase cells that have two round, clearly separated nuclei; *early S*, with initial bud emergence, cells are in early S; *mid-to-late S*, cells with a bud big enough to form a ring at the bud neck, in which nuclei are still round and centred in the mother cell; *G2 phase*, large budded cells (bud ≥ two-thirds of mother) with the nucleus at the bud neck; *mitosis (M)*, large budded cells in which the nucleus extends into the daughter cell due to spindle extension; *telophase (T)*, two globular cells with two distinct nuclei that remain connected by residual NE structures.

z-Stacks

Wide-field microscopy is well adapted to experiments in which a large number of cells (200–300) need to be scored, e.g., when determining the subnuclear position of a given locus relative to the nuclear envelope or another tagged locus or landmark (e.g., spindle pole body or nucleolus). The reference point should optimally be tagged with a different fluorescent protein. If two loci bind the same fluorescent fusion proteins, then their intensities should be significantly different. Rapid through-focus stacks of images using the full chip capacity of the camera are taken of cells growing on agar or in a Ludin chamber (such that 20–30 individual cells are resolved per field). Optimal parameters for GFP are as follows: exposure time, 100–200 ms; *z* spacing of 200 nm for 18 focal planes, excitation wavelength 475 nm. For dual-wavelength capture, images of both wavelengths (CFP: 432 nm, ~300 ms; YFP: 514 nm, ~150 ms) must be acquired before the focal plane changes. A phase image is taken after every stack of fluorescence images. Wide-field images have out-of-focus haze and deconvolution of the *z* stack is often necessary to reassign blurred intensities back to their

original source. Use Metamorph software or other available deconvolution packages.

Three-Dimensional Time Lapse

The conditions for capturing 3D time-lapse series are as follows: 5–11 optical *z* slices taken every 1 to 4 min, *z* sections are 200 to 400 nm in depth, and the exposure time is ~50 ms. Using these settings, up to 300 stacks of five sections each (1500 frames) at 1-min intervals can be captured without affecting cell cycle progression. More rapid sampling with this system, however, leads to bleaching and potential cellular damage. Until this can be remedied by more rapid and more sensitive CCD cameras, wide-field microscopy is recommended for less rapid time-lapse imaging (intervals ≥60 s) on larger fields and confocal microscopy (see later) for very rapid time-lapse imaging (intervals ≤2 s) on small regions of interest (typically one yeast nucleus).

For very long imaging times (>1 h), stray light should be suppressed by inserting an additional shutter. Deconvolution is performed using the Metamorph fast algorithm with five iterations, a sigma parameter of 0.7, and a frequency of 4.

3. Confocal Microscopy

To follow chromatin dynamics in individual cells with rapid time-lapse microscopy, the Zeiss LSM510 scanning confocal microscope is particularly well adapted, although the laser and acousto-optic tuneable filter (AOTF) system is limited in activation wavelengths. Its positive attributes are an ability to limit scanhead motion to a minimal region of interest (ROI), rapid and well-regulated scanning speeds, and the possibility to adjust pinhole aperture and laser intensities to very low levels, while maintaining maximal sensitivity.

General Settings

To reduce the risk of damage by illumination, the laser transmission is kept as low as possible, and the cells are imaged as rapidly as possible within a minimal ROI. Useful settings for the Zeiss LSM510 are as follows.

Laser: argon/2 458, 488, or 514 nm tube current 4,7 amp. Output 25%.

Filters: Channel 1: Lp 505 for GFP alone; channel 1 Lp 530, channel 3 Bp 470–500 for YFP/CFP single track acquisition.

Channel setting: Pinhole 1–1.2 airy unit (corresponding to optical slice of 700 to 900 nm); detector gain: 930 to 999; amplifier gain: 1–1.5; amplifier offset: 0.2–0.1 V; laser transmission AOTF = 0.1–1% for GFP alone, 1–15% for YFP, and 10–50% for CFP in single track acquisition. In order to use minimal laser transmission the pinhole must be aligned regularly.

Scan setting: Speed 10 (0.88 µs/pixel); 8 bits one scan direction; 4 average/mean/line; zoom 1.8 (pixel size: 100 × 100 nm)

Imaging intervals: 1.5 s

Note: If CFP and YFP signals are very weak, images can be acquired sequentially using the more sensitive LSM 510 channel 1 in multitrack mode. This allows the use of broader filters: long-pass filter Lp 475 for CFP and Lp 530 for YFP. Alternatively, and to avoid any cross talk, recover the YFP signal as before and use Bp 470–500 on channel 3 for CFP. These latter parameters will slow the imaging process.

Two- or Three-Dimensional Time Lapse

If maximal capture speed is desired, only one image per time point can be taken, as long as the GFP spot stays in the imaged plane of focus (called 2D time lapse). Often the plane of focus has to be changed manually to follow the spot. Image acquisition in 3D has two main advantages. (1) The GFP spot does not have to be followed manually as it is always present in one of the focal planes. A subsequent maximal projection along the *z* axis produces a complete 2D time sequence without loss of focus on the GFP spot. (2) After image reconstruction, one can visualise the nucleus and calculate distances in 3D. Such measurements are nonetheless compromised by the reduced optical resolution in *z* (≥0.5 µm for 488-nm light).

Specific 3D time-lapse settings are as follows: six to eight optical slices in *z*, 300- to 450-nm spacing in *z* with Hyperfine HRZ 200 motor using a ROI of 3 × 3 to 4 × 4 µm and time intervals of 1.5 s. A 12-min time-lapse series at 0.2% laser transmission did not influence cell cycle progression.

C. Image Analysis

1. z Stacks

Determination of the subnuclear position of a GFP-tagged locus is monitored relative to the centre of the Nup49-GFP ring. Nuclei in which the tagged locus is at the very top or bottom of the nucleus are not scored because the pore signal no longer forms a ring but a surface and a peripheral spot will appear internal.

1. Measure the distance from the centre of intensity of the GFP spot to the nearest pore signal along the nuclear diameter, as well as the nuclear diameter itself, using the middle of the GFP-Nup49 ring as the periphery (Fig. 4). Several programs can export coordinates

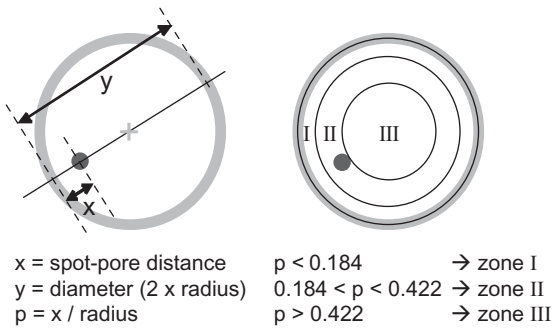

FIGURE 4 Analysis of DNA locus position. Relative locus position is calculated by normalising measured distance × by the radius (0.5 × measured distance *y*). The relative radial distances can then be classified and attributed to three groups of equal surface. The peripheral zone (zone I) is a ring of width = 0.184 × the nuclear radius (*r*). Zone II lies between 0.184 and 0.422*r*, and zone III is the centre of the nucleus with radius = 0.578*r*. In a predicted random distribution every group would contain one-third of the cells.

of points of interest, and the publicly available point picker plug in for ImageJ (Rasband) is useful.

2. Calculate the distances/diameter ratio, e.g., using Excel. Determine the precise relative radial position by dividing the distance between pore and the spot by half of the calculated diameter, thus normalising distances.

3. Classify the position of each spot with respect to three concentric zones of equal surface (Fig. 4). The peripheral zone (zone I) is a ring of width = 0.184 × the nuclear radius (*r*). Zone II lies between 0.184 and 0.422*r* and zone III is the core of the nucleus with radius = 0.578*r*. The three zones are of equal surface no matter where the nuclear cross section is taken.

4. Compare the measured distribution to another (e.g., other cell cycle phase, another condition or a random distribution) with a χ^2 analysis. If only percentages of one zone (e.g., the outermost zone) are compared for different conditions (or to a random distribution), a proportional test should be applied. Statistical significance is determined using a 95% confidence interval.

2. *Three-Dimensional Time Lapse Locus Tracking*

A prerequisite for the precise description of chromatin movement is the knowledge of the coordinates of the locus and of the nuclear centre for each frame of a time-lapse movie. In collaboration with D. Sage and M. Unser (Swiss Federal Institute of Technology, Lausanne), a best-fit algorithm has been developed that reliably tracks a moving spot in 2D time-lapse movies or in maximal projections of *z* stacks in 3D time lapse using nuclei carrying Nup49-GFP or expressing *tetR*-GFP to detect the nucleoplasmic signal. This system is complete and dramatically improves reproducibility and the speed of analysis, while allowing user intervention at several stages. The algorithm has been implemented as a Java plug in for the public domain ImageJ software (Rasband; Sage *et al*., 2003). The spatiotemporal trajectory is exported as *x*,*y* coordinates for each time point in a spreadsheet. An implementation for 3D image stacks over time is also available (Sage et al, 2005). Automated image analysis requires three steps.

a. Alignment phase. The first step is an alignment module that compensates for the translational movement of the nucleus, cell, or microscope stage. This is achieved by a modifiable threshold on the image. The extracted points are then fitted within an ellipse using the least-squares method. Finally, each image is realigned automatically with respect to the centre of the ellipse.

b. Preprocessing phase. To facilitate the detection of the tagged locus, the images are convolved with a Mexican-hat filter. This preprocessing compensates for background variations and enhances small spot-like structures.

c. Tracking phase. The final step is the tracking algorithm. Using dynamic programming, which takes advantage of the strong dependency of the spot position in one frame on its position in the next, the optimal trajectory over the entire period of the movie is determined. The following three criteria influence spot recognition: (1) maximum intensity (i.e., the tagged DNA is usually brighter than the pore signal), (2) smoothness of trajectory, and (3) position relative to the nuclear centre. This latter criterion is necessary because Nup49-GFP staining can be confused with a weak perinuclear locus. All three parameters can be modulated individually in order to optimise the tracking for different situations (loci that are more mobile, more peripheral, of variable intensity, etc). Most importantly, the program has the option of further constraining the optimisation by forcing the trajectory to pass through a manually defined pixel. In that way mistracked spots can again be added manually to the correct trajectory, which is recalculated quasi-instantaneously. This tracking method proves to be extremely robust and reproducible due to its global approach.

Note: Some commercially available software are also able to track objects [e.g., Imaris (Bitplane), Volocity (Improvision)], although tracking efficiency is variable and usually requires uniformly high-quality images. The algorithms are mostly based on threshold principles, which are rarely modifiable or interactive, and which are ill-suited for noisy images.

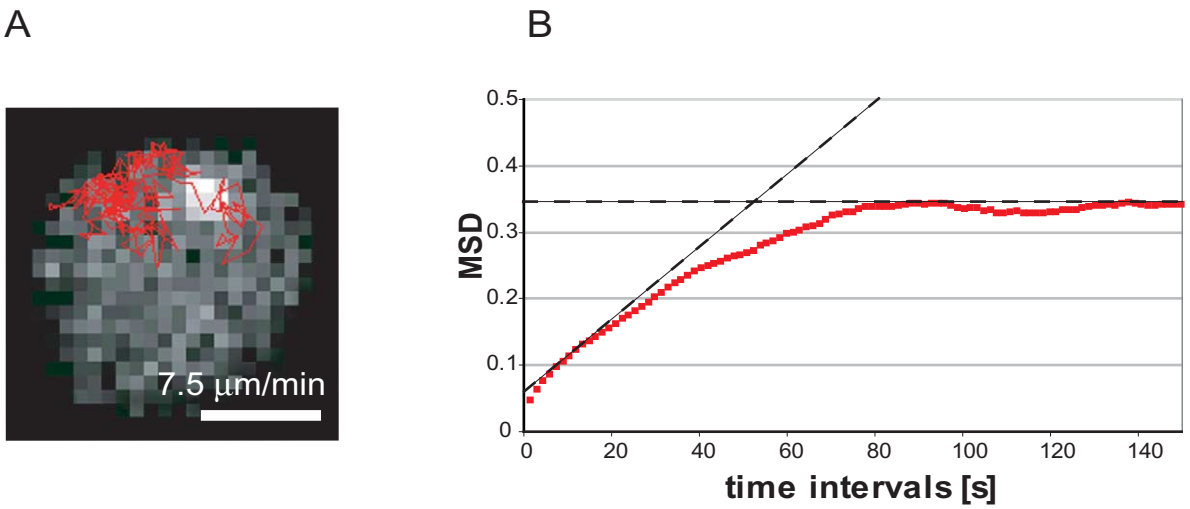

FIGURE 5 Analysis of DNA locus dynamics. (**A**) The projected trace of 300 images of a movie of the *LYS2* locus. The average track length in 5 min is 37.4 µm. Bar: 1 µm. (**B**) A mean square displacement (MSD, $\langle \Delta d^2 \rangle$ in [µm^2]) analysis on an average of 8 movies of the *LYS2* locus. All cells were observed in G1 phase.

Characterisation of Movement

Because each time-lapse series represents a single cell, it is indispensable to average 8–10 movies over a total time >40 min for a given strain or condition. Subtle differences require a larger data source. Useful parameters for quantitative analysis include the following.

a. Track length. The projected track of the tagged locus can be visualised using LSM software, ImageJ, Excel, or other programs (Fig. 5A). The sum of all 1.5-s step lengths within a time-lapse series yields the total track length of that movie. From this, average track length and velocity (µm/min) can be calculated, but often this parameter is not very revealing.

b. Step size. A histogram of step size distribution describes the nature of the movement more precisely. Statistical parameters such as mean, median, and standard deviation of individual and groups of movies can be calculated and compared with statistical tests (e.g., ANOVA). Even small but reproducible significant differences can be documented due to the large number of measurements.

c. Large movements. Often differences in mobility are not obvious by comparing average speed, yet the frequency of large steps >500 nm will vary significantly. These indicate transient high velocity movements. We generally score for steps larger than 500 nm during seven frames (10.5 s), an interval that has proven useful for distinguishing patterns of mobility between different physiological states and stages of the cell cycle (Heun *et al.*, 2001b). These are reported as the number of large steps per 10 min, averaged over at least 50 min of time-lapse imaging. Although a 500 nm is a meaningful cutoff, any threshold over 300 nm can be used.

d. Mean square displacement (MSD). Observing the movement of a DNA locus over time not only gives information about its velocity, but also about the subvolume of the nucleus that it occupies during a given period of time. It has been shown for several chromosomal loci that chromosomal domains are able to move apparently randomly in a given subvolume (Gasser, 2002). This constraint can be quantified by MSD analysis, assuming that the movement of the spot follows a random walk. Ideally it describes a linear relationship between different time intervals and the square of the distance travelled by a particle during this period of time (MSD or $\langle \Delta d^2 \rangle$, where $\Delta d^2 = \{d(t) - d(t + \Delta t)\}^2$ (Berg, 1993; Marshall *et al.*, 1997; Vazquez *et al.*, 2001). In order to get the numbers, one must calculate the distances travelled by the spot for each time interval (1.5, 3, 4.5 s . . .) and plot the square of the mean against increasing time intervals. These calculations and the corresponding graphs can be performed easily in Excel (Microsoft) or Mathematica (Wolfram Research). A representative MSD graph is shown in Fig. 5B. In these curves, the slope reflects the diffusion coefficient of the particle, and the linearity of the curve is usually lost at larger time intervals due to spatial constraint on the freedom of movement of the locus, i.e., the random walk of the particle is obstructed by the nuclear envelope or other subnuclear constraints, leading to a plateau (horizontal dashed line in Fig. 5B). The height of this plateau is related to the volume in which the particle is restricted. The slope of the MSD relation is directly correlated with diffusion coefficient. As

explained earlier, in enclosed systems, the diffusion coefficient decreases with increasing Δt due to space constraints exerted on the particle dynamics. Nevertheless, the maximal diffusion coefficient can be calculated for very short time intervals and reflects the intrinsic mobility of particles (see sloping dashed line in Fig. 5B). For chromosomal loci in yeast, we observed a maximal diffusion coefficient in the range of 1×10^{-4} to $1 \times 10^{-3} \mu m^2/s$ based on short time intervals. If distances are measured between two separate moving loci, $\langle \Delta d^2 \rangle$ reflects two times the MSD of an individual spot or locus moving relative to a fixed point (Vazquez *et al*., 2001). A more theoretical discussion of these parameters is found in Berg (1993).

IV. COMMENTS

It is very difficult to accurately quantify the intensity of a small, mobile GFP-lac^i focus. Even in deconvolved images it can differ by twofold in sequential images.

This protocol shows the optimal method for the described microscope setups. For different microscopes, the values and methods of this protocol are simply a starting point for further optimisation. As improvements in technology (e.g., more sensitive and rapid CCD cameras) and reagents (e.g., more stable or more intense GFP variants) evolve, future adjustments of this protocol will be indispensable.

The method described here can also be applied to *Schizosaccharomyces pombe* with a few changes, one being immobilisation on a coverslip with isolectin B (1 mg/ml) (Williams *et al*., 2002) or lectin from *Bandeiraea simplicifolia* (lyophilized powder, Sigma Cat. No. L2380).

V. PITFALLS

1. To ensure that DNA movements are not the result of nuclear rotation, fluorescence recovery after photobleaching on GFP nuclear pore components should be performed over the same time intervals used to monitor DNA movement.

2. To increase oxygen concentration and to prevent massive production of CO_2 under the cover slide, vortex the agarose/medium before making the patch.

3. Growth conditions must be standardised thoroughly, because both choice of carbon source and its concentration significantly influence subnuclear position and dynamics of tagged loci.

4. Cells grown in minimal medium may not pellet as well as cells grown in YPD. Concentrate cells by centrifuging 2 volumes of culture in the same 1.5-ml tube.

5. In the Ludin chamber yeast cells often bud upwards into the medium (i.e., parallel to the optical axis). Thus it is important to scan the entire cell in transmission mode not to miss the presence of a bud.

6. Observations made on individual cells are often not representative of entire populations. It is crucial to verify observed differences with the appropriate statistical tests.

References

Belgareh, N., and Doye, V. (1997). Dynamics of nuclear pore distribution in nucleoporin mutant yeast cells. *J. Cell Biol.* **136**(4), 747–759.

Belmont, A. S. (2001). Visualizing chromosome dynamics with GFP. *Trends Cell Biol*. **11**(6), 250–257.

Berg, H. C. (1993). "*Random Walks in Biology*." Princeton Univ. Press, Princeton, NJ.

Campbell, R. E., Tour, O., Palmer, A. E., Steinbach, P. A., Baird, G. S., Zacharias, D. A., and Tsien, R. Y. (2002). A monomeric red fluorescent protein. *Proc. Natl. Acad. Sci. USA* **99**(12), 7877–7882.

Fuchs, J., Lorenz, A., and Loidl, J. (2002). Chromosome associations in budding yeast caused by integrated tandemly repeated transgenes. *J. Cell Sci*. **115**(Pt 6), 1213–1220.

Gasser, S. M. (2002). Visualizing chromatin dynamics in interphase nuclei. *Science* **296**(5572), 1412–1416.

Guthrie, C., and Fink, G. R. (1991). "*Guide to Yeast Genetics and Molecular Biology*." Academic Press, San Diego.

Hediger, F., Neumann, F. R., Van Houwe, G., Dubrana, K., and Gasser, S. M. (2002). Live Imaging of Telomeres: yKu and Sir Proteins Define Redundant Telomere-Anchoring Pathways in Yeast. *Curr. Biol*. **12**(24), 2076–2089.

Heun, P., Laroche T., Raghuraman, M. K., and Gasser, S. M. (2001a). The positioning and dynamics of origins of replication in the budding yeast nucleus. *J. Cell Biol*. **152**, 385–400.

Heun, P., Laroche, T., Shimada, K., Furrer, P., and Gasser, S. M. (2001b). Chromosome dynamics in the yeast interphase nucleus. *Science* **294**(5549), 2181–2186.

Lisby, M., Mortensen, U. H., and Rothstein, R. (2003). Colocalization of multiple DNA double-strand breaks at a single Rad52 repair centre. *Nature Cell Biol*. **5**(6), 572–577.

Marshall, W. F., Straight, A., Marko, J. F., Swedlow, J., Dernburg, A., Belmont, A., Murray, A. W., Agard, D. A., and Sedat, J. W. (1997). Interphase chromosomes undergo constrained diffusional motion in living cells. *Curr. Biol*. **7**(12), 930–939.

Michaelis, C., Ciosk, R., and Nasmyth, K. (1997). Cohesins: Chromosomal proteins that prevent premature separation of sister chromatids. *Cell* **91**(1), 35–45.

Rasband, W. ImageJ. National Institute of Health, Bethesda, MD.

Sage, D., Neumann, F. R., Hediger, F., Gasser, S. M., and Unser, M. (2005). "*Automatic Tracking of Individual Fluorescent Particles: Application to Chromatin Dynamics*." in IEEE Transactions on Image Processing., in press.

Straight, A. F., Belmont, A. S., Robinett, C. C., and Murray, A. W. (1996). GFP tagging of budding yeast chromosomes reveals that protein-protein interactions can mediate sister chromatid cohesion. *Curr. Biol*. **6**(12), 1599–1608.

Straight, A. F., Sedat, J. W., and Murray, A. W. (1998). Time-lapse microscopy reveals unique roles for kinesins during anaphase in budding yeast. *J. Cell Biol.* **143**(3), 687–694.

Vazquez, J., Belmont, A. S., and Sedat, J. W. (2001). Multiple regimes of constrained chromosome motion are regulated in the interphase Drosophila nucleus. *Curr. Biol.* **11**(16), 1227–1239.

Williams, D. R., and McIntosh, J. R. (2002). mcl1+, the *Schizosaccharomyces pombe* homologue of CTF4, is important for chromosome replication, cohesion, and segregation. *Eukaryot Cell* **1**(5), 758–773.

SECTION

10

Assays and Models of *in vitro* and *in vivo* Motility

CHAPTER

47

Microtubule Motility Assays

N. J. Carter and Robert A. Cross

I. INTRODUCTION

As the pivotal role of microtubule (MT) motors in the cell cycle becomes more widely recognized, so the demand for motility assays will increase. This article presents a robust and straightforward set of protocols based on experience gained in our laboratory. Readers seeking to set up more specialised assays should refer to one of the excellent methodological compendia that are available (Inoue and Spring, 1997; Cross and Kendrick Jones, 1991; Scholey, 1993).

II. MATERIALS AND INSTRUMENTATION

A. Hardware

1. Microscope

Unstained MTs are visualized most conveniently by video microscopy using computer-enhanced differential interference contrast (DIC). MTs assembled from fluorescently labeled tubulin can be visualized using epifluorescence. This article concentrates on these two contrast modes. It is also possible to visualise microtubules by dark field, which gives a high contrast image of unstained microtubules, or by phase contrast, but both modes are susceptible to dirt in the solutions and so may be inconvenient for routine work. Interference reflection produces higher contrast than DIC and gives information in the *Z* direction, but again is susceptible to dirt.

For all modes of contrast the main requirement of the microscope is that it should be as simple as possible. It should also be big and heavy to give it some vibration resistance. Uprights are less expensive, optically straightforward, and more convenient if the bathing solution is to be exchanged during observation (which is often the case). Inverted scopes are more stable and provide much better access to the specimen if other inputs (micromanipulators, flash-photolytic lasers, evanescence prisms) are envisioned.

Human eyes work in colour and have a higher dynamic range, better spatial resolution, and a bigger view field than a video camera. It is very useful to be able to use them to find focus. To do this the microscope needs to incorporate some sort of device to switch the light between the eyepieces and the camera.

2. Illumination

One hundred Watt Hg lamps generate large amounts of heat and it is necessary to remove this heat from the illuminating light. Glass heat filters may be used, but the best way to filter out heat is to use a hot mirror, a mirror that transmits infrared but reflects visible light (technical video).

DIC optics are optimised for visible wavelengths, and it is conventional to use a green interference filter to give narrow band illumination. In practice the improvement this brings is often too slight to be obvious by eye, and removing the green filter can be a convenient way to brighter illumination. The UV emitted by Hg lamps is removed substantially removed by optical (lead) glass, but for DIC an in-line UV filter is nonetheless a sensible precaution.

A useful improvement in both fluorescence and DIC image quality can be achieved by sending the illuminating light through a fibre-optic light scrambler (Technical Video). Light from the lamp is focussed into one end of the fibre (Fig. 1), and the other end emits a

Copyright 2006, Elsevier Science (USA).
All rights reserved.

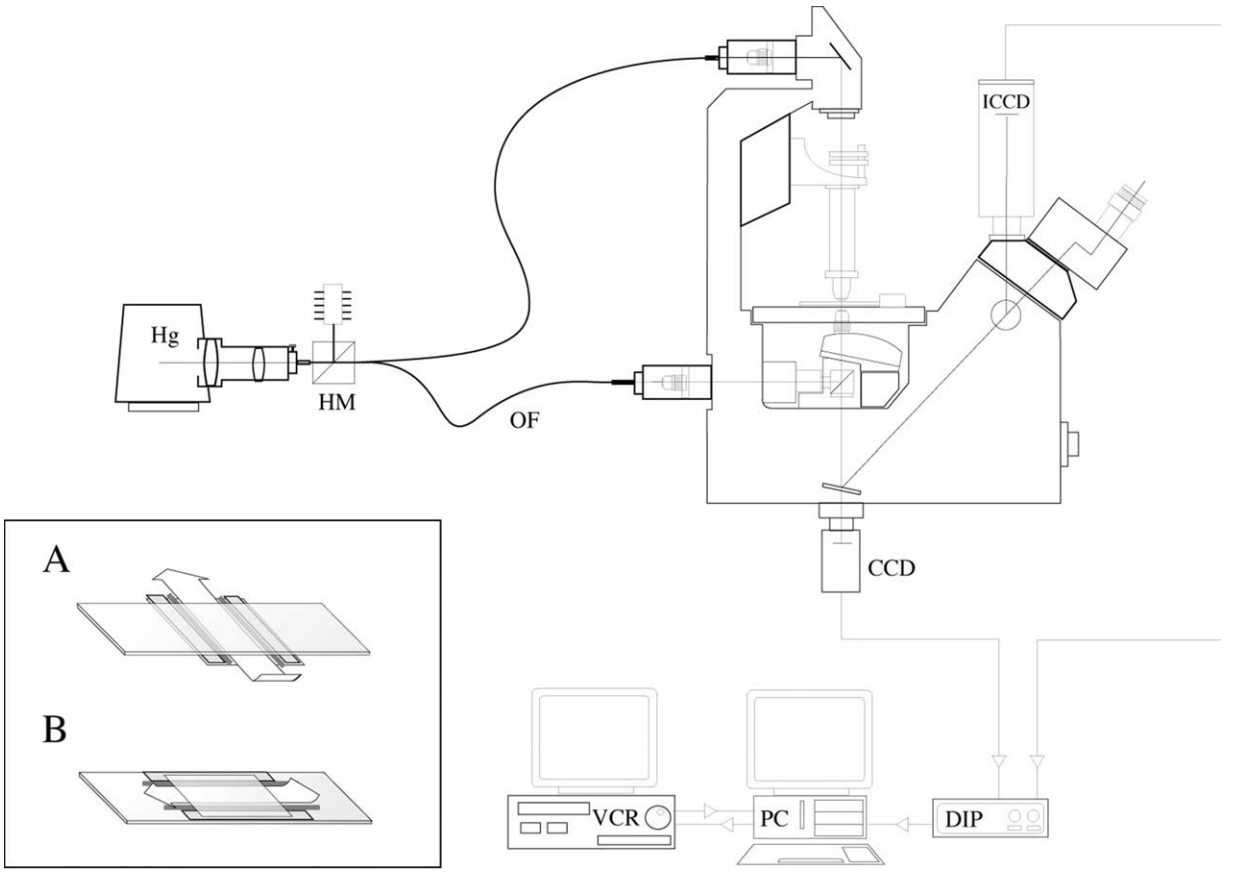

FIGURE 1 Video microscope. An inverted microscope set up for both fluorescence and DIC microscopy. Hg, mercury lamp; HM, hot mirror; OF, optical fibre; CCD charge-coupled device camera (for DIC); ICCD, intensified CCD (for fluorescence); DIP, digital image processor; PC, personal computer; VCR, video cassette recorder.

uniform disc of light (of Gaussian intensity profile), which is used to illuminate the microscope.

3. Optical Train

For maximum image quality in all contrast modes, it is advisable to reduce the number of optical components between the objective and the camera to a minimum. The most critical component is the objective. The light intensity transmitted by a lens is proportional to the square of its numerical aperture (NA), whilst resolution rises linearly with the NA. It is important therefore to use a 1.4 NA (therefore oil immersion) 60 or 100× planapo objective in order to maximise light-gathering power and resolution, particularly so in epifluorescence, where the objective doubles as the condensor.

We use a novel configuration that replaces the condensor on a Zeiss Axiovert with a home-built fitting that improves light collection from the Zeiss tungsten lamp and mounts a second objective in place of the condensor. This arrangement (Fig. 1) gives good MT DIC with a field about 40 µm and brings the considerable advantages of the tungsten lamp, which is much more stable than the Hg lamp. For smaller view fields, the higher radiant intensity of the Hg lamp is necessary.

4. Antivibration Hardware

Vibration will degrade the highly magnified image. Low frequencies (people walking across the floor) will cause the image to bounce around, whilst high frequencies will be averaged out by the video framing rate and cause the image to blur. The extent of this problem is, however, often overemphasized. Before purchasing an expensive and awkward vibration-damping equipment, try placing a few layers of bubble wrap under the microscope baseplate.

5. Temperature Control Hardware

Motility rates for several motors are extremely temperature sensitive in the range of room temperature, and temperature control is consequently important if

measurements taken at different times are to be compared. The best way is to temperature clamp the entire microscope. If you have air conditioning this will already be happening. To warm specimens above ambient temperature, we use a homemade plexiglass box with a warm-air blower coupled to the side. Another option is to use water jackets for the objective and stage. These are readily fashioned by wrapping flexible, narrow-bore copper tubing around several times and connecting the ends to a water bath with a circulator (e.g., Techne) using silicon tubing. If cooling is necessary, we find it useful to wrap the microscope in a tent made of cling film, reducing condensation.

6. Camera

For fluorescence of moving objects, two types of low-light level / high-contrast / high-framing rate cameras are suitable: intensified charge-coupled device (ICCD) and intensified silicon-intensified tube (ISIT) cameras. ICCD cameras are better for current purposes because ISIT cameras, although more sensitive, introduce spatial and intensity distortions across the view field that are tedious to correct for. All the aforementioned produce an analogue video signal, e.g., ISIT Hamamatsu C2400-08 and ICCD Hamamatsu C2400-97E. An alternative approach that is becoming feasible uses a digital camera to record direct to computer hard disc in time lapse. A cooled CCD camera coupled to a generation 4 intensifier gives excellent sensitivity for fluorescence work, but is limited by the quantum efficiency of the intensifier (about 30%) and is currently very expensive and the digital data can be awkward to archive. If considering this route, be sure to test the software, which in our experience can place more severe limits on performance than the specifications of the hardware.

For DIC, a nonintensified scientific grade CCD is fine, e.g., grey-scale CCD camera Hamamatsu C2400 77e.

7. Camera Coupling/Magnification

The ideal magnification sets four or more camera pixels across the width of the MT. For a 512×512 pixels (2/3 in.) CCD, this corresponds to a square field with sides of 20–25 μm. Zoom couplings are wonderfully convenient but are not always a good idea because they absorb a lot of light. Magnification must be calibrated using a stage micrometer.

8. Image Processor

CCD cameras are often offered with a hardware box providing real time analogue enhancement of the video signal (any or all of gain, back-off and shading correction). A digital video processor is better, which is able to digitise incoming video frames, perform frame averaging, contrast enhancement, background subtraction, and caption overlay and then re-encode the image as an analogue video signal, all in real time. The Hamamatsu Argus 20 is so well thought out that it is virtually standard equipment for video microscopy laboratories. The best and most flexible arrangement is to adjust the gain and backoff on an Argus 20 or similar processor controls such that there are no areas in the image that are completely saturated and then apply further digital enhancement. The resulting signal is displayed on a monitor and is fed to the PC for direct grabbing of video clips and to the VCR for archiving.

9. Monitor

It is worth investing in a high-quality 14-in. multiformat monitor. Larger monitors look impressive but are only helpful if they have to be placed a long distance from the operator.

10. Video Recording

At the time of writing, the most convenient and practical way to store large amounts of video is still to use video tape. Recording to VCRs inevitably involves some degradation of the image (loss of spatial resolution, noise, contrast effects). For practical purposes the resolution loss is potentially the most serious problem. The effective resolution following recording can be visualised by recording and replaying a test card image having black and white lines at various spatial frequencies. Currently the best option is digital recording to video tape. Digital video tape recorders input and output an analogue signal, but encode data digitally to tape. The digitization involves some compression of the incoming video signal, but most of the compression is on the chrominance rather than the luminance, with the result that spatial information is relatively well preserved, particularly for grey-scale signals. Unlike other compression schemes such as DVD, there is no compression along the temporal axis. There are currently two sizes of tape: digital video (DV) and mini-DV. There are also two different formats: DVCAM (Sony) and DVCPRO (Panasonic). These two formats use the same compression scheme but DVCPRO spaces the tracks further apart on the tape, giving (arguably) better reliability and accuracy for editing, but with correspondingly less recording time on the tapes. Digital video recorders tend to be built for the pro market and are more robustly engineered than consumer machines, but are also more expensive.

We have evolved a video-recording strategy that offers maximum flexibility: Time-lapse digital

recording of grabbed video frames to computer hard disc (with no resolution loss) and simultaneous real-time recording to digital VCR. The VCR runs uninterrupted in the background and generates an archive. The operator is free to go back to this archive at a later date and transfer interesting sequences to the computer for analysis. Captured digital sequences can be archived to external hard discs. We now have a fast digital capture and analysis application RETRAC II, which allows batch digitisation of video clips from tape for subsequent analysis. RETRAC II can be downloaded from our website (http://mc11.mcri.ac.uk/Retrac/index.html).

Analogue video recording is still in widespread use. Different video formats unfortunately operate in different countries. In the United States and Japan, NTSC format applies (525 lines per frame; 30 frames/s, typically captured at 640 × 480 pixels). European countries use PAL, which has higher spatial resolution but lower time resolution (625 lines per frame, 25 frames per sec, typically captured at 768 × 576 pixels).

11. Computing

The most convenient way to analyse motility is to capture a sequence of frames into computer memory and to track objects using a mouse-driven cursor. It helps to have a hard disc big enough to hold 2 day's work (more is dangerous because of the temptation not to back up) and enough hard memory to hold the stack of captured frames. A typical 20 frame stack uses about 8 Mb of application memory; if you want to use larger stacks then you need more memory. Processed stacks can conveniently be archived to removable discs. We use 100-Mb zip discs or 230-Mb magneto-optical discs. CD writers are getting less expensive and are worth considering if a permanent archive is required. Video compression protocols (JPEG, MPEG) are best avoided, as all involve some data loss. That said, Quicktime has become a standard for digital video and can use a variety of compressors, some of which are lossless.

12. Frame Grabber Card

Large numbers of video grabbing cards are available. Only a few are supported by Retrac and NIH Image, the freeware software packages that are recommend later. Because the situation is fluid, please check the software documentation for a list of supported cards.

13. Software

On the Mac, the best route for analysis is NIH Image, which can be customised using macros to track objects and output data in spreadsheet-compatible format. Macros for basic tracking through NIH Image stacks are available for download from our web page http://mc11.mcri.ac.uk/retrac.html. NIH Image runs on system 9 macs, with support for the Scion LG3 frame capture board, or in classic in OSX but without the Scion support. Wayne Rasband is continuing development of ImageJ, an NIH image—inspired java programme that runs in OSX and currently has partial support for the LG3 board (http://rsb.info.nih.gov/ij/). NIH Image and ImageJ are both available for the PC.

RETRAC 2 for Windows is purpose-written for the analysis of motility assay data. The latest version supports time-lapse frame grabbing from either VCR or live video, autofocus, autocontrast, tracking (including drift correction) spatial filtration, and magnification. The programme now incorporates a powerful file manager. Figure 2 shows a screenshot during tracking.

14. Glassware

The type of slide used does not matter. The type of coverslip does. The thickness of the coverslip should be matched to the objective. The objective will be marked appropriately [e.g., 60/planapo DIC 1.4 0.17/160 means a 60× objective selected as strain free for DIC, aplanatic (flat field); apochromatic (low chromatic aberration for blue yellow and green); optimised for cover glasses 0.17 mm thick and with a 160-mm focal length]. We use Chance 22 × 22-mm No.1.5 coverslips. In the past we have used these without any special cleaning treatment and rejected "bad" batches of coverslips that show poor binding of motor and/or a poor image because of surface contamination. This is still a workable approach, but we have begun to use a cleaning procedure that appears effective in removing contamination and making the coverslip reproducibly hydrophilic, as evidenced by the spreading of a drop of buffer placed on the surface so that it wets the entire surface. This coverslip cleaning procedure is based heavily on that given on the Technical Video website (http://www.technicalvideo.com/Products/CCP.html). Our localized variant is on our website (http://mc11.mcri.ac.uk/protocols.html).

III. PROCEDURES

A. Taxol-Stabilised Microtubules

Solutions

1. *1 M K–PIPES:* PIPES dissolves around its isoelectric point of about pH 6.5. Take 500 ml water, add 65 g solid KOH, and then, after cooling if necessary, slowly add 302 g PIPES buffer (Sigma P-6757). Once everything is dissolved, monitor pH and roughly adjust by

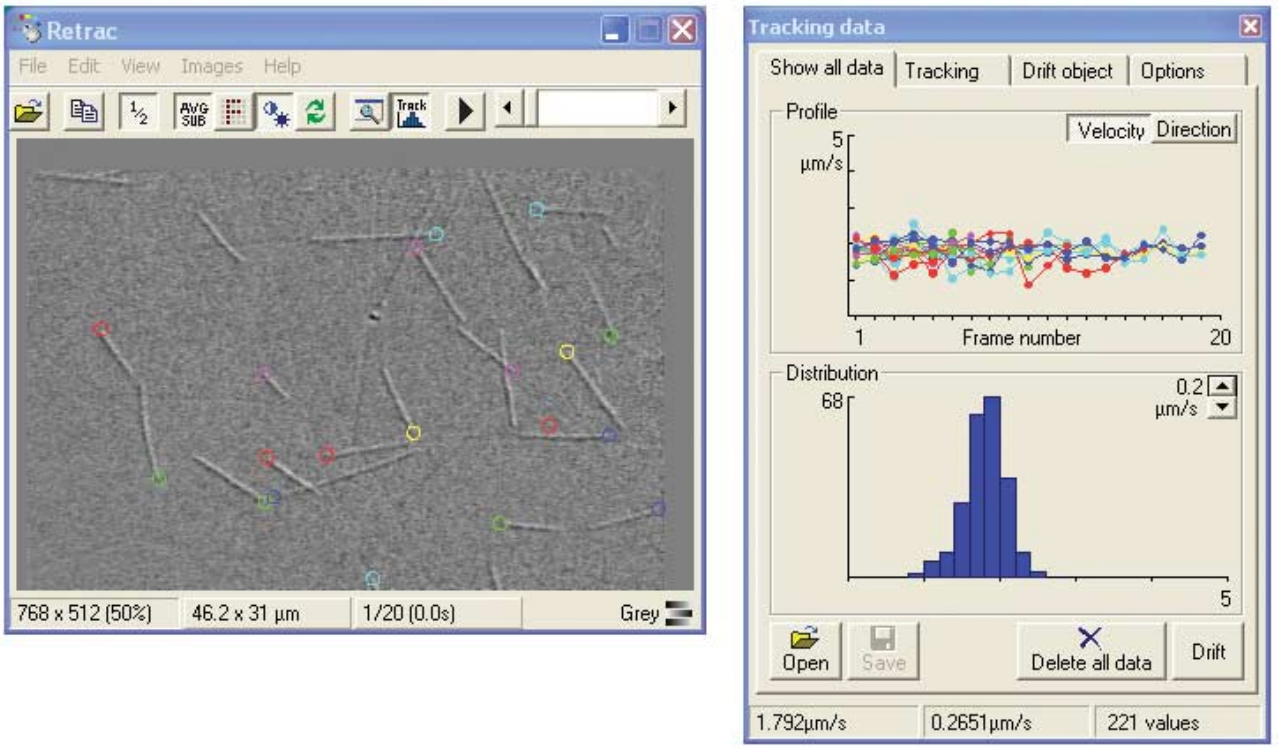

FIGURE 2 A screenshot from RETRAC 2.

adding more KOH pellets as necessary. Allow the warm solution to cool and then fine-adjust pH using 5 *M* KOH. Be careful not to overshoot, as there is no way back.

2. *100 mM NaGTP stock solution:* Because nucleoside triphosphates such as GTP and ATP undergo rapid hydrolysis at acidic pH, efforts should be made to control pH when dissolving and storing them. Dissolve 1 g NaGTP (Sigma G8877) in 15 ml 10 m*M* Na-PIPES, pH 6.9, monitoring pH. Rapidly reneutralise pH by titrating in 5 *M* KOH. Fine adjust pH and then make volume up to 19.11 ml. Store frozen at –20°C in aliquots of 5–2000 µl. Do not add $MgCl_2$ to the stock solution (it precipitates).

3. *100 mM MgATP stock solution:* Dissolve 5.87 g NaATP (Sigma A7699 ATP ultra or Boehringer 519 987) in 60 ml 10 m*M* K-PIPES, pH 6.9, monitoring pH continuously and holding as close as possible to neutral using concentrated KOH. Once the ATP is dissolved, add 10 ml of 1 *M* $MgCl_2$ and readjust pH to 6.9. Adjust volume to 100.0 ml and freeze in aliquots of 5–5000 µl.

4. *Taxol stock solution:* Wear gloves and work in the fume hood. Inject 2.93 ml anhydrous dimethyl sulfoxide (DMSO, Aldrich 27685-5) into a 25-mg bottle of taxol (Sigma T 7402). Dissolve by vortexing and store as 2- to 20-µl aliquots at –20°C. Taxol is stable in DMSO but unstable in water. It is insoluble in aqueous buffers above about 18 µ*M*. DMSO is explosive if it gets wet. Store small volumes at room temperature over beds of Sephadex G-50.

5. *0.2 M NaEGTA:* Dissolve 15.2 g EGTA (Sigma E 4378) in 190 ml water. Adjust pH to neutral by adding concentrated NaOH and then make volume to 200.0 ml. Store at room temperature.

6. *1 M* $MgCl_2$: 20.33 g $MgCl_2 \cdot 6H_2O$ to 100 ml water. Sterile filter and store at room temperature.

7. *BRB 80 (Brinkley reassembly buffer):* 80 m*M* K-PIPES, 1 m*M* $MgCl_2$, 1 m*M* EGTA, pH 6.9. Make up as a 10× stock, store at 4°C, and dilute freshly for use.

Purified tubulin at about 100 µ*M* (protocol for tubulin preparation on our web page) in BRB80 should be flash frozen in 10- to 25-µl aliquots in the presence of 30% glycerol by immersion in liquid nitrogen and stored either at –70°C or preferably in liquid nitrogen.

Steps

1. Thaw an aliquot of tubulin (typically 200 µ*M*) and add stock 100 m*M* NaGTP to 1 m*M* and $MgCl_2$ to 2 m*M*. Warm to 37°C and incubate for 20 min.
2. After 20 min, add taxol from a 10 m*M* stock in DMSO to 20 µ*M* final. Dilute microtubules 1000-fold for use using BRB80 buffer supplemented with 20 µ*M* taxol.

B. Preparation of Flow Cells

Steps

1. Apply single-sided Scotch tape to the long edges of a microscope slide such that the strip of glass surface between the two pieces of tape is 8–10 mm wide. Trim away overhangs with a razor blade.

2. Extrude two parallel stripes of Apiezon M grease from a syringe with a squared-off wide-bore needle along the inner edges of the tape strips.

3. Press a clean coverslip onto the grease. The volume of the flow cell can be adjusted by spacing the grease strips apart and/or by placing spacers between the coverslip and the slide. Single-sided Scotch magic tape is about 50 µm thick, giving a flow cell of about 10 mm × 5 mm × 50 µm, or 25 µl. Thinner metal or cellophane foils can be used to make a shallower flow cell and conserve sample. It is helpful to make the flow cell shallow because the microtubules below the top surface scatter light and reduce contrast. For inverted scopes, it is convenient to arrange flow crosswise. The inset to Fig. 1 illustrates flow cells for inverted (A) and upright (B) microscopes.

C. Surface Adsorption of Motor

Solutions

1. *Motility buffer:* BRB 80 plus 1 m*M* MgATP. For fluorescence work only, degas and add 1% of 100× antibleach mix (GOC), which is 100 mg/ml glucose oxidase (Sigma G7016), 18 mg/ml catalase (Sigma C100), and 300 mg/ml glucose (Sigma G7528) in BRB80 plus 50% glycerol. When aliquoting, fill tubes to exclude oxygen, cap, and store at –20°C.

2. *100× diluted MTs:* either motility buffer or motility buffer plus GOC.

Steps

1. Place the flow cell flat. Using a Gilson, inject into the cell 1 chamber volume of motor solution. The solution is drawn into the cell by capillarity. Incubate the slide in a moisture chamber for 2–5 min at 20°C to allow the motor to adsorb to the glass.

2. Wash the cell with 2 chamber volumes of assay buffer, applying the solution to one side of the chamber using a micropipette and drawing the solution gently through the cell using the capillary action of the torn edge of a strip of Whatman 3 MM, placed at the exit of the chamber.

3. Flow in 1 volume of MTs in motility buffer + taxol and mount the slide on the microscope stage, oiling the condensor to the bottom of the slide (it may be possible to use a dry condensor for quick-and-dirty assays).

4. Extra for fluorescence work 1. Degas some BRB80. To 10 ml, add 100 µl of 100× GOC. Take another 3 ml and add MgATP to 2 m*M*. Fill and cap tubes to exclude oxygen and hold buffers on ice. Add taxol to 20 µ*M* freshly before use.

D. Microscope Setup

1. DIC

Before the day's work, align the microscope roughly using a test specimen (a slide made using a suspension of plastic beads provides a stable and realistic test specimen). Switch on the lamp and allow a few minutes for the arc to stabilise. Rack down the objective and oil it to the slide. Insert some neutral density filtration to protect your eyes from the intensely bright light, focus roughly on the top surface of the grease at the edge of the chamber, and then drive the stage to centre the sample below the objective. Find some beads attached to the undersurface of the coverslip. Open the condensor aperture and close the field aperture. Obtain Koehler illumination by focussing and centring the condensor so that a sharp image of the field diaphragm appears in the view field. Open the field diaphragm again and adjust DIC sliders close to extinction.

Focussing on MTs in the experimental flow cell is also best done using the grease surface as a guide. Focus as described earlier and then remove neutral density filters and switch in the video system. Adjust fine focus to image the surface. Adjust light intensity to almost saturate the camera (this is the point where signal to noise is maximal). With the contrast on the Argus set to maximum, microtubules should be visible without background subtraction. Defocus slightly, collect a background image, and subtract. Microtubules should now be clearly visible.

2. Epifluorescence

A test sample of multispectral fluorescent beads is very useful (Molecular Probes multispeck M-7900). Switch on the arc lamp and allow a few minutes for the arc to stabilise. Once the lamp is stable, align the microscope for epifluorescence: Remove an objective and place a piece of paper on the stage. Inset some neutral density filtration. Close the field diaphragm slightly and focus and centre the image of the lamp filament that appears on the paper. Replace the objective.

Focussing on microtubules in the experimental cell is much easier with dark-adapted eyes. Using the full intensity of the mercury lamp, rack the objective down until MTs are visible, first as a dim red glow, and then as sharply defined bright red lines on a black back-

ground. Immediately reduce the illumination intensity to protect against photobleaching, switch in the intensified camera, and start recording.

E. Recording Data

The most flexible arrangement for data recording is to set up time-lapse digital recording of video frames to a computer hard disc (with no resolution loss) and simultaneous recording to VCR. The VCR runs uninterupted in the background for 3 h per tape and generates an archive. The operator is free to go back to this archive at a later date and recapture interesting sequences for analysis.

F. Analysing Data Calibration

Image a stage graticule, a slide with etched lines at 1- or 10-μm intervals (from microscope manufacturers). It is important to calibrate both in X and Y; simply rotate the camera 90°. Most systems will give a different number of pixels per micrometer in X and Y. Tracking software compensates for this effect.

The best way to track is to follow the tip of a moving microtubule: tracking the centroids, as common in cell tracking, for example, will give you the wrong answer as soon as the microtubule bends. For maximum accuracy, the time lapse between frames should be adjusted to minimise the effects of operator error when tracking using the mouse. In practice we try to collect 20 frames and adjust the time lapse so that the microtubules move across the full field (22 μm) during this time.

IV. COMMENTS

A. Archiving Data

It is very important to have a formal system for identifying every video frame on every tape. In this way there is no possibility of confusing data sets. The simplest way to do this is to time and date stamp the frames as they are generated, using the overlay feature of the Argus. As ever, keeping careful written notes also helps a lot. For complex experiments it can be useful to speak notes onto the audio track of the tape. Digital clips are archived most conveniently on external.

B. Imminent Technology

As computers get quicker, it is realistic to start recalculating images in real time. Autocontrast is one interesting possibility, whereby the pixels of each incoming frame are parsed and the look-up table is stretched to optimise contrast. It will be some time before we can dispense with the VCR. Real-time recording of uncompressed grey-scale video to disc is pushing the limits at present, but sufficiently fast sustained data transfer rates will soon be available. This is not the real problem, however. One frame of PAL video is 768 × 512 pixels, which, with 8 bit (256 greys) data, means that each frame is 384 kb. Real-time recording to hard disc fills the disc up at about 0.5 Gb per minute, and it soon becomes necessary to archive data to video tape.

C. Workstation Ergonomics

It is worth paying some attention to the ergonomics of your microscope workstation. Microscope focus, mouse, keyboard video, and contrast-adjustment electronics all need to be within easy reach of a seated operator. Screens should be visible with only a slight turn of the head. It is very helpful to have a foot switch to dim the room lights and blinds on windows.

D. Best Practice

Because of inherent uncertainties about the way a particular protein attaches to a particular glass, motility assays are at their strongest when used to measure the relative motility in different treatments of samples. It is commonly assumed that motility assays measure motor-driven microtubule sliding under zero load. It is probably more correct to assume that an unspecified, variable, (but low) load applies.

V. PITFALLS

A. Computerphilia

The most common fault in video microscopy is to overprocess an indifferent optical image. Too much processing can seriously degrade the amount of information in the image. A good primary image has high spatial resolution (sharpness), high contrast, and low background noise. Obtaining one is partly a function of specimen preparation and partly of microscope setup.

B. Lamp Intensity Fluctuates

In DIC, a troublesome problem is sudden variations in light intensity caused by the arc of the mercury lamp wandering. These are not noticeable in normal modes

of microscopy, but with electronic amplification of contrast they become annoying. The only solution is to change the lamp. Cooling the lamp using a fan may help. Mercury lamps typically need changing after 100 h, because after that their intensity drops fairly rapidly.

C. Microtubules Fishtail or Do Not Move At All

Some motor proteins bind better to the glass surface than others. Erratic motility may be due to your protein denaturing on the glass or binding in such a way that its force-generating conformational change is inhibited. Areas of uncoated glass can also bind microtubules and inhibit sliding. Increase motor concentration if possible or try infusing the motor twice over and/or reducing or eliminating the wash step prior to infusing microtubules. Including casein at 0.1–1 mg ml in the assay buffer efficiently protein coats glass. Because motor activity can also be sensitive to thiol oxidation, try including 5 m*M* DTT in your motility buffer.

References

Cross, R. A., and Kendrick, Jones J. (1991). Motor proteins. *J. Cell. Sci.* Suppl. 14.

Inoué, S., and Spring, K. R. (1997). "*Video Microscopy*." Plenum Press, New York.

Kron, S. J., Toyoshima, Y. Y., Uyeda, T. Q. R., and Spudich, J. A. (1991). *Assays for actin sliding movement over myosin-coated surfaces*. *Methods Enzymology* **196**, 399–416.

Scholey, J. M. (1993). *Motility assays for motor proteins*. *Methods Cell Biol* **39**.

CHAPTER

48

In vitro Assays for Mitotic Spindle Assembly and Function

Celia Antonio, Rebecca Heald, and Isabelle Vernos

I. INTRODUCTION

During the past two decades, cell biology has entered a phase in which technology is so powerful that fundamental questions concerning the morphogenesis and function of cellular organelles can be addressed. One essential and beautiful structure is the mitotic spindle. The work of Lohka and Maller (1985), followed by that of a few other laboratories (Murray and Kirschner, 1989; Sawin and Mitchison, 1991; Shamu and Murray, 1992), opened up a novel approach to studying such a complex and dynamic structure. The idea is not to purify individual spindle components and put them back together hoping that a spindle will assemble, it is rather to open up the cell and prepare a cytoplasmic extract as crude and concentrated as possible to keep the conditions close to the *in vivo* situation. At first sight, this approach seems uninformative: one merely mimics *in vitro* what happens *in vivo*. However, several methods have been developed to manipulate the system, such as the addition of reagents and depletion of proteins. Also the microscopy techniques have evolved and now allow the study of different aspects of spindle formation and function (Desai *et al*., 1998; Kalab *et al*., 2002). Thus, this system can be used both to analyze the mechanism of spindle assembly and function and to evaluate the role of individual molecules in the process. More methods are still being developed or improved that will increase the usage and the utility of these extracts even more.

II. MATERIALS AND INSTRUMENTATION

A. Preparation of *Xenopus laevis* Egg Extracts

Incubator at 16°C, clinical centrifuge, DuPont Sorvall RC-5 centrifuge, HB-4 or HB-6 rotor with rubber adaptors (Sorvall Cat. No. 00363), Beckman ultraclear SW50 tubes (Cat. No. 344057), Sarstedt 13-ml adaptor tubes (Cat. No. 55.518), 1-ml syringes, 18- and 27-gauge needles, glass pasteur pipettes.

Mature female frogs are from African Reptile Park. Pregnant mare serum gonadotropin (Intergonan) is from Intervet. Human chorionic gonadotropin (HCG, Cat. No. CG-10), cytochalasin D (Cat. No. C-8273), EGTA (Cat. No. E-4378), 4.9 *M* $MgCl_2$ (Cat. No. 104.20), and ATP (Cat. No. A-2383) are from Sigma. $CaCl_2$ (Cat. No. 2383), KCl (Cat. No. 1.04936.1000), NaCl (Cat. No. 1.06404.1000), and L-cysteine (Cat. No. 1.02838.1000) are from Merck. Leupeptin (Cat. No. E18) and pepstatin (Cat. No. E19) are from Chemicon. Aprotinin (Cat. No. 981532) and creatine phosphate (Cat. No. 0621714) are from Roche. HEPES is from Biomol. Sucrose is from USB (Cat. No. 21938).

B. Preparation of DNA Beads

Biotin-21-dUTP (Cat. No. 5201-1) is from Clontech. Biotin-14-dATP (Cat. No. 19524-016) is from Invitrogen. Thio-dCTP (Cat. No. 27-7360-02), thio-dGTP (27-7370-04), and G-50 gel-filtration (NICK) columns

Copyright 2006, Elsevier Science (USA).
All rights reserved.

(17-0855-01) are from Amersham Pharmacia Biotech. Restriction enzymes and Klenow (Cat. No. M02125) are from New England Biolabs. The magnetic particle concentrator (MPC) and Kilobase BINDER kit containing Dynabeads M-280 Streptavidin, washing, and binding solutions can be obtained from Dynal. Trizma base (Cat. No. T-1503) is purchased from Sigma, and EDTA (Cat. No. 1.08418.1000) is from Merck.

C. Spindle and Aster Assays

Freshly prepared CSF extract, sperm nuclei (3000/µl)(Murray, 1991), rhodamine-labelled tubulin (2–3 mg/ml) (Hyman *et al*., 1991), 76 × 26-mm microscope slides, 22 × 22-mm coverslips, fluorescence microscope. PIPES (Cat. No. P-6757), Triton X-100 (Cat. No. T-8787), glutaraldehyde (Cat. No. G-5882), $NaHB_4$ (Cat. No. S-9125), GTP (Cat. No. G-8877), and Hoechst dye (bisbenzimide, Cat. No. H33342) are from Sigma. Glycerol (Cat. No. 1.04093.2500) and formaldehyde (Cat. No. 1.04003) are from Merck. Protein A dynabeads (Cat. No. 100.02) are from Dynal. Dimethyl sulfoxide (DMSO, Cat. No. 27,685-5) is from Sigma-Aldrich, and Paclitaxel (taxol equivalent) (Cat. No. P-3456) is from Molecular Probes. For sedimentation and immunofluorescence experiments, corex tubes (15 ml) are equipped with plastic adaptors (home-made, see Evans *et al*., 1985) to support 12-mm round coverslips. The tubes are centrifuged in an HB-4 rotor containing rubber adaptors. pGEX expression vectors are from Amersham Pharmacia Biotech.

III. PROCEDURES

A. Preparation of *X. laevis* CSF Egg Extracts

Good protocols detailing the preparation of Xenopus egg extracts and sperm nuclei have already been published (Murray, 1991). We describe here only the preparation of metaphase cytostatic factor-arrested "CSF" extracts as optimized in our laboratory for spindle assembly reactions.

Solutions

1. *Pregnant mare serum gonadotropin (PMSG)*: Dissolve in sterile water to a final concentration of 200 units/ml. Store at 4°C
2. *Human chorionic gonadotropin (HCG)*: Dissolve in sterile water to a final concentration of 2000 units/ml. Store at 4°C.
3. *MMR*: 100 m*M* NaCl, 2 m*M* KCl, 1 m*M* $MgCl_2$, 2 m*M* $CaCl_2$, 0.1 m*M* EDTA, 5 m*M* HEPES, pH 7.8. Prepare a 20X MMR stock solution. Adjust pH with NaOH, autoclave, and store at room temperature. Before use make 1X MMR from the 20X stock solution and adjust pH again if necessary.
4. *Dejellying solution*: 2% L-cysteine, pH 7.8. Prepare in water and adjust pH with NaOH. Make fresh just before use.
5. *LP*: dissolve leupeptin and pepstatin in DMSO to a final concentration of 10 mg/ml. Store in 50-µl aliquots at –20°C.
6. *Aprotinin*: Dissolve in sterile water to a final concentration of 10 mg/ml. Store in 50-µl aliquots at –20°C.
7. *Cytochalasin D*: Dissolve in DMSO to a final concentration of 10 mg/ml. Store in 50-µl aliquots at –20°C.
8. *20X XB salts*: 2 *M* KCl, 20 m*M* $MgCl_2$, 2 m*M* $CaCl_2$. Filter sterilize and store at 4°C.
9. *XB*: 1X XB salts containing 50 m*M* sucrose and 10 m*M* HEPES. Adjust pH to 7.7 with KOH. Prepare fresh before use.
10. *CSF-XB*: Prepare from XB buffer by adjusting $MgCl_2$ to 2 m*M* and adding 5 m*M* EGTA. To prepare CSF-XB with protease inhibitors (CSF-XB with PI), add LP stock solutions and aprotinin to a final concentration of 10 µg/ml.
11. *Energy Mix*: 20X stock contains 150 m*M* creatine phosphate, 20 m*M* ATP, 2 m*M* EGTA, 20 m*M* $MgCl_2$. Store in 100-µl aliquots at –20°C.

Steps

1. Inject four to six frogs subcutaneously with 0.5 ml (1000 units) PMSG each using 1-ml syringes and a 27-gauge needle at least 4 days before planning to make an extract. They should be used within 2 weeks after the priming injection. The number of frogs required depends on the quantity and quality of eggs. Five milliliters of eggs (one SW50 tube) gives approximately 1 ml of extract.

2. Sixteen to 18 h before use, inject frogs subcutaneously with 0.25–0.5 ml (500–1000 units) HCG. Place the frogs in individual boxes containing 500 ml MMR at 16°C.

3. Prepare all solutions before starting collecting the eggs: 2 liters MMR, 500 ml XB, 400 ml CSF-XB, 100 ml CSF-XB with PI, and 500 ml of dejellying solution. Rinse all glassware with distilled water (eggs stick to plastic dishes). Cut off the end of a glass pasteur pipette and fire polish it to make a wide-mouth pipette.

4. Collect laid eggs in MMR. Frogs can also be squeezed, which often gives the highest quality eggs. Keep eggs from different frogs in separate batches. Discard batches of eggs containing more than 5% of lysed, ugly, or stringy eggs.

5. Wash a few times with MMR to take away skin and other detritus and remove bad eggs. Pour off MMR and add 250 ml dejellying solution. When laid, eggs are enveloped in a transparent jelly coat and do not pack closely together. Swirl the beaker frequently and change the dejellying solution. After removal of the jelly coat, eggs pack together. This takes about 5 min. Eggs left for too long in cysteine will lyse.

6. Pour off the dejellying solution and add 500 ml MMR. Repeat the rinse one more time. After removal of the jelly coat, the eggs become fragile. They lyse easily and can activate if in contact with air. They must always remain immersed in buffer. Remove all bad-looking eggs: white and puffy, flattened, or activated ones (darker pole retracted), and those with mottled pigmentation.

7. Wash three times with 100–200 ml XB.

8. Remove as much buffer as possible, keeping all eggs immersed. Wash three times with 100–200 ml CSF-XB and finally keep eggs in CSF-XB with PI.

9. Transfer eggs using the cut glass Pasteur pipette to SW50 tubes containing 1 ml CSF-XB with PI plus 3 µl cytochalasin D (30 µg/ml). Always immerse the pipette tip in solution before expelling eggs to prevent contact with air. Transfer the SW50 tubes to 13-ml Sarstedt adaptor tubes, which contain 0.5 ml of water to prevent the tubes from collapsing.

10. Centrifuge in a clinical centrifuge at 16°C at 600 *g* for 1 minute and then immediately increase the speed to 1200 *g* for an additional 30 s. After centrifugation, remove all excess buffer from the top of the packed eggs. Removal of buffer is critical to obtain a concentrated cytoplasm.

11. Place the tubes in an HB-4 or HB-6 rotor containing rubber adaptors. Centrifuge at 10,500 rpm for 15 min at 16°C to crush the eggs.

12. Place the tubes on ice. A yellow lipid layer is at the top of the tube. Underneath is the cytoplasmic layer, then heavy membranes, and yolk particles at the bottom of the tube. Wipe the sides of the tubes with a tissue before piercing with a 18-gauge needle at the bottom of the cytoplasmic layer. Slowly and carefully aspirate the cytoplasm using a 1-ml syringe with the needle opening facing upward. Remove needle from syringe and carefully expel the cytoplasm into a 1.5-ml tube. Place on ice.

13. Add LP and aprotinin to 10 µg/ml (1:1000 dilution of stocks) and cytochalasin D to 20 µg/ml (1:500 dilution of stock). Add energy mix (1:20 dilution of stock) and mix gently.

Comments on Sperm Nucleus Preparation

Based on Gurdon (1976) and modified by Murray (1991), our only modification is to mash fragments of testes between two frosted (rough) slides before filtering through a cheesecloth mesh.

B. Preparation of DNA Beads

For preparation of DNA beads, linearized couple plasmid DNA and fill in with nucleotides so that one end contains biotinylated bases and the other thio-nucleotides to inhibit exonuclease activity and the formation of large aggregates of beads. Couple the DNA to 2.8 µm magnetic beads. Incubation in the extract will allow the association of chromatin proteins and the consequent formation of chromatin (Heald *et al*., 1996).

Solutions

1. *TE*: 10 m*M* Tris, 1 m*M* EDTA, pH 8. Adjust pH with HCl, autoclave, and store at room temperature.
2. *Washing and binding solutions*: Included with Kilobase BINDER kit.
3. *Bead buffer*: 2 *M* NaCl, 10 m*M* Tris, 1 m*M* EDTA, pH 7.6. Adjust pH with HCl and store at room temperature.
4. *Hoechst dye solution*: Dissolve bisbenzimide in water to a final concentration of 10 mg/ml. Store in the dark at 4°C.

Steps

1. Prepare plasmid DNA by Qiagen column purification. While the sequence of the DNA is not important, the plasmid should be more than 5 kb to effectively induce chromatin assembly. Cut 50 µg of the DNA with two restriction enzymes that have unique sites in the polylinker to produce one short and one long DNA fragment. One end of the long fragment should terminate in an overhang containing Gs and Cs and the other should contain only As and Ts (e.g., *Not*1, *Bam*H1). See Fig. 1.

2. Ethanol precipitate the DNA and resuspend in 25 µl TE. Quantify recovery by OD_{260} measurement.

3. Prepare fill-in reaction in 70 µl containing 1X Klenow buffer, 30 µg DNA, 50 µ*M* nucleotides (biotin-dATP, biotin-dUTP, thio-dCTP, and thio-dGTP) and 20 units Klenow. Incubate for 2 h at 37°C.

4. Remove unincorporated nucleotides, following instructions supplied with the Sephadex G-50 gel filtration column (NICK column). The DNA is eluted in a large volume (400 µl), but the recovery is better than with spin columns. Quantify recovery by OD_{260} measurement.

5. Prepare coupling mix by combining 400 µl biotinylated DNA and 400 µl binding solution. Set aside 25 µl of the coupling mix for later evaluation of coupling efficiency.

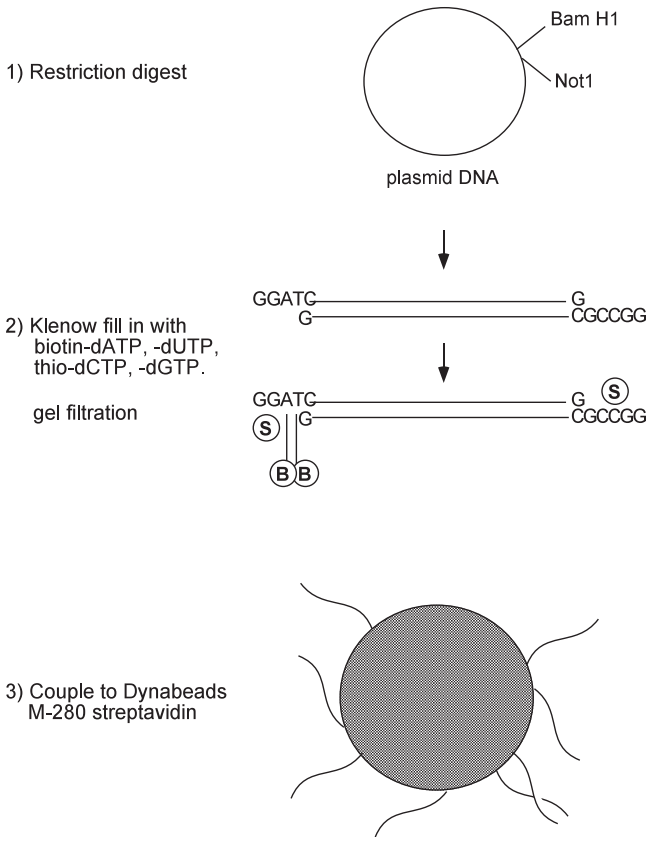

FIGURE 1 Steps in preparation of DNA beads.

6. Prepare 3µl of streptavidin-conjugated dynabeads for each microgram of DNA recovered, so 120µl for 30µg. Retrieve beads using the MPC (magnet) and wash once with 5 volumes of binding solution (600µl for 120-µl beads). Retrieve the beads and resuspend them in coupling mix containing DNA.

7. Incubate bead/coupling mixture for several hours (or overnight) on a rotating wheel at 4°C.

8. Retrieve the beads and save the supernatant. Compare the OD_{260} of the supernatant to the sample taken before coupling to determine the amount of DNA immobilized. Typically two-thirds of the DNA is coupled. Stain 1µl of beads with 5µg/ml Hoechst dye and observe them by fluorescence microcopy. The beads should appear as very bright dots with no dark patches. If the amount of DNA coupled in the first round does not seem sufficient, incubate the beads a second time with biotinylated DNA.

9. Wash beads twice with washing solution and then twice with bead buffer. After the last wash, resuspend the beads in bead buffer so that the final concentration of immobilized DNA is 1µg/5µl of beads. Store at 4°C.

C. Spindle and Aster Assembly *in vitro*

Chromatin triggers spindle assembly in CSF Xenopus egg extract. Experimentally there are two ways to induce formation of the spindle: by the addition of sperm nuclei (Desai *et al.*, 1999) or DNA beads to the extract (Heald *et al.*, 1996). To decide on which method to use it is important to understand the characteristics of the two systems. Each sperm nucleus is tightly associated to a centriole. In a very simple process, half spindles can assemble around sperm nuclei just by incubation of the sperm nuclei in extract. Over time these half spindles fuse to form bipolar spindles. If the extract is cycled through interphase the DNA replicates and each centrosome duplicates. The addition of fresh CSF extract sends the extract back into mitosis, chromosomes with their paired kinetochores condense, the duplicated centrosomes move apart, and a bipolar spindle assembles. Anaphase can be induced at this point by the addition of calcium to the system.

DNA beads are made from any kind of plasmid DNA that is long enough to induce chromatin assembly. They are unlikely to assemble kinetochores, as centromere sequences are not present. Spindle assembly around DNA beads is achieved by first assembling chromatin on the beads in an extract that is cycled through interphase. The beads are then retrieved and resuspended in fresh CSF extract. Using this method, spindles assemble in the absence of kinetochores and centrosomes. It is then ideal to study certain processes of spindle assembly that are independent of these structures.

A simplified method to study microtubule dynamics and focusing of microtubule minus ends is the assembly of asters in CSF extract. Asters can be assembled by the addition of human centrosomes purified from KE37 lymphoid cells (Bornens *et al.*, 1987), DMSO, or taxol to the extract (Wittmann *et al.*, 1998).

Solutions

1. *10X calcium solution*: 4 m*M* $CaCl_2$, 100 m*M* KCl, 1 m*M* $MgCl_2$. Store in aliquots at –20°C.
2. *4.9 M $MgCl_2$ stock solution (Sigma)*
3. *10X MMR*: See Section III,A.
4. *Hoechst dye solution*: See Section III,B.
5. *Spindle fix*: 48% glycerol, 11.1% formaldehyde, 5µg/ml Hoechst dye in 1X MMR. Always prepare fresh on day of use.
6. *BRB80*: 80 m*M* PIPES, 1 m*M* $MgCl_2$, 1 m*M* EGTA, pH 6.8. Prepare a 5X BRB80 solution. Dissolve components in sterile water and, while stirring, add KOH pellets until the PIPES dissolves. Adjust to pH 6.8 with KOH solution. Sterilize by filtration and store at 4°C.

7. *Dilution buffer*: 1X BRB80 containing 30% glycerol and 1% Triton X-100. Store at room temperature. Better preservation of the spindles can be achieved by adding 0.25% glutaraldehyde to the dilution buffer. Use a full vial of glutaraldehyde and store in aliquots at –20°C.

8. *Aster dilution buffer*: BRB80 containing 10% glycerol, 0.25% glutaraldehyde, 1 m*M* GTP, 0.1% Triton X-100. Use a fresh vial of glutaraldehyde to prepare buffer and store in aliquots at –20°C.

9. *Cushion*: 40% glycerol, BRB80. Store at 4°C.

10. *Aster cushion*: 25% glycerol, BRB80. Store at 4°C.

11. *PBS*: 137 m*M* NaCl, 2.7 m*M* KCl, 4.3 m*M* Na_2HPO_4, 1.4 KH_2PO_4 m*M*, pH 7.4. Sterilize by autoclaving and store at room temperature.

12. *Immunofluorescence buffer (IF buffer)*: PBS containing 2% BSA and 0.1% Triton X-100. Add azide and store at 4°C.

13. *Mowiol*: 10% Mowiol 4–88, 25% glycerol, and 0.1 *M* Tris, pH 8.5. To prepare, mix 6 g Mowiol with 6 g glycerol. Add 6 ml sterile water and stir for several hours at room temperature. Add 12 ml 0.2 *M* Tris, pH 8.5, and place the mixture in a heating plate at 50°C for 10 min with continues stirring. After the Mowiol dissolves, centrifuge at 5000 *g* for 15 min. Store in aliquots at –20°C.

Steps for Spindle Assembly around Sperm Nuclei (see Fig. 2)

1. Before using an extract to assemble spindles, its quality should be tested by setting up a "half spindle" reaction. Combine 20 µl CSF extract, 0.2 µl rhodamine-labelled tubulin and 0.8 µl sperm nuclei (about 75 nuclei/µl extract) in a 1.5-ml tube and mix. The extract can be mixed by gently moving the pipette in circles

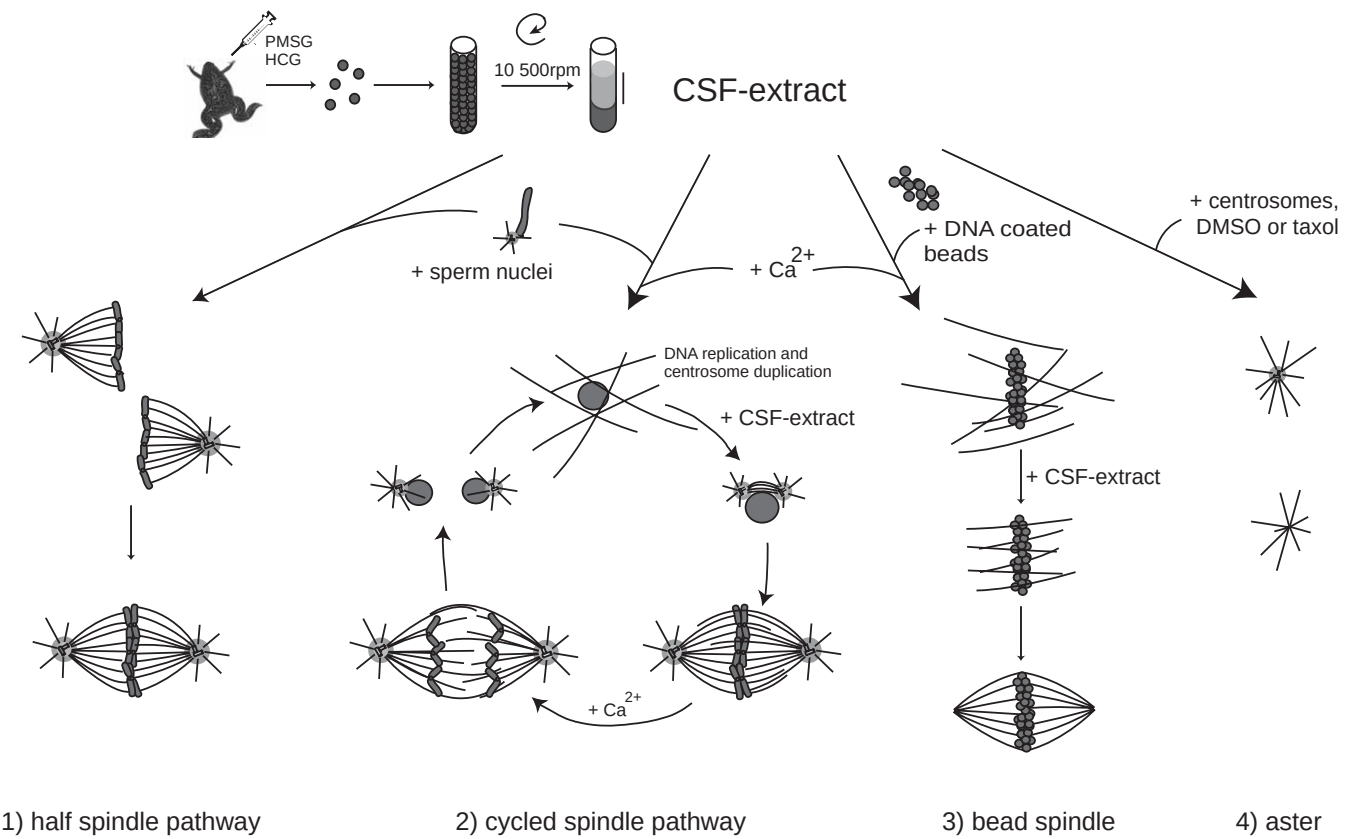

FIGURE 2 Preparation of CSF Xenopus egg extract and structures that assemble after addition of different components. (1) Addition of sperm nuclei to the CSF extract leads to the formation of half spindles that can fuse to form bipolar spindles. (2) Addition of calcium together with sperm nuclei sends the system into interphase, allowing DNA replication and centrosome duplication to occur. Addition of fresh CSF extract sends the system back to mitosis and bipolar spindles form. Calcium addition at this point induces chromosome segregation and entry into interphase. (3) Bead spindle: addition of DNA-coated beads and calcium to an extract leads to the formation of chromatin and nuclei around beads. Addition of CSF extract followed by incubation in fresh CSF extract allows the formation of bipolar spindle. (4) Asters: Addition of purified centrosomes or DMSO or taxol leads to the formation of microtubule asters with microtubule minus ends focused at the centrosome or at the center of the aster.

or by pipetting up and down, always avoiding making bubbles. Incubate the reaction mixture at 20°C and take a squash at 30–40 min. To make a squash, using a cut-off tip, transfer 1 µl of reaction mixture to a microscope slide, carefully place 5 µl of spindle fix solution on top, and gently place a 18 × 18-mm coverslip on top. Analysis of the squash by fluorescence microscopy should reveal half spindles with condensed chromosomes and occasionally also spindles. There should be no free microtubule nucleation.

2. If the extract is good, proceed with the spindle assembly protocol. For each reaction add on ice 0.2 µl rhodamine-labelled tubulin and 0.8 µl sperm nuclei to 20 µl CSF extract in a 1.5-ml tube and mix. Incubate for 10 min at 20°C and then release extract into interphase by the addition of 2 µl 10X calcium solution. Mix gently.

3. Incubate for 80 min at 20°C. Check that the extract is in interphase by taking a squash as described in step 1. If the sample is to be saved, seal the coverslip to the slide with nail polish. At this stage, nuclei should appear large, round, and uniform, and microtubules should be long and abundant.

4. At 90 min postcalcium addition, add 20 µl of fresh CSF extract containing 0.2 µl rhodamine-labelled tubulin to the reaction.

5. Incubate further at 20°C. Take squashes (step 1) at different time points to assess the stage of spindle formation. During the incubation, prepare 15 ml Corex tubes with plastic adapters, a round 12-mm coverslip, and 5 ml of cushion.

6. Forty-five to 60 min after mitosis reentry (step 4), quickly add 1 ml dilution buffer and mix by gently inverting the tube a couple of times. Carefully layer the mixture over the cushion using a cut pipette tip. Centrifuge at 16°C for 12 min at 12,000 rpm in an HB-4 or HB-6 rotor. Aspirate supernatant and cushion before removing the coverslip. Fix coverslips in –20°C methanol for 5 minutes. Rehydrate samples by placing the coverslips in PBS. If dilution buffer contains glutaraldehyde, incubate the coverslips twice for 10 min in 0.1% $NaHB_4$ in PBS and wash with PBS.

7. To perform immunofluorescence, place the coverslip face up on a surface covered with parafilm. Incubate the coverslips with primary antibodies diluted in IF buffer for 20–30 min. Wash the coverslips two times for 5 min with PBS and incubate with IF buffer containing the secondary antibody and 5 µg/ml Hoechst for 20–30 min. Wash three times for 5 min with PBS and carefully place the coverslips upside down on a 3- to 4-µl drop of Mowiol on a microscope slide, avoiding air bubbles. Prior to observation, allow the Mowiol to set for 15 min at 37°C or at room temperature for several hours.

8. To visualize the early steps of anaphase, add 4 µl 10X calcium solution to the metaphase spindles before step 6. Take samples before calcium addition and every 5 min after calcium addition for 20–30 min and process them as described earlier. It is not always possible to visualize separation of the sister chromatids and only high-quality extracts can be used successfully to study anaphase.

Steps for Spindle Assembly around Chromatin Beads (see Fig. 2)

1. Transfer 3 µl of DNA beads (about 0.5 µg DNA) to a 0.5-ml Eppendorf tube and place on a magnet. Remove supernatant, and wash beads by resuspending them in 20 µl of extract.

2. Retrieve beads and resuspend in 100 µl CSF extract. Transfer to a 1.5-ml Eppendorf tube and incubate at 20°C.

3. After 10 min, release the CSF extract into interphase by adding 10 µl of calcium solution. Incubate for 2 h at 20°C.

4. Return the extract containing the beads to mitosis by adding 50 µl of fresh CSF extract. Incubate for 30 more min at 20°C. The procedure can be continued or stopped at this point by freezing the beads in the extract using liquid ethane and storing them in liquid nitrogen.

5. Incubate the bead mixture on ice for several minutes. Retrieve the beads on ice over 10–15 minutes. Due to the viscosity of the extract, bead retrieval is slow. Pipette the mixture every several minutes, keeping the tube on the magnet.

6. Remove the supernatant and resuspend the beads in 150 µl of fresh CSF extract containing 1.5 µl rhodamine-labelled tubulin.

7. Incubate at 20°C. Monitor the spindle assembly by taking 1-µl samples and squashing with fixative as described earlier. Spindle assembly requires between 30 and 90 min, depending on the extract. For immunofluorescence studies, spin the bead spindles through a cushion onto a coverslip and perform immunofluorescence as described previously for spindle assembled around sperm nuclei.

Steps for Aster Formation (see Fig. 2)

1. For each reaction, add on ice 0.2 µl rhodamine-labelled tubulin to 20 µl CSF extract in a 1.5-ml tube. To assemble asters, add either purified human centrosomes (Bornens *et al.*, 1987) or 5% DMSO or 1 µ*M* taxol.

2. Incubate the reaction for 30–60 min in a 20°C water bath. During this incubation, prepare as before 15-ml Corex tubes with plastic adapters, round 12-mm coverslip, and 5 ml aster cushion.

3. At the end of the incubation time, dilute the reactions with aster dilution buffer and carefully layer them on top of the cushion using a pipette with a cut tip and subsequently centrifuge onto the coverslips in a HB4 or HB6 rotor at 12,000 rpm for 12 min at 16°C.

4. As before, remove the cushion with a vacuum pump and postfix the coverslips in –20°C methanol for 5 min. To quench the glutaraldehyde, incubate twice for 10 min in 0.1% $NaHB_4$ in PBS and process for immunofluorescence.

D. Functional Studies of Proteins Involved in Spindle Assembly

The Xenopus egg extract system is a powerful tool to assess the involvement of individual proteins in the process of spindle assembly. Different methods have been developed to address specific questions.

Localization studies can be performed by classical immunofluorescence methods or by direct visualization of GFP-tagged proteins added to the reaction mixture or by a combination of both by adding GST-tagged proteins followed by immunofluorescence with anti-GST antibodies.

Functional studies can be performed by adding dominant-negative constructs to the reaction mixture or by depleting the protein or antibodies under study from the extracts before use (Antonio *et al.*, 200••; Boleti *et al.*, 1996). Depletion experiments should be complemented by "add back" or rescue experiments in which a recombinant protein is added to the depleted extracts (Fig. 3). In all tree cases, a careful quantification of the structures found in control or treated samples has to be performed.

Solutions

1. *CSF-XB with PI*: See Section III,A.
2. *PBS-TX*: PBS containing 0.1% Triton X-100. Store at 4°C.

Steps for Immunodepletion

1. Usually around 10 µg of specific antibody is needed to deplete 150 µl of extract. The amount of antibody has to be adjusted for each case depending on the antibody itself and on the abundance of the protein in the extract. Prepare a control mock-depleted extract using the same amount of unspecific purified IgG.

2. Transfer 40 µl of Dynal beads coupled to protein A to a 1.5-ml tube and retrieve them using a magnet. Wash them twice by resuspending the beads in 500 µl PBS-TX and retrieving them with the magnet.

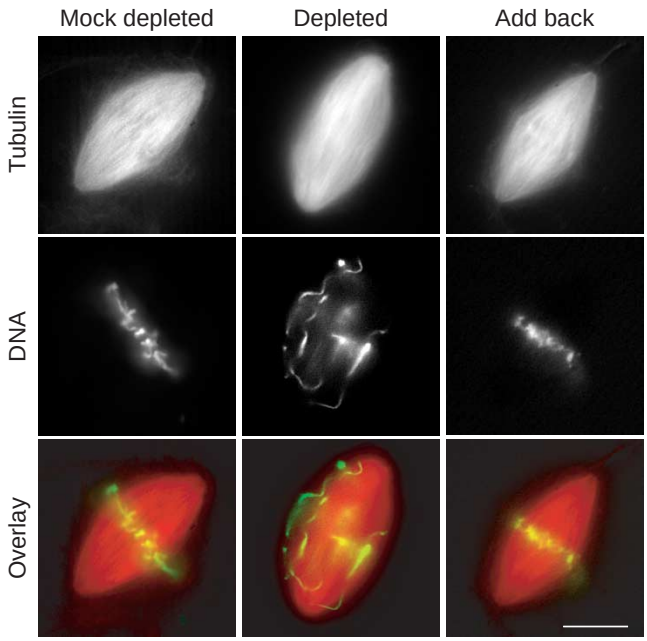

FIGURE 3 Spindles assembled in CSF Xenopus egg extract following the cycled spindle pathway. The extract was mock depleted, Xkid depleted, or Xkid depleted supplemented with recombinant Xkid protein (add back). When Xkid was depleted, mitotic chromosomes failed to align at the metaphase plate. Alignment of chromosomes was rescued by the addition of recombinant protein to the extract. Scale bar: 10 µm.

3. Incubate the beads with 10 µg of antibody diluted in 200 µl of PBS-TX for 1 h on a rotating wheel at 4°C

4. Wash twice as just described with PBS-TX and once with CSF-XB containing PI. Remove as much wash buffer as possible and carefully resuspend the beads in 150 µl of extract by pipetting up and down. Keep the extract (containing the beads) on ice for 90 min with occasional mixing by pipetting up and down.

5. Retrieve the beads by placing the tube on the magnet for 5 min on ice. Collect the extract into a new tube and keep it on ice. To remove the beads more efficiently, repeat this procedure once more. Check the efficiency of depletion by Western blot analysis of mock and protein-depleted extracts. To visualize the immunoprecipitated protein, wash the beads once with CSF-XB containing PI and three times with PBS-TX. Resuspend the beads in Laemmli sample buffer and incubate at room temperature for 5 min. Retrieve the beads on a magnet and boil the supernatant before loading on SDS–PAGE.

6. An important control to include in depletion experiments is the add back of the purified recombinant protein to the depleted extract in a range of concentrations close to that of the endogenous protein. In case the protein is degraded during interphase, the

recombinant protein should be added only at mitosis reentry.

7. The depleted, the control mock depleted, and add-back extracts can now be used in parallel to assemble asters and spindles following the methods described in Section III,C.

6. Compare the spindles or asters formed in each reaction either by taking samples and squashing them in a slide with fixative solution or by centrifuging them onto coverslips and performing immunofluorescence.

Steps for Specific Antibodies or Dominant-Negative Protein Addition

1. In the case of addition of specific antibodies, prepare a concentrated solution (at least 2 mg/ml) of an affinity-purified polyclonal or monoclonal antibody in PBS or CSF-XB. It is a good idea to try different concentrations of antibody (ranging from 200 to 400 µg/ml). For dominant-negative addition, prepare constructs expressing different fragments of the protein under study fused to GFP or GST. Purify the fusion proteins and dialyze them extensively against CSF-XB.

2. Add the antibodies or dominant-negative protein to the extract in a volume corresponding to one-tenth of the total volume and follow the protocol for spindle assembly or aster formation as described in Section III,C. The antibodies or dominant negative can be added at the beginning of the spindle assembly procedure or at mitosis reentry.

3. When adding antibodies, two control samples should be run in parallel: one containing a similar amount of a control antibody and another containing the same volume of buffer. In the case of dominant-negative addition, include also the same volume of buffer as control and a sample containing GST or GFP protein.

4. Samples taken at different time points are fixed and analyzed as before. To examine the localization of the antibody, process the samples by immunofluorescence using a fluorochrome-conjugated secondary antibody. Localization of the dominant negative can be observed directly if the tag is GFP or by using an anti-GST antibody.

IV. PITFALLS

The biggest pitfall in studying spindle assembly with this system is the problem of reproducibility in Xenopus egg extracts. To obtain good eggs, the frog colony must be healthy and well cared for. This requires a substantial commitment on the part of the laboratory. Even with healthy frogs, there is seasonal variation in the quality of eggs, with summer being the off season. Furthermore, even experienced extract makers do not manage to prepare functional extracts every time, which can be frustrating. Therefore, experiments must be repeated several times to ensure a valid interpretation.

References

Antonio, C., Ferby, I., Wilhelm, H., Jones, M., Karsenti, E., Nebreda, A. R., and Vernos, I. (2000). Xkid, a chromokinesin required for chromosome alignment on the metaphase plate. *Cell* **102**(4), 425–435.

Boleti, H., Karsenti, E., and Vernos, I. (1996). Xklp2, a novel Xenopus centrosomal kinesin-like protein required for centrosome separation during mitosis. *Cell* **84**, 49–59.

Bornens, M., Paintrand, M., Berges, J., Marty, M. C., and Karsenti, E. (1987). Structural and chemical characterization of isolated centrosomes. *Cell Motil. Cytoskel.* **8**(3), 238–249.

Desai, A., Maddox, P. S., Mitchison, T. J., and Salmon, E. D. (1998). Anaphase A chromosome movement and poleward spindle microtubule flux occur at similar rates in Xenopus extract spindles. *J. Cell Biol.* **141**(3), 703–713.

Desai, A., Murray, A., Mitchison, T. J., and Walczak, C. E. (1999). The use of Xenopus egg extracts to study mitotic spindle assembly and function *in vitro*. *Methods Cell Biol.* **61**, 385–412.

Evans, L., Mitchison, T. J., and Kirschner, M. W. (1985). Influence of the centrosome on the structure of nucleated microtubules. *J. Cell Biol.* **100**, 1185–1191.

Gurdon, J. B. (1976). Injected nuclei in frog oocytes: Fate, enlargement, and chromatin dispersal. *J. Embryol. Exp. Morphol.* **36**, 523–540.

Heald, R., Tournebize, R., Blank, T., Sandaltzopoulos, R., Becker, P., Hyman, A., and Karsenti, E. (1996). Self organization of microtubules into bipolar spindles around artificial chromosomes in Xenopus egg extracts. *Nature* **382**, 420–425.

Hyman, A., Drechsel, D., Kellogg, D., Salser, S., Sawin, K., Steffen, P., Wordeman, L., and Mitchison, T. (1991). Preparation of modified tubulins. *Methods Enzymol.* **196**, 478–485.

Kalab, P., Weis, K., and Heald, R. (2002). Visualization of a Ran-GTP gradient in interphase and mitotic Xenopus egg extracts. *Science* **295**(5564), 2452–2456.

Lohka, M., and Maller, J. (1985). Induction of nuclear envelope breakdown, chromosome condensation, and spindle formation in cell-free extracts. *J. Cell Biol.* **101**, 518–523.

Murray, A. (1991). Cell cycle extracts. *In* "*Methods in Cell Biology*" (B. K. Kay, H. B. Peng, eds.), vol. 36, pp. 581–605. Academic Press, San Diego.

Murray, A. W., and Kirschner, M. W. (1989). Cyclin synthesis drives the early embryonic cell cycle. *Nature* **339**, 275–280.

Sawin, K. E., and Mitchison, T. J. (1991). Mitotic spindle assembly by two different pathways *in vitro*. *J. Cell Biol.* **112**, 925–940.

Shamu, C. E., and Murray, A. W. (1992). Sister chromatid separation in frog egg extracts requires DNA topoisomerase II activity during anaphase. *J. Cell Biol.* **117**, 921–934.

Wittmann, T., Boleti, H., Antony, C., Karsenti, E., and Vernos, I. (1998). Localization of the kinesin-like protein Xklp2 to spindle poles requires a leucine zipper, a microtubule-associated protein, and dynein. *J. Cell Biol.* **143**(3), 673–685.

CHAPTER

49

In vitro Motility Assays with Actin

James R. Sellers

I. INTRODUCTION

The interaction between actin and myosin has been studied for years using a variety of techniques, including ultracentrifugation, light scattering, chemical cross-linking, fluorescence, and measurement of the effect of actin on the MgATPase activity of myosin. The sliding actin *in vitro* motility assay constitutes a relatively recent technique for studying actin–myosin interaction. This assay, developed by Kron and Spudich (1986), takes advantage of the ability to image rhodamine–phalloidin-labeled actin filaments by fluorescence microscopy as they interact with and are translocated by myosin bound to a coverslip surface. The sliding actin *in vitro* motility assay is among the most elegant biochemical assays, reproducing the most fundamental property of a muscle, the ability of myosin to translocate actin using only the two highly purified proteins. It is a close *in vitro* correlate of the maximum unloaded shortening velocity of muscle fibers (Homsher *et al.*, 1992). As shown here, it is simple to set up, reproducible, quantitative, and utilizes as little as 1 µg of myosin per assay. The assay is now used routinely in a large number of laboratories studying myosin and actin biochemistry. Although originally developed for studying the conventional class II myosin, it can be adapted to study unconventional myosins also.

This article discusses the design of the assay, describes the equipment required for its setup, and deals with methods for quantification and presentation of the results. Because different myosins exhibit a range of actin translocation speeds from 0.02 to 60 µm/s (Sellers, 1999), it will be necessary to discuss modification of the experimental setup for fast and slow myosins. Also, differences between low- and high-duty cycle myosins are discussed. We will describe the instrumentation that we use in our system and elaborate on other options where applicable.

II. MATERIALS AND INSTRUMENTATION

The following reagents are from Sigma Chemical Company (www.sigmaaldrich.com): MOPS (Cat. No. M-5162), EGTA (Cat. No. E-4378), ATP (Cat. No. A-5394), glucose (Cat. No. G-7528), glucose oxidase (Cat. No. G-6891), catalase (Cat. No. C-3155), and methylcellulose (Cat. No. M-0512). Rhodamine–phalloidin (Cat. No. R415) is from Molecular Probes, Inc. (www.probes.com). Nitrocellulose (superclean grade, Cat. No. 11180) is from Ernest F. Fullam, Inc. (www.fullam.com). Bovine serum albumin (BSA, Cat. No. 160069) and dithiothreitol (DTT, Cat. No. 856126) are from ICN (www.icnbiomed.com). The following items are from Thomas Scientific (www.thomassci.com): microscope slides (Cat. No. 6684-H30) and microscope 18-mm^2 No. 1 thickness coverslips (Cat. No. 6667-F24). Double sticky cellophane tape (Scotch Brand) and Sony sVHS videotapes (ST120) are from local suppliers.

The following instrumentation is used in our laboratory for the following procedures. Zeiss Axioplan microscope and objectives (www.zeiss.com), Air Therm Heater (www.wpiinc.com), intensified CCD camera from Videoscope, International (www.videoscopeintl.com), TR black-and-white videomonitor and sVHS videotape recorder (Model AG7350) from Panasonic (www.panasonic.com), Argus 10 image

Copyright 2006, Elsevier Science (USA).
All rights reserved.

processor from Hamamatsu Photonics (www.hamamatsu.com), and VP110 digitizer from Motion Analysis (www.motionanalysis.com).

III. PROCEDURES

A. Construction of Flow Cells

Steps

1. Prepare nitrocellulose-coated coverslips by first placing 3 µl of a 1% solution of nitrocellulose in isoamylacetate directly on a No. 1 thickness 18-mm^2 coverslip and spreading with the broad side of the micropipette tip. Dry the coverslip to create the film and use within 1 day. Some investigators use silicon coating of the coverslips (Fraser and Marston, 1995)
2. Place two 5 × 25-mm strips of double sticky Scotch cellophane tape about 10 mm apart on a 25 × 75-mm glass microscope slide. Place a nitrocellulose-coated coverslip with the coated side down onto the tracks. Press gently to create a tight seal.

B. Preparation of Rhodamine–Phalloidin-Labeled Actin

1. Place 60 µl of 3.3 µ*M* rhodamine–phalloidin (in methanol) into an Eppendorf tube and dry using a Speed-Vac concentrator.
2. Redissolve the rhodamine–phalloidin powder in 3–5 µl of methanol.
3. Add 85 µl of 20 m*M* KCl, 20 m*M* MOPS (pH 7.4), 5 m*M* $MgCl_2$, 0.1 m*M* EGTA, and 10 m*M* DTT (buffer A). To make 100 ml of buffer A, add 1 ml of 2 *M* KCl, 1 ml of 2 *M* MOPS (pH 7.4), 0.5 ml of 1 *M* $MgCl_2$, 0.02 ml of 0.5 *M* EGTA, and 154 mg DTT. Bring to 100 ml with H_2O and adjust pH to 7.4.
4. Add 10 µl of a freshly diluted 20 µ*M* F-actin solution (in buffer A) and incubate for an hour on ice. The rhodamine–phalloidin actin can routinely be used as is at this stage.
5. If a lower background fluoresence is desired, centrifuge for 15 min at 435,000 *g* in a TL-100 ultracentrifuge (Beckman Instruments), remove the supernatant, and gently resuspend the pink rhodamine–phalloidin-labeled actin pellet in buffer A using a pipettor tip that has been cut to widen the bore size.
6. The rhodamine–phalloidin-labeled actin solution is stable for several weeks.

C. Preparation of Sample for Motility Assay

Solutions

1. *Wash solution:* 50 m*M* KCl, 20 m*M* MOPS (pH 7.4), 5 m*M* $MgCl_2$, 0.1 m*M* EGTA, and 5 m*M* DTT; to make 100 ml, add 2.5 ml of 2 *M* KCl, 1 ml of 2 *M* MOPS, (pH 7.4), 0.5 ml of 1 *M* $MgCl_2$, 0.02 ml of 0.5 *M* EGTA, and 77 mg of DTT. Bring volume to 100 ml with H_2O and pH to 7.4.
2. *Blocking solution:* 1 mg/ml BSA in 0.5 *M* NaCl, 20 m*M* MOPS (pH 7.0), 0.1 m*M* EGTA, and 1 m*M* DTT solution. To make 100 ml of blocking solution, add 10 ml of 5 *M* NaCl, 1 ml of 2 *M* MOPS (pH 7.4), 0.02 ml of 0.5 *M* EGTA, 15.4 mg of DTT, and 100 mg of BSA. Bring to 100 ml with H_2O and pH to 7.0.
3. *Rhodamine–phalloidin-labeled actin solution:* 20 n*M* rhodamine–phalloidin-labeled actin. To make 1 ml, take 10 µl of 2 µ*M* rhodamine–phalloidin-labeled actin, 10 µl of 500 m*M* DTT, and 980 µl of wash solution.
4. *ATP–actin wash:* 1 m*M* ATP and 5 µ*M* F-actin (unlabeled) in wash solution. To make 1 ml, add 10 µl of 0.1 *M* ATP and 50 µl of 100 µ*M* F-actin to 940 µl of wash solution.
5. *4X stock solution:* 80 m*M* MOPS (pH 7.4), 20 m*M* $MgCl_2$, and 0.4 m*M* EGTA. To make 100 ml, add 4 ml of 2 *M* MOPS (pH 7.4), 2 ml of 1 *M* $MgCl_2$, and 0.08 ml of 0.5 *M* EGTA. Bring volume to 100 ml with H_2O and pH to 7.4.
6. *1.4% methycellulose solution:* Dissolve 1.4 g of methylcellulose in a final volume of 100 ml of H_2O by stirring overnight. Occasionally it is necessary to homogenize the solution with a glass–Teflon homogenizer to aid in solubilization. Dialyze the dissoved methylcellulose against 4 liters of H_2O overnight. Divide into 10-ml aliquots and freeze at –20°C.
7. *Motility buffer:* 50 m*M* KCl, 20 m*M* MOPS (pH 7.4), 5 m*M* MgCl2, 0.1 m*M* EGTA, 1 m*M* ATP, 50 m*M* DTT, 2.5 mg/ml glucose, 0.1 mg/ml glucose oxidase, and 0.02 mg/ml catalase. To make 1 ml, add 250 µl of 4X stock solution, 10 µl of 0.1 *M* ATP, 25 µl of 2 *M* KCl, 100 µl of 0.5 *M* DTT (prepare fresh each day by adding 77 mg DTT to 1 ml of H_2O), 20 µl of 125 mg/ml glucose, 20 µl of 5 mg/mol glucose oxidase, 1 µl of 20 mg/ml catalase, and 573 µl of H_2O. If methylcellulose is to be used in the motility buffer (see later), then add 500 µl of 1.4% methylcellulose and 73 µl of H_20.

Steps

1. Apply 0.2 mg/ml myosin in 0.5 *M* NaCl, 20 m*M* MOPS (pH 7.0), 0.1 m*M* EGTA, and 1 m*M* DTT to fill the flow chamber. Wait 1 min.
2. Wash with 75 µl of blocking buffer. Wait 1 min.

3. Wash with 75 µl of wash solution, followed by 75 µl of ATP–actin wash solution. Wait 1 min. This step is optional.
4. Wash with 75 µl of wash solution, followed by 75 µl of rhodamine–phalloidin-labeled actin solution. Wait 1 min.
5. Initiate reaction by the addition of 75 µl of motility buffer.
6. Place slide on microscope stage and image.

Comments

In the protocol just described, myosin is bound to the surface as monomers. If myosin is to be bound as filaments, it is necessary to block with BSA that is in a low ionic strength solution, such as the wash solution. Alternatively, heavy meromyosin or a soluble unconventional myosin can be applied to the flow chamber at either low or high ionic strength. In some cases, myosin or HMM can be attached to the surface via specific antibodies against their carboxyl-terminal sequence (Winkelmann *et al*., 1995; Cuda *et al*., 1993; Reck-Peterson *et al*., 2001), which may also serve the purpose of further purifying the desired isoform of myosin. If actin filaments are binding poorly to the surface, the motility buffer can be augmented with 0.7% methylcellulose (modify motility buffer preparation to add 0.5 ml of 1.4% methylcellulose and add less water to bring the final volume to 1 ml. Note that this solution is very viscous and must be mixed well).

Although each myosin has its own characteristic velocity, the velocity of a given myosin can vary with ionic and assay conditions. In general the velocity tends to increase as the ionic strength is raised from 20 to 100 m*M* and increases with temperature. At higher ionic strengths the actin filaments typically begin to become weakly associated with the myosin-coated surface and move erratically. The velocity of actin filament translocation by some myosins, such as vertebrate smooth muscle myosin and *Limulus*-striated muscle myosin, is increased markedly (two to four times) by the inclusion of 200 n*M* tropomyosin in the motility buffer (Wang *et al*., 1993; Umemoto and Sellers, 1990). However, tropomyosin inhibits the movement of brush border myosin I (Collins *et al*., 1990).

Step 3 is optional. It is often included to improve the "quality" of movement by binding unlabeled actin to noncycling myosin heads that would otherwise bind and tether the labeled actin added subsequently. This step can be omitted if the myosin is capable of moving actin filaments smoothly. For myosin V, better quality movement can be obtained by first blocking the surface with 0.1–1.0 mg/ml of BSA before adding the myosin.

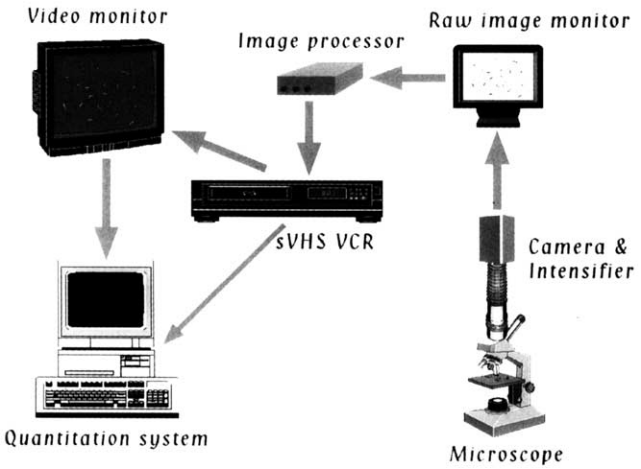

FIGURE 1 Schematic diagram of equipment setup.

D. Recording and Quantifying Data Steps and Equipment

A schematic diagram of the equipment setup is shown in Fig. 1. The following describes the equipment used in our laboratory. There is a wide selection of video microscopy equipment represented by many manufacturers.

1. Place the microscope slide under a 100X, 1.4 NA Plan-Neofluor objective in an Axioplan microscope (both from Carl Zeiss, Germany) equipped for epifluorescence. Other microscopes, including ones with an inverted format, are also suitable and a variety of objectives can be used, but note that high numerical apertures are required for maximal brightness. Illumination is via a 100-W mercury lamp. An IR filter should be placed between the source and the sample to attenuate heat; neutral density filters are useful to attenuate light intensity if needed. A filter set designed for rhodamine fluorescence measurements should be utilized in the filter cube. For quantitative work it is necessary to control the temperature of the assay. This can be accomplished in several ways. The most inexpensive way is to create an air curtain using a hair dryer. Other methods include fabricating a water jacket for the objective and to use a circulating water bath to regulate temperature or creating an environmental box heated with an Airtherm heater (World Precision Instruments). In our experience, commercial stage heaters are not sufficient as oil immersion objectives act as large heat sinks.

2. Image actin filaments using an ICCD 350F intensified CDD camera (Videoscope International). Other low-light systems are possible, such as an SIT camera or intensified SIT camera. Several

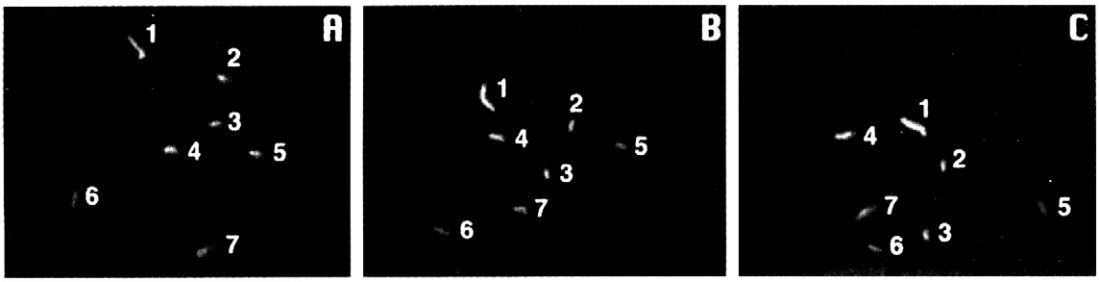

FIGURE 2 One-second intervals of actin filaments moving over a myosin-coated surface.

manufacturers sell this equipment. These camera systems produce an analog output that can be viewed on a standard black-and-white video monitor (TR Panasonic) and recorded on an AG7350 sVHS recorder (Panasonic). It is also possible to collect data digitally using a cooled CCD camera linked to a computer.

3. It is useful to process the raw image using an image processor such as the Argus 10 or Argus 20 (Hamamatsu Photonics) to perform frame averaging and/or background subtraction. There are several commercial software packages that can do this also. Display the processed image on another video monitor.

4. Determine the movement of individual actin filaments using an automated tracking system equipped with a VP110 digitizer from Motion Analysis. Many investigators have created there own software routines to track actin filaments in a semiautomated manner.

Comments

Given the range of motility rates of different myosins, there is no standard number of frames to average in order to get a good image. If the myosin is moving at 5 μm/s, a 2 or 4 frame average is used along with high illumination levels that can be tolerated because of the short exposure time needed to define a filament path. With slow myosins that may move at rates of less than 0.1 μm/s, it is possible to average 64 frames and to reduce the light intensity so that longer recording periods are possible.

The quantification of the rate of actin filament sliding is perhaps the most difficult part of the motility assay. The method just described requires a fairly expensive apparatus that is accurate, very fast, and can give unbiased results (for an extensive discussion of quantification of data, see Homsher *et al.*, 1992). The user inputs the desired sampling rate and sampling time to collect data from either the live image or a prerecorded image. The computer determines the centroid position of each actin filament in each frame, connects the centroids to form paths, calculates the incremental velocity between each successive data point in a path, and, finally, calculates a mean ± SD for each filament path. This process takes only seconds for a field of 25–30 actin filaments. Several investigators use commercial frame grabbers and write their own software for semiautomated tracking of actin filaments (Work and Warshaw, 1992; Marston *et al.*, 1996). There is at least one free downloadable source of semiautomatic tracking software available (http://mc11.mcri.ac.uk/retrac/).

E. Presentation of Data

Figure 2 shows three frames taken at 1-s intervals of actin filaments moving over a myosin-coated surface as it would appear on the video monitor. Data from such an experiment are presented most commonly as the mean ± SD of the velocity of the population of actin filaments. In general, the SD is typically 10–20% of the mean. There are two cases where merely reporting this number does not always accurately describe what is occurring in the assay. One such case is when something (perhaps a regulatory protein) is affecting the number of filaments that are moving. If, in the absence of the regulatory protein, >95% of the actin filaments are moving at 1 μm/s whereas only 5% of the filaments move at any velocity in the presence of the regulatory protein, reporting only the mean value for the velocity in each case does not reflect the difference that is observed in the assay between the two conditions. A better method for data display for this example is to display all data in the form of a histogram so that one can see that most of the actin filaments are not moving in the presence of the regulatory protein. This display also allows the reader to see whether the regulatory protein affects the speed of movement of the few actin filaments that remain moving. The other case where more complex data display is necessary is if the filaments are moving erratically. Here the mean velocity will underestimate the "instantaneous" velocity and will have a considerably larger standard deviation than that of smoothly moving filaments. One way to display these data graphically is to show a path plot

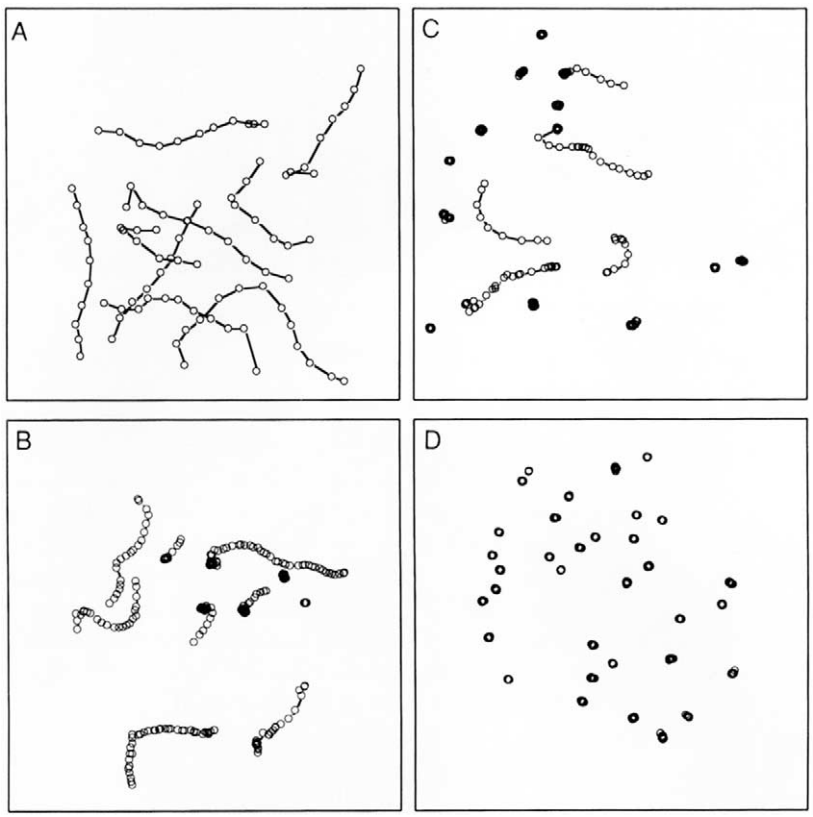

FIGURE 3 Actin filaments plotted in two-dimensional space as a function of time. A) smoothly moving actin filaments; B) actin filaments moving more erratically; C) a mixture of moving and nonmoving actin filaments; D) nonmoving actin filaments.

in which the centroid position of the moving actin filaments is plotted in two-dimensional space as a function of time (Fig. 3).

IV. PITFALLS

1. Actin filaments are moving erratically or only a fraction of the actin filaments are moving. The cause of this phenomena is usually noncycling heads in the preparation. Using the actin–ATP wash solution described in Section III,C,3 usually helps or eliminates the problem, but if erratic motility persists, do the following. Bring the myosin solution to 0.5 *M* in NaCl and add actin to a final concentration of 10 μM, ATP to 2 m*M*, and $MgCl_2$ to 5 m*M*. Immediately sediment at 435,000 *g* for 15 mn in a Beckman TL-100 ultracentrifuge. Remove the supernatant and use it for the motility assay.

2. Actin filaments shear quickly into small dots. Several things can contribute to this phenomenon. Poor-quality myosin containing a significant number of noncycling heads might be a problem. See Pitfall 1 for advice on how to remove these. Decreasing the density of myosin heads on the surface and/or increasing the ionic strength of the assay solution also sometimes helps, as does decreasing the light intensity. In general, myosin bound to the surface as monomers tend to shear less than myosin bound as filaments.

3. Actin filaments appear wobbly when they move or are moving in a back and forward type manner. If the assay does not contain methylcellulose, any portion of the actin filament that is not bound along its length by myosin will experience Brownian motion and appear very wobbly. Even though these filaments may be moving, their movement will be erratic and difficult to quantify. Increasing the density of myosin on the surface, decreasing the ionic strength of the assay, or using methylcellulose in the assay buffer usually helps. The back and forward motion of the actin filaments seen in the presence of methylcellulose is merely Brownian motion in the presence of the viscous solution where the actin filament is restricted to move mostly along its long axis. If the actin filament is not bound it will move back and forward. Increasing the density of myosin or decreasing the ionic strength of the solution should help.

4. Actin filaments photobleach rapidly. Decrease the light intensity if possible and use image processing

to do frame averaging to improve the signal-to-noise ratio. Degas the solutions. Make sure the glucose, glucose oxidase, and catalase components of the motility buffer are good. The presence of 50 m*M* DTT also aids in preventing photobleaching.

5. Actin filaments leave comet tail-like images as they move. If you are frame averaging, merely decrease the number of frames averaged. If not, the problem is likely to be encountered when the actin filaments are moving fast and a non-CCD type camera is used. The streaking or persistence in this case is related to the fact that the tube cameras effectively average about four frames in producing their image. The persistence can be attenuated by increasing the light level or by switching to a lower magnification objective.

Acknowledgments

I thank Qian Xu and Takeshi Sakamoto for critical reading of the manuscript.

References

Collins, K., Sellers, J. R., and Matsudaira, P. (1990). Calmodulin dissociation regulates brush border myosin I (110-kD-calmodulin) mechanochemical activity *in vitro*. *J. Cell Biol.* **110**, 1137–1147.

Cuda, G., Fananapazir, L., Zhu, W.-S., Sellers, J. R., and Epstein, N. D. (1993). Skeletal muscle expression and abnormal function of β-myosin in hypertrophic cardiomyopathy. *J. Clin. Invest.* **91**, 2861–2865.

Fraser, I. D. C., and Marston, S. B. (1995). *In vitro* motility analysis of smooth muscle caldesmon control of actin-tropomyosin filament movement. *J. Biol. Chem.* **270**, 19688–19693.

Homsher, E., Wang, F., and Sellers, J. R. (1992). Factors affecting movement of F-actin filaments propelled by skeletal muscle heavy meromyosin. *Am. J. Physiol. Cell Physiol.* **262**, C714–C723.

Kron, S. J., and Spudich, J. A. (1986). Fluorescent actin filaments move on myosin fixed to a glass surface. *Proc. Natl. Acad. Sci. USA* **83**, 6272–6276.

Marston, S. B., Fraser, I. D. C., Bing, W., and Roper, G. (1996). A simple method for automatic tracking of actin filaments in the motility assay. *J. Musc. Res. Cell Motil.* **17**, 497–506.

Reck-Peterson, S. L., Tyska, M. J., Novick, P. J., and Mooseker, M. S. (2001). The yeast class V myosins, Myo2p and Myo4p, are nonprocessive actin- based motors. *J. Cell Biol.* **153**, 1121–1126.

Sellers, J. R. (1999). "Myosins." Oxford Univ. Press, Oxford.

Umemoto, S., and Sellers, J. R. (1990). Characterization of *in vitro* motility assays using smooth muscle and cytoplasmic myosins. *J. Biol. Chem.* **265**, 14864–14869.

Wang, F., Martin, B. M., and Sellers, J. R. (1993). Regulation of actomyosin interactions in *Limulus* muscle proteins. *J. Biol. Chem.* **268**, 3776–3780.

Winkelmann, D. A., Bourdieu, L., Kinose, F., and Libchaber, A. (1995). Motility assays using myosin attached to surfaces through specific binding to monoclonal antibodies. *Biophys. J.* **68**(*Suppl.*), 72S.

Work, S. S., and Warshaw, D. M. (1992). Computer-assisted tracking of actin filament motility. *Anal. Biochem.* **202**, 275–285.

CHAPTER

50

Use of Brain Cytosolic Extracts for Studying Actin-Based Motility of *Listeria monocytogenes*

Antonio S. Sechi

I. INTRODUCTION

Cell motility is essential for numerous biological events. Unicellular organisms, for instance, use directed movement to find and ingest food. In multicellular organisms, cell motility is required for the morphogenetic movements that accompany embryogenesis, fibroblast migration during wound healing, and the chemotactic movement of immune cells during an immune response. Cell motility is characterised by the formation of cellular extensions that, depending on their morphology and cellular context, are called lamellipodia, ruffles, or filopodia. In recent decades many cell biological, biochemical, and biophysical studies have established that the formation of these structures depends on the activity of the actin cytoskeleton and its associated proteins. More specifically, the assembly of a network of actin filaments at the leading edge of motile cells provides the propulsive force for the extension of these structures (see Small *et al*., 2002). Despite much effort, however, the complexity of cell motility has precluded the detailed analysis of the molecular mechanisms and components that govern this process.

Since the mid-1980s, much work focused on the intracellular actin-based motility of the gram-positive bacterium *Listeria monocytogenes*. *Listeria* can induce its own uptake by phagocytic and nonphagocytic cells and, once free in the cytoplasm, recruits host cell cytoskeletal components, which are then rearranged into phase-dense actin tails. The assembly of actin monomers at the actin filament (+) ends abutting the bacterial surface provides the propulsive force that allows *Listeria* to move within the infected cells and spread to adjacent cells while avoiding exposure to the host's humoral immune system. As these bacteria imitate the protrusive behaviour of lamellipodial edges, *Listeria* motility is considered a simplified model system for actin filament dynamics during cell motility (Cossart and Bierne, 2001; Frischknecht and Way, 2001). As one approach towards defining the molecular basis of bacterial motility, we and others have developed simple *in vitro* systems that support actin-based *Listeria* motility based on *Xenopus*, platelets, and mouse brain extracts (Theriot *et al*., 1994; Marchand *et al*., 1995; Laurent and Carlier, 1998; Laurent *et al*., 1999; May *et al*., 1999). These cell-free systems in combination with bacterial genetics and cell biological studies have been essential for the characterisation of two key regulators of actin cytoskeleton dynamics: Ena/VASP proteins and the Arp2/3 complex (Pistor *et al*., 1995, 2000; Smith *et al*., 1996; Niebuhr *et al*., 1997; May *et al*., 1999; Skoble *et al*., 2000, 2001; Geese *et al*., 2002). They also provided the basis for further development of *in vitro* motility systems that culminated in the reconstruction of bacterial motility using a limited set of purified proteins (Loisel *et al*., 1999). This article describes procedures for the preparation and use of mouse brain extracts for studying *Listeria* motility.

Copyright 2006, Elsevier Science (USA).
All rights reserved.

II. MATERIALS AND INSTRUMENTATION

Calcium chloride (Cat. No. 102378), magnesium chloride hexahydrate (Cat. No. 105832), potassium chloride (Cat. No. 4936), HEPES (Cat. No. 10110), sucrose (Cat. No. 1.07654), sodium chloride (Cat. No. 1.06404), disodium hydrogen phosphate dihydrate (Cat. No. 1.06580), sodium dihydrogen phosphate hydrate (Cat. No. 6346), and paraffin (Cat. No. 1.07160) are from Merck. EGTA (Cat. No. E-3889), methylcellulose (Cat. No. M-0555), ATP (Cat. No. A-2383), erythromycin (Cat. No. E-6376), and lanoline (Cat. No. L-7387) are from Sigma. Chymostatin (Cat. No. 17158), leupeptin (Cat. No. 51867), pepstatin (Cat. No. 52682), PEFABLOCK (Cat. No. 31682), aprotinin (Cat. No. 13178), and creatine kinase (Cat. No. 127566) are from Boehringer-Ingelheim. Dithiothreitol (DTT, Cat. No. 43815), Tris–HCl (Cat. No. 93363), and glycerol (Cat. No. 49770) are from Fluka. Cell-Tak (Cat. No. 354241) is from BD Biosciences. Creatine phosphate (Cat. No. 621714) is from Roche. Vaseline (Cat. No. 16415) is from Riedel-de Haen. Brain heart infusion (BHI) culture medium and Bacto agar are from Difco Laboratories. Rhodamine-labelled actin (Cat. No. AR05) is from Cytoskeleton. A glass homogeniser equipped with a Teflon piston, glass slides (76 × 26 mm), glass coverslips (22 × 22 mm), forceps, scissors, and razor blades are from local suppliers. Bacterial motility is observed using an Axiovert 135TV microscope (Zeiss) equipped with a Plan-Apochromat 100×/1.4 NA oil immersion objective. Images can be acquired with a cooled, back-illuminated CCD camera (TE/CCD-1000 TKB; Roper Scientific) driven by IPLab Spectrum software (Scanalitics).

III. PROCEDURES

A. Explantation of Mouse Brains

Solution

Phosphate-buffered saline (PBS): 130 m*M* NaCl, 1.5 m*M* $NaH_2PO_4 \cdot H_2O$, and 4 m*M* $Na_2HPO_4 \cdot 2H_2O$, pH 7.4. For 1 litre, weigh out 7.65 g NaCl, 0.21 g $NaH_2PO_4 \cdot H_2O$, and 0.72 g $Na_2HPO_4 \cdot 2H_2O$. Dissolve in 900 ml H_2O, adjust pH to 7.4 with 1 *N* NaOH, and bring volume to 1 litre. Store at 4°C.

Steps

1. Kill mice using CO_2 or by cervical dislocation.
2. Remove skin and fur from the head using thin-tipped scissors and discard.
3. Cut the skull bone by sliding the scissors along the sagittal suture (Fig. 1a, dashed red line).
4. Cut the frontal, parietal, and interparietal bones along their sutures and remove them (Fig. 1a, dashed green line).
5. Gently pinch the surface of the brain to lift the meninges up and gently ease the brain out of the skull.
6. Put explanted brains in ice-cold PBS.
7. Wash brains three times in ice-cold PBS to remove tissue debris and blood residues.

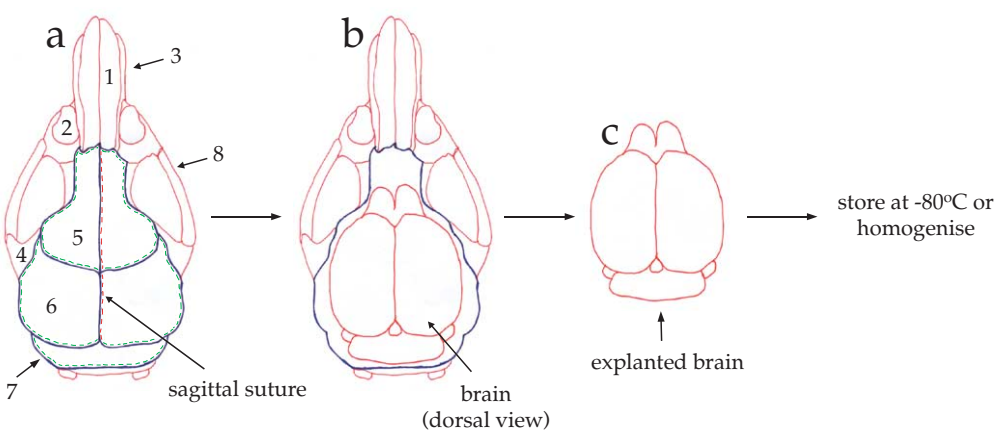

FIGURE 1 Diagram of the explantation of mouse brains. (a) Dorsal view of mouse skull showing the nasal bone (1), eye socket (2), nasal process of incisive bone (3), zygomatic process (4), frontal bone (5), parietal bone (6), interparietal bone (7), and zygomatic bone (8). (b) Dorsal view of skull after cutting (along the dashed green and red lines) and removing the frontal, parietal, and interparietal bones. (c) Dorsal view of explanted brain.

8. Proceed to Section III,B or flash freeze the brains in liquid nitrogen. Store frozen brains at –80°C.

B. Preparation of Cytosolic Extracts

Solutions

1. *Homogenisation buffer (HB)*: 20 m*M* HEPES, pH 7.5, 100 m*M* KCl, 1 m*M* $MgCl_2 \cdot H_2O$, 1 m*M* EGTA, and 0.2 m*M* $CaCl_2$. For 1 litre, weigh out 4.76 g HEPES, 7.45 g KCl, 0.2 g $MgCl_2 \cdot H_2O$, 0.38 g EGTA, and 0.02 g $MgCl_2$. Dissolve in 900 ml H_2O, adjust pH to 7.5 with 1 *N* NaOH, and bring volume to 1 litre. Store at 4°C.

2. *Protease inhibitors*: 20 mg/ml chymostatin, 1 mg/ml leupeptin, 1 mg/ml pepstatin, 167 m*M* Pefabloc, and 10 mg/ml aprotinin. To prepare stock solutions, dissolve 1 mg chymostatin in 50 µl dimethyl sulfoxide, 0.5 mg leupeptin in 500 µl H_2O, 0.5 mg pepstatin in 500 µl methanol, 20 mg Pefabloc in 500 µl H_2O, and 0.5 mg aprotinin in 50 µl H_2O. Aliquot and store at –20°C.

3. *0.1 M ATP*: For 50 ml, weigh out 2.75 g ATP. Dissolve in H_2O, aliquot, and store at –20°C.

4. *0.1 M DTT*: For 50 ml, weigh out 0.77 g DTT. Dissolve in H_2O, aliquot, and store at –20°C.

5. *2 M sucrose*: For 20 ml, weigh out 13.69 g sucrose. Dissolve in H_2O, aliquot, and store at –20°C.

6. *Homogenisation buffer supplemented with protease inhibitors (HBI)*: HB containing 60 µg/ml chymostatin, 5 µg/ml leupeptin, 10 µg/ml pepstatin, 4 m*M* Pefabloc, 2 µg/ml aprotinin, 0.5 m*M* ATP, and 1 m*M* DTT. Shortly before use add to 20 ml of HB 60 µl of 20 mg/ml chymostatin, 100 µl of 1 mg/ml leupeptin, 200 µl of 1 mg/ml pepstatin, 476 µl of 167 m*M* Pefabloc, 4 µl of 10 mg/ml aprotinin, 200 µl of 0.1 *M* DTT, and 50 µl of 0.1 *M* ATP.

Steps

1. After the last wash in PBS (see Section III,A, step 7) remove PBS and weigh the brains.
2. Cut the brains into small pieces using a razor blade (keep brains on ice).
3. Add 0.75 ml of HBI per gram of wet tissue (keep brain suspension on ice).
4. Transfer brain suspension into a glass homogeniser on ice.
5. Grind brain tissue for 20 passages of the pestle on ice.
6. Centrifuge crude extract at 15,000 *g* for 1 h at 4°C.
7. Recover clarified supernatant (cytosolic brain extract) and supplement it with 150 m*M* sucrose, 50 mg/ml creatine kinase, 30 m*M* creatine phosphate, and 0.5 m*M* ATP.
8. Aliquot and flash freeze in liquid nitrogen. Store frozen aliquots at –80°C.

C. Preparation of Bacteria

Solutions

1. *Brain heart infusion (BHI) broth*: Prepare liquid medium according to the manufacturer's instruction, autoclave, filter, and store at 4°C. For agar plates, add Bacto-agar (15 g/liter of BHI broth), autoclave, and pour 30 ml in a 10-cm petri dish. Store plates at 4°C.
2. *Erythromycin stock solution*: Dissolve 50 mg of erythromycin in 10 ml of pure ethanol. Store at 4°C.

Bacterial Culture

1. Streak the bacteria onto BHI agar plates. Incubate at 37°C for 24 h.

2. Put 5 ml of BHI (supplemented with 50 µg/ml erythromycin) in a 15-ml sterile Falcon tube. Scrape a few colonies off the BHI plate using a sterile pipette tip or a flamed bacteriological loop. Inoculate the broth and grow bacteria overnight at 37°C with vigorous shaking.

3. Transfer bacterial culture to a centrifuge tube and pellet the bacteria at 10,000 *g* for 3 min.

4. Wash bacterial pellet three times in homogenisation buffer. After the final washing step, resuspend pellet in a final volume of homogenisation buffer corresponding to the initial volume of bacterial culture.

5. Alternatively, supplement the overnight culture with 20% glycerol, aliquot, and store at –80°C.

D. Listeria Motility Assay

Solutions

1. *2% methycellulose in homogenisation buffer (stock solution)*: Heat 100 ml of HB to 60°C and then add 2 g of methylcellulose. Stir vigorously until the methycellulose dissolves. Cool down and store at room temperature.

2. *0.5% methycellulose in homogenisation buffer (working solution)*: To make 10 ml, mix 7.5 ml of HB with 2.5 ml of 2% methycellulose. Store at 4°C.

3. *VALAP*: Mix vaseline, lanoline, and paraffin in a 1:1:1 ratio (w/w/w) and homogenise at 75°C. Store at room temperature.

4. *G buffer*: 5 m*M* Tris–HCl, pH 7.6, 0.5 m*M* ATP, 0.1 m*M* $CaCl_2$, and 0.5 m*M* DTT. For 1 litre, weigh out 0.8 g Tris–HCl, 0.01 g $CaCl_2$, and then add 5 µl of 0.1 *M* ATP and 5 µl of 0.1 *M* DTT. Dissolve in 900 ml H_2O,

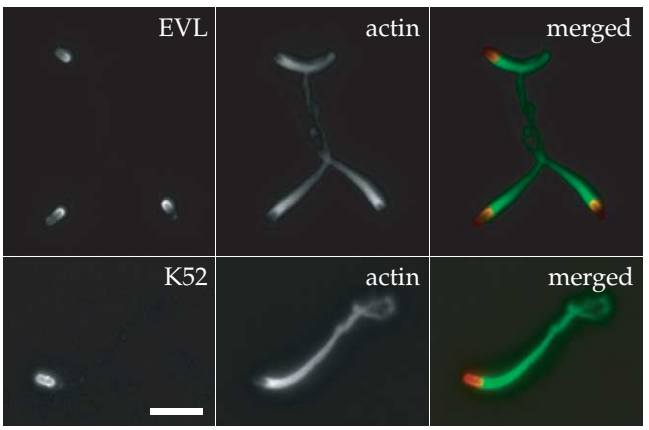

FIGURE 2 Immunofluorescence microscopy showing *Listeria* actin tails formed in mouse brain extracts. Bacteria were incubated in mouse brain extract for 30 min at room temperature and then 5 µl of motility mixture was applied onto Cell Tak-coated cover slips (the coating procedure was done according to the manufacturer's instructions) and incubated for 5 min on ice. Afterwards, bacteria were fixed with 4% PFA for 20 min at room temperature. Immunolabelling was done according to Geese *et al*. (2002) using the affinity-purified polyclonal antibody K52 to label bacterial surface, the monoclonal antibody 84H1 to label EVL, and Texas red-labelled phalloidin to label the actin tails. Primary antibodies were detected using Alexa 488-conjugated secondary antibodies. Scale bar: 5 µm.

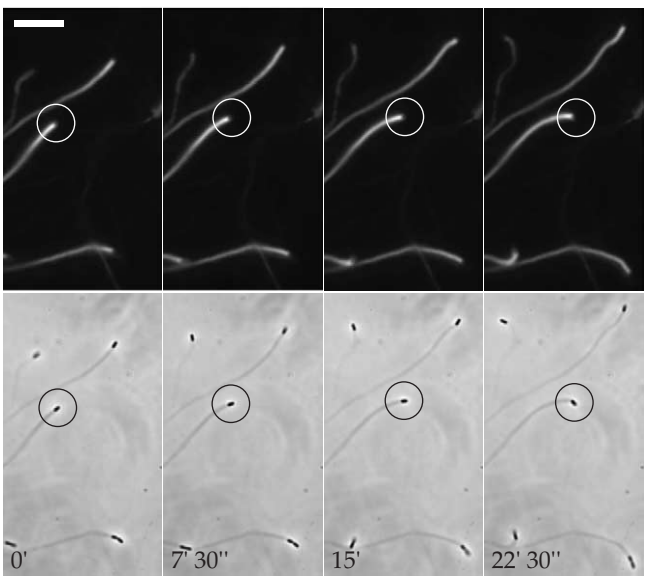

FIGURE 3 Dynamics of *Listeria* motility in mouse brain extracts. Bacteria were mixed with 4 µl brain extract, 4 µl of 0.5% methycellulose, and 0.2 µl rhodamine-labelled actin and were incubated at room temperature for 10 min. Thereafter, 1.7 µl of motility mixture was spotted onto a glass slide and a 22 × 22-mm glass coverslip overlaid on it. Bacterial motility was observed using a Axiovert 135 TV inverted microscopy equipped with phase-contrast and epifluorescence optics using a Plan-Apochromat 100×/1.4 NA oil immersion objective. Images were acquired using a cooled, back-illuminated CCD camera (TE/CCD-1000 TKB; Roper Scientific) driven by IPLab Spectrum software (Scanalitics). (Top) Rhodamine-labelled actin and (bottom) the corresponding phase-contrast images. Scale bar: 10 µm.

adjust pH to 7.6 with 1 *N* NaOH, and bring volume to 1 litre. Store at 4°C.

5. *Rhodamine-labelled actin*: Add 6 µl of G buffer to one aliquot of rhodamine-labelled actin. Mix gently and store on ice.

Steps

1. Wash bacteria three times in homogenisation buffer. Resuspend pellet in 20 µl homogenisation buffer.

2. In a small Eppendorf tube, mix 4 µl brain extract, 4 µl of 0.5% methycellulose, 0.5 µl bacteria suspension, and 0.2 µl rhodamine-labelled actin. Mix by pipetting up and down gently. Do not vortex. Incubate mixture at room temperature for 10 min.

3. Remove 1.7 µl of motility mixture and spot it onto a glass slide. Gently place a 22 × 22-mm glass coverslip over the drop and press down until the drop spreads to the edges. Seal the coverslip edges with VALAP.

4. Observe slide with an upright or inverted microscope. Actin comet tails can be observed easily by phase contrast or epifluorescence using a Plan-Apochromat 100×/1.4 NA oil immersion objective (Figs 2 and 3).

IV. COMMENTS AND PITFALLS

Although cell-free systems based on egg extracts of *Xenopus laevis* or human platelet extracts provide excellent *in vitro* systems for supporting actin-based bacterial motility, their ability to do so can be affected negatively by various factors, such as health of eggs or quality and age of platelet preparations. In this context, mouse brain extracts offer a more "robust" *in vitro* system that does not seem to be influenced by external factors such as mouse strain and age.

The reconstitution of *Listeria* motility using mouse brain extracts can have a variety of uses. For instance, it can be used to study the role of actin cytoskeletal components involved in *Listeria* motility by interfering with their function using specific inhibitors or antibodies, as described in May *et al*. (1999). Moreover, the procedure described here may be further developed and adapted to obtain cell-free extracts from normal cultured cells or cells that lack or express mutated ver-

sions of the actin cytoskeletal proteins of interest, thus widening the spectrum of *in vitro* systems available for studying bacterial motility.

Three main parameters have to be considered to achieve optimal *Listeria* motility with mouse brain extracts. First, the protein ActA must be expressed at high levels on the bacterial surface. As most wild-type strains express low levels of this protein under standard culture conditions, a *Listeria* strain (see Lingnau *et al*., 1996) that constitutively expresses high levels of this protein must be used in this assay. The second critical parameter is the total protein concentration of the brain extract, which must be at least 10 mg/ml. The total protein concentration can be increased by reducing the amount of homogenisation buffer per gram of wet tissue. Moreover, mouse brain extracts should not be diluted more than fourfold as further dilution leads to loss of activity in the motility assay. Finally, the high amount of actin present in these extracts induces its spontaneous polymerisation, characterised by the formation of short actin bundles. As this actin network may affect bacterial motility, mouse brain extracts must be kept on ice to reduce the tendency of actin to polymerise.

Acknowledgments

I thank David A. Monner and Jürgen Wehland (GBF, Department of Cell Biology) for helpful discussions and valuable support.

References

Cossart, P., and Bierne, H. (2001). The use of host cell machinery in the pathogenesis of Listeria monocytogenes. *Curr. Opin. Immunol.* **13**, 96–103.

Frischknecht, F., and Way, M. (2001). Surfing pathogens and the lessons learned for actin polymerization. *Trends Cell Biol.* **11**, 30–38.

Geese, M., Loureiro, J. J., Bear, J. E., Wehland, J., Gertler, F. B., and Sechi, A. S. (2002). Contribution of Ena/VASP proteins to intracellular motility of Listeria requires phosphorylation and proline-rich core but not F-actin binding or multimerization. *Mol. Biol. Cell* **13**, 2383–2396.

Laurent, V., and Carlier, M. F. (1998). Use of platelet extracts for actin-based motility of Listeria monocytogenes. *In* "Cell Biology: A Laboratory Handbook" (J. Celis, ed.), pp. 359–365. Academic Press, New York.

Laurent, V., Loisel, T. P., Harbeck, B., Wehman, A., Grobe, L., Jockusch, B. M., Wehland, J., Gertler, F. B., and Carlier, M. F. (1999). Role of proteins of the Ena/VASP family in actin-based motility of Listeria monocytogenes. *J. Cell Biol.* **144**, 1245–1258.

Lingnau, A., Chakraborty, T., Niebuhr, K., Domann, E., and Wehland, J. (1996). Identification and purification of novel internalin-related proteins in Listeria monocytogenes and *Listeria ivanovii*. *Infect. Immun.* **64**, 1002–1006.

Loisel, T. P., Boujemaa, R., Pantaloni, D., and Carlier, M. F. (1999). Reconstitution of actin-based motility of Listeria and Shigella using pure proteins. *Nature* **401**, 613–616.

Marchand, J. B., Moreau, P., Paoletti, A., Cossart, P., Carlier, M. F., and Pantaloni, D. (1995). Actin-based movement of Listeria monocytogenes: Actin assembly results from the local maintenance of uncapped filament barbed ends at the bacterium surface. *J. Cell Biol.* **130**, 331–343.

Niebuhr, K., Ebel, F., Frank, R., Reinhard, M., Domann, E., Carl, U. D., Walter, U., Gertler, F. B., Wehland, J., and Chakraborty, T. (1997). A novel proline-rich motif present in ActA of Listeria monocytogenes and cytoskeletal proteins is the ligand for the EVH1 domain, a protein module present in the Ena/VASP family. *EMBO J.* **16**, 5433–5444.

Pistor, S., Chakraborty, T., Walter, U., and Wehland, J. (1995). The bacterial actin nucleator protein ActA of Listeria monocytogenes contains multiple binding sites for host microfilament proteins. *Curr. Biol.* **5**, 517–525.

Pistor, S., Grobe, L., Sechi, A. S., Domann, E., Gerstel, B., Machesky, L.M., Chakraborty, T., and Wehland, J. (2000). Mutations of arginine residues within the 146-KKRRK-150 motif of the ActA protein of Listeria monocytogenes abolish intracellular motility by interfering with the recruitment of the Arp2/3 complex. *J. Cell Sci.* **113**, 3277–3287.

Skoble, J., Auerbuch, V., Goley, E. D., Welch, M. D., and Portnoy, D. A. (2001). Pivotal role of VASP in Arp2/3 complex-mediated actin nucleation, actin branch-formation, and Listeria monocytogenes motility. *J. Cell Biol.* **155**, 89–100.

Skoble, J., Portnoy, D. A., and Welch, M. D. (2000). Three regions within ActA promote Arp2/3 complex-mediated actin nucleation and Listeria monocytogenes motility. *J. Cell Biol.* **150**, 527–538.

Small, J. V., Stradal, T., Vignal, E., and Rottner, K. (2002). The lamellipodium: Where motility begins. *Trends Cell Biol.* **12**, 112–120.

Smith, G. A., Theriot, J. A., and Portnoy, D. A. (1996). The tandem repeat domain in the Listeria monocytogenes ActA protein controls the rate of actin-based motility, the percentage of moving bacteria, and the localization of vasodilator-stimulated phosphoprotein and profilin. *J. Cell Biol.* **135**, 647–660.

Theriot, J. A., Rosenblatt, J., Portnoy, D. A., Goldschmidt-Clermont, P. J., and Mitchison, T. J. (1994). Involvement of profilin in the actin-based motility of L. monocytogenes in cells and in cell-free extracts. *Cell* **76**, 505–517.

CHAPTER

51

Pedestal Formation by Pathogenic *Escherichia coli*: A Model System for Studying Signal Transduction to the Actin Cytoskeleton

Silvia Lommel, Stefanie Benesch, Manfred Rohde, and Jürgen Wehland

I. INTRODUCTION

Dynamic rearrangement of the actin cytoskeleton in response to signal transduction plays a fundamental role in the regulation of cellular functions. Understanding actin dynamics therefore represents one of the challenges of modern cell biology. Several pathogens have evolved diverse strategies to trigger rearrangement of the host actin cytoskeleton to facilitate and enhance their infection processes. By manipulating the actin assembly machinery or signalling routes leading to its activation, pathogens can either block or induce phagocytosis, drive intracellular motility, and exploit their host cells in other ways. Analyses of host pathogen interactions have not only broadened our knowledge of how these pathogens cause disease, but have also emerged as model systems in the study of cellular actin dynamics (for examples, see Frischknecht and Way, 2001). The focus of this article is on the formation of cytoskeletal rearrangements called actin pedestals induced by the diarrhoeagenic extracellular bacterial pathogens enteropathogenic *Escherichia coli* (EPEC) and enterohaemorrhagic *E. coli* (EHEC) as systems to study signalling and actin assembly at the plasma membrane.

During infection of the intestinal mucosa, EPEC and EHEC induce specific, so-called attaching and effacing (A/E) lesions on intestinal epithelial cells (for review, see Nataro and Kaper, 1998). A/E lesions are characterized by a localized loss of microvilli and intimate adherence of bacteria to the cell surface followed by recruitment of the cellular actin assembly machinery to sites of bacterial attachment, resulting in the formation of actin-rich pseudopod-like structures termed pedestals to which the bacteria intimately adhere.

Importantly, the histopathological changes associated with the A/E phenotype *in vivo* can be mimicked in cell culture [(Knutton *et al.*, 1987), see Fig. 1], which allows to define the molecular mechanisms employed by EPEC and EHEC to induce cytoskeletal rearrangements. The ability to form actin pedestals on cultured cells furthermore correlates with the ability of EPEC and EHEC to colonize the intestine and cause disease in human and other animal hosts (e.g., Donnenberg *et al.*, 1993).

The genes necessary for A/E lesion formation in EPEC map to an about 35-kb chromosomal pathogenicity island, designated the locus of enterocyte effacement (LEE), which is highly conserved in EHEC. Although EPEC and EHEC produce highly similar lesions, EPEC in the small intestine and EHEC in the large intestine, the molecular mechanisms of pedestal formation employed by EPEC versus EHEC differ (for review, see Campellone and Leong, 2003).

Both pathogens translocate their own receptor, the translocated intimin receptor (Tir, EspE), which binds to the bacterial surface protein intimin, via a type III secretion system into the underlying host cell. EPEC Tir becomes tyrosine phosphorylated upon insertion

Copyright 2006, Elsevier Science (USA).
All rights reserved.

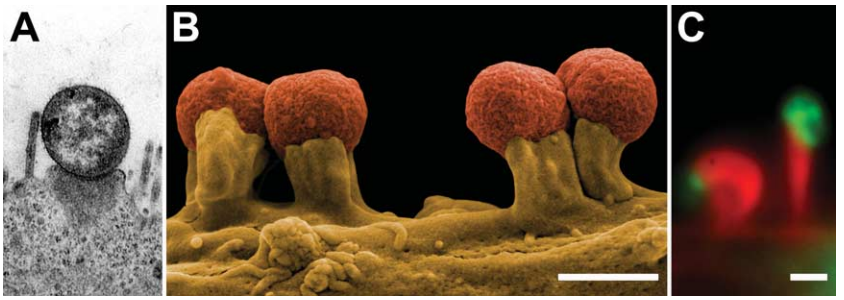

FIGURE 1 Actin pedestal formation induced by EHEC and EPEC *in vivo* and on the surface of cultured cells. (A) Transmission electron micrograph showing the characteristic attaching and effacing (A/E) lesion formation of the enterohaemorrhagic *Escherichia coli* (EHEC) O157:H7 strain 86/24 observed in piglet colon. Note the intimate attachment, localized loss of microvilli, and formation of a raised, pedestal-like structure beneath the bacterium that characterizes this lesion (courtesy of Florian Gunzer, Institute of Medical Microbiology, Hannover Medical School, Germany). **(B)** Scanning electron micrograph of enteropathogenic *E. coli* (EPEC) O127:H6 strain E2348/69 (pseudocoloured in red) sitting on top of pedestals induced on the surface of cultured murine embryonic fibroblast cells upon infection that resemble A/E lesions formed by EPEC *in vivo*. **(C)** EHEC O157:H7 strain 86/24-induced actin pedestal formation as visualized by fluorescence actin staining using AlexaFluor 594 phalloidin to specifically label F-actin (shown in red). EHEC bacteria shown in green were detected with monoclonal antibodies against EspE (Deibel *et al*., 1998) and AlexaFluor 488-conjugated goat antimouse secondary antibodies. Bars: 1 µm.

into the host cell membrane and binding to intimin. This phosphorylation is critical for actin pedestal formation by EPEC (Kenny, 1999), as it allows recruitment of the cellular signalling adaptor protein Nck to bacterial attachment sites. Nck, in turn, triggers by a so far unknown mechanism recruitment and activation of N-WASP. Both Nck and N-WASP are essential host proteins for pedestal formation induced by EPEC, as cells lacking either Nck or N-WASP are resistant to actin pedestal formation by EPEC (Gruenheid *et al*., 2001; Lommel *et al*., 2001) (for N-WASP, see Fig. 2). N-WASP is a member of the WASP/Scar family of cellular nucleation-promoting factors and has emerged as a central node protein that regulates actin polymerisation by activating the Arp2/3 complex, a main factor for nucleation of actin filaments in response to multiple upstream signals.

In contrast, EHEC Tir is not tyrosine phosphorylated and pedestals are formed independently of Nck. Despite that, EHEC-induced pedestal formation still depends on N-WASP function (Lommel *et al*., 2004) to promote Arp2/3 complex-mediated actin polymerisation. Thus, EPEC and EHEC have evolved different strategies to trigger cellular signalling routes leading to actin assembly, which converge in recruitment and activation of N-WASP to promote Arp2/3-mediated actin polymerisation.

The aim of this article is to outline a methodology for the analysis of actin pedestal formation by EPEC and EHEC using cultured cells as model systems to study regulatory mechanisms controlling actin assembly at the plasma membrane. This article describes

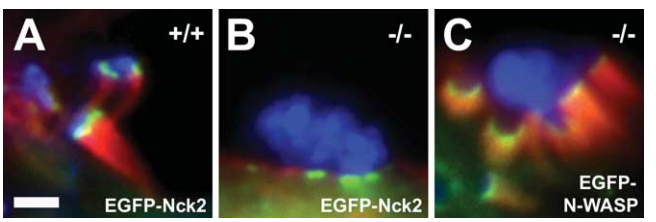

FIGURE 2 EGFP-tagging and knockout cell lines as tools for analysis of the molecular mechanism of actin pedestal formation induced by EPEC. Cultured murine embryonic fibroblasts expressing (+/+, **A**) or lacking N-WASP (–/–, **B** and **C**) were infected with EPEC and examined by immunofluorescence microscopy. F-actin is shown in red as detected by fluorescence actin staining with AlexaFluor 594 phalloidin, bacteria are shown in blue as detected with anti-EspE monoclonal antibodies in combination with AlexaFluor 350-conjugated goat antimouse secondary antibodies, and the host proteins Nck2 **(A** and **B)** and N-WASP **(C)** expressed ectopically with an EGFP tag are shown in green. Whereas EPEC induced the formation of prominent pedestals in N-WASP-expressing cells (+/+, **A**), they were unable to trigger actin accumulation on N-WASP-defective cells (–/–, **B**). The bacterial ability to direct actin reorganisation in N-WASP-defective fibroblasts was restored by providing EGFP-tagged N-WASP by transient transfection (**C**). Together, this clearly demonstrates that N-WASP is a host cell protein essential for pedestal formation induced by EPEC. Recruitment of the host cell signalling adaptor protein Nck2 is triggered by EPEC independently of actin accumulation, as was revealed by ectopic expression of EGFP-tagged Nck2 in either N-WASP-expressing (+/+, **A**) or N-WASP-defective cells (–/–, **B**). Bar: 2 µm, (valid for A–C).

protocols for the coculture of bacteria with cell lines and for basic immunofluorescence microscopy techniques that are used to examine bacterial–host cell interactions in terms of bacterial attachment and

effects on the actin cytoskeleton. These may be combined with ectopical expression of host cell proteins tagged with green fluorescent protein (GFP) for analysis of subcellular localisation and dynamic reorganisation of a protein during the infection process using digital fluorescence microscopy (for examples, see Fig. 2). A further advance to unravel the molecular mechanism of pedestal formation is the use of cell lines derived from knockout mice. Cell lines derived from such mice can be reconstituted by expressing wild-type or mutated proteins tagged with GFP, which facilitates the analysis of the contribution of specific protein domains to actin pedestal formation (for examples, see Fig. 2).

II. MATERIALS AND INSTRUMENTATION

A Cell Lines, Bacterial Pathogen Strains, and Culture Media Reagents

1. Cells

Epithelial cell lines used commonly for EPEC and EHEC infection experiments are HeLa and HEp-2 cells, as well as the intestinal epithelial cell lines T84 or Caco-2 (available from American Type Culture Collection). EPEC and EHEC will also adhere and induce the formation of actin pedestals on mouse embryonic fibroblast cell lines (MEFs), which are used routinely in our laboratory. Embryonic fibroblast cell lines offer the advantage that such cell lines can be established quite easily from conditional or conventional knockout mice, thus allowing the analysis of specific host proteins in actin pedestal formation induced by EPEC and EHEC.

2. Bacterial Pathogen Strains

Prototype enteropathogenic and enterohaemorrhagic *E. coli* strains used in analyses of the molecular mechanism of actin pedestal formation are enteropathogenic *E. coli* strain E2348/69 (O127:H6) (Levine *et al*., 1978), enterohaemorrhagic *E. coli* strain 86/24 (O157:H7) [isolated from an outbreak in Walla Walla, WA., U.S.A. (Griffin *et al*., 1988)], and enterohaemorrhagic *E. coli* strain EDL933 (O157:H7) (American Type Culture Collection #700927; for genome sequence information, see Perna *et al*., 2001).

3. Cell and Bacterial Culture Reagents

Dulbecco's modified eagle medium (DMEM), low glucose (Invitrogen Corp., GIBCO #31885-023), fetal bovine serum (Sigma-Aldrich #F 7524), L-glutamine (Invitrogen Corp., GIBCO #25030-024), penicillin/streptomycin (Invitrogen Corp., GIBCO #15070-063), Luria-Bertani (LB) broth agar (e.g., BD #244520), LB broth (e.g., BD #244620), and HEPES (Sigma-Aldrich #H 3375), fibronectin (pure) (Roche #1051407).

B. Constructs and Reagents for Expression of GFP-Tagged Host Proteins

1. *Transfection reagent*, e.g., FuGENE 6 (Roche #1 814 443)
2. A set of vectors for construction of EGFP fusions is available from Clontech (BD Biosciences).
3. *EGFP-N-WASP*: as described (Lommel *et al*., 2001)
4. *EGFP-Nck2*: as described (Scaplehorn *et al*., 2002)

C. Additionally Needed Reagents and Plasticware

1. Basics

General equipment and plasticware for molecular biology and cell culture techniques.

2. Cell Culture and Immunofluorescence Microscopy

Twenty-four-well cell culture plates (e.g., Corning Inc. #3524), 12-mm round glass coverslips (e.g., Assistent #1001, thickness 0.17 mm), absolute ethanol (Sigma-Aldrich #E 7023), HCl (37%) (Sigma-Aldrich #H 7020), lint-free absorptive paper [e.g., GB002, Schleicher&Schuell #10427736 (58 × 68 cm) and #10485285 (22.2 × 22.2 cm)], large square plastic dish (e.g., 24.5 × 24.5-cm polystyrene dish with lid, Sigma-Aldrich #Z37,165-3), Parafilm M (e.g., Fisher Scientific #917 00 02), forceps with curved fine tips (e.g., coverslip forceps Dumont #11251-33), NaCl (Sigma-Aldrich #S 7653), KCl (Sigma-Aldrich #P 1338), Na_2HPO_4 (Sigma-Aldrich #S 7907), KH_2PO_4 (Sigma-Aldrich #P 0662), paraformaldehyde (PFA), (Sigma-Aldrich #P 6148), NaOH (Merck/VWR International #109913), Triton X-100 (Sigma-Aldrich #T 8532), normal goat serum (Invitrogen Inc.: GIBCO #16210-064), bovine serum albumin (BSA, Sigma-Aldrich #A 2153), goat anti-mouse Alexa Fluor 350- or Alexa Fluor 488-conjugated secondary antibodies (Molecular Probes #A-11045 and #A-11001), DAPI (e.g., Molecular Probes, #D-1306), fluorophore-coupled phalloidin [e.g., Alexa Fluor 594 phalloidin (red fluorescence, Molecular Probes #A-12381)], glycerol (87%, analytical grade) (e.g., Merck/VWR International #104094), Mowiol 4-88 (Calbiochem #475904), Tris base (e.g., Trizma base, Sigma-Aldrich #T 1503), *n*-propyl gallate (Sigma-

Aldrich #P 3130), and SuperFrost microscope glass slides (Fisher Scientific #9161161).

D. Instrumentation and Laboratory Equipment

1. Centrifuges

Tabletop centrifuge (e.g., centrifuge 5414D, Eppendorf #5425 000.219), centrifuge equipped with rotor suitable for microtiter plates, and 15- and 50-ml polypropylene tubes (e.g., centrifuge 5810, Eppendorf #5810 000.017 with rotor A-4-81 and A-4-81-MTP).

2. Clean Benches and Cell Incubators

Clean bench and cell culture incubator suitable for work with EPEC and EHEC pathogens in accordance with respective national safety regulations.

3. Microscope

Inverted microscope (e.g., Axiovert 135TV, Carl Zeiss Jena GmbH) equipped for epifluorescence microscopy with 40×/1.3 NA and 100×/1.3 NA Plan-NEOFLUAR oil immersion objectives, 1.6 and 2.5 optovar magnification, electronic shutters (e.g., Uniblitz Electronic 35-mm shutter including driver Model VMMD-1, BFI Optilas) to allow for computer-controlled opening of the light paths, excitation and emission filters (Omega Optical Inc. or Chroma Technology Corp.) to enable three-colour epifluorescence, and mercury short arc lamp (Osram, HBO103W/2) for fluorescence light path.

4. Data Acquisition

Preferably a back-illuminated, cooled charge-coupled device (CCD) camera (e.g., Princeton Research Instruments TKB 1000×800, SN J019820; Controller SN J0198609) driven, for instance, by IPLab (Scanalytics Inc.) or Metamorph software (Universal Imaging Corporation).

III. PROCEDURES

Solutions

1. *Cell culture growth media*: Cell culture growth medium suitable for the propagation of the cell line chosen. We use DMEM, low glucose supplemented with 10% heat-inactivated fetal bovine serum, 2 m*M* L-glutamine, and 50 U/ml each of penicillin and streptomycin for propagation of our embryonic fibroblast cell lines.

2. *Cell culture growth media for bacterial infection experiments*: For bacterial infection experiments, omit penicillin and streptomycin from growth media starting a day prior to infection.

3. *Standard bacterial cultures*: Prepare LB broth and LB agar plates according to standard protocols (e.g., Maniatis *et al*., 1982).

4. *Preactivating culture of EPEC*: DMEM, low glucose for culturing EPEC prior to infection of cell monolayers.

5. *Preactivating culture of EHEC*: DMEM, low glucose, supplemented with 100 m*M* HEPES, pH 7.4, for culturing EHEC prior to infection of cell monolayers.

6. *Phosphate-buffered saline (PBS)*: 140 m*M* NaCl, 2.7 m*M* KCl, 10 m*M* Na_2HPO_4, 1.8 m*M* KH_2PO_4, pH 7.4

7. *Fixative*: Prepare a 4% solution of PFA in PBS, pH 7.4. Paraformaldehyde is very toxic, work in fumehood when preparing stock, do not inhale, and wear gloves. To prepare 100 ml, add 4 g PFA to 90 ml PBS. In order for the PFA to dissolve, heat the solution to 60–65°C with continuous stirring. If necessary, adjust the pH to 7.4 by adding NaOH (be patient!). Do not heat solution above 70°C, as PFA will degrade. Let cool to room temperature, check the pH, and adjust with PBS to full volume. Filter through paper filter to remove insoluble aggregates and store in aliquots (e.g., 15 and 50 ml) at –20°C.

8. *Cell permeabilization*: Fixative supplemented with 0.1% Triton X-100 just prior to use. Make up a 10% stock solution of Triton X-100 in PBS and store at 4°C.

9. *Antibody diluent*: 1% BSA in PBS. Prepare and store in suitable aliquots (1–2 ml) at –20°C.

10. *Blocking solution*: 10% normal goat serum in PBS. Prepare from frozen aliquots of serum just prior to use.

11. *Antibody Mixtures*: Dilute antibodies just prior to use to appropriate working concentration in 1% BSA in PBS. The ideal concentration will result in a strong signal with no or little background staining and has to be established experimentally for each new antibody. To start, follow instructions given by the supplier. When using a concentrated primary antibody, a 1:100 dilution resulting in about 10 µg/ml should be a good starting point for immunofluorescence microscopy. Secondary antibodies conjugated to fluorophores are available from numerous suppliers. In our hands, secondary reagents coupled to Alexa Fluor dyes from Molecular Probes have worked very well. Note, however, that most polyclonal antisera will exhibit unspecific cross-reaction with EPEC and EHEC bacteria. A way to avoid problems associated with unspe-

cific labelling of bacteria is to use monoclonal reagents (see general comment in Section IV). We store our antibodies in the dark at 4°C in a refrigerator. For long-term storage, antibodies may be stored at –20 or –80°C. Follow the recommendations given by the supplier.

12. *Mounting medium*: Weigh out 6 g glycerol and add 2.4 g Mowiol 4-88. Stir thoroughly. Add 6 ml aqua dest and mix for several hours at room temperature. Add 0.2 ml 0.2 *M* Tris–Cl, pH 8.5, and heat to 60°C for 10 min. Remove insoluble material by centrifugation at 6000 g for 30 min. Store in aliquots at –20°C. In order to reduce photobleaching during fluorescence microscopy, add 2.5–5 mg/ml *n*-propyl gallate prior to use (Giloh and Sedat, 1982).

A. Basic Protocol: Infection of Cell Monolayers with EPEC or EHEC

EPEC and EHEC pose a significant threat to human health, especially EHEC with its low infectious dose of ~10–100 cfu. When working with EPEC and EHEC, always wear protective clothing and work under an appropriate clean bench in accordance with national safety regulations. Decontaminate all materials that have been in contact with the pathogen.

Steps

1. Pretreat 12-mm round glass coverslips as follows: wash coverslips in a mixture of 60% absolute ethanol and 40% concentrated HCl for 30 min and rinse extensively with aqua dest (heating in a microwave oven is helpful). To dry coverslips, spread on lint-free absorptive paper. Sterilize for tissue culture either by autoclaving on the dry cycle at 220°C or by exposing to ultraviolet light for 45 min in a culture dish.

2. On day 1, streak EPEC and EHEC from frozen glycerol stocks onto fresh LB agar plates and incubate overnight at 37°C. Keep plates in the refrigerator until liquid overnight cultures are started.

3. On day 2, seed cells onto 12-mm pretreated coverslips in a 24-well tissue culture plate in cell culture growth media without antibiotics. Incubate overnight in a tissue culture incubator supplemented with CO_2 to allow the cells to adhere to the coverslips. For MEFs, we find microscopic analysis of actin pedestal formation easiest if cells have reached about 80% confluency at the time of analysis; the number of cells seeded should be adjusted accordingly. To reduce detachment of MEFs infected with EHEC, use fibronectin coated coverslips.

4. Start an overnight liquid culture of EPEC or EHEC in 5 ml LB medium with bacteria from the streaked plate. In our experience, small inoculation loads result in a higher infection efficiency. Grow overnight with aeration at 37°C on a rotary shaker at 180 rpm.

5. On day 3, collect bacteria from the 0.5-ml overnight culture by centrifugation for 3 min at 4500 rpm in a tabletop centrifuge. Wash bacterial pellet twice in DMEM and inoculate 25 ml DMEM (EPEC) or 25 ml DMEM supplemented with 100 m*M* HEPES, pH 7.4 (EHEC). Grow at 37°C at 180 rpm for 3 h.

Environmental cues such as temperature, pH, and osmolarity, as well as growth phase, have been described to influence the transcriptional regulation of expression of virulence factors, e.g., of the type III secretion system. Media conditions that appear to stimulate virulence are those considered to mimic the gastrointestinal tract (e.g., Beltrametti *et al*., 1999; Kenny *et al*., 1997). In our experience, preactivation of EPEC and EHEC by growth for 3 h in DMEM for EPEC or DMEM supplemented with 100 m*M* HEPES, pH 7.4, for EHEC is sufficient for reproducible efficient bacterial infection of cultured cell monolayers. In our hands, the morphological appearance of preactivated bacterial cultures correlates with their infectious capability: After 3 h, EPEC should be found aggregated to small clumps of bacteria but should not grow in long rows. Aggregation likely reflects the expression of type IV bundle-forming pili, rope-like appendages that represent an important additional virulence factor found to enhance initial adherence and virulence of EPEC (Bieber *et al*., 1998). EHEC, which lack bundle-forming pili, should be present as single bacteria in preactivation cultures, but again should not grow in long rows.

6. In the meantime, exchange cell culture medium of cell monolayers with 1 ml per well of fresh cell culture medium without antibiotics.

7. Add 10 µl of the bacterial 3-h preactivation culture into each well. Initiate infection by brief centrifugation for 5 min at 650 g in a centrifuge prewarmed to at least room temperature, allowing bacteria and cells to make contact with each other.

8. Place in an incubator supplemented with 7.5% CO_2 at 37°C for 1 h. Incubation at lower temperatures results in a reduced infection efficiency.

9. Remove media containing nonattached bacteria by aspiration and gently replace with 1 ml of fresh prewarmed culture medium without antibiotics per well. Be careful not to let the cells dry out when exchanging the medium.

10. Repeat medium changes every hour until a total infection time of 4.5 to 5 h has been reached.

In our hands, longer infection times generally result in pedestals of increased length, facilitating analysis of

pedestal composition. In addition, after short incubation times, EPEC bacteria are found mostly adhered in aggregates, which may confound analysis. Later during infection, EPEC bacteria will distribute from aggregates, making it easier to distinguish single pedestals. However, too long incubation results in increased cell death and detachment of cells, especially when working with EHEC.

11. After the incubation period, remove the medium by aspiration and gently wash the coverslips twice with PBS prewarmed to 37°C to remove unattached bacteria.
12. For fixation, immerse each coverslip with 500 µl of fixative prewarmed to 37°C and incubate at room temperature for 20 min.
13. After fixation, gently wash twice with PBS and store in PBS at 4°C until proceeding to cell permeabilization and immunostaining.

B. Alternative Protocol: EPEC and EHEC Infections of Transiently Transfected Cell Monolayers

For experiments involving ectopic expression of host cell molecules, e.g., tagged with GFP, designed to analyse their role in actin pedestal formation induced by EPEC or EHEC (see general comments, Section IV), follow the basic protocol with the exceptions that cells are already seeded on day 1, and day 2 will be required for transfection of host cell monolayers with plasmid DNA in addition to starting bacterial overnight cultures.

Steps

1. On day 1, seed cells in regular cell culture growth media on coverslips as described in the basic protocol with the modification that the number of cells seeded should be reduced to allow for the additional day needed for transfection. Again, about 80% confluency of MEFs should be reached at the time of bacterial infection.
2. On day 2, prior to transfection, exchange the cell culture growth medium for 0.5 ml growth medium without antibiotics. Transfect cells growing on coverslips in 24-well plate 12–24 h overnight according to standard protocols, e.g., using FuGENE 6 transfection reagent. We use 0.2 µg of DNA per well of a 24-well plate with a ratio of FuGENE 6 to DNA of 3:1. In our hands, plasmid DNA prepared with MaxiPrep kits, e.g., from Qiagen or Invitrogen Corp. is sufficiently pure for cell transfection.

Good transfection efficiency is a prerequisite for analyses involving bacterial infections, as the number of cells that are both transfected and infected may be too low. You may want to consider testing different lots of fetal bovine serum, as we have detected great variability in transfection rates using different sera. Alternatively, you may have to resort to fluorescence-assisted cell sorting to enrich for the population expressing the GFP-tagged protein of interest. In this case, transfect cells in regular cell culture plates and seed onto coverslips after sorting.

C. Immunofluorescence Microscopy

See general comments about immunofluorescence microscopy analysis of EPEC- and EHEC-infected cells.

Steps

1. Permeablize cells in 0.1% Triton X-100 in PBS for 1 min.
2. Gently wash twice with PBS.
3. Prepare a humid chamber: Lay out a large square plastic dish (e.g., 24.5 × 24.5-cm polystyrene dish with lid) with a moistened piece of absorptive filter paper and coat with a layer of Parafilm M.

Perform all blocking and immunolabelling steps as follows: Using forceps, place coverslips with the cell side facing downward onto a drop of about 20 µl of blocking or antibody mixture spotted onto parafilm in the humid chamber. This helps minimize the amount of antibody needed without letting the cells dry out. In order to minimize the loss of cells when moving the coverslips after each incubation step, pipette a small amount of PBS right next to the edge of each coverslip after each incubation step. This will cause the coverslips to float on top of the PBS and will allow easy removal of the coverslips using forceps. Wash coverslips by carefully submerging them successively into three small beakers filled with PBS. In between individual washing steps, drain residual PBS by carefully streaking the edge of the coverslips across thin absorptive filter paper without allowing the cells to dry out.

4. Block with 10% normal goat serum in PBS for 20 min in humid chamber.
5. Stain with primary antibody mixture for 1 h at room temperature in humid chamber.
6. Wash three times with PBS. For polyclonal primary antibodies, include 0.1% Triton-X100 during first two washing steps.
7. Stain with secondary antibody mixture for 1 h at room temperature in humid chamber in the dark. To specifically label F-actin, use fluorescent dye-coupled

phalloidin, e.g., Alexa Fluor 594 phalloidin (red fluorescence), added at a concentration of 1–2.5 U/ml. To detect Leatuis by staining bacterial DNA, blue fluorescent DAPI may be added.

8. Wash three times with PBS. For polyclonal primary antibodies, include 0.1% Triton-X100 during first two washing steps.

9. To mount coverslips onto microscope glass slides, place drops of about 5 µl mounting medium on ethanol-wiped slides. Avoid air bubbles. Using forceps, gently place coverslips on mounting medium with the cell side facing downward. Once in contact with the mounting medium, avoid moving the coverslips as this will cause cells to be ripped off. Carefully remove access mounting media or residual PBS by placing a piece of absorptive filter paper onto the glass slides without moving the coverslips.

10. Dry mount coverslips for 3–4 h at room temperature in the dark or overnight prior to microscopic observation when using oil immersion lenses.

11. Store samples in the dark at 4°C. It is advisable to complete photography of samples within 1–2 weeks, as background fluorescence increases over time.

12. Using epifluorescence and appropriate emission filters, infected cells are detected readily by fluorescence actin staining (FAS) of actin pedestals. Search for interesting cells (e.g., both transfected and infected) using low magnification (e.g., 40×). To resolve subcellular structures such as pedestals, switch to higher magnification (100×) with or without optovar magnification. Always use minimal exposure time required to get a good signal-to-noise ratio.

IV. GENERAL COMMENTS ON IMMUNOFLUORESCENT ANALYSIS OF EPEC- AND EHEC-INFECTED CELLS

It is important to consider that polyclonal antibodies are likely to exhibit cross-reactivity against *E. coli*, which will lead to unspecific labeling of EPEC or EHEC bacteria and may confound the analysis of the role of a specific protein in actin pedestal formation by immunofluorescence microscopy. Thus, it may be difficult to discern between recruitment of a protein to the very tips of pedestals or bacterial attachment sites and unspecific labeling of bacteria, especially when using low magnification. Always test secondary reagents for unspecific labeling of bacteria. Consider using affinity-purified reagents. For polyclonal primary reagents, try addition of 0.1% Triton-X100 to PBS during washing steps. Cross-reaction of polyclonal reagents is no problem when immunolabelling is only performed to detect bacteria, as is the case in the examples shown in Fig. 2, in which EPEC bacteria were detected with monoclonal antibodies against bacterial EspE (Deibel *et al*., 1998) and Alexa Fluor 350 fluorescent-labelled goat antimouse secondary antibodies, whereas F-actin was stained with fluorescent Alexa Fluor 594 phalloidin, and the host cell protein Nck was visualized with the help of an EGFP tag. There are reports in the literature about preabsorption of antibodies against fixed bacteria prior to immunolabelling, which when tried in our laboratory was of little success. Another possible solution to overcome the problem may be the use of monoclonal secondary reagents (e.g., rat antimouse), which are available from various suppliers (e.g., Zymed Laboratories), although so far not as conjugates with AlexaFluor dyes.

An alternative approach to detect the subcellular localisation of a given protein during EPEC- or EHEC-induced pedestal formation is the use of the enhanced green fluorescent protein (EGFP) as a tag (see Fig. 2). It is important to keep in mind that tagging may significantly alter folding, activity, and proper subcellular localisation of the protein of interest. Thus, we recommend testing N- and C-terminal fusions and confirming that the localization pattern of an EGFP fusion protein equals the localization pattern of the untagged protein as detected by immunofluorescence microscopy. In addition, with the increasing availability and use of knockout cell lines, testing an EGFP-tagged protein for its ability to complement a null mutation may become a feasible possibility to ensure proper function of the EGFP-tagged protein.

Acknowledgments

We thank Florian Gunzer for the transmission electron micrograph of EHEC-infected piglet colon for Fig. 1, Klemens Rottner and Theresia Stradal for support and helpful discussions, and Brigitte Denker for excellent technical assistance. J.W. was supported by the DFG (SFB 621) and the Fonds der Chemischen Industrie.

References

Beltrametti, F., Kresse, A. U., and Guzman, C. A. (1999). Transcriptional regulation of the esp genes of enterohemorrhagic *Escherichia coli*. *J. Bacteriol.* **181**, 3409–3418.

Bieber, D., Ramer, S. W., Wu, C.-Y., Murray, W. J., Tobe, T., Fernandez, R., and Schoolnik, G. K. (1998). Type IV pili, transient bacterial aggregates, and virulence of enteropathogenic *Escherichia coli*. *Science* **280**, 2114–2118.

Campellone, K. G., and Leong, J. M. (2003). Tails of two Tirs: Actin pedestal formation by enteropathogenic *E. coli* and enterohemorrhagic *E. coli* O157:H7. *Curr. Opin. Microbiol.* **6**, 82–90.

Deibel, C., Kramer, S., Chakraborty, T., and Ebel, F. (1998). EspE, a novel secreted protein of attaching and effacing bacteria, is directly translocated into infected host cells, where it appears as a tyrosine-phosphorylated 90 kDa protein. *Mol. Microbiol.* **28**, 463–474.

Donnenberg, M. S., Tzipori, S., McKee, M. L., O'Brien, A. D., Alroy, J., and Kaper, J. B. (1993). The role of the eae gene of enterohemorrhagic *Escherichia coli* in intimate attachment *in vitro* and in a porcine model. *J. Clin. Invest.* **92**, 1418–1424.

Frischknecht, F., and Way, M. (2001). Surfing pathogens and the lessons learned for actin polymerization. *Trends Cell Biol.* **11**, 30–38.

Giloh, H., and Sedat, J. W. (1982). Fluorescence microscopy: Reduced photobleaching of rhodamine and fluorescein protein conjugates by n-propyl gallate. *Science* **217**, 1252–1255.

Griffin, P. M., Ostroff, S. M., Tauxe, R. V., Greene, K. D., Wells, J. G., Lewis, J. H., and Blake, P. A. (1988). Illnesses associated with *Escherichia coli* O157:H7 infections: A broad clinical spectrum. *Ann. Intern. Med.* **109**, 705–712.

Gruenheid, S., DeVinney, R., Bladt, F., Goosney, D., Gelkop, S., Gish, G. D., Pawson, T., and Finlay, B. B. (2001). Enteropathogenic *E. coli* Tir binds Nck to initiate actin pedestal formation in host cells. *Nature Cell Biol.* **3**, 856–859.

Kenny, B. (1999). Phosphorylation of tyrosine 474 of the enteropathogenic *Escherichia coli* (EPEC) Tir receptor molecule is essential for actin nucleating activity and is preceded by additional host modifications. *Mol. Microbiol.* **31**, 1229–1241.

Kenny, B., Abe, A., Stein, M., and Finlay, B. (1997). Enteropathogenic *Escherichia coli* protein secretion is induced in response to conditions similar to those in the gastrointestinal tract. *Infect. Immun.* **65**, 2606–2612.

Knutton, S., Lloyd, D. R., and McNeish, A. S. (1987). Adhesion of enteropathogenic *Escherichia coli* to human intestinal enterocytes and cultured human intestinal mucosa. *Infect. Immun.* **55**, 69–77.

Levine, M. M., Bergquist, E. J., Nalin, D. R., Waterman, D. H., Hornick, R. B., Young, C. R., and Sotman, S. (1978). *Escherichia coli* strains that cause diarrhoea but do not produce heat-labile or heat-stable enterotoxins and are non-invasive. *Lancet* **1**, 1119–1122.

Lommel, S., Benesch, S., Rottner, K., Franz, T., Wehland, J., and Kuhn, R. (2001). Actin pedestal formation by enteropathogenic *Escherichia coli* and intracellular motility of *Shigella flexneri* are abolished in N-WASP-defective cells. *EMBO Rep.* **2**, 850–857.

Lommel, S., Benesch, S., Rohde, M., Wehland, J., and Rottner, K. (2004) Enterohaemorrhagic and enteropathogenic Escherichla coli use different mechanisms for actin pedestal formation that converge on N-WASP, *Cell Microbiol*. **6**, 243–254.

Maniatis, T., Fritsch, E. F., and Sambrook, J. (1982). "*Molecular Cloning: A Laboratory Manual*." Cold Spring Harbor Laboratory, Cold Spring Harbor, NY.

Nataro, J. P., and Kaper, J. B. (1998). Diarrheagenic *Escherichia coli*. *Clin. Microbiol. Rev.* **11**, 142–201.

Perna, N. T., Plunkett, G., 3rd, Burland, V., Mau, B., Glasner, J. D., Rose, D. J., Mayhew, G. F., Evans, P. S., Gregor, J., Kirkpatrick, H. A., Posfai, G., Hackett, J., Klink, S., Boutin, A., Shao, Y., Miller, L., Grotbeck, E. J., Davis, N. W., Lim, A., Dimalanta, E. T., Potamousis, K. D., Apodaca, J., Anantharaman, T. S., Lin, J., Yen, G., Schwartz, D. C., Welch, R. A., and Blattner, F. R. (2001). Genome sequence of enterohaemorrhagic *Escherichia coli* O157:H7. *Nature* **409**, 529–533.

Scaplehorn, N., Holmstrom, A., Moreau, V., Frischknecht, F., Reckmann, I., and Way, M. (2002). Grb2 and Nck act cooperatively to promote actin-based motility of vaccinia virus. *Curr. Biol.* **12**, 740–745.

CHAPTER

52

Listeria monocytogenes: Techniques to Analyze Bacterial Infection *in vitro*

Javier Pizarro-Cerdá and Pascale Cossart

I. INTRODUCTION

Listeria monocytogenes is a gram-positive food-borne pathogen responsible for listeriosis, a human infection with an overall 30% mortality rate, ranging from a clinically nonapparent fecal carriage to sever gastroenteritis, mother-to-child infections, and central nervous system infections (Dussurget *et al*., 2004; Lecuit and Cossart, 2002; Vazquez-Boland *et al*., 2001). At the individual level, *Listeria* has the capability to cross three internal barriers: the intestinal barrier, the blood–brain barrier, and the feto–placental barrier. At the cellular level, *Listeria* is able to enter macrophages, as well as nonprofessional phagocytes, such as epithelial cells. Within infected cells, *Listeria* disrupts its internalisation vacuole and escapes the phagocytic cascade by proliferating in the cytoplasm. In this environment, *Listeria* promotes actin polymerisation in order to move inside infected cells and induces its translocation to neighbouring cells, where the intracellular infectious cycle starts again (Fig. 1). *Listeria* has become a paradigm of bacterial pathogenesis at both cellular and individual levels due to the extensive study of the bacterial virulence factors and of the cellular machinery necessary for the infectious process (Gaillard *et al*., 1991; Kocks *et al*., 1992; Dramsi *et al*., 1995; Ireton *et al*., 1996; Mengaud *et al*., 1996; Lecuit *et al*., 1999; Braun *et al*., 2000; Shen *et al*., 2000). This article describes some basic methods in cellular microbiology that have been used routinely to study the infection process of *Listeria in vitro* that can be adapted to study the pathogenesis of other intracellular bacteria.

II. MATERIALS AND INSTRUMENTATION

Listeria monocytogenes wild-type strain EGD (serovar 1/2a) comes from the bacterial collection in our laboratory at the Pasteur Institute. Lovo cells (Cat. No. CCL-229) are from the American Type Culture Collection. F-12K nutrient mixture (Kaighn's modification, Cat. No. 21127-022), L-glutamine (200 m*M*, 100×, Cat. No. 25030-024), fetal calf serum (Cat. No. 16000-044), trypsin/EDTA (1×, Cat. No. 25300-054), trypan blue (0.4% solution, Cat. No. 15250-061), and phosphate-buffered saline (PBS, pH 7.4, 10×, Cat. No. 70011-036) are from Gibco. Gentamicin (10 mg/ml, Cat. No. G-1272), bovine serum albumin (BSA, Cat. No. A-7030), saponin (Cat. No. S-7900), $CaCl_2$ (Cat. No. C-4901), $MgCl_2$ (Cat. No. M-8266), NaOH (Cat. No. 930-65), Tris (Cat. No. T-6066), paraformaldehyde (Cat. No. P-6148), and NH_4Cl (Cat. No. A-5666) are from Sigma. Malassez cell counting chamber (Cat. No. 99501.01), glass slides (Cat. No. 79703.01), coverslips (Cat. No. 79720.02), plastic boxes (Cat. No. 96496.02), curved forceps (Cat. No. 24434.01), Whatmann 3 mm chromatography paper (Cat. No. 10343.01), absorbant paper (Cat. No. 62908.01), Parafilm (Cat. No. 97949.01), orbital shaker (Cat. No. 08242.107), beakers (Cat. No. 11362.01), and

Copyright 2006, Elsevier Science (USA).
All rights reserved.

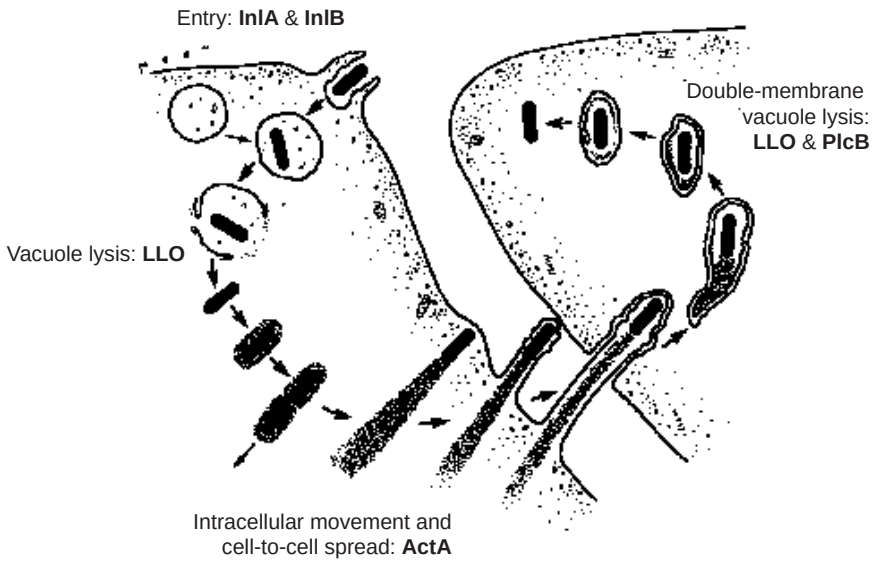

FIGURE 1 Intracellular cycle of *Listeria monocytogenes*. *Listeria* induces its own internalisation in non-phagocytic cells through interaction of the bacterial invasion proteins InlA and InlB with their cellular receptors E-cadherin and c-Met, respectively. Bacteria are initially located in a phagocytic vacuole that is disrupted by the lytic enzyme listeriolysin O (LL0), enabling *Listeria* to reach the cytoplasm and to proliferate in this environment. Intracellular actin-based movement is then induced due to the expression of the bacterial product ActA, which recruits several key players involved in actin polymerisation. Those *Listeria* that have reached the plasma membrane can form protrusions that extend to neighbouring cells. Bacteria are contained in a double-membrane phagosome that is lysed through the action of listeriolysin O and the phosphatidylcholine phospholipase C PlcB, allowing the infectious cycle to start again.

pH meter (Cat. No. 71519.01) are from Merck-Eurolab. Twenty-four-well plates (Cat. No. 351157), 15-ml polystyrene conical tubes (Cat. No. 352099), petri dishes (Cat. No. 343633), 75-cm^2 vented cell culture flasks (Cat. No. 353110), brain–heart infusion agar (Cat. No. 241830), and brain–heart infusion broth (Cat. No. 299070) are from Becton-Dickinson Biosciences. Anti-*Listeria* rabbit polyclonal serum was developed in our laboratory at the Pasteur Institute (clone R69). The mouse monoclonal anti-E cadherin BTA-1 antibody is from R&D Systems. Rabbit polyclonal antihuman c-Met (Cat. No. C-28) is from Santa Cruz Biotechnology. Goat antirabbit antibodies coupled with Alexa Fluor 488 (Cat. No. A-11008) or Alexa Fluor 546 (Cat. No. A-11010) and goat antimouse antibodies coupled with Alexa Fluor 488 (Cat. No. A-11001) and Alexa Fluor 488 phalloidin (Cat. No. A-12379) are from Molecular Probes. Mowiol 4-88 (Cat. No. 475904) is from Calbiochem. The tabletop 5415D centrifuge is from Eppendorf. Spectrophotometer Ultrospec 3000 Pro is from Amersham Pharmacia Biotech. The axiovert 135 microscope is from Zeiss. Image acquisition is performed with a RTE/CDD-1300 camera by Princeton Scientific Instruments. Image analysis and processing are done with Metamorph software from Universal Imaging Corporation.

III. PROCEDURES

A. Measurement of Bacterial Invasion: The Gentamicin Survival Assay

This procedure is a classical method that can be adapted to study the intracellular survival kinetics of different intracellular pathogens.

Solutions

1. *Cell culture medium*: F-12K nutrient mixture (Kaighn's modification) without supplements. Store at 4°C. Warm at 37°C just before use.

2. *Complete cell culture medium*: F-12K nutrient mixture (Kaighn's modification) supplemented with 2 m*M* L-glutamine and 10% fetal bovine serum. To make 500 ml, add 5 ml of a 200 m*M* L-glutamine stock solution and 50 ml of fetal bovine serum to 445 ml of F-12K nutrient mixture (Kaighn's modification). Store at 4°C and use within 7 to 8 weeks. Warm at 37°C just before use.

3. *Complete cell culture medium supplemented with gentamicin*: Complete cell culture medium supplemented with 10 µg/ml gentamicin. To make 50 ml, add 50 µl of the gentamicin stock solution (at

10 mg/ml) to 50 ml of F-12K nutrient mixture. Prepare fresh and warm at 37°C just before use.

4. *1× PBS*: To make 500 ml, add 50 ml of the PBS, pH 7.4, 10× solution to 450 ml of sterile distilled water. Store at room temperature. Warm at 37°C just before use.

5. *Trypsin/EDTA*: Aliquot in 5-ml portions in sterile 15-ml tubes. Keep at –20°C. Warm at 37°C just before use.

6. *Trypan blue solution*: Keep at room temperature.

7. *Brain–heart infusion agar*: Suspend 52 g of the powder in 1 liter of water and dissolve by frequent agitation. Autoclave at 121°C for 15 min, cool down at 50°C, and distribute in petri dishes. Keep at 4°C.

8. *Brain–heart infusion broth*: Suspend 37 g of the powder in 1 liter of water and dissolve by frequent agitation. Autoclave at 121°C for 15 min. Cool down and keep at room temperature.

Steps

1. Two days before the invasion assay, wash the LoVo cells (grown to 90% confluence in a 75-cm^2 flask) by removing the cell culture medium and adding 10 ml of PBS. Remove the PBS, add 1 ml of trypsin/EDTA, and incubate the cells for 5 min at 37°C in a 10% CO_2 atmosphere. After this incubation, carefully hit the flask to release the cells and dilute them in 10 ml of fresh complete cell culture medium. Take 10 µl of this solution and mix with 90 µl of a 0.4% trypan blue solution. With a visible light microscope, count viable cells (the ones not stained by the dye) on a Malassez cell counting chamber (100 squares = 1 µl) and dilute them to a final concentration of 10^5 cells/ml with complete cell culture medium. Add 500 µl of this solution to each of three wells of a 24-well plate and incubate for 48 h at 37°C in a 10% CO_2 atmosphere.

2. The evening before the invasion assay, take a colony of *L. monocytogenes* from a brain–heart infusion agar plate and inoculate in 5 ml of brain–heart infusion broth contained in a 15-ml tube. Incubate overnight on a rocking platform at 37°C.

3. The day of the assay, dilute 400 µl of the bacterial overnight culture in 5 ml of fresh brain–heart infusion broth contained in a 15-ml tube and incubate it on a rocking platform at 37°C to an OD_{600} of 0.8 (approximately 8×10^8 bacteria/ml).

4. Centrifuge 1 ml of the bacterial culture for 2 min at 6000 rpm and resuspend the pellet in 1 ml of PBS. Repeat this step twice; the second time resuspend the bacterial pellet in 1 ml of cell culture medium. Measure the OD and dilute bacteria to a final solution of 10^7 bacteria/ml with cell culture medium.

5. Wash LoVo cells in each well once with 1 ml of cell culture medium and add 500 µl of the bacterial dilution (MOI of 50, as we assume that cells have grown to a final density of 10^5 cells/well). Incubate for 1 h at 37°C in a 10% CO_2 atmosphere.

6. Make a 10-fold dilution of the initial bacterial solution by adding 100 µl of this preparation to 900 µl of sterile distilled water contained in an Eppendorf tube. Make another 10-fold dilution by adding 100 µl of the first 10-fold dilution to 900 µl of sterile distilled water contained in a different Eppendorf tube. Repeat this operation twice. Take a brain–heart infusion agar plate, divide the surface into four equal parts (by tracing a cross on the bottom of the plate), and plate 50 µl of each 10-fold dilution on each part. Incubate the plate overnight at 37°C in order to have an exact record of the precise number of bacteria that were inoculated on LoVo cells.

7. After 1 h of bacterial inoculation, wash LoVo cells carefully three times with 1 ml of PBS and then add 1 ml of the cell culture medium supplemented with gentamicin. Incubate the cells for another hour at 37°C in a 10% CO_2 atmosphere.

8. Wash the cells twice with 1 ml of PBS and add 1 ml of sterile distilled water to each well. Disrupt the cells by pipetting up and down water several times. Make a 10-fold dilution by adding 100 µl of the disrupted cell solution contained in each well to a different Eppendorf containing 900 µl of steriled distilled water. Make another 10-fold dilution for each tube by adding 100 µl of the first 10-fold dilution to 900 µl of sterile distilled water contained in a different Eppendorf tube. Repeat this operation once for each individual series of tubes. Take three brain–heart infusion agar plates, divide their surface in four equal parts (by tracing a cross on the bottom of the plate), and for each series of tubes, plate 50 µl of each 10-fold dilution on a different part of the agar plate (also plate 50 µl of the initial disrupted cell solution contained on the wells). Incubate the plate overnight at 37°C.

9. The day after the invasion assay, count the colony-forming units (CFU) on the agar plates at a dilution that allows a clear discrimination of individual bacterial colonies. The percentage of *Listeria* that were able to invade the LoVo cells (and which survived the gentamicin treatment) is evaluated as the ratio of bacteria recovered from the disrupted cell solution divided by the total number of bacteria added to the monolayers (results are expressed as the mean of bacterial counts obtained from the three different wells ± standard deviation).

Comments

1. Cells are grown preferentially without antibiotics.

2. *Listeria* are P2 microorganisms and should be manipulated in a microbiological hood.

3. The replication of bacteria inside cells can be analysed over time if different subsets of cells are infected initially at the same time and then each subset of cells is lysed at different time points after inoculation. This procedure is helpful in order to track the proliferation or killing of bacteria in the intracellular environment.

B. Measurement of Bacterial Invasion: Differential Immunofluorescence Labeling of Intracellular versus Extracellular Bacteria

Visualisation of bacteria allows evaluation of several parameters, such as the proportion of cells in the inoculated monolayer to which bacteria attach, as well as the proportion of adherent versus invasive bacteria.

Solutions

1. *Cell culture medium, complete cell culture medium, 1× PBS, trypsin/EDTA, trypan blue solution, brain–heart infusion agar, and brain–heart infusion broth*: Prepare as described in the Section III,A.

2. *Fixation solution*: 3% paraformaldehyde in PBS. To prepare 100 ml, heat 80 ml of PBS to 80°C and then add 3 g of paraformaldehyde while stirring. Mix until clear (add a few drops of 1 *N* NaOH to help dissolution if the liquid does not become clear after several minutes of stirring). Add 100 µl of 100 m*M* $CaCl_2$ and 100 µl of 100 m*M* $MgCl_2$, cool down at room temperature, add PBS up to 100 ml, and check pH (should be about 7.4). Aliquot in 5-ml portions and store at –20°C. Use only freshly thawed solution.

3. *Quenching solution*: 50 m*M* NH_4Cl in PBS. Prepare 100 ml of a stock solution of 1 *M* NH_4Cl in PBS by adding 5.35 g of NH_4Cl to 80 ml of PBS. Mix until clear and add PBS up to 100 ml. Keep at room temperature. The quenching solution used in the experiment will be prepared freshly by diluting 500 µl of the 1 *M* NH_4Cl stock solution in 9.5 ml of PBS.

4. *Blocking solution*: 1% BSA in PBS. To prepare 200 ml, add 2 g of BSA to 200 ml of PBS. Mix until clear. Prepare fresh just before performing the experiment.

5. *Permeabilising/blocking solution*: 0.05% saponin in blocking solution (1% BSA in PBS). To prepare 100 ml, add 50 µg of saponin to 100 ml of blocking solution. Prepare fresh just before performing the experiment.

6. *First primary antibody solution*: 1/500 dilution of R11 anti-*Listeria* rabbit polyclonal serum in blocking solution. To prepare 500 µl, add 1 µl of the R11 serum in 499 µl of blocking solution (1% BSA in PBS). Prepare fresh before performing the experiment.

7. *First secondary antibody solution*: 1/500 dilution of Alexa 546 antirabbit serum in blocking solution. Prepare as in step 6.

8. *Second primary antibody solution*: 1/500 dilution of R11 anti-*Listeria* rabbit polyclonal serum in permeabilising solution. Prepare as in step 6, using permeabilising/blocking solution instead of blocking solution.

9. *Second secondary antibody solution*: 1/500 dilution of Alexa 488 antirabbit serum in permeabilising solution. Prepare as in step 7, using permeabilising/blocking solution instead of blocking solution.

10. *Mounting solution*: 2.4% Mowiol/6% glycerol in 20 m*M* Tris buffer. To prepare 100 ml, add 2.4 g of Mowiol and 6 g of glycerol to 6 ml of distilled water. Keep at room temperature overnight. Add 90 ml of 0.2 *M* Tris, pH 8.5, warm in a water bath at 50°C, and mix regularly until total dissolution. Spin 15 min at 4000 rpm and aliquot supernatant in 1-ml portions at –20°C. Once an aliquot is thawed, keep at 4°C.

Steps

1. Infect LoVo cells following steps 1 to 5 described in Section III,A, adding 12-mm-diameter glass coverslips to the wells before seeding the cells (step 1).

2. After 1 h of bacterial inoculation, wash LoVo cells carefully three times with 1 ml of PBS and then add 500 µl of the fixation solution. Incubate for 15 min (all steps are now performed at room temperature).

3. Wash LoVo cells carefully once with 1 ml of PBS and add 500 µl of the quenching solution in order to block free aldehyde groups. Incubate for 10 min.

4. Prepare a wet incubation chamber by humidifying a 10 × 10-cm piece of Whatman 3 mm chromatographic paper. Add a sheet of Parafilm over the Whatman paper and, for each coverslip that is going to be labelled, add a drop of 30 µl of the first primary antibody solution to the Parafilm sheet.

5. Take carefully each coverslip from the wells with the forceps, carefully remove the excess of liquid from the coverslip by touching gently the tip of the coverslip with absorbant paper, and label extracellular bacteria by putting the coverslip (cells downwards) over the drop of the first primary antibody solution. Cover with a plastic lid and incubate for 30 min.

6. Prepare a second wet incubation chamber as described in step 4 and add a drop of 30 µl of the first secondary antibody solution to the Parafilm sheet for each coverslip that is going to be labeled.

7. Take carefully each coverslip with the forceps and, in order to wash the first primary antibody solution, dip it gently 10 times in a 50-ml beaker containing 40 ml of the blocking solution. Remove excess

liquid as described in step 5 and label the first primary antibody by putting the coverslip (cells downwards) over the drop of the first secondary antibody solution. Cover with the plastic lid and incubate for 25 min.

8. Prepare a third wet incubation chamber as described in step 4 and, for each coverslip that is going to be labelled, add a drop of 30 µl of the second primary antibody solution to the Parafilm sheet.

9. Take carefully each coverslip with the forceps and wash the first secondary antibody solution by dipping the coverslip 10 times in a 50-ml beaker containing 40 ml of the blocking solution and then dipping it again 10 times in a 50-ml beaker containing 40 ml of the permeabilising/blocking solution. Remove excess liquid from the coverslip as described in step 5 and label intracellular and extracellular bacteria by putting the coverslip (cells downwards) over the drop of the second primary antibody solution. Cover with the plastic lid and incubate for 30 min.

10. Prepare a fourth wet incubation chamber as described in step 5 and add a drop of 30 µl of the second secondary antibody solution to the Parafilm sheet for every coverslip that is going to be labelled.

11. Take carefully each coverslip with the forceps and wash the second primary antibody solution by dipping the coverslip 10 times in a 50-ml beaker containing 40 ml of the permeabilising/blocking solution. Remove excess liquid as described in step 5 and label the second primary antibody by putting the coverslip (cells downwards) over the drop of the second secondary antibody solution. Cover with the plastic lid and incubate for 25 min.

12. Take carefully each coverslip and wash the second secondary antibody solution by dipping it 10 times in a 50-ml beaker containing 40 ml of the permeabilising/blocking solution, 10 times in a different 50-ml beaker containing 40 ml of PBS, and 10 times in a third 50-ml beaker containing 40 ml of distilled water. Remove excess water and put the coverslip carefully over a 10-µl drop of mounting medium on top of a glass slide.

13. Visualise the preparation with a fluorescence microscope (Fig. 2). Extracellular bacteria, labelled with the first and second primary antibodies and, accordingly, also labelled with the first and second secondary antibodies, will appear yellow (due to the superposition of the green signal of the Alexa 488 fluorochrome and of the red signal of the Alexa 546 fluorochrome). Intracellular bacteria, however, labelled only with the second primary antibody and, consequently, labelled only with the second secondary antibody, will appear green. Count extracellular and intracellular *Listeria* in at least 100 LoVo cells and express the results in a histogram standardising the

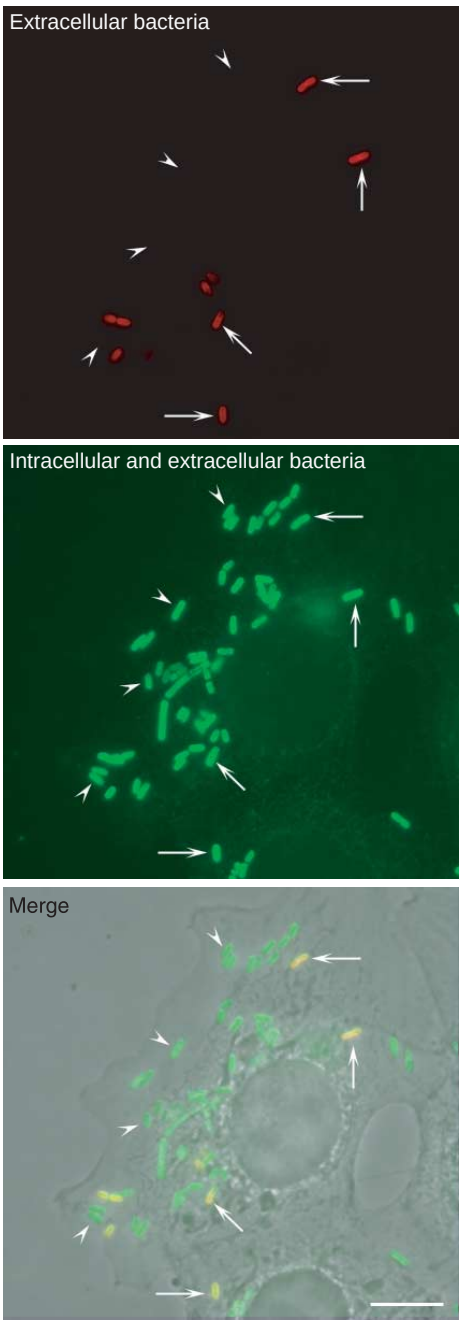

FIGURE 2 Differential immunolabeling of intracellular versus extracellular bacteria. LoVo cells were infected with *L. monocytogenes* as described in the text, and extracellular bacteria were distinguished from intracellular microorganisms by differential immunolabeling. (Top) Extracellular bacteria were labeled with an anti-*Listeria* serum without permeabilising LoVo cells. (Middle) The total population of bacteria (both extracellular and intracellular) was labeled with the same anti-*Listeria* serum after permeabilising LoVo cells. Intracellular bacteria are identified as those bacteria that are labeled only after the permeabilisation treatment. (Bottom) Phase image of LoVo cells and *Listeria*. Bar: 5 µm. Arrowheads, intracellular bacteria; arrows; extracellular bacteria.

total number of bacteria to 100% and expressing accordingly the corresponding proportions of extracellular and intracellular *Listeria*.

Comments

1. Never allow cells to dry.
2. As fluorochromes are sensitive to light, perform incubations in the dark by covering with a plastic lid enveloped in aluminum foil.
3. Antibody dilutions are suggested accordingly to their use in our own laboratory. They could need finer adjustment depending on the batch used.

C. Visualisation of the Interaction of *Listeria* with Its Receptors E-Cadherin and c-Met

Two bacterial proteins, InlA (internalin) and InlB, are known to mediate the internalisation process of *Listeria* into target cells (Gaillard *et al*., 1991; Dramsi *et al*., 1995; Cossart *et al*., 2003). InlA promotes entry into a subset of epithelial cells that express its cellular receptor, the adhesion molecule E-cadherin (Mengaud *et al*., 1996; Lecuit *et al*., 1999), a transmembrane protein that is normally involved in homophilic cell/cell interactions. Two different cellular receptors have been identified for InlB: the receptor for the globular part of the complement component C1q (gC1q-R) (Braun *et al*., 2000) and c-Met, the receptor for the hepatocyte growth factor (Shen *et al*., 2000). Interaction of InlA and InlB with their respective cellular receptors induces the recruitment to the site of bacterial entry of intracellular molecules that mediate cytoskeletal rearrangements necessary to induce bacterial invasion (Ireton *et al*., 1996, 1999; Lecuit *et al*., 2000; Bierne *et al*., 2001). By immunofluorescence it is possible to visualise the recruitment of E-cadherin and c-Met at the site of bacterial invasion.

Solutions

1. *Cell culture medium, complete cell culture medium, 1× PBS, trypsin/EDTA, trypan blue solution, brain–heart infusion agar, and brain–heart infusion broth*: Prepare as described in Section III,A.

2. *Fixation solution, quenching solution, permeabilising/blocking solution, and mounting medium*: Prepare as described in Section III,B.

3. *Primary antibody solution*: 1/100 dilution of both the anti-E-cadherin mouse monoclonal serum BTA-1 and the anti-C-Met polyclonal serum C-28. To prepare 500 µl, add 5 µl of the anti-E-cadherin BTA-1 serum and 5 µl of the anti-C-Met C-28 serum to 490 µl of permeabilising/blocking solution. Prepare fresh before performing the experiment.

4. *Secondary antibody solution*: 1/500 dilution of both Alexa 488 antimouse serum and Alexa 546 antirabbit serum in permeabilising/blocking solution. To prepare 500 µl, add 1 µl of each secondary antibody to 498 µl of permeabilising/blocking solution freshly before use.

Steps

1. Infect LoVo cells following step 1 in Section III,B.
2. Fix and quench LoVo cells following steps 2 and 3 in Section III,B.
3. Label LoVo cells following steps 4 to 7 in Section III,B, taking into account that in the present experiment there is only one primary antibody solution (containing actually a mix of two different primary antibodies) and only one secondary antibody solution (containing a mix of two different secondary antibodies).
4. Wash and mount the cells following step 12 in Section III,B.
5. Visualise the preparation with a fluorescence microscope (Fig. 3). c-Met will be recognised by the red signal (from the Alexa 546 fluorochrome) and will be observed at different locations of the plasma membrane of LoVo cells. E-cadherin will be detected by the green signal (from the Alexa 488 fluorochrome) and will be found essentially at adherens junctions located in the borderline region between two different adjacent cells. *Listeria* can be visualised by light microscopy (phase contrast). Both receptors can also be detected at the site of entry of invading *Listeria*.

D. Visualisation of *Listeria*-Induced Actin Comet Tails and Protrusions

A hallmark of *Listeria* infection is the polymerisation of cellular actin: bacteria that have escaped their internalisation vacuoles take advantage of this actin-based motility mechanism to reach and infect neighbouring cells without leaving the intracellular environment. A single bacterial product, the protein ActA, is responsible for this phenomenon by recruiting to the bacterial rear end two cellular key players of the actin nucleation process: VASP and the Arp2/3 complex (Cossart, 2000). Polymerised actin can be visualised as a structure that extends from the rear end of the moving *Listeria* to the cell cytoplasm, which has been named the actin comet tail. Bacteria that have reached the plasma membrane of a primary infected cell form protrusions that extend into the cytoplasm of neighbouring cells (or that extend simply to the extracellular space in the case of cells that do not have adjacent neighbours). These structures can be visualised by labelling the cel-

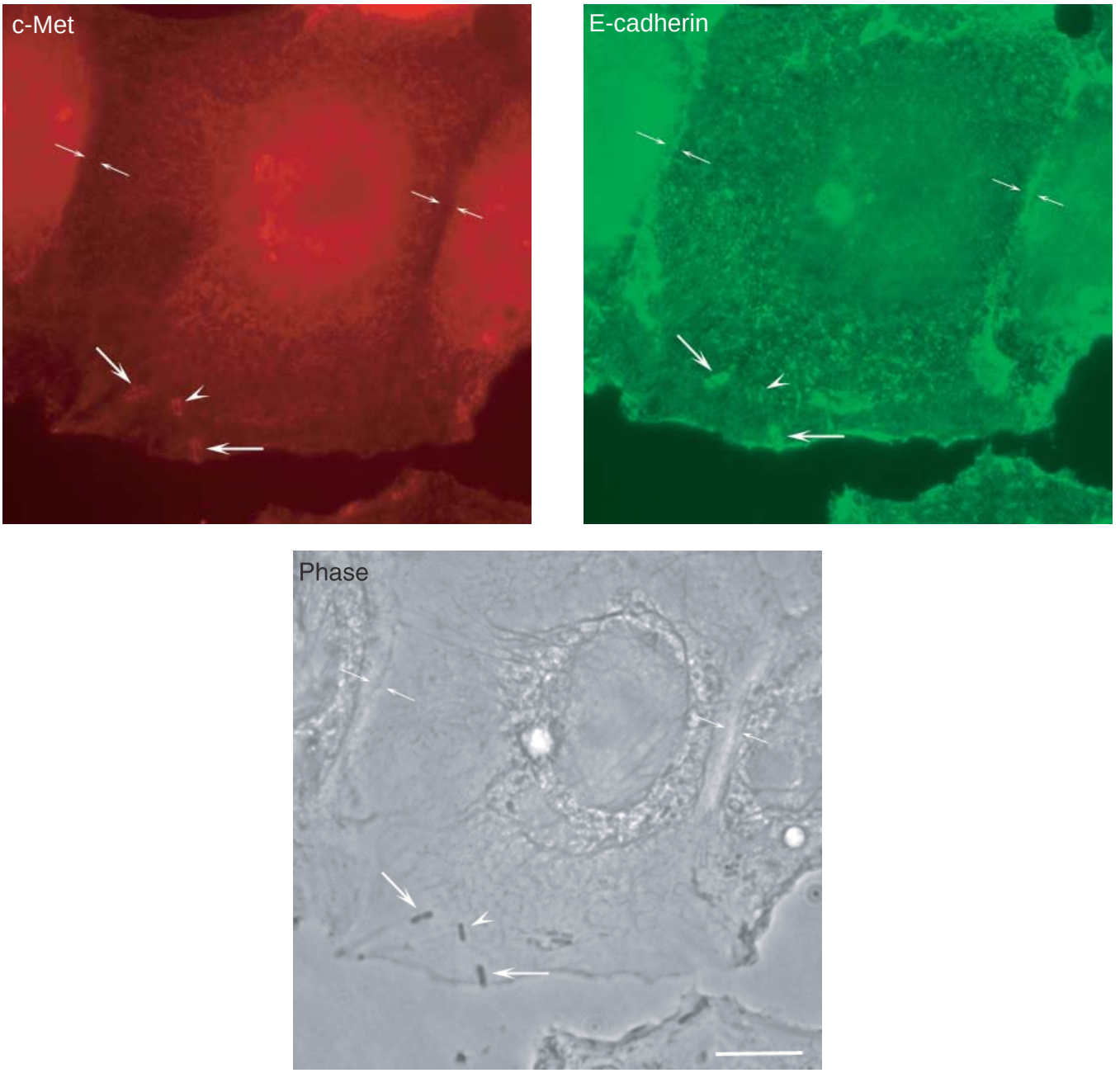

FIGURE 3 Interaction of *Listeria* with its receptors E-cadherin and c-Met. LoVo cells were infected with *L. monocytogenes* as described in the text, and its receptors E-cadherin and c-Met were immunolabelled. (Top left) c-Met shows a diffuse distribution in LoVo cells and is clearly absent at sites of adherens junctions formation, but is clearly recruited at sites of bacterial invasion. While some of the invading *Listeria* colocalise with both E-cadherin and c-Met, one bacterium is shown that only colocalises with c-Met and not with E-cadherin (arrowhead), suggesting that the interaction of *Listeria* with each one of their receptors can be uncoupled, as observed in cells lines such as Caco-2 (in which invasion is mediated mainly by the InlA/E-cadherin interaction) or Vero (in which invasion is driven exclusively by the InlB/c-Met interaction). (Top right) E-cadherin distribution at the plasma membrane of LoVo cells can be clearly seen at sites of adherens junction formation as well as at sites of bacterial entry. (Bottom) Phase image of LoVo cells and *Listeria*. Bar: 5µm. Opposing arrows, adherens junction; large arrows, bacteria that recruit E-cadherin and c-Met at their site of entry; arrowheads, bacterium that only recruits c-Met at its site of entry.

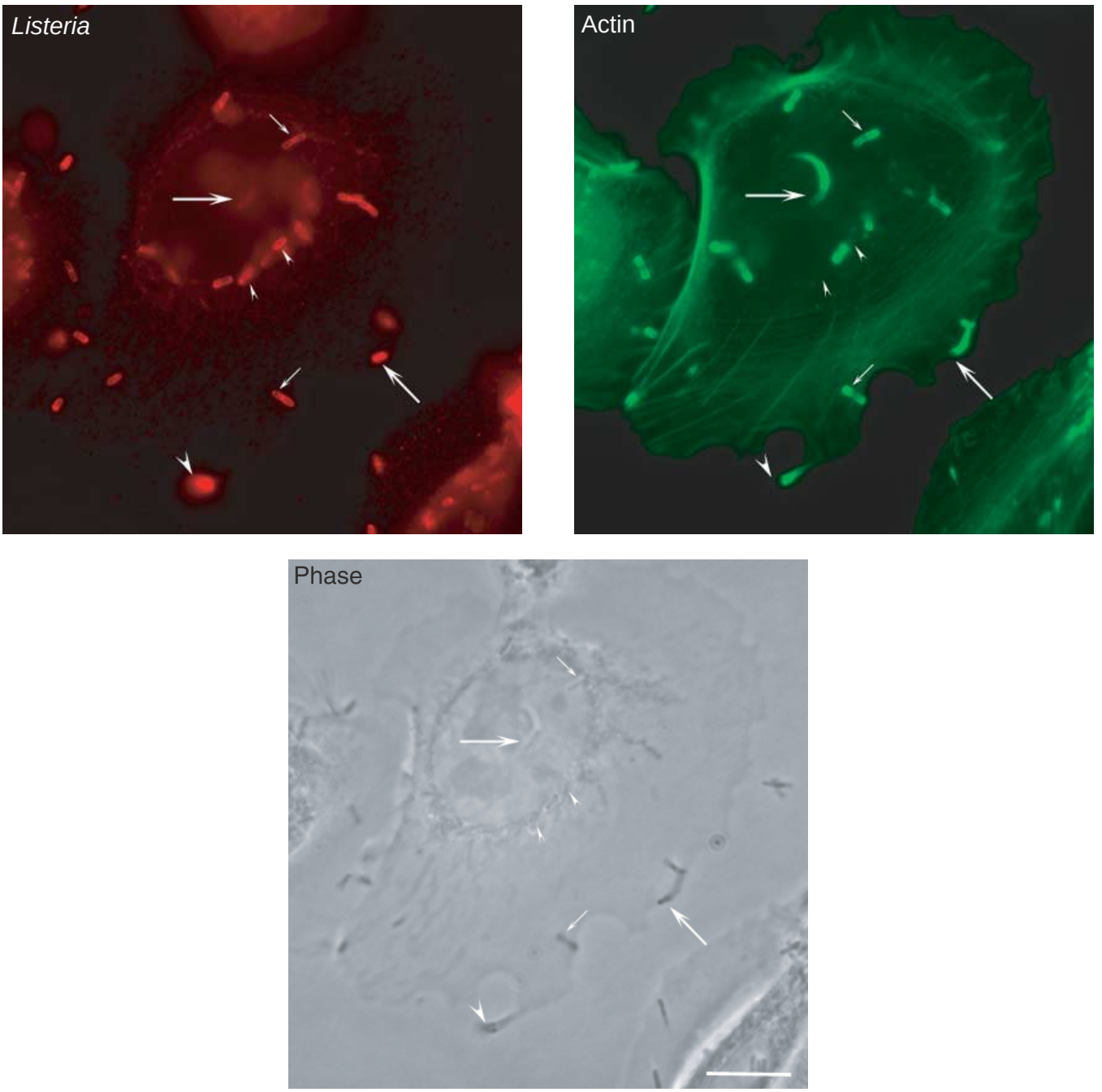

FIGURE 4 Actin polymerisation and protrusion formation by *Listeria*. LoVo cells were infected with *Listeria* as described in the text. Both bacteria and the actin cytoskeleton were labelled for immunofluorescence analysis. (Top left) Labelling of the total population of bacteria associated to LoVo cells. (Top right) Actin labelling with the fungal drug phalloidin. While some bacteria are not associated with actin (small arrowheads), other bacteria are detected at early phases of actin polymerisation (small arrows). Bacteria at later stages of their intracellular cycle can be observed at the tip of actin comet tails (big arrows). *Listeria* that have reached the plasma membrane can form protrusions that extend beyond the infected cell (big arrowhead). (Bottom) Phase image of LoVo cells and *Listeria*. Bar: 5µm.

lular actin with the fungal drug phalloidin in cells that have been infected with *Listeria* for at least 5 h.

Solutions

1. *Cell culture medium, complete cell culture medium, 1× PBS, trypsin/EDTA, trypan blue solution, brain–heart infusion agar, and brain–heart infusion broth*: Prepare as described in Section III,A.

2. *Fixation solution, quenching solution, permeabilising/blocking solution, and mounting medium*: Prepare as described in Section III,B.

3. *Primary antibody solution*: 1/500 dilution of R11 anti-*Listeria* rabbit polyclonal serum in permeabilising/blocking solution. To prepare 500 µl, add 1 µl of the R11 serum in 499 µl of permeabilising/blocking solution. Prepare fresh before performing the experiment.

4. *Secondary antibody and probe solution*: 1/500 dilution of Alexa 546 antirabbit serum in permeabilising/blocking solution and 1/100 dilution of phalloidin Alexa 488. To prepare 500 µl, add 1 µl of the Alexa 546 serum and 5 µl of the phalloidin Alexa 488 probe to 496 µl of permeabilising/blocking solution. Prepare freshly before use.

Steps

1. Infect LoVo cells following steps 1 to 5 and step 7 in Section III,A, adding 12-mm-diameter glass coverslips to the wells before seeding the cells (step 1) and incubating the LoVo cells in the presence of cell culture medium supplemented with gentamicin for 5 h insted of 1 h (step 7).

2. Fix and quench LoVo cells following steps 2 and 3 in Section III,B.

3. Label LoVo cells following steps 4 to 7 in Section III,B, taking into account that in the present experiment there is only one primary antibody solution (containing one primary antibody) and only one secondary antibody solution (containing a mix of one secondary antibody and one cytoskeletal probe).

4. Wash and mount the cells following step 12 in Section III,B.

5. Visualise the preparation using a fluorescence microscope (Fig. 4). Actin will be detected by the green signal (from the Alexa 488 fluorochrome) and will be observed at different cellular locations, such as stress fibres or cortical filaments near the plasma membrane. *Listeria* will appear as red (due to the signal of the Alexa 546 fluorochrome). Bacteria that have just lysed their phagosomal membrane and that have already started to polymerise actin will also be surrounded uniformly with the Alexa 488 fluorochrome. Those *Listeria* that broke their vacuole early will be associated with comet tails, which can be visualised starting at the rear pole of red bacteria and projecting into the cell cytoplasm. In the case of those *Listeria* that have reached the plasma membrane of an infected cell, a protrusion can be seen as a protruding structure that contains a red bacteria at its tip and a green actin comet tail following behind.

References

Bierne, H., Gouin, E., Roux, P., Caroui, P., Yin, H.L., and Cossart, P. (2001). A role for cofilin and LIM Kinase in Listeria induced phagocytosis. *J. Cell Biol.* **155**, 101–112.

Braun, L., Gebrehiwet, B., and Cossart, P. (2000). gC1q-R/p32, a C1q binding protein, is a novel receptor for *Listeria monocytogenes*. *EMBO J.* **19**, 1458–1466.

Cossart, P. (2000). Actin-based motility of pathogens: The Arp2/3 complex is a central player. *Cell. Microbiol.* **2**, 195–205.

Cossart, P., Pizarro-Cerda, J., and Lecuit, M. (2003). Invasion of mammalian cells by Listeria monocytogenes: Functional mimicry to subvert cellular functions. *Trends Cell Biol.* **13**, 23–31.

Dramsi, S., Biswas, I., Maguin, E., Braun, L., Mastroeni, P., and Cossart, P. (1995). Entry of *L. monocytogenes* into hepatocytes requires expression of InlB, a surface protein of the internalin multigene family. *Mol. Microbiol.* **16**, 251–261.

Dussurget, O., Pizarro-Cerda, J., and Cossart, P. (2004). Molecular determinauts of Listeria monocytogeues virulence. *Annu. Rev. Microbiol.* **58**, 587–610.

Gaillard, J.-L., Berche, P., Frehel, C., Gouin, E., and Cossart, P. (1991). Entry of *L. monocytogenes* into cells is mediated by internalin, a repeat protein reminiscent of surface antigens from Gram-positive cocci. *Cell* **65**, 1127–1141.

Ireton, K., Payrastre, B., and Cossart, P. (1999). The Listeria monocytogenes protein InlB is an agouist of manmalian phosphoinositide 3-kinase. *J. Biol. Chem.* **274**, 17025–17032.

Ireton, K., Payrastre, B., Chap, H., Ogawa, W., Sakaue, H., Kasuga, M., and Cossart, P. (1996). A role for phosphoinositide 3-kinase in bacterial invasion. *Science* **274**, 780–782.

Kocks, C., Gouin, E., Tabouret, M., Berche, P., Ohayon, H., and Cossart, P. (1992). *L. monocytogenes*-induced actin assembly requires the actA gene product, a surface protein. *Cell* **68**, 521–531.

Lecuit, M., and Cossart, P. (2002). Genetically-modified animal models for human infections: The *Listeria* paradigm. *Trends Mol. Med.* **8**, 537–542.

Lecuit, M., Dramsi, S., Gottardi, C., Fedor-Chaiken, M., Gumbiner, B., and Cossart, P. (1999). A single amino-acid in E-cadherin is responsible for host specificity towards the human pathogen *Listeria monocytogenes*. *EMBO J.* **18**, 3956–3963.

Lecuit, M., Hurme, R., Pizaro-Cerda, J., Ohayon, H., Geiger, B., and Cossart, P. (2000). A role for alpha- and beta-catenins in bacterial uptake. *Proc. Natl. Acad. Sci. USA* **97**, 10008–10013.

Mengaud, J., Ohayon, H., Gounon, P., Mège, J.-M., and Cossart, P. (1996). E-cadherin is the receptor for internalin, a surface protein required for entry of *Listeria monocytogenes* into epithelial cells. *Cell* **84**, 923–932.

Shen, Y., Naujokas, M., Park, M., and Ireton, K. (2000). InlB-dependent internalization of *Listeria* is mediated by the met receptor tyrosine kinase. *Cell* **103**, 501–510.

Vazquez-Boland, J.A., Kuhn, M., Berche, P., Chakraborty, T., Dominguez-Bernal, G., Goebel, W., Gonzalez-Zorn, B., Wehland, J., and Kreft, J. (2001). Listeria pathogenesis and molecular virulence determinants. *Clin. Microbiol. Rev.* **14**, 584–640.

SECTION

11

Mechanical Stress in Single Cells

CHAPTER

53

Measurement of Cellular Contractile Forces Using Patterned Elastomer

Nathalie Q. Balaban, Ulrich S. Schwarz, and Benjamin Geiger

1. INTRODUCTION

The adhesive interaction of cells with their neighbors and with the extracellular matrix is a characteristic feature of all metazoan organisms. Cell adhesion is essential for cell migration, tissue assembly, and the direct communication of cells with their immediate environment. These interactions are mediated via specific cell surface receptors that specifically interact with the external surface, and link it, across the membrane, with the actin cytoskeleton (Geiger *et al.*, 2001). These multimolecular complexes are subjected to constant mechanical perturbation, generated either by the cellular contractile system or by changes in the neighborhood of the cell. To list just a few examples, in the course of cell migration, focal adhesions (FA) are formed, where contractile microfilament bundles, consisting of actin and myosin, are anchored. Their pulling on the substrate is involved in regulating the adhesion itself, as well as in coordinating the persistent forward movement of the cell. Mechanical perturbations are generated by diverse external factors, such as muscle contraction, blood flow, gravitational forces, and acoustic waves. Both internal and external forces apparently act at adhesion sites and modulate their organization and signaling activity (Geiger and Bershadsky, 2001; Riveline *et al.*, 2001; Galbraith *et al.*, 2002). In view of the major physiological significance of these cellular forces, it appears important to develop approaches for the accurate measurement of cellular forces with an appropriate sensitivity and spatial resolution (Beningo and Wang, 2002; Roy *et al.*, 2002). This article describes an approach for measuring such forces using the patterned polydimethylsiloxane (PDMS) elastomer as an adhesive substrate and cells expressing fluorescent focal adhesion molecules (Balaban *et al.*, 2001). These experiments demonstrated that cells maintain a constant stress at focal adhesion sites, of the order of ~5 n$N/\mu m^2$, and that changes in cellular contractility lead rapidly to changes in FA organization. This article describes the technique used for the preparation of the patterned elastomeric substrate and for measuring the cellular forces.

II. MATERIALS AND EXPERIMENTATION

A. Lithography

Silicone wafer
Photoresist: Microposit S1805 (Shipley, Marlborough, MA)
Developer: Microposit MF-319 (Shipley)
HMDS or tridecafluorooctyltrichlorosilane (UCT, Bristol, PA)
Acetone, methanol
Spinner (Headway Research, Inc., Garland TX)
Mask aligner (Karl Suss, MJB3, Germany)
Chrome mask with desired pattern, or transparency
Digital hot plates
Oven
Scriber

B. Elastomer

PDMS: Sylgard 184, Dow Corning
No. 1 glass coverslips (diameter 25 mm)
Oven

Copyright 2006, Elsevier Science (USA).
All rights reserved.

C. Microscopy

The DeltaVision microscopy system (Applied Precision Inc., Issaquah, WA) is used in these experiments. Similar microscopy systems could be used for such purpose, provided that they are capable of accurately acquiring high-resolution images (512 × 512 pixels or better) at a high sensitivity (allowing for low-dose recording) and high dynamic range (12 bit or better).

D. Calibration

Bulk calibration: weights, clamps

Calibrated micropipettes with elastic constants 10–50 n$N\,\mu m^{-1}$

E. Image Analysis

Image analysis software: Priism (Applied Precision Inc.)

Data analysis software: Matlab (The Mathworks, Natick, MA) (This software can be purchase with image analysis toolbox and used to perform the image analysis as well)

F. Calculation of Forces

A detailed description of this calculation is provided in a web site established by Dr. Ulrich Schwartz (see later).

III. PROCEDURES

A. Lithography

This step provides molds consisting of a pattern of photoresist on silicon wafer that will be used for the patterning of elastomer substrates, a technique termed "soft lithography" (Whitesides *et al.*, 2001). It relies on access to a clean room with basic optical lithography. It also assumes the availability of the chrome mask with the pattern of interest. For high-resolution patterns (features below 1 µm), such masks are produced by electron beam lithography (also available in many clean room facilities). For low-resolution patterns (5 µm features and more), transparencies with appropriate resolution (5080 dpi) can be used.

1. Clean silicon wafer in acetone and then immediately wash with methanol and blow dry.
2. (Optional) Bake for 20 min in a 120°C oven.
3. Dispense HMDS in the middle of the wafer until full coverage and spin at 6000 rpm for 1 min.
4. Dispense S1805 photoresist in the middle of the wafer covering approximately one-third of the wafer and spin at 5000 rpm for 30 s.
5. Soft bake on hot plate at 80°C for 5 min.
6. Make sure the wafer and the mask are in contact in the mask aligner.
7. Expose for 10 s. This number is only an estimate; exposure and development times have to be adjusted for the specific exposure system. Typically an exposure of 100–140 mJ/cm^2 is recommended.
8. Develop for 10 s (see aforementioned comment).
9. Hard bake for 5 min in a 120°C oven.
10. In order to prevent sticking between the mold and the PDMS, an additional spin of HMDS can be performed at this stage. Alternatively, overnight exposure to vapors of tridecafluorooctyltrichlorosilane can be done.
11. Dice the wafer with a scriber in small pieces of about 5 × 5 mm. Each of these pieces can be reused as a mold many times for patterning of the PDMS substrates.

B. Elastomer Substrates

1. Pour about 30 ml of part A of the Sylgard 184 kit. Add 1 part of B (cross-linker) for 50 parts of A (in weight). Mix thoroughly.

2. Cover and let stand on bench until bubbles are scarce (typically 30 min).

3. Coat glass coverslips with the PDMS mixture. For large patterns that can be seen with low-resolution, long working distance objectives, put a few drops of the mixture in the middle of the coverslip on a flat surface covered with aluminium foil and let flow until the whole coverslip is covered. For short working distance objectives, a thinner layer is needed. This can be achieved by spinning No.1 coverslips at 1000 rpm on a spinner equipped with a 0.05-in. rotating head or "chuck." Alternatively, coverslips coated with PDMS can be put vertically to allow the flow of excess PDMS and attain a thinner thickness (typically 0.05 mm).

4. Place the coated coverslips on aluminium foil and bake in an oven at 65°C for 25 min until the top layer of the PDMS has started to solidify.

5. Place the rest of the PDMS mixture in the oven for bulk calibration purposes (see Section III,D).

6. Place a piece of the mold in the center of each coverslip (the patterned side of the mold should be in contact with the PDMS) and put back in oven overnight.

7. Delicately separate the mold from the patterned coverslip.

8. Glue each patterned coverslip to the botton of a 35-mm tissue culture plate with a 15-mm hole. This step can be done with melted paraffin.

9. Wash the coverslip and dish extensively with phosphate-buffered saline (PBS).

10. Incubate at 4°C overnight with a solution of 10 µg/ml of fibronectin in PBS.

11. Before plating the cells, wash the fibronectin solution with fresh plating medium twice and incubate the substrates with medium at 37°C for 1 h.

12. Plate cells at appropriate dilution and incubate immediately until observation.

C. Microscopy

Images are recorded, using phase-contrast or fluorescence optical mode, with a DeltaVision system digital microscopy system. This system is based on a Zeiss inverted microscope equipped with filter sets for multiple color microscopy and a high-resolution, scientific-grade CCD camera. Images are acquired using high numerical aperture oil objectives for the high-resolution pattern and focal adhesion detection (Fig. 3); long distance objectives are used for semiquantitative estimates of force using large patterns (Fig. 2). Image processing is conducted primarily using the Prism software of the DeltaVision system.

D. Calibration of Elastic Properties of the Elastomer

The aim of this step is to determine whether the cured PDMS is an elastomer and to obtain the two parameters that characterize its elasticity, namely the Young modulus (Y) and the Poisson ratio (σ) (Feynman, 1964).

1. *Bulk Calibration*

Cut strips of cured elastomer (see Section III,B, step 5). Typically a strip of 100 × 30 × 5 mm can be used. Hold each side with clamps wider than the strip. With a marker, draw two lines on the elastomer, away from the clips, separated by about 50 mm. The distance between the lines is marked as L in Fig. 1. Add increasing masses, m, to the lower clamp and measure the total increase in length, dL, until $dl > L$. Plot the relation $\frac{dl}{L}(m)$ with m expressed in kilograms. Verify that the relation is linear and extract the linear coefficient, α. The Young modulus (in Pa) is given by

$$Y = \frac{g}{A\alpha}$$

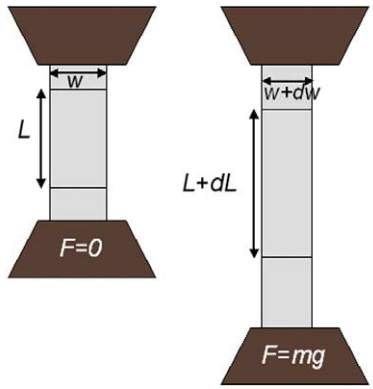

FIGURE 1 **Bulk calibration of the elastomer.** A stripe of PDMS prepared in parallel to preparation of elastomer substrates is checked for its elastic properties. The procedure consists of subjecting the stripe to increasing masses while measuring the force–extension response.

with $A = w*h$, the cross section of the strip (in m^2), and $g = 9.8\,m\,s^{-2}$.

The Poisson ration, σ, is given by measuring the contraction in w and h:

$$\frac{dw}{w} = \frac{dh}{h} = -\sigma\frac{dl}{L}$$

The strips should be stretched overnight to verify that they relax to their original length, L, once the weights are removed.

2. In Situ *Calibration*

In order to verify that the plating of cells does not modify the elastic characteristics of the surface, *in situ* calibration of the elasticity of the patterned substrate is performed under a microscope.

Mount the calibrated micropipette on a micromanipulator. Approach the surface slowly, keeping the micropipette parallel to the patterned elastomer surface. Once the tip of the micropipette is in contact with the surface, acquire an image of the patterned elastomer and of the tip of the pipette. Slowly move the stage by 2–3 µm in order to create a stress between the micropipette and the surface. Acquire a new image of the deformed pattern and of the micropipette bending. Usually, images at different magnifications are necessary in order to visualize the distortions of the pattern and of the micropipette. The force exerted by the micropipette is measured directly by quantifying the deflection of the pipette in the image. Verify that the calculation of force using the bulk Young modulus agrees with the known force exerted by the calibrated micropipette.

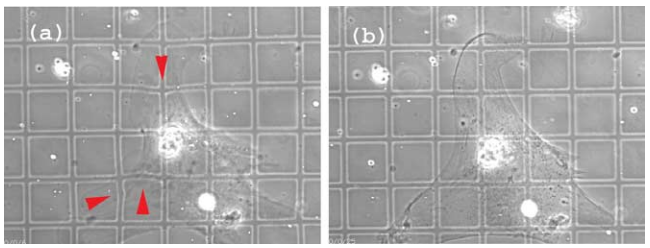

FIGURE 2 **Rapid semiquantitative estimate of forces (Balaban *et al.*, 2001).** A large grid-patterned elastomer is used for the easy visualization of distortions. (a) A rat cardiac fibroblast exerts forces on the elastomer substrates, which result in deformations of the grid (marked by arrows). (b) Once the forces are relaxed by adding an inhibitor of contractility, the grid returns to its original regular shape. Grid size: 30 μm.

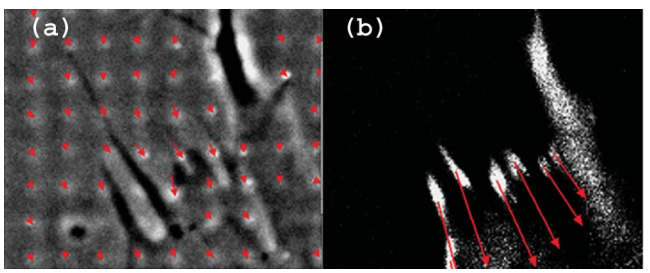

FIGURE 3 **From displacements to forces (Balaban *et al.*, 2001).** (a) Phase-contrast image of a small part of a fibroblast on the high-resolution dot pattern. Arrows denote displacements of the center of mass of the dots relative to the relaxed image. Pitch size: 2 μm. (b) Fluorescence image of the same field of view showing locations of the focal adhesions. The length of the arrows here indicates the forces at each focal adhesion, calculated from displacement data.

E. Image Analysis

Substrates with low resolution patterns such as the 30-μm grid shown in Fig. 2 can provide semiquantitative estimates of the mechanical perturbation due to cells and is useful for the rapid comparison between different cell types or conditions. However, for the quantitative measurement of the forces at single adhesion sites, high-resolution patterns of dots (Fig. 3a), as well as fluorescence tagging of adhesion sites, are needed (Fig. 3b). In this section, it is assumed that the following images are available for the same field of view.

a. Phase contrast of cells on a high-resolution pattern of dots ("dot_force.tif").

b. Phase contrast of the high-resolution pattern of dots, after forces have been relaxed ("dot_relaxed.tif"), namely after treatment with acto-myosin inhibitors or trypsinization. Alternatively, locations of the dots in the relaxed pattern can be generated directly as ("center_relaxed.dat") by assuming the regularity of the pattern.

c. Fluorescence image of adhesion sites ("focals.tif").

Registration of Images

In order to correct for eventual shifts during image acquisitions, all three images should be aligned using fixed reference points. Typically, corrections of a few pixels shift in x or y might be needed; angular shift are infrequent.

The step is performed using the registration option of the image analysis software.

Detection of the Pattern

This step automatically detects the dots in the two phase-contrast images and outputs their center-of-mass coordinates to an ASCII file. It is important to use the same parameters for both images.

a. Filter "dot_force.tif " and dot_relaxed.tif" with a large kernel in order to correct for background unevenness.

b. Depending on the image quality, use a high pass filter with a small kernel to enhance the dots contrast on both images.

c. Perform segmentation for the detection of the dots. Verify that the segmentation detected the dots properly. Correct manually for eventual defects.

d. Save the center of mass coordinates of the dots in each picture in two separate ASCII files ("center_relaxed.dat" and "center_force.dat").

e. Using Matlab, load the two ASCII files and arrange in pairs nearest neighbors according to their center of mass coordinates to identify equivalent dots between the two files. This will work for most of the image where there are no displacements. In areas where displacements are larger than the distance between dots, manual corrections might be needed (see Section III,F). Save data as an ASCII file ("lines.dat") whose first two columns are the x and y coordinates of the dots in "center_relaxed.dat" and the last two columns are the x and y coordinates of the equivalent dots from "center_force.dat".

f. Visualization of the displacements: load "lines.dat" using a procedure for drawing arrows in the image analysis software (DrawArrows in Prism) on top of the phase-contrast images. Correct for wrong or missing arrows. Save corrections.

3. Detection of Focal Adhesions

This step automatically detects focal adhesions in the fluorescence image of cells with GFP-tagged focal adhesion protein (Zamir *et al.*, 1999). ("focals.tif") and

outputs their center-of-mass coordinates to an ASCII file ("focals.dat"). The segmentation procedure is analogous to the detection of dots in the pattern.

F. Calculation of Forces

The main advantage of flat elastic substrates is that they interfere little with cell adhesion as traditionally studied on glass or plastic surfaces. In particular, by using transparent elastomers such as PDMS, one can use the normal setups for light microscopy. The main disadvantage of flat elastic substrates is that a computational technique has to be implemented to calculate force from displacement. For the procedure described here, a package with Matlab routines can be downloaded from http://www.mpikggolm.mpg.de/th/people/schwarz/ElasticSubstrates/. For well-spread cells, one can assume that forces are applied to the top side of the elastic film mainly in a tangential fashion. Because the PDMS film is much thicker than typical displacements on its top side, one can moreover assume that displacements follow from forces as in the case of an elastic half-space. Because we focus on forces from single focal adhesions, where force is localized to a small region of space (namely the focal adhesion), we finally assume that each focal adhesion corresponds to one point force. Then displacement follows from force as described by the well-known Boussinesq solution for the Green function (Landau and Lifshitz, 1970). Since we only consider the case of small deformations (i.e., magnitude of strain tensor $|u_{ij}| < 1$), we deal with linear elasticity theory, and deformations resulting from different force centers can be simply added up to give overall deformation at a given point. However, because the Green function of a point force diverges for small distance r as $1/r$, we first use the Matlab program "data.m" to clear the file "lines.dat" from all displacement data points, which are closer to the positions of the focal adhesions in "focals.dat" than a distance of the order of the size of focal adhesions [this procedure can be justified with the concept of a force multipolar expansion (Schwarz *et al.*, 2002)]. This gives a new file "newlines.dat", which together with "focals.dat" is used by our main Matlab program, "inverse.m". Since we are interested in force as a function of displacement, but the Boussinesq solution from linear elasticity theory describes deformation as a function of force, we now have to solve an inverse problem. Because the elastic kernel effectively acts as a smoothing operation that removes high-frequency data, this inversion is ill posed in presence of noise in displacement data: small differences in displacement data can result in large differences in the force pattern. Due to the noise problem, we only can estimate force through a χ^2 minimization. Moreover, the target function has to be extended by a so-called regularization term, which prevents the program from reproducing every detail of displacement data through a force estimate with unrealistically large forces. Therefore, we add a quadratic term in force to the target function, which guarantees that forces do not become exceedingly large. The regularization procedure introduces an additional variable, the regularization parameter λ, whose value is fixed by the program "inverse.m" with the help of the so-called discrepancy principle, which states that the difference between measured displacement and displacement following from the force estimate should attain a certain nonvanishing value. Because the target function remains quadratic for the simple regularization term used, it can be inverted easily by singular value decomposition. For this purpose, the Matlab program "inverse.m" uses the freely available package of Matlab routines *Regularization Tools* by P. C. Hansen. Finally the force estimate is saved in a new ASCII file "forces.dat", which for each entry in "focals.dat" gives the corresponding force estimate. Force calibration assumes the value $\sigma = 0.5$ for the Poisson ratio and requires values for Young modulus Y and microscope resolution. The resolution of this procedure depends on the details of the force pattern under consideration, but can be estimated by data simulation. Even under the most favorable conditions, which can be achieved experimentally in regard to quality of displacement data, the original force cannot be reproduced completely and regularization is required to arrive at a reasonable estimate. Spatial and force resolutions have been found to be better than $4\,\mu m$ and $4\,nN$, respectively. Therefore the calculated point force should be correlated with other properties of a focal adhesion only when no other focal adhesions are closer than the spatial resolution of our method.

IV. PITFALLS

1. The mixing of the PDMS should be done in many strokes (typically for a few minutes) and preferably in plastic dishes with lids.

2. Because of variations between batches, the 50:1 ratio of the Sylgard kit might need adjustment.

3. The first bake of the PDMS layer should be fine tuned: too much baking before putting the mold will result in a poor pattern, whereas insufficient baking will result in difficulties separating the mold from the PDMS. Baking times can be reduced by increasing the temperature.

4. Before dicing the patterned wafer, make sure the scriber is good by practicing on a similar unpatterned wafer.

5. The choice of the cells to use is important: immortalized cell lines often exert forces that are below the force resolution of this method.

6. Focal adhesions formed on PDMS may differ, at the molecular level, from those formed on other substrates and their composition (e.g., type of integrin) should be examined.

Acknowledgments

BG is the E. Neter Prof. for cell and tumor biology.

NQB is supported by the Bikura program of the Israel Science foundation and is a fellow of the Center for Complexity; The Horowitz Foundation.

References

Balaban, N. Q., Schwarz, U. S., *et al.* (2001). Force and focal adhesion assembly: A close relationship studied using elastic micropatterned substrates. *Nature Cell Biol.* **3**(5), 466–472.

Beningo, K. A., and Wang, Y. L. (2002). Flexible substrata for the detection of cellular traction forces. *Trends Cell Biol.* **12**(2), 79–84.

Feynman, R. P. (1964). *The Feynman Lecture on Physics*. Addison & Wesley.

Galbraith, C. G., Yamada, K. M., *et al.* (2002). The relationship between force and focal complex development. *J. Cell Biol.* **159**(4), 695–705.

Geiger, B., and Bershadsky, A. (2001). Assembly and mechanosensory function of focal contacts. *Curr. Opin. Cell Biol.* **13**(5), 584–592.

Geiger, B., Bershadsky, A., *et al.* (2001). Transmembrane crosstalk between the extracellular matrix–cytoskeleton crosstalk. *Nature Rev. Mol. Cell Biol.* **2**(11), 793–805.

Landau, L. D., and Lifshitz, E. M. (1970). "*Theory of Elasticity*." Pergamon Press, Oxford.

Riveline, D., Zamir, E., *et al.* (2001). Focal contacts as mechanosensors: Externally applied local mechanical force induces growth of focal contacts by an mDia1-dependent and ROCK-independent mechanism. *J. Cell Biol.* **153**(6), 1175–1186.

Roy, P., Rajfur, Z., *et al.* (2002). Microscope-based techniques to study cell adhesion and migration. *Nature Cell Biol.* **4**(4), E91–E96.

Schwarz, U. S., Balaban, N. Q., *et al.* (2002). Calculation of forces at focal adhesions from elastic substrate data: The effect of localized force and the need for regularization. *Biophys. J.* **83**(3), 1380–1394.

Whitesides, G. M., Ostuni, E., *et al.* (2001). Soft lithography in biology and biochemistry. *Annu. Rev. Biomed. Eng.* **3**, 335–373.

Zamir, E., Katz, B. Z., *et al.* (1999). Molecular diversity of cell-matrix adhesions. *J. Cell Sci.* **112**(Pt. 11), 1655–1669.

PART

C

APPENDIX

CHAPTER

54

Resources

José M.A. Moreira and Emmanuel Vignal

I. INTRODUCTION

In the past decade, researchers have witnessed an explosive growth in the amount of information available to them at internet-based sites. In this day and age, researchers requiring supplementary information to a particular aspect of a research technique can do so by using a search engine or browsing through the internet, but this is more often than not a time-consuming and frustrating endeavour where one ends up having to deal with thousands of hits that are not relevant to the initial query.

This section lists outstanding resources for cell and molecular biology research that complement and extend the usefulness of the research protocols described in the previous sections. We have found the sites listed here to be comprehensible, useful, and generally well run and consequently we recommend them as good starting points for any researcher rummaging around for information. Nonetheless, this compilation is intended solely as a valuable aid to the research techniques described throughout this book rather than a stand-alone guide of laboratory procedures or an exhaustive listing of Web resources.

II. INTERNET RESOURCES FOR CELL BIOLOGISTS

A. Cells and Tissue Culture

1. The World Federation for Culture Collections (WFCC)

http://wdcm.nig.ac.jp/wfcc

The WFCC is a federation concerned with the collection, authentication, maintenance, and distribution of cultures of microorganisms and cultured cells. The WFCC, through the World Data Center for Microorganisms (WDCM), developed an international database on culture resources worldwide. This data resource is now maintained at the National Institute of Genetics (NIG, Japan) and has records of nearly 469 culture collections from 62 countries (http://wdcm.nig.ac.jp/hpcc.html). The records contain data on the organisation, management, services, and scientific interests of the collections. Each of these records is linked to a second record containing the list of species held.

2. European Collection of Cell Cultures (ECACC)

http://ecacc.org.uk

In addition to being a bank of cell lines and hybridomas, ECACC also provides an EBV immortalisation service to establish lymphoblastoid cell lines from patients and their families with genetic and chromosomal abnormalities. This site boasts a full 25,000 cell lines and approximately 420 hybridomas.

3. RIKEN Cell Bank

http://www.rtc.riken.go.jp

The RIKEN cell bank has been organized as a unique, nonprofit public collection for deposit, isolation, preservation, and distribution of cultured animal cell lines produced by the life science research community. It houses a large number of cell lines as well as hybridomas established by its staff.

4. American Type Culture Collection (ATCC)

http://www.atcc.org

The ATCC Cell Biology Collection (http://www.atcc.org/SearchCatalogs/CellBiology.cfm) includes a very comprehensive and diverse cell bank, consisting of 4000 cell lines from more than 150 different species.

Copyright 2006, Elsevier Science (USA).
All rights reserved.

It holds 950 cancer cell lines (including 700 human cancer cell lines) and over 1200 hybridomas for the production of monoclonal antibodies, as well as a variety of special collections.

5. The Mammalian Genetics Unit at Harwell (MGU)

http://www.mgu.har.mrc.ac.uk

Home page of an integrated campus for mouse genetics research with facilities for molecular genetics, genomics, mutagenesis, transgenesis, and bioinformatics. The MGU has a large collection of mouse stocks containing over 200 mutant, chromosome abnormality, and inbred lines. The stocks are maintained for experimental and breeding purposes and are available to investigators on request.

6. Stem Cell Information at NIH

http://escr.nih.gov

A Web site provided by the National Institutes of Health (NIH) hosting information and links on stem cells.

7. The Stem Cell Database (SCD)

http://stemcell.princeton.edu/index.html

A joint project of the laboratories of Ihor R. Lemischka (Princeton University) and G. Christian Overton (University of Pennsylvania), the SCD contains data on the molecular phenotype of hematopoietic stem cells.

B. Viruses

1. All the Virology on the WWW

http://www.tulane.edu/~dmsander/garryfavweb.html

A site that collects many virology-related Web sites of interest for virologists and others interested in learning more about viruses.

2. The Universal Virus Database (ICTVdB)

http://ictvdb.bio2.edu/index.htm

The directory of ICTVdB is an index of viruses, a list of approved virus names linked to virus descriptions coded from information in "Virus Taxonomy: The Seventh Report of the International Committee on Taxonomy of Viruses" by van Regenmortel *et al.* (eds.), Academic Press (2000), and includes updates subsequently approved by ICTV. It also incorporates the plant virus database VIDEdB and is illustrated with EM pictures, diagrams, and images of symptoms contributed by virologists around the world.

C. Antibodies

1. The Antibody Resource Page

http://www.antibodyresource.com

A site that provides a broad collection of links to companies that sell antibodies or antibody-related products on the internet. Furthermore, it also presents sections containing links to online educational resources about antibodies and databases and software with immunological relevance.

2. AbCam

http://www.abcam.com

AbCam features an extensive compilation of antibody information and advice for locating specific antibodies with a large selection of antibodies available online and a search engine to other antibody companies. In addition, AbCam provides a conference calendar, a database of conferences that have been submitted by research scientists.

3. KabatMan

http://www.bioinf.org.uk/abs

A site that provides information on antibody structure and sequence as well as other useful links.

4. Information Resources for Adjuvants and Antibody Production

http://www.nal.usda.gov/awic/pubs/antibody

A very useful Web page for any researcher interested in antibody production. A rather comprehensive set of references is an added value.

5. Developmental Studies Hybridoma Bank (DSHB), at the University of Iowa

http://www.uiowa.edu/~dshbwww

The DSHB supplies investigators with low-cost monoclonal antibodies useful for studies in developmental and cell biology. They may be ordered as tissue culture supernatants, ascites, or partially purified immunoglobulins. Certain selected hybridomas are also available as frozen or growing cells.

6. IMGT, the International ImMunoGeneTics Information System

http://imgt.cines.fr

An integrated information system specializing in immunoglobulins, T-cell receptors, major histocompatibility complex, and related proteins of the immune system of human and other vertebrate species. This

site contains standardized and annotated data on proteins of the immune system, which include databases of nucleotide and protein sequences, gene maps, genetic polymorphisms, specificities, 2D and 3D structures, and a collection of interactive tools.

D. Flow Cytometry

1. Flow Cytometry Core Laboratory at the University of Florida

http://www.biotech.ufl.edu/FlowCytometry

One of the core laboratories that compose the Interdisciplinary Center for Biotechnology Research at the University of Florida in Gainesville, Florida. This Web page provides a wealth of information and links related to flow cytometry. Included is the database for antibody cross-reactivity (http://www.keithbahjat.com/abcxr/), a repository for flow cytometry software, and protocols for FACS-based analysis.

2. Flow Cytometry on the Web

http://flowcyt.salk.edu/sitelink.html

A collection of links for those interested in flow cytometry. A good starting point if one is looking for software, protocols, instrumentation, protocols, or any flow cytometry-related subject.

E. Immunohistochemistry

1. ImmunoQuery

http://www.immunoquery.com

An immunohistochemistry database query system to help determine the best panel of immune stains that will aid in the differential diagnosis of tumors. It lists antibodies that can differentiate between tumors entered by the user (e.g., lung adenocarcinoma vs breast carcinoma), ranks the antibodies in terms of their ability to differentiate between tumors, and provides instant references to journal articles describing the reactivity of these antibodies.

2. IHC World

http://www.ihcworld.com

A Web site dedicated to everything related to immunohistochemistry. Provides comprehensive and updated information regarding tissue processing, antigen retrieval, antibody selections, antibody protocol database, image analysis, protocol links, books, and journals.

3. DAKOCytomation's Immunochemical Staining Methods Online Handbook (3rd Ed.)

http://ca.us.dakocytomation.com/ihcbook/hbcontent.htm

This site features a pdf-based online version of DAKO's IHC handbook. A very useful book, with detailed information on basic immunohistochemistry techniques including protocols and reviews of alternative methods.

4. PathBase: The European Mutant Mouse Pathology Database

http://eulep.anat.cam.ac.uk

Pathbase is a database of histopathology photomicrographs and macroscopic images derived from mutant or genetically manipulated mice. This site containes a searchable database of histopathological images mainly from transgenic and knockout mice with effects on cell proliferation and cancer, and the response of adult and fetal animals to environmental insults such as radiation at high and low doses relevant to accidental, environmental, and medical irradiation of humans.

5. Histosearch

http://www.histosearch.com

A site comprising a histology search engine for searches over 20,000 Web pages from histology-related sites on the internet, hyperlinks to other histology sites, and to relevant newsgroups and archives.

F. Transgenes and Gene Knockout and -down Technology

1. C. elegans Gene Knockout Consortium

http://www.celeganskoconsortium.omrf.org

This consortium aims at facilitating genetic research of this important model system through the production of deletion alleles at specified gene targets. Targets are chosen based on investigator requests. Strains produced by the consortium are freely available with no restrictions to any investigator.

2. BioMedNet's Mouse Knockout and Mutation Database

http://research.bmn.com/mkmd

A comprehensive database of phenotypic and genotypic information on mouse knockouts and classical mutations with more than 8000 database entries covering over 3000 unique genes.

3. The Nagy Laboratory Cre Transgenic Database

http://www.mshri.on.ca/nagy/cre.htm

This Web site contains a database of published as well as unpublished and in the making Cre transgenic lines. Also some mouse genetics protocols and links. All in all, a good site for those researchers with an interest in ES cell-mediated rodent genome alterations.

4. Database of Gene Knockout

http://www.bioscience.org/knockout/knochome.htm

A mouse gene knockout database with strains classified alphabetically or according to the viability of the knockout: viable mice, or resulting in prenatal, postnatal, or perinatal mortality.

5. Gene Targeting Protocols

http://www.biowww.net/index.php/article/articleview/125/1/16/

A set of 23 gene targeting protocols from Practical Approach Online (in pdf format).

6. Antisense Gene Targeting

http://www.gene-tools.com

GeneTools produces antisense morpholino oligosnucleotides to shut down selected RNA sequences. Provides a very good alternative to phosphorothioates. Microinjection or electroporation of Morpholino oligosnucleotides into the embryos of frogs, zebrafish, chicks, and sea urchins has been shown to successfully and specifically shuts down the expression of desired mRNAs. Another alternative is locked nucleic acid oligosnucleotides that can be obtained through http://www.exiqon.com.

7. RNA Interference Resources

http://www.ambion.com/techlib/resources/RNAi

A resource containing a wealth of information on siRNA-mediated gene silencing, with many useful reviews, references, and links to other sites of interest. An additional site of interest is McManus home page (http://web.mit.edu/mmcmanus/www/RNAi.html), a very good Web site for researchers interested in the process of RNA interference.

G. Organelle Systems

1. Cell Biology Topics: Organelles

http://cellbio.utmb.edu/cellbio

A collection of links to Web pages providing basic information on organelle systems. Most of the topics focus on structure/function correlations.

2. The Virtual Cell Web Page

http://personal.tmlp.com/Jimr57/textbook/chapter3/chapter3.htm

A nice presentation on cell organization and function/structure relations. A similar resource can be found at http://www.life.uiuc.edu/plantbio/cell.

H. Genomics

1. DNA Microarray Web Site

http://www.gene-chips.com/GeneChips.html#proteinchip

A Web page boasting a collection of links to academic and industrial sites of interest for researchers with an interest in microarrays (DNA as well as protein chips).

2. Grid It

http://www.bsi.vt.edu/ralscher/gridit

A useful resource for researchers interested in microarray technology. Includes an introduction to microarray technology and links to sources of equipment, analysis software, and other microarray sites.

3. LGM Microarray Links

http://www.biologie.ens.fr/en/genetiqu/puces/links.html

A collection of links to microarray resources.

4. Genomics: A Global Resource

http://www.biopad.org

A gateway to a plethora of genomic resources.

I. Proteomics

1. Meta-Database Catalog of Two-Dimensional Gel Images Found in Web Databases (2DWG)

http://www-lmmb.ncifcrf.gov/2dwgDB/2DWG.html

A catalog of some of the 2D gel images that can be found in 2D gel databases on the Web.

2. Two-Dimensional Gel Electrophoresis Tutorial

http://www.aber.ac.uk/parasitology/Proteome/Tut_2D.html

A tutorial written by Dr James R. Jefferies. Sections covering this topic include 2D gel electrophoresis, immobilized pH gradients, 2D procedure, sample preparation, sample solubilisation, chaotrophe, reductants, detergents–surfactants, ampholytes, interfering substances, protein estimation, gel electrophoresis, IEF

run, strip equilibration, SDS–PAGE run, staining, general considerations, and references.

3. The Danish Centre for Human Genome Research's 2D PAGE Databases

http://proteomics.cancer.dk

A site containing proteomic databases developed for the study of global cell regulation in health and disease, focusing on skin biology and bladder cancer. Procedures are illustrated with still images and videos. The site also features a gallery of 2D gels of cells, tissues, and fluids, as well as 2D gel immunoblots.

4. EXPASy World 2DPAGE Index

http://www.expasy.ch/ch2d/2d-index.html

A site containing references to known 2D PAGE database servers, as well as to 2D PAGE-related servers and services.

J. Spectroscopy

1. Spectroscopy Now

http://www.spectroscopynow.com/Spy/basehtml/SpyH

A gateway to various spectroscopy resources, including mass spectrometry, RAMAN, and NMR.

2. Protein Prospector

http://prospector.ucsf.edu

A collection of proteomics tools for mining sequence databases in conjunction with mass spectrometry experiments.

K. Cell Signaling

1. The Alliance for Cell Signaling

http://www.signaling-gateway.org

The AfCS-Nature Signaling Gateway is a comprehensive and up-to-the-minute resource for anyone interested in cell signaling. The AfCS is an initiative with the aim of performing comprehensive experimental analyses of selected signaling systems, providing these data freely to the research community. Several tools of interest to investigators within the signalling community are also available here.

2. Phosphobase

http://www.cbs.dtu.dk/databases/PhosphoBase

A database of phosphorylation sites, including two implementations of algorithms for prediction of potential phosphorylation sites.

3. List of Apoptosis Regulators

http://www-personal.umich.edu/~ino/List/AList.html

A Web site providing general and specific information of apoptosis regulators and signalling pathways, as well as quick access to relevant papers and sequences.

4. Science's Signal Transduction Knowledge Environment

http://stke.sciencemag.org

A global resource useful to scientists who specialize in signal transduction, as well as the many scientists who need to follow and apply the current findings of this field even though their primary interest may not be in signal transduction mechanisms themselves.

5. Inositols.com

http://www.inositols.com

A Web-based resource for inositols, phosphoinositides, phosphatidylinositols, and other essential cell-signaling molecules.

6. BioCarta's Pathways

http://www.biocarta.com/genes/index.asp

A Web site containing interactive graphic models of molecular and cellular pathways.

L. Databases of Molecular Interactions and Pathways

1. Biomolecular Interaction Network Database (BIND)

http://www.bind.ca

This site consists of a search engine, PreBIND, that allows the user to mine the biomedical literature for protein–protein interactions and a database, BIND, that stores descriptions of interactions, molecular complexes, and pathway records.

2. General Repository of Interaction Databases (GRID)

http://biodata.mshri.on.ca/grid/servlet/Index

A database of genetic and physical interactions containing interaction data from many different sources. This site is also home to the Osprey Network Visualization System (http://biodata.mshri.on.ca/osprey/servlet/Index), a powerful application for graphically representing physical and genetic biological interactions that is coupled to the GRID database.

3. Database of Interacting Proteins (DIP)

http://dip.doe-mbi.ucla.edu

A database of experimentally determined interactions between proteins. It combines information from a variety of sources to create a single, consistent set of protein–protein interactions.

4. Molecular Interactions Database (MINT)

http://cbm.bio.uniroma2.it/mint

A database of functional interactions between biological molecules (proteins, RNA, DNA). Beyond cataloguing the formation of binary complexes, MINT also stores other type of functional interactions, namely enzymatic modifications of one of the partners.

5. Curagen's PathCalling Yeast Interaction Database

http://portal.curagen.com/extpc/com.curagen.portal.servlet.Yeast

PathCalling is a proteomic technology designed to identify protein–protein interactions on a genome-wide scale.

6. Biomolecular Relations in Information Transmission and Expression (BRITE)

http://www.genome.ad.jp/brite

BRITE is a database of binary relations for computation and comparison of graphs involving genes and proteins. It contains diverse sets of binary relations, including the generalized protein interactions that underlie the KEGG pathway diagrams, systematic experimental data on protein–protein interactions by yeast two-hybrid systems, sequence similarity relations by SSEARCH, expression similarity relations by microarray gene expression profiles, and cross-reference links between database entries.

7. KEGG Pathway Database

http://www.genome.ad.jp/kegg/kegg2.html#pathway

A part of the Kyoto Encyclopedia of Genes and Genomes, this graphical interface for pathway diagrams is very user friendly and a boon of information for any researcher looking for relational information for a given protein. Two diagrammatical databases are available, a metabolic pathway database (http://www.genome.ad.jp/kegg/metabolism.html) and a regulatory pathway database (http://www.genome.ad.jp/kegg/regulation.html); each one of these divided in subsections. In addition to the possibility to perform searches on particular objects or sequences in the various pathways, one can also generate possible reaction pathways.

8. Yeast Interacting Proteins Database

http://genome.c.kanazawa-u.ac.jp/Y2H

A companion site to a publication reporting on the comprehensive two-hybrid analysis of the budding yeast proteome. One can download the complete datasets or analyse them as well as previously reported protein–protein interactions using a graphical system for viewing gene regulatory networks.

M. Gateways to Scientific Resources

1. The DEAMBULUM–BIONETosphere Thematic Exploration

http://www.infobiogen.fr/services/deambulum/english

A gateway to useful online resources for molecular biology, biocomputing, medicine, and biology. It includes hyperlinks to databases (sequence, bibliographic, organisms, etc.), sequence analysis tools, software, and many others.

2. The WWW Virtual Library of Cell Biology

http://vlib.org/Science/Cell_Biology/index.shtml

A very large repository of cell biology information. It includes numerous sections with hyperlinks to various cell biology laboratories, databases, journals, methods, organizations, and meetings, among others.

3. Pedro's Biomolecular Research Tools

http://www.public.iastate.edu/~pedro/research_tools.html

An extensive and quite comprehensive collection of links to resources useful to molecular and cell biologists.

4. The Canadian Bioinformatics Resource

http://cbr-rbc.nrc-cnrc.gc.ca/index_e.php

A Web site providing convenient, effective access to widely used bioinformatic tools and databases.

5. Atelier BioInformatique, aBi Online Analysis Tools

http://www.up.univ-mrs.fr/~wabim/english/logligne.html

An extensive collection of hyperlinks to various bioinformatics tools available online. A similar but complementary Web site is the home page of Dr. Andrew Kropinski (http://molbiol-tools.ca/).

6. bioWWW a Resource for Life Science Researchers

http://www.biowww.net/index.php

A forum for life science researchers containing information and links to protocols, news groups, and many other resources.

7. Molecular Biology Gateway

http://www.horizonpress.com/gateway

A gateway to Web resources for molecular biology, genetics, microbiology, and biochemistry.

N. Sequence Databases and Analysis Tools

This is arguably the largest single group of scientific Web sites in existence. The number of sites featuring sequence analysis tools (of proteins as well as nucleic acids), database queries, and prediction algorithms, among others, is overwhelming and many times the hardest task is to choose which one to use. Listing of even just the most interesting and relevant sites would exceed by far the scope of this resource section. We have chosen instead to provide a few select Web pages of major biology servers containing a large and well-curated collection of databases and tools that allow them be used as entry points for broader searches.

1. The European Bioinformatics Institute (EBI)

http://www.ebi.ac.uk/services

The European Bioinformatics Institute is a nonprofit academic organisation that forms part of the European Molecular Biology Laboratory (EMBL). The EBI manages databases of biological data and provides a comprehensive range of very useful bioinformatics tools.

2. The Catalog of Databases (DBCAT)

http://www.infobiogen.fr/services/dbcat

A near-exhaustive list of existent databases for various application fields, such as DNA, RNA, and proteins.

3. The National Center for Biotechnology Information (NCBI)

http://www.ncbi.nlm.nih.gov

One of the major bioinformatics servers, NCBI creates public databases, conducts research in computational biology, develops software tools for analyzing genome data, and disseminates biomedical information. It provides an extensive collection of tools and resources, including, but not limited to, molecular databases such as GenBank, Entrez, and dbEST; literature databases such as PubMed and OMIM; and tools such as BLAST, Cn3D, and LinkOut.

4. Genome Net

http://www.genome.ad.jp

A Japanese network of database and computational services for genome research and related research areas in molecular and cellular biology. A gateway providing entry points to resources, including, but not limited to, DBGET (Integrated Database Retrieval System), KEGG (Kyoto Encyclopedia of Genes and Genomes), and SSDB (Sequence Similarity Database) (http://www.genome.ad.jp/dbget/dbget.links.html).

5. The Protein DataBank at Brookhaven (PDB)

http://www.rcsb.org/pdb

PDB is the repository for the processing and distribution of 3D biological macromolecular structure data. In addition to containing structural data deposited by crystallographers and spectroscopists (NMR), worldwide PDB also presents a large collection of software for structural work and educational resources.

6. Center for Biological Sequence Analysis Server (CBS)

http://www.cbs.dtu.dk/services

The server at CBS provides a set of very useful tools for sequence analysis, such as *TMHMM* for the identification of transmembrane helices in proteins; *TargetP* for the determination of subcellular location of proteins; and *NetNGlyc* for the identification of N-linked glycosylation sites in human proteins, as well as a very nice collection of links to other sites of interest.

7. The Expert Protein Analysis System (ExPASy) Molecular Biology Server

http://www.expasy.org

The ExPASy proteomics server of the Swiss Institute of Bioinformatics (SIB) is dedicated to protein analysis and contains a large number of tools as well as links to biology servers. The Amos Bairoch's WWW links page within the ExPASy server (http://www.expasy.org/alinks.html) contains pointers to information sources for life scientists with an interest in biological macromolecules. Additionally, this site is also home to Biohunt (http://www.expasy.org/BioHunt), a molecular biology search engine.

8. The Institute for Genomic Research (TIGR)

http://www.tigr.org

A not-for-profit research institute whose primary research interests are in structural, functional, and

comparative analysis of genomes and gene products from a wide variety of organisms. This site contains a collection of curated databases containing DNA and protein sequence, gene expression, cellular role, protein family, and taxonomic data for microbes, plants, and humans. Particularly interesting is the TIGR microarray resources page, where one can find many software tools available for free download.

9. GeneCards

http://discover.nci.nih.gov/textmining/filters.html

A database of human genes, their products, and their involvement in diseases. A search engine useful for people who wish to find information about genes of interest.

O. Educational and General Information Resources

1. Cell and Molecular Biology Online

http://www.cellbio.com

A site containing general information and links for cell and molecular biologists. It features several hyperlinks to many resources such as online journals, methods, protocols, and laboratories.

2. The Glossarist

http://www.glossarist.com/glossaries/science/life-sciences

A searchable glossary directory. Looking for the definition of a term in a particular subject can be difficult and time-consuming. That is where the Glossarist can help you look. This Web page contains links to several online dictionaries and glossaries, including, but not limited to, the online version of the book published by Lackie and Dow (1999) (http://on.to/dictionary) and BioABACUS (http://www.nmsu.edu/~molbio/bioABACUShome.htm), a searchable database of abbreviations and acronyms in biotechnology.

3. Kimball's Biology Pages

http://biology-pages.info

A Web site containing an online biology textbook. Even though some of the information in this Web site has been taken from the sixth edition of the author's general biology text "Biology" published in 1994 by Wm. C. Brown, frequent updates make this site well worth a visit.

4. Online Biology Book

http://www.emc.maricopa.edu/faculty/farabee/BIOBK/BioBookTOC.html

A college-level introduction biology text with an interesting set of lectures with many illustrations.

5. The Biology Project

http://www.biology.arizona.edu

An online interactive resource for biology. This site consists of student-oriented, highly interactive learning materials that can be used to support lectures for laboratory meetings, and discussion sessions of general education courses.

6. Biotech's Scientific Dictionary

http://biotech.icmb.utexas.edu/search/dict-search.html

A dictionary on general terminology of biochemistry, biotechnology, botany, cell biology, and genetics, as well as more specific brief definitions of the cell constituents.

7. Biology Online

http://www.biology-online.org

A source of basic biological information, with tutorials and a dictionary of biology, as well as links to hundreds of related biology sites.

8. The Visible Mouse

http://ccm.ucdavis.edu/tvmouse/index.html

A Web site providing a very nice introduction to the anatomy, physiology, histology, and pathology of the laboratory mouse with emphasis on genetically engineered mice.

9. Lee M. Silver's Mouse Genetics

http://www.informatics.jax.org/silver

The electronic version of Silver's book.

10. The Zebrafish Book

http://zfin.org/zf_info/zfbook/zfbk.html

A guide for the laboratory use of zebrafish (*Danio rerio*).

11. Mark Blaxter's Home Page

http://nema.cap.ed.ac.uk/Caenorhabditis/C_elegans_genome/Celegansgenome.html

It contains "The Genetics of *Caenorhabditis elegans*, an Introduction," a very well-written introduction to the biology of *C. elegans*.

12. BioResearch

http://bioresearch.ac.uk

A gateway to evaluated internet resources in the basic biological and biomedical sciences, aimed at students, researchers, academics, and practitioners in biological or biomedical science.

P. Safety, Ethical Issues, Legislation, and Patents

1. International Centre for Genetic Engineering and Biotechnology–Biosafety

http://www.icgeb.org/~bsafesrv

The ICGEB Biosafety Web pages, containing information on biosafety, international biosafety regulations (USA, Europe and others), handling of GMOs, and links to other related sites.

2. European Agency for Safety and Health at Work (OSHA)

http://agency.osha.eu.int

This is the corporate Web site of the OSHA. It provides useful information and access to full-text versions of all OSHA's publications.

3. European Chemical Bureau (ECB)

http://ecb.jrc.it

The ECB is the focal point in Europe for data and the assessment procedure on dangerous chemicals. This site provides information on the classification and labelling of substances, import/export of dangerous chemicals, legislation, and a collection of links to other related sites.

4. Material Safety Data Sheet (MSDS) Databases Search

http://www.msdssearch.com/DBLinksN.htm

A search engine for MSDS libraries. MSDSSEARCH is a reliable starting point for obtaining the most updated MSDS documents from the manufacturer and provides a single, international, database with all MSDSs available in text format at no cost to users.

5. EUROPA Steering Committee on Bioethics

http://www.coe.int/T/E/Legal_Affairs/Legal_co-operation/Bioethics/CDBI

This Web site contains information concerning meetings and documentation produced by the CDBI as well as links to other relevant sites.

6. The International Bioethics Committee (IBC)

http://portal.unesco.org/shs/en/ev.php@URL_ID=1372&URL_DO=DO_TOPIC&URL_SECTION=201.html)

The Bioethics Programme is part of UNESCO's Division of the Ethics of Science and Technology in the Social and Human Sciences Sector and, through its committees, produces advice, recommendations, and proposals to submit to the Director-General for consideration by UNESCO's governing bodies. In addition to providing access to IBC's documents, this Web site has various links to legislative institutions, databases of bioethics institutions, and other related websites.

7. Institutional Animal Care and Use Committee at University of Iowa

http://research.uiowa.edu/animal

This Web site has a very descriptive collection of basic biomethodology for mouse, rat, rabbit, and guinea pig animal husbandry, as well as a large number of established guidelines/regimens for various animal uses (e.g., recommendations for the production of ascitic fluid; regimens for anesthesia and analgesia of laboratory animals).

8. Animal Care at Johns Hopkins

http://www.jhu.edu/animalcare/committee1.html

A lot of useful information on regulations and polices on animal care and use.

9. UCAR Manual on the Responsible Care and Use of Laboratory Animals

http://www.urmc.rochester.edu/ucar/manual/index.htm

A resource from the University of Rochester Medical Center. It includes a manual on care and use of laboratory animals and links to other resources, such as the dosage calculator (http://www.fda.gov/cder/cancer/animalframe.htm).

10. OECD Principles of Good Laboratory Practices

http://www.oecd.org/EN/home/0,,EN-home-526-14-no-no-no-no,00.html

A Web site containing information on OECD guidelines for GLP, and principles of GLP, as well as links to national GLP sites.

11. U.S. Environmental Protection Agency (EPA)

http://www.epa.gov/Compliance/monitoring/programs/glp/index.html

EPA's home page to the Good Laboratory Practice Standards (GLPs) compliance monitoring program.

12. *Esp@cenet*

http://gb.espacenet.com

Europe's network of patent databases. Search published worldwide patent applications with an English abstract and title as well as published patent applications in their original language from various European countries. A real trove of information, reagents, and sequences is sometimes buried in patent applications.

Q. Literature Datasets

1. *BioMed Central*

http://www.biomedcentral.com

An open access, independent publishing house committed to providing immediate free access to peer-reviewed biomedical research.

2. *PubMed*

http://www.ncbi.nlm.nih.gov/PubMed

PubMed is a service of the National Library of Medicine providing access to over 12 million MEDLINE citations back to the mid-1960s and additional life science journals. PubMed also includes links to many sites providing full text articles and other related resources. A similar service is provided by *HighWire* (http://highwire.stanford.edu).

3. *Online Mendalian Inheritance in Man (OMIM)*

http://www.ncbi.nlm.nih.gov/entrez/query.fcgi?db=OMIM

A resource provided by NCBI containing curated reviews on human genes of interest with many references and embedded hyperlinks to other resources.

4. *The Cochrane Library*

http://www.update-software.com/cochrane

This site consists of a regularly updated collection of evidence-based medicine databases, including The Cochrane Database of Systematic Reviews, which provide high-quality information to people providing and receiving care and those responsible for research, teaching, funding, and administration at all levels. The Cochrane Library is available on a subscription basis, but there are several countries that have arranged national provisions and thus allow all residents to access The Cochrane Library for free (e.g., Australia, England, Norway, Finland).

5. *The Wellcome Library*

http://library.wellcome.ac.uk

One of the world's greatest collections of books, manuscripts, pictures, and films around the meaning and history of medicine.

6. *LOCATORplus*

http://locatorplus.gov

A catalog of books, journals, and audiovisuals in the National Library of Medicine collections.

7. *MedBioWorld*

http://www.sciencekomm.at/index.html

A large medical reference site including an exhaustive list of medical journals and medical associations and similar resources in the biological sciences. Other research tools include medical glossaries, disease databases, clinical trials and guidelines, and medical journals offering full-text article.

8. *BioMail Service*

http://www.biomail.org

Biomail is an automatic service that regularly (weekly by default) searches for articles, that have recently appeared in the PubMed Medline database using customized search terms. Then it emails lists of the found articles to the user.

R. General Protocols

1. *bioProtocol*

http://www.bio.com/protocolstools

This Web site features a collection of protocols contributed by scientists from over 125 academic laboratories covering a variety of life science disciplines. A large site with a plethora of links and many useful protocols.

2. *iProtocol*

http://iprotocol.mit.edu

An initiative by a team of MIT-affiliated researchers and local software engineers to develop a free Web site containing research protocols used in biological sciences.

3. *BioVisa.net*

http://www.biovisa.net

A specialized Web site containing a collection of links to more than 2000 online protocols. You can discuss these protocols with researchers that share a

similar interest. The protocols are indexed into eight categories: anatomy and histology, biochemistry and molecular biology, biotechnology, cell biology, developmental biology, genetics, immunology, and neuroscience.

4. Protocol Online

http://www.protocol-online.org

A database of research protocols in a variety of life science fields. It features user-submitted protocols as well as links to other Web sites.

S. General Reagents and Techniques

1. The Biocurrents Research Center—Database of Pharmocological Compounds

http://zeus.mbl.edu/public/BRC

A NIH-funded database providing its user with a useful forum on the use of pharmacological compounds in cellular research. It lists over 500 compounds with details on their mode of action and employ, including references.

2. Biocompare

http://www.biocompare.com

A buying guide for life sciences. Even though this site is commercially oriented it allows one to search a wide range of product-related technical information for the life science researcher in a rather comprehensive manner. If you need something and do not know where to buy it and whom to buy it from, this site may be just what you need. Included is Biocompare's Antibody Search, which allows you to search over 60,000 antibodies from various antibody suppliers. A similar service provider is BioSupplyNet (http://www.biosupplynet.com/) where you can browse and search for suppliers in a variety of areas of life science research.

3. Bioresearch Online

http://www.bioresearchonline.com/content/homepage

A sourcing site for bioresearch. In addition to it belong a buyer's guide and a free newsletter, it contains a search engine for product information.

4. LabVelocity's Biowire

http://home.labvelocity.com/scientists/index.jhtml?subSection=biowire

A Web site containing user-written laboratory product reviews pertaining to the life sciences community. It holds a very large number (ca. 25,000) of product reviews, which are a good aid not only when deciding on purchasing a particular item, but also if you are searching for a specific product. A complementary site is SciQuest (http://www.sciquest.com/commerce/CommerceRouter/Index), a site providing search possibilities for scientific products.

5. MedWebPlus

http://medwebplus.com

A search engine for finding health sciences information.

T. Model Organisms

1. The Mouse Genome Resources

http://www.ncbi.nlm.nih.gov/genome/guide/mouse

A gateway to mouse resources. This site is an entry point to access information pertaining to the NCBI mouse genome sequence as well as other extramural mouse resources.

2. Whole Mouse Catalog

http://www.rodentia.com/wmc/index.html

A collection of links to internet resources of particular interest to scientific researchers using mice or rats in their work.

3. The Jackson Laboratory Home Page

http://www.jax.org

JAX online consists of a series of resources of interest for mouse researchers, including databases (http://www.jax.org/resources/search_databases.html) and a mouse strain repository (http://jaxmice.jax.org/index.html) for the collection and distribution of genetically engineered mice, as well as a Mouse Genome Informatics (MGI) site that provides integrated access to data on the genetics, genomics, and biology of the laboratory mouse.

4. The Mouse Phenome Database

http://aretha.jax.org/pub-cgi/phenome/mpdcgi?rtn=docs/home

A collection of comprehensive phenotypic and genotypic data on inbred laboratory mouse strains.

5. The Edinburgh Mouse Atlas Project (EMAP)

http://genex.hgu.mrc.ac.uk/intro.html

This Web site is the home page of a collaborative project within the University of Edinburgh aiming at the creation of a digital atlas of mouse embryonic development. It consists of a series of interactive three-dimensional computer models of mouse embryos at

successive stages of development with defined anatomical domains linked to a stage-by-stage ontology of anatomical names. Additionally, the EMAP atlas underlies an image-mapped gene-expression database (EMAGE; http://genex.hgu.mrc.ac.uk/Emage/database/intro.html). These two databases are interoperable.

6. ARKdb

http://www.thearkdb.org

This database system provides access to comprehensive public repositories for genome mapping data from farmed and other animal species (e.g., cat, chicken, cow, deer, horse, pig, salmon, sheep, tilapia, turkey). Data stored include details of loci and markers, references/papers, authors, genetic linkage map assignments, cytogenetic map assignments, experimental techniques, PCR primers and conditions, and any other data pertaining to genome mapping.

7. Rat Genome Database (RGD)

http://rgd.mcw.edu

A Web site providing a large amount of rat genetic and genomic resources. It includes curated data on rat genes, quantitative trait loci (QTL), microsatellite markers, and rat strains used in genetic and genomic research. In addition, RGD provides a large number of tools for gene prediction, radiation hybrid mapping, polymorphic marker selection, and more.

8. FlyBase

http://flybase.bio.indiana.edu

A database of genetic and molecular data for *Drosophila*. FlyBase includes data on all species from the family Drosophilidae, but the primary species represented is *Drosophila melanogaster*. This site also contains several links to resources of interest for *Drosophila* researchers.

9. The Zebrafish Information Network (ZFIN)

http://zfin.org

ZFIN is a database resource for the laboratory use of zebrafish. It provides integrated zebrafish genetic, genomic, and developmental information, together with links to corresponding data in other model organism and human databases.

10. The HGMP-RC Fugu Genome Project

http://fugu.hgmp.mrc.ac.uk

In addition to containing the publicly available draft sequence of the Fugu genome, this site also provides a collection of protocols, publications, and much data for the scientific community with an interest in *Fugu rubripes* (the Japanese puffer fish).

11. Caenorhabditis elegans WWW Server

http://elegans.swmed.edu

A Web site aimed at the community of *C. elegans* researchers. This site boasts a large number of resources, including literature search, methods, a list of meetings, labs, and researchers, links to Bionet.celegans, etc. A companion site is WormBase (http://www.wormbase.org/). A Web site displaying a large amount of relevant information and hyperlinks for the *C. elegans* scientific community.

12. WWW Virtual Library for Xenopus

http://www.xenbase.org/xmmr/frog.html

A site dedicated to *Xenopus laevis*, a commonly used model system for studying vertebrate early development. One of the main uses of this site is as a reference for researchers looking for molecular probes. It also contains a collection of whole mount staining patterns using both antibody and nucleic acid probes, a methods book, supplier listing, Xenopus scientific community white pages, and more.

13. dictyBase

http://dictybase.org

An informatics resource for *Dictyostelium discoideum*, it consists of a comprehensive genomic *Dictyostelium* database, lab protocols and strain availability, and a list of researchers, among many other links.

14. The Arabidopsis *Information Resource (TAIR)*

http://www.arabidopsis.org

A comprehensive resource for the scientific community working with *Arabidopsis thaliana*, a widely used model plant. TAIR consists of a searchable relational database, which includes many different data types. In addition, pages on news, information on the Arabidopsis Genome Initiative (AGI), Arabidopsis lab protocols, and useful links are provided.

Additional sites and nonlisted model organisms can be found at the following sites:

The WWW Virtual Library: Model Organisms (http://ceolas.org/VL/mo/)

The Sanger Institute's Model Organisms Resources Links (http://www.sanger.ac.uk/Info/Links/modelorgs.shtml)

Infobiogen's list of genomes and organisms (http://www.infobiogen.fr/services/deambulum/english/genomes1.html)
NIH's Model Organisms for Biomedical Research website (http://www.nih.gov/science/models/).

III. IMAGING TECHNIQUES IN CELL BIOLOGY

One of the paramount interests of cell biologists is to observe cellular themes, temporally as well as spatially resolved. No longer just structures, but also proteins and their cellular localisation, dynamics, and interaction(s). The field of cellular imaging is currently one of the cornerstones of cell biology and microscopy constitutes arguably its single most important technique. For this reason, we have chosen to list and highlight Web sites dealing with the subject of microscopy in a more comprehensive manner then hitherto. This part of the resources section is thus devoted to microscopy techniques and covers the subject in a broad manner with sites that should be of great use to the novice and experienced user alike.

A. Light Microscopy

1. A Brief History of Optics

http://members.aol.com/WSRNet/D1/hist.htm

A part of the laser-optics UK Web site giving a historical summary of the important discoveries in the field of optics.

2. Properties of Light and Introductory Optics

http://micro.magnet.fsu.edu/primer/lightandcolor/index.html

The Molecular Expressions Microscopy Primer is an excellent microscopy Web site from Florida State University (principal authors: Michael W. Davidson, FSU and Mortimer Abramowitz—http://micro.magnet.fsu.edu/). An extensive series of tutorials on light and colours can be found on this Web site: nature of light (electromagnetic radiation, duality of light, definition of colours), physical properties (reflection, refraction, diffraction, polarisation, interference), and fundamental tools to generate and direct light (lenses, filters, sources of light, laser). A good introduction about light microscopy written by these authors can be downloaded at: http://screensavers.magnet.fsu.edu/pdfs/microscopy.pdf.

3. Anatomy of a Light Microscope and Basic Concepts in Optical Microscopy

http://micro.magnet.fsu.edu/primer/anatomy/components.html

http://micro.magnet.fsu.edu/primer/anatomy/anatomy.html

The complete description of the different parts of a microscope can be found within this link: microscope components configuration, optical train components, perfect lens characteristics, objectives, and other important parts of the microscope.

4. Concepts and Formulas in Microscopy

http://www.microscopyu.com/articles/formulas/formulasindex.html

A part of the Nikon's MicroscopyU Web site (http://www.microscopyu.com/). This Web site was originally designed to provide an educational forum for all aspects of optical microscopy, digital imaging, and photomicrography and complements the Molecular Expressions Microscopy Primer microscopy Web site (http://micro.magnet.fsu.edu/). This Web site part covers concepts and formulas in microscopy and includes definitions on some very important and often not well-understood parameters (numerical aperture, depth of field, resolution, and many others).

5. Sources of Visible Light

http://micro.magnet.fsu.edu/optics/lightandcolor/sources.html

Description of various sources of light used for fluorescence microscopy.

6. Köhler Illumination

http://micro.magnet.fsu.edu/primer/anatomy/kohler.html

Köhler illumination is a basic requirement of all modern light microscopy. The purpose is to obtain an evenly lit field of view and as wide a cone of radiation as possible in order to achieve maximum resolution. This Web page explains clearly what the Köhler illumination is and how to set it up.

7. Specialised Microscopy Techniques

http://micro.magnet.fsu.edu/primer/techniques/index.html

Microscopic techniques can be separated into two categories: microscopy using polychromatic light (basic light microscopy) and microscopy using specific wavelength (fluorescence microscopy) that need specific filters. Here you will find a description of

different nonfluorescent microscopy techniques: bright-field and dark-field microscopy, Nomarski (or DIC), phase contrast, and so on.

B. Fluorescence Microscopy

1. What Is Fluorescence? The Stokes Law

http://micro.magnet.fsu.edu/primer/techniques/fluorescence/introduction.html

Cell biologists want to observe the localisation, dynamics, and relocalisation of proteins. Unfortunately, proteins are not directly visible; in order to monitor their localisation they need to be tagged with fluorescent probes. This site gives the necessary background about how fluorescence is generated.

http://micro.magnet.fsu.edu/optics/timeline/people/stokes.html

A link about George Gabriel Stokes.

2. Fluorescence Microscopy Tutorials

http://micro.magnet.fsu.edu/primer/techniques/fluorescence/fluorhome.html

Fluorescence microscopy is the most common technique today in medical and biological sciences. This link focuses on excitation and emission fundamentals, light sources, lasers, and filter cubes. The section interactive Java tutorials give very useful information about fluorochrome data tables, excitation/emission wavelengths, and filter cube suggestions listed by applications.

3. Laser and Fluorescence Microscopy

http://www.olympusmicro.com/primer/lightandcolor/laserhome.html

Section about laser fundamentals from the Olympus Web site. Lasers can be found in CD players and various other commonly used objects. In the field of microscopy, lasers are used for their monochromatic properties, light coherence, and power. This link gives useful and accessible information about laser physics. Many Java tutorials are also available.

C. Image Acquisition

1. Cameras and CCD Detectors

http://www.olympusmicro.com/primer/digitalimaging/index.html

Originally, mechanisms of image capture were restricted to photomicrography on film. Currently, the development of sensitive and low noise cameras gives the possibility to acquire digitally images from the microscope. These cameras with high sensitivity are at the core of the development of video microscopy. Digitalized images, as an ordered matrix of integers rather than a series of analog variations in colour and intensity, give the interesting possibility to post process images in order to enhance features and extract information. This section addresses a variety of current topics in image acquisition and processing.

http://www.roperscientific.com/library_encyclopedia.shtml

A part of the Roper scientific Web site (http://www.roperscientific.com) called encyclopedia and describing many camera concepts, such as binning, gain, and dynamic range, among others. A very useful reference to understand basic principles of cameras and CCD detectors.

http://helios.mol.uj.edu.pl/camera.html

Comparison of technical characteristics of several cameras.

D. Filter Sets and Fluorescence Filter Cubes

http://micro.magnet.fsu.edu/primer/techniques/fluorescence/filters.html

Filter sets are designed to select a specific wavelength for specimen illumination with polychromatic light sources and are essential for selectively collecting fluorescent light coming from the sample. Proper selection of filters is the key to successful fluorescence microscopy. This section describes characteristics of excitation and emission filters used in combination with dichroic mirrors to design filter cubes.

http://www.omegafilters.com/front/curvomatic/spectra.php

The Curvomatic application from the Omega Web site (http://www.omegafilters.com) is a tool helping microscopists to choose their filters set according to fluorophores used. A very useful application.

E. Fluorescence Tables

http://micro.magnet.fsu.edu/primer/techniques/fluorescence/fluorotable2.html

This link provides a table that summarizes several peak excitation and emission wavelengths of commonly used fluorochromes. These different fluorescence tags can be coupled with proteins or drugs (e.g., phalloidin or taxol) to monitor localisation of proteins in cells.

http://fluorescence.nexus-solutions.net/frames6.htm

The Bio-Rad fluorescence database has been designed to allow the user to superimpose graphical fluorochrome data from various fluorochromes onto a normalised axis. Both emission and excitation spectra can be plotted from any fluorochrome in the database. These can subsequently be overlaid with filter data curves and laser lines, which aids the microscopist in selection of the correct fluorochrome for use with their samples and microscope.

http://www.bdbiosciences.com/spectra/

The fluorescence spectrum viewer from bdbiosciences. This can be used as an alternative to Bio-Rad fluorescent database and the curvomatic application from Omega.

F. Fluorescent Probes for Light Microscopy

1. Fluorophores and Fluorescents Reagents

http://www.probes.com/handbook/

An electronic version of the Molecular Probes Handbook. Molecular Probes is one of the most interesting providers of fluorescent probes for cell biology. This Web edition of the handbook is an updated version of the 9th edition and is presented in two formats. Very useful information can be found in this Web handbook, such as cross-linking techniques, photoreactives reagents, probes for cytoskeletal proteins, membranes, organelles, and endocytosis, as well as pH indicators, and ions indicators.

http://www.probes.com/servlets/spectra/

This link points to the complete list of fluorescent Probes available from Molecular Probes. For each probe a sheet summarizes some characteristic of the probe (emission and excitation spectra, physical properties, etc . . .). Spectra are also available for download.

http://www.probes.com/resources/calc/basedyeratio.html

A base/dye ratio calculator from molecular probes. This applet allows the possibility to calculate fluorescence characteristics (maximum wavelength, extinction coefficient) of a nucleotide coupled to a fluorescent dye.

2. Secondary Antibodies for Immunohistochemistry

http://www.aecom.yu.edu/aif/instructions/immunofluor/controls/abodies.htm

A part of the analytical imaging facility Web site from Albert Einstein college of medicine (New York, http://www.aecom.yu.edu/aif/). This link points to a troubleshooting guide on immunofluorescence nonspecific labelling; very useful for understanding staining problems in immunofluorescence experiments.

http://www.jacksonimmuno.com/, http://www.zymed.com/pindex/index64.html and http://www.probes.com/

Jackon immunoresearch and Zymed are providers (although not unique) of secondary antibodies used in fluorescence microscopy. Secondary antibodies are classical tools used in cell biology to reveal localisation of proteins by fluorescence microscopy. Molecular Probes also provides some secondary antibodies.

3. GFP. Background and Properties of GFP and Related Tags

http://www.biochemtech.uni-halle.de/PPS2/projects/jonda/index.htm

These Web pages about green fluorescent protein (GFP) have been developed as a dissertation project for the principles of protein structure using the internet course (http://www.cryst.bbk.ac.uk/PPS2/top.html). You will find the *in vivo* role of the GFP and some basic properties. Biosynthesis, chemical structure of the fluorophore, and spectrum characteristics of this protein are also available.

4. Commercial Web site of Fluorescent Proteins

http://www.clontech.com/gfp/index.shtml

This link points to the Clontech Web site, with emphasis on GFP vectors. Clontech is historically the first provider of GFP-expressing vectors.

G. Immunohistochemistry and Immunofluorescence Protocols

1. Protocols Database

http://www.ihcworld.com/protocols.htm

Protocol Links Web page of IHC world Web site (http://www.ihcworld.com/; online information center for immunohistochemistry). An extensive list of Web sites, pdf files, and protocols covering fields of general histology, immunohistochemistry, immunofluorescence, *in situ* hybridisation, and electron microscopy protocols.

http://www.ihcworld.com/protocol_database.htm

Link to the protocols database of the IHC Web site. You can query the protocol database for a specific antibody-staining protocol.

2. Immunohistochemistry and in situ *Hybridization*

http://home.no.net/immuno

Link to a Web site explaining theory and techniques of immunolabelling. Some protocols are available and many Powerpoint presentations are downloadable. Useful teaching resource.

3. Other Immunofluorescence Protocols

http://www.itg.uiuc.edu/publications/techreports/99-006/

Web site of the imaging technology group from the Beckman Institute for Advanced Science and Technology (http://www.itg.uiuc.edu/). Link includes technical bulletin providing an introduction to fluorescent microscopy and a collection of various protocols for specific applications of fluorescence.

H. Other Microscopy Techniques

1. Three-Dimensional Laser Confocal Microscopy

http://www.cs.ubc.ca/spider/ladic/overview.html

Web site from Lance Ladic, Department of Physiology, University British Columbia, giving a basic introduction to 3D laser-scanning microscopy.

http://www.mih.unibas.ch/Booklet/Booklet96/Chapter1/Chapter1.html

Link to the course "Looking inside cells and tissues by optical sectioning with a confocal laser scanning microscope" prepared by M. Dürrenberger and R. Sütterlin. Also some basics about confocal microscopy.

http://www.science.uwaterloo.ca/physics/research/confocal/intro.html

Home page of the scanning laser microscopy lab (also known as the confocal microscopy group) of the physics department at the University of Waterloo. This site is designed for researchers who use (or might like to use) confocal microscopes. This Web site describes optical design, problems of lateral and axial resolution, and problems of confocal slicing in confocal microscopy. Some formulae can also be found.

http://micro.magnet.fsu.edu/primer/techniques/confocal/index.html

A complete section about confocal microscopy from the Molecular Expressions Microscopy Primer Web site. Basic concepts, imaging modes, specimen preparation and imaging, laser systems for confocal microscopy, etc . . . A very nice interactive java tutorial showing how a confocal microscope is working. This tutorial also shows effects of pinhole aperture on the quality of the confocal image.

2. Spinning Disk Confocal Microscopy

http://www.atto.com/Carv/confocaldesc.htm

A short Web page that describes differences between confocal scanning microscopy and the new technique of spinning disk confocal microscopy.

3. Multiphoton Fluorescence Microscopy and Two Photon Theory

http://microscopy.fsu.edu/primer/techniques/fluorescence/multiphoton/multiphotonhome.html

Multiphoton fluorescence microscopy is a powerful research tool that combines the advanced optical techniques of laser-scanning microscopy with long wavelength multiphoton fluorescence excitation. Multiphoton microscopy is generally used to specifically excitate fluorophores in a specific Z location. This link gives much information about this technique complementary to confocal microscopy.

4. Fluorescence Resonance Energy Transfer (FRET) Microscopy

http://www.anatomy.usyd.edu.au/mru/fret/abot.html

FRET microscopy uses the same physical principle as FRET spectroscopy. FRET is a technique used to determine the interaction (or proximity) of two fluorescent labelled molecules. This site gives the mathematical background necessary to explain FRET spectroscopy. Observations and equations described here are applicable to FRET microscopy.

http://www.probes.com/handbook/boxes/0422.html

Molecular Probes Web page about fluorescence resonance energy transfer microscopy. Information about primary conditions of FRET, Förster radius, and fluorophore pairs used for FRET can be found.

5. Fluorescent Lifetime Imaging Microscopy (FLIM)

http://www.cci.virginia.edu/flim/

Time-resolved fluorescence emission spectroscopy of a photoexcited sample is a powerful tool for the study of living cells in both space and time of their internal biochemistry. The Web page of the W.M. Reck Center for Cellular Imaging (University of Virginia) provides theory, images, and references about FLIM.

6. Fluorescent Recovery after Photobleaching (FRAP) Microscopy

http://www.bio.davidson.edu/courses/Molbio/FRAPx/FRAP.html

Link about FRAP to the Department of Biology, Davidson College, US. FRAP is used to measure the ability of a molecule to move around over time. This link provides information about this technique.

7. Fluorescence Correlation Microscopy

http://imd-www.es.hokudai.ac.jp/~gnishi/fcs/fcs.html

Web page of fluorescence correlation spectroscopy and its application, maintained by Goro Nishimura from Hokkaido University. The principle of fluorescence correlation spectroscopy is described in this Web page.

8. Fluorescence Speckle Microscopy

http://www.scripps.edu/cb/waterman/Flurorescent_speckle_categories.htm

Part of Clare Waterman-Storer Web site (http://www.scripps.edu/cb/waterman/) related to speckle microscopy. Everything needed to perform speckle microscopy is described: introduction to this technique, design and building of a fluorescent speckle microscope system, theory of fluorescent speckle microscopy image formation, preparation of living cell for speckle microscopy, and analysis of time-lapse FSM image series. A very informative Web site.

I. Electron Microscopy

1. Electron Microscopy for Dummies

http://cryoem.berkeley.edu/~nieder/em_for_dummies/

These pages have been designed and written by Hanspeter Niederstrasser of the laboratory of Dr. Eva Nogales, University of California, Berkeley. As the title implies, this Web site gives a good overview of electron microscopy techniques (transmission and scanning electron microscopy). A brief description of basic methods of preparation of samples can also be found.

2. What Are Electron Microscopes?

http://www.unl.edu/CMRAcfem/em.htm

This Web site from the Center for Materials Research and Analysis University of Nebraska–Lincoln gives more information about how electron microscopes work: descriptions of electron source, magnetic lenses, apertures, and interaction with the specimen leading to EM "image" formation.

3. Transmission Electron Microscope (TEM)

http://em-outreach.sdsc.edu/web-course/toc.html

A very complete Web course on TEM from the Electron Microscopy Outreach Program (http://em-outreach.sdsc.edu/). Principle of TEM, microscope design, microscope operation, specimen preparation, and so on are described in this Web course. Essential as a teaching resource.

4. Transmission Electron Microscope Sample Preparation

http://bama.ua.edu/~hsmithso/class/bsc_656/websites/sample_tem.html

A Web site about TEM sample preparation maintained by H.E. Smith Somerville (http://bama.ua.edu/~hsmithso/index.shtml) from the University of Alabama. Fixation and processing protocols, embedding, and immunocytochemistry are described.

5. Scanning Electron Microscopy

http://www.jeol.com/sem_gde/tbcontd.html

A guide to scanning microscope observation, part of the Jeol Web site (a company manufacturing electron microscopes). Good overview about scanning electron microscopy.

6. Electron Microscopy Protocols

http://biousa.hypermart.net/cellbio/microscopy/electron_microscopy.htm

This site was originally created and is maintained by Dr. Longcheng Li while doing postdoctoral research at UCSF. Some electron microscopy protocols can be found.

J. Miscellaneous

1. Image Galleries

http://www.cellsalive.com/toc.htm

Cell Alive Web site is a virtual museum of microscopic images (light microscopy and electron microscopy) of various organisms (eukaryotic, prokaryotic cells, plants, etc . . .).

http://www.microscopyu.com/galleries/index.html

Microscopy image gallery from Nikon microscopy Web site. Different sections showing images obtained using different techniques (wide field, confocal, etc . . .).

2. An Archive of Electron Micrographs

http://www.biochem.wisc.edu/inman/empics/

A collection of electron micrography images from the Institute for Molecular Virology, University of Wisconsin–Madison.

3. Atlas of Microscopy Anatomy

http://www.vh.org/adult/provider/anatomy/MicroscopicAnatomy/MicroscopicAnatomy.html

Electronic version of the Atlas of Microscopic Anatomy: A Functional Approach: Companion to Histology and Neuroanatomy, second edition.

4. A Video Tour of Cell Motility

http://cellix.imolbio.oeaw.ac.at/Videotour/video_tour.html

Contribution to the EAMNET network (http://www.embl.de/eamnet) from the John Victor Small laboratory. An original gallery of video microscopies describing the phenomenon of cell motility.

5. Free Software for Microscopy

http://www.cs.ubc.ca/spider/ladic/software.html

A part from Lance Ladic Web site (Department of Physiology, University British Columbia) giving many links for microscopy and image processing softwares.

6. ImageJ–Freeware Java Image Processing Software

http://rsb.info.nih.gov/ij/

ImageJ is a very good image processing software, written in Java and available for all types of platforms (Linux/UNIX, Windows and Mac-based computer).

7. Power Point Presentations on Microscopy

http://www.cyto.purdue.edu/flowcyt/educate/pptslide.htm

General teaching resource about light microscopy available as powerpoint presentations.

8. The European Advanced Light Microscopy Network (EAMNET) Network

http://www.embl.de/eamnet

EAMNET is a EU-funded network of eight European laboratories and two industrial partners working in the field of light microscopy. The aim of EAMNET is to assist scientists in exploiting the power of imaging by organizing practical teaching courses, creating online teaching modules, and offering software packages for microscopy.

9. Cell Migration Consortium

http://www.cellmigration.org/sciMovies.html

Movies and photo from the cell migration consortium (http://www.cellmigration.org/).

References

Ito, T., Chiba, T., Ozawa, R., Yoshida, M., Hattori, M., and Sakaki, Y. (2001). A comprehensive two-hybrid analysis to explore the yeast protein interactome. *Proc. Natl. Acad. Sci. USA* **98**, 4569–4574.

Lachie, J. M., and Dow, J. A. T. (1999). "The Dictionary of Cell and Molecular Biology," 3rd Ed. Academic Press, London.

CELL BIOLOGY

A LABORATORY HANDBOOK

Third Edition
Volume 3

Editor-in-chief
Julio E. Celis, Institute of Cancer Biology, *Danish Cancer Society, Copenhagen, Denmark*

Associate Editors
Nigel P. Carter, *The Sanger Center, Wellcome Trust, Cambridge, UK*
Kai Simons, *Max-Planck Institute of Molecular Cell Biology and Genetics, Dresden, Germany*
J. Victor Small, *Austrian Academy of Sciences, Salzburg, Austria*
Tony Hunter, *The Salk Institute, La Jolla, California, USA*
David M. Shotten, *University of Oxford, UK*

CELL BIOLOGY

A LABORATORY HANDBOOK

Third Edition
Volume 3

Edited by

Julio E. Celis
Institute of Cancer Biology, Danish Cancer Society,
Copenhagen, Denmark

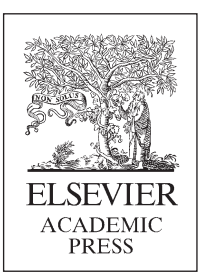

AMSTERDAM • BOSTON • HEIDELBERG • LONDON
NEW YORK • OXFORD • PARIS • SAN DIEGO
SAN FRANCISCO • SINGAPORE • SYDNEY • TOKYO

Elsevier Academic Press
30 Corporate Drive, Suite 400, Burlington, MA 01803, USA
525 B Street, Suite 1900, San Diego, California 92101–4495, USA
84 Theobald's Road, London WC1X 8RR, UK

This book is printed on acid-free paper.

Copyright © 2006, Elsevier Inc. All rights reserved.

No part of this publication may be reproduced or transmitted in any form or by any means, electronic or mechanical, including photocopy, recording, or any information storage and retrieval system, without permission in writing from the publisher.

Permissions may be sought directly from Elsevier's Science & Technology Rights Department in Oxford, UK: phone: (+44) 1865 843830, fax: (+44) 1865 853333, E-mail: permissions@elsevier.co.uk. You may also complete your request on-line via the Elsevier homepage (http://elsevier.com), by selecting "Customer Support" and then "Obtaining Permissions."

Library of Congress Cataloging-in-Publication Data
Application Submitted

British Library Cataloguing in Publication Data
A catalogue record for this book is available from the British Library

ISBN 13: 978-0-12-164733-9
ISBN 10: 0-12-164733-1
Set ISBN 13: 978-0-12-164730-8
Set ISBN 10: 0-12-164730-7

For all information on all Elsevier Academic Press publications
visit our Web site at www.books.elsevier.com

Printed in China
05 06 07 08 09 10 9 8 7 6 5 4 3 2 1

Working together to grow
libraries in developing countries
www.elsevier.com | www.bookaid.org | www.sabre.org
ELSEVIER BOOK AID International Sabre Foundation

Contents of Volume 3

Contents of other Volumes

VOLUME 1

PART A. CELL AND TISSUE CULTURE: ASSOCIATED TECHNIQUES

Section 1. General Techniques

Section 2. Culture of Specific Cell Types: Stem Cells

Section 3. Culture of Specific Cell Types: Haemopoietic, Mesenchymal, and Epithelial

Section 5. Membranes

Section 6. Mitochondria

Section 7. Nuclear Transport

Section 8. Chromatin Assembly

Section 9. Signal Transduction Assays

Section 7. Sample Fractionation for Proteomics

Section 8. Gel Electrophoresis

Section 9. Detection of Proteins in Gels

Section 10. Gel Profiling of Posttranslationally Modified Proteins

Section 11. Protein/Protein and Protein/Small Molecule Interactions

Contributors

Numbers in parenthesis indicate the volume (bold face) and page on which the authors' contribution begins.

Mads Aaboe (**4**: 83) Clinical Biochemical Department, Molecular Diagnostic Laboratory, Aarhus University Hospital, Skejby, Brendstrupgaardvej, Aarhus N, DK-8200, DENMARK

Tanja Aarvak (**1**: 239) Dynal Biotech ASA, PO Box 114, Smestad, N-0309, NORWAY

Harindra R. Abeysinghe (**3**: 345) Department of Pathology and Laboratory Medicine, University of Rochester School of Medicine, 601 Elmwood Ave., Rm 1-6337, Rochester, NY 14642

Ruedi Aebersold (**4**: 437) The Institute for Systems Biology, 1441 North 34th Street, Seattle, WA 98103-8904

Ueli Aebi (**3**: 233, 241) ME Muller Institute for Microscopy, Biozentrum, University of Basel, Klingelbergstr. 50/70, Basel, CH-4056, SWITZERLAND

Cheol-Hee Ahn (**4**: 29) School of Materials Science and Engineering, Seoul National University, Seoul, 151-744, SOUTH KOREA

Natalie G. Ahn (**4**: 443) Department of Chemistry & Biochemistry, University of Colorado, 215 UCB, Boulder, CO 80309

Ramiro Alberio (**4**: 45) School of Biosciences, University of Nottingham, Sutton Bonington, Loughborough, Leics, LE12 5RD, UNITED KINGDOM

Donna G. Albertson (**3**: 445) Cancer Research Institute, Department of Laboratory Medicine, The University of California, San Francisco, Box 0808, San Francisco, CA 94143-0808

Heiner Albiez (**1**: 291) Department of Biology II, Ludwig-Maximilians University of Munich, Munich, GERMANY

Terence Allen (**3**: 325) CRC Structural Cell Biology Group, Paterson Institute for Cancer Research, Christie Hospital NHS Trust, Wilmslow Road, Withington, Manchester, M20 4BX, UNITED KINGDOM

Noona Ambartsumian (**1**: 363) Department of Molecular Cancer Biology, Danish Cancer Society, Institute of Cancer Biology, Strandboulevarden 49, Copenhagen, DK-2100, DENMARK

Øystein Åmellem (**1**: 239) Immunosystems, Dynal Biotech ASA, PO Box 114, Smestad, N-0309, NORWAY

Patrick Amstutz (**1**: 497) Department of Biochemistry, University of Zürich, Winterthurerstr. 190, Zurich, CH-8057, SWITZERLAND

Jens S. Andersen (**4**: 427) Protein Interaction Laboratory, University of Southern Denmark—Odense, Campusvej 55, Odense M, DK-5230, DENMARK

Mads Hald Andersen (**1**: 97) Tumor Immunology Group, Institute of Cancer Biology, Danish Cancer Society, Strandboulevarden 49, Copenhagen, DK-2100, DENMARK

Helena Andersson (**4**: 63) Bioscience at Novum, Karolinska Institutet, Halsovagen 7-9, Huddinge, SE-141 57, SWEDEN

Peter W. Andrews (**1**: 183) Department of Biomedical Science, The University of Sheffield, Rm B2 238, Sheffield, S10 2TN, UNITED KINGDOM

Elsa Anes (**2**: 57) Faculdade de Farmacia, Universidade de Lisboa, Av. Forcas Armadas, Lisboa, 1649-019, PORTUGAL

James M. Angelastro (**1**: 171) Department of Pathology and Center for Neurobiology and Behavior, Columbia University College of Physicians

and Surgeons, 630 West 168th Street, New York, NY 10032

Sergey V. Anisimov (**4**: 103) Molecular Cardiology Unit, National Institute on Aging, NIH, 5600 Nathan Shock Drive, Baltimore, MD 21224

Celia Antonio (**2**: 379) Department of Biochemistry & Molecular Biophysics, College of Physicians & Surgeons, Columbia University, 701 W 168ST HHSC 724, New York, NY 69117

Shigehisa Aoki (**1**: 411) Department of Pathology & Biodefence, Faculty of Medicine, Saga University, Nebeshima 5-1-1, Saga, 849-8501, JAPAN

Ron D. Appel (**4**: 207) Swiss Institute of Bioinformatics, CMU, Rue Michel Servet 1, Geneva 4, CH-1211, SWITZERLAND

Rolf Apweiler (**4**: 469) EMBL Outstation, European Bioinformatics Institute, Wellcome Trust Genome Campus, Hinxton, Cambridge, CB10 1SD, UNITED KINGDOM

Nobukazu Araki (**2**: 147) Department of Histology and Cell Biology, School of Medicine, Kagawa University, Mki, Kagawa, 761-0793, JAPAN

Christopher M. Armstrong (**4**: 295) Dana Faber Cancer Institute, Harvard University, 44 Binney Street, Boston, MA 02115

Anthony J. Ashford (**2**: 155) Antibody Facility, Max Planck Institute of Molecullar Cell Biology and Genetics, Pfotenhauerstrsse 108, Dresden, D-01307, GERMANY

Daniel Axelrod (**3**: 19) Dept of Physics & Biophysics Research Division, University of Michigan, Ann Arbor, MI 48109-1055

Sheree Bailey (**1**: 475) Dept of Immunology, Allergy and Arthritis, Flinders Medical Centre and Flinders University, Bedford Park, Adelaide, SA, 5051, SOUTH AUSTRALIA

Nathalie Q. Balaban (**2**: 419) Department of Physics, The Hebrew University-Givat Ram, Racah Institute, Jerusalem, 91904, ISRAEL

William E. Balch (**2**: 209) Department of Cell and Molecular Biology, The Scripps Research Institute, 10550 North Torrey Pines Road, La Jolla, CA 92037

Debabrata Banerjee (**1**: 315) Department of Medicine, Cancer Institute of New Jersey, 195 Little Albany Street, New Brunswick, NJ 08903

Jiri Bartek (**4**: 253) Department of Cell Cycle and Cancer, Danish Cancer Society, Strandboulevarden 49, Copenhagen, DK-2100, DENMARK

Werner Baschong (**3**: 5) ME Muller Institute for Microscopy, Biozentrum, University of Basel, Klingelbergstrasse 50/70, Basel, CH-4056, SWITZERLAND

Philippe I. H. Bastiaens (**3**: 153) Cell Biology and Cell Biophysics Program, European Molecular Biology Laboratory, Meyerhofstrasse 1, Heidelberg, 69117, GERMANY

Jürgen C. Becker (**1**: 103) Department of Dermatology, University of Würzburg, Sanderring 2, Würzburg, 97070, GERMANY

Martin Béhé (**4**: 149) Department of Nuclear Medicine, Philipp's-University of Marburg, Baldingerstraße, Marburg/Lahn, D-35043, GERMANY

Thomas M. Behr (**4**: 149) Department of Nuclear Medicine, Philipp's-University of Marburg, Baldingerstraße, Marburg, D-35043, GERMANY

Stefanie Benesch (**2**: 399) Department of Cell Biology, Gesellschaft fur Biotechnoogische Forschung, Mascheroder Weg 1, Braunschweig, D-38124, GERMANY

Aaron Bensimon (**3**: 429) Laboratoire de Biophysique de l'ADN, Departement des Biotechnologies, Institut Pasteur, 25 rue du Dr. Roux, Paris Cedex 15, F-75724, FRANCE

John J. M. Bergeron (**2**: 41) Department of Anatomy and Cell Biology, Faculty of Medicine, McGill University, STRATHCONA Anatomy & Dentistry Building, Montreal, QC, H3A 2B2, CANADA

Michael W. Berns (**3**: 351) Beckman Laser Institute, University of California, Irvine, 1002 Health Sciences Road E, Irvine, CA 92697-1475

Joseph R. Bertino (**1**: 315) The Cancer Institute of New Jersey, 195 Little Albany Street, New Brunswick, NJ 08901

Paulo Bianco (**1**: 79) Dipartimento di Medicina Sperimentale e Patologia, Universita 'La Sapienza', Viale Regina Elena 324, Roma, I-00161, ITALY

Hans Kaspar Binz (**1**: 497) Department of Biochemistry, University of Zürich, Winterthurerstr. 190, Zürich, CH-8057, SWITZERLAND

R. Curtis Bird (**1**: 247) Department of Pathobiology, Auburn University, Auburn, AL 36849

Mina J. Bissell (**1**: 139) Life Sciences Division, Lawrence Berkeley National Laboratory, 1 Cyclotron Road, Bldg 83-101, Berkeley, CA 94720

Stephanie Blackwood (**3**: 445) Cancer Research Institute, University of California San Francisco, PO Box 0808, San Francisco, CA 94143-0808

Blagoy Blagoev (**4**: 427) Protein Interaction Laboratory, University of Southern Denmark—Odense, Campusvej 55, Odense M, DK-5230, DENMARK

Kenneth R. Boheler (**4**: 103) Laboratory of Cardiovascular Science, National Institute on Aging, NIH, 5600 Nathan Shock Drive, Baltimore, MD 21224-6825

Michelle A. Booden (**1**: 345) Lineberger Comprehensive Cancer Center, University of North Carolina at Chapel Hill, Chapel Hill, NC 27599-7295

Gary G. Borisy (**3**: 277) Department of Cell and Molecular Biology, Northwestern University Medical School, Chicago, IL 6011-3072

Elliot Botvinick (**3**: 351) Beckman Laser Institute, University of California, Irvine, 1002 Health Sciences Road, East, Irvine, CA 92697-1475

Gérard Bouchet (**4**: 207) Swiss Institute of Bioinformatics (SIB), CMU, rue Michel-Servet 1, Genève 4, CH-1211, SWITZERLAND

Rosemary Boyle (**4**: 437) The Institute for Systems Biology, 1441 North 34th St., Seattle, WA 98109

Susanne Brandfass (**1**: 563) Department of Biochemistry and Cell Biology, Max Planck Institute of Biophysical Chemistry, Am Faßberg 11, Gottingen, D-37077, GERMANY

Pascal Braun (**4**: 73) Department of Chemistry and Chemical Biology, Harvard University, 12 Oxford Street, Cambridge, MA 02138

Steven A. Braut (**4**: 121) Department of Anatomy and Structural Biology, Golding # 601, Albert Einstein College of Medicine of Yeshiva University, 1300 Morris Park Avenue, Bronx, NY 10461

Alvis Brazma (**4**: 95) EMBL Outstation—Hinxton, European Bioinformatics Institute, Wellcome Trust Genome Campus, Hinxton, Cambridge, CB10 1SD, UNITED KINGDOM

J. David Briley (**3**: 471) Department of Genomic Sciences, Glaxo Wellcome Research and Development, 5 Moore Drive, Research Triangle Park, NC 27709-3398

Simon Broad (**1**: 133) Keratinocyte Laboratory, London Research Institute, 44 Lincoln's Inn Fields, London, WC2A 3PX, UNITED KINGDOM

Nicholas H. Brown (**3**: 77) Wellcome Trust/Cancer Research UK Institute and Departmentt of Anatomy, University of Cambridge, Tennis Court Road, Cambridge, CB2 1QR, UNITED KINGDOM

Heather L. Brownell (**2**: 329, 341) Office of Technology Licensing and Industry Sponsored Research, Harvard Medical School, 25 Shattuck Street, Gordon Hall of Medicine, Room 414, Boston, MA 02115

Damien Brunner (**3**: 69) Cell Biology and Cell Biophysics Programme, European Molecular Biology Laboratory, Meyerhofstrasse 1, Heidelberg, D-69117, GERMANY

Suzannah Bumpstead (**3**: 463) Genotyping / Chr 20, The Wellcome Trust Sanger Institute, The Wellcome Trust Genome Campus, Hinxton, Cambridge, CB10 1SA, UNITED KINGDOM

Deborah C. Burford (**3**: 403) Wellcome Trust, Sanger Institute, The Wellcome Trust Genome Campus, Hinxton, Cambridge, CB10 1SA, UNITED KINGDOM

Gerald Burgstaller (**2**: 161) Department of Cell Biology, Institute of Molecular Biology, Austrian Academy of Sciences, Billrothstrasse 11, Salzburg, A-5020, AUSTRIA

Ian M. Caldicott (**1**: 157)

Angelique S. Camp (**1**: 457) Gene Therapy Centre, University of North Carolina at Chapel Hill, 7119 Thurston-Bowles (G44 Wilson Hall), Chapel Hill, NC 27599-7352

Keith H. S. Campbell (**4**: 45) School of Biosciences, Sutton Bonington, Loughborough, Leics, LE12 5RD, UNITED KINGDOM

Yihai Cao (**1**: 373) Microbiology & Tumor Biology Center, Karolinska Institute, Room: Skrivrum (G415), Box 280, Stockholm, SE-171 77, SWEDEN

Maria Carmo-Fonseca (**2**: 277, **3**: 419) Institute of Molecular Medicine, Faculty of Medicine, University of Lisbon, Av. Prof. Egas Moniz, Lisbon, 1649-028, PORTUGAL

T. Carneiro (**3**: 419) Faculty of Medicine, Institute of Molecular Medicine, University of Lisbon, Av. Prof. Egas Moniz, Lisboa, 1649-028, PORTUGAL

Nigel P. Carter (**2**: 133) The Wellcome Trust, Sanger Institute, The Wellcome Trust, Genome Campus, Hinxton, Cambridge, CB10 1SA, UNITED KINGDOM

Célia Carvalho (**3**: 419) Faculty of Medicine, Institute of Molecular Medicine, University of Lisbon, Av. Prof. Egas Moniz, Lisboa, 1649-028, PORTUGAL

Lucy A. Carver (**2**: 11) Cellular and Molecular Biology Program, Sidney Kimmel Cancer Center, 10835 Altman Row, San Diego, CA 92121

Doris Cassio (**1**: 231, **3**: 387) INSERM U-442: Signalisation cellulaire et calcium, Bat 443, Universite Paris-Sud, Street George Clemenceau Pack, 444, Orsay, Cedex, F-91405, FRANCE

Chris Catton (**3**: 207) Department of Zoology, University of Oxford, South Parks Road, Oxford, OX1 3PS, UNITED KINGDOM

Julio E. Celis (**1**: 527, **4**: 69, 165, 219, 243, 289) Danish Cancer Society, Institute of Cancer Biology and Danish Centre for Translational Breast Cancer Research, Strandboulevarden 49, Copenhagen O, DK-2100, DENMARK

Pierre Chambon (**3**: 501) Institut de Génétique et de Biologie Moléculaire et Cellulaire, 1 rue Laurent Fries, B.P.10142, Illkirch CEDEX, F-67404, FRANCE

Francis Ka-Ming Chan (**2**: 355) Department of Pathology, University of Massachusetts Medical School, Room S2-125, 55 Lake Avenue North, Worcester, MA 01655

Ming-Shien Chang (**3**: 87) Department of Physics, Duke University, 107 Physics Bldg, Durham, NC 27708-1000

Samit Chatterjee (**2**: 241) Margaret M. Dyson Vision Research Institute, Department of Ophthalmology, Weill Medical College of Cornell University, 1300 York Avenue, New York, NY 10021

Sandeep Chaudhary (**1**: 121) Veterans Affairs Medical Center, San Diego (V111G), 3350 La Jolla Village Drive, San Diego, CA 92161

Jingwen Chen (**3**: 471) Department of Genomic Sciences, Glaxo Wellcome Research and Development, 5 Moore Drive, Research Triangle Park, NC 27709

Yonglong Chen (**1**: 191) Institute for Biochemistry and Molecular Cell Biology, University of Goettingen, Justus-von-Liebig-Weg 11, Göttingen, D-37077, GERMANY

Yong Woo Cho (**4**: 29) Akina, Inc., Business & Technology Center, 1291 Cumberland Ave., #E130, West Lafayette, IN 47906

Juno Choe (**1**: 269) Institute for Systems Biology, 1441 N. 34th St, Seattle, WA 98103

Claus R. L. Christensen (**1**: 363) Department of Molecular Cancer Biology, Danish Cancer Society, Institute of Cancer Biology, Strandboulevarden 49, Copenhagen, DK-2100, DENMARK

Theodore Ciaraldi (**1**: 121) Veterans Affairs Medical Center, University of California, San Diego, 9500 Gilman Drive, La Jolla, CA 92093-9111

Aaron Ciechanover (**4**: 351) Center for Tumor and Vascular Biology, The Rappaport Faculty of Medicine and Research Institute, Technion-Israel Institute of Technology, POB 9649, Efron Street, Bat Galim, Haifa, 31096, ISRAEL

Mark S. F. Clarke (**2**: 233, **4**: 5) Department of Health and Human Performance, University of Houston, 3855 Holman Street, Garrison—Rm 104D, Houston, TX 77204-6015

Martin Clynes (**1**: 335) National Institute for Cellular Biotechnology, Dublin City University, Glasnevin, Dublin, 9, IRELAND

Philippe Collas (**1**: 207) Institute of Medical Biochemistry, University of Oslo, PO Box 1112 Blindern, Oslo, 0317, NORWAY

Kristen Correia (**4**: 35) Krumlauf Lab, Stowers Institute for Medical Research, 1000 East 50th Street, Kansas City, MO 64110

Pascale Cossart (**2**: 407) Unite des Interactions Bacteries-Cellules/Unité INSERM 604, Institut Pasteur, 28, rue du Docteur Roux, Paris Cedex 15, F-75724, FRANCE

Thomas Cremer (**1**: 291) Department of Biology II, Ludwig-Maximilians University of Munich, Munich, 80333, GERMANY

Robert A. Cross (**2**: 371) Molecular Motors Group, Marie Curie Research Institute, The Chart, Oxted, Surrey, RH8 0TE, UNITED KINGDOM

Matthew E. Cunningham (**1**: 171) Hospital for Special Surgery, New York Hospital, 520 E. 70th Street, New York, NY 10021

Noélia Custódio (**3**: 419) Faculty of Medicine, Institute of Molecular Medicine, University of Lisbon, Av. Prof. Egas Moniz, Lisboa, 1649-028, PORTUGAL

Zbigniew Darzynkiewwicz (**1**: 279) The Cancer Research Institute, New York Medical College, 19 Bradhurst Avenue, Hawthorne, NY 10532

Ilan Davis (**3**: 187) Wellcome Trust Centre for Cell Biology, Institute of Cell and Molecular Biology, The University of Edinburgh, Michael Swann Building, The King's Buildings, Mayfield Road, Edinburgh, EH9 3JR, SCOTLAND

Stephen C. De Rosa (**1**: 257) Vaccine Research Center, National Institutes of Health, 40 Convent Dr., Room 5610, Bethesda, MD 20892-3015

Nicholas M. Dean (**3**: 523) Functional Genomics, GeneTrove, GeneTrove (a division of Isis Isis Pharmaceuticals, Inc.), 2292 Faraday Avenue, Carlsbad, CA 92008

Anne Dell (**4**: 415) Department of Biological Sciences, Biochemistry Building, Imperial College of Science, Technology & Medicine, Biochemistry Building, London, SW7 2AY, UNITED KINGDOM

Panos Deloukas (**3**: 463) The Wellcome Trust, Sanger Institute, Hinxton, Cambridge, CB10 1SA, UNITED KINGDOM

Nicolas Demaurex (**3**: 163) Department of Cell Physiology and Metabolism, University of Geneva Medical Center, 1 Michel-Servet, Geneva, CH-1211, SWITZERLAND

Chris Denning (**4**: 45) Division of Animal Physiology, School of Biosciences, Institute of Genetics Room C15, University of Nottingham, Queens Medical Centre, Nottingham, NG7 2UH, UNITED KINGDOM

Ami Deora (**2**: 241) Margaret M. Dyson Vision Research Institute, Department of Ophthalmology, Weill Medical College of Cornell University, 1300 York Avenue, New York, NY 10021

Julien Depollier (**4**: 13) Centre de Recherche en Biochimie Macromoléculaire (UPR 1086), Centre National de la Recherche Scientifique (CNRS), 1919 Route de Mende, Montpellier Cedex 5, F-34293, FRANCE

Channing J. Der (**1**: 345) Department of Pharmacology, University of North Carolina at Chapel Hill, Lineberger Comprehensive Cancer Center, Chapel Hill, NC 27599

Bart Devreese (**4**: 259) Department of Biochemistry, Physiology and Microbiology, University of Ghent, K.L. Ledeganckstraat 35, Ghent, B-9000, BELGIUM

Alberto Diaspro (**3**: 201) Department of Physics, University of Genoa, Via Dodecaneso 33, Genoa, I-16146, ITALY

James Fred Dice (**4**: 345) Department Physiology, Tufts University School of Medicine, 136 Harrison Ave, Boston, MA 02111

Thomas J. Diefenbach (**4**: 307) Department of Physiology, Tufts University School of Medicine, 136 Harrison Avenue, Boston, MA 02111

Chris Dinant (**2**: 121) Biomolecular Sciences, UMIST, PO Box 88, Manchester, M60 1QD, UNITED KINGDOM

Da-Qiao Ding (**3**: 171) Structural Biology Section and CREST Research Project, Kansai Advanced Research Center, Communications Research Laboratory, 588-2 Iwaoka, Iwaoka-cho, Nishi-ku, Kobe, 651-2492, JAPAN

Gilles Divita (**4**: 13) Centre de Recherche en Biochimie Macromoléculaire (UPR 1086), Centre National de la Recherche Scientifique (CNRS), 1919 Route de Mende, Montpellier Cedex 5, F-34293, FRANCE

Eric P. Dixon (**1**: 483) TriPath Oncology, 4025 Stirrup Creek Drive, Suite 400, Durham, NC 27703

Bernhard Dobberstein (**2**: 215) Zentrum fur Molekulare Biologie, Universitat Heidelberg, Im Neuenheimer Feld 282, Heidelberg, D-69120, GERMANY

Lynda J. Donald (**4**: 457) Department of Chemistry, University of Manitoba, Room 531 Parker Building, Winnipeg, MB, R3T 2N2, CANADA

Wolfgang R. G. Dostmann (**2**: 299) Department of Pharmacology, University of Vermont, Health Science Research Facility 330, Burlington, VT 05405-0068

Adam Douglass (**3**: 129) Department of Cellular and Molecular Pharmacology, The University of California, San Francisco, School of Medicine, Medical Sciences Building, Room S1210, 513 Parnassus Avenue, San Francisco, CA 94143-0450

Kate Downes (**3**: 463) Genotyping / Chr 20, The Wellcome Trust, Sanger Institute, The Wellcome Trust Genome Campus, Hinxton, Cambridge, CB10 1SA, UNITED KINGDOM

Harry W. Duckworth (**4**: 457) Department of Chemistry, University of Manitoba, Room 531 Parker Building, Winnipeg, MB, R3T 2N2, CANADA

Derek M. Dykxhoorn (**3**: 511) CBR Institute for Biomedical Research, Harvard Medical School, 200 Longwood Ave, Boston, MA 02115

Lars Dyrskjøt (**4**: 83) Clinical Biochemical Department, Molecular Diagnostic Laboratory, Aarhus University Hospital, Skejby, Brendstrupgaardvej, Aarhus N, DK-8200, DENMARK

Christoph Eckerskorn (**4**: 157) Protein Analytics, Max Planck Institute for Biochemistry, Klopferspitz 18, Martinsried, D-82152, GERMANY

Glenn S. Edwards (**3**: 87) Department of Physics, Duke University, 221 FEL Bldg, Box 90305, Durham, NC 27708-0305

Andreas A. O. Eggert (**1**: 103) Department of Dermatology, Julius-Maximillians University, Josef-Schneider-Str. 2, Würzburg, 97080, GERMANY

Maria Ekström (**4**: 63) Bioscience at Novum, Karolinska Institutet, Huddinge, SE-141 57, SWEDEN

Andreas Engel (**3**: 317) Maurice E. Müller Institute for Microscopy at the Biozentrum, University of Basel, Klingelbergstrasse 70, Basel, CH-4056, SWITZERLAND

Anne-Marie Engel (**1**: 353) Bartholin Institutte, Bartholinsgade 2, Copenhagen K, DK-1356, DENMARK

José A. Enríquez (**2**: 69) Department of Biochemistry and Molecular and Cellular Biology, Universidad de Zaragoza, Miguel Servet, 177, Zaragoza, E-50013, SPAIN

Rachel Errington (**1**: 305) Department of Medical Biochemistry and Immunology, University of Wales College of Medicine, Heath Park, Cardiff, CF14 4XN, UNITED KINGDOM

Virginia Espina (**3**: 339) Microdissection Core Facility, Laboratory of Pathology, National Cancer Institute, 9000 Rockville Pike, Building 10, Room B1B53, Bethesda, MD 20892

H. Dariush Fahimi (**2**: 63) Department of Anatomy and Cell Biology II, University of Heidelberg, Im Neuenheimer Feld 307, Heidelberg, D-69120, GERMANY

Federico Federici (**3**: 201) Department of Physics, University of Genoa, Via Dodecaneso 33, Genoa, I-16146, ITALY

Daniel L. Feeback (**2**: 233, **4**: 5) Space and Life Sciences Directorate, NASA-Johnson Space Center, 3600 Bay Area Blvd, Houston, TX 77058

Patricio Fernández-Silva (**2**: 69) Dept of Biochemistry and Molecular and Cellular Biology, Univeridad de Zaragoza, Miguel Servet 177, Zaragoza, E-50013, SPAIN

Erika Fernández-Vizarra (**2**: 69) Dept of Biochemistry and Molecular and Cellulary Biology, Universidad de Zaragoza, Miguel Servet, 177, Zaragoza, E-50013, SPAIN

Patrick F. Finn (**4**: 345) Department of Physiology, Tufts University School of Medicine, 136 Harrison Ave, Boston, MA 02111

Kevin L. Firth (**2**: 329, **2**: 341) ASK Science Products Inc., 487 Victoria St, Kingston, Ontario, K7L 3Z8, CANADA

Raluca Flükiger-Gagescu (**2**: 27) Unitec—Office of Technology Transfer, University of Geneva and University of Geneva Hospitals, 24, Rue Général-Dufour, Geneva 4, CH-1211, SWITZERLAND

Leonard J. Foster (**4**: 363, 427) Protein Interaction Laboratory, University of Southern Denmark, Odense, Campusvej 55, Odense M, DK-5230, DENMARK

Dimitrios Fotiadis (**3**: 317) M. E. Müller Institute for Microscopy at the Biozentrum, University of Basel, Klingelbergstrasse 70, Basel, CH-4056, SWITZERLAND

Patrick L. T. M. Frederix (**3**: 317) M. E. Müller Institute for Microscopy at the Biozentrum, University of Basel, Klingelbergstrasse 70, Basel, CH-4056, SWITZERLAND

Marcus Frohme (**4**: 113) Functional Genome Analysis, German Cancer Research Center, Deutsches Krebsforschungszentrum, Im Neuenheimer Feld 580, Heidelberg, D-69120, GERMANY

Masanori Fujimoto (**4**: 197) Department of Biochemistry and Biomolecular Recognition, Yamaguchi University School of Medicine, 1-1-1, Minami-kogushi, Ube, Yamaguchi, 755-8505, JAPAN

Margarida Gama-Carvalho (**2**: 277) Faculty of Medicine, Institute of Molecular Medicine, University of Lisbon, AV. Prof. Egas Moniz, Lisbon, 1649-028, PORTUGAL

Henrik Garoff (**1**: 419, **4**: 63) Unit for Cell Biology, Center for Biotechnology. Karolinska Institute, Huddinge, SE-141 57, SWEDEN

Susan M. Gasser (**2**: 359) Friedrich Miescher Institute fr Biomedical Research, Maulbeerstrasse 66, Basel, CH-1211, SWITZERLAND

Kristine G. Gaustad (**1**: 207) Institute of Medical Biochemistry, University of Oslo, PO Box 1112 Blindern, Oslo, 0317, NORWAY

Benjamin Geiger (**2**: 419) Dept. of Molecular Cell Biology, Weizman Institute of Science, Wolfson Building, Rm 617, Rehovot, 76100, ISRAEL

Kris Gevaert (**4**: 379, **4**: 457) Dept. Medical Protein Research, Flanders Interuniversity Institute for Biotechnology, Faculty of Medicine and Health Sciences, Ghent University, Instituut Rommelaere—Blok D, Albert Baertsoenkaai 3, Gent, B-9000, BELGIUM

Jilur Ghori (**3**: 463) Genotyping / Chr 20, The Wellcome Trust, Sanger Institute, The Wellcome Trust, Genome Campus, Hinxton, Cambridge, CB10 1SA, UNITED KINGDOM

Alasdair J. Gibb (**1**: 395) Department of Pharmacology, University College London, Gower Street, London, WC1E GBT, UNITED KINGDOM

Mario Gimona (**1**: 557, **2**: 161, **4**: 145) Department of Cell Biology, Institute of Molecular Biology, Austrian Academy of Sciences, Billrothstrasse 11, Salzburg, A-5020, AUSTRIA

David A. Glesne (**1**: 165) Biosciences Division, Argonne National Laboratory, 9700 South Cass Avenue, Argonne, IL 60439-4844

Martin Goldberg (**3**: 325) Science Laboratories, University of Durham, South Road, Durham, DH1 3LE, UNITED KINGDOM

Kenneth N. Goldie (**3**: 267) Structural and Computational Biology Programme, EMBL, Meyerhofstrasse 1, Heidelberg, D-69117, GERMANY

Jon W. Gordon (**3**: 487) Geriatrics and Adult Development, Mount Sinai School of Medicine, One Gustave L. Levy Place, New York, NY 10029

Angelika Görg (**4**: 175) Fachgebiet Proteomik, Technische Universität München, Am Forum 2, Freising Weihenstephan, D-85350, GERMANY

Martin Gotthardt (**4**: 149) Department of Nuclear Medicine, Philipp's-University of Marburg, Baldingerstraße, Marburg/Lahn, D-35043, GERMANY

Frank L. Graham (**1**: 435) Department of Biology, McMaster University, Life Sciences Building, Room 430, Hamilton, Ontario, L8S 4K1, CANADA

Claude Granier (**1**: 519) UMR 5160, Faculté de Pharmacie, 15 Av. Charles Flahault, Montpellier Cedex 5, BP 14491, 34093, FRANCE

Lloyd A. Greene (**1**: 171) Department of Pathology and Center for Neurobiology and Behavior, Columbia University, College of Physicians and Surgeons, 630 W. 168th Street, New York, NY 10032

Susan M. Gribble (**3**: 403) Sanger Institute, The Wellcome Trust, The Wellcome Trust Genome Campus, Hinxton, Cambridge, CB10 1SA, UNITED KINGDOM

Gareth Griffiths (**2**: 57, **3**: 299) Department of Cell Biology, EMBL, Postfach 102209, Heidelberg, D-69117, GERMANY

Sergio Grinstein (**3**: 163) Cell Biology Program, Hospital for Sick Children, 555 University Avenue, Toronto, Ontario, M5G 1X8, CANADA

Pavel Gromov (**1**: 527, **4**: 69, 165, 243, 289) Institute of Cancer Biology and Danish Centre for Translational Breast Cancer Research, Danish Cancer Society, Strandboulevarden 49, Copenhagen, DK-2100, DENMARK

Irina Gromova (**4**: 219) Department of Medical Biochemistry and Danish Centre for Translational Breast Cancer Research, Danish Cancer Society, Strandboulevarden 49, Copenhagen, DK-2100, DENMARK

Dale F. Gruber (**1**: 33) Cell Culture Research and Development, GIBCO/Invitrogen Corporation, 3175 Staley Road, Grand Island, NY 14072

Markus Grubinger (**4**: 145) Institute of Physics and Biophysics, University of Salzburg, Hellbrunnerstr. 34, Salzburg, A-5020, AUSTRIA

Jean Gruenberg (**2**: 27, 201) Department of Biochemistry, University of Geneva, 30, quai Ernest Ansermet, Geneva 4, CH-1211, SWITZERLAND

Stephanie L. Gupton (**3**: 137) 10550 North Torrey Pines Road, CB 163, La Jolla, CA 92037

Cemal Gurkan (**2**: 209) Department of Cell and Molecular Biology, The Scripps Research Institute, 10550 North Torrey Pines Road, La Jolla, CA 92037

Martin Guttenberger (**4**: 131) Zentrum für Molekulariologie der Pflanzen, Universitat Tübingen, Entwicklungsgenetik, Auf der Morgenstelle 3, Tübingen, D-72076, GERMANY

Thomas Haaf (**3**: 409) Institute for Human Genetics, Johannes Gutenberg-Universität Mainz, 55101, Mainz, D-55131, GERMANY

Christine M. Hager-Braun (**1**: 511) Health and Human Services, NIH National Institute of Environmental Health Sciences, MD F0-04, PO Box 12233, Research Triangle Park, NC 27709

Anne-Mari Håkelien (**1**: 207) Institute of Medical Biochemistry, Institute of Medical Biochemistry, University of Oslo, PO Box 1112 Blindern, Oslo, 0317, NORWAY

Fiona C. Halliday (**1**: 395) GlaxoSmithKline, Greenford, Middlesex, UB6 OHE, UNITED KINGDOM

Gerald Hammond (**2**: 223) Molecular Neuropathobiology Laboratory, Cancer Reasearch UK London Research Institute, 44 Lincoln's Inn Fields, London, WC2A 3PX, UNITED KINGDOM

Klaus Hansen (**4**: 253)

Hironobu Harada (**1**: 367) Department of Neurosurgery, Ehime University School of Medicine, Shitsukawa, Toon-shi, Ehime, 791-0295, JAPAN

Robert J. Hay (**1**: 43, 49, 573) Viitro Enterprises Incorporated, 1113 Marsh Road, PO Box 328, Bealeton, VA 22712

Izumi Hayashi (**1**: 151) National Medical Center and Beckman Research Institute, Division of Neurosciences, City of Hope, 1500 E. Duarte Rd, Duarte, CA 91010-3000

Timothy A. Haystead (**4**: 265) Department of Pharmacology and Cancer Biology, Duke University Medical Center, Box 3813 Med Ctr, Durham, NC 27710

Rebecca Heald (**2**: 379) Molecular and Cell Biology Department, University of California, Berkeley, Berkeley, CA 94720-3200

Florence Hediger (**2**: 359) Department of Molecular Biology, University of Geneva, 30, Quai Ernest Ansermet, Geneva, CH-1211, SWITZERLAND

Rainer Heintzmann (**3**: 29) Randall Division of Cell and Molecular Biophysics, King's College London, Guy's Campus, London, SE1 1UL, UNITED KINGDOM

Frederic Heitz (**4**: 13) Centre de Recherche en Biochimie Macromoléculaire (UPR 1086), Centre National de la Recherche Scientifique (CNRS), 1919 Route de Mende, Montpellier Cedex 5, F-34293, FRANCE

Johannes W. Hell (**2**: 85) Department of Pharmacology, University of Iowa, 2152 Bowen Science Building, Iowa City, IA 52242

Kai Hell (**4**: 269) Adolf-Butenandt-Institut fur Physiologische Chemie, Lehrstuhl: Physiologische Chemie, Universitat Munchen, Butenandtstr. 5, Gebäude B, Munchen, D-81377, GERMANY

Robert R. Henry (**1**: 121) Veterans Affairs Medical Center, San Diego (V111G), 3350 La Jolla Village Drive, San Diego, CA 92161

Johan Hiding (**2**: 45) Göteborg University, Institute of Medical Biochemistry, PO Box 440, Göteborg, SE-403-50, SWEDEN

Yasushi Hiraoka (**3**: 171) Structural Biology Section and CREST Research Project, Kansai Advanced Research Center, Communications Research Laboratory, 588-2 Iwaoka, Iwaoka-cho, Nishi-ku, Kobe, 651-2492, JAPAN

Mary M. Hitt (**1**: 435) Department of Pathology & Molecular Medicine, McMaster University, 1200 Main Street West, Hamilton, Ontario, L8N 3Z5, CANADA

Julie Hodgkinson (**3**: 307) School of Crystallography, Birkbeck College, Unversity of London, Malet Street, London, WC1E 7HX, UNITED KINGDOM

Klaus P. Hoeflich (**2**: 307) Division of Molecular and Structural Biology, Ontario Cancer Institute, Department of Medical Biophysics, University of Toronto, 610 University Avenue, 7-707A, Toronto, Ontario, M5G 2M9, CANADA

Tracy L. Hoffman (**1**: 21) ATCC, P.O. Box 1549, Manassas, VA 20108

Jörg D. Hoheisel (**4**: 113) Functional Genome Analysis, German Cancer Research Center, Deutsches Krebsforschungszentrum, Im Neuenheimer Feld 580, Heidelberg, D-69120, GERMANY

Thomas Hollemann (**1**: 191) Institute for Biochemistry and Molecular Cell Biology, University of Goettingen, Justus-von-Liebig-Weg 11, Göttingen, D-37077, GERMANY

Caterina Holz (**4**: 57) PSF biotech AG, Huebnerweg 6, Berlin, D-14059, GERMANY

Akira Honda (**2**: 299) Department of Pharmacology, University of Vermont, Health Science Research Facility 330, Burlington, VT 05405-0068

Masanori Honsho (**2**: 5) Max Planck Institute of Molecular Cell Biology and Genetics, Pfotenhauerstrasse 108, Dresden, D-01307, GERMANY

Andrew N. Hoofnagle (**4**: 443) School of Medicine, University of Colorado Health Sciences Center, Denver, CO 80262

Eliezer Huberman (**1**: 165) Gene Expression and Function Group, Argonne National Laboratory, 9700 South Cass Avenue, Argonne, IL 60439-4844

M. Shane Hutson (**3**: 87) Department of Physics, Duke University, 107 Physics Bldg, Durham, NC 27708-1000

Andreas Hüttmann (**1**: 115) Abteilung für Hämatologie, Universitäkrankenhaus Essn, Hufelandstr. 55, Essen, 45122, GERMANY

Anthony A. Hyman (**2**: 155) Max Planck Institute of Molecular Cell Biology and Gene Technology, Pfotenhauerstrasse 108, Dresden, D-01307, GERMANY

Sherrif F. Ibrahim (**1**: 269) Institute for Systems Biology, 1441 N. 34th St, Seattle, WA 98103

Kazuo Ikeda (**1**: 151) National Medical Center and Beckman Research Institute, Division of Neurosciences, City of Hope, 1500 East Duarte Road, Duarte, CA 91010-3000

Elina Ikonen (**2**: 181) The LIPID Cell Biology Group, Department of Biochemistry, The Finnish National Public Health Institute, Mannerheimintie 166, Helsinki, FIN-00300, FINLAND

Pranvera Ikonomi (**1**: 49) Director, Cell Biology, American Type Culture Collection (ATCC), 10801 University Blvd., Manassas, VA 20110-2209

Mitsuhiko Ikura (**2**: 307) Division of Molecular and Structural Biology, Ontario Cancer Institute, Department of Medical Biophysics, University of Toronto, 610 University Avenue 7-707A, Toronto, Ontario, M5G 2M9, CANADA

Arup Kumar Indra (**3**: 501) Institut de Génétique et de Biologie Moléculaire et Cellulaire (IGBMC), 1 rue Laurent Fries, B.P.10142, Illkirch CEDEX, F-67404, FRANCE

Takayoshi Inoue (**4**: 35) National Institute for Neuroscience, 4-1-1 Ogawahigashi, Kodaira, Tokyo, 187-8502, JAPAN

Kumiko Ishii (**2**: 139) Supra-Biomolecular System Research Group, RIKEN (Institute of Physical and Chemical Research), 2-1, Hirosawa, Wako-shi, Saitama, 351-0198, JAPAN

Dean A. Jackson (**2**: 121) Department of Biomolecular Sciences, UMIST, PO Box 88, Manchester, M60 1QD, UNITED KINGDOM

Reinhard Jahn (**2**: 85) Department of Neurobiology, Max-Planck-Institut for Biophysical Chemistry, Am Faßberg 11, Gottingen, D-37077, GERMANY

Kim D. Janda (**1**: 491) Department of Chemistry, BCC-582, The Scripps Research Institute, 10550 N. Torrey Pines Road, La Jolla, CA 92037

Harry W. Jarrett (**4**: 335) Department of Biochemistry, University of Tennessee Health Sciences Center, Memphis, TN 38163

Daniel G. Jay (**4**: 307) Dept. Physiology, Tufts University School of Medicine, 136 Harrison Avenue, Boston, MA 02111

David W. Jayme (**1**: 33) Cell Culture Research and Development, GIBCO/Invitrogen Corporation, 3175 Staley Road, Grand Island, NY 14072

Ole Nørregaard Jensen (**4**: 409) Protein Research Group, Department of Biochemistry and Molecular Biology, University of Southern Denmark, Campusvej 55, Odense M, DK-5230, DENMARK

Jae Hyun Jeong (**4**: 29) Department of Chemical & Biomolecular Engineering, Center for Ultramicrochemical Process Systems, Korea Advanced Institute of Science and Technology, Daejeon, 305-701, SOUTH KOREA

Jeff A. Jones (**2**: 233) Space and Life Sciences Directorate, NASA-Johnson Space Center, TX 77058

Gloria Juan (**1**: 279) Research Pathology Division, Room S-830, Memorial Sloan-Kettering Cancer Center, 1275 York Avenue, New York, NY 10021

Melissa S. Jurica (**2**: 109) Molecular, Cell & Developmental Biology, Center for Molecular Biology of RNA, UC Santa Cruz, 1156 High Street, Santa Cruz, CA 95064

Eckhart Kämpgen (**1**: 103) Department of Dermatology, Friedrich Alexander University, Hartmannstr. 14, Erlangen, D-91052, GERMANY

Roger Karlsson (**2**: 165) Department of Cell Biology, The Wenner-Gren Institute, Stockholm University, Stockholm, S-10691, SWEDEN

Fredrik Kartberg (**2**: 45) Göteborg University, Institute of Medical Biochemistry, PO Box 440, Gothenburg, SE, 403-50, SWEDEN

Irina N. Kaverina (**3**: 111) Institute of Molecular Biotechnology, Austrian Academy of Sciences, Dr. Bohrgasse 3-5, Vienna, A-1030, AUSTRIA

Ralph H. Kehlenbach (**2**: 267) Hygiene-Institut-Abteilung Virologie, Universitat Heidelberg, Im Neuenheimer Feld 324, Heidelberg, D-69120, GERMANY

Daniel P. Kiehart (**3**: 87) Department of Biology, Duke University, B330g Levine Sci Bldg, Box 91000, Durham, NC 27708-1000

Katherine E. Kilpatrick (**1**: 483) Senior Research Investigator, TriPath Oncology, 4025 Stirrup Creek Drive, Suite 400, Durham, NC 27703

Jong-Duk Kim (**4**: 29) Department of Chemical & Biomolecular Engineering, Center for Ultramicrochemical Process Systems, Korea Advanced Institute of Science and Technology, Daejeon, 305-701, SOUTH KOREA

Maurice Kléber (**1**: 69) Institute of Cell Biology, Department of Biology, Swiss Federal Institute of Technology, ETH—Hönggerberg, Zurich, CH-8093, SWITZERLAND

Toshihide Kobayashi (**2**: 139) Supra-Biomolecular System Research Group, RIKEN (Institute of Physical and Chemical Research) Frontier Research System, 2-1, Hirosawa, Wako-shi, Saitama, 351-0198, JAPAN

Stefan Kochanek (**1**: 445) Division of Gene Therapy, University of Ulm, Helmholtz Str. 8/I, Ulm, D-89081, GERMANY

Anna Koffer (**2**: 223) Physiology Department, University College London, 21 University Street, London, WC1E 6JJ, UNITED KINGDOM

Antonius Koller (**4**: 383) Department of Cell Biology, Torrey Mesa Research Institute, 3115 Merryfield Row, San Diego, CA 92121

Erich Koller (**3**: 523) Functional Genomics, GeneTrove, Isis Pharmaceuticals, Inc., 2292 Faraday Ave., Carlsbad, CA 92008

Robert L. Kortum (**1**: 215) The Eppley Institute for Research in Cancer, The University of Nebraska Medical Center, 986805 Nebraska Medical Center, Omaha, NE 68198-6805

Irina Kratchmarova (**4**: 427) Protein Interaction Laboratory, University of Southern Denmark—Odense, Campusvej 55, Odense M, DK-5230, DENMARK

Geri E. Kreitzer (**2**: 189) Cell and Developmental Biology, Weill Medical College of Cornell University, LC-300, New York, NY 10021

Florian Kreppel (**1**: 445) Division of Gene Therapy, University of Ulm, Helmholtz Str. 8/I, Ulm, D-89081, GERMANY

Mogens Kruhøffer (**4**: 83) Molecular Diagnostic Laboratory, Clinical Biochemical Department, Aarhus University Hospital, Skejby, Brendstrupgaardvej, Aarhus N, DK-8200, DENMARK

Robb Krumlauf (**4**: 35) Stowers Institute for Medical Research, 1000 East 50th Street, Kansas City, MO 64110

Michael Kühl (**1**: 191) Development Biochemistry, University of Ulm, Albert-Einstein-Allee 11, Ulm, D-89081, GERMANY

Mark Kühnel (**2**: 57) Department of Cell Biology, EMBL, Postfach 102209, Heidelberg, D-69117, GERMANY

Anuj Kumar (**3**: 179) Dept. of Molecular, Cellular, and Developmental Biology and Life Sciences Institute, University of Michigan, 210 Washtenaw Avenue, Ann Arbor, MI 48109-2216

Thomas Küntziger (**1**: 207) Institute of Medical Biochemistry, Institute of Medical Biochemistry, University of Oslo, PO Box 1112 Blindern, Oslo, 0317, NORWAY

Yasuhiro Kuramitsu (**4**: 197) Department of Biochemistry and Biomolecular Recognition, Yamaguchi University School of Medicine, 1-1-1 Minami-kogushi, Ube, Yamaguchi, 755-8505, JAPAN

Sergei A. Kuznetsov (**1**: 79) Craniofacial and Skeletal Disease Branch, NIDCR, NIH, Department of Health and Human Services, 30 Convent Drive MSC 4320, Bethesda, MD 20892

Joshua Labaer (**4**: 73) Harvard Institute of Proteomics, 320 Charles Street, Boston, MA 02141-2023

Frank Lafont (**2**: 181) Department of Biochemistry, University of Geneva, 30, quai Ernest-Ansermet 1211, Geneva 4, CH-1211, SWITZERLAND

Yun Wah Lam (**2**: 103, 115) Wellcome Trust Biocentre, MSI/WTB Complex, University of Dundee, Dow Street, Dundee, DD1 5EH, UNITED KINGDOM

Angus I. Lamond (**2**: 103, 115) Wellcome Trust Biocentre, MSI/WTB Complex, University of Dundee, Dow Street, Dundee, DD1 5EH, UNITED KINGDOM

Lukas Landmann (**3**: 5) Institute for Anatomy (LL), Anatomisches Institut, University of Basel, Pestalozzistrasse 20, Basel, CH-4056, SWITZERLAND

Helga B. Landsverk (**1**: 207) Institute of Medical Biochemistry, Institute of Medical Biochemistry, University of Oslo, PO Box 1112 Blindern, Oslo, 0317, NORWAY

Christine Lang (**4**: 57) Department of Microbiology and Genetics, Berlin University of Technology, Gustav-Meyer-Allee 25, Berlin, D-13355, GERMANY

Paul LaPointe (**2**: 209) Department of Cell and Molecular Biology, The Scripps Research Institute, 10550 North Torrey Pines Road, La Jolla, CA 92037

Martin R. Larsen (**4**: 371) Department of Biochemistry and Molecular Biology, University of Southern Denmark, Campusvej 55, Odense M, DK-5230, DENMARK

Pamela L. Larsen (**1**: 157) Department of Cellular and Structural Biology, University of Texas Health Science Center at San Antonio, San Antonio, TX 78229-3900

Eugene Ngo-Lung Lau (**1**: 115) Leukaemia Foundation of Queensland Leukaemia Research Laboratories, Queensland Institute of Medical Research, Royal Brisbane Hospital Post Office, Brisbane, Queensland, Q4029, AUSTRALIA

Sabrina Laugesen (**4**: 371) Department of Biochemistry and Molecular Biology, University of Southern Denmark, Campusvej 55, Odense M, DK-5230, DENMARK

Daniel Laune (**1**: 519) Centre de Pharmacologie et Biotechnologie pour la Santé, CNRS UMR 5160, Faculté de Pharmacie, Avenue Charles Flahault, Montpellier Cedex 5, F-34093, FRANCE

Andre Le Bivic (**2**: 241) Groupe Morphogenese et Compartimentation Membranaire, UMR 6156, IBDM, Faculte des Sciences de Luminy, case 907, Marseille cedex 09, F-13288, FRANCE

Ronald Lebofsky (**3**: 429) Laboratoire de Biophysique de l'ADN, Departement des Biotechnologies, Institut Pasteur, 25 rue du Dr. Roux, Paris Cedex 15, F-75724, FRANCE

Chuan-PU Lee (**2**: 259) The Department of Biochemistry and Molecular Biology, Wayne State University School of Medicine, 4374 Scott Hall, 540 E. Canfield, Detroit, MI 48201

Eva Lee (**1**: 139) Life Sciences Division, Lawrence Berkeley National Laboratory, 1 Cyclotron Road, Bldg 83-101, Berkeley, CA 94720

Joon-Hee Lee (**4**: 45) School of Biosciences, University of Nottingham, Sutton Bonington, Loughborough, Leics, LE12 5RD, UNITED KINGDOM

Kwangmoon Lee (**1**: 215) The Eppley Institute for Research in Cancer, The University of Nebraska Medical Center, 986805 Nebraska Medical Center, Omaha, NE 68198-6805

Thomas Lee (**4**: 443) Dept of Chemistry and Biochemistry, Univ of Colorado, 215 UCB, Boulder, CO 80309-0215

Margaret Leversha (**3**: 395) Memorial Sloan Kettering Cancer Center, 1275 York Avenue, New York, NY 10021

Jeffrey M. Levsky (**4**: 121) Department of Anatomy and Structural Biology, Golding # 601, Albert Einstein College of Medicine of Yeshiva University, 1300 Morris Park Avenue, Bronx, NY 10461

Alexandre Lewalle (**3**: 37) Randall Centre, New Hunt's House, Guy's Campus, London, SE1 1UL, UNITED KINGDOM

Chung Leung Li (**1**: 115) Experimental Haematology Laboratory, Stem Cell Program, Institute of Zoology/Genomics Research Center, Academia Sinica, Nankang 115, Nankang, Taipei, 11529, R.O.C.

LiQiong Li (**3**: 345) Department of Pathology and Laboratory Medicine, University of Rochester School of Medicine, 601 Elmwood Ave., Rm 1-6337, Rochester, NY 14642

Mei Li (**3**: 501) Institut de Génétique et de Biologie Moléculaire et Cellulaire (IGBMC), 1 rue Laurent Fries, B.P.10142, Illkirch CEDEX, F-67404, FRANCE

Siming Li (**4**: 295) Dana Faber Cancer Institute, Harvard University, 44 Binney Street, Boston, MA 02115

Lih-huei Liaw (**3**: 351) Beckman Laser Institute, University of California, Irvine, 1002 Health Sciences Road E, Irvine, CA 92697-1475

Antonietta M. Lillo (**1**: 491) Department of Chemistry, BCC-582, The Scripps Research Institute, 10550 N. Torrey Pines Road, La Jolla, CA 92037

Uno Lindberg (**2**: 165) Department of Cell Biology, Stockholm University, The Wenner-Gren Institute, Stockhólm, S-10691, SWEDEN

Christian Linden (**1**: 103) Department of Virology, Julius-Maximillins University, Versbacher Str. 7, Würzburg, D-97080, GERMANY

Robert Lindner (**2**: 51) Department of Cell Biology in the Center of Anatomy, Hannover Medical School, Hannover, D-30625, GERMANY

Lance A. Liotta (**3**: 339) Chief, Laboratory of Pathology, National Cancer Institute Building 10, Room 2A33, 9000 Rockville Pike, Bethesda, MD 20892

Adam J. Liska (**4**: 399) Max Planck Institute of Molecular Cell Biology and Genetics, Pfotenhauerst 108, Dresden, D-01307, GERMANY

Hong Liu (**1**: 139) Life Sciences Division, Lawrence Berkeley National Laboratory, 1 Cyclotron Road, Bldg 83-101, Berkeley, CA 94720

Silvia Lommel (**2**: 399) Department of Cell Biology, German Research Center for Biotechnology (GBF), Mascheroder Weg 1, Braunschweig, D-38124, GERMANY

Giuseppe S. A. Longo-Sorbello (**1**: 315) Centro di Riferimento Oncologico, Ospedale "S. Vincenzo", Taormina, Contradra Sirinam, 08903, ITALY

Lovisa Lovmar (**3**: 455) Department of Medical Sciences, Uppsala University, Akademiska sjukhuset, Uppsala, SE-75185, SWEDEN

Eugene Lukanidin (**1**: 363) Department of Molecular Cancer Biology, Institute of Cancer Biology, Danish Cancer Society, Strandboulevarden 49, Copenhagen, DK-2100, DENMARK

Jiri Lukas (**4**: 253) Department of Cell Cycle and Cancer, Danish Cancer Society, Strandboulevarden 49, Copenhagen, DK-2100, DENMARK

Peter J. Macardle (**1**: 475) Department of Immunology, Allergy and Artritis, Flinders Medical Centre and Flinders University, Bedford Park, Adelaie, SA, 5051, SOUTH AUSTRALIA

Peder S. Madsen (**4**: 69) Institute of Medical Biochemistry, University of Aarhus, Ole Worms Alle, Building 170, Aarhus C, DK-8000, DENMARK

Nils E. Magnusson (**4**: 83) Clinical Biochemical Department, Molecular Diagnostic Laboratory, Aarhus University Hospital, Skejby, Brendstrupgaardvej, Aarhus N, DK-8200, DENMARK

Asami Makino (**2**: 139) Supra-Biomolecular System Research Group, RIKEN (Institute of Physical and Chemical Research) Frontier Research System, 2-1, Hirosawa, Wako-shi, Saitama, 351-0198, JAPAN

G. Mike Makrigiorgos (**3**: 477) Department of Radiation Oncology, Dana Farber-Brigham and Women's Cancer Center, 75 Francis Street, Level L2, Boston, MA 02215

Matthias Mann (**4**: 363, 427) Protein Interaction Laboratory, University of Southern Denmark, Odense, Campusvej 55, Odense M, DK-5230, DENMARK

Edward Manser (**4**: 285) Glaxo-IMCB Group, Institute of Molecular and Cell Biology, Singapore, 117609, SINGAPORE

Ahmed Mansouri (**3**: 491) Department of Molecular Cell Biology, Max-Planck-Institute of Biophysical Chemistry, Am Fassberg 11, Göttingen, D-37077, GERMANY

Alan D. Marmorstein (**2**: 241) Cole Eye Institute, Weill Medical College of Cornell Cleveland Clinic, 9500 Euclid Avenue, i31, Cleveland, OH 44195

Bruno Martoglio (**2**: 215) Institute of Biochemistry, ETH Zentrum, Building CHN, Room L32.3, Zurich, CH-8092, SWITZERLAND

Susanne E. Mason (**1**: 407) Department of Physiology, University of Maryland School of Medicine, 655 W. Baltimore St., Baltimore, MD 21201

Stephen J. Mather (**1**: 539) Dept of Nuclear Medicine, St Bartholomews Hospital, London, EC1A 7BE, UNITED KINGDOM

Arvid B. Maunsbach (**3**: 221, 289) Department of Cell Biology, Institute of Anatomy, Aarhus University, Aarhus, DK-8000, DENMARK

William Hayes McDonald (**4**: 391) Department of Cell Biology, The Scripps Research Institute, 10550 North Torrey Pines Rd, La Jolla, CA 92370

Kathleen M. McKenzie (**1**: 491) Department of Chemistry, BCC-582, The Scripps Research Institute, 10550 N. Torrey Pines Road, La Jolla, CA 92037

Alexander D. McLellan (**1**: 103) Department of Microbiology & Immunology, University of Otago, PO Box 56, 720 Cumberland St, Dunedin, NEW ZEALAND

Scott W. McPhee (**1**: 457) Department of Surgery, University of Medicine and Dentistry of New Jersey, Camden, NJ 08103

Jill Meisenhelder (**4**: 139) Molecular and Cell Biology Laboratory, The Salk Institute, 10010 North Torrey Pines Road, La Jolla, CA 92037

Paula Meleady (**1**: 13) National Institute for Cellular Biotechnology, Dublin City University, Glasnevin, Dublin, 9, IRELAND

Nicholas T. Mesires (**4**: 345) Department of Physiology, Tufts University School of Medicine, 136 Harrison Ave, Boston, MA 02111

Daniel Metzger (**3**: 501) Institut de Génétique et de Biologie Moléculaire et Cellulaire (IGBMC), Institut Clinique de la Souris (ICS), 1 rue Laurent Fries, B.P.10142, Illkirch CEDEX, F-67404, FRANCE

Martina Mirlacher (**3**: 369) Division of Molecular Pathology, Institue of Pathology, University of Basel, Schonbeinstrasse 40, Basel, CH-4031, SWITZERLAND

Suchareeta Mitra (**4**: 335) Department of Biochemistry, University of Tennessee Health Sciences Center, Memphis, TN 38163

Atsushi Miyawaki (**2**: 317) Laboratory for Cell Function and Dynamics, Advanced Technology Center, Brain Science Institute, Institute of Physical and Chemical Research (RIKEN), 2-1 Horosawa, Wako, Saitama, 351-0198, JAPAN

Dejana Mokranjac (**4**: 269) Adolf-Butenandt-Institut fur Physiologische Chemie, Lehrstuhl: Physiologische Chemie, Universitat Munchen, Butenandtstr. 5, Gebäude B, Munchen, D-81377, GERMANY

Peter L. Molloy (**4**: 325) CSIRO Molecular Science, PO Box 184, North Ryde, NSW, 1670, AUSTRALIA

Richard A. Moravec (**1**: 25) Promega Corporation, 2800 Woods Hollow Road, Madison, WI 53711-5399

José M. A. Moreira (**1**: 527) Institute of Cancer Biology and Danish Centre for Translational Breast Cancer Research, Danish Cancer Society, Strandboulevarden 49, Copenhagen O, DK-2100, DENMARK

May C. Morris (**4**: 13) Centre de Recherche en Biochimie Macromoléculaire (UPR 1086), Centre National de la Recherche Scientifique (CNRS), 1919 Route de Mende, Montpellier Cedex 5, F-34293, FRANCE

Robert A. Moxley (**4**: 335) Department of Biochemistry, University of Tennessee Health Sciences Center, Memphis, TN 38163

Anne Muesch (**2**: 189) Margaret M. Dyson Vision Research Institute, Department of Opthalmology, Weill Medical College of Cornell University, New York, NY 10021

Peggy Müller (**1**: 325) Zentrum für Angewandte Medizinische und Humanbiologische Forschung, Labor für Molekulare Hepatologie der Universitätsklinik und Polikinik für Innere Medizin I, Martin Luther University Halle-Wittenburg, Heinrich-Damerow-Street 1, Saale, Halle, D-06097, GERMANY

Steve Murray (**3**: 325) CRC Structural Cell Biology Group, Paterson Institute for Cancer Research, Christie Hospital NHS Trust, Wilmslow Road, Withington, Manchester, M20 4BX, UNITED KINGDOM

Connie Myers (**1**: 139) Life Sciences Division, Lawrence Berkeley National Laboratory, 1 Cyclotron Road, Bldg 83-101, Berkeley, CA 94720

Kazuyuki Nakamura (**4**: 197) Department of Biochemistry and Biomolecular Recognition, Yamaguchi University School of Medicine, 1-1-1 Minami-kogushi, Ube, Yamaguchi, 755-8505, JAPAN

Maithreyi Narasimha (**3**: 77) Wellcome Trust/Cancer Research UK Institute and Dept of Anatomyaraki, University of Cambridge, Tennis Court Road, Cambridge, CB2 1QR, UNITED KINGDOM

Dobrin Nedelkov (**4**: 279) Intrinsic Bioprobes, Inc., 625 S. Smith Road, Suite 22, Tempe, AZ 85281

Randall W. Nelson (**4**: 279) Intrinsic Bioprobes Inc., 625 S. Smith Road, Suite 22, Tempe, AZ 85281

Frank R. Neumann (**2**: 359) Department of Molecular Biology, University of Geneva, 30, Quai Ernest Ansermet, Geneva, CH-1211, SWITZERLAND

Walter Neupert (**4**: 269) Adolf-Butenandt-Institut fur Physiologische Chemie, Lehrstuhl: Physiologische Chemie, Universitat Munchen, Butenandtstr. 5, Gebäude B, Munchen, D-81377, GERMANY

Axl Alois Neurauter (**1**: 239) Immunosystem R & D, Dynal Biotech ASA, PO Box 114, Smestad, N-0309, NORWAY

Phillip Ng (**1**: 435) Dept of Molecular and Human Genetics, Baylor College of Medicine, One Baylor Plaza, Houston, TX 77030

Garth L. Nicolson (**1**: 359) The Institute for Molecular Medicine, 15162 Triton Lane, Huntington Beach, CA 92649-1041

Trine Nilsen (**4**: 275) Department of Biochemistry, Institute for Cancer Research, The Norwegian Radium Hospital, Montebello, Oslo, N-0310, NORWAY

Tommy Nilsson (**2**: 45) Göteborg University, Institute of Medical Biochemistry, PO Box, Göteborg, SE-403 50, SWEDEN

Lars Norderhaug (**1**: 239) Dynal Biotech ASA, PO Box 114, Smestad, N-0309, NORWAY

Robert O'Connor (**1**: 5, 13, 335) National Institute for Cellular Biotechnology, Dublin City University, Glasnevin, Dublin, 9, IRELAND

Lorraine O'Driscoll (**1**: 5, 335) National Institute for Cellular Biotechnology, Dublin City University, Glasnevin, Dublin, 9, IRELAND

Martin Offterdinger (**3**: 153) Cell Biology and Cell Biophysics Program, European Molecular Biology Laboratory, Meyerhofstrasse 1, Heidelberg, D-69117, GERMANY

Philip Oh (**2**: 11) Cellular and Molecular Biology Program, Sidney Kimmel Cancer Center, 10835 Altman Row, San Diego, CA 92121

Takanori Ohnishi (**1**: 367) Department of Neurosurgery, Ehime University School of Medicine, Shitsukawa, Toon-shi, Ehime, 791-0295, JAPAN

Sjur Olsnes (**4**: 19, 275) Department of Biochemistry, The Norwegian Radium Hospital, Montebello, Oslo, 0310, NORWAY

Shao-En Ong (**4**: 427) Protein Interaction Laboratory, University of Southern Denmark—Odense, Campusvej 55, Odense M, DK-5230, DENMARK

Akifumi Ootani (**1**: 411) Department of Internal Medicine, Faculty of Medicine, Saga University, Nebeshima 5-1-1, Saga, 849-8501, JAPAN

Valerio Orlando (**4**: 317) Dulbecco Telethon Institute, Institute of Genetics & Biophysics CNR, Via Pietro Castellino 111, Naples, I-80131, ITALY

Torben Faeck Ørntoft (**4**: 83) Clinical Biochemical Department, Molecular Diagnostic Laboratory, Aarhus University Hospital, Skejby, Brendstrupgaardvej 100, Aarhus N, DK-8200, DENMARK

Mary Osborn (**1**: 549, 563) Department of Biochemistry and Cell Biology, Max Planck Institute of Biophysical Chemistry, Am Faßberg 11, Gottingen, D-37077, GERMANY

Lawrence E. Ostrowski (**2**: 99) Cystic Fibrosis/Pulmonary Research and Treatment Centre, University of North Carolina at Chapel Hill, Thurston-Bowles Building, Chapel Hill, NC 27599-7248

Hendrik Otto (**2**: 253) Institut für Biochemie und Molekularbiologie, Universität Freiburg, Hermann-Herder-Str. 7, Freiburg, D-79104, GERMANY

Kerstin Otto (**1**: 103) Department of Dermatology, Julius-Maximillians University, Josef-Schneider-Str. 2, Würzburg, 97080, GERMANY

Michel M. Ouellette (**1**: 215) Department of Biochemistry and Molecular Biology, Eppley Institute for Research in Cancer, The University of Nebraska Medical Center, 986805 Nebraska Medical Center, Omaha, NE 68198-6805

Jacques Paiement (**2**: 41) Département de pathologie et biologie cellulaire, Université de Montréal, Case postale 6128, Succursale "Centre-Ville", Montreal, QC, H3C 3J7, CANADA

Patricia M. Palagi (**4**: 207) Swiss Institute of Bioinformatics, CMU, 1 Michel Servet, Geneva 4, CH-1211, SWITZERLAND

Kinam Park (**4**: 29) Department of Pharmaceutics and Biomedical Engineering, Purdue University School of Pharmacy, 575 Stadium Mall Drive, Room G22, West Lafayette, IN 47907-2091

Helen Parkinson (**4**: 95) EMBL Outstation—Hinxton, European Bioinformatics Institute, Wellcome Trust Genome Campus, Hinxton, Cambridge, CB10 1SD, UNITED KINGDOM

Richard M. Parton (**3**: 187) Wellcome Trust Centre for Cell Biology, Institute of Cell and Molecular Biology The University of Edinburgh, Michael Swann Building, The King's Buildings, Mayfield Road, Edinburgh, EH9 3JR, SCOTLAND

Bryce M. Paschal (**2**: 267) Center for Cell Signaling, University of Virginia, 1400 Jefferson Park Avenue, West Complex Room 7021, Charlottesville, VA 22908-0577

Wayne F. Patton (**4**: 225) Perkin-Elmer LAS, Building 100-1, 549 Albany Street, Boston, MA 02118

Staffan Paulie (**1**: 533) Mabtech AB, Box 1233, Nacha Strand, SE-131 28, SWEDEN

Rainer Pepperkok (**3**: 121) Cell Biology and Cell Biophysics Programme, European Molecular Biology Laboratory (EMBL), Meyerhofstrasse 1, Heidelberg, D-69117, GERMANY

Xomalin G. Peralta (**3**: 87) Department of Physics, Duke University, 107 Physics Bldg, Durham, NC 27708-1000

Martha Perez-Magallanes (**1**: 151) National Medical Center and Beckman Research Institute, Division of Neurosciences, City of Hope, 1500 E. Duarte Rd, Duarte, CA 91010

Stephen P. Perfetto (**1**: 257) Vaccine Research Center, National Institutes of Health, 40 Convent Dr., Room 5509, Bethesda, MD 20892-3015

Hedvig Perlmann (**1**: 533) Department of Immunology, Stockholm University, Biology Building F5, Top floor, Svante Arrhenius väg 16, Stockholm, SE-10691, SWEDEN

Peter Perlmann (**1**: 533) Department of Immunology, Stockholm University, Biology Building F5, Top floor, Svante Arrhenius väg 16, Stockholm, SE-10691, SWEDEN

Timothy W. Petersen (**1**: 269) Institute for Systems Biology, 1441 N. 34th St, Seattle, WA 98103

Patti Lynn Peterson (**2**: 259) Department of Neurology, Wayne State University School of Medicine, 5L26 Detroit Receiving Hospital, Detroit Medical Center, Detroit, MI 48201

Nisha Philip (**4**: 265) Department of Pharmacology and Cancer Biology, Duke University, Research Dr. LSRC Rm C115, Box 3813, Durham, NC 27710

Thomas Pieler (**1**: 191) Institute for Biochemistry and Molecular Cell Biology, University of Goettingen, Humboldtallee 23, Göttingen, D-37073, GERMANY

Daniel Pinkel (**3**: 445) Department of Laboratory Medicine, University of California San Francisco, Box 0808, San Francisco, CA 94143-0808

Javier Pizarro Cerdá (**2**: 407) Unite des Interactions Bacteries-Cellules/Unité INSERM 604, Institut Pasteur, 28, rue du Docteur Roux, Paris Cedex 15, F-75724, FRANCE

Andreas Plückthun (**1**: 497) Department of Biochemistry, University of Zürich, Winterthurerstrasse 190, Zürich, CH-8057, SWITZERLAND

Helen Plutner (**2**: 209) Department of Cell and Molecular Biology, The Scripps Research Institute, 10550 North Torrey Pines Road, La Jolla, CA 92037

Piotr Pozarowski (**1**: 279) Brander Cancer Research Institute, New York Medical College, Valhalla, NY 10595

Johanna Prast (**1**: 557) Institute of Molecular Biology, Austrian Academy of Sciences, Billrothstrasse 11, Salzburg, A-5020, AUSTRIA

Brendan D. Price (**3**: 477) Department of Radiation Oncology, Dana Farber-Brigham and Women's Cancer Center, 75 Francis Street, Level L2, Boston, MA 02215

Elena Prigmore (**3**: 403) Sanger Institute, The Wellcome Trust, The Wellcome Trust Genome Campus, Hinxton, Cambridge, CB10 1SA, UNITED KINGDOM

Gottfried Proess (**1**: 467) Eurogentec S.A., Liege Science Park, 4102 Seraing, B-, BELGIUM

David M. Prowse (**1**: 133) Centre for Cutaneous Research, Barts and The London Queen Mary's School of Medicine and Dentistry, Institute of Cell and Molecular Science, 2 Newark Street, Whitechapel London, WC2A 3PX, UNITED KINGDOM

Manuela Pruess (**4**: 469) EMBL outstation—Hinxton, European Bioinformatic Institute, Welcome Trust Genome Campus, Hinxton, Cambridge, CB10 1SD, UNITED KINGDOM

Eric Quéméneur (**4**: 235) Life Sciences Division, CEA Valrhô, BP 17171 Bagnols-sur-Cèze, F-30207, FRANCE

Leda Helen Raptis (**2**: 329, 341) Department of Microbiology and Immunology, Queen's University, Room 716 Botterell Hall, Kingston, Ontario, K7L3N6, CANADA

Anne-Marie Rasmussen (**1**: 239) Dynal Biotech ASA, PO Box 114, Smestad, N-0309, NORWAY

Andreas S. Reichert (**4**: 269) Department of Physiological Chemistry, University of Munich, Butenandtstr. 5, München, D-81377, GERMANY

Siegfreid Reipert (**3**: 325) Ordinariat II, Institute of Biochemistry and Molecular Biology, Vienna Biocenter, Dr. Bohr-Gasse 9, Vienna, A-1030, AUSTRIA

Guenter P. Resch (**3**: 267) Institute of Molecular Biology, Dr. Bohrgasse 3-5, Vienna, A-1030, AUSTRIA

Katheryn A. Resing (**4**: 443) Dept of Chemistry and Biochemistry, University of Colorado, 215 UCB, Boulder, CO 80309-0215

Donald L Riddle (**1**: 157) Division of Biological Sciences, University of Missouri, 311 Tucker Hall, Columbia, MO 65211

Mara Riminucci (**1**: 79) Department of Experimental Medicine, Universita' dell' Aquilla, Via Vetoio, Coppito II, L'Aquila, I-67100, ITALY

Terry L. Riss (**1**: 25) Promega Corporation, 2800 Woods Hollow Road, Madison, WI 53711-5399

Pamela Gehron Robey (**1**: 79) Craniofacial and Skeletal Disease Branch, NIDCR, NIH, Department of Health and Human Services 30 Convent Dr, MSC 4320, Bethesda, MD 20892-4320

Linda J. Robinson (**2**: 201)

Philippe Rocca-Serra (**4**: 95) EMBL Outstation—Hinxton, European Bioinformatics Institute, Wellcome Trust Genome Campus, Hinxton, Cambridge, CB10 1SD, UNITED KINGDOM

Alice Rodriguez (**3**: 87) Department of Biology, Duke University, Durham, NC 27708-1000

Enrique Rodriguez-Boulan (**2**: 189, 241) Margaret M Dyson Vision Research Institute, Department of Opthalmology, Weill Medical College of Cornell University, New York, NY 10021

Mario Roederer (**1**: 257) ImmunoTechnology Section and Flow Cytometry Core, Vaccine Research Center, National Institute for Allergy and Infectious Diseases, National Institutes of Health, 40 Convent Dr., Room 5509, Bethesda, MD 20892-3015

Peter Roepstorff (**4**: 371) Department of Biochemistry and Molecular Biology, University of Southern Denmark, Campusvej 55, Odense M, DK-5230, DENMARK

Manfred Rohde (**2**: 399) Department of Microbial Pathogenicity, Gesellschaft fur Biotechnoogische Forschung, Mascheroder Weg 1, Braunschweig, D-38124, GERMANY

Norbert Roos (**3**: 299) Electron Microscopical Unit for Biological Sciences, University of Oslo, Blindern, Oslo, 0316, NORWAY

Sabine Rospert (**2**: 253) Institut für Biochemie und Molekularbiologie, Universität Freiburg, Hermann-Herder-Str. 7, Freiburg, D-79104, GERMANY

Klemens Rottner (**3**: 111) Cytoskeleton Dynamics Group, German Research Centre for Biotechnology (GBF), Mascheroder Weg 1, Braunschweig, D-38124, GERMANY

Line Roy (**2**: 41) Department of Anatomy and Cell Biology, Faculty of Medicine, McGill University, STRATHCONA Anatomy & Dentistry Building, Montreal, QC, H3A 2B2, CANADA

Sandra Rutherford (**3**: 325) CRC Structural Cell Biology Group, Paterson Institute for Cancer Research, Christie Hospital NHS Trust, Wilmslow Road, Withington, Manchester, M20 4BX, UNITED KINGDOM

Beth Rycroft (**1**: 395) Department of Pharmacology, University College London, Gower Street, London, WC1E GBT, UNITED KINGDOM

Patrick Salmon (**1**: 425) Department of Genetics and Microbiology, Faculty of Medicine, University of Geneva, CMU-1 Rue Michel-Servet, Geneva 4, CH-1211, SWITZERLAND

Paul M. Salvaterra (**1**: 151) National Medical Center and Beckman Research Institute, Division of Neurosciences, City of Hope, 1500 E. Duarte Rd, Duarte, CA 91010-3000

R. Jude Samulski (**1**: 457) Gene Therapy Centre, Department of Pharmacology, University of North Carolina at Chapel Hill, 7119 Thurston Bowles, Chapel Hill, NC 27599-7352

Susanna-Assunta Sansone (**4**: 95) EMBL Outstation—Hinxton, European Bioinformatics Institute, Wellcome Trust Genome Campus, Hinxton, Cambridge, CB10 1SD, UNITED KINGDOM

Ugis Sarkan (**4**: 95) EMBL Outstation—Hinxton, European Bioinformatics Institute, Wellcome Trust Genome Campus, Hinxton, Cambridge, CB10 1SD, UNITED KINGDOM

Moritoshi Sato (**2**: 325) Department of Chemistry, School of Science, University of Tokyo, 7-3-1 Hongo, Bunkyo-Ku, Tokyo, 113-0033, JAPAN

Guido Sauter (**3**: 369) Institute of Pathology, University of Basel, Schonbeinstrasse 40, Basel, CH-4003, SWITZERLAND

Carolyn L. Sawyer (**2**: 299) Department of Pharmacology, University of Vermont, Health Science Research Facility 330, Burlington, VT 05405-0068

Guray Saydam (**1**: 315) Department of Medicine, Section of Hematology, Ege University Hospital, Bornova Izmir, 35100, TURKEY

Silvia Scaglione (**3**: 201) BIOLab, Department of Informatic, Systemistic and Telematic, University of Genoa, Viale Causa 13, Genoa, I-16145, ITALY

Lothar Schermelleh (**1**: 291, 301) Department of Biology II, Biocenter of the Ludwig-Maximilians University of Munich (LMU), Großhadernerstr. 2, Planegg-Martinsried, 82152, GERMANY

Gudrun Schiedner (**1**: 445) CEVEC Pharmaceuticals GmbH, Gottfried-Hagen-Straße 62, Köln, D-51105, GERMANY

David Schieltz (**4**: 383) Department of Cell Biology, Torrey Mesa Research Institute, 3115 Merryfield Row, San Diego, CA 92121

Jan E. Schnitzer (**2**: 11) Sidney Kimmel Cancer Center, 10835 Altman Row, San Diego, CA 92121

Morten Schou (**1**: 353) Bartholin Institute, Bartholinsgade 2, Copenhagen K, DK-1356, DENMARK

Sebastian Schuck (**2**: 5) Max Planck Institute of Molecular Cell Biology and Genetics, Pfotenhauerstrasse 108, Dresden, D-01307, GERMANY

Herwig Schüler (**2**: 165) Department of Cell Biology, The Wnner-Gren Institute, Stockholm University, Stockholm, S-10691, SWEDEN

Michael Schuler (**3**: 501) Institut de Génétique et de Biologie Moléculaire et Cellulaire (IGBMC), 1 rue Laurent Fries, B.P.10142, Illkirch CEDEX, F-67404, FRANCE

Ulrich S. Schwarz (**2**: 419) Theory Division, Max Planck Institute of Colloids and Interfaces, Potsdam, 14476, GERMANY

Antonio S. Sechi (**2**: 393) Institute for Biomedical Technology-Cell Biology, Universitaetsklinikum Aachen, RWTH, Pauwelsstrasse 30, Aachen, D-52057, GERMANY

Richard L. Segraves (**3**: 445) Comprehensive Cancer Center, University of California San Francisco, Box 0808, 2400 Sutter N-426, San Francisco, CA 94143-0808

James R. Sellers (**2**: 387) Cellular and Motility Section, Laboratory of Molecular Cardiology, National Heart, Lung and Blood Institute (NHLBI), National Institutes of Health, 10 Center Drive, MSC 1762, Bethesda, MD 20892-1762

Nicholas J. Severs (**3**: 249) Cardiac Medicine, National Heart and Lung Institute, Imperial College, Faculty of Medicine, Royal Brompton Hospital, Dovehouse Street, London, SW3 6LY, UNITED KINGDOM

Jagesh Shah (**3**: 351) Laboratory of Cell Biology, Ludwig Institute for Cancer Research, University of California, 9500 Gilman Drive, MC 0660, La Jolla, CA 92093-0660

Norman E. Sharpless (**1**: 223) The Lineberger Comprehensive Cancer Center, The University of North Carolina School of Medicine, Lineberger Cancer Center, CB# 7295, Chapel Hill, NC 27599-7295

Andrej Shevchenko (**4**: 399) Max Planck Institute for Molecular Cell Biology and Genetics, Pfotenhauerstrasse 108, Dresden, D-01307, GERMANY

David M. Shotton (**3**: 207, 249, 257) Department of Zoology, University of Oxford, South Parks Road, Oxford, OX1 3PS, UNITED KINGDOM

David I. Shreiber (**1**: 379) Department of Biomedical Engineering, Rutgers, the State University of New Jersey, 617 Bowser Road, Piscataway, NJ 08854-8014

Snaevar Sigurdsson (**3**: 455) Department of Medical Sciences, Uppsala University, Akademiska sjukhuset, Uppsala, SE-751 85, SWEDEN

Stephen Simkins (**1**: 483) TriPath Oncology, 4025 Stirrup Creek Drive, Suite 400, Durham, NC 27703

Ronald Simon (**3**: 369) Division of Molecular Pathology, Institute of Pathology, University of Basel, Schonbeinstrasse 40, Basel, CH-4031, SWITZERLAND

Kai Simons (**1**: 127, **2**: 5, 181) Max Planck Institute of Molecular Cell Biology and Genetics, Pfotenhauerstrasse 108, Dresden, D-01307, GERMANY

Jeremy C. Simpson (**3**: 121) Cell Biology and Cell Biophysics Programme, European Molecular Biology Laboratory (EMBL), Meyerhofstrasse 1, Heidelberg, D-69117, GERMANY

Robert H. Singer (**4**: 121) Department of Anatomy and Structural Biology, Golding # 601, Albert Einstein College of Medicine of Yeshiva University, 1300 Morris Park Avenue, Bronx, NY 10461

Mathilda Sjöberg (**1**: 419) Department of Biosciences at Novum, Karolinska Instituet, Huddinge, SE-141-57, SWEDEN

Camilla Skiple Skjerpen (**4**: 275) Department of Biochemistry, Institute for Cancer Research, The Norwegian Radium Hospital, Montebello, Oslo, N-0310, NORWAY

John Sleep (**3**: 37) Randall Division, Guy's Campus, New Hunt's House, London, SE1 1UL, UNITED KINGDOM

J. Victor Small (**1**: 557) Department of Cell Biology, Institute of Molecular Biology, Austrian Academy of Sciences, Billrothstrasse 11, Salzburg, A-5020, AUSTRIA

Joél Smet (**4**: 259) Department of Pediatrics and Medical Genetics, University Hospital, De Pintelaan 185, Ghent, B-9000, BELGIUM

Kim Smith (**3**: 381) Director of Cytogenetic Services, Oxford Radcliffe NHS Trust, Headington, Oxford, OX3 9DU, UNITED KINGDOM

Paul J. Smith (**1**: 305) Dept of Pathology, University of Wales College of Medicine, Heath Park, Cardiff, CF14 4XN, UNITED KINGDOM

Antoine M. Snijders (**3**: 445) Comprehensive Cancer Center, Cancer Research Institute, The University of California, San Francisco, Box 0808, 2340 Sutter Street N-, San Fransisco, CA 94143-0808

Michael Snyder (**3**: 179) Department of Molecular, Cellular and Developmental Biology, Yale University, P. O. Box 208103, Kline Biology Tower, 219 Prospect St., New Haven, CT 06520-8103

Irina Solovei (**1**: 291) Department of Biology II, Anthropology & Human Genetics, Ludwig-Maximilians University of Munich, Munich, GERMANY

Marion Sölter (**1**: 191) Institute for Biochemistry and Molecular Cell Biology, University of Goettingen, Justus-von-Liebig-Weg 11, Göttingen, D-37077, GERMANY

Lukas Sommer (**1**: 69) Institute of Cell Biology, Department of Biology, Swiss Federal Institute of Technology, ETH—Hönggerberg, Zurich, CH-8093, SWITZERLAND

Simon Sparks (**3**: 207) Department of Zoology, University of Oxford, South Parks Road, Oxford, OX1 3PS, UNITED KINGDOM

Kenneth G. Standing (**4**: 457) Department of Physics and Astronomy, University of Manitoba, 510 Allen Bldg, Winnipeg, MB, R3T 2N2, CANADA

Walter Steffen (**3**: 37, 307) Randall Division, Guy's Campus, New Hunt's House, London, SE1 1UL, UNITED KINGDOM

Theresia E. B. Stradal (**3**: 111) Department of Cell Biology, German Research Centre for Biotechnology (GBF), Mascheroder Weg 1, Braunschweig, D-38124, GERMANY

Per Thor Straten (**1**: 97) Tumor Immunology Group, Institute of Cancer Biology, Danish Cancer Society, Strandboulevarden 49, Copenhagen, DK-2100, DENMARK

Hajime Sugihara (**1**: 411) Department of Pathology & Biodefence, Faculty of Medicine, Saga University, Nebeshima 5-1-1, Saga, 849-8501, JAPAN

Chung-Ho Sun (**3**: 351) Beckman Laser Institute, University of California, Irvine, 1002 Health Sciences Road E, Irvine, CA 92697-1475

Mark Sutton-Smith (**4**: 415) Department of Biological Sciences, Imperial College of Science, Technology and Medicine, Biochemistry Building, London, SW7 2AY, UNITED KINGDOM

Tatyana M. Svitkina (**3**: 277) Department of Cell and Molecular Biology, Northwestern University Medical School, Chicago, IL 60611

Ann-Christine Syvänen (**3**: 455) Department of Medical Sciences, Uppsala University, Forskningsavd 2, ing 70, Uppsala, SE-751 85, SWEDEN

Masako Tada (**1**: 199) ReproCELL Incorporation, 1-1-1 Uchisaiwai-cho, Chiyoda-ku, Tokyo, 100-0011, JAPAN

Takashi Tada (**1**: 199) Stem Cell Engineering, Stem Cell Research Center, Institute for Frontier Medical Sciences, Kyoto University, 53 Kawahara-cho Shogoin, Sakyo-ku, Kyoto, 606-8507, JAPAN

Angela Taddei (**2**: 359) Department of Molecular Biology, University of Geneva, 30, Quai Ernest Ansermet, Geneva 4, CH-1211, SWITZERLAND

Tomohiko Taguchi (**2**: 33) Department of Cell Biology, Yale University School of Medicine, 333 Cedar Street, PO Box 208002, New Haven, CT 06520-8002

Kazusuke Takeo (**4**: 197) Department of Biochemistry and Biomolecular Recognition, Yamaguchi University School of Medicine, 1-1-1, Minami-kogushi, Ube, Yamaguchi, 755-8505, JAPAN

Nobuyuki Tanahashi (**2**: 91) Laboratory of Frontier Science, Core Technology and Research Center, The Tokyo Metropolitan Institute of Medical Sciences, 3-18-22 Honkomagome, Bunkyo-ku, Tokyo, 113-8613, JAPAN

Keiji Tanaka (**2**: 91) Laboratory of Frontier Science, Core Technology and Research Center, The Tokyo Metropolitan Institute of Medical Sciences, 3-18-22 Honkomagome, Bunkyo-ku, Tokyo, 133-8613, JAPAN

Chi Tang (**2**: 121) Dept of Biomolecular Sciences, UMIST, PO Box 88, Manchester, M60 1QD, UNITED KINGDOM

Kirill V. Tarasov (**4**: 103) Molecular Cardiology Unit, National Institute on Aging, NIH, 5600 Nathan Shock Drive, Baltimore, MD 21224

J. David Taylor (**3**: 471) Department of Genomic Sciences, Glaxo Wellcome Research and Development, 5 Moore Drive, Research Triangle Park, NC 27709-3398

Nancy Smyth Templeton (**4**: 25) Department of Molecular and Cellular Biology & the Center for Cell and Gene Therapy, Baylor College of Medicine, One Baylor Plaza, Alkek Bldg., Room N1010, Houston, TX 77030

Kenneth K. Teng (**1**: 171) Department of Medicine, Wiell Medical of Cornell University, 1300 York Ave., Rm-A663, New York, NY 10021

Patrick Terheyden (**1**: 103) Department of Dermatology, Julius-Maximillians University, Josef-Schneider-Str. 2, Würzburg, D-97080, GERMANY

Scott M. Thompson (**1**: 407) Department of Physiology, University of Maryland School of Medicine, 655 W. Baltimore St., Baltimore, MD 21201,

John F. Timms (**4**: 189) Department of Biochemistry and Molecular Biology, Ludwig Institute of Cancer Research, Cruciform Building 1.1.09, Gower Street, London, WC1E 6BT, UNITED KINGDOM

Shuji Toda (**1**: 411) Department of Pathology & Biodefence, Faculty of Medicine, Saga University, Nebeshima 5-1-1, Saga, 849-8501, JAPAN

Yoichiro Tokutake (**3**: 87) Department of Physics, Duke University, 107 Physics Bldg, Durham, NC 27708-1000

Evi Tomai (**2**: 329) Department of Microbiology and Immunology, Queen's University, Room 716 Botterell Hall, Kingston, Ontario, K7L3N6, CANADA

Kenneth B. Tomer (**1**: 511) Mass Spectrometry, Laboratory of Structural Biology, National Institute of Environmental Health Sciences NIEH/NIH, 111 Alexander Drive, PO Box 12233, Research Triangle Park, NC 27709

Derek Toomre (**3**: 19) Department of Cell Biology, Yale University School of Medicine, SHM-C227/229, PO Box 208002, 333 Cedar Street, New Haven, CT 06520-8002

Sharon A. Tooze (**2**: 79) Secretory Pathways Laboratory, Cancer Research UK London Research Institute, 44 Lincoln's Inn Fields, London, WC2A 3PX, UNITED KINGDOM

David Tosh (**1**: 177) Centre for Regenerative Medicine, Department of Biology and Biochemistry, University of Bath, Claverton Down, Bath, BA2 7AY, UNITED KINGDOM

Yusuke Toyama (**3**: 87) Department of Physics, Duke University, 107 Physics Bldg, Box 90305, Durham, NC 27708-0305

Robert T. Tranquillo (**1**: 379) Department of Biomedical Engineering and Department of Chemical Engineering and Materials Science, University of Minnesota, Biomedical Engineering, 7-112 BSBE. 312 Church St SE, Minneapolis, MN 55455

Signe Trentemølle (**4**: 165) Institute of Cancer Biology and Danish Centre for Translational Breast Cancer Research, Danish Cancer Society,

Strandboulevarden 49, Copenhagen, DK-2100, DENMARK

Didier Trono (**1**: 425) Department of Genetics and Microbiology, Faculty of Medicine, University of Geneva, CMU-1 Rue Michel-Servet, Geneva 4, CH-1211, SWITZERLAND

Kevin Truong (**2**: 307) Division of Molecular and Structural Biology, Ontario Cancer Institute, Department of Medical Biophysics, University of Toronto, 610 University Avenue, 7-707A, Toronto, Ontario, M5G 2M9, CANADA

Jessica K. Tyler (**2**: 287) Department of Biochemistry and Molecular Genetics, University of Colorado Health Sciences Center at Fitzsimons, PO Box 6511, Aurora, CO 80045

Aylin S. Ulku (**1**: 345) Department of Pharmacology, University of North Carolina at Chapel Hill, Lineberger Comprehensive Cancer Center, Chapel Hill, NC 27599-7295

Yoshio Umezawa (**2**: 325) Department of Chemistry, The School of Science, University of Tokyo, 7-3-1 Hongo, Bunkyo-ku, Tokyo, 113-0033, JAPAN

Ronald Vale (**3**: 129) Department of Cellular and Molecular Pharmacology, The Howard Hughes Medical Institute, The University of California, San Francisco, N316, Genentech Hall, 1600 16th Street, San Francisco, CA 94107

Jozef Van Beeumen (**4**: 259) Department of Biochemistry, Physiology and Microbiology, University of Ghent, K.L. Ledeganckstraat 35, Ghent, B-9000, BELGIUM

Rudy N. A. van Coster (**4**: 259) Department of Pediatrics and Medical Genetics, University Hospital, University of Ghent, De Pintelaan 185, Ghent, B-9000, BELGIUM

Ger van den Engh (**1**: 269) Institute for Systems Biology, 1441 North 34th Street, Seattle, WA 98103-8904

Peter van der Geer (**4**: 139) Department of Chemistry and Biochemistry, University of California, San Diego, 9500 Gilman Dr., La Jolla, CA 92093-0601

Joël Vandekerckhovr (**4**: 379, 457) Department of Medical Protein Research, Flanders Interuniversity Institute for Biotechnology, KL Ledeganckstraat 35, Gent, B-9000, BELGIUM

Charles R. Vanderburg (**4**: 5) Department of Neurology, Massachusetts General Hospital, 114 Sixteenth Street, Charlestown, MA 02129

John Venable (**4**: 383) Department of Cell Biology, Scripps Research Institute, 10550 North Torrey Pines Road, La Jolla, CA 92037

Isabelle Vernos (**2**: 379) Cell Biology and Cell Biophysics Programme, European Molecular Biology Laboratory, Meyerhofstrasse 1, Heidelberg, D-69117, GERMANY

Peter J. Verveer (**3**: 153) Cell Biology and Cell Biophysics Program, European Molecular Biology Laboratory, Meyerhofstrasse 1, Heidelberg, D-69117, GERMANY

Marc Vidal (**4**: 295) Cancer Biology Department, Dana-Farber Cancer Institute, 44 Binney Street, Boston, MA 02115

Emmanuel Vignal (**2**: 427) Department Genie, Austrian Academy of Sciences, Billrothstrasse 11, Salzbourg–Autriche, A-520, 5020, AUSTRIA

Sylvie Villard (**1**: 519) Centre de Pharmacologie et Biotechnologie pour la Santé, CNRS—UMR 5094, Faculté de Pharmacie, Avenue Charles Flahault, Montpellier Cedex 5, F-34093, FRANCE

Hikka Virta (**1**: 127) Department of Cell Biology, European Molecular Biology Laboratory, Cell Biology Programme, Heidelberg, D-69012, GERMANY

Alfred Völkl (**2**: 63) Department of Anatomy and Cell Biology II, University of Heidelberg, Im Neuenheimer Feld 307, Heidelberg, D-69120, GERMANY

Sonja Voordijk (**4**: 207) Geneva Bioinformatics SA, Avenue de Champel 25, Geneva, CH-1211, SWITZERLAND

Adina Vultur (**2**: 329, 341) Department of Microbiology and Immunology, Queen's University, Room 716 Botterell Hall, Kingston, Ontario, K7L3N6, CANADA

Teruhiko Wakayama (**1**: 87) Center for Developmental Biology, RIKEN, 2-2-3 Minatojima-minamimachi, Kobe, 650-0047, JAPAN

Daniel Walther (**4**: 207) Swiss Institute of Bioinformatics (SIB), CMU, rue Michel-Servet 1, Genève 4, 1211, SWITZERLAND

Gang Wang (**3**: 477) Department of Radiation Oncology, Dana Farber-Brigham and Women's Cancer Center, 75 Francis Street, Level L2, Boston, MA 02215

Nancy Wang (**3**: 345) Department of Pathology and Laboratory Medicine, University of Rochester School of Medicine, 601 Elmwood Ave., Rm 1-6337, Rochester, NY 14642

Xiaodong Wang (**2**: 209) Department of Cell and Molecular Biology, The Scripps Research Institute, 10550 North Torrey Pines Road, La Jolla, CA 92037

Yanzhuang Wang (**2**: 33) Department of Cell Biology, Yale University School of Medicine, 333 Cedar Street, PO BOX 208002, New Haven, CT 06520-8002

Yu-Li Wang (**3**: 107) Department of Physiology, University of Massachusetts Medical School, 377 Plantation St., Rm 327, Worcester, MA 01605

Graham Warren (**2**: 33) Department of Cell Biology, Yale University School of Medicine, 333 Cedar Street, PO Box 208002, New Haven, CT 06520-8002

Clare M. Waterman-Storer (**3**: 137) 10550 North Torrey Pines Road, CB 163, La Jolla, CA 92037

Jennifer C. Waters (**3**: 49) Department of Cell Biology, Department of Systems Biology, Harvard Medical School, 240 Longwood Ave, Boston, MA 02115

Fiona M. Watt (**1**: 133) Keratinocyte Laboratory, London Research Institute, 44 Lincoln's Inn Fields, London, WC2A 3PX, UNITED KINGDOM

Gerhard Weber (**4**: 157) Protein Analytics, Max Planck Institute for Biochemistry, Klopferspitz 18, Martinsried, D-82152, GERMANY

Peter J. A. Weber (**4**: 157) Proteomics Division, Tecan Munich GmbH, Feldkirchnerstr. 12a, Kirchheim, D-, 85551, GERMANY

Paul Webster (**3**: 299) Electron Microscopy Laboratory, House Ear Institute, 2100 West Third Street, Los Angeles, CA 90057

Jürgen Wehland (**2**: 399) Department of Cell Biology, Gesellschaft fur Biotechnoogische Forschung, Mascheroder Weg 1, Braunschweig, D-38124, GERMANY

Dieter G. Weiss (**3**: 57) Institute of Cell Biology and Biosystems Technology, Department of Biological Sciences, Universitat Rostock, Albert-Einstein-Str. 3, Rostock, D-18051, GERMANY

Walter Weiss (**4**: 175) Fachgebiet Proteomik, Technische Universität Muenchen, Am Forum 2, Freising Weihenstephan, D-85350, GERMANY

Adrienne R. Wells (**3**: 87) Department of Biology, Duke University, Durham, NC 27708-1000

Jørgen Wesche (**4**: 19) Department of Biochemistry, The Norwegian Radium Hospital, Montebello, Oslo, 0310, NORWAY

Pamela Whittaker (**3**: 463) Genotyping / Chr 20, The Wellcome Trust Sanger Institute, The Wellcome Trust Genome Campus, Hinxton, Cambridge, CB10 1SA, UNITED KINGDOM

John Wiemann (**3**: 87) Department of Biology, Duke University, B330g Levine Sci Bldg, Box 91000, Durham, NC 27708-1000

Sebastian Wiesner (**2**: 173) Dynamique du Cytosquelette, Laboratoire d'Enzymologie et Biochimie Structurales, UPR A 9063 CNRS, Building 34, Bat. 34, avenue de la Terrasse, Gif-sur-Yvette, F-91198, FRANCE

Ilona Wolff (**1**: 325) Prodekanat Forschung, Medizinnishce Fakultät, Martin Luther University Halle-Wittenburg, Magdeburger Str 8, Saale, Halle, D-06097, GERMANY

Ye Xiong (**2**: 259) The Department of Biochemistry and Molecular Biology, Wayne State University School of Medicine, 4374 Scott Hall, 540 E. Canfield, Detroit, MI 48201

David P. Yarnall (**3**: 471) Department of Metabolic Diseases, Glaxo Wellcome Inc, 5 Moore Drive, Research Triangle Park, NC 27709-3398

Hideki Yashirodas (**2**: 91) Laboratory of Frontier Science, Core Technology and Research Center, The Tokyo Metropolitan Institute of Medical Sciences, 3-18-22 Honkomagome, Bunkyo-ku, Tokyo, 133-8613, JAPAN

John R. Yates III (**4**: 383, 391) Department of Cell Biology, Scripps Research Institute, 10550 North Torrey Pines Road, La Jolla, CA 92037

Charles Yeaman (**2**: 189) Department of Cell and Developmental Biology, Weill Medical College of Cornell University, New York, NY 10021

Robin Young (**2**: 41) Département de pathologie et biologie cellulaire, Université de Montréal, Case postale 6128, Succursale "Centre-Ville", Montreal, QC, H3C 3J7, CANADA

Christian Zahnd (**1**: 497) Department of Biochemistry, Univerisity of Zürich, Winterthurerstr. 190, Zürich, CH-8057, SWITZERLAND

Zhuo-shen Zhao (**4**: 285) Glaxo-IMCB Group, Institute of Molecular and Cell Biology, Singapore, 117609, SINGAPORE

Huilin Zhou (**4**: 437) Department of Cellular and Molecular Medicine, Ludwig Institute for Cancer Research, University of California, San Diego, 9500 Gilman Drive, CMM-East, Rm 3050, La Jolla, CA 92093-0660

Timo Zimmermann (**3**: 69) Cell Biology and Cell Biophysics Programme, EMBL, Meyerhofstrasse 1, Heidelberg, D-69117, GERMANY

Chiara Zurzolo (**2**: 241) Department of Cell Biology and Infection, Pasteur Institute, 25,28 rue du Docteur Roux, Paris, 75015, FRANCE

Preface

Scientific progress often takes place when new technologies are developed, or when old procedures are improved. Today, more than ever, we are in need of complementary technology platforms to tackle complex biological problems, as we are rapidly moving from the analysis of single molecules to the study of multifaceted biological problems. The third edition of *Cell Biology: A Laboratory Handbook* brings together 236 articles covering novel techniques and procedures in cell and molecular biology, proteomics, genomics, and functional genomics. It contains 165 new articles, many of which were commissioned in response to the extraordinary feedback we received from the scientific community at large.

As in the case of the second edition, the *Handbook* has been divided in four volumes. The first volume covers tissue culture and associated techniques, viruses, antibodies, and immunohistochemistry. Volume 2 covers organelles and cellular structures as well as assays in cell biology. Volume 3 includes imaging techniques, electron microscopy, scanning probe and scanning electron microscopy, microdissection, tissue arrays, cytogenetics and in situ hybridization, genomics, transgenic, knockouts, and knockdown methods. The last volume includes transfer of macromolecules, expression systems, and gene expression profiling in addition to various proteomic technologies. Appendices include representative cultured cell lines and their characteristics, Internet resources in cell biology, and bioinformatic resources for in silico proteome analysis. The Handbook provides in a single source most of the classical and emerging technologies that are essential for research in the life sciences. Short of having an expert at your side, the protocols enable researchers at all stages of their career to embark on the study of biological problems using a variety of technologies and model systems. Techniques are presented in a friendly, step-by-step fashion, and gives useful tips as to potential pitfalls of the methodology.

I would like to extend my gratitude to the Associate Editors for their hard work, support, and vision in selecting new techniques. I would also like to thank the staff at Elsevier for their constant support and dedication to the project. Many people participated in the realization of the *Handbook* and I would like to thank in particular Lisa Tickner, Karen Dempsey, Angela Dooley, Carl Soares, and Tari Paschall for coordinating and organizing the preparation of the volumes. My gratitude is also extended to all the authors for the time and energy they dedicated to the project.

Julio E. Celis
Editor

PART

A

IMAGING TECHNIQUES

SECTION

1

Light Microscopy

CHAPTER

1

Fluorescence Microscopy

Werner Baschong and Lukas Landmann

I. ABOUT FLUORESCENCE

A. Luminescence, Fluorescence, and Phosphorescence

Luminescent substances emit light when irradiated, in contrast to most other light-absorbing substances, which merely heat up. Luminescence is usually induced by light, but can also be initiated by other electromagnetic radiation or by chemical reactions. In any case, bound or free electrons or atoms or molecules are temporarily excited to a higher energy state. When falling back to a lower state they emit part of the energy in the form of light. Since this excitation/relaxation process itself consumes energy, the wavelength of the emitted light is always longer than that required for excitation (Stoke's law). Fluorescence is emitted within nanoseconds after irradiation, i.e., in biological terms immediately. Phosphorescence manifests rather as an afterglow lasting between fractions of a second and several months.

B. Primary Fluorescence

A number of substances such as oils, optical brighteners, and plastic material but also many tissue components such as chlorophyll or bone intrinsically emit fluorescent light when irradiated with shortwave radiation. This kind of fluorescence is called primary fluorescence (1°-fluorescence) or inherent autofluorescence.

C. Secondary Fluorescence

Most of the objects to be investigated with a light microscope, i.e., cells, tissues, and bacteria, do not show an inherent fluorescence. These objects or specific details of these objects are rendered fluorescent either by fluorescent dyes or by tissue processing, e.g., fixation. Light emission caused by fluorochromes added to the specimen is called secondary fluorescence (2°-fluorescence) or just fluorescence. Processing-induced 2°-fluorescence is also called processing-related autofluorescence or, often and also together with inherent autofluorescence, simply autofluorescence.

D. Fluorophores (Fluorochromes)

Fluorophores are, in analogy to chromophores, the chemical groups responsible for the colour of a molecule, the groups responsible for a molecule's fluorescence. Fluorochromes are fluorescent molecules, often dyes. The expressions "fluorophore" and "fluorochrome" are often used equivalently. Each fluorophore has a specific (often overlapping) excitation and emission spectrum with distinct maxima.

Calcein, fluorescein, and, in the wider sense, tetracyclines, which accumulate in bone and teeth, are typical fluorochromes. Site-specific fluorescent dyes include the widely used DNA probes 4,6-diamino-2-phenylindole (DAPI), ethidium iodide, Hoechst 33342, and acridine orange, but also include fluorescent analogues of specific membrane lipids (e.g., www/probes.com/site-specific).

E. Direct and Indirect Immunofluorescence

Immunofluorescence (IF) is used to reveal the presence of specific antigens in body fluid, cells, or tissue by means of the corresponding fluorophore-conjugated antibodies and illumination with an

Copyright 2006, Elsevier Science (USA).
All rights reserved.

appropriate light source. The technique relies on the strong binding between antibodies and corresponding antigens, which allows for washing off nonbound label, thus displaying fluorescent objects against a dark background.

The principle of IF has found wide application in diagnostics, directly for the detection of antigens or indirectly for that of antibodies. In the former case, the presence of an antigen is directly visualized via the corresponding fluorescence-labeled (F-) antibody. Antigens may be viruses, bacteria fungi, etc. In the latter case, a specific—often immobilized—antigen is incubated, e.g., with a patient's serum, and in a second step, a F-labeled antihuman immunoglobulin antibody is used to detect the presence of antigen-specific antibodies. The indirect test reveals the presence of antibodies directed against a specific virus or a marker-protein typical for a specific disease.

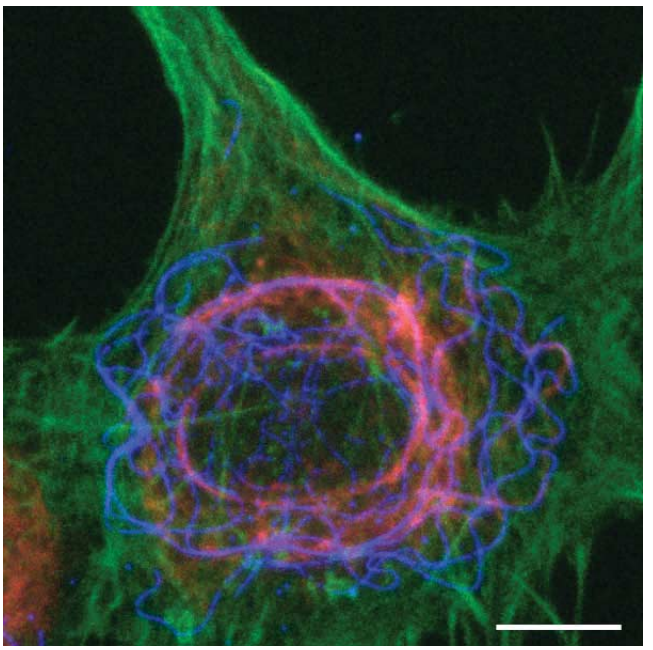

FIGURE 1 Localization of F-actin, vimentin, and tubulin in fibroblasts by fluorescence microscopy and photographical overlay. Rat 2sm6 fibroblasts (Leavitt, and Kakunaga, *J. Biol. Chem.* (1980)) were grown as monolayer on glass coverslips. *Prefixation*: 2% octyl-POE (*n*-octylpolyethoxyethylene)/0.125% glutaraldehyde, 5 min in MHB (Hanks buffer, Ca-free, containing 2 m*M* EGTA and 5 m*M* MES, pH 7. *Postfixation*: 1% glutaraldehyde in MHB (20 min) at ~20°C. Removal of background fluorescence with 0.5 mg/ml $NaBH_4$ (2 × 10 min at 0°C). *Labeling:* Filamentous actin (green): phalloidin Alexa-488 (www.probes.com); vimentin (blue): mouse anti-vimentin-Cy3 (monoclonal, www.sigma-aldrich.com); and tubulin (red): 1°-antibody, mouse anti-β-tubulin (monoclonal, www.sigma-aldrich.com) and 2°-antibody, goat antimouse IgG-Cy5. Composite image by triple exposure. Scale bar: 25 µm.

II. PRINCIPLES OF EPIFLUORESCENCE MICROSCOPY

A. Fluorescence Microscopy (FM)

Conventional bright-field microscopy visualizes structures of cells and tissues via the absorption and diffraction of light. In contrast, in FM, fluorochromes become independent light sources when irradiated with the appropriate exciting wavelengths, while the nonfluorescent surroundings remain dark. FM takes advantage of (i) Stoke's law, i.e., the difference of wavelength between exciting and emitted light, and (ii) the high visibility of fluorescent objects in the dark.

The fluorescence microscope is designed to induce the strongest possible fluorescence in the fluorescent object and the least interference from light of other wavelengths. This is achieved by (i) physically filtering the irradiating light so that it matches the exciting wavelength of the fluorophore and (ii) filtering the light emitted by the specimen in a fashion that only the fluorescent light emitted by the excited fluorophore will enter the optical path. Light of other wavelengths, including the exciting light, is barred off, thus generating a dark background, i.e., "good" image contrast.

The F-labeled object compares to a torch at night: The light is well visible, whereas the structure of the torch itself not. This manifests in the virtual resolution of FM. (i) Even cytoskeletal elements, e.g., microfilaments (6 nm), intermediate filaments (8–10 nm), and microtubules (25 nm), become well discernible when F-labeled, despite the theoretical resolution of ~200 nm of the microscopes (Fig. 1; cf. Baschong *et al*., 1999). (ii) However, it is difficult to decide whether two different fluorescent labels observed at the same spot really colocalize or whether they only appear to overlap because they cross over in space.

1. Fluorescence Microscopes for Transmitted Light Excitation

Initially, in fluorescence microscopes the beam of the exciting light was transmitted to the object through a bright-field condenser. This type of fluorescence microscope is practically no longer used in biology because the transmitted light causes considerable brightening of the specimen background and, consequently, low image contrast.

2. Fluorescence Microscopes for Incident Light Excitation (Epifluorescence)

Today's fluorescence microscopes work as epifluorescence microscopes and illuminate the object from

above, comparable to illumination in reflection microscopy (Fig. 2). Typically, the light source is placed perpendicular to the optical path. The light then passes through an "excitation" filter and hits at an angle of 45° a reflection short pass filter (dichroic beam-splitting mirror) placed in the optical path. As a mirror it deflects the excitation light to the objective (which also functions as a condenser) and ultimately to the specimen. Fluorescent light emitted by the irradiated specimen is collected by the objective lens and transmitted to the reflection long-pass filter (dichroic beam-splitting mirror) again. As a long-pass filter the latter now blocks any reflected excitation light and is translucent only for the longer-waved light emitted by the specimen. This emitted light is further filtered through a barrier or suppression filter before reaching the eyepiece.

Epifluorescence imaging can be complemented with visualization by transmitted light bright-field, dark-field, phase contrast, interference contrast, or by polarized light. Most conventional bright-field microscopes, including inverted microscopes or ster-eomicroscopes, can be adapted to FM (fore details, see, e.g., www.leica.com; www.nikon.com; www.olympusbiosystems.com; www.zeiss.com).

B. Components of the Fluorescence Microscope

1. Light Sources

Fluorescence microscopes require a light source, which illuminates the field of view (i) evenly and uniformly (ii) at the exciting wavelength dictated by the fluorochrome and (iii) with high intensity, as the fluorescence yield amounts only to a few percent of the excitation energy. High-pressure gas discharge lamps such as mercury (HBO) or xenon (XBO) arcs are most suitable. HBO burners emit a spectrum of a background continuum with the typical high-intensity mercury lines (Fig. 3). The XBO spectrum is also continuous. It is more intense in the red and far-red and comes closer to the spectrum of daylight (Fig. 4). HBO are usually preferred for conventional FM because of the higher radiation output in the ultraviolet to green region.

For even and uniform illumination, proper alignment of the arc is prerequisite. Since gas discharge lamps (50–400 W) operate at 10–15 bars and generate a substantial amount of heat, manufacturers instructions on alignment, installation, and safety are compulsory. (For light sources and spectra, see, e.g., www.esrf.fr, www.heraeusnoblelight.com; www.osram.com; www.olympusbiosystems.com.)

2. Optical Filters and Dichroic Mirrors

Filters for FM are designed to selectively transmit light matching the excitation wavelength of a given fluorochrome (exciter, excitation filter), to transmit only the light emitted by fluorochrome fluorescence (emitter, emitter barrier filter), or to separate the exciting and emitted light (dichroic mirror).

The three elements are usually mounted in blocks (Fig. 2) and are inserted into sliders or filter wheels. This allows for rapid switching of filter sets and facilitates operation at multiple channels. Exciter and emitter filter have to be oriented exactly at 45° to the dichroic mirror and the emitter filter perpendicular to the optical axis. Moreover, precision of the sliding mechanism is prerequisite (shift free), as the images of different filter sets will be displaced laterally, a phenomenon typically manifested when recording multi-fluorescence images via supraexposure.

Filters are characterized by their transmission and absorption or reflection properties: Short-pass (KP, SP) filters transmit light up to a certain cut-off wavelength and absorb longer wavelength light. Absorption of short wavelength and transmission of long wavelength light are provided by long-pass (LP) or barrier filters. Today, band-pass (BP) filters (Fig. 2) or multiple band-pass filters, which are translucent for one or several specific bands of wavelength, are most widely used. Dichroic mirrors (dichroic beam-splitting mirrors, color dividers, or reflection long-pass filters) also display LP characteristics. Multiple dichroic mirrors are translucent for several specific bands of wavelengths.

KP and LP filters and dichroic mirrors are characterized by their cut-off wavelength in nanometers, BP filters by the wavelength at maximal transmission, and the bandwidth at 50% transmission in nanometers. The smaller the overlap (crosstalk; Fig. 2) of the transmission curves of exciter and barrier filters, the better the image contrast. Occasionally, standard filter sets are offered where spectral separation may have been traded in for brightness of the fluorescent image: Brightness appeals to the naked eye but not to the charge-coupled device (CCD) camera, which discloses deficient channel separation rigorously.

3. Objective Lenses

The numerical aperture of the objective is the single most important factor for the brightness of the fluorescent image: Objectives with larger apertures concentrate more of the exciting light (illumination) on the specimen and collect more of the emitted light forming the fluorescence image. Because both the intensity of excitation and that of the emitted image

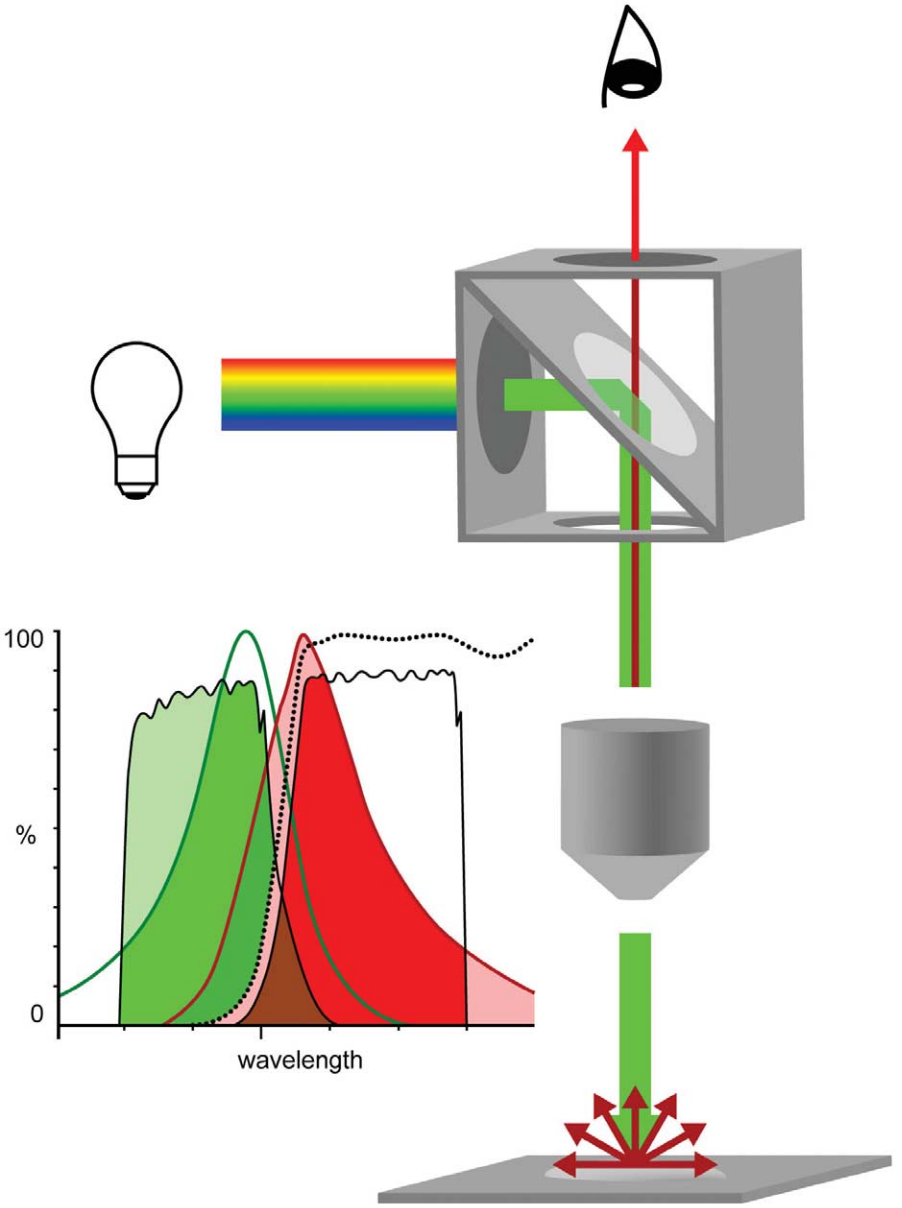

FIGURE 2 The epifluorescence microscope. Light source, positioned perpendicular to the optical axis of the fluorescence microscope, irradiates a cube that is placed in the axis and that comprises an exciter filter (ExF), a dichroic mirror (DM), and an emitter filter (EmF). Only light corresponding to the exciting wavelengths (green) passes ExF and reaches the DM placed at an angle of 45°, where light is deflected along the optical axis to be condensed by the objective (Oj) and focused onto the specimen. Corresponding fluorophores are excited and emit longer-waved fluorescent light (red). The Oj collects the emitted light (red) together with reflected exciting light (green). The DM is transparent for the longer-waved light, but not for the reflected exciting light, i.e., it functions as a long-pass filter. The EmF band pass filter is transparent only for light corresponding to the bandwidth of the emitted light (EmF filters off interfering shorter and longer-waved frequencies) and reaches the eye or the registration device, respectively.

Spectral separation by band-pass filters (Exm, EmF) and DM (dotted line) of exciting (green line) light and emitted (red line) fluorescence light, and cross talk.

The DM reflects most of the light passing the ExF (light green). This light corresponds mainly to the exciting spectrum of the fluorophore (green). Most of the emitted light (light red and red) passes the DM. The EmF further restrains this light (red) and filters off interfering light of lower or higher wavelength. However, because the transparence of ExF and EmF and the spectra of exciting and emission spectra are rarely separated but overlap to some extent, separation is not complete. Part of the higher wavelength light confined by the ExF passes the DM and also the EmF, where it adds as cross talk to the emitted signal (brown). Comparably, a part of the emitted light passes in the exciter channel.

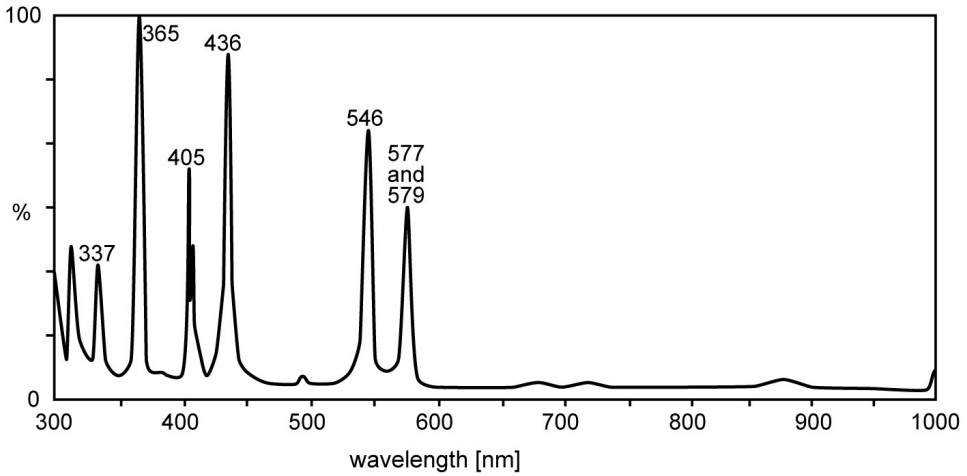

FIGURE 3 Relative spectral radiation of a high-pressure mercury lamp (HBO). Note the typical mercury lines of intense radiance. Courtesy of www.osram.com.

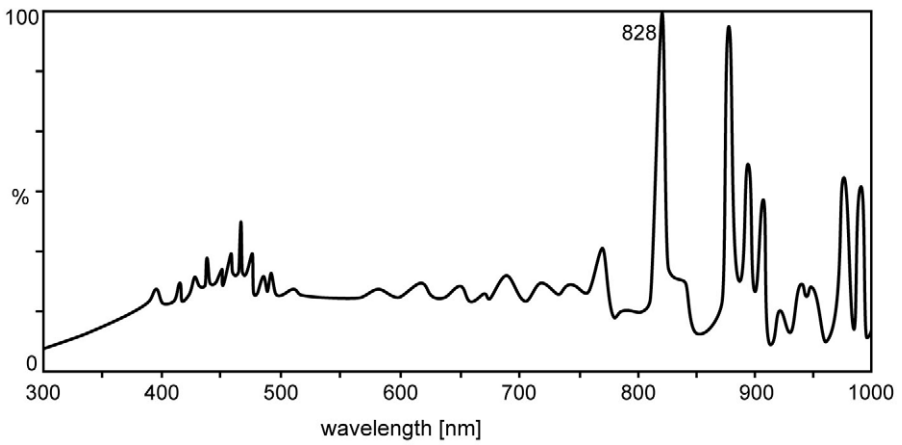

FIGURE 4 Relative spectral radiation of a high-pressure xenon lamp (XBO).

are proportional to the square of the numerical aperture (NA) of the objective lens and inverse proportional to the overall magnification (Mag_{tot}), the brightness (B) of the image increases with the fourth power of the NA,

$$B = \frac{(NA_{obj})^4}{(Mag_{tot})^2}$$

i.e., the higher the NA of an objective and the lower its magnification, the brighter the resulting image. Consequently, immersion objectives with their high numerical aperture are preferred even for low magnifications and they are combined with an eyepiece or with intermediary optics of the lowest magnification needed to detect the details of interest.

For excitation in the visible most of the objective lenses have good transmission properties and lack fluorescent components, including cements. For near UV excitation down to 360 nm, plan-fluorite objectives specifically coated against internal reflection and designed for use with oil, glycerol, or water immersion, with and without coverslips, are available from all major manufacturers. Typically, oil immersion objectives have numerical apertures of up to 1.4 and water immersion objectives up to 1.2. The latter have longer working distances, which make them well suitable for the observation of living cells in culture. Plan-apochromat lenses (63/1.4 and 100/1.4) suitable for UV excitation are also available.

When working with tissue, where overview images are essential, low magnification objectives (0.5–4×) should be accessible. Note that phase rings in an objective lens will reduce light throughput by up to 25%.

4. Recording Systems

a. Photomicrography. High-quality photographic recording of fluorescent images is not trivial. Because the emitted light is of low intensity, fast, i.e., highly sensitive, and therefore grainy, films have to be used. Nonetheless, exposure times will be long, which requires correction of the automatic exposure measurements by a film-specific reciprocity factor. Automatic illumination measurements are deceived by the nature of the fluorescent image, which is made up of a small bright signal against a large dark background, thus rendering integrated and spot measurements equally ineffective.

b. Charge-Coupled Device Imaging. With CCD imaging by solid state or video cameras, image quality and settings can be monitored on screen and adjusted accordingly. The single most important factor is sensitivity, defined by quantum efficiency, which is a measure of the efficiency of the detector to generate electric charge from incident photons. For weak fluorescence it is crucial that the imaging device is able to integrate and add up several frames.

Image resolution depends directly on the number of pixels registered per frame. For most applications, 1 megapixel, which yields images with a resolution roughly equivalent to 35-mm photographic film, is sufficient. Because CCD cameras are most sensitive in the red and far-red parts of the spectrum, auto gain control (AGC) should be switched off except when an infrared blocking filter is used.

Digital registration facilitates image processing and analysis. However, image files are of considerable size and require appropriate space for storage.

III. PRACTICAL CONSIDERATIONS

A. Choice of Filters

The selection of filters is dictated by the fluorophores intended to use (or vice versa). The latter have been roughly divided into four classes: (i) ultraviolet dyes, which are excited by UV light (~350 nm) and emit in the blue spectrum (~450 nm), (ii) fluorophores of the fluorescein isothiocyanate (FITC) class excited in the blue (~490 nm) and emitting in the green (~520 nm), (iii) rhodamine class dyes excited in the green (~560 nm) and emitting in the red (~580 nm), and (iv) fluorochromes such as Cy5 excited by red light (~630 nm) and emitting in the far red (~660 nm). For each class of fluorochromes, specific exciter/emitter filter blocks are available. Lists of fluorochromes, their spectral characteristics, and the appropriate filter sets are displayed by all major manufactures (e.g. www.chroma.com; www.seojinft.co.kr; www.omegafilters, www.schott.com).

Combinations of multiband-pass filters for the simultaneous observation and recording of two to three fluorochromes are also available. The latter are excellent for the observation of moving live specimens, but are generally more prone to cross talk than single channel filters. Alternatively, multiple fluorescence imaging can be performed by single channel imaging in conjunction with multiple photographic supraexposure.

B. Plasticware, Immersion Media, Embedding Resins, Mounting

For FM of cultured cells, culture medium and plasticware should not contain fluorescent compounds. Immersion oils, embedding resins, and mounting media should not fluoresce. Manufacturers often specify products as "safe to use for FM." Nonetheless, a quick check under the FM possibly together with the fluorochrome intended for use is never a waste of time.

For mounting of the specimen, various permanent water-soluble and water-insoluble resins (Kagayama and Sasano, 1999) containing an antifading compound are in use (Berrios *et al.*, 1999). Mounting media prepared on the basis of glycerol are very common because they are quick and simple to prepare. Sealing the coverslip after glycerol mounting with nail polish onto the slide provides mechanical stability and excludes oxygen.

Polymerizing mounting media such as Mowiol (Hoechst 1188, www.sigma-aldrich.com) generate stable mounts and exclude oxygen better than glycerol. In both cases, specimens should be stored in the dark, preferentially at 4°C.

C. Fading

In chemical terms, fading is caused by light-induced oxidation and decay of the fluorochrome, i.e., fluorescence underlies continuously progressing and irreversible destruction (Berrios *et al.*, 1999). Fluorochromes vary considerably with respect to fading; whereas FITC and green fluorescent protein (GFP) are highly sensitive, more recently introduced fluorochromes, such as indol-cyanine-based Cy dyes (www.amersham.com) and coumarin- or rhodamin-derived Alexa dyes (www.probes.com), are extremely stable toward light and oxygen. Nonetheless, exposition of a F-labeled specimen to light and oxygen should

be minimized and radical scavengers, e.g., *n*-propylgallate (www.sigma-aldrich.com), added to the mounting medium. The shutter at the light source should be used as often as possible. In addition, excitation intensity should be adjusted to the lowest possible level. Samples should be stored in the dark at 4°C.

D. Autofluorescent Compounds in Cells and Tissue

Inherent 1°-autofluorescence in cells often relates to the presence of NADH, riboflavin, or lysosomal residual material (lipofuscin) that are excited by near UV and blue light. If fluorescence labeling is expected to be weak, using fluorochromes emitting in the red or far-red may thus be advantageous. Furthermore, specific cell and tissue constituents such as chlorophyll in plants, hemoglobin in red blood cells, and elastic fibers, mast cell granules, bone, and so on in tissue typically exhibit 1°-autofluorescence.

2°-processing-related autofluorescence is essentially caused by fluorescent contaminants either due to unspecific adsorption of fluorescent molecules, e.g., fluorescent probes during processing, or generated by fixation, e.g., due to binding of fluorescent probes by nondeactivated aldehydes or by generation of glutaraldehyde or acrolein-derived polymers.

E. Poor Fluorescence Contrast

Poor contrast in a fluorescent image can be the effect of various causes: (i) autofluorescent contaminants in the immersion oil or (mounting) medium and (ii) inadequate filter combination with cross talk between excitation and emission wavelengths. (iii) If spectral properties seem to be adequate, poor contrast may be due to "minidefects" in the exciting filter. (iv) In thicker specimens, fluorescence generated above and below the focal plane may obscure the image. Those specimens need deconvolution and/or examination by confocal microscopy.

IV. IMMUNOFLUORESCENCE MICROSCOPY

A. Principle

Immunofluorescence microscopy (IMF) takes advantage of both fluorescence microscopy, as initiated about hundred years ago by Köhler and others for the documentation of autofluorescent or fluorescence-stained structures, and detection of fluorophore-conjugated antibodies, as introduced by Coons and Kaplan (1950). Specific cell and tissue constituents are visualized by IF either (i) directly (direct IF, primary fluorescence, 1°-IF) by fluorophore-conjugated antibodies (F-antibody) raised against the antigen of interest or (ii) indirectly (indirect IF, secondary IF, 2°-IF) via incubating a specimen, e.g., with a serum containing specific antibodies and revealing their presence by means of F-antibodies against the class and species of the first antibody (Fig. 5). Indirect IF is usually preferred because the 2° F-antibodies can be used against any primary antibodies of the appropriate class. Moreover, 2°-IF seems to provide brighter signals, as a 1°-antibody can bind more than one 2°-F-antibody. For multiple labeling 1°-IF, 2°-IF and site-specific fluorescent stains such as DAPI and F-phalloidin, are frequently combined.

B. Specimen Preparation

1. Objective Slides

Sample processing for IFM involves several steps of extensive washing and may be preceded by deparaffination. Specimen sections may not adhere enough to withstand such manipulations and get lost during washing. Adhesion of sections can be improved by using silanized or polylysine-treated slides (e.g., www.emsdiasum.com/ems/histology/slides.html) (see also article by Osborn and Brandfass).

2. Permeabilization

In specimens involving whole cell preparations or thicker tissue sections (e.g., cryostat sections), cytosolic proteins may be hardly accessible for antibodies because of the cell membrane (Fig. 6). In order to preserve the three-dimensional architecture of intracellular elements, e.g., of the cytoskeleton, the membrane lipids should be removed without interfering with the intracellular architecture. This is achieved either by chilled alcohol or acetone or by detergents used together with aldehydes. The principal steps are the same: During extraction of the membrane lipids by the solvent, e.g., ethanol, the detergent solution, or even the aldehyde solution itself, the solvent penetrates into the cell interior and immediately stabilizes the interior elements either by alcohol precipitation or by aldehyde cross-linking, respectively.

Permeabilization has to be adapted to the specific requirements of the cells and tissue in question and to the specific elements to be visualized; e.g., for cytoskeletal labeling permeabilization of cells with buffered solutions of 0.5–2% Octyl-POE (*n*-octylpolyethoxyethylene, www.alexis-corp-com) or of 1–2% Triton X-100 (e.g., www.sigma-aldrich-com) both

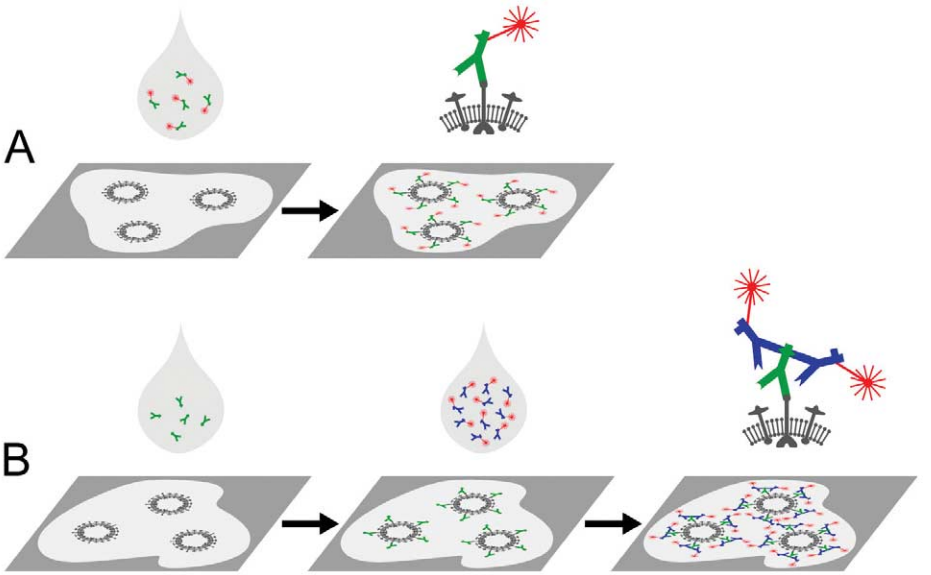

FIGURE 5 Primary and secondary immunofluorescence labeling. Primary immunofluorescence (A): A specimen with the antigen to be visualized (e.g., a viral surface protein) is incubated with the specific antibody conjugated to a fluorophore. Excess antibodies are washed off. Fluorescence microscopy reveals the presence of the antigen (e.g., the virus) directly as fluorescent signals. Secondary immunofluorescence (B): The same specimen is first incubated with antigen-specific antibodies (e.g., a rabbit serum) and excess is washed off. The specimen is then incubated with fluorophore-conjugated antibodies directed against the species and type of the primary antibody (e.g., antirabbit IgG antibodies raised in goat) and excess is washed off. The presence of the antigen manifests in the fluorescence microscope as a fluorescent signal. Since more than one secondary antibody may bind to each primary antibody, the signal may be stonger than obtained by primary immunolabeling.

containing 0.125–0.25% glutaraldehyde, and subsequent post-fixation with 1% glutaraldehyde or 1% formaldehyde proved efficient between pH 5.5 and 9.5 (Baschong *et al*., 1999).

3. *Physical Fixation*

While cryofixation and cryosectioning have become state of the art, microwave fixation, i.e., heat-related denaturation and stabilization of tissue and cells, comparable to boiling an egg, has not yet reached general applicability. In connection with FM it is used preferentially in a clinical environment. Preservation of morphology and antigenicity by microwave fixation is apparently comparable to cryopreservation or to chemical fixation, yet it can be achieved within several orders of magnitude faster and in tissue probes as large as 1 cm^3. However, extensive calibration and preferably specific microwave devices are prerequisites for proper performance. Employing common large-cavity microwave devices (e.g., household) will lead to irreproducible results if not calibrated properly (for details, see Login and Dvorak, 1994; Giberson and Demaree, 1995).

4. *Chemical Fixation*

a. Fixation by Solvents. Fixation by solvents is common in immunohistochemistry. These organic solvents—most often methanol or acetone chilled to –20°C—disrupt the membrane and simultaneously precipitate the proteins in the cytosol. Protein precipitation of intracellular elements might displace intracellular structures and induce cytoskeletal elements to coalesce. However, especially when using cryo sections, solvent fixation may dissolve lipophilic surface layers that interfere with antibody access or may denature proteins and make them more accessible for antibodies prepared from denatured antigens. For processing plant and yeast material and also for certain endoparasites (W. Baschong, personal communication), solvent fixation has proven advantageous.

b. Fixation by Aldehydes. Formaldehyde and, to a lesser extent, glutaraldehyde and acrolein are used routinely for the stabilization of supramolecular assemblies, e.g., of cytoskeletal and cytoskeleton-associated elements, i.e., for preserving the three-

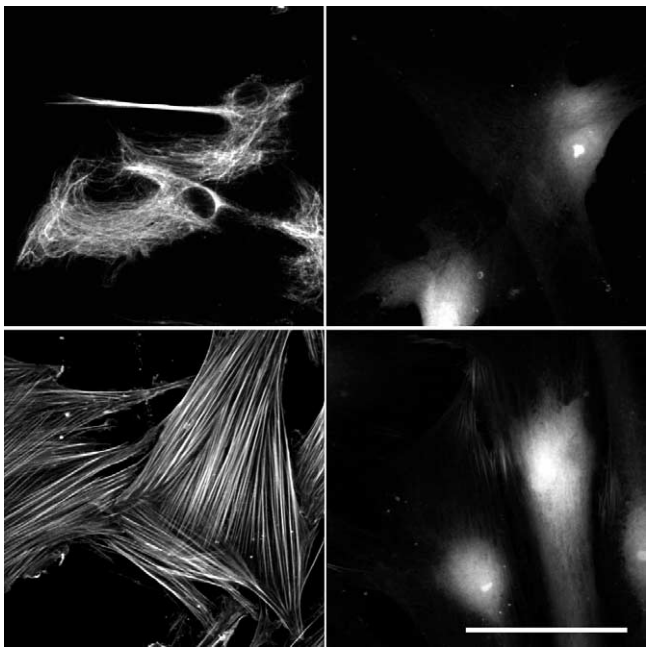

FIGURE 6 Effect of permeabilization/prefixation on cytoskeletal labeling. Human dental ligament cells on glass coverslips. Top, bottom (left) with and top, bottom (right) without permeabilization/prefixation as described in Fig. 1. *Labeling*: vimentin (top): Cy3 antivimentin (monoclonal mouse, www.amershambiosciences.com). F-actin (bottom): TRITC-phalloidin (www.sigma-aldrich.com). Cytoskeletal labeling only in permeabilized cells. In non-permeabilized cells actin is partially accessible for small phalloidin (1250 Da) but not for large anti-vimentin IgG (~150,000 Da). Scale bar: 25 µm. From Baschong *et al*. (1999).

dimensional (3D) architecture of cell and tissue constituents. Formaldehyde is usually diluted to a final concentration of 4–5%, either from a concentrated 37% stock or from freshly dissolved paraformaldehyde (so far we have not experienced differences in performance of one or the other), acrolein, or glutaraldehyde to a final concentration of 1%. Indeed, at the electron microscopic level, structural preservation of pure protein assemblies by either solution proved comparable (Baschong *et al*., 1984). Glutaraldehyde seems to react faster and to polymerize in the presence of oxygen to a large network, whereas formaldehyde seems to react slower and via oligomeric HCHO chains (Baschong *et al*., 1983). In fact, this is also reflected in the depth of antibody penetration: While immunolabeling of liver tissue fixed with 0.1% glutaraldehyde tissue was confined to a surface zone of about 1 µm, labeling of the same tissue fixed with 4% paraformaldehyde proved to be regular and intense down to 5 µm (L. Landmann personal communication). In our hands, 4–5% HCHO for routine microscopy or 1% glutaraldehyde postfixation in conjunction with permeabilization provided acceptable results in most cells and tissue. Nonetheless, it should be kept in mind that the mode of fixation can affect the antigenicity (see Section IV,B,4), i.e., optimal fixation conditions for immunolabeling an antigen in a specific tissue have to be established by trial and error. Tris buffers should not be used. They react with aldehydes under liberation of HCl, which may destroy the specimen.

4. Antigen Preservation

Preservation of antigenicity is of major concern in IFM. However, tissue preservation and embedding involves denaturation (microwave and solvent fixation) or chemical cross-linking of proteins, i.e., processes that may, and often do, affect the epitopes an antibody had been raised against. Moreover, in cryopreserved specimens, where denaturation is least, epitopes may become degraded by nondeactivated proteases. In short, there are no rules indicating how to minimize loss of antigenicity other than trial and error. At least, most suppliers of antibodies now indicate at which conditions successful labeling had been achieved with their products, thus providing the first step toward optimal labeling.

5. Managing Autofluorescence

Secondary preparation-related autofluorescence mostly relates to chemical fixation: Nonreacted aldehyde groups [e.g., of glutaraldehyde or (paraformaldehyde)] bind fluorescence markers either directly or via binding antigens or primary antibodies, thus creating substantial background fluorescence. Binding can be prevented by blocking aldehyde groups with amines such as glycine and ethanolamine, or by reducing them to OH-groups by sodium borohydride. The latter also considerably reduces the fluorescence of glutaraldehyde-derived polymers (Fig. 7).

For controlling autofluorescene in more complex tissue, e.g., bone marrow, multiple strategies such as NH_3 and $NaBH_4$ treatment before and Sudan black B counterstaining after labeling may be required (Baschong *et al*., 2001). In any case, an unlabeled specimen should be examined at the start of any study.

C. Antibody Conjugates

1. Preparation of Fluorescent Antibody Conjugates

Historically, fluorochromes, e.g., carboxyfluorescein, were coupled directly to the antibody of interest. Nowadays, not only antibodies coupled to a variety of fluorochromes and against practically all types of primary antibodies, but also a lot of fluorophore-tagged primary antibodies against many structural and pathological markers are available from a multi-

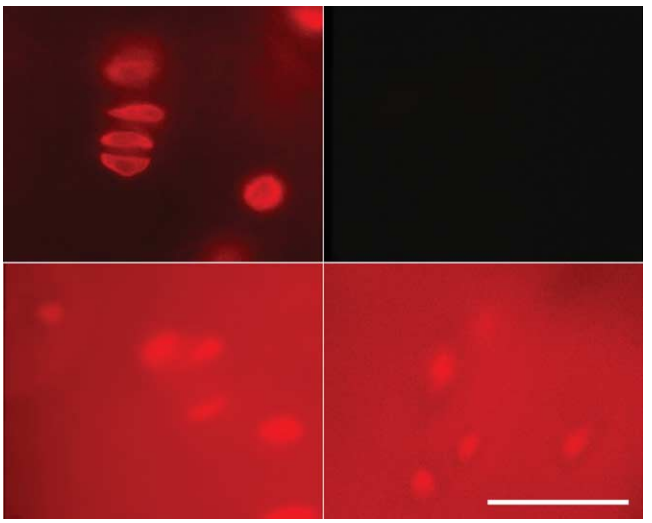

FIGURE 7 Control of background fluorescence by $NaBH_4$. Bovine articular cartilage (100-µm-thick sections). Fixation as described in Fig. 1, but prefixation 40 min and postfixation 60 min. Top (left and right): Treatment with 5 mg/ml $NaBH_4$, 2 × 30 min. Bottom (left and right): Control without NaBH4-treatment. *Labeling*: Left (top and bottom): Cy3 antivimentin; right (top and bottom): nonlabeled control. Top: exposure time 2 s, bottom: exposure time 0.2 s. From Baschong *et al*. (1999).

tude of suppliers. For specific fluorescence labeling of antibodies, e.g., in conjunction with primary IFM, specific labeling kits comprising a variety of fluorochromes are on the market (e.g., www.amersham.com).

2. *Antibody Titration*

For FM, the antibody titer is defined as the highest dilution, which results in optimal specific staining with the lowest possible background. This dilution has to be determined empirically for each antibody. Typically, titers vary from 1:5 to 1:100 for monoclonals in cell culture supernatant, from 1:100 to 1:2000 for polyclonal antisera, and up to 1:100,000 for monoclonals in ascites fluid. Manufacturers occasionally indicate a dilution range that may serve as a starting point for titration. Typically, checkerboard titrations (Table I) are used to determine the optimal dilutions of more than one reagent simultaneously, e.g., of a primary and the corresponding secondary antibody.

One slide is prepared for each pairing, i.e., nine (3^2) slides if three dilutions of the 1° and the 2° antibody have to be tested. Test slides are judged visually for both specific staining/labeling (ss) and background fluorescence (bg). If different dilutions show identical or similar results (indicated by oblique line in Table I), antibody costs can become a criterion for selection.

TABLE I

I AB/II Ab	1:50	1:100	1:200
1:250	ss:	ss:	ss:
	bg:	bg:	bg:
1:500	ss:	ss:	ss:
	bg:	bg:	bg:
1:1000	ss:	ss:	ss:
	bg:	bg:	bg:

Negative controls carried out in parallel, i.e., performing the labeling protocol without the 1° antibody or without 2° antibody, indicate unspecific binding of the 2° antibody or autofluorescence, respectively.

3. *Labeling with Primary or Secondary Fluorescence Antibodies*

Incubation time and incubation temperature are interdependent with the antibody titer, although with less influence on the quality of labeling than the latter. Generally, incubation times between 30 and 120 min at ambient temperature are sufficient. When labeling intracellular elements, e.g., cytoskeletal structures, in permeabilized 3D-cell cultures or tissue, 3–4 h of incubation with the 1° antibody at 20°C followed by three to four washes for 10 min each and subsequent incubation with the 2°F-antibody and four to five washes for 10–20 min is adequate (Baschong *et al*., 1999). Antibodies with lower affinity may perform better if incubated overnight at 4°C.

To avoid drying out of the specimen, incubations should always be performed in a moist chamber.

Occasionally, incubation at an elevated temperature (e.g., 37°C) in combination with microwave treatment is reported. Such conditions may be optimal for the specific antibody and tissue described, yet difficult to transform to other experiments without extensive calibration (see also microwave fixation).

Unspecific binding of 1° or 2° antibodies or both results in background labeling. Underlying mechanisms are manifold and difficult to elucidate. Nonetheless, some general precautions will reduce the risk. Unspecific binding of polyclonal antisera can be reduced by employing only its immunoglobulin G fraction isolated via affinity chromatography, e.g., over a protein A column (e.g. www. amersham.com; www. bio-rad.com). Unspecific binding can be reduced further by cross-absorption of antibodies against preimmune serum from the species providing the antibody and—in case of multiple labeling—against the antibodies used for labeling in other channels.

Unspecific binding due to hydrophobic interactions can be reduced by incubation with a 1% solution of a blocking protein such as albumin, ovalbumin, or gelatin, either prior to the primary antibody step and/or together with the antibody solution.

4. Commercial Antibodies

As indicated previously, antibodies are available from a multitude of suppliers, be it nonlabeled as antisera, as affinity-purified immunoglobulines, as monoclonal antibody preparations, or as F-labeled 1° and 2° antibodies (e.g., www.amersham.com; www.jacksonimmuno.com; www.probes.com; www.sigma-aldrich.com; www.dianova.de). Such preparations may be supplied in buffer as concentrated or diluted solutions, as frozen or freeze-dried preparations, etc. There are no standard conditions for supplying antibody preparations. The form in which they are supplied is at least in part dictated by the environment wherein they best maintain their activity. Antibody preparations may be sensitive to high salt or low salt concentrations and to high or low pH. They may contain traces of proteases, limiting their shelf life. Other preparations may be sensitive to freezing and should definitively be stored above 0°C. Some freeze-dried preparations may already contain the amount of salts required for yielding the appropriate buffer solution upon reconstitution; then reconstitution with phosphate-buffered saline (PBS) instead of the indicated water may turn out detrimental. In consequence, keeping antibodies at other conditions than indicated by the provider may interfere with their activity. Fluorescent probes should always be kept in the dark. Antibody solutions should be protected against microorganisms (e.g., by 0.1–0.05% sodium azide).

V. MISCELLANEOUS

A. Green Fluorescent Protein and Analogues

The discovery of GFP of the jellyfish *Aequorea victoria* less than 10 years ago has added a new dimension to the study of cells and their molecular organization (Miswender *et al*, 1995; Wouters *et al*., 2001). Directly engineering the GFP sequence into the protein of interest not only reveals its topology, but also allows for the visualization of dynamic processes, such as polymerization/depolymerization reactions, intracellular transport, and ligand binding and in living cells and by time-lapse FM.

A GFP fusion protein is characterized by its brilliant green fluorescence (excitation 484 nm, emission 510 nm). More photostable genetic variants such as EGFP (enhanced GFP, 10–35 × brighter signal) and with different spectral properties such as cyan fluorescent protein (CFP; excitation 439 nm, emission 476 nm) and yellow fluorescent protein (YFP; excitation 512 nm, emission 529 nm) have been introduced consecutively. For the visualization of these markers, specific filter sets are available. However, because of the closeness of exciting and emitting wavelengths, cross talk is difficult to avoid.

CFP and YFP are the most widely used pairs for multifluorescence imaging. Corresponding multipass filters for simultaneous imaging are available. Because of the cross talk, weak signals are best visualized by the consecutive application of single channel filters or, more accurately, by "spectral fingerprinting" using confocal microscopy.

The recent introduction of reef coral fluorescent proteins (RCFPs), which include variants with emissions in the cyan, green, yellow, red, and far-red part of the spectrum, has increased experimental flexibility greatly. RCFPs make powerful tools for monitoring promoter activity, labeling whole cells, and, in some cases, visualizing organelles. The RCFP "DsRed" has been combined with GFP or with YFP and CFP, respectively (www.bdbiosciences.com) (see also article by Rottner *et al*.).

B. Multiparameter Strategies

1. Double Labeling–Multiple Labeling

Several antigens or specific sites in a specimen can be labeled as long as the fluorescent probes comprise fluorophores of different classes. For multifluorescence labeling it is advisable to use the more stable fluorochromes of the Cy (www.amersham.com) or Alexa (www.probes.com) series. The sequence of labeling may be crucial in limiting cross-reactions and weak labeling due to steric hindrance. As a rule of thumb, indirect labeling using 2°-F-antibodies should precede direct labeling with 1°-F-antibodies, F-phalloidin, DAPI, etc., and polyclonal antibodies should be used prior to monoclonal antibodies.

Double labeling can also be performed using a solution of a monoclonal antibody (raised in mouse) in a polyclonal antiserum (raised in rabbit) followed by incubation with a mixture of the corresponding 2°-F-antibodies carrying fluorophores of different classes. If two antibodies raised in the same species—normally mouse monoclonal antibodies—have to be used, at least one antibody should be applied directly as 1°-F-antibody (see Section IV,C,1). Alternatively, two different monoclonal antibodies can be visualized by the sequential addition of fluorescence-labeled antimouse

Fab-fragments carrying fluorophores of different classes (F_1 and F_2). The first mouse monoclonal antibody is visualized by F_1-antimouse Fab fragments and after thorough washing, the second mouse monoclonal is applied and visualized by a F_2-antimouse antibody or by F2-antimouse Fab-fragments (e.g., www.dianova.de) (see also article by Prast *et al*.).

2. *Multipass Filters Versus Sequential Recording*

Multichannel fluorescence (e.g., double or triple label IF) can be monitored with specific filter sets that are designed to visualize up to four fluorochromes simultaneously. Multichannel imaging is ideal for imaging dynamic processes and for live cell imaging, as the time-consuming switching of channels is obsolete. In general, multipass filters are more prone to cross talk and less sensitive than single channel filter sets.

Subsequent recording of each fluorochrome with its appropriate filter set yields better separation of channels and higher sensitivity. It permits also to manually balance brightness of the different channels. However, the perfect x/y register (shift free) of the different images is crucial. In case of need, the filter alignment can be tested with special fluorescent beads (alignment beads, e.g., www.probes.com; www.bio-rad.com).

Appendix

Immunofluorescence labeling of cytoskeletal elements in cultured cells (cf. Fig. 1). Cells [rat SM2 fibroblasts (Leavitt and Kakunaga, (1980)] were seeded onto glass coverslips (ca. 12 mm diameter) placed in 24-well culture plates and grown in culture medium for 24 h.

Solutions

1. *PBS* (*without magnesium and calcium*):

NaCl	140 m*M*	8.19 g
KCl	14 m*M*	1.05 g
$Na_2HPO_4 \cdot 12H_2O$	11 m*M*	4.8 g
KH_2PO_4	4 m*M*	0.6 g

Make up to 1 liter with double-distilled water and adjust with 1 *N* HCl to pH 7.2–7.4; alternatively, purchase (e.g., www.sigma-aldrich). Pass through a 0.22-µm filter and store at 4°C. If not used for living cells, preserve buffers with 0.05% NaN_3.

2. *MHB buffer (modified Hank's buffer according to Small and Celis, 1978)*:

NaCl	137 m*M*	8 g
KCl	5 m*M*	0.4 g
$Na_2HPO_4 \cdot 12H_2O$	1.1 m*M*	0.48 g
KH_2PO_4	0.4 m*M*	0.06 g
$NaHCO_3$	4 m*M*	0.35 g
Glucose	5.5 m*M*	1 g
$MgCl_2$	2 m*M*	2 ml from 1 M stock
EGTA	2 m*M*	8 g
MES (e.g., www.sigma-aldrich.com)	5 m*M*	1.065 g

Make up to 1 liter with double-distilled water and adjust with 1 *N* HCl to pH 7. Pass through a 0.22-µm filter and store at 4°C. If not used for living cells, preserve buffer with 0.05% NaN_3.

3. *Permeabilization/prefixation solution*: 2% *n*-octylpolyethoxyethylene (www.alexis-corp-com) and 0.125% glutaraldehyde in MHB.

4. *Fixation solution*: 1% glutaraldehyde in MHB.

5. *$NaBH_4$ solution (for aldedhyde reduction and removal of autofluorescence)*: 0.5% (w/v) of $NaBH_4$ dissolved in cold PBS. Prepare freshly before use. Keep on ice.

6. *Incubation buffer*: 0.5% (w/v) bovine serum albumin (BSA, e.g., fraction V, www.sigma-aldrich.com) in MHB.

Mounting Solutions

1. *Glycerol*: Dissolve 0.75% *n*-propyl gallate (www.sigma-aldrich.com) or 2.5% MHB DABCO (diazabicyclo[2.2.2.] octane, www.sigma-aldrich.com) in 10 ml PBS and stir vigorously at room temperature. Add 90 ml glycerol and stir until homogeneous.

2. *Mowiol*: Dissolve 20 g of Mowiol (Hoechst 1188, www.aventis.com) at roomtemperature in 80 ml PBS (pH 7.2) or MHB [pH. 6.5 (Small and Celis 1978)]. Add while stirring 40 ml glycerol and stir for another 8–24 h. Remove insoluble particles by centrifugation (20,000 *g*, 15 min). Then dissolve 0.75% *n*-propyl gallate or 2.5% DABCO by stirring for another 4 h in the dark. Divide the solution in aliquots and store airtight and at 4°C in the dark.

3. *Mowiol for fluorescence staining of DNA*: Supplement 100 *ml* Mowiol solution with 5 µl of a DAPI (4,6-diamino-2-phenylindole, e.g., www.sigma-aldrich.com) stock solution (1 mg/ml in distilled water). Use this solution when mounting the specimen instead of the conventional Mowiol solution in order to stain nuclear and possibly also mitochondrial DNA.

Labeling Protocol

Permeablization, fixation, and blocking of free aldehyde groups can be performed in a 24-well culture dish.

1. Rinse coverslips with cells shortly with PBS.
2. Replace with permeabilization solution and incubate for 5 min at room temperature.
3. Rinse with MHB (1 × 3 min).
4. Incubate with fixation solution for 20 min at room temperature.

5. Rinse with PBS or MHB (3 × 3 min).
6. Place dish on ice and add precooled $NaBH_4$ for 10 min.
7. Change $NaBH_4$ and incubate again for 10 min on ice.
8. Replace solution with PBS or MHB solution (3 × 10 min) while agitating dish at room temperature using a shaker.

The following fluorescence markers and antibodies are used for immunolabeling.

Antigen	Marker	Dilution	Source
Actin filaments	Phalloidin Alexa-488	1:400	www.probes.com
Vimentin	Mouse antivimentin-Cy3 (IgG_1)	1:1000	www.sigma-aldrich.com
Tubulin	1°antibody Mouse anti-β-tubulin (IgG_1)	1:50	www.sigma-aldrich.com
Mouse IgG_1	2°antibody Goat antimouse IgG-Cy5	1:500	www.amersham-biosciences-com

Dilute all antibodies in incubation buffer.

All steps involving fluorochromes should be carried out in the dark (e.g., keep dishes in a black box).

1. Rinse with incubation buffer for 10 min at room temperature.
2. Incubate with normal goat serum (i.e., species in which the 2° antibodies were raised) diluted 1:20 in incubation buffer for 30 min at room temperature.
3. Incubate with primary antibody (i.e., mouse anti-β-tubulin) for 60 min at room temperature.
4. Wash with PBS (3 × 5 min).
5. Incubate with a mixture of the secondary antibody (i.e., goat antimouse IgG-Cy5) and phalloidin Alexa-488 for 60 min at room temperature.
6. Wash with PBS (3 × 5 min).
7. Incubate with antivimentin-Cy3 for 60 min at room temperature.
8. Wash with PBS (3 × 5 min).

Mount coverslips with Mowiol on slides. Cells must not be allowed to dry out. Certain antibodies may require incubation overnight at 4°C to yield better results. Specimens can be stored for several weeks at 4°C.

Acknowledgments

We thank Markus Dürrenberger and Rosmarie Sütterlin for continuous help and critical discussions. This work was supported by the M.E. Müller-Foundation (WB) and by the Kanton of Baselstadt (LL, WB).

References

Baschong, W., Baschong-Prescianotto, C., and Kellenberger, E. (1983). Reversible fixation for the study of morphology and macromolecular composition of fragile biological structures. *Eur. J. Cell Biol.* **35,** 1–6.

Baschong, W., Baschong-Prescianotto, C., Wurtz, M., Carlemalm, E., Kellenberger, C., and Kellenberger, E. (1984). Preservation of protein structures for electron microscopy by fixation with aldehydes and/or OsO4. *Eur. J. Cell Biol.* **35,** 21–26.

Baschong, W., Dürrenberger, M., Mandinova, A., and Suetterlin, R. (1999). Three dimensional visualization of the cytoskeleton by confocal laser scanning microscopy. *Methods Enzymol.* **307**, 173–189.

Baschong, W., Suetterlin, R., and Laeng, R. H. (2001). Control of autofluorescence of archival formaldhehyde-fixed, paraffin-embedded tissue in confocal laser scanning microscopy (CLSM). *J. Histochem. Cytochem.* **49,** 1565–1571.

Berrios, M., Conlon, K. A., and Colflesh D. E. (1999). Antifading agents for confocal fluorecence microscopy. *Methods Enzymol.* **307**, 55–79.

Coons, A. H., and Kaplan, M. H. (1950). Localization of antigen in tissue cells. II. Improvements in a method for the detection of antigen by means of fluorescent antibody. *J. Exp. Med.* **91**, 1–13.

Giberson, R. T., and Demaree, R. S., Jr. (1995). Microwave fixation: Understanding the variables to achieve rapid reproducible results. *Microsc. Res. Tech.* **32**, 246–254.

Kagayama, M., and Sasano, Y. (1999). Mounting techniques for confocal microscopy. *Methods Enzymol.* **307**, 79–84.

Leavitt, J., and Kakunaga, T. (1980). Expression of a variant form of actin and additional polypeptide changes following chemical-induced *in vitro* neoplastic transformation of human fibroblasts. *J. Biol. Chem.* **255**, 1650–1661.

Login, G. R., and Dvorak, A. M. (1994). Methods of microwave fixation for microscopy: A review of research and clinical applications: 1970–1992. *Prog. Histochem. Cytochem.* **27**, 1–127.

Miswender, K. D., Blackman, S. M., Rohde, L., Magnuson, M. A., and Piston D. W. (1995) Quantitative imaging of Green Fluorescent Protein in cultured cells: Comparison of microscopic techniques, use in fusion proteins and detection limits. *J. Microsc.* **180**, 109–116.

Small, J. V., and Celis, J. E. (1978). Direct visualization of the 10 nm (100 A) filament network in whole and enucleated cells. *J. Cell Sci.* **31**, 393–409.

Wouters, F. S., Verweer, P. J., and Bastiaens, P. P. (2001). Imaging biochemistry inside cells. *Trends Cell Biol.* **11**, 203–211.

CHAPTER

2

Total Internal Reflection Fluorescent Microscopy

Derek Toomre and Daniel Axelrod

I. INTRODUCTION

A. Overview and Applications

Total internal reflection fluorescent microscopy (TIRFM), also called evanescent wave microscopy, selectively excites fluorophores in a very thin (<100 nm) optical plane near the cell/coverslip interphase; the intensity of this evanescent field drops off exponentially away from the coverslip (Axelrod, 2003). The net effect is that there is virtually no out-of-focus background fluorescence and the vertical resolution and signal-to-noise are excellent, unmatched by any other light microscopy technique. These attributes make TIRFM ideal for sensitive and quantitative imaging of processes near the ventral (or basal) cell surface. The advent of a multicolor pallet of green fluorescent proteins tags (e.g., CFP, GFP, YFP, and dsRed) and other fluorophores (e.g., FlAsH), new very high numerical aperture (NA) lens, and "turn-key" commercial TIRFM systems has made TIRFM increasingly popular with cell biologists.

Its applications include studies of exocytosis (Steyer and Almers, 2001; Toomre and Manstein, 2001; Zenisek *et al*., 2000; John *et al*., 2001), endocytosis (Merrifield *et al*., 2002), cytoskeleton dynamics (Merrifield *et al*., 2002; Vale *et al*., 1996), and *in vivo* and *in vitro* single molecule studies (Ishijima and Yanagida, 2001; Pierce, 1999; Sako and Uyemura, 2002). For example, exocytic fusion of single vesicles can be observed directly by TIRFM as a fluorescent "flash" and cytoskeleton elements near the "footprint" of the cell are selectively illuminated (Fig. 1). Moreover, it can be combined with other microscopy techniques, including bright-field and epifluorescence microscopy (Toomre and Manstein, 2001), fluorescent resonance energy transfer (FRET) (Sako and Uyemura, 2002), fluorescent recovery after photobleaching (FRAP) (Sund and Axelrod, 2000), fluorescence correlation spectroscopy (FCS) (Starr and Thompson, 2001), and atomic force microscopy (AFM) (Nishida *et al*., 2002). In-depth reviews of TIRFM theory (Axelrod, 2003), implementation (Axelrod, 2003; Oheim, 2001), and applications (Axelrod, 2001; Ishijima and Yanagida, 2001; Steyer and Almers, 2001; Toomre and Manstein, 2001) are available, and excellent interactive tutorials can be found at http://www.olympusmicro.com/primer/techniques/fluorescence/tirf/tirfhome.html.

B. Theoretical Principles

The following is a condensed summary of total internal reflection (TIR) theory; for brevity, specialized properties of TIR illumination, such as the effects of polarized light and the use of metal films for creating surface plasmon resonance effects, can be found elsewhere (Axelrod, 2003; Sund *et al*., 1999).

TIRFM is based on how light behaves at an interface of two mediums of different refractive index (see Fig. 2). Specifically, if a beam of light traveling in a medium of high refractive index, such as glass (n_3 ~1.51), enters a lower refractive index medium, such as water (n_1~1.33) or the cytosol of a cell (n_1 ~1.36–1.38), beyond a certain critical angle, θ_c (measured from the normal), it is totally internally reflected, rather than simply refracted. For TIR to occur, two conditions must be met: $n_3 > n_1$ *and* the incidence angle of the light, θ, must be greater than the critical angle, θ_c. This critical angle can be derived from Snell's law of

Copyright 2006, Elsevier Science (USA).
All rights reserved.

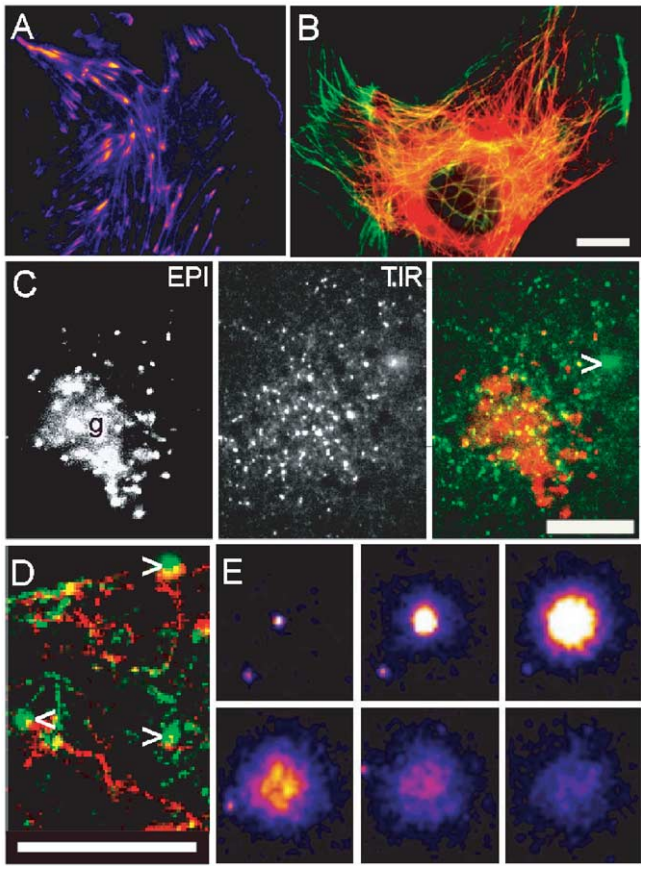

FIGURE 1 Images of cell cytoskeleton and membrane traffic with TIRFM. (**A** and **E**) Images of the TIR fluorescent signal that have been false colored; bright to dimmest signal is white > yellow > red > purple. (**B–D**) The normal epifluorescent signal (EPI) is colored red and the TIR fluorescent signal (TIR) is shown in green. All images are from PtK_2 epithelial-like cells labeled with various YFP constructs. (**A**) Actin-YFP. Note that the ends of stress fibers (likely focal adhesions) are particularly bright. (**B**) Tubulin-YFP. Tubulin near the coverslip is yellowish-green. Note that single microtubules can be observed clearly by TIRFM (green) even under dense areas of microtubules (red). (**C**) Different views of membrane cargo. VSVG-YFP, a membrane protein, was accumulated in the Golgi (g) and then released. The cursor indicates a vesicle that has just fused with the plasma membrane (PM). Note that EPI and TIR images of the cell are very different (even though the focal plane was not changed). In EPI the Golgi area is stained brightly, whereas in TIR vesicles near the membrane are brightest; there is weak PM staining due to VSVG-YFP that has already fused. (**D**) Tracking trafficking and fusion. A series of ~200 frames were back subtracted and the difference image was projected. Vesicles that moved out gave a red EPI "track," turned yellow/green as they approached the membrane, and fusion itself gave a green circular "flash," indicated by the cursors. (**E**) Collage of a vesicle undergoing fusion. Starting in the top left, 1 sec intervals are shown from left to right. The fading of the signal in frames 4–6 is due to lateral diffusion of protein in the membrane. All images were taken with a TIRFM microscope similar to that in Fig. 4A, but with a hemicylinder prism. Scale bars: 5 μm (B–D) and 2 μm width of Box in (E). Reprinted from Toomre and Manstein (2001).

refraction ($n_3 \sin\theta_3 = n_1 \sin\theta_1$). By definition, at the critical angle $\theta_1 = 90°$, giving $n_3 \sin\theta_c = n_1(1)$, θ_c is thus expressed as

$$\theta_c = \sin^{-1}(n_1/n_3)$$

where n_1 and n_3 are the refractive indices of the liquid and solid, respectively. In the example with cells attached to glass, $\theta_c = 64.2°$ (if n_1~1.36). In reality, there is often a thin intermediate layer(s) such as the cellular plasma membrane (n_2), but for many purposes these can be disregarded as the effects are often nominal (Axelrod, 2003).

Although the TIR beam does not propagate into and through the low density medium (e.g., the cell interior), it does create an electromagnetic field in a thin zone in that region near the solid surface. This "evanescent field" decays exponentially in intensity with distance from the surface (z axis) and only fluorophores in the aqueous medium near the glass are excited, as illustrated in Fig. 2; this assumes that the coherent light beam acts as an "infinitely" extended plane wave, which is a fair approximation in most TIRFM setups. The intensity of the evanescent field, I, at various distances, z, from the coverslip and its penetration depth, d (defined as a decay of I_z to 1/e or ~37% intensity), can be expressed by the following equations:

$$I(z) = I(0)e^{-z/d} \quad \text{where} \quad d = \frac{\lambda_o}{4\pi}\left(n_3^2 \sin^2\theta_3 - n_1^2\right)^{-1/2}$$

Shallower penetration depths occur with large differences in refractive index of the two mediums, short wavelength light (λ_o), and steep angles of incident light. Practically, d can be as low as ~20 nm with exotic high refractive index materials, but ~50–200 nm is typical with common materials, wavelengths, and setups. It is worth noting that the emitted light can also experience near field effects, causing significant anisotropic deviations from a simple exponential curve; this deviation will vary depending on the NA of the objective lens and its location. For "objective-type" TIRFM setups, the field decays quicker, whereas it is slower in "prism-type" setups (these setups are described in detail later) (Axelrod, 2003; Steyer and Almers, 2001).

C. Advantages of TIRFM over Confocal Microscopes

A principal advantage of TIRFM is excellent signal to noise, achieved by limiting the illumination to a thin focal plane. High-contrast images can be imaged quickly with minimal photobleaching. In contrast, confocal laser scanning microscopes are slower and

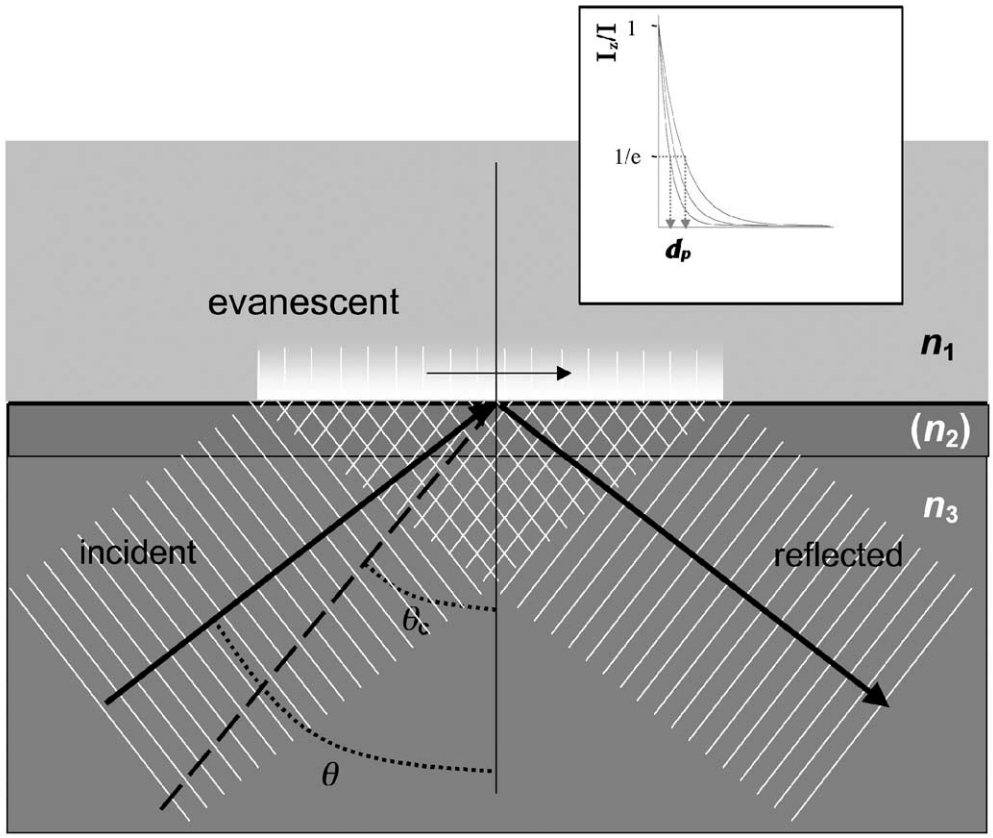

FIGURE 2 Geometrical scheme of TIR. Refractive index n_3 must be greater than n_1. The intermediate layer (consisting of metal or a dielectric material of refractive index n_2) is not necessary for TIR to occur, but can introduce useful optical properties. Most applications of TIRFM do not use an intermediate layer. The incidence angle θ must be larger than the critical angle θ_c for TIR to occur. The exponentially decaying evanescent field in the n_1 material is used to excite fluorophores. The inserted box shows examples of exponential decay curves of the intensity of the evanescence field at various penetration depths (d). Adapted from Axelrod (2003).

less sensitive, but can image the entire depth of the cell, one slice at a time (Table I).

II. MATERIALS AND INSTRUMENTATION

A. Illumination

In practice, most TIRFM systems employ lasers, which allow for an intense colliminated beam of light. Typically lasers that provide 10 s to 100 s of milliwatts per line(s) of interest are used. For imaging GFP proteins, an air-cooled argon laser (e.g., 100 mW, 488 nm, Melles Griot) or, alternatively, an optically pumped-diode laser (e.g., "Sapphire", 20–200 mW, 488 nm, Coherent) can be used; multicolor samples generally require stronger lasers to "pick" a weaker line or multiple lasers coupled with dichroic filters. In some configurations, mentioned later, an arc lamp may be feasible.

B. Light Path to the Microscope

The beam of laser light must be redirected to the microscope (prism or objective) and focused. Traditionally, an optical chain of mirrors and lens are employed, requiring an "optical table." An alternative is to couple the light into a single mode fiber optic, providing a more flexible configuration (the laser need not be on the optical table and the fiber can be positioned easily). The fiber is generally coupled to a focusing lens or TIR condenser. A set of XY[1] and possibly Z micro-

[1] For convention here, the Z axis is parallel to the laser and optical axis and XY is perpendicular to it.

TABLE I A Comparison of TIRFM and Confocal Microscopes

	TIRFM	Confocal microscope (laser scanning)
Illumination depth (*z* axis)	~50- to 100-nm penetration depth (1/e)	~500 nm
Detector	Cooled CCD or intensified camera	Photomultiplier tube
Quantum Efficiency of detector	~40–90%	~10–20%
Acquisition speed	Fast; can capture the image in milliseconds, depending on the camera and signal to noise	Slow; scanning a frame typically takes seconds
Contrast	Excellent: signal to noise is ~10–100× better than confocal or ~1000× better than wide-field microscopes	Moderate to good
Sensitivity	Single molecule capable	Hundreds of molecules
Bleaching	Low	Considerable
Cellular imaging	Cell surface only	Entire cell
Approximant cost	~$1–50 K+ for conversion of a wide-field fluorescent microscope, depending on the method used	~$300–500 K

TABLE II Comparison of Objective-Type and Prism-Type TIRFM Setups

	Objective type	Prism type
Illumination angle	Fixed or limited range	Variable
Access to top of sample?	Yes (inverted scope)	Limited (upright scope) None (inverted scope)
Objective lens	Oil immersion (1.4 NA, 1.45 NA, 1.65 NA[a])	Water immersion (~1.0–1.2 NA)
Light path for excitation and emission light	Same (coupled)	Separate (uncoupled)
Signal to noise	Very good; but some noise due to internal reflections of excitation light in the objective lens	Better; less background light
Commercial system?	Yes	No
Object brightness	Collected light varies approximately monotonically with distance[b]	Collected light varies nonmonotonic with distance[b]
XY resolution	Excellent (higher NA lens)	Good to very good

[a] Requires expensive coverslips and special immersion oil.
[b] See Axelrod (2003) and Steyer and Almers (2001).

manipulaters are used to control the angle and position of the beam (e.g., where it strikes the prism or the back focal plane of the objective).

C. TIRFM Optical Configurations

There are basically two kinds of TIRFM setups: an "objective type" (also called "prismless") and a "prism type." Both can be mounted in numerous configurations; for simplicity, a few common configurations are shown in Figs. 3 and 4. Both setups have advantages and disadvantages as outlined in Table II.

1. Objective-Type TIRFM

Principle

The recent development of very high NA objectives has made objective-type TIRFM feasible. The microscope can be configured in several variations by use of commercial accessories or straightforward modifications (e.g., Fig. 3). To achieve TIR, a beam of light, usually from a laser, is focused off-axis at the back focal plane (BFP) of the objective. The greater the off-axis radial position of the focus, the greater the angle of incidence θ_3 of the beam in the glass. The maximal angle of incidence, θ_m ($\geq\theta_3$), depends on the NA of the

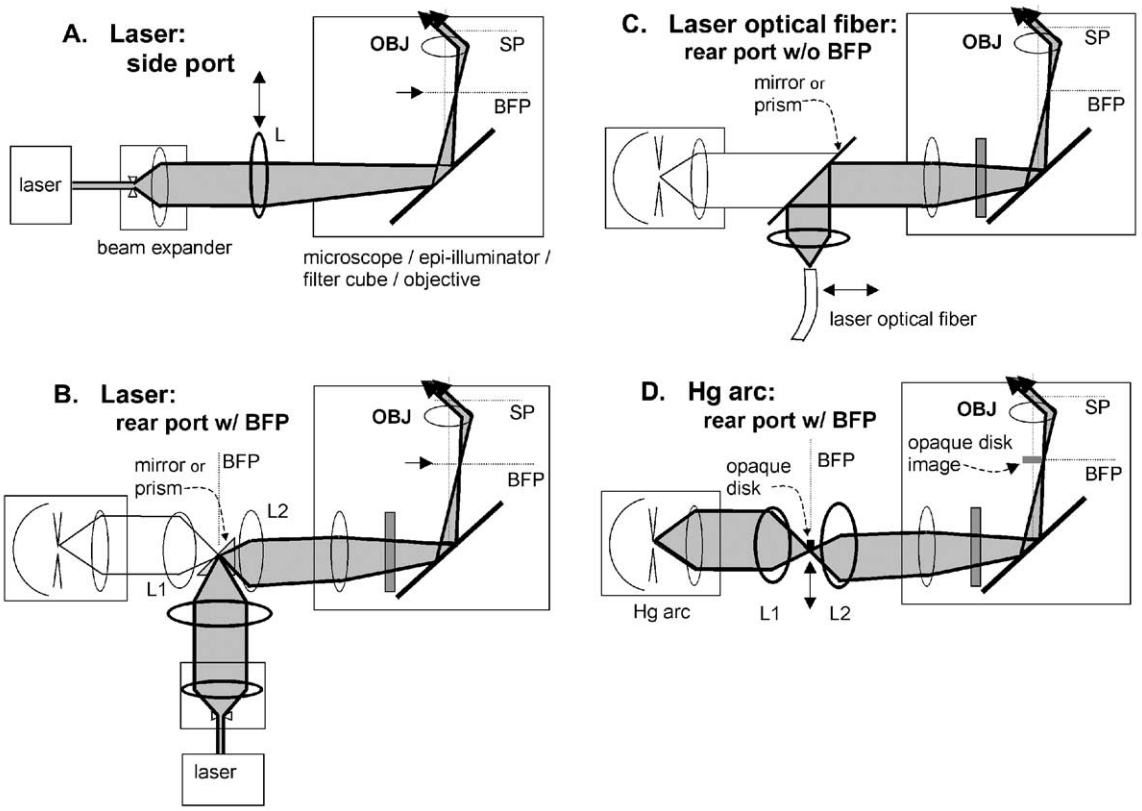

FIGURE 3 Four arrangements for objective-type (prismless) TIRFM in an inverted microscope. In all these configuration, OBJ refers to the objective, SP refers to sample plane, and BFP refers to the objective's back focal plane or its equivalent or "aperture" planes. Components drawn with heavier lines need to be installed; components in lighter lines possibly preexist in the standard microscope. (**A**) Laser illumination through a side port (requires a special dichroic mirror cube facing the side, available for the Olympus IX-70 microscope). The beam is focused at the back focal plane at a radial position sufficient to lead to supercritical angle propagation into the coverslip. Moving the focusing lens L transversely changes the angle of incidence at the sample and allows switching between subcritical (EPI) and supercritical (TIR) illumination. (**B**) Laser illumination in microscope systems containing an equivalent BFP in the rear path normally used by an arc lamp. The laser beam is focused at the BFP where the arc lamp would normally be imaged. The Zeiss Axiovert 200 provides this BFP, marked as an "aperture plane." If (as in the Olympus IX-70) an aperture plane does not exist in the indicated position, it can be created with the pair of lens L1 and L2. (**C**) Laser illumination introduced by an optical fiber through the rear port normally used by the arc lamp. This scheme is employed in the commercial Olympus TIR device. (**D**) Arc lamp TIR illumination with no laser at all. The goal is to produce a sharp-edged shadow image of an opaque circular disk at the objective back focal plane such that only supercritical light passes through the objective. The actual physical opaque disk (made ideally of aluminized coating on glass) must be positioned at an equivalent upbeam BFP, which, in Kohler illumination, also contains a real image of the arc. The Zeiss Axiovert 200 provides this BFP, marked as an "aperture plane." If (as in the Olympus IX-70) an aperture plane does not exist in the indicated position, it can be created with the pair of lens L1 and L2. Illumination at the back focal plane is a circular annulus; it is shown as a point on one side of the optical axis for pictorial clarity only. Adapted from Axelrod (2003).

objective (by definition NA = $n_{oil} \sin \theta_m$). Snell's law ($n_3 \sin \theta_3 = n_1 \sin \theta_1$) leads NA $\geq n_1 \sin \theta_1$. At the critical angle, θ_c, $\theta_1 = 90°$ and thus NA $\geq n_1$. In the cellular context, for TIR to occur, we must have NA $> n_{cytosol}$. For a 1.4 NA oil lens and $n_{cytosol} = 1.38$, only a very thin cone at the outer edge of the back focal plane of the objective barely (<3% of the aperture) allows TIR excitation. (Of course, the whole aperture is still used to gather emitted light.) Practically, TIR is easier to obtain with 1.45 and 1.65 NA objectives that allow θ_c to be surpassed more easily and TIR can occur in ~10 and 25% of the aperture, respectively.

An arc-lamp illumination system can also be configured for TIRFM illumination by use of an opaque

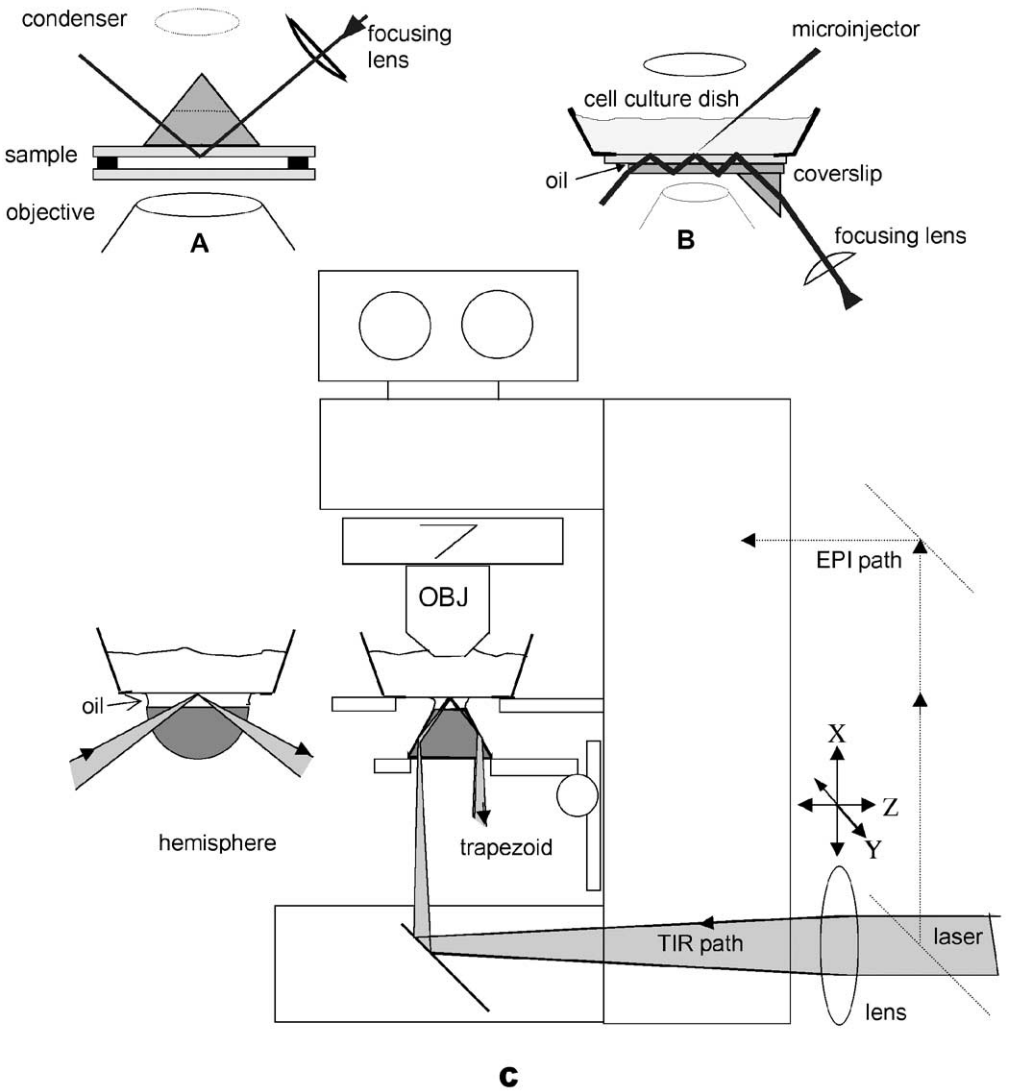

FIGURE 4 Schematic drawings for prism-based TIRFM using a laser as a light source. The vertical distances are exaggerated for clarity. (**A**) This configurations uses a TIR prism above the sample. The buffer-filled sample chamber sandwich consists of a lower bare glass coverslip, a spacer ring (made of 60 μm-thick Teflon or double-stick cellophane tape), and the cell coverslip inverted so the cells face down. The upper surface of the cell coverslip is put in optical contact with the prism lowered from above by a layer of immersion oil or glycerol. The lateral position of the prism is fixed but the sample can be translated while still maintaining optical contact. The lower coverslip can be oversized and the spacer can be cut with gaps so that solutions can be changed by capillary action with entrance and exit ports. (**B**) This configuration places the prism below the sample and depends on multiple internal reflections in the substrate, thus allowing complete access to the sample from above for solution changing and/or electrophysiology studies. However, only air or water immersion objectives may be used because oil at the lower surface of the substrate will thwart the internal reflections. (**C**) TIRFM on an upright microscope utilizing the integral optics in the microscope base and a trapezoidal prism on the vertically movable condenser mount. The position of the beam is adjustable by moving the external lens. An alternative hemispherical prism configuration for variable incidence angle is also indicated to the left. Vertical distances are exaggerated for clarity. An extra set of mirrors can be installed to deflect the beam into an epi-illumination light path (shown with dashed lines). Adapted from Axelrod (2003).

disk of the correct diameter inserted in an "upbeam" plane equivalent of the BFP of the objective (Fig. 3D). It is less expensive, gives freedom in the choice of excitation wavelengths, and avoids interference fringes, but it is considerably dimmer as much of the excitation light is necessarily blocked; this can be improved somewhat by employing a conical prism in the arc-lamp light path (Axelrod, 2003).

Materials

1. Microscope: usually inverted (this allows complete access to the cells). Objectives: high NA "TIRFM" objective(s), typically 1.45–1.65 NA, 60–100× magnification: currently available from Olympus, Zeiss, and Nikon (1.65 NA only from Olympus).
   a. 1.45 NA objectives use regular #1.5 coverslips (n = 1.52), possibly premounted in a 30-mm petri dish (e.g., Mattek, Ashland, MA).
   b. 1.65 NA objective requires "special" high refractive index oil (n = 1.78), really iodomethane, that is volatile and potentially toxic (Cargille, USA). Similarly, high refractive index coverslips are needed, e.g. n = 1.78 coverslips made of LAFN21 glass (Olympus) or SF11 glass (custom cut by VA Optical Co, San Anselmo, CA). Unfortunately, such coverslips are expensive (>$20/coverslip), fragile, and practically are only reusable a few times. It is, however, a good choice when a thin d is needed.
2. Filters: dichroic filters and emission filters appropriate for the laser line(s): These must block scattered light from the laser and generally require high band-pass filters (e.g., Chroma Corp., USA).
3. *Optional*: commercial objective-type TIRFM condensers are available from Till Photonics, Olympus, Zeiss, and Nikon for mounting to their respective microscopes. Generally lasers are coupled into them via a fiber optic.

Configuration

1. Focus the laser beam (using an external focusing lens) to a point on the BFP of a high NA objective (1.45–1.65 NA) so that it emerges from the objective as a collimated "beam" of light, (*Caution: Use safety glasses*.)
2. Using XY micromanipulators adjust the point of focus radially off-axis in the BFP so as to achieve TIR (see protocol later). There is a one-to-one correspondence between the off-axis radial distance ρ and the angle θ. At a sufficiently high ρ, the critical angle for TIR can be exceeded; further increases in ρ reduce the penetration depth, d.

2. Prism-Type TIRFM

Principle

Some typical TIRFM setups are shown in Fig. 4. Note that TIR illumination of cells is achieved on the coverslip side with the aid of an optically coupled prism, whereas emitted light is detected with a conventional water-immersion lens on the opposite side. This restricts access to the sample, but allows for TIR to be achieved over a greater range of angles and hence greater flexibility in d.

Materials

1. Microscope (upright will provide some access to sample)
2. ~1.0–1.25 NA water immersion objective (~20×–60×). If access to the sample is desired, a long working distance "dip-in" objective may be best.
3. Prism: triangular, trapezoidal, or hemispherical, depending on the setup. Equilateral prisms made from flint glass (n = 1.648) are available commercially (Rolyn Optics, USA) and will provide a sufficiently high n for TIR to occur at the aqueous interface. A hemispherical prism (e.g., quartz) allows for variable incidence angles over a continuous range but requires external optical elements (vertical optical rail with XYZ translators).
4. A mount for holding and positioning (XY) the prism (see Fig. 4)
5. Dichroic filters and emission filters appropriate for the laser line(s): These must block the scattered or propagating laser light (usually less than in "objective-type" setups)
6. Cells are usually grown on disposable glass coverslips/slides, but more exotic high n_3 materials such as sapphire, titanium dioxide, and strontium titanate (with n as high as 2.4) can yield exponential decay depths d as low as $\lambda_o/20$.
7. Optical coupling of prism to coverslip/slide: This may be optically coupled with glycerol, cyclohexanol, or microscope immersion oil, among other liquids, and need not exactly match in refractive index.

Configuration

Figures 4A and 4B show representative schematic drawings for setting up prism-based TIR in an inverted microscope. Figure 4C shows a convenient low-cost prism-based TIRFM setup for an upright microscope. Specifically, the laser beam is introduced in the same port in the microscope base as intended for the transmitted light illuminator (which should be removed), thereby utilizing the microscope's own in-

base optics to direct the beam vertically upward. The prism, in the shape of a trapezoid, is mounted on the microscope's condenser mount, in optical contact (through a layer of immersion oil) with the underside of the glass coverslip. An extra lens, just upbeam from the microscope base, allows the incident beam to be adjusted to totally reflect off one of the sloping sides of the prism, from which the beam continues up at an angle toward the cells grown on the coverslip where it is weakly focused.

In all the prism-based methods, the TIRF spot should be focused to a width no larger than the field of view and θ should exceed θ_c by at least a couple of degrees. At incidence angles very near θ_c, the cells cast a noticeable "shadow" along the surface.

C. Camera

A good cooled CCD camera should be adequate for most TIRFM imaging of cells. For instance, current "extended range" (ER) front-illuminated CCD cameras have quantum efficiencies up to ~65% (available from Hamamatsu, PCO, Roper, etc.). Back-thinned cameras are more sensitive but generally slower and more expensive. Intensified or electron multiplying (EM) CCD cameras are typically used for rapid single molecule imaging (Pierce, 1999).

D. Accessories

Cells grown on coverslips are placed in cell imaging chamber (e.g., Mattek dishes with glued in coverslip). Focus drift along the *z* axis can be problematic, especially when heating cells to 37°C, as even minor drifts are very noticeable in TIRFM. To minimize drift, an environmental chamber or heated "plexiglass" box is helpful. A number of commercial based ones are available; however, this can also be homebuilt for much less using a "Air-therm" (World Precision Instruments; England) or similar hot-air blower and a self-built box. Another solution is to use an active autofocusing device connected to a piezoelectric device.

III. PROCEDURES

Caution! *The use of lasers should be considered potentially hazardous to the eyes and proper laser safety should be followed. Precautions include (but not limited to) using appropriate laser safety glasses/goggles, attenuating the laser power while making adjustments, never looking directly into the beam or its reflections, and not looking into the eyepiece unless adequate dichroic and emission filters are in place (and even then use extreme caution). Indirect imaging of the beam and sample image can be accomplished with CCD cameras and is much safer.*

A. Objective-Type TIRFM Setup: A Practical Protocol

This description is for the setup in Figs. 3A–3C, but is similar for other configurations.

1. Prepare a test sample consisting of a film of fluorescent lipid adsorbed to the coverslip. Dissolve dioctadecylindocarbocyanine ("diI"; Molecular Probes) in ethanol at ~0.5 mg/ml, place a droplet on the coverslip, and rinse with distilled water before it dries and a diI monolayer will remain on the coverslip. When excited at 488 nm and observed with a fluorescein dichroic and "long-pass" emission filter, the diI will appear orange. Add an aqueous dilute fluorescein solution (faint yellow) to the sample chamber, which will emit in green. Alternatively, add an aqueous suspension of fluorescent microbeads (~100 nm diameter, 488 nm, Molecular Probes, USA). Some of the beads will adhere to the surface, whereas bulk suspended beads will jitter with Brownian motion.

2. Carefully place a drop of immersion oil on the objective lens, set the sample on the microscope stage, and slowly raise the objective to establish optical contact.

3. Remove the excitation filter from the filter cube if it were present for arc illumination, leaving only the appropriate dichroic and emission filters, or instead use a laser "clean-up" excitation filter (e.g., laser line wavelength ± ~10 nm; Chroma).

4. Remove all obstructions between the test sample and the ceiling. Allow a collimated "raw" laser beam to enter the side or rear epi-illumination port along the optical axis. A large area of laser illumination should be seen on the ceiling, roughly straight up. *(Make sure to keep your eyes out of the laser beam path! Ideally use laser safety glasses.)*

5. Place a focusing lens (~100 mm focal length plano- or double-convex lens mounted on a XY microtranslator) at a position ~about 20 cm "upbeam" from where the beam enters the microscope illumination port. The illuminated region on the ceiling will now be a different size, probably smaller.

6. Move the focusing lens longitudinally (along the *z* axis) to minimize the illuminated region on the ceiling. This will occur where the converging lens focal point falls exactly at the objective's back focal plane. At this position, the beam is thereby also focused at the

objective's actual back focal plane and emerges from the objective in a roughly collimated form.

7. Fine tune the lateral position of the focusing lens so that (as you face the microscope) the beam spot on the ceiling moves down a wall to the right or left. The inclined path of the beam through the fluorescent aqueous medium in the sample will be obvious to the eye. Continue to adjust the focusing lens lateral position until the beam traverses almost horizontally through the fluorescent medium and then farther, past where it just disappears. The beam is now totally reflecting at the substrate/aqueous interface.

8. Carefully view the sample through the microscope eyepieces (or with a color CCD camera). The diI/fluorescein sample should appear orange, not green, as only the surface is being excited; the beads should look like high contrast immobilized dots, occasionally some will "blink" as they diffuse into and out of the evanescent field. Back off the focusing lens to where the beam reappears in the sample (i.e., subcritical incidence). When viewed through the eyepieces, the diI/fluorescein sample should now appear very bright green or beads will have lots of background as they jiggle through multiple focal planes and emit out-of-focus light.

9. If the illuminated region in the field of view is not centered, adjust the lateral position of the "raw" laser beam before it enters the focusing lens and repeat Steps 7 and 8. If the illuminated region thereby approaches the center, continue to readjust the raw beam in the same direction and repeat the steps until centering is achieved. If the illuminated region moves even farther to the side, then adjust the raw beam in the opposite direction and repeat the steps. The final position will be a laser beam entering the focusing lens parallel to its optical axis but somewhat off center.

10. If the illuminated region is too small, increase the width of the beam before it enters the focusing lens with a beam expander or long focal length diverging lens. At best, about two-thirds of the whole field of view can be illuminated by TIR (which includes the entire central region typically viewed by a CCD camera).

11. Replace the test sample with the sample of interest and focus the microscope. As the lateral position of the external focusing lens is adjusted through the critical angle position, the onset of TIR fluoresence should be obvious as a sudden darkening of the background and a flat two-dimensional look to the features near the surface. Importantly the entire field of view has only one plane of focus. A good control is to take one image by TIR and then, without adjusting the focus, take another fluorescent image by conventional epi-illumination (see Fig. 1). For most cellular objects, these two images, when overlaid, should look very different. As one's experience increases, the test sample can be skipped and all the adjustments made directly on the actual sample of interest (although this can be tricky if, say, there are only a few transfected GFP cells that one must "hunt" down).

B. Prism-Type TIRFM Practical Protocol

This description is for the setup in Fig. 4C, but is basically similar for other configurations.

1. Mount the prism on the condenser mount carrier, if possible. Alternatively, the prism holder can be fixed directly to the optical table or microscope.

2. Depending on the configuration, a system of mirrors with adjustable angle mounts fixed to the table must be used to direct the beam toward the prism.

3. Place a test sample (e.g., a diI-coated coverslip and fluorescein or bead solution; see earlier) in the same kind of sample holder as to be used for real cell-based experiments.

4. With the test sample on the stage, focus on the fluorescent surface with bright-field or fluorescent epi-illumination. Usually, dust and defects can be seen well enough to find the focal plane by the coverslip/medium interface.

5. Place a small droplet of immersion oil directly on the prism and carefully translate the prism vertically so it touches and spreads the oil, but does not inhibit lateral sliding; too much oil may interfere with the illumination path.

6. Rough adjustments: Using safety goggles to attenuate errant reflections and without the focusing lens in place, adjust the "raw" collimated laser beam position with the mirrors so that TIR occurs directly in line with the objective's optical axis, as seen from the scatter of the laser light as it traverses through the prism, oil, and TIR surface.

7. Insert the focusing lens so that the focus is roughly at the TIR area under observation. By eye, using XY translators on the focusing lens, adjust its lateral position so that the TIR region occurs directly in line with the objective. Look for three closely aligned spots of scattered light, corresponding to where the focused beam first crosses the immersion oil layer, where it totally reflects off the sample surface, and where it exits and recrosses the oil.

8. Fine adjustments: The yellow-orange TIR elliptical region should now be in view but not centered. Make final adjustments with the focusing lens (XY) to center this area and move it along the z axis to achieve the desired size. TIR can be distinguished from two out-of-focus blurs past either end of the ellipse. The

TIR spot contains sharply focused images of defects in the diI coating or sharp dots of adsorbed beads and flashes as diffusing beads drift into the evanescent wave; as a negative control the green-emitting fluorescein is hardly seen.

9. With the optics now aligned correctly for TIR, lower the prism vertically to remove the diI sample and replace it with the actual cell sample. Raise the prism to make optical contact. Although the TIR region will be slightly off, it will be close enough to make final adjustments while observing fluorescent cells.

IV. COMMENTS

1. A "homebuilt" TIRFM system can be ideal in terms of flexibility and cost; however, commercial "turn-key" systems may be quicker or easier to implement.

2. Even "thick cells" can be imaged by TIRFM, but one will only "see" where the cell contacts the coverslip. In theory, it is sometimes possible to image deeper in the cell if there is a big refractive index difference of organelles/membranes, but in practice this is rarely implemented. Also, if the penetration is too deep (e.g., past 150 nm), higher refractive index organelles such as granules can scatter the TIR light, producing artifacts.

3. TIRFM is different from the nonfluorescent technique called "reflection internal microscopy" (RIM or also IRM) that uses bright-field illumination to visualise cell–substrate contacts.

V. PITFALLS

A common problem is adjusting the system so that a homogeneous evanescent field is achieved. If alignment on a single mode fiber is off, output light may give a speckled appearance from hitting the cladding and will require realignment. Laser illumination can produce interference fringes, manifested as intensity variations over the sample area. In this case, it may be advisable to scramble the light (e.g., in a commercially optical fiber phase scrambler).

References

Axelrod, D. (2001). Total internal reflection fluorescence microscopy in cell biology. *Traffic* **2**, 764–774.

Axelrod, D. (2003). Total internal reflection fluorescence microscopy in cell biology. *Methods Enzymol* **361**, 1–33.

Ishijima, A., and Yanagida, T. (2001). Single molecule nanobioscience. *Trends Biochem. Sci.* **26**, 438–444.

Johns, L. M., Levitan, E. S., Shelden, E. A., Holz, R. W., and Axelrod, D. (2001). Restriction of secretory granule motion near the plasma membrane of chromaffin cells. *J. Cell Biol.* **153**, 177–190.

Merrifield, C. J., Feldman, M. E., Wan, L., and Almers, W. (2002). Imaging actin and dynamin recruitment during invagination of single clathrin-coated pits. *Nature Cell Biol.* **4**, 691–698.

Nishida, S., Funabashi, Y., and Ikai, A. (2002). Combination of AFM with an objective-type total internal reflection fluorescence microscope (TIRFM) for nanomanipulation of single cells. *Ultramicroscopy* **91**, 269–274.

Oheim, M. (2001). Imaging transmitter release. II. A practical guide to evanescent-wave imaging. *Lasers Med. Sci.* **16**, 159–170.

Pierce, D. V. R. D. (1999). Single-molecule fluorescence detection of green fluorescent protein and application to single proteins dynamics. *Methods Cell Biol.* **58**, 49–73.

Sako, Y., and Uyemura, T. (2002). Total internal reflection fluorescence microscopy for single-molecule imaging in living cells. *Cell Struct. Funct.* **27**, 357–365.

Starr, T. E., and Thompson, N. L. (2001). Total internal reflection with fluorescence correlation spectroscopy: Combined surface reaction and solution diffusion. *Biophys. J.* **80**, 1575–1584.

Steyer, J. A., and Almers, W. (2001). A real-time view of life within 100 nm of the plasma membrane. *Nature Rev. Mol. Cell Biol.* **2**, 268–275.

Sund, S. E., and Axelrod, D. (2000). Actin dynamics at the living cell submembrane imaged by total internal reflection fluorescence photobleaching. *Biophys. J.* **79**, 1655–1669.

Sund, S. E., Swanson, J. A., and Axelrod, D. (1999). Cell membrane orientation visualized by polarized total internal reflection fluorescence. *Biophys. J.* **77**, 2266–2283.

Toomre, D., and Manstein, D. J. (2001). Lighting up the cell surface with evanescent wave microscopy. *Trends Cell Biol.* **11**, 298–303.

Vale, R. D., Funatsu, T., Pierce, D. W., Romberg, L., Harada, Y., and Yanagida, T. (1996). Direct observation of single kinesin molecules moving along microtubules. *Nature* **380**, 451–453.

Zenisek, D., Steyer, J. A., and Almers, W. (2000). Transport, capture and exocytosis of single synaptic vesicles at active zones. *Nature* **406**, 849–854.

CHAPTER

3

Band Limit and Appropriate Sampling in Microscopy

Rainer Heintzmann

I. INTRODUCTION

A. What Is "Sampling?"

In microscope images obtained with the help of electronic devices (e.g., CCD camera) or in a scanning microscope system, data are usually obtained (sampled) at equidistant coordinates in object space. The distance between these measurement positions is usually denoted as the "sampling distance." Current technology samples on orthogonal coordinates (rectilinear sampling) with appropriate sampling distances along the in-plane coordinates X, Y and the axial coordinate Z (for three-dimensional imaging).

For a deeper understanding of how to choose these distances correctly, it is useful to assume the intensity distribution near the detector (translated back to sample coordinates) to be a continuous function (Fig. 1). The equidistant sampling coordinates, at which the values of the image function are recorded, are depicted as dashed lines in Fig. 1. The fact that pixels have a discrete physical size is not considered here to keep the discussion simple. This pixel-size effect is described by a convolution and can be considered as a multiplicative modification of the optical transfer function (Sheppard *et al.*, 1995). In the considerations given in this article, noise resulting from photons and/or the detector system is neglected.

B. Spatial Frequencies

Any physical function (e.g., as shown in Fig. 1) can be decomposed into a sum of sine waves, each with a different frequency, amplitude, and zero position (so-called phase). To exactly represent a function, this sum generally contains an infinite amount of components. Such decomposition is useful especially in optics, as images of (linear) optical systems have the interesting property of only transmitting sine waves of the sample up to a fixed limiting frequency. A periodic fluorescence distribution with a count of maxima per µm above this limit frequency will appear as a uniform constant in the image. Such systems are often called "band-limited" systems, as only a compact, limited band of frequencies (from zero to the maximal transmittable frequency) is transferred. How well a defined frequency is transferred is depicted in the "optical transfer function (OTF)" as outlined in Fig. 2 for in-plane imaging in a fluorescence wide-field microscope.

The "spatial frequency" given on the X axis of this graph denotes the number of maxima per meter for each sine wave. The sum of all sine waves yields the perfect image. The transfer strength of the OTF (Y axis) denotes how well a sample consisting of only one spatial frequency (one such sine wave) would be transferred to the detector.

C. Band Limit of Optical Systems

1. Fluorescence Microscopy

When considering the sampling properties of microscopic imaging, a physical model (Young, 1985) of the microscope system has to be constructed. Due to the laws of physics, this OTF is zero beyond a well-defined limiting frequency (see Appendix or Sheppard *et al.*, 1994). In the case of wide-field fluorescence microscopy, the limiting frequency is as follows:

$$k_{xy,\max} = \frac{2NA}{\lambda_{\mathrm{em}}},$$

with $k_{xy,\max}$ denoting the maximal in-plane spatial frequency, λ_{em} the shortest detected vacuum wavelength

Copyright 2006, Elsevier Science (USA).
All rights reserved.

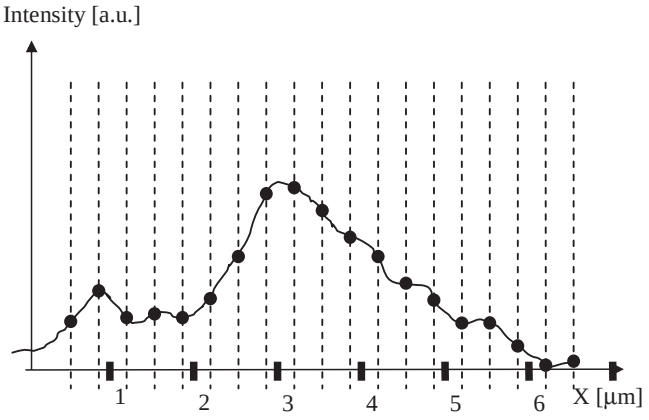

FIGURE 1 Diagram of a microscope image as a continuous function over space (here indicated as the *X* coordinate). Dashed lines indicate the points at which the function is sampled (its value is recorded).

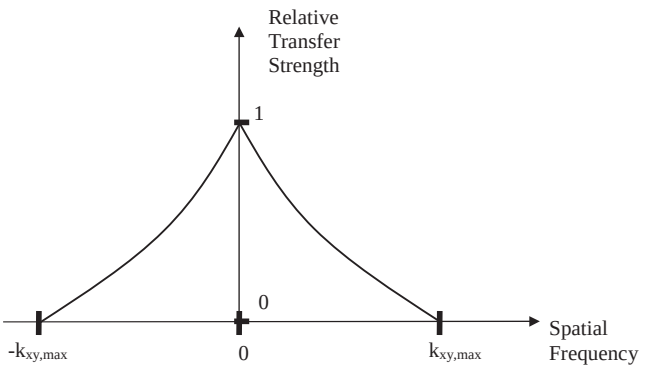

FIGURE 2 The approximate shape of the in-plane optical transfer function of a fluorescence wide-field microscope. For spatial frequencies above the limiting frequency ($k_{xy,max}$), no information can be transferred from the object to the microscope image.

of the fluorescence emission light, and $NA = n\sin(\alpha)$ the numerical aperture defined by the refractive index n of the medium immersing the sample and the objective detecting light at an aperture half-angle of α.

Similarly, a limiting maximal transmittable axial spatial frequency $k_{z,max}$ can be given for sine waves with Z components as:

$$k_{z,\max} = \frac{NA}{\lambda_{em}} \frac{[1-\cos(\alpha)]}{\sin(\alpha)}.$$

In confocal fluorescence microscopy, the illumination is confined to a diffraction-limited spot. At very small pinhole size, detection is also diffraction limited. A fluorophore needs to be excited and detected by the system, leading to a multiplicative process of excitation and detection. As a result, the aforementioned

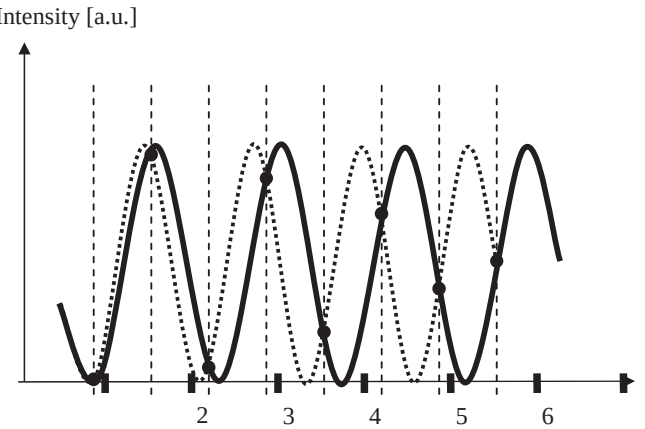

FIGURE 3 Aliasing. Two sine waves with different spatial frequencies yield identical sampled values. A distinction based on the measured values is only possible when the dashed alternative wave can be excluded, as its frequency lies above the transfer limit. This gives rise to the Nyquist theorem stating that the maximal possible frequency in the image has to be sampled with more than two positions per wavelength.

frequency limits have to be extended for the case of confocal fluorescence microscopy (see Appendix for details).

It should be noted that for larger pinhole sizes (>0.3 Airy discs, definition see Section III,B), the in-plane transfer function reaches values very close to zero above the spatial frequency stated by the wide-field limit. This explains why the in-plane resolution of confocal images achievable in practice is rarely substantially superior to wide-field images.

2. *Aliasing*

Because the images can be decomposed into the sine waves, it is useful to consider how an individual sine wave is sampled by the equidistant measurements. Figure 3 shows such a sine wave (solid black line) along with its values marked at equidistant sampling positions. Does such a measurement determine the frequency of the measured sine wave uniquely? As evident from Fig. 3 (dotted line), this is not the case, as multiple sine waves (these are called aliases) could possibly give the same measured values. However, if it is known that a maximal transmittable frequency exists, frequencies of sine waves in the image beyond that limit can be excluded as possible sources for this measurement. To guarantee a unique interpretation of a given measurement, all that needs to be done is to ensure all aliasing frequencies lie beyond the *a priori* known transmittable frequency limit.

In an acquired image, multiple frequencies are measured simultaneously, and the aforementioned

should be true for all spatial frequencies possibly present in the image. The highest frequencies in the image (just below the frequency limit, e.g., $k_{img} < k_{max} = 5\,\mu m^{-1}$) turn out to be most critical, as their lowest frequency alias ($k_{alias} = k_s - k_{img}$, e.g., at $k_s = 11\,\mu m^{-1}$, k_{alias} is $6\,\mu m^{-1}$) appears at lower frequencies than aliases of other lower frequency image contributions. If the image is sampled at least at twice its highest contained spatial frequency ($k_s > 2k_{img}$), aliasing can be avoided, as interpretation of the sampled values is unique because k_{alias} is above the limiting frequency k_{max}. In other words, the sampling frequency ($k_s = 1/D$), as defined by the sampling distance D, has to exceed the maximal transmittable frequency by a factor of two ($k_s > k_{Nq} = 2k_{max}$). This limiting sampling frequency k_{Nq} is called the Nyquist frequency.

This means that all values of the continuous band-limited function in between the sampled values can theoretically be predicted solely based on the knowledge of the band limit of the system and the sampled values (assuming an infinite amount of them and not considering noise). Sampling denser than this requirement stated earlier is termed oversampling; sampling sparser than the limit is termed undersampling.

II. INSTRUMENTATION

Selection of the appropriate sampling distances is crucial for almost all optical systems with computerized image acquisition. In the field of optical microscopy, one has to discriminate among *fluorescence-*, *transmission-*, and *reflection-based* systems.

III. PROCEDURES

In the procedures suggested here, equations are stated for different microscopy arrangements. They are derived from Fourier theory in the Appendix.

A. CCD-Based Imaging Systems (in Plane)

Many imaging systems do not allow for any direct control over the size of the detector bins. CCD camera-based systems and digitizing micrographs on a scanner fall in this category. To select the appropriate sampling distance:

1. Obtain the pixel pitch (P) of your CCD camera from the manufacturer/supplier. The pixel pitch is the distance in X and Y directions between successive pixels. Usually this is in the range of 5 to 20 µm. When binning is used during image acquisition, the pixel pitch has to be multiplied with the binning factor (e.g., with 2×2 binning: multiply the pixel pitch by 2). When digitizing micrographs, a corresponding value is given by either the pixel-to-pixel distance after scanning or the resolution of the micrograph, whichever value is bigger. When a micrograph is scanned, care has to be taken to account for all magnification factors to finally obtain a pixel size corresponding to the image plane.

2. Make a list of available objectives. Note magnification (e.g., 40 or 63×) and numerical aperture (e.g., 0.9 or 1.3) for each of them. These values are usually engraved on the side of the objectives. If any post-magnification system (e.g., Zeiss Optovar) is available on your microscope, multiply the objective magnification with the appropriate factor. The obtained total magnification is called M.

3. Calculate the in-plane sampling distance (D_{xy}) as dictated by the detector pixel pitch in the object plane for each objective, dividing the pixel pitch by the magnification:

$$D_{xy} = \frac{P}{M}$$

4. Calculate the maximum sampling distance (d_{max}) in the object plane from the numerical aperture of the objective and the vacuum wavelength of light used for imaging:

Wide-field fluorescence: $$d_{xy,\max} = \frac{\lambda_{em}}{4NA_{obj}}$$

Transmission or phase microscopy:

$$d_{xy,\max} = \frac{\lambda}{2\left(NA_{obj} + NA_{cond}\right)}$$

In wide-field illumination microscopy systems, λ_{em} should be the shortest detected emission wavelength (e.g., FITC $\lambda_{em} = 500$ nm); in transmission microscopy, the shortest transmitted wavelength should be used (e.g., blue at $\lambda = 400$ nm). Note that the numerical aperture of the condensor (NA_{cond}) contributes equally as the objective numerical aperture to the final resolution, although the contrast may suffer in transmission microscopy with a high condensor numerical aperture. Also note that the value NA_{cond} is taken for a fully open condensor aperture; a closed condensor aperture enhances the contrast but reduces NA_{cond} and thus the resolution.

5. Ensure that $D_{xy} < d_{xy,max}$ by selecting the appropriate objective and/or postmagnification optics from the list.

CCD Example

Let's say the pixel pitch of your camera is 7 µm and you are using no binning. The question is whether using a 100×, 1.3 NA oil ($n = 1.516$) immersion objective with the standard microscope tube lens (i.e., $M = 100$), the sampling distance in the focal plane corresponding to $D_{xy} = \frac{7\mu m}{100} = 70\ nm$ satisfies the Nyquist limit. The maximum sampling distance for wide-field fluorescence microscopy (e.g., detecting FITC at 500 nm shortest detection wavelength) is $d_{xy,\max} = \frac{500\ nm}{4 \cdot 1.3} \approx 96.15\ nm > 70\ nm$, thus your system respects the Nyquist limit. A 2 × 2 binning on the CCD, however, would undersample the image.

B. Confocal Systems (in Plane)

Confocal microscopy usually allows for free control over the sampling distance in the object plane by selecting an appropriate magnification ("zoom") and image size in pixels. A notable exception to this is a Nipkov-type disc-scanning system employing a CCD camera. For such systems, the maximum sampling distances ($d_{xy,\max}$ and $d_{z,\max}$) corresponding to a confocal system have to be selected, although the protocol for the CCD camera should be followed.

1. Calculate the maximum sampling distance (Sheppard, 1989; Wilson, 1990; Sheppard *et al*., 1994) from the parameters of the objective (see CCD procedure for definitions):

Confocal fluorescence (small pinhole):

$$d_{xy,\max} = \frac{\lambda_{eff}}{4NA_{obj}},\ \lambda_{eff} = \frac{1}{\frac{1}{\lambda_{ex}} + \frac{1}{\lambda_{em}}}$$

Confocal fluorescence (large pinhole):

$$d_{xy,\max} = \frac{\lambda_{eff}}{4NA_{obj}}$$

Confocal two-photon fluorescence (no pinhole):

$$d_{xy,\max} = \frac{\lambda_{ex}}{8NA_{obj}},$$

with λ_{ex} being the irradiating wavelength (usually in the infrared).

Confocal reflection: $d_{xy,\max} = \frac{\lambda}{4NA_{obj}}$

The strict theoretical limit even for large pinholes is the value given for small pinhole size. However, because the lateral high-frequency content for larger pinholes is negligible and usually lies well below the noise level, the "wide-field fluorescence" in-plane equation (as given earlier) can be applied, replacing the emission wavelength with the excitation wavelength. As a rule of thumb, consider pinhole sizes below 0.5 Airy discs in the pinhole plane as being small and sizes above 1.5 Airy discs as being large. In object space coordinates one Airy disc diameter (the first dark ring of a diffraction limited spot, assuming low *NA*) is

$$1.22\frac{\lambda_{em}}{NA_{obj}}.$$

To compare with actual pinhole sizes, the pinhole has to be translated to the object space coordinates by the appropriate demagnification factor, if the pinhole size is not stated in Airy disc units in the microscope operating software.

2. For beam-scanning or object-scanning confocal systems, the in-plane sampling distance (D_{xy}) is usually stated somewhere on the screen. It can also be calculated from the image size in the object plane (S_{img}) and the number of pixels (N_{pix}) along *X* or *Y*: $D_{xy} = \frac{S_{img}}{N_{pix} - 1}$.

This distance should be selected to be below the $d_{xy,\max}$ calculated earlier.

Confocal Example

With the microscope parameters as stated in the wide-field example in Section III,A, confocal microscope illuminating at 488 nm

$$\left(\lambda_{eff} = \frac{1}{\frac{1}{488\ nm} + \frac{1}{500\ nm}} \approx 247.0\ nm \right),$$

with a small detection pinhole setting, would allow a maximum in-plane sampling distance of

$$d_{xy,\max} \approx \frac{247\ nm}{4 \cdot 1.3} = 47.5\ nm$$

and the pixel-to-pixel spacing D_{xy} should be adjusted to a smaller value. For large pinholes, the following sampling distance should be acceptable:

$$d_{xy,\max} = \frac{488\ nm}{4 \cdot 1.3} \approx 93.8\ nm.$$

C. Focus Series

For the acquisition of focus series (Z stacks), an additional sampling limit along the axial direction also needs to be obeyed by choosing an appropriate distance between neighboring image planes. To calculate the corresponding maximum plane-to-plane distance ($d_{z,\max}$), the aperture half-angle of the objective (α_{obj}) has to be known. Because this value is often not stated, it has to be calculated from the numerical aperture and the refractive index (n) of the immersion medium:

1. Calculate the aperture half-angle of the objective as

$$\alpha_{obj} = \arcsin\left(\frac{NA}{n}\right).$$

   Approximate values for the refractive index are stated in Table I.
2. Once the aperture half-angle is known, the maximum plane-to-plane distance is calculated as

Wide-field fluorescence:

$$d_{z,\max} = \frac{\lambda_{em}}{2NA_{obj}} \frac{\sin(\alpha_{obj})}{(1-\cos(\alpha_{obj}))}$$

Transmission or phase microscopy:

$$d_{z,\max} = \frac{\lambda}{2NA_{\max}} \frac{\sin(\alpha_{\max})}{(1-\cos(\alpha_{\max}))}$$

Confocal fluorescence:

$$d_{z,\max} = \frac{\lambda_{eff}}{2NA_{obj}} \frac{\sin(\alpha_{obj})}{(1-\cos(\alpha_{obj}))}, \lambda_{eff} = \frac{1}{\frac{1}{\lambda_{ex}} + \frac{1}{\lambda_{em}}}$$

Confocal two-photon fluorescence:

$$d_{z,\max} = \frac{\lambda_{ex}}{4NA_{obj}} \frac{\sin(\alpha_{obj})}{(1-\cos(\alpha_{obj}))},$$

   with λ_{ex} being the irradiating wavelength (usually in the infrared).

Reflection confocal: $d_{z,\max} = \frac{\lambda}{4n}$

TABLE I List of Refractive Indices

Medium	Refractive index n
Air or vacuum	1
Water	1.33
Oil	1.516
Glycerin (100%)	1.47

   For transmission or phase microscopy, $NA_{\max}$ and $\alpha_{\max}$ denote the corresponding values of the greater of the condensor and objective numerical aperture.
3. Ensure that the distance between successive image planes (D_z) in object coordinates is below $d_{z,\max}$.

Focus Series Examples

For the parameters of the wide-field fluorescence example just given, the appropriate spacing between successive image planes should be chosen to be below

$$d_{z,\max} \approx \frac{500\,nm}{2 \cdot 1.3} \frac{\sin(59°)}{(1-\cos(59°))} \approx 339.6\,nm$$

with the aperture half angle being estimated from the NA (1.3) and the refraction index of oil (n = 1.516):

$$\alpha_{obj} = \arcsin\left(\frac{1.3}{1.516}\right) \approx 59.0°$$

Accordingly, the maximum spacing for confocal fluorescence microscopy (parameters as given in Section III,B) is calculated as

$$d_{z,\max} \approx \frac{247\,nm}{2 \cdot 1.3} \frac{\sin(59°)}{(1-\cos(59°))} \approx 167.8\,nm$$

IV. PITFALLS: CONTRAST AND SAMPLING

Suppose the object and its image consist of a sine wave with a single spatial frequency (e.g., 200 nm distance between two maxima). The sampling limit requires sampling at more than the double frequency (i.e., D_{xy} < 100 nm). If this image is sampled too close to the limiting frequency, there may be a problem. Depending on the exact position of the object, one may be fortunate enough to sample a maximum, then a minimum, a maximum again, and so on or, if unlucky, always sample half the maximum (see example in Fig. 4). In the latter case, the result would be indistinguishable from an object with zero frequency. Even when sampling at distances slightly below the required minimum distance, a very low contrast can result for images of small size. Therefore, one should oversample, such that at least one full period of the resulting envelope amplitude modulation is captured. In other words, with M pixels along a spatial direction, the stated maximum sampling distance should be lowered by multiplication with the factor $M/(M+1)$. For common image sizes (e.g., 512×512), this factor is negligible, but it can be substantial when acquiring only few Z sections (in which case M is the number of sections).

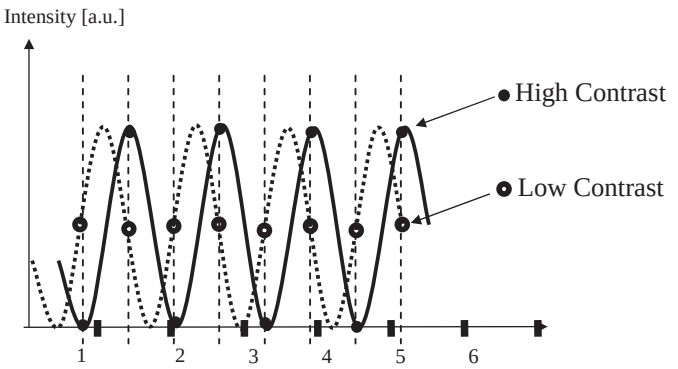

FIGURE 4 For images containing only a few measured values, the measured contrast can be dependent on the exact phase of the sine wave to perform measurements even when the Nyquist limit frequency is obeyed (compare the contrast of closed and open circles). To ensure that at least one full variation of contrast is recorded, oversampling is recommended, as it leads to a required sampling frequency enhanced by a factor of $(M + 1)/M$ with M measured sampled points.

A. When to Use Undersampling

For some applications the sampling limit does not need to be obeyed. If, for example, the task is to count homogeneously filled cells with a fluorescent dye using a 20×, 0.9 NA objective, it makes a lot of sense to seriously undersample the data. For a cell to be identified it might suffice to detect two adjacent bright pixels. Thus the required sampling can, in some cases, depend on the size of the object structure to image. Undersampling (e.g., by binning) can reduce the amount of acquired data (important in screening applications), reduce the readout noise, dark current, and sometimes enlarge the field of view. In the mentioned application the introduced aliasing effects should be tolerable.

In other applications (e.g., neuronal imaging of dendrites) it may be very tempting to undersample the data. However, thin structures (such as dendrites) may occasionally be lost in some pixels because they happen to lie between two sample points. Such missing gaps can then render a computer-based analysis difficult, as the structures appear ruptured and will also cause serious problems when successive computerized deconvolution is applied to data. In these cases it can even be better to reduce the numerical aperture of the objective than to seriously undersample at high *NA*.

B. When to Use Oversampling

For some gray value-based image processing tasks, oversampling is recommendable (Young, 1996, 1988; Verbeek, 1985; Verbeek and vanVliet, 1993); e.g., if the aim is the precise determination of object positions, one should oversample data by a factor of at least 1.5 (sample at a 1.5 times smaller pixel pitch as compared to the limits given earlier). Simulations revealed (Heintzmann, 1999) that determination of the center of mass can result in a significant systematical error even when sampled according to the stated sampling limits. Furthermore, a smaller sampling distance determines more precisely where each photon hits the detector, thus leading to a slightly more precise estimate of the particle position (Heintzmann, 1999). Oversampling can also be useful when successive deconvolution of data is planned (see below). Note that with oversampling, the photon dose delivered to the sample can still be kept constant. Acquired images may look inferior at a first glance, but they still contain all the necessary information. Such data always allow for successive binning, resampling, and/or smoothing to enhance the visual appearance.

C. Deconvolution: Out-of-Band Reconstruction Possibilities

When the computerized deconvolution is applied to data, it is often useful to oversample data during data acquisition. The reason is that constrained deconvolution is capable of "guessing" high-frequency components in the object structure that have not been acquired. This is enabled by the use of prior knowledge about the object, e.g., its positivity or smoothness (Sementilli *et al.*, 1993). In principle, acquired data can be resampled, but this always involves loss of information about the photon statistics, or even interpolation errors can result. Although software might be able to reconstruct on a denser grid than raw data, there may be (depending on the algorithm) some resampling involved, which in turn can skew the statistics of the deconvolution procedure, thus leading to inferior results. As a rule of thumb, a two-fold oversampling (two times smaller sampling distances as compared to the given limits) should suffice even for advanced deconvolution software.

Appendix: Derivation of Cut-Off Frequencies

To obtain the equations given in the text, an expression for the cut-off spatial frequency was derived and the Nyquist theorem applied, calculating the maximum sampling distance as half the distance corresponding to this cut-off spatial frequency. Note that this derivation is valid for high NA vector theory.

Electric field components of a plane wave can be described by a single point in Fourier space. Its dis-

tance to the origin is proportional to the inverse wavelength. A lens forms its image by the constructive interference of converging parallel beams. It can thus be described by a "cap" (Gustafsson *et al*. 1995) in Fourier space (Fig. 5a).

For incoherent **fluorescence wide-field** imaging, the intensity in focus describing the point spread function (PSF) is obtained as the square of the absolute magnitude of the electric field distribution. Because the optical transfer function (OTF) is the Fourier transformation of the PSF, it can be obtained as an autocorrelation of Fig. 5a, which is identical to the convolution with itself mirrored at the origin in Fourier space. The resulting region of support is depicted in Fig. 5b. The corresponding distances are the reciprocal values, which have to be halved, yielding the respective maximum sampling distance in *XY* and *Z* directions.

In the case of confocal microscopy, photons have to be excited and detected. This leads to a multiplication of the probabilities of excitation PSF (corresponding to the OTF in Fig. 5b, but for λ_{ex}) and the emission PSF (corresponding to the OTF in Fig. 5b). In Fourier space, this translates to a convolution of Fig. 5b as depicted in Fig. 6, yielding the appropriate equations for the confocal closed pinhole case. The size and shape of the pinhole is described by a multiplicative modification of the detection OTF with the Fourier transformed pinhole. The two-photon (no detector pinhole) derivation follows in a similar fashion, as its PSF is the square of the excitation PSF, which can be described by autocorrelation of Fig. 5b for λ_{ex}.

When dealing with wide-field transmission, the situation is different. The image can no longer strictly be described as a convolution of the object with a point spread function. However, for incoherent imaging in transmission, such approximation still holds. Nevertheless it is preferable to think of this as a scattering problem. Neglecting multiple scattering, one can look for the scattering object vectors in Fourier space, which should be imaged by the system. Scattering theory states that the incoming wave vector plus the object vector yields the outgoing wave vector. Incoming and outgoing vectors are restricted by the Ewald sphere and the numerical aperture of the condensor and objective, respectively. As depicted in Fig. 7a the range of possible scattering vectors depends on both, the incoming light as defined by the numerical aperture of the condensor and the outgoing light as restricted by the objective.

The equation for confocal reflection microscopy is obtained by considering the possible scattering vectors when illuminating and detecting through the same objective (Fig. 7b).

Acknowledgments

B. Rieger, S. Höppner, E. Lemke, I. T. Young, and T. M. Jovin are thanked for their help in revising this manuscript and C. J. R. Sheppard for fruitful discussions on sampling.

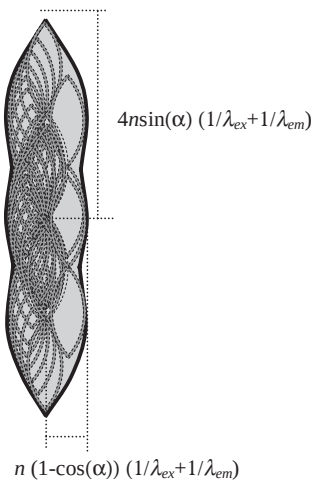

FIGURE 6 Support of the optical transfer function for a confocal fluorescence microscope obtained by autocorrelation of Fig. 5b.

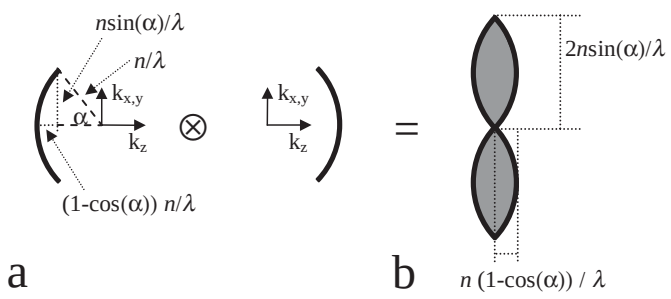

FIGURE 5 Derivation of the region of support of the fluorescence wide-field optical transfer function (b) from an autocorrelation of interfering plane waves (a), all depicted in Fourier space.

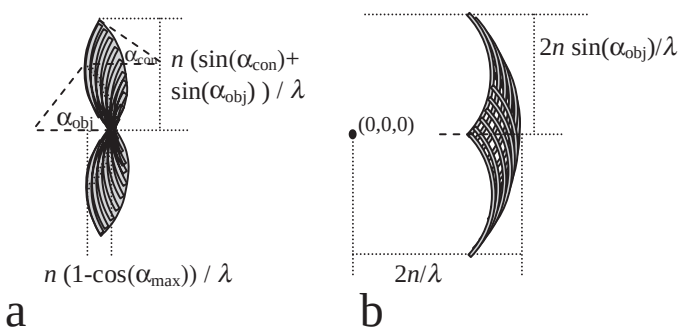

FIGURE 7 Shape of object frequencies (scattering vectors) that can possibly be imaged with an incoherent wide-field transmission microscope (a) and a confocal reflection microscope (b).

References

Gustafsson, M. G. L., Agard, D. A., and Sedat, J. W. (1995). Sevenfold improvement of axial resolution in 3D widefield microscopy using two objective lenses. *Proc. SPIE* **2412**, 147–156.

Heintzmann, R. (1999). "Resolution Improvement of Biological Light Microscopic, data." *Ph.D. thesis*, Institute of Applied Physics, University of Heidelberg, Germany.

Sementilli, P. J., Hunt, B. R., and Nadar, M. S. (1993). Analysis of the limit to superresolution in incoherent imaging. *J. Opt. Soc. Am. A* **10**, 2265–2276.

Sheppard, C. J. R. (1989). Axial resolution in confocal fluorescence microscopy. *J. Microsc.* **154**, 237–241.

Sheppard, C. J. R., Gu, M., Kawata Y., and Kawata, S. (1994). Three-dimensional transfer functions for high-aperture systems. *J. Opt. Soc. Am. A* **11**, 593–598.

Sheppard, C. J. R., Gan, X., Gu, M., and Roy, M. (1995). Signal-to-noise in confocal microscopes. *In "Handbook of Biological Confocal Microscopy"* (J. B. Pawley, ed.), pp. 363–371. Plenum Press, New York.

Verbeek, P. W. (1985). A class of sampling-error free measures in oversampled band-limited images. *Pattern Recogn. Lett.* **3**, 287–292.

Verbeek, P. W., and van Vliet, L. J. (1993). Estimators of 2D edge length and position, 3D surface area and position in sampled grey-valued images. *BioImaging* **1**, 47–61.

Wilson, T. (1990). Confocal microscopy. *In "Confocal Microscopy"* (T. Wilson, ed.), pp. 1–64. Academic Press, London.

Young, I. T. (1985). Estimation of sampling errors. *Cytometry* **6**, 273–274.

Young, I. T. (1988). Sampling density and quantitative microscopy. *Anal. Quant. Cytol. Histol.* **10**, 269–275.

Young, I. T. (1996). Quantitative microscopy. *IEEE Engineer. Med. Biol. Mag.* **15**, 59–66.

CHAPTER

4

Optical Tweezers: Application to the Study of Motor Proteins

Walter Steffen, Alexandre Lewalle, and John Sleep

I. INTRODUCTION

Optical tweezers allow the study of interactions of single molecules of motor proteins with the track, actin or microtubules, on which they run. The mechanical properties of cellular motors can only be studied at the single molecule level, and for those that act in organised structures, notably muscle, study at this level avoids the complexity of interpreting the effect of large numbers of motors acting in parallel and asynchronously. This article concentrates primarily on the use of the "bead–actin–bead dumbbell" method (Finer *et al.*, 1994, Fig. 1) for studying actomyosin interactions, which necessitates the use of a dual-beam trap. This approach is particularly useful for nonprocessive actin-based motors, but many of the principles are equally applicable to processive actin and microtubule-based motors. Sheetz (1998) has edited a useful volume of articles on laser tweezers in biology.

II. MATERIALS AND INSTRUMENTATION

1. Optical table (~4 × 3 ft).
2. Research-quality inverted microscope with provision for epi-illumination, a xenon light source for bright-field imaging, and an objective >60× and ≥1.25 NA with good transmission properties at 1064 nm.
3. A high-quality piezo-controlled stage (e.g., Physik Instrumente P-528) and a piezo-controlled focussing device (e.g., Physik Instrumente P-723 or with superior capacitative position sensor P-725).
4. Nd : YAG laser ≥ 1 W.
5. Two 2-mm aperture electro-optic deflectors (EOD) (Leysop) with associated high-voltage amplifiers (Apex sells inexpensive high-voltage hybrid amplifiers).
6. Two CCD cameras and one intensified camera for fluorescence.
7. Dual-photodiode quadrant detector (QD) and associated electronics with a frequency response >10 kHz.
8. One computer with DAQ board for primary data acquisition and one with frame grabber for servo-controlled stage feedback. (A single computer might suffice for these two applications.) We use National Instruments DAQ boards and frame grabbers in association with Labview software.

III. OVERVIEW OF OPTICAL TWEEZERS

The standard single-beam gradient setup is capable of trapping small particles, e.g., 1-μm latex beads, of higher refractive index than the surrounding medium. The mode of operation has been explained in varying degrees of detail in many review articles, including the compilation by Sheetz (1998). Most modern microscopes use infinity-corrected optics and we will assume this to be the case in this article. To form a trap, a parallel beam must fill the back focal plane of the objective, i.e., be ~5 mm in diameter. Most of the common lasers used for trapping emit narrower beams than this, which necessitates the use of a beam-expanding telescope. This could be a proprietary item but in order to place all the optical components in their

Copyright 2006, Elsevier Science (USA).
All rights reserved.

correct positions, it is more convenient to use two separate lenses for this purpose (Figs. 2 and 4). Outside the beam-expanding telescope, it is the angle of the laser beam that controls the position of the trap, whereas within the beam-expanding telescope, i.e., between **L1** and **L2**, it is the lateral displacement of the beam. The mirror in Fig. 2 is in a plane that is conjugate to the back focal plane of the microscope so that the amount of light entering the objective is independent of the angle of the mirror. This mirror allows initial positioning of the trap at the beginning of the experiment. An electro-optic or acousto-optic deflector at or near this position allows rapid control of trap position.

IV. PRACTICAL DESIGN

An optical trap setup has to fulfill several other functions besides trapping. For actomyosin experiments, a bright-field image is required to visualise the beads for trapping and a video-rate fluorescence image is required for attaching the actin filaments to the beads, which necessitates an intensified CCD camera. The positions of the two beads of the dumbbell must be measured with a precision of ≤1 nm with a frequency of >10 kHz, which is achieved most readily by projecting a bright-field image of the beads onto two QDs. A xenon arc is a favourable light source for this purpose. If the position of the stage is to be servo controlled to overcome drift, a CCD camera with a field width of about 10 µm is also required. Figure 3 shows the various light paths.

An inverting microscope is generally preferred because it allows the majority of optical components to be close to the optical table and is generally more stable. Furthermore, beads floating in solution tend to fall towards the coverslip, the region useful for exploring myosin interactions. The trapping beam is introduced into the optical system via a dichroic mirror (**d1** in Figs. 3 and 4). The best location for this dichroic is

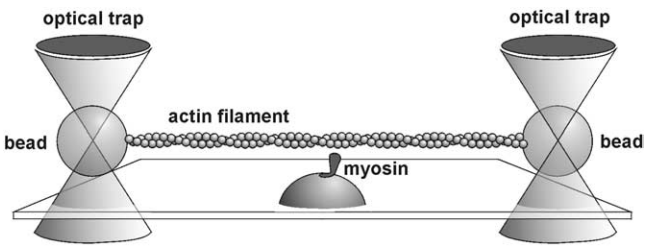

FIGURE 1 The dumbbell setup.

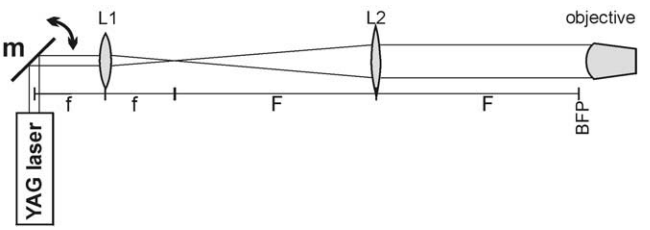

FIGURE 2 Basic optics of the trapping beam (**m** = **m3** in Fig. 3). Focal lengths are f and F and BFP is the back focal plane of the objective.

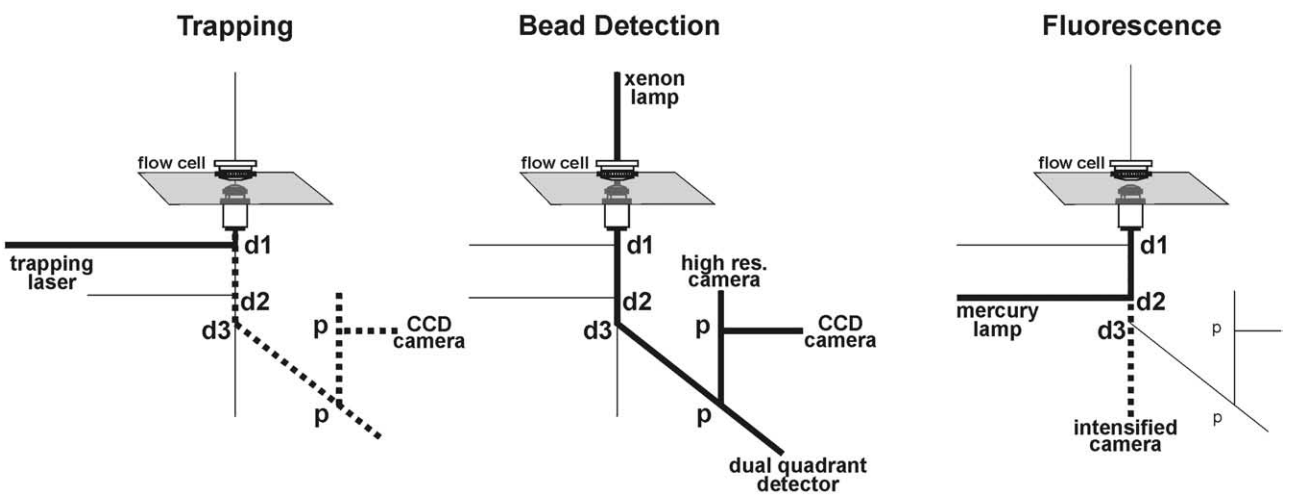

FIGURE 3 The main light paths. Dotted lines in the trapping panel correspond to the reflected light, which is useful for alignment and in the fluorescence panel to the emitted fluorescence. d are dichroic mirrors and p are beam splitting prisms.

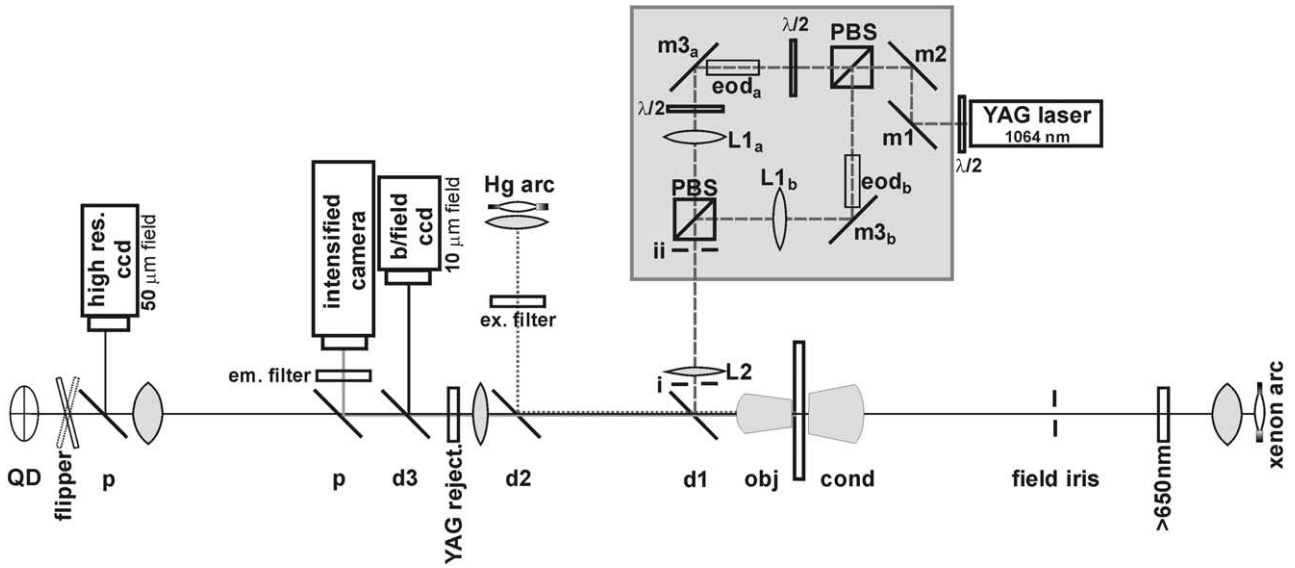

FIGURE 4 Diagram of the trap setup.

immediately below the objective (Lang *et al*., 2002), but can be combined with the fluorescence excitation beam or before the dichroic of the fluorescence cube. The dumbbell assay requires two traps that can be created either by temporal sharing of a single beam (Visscher *et al*., 1993) or by using polarising beam splitters. We will describe the simplest possible version of the latter approach (Fig. 4). The wavelength of Nd:YAG lasers (1064 nm) is suitably distant from the absorption of most biological materials, yet near enough to the visible spectrum for the performance of standard microscope objectives to be adequate. The first $\lambda/2$ waveplate controls the relative intensities of the two beams. Mirrors **m1** and **m2** control the position and angle of the laser beam. Mirrors **m3** are at a distance f away from lenses **L1** and are thus conjugate with the back focal plane of the objective. They allow positioning of the two traps at the beginning of the experiment to tension the dumbbell to the desired level. Because the angular deviation from the EODs is small, the entry of the beam into the back focal plane of the microscope is affected negligibly, provided that they are positioned close to the mirrors **m3**. Path **a** needs a $\lambda/2$ wave plate on both sides of the EOD to rotate the plane of polarisation by 90° and back again as the EODs have a preferred polarisation direction. The dichroic **d1** reflects wavelengths above 900 nm. The YAG rejection filter avoids reflected trapping laser light, contributing to the bright-field QD signal. The dichroic **d2** reflects below 550 nm for the exciting Hg lamp. Pellicle beam splitters **p** provide light for the low and high magnification bright-field cameras. The dichroic **d3** reflects light >555 nm to pick out the emitted fluorescence, which then passes through the emission filter. The light path of the trapping laser must be enclosed to avoid movement of the laser beam due to air currents in the room. This is done most easily by a combination of tubes and a box around the square of the beam splitting prisms (grey box in Fig. 4).

V. ALIGNMENT

On the first occasion, alignment of the two trapping beam can cause frustration, but the following protocol works even if the trap is being constructed from scratch rather than being based on a microscope. It is based on the principle of sending a HeNe or similar visible laser beam backwards through the microscope to define the optical axes of the various light paths. Laser safety glasses are required during the alignment procedure.

1. Check that the microscope stage is horizontal with a spirit level.
2. Establish a rough vertical optical axis by dropping a plumb line from the ceiling to the centre of the objective holder.
3. To refine the line of the beam, attach a tiltable mirror at the ceiling so that the HeNe beam can be reflected back to the objective. Place a mirror on the stage and adjust the position of the HeNe beam on the ceiling mirror and the angle of that mirror so that

the beam is hitting the centre of the objective and is being reflected back along itself.

4. Before extension of the optic axis to the trapping laser, remove lenses **L1** and **L2** and the EODs from their provisional positions. Replace the microscope objective with a ~4-mm aperture (readily made from an old objective) to let the reference beam through. This defines the back aperture of the objective.

5. Centre two apertures on the HeNe beam, as widely spaced as possible between the microscope and the recombining prism (positions i and ii in Fig. 4).

6. Switch on the trapping laser and make the two paths collinear with the HeNe laser beam. For path **a**, orientation of **m1** allows the trapping beam to be made coincident with the reference beam at **m2**, and the orientation of **m2** allows it to be made collinear with the reference beam. For path **b**, a small rotation of the first polarising beam splitter together with orientation of its prism table allows the trapping beam of path **b** to be made concident with the reference beam at **m3b**, and orientation of **m3b** allows the beams in path **b** to be made collinear. Any CCD cameras attached to microscope ports now show the beam in the centre and those not on microscope ports should be centred at this time. The focus of the cameras should be adjusted to correspond to that of the microscope eyepiece.

7. Replace the objective aperture with the objective, place a dry flow cell (construction described later) on the stage and focus on the inner surface of the cover slip. The alignment should be adequate to see the reflected laser beam with a low-magnification, infrared-sensitive CCD camera. Fine-tune the alignment of the trapping beams to make the diffraction pattern around the reflected image symmetrical.

8. Lens **L2** can now be inserted at its focal length F (~300 mm) from the back focal plane of the objective and positioned laterally so that the reversed beam still impinges on the trapping laser and the reflected image remains symmetrical. Note that **L2** focusses the trapping beam at the back focal place of the objective. The laser beam should be turned down to minimum intensity to avoid damage.

9. Insert the two lenses **L1** at a distance (f + F) further back from **L2** so that **L1** and **L2** form beam-expanding telescopes (Fig. 2). Adjust their lateral position so that the reflected image is again symmetrical. If the objective is replaced by the aperture, the parallel beam should hit the ceiling mirror at the same point as the HeNe laser.

10. The apparatus should now be able to trap 1-μm beads. A small adjustment of axial position of lenses **L1** can be used to fine control the z position of each trap.

11. Adjust the orientation of the mirrors **m3** to position the two traps for the dumbbell experiment ~6 μm apart.

12. Position the electro-optic deflectors (EOD) as near as possible to the mirrors **m3**. EODs are convenient because, in the absence of an applied voltage, the beam is not deflected. If an AOD is used rather than an EOD, typically the angle of the beam will change at this point, which will need some realignment. Some AODs are more convenient in that they have the far face cut so that refraction compensates for the diffraction and at the centre frequency the first-order beam remains parallel to the input beam.

13. The relative intensities of the two beams can be monitored using an adequately large (~1 cm) photodiode mounted above the field stop of the condenser and equalised by rotation of the $\lambda/2$ plate positioned prior to the first beam splitter. The stiffness of the two traps should now be roughly equal.

14. Equalise the height at which the two beads are trapped by final positioning of the lenses **L1**. Move the lenses **L1** closer to the microscope to move the trapped bead further from the surface of the coverslip.

VI. CALIBRATION

1. Transimpedance amplifiers are used to convert the currents from the individual quadrants of the photodetector to voltages. A signal that is almost linearly proportional to, for example, the horizontal bead displacement for movements up to about one-third of a bead diameter is gained by summing the two left-hand and the two right-hand quadrants and taking the difference signal between these values. This signal needs to be converted from volts into bead movement in nanometers. First, it is necessary to convert volts to micrometers movement of the bead image at the quadrant detector by moving the QD to a series of positions with a micrometer-driven slide. Magnification of the microscope from the stage to the quadrant detector then allows conversion of QD volts to bead movement in nanometers. As an accurate calibration using the micrometer is time-consuming, we apply a 2-Hz square wave to a stepper motor to rotate a thin (~0.5 mm) microscope slide ± 7.5° so as to give a constant lateral displacement of the bead image (see Fig. 5), which can be measured.

2. A variety of methods have been described for measuring the trapping strength, but probably the most robust one for routine use is to apply a square wave to the traps. The bead position record is then averaged over a sufficient number of cycles to give a

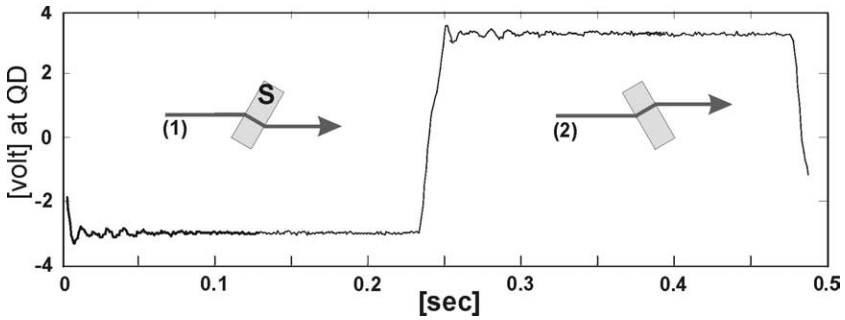

FIGURE 5 Calibration using the "flipper" to provide known lateral movement of the bead image.

smooth trace and a rate λ fitted to the exponential decay. The trap stiffness is then $6\pi r\eta\lambda$ (r being the radius of bead and η the viscosity). It should be noted that η is quite temperature dependent and also that the bulk value is only applicable if the trapped bead is a few bead diameters away from the coverslip. Other methods of measuring trap stiffness have been described by Svoboda and Block (1994).

VII. THE DUMBBELL EXPERIMENT

A. Assembling the Dumbbell

Preparation of the components is described in Section X. The first step is to trap two beads: if one can be found that has already stuck near to the end of a 5- to 8-mm-long actin filament, so much the better. In the absence of such good fortune, the piezo stage is moved in order to catch a suitable filament near its end. The spacing of the beads is then adjusted to match the filament prior to attaching the loose end by aligning the actin filament using movement of the stage to induce flow past the stationary beads. If the beads and actin filaments have been prepared properly, attachment to the second bead should occur almost instantly because of the constraining influence of the flow. It soon becomes apparent that the correct concentration of beads and actin filaments is critical for successful assembly and use of dumbbells. If there is an inadequate supply of either, too much time is spent searching for beads or actin, if the concentration of one of these is too high, the perfect dumbbell is liable to be spoilt by the capture of extra beads or actin filaments. Due to the effect of radiation pressure, beads enter the trap from the objective side (beads about to be caught look blacker than in their trapped position), which has the fortunate repercussion that the required beads are normally caught ~10 µm deep, whereas in the operating position, 1.5 µm above the surface of the coverslip, uninvited beads rarely enter the trap. However, actin filaments can float past and become attached. The traps naturally accumulate all forms of small particles that can seriously increase the noise when measuring bead position. All solutions should be filtered and/or centrifuged prior to use.

B. Tensioning the Dumbbell

The success of an experiment is dependent upon the movement of the actin filament being transmitted to the trapped beads, which requires that the compliance between the segment of actin interacting with the myosin and the bead be low compared to that of the myosin head. The compliance of actin itself is low, and the limiting feature is the link between the actin and the bead. The compliance of this link is very nonlinear, and to achieve the required value (>1 pN/nm), a significant pretension (>5 pN) is necessary. One way of doing this is to align the quadrant detectors, apply a triangular wave to one of the traps, and monitor whether the other bead faithfully follows the first. If not, the dumbbell tension is increased using one of the mirrors **m3**. One problem is that for a weak trap (0.02 pN/nm) and a 1-µm bead this is quite close to the maximum force. Moreover, the stiffness along the beam (z) axis is several times weaker than the x,y stiffness and is reduced further when the bead is at the edge of the trap. The overall result is that the beads become rather unstable, particularly in the z direction, and the quality of the results is degraded. The application of positive feedback, outlined later, significantly helps limit this problem.

A myosin, suitably positioned near the top of a fixed 1.5-µm glass bead, now needs to be found to allow interaction with the actin. The initial search can be done with a mouse-driven stage but it is very convenient to be able to move the actin ±300 nm along the y

axis (regarding the axis of the actin filament as x) using a potentiometer so that the filament can be placed exactly above the myosin to get the maximum rate of interaction. At realistic values of dumbbell tension, thermal motion results in the standard deviation of the position of the middle of the actin filament being about 40 nm, so the actin needs to be positioned in the y and z axes to within ~20 nm of its optimal position. At this point it is desirable to servo control the position of the stage relative to the traps so that the rate of interaction becomes reasonably constant. Typically 100 second data files are recorded (normally at 10 kHz with a 5-kHz antialias filter).

VIII. IMPROVEMENT OF PERFORMANCE

A. Positive Feedback of Bead Position to Trap Position

For a simple trap the maximum force provided by a trap is directly related to its stiffness, with the width of the energy well being controlled by the size of the trapped bead and of the diffraction limited spot. It is advantageous to carry out actomyosin experiments with traps that are considerably more compliant than the myosin head to provide a good contrast in the variance of bead position between periods of actin attachment and detachment, which limits the extent that the dumbbell can be pretensioned to a somewhat suboptimal level. One way to get around this problem is to feedback a fraction α of the bead position to the trap position ($X_t = \alpha X_b$) (Steffen *et al.*, 2001). Such positive feedback broadens the energy well and reduces the stiffness by a factor of α, which allows the intensity of the trapping beam to be increased by this factor to restore the stiffness to its original value. Both the maximum force and the stiffness in the y and, more importantly, the z directions are increased due to this increase in beam intensity. This procedure works well for modest values of α (~2), but considerable care needs to be taken if larger values are used because noise other than that arising from the thermal motion of the bead is also amplified.

B. Stage Feedback

The stability of optical microscopes is comparable to the resolution, i.e., slightly submicrometer. The monomer periodicity of actin is 5.5 nm and this will not be resolved unless the stability of the position of the stage with respect to the objective is around the 1-nm level during the period of data collection. This is only possible by servo-controlling the stage position. We have used a combination of piezo-positioned stage and objective, but piezo stages, which have adequate movement in the z as well as the x,y directions, are now available (e.g., Physik Instrumente: P-562.3CD) and are probably the most convenient solution. It is advantageous to bolt the objective directly below the stage so as to minimise thermal drift. Positioning in all three directions can be controlled on the basis of video images, but the noise level is probably slightly lower if an image of the fixed, myosin-bearing bead is projected onto a third quadrant detector to control the x,y position. For most applications, speed of the feedback loop is not the issue. A simple Labview program is available for download from traps.rai.kcl.ac.uk.

IX. ANALYSIS OF DATA

The activity of nonprocessive motors is usually detected on the basis of the reduction of variance of bead position during periods of attachment (Molloy *et al.*, 1995). If both the compliance of at least one of the actin bead links and of the myosin is more than five times the combined stiffness of the traps, at least the longer events will be readily visible on an oscilloscope trace. In these circumstances, detection of events on the basis of reduction of the variance of the bead position is relatively straightforward. We use a program developed by Smith *et al.* (2001), which carries out a maximum-likelihood analysis of the whole trace and assigns the rates of attachment, f, and detachment, g, as well as the periods of attachment. By comparison of the covariance and autovariance of the bead positions during periods of attachment and detachment, the program also deduces the compliance of the two actin bead links and of the myosin link and corrects the observed working stroke for the effect of these compliances. The core Fortran program and a Matlab program that calls them and analyses batches of files and plots out the most useful aspects of the analysis is available from traps.rai.kcl.ac.uk.

Two parts of the standard output are shown in Fig. 6 (obtained from separate experiments). Figure 6a shows a histogram of the positions of interactions for a dumbbell that is kept stationary with respect to the myosin for the duration of the 100-s record. In general, it is necessary to servo control the stage position to be able to associate each interaction as being with a specific actin monomer. Patlak (1993) proposed a method of analysis of ion channel data based on mean-variance histograms and he has adapted the method for acto-

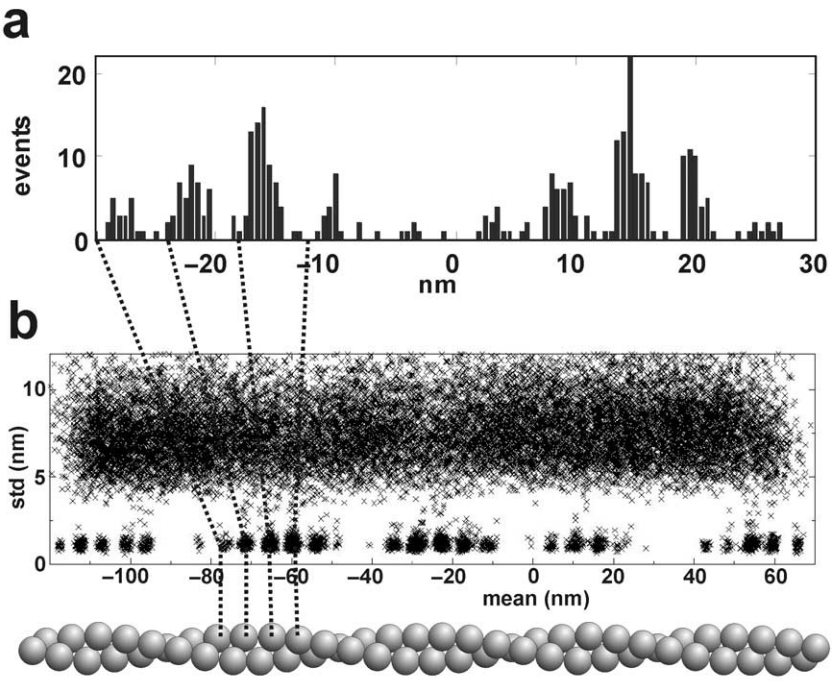

FIGURE 6 (a) Histogram of the position of interactions with a stationary dumbbell and a relatively weak trap so that two target zones are accessed. The myosin is halfway between the two target zones. (b) A plot of the standard deviation versus the mean position of 5-ms time slices of a data record in which the dumbbell is moved past five target zones during the 100 s of data collection.

myosin data (Guilford *et al.*, 1997). We have not used the method for final analysis of data but find that plotting the standard deviation against the mean for time slices of bead position data provides a very valuable initial check on data quality. Such a plot is shown in Fig. 6b. In this record the dumbbell has been moved past five target zones of the actin filament (a target zone is a region in which monomers are suitably oriented to interact with actin). The plot readily identifies both the target zones and the underlying actin monomers. Such plots reveal inhomogeneities among target zoned and monomers. Analysis methods have been reviewed by Knight *et al.* (2001).

X. PROCEDURES

A. Preparation of Latex Beads

The preparation of neutravidin-coated latex beads is a straightforward procedure and, in our hands, appears to be superior to commercial products. By first generating latex beads covalently cross-linked to biotin, one can generate a stock of beads that can be stored for many months. Once coated with neutravidin the beads are used for a period of 2–3 weeks.

Buffer, Solutions, and Materials

Carboxylated latex beads (Sigma, L3905, 1 µm in diameter, 2.5% solids)
Eppendorf reaction vials, screw top
1-Ethyl-3-(3-dimethylaminopropyl)carbodiimide (EDAC) (Sigma, E1769)
50 m*M* phosphate buffer, pH 7.0
2 mg/ml biotin-x-cadaverine (Molecular Probe, A1594) in dimethyl sulfoxide, aliquots stored at –80°C
10% NaN_3
1 *M* glycine
5 mg/ml neutravidin (Molecular Probe, A-2666, aliquots stored at –80°C)

Biotinylated Latex Beads

1. Centrifuge 250-µl latex beads in a 1.5-ml Eppendorf reaction vial at 6000 *g* preferably in a swing-out rotor (e.g., Sorvall RSA) for 10 min.
2. Aspirate supernatant without disturbing the pellet.
3. Resuspend beads in 500 µl of 50 m*M* phosphate buffer, pH 7.0, place in sonicating bath for 10 seconds, and centrifuge as in step 1.
4. Repeat washing step.
5. Resuspend beads in 250 µl of phosphate buffer, pH 7.0.

6. Add 25 µl of 2 mg/ml biotin-x-cadaverine and vortex.
7. Add ~2 mg of EDAC cross-linker, mix, and incubate at room temperature for 30 min.
8. Add 500 µl of phosphate buffer and centrifuge as in step 1.
9. For the washing step, resuspend beads in 500 µl phosphate buffer, sonicate in a bath for 10 s, and centrifuge as in step 1.
10. Repeat washing step at least five-times.
11. After final wash, resuspend beads in 500 µl phosphate buffer containing 0.02% NaN_3 and store in a refrigerator.

Neutravidin – Biotin Latex Beads

1. Resuspend 25 µl of biotinylated 1-µm latex beads (see earlier discussion) in 175 µl phosphate buffer.
2. Centrifuge at 6000 *g* for 10 min.
3. Aspirate supernatant.
4. Resuspend beads in 100 µl of phosphate buffer containing 0.1 *M* glycine.
5. Add 15 µl of 5 mg/ml neutravidin and incubate at room temperature for 20 min (mix intermittently).
6. Add 100 µl phosphate buffer and centrifuge as in step 2.
7. For the washing step, resuspend beads in 500 ml phosphate buffer, sonicate in a bath for 10 s, and centrifuge as in step 2.
8. Repeat washing step at least five-times.
9. After final wash, resuspend beads in 200 ml phosphate buffer containing 0.02% NaN_3 and store in a refrigerator.
10. Test beads in a binding assay (fluorescence microscopy) by mixing beads with 1–4 µg/ml biotinylated F-actin at a ratio of 1:50.

B. Preparation of Biotin-Tetramethyl Rhodamine-Actin

F-actin (~50 µ*M*) is modified with a 0.5–1 molar ratio of biotin–$PEAC_5$–maleimide (Dojindo) in a buffer consisting of 10 m*M* $NaHCO_3$, basically as described by Ishijima *et al*. (1998). It is taken through two depolymerisation cycles before adding 2 mg/ml trehalose and flash freezing 10-µl aliquots. An aliquot is polymerised with a small molar excess of tetramethyl rhodamine phalloidin overnight. The next morning, excess dye and any monomeric actin are removed by spinning through 200 µl of 10% sucrose (29,000 *g*, 30 min: 30,000 rpm in Beckman TLA 100.1 rotor) to remove monomeric actin, and the filamentous actin is resuspended with 0.1 mole rhodamine phalloidin per mole of actin.

C. Preparation of Fixed-Bead Microscope Slides (Flow Cell)

To allow myosin to access the actin of the dumbbell, it must be raised above the surface of the cover slip. This is achieved most simply by applying a suspension of 1.5-µm glass beads in a nitrocellulose solution to the coverslip surface.

Steps

1. Apply 2 µl of glass microspheres (1.5 µm) suspended in 0.05% nitrocellulose in amyl acetate to coverslips (#1.5: 22 × 22 mm). Spread the suspension evenly using the edge of a second coverslip mounted on a cocktail stick. Allow to dry.
2. On a microscope slide lay down two thin strips of vaseline (spacing ~8 mm) using a syringe (~22-gauge needle).
3. Place nitrocellulose-coated coverslips on top of the slide and press down lightly to produce a gap of about 30 µm. (Thick aluminium foil can be used as a spacer.)
4. Secure the four corners of the coverslip with Superglue.

D. Sample Preparation

Buffers and Solutions

Deoxygenation system (Harada *et al*., 1990):
1 mg/ml catalase (Sigma, C-100) and
5 mg/ml glucose oxidase (Sigma, G7141)
1 m*M* phalloidin (Sigma, P2141) in methanol, store at –20°C
100 m*M* Na-ATP
Buffer A: 25 m*M* K–HEPES, pH 7.6, 25 m*M* KCl, 4 m*M* $MgCl_2$, 0.02% NaN_3
Reaction mix (RM) freshly prepared before every experiment: 1 ml buffer A, 20 µl of 5 mg/ml glucose oxidase, 20 µl of 1 mg/ml catalase, 20 µl of 100 mg/ml glucose, 1 µl β-mercaptoethanol (BME), 0.5 µl of 1 µ*M* phalloidin, and 1 µ*M* ATP or other nucleotides at concentration of choice
Blocking solution: 1 ml buffer A and 20 µl of 50 mg/ml bovine serum albumin
Buffer B (make fresh every day):
1 ml buffer A,
1 µl of 1 m*M* phalloidin, and
2 µl BME
Actin freshly diluted 1:200 in buffer B
10× actin polymerisation buffer: 50 m*M* phosphate, pH 7.5, 500 m*M* K–acetate, 20 m*M* Mg-acetate, and 20 m*M* NaN_3

Procedure

1. Add 1–5 µg/ml of myosin in buffer B to flow cells and incubate for 1 min.
2. Wash out excess myosin with 30 µl of buffer B followed by 30 µl of blocking solution. Incubate with blocking solution for 1 min.
3. Wash with 30 ml of buffer B.
4. Apply 30 µl of final reaction mix containing 1-µl neutravidin-coated latex beads, 1–2 n*M* biotinylated actin, and the chosen concentration of ATP. If the ATP concentration is less than 10 µ*M*, addition of a regenerating system (1 m*M* phosphocreatine, 20 µg/ml creatine phosphokinase) is advisable.

References

Finer, J. T., Simmons, R. M., and Spudich, J. A. (1994). Single myosin molecule mechanics: Piconewton forces and nanometre steps. *Nature* **368**, 113–119.

Guilford, W. H., Dupuis, D. E., Kennedy, G., Wu, J., Patlak, J. B., and Warshaw, D. M. (1997). Smooth muscle and skeletal muscle myosins produce similar unitary forces and displacements in the laser trap. *Biophys. J.* **72**, 1006–1021.

Harada, Y., Sakurada, K., Aoki, T., Thomas, D. D., and Yanagida, T. (1990). Mechanochemical coupling in actomyosin energy transduction studied by *in vitro* movement assay. *J. Mol. Biol.* **216**, 49–68.

Ishijima, A., Kojima, H., Funatsu, T., Tokunaga, M., Higuchi, H., Tanaka, H., and Yanagida, T. (1998). Simultaneous observation of individual ATPase and mechanical events by a single myosin molecule during interaction with actin. *Cell* **92**, 161–171.

Knight, A. E., Veigel, C., Chambers, C., and Molloy, J. E. (2001). Analysis of single-molecule mechanical recordings: Application to actomyosin interactions. *Prog. Biophys. Mol. Biol.* **77**, 45–72.

Lang, M. J., Asbury, C. L., Shaevitz, J. W., and Block, S. M. (2002). An automated two-dimensional optical force clamp for single molecule studies. *Biophys. J.* **83**, 491–501.

Molloy, J. E., Burns, J. E., Kendrick-Jones, J., Tregear, R. T., and White, D. C. (1995). Movement and force produced by a single myosin head. *Nature* **378**, 209–212.

Patlak, J. B. (1993). Measuring kinetics of complex single ion channel data using mean-variance histograms. *Biophys. J.* **65**, 29–42.

Sheetz, M. P. (1998). Laser tweezers in cell biology: Introduction. *Methods Cell Biol.* **55**, xi–xii.

Smith, D. A., Steffen, W., Simmons, R. M., and Sleep, J. (2001). Hidden-Markov methods for the analysis of single-molecule actomyosin displacement data: The variance-Hidden-Markov method. *Biophys. J.* **81**, 2795–2816.

Steffen, W., Smith, D., Simmons, R., and Sleep, J. (2001). Mapping the actin filament with myosin. *Proc. Natl. Acad. Sci. USA* **98**, 14949–14954.

Svoboda, K., and Block, S. M. (1994). Biological applications of optical forces. *Annu. Rev. Biophys. Biomol. Struct.* **23**, 247–285.

Visscher, K., Brakenhoff, G. J., and Krol, J. J. (1993). Micromanipulation by "multiple" optical traps created by a single fast scanning trap integrated with the bilateral confocal scanning laser microscope. *Cytometry* **14**, 105–114.

SECTION

2

Digital Video Microscopy

CHAPTER

5

An Introduction to Electronic Image Acquisition during Light Microscopic Observation of Biological Specimens

Jennifer C. Waters

I. INTRODUCTION

This article introduces the reader to the choices and considerations that need to be made when designing an image acquisition system. It focuses on the use of electronic cameras to record images of biological specimens generated with light microscopy techniques. There is no one image acquisition system that will work for every light microscopy application. To make the best choices for your application, you should understand your needs, as well as the strengths and limitations of the equipment available.

II. UNDERSTANDING YOUR NEEDS

The ideal image acquisition system would be sensitive enough to acquire beautiful images of very dim fluorescence specimens, fast enough to record the most dynamic processes, have high resolution to capture the finest detail, and have enough useful dynamic range to accurately measure minute differences in intensity. However, optimizing any one of these criteria can only be accomplished by limiting one or more of the others (Shotton, 1993; Spring, 2000). It is therefore impossible to design one image acquisition system that will be ideal for the wide range of light microscopy applications in cell biology. Instead, one should determine how best to meet the needs of the majority of system users, with an understanding that some compromises will probably need to be made.

To begin, it is useful to recognize the demands that the mode of microscopy used to generate the images imposes on the image acquisition system. In their research, cell biologists most commonly use fluorescence microscopy and various forms of transmitted light microscopy. Fluorescence microscopy techniques include standard wide-field epifluorescence (i.e., where the fluorescence excitation light reaches the specimen through the same objective lens that is used to image the fluorescence emission) (Herman, 1998), laser-scanning confocal (Inoué, 1995), and Nipkow spinning disk confocal (see article by Waterman-Storer and Gupton; Maddox, 2003). Laser-scanning confocal systems use photomultiplier tubes, not electronic cameras, to collect photons sequentially from the pixels that are used to generate images. Transmitted light techniques include standard bright-field microscopy (Murphy, 2001) and contrast generation methods such as phase contrast and differential interference contrast (DIC, Nomarski) (Inoué and Spring, 1997; Murphy, 2001).

A. Fluorescence Microscopy

In fluorescence microscopy, cellular components are labeled with molecules that emit photons when illuminated with excitatory light of the appropriate wavelength (Berland, 2001; Herman, 1998). Its high level of molecular specificity and relative ease of use have made fluorescence microscopy the most commonly used mode of light microscopy in cell biology research today. The use of fluorescence microscopy to visualize the dynamics of specific molecules in live cells over

Copyright 2006, Elsevier Science (USA).
All rights reserved.

time has increased greatly since the discovery and cloning of green fluorescent protein (GFP) (Tsien, 1998).

Acquiring fluorescence images presents a special challenge because of the relatively low number of photons emitted by the specimen that must be collected by the microscope optics and detected by the camera (Herman, 1998; Spring, 2001). The number of photons emitted by the specimen is limited by the concentration of fluorophore and the efficiency with which the fluorophore emits photons when exposed to excitation wavelengths of light. Fluorescence image acquisition is further complicated by the gradual decrease in fluorescence known as photobleaching. When fluorophores are exposed to excitation photons, they can and do undergo chemical modifications that irreversibly inhibit further emission of light (Herman, 1998). Therefore, when choosing microscope optics and a camera for a fluorescence microscopy image acquisition system, attention should be paid to light efficiency: achieving the highest image quality with the smallest number of excitation photons (Salmon and Waters, 1996). Light efficiency is particularly critical when the acquisition system will be used for imaging fluorescence in live cells over time, where the rate of photobleaching imposes limits on the length of an experiment, and where overexposure to excitation light can also induce phototoxicity in the illuminated cells.

B. Bright-Field-Transmitted Light Microscopy

There are several different types of transmitted light microscopy that are routinely used by cell biologists (Murphy, 2001). Most of the thin specimens that cell biologists examine with transmitted light microscopy absorb very little light and are therefore essentially transparent. Standard bright-field microscopy is consequently used primarily in conjunction with histology stains that bind with some specificity to cellular components and absorb particular wavelengths of light. When illuminated with white light, these stains result in a bright high-contrast color image. A camera capable of recording color images (Spring, 2000) is usually preferred when working with such histology-stained slides in bright-field mode.

Even though thin biological specimens usually absorb little light, they do cause changes in the optical path of the light rays that pass through them because of refractive index changes; these changes, however, are invisible to our eyes and to electronic cameras. A variety of optical contrast generation methods use additional components in the transmitted light path that translate changes in refractive index into contrast that our eyes and electronic cameras can detect (Murphy, 2001; Inoué and Spring, 1997). The contrast generation methods used most commonly by cell biologists are phase contrast and differential interference contrast. These methods have the benefit of generating contrast in transparent specimens in a noninvasive manner that allows them to be used with living cells and tissues without the need for chemical treatments or the application of stains.

The light efficiency of the image acquisition system that is of such concern to the fluorescence microscopist matters less for the various transmitted light-imaging techniques, which are usually not photon limited. In transmitted bright-field microscopy, briefly increasing the intensity of illumination light will increase the brightness of the image without inducing specimen damage, allowing the user to meet the requirements of a less sensitive and less expensive camera, although it should be noted that prolonged exposure to intense light below 500 nm in wavelength (i.e., blue and ultraviolet) is phototoxic to cells. Cameras optimized for fast acquisition can be used to record transmitted light images of dynamic processes, such as cell motility, or changes in cell or organelle morphology with the high temporal resolution (Shotton, 1993; see article by Weiss).

III. THE IMAGE ACQUISITION SYSTEM

An image acquisition system minimally consists of a microscope and a camera, but may also include a computer, imaging software, and a variety of motorized components for automated acquisition (Salmon and Waters, 1996). Selection of the appropriate equipment for your application requires a basic knowledge of the parameters used to evaluate the equipment and how they affect performance.

A. Electronic Cameras

There are many different electronic cameras available for acquiring images from light microscopes. The basics of choosing the appropriate camera for your application will be introduced here, while subsequent articles will discuss the details of video-enhanced light microscopy (see article by Weiss) and cooled charge-coupled device (CCD) camera technology.

1. Analog Video Cameras versus Digital CCD Cameras

The majority of video and digital cameras produced today use a charge-coupled device, comprising a two-

dimensional array of on-chip single pixel photodiodes to sense incident photons (Spring, 2000; Hiraoka *et al*., 1987). However, video and digital cameras differ in their final signal output; a video camera has an analog output corresponding to one of the video standards (PAL, SECAM, or NTSC) while a digital camera has digital output. The analog signal from a video camera can be viewed in real time on a conventional video monitor and is usually recorded onto analog videotape, which is a very inexpensive medium. A CCD camera is referred to as a digital camera when the analog signal is digitized prior to output from the camera or camera controller. In a 12-bit camera, for example, the analog signal is converted into gray scale values ranging from 0 (equivalent to black) to 4095 (equivalent to white), giving a total of 2^{12} gray levels. The digital image information can be recorded on digital videotape in DV format or can be output to a computer RAM or hard drive and archived onto other digital media, such as the hard drives of network servers, CD-ROMs, and DVDs.

Digital imaging has now become the norm in many research laboratories. Digital images can be viewed and inspected immediately, processed and analyzed using specialized software packages, and inserted easily into digital documents or shared via the Internet. Significant advances in camera technology, software capabilities, computer speed, and storage capacity have made digital imaging favorable and affordable for a wide range of light microscopy applications (Spring, 2001; Salmon and Waters, 1996; Mason, 1999).

2. *Video-Enhanced Microscopy*

Analog video microscopy has some unique advantages over digital imaging that make it preferable for select applications, particularly video-enhanced contrast microscopy where electronic adjustment of the contrast and background "black level" are required during real-time recording (Inoué and Spring, 1997; Murphy, 2001; Shotton, 1993; see article by Weiss). Video cameras are also useful and economical for bright-field applications that require continuous monitoring over long periods of time, without worrying about the memory limitations of computer RAM and hard disk space. Video cameras have high temporal resolution, with their images being recorded onto videotape at 25 frames per second (PAL and SECAM) or 30 frames per second (NTSC). Alternatively, time-lapse VCRs can be used to slow the rate at which the video signal is sampled and recorded. However, videotape fails to capture the full resolution of the video signal. Full resolution digital images can be recorded directly from a video camera to disk using a specialized frame-grabber board containing an analog-to-digital converter installed in a computer (Inoué and Spring, 1997; Shotton, 1993).

Video cameras are commonly used to record movement and changes in specimen shape, including processes such as cell motility, chromosome movement during mitosis, cytokinesis, early embryonic development, chemotaxis, and wound healing. In the early 1980s, Shinya Inoué, Robert Allen, and others demonstrated that using video camera controls to manipulate the analog signal electronically can increase the dynamic range and contrast of very low contrast images that would otherwise be invisible to the eye (Inoué and Spring, 1997). Digital image processors can be used in conjunction with video camera controls to reduce noise and further improve image contrast by real-time digital subtraction of a background image. For example, high-resolution video-enhanced DIC microscopy can be used to image the dynamics of individual microtubules in real time: individual microtubules, which at a diameter of 25 nm are about 10 times below the resolution limit of the light microscope, can be visualized clearly (Inoué and Spring, 1997; see article by Weiss).

3. *Digital-Cooled CCD Cameras*

Slow scan-cooled CCD cameras record full size images at a slower rate (1–10 frames per second) than video cameras, but have superior light sensitivity, low noise, large dynamic range, linear response, and high spatial resolution (Spring, 2000; Inoué and Spring, 1997; Murphy, 2001). These properties make cooled CCDs the detector of choice for acquisition of fluorescence microscopy images (Spring, 2001; Hiraoka *et al*., 1987) and are used routinely to collect images of fixed specimens labeled with fluorescent antibodies and dyes. Cooled CCDs are also used to record the dynamics of live fluorescent cells, including cells loaded with calcium indicators (Mason, 1999) and cells expressing GFP-tagged proteins (Tsien, 1998), and to collect images from Nipkow spinning disk confocals. The Yokogawa CSU-10 dual Nipkow spinning disk confocal (Maddox *et al*., 2003; Mason, 1999) can be used to collect high-resolution confocal images of weakly fluorescent specimens with greater speed and signal to noise than traditional laser-scanning confocals. This is probably due in part to the use of a low noise-cooled CCD as a detector instead of the photomultiplier tube used by laser-scanning confocals. There are many different cooled CCD cameras available that can be used for these types of fluorescence applications, with a wide range in price and performance. Comparison shopping for a cooled CCD camera requires a basic

understanding of the properties used to describe performance (Spring, 2000).

Quantum efficiency is a measure of the percentage of incident photons that are recorded by a CCD camera (Spring, 2000; Inoué and Spring, 1997; Murphy, 2001). The higher the quantum efficiency, the more sensitive the camera will be to photons emitted from the specimen, which translates into shorter exposure times and better temporal resolution. Quantum efficiency of a CCD chip varies with the wavelength of light. Back-thinned CCD chips can have a maximum quantum efficiency as high as 90%, but are relatively delicate and expensive detectors. The more commonly used CCD chips have a maximum quantum efficiency in the range of 50–70%. The camera manufacturers provide graphs of the quantum efficiency of the CCD chips used in their camera at different wavelengths of light. For very low-light applications, image intensifiers can be used in conjunction with the CCD chip to increase the intensity of the signal (Inoué and Spring, 1997), while limiting spatial resolution and dynamic range. Dynamic range is a measure of the range of intensities that can be detected by the CCD chip and is defined by the full well capacity of a single pixel on-chip photodiode divided by the mean camera pixel noise (Spring, 2000; Inoué and Spring, 1997; Murphy, 2001). A new class of back-thinned CCD chip, called an electron multiplying charge-coupled device (EMCCD), which has built-in amplification of the signal from each pixel before readout, gives a sensitivity that exceeds even that of avalanche photodiodes, while retaining the benefits of fast CCD array readout, and promises to bring additional benefits to low-light imaging applications.

All CCD cameras contribute some amount of noise to the images they create (Inoué and Spring, 1997; Spring, 2000). Excessive noise can drown out the signal coming from a specimen, effectively decreasing the sensitivity and dynamic range of the camera. For fluorescence microscopy, in which the level of signal is inherently low, it is important to choose a camera that has been designed to minimize noise. The two main types of CCD camera noise are thermal noise and readout noise (Spring, 2000). Thermal noise (also known as dark noise) is reduced greatly by cooling the CCD chip below ambient temperature, making cooled CCD cameras optimal for fluorescence applications. Readout noise is generated as the signal is read from the CCD chip and is proportional to the readout speed: the faster the CCD chip is read, the greater the probability of error in the A-to-D converter and thus the higher the readout noise. Slow scan-cooled CCD cameras are preferable for low-light level fluorescence microscopy applications (Spring, 2001), as long as the speed of acquisition can be sacrificed.

The spatial resolution of a CCD camera is determined by the size of the photon-sensitive photodiodes that make up the CCD chip relative to the optical magnification of the microscopic image focused upon it (Shotton, 1993, 1997; Inoué and Spring, 1997; Spring, 2000). Cooled CCD cameras usually have at least 1024^2 light-sensing photodiodes (i.e., pixels), which range in size on CCDs from different manufacturers from $5 \times 5\,\mu m$ to $25 \times 25\,\mu m$ each. (The pixels on some CCDs, particularly those on three-color CCD chips, are oblong rather than square, but these should be avoided for scientific imaging applications because of the potential problems caused in subsequent image processing.) The optical resolution of the microscope will be adequately preserved by the camera only if each resolvable point in the magnified image is sampled by at least two photodiodes (the Nyquist criterion) (Shotton, 1993; Inoué and Spring, 1997; Shotton, 1997; Stelzer, 1998). For example, the Abbe diffraction resolution limit (Inoué, 1995; Inoué and Spring, 1997) of an objective lens with a numerical aperture of 1.4 at 510 nm (the peak emission wavelength of GFP) is 0.22 µm. With 60× magnification by the objective lens and no secondary magnification between this lens and the CCD camera, this would be projected to 13.2 µm at the CCD chip. Therefore, a photodiode size of 6.5 µm or smaller would be necessary to match the resolution of the objective lens and prevent loss of specimen detail by digital undersampling of the optical image.

For live cell fluorescence applications, in which greater temporal resolution is needed, some cooled CCD cameras allow the user to increase the acquisition rate by binning adjacent photodiodes together and/or reading only a subarray of the chip (Inoué and Spring, 1997; Shotton, 1997; Spring, 2000; Salmon and Waters, 1996). Binning photodiodes 2×2, for example, results in a fourfold increase in image intensity, allowing for shorter exposure times. Binning also decreases the number of pixels in the output image, using less computer memory and allowing for faster image transfer. The increase in image intensity and acquisition times does come at a price: such 2×2 binning of adjacent pixels results in a twofold loss in spatial resolution. For many fluorescence applications, however, where the critical parameter is usually the ability to detect faint fluorescent objects rather than to resolve them spatially, the increase in image intensity and speed of acquisition are well worth the decrease in spatial resolution (Salmon and Waters, 1996). Some cameras allow the user to increase the image transfer time by reading only a subarray, or region-of-interest, of the full CCD chip. When the interesting area of the specimen does not fill the entire camera field of view, this

is an easy way to increase image acquisition speed and decrease the image file size.

4. Color Cameras

Because CCD chips cannot differentiate between different wavelengths of light, color CCD cameras must use wavelength selection components within the camera itself to produce red, green, and blue images of the specimen from subarrays of pixels, which are then combined into the resulting color image (Spring, 2000). Color CCD cameras are significantly less sensitive and have lower spatial resolution than monochromatic cameras because of the additional filters and beam splitters used for wavelength selection and because of the division of the pixels to image the three primary colors. Color CCD cameras are useful for recording bright-field colored specimens and may be necessary for fluorescence imaging in the rare case that the color of light emitted by the fluorophore is diagnostic. However, for the majority of fluorescence microscopists, the best solution is a monochromatic CCD camera used in conjunction with appropriate wavelength-specific filters within the microscope and with image processing software to pseudo-color and merge the wavelength-specific monochrome images subsequent to acquisition.

B. Computers and Software for Digital Imaging

Digital cameras output the signal in a format that can be interfaced directly to the computer (IEEE-1394 "FireWire," RS-422, and SCSI interfaces are commonly used; Inoué and Spring, 1997). The necessary computer boards are usually purchased from the manufacturer of the camera or the image acquisition software. The software manufacturer may recommend purchasing the computer as well as necessary boards for image acquisition directly from them; this is usually preferable because the software manufacturer will install the boards into the computer and make sure that all of the components are compatible before they arrive in your laboratory. A computer dedicated to image acquisition will need a fast processor and a significant amount of RAM and hard drive space, as a single full frame image from a high-resolution 12-bit monochrome CCD camera can easily exceed 2 MB. At least 512 MB of computer RAM will be needed for most live cell applications. A CD-ROM or DVD writer is also useful.

Image acquisition software is used to manipulate camera settings such as gain, exposure time, and binning. An image acquisition and processing software package should minimally provide such useful features as pseudo-coloring, image merging/overlay, and manipulation of image brightness, contrast, and gamma for optimal display. Advanced software packages will also drive additional hardware, such as shutters and filter wheels, necessary for automated imaging (see Section IIID), and will provide tools for postacquisition image analysis. For a live cell image acquisition system, a software package that allows full customization will provide the most flexibility in designing experiments. For example, the software package MetaMorph (Universal Imaging Corp., a subsidiary of Molecular Devices) allows customized control of the parameters, sequence, and timing of image acquisition via "journals," a sequence of instructions to the software that are easily generated by recording selections from the program menus (Salmon and Waters, 1996). When choosing a software package, it is important to consider the long-term imaging and analysis goals of the user group. A software package that can meet the growing needs of the users may cost more up front, but will be well worth the investment in the long run. The long-term benefits that accrue from use of a digital asset management system for the organization of all image data within a laboratory, such as the freely available Open Microscopy Environment (www.openmicroscopy.org), which permits recording of descriptive metadata and image analysis results in a database together with raw and processed image files (Swedlow *et al*., 2003), should not be underestimated.

C. Microscope and Optics

To prevent vibration from degrading images, a stable, high-quality microscope stand is needed, preferably mounted on a vibration isolation table. Microscope optics should be kept clean, and every effort should be made to keep the environment dust free (for instructions on how to clean optics, see Inoué and Spring, 1997). The microscope illumination pathway should be aligned using the principles of Koehler illumination (Murphy, 2001; Inoué and Spring, 1997; http://www.microscopyu.com). All of the modern advances in image processing cannot compensate for dirty, misaligned optics.

Electronic cameras can be mounted on either an upright or an inverted microscope stand. An inverted microscope is usually preferable for live cell work, as the design allows easy access to the specimen during image acquisition for microinjection or perfusion and accommodates most heated incubation chambers. Inverted stands also have the added benefit of being particularly stable and resistant to focus drift.

Electronic cameras are usually mounted onto light microscopes via a camera port. An additional adapter, available from the microscope manufacturer, is used to couple the camera to the port. Research grade light microscopes can be equipped with multiple camera ports for attaching more than one camera. This is particularly useful on microscopes that are used for different modes of light microscopy so that cameras optimally suited for each mode can be mounted on the microscope simultaneously. For example, a microscope used for both bright-field histology-stained slides and fluorescence microscopy would be best outfitted with a color CCD camera as well as a cooled CCD camera. While cameras can be taken on and off of microscopes with relative ease, it is preferable to leave cameras mounted on the microscope to prevent dust from entering the body of the microscope and from adhering to the camera faceplate. Microscopes with camera ports come with a set of mirrors and/or prisms that are used to reflect to the camera image-forming light that would otherwise go to the eyepieces. Any light sent to the eyepieces during image acquisition is done so at the expense of light sent to the camera. Therefore, it is preferable to use a 100% reflecting mirror to send all of the light to the camera when acquiring photon-limited fluorescence microscopy images.

Provided that the optical image is adequately sampled by the camera, the spatial resolution of an image acquisition system is determined primarily by the microscope optics (Inoué and Spring, 1997; Shotton, 1997; Murphy, 2001). For transmitted light microscopy techniques, the spatial resolution limit is defined as the minimum distance two objects must be separated in order from them to be distinguished as separate and, according to Rayleigh's criterion, is equal to 1.22λ divided by the condenser NA plus the objective NA, where λ is the wavelength of the light source and NA is the numerical aperture (Inoué, 1995). For fluorescence microscopy, the optical resolution limit is defined as the radius of an image of an infinitely small point source of light and is equal to 0.61λ divided by the NA of the objective lens, where λ is the fluorescence emission wavelength (Inoué, 1995). However, for two-photon confocal microscopy, the resolution is limited by the longer infrared excitation wavelength. To ensure that spatial resolution is limited by the optics and not by the pixel size in the CCD chip, the minimum total magnification used from specimen to image plane should be equal to twice the photodiode width divided by the optical resolution limit (Shotton, 1997; Spring, 2000, 2001), as explained earlier. For low-light (and therefore low-contrast) specimens, it is ideal to oversample the image by using a magnification equal to three times the photodiode width divided by the optical resolution limit (Maddox *et al*., 2003; Stelzer, 1998), although, as explained earlier, it may alternatively be necessary to sacrifice spatial resolution in order to capture enough photons per pixel to render the objects under study visible at all. Microscopes can be equipped with relay lenses that increase the magnification of the image to the camera in order to meet these requirements.

For some applications, spatial resolution is less important than capturing a large field of view. The rectangular CCD chip in a camera does not capture the entire round field of view seen through the microscope eyepiece—usually only 50–70% of the field of view is collected by the camera. If a larger field of view is required, magnification-reducing lenses can be placed in front of the camera. A 0.6× relay lens will usually come close to matching the camera field of view with the eyepiece field of view, while sacrificing image resolution. Alternatively, to maintain high resolution, multiple images of adjacent fields of view can be collected at high magnification, ideally using a scanning specimen stage on the microscope, and then "stitched" together into a larger image using image processing software.

For fluorescence microscopy in particular, it is important that the microscope is optimized for maximum collection and transmission of light. The single most important parameter in determining the amount of image forming light that reaches the camera is the numerical aperture of the objective lens (Murphy, 2001; Abramowitz *et al*., 2002). The brightness of an image formed by an objective lens can be defined by $B = 10^4 NA^4/M^2$, where NA and M refer to the numerical aperture and the magnification of the objective lens, respectively (Abramowitz *et al*., 2002). The numerical aperture, which is usually marked on the barrel of an objective lens just to the right of the magnification, is a measure of the half angle of the cone of light accepted by the objective lens times the refractive index of the medium between the lens and the specimen. The higher the numerical aperture, the more light the lens is capable of collecting. Conversely, the brightness of an image is inversely proportional to the square of the magnification. Therefore, a 60×/1.4 NA objective lens will create a brighter image than a 100×/1.4 NA objective, while having the same optical resolution. The actual light transmission of a lens is also affected by the extent to which the lens is corrected for aberrations, a highly corrected plan apochromat objective with many internal lens elements transmitting less light than a more simple fluorite lens (Abramowitz *et al*., 2002). Phase-contrast objective lenses are not optimal for low-light fluorescence imaging, as these objectives have a light-attenuating

phase annulus in the back focal plane that decreases the intensity of the signal by 10–15%.

To perform fluorescence microscopy effectively, the optimal fluorophore, filters, and illuminator should be chosen for a given application (Kinoshita, 2002; Reichman, 2000). It is also important to minimize the number of filters and prisms in the light path that absorb the excitation or emission light and decrease the intensity of the signal. For example, on a microscope with both fluorescence and DIC optics, the polarization analyzer (Murphy, 2001) is usually situated in the shared light path just behind the objective lens and should be removed when using the microscope for fluorescence to prevent attenuation of the signal.

D. Automated Live Cell Image Acquisition

Motorized microscope components allow the user to automate image acquisition and are particularly useful for live cell time-lapsed studies (Salmon and Waters, 1996; Mason, 1999). Components such as electronic shutters, filter wheels, motorized stages, and focus motors can be attached to a research grade microscope and controlled through a computer using image acquisition software. Electronic shutters, which are used to block the light source from illuminating the specimen between camera exposures, are particularly important for fluorescence specimens as a means of minimizing photobleaching and phototoxicity, thereby increasing image quality and cell viability over long periods of time-lapse recording. For live cell studies in which the localization of more than one fluorophore is to be time-lapse recorded, automated switching between fluorescence filter sets is necessary. Microscopes are now available that come equipped with a motorized fluorescence filter set slider or turret; however, they tend to be too slow for live cell applications in which the time between acquisition of the different fluorophores needs to be minimized. A faster solution is the addition of motorized filter wheels to the fluorescence light path (Salmon and Waters, 1996; Mason, 1999). In this setup, the standard fluorescence filter set (Herman, 1998) is replaced with a multiple band-pass dichroic mirror (Reichman, 2000). Excitation illumination is then controlled with a motorized wheel filled with single band-pass excitation filters placed in front of the light source. Either a single multiple band-pass emission filter or a set of single band-pass emission filters in a second motorized wheel (placed just before the camera) is then used to select emission wavelengths. Filter wheels are available that can move between adjacent positions in 30–50 ms, allowing rapid switching between fluorophores.

Focus motors attach to the fine focus mechanism of the microscope and allow automated focus control through image acquisition software. Focus motors can be used in conjunction with autofocus functions in the software or to collect a stack of optical sections for subsequent deconvolution and/or 3D reconstruction. Motorized stages can be used with image acquisition software to automate movement of the stage between more than one field of view or between wells in a culture dish. An image acquisition system equipped with a focus motor, a motorized stage, and advanced image acquisition software can be used for "4D" (*x*, *y*, *z* and *time*), "5D" (*x*, *y*, *z*, *time*, and *wavelength*), and "6D" (multiple *x*, *y* areas, *z*, *time*, and *wavelength*) live cell imaging.

It is often useful to collect both fluorescence and bright-field transmitted light images of the same specimen (Salmon and Waters, 1996). For many experiments, it is sufficient to acquire a phase or DIC image at the beginning and end of the fluorescence time lapse. When automated switching between fluorescence and bright field is required, both illumination pathways must have an electronic shutter in front of the light source. For DIC and fluorescence microscopy, a motorized polarization analyzer is also desirable so that this light-attenuating filter can be automatically removed from the light path while the fluorescence image is acquired. This DIC analyzer can alternatively be placed into a motorized wheel in front of the camera, alongside fluorescence emission filters.

IV. PREPARING YOUR SPECIMEN FOR IMAGING

An important part of generating excellent images of fluorescence specimens is to learn to evaluate critically the quality of the fluorescence signal relative to background fluorescence. It is difficult, and in many cases impossible, to use subsequent image processing to remove noise that comes from nonspecific fluorescence staining from the collected image. Fluorophores with high quantum efficiency and low photobleaching should be chosen whenever possible (Herman, 1998). It is well worth the time and effort of optimizing your labeling protocol to maximize signal while minimizing background fluorescence (Harper, 2001).

For high-resolution fluorescence work it is also important that specimens are mounted properly for viewing. The majority of high numerical aperture objectives are marked "0.17" on the objective barrel, indicating that they are designed to image through a 0.17-μm-thick coverslip (Murphy, 2001; Abramowitz

et al., 2002). This means that there should be nothing between the specimen and the front of the objective lens except a 0.17-µm-thick glass coverslip and the appropriate immersion medium (usually immersion oil). This means that the specimen to be imaged must be located adjacent to the coverslip, not at a great distance into its aqueous support medium. If the latter situation is unavoidable, a suitable water-immersion objective designed for confocal imaging deep within the aqueous specimen should be used. High-resolution light microscopy cannot be performed through a plastic petri dish or 16-well plate. Live cells should instead be grown in petri dishes or welled chambers that have a glass coverslip cemented into the bottom. There are also commercially available viewing chambers for live cell work that are designed to hold a coverslip and a volume of media. Similar chambers can be built with the help of a clever machine shop (for one such design, see Rieder and Cole, 1998). Fixed fluorescence specimens should be mounted in a glycerol-based media with an antiphotobleaching reagent. There are many commercially available mounting media, but it is also easy and inexpensive to make your own (one reliable recipe is a 1:1 mixture of double-strength phosphate-buffered saline and glycerol containing 0.5% *n*-propyl gallate). For live cell work, reducing the concentration of oxygen in media will also help prevent photobleaching. The product Oxyrase (http://www.oxyrase.com) works very well when used with a closed viewing chamber. However, it should be realized that lack of oxygen may compromise the long-term survival of the cells.

Focus drift while filming live cells can be disruptive and frustrating. A small amount of focus drift (1–2 µm per hour) is usual and must be tolerated, but steps can be taken to minimize the amount of focus drift in your image acquisition system. It is important to be sure that coverslips are mounted securely to the slide or viewing chamber and that the slide or viewing chamber itself is clamped tightly onto the microscope stage. With oil objectives, some amount of focus drift will occur within the first few minutes of viewing as the oil settles across the objective lens. It is thus often preferable to wait several minutes after placing a specimen on the microscope before beginning filming. Heated stage chambers can also lead to focus drift by causing fluctuations in temperature that make microscope components expand. Heated incubation chambers that totally enclose and heat the entire body of the microscope as well as the specimen are often the best way to maintain temperature and focus during image acquisition, especially during long-term experiments. Use of a fixed, permanently mounted specimen and monitoring focus over time will help determine whether focus drift is coming from your equipment or your specimen.

References

Abramowitz, M., Spring, K. R., Keller, H. E., and Davidson, M. W. (2002). Basic principles of microscope objectives. *BioTechniques* **33**, 772–781.

Berland, K. (2001). Basics of fluorescence. *In* "*Methods in Cellular Imaging*" (A. Periasamy, ed.). Oxford Univ. Press, New York.

Harper, I. (2001). Fluorophores and their labeling procedures for monitoring various biological signals. *In* "*Methods in Cellular Imaging*" (A. Periasamy, ed.). Oxford Univ. Press, New York.

Herman, B. (1998). "Fluorescence Microscopy." 2nd Ed. Springer Verlag, Hiedelberg.

Hiraoka, Y., Sedat, J. W., and Agard, D. A. (1987). The use of a charged-couple device for quantitative optical microscopy of biological structures. *Science* **238**, 36–41.

Inoué, S. (1995). Foundations of confocal scanned imaging in light microscopy. *In* "*Handbook of Biological Confocal Microscopy*" (J. Pawley, ed.), 2nd Ed. Plenum Press, New York.

Inoué, S., and Spring, K. R. (1997). "Video microscopy," 2nd Ed. Plenum Press, New York.

Kinoshita, R. (2002). Optimize your system with the right filter set. *Biophoton. Int.* **9**(9), 46–50.

Maddox, P. S., Moree, B., Canman, J. C., and Salmon, E. D. (2003). A spinning disk confocal microscope system for rapid high resolution, multimode, fluorescence speckle microscopy and GFP imaging in living cells. *Methods Enzymol.* **360**.

Mason, W. T., Dempster, J., Hoyland, J., McCann, T. J., Somasundaram, B., and O'Brien, W. (1999). Quantitative digital imaging of biological activity in living cells with ion-sensitive fluorescent probes. *In* "*Fluorescent and Luminescent Probes*" (W. T. Mason, ed.), 2nd Ed. Academic Press, London.

Murphy, D. B. (2001). "Fundamentals of Light Microscopy and Digital Imaging." Wiley-Liss, New York.

Reichman, J. (2000). "Handbook of Optical Filters for Fluorescence Microscopy." Download from http://www.chroma.com.

Rieder, C. L., and Cole, R. (1998). Perfusion chambers for high-resolution video light microscopic studies of vertebrate cell monolayers: Some considerations and a design. *Methods Cell Biol.* **56**, 253–275.

Salmon, E. D., and Waters, J. C. (1996). A high resolution multimode digital imaging system for fluorescence studies of mitosis. *In* "*Analytical Use of Fluorescent Probes in Oncology*" (Kohen and Hirschberg, eds.), pp. 349–356. Plenum Press, New York.

Shotton, D. M. (1993). An introduction to the electronic acquisition of light microscope images. *In* "*Electronic Light Microscopy*" (D. M. Shotton, ed.), pp. 2–35. Wiley-Liss, New York.

Shotton, D. M. (1997). Image resolution and digital image processing in electronic light microscopy. *In* "*Cell Biology: A Laboratory Handbook*" (J. E. Celis, ed.), 2nd Ed., Vol. 3, pp. 85–98. Academic Press, San Diego.

Spring, K. (2000). Scientific imaging with digital cameras. *BioTechniques* **29**, 70–76.

Spring, K. (2001). Detectors for fluorescence microscopy. *In* "*Methods in Cellular Imaging*" (A. Periasamy, ed.). Oxford Univ. Press, New York.

Stelzer, E. H. K. (1998). Contrast, resolution, pixilation, dynamic range, and signal-to-noise ratio. *J. Microsc.* **189**, 15–24.

Swedlow, J. R., Goldberg, I., Brauner, E., and Sorger, P. K. (2003). Informatics and quantitative analysis in biological imaging. *Science* **300**, 100–102.

Tsien, R. Y. (1998). The green fluorescent protein. *Annu. Rev. Biochem.* **67**, 509–544.

CHAPTER

6

Video-Enhanced Contrast Microscopy

Dieter G. Weiss

I. INTRODUCTION

Video contrast enhancement is a technique that considerably improves images obtained by a large variety of video-based imaging systems used in light, electron, and confocal microscopy. It requires a camera system with manually adjustable "gain" and "offset" (also called "pedestal" or "black level" by some manufacturers). Much better results are obtained if digital image processing can be applied in addition. In light microscopy the most striking image improvements are possible if the technique is applied to images obtained by polarized light methods. In such cases the improvement in true resolution is almost 2-fold and in visualization is 10-fold over conventional light microscopy by eye. The specimens most suitable for observation by this technique are unstained, low-contrast objects, such as living cells, uncontrasted semithin electron-microscopic sections, or gels and colloidal material. The objects made additionally accessible to observation include organelles, especially small vesicles, isolated microtubules (25 nm), latex beads 20 nm in size and larger, and colloidal gold particles of 5 nm in diameter and larger. The basic principles and theory are described in detail elsewhere (Weiss *et al*., 1999; Weiss and Maile, 1993).

II. EQUIPMENT

Video-enhanced contrast (VEC) microscopy requires the combination of a versatile, high-quality research microscope with an analog and digital real-time image processor. The parts required were discussed in detail elsewhere (Inoué and Spring, 1997; Weiss *et al*., 1999; Weiss and Maile, 1993) so that a short summary may suffice here.

To utilize the technique to its full extent, a massive, stable microscope preferably equipped with differential interference contrast (DIC), and if required additional epi-illumination fluorescence, transmitted light bright-field, dark-field, or other techniques, is used. The illumination should be as bright and even as possible to provide enough light for working at the highest magnifications. A stabilized DC mercury arc or xenon lamp with a narrow band filter (e.g., green 546 ± 10 nm for mercury arc lamps) is recommended; with some microscopes it may preferably be equipped with a light-scrambling fiber optic connection (Ellis, 1985; Inoué, 1986) (Technical Video Ltd.). The condenser and objective should be of the oil immersion type when working with objective magnifications of 40× and more. The numerical aperture (NA) of the condenser front lens must match that of the objective; for 60 and 100× objectives, a 1.4 NA oil condenser front lens is required. An exit port projecting 100% of the light to the video camera is essential for fluorescence and high magnification DIC work. In order to visualize objects of sizes near and below the limit of resolution, optical magnification of 2 or 4× is in addition to 100 or 60X, NA 1.3–1.4 objectives required and is obtained by the use of high oculars (16, 25×) and a video camera objective (50 or 63 mm) or, preferably, by direct projection of the image to the camera and additional magnification changers. This yields magnifications on a monitor with a 25-cm screen width of 10,000× and more. A temperature-controlled box is needed for work with cultured cells. The use of at least one heat-absorbing and one heat-reflecting filter is essential; a narrow band green filter and a UV filter are recommended for DIC work with most cell types.

Copyright 2006, Elsevier Science (USA).
All rights reserved.

Because VEC microscopy is best applied with DIC, it should be noted that DIC microscopes differ in the separation of the two orthogonally polarized wave trains. If this so-called shear is high (250 nm) the bright and dark rims of the object are also wide and have high contrast differences so that a crisp, very high contrast image appears when inspected by eye. However, in this case the true resolution cannot be increased over 250 nm, which is also the conventional limit. Most high magnification oil optics are designed with medium shear so that there will be a gain in resolution with VEC-DIC. Low-shear DIC optics would yield poor visual contrast but best improvement of resolution with VEC microscopy. Although microscope manufacturers intended up to now to design their DIC prism systems for bright shadow-cast visual contrast, Nikon was the first to offer a design better suitable for VEC-DIC in their new line of Eclipse microscopes with low-shear Wollaston prisms and the de Sénarmont compensator recommended by Allen *et al.* (1981a,b).

The image is picked up by a high-quality video camera, usually a chalnicon or newvicon tube camera. Charge-coupled device (CCD) cameras are equally suitable only if they have a comparable dynamic range. The cameras need to have a manually adjustable offset (black level) and gain to allow for analog contrast enhancement. Automatic gain control (AGC), if present, must be disabled. The digital image processor needs to have the following features to be performed in real time, i.e., at video rate: digitization with 512 × 512 pixels of 256 possible gray levels or better, arithmetic frame operations such as subtraction of the out-of-focus background (mottle) pattern, accumulation, rolling averaging (recursive filtering) of images in order to increase the signal-to-noise ratio, scaling, frame counting, and finally selecting of the desired range of gray levels (histogram stretching or digital contrast enhancement). In addition, controls signaling camera saturation and excessively high light levels, digital filters, or pseudo-color option are also useful. The cameras and processors developed for microscopy from Hamamatsu Photonics (e.g., Hamamatsu Photonics Deutschland) and Dage-MTI, Inc. are the most widely used ones.

III. STRATEGY OF IMAGE GENERATION

Video contrast enhancement of microscopic images obtained using bright-field, dark-field, anaxial illumination including Varel contrast, fluorescence, reflected light confocal, or fluorescence confocal optics, rather than DIC and polarization optics, is very straightforward. It is performed by following the steps in Table I with the exception of step 4.

For special aspects of video enhancement **in** fluorescence microscopy, refer to Lange *et al.* (1996). High-resolution VEC microscopy can also be used simultaneously with fluorescence if appropriate beam

TABLE I Steps in AVEC-DIOC Microscopy[a]

Step		Manipulation	Result
1[b]	M[c]	Focus specimen	Image appears
2	M	Adjust microscope correctly for Köhler illumination	Image improves
3	M	Open iris diaphragm fully	Optical image becomes too bright
4	M	Set compensator up to 20° from extinction[d]	Optical image worsens
5	C	Analog enhance by manually adjusting gain and offset	High-contrast video image with often disturbing mottle pattern appears
6	M	Defocus or move specimen laterally out of field of view	Object disappears, mottle remains
7	P	Average and store mottle image, then subtract mottle image from incoming video images	Absolutely homogeneous, light gray ("empty") image appears
8	M	Return specimen to focal plane	Clear image appears; if contrast is weak go to step 9
9	P	Contrast enhance digitally (histogram stretching)	Contrast becomes optimal; if pixel noise is high go to step 10
10	P	Use rolling or jumping averaging or digital filtering	Clear, low noise, and high-contrast image appears

[a] Reprinted from Weiss and Maile (1993) by permission of Wiley-Liss, Inc., a subsidiary of John Wiley & Sons, Inc.

[b] Before step 1, one should set the "brightness" and "contrast" controls of the monitor showing the processed image to their intermediate positions because the degree of enhancement will not be adequate in the recorded sequence if the monitor had been adjusted to an extreme setting. To use VEC microscopy to its full extent, make sure that the microscope objective and condenser front lenses are absolutely clean (check at least once daily) and that the lamp is always optimally adjusted and centered.

[c] Manipulations are performed at the microscope (M), camera control (C), or image processor (P), respectively.

[d] Particles need to appear in DIC microscopy images as if illuminated from above, i.e., with their bright part up, whereas vacuoles have the opposite shadows. If this is not the case, the camera has to be rotated 180° or the compensator or Wollaston prism has to be set to the opposite side with respect to the extinction position.

splitters and filters are used. When applied to live cells stained with vital dyes, this allows observation of organelle morphology and dynamics in parallel with the identification of the types of organelles or with measurements of ion concentrations (Foskett, 1993).

Most striking image improvements are usually gained with DIC and polarization microscopy, but special attention and some explanations are required for step 4. Allen *et al.* (1981a,b) and lnoué (1981, 1989; Inoué and Spring, 1997) simultaneously developed procedures of video contrast enhancement for polarized-light techniques that differed considerably in their approach but yielded very similar results. Although this is not the place to judge which one is more appropriate, we have to distinguish clearly between the two strategies to avoid confusion.

Allen named his techniques "Allen video-enhanced contrast" differential interference contrast and polarization (AVEC-DIC and AVEC-POL, respectively) microscopy. AVEC techniques involve the introduction of additional bias retardation by setting the polarizer and analyzer relatively far away from extinction to gain a high specimen signal. Allen suggested the use of a de Sénarmont compensator (Bennett, 1950), which consists of a quarter-wave plate (specific for the wavelength used) in front of a rotatable analyzer. In DIC microscopy, alternatively but less accurately, the desired bias retardation can also be introduced by shifting the adjustable Wollaston prism. Allen recommended a bias retardation of one-quarter to one-ninth of a wavelength away from extinction, with one-ninth (20°) as the best compromise between high signal and minimal diffraction anomaly of the Airy pattern (Allen *et al*., 1981b). The enormous amount of stray light introduced at such settings is removed by an appropriately large setting of analog and/or digital offset.

The technique recommended by lnoué, which in this article is called IVEC microscopy for distinction, aims to optically reduce stray light and diffraction anomaly arising from curved lens surfaces and other sources by employing selected, extremely strain-free objectives and the special rectifying lenses developed by Inoué (1961). The latter are available commercially only for few microscopes (some lines of Nikon) and are expensive. Inoué's special optimized microscope (Inoué and Spring, 1997) is used at a polarizer setting very close to extinction, which cannot be used for VEC micro-scopy with many other instruments because insuf-ficient light is passed for near-saturation of the video camera.

Thus in IVEC microscopy, stray light is not admitted, as the polarizers stay close to extinction and the special rectifying optics further reduce the stray light. Consequently, filters to reduce brightness are not required. On the contrary, a very bright arc lamp, ideally with a fiber-optic illuminator, is necessary to saturate the camera. The AVEC technique, however, electronically improves primary optical images characterized by low contrast and relatively high stray light content, arising from a "non-optimal" optical arrangement. In IVEC microscopy, no compromise is made regarding the optics, and consequently less demanding electronic steps are required to rescue the image. The AVEC technique is, however, one that can be used with any good research microscope equipped with commercial film polarizers.

The steps required for image generation and improvement by VEC microscopy are summarized in Table I and are explained later. They include procedures different from those used in conventional microscopy, which are, however, required for the highest resolution and visualization of subresolution objects. The procedure described is that for AVEC-DIC, but if DIC or other polarized light techniques are not required, step 4 should simply be omitted. Steps 1–5 of the procedure given here yield the final image if digital processing is not possible or if only analog enhancement is required. In this situation, analog enhancement has to be stopped just before mottle or uneven illumination becomes annoying. Analog shading correction and other types of analog image improvement may be applied if the camera control unit offers them. The use of a light scrambler and meticulous cleaning of the microscope and the lens surfaces in the projecting system to the camera (see step 5) help considerably in permitting high levels of analog enhancement.

Generally, it is most desirable in video microscopy to obtain near-saturation of the video camera prior to applying analog or digital enhancement. *If there is insufficient light*, the following measures are recommended: use brighter lamps (mercury or xenon lamp); redo the illumination adjustments such as setting Köhler illumination and centering the filament or arc, possibly while observing the image on the monitor to improve; remove ground glass diffusers from the light path; make sure that the video exit port receives 100% of the light; reduce magnification slightly; or replace the otherwise highly recommended narrow band-pass filter by a wider one.

In AVEC microscopy, near-saturation should be reached at a retardation setting of about one-ninth of a wave (20°), as this provides the best resolution (Hansen *et al*., 1988). Further opening of the crossed polarizers far beyond 20° will rarely improve the image further, but it may introduce amounts of stray light no longer manageable by offset, leading to a bright-field type of appearance.

In the case of excessive light reaching the camera, the following steps are recommended: apply weak neutral density gray filters, employ high-power light sources that can be attenuated (e.g., the Atto-Arc system from Carl Zeiss or metal halide burners, e.g., from Nikon), or increase magnification slightly.

Reducing light intensity by closing diaphragms is not recommended as it reduces resolution. In AVEC microscopy, if the one-ninth setting yields too much light for the camera, this could be reduced by setting the compensator or Wollaston prism to a position of less than 20°. Although widely used, this does somewhat compromise image quality, especially if settings of less than 15° or 10° are used (Allen *et al*., 1981a,b; Hansen *et al*., 1988).

IV. SAMPLE PREPARATION

Live cells from tissue cultures should preferentially be grown on a cover glass. The specimen's region of interest should be close to the cover glass surface, where the best image is obtained. If the highest magnifications are intended, it may be that the optics can be adjusted for Köhler illumination only at this surface and a few tens of micrometers below (upright microscope), as high-magnification objectives are usually designed for best optical imaging of objects only near a distance of 170 µm from the front element, i.e., 10–20 µm from the inner surface of a regular cover glass (No. I glasses, approximately 170 µm thick). To identify objectives for which this distance and the presence of a 170-µm-thick cover glass is critical, look for the "0.17" engraved or refer to the manufacturer's data sheet. If thick cells or other extended specimens must be observed with such objectives, No. 0 cover glasses (80–120 µm thick) and/or thinner glass slides (0.9 instead of 1 mm) (both available from O. Kindler GmbH or Scholt North America) may have to be used instead of the regular ones to allow the setting up of Köhler illumination with oil immersion of both condenser and objective lens and to permit a greater working distance within the specimen. The use of a slide preparation made of two cover glasses mounted in a frame as depicted in Fig. I would serve the same purpose.

Note, however, that if the oil immersion objectives are focusing through water rather than through glass and oil only, spherical aberration will be introduced. The use of monochromatic illumination or of immersion oils of different refractive indices (R. P. Cargille Laboratories) is recommended to overcome this problem. Alternatively, for imaging deep within an aqueous sample, water immersion objectives must be used. Special water immersion objectives have become available from major manufacturers for confocal microscopy. They combine high numerical aperture (e.g., 60×, NA 1.2) with correction for extreme working distances of up to 220 µm below the cover glass (Brenner, 1994).

Aqueous samples have to be prevented from drying out by completely sealing the cover glass to the microscope slide. Nail polish may be used for this or, if live or other solvent-sensitive specimens, such as microtubules, extruded cytoplasm, or cultured cells, are being observed, VALAP is recommended. This consists of equal parts by weight of Vaseline, lanolin, and paraffin (MP 51–53°C); it liquefies at around 65°C. It may be applied around the cover glass with a cotton tip applicator or fine paint brush and hardens rapidly. If the specimen is small enough or in suspension, sample volumes of no more than 5–10 µl should be used with 22 × 22-mm cover glasses and without spacers to produce very thin specimens (ca. 10 µm thick) for best image quality.

If working with an inverted microscope, the specimen slide has to be inverted for fitting to the microscope with the cover glass underneath. With most microscope stages, this will interfere with the VALAP sealant, and flat positioning of the slide will not be possible. Instead, use of a metal frame the size of a regular slide and 0.8 to 1 mm thick to hold a sandwich of two cover glasses of dissimilar sizes separated by tape or cover glass spacers is recommended (Schnapp, 1986; Weiss *et al*., 1999, 1990) (Fig. 1).

If thick specimens, such as tissue slices, vibratome sections, or nerve bundles, are to be observed at high magnifications that require oil immersion, only contrasting techniques that allow optical sectioning such as DIC, Hoffman modulation contrast, or anaxial illumination (including Varel) contrast are recommended. Only the first 10 or 20 µm behind the cover glass will yield perfect images. However, even if expensive long working distance water immersion objectives are not available, part of the loss of image quality can be compensated for by video enhancement with good results down to a depth of 100 µm or more, with respect to both visibility and contrast, sometimes also to resolution (Kachar, 1985). The opacity of live tissues such as brain slices is reduced greatly when 700 to 800 nm light is used because they are transparent for infrared or near-infrared light (Dodt and Zieglgänsberger, 1990).

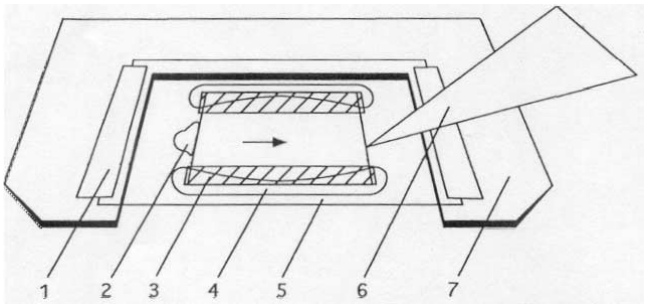

FIGURE 1 Slide preparation suitable for highest magnification VEC microscopy with upright and inverted microscopes and for superfusion of live cells or suspension specimens: (1) adhesive tape attaching the cover glass to the metal frame (7); (2) drop of medium to replace the original medium; (3) VALAP sealant; (4) small cover glasses or thin adhesive tape as spacers (e.g., double-sticky Scotch Tape); (5) carrier cover glass [e.g., No. 2 (extra thick) 24 × 50 or 60 mm]; (6) filter paper wick to induce medium flow (arrow); and (7) metal frame of the size of regular microscope slides made of brass or aluminum 0.8 to 1 mm thick and absolutely flat. For use with inverted microscopes the preparation should be mounted on the lower side of the carrier glass (5). Reproduced from Weiss *et al*. (1990) with permission by Plenum Press.

V. GENERATION OF THE IMAGE

Step 1: Focusing the Specimen

We find the specimen preferably by looking through the oculars or, alternatively, by looking at reduced magnification at the monitor. Only if the entire specimen consists of subresolution size material (density gradient fractions, microtubule suspensions, unstained EM sections) will it be difficult to find the specimen plane. Use a relatively dark setting of the condenser diaphragm and/or polarizers or prisms and look for contaminating larger particles. If there are none, routinely apply a fingerprint to one corner of the specimen side of the cover glass and use this for focusing.

Step 2: Adjusting Köhler Illumination

After finding a coarse setting for the illumination, the desired plane for the specimen is selected exactly. Then the condenser is finely adjusted, but now in relation to the image on the monitor (make sure the light is reduced to avoid damage of the camera!). The field diaphragm must be centered on the monitor and opened until it becomes just invisible. If the field diaphragm is opened too much, most microscope–camera adapter tubes or high-power projectives and oculars will create a very annoying central hot spot. If this persists at the adjustment for proper illumination, closing the projective diaphragm or inserting a self-made diaphragm cutting the peripheral light at the microscope exit usually helps. Note that at the high magnifications and numerical apertures used here, Köhler illumination has to be readjusted once the focus is changed more than a few micrometers.

As we will apply extreme contrast enhancement later, we have to start out with as even an illumination setting as possible (Fig. 2a). Proper centering of the lamp and setting of the collector lens are therefore important. At high magnifications as much light as possible needs to be collected. Some workers have therefore used critical illumination, i.e., focusing the light source onto the specimen plane instead of Köhler illumination (Schnapp, 1986). This is counter to good microscopical practice and can lead to very uneven illumination as the filament or arc a will be superimposed onto the image of the specimen and, subsequently, has to be subtracted digitally by mottle subtraction. Critical illumination might be useful, however, in those cases where the illuminating light is made extremely homogeneous by light scrambling with a light fiber device (Ellis, 1985; Inoué, 1986; Schnapp, 1986) (Technical Video Ltd.).

Step 3: Full Numerical Aperture for Highest Resolution

Open the condenser diaphragm fully in order to utilize the highest possible numerical aperture to obtain highest resolution. Also, any iris diaphragm of the objective should be opened fully. The result of opening the condenser diaphragm will usually be that the optical image worsens because it becomes too bright and flat for the eye. This setting will result in a small depth of focus, especially with DIC (optical sections of 0.3 µm or less with 100× NA 1.4 oil objectives). If collection of information from a large depth of focus is desired (e.g., viewing very dilute suspensions) and resolution can be sacrificed, the condenser diaphragm may be closed down as desired.

Be careful to protect the camera from too high light intensity prior to this step. However, at this point you have to make sure that the camera receives the proper amount of light to work near its saturation end. Some manufacturers have red and green control lamps built in to indicate this. In any case you should see a moderately modulated image on the monitor, whereas a very flat or no image indicates insufficient light. In this case, follow the recommendations on how light intensity can be increased (see Section III). If the illumination has to be reduced to protect the camera, this should not be done by closing diaphragms, as this compromises resolution (see Section III).

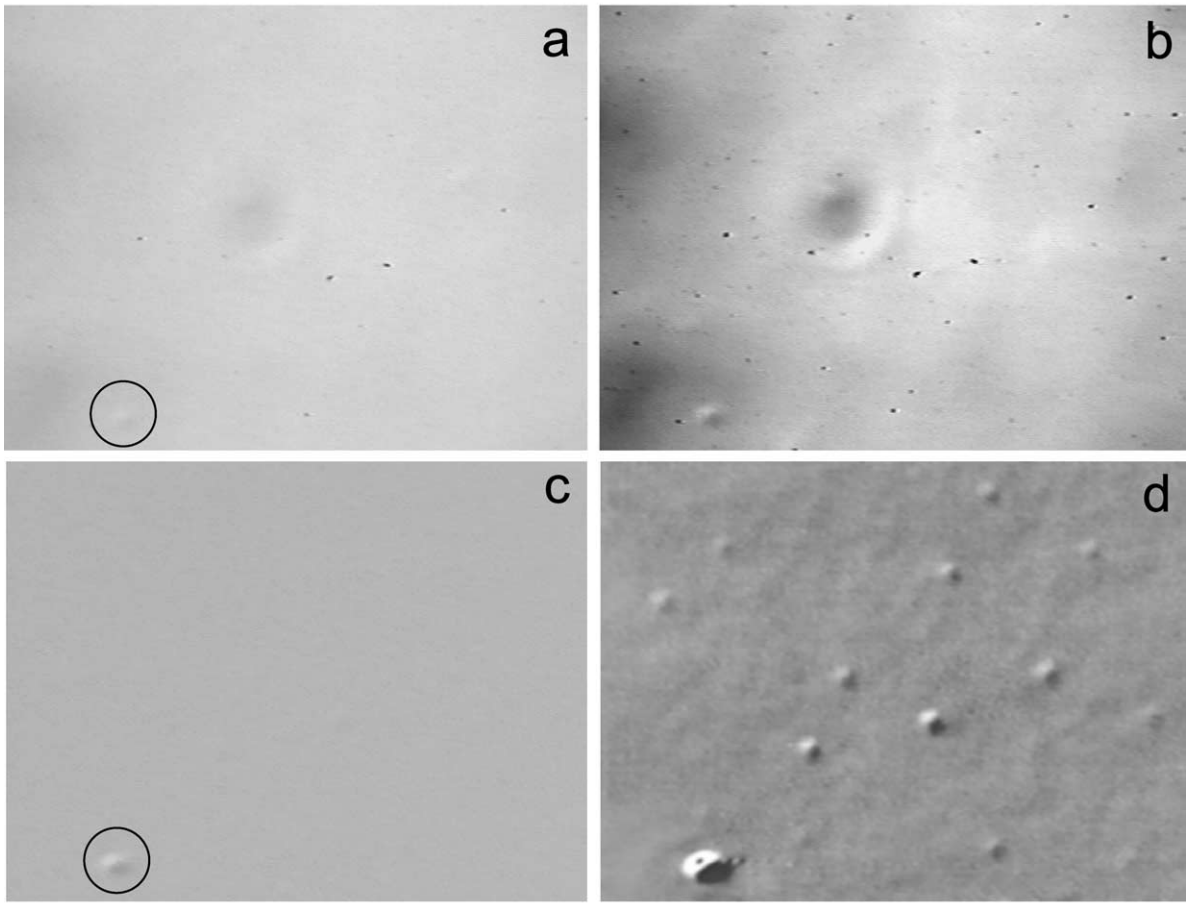

FIGURE 2 VEC microscopy of a specimen with very weak contrast. The steps of image generation and contrast enhancement in VEC microscopy are demonstrated using subresolution size latex beads (50 nm diameter). (a and b) Analog contrast enhancement. (c and d) Digital background subtraction and digital contrast enhancement. (a) In focus, not enhanced; only the large aggregate of a size above the limit of resolution is visible (circle); (b) in focus, analog-enhanced; the mottle becomes annoying; (c) in focus, mottle subtracted; (d) the same digitally enhanced. Microscope: Reichert-Leica Polyvar; image processor: Hamamatsu Argus 10; width of frames: 22 µm.

Step 4: Setting the Compensator (Polarized Light Techniques Only)

Set the compensator or main prism (AVEC-DIC) or the polarizer (AVEC-POL) to about 1/9 λ, i.e., one-ninth of a wavelength. The optical image, i.e., that seen in the oculars, will disappear due to excessive stray light.

If you have the accessories for de Sénarmont compensation as recommended by Allen *et al*. (1981a,b; see also Weiss and Maile, 1993; Weiss *et al*., 1999), set them at 20'° off extinction. The basic setup for the de Sénarmont compensator is as follows: Remove both Wollaston prisms and quarter-wave plate from the light path; set analyzer and polarizer to best extinction; insert quarter-wave plate at 0° (best extinction); insert Wollaston prisms and set the adjustable one to best symmetrical extinction (if possible, check with a phase telescope for symmetry of the pattern); and use the rotatable analyzer as a compensator and set it as desired (one-ninth of a wave is 20°, one-quarter is 45°).

If you do not have such a calibrated system, first determine the distance between extinction (0°) and maximum brightness (90° or one-half of a wavelength)

by moving the adjustable Wollaston prism and then estimate and select approximately the ninth of a wave or 20° position. Many microscopes equipped with DIC for biological applications do not allow a phase shift of 90° and some may not even allow 20° because for observation by eye, phase shifts of a few degrees already yield good contrast. Microscope manufacturers will, however, have the proper parts in their mineralogy programs.

At this point you have to again make sure that the camera is protected from excessive light but receives enough light to work near its saturation end. Ideally this should be near the one-ninth setting. Light adjustment should be done as explained in Section III. Opening the compensator or the crossed polarizers beyond 20°, although perhaps leading to a better saturation of the camera, will hardly improve the resolution of DIC or polarization images and will yield a poor image resembling the bright-field type.

In IVEC microscopy, stray light is not admitted, i.e., the polarizers stay close to extinction and the special rectifying optics further reduce the stray light. Filters to reduce brightness will not be required, but very bright lamps will be necessary to saturate the camera.

Step 5: Analog Enhancement

Increase the gain on the camera to obtain good contrast. Then apply offset (pedestal). Always stop before you lose parts of the image that become too dark or too bright. Repeat this procedure several times, if necessary and helpful. Make sure that the monitor for watching the changes is not set to extreme contrast or brightness and is terminated properly (75 Ω setting). Analog enhancement improves the contrast of the specimen, but unfortunately also emphasizes dust particles, uneven illumination, and optical imperfections. These artifacts, called "mottle," are superimposed on the image of the specimen and may, in some cases, partially or totally obscure it (Fig. 2). Disturbing contributions from fixed pattern noise (mottle) or excessive amounts in unevenness of illumination (Fig. 2b) can, however, be tolerated if digital processing is performed later (Fig. 2c and d).

If digital processing is not possible, stop enhancement just before mottle or uneven illumination becomes annoying. Optimal adjustment of the lamp and thorough cleaning of the inner optical surfaces of the microscope, oculars, and camera lens usually result in images that allow the application of considerably higher analog contrast enhancement. Apply analog shading correction and other types of analog image improvement if your camera control unit offers these features.

Finding Dust When the imaged dust particles or the mottle pattern rotates when the camera head is rotated, they are in the optical path before the camera, while the immobile dust is to be found on the camera face plate. Rotate the ocular or camera objective lens to find dust located there. Dust should be removed with a low-pressure air gun or an optical cleaning brush. If this does not help, use lens paper or a fat-free cotton tip applicator (wooden stick, no plastic!) with ethanol or ether (in the fume hood only!). Work from the center to the periphery in a circular fashion while carefully avoiding to apply any pressure. Dust or mottle that is defocused if the specimen is defocused is part of the specimen.

Step 6: Finding a "Background" Scene

Try removing the specimen laterally out of the field of view or (when using DIC) defocus to render it just invisible (preferably toward the cover glass). The result is an image containing only the imperfections of your microscope system (mottle pattern). This step may not be satisfactory, however, with such techniques as phase contrast or bright field.

Step 7: Background (Mottle) Subtraction

Freeze, i.e., store, the mottle image, preferably averaged over several frames, and subtract it from all incoming video frames.

Step 8: Return Specimen to Focal Plane

When returning the specimen to the focal plane, you should see an absolutely even and clean image, which may, however, be weak in contrast (Fig. 2c). If there are regions "missing" that are gray and flat, there is too much contrast in the mottle of the raw image to be subtracted properly. Reduce gain, adjust offset, and repeat the procedure.

Step 9: Digital Enhancement

This is done in a similar manner to step 5. Alternate between stretching a selected range of gray levels (setting "width") and shifting the image obtained up and down the scale of gray levels (setting "level" or "lower level") until a pleasing result is found (Fig. 2d). If available on your equipment, display the gray level histogram and select the upper and lower limits, which are to be defined as bright white and saturated black, respectively. If the image is noisy (pixel noise), go to step 10.

Step 10: Temporal Filtering (Frame Averaging)

Use an averaging function in a rolling (recursive filtering) or jumping mode over two or four frames. This

will still allow the observation of fairly rapid movements in your specimen, whereas very fast motions and noise due to pixel fluctuations will be averaged out. Averaging over a large number of frames will filter out all undesired motion and may be used with a fixed specimen or in order to remove, for example, distracting Brownian motion of small particles in suspension. The image will then contain the immobile parts of the object exclusively.

Please note that not all image processors are capable of performing background subtraction and the rolling average function simultaneously, as desired here. In this case, averaging generally yields the better image improvement for low light applications (fluorescence), whereas background subtraction is more advantageous in VEC microscopy, although this should be determined experimentally.

Step 11: Spatial Filtering

A large number of digital procedures for spatial filtering are available that can be used to reduce noise, to enhance edges of objects, or to reduce shading (Shotton, 1993; Russ, 1995). Some image processors offer such filters at video rate so that live sequences can be accentuated by filtering prior to recording.

Step 12: Printing Pictures

For publication purposes, pictures may be photographed or filmed off the video screen by observing special procedures and hints to remove video lines as discussed in detail by Inoué and Spring (1997) or Weiss *et al*. (1999). Alternatively, video printers are available with near-photographic or, at higher cost, with true pho-tographic quality that can be directly connected to the analog video output. Very good results are also obtained if all analog and photographic steps for printing can be avoided and the selected frame is directly transferred in digital form to a computer and from there to a high-resolution printer.

VI. INTERPRETATION OF IMAGES

Unlike in EM images, which truly resolve the submicroscopic objects depicted, the sizes of objects seen by AVEC-DIC microscopy may not necessarily reflect their real size. When AVEC-DIC is used, the limit of true resolution is shifted to almost one-half of that obtained conventionally. Objects smaller than the limit of resolution, i.e., 100–250 nm, depending on the optics and the wavelength of light used, are inflated by diffraction to the size of the resolution limit. The orientation of birefringent objects may also somewhat affect their apparent thickness if they are oriented at angles very close to 45° or 135°. Whereas the size of the image does not enable a decision on whether one or several objects of a size smaller than the limit of resolution are pre-sent, the contrast sometimes permits this judgment to be made. A pair of microtubules would, for example, have the same thickness as a single one, but the contrast would be about twice as high. If large numbers of subresolution objects are separated by distances of less than 200 nm from each other (e.g., microtubules in concentrated suspensions or vesicles in a synapse), they will remain invisible, but they will be depicted clearly if they are separated by more than the resolution limit.

Also remember that if in-focus subtraction or averaging over time is used, the immobile or the moving parts of the specimen, respectively, may have been completely removed from the image.

References

Allen, R. D., Allen, N. S., and Travis, J. L. (1981a). Video-enhanced contrast, differential interference contrast (AVEC-DIC) microscopy: A new method capable of analyzing microtubule-related motility in the reticulopodial network of *Allogromia laticollaris*. *Cell Motil*. **1**, 291–302.

Allen, R. D., Travis, J. L., Allen, N. S., and Yilmaz, H. (1981b). Video-enhanced contrast polarization (AVEC-POL) microscopy: A new method applied to the detection of birefringence in the motile reticulopodial network of *Allogromia laticollaris*. *Cell Motil*. **1**, 275–288.

Bennett, H. S. (1950). Methods applicable to the study of both fresh and fixed materials: The microscopical investigation of biological materials with polarized light. *In "Handbook of Microscopical Technique"* (C. E. McClung, ed.), pp. 591–677. Harper and Row (Hoeber), New York.

Brenner, M. (1994). Imaging dynamic events in living tissue using water immersion objectives. Am. Lab. April, 38–44 (also as Technical Bulletin from Nikon Inc. Melville, NJ).

Dodt, H. U., and Zieglgänsberger, W. (1990). Visualizing unstained neurons in living brain slices by infrared DIC-video microscopy. *Brain Res*. **537**, 333–336.

Ellis, G. W. (1985). Microscope illuminator with fiber optic source integrator. *J. Cell Biol*. **101**, 83a.

Foskett, J. K. (1993). Simultaneous differential interference contrast and quantitative low-light fluorescence video imaging of cell function. *In "Optical Microscopy: Emerging Methods and Applications"* (B. Herman and J. J. Lemasters, eds.), pp. 237–261. Academic Press, New York.

Hansen, E. W., Conchello, J. A., and Allen, R. D. (1988). Restoring image quality in the polarizing microscope: Analysis of the Allen video-enhanced contrast method. *J. Opt. Soc. Am*. **A5**, 1836–1847.

Inoué, S. (1961). Polarization microscope. *In "The Encyclopedia of Microscopy"* (G. L. Clark, ed.), pp. 480–485. Reinhold, New York.

Inoué, S. (1981). Video image processing greatly enhances contrast, quality, and speed in polarization-based microscopy. *J. Cell Biol*. **89**, 346–356.

Inoué, S., and Spring, K. R. (1997). "Video Microscopy", 2nd Ed., Plenum Press, New York, 741 pp.

lnoué, S. (1989). Imaging of unresolved objects, superresolution, and precision of distance measurement with video microscopy. *In* "*Methods in Cell Biology*" (D. L. Taylor and Y.-L. Wang, eds.), Vol. 30, pp. 85–112. Academic Press, New York.

Kachar, B. (1985). Asymmetric illumination contrast: A method of image formation for video light microscopy. *Science* **277**, 766–768.

Lange, B. M. H., Sherwin, T., Hagan, I. M., and Gull, K. (1996). The basics of immunofluorescence video-microscopy for mammalian and microbial systems. *Trends Cell Biol*. **5**, 328–332.

Russ, J. C. (1995). "The Image Processing Handbook," 2nd Ed. CRC Press, Boca Raton, FL.

Schnapp, B. J. (1986). Viewing single microtubules by video light microscopy. *Methods Enzymol*. **134**, 561–573.

Shotton, D. (1993). An introduction to digital image processing and image display in electronic light microscopy. *In* "*Electronic light Microscopy*" (D. Shotton, ed.), pp. 39–70. Wiley-Liss, New York.

Weiss, D. G., and Maile, W. (1993). Principles, practice, and applications of video-enhanced contrast microscopy. *In* "*Electronic Light Microscopy*" (D. Shotton, ed.), pp. 105–140. Wiley-Liss, New York.

Weiss, D. G., Maile, W., Wick, R. A., and Steffen, W. (1999). Video microscopy. *In* "*Light Microscopy in Biology*. *A Practical Approach*" 2nd Ed. (A. J. Lacey, ed.), pp. 73–149. Oxford University Press, Oxford.

Weiss, D. G., Meyer, M., and Langford, G. M. (1990). Studying axoplasmic transport by video microscopy and using the squid giant axon as a model system. *In* "*Squid as Experimental Animals*" (D. L. Gilbert, W. J. Adelman, Jr., and J. M. Arnold, eds.), pp. 303–321. Plenum Press, New York.

SECTION

3

Confocal Microscopy of Living Cells and Fixed Cells

CHAPTER

7

Spinning Disc Confocal Microscopy of Living Cells

Timo Zimmermann and Damian Brunner

I. INTRODUCTION

Confocal laser-scanning microscopy (CLSM) has in the last decade significantly extended our ability to visualise highly complex biological samples as multi-dimensional datasets (with dimensions of space and time, and different pseudocolours representing monochrome images collected from different fluorophores emitting at different wavelengths). In parallel, the introduction of fluorescent proteins such as green fluorescent protein (GFP) and its variants, as tags for structures of interest, has opened up new ways to observe intracellular processes *in vivo*. This article presents and discusses a variant of confocal microscopy, the spinning disc microscope, which is particularly well suited for fast three-dimensional (3D) real-time imaging of living cells, and describes its application to the imaging of yeast cells.

The most common type of confocal microscope uses a single focused laser beam to sequentially point scan a region of a sample. Spinning disc confocal microscopes (SDCMs) instead use a parallelised scanning approach with multiple confocal beams that simultaneously illuminate the sample. This overcomes the severe speed disadvantage that is inherent in the approach of sequentially scanning with a single beam. SDCM has thus become a powerful tool, especially for the time-limited requirements of *in vivo* imaging in combination with GFP technology.

A spinning disc confocal microscope consists of the confocal scanning unit containing the light source (a laser or fluorescence lamp), a rotating Nipkow disc with thousands of pinholes arranged in a geometric spiral, and a CCD camera, all of which are attached to a conventional light microscope (Fig. 1A). The light passes through the pinholes and then, when focused into the specimen by the objective lens, creates a set of confocal minibeams that sweep the chosen focal plane of the specimen as the disc rotates. The pinholes all have an identical, fixed aperture, and, in most commonly used setups, the excitation and emission light of each minibeam passes through the same pinhole (Inoué and Inoué, 2002; Kino, 1995). Because the pinholes only cover a small percentage of the disc surface, most of the excitation light would normally not pass the disc to reach the sample. This has for a long time been a limitation in the applicability of SDCM for weak fluorescence signals. However, Yokogawa Corp. overcame this problem by attaching a second disc on top of the pinhole disc that contains an identical array of microlenses, each of which covers a pinhole on the lower disc (Fig. 1A). Because each microlens focuses the excitation light of a larger region into its corresponding pinhole, this increases the efficiency of use of the excitation light from 1–4% (pinhole area) to 40–60% (Inoué and Inoué, 2002). This results in higher fluorescence emission signals due to the significant increase in excitation.

The fluorescence emission passes the pinholes and is then deflected onto the camera by a dichroic beam splitter, which is situated inbetween the two discs (Fig. 1A). Furthermore, because the unused excitation light is rejected already by the microlens disc, it cannot interfere with the detection signal, as would be the case in single disc designs.

In the Yokogawa scan unit, approximately 1000 of the 20,000 pinholes in the Nipkow disc cover the field of view of the microscope at any one time (Fig. 1B). The pinholes are arranged such that every region of the image is covered during one-twelfth of a disc rotation. Because the disc rotates at 1800 rpm, 360 full

Copyright 2006, Elsevier Science (USA).
All rights reserved.

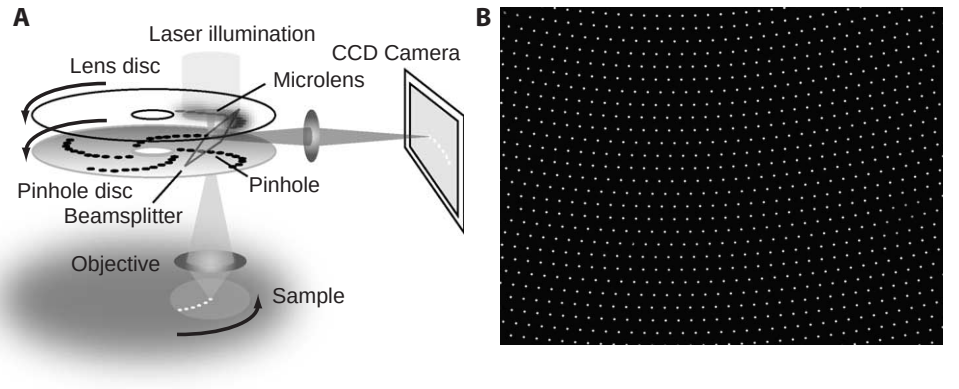

FIGURE 1 (A) Schematic of an SDCM setup. (B) Approximately 1000 of the 20,000 pinholes on the Nipkow disc cover the field of view of the microscope at any one time.

frames are scanned per second. This fast image acquisition rate means that two features of the CCD camera used for image detection become limiting: the sensitivity of the camera and its readout time.

Two alternative spinning disc designs use xenon or mercury arc lamps instead of laser light for excitation (ATTO Bioscience, Olympus). They can be added onto existing wide-field microscope systems and can be switched easily between wide-field and confocal imaging modes. Because they use lamps with a continuous emission spectrum, the excitation light can be controlled and varied with excitation filters. This flexibility is not available with systems employing lasers because there the excitation is limited to lines provided by the installed lasers.

II. MATERIALS AND INSTRUMENTATION

A. Materials

1. Media

All cell culture media are prepared in bulk and sterilised by autoclaving at 10 psi for 20 min. At this pressure, very little caramelisation of glucose takes place, which can cause background fluorescence. However, for live imaging we alternatively use sterile filtered medium to keep background fluorescence to an absolute minimum. The media is stored in 500-ml bottles, and agar is remelted in a microwave oven before using.

Yeast extract (YE): 0.5% (w/v) yeast extract (Bio 101 Systems—Q Biogene, 4018-022); 3.0% (w/v) glucose (Merck, 104074.1000)

Yeast extract + supplements (YES): YE plus 225 mg/l each of adenine, histidine, leucine, uracil, and lysine hydrochloride (all Sigma, A 9126, H 8125, 61820, U 0750, L 5626).

Edinburgh minimal medium (EMM 2): 3 g/liter potassium hydrogen phthallate (14.7 m*M*) (Sigma, P 3792); 2.2 g/liter Na_2HPO_4 (15.5 m*M*) (Merck, 106586.0500); 5 g/liter NH_4Cl (93.5 m*M*) (Merck, 101145.1000); 2% (w/v) glucose (111 m*M*) (Merck, 104074.1000); 20 ml/liter salts (stock "salts ×50"); 1 ml/liter vitamins (stock "vitamins ×1000"); and 0.1 ml/liter minerals (stock "minerals ×10,000").

"Salts ×50": 52.5 g/liter $MgCl_2{\cdot}6H_20$ (0.26 *M*) (Merck, 105833.1000); 0.735 mg/liter $CaCl_2{\cdot}2H_20$ (4.99 m*M*) (Merck, 102382.1000); 50 g/liter KCl (0.67 *M*) (Merck, 104936.1000); and 2 g/liter Na_2SO_4 (14.1 m*M*) (Merck, 106649.1000)

"Vitamins ×1000": 1 g/liter pantothenic acid (4.20 m*M*) (Sigma, P 2250); 10 g/liter nicotinic acid (81.2 m*M*) (Sigma, N 0761); 10 g/liter inositol (55.5 m*M*) (Sigma, P 7508); and 10 mg/liter biotin (40.8 µ*M*) (Sigma, B 4639)

"Minerals ×10,000": 5 g/liter boric acid (80.9 m*M*) (Merck, 100165.1000); 4 g/liter $MnSO_4$ (23.7 m*M*) (Sigma, M 1144); 4 g/liter $ZnSO_4{\cdot}7H_2O$ (13.9 m*M*) (Sigma, Z 0251); 2 g/liter $FeCl_2{\cdot}6H_2O$ (7.40 m*M*) (Sigma, F 2130); 0.4 g/liter molybdic acid (2.47 m*M*) (Sigma, M 1019); 1 g/liter KI (6.02 m*M*) (Sigma, P 5686); 0.4 g/liter $CuSO_4{\cdot}5H_2O$ (1.60 m*M*) (Merck, 1027900250); and 10 g/liter citric acid (47.6 m*M*) (Merck, 100244).

Minimal supplemented medium (used for vegetative growth): EMM2 plus 225 mg/liter each of adenine, histidine, leucine, uracil, and lysine hydrochloride (all Sigma, A 9126, H 8125, 61820, U 0750, L 5626), as described earlier for YES

Solid media: add 2% Difco Bacto agar (BD, 214010) to the appropriate liquid media before autoclaving

These media, and the fission yeast growth conditions employed, are described online under http://www-rcf.usc.edu/~forsburg/lab.html and in H. Gutz (1974) and Moreno *et al*. (1991).

2. *Other Materials*

Culture dishes (MatTec Corporation, P35G-1.5-10-C). Lectin BS-1 from *Bandeiraea simplicifolia* (Sigma, L-2380). Flow chamber (EMBL custom made, can be ordered from EMBL workshop). Silicon paste (Baysilone-Paste 35 g, hochviskos, GE Bayer Silicones).

B. Instrumentation

Spinning Disc Setups

Yokogawa scanheads: Two confocal scanning unit (CSU) designs by Yokogawa Corp. are available in our laboratory. The CSU-10 (Inoué and Inoué, 2002) is incorporated into several commercially available spinning disc setups (Perkin Elmer, VisiTech/Solamere). In addition to the CSU-10, we now also use a CSU-21 unit with higher and variable disc rotation speeds and with switchable filter sets. In our experiments, we use two Perkin Elmer setups with Hamamatsu Orca-ER CCD cameras and a 488/568/647-nm argon krypton laser, or 488/568/647-nm argon krypton, 442 helium/cadmium, and 488/514-nm Argon lasers, respectively. For switching between fluorescence channels, we use filter wheels (Ultraview LCI system) or acousto-optical tunable filters (AOTFs, Ultraview RS system).

III. PROCEDURES

In principle, there are no SDCM-specific restrictions, with respect either to the cell type or organism used or to the preparation/mounting procedures applied. Whatever specimen is mountable on an epifluorescence microscope or a single beam laser-scanning confocal setup can also be imaged using an SDCM. Here we present the mounting methods used for live imaging of fission yeast cells that express tubulin or microtubule-associated proteins tagged with GFP, CFP, and YFP (Brunner and Nurse, 2000; Ding *et al*., 1998; Drummond and Cross, 2000; Busch *et al*., 2004) and we describe the way we usually approach the task. To a large extent this approach would also be applicable to live imaging of yeast with epifluorescence and single beam confocal microscope setups.

A. Mounting Cells

Fission yeast cells can be mounted in a variety of ways for live imaging. However, for 3D imaging of intracellular structures over extended periods of time, it is important that the cells are absolutely immobile. Special attention therefore has to be given to immobilising the cells such that movements that would otherwise be created by medium flow cannot displace the cells during the acquisition process.

1. *Mounting Cells in Petri Dishes*

This method of adhering yeast cells to a coverslip allows imaging over short and intermediate time periods in liquid medium. Dividing cells will often disconnect from the glass surface and move out of the focal plane.

Steps

1. Use culture dishes with glass bottoms formed by 0.17-mm-thick microscope coverslips of 10 mm diameter. Be aware that their use is restricted to inverted microscopes! Wipe the glass surface inside the dish with a "cotton-bud" stick soaked in 70% ethanol containing one drop of glacial acetic acid per milliliter to remove the oil coating that is present on most glass surfaces. Rinse with double distilled water and dry with a Kimwipe.
2. Coat the cleaned glass surface by distributing 0.5 µl of 2 mg/ml lectin in H_2O with a pipette tip and allow to air dry.
3. Pipet 300 µl of cell suspension onto the coated glass and allow 5–10 min for cells to adhere to the lectin-treated glass surface.
4. Remove the medium and any unattached cells with a pipette, wash with 2 ml of fresh medium, and finally add 200 µl fresh medium for imaging.

2. *Mounting Cells on Solid Medium*

This method of embedding yeast cells in agar medium allows imaging over long time periods. Dividing cells will remain in the selected focal planes.

Steps

1. Stick one or more layers of narrow adhesive tape along the long axis of two slides, near one of their edges. The thickness of the tape will define the thickness of the agar pad and thus the amount of nutrients available. We usually make pads of about 0.25 mm thickness.
2. Place the slides on a flat surface to the left and the right of a third clean untreated, empty slide, leaving small gaps between the parallel slides (Fig. 2).

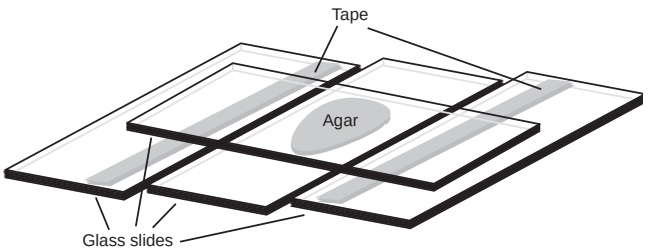

FIGURE 2 Setup for making agar pads.

3. Melt previously prepared agar medium in the microwave (open the lid of the container as it may explode) and apply a drop of the hot medium onto the middle of the central slide.

4. Place a fourth slide perpendicular to the other three, centred on top of the agar drop, and push its ends down onto the flanking slides in the taped area (Fig. 2). Keep pressing for about 30 s to allow cooling and repolymerisation of the agar.

5. Carefully remove the top slide (slow sideward sliding helps) and then, with a scalpel, trim away the edges of the remaining agar pad to make it slightly smaller than the square coverslip that will be used subsequently to cover the preparation.

6. Add a drop of yeast cell suspension onto the agar pad. Make sure that the cells are not too dense. Usually, the aim is to have isolated single cells distributed all over the agar surface, with clear areas between them.

7. Let the preparation stand until the agar has absorbed the fluid medium. Place a coverslip on top of the agar (avoid trapping air bubbles) and seal between the edges of the coverslip and the slide with a preparation of melted VALAP (a 1:1:1 mixture of vaseline, lanolin, and paraffin wax). The duration of usage of such a preparation depends on the thickness of the agar pad and on the density of the cells.

3. Mounting Cells in a Flow Chamber

This method allows imaging of cells over short and intermediate time periods. It is particularly suitable for applications where media are exchanged during image acquisition (i.e., drug wash-in/wash-out experiments).

Steps

1. The flow chamber (Fig. 3) consists of a closed cylindrical space (0.5 mm high) with connected inlet and outlet tubes for medium exchange, the ends of which, separated by 10 mm, can be sealed by circular coverslips of 15 mm diameter that form observation windows through which cells attached to the lower or upper coverslip can be observed using an inverted or upright microscope, respectively. Prepare the flow chamber for adhesion of the coverslips by covering the edges that will support them with silicon paste.

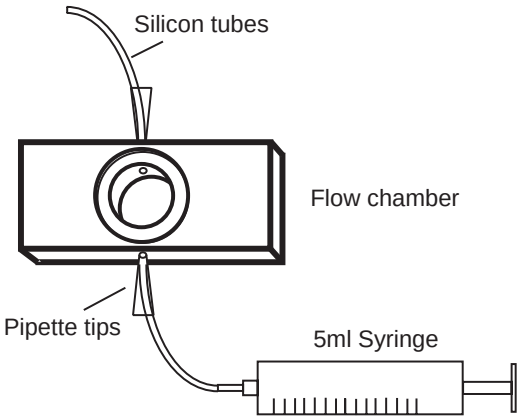

FIGURE 3 Design of a simple flow chamber. The core made of aluminium has the size of a standard microscopy slide except that it is slightly thicker. However, multiple sizes are available to suit the experimental requirements.

2. Clean two coverslips in 70% ethanol containing a drop or two of glacial acetic acid/ml as described previously. Rinse slides with water and dry with a Kimwipe.

3. Coat one coverslip with lectin as described earlier and place it on the silicon paste to form a window on the lower surface of the flow chamber, with the lectin-coated side facing inward.

4. Apply the cell suspension to the lectin-coated surface of the coverslip, let cells settle for 5 min, remove the medium, and wash once with fresh medium.

5. Immediately proceed to close the chamber by applying the second clean coverslip to form the upper window and flow in the required medium to fill the chamber and prevent the cells from drying out.

6. Exchange the medium as desired during image acquisition using the attached syringe.

B. Imaging Procedure

Several requirements have to be carefully considered to optimally resolve a dynamic process of interest in space and time. Above all, the total amount of light required for imaging should be kept to a minimum because the strong illumination needed for fluorescence microscopy observation will invariably affect the living sample, particularly if of a wavelength below 500 nm. The microscope setup should therefore be optimised to collect as much of the fluorescence signal as possible. Use high NA objectives and match

the refractive indices of the sample and the objective. Also the selected camera type is important. The more sensitive it is, the less excitation light is required for a viable signal. What should also be considered in the choice of camera is that for imaging very fast events, its readout time can become a limiting factor.

After optimizing the microscope setup, the first challenge is to set the imaging parameters such that your structure of interest can be unambiguously detected with sufficient contrast for the duration of the experiment, during which the signal intensity will decrease over time due to photobleaching. The observation intervals and the total experiment duration will therefore influence the initial image acquisition settings. Setting up such *in vivo* experiments thus means finding an optimal compromise between these variables.

Four relevant imaging parameters can be manipulated on an SDCM. (1) The excitation intensity defines the amount of photons that reach the sample and excite the fluorophores. (2) The exposure time defines the amount of emission light being collected by the CCD camera prior to each image readout. (3) The degree of CCD binning defines how many photons are sampled into a single image point (pixel), and also the spatial resolution. (4) Finally, the camera gain setting defines the overall sensitivity of the camera. How changing these parameters affects the image acquisition is shown in Fig. 4A. Figure 4B illustrates the interdependence of the parameters for three-dimensional (*x*, *y*, and *time*) temporal imaging experiments. For example, if the amount of excitation light (*n* photons) to be used for the complete duration of the experiment is defined, an increase in the number of time points has to be compensated for by decreasing the amount of excitation per image, either by shortening each exposure time or by reducing the excitation intensity. This will be perceived as a lower signal (compare a and b). If the signal level cannot be reduced, an increase in the number of time points for an experiment will be brought about by an increase in total irradiation (compare a and c), with concomitant increases in photobleaching (not shown in Fig 4B) and phototoxicity. An alternative possibility, which is not demonstrable in the illustration, is to increase CCD binning, which allows one to keep the irradiation dose low, but results in a loss of spatial resolution and thus of structural information.

The considerations we have discussed can be easily extended to four-dimensional (*x*, *y*, *z*, and *time*) temporal imaging, which is one of the strong points of SDCM. To collect a *z* stack of confocal *x*, *y* images spanning the relevant *z*-axis range of an object at each of several time points, three simple points have to be considered. (1) The range along the *z* axis should be set according to the thickness and expected movement of

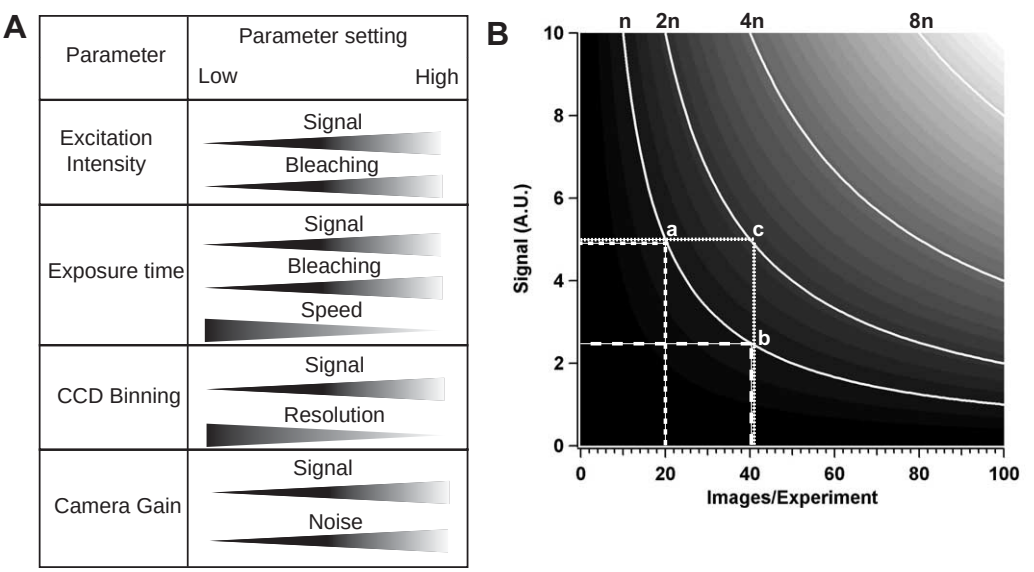

FIGURE 4 (A) Variables that can be changed on an SDCM and effects of the respective changes on other parameters that are relevant for live imaging. (B) The diagram shows interdependence among the number of frames taken in an experiment (*X* axis), the signal intensity per image (a function of exposure time and excitation intensity; *Y* axis), and the number of photons exciting the sample (*n* curves). A.U., arbitrary units of signal intensity.

the structures of interest. (2) It should not cover non-relevant regions. (3) The number of optical sections should be set according to the required z axis resolution and, to avoid unnecessary oversampling, should not be set smaller than half the z axis resolution of the confocal microscope itself. It is possible that ones initial ideal image acquisition settings have to be adjusted if the number of exposures required for the complete time series would otherwise result in unacceptable levels of photobleaching.

Steps for Setting up a SDCM in Vivo Experiment

1. Plan all general settings (time intervals, duration, camera settings) for the experiment using existing comparable images and sequences before putting the sample on the microscope. This minimises setup and fine-tuning time.
2. Use as little light as possible for finding the sample! Find the focal plane and, if possible, also your object of interest using phase contrast or DIC. This reduces unnecessary photobleaching prior to imaging. If you need to see the fluorescence to identify your object, first reduce the fluorescence excitation as much as possible.
3. Optimise the settings for image acquisition on the chosen object as discussed earlier and illustrated in Fig. 4A.
4. Once you find the optimal conditions, choose a new object. Set upper and lower z limits. With sufficient preexisting knowledge of the sample (e.g., the diameter of fission yeast cells is around 4 µm), upper and lower z limits can be set by focusing on the middle of the sample and setting the z limits around it without further imaging (e.g.) ±2.2 µm for fission yeast cells).
5. Always store all the raw image data before further processing the images.

C. Multicolor Imaging

SDCMs allow multicolor imaging from multiple fluorochromes. This is usually done by sequentially acquiring the appropriate fluorescence channel images. The switching between different detection settings can be done with filter wheels or (just for the excitation) with acousto-optical tunable filters. AOTFs are provided by the manufacturers of some of the new spinning disc setups (Perkin Elmer, VisiTec/Solamere). Sequential "multichannel" image acquisition at multiple wavelengths involves a significant reduction in the frame rate (at least by a factor of two) because at least two wavelength-specific images have to be acquired for every time point. This can be a limitation when observing very fast processes. Furthermore, fast structures might move during the time intervals between acquisition of the different wavelength images, leading to spatial mismatches between the different image channels. If this is the case, an alternative parallel acquisition approach, where the image channels are detected simultaneously, has to be implemented. For this, the emitted fluorescence is split into longer and shorter wavelength components by an appropriate dichroic beam splitter and is projected either onto separate CCD cameras or onto different regions of the same CCD chip. The recent introduction of sensitive color CCD cameras (such as the Orca 3CCD camera by Hamamatsu Photonics) increases the potential for fast multichannel imaging (T. Nagai, personal communication).

IV. COMMENTS

In imaging, as in all experiments, the tools should match the task. It is therefore important to understand the specific properties and advantages of the available imaging approaches. The following discussions highlight the abilities and shortcomings of SDCM versus single beam confocal and wide-field microscopes.

A. SDCM versus Single Beam Scanning Confocal Microscopy (see Table I)

1. Sensitivity

An essential point to be taken into consideration is the sensitivity of the detection devices. These are CCD cameras for SDCMs and PMTs for single beam confocal microscopes. CCD cameras have higher intrinsic quantum efficiencies than PMTs and therefore collect the available emission photons more efficiently, resulting in increased sensitivity (Inoué and Inoué, 2002). In practice, this significantly reduces the required exposure times in SDCM experiments, permitting higher frame rates and accordingly a speed advantage for equivalent signals when compared to single beam systems. This makes SDCM more suitable for imaging fast phenomena, although both types of confocal microscope are equally suited for time-lapse applications, where observations may be extended over several hours, with significant pauses between the acquisition of each 2D (x, y) image or each 3D (x, y, z) image stack.

2. Imaging Speed

SDCMs are particularly well suited for fast 3D (x, y, and *time*) and 4D (x, y, z, and *time*) temporal imaging. This is due to the almost instantaneous image generation by the spinning disc and the very sensitive CCD

TABLE I Comparison of Single and Multibeam Confocal Microscopes for *in Vivo* Imaging

	Single beam scanning confocal microscope	Multibeam scanning confocal microscope
Speed and temporal resolution	Frame rate limited to ~1 Hz at maximal spatial resolution +	High frame rate +++
Detection sensitivity	Photomultiplier tube +	CCD camera ++
Avoidance of photobleaching for equal image signals	More excitation required +	Less excitation required ++
Multichannel imaging	Simultaneous detection ++	Sequential detection usual +
Region bleaching or photoactivation	Possible ++	Not possible without additional hardware –
Optical sectioning efficiency (*z* resolution)	Adjustable pinhole diameter, giving optimal exclusion of out-of-focus blur ++	Fixed pinhole diameter, allowing possible contribution of unwanted out-of-focus blur +

cameras that can be used. The frame acquisition rate is determined by the exposure time required by the CCD camera. With sensitive cameras this can be lowered considerably. In this way, the high frame rates required for resolving fast events can be achieved. Generally, an image of equal quality and resolution can be generated significantly faster on an SDCM than on a single beam scanning confocal microscope. The speed disadvantage of single beam systems can, however, be partially overcome by scanning only a small subregion of the total image field. Furthermore, if only a single line is read out [e.g., acquisition of a 2D (*x* and *time*) image, suitable for certain types of Ca^{2+} imaging], the scan rate of a single beam confocal microscope can significantly exceed the frame rate of an SDCM.

3. *Photobleaching and Phototoxicity*

An observation made by many researchers working with both single beam and multibeam confocal systems is that photobleaching seems to be reduced in multibeam systems, permitting the same kind of sample to be observed over a longer period of time. However, it has been shown that the absolute rate of bleaching in SDCMs is similar to that using other confocal microscopes (Inoué and Inoué, 2002). The difference seems to be mainly due to the increased sensitivity of detection, which allows less excitation light to be used in SDCM.

4. *Optical Sectioning*

Adjusting the diameter of the detection pinhole varies the thickness of an optical section in a single beam confocal microscope, and hence *z* resolution. This is not possible with an SDCM. Here, the pinhole diameter is fixed because the holes in the disc cannot be modified. The numerical aperture of the objective employed therefore defines the thickness of the optical section. With high NA objectives (>1.3), this is in the range of <1 µm at 488 nm excitation. Furthermore, when imaging within thick specimens, out-of-focus fluorescence from an excitation minibeam can reach into neighbouring pinholes, which will compromise confocality (Inoué and Inoué, 2002). For such specimens, the optical sectioning will therefore be better if a single beam confocal microscope is used. For dynamic *in vivo* applications, however, these sectioning considerations are usually outweighed by the superior acquisition performance of multibeam systems.

B. SDCM versus Wide-Field Microscopy

Almost all of the mentioned positive features of SDCM (speed, sensitivity) also apply to wide-field microscope setups, which in principle are even faster due to the fact that the entire field of view is illuminated simultaneously. In addition, wide-field systems collect more of the emission light than SDCMs (since no emitted light is rejected by the disc of confocal pinholes), which is important for extremely weak fluorescence signals. However, due to the lack of confocality, deconvolution has to be applied to images generated on wide-field systems in order to gain a reasonable 3D resolution. Deconvolution is time-consuming and is

not trivial, as it critically depends on optimised system setups and image acquisition parameters in order to avoid the creation of artefacts, as well as requiring careful measurement of the point spread function of the microscope.

Furthermore, a z stack of wide-field images has to be acquired to enable deconvolution to be applied, and motion artefacts can be created in such a z stack when imaging fast processes. This is not the case for SDCM, as a single unprocessed image already constitutes a reasonably blur-free optical section. This means that SDCM has a significant speed and sample illumination advantage over a conventional wide-field microscope for fast temporal imaging of a single focal plane.

It should be noted that deconvolution can also be applied to z stacks acquired by SDCM, which can further increase the z resolution.

V. PITFALLS

Although most SDCMs use laser light for excitation, the laser cannot be used for spot or region bleaching as in single beam confocal microscopes. Powerful applications such as fluorescence recovery after photobleaching, photoconversion, or photoactivation, which are used to analyze protein dynamics in living cells, are therefore not possible. However, regional bleaching could, in principle, be made possible by implementing an additional positionable laser.

References

Brunner, D., and Nurse, P. (2000). CLIP170-like tip1p spatially organizes microtubular dynamics in fission yeast. *Cell* **102**, 695–704.

Busch, K. E., Hayles, J., Nurse, P., and Brunner, D. (2004). Tea2p Kinesin is involved in spatial microtubule organization by transporting tip1p on microtubules. *Dev. Cell* **6**, 831–843.

Ding, D.-Q., Chikashige, Y., Haraguchi, T., and Hiraoka, Y. (1998). Oscillatory nuclear movement in fission yeast meiotic prophase is driven by astral microtubules as revealed by continuous observation of chromosomes and microtubules in living cells. *J. Cell Sci.* **111**, 701–712.

Drummond, D. R., and Cross, R. A. (2000). Dynamics of interphase microtubules in *Schizosaccharomyces pombe*. *Curr. Biol.* **10**, 766–775.

Gutz, H. H., Leupold, U., and Loprieno, N. (1974). *Schizosaccharomyces pombe*. *In "Handbook of Genetics"* (R. C. King, ed.), pp. 395–445. Plenum Press, New York.

Inoué, S., and Inoué, T. (2002). Direct-view high-speed confocal scanner: The CSU-10. *Methods Cell Biol.* **70**, 87–127.

Kino, G. S. (1995). Intermediate optics in Nipkow disc microscopes. *In "Handbook of Biological Confocal Microscopy"* (J. B. Pawley, ed.), pp. 155–165. Plenum Press, New York.

Moreno, S., Klar, A., and Nurse, P. (1991). Molecular genetic analysis of fission yeast *Schizosaccharomyces pombe*. *Methods Enzymol.* **194**, 795–823.

CHAPTER

8

Confocal Microscopy of *Drosophila* Embryos

Maithreyi Narasimha and Nicholas H. Brown

I. INTRODUCTION

The genetically tractable organism *Drosophila melanogaster* is proving to be an excellent model system for cell biological analysis in the context of the whole organism. The relative ease with which embryos can be obtained in large numbers and processed for high-resolution light microscopy has facilitated many recent advances at the interface between cell and developmental biology. Fine subcellular structures previously impossible to visualise by conventional fluorescence microscopy, on account of high noise resulting from out-of-focus signals, are revealed with clarity on a confocal microscope.

There are several reasons why scientists who have not used *Drosophila* before may wish to use Drosophila embryos for the analysis of protein localisation and expression. The embryo contains representatives of each cell type and is small enough ($500 \times 100\,\mu m$) to fit within the field of view of a 20X objective lens. The embryos are nearly transparent, permitting visualisation of all cells in whole mount preparations. These features allow one to assay the tissue distribution of a particular protein in a single specimen. The tissues have a relatively simple structure, with the epithelia being made up of a single layer of cells. In general, there are fewer copies of each protein encoded by the genome compared with vertebrates, e.g., one α-actinin rather than four, further simplifying the analysis of the distribution of a particular kind of protein. Injection of double-stranded RNA can be an effective way to knock down protein expression, provided the bulk of the protein in the embryo comes from new synthesis. Sophisticated manipulation of the proteins is possible using the powerful molecular genetic techniques available in this organism.

While *Drosophila* has many advantages for cell biological analysis, it also has some drawbacks. The cells are small: an embryonic epidermal cell, for example, has dimensions of only $2 \times 5\,\mu m$ compared to a vertebrate epidermal cell of $10 \times 20\,\mu m$, which can make it difficult to resolve different intracellular compartments. The embryo is the only stage where the whole animal can be stained in its entirety; at late stages of development, antibody penetration is blocked by the secreted exoskeleton [although the use of proteins tagged with green fluorescent protein (GFP) circumvents this problem]. Therefore, the most easily generated samples for analysis are the embryo or tissues, that are easily dissected from the larva or adult, such as the imaginal discs and ovaries. Only a small number of *Drosophila* cell lines are available for *in vitro* culture and experimentation. These represent just a few cell types and are also small. Finally, antibodies raised against vertebrate proteins rarely bind to *Drosophila* orthologues, even when they are highly conserved. Therefore, new antibodies need to be raised to see the distribution of a given protein in *Drosophila*. An important exception to this are antibodies raised to specific motifs of proteins, such as those recognising particular phosphorylated residues. A growing number of antibodies against *Drosophila* proteins are available, either from the Developmental Studies Hybridoma Bank or directly from the laboratory that has generated them; few are available commercially.

This article describes the techniques used to look at cell junctions and cytoskeletal structures in the developing embryo, using both antibodies against

Copyright 2006, Elsevier Science (USA).
All rights reserved.

Drosophila proteins and GFP-tagged proteins expressed from transgenes.

The embryo is surrounded by two proteinaceous layers: the egg shell or chorion, which is removed easily; and the vitelline membrane, which is impermeable and more difficult to remove. The vitelline membrane can be permeabilised by treatment with heptane, permitting fixatives to reach the embryo. The vitelline membrane is generally removed by "popping" the embryos with a rapid osmotic shock produced by adding methanol to create a heptane–methanol interface and shaking vigorously. The fixation/devitellinisation steps are the part of the procedure most likely to go wrong, but with practice become routine. Once the embryos are fixed and the vitelline membrane removed, antibody staining is straightforward. Simple mounting of embryos is sufficient in most cases, which, due to the elongated shape of the embryo, allows many optical section views except a cross section of the embryo (i.e., cutting a slice from the middle of loaf of bread). As this can be very informative, we also describe a more labour-intensive method that allows such a view. We also make some recommendations for getting the best confocal images of *Drosophila* embryos. Additional references describing these methods are found in Davis (1999), Hazelrigg (2000), and Rothwell (2000).

II. INSTRUMENTATION AND MATERIALS

A. Equipment

Fly bottles or vials (250-ml bottles and 30/40 ml vials, Scientific Lab Supplies)
Egg collection cages (see Fig. 1, I)
Apple juice agar plates (see solutions)
Embryo collection baskets (see Fig. 1, I)
Scintillation vials (4 ml, 908-054, Jencons; 20 ml, 215/0079/00, BDH)
Rollers (Denley Spiramix 5 or equivalent)
Rotary shakers (Labinco BV or equivalent)
Microscope glass slides 76 × 26 mm (Menzel Glaeser, Superfrost Color)
Coverslips 22 × 22 mm, 22 × 40 mm (Menzel Glaeser)
Forceps (Watkins and Doncaster)
A001 size dissecting tungsten needles (E6871, Watkins and Doncaster)
Needle holder (Watkins and Doncaster)
$26G^{3/8}$, 0.45 × 10 syringe needle (Industrial and Scientific)
Artist's paintbrushes 00, 000

B. Reagents

Bleach (commercial)
Heptane (27051-2, Sigma)
Methanol (M/4000/PC17, Fischer Chemicals)
Ethanol (E/0555DF/17, Fischer Chemicals)
Formaldehyde (37–40%, 101134-A, AnalaR /BDH, reagent grade)
Paraformaldehyde (40% EM grade, 15715, Electron-microscopy Sciences)
Triton X-100 (T-9284, Sigma)
Bovine serum albumin (BSA) fraction IV (A-2153, Sigma)
NaCl (102415K, AnalaR/BDH)
KCl (101984L, AnalaR/BDH)
NaH_2PO_4 (301324Q, AnalaR/BDH)
Na_2HPO_4 (S-9390, Sigma)
KH_2PO_4 (102034B, AnalaR/BDH)
$MgCl_2$ (63064 Fluka Biochemika)
EGTA (E-4378, Sigma)
PIPES (P-8203, Sigma)
SDS (Ultrapure, Melford Labs Ltd.)
Glycerol (101184K, AnalaR/BDH)
Sucrose (S-0389, Sigma)
Apple juice (commercial)
Bactoagar (0140-01, Difco laboratories)
Nipagin (Nipa Laboratories Inc.)
Baker's yeast blocks (Commercial)
Vectashield (H-1000,Vector Labs, Burlingame)
Voltalef H10S Halocarbon oil (Elf Atochem, France)
Fly food (Instant *Drosophila* medium, Phillip Harris Scientific)

C. Solutions

1. *10× phosphate-buffered saline (PBS) (1 litre) (adapted from Sambrook and Russell, 2001):* 80 g (137 m*M* final) NaCl, 2 g (2.7 m*M* final) KCl, 14.4 g (10 m*M* final) Na_2HPO_4, 2.4 g (2 m*M* final) KH_2PO_4, and distilled water up to 1 litre. Dissolve all components in 800 ml of H_2O and make volume up to 1 litre. Adjust pH to 7.4 with HCl/NaOH. Sterilise by autoclaving.

2. *PBT (500 ml) PBS with 0.3% Triton X-100:* 50 ml 10× PBS, 750 µl Triton X-100 (0.3% v/v), 0.1 g (optional) sodium azide, and distilled water to 500 ml

3. *PBTB (500 ml) PBS with 0.3% Triton X-100 and 0.5% BSA:* 50 ml 10× PBS, 2.5 g BSA (0.5% w/v), 750 µl Triton X-100 (0.3% v/v), 0.1 g (optional) sodium azide, and distilled water to 500 ml.

4. PB: 77.4 ml (100 m*M* final) Na_2HPO_4 (1 *M*) and 22.6 ml (100 m*M* final) NaH_2PO_4 (1 *M*). Dissolve in distilled water to 1000 ml. Adjust pH to 7.4.

5. *PEM (4 ml) (adapted from Ashburner, 1989)*: 400 µl (100 m*M* final) 1 *M* PIPES (pH 6.9), 4 µl (1 m*M* final)

1 *M* $MgCl_2$, and 20 µl (1 m*M* final) 200 m*M* EGTA (pH 8.0). Adjust to pH 6.9 with 10 *M* KOH to final volume of 4 ml.

6. *4% formaldehyde in PBS (100 ml)*: 10 ml 10× PBS, 10.8 ml 37% formaldehyde, and 79.2 ml distilled water.

7. *Apple juice agar plates (1.6 litre)*: 36 g Bactoagar and 1200 ml distilled water. Dissolve the agar in a microwave oven or on a heating pad until the solution is clear. Dissolve 40 g sucrose in 400 ml apple juice in a microwave oven or on a heating pad until the solution is clear. Mix the two solutions once clear on a stirrer. Add 20 ml of 20% Nipagin when the solution has cooled below 60°C. Stir again and pour while still liquid into 5-cm/9-cm petri dishes. When set, store at 4°C. Allow to reach room temperature before use.

III. PROCEDURES

A. Producing Embryos for Confocal Microscopy

Steps

1. Grow up flies. If you are not a fly laboratory, try to obtain a few bottles from a fly colleague. Alternatively, make simple bottles with instant fly food, topped with cotton or a foam plug. Try to get the density of flies such that they are neither under- nor overcrowded. For 250-ml bottles, 20 females and 10 males will lay the ideal number of eggs per bottle in a 24-h period, after an initial lag of a couple of days while they feed and mate. Such a bottle will produce about 500 flies after 10 days at 25°C, depending on the food and the fly strain. Ideally, collect adult flies within 1–2 days after eclosion from the pupal case. For the egg collection cages described later, 25–200 females and about half the number of males is a good number.

2. Set up an egg collection cage containing an apple juice agar plate at the bottom, fixed on with tape, and a ventilation screen at the top (Fig. 1, IA). The plate should have an approximately 50 µl dab of yeast paste in the centre. Make yeast paste by stirring in a bit of water into the baker's yeast to make it the consistency of toothpaste. This is the food for the flies and is essential for the females to lay large numbers of eggs. Ensure that there is no excess moisture in the cage or plate (usually resulting from condensation on the plate). Put the flies into the cage and incubate at the desired temperature (usually 25°C). It will take a couple of days before the females lay substantial numbers of eggs, but once they get going each female can lay 100 eggs a day. Replace the yeasted apple juice plates at least once a day. To do this, invert the cage and peel back the tape holding the plate. Gently tap the flies down on the bench and quickly swap the plate. Even for the most practiced of us, this usually results in a few flies gaining freedom.

3. Collect embryos for analysis. Place a new yeasted apple juice plate on the cage. After the appropriate time period (e.g., 4 hs), remove the plate from the cage, replacing with a fresh one, and age the plate containing the embryos at 25°C for the desired length of time. Such short collections are an advantage when one is interested in a particular developmental event (for staging, see Wieschaus and Nuesslein-Volhard, 1998; Campos-Ortega and Hartenstein, 1997), and for the novice who has not yet learned how to stage embryos by visual examination. Embryogenesis lasts 22 h at 25°C, but the exoskeleton becomes secreted at about 16 h, making embryos older than this inaccessible to antibody staining using standard methods. Development takes twice as long at 18°C, allowing some adjustment to more convenient hours. The embryo plates can also be stored at 4°C for up to 24 h, but this has been known to cause subtle phenotypes. Overnight collections allow the examination of all stages of embryogenesis, but the distribution of embryos at the different stages is rarely even.

B. Removal of Chorion (Dechorionation)

In this step, the embryos are collected from the plate, washed well to remove yeast and other detritus from the plate and the eggshell (chorion) removed. You should prepare vials ready for the fixation step (**C**1) before starting this step.

Steps

1. Add about 2 ml water to each plate and, with the aid of a paintbrush, gently release the embryos from the agar (the eggs are usually partially pushed into the agar when they are laid).

2. Rinse/pour embryos into a meshed basket, made as shown in Fig. 1, IB.

3. Place the basket in a dish (the lids from the apple juice plates are useful for this) containing 50% bleach (1:1, water:commercial bleach). It should be made fresh and can be used for a maximum of 2 days. If older, the bleach still removes the chorion, but affects devitellinisation adversely. Swirl the basket in the dish and add more bleach into the basket. After 2–5 mins, most embryos will have risen to the surface, indicative of successful dechorionation. Do not extend the period in bleach beyond 5 min; prolonged exposure can destroy tissue architecture.

4. Wash the embryos thoroughly while in the basket by swirling embryos under running tap water or water from a squirt bottle.

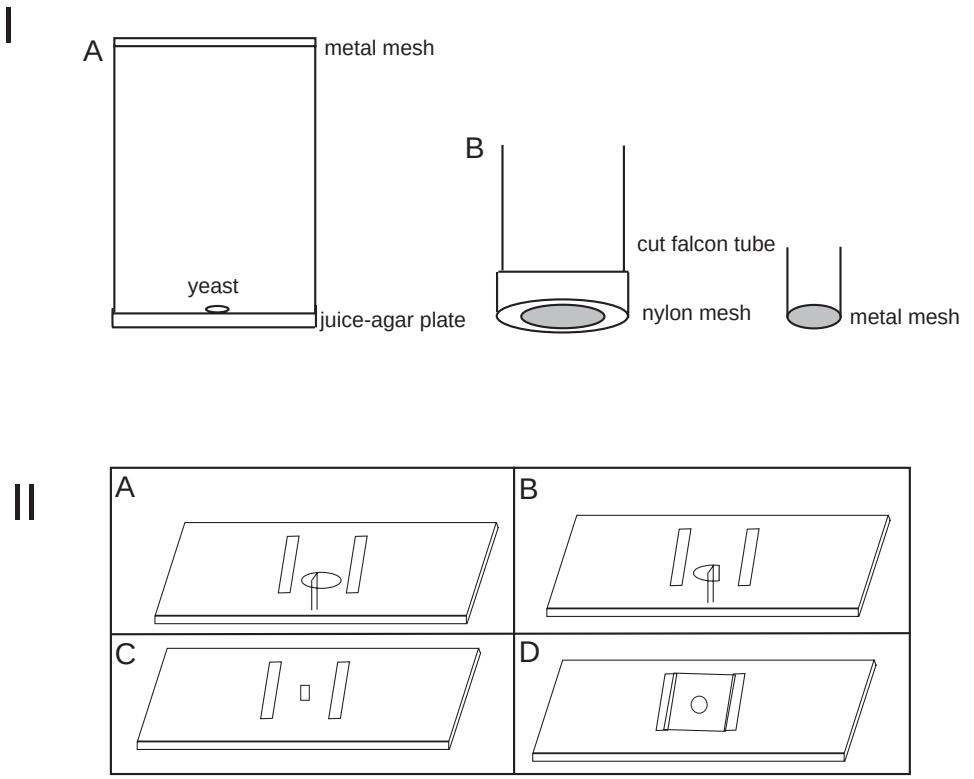

FIGURE 1 Schematic showing the parts that make up an egg-laying cage (IA). Apple juice agar is poured and allowed to set in petri plates. A dab of yeast is placed on warmed plates that are placed on top of cages containing flies. The plate is strapped onto the cage and the contraption is placed inverted in an incubator. The parts that make up an egg collection basket are shown in IB. A nylon mesh/sieve is screwed onto a cut 50-ml Falcon tube by the cap in which a hole has been cut using a hot scalpel blade. A 15-ml cut Falcon tube can also be used to make smaller baskets using metal wire mesh that is cut into rounds of the appropriate diameter and fastened onto the tube by melting the end of the tube with a hot scalpel blade. (II) Schematic showing how sections are cut. See text for details.

5. Briefly dry embryos by placing them on a paper towel. Do not overdry.

C. Standard Fixation and Removal of Vitelline Membrane (Devitellinisation)

Steps

1. Label a scintillation vial for each different sample of embryos (stage or genotype) and add 0.8 ml of 4% formaldehyde in PBS.

2. Transfer the basket of embryos into a dish containing heptane. Using a Pasteur pipette, transfer the embryos with the heptane into the scintillation vial containing 4% formaldehyde in PBS. The amount of heptane should be equal to or greater than the volume of fixative solution. Mix for 20–30 mins at room temperature or at 37°C on a roller or other device.

3. Remove the aqueous phase from the bottom with a Pasteur pipette and then remove the heptane. Add 1 ml of new heptane and then rapidly add 1–3 ml of methanol and shake by vigorous inverting/vortexing for 1 min. (If you want to stain the embryos with phalloidin, use 80–90% ethanol rather than methanol at this and the next two steps; this has the disadvantage that reduced number of embryos are successfully devitellinised.)

4. Let the embryos settle for about 10 s and then transfer the embryos from the bottom of the vial to an Eppendorf tube with a Pasteur pipette. Any embryos still at the interface between the heptane and the methanol have not popped out of the vitelline membrane and therefore will not stain well and should be left behind. An alternative method for this step is remove all of the liquid phase, including embryos that have not settled, leaving only the devitellinised embryos at the bottom of the vial. Add 1–2 ml of methanol to the embryos and vortex/shake for 30 s. Remove methanol.

5. Wash in methanol three times. For each wash, squirt in 1 ml of methanol so that the embryos disperse. Let the embryos settle by gravity and remove the methanol (this is called a gravity wash). Either proceed to the next step or add 1 ml methanol and store at –20°C (for embryos that will be stained with phalloidin store in 100% ethanol).

Comments

Embryos can be stored in methanol or ethanol at –20°C for several months and will continue to be successfully stained by most antibodies. However, detection of some antigens and GFP fluorescence are affected adversely by exposure to ethanol or methanol. In these cases, do steps 3–5 as rapidly as possible and proceed quickly to step **D**1. Some antibodies will not recognise their antigen in embryos fixed by this method, but will when one of the alternative methods described in Section III,**G** is used.

D. Antibody Staining of Embryos

Steps

1. Wash embryos in PBT (PBS with 0.3% Triton X-100): First give three to five quick washes, where 1 ml is squirted in so the embryos are dispersed, the embryos are allowed to settle by gravity, and then the PBT is removed (a gravity wash) and then give one longer wash (15 mins) with mixing. We use a device that gently inverts the tubes for this and all subsequent steps, but a variety of mixing devices should work. If mixing is not sufficient, it will result in variable staining of embryos in the tube.

2. (Optional) Staining with some antibodies is improved by a 15-min incubation in 0.1% SDS with mixing, followed by three washes in PBT. This may help those antibodies raised against bands from SDS gels.

3. Block nonspecific binding sites on the embryos by incubating in PBTB for 30 min. Transfer 15 µl (5–20 µl) of embryos to a 0.5-ml Eppendorf tube for each staining with a Pipetteman and a yellow tip with the last couple of millimeter of the end cut off with a razor blade. Rinse the tip with some PBT before taking up the embryos. While the volume of embryos is not critical, larger volumes can result in uneven staining. The volume of 15 µl of embryos corresponds to about 100 embryos, which is sufficient for most purposes. If more embryos are desired, use multiple tubes or a larger tube for staining.

4. Incubate embryos with 250–500 µl of PBTB containing an appropriate dilution of each primary antibody at 4°C overnight. Optimal timing depends on the antibody and whether staining of internal tissues is important, in which case longer incubations are recommended. We have successfully used a range from 2 h at room temperature to 2 days at 4°C. If the appropriate dilution is not known, a good starting point is 1 : 1000 for antisera and 1 : 10 for monoclonal antibody supernatants.

5. Wash off the primary antibody with PBT with three to five gravity washes and one to three longer (at least 15 min) washes.

6. Incubate with fluorochrome-conjugated secondary antibodies diluted in PBTB as suggested by the manufacturer (usually 1 : 100–300) at room temperature for 2 h or overnight at 4°C. The choice of fluorochrome coupled will depend on the laser lines of the confocal you are using. Our preferred ones are Alexa488, Alexa568 or Cy3, and Cy5. We tend to keep the embryos in the dark during the incubation.

7. Wash secondary antibodies off with three to five gravity washes and three longer (5–30 min each) washes in PBT. Washing overnight is also fine. The embryos can be left for a day or two in PBT at 4°C, but it is better to store them after step **F**1 or once mounted on microscope slides.

E. Staining with Phalloidin to Visualise Actin

Steps

1. Embryos that have been exposed to methanol will not stain with phalloidin, so use 90% ethanol rather than methanol during devitellinisation.

2. Dissolve rhodamine-conjugated phalloidin in methanol (methanol harms the actin, not the phalloidin) and store at –20°C in aliquots of 6 units. To stain embryos, vacuum dessicate the required number of aliquots and resuspend in PBTB at 1 unit/100 µl.

3. Follow sections **D**1 and **D**2. (If phalloidin staining is to be combined with antibody staining, proceed through sections **D**3 to **D**5 and then go to **E**4. Phalloidin can be combined with the secondary antibodies at **D**6, at the concentration described later.

4. Incubate embryos with 1 unit of phalloidin (100 µl of the aforementioned solution, plus 400 µl PBT or PBTB)/0.5 ml tube containing approximately 20 µl of embryos for at least 30 min.

5. Wash twice with PBT (if combined with secondary antibodies, wash more thoroughly).

F. Standard Mounting on a Microscope Slide

Steps

1. After the final wash, replace PBT with 50–200 µl of Vectashield or similar glycerol-based mounting

medium containing antibleaching agents. The embryos can be stored at 4°C for a couple of days or, for longer periods, allow 30 min to equilibrate in the Vectashield and store at –20°C.

2. Using a Pipetteman and a yellow tip with the end cut off, transfer some of the embryos onto a slide. First suck up approximately 5 µl of Vectashield alone and then the embryos, as this reduces sticking of the embryos to the inside of the yellow tip. For a 22 × 22-mm coverslip, use 20–30 µl per slide. The lower volume will lead to a mild flattening of the embryos, which can be an advantage, but is trickier to mount without air bubbles. As you add the embryos to the slide, move the tip to spread them out over a square region a bit smaller than the coverslip. Using a needle or similar instrument (such as plastic Pipetteman tip with a very small diameter), gently distribute the embryos more evenly and separate them from each other. (Do not fiddle too long with this, as they will generally distribute into a monolayer when the coverslip is placed on top, but this step helps reduce or eliminate the number of embryos lying on top of each other.) The goals of the experiment will dictate the optimal number of embryos per slide. For staged embryos, it is better to have fewer embryos, less than 30 per slide. You can then in a single session on the confocal completely examine all embryos on the slide and start a new session with a new slide. This is helpful because it is easier to find the best embryos at low power and then add oil for the image collection. If you have embryos from an overnight collection, a larger number of embryos improves the chance of finding each stage on a given slide. With a forceps, gently place a coverslip over the embryos, starting at one end to avoid introducing air bubbles and gently let go of the forceps as the Vectashield spreads. If a small volume has been used to flatten the embryos, let sit for 10 min and then if there is still air under the coverslip, add a little more Vectashield to an edge.

3. (Optional) Seal the edges with nail varnish (but see Section III,G,5).

General Comments

Almost every aspect of this procedure will vary from fly laboratory to fly laboratory and even within our laboratory there are a number of variations. None of the following are critical: which recipe is used for the egg collection plates (some laboratories prefer grape juice), the tubes used for fixation and staining, the solutions used for antibody staining, the timing of the incubations and the number of washes, and the medium for mounting the embryos. As mentioned at the beginning, the key steps are fixation and devitellinisation. Again there are many variants of this, and the important thing is to get a method that works well for the antibodies you are using. Once you have a method that works, try to do this step as identically as possible each time. This will give you reproducibly good staining. Generally, the first time a new person in the laboratory does this technique it does not work well. However, after a few times, it is hard to understand how you could have failed the first time. A simple check is to look at a few embryos at step **C**4 or **D**1 down a dissecting microscope. If the embryos are still surrounded by the transparent shiny vitelline membrane, throw them away and try again. Before moving onto microscopy, we will mention some useful variants of this technique.

G. Alternative Methods for Embryo Fixation and Devitellinisation

1. Alternative Fixation Solutions

In these the method is identical to that described earlier, but instead of 1:1 4% formaldehyde in PBS:heptane, and 20–30 min at room temperature, use the following alternatives.

1:1 4% formaldehyde in PEM:heptane, 20–30 min at room temperature.
1:1 4% formaldehyde in PB:heptane, 20–30 minutes (Uemura *et al*., 1996).
1:1 37% formaldehyde:heptane, 2–5 min at 25–37°C with gentle mixing

This can improve the preservation of cytoskeletal structures present in membrane compartments [e.g., scribble, β-heavy spectrin (Bilder *et al*., 2000)] and gives the best preservation of microtubules (Foe *et al*., 2000).

2. Heat Fixation (Muller et al., 1996)

Heat fixation improves the penetration of antibodies into late stage embryos and larvae (when the exoskeleton normally blocks antibodies).

Steps

1. With a paintbrush, transfer dechorionated embryos from the dechorionation basket into a scintillation vial containing 1–2 ml of 0.4% NaCl and 0.3% Triton X-100 solution that has been heated in a boiled, but no longer boiling, water bath with its cap half screwed on.
3. Pull the vial out of the hot water bath, screw cap tightly, and shake once vigorously.
4. Uncap the vial and fill up with ice-cold 0.4% NaCl and 0.3% Triton X-100.
5. Leave on ice until cooled.

6. Pour off the solution, add heptane and methanol in equal volumes, and vortex to devitellinize.
7. Remove embryos from bottom, transfer to new tube, and wash twice with methanol.
8. Incubate in methanol for an additional hour and proceed as usual for antibody staining.

3. Fixation Conditions for Visualising Nonmuscle Myosin (Foe et al., 2000)

Steps

1. Transfer dechorionated embryos to 4 ml of fixation solution: 1 volume 40% formaldehyde (EM grade) and 3 volumes PBS.
2. Vortex for 45 s and add 4 ml heptane.
3. Shake vigorously for 25 min.
4. To devitellinise the embryos, use either 80–90% ethanol (as for phalloidin described earlier) or hand peel embryos after replacing the fixation solution with PBS many times (see Section III,J,1).

4. Methanol Fixation

Steps

1. Transfer dechorionated embryos to 1:1 heptane: (97% methanol, 3% 0.5 *M* NaEGTA, pH 8.0)
2. Shake hard for 2 min.
3. Transfer embryos from the bottom of the vial to a 1.5-ml Eppendorf tube.
4. Wash three times with methanol
5. Incubate in methanol overnight at 4°C.

This is a good alternative when a new antibody fails to stain embryos fixed under standard conditions, as a number of antibodies have been found to only work on embryos prepared by this method. Other antibodies will work with both this method and standard fixation, while some will not stain with this method.

5. Fixation Conditions for Visualising GFP

If you are planning to visualise GFP fluorescence, keep exposure of the embryos to methanol or ethanol to a minimum and do not seal the slides with clear nail varnish. Organic solvents quench GFP fluorescence or severely affect its ability to fluoresce.

H. Embryo Thick Sections (Adapted from Grosshans and Wieschaus, 2000)

To get a good cross-sectional view of the embryo by confocal microscopy it is necessary to cut sections. They give far better resolution than optical *X-Z* scans (see later and Figs. 2E and 2F). We have used a relatively crude method that does not require a microtome and is compatible with our standard methods for antibody staining. These sections are particularly useful for the visualisation of morphogenetic events that occur in the midline and in the interior of the embryo, such as invagination of the mesoderm, formation of the midgut, and dorsal closure.

Steps

1. Fix and stain the embryos according to the desired protocol. It is hard to combine this method on phalloidin-stained embryos, because the ethanol (rather than methanol) treatment results in embryos that are harder to cut and the morphology is not as well preserved.

2. Follow the antibody staining protocol described in Section III,**C**. Keep embryos in PBT after the secondary antibody has been washed off.

3. Refix the stained embryos in 4% formaldehyde in PBT for 30–60 min at 37°C.

4. Wash the embryos in PBT, do three gravity washes, and one 15-min wash with mixing.

5. Take the embryos through a glycerol series comprising of 10, 20, and 30% glycerol in PBT for 1 h each followed by 40% overnight. (This is the optimal concentration, do not go higher.)

6. On clean dusted microscope slides, make bridges with strips of coverslips cut using a diamond knife. These are stuck to the slide using clear nail varnish.

7. Place an embryo on the slide in a drop of Vectashield between the bridges (see Fig. 1, IIA).

8. To cut the embryo, use a $26G^{3/8}$ hypodermic needle fitted to a 2.5-ml syringe whose plunger has been removed. Cut at one end in one clean sweep with the bevelled edge facing away from the slice you wish to keep. Turn the embryo around with the dissecting needle. Once again, with the bevelled edge of the needle pointing away from the slice you want to keep, cut the embryo to obtain a slice of the desired region (Fig. 1, IIB). The thickness of the section must be approximately the same thickness as the bridges; that is the thickness of a coverslip, which is about one-fifth the length of the embryo. If the sections are thinner, they are hard to orient and most of the section is beyond the depth of focus of the 60× objective; if they are thicker, the morphology is distorted by the resulting squashing. With practice you can cut more than one section from the same embryo, but each should be mounted on a separate slide due to slight differences in thickness.

9. Remove the undesired embryo pieces with the dissecting needle (Fig. 1, IIC) and orient the desired slice so that it lies at the bottom of the drop of Vectashield with its anterior face up.

10. Place a 22 × 22-mm coverslip over the section and the bridges (Fig. 1, IID). Do not seal the sides to

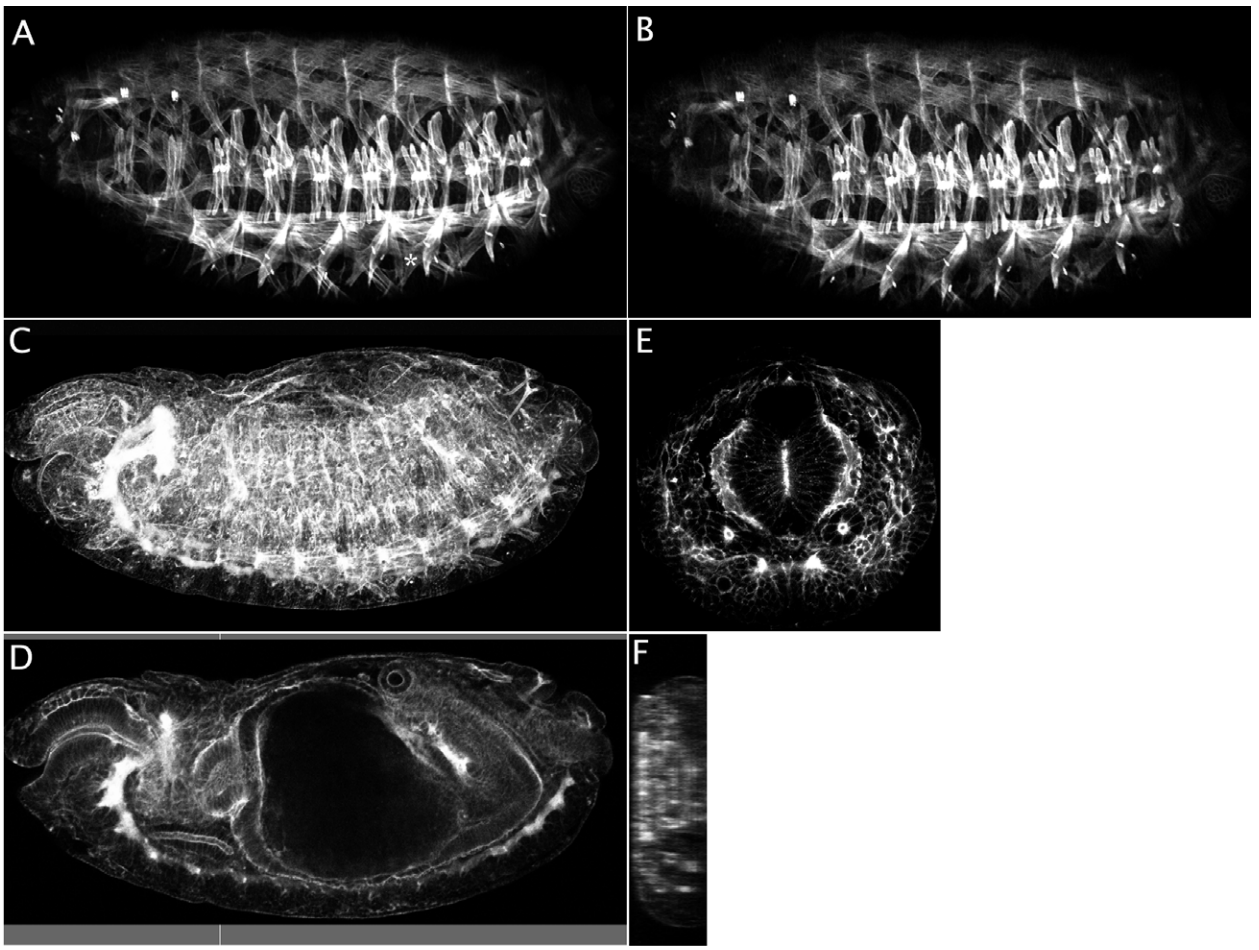

FIGURE 2 A projection of four optical sections of a late *Drosophila* embryo stained with phalloidin to highlight actin in somatic muscles (A) is compared to a single optical section (B). Note that some muscles (asterisk in A) are not visualised in the single optical section. A projection of 42 sections of a *Drosophila* embryo stained with phalloidin is used to visualise actin in the whole embryo (C). A single optical section through the same embryo (D) reveals staining in internal structures that are obscured by the extensive surface staining in C. A confocal generated *X*–*Z* section along the *Z* axis depicted by the white line in D is shown in F. Such a scan provides very poor resolution. A single optical section of a thick section cut (as described in Section III,H) to include the same region of the embryo as shown in D is shown in E. Such a section resolves the apicobasal extension of actin especially in internal organs that are obscured in whole embryos. In all images, the dorsal surface of the embryo is on top. In A–D, the anterior end of the embryo is on the left.

allow for reorientation. If the section is slightly thinner than the thickness of the coverslip, it may move/turn in the drop of Vectashield. Slight pressure on the corner of the coverslip can then bring the section back to its right orientation. If the section moves under the coverslip during imaging, abandon that section and proceed to the next.

11. View under a 60× oil immersion objective lens.

I. Confocal Microscopy

Drosophila embryos can be examined with a variety of confocal microscope setups. Both inverted and upright microscopes are appropriate. The key variable is the available laser lines; this will dictate the optimal choice of fluorochrome-conjugated secondary antibodies that one should use. A detailed description of confocal microscopy is clearly beyond the scope of this article (a good reference is Centonze and Pawley, 1995), but we hope to provide a few helpful hints.

Once one has obtained an initial quick view of the result of the staining, which is often possible by conventional fluorescence microscopy if the signal is strong, the usual goal is to produce a set of images for publication. The biggest challenge is to produce a set of comparable images of different embryos. For

example, for a general description of the distribution of a new protein one would like comparable views of embryos at different stages; generally a lateral view. There is a strong convention in the fly field regarding images of embryos: they should always have anterior to the left and dorsal up. Similarly, for a comparison of staining in different mutants, it is essential to obtain a suitable micrograph from wild type and each mutant at the same stage and with the same view: this can often require looking through many embryos. Clearly, to be able to achieve this you must be able to tell the stage of the embryo and which way is up, which is not as easy as it sounds. The only way to achieve this is to spend time looking at embryos down the microscope. To learn your way around embryonic development, it helps to examine embryos that are stained with antibodies that highlight the development of a particular tissue. The following antibodies are recommended for this: Fasciclin III (available from the Developmental Studies Hybridoma Bank) and phosphotyrosine (available from Sigma). For an overall view of the embryo, phalloidin (rhodamine conjugated, Molecular Probes) is very useful (see Fig. 2).

In general, we start our confocal session by first scanning through the slide by conventional fluorescence, taking note of the approximate position on the slide of embryos of the right stage and orientation that have stained well. Next we find a well-stained embryo that is not one of the best ones and use it to work out the appropriate settings for each channel on the confocal. When it is essential that there is minimal mixing between the outputs of each channel, then it is advisable to do sequential scanning rather than simultaneous. Use the channel with the brightest signal to get started. In most cases we use a collection area of 1024 $\times$ 768 pixels. Using rapid scanning, find the best focal plane, adjusting the focus by hand (adjustments to the eyepieces often result in the view by eye being at a different focal plane than the resultant scan). Using intermediate scan rates, set the laser power, iris, gain, and background levels appropriately for the first channel and then proceed to the next channel. We keep the iris similar in the different channels so that they all capture the same depth of focus. Some confocal setups have this feature built into the software.

Once all channels are set up, adjust the focus to obtain the optimal image. Collect images using Kalman scanning to improve the signal-to-noise ratio. We use either 166 lines per second with three to five scans or 50 lines per second and two scans. Make a note of the orientation of the embryo, especially if you are just focused on a small region.

Because the embryo is curved, in many cases a single section will not capture all of the relevant tissue. In this case, collect a series of sections at different focal planes and combine them into a single image using the projection software. The first step is to find the top and bottom of the series you wish to collect. Turn on the focus motor, doing fairly rapid scans in a channel with the most robust signal, and vary the focal plane to find the top and bottom. Be aware that with an oil objective lens, the new focal plane can take a minute to "settle." Set up the software to collect the Z series. Generally we use a step of 1 µm, with a range from 0.5 to 2.0 µm. Collect the Z series and project the image. For some tissues, e.g., the somatic muscles, it helps if the embryos are mildly flattened by mounting in a minimal amount of Vectashield, as described in Section III,**F**,2; then fewer scans are required to visualise all the muscles (Figs.2A and 2B).

One other variable to keep an eye on is the zoom. We standardly keep this at 1 (no zoom), and it is helpful to check that it has not been varied by a previous worker, as your images from session to session will not be comparable. Some judicious use of the zoom function can improve resolution. In practice we have found that a zoom factor of greater than two provides no further improvement in resolution and may even lead to loss of resolution.

J. Examination of GFP in Living Embryos

Steps

1. For imaging live embryos, briefly dry embryos over a paper towel after dechorionation. Alternatively, the embryos can be dechorionated by hand by gently rolling on double-stick 3MM Scotch tape with a forceps.
2. Transfer embryos in their vitelline membranes with a paintbrush or forceps to a drop of halocarbon oil. Cover with a coverslip and leave the slides unsealed. For time-lapse analysis it is essential to use a method that allows better access of air to the embryo. We use a microscope slide consisting of an air-permeable Teflon membrane in a holder (Edwards *et al.*, 1997; Kiehart *et al.*, 1994).

IV. COMMON PROBLEMS

A. Nonstaining Embryos

The most common causes are (i) use of inappropriate fixation method, (ii) inefficient devitellinisation, (iii) inappropriate primary and/or secondary antibody, and (iv) faulty laser, either nonfunctioning or unsuitable for the fluorochrome coupled to the secondary antibody.

B. Bleaching

This is a common problem inherent to confocal microscopy, especially during the acquisition of a Z series at high laser power and high magnification. It can be reduced by ensuring that the laser power is set to the minimum value that is optimal for the image.

C. Low-Resolution Images

Low-Resolution Images can result from faulty image processing of the original image. Obtain the highest resolution image possible on the confocal. Information that does not exist in the acquired data cannot be added by image processing software. Too high a gain can result in too much noise. Such noisy images may be improved by increasing either the iris or the laser power. Out of focus signals resulting from inappropriate mounting and from inappropriate thickness of sections are the cause of low-resolution images from sections.

Acknowledgments

We thank Sylvia Erhardt, Anja Hagting, Jasmin Kirchner, Jordan Raff, Katja Roeper, Alex Sossick, and Christos Zervas for comments and suggestions.

References

Ashburner, M. (1989). "*Drosophila*, a Laboratory Manual," p. 372. Cold Spring Harbor Laboratory Press, Cold Spring Harbor, NY.

Bilder, D., Li, M., and Perrimon, N. (2000). Cooperative regulation of cell polarity and growth by *Drosophila* tumor suppressors. *Science* **289**(5476), 113–116.

Campos-Ortega, J., and Hartenstein, V. (1997). "The Embryonic Development of *Drosophila melanogaster*," pp. 1–102. Springer-Verlag, Berlin.

Centonze, V., and Pawley, J. (1995). Tutorial on confocal microscopy and use of the confocal test specimen. *In* "*Handbook of Biological Confocal Microscopy*" (J. Pawley. ed), pp. 549–569. Plenum Press, New York.

Davis, I. (1999). Visualising fluorescence in *Drosophila*: Optimal detection in thick specimens. *In* "*Protein Localization by Fluorescence Microscopy*" (J. V. Small, ed.), pp. 133–161. Oxford Univ. Press, Oxford.

Edwards, K. A., Demsky, M., Montague, R. A., Weymouth, N., and Kiehart, D. P. (1997). GFP-moesin illuminates actin cytoskeleton dynamics in living tissues and demonstrates cell shape changes during morphogenesis in *Drosophila*. *Dev Biol*. **191**, 103–117.

Foe, V. E., Field, C. M., and Odell, G. M. (2000). Microtubules and mitotic cycle phase modulate spatiotemporal distributions of F-actin and myosin II in *Drosophila* syncytial blastoderm embryos. *Development* **127**(9), 1767–1787.

Grosshans, J., and Wieschaus, E. (2000). A genetic link between morphogenesis and cell division during formation of the ventral furrow in *Drosophila*. *Cell* **101**(5), 523–531.

Hazelrigg, T. (2000). GFP and other reporters. *In* "*Drosophila Protocols*" (W. Sullivan, M. Ashburner, and W. Scott Hawley, eds.), pp. 313–344. Cold Spring Harbor Laboratory Press, Cold Spring Harbor, NY.

Kiehart, D. P., Montague, R. A., Rickoll, W. L., Foard, D., and Thomas, G. H. (1994). High resolution microscopic methods for the analysis of cellular movements in *Drosophila* embryos. *Methods Cell Biol*. **44**, 507–532.

Muller, H. A., and Wieschaus, E. (1996). armadillo, bazooka, and stardust are critical for early stages in formation of the zonula adherens and maintenance of the polarized blastoderm epithelium in *Drosophila*. *J Cell Biol*. **134**(1), 149–163.

Rothwell, W. F., and Sullivan, W. (2000). Fluorescent analysis of embryos. *In* "*Drosophila Protocols*" (M. Ashburner, W. Sullivan, and R. Scott Hawley, eds.), pp. 141–158. Cold Spring Harbor Laboratory Press, Cold Spring Harbor, NY.

Sambrook, J., and Russell, D. W. (2001). "Molecular Cloning: A Laboratory Manual," A1.7. Cold Spring Harbor Laboratory Press, Cold Spring Harbor, NY.

Uemura, T., Oda, H., Kraut, R., Hayashi, S., Kotaoka, Y., and Takeichi, M. (1996). Zygotic *Drosophila* E-cadherin expression is required for processes of dynamic epithelial cell rearrangement in the *Drosophila* embryo. *Genes Dev*. **10**(6), 659–671.

Wieschaus, E., and Nuesslein-Volhard, C. (1998). Looking at embryos. *In* "*Drosophila, a Practical Approach*" (D. Roberts, ed.), pp. 179–213. IRL Press (Oxford Univ. Press), Oxford.

CHAPTER

9

Ultraviolet Laser Microbeam for Dissection of *Drosophila* Embryos

Daniel P. Kiehart, Yoichiro Tokutake, Ming-Shien Chang, M. Shane Hutson, John Wiemann, Xomalin G. Peralta, Yusuke Toyama, Adrienne R. Wells, Alice Rodriguez, and Glenn S. Edwards

I. INTRODUCTION

Laser microbeams provide a unique opportunity to augment traditional genetic and cell biological analysis of biological phenomena with surgical studies that selectively damage cells, allowing us to "interrogate" the mechanical properties of adjacent tissues. By applying biophysical and quantitative reasoning to the results of microbeam surgery on wild-type and mutant embryos, we gain insight into the molecular basis of changes in cell and tissue structure during processes such as morphogenesis and wound healing. Previously, microbeams have been used for a wide variety of applications, including surgery, ablation, chromophore-assisted laser inhibition, and molecular uncaging (e.g., Berns *et al*., 1991, 1998; Bargmann and Avery, 1995; Lin *et al*., 1995; Skibbens *et al*., 1995; Wang and Augustine, 1995; Buchstaller and Jay, 2000; Grill *et al*., 2003). This article describes the use of ultraviolet (UV) laser microbeam interrogation strategies, combined with confocal microscopy, to investigate the developmental process of dorsal closure (Figs. 1 and 2; see also Kiehart *et al*., 2000; Harden, 2002; Jacinto *et al*., 2002; Hutson *et al*., 2003).

Dorsal closure can be summarized as follows. In the early stages of closure, the dorsal surface of the embryo is covered by the large, flat polygonal cells of the amnioserosa. The rest of the embryo is covered by smaller, cuboidal-to-columnar cells of the lateral and ventral epidermis. The visible area of the amnioserosa is shaped roughly like a human eye, with a wide central section that tapers to canthi, the corners of the eye (see Kiehart *et al*., 2000; Bloor and Kiehart, 2002). With time, this eye-like structure "closes." A single row of amnioserosa cells is tucked under the lateral epidermis throughout closure (Kiehart *et al*., 2000). Where these cell sheets overlap, the dorsalmost row of lateral epidermis cells comprise a third, distinct tissue known as the leading edge of the lateral epidermis (see later and Foe, 1989; Kiehart *et al*., 2000; Stronach and Perrimon, 2001). The cells of the leading edge on each flank of the embryo contain an actomyosin-rich "purse string" or "actin cable" (Young *et al*., 1993; Kiehart, 1999; Kiehart *et al*., 2000). In addition, these cells extend dynamic finger-like filopodia ~10 μm in length (Jacinto *et al*., 2000). At the canthi, pairs of these filopodia can span the gap between opposing leading edges. As dorsal closure progresses, the actin cytoskeleton is remodeled and each structure changes (Young *et al*., 1993; Jacinto *et al*., 2000; Kiehart *et al*., 2000; Wood *et al*., 2002). Cells of the lateral epidermis are stretched (or elongate) toward the dorsal midline; the purse string contracts along their length; and cells of the amnioserosa actively change shape as their apical surfaces contract to help draw the lateral epidermal sheets together. The two flanks of the lateral epidermis adhere to one another or are zipped together—filopodia and lamellipodia from opposing leading edges interdigitate and a seam is formed (Jacinto *et al*., 2000; Bloor and Kiehart, 2002). At the end stages, the arcs flatten out and closure occurs "edge to edge" as numerous contacts are made simultaneously between the opposing sheets. Once the tissues from opposing flanks are sutured together, the actin-rich purse string dissolves. Ultimately, the dorsal surface is covered by

Copyright 2006, Elsevier Science (USA).
All rights reserved.

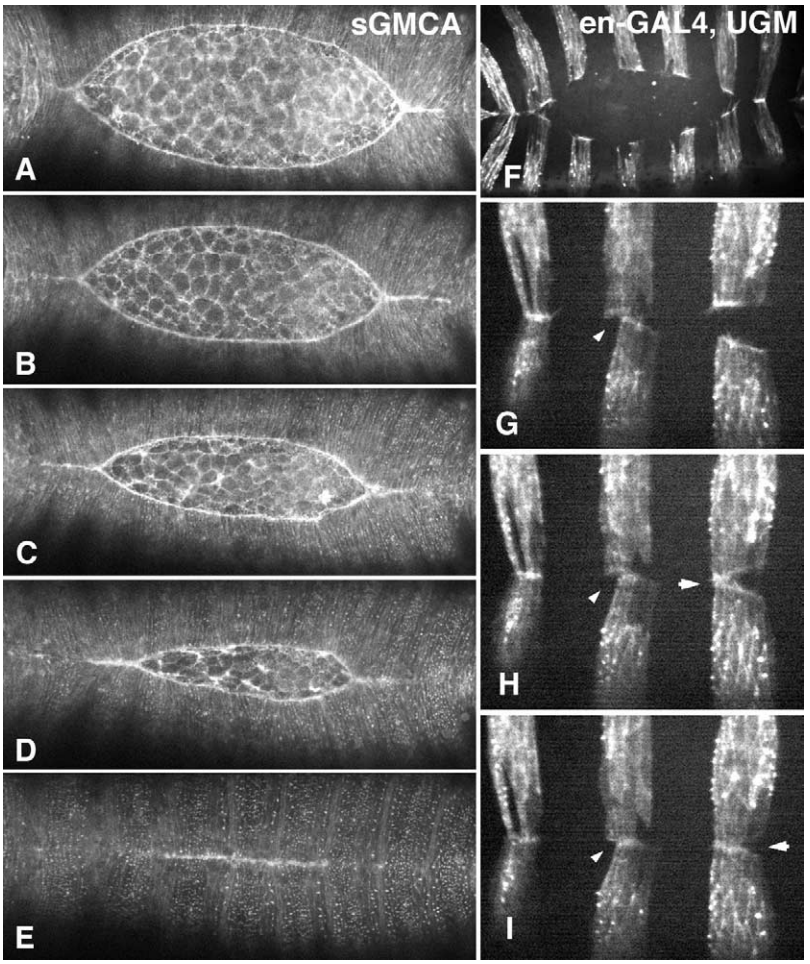

FIGURE 1 Native dorsal closure. (A–E) A time-lapsed sequence of dorsal closure in an embryo that expresses GFPmoe ubiquitously under the control of the heterologous *spaghetti-squash* (encodes nonmuscle myosin regulatory light chain) promoter/enhancer cassette (from Kiehart *et al*., 2000). (F–I) A time-lapsed series from an embryo in which the GFPmoe is expressed in epidermal stripes. The yeast transcriptional activator GAL4 was expressed under the control of an *engrailed* enhancer/promoter cassette, which in turn drives the expression of UAS-GFPmoe (Bloor and Kiehart, 2002). The GAL4/UAS expression system was developed by Brand and Perrimon (1994).

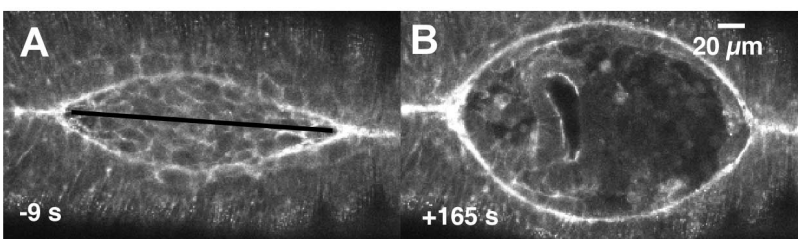

FIGURE 2 Confocal fluorescent images of native and laser perturbed dorsal closure. (A) An image of the dorsal opening just prior to laser surgery. (B) The full recoil of the dorsal opening, which occurs 165 s after a mechanical jump experiment, i.e., where the laser microbeam cuts from canthus to canthus (along black line in A) to remove the force due to the amnioserosa. Taken from Hutson *et al*. (2003).

a continuous epithelium that appears seamless. The main process of closure requires ~2–3 h. The focus of our research is to understand the molecular basis of force production and regulation for these movements that are well choreographed in space and time.

We perform laser surgery on fly embryos that carry green fluorescent protein (GFP) transgenes and can be imaged by confocal microscopy (see Hutson *et al*., 2003). Hutson *et al*. (2003) used optical methods to generate a near diffraction-limited spot of UV light and added the capability of steering that beam under computer control that is detailed later. By modifying our imaging systems, we can record high-resolution, time-lapsed image sequences of embryos before, during, and after UV surgery. We detail methods for automated processing of digitally acquired images and describe analytic strategies designed to reduce large data sets in the form of high-resolution image stacks to a small number of geometric parameters. With the help of QuickTime videos of the time-lapsed image stacks, changes in specimen morphology that result from laser surgical interrogation are therefore described both qualitatively and quantitatively. This provides unique insight into the morphogenic process and tissue response to laser surgery. By using these approaches and comparing wild-type and mutant embryos, we gain insight into the molecular basis of cell and tissue structure and behavior.

II. GFPMOE EMBRYOS

*Drosophil*a embryos that carry GFP-fusion transgenes are mounted to allow high spatial and temporal resolution imaging under conditions that allow development to proceed unimpeded. We use GFP fused to the actin-binding region of moesin (here called GFPmoe; Edwards *et al*., 1997; Kiehart *et al*., 2000; Bloor and Kiehart, 2002; Dutta *et al*., 2002; Hutson *et al*., 2003), which functions as a fluorescent marker for F-actin-rich regions of cells in the embryos. We can express these GFPmoe transgenes under the control of a variety of different promoter/enhancer cassettes (Fig. 1) and find that they are benign under all conditions examined so far: fly development is completely normal from egg lay to the formation of healthy, fertile adults such that we can maintain homozygous stocks of the fluorescently marked flies. Because of the high concentration of filamentous actin in the cortex of virtually all fly cells, these constructs provide a particularly efficacious way of imaging cell boundaries, thereby revealing the structural complexity of the embryo at the cellular level. Other GFP-fusion constructs (e.g., GFP–α-catenin, GFP–actin, GFP–src, GFP–DE-cadherin, Oda and Tsukita 1999; Verkhusha *et al*., 1999; Kaltschmidt *et al*., 2000; Oda and Tsukita, 2001) are applicable to imaging and may even prove superior for certain applications, but the GFPmoe has the advantage of being stable, bright, and benign.

III. EMBRYO OBSERVATION CHAMBER

We mount specimens in an environment that does not perturb progress in development (i.e., allows ready access to oxygen, prevents dessication) yet allows for high-resolution imaging (Fig. 3). We sandwich specimens between a gas-permeable membrane (a thin sheet of transparent Teflon that is available commercially and inexpensive, Fisher Scientific, Cat. No. 13-298-82) and a glass coverslip (Kiehart *et al*., 1994). The most recent version of our chamber allows the embryo, surrounded by inert, nontoxic halocarbon oil, to be

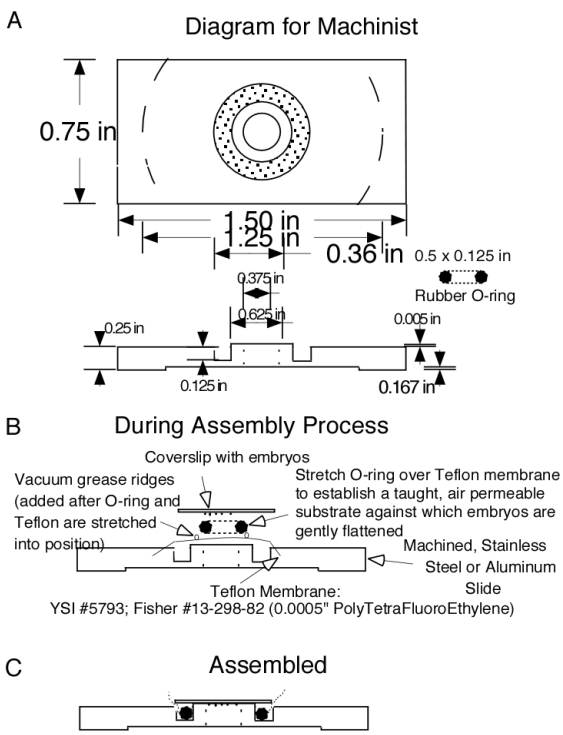

FIGURE 3 Teflon window chamber for the observation of embryos. The chamber is as described in the text. (A) A mechanical drawing to scale that can be used by an appropriately skilled shop to machine the stainless steel or aluminum chamber required to hold the gas-permeable membrane and the coverslip with embryos affixed. (B and C) How the chamber looks during and after assembly with a coverslip and embryos.

gently and slightly flattened, thereby improving our ability to image movements in a single (or relatively few) optical sections. These slightly flattened embryos hatch into larvae and, if removed from the halocarbon oil, proceed through development to form healthy and fertile flies.

IV. CONFOCAL MICROSCOPY

We perform laser surgery using one of three commercially available confocal microscope systems in which visible [e.g., continuous wave (CW) argon ion, krypton–argon ion, HeCd], lasers excite GFP (or its spectral variants, e.g., Heim and Tsien, 1996; Ormo *et al*., 1996; Miyawaki *et al*., 1997) and provide imaging contrast. We have mounted the surgical UV lasers on both upright and inverted microscope systems. Thus far we have used a Zeiss Axioscope (upright) microscope equipped with a Bio-Rad 600 scanning laser confocal imaging system (Kiehart *et al*., 2000), a Zeiss Axiovert (inverted) outfitted with a Zeiss 410 scanning laser confocal imaging system (Hutson *et al*., 2003), and a Zeiss Axioplan (upright) outfitted with a Perkin Elmer/Yokogawa spinning disk confocal imaging system using a Hamamatsu Orca ER camera (unpublished). Confocal microscopy is essential for imaging the thick (150 µm diameter; 450 µm long), optically challenging (yolky and light scattering) embryos.

For each confocal microscope system, modifications to the optical path of the microscope were necessary to allow *simultaneous* imaging and laser surgery. Thus, at an appropriate location (see later), we introduced a dichroic filter that reflects UV ablating light and passes visible imaging light (or *vice versa*), depending on the microscope system. This allows the morphology of the embryos before, during, and after a laser incision to be observed and recorded at image acquisition frequencies of 0.1 to 1 Hz with scanning laser confocals, or better than 1 Hz with spinning disk confocals.

For the Zeiss Axioscope/Bio-rad 600 system and the Zeiss Axioplan/spinning disk system, which are both upright microscopes, the imaging systems are introduced from above, through the trinocular heads. As a consequence, on these systems we required a long-pass dichroic filter that transmits the 488-nm excitation light and the 508-nm light emitted from EGFP and reflects the 337.1- or 355-nm ablating wavelengths (Model 400DCLP, Chroma Technology Corp., Rockingham, VT). On the Axioscope/Bio-rad system, the UV laser was introduced through the epiport (the mercury arc illuminator and associated collectors and diaphragms used conventionally for wide-field fluorescence work having been removed) so that the unmodified 337.1-nm surgical laser beam illuminated first the dichroic and then the objective, in that order. Unfortunately, the epiport on the Zeiss Axioplan includes a "drop-down" prism that does not transmit or transmits only poorly in the UV so we had to devise an alternate strategy for introducing the ablating beam. We modified an epifilter holder to accept light orthogonal to the nominal axis of incidence by drilling out the end of an epi slider and rotating the dichroic filter holder about the optic axis so that it remains positioned at 45° to the optic axis, but can reflect the UV light passing through the end of the slider onto the optic axis (Fig. 4). Most competent university machine shops should be able to modify an existing Zeiss slider in this manner satisfactorily. More recent Zeiss microscopes do not have this transmission problem, so that the standard epiport can be used to introduce the ablating beam—one of the fluorescent filter sets is simply replaced with the appropriate dichroic filter.

For the Zeiss 410 scanning laser confocal system mounted on the Zeiss Axiovert inverted scope, we required two modifications. Normally, a first surface mirror mounted in the epifluorescence filter slider is designed to reflect the imaging beam path. Our first modification was to replace this mirror with a short-pass dichroic filter (Model 360DCSX, Chroma Technology Corp.) that reflects 488- and 508-nm imaging wavelengths but transmits the 355-nm UV ablating beam. In practice, we left the first surface mirror in place and inserted the required dichroic in one of the other filter positions. To image from a nonstandard filter slider position, we defeated the interlocking system, which prevents the imaging laser from accidentally being projected through the binocular eyepieces, by taping two rare earth magnets (Cat. No. 64-1895, RadioShack Corp.) over the detector that senses the position in which the slider is located. This allows imaging with the slider in any position. The second modification was to the mount of the tube lens required for image formation by the binocular eyepieces and the Keller port (an optical port on the bottom of the Zeiss Axiovert that allows a straight optical path through the bottom of the inverted scope). This tube lens does not transmit UV and is mounted in a fixed position between the Keller port and the objective. We removed the lens from its fixed mount, machined a new mount for it, and attached the mounted lens to the sliding first surface mirror that is used to select between access to the Keller port and access to the binocular eyepieces. Thus, this modification allows imaging with the binocular eyepieces, but the tube lens slides out of the way when the Keller port

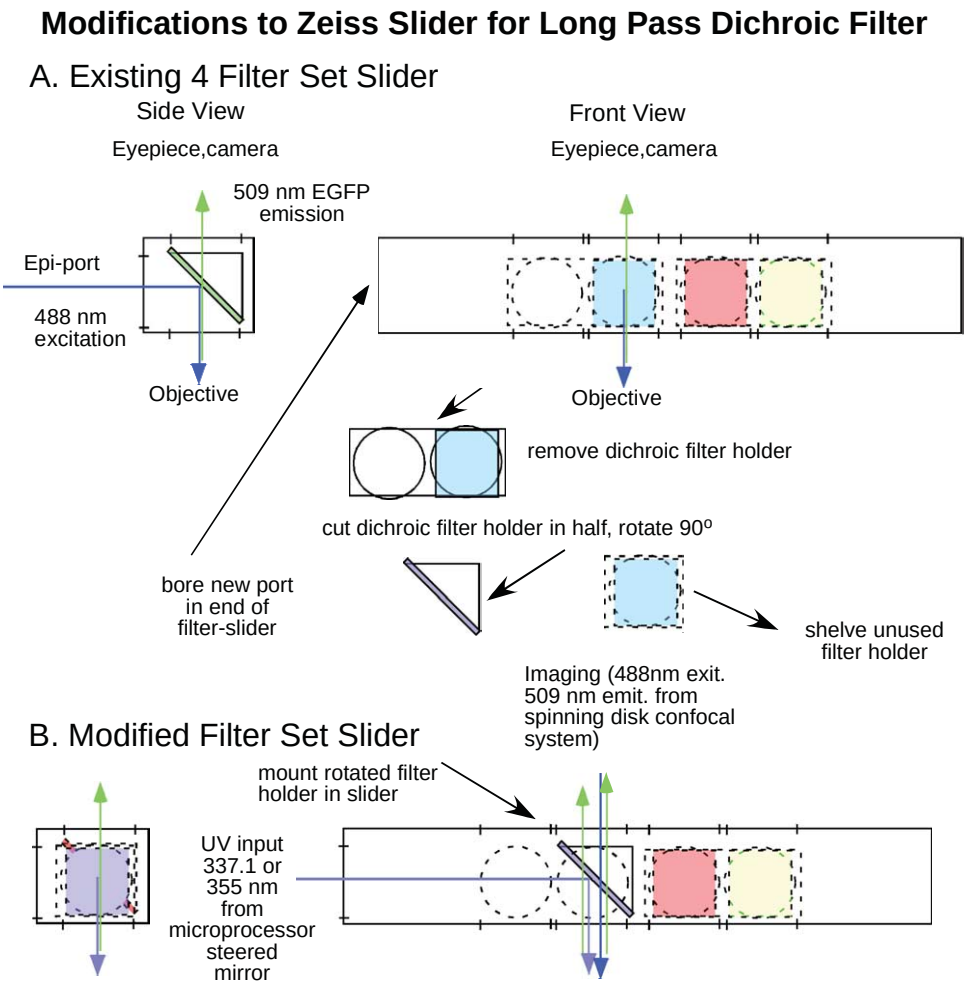

FIGURE 4 Modifications required so that a Zeiss epifluorescent filter holder/slider can be used to introduce UV ablating light onto the optic axis of a Zeiss Axioplan microscope (see text). (A) A schematic of the unmodified four-position slider with filter sets. It diagrams removal and modification of one of the dichroic filter mounts. (B) A schematic of the modified holder with the appropriate dichroic mounted. UV ablating light enters through a hole bored in the end of the slider.

is selected. With these modifications in place, the first optical components encountered by the expanded, UV ablating beam are the dichroic and the objective, in that order. Clearly, the configuration we describe is independent of the use of laser scanning versus spinning disk microscope technology. The advent of spectral variants of GFP mentioned earlier, the proliferation of other unrelated fluorescent proteins, each with different excitation and emission characteristics (Lippincott-Schwartz and Patterson, 2003), and the use of UV microbeams over a range of wavelengths may require selection of dichroic filters with different spectral characteristics.

V. ULTRAVIOLET MICROBEAM

Originally, we used a nitrogen laser to produce a UV beam on the Zeiss Axioscope/Bio-rad 600 imaging system that, as implemented, can be described more appropriately as a "UV macrobeam" (see later). The N_2 laser (Model VSL-337ND-S, 337.1 nm, 300 µJ, 75-kW peak power, 4-ns pulse width, 0–60 Hz repetition rate, Laser Science, Inc., Franklin, MA) was introduced without modification through the wide-field epiport of our microscope as described earlier. The beam produced by this laser does not have a Gaussian spatial

profile nor did it fill the back aperture of the 25× (NA 0.8) or 40× (NA 0.9, 1.0, 1.2, or 1.3) objectives commonly used for our experiments. As a consequence, lesions that result are larger than 5–10 µm in diameter. Furthermore, the N_2 laser is an unstable resonator. Consequently, introduction of a spatial filter designed to produce a Gaussian spatial profile proved impractical due to damage to the spatial filter and insufficient transmitted intensity for microsurgery. Nevertheless, the original system provided a useful tool for introducing spot lesions and did yield biologically significant observations (Kiehart *et al.*, 2000). Fiber adapters that couple this N_2 laser to various microscope systems are available commercially through Laser Science, Inc. However, we have found that the flexibility offered by individual optical components offsets the disadvantage of the extra space they require. Thus, we chose an alternate strategy to improve the quality of our microbeam.

To achieve the near diffraction-limited spot that we required, we upgraded to a Q-switched Nd:YAG laser, operating at the third harmonic, with considerably more power and an extremely stable Gaussian output (Model MiniLight II, 355 nm, 8 mJ, 1.0 MW peak power, 3–5 ns pulse duration, 1–15 Hz repetition rate; Continuum, Santa Clara, CA). We had previously used earlier Nd:YAG laser technology manufactured by Continuum (Model Quantel YSG571C, 355 nm, 300–700 nJ, 10 MW peak power, 8 ns pulse duration, 10 Hz repetition rate, no longer available commercially), but this laser was relatively large, required a spatial filter (R1,2 in Fig. 6), and required daily, tedious alignment. In contrast, the Minilite II is substantially easier to maintain and is essentially a turnkey system. Moreover, it has improved beam quality, thereby eliminating the need for a spatial filter. Currently we have two complete Minilite II laser surgical systems set up, one mounted on the Zeiss Axiovert/410 imaging system and the other on the Zeiss Axioplan/spinning disk system. The optical trains for the two systems are essentially identical and are detailed later.

To produce a near diffraction-limited spot, the laser beam is steered into the optical path of the microscope using an "optical train" that consists of individual

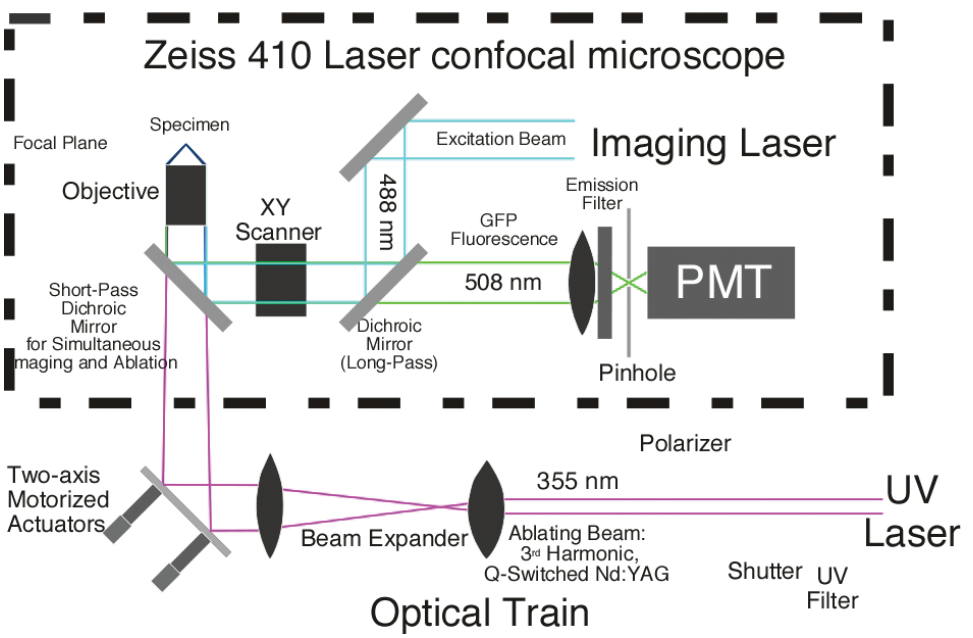

FIGURE 5 Schematic diagram of the Zeiss 410 scanning laser confocal microscope/UV laser surgical system. Part of the interior of the microscope (dotted box) showing how the internal excitation beam (visible argon ion laser) and the external microbeam (third harmonic of a Nd:YAG laser) are combined by a short-pass dichroic mirror to simultaneously direct both laser beams onto the sample. In order that the visible and UV focal planes coincide, the microbeam converges slightly in this case to compensate for the chromatic aberration of the microscope objective (see text). The long-pass dichroic mirror shown is an integral part of the Zeiss 410 imaging system and is left unmodified. It reflects excitation light scattered from the specimen while transmitting fluorescent light to the pinhole and onto the photomultiplier tube (PMT). Note that our laser confocal system utilizes an inverted microscope, with the specimen set above the objective. A comparable system, mounted on a standard upright microscope, is very similar and is described in the text.

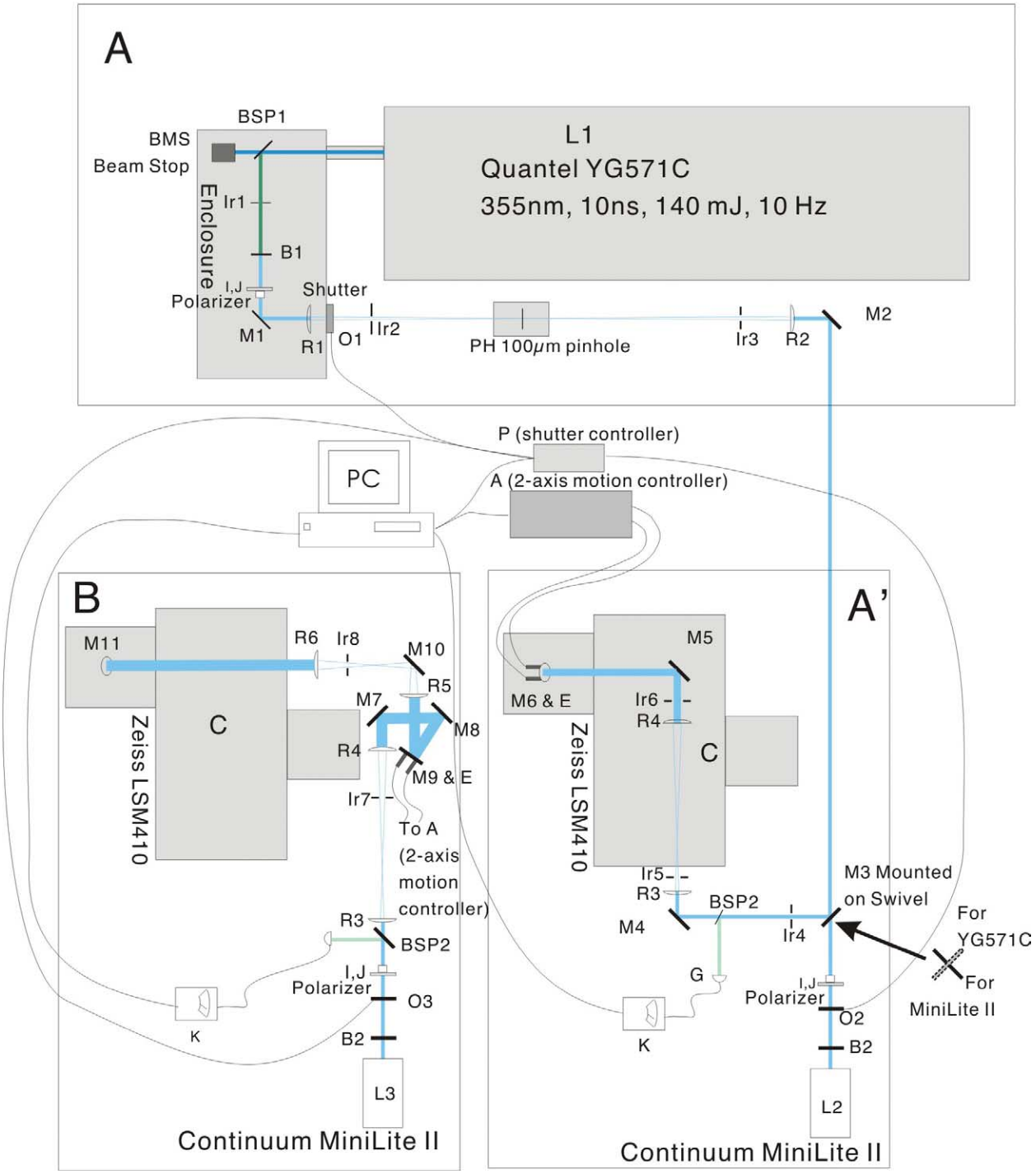

FIGURE 6 Optical layout for the UV microbeam, scanning laser confocal microscope system. Sketch of the optical train of the UV ablating laser system mounted on the Zeiss 410 imaging system is drawn roughly to scale. (A and A′) Layout for Quantel and Minilite II. (B) Layout for Minilite II with telescope included. Major components are labeled and letters are described in Table I and in the text.

components (mirrors, lenses, filters, and diaphragms) mounted on an vibration isolation table (e.g., Micro-G, Technical Manufacturing Corp., Peabody, MA). By implementing a beam expander, the back aperture of the objective can be filled and a near diffraction-limited microbeam generated so that the area of a lesion can be reduced to the submicrometer scale, achieving our goal of ablating a single cell (Figs. 5 and 6).

VI. ASSEMBLY OF THE OPTICAL TRAIN

The optical train required to achieve a near diffraction-limited spot in the specimen plane is shown schematically and approximately to scale for the two generations of Continuum Nd:YAG lasers that we used (Fig. 6). The individual components are described later, their position is specified by an appropriate letter in Fig. 6, and the suppliers and part numbers for the various components are specified in Table I. The specific components were chosen based on a number of factors, including compatibility with other components, cost, and availability. In most if not all cases, equivalent lenses, mirrors, and filters and ancillary components such as rails, sliders, posts, lens, and mirror mounts are available from any one of a number of suppliers (e.g., Melles Griot, www.mellesgriot.com; Oriel, www.oriel.com, Newport, www.newport.com; Edmund Industrial Optics, www.edmundoptics.com; CVI Laser, www.cvilaser.com; Chroma, www.chroma.com; and Omega, www.omegafilters.com). Lenses and mirrors were mounted in appropriate mounts and positioned via posts, sliders, and optical rails as shown schematically.

To set up the optical train, we first mount the laser on the optical table at an appropriate height (beam approximately 18 cm from the table surface) and then position the shutter. Next we mount and align individual mirrors in order to maintain the UV beam parallel or perpendicular to the surface of the table and guide it to the dichroic filter that merges the optic axis of the UV optical train with the visible light optic axis of the imaging microscope. Mirrors closest to the laser are added first. Many commercially available white index cards, business cards, or "post it" notes fluoresce sufficiently to allow the beam to be visualized during this alignment process. Alternatively, cards can be doped with a dilute solution of DAPI to improve visualization of the beam. Once the mirrors are aligned properly to guide the unmodified beam through the objective, the polarizer, the individual lenses that comprise the beam expander and the telescope are added, in that order. In each case, one needs to verify that they are mounted centrally and orthogonal to the optical train. Again, the lens closest to the laser is inserted first.

Downstream of the laser and upstream of the beam expander are the following key components: A UV band-pass filter (B1 and B2 in Fig. 6, peak transmission

TABLE I Optical Instrumentation

The following is a list of the optical components comprising the optical trains shown in Fig. 6.

A	Two-axis motion controller (Newport ESP300-11N11N) to operate the motorized actuators
B1,2	Band-pass filters (Newport FSR-UG11), transmission peak at ~340 nm
BMS	Beam stop
BSP1	Optical flat beam splitter, reflects approximately 10%
BSP2	Thin glass plate (coverslip) beam splitter, reflects approximately 10%
C	Confocal microscopes: Zeiss Axiovert/LSM410; Zeiss Axioplan or Axioscope with PerkinElmer/Yokogawa spinning disk confocal
E	Motorized actuator (Newport CMA-12PP) for beam steering
G	Detector (Ophir Optronics, Model PD10) for power measurement
I	Polarizer (Newport 10GL08)
Ir1–8	Iris diaphragms
J	Polarizer stage (Newport RSP-1T) for holding and rotating the polarizer
K	Power meter (Ophir Optronics, NOVA)
L1–3	Q-switched UV laser (Continuum Quantel or MiniLite II)
M1–8	Mirrors (Newport 10D10AL.2) aluminum coated
M9,11	Mirrors (CVI PAUV-PM-2037-C) aluminum coated
O1–3	Shutters (Uniblitz VS25S2ZM0)
P	Shutter controller (Uniblitz D122)
PH	Pinhole for spatial filter
R1,2	UV-fused silica lens for spatial filter (CVI PLCX-25.4-360.6-UV, f = 700.0 mm)
R3,4	UV-fused silica lens for beam expander (Newport SPX019, f = 75.6 mm and SPX028, f = 200 mm)
R5,6	UV-fused silica lenses for telescope (CVI PLCX-50.8-180.3-UV-3555-532, f = 378 mm)

at 340 or 355 nm) is positioned at the exit of the laser and transmits only the third harmonic (355 nm) while blocking the fundamental and second harmonic. To control sample exposure to the microbeam, a shutter (O1-3) and a calcite polarizer (I) mounted on a rotary stage (J) are situated after the UV band-pass filter. The shutter is operated by a shutter controller (P) connected to the same computer that steers the beam (see later) via an RS-232 interface. Note that this computer is distinct from the imaging PC required for either laser scanning or spinning disk confocal imaging of the samples. Control of the shutter is achieved through custom plug-ins written for ImageJ, a free software package available from the Web site of the National Institutes of Health (NIH), http://rsb.info.nih.gov/ij/. The custom plug-ins that we have written are available on our Web site: http://www.biology.duke.edu/kiehartlab/biopdc/.

Continuous attenuation of the filtered UV laser beam, which is polarized linearly, is achieved by rotating the polarizer. To measure the intensity of the beam, a small fraction of the ablating beam is diverted to a detector by positioning a partially reflecting glass surface (BSP2)—in our case a glass coverslip—in the optical train of the ablating beam. The transmitted beam is for dissection and the reflected beam is for monitoring the power. Calibrating the energy ratio between the two beams (ratio ~0.1), we can unambiguously determine the energy per pulse incident on the specimen.

VII. FINE-TUNING THE OPTICAL TRAIN TO OPTIMIZE THE MICROBEAM

Minimization of the microbeam spot size at the imaging focal plane is achieved by optimizing two beam parameters: beam diameter and divergence. Our first problem is that the diameter of the emitted laser beam (<3 mm) is considerably smaller than the back aperture (~10 mm) of the objective lenses typically used for imaging and surgery. A second complication arises because the index of refraction of the lenses in the objective is wavelength dependent. Although the objectives used are neofluars (fluorite lenses sometimes called semiapochromats; Inoue and Spring, 1997; Murphy, 2001) or apochromats in the visible spectral region, the index of refraction varies with wavelength in the UV. The resulting longitudinal chromatic aberration causes a discrepancy in the position along the optical axis between the focal points of the visible light and the UV light.

To expand the beam, to permit correction of this chromatic aberration, and to deliver a near diffraction-limited spot, two fused silica lenses (R3, R4, Fig. 6) that transmit UV are introduced. We fix the position of the second lens and adjust the distance between these two lenses by moving the first lens. The focal lengths of these lenses were chosen so that the diameter of the laser beam is expanded by three times, thus nearly filling the back aperture of the objective with plane parallel light. However, as explained earlier, this plane parallel beam will not be focused in the same plane as the visible, imaging laser. To correct for chromatic aberration of the objective for the UV light, we increase the length between the two lenses of the beam expander. This introduces a slight convergence to the UV beam and alters the focal plane of the ablating laser. Due to this convergence, the expanded beam did not completely fill the back aperture of the objective. Because the Nd:YAG laser is not power limited, alternate lenses could be used to expand the beam further and overcome this limitation. Nevertheless it is important to note that we achieved our goal of providing a microbeam that was sufficiently small to ablate a single cell.

In practice, to optimize alignment of the beam expander, we made test samples constisting of a thin layer (~150 μm thick) of 1–2% agarose (in deionized water) sandwiched between a slide and a coverslip. For visible light the agarose was supplemented with 0.2% rhodamine dye, for UV light no dye was used. In each case, the focused beam cavitates the gel in a small region defined by the focus, causing a small bubble to form. Fine adjustment of the two beam expander lenses is performed by iteratively reducing the power such that it is just sufficient to cavitate the gel and then readjusting the lenses such that the focal planes of the visible, imaging light and the UV ablating light coincide. The process is repeated until minimum power is required to ablate the gel adjacent to the coverslip. Near diffraction-limited spot size is confirmed by using the laser to ablate holes in a thin film of aluminum evaporated onto glass, which forms an ideal and stable test specimen (Fig. 7A).

The ablating UV laser is pulsed and the dose of UV light delivered to the specimen can be adjusted with the computer-controlled shuttering system. By adjusting the duration for which the shutter is open, a specimen is exposed to the desired number of pulses, N. However, for small values of N, there is potentially some ambiguity in the number of UV pulses to which the specimen is exposed because the laser pulses are not synchronized to the shuttering system. In practice, the repetition rate of the laser pulses is 10 Hz, so we set the shutter-open duration to 0.1 N–0.005 s,

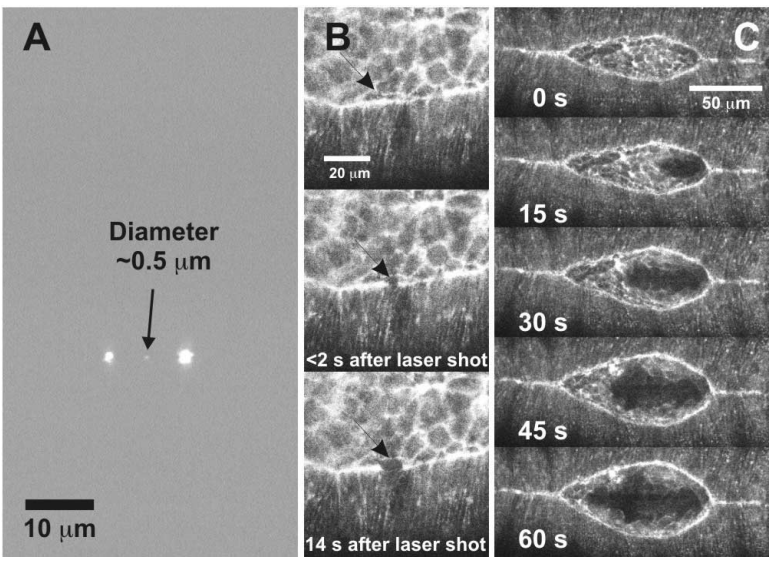

FIGURE 7 Performance of the UV microbeam. (A) Demonstration of the near diffraction-limited spot size as measured on a thin film of aluminum. The smallest spot was made by a single pulse of ~50 nJ on the film. The left and the right incisions received single pulses of ~100 and ~200 nJ, respectively. (B) Application of the near diffraction-limited microbeam to surgery on the leading edge of the lateral epidermis. The microbeam was aimed at the center of the field, a specimen was brought into position, and the supracellular purse string at the leading edge was nicked by a single pulse of ~200 nJ. (C) Demonstration of beam steering: the microbeam is steered from canthus to canthus to make a linear incision. Elapsed time is shown in seconds and starts at first lasing. Reproduced from Edwards *et al*. (2003).

i.e., slightly smaller than the period times the number of pulses. This eliminates the possibility of $N + 1$ pulses passing the shutter, but with low probability (~5%), only $N - 1$ pulses may pass. Here, the pulse duration is only 10 ns and 3 ms is needed for completion of opening or closing the shutter. Typically, more than ten pulses are used to perturb the embryo so the expected dose was constant (except for the rare occasion when it was 5–10% less than the expected value).

VIII. BEAM STEERING

By introducing two computer-controlled linear actuators (E's in Fig. 6) to angularly position one of the mirrors in the optical path, the beam can be steered systematically in two dimensions, thus converting a spot ablation tool into a precise UV-scalpel for tissue surgery (see results: Figs. 2 and 7). The actuators replace adjustment screws of a kinematic optical mount. The two motorized actuators are positioned by a two-axis motion controller (A in Fig. 6), which offers a step size of 0.1 μm. With this step size, the resolution of the laser trajectory is not limiting and is instead determined by the coarseness of the image, i.e., the number of pixels in a frame (512 × 512). With the 40× objective that we typically use, we achieve subcellular resolution in the specimen. The controller communicates via an RS-232 interface with the microbeam computer running ImageJ with custom Java plug-ins. The plug-ins allow PC-controlled steering of the microbeam at a constant velocity along any defined trajectory in the specimen plane.

When it is steered off axis, the UV laser beam may be cropped by the back aperture of the objective, thereby restricting the region in the specimen plane that is accessible to surgery (Fig. 8B). Initially, to achieve a large area for incisions, we set the final mirror (M6, M9 in Fig. 6) mounted on linear actuators (E's) as close to the back aperture of the objective as possible. In our system, this length is ~20 cm. Using the 40X objective (1.3 NA oil immersion objective), a roughly circular region with a radius of ~70 μm can be targeted for ablation. To overcome this limitation, to improve flexibility in the overall design of the optical train, and to increase the area of the specimen that is accessible to the UV microbeam, we inserted a telescope into the optical train designed to project the expanded beam onto the back aperture of the objective (Figs. 6 and 8A). The telescope is composed of one mirror (M10) and two plano-convex fused silica lenses, $f = 350$ mm (R5, R6 shown in Fig. 6). To accommodate

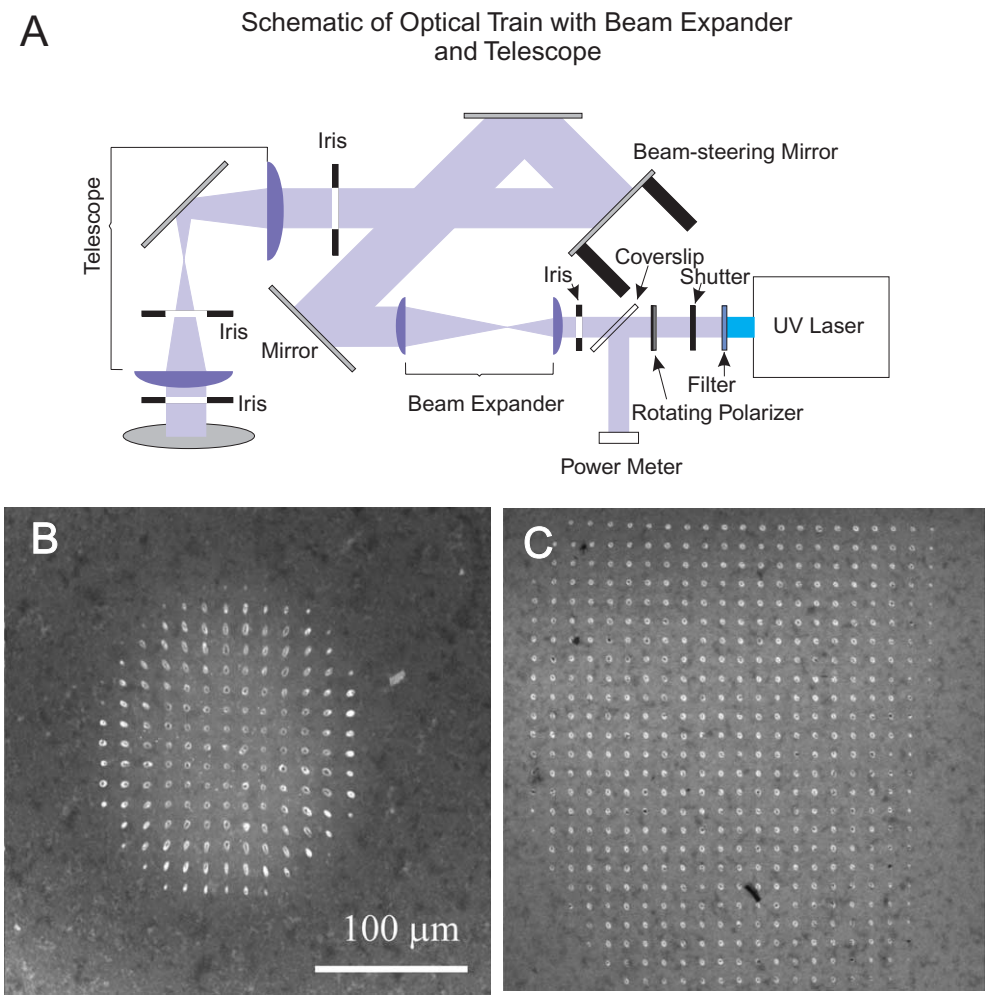

FIGURE 8 An optical telescope improves the effective area of laser ablation. (A) UV optical train using a telescope to avoid vignetting at the back aperture of the objective (see text). (B) Effective area of laser ablation without the telescope is limited due to clipping of the UV microbeam using the UV optical train shown in Fig. 5. Only the region within the circle of radius ~70 µm about the optical axis can be ablated on a target specimen (rhodamine dye in agarose gel). (C) Effective area of UV laser ablation after installation of the telescope. Note that the area is expanded significantly, covering the major part of the image plane, and that the lesions maintain a round morphology farther from the optical axis. Scale bar is for both B and C.

the travel range of the steered beam, the diameter of these optical components (2 in.) is two times larger than that of other lenses in the optical train. With this telescope, the incident laser beam can be steered off axis and yet remain centered on the back aperture of the objective, thereby increasing the area accessible to the ablating beam at the specimen plane. Moreover, the mirror that is used for beam steering no longer needs to be as close to the back aperture of the objective as possible.

The protocol for executing a laser incision is as follows. An image of the embryo from the laser scanning confocal microscope is captured by the imaging software, transferred, and displayed on the screen of the PC that controls the ablating microbeam. The pattern of a user-defined incision is drawn on this image with the PC's mouse or cursor. The desired laser incision is then executed by running custom Java plug-ins for ImageJ that coordinate opening and closing of the upstream shutter with the two motorized actuators that position the beam steering mirror. Trial and error is used to determine an appropriate rate of movement for the mirror. Typically, scan rates correspond to about 10 µm per second on the surface of the embryo. The longest incisions typically required 10 s of 10-Hz pulsed UV laser exposure.

IX. AUTOMATED ACQUISITION OF GEOMETRIC PARAMETERS

High-resolution time-lapsed analysis of morphogenesis can rapidly generate vast quantities of images that can quickly overwhelm the researcher's ability to store and interpret data. In particular, data analysis that requires manual intervention becomes a critical rate-limiting step. As a consequence, we apply automated methods designed to extract a small number of key geometric parameters from stacks of several hundred images, each 2–4 Mbytes in size. First, confocal images of dorsal closure are saved as TIFF files directly or are exported from proprietary software into TIFF or AVI format. Such images are then loaded into the ImageJ image processing software. Several basic processing functions, such as measurement of the length or the area of a designated region, are built into the software, but additional customized routines have been implemented as custom Java plug-ins.

Thus far, we have been most successful with automated methods designed to recover the shape of the exposed amnioserosa, as outlined by the bright, actin-rich, supracellular purse string that forms at the leading edge of the lateral epidermis (Figs. 1, 7, and 9).

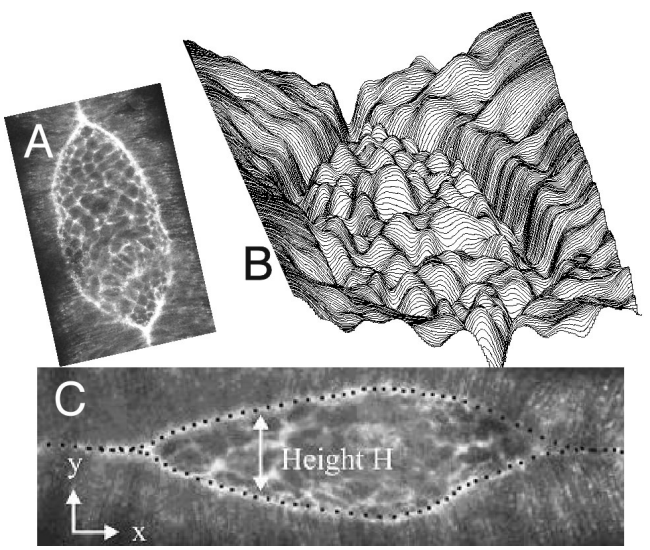

FIGURE 9 The leading edge of the lateral epidermis, the inverse intensity landscape, and the application of the snakes algorithm for the automated identification of the leading edge of the lateral epidermis. (A) Fluorescent image of the dorsal opening about two-thirds of the way through closure. (B) An inverse intensity landscape for a comparably staged embryo (see text). (C) Snakes fit to the two leading edges of the dorsal opening for an embryo at a later stage. The 50 fitting points on each edge are apparent.

To quantify how the tissue geometry changes with time in native embryos or in those cut with the UV laser microbeam, we extract the contour of the leading edge in each image as digitized information as follows: in our system, the original size of an image is typically 512 × 512 pixels, but can be as large as 2048 × 2048 pixels. To optimize handling of the large data sets, the first image is cropped to reduce its size so that it contains only the region of interest (typically the entire embryo). By treating the set of TIFF images as a stack, all of the following images are automatically cropped using the same frame. To capture the contour of the leading edge, which is represented as bright pixels forming a closed geometry, we employ the technique of active contour models, also known as "snakes" (Kass *et al.*, 1987). This method is generally used for recognizing the boundary of an object in an image and, in our images, readily identifies the supracellular purse string or actin-rich cable at the leading edge as the bright pixels due to GFPmoe fluorescence (Fig. 9). In practice, each stack of images is processed with a custom Java plug-in that executes the snakes analysis.

The snake method can be understood in terms of an "energy" landscape as follows. This landscape corresponds to the inverse image intensity, i.e., the brightest regions correspond to minimum energies (Fig. 9B). In an original image, the brightness of each pixel is stored as 8 or 12 bit intensity information (depending on the imaging system), where the dimmest pixels approach 0 and the brightest pixels approach either 255 or 4095, respectively. For the inverse intensity plot, the brightest pixels approach 0 and the dimmest, 255 or 4095, respectively. Consequently, fitting the snake corresponds to minimizing a multiterm energy equation associated with the contour in the inverse intensity landscape. The energy of a snake is determined by its length, curvature, and the brightness along a contour described by 100 discrete points. This number of points is chosen to balance accuracy with computational demands. The energy E_{total} of the snake is given by the following algorithm, implemented as a plug-in to ImageJ:

$$E_{\text{total}} = E_{\text{internal}} + E_{\text{image}} + E_{\text{constraint}} \quad (1)$$

where E_{internal} and E_{image} are integrals of $(a\,|\,d\mathbf{v}/ds\,|^2 + b\,|\,d^2\mathbf{v}/ds^2\,|)$ and $c\ \mathrm{I}(s)$, respectively. The parameter s runs from 0 to 1 and $\mathbf{v}$ is a vector in the x, y plane as shown in Fig. 9. The parameters a, b, and c weight the contributions from the terms to achieve acceptable curve fitting and are chosen by user intervention. The first term of E_{internal}, $a\,|\,d\mathbf{v}/ds\,|^2$, is analogous to the energy due to stretching of an elastic rod. Note that the 100 points are approximately distributed uniformly along the leading edge, as if "springs" that connect

these points are of nearly uniform, minimal length (Fig. 9). The second term of $E_{internal}$, $b|d^2\mathbf{v}/ds^2|$, is analogous to the bending energy of a rod and here is minimized as well: as a consequence, steep bends are energetically expensive and selected against in the energy minimization process. The image energy E_{image} is the value of the experimentally determined inverse intensity, described previously. The final energy term, $E_{constraint}$, addresses the complications of fitting the leading edges where they converge near the canthi and beyond where they are already sutured into seams. In our implementation, these constraints mimic the connection of two additional springs. One spring connects the 1st snake point to the right edge of the image; the second connects the middle (50th) snake point to the left edge. Mathematically, $E_{constraint}$ is given by $k(x_1 - w)^2 + kx_{50}^2$, where w is the width of the cropped image. Similar to a, b, and c, the parameter k is chosen by user intervention to achieve acceptable curve fitting.

Energy minimization is optimized by allowing the snake, *i.e.*, a mathematical contour, to computationally wiggle about the inverse intensity landscape using the methods of gradient descent (Kass *et al.*, 1987). There is a competition between the various terms in the energy equation. In isolation, the contribution from rods and springs favors being unstretched, the contribution from rods also favors being straight, and the contribution of E_{image} seeks out the twists and turns of the deeper valleys of the inverse intensity landscape. The computational refinement of the overall positioning of the snake is an iterative process that strikes a balance of the energy terms via the choice of parameters a, b, c, and k. Essential to the method of gradient descent is determining the derivative of change in each of the energy terms for each repositioning (wiggle) of the snake to identify the term(s) that should dominate the next choice of position in this refinement process. Consequently, successive iterations ideally optimize positioning the snake in the valley of the inverse intensity landscape that corresponds to the two leading edges. This computational approach proved quite satisfactory in practice, provided sufficient brightness and contrast are available in the individual images. Under these conditions, it takes several minutes to analyze a stack of 500 sequential images when using a Pentium IV desktop computer with a 2.4-GHz processor. The positions of points fit to the upper and lower leading edges are stored in a text file as a digitized data set that can be imported into other programs for further analysis.

We are currently developing additional strategies designed to rapidly and automatically identify other structural features (e.g., the shape and position of individual cells, the number and distribution of filopodia). Our goal is to devise methods that parallel those developed for the acquisition and mathematical description of the supracellular purse string using the snakes strategy described earlier. Thus, parameters are to be analyzed automatically as a function of time (i.e., measured on sequential images in the time-lapsed image stack), tabulated into a spreadsheet program, and analyzed and evaluated quantitatively for statistical reliability. Extracted data are reviewed on a frame-by-frame basis to verify that the imaging software accurately identified relevant structures. Together, QuickTime videos constructed from image stacks and the extracted geometric parameters constitute analysis of the experimental data sets. The reproducibility of our observations is confirmed by comparing the results from a set of at least six individual embryos that were manipulated genetically and/or surgically in an identical fashion.

X. PUTTING IT ALL TOGETHER: EMBRYO MICROSURGERY

Preparation of the Embryos for Observation

Small population cages containing 30–300 adult flies of the appropriate genotype are used to collect embryos on grape juice agar plates by standard methods (Roberts, 1998). To improve the optical qualities of the embryo, the chorion is removed mechanically by rolling an embryo on double-sided adhesive tape or is removed chemically by immersing the embryo in 50% bleach using standard methods (Roberts, 1998). This leaves behind a transparent protective layer, the vitelline envelope. With the aid of a dissecting microscope, the dechorionated embryos are oriented dorsal side up in an orthogonal array (e.g., three rows of 10 embryos each) on a pad of 1% agar. The embryos are spaced so that they are at least 1–2 embryo diameters apart. The array is then picked up on a #1.5 22 × 22-mm glass coverslip coated with a thin layer of "embryo glue" (Roberts, 1998). We find that arranging the embryos on the agar pad allows more flexibility in getting their orientation just right and dramatically reduces the number of embryos that are damaged when compared to protocols that call for aligning the embryos directly on the glue-coated coverslip. The coverslips are made in advance by putting a few drops of adhesive, solubilized from double-stick tape (type 415, 3M Company, St. Paul, MN; Whiteley and Kassis 1993) with hexane and allowing the glue to air dry for at least 5–10 minutes (we typically store the coated coverslips in a closed box to avoid accumula-

tion of dust and use them within 1–2 days of coating them). To prevent desiccation, the embryos are covered immediately with a few drops of halocarbon oil (#27 or #700, or a mixture of the two, Sigma, St. Louis, MO), which is chemically inert and allows ready access to O_2. An observation slide is prepared in advance as follows: Stretch a sheet of optically transparent oxygen-permeable Teflon membrane (Fisher Scientific, Cat. No. 13-298-82) across the opening in a machined metal slide (see later and Fig. 3) fixed into place with an O ring and then extrude, from a number 18 hypodermic needle, two low (0.1–0.5 mm) parallel ridges of high-vacuum silicone grease (Dow Corning, Midland, MI) on either side of the opening. The coverslip with its embryo array and oil is rapidly inverted onto and is then compressed gently against the ridges of vacuum grease. The vacuum grease helps hold the coverslip in place and functions as a spacer that prevents overflattening of the embryos. Together with the halocarbon oil, the silicone grease also prevents desiccation of the sample. By positioning the array of embryos over a hole in the metal slide, the embryos can be observed by transmitted light microscopy. The Teflon membrane used is extremely birefringent, such that it interferes with phase contrast and differential interference imaging systems. The thickness of the slide further precludes achieving Köhler illumination with a high NA condenser. Nevertheless, because the embryos are flattened gently against the coverslip, excellent high-resolution confocal epifluorescence images can be collected. Moreover, wild-type embryos that are unperturbed will hatch into larvae, and if such larvae are removed from the oil and treated appropriately, these will readily develop into adult flies.

XI. LASER SAFETY

Note that it is important to wear appropriate protective eyewear when working with the pulsed UV laser beam. Although we typically use the UV laser in its low-energy mode, the pulses still contain significant intensity, especially before they reach the calcite polarizer. Keep in mind that this polarizer attenuates the beam via reflection. To eliminate a potentially dangerous reflection, we cover the reflection ports of the polarizer housing with opaque electrical tape. The Continuum Minilite II is a class IV laser and special precautions and training are appropriate for personnel involved in setting up the microbeam system (Marshall and Sliney, 2000; Sliney, 2000). In practice, the UV ablating beam is attenuated by glass elements throughout the optical path of the microscope system; nevertheless, we never observe the specimen through the microscope eyepieces while it is being illuminated by the UV laser. A visible microbeam would be a significant eye hazard and safety interlocks are required.

XII. MICROBEAM OPTIMIZATION

A. Daily Protocol

To optimize the system and dissect the surface of an embryo effectively, we describe general procedures that should typically be performed daily before laser surgery on embryos is attempted. However, if the laser exhibits a Gaussian spatial profile and is stable, several steps (2, 3, 4, and 10) can be skipped. Note that the third harmonic generated by the laser is polarized horizontally and rotating the polarizer set in the optical train attenuates the power as a function of the angle ψ between the beam's polarization and the crystal polarization ($\sim\cos^2\psi$).

B. Startup and Calibration of Beam Intensity

1. Turn on the microscope, the imaging system including the imaging laser, and the computer. Turn on the ablating laser and its computer. Verify that the ablating shutter is in the closed position and that the ablating laser is in the low-energy mode. Allow all systems to warm up for several minutes.

2. To estimate the intensity of the laser and evaluate the dose delivered to the specimen plane, deflect a small fraction of the energy to a power meter (Model PD10, Ophir Optronics, Wilmington, MA) with a partially reflecting surface (a coverslip) placed in the optical train (BSP2 in Fig. 6). The steps that follow calibrate the optical train by comparing the power of the deflected light to the power measured at the specimen plane. If two calibrated detectors are available, measurements can be taken simultaneously: one detector is positioned to measure the deflected light and the other is positioned on the microscope stage (it replaces the specimen) at or near the focal point of the objective. If only one detector is available, power at the two positions is measured sequentially (we find that in practice the output from the Continuum Minilite II is very stable and that this approach is quite satisfactory).

3. Open the UV laser shutter and read the energy per pulse at each detector. Because the amount of energy deflected to the power meter by reflection from the coverslip is a function of the angle of incidence and the azimuth angle of the polarized 355-nm ablating light, the ratio of these readings shows slight depend-

ence on the angle of the calcite polarizer. Check and record the ratios for several angles. Later, during embryo surgery, observe the angle of the polarizer and use the appropriate ratio to estimate the energy incident on the sample.

4. Close the UV laser shutter.

C. Ablation on a Test Sample to Optimize the Beam

5. Remove the detector at the specimen plane and place a slide of an agarose gel made by sandwiching a drop of molten agarose or agar (1–2% in deionized H_2O containing 0.02% NaN_3 as a preservative and, for use in fluorescent mode, 0.02% rhodamine B or fluorescein) between a slide and a coverslip and sealing the coverslip (nail polish is convenient—this preparation lasts indefinitely). To aid in determining the plane of focus during subsequent steps, we first make fine scratches on the inside surface of the coverslip with a diamond-tipped marker prior to assembling the agar sandwich. We adjust the thickness of the agarose so that it is approximately 150 µm, thereby simulating the optical properties of an embryo sample chamber. For our applications, laser surgery typically occurs close to the surface of the embryo, <15 µm deep.

6. Block the UV laser beam from entering the microscope with a beam stop (not shown in Fig. 6) positioned somewhere after the coverslip beam splitter (BSP2 in Fig. 6) and then open the UV laser shutter. A small fraction of the beam will be reflected by the coverslip beam splitter (BSP2) to illuminate the detector G. Rotate the polarizer until the estimated value of the energy per pulse that would reach the sample when the beam stop is removed reaches the threshold required to cavitate the gel—for our system, this threshold, using either a 40×, 1.3 NA oil immersion lens or a 40×, 1.2 NA water immersion lens, is ~200 nJ/pulse. The angle of the polarizer and the ratio of intensities at detector G and at the specimen position for this particular angle, previously measured in step 3, are used to estimate the energy at the sample.

7. Close the UV laser shutter and remove the beam stop.

8. While monitoring the surface of the gel on the monitor screen of the confocal system using transmitted light mode, use the shutter to let a single laser pulse illuminate the gel. This procedure is repeated in steps 9 and 10.

9. Adjust the orientation of the mirror using the two-axis motion controller so that the ablation beam hits the center of the gel on the screen. Specifically, record the x, y position of the ablated spot, execute the "Center_Microbeam" custom ImageJ plug-in to recalibrate the beam steering computer's coordinate system, and set the position of the spot to the origin at the center of the imaging field.

10. Optimize the position of the two lenses in the beam expander by adjusting them so that diameter of the ablated spot is minimal. Two factors—the distance between the two lenses and between the objective and the second lens—determine the size of the lesion produced by the laser beam. For the objectives we have used, the smallest possible lesion is achieved with a slightly converging beam. Initially, align the beam expander to transmit plane parallel light and set the laser power so that a single pulse is more than sufficient to ablate a spot in the gel at the focal plane. Next, carry out an iterative process whereby the distance between the two lenses of the beam expander is increased, typically in several millimeter steps, to introduce a convergence to the transmitted light. In practice, the lens closest to the back aperture of the objective remained fixed and we moved the first lens to increase the distance between the lenses, a few millimeters at a time. This initially reduces and then expands the UV spot size in the focal plane. As a consequence, the adjustment moves the lenses through the optimal convergence—once that occurs, reduce the increment and step back to the point that gives the apparent minimum spot size. Reduce the energy per pulse and then repeat the protocol just described to fine-tune the beam expander. Typically three to five iterations are sufficient to minimize the spot size. Measured on the agarose gel, the lesion diameter is typically 1–3 µm.

11. Once the microbeam alignment has been completed, the near diffraction-limited spot size is confirmed by replacing the gel sample with a thin aluminum film. By rotating the polarizer to attain the minimum exposure that ablates with a single shot, the lesion radius approaches the diffraction limit.

D. Dissection and Imaging of the Embryo

12. Replace the aluminum film with an observation slide of appropriately staged *Drosophila* embryos. Set the laser power to below that which is expected to be a threshold dose for creating a lesion (e.g., 200 nJ per pulse) and use a target embryo to empirically define the power required to generate a lesion of desired magnitude by gradually increasing the dose until the appropriate response is seen in the confocal image of the embryo. Once a desired dose has been defined, verify this on a different region of the same target embryo or on a new embryo. Then, select a new specimen, record an image, and transfer the image from the

imaging computer to the beam steering computer. Using the beam steering computer, specify the pattern you wish to cut on the embryo.

13. On the imaging computer, initiate a time-lapsed series. Verify that the intensity in the image does not exceed the dynamic range of the digital acquisition system. With collection of the confocal time-lapse series underway, use the beam steering computer to initiate the laser surgical cut(s). Process and analyze images later.

XIII. TIPS AND PITFALLS

When choosing mirrors, one should consider their damage threshold and the reflection coefficient at the appropriate laser wavelength. Broadband aluminum-coated mirrors have been selected for all mirrors in the optical train.

For UV-transmitting lenses, those made of UV-fused silica have excellent transmission from 180 nm up to 2100 nm at moderate cost. To allow flexibility in choosing the wavelength of the beam, lenses without optical coating may be preferable.

Generally, the transmission of standard microscope objectives shows a steep drop off in the UV. If UV lasers with shorter wavelengths are selected, make sure that the objective is designed for this range and that the energy of the beam after transmission through the objective lens is sufficient for incisions. In particular, avoid laser damage to the objective itself due to UV absorption.

XIV. CLOSING REMARKS

Laser microbeams have become an essential tool to investigate dynamics in cell biology. We have presented details of our specific application to microsurgery using computer steering of near diffraction-limited UV beams. We have applied this approach, together with mathematical modeling and biophysical reasoning, to probe the forces responsible for morphogenesis in *Drosophila*, where the wide array of mutations that affect such processes allow us to investigate the molecular bases for such forces (Hutson *et al*., 2003; unpublished observations). We are extending our studies to other morphogenetic movements in *Drosophila* (e.g., thoracic closure) and are exploring the use of these approaches in other model species—*Caenorhabditis elegans* (nematode), *Danio rerio* (zebrafish), and *Mus musculus* (mouse). As described in the introduction, microbeams, particularly computer-steered microbeams, might also be applied to other approaches that use optical methods to probe molecular function, e.g., fluorescent resonance energy transfer, fluorescence recovery after photobleaching, or chromophore-assisted laser inactivation.

References

Bargmann, C. I., and Avery, L. (1995). Laser killing of cells in *Caenorhabditis elegans*. *Methods Cell Biol*. **48**, 225–250.

Berns, M. W., Tadir, Y., Liang, H., and Tromberg, B. (1998). Laser scissors and tweezers. *Methods Cell Biol*. **55**, 71–98.

Berns, M. W., Wright, W. H., and Wiegand Steubing, R. (1991). Laser microbeam as a tool in cell biology. *Int. Rev. Cytol*. **129**, 1–44.

Bloor, J. W., and Kiehart, D. P. (2002). *Drosophila* RhoA regulates the cytoskeleton and cell-cell adhesion in the developing epidermis. *Development* **129**, 3173–3183.

Brand, A. H., Manoukian, A. S., and Perrimon, N. (1994). Ectopic expression in *Drosophila*. *In* "Drosophila melanogaster: Practical Uses in Cell and Molecular Biology." (L. S. B. Goldstein, E. A. Fyrberg, eds.), pp. 635–654. Academic Press, San Diego.

Buchstaller, A., and Jay, D. G. (2000). Micro-scale chromophore-assisted laser inactivation of nerve growth cone proteins. *Microsc. Res. Tech.* **48**, 97–106.

Dutta, D., Bloor, J. W., Ruiz-Gomez, M., VijayRaghavan, K., and Kiehart, D. P. (2002). Real-time imaging of morphogenetic movements in *Drosophila* using Gal4-UAS-driven expression of GFP fused to the actin-binding domain of moesin. *Genesis* **34**, 146–151.

Edwards, G. S., Austin, R. H., Caroll, F. E., Copeland, M. L., Couprie, M. E., Gabella, W. E., Haglund, R. F., Hooper, B. A., Hutson, M. S., Jansen, E. D. *et al*. (2003). FEL-based-biophysical and biomedical instrumentation. *Rev. Sci. Instrum.* **74**, 3207–3245.

Edwards, K. A., Demsky, M., Montague, R. A., Weymouth, N., and Kiehart, D. P. (1997). GFP-moesin illuminates actin cytoskeleton dynamics in living tissue and demonstrates cell shape changes during morphogenesis in *Drosophila*. *Dev. Biol.* **191**, 103–117.

Foe, V. E. (1989). Mitotic domains reveal early commitment of cells in *Drosophila* embryos. *Development* **107**, 1–22.

Grill, S. W., Howard, J., Schaffer, E., Stelzer, E. H., and Hyman, A. A., (2003). The distribution of active force generators controls mitotic spindle position. *Science* **301**, 518–521.

Harden, N. (2002). Signaling pathways directing the movement and fusion of epithelial sheets: Lessons from dorsal closure in *Drosophila*. *Differentiation* **70**, 181–203.

Heim, R., and Tsien, R. Y. (1996). Engineering green fluorescent protein for improved brightness, longer wavelengths and fluorescence resonance energy transfer. *Curr. Biol*. **6**, 178–182.

Hutson, M. S., Tokutake, Y., Chang, M. S., Bloor, J. W., Venakides, S., Kiehart, D. P., and Edwards, G. S. (2003). Forces for morphogenesis investigated with laser microsurgery and quantitative modeling. *Science* **300**, 145–149.

Inoue, S., and Spring, K. R. (1997). "Video Microscopy." Plenum Press, New York.

Jacinto, A., Wood, W., Balayo, T., Turmaine, M., Martinez-Arias, A., and Martin, P. (2000). Dynamic actin-based epithelial adhesion and cell matching during *Drosophila* dorsal closure. *Curr. Biol*. **10**, 1420–1426.

Jacinto, A., Woolner, S., and Martin, P. (2002). Dynamic analysis of dorsal closure in *Drosophila*: From genetics to cell biology. *Dev. Cell* **3**, 9–19.

Kaltschmidt, J. A., Davidson, C. M., Brown, N. H., and Brand, A. H. (2000). Rotation and asymmetry of the mitotic spindle direct

asymmetric cell division in the developing central nervous system. *Nature Cell Biol*. **2**, 7–12.

Kass, M., Witkin, D., and Terzopoulos, D. (1987). Active contour models. *Int. J. Comput Vision* **1**.

Kiehart, D., Galbraith, C., Edwards, K., Rickoll, W., and Montague, R. (2000). Multiple forces contribute to cell sheet morphogenesis for dorsal closure in *Drosophila*. *J. Cell Biol*. **149**, 471–490.

Kiehart, D. P. (1999). Wound healing: The power of the purse string. *Curr. Biol*. **9**, R602–R605.

Kiehart, D. P., Montague, R. A., Rickoll, W. L., Foard, D., and Thomas, G. H. (1994). High-resolution microscopic methods for the analysis of cellular movements in *Drosophila* embryos. *Methods Cell Biol*. **44**, 507–532.

Lin, D. M., Auld, V. J., and Goodman, C. S. (1995). Targeted neuronal cell ablation in the *Drosophila* embryo: Pathfinding follower growth cones in the absence of pioneers. *Neuron* **14**, 707–715.

Lippincott-Schwartz, J., and Patterson, G. H. (2003). Development and use of fluorescent protein markers in living cells. *Science* **300**, 87–91.

Marshall, W., and Sliney, D. (eds.) (2000). "Laser Safety Guide." Orlando, FL.

Miyawaki, A., Llopis, J., Heim, R., McCaffery, J. M., Adams, J. A., Ikura, M., and Tsien, R. Y. (1997). Fluorescent indicators for Ca^{2+} based on green fluorescent proteins and calmodulin. *Nature* **388**, 882–887.

Murphy, D. B. (2001). "Fundamentals of Light Microscopy and Electronic Imaging," Wiley-Liss, New York.

Oda, H., and Tsukita, S. (1999). Dynamic features of adherens junctions during *Drosophila* embryonic epithelial morphogenesis revealed by a Dalpha-catenin-GFP fusion protein. *Dev. Genes Evol*. **209**, 218–225.

Oda, H., and Tsukita, S. (2001). Real-time imaging of cell-cell adherens junctions reveals that *Drosophila* mesoderm invagination begins with two phases of apical constriction of cells. *J. Cell Sci*. **114**, 493–501.

Ormo, M., Cubitt, A. B., Kallio, K., Gross, L. A., Tsien, R. Y., and Remington, S. J. (1996). Crystal structure of the *Aequorea* victoria green fluorescent protein. *Science* **273**, 1392–1395.

Roberts, D. B. (1998). "*Drosophila*: A Practical Approach." IRL Press at Oxford University Press, New York.

Skibbens, R. V., Rieder, C. L., and Salmon, E. D. (1995). Kinetochore motility after severing between sister centromeres using laser microsurgery: Evidence that kinetochore directional instability and position is regulated by tension. *J. Cell Sci*. **108**(Pt 7), 2537–2548.

Sliney, D. (ed.) (2000). *LIA Guide for the Selection of Laser Eye Protection*. Orlando, FL.

Stronach, B. E., and Perrimon, N. (2001). Investigation of leading edge formation at the interface of amnioserosa and dorsal ectoderm in the *Drosophila* embryo. *Development* **128**, 2905–2913.

Verkhusha, V. V., Tsukita, S., and Oda, H. (1999). Actin dynamics in lamellipodia of migrating border cells in the *Drosophila* ovary revealed by a GFP-actin fusion protein. *FEBS Lett*. **445**, 395–401.

Wang, S. S., and Augustine, G. J. (1995). Confocal imaging and local photolysis of caged compounds: Dual probes of synaptic function. *Neuron* **15**, 755–760.

Whiteley, M., and Kassis, J. A. (1993). Double-sided sticky tape for embryo injections. *Drosophila Information Newsletter* **11**: http://flybase.bio.indiana.edu/docs/news/DIN/dinvol11.txt.

Wood, W., Jacinto, A., Grose, R., Woolner, S., Gale, J., Wilson, C., and Martin, P. (2002). Wound healing recapitulates morphogenesis in *Drosophila* embryos. *Nature Cell Biol*. **4**, 907–912.

Young, P. E., Richman, A. M., Ketchum, A. S., and Kiehart, D. P. (1993). Morphogenesis in *Drosophila* requires nonmuscle myosin heavy chain function. *Genes and Dev*. **7**, 29–41.

SECTION

4

Fluorescent Microscopy of Living Cells

CHAPTER

10

Introduction to Fluorescence Imaging of Live Cells: An Annotated Checklist

Yu-li Wang

It is becoming clear that most biological molecules in living cells are in a highly dynamic state, changing their interactions and spatial organizations in response to signals. With recent advances in optics, probe design, and photon detection, there are few approaches as suitable as fluorescence imaging for investigating dynamic events in living cells. However, successful execution of fluorescence imaging relies heavily on proper setup of facilities. The purpose of this article is to provide a comprehensive list of the equipment, with associated notes, for those setting up new imaging facilities.

There are many options in setting up a fluorescence imaging facility, each with its advantages and disadvantages. The decision is usually dictated by a combination of experimental goals and personal preferences. While this article attempts to provide some useful guidelines, it is important not to equip much beyond what is necessary, as excess equipment wastes money, creates confusion, and often becomes obsolete when one finally finds the opportunity to use it.

Microscope Stand

An inverted microscope generally allows more flexibility and workspace for the culture (see later) and manipulation of live cells than an upright microscope. In addition, while inverted stands by major manufacturers give comparable performances, it is important to take into consideration the feasibility, accessibility, and convenience for special third-party accessories, such as the culture chamber, micromanipulator, filter wheels, and confocal optics to be used. Therefore, choice of the stand should not be made until the design of the rest of the system becomes largely clear.

One aspect particularly relevant to living cell imaging is the stability of the microscope stand. Some old microscopes are prone to stage drift, particularly at an elevated temperature. They require either extensive manual input or an autofocusing mechanism for time-lapse imaging. However, it is often difficult to obtain reliable information on the stability through manufacturers or on-site demonstration, and experience of colleagues is often the most reliable source.

Several current microscope designs incorporate useful automatic features, such as lamp shutters (see later) and motorized magnification and stage controls, which may alleviate the need to incorporate third-party components and facilitate automated multimode time-lapse imaging.

Objective Lenses and Contrasting Method

A basic set of objectives consists of 10×, 40× dry, 40× immersion, 100× immersion lenses and possibly a 60 or 63× immersion lens. Dry lenses are used primarily for scanning the samples and do not have to be expensive. However, immersion lenses should have as high a numerical aperture and light transmission efficiency as possible. Because images are typically collected near the center of the field, lenses highly corrected for flat field usually provide no detectable benefit and are more costly and less light efficient than simpler lenses such as Fluar lenses. All lenses for fluorescence imaging should be checked upon delivery for the quality of point-spread function, using fluorescent beads as the sample (see later).

For most applications, phase-contrast optics should suffice for scanning the sample and for collecting paired fluorescence and transmission images. The presence of quarter-wave plate in the phase lens does cause some (~<5%) light loss, although it is usually not serious enough to defeat the use of phase-contrast optics. The alternative is DIC optics, which requires

Copyright 2006, Elsevier Science (USA).
All rights reserved.

the repeated insertion and removal of an analyzer in the optical path when one shifts between DIC and fluorescence optics. This, and the higher cost, makes DIC optics less desirable in most cases.

Condenser

Unless the experiment involves high-resolution transmission optics or dark-field optics, a condenser with a long working distance should be used in conjunction with an inverted stand.

Control of Projection Magnification

It is critical to choose an optimal magnification for live cell imaging, balancing between signal intensity (favored by low magnification) and resolution (favored by high magnification). It is particularly important to match the final magnification with the pixel size of the detector (see later). Projection magnification may be controlled conveniently in some microscopes by switching the tube lens or by adding additional lenses (referred to as Optovar for Zeiss microscopes). New stands allow changes of magnification to be controlled automatically in time-lapse imaging.

Epi-illuminator and Fluorescence Filter Sets

Some new epi-illumination systems provide a light trap, which reduces the background stray light, and standard Kohler illumination with both field and aperture diaphragms. The aperture diaphragm may be used to control the lamp intensity as well as the angular span and depth of illumination. The light trap is useful for single molecular imaging, which is typically limited by the background.

There are several commercial sources of high-quality fluorescence filter sets. A handbook on the selection of filter sets may be found at the Web site of Chroma Optics. The main consideration is to balance signal strength (favored by cuton/cutoff filters or wide band-pass filters) against the reduction of signal crossover from probes of different colors (favored by narrow band-pass filters). The latter consideration is particularly important when an intense, long wavelength probe is used in conjunction with a weak, short wavelength probe. In addition to standard filter sets, multiband filters are now readily available that allow simultaneous illumination and/or detection of multiple fluorophores.

Heater Filter or Heat Mirror

When imaging living cells it is critical to remove the infrared component from the light source, as the fluorescence filter set may not be able to block infrared light. Failure to do so may cause not only heat damage to the cell, but also high background with some infrared-sensitive cameras. The filter (e.g., BG38) or heat-reflecting mirror may be placed either in front of the lamp or in the epi-illuminator. Attention should be paid to the UV transmission of these filters if UV excitation is to be used for imaging.

Lamps and Lamp Power Supplies

The system should include both a mercury arc lamp and a 100-W quartz-halogen lamp for epi-illumination, coupled through a selection mirror to the microscope. Contrary to common practice, the most suitable lamp for fluorescence imaging of live cells is often a 100-W quartz-halogen lamp. Unless the experiment involves single molecule or speckle imaging, quartz-halogen lamps are much more cost effective and are sufficiently intense for imaging most cellular structures while minimizing radiation damage. They also allow easy adjustment of the light intensity, using a variable, stabilized DC power supply.

The mercury arc lamp should consist of a well-shielded housing, power supply, and power supply cable to minimize the potentially damaging electromagnetic wave during ignition. Although some power supplies allow adjustment of the light intensity, the range of adjustment is limited. Therefore, it is often necessary to attenuate the light from mercury arc lamps using a set of neutral density filters to avoid radiation damage. Alternatively, the intensity may be controlled using the aperture diaphragm in the epi-illuminator as mentioned earlier.

Shutters

Electronic shutters should be used to control fluorescence excitation. These shutters should be used as much as possible to minimize the duration of illumination and should have the interface for computer control during automated time-lapse recording.

Cameras

Cooled CCD cameras are used for most fluorescent imaging applications. In choosing a camera, important parameters include quantum efficiency, noise level, pixel size and full-well capacity, and scanning frequency. In order to minimize the excitation light for imaging live cells, the camera should be as "sensitive" as possible, which generally means a high quantum efficiency, low noise, large pixel size, and slow scan rate. The sensitivity requirement must therefore be balanced against the required resolution (favored by a larger number of small pixels) and imaging rate (favored by a higher scanning frequency).

Slow-scan CCD cameras are generally limited in their frame rate. In addition, unless the sample is very intense, the signal-to-noise ratio is poor under short

exposures. This limits both their use for high-speed imaging and the ease in focusing the images. Focusing is facilitated with cameras using the shutterless, frame-transfer or interline CCDs, which are able to provide a continuous stream of images at video rate in addition to slow-scan digital signals.

Intensified CCD cameras are generally more suitable for high-speed imaging, although usually with a compromised quantum efficiency. Of particular interest are cameras that use CCD chips with the new electron amplification technology (e.g., photometric Cascade and Andor Ixon cameras), which allow both long-exposure and high-speed imaging at a high quantum efficiency.

Optical Coupling of Cameras

Coupling with the detector should be achieved with as few lens elements as possible. It is recommended to have several couplers with different magnification factors. In conjunction with different objective lenses and projection magnifications mentioned earlier, they allow a wide range of magnifications for both light-limiting and high-resolution applications. The Nyquist resolution criterion should be considered when choosing the magnification: each pixel should correspond to no more than half the required resolution limit on the sample. Due to the diffraction limit of the microscope, this distance needs not be smaller than 50 nm for most applications. The actual area imaged onto each pixel may be determined easily by taking an image of a scale standard (see later).

Vibration Isolation Table

A full-fledged vibration isolation table is necessary in adverse environment, e.g., in areas of heavy traffic or in high-rise buildings, or for demanding experiments of micromanipulations or single molecular imaging. Simple isolation measures may suffice otherwise. These include inner tires under the table or rubber isolation pads (Edmond Scientific) or tennis balls under a slab tabletop.

Motorized Stage and Focusing Control

A motorized XY stage is optional. It allows one to monitor multiple cells in separate regions and may increase the output greatly in time-lapse experiments. A motorized focusing control is required for optical sectioning, three-dimensional imaging, and automatic focusing. However, many simple imaging experiments may be better served without the complications of motorized stage controls.

Computer Hardware and Software

A high-end personal computer is required not only for image acquisition, but also for device control and data analysis. The system should have a high-capacity hard disk, a recordable CD/DVD drive for archiving and porting data, and double monitors to accommodate all the images and control windows. Before making a decision on the software package, it is advisable to prepare a list of application requirements, as many features seen in software demonstrations are visually dazzling but practically useless. The efficiency of a package should be judged by counting the number of mouse clicks or key strokes for setting up and triggering the most frequently used functions.

As a minimum for live cell imaging, the program should be able to control the camera, shutters, and motorized devices, to perform time-lapse recording, and to allow changes of recording parameters without stopping the recording. In addition, the user should be able to review dynamic processes as movies even during the recording. The program should also be able to perform automatic contrast enhancement (without losing the original intensity values) and to save images in a nonlossy file format with automatically generated or manually entered file names.

Microscope Incubators

There are a number of options available through microscope manufacturers and independent companies such as Bioptechs. Discussions of cell culture on microscopes may be found at the Web site of Bioptechs and in McKenna and Wang (1989).

There is no "ideal" culture device for all the applications. The range of possible devices varies from a heated stage, a heating collar for the objective lens, a small heated culture chamber, to a large enclosure that fits over the entire microscope. A heated stage is the most convenient but the least functional, as the point of observation is over an open area far away from the heat source. A heating collar for the objective lens applies heat much closer to the sample. However, it works only in conjunction with immersion lenses and has a limited area of heating. It is usually used in conjunction with an additional chamber or enclosure. Large microscope enclosures provide the most stable temperature; however, it must be designed carefully to provide convenient access. There are also a number of perfusion and heated culture chambers for microscopy. These chambers generally provide excellent optical and culture conditions; however, the associated wires and tubing may add to the inconvenience, and the sealed environment may not be compatible with micromanipulation experiments.

It is important to maintain the temperature stability to within a fraction of a degree, as even minor drifts in temperature can cause severe drifts in focusing and

sample positioning. In addition to heating, it is important to maintain the pH and osmolarity of the culture medium. While this should not be a problem with sealed chambers or perfusion chambers, open chambers should be used in conjunction with either a CO_2-independent medium (e.g., L-15) or injection of CO_2 into the incubator. It should be noted that HEPES-buffered media only slow down pH drift and are not suitable for long-term cultures by themselves. Osmolarity may also be a serious problem with open dishes in a heated environment. It may be controlled by replacing the medium periodically or by covering the medium with a layer of mineral oil (Sigma).

Testing Samples

Several testing samples should be prepared for characterizing the imaging system. First, a micrometern scale is essential for all microscopy laboratories for determining the final magnification. Second, a "flat field" sample is prepared by spreading a drop of appropriate fluorophores in 50% glycerol under a coverslip. It is useful for checking the uniformity of epi-fluorescence illumination and for setting the field diaphragm. Also essential is a sample of fluorescent beads. It is prepared by diluting 0.1-μm-diameter fluorescent latex beads (Molecular Probes) by ~10^5 into melt 1% agarose, and mounting a small volume (~20–50 μl) of the suspension on a heated glass slide under a coverslip, before letting the sample cool down. The bead sample is used for checking the combined optical quality of the imaging system. Defects not readily visible with cell samples are often recognized easily when one examines the images of single beads. Defocused beads should appear as radially symmetric disks or concentric rings.

Additional Equipment

Additional equipment may be required for special purposes. Multiwavelength imaging is often achieved with filter wheels at the illumination and/or detection optical path. In addition, devices such as Dual-View and Quad-View from Optical Insights generate composite images at different wavelengths. Spinning disk confocal heads have been used extensively for imaging fine structures in single cells. Its balance between light efficiency and resolution proves particularly suitable for cultured cells. Finally, total internal reflection fluorescence optics is being used extensively for imaging structures near the cell–glass interface, such as focal adhesions. Details of these approaches and devices are beyond the scope of this article; however, their potential use should be considered when designing the imaging system.

Reference

McKenna, N. M., and Wang, Y.-L. (1989). Culturing cells on the microscope stage. *Methods Cell Biol.* **29**, 295–305.

CHAPTER

11

Cytoskeleton Proteins

Klemens Rottner, Irina N. Kaverina, and Theresia E. B. Stradal

I. INTRODUCTION

The visualisation of cytoskeletal proteins and their dynamics in live cells has led to invaluable insights into cytoskeleton-driven processes as various as cell migration, chromosome segregation during division, cytokinesis, and phagocytosis, as well as the establishment of cell–substrate or cell–cell adhesion. The cytoskeleton of eukaryotic cells can be grossly divided into three filamentous systems: actin filaments, microtubules, and intermediate filaments.

This article focuses on revealing the dynamics of the actin cytoskeleton and the microtubule system, as well as some proteins associating with them in interphase cells. It compares classical approaches with more recent advancements in this enormously growing field.

More specifically, this article discusses visualisation of the cytoskeleton using purified components chemically modified with fluorescent dyes and compares this method with ectopic expression of cytoskeletal genes fused to fluorescent protein tags such as green fluorescent protein (GFP). While the efficient introduction of fluorescently labelled cytoskeletal proteins is usually achieved by microinjection, which requires additional equipment and experimental effort, the expression of genes tagged to fluorescent proteins is obtained by transfection of the respective fusion constructs. We will show that both methods can lead to equally satisfying results, but as the transfection of nucleic acids seems to be continuously improved and developed further, the latter method may be used more frequently for most common tissue culture cells. However, because studies on cytoskeleton dynamics are sometimes performed on cell types that have so far not been reported to mediate the expression of ectopic genes, such as epidermal fish keratocytes, protein microinjection and subsequent analysis are still performed. In addition, we briefly mention the microinjection of specific antibodies to monitor the dynamics of cytoskeletal components.

Finally, this article gives examples of how to approach the visualisation of two distinct cytoskeletal components in the same living cell using two-colour fluorescence video microscopy.

II. MATERIALS AND INSTRUMENTATION

A. Equipment

1. Microscope

Inverted microscope (e.g., Axiovert 135TV, Carl Zeiss Jena GmbH) equipped for epifluorescence and phase-contrast microscopy with 40×/1.3NA and 100×/1.4NA oil immersion objectives, 1.6 and 2.5 optovar intermediate magnification, electronic shutters (e.g., Uniblitz Electronic 35-mm shutter including driver Model VMMD-1, BFI Optilas) to allow for computer-controlled opening of the light paths, filter wheel (e.g., LUDL Electronic Products LTD, SN: 102691 and driver SN: 1029595) to enable two-colour epifluorescence in combination with appropriate dichroic beam splitters and emission filters (Omega Optical Inc. or Chroma Technology Corp.), and tungsten lamps (Osram, HLX64625, FCR 12V, 100W) for both phase contrast and fluorescence light paths. Tungsten lamps are not as bright as mercury lamps, but the latter cause photodamage and bleaching with higher probability.

Copyright 2006, Elsevier Science (USA).
All rights reserved.

2. Data Acquisition

Preferably by a back-illuminated, cooled charge-coupled-device camera (e.g., Princeton Research Instruments TKB 1000 × 800, SN:J019820; Controller SN:J0198609) driven, for instance, by IPLab (Scanalytics Inc.) or Metamorph software (Universal Imaging Corporation). Dependent on cell types and/or processes studied, this "epifluorescence setting" can be extended to the various options of confocal microscopy (see contributions on confocal imaging within this volume).

3. Microinjection

Commercial microinjection capillaries (Femtotips I; Cat. No.: 5242952.008, Eppendorf AG) or, alternatively, self-made needles requiring a "needle puller" (e.g., Model PN-30, Narishige International LTD), mechanical (Cat. No.: 520137, Leica Microsystems), oil-pressure-driven (e.g., Model M0188NE, SN:99069, Narishige International LTD), or electronic (e.g., Model 5171, Eppendorf AG) micromanipulators used in combination with an air pressure device (e.g., Transjector 5246, Eppendorf AG); flexible microloaders for loading microinjection capillaries (Cat. No.: 5242956.003, Eppendorf AG).

4. Centrifuges

Cooled high-speed benchtop centrifuges (e.g., Biofuge *fresco*, Heraeus) to pellet protein aggregates prior to injection.

5. Heating

Open (e.g., Series 20 chamber platform, Model PH4, Warner Instruments used with heater controller model TC-324B, SN:1176) or, alternatively, closed heating chambers (e.g., Model FCS2, Bioptechs Inc.).

Cells growing at room temperature are observed on coverslips mounted to the bottom of plastic dishes harbouring a central hole or in comparable commercial devices.

6. Coverslips

Round glass coverslips, 15 or 40 mm in diameter, cleaned in 6/4 ethanol/HCl (37%), washed extensively with H_2O, dried, and sterilised by exposure to ultraviolet light or in a dry heat sterilizer at 220°C (ethanol: Sigma, Cat. No.: E-7023; HCl: Sigma, Cat. No.: H-7020).

7. Basics

General equipment and plastic-ware (e.g., from Becton Dickinson Biosciences or Greiner Bio-One GmbH) for molecular biology techniques and tissue culture.

B. Cells and Media

1. Cells

Mouse melanoma cells B16-F1 (American Type Culture Collection: CRL-6323) and goldfish fin fibroblasts (CAR, American Type Culture Collection: CCL-71).

2. Growth

All reagents are from Invitrogen Corp. unless stated otherwise. For B16-F1: Dulbecco's modified Eagle's medium (Cat. No.: 41965-039) supplemented with 10% fetal calf serum (FCS, PAA Laboratories, Clone, Cat. No.: A11-041), 2 m*M* glutamine (Cat. No.: 25030-024), 1% antibiotics (Cat. No.: 15070-063). For CAR: basal Eagle's medium with Hank's balanced salt solution (Cat. No.: 21370-028), 15% serum (Hyclone, Cat. No.: SH30070.03), 1 m*M* glutamine, 1 m*M* nonessential amino acids (Cat. No.: 11140-035), and 1% antibiotics. Upon confluence, cells are detached using trypsin (Cat. No.: 25300-054) and seeded according to standard protocols.

3. B16 Medium for Microscope

Ham's F12 HEPES-buffered medium (Sigma, Cat. No.: N8641) including complete supplements of the regular growth medium (see point **2**).

4. Substrates

Laminin (Sigma, Cat. No.: L2020) or fibronectin (Roche, Cat. No.: 1051407).

5. Lipofection

With Superfect transfection reagent (Qiagen GmbH, Cat. No.: 301305) or FuGENE6 (Roche, Cat. No.: 1 814 443).

C. Proteins and Constructs

1. *TAMRA-vinculin*: From turkey gizzard, coupled to carboxytetramethylrhodamine (5'-TAMRA) succinimidyl ester (Molecular Probes, Cat. No.: C-2211) as described (Rottner *et al.*, 1999) and upon addition of 2 mg sucrose/mg protein stored in 30-µl aliquots at 1 mg/ml at –70°C
2. *TAMRA-α-actinin*: From turkey gizzard, kindly provided by M. Gimona (Salzburg) and fluorescently modified and stored as described for vinculin
3. *Cy3-tubulin*: As described (Hyman, 1991); for a protocol of tubulin labelling (by John Peloquin) we recommend http://www.borisylab.nwu.edu/pages/protocols/cy3tub.html
4. *EGFP-tubulin*: Kindly provided by M. Geese (Braunschweig), comprises murine β3-tubulin fused into EGFP-C2 (Clontech, Cat. No.: 6083-1)

5. *EGFP-EB1*: As described (Stepanova *et al*., 2003)
6. *EGFP-p16-B*: p16B-cDNA, also known as ARPC5B (Millard *et al*., 2003), was amplified from a human EST clone (Acc. No.: 12652556, RZPD cloneID IRALp962P167) and subcloned into EGFP-C1 (Clontech; Cat. No.: 6084-1)
7. *Zyxin-EGFP*: As described (Rottner *et al*., 2001)
8. *Zyxin-dsRED*: As described (Bhatt *et al*., 2002)

III. PROCEDURES

Solutions

All chemicals are from Sigma-Aldrich.

1. *Phosphate-buffered saline (PBS) working solution*: 140 m*M* NaCl (Cat. No.: S-7653), 2.7 m*M* KCl (Cat. No.: P-1338), 10 m*M* Na_2HPO_4 (Cat. No.: S-7907), 1.8 m*M* KH_2PO_4 (Cat. No.: P-0662), pH 7.4
2. *Urea*: 2 *M* in H_2O (Cat. No.: U-0631)
3. *Laminin coating buffer*: 50 m*M* Tris (Cat. No.: T-1503) adjusted with HCl to pH 7.5, 150 m*M* NaCl
4. *Microinjection buffer (for vinculin and α-actinin)*: 2 m*M* Tris–acetate (acetic acid: Cat. No.: A-0808), 50 m*M* KCl (Cat. No.: P-1338), 0.1 m*M* dithioerythritol (DTE, Cat. No.: D-8255), pH 7.0. Note that microinjection buffers vary significantly depending on the cytoskeletal protein injected [e.g., buffers for microinjecting actin generally lack KCl (Wang, 1984), whereas buffers for injecting myosin II require KCl (up to 450 m*M*) in order to avoid polymerisation of the respective component in the needle (Verkhovsky and Borisy, 1993)].
5. *Microinjection buffer (for tubulin)*: 80 m*M* PIPES (Cat. No.: P-6757) adjusted with KOH (Cat. No.: P-6310) to pH 6.8, 1 m*M* $MgCl_2$ (Cat. No.: M-2670), 1 m*M* EGTA (Cat. No.: E-1644) (Fig. 1).

A. Visualisation Using a Fluorescently Conjugated Protein

Steps

1. Various different fibroblast cell lines survive microinjections better when grown on fibronectin. For coating of coverslips, dissolve fibronectin at a concentration of 1 mg/ml in 2 *M* urea and store at 4°C.
2. Dilute fibronectin stock 1:20 to 50 µg/ml with PBS and coat sterile coverslips for 1 h at room temperature (150 µl for 15-mm-diameter coverslips). Before seeding the cells, wash thoroughly with PBS to remove urea (two to three times).
3. Upon washing, seed the cells onto coverslips in a petri dish and let them attach and spread for 12–72 h in an incubator.
4. Thaw an aliquot of fluorescently coupled protein. If not in appropriate buffer, dialyse the sample into microinjection buffer using Slide-A-Lyzer (e.g., Pierce, 10 kDa cutoff Cat. No.: 66415) or a similar device for the dialysis of small volumes and concentrate using microcon concentrators (Amicon, YM-10, Cat. No.: 42407) (for proteins such as vinculin or α-actinin, concentrations of 0.5–1 mg/ml are ideal for injections).
5. Spin the probe for microinjection in a cooled centrifuge at maximum speed (approximately 10,000 *g*) for at least 30 min before loading the needle in order to remove protein aggregates that may clog up the needle tip.
6. Mount cells onto the microscope in a chamber freely accessible to the microinjection needle.
7. Upon loading of the needle from the back using a flexible pipette tip, carefully inspect the needle tip for the absence of air bubbles. If required, remove them by gently hitting the needle shaft, but proceed rapidly in order to avoid drying of the tip.
8. Apply pressure (20–100 hPa) to the needle holder, attach needle, and rapidly move needle into the medium. (The "background pressure" applied before entering the medium is required to avoid sucking up of the medium due to capillary force of the needle tip.)
9. Bring the needle close to the cells.
10. Before injections, check the needle flow by fluorescence.
11. In case of flow, gently inject the cells, manually or using a so-called half-automatic system (Eppendorf AG, see earlier discussion). For manual injections, carefully approach the membrane and remove immediately upon needle flow into the cell.
12. Upon injection of a sufficient number of cells, allow the cells to recover and the cytoskeletal proteins to incorporate (e.g., 30–60 min). For actin, full incorporation into the cytoskeleton may take up to 2 h. In contrast, vinculin targets to focal adhesions within minutes.
13. After incorporation of the injected protein, darken the room and search for interesting cells using epifluorescence and preferably a 40× oil immersion lens. In case no fluorescent cells can be found by eye, it will be difficult to pick up a satisfying signal using a back-illuminated CCD camera.
14. After selection of an interesting cell, switch to higher magnification (100×) with or without optovar intermediate magnification and test for the minimal exposure time required to get a good signal/noise ratio. (For important details on fluorescence imaging and image processing, see articles by Anderson and by Wang.)
15. In order to record a stack of fluorescent images, set the appropriate number of images to be taken and

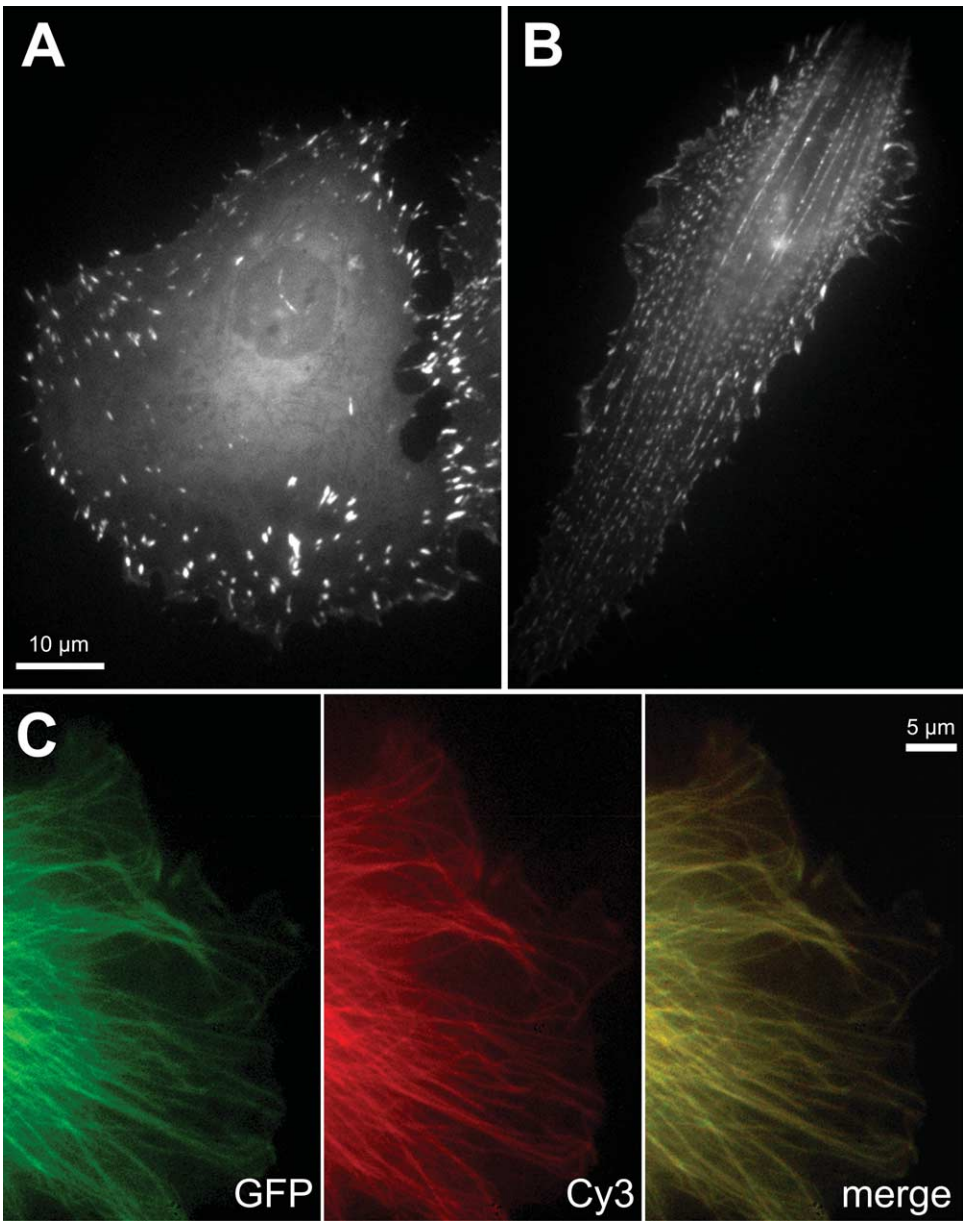

FIGURE 1 Examples for specific incorporation of fluorescently tagged, microinjected proteins: CAR fish fibroblasts microinjected with TAMRA-vinculin (**A**) or TAMRA-α-actinin (**B**). Note the specific recruitment of both probes to focal adhesions and the additional periodic incorporation of α-actinin into stress fibres. (**C**) EGFP-β-tubulin (kind gift of M. Geese, Braunschweig) expression (green) in a CAR cell additionally microinjected with Cy3-tubulin (kind gift of F. Severin, Dresden; red). Note that both probes reveal an identical microtubule pattern (merge) and can therefore be used equally to study microtubule dynamics.

the time period in between individual frames (dependent on experiment). In order to avoid photodamage, illuminate cells with strong fluorescent light as rarely as possible. Avoid focusing in between frames using epifluorescence; focus using transmitted light, for example, in phase contrast, because for transmitted optics, much lower lamp intensities are required.

B. Visualisation Using a GFP-Tagged Protein (upon Transient Expression)

Steps

1. Purify the expression vector for your GFP-tagged open reading frame of interest using standard DNA purification columns (e.g., Qiagen-tip 500); dilute the

construct in H_2O in concentrations of not less than 0.5 µg/µl.

2. Seed the cells into 3.5-cm-diameter dishes (Falcon, Cat. No.: 35.3001) and allow them to attach and spread for 12–24 h.

3. Transfect cells in 3.5-cm dishes 12–24 h according to standard protocols, e.g., using FuGENE (Roche; 3 µl FuGENE/µg DNA) or Superfect transfection reagent (Qiagen; 6 µl Superfect/µg DNA). In our hands, 1–2 µg of DNA is sufficient per 3.5-cm-diameter dish.

4. Detach transfected cells using trypsin and seed onto coverslips. For studying the dynamics of GFP-tagged proteins during the actin-based motility of B16-F1 melanoma cells, we coat coverslips with 25 µg/ml laminin in laminin-coating buffer (1 h at room temperature); laminin stock (1 mg/ml) is stored in small aliquots at –20°C.

5. Upon spreading (for B16-F1 cells, wait 3–5 h), mount coverslips on the microscope using an appropriate open or closed chamber system, including a heating device if required. Compensate for lack of CO_2 by using HEPES-buffered growth media if needed. Changing to HEPES-buffered media may require some adaption time (dependent on cell type).

6. Darken the room and search for transfected cells with your eyes with epifluorescence preferably using a 40×/1.3NA oil immersion lens.

7. Upon identification of an interesting cell, proceed as in steps **13** and **14** in Section III,A.

IV. GENERAL COMMENTS ON FLUORESCENT TAGGING

In order to obtain reliable data on the dynamics of any given cytoskeletal protein, it is important to consider potential interference of the fluorescent tag with proper subcellular targeting of the protein or with general protein function. It is therefore essential to make sure that the fluorescent analogue of a given protein incorporates identically to the endogenous protein, which can be tested for by cross-staining with appropriate antibodies. Chemical coupling of a purified protein to a conventional fluorescent tag such as fluoresceine or rhodamine can be advantageous over a fluorescent protein tag (such as GFP) due to the much lower molecular size of the former. However, certain coupling buffers (dependent on coupling chemistry) may affect proper protein folding and therefore lead to irreversible damage to a given protein avoiding its proper incorporation into the cytoskeleton. In general, monovalent dyes are advantageous over bi- or tetravalent dyes because the latter can cause irreversible protein multimerisation due to the coupling reaction (which can be tested for by SDS–PAGE).

For the fusion of cDNAs to fluorescent protein tags, the most common of which currently is the enhanced green fluorescent protein (EGFP, Clontech), also known as GFPmut1 (Cormack *et al*., 1996), we recommend always comparing the fusion of the given cDNA to both the N and the C terminus of the tag because it is difficult to predict whether the fusion to the protein tag on either side may interfere with protein function. For instance, in order to generate reliable fusion proteins for the visualisation of the actin nucleating complex Arp2/3 (Higgs and Pollard, 2001), we have so far generated N- and C-terminal fusions to each of the seven components and tested their incorporation in cells, with varying results. Some of the constructs showed poor incorporation or even interfered with lamellipodia protrusion (p34-EGFP). Good results were obtained with small molecular weight components of the complex (p16 and p21), although both N- and C-terminally tagged Arp3 also proved useful (Stradal *et al*., 2001). Figure 2 shows the dynamics of p16B (ARPC5B), a novel isoform of p16 (Millard *et al*., 2003) fused to the C terminus of EGFP in B16-F1 cells. In addition, spacers between EGFP and the gene of interest can be crucial for incorporation of the fusion constructs (Geese *et al*., 2000).

As an alternative possibility to follow the dynamics of cytoskeletal proteins, it is worth mentioning purification, fluorescent coupling, and microinjection of monoclonal antibodies directed against a cytoskeletal protein, which has been used in the past for zyxin (Rottner *et al*., 2001). This requires that the epitopes are freely accessible in the native protein and that injected antibodies do not interfere with proper protein positioning and function, prerequisites that can again only be evaluated experimentally.

V. CHOICE OF COMBINATIONS FOR DUAL LABELING

As with conventional fluorescent dyes, fluorescent protein tags today also come in different colours. As opposed to multiple labellings of fixed samples (see article by Prast *et al*.), for live cell imaging as described here, only dual-labelling experiments have proven practical so far, probably due to the lack of sufficiently bright dyes excitable by UV excitation. We provide examples here for imaging EGFP-tagged proteins together with injected proteins tagged to rhodamine derivatives or to Cy3 (see Fig. 3). An important

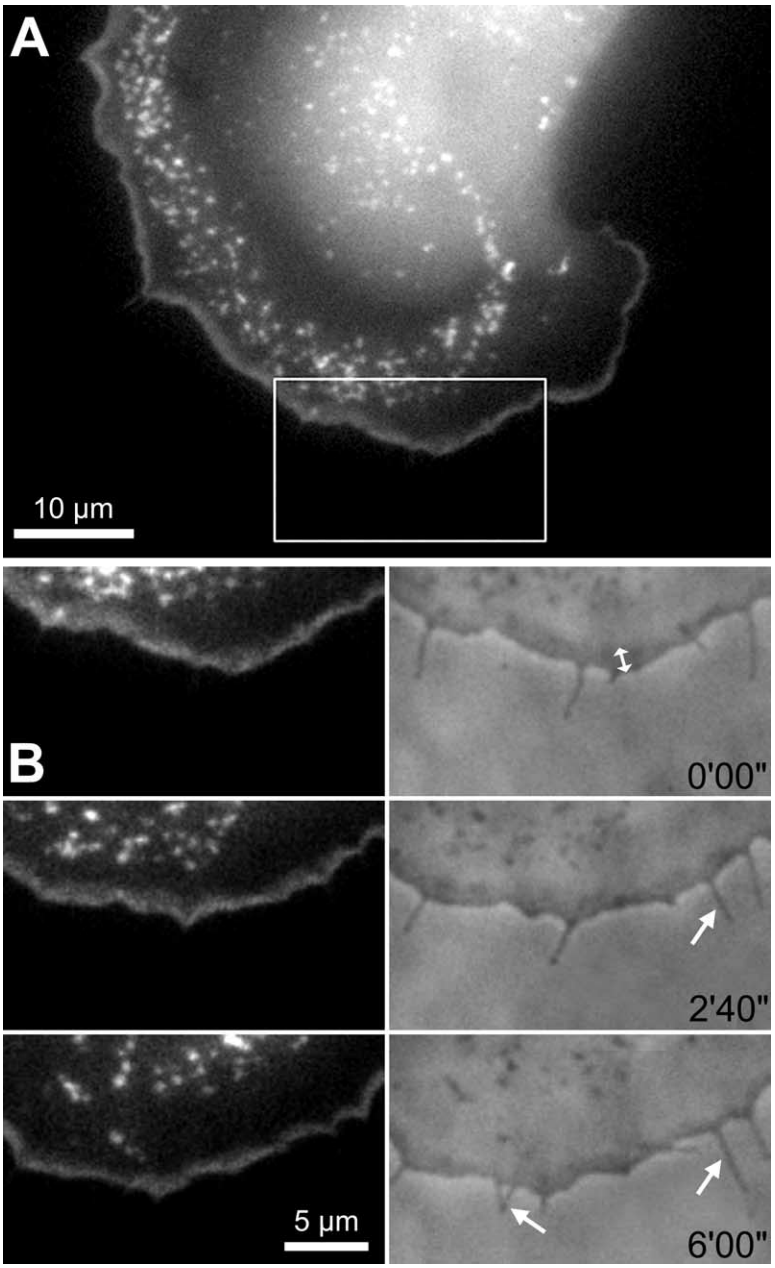

FIGURE 2 Arp2/3 dynamics in motile B16-F1 melanoma cell as revealed by transient expression of the GFP-tagged novel isoform p16B (ARPC5B). (**A**) Note that EGFP-p16B incorporated into the lamellipodial actin meshwork at the cell periphery and into highly dynamic surface ruffles, also known as actin flowers or clouds, as expected. (**B**) The time-lapse sequence from the region boxed in **A** (right panel: phase contrast) reveals reorganisation of the Arp2/3 complex during advancement of the cell periphery. Time is in minutes and seconds. Note the relatively constant lamellipodium width (double-headed arrow in **B**) during forward movement and the virtual exclusion of this Arp subunit from protruding filopodia (arrows).

alternative is the use of the red fluorescent protein from *Discosoma* sp. (dsRED), exemplified here by a dsRED-zyxin probe combined with EGFP-tubulin (Fig. 4). However, in contrast to EGFP, dsRED and even the improved variant termed dsRED2 (Clontech) are known to form a tetramer when fluorescent (Baird *et al*., 2000). Unfortunately, this feature can interfere with the function of certain cytoskeletal proteins. For instance, expression of a dsRED-calmodulin fusion protein was reported to cause severe aggregation and

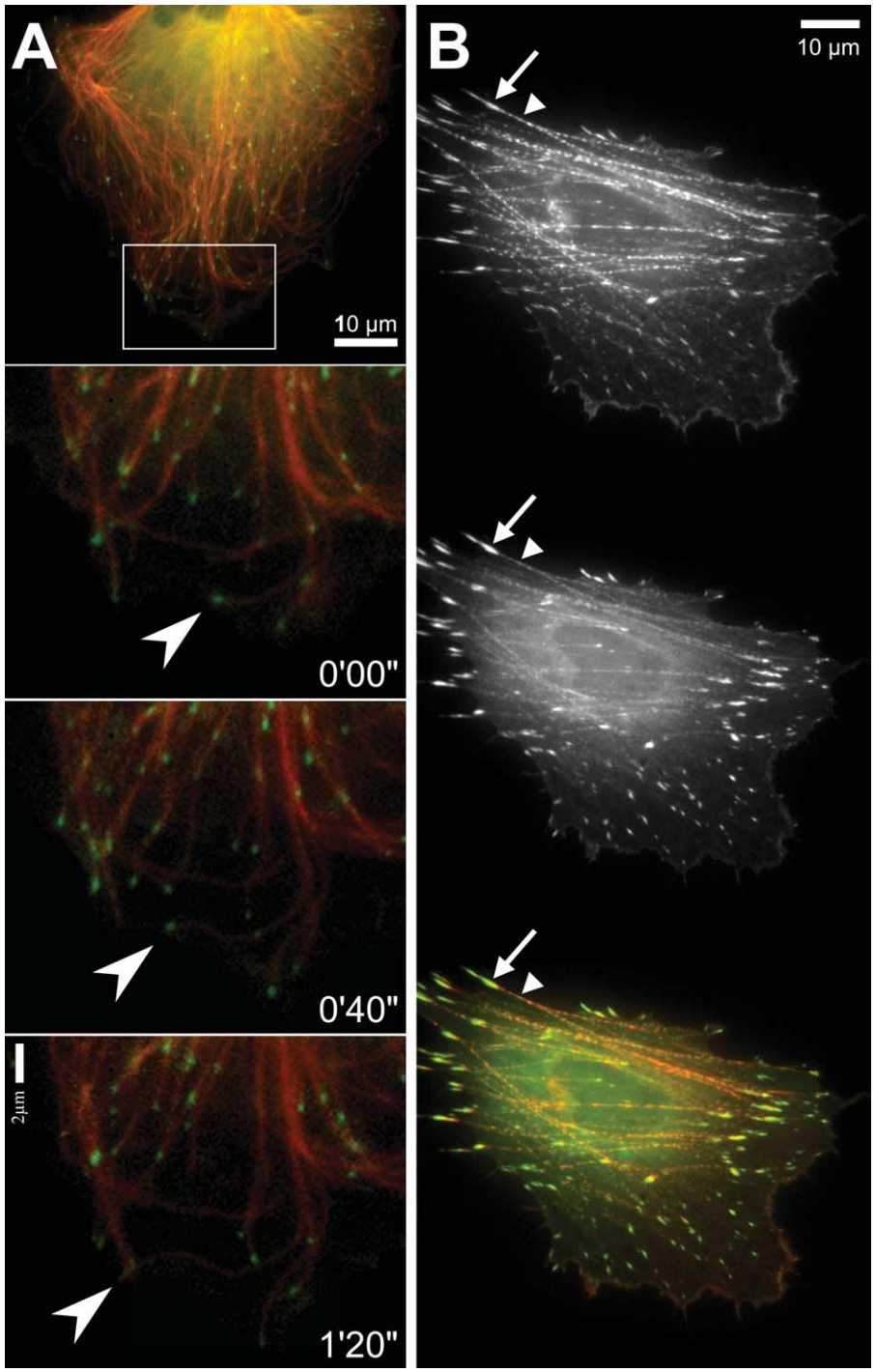

FIGURE 3 Examples of simultaneous visualisation of two distinct cytoskeletal components in the same cell. (**A**) Dynamics of microtubule plus ends in fish fibroblast CAR. Microinjected Cy3-tubulin (red) combined with ectopically expressed EGFP-EB1 (kind gift of A. S. Akhmanova, Rotterdam; green). Top image, overview. Bottom images, zoom into the boxed region in the overview, subsequent frames, time shown in minutes and seconds. Note that EB1 localises to the tips of growing microtubules (e.g., arrowheads in frames 0′00″ and 0′40″), but is absent from pausing or shrinking microtubule ends (e.g., arrowhead in frame 1′20″). (**B**) EGFP-zyxin expressing CAR cell microinjected with TAMRA-α-actinin: As shown in Fig. 2B, the α-actinin probe (top panel and red in the merged image at the bottom) mainly incorporates along stress fibers (arrowheads) and in focal adhesions (arrows). Zyxin (middle panel and green at the bottom), thought to be recruited to the cytoskeleton via α-actinin binding (Reinhard *et al.*, 1999), shows a similar, although not identical distribution. The merged image (bottom) reveals that zyxin (green) is enriched in focal adhesions, whereas α-actinin (red) targets more prominently to stress fibres, indicating that the subcellular positioning of zyxin is more complex than simple α-actinin-mediated recruitment.

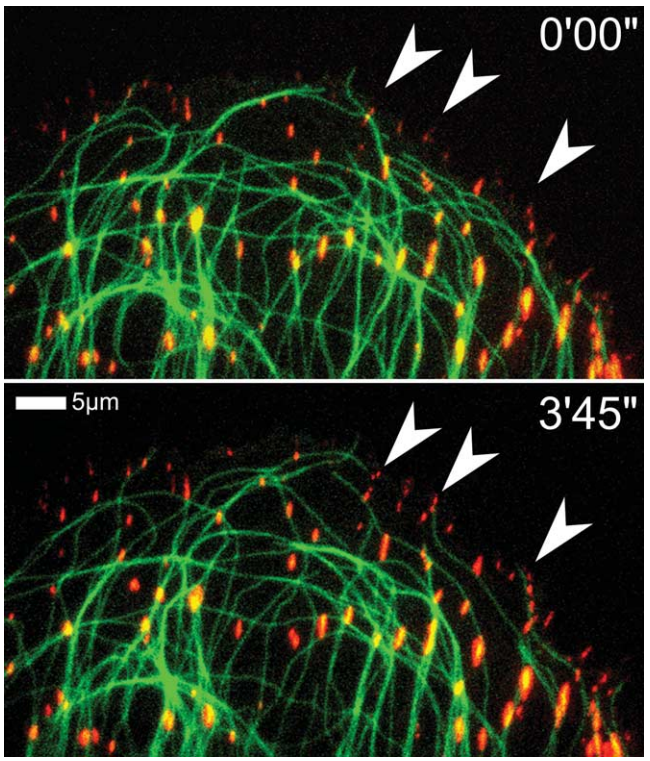

FIGURE 4 Simultaneous visualisation of two cytoskeletal components using two distinct fluorescent protein tags. Combination of EGFP-β-tubulin (pseudocoloured red) and dsRED-zyxin (kind gift of A. Huttenlocher, Madison; green) expressed ectopically in a CAR fish fibroblast. The combination reveals the formation and microtubule targeting of focal adhesions on this slowly protruding cell edge. Subsequent frames, time shown in minutes and seconds. Note newly formed adhesions (frame 3'45") and microtubules associated with them (arrowheads).

therefore mislocalisation of the tagged protein (Mizuno *et al.*, 2001).

As an alternative, mutations in EGFP have led to spectrally separable variants, ECFP (cyan) (Heim and Tsien, 1996) and EYFP (yellow) (both Clontech), which were used successfully for dual-labelling experiments of cytoskeletal proteins in the past (Geese *et al.*, 2002). However, the excitation and emission maxima of both dyes are relatively close, making it more difficult to separate them clearly. In addition, ECFP is significantly dimmer than EYFP, hence the simultaneous imaging of complex cytoskeletal structures may prove more difficult using these variants as compared to the red/green combinations given earlier.

Exciting more recent developments include far red fluorescent proteins, which appear separable not only from EGFP, but also from ECFP and EYFP. One was obtained from mutating a nonfluorescent chromoprotein from *Heteractis crispa*, termed HcRED-2A in (Gurskaya *et al.*, 2001), and is available as HcRED-1 (Clontech). The protein is a dimer and can now also be obtained as a "monomeric" tandem variant (evrogen.com).

In addition, Tsien and colleagues have developed a true monomeric red fluorescent protein (termed mRFP1) with excitation and emission peaks at 584 and 607, respectively, by introducing multiple mutations into dsRED (Campbell *et al.*, 2002). Comparisons of HcRED-1, its tandem variant, and mRFP1 as fusion proteins with actin and other cytoskeletal components revealed that mRFP1—at least in fusion with the components tested—was superior to the former red variants, mainly due to the lack of aggregation (not shown). Hence, although about 25% of the brightness of the original dsRED, the mRFP1 probe in combination with EGFP is expected to prove very useful for live cell dual imaging.

Acknowledgments

We thank Drs. Mario Gimona and Fedor Severin for kindly providing purified smooth muscle proteins and Cy3-tagged tubulin, respectively, Dr. R. Y. Tsien for mRFP1 cDNA, Drs. Anna S. Akhmanova, Marcus Geese, and Anna Huttenlocher for expression constructs, and Petra Hagendorff for excellent technical assistance.

References

Baird, G. S., Zacharias, D. A., and Tsien, R. Y. (2000). Biochemistry, mutagenesis, and oligomerization of DsRed, a red fluorescent protein from coral. *Proc. Natl. Acad. Sci. USA* **97**, 11984–11989.

Bhatt, A., Kaverina, I., Otey, C., and Huttenlocher, A. (2002). Regulation of focal complex composition and disassembly by the calcium-dependent protease calpain. *J. Cell Sci.* **115**, 3415–3425.

Campbell, R. E., Tour, O., Palmer, A. E., Steinbach, P. A., Baird, G. S., Zacharias, D. A., and Tsien, R. Y. (2002). A monomeric red fluorescent protein. *Proc. Natl. Acad. Sci. USA* **99**, 7877–7882.

Cormack, B. P., Valdivia, R. H., and Falkow, S. (1996). FACS-optimized mutants of the green fluorescent protein (GFP). *Gene* **173**, 33–38.

Geese, M., Loureiro, J. J., Bear, J. E., Wehland, J., Gertler, F. B., and Sechi, A. S. (2002). Contribution of Ena/VASP proteins to intracellular motility of listeria requires phosphorylation and proline-rich core but not F-actin binding or multimerization. *Mol. Biol. Cell* **13**, 2383–2396.

Geese, M., Schluter, K., Rothkegel, M., Jockusch, B. M., Wehland, J., and Sechi, A. S. (2000). Accumulation of profilin II at the surface of Listeria is concomitant with the onset of motility and correlates with bacterial speed. *J. Cell Sci.* **113**(Pt. 8), 1415–1426.

Gurskaya, N. G., Fradkov, A. F., Terskikh, A., Matz, M. V., Labas, Y. A., Martynov, V. I., Yanushevich, Y. G., Lukyanov, K. A., and Lukyanov, S. A. (2001). GFP-like chromoproteins as a source of far-red fluorescent proteins. *FEBS Lett.* **507**, 16–20.

Heim, R., and Tsien, R. Y. (1996). Engineering green fluorescent protein for improved brightness, longer wavelengths and fluorescence resonance energy transfer. *Curr. Biol.* **6**, 178–182.

Higgs, H. N., and Pollard, T. D. (2001). Regulation of actin filament network formation through ARP2/3 complex: Activation by a diverse array of proteins. *Annu. Rev. Biochem.* **70**, 649–676.

Hyman, A. A. (1991). Preparation of marked microtubules for the assay of the polarity of microtubule-based motors by fluorescence. *J. Cell Sci. Suppl.* **14**, 125–127.

Millard, T. H., Behrendt, B., Launay, S., Futterer, K., and Machesky, L. M. (2003). Identification and characterisation of a novel human isoform of Arp2/3 complex subunit p16-ARC/ARPC5. *Cell Motil. Cytoskel.* **54**, 266.

Mizuno, H., Sawano, A., Eli, P., Hama, H., and Miyawaki, A. (2001). Red fluorescent protein from Discosoma as a fusion tag and a partner for fluorescence resonance energy transfer. *Biochemistry* **40**, 2502–2510.

Reinhard, M., Zumbrunn, J., Jaquemar, D., Kuhn, M., Walter, U., and Trueb, B. (1999). An alpha-actinin binding site of zyxin is essential for subcellular zyxin localization and alpha-actinin recruitment. *J. Biol. Chem.* **274**, 13410–13418.

Rottner, K., Hall, A., and Small, J. V. (1999). Interplay between Rac and Rho in the control of substrate contact dynamics. *Curr. Biol.* **9**, 640–648.

Rottner, K., Krause, M., Gimona, M., Small, J. V., and Wehland, J. (2001). Zyxin is not colocalized with vasodilator-stimulated phosphoprotein (VASP) at lamellipodial tips and exhibits different dynamics to vinculin, paxillin, and VASP in focal adhesions. *Mol. Biol. Cell* **12**, 3103–3113.

Stepanova, T., Slemmer, J., Hoogenraad, C. C., Lansbergen, G., Dortland, B., De Zeeuw, C. I., Grosveld, F., van Cappellen, G., Akhmanova, A., and Galjart, N. (2003). Visualization of microtubule growth in cultured neurons via the use of EB3-GFP (end-binding protein 3-green fluorescent protein). *J. Neuroscience* **23**, 2655–2664.

Stradal, T., Courtney, K. D., Rottner, K., Hahne, P., Small, J. V., and Pendergast, A. M. (2001). The Abl interactor proteins localize to sites of actin polymerization at the tips of lamellipodia and filopodia. *Curr. Biol.* **11**, 891–895.

Verkhovsky, A. B., and Borisy, G. G. (1993). Non-sarcomeric mode of myosin II organization in the fibroblast lamellum. *J. Cell Biol.* **123**, 637–652.

Wang, Y. L. (1984). Reorganization of actin filament bundles in living fibroblasts. *J. Cell Biol.* **99**, 1478–1485.

CHAPTER

12

Systematic Subcellular Localization of Novel Proteins

Jeremy C. Simpson and Rainer Pepperkok

I. INTRODUCTION

The completion of several genome sequencing projects now reveals many thousand open reading frames (ORFs) encoding novel proteins of unknown function. One of the major challenges in the next years will be to allocate functional data to each of these new proteins and to determine how they interact with each other to form the complex regulatory networks underlying fundamental processes of life and disease. Determining the subcellular localisation of these novel ORFs is one important step to be taken in order to bridge the gap between known sequence and unknown function. One way to achieve this may be to systematically raise protein specific antibodies and use them subsequently to determine localisation by immunofluorescence microscopy. However, raising antibodies on such a scale is laborious and expensive. A good alternative to subcellular localisation by immunofluorescence using antibodies is the tagging of the novel ORFs with the green fluorescent protein (GFP) or its spectral variants (Tsien, 1998, 1998, 2002; Zhang *et al*., 2002) followed by subcellular localisation of the GFP-tagged fusion proteins in living cells or multicellular organisms (Ding *et al*., 2000; Simpson *et al*., 2000). This approach has now become much simpler and faster by advances in restriction enzyme-free cloning methods, such as the Gateway system from Invitrogen (Walhout *et al*., 2000), which enable hundreds of defined ORFs to be transferred into GFP vectors in a matter of days. GFP tagging is not only less expensive and perhaps faster, but has the critical advantage compared to immunofluorescence that the expressed GFP fusion proteins can be localised in living samples, which reduces the risk of artefacts caused by fixation and subsequent permeabilisation as is necessary for immunofluorescence. The GFP tag further enables determination of the dynamics of the fluorescent protein, e.g., by time-lapse fluorescence microscopy or fluorescence recovery after photobleaching (FRAP; Bastiaens and Peppperkok, 2000), and thus permits a further level of functional characterisation. This article describes the basic methodology used to systematically determine the subcellular localisation of novel human proteins as they have been derived by past and current cDNA sequencing projects worldwide.

II. EXPERIMENTAL STRATEGY

Our experimental strategy to systematically localise novel proteins is summarised schematically in Fig. 1. It is based on tagging of the respective cDNAs with the GFP and subsequent expression and localisation of the GFP fusion proteins in living and fixed cells. We start the subcellular localisation procedure with bioinformatic analyses of the sequences under study in order to identify organelle-specific targeting sequences or related proteins of which the localisation has already been determined. These data are always considered alongside the final experimental results obtained.

Because localisation is wholly dependent upon targeting sequences within the protein of interest, tagging of a protein with GFP always carries the risk that these targeting sequences become masked, which will finally lead to a mislocalisation of the tagged protein. We address this problem by tagging the proteins separately at their N and C termini and determining the localisation of both fusion proteins. If N- and C-

Copyright 2006, Elsevier Science (USA).
All rights reserved.

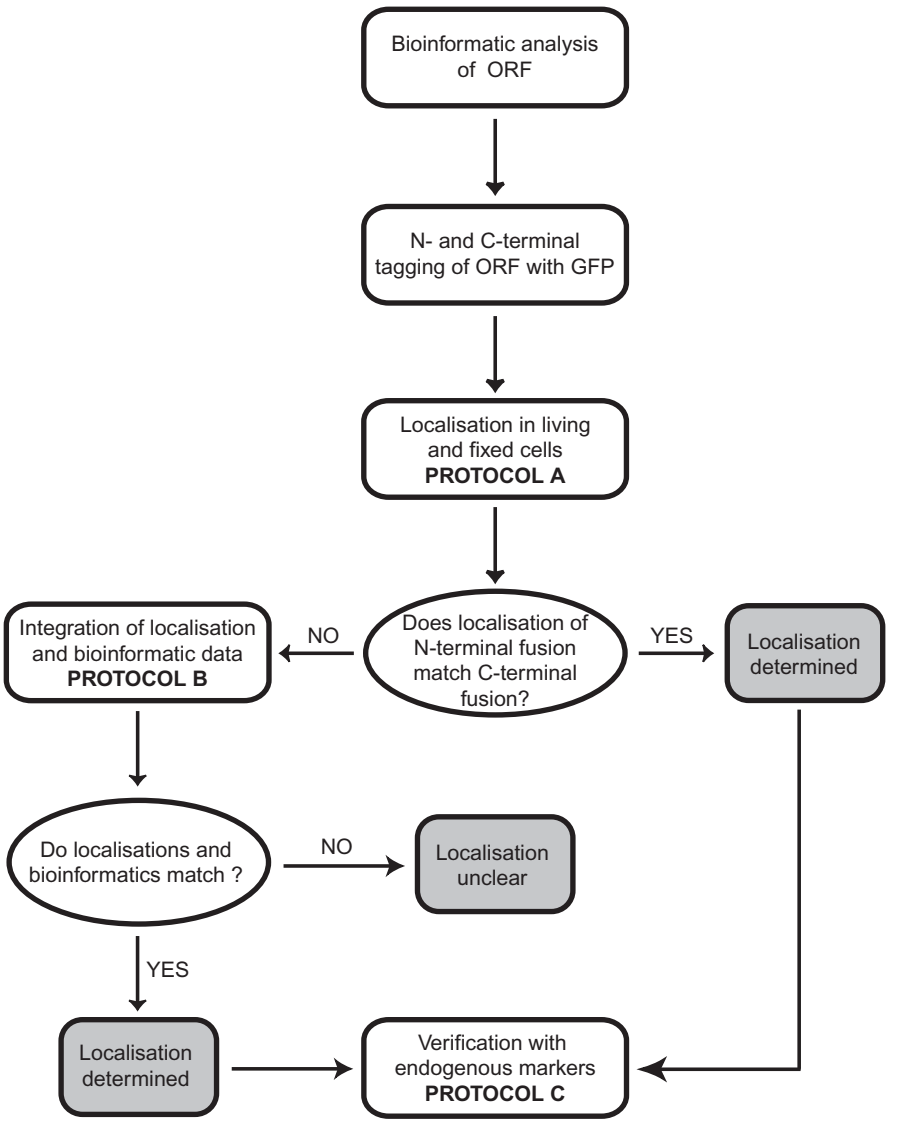

FIGURE 1 Experimental strategy to systematically localise novel proteins in cells. For details, see text.

terminal fusions show identical localisation patterns, one can be confident that the subcellular localisation determined is correct. If the N- and C-terminal fusions give different results, data are considered with respect to the bioinformatic predictions. The localisation that best matches the bioinformatic data is then considered as the correct one. Finally, data are verified by colocalisation of the GFP fusion proteins with established endogenous organelle-specific markers.

Localisation studies can be performed in a variety of cultured cell lines, the choice of which should preferably match the source of the ORFs. However, we prefer to use the monkey kidney fibroblast cell line, Vero (ATCC CCL-81), as these cells have the advantages that they are large in diameter (about 60 µm), display a very clear subcellular morphology (see examples shown in Fig. 2), and are particularly flat, which makes them ideal for imaging using wide-field fluorescence microscopy. Furthermore, we have so far observed no discrepancies of protein localisations in these cells compared to HeLa (ATCC CCL-2) cells, which are of human origin. In cases where a clear localisation of the GFP-tagged fusion protein to a cellular compartment or structure is difficult to achieve in Vero or HeLa cells, we use more specialised cell types for the localisation experiments, such as rat primary hippocampal neurons or SH-SY5Y human neuroblastoma cells (ATCC CRL-2266), when the protein under investigation is, for example, derived from a brain-specific cDNA library.

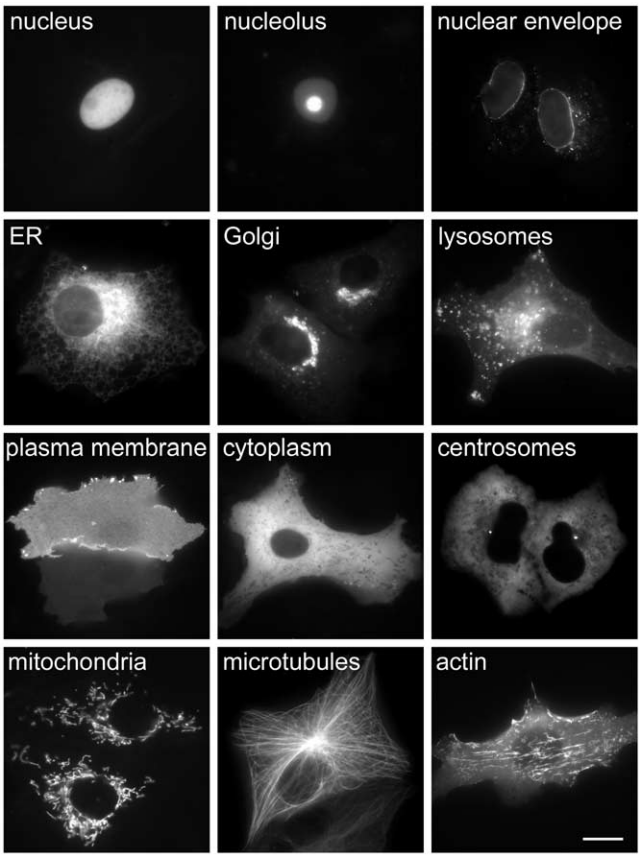

FIGURE 2 Examples of subcellular localise observed in live Vero cells. Vero cells expressing a variety of GFP-tagged proteins localise to different sub-cellular compartments. More examples of localisations can be seen at http://gfp-cdna.embl.de. Bar: 10 µm.

III. MATERIALS AND INSTRUMENTATION

Vero cells (ATCC CCL-81) are grown in minimal essential medium (MEM) containing Earle's salts (Cat. No. 21090-022) with the addition of 2 m*M* L-glutamine (Cat. No. 25030-024) and 100 U/ml penicillin/100 µg/ml streptomycin (Cat. No. 15140-122) all from Invitrogen and 10% foetal calf serum (FCS) (Cat. No. A15-043) from PAA Laboratories. Trypsin–EDTA (Cat. No. 25300-054) is from Invitrogen. Live cell imaging is performed in "Imaging Medium," consisting of MEM containing Earle's salts but lacking phenol red, FCS, and antibiotics (Cat. No. M3024) from Sigma. For transfections, OptiMEM with Glutamax (Cat. No. 51985-026) is from Invitrogen and the FuGENE6 transfection reagent (Cat. No. 1814443) is from Roche. High-purity cycloheximide powder (Cat. No. 239764) is from Calbiochem. Methanol (Cat. No. 106009) and glycine (Cat. No. 104201) are from Merck. Paraformaldehyde (PFA) (Cat. No. P6148) and Triton X-100 (Cat. No. T9284) are from Sigma. Cy5-conjugated secondary antibodies (antimouse, Cat. No. PA45002, and antirabbit, Cat. No. PA45004) are from Amersham Biosciences. Alexa Fluor647-conjugated secondary antibodies (antisheep, Cat. No. A-21448, and antigoat, Cat. No. A-21447) are from Molecular Probes. Standard cell culture plasticware is from Falcon / BD Biosciences. Glass-bottomed live cell imaging dishes (35 mm, with 10 mm number 1.5 coverglass) (Cat. No. P35G-1.5-10-C) are available from MatTek, and Lab-Tek 8-well chambered cover glass dishes (Cat. No. 155411) are from Nalge Nunc. Cells are imaged on a Zeiss Cell Observer System consisting of a Zeiss Axiovert 200 inverted microscope equipped with a Zeiss Plan-apochromat 63×/1.4 NA objective and standard CFP (Cat. No. 1196-682), GFP (Cat. No. 1114-459), YFP (Cat. No. 1196-681), and Cy5/Alexa647 (Cat. No. 488026) filter sets. Images are captured with a CCD camera (Zeiss Axiocam) using Zeiss Axiovision 3.1 software. Images are contrast adjusted and merged using Photoshop 6.0 from Adobe.

IV. PROCEDURES

A. Localisation of GFP-Fusion Proteins in Living and Fixed Cells

Solutions

1. Prepare imaging medium by dissolving 9.4 g of the powder in 900 ml water. Add 0.5 g of $NaHCO_3$, HEPES pH 7.4 to 25 m*M*, and L-glutamine to 2 m*M* final concentration. Adjust the pH to 7.0 with 1 *N* NaOH, make up volume to 1 litre, and then sterilise by filtration through a 0.22-µm filter. Store in 50-ml aliquots at 4°C for up to 3 months.
2. Prepare a 3% solution of PFA by dissolving 15 g of PFA powder in 400 ml of phosphate buffered saline (PBS) and heating the solution to 65°C whilst stirring. When dissolved, add 50 µl of 1 *M* $CaCl_2$ and 50 µl of 1 *M* $MgCl_2$. Adjust pH to 7.4 with 1 *N* NaOH, make up volume to 500 ml, filter through Whatman filter paper (No. 1), and store in 10-ml aliquots at –20°C. Aliquots should not be refrozen after use.

1. Plating Cells on Live Cell Imaging Dishes

Steps

1. The day prior to transfection, take a 90% confluent 10-cm dish of Vero cells and harvest the cells with 3 ml of trypsin–EDTA solution.

2. Resuspend the cells in a total volume of 20 ml of complete MEM growth medium.
3. Use this cell suspension to prepare either individual 35-mm live cell dishes or 8-well chambered cover glass dishes.
4. For the individual live cell dishes, mix 0.5 ml of the cell suspension with 1.5 ml of complete MEM for each dish. For 8-well dishes, mix 0.05 ml of the cell suspension with 0.25 ml of complete MEM for each well.
5. Incubate dishes in a humidified CO_2 incubator at 37°C overnight.

2. *Transfection of Cells*

Steps

1. On the day of transfection prepare the DNA and transfection reagent. Aliquot each DNA to be tested into a fresh tube, using 1 µg for the individual dishes and 0.1 µg for each well of the 8-well dishes.
2. Into fresh tubes aliquot OptiMEM (100 µl) followed by 3 µl of the FuGENE6 reagent (35-mm dishes) or OptiMEM (50 µl) followed by 0.3 µl of FuGENE6 (8-well dishes). Ensure that the transfection reagent does not come into contact with the side of the tube.
3. Mix briefly by pipetting only and then incubate at room temperature for 5 min.
4. Transfer the FuGENE6-OptiMEM mixture into the DNA, mix by pipetting, and incubate at room temperature for 30 min.
5. Add the complete transfection mixture dropwise to the cells and then mix by swirling the dishes.
6. Incubate in a humidified CO_2 incubator at 37°C.

3. *Imaging of Living Cells*

Localisations of GFP-tagged proteins may change due to the expression levels and therefore we use cells expressing low and moderate levels of the protein under investigation for our localisation experiments.

Therefore, cells are imaged at various times, typically 14, 20, and 40 h after transfection. This results in cells expressing low, moderate, and high amounts of the GFP-tagged proteins and gives further information how the expression level might influence localisation.

Steps

1. Replace the transfection medium with an equal volume of imaging medium.
2. Observe the cells on an inverted microscope using a 63× objective, taking multiple images for each plasmid transfected.
3. Replace the imaging medium with the MEM growth medium and continue incubating cells in a humidified CO_2 incubator at 37°C.
4. Repeat steps 1 to 3 at various time points after transfection.

4. *Imaging of Fixed Cells*

In parallel cultures or following image acquisition from live cells it is important to fix the cells and remove any soluble GFP signal that may be obscuring more subtle localisation patterns. The choice of fixation reagent is largely determined by the localisation pattern observed in the live cells. Paraformaldehyde, for example, allows for better fixation of small membrane structures such as endosomes. However, when appropriate, we prefer methanol as the fixative, as this is rapid and effectively removes soluble cytoplasmic GFP-tagged proteins, but leaves structures largely intact.

Steps

Methanol Fixation

1. Remove the entire growth medium from the dishes.
2. Plunge the entire culture dish into a glass trough containing methanol at –20°C.
3. Incubate at –20°C for 4 min.
4. Remove dishes from the methanol and wash cells twice, 3 min each time, with room temperature PBS.
5. Observe the cells still covered in PBS on an inverted microscope using a 63× objective, taking multiple images for each plasmid transfected.

Paraformaldehyde Fixation

1. Replace the growth medium with a similar volume of freshly thawed PFA at room temperature.
2. Incubate for 20 min.
3. Quench the reaction by replacing the PFA with PBS containing 30 m*M* glycine in order to remove cell autofluorescence due to PFA fixation.
4. After a 5-min incubation, wash the cells twice with PBS.
5. Observe the cells on an inverted microscope using a 63× objective, taking multiple images for each plasmid transfected.

5. *Classification of Localisations*

Images obtained from living and fixed cells are then inspected manually and compared to images obtained in living and fixed cells with already established GFP-tagged organelle-specific markers (see examples in Fig. 2; more examples for organelle-specific localisations can be seen at http://gfp-cdna.embl.de.

B. Integration of Localisations with Bioinformatic Predictions

Having classified localisation of the GFP-tagged protein in live and fixed cells (Section IV,A), and if the N- and C-terminal fusions give the same localisation pattern, one can be relatively confident that this represents the localisation of this protein and therefore one can proceed with confirmation of the results by colocalisation of the GFP-tagged proteins with endogenous organelle-specific markers (Section IV,C). When the N- and C-terminal localisation patterns differ, bioinformatic data about the protein of interest should be consulted. In our experience, for over two-thirds of the proteins we have screened, combination of bioinformatic predictions with experimental cell localisations allows a final localisation to be concluded.

Steps

1. Compare the protein sequence under investigation with all known sequences in worldwide databases. Such BLAST searches, for example, available from the NCBI (http://www.ncbi.nlm.nih.gov/BLAST), may reveal similar proteins from other organisms for which the localisation may have already been characterised.

2. Analyse the sequence for potential N-terminal targeting peptides known to direct proteins into either the secretory pathway or the mitochondria. The PSORT programme (http://psort.nibb.ac.jp) is very useful in this respect.

3. Scan for any known domains within the protein of interest. The SMART programme (http://smart.embl-heidelberg.de) provides a graphical interface whereby all known proteins containing any detected domains and likely transmembrane sequences can be visualised. The links provided from these results allow the unknown protein to be put into context of other proteins of potentially similar function.

4. Analyse the protein sequence for any other possible posttranslational targeting motifs such as myristoylation or prenylation consensus sites, which may also be used to target the protein to defined subcellular structures. The PROSITE programme is useful in this respect (http://www.expasy.org/prosite).

5. Determine the final localisation by considering for which of the GFP fusion protein orientations (N- or C-terminal fusions) most of the bioinformatic predictions are consistent with the experimental localisation data. For example, if proteinX-GFP was seen to localise in the mitochondria, whereas GFP-proteinX displays a diffuse localisation and a mitochondrial targeting sequence is predicted, the localisation is concluded to be mitochondrial.

C. Verification of Results by Colocalisation with Endogenous Organelle-Specific Markers

1. Immunostaining of Cells

Before staining, cells are fixed with methanol or paraformaldehyde as described in Section IV,A. For verification of the localisations, we use commercially available primary antibodies recognising organelle-specific marker proteins. The suppliers of these antibodies, the host animals in which they have been raised, the preferred cell fixation method giving best results, and the required antibody dilutions are summarised in Table I. The secondary antibodies we use are conjugated with Cy5 or Alexa647, which can be separated easily from YFP or CFP fluorescence using standard filter sets.

Steps

1. Prior to immunostaining, those cells fixed with PFA must be permeabilised. For this, incubate the cells with PBS containing 0.1% Triton X-100 at room temperature for 5 min and then wash twice with PBS.
2. Prepare the organelle-specific primary antibodies in PBS at the appropriate dilution (see Table I).
3. Overlay the cells with 50 µl (35-mm dishes) or 75 µl (8-well dishes) of these dilutions and incubate at room temperature for 30 min.
4. Remove the antibodies and wash the cells twice with PBS.
5. Dilute the appropriate secondary antibodies in PBS.
6. Overlay the cells with secondary antibodies as described in step 3.
7. Incubate for 20 min. Finally, wash cells twice with PBS, leaving them covered in PBS for imaging.

2. Analysing Colocalisation

For colocalisation of the double-labelled samples we use a Zeiss Cell Observer System for image acquisition. It is equipped with filter sets for CFP, GFP, YFP, and Cy5/Alexa647. Imaging of the two colour channels (GFP-tagged protein and Cy5/Alexa647-stained organelle marker) is performed sequentially, which has the advantage of minimising bleed through of the channels. We analyse colocalisation by merging the images acquired for the GFP-tagged protein (green) and the organelle marker (red). This is usually sufficient to accurately determine whether the suspected localisation of the GFP-tagged protein matches the one of the reference marker. However, for reasons of reliability, it is important that during image acquisition the exposure time is set such that the camera is not saturated and that the range of grey levels of the captured images covers the entire dynamic range of the imaging system (e.g., 256 on an 8-bit camera). Some image

TABLE I Commercially Available Antibodies and Stains as Organelle-Specific Markers Used for Colocalisation Experiments

Organelle	Host[a]/antigen	Supplier/Cat. No.	Fixation,[b] dilution
Endoplasmic reticulum	rb-calnexin	Santa Cruz Biotech sc11397	M/P, 1:300
Golgi complex	mo-golgin97	Molecular Probes A-21270	M/P, 1:200
trans-Golgi network	sh-TGN46	Serotec AHP500	M/P, 1:1000
Early endosomes	mo-EEA1	BD Biosciences 610456	P, 1:100
Late endosomes	mo-CI M6PR	Affinity Bioreagents MA1-066	P, 1:50
Lysosomes	mo-LAMP1	BD Biosciences 611042	P, 1:50
Peroxisomes	rb-PMP70	Zymed 71-8300	P, 1:500
Plasma membrane	go-cadherin	Santa Cruz Biotech sc1499	M/P, 1:100
Mitochondria	mo-HSP60	Sigma H4149	M, 1:200
Centrosome	rb-γ-tubulin	Santa Cruz Biotech sc10732	M/P, 1:300
Microtubules	mo-α-tubulin	Neomarkers MS581	M/P, 1:500
Intermediate filaments	mo-vimentin	Sigma V6630	P, 1:50
Stains			
Actin[c]	Alexa-647 phalloidin	Molecular Probes A-22287	P, 1:40
Nucleus[d]	Hoechst 33342	Sigma B2261	M/P, 1:1000

[a] go, goat; mo, mouse; rb, rabbit; sh, sheep.
[b] M, methanol; P, paraformaldehyde.
[c] Phalloidin stains the actin cytoskeleton directly without the need for secondary antibodies. Phalloidin conjugated to other dyes is also available; however, the Alexa 647 dye can be used with CFP-, GFP-, or YFP-tagged proteins.
[d] Stock solutions of Hoechst can be prepared in water at 1 mg/ml and stored at –20°C. It can be included in the final PBS wash step after fixation of cells. Following a 5-min incubation, cells should be washed a further time with PBS. Dilutions of Hoechst to 1:5000 may be required to avoid bleed through between this colour and CFP.

acquisition software (e.g., Axiovision) contains an autoexposure feature to ensure that this occurs.

Steps

1. Position the GFP-positive cells to be imaged within the field of view and focus on the structure(s) of interest.
2. Acquire an image using the autoexposure procedure.
3. Change to the Cy5/Alexa647 filter position.
4. Acquire an image using the autoexposure procedure. It is important not to change the focus position in steps 3 and 4.
5. Overlay the two images using the Axiovision software with the GFP image as the green channel and the Cy5/Alexa647 image as the red channel.
6. Inspect the overlay image visually. Colocalising structures appear yellow.

V. COMMENTS

1. High-quality glass-bottomed 96-well plates are now becoming more widespread and although they are still relatively expensive, they offer the clear advantage that many more DNA-GFP constructs can be screened consecutively using less material. In our experience, however, some cell types find these plates toxic for growth, and transfection efficiencies are often significantly lower than in other dish formats, presumably due to liquid mixing problems in this shape of well.

2. A wide variety of transfection reagents are available from different suppliers, with the choice of which reagent to use being largely governed by the cell line. Generally we have found that when screening large numbers of DNA molecules, it is best to choose a reagent with a simple protocol that works efficiently in the presence of serum.

3. Novel proteins of the secretory pathway often display heterogeneity of localisations (endoplasmic reticulum, Golgi complex, endosomal / lysosomal system, plasma membrane) when examined. In such cases it is important to perform a cycloheximide chase of the newly synthesised GFP-tagged proteins to try to determine their final compartment of residence. This is achieved by the addition of 100 μg/ml cycloheximide to the growth medium (stock solutions are prepared at 100 mg/ml in methanol or ethanol and stored at –20°C) followed by imaging the cells at regular intervals (every 2 h) up to 8 h after drug treatment. This

chase time is usually sufficient to ensure that even large cell surface proteins have time to fold and are able to transit the entire secretory pathway, reaching their final destination.

References

Bastiaens, P. I., and Pepperkok, R. (2000). Observing proteins in their natural habitat: The living cell. *Trends Biochem. Sci.* **25**, 631–637.

Ding, D. Q., Tomita, Y., Yamamoto, A., Chikashige, Y., Haraguchi, T., and Hiraoka, Y. (2000). Large-scale screening of intracellular protein localization in living fission yeast cells by the use of a GFP-fusion genomic DNA library. *Genes Cells* **5**, 169–190.

Simpson, J. C., Wellenreuther, R., Poustka, A., Pepperkok, R., and Wiemann, S. (2000). Systematic subcellular localisation of novel proteins identified by large-scale cDNA sequencing. *EMBO Rep.* **1**, 287–292.

Tsien, R. Y. (1998). The green fluorescent protein. *Annu. Rev. Biochem.* **67**, 509–544.

Walhout, A. J. M., Sordella, R., Lu, X., Hartley, J. L., Temple, G. F., Brasch, M. A., Thierry-Mieg, N., and Vidal, M. (2000). Protein interaction mapping in *C. elegans* using proteins involved in vulval development. *Science* **287**, 116–122.

Zhang J., Campbell, R. E., Ting, A. Y., and Tsien, R. Y. (2002). Creating new fluorescent probes for cell biology. *Nature Rev. Mol. Cell Biol.* **3**, 906–918.

CHAPTER

13

Single Molecule Imaging in Living Cells by Total Internal Reflection Fluorescence Microscopy

Adam Douglass and Ronald Vale

I. INTRODUCTION

Traditional approaches to molecular and cell biology rely on techniques that infer the behavior of biomolecules based on the properties of a large ensemble. While using such methods to derive the average behavior of a system clearly has been valuable in developing our understanding of biology, bulk measurements often fail to provide information on heterogeneity within the population. The development of methods to measure the electrical activity of single ion channels (Neher *et al*., 1978) first illustrated this point quite clearly, and the ensuing years have seen an explosion of interest in expanding our ability to study biological materials on a single molecule level, especially using optical techniques. Early studies in the field focused primarily on *in vitro* systems containing a limited number of purified components (Funatsu *et al*., 1995; Dickson *et al*., 1997; Pierce *et al*., 1997) and greatly advanced our ability to detect variations not only within a population of molecules, but within the behavior of individual molecules over time. More recently, several groups have demonstrated the possibility of adapting single molecule techniques to living cells (Sako *et al*., 2000; Ueda *et al*., 2001).

These new abilities have been facilitated by several factors, including (1) the advent of green fluorescent protein (GFP) as a fluorescent tag for proteins in their natural environment, (2) the improved sensitivity of intensified charge-coupled devices (ICCDs) and other detectors, and (3) the development and refinement of total internal reflection fluorescence (TIRF) microscopy (Axelrod, 2003). While other techniques, such as near-field scanning optical microscopy (NSOM) and more traditional wide-field approaches, have been used for single molecule imaging in cells (Schutz *et al*., 1997; de Lange *et al*., 2001), TIRF is by far the most commonly used. In TIRF illumination, the excitation light is directed at the sample at a sufficiently large angle that it is totally internally reflected when it strikes the interface between the aqueous buffer and the glass substrate upon which it lies. This creates an exponentially decaying evanescent wave that penetrates into the sample to a depth of only 100–200 nm, the exact distance depending on the refractive indices of the two materials. As a result, only fluorophores lying near the interface are excited efficiently. This greatly decreases the background signal contributed by out-of-focus fluorescence and helps increase the signal-to-noise ratio in the output image to the level required for single molecule detection. Ready-built TIRF systems are available from several microscope vendors (Olympus, Nikon); however, it is relatively simple to add TIRF optics to an ordinary, inverted microscope, which is often preferable to commercial options due to the greater flexibility such an approach provides for later modifications to the system. This chapter provides an overview of how to construct, align, and use a TIRF system for single molecule imaging in live cells.

II. MATERIALS AND INSTRUMENTATION

Several commercial sources exist for optical devices and accessories. Some that are used commonly in our laboratory include the following.

Copyright 2006, Elsevier Science (USA).
All rights reserved.

Newport Scientific: Vibration isolation tables, optical mounts, lenses (www.newport.com)
Chroma: Excitation and emission filters (www.chroma.com)
New Focus: Optics and optical mounts (www.newfocus.com)
Stanford Photonics: ICCD cameras (www.solameretech.com)
Oriel: Optical fibers and accessories (www.oriel.com)
Melles Griot: Argon-ion and HeNe lasers (www.mellesgriot.com)
MatTek: Glass-bottom cell culture dishes (www.mattek.com)
Bioptechs: Temperature control and perfusion equipment (www.bioptechs.com)
Optical Insights: Beam splitters for simultaneous, two-color imaging (www.optical-insights.com)

In addition, some manufacturers provide prebuilt TIRF systems:

Olympus: www.olympusamerica.com
Nikon: www.nikonusa.com

III. PROCEDURES

A. Illumination Strategies

TIRF can be achieved using one of a number of illumination schemes, but most researchers use either prism- or objective-type configurations. In prism-type TIRF, the excitation laser does not enter the internal optical path of the microscope, but rather is directed at the sample from above, through a prism that is optically coupled to the glass slide via a layer of glycerol. Total internal reflection occurs at the interface between the slide and the sample medium, and the excitation beam is completely reflected away from the sample volume. In order to be visible, samples must be firmly attached to the glass slide, which is then affixed with a coverslip and inverted. This results in the major limitation of prism-type illumination, which is that the sample becomes completely enclosed between the two glass surfaces. Since the plane of illumination lies a distance equal to the thickness of the coverslip plus that of the sample away from the objective, one must use a very small sample volume in order to obtain images with high numerical aperture (NA), short working distance objectives. These considerations make it a poor choice for live cell applications in which cell health might be compromised by extended isolation in a confined, oxygen-poor environment. It is primarily for this reason that we perform the majority of our live cell, single molecule imaging using an objective-type microscope.

In objective-type TIRF, the excitation beam enters the microscope through one of its illumination ports and is directed at the sample through the microscope objective, as in epifluorescence illumination. To achieve TIR, the beam is brought into focus at the back focal plane of the objective, but is aligned at the peripheral edge of the objective rather than at the center, as in epifluorescence microscopy. This offset changes the illumination angle as the beam approaches the sample. The maximum angle of illumination depends on the numerical aperture of the objective, and for 1.4 NA objectives is 67°. Since the critical angle for TIR at the cell–glass interface is roughly 65°, this makes it difficult to position the beam so that it will be totally internally reflected. Several microscope manufacturers have begun to produce larger NA objectives that increase the ease of aligning the beam in an objective-type system. In our microscope, we use a 1.45 NA objective (Zeiss), which has a maximum cone angle of approximately 71°. Olympus sells a 1.65 NA objective that offers great flexibility in aligning TIRF systems, but carries the liability of requiring specially designed coverslips and immersion oils of a high refractive index. The major disadvantage to using objective-type configurations is that they are more prone to background signals arising from the excitation beam, as it is reflected toward the detector, and can also generate spurious reflections or fluorescence within the objective itself. However, these tradeoffs are minor in comparison to the gain in cell health offered by objective-type illumination.

B. Choice of Detector

Due to their extreme sensitivity and high readout speed, intensified charge-coupled device-based cameras are excellent for single molecule imaging. High-end ICCDs have single photon sensitivity under ideal conditions and can acquire 640 × 480 images directly to digital storage media at rates of over 100 frames per second. At these speeds, the rate of photon emission by a single fluorophore becomes a limiting factor in obtaining a reasonable signal-to-noise ratio. There are, however, several disadvantages to ICCDs. The intensification process can result in noise due to ion feedback events and dark current in the intensifier, as well as the emergence of low-intensity "valleys" at boundary points in the image, such as those surrounding single fluorophores. The intensifier also introduces nonlinearity in the response of the detector to light, and so care must be taken to ensure that one is working within the linear range of the camera if

quantitative measurements of fluorescence intensity are to be made. Advances in camera technology are changing these limitations, however. For instance, Stanford Photonics now produces a dual-intensifier camera that is cooled by a water jacket, which shows great promise for single molecule imaging due to its extremely low noise levels.

Traditional, cooled CCDs are a feasible alternative in some applications and are desirable for their high image quality and the strong linearity of their response. Unfortunately, they also have slow readout speeds, a problem that some researchers have overcome by reading from only a small region of the detector. This is of course not an option if one wishes to image a relatively large area such as an entire cell surface, and even under ideal conditions the temporal resolution provided by cooled CCDs might not be great enough to observe more rapid phenomena, such as the lateral diffusion of certain membrane proteins or lipids. Still, cooled CCDs have been extremely useful in some cases. For example, Yildiz *et al*. (2003) used this approach to track single myosin motors walking along actin filaments to a precision of 1.5 nm.

C. Microscope Layout

The configuration of our objective-type TIRF microscope is shown in Fig. 1. In this geometry, excitation light from the HeNe and argon-ion lasers is combined at the first dichroic mirror and is coaligned through the remaining optical elements. The filter wheel placed outside the argon laser allows rapid selection of the excitation wavelength from the multiwavelength source. To avoid selective excitation of fluorophores with a given orientation, the illumination light is depolarized by a quarter-wave plate placed in each beam path. Lateral positioning of the excitation beams within the objective is controlled through the movements of TM1, which regulates the incidence angle at the sample. Rotation of mirror M3 180° allows the user to switch between TIRF and epifluorescence illumination. Optics shown inside the microscope housing are all fixed components, supplied by the manufacturer.

D. Laser Alignment

1. Bring the two beams (Argon and HeNe) into alignment with one another. Irises fixed at the desired height and placed at various points in the optical path can be enormously useful in this step. Using the beam riser mirrors, align both beams to the horizontal axis at the same height, as measured at at least two points before DM1 along each path. Ensure that the beam spots at DM1 and M1 overlap completely with one another. In all alignment steps, make efforts to align the beams as close to the center of each optical element as possible.

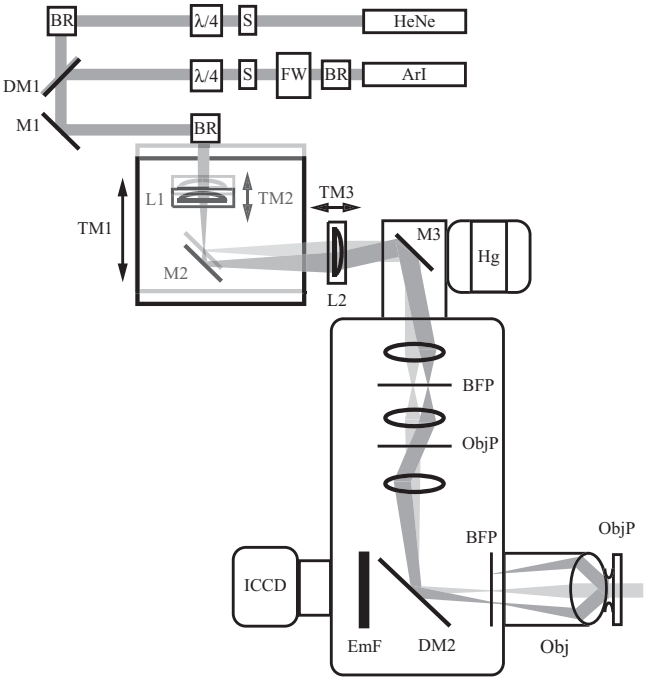

FIGURE 1 Optical configuration of the objective-type TIRF microscope used in our laboratory. The excitation light paths are indicated for both lasers in one of two configurations. In one (light gray), beams are aligned with the optical axis of the excitation port of the microscope and travel up the center of the objective, generating transmitted fluorescence illumination of the sample. In the second, beams enter the illumination port off axis, traveling up the edge of the objective, and are totally internally reflected at the sample. Switching between the two types of illumination can be accomplished by moving the translation mount TM1. Beam size, and thus the size of the TIRF illumination spot, is determined by the relative positions of lenses L1 and L2. HeNe, helium–neon laser; ArI, mixed wavelength argon–ion laser; S, shutter; BR, beam riser; FW, filter wheel; λ/4, quarter-wave plate; DM1–2, dichroic mirrors; M1–3, mirrors; L1–3, lenses; TM1–3, translation mounts; Hg, mercury arc lamp; BFP, back focal plane of the objective; ObjP, object plane; Obj, objective; EmF, emission filter; ICCD, intensified charge-coupled device-based camera.

2. Center the combined beams at L1, M2, L2, and M3.

3. Remove L1, L2, and the objective from their positions and center the beam in the microscope cavity by watching the projected illumination spot above the microscope housing. A piece of white paper placed above the microscope can be useful in this step. To achieve the best possible alignment, make sure that the beam profile is not clipped when the microscope's field and aperture diaphragms are closed.

4. Replace L2 and adjust its position to minimize the size of the projected beam spot.

5. Replace L1 and the objective, and mount a fluorescently labeled sample (preferably cells or fluorescent beads). Bring the ventral surface of the sample into focus as viewed through the eyepieces. (See Section IVD).

6. Remove the sample and clean the immersion oil from the objective. Adjust L1 to minimize the size of the projected beam spot. Ensure that the beam is collimated as it emerges from the objective.

7. Apply immersion oil to the objective and place a glass coverslip on top of it. Optically couple a plano-convex lens to the coverslip with more immersion oil. This will frustrate total internal reflection at the glass–air interface and allow one to follow the projected beam position over a wide range of incidence angles. Move TM1 to deflect the beam until it begins to be clipped by the back focal plane of the objective. This indicates that the largest possible incidence angle has been reached. Readjust TM1 to barely eliminate clipping and remove the coverslip and lens.

8. Place a fluorescent sample (in our experience, either 200-nm fluorescent beads or an aqueous solution of a fluorophore at high concentration are best) on the microscope and observe through the eyepieces to ensure that TIRF has been attained. The success of the alignment can be assessed by the presence of a very shallow focal plane and low fluorescent background from nonsurface-adsorbed fluorophores. It might be necessary at this point to center the illumination spot by moving M1 or M2.

E. Imaging Single GFPs

The greatest difficulty with imaging single fluorescent proteins lies in titrating their expression. At high levels of GFP expression, the density of tagged protein can result in multiple fluorophores being closer to one another than the diffraction limit of light, which prevents the identification of single molecules. Because most vectors are designed to drive high levels of protein expression, obtaining a suitable density of GFP can be difficult. As a long-term solution, it is desirable to create a cell line that stably expresses very low levels of GFP (Fig. 2). This is usually possible, but requires the labor-intensive screening of clonally derived cell lines (most of which will express too much of the transgene) by TIRF. Alternatively, cells can be imaged either very early (several hours) or very late (over a week) after transfection, which will enrich the number of low-expressing cells, although cells will be extremely variable in their fluorescence levels. Another approach is to sort the transfectants by FACS and collect only the lowest expression group for imaging. It is also possible to place the transgene under the control of an inducible promoter element and titrate the level of inducer to optimize expression levels. In many cases, basal levels of expression from the uninduced promoter suffice for single molecule imaging. We have found this to be true for uninduced metallothionine promoters in a Drosophila cell culture system.

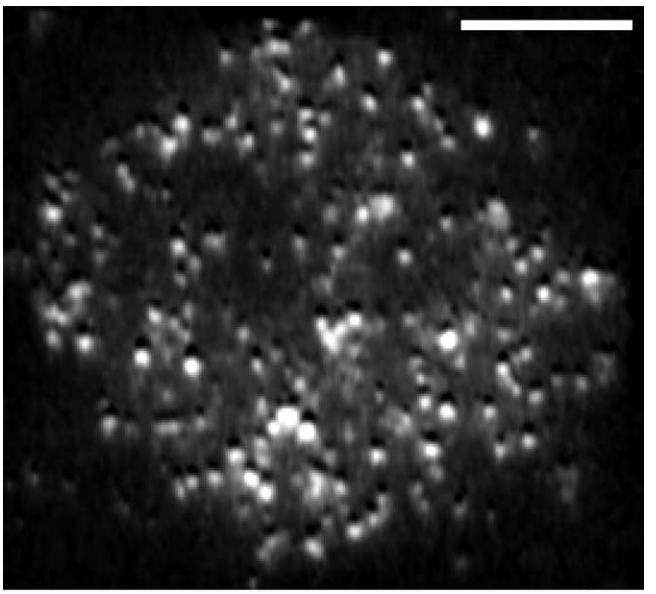

FIGURE 2 Single molecules of Lck-GFP in a T-cell membrane. Objective-type TIRF was used to image Jurkat T cells that were stably transfected with a GFP fusion of the membrane-associated, tyrosine kinase, Lck, and selected for low expression levels. Scale bar: 10 μm. The bright punctae in the image correspond to single molecules. This image was taken from a single frame of a sequence acquired at video rate (30 fps).

As the first single molecule studies of GFP demonstrated (Dickson *et al.*, 1997; Pierce *et al.*, 1997), emission from fluorescent proteins is often unstable, a property that is not usually shared by their small organic counterparts. This can result in the molecule disappearing for short intervals, thereby complicating single molecule tracking. In most situations, however, the dark states of GFP are short-lived, typically lasting only a frame or two at video rate, and are infrequent enough that they do not pose an insurmountable problem to obtaining useful data.

F. Sample Preparation

There are several options for systems in which to mount cells for single molecule imaging. A luxury afforded by objective-type TIRF is the ability to use glass-bottom tissue culture dishes, which allow one to grow cells on a surface that is suitable for microscopy. Alternatively, cells can be adhered to glass coverslips and imaged in a perfusion chamber, such as the closed

configuration system available from Bioptechs. When used in conjunction with objective and sample heating elements, the latter solution allows for the greatest degree of control over environmental parameters that affect cell health and makes it possible to change buffer conditions rapidly (e.g., by perfusing pharmacological agents, antibodies, or chemoattractants). Heating the sample with an external heat source (such as a hot air blower pointed at the stage assembly) is possible, but resulting oscillations in stage position can make in quite difficult to maintain the tight control over the focal plane that is needed for single particle tracking.

In all cases, it is advisable to clean the glass substrate before use in order to remove fluorescent impurities that would complicate imaging and to impart an electrical charge to the glass to facilitate cell adhesion or surface functionalization. This can be accomplished in a number of ways. We immerse the glass overnight in an aqueous solution of 70% sulfuric acid and 9% hydrogen peroxide. The mixture will evolve a good deal of heat when prepared and should be applied to the glass while still hot. This combination of reagents is predictably quite volatile and should only be used in a fume hood by persons wearing appropriate protective attire.

It is often useful to coat the glass with various substances prior to use. Such treatments do not appear to adversely affect the quality of single molecule images obtained by TIRF. In our experiments, we have successfully imaged various cell types adhering to a variety of materials on the coverslip surface, including antibodies, concanavalin A, and polylysine. Good cell adhesion is a prerequisite for TIRF, as the cell membrane must lie within the evanescent wave to be visible. However, in our experience with many cell types, polylysine coating is not necessary for adhesion if the glass has been cleaned thoroughly first.

Finally, the choice of imaging buffer can be tremendously important for obtaining high-quality, single molecule images. Buffers should be free of substances with appreciable fluorescence in the desired wavelength range, which eliminates the use of most tissue culture media (especially those containing serum or colorimetric pH indicators) during the imaging process. For the majority of our experiments, we have used a modified HEPES-buffered saline solution (20 m*M* HEPES, 135 m*M* NaCl, 4 m*M* KCl, 1 m*M* Na_2HPO_4, 10 m*M* glucose, 1 m*M* $CaCl_2$, 0.5 m*M* $MgCl_2$, pH 7.4). All cell types should be washed with imaging buffer one or two times before beginning the experiment. Adherent cultures should be washed especially thoroughly if they have been grown on the imaging surface, as they tend to produce debris that can complicate single molecule imaging.

G. Simultaneous Imaging of Multiple Fluorophores

The discovery and development of fluorescent proteins with a wide variety of excitation and emission properties have provided researchers with the ability to simultaneously observe the behavior of two or more types of protein in living cells. The combination of GFP and DsRed is of particular interest for single molecule imaging. Both proteins can be excited by the 488-nm line of an argon-ion laser quite efficiently, and yet emit light of widely disparate wavelengths that can be separated using conventional dichroic mirrors and filtersets. For real time, simultaneous imaging of both proteins at video rate, a beam splitter module is available from Optical Insights that projects the two emission wavelengths onto different halves of the detector, eliminating the need for multiple cameras and emission paths. This allows one to acquire both color components of the image without switching excitation sources, which is often essential due to the rapid timescale on which changes can occur at the single molecule level (Campbell *et al.*, 2002). For dual-color imaging with GFP, the most suitable version of DsRed is a dimeric variant, termed the "tandem dimer," in which two identical copies of the modified DsRed transcript are connected to one another by a short linker region. The high effective concentration of the linked fluorophores in the translated protein is thought to favor the formation of intra- rather than intermolecular contacts and prevents aggregation effects from interfering with the function of the protein to which the tag is attached. The tandem dimer is preferable to the monomeric version of the protein in that it retains the ability to be excited at 488 nm, while the monomer does not. We have imaged single molecules of GFP and the tandem dimer in the same sample using 488-nm excitation and have found the two fluorophores to be quite spectrally separable from one another. It remains to be seen how generally valuable DsRed will be for live cell, single molecule imaging, as it is significantly dimmer than GFP at 488-nm excitation and might not provide a high enough signal for the detection of rapidly moving proteins. At the very least, the tandem dimer should provide a useful counterstain to mark one component at the population level while imaging single molecules of a GFP-tagged protein.

Dual-color imaging of small organic fluorophores is also possible, but the majority of such combinations require the simultaneous use of two excitation sources. This is made relatively easy by excitation filter sets that are designed to deal with two wavelengths, but it demands that careful attention be paid to the

coalignment of the two sources with one another. We, for example, have obtained dual-color images of Cy3- and Cy5-labeled proteins diffusing in artificial lipid bilayers and interacting with Jurkat T cells. Experiments done *in vitro* have also shown this fluorophore combination to be useful for single molecule FRET, a technique that several groups have applied to living cells (Sako *et al*., 2000). Finally, although it is a nascent technology, the application of semiconductor quantum dots as single molecule tags (Dahan *et al*., 2003) promises to simplify illumination schemes greatly for multicolor, single molecule experiments.

H. Image Analysis

The precise method of analysis to choose will of course depend on the information that is desired, but there are a few analytical issues that apply to most single molecule experiments. Most prominent among these is the systematic, automated identification of single fluorophores. The relatively low signal-to-noise level achieved in single molecule images poses a problem in this regard, as it is sometimes impossible to distinguish between a fluorophore and a region of high background fluorescence based solely on a static intensity threshold. Furthermore, if the molecules of interest are moving rapidly in the *X-Y* plane, as they often are in studies of membrane proteins, it can be quite difficult to follow single molecules through consecutive frames. Several groups have developed tracking algorithms to overcome these problems, and most of these utilize some measure of the molecule's shape or *X-Y* intensity distribution to identify relevant spots in an image (Gelles *et al*., 1988; Cheezum *et al*., 2001). In our laboratory, we have developed a tracking routine that uses cross-correlation between an idealized molecule and the TIRF image to find spots (Klopfenstein *et al*., 2002). Continuity of molecular trajectories between frames is obtained by ensuring that the fluorophores are at a very low density in the cell surface (to prevent confusion between neighboring molecules) and by including a search radius as a tracking parameter. The latter point restricts the search to a small area around the initial location of the molecule, under the assumption that it is moving with a fairly predictable speed. We have implemented this routine using the commercially available MATLAB software, but similar procedures could easily be developed in other programming environments.

While cross-correlation is a great improvement over manual tracking, it is computationally inefficient, requiring a relatively large amount of CPU time to track a single spot. This makes it impractical for the automated detection and tracking of every molecule in an image, and in our analyses we manually indicate which spot to follow by providing its initial Cartesian coordinates to the tracking algorithm. Complete automation of the procedure for all spots in an image sequence might be achievable by more efficient algorithms, such as fitting to a theoretical function (e.g., a Gaussian distribution), line-based routines, or segmentation analysis. We have applied a set of particle tracking routines maintained by Dr. Eric Weeks (available at www.physics.emory.edu/~weeks/idl) to this task, with extremely promising results.

Positional information is not the only parameter that can be obtained from single molecule images. The quantized nature of single molecule fluorescence makes the technique suitable for obtaining estimates of oligomerization state based on spot intensity and has been used to this end in studies of GFP-tagged E-cadherin in living fibroblasts (Iino *et al*., 2001). The addition of polarization optics to a TIRF microscope enables measurements of molecular orientation at the single molecule level and can provide striking information about dynamic changes in parameters such as protein conformation and binding events (Khan *et al*., 2000). Single molecule FRET is also just beginning to be explored and holds great promise for measuring protein–protein interactions in living cells.

IV. PITFALLS

A. Visualization of Internal Structures

While the evanescent wave created in TIRF microscopy penetrates to a shallow depth, it is still possible to visualize structures that are inside the cell, rather than at its surface. Several studies have exploited this to monitor the dynamics of vesicle fusion with the plasma membrane (Toomre *et al*., 2000), but it can be a source of complication in single molecule experiments. This is particularly problematic with proteins that partition into both plasma membrane and vesicular pools and can lead to spurious conclusions about protein behavior. Due to the low intensity of the excitation light at the cell interior, however, it is very unlikely that single molecules on vesicle surfaces will be visible. It is more probable that signals from the cell interior will represent clusters of several fluorophores, although internal structures might show fluorescence intensities similar to those of single molecules. To avoid confusion between surface and internal components then it is important to only

analyze spots that can be attributed to single molecules, i.e., that photobleach in a single step. Alternatives might include performing TIRF with a system in which the illumination depth is reduced—for instance, by the use of substrates with higher refractive indices or by the imposition of an intermediate layer, acting as a spacer, between the glass and the sample. However, these require a significant investment of time and effort to implement.

B. Objective Fluorescence

Materials used in construction of the high NA objectives used in objective-type TIRF fluoresce at certain excitation wavelengths, an effect that was ignored in their development because the fluorescence is small compared to the signal generated by traditional epifluorescence and confocal microscopies. Unfortunately, this background fluorescence is detectable in systems with single molecule sensitivity, and while it does not prevent the detection of single molecules, it does reduce the signal-to-noise ratio. We have noticed this effect with a number of different objectives from several manufacturers. There is at present no solution to this problem, but in our hands the effect is only noticeable when simultaneously imaging dyes with wavelengths similar to Cy3 and Cy5. Excitation with the 514-nm line used for Cy3 causes the objective to fluoresce in the far red end of the spectrum, where Cy5 emits, and this contributes to the background in the Cy5 channel.

C. Inhomogeneous Illumination

A problem with coherent light such as that emitted by lasers is its tendency to generate interference patterns. The problem is compounded by imperfections in the optical elements used to route the laser to its destination, and in TIRF systems this can result in local intensity minima and maxima within the illumination spot. A number of methods can be employed to homogenize the spot profile. Holographic beam diffusers and ground glass elements accomplish this quite completely, but the resulting beam divergence is typically too severe to allow proper TIR alignment, even when a downbeam lens is used to attempt to regain collimation. A more suitable approach is to route the excitation light through a multimode optical fiber that has been bent at a narrow angle. Alignment of the beam into and out of the fiber can be laborious, but once achieved it results in a homogeneous and well-collimated beam.

D. Changes in Incidence Angle while Focusing

If the microscope utilizes a translatable objective mount to adjust the image focus, another problem will arise when implementing TIRF. As the objective is moved vertically, the position of its back focal plane will change, resulting in a loss of collimation in the beam as it passes through the objective. This is not normally a problem if the beam has been aligned such that it propagates into the edge of the objective lens, as the incidence angle will already be well beyond the critical angle required for total internal reflection, and changes in collimation will be small. It must be emphasized, however, that the objective should be as close to its in-focus location as possible before aligning the laser to achieve TIRF. Otherwise, subsequent focusing on the bottom surface of the sample can greatly disrupt the incidence angle of the laser, leading to transmission of a substantial portion of the light through the objective and into the cell. The ideal method of avoiding this is to control image focus by moving the microscope stage, rather than the objective, but it is not completely necessary.

Acknowledgments

The authors thank Nico Stuurman and Reed Kelso for valuable discussions relevant to the manuscript.

References

Axelrod, D. (2003). Total internal reflection fluorescence microscopy in cell biology. *Methods Enzymol* **361**, 1–33.

Campbell, R. E., Tour, O., Palmer, A. E., Steinbach, P. A., Baird, G. S., Zacharias, D. A., and Tsien, R. Y. (2002). A monomeric red fluorescent protein. *Proc. Natl. Acad. Sci. USA* **99**(12), 7877–7882.

Cheezum, M. K., Walker, W. F., and Guilford, W. H. (2001). Quantitative comparison of algorithms for tracking single fluorescent particles. *Biophys J.* **81**(4), 2378–2388.

Dahan, M., Levi, S., Luccardini, C., Rostaing, P., Riveau, B., and Triller, A. (2003). Diffusion dynamics of glycine receptors revealed by single-quantum dot tracking. *Science* **302**(5644), 442–445.

de Lange, F., Cambi, A., Huijbens, R., de Bakker, B., Rensen, W., Garcia-Parajo, M., van Hulst, N., and Figdor, C. G. (2001). Cell biology beyond the diffraction limit: Near-field scanning optical microscopy. *J. Cell. Sci.* **114**(Pt. 23), 4153–4160.

Dickson, R. M., Cubitt, A. B., Tsien, R. Y., and Moerner, W. E. (1997). On/off blinking and switching behaviour of single molecules of green fluorescent protein. *Nature* **388**(6640), 355–358.

Funatsu, T., Harada, Y., Tokunaga, M., Saito, K., and Yanagida, T. (1995). Imaging of single fluorescent molecules and individual ATP turnovers by single myosin molecules in aqueous solution. *Nature* **374**(6522), 555–559.

Gelles, J., Schnapp, B. J., and Sheetz, M. P. (1988). Tracking kinesin-driven movements with nanometre-scale precision. *Nature* **331**(6155), 450–453.

Iino, R., Koyama, I., and Kusumi, A. (2001). Single molecule imaging of green fluorescent proteins in living cells: E-cadherin forms oligomers on the free cell surface. *Biophys J.* **80**(6), 2667–2677.

Khan, S., Pierce, D., and Vale, R. D. (2000). Interactions of the chemotaxis signal protein CheY with bacterial flagellar motors visualized by evanescent wave microscopy. *Curr. Biol.* **10**(15), 927–930.

Klopfenstein, D. R., Tomishige, M., Stuurman, N., and Vale, R. D. (2002). Role of phosphatidylinositol(4,5)bisphosphate organization in membrane transport by the Unc104 kinesin motor. *Cell* **109**(3), 347–358.

Neher, E., Sakmann, B., and Steinbach, J. H. (1978). The extracellular patch clamp: A method for resolving currents through individual open channels in biological membranes. *Pflug. Arch.* **375**(2), 219–228.

Pierce, D. W., Hom-Booher, N., and Vale, R. D. (1997). Imaging individual green fluorescent proteins. *Nature* **388**(6640), 338.

Sako, Y., Minoghchi, S., and Yanagida, T. (2000). Single-molecule imaging of EGFR signalling on the surface of living cells. *Nature Cell Biol.* **2**(3), 168–172.

Schutz, G. J., Schindler, H., and Schmidt, T. (1997). Single-molecule microscopy on model membranes reveals anomalous diffusion. *Biophys J.* **73**(2), 1073–1080.

Toomre, D., Steyer, J. A., Keller, P., Almers, W., and Simons, K. (2000). Fusion of constitutive membrane traffic with the cell surface observed by evanescent wave microscopy. *J. Cell Biol.* **149**(1), 33–40.

Ueda, M., Sako, Y., Tanaka, T., Devreotes, P., and Yanagida, T. (2001). Single-molecule analysis of chemotactic signaling in Dictyostelium cells. *Science* **294**(5543), 864–867.

Yildiz, A., Forkey, J. N., McKinney, S. A., Ha, T., Goldman, Y. E., and Selvin, P. R. (2003). Myosin V walks hand-over-hand: single fluorophore imaging with 1.5-nm localization. *Science* **300**(5628), 2061–2065.

CHAPTER

14

Live-Cell Fluorescent Speckle Microscopy of Actin Cytoskeletal Dynamics and Their Perturbation by Drug Perfusion

Stephanie L. Gupton and Clare M. Waterman-Storer

I. INTRODUCTION

Fluorescent speckle microscopy (FSM) is a method used to analyze the movement, assembly, and disassembly dynamics of macromolecular structures *in vivo* and *in vitro* (Waterman-Storer *et al*., 1998). FSM capitalizes on the well-established method of fluorescent analog cytochemistry, in which purified protein is covalently linked to a fluorophore and microinjected or expressed as a green fluorescent protein (GFP) fusion in living cells, incorporated into cellular structures, and whose dynamics are visualized by time-lapse or video wide-field epifluorescence microscopy (Wang *et al*., 1982; Prasher, 1995). This approach has been limited in its ability to report protein dynamics because of inherently high background fluorescence from unincorporated and out-of-focus incorporated fluorescent subunits and the difficulty in detecting movement or turnover of subunits because of their uniform labeling of fluorescent structures. In contrast, FSM offers the capability to measure variations in molecular dynamics in living cells at high spatial and temporal resolution. In addition, FSM reduces out-of-focus fluorescence and improves the visibility of fluorescently labeled structures and their dynamics in three-dimensional polymer arrays such as the mitotic spindle (Waterman-Storer and Salmon, 1999; Maddox *et al*., 2002, 2003).

This article describes how to use FSM for measuring actin cytoskeletal dynamics in living cells using microinjected fluorescently labeled skeletal muscle actin and the manipulation of actin dynamics during high-resolution FSM imaging by drug perfusion. This allows measurement of the kinetic evolution of the response of the actin cytoskeleton to the effects of drugs with unknown or known molecular targets, including actin and its associated proteins. We have used this technique to study changes in actin dynamics in response to perfusion of cytochalasin D (an actin filament capping drug) (see Fig. 5), latrunculin A [an actin monomer sequestering drug (Ponti *et al*., 2002)], and ML-7 and calyculin-A [myosin II inhibitors and activators, respectively (Gupton *et al*., 2002)]. These experiments have provided insight into how the actin cytoskeleton is organized into functionally distinct zones in migrating cells, with an exploratory lamellipodium at the leading edge whose actin dynamics are sensitive to filament capping, and a lamellum where traction forces are generated by myosin II-mediated actin dynamics. Using FSM analysis during perfusion of drugs that specifically affect signaling molecules or other structural components of the actin cytoskeleton will be a valuable approach for understanding the molecular regulation of the cytoskeleton during cell morphogenesis.

Principles of FSM Imaging

In its initial development in 1998, FSM utilized conventional wide-field epifluorescence light microscopy and digital imaging with a sensitive, low-noise cooled

Copyright 2006, Elsevier Science (USA).
All rights reserved.

charge-coupled device (CCD) camera and was applied to study the assembly dynamics and movement of microtubule polymers (Waterman-Storer and Salmon, 1997). Since then, FSM has seen new applications in answering various questions about actin and microtubule cytoskeletal function *in vivo* during cell motility, neuronal pathfinding, and mitosis, as well as given insight into cytoskeletal dynamics *in vitro*. It also has been transferred from widefield epifluorescent microscopes to confocal and total internal reflection fluorescence (TIRF) microscopes, which reduce the out-of-focus contribution further and thus increase the speckle contrast (Grego *et al.*, 2001; Maddox *et al.*, 2002; Adams *et al.*, 2002; Adams *et al.*, 2004). Computer-based analysis of FSM image series has begun to be developed so that the use of dynamic speckles as quantitative reporters of polymer trajectory, velocity, assembly rate, lifetime, and disassembly rate can be realized (Ponti *et al.*, 2003).

FSM was initially discovered by accident when it was noticed in high-resolution images of cells injected with X-rhodamine-labeled tubulin that some microtubules exhibited variations in fluorescence intensity along their lattices, i.e., they looked speckled (Waterman-Storer and Salmon, 1997). These speckles were used as marks of the microtubule lattice to allow differentiation between mechanisms of microtubule movement in living cells.

To understand the origin of speckles on microtubules as an example, one must consider how the images of fluorescent microtubules are formed by the optics of the microscope. Microtubules assemble from tubulin dimers into polymers with 1625 dimers per micrometer of microtubule (Desai and Mitchison, 1997). In an image made by a microscope, a fluorescent microtubule appears as wide as the smallest region that the microscope is capable of resolving, defined by geometrical optics of light as $r = 0.61\lambda/\mathrm{NA}_{\mathrm{obj}}$ (Inoué and Spring, 1997), where λ is the emission wavelength of the fluorophore and $\mathrm{NA}_{\mathrm{obj}}$ is the numerical aperture of the microscope objective lens. For example, for X-rhodamine (602 nm emission)-labeled microtubules imaged with the best available 1.4 NA optics, the smallest resolvable region of a microtubule is 270 nm, which contains 440 tubulin dimers. A low fraction of fluorescent dimers, $f = 1\%$, will produce a mean number n of 4 fluorescent dimers ($n = 440 \times f$) per resolvable image region. In FSM images, the speckle pattern along the microtubule is produced by variations in the number of fluorescent dimers per resolvable image region relative to this mean. Thus, the "contrast" of the speckle pattern can be expressed as the ratio between the standard deviation and the mean of a binomial distribution with n elements: $c = \sqrt{n \cdot f \cdot (1-f)}/(n \cdot f)$. This formula indicates (i) that the contrast c increases with lowering f and (ii) that it decreases with growing n, indicating the requirement for optics with the highest NA possible.

For example, during assembly of a microtubule with 1% fluorescent-labeled tubulin and 99% unlabeled tubulin in an image taken with 1.4 NA optics, one 270-nm segment of the microtubule may contain 1 fluorescent dimer and 339 nonfluorescent dimers, while the adjacent resolvable segment of the microtubule could contain 7 fluorescent dimers, producing a 7× difference in image brightness between adjacent resolvable regions, and thus high speckle contrast. By comparison, at $f = 50\%$, adjacent minimally resolvable image regions may contain 212 and 234 fluorescent dimers, a 1.1× difference in image brightness and thus very low speckle contrast.

Thus, time-lapse FSM requires the ability to visualize high-resolution image regions (~0.25 µm) containing few (1–10) fluorophores and the capacity to inhibit fluorescence photobleaching. This requires a very sensitive imaging system with little extraneous background fluorescence, very efficient photon collection, a camera with low noise, high quantum efficiency, high dynamic range, high resolution, and suppression of fluorescence photobleaching and photodamage in the specimen with illumination shutters and/or oxygen scavengers (Waterman-Storer *et al.*, 1993, 1998; Mikhailov and Gundersen, 1995).

Since the original analysis of microtubules, the "speckle" method has been applied to other cytoskeletal systems. When injected with low levels of fluorescently labeled actin, actin-rich structures such as the lamellipodium of migrating cells appear speckled in high-resolution fluorescence images (see Fig. 1) (Waterman-Storer *et al.*, 1998, 2000; Verkhovsky *et al.*, 1999; Watanabe and Mitchison, 2002). Also, a GFP fusion of a microtubule-binding protein, ensconsin, when expressed in cells at very low levels, gave a speckled distribution along microtubules (Bulinski *et al.*, 2001). These actin and ensconsin speckles formed in different ways from those in a single microtubule polymer. For actin, the lamellipodium is filled with a cross-linked and dense three-dimensional meshwork of actin filaments (see Fig. 1), and each filament is made up of a paired helix of 360 actin monomers per micrometer (Pollard *et al.*, 2000; Small 1981; Svitkina *et al.*, 1997). Here, a fluorescent speckle may arise from fluorescently labeled actin monomers within multiple different actin filaments of the meshwork falling into the same minimally resolvable image region (Fig. 2a); however, none of the filaments are detected individually. Thus, the entire meshwork appears as a relatively even distribution of fluorescent speckles in images. For ensconsin, binding of few diffusible GFP–ensconsin

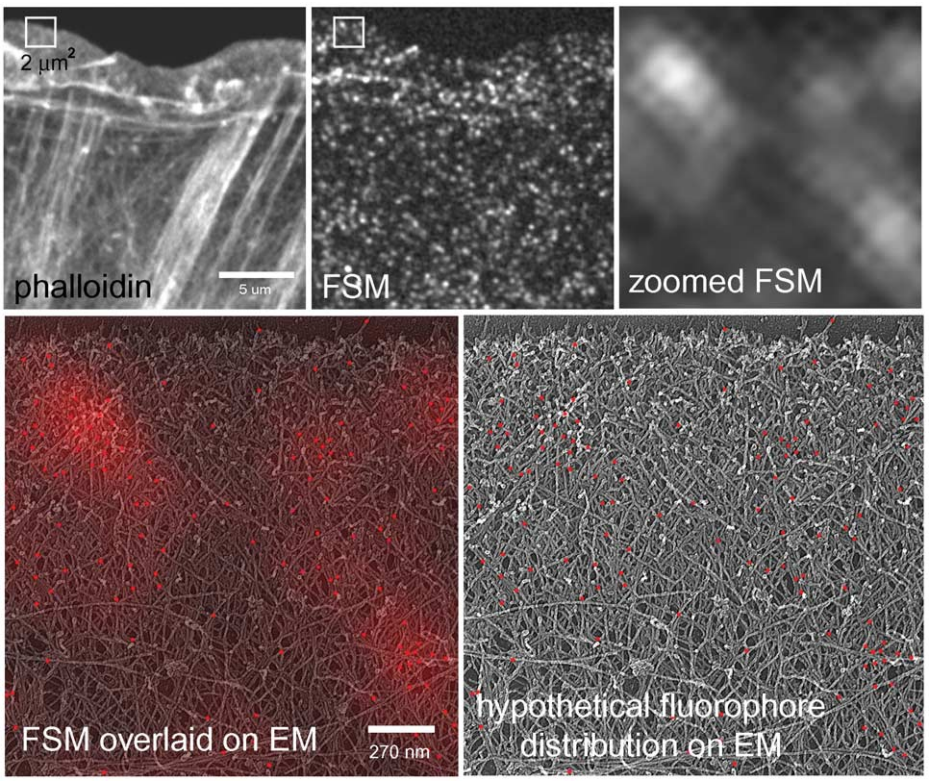

FIGURE 1 FSM of the actin cytoskeleton. (Top) A newt lung epithelial cell was microinjected with a low level of X-rhodamine-labeled actin, fixed, and stained with Alexa-488 phalloidin. In the phalloidin image, all actin filaments are labeled and can be visualized, giving much information about the higher order structural organization, including the location of filament meshworks in the lamellipodium and filament bundles in the cell body. In the single FSM image, much of the structural information is lost, but in time-lapse FSM series, dynamic information is gained that cannot be obtained with higher level labeling of the cytoskeleton. The 2 × 2-μm box in the middle panel is zoomed up in the right-hand panel, and in the bottom right it is colorized red and overlaid onto a quick-freeze deep-etch image of the same-sized region of the actin cytoskeleton in the leading edge of a fibroblast (kindly provided by Tatiana Svitkina, Northwestern University). This gives a sense of the scale of FSM compared to EM so that you can see how many filaments actually fit within the 270-nm resolution-limited image region. In the bottom right panel, a hypothetical fluorophore distribution that could give rise to the speckle pattern is shown, demonstrating the very small proportion of the total actin that is utilized for gaining information in FSM images.

molecules to the microtubule lattice, together with many unlabeled ensconsin molecules, results in GFP–ensconsin speckles along microtubules.

Thus, a "speckle" in general terms is defined as a minimally resolvable image region that is significantly higher in fluorophore concentration (i.e., fluorescence intensity) than its immediately neighboring minimally resolvable image region. In addition, for a speckle to be detected, the fluorescent molecules must be immobilized for the time required for image acquisition. The rapid motion of a small number of mobile (diffusible) fluorescent molecules results in a low level of evenly distributed background signal in the many pixels the molecules visit during the 0.5- to 3-s exposure time required by the camera to acquire an image of the dim FSM specimen (e.g., for our imaging system, actin monomers move at 63 pixels/s in the image space). This concept was demonstrated nicely by Watanabe and Mitchison (2002), who showed that diffusible GFP expressed at very low levels in cells produced an even distribution of fluorescence in high-resolution images, while a similar expression level of GFP–actin produced a speckled fluorescence image.

Speckle patterns in macromolecular assemblies act as a "bar code" pattern on structures that only change with assembly or disassembly of the structure over time (Waterman-Storer and Salmon, 1998). The pattern also serves as fiducial marks on macromolecular assemblies, which in time-lapse movies can be tracked and measured, with translation of the speckle pattern

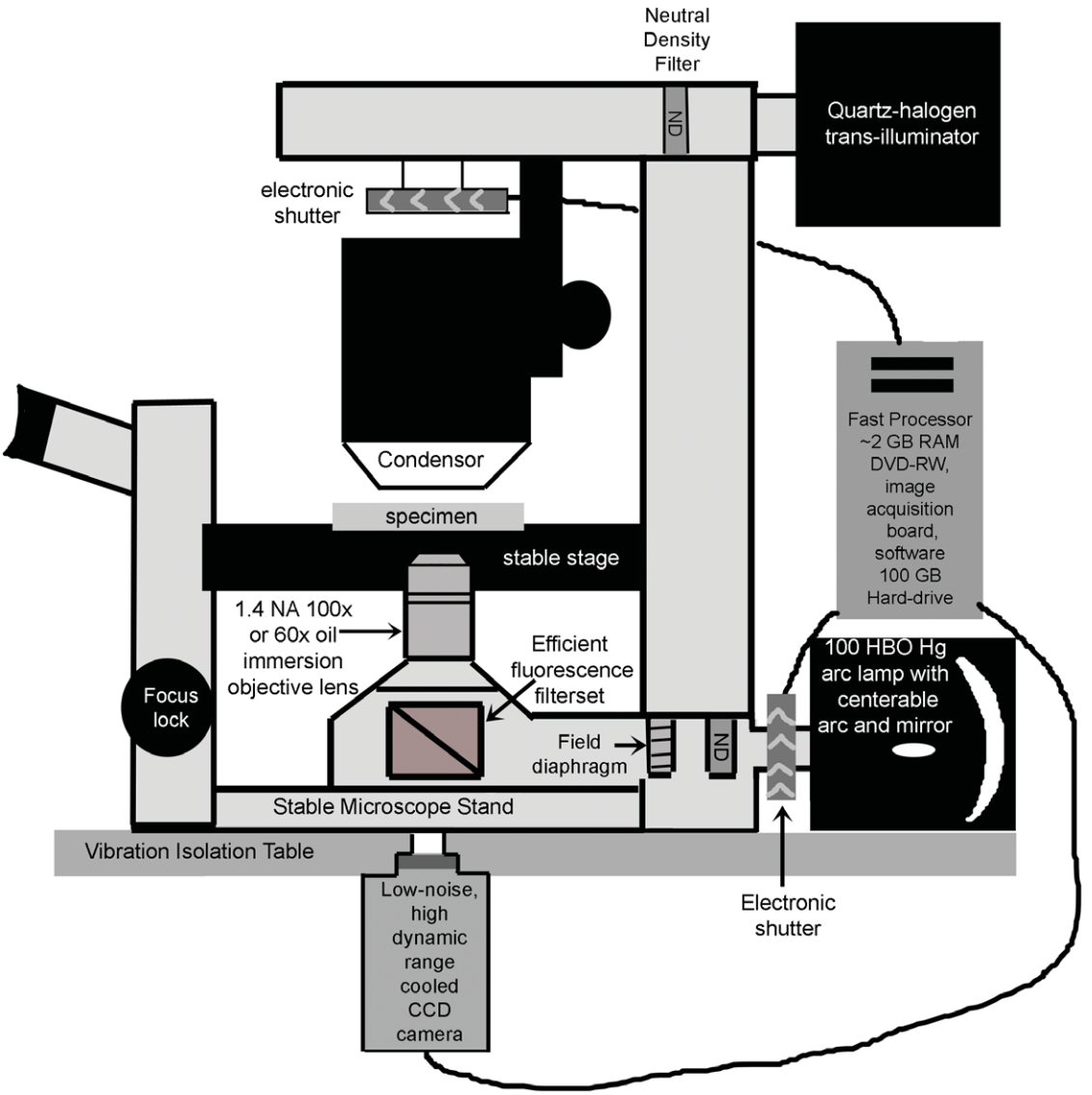

FIGURE 2 Schematic diagram of the important components of an inverted microscope optimized for FSM.

encoding trajectory and velocity and appearance/disappearance of speckles relating to assembly/disassembly dynamics. FSM therefore provides an exceptional tool for studying the actin cytoskeleton during processes such as cell migration, division, morphogenesis, and neuronal pathfinding. Furthermore, FSM can serve as the quantitative readout to link pharmacological, molecular, or genetic interventions to changes in cytoskeleton dynamics to permit a systematic deciphering of molecular regulation of the actin cytoskeleton.

This chapter article gives guidelines for designing a microscope imaging system for performing time-lapse FSM and protocols for achieving time-lapse FSM imaging of the actin cytoskeleton in living tissue cells cultured on glass coverslips. Finally, it also describes a perfusion system for temporally controlled application of drugs during time-lapse FSM of actin to observe the kinetic evolution of their effects on the dynamics and organization of the actin cytoskeleton.

II. MICROSCOPY INSTRUMENTATION

As opposed to a step-by-step protocol, this section discusses the basic components needed to set up an FSM system, giving the recommendations for critical requirements in each type of component (see Fig. 2).

The following *materials* are needed: upright or inverted epifluorescent microscope and optics, including epi-illuminator, objective lens, excitation filter, emission filter, and dichromatic mirror; electronically controlled shutter; cooled CCD camera; and computer, digital image acquisition board, and software for control of shutter and image acquisition.

A. Upright or Inverted Epifluorescent Microscope and Optics

1. The microscope stand should be of biological research quality, with a substantial mass that resists vibration. If possible, the microscope should be mounted on a vibration isolation table (available from Newport or TMC). Either upright or inverted configurations can be used, although inverted microscopes offer more flexibility in choosing imaging chambers for living cells and accommodating open petri dishes. The focusing system should be lockable during long-term time-lapse imaging, as slight shifts in focus result in changes in speckle intensity that can be interpreted artifactually as actin dynamics. Acceptable recent-model uprights include Nikon Eclipse E400, 600, 800, or 1000; Olympus BX series; or Zeiss Axioplan 2. Inverteds include Nikon Eclipse TE-2000 series, Olympus IX series, Zeiss Axiovert 200, or Leica DM IRB.

2. The microscope should be equipped with a high-quality epi-illuminator. The lamp should be a 100HBO mercury arc, and the lamp housing should include a parabolic mirror and should allow manual control of bulb and mirror centration for proper alignment of Koehler epi-illumination. It is very helpful, although not necessary, to have manual control of centration and size of the field diaphragm of the epi-illuminator. Closing down the field diaphragm to just the area of the specimen being imaged reduces photodamage to the whole specimen and reduces out-of-focus fluorescent flare in the image. Similarly, it is helpful if the epi-illuminator is equipped with slots in which to insert neutral density filters to control specimen illumination and an infrared blocking filter to minimize exposure of the specimen to damaging heat.

3. The objective lens (which also acts as the condenser in epi-illumination) should be of the highest numerical aperture available, i.e., 1.4 NA oil immersion. Magnification should be either 60, 63, or 100×, the choice being dependent on the spatial resolution of your camera detector (see Section II,6). Keep in mind that 60 or 63× lenses are often more efficient at transmitting light than 100× lenses. However, you should ***never*** sacrifice system resolution for this small gain in light detection. The lens should not contain contrast-forming elements such as phase rings that block transmission of photons. The lens should be corrected for chromatic aberration (apochromatic) and flat-field corrected (Plan). We have had good luck using DIC plan apochromat objectives.

4. The excitation and emission filters and dichromatic mirror should be as efficient as possible at exciting the fluorophore, separating the excitation from emission, and collecting the emission of the fluorophore of your choice. The use of long-pass instead of band-pass filters may maximize this efficiency. High-quality filter/mirror sets for commonly used fluorophores are available from Chroma Technologies or Omega.

5. The path from the objective lens to the detector should be simple and contain as few intervening components as possible to allow maximum photon collection. Removal of analyzers, wave plates, and Wollaston prisms that are used for various modes of polarization microscopy is required. Optovars or magnification changers should optimally be removed; however, if they are needed to match the microscope resolution to the detector resolution (see later), this is a source of light loss that will have to be lived with. The camera port should utilize the most direct path from the specimen. For an upright microscope, this would be directly over the objective, and for an inverted configuration, a bottom port underneath the microscope is the best bet. The bottom port requires a hole in the table upon which the microscope is seated in order to accommodate the camera. If this is impractical, a side camera port, which requires one mirror to direct the image to the camera, is better than a front port that requires at least two mirrors. Finally, prisms that split the image between the ocular and camera port should be removed from the light path.

B. Electronically Controlled Shutter

1. The electronically controlled shutter should be mounted with proper adapters in the light path between the lamp house and the epi-illuminator.

2. The shutter should be mirrored on the surface facing the lamp to reflect heat away from the specimen.

3. The shutter should operate quietly, quickly, reliably, and without excessive vibration. Shutters can be obtained from Vincent Instruments that are actuated from a software-triggered pulse via the serial or parallel port of the computer.

C. Cooled CCD Camera

Choice of the camera is one of the critical, make-or-break decisions in the design of an FSM imaging system. For imaging the low fluorescence of dim FSM

specimens, the camera demands are steep: it should be highly sensitive, extremely low noise (remember that speckles look a lot like noise!), high spatial resolution, high dynamic range, and, depending on your biological application, it may need high speed as well. The camera should be a scientific grade slow-scan cooled charge-coupled device camera. To date, most intensified cooled CCD we have tested (both microchannel plate type or on-chip type) have had noise characteristics that obfuscate speckle detection, although on-nip electron multiplication LCDs appear promising. Cameras are available from several manufacturers (Hamamatsu Photonics, Roper Scientific, Cohu, Andor) at prices ranging from ~$9000 to $30,000 USD. We give an example of the specifications of the camera of choice in our laboratory, the Hamamatsu Orca II ER, as a benchmark.

D. The CCD Chip

1. Spatial Resolution

Spatial resolution is determined by the physical size of the silicon photodiodes ("pixels") that convert photons to charge on the CCD chip. These currently range in size from about 6×6 to $30 \times 30\,\mu m$. The larger the pixel size, the more magnification from the microscope will be needed to ensure resolution-limited images. Thus, smaller pixel size is better for FSM, as it will not require photon-robbing magnification changers or optovars in the light path. The total number of pixels making up the CCD and the pixel size will determine the imaging area. For example, our Orca II ER has a 1344×1024 array of $6.4 \times 6.4 = 41\,\mu m^2$ pixels, resulting in a 8.67×6.60-mm CCD capable of imaging an 87×66-μm area of the specimen at 100× magnification.

2. Pixel Well Capacity

Based on the physical composition of the silicon photodiodes, pixels will have a maximal number of photoelectrons that it can "hold" before it is saturated with charge, which will correspond to white saturation in the image. The greater this "full well capacity," the greater the potential for a high dynamic range, after taking noise into consideration (see later). The full well capacity is also a function of the pixel size, so for FSM imaging one should consider the best full well capacity per micrometer of pixel area. The Orca II ER has a full well capacity of 18,500 electrons/$41\,\mu m^2$ = 45 electrons per μm^2.

3. Illumination Geometry

CCDs can be illuminated from their front or back sides. Front-side illumination requires that the light pass through substrate materials to reach the photosensitive area, reducing quantum efficiency (QE). This is the configuration of our Orca II ER. Back-illuminated CCDs are physically thinned (also called "back-thinned") to allow illumination directly on the photosensitive surface, making them much more sensitive (and much more fragile and expensive!). However, because of the thinning process, there are limits to the size of the pixels, with the smallest currently available at $13 \times 13\,\mu m$. Thus, one has to weigh whether the increased sensitivity is worth the photon loss in having an optavar in the image path, as well as whether one can afford the expense. For FSM applications, sensitive front illuminated CCDs, such as the Orca II ER, work quite well.

4. Spectral Sensitivity

Different types of CCDs have specific probabilities at any given wavelength of converting a photon striking the pixel to an electron that is counted as signal by the camera (quantum efficiency). Manufacturers supply graphs of the wavelength vs QE for their available CCDs. A CCD should be chosen that has a high (>50%) QE in the wavelength range of your fluorophore of choice. The Orca II ER has ~70% QE between 450 nm (blue-green) and 600 nm (orange-red). Some back-illuminated cameras achieve ~90% QE throughout the visible spectrum, but have excessively large pixels and terribly slow readout (see later).

5. Readout Geometry

Once photons are converted to charge in the array of pixels, the charges must be read out to an image acquisition board so that the image can be reconstructed in the computer by assigning a gray value to the relative charge at each pixel position. Charges are transferred out of the CCD in three basic ways. Full-frame readout occurs as each row of pixel charges is transferred serially out of the CCD one row after another. This type is the slowest and introduces the most noise (nonphoton-associated charge) into the image, although can still acceptable for FSM if other camera electronics do not introduce sources of noise. In contrast, in frame transfer and interline transfer CCDs, either the entire pixel charge array or whole rows of pixels are transferred simultaneously to an array of pixels that are masked from light. The charges are then read out from the masked area while the imaging area is being exposed to light again. These types are much faster and less noisy than the full-frame readout type. All three geometries are acceptable for FSM, although attention should be given to the manufacturer's specifications for the noise introduced during readout ("readout noise") as this will deter-

mine the dynamic range of the camera (see later). Our Orca II ER is the interline transfer type, giving a good balance of higher speed and low readout noise (three to five electrons).

E. Camera Electronics

1. Cooling

Heat on the CCD can cause nonphoton-associated charge to build up in pixels, thus contributing to image noise. The coldest camera possible within a reasonable budget should be chosen. Manufacturers will house the same CCD in cameras with different degrees of cooling, ranging from 20°C below ambient temperature to –50 or –60°C. Do not try to go the inexpensive route here because heat is an avoidable source for noise that can easily mask your very faint FSM signal. The Orca II ER is cooled to –60°C, contributing to its exceptionally low readout noise (see earlier discussion).

2. Readout Speed

In general, the faster the readout speed, the more error is introduced during charge transfer, which translates to noise in your image. Speeds in modern cameras range from 100 kHz/pixel in some low-noise back-illuminated cameras to 14–15 MHz/pixel in interline and frame transfer cameras. For quantitative FSM imaging of cytoskeletal dynamics, image acquisition rates of 1–2 images/s may be required, which cannot be accomplished by the slower cameras. Here, a reasonable compromise of speed and low noise must be sought, but it is recommended not to buy a camera much slower than 1 MHz. The Orca II ER has a choice of readout speeds, a higher noise, fast readout at 10 mHz/pixel or a slower low-noise (quoted earlier) 1.25-mHz/pixel readout rate.

3. Dynamic Range

For FSM imaging of very dim specimens, it is important to have the biggest dynamic range possible (again, within a reasonable budget). Although pixel full-well capacity is set for a given CCD, the number of gray levels this amount of charge is divided up into is not fixed. It can be encoded by 8, 10, 12, 14, or 16 bits of information per pixel, corresponding to 256, 1024, 4096, 16,384, or 65,536 (2^8, 2^{10}, 2^{12}, 2^{14}, 2^{16}) gray levels. However, statistically, it is not possible to distinguish between two gray levels that differ by less than the noise level. Thus the actual dynamic range is determined by the pixel full-well capacity divided by the readout noise. For example, our Orca II ER camera advertises 14 bit dynamic range (16,384 gray levels) and has a full-well capacity of 18,500 photoelectrons. Thus, it must have a noise level of 18,500/16,384 = 1.1 electrons per pixel or less to make use of the full 14 bit range. Because the Orca II ER has a minimum of three electrons noise, the actual dynamic range is 18,500/3 = 6166 discernible gray levels. For FSM imaging, a bigger dynamic range (at least 12 bit) is required so that differences between the intensity of two or three fluorophores can be detected quantitatively.

4. Subarraying and Binning

Being able to read out only a specified portion of the CCD (subarraying) can increase image acquisition speed for imaging small areas of a cell, but it is not necessary. Binning, in which the charges in a group of pixels are combined and read out as a single pixel to increase sensitivity, should not be done in FSM, as this effectively increases pixel size and decreases CCD resolution.

F. Computer, Digital Image Acquisition Board, and Software for Control of Shutter and Image Acquisition

1. Computer

A computer with the fastest processor and most random access memory (RAM) affordable should be used. Currently, computers with ~2-GHz processors and 2-GB RAM can be had for ~$3000 USD. Time-lapse FSM image series are large files often on the order of 500 MB or more and computer "horsepower" is necessary to view and manipulate these. A large hard drive (100 GB) is useful for temporary file storage.

2. File Storage

A DVD R/W device is the most economical choice recommended to archive the large files generated by time-lapse FSM. The fastest write speed available within budget should be chosen. A portable USB-based hard drives allow rapid transfer between computers. However, in the best case, a large networked file server is preferred.

3. Image Acquisition Board

Use the board recommended by your camera and software manufacturer, making sure that the board can handle the bit depth of the camera. Many cameras come with their own boards.

4. Software

Software should be capable of time-lapse digital image acquisition and triggering the shutter during camera exposure. The software should allow easy

viewing of time-lapse series as movies, with control of play-back rate and adjustment of brightness and contrast in the entire image series. Basic image processing, including the ability to perform low-pass filtering and image arithmetic (subtraction, multiplication, etc.), is required. The software should provide the ability to perform quantitative analysis of intensity, position, and distance. We have used Metamorph (Universal Imaging) with outstanding success. However, NIH-Image freeware (available at http://rsb.info.nih.gov/nih-image/) is also very versatile and many free macros are available.

G. Matching Microscope and Detector Resolution

A critical key to obtaining resolution-limited images of fluorescent speckles is matching microscope and camera resolution. The resolution-limited image region has to be magnified to an area on the CCD large enough to achieve a sampling frequency that is high enough to be able to digitally resolve structures at the resolution limit (Stelzer, 1998). As a rule of thumb, magnifying the resolution limited image region to the size of 3×3 pixels on the CCD is sufficient so that the CCD does not limit imaging system resolution or produce aliasing between pixel rows. This is referred to as the Nyquist sampling criterion. Any magnification over this value does not contain significantly more information and simply reduces the area of the specimen that is imaged. The magnification (M) required to achieve this is given by

$$M = 3 P_{width}/r$$

where P_{width} is the width of a pixel and r is the size of the resolution-limited image region. Thus, for red fluorescence with a resolution limit of 0.27 µm and a camera with 6.7 µm pixels and a 1.4 NA objective lens, the magnification required to satisfy the Nyquist criterion is 75×. Thus either a 100× objective or a 60× with 1.25× intermediate magnification should be used, whichever transmits more light.

III. MATERIALS AND INSTRUMENTATION FOR CELL PREPARATION, DRUG PERFUSION, AND FSM IMAGING

Successful time-lapse FSM imaging of actin dynamics is highly dependent on the choice of cell type. Cells should grow in tissue culture well adhered to glass coverslips and should be relatively large (>50 µm diameter), well spread, flat, and thin (<1.0 µm). We routinely use PtK_1 cells, an epithelial line from rat-kangaroo kidney (American Type Culture Collection, Manassas, VA, ccl-35). These cells are optimal as they are large, thin cells and are relatively easy to microinject. PtK_1 cells are maintained in F-12 Hams media (Sigma, St. Louis, MO, Cat. No. N-4388) and plated on 22× 22-mm #1.5 cover glasses (Corning, Kennebunk, ME, Cat. No. 2870-22) in 35-mm tissue culture dishes and maintained in a humidified incubator at 37°C supplemented with 5% CO_2. Use of this type of coverslips is critical, as high-resolution optics are specifically corrected for this thickness (#1.5 = 0.17 mm. thick), and our custom-made perfusion chamber described in Fig. 2 is specifically designed for them. Prior to plating cells, the coverslips are cleaned by sequential washes and sonications in detergent, water, and ethanol, as described in detail in Waterman-Storer (1998). This level of coverslip cleanliness is of paramount importance, as coverslip dirt results in background fluorescence that degrades speckle contrast.

Fluorescently labeled skeletal muscle actin can be bought (Cytoskeleton, Denver, CO, Cat. No. APHR-A) or made using the detailed protocol published elsewhere (Waterman-Storer, 2001). A labeling ratio of 0.3–1.0 fluorescent dye molecules per protein molecule is acceptable. We recommend using longer wavelength fluorophores, such as Texas red (ex 596 nm, em 615 nm), X-rhodamine (ex 575 nm, em 602 nm), Alexa 568 (ex 578 nm, em 603 nm), or tetramethyl rhodamine (ex 541 nm, em 572 nm), as cellular autofluorescence that degrades speckle contrast tends to be at shorter emission wavelengths (~500–550 nm). Very short wavelength excitation fluorophores (i.e., <400 nm) should not be used, as the UV light required for their excitation is very damaging to living cells. In addition, we have found no qualitative difference in FSM of actin dynamics using actin coupled to fluorescent dyes via either lysine residues (i.e., succimidyl ester fluorophore derivates) or cysteine residues (malemide derivates).

Labeled actin should be stored long term (up to 2 years) in flash-frozen aliquots at higher protein concentrations (5–10 mg/ml) at –70°C and can be diluted to the working concentration of 1 mg/ml in G buffer (2 m*M* Tris–Cl, pH 8.0, and 0.2 m*M* $CaCl_2$; just before use add 0.2 m*M* ATP and 0.5 m*M* 2-mercaptoethanol; store up to 1 day at 4°C), refrozen in 5-µl aliquots, and stored for several months before use. To prevent problems of clogged microinjection needles, prior to microinjection into cells, fluorescent actin must be clarified by centrifugation in a swinging bucket rotor (Sorvall, Newtown, CT, Cat. No. S55-S or Beckman Cat. No. TLS-55) in a microultracentrifuge (Sorval, Cat.

No. RCM120 or Beckman Cat. No. TL-100). If possible, keep the rotor stored at 4°C for convenience. Microinjection needles can be bought from Eppendorf (Femtotip II, Brinkman, Westbury, NY, Cat. No. 930000043), although we pull our own from thin wall borosilicate glass capillaries with an outer diameter of 1.00 mm, an inner diameter of 0.78 mm, and a length of 10 cm (Sutter, Novato, CA, Cat. No. BF100-78-10) using a Sutter Instruments P-87 needle puller with a 2.5 × 4.5-mm box filament (Sutter, Cat. No. FB245B). Needles are treated further with hexamethyldisilazane (HMDS, Pierce, Rockford, IL, Cat. No. 999-97-3) to prevent clogging caused by protein adhering to the insides of the needle. A 10-µl Hamilton syringe (Hamilton, Reno, NV, Cat. No. 80008) is used to back load needles with fluorescent actin.

Coverslips of cells are injected in 35-mm tissue culture dishes using an Eppendorf Injectman (Cat. No. 5179 000.018), microneedle holder and grip heads (Cat. No. 5176 190.002, Cat. No. 5176 210.003), and transinjector (Cat. No. 5246 000.010) (Brinkman, Westbury, NY) system mounted stably on a microscope. Although many fine-control microinjectors are acceptable, be sure that they are designed for mammalian cell injection, as those designed for *in vitro* fertilization of larger eggs may not have fine enough positional control. For back pressure in the needle, systems capable of repeatable femtoliter injection volumes are needed; other systems including those made by Picospritzer are acceptable. The microscope on which the microinjector is mounted must be a stable platform-inverted configuration. Although we use a Nikon TE-2000-S, all those mentioned previously are suitable, as well as less expensive "clinical" models. The microscope must be equipped with a quartz-halogen transilluminator and a long working distance phase-contrast condenser lens system that allows room for an open tissue culture dish on the stage (we use a Nikon 0.35 NA extra-long working distance condenser lens). A long working distance dry (nonimmersed) 40× phase contrast objective lens is required to image cells through the thickness of the plastic dish and coverslip during microinjection (we use a Nikon 40× 0.55 NA objective with a 2.1-mm working distance).

In order to keep cells happy and healthy during FSM imaging over time, it is necessary to keep the cells in an optimum environment on the microscope stage. This includes proper temperature and pH regulation and minimizing photodamage and photobleaching caused by exposure to excitation light. Because suppression of fluorescence photobleaching is one of the most critical aspects of successful FSM imaging, when filming PtK_1 cells, we supplement their F-12 Hams media with Oxyrase (Oxyrase Inc., Mansfield, OH, Cat. No. ES-50), an oxygen-scavenging enzyme purified from *Escherichia coli*, which decreases photobleaching and photodamage to the cell. To make this reagent effective, cells and their surrounding media must be sealed from exposure to air. In order to minimize deleterious effects of pH, one might consider adding 5 m*M* HEPES buffer (pH 7.0) to the medium. However, because we use F-12 Ham's media for PtK_1 cells, which is already buffered, this does not require extra HEPES. For temperature control, we find that an airstream stage incubator, such as those produced by Nevtek instruments (ASI-400), is the best bet. One should experiment ahead of time to determine the setting on the thermostat that gives a sample temperature ***(with the objective lens coupled by immersion oil!)*** of 37°C and keeps cells viable over several hours.

For drug treatment studies we have custom designed a live-cell perfusion chamber that allows use of high-resolution oil-immersion objective and condenser lenses and gives near laminar flow for complete exchange of media in a minimal volume while remaining sealed from the environment (Fig. 3). The chamber portion comes in direct contact with media that washes over cells, and thus must be made of inert stainless steel. The chamber top that holds down the coverslip of cells on the chamber has no contact with media, and thus can be made of less inert aluminum, while the coverslip gasket is made of 0.005-in. thick Teflon sheet, for flexibility. A 24 × 60-mm coverslip (Corning, Cat. No. 2940-246) must be sealed to the bottom of the chamber with hot VALAP (a 1:1:1 mixture of Vaseline, paraffin, and lanolin prepared in the laboratory) to complete the condenser lens-facing side of the imaging chamber. Any good machine shop should be capable of reproducing this chamber based on the diagram in Fig. 3.

IV. PROCEDURES

A. Microinjection of Fluorescent Actin

Microinjection of 1 mg/ml fluorescently labeled actin allows later visualization of protein dynamics by time-lapse FSM.

1. Plate cells onto cleaned coverslips (Waterman-Storer, 1998) at least 24 h before microinjection.

2. Pull microinjection needles from borosilicate glass capillaries (1.0 mm outer and 0.78 mm inner diameter). Proteins that polymerize, such as actin, are notoriously difficult to microinject, as the large polymers will clog the needle tips. We have ascertained that

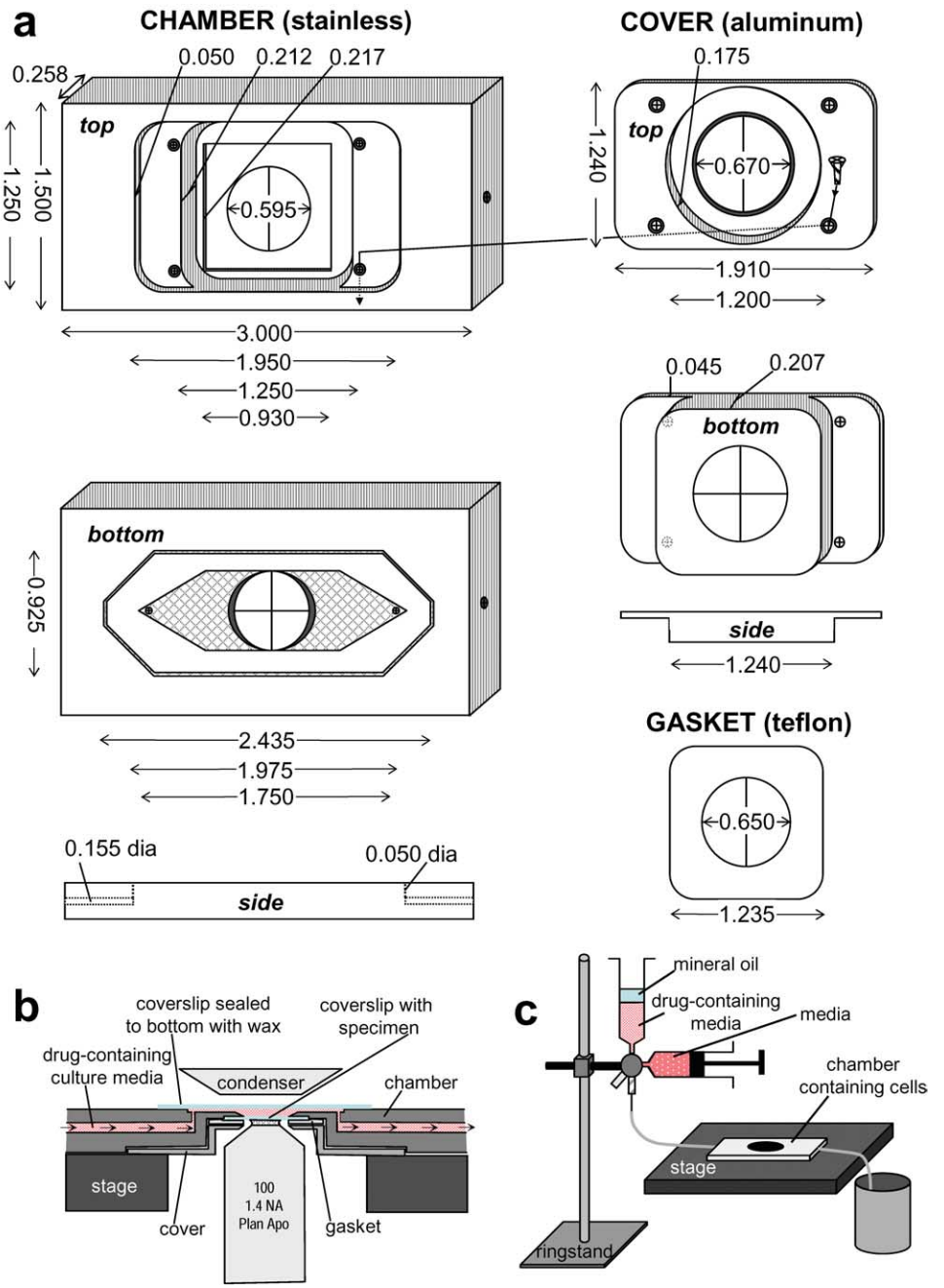

FIGURE 3 A custom-designed perfusion system for drug application during high-resolution FSM imaging. (a) Specifications for chamber design. The chamber is made of stainless steel, the top of aluminum, and the gasket of a 0.005-in. Teflon sheet. Forty-five degree beveled areas are shown in dark gray, holes have crosses across them, and on the bottom of the chamber, the hatched areas are machined-in 0.007 in. to create the imaging chamber. (b) Cutaway side view of the chamber in operation on the microscope stage (not to scale). (c) Schematic of the setup used for drug perfusion.

needles efficient for injecting actin and other polymerizing protein such as tubulin consist of an inner tip diameter of less than 1 µm, and a short, relatively blunt taper to prevent clogging, breaking, or overflexible needles. By experimenting with the parameters of the needle puller, one can adjust the shape of the needle. The following four-step program may serve as a starting point for achieving good needles on the Sutter needle puller, but depending on the age and capabilities of the glass-heating filament in the needle puller,

the needle-pulling program will necessitate some variation according to the guidelines in the owner's manual.

Heat	Pull	Velocity	Time	Pressure
Ramp + 10	100	10	250	500
Ramp	100	10	250	500
Ramp	100	10	250	500
Ramp + 10	100	15	250	500

Commercially available microinjection needles such as Eppendorf Femtotips II work well for actin microinjection and thus are an alternative to pulling your own needles; however, they are expensive and can only be used with Eppendorf injection systems.

3. In a closed petri dish, rest freshly pulled (or freshly opened commercial) needles on a small cylinder of modeling clay to immobilize them and prevent breaking of the tip. In a chemical fume hood, add a few drops of HMDS to the bottom of the petri dish and close the dish immediately. This silanization vapor on the glass will prevent absorption of protein, therefore reducing needle clogging. Allow at least 2 h incubation of needles in the hood with HMDS before use.

4. Just prior to microinjection, chill the microultracentrifuge to 4°C. Thaw an aliquot of labeled actin at body temperature and transfer it to ice immediately. Centrifuge for 20 min at 30,000 *g* in a swinging bucket rotor to remove aggregates that may clog the needle.

5. Following centrifugation, transfer the tube of labeled actin to ice. Using a Hamilton syringe, back load approximately 1 µl of clarified fluorescent actin (being careful not to touch the syringe needle to the pellet!) into a microinjection needle inserted as close as possible to the microneedle tip. Insert the microneedle into the needle holder of the microinjection device. The needle holder should be at an angle of approximately 45° relative to the microscope stage. The back pressure should be set to ~0.8 psi. To rid the needle of air bubbles, use the clean button (which transiently increases the back pressure to a maximum of 65 psi) to push solution through the needle tip.

6. Center the needle over the objective lens as well as possible by eye and lower the needle into the medium in the 35-mm tissue culture dish, stopping immediately when the needle comes in contact with the medium. Close the condensor diaphragm down and move the needle in the *x*–*y* plane so that the very tip of the needle is in the centered cone of light. The needle should be well above the cells, so open the condensor diaphragm and look through the microscope, moving the needle slowly in the *xy* direction and looking for the out-of-focus shadow of the needle in the image field of view. Once the shadow of the needle is in the field, focus up until the needle is in focus. Now slowly alternate between moving the focus down and then the needle down until the needle is in focus just above the cells. Alternatively, using a Bertrand lens, view the objective lens back aperture, where the tip of the needle will be in focus when the needle has just entered the medium. Center the needle tip in the image of the phase ring, then view the image, and lower the needle until it is in focus. Quickly getting needles in focus at the plane of the specimen without breaking their tips will likely take some practice.

7. We find it most simple to keep constant slow flow of labeled actin from the needle tip to help prevent clogging. Bring the flowing needle tip over the cell that you want to inject and lower the needle until it touches the cell just adjacent to the nucleus. As the solution flows into the cell, you will see a change in the contrast of the cell around the nucleus. Rapidly remove the needle from the cell before it blows up.

8. After microinjecting approximately 40 cells in a dish successfully, replace the medium with fresh medium, and place the dish back into the incubator for at least 2 h to allow the cells to recover from injection and to incorporate fluorescently labeled actin into the cytoskeleton.

B. Live-Cell Imaging and Drug Perfusion

1. After microinjection of cells, begin preparing for live-cell imaging and drug perfusion. Turn on the heater to preequilibrate stage and objective lens temperatures several hours before you plan on imaging the cells. This will minimize focus drift caused by temperature shifts that expand/contract the metal in the microscope body. Prepare 20 ml of media (buffered with 10 m*M* HEPES if necessary) containing 30 µl of Oxyrase/ml of media.

2. Right before mounting cells in the perfusion chamber, prepare the perfusion setup (see Fig. 3c). Our custom-designed perfusion setup uses two 10-ml syringes mounted into a two-way luer-lock syringe stopcock (available from medical supply houses) with a 25-gauge needle at the bottom, feeding into a tube that connects to the perfusion chamber (Fig. 3). One syringe should be filled with 10 ml of drug-free media containing 30 µl of Oxyrase/ml of media. Be sure to tap out all bubbles from the syringe to maintain Oxyrase activity. This syringe should be mounted on the stopcock valve parallel to the tabletop. The second syringe will be used for drug-containing media. Remove the plunger from this syringe and place into the stopcock valve perpendicular to the first syringe (perpendicular to the tabletop). Fill it with 8 ml of drug-treated media

supplemented with oxyrase and then cover with mineral oil to protect the oxyrase from the air. The drug perfusion will be done by gravity, as opposed to pushing a syringe.

3. To prepare the perfusion chamber, melt VALAP and heat the perfusion chamber on a heating block for a few minutes. Using a cotton-tipped applicator swab, place a thin layer of VALAP around the outer ring on the bottom of the perfusion chamber and adhere a 24 × 60-mm coverslip onto this. Allow the valap to solidify under the cover glass and place on a cool surface to return the perfusion chamber to room temperature.

4. Once the perfusion chamber is at room temperature, place vacuum grease around the perimeter of the coverslip-mounting surface of the top side of the chamber. Place the chamber on the microscope stage to allow it to heat to 37°C. Once the perfusion chamber is warm, place the coverslip with injected cells face down onto the chamber. Put the gasket on top of the coverslip, making sure it seals the chamber; an additional layer of vacuum grease may aid in this. Then place the aluminum chamber cover over the gasket and attach it to the chamber by screwing down opposite corners in turns, being careful not to crack the coverslip.

5. Once the perfusion chamber is set up, insert the drug-free media inlet tube into one end of the perfusion chamber and hold the chamber so the inlet end is facing down so that when the chamber is filled with media, all air bubbles will be pushed up through the upper outlet. Slowly push the drug-free media through the perfusion chamber. Avoid trapping bubbles by lightly tapping the chamber on a hard surface as you fill it.

6. Insert another tube into the outlet end of the perfusion chamber for discarded media to flow into a waste beaker.

7. Back the microscope focus all the way down and then place a small drop of the appropriate immersion oil on the 100× 1.4 NA objective lens front element. Place the filled perfusion chamber cell side down on the microscope stage and bring the focus up until the oil on the objective is in contact with the coverslip.

8. Bring the cells into focus using phase-contrast or DIC optics, being careful not to smash the objective lens into the coverslip. If using DIC, remember to remove the Wollaston prism and analyzer from the imaging path after finding the cells! Search the coverslip using epifluorescence for the injected cells and verify their viability by seeing if fluorescent actin is excluded from the nucleus. Be careful to keep your cell-gazing time to the absolute minimum, as you will be photobleaching the fluorescent actin. Choose a cell to image that is very dimly fluorescent. Getting the cells in focus with a high-magnification oil-immersed lens and finding the injected cells will take practice and patience.

9. Begin FSM image acquisition. Using the microscope system described in Section II with a mercury arc bulb with <200 h of use on it, exposure times for FSM images taken with unattenuated (neutral density filters removed) light of 500–1000 ms should provide a signal of around 0.3–0.6% of the total gray scale. This translates to a signal of 50–100 gray levels above background for a 14 bit camera or 10–20 for a 12 bit camera. We find that maximizing the gain setting of the camera (if available) is very helpful when taking images of actin speckles. For imaging processes such as actin flow in a PtK_1 cell, an acquisition rate of one image every 5–10 s will allow accurate actin flow velocity analysis. Microscope control software such as Metamorph can be set up easily to acquire images with specific camera parameters and light exposure times at regular intervals for a prescribed total length of time. Plan on taking predrug images for 5–10 min and postdrug images for several tens of minutes.

10. After an appropriate accumulation of images of actin dynamics in the untreated cell, switch the stopcock position to allow drug-containing media to flow through the chamber at a rate of ~2–4 ml/min. Drug perfusion should take approximately 30 s. Continue to acquire images before, during, and after drug perfusion.

11. Continue imaging until the process of interest has terminated or the fluorescent actin is photobleached.

C. Interpreting Speckle Dynamics

Interpretation of actin speckle dynamics provides information about actin turnover and actin flow in a cell and how this relates to cell behavior. Using image analysis software such as Metamorph, images can be processed and analyzed.

1. After acquiring a time series of actin FSM images for at least 5 to 10 min, observe the actin movement by simply watching the time series as a movie. This can be done using Metamorph, Quicktime (Apple, Cupertino, CA), or NIH Image. Pay careful attention to the trajectories of actin movement, convergence of actin in different regions of the cell, and speeds of actin movement in different regions of the cell.

2. Use kymograph analysis to obtain information about the rate of actin retrograde flow and/or the activity of the leading edge. Kymographs are time–distance plots created by extracting the same row of pixels from each image in a time series and laying them side by side in a montage (see Figs. 4 & 5). For measuring

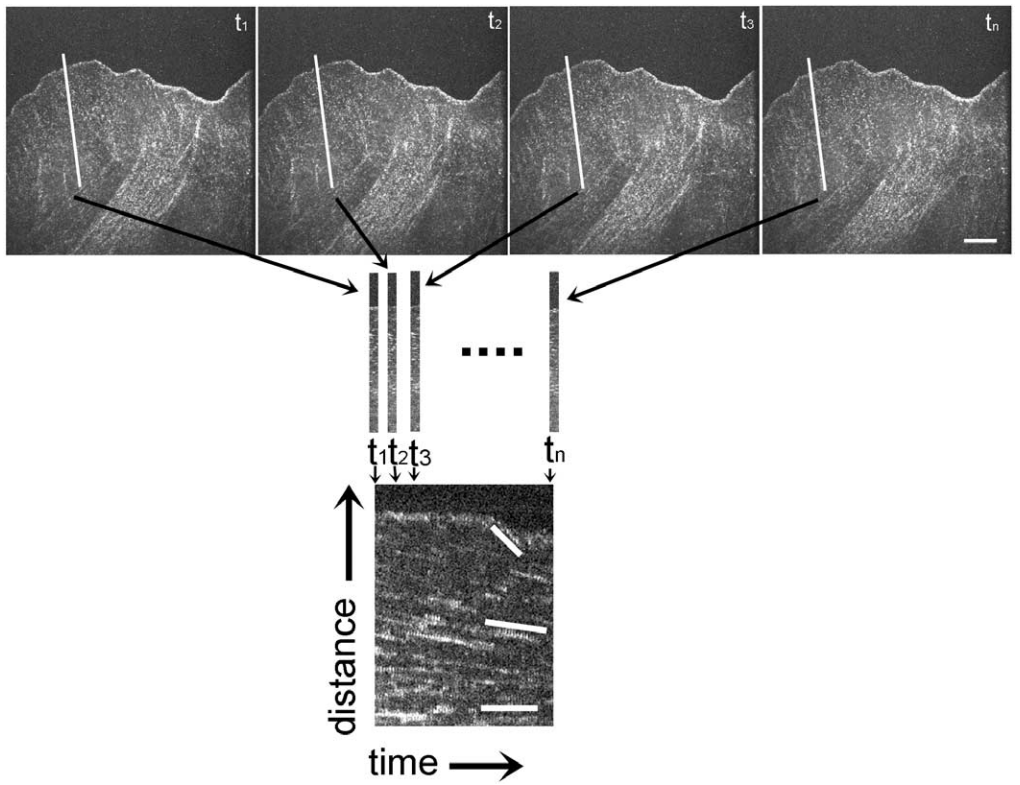

FIGURE 4 Kymograph construction from an FSM time series. The first row of images is taken from a FSM time series. The white line in each image depicts the row of pixels along the trajectory of actin movement (as determined from watching the series as a movie) extracted to construct the kymograph to show actin dynamics, seen below the images. Rows of pixels are laid side by side in a montage to create a time vs distance plot, seen on the bottom of the figure. This kymograph allows analysis of the rates of actin movement within different regions of the cell. Lines in the kymograph on the bottom highlight discreet rates of actin flow in which the magnitude of the slope of the lines relates to the velocity of actin movement. Bar: 10 μm.

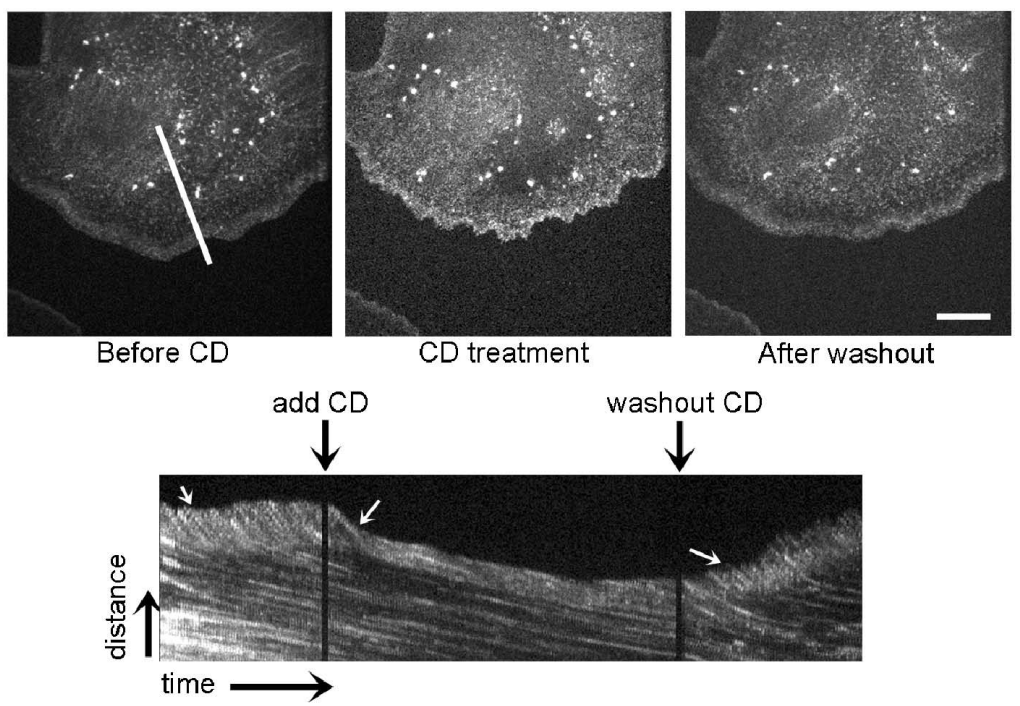

FIGURE 5 FSM reveals that cytochalasin D (CD) halts actin polymerization and fast retrograde flow in the lamellipodium. Images are taken from a time series before CD treatment, during CD treatment, and after washing out CD. (Bottom) A kymograph taken from the time series along the white line indicated in the first image. Perfusion and washing out of CD are marked by black arrows over the kymograph. White arrows on the kymograph indicate the region of rapid retrograde flow inhibited by CD treatment and relieved after CD washout. Bar: 15 μm.

actin dynamics, choose a row of pixels along the trajectory of actin movement as determined from watching the movie. For measuring leading edge activity, choose a row of pixels perpendicular to the leading edge.

V. PITFALLS

Successful FSM imaging of live cells requires several critical components, such as proper fluorescent protein concentration, successful suppression of photobleaching, and high-quality, well-labeled, fully functional fluorescent protein. Fluorescent actin speckles cannot be detected if the concentration of fluorescent protein in the cell is too high, which can occur if the microneedle concentration is >1 mg/ml. Even at proper needle concentrations, too much fluorescent actin can get into the cell if the microinjection technique is not optimized. Conversely, if there is not enough fluorescent protein injected into cells, the camera exposures required to acquire a decent image will be excessively long and may result in motion artifacts within the image. Photobleaching is also a major pitfall in FSM imaging. This can occur if the imaging chamber is not fully sealed, if there are air bubbles present in the chamber, or if the Oxyrase has begun to lose its potency. Ensuring an airtight chamber with fresh Oxyrase will reduce photobleaching greatly. Finally, ensuring that the actin remains functional during the labeling process is an extremely important consideration for quality FSM imaging. If you are making your own fluorescent actin, be sure to use high-quality acetone powder that is finely powdered or "fluffy" and that the dye is fresh and has been stored in dessicant at –20°C. Old dye will render actin nonpolymerizable, so avoid using dye that is not fresh.

References

Adams, M. C., Matov, A., Yarar, D., Gupton, S. L., Danuser, G., and Waterman-Storer, C. M. (2004). Siginal analysis of total internal reflection fluorescent speckle microscopy (TIR-FSM) and wide-field epi-fluorescence FSM of the actin cytoskeleton and focal adhesions in living cells. *J Microsc.* **216**, 138–52.

Adams, M. C., Salmon, W. C., Gupton, S. L., Cohan, C. S., Wittmann, T., Prigozhina, N., and Waterman-Storer, C. M. (2003). A high-speed multispectral spinning-disk confocal microscope system for fluorescent speckle microscopy of living cells. *Methods.* **29**(1), 29–41.

Bulinski, J. C., Odde, D. J., Howell, B. J., Salmon, T. D., and Waterman-Storer, C. M. (2001). Rapid dynamics of the microtubule binding of ensconsin *in vivo*. *J. Cell Sci.* **114**(Pt 21), 3885–3897.

Desai, A., and Mitchison, T. J. (1997). Microtubule polymerization dynamics. *Annu. Rev. Cell Dev. Biol.* **13**, 83–117.

Grego, S., Cantillana, V., and Salmon, E. D. (2001). Microtubule treadmilling *in vitro* investigated by fluorescence speckle and confocal microscopy. *Biophys. J.* **81**(1), 66–78.

Gupton, S. L., Salmon, W. C., and Waterman-Storer, C. M. (2002). Converging populations of f-actin promote breakage of associated microtubules to spatially regulate microtubule turnover in migrating cells. *Curr. Biol.* **12**(22), 1891–1899.

Inoué, S., and Spring, K. R. (1997). "Video Microscopy." Plenum Press, New York.

Maddox, P., Desai, A., Oegema, K., Mitchison, T. J., and Salmon, E. D. (2002). Poleward microtubule flux is a major component of spindle dynamics and anaphase in mitotic Drosophila embryos. *Curr. Biol.* **12**(19), 1670–1674.

Maddox, P., Straight, A., Coughlin, P., Mitchison, T. J., and Salmon, E. D. (2003). Direct observation of microtubule dynamics at kinetochores in Xenopus extract spindles: Implications for spindle mechanics. *J. Cell Biol.* **162**(3), 377–382.

Maddox, P. S., Moree, B., Canman, J. C., and Salmon, E. D. (2003). Spinning disk confocal microscope system for rapid high-resolution, multimode, fluorescence speckle microscopy and green fluorescent protein imaging in living cells. *Methods Enzymol.* **360**, 597–617.

Mikhailov, A. V., and Gundersen, G. G. (1995). Centripetal transport of microtubules in motile cells. *Cell Motil. Cytoskel.* **32**(3), 173–186.

Pollard, T. D., Blanchoin, L., and Mullins, R. D. (2000). Molecular mechanisms controlling actin filament dynamics in nonmuscle cells. *Annu. Rev. Biophys. Biomol. Struct.* **29**, 545–576.

Ponti, A., Vallotton, P., Salmon, W. C., Waterman-Storer, C. M., and Danuser, G. (2003). Computational analysis of f-actin turnover in cortical actin meshworks using fluorescent speckle microscopy. *Biophys. J.* **84**(5), 3336–3352.

Prasher, D. C. (1995). Using GFP to see the light. *Trends Genet.* **11**(8), 320–323.

Small, J. V. (1981). Organization of actin in the leading edge of cultured cells: Influence of osmium tetroxide and dehydration on the ultrastructure of actin meshworks. *J. Cell Biol.* **91**(3 Pt 1), 695–705.

Stelzer, E. H. K. (1998). Contrast, resolution, pixelation, dynamic range and signal-to-noise ratio: Fundamental limits to resolution in fluorescence light microscopy. *J. Microsc.* **189**, 15–24.

Svitkina, T. M., Verkhovsky, A. B., McQuade, K. M., and Borisy, G. G. (1997). Analysis of the actin-myosin II system in fish epidermal keratocytes: Mechanism of cell body translocation. *J. Cell Biol.* **139**(2), 397–415.

Verkhovsky, A. B., Svitkina, T. M., and Borisy, G. G. (1999). Self-polarization and directional motility of cytoplasm. *Curr. Biol.* **9**(1), 11–20.

Wang, Y. L., Lanni, F., McNeil, P. L., Ware, B. R., and Taylor, D. L. (1982). Mobility of cytoplasmic and membrane-associated actin in living cells. Proc. *Natl. Acad. Sci. USA* **79**(15), 4660–4664.

Watanabe, N., and Mitchison, T. J. (2002). Single-molecule speckle analysis of actin filament turnover in lamellipodia. *Science* **295**(5557), 1083–1086.

Waterman-Storer, C. M. (2002a). Fluorescent speckle microscopy (FSM) of microtubules and actin in living cells. *In "Current Protocols in Cell Biology"* (K. S. Morgan, ed.) Wiley, New York.

Waterman-Storer, C. M. (2002b). Microtubule/organelle motility assays. *In "Current Protocols in Cell Biology"* (J. S. Bonifacio, M. Dasso, J. B. Harford, J. Lippincott-Schwartz, and K. M. Yamada, eds.). Wiley, New York.

Waterman-Storer, C. M., Desai, A., Bulinski, J. C., and Salmon, E. D. (1998). Fluorescent speckle microscopy, a method to visualize the

dynamics of protein assemblies in living cells. *Curr. Biol.* **8**(22), 1227–1230.

Waterman-Storer, C. M., and Salmon, E. D. (1997). Actomyosin-based retrograde flow of microtubules in the lamella of migrating epithelial cells influences microtubule dynamic instability and turnover and is associated with microtubule breakage and treadmilling. *J. Cell Biol.* **139**(2), 417–434.

Waterman-Storer, C. M., and Salmon, E. D. (1998). How microtubules get fluorescent speckles. *Biophys. J.* **75**(4), 2059–2069.

Waterman-Storer, C. M., and Salmon, E. D. (1999). Fluorescent speckle microscopy of microtubules: How low can you go? *FASEB J.* **2**, S225–S230.

Waterman-Storer, C. M., Salmon, W. C., and Salmon, E. D. (2000). Feedback interactions between cell-cell adherens junctions and cytoskeletal dynamics in newt lung epithelial cells. *Mol. Biol. Cell* **11**(7), 2471–2483.

Waterman-Storer, C. M., Sanger, J. W., and Sanger, J. M. (1993). Dynamics of organelles in the mitotic spindles of living cells: Membrane and microtubule interactions. *Cell Motil. Cytoskel.* **26**(1), 19–39.

CHAPTER

15

Imaging Fluorescence Resonance Energy Transfer between Green Fluorescent Protein Variants in Live Cells

Peter J. Verveer, Martin Offterdinger, and Philippe I. H. Bastiaens

I. INTRODUCTION

In recent years, the measurement of fluorescence resonance energy transfer (FRET) between variants of fluorescent proteins has emerged as a powerful tool for intracellular measurements of protein reactions (Heim and Tsien, 1996; Matz *et al*., 1999; Tsien, 1998; Wouters *et al*., 2001). For FRET assays in living cells, the green fluorescent protein (GFP), cyan fluorescent protein (CFP), and yellow fluorescent protein (YFP) variants are used most frequently. These GFP variants are intrinsically fluorescent and do not require any exogenous cofactors or substrates, rendering them particularly useful as genetically encoded fluorescent tags to participate as a donor or acceptor fluorophore in a FRET pair. FRET is a photophysical effect where energy is transferred from an excited donor to an acceptor fluorophore; it is a process that is mediated by a direct electromagnetic interaction and does not involve the emission and subsequent absorption of a photon (Clegg, 1996). The efficiency of the transfer depends on the spectral properties of the donor and acceptor and on their relative orientation and distance. Most importantly, the energy transfer efficiency has an inverse sixth order dependency on the distance between the two fluorophores, and therefore FRET only occurs at distances that are typically less than 10 nm. As a result, FRET can be used to specifically image molecular interactions or conformational changes as these events may bring donor and acceptor fluorophores within this distance range, providing they are attached to the same macromolecule or to the interacting molecules.

FRET cannot be measured directly, but its occurrence is reflected by changes in the fluorescence kinetics of both the donor and the acceptor molecules that can be measured by optical means. Due to the direct transfer of energy from the donor to the acceptor, the rate at which the donor returns to its ground state after excitation increases and therefore its fluorescence lifetime decreases. Since the quantum yield of a fluorophore is proportional to its lifetime, the steady-state intensity of the donor molecule also decreases if FRET occurs. However, the steady-state fluorescence of the acceptor increases due to the sensitized emission induced by the energy transfer. Here we outline two methods to detect FRET that are based on the measurement of these effects: (1) fluorescent lifetime imaging microscopy (FLIM) and (2) sensitized emission measurements.

The fluorescent lifetime of a fluorophore is a measure of the time that the fluorophore spends in the excited state and is independent of probe concentration and light path length (Bastiaens and Squire, 1999). FRET reduces the fluorescence lifetime of the donor molecule since it depopulates its excited state. Thus, the measurement of the fluorescence lifetime of the donor can be used as an indicator for FRET. In such an assay, the donor–acceptor pair is chosen such that the donor fluorescence can be detected specifically without detecting any acceptor fluorescence. Therefore absolute specificity of the acceptor probe is not required, and experiments can be carried out with an

Copyright 2006, Elsevier Science (USA).
All rights reserved.

excess of acceptor. The reduction of the fluorescence lifetime due to FRET should be judged in comparison to the fluorescence lifetime of the donor in the absence of FRET. This can be achieved using an internal control where at the end of the experiment the acceptor is photobleached (Bastiaens and Jovin, 1998). This may require illumination of the acceptor for an extended period during which relocation of the proteins may occur. However, because the fluorescence lifetime of the donor is independent of probe concentration, this poses no problem because only the average value of the lifetime after photobleaching is required. FLIM can be implemented in two conceptually different ways (Bastiaens and Squire, 1999). In the first approach, the sample is illuminated with a short laser pulse, and the resulting fluorescence decay is sampled using a fast, gated detector. The measured curve is a direct reflection of the fluorescence decay from which the fluorescent lifetime can be derived. The second approach uses sinusoidally modulated laser light to illuminate the sample at a high frequency (typically ~80 MHz). The resulting fluorescence is also sinusoidally modulated but phase shifted and demodulated compared to the excitation. This phase shift and demodulation depend on the fluorescent lifetime, which can therefore be derived if these quantities can be measured. This can be achieved with a sinusoidally modulated detector whose phase is shifted systematically with respect to the phase of the illumination. The result is a sinusoidally shaped curve from which the phase shift and demodulation, and thus the lifetime, can be derived. Although this approach appears more complex, it requires a less expensive and complicated laser setup and has proven to be a reliable approach in biological applications.

Sensitized emission measurements can be achieved using standard wide-field or confocal microscopes if the appropriate excitation sources are available and the fluorescence emissions of the donor and acceptor can be detected. Generally it is not possible to image the sensitized emission directly, as excitation of the donor cannot be achieved without also directly exciting the acceptor. In addition, bleed through from the donor fluorescence also contributes to the signal that is detected in the acceptor channel upon excitation of the donor. Thus, the signal that is measured upon excitation of the donor consists of three components: bleed through from donor emission, acceptor emission due to direct excitation of the acceptor, and sensitized emission from the acceptor due to energy transfer. Thus the measurement must be corrected for bleed through and direct excitation, which can be achieved using an additional specific measurement of the donor fluorescence upon donor excitation and a measurement of the acceptor fluorescence upon specific excitation of the acceptor. These corrections require scalar calibration factors that can be found using two reference samples that contain either donor or acceptor molecules alone.

The use of green fluorescent protein variants as partners in a FRET pair requires consideration of the relative expression levels of the two protein–GFP fusions in the light of the measurement method that is being used. Using FLIM implies that only the donor fluorophore is being used to measure FRET, which makes this method eminently useful in the case that the acceptor is expressed in a saturating excess over the donor. This is an advantage if the acceptor-tagged protein is used as a sensor to report on the activity or covalent state of the donor-tagged protein, as it is then ensured that any donor-tagged protein can bind to at least one sensor molecule. In sensitized emission measurements the use of excess amounts of acceptor may lead to problems, as the contribution of sensitized emission may then be low compared to the direct excitation of the acceptor. Thus, care should then be taken that the expression levels of acceptor and donor are comparable.

This article uses an example of an assay for the detection of the phosphorylation state of the epidermal growth factor receptor (EGFR). YFP was fused to a phosphotyrosine-binding domain (PTB-YFP) from Shc, which recognizes three high-affinity binding sites on the intracellular part of the EGFR upon phosphorylation (Zhou *et al.*, 1996). We used the citrine variant of YFP that, compared to previous variants, has a reduced sensitivity to pH due to a much lower p*K*a (5.7), has twice the photostability, and exhibits much better expression at 37°C (Griesbeck *et al.*, 2001). CFP was fused to EGFR (EGFR-CFP) and FRET between CFP and YFP was used to detect the binding of PTB to EGFR and thereby the phosphorylation of EGFR.

II. MATERIALS AND INSTRUMENTATION

A. Materials

Dulbecco's modified Eagle's medium

CO_2-independent imaging medium, containing no components that are autofluorescent. Available commercially from Life Technologies or prepared using the standard formulation of Dulbecco's modified Eagle's medium by omitting pH indicator phenol red, penicillin, streptomycin, folic acid, and riboflavin.

Glass-bottomed tissue culture dishes (35-mm, MatTek Corporation)

Transfection reagent, e.g., Superfect, Qiagen; Lipofectamine, Invitrogen; FuGENE-4, Roche
Plasmids encoding the CFP- and YFP-tagged proteins of interest

B. Instrumentation

Fluorescence lifetime imaging microscope suitable for measuring the lifetime of CFP and equipped with a filter set suitable for specifically exciting and imaging YFP. For the experiments described here, we used a home-built wide-field system (Squire and Bastiaens, 1999). CFP excitation: Ar laser at 457.9 nm, CFP filter set (dichroic beam splitter 467; DELTA, Lyngby, Denmark, emission filter HQ480/20; Chroma). YFP excitation: 100-W mercury lamp, YFP filter set (dichroic filter 530 long pass, excitation 510/25, emission filter HQ560/50).
Leica SP2 confocal microscope, equipped with Ar laser with 457.9-nm laser line for CFP excitation and a 514-nm line for YFP excitation
Wide-field fluorescence microscope with appropiate filter sets. For example (from Sorkin *et al.*, 2000): YFP filter set (excitation 500/20 nm, emission 535/30 nm), CFP filter set (excitation 436/10 nm, emission 470/30 nm), FRET filter set (excitation 436/10 nm, emission 535/30 nm).
Computer with image processing software, such as IPLab (Scanalytics)

III. PROCEDURES

A. Cell Preparation

To prepare cells for FRET experiments with either FLIM or sensitized emission, the donor and acceptor plasmid DNA must be introduced into the cells. This is accomplished using standard transfection methods or, alternatively, using nuclear microinjection. The following steps are used to prepare adherent cells for imaging using transient transfection:

1. Day 1: Seed the cells onto glass-bottomed dishes.
2. Day 2: Cell transfection.
   a. Transfect a number of dishes with both plasmids encoding CFP- and YFP-tagged protein, according to the protocol provide by the supplier of the transfection agent.
   b. For sensitized emission measurements only: transfect a number of dishes with plasmids encoding the CFP-tagged protein.
   c. For sensitized emission measurements only: transfect a number of dishes with plasmids encoding the YFP-tagged protein.
3. Incubate the transfected cells under the appropriate conditions for 15–24 h (e.g., 37°C, 5% CO_2) to allow the cells to express the proteins.
4. Day 3: Before imaging, proceed optionally with any necessary cell-handling protocols such as starvation in medium without growth factors.
5. Immediately before imaging replace the culture medium with CO_2-independent imaging medium.

B. Fluorescence Lifetime Microscopy

Fluorescence lifetime microscopy is well suited for FRET experiments where the acceptor is present in excess, as only the fluorescence of the donor needs to be measured. Figure 1 shows an example where FRET between EGFR-CFP and PTB-YFP was measured with FLIM before and after stimulation with epidermal growth factor (EGF). An experiment on living cells requires following the response of the cells to a stimulus in time. At selected time points, a FLIM data set is acquired that contains fluorescence intensity and lifetime information of the donor. Additionally, a fluorescence intensity image of the distribution of the acceptor is acquired. Finally, a control measurement is performed to obtain the lifetime of the donor in the absence of FRET. A detailed description of the FLIM data acquisition itself falls outside the scope of this article. Acquisition of a single data set that captures the spatially resolved lifetimes at a given time is therefore assumed to be a single step in our protocol. More details can be found in the relevant literature (Clegg and Schneider, 1996; Gadella *et al.*, 1993; Squire and Bastiaens, 1999). An experiment involves the following steps.

1. Acquire a FLIM data set using the 457.9-nm line to excite the CFP donor.
2. Acquire an image of the YFP fluorescence using the 100-W mercury lamp and the YFP filter set.
3. Optionally, repeat steps 1 and 2 for several time points to require a time-lapse series.
4. Illuminate the acceptor extensively with the YFP filter set until the fluorescence from YFP is abolished completely.
5. Acquire a final FLIM data set to find the lifetime of the donor in the absence of acceptor.

C. Fluorescence Lifetime Imaging Microscopy Data Analysis

Analysis of fluorescence lifetime imaging microscopy data is an extended subject that is described

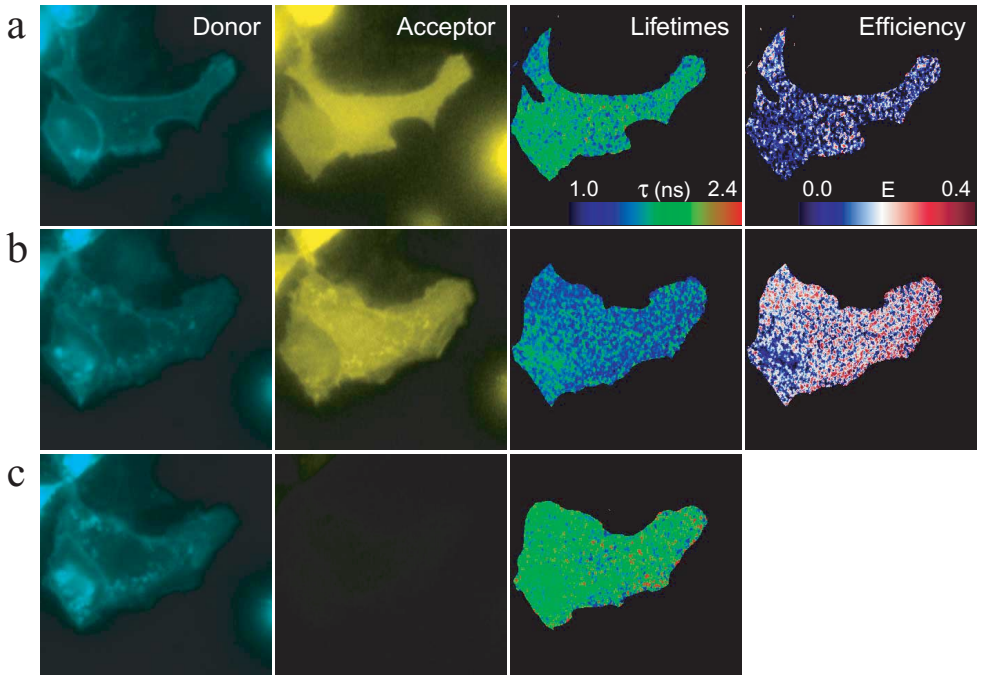

FIGURE 1 Fluorescence lifetime imaging microscopy of CFP-tagged epidermal growth factor receptor (EGFR-CFP) cotransfected with YFP-tagged phosphotyrosine-binding domain (PTB-YFP) stimulated with epidermal growth factor (EGF). Measurements are made before and after stimulation, and finally after photobleaching of the acceptor. The lifetime of the donor in the absence of FRET is calculated from the average lifetime after photobleaching and is used to calculate the energy transfer efficiencies for the other measurements as described in the text. From left to right: CFP fluorescence (donor), YFP fluorescence (acceptor), fluorescence lifetime, and apparent energy transfer efficiency. (a) Results before stimulation with EGF. (b) Results after stimulation with EGF for 18 min. (c) Results after destruction of the acceptor fluorophores by photobleaching. The average apparent lifetime of the donor after photobleaching of the acceptor was 1.9 ns.

elsewhere (Gadella *et al.*, 1994; Verveer *et al.*, 2001). We will therefore assume that the FLIM data analysis software is provided as a part of the instrumental setup and calculates a lifetime value at each pixel position from the measured FLIM data. The result found at a given pixel location is a weighted summation of the fluorescence lifetimes of the individual molecular components present, and if a significant proportion of those components have a short lifetime due to FRET, this is reflected in a decrease in the measured lifetime. This measured value should be compared to the lifetime of the donor fluorophore in the absence of FRET, which can be found from the sample itself by photobleaching the acceptor. Given the measured lifetime at each pixel $\tau_{DA}(i)$, and the donor lifetime τ_D, an apparent energy transfer efficiency can be calculated in each pixel:

$$E(i) = 1 - \frac{\tau_{DA}(i)}{\tau_D}.$$

The analysis consist of the following steps.

1. Calculated the fluorescence lifetime image for the FLIM data set that was obtained after acceptor photobleaching. Calculate the average value to obtain the lifetime of the donor τ_D in the absence of acceptor.
2. Calculate the fluorescent lifetime images for all the other measured FLIM data sets.
3. Divide each pixel of the fluorescent lifetime images by τ_D.
4. Multiply the resulting pixel values by –1 and add 1 to obtain $E(i)$.

D. Sensitized Emission Measurements

Sensitized emission measurements are well suited for cases where donor and acceptor are expressed at similar levels. Detecting FRET by sensitized emission requires correction for fluorescence bleed through and unmixing of direct and sensitized acceptor emission (Gordon *et al.*, 1998; Nagy *et al.*, 1998). For illustration purposes we will assume the use of a Leica SP2 micro-

scope, but the discussion generalizes to any microscope equipped with the proper excitation and emission filters. Figure 2 shows an example where FRET between EGFR-CFP and PTB-YFP was measured using sensitized emission before and after stimulation with EGF. This article limits itself to donor and acceptor pairs with the following spectral properties: (1) upon donor excitation the donor fluorescence can be detected specifically; and (2) the acceptor can be excited specifically (i.e., no donor fluorescence upon acceptor excitation). The CFP-YFP FRET pair that we use in this article meets these requirements. The CFP was excited at 457.9 nm, which yields also significant direct excitation of YFP, and the YFP was excited specifically at 514 nm. The Leica SP2 microscope allows flexible settings for measurements of the emission with up to four detectors simultaneously. We simultaneously detected fluorescence at 460–495 nm (CFP channel) and at 520–570 nm (YFP channel). In the CFP channel, no significant YFP emission is detected, but in the YFP channel, a significant contribution of CFP fluorescence is present upon excitation of CFP. Measurement of the CFP channel upon CFP excitation allows for estimation of the amount of bleed through if it is known how much CFP emission is detected in the YFP channel. This can be calibrated by excitation of CFP in a reference sample transfected with CFP-tagged protein only. Dividing the total signal in the YFP channel by the total signal in the CFP channel gives the scalar bleed-through correction factor. To calculate the bleed-through image in a sample with both CFP and YFP, each pixel in the image from the CFP channel is multiplied with the scalar bleed-through correction factor obtained from a reference sample. In a similar fashion, the amount of direct excitation is calibrated from a reference sample that expresses only the YFP-tagged protein. The total signal detected in the YFP signal upon CFP excitation is divided by the total

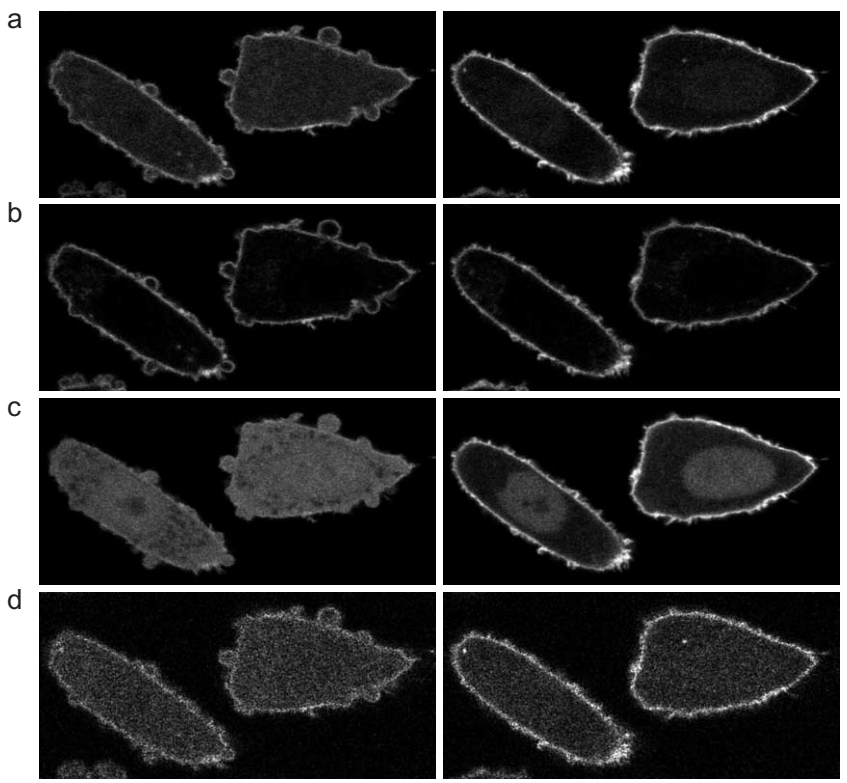

FIGURE 2 Sensitized emission measurement of FRET between CFP-tagged epidermal growth factor receptor (EGFR-CFP) cotransfected with YFP-tagged phosphotyrosine-binding domain (PTB-YFP) stimulated with epidermal growth factor (EGF). Measurements were made before stimulation and after 90 s of stimulation with EGF. Different images and the calculated result before (left) after (right) stimulation. (a) Images measured in the acceptor channel upon excitation of the donor. (b) Images measured in the donor channel upon donor excitation. (c) Images measured in the acceptor channel upon acceptor excitation. (d) Sensitized emission calculated by subtracting the images in b and c from the images in a after scaling with the appropriate scalar correction factors for bleed through and direct excitation.

signal upon YFP excitation to obtain the scalar direct excitation correction factor. To calculate the direct excitation image in a sample with both CFP and YFP, each pixel in the image measured in the YFP channel upon specific YFP excitation is multiplied with the scalar direct excitation correction factor. An image of the sensitized emission is then calculated by pixel-wise subtraction of the bleed-through and direct excitation images from the image that is measured in the YFP channel upon excitation of CFP.

The reference measurements should be taken at the same instrumental settings (detector gains and offsets, illumination power) as used for the sensitized emission measurements itself. Results of the reference measurements for a given setting should be reproducible and it is advisable to check this by repeating the reference measurement procedure a few times. Reference measurements are done using the following steps.

1. A sample with only donor molecules is used to calibrate the contribution of bleed through.
   a. Excite the donor and acquire an image of the donor channel, yielding image $D_{DD}(i)$, where i is the pixel index.
   b. Excite the donor and acquire an image of the acceptor channel, yielding image $D_{DA}(i)$.

Care should be taken that the sample is not moved between acquisitions. In live cells the images should be taken in quick succession to avoid artifacts due to relocation of the donor-tagged protein or movement or deformation of the cell. In some instruments (e.g., the Leica SP2 used by us) it is possible to acquire the two images simultaneously, which is preferable.

2. The contributions of direct excitation are calibrated using a sample that has only acceptor molecules.
   a. Excite the donor and acquire an image of the acceptor channel, yielding image $A_{DA}(i)$.
   b. Excite the acceptor and acquire an image of the acceptor channel, yielding image $A_{AA}(i)$.

These images must be taken separately, but the same concerns about sample movement, as described in point 1, are valid. The Leica SP2 microscope allows switching between donor and acceptor excitation sources on a line-by-line basis or on a frame-by-frame basis. The former is preferable, as less movement will occur between acquisitions of successive lines than between acquisitions of successive images.

For sensitized emission measurements with samples that have both donor and acceptor molecules, the following steps are taken.

1. Excite the donor and acquire an image of the donor, yielding image $F_{DD}(i)$.
2. Excite the donor and acquire an image of the acceptor, yielding image $F_{DA}(i)$.
3. Excite the acceptor and acquire an image of the acceptor channel, yielding image $F_{AA}(i)$.

Again, care should be taken that the sample is not moved between image acquisition or that significant relocation of the proteins of interest or the cell as a whole takes place. Using a Leica SP2 microscope, steps 1 and 2 can be done simultaneously and switching between illumination sources should be done on a line-by-line basis.

When possible, the detector used should have a high dynamic range for all measurements. For instance, modern confocal microscopes allow recording data with 12-bit precision.

E. Sensitized Emission Data Analysis

The data analysis steps for sensitized emission measurements are fairly simple and can be performed with many commercially available image processing packages. The following steps are used for calculating the sensitized emission image from the measured images.

1. Background correction, applied to all images:
   a. Select a small region of interest in the background of the image.
   b. Calculate the mean intensity with the region of interest to obtain the background value.
   c. Subtract the background value from each pixel the image.
2. Calculate the correction factor for the bleed through from the reference measurements by taking the ratio between the signal in the acceptor channel to the donor channel.
   a. Create a mask from the pixels with high signal within image $D_{DD}(i)$, by thresholding, or interactive selection. It is important to exclude saturated pixels from the mask, as the calculated result from such pixels will be incorrect.
   b. Calculate the sum of the pixel intensities in image $D_{DD}(i)$, within the mask:

$$sum(D_{DD}) = \sum_{i \in mask} D_{DD}(i).$$

   c. Calculate the sum of the pixel intensities in image $D_{DA}(i)$, within the mask:

$$sum(D_{DA}) = \sum_{i \in mask} D_{Da}(i).$$

   d. Calculate the scalar bleed-through correction factor

$$C_{\text{bleed-through}} = \frac{sum(D_{DA})}{sum(D_{DD})}.$$

3. Calculate the correction factor for direct excitation from the reference measurements by taking the ratio of the signals in the acceptor channel upon excitation of the donor and acceptor, respectively.

a. Create a mask from the pixels with high signal within image $A_{AA}(i)$ by thresholding or interactive selection. Exclude saturated pixels.

b. Calculate the sum of the pixel intensities in image $A_{DA}(i)$, within the mask:

$$sum(A_{DA}) = \sum_{i \in mask} A_{DA}(i).$$

c. Calculate the sum of the pixel intensities in image $A_{AA}(i)$ within the mask:

$$sum(A_{AA}) = \sum_{i \in mask} A_{AA}(i).$$

d. Calculate the scalar direct excitation correction factor:

$$C_{\text{direct-excitation}} = \frac{sum(A_{DA})}{sum(A_{AA})}.$$

4. Calculate the bleed-through correction in each pixel by multiplying the image in the donor channel upon donor excitation with the correction factor obtained in step 2:

$$BT(i) = C_{\text{bleed-through}} \cdot F_{DD}(i)$$

5. Calculate the correction for direct excitation of the acceptor in each pixel by multiplying the image in the acceptor channel upon acceptor excitation with the correction factor obtained in step 3:

$$DE(i) = C_{\text{direct-excitation}} \cdot F_{AA}(i)$$

6. Calculate the sensitized emission image by subtracting the corrections for bleed-through and direct excitation calculated in steps 4 and 5 from the image that was measured in the acceptor channel upon donor excitation:

$$S(i) = F_{DA}(i) - BT(i) - DE(i).$$

This image represents the fluorescent light due to energy transfer that is directly proportional to the concentration of donor–acceptor complexes.

7. *Optional*: Calculate an apparent energy transfer efficiency using

$$E_A = \frac{S(i)}{F_{AA}(i)}.$$

This equation normalize the sensitized emission with the emission of the acceptor only, and therefore the result is proportional to the fraction of interacting molecules with respect to the total amount of acceptor-tagged molecules (Wouters *et al.*, 2001). It is also possible to normalize the sensitized emission with the donor fluorescence; however, because the donor emission is quenched by FRET, this is *not* proportional to the relative fraction of donor-tagged molecules that is in an interacting pair.

References

Bastiaens, P. I. H., and Jovin, T. M. (1998). Fluorescence resonance energy transfer microscopy. *In "Cell Biology: A Laboratory Handbook"* (J. E. Celis, ed.), pp. 136–146. Academic Press, New York.

Bastiaens, P. I. H., and Squire, A. (1999). Fluorescence lifetime imaging microscopy: Spatial resolution of biochemical processes in the cell. *Trends Cell Biol.* **9**, 48–52.

Clegg, R. M. (1996). Fluorescence resonance energy transfer. *In "Fluorescence Imaging Spectroscopy and Microscopy"* (X. F. Wang and B. Herman, eds.), pp. 179–252. Wiley, New York.

Clegg, R. M., and Schneider, P. C. (1996). Fluorescence time-resolved imaging microscopy: A general description of lifetime-resolved imaging measurements. *In "Fluorescence Microscopy and Fluorescence Probes"* (J. Slavik, ed.), pp. 15–33. Plenum Press, New York.

Gadella, T. W. J., Jr., Clegg, R. M., and Jovin, T. M. (1994). Fluorescence lifetime imaging microscopy: Pixel-by-pixel analysis of phase-modulation data. *Bioimaging* **2**, 139–159.

Gadella, T. W. J., Jr., Jovin, T. M., and Clegg, R. M. (1993). Fluorescence lifetime imaging microscopy (FLIM). Spatial resolution of microstructures on the nanosecond time-scale. *Biophys. Chem.* **48**, 221–239.

Gordon, G. W., Berry, G., Liang, X. H., Levine, B., and Herman, B. (1998). Quantitative fluorescence energy transfer measurements using fluorescence microscopy. *Biophys. J.* **74**, 2702–2713.

Griesbeck, O., Baird, G. S., Campbell, R. E., Zacharias, D. A., and Tsien, R. Y. (2001). Reducing the environmental sensitivity of yellow fluorescent protein: Mechanism and applications. *J. Biol. Chem.* **276**, 29188–29194.

Heim, R., and Tsien, R. Y. (1996). Engineering green fluorescent protein for improved brightness, longer wavelengths and fluorescence resonance energy transfer. *Curr. Biol.* **6**, 178–182.

Matz, M. V., Fradkov, A. F., Labas, Y. A., Savitsky, A. P., Zaraisky, A. G., Markelov, M. L., and Lukyanov, S. A. (1999). Fluorescent proteins from nonbioluminescent Anthozoa species. *Nature Biotechnol.* **17**, 969–973.

Nagy, P., Vámosi, G., Bodnár, A., Locket, S. J., and Szöllösi, J. (1998). Intensity-based energy transfer measurements in digital imaging microscopy. *Eur. Biophys. J.* **27**, 377–389.

Sorkin, A., McClure, M., Huang, F., and Carter, R. (2000). Interaction of EGF receptor and Grb2 in living cells visualized by fluorescence resonance energy transfer (FRET) microscopy. *Curr. Biol.* **10**, 1395–1398.

Squire, A., and Bastiaens, P. I. H. (1999). Three dimensional image restoration in fluorescence lifetime imaging microscopy. *J. Microsc.* **193**, 36–49.

Tsien, R. Y. (1998). The green fluorescent protein. *Annu. Rev. Biochem.* **67**, 509–544.

Verveer, P. J., Squire, A., and Bastiaens, P. I. H. (2001). Frequency-domain fluorescence lifetime imaging microscopy: A window on the biochemical landscape of the cell. *In "Methods in Cellular Imaging"* (A. Periasamy, ed.), pp. 273–292. Oxford Univ. Press, Oxford.

Wouters, F. S., Verveer, P. J., and Bastiaens, P. I. H. (2001). Imaging biochemistry inside cells. *Trends Cell Biol.* **11**, 203–211.

Zhou, M. M., Harlan, J. E., Wade, J. S., Crosby, S., Ravichandran, K. S., Burakoff, S. J., and Fesik, S. W. (1996). Binding affinities of tyrosine-phosphorylated peptides to the COOH-terminal SH2 and NH2-terminal phosphotyrosine binding domains of Shc. *J. Biol. Chem.* **271**, 31119–31123.

SECTION

5

Use of Fluorescent Dyes for Studies of Intracellular Physiological Parameters

CHAPTER

16

Measurements of Endosomal pH in Live Cells by Dual-Excitation Fluorescence Imaging

Nicolas Demaurex and Sergio Grinstein

I. INTRODUCTION

The pH of endosomes can be measured with minimal interference to cellular function using internalized ligands or antibodies labeled with pH-sensitive fluorescent probes. Following internalization of receptor-bound or fluid phase probes, a rapid acidification can be detected along the endosomal pathway, with the pH decreasing within minutes by nearly one pH unit (Fig. 1). Cargo can then recycle back to the plasma membrane, reach the Trans-Golgi-Network (TGN) (pH~6.0), or be targeted for degradation through late endosomes (pH < 6.0) and lysosomes (pH < 5.5). Determination of the vesicular pH thus allows one to establish whether, at a specific time point, the cargo resides within a sorting, recycling, or degradation compartment (Demaurex, 2002). Repeating such pH measurements at different times during the internalization provides a functional readout of the pathway followed by internalized compounds.

The most convenient indicator for such measurements is Fluorescein Isothiocyanate (FITC), and numerous specific antibodies and ligands labeled with FITC are readily available. Covalent labeling of specific proteins or antibodies with FITC is relatively easy to perform, at low cost (Grinstein and Furuya, 1988). From a measurement standpoint, the most important feature is that the bright fluorescence of FITC is strongly pH dependent at its peak excitation wavelength of λ_{ex} = 490 nm, but is almost completely pH insensitive at λ_{ex} = 440 nm, thus allowing dual-excitation ratio fluorescence imaging. The ratio λ_{ex} = 490/λ_{ex} = 440 normalizes the measurements for the amount of fluorophore, as well as for differences in refractive index and changes in focus, and truly represents pH. The fluorescence ratio can be calibrated *in situ* by equilibrating the pH of the vesicle with the extracellular pH using nigericin, a K^+/H^+ ionophore, and monensin, a Na^+/H^+ ionophore (for details, see Thomas *et al*. (1979)). Using a standard fluorescence microscopy apparatus, such as the one described in Fig. 2 and the protocol and image analysis techniques described here, the pH of endocytic compartments can be measured simply by incubating cells with FITC-labeled ligands or antibodies (Demaurex *et al*., 1998; Gagescu *et al*., 2000; Piguet *et al*., 1999, 2000).

II. MATERIALS AND INSTRUMENTATION

MES, HEPES, and RPMI 1640 medium (bicarbonate free) are obtained from Sigma. Ionophores (sodium salts) are from Fluka (nigericin, Cat. No. 72445; monensin Cat. No. 69864).

The open perfusion microincubator, Leiden coverslip holder, and temperature controller are from Harvard Apparatus (refs. PDMI-2 and TC-202A). Glass coverslips are "Assistent" circular cover glasses No. 1001, Ø 25 mm, thickness 0.16 mm from Karl Hecht Glaswarenfabrik, D-97647 Sondheim/Rhön, Germany.

Copyright 2006, Elsevier Science (USA).
All rights reserved.

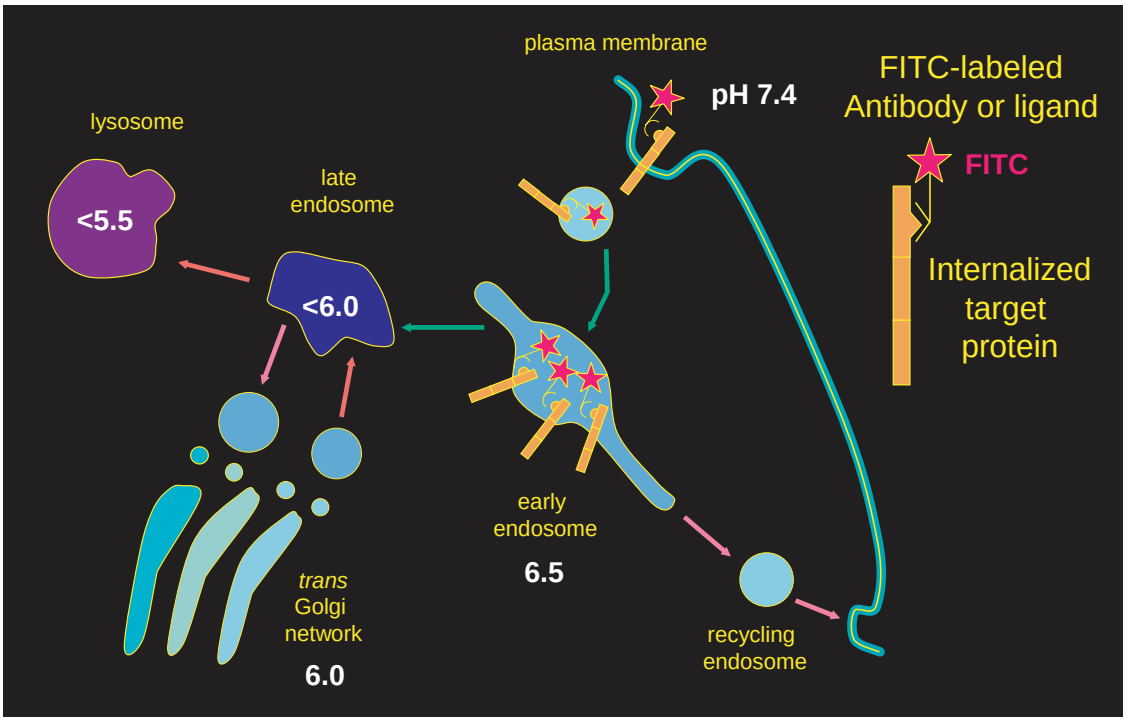

FIGURE 1 **Measuring the pH of endocytic organelles with internalized FITC.** Organelles acidify rapidly as they progress along the endocytic pathway. The pH of endocytic compartments can be measured simply by allowing cells to internalize FITC-labeled antibodies or ligands (red stars). The fluorescence of the FITC-labeled compartments is then imaged at the pH-dependent (λ_{ex} = 490 nm) and pH-independent (λ_{ex} = 440 nm) FITC excitation wavelength to determine the pH of the organelle.

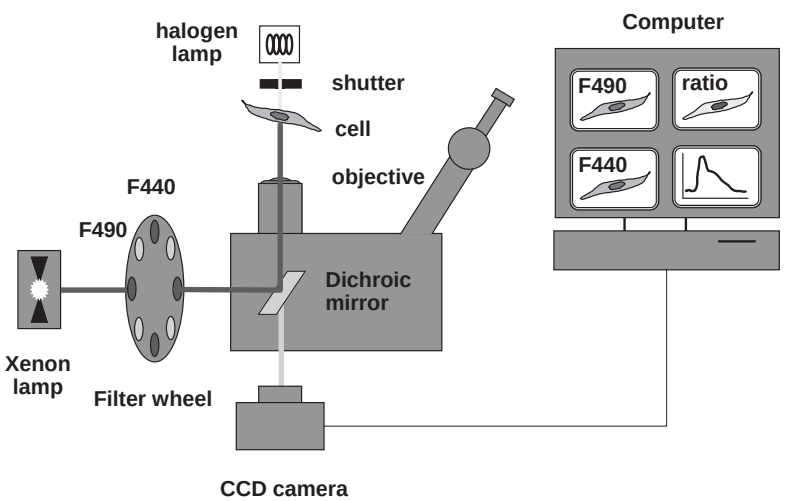

FIGURE 2 **Optical and hardware components used for endosomal pH measurements.** The key components are (1) an objective with high (1.4) numerical aperture (2) high-quality filters and dichroic mirrors, and (3) a fast, low-noise, highly sensitive CCD camera. The camera is attached at the bottom port of the microscope to maximize light collection. High-quality optics and a sensitive camera are required to capture the faint fluorescence of small moving endosomes with sufficient signal to noise.

The setup for ratio fluorescence imaging is illustrated in Fig. 1. We use a Axiovert S100TV microscope and a 100X, 1.3 NA oil-immersion objective (Carl Zeiss AG, Feldbach, Switzerland). Alternate excitation at 440 ± 10 and 490 ± 10 nm is achieved using a fast monochromator (Deltaram, Photon Technology International Inc., Monmouth Junction, NJ) or a filter wheel equipped with excitation filters 440DF20 (Cat. No. XF1010) and 490DF20 (Cat. No. XF1011, both from Omega Optical, Brattleboro, VT). The light path comprises a 515DRLPXR dichroic mirror (Cat. No. XF 2058) and 535DF25 emission filter (Cat. No. XF3001) inserted into the microscope filter slider. Images are captured with a back-illuminated CCD frame transfer camera (MicroMax 512 BFT; Roper Scientific; Trenton, NJ) attached to the bottom port of the microscope.

III. PROCEDURES

A. Preparation

Solutions

1. *Recording solution:* 140 m*M* NaCl, 5 m*M* KCl, 1 m*M* $MgCl_2$, 1 m*M* $CaCl_2$, 10 m*M* glucose, 20 m*M* HEPES, pH 7.4, with NaOH. To make 100 ml, add 14 ml NaCl 1 *M*, 0.5 ml KCl 1 *M*, 0.1 ml $MgCl_2$ 1 *M*, 0.1 ml $CaCl_2$ 1 *M*, 0.5 ml 40% glucose, 2 ml HEPES 1 *M*, and complete to 100 ml with distilled water.

2. *Calibration solution:* 140 m*M* KCl, 1 m*M* $MgCl_2$, 0.2 m*M* EGTA, 20 m*M* HEPES (pH 7.0–8.0) or MES (pH 5.5–6.5), 5 µg/ml nigericin, 5 µ*M* monensin. To make 50 ml of each, add 28 ml KCl 1 *M*, 4 ml MES 1 *M*, 200 µl $MgCl_2$ 1 *M*, 200 µl EGTA 0.4 *M*, and complete to 200 ml with distilled water. Divide in 50-ml aliquots labeled "5.5," "6.0," and "6.5." Repeat the same procedure using HEPES instead of MES as buffer and divide in 50-ml aliquots labeled "7.0," "7.5," and "8.0." Adjust the pH to 5.5, 6.0, 6.5, 7.0, 7.5, and 8.0 with KOH or HCl using a pH electrode precalibrated at 37°C under continuous magnetic stirring. These solutions can be kept at 4°C for 1–2 weeks. On the day of the experiment, take 10 ml of each calibration solution and add 10 µl nigericin (stock 5 mg/ml) and 1 µl monensin (stock 50 m*M*) to each vial. Measure the pH precisely with the pH electrode (at 37°C) and write down the pH value to two decimals (e.g., pH 5.54; 5.92; 6.02; 6.54; 7.04). These solutions must be used the same day.

3. *Nigericin stock:* Add 1 ml ethanol 100% to 5 mg nigericin and store at –20°C for no more than 3 months.

4. *Monensin stock:* Add 1.44 ml ethanol 100% to 50 mg monensin and store at –20°C for no more than 3 months.

Steps

1. In a hood, wash the coverslips separately with ethanol and rinse with distilled water. Place coverslips into a tank filled with distilled water. Autoclave. Clean coverslips can be stored in sterile water for 1–2 months.

2. If necessary, coat the coverslips with an agent that promotes attachment of weakly adherent cells. Poly-L-lysine and Cell Tak (collaborative Research Inc) have been used extensively. Wash excess adhesive agent.

3. Place each coverslip into a 35-mm petri culture dish (single or multiwell). Close the lid and leave for 20 min under UV illumination. The culture dishes "loaded" with clean coverslips can be used for 1–2 weeks.

4. Two to 3 days prior to the measurements, plate cells on the glass coverslip at low density (~10^4 cells). Fill the petri dish with 3 ml of culture medium.

5. *Optional*: One to 2 days before measurements, transfect cells with the receptor or recombinant protein bearing the cognate epitope for the FITC-labeled ligand or antibody.

B. Loading Cells with the FITC-Labeled Ligand or Antibody

The example given here is for endosomal pH measurements with internalized FITC-transferrin. Optimal concentrations, requirement for serum depletion, and incubation times have to be determined for each particular ligand or antibody.

Steps

1. Incubate cells in their appropriate culture medium with 25 µg/ml of FITC-labeled ligand for 20 min at 37°C.

2. Wash the cells twice with phosphate-buffered saline (PBS) to remove extracellular FITC. Maintain cells in recording medium until use. Measurements should be performed within 30 min of loading.

3. If necessary, wash the cells twice with acidic solution (pH 4.0) at 4°C to remove FITC bound to the plasma membrane.

4. Using fine tweezers, place the coverslip into the Leiden chamber, orienting the coverslip so that cells face upward. Ensure that a good seal exists between the coverslip and the O ring by wiping away excess medium from the underside of the coverslip and

checking for leaks. The underside should remain dry and clean to allow oil-immersion microscopy.

5. Add 2 ml of recording solution to the dish and proceed to the experiment.

C. Measurements of FITC Fluorescence Ratio

1. Place a drop of oil on the immersion objective and position the loaded Leiden dish in an open perfusion microincubator over the objective.

2. Turn off room lights or use a dark curtain around the microscope to eliminate stray light from entering the optical system. Red light can be used for dim illumination of the room if a red-blocking filter (550CFSP-Omega Optical) is mounted in front of the camera.

3. Turn on the lamp power supply and then start the arc lamp. It is important to start the lamp before turning the computer on to eliminate possible damage due to power surges.

4. Turn on the computer and other external hardware devices. Verify that the temperature controller of the microincubator is set to the appropriate value (e.g., 37°C).

5. Launch the software designed for time-lapse ratio fluorescence measurements and initiate a new experiment. We use Metafluor 5.0 from Universal Imaging Corp. Using the illumination control panel, install the correct hardware drivers for the external devices, and configure them with the appropriate settings. Through the use of "Metadevices," Metafluor allows the user to create a variety of hardware configurations with different names.

6. In the "configure acquisition" window set the experiment-specific parameters such as exposure time, pixel binning, and Metadevice selection for each wavelength. Typical exposure times range from 0.5 to 1 s and should not exceed 2 s (see Section V). Keep in mind that wavelength 1 is always the numerator of ratio 1. After configuring these settings, save them as a protocol file that can be retrieved for subsequent use.

7. In the "configure experiment" menu, choose the wavelengths to acquire (W1 and W2) and ratio to be calculated (W1 over W2). Make sure that the acquired images and calculated ratio are displayed and updated continuously.

8. Observe the sample using transmission light to bring the cells in focus and then switch to fluorescence illumination to select cells that express the internalized probe correctly. Open the camera port and acquire a set of images. If necessary, reset the "configure acquisition" parameters to optimize the exposure times.

9. In the "reference image" menu, acquire a set of images with the illumination shutter closed to subtract the background noise of the camera. Then reopen the shutter and acquire updated images with background subtraction.

10. Use the "region" tool to define regions of interest around individual cells. For each region, spatially averaged fluorescence and ratio data will be graphed only for pixels with absolute values higher than the preset threshold. Once the regions are defined, return to the image windows and set the threshold levels to separate the labeled structures from the background fluorescence.

11. From the "experiment control panel," select "save image" to save the fluorescence images. Always save the original fluorescence images during acquisition, not the calculated ratios.

12. Open the "event mark" window to define and reuse markers associated with a specific experiment. Markers applied during drug addition and calibration facilitate the analysis of the experiment during playback.

13. Acquire a series of fluorescence images from several individual cells (~50) to obtain the steady-state ratio value of the labeled organelle. Do not perform more than two to three image acquisitions per field to avoid bleaching of FITC. Check on the ratio graph that the spatially averaged ratio values are homogeneous between cells.

D. Calibration of pH vs Fluorescence

1. At the end of the acquisition period, select one representative field and perfuse the dish sequentially with the calibration solutions. Monitor the fluorescence to ensure establishment of a stable ratio, indicating equilibration of the vesicular pH with the external pH.

2. Once a steady-state ratio has been collected, change to the next solution and repeat step 1. Continue until fluorescence ratios have been recorded for all the calibration solutions.

3. Using the Metamorph software, create a titration calibration table to convert fluorescence ratio values to pH. The calibration table can be used to plot real-time pH change and to create a pH "map" of the labeled structures.

E. Image Analysis: Determining the pH of Individual Endosomes

Preparation

Using Metamorph, create the following analysis "Journals," "table," and "state file":

1. Journal "Initialize Ratio.jnl"

Line	Function	Value	Description
1	Load gray calibration table	File: 256.GRY	Load predefined calibration table
2	Apply gray calibration table		Rescale the 8-bit ratio image from 256 digits into ratio units
3	Threshold image	Image: current at start Threshold: 1; 255; inclusive	Select labeled structures on the ratio image
4	Integrated morphometry-load state	File: Ratio.IMA	Load predefined object selection and measurement criteria

2. Calibration Table "256.GRY"

Image depth: 8 bit; gray vs calibration values: 0 → 0.5; 256 → 3.5; interpolation: linear

3. State file "Ratio.IMA"

Setup parameters for classifying: *Enable*: pixel area: 10 <= N <= 500; hole area: 0 <= N <= 0

Setup parameters for measuring: *Enable*: area; average gray value; format: #.###

Configure log: *Enable*: image name; image plane; object #; average gray value; area

Preferences: Measure objects: *Disable*: "warn user when measurements data will be erased"

4. Journal "Measure ratio.Jnl"

Line	Function	Value	Description
1	Integrated morphometry-measure	Image: current at start Plane: current	Measure all thresholded objects meeting criteria on current plane
2	Integrated morphometry-log data	Image: current at start	Log measurement data to spreadsheet

Steps

1. Using the MetaFluor program, open a previous experiment and create a series of ratio images. In the "Image display controls," check that the minimal and maximal ratio values are set to 0.5 and 3.5, respectively. Adjust the threshold on the 440-nm image (W2) to separate the fluorescent vesicles from the background. If possible, the same threshold should be used for all images. From the "experiment control panel," select "save ratios" to save the ratio images as 8-bit TIF images. Make sure to save only one ratio image for each field acquired during the steady-state measurement period.

2. Launch the MetaMorph program. In the "File" menu, use the function "Build stack: numbered name" to load a stack of ratio image from the desired experiment. Use the "Stack: Montage" function to create and print an image gallery. Check for duplicates.

3. In the "Journal" menu, use the function "Run" with journal "Initialize Ratio.jnl" to rescale the 8-bit ratio image and load the object selection and measurement criteria. *Tip*: Journal playback can be simplified by defining journals as button on the "Journal Taskbar."

4. In the "Log" menu, use the function "Open object log" to create the connection with the spreadsheet program (e.g., Microsoft Excel).

5. In the "Journal" menu, use the function "Loop for all planes," with journal "Measure ratio.Jnl." This will extract the average ratio value of all objects that meet the criteria (area size between 10 and 500 pixels, devoid of holes) in every image from the ratio stack. Check the quality of the segmentation by comparing the measurement images with the original fluorescence images. Most individual vesicles should be included as well as aggregates of <10 vesicles. Spots and very large compound structures should not be included (Fig. 3).

6. Switch to the spreadsheet program. Check the quality of the measurements by displaying ratio data as a histogram. The distribution should be gaussian if the population of vesicles has a homogeneous pH.

7. Using the spreadsheet program, create a calibration curve for the experiment. Enter the ratio values measured during the calibration procedure as X column and the pH values of the calibration solutions (measured at two decimals) as Y column. Display the resulting points on a dot graph. Fit a linear equation to the points and copy the parameters. Use these values to apply a calibration equation to ratio data. A pH histogram can now be generated and the average pH values of the population of vesicles determined.

IV. COMMENTS

Even for experienced users, a few minutes are required to collect enough images of FITC-labeled cells to construct a pH histogram. Within the acquisition period, the pH of endosomes can change significantly, particularly during the early phases of endocytosis. For this reason, it is important to check that the pH is at steady state by graphing the ratio values during the

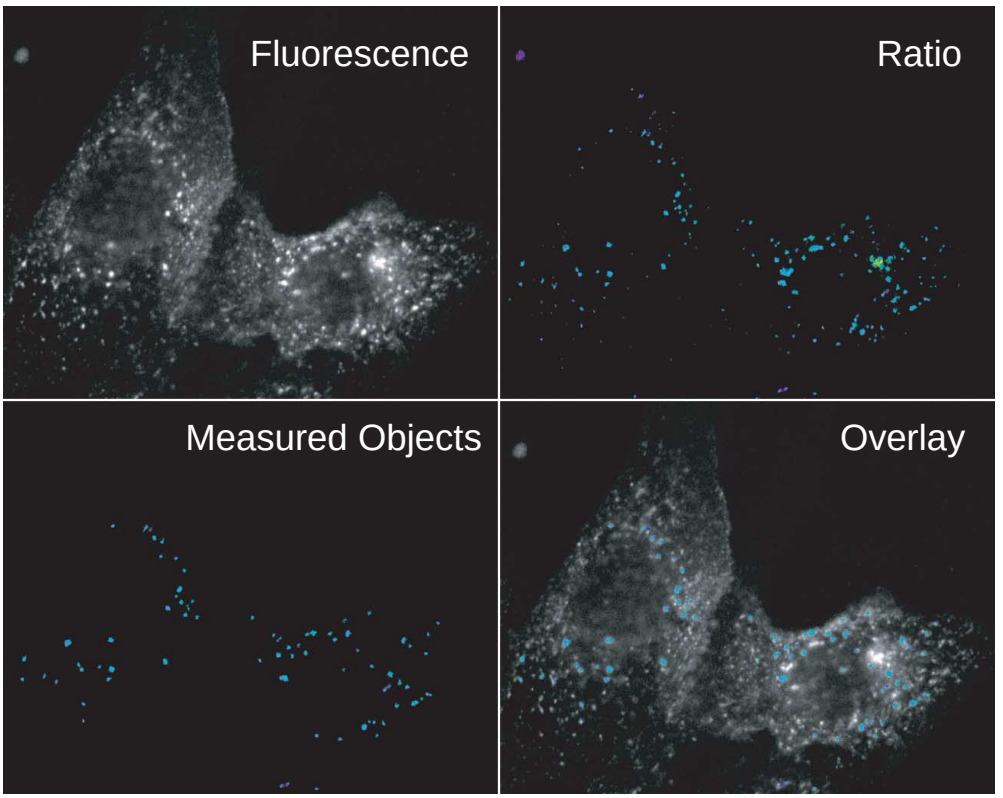

FIGURE 3 Fluorescence and ratio images of early endosomes in MDCK cells. MCDK cells were allowed to internalize FITC-labeled transferrin for 5 min at 37°C. (Top left) A 490-nm fluorescence image, exposure time 1 s. (Top right) A 490/440-nm ratio image. A low-intensity threshold of 30/4095 was used to separate fluorescent vesicles from background. (Bottom left) Vesicles recognized as individual endosomes by the image analysis routine. Seventy-three individual objects met selection criteria (pixel area 10–500, no holes). (Bottom right) Composite image of the vesicles selected by the image analysis routine and the original fluorescence image.

acquisition period. In any case, the acquisition period should be kept as short as possible and should not exceed 20 min.

When counting individual vesicles, small and large structures have the same "weight" in the pH histogram. This biases the readout toward the pH value of the smallest, most numerous vesicles. If the vesicles are highly heterogeneous in size, the pH values should be normalized to the vesicle area.

Failure to wash carefully extracellular FITC might result in a large contribution of the plasma membrane to the ratio images. These structures are normally excluded by the size criteria, but will otherwise appear as a second peak around pH 7.4 on the histogram.

V. PITFALLS

1. Do not use exposure times longer than 2 s to avoid distortions caused by the movement of endosomes. The division of two fluorescence images acquired sequentially will invariably produce "hot" or "cool" pixels on the ratio images, mainly at the organelle edges. Most irrelevant pixels are removed by the intensity threshold, but this procedure discards many small moving vesicles, resulting in a significant loss of information. Using short exposures is the best way to capture the rapidly moving endosomes and to avoid such distortions. The gain in resolution allows to better quantify the ratio images so that a fast, sensitive camera is highly desirable to obtain accurate pH data.

2. Use minimal illumination to prevent photobleaching and cellular damage. Do not make repeated measurements of the same field, but instead perform separate measurements on different fields. The best procedure is to select the cells at random, using bright-field illumination. If only a few cells are labeled with the FITC ligand, the labeled cells should be selected using 440-nm illumination to avoid selection bias induced by the pH dependency of FITC—a bright 490-

nm fluorescence reflecting not only a successful labeling, but also an elevated pH.

References

Demaurex, N. (2002). pH Homeostasis of cellular organelles. *News Physiol Sci*. **17**, 1–5.

Demaurex, N., Furuya, W., D'Souza, S., Bonifacino, J. S., and Grinstein, S. (1998). Mechanism of acidification of the trans-Golgi network (TGN): In situ measurements of pH using retrieval of TGN38 and furin from the cell surface. *J. Biol. Chem*. **273**(4), 2044–2051.

Gagescu, R., Demaurex, N., Parton, R. G., Hunziker, W., Huber, L. A., and Gruenberg, J. (2000). The recycling endosome of Madin–Darby canine kidney cells is a mildly acidic compartment rich in raft components. *Mol. Biol. Cell*. **11**(8), 2775–2791.

Grinstein, S., and Furuya, W. (1988). Assessment of Na+-H+ exchange activity in phagosomal membranes of human neutrophils. *Am. J. Physiol*. **254**(2 Pt 1), C272–C285.

Piguet, V., Gu, F., Foti, M., Demaurex, N., Gruenberg, J., Carpentier, J. L., and Trono, D. (1999). Nef-induced CD4 degradation: A diacidic-based motif in Nef functions as a lysosomal targeting signal through the binding of beta-COP in endosomes. *Cell* **97**(1), 63–73.

Piguet, V., Wan, L., Borel, C., Mangasarian, A., Demaurex, N., Thomas, G., and Trono, D. (2000). HIV-1 Nef protein binds to the cellular protein PACS-1 to downregulate class I major histocompatibility complexes. *Nature Cell Biol*. **2**(3), 163–167.

Thomas, J. A., Buchsbaum, R. N., Zimniak, A., and Racker, E. (1979). Intracellular pH measurements in Ehrlich ascites tumor cells utilizing spectroscopic probes generated in situ. *Biochemistry* **18**(11), 2210–2218.

CHAPTER

17

Genome-Wide Screening of Intracellular Protein Localization in Fission Yeast

Da-Qiao Ding and Yasushi Hiraoka

I. INTRODUCTION

Intracellular localization is an important part of the characterization of a gene product. In order to search for genes based on the intracellular localization of their products, we constructed a green fluorescent protein (GFP)–fusion genomic DNA library of the fission yeast *Schizosaccharomyces pombe* (Ding *et al*., 2000). This was accomplished by fusing random fragments of genomic DNA to the 5′ end of the GFP gene in such a way that the expression of potential GFP–fusion proteins would be under the control of the endogenous promoters contained in the genomic DNA fragments. The intracellular localization of the fusion proteins was determined by microscopic observation of individual transformants. As genes fused to GFP are expressed under their native promoters, the intracellular localization of gene products can be examined under physiological conditions in both mitotic and meiotic cells. This library provided the foundation for a survey of the intracellular localization of *S. pombe* proteins. Now that the *S. pombe* genome project is completed, genes can be searched from the intracellular locations of their protein products using our image database. Our library of GFP–fusion constructs also provides useful fluorescent markers, which can be used readily for microscopic observation in living cells and for various intracellular structures and cellular activities.

II. MATERIALS AND INSTRUMENTATION

Polypeptone is from Nihon Pharmaceutical (Cat. No. 394-00115), yeast extract is from Difco (Cat. No. 212750), agar is from Wako (Cat. No. 010-15815), ampicillin is from Wako (Cat. No. 016-10373/TWK6416), glucose is from Wako (Cat. No. 041-00595), Zymolyase-100T is from Seikagaku (Cat. No. 120493/109406), novozym 234 is from Novo Nordisk (Cat. No. 2880/PPM4356), proteinase K is from Merck (Cat. No. 24658-0100/V354968 92), and T4 DNA ligase is from TaKaRa (Cat. No. 2011A/1511). Water used for the preparation of the culture medium and all of the solutions is first treated using the Elix 5 water purification system (Millipore) and then the MilliQ ultrapure water purification system (Millipore).

Ten-well 25 × 75-mm glass slides are from Polyscience (Cat. No. 18357), and glass-bottom culture dishes are from MatTek (Cat. No. P35G-1.5-10-C). The DNA sequencer used is the ABI377 from Perkin-Elmer. A computer-controlled, fluorescence microscope system (DeltaVision, Applied Precision; Haraguchi *et al*., 1999) is used for visual screening of the GFP library. This microscope system is based on an inverted fluorescence microscope (IX70, Olympus Optical) equipped with a Peltier-cooled, charge-coupled device (CCD) (CH250 or CH350, Photometrics Ltd., Tucson,

Copyright 2006, Elsevier Science (USA).
All rights reserved.

AZ). The objective lens used is an Olympus oil immersion lens (SPlan Apo 60/NA 1.4).

III. PROCEDURES

A. Construction of the GFP–Fusion Genomic DNA Library

Figure 1 summarizes our strategy for the construction and screening of a gene library in which *S. pombe* genomic DNA fragments from a wild-type strain were fused to the 5′ end of the GFP–S65T gene.

1. Construction of Plasmid Vectors for the Library

The construction of one such library is described in detail in Ding *et al*. (2000). The multicopy plasmid used as a vector for our library was created by modification of a popular vector for fission yeast, pREP1 (Maundrell, 1993). In order to express GFP–fusion genes under the control of endogenous yeast promoters, the nmt1 promoter region in pREP1 was deleted; therefore, only genes in DNA fragments that also contained the genes' endogenous promoters would be expressed. Next, the coding sequence of GFP–S65T (Heim and Tsien, 1996) was amplified by polymerase chain reaction (PCR), and inserted upstream of the nmt1 terminator. Linker oligonucleotides were then designed such that all three reading frames of the restriction DNA fragments were fused to the GFP-coding sequence. Each of the resultant plasmids contained the *S. pombe* ars1 as a replication origin and the *S. cerevisiae* LEU2 gene as a selection marker, both of which were derived from the pREP1 plasmid (Fig. 1).

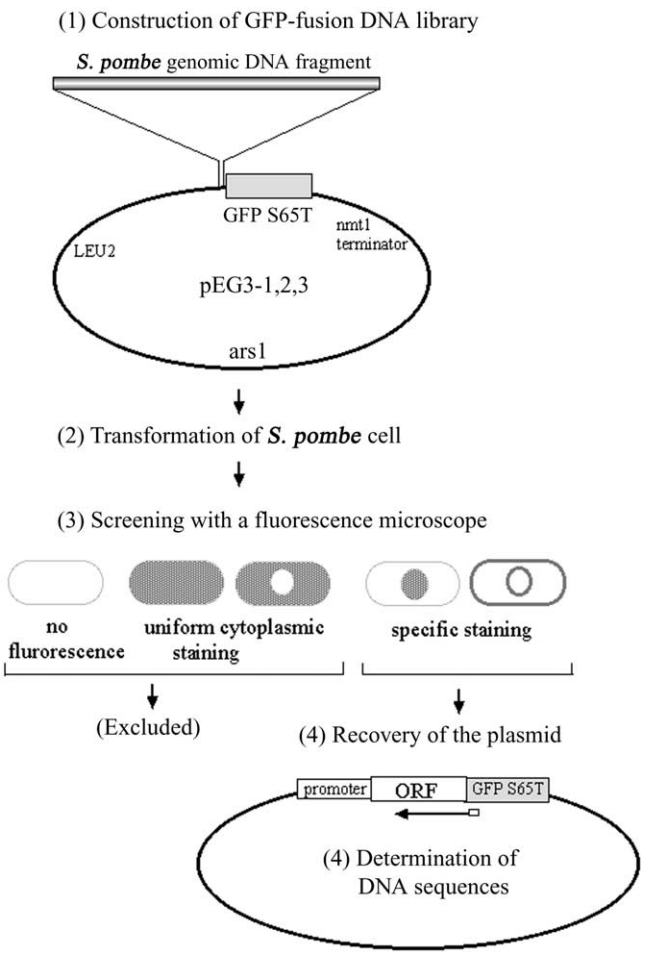

FIGURE 1 Strategy for construction and screening of the GFP–fusion genomic DNA library. Modified from Ding *et al*. (2000).

Insertion of the GFP PCR product into the nmt1 promoter deleted pREP1, resulting in pEG3-1. This plasmid has a *Bam*HI site immediately 5′ to GFP and was used as the first frame library plasmid. The second frame plasmid, pEG3-2, was constructed by inserting a 12 base (CCCAGATCTGGG) *Bgl*II linker into pEG3-1 that had been digested with *Bam*HI and blunt-ended. The third frame plasmid, pEG3-3, was constructed by inserting a 10 base (CCAGATCTGG) *Bgl*II linker into *Bam*HI digested, blunt-ended pEG3-1. Importantly, restriction enzyme sites that can be used for recloning of the yeast gene into other GFP–fusion vectors must be present. In our library, DNA restriction fragments were cloned into the *Bam*HI site of pEG3-1. In pEG3-2 and pEG3-3, however, the *Bam*HI site was absent, as the *Bgl*II linkers were blunt ended into this site. Therefore, the *Bam*HI site present in pEG3-1 was used to reclone genes from this plasmid, while *Bgl*II restriction sites were used to reclone genes present in pEG3-2 and pEG3-3.

Insertion of the library of DNA restriction fragments into each of the three plasmids, pEG3-1, pEG3-2, and pEG3-3, resulted in a library of random fragments of genomic DNA fused to the GFP-coding sequence. Microscopic observation was used to eliminate transformants that did not express GFP–fusion proteins (Fig. 1). These included transformants that did not express a GFP–fusion protein due to the absence of an endogenous promoter to drive the expression of the fusion gene or because the GFP-coding sequence was not in-frame with the fission yeast protein-coding sequence. Thus, after visual screening, a significant proportion of the library consisted of fission yeast genes fused in-frame with GFP and driven by their natural biological promoters.

An important point that needs to be taken into consideration in this type of library is that the linker oligonucleotides used to generate alternative GFP

reading frames introduce a spacer between GFP and the yeast gene, and this spacer may affect the localization of the GFP–fusion protein (see Section IV).

2. Preparation of Genomic DNA

The *S. pombe* strain 968 h^{90} was used to prepare genomic DNA. Genomic DNA was isolated according to Matsumoto *et al*. (1987), which involves two centrifugation steps for the isolation of nuclei to reduce mitochondrial DNA contamination.

Solutions

1. *YEade culture medium*: 0.5% yeast extract, 3% glucose, 75 µg/ml adenine sulfate dihydrate
2. *CPS buffer*: 50 m*M* citrate/phosphate, pH 5.6, 40 m*M* EDTA, 1 *M* sorbitol
3. *10 mM TE buffer*: 10 m*M* Tris–HCl, pH 7.5, 1 m*M* EDTA
4. *50 mM TE buffer*: 50 m*M* Tris–HCl, pH 7.5, 50 m*M* EDTA

Steps

1. Prepare a 200-ml liquid culture of *S. pombe* cells in a rich medium (YEade) and grow to midlog phase (1×10^7 cells/ml) with shaking at 33°C.
2. Harvest by centrifugation at 2500 rpm for 5 min.
3. Wash cells in 10 ml of 10 m*M* TE buffer. Centrifuge at 2500 rpm for 5 min.
4. Resuspend cells in CPS buffer at 3.4×10^8 cells/ml, add Zymolase-100T and Novozym to a final concentration of 0.2 mg/ml, and incubate at 36°C with gentle shaking for 30 min to digest the yeast cell walls.
5. Check digestion of cell walls using a phase-contrast microscope. Continue the digestion until 80% of the cells become round-shaped protoplasts.
6. Spin down at 2000 rpm for 5 min.
7. Wash with 5 ml CPS buffer and resuspend in 5 ml ice-cold 10 m*M* TE buffer containing 1% Triton X-100.
8. Spin down at 2000 rpm for 5 min at 0°C. Transfer the supernatant to a new tube and centrifuge at 10,000 rpm for 30 min at 4°C. Discard the supernatant and dry the pellet.
9. Resuspend the pellet in 5 ml of 50 m*M* TE buffer. Add 0.5 ml 10% SDS, 0.375 ml 4 *M* sodium chloride, and 0.5 mg protease K and incubate overnight at 50°C.
10. Add 5 ml of phenol/chloroform (1:1) and mix well. Spin down at 10,000 rpm for 10 min.
11. Transfer the upper aqueous phase to a new tube and repeat step 10.
12. Transfer the upper aqueous phase to a new tube and precipitate DNA with 2 volumes of ethanol. Wash the pellet with ice-cold 70% ethanol and dry under vacuum.
13. Finally, resuspend DNA in 0.1 ml of 10 mM TE buffer containing 100 µg/ml RNase A. The DNA can be quantified by running an aliquot on an agarose gel alongside a calibrated DNA sample. Typical yields are about 5–15 µg per a starting culture of 200 ml at midlog phase.

3. Partial Digestion of Genomic DNA

Genomic DNA is partially digested with a four-base cutter restriction enzyme, e.g., *Sau*3AI (Ding *et al*., 2000). A combination of several four- or six-base cutter restriction enzymes is also applicable (Sawin and Nurse, 1996). Considering the average size of fission yeast genes, including their promoters, 3- to 6-kb DNA fragments are appropriate. A suitable digestion time should be determined empirically in a small-scale pilot experiment. Centrifuge the partially digested DNA through a sucrose gradient (10–40%) at 50,000 rpm for 15 min using a RP-50T2 rotor in a Hitachi ultracentrifuge (Himac CP70G). Collect fractions and run aliquots out on an agarose gel. Pool the fractions that contain DNA fragments with the preferred length. Recover the DNA by ethanol precipitation.

4. Construction of Plasmid Libraries in Escherichia Coli

Digest each plasmid vector—when constructing our library, these were pEG3-1, pEG3-2, and pEG3-3—with an appropriate restriction enzyme and treat with alkaline phosphatase to inhibit self-ligation of the plasmid. Run small-scale pilot ligation experiments to find ligation conditions that minimize background transformants derived from self-ligation. In our large-scale experiments, 30 ng of the alkaline phosphatase-treated vector and 150 ng of DNA fragments were incubated with 350 units of T4 ligase in a total volume of 30 µl overnight at 16°C. Competent *E. coli* (DH5α) were transformed with 30 µl of each of the three plasmid DNA libraries and were plated on LB plates containing 50 µg/ml ampicillin at a dilution suitable for the appearance of isolated single colonies. This procedure yielded approximately 12,000 *E. coli* transformants for each library. Ampicillin-resistant colonies were scraped from plates with LB medium. A portion of this pool of cells (1/10 volume) was saved in small aliquots at –80°C as a frozen stock. DNA was prepared from the remaining cells. Small-scale preparations of DNA from 30 individual transformants showed that 76–85% of the plasmids had insert DNAs with an average length of 5 kbp.

B. Transformation of *S. pombe* Cells with the Library

Three sets of transformation were carried out using the libraries based on the three plasmid vectors, pEG3-1, pEG3-2, and pEG3-3. Homothalic *S. pombe* strains CRL126 (h^{90} leu1-32 ura4 his2) and CRL152 (h^{90} leu1-32 ura4 lys1) were used for transformation with the GFP–fusion genomic DNA libraries. Homothalic (h^{90}) strains can readily be induced to undergo meiosis and thus can be conveniently screened for mitotic and meiotic localization of fluorescently labeled proteins. A standard lithium chloride method (Moreno *et al.*, 1991) can be used for the transformation of fission yeast cells with the library DNA. Transformants were selected on plates of EMM2 (Edinburgh minimal medium; Moreno *et al.*, 1991) lacking leucine. In our experiments, 50 μg of one library transformed into 7×10^8 cells generated about 40,000 fission yeast transformants on 45 plates of EMM2 in 90-mm dishes.

C. Microscopic Screening of *S. pombe* Transformants

A total of about 50,000 transformants from the three libraries were selected for microscopic screening (Table I). Single colonies were picked with toothpicks and transferred onto new plates of EMM2. Cells were grown for 24 h at 33°C and then for 12 h at 26°C. Culture of the cells at 26°C enhances GFP fluorescence. Cells were then suspended in liquid EMM2 lacking a nitrogen source on a 10-well glass slide (Polysciences) and were observed with our CCD microscope system using an Olympus oil immersion objective lens (SPlan Apo 60/NA 1.4) and high-selectivity excitation and barrier filters for fluorescence (Chroma Technology, Brattleboro, VT). GFP signals are usually bright and easily detected by eye, but when the signal is weak it is recommended that images be taken on the CCD with relatively long exposure times (a few seconds on our system). Note that dead cells often produce strong autofluorescence at the emission wavelength of GFP and should therefore be avoided when ascertaining the intracellular localization of GFP–fusion proteins.

D. Recovery of Plasmids from Selected Transformants and Determination of Nucleotide Sequences of a DNA Insert

Out of 50,000 transformants, 728 transformants exhibited distinct patterns of GFP fluorescence (Table I). Examples of localizations of GFP–fusion proteins are shown in Fig. 2. Plasmids from these transformants were recovered using standard methods (Moreno *et al.*, 1991). Isolated plasmids were retransformed into fission yeast cells to confirm the intracellular localizations determined from the first screening. Partial nucleotide sequencing of the ORF of the inserted yeast gene was performed using a portion of the GFP gene

TABLE I Summary of GFP–Fusion Library[a]

	Frame 1	Frame 2	Frame 3	Total
Total clones screened	25,494	12,084	12,267	49,845
Clones with GFP staining	3,295	1,279	2,380	6,954
Clones with discrete GFP-staining patterns	302	130	296	728

Localization pattern	Total number	Sequenced clone	Independent gene
Nucleus (general nuclear staining)	307	236	98
Nuclear dots	31	26	10
Nucleolus	29	29	22
Nuclear rim	26	26	15
Membrane (nuclear and plasma membrane, ER)	180	115	57
SPB	6	6	3
Microtubule	22	22	5
Cell pole, septum	10	12	8
Cell periphery	26	14	11
Cytoplasmic structures	85	25	19
Spore rim	6	5	2
Total	728	516	250

[a] Reproduced from Ding *et al.* (2000).

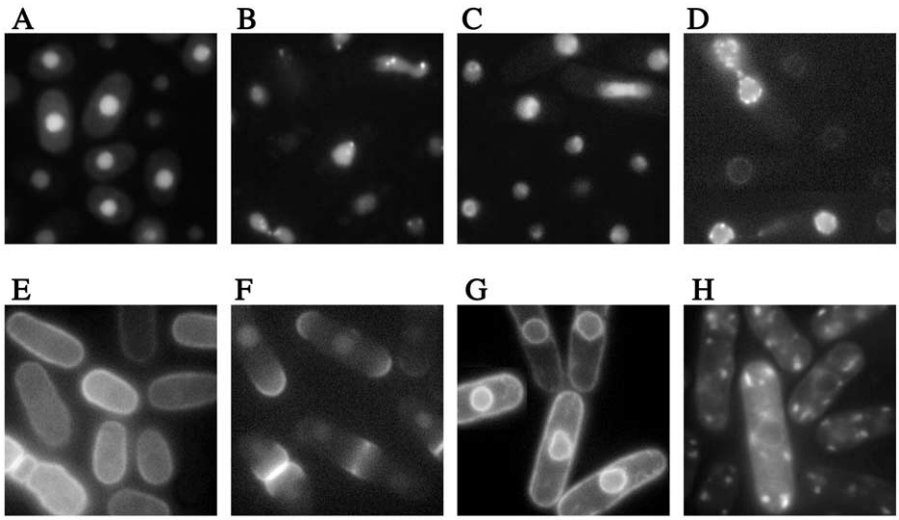

FIGURE 2 Examples of localizations of GFP–fusion proteins. (A) General nuclear staining, (B) nuclear dots, (C) nucleolus, (D) nuclear rim, (E) cell periphery, (F) cell pole and septum, (G) membrane, and (H) cytoplasmic dots. Scale bar: 10 μm.

as a sequencing primer (Fig. 1). Sequencing identified 250 independent genes (Ding *et al.*, 2000).

E. Construction of Image Database of Intracellular Localization

We constructed an image database of the intracellular localization of these 250 gene products and categorized them into 11 groups as shown in Table I (Ding *et al.*, 2000). Occasionally, a GFP–fusion protein was observed in more than one intracellular localization, as some proteins localize to several structures simultaneously or localize to various different structures during passage through the cell cycle. In these cases, we categorized the gene by the intracellular location that exhibited the most prominent staining. Secondary localizations are also listed in the database and genes can be searched for by any of their detected locations. Using this database, DNA sequences can be searched based on the localization of their products (see our Web site, http://www.karc.crl.go.jp/d332/CellMagic/index.html).

F. Time-Lapse Observation in Living Cells

Time-lapse images of GFP fluorescence in living cells were obtained on a cooled CCD using our computer-controlled fluorescence microscope system (Ding *et al.*, 1998; Haraguchi *et al.*, 1999). For time-lapse observation, living fission yeast cells expressing a GFP–fusion construct are mounted between two coverslips (Method 1) or in a 35-mm glass-bottom culture dish (MatTek Corp., Ashland, MA) coated with concanavalin A (Method 2), and observed in EMM2 medium. Sandwiching between coverslips generates clearer images, but allows observation for only about 2 h due to the limited amount of nutrition and oxygen available to the cells in such an arrangement. For longer observation, the use of glass-bottom culture dishes is recommended.

Solution

To make 1 liter of EMM2, add 20 g glucose, 5 g NH_4Cl, 2.2 g Na_2HPO_4, 3 g potassium hydrogen phthalate, 20 ml salts,[1] 0.1 ml trace elements,[2] 1 ml vitamins,[3] and 20 ml amino acids[4].

Complete EMM2 medium containing NH_4Cl as the nitrogen source generates optical turbidity after autoclaving, disturbing microscopic observation. The use of EMM2 depleted of NH_4Cl (EMM2-N) is recommended because of its optical clarity. Usually EMM2-N is used for the induction of meiosis and the observation of meiotic cells. For mitotic growth,

[1] Salts (50× stock): 52.5 g/liter $MgCl_2{\cdot}6H_2O$, 0.735 g/liter $CaCl_2{\cdot}2H_2O$, 50 g/liter KCl, and 2 g/liter Na_2SO_4.

[2] Trace elements (10,000× stock): 5 g/liter boric acid (H_3BO_3), 4 g/liter $MnSO_4$, 4 g/liter $ZnSO_4{\cdot}7H_2O$, 2 g/liter $FeCl_2{\cdot}6H_2O$, 0.4 g/liter molybdic acid (H_2MoO_4), 1 g/liter KI, 0.4 g/liter $CuSO_4{\cdot}5H_2O$, and 10 g/liter citric acid.

[3] Vitamins (1000× stock): 1 g/liter pantothenic acid, 10 g/liter nicotinic acid, 10 g/liter *myo*-inositol, and 10 mg/liter biotin.

[4] Amino acids (50× stock): 10 mg/ml L-leucine, 3.75 mg/ml adenine sulfate dihydrate, 3.75 mg/ml uracil, 3.75 mg/ml L-histidine hydrochloride monohydrate, and 3.75 mg/ml L-lysine hydrochloride.

however, a nitrogen source is necessary; in this case, autoclave EMM2-N and add a filtered 50x stock solution of NH_4Cl to the autoclaved EMM2-N.

Method 1: Sandwiching between Coverslips (Fig. 3)

Steps

1. Prepare two coverslips (60 × 24 mm and 18 × 18 mm).
2. Suspend fission yeast cells in the EMM2 medium.
3. Place 2.5 µl of cells on the larger coverslip (60 × 24 mm).
4. Cover with the smaller coverslip (18 × 18 mm) carefully so as not to introduce air bubbles.
5. Seal with silicon grease to avoid evaporation during observation (Fig. 3A). Do not use organic solvent-containing sealing reagents such as nail enamel as they are toxic to living cells. If the sealing is poor, cells can move due to streaming of media caused by evaporation.
6. Observe the specimen on an inverted microscope (Fig. 3B).

Method 2: Glass-Bottom Culture Dishes (Fig. 4)

Steps

1. Coat a glass-bottom culture dish (Fig. 4A) with concanavalin A shortly before use. Spread 50 µl of 1 mg/ml concanavalin A solution on the glass bottom of the dish. Then, remove excess solution and dry.
2. Suspend fission yeast cells in EMM2 medium.
3. Place 50 µl of cells on the glass bottom in the center of the dish. The cell wall will adhere to the concanavalin A.
4. Place small drops of water, or small pieces of wet paper or cotton, at the periphery of the dish to avoid evaporation during observation. Seal the lid of the dish with parafilm.
5. Place the dish on an inverted microscope (Fig. 4B). Leave the specimen on the microscope stage for about 10 min before observation to allow the cells to settle down in the dish.

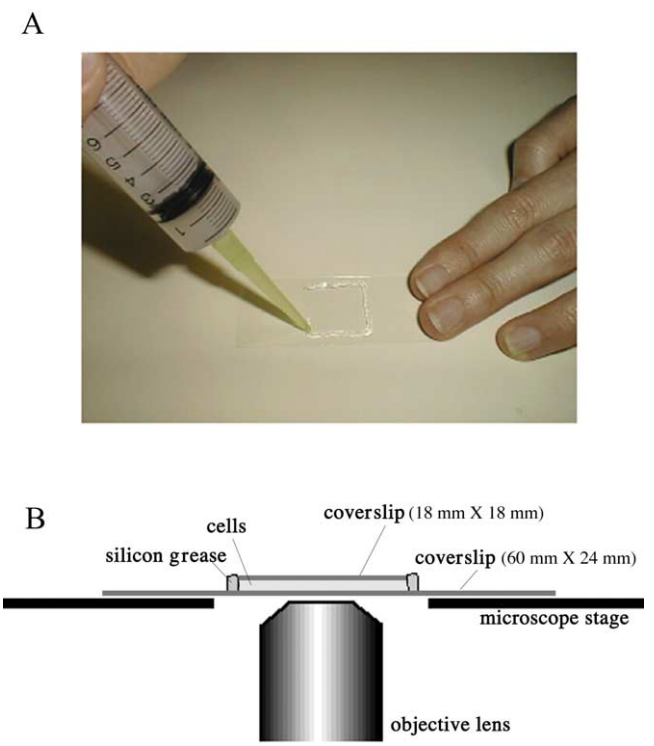

FIGURE 3 Living cells between coverslips. (A) Living fission yeast cells are mounted between coverslips and sealed with silicon grease. Silicon grease is packed in a syringe capped with a micropipette tip and applied to the edges of the smaller, upper coverslip. (B) A side view of a specimen on the microscope stage.

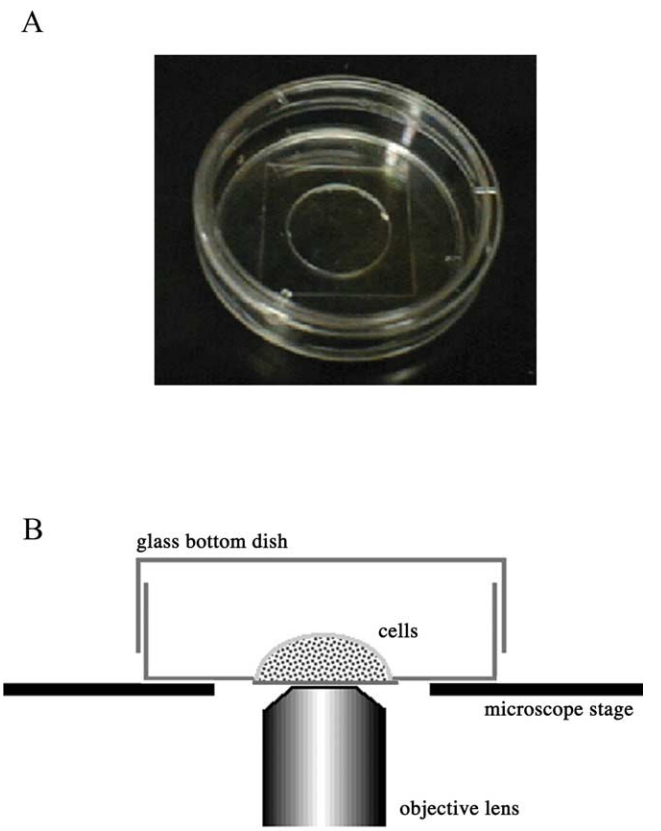

FIGURE 4 Living cells in a glass-bottom culture dish. (A) A 35-mm glass-bottom culture dish. (B) A side view of a specimen on the microscope stage.

IV. COMMENTS

A spacer between GFP and the gene may affect the localization of the GFP–fusion protein. We constructed our library using three plasmid vectors, pEG3-1, pEG3-2, and pEG3-3. In pEG3-1, there was no spacer codon between GFP and the yeast coding sequence, whereas in pEG3-2, three amino acid residues, Trp, Gly, and Ser, were inserted between GFP and the yeast coding sequence, and in pEG3-3 three amino acid residues, Leu, Gly, and Ser, were inserted. The best results were obtained when Leu, Gly, and Ser were inserted between GFP and the fission yeast coding sequence (Ding *et al*., 2000). Fusing the GFP directly to the protein backbone or with a spacer made of a heterocyclic aromatic amino acid, such as tryptophan, may affect the secondary structure of the fusion protein and, consequently, may disturb its intracellular localization.

An obvious limitation of our library is that those gene fragments that abate cell viability cannot be obtained. Another limitation of our library is occasional mislocalization of the fusion gene products. Because we fused GFP to random fragments of the genomic DNA, the C-terminal portion of the gene product was truncated to various extents and replaced by GFP. Gene products that have localization signals at their C termini could be mislocalized or excluded during screening. Also, cryptic localization signals can occasionally be contained within the amino acid sequences fused to GFP. Now that all the protein-coding genes of *S. pombe* have been identified by the completion of the *S. pombe* genome project (Wood *et al*., 2002), these limitations can be partly eliminated by constructing an ordered library in which the GFP gene is fused to full-length open reading frames. In the budding yeast *S. cerevisiae*, a collection of strains have been constructed, in which the GFP–fusion construct is integrated into the native chromosomal locus and expressed under their own promoter (Huh *et al*., 2003).

V. PITFALLS

1. For observing living fluorescently stained cells, use a high-sensitive camera to avoid damage to the cells caused by the excitation light and also minimize the excitation by the use of a shutter.

2. Occasionally an isolated plasmid will contain two different GFP–fusion genes, presumably as a result of heterodimer formation. This is seen during nucleotide sequence determination as two sequences overlapping each other. In such cases, the fusion proteins must be recloned into separate plasmids and the intracellular localization of the GFP–fusion products examined individually.

3. Because the GFP–fusion constructs are expressed on a multicopy plasmid, overexpression of the GFP–fusion protein may occur and affect its intracellular localization. To minimize this problem, it is recommended to use fresh preparations of exponentially growing cells for observation. Cells with physiological perturbations tend to fluoresce brightly or to accumulate fluorescent protein aggregates in the cell. Avoid observing such cells that give atypically bright fluorescence. In principle, localization patterns representative of the major population of cells in a microscope field are reliable.

References

Ding, D. Q., Chikashige, Y., Haraguchi, T., and Hiraoka, Y. (1998). Oscillatory nuclear movement in fission yeast meiotic prophase is driven by astral microtubules, as revealed by continuous observation of chromosomes and microtubules in living cells. *J. Cell Sci.* **111**(Pt. 6), 701–712.

Ding, D. Q., Tomita, Y., Yamamoto, A., Chikashige, Y., Haraguchi, T., and Hiraoka, Y. (2000). Large-scale screening of intracellular protein localization in living fission yeast cells by the use of a GFP–fusion genomic DNA library. *Genes Cells* **5**, 169–190.

Haraguchi, T., Ding, D. Q., Yamamoto, A., Kaneda, T., Koujin, T., and Hiraoka, Y. (1999). Multiple-color fluorescence imaging of chromosomes and microtubules in living cells. *Cell Struct. Funct.* **24**, 291–298.

Heim, R., and Tsien, R. Y. (1996). Engineering green fluorescent protein for improved brightness, longer wavelengths and fluorescence resonance energy transfer. *Curr. Biol.* **6**, 178–182.

Huh, W. K., Falvo, J. V., Gerke, L. C., Carroll, A. S., Howson, R. W., Weissman, J. S., and O'Shea, E. K. (2003). Global analysis of protein localization in budding yeast. *Nature* **425**, 686–691.

Matsumoto, T., Fukui, K., Niwa, O., Sugawara, N., Szostak, J. W., and Yanagida, M. (1987). Identification of healed terminal DNA fragments in linear minichromosomes of *Schizosaccharomyces pombe*. *Mol. Cell. Biol.* **7**, 4424–4430.

Maundrell, K. (1993). Thiamine-repressible expression vectors pREP and pRIP for fission yeast. *Gene* **123**, 127–130.

Moreno, S., Klar, A., and Nurse, P. (1991). Molecular genetic analysis of fission yeast *Schizosaccharomyces pombe*. *Methods Enzymol.* **194**, 795–823.

Sawin, K. E., and Nurse, P. (1996). Identification of fission yeast nuclear markers using random polypeptide fusions with green fluorescent protein. *Proc. Natl. Acad. Sci. USA* **93**, 15146–15151.

Wood, V., *et al*. (2002). The genome sequence of *Schizosaccharomyces pombe*. *Nature* **415**, 871–880.

CHAPTER

18

Large-Scale Protein Localization in Yeast

Anuj Kumar and Michael Snyder

I. INTRODUCTION

Proteomics has contributed significantly to our knowledge of eukaryotic cell biology through large-scale studies describing protein–protein interactions, protein complex composition, and relative protein abundance. Recent work in the budding yeast *Saccharomyces cerevisiae* (Kumar *et al*., 2002) has extended the scope of proteomics to encompass the genome-wide analysis of protein localization—the large-scale and systematic identification of the subcellular compartment or organelle to which a protein localizes. The subcellular localization of a protein can be of fundamental importance in characterizing the function and regulation of that protein. For example, an uncharacterized protein that localizes to the mitochondria may be inferred to function directly or indirectly in cellular respiration. Many transcription factors are regulated through subcellular compartmentalization: nuclear export of the transcription factor Pho4p is tightly regulated such that it is only localized within the nucleus (and therefore capable of activating transcription) in response to phosphate starvation (O'Neill *et al*., 1996). Protein function can also be addressed on a global scale by integrating protein localization data with a variety of other proteomic data sets. In particular, protein localization data are a strong complement to large-scale protein–protein interaction studies, corroborating many putative interactions while also highlighting potential false-positive results (Gerstein *et al*., 2002). Ultimately, genome-wide protein localization data will be helpful in identifying the constituent proteins of each cellular organelle and, potentially, mechanisms by which some of these proteins are regulated.

Yeast proteins may be localized through any of several approaches. By one common strategy, antibodies against a target protein can be used to immunolocalize that protein within a fixed cell. Antibodies against native proteins may be prepared by standard immunology; however, the feasibility of applying this approach on a proteome-wide scale has yet to be demonstrated. Alternatively, yeast proteins may be epitope tagged for subsequent immunolocalization. Tagged proteins can be localized by indirect immunofluorescence using monoclonal antibodies directed against the epitope tag. Epitope tags may be introduced into a protein-coding sequence by several methods. Many yeast vectors are available by which epitope tags may be fused to the amino (N) terminus or carboxy (C) terminus of a cloned gene (Longtine *et al*., 1998). In addition, epitope tags may be introduced at random within a protein-coding sequence by insertional mutagenesis using a modified epitope-bearing transposon (Hoekstra *et al*., 1991; Ross-Macdonald *et al*., 1997, 1999). A combination of random and directed tagging methods has been used successfully in *Saccharomyces* to epitope tag approximately 3600 yeast genes; subsequent immunolocalization of this protein set has defined the subcellular localization of nearly 2800 yeast proteins (Kumar *et al*., 2002).

As an alternative to immunolocalization, proteins may be localized by fluorescence microscopy using yeast open reading frame (ORF)–fluorescent protein chimeras. Coding sequence for a fluorescent protein [e.g., green fluorescent protein (GFP)] can be fused to a protein of interest using any number of appropriate tagging vectors (e.g., GFP-tagging vectors of the pFA6a series) (Longtine *et al*., 1998). Yeast ORF–GFP fusions may be constructed as integrated chromosomal alleles using these vectors in conjunction with standard

Copyright 2006, Elsevier Science (USA).
All rights reserved.

polymerase chain reaction (PCR)-based methods. GFP tagging has been used extensively in *S. cerevisiae* for the localization of individual target proteins; ongoing efforts to tag all annotated yeast ORFs with GFP should enable large-scale analysis of protein localization by fluorescence microscopy in living yeast cells.

This article presents detailed protocols by which yeast ORFs may be epitope tagged and yeast strains containing tagged proteins prepared for immunofluorescence analysis in a 96-well format. The protocols presented here utilize the PCR-based tagging method of Longtine *et al.* (1997) to generate C-terminal chromosomal gene fusions with a sequence encoding three copies of the hemagglutinin (HA) epitope. The resulting HA-tagged yeast proteins can be immunolocalized by indirect immunofluorescence as described; the immunofluorescence protocol is adapted for performance in a 96-well format, facilitating proteome-scale analysis of protein localization.

II. MATERIALS AND INSTRUMENTATION

G418 sulfate (geneticin) may be purchased from Invitrogen Corp. (Cat. No. 11811023). Glusulase is a trademarked preparation of β-glucuronidase / sulfatase, each available from Sigma (Cat. Nos. G0258 and S8504). Zymolyase-100T is from Seikagaku America; Lyticase from Sigma may be substituted (Cat. No. L4025). The mouse anti-HA monoclonal antibody 16B12 is from Covance (Cat. No. MMS-101R-1000). Cy3-conjugated affinity-purified goat antimouse IgG is from the Jackson Laboratories (Cat. No. 115-165-146). 4,6-Diamidino-2-phenylindole (DAPI) is available from Sigma (Catalog No. D-9542). Poly-L-lysine is from Sigma (Cat. No. P1524). Microscope slides are from Carlson Scientific (Cat. No. 101805).

III. PROCEDURES

A. Epitope-Tagging Yeast Genes

Yeast genes may be epitope tagged through a variety of methods: the protocol described here is essentially that of Longtine *et al.* (1997) in which PCR is used to amplify a cassette from the vector pFA6a-3HA-kanMX6 suitable for generating an integrated C-terminal HA-tagged allele of any nonrepeated yeast gene. The HA-tagging cassette (Fig. 1A) consists of a sequence encoding three copies of the HA epitope, the *S. cerevisiae ADH1* terminator, and the *kanMX6* module encoding resistance to G418. Tagging cassettes are amplified using primers with 5′ ends corresponding to the target gene and 3′ ends corresponding to the

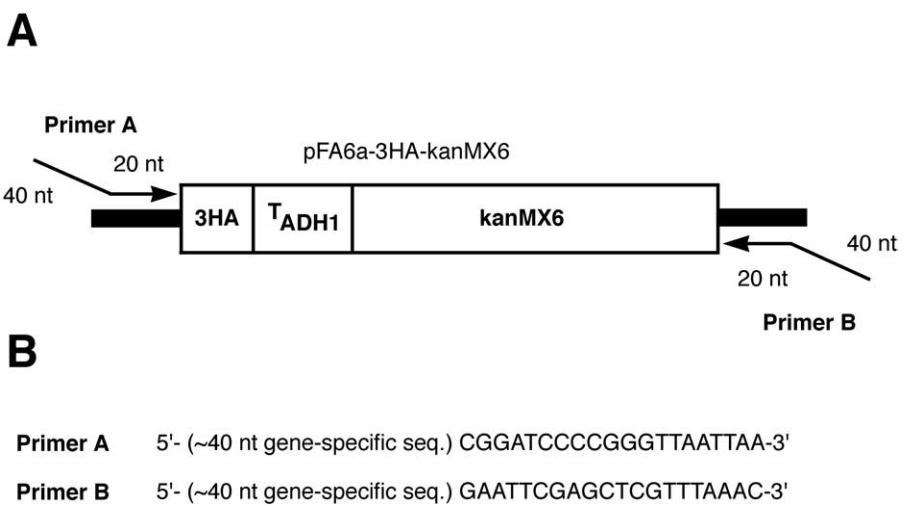

Figure 1 (A) HA-tagging cassette amplified from the yeast vector pFA6a-3HA-kanMX6. The tagging cassette contains a sequence encoding three copies of the influenza virus hemagglutinin epitope (3HA), the *S. cerevisiae ADH1* terminator, and the sequence encoding the kanMX6 cassette (encoding resistance to G418 sulfate). PCR primers for amplification of this cassette are designed such that the 5′ end of each primer consists of approximately 40 nucleotides of a gene-specific sequence, whereas the 3′ end consists of approximately 20 nucleotides of sequence from the polylinker immediately flanking the tagging cassette. (B) Example of PCR primers suitable for C-terminal HA tagging of target genes.

cassette; primer design is discussed later. Amplified cassettes are subsequently introduced into yeast by standard methods of DNA transformation (Gietz *et al*., 1992). By homologous recombination, the tagging cassette integrates at its intended genomic locus; transformants containing this cassette are selected on medium supplemented with G418. By this PCR-based approach, yeast genes may be systematically epitope tagged for subsequent large-scale immunolocalization.

Solutions

1. *YPD medium:* 1% Bacto-yeast extract, 2% Bacto-peptone, 2% glucose, 2% Bacto-agar, distilled water. Autoclave at 121°C and 15 lb/inz. in of pressure for 15 min; cool to ~55°C and pour plates. Omit agar for liquid media.

2. *YPD-G418 plates:* Prepare YPD medium. After cooling, supplement YPD with 150 mg/liter G418. To prepare a stock solution of G418 (geneticin), dissolve in water at a concentration of 80 mg dry weight per milliliter and filter sterilize.

Steps

1. Design primers enabling targeted integration of the amplified tagging cassette at its intended genomic locus. Example primers are shown in Fig. 1B. Design the 5′ end of each primer such that it consists of 40–50 nucleotides of sequence from the target gene. Choose the gene-specific sequence of the forward primer (A) such that it ends just upstream of the stop codon; choose the gene-specific sequence of the reverse primer (B) such that it ends just downstream of the stop codon.

2. Amplify the HA-tagging cassette from plasmid pFA6a-3HA-kanMX6 using PCR primers A and B. Use standard cycling conditions; vary conditions and primer/template concentrations as needed. Repeat PCR reaction four or more times. Pool reactions, extract once with phenol:chloroform:isoamyl alcohol (25:24:1), precipitate, and resuspend in a small volume of water (~10 µl).

3. Introduce concentrated PCR product into *S. cerevisiae* by any standard DNA transformation protocol (e.g., the lithium acetate protocol of Gietz *et al*., 1992). This process may be performed in 96-well format as described previously (Kumar *et al*., 2000).

4. Select transformants on YPD medium supplemented with G418. Wash cells in water (~1 ml), and resuspend in 200 µl of water. Spread onto YPD plates; incubate overnight at 30°C and replicate onto YPD-G418 plates. Pick individual G418-resistant colonies. Alternatively, G418 selection may be performed in large scale. Wash, precipitate, and resuspend transformants in 400 µl YPD in 96-well plates. Incubate at 30°C for 4–6 h with shaking. Streak transformant mixtures onto rectangular 86 × 128-mm YPD plates supplemented with G418. Use an eight-pronged replicator, such that 24 streaks (correponding to 24 transformant cultures) may be produced per plate. Pick G418-resistant colonies as described previously.

5. Using PCR, confirm that the HA-tagging cassette has integrated by homologous recombination with the target gene. Choose one primer such that it anneals within the HA-tagging cassette and another primer that anneals to the target gene locus outside of the insertion region. Identify a PCR product of the expected size as evidence of homologous integration.

B. Large-Scale Immunolocalization of Epitope-Tagged Proteins

Strains containing HA-tagged proteins may be immunolocalized by indirect immunofluorescence using monoclonal antibodies directed against the HA epitope (primary antibody) and the Cy3-conjugated secondary antibody. Immunolocalization in yeast necessitates permeabilization of the cell wall; here, yeast cells are spheroplasted using the trademarked enzyme preparations glusulase and Zymolyase-100T. The provided immunolocalization protocol is tailored for implementation in a 96-well format. Using this procedure, a single researcher can easily prepare 192 samples (two 96-well microtiter plates) for immunofluorescence in a period of 3 days (Kumar *et al*., 2000). Sample immunofluorescence patterns in cells containing HA-tagged proteins are presented in Fig. 2.

Solutions

1. *Solution A:* 1.2 *M* sorbitol, 50 m*M* KPO_4, pH 7. Prepare sorbitol as a 2 *M* stock solution in water. Store solution A up to 1 week at 4°C.

2. *Solution A / glusulase / Zymolyase:* Supplement solution A with 1 µl/ml 2-mercaptoethanol, 1 µl/ml glusulase, 1 µl/ml Zymolyase (at a concentration of 10 mg/ml). Prepare a stock solution of 10 mg/ml Zymolyase in 5% glucose in 20 m*M* phosphate buffer, pH 7.4. Store stock solution of Zymolyase at –20°C. Add 2-mercaptoethanol under a chemical fume hood. Prepare this mixture immediately before use.

3. *Phosphote-buffened Saline (PBS) buffer:* 20× PBS buffer per liter, 160 g NaCl, 4 g KCl, 28.8 g Na_2HPO_4, 4.8 g KH_2PO_4, 800 ml water. Adjust pH to 7.4; adjust volume to 1 liter. Autoclave and store at room temperature. Dilute 20-fold prior to use. PBS buffers supplemented with BSA may be stored for approximately 1 week at 4°C.

4. *Antibody solutions:* Primary and secondary antibodies should be added to PBS buffer immediately

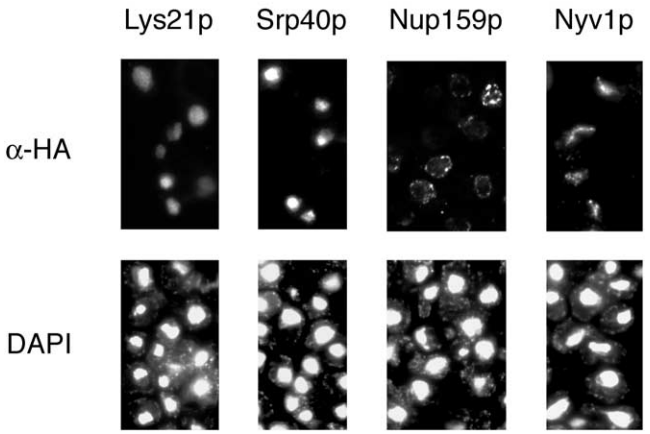

Figure 2 Examples of immunofluorescence patterns from large-scale protein localization studies in *S. cerevisiae*. (Top) Immunofluorescence patterns in vegetative yeast cells stained with monoclonal antibodies directed against HA. (Bottom) The same cells stained with the DNA-binding dye 4,6-diamidino-2-phenylindole (DAPI). Staining of the nucleus is evident in cells carrying a tagged allele of the homocitrate synthase Lys21p, while nucleolar staining can be seen in cells HA tagged for the chaperone Srp40p. HA-tagged Nup159p localizes to the nuclear rim, while staining of the vacuole may be observed in cells containing a tagged form of the v-SNARE Nyv1p.

prior to use. Centrifuge antibodies at 4°C for 10 min at maximum speed in a variable-speed microcentrifuge (e.g., Eppendorf Model 5415C centrifuge). Store the Cy3-conjugated secondary antibody in the dark at –20°C.

5. *Poly-L-lysine solution:* 0.5 mg/ml poly-L-lysine. Dissolve 50 mg poly-L-lysine powder in 10 ml H_2O; dilute 10-fold in H_2O. Filter sterilize if desired and aliquot into 1.5-ml tubes. Store at –20°C. Centrifuge poly-L-lysine solution for 10 min prior to use.

6. *DAPI stock solution:* Dissolve DAPI at a concentration of 1 mg/ml in sterile H_2O. Wear gloves and safety glasses when working with DAPI, as it is a possible carcinogen. Store at –20°C.

7. *Mount medium with DAPI:* 1 mg/ml *p*-phenylenediamine in PBS supplemented with DAPI (final concentration of 1 µg/ml). Dissolve 100 mg *p*-phenylenediamine in 10 ml PBS buffer; prepare solution in a small beaker covered with aluminum foil. Add 90 ml glycerol and continue stirring. Aliquot into 1.5-ml tubes and store at –70°C. Before use, add 1 µl DAPI stock / ml mount medium. Mount medium with DAPI may be stored for up to 2 weeks.

Steps

1. Inoculate strains containing HA-tagged proteins in 96-well microtiter plates containing 75 µl YPD media per well. Grow cultures overnight (approximately 12 h) at 30°C with gentle shaking on an orbital platform shaker (240 rpm). Alternatively, incubate plates on a vortex shaker set to its lowest speed. After overnight growth, add 45 µl YPD; grow for an additional 90 min to an OD_{600} of 0.75–1.

2. Fix cells in formaldehyde at a final concentration of 3.75% (v/v). Agitate cells gently for 30 min using a vortex shaker set to its lowest speed. Collect cells by centrifugation at 2000 rpm for 4 min in a Sorvall H-1000B rotor. Wash pelleted cells three times in 100 µl solution A. Resuspend cells in 100 µl of solution A supplemented with 0.1% (v/v) 2-mercaptoethanol, 0.02% (w/v) glusulase, and Zymolyase-100T (5 µg/ml).

3. Spheroplast cells in this mixture at 37°C with gentle shaking for 13–20 min (optimal incubation times must be determined empirically). Check cells periodically during this incubation; once translucent, recover cells and wash in 100 µl solution A. Resuspend pelleted cells in 100 µl PBS buffer supplemented with 0.1% (v/v) Nonidet P-40 and 0.1% (w/v) bovine serum albumin (BSA). Incubate samples at room temperature without shaking for 15 min. Pellet cells by centrifugation as before. Remove excess liquid by aspiration, and resuspend pellets in 100 µl PBS supplemented with 3% (w/v) BSA. Gently shake cells at room temperature for 30 min to 1 h.

4. Add 40 µl of mouse anti-HA monoclonal antibody 16B12 at a final dilution of 1:1000 in PBS supplemented with 3% (w/v) BSA. Incubate overnight at 4°C with gentle shaking.

5. Wash cells as follows: once in 150 µl PBS supplemented with 0.1% (w/v) BSA, once with 100 µl PBS supplemented with 0.1% (w/v) BSA and 0.1% (v/v) Nonidet P-40, and once in 100 µl PBS supplemented with 0.1% (w/v) BSA. During this final wash, gently shake cells for 5 min at room temperature prior to centrifugation.

6. Treat pelleted cells with Cy3-conjugated affinity-purified goat antimouse IgG (secondary antibody) at a final dilution of 1:200 in 40 µl of PBS supplemented with 3% (w/v) BSA. Shake cells gently at room temperature for 2 h in the dark (to minimize Cy3 exposure to light).

7. Prepare poly-L-lysine-coated slides for use in step 9. To prepare two slides, add a total volume of 40 µl poly-L-lysine solution (0.5 mg/ml in H_2O) to one slide; distribute the poly-L-lysine in five or six wells spaced evenly over the surface of the slide. Place the other slide (with no added polylysine) onto the poly-L-lysine-treated slide such that the two faces of the slides are sandwiched together. Wait 15 min. Separate slides and rinse in H_2O; allow slides to air dry before use in step 9.

8. Wash cells (from step 6) as follows: once in 150 µl PBS plus 0.1% (w/v) BSA, once in 100 µl PBS plus 0.1%

(w/v) BSA with gentle shaking for 5 min, twice in 100 µl PBS plus 0.1% (w/v) BSA and 0.1% (v/v) Nonidet P-40, and once in 100 µl PBS plus 0.1% (w/v) BSA.

9. Resuspend cells in 75 µl PBS. Using a multichannel pipetter, transfer 15 µl of this cell suspension into 12 individual wells on a poly-L-lysine-treated slide. Allow cells to sit for a minimum of 15 min before removing excess solution by aspiration. Add mounting medium supplemented with DAPI such that a total volume of 40 µl is spotted at five or six locations in between the wells. Place a coverslip on the slide; avoid air bubbles and ensure that mounting medium is spread over all wells. Seal slides with nail polish and store in the dark at –20°C; do not store slides longer than 1 month prior to examination.

PITFALLS

In designing protein localization studies, consideration should be paid to the placement of reporter/epitope tags relative to each target open reading frame. Typically, reporters and epitope tags are fused to either N or C termini of target genes; however, each tagging strategy possesses associated advantages and drawbacks. Organelle-specific targeting signals (e.g., mitochondrial targeting peptides and nuclear localization signals) are often located at the N terminus (Silver, 1991). N-terminal reporter fusions may disrupt these sequences, resulting in aberrant protein localizations. In other cases, C-terminal sequences may be important for proper function and regulation. For example, isoprenylation motifs are typically C-terminal, and sequences important for plasma membrane localization may be found throughout the gene-coding sequence (Nakai and Horton, 1999). While no single tagging strategy can be all-encompassing, a greater proportion of the yeast proteome should remain functional as C-terminal fusions: several studies have generated genome-wide C-terminal fusions for large-scale protein localization (Ding *et al*., 2000; Kumar *et al*., 2002).

Gene copy number may also impact upon the accuracy with which a tagged protein is localized. Overexpressed protein products can saturate intracellular transport mechanisms, potentially resulting in anomalous protein localization. However, weakly expressed single copy genes may yield insufficient protein levels for analysis, although the protocol presented here—in which tagged proteins are expressed endogenously under control of their native promoters—has been used successfully to localize nonabundant proteins (Kumar *et al*., 2002).

The immunofluorescence protocol presented here is reliable, but care should be taken to empirically determine optimal incubation times for spheroplasting (Zymolyase/glusulase treatment). The efficiency of spheroplasting may be monitored by phase-contrast microscopy. Ideally, cells should be a dark, translucent gray. Bright cells may have been insufficiently digested, whereas pale gray cells with little internal structure have likely been overdigested (Adams *et al*., 1998). In our hands, cells spheroplasted for 13–20 min yield good staining patterns upon subsequent antibody treatment.

References

Adams, A., Gottschling, D. E., Kaiser, C. A., and Stearns, T. (1998). Methods in Yeast Genetics, pp. 135–137. Cold Spring Harbor Laboratory Press, Plainview, NY.

Ding, D. Q., Tomita, Y., Yamamoto, A., Chikashige, Y., Haraguchi, T., and Hiraoka, Y. (2000). Large-scale screening of intracellular protein localization in living fission yeast cells by the use of a GFP-fusion genomic DNA library. *Genes Cells* **5**, 169–190.

Gerstein, M., Lan, N., and Jansen, R. (2002). Proteomics: Integrating interactomes. *Science* **295**, 284–287.

Gietz, D., St. Jean, A., Woods, R. A., and Schiestl, R. H. (1992). Improved method for high efficiency transformation of intact yeast cells. *Nucleic Acids Res*. **20**, 1425.

Hoekstra, M. F., Burbee, D., Singer, J., Mull, E., Chiao, E., and Heffron, F. (1991). A Tn*3* derivative that can be used to make short in-frame insertions within genes. *Proc Natl Acad Sci USA* **88**, 5457–5461.

Kumar, A., Agarwal, S., Heyman, J. A., Matson, S., Heidtman, M., Piccirillo, S., Umansky, L., Drawid, A., Jansen, R., Liu, Y, Cheung, K.-H., Miller, P., Gerstein, M., Roeder, G. S., and Snyder, M. (2002). Subcellular localization of the yeast proteome. *Genes Dev*. **16**, 707–719.

Kumar, A., des Etages, S. A., Coelho, P. S. R., Roeder, G. S., and Snyder, M. (2000). High-throughput methods for the large-scale analysis of gene function by transposon tagging. *Methods Enzymol*. **328**, 550–574.

Longtine, M. S., McKenzie, A., III, Demarini, D. J., Shah, N. G., Wach, A., Brachat, A., Philippsen, P., and Pringle, J. R. (1998). Additional modules for versatile and economical PCR-based gene deletion and modification in *Saccharomyces cerevisiae*. *Yeast* **14**, 953–961.

Nakai, K., and Horton, P. (1999). PSORT: A program for detecting sorting signals in proteins and predicting their subcellular localization. *Trends Biochem Sci*. **24**, 34–36.

O'Neill, E. M., Kaffman, A., Jolly, E. R., and O'Shea, E. K. (1996). Regulation of PHO4 nuclear localization by the PHO80-PHO85 cyclin-CDK complex. *Science* **271**, 209–212.

Ross-MacDonald, P., Coelho, P. S. R., Roemer, T., Agarwal, S., Kumar, A., Jansen, R., Cheung, K.-H., Sheehan, A., Symoniatis, D., Umansky, L., Heidtman, M., Nelson, F. K., Iwasaki, H., Hager, K., Gerstein, M., Miller, P., Roeder, G. S., and Snyder, M. (1999). Large-scale analysis of the yeast genome by transposon tagging and gene disruption. *Nature* **402**, 413–418.

Ross-Macdonald, P., Sheehan, A., Roeder, G. S., and Snyder, M. (1997). A multipurpose transposon system for analyzing protein production, localization, and function in *Saccharomyces cerevisiae*. *Proc Natl Acad Sci USA* **94**, 190–195.

Silver, P. A. (1991). How proteins enter the nucleus. *Cell* **64**, 489–497.

SECTION

6

Digital Image Processing, Analysis, Storage, and Display

CHAPTER

19

Lifting the Fog: Image Restoration by Deconvolution

Richard M. Parton and Ilan Davis

I. INTRODUCTION

Deconvolution is a data processing technique that is very widely used in science and engineering. Biologists first applied this method to fluorescence microscopy in the early 1980s (Agard, 1984), but it was already in common use by astronomers for sharpening images acquired using telescopes. The term deconvolution is derived from the fact that it reverses the distortion (convolution) of data introduced by a recording system, such as a microscope when it forms an image of the specimen. Any microscope image of a fluorescent specimen can, in principle, be deconvolved after acquisition in order to improve contrast and resolution. The most common application in biology is for deblurring images acquired as three-dimensional (3D) image stacks using a wide-field fluorescence microscope, where each image includes considerable out-of-focus light or blur originating from regions of the specimen above and below the plane of focus. In essence, deconvolution techniques use information describing how the microscope produces a blurred image in the first place as the basis for a mathematical transformation that refocuses or sharpens the image. Deconvolution of wide-field data can provide results resembling the blur-free "optical sectioning" achieved with confocal microscopes, which remove the out-of-focus light optically before image acquisition by placing a pinhole in the appropriate position in the light path. Deconvolution is also applicable to confocal or multiphoton images as they too involve a convolution of data and, in practice, rarely exclude all out-of-focus information. The best deconvolution techniques attempt to correctly reassign each photon of the out-of-focus light from the blurred optical sections being processed to their points of origin within the image state. When successful, this gives wide-field microscopy an advantage over confocal optics, particularly with live-cell work, as all the available emitted fluorescent light, including that coming from out of focus regions, is collected in parallel and is then reassigned to its correct location in the 3D image. This affords the wide-field microscope its faster imaging speeds and flexibility. In contrast, the out-of-focus fluorescence blur removed optically by confocal microscopy can never be recovered, resulting in lower light capture efficiency. However, deconvolution requires powerful computers, thus introducing additional cost and delay before the sharpened image can be viewed. Nevertheless, if one is required to resolve and analyse fine structural details and carry out true volume analysis, deconvolution is an option that should be seriously considered.

This technical guide is intended both for those researchers who are completely new to the method and for those who use deconvolution, but would like a better appreciation of how the method works and the present state of the art. We will first briefly explain the principles of deconvolution and then describe the different types of deconvolution methods currently available. Next we discuss practical considerations and limitations in applying the techniques. Finally, we describe improved deconvolution algorithms, which are currently being developed.

II. CONVOLUTION AND DECONVOLUTION

The magnified image of a specimen observed by eye or a digital camera mounted on a microscope is not a

Copyright 2006, Elsevier Science (USA).
All rights reserved.

perfect representation of the specimen. The image is blurred or **convolved** by the microscope optics and some information is lost (Fig. 1A). This is an inevitable consequence of how objective lenses work and there are no simple ways round the problem (Hecht, 2002). The nature of image convolution in fluorescence microscopy is appreciated most easily by viewing small spherical fluorescent beads (with diameters in the order of hundreds of nanometers; Figs. 1B–1D). When the beads used are smaller than the smallest detail that the optics can resolve (i.e., **subresolution**, 50 to 200 nm), they form effective single point sources of light and the image resulting from a single bead is known as the **point spread function (PSF)**, being a record of how much the microscope has spread or blurred a single point while imaging it (Jonkman *et al*., 2003; Figs. 1B–1D). Such images consist of a series of concentric rings in three dimensions (so-called **airy rings**) of out-of-focus light around points of light (Figs. 1B and 2A). The PSF is a three-dimensional function, describing how the image of a subresolution point is blurred in the z dimension as well as in x and y, and it varies between different objectives, those with higher numerical apertures giving less blurring (Figs. 1B–1D). Wide-field, confocal, and multiphoton imaging configurations all have their own characteristic PSFs. A biological specimen may be thought of as a collection of subresolution points, each of which is convolved by the objective's PSF independently. Mathematically, convolution involves replacing each point in the specimen by a point spread function during the process of image formation. It is the combination of out-of-focus

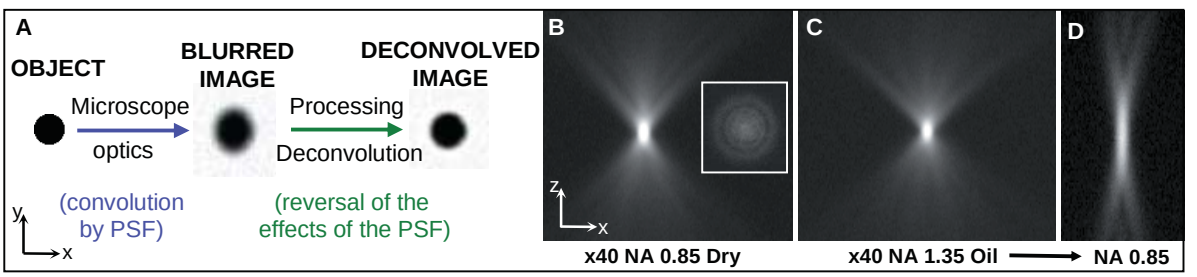

FIGURE 1 Convolution, deconvolution, and the point spread function (PSF). (A) Interpretive diagram of the principles of convolution and deconvolution based upon a simple spherical object. (B–D) Wide-field fluorescence PSFs obtained by imaging 100-nm fluorescent beads (excitation 520 nm; emission 617 nm) with a ×40/NA 0.85 dry objective and with a ×40/NA 1.35 oil immersion with adjustable collar set at NA 1.35 and NA 0.85. Images shown are single median x, z planes from 3D data sets, step size 0.1 µm. (Inset) An x, y view 20 µm from the centre. Deterioration of the PSF from C to D is a consequence of mismatch of the immersion oil refractive index with the reduced numerical aperture set. Resolution in z depends upon both RI and NA.

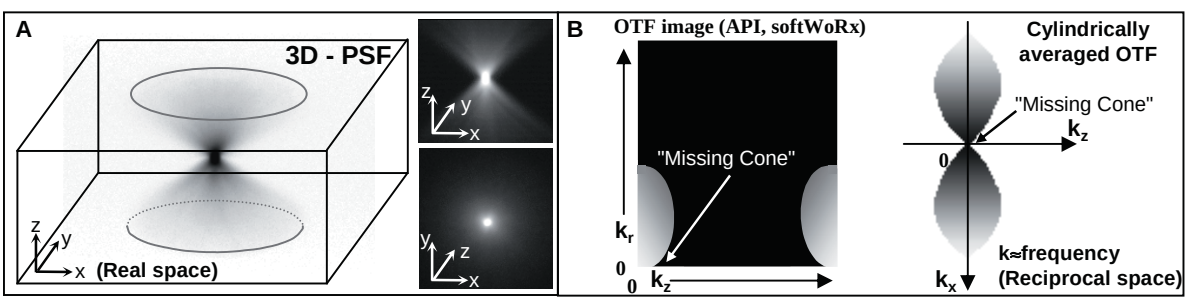

FIGURE 2 (A) Three-dimensional (x, y, z) view of a wide-field fluorescence point spread function. For clarity, the volume representation is shown as a negative image. (B) Two different representations of the Fourier transform of a PSF—an optical transfer function (OTF). In the OTF, frequency information is plotted in "k space" or reciprocal space (where k_z is reciprocally related to z and k_r to x and y in real space, see Technical Summary 2). OTFs are often averaged radially over x, y, hence the axis k_r. The area covered by the OTF corresponds to the frequency information collected by the optics. The "missing cone" region (arrows) corresponds to lost frequencies due to the limited size of the objective pupil, a consequence of this being the far greater blurring of an object along the z axis than in x and y.

light from these overlapping PSFs in and beyond the plane of focus that leads to the familiar blur in wide-field fluorescence images (Figs. 3A and 4A).

Image **deconvolution** refers to a mathematical process by which the effects of image convolution by the microscope are reduced or reversed to allow one to reproduce more closely the detail present in the original specimen (Agard, 1984; Hiraoka *et al*., 1990; Figs. 3B and 4B–4H). The more advanced deconvolution methods attempt to reassign this out-of-focus light to its point of origin (i.e., converting airy rings back into single point sources of light); the resulting image

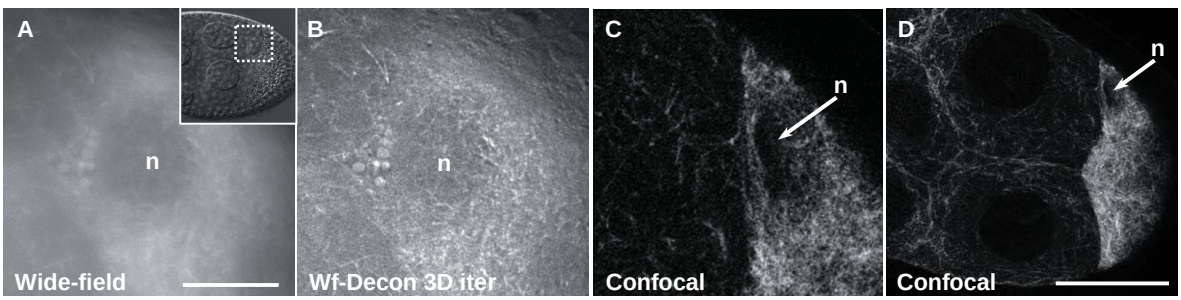

FIGURE 3 Comparison of wide-field and confocal imaging of living *Drosophila* egg chambers (stage 8) expressing Tau-GFP localised to the tubulin cytoskeleton. (A) Wide-field image of the area surrounding the oocyte nucleus (see insert: DIC image of the egg chamber). The image required 200 ms exposure. (B) Image A after 3D iterative deconvolution using the Applied Precision *Resolve 3D* algorithm (*softWoRx*, API). (C) Point scanning confocal optical section of a similar egg chamber, which took 2 s to collect. (D) Wider view of the confocal image of the egg chamber from C. All images were collected with ×60/1.2 NA water immersion objectives. Scale bars: 100 µm (A–C) and 50 µm (D). The oocyte nucleus (n) is indicated in each case.

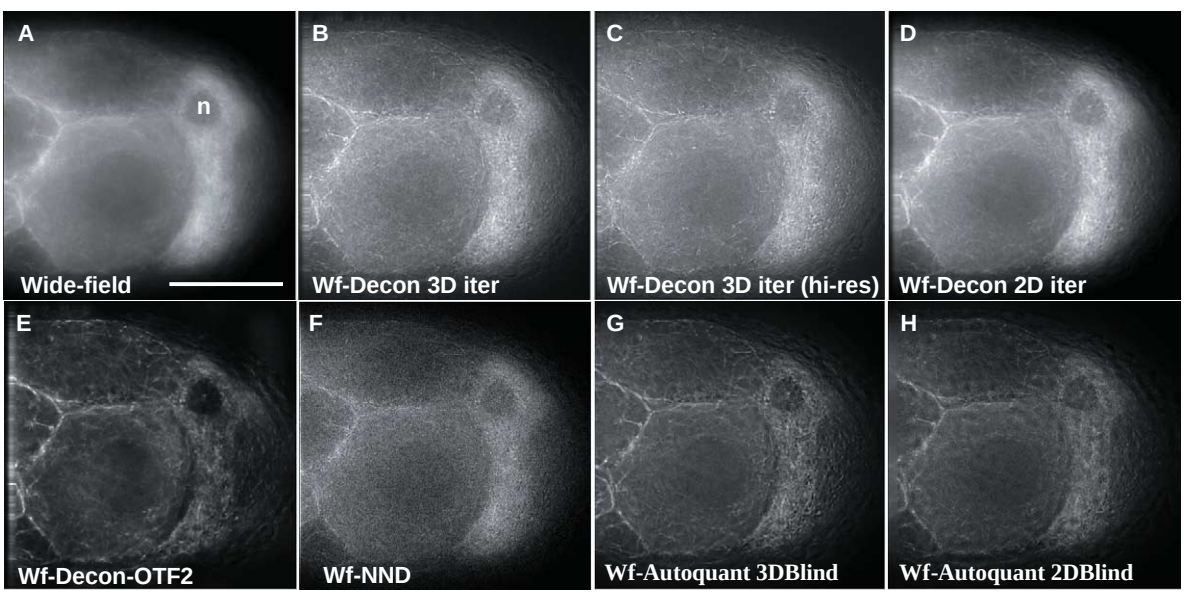

FIGURE 4 Comparing the results of different deconvolution methods on a challenging 3D (60 image) wide-field data set of a *Drosophila* egg chamber (*z*-step 0.2 µm, *x*, *y* pixel size 0.212 µm; a ×60 1.2 NA water objective). (A) Single unprocessed wide-field image. (B) The corresponding image plane after 3D iterative, constrained deconvolution of the data set (*softWoRx*, API: empirical PSF). (C) Deconvolution as in B using a second 60 image 3D data set of the same tissue collected at an *x*, *y* pixel size of 0.106 µm—higher sampling rate. (D) Two-dimensional iterative constrained deconvolution of the first image data set (*softWoRx*, API: empirical PSF). Each *z* plane is deconvolved independently as if it were part of a time-series data set. (E) Deconvolution as in B but using a different PSF (OTF) and more severe smoothing. (F) Using the "nearest neighbours" deconvolution algorithm (*softWoRx*, API). (G) Using the 3D iterative, "adaptive blind" deconvolution algorithm (*Autodeblur*, Autoquant—10 iterations; low noise; no spherical aberration; recommended expert settings). (H) Using the 2D iterative, adaptive blind deconvolution algorithm (*Autodeblur*, Autoquant—15 iterations; low noise; no spherical aberration; recommended expert settings). Scale as for Fig. 3D. Raw data were 12 bit saved as 16 bit; the images shown are 8 bit; with contrast stretched to fill the full dynamic range.

should be sharper with increased contrast and, under certain circumstances, increased *Z* resolution (Figs. 3B, 4B, 4C, 4E, and 4G; Agard, 1984; Agard *et al*., 1989).

III. DECONVOLUTION, DEBLURRING, AND IMAGE RESTORATION

Given the raw image and the PSF for the imaging system it should, in principle, be possible to reverse the convolution of an object by the microscope mathematically, according to a simple relationship—the so-called "linear inverse filter" (Technical Summary 1). However, in practice, simple reversal of convolution is not possible, primarily because of the confounding effect of noise in image data, which becomes amplified during this process (Technical Summary 1). Several fundamentally different deconvolution approaches of varying complexity have been developed to overcome this problem (see Table I; Agard, 1984; Agard *et al*., 1989; Holmes *et al*., 1995; van Kempen *et al*., 1997).

For the biologist, it is important to be able to recognise the different algorithms and appreciate the consequences of those differences to processed data (noted in Table I). The differences are significant: from simple rapid contrast enhancement by deblurring algorithms such as "nearest neighbours" to the much slower restoration procedures such as the constrained iterative algorithms, which can, under ideal conditions, "recover" information lost through convolution by the microscope optics (see later).

Technical Summary 1: Convolution Theory and Fourier Space

Convolution refers to the effect that the microscope optics has in forming the image of an object viewed through the microscope. The microscope image is the result of the convolution (symbolised by ⊗) of the object by the PSF of the microscope (Fig. 1). Mathematically, convolution involves applying the function that relates object to image to each point of the function defining the image (Hecht, 2002). The PSF empirically defines the function relating an object to its image:

$$\text{Microscope image} = \text{object} \otimes \text{PSF}$$

In theory, determing what the object should look like, given the microscope image and the PSF, simply requires reversal of this convolution. Performing this calculation using image data directly (known as calculating in "**real space**") is computationally very time-consuming. This limitation may be overcome by carrying out calculations in "**Fourier space"** by computing the Fourier transform (FT) of both image data and the PSF (see Technical Summary 2). The Fourier-transformed PSF is also known as an optical transfer function (**OTF**). In Fourier space, the convolution relationship described earlier becomes a simple multiplication:

$$\text{FT (microscope image)} = \text{FT (object)} \times \text{FT (PSF)}, \text{ or equivalently}$$

$$\text{FT (microscope image)} = \text{FT (object)} \times \text{OTF (Van der Voort and Hell)}$$

Deconvolution on the basis of the aforementioned equation is known as a simple linear inverse filter (Table I). However, the simple linear inverse filter is of very little practical use, as the relationship between image and object is invalidated by **noise** in the collected image. The simple linear inverse filter does, however, provide the theoretical basis for more complex deconvolution algorithms that take account of real imaging situations (Hiraoka *et al*., 1990).

A. Classification of Algorithms

There is considerable confusion caused by the existence of different names for deconvolution algorithms due to the history of development of this method (Agard, 1989; van Kempen *et al*., 1997). Currently, only a few algorithms are routinely employed in biological image processing (Table I). In an article by Wallace *et al*. (2001), algorithms are classified into (1) "**deblurring**" methods (Table I), which are said to act two-dimensionally, on one *z* plane at a time, and (2) "**image restoration**" or "true deconvolution" methods, which act in a truly three-dimensional way on all planes simultaneously. In general, deblurring methods may be useful for a rapid qualitative improvement in image contrast, e.g., to aid data screening (Fig. 3F, nearest neighbour deconvolution). However, the most powerful algorithms are the constrained iterative procedures of the second class: considered as the method of choice for quality 3D data processing, these will be the focus of the remainder of this article. Within the family of constrained iterative approaches, different algorithms vary in the way noise is modelled and how PSF information is dealt with (Table I; Agard *et al*., 1989; Holmes *et al*., 1995; van Kempen *et al*., 1997).

B. Constrained Iterative Deconvolution

The constrained iterative deconvolution approach (Agard, 1984; Agard *et al*., 1989) is truly restorative, in

TABLE I Deconvolution Algorithms Used in Biological Fluorescence Image Processing[a]

	Algorithm/product name[b]	Features
Deblurring class		
Subtractive	Widely available in image processing software as "nearest neighbours" or "no neighbours" processing. (e.g., *Metamorph*, Universal Imaging; *Autodeblur*, Autoquant)	Works on the basis that most of the out-of-focus blur originates in the neighbouring planes in *z* (when sampling at approximately the *z* resolution). The nearest *z* sections above and below the section being corrected are blurred with a filter and these blurred images are then subtracted from the plane of interest to give the deblurred section. "No neighbours" extrapolates only from a single plane. • Computationally inexpensive and therefore useful for quick results • Prone to creating artefacts • Signal is reduced by the subtractions and noise is propagated • Affects quantification: should be used only for qualitative contrast enhancement
Image restoration class		
Linear inverse filter	For example, the Tikhonov-Miller filter used in *analySIS*	The simplistic approach of reversing convolution by the optics. Does not take account of the effects of noise. Often used as the "first guess" for iterative deconvolution. Still a true 3D method requiring a PSF, which attempts to reassign out of focus information to its point of origin. • Computationally inexpensive and therefore useful for quick results • Prone to creating artefacts • Noise is propagated, thus tends to be used only as a qualitative method • Not capable of super resolution but can restore information supported by the OTF coverage.
Regularised inverse filter	For example, the regularised Wiener filter. Found in several applications, e.g., *DeconvolveJ*, NIH image,[c] *Autodeblur-inverse filter* from Autoquant and *AxioVision 3D-Deconvolution* from Carl Zeiss	A refinement of the above employing regularisation so that the deconvolution solutions are physically realistic and artifacts are suppressed. **Regularisation** involves limiting the possible solutions that are accepted in accordance with certain assumptions made *a priori* about the object, such as the degree of smoothness, essential when dealing with real, noisy data. Limiting the contribution of noise by regularisation comes at the expense of resolution, and to optimise this trade-off between image sharpness and noise amplification, different values of the **regularisation parameter** must be assessed.
Constrained Iterative Additive (Gaussian) noise model	For example, the modified Jansson van Cittert algorithm (Agard *et al*., 1989) implemented in modified form in *softWoRx* from API	A further refinement on the aforementioned; an additional positivity constraint is applied that restricts output image intensities to be positive (see main text). • Computationally expensive and therefore slow • Less prone to artifacts • Signal is reassigned, increasing the brightness of features and the signal-to-noise level • Works very well when the OTF is matched to data, suffers when data is affected by spherical aberration • Quantitative and capable of superresolution in *z* (beyond the *z* optical resolution limit of the microscope)
Constrained Iterative Maximum Likelihood estimation (Poisson noise model)	For example, the Richardson–Lucy algorithm implemented in *Huygens Essential* from Scientific Volume Imaging. Also *AxioVision 3D-Deconvolution* from Carl Zeiss	A variant of the constrained, iterative algorithms that assumes a Poisson model to quantify the noise present during imaging. Huygens essential uses the classical maximum likelihood estimation method and either optimised empirical or theoretical PSFs. • Computationally even more expensive, requiring more iterations and therefore slower • More recent than the Agard/Sedat-modified Jansson van Cittert algorithm • Quantitative (but see main text) and capable of superresolution in *Z* • Useful for noisy, photon-limited confocal imaging data (e.g., van Kempen *et al*., 1997)
Constrained Iterative Adaptive Blind deconvolution	Includes the EM-MLE (expectation minimisation algorithm) of Autoquant's *Autodeblur-2D* and *3D blind* deconvolution options	Blind deconvolution is also iterative and constrained but it determines an estimate of both the object and the PSF of the imaging system based upon raw image data and certain *a priori* assumptions about the PSF. These algorithms also assume a Poisson model of noise in the image. • Determining two unknowns is computationally more expensive and therefore even slower • Does not require an empirical PSF and is more tolerant of spherical aberration and asymmetry • Can generate a derived calculated PSF that can be used to speed up subsequent processing • May not be able to restore to as high resolution as when using an optimised empirical PSF • Better at dealing with signal-limited noisy data (such as confocal images) • May affect image data such that it is no longer absolutely quantitative

[a] Represents a summary of commonly used algorithms and is not intended to be exhaustive.
[b] These products may be sold (under license) by other agents.
[c] National Institute of Health Image-J software is free to download from http://rsb.info.nih.gov/ij.

that it attempts to reassign (put back) the out-of-focus light to its expected point of origin rather than simply subtract it from the image as with the deblurring methods (Table I; Figs. 3 and 4). This not only increases the brightness of features in the object, thus improving signal-to-noise levels, but also improves contrast and apparent resolution. Furthermore, these algorithms are capable, under ideal circumstances, of deconvolution solutions with so-called **superresolution** along the *Z* axis—the recovery of detail lost from the image by the convolution of the optics (i.e., beyond diffraction-limited resolution). This phenomenon is usually explained in terms of "the recovery of lost spatial frequencies" or the "**missing cone**" of *z* information (Hiraoka *et al*., 1990; Goodman, 1996), a reference to the shape of the PSF in **Fourier space** (Fig. 2B; Technical Summary 2).

Technical Summary 2: Fourier Transformation and Fourier Space

Fourier transformation represents an image in terms of the spatial frequency information it contains. Sharp edges or fine details correspond to high spatial frequencies; large areas of slowly changing intensity have low spatial frequencies. The entire image can be considered to be the result of the combination of a set of complex "waves." The summation of these waves to create the image is described mathematically as the three-dimensional integral of many simple sinusoidal wave functions, each having specific frequencies, phases, and amplitudes. The Fourier transform of the image (a "discrete Fourier transform" in the case of image data) is a plot of the frequency information present in the real space image, each point representing a particular spatial frequency (see figure below; Hecht, 2002).

1. Fourier transformation is used in deconvolution processing simply because the convolution calculation is much faster in Fourier space (*Frequency*$_x$, *Frequency*$_y$, *Frequency*$_z$) than in real space *x*, *y*, *z* (Van der Voort and Hell, 1997).

2. In Fourier space, the dimensions along the axes are spatial frequency. These reciprocal space coordinates do not map directly to *x*, *y*, *z* positions in real space, but are related to them reciprocally, i.e., things that are closer together in real space (fine details) give high spatial frequency components that are further from the mathematical origin of the Fourier transform in Fourier space and *vice versa*. For this reason, Fourier space is often referred to as "reciprocal space." Amplitudes in a real space image result from the summed amplitudes of each spatial frequency component (effectively how often a particular frequency occurs).

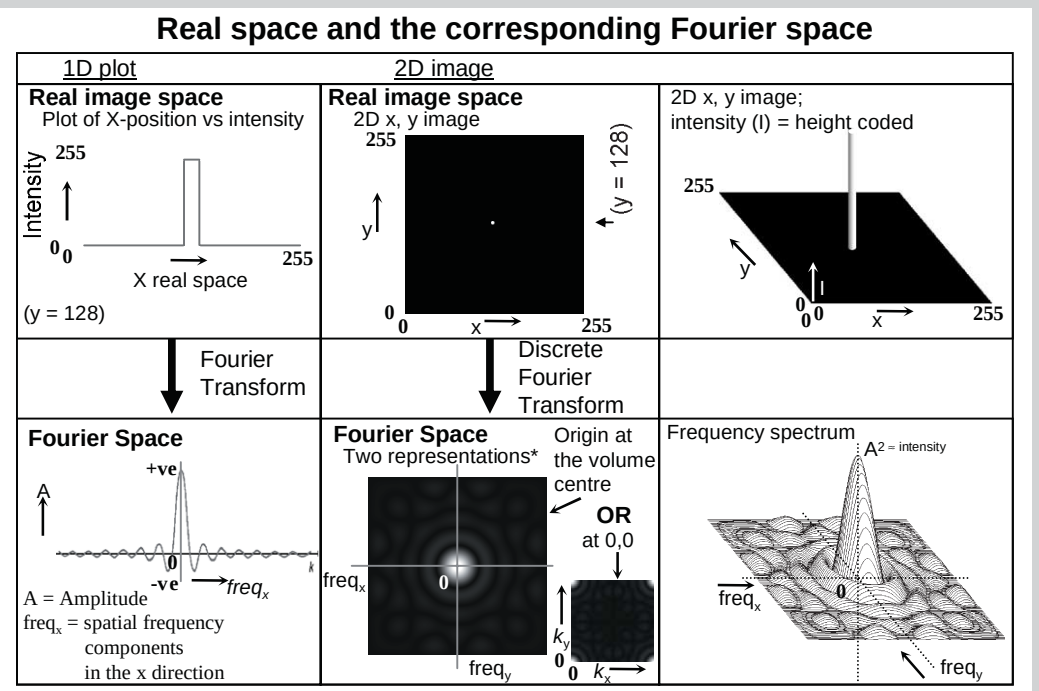

* Note the two different ways that the Fourier space image can be represented depending upon where the origin is located (see also Fig. 2B). The lack of complete radial symmetry in the discrete Fourier transform of the 2D image is an artefact of the discrete Fourier transform algorithm used (Image-J, FFT; NIH).

The name used for the "constrained iterative" class of deconvolution refers to the two critical features that define it: "constrained" and "iterative." The term "**constrained**" refers to the use of the "**positivity constraint**." "**Iterative**" refers to the way in which these algorithms are implemented by repeated cycles of comparison and revision.

The positivity constraint is simply a mathematical term in the algorithm that rejects solutions for the image intensity at any point that give negative values. This limits possible solutions to more realistic outcomes—photons are there or not there, but are never negative. The positivity constraint means that there is no longer a simple linear relationship between the collected image and the deconvolved result, as with the inverse linear filter. Such algorithms are, therefore, also known as **nonlinear methods**. [The positivity constraint is similar in concept to **regularisation** (Table I), which also imposes constraints on possible solutions, but should not be confused with it.] A consequence of the positivity constraint is that it confers the superresolution capabilities of these algorithms by allowing meaningful extrapolation to "recover" some of the z information missing from raw data due to the convolution by the PSF of the microscope (Hiraoka *et al*., 1990; Goodman, 1996).

The iterative process of these deconvolution algorithms may be described in simplified empirical terms as follows. An "**initial guess"** at the deconvolved solution (i.e., the true object) is generated from raw image data. This **initial guess** can be different depending upon the actual algorithm used and may be raw image data transformed with a fast, simple, linear inverse filter step (see Table I) or simply raw image data itself after smoothing. The next step assesses the success of the initial guess as an estimate of the true object by comparing the guess convolved with the PSF of the microscope with the raw original image data. If the guess is correct, then convolving it according to the expected relationship between the true image and collected image (on the basis of the appropriate PSF, see Technical Summary 1) should yield values equivalent to raw image data, i.e., the difference between the two should be minimal. Iterative processing then begins: repeated cycles of calculating a revised convolved guess and comparing with original data operate to incrementally minimise the difference between the two. The positivity constraint is imposed at each revision of the guess. In practice, the number of iterations is predetermined either as a definite number of cycles (which can be from tens to hundreds depending upon data and algorithm, Table I) or when a predefined limit is reached in terms of the difference found upon comparison. Generally, excessive numbers of cycles are nonproductive and an optimum can be found for one's particular data type, this is commonly between 10 and 40. The final guess is taken to be the optimally deconvolved image.

A consequence of all this processing is that implementation is very computationally demanding and so potentially slow. However, modern computers have become so fast and relatively inexpensive that a large deconvolution task, such as a stack of 64 z sections, each of 512 × 512 pixels, can be completed in a few minutes.

C. Using Deconvolution

To achieve the best image quality from a wide field imaging system (i.e., resulting in features sharply defined by high contrast and with a resolution approaching the diffraction limit), deconvolution is almost indispensable.

Wide-field deconvolution is appropriate to many imaging applications. However, it works best for 3D image sets obtained from thin (>50 μm) culture cells or optically very transparent material with low background fluorescence. These criteria are most usually met with fixed material. Live cell imaging is far more challenging for deconvolution, as it introduces problems such as motion blur and increased scattering, bleaching, and **spherical aberration** (SA) made worse by the constraints on excitation exposure due to phototoxicity. Deconvolution can be used to assist visualization of fine structures (Figs. 3 and 4), for calculating z projections (extended focus images), for 3D rendering and quantitative volume analysis, for colocalisation studies (Landmann, 2002), and for fast quantitative tracking of dynamic structures (MacDougall *et al*., 2003).

Wide-field deconvolution can provide a similar degree of reduction in out-of-focus blur as does confocal microscopy, but without the elimination and loss of signal associated with passing the emitted light through a confocal pinhole (Swedlow *et al*., 2002; Pawley and Czymmek, 1997). Aided by the high quantum efficiency (QE) charge-coupled device (CCD) detectors used (Amos, 2000), wide field is both fast and sensitive compared to point scanning confocal imaging, making it especially useful for rapid imaging of labile, dynamic processes in live material (Periasamy *et al*., 1999; Wallace *et al*., 2001; Swedlow *et al*., 2002).

Confocal microscopes, however (particularly in the special case of multiphoton imaging), are better at imaging thick, opaque, and scattering specimens with higher background fluorescence (Periasamy *et al*., 1999; Diaspro, 2001; Swedlow *et al*., 2002).

Confocal systems also tend to have simultaneous multichannel imaging, which is not common for wide field. On the down side, confocals are usually photon limited and so can only be used effectively with samples that are bright enough to see clearly by eye and that have a narrow dynamic range of signal strength, as dim samples require intense illumination (which promotes bleaching) and high photomultiplier (PMT) gain settings (which increase noise). Point scanning confocals also tend to be slow, which means that they suffer from motion blur artefacts when imaging dynamic processes in living cells.

Deconvolution and confocal imaging are by no means mutually exclusive: confocal imaging can nearly always benefit from the improvements in contrast, signal-to-noise ratio, and resolution afforded by restorative deconvolution methods (Wiegand *et al*., 2003). Furthermore, while excluded photons cannot be restored, the application of deconvolution to confocal images does allow the confocal pinhole to be opened slightly during imaging, sacrificing confocality but increasing signal and reducing spherical aberration effects (Pawley, 1995). The brighter but more blurry images are then restored by deconvolution. This is particularly helpful where SA precludes the use of small pinhole settings, e.g., when imaging deep within a specimen (>10 μm). However, one of the biggest limitations when deconvolving confocal images is that they tend to be very noisy because of the low signal available due to the low light throughput and low quantum efficiency of photon multipliers used as detectors in confocal imaging. This problem can best be dealt with either by averaging frames or decreasing scan rate, both at the expense of speed, rather than by increasing the gain on the PMT (which merely introduces more noise). The *Huygens Professional* software from scientific volume imaging (SVI) addresses the noise content of raw data and makes use of this information during restoration. Another potential problem with deconvolution of laser scanning confocal images is that the pinhole size affects the point spread function. SVI's *Huygens* deconvolution software or Autoquant's *Autodeblur* program both offer solutions to this problem in that they have options to take account of the effect of the confocal pinhole on the PSF.

The issues of limited signal to noise and slow scan speed of point scanning confocals means that the generation of image data of sufficient quality to fully benefit from deconvolution is not well suited to fast live-cell imaging. A spinning disc (or "multifocal") confocal microscope, however, uses multiple pinholes for high-speed scanning and captures images on a highly sensitive CCD camera, which is inherently much less noisy than a PMT, combining the advantages of increased contrast of confocal imaging with the efficiency of the CCD detector and speed of wide field. *Huygens* (SVI) provides a deconvolution algorithm specifically tailored to the multiple scanning spots of this form of imaging.

While true deconvolution is a spatial 3D (x, y, z) phenomenon, often the need is to process tme-lapse data (x, y, and *time*). Algorithms exist that are specifically designed to deal with such data (see later for details); however, deconvolution with only spatial 2D data is necessarily not as effective as with a full 3D stack of z sections, as it lacks information to take proper account of distortion in the z dimension. It is also important to note that deconvolution cannot take account of "motion blur" during image capture so suitably short exposure times are essential.

IV. PRACTICAL IMPLEMENTATION OF DECONVOLUTION

Deconvolution, particularly the more advanced approaches, is implemented through a software package where the algorithm is generally assisted by data correction before and noise reduction steps both before and between iterations. With a given deconvolution package, the quality of results obtained will depend foremost upon the quality of raw image data and upon the accuracy of PSF data. Next in importance is the algorithm used and how well it is implemented: noise handling, background or dark signal correction, the initial guess, the regularisation parameter, and filtering and smoothing steps. As different settings, algorithms, or packages may have varying success with different data, it is invaluable to test different programs to understand how a program behaves with your own raw data (Fig. 4A–4H) and to pay close attention to software manufacturers' criteria for raw data and data collection.

A. Collection of Raw Image Data

The quality of raw data is arguably the most important determinant in obtaining good deconvolution results. Essentially, improving raw data involves improving the **useful** signal-to-noise ratio of images (Pawley, 1995). The most important factors relating to this are given in Technical Summary 3. In our experience, it is always easier to meet criteria for good imaging in fixed material than it is for living material

where compromises must be made (Davis and Parton, 2004).

In some situations, such as rapid time-lapse experiments with live material, it is desirable to collect 2D x, y images rather than full 3D x, y, z data sets at each time point. Some 3D iterative algorithms will permit limited processing of 2D data sets by effectively ignoring the z dimension (e.g., Applied Precision's *softWoRx*; Figs. 4D and 4H). In such cases, "displaced" out-of-focus light in the plane of imaging is effectively reassigned to its point of origin within the same plane, but out-of-focus light originating from other planes of focus is ignored. Accordingly, this works best when the out-of-focus blurring effect in z is least detrimental, i.e., with low numerical aperture, low magnification objectives, or thin, optically transparent specimens. Autoquant's *Autodeblur* program suite offers an iterative blind algorithm for use with 2D images that similarly tackles x, y data on the assumption that everything is in one plane of focus, which is acceptable for thin specimens. This should not be confused with the no-neighbours algorithm (Table I), a simple deblurring method for 2D data, which is essentially a contrast enhancement algorithm.

Technical Summary 3: Data Collection Procedures

1. Use a correctly set up and aligned microscope with high-quality objective lenses, accurate z control (by Piezo focusing or motorised stage, Fig. 5), and low noise detectors of good dynamic range and high QE (proportion of photons arriving at the detector that go to produce an output signal).

The quality of deconvolution is dependent upon correct positional information. Pixel sizes should be determined by accurate calibration of the image in x and y, and the z drive should be as precise and reproducible as possible. [For example, the nanomovers offered by Applied Precision Inc. (API) for their *Deltavision* system have 4 nm precision and 30 nm repeatability. Pifoc drives supplied by Precision Instruments are more accurate and reproducible, depending on the speed of movement and the time allowed to settle (Fig. 5), but alter the point spread function and can only be mounted on objection at a time.]

In general, current deconvolution methods are poor at taking account of aberrations in the imaging optics or distortions produced by imaging in thick specimens (primarily SA) or by motion blur. Sample preparation using appropriate mounting media to match the refractive index (RI) of the specimen and the use of correct immersion medium for the objective used (dry, oil, water, or glycerol) can reduce spherical aberration. It is also important to use the correct coverslip thickness or correction collar setting for the objective (default 0.17 mm; #1.5) and to ensure that as far as possible the specimen is immediately adjacent to the coverslip. Imaging deep into specimens (>10 µm) increases SA, which can be partly corrected using objectives with correction collars or by using immersion oils of higher than normal RI (Fig. 6; Davis, 2000).

2. To realise the optical resolution of your imaging system, it is important to follow the **Nyquist** sampling rule by using a pixel size in the electronic imaging device at least two times smaller (ideally, a minimum 2.3 times) than the expected optical resolution in x, y, and z (Pawley, 1995; Jonkman *et al*., 2003). It is possible to determine the theoretical optical resolution based upon the numerical aperture of the objective and emission wavelength using the equation below. The values obtained should be used as an estimate on which to base the digital sampling size. However, in reality it may benefit the final result to make a small

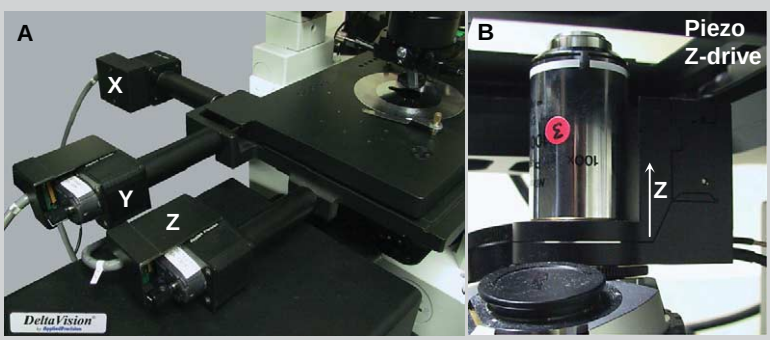

FIGURE 5 Different approaches to z movement control. (A) An x, y, z motorised stage from the API *Deltavison* system. (B) A piezo z-drive nosepiece from Precision Instruments. Note that use of a nosepiece under an objective may alter its PSF.

RI	1.502	1.506	1.510	1.514	1.532

	RI		RI
Air	1.00	Cargille Oils	1.33–1.53
Water	1.33	Vectashield	1.46
Glycerol	1.47	Cytoplasm	1.35–1.45
Glass	1.515	Membrane	1.46–1.6

FIGURE 6 Cargille immersion oils of varying refractive index (RI) and several useful RI values. Note that dilutions of glycerol (80 to 40%) give RI of 1.446 to 1.391.

sacrifice in the sampling rate by binning pixels on a CCD readout to boost signal-to-noise ratio, increase imaging speed, or avoid fluorochome photobleaching. Figure 4C shows deconvolution result improvement with better x, y spatial sampling (0.106 µm pixel) compared to Fig. 4B (0.212 µm), despite the lower fluorescence signal.

Calculation to determine theoretical resolution limits:

$$\text{Lateral } (XY) \text{ resolution} = 0.61 * \text{wavelength}_{\text{emision}} / \text{numerical aperture}_{\text{objective}}$$

$$\text{Axial } (Z) \text{ resolution} = 2 * \text{wavelength}_{\text{em}} * \text{refractive index} / (\text{numerical aperture}_{\text{obj}})^2$$

(refractive index in this case refers to the **specimen immersion medium** RI)

3. In general, it is not advisable to collect Z planes so far below or above the best focus that only blur is seen, as you only end up bleaching the sample.

4. Noise is a significant problem for deconvolution and should be reduced during collection as much as possible. Noise is generally given as the signal-to-noise ratio (S/N; Sheppard, 1995). Poisson distributed Shot noise ($S/N = n/\sqrt{n}$ or simply $\sqrt{n}$, where n may be approximated as the image signal) is the fundamental limitation in S/N. As the number of photons detected increases, the signal-to-noise ratio improves according to the Poisson statistics of photon detection. The signal should not, of course, be so high as to saturate the detector. Both the *Huygens* (SVI) and *Autodeblur* (Autoquant) programs make use of "roughness penalty factors," which, unlike smoothing filters, can be set by the user to constrain their deconvolved solutions to reduce noise while preserving edge features.

The detector should have good dynamic range, high quantum efficiency (QE), low dark signal, and low readout noise (Amos, 2000). When taking short exposures with CCD detectors, readout noise tends to be the most important source of detector noise, whereas when taking long exposure, dark current predominates.

Slow-scan cooled CCD detectors with low dark current and readout noise, reading out pixel intensities as 12–16 bit images (2^{14} = 4096, 2^{16} = 65,536 intensity levels), are used most commonly in wide-field fluorescence imaging systems. They can produce images with a large dynamic range (total intensity levels/intensity levels of noise) and favourable overall S/N ratio.

Confocal systems are less light efficient, and the images they produce are generally photon limited and most commonly recorded as only 8 bit data (= 256 intensity levels). Therefore confocals are more prone to noise problems. Point scanning confocals use relatively low QE photomultipliers, whereas disc scanning systems use CCDs. Imaging only bright signals or averaging several frames to count more photons can help reduce such noise problems.

5. Generally a **dark signal** should be determined (by collecting an image without illumination). However, as different algorithms deal with this parameter differently, which can have significant effects on deconvolution, its use requires careful consideration. In certain algorithms, if too little subtraction correction is made the positivity constraint is not implemented correctly, too much and genuine signal is lost. *Huygens* Professional (SVI) permits automatic estimation or manual input of this information. Some programs correct for **background** signal from part of an image that does not include the specimen (but which can, however, include certain sources of **autofluorescence** from slide preparations and evenly distributed **non-specific staining**).

6. Intensity fluctuations due to light source flicker or bleaching during the collection of z sections or time series images have an adverse affect on deconvolution. Using stable power supplies, regularly changing **mercury arc lamps**, or measuring fluctuations and correcting collected data can help significantly (*DeltaVision* System, API). Bleaching may be reduced by the use of an antifade reagent, which are available commercially or can be home made. Some algorithms include bleaching correction based upon an expected theoretical rate of decline in fluorescence.

B. The PSF (and Its Fourier Transform the OTF)

In addition to optimising raw image quality, using the correct PSF for the image being deconvolved is fundamental to the final result, as one might expect

from the convolution relationship discussed in detail earlier (Fig. 1; Fig. 4B compared to Fig. 4E). A PSF may be empirical (i.e., measured; Hiraoka *et al*., 1990; but see Van der Voort and Strasters, 1995; Davis, 2000) or theoretical (calculated). The former is generally recorded by 3D imaging of subresolution beads using exactly the same optics as used to image the specimen, whereas the latter is generated by the software package used, after inputting the emission wavelength, objective lens details, and refractive index of the immersion medium and mounting medium (e.g., *Huygens* from SVI; *Zeiss 3D Deconvolution Module* from Zeiss; *Autodeblur* from Autoquant). Important considerations relating to PSFs are given in Technical Summary 4.

Technical Summary 4: Use of PSF (OTF)

Empirical PSFs

1. If collected correctly, these have the greatest potential for high-quality deconvolution of images taken with high numerical aperture lenses. However, a poor empirical PSF is certainly worse than a theoretical one (Hiraoka *et al*., 1990).
2. Are often collected at 488-nm excitation and 520-nm emission wavelengths. Software packages usually make adjustments when the actual imaging situation is at a different wavelength. *Huygens* (SVI) offers the possibility of multiwavelength PSF processing as an aid to chromatic aberration correction in colocalisation.
3. Experience reveals that collecting a PSF to match the true aberrated imaging situation *in vivo* (e.g., by injecting fluorescent beads into a cell or by mounting beads so that they are imaged through a particular depth of media of refractive index close to that of a cell) is less effective than using a PSF corresponding to optimal imaging conditions and aspiring to match *in vivo* imaging conditions to that situation.
4. Some software packages come with prerecorded optimised (e.g., averaged over many beads or "processed" by averaging, smoothing, or deconvolving) empirical OTF's for particular objectives, and using these is often preferable to collecting your own (e.g., API's *softWoRx* package; Fig. 2B). *Huygens* (SVI) permits optimisation of your own empirical PSF data by registering and averaging images of multiple beads and correcting for the fact that a bead is, in reality, not an infinitely small point source.
5. In the case of objective lenses with numerical aperture collars, it may be necessary to collect specific PSFs for each setting of the collar (Figs. 1C and 1D), similarly for different confocal pinhole apertures.

Theoretical PSFs

1. These work well with low NA, low magnification objectives.
2. They are usefully employed in some software packages for use with confocal (and MP) imaging, as they can be optimised for different confocal pinhole settings by calculation.

Blind Deconvolution, Estimated, or Adaptive PSF

1. "Blind deconvolution" methods (Table I; renamed "adaptive blind deconvolution," Autoquant, Autodeblur) offer an effective way to circumvent some of the issues mentioned earlier. Instead of using an empirical or calculated PSF, an estimate of the "true" PSF is generated iteratively from the image data itself at the same time as image restoration (Holmes *et al*., 1995).
2. Adaptive blind deconvolution can be useful where a representative PSF is not easy to obtain, such as with confocal imaging using variable pinhole settings, multiphoton imaging, or imaging in the presence of SA.
3. Adaptive blind deconvolution is not a perfect solution, as it is only an estimate determined on the basis of severe constraints imposed upon possible solutions.

Ultimately, it is necessary to determine by trial and error the approach that works best for any particular data type. In virtually all cases, the use of a single PSF for an entire 3D image set is a compromise, especially with live material. Generally, the optical conditions vary between parts of the same image or at different z planes (i.e., the PSF itself varies spatially). However, most current algorithms assume a spatially invariant PSF to simplify processing (Hiraoka *et al*., 1990).

C. Computer System Organisation

Advances in computer technology have had a great impact upon deconvolution, largely because of the computational demands of this approach (Holmes *et al*., 1995; Wallace *et al*., 2001). Be aware that with the requirements of deconvolution for multiple z planes and with CCD image detection now able to generate $1024 \times 1024 \times 16$ bit images many times a second, computer systems must deal with many gigabytes of information within relatively short periods of time. Implementation of deconvolution algorithms requires appropriate processor power and adequate data transfer, short-term storage, and archiving capabilities. While in the past deconvolution required special high-performance workstations, dual processor personal computers with at least 1 Gb of RAM, greater than 50-

Gb hard drives, CD, or DVD-R writers and network connection speeds of 100 Mbit/s to 1 Gbit/s are now standardly used for deconvolution. To increase the efficiency of a laboratory, it is desirable to have separate computers dedicated to image capture and image analysis. A high-quality properly set up monitor (24- or 32-bit colour; calibrated to set contrast and brightness) is necessary for viewing image data. Where many users are involved, it is desirable to have a rack-mounted cluster of many computers linked to a RAID disk (redundant array of independent discs), networked to stand-alone acquisition and processing stations for individual user access.

V. ASSESSMENT OF DECONVOLVED IMAGES

Deconvolution works best when imaging conditions are near optimal, which is possible for fixed material but rarely achieved in living specimens (Kam *et al*., 2000). If the raw images are poor, deconvolution can perform poorly or even produce artefacts that degrade the images. Visual assessment of the removal of out-of-focus blur is a useful guide of success, taking care to correctly set the brightness and contrast of the image display. Features should emerge sharpened with increased brightness after processing. However, as a general guide, you should only trust features observed in the deconvolved image when they are also present, however faintly, in the unprocessed original image. Comparison of the deconvolved results with images acquired by an independent technique, such as electron microscopy or confocal imaging, is also useful. Detailing deconvolution artefacts and their basis is beyond the scope of this article and are dealt with elsewhere (e.g., Wallace *et al*., 2001). In general, small punctate or ring-like features should be viewed with scepticism, while excessive noise suggests poor initial data or problems with the parameters used. If detail appears to be lost after processing, then initial background subtraction may have been too high or filtering and noise suppression steps too aggressive.

VI. QUANTIFICATION

As true deconvolution algorithms (but not deblurring methods) relocate signal to the point of origin within 3D features, while decreasing intensity in the background, they should conserve the sum of the fluorescence signal and permit or even improve quantitative analysis of data (van Kempen *et al*., 1997; Wiegand *et al*., 2003). However, some argue that the reassignment of distant, dim light where noise dominates (Pawley and Czymmek, 1997) and also the processing by which noise is dealt with [particularly in the case of blind deconvolution (Van der Voort and Strasters, 1995)] result in absolute conservation being compromised. If strict quantitative intensity comparison (or intensity ratio calculation) is required, undeconvolved data should always be analysed as well for comparison and independent controls sought. As with all image analysis, caution should be exercised when making direct comparisons between different images—initial imaging conditions and deconvolution processing should be comparable between data sets.

Quantitative positional and structural analysis, which is not so dependent upon absolute intensity values, including centroid determination, movement tracking, volume analysis, and colocalisation, have all been performed successfully on deconvolved data (e.g., Van Der Voort and Strasters, 1995; Wallace *et al*., 2001; Landmann, 2002; Wiegand *et al*., 2003; Macdougall *et al*., 2003). Where quantitative analysis is intended, it is essential to apply deconvolution systematically, with an understanding of possible artefacts and, if possible, with confirmation by an independent technique.

VII. FUTURE DEVELOPMENTS

Improvement in the quality of the initial imaging is the most effective way to enhance deconvolution. For example, correct sampling, noise reduction, use of photon limited (rather than noise limited) detectors, precise and rapid piezo *z* movers, and better corrected objectives all help to improve the quality of imaging and hence the deconvolution result. However, advances are also being made in the quality of processing. Faster computers are allowing the use of increasingly more complex calculations within realistic timescales. More advanced deconvolution algorithms are being developed to deal with the poor signal to noise and with the aberrations associated with imaging *in vivo* (Holmes *et al*., 1995; Kam *et al*., 2000). **Pupil functions**, which are in use in astronomy, are beginning to be used in biology (Hanser *et al*., 2003) in order to correct for asymmetries in the PSF (current deconvolution algorithms assume that the PSF is radially symmetric in *x* and *y* and bilaterally symmetric in *z*). Iterative constrained algorithms aided by **wavelet analysis** may allow us to tackle situations of poor

signal to noise and distorted PSF when imaging deep *in vivo* using confocal and multiphoton techniques (Boutet de Monvel, 2001; Gonzalez and Woods, 2002).

Acknowledgments

We thank John Sedat, Satoru Uzawa, Sebastian Haase, Lukman Winito, and Lin Shao (University of California San Francisco) and also Zvi Kam (Weizmann Institute of Science) for interesting discussions relating to deconvolution. We are also indebted to Jochen Arlt and the COSMIC imaging facility (Physics Department, University of Edinburgh) for invaluable technical advice and access to advanced imaging equipment and also to Simon Bullock, David Ish-Horowicz, Daniel Zicha, and Alastair Nicol (Cancer Research-UK, London) for allowing access to their imaging equipment and for the introduction to wavelet analysis. Thanks for technical advice must also go to the many contributors to the Confocal List (URL: http://listserv.acsu.buffalo.edu/cgi-bin/wa?S1=confocal); Carl Brown of Applied Precision Inc. (USA); Jonathan Girroir of AutoQuant Imaging (USA); and Rory R. Duncan, University of Edinburgh Medical School. We are grateful to Renald Delanoue, Veronique van De Bor, and Sabine Fischer-Parton (University of Edinburgh) for critical reading of the manuscript.

Useful Web Sites

Andor Technology (EMCCD cameras) www.andor-tech.com

Applied Precision (Deltavision) www.api.com/lifescience/dv-technology.html

Autoquant (see education pages) www.aqi.com also www.leica.com

Carl Zeiss (3D Deconvolution) www.zeiss.co.uk (*AxioVision, 3D-Deconvolution*)

Huygens (see essential user guide) www.svi.nl also www.bitplane.com and www.vaytek.com

Image J (FFTJ and Deconvolution-J) http://rsb.info.nih.gov/ij/plugins/fftj.html

Mathematica for wavelet analysis www.hallogram.com.mathematica.waveletexplorer/www.wolfram.com/products/applications/wavelet/

Power Microscope On-line deconvolution www.powermicroscope.com

References

Agard, D. A. (1984). Optical sectioning microscopy: Cellular architecture in three dimensions. *Ann. Rev. Biophys. Bioeng.* **13**, 191–219.

Agard, D. A., Hiraoka, Y., Shaw, P., and Sedat, J. W. (1989). Fluorescence microscopy in three dimensions. *Methods Cell Biol.* **30**, 353–377.

Amos, W. B. (2000). Instruments for fluorescence imaging. *In* "*Protein Localization by Fluorescence Microscopy*" (V. J. Allan, ed.), pp. 67–108. OUP, Oxford.

Boutet de Monvel, J., Le Calvez, S., and Ulfendahl, M. (2001). Image restoration for confocal microscopy: Improving the limits of deconvolution, with application to the visualization of the mammalian hearing organ. *Biophys. J.* **80**(5), 2455–2470.

Davis, I. (2000). Visualising fluorescence in *Drosophila*: Optimal detection in thick specimens. *In* "*Protein Localisation by Fluorescence Microscopy: A Practical Approach*" (V. J. Allan, ed.), pp. 131–162. OUP, Oxford.

Davis, I., and Parton, R. M. (2004). Time-lapse cinematography in living *Drosophila* tissues. *In* "*Live Cell Imaging: A Laboratory Manual*." (R. O. Goldman and D. L. Specktor, eds.), pp. 385–407. Cold Spring Harbor Laboratory Press, Cold Spring Harbor, NY.

Diaspro, A. (2001). "*Confocal and Two-Photon Microscopy: Applications and Advances*." Wiley-Liss, New York.

Gonzalez, R. C., and Woods, R. E. (2002). "*Digital Image Processing*," 2nd Ed. Addison-Wesley, San-Francisco.

Goodman J. W. (1996). "*Introduction to Fourier Optics*," Chap. 6. McGraw-Hill, New York.

Gusstafsson, M. G. L. (1999). Extended resolution fluorescence microscopy. *Curr. Opin Struct. Biol.* **9**, 627–634.

Hanser, B. M., Gustafsson, M. G. L., Agard, D. A., and Sedat, J. W. (2003). Phase retrieval of high-numerical-aperture optical systems. *Optics Lett.* **28**, 801–803.

Hecht, E. (2002). "*Optics*," 4th Ed., pp. 281–324 and 519–559. Addison Wesley, San Francisco.

Hiraoka Y., Sedat J. W., and Agard D. A. (1990). Determination of three-dimensional imaging properties of a light microscope system: Partial confocal behaviour in epifluorescence microscopy. *Biophys. J.* **57**, 325–333.

Holmes J. H., Bhattacharyya, S., Cooper, J. A., Hanzel, D., Krishnamurthi, V., Lin, W., Roysam, B., Szarowski, D. H., and Turner, J. N. (1995). Light microscope images reconstructed by maximum likelihood deconvolution. *In* "*The Handbook of Biological Confocal Microscopy*" (J. B. Pawley, ed.), 2nd Ed., pp. 389–402. Plenum Press, New York.

Jonkman, J. E. N., Swoger, J., Kress, H., Rohrbach, A., and Stelzer E. H. K. (2003). Resolution in optical microscopy. *Methods Enzymol.* **360**, 416–446.

Kam, Z., Hanser, B., Gustafsson, M. G. L., Agard, D. A., and Sedat, J. W. (2000). Computational adaptive optics for live three-dimensional biological imaging. *Proc. Natl. Acad. Sci. USA* **98**, 3790–3795.

Landmann, L. (2002). Deconvolution improves colocalisation analysis of multiple fluorochromes in 3D confocal data sets more than filtering techniques. *J. Microsc.* **208**(2), 134–147.

MacDougall, N., Clark, A., MacDougall, E., and Davis, I. (2003). *Drosophila* gurken (TGFalpha) mRNA localises as particles that move within the oocyte in two dynein-dependent steps. *Dev. Cell* **4**, 307–319.

Pawley, J. B. (1995). "*Handbook of Biological Confocal Microscopy*," 2nd Ed. Plenum Press, New York.

Pawley, J. B. (2000). The 39 steps: A cautionary tale of quantitative 3-D fluorescence microscopy. *BioTechniques* **28**, 884–888.

Pawley, J. B., and Czymmek, K. J. (1997). 3D microscopy: Confocal, deconvolution or both. Online at URL: http://www.biotech.ufl.edu/sems/183.pdf (accessed July 5th 2004).

Periasamy, A., Shoglund, P., Noakes, C., and Keller, R. (1999). An evaluation of two-photon versus confocal and digital deconvo-

lution fluorescence microscopy imaging in *Xenopus* morphogenesis. *Microsc. Res. Techn.* **47**, 172–181.

Scalettar, B. A., Swedlow, J. R., Sedat, J. W., and Agard, D. A. (1996). Dispersion, aberration and deconvolution in multi-wavelength fluorescence images. *J. Microsc.* **182**(1), 50–60.

Sheppard, C. J. R., Gan, X., Gu, M., and Roy, M. (1995). Signal-to-noise in confocal microscopes. *In "The Handbook of Biological Confocal Microscopy"* (J. B. Pawley, ed.), 2nd Ed., pp. 363–371. Plenum Press, New York.

Swedlow, J. R., Hu, K., Andrews, P. D., Roos, D. S., and Murray, J. M. (2002). Measuring tubulin content in *Toxoplasma gondii*: A comparison of laser-scanning confocal and wide-field fluorescence microscopy. *Proc. Natl. Acad. Sci. USA* **99**, 2014–2019.

Van der Voort, H. T. M. (1997). Image restoration in one- and two- photon microscopy. Online at URL: http://www.svi.nl/education/#Discussions (accessed July 5th 2004).

Van der Voort, H. T. M., and Strasters, K. C. (1995). Restoration of confocal images for quantitative image analysis. *J. Microsc.* **178**(2), 165–181.

VanKempen, G. M. P., vanVliet, L. J., Verveer, P. J., and vanderVoort, H. T. M. (1997). A quantitative comparison of image restoration methods for confocal microscopy. *J. Microsc.* **185**(3), 354–365.

Wallace, W., Schaefer, L. H., and Swedlow, J. R. (2001). A working person's guide to deconvolution in light microscopy. *BioTechniques* **31**, 1076–1097.

Wiegand, U. K., Duncan, R. R., Greaves, J., Chow, R. H., Shipston, M. J., and Apps, D. K. (2003). Red, yellow, green go! A novel tool for microscopic segregation of secretory vesicle pools according to their age. *Biochem. Soc. Trans.* **31**, 851–856.

CHAPTER

20

The State of the Art in Biological Image Analysis

Federico Federici, Silvia Scaglione, and Alberto Diaspro

I. INTRODUCTION

The general chain of image acquisition and treatment can be sketched as shown in Fig. 1. Before undertaking analysis of a collected set of images, one should identify the most suitable procedure to be followed. In particular, two different approaches can be outlined:

1. An image *processing* procedure (whose output is an image) requiring the use and development of tools for image enhancement.
2. An image *analysis* procedure in which further quantitative statistics of both morphological and fluorescence intensity parameters are determined, leading to numerical data output.

II. IMAGE PROCESSING

The first steps to be performed are noise reduction, shading correction, contrast, and edge enhancement. Depending on the noise sources and the hardware devices involved, images can be processed via software or hardware. Different standard image processing routines can be run and eventually adapted according to the kind of captured and stored data input (RGB, grey scale, or binary color space, multilayered or single-layered, compressed or uncompressed).

For software data treatment, special algorithms (filters) are used or developed, either directly acting on the original numerical matrix (representative of the image) or within the frequency domain obtained by a particular mapping of the spatial data set through the Fourier transform (Diaspro *et al.*, 2002). Although automated software with a wide range of standard and optimised filters is available, the use of these tools as black boxes can cause new unexpected artefacts to be added to images. This can be particularly risky when dealing with biological samples whose degree of complexity may often prevent the user from relying on his common sense. The final goal of these procedures is that of improving the signal to noise ratio (SNR), leading to better image visualisation without any loss of intrinsic amount of information.

III. IMAGE ANALYSIS

Quantitative image analysis deals with both collecting information from fluorescence intensity signals and obtaining morphological–geometrical parameters from the sample. Different biological treatments and data acquisition procedures (using specific off-line processing) are typically required, according to the topic under study. It is worth listing some of the most commonly used procedures: *colocalization, morphological analysis [geometrical parameter estimation on three-dimensional (3D) and two-dimensional (2D) samples], image classification (fractal analysis and feature extraction), and frequency domain analysis* (Diaspro *et al.*, 1990; Castleman, 1996).

IV. COLOCALIZATION

The observations of *in vivo* cellular details and events often involve the use of single or multifluorescence labelling with a high degree of specificity with the respect of the structures under investigation. The

Copyright 2006, Elsevier Science (USA).
All rights reserved.

necessity of simultaneously imaging different functional parts of samples (such as microtubules, nuclei or mitochondria) demands the use of multiple distinct fluorescence dyes in order to reveal the parts of interest by keeping them visually distinct from one another. In this situation, image acquisition is typically carried on separately at the different excitation wavelengths and the later offline analysis may deal, among other things, with one more problem: that of extracting information about the eventual overlap (colocalization) between the different fluorescence signals expressed by the various part of the sample, which thus occupy the same physical location. This is a crucial task, especially in biological and medical studies where one is interested in studying the molecules distribution with the respect of particular functional structures such as receptors.

Provided that the probes' emission spectra are sufficiently separated and correct filter sets are used during the data acquisition, colocalization means that the emitted fluorescence signals (colors) are pictured within the same pixels. In the case of two-probe labelling (Fig. 2), data analysis can be performed by generating a scatter plot in which x-y coordinates represent, respectively, red and green intensity values, and the intensity of each point (according to a suitable color code) represents the number of pixels with that intensity value (Fig. 3).

In addition to this visualisation, a proper quantification of the degree of colocalization can be obtained by comparing each of the acquired images by means of suitable coefficients (Fig. 4), which may account either for the similarity of shapes between the two images (without considering intensities) or for the

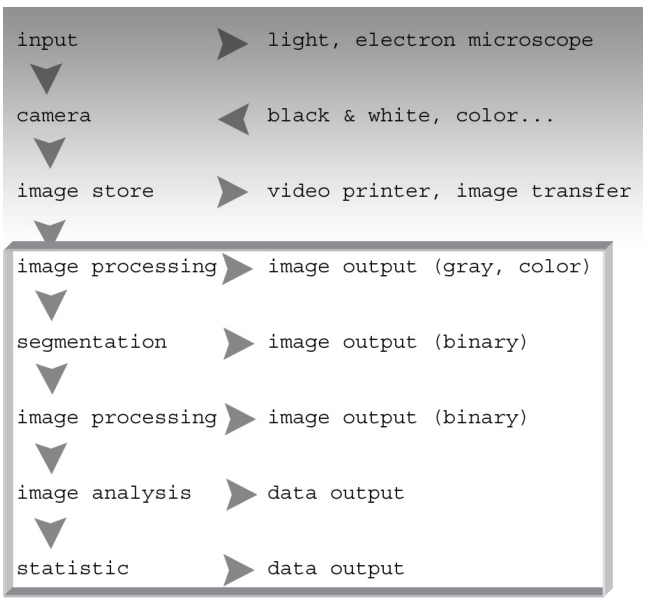

FIGURE 1 Chain of image acquisition and treatment.

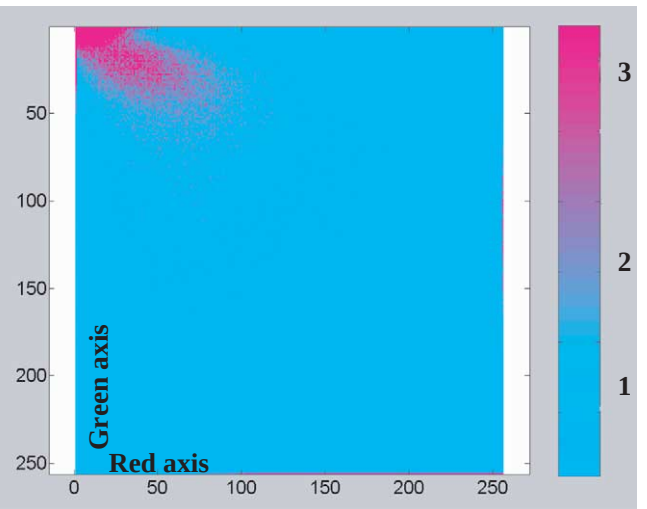

FIGURE 3 Scatter plot: purple dots represent highly colocalized red–green intensity pixels.

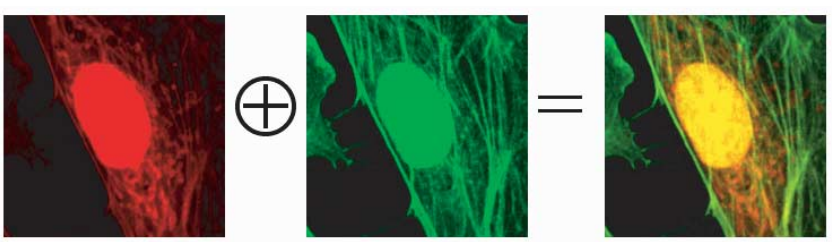

FIGURE 2 Two-photon imaging (750-nm wavelength) of an artery endothelial bovine pulmonary cell. Mitochondria (labelled with MitoTracker) are visible in the red channel, actin filaments (labelled with BODIPY) in the green one, and nuclei (labelled with DAPI) in both. The emission intensity of the nucleus is much higher than the others due to the strong concentration of DNA-bounded DAPI inside the cell with respect to the other dyes. Colocalized pixels are yellow ones in the RGB image (Diaspro, 2001).

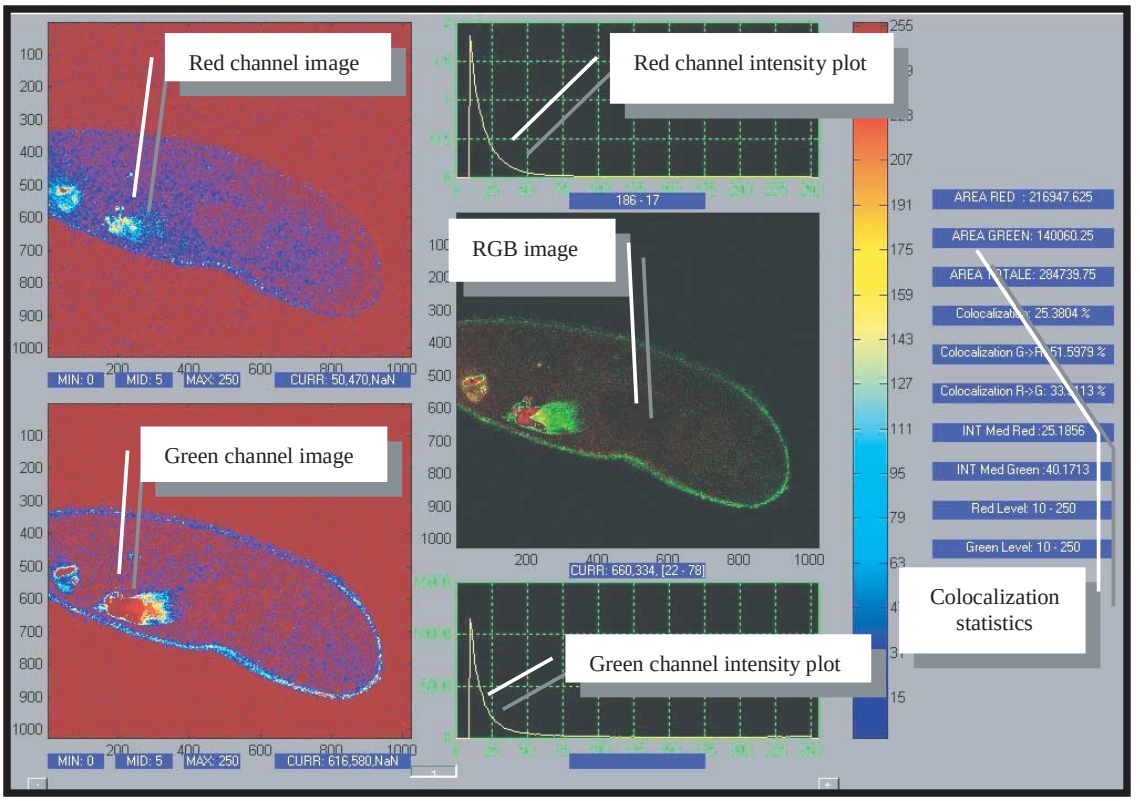

FIGURE 4 Snapshot of a typical image analysis user interface for colocalization analysis. Courtesy of Marco Raimondo and Paola Ramoino, LAMBS, http://www.lambs.it.

difference of intensity between colocalized pixels, depending on the kind of information one is interested in.

A. Morphological Analysis and Classification

Morphological investigations of images are strictly connected to the idea of topological space due to the mathematical environment wherein tools for quantitative analysis are developed. As a first step, this requires a unequivocal relationship between each image array and a set of real space coordinates to be established. For single-layered images, this goal can be accomplished by dividing the field of view (i.e., the real dimension of the region within the image) by the number of pixels, thus getting the effective size of the elementary dot in the image. This is all one typically needs for geometrical calculations in the plane. Multilayered images naturally involve a third dimension so that one more relationship needs to be established between the optical sections and their real world distance from one another. The simplest approach for solving this task consists of assigning the optical sectioning distance (eventually scaled to account for further data acquisition artefacts) to two contiguous slices. Once these correspondences are established between the images and the topological space, further and more complex computer-based processing can be performed, including 3D sample reconstruction (Fig. 5), morphometrical estimations, object counting, and localization (Bianco and Diaspro, 1989; Diaspro *et al*., 1990).

The need of morphometrical measurements is often the main prerequisite in most biological and medical comparative studies where the shape and dimension of structural components of the samples (such as tissues, cells, and organlets) are strictly related to their functions. In these cases, an effective 3D visualization may be nice looking while failing to provide accurate results in terms of accurate characterization of the structural properties of interest. It is far better to use suitable stereological methods, implemented using highly efficient software, involving single slices. These procedures can be either semi-interactive or completely automated. The main difference between these two approaches is that the latter ones are faster but require reliable automatic thresholding and segmentation routines for the recognition of the objects of interest within the images.

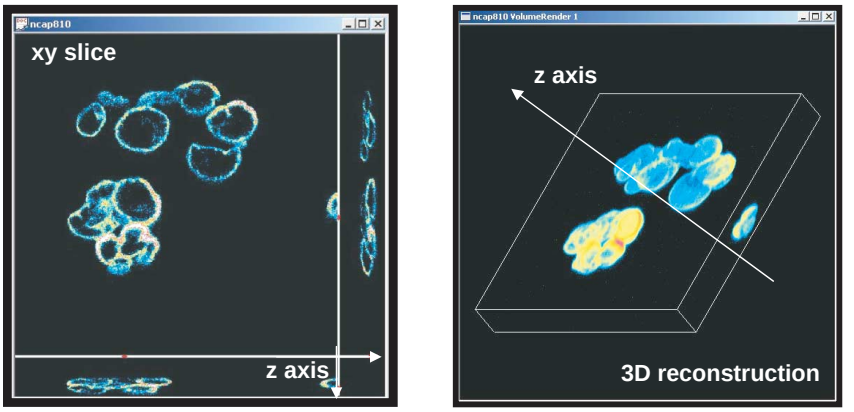

FIGURE 5 Snapshot of a 3D sample data acquisition (left) and 3D sample reconstruction (right).

Several different stereological methods have been tested and improved over the years: the optical dissector principle (Gundersen, 1986; Sterio, 1984) or the unbiased sampling brick rule (Howard *et al*., 1985) for particles counting; the nucleator (Gundersen, 1988) and the planar rotator (Jensen and Gundersen, 1993) applied to a stack of optical sections for estimating the mean particle volume; the optical rotator (Kieu and Jensen, 1993; Tandrup *et al*., 1997), spatial grid method (Sandau, 1987), and "Fakir method" (Kubinova and Janacek, 1998) for surface area estimation; and the vertical slices method (Gokhale, 1990) and global spatial sampling (Larsen *et al*., 1998) for length estimation. Moreover, volume and surface area or curve length estimation can be obtained with known precision and are considered to be free from any systematic error (bias) relating to the sample strategy. Furthermore, they can be undertaken without any previous assumptions about the shape or the structure of the objects under investigation, thus allowing the user to get a realistic average value of the parameters of interest as a result of an average obtained from repeated measurement processes. One more important parameter for many computer vision tasks, such as image classification, is texture segmentation, consisting of splitting an image into regions of similar texture. This task is usually performed in two stages: texture feature extraction (to characterize each texture) and further texture segmentation (to determine homogeneous regions), allowing a proper segmentation of the image.

The limiting factors for all these investigations are the resolution of the imaging system, determined by its point spread function (PSF), and the intrinsic reproducibility of the observed phenomenon itself, which if poor might demand an improvement in the accuracy of the data acquisition protocol (Bianco and Diaspro, 1989; Castleman, 1996).

The approaches discussed so far mainly rest on some common properties of the familiar topological space, but there exist in nature objects whose properties are not fully analysable by any possible set of standard topological parameters. When considering the morphology of samples, for instance, it is very common to take into account those geometrical parameters suggested by a suitable modelling of structures, involving elementary shapes such as lines, circles, spheres, or simple polygon. This allows one both to obtain a preliminary quantitative analysis of the geometrical properties of the samples and to cluster them according to the values of some characteristic parameters. Unfortunately, this method cannot always be applied successfully, as most of the complex biological structures cannot be modelled easily by simple shapes. One popular example is that of the branching structure of many biological structures, such as the arteries, veins, nerves, the parotid gland ducts, or the bronchial tree in the human body. The presence of a certain self-similarity and the lack of a well-defined scale suggest that a complete characterization cannot be based simply on a conventional surface/volume estimation, as such a numerical value does not convey any further information about the degree of complexity of the shape to which it is related. These empirical evidences lead to the idea that some other independent parameter might exist, something like a space-filling factor: this is the fractal dimension (*fd*), existing somewhere between the usual topological dimensions, whose value ranges between 1 and 2, respectively, depending on whether the object fills almost no space (such as in the case of a line) or fills all the available space (such as in the case of a square or a circle). A combination of fractal dimension and standard texture features has been shown to provide better discrimination than standard texture features alone. An example of this

application is that related to the study of the breaking strength of bones. Despite the fact that there is a strong dependence of breaking strength on mineral density, more refined models are required to explain variations in the strength of bones having identical densities. Consideration of the way in which mineral density is arranged within the bones, thus influencing their structural resistance, has led to the use of the fractal index as a parameter, which is both calculated easily from images and particularly efficient for their classification. Other studies employing fractal analysis have involved the characterization of mammographic patterns (Caldwell *et al*., 1990), colorectal polyps (Cross *et al*., 1994), trabecular bones (Cross *et al*., 1993a; Majumdar *et al*., 1993; Benhamou *et al*., 1994), retinal vessels (Mainster, 1990), renal arteries (Cross *et al*., 1993b), Papanicolaou-stained cervical samples (MacAulay *et al*., 1990), and epithelial lesions (Landini *et al*., 1990).

It is worth pointing out here that a variety of procedures have been proposed for estimating the *fd* of images, such as the box-counting method (BC) or the fractional Brownian motion method (FBM); the best algorithm for the job will vary according to the kind of images under study. It can be shown that the BC method is ineffective if applied to low-resolution images, whereas the FBM one reveals its limits when applied to noisy images or to systems with strong local scaling factors.

Moreover, because every *fd* calculation needs a threshold level to be set in order to discriminate different regions within the same image, this implies the existence of a fractal spectrum in which the value of *fd* depends on the threshold level. The best choice for this threshold can be made either from prior knowledge about the inner structure of the sample or through some parameters (such as the linear correlation coefficient for the BC method), intrinsic to the particular *fd* algorithm used, which may somehow account for the fractal dimension.

B. Frequency Domain

Some image analysis techniques employed in a wide range of applications, such as image filtering, reconstruction and compression, turn time domain inputs into frequency domain outputs. A representation of a given multidimensional signal in the frequency domain is often useful for identifying periodical components within signals.

The Fourier transform provides a unique and invertible mapping of original data to frequency domain data represented as complex numbers, termed structure factors, in which the frequency characteristics are displayed in terms of their magnitudes and phases. Both the magnitude and the phase functions of the structure factors are necessary for the complete reconstruction of an image from its Fourier transform. The magnitude-only image is unrecognizable and has severe dynamic range problems. The phase-only image is barely recognizable, i.e., severely degraded in quality. The advantage of using the Fourier transform lies in its invariant properties. It is easy to demonstrate, for instance, that rotating the object merely causes a phase change to occur and that the same phase change is caused to all the structure factors. The magnitude is independent of the phase and so is unaffected by rotation. (This is an example of the very important property of shift invariance.) Second, consider a change of size of the object. This does not change any of the phases and changes the magnitudes of all the structure factors by the same factor. If the magnitude of the spectrum is normalised, then it is invariant to object size as well. Finally, consider the effect of noise and quantisation errors on the boundary. This will cause local variation of high frequency components and will not change the low frequencies. Hence, if the high frequency components of the spectrum are ignored, the rest of the spectrum is unaffected by noise. Thus, for object recognition, the Fourier descriptor offers many advantages and is very useful not only in comprehensively understanding digital image analysis, but also in digital image processing. It could be a useful tool to deal with texture analysis, which is an important field in remote sensing, and it is fast to compute.

V. CONCLUSIONS

This article outlined the fundamental concepts of image processing and image analysis, addressing the main methods and giving a full list of references for deeper insights on topics of interest.

References

Benhamou, C. L., Lespessailles, E., Jacquet, G., Harba, R., Jennane, R., Loussot, T., Tourliere, D., and Ohley, W. (1994). Fractal Organization of Trabecular Bone Images on Calcaneus Radiographs. *J Bone Min. Res.* **9**, 1909–1918.

Bianco, B., and Diaspro, A. (1989). Analysis of three-dimensional cell imaging obtained with optical microscopy techniques based on defocusing. *Cell Biophys.* **15**(3), 189–199.

Caldwell, C. B., Stapleton, S. J., Holdsworth, D. W., Jong, R. A., Weiser, W. J., Cooke, G., and Yaffe, M. J. (1990). Characterisation of mammographic parenchymal pattern by fractal dimension. *Phys. Med. Biol.* **35**, 235–247.

Castleman, K. R. (1996)."Digital Image Processing." Prentice Hall, Englewood Cliffs, NJ.

Cross, S. S., Bury, J. P., Silcocks, P. B., Stephenson, T. J., and Cotton, D. W. K. (1994). Fractal geometric analysis of colorectal polyps. *J. Pathol.* **172**, 317–323.

Cross, S. S., *et al.* (1993a). Trabecular bone does not have a fractal structure on light microscopic examination. *J. Pathol.* **170**, 311–313.

Cross, S. S., Start, R. D., Silcocks, P. B., Bull, A. D., Cotton, D. W. K., and Underwood, J. C. E. (1993b). Quantitation of the renal arterial tree by fractal analysis. *J. Pathol.* **170**, 479–484.

Diaspro, A. (ed.) (2002). "Confocal and Two-photon Microscopy: Foundations, Applications and Advances." Wiley-Liss, New York.

Diaspro, A., Adami, M., Sartore, M., and Nicolini, C. (1990). IMAGO: A complete system for acquisition, processing, two/three-dimensional and temporal display of microscopic bio-images. *Comput. Methods Programs Biomed.* **31**(3–4), 225–236.

Gokhale, A. M. (1990). Unbiased estimation of curve length in 3D using vertical slices. *J. Microsc.* **159**, 133–141.

Gundersen, H. J. G. (1986). Stereology of arbitrary particles: A review of unbiased number and size estimators and the presentation of some new ones, in memory of William R. Thompson. *J. Microsc.* **143**, 3–45.

Gundersen, H. J. G. (1988). The nucleator. *J. Microsc.* **151**, 3–21.

Howard, C. V., Reid, S., Baddeley, A., and Boyde, A. (1985). Unbiased estimation of particle density in the tandem scanning reflected light microscope. *J. Microsc.* **138**, 203–212.

Kieu, K., and Jensen, E. B. V. (1993). Stereological estimation based on isotropic slices through fixed points. *J. Microsc.* **170**, 45–51.

Kubinova, L., and Janacek, J. (1998). Estimating surface area by isotropic fakir method from thick slices cut in arbitrary direction. *J. Microsc.* **191**, 201–211.

Jensen, E. B. V., and Gundersen, H. J. G. (1993). The rotator. *J. Microsc.* **170**, 35–44.

Landini, G., and Rippin, J. W. (1993). Fractal dimensions of the epithelial-connective tissue interfaces in premalignant and malignant epithelial lesions of the floor of the mouth. *Anal. Quant. Cyt. Hist.* **15**, 144–149.

Larsen, J. O., Gundersen, H. J. G., and Nielsen, J. (1998). Global spatial sampling with isotropic virtual planes: Estimators of length density and total length in thick, arbitrarily orientated sections. *J. Microsc.* **191**, 238–248.

MacAulay, C., and Palcic (1990). Fractal texture features based on optical density surface area. *Anal. Quant. Cyt. Hist.* **12**, 394–398.

Mainster, M. A. (1990). The fractal properties of retinal vessels: Embryological and clinical implications. *Eye* **4**, 235–241.

Majumdar, S., Weinstein, R. S., and Prasad, R. R. (1993). Application of fractal geometry techniques to the study of trabecular bone. *Med. Phys.* **20**, 1611–1619.

Manders, E. M. M., Verbeek, F. J., and Aten, J. A. (1993). Measurement of co-localization of objects in dualcolor confocal images. *J. Microsc.* **169**, 375–382.

Puig, D., and García, M. A. (2001). Determining optimal window size for texture feature extraction methods. *In* "IX Spanish Symposium on Pattern Recognition and Image Analysis," Vol. 2, pp. 237–242.

Robert, N., Puddephat, M. J., and McNulty, V. (2000). The benefit of stereology for quantitative radiology. *Br. J. Radiol.* **73**, 679–697.

Sandau, K. (1987). How to estimate the area of a surface using a spatial grid. *Acta Stereol.* **6**, 31–36.

Sterio, D. C. (1984). The unbiased estimation of number and sizes of arbitrary particles using the disector. *J. Microsc.* **134**, 127–136.

Tamames, J., Clark, D., Herrero, J., Dopazo, J., Blaschke, C., Fernandez, J. M., Oliveros, J. C., and Valencia, A. (2002). Bioinformatics methods for the analysis of expression arrays: Data clustering and information extraction. *J. Biotechnol.* **98**, 269–283.

Tandrup, T., Gundersen, H. J. G., and Jensen, E. B. V. (1997). The optical rotator. *J. Microsc.* **186**, 108–120.

CHAPTER

21

Publishing and Finding Images in the BioImage Database, an Image Database for Biologists

Chris Catton, Simon Sparks, and David M. Shotton

I. INTRODUCTION: THE NEED FOR IMAGE DATABASES

Images and videos form a vital part of the scientific record. While the significance of the various genome publications is beyond dispute, attention has now shifted to the organization and integration of information within cells, where the need for functional analysis of gene products is universally recognised. The significance of microscopy images in the process of determining the spatiotemporal expression patterns of gene products cannot be overestimated. The volume of such images is also significant. In a single day, an active cell biology lab may generate between 5 and 50 Gbytes of multidimensional confocal image data or digital video data.

We recently wrote to a colleague requesting a copy of a beautiful confocal image that he had collected some years ago while a graduate student in Heidelberg, which showed the expression sites of a particular gene in the developing mouse embryo. His reply typifies the wasteful fate of an unfortunately large proportion of biological research images, and is perhaps the best possible argument for a publicly funded image database that can provide free access to and a safe repository for such images:

> Concerning the image data you requested—this is a tough one. The image was recorded about ten years ago, and I never managed to write a paper about the work so it was never published. The original data (if they still exist) must be on some magneto-optical disk in one of many boxes in my flat—quite hopeless to find at short notice. All I can promise is that I'll look into this once I am back from my travels, but that will take a few months. Whether anyone still has hardware capable of reading the disc is quite another matter! Sorry about this.

The European Commission-funded ORIEL Project (*Online Research Information Environment for the Life Sciences*; www.oriel.org), coordinated from the European Molecular Biology Organization in Heidelberg, is developing tools and procedures to promote access to and integrated retrieval of various types of digital biological information. Within this umbrella project, the BioImage Database project (www.bioimage.org) has four purposes: to provide the scientific community with a freely accessible database and archive of high-quality multidimensional digital images of biological research relevance, with deep descriptive metadata; to make the images and their metadata available electronically via the Internet for personal study, educational, commercial, medical, and scientific research purposes; to provide tools to assist in the submission, downloading and visualization of such images, and in making comparisons between them; and to provide links between these image data and other relevant digital items of biological information (Shotton, 2003; Shotton *et al.*, 2003).

Taking its name and concept from an earlier BioImage Database prototype (Carazo *et al.*, 1999; Carazo and Stelzer, 1999; Lindek *et al.*, 1999), the BioImage

Copyright 2006, Elsevier Science (USA).
All rights reserved.

Database has been completely redesigned and rewritten within the Image Bioinformatics Laboratory of the Department of Zoology at Oxford University and it is now standards-based, using open source components throughout and employing semantic web technologies to provide a semantic reasoning layer between the users and the stored metadata. Central to these is a newly written ImageStore Ontology that defines the metadata descriptors used for the images and through which all user interactions with the database occur (Catton and Shotton, 2002; Sparks and Shotton, 2003). We are now starting to populate this publicly accessible BioImage Database with images from biological journals, individual researchers, learned societies, and research collections, with the intention that it should become for biological images what the standard bioinformatics databases are for sequences and structural data, with an emerging culture of image submission to the BioImage Database of high-quality research imagery arising from publicly funded biological research.

Our motivation in creating the BioImage Database is the belief that images are important assets created by the scientific process, but that they are only useful if they can be found by those interested in viewing or using them. Images held on unlabelled slides in desk drawers, dusty stacks of CDs, or forgotten discs in cardboard boxes are not scientific assets but liabilities. The purpose of this article is to bring the BioImage Database to your attention and to invite you both to submit your image collections for publication in the BioImage Database and to use its contents for your own research and teaching activities.

II. METADATA IN BIOIMAGE

Accurate and detailed metadata (data about data) are essential for finding images in a databse because, unlike sequences and text, images are not self-describing. While it is possible to scan through a sequence and recognise particular codons or transcription factor binding sites or to search a text document and extract key words that can be used to rank the relevance of a document to a query, the development of software that can identify the contents of an image by analysing its pixels is in its infancy. Thus without appropriate metadata, images are difficult or impossible to find, and online databases become little more than meaningless and costly data graveyards. Unfortunately, the process of manual metadata submission can be time-consuming, which is a disincentive to sharing information. Traditionally, there has been a tension between the cost of investing this effort "up front" at the time of image creation and storage and the subsequent benefits gained in terms of ease of image location and retrieval. The BioImage Database attempts to assist in the metadata submission process both by simplifying the submission of metadata by authors and by automating the harvesting of prerecorded metadata from image files, as described later.

The image metadata within the BioImage Database relate to several domains.

A. People and Institutions

With the consent of the authors, the BioImage Database holds contact information (names, postal and e-mail addresses, phone and fax numbers, etc.) about the people responsible for conducting experiments and creating the submitted images, the institutions in which they work, and the agencies that have funded their research. The data structure is flexible enough to record individuals' affiliations to several institutions, either simultaneously or sequentially, as appropriate.

B. Studies, Publications, and External Databases

Within the BioImage Database, the fundamental unit of record is the BioImage Study, roughly equivalent in scope to a peer-reviewed scientific paper. Indeed, a BioImage Study will normally be hyperlinked to one or more scientific papers based upon the image data contained within the study. From these studies, users may also make direct links to the principal taxonomic, structural, and sequence databases, permitting the BioImage Database to be used for lateral access to the wider scientific literature and other relevant factual data.

C. Experiments, Data Sets, and Images

The findings included within a BioImage Study may have been obtained from several experiments. All the images resulting from a single experiment, typically obtained from observation of similar specimens (or a single one), constitute a single BioImage image set. However, image sets do not necessarily have to be associated with particular scientific experiments. Collections of images on a related theme, e.g., historical time-lapse cine footage of mitosis in *Haemanthus*, may be grouped together into a single image set, even though they were not all obtained during a particular experiment.

D. Media Objects

An experiment may result in the creation of one or more media objects, e.g., images, videos, and models, which may be of any type or dimensionality—conventional 2D images, 3D, or 4D (*x*, *y*, *z*, and *time*) images comprising one or more fluorescence channels, videos, animations, surface reconstructions, etc. Ancillary data in the form of interpretive diagrams, graphs, tables, etc. may also be included. The BioImage data model is capable of recording all the basic details concerning these media objects. For example, for a conventional 3D confocal image, metadata would include the file format and size, the compression codec and quality settings, the *x*, *y*, and *z* pixel resolutions and pixel dimensions at the image plane, the corresponding optical resolutions at the image plane, the *x*, *y* and *z* data acquisition speeds, and the wavelength characteristics of each separate imaging channel. The provenance of the image is also recorded, showing when and by whom it was created and entered into the BioImage Database, how it may have been derived from another image, and, if so, the image processing and/or compression algorithms that have been used. Thus, for example, one might record the algorithm and point spread function parameters used to produce a blur-free deconvolved 3D image from a set of raw fluorescence optical sections showing out-of-focus blur. Similarly, if a section of video is submitted for publication, the BioImage Database can record details about the source file from which it was edited and the original tape or disc upon which that original was recorded.

E. Semantic Metadata

The metadata domains described so far cover only *who* created an image and *when*, *where*, *how*, and *why* it was made. They do not tell us *what* the image actually represents, and its *significance*, and these are arguably the most important kind of metadata (Shotton *et al.*, 2002). Many image databases fail to distinguish adequately between the content and the meaning of an image or to take into account different interpretations of the same data. Within the ImageStore ontology, we make a clear distinction between what the image represents (i.e., what is being denoted in the image—the species, cell type and preparation conditions of the specimen, and the identifiable features within the image) and the connotations attached to the image (the interpreted meaning, purpose, or significance of the image, its relevance to its creator and others, and its semantic relationship to other images) (Catton and Shotton, 2002, 2003). In addition, we use external ontologies and taxonomies to assist in the description of image content, instead of relying solely on conventional key words. Currently we are using GO ontology (http://www.geneontology.org) to describe genes and gene products and NCBI taxonomy (http://www.ncbi.nlm.nih.gov/Taxonomy/) to identify species.

III. HOW TO SUBMIT IMAGES TO THE BIOIMAGE DATABASE

Via the BioImage home page (www.bioimage.org), users may apply for a submission account to the BioImage Database. They will then be supplied with a username and password that will permit them to use the submission service. On entering the service, the user may enter or update personal details and is presented with a list of previously submitted BioImage Studies that may be edited and the option to submit more.

While at the time of writing the details have yet to be fully worked out, the BioImage Database intends to adopt two complementary approaches to submission—manual and semiautomatic. The manual submission interface is interactively customized for the type of submission to be made (e.g., entry of the accelerating voltage will be requested for submissions of electron micrographs but not of light micrographs), with the submission forms being generated dynamically as appropriate from the structures within the ImageStore ontology and any approved auxiliary ontologies. Any new submission starts at the BioImage study page and progresses to subsequent pages according to related resources required. Each page allows the user to enter appropriate values for that resource's attributes.

For example, a user may start the submission of a new study by entering its title and a brief textual description in the study page. The user may then wish to describe an experiment within that study, bringing up the experiment page within which (s)he can enter details of the technique used and specify the parameters used for image capture and subsequent digital image processing. The user effectively creates a tree of resources, each with its own defining attributes, which may be navigated, modified, pruned, and expanded before being finally committed to the database. An example is shown in Fig. 1.

Many of the metadata required to document an image may already be available in digital form, e.g., in the headers of image files generated by modern research microscopes and digital cameras. By captur-

FIGURE 1 A BioImage database submission interface.

ing this information at source, the process of managing images locally and submitting them to BioImage can be streamlined significantly, since BioImage can read the image header files, extract the relevant metadata, and use these to populate the submission forms, easing the task of manual submission.

The ultimate extension of this rationale will be the automated uploading of the entire metadata content of studies recorded in a local image asset management database using open source software provided by the Open Microscopy Environment (www.openmicroscopy.org; Swedlow *et al.*, 2003), together with any analytical results associated with such studies. To achieve this, we are working with the developers of the Open Microscopy Environment in two ways. First, BioImage will directly import and export image files and associated metadata recorded in OME-XML, a format that has been adopted as a common image exchange format by the European Light Microscopy Initiative and a number of leading microscope and software manufacturers. Second, we plan to develop a cross-mapping ontology and a BioImage plug-in for the OME system that will allow the automated uploading of selected OME studies from a researcher's local OME database direct to BioImage using Web services protocols, permitting OME users to publish the best of their images and associated analytical results to the BioImage Database without hassle, with the submitters being required to add manually only a minimum amount of additional information for each study.

It is important to note that while most original high-resolution multidimensional images will be directly available from the BioImage Database server, this does not have to be the case. Provided that URLs for these original high-resolution multidimensional images are provided and that these images themselves are made

permanently available on a stable server elsewhere, they need not reside on the BioImage Database server. However, medium-resolution "Web quality" 2D representative versions of the original images, of at least 512 by 512 pixels, must be submitted to the BioImage Database in PNG, TIFF, or JPEG format at the same time as the metadata relating to them. This permits authors to maintain copyright control over their high-resolution images if so desired (see Section VI). However, the BioImage staff will need initial access to any multidimensional high-resolution images that they will not be hosting directly in order both to check image quality and to extract metadata from the image header files.

IV. HOW TO FIND IMAGES IN THE BIOIMAGE DATABASE

Users can employ several strategies to find images described in the BioImage Database—browsing, searching, or a combination of both.

A. Browsing

After logging on to the BioImage Database, users will immediately be presented with the main browse interface (Fig. 2). This page will allow users to start their search by selecting an organism type (e.g., plant),

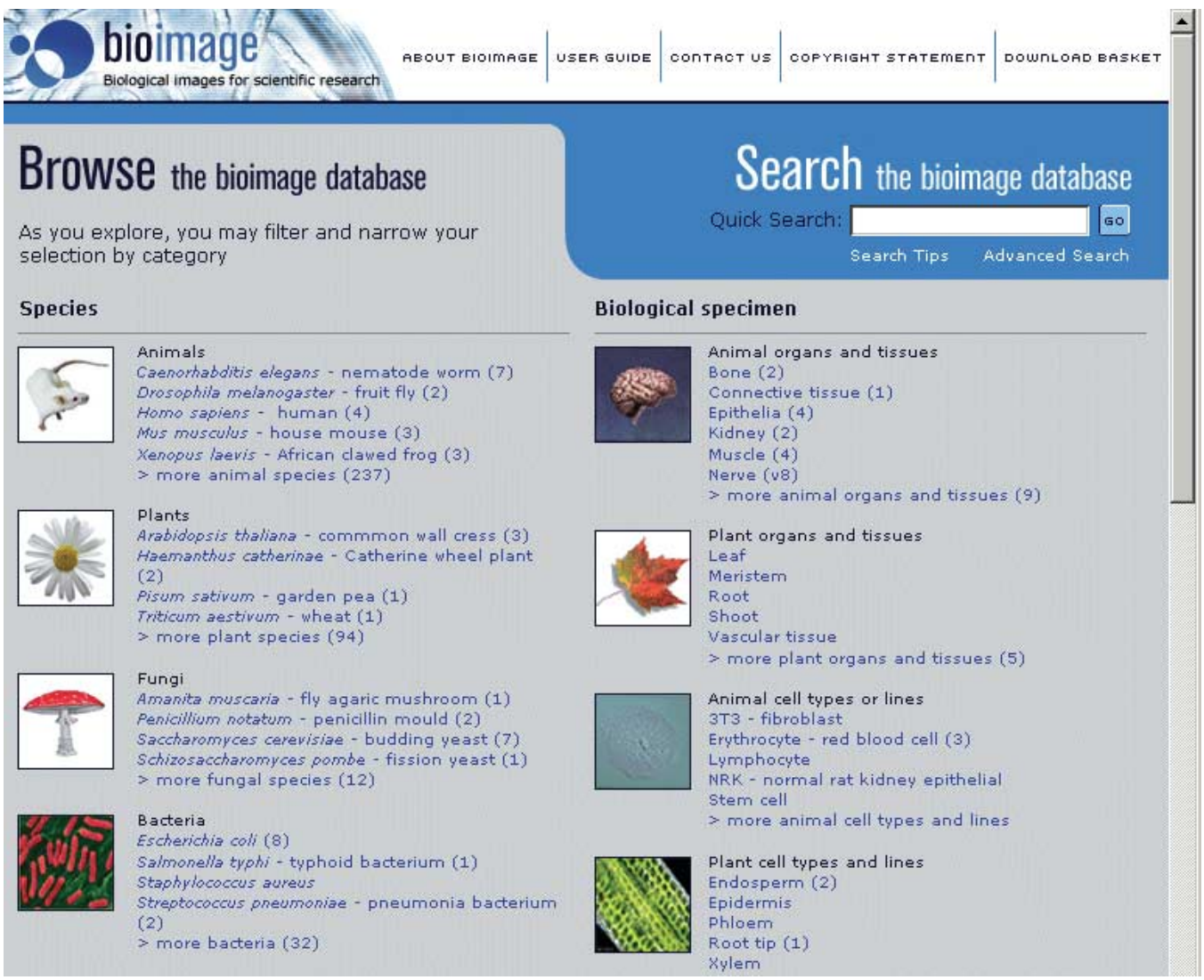

FIGURE 2 Design for the BioImage Database home page and browse interface.

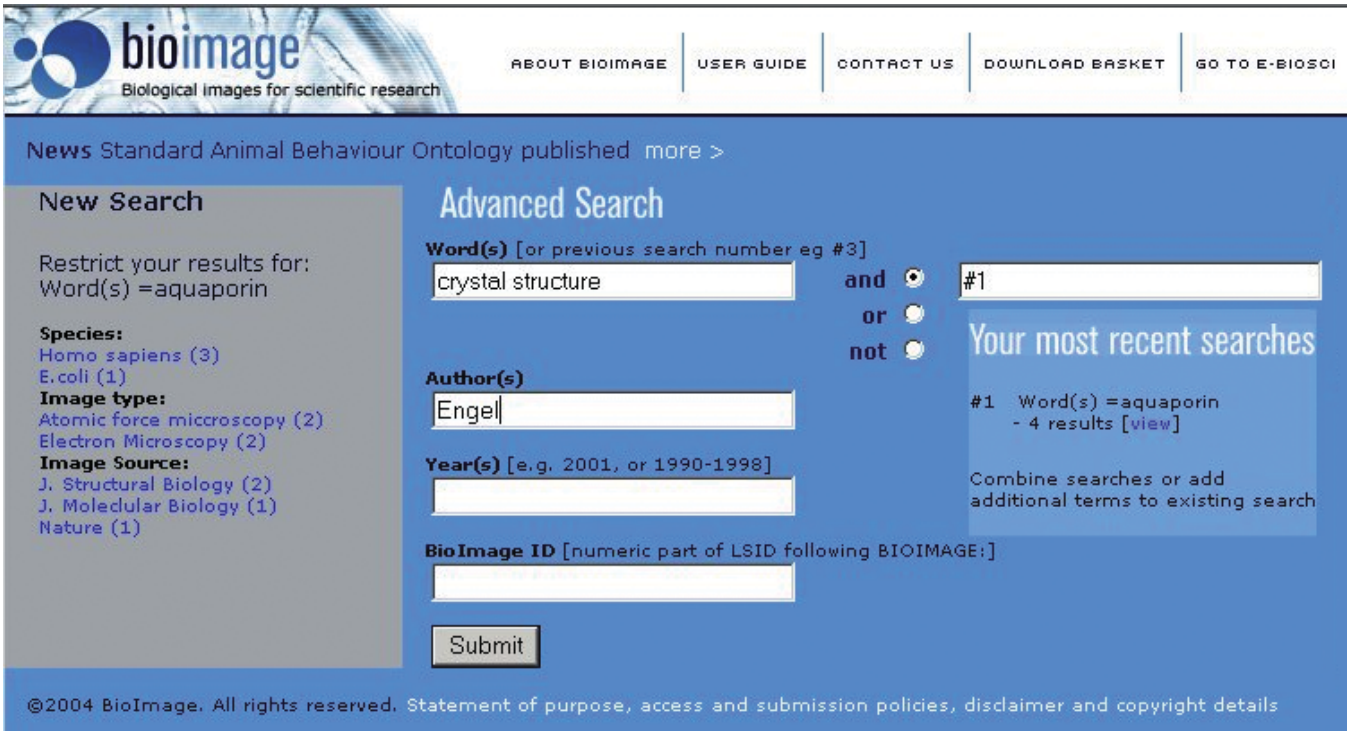

FIGURE 3 The BioImage Database advanced search interface.

a biological process (e.g., cell cycle, reproduction, or motility), a biological specimen (e.g., an organ, tissue, cell type, or organelle), an image type (e.g., electron micrograph), or an image source (e.g., *EMBO Journal* or University of Oxford). Each main section has several subheadings, and under each subheading the most commonly requested categories in the database are listed. Selecting ">other . . ." will list all the categories under that subheading. Selecting the "*Homo sapiens*—human" category, for example, will immediately list for the user all BioImage studies that contain images of humans, of human tissues, of human cells, and of organelles or macromolecules of human origin.

The results set can be refined at any stage using the grey "Refine Results" panel to the left of the screen—so that, for example, selecting Biological Specimen>Organelle>Golgi apparatus will restrict the results to those that show the human Golgi apparatus.

B. Searching

Browsing and searching within the BioImage Database are complementary and mutually supportive activities, with a search tab always available within the browse window (Fig. 2).

Users can employ two modes of searching:

1. Quick Search Interface, Available from the Browse Window

This permits simple key word or key phrase searching for matching text in all titles, descriptions, categories, and author records.

2. Advanced Search Interface

This window (Fig. 3) appears after clicking the "Advanced search" button beneath the Quick Search box. It permits the use of Boolean operators (and, or, not) between search terms applied to BioImage study titles, descriptions and categories, and enables restriction by author, date, and BioImage identifier. It further permits iterative refinement by reusing previous search results in a manner familiar to users of the bibliographic database software WinSPIRS, as all search results are saved automatically for the duration of a session.

The advanced search interface thus enables users to enter queries of the type: "Retrieve all studies containing images of Drosophila testes showing expression of the gene *always early* (*aly*)" by combining the terms "*Drosophila testis*" and "*aly*." The user can then link out from the retrieved BioImage studies both to the relevant gene sequences and to literature publications about them.

BioImage text searches should not include "wild cards," as the BioImage text search engine is a reasonably sophisticated tool that looks for matches in word stems and will automatically identify plural forms and other grammatical variants. So, for example, a search for "Kills," "Killing," or "Killed" will all return the study "Killing of mouse L929 fibroblasts by mouse HA-8 cytotoxic lymphocytes (CTL)" but not a study on killifish.

A major goal of the current BioImage Database development is to move away from conventional searching by exact key word matching and instead use ontologies to provide the ability to undertake semantically rich searches that can handle synonyms ("yeast" and "*S. cerevisiae*"), homonyms ("G protein": does it mean a GTP-binding protein or the coat glycoprotein from Semliki forest virus?), related terms ("cell division" and "mitosis"), and hierarchies ("*Mus musculus*," "rodent," and "mammal"). A search for "yeast" would thus return studies of *S. cerevisiae* even if the term "yeast" appears nowhere in the study metadata. The improved accuracy of search and browse results will become increasingly apparent to users of the BioImage Database as these improvements are introduced. Users should check the online "Development status" page for the current status of this work.

C. Viewing Browse and Search Results

Results can be displayed in one of three ways by using the tabs shown at the top of the results page.

1. *As a List of Studies*

For each study retrieved, the user is shown a representative thumbnail image, the study title, and its brief textual description, the study ID [in the form of a Life Science Identifier (LSID; http://www.i3c.org)], the authors' names, the categories into which the study falls, and the number of image sets and images within the study, as shown in Fig. 4.

2. *As a List of Image Sets*

For each image set, the user is similarly shown a representative thumbnail image, the image set title, and its brief textual description, the image set ID, the authors' names, the categories into which the image set falls, the ID and title of the study to which the image set belongs, and the number of images contained within the image set.

3. *As an Array of Images*

For each image, the user is simply shown a thumbnail image, with the image title and ID, and a list of the versions of that image that are available for download (e.g., for a 3D confocal data set: there may be a Web resolution 2D representative image, a high-resolution 2D representative image, a Web resolution 3D image stack, or the original high-resolution 3D image dataset), with check boxes against each option that allows the user to select one or more for downloading, in one or more formats. Mousing over each option will open a transient display giving details of the formats, file sizes, and so on available for each version of the image. For each type of display, clicking on a thumbnail image opens a larger version of the image, whereas clicking on a title will take the user to another page showing more complete metadata relating to the study, the image set, or the image, as appropriate.

The best way of viewing results depends to some extent on the purpose of the search. Users looking for a striking image to illustrate a particular biological topic will probably want to scan the array of images visually, matching their search criteria displayed by using the "Image" tab, whereas users more interested in the significance of the images may prefer the study or image set displays, with their richer metadata descriptors.

Users can move between these alternative display modes by clicking on the relevant tabs (Figs. 4 and 5), and the range of results displayed may be progressively refined using the "Refine Results" panel. For example, after an initial selection for all studies relevant to the "*Homo sapiens*—human" category, it may be that not all the image sets in a particular returned study involved human material. If the study involved a comparison between cellular structures in human and mouse brain, it would be quite likely to contain separate image sets for each. If mouse data were irrelevant to the user's requirements, they could be removed from the image set or image result displays by restricting the display, using the Refine Results panel, to show only "*Homo sapiens*—human" results. This area of the database functionality is currently under development, but the ultimate aim is to allow users to navigate hierarchically through each set of categories using taxonomies and ontologies provided by third parties, permitting both restriction and expansion of the scope of displayed results. Again, users should refer to the BioImage online "Development status" page for the current status of this facility.

V. DOWNLOADING IMAGES AND VIDEOS

A. Downloading Images

When viewing image search/browse results, users may mark individual images to be added to their

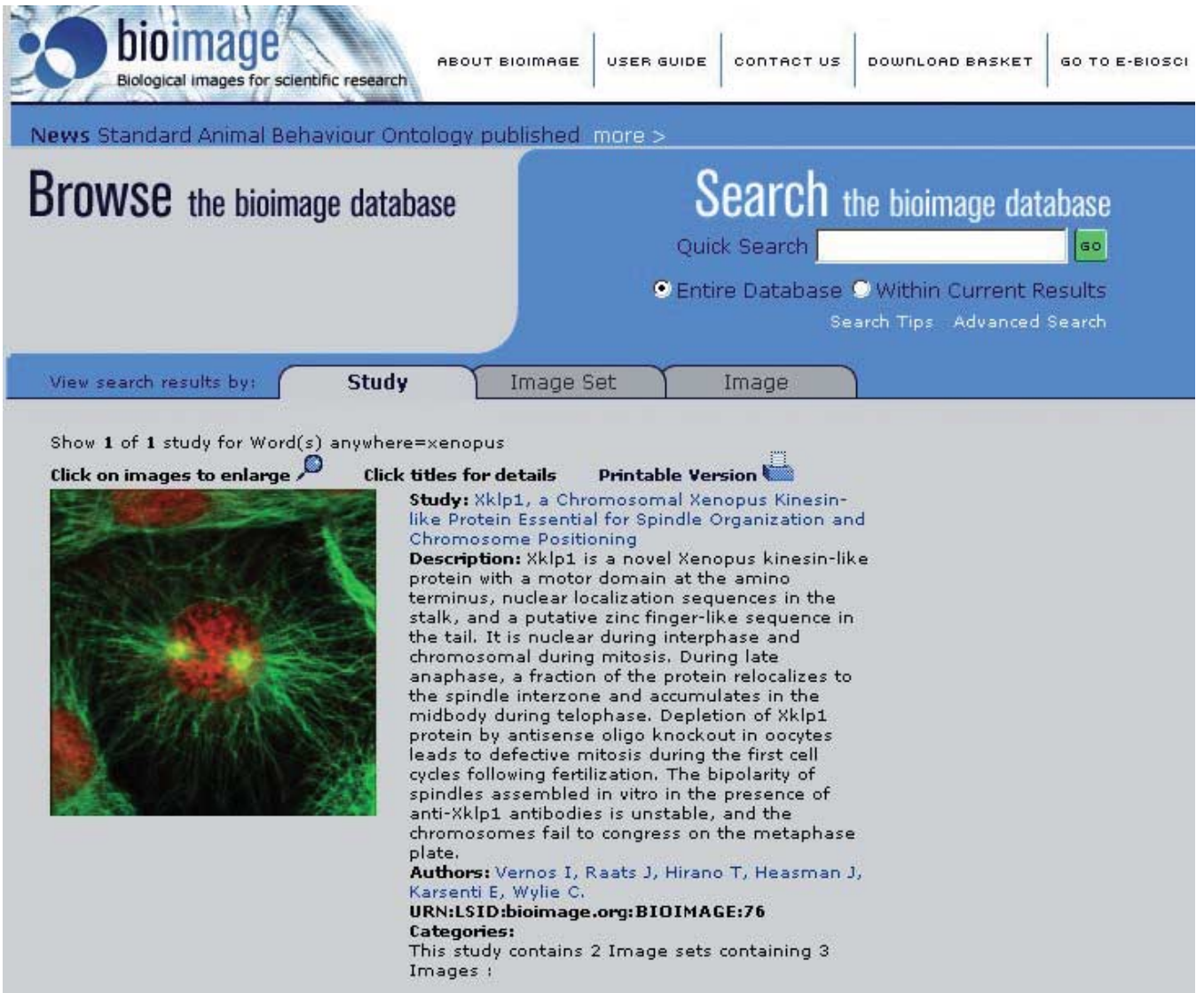

FIGURE 4 The BioImage Database results interface, showing study results.

download basket. To review the selected images and to initiate the download, users must select "Download Basket" from the main menu at the top of the browser window. Users will then be asked to confirm their agreement to the BioImage Database conditions of use before beginning the download process. Currently the download process begins immediately once these options have been specified and the download button is clicked, although it may be necessary in the future to schedule downloads to later times if current traffic is high and the requested files are large. Users may wish to check the online "System status" page to determine the current workload on the system.

Together with the downloaded images, users will be sent XML documents containing core metadata relating to the selected images, and to the image sets and studies of which they are a part, unless these are already bundled with the image as an OME-XML file.

B. Customizing Videos

For videos stored within the BioImage Database, we hope shortly to provide two possibilities for customising selected videos before downloading them, both of which depend upon a separate software service entitled VIDOS (Boudier and Shotton, 2000), which is part of a suite of on-line video services that we are developing under the umbrella title of VideoWorks (www.videoworks.ac.uk).

In interactive mode, a BioImage user, having selected a video, can choose the "Customize the video using VIDOS" button. In this case, the video will

automatically be made available to the VIDOS server, which will cause a VIDOS customization applet to open in a new browser window on the user's machine. The user can then interactively select the desired spatial and temporal editing parameters for the video and choose the required download format, codec, and compression quality. The VIDOS server then commissions a conversion job that runs on a VIDOS slave processor and finally delivers the customised video file to the user.

The alternative method of using VIDOS is more sophisticated, although less flexible, and depends upon the presence of prerecorded semantic content metadata for the video within the BioImage Database (Shotton *et al.*, 2000; Machtynger and Shotton, 2002; Rodriguez *et al.*, 2004). This permits users to search not just for entire videos, but also for clips from videos containing particular scenes, events, objects, or actors specified in the search. For example, a search might be for any clip showing apoptotic death of a fibroblast induced by a cytotoxic T lymphocyte. The images within any BioImage study returned by this search would include not only the entire video(s) containing such events, which could be downloaded directly or customised interactively as described earlier, but also those named video clips within the complete video(s) containing the specified events. Streaming previews of each such video or video clip could be viewed by clicking on the appropriate thumbnail keyframe image, while selection of a particular clip for downloading in a selected format would trigger a sequence of automated interactions between the BioImage server and the VIDOS sever using Web services protocols that would pass predetermined spatiotemporal editing and format customization parameters to the VIDOS server, commissioning an appropriate VIDOS customization job, and finally returning the requested clip to the user. For efficiency, such clips, once created, would be cached so that they would be available immediately for downloading upon a second request by a different user. While this Web services version of VIDOS has been tested and shown to work in prototype, it has yet to be fully implemented within the BioImage system, and potential users should consult the BioImage online "Development status" page for further information.

VI. COPYRIGHT ISSUES AND LICENSING AGREEMENTS

BioImage encourages users to submit their images under the Creative Commons Public Licence (http://creativecommons.org) that is also used by the Public Library of Science (www.plos.org). This licence, the terms of which are viewable at http://creativecommons.org/licenses/by/1.0/legalcode, grants to the BioImage Database and its end users "a worldwide, royalty-free, nonexclusive, perpetual (for the duration of the applicable copyright) license to exercise the rights in the Work." This effectively provides open access for BioImage Database users to view, download, and use the images, provided that copyright is acknowledged by including the name of the author and the original title of the image in any reproduction or derivative work and by insisting that any subsequent distribution of the image or derivative work is made under the same Creative Commons Public Licence. We believe this approach to be the most appropriate for images created as part of research projects undertaken using public funds and will maximise the potential usefulness of the images.

However, because some people may wish to submit images to the database that may have been created primarily for commercial purposes or may have significant commercial value that the copyright holders wish to retain, the Creative Commons Public Licence is not always appropriate. We therefore alternatively allow images to be submitted and licensed to the BioImage Database for noncommercial use only. Under this agreement, contributing authors retain full copyright to their material. However, they licence to the BioImage Database the right to make the image available to BioImage users, but only for noncommercial purposes and not for financial gain. End users must acknowledge the name of the original author and the source of the images as being the BioImage Database Web site and are legally obliged to contact the copyright holders for permission to reproduce the image outside the terms of this license.

As a further safeguard, authors may submit to the BioImage Database only thumbnail and Web resolution images, as defined earlier, while retaining the original high-resolution image files on their own Web sites, to which potential users must go for access to them, with whatever access and payment regulations that the user requires. The BioImage Database itself will take no part in such commercial transactions.

An alternative safeguard for those submitting images to the BioImage Database under either of the aforementioned licences is the ability to embargo publication of the images until some future date, e.g., until after the publication of that important *Nature* paper that is dependent upon the information contained within the images. For full details of these licenses and how they are applied, please see the BioImage Web site.

VII. VALUE AND FUTURE POTENTIAL OF THE BIOIMAGE DATABASE

The biological community is currently suffering form a surfeit of information in digital form, including journal publications, sequences and sequence-related information, three-dimensional structures, and digital image data. In 1999, an advisory committee to the U.S. National Institutes of Health estimated that some biomedical laboratories were already producing 100 terabytes of information a year. In the same year, the NCBI reported that 600,000 searches a day were being carried out on its collection of databases (Botstein and Smarr, 1999). In the time since that report, the volume of sequence data to be searched has increased by almost an order of magnitude and the volume of requests has approximately doubled every year. The EMBO DNA sequence database run by the EBI now receives over a million queries a day and is updated once a second (G. Cameron, personal communication, 2003). As David Roos (2001) has said: "We are swimming in a rapidly rising sea of data . . . how do we keep from drowning?"

With the advent of high-throughput cellular screening systems capable of generating 40,000 images a day and of functional MRI scans generating 100 Gb of data with each experiment, images are adding significantly to the scale of this data deluge. The integration of such multidimensional image data with the scientific literature and with a rapidly growing set of disparate bioinformatics resources, it is rapidly becoming one of the most demanding challenges for information science. There is an urgent need to better exploit the potential of the Internet and other communication networks to help researchers navigate through what is becoming an intricate and confusing information landscape. This need can be met in part by providing research communities with sophisticated tools to manage large complex multimedia datasets. The BioImage Database is one such tool.

We therefore invite you to use and to tell your colleagues about the BioImage Database and to submit your best images for publication within it, thereby not only maximizing exposure of your research achievements, but also ensuring that in 10 year's time *you* will know where to find your images in a format in which they can still be viewed!

References

Botstein, D., and Smarr, L. (co-chairs) (1999). Report of the Advisory Committee to the Director, NIH Working Group on Biomedical Computing. Available online at http://www.nih.gov/about/director/060399.htm.

Boudier, T., and Shotton, D. M. (2000). VIDOS, a system for video editing and format conversion over the Internet. *Comput. Networks* **34**, 931–944.

Carazo, J. M., and Stelzer, E. H. K. (1999). The BioImage Database Project: Organizing multidimensional biological images in an object-relational database. *J. Struct. Bio.* **125**, 97–102.

Carazo, J. M., Stelzer, E., Fita, I., Henn, C., Machtynger, J., McNeil, P., Shotton, D. M., Chagoyen, M., Alarcon, P. A., Lindek, S., Fritsch, R., Heymann, B., Kalko, S., Pittet, J.-J., Rodriguez-Tome, P., and Boudier, T. (1999). Organizing multidimensional biological microscopic image information: The BioImage database. *Nucleic Acid Res.* **27**, 280–283.

Catton, C., and Shotton, D. M. (2002). Making sense of images: Ontologies and the BioImage database. *Proc. Standards and Ontologies for Functional Genomics*, Hinxton, November, 2002. Available at http://www.bioimage.org/publications.do.

Catton, C., and Shotton, D. M. (2003). "What is that crow thinking?" Separating fact and hypothesis in the BioImage Database. Proc. 2nd e-BioSci/ORIEL Summer Conference *Beating the Data Deluge*, Varenna, Italy, Sept 2–5, 2003. Available online at http://www.bioimage.org/publications.do.

Lindek, S., Fritsch, R., Machtynger, J., de Alarcon, P. A., and Chagoyen, M. (1999). Design and realization of an on-line database for multidimensional microscopic images of biological specimens. *J. Struct. Bio.* **125**, 103–111.

Machtynger, J., and Shotton, D. M. (2002). VANQUIS, a system for the interactive semantic content analysis and spatiotemporal query by content of videos. *J. Microsc.* **205**, 43–52.

Rodriguez, A., Guil, N., Shotton, D. M., and Trelles, O. (2004). Automatic analysis of the content of cell biological videos, and database organization of their metadata descriptors. *IEEE Transact. Multimedia* **6**, 119–128.

Roos, D. S. (2001). Computational biology: Bioinformatics—trying to swim in a sea of data. *Science* **291**, 1260–1261.

Shotton, D. M. (2003). The BioImage Database: Multidimensional research images and their relationship to the wider online research information environment for the life sciences. Proc. E-BioSci Mtg. Biological Information Management: Challenges and Choices. NeSC, Edinburgh, 28/4/03. Online at http://www.bioimage.org/publications.do.

Shotton, D. M., Catton, C., and Sparks, S. (2003). BioImage: From image database to Grid service. Proc. 2nd e-BioSci/ORIEL Summer Conference *Beating the Data Deluge*, Varenna, Italy. Available online at http://www.bioimage.org/publications.do.

Shotton, D. M., Rodriguez, A., Guil, N., and Trelles, O. (2000). Object tracking and event recognition in biological microscopy videos. *In "Proc. 15th International Conference on Pattern Recognition: ICPR 2000,"* Barcelona, Spain (3–8 September 2000) **4**, 226–229.

Shotton, D. M., Rodriguez, A., Guil, N., and Trelles, O. (2002). A metadata classification schema for semantic content analysis of videos. *J. Microsc.* **205**, 33–42.

Sparks, S., and Shotton, D. M. (2003). The application of ontologies to the BioImage database. Proc. 2nd e-BioSci/ORIEL Summer Conference *Beating the Data Deluge*, Varenna, Italy. Available online at http://www.bioimage.org/publications.do.

Swedlow, J. R., Goldberg, I., Brauner, E., and Sorger, P. K. (2003). Informatics and quantitative analysis in biological imaging. *Science* **300**, 100–102.

PART

B

ELECTRON MICROSCOPY

SECTION

7

Specimen Preparation Techniques

CHAPTER

22

Fixation and Embedding of Cells and Tissues for Transmission Electron Microscopy

Arvid B. Maunsbach

I. INTRODUCTION

Chemical fixation is the first step in most procedures for the preparation of cells and tissues for transmission electron microscopy. It is a very critical step, as the quality of fixation is of fundamental importance for results of the electron microscopical analysis. The main purposes of chemical fixation are to stop metabolic processes, to preserve cellular fine structure, and to stabilize the cells for subsequent steps in the preparatory procedure. In some studies, care must also be taken to preserve enzyme activity and/or tissue antigenicity. The choice of chemical fixation procedure requires careful consideration of three main factors:

1. Selection of the fixing agent itself, e.g., glutaraldehyde, formaldehyde, osmium tetroxide, or mixtures or sequences thereof.
2. Selection of the proper vehicle for the fixative, e.g., choice of buffer, pH, added salts, or other substances.
3. Selection of the procedure for applying the fixative to the cells or tissues.

No single standard fixation method is suitable for all types of cells and tissues. The aforementioned three factors usually have to be adjusted for each specific cell type, tissue, or experimental situation and, consequently, a very large number of fixation procedures have been described. The literature on chemical fixation for electron microscopy is extensive (see Sabatini *et al*., 1963; Maunsbach, 1966a,b; Griffith, 1993; Glauert and Lewis, 1998; Maunsbach and Afzelius, 1999). It is nevertheless possible to point at some general principles and procedures with wide applicability. This chapter describes such procedures found useful for different applications in cell biology in our laboratory.

Tissues to be analyzed in the electron microscope are usually embedded in resins for ultramicrotomy. The embedding procedures vary with respect to chemical composition of resins, protocols for dehydration, and procedures for infiltration with resins, as well as the properties of the embedded tissue with respect to sectioning quality, tissue shrinkage, and tissue contrast in the electron microscope. Epoxy resins are the most commonly used embedding media in biological electron microscopy (Luft, 1961; Glauert and Lewis, 1998). They combine good ultrastructural preservation of the tissues, ease of sectioning, reproducibility, and relative ease of handling. However, they preserve tissue antigenicity only to a very limited extent. Acrylic resins, such as the Lowicryls (Carlemalm *et al*., 1985), provide both good ultrastructural preservation and preserve, to a larger extent, tissue antigenicity. Embedding in acrylic resins is carried out at low temperature either by progressively lowering the temperature during dehydration and resin infiltration or by cryofixation followed by freeze substitution and UV polymerization at low temperature (see article by Maunsbach).

Copyright 2006, Elsevier Science (USA).
All rights reserved.

II. MATERIALS AND INSTRUMENTATION

A. Fixation

Agar (Merck 101615)
Glutaraldehyde, 25% aqueous stock solution EM grade (Merck 104239)
Sodium cacodylate ($C_2H_6AsNaO_2 \cdot 3H_2O$, Merck Art 820670)
Osmium(VIII) tetroxide ($Os0_4$, 76028 Johnson Matthey Materials Technology)
Paraformaldehyde powder (Merck 104005)
Operating table
Anesthetic
Scissors, forceps, scalpels, and clamps for surgical procedures
Small forceps with fine claws
Gauze swabs
Plastic petri dishes
Thin razor blades
5- to 10-ml vials with lids for specimens
Gloves
Short-beveled syringe needle for perfusion of rat aorta, length about 50 mm, outer diameter 1.3–1.5 mm
Blunt syringe needle for heart perfusion, length about 100 mm, outer diameter 2.0–2.4 mm
Perfusion set with drip chamber as used for intravenous blood infusions (Fig. 1)
Flask to which the perfusion set fits
10- to 15-cm-thick syringe needle to ventilate the flask
Stand to hold the fixative flask upside down about 150 cm above the operating table
Adequate ventilation

B. Dehydration and Embedding in Epoxy Resin

Epoxy resin kit (TAAB TO24) containing epoxy resin (TAAB 812), dodecenyl succinic anhydride (DDSA), methyl nadic anhydride (MNA), and 2,4,6-tri(dimethylaminomethyl)phenol (DMP-30)
Ethanol
Maleic acid ($C_4H_4O_4$, Merck 800380)
Uranyl acetate dihydrate [$(CH_3COO)_2UO_2 \cdot 2H_2O$, TAAB 1001]
Propylene oxide (C_3H_6O, Merck 112492).
5- to 10-ml glass vials with lids (Fig. 2a).
Gloves
Disposable beaker for mixing resin
Disposable Pasteur pipettes
Flat embedding molds in resistant rubber (G3690, Agar Scientific Ltd., Fig. 2b)
Fine forceps
Wooden stick

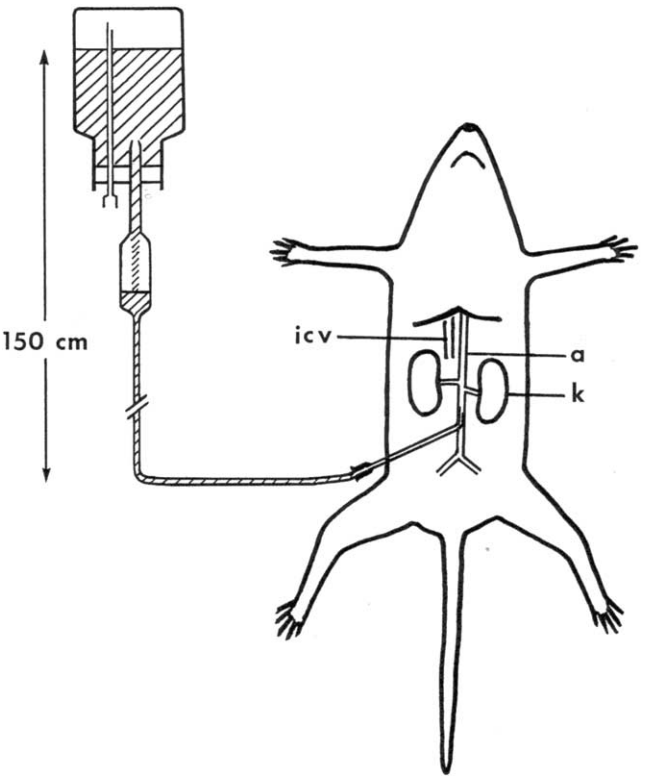

FIGURE 1 Schematic drawing of perfusion fixation of rat through the abdominal aorta. The flask with the fixative and the drip chamber is placed about 150 cm above the animal. a, aorta; icv, inferior caval vein; k, kidney.

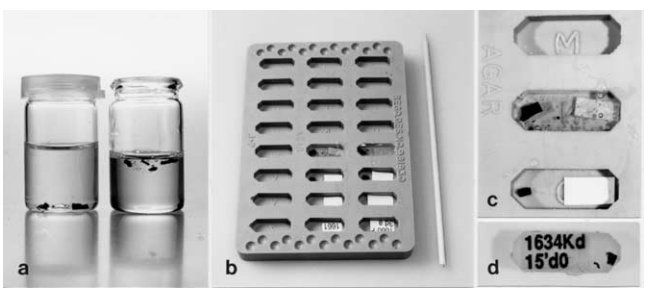

FIGURE 2 Embedding in epoxy resin. (a) Vials with specimens during ethanol dehydration (left) and infiltration in pure epoxy resin (right). At the start of infiltration the tissue blocks are placed on top of the resin and allowed to sink to the bottom. (b) Flat embedding mold used for epoxy embedding. Specimens and labels are placed in the wells. The wooden stick (right) is used to orient blocks and labels in the resin. (c) Enlargement of central wells showing specimen and label without resin (below), specimen with label and epoxy (middle), and empty well (top). (d) Polymerized epoxy block with label seen from back side.

III. PROCEDURES

For many purposes, adequate fixation is obtained by simple immersion of small tissue pieces into the fixative solution. This is the only mode of fixation possible for many tissues and for biopsies. However, a more rapid and uniform fixation is usually obtained if the fixative solution is perfused via the vascular system, either through the heart or through the abdominal aorta (Fig. 1) or, in some cases, through the venous system. Perfusion fixation (Figs. 3a and 4) should be preferred over immersion fixation (Figs. 3b and 5) whenever possible. For most tissues, 1% glutaraldehyde is sufficient for general ultrastructural studies. This concentration does not require a preceding rinse of the vascular system with a salt solution. For cytochemical or immunocytochemical studies, 4% formaldehyde plus 0.1% glutaraldehyde is preferable (Fig. 3b), but the glutaraldehyde should be omitted if the enzymes or antigens are inhibited by glutaraldehyde.

A. Perfusion Fixation of Rats through the Abdominal Aorta

The following procedure (Maunsbach, 1966a) results in efficient fixation of kidney, liver, pancreas, and small intestines. In the kidney, which is very sensitive to variations in the mode of applying the fixative, it preserves open tubules and normal relationships between tubule cells. The procedure is described for rats but can also be adapted for other animals.

Solutions

1. *0.2 M sodium cacodylate buffer*: To make 1000 ml, dissolve 42.8 g sodium cacodylate in 900 ml of distilled water. Adjust pH to 7.2 with 1 *N* HCl. Complete to 1000 ml with distilled water.
2. *0.1 M sodium cacodylate buffer*: Dilute 0.2 *M* sodium cacodylate buffer with an equal amount of distilled water.
3. *1% glutaraldehyde in 0.1 M sodium cacodylate buffer*: To make 500 ml of fixative solution, mix 250 ml 0.2 *M* sodium cacodylate buffer and 20 ml 25% aqueous glutaraldehyde and add distilled water to 480 ml. Adjust pH to 7.2 with 0.1 *N* NaOH or 0.1 *N* HCl. Complete with distilled water to 500 ml.
4. *20% stock solution of formaldehyde*: To make a 100-ml solution, mix 20 g of paraformaldehyde powder with 80 ml of distilled water in a glass flask. Heat to 60°C while gently agitating the milky solution. Add 1 *N* sodium hydroxide dropwise until the solution clears up. Complete to 100 ml with distilled water. This procedure should be carried out in a well ventilated hood and with protection for the face. The solution can be stored for a few days in the refrigerator.
5. *4% formaldehyde plus 0.1% glutaraldehyde in 0.1 M sodium cacodylate buffer for immunocytochemistry*: To make a 500-ml solution, mix 100 ml of 20% formaldehyde stock solution, 2 ml 25% glutaraldehyde, and 250 ml 0.2 *M* sodium cacodylate buffer. Add distilled water to 480 ml. Adjust pH to 7.2 with 0.1 *N* NaOH or 0.1 *N* HCl. Complete with distilled water to 500 ml. For sensitive antigens, omit the glutaraldehyde.
6. *2% osmium tetroxide stock solution*: 1 g crystalline osmium tetroxide is obtained preweighed in closed glass ampules. Wash the ampule carefully and score the vial around its perimeter with a diamond or a fine file. Break the vial cautiously and empty the crystals into 50 ml of distilled water in a glass vial with a tight lid. The crystals dissolve very slowly and the solution should be prepared at least the day before use. Shaking and/or ultrasonic treatment speeds up the process. All steps should be carried out in a well-ventilated hood. Always wear gloves when handling osmium tetroxide solutions. The solution is stable if kept in the cold and protected from strong light.
7. *1% buffered osmium tetroxide*: To make 10 ml of fixative solution, mix 5 ml of 0.2 *M* cacodylate buffer and 5 ml of 2% osmium tetroxide stock solution.

Steps

1. Place the closed flask containing the fixative upside down about 150 cm above the level of the aorta in the animal. The fixative has room temperature.
2. Connect the flask to the perfusion needle via the administration set for intravenous solutions and ventilate the flask (Fig. 1).
3. The size of the needle has a 1.3- to 1.5-mm outer diameter for a 300-g rat and is proportionally smaller for lighter animals. The needle is bent at an angle of about 45° with the beveled side out (i.e., down during perfusion).
4. Connect the perfusion needle via the infusion set to the flask containing the fixative. Check that there are no air bubbles in the tubing of the infusion set.
5. Fix the anesthesized animal onto the operating table with its back down. No artificial respiration is used.
6. Open the abdominal cavity by a long midline incision with lateral extension and move the intestines gently to the left side of the animal.
7. Carefully expose the aorta below the origin of the renal arteries and very gently free the aorta from overlaying adipose and connective tissues.

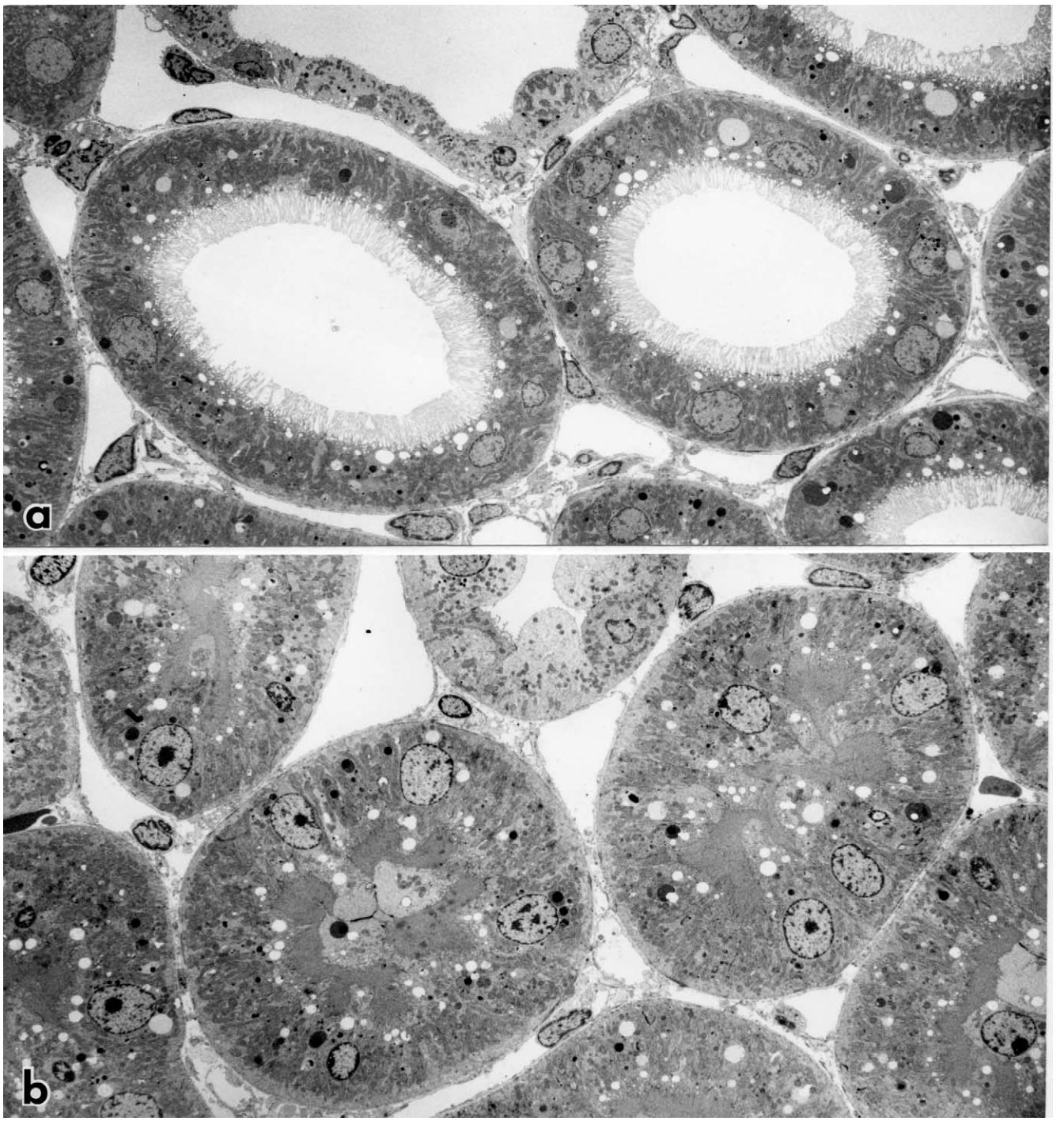

FIGURE 3 Transmission electron micrograph of rat kidney cortex perfusion fixed through the abdominal aorta with 1% glutaraldehyde (a). Tubule lumens are open and brush borders of proximal tubules are arranged uniformly. (b) Comparable area of rat kidney cortex immersion fixed with 1% glutaraldehyde. All proximal tubules are collapsed with portions of cytoplasm occupying the tubule lumen, and nuclei have moved away from the basement membrane. Both specimens were postfixed in 1% osmium tetroxide in 0.1 *M* cacodylate buffer, block stained with 1% uranyl acetate in sodium maleate buffer at pH 5.5, dehydrated in ethanol, and embedded in Epon resin, and sections were double stained with uranyl acetate and lead citrate. 1200×.

8. Hold the wall of the aorta firmly with the small forceps with fine claws about 0.5–1.0 cm from its distal bifurcation. Insert the bent needle close to the forceps toward the heart into the lumen of the aorta (with the beveled side of the tip down).

9. In very rapid succession (a) cut a hole in the inferior caval vein with fine scissors, (b) start the perfusion, and (c) clamp the aorta below the diaphragm, but above the origin of the renal arteries. When performing these manipulations, accuracy and speed are essential and the fixation procedure is preferably carried out by two persons. It is particularly important to clamp the aorta rapidly after the perfusion has been started. This is done most easily by compressing the aorta toward the posterior wall of the peritoneal cavity with a finger (wear gloves), which is then replaced by a clamp. Finally, cut the aorta above the compression.

10. The kidney surface must blanch immediately and show a uniform, pale color. The flow rate should be at least 60–100 ml/min for an adult rat. Perfuse for 3 min. Stop the perfusion and excise and trim the tissues with a razor blade. Store the tissue in vials and immersion fix in the same fixative for 2 h.

11. Rinse the tissue two times for 30 min in 0.1 *M* sodium cacodylate buffer.

12. Postfix the tissue in 1% osmium tetroxide for 1 h in the cold. Swirl the vial occasionally to secure uniform penetration of the fixative.

13. Rinse two times for 30 min in 0.1 *M* sodium cacodylate buffer. The tissue is now ready for dehydration and embedding.

B. Perfusion Fixation through the Heart

The following procedure provides fixation of most rat organs with 1% glutaraldehyde. For some organs the glutaraldehyde concentration should be increased (e.g., to 5% for the brain) and the fixative preceded by a brief rinse with a balanced salt solution such as Tyrode. For immunocytochemistry, use 4% paraformaldehyde with or without 0.1% glutaraldehyde .

Solutions

1. *1% glutaraldehyde in 0.1 M sodium cacodylate buffer*: See Section III,A.

2. *4% paraformaldehyde plus 0.1% glutaraldehyde in 0.1 M sodium cacodylate buffer*: See Section III,A.

3. *0.1 M sodium cacodylate buffer*: See Section III,A.

Steps

1. Place the closed flask containing the fixative upside down about 150 cm above the level of the aorta in the animal.

2. Connect the perfusion needle via the infusion set to the flask containing the fixative and ventilate the flask. Check that there are no air bubbles in the tubing of the infusion set.

3. Fix the anesthetized animal onto the operating table with its back down.

4. Open the thoracic cavity of the animal without giving artificial respiration.

5. Grasp the heart close to its apex with a forceps. Cut a small hole in the wall of the left ventricle close to the apex with fine scissors. Rapidly insert a blunt syringe needle (2.0–2.4 mm outer diameter for a 300-g rat and proportionally smaller for lighter animals) and move it into the ascending aorta. Place a clamp on the aorta to hold the needle.

6. Cut a hole in the right atrium of the heart and start perfusion immediately.

7. Check the flow rate in the drip chamber and flask. The flow rate should be at least 150 ml/min for an adult rat. Perfuse for 3 min. Stop the perfusion and remove pieces of tissue. Subdivide the tissue and fix it additionally for 2 h in the same fixative.

8. Proceed as described earlier for perfusion fixation through the abdominal aorta (steps 11–13).

C. Immersion Fixation

Immersion fixation of tissues for general ultrastructural studies is carried out with 1 or 2% glutaraldehyde for small tissue blocks. If the size of the tissue in one dimension is about 0.5 mm or more, the concentration should be increased to 3%, which is recommended for renal biopsies. For large specimens, an alternative solution is 2% formaldehyde plus 2.5% glutaraldehyde fixative (Fig. 4b). For immunocytochemical studies, use 4% formaldehyde with or without 0.1% glutaraldehyde fixative. If the antigen is sensitive to fixation, glutaraldehyde should be excluded.

Solutions

1. *1% glutaraldehyde in 0.1 M sodium cacodylate buffer*: See Section III,A.

2. *3% glutaraldehyde in 0.1 M sodium cacodylate buffer*: To make 100 ml of fixative solution, mix 50 ml 0.2 *M* sodium cacodylate buffer, 12 ml 25% aqueous glutaraldehyde, and add distilled water to 90 ml. Adjust pH to 7.2 with 0.1 *N* NaOH or 0.1 *N* HCl. Complete with distilled water to 100 ml.

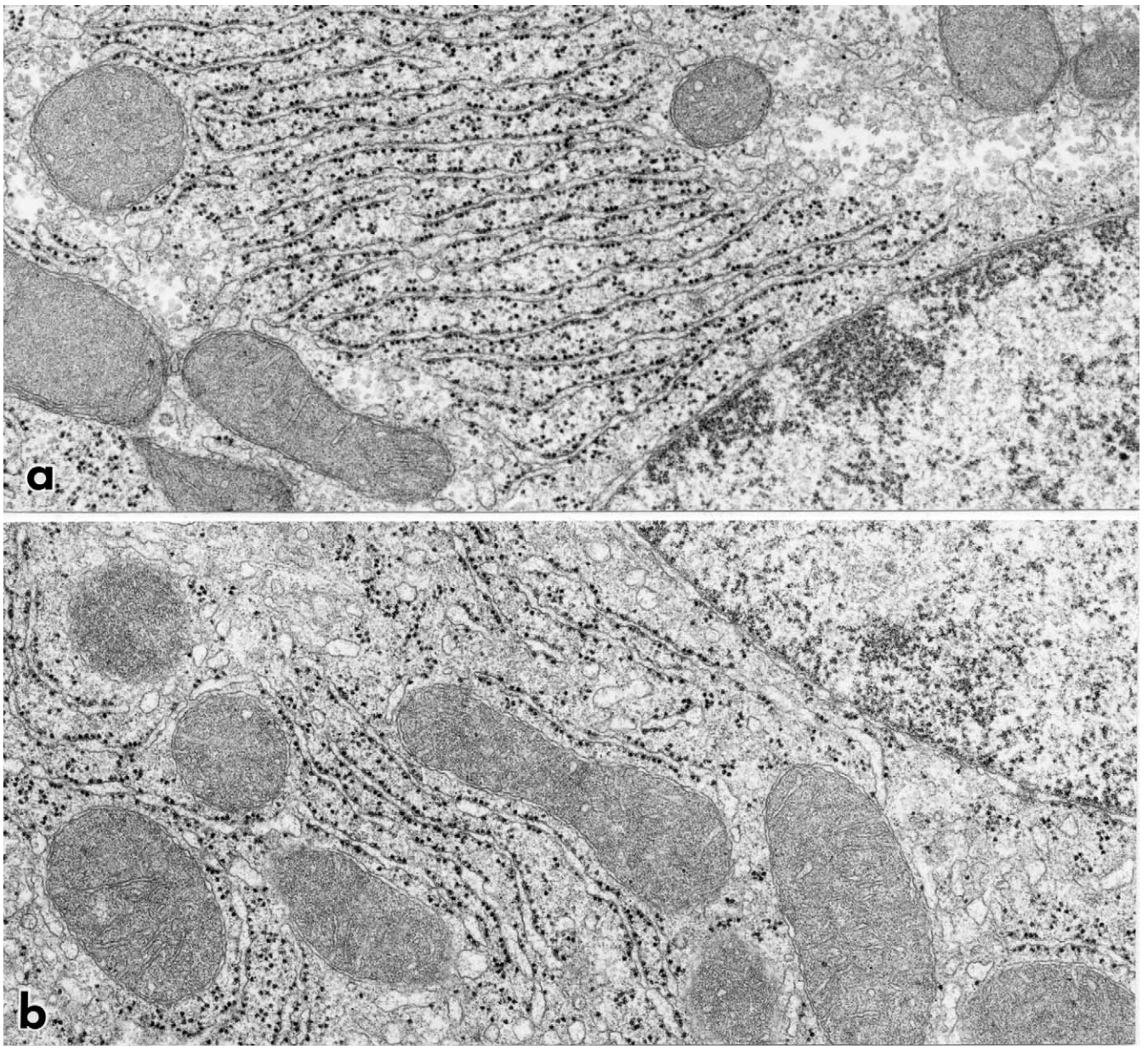

FIGURE 4 Parts of liver cells from rats perfusion fixed through the heart with 1% glutaraldehyde (a) and 4% formaldehyde plus 0.1% glutaraldehyde (b). Cell ultrastructure is similar but small focal expansions of the endoplasmic reticulum occur (b). 32,500×.

3. *4% formaldehyde plus 0.1% glutaraldehyde in 0.1 M sodium cacodylate buffer*: See Section III,A.

4. *2% formaldehyde plus 2.5% glutaraldehyde in 0.1 M sodium cacodylate buffer, often referred to as half-strength "Karnovsky's fixative" (Karnovsky, 1965)*: To make 250 ml of fixative solution, mix 25 ml 25% aqueous glutaraldehyde stock solution, 25 ml 20% formaldehyde stock solution, and 125 ml 0.2 *M* sodium cacodylate buffer; add distilled water to about 240 ml and adjust pH to 7.2 with 0.1 *N* NaOH or 0.1 *N* HCl. Complete with distilled water to 250 ml.

5. *1% osmium tetroxide in 0.1 M sodium cacodylate buffer*: See Section III,A.

6. *0.1 M sodium cacodylate buffer*: See Section III,A.

Steps

1. Cut out a piece of tissue from the organ under study and place it in a precold, empty petri dish.

2. Hold the tissue gently with a forceps and cut thin slices with a thin razor blade using sawing movements. The slices should not exceed 0.5 mm in thickness. Great care should be taken not to strain the tissue mechanically. Areas where the forceps have touched the tissue should be discarded.

3. Trim the slices to less than than $0.5 \times 5 \times 5$ mm and immerse them into the fixative solution.

4. Swirl the vial occassionally during fixation to secure uniform penetration of the fixative from all sides into the tissue. Fixation should last at least 2 h. In most cases the temperature of the fixative is not important. Initial fixation can be carried out at room temperature and followed by fixation in the cold.

5. Trim down the dimensions of the tissue slices while in the fixative solution in order to get small blocks suitable for embedding. It is absolutely essential that only tissue from the surface of the tissue is used, as the quality of fixation deteriorates with increasing distance from the surface of the immersion fixed slice (Fig. 5).

6. Proceed as described earlier for perfusion fixation through the abdominal aorta (see Section III,A, steps 11–13).

D. Fixation of Tissue Cultures

Solutions

1. *2% glutaraldehyde in 0.1 M sodium cacodylate buffer*: To make 100 ml, mix 50 ml 0.2 *M* sodium cacodylate buffer, 8 ml 25% glutaraldehyde, and 30 ml distilled water. Adjust pH to 7.2 with 0.1 *N* NaOH or 0.1 *N* HCl. Complete with distilled water to 100 ml.
2. *0.1 M sodium cacodylate buffer*: See Section III,A.

Steps

1. Gently decant the tissue culture medium.
2. Immediately add 2% glutaraldehyde in 0.1 m*M* cacodylate buffer. Very gently swirl the fixative in the culture dish.
3. Fix for 1 h.
4. Proceed as described earlier for perfusion fixation through the aorta (see Section III,A, steps 11–13).

E. Fixation of Cell Suspensions

Solutions

1. *2% glutaraldehyde in 0.1 M sodium caocdylate buffer*: See Section III,D.
2. *2% agar in 0.1 M sodium cacodylate buffer*: Dissolve during stirring 2 g agar in 100 ml 0.1 *M* sodium cacodylate buffer. Heat to close to 100°C until dissolved.

Steps

1. Mix the cell suspension rapidly with an equal volume of 2% glutaraldehyde in 0.1 *M* cacodylate buffer.
2. Fix for 1 h.
3. Sediment the cells in a centrifuge tube by centrifugation at approximately 1000 *g* for 5 min. Decant the supernatant.
4. Resuspend the cells in an excess of 0.1 *M* cacodylate buffer. Repeat step 3 after 15 min.
5. Add 1% osmium tetroxide in 0.1 *M* cacodylate buffer and resuspend the cells. Fix for 30 min. Repeat step 3.
6. Add 0.1 *M* sodium cacodylate buffer and resuspend the cells. Repeat step 3.
7. To the pellet add an equal volume of 2% agar in 0.1 *M* sodium cacodylate buffer, which has been heated to about 40°C. Mix the agar and the pellet rapidly with a fine glass rod. Allow the pellet to cool. Thereafter treat the pellet as a tissue block during dehydration and further processing. Take care not to resuspend the cells.

F. Dehydration and Embedding in Epoxy Resin

The following procedure results in embedded tissue blocks with good cutting properties from a variety of tissues. It includes *en bloc* staining with uranyl acetate, which improves contrast in subsequent section staining. If *en bloc* staining is not desired, steps 2–4 should be omitted (compare Figs. 6a and 6b).

Solutions

1. *70, 90, and 95% ethanol in water*
2. *0.05 M maleate buffer*: To make 100 ml, dissolve 0.58 g maleic acid in about 80 ml water and adjust pH to 5.2 with 1 *N* NaOH. Fill up to 100 ml with water.
3. *0.5% uranyl acetate in 0.05 M sodium maleate buffer*: To make 100 ml, dissolve 0.58 g maleic acid in 80 ml water and adjust pH to 6.0 with 1 *N* NaOH. Dissolve 0.5 g uranyl acetate dihydrate in this solution and adjust (if necessary) pH to 5.2 with NaOH. Fill up to 100 ml with water.
4. *Epoxy resin*: To make 100 g resin, mix 48 g TAAB 812, 19 g DDSA, and 33 g MNA. Stir continuously for 5 min. Add 2 g DMP-30 and stir continuously for another 5 min. The complete epoxy mixture should be used for initial infiltration within the next few hours, as it will slowly start to polymerize at room temperature. The freshly mixed complete resin can be stored in the freezer (e.g., –20°C) for months in closed vials. The vials must attain room temperature before being opened and used for embedding.

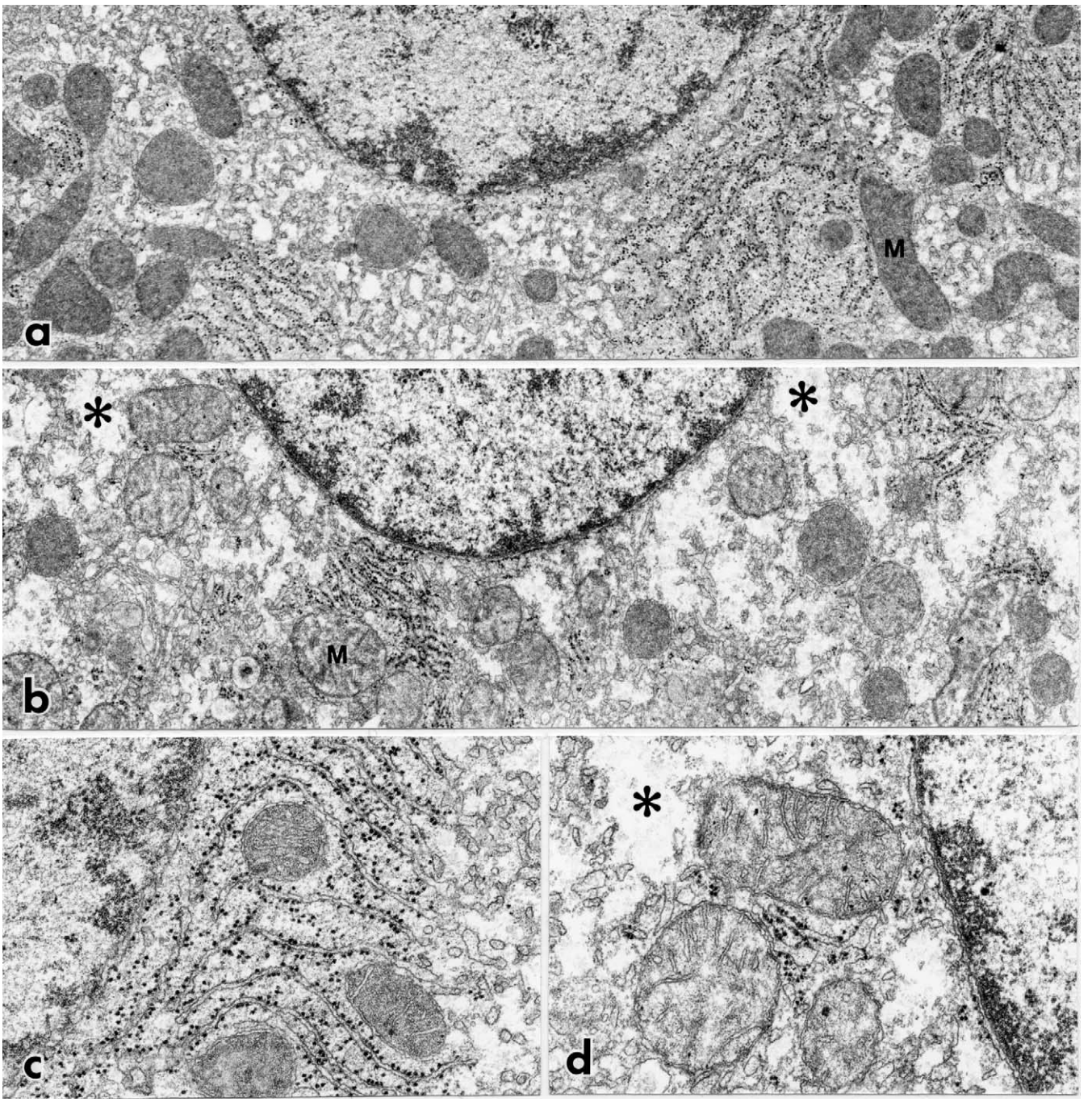

FIGURE 5 Liver cells fixed by immersion in 1% glutaraldehyde and observed in a section cut at a right angle to the liver surface. (a) The cell is located at the very surface of the liver. (b) The cell is located about 200 µm from the surface and thus fixed with some delay. The cytoplasm of the superficial cell, shown at higher magnification (c), is well preserved, but the cytoplasm of interior cells shows evidence of cell swelling with almost empty regions (*). Mitochondria (M) are well preserved (a, c), but dilated with a partly empty matrix (b and d). a and b: 15,000×; c and d: 32,500×.

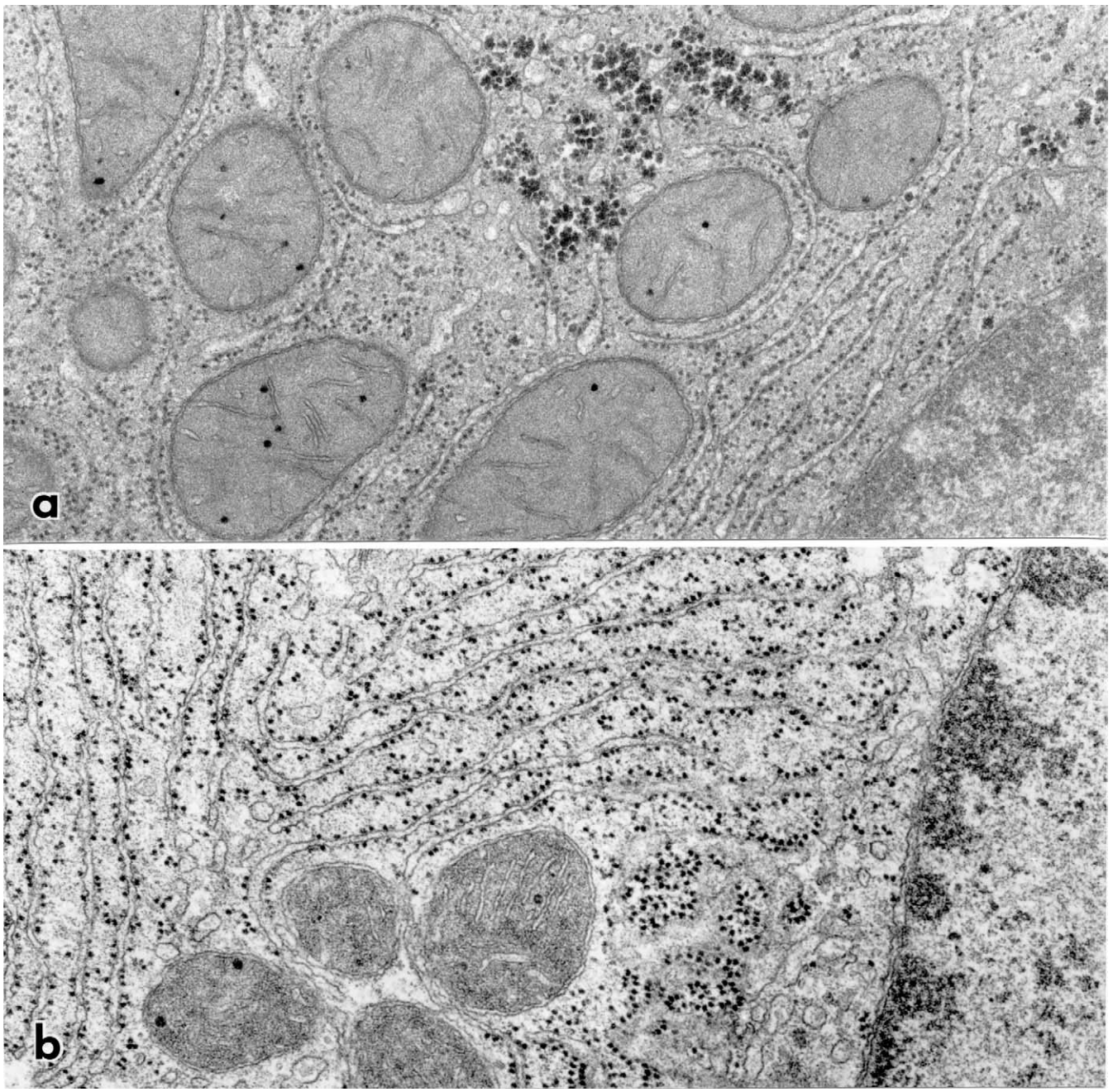

FIGURE 6 Electron micrographs of cells in liver perfusion fixed with 1% glutaraldehyde, postfixed in osmium tetroxide, and embedded in epoxy resin. (a) Embedding without *en bloc* staining but section staining with lead citrate. This preparation gives a good overall image of subcellular architecture. (b) Same fixation and embedding except that the tissue was *en bloc* stained with uranyl acetate and the section was double stained with uranyl acetate and lead citrate. The micrograph shows considerable contrast with emphasis on membranes, ribosomes, and nuclear components. 40,000×.

Steps

1. Rinse tissue fixed in aldehydes and/or osmium tetroxide for 2 × 30 min in buffer (e.g., same buffer used for fixation). Keep the tissue at 0–4°C until step 6. If *en bloc* staining is not desired, proceed to step 5.

2. For *en bloc* staining, rinse for 2 × 15 min with sodium maleate buffer. As in all the following steps up to step 10, remove fluid with a Pasteur pipette before adding new fluid. The tissue must never be allowed to dry.

3. Stain for 60 min in uranyl acetate in maleate buffer.
4. Rinse for 2 × 15 min in sodium maleate buffer.
5. Dehydrate for 2 × 15 min in 70% ethanol.
6. Dehydrate for 2 × 15 min in 90% ethanol. This and the following steps of dehydration and infiltration are carried out at room temperature.
7. Dehydrate for 2 × 15 min in 95% ethanol.
8. Dehydrate for 2 × 15 min in absolute ethanol. Repeat for large specimens.
9. Place the tissue for 2 × 15 min in propylene oxide, which acts as a transition medium. Take particular care that the tissue does not dry, as propylene oxide evaporates very rapidly. Because propylene oxide is toxic and very volatile, this and all subsequent steps should be carried out in a well-ventilated hood with gloves.
10. Infiltrate the tissue for 60 min in a mixture of 50% propylene oxide and 50% completely mixed epoxy resin.
11. Transfer the specimens to the surface of the epoxy resin in a clean vial containing 100% resin (Fig. 2a). Use a fine forceps or a wooden stick. Propylene oxide gradually diffuses out of the tissue blocks when they sink through the resin. Leave the specimens in the epoxy resin overnight at room temperature.
12. Fill the flat embedding mold with epoxy resin (Fig. 2b). Place a small piece of paper with the identification number of the specimen upside down in the resin next to the specimen (Figs. 2c and 2d). If necessary, adjust the location of the tissue block and/or the paper with a wooden stick.
13. Polymerize the specimens at 60°C for 2 days.

IV. COMMENTS

1. Chemicals used in fixation for electron microscopy, notably aldehydes, osmium tetroxide, and cacodylate, are toxic and should be handled with adequate safety precautions. Exposure to formaldehyde may lead to allergic reactions. Also, chemicals used during dehydration and embedding in epoxy or acrylic resins are toxic (mutagenic, allergenic, and, in some cases, perhaps carcinogenic) and should be handled with adequate safety precautions (Ringo *et al.*, 1982). Work in a well-ventilated hood and use gloves. Note that resins can penetrate most types of gloves within a short time.

2. For immunocytochemistry the sensitivity of the antigen to aldehydes determines the compositions of the fixative. As a rule of thumb, insensitive antigens can be fixed with 1% glutaraldehyde, sensitive antigens with 4% formaldehyde plus 0.1% glutaraldehyde, and very sensitive antigens with 4% formaldehyde only. In the latter case the formaldehyde concentration may be increased to 8%.

3. Cells tend to swell if the osmolality of the fixative vehicle (buffer) is low, whereas they shrink if the fixative solution has a high solute concentration (Maunsbach, 1966b). For this reason the osmotic composition of the fixative vehicle has to be adjusted for some tissues. In the outer renal medulla, where extracellular osmolality is high, the normal perfusion fixative (1% glutaraldehyde in 0.1 *M* cacodylate buffer) should be supplemented with 0.2 *M* sucrose, whereas for amphibian tissues, the vehicle osmolality should be decreased slightly.

4. The pH of aldehyde fixatives is normally 7.0–7.5 and fine adjustments of pH are not crucial in most ultrastructural studies. The choice of buffer in the fixative may influence the appearance of the tissue but in most tissues only to a moderate degree. Phosphate buffers are often used instead of cacodylate but in some tissues give a fine precipitate at concentrations around 0.1 *M* or more.

5. In highly vascularized organs, such as the pancreas, perfusion fixation leads to a distension of the extravascular space. Such swelling can be prevented by the addition of 2% dextran (molecular weight around 40,000) to the perfusion solution (Bohman and Maunsbach, 1970).

6. Storage of cells and tissues in glutaraldehyde fixatives has very little influence on the final appearance of the tissue in the transmission microscope. Except for immunocytochemical studies, the preparation procedure can be halted for days, sometimes even months, while the tissue is in the aldehyde fixative. Pieces of aldehyde-fixed tissue can therefore be transported easily in fixative between laboratories.

7. The protocol for ethanol dehydration in connection with epoxy resin embedding can be varied considerably without great effects on the final result. In most cases, short dehydration times seem preferable but storage of the specimens overnight at 4°C is usually without problems.

8. Acetone is often used as an alternative to ethanol for dehydration but the results are in most cases essentially the same. Both ethanol and acetone dehydration lead to extraction of tissue lipids and shrinkage of tissue dimensions. These effects vary between tissues and may be slightly different in different protocols but cannot be eliminated.

9. The chemical composition of epoxy resins from different manufacturers varies considerably (see Mollenhauer, 1993; Glauert and Lewis, 1998). Consequently, the properties of the different epoxy resins also vary with respect to viscosity and flow rate, hard-

ness after polymerization, stainability, and stability in the electron beam. However, ultrastructural observations using presently available epoxy resins are quite comparable and in fact are often indistinguishable.

10. The hardness of the polymerized epoxy blocks can be modified by changing the ratio of DDSA/MNA in the epoxy-embedding medium. Thus, an increase of DDSA gives softer blocks and an increase of MNA given harder blocks. However, adjustment of the anhydride : epoxide ratio is not necessary, although this was previously considered important for controlling the properties of the resin. While polymerization is normally carried out at 60°C, a higher curing temperature (80–100°C) can be used for very rapid polymerization, although this may lead to structural derangement of membranes.

V. PITFALLS

1. If the fixative flow is compromised during perfusion fixation, sufficient concentration of fixative is not obtained throughout the tissue and cells may undergo various abnormal alterations before they are fixed. In a successful perfusion the surfaces of the organs blanch very rapidly, the kidney surface within less than a second, and the tissues harden quickly. There is usually a good correlation among the speed of tissue blanching, fixative flow as observed in the drip chamber, absence of blood in dissected tissues, and final quality of tissue preservation as observed in the electron microscope.

2. It is very important that the tissues are not damaged mechanically when dissected and trimmed before immersion fixation or after fixation. Small pieces cut out with a razor blade should only be transferred between vessels with a fine forceps holding onto corners of the tissue blocks or with a Pasteur pipette.

3. Following immersion fixation it is necessary to secure that the tissue analyzed in the electron microscope originates from the surface layers of the tissue block, as there is a gradient in the quality of fixation from the surface to the center of the block (Fig. 4). In the center of tissue slices, where the fixative has arrived with some delay, there is swelling of cytoplasm and organelles. Thus, before cutting thin sections it is practical first to examine thick (1–3 µm) sections of the same tissue block by light microscopy to select the optimal location of tissue for electron microscope analysis.

4. Difficulties in sectioning of tissue embedded in epoxy resin are often due to soft resin blocks. This condition may originate from one or more deviations from the dehydration/infiltration protocol: (a) Wrong epoxy resin composition, (b) insufficient stirring of the components of the resin, (c) too short an infiltration time in pure resin, (d) too large a specimen (all dimensions exceeding 1 mm), (e) too short a polymerization time, (f) incomplete dehydration, or (g) incomplete removal of ethanol.

References

Bohman, S.-O., and Maunsbach, A. B. (1970). Effects on tissue fine structure of variations in colloid osmotic pressure of glutaraldehyde fixatives. *J. Ultrastruct. Res.* **30**, 195–208.

Carlemalm, E., Villiger, W., Hobot, J. A., Acetarin J.-D., and Kellenberger, E. (1985). Low temperature embedding with Lowicryl resins: Two new formulations and some applications. *J. Microsc.* **140**, 55–63.

Glauert, A. M., and Lewis, P. R. (1998). Biological specimen preparation for transmission electron microscopy. *In* "Practical Methods in Electron Microscopy" (A. M. Glauert, ed.), Vol. 17. Portland Press, London.

Griffiths, G. (1993). "Fine Structure Immunocytochemistry." Springer-Verlag, Berlin.

Karnovsky, M. J. (1965). A formaldehyde-glutaraldehyde fixative of high osmolality for use in electron microscopy. *J. Cell Biol.* **27**, 137A.

Luft, J.H. (1961). Improvements in epoxy resin embedding methods. *J. Biophys. Biochem. Cytol.* **9**, 409–414.

Maunsbach, A. B. (1966a). The influence of different fixatives and fixation methods on the ultrastructure of rat kidney proximal tubule cells. I. Comparison of different perfusion fixation methods and of glutaraldehyde, formaldehyde and osmium tetroxide fixatives. *J. Ultrastruct. Res.* **15**, 242–282.

Maunsbach, A. B. (1966b). The influence of different fixatives and fixation methods on the ultrastructure of rat kidney proximal tubule cells. II. Effects of varying osmolality, ionic strength, buffer systems and fixative concentration of glutaraldehyde solutions. *J. Ultrastruct. Res.* **15**, 283–309.

Maunsbach, A. B., and Afzelius, B. A. (1998). "Biomedical Electron Microscopy. Illustrated Methods and Interpretations." Academic Press, San Diego.

Mollenhauer, H.H. (1993). Artifacts caused by dehydration and epoxy embedding in transmission electron microscopy. *Microsc. Res. Technique* **26**, 496–512.

Ringo, D. L., Brennan, E. F., and Cota-Robles, E. H. (1982). Epoxy resins are mutagenic: Implications for electron microscopists. *J. Ultrastruct. Res.* **80**, 280–287.

Sabatini, D. D., Bensch, K., and Barnett, R. J. (1963). Cytochemistry and electron microscopy. The preservation of cellular ultrastructure and enzymatic activity by aldehyde fixation. *J. Cell Biol.* **17**, 19–58.

CHAPTER

23

Negative Staining

Werner Baschong and Ueli Aebi

I. INTRODUCTION

Heavy metal negative staining, a now widely used routine technique to prepare biological material for imaging in the transmission electron microscope (TEM), was introduced almost 50 years ago (Brenner and Horne, 1959; for reviews, see Oliver, 1973; Horne, 1991). Suitable specimens may either be in solution or in suspension and thus include the whole spectrum of structural organization of biomolecules, ranging from monomeric and oligomeric proteins [e.g., RNA polymerase (Fig. 1a) or glutamine synthetase (Fig. 1b, bottom)], to protein polymers [e.g., cytoskeletal filaments or the multistranded helical cables of glutamine synthetase (Fig. 1b, top)], and eventually to large multicomponent supramolecular assemblies [e.g., nuclear pore complexes or bacteriophages (Fig. 1c)]. Compared to other electron microscopic techniques, negative staining is remarkably simple and can easily provide reliable structural information as quickly as 2 min after preparing the specimen down to resolutions of 2.0 nm (reviewed by Bremer *et al*., 1992) and below (Harris, 1999).

As shown schematically in Fig. 2a, a negatively stained specimen is embedded in a microcrystalline heavy atom salt replica that portrays its molecular architecture. Because heavy metal atoms (e.g., U, V, W, Au, Mo, Pt, Pb, Os) scatter electrons much more strongly than elements constituting the biomolecules (i.e., C, H, O, N, P, S), the contrast of negatively stained specimens (Fig. 2b) is much higher than that of unstained specimens and reversed (hence "negative" staining). In addition, the heavy metal salt replica stabilizes the specimen against collapse and distortion and substitutes, at least partially, for the aqueous environment typical for biomolecules. It also serves as a radiation protectant in the sense that it is more radiation resistant than biological matter (cf. Aebi *et al*., 1984; Bremer and Aebi, 1992).

II. MATERIALS AND INSTRUMENTATION

Negative staining requires only minor investment for instrumentation and supplies. For routine applications, the following items are needed.

1. *Specimen support grids* (Fig. 3a): For example, from Pelco International (www.pelcoint.com). Typically 200–400 mesh/in. copper grids, 3.05 mm in diameter and 0.7 mm thick, coated with a specimen support film (mostly either a carbon/collodion composite film, or a thin carbon film). The specimen grids should be stored dust free, e.g., in a petri dish (Fig. 3b) that is kept at relatively low humidity.
2. *Precision forceps* (Fig. 3c): For example, from Electron Microscopy Sciences (www.emsdiasum.com). It is advisable to bend the jaws of the forceps slightly inwards to prevent surface tension from trapping buffers and solutes between the jaws. A tightly fitting rubber band or piece of plastic tubing allows the jaws to be fixed in the closed state.
3. *Glow discharge unit* (Fig. 3d). It is used to render the support film of the specimen grids hydrophilic and can be built as detailed by Aebi and Pollard (1987). The specimen grid is glow discharged on a small glass block coated with Parafilm (Fig. 3d, arrowhead).
4. A *metal* or *plastic tray* (Fig. 3e) serves as the "workbench." Drops of water and stain, typically 100 µl each, can be placed on a piece of Parafilm (Fig. 3e,

Copyright 2006, Elsevier Science (USA).
All rights reserved.

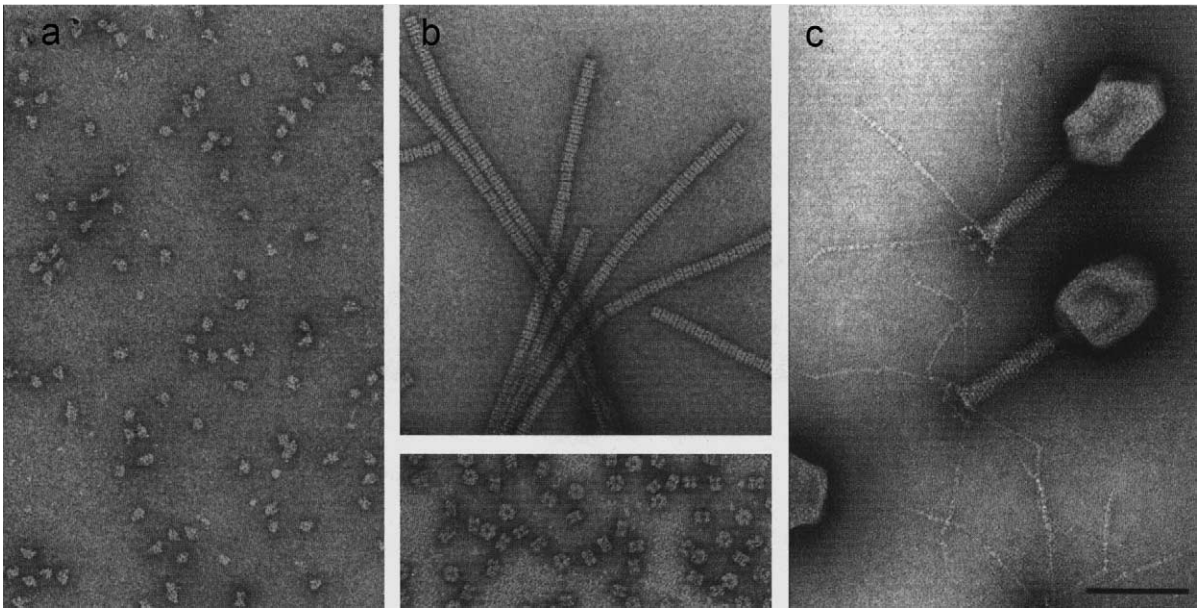

FIGURE 1 From molecules to replicating molecular machines—examples of negatively stained preparations. **(a)** Monomers of *Escherichia coli* RNA polymerase holoenzyme. **(b)** Glutamine synthetase from *E. coli.* (Top) Helical filaments are formed in the presence of millimolar amounts of Co^{2+} ions. (Bottom) The intact enzyme molecule is composed of 12 identical 50-kDa subunits that associate with 622 symmetry: i.e., end-on views display a typical blossom-like appearance with six-fold symmetry, whereas side views reveal twofold symmetry. **(c)** *E. coli* bacteriophage T4: organization into a distinct prolate icosahedral head and a contractile helical tail to which a base plate with extended fibers is attached at the bottom are evident. RNA polymerase (a) and glutamine synthetase (b) were stained with 0.75% uranyl formate; and bacteriophage T4 (c) was stained with 1% uranyl acetate. Scale bar: 100 nm.

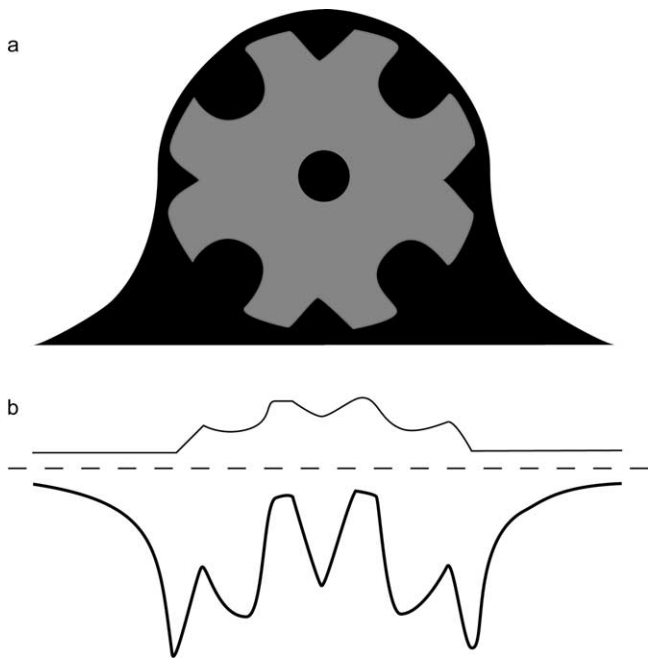

FIGURE 2 Schematic representation of a "negatively stained" model specimen. **(a)** The schematic view represents a cross section through a model specimen (light grey) that has been embedded in an ideal negative stain (dark grey). **(b)** The schematic view in a was projected by adding the pixel values along the vertical axis. The projection profile of the "negatively stained" model specimen is represented by a thick black trace, whereas the projection profile of the "unstained" model specimen is depicted by a thinner grey trace. In the case of the "negatively stained" specimen, its projection profile was inverted, i.e., multiplied by –1, to compare it directly with the corresponding profile of the "unstained" specimen.

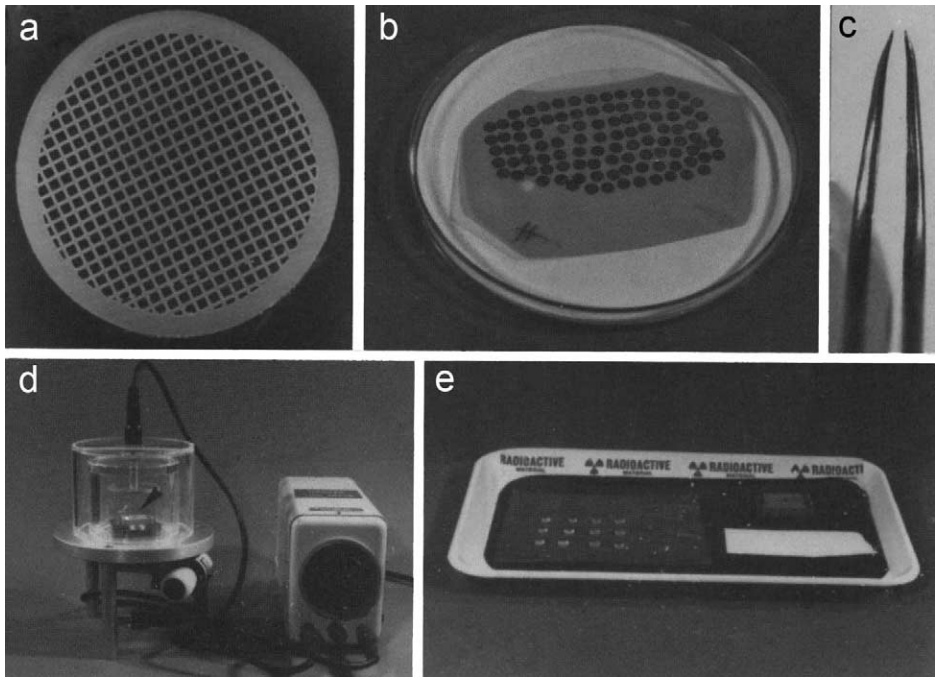

FIGURE 3 Materials and equipment required for negative staining. **(a)** Specimen support grid (e.g., 200 mesh/in. copper grid, 3.05 mm in diameter and 0.7 mm thick) coated with a collodion-carbon composite film (the support film is particularly evident at the edges). **(b)** The specimen support grids are stored on filter paper in a covered petri dish (the cover is removed for clarity). **(c)** Precision forceps with the jaws slightly bent inwards are used for all manipulations. **(d)** The specimen grids are rendered hydrophilic in a reduced atmosphere of air using a custom-built glow-discharge unit (for the design, see Aebi and Pollard, 1987). The specimen grids are glow discharged on a small glass block that is covered with Parafilm (see arrowhead). **(e)** A plastic or metal tray serves as the "workbench" for staining. The water and stain drops are placed on a piece of Parafilm on the left, the glass block with a glow discharged grid is seen on right at the back, and a piece of filter paper is depicted in the front.

left). Filter or blotting paper (Fig. 3e, right) is required for removing excess liquid from the specimen grid.

5. *Micropipettes*: 5 µl and adjustable to 20–200 µl or similar.

6. A *stopwatch* is required to control adsorption and staining times.

7. A *Pasteur pipette* drawn out into a capillary and connected to a suction device such as a water jet pump serves to remove excess stain from the specimen grid (Fig. 4f).

III. PROCEDURES

Solutions

The following solutions are required for negative staining.

1. *Specimen solution/suspension*
2. *Deionized or, even better, double-distilled water*. Water is required for washing the specimen grid after specimen adsorption.
3. *Negative stain, i.e., heavy metal solution*. For instance, uranyl acetate or sodium phosphotungstate.

A. Preparation of Negative Stain Solution

For the properties of various negative stains, along with references on their preparation, see Bremer *et al.* (1992). Here, the preparation of uranyl formate, one of the more delicate procedures, is described as an example:

(Mind, uranyl salts are radioactive, cf. p xxx)

Steps

1. Weigh out uranyl formate to obtain a final concentration of 0.75% (i.e., 7.5 mg/ml).
2. Boil an appropriate amount of water to remove CO_2 and to increase the solubility of the uranyl formate in the boiling water.
3. Pour the boiling water into a small beaker containing the weighed uranyl formate.
4. Stir slowly for 5–10 min in the dark (i.e., with the beaker wrapped into aluminum foil).

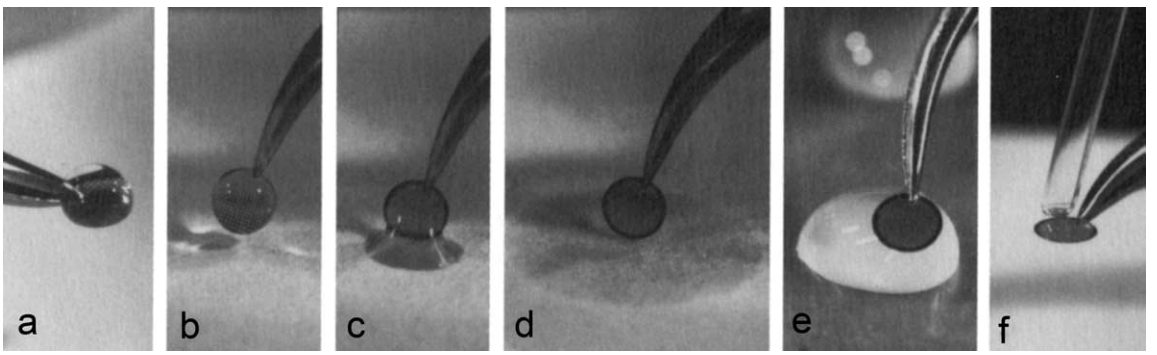

FIGURE 4 Negative staining. **(a)** A ~5-µl drop of sample solution/suspension is placed onto a glow-discharged specimen support grid that is held horizontally by a pair of forceps and allowed to adsorb for 30–60 s. **(b)** The specimen grid is then turned vertically and **(c)** allowed to gently touch the filter paper, which **(d)** removes excess liquid. **(e)** The adsorbed specimen is then washed by carefully placing it sideways onto a drop of water for 1 s, blotted as shown in b–d, and washed a second time. The actual staining is performed similarly by first washing the specimen grid on a drop of negative stain as described in **e**, blotting and repeating this step once more, this time leaving the specimen grid for 10 s on the drop of negative stain solution. **(f)** After blotting off excess stain, the residual stain is removed by gently moving a capillary (drawn-out and shaped from a Pasteur pipette) around the edge of the grid. The capillary is connected to a low-vacuum suction device (e.g., a water jet pump).

5. Filter the solution through a 0.2-µm membrane filter [e.g., a Supor 0.2-µm *Acrodisc 32* from Gelman Sciences (www.pall.com)].
6. Adjust the pH to 4.25 by adding 10 *N* NaOH (about 2 µl per 1 ml negative stain solution). The uranyl formate solution should turn into a moderately intense yellow (*Caution*: Increasing the pH toward neutral rapidly leads to precipitation of uranyl salts.)
7. Stir for another 5 min in the dark.
8. Filter a second time.
9. Readjust the volume with double-distilled water to compensate for water loss due to evaporation, filtration, etc.
10. Store stain in the dark (e.g., in a tube wrapped into aluminum foil). It will keep stable for 1–2 days.

Note: Uranyl formate may be difficult to purchase: Try, e.g., www.pfaltzandbauer.com (Pfaltz & Bauer Inc., Waterbury, CT 06708).

B. Staining

Our standard staining procedure for soluble proteins and their supramolecular assemblies is illustrated in Fig. 4. As might be appreciated, this procedure is quick, simple, and straightforward.

Steps

1. Glow discharge specimen grids in a unit such as shown in Fig. 3d, e.g., for 15 s (for details, see Aebi and Pollard, 1987).

2. To the freshly glow-discharged specimen grid, apply a 5-µl drop of the sample solution/suspension (Fig. 4a). Let it adsorb for 30–60 s, and then blot off the drop as illustrated in Figs. 4b–4d. For blotting, hold the specimen grid vertical (Fig. 4b) and allow it to touch the filter paper gently (Fig. 4c). The drop will be removed by capillary forces (Fig. 4d).

3. Next, wash the specimen grid on a drop of double-distilled water by carefully lowering it sideways onto the surface of the drop (Fig. 4e). After 1 s, carefully remove the specimen grid from the water drop, blot as shown in Figs. 4b–4d, and repeat this washing regimen once more.

4. Finally, stain the specimen for 1 s by lowering the specimen grid onto a drop of negative stain solution as described for the washing regimen (Fig. 4e) and then blot the specimen grid as described in Figs. 4b–4d. Repeat this step once; this time, however, leave the specimen grid for 10–15 s on the negative stain drop (as illustrated in Fig. 4e) before blotting.

5. After blotting off excess stain (Figs. 4b–4d), further reduce the residual stain layer to just a thin (i.e., 50–100 nm thick) liquid film prior to air drying. This should be achieved in a controlled fashion; a drawn-out and shaped into a slightly bent capillary Pasteur pipette, connected to a suction device such as a water jet pump, is moved gently around the edge of the specimen grid (Fig. 4f). The preparation is now ready for inspection in the EM.

IV. COMMENTS

The quality of a negatively stained preparation (i.e., the interpretable structural detail captured on the EM

screen, depicted on an electron micrograph, or monitored by a video or slow-scan camera attached to the EM) depends primarily on the penetration properties (e.g., size, charge, and hydrophobicity) of the heavy metal salt used for negative staining and on the physicochemical properties (e.g., solubility, charge, and hydrophobicity) of the specimen. Because some negative stains have a relatively acidic pH, whereas others are neutral or moderately basic and because they may be neutral, anionic, or cationic (for review, see Bremer *et al.*, 1992), negative staining is quite versatile and can be tailored to specific needs.

When visualizing structures comprising components of different electron densities, e.g., colloidal gold-labeled proteins, the electron density of the heavy metal may become crucial. While 2- to 3-nm Au particles associated to bacteriophage T4 polyheads, i.e., aberrant tubular assemblies constituted exclusively of the major viral head protein gp23, are barely discernible from the uranyl acetate acetate-stained protein units (Fig. 5a), 3-nm Au-labled immunoglobulin G binding to the appropriate haemaglutinin antigen (Fig. 5b) and even 1- to 2-nm Au-labeled Fab fragments binding to haemaglutine assemblies (Fig. 5c), are still well discernible when stained with $NaSiO_4WO_4$, a less electron dense and intrinsically neutral negative stain (Baschong and Wrigley, 1990). *A priori*, the optimal stain for a particular specimen has to be chosen and evaluated by trial and error.

In our laboratory, starting in a first trial with an uranyl salt [we still favour uranyl salts and formate over acetate for it is slightly more stable in the electron beam (cf. Bremer *et al.*, 1992)] or with a tungstate (e.g., NaPT, i.e., sodium phosphotungstate) proved successful with a wide variety of specimens, including cytoskeletal, membrane and soluble cytosolic proteins, and their supramolecular assemblies (for examples, see Aebi *et al.*, 1983, 1984, 1988; Bremer *et al.*, 1991, 1992, 1994; Hoenger and Aebi, 1996). Within this respect, it may be noteworthy that uranyl acetate can also act as a primary fixative: It was observed to stabilize bacteriophage T4 polyheads against dilution-induced dissassembly in an aldehyde-like manner (Baschong *et al.*, 1983; W. Baschong unpublished results) and was more recently documented to act as a primary fixative for skeleton muscle (Fassel and Graeser, 1997).

With tightening safety rules for the use of radioactive substances—uranyl salts are radioactive—ordering, handling, and disposal of uranyl salts usually have specific guidelines (check with your safety responsible). In turn, the availability of uranyl salts may become more restricted, while novel ready-made commercial methylamine–vanadate (Tracz *et al.*, 1997) and methylamine–tungstate-based stains (Shayakhmetov *et al.*, 2000) have been introduced (www.nanoprobes.com, Nanoprobes Inc., Yaphank, NY 11980-9710). As a consequence, nonradioactive metal salts such as tungstates, molybdates and vanadates may be given preference. The performance of such alternatives is best evaluated by trial and error, as illustrated in Figs. 6a–6e by staining bacteriophage T4 polyheads with uranyl formate (a) and prospective alternatives, i.e., with NH_4MoO_4 (b), NH_4VO_4 (c), Na_2WO_4 (d), and $RhCl_3$ (e), and liposomes with methylamine vanadate (f).

The negative staining protocol described earlier is suitable for most specimens and stains. With delicate proteins, an additional washing step of the grid with water or sample buffer *prior* to applying the specimen may be included to wet the specimen support film and to minimize surface tension and/or denaturation of the specimen. The optimal sample concentration, which obviously has to be determined experimentally, should yield well-dispersed and evenly distributed particles adsorbed to the specimen support film. It is determined by the size, shape, and adsorption properties of the biomolecules or supramolecular assem-

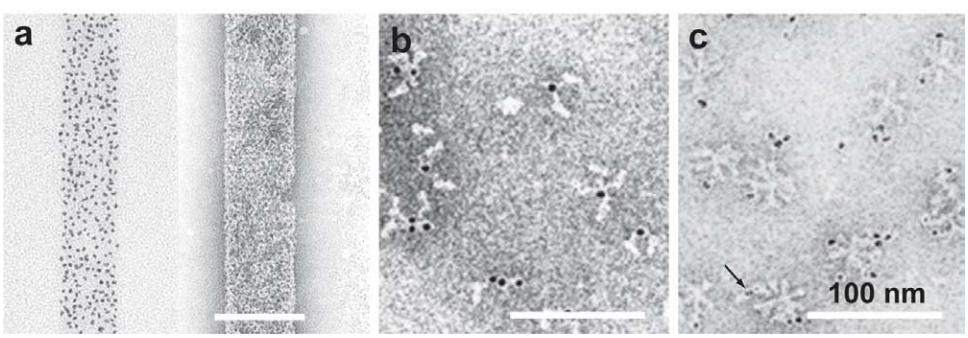

FIGURE 5 Negative staining of Fab–gold and antibody–gold complexes: (**a**) Bacteriophage T4 polyheads labeled with Fab-$Au_{2.5\,nm}$ unstained (left) and stained with 1% uranyl acetate. (**b**) Au_3-labled immunoglobulin G bound to bromelain-treated haemagglutinin. (**c**) $Au_{1–2\,nm}$-labeled Fab bound to haemagglutinin rosettes. Arrow: $Au_{1–2\,nm}$ colloid. (Adapted from Baschong & Wrigley, 1990)

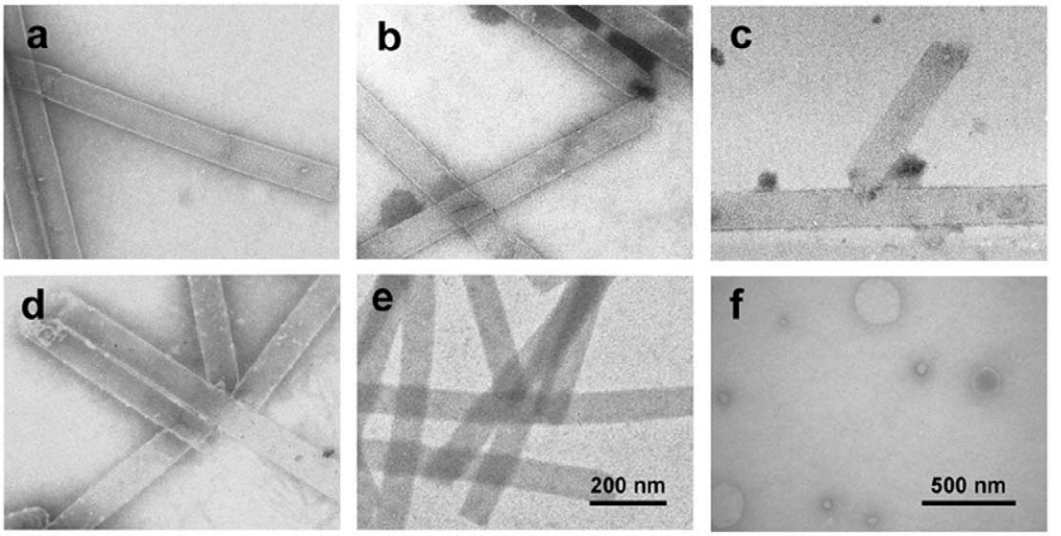

FIGURE 6 Comparative series of prospective negative stains used on bacteriophage T4 polyheads: (**a**) with 1% uranyl formate, (**b**) with 2% NH_4MoO_4, (**c**) with half-saturated NH_4VO_4, (**d**) with 1% Na2WO_4, and (**e**) with 2% $RhCl_3$. (**f**) Liposomes stained with metylamine–vanadate, courtesy of C. Prescianotto-Baschong.

blies under investigation, but also by the washing and staining regimen employed. For oligomers or polymers (e.g., such as filaments), crystalline, or paracrystalline specimens, a higher concentration than for individual biomolecules is required. As a rule of thumb, a few micrograms per milliliter for single particles (see Fig. 1a and bottom of Fig. 1b) and a few hundred micrograms per milliliter for supramolecular assemblies such as filaments (see top of Fig. 1b) or virus particles (see Fig. 1c) usually yield a reasonable particle density on the EM grid. The ionic conditions of the sample buffer and the presence of detergents, while strongly interfering with specimen adsorption, may have little effect on the quality of the negative stain replica surrounding the biomolecules, as long as a sufficient number of washing steps (usually two to six for most compounds) are employed prior to applying the negative stain solution to the specimen.

Heavy metal salts may not be inert but may interact physically or chemically with the specimen. Such sample–stain interactions may not explicitly produce "preparation artifacts" but sometimes unveil biologically significant information about the specimen going beyond purely structural aspects. For instance, human epidermal keratin filaments (cf. Aebi *et al*., 1983), after negative staining with uranyl formate (UF; pH 4.25), appear rather compact and featureless with a fairly uniform width (Fig. 7a). By contrast, when the same filaments are stained negatively with sodium phosphotungstate (NaPT; pH 7.0), they partially unravel and thereby unveil their protofibrillar substructure (Fig. 7b). This local unraveling becomes even more pronounced after washing the filaments briefly with 10 m*M* phosphate buffer (NaP_i; pH 7.0) prior to staining them negatively with UF (Fig. 7c). Most likely, the inorganic phosphate (P_i) acts as a modulator of the lateral interaction of the protofilaments and/or protofibrils constituting the filament (cf. Aebi *et al*., 1983, 1988). In fact, a similar response to different negative stains has also been observed with F-actin filaments where inorganic phosphate appears to modulate the relative strength of the intersubunit bonds *along* and *between* the two long-pitch helical strands of actin subunits defining the filament (cf. Bremer *et al*., 1991, 1994; Bremer and Aebi, 1992).

V. PITFALLS

A. Poor Specimen Adsorption

1. *Specimen support film is wrongly charged:* Highly negatively charged proteins or DNA do adsorb poorly to support films exhibiting a net negative charge as produced by glow discharge in a reduced atmosphere of air. By contrast, glow-discharging specimen grids in a reduced atosphere of pentylamine yield a *net positive charge* of the support film (cf. Aebi and Pollard, 1987).

2. *Specimen support film is not properly glow discharged:* Try longer glow discharge, and glow discharge only one grid at a time and use it immediately.

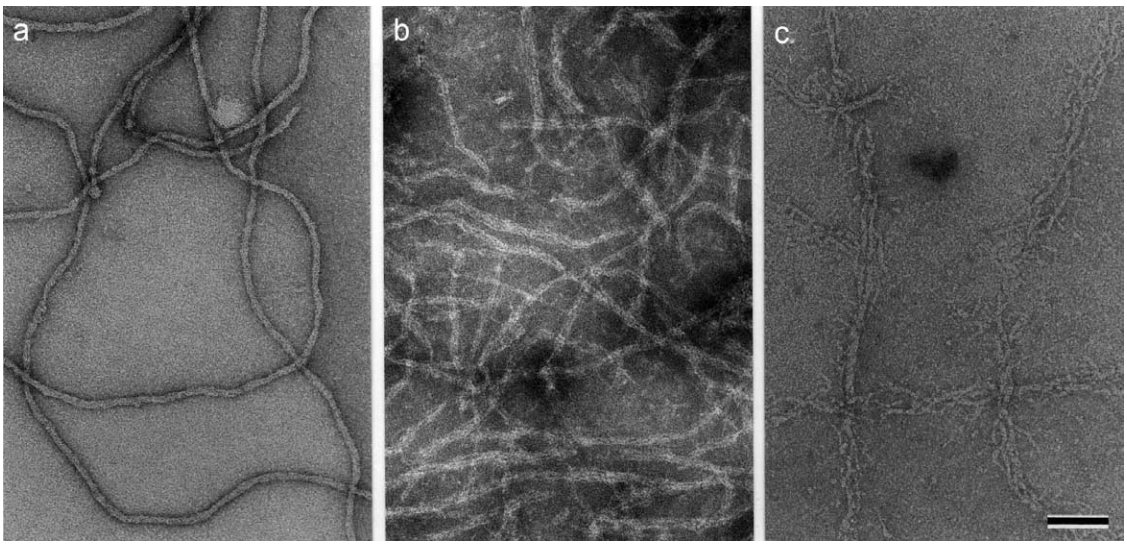

FIGURE 7 Negatively stained human epidermal keratin filaments. **(a)** Keratin filaments in 10 m*M* Tris, pH 7.5, stained negatively with 0.75% uranyl formate (UF; pH 4.25) appear relatively featureless and compact with a fairly uniform width. **(b)** In contrast, when the same keratin filaments are stained negatively with 2% sodium phosphotungstate (NaPT; pH 7.0) instead, they locally unravel and exhibit their protofibrillar substructure. **(c)** Even more dramatic unraveling into their protofibrils occurs when the adsorbed filaments are washed briefly with 10 m*M* phosphate buffer (NaP_i; pH 7.0) prior to staining them with 0.75% UF, pH 4.25. Scale bar: 100 nm.

B. Patchy, Poor, or Bad Staining

1. *Specimen concentration is too high:* A high density of particles adsorbed to the specimen support film renders quantitative and/or controlled removal of excess stain more difficult, thereby resulting in inhomogeneities in the staining even in particle-free areas. Try lower specimen concentration.

2. *Stain is not sufficiently removed:* Try removing stain more quantitatively by suction with a capillary as illustrated in Fig. 4f.

3. *Suboptimal stain for the specimen:* Try a different stain.

4. *Suboptimal wetting properties of the specimen support film:* Try longer glow discharge times or switch to a different sample buffer, assuming that this does not compromise the specimen.

5. *Incompatibilities between stain and buffers:* For instance, uranyl salts precipitate in the presence of inorganic phosphate. Hence avoid using phosphate buffers.

6. *Buffer contains high molar salt or detergent:* Try including more washing steps.

C. "Bubbling" of Stain Upon Irradiation

1. *Strong recrystallization or water content of stain is too high:* Try "prebaking" specimen at a low magnification (e.g., at 1000×) for 3–5 s before using higher magnifications.

D. Disintegration of Specimen During Preparation

1. *Specimen is instable in water* (washing steps!): Wash and preequilibrate the specimen with sample buffer instead of water. Replace the conventional buffer with a buffer that will dry off by sublimation when in the electron microscope, such as ammonia acetate. Alternatively, use such a volatile buffer at least for the washing steps. Mild cross-linking with, e.g., 0.05–0.25% glutaraldehyde for 2 min on ice (quench with 1% glycine, pH 7.0, or with 1% freshly made $NaBH_4$) may also stabilize the specimen.

E. Significant Background of Monomers and/or Small Oligomers with a Specimen Containing Supramolecular Assemblies

1. *Specimen is in steady-state equilibrium with monomers and/or oligomers:* Pellet the specimen (e.g., in a tabletop or air fuge at 100,000 *g*), discard the supernatant, resuspend the pellet in sample buffer, and immediately prepare the grid. Alternatively, fix, e.g., the protein assembly, with 4% formaldehyde while in

equilibrum and purify on a sucrose gradient (Baschong *et al*., 1991).

Acknowledgments

We thank Rosmarie Suetterlin and Daniel Mathys for their help. This work was supported by the Canton Basel-Stadt and the M.E. Müller Foundation of Switzerland)

References

Aebi, U., Fowler, W. E., Buhle, E. L., and Smith, P.R. (1984). Electron microscopy and image processing applied to the study of protein structure and protein-protein interactions. *J. Ultrastruct. Res.* **88**, 143–176.

Aebi, U., Fowler, W. E., Rew, P., and Sun, T.-T. (1983). The fibrillar structure of keratin filaments unraveled. *J. Cell Biol.* **97**, 1131–1143.

Aebi, U., Haener, M., Troncoso, J. C., and Engel, A. (1988). Unifying principles in intermediate filament structure and assembly. *Protoplasma* **145**, 73–81.

Aebi, U., and Pollard, T. D. (1987). A glow discharge unit to render electron microscope grids and other surfaces hydrophilic. *J. Electron. Microsc. Tech.* **7**, 29–33.

Baschong, W., Baschong-Prescianotto, C., Engel, A., Kellenberger, E., Lustig, A., Reichelt R., Zulauf, M., and Aebi U. (1991). Mass analysis of bacteriophage T4 proheads and mature heads by scanning transmission electron microscopy and hydrodynamic measurements. *J. Struct. Biol.* **106**, 93–101.

Baschong, W., Baschong-Prescianotto, C., and Kellenberger, E. (1983). Reversible fixation for the study of morphology and macromolecular composition of fragile biological structures. *Eur. J. Cell Biol.* **32**, 1–6.

Baschong, W., and Wrigley, N. G. (1990). Small colloidal gold conjugated to Fab fragments or to immunoglobulin G as high-resolution labels for electron microscopy: A technical overview. *J. Electron. Microsc. Tech.* **14**, 313–323.

Bremer, A., Henn, C., Engel, A., Baumeister, W., and Aebi, U. (1992). Has negative staining still a place in biomacromolecular electron microscopy? *Ultramicroscopy* **46**, 85–111**.**

Bremer, A., Henn, C., Goldie, K. N., Engel, A., Smith, P. R., and Aebi, U. (1994). Towards atomic interpretation of 3-D reconstructions of F-actin filaments. *J. Mol. Biol.* **242**, 683–700.

Brenner, S., and Horne, R. W. (1959). A negative staining method for the high resolution electron microscopy of viruses. *Biochim. Biophys. Acta* **34**, 103–110.

Fassel, T. A., and Graeser, M. L. (1997). Uranyl acetate as a primary fixative for skeletal muscle. *Microsc. Res. Tech.* **37**, 600–601.

Harris, J. R. (1999). Negative staining of thinly spread biological particulates. *Methods Mol. Biol.* **117**, 13–30.

Horne, R. W. (1991). Early developments in the negative staining technique for electron microscopy. *Micron Microsc. Acta* **22**, 321–326.

Oliver, R. M. (1973). Negative stain electron microscopy of protein macromolecules. *Methods Enzymol.* **27**, 616–672.

Shayakhmetov, D. M., Papayannopoulou, T., Stamatoyannopoulos, G., and Lieber, A. (2000). Efficient gene transfer into human CD34+ cells by a retargeted adenovirus vector. *J. Virol.* **74**, 2567–2583.

Tracz, E., Dickson, D. W., Hainfeld, J. F., and Ksiezak-Reding, H. (1997). Paired helical filaments in corticobasal degeneration: The fine fibrillary structure with NanoVan. *Brain Res.* **773**, 33–44.

CHAPTER

24

Glycerol Spraying/Low-Angle Rotary Metal Shadowing

Ueli Aebi and Werner Baschong

I. INTRODUCTION

Heavy-metal replication (Williams and Wyckoff, 1945) is one of the oldest and yet most effective methods to provide enhanced contrast when imaging biological specimens in a transmission electron microscope (TEM) (for review, see Fowler and Aebi, 1983; Mould *et al*., 1985; Nermut and Eason, 1989). This technique requires efficient adsorption of the sample to a specimen support so that the biomolecules or particles to be visualized become well dispersed and distributed evenly. Moreover, to minimize shadow-casting artifacts produced by corrugations of the specimen support, it should ideally be smooth at atomic dimensions. Mica fulfills both these requirements and hence emerges as an ideal specimen support. For a good replica, the contrast-enhancing metal should produce a fine grain, detach easily from the specimen support, and be stable in the electron beam. An example of a metal that favorably meets these three criteria is platinum (Pt).

The combination of mica and platinum was first proposed by Hall (1956) in his 'mica replication' technique. Hall sprayed different solutions of biomolecules (i.e., an adenosine phosphate polymer, collagen, DNA, and fibrinogen) onto a piece of freshly cleaved mica. The mica was then dried in a vacuum evaporator and subsequently metal casted at a low angle (i.e., 5–15°) with platinum. The metal layer on the mica was stabilized by backing it with a layer of each of SiO and collodion. The resulting replica was then floated off the mica onto distilled water, picked up on a specimen support grid, and imaged in a TEM (Hall, 1956). More disperse spreading and even distribution of the biomolecules on the mica surface were achieved by adding glycerol to the sample before spraying it (Tyler and Branton, 1980; Fowler and Erickson, 1983). For their modification of Hall's technique, Tyler and Branton coined the term *glycerol drying*. Specifically, they added glycerol to the sample before spraying it onto the mica and backed the metal replica with carbon only. The more accurate and appropriate term used now is *glycerol spraying/low-angle rotary metal shadowing*.

Glycerol spraying/low-angle rotary shadowing has been claimed to preserve native conformations comparably to cryotechniques (Mould *et al*., 1985; Nermut and Eason, 1989). It has been used time and again to characterize complex macromolecules at near-native conditions and especially also proteoglycans (Moergeli *et al*., 1985; Rodriguez *et al*., 1995; Scheel *et al*., 1999, Hofmann *et al*., 2000; Griffith *et al*., 2002). Indeed, a stabilization of the native confirmation by glycerol against temperature-, pH-, or organic solvent-induced changes was corroborated by electron spray mass spectrometry (Grandori *et al*., 2001).

For glycerol spraying, droplets of a glycerol-containing solution are vaporized using air pressure and sprayed against a mica surface. The droplets spread on impact and retract rapidly due to the high surface tension of the glycerol-containing solution. Molecules or particles adsorbed to the mica surface are left behind with little or no solvent surrounding them. Therefore, they dry almost instantaneously. The dried, retracted sample droplets produce the characteristic "droplet centers" (see Fig. 3a) that are observed with glycerol-sprayed preparations at low magnification. These droplet centers represent a residue that is formed by the salts in the sample buffer and by unabsorbed protein and other debris that is swept off the mica by the advancing or retracting drop (Tyler and Branton, 1980).

Copyright 2006, Elsevier Science (USA).
All rights reserved.

Specimens that are suitable for glycerol spraying/low-angle rotary metal shadowing range from single protein (e.g., myosin) and DNA molecules to relatively stable biopolymers or supramolecular assemblies such as intermediate filaments or protein/glycosaminoglycan complexes. The achievable resolution is a few nanometers and thus sufficient to reveal the overall size and shape and/or the principal domain architecture of many biomolecules.

II. MATERIALS AND INSTRUMENTATION

For routine applications of glycerol spraying/low-angle rotary metal shadowing, the following items, gadgets, and equipment are required.

1. Gilson Pipetman adjustable pipette P20, with tips (Fig. 1a), and Gilson Microman adjustable pipette M25, with tips (Fig. 1b) (http://www.gilson.com/)
2. Vortex apparatus
3. Pair of scissors (Fig. 1c).
4. Double-sided adhesive Scotch tape
5. Specimen support grids (Fig. 1d): For example, from Pelco International (http://www.pelcoint.com/) (typically, 400 mesh/in. copper grids, 3.05 mm in diameter and 0.7 mm thick)
6. Spot plate (Fig. 1e): For example, from BAL-TEC (http://www.bal-tec.com/) (Cat. No. B 8010 030 83)

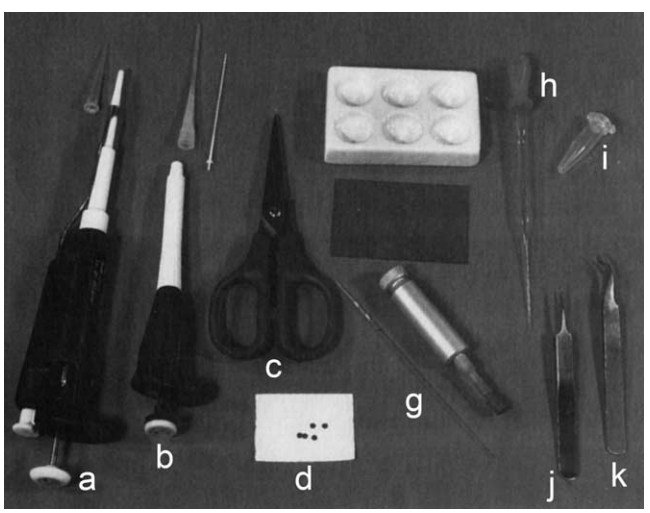

FIGURE 1 *Standard equipment for glycerol spraying/low-angle rotary metal shadowing*. Two adjustable pipettes: (**a**) Gilson Pipetman P20, and (**b**) Gilson Microman M25, together with their respective tips; (**c**) a pair of scissors; (**d**) copper specimen grids; (**e**) spot plate; (**f**) mica sheet; (**g**) 25-µl glass micropipettes with pipettor; (**h**) Pasteur pipettes; (**i**) Eppendorf tubes; and a pair each of (**j**) fine, straight forceps, and of (**k**) fine, bent forceps.

7. Mica sheets (Fig. 1f): For example, from BAL-TEC (Cat. No. BU 006 027-T)
8. 25-µl glass micropipettes with pipetter (Fig. 1g)
9. Pasteur pipettes (Fig. 1h)
10. Eppendorf tubes (Fig. 1i)
11. Precision forceps: For example from Electron Microscopy Sciences (http://www.emsdiasum.com/ems/). A pair of fine, straight forceps (Fig. 1j) and a pair of fine, bent forceps (Fig. 1k).
12. Compressed air at a pressure of 0.8 bar (80 psi)
13. Custom-built spray apparatus with air-pressure controller (Figs. 2d and 2e). The major elements or pieces to be manufactured or purchased include
    - A polyvinyl chloride (PVC) frame mounted onto an aluminum base
    - A Pasteur pipette connected to a compressed air supply via an air pressure/volume controller unit so that a set volume of a fine stream of air is produced at its nozzle by the push of the release button on the controller
    - A clamp mounted on a post to fasten a 25-µl glass micropipette containing the sample so that it points to the center of the stream of pressurized air
    - A metal sphere on a height-adjustable post so that it can be placed into the center of the fine air stream and disperse the sample drops evenly
    - A curved glass tube that traps the large sample droplets, aggregates, and other heavy particles
    - A square piece of freshly cleaved mica that is fastened with a piece of double-sided adhesive tape below the curved glass tube
14. Glow-discharge apparatus: For example, custom built as detailed by Aebi and Pollard (1987) (see also article by Baschong and Aebi) or SCD 005 (Cat. No. BU GO5 750 116-T) from BAL-TEC.
15. High-vacuum evaporation unit: For example, BAE 080-T (Cat. No. BU P03 527) from BAL-TEC specifications:
    a. High-vacuum pumping unit with rotary vane pump
    b. Vacuum measuring device for rough and high vacuum
    c. Evaporation unit with controller, high current supply, and cross-shaped vacuum chamber
16. Accessories for BAL-TEC high-vacuum evaporation unit:
    a. Cold trap for BAE 080-T (Cat. No. BB 176 942-W)
    b. Quick-release flange WF 206, including EK-030 electron gun (Cat. No. BU 007 038-T)
    c. Quick-release flange WF 211, rotary table (Cat. No. BB 192 281-T)

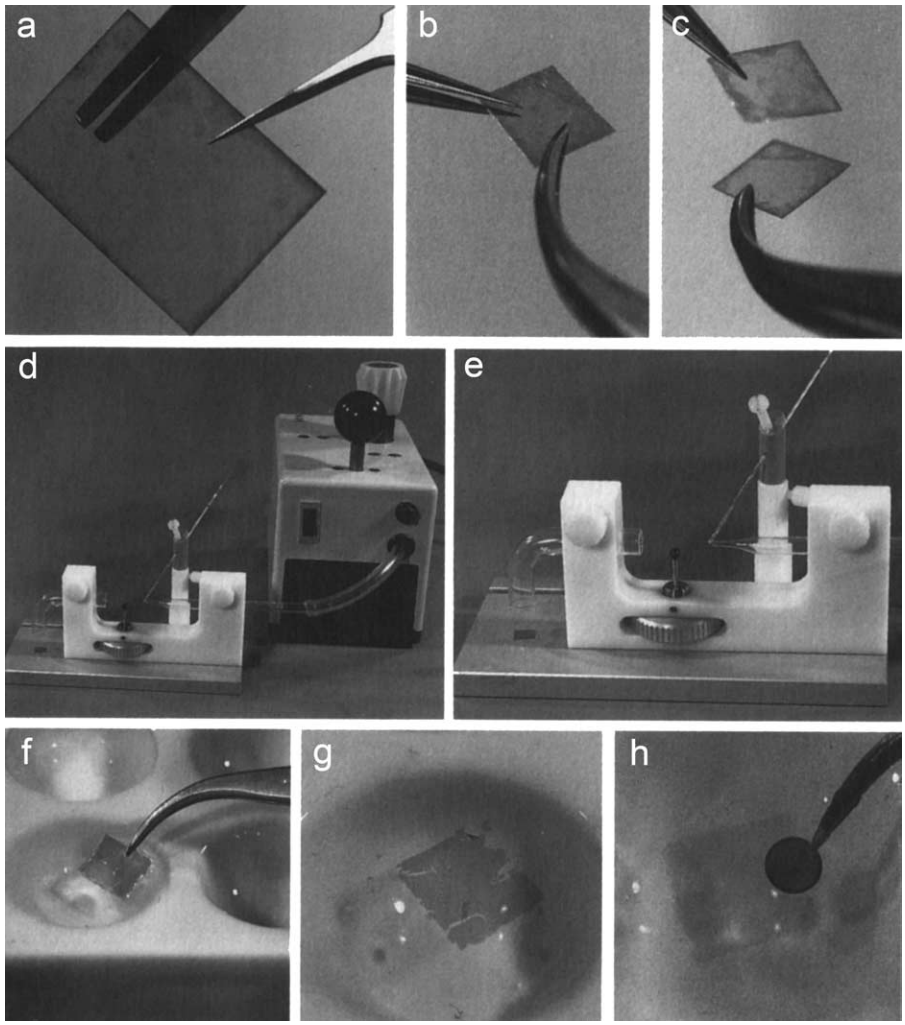

FIGURE 2 *Selected steps of the glycerol spraying/low-angle rotary metal shadowing technique.* (**a**) A piece of mica held with a pair of straight forceps is cut into square pieces with a pair of scissors. (**b and c**) Using forceps, the mica is next cleaved into two sheets. (**d and e**) The glycerol-containing solution is drawn into a 25-µl glass micropipette that is mounted on the spray apparatus such that it points to the center of the stream of pressurized air that is focused by a Pasteur pipette. (**f**) The Pt/C-shadowed and C-backed mica is slowly immersed into water, and (**g**) the mica sheet is removed once the Pt/C+C-replica is floated off. (**h**) The replica is then placed on a specimen grid with a pair of forceps.

d. Quick-release flange WF 204, C-evaporator (Cat. No. BB 192 276-T)
e. Digital quartz-crystal thickness meter QSG 060 (Cat. No. BU M01 259)
f. Electron beam evaporation device EVM 030, (Cat. No. BU S04 000)

17. Materials for BAL-TEC high-vacuum evaporation unit:
    a. Carbon rods for Pt/C evaporator (Cat. No. BU 006 101-T)
    b. Platinum inserts (Cat. No. BU 006 103-T)
    c. Carbon rods for C-evaporator (Cat. No. BU 006 115)
    d. Tungsten cathodes (Cat. No. BU 020 023-T)
18. Liquid nitrogen

III. PROCEDURES

Solutions

1. *Glycerol 100% anhydrous*: For example, from Fluka (http://www.sigmaaldrich.com/)(Cat. No. 49770)
2. *Sodium hypochlorite solution, 13–15%, technical grade*: For example, from Siegfried (http://www.siegfried.ch/) (Cat. No. 180550–01)

A. Spraying

Steps

1. Hold a piece of mica with a pair of straight forceps and cut it into square pieces (5–7 mm side length) with a pair of scissors (Fig. 2a).
2. Dilute the sample to a concentration of about 10–100 n*M* (0.1–1.0 mg/ml for most proteins) and pipette 20 µl into an Eppendorf tube.
3. Add 8.6 µl of 100% glycerol to the sample (i.e., 30% final glycerol concentration) using the Gilson Microman M25. Mix thoroughly with the pipette and vortex.
4. Draw 10 µl of the glycerol-containing solution into a 25-µl glass micropipette and mount it on the spray apparatus (Figs. 2d and 2e).
5. With two pairs of forceps, cleave the mica into two sheets (Figs. 2b and 2c).
6. With its freshly cleaved side up, place the mica below the bent glass tube of the spray apparatus. During spraying, the mica sheet should either be fixed with a piece of double-sided adhesive tape as shown in Fig. 2e or held in position with a pair of forceps.
7. Briefly (i.e., for about 1 s) press the button of the air-pressure control unit (depicted in Fig. 2d) to spray the sample suspension onto the freshly cleaved mica.

Note: The metal sphere placed in the spray path disperses the sample droplets evenly. The curved glass tube traps remaining large droplets, aggregates, and other heavy particles that will not follow the air flow when the spray path changes its direction by 90°.

8. Repeat spraying in the same way with another 10 µl of suspension onto the second piece of mica, etc.

B. Metal Evaporation

Steps

1. Switch on the thin film quartz monitor.
2. Set up the electron gun for Pt/C evaporation and the carbon evaporation unit for C-evaporation according to the instruction manual of the supplier.
3. The recommended working distance between the Pt/C tip in the electron gun and the middle of the table is 12 cm and the tilt angle of the table relative to the evaporation axis should be around 5°. For the C tips in the C evaporation unit, the recommended working distance is the same but the tilt angle should be 80–90°.
4. Mount the mica with double-sided adhesive tape onto the table. Make sure that the sprayed side of the mica is up!
5. Mount the table onto the rotating base in the vacuum chamber and start evacuating.
6. After 30 min, the vacuum meter should read better than 2×10^{-5} mbar.
7. Pour liquid nitrogen into the Meissner trap.
8. After an additional 5 min, the vacuum meter should read better than 6×10^{-6} mbar.
9. Degas Pt/C tip according to the instruction manual of the supplier.
10. Start the motor of the rotating base (set to about 120 rpm).
11. Set the thin film quartz monitor to zero.
12. Start evaporating Pt/C according to the instruction manual. Open the manual shutter.
13. Read the frequency on the thin film quartz monitor.
14. After the frequency has changed by 300 Hz, close the manual shutter and stop evaporation.
15. Evaporate C according to the instruction manual of the supplier.
16. On a white reference the carbon layer should look deep brown (cf. Figs. 2f and 2g).

Note: It is advisable to calibrate current and evaporation times of the power supply so that standard settings can be used.

17. Turn the rotating table off, break the vacuum, and remove the rotating table from the vacuum chamber.

C. Floating off the PT/C+C Replica

Steps

1. Fill the wells of the spot plate (Fig. 1e) with distilled water (Fig. 2f).
2. As illustrated in Fig. 2f, slowly immerse the mica at an angle of ~45° holding it firmly with the forceps.
3. Submerge the mica completely and remove it when the Pt/C+C-replica is floating on the water surface (Fig. 2g).
4. With a pair of forceps, submerge a freshly glow-discharged specimen grid, place it underneath the Pt/C+C-replica, and use it as a sieve to collect the replica piece by piece.
5. Dry the specimen grids by layering them with the film side up onto a piece of filter paper.
6. The specimen grids are now ready for inspection in the EM.

D. Electron Microscopy

Steps

1. Identify droplet centers as shown in Fig. 3a at a low magnification of, e.g., 5000×. *Note:* The droplet

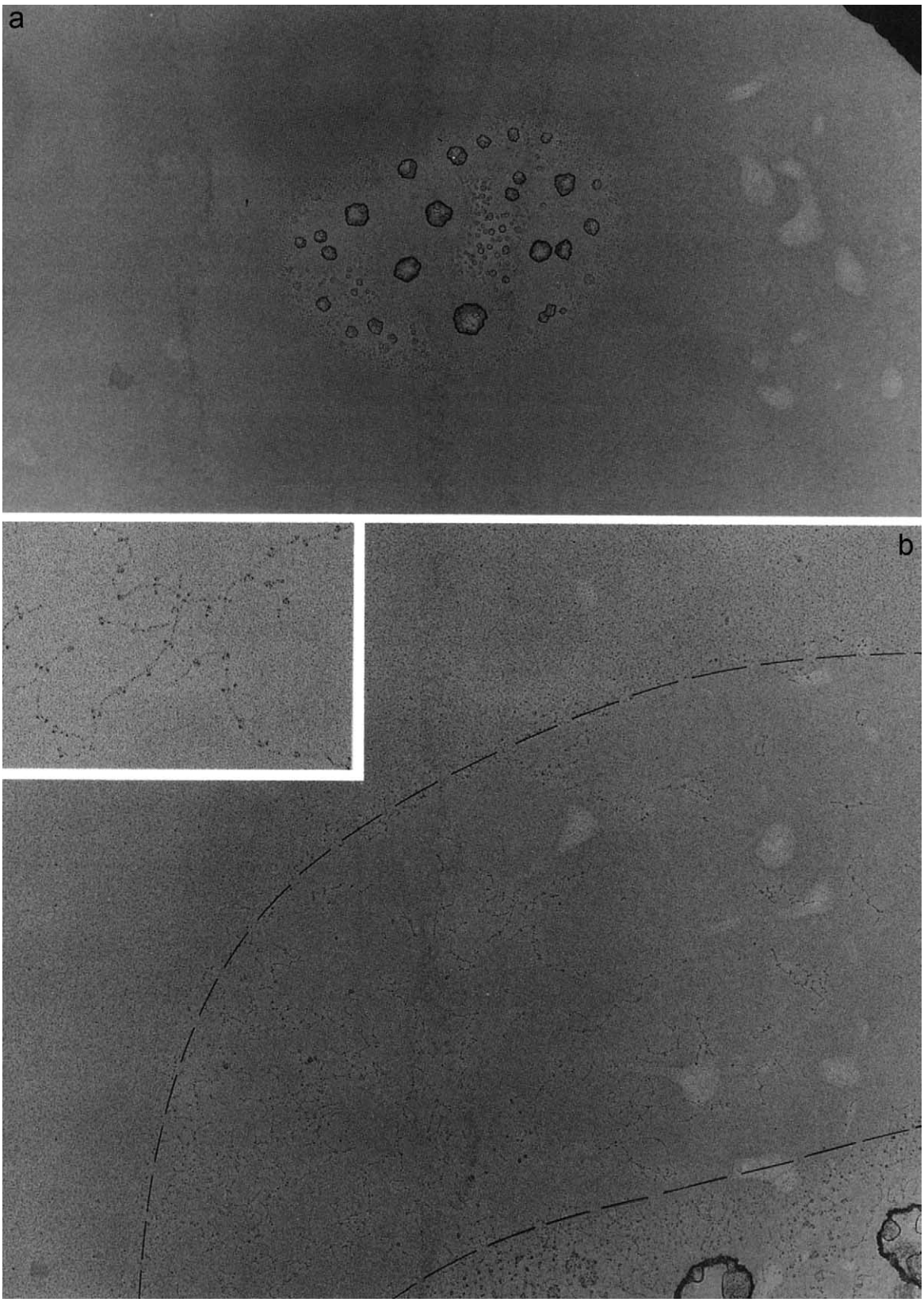

FIGURE 3 *Electron microscopy of glycerol-sprayed/low-angle rotary metal-shadowed preparations.* (**a**) At low magnification, very prominent features of glycerol-sprayed/low-angle rotary metal-shadowed preparations are the "droplet centers" formed by the salts in the buffer, unabsorbed protein, and debris that are swept off the mica by the advancing and/or retracting drop of the specimen/glycerol solution. (**b**) When moving from the center of such a droplet center outward, a transition from a coarse and irregular to a smooth and clean background is observed. Well-spread molecules are found in the zone that shows a clean background (demarcated by dashed lines). (Inset) A higher magnification view that reveals head-to-tail polymers of myosin-like lamin dimers (see Heitlinger *et al*., 1991).

centers are easy to find if your sample is kept in non-volatile buffers and/or contains salts. The droplet center size varies from 5 to 50 µm in diameter. Choose droplet centers with a size of about 5–10 µm.

2. Increase the magnification to about 20,000–50,000×. Set coarse focusing and then slowly move from the center toward the edge of the droplet.

3. Dashed lines in Fig. 3b highlight the sharp transition from salt crystals to a clean background that is typically observed over increments of the droplet center distance by 0.5–2 µm. In this "clean belt" around the droplet center well-spread and well-preserved protein particles are usually found readily (Fig. 3b, inset).

IV. PITFALLS

1. ***Replica resists detaching from the mica.*** Occasionally, the Pt/C+C replica sticks to the mica. The replica usually detaches more easily after the mica has been incubated in a moist atmosphere at 37°C for 30 min. Alternatively, the replica may also be floated off onto 6% sodium hypochlorite rather than water; however, after this treatment, the replica has to be transferred with a platinum loop to distilled water and allowed to incubate for 10 min. One reason for frequent sticking of the Pt/C+C replica to the mica may be too good a vacuum during C evaporation. Breaking the vacuum after Pt/C evaporation, reevacuation to 7×10^{-5} mbar, and subsequent C evaporation may solve this problem.

2. ***Preparation not satisfactory*:** (a) *Specimen dependent*: The specimen may not be optimal for glycerol spraying. Some specimens, including actin filaments, are relatively sensitive to shearing forces and may thus break into small pieces on spraying. (b) *Buffer dependent*: Many buffers and solutions can be used but detergents or high concentrations (i.e., ≥2 *M*) of urea or guanidine hydrochloride cause problems through eutectic effects. In this case, the buffer should be changed or diluted.

3. ***Phase separation after addition of glycerol.*** For good results, it is essential that the sample is a solution that contains glycerol. In case of phase separation, different buffers should be tried. If volatile buffers (e.g., ammonium acetate) are used, the evaporating unit should be evacuated for 2–3 h rather than for 30 min before metal evaporation (see earlier discussion).

Acknowledgments

This work was supported by the M. E. Mueller Foundation of Switzerland and the Canton Basel-Stadt.

References

Aebi, U., and Pollard, T. D. (1987). A glow discharge unit to render electron microscope grids and other surfaces hydrophilic. *J. Electron. Microsc. Tech.* **7**, 29–33.

Fowler, W. E., and Aebi, U. (1983). Preparation of single molecules and supramolecular complexes for high-resolution metal shadowing. *J. Ultrastruct. Res.* **83**, 319–334.

Fowler, W. E., and Erickson, H. P. (1983). Electron microscopy of fibrinogen, its plasmic fragments and small polymers. *Ann. N. Y. Acad. Sci.* **408**, 146–163.

Grandori, R., Matecko, I., Mayr, P., and Mueller, N. (2001). Probing protein stabilization by glycerol using electrospray mass spectroscopy. *J. Mass Spectrom.* **36**, 918–922.

Griffith, J. D., Lindsey-Boltz, L. A., and Sancar, A. (2002). Structures of the human Rad17-replication factor C and checkpoint Rad 9-1-1 complexes visualized by glycerol spray/low voltage microscopy. *J. Biol. Chem.* **277**, 15233–15236.

Hall, C. E. (1956). Visualization of individual macromolecules with the electron microscope. *Proc. Natl. Acad. Sci. USA* **42**, 801–806.

Heitlinger, E., Peter, M., Haener, M., Lustig, A., Aebi, U., and Nigg, E. A. (1991). Expression of chicken lamin B2 in *Escherichia coli*: Characterization of its structure, assembly and molecular interactions. *J. Cell Biol.* **113**, 485–495.

Hofmann, I., Mucke, N., Reed, J., Herrmann, H., and Langowski, J. (2000). Physical characterization of plakophilin 1 reconstituted with and without zinc. *Eur J. Biochem.* **267**, 4381–4389.

Mould, A. P., Holmes, D. F., Kadler, K. E., and Chapman, J. A. (1985). Mica sandwich technique for preparing macromolecules for rotary shadowing. *J. Ultrastruct. Res.* **91**, 66–76.

Moergelin, M., Paulsson, M., Malmstrom, A., and Heinegard, D. (1989). Shared and distinct structural features of interstitial proteoglycans from different bovine tissues revealed by electron microscopy. *J. Biol. Chem.* **264**, 12080–12090.

Nermut, M. V., and Eason, P. (1989). Cryotechniques in macromolecular research. *Scan. Microsc. Suppl.* **3**, 213–224; discussion 224–225.

Roughley, P. J., Rodriguez, E., and Lee, E. R. (1995). The interactions of "non-aggregating" proteoglycans. *Osteoarthritis Cartilage* **3**, 239–348.

Scheel, J., Pierre, P., Rickard, J. E., Diamantopoulos, G. S., Valetti, C., van der Goot, F. G., Haener, M., Aebi, U., and Kreis, T. E. (1999). Purification and analysis of authentic CLIP-170 and recombinant fragments. *J. Biol. Chem.* **274**(36), 25883–25891.

Tyler, J. M., and Branton, D. (1980). Rotary shadowing of extended molecules dried from glycerol. *J. Ultrastruct. Res.* **71**, 95–102.

Williams, R. C., and Wyckoff, R. G. W. (1944). The thickness of electron microscopic objects. *J. Appl. Phys.* **15**, 712–716.

SECTION

8

Cryotechniques

CHAPTER

25

Rapid Freezing of Biological Specimens for Freeze Fracture and Deep Etching

Nicholas J. Severs and David M. Shotton

I. PRINCIPLES OF RAPID FREEZING

Stabilization of biological structure by the physical process of freezing (cryofixation) forms the starting point for freeze fracture and deep etching (see article by Shotton) and for freeze substitution, cryoultramicrotomy, and cryoelectron microscopy (see articles by Roos *et al.*, and Resch *et al.*). To avoid ultrastructural damage to the specimen caused by the growth of large ice crystals, rapid freezing is essential. True vitrification (i.e., formation of amorphous, noncrystalline ice) can be achieved only by cooling rates of greater than 2×10^5 °C/s over the critical range of 20 to –100 °C, i.e., cooling over this range in a fraction of a millisecond. Rates of this magnitude can be attained in very thin (<3 μm) films of suspended liquid that are plunged rapidly into liquid nitrogen-cooled liquid propane or ethane, and particulate specimens (e.g., viruses) embedded in such frozen thin films may be observed directly in the vitrified state on the cold stage of a cryoelectron microscope. For freeze fracture and deep etching, however, the requirement for a larger specimen size precludes true vitrification throughout the specimen because the maximal cooling rate possible within the sample is limited by the rate of heat conduction through it. Thus, for most practical purposes, the goal when applying cryofixation for freeze fracture and deep etching is to apply cooling conditions that reduce ice crystal size sufficiently that there is no visible distortion of cellular structure. The techniques employed for such rapid freezing may be divided into three groups: conventional rapid freezing techniques, with cooling rates of between 10^3 and 10^4°C/s; ultrarapid freezing techniques, with rates in excess of 10^4°C/s; and hyperbaric freezing in which, although a relatively slow cooling rate is employed, ice crystal nucleation and growth are retarded by high pressure. This article gives a brief account of the principles and practical applications of these techniques. Comprehensive reviews of the field as a whole can be f ound in Robards and Sleytr (1985), Steinbrecht and Zierold (1987), Echlin (1992), and Severs and Shotton (1995).

Working with cryogenic liquids is potentially hazardous. Novices should ensure that they are fully conversant with appropriate safety precautions by consulting their institutional safety advisor. For further guidance articles on safety in Robards and Sleytr (1985), Ryan and Liddicoat (1987), and Steinbrecht and Zierold (1987).

II. CONVENTIONAL RAPID FREEZING FOR FREEZE FRACTURE

A. Chemical Fixation and Glycerination

Ice crystal damage can be avoided at relatively slow cooling rates if the specimen is first infiltrated with a buffered cryoprotectant. Glycerol, used at concentrations of 20–30%, is by far the most commonly used cryoprotectant. Prior fixation with aldehydes (usually glutaraldehyde) is routinely carried out with the aim of minimizing cryoprotectant-induced artifacts, although such aldehyde fixation may itself induce artifacts. A few specimens (e.g., cells of low water content such as yeast or bacteria, or concentrated membrane preparations such as erythrocyte ghosts) may be successfully frozen by conventional methods without prior chemical pretreatment.

Copyright 2006, Elsevier Science (USA).
All rights reserved.

B. Mounting of Specimens Prior to Freezing

To enable processing through the various subsequent steps of freeze fracture or deep etching, specimens are first mounted on specially designed supports (Fig. 1). Standard specimen supports are made from metals of high thermal conductivity and are as small as is compatible with ease of handling. The precise design of support used will vary according to the nature of the specimen, the type of freeze-fracture apparatus, and the manner in which fracturing is executed. Careful mounting is critical and should always be done with the aid of a binocular microscope.

For conventional knife fracture of cell suspensions (see article by Shotton), a droplet of concentrated cell suspension is placed on the central raised portion of a cleaned flat-topped specimen support (Figs. 1a and 1c). Care should be taken to avoid bubbles and to avoid getting liquid on the rim of the holder (which will prevent it fitting the specimen table after freezing). Tissue blocks for knife fracture are conventionally mounted in similar supports that have a central well (Fig. 1b). The tissue is held securely in the well with a portion protruding for subsequent fracture. Flat-type holders without wells can also be used as mounts for tissue pieces; in this case, polyvinyl alcohol (PVA) mounting medium is recommended to attach the sample firmly to the holder. PVA mounting medium consists of 20–30% PVA in phosphate-buffered saline (PBS) containing 20–33% glycerol. A simple recipe is to dissolve the PVA powder (mean molecular mass 10 kDa) to 45% in PBS by prolonged heating at below 100°C in a double boiler and then to dilute with half the volume of glycerol to give a solution containing 30% PVA and 33% glycerol. PVA is conveniently applied from a syringe or using a sharpened applicator stick and should be kept at 4°C or, for prolonged storage, at –20°C.

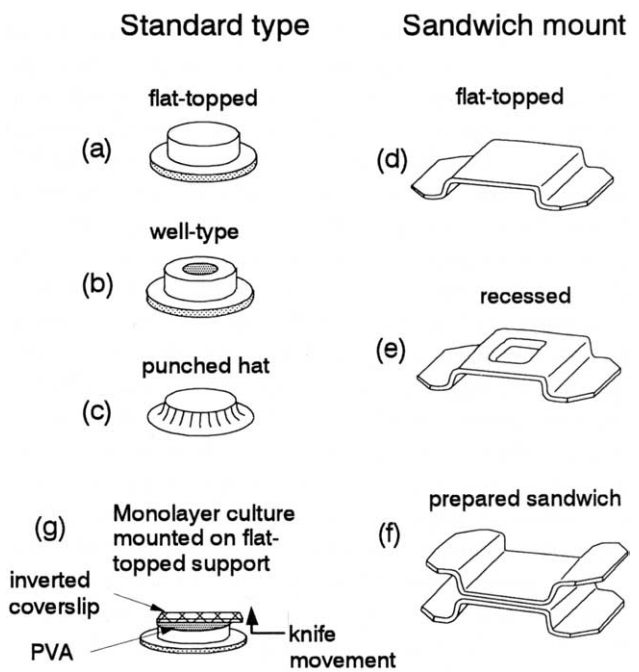

FIGURE 1 Examples of supports used for mounting specimens prior to freezing. (a and b) Standard supports for knife fracturing made either from a gold–nickel alloy (Balzers) or from copper (e.g., Reichert Cryofract, Polaron). (c) An inexpensive alternative, compatible with the same type of specimen table, punched out from a copper sheet. (d–f) Mounting systems for fracturing specimens in double-replica devices. Different designs of these mounts are used in different freeze-fracture plants. (d and e) Different types of mount used to sandwich thin specimens as shown in f. When a pair of flat-topped mounts (d) is used, a spacer may be included to prevent compression of the sample. (g) Use of a standard flat-topped support and PVA for mounting of cells cultured on a plastic coverslip. Reproduced from Severs and Shotton (1995), with permission.

As an alternative to fracturing by knife, specimens may be fractured by being broken apart in a hinged double-replica device. This dictates use of a pair of mounts between which the specimen is sandwiched (Figs. 1d–1f). The double—mount principle was originally devised for making complementary P- and E-face replicas, but is often convenient for routine preparation.

Various techniques have been developed for mounting cultured cells for freeze fracture. A particularly versatile approach, suitable for cells grown on plastic coverslips, is that of Pauli *et al*. (1977). A piece of the coverslip is mounted cell side down on a droplet of PVA placed on a standard flat-topped support, leaving a portion of the coverslip projecting horizontally by about 0.5 mm (Fig. 1g). Fracturing is done by raising the tip of the knife from below the coverslip; this flips the coverslip off the frozen PVA, directing the fracture plane through the cells.

C. Freezing

Conventionally fixed and cryoprotected specimens are normally frozen by simple immersion in a liquid cryogen. However, direct immersion of specimens into liquid nitrogen (which at atmospheric pressure is at its boiling point, –196°C) leads to formation of an insulating layer of evaporated nitrogen gas around the specimen, preventing rapid cooling (the *leidenfrost* effect). This problem is avoided by using nitrogen slush, a mixture of solid and liquid nitrogen at its freezing point (–210°C).

A simple way to make nitrogen slush is to fill a small, well-insulated styrofoam container with liquid nitrogen, place it in a desiccator, and evacuate it using

a water pump or rotary pump until, through loss of latent heat of evaporation, the nitrogen ceases to bubble and solidifies. After a further 30 s, the vacuum is released, and some of the solid nitrogen melts, giving a slush at –210°C. By repeating this process several times, the entire volume of nitrogen is brought down to the same temperature before removal for use. Slush can be made similarly using a standard vacuum evaporator unit or a commercially available slusher. Once made, the slush must be used immediately. The mounted specimen, held in fine forceps, is inserted swiftly into the nitrogen slush and is then transferred into a separate container of liquid nitrogen for storage or further processing. After a few minutes the solid nitrogen will have melted and a new batch of slush must be prepared.

The traditional alternative method for freezing specimens is to immerse them manually into a secondary cryogenic liquid cooled to near its freezing point using liquid nitrogen as the primary cryogen. Such a secondary cryogenic liquid ideally combines the properties of high thermal conductivity, a high heat capacity, a freezing point close to the boiling point of liquid nitrogen, and a large temperature difference between its freezing and boiling points. The nonflammable refrigerant gases freon 22 (chlorodifluoromethane, $CHClF_2$; melting point –160°C, boiling point –40°C) and freon 12 (CCl_2F_2; melting point –155°C, boiling point –30°C) fit these requirements and were, for many years, used as the standard secondary cryogens for the freezing of cryoprotected specimens. However, freons are no longer used due to their deleterious effects on the earth's ozone layer. The cooling rates obtainable with nitrogen slush are comparable to those achieved with the fluorocarbon cryogens and are certainly adequate for the freezing of cryoprotected specimens.

III. ULTRARAPID FREEZING

Ultrarapid freezing techniques opened a new chapter in biological ultrastructure research, permitting the examination of specimens that had been frozen directly from the living state, without prior chemical treatment. There are four principal methods for the ultrastructural preservation of biological specimens by extremely rapid freezing in the absence of cryoprotectants: plunging, spraying, jetting, and metal block-impact freezing (reviewed by Gilkey and Staehelin, 1986). With all these methods, good ultrastructural preservation is confined to a 10- to 20-µm surface layer. Further from the surface, the inherently low thermal conductivity of biological tissue limits the rate of heat loss and leads unavoidably to the growth of large ice crystals and consequent ultrastructural damage, similar to that observed if noncryprotected samples are frozen directly by standard immersion freezing.

A. Plunge Freezing

By optimizing conditions for the traditional approach of immersing specimens in a liquid nitrogen-cooled cryogen, cooling rates can be improved sufficiently to permit observation of a well-frozen structure in the absence of chemical cryoprotection. Numerous pneumatic, solenoid-operated and spring-driven devices incorporating these features have been developed; one example is illustrated in Fig. 2a. Key conditions for efficient cooling are that the specimen should have a maximal surface to volume ratio and be mounted in thin supports of low mass, and that its entry velocity into the cryogen should be high (hence the term *plunge* freezing). The stirred cryogen should fill a deep container to the brim so that the specimen does not undergo precooling before entry and completes its cooling over the critical range from 20°C to –100°C while still in motion through the liquid.

Liquid propane (C_3H_8; melting point –189°C, boiling point –42 °C) and liquid ethane (C_2H_6; melting point –172 °C, boiling point –89 °C), cooled with liquid nitrogen to close to their freezing points, are the most efficient cryogens for plunge freezing; they are, however, potentially hazardous and need special care in handling.[1] The usual mounting method is to sandwich the specimen between a pair of thin supports; not only can these mounts be adapted readily to fulfill the criteria given earlier, but, upon their separation during fracturing in a double-replica device, the fracture plane tends conveniently to follow

[1] Extreme care must always be taken to eliminate any possibility of explosion hazard when working with liquified flammable gases, as ignition of even a small volume of liquid can have devastating consequences. The flash point of liquid propane is –104°C; that of liquid ethane is –130°C. These gases create explosive mixtures in air at concentrations above 3% (ethane) or 2.2% (propane). Beware also that below –183°C oxygen will condense from the air, forming a potentially explosive mixture. All work involving liquified flammable gases must be undertaken within the confines of an extraction fume cupboard suitable for flammable vapours, and naked flames and electrical switches that might generate sparks must be totally excluded from the work area. The liquified cryogens should not be stored, but should be safely discarded after each experiment either by evaporation within the fume cupboard or, if direct access to outdoors is available, by carefully pouring the liquid onto the ground at a site distant from people, cars, buildings, and other man-made installations. Liquified gases should never be poured down a drain.

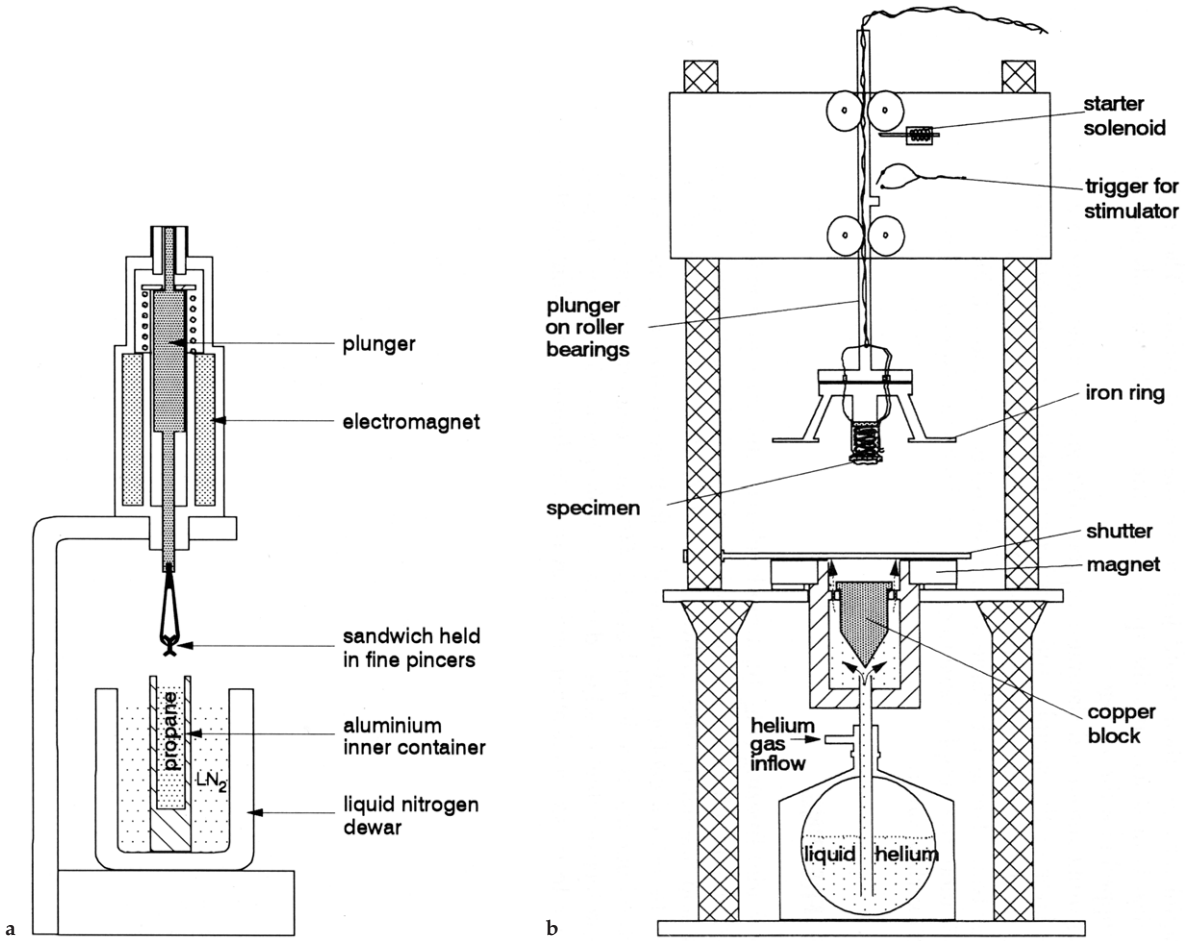

FIGURE 2 Examples of rapid freezing apparatus. (**a**) An example of a solenoid-operated plunge-freezing apparatus [adapted from Escaig (1982), with permission]. (**b**) A metal block slam-freezing device (Heuser version). The specimen is mounted on a detachable freezing head, which plugs into the plunger, the highly polished pure copper block is cooled from below with a spray of liquid helium, and the plunger is allowed to fall onto the block under gravity. The original device was set up to permit stimulation in nerve muscle preparations. From Heuser *et al.* (1979), with permission.

a superficial well-frozen layer of the specimen, adjacent to the support. If a mechanical plunge-freezing machine is not available, simple manual plunge freezing of specimens into propane under optimized conditions is always worth trying. Sandwich-mounted cell and membrane suspensions, in particular, lend themselves to this approach, and satisfactory results have been obtained in some animal and plant tissues (Severs and Green, 1983; Galway *et al.*, 1995). The entry velocity attainable by manual plunging will not be as high or as reproducible as that achieved using a mechanical device, but the method is simple, has negligible cost, and, with practice, can give satisfactory results.

B. Spray Freezing

Spray freezing is essentially a version of immersion freezing in which the specimen size is reduced to microscopic droplets and, as such, this method is only suitable for suspensions of single cells, organelles, or membranes (Bachmann and Schmitt-Fumian, 1973). The low thermal mass of the individual droplets permits satisfactory freezing in the absence of cryoprotection. Minute droplets of the suspension are sprayed into liquid nitrogen-cooled propane. The propane is then warmed to –85°C and removed using a vacuum pump. The frozen droplets are mixed with butyl benzene at –85°C and transferred to a standard flat-topped specimen support, which is finally immersed in liquid nitrogen to solidify the specimen. Although, as a freezing method for particulate specimens, spray freezing was superseded by other more straightforward methods (e.g., plunge freezing a sandwich-mounted suspension into propane), it forms an integral part of *quenched flow* devices designed to capture very rapid dynamic cellular events, on a

millisecond time scale, at defined intervals after rapid mixing cells with a stimulating agent. A spray-freezing device based on this quench flow principle is available commercially (Balzers Model SFD 010). After spraying the stimulated cells into vigorously stirred propane and evaporating the cryogen, samples may be processed by freeze substitution in methanol containing glutaraldehyde and then either embedded and sectioned or rehydrated and refrozen for freeze fracture (Knoll, 1995).

C. Jet Freezing

In *jet freezing*, instead of moving the specimen rapidly through the cryogen, the reverse is done; cold propane is squirted at high velocity onto the stationary specimen (for review, see Gilkey and Staehelin, 1986). Most versions of commercially available equipment have dual jets, which simultaneously squirt liquid propane at each side of a sample (typically a cell or membrane suspension) sandwich mounted between a pair of thin copper supports. A double-jet machine from Balzers (Model JFD 030) incorporates a thermostatically controlled specimen environmental chamber, allowing freezing of the specimen from any chosen starting temperature between +10 and +90°C, a feature of particular importance for lipid research. As an alternative, one-sided propane jet freezers may be constructed with the aid of workshop facilities and have been used successfully in a number of laboratories. The safety precautions outlined in Section III,A apply equally to this freezing method.

D. Metal Block Freezing

The *metal block freezing technique*, also known as *slam freezing* or *metal mirror freezing*, has seen wide application in cell biology. The principle of the technique is to bring the biological specimen into rapid and firm contact with the highly polished surface of a pure copper block, cooled by liquid helium (boiling point 4 K; –269°C) to a temperature of ~18 K (–255°C). Variations on this theme include the use of a silver block in place of copper and cooling by means of liquid nitrogen instead of liquid helium. Various designs of slam freezing machine have been developed, notably by Heuser *et al.* (1979) and Escaig (1982), and made available commercially. In the Heuser-type apparatus (Fig. 2b), the specimen is fixed beneath the lower end of a vertical plunger, which is then allowed to fall under the influence of gravity. As the specimen falls, a shutter (which protects the liquid helium-cooled copper block from condensation) is opened, the specimen strikes the copper block, and freezing of the surface layer of the specimen is completed within 2 ms. The Escaig device is more sophisticated, using an electromagnetic plunger to propel the specimen, and protection of the helium-cooled block under vacuum until the instant the shutter opens just prior to specimen contact. Both machines are designed to ensure that the specimen does not bounce on impact, but remains applied firmly to the block until removed into liquid nitrogen. Specimen-mounting systems for slam freezing vary according to the apparatus employed, the requirements of the specimen, and its subsequent processing. Most incorporate features to cushion the specimen from the full force of the impact and to limit its flattening, e.g., by mounting within a spacer ring on a piece of rubber foam or fixed lung tissue.

If a sophisticated automated slam freezer is not available, an effective alternative is to use a simple, hand-held copper block (Dempsey and Bullivant, 1976). The block, fitted with a handle, is cooled in liquid nitrogen and is then raised just above the liquid surface. The upper surface is wiped with absorbent tissue and the specimen is then rapidly pushed onto it manually before being dropped into the nitrogen.

Metal block freezing using automated slammers reproducibly gives excellent cryofixation in the surface 10-μm layer of the sample, and satisfactory results can, with experience, also be obtained using simple manual-freezing blocks. Deeper regions of noncryoprotected specimens will always be badly damaged by large ice crystals and compression shock, and so, for freeze-fracture replication, the samples have to be fractured with precision by microtome through the well-frozen surface layer.

IV. HIGH-PRESSURE FREEZING

In high-pressure (hyperbaric) freezing, a sandwich-mounted specimen is frozen by double-sided jetting with liquid nitrogen while briefly being subjected to a pressure of 2100 bar (Galway *et al.*, 1995; Kiss and Staehelin, 1995). At such high-pressure, the critical cooling rate needed to limit ice crystals to a size below that causing ultrastructural damage is reduced from 10,000°C/s to approximately 100 to 500°C/s. This cryoprotective effect is achieved because high-pressure lowers the freezing point and reduces the rate of ice nucleation and growth to a degree equivalent to that achieved by using 20% glycerol for cryoprotection with conventional immersion freezing. Although high pressure is potentially lethal to cells, major artifacts from this source appear to be avoidable. High-pressure freezing requires specialist equipment, available from Balzers Union (Model HPM 010) and from Leica

(Model PI 32-165). The former device freezes specimens up to 0.5 mm in thickness and 1 mm^3 in volume; the latter use specimens of up to 0.6 mm in thickness and 1.5 mm^3 in volume.

The major advantage of high-pressure freezing is that structure is well preserved to a much greater depth than is possible with any of the ultrarapid freezing techniques discussed previously. True vitrification to an average depth of 200 μm has been reported in test specimens [catalase crystals in sugar solutions; Sartori *et al.* (1993)]; in plant specimens, no ice crystal damage is apparent to a depth of 600 μm in planar samples and 1 mm in spherical samples (Gilkey and Staehelin, 1986). High-pressure freezing is thus of particular value in the direct freezing of solid tissue specimens.

V. ADVANTAGES OF ULTRARAPID AND HIGH-PRESSURE FREEZING METHODS

Ultrarapid and high-pressure freezing methods offer a multitude of advantages as preparation methods in cell biology. By avoiding the need for chemical fixation, these cryofixation techniques potentially permit the study of cell structure in a condition close to that existing in life. Because one particular instant in a biological process can be captured, the accumulation of intermediate stages, which may occur during slow death in aldehyde fixatives, is avoided. Living specimens can thus be frozen for ultrastructural examination at known intervals after application of a biological stimulus. This has made it possible to use the electron microscope for studies of transient biological events that are completed within a few seconds or even, in favorable instances, within a few milliseconds. The ability to undertake such direct kinetic studies was a significant breakthrough in cell biology, as previously, sequences of such rapid events could only be guessed at indirectly from images of chemically fixed specimens. Metal block impact freezing, spray freezing, plunge freezing, and jet freezing methods have all been adapted to permit time-resolved analysis of rapid events (for review, see Knoll, 1995).

Another important advantage is that ultrarapid-frozen specimens can be subjected to *deep etching* or freeze drying, a technique in which water molecules are allowed to sublime from the frozen surface of a fractured (or, in some cases, unfractured) specimen before replication (see article by Shotton). Glycerol cannot be sublimed, but by directly freezing specimens in dilute aqueous solutions, the outer surfaces of membranes, extracellular matrix components, and intracellular cytoskeletal elements can be exposed by deep etching or freeze drying. For deep-etch observations of the cytoskeleton and internal membrane surfaces of cells, a compromise has to be made in order to obtain clean views unobscured by cytoplasmic components. Typical procedures for cultured cells attached to a substrate involve lysing them with Triton X-100 or physically tearing them open by peeling off a strip of nitrocellulose membrane that has been allowed to adhere to their dorsal surfaces. This is followed by rinsing in dilute buffer to remove cytoplasmic components, light fixation with aldehydes, and then immersion in 10–15% methanol immediately prior to freezing. The methanol acts as a cryoprotectant, increasing the depth of adequate freezing, and also has the advantage of being volatile under vacuum at –100°C, thus facilitating the etching process. This application is thus quite distinct from studies aiming to preserve structure in the native state, but it is a fundamentally important one, as it provides access to structural information that cannot be obtained by other electron microscopical methods (Heuser, 1981). Deep etching has also been adapted to study macromolecules absorbed to microscopic mica flakes and other substrates (Heuser, 1989).

In addition to freeze fracture, deep etching, and cryoelectron microscopy, other key routes to the examination of ultrarapid-frozen specimens are freeze substitution and cryoultramicrotomy. Here the ability to preserve epitopes is of prime importance for immunocytochemical studies (see article by Roos *et al.*). The complementary application of these approaches, together with freeze-fracture cytochemistry (Severs, 1995; Fujimoto, 1997), has wide application in cell biology today.

Acknowledgment

We thank Stephen Rothery for preparation of the figures.

References

Bachmann, L., and Schmitt-Fumian, W. W. (1973). Spray-freezing and freeze-etching. *In "Freeze-Etching: Techniques and Applications"* (E. L. Benedetti and P. Favard, eds.), pp. 73–80. Société Française de Microscopie Électronique, Paris.

Dempsey, G. P., and Bullivant, S. (1976). A copper block method for freezing non-cryoprotected tissue to produce ice-crystal-free regions for electron microscopy. *J. Microsc.* **106**, 251–271.

Echlin, P. (1992). "*Low-Temperature Microscopy and Analysis*." Plenum, New York.

Escaig, J. (1982). New instruments which facilitate rapid freezing at 83K and 6K. *J. Microsc.* **126**, 221–230.

Fujimoto, K. (1997). SDS-digested freeze-fracture replica labeling electron microscopy to study the two-dimensional distribution of integral membrane proteins and phospholipids in biomembranes: Practical procedure, interpretation and application. *Histochem. Cell Biol.* **107**, 87–96.

Galway, M. E., Heckman, M. E., Hyde, G. J., and Fowke, L. C. (1995). Advances in high-pressure and plunge-freeze fixation. *Methods Cell Biol.* **49**, 3–19.

Gilkey, J. C., and Staehelin, L. A. (1986). Advances in ultrarapid freezing for the preservation of cellular ultrastructure. *J. Electron Microsc. Tech.* **3**, 177–210.

Heuser, J. (1989). Protocol for 3-D visualization of molecules on mica via the quick freeze, deep etch technique. *J. Electron Microsc. Tech.* **13**, 244–263.

Heuser, J. E. (1981). Preparing biological specimens for stereo microscopy by the quick-freeze, deep-etch, rotary-replication technique. *Methods Cell Biol.* **22**, 97–122.

Heuser, J. E., Reese, T. S., Dennis, J., Jan, Y., Jan, L., and Evans, L. (1979). Synaptic vesicle exocytosis captured by quick freezing and correlated with quantal transmitter release. *J. Cell Biol.* **81**, 275–300.

Kiss, J. Z., and Staehelin, L. A. (1995). High pressure freezing. *In* "*Rapid Freezing, Freeze Fracture and Deep Etching*" (N. J. Severs and D. M. Shotton, eds.), pp. 89–104. Wiley-Liss, New York.

Knoll, G. (1995). Time resolved analysis of rapid events. *In* "*Rapid Freezing, Freeze Fracture and Deep Etching*" (N. J. Severs and D. M. Shotton, eds.), pp. 105–126. Wiley-Liss, New York.

Pauli, B. U., Weinstein, R. S., Soble, L. W., and Alroy, J. (1977). Freeze-fracture of monolayer cultures. *J. Cell Biol.* **72**, 763–769.

Robards, A. W., and Sleytr, U. B. (1985). Low temperature methods in biological electron microscopy. *In* "*Practical Methods in Electron Microscopy*" (A. M. Glauert, ed.), Vol. 10. Elsevier, Amsterdam.

Ryan, K. P., and Liddicoat, M. I. (1987). Safety considerations regarding the use of propane and other liquified gases as coolants for rapid freezing purposes. *J. Microsc.* **147**, 337–340.

Sartori, N., Richter, K., and Dubochet, J. (1993). Vitrification depth can be increased more than 10-fold by high pressure freezing. *J. Microsc.* **172**, 55–61.

Severs, N. J. (1995). Freeze-fracture cytochemistry: An explanatory survey of methods. *In* "*Rapid Freezing, Freeze Fracture and Deep Etching*" (N. J. Severs, and D. M. Shotton, eds.), pp. 173–208. Wiley-Liss, New York.

Severs, N. J., and Green, C. R. (1983). Rapid freezing of unpretreated tissues for freeze-fracture electron microscopy. *Biol. Cell.* **47**, 193–204.

Severs, N. J., and Shotton, D. M. (1995). "*Rapid Freezing, Freeze Fracture and Deep Etching*." Wiley-Liss, New York.

Steinbrecht, R. A., and Zierold, K. (1987). "*Cryotechniques in Biological Electron Microscopy*." Springer-Verlag, Berlin.

CHAPTER

26

Freeze Fracture and Freeze Etching

David M. Shotton

I. PRINCIPLES OF FREEZE-FRACTURE TECHNIQUE

The technique of freeze fracture is unique among electron microscopic (EM) methods in that it gives *en face* views of the internal organisation of biological membranes, allowing the study of the in-plane distribution of integral proteins spanning the lipid bilayer and of other membrane features, as a function of developmental stage, experimental conditions, or onset of disease. Although freeze fracture can be undertaken using very simple equipment that can be constructed in any workshop, in conjunction with a standard vacuum coating unit (Bullivant and Ames, 1966; Bullivant *et al.*, 1979), or using a commercial attachment to such a coating unit, it is normally performed within a specialized high vacuum freeze-fracture apparatus, with a temperature-controlled, liquid nitrogen-cooled holder for specimens. The standard procedure for specimen preparation by freeze fracture in such an apparatus is summarised in Fig. 1 and can be described briefly as follows.

A. Freezing

Conventionally, a small block of biological tissue (approximately $2 \times 2 \times 1$ mm) or a droplet of cell suspension on a copper or gold support (Fig. 1a), stabilised by glutaraldehyde fixation and cryoprotected by infiltration with 25–30% glycerol, is first rapidly frozen by plunging it manually into nitrogen slush or a liquified cryogen cooled to near its freezing point by liquid nitrogen (Fig. 1b). Full details of specimen supports and alternative rapid freezing methods are found in the article by Severs and Shotton and in Severs *et al.* (1995).

B. Fracturing

After storage for an unlimited period in liquid nitrogen, the frozen specimen is transferred quickly to the precooled, temperature-controlled specimen table within the high vacuum chamber of a freeze-fracture apparatus, either via an airlock or, more usually, after venting the chamber with dry nitrogen gas, which is then reevacuated to better than 2×10^{-6} mbar (Fig. 1c) (1 mbar = 100 pa = 0.75 torr). Freeze fracture is traditionally achieved by striking the specimen, maintained at –110°C, with a cold razor blade clamped within the jaws of the hollow microtome knife blade holder, which is itself filled and cooled to below –150°C with circulating liquid nitrogen. As when a log of wood is cleaved by an axe, a plane of free fracture precedes the blade edge, following a line of least resistance through the frozen specimen (Fig. 1d). When this fracture plane encounters a cell, it frequently passes along the centre of the lipid bilayer of the plasma membrane, as this is a line of weakness at cryogenic temperatures, splitting the asymmetric membrane into an extracellular (E) half and a protoplasmic (P) half (nomenclature of Branton *et al.*, 1975). Integral proteins, which span the membrane, may partition with one or other half of the membrane, from which they will protrude to form small freeze-fracture intramembrane particles (IMPs), leaving complementary pits in the other half membrane from which they were wrenched. Internal cell membranes may be similarly fractured, if the fracture plane initially passes through the plasma membrane and into the cell. Alternative specimen supports, including "double replica" specimen holders that provide tensile fracture of the frozen specimen, are detailed in the article by Severs and Shotton.

Copyright 2006, Elsevier Science (USA).
All rights reserved.

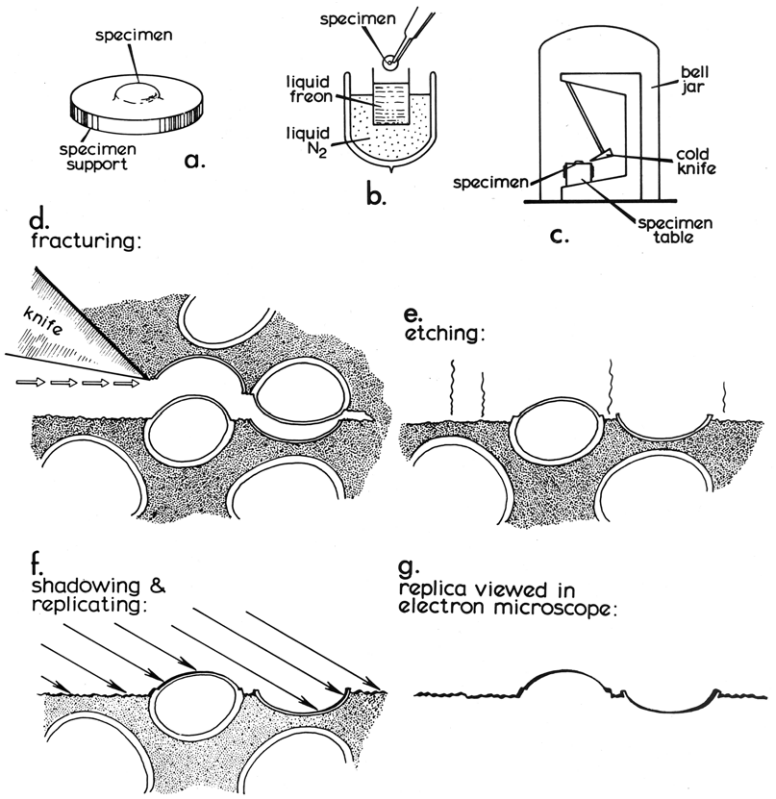

FIGURE 1 Basic steps in the conventional freeze-fracture procedure described in the text. Diagram courtesy of Daniel Branton, first published by Shotton (1982), reproduced by permission.

C. Etching

The specimen may then optionally be etched after fracturing (Fig. 1e). During etching, water molecules are allowed to sublime from the frozen surface of the fractured specimen, which for this purpose is fractured at a slightly higher temperature, at which the sublimation pressure of ice exceeds the partial pressure of the residual water molecules in the vacuum atmosphere by about 10-fold (typically –100°C for a vacuum of 2×10^{-6} mbar), leading to an etching rate of about 2 nm per second. The sublimed water molecules are condensed on a nearby cold trap, typically the underside of the cooled knife, which is positioned for this purpose above the fractured specimen. Etching lowers the specimen ice table and exposes the true surfaces of freeze-fractured membranes, thereby revealing membrane surface features of interest that were obscured previously by the overlying ice. The introduction of ultrarapid freezing techniques (see previous article by Severs and Shotton) has made it possible to freeze a wide variety of living tissue sufficiently rapidly to achieve good cryofixation of the surface layer of cells in the absence of chemical fixation and glycerol cryoprotection, enabling their subsequent etching. More extensive etching for up to 30 min at –100°C (deep etching or freeze drying) may be used to reveal more extensive cytoskeletal, extracellular, or membrane features or macromolecular structure (see Heuser, 1989; Hawes and Martin, 1995; and chapters in Severs and Shotton, 1995).

D. Replication

The frozen surface of a freeze-fractured or freeze-etched specimen is rich in topographical detail, but is extremely labile. In order to convert this labile structural information into stable contrast information accessible in the electron microscope, the specimen is obliquely shadowed with a thin layer of atomic platinum (typically with an average thickness of 1.5 to 2 nm), deposited from an evaporative source, usually an electron bombardment gun (Fig. 1f). The platinum atoms landing upon the frozen surface of the replica do not form a homogeneous layer, even upon smooth surfaces. Instead, after travelling short distances laterally on the membrane surface as they lose kinetic energy, the atoms coalesce to form small platinum

grains, about 1 nm in diameter, leaving the immediately adjacent surface free from platinum. The deposited film contains 5% (w/w) carbon with the platinum, which limits the maximum size of the grains to about 1.5 nm. These frequently form upon existing surface particles, giving a "decoration" effect, which may accentuate specimen detail in a useful way. The presence of these grains effectively limits the resolution of the replica to approximately 2.5 nm.

Alternative shadowing materials may be used, most commonly a mixture of tantalum and tungsten (approximate stoichiometry 80:20, w/w), which provides replicas of somewhat smaller grain size and higher resolution. However, such replicas are hard to make reproducibly, as the composition of the tantalum–tungsten anode of the electron bombardment gun changes from one evaporative shadowing run to the next due to the higher vapour pressure of the molten tantalum. The replicas are also of much lower contrast and have more limited chemical stability than conventional platinum replicas, and hence their use is confined almost exclusively to high-resolution ultrastructural studies (e.g., Abermann *et al.*, 1972; Zingsheim and Plattner, 1976; Gross, 1987).

With conventional unidirectional platinum shadowing of stationary specimens, the platinum atoms accumulate on the near side of protrusions, leaving platinum-free "shadows" in their lee. Alternatively, the specimen may be rotated during replication while maintaining the platinum deposition angle constant relative to the plane of fracture. Such rotary shadowing, which results in a uniform distribution of platinum grains around protrusions and an absence of shadows, is particularly useful for deep etched specimens. In either case, this discontinuous and physically fragile platinum surface replica is then strengthened by a uniform backing of electron-translucent carbon (about 15 to 20 nm thick; not shown in Fig. 1), deposited either unidirectionally from above or, for additional strength, from an angle of 80° while the specimen is rotating. This combined platinum–carbon replica is then removed from the vacuum chamber, is cleaned free of all the original biological material by digestion of the underlying thawed specimen with bleach or chromic acid followed by washing with distilled water, and is viewed directly in the transmission electron microscope (Fig. 1g).

II. TECHNICAL ADVICE

Precise details of the operation of the freeze-fracture apparatus, replication conditions, gun adjustments, and so on will vary between different models of freeze-fracture apparatus and should be conducted according to the manufacturers' instructions. Detailed comparative descriptions of different types of freeze-fracture equipment are given by Newman (1995). The following advice, based on experience with the Balzers BAF 300 machine, should be of general applicability.

A. Before the Freeze-Fracture Run

Check that there is enough liquid nitrogen to complete the run and prepare the electron bombardment guns for use according to the manufacturer's instructions. Check the incident shadowing angle of the platinum gun, changing it if necessary. The normal angle of incidence for unidirectional platinum shadowing of freeze-fracture replicas is 45°; from 6° to 26° is most useful for rotary shadowing of deep-etched specimens, depending upon the nature of the specimen; and 9° and 6° are used for unidirectional and rotary low-angle shadowing, respectively, of individual macromolecules absorbed onto mica sheets. For microtome fracture, fit an appropriate specimen stage and a reusable tungsten blade or a new single-edged carbon steel razor blade. Do not use stainless steel razor blades, as their edges bend on contact with ice and thus do not fracture well. Using a binocular dissecting microscope, ensure that the blade is horizontal above the specimen positions. Alternatively, fit a double-replica opening device in place of the blade and an appropriate double-replica specimen stage. Good thermal contacts should be ensured by the use of small amounts of a thermal conductive paste or high vacuum grease. If appropriate for your machine, prepare and fit a "shadow paper" (a piece of thin card with a central cutout, placed as a collar around the specimen stage where it will intercept some of the evaporated material), which will provide a permanent record of the replication run, to supplement any chart recorder trace made of the stage temperature and quartz crystal replica thickness monitor output.

B. Precooling the Stage and Specimen Preparation

Close and evacuate the chamber. Turn on the quartz crystal replica thickness monitor to warm up. At a vacuum of 10^{-4} mbar or better, turn on the chart recorder (if used), start the stage cooling, and briefly test fire both guns. Under liquid nitrogen, mount the specimen supports bearing the frozen specimens in the appropriate specimen holder in preparation for transfer to the specimen stage of the apparatus.

C. Loading Specimens

After the stage has been allowed to equilibrate at its minimum temperature (below –170°C) for 5 min, turn off the high vacuum gauge, vent the chamber with dry nitrogen gas (conveniently generated by running liquid nitrogen through a length of uninsulated copper tubing) in order to prevent the water vapour contamination that would otherwise occur if venting with air, open the chamber door or specimen access port, quickly transfer the specimens from liquid nitrogen to the cold specimen table, close the chamber, and immediately reevacuate. Modern freeze-fracture machines are often equipped with an airlock so that specimens may alternatively be loaded directly into the chamber without breaking the vacuum.

D. Specimen Temperature Adjustment

At a vacuum of 10^{-4} mbar or better, start the knife cooling and raise the specimen temperature to –110°C (for freeze fracture) or –100°C (for freeze etching). For the standard specimen stage, the indicated temperature and the actual stage temperature should correspond fairly exactly. However, the poor thermal contacts that may occur when using certain designs of double-replica specimen holders mean that the specimens may in practice be 5 to 15° warmer than indicated so that the indicated specimen stage temperature must be set low to compensate. One should predetermine these temperatures, etching rates, and contamination conditions using test specimens such as erythrocyte ghosts frozen in distilled water (ghost preparation is described by Shotton, 1998) and/or a digital thermometer with the thermocouple clamped in place of one of the specimens for direct measurements. Note that the specimens may take 10 min to reach temperature equilibrium after a large change in temperature and 5 min to reach equilibrium after a small (<10°C) change.

E. Fracture Process

When fracturing with a microtome blade, observe the specimens with the binocular microscope and use the microtome controls to lower the knife blade until it is just clear of the tops of the specimens. Then make a series of progressively lower passes of the blade over the specimens. If possible, it is preferable to make the actual cuts slowly by hand rather than using the motor drive, thus enabling one to get a feel of the blade passing through the ice of the specimens. Reduce the cutting depth to a minimum as soon as any appreciable area of specimen is being cut and continue cutting until all specimens show large smooth fractured areas. For elongated cells such as nerve and muscle fibres, extensive fracture planes are best obtained by orienting the specimens so that the fibres are parallel with the edge of the blade and by cutting fast by motor using only a few deep cuts. When using a double-replica device, fracturing is a single event that should be done after temperature equilibration and preparation for shadowing.

Prior to the final cut (or to fracture in the double-replica device), check the specimen temperature, ensure that the vacuum is better than 2×10^{-6} mbar, and prepare for shadowing. (Modern freeze-fracture machines may achieve vacuum of 2×10^{-7} mbar or better.) Then make the final cut, check through the binoculars that the specimen surfaces are clear of debris, and either shadow immediately or reverse the knife over the specimens to act as a cold trap while etching.

F. Etching

Normally, etching is conducted immediately after fracture at –100°C for 60 s in a vacuum of better than 2×10^{-6} mbar, with a cold trap (below –160°C) in close proximity to the specimen surfaces. This lowers the ice level approximately 120 nm. Deep etching, used, for example, to expose macromolecules adsorbed to the surfaces of mica flakes or to reveal the cytoskeleton of permeabilized cells, is performed for longer, at a higher temperature (–95°C), or both. If taken to completion, this is equivalent to freeze drying.

G. Replication

A quartz crystal replica thickness (thin film) monitor, positioned adjacent to the specimen stage in the path of the shadowing beams, is usually used to monitor replica deposition rates and amounts. Sequentially, operate the platinum and carbon guns according to the manufacturer's instructions to deposit the desired thickness of material, with the specimen stage stationary or rotating, as required. It is usual for unidirectional shadowing to deposit 1.5 to 2 nm thickness of a 95% Pt – 5% C mixture from the platinum gun. The amount of platinum deposited is critical and should not be more than the minimum required to generate good contrast. It is best to deposit the platinum at as rapid a rate as possible, starting to fire the platinum gun immediately prior to moving the knife away from its position over the specimens or just before opening a double-replica device, thus immediately exposing the specimens to a stream of platinum

vapour, reducing to a minimum the time during which contamination might occur.

Immediately after platinum shadowing, strengthen the replica with a 10- to 20-nm-thick layer of carbon from the carbon gun. Quite large differences in the amount of carbon deposited make little obvious difference to the final appearance of the replica, except in the case of deep-etched filamentous structures, where too much carbon creates a large semitransparent "ghost" replica surrounding the thin carbon replica. However, for maximum contrast, the carbon thickness should be kept to the minimum required to maintain the structural integrity of large replica fragments during the subsequent cleaning process. During the carbon deposition, heating of the crystal by radiation from the carbon gun, which has a larger anode and uses a higher electron bombardment current, is significant and will lead artifactually to a competing increase in the crystal frequency, which is "recovered" after the carbon evaporation ceases. Once this behaviour is recognised, it can be accommodated for easily by starting the carbon shadowing as a small positive beat frequency. On initial heating the beat frequency will drop. It will then rise to a predetermined cutoff point as carbon is deposited and will finally "overshoot" by an amount equal to the initial drop as the crystal cools at the end of the carbon deposition.

Rotary shadowing is conducted as for unidirectional shadowing except that a commutator unit is used to rotate the specimen about an axis perpendicular to the fracture plane during both platinum and carbon deposition. A little over half the amount of platinum normally used for unidirectional shadowing is usually sufficient to give good contrast for rotary-shadowed freeze-etch replicas, with the normal amount of carbon.

After carbon shadowing, return all gun controls to zero, switch off the high tension supply, the monitor and recorder, the knife cooling and the high vacuum gauge, and prepare to remove the specimens. Stage cooling may be continued until the specimens have been removed.

H. Specimen Removal and Apparatus Shutdown

Vent the chamber and remove the specimens, minimising frosting on the specimens after venting by working fast. Then treat the specimens for replica removal as described later. Only when this has been done, shut down the apparatus. Turn off the stage cooling and reevacuate the chamber. If appropriate, turn on the stage and knife heating. When both are warm, revent the chamber, safely discard the disposable razor blade (if used), remove any water condensation droplets from the stage or microtome with paper tissues, and complete the drying process with a hot air gun. Finally, close the chamber and reevacuate. If appropriate, raise the knife to its upper limit, ready for the next run. When the vacuum is better than 10^{-5} mbar, the pumping unit may be turned off, following the manufacturer's instructions. Complete the run record log sheet.

I. Retrieval and Cleaning of Replicas

Replica cleaning is often the most difficult stage of the entire procedure, during which replica fragmentation is frequently experienced. All dishes, implements, and solutions must be scrupulously clean to avoid replica contamination.

For replicas of cell suspensions, hold the specimen support above or just in contact with the surface of clean distilled water in a white ceramic spotting tray or a small petri dish, wait for it to thaw and the frost on top of the replica to evaporate, and then slowly immerse the specimen support into the water at approximately a 30° angle to the horizontal. The hydrophobic replica of the fractured surface will float off intact onto the water surface, surrounded by junk from the surrounding nonfractured (and hence rough) surfaces of the specimen, from which it may be separated easily. Transfer the floating replica (without any of the surrounding junk) onto the surface of a solution of sodium hypochlorite [technical grade, 10–14% (w/v) available chlorine] diluted to 50% with 10 mM sodium hydroxide, and leave covered at room temperature for at least 30 min (or overnight). (Commercial bleach should only be used if free from detergents, which tend to wet the replica and cause it to sink.) Then rinse the cleaned replica by transferring it sequentially onto two changes of distilled water and finally mount on an EM grid. Replica fragmentation upon transferring to and from cleaning solution is minimised if the replica is picked up on the upper surface of a bent round-ended glass rod formed using a Bunsen flame or the bent sealed tip of a Pasteur pipette formed in the flame of a small alcohol lamp to resemble an ice-hockey stick in shape. This method transfers less liquid than the use of a platinum loop, and any violent mixing of cleaning solution and water occurs at the underside of the rod while the replica is still safe on the upper surface. More thorough replica cleaning may be achieved, if necessary, by acidifying the hypochlorite with concentrated hydrochloric acid to form a stronger oxidising solution, by warming the hypochlorite to 60°C, or by using chromic acid. Concentrated sulphuric acid alone will digest the cellulose

of plant specimens. Replicas of deep-etched, rotary-replicated specimens are among the most difficult to clean, having a layer of platinum–carbon almost totally enveloping many of the biological structures, and prolonged exposure to strong acids may be required to achieve complete cleaning. Swelling of enclosed structures during this cleaning process can lead to severe replica fragmentation, but even the smallest of visible replica fragments can hold valuable structural information and so should all be kept, washed, and mounted on formvar-coated grids (see Section II,J). Other methods of cleaning replicas of difficult specimens are described in Shotton (1998b).

J. Mounting of Replicas

Floating replicas may be picked up from the meniscus of distilled water on bare EM grids either from above or from below. In the latter case, the EM grids should first be made hydrophilic by glow discharge, by brief immersion in a 0.1-mg/ml bacitracin solution, or by washing in alcoholic sodium hydroxide (30 g NaOH dissolved in 30 ml distilled H_2O, added to 250 ml 98% EtOH) followed by vigorous agitation in two changes of distilled water. Replicas are then mounted by careful manipulation of the submerged grid below the replica fragment, followed by slow withdrawal of the grid through the water surface. If, during this withdrawal, the grid is rotated to be at ~90° to the meniscus, with the replica fragment centrally located on it, little water will accompany removal of the grid. This can subsequently be removed by gently blotting the back of the grid onto a circle of filter paper and then by drying between the tips of the forceps holding the grid with a pointed piece of the filter paper, before placing the grid box. If the replica is to be picked up from above, the EM grid should be brought down flat onto the replica and then removed

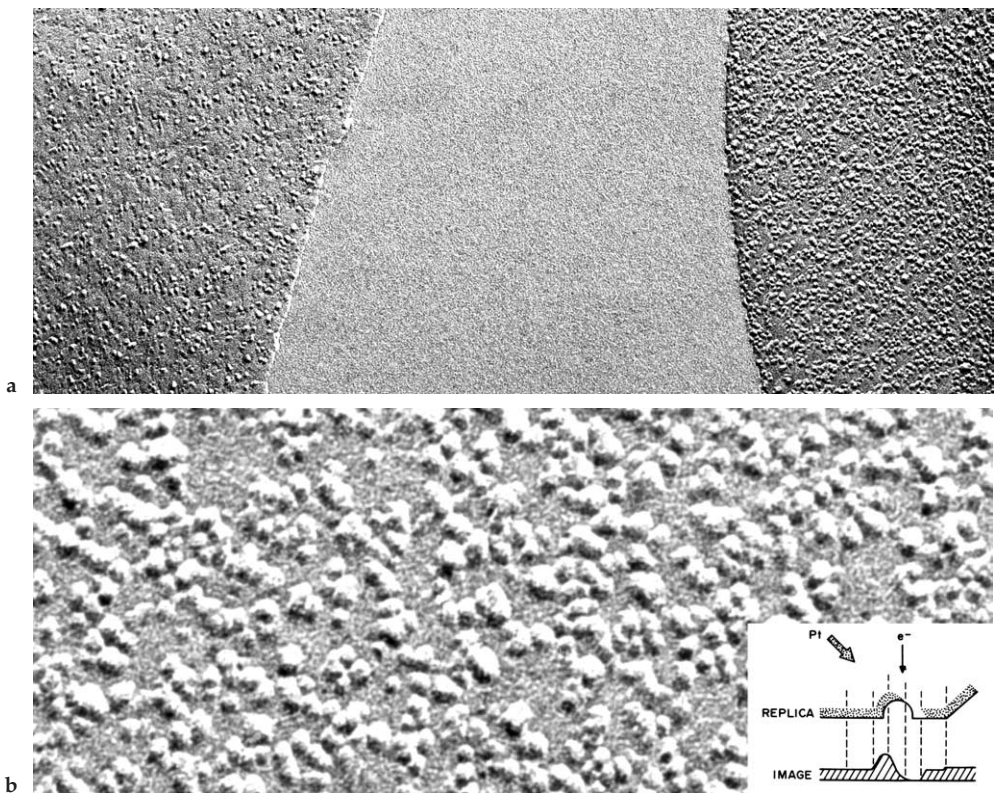

FIGURE 2 Freeze-fracture replica showing the appearance of erythrocyte fracture faces and intramembrane particles. (a) On the right, the protoplasmic fracture face (P face), and on the left, the extracellular fracture face (E face) of normal erythrocyte ghost membranes from two adjacent cells separated by a region of ice. Positive contrast image with the platinum shadowing direction from below. Magnification ×67,200 (b) An erythrocyte P face shown at a higher magnification to reveal individual intramembrane particles (IMPs), which throw short white shadows upward. Magnification ×255,000. (*Inset*) Diagrammatic view of a single platinum-replicated IMP and of its projected electron scattering power, which determines the optical density of its positive photographic image when viewed with the electron beam normal to the replica. From Steere and Rash (1979), reproduced by permission of Raven Press.

with a twist of the wrist to rotate it upside down at the meniscus, with partial submersion to ensure good adhesion of the replica with the grid. For certain investigations, it is important to know the orientation of the replica and hence the handedness of its projected image. For this, one should adopt a convention of always mounting replicas in the same orientation on one of the surfaces of the EM grid (either the dull or the shiny surface) and of orienting this surface facing to the right in one's grid storage box.

Bare 400 mesh hexagonal thin-bar EM grids are ideal for observing replicas of cell suspensions, but do not allow uninterrupted observation of extensive fracture faces of long myotubes or other large cells. For such replicas, formvar-coated 150-mesh or slot EM grids may be used, which have been coated lightly with carbon on their reverse side (i.e., on the side of the grid bars not covered with formvar, as opposed to the conventional method of depositing the carbon on top of the formvar layer, out of contact with the metal grid itself). This has the advantage that the flat surface of the formvar film remains hydrophilic and can be used to pick up floating replicas from below with ease.

Replicas should be observed at an intermediate magnification (×20,000–×90,000) in a transmission electron microscope and should appear crisp, clean, and of high contrast (Fig. 2). More in-depth descriptions of the technique, of the interpretation of freeze-fracture images, and of the potential artefacts that accompany the freeze-fracture technique, involving variations in replica quality, etching artifacts, specimen contamination, and plastic distortion, are discussed more fully in the longer original edition of this article in Shotton (1998b) and in earlier publications by Fisher and Branton (1974), Southworth *et al*. (1975), Sleytr and Robards (1977), Rash and Hudson (1979), Robards and Sleytr (1985), Abysekera and Robards (1995), and Shotton and Severs (1995).

References

Abermann, R., Salpeter, M. M., and Bachman, L. (1972). High resolution shadowing. *In* "*Principles and Techniques of Electron Microscopy*" (M. A. Hudson, ed.), pp. 197–217. Van Nostrand Reinhold, New York.

Abeysekera, R. M., and Robards, A. W. (1995). Freeze-fracture artifacts: How to recognise and avoid them. *In* "*Rapid Freezing, Freeze Fracture and Deep Etching*" (N. J. Severs and D. M. Shotton, eds.), pp. 69–88. Wiley-Liss, New York.

Branton, D., Bullivant, S., Gilula, N. B., Karnovsky, M. J., Moor, H., Mühlethaler, K., Northcote, D. H., Packer, L., Satir, B., Satir, P., Speth, V., Staehlin, L. A., Steere, R. L., and Weinstein, R. S. (1975). Freeze-etch nomenclature. Science 190, 54–56.

Bullivant, S., and Ames, A. (1966). A simple freeze-fracture replication method for electron microscopy. J. Cell Biol. 29, 435–447.

Bullivant, S., Metcalfe, P., and Warne, K. P. (1979). Fine structure of yeast plasma membrane after freeze fracturing in a simple shielded device. *In* "*Freeze Fracture: Methods, Artifacts and Interpretations*" (J. E. Rash and C. S. Hudson, eds.), pp. 141–147. Raven Press, New York.

Fisher, K., and Branton, D. (1974). Application of the freeze-fracture technique to natural membranes. Methods Enzymol. 32, 35–44.

Gross, H. (1987). High resolution metal replication of freeze-dried specimens. *In* "*Cryotechniques in Biological Electron Microscop*" (R. A. Steinbrecht and K. Zierold, eds.), pp. 205–215. Springer-Verlag, Berlin.

Newman, T. M. (1995). A guide to equipment for production of freeze-fracture replicas. *In* "*Rapid Freezing, Freeze Fracture and Deep Etching*" (N. J. Severs and D. M. Shotton, eds.), pp. 51–68. Wiley Liss, New York.

Rash, J. E., and Hudson, C. S. (1979). "Freeze Fracture: Methods, Artifacts and Interpretations." Raven Press, New York.

Robards, A. W., and Sleytr, U. B. (1985). Low temperature methods in biological electron microscopy. *In* "*Practical Methods in Electron Microscopy*" (A. M. Glauert, ed.), Vol. 10. Elsevier, Amsterdam.

Severs, N. J., Newman, T. M., and Shotton, D. M. (1995). A practical introduction to rapid freezing techniques. *In* "*Rapid Freezing, Freeze Fracture and Deep Etching*" (N. J. Severs and D. M. Shotton, eds.), pp. 31–50. Wiley-Liss, New York.

Severs, N. J., and Shotton, D. M. (1995). "Rapid Freezing, Freeze Fracture and Deep Etching." Wiley-Liss, New York.

Shotton, D. M. (1998a). Preparation of human erythrocyte ghosts. *In* "*Cell Biology: A Laboratory Handbook*" (J. E. Celis, ed.), 2nd Ed. Vol. 2, pp. 26–33. Academic Press, San Diego.

Shotton, D. M. (1998b). Freeze fracture and freeze etching. *In* "*Cell Biology: A Laboratory Handbook*" (J. E. Celis, ed.), 2nd Ed., Vol. 3, pp. 310–322. Academic Press, San Diego.

Shotton, D. M., and Severs, N. J. (1995). An introduction to freeze fracture and deep etching. *In* "*Rapid Freezing, Freeze Fracture and Deep Etching*" (N. J. Severs and D. M. Shotton, eds.), pp. 1–30. Wiley-Liss, New York.

Sleytr, U. B., and Robards, A. W. (1977). Freeze fracturing: A review of methods and results. J. Microsc. 111, 77–100.

Southworth, D., Fisher, K., and Branton, D. (1975). Principles of freeze fracturing and etching. *In* "*Techniques of Biochemical and Biophysical Morphology*" (D. Glick and R. Rosenbaum, eds.), Vol. 2, pp. 247–282. Wiley, New York.

Steere, R. L., and Rash, J. E. (1979). Use of double-tilt device (goniometer) to obtain optimum contrast in freeze-fracture replicas. *In* "*Freeze Fracture: Methods, Artifacts and Interpretations*" (J. E. Rash and C. S. Hudson, eds.). Raven Press, New York.

Zingsheim, H. P., and Plattner, H. (1976). Electron microscopic methods in membrane biology. *In* "*Methods in Membrane Biology*" (E. D. Korn, ed.), Vol. 7, pp. 1–146. Plenum Press, New York.

SECTION

9

Electron Microscopy Studies of the Cytoskeleton

CHAPTER

27

Electron Microscopy of Extracted Cytoskeletons: Negative Staining, Cryoelectron Microscopy, and Correlation with Light Microscopy

Guenter P. Resch, J. Victor Small, and Kenneth N. Goldie

I. INTRODUCTION

Our understanding of the function of the cytoskeleton and its associated proteins has been much advanced by developments in imaging methods for light microscopy. With the advent of probes, such as green fluorescent protein, the localisation of gene products in living cells under different physiological conditions is now readily feasible (e.g., Vignal and Resch, 2003). However, to extend our understanding of the functional interactions taking place, parallel information about cellular ultrastructure is essential. Here, electron microscopy (EM) is required to provide information about cell architecture at the nanometre level.

Three major filament systems make up the cytoskeleton: actin filaments, microtubules, and intermediate filaments. When not in organised bundles, actin filaments are poorly preserved after dehydration and embedding in plastic. This fact, taken together with the open, three-dimensional nature of the cytoskeleton networks, has limited the information obtainable by conventional EM methods based on thin sectioning. The methods of choice for studying the cytoskeleton of cultured cells have therefore centered on "whole mount" procedures, involving the culturing of cells on plastic films or coverslips and the preparation of entire cytoskeletons, or their replicas, for electron microscopy. Methods that deliver useful structural information about cytoskeleton organisation include quick freezing and deep etching (Heuser and Kirschner, 1980), critical point drying followed by metal shadowing (Svitkina *et al*., 1995), and negative staining (reviewed in Small, 1988; Small *et al*., 1999). More recently, advances in cryoelectron microscopy have opened the way to the study of cytoskeletal structures under conditions that obviate processing steps that could produce artefactual distortions of filament networks (Resch *et al*., 2002; Medalia *et al*., 2002). In particular, these latter approaches, involving cryoelectron tomography, promise to deliver new information about ultrastructural interactions in three-dimensional space unobtainable by other means.

This article describes the application of negative staining and cryo-EM to studies of the cytoskeleton; taking advantage of the developments in light microscopy, we also highlight the feasibility of correlating information on the living cell with electron microscopy (see also Svitkina and Borisy, 1999) for delivering meaningful structural information.

II. MATERIALS AND INSTRUMENTATION

A. General

Chloroform (Cat. No. 1.02445.1000), disodium hydrogen phosphate (Cat. No. 1.06580.1000), ethanol (Cat. No. 1.00983.2511), glucose (Cat. No.

Copyright 2006, Elsevier Science (USA).
All rights reserved.

1.04074.1000), sodium chloride (Cat. No. 1.06404.1000), and sodium dihydrogen phosphate (Cat. No. 1.06345.1000) are from Merck EGTA (Cat. No. E3889), MES (Cat. No. M2933), taxol ("paclitaxel," Cat. No. T7402), and Triton X-100 (Cat. No. X100) are from Sigma. Phalloidin was a generous gift from Professor H. Faulstich (Heidelberg) and is obtainable from Sigma (Cat. No. P2141). EM-grade glutaraldehyde (Cat. No. R1020) and Formvar (Cat. No. R1201) are from Agar Scientific, Stanstead, UK; nickel 200 mesh hexagonal or nickel H2 finder grids are from Graticules Ltd., Tonbridge, UK; and steel and titanium forceps (number 5) are from Dumont & Fils., Switzerland. Thirteen-millimeter-diameter plastic coverslips (Cat. No. 174950) are from Nunc, Rochester. Further materials required include Dow Corning silicone-based high vaccum grease and Whatman Qualitative No. 1 filter paper. The following are from local suppliers: glassware (50-ml bottle, measuring cylinder, a glass through minimum 7 cm deep, a rod or pipette), object slides with frosted ends, Parafilm, transfer pipets, scalpels, and blades. Additionally, cell culture equipment (media, incubators, inverted phase contrast microscope), a basic workshop setup (for producing coverslips with holes), and a routine transmission electron microscope are required.

B. Negative Staining

Sodium silicotungstate (Cat. No. R1230) is from Agar Scientific, Stanstead, UK. Minisart 0.2-µm filters are from Sartorius.

C. Cryo-EM

1,2-Dichlorethane (Cat. No. 8.22346.2500) and methanol (Cat. No. 1.06009.2511) are from Merck, and 87% glycerol (Cat. No. G7757) is from Sigma. Additional laboratory equipment required for producing holey films is a microprobe sonicator and a vacuum evaporator for carbon coating (e.g., Edwards E306).

A freeze-plunging device, either home made (drawings and materials list available upon request) or a commercial apparatus housed in a chemical extractor hood, is needed. At the base of the plunger is a polystyrene box for liquid nitrogen and into this sits a small container for condensing ethane (see Fig. 3). Frost-free liquid nitrogen, gaseous ethane, and a regulator valve with a length of silicon tubing, 4 mm inner diameter and 6 mm outer diameter (Tygon 3603, Norton Performance Plastics Corporation, Akron, OH), with one end fitted with a pipette tip with its end cut at a 45° angle, are needed. *Note: Remove any sources of ignition from the working area as ethane is highly flammable and explosive.* Safety glasses for eye protection or a Plexiglas full face shield, which additionally helps prevent inadvertent breathing onto the cold surfaces, a cause of ice contamination, are required.

Use Whatman qualitative No. 1 filter paper (Cat. No. 1001055), cut to rectangular strips of approximately 1 × 4 cm. Grid box (Agar Scientific, Cat. No. G276A) cut into small squares of 15 mm so that there are four grid holes arranged symmetrically within the square, fitted with a clear plastic lid, 13 mm circular diameter and 1 mm thick, with a 4-mm square notch cut out to allow access to one grid hole at a time is required. This is fitted with metal or nylon screw attached through the center to the grid box base so it can be rotated from one hole to the next and fixed tight for storage. Obtain 50-ml polypropylene conical tube with two approximately 8-mm-diameter holes in the lid to allow nitrogen to enter the tube and for retrieval using long tweezers. Small, portable industrial quality vacuum dewars (do *not* use houshold vacuum flasks as they can dangerously implode) or a polystyrene container for transporting grids in the grid box is needed. Purchase a large vacuum dewar for long-term storage; it is useful to have a dewar that has numbered and colour-coded holders of the correct size to hold storage tubes.

Additional tools needed are large tweezers (200 mm long; Bochem, Weilberg, Germany) and small screwdrivers. At least two sets of tools that contact liquid nitrogen should be available, as they will frost after they have been cooled in the nitrogen and then removed and left on a bench. If you then reintroduce them back into the liquid nitrogen, they will contaminate the nitrogen with the ice crystals.

For electron microscopy, a transmission electron microscope fitted with cryo blades to protect the frozen grid from ice contamination, as well as a cryo holder, cryo transfer station, and temperature controller (Gatan, Pleasanton, USA), are needed.

III. PROCEDURES

A. Negative Staining

1. Preparation of Formvar-Coated Grids

Thin plastic films on grid supports, as used for conventional EM, can be used as a growth substrate for cultured cells. For alternative protocols, see Small and Herzog (1994) and Small and Sechi (1998).

Solution

Dissolve 0.4 g Formvar in 50 ml chloroform and stir vigorously in a tightly closed bottle for at least 1 h. To produce films without holes, this solution and all glassware used should be kept as dry as possible.

Steps

1. Clean an object slide with a frosted end first with distilled water and then with 70% ethanol and allow to dry completely.
2. Transfer the Formvar solution into a measuring cylinder wide enough for the slide and submerge the slide, holding it on the frosted end by a clamp or peg attached to a thread, to just below the frosted area. After 30 s, lift the slide smoothly out of the solution and let it dry for 3 min hanging just above the solution surface.
3. Drain the excess solution at the bottom of the slide with filter paper and cut the film at the bottom, the left and the right edges, around 1–2 mm inside the edge of the slide. (Do the same for the back side *before* wetting the film, if both films are to be floated off together.)
4. Prepare a large vessel filled to the lip with distilled water, clean the surface with a glass rod from dust, and float off either one or both of the films simultaneously at an angle of 45° resp. 90° onto the surface. A black background below the vessel improves visualisation for this and the following steps. (*Note*: If difficulties are encountered with floating off the film, try another brand of slides or a different washing protocol; see also Small and Herzog, 1994.)
5. Place 200 mesh Ni grids with the dull side downwards onto the film. For easy handling of the magnetic nickel grids, the use of titanium forceps is recommended. Retrieve the film from the water surface with a piece of Parafilm that is put on top of the floating grids/film assembly and then lifted up carefully from one end. (An alternative way to do this is to use a microscope slide: with an address sticker adhered to one side and trimmed at the the edges, hold the slide at a 45° angle (paper side down), touch the film a few millimetres within one of the narrow ends, and slowly submerge the slide into the water. The film with the grids will follow the slide and stick very well.)
6. Remove excess water by blotting carefully with filter paper and allow the filmed grids to dry completely. To separate them without damaging the film, cut the film around each individual grid with the tip of a pair of forceps.

2. Cell Culture

Cells are plated onto the grids the same as for coverslips, and the density is chosen to give one or two cells per grid square after attachment and spreading. In general, cells spread more slowly on plastic film than on glass; to encourage attachment and spreading, the filmed grids may be coated with matrix molecules or serum (depending on cell type) prior to plating. Check for adequate cell spreading in an inverted microscope with phase-contrast optics prior to further processing.

In order to render the film more stable in the electron beam, an additional layer of carbon deposited onto the grid can be used. However, under these conditions, we experience a decrease in quality of the negative stain so that we usually apply a thin carbon layer *after* staining (see later).

To avoid the problem of loose, floating grids, it is an advantage to immobilise them in one way or another (see also Small and Sechi, 1998). To immobilise single grids, we sandwich them between a plastic coverslip with a 2.5- to 2.7-mm hole in the center of a petri dish. Dots of vacuum grease are used to fix the plastic coverslip to the petri dish.

Steps

1. Prepare plastic coverslips >12 mm diameter with a central hole of 2.5–2.7 mm; this is best done by fixing a stack of them tightly in a holder prepared separately for this purpose (Fig. 2a) before drilling. Clean the coverslips by washing them twice with 70% EtOH and once with water, both of them heated in a microwave oven until boiling.
2. For cell culture over periods of more than 12 h, sterilise grid sets under UV light in an open petri dish for 5 min. Air bubbles get trapped easily in the mesh, which makes observation of the spreading cells (e.g., in phase contast) difficult. This can be avoided by incubating the grids in sterile water in the fridge overnight before use. This step should be performed individually for each grid in grid boxes (volume per slot approximately 15 µl) to avoid the grids adhering to each other.
3. Transfer the grids, with the filmed side up, to sterile (and dry) petri dishes and fasten them with the plastic coverslips: Apply small spots of high vacuum grease onto the edge of the coverslips and press them down into the petri dishes, with the grid trapped below the hole. Only coverslips with a regular hole and flat edge should be used.
4. After they are mounted, the films can be protein coated and cell culture can be carried out as usual.

3. Extraction/Fixation

Solutions

1. Prewarmed phosphate-buffered Saline (PBS, 150 m*M* NaCl, 3 m*M* NaH_2PO_4, 8 m*M* Na_2HPO_4, pH 7.4)

2. Prewarmed extraction buffer [0.25% Triton X-100 (diluted from a 20% stock) and 0.5% EM-grade glutaraldehyde (diluted from a 25% stock) in CB: 10 m*M* MES, 150 m*M* NaCl, 5 m*M* EGTA, 5 m*M* $MgCl_2$, 5 m*M* glucose, pH 6.1]
3. Fixation buffer at room temperature (1.0% EM-grade glutaraldehyde from a 25% stock in CB)
4. Phalloidin, 1 mg/ml in MeOH, stored at –20°C
5. Taxol, 10 m*M* in dimethyl sulfoxide, stored at –20°C

Steps

1. Remove cover glasses and transfer grids to a small petridish with prewarmed PBS for a brief wash. To avoid bending in the transfer step, a magnetised steel forceps is useful for initially lifting the grid so that it can be grabbed more easily with another pair of (titanium) forceps.

2. Aspirate the PBS carefully, do not allow to dry, and replace it with prewarmed extraction buffer; incubate for 1 min.

3. Replace the extraction buffer with fixation buffer and fix for >20 min up to overnight at 4°C; to improve the preservation of actin and microtubules, 10 µg/ml phalloidin or 10 µg/ml taxol can be added.

4. Negative Staining and Electron Microscopy

Solution

2% sodium silicotungstate in ddH_2O, adjusted to pH 7 with NaOH (equilibration of pH can take a long time) and filtered through a 0.20-µm filter.

Steps

1. Clamp the grid in a pair of forceps using a large paper clip over the shaft to hold the tips together; do not allow the sample to dry at this step!

2. Rinse with a few drops of the negative stain from a transfer pipette. After a few seconds, drain the stain from the *entire* back side of the grid with filter paper to remove it as completely as possible. On the front, drain only from the edges to leave a thin film so as not to damage the sample. Special care has also to be taken to drain excess stain from between the tips of the forceps: Bring the edge of the filter paper into contact with the edge of the grid at the contact point with the forceps.

3. Allow to air dry and observe in a routine TEM (Fig. 1a). To avoid drift of the plastic film upon exposure to the electron beam, a thin layer of carbon can be deposited onto the film in a vacuum evaporator.

B. Cryo-EM

This section describes the method from Resch *et al*. (2002) in more detail.

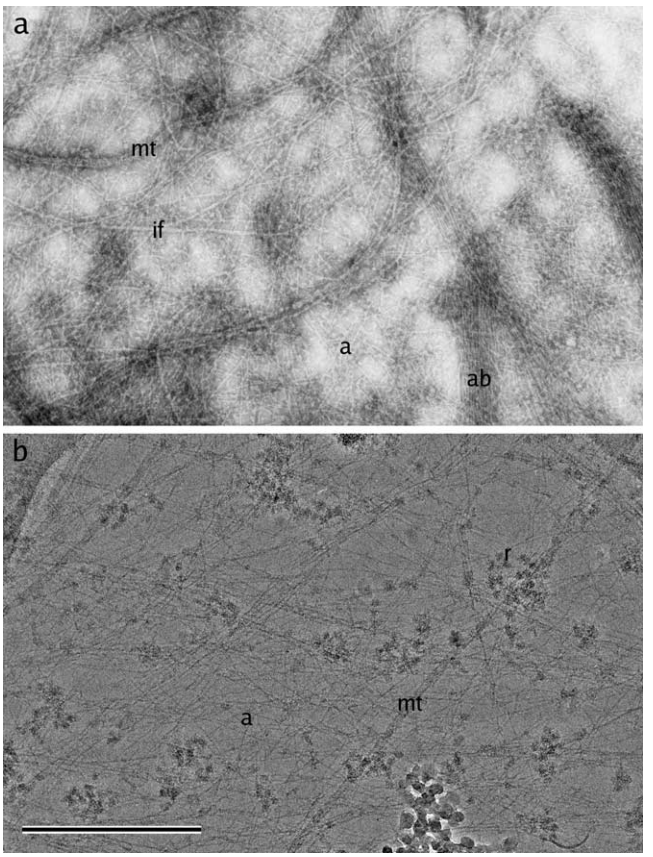

FIGURE 1 Extracted cytoskeletal networks in thin regions of cells visualised by (a) negative staining with sodium silicotungstate and (b) cryoelectron microscopy. a, actin; ab, actin bundle; mt, microtubule; if, intermediate filaments; r, ribosome aggregation. Bar: 500 nm.

1. Preparation of Holey Films

For unstained specimens, the support film itself contributes a significant background noise in the electron microscope image. To improve contrast conditions in the cryo-EM, we have therefore used holey films to support cells and have selected areas for structural analysis where parts of cells span the holes. The method for making holey films was derived from that described in Hodgkinson and Steffen (2001); it was optimised for a hole/film ratio that was significantly lower than for films used for molecular suspensions to allow the cells to attach and spread.

Solution

Dissolve 0.25 g Formvar in 50 ml chloroform and stir in a tightly closed bottle for at least 1 h. After the Formvar is dissolved, add 150 µl of 50% glycerol in water; shake the solution vigorously for 1 min.

Steps

1. Prepare a clean object slide as described previously.
2. Sonicate the Formvar/glycerol solution for 3 min.
3. Rapidly transfer the solution to a staining jar, dip the slide into it, remove, and allow to air dry for a few minutes.
4. Float off both sides of the film as described earlier and place 200 mesh Ni grids with the dull side facing the film on top. In this case, the grids should not be placed too close together on the film, as the filter paper used to retrieve the grids will not adhere sufficiently!
5. Retrieve the grids and the film with a piece of filter paper, *not* with Parafilm or a slide, and allow to dry.
6. Prepare a stack of filter paper in a large glass petri dish saturated with MeOH and incubate the grid set on this, with the film up, for 10 min. This serves to perforate the pseudoholes. Remove and allow to air dry completely before proceeding.
7. At this stage, we recommend checking the film with a phase-contrast microscope for the size and distribution of holes, which is affected by the amount of glycerol as well as by the power and duration of the sonication. If neccessary, vary these factors.
8. Coat the grids with a thick (dark grey) layer of carbon in a high vacuum evaporator.
9. Prepare a bed of filter paper saturated with 1,2-dichlorethane. Place the set of grids, film side up, onto the filter paper and leave for 2 h to dissolve the plastic film. If the filter paper bends up at the edges, either cut it into smaller pieces or use small pieces of glass to hold it down.
10. After final drying, check a few grids in the EM (see Fig. 2b) and store them individually in grid boxes.

2. *Cell Culture*

For preparation of cells for cryo-EM, the same procedure is used as for negative staining. However, making the cells attach and spread on perforated films might require additional steps, including coating with matrix molecules (for general strategies, see also Resch *et al*., 2002; and Vignal and Resch, 2003).

It can save a lot of time and effort prior to preparing the cryo-frozen grids if they are screened beforehand in a phase-contrast microscope. This allows the possibility to roughly assess the quality and number of cells grown on the surface. The proximity of likely cell candidates for the electron microscopy can also be mapped at this stage (see later).

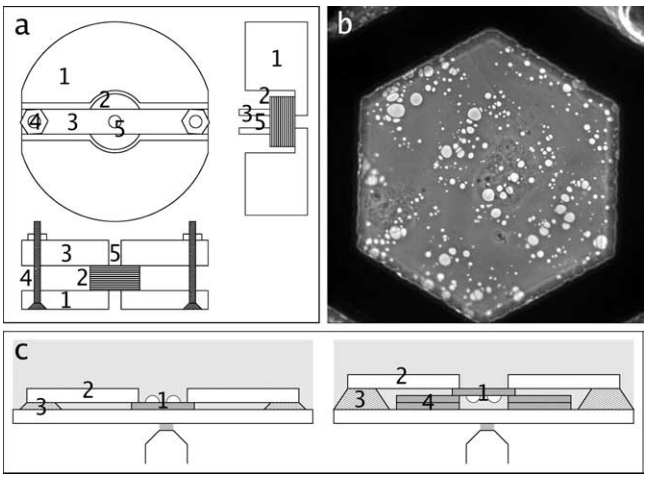

FIGURE 2 (a) Device used for mounting the plastic coverslips for drilling consists of a plastic body (1) with an elongated grove (here horizontal) and a central round indentation (2) in which a stack of cover glasses sit. They are mounted by a Plexiglas bar (3) on top of the groove, which is pressed down firmly onto them by two screws at its end (4). Drilling is done via a central hole (5) in the Plexiglas bar. (b) Perforated carbon film as typically used for cultivating cells for cryo-EM on a 200 mesh hexagonal Ni grid. (c) Two setups to mount grids for correlative LM/EM in petri dishes with a coverslip inset in the bottom on an inverted microscope; samples are covered with medium, the objective is coming from below. (Left) Upright setup: The grid with cells up (1) is mounted by a plastic coverslip with a central hole (2) that is attached via high vaccuum grease (3). (Right) Inverted setup for fluorescence microscopy: The grid with cells on it facing downwards (1) is put on top of two other nickel grids (4) that serve as spacers for the cells and fixed with the coverslip as described earlier.

3. *Extraction/Fixation*

For cryo-EM as outlined here, removal of the membrane and cytosolic protein is necessary to visualise the cytoskeletal networks and actin filament subunit structure clearly. It is also necessary to fix the cytoskeletons lightly during this extraction process to stabilise the networks. Medalia *et al*. (2002) have applied cryoelectron tomography to unextracted cells, in which case filament networks are visible only after complex image-processing regimes.

Here, the extraction/fixation protocol is the same as for negative staining, except that postfixation seems not to be neccessary.

4. *Cryo Plunging of Specimen Grids*

The objective of plunge freezing is to obtain a well distributed, quick frozen specimen in a homogeneously thin layer of vitrified ice uncontaminated with frost. For this, the blotting regime is critical. The amount of blotting required can be sample/buffer dependent so this might have to be adapted for dif-

ferent preparations. It is important to remain consistent but because in some cases even subsecond differences in blotting times can cause variability with ice thickness, differences between grids are unavoidable. In order to counter this, make several grids at each session.

If a washing buffer is to be used, it is important that it is at the same osmolarity as the cell culture media, as the integrity of the cells could be compromised.

Steps

1. Set up your workspace with all the required tools close at hand prior to freezing (Fig. 3). It is important to have good light and it is useful to have additional light (e.g., equipoise lamp) that can be positioned facing toward the grid for observing the blotting step when plunging. Frost in the liquid nitrogen and ethane can be a source of contamination on your grids so always try to minimise exposure to water vapour. Always keep the nitrogen containers sealed with lids and do not breathe onto the nitrogen or ethane surfaces. Precool all tools that come into contact with the grid or grid box, as they may heat the specimen, causing cubic or hexagonal ice to form.

2. Set up the plunger. Check the alignment of the forceps in the plunging arm so that the forceps will plunge the grid a few millimetres below the surface of the liquified ethane. Do not adjust the drop height so that the grid gets too near the base of the ethane container as ethane ice forms there, which will damage the grid if it comes into contact with it.

3. Put on eye protection or a face shield and fill the polystyrene container with liquid nitrogen. Also fill the portable transfer dewar with liquid nitrogen and submerge the polypropylene conical tube into this. Keep a lid on the transfer dewar to minimise contamination.

4. Precool the small ethane container with liquid nitrogen. Make sure all liquid nitrogen is removed from the inside of the container as it interferes with the liquifying of the ethane. Place one of the grid storage boxes into the liquid nitrogen.

5. Place the pipette tip from the ethane supply into the bottom of the small ethane container and slowly open the regulator valve. After a short time, the ethane gas will start to condense on the bottom of the container. This is normally accompanied by a high-pitched squeal. Keeping the pipette tip just below the surface of the liquid ethane and gently moving it around the inner walls allow the level to rise to the top of the ethane container. Keep the tip moving in the ethane so that the tip does not ice up and block. Do not allow the liquid ethane to spill over into the nitrogen. You can use a double-walled ethane container with a small gap between the walls to avoid this. *Note: Liquid ethane can cause serious burns if it comes into contact with your skin or eyes so always exercise caution and regulate the ethane to a slow and gentle flow.*

6. After a short time, the liquified ethane will start to solidify. If this happens, you must deice by inserting the pipette tip into the ethane. Slowly open the ethane gas supply as you do not want to splash ethane into the nitrogen. Gently move the pipette tip around the edges of the ethane container until the ethane liquifies.

7. Pick up a grid by the edge, sample side up with forceps. The samples are usually washed briefly, immediately prior to plunging. Cut a piece of Parafilm, place on a flat surface, and apply 2 × 50-µl drops of washing buffer, e.g., prewarmed PBS. Keeping the grid in the tweezers, blot the grid side on with a piece of filter paper. Apply the grid, sample side down to the surface of the washing droplet, blot, and place onto the second drop. Remove the grid; a droplet from the washing buffer should remain on the grid surface. Place the forceps into the clamp of the plunger arm with the sample (and droplet) facing towards you.

8. Using a strip of the Whatman qualitative No. 1 filter paper, carefully blot the surface of the grid. Use a visual assessment to roughly gauge the degree of blotting (Fig. 4): When first touching the grid, the filter paper will pull onto the droplet by surface tension and you should see the outline image of the grid, through the paper. Once most of the surface liquid is adsorbed

FIGURE 3 Working setup as typically used for freeze plunging. (1) Gaseous ethane bottle, (2) regulator valve with Tygon tubing and pipette tip, (3) full face shield, (4) filter paper strips, (5) polystyrene box for liquid nitrogen, (6) small container (sitting on an aluminum block) for condensing ethane, (7) plunger arm, fixed with a pair of forceps holding the grid (arrowhead), (8) 50-ml conical tube for grid box storage, (9) tools (fine and large forceps, screwdrivers), and (10) sample transport dewar. For details, see text.

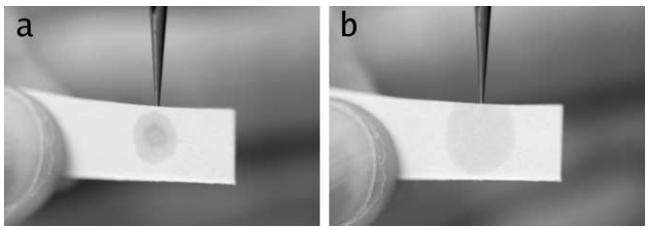

FIGURE 4 Blotting of the grid immediately prior to freeze plunging: (a) when first touching the grid and droplet with a strip of filter paper, an outline of the grid is clearly visible through the paper and (b) as the liquid is absorbed by the filter paper, the droplet imprint will increase in diameter until most of the liquid is removed from the grid surface. The grid outline will disappear and the paper will pull away from the grid. At this moment, plunge the grid immediately. For more details, see text.

by the paper you will reach a point where the grid outline will suddenly disappear and the paper will also pull away. This is the time when the sample should be plunged rapidly into the ethane. Waiting even a few seconds after the pull-away point can result in excess removal of liquid, sample damage, and drying.

9. While keeping the grid under the surface of the ethane, remove the tweezers from the plunging arm. Raise the plunging arm away from the tweezers. Carefully remove the tweezers and grid from the ethane and immediately hand plunge the grid into the liquid nitrogen. Make sure the grid stays under the cold nitrogen vapour cloud to keep it from warming and frosting. This can be achieved by having sides on the polystyrene liquid nitrogen box that are higher than the top level of the liquid ethane container.

10. Transfer the grid, keeping it submerged under the liquid nitrogen, into one of the storage slots in the grid box. After all samples have been loaded, close the lid firmly with a screwdriver. Place the liquid nitrogen-filled transfer dewar containing the polypropylene tube close to the plunger. Using a large pair of tweezers, quickly transfer the grid box from the plunger into the tube. Screw the lid onto the tube.

11. Move the tube and grid boxes holding the samples into a long-term storage dewar. As long as the nitrogen is kept topped off the grids can remain here for long periods (sometimes years) without deterioration until you are ready to view them in the microscope. We totally dry our dewars once a year with a stream of dry nitrogen gas to remove any frost that may accumulate with time. Transfer all grids to another frost-free container while drying the original dewar.

5. Electron Microscopy

Steps

1. Using a precooled pair of large tweezers, remove the grid storage box holding the frozen grids and place in a liquid nitrogen-filled transfer dewar.

2. At the electron microscope, fill the anti-contaminator and cryo-blade dewars.

3. If the cryo holder has been pumped (it is recommended to continually vacuum pump the cryo holder dewar when not being used), remove it from the vacuum pump stand. Insert the holder carefully into the loading station. Connect the cable for temperature measurement between the cryo holder and the temperature controller.

4. Remove the clip ring from the cryo holder with the clip ring tool.

5. Put on eye protection or a face shield.

6. Fill the specimen holder dewar and the loading station dewar with liquid nitrogen. After each filling with liquid nitrogen, replace the Plexiglas lid on the loading station dewar to minimise frost contamination. Keep the cap on the holder dewar, as it keeps the outer sides from cooling. Make sure you open and close the tip shutter as you cool as this prevents the shutter from jamming. You will need to keep topping off the level so that nitrogen sits just below the tip of the sample holder. Wait for the temperature controller to read at least –160°C before loading your sample.

7. Placing the transfer dewar as close as possible to the specimen holder dewar, rapidly transfer the grid box holding the frozen specimens to the specimen holder dewar. Use a precooled pair of large tweezers.

8. Precool a screwdriver and loosen the lid of the grid box.

9 Check that the level of the liquid nitrogen is just below the tip of the holder; cool a pair of No. 5 forceps and the clip ring tool in the loading station dewar.

10. Using the forceps, remove a grid from the grid box. Making sure you keep the grid within the cold nitrogen vapour, place the grid into the recess in the cryo holder tip. Centre the grid in the recess and fasten with the clip ring. Immediately close the holder tip shutter.

11. Replace the Plexiglas lid on the loading station dewar and lift the loading station and cryo holder and place onto the console desk of the microscope. We protect the console surface from nitrogen damage with a metal splash guard (Gowen and Burger, 1998).

12. Cycle the roughing pump on the microscope so that the pump lines to the microscope sample stage (e.g., compustage on an FEI machine) are under good vacuum before insertion of the cryo holder.

13. Remove the holder from the loading station and carefully insert into the microscope stage for preevacuation. (It can be useful to pretilt the stage to around –60° so that the holder dewar neck is positioned at "3 o'clock" instead of "6 o'clock" to lessen nitrogen spillage when the holder is introduced.) Wait for the vacuum to be restored and then insert the holder all the way into the microscope.

14. Allow at least 20 min for the temperature to stabilise and the vacuum to recover. Temperature variations cause the holder to drift. Connect the cable from the temperature controller and monitor the temperature. During the transfer the temperature should not warm to above about –150°C. Normally the holder will stabilise at around –180°C. Do not leave the cable connected to the holder as this can also cause drift effects.

6. Image Acquisition

To reduce damage when viewing cryo grids in the electron microscope, it is necessary to have low-dose software, which allows you to minimise the electron dose applied to the sample. Always use the beam blanker when you are not observing the specimen. The microscope should be well aligned and set up for low-dose conditions. To lower the electron intensity at the sample, you can use a small condenser aperture, small spot size, and low emission settings.

Steps

1. Once the holder temperature has equilibrated and drift minimised, the grid should be screened at low magnification (usually at around 3000× or less) to find promising cell areas for imaging.

2. Images can be acquired either digitally using a CCD camera system or taken onto plate film. If required, images on plate film can be scanned digitally using a suitable high-resolution film scanner.

3. In some instances, micrographs may appear to have an uneven intensity difference across the image due to local variations in ice thickness. Applying a high-pass filter helps even the intensity, which allows subsequent contrast adjustments to be made more easily (Fig. 1b).

C. Correlation with Light Microscopy

For situations in which the cell shape cannot be visualised clearly (e.g., frozen hydrated samples) or in which the function cannot be deduced solely from the morphology but only from a marker protein (e.g., GPF-VASP for protruding lamellipodia; Rottner *et al*., 1999), correlative light and electron microscopy on the same cell can be very helpful in establishing the structure–function link as discussed earlier. This correlation should be relatively straightforward for the classical methods, where cells are grown directly on glass coverslips with etched finder patterns; appealing examples can be found in Svitkina and Borisy (1999). For negative staining and cryo-EM, where cells are grown directly on grids, finder grids with indexed grid holes have to be used (Fig. 5).

Steps

1. Prepare grids with a Formvar or a holey carbon film as described earlier; use H2 Ni finder grids instead of hexagonal 200 mesh grids to be able to relocate your samples.

2. Spread cells on these grids. For correlative LM/EM, it is essential to remove any air bubbles trapped in the mesh by preincubating them in water as described previously.

3. Mount the grids individually for light microscopy; how exactly this is done depends on the setup and the cell line used. As a general guide, care has to be taken to (1) mount the grid flat (e.g., by using the method described earlier with coverslips with a hole drilled in the center), (2) have the cells as close to the objective to avoid problems with focus, and (3) mount grids with a carbon film upside down for epifluorescence to avoid loss of intensity. Two sample setups using petri dishes with a glass coverslip at the bottom are shown in Fig. 2c.

4. For the light optical observation of the cells, there are several possibilities available: (1) living cells in phase contrast, (2) living cells expressing a fluorescent protein (conjugate), and (3) fixed cells after staining with a fluorescent probe. For the latter method, it is essential to minimise the damage of the substructure

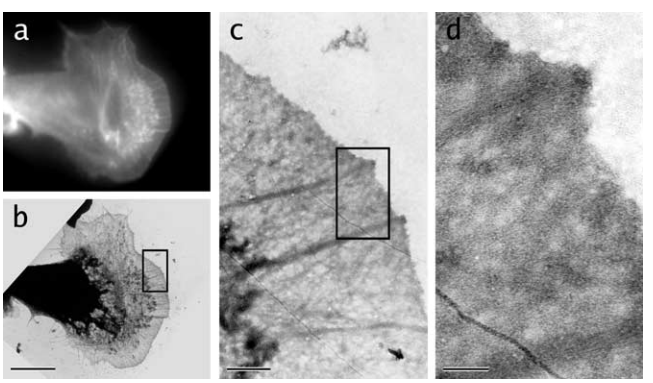

FIGURE 5 Correlative light and electron microscopy as demonstrated by a B16 mouse melanoma cell: (a) Cell stained with fluorescently labelled phalloidin and visualised by epifluorescence microscopy, (b) corresponding view of the same cell afer negative staining, (c and d) higher magnification insets of the previous images. Bars (a and b) = 10 µm, (c) = 1 µm, (d) = 250 nm.

by prolonged incubation steps in the staining protocol, e.g., fluorescently labelled phalloidin can be included directly in the fixative.

5. Record the position of each cell observed in a map of the finder grid; such a map for the H2 grids is provided by the authors at ftp://cellix.imba.oeaw.ac.at/Protocols/findergrids.zip.

6. Proceed as described earlier for negative staining or cryo-EM.

Acknowledgments

The authors thank Johanna Prast, Institute of Molecular Biology, Salzburg, for her continuous support, Marietta Schupp, Photo Lab, EMBL Heidelberg, for her contributions (Figs. 3 and 4), and Johann Diendorfer, Institute of Molecular Biology, Salzburg, for his help with producing coverslips with holes. GPR is supported by project P-15710 of the Austrian Science Foundation.

References

Gowen, B. E., and Burger, L. (1998). Cryo-TEM liquid nitrogen splash guard. *J. Micros.* **191**, 320–322.

Heuser, J. E., and Kirschner, M. W. (1980). Filament organization revealed in platinum replicas of freeze-dried cytoskeletons. *J. Cell Biol.* **86**, 212–234.

Hodgkinson, J. L., and Steffen, W. (2001). Direct labeling of components in protein complexes by immuno-electron microscopy. *Methods Mol. Biol.* **161**, 133–139.

Medalia, O., Weber, I., Frangakis, A. S., Nicastro, D., Gerisch, G., and Baumeister, W. (2002). Macromolecular architecture in eukaryotic cells visualized by cryoelectron tomography. *Science* **298**, 1155–1157.

Resch, G. P., Goldie, K. N., Krebs, A., Hoenger, A., and Small, J. V. (2002). Visualisation of the actin cytoskeleton by cryo-electron microscopy. *J. Cell Sci.* **115**, 1877–1882.

Rottner, K., Behrendt, B., Small, J. V., and Wehland, J. (1999). VASP dynamics during lamellipodia protrusion. *Nature Cell Biol.* **1**, 321–322.

Small, J. V. (1988). The actin cytoskeleton. *Electr Microsc. Rev.* **1**, 155–174.

Small, J. V., and Herzog, M. (1994). Whole-mount electron microscopy of the cytoskeleton: Negative staining methods. *In* "*Cell Biology: A Laboratory Handbook*" (J. E. Celis, ed.), Vol. 2, pp. 135–139. Academic Press, San Diego.

Small, J. V., Rottner, K., Hahne, P., and Anderson, K. I. (1999). Visualising the actin cytoskeleton. *Microsc. Res. Tech.* **47**, 3–17.

Small, J. V., and Sechi, A. (1998). Whole-mount electron microscopy of the cytoskeleton: Negative staining methods. *In* "*Cell Biology: A Laboratory Handbook*" (J. E. Celis, ed.), 2nd ed., Vol. 3, pp. 285–291. Academic Press, San Diego.

Svitkina, T. M., and Borisy, G. G. (1999). Arp2/3 complex and actin depolymerizing factor/cofilin in dendritic organization and treadmilling of actin filament arrays in lamellipodia. *J. Cell Biol.* **145**, 1009–1026.

Svitkina, T. M., Verkhovsky, A. B., and Borisy, G. G. (1995). Improved procedure for electron microscopic visualization of the cytoskeleton of cultured cells. *J. Struct. Biol.* **115**, 290–303.

Vignal, E., and Resch, G. P. (2003). Shedding Light and Electrons on the Lamellipodium: Imaging the Motor of Crawling Cells. Biotechniques **34**(4), 780–789.

CHAPTER

28

Correlative Light and Electron Microscopy of the Cytoskeleton

Tatyana M. Svitkina and Gary G. Borisy

I. INTRODUCTION

Light and electron microscopy (EM) each have certain advantages and limitations for the investigation of the cytoskeleton. Light microscopy allows for kinetic observations in living cells; in particular, modern fluorescence technology affords imaging of single fluorophores with high temporal resolution. However, the spatial resolution of light microscopy is limited to approximately 200–300 nm. In contrast, EM affords high spatial resolution but provides only static images and is not applicable to living cells. Correlative light and EM is a way to combine the advantages of these two techniques and link cell structure and dynamics. The main strategy of this approach is to follow the dynamics of a living cell by time-lapse imaging and subsequently analyze the same cell by EM.

The success of correlative microscopy imposes special demands at both the light and the EM level. To allow for precise identification of corresponding features in EM, light microscopy should be performed at the highest possible resolution and allow for the fast cessation of dynamic cellular processes at the end of the light microscopic observation. For fluorescence light microscopy, issues of photodamage and phototoxicity become more critical, as EM is able to reveal damage not recognizable at the light microscopic level. The key requirements for the EM procedure are quality, reproducibility, and yield. Yield is essential because detailed observation of individual living cells places a high investment of investigator time and effort in a single cell. If the efficiency of recovering a cell for EM is low, the investment is lost.

For studying cytoskeletal components, we have chosen detergent extraction–chemical fixation–critical point drying (CPD)–TEM of platinum replicas as a basic procedure (Svitkina *et al.*, 1995) because it allows a higher yield of successful results in comparison with alternative approaches. In the replica EM technique, the contrast is created by shadowing of three-dimensional (3D) samples with metal. The purpose of detergent extraction is to uncover the cytoskeleton and make it available to metal coating, yet to preserve it in its entirety as in the living state (Lindroth *et al.*, 1992). The composition of the extraction solution is designed to achieve this goal. Chemical fixation provides cell structures with physical resistance against subsequent harsh procedures. Our fixation procedure includes consecutive treatment with glutaraldehyde, tannic acid, and uranyl acetate. Drying exposes surfaces of the specimen for vacuum shadowing. The preservation of 3D structure is the major concern during EM processing, especially during drying. The main source of problems is the surface tension at the liquid–gas interface, which will crush fragile cytoskeletal structures if the interface passes through the sample. CPD is a simple and reliable technique, which circumvents this problem and preserves the complicated 3D structure of the cytoskeleton (Ris, 1985).

This article describes the procedure for preparation of cells for correlative EM after light microscopic observation, as well as the combination of this approach with immunostaining. Direct comparison of

Copyright 2006, Elsevier Science (USA).
All rights reserved.

living cells and platinum replicas of their cytoskeletons using a number of different markers demonstrated that our protocol does not introduce alterations in the distribution of several cytoskeletal elements (Svitkina *et al*., 1997; Svitkina and Borisy, 1998, 1999).

II. MATERIALS AND INSTRUMENTATION

1. Leibovitz's L-15 medium (Cat. No. 21083-027, GIBCO)
2. Phosphate-buffered saline (PBS) (Cat. No. 21-040-CV, Cellgro)
3. PIPES (Cat. No. 528131, Calbiochem)
4. Triton X-100 (Surfact-Amps X-100, Cat. No. 28314, Pierce)
5. Polyethelene glycol (PEG), MW 40,000 (Cat. No. 33139, Serva Electrophoresis) or MW 35,000 (Cat. No. 81310, Fluka)
6. Taxol (paclitaxel) (Cat. No. T7402, Sigma)
7. Phalloidin (Cat. No. P2141, Sigma)
8. Glutaraldehyde (Cat. No. 01909-10, Polysciences)
9. Sodium cacodylate (Cat. No. C-4945, Sigma)
10. Tannic acid (Cat. No. 1764, Mallinckrodt)
11. Uranyl acetate (J. T. Baker Chemical Co.)
12. $NaBH_4$ (Cat. No. 213462, Aldrich)
13. Bovine serum albumin (BSA) (Cat. No. A-7906, Sigma)
14. Tween 20 (Cat. No. X251-7, J. T. Baker Chemical Co.)
15. Tris (Trizma–HCl) (Cat. No. T-3253, Sigma)
16. Gold-conjugated antibodies (Cat. Nos. G-7777, G-3779, G-5527, G-5652, Sigma; Cat. Nos. 115-215-068, 111-215-144, Jackson Immunoresearch Laboratories)
17. Ethanol (Cat. No. 15055, Electron Microscopy Sciences)
18. Molecular sieves (4 Å, 8–12 mesh) (Cat. No. M514-500, Fisher)
19. Hydrofluoric acid (HF) (Cat. No. A147-1, Fisher)
20. 35-mm tissue culture dishes
21. 22 × 22-mm glass coverslips (No. 1.5)
22. Silicon vacuum grease (Dow Corning)
23. Gold wire (Cat. No. 21-10, Ted Pella)
24. Platinum wire (Cat. No. 23-10, Ted Pella)
25. Tungsten wire (Cat. No. 27-3-20, Ted Pella)
26. Carbon rods (Cat. No. 61-13, Ted Pella)
27. Platinum loop
28. Diamond pencil
29. Double-sided tape (Scotch)
30. Lens tissue (Kodak)
31. Post-It notes
32. Electron microscopic grids (e.g., Cat. No. G50, Ted Pella)
33. Locator grids (e.g., 7GC200, Ted Pella)
34. Holders for critical point drying. We use a homemade holder (Fig. 1), which consists of a wire basket that fits the size of the critical point dryer's chamber. Such a design is good for correlative EM, as it is not very demanding to the shape and size of the coverslips. For noncorrelative EM, commercially available holders can be used (e.g., Cat. No. 8762 for coverslips under 7 mm or Cat. No. 8766 for round 12-mm coverslips, Tousimis).
35. 50-ml glass beakers
36. Homemade scaffolds (Fig. 1)
37. Stirrer bars (Fig. 1)
38. Fine tip forceps
39. Dissection microscope
40. Critical point dryer. We use a semiautomatic Samdri-795 or manual Samdri PVT-3 (Tousimis). Other devices have also been used successfully. As a source of liquid CO_2, we use high-quality carbon dioxide (Cat. No. CD 4.8SE, Praxair); however, lower quality grades can also be used if they have low water and carbohydrate contamination. The cylinder should be equipped

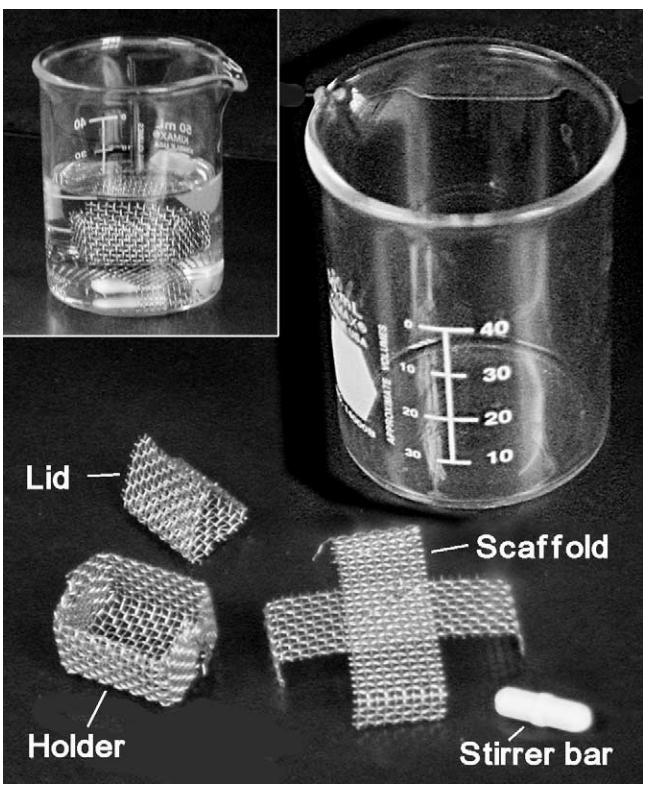

FIGURE 1 Accessories for CPD: specimen holder, lid for holder, and scaffold are made from stainless steel mesh. Inset shows an assembled set.

with water and oil absorbing filter (Cat. No. 8781/82A, Tousimis).

41. Vacuum evaporator. We use an Edwards 12E1 evaporator equipped with rotary and diffusion pumps, power supply, rotary stage, and thickness monitor (Cat. No. QM-311, Kronos, Inc.). Newer models with suitable configuration are now available from Edwards and other sources.

III. PROCEDURES

A. Cell Culture and Light Microscopy

Details of cell cultivation, introduction of fluorescent probes into cells, and light microscopic observation are beyond the scope of the present description. However, certain issues are specific to correlative microscopy and these we discuss.

1. Preparation of Locator Coverslips

Locator coverslips are helpful in facilitating the relocalization of the same cells. The reference marks on the coverslip should be recognizable by both light and EM. We use glass coverslips coated with a thin layer of gold through a locator grid (Fig. 2). Cells are selected within clear uncoated glass areas corresponding to the solid parts of the locator grid.

Steps

1. Put one or two locator grids in the center of 22 × 22-mm glass coverslip. Place coverslips onto the stage of vacuum evaporator.
2. Evaporate gold onto coverslips using a procedure suitable for the particular evaporator. Thickness of gold coating may vary. It should be clearly visible by eye as a purple transparent deposit. Avoid too thick of a coating because the gold may then contaminate the clear glass area under the grid.
3. Remove grids, collect coverslips, and bake them at 160°C overnight. Baking prevents dislocation of gold grains by cultured cells.

2. Cultivation chambers

The locator coverslips may be mounted into different types of chambers suitable for cell cultivation and observation. For correlative microscopy, the chamber design should allow for the fast exchange of media. In our laboratory, we typically mount coverslips onto the hole in the bottom of 35-mm tissue culture dishes (Fig. 2) and perform light microscopic observations in open dishes. Compared to any kind of sealed chambers, this design allows faster processing for EM and decreases the lapse between light and EM observations. To prevent pH shift in the medium during observation, we use Leibovitz's L-15 medium.

Steps

1. Smooth edges of the hole before mounting the coverslip.
2. Apply a thin line of vacuum grease along the edges of the hole inside the dish. Use the minimum amount of grease required to prevent leakage to avoid complications during subsequent excision of the central area of the coverslip with the desired cells (see later).
3. Mount the coverslip with gold-coated side facing upward. Press firmly along the line of grease until grease forms a continuous clear circle around the hole without any air bubbles, which may cause

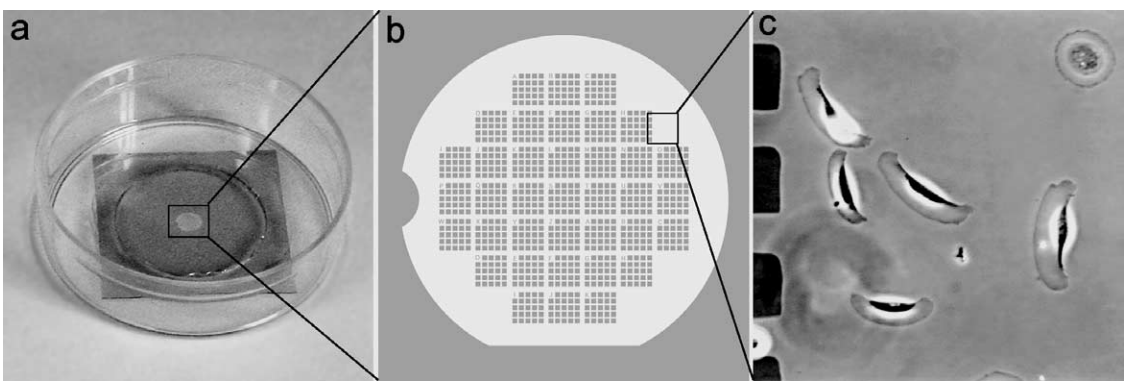

FIGURE 2 Locator coverslip for relocalization of cells. (a) A 22 × 22-mm coverslip was coated with gold through the locator grid and mounted over the 18-mm hole in a 35-mm plastic dish with vacuum grease. (b) Diagram showing gold pattern on the coverslip. (c) Xenopus epidermal keratocytes growing on a coverslip with gold pattern. The imaged area corresponds to the box in b. Dark squares at left are gold islands corresponding to holes in the locator grid, which was used for shadowing.

leakage. Sterilize with UV irradiation before plating cells.

B. Preparation of Cytoskeletons

1. Extraction and Fixation

Solutions

1. *PEM buffer:* 100 m*M* PIPES, pH 6.9; 1 m*M* $MgCl_2$; and 1 m*M* EGTA. To make 100 ml of 2× stock solution, mix ~70 ml of distilled water and 6 g of PIPES. While stirring, add concentrated KOH to this turbid solution until it almost clears. Add 76 mg of EGTA and 200 µl of 1 *M* stock of $MgCl_2$, adjust pH to 6.9 with 1 *N* KOH, and complete with distilled water until 100 ml. Store at 4°C.
2. *Extraction solution:* 1% Triton X-100, 4% PEG in PEM buffer supplemented (optionally) with 2 µM taxol and/or 2 µ*M* phalloidin. To make 10 ml, combine 5 ml of 2× PEM, 1 ml of 10% Triton X-100, 400 mg PEG, and complete to 10 ml with distilled water. Stir for ~10–15 min until dissolved. Store at 4°C and use within 1 week. Add 10 µl of 2 m*M* taxol (paclitaxel) in dimethyl sulfoxide (DMSO) or 10 µl of 2 m*M* phalloidin in DMSO before use.
3. *Sodium cacodylate stock:* 0.2 *M* Na-cacodylate, pH 7.3. Dissolve 4.28 g of Na-cacodylate in distilled water, adjust pH to 7.3 with HCl, and complete until 100 ml. Store at 4°C.
4. *Glutaraldehyde:* 2% glutaraldehyde in 0.1 *M* sodium cacodylate, pH 7.3. To make 10 ml, combine 5 ml of 0.2 *M* Na-cacodylate, 0.8 ml of 25% glutaraldehyde, and 4.2 ml of distilled water. Store at 4°C and use within a week.
5. *Tannic acid:* 0.1% aqueous tannic acid. Weigh 10 mg of tannic acid and dissolve in 10 ml of distilled water. Use within a day.
6. *Uranyl acetate:* 0.1% aqueous uranyl acetate. Weigh 10 mg of uranyl acetate and dissolve in 10 ml of distilled water. Remove undissolved salt by centrifugation. Store at room temperature.

Steps

1. Using a pipette or vacuum aspirator, aspirate culture medium from a dish while it is on the microscope stage. Immediately, but gently, add prewarmed to 37°C PBS with a wide-mouth pipette or pour from a beaker.
2. Aspirate PBS and immediately add extraction solution at room temperature. Exchange of media should be fast to avoid cell damage by drying and to decrease the lapse between living and lysed state of the cell. Incubate for 3–5 min at room temperature.
3. Rinse cells with PEM buffer at room temperature two or three times, 1 min each.
4. Add glutaraldehyde and incubate for at least 20 min at room temperature. If necessary, specimens can be refrigerated at this stage and stored for several days in sealed dishes to prevent drying. Before further processing, specimens should be brought back to the room temperature. If immunogold staining is required, it is best to do it after this step (see later).
5. Remove glutaraldehyde and add tannic acid. No washing is necessary before application of tannic acid, although it is not contraindicated. Incubate for 20 min at room temperature, rinse in three changes of distilled water, and incubate for 5 min in the last change of water.
6. Remove water and add uranyl acetate; incubate for 20 min at room temperature. Replace uranyl acetate with distilled water.

2. Immunostaining

Platinum replica EM is compatible with immunoelectron cytochemistry and with the use of colloidal gold as an electron-dense marker. The difference in electron density between colloidal gold particles and the platinum layer is sufficient for detection of the immune reaction in coated specimens. The specific protocol for immunogold EM depends on the primary antibody and its ability to recognize antigen under particular conditions. Initial evaluation of the quality of staining at the light microscopic level is strongly recommended. For most antibodies we use immunostaining after glutaraldehyde fixation because it provides the best structural preservation. We do not recommend using formaldehyde or methanol fixation, as they are generally inadequate for preserving structure at the EM level.

Solutions

1. *Sodium borohydrate $NaBH_4$:* 2 mg/ml $NaBH_4$ in PBS. Weigh 20 mg of $NaBH_4$ and complete with 10 ml of PBS. Use immediately.
2. *Primary antibody:* The required antibody concentration should be estimated in preliminary light microscopic experiments. For EM, use the antibody concentration that produces a bright immunofluorescence signal.
3. *Buffer A:* 20 m*M* Tris–HCl, pH 8.0, 0.5 *M* NaCl, and 0.05% Tween 20. To make 100 ml of 5× stock solution, dissolve 1.2 g Trizma–HCl and 14.5 g NaCl in distilled water. Adjust pH to 8.0. Add 250 µl of Tween 20 and complete to 100 ml with distilled water. Store at 4°C.

4. *Buffer A with 0.1% BSA:* To make 50 ml, combine 10 ml of 5× stock buffer A, 50 mg BSA, and 40 ml of distilled water. Store at 4°C for 1 month.
5. *Buffer A with 1% BSA:* To make 10 ml, combine 2 ml of 5× stock buffer A, 100 mg BSA, and 8 ml of distilled water. Store at 4°C for 1 month.
6. *Secondary antibody:* Colloidal gold-conjugated secondary antibody diluted 1:5 to 1:10 in buffer A with 1% BSA.

Steps

1. After glutaraldehyde fixation (step 4 of Section III.B.1), wash specimens with PBS (two brief rinses and 5 min in the third change of PBS).

2. Quench specimens by $NaBH_4$ for 10 min at room temperature. Shake off bubbles occasionally. Rinse in PBS (three changes, 5 min in the last change).

3. Remove PBS from the dish. Using cotton swabs, wipe the buffer from the dish and coverslip, leaving wetness on only a small (approximately 5–7 mm) central area containing the locator grid. However, be careful to avoid allowing this area to dry out. Apply primary antibody and incubate for 30–45 min at room temperature. Rinse in PBS (three changes, 5 min in the last change).

4. Rinse once in buffer A with 0.1% BSA. Wipe coverslips as before and apply colloidal gold-conjugated antibody. Incubate overnight at room temperature in a sealed dish in moist conditions. Rinse in buffer A containing 0.1% BSA (three changes, 5 min in the last change) and fix with glutaraldehyde, tannic acid, and uranyl acetate (steps 4–6 in the Section III.B.1) (Fig. 3).

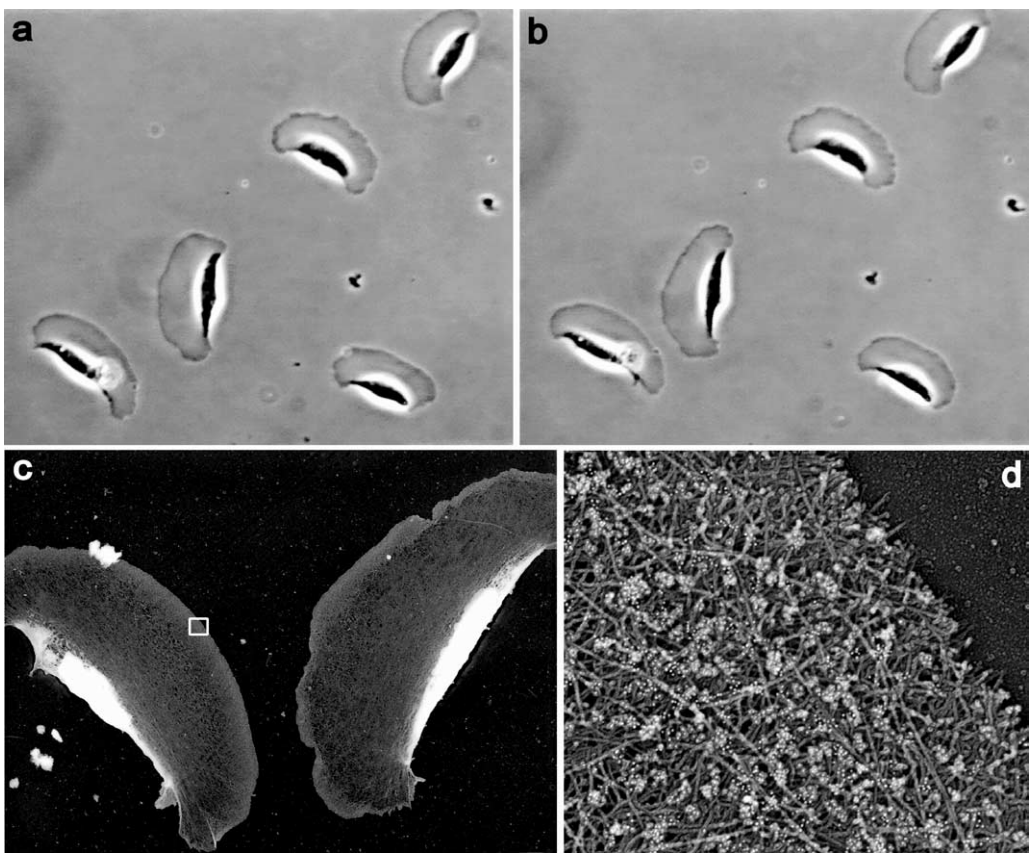

FIGURE 3 Correlative immuno-EM of locomoting Xenopus keratocytes. The phase-contrast time-lapse sequence was acquired with 6-s intervals. The two phase-contrast images shown (**a** and **b**) were taken 1 min apart. After acquisition of the second image, cells were immediately extracted, fixed with glutaraldehyde, quenched with $NaBH_4$, stained with rabbit antibody to Xenopus ADF/cofilin and secondary antibody conjugated with 10 nm colloidal gold, and processed for platinum replica EM. Low-magnification EM (**c**) shows two keratocytes from lower left corner in **b**. Boxed region from **c** is enlarged in **d**. Gold particles appear as white dots because of the reversed contrast of the original image. Distribution of gold particles demonstrates that ADF/cofilin is excluded from the narrow zone at the extreme leading edge (Svitkina and Borisy, 1999).

C. Critical Point Drying

The idea of the technique is to remove liquid from the sample without exposing it to high surface tension. This is accomplished by bringing the sample to or above the critical point, a specific combination of temperature and pressure for the particular liquid where phase boundary does not exist. For most liquids, including water, the critical point is too extreme to be of practical use. In contrast, carbon dioxide has a critical point at 31.3°C and 1072 psi (72.9 atm) and represents the fluid of choice for CPD of biological samples. Because CO_2 has limited solubility in water, ethanol (or acetone) is used as a transitional liquid, which is miscible with either water or CO_2 in any proportion.

Solutions

1. *Graded ethanols:* 10, 20, 40, 60, or 80% ethanol. Combine 10, 20, 40, 60, or 80 ml of 100% ethanol, respectively, with distilled water until a final volume of 100 ml. Allow to stand until all air bubbles are gone and temperature is equilibrated to ambient conditions.
2. *Uranyl acetate in ethanol:* 0.1% uranyl acetate in 100% ethanol. Weigh 25 mg of uranyl acetate, add 25 ml of 100% ethanol, and stir until dissolved. Use within several hours.
3. *Dried ethanol:* 100% ethanol dried over molecular sieves. Wash molecular sieves free of dust with multiple changes of water and bake overnight at 160°C. After cooling, combine 50–100 g of molecular sieves with 500 ml of 100% ethanol. Seal with Parafilm. Store at room temperature for 2 days before use.

Steps

1. If oil objectives are used for light microscopy, remove the immersion oil from the bottom of the coverslip with cotton swabs soaked in ethanol.

2. Detach the coverslip from the bottom of a dish and quickly transfer it into a wide petri dish filled with water. Some silicone grease will remain on the lower side of the coverslip. Lightly press the coverslip down to the petri dish bottom, making sure that the grease does not contaminate the central area of the coverslip containing the cells of interest. Using a diamond pencil, cut off the greased edges of the coverslip to obtain a clean central part of the coverslip with the locator grid. It is helpful to use a razor blade as a guide for making cuts. Use a sharp diamond pencil and avoid glass crumbs around the cutting area to prevent coverslips from shattering. The optimal size of the central piece of the coverslip containing cells of interest is 6–8 mm.

3. Place a specimen holder for CPD into a wide beaker filled with water. Cut lens tissue into pieces fitting the size of the holder. Put a sheet of lens tissue on the bottom of the holder and place the coverslip onto it. Load other coverslips one after another using additional lens tissue sheets as spacers. The lens tissue separates samples and helps retain a layer of liquid over the specimens during transfer. Keep the whole stack loose to allow for easy liquid exchange. Up to 12 coverslips with dimensions 6–8 mm may be processed simultaneously. Overloading the holder makes the exchange of liquid difficult. Loosely put on a lid to prevent the last sheet of lens tissue from flowing away.

4. Put a stirrer bar into a 50-ml beaker. Place a wire scaffold over the stirrer. Add 10% ethanol in amount sufficient to cover the specimen holder when it is placed onto the scaffold. Quickly transfer the holder from water to the beaker (Fig. 1). Stir for 5 min.

5. Prepare another beaker with 20% ethanol in the same way. Transfer the holder and stir for 5 min. Repeat this step for 40, 60, 80, and twice for 100% ethanol. Two sets of beaker/stirrer bar/scaffold are sufficient for dehydration, as they can be alternated in successive steps.

6. Place holder into uranyl acetate in ethanol and incubate for 20 min. No stirring is necessary.

7. Prepare beaker as in step 4 but with 100% ethanol, put in holder, and stir for 5 min. Repeat once more. Then, repeat twice with dried 100% ethanol.

8. Fill the specimen chamber of the CPD device with dried 100% ethanol. The amount of ethanol in CPD chamber should be just enough to cover the holder. Place holder into the chamber. If the CPD device is equipped with a stirrer, put a stirrer bar underneath the holder. Close chamber and open CO_2 cylinder and inlet valve on CPD machine. Cool down the chamber to 10–15°C to keep CO_2 in liquid state. Maintain this temperature until the heating step. Turn stirrer on. Wait until the chamber is filled.

9. Slightly open exhaust valve for 30 s, keeping inlet valve open to allow for exchange of ethanol to liquid CO_2. If the CPD is not equipped with a stirrer, shake CPD manually during this step. Close exhaust valve. Repeat this washing step 10 times every 5 min to remove all traces of ethanol. Keep the level of CO_2 always above the upper edge of the holder.

10. Turn off stirrer and cooler. Turn on heat to raise pressure and temperature above the critical point for CO_2, usually until 40°C and 1200 psi (80 atm). Then slowly release pressure by opening exhaust valve. A fast decrease of pressure may cause condensation of CO_2 back to liquid and ruin the dried samples.

11. Remove holder from the CPD chamber and immediately place it in a sealed desiccated container.

Dried cells can easily absorb moisture from air, which will introduce artifacts similar to those created by air drying. Therefore, it is important to keep samples inside the desiccator until ready for replica preparation.

D. Platinum Replica Preparation

1. Shadowing

Rotary shadowing at an angle creates a gradation of metal thickness depending on the 3D organization of the sample. Platinum is a popular metal for vacuum evaporation because it represents a reasonable compromise between melting temperature and grain size. Platinum grains deposited onto the specimen surface are not cohesive and can be distorted easily during subsequent manipulations or under the electron beam. The platinum layer should be stabilized by carbon, which forms a cohesive film and thus keeps platinum grains in place. The specific procedures for platinum and carbon shadowing depend on the particular device. Therefore, we describe just some important issues.

Mounting of Coverslips

Rotation of the stage will dislodge samples if they are not secured on the stage. Double-sided sticky tape is too strong and does not permit easy and safe detachment of samples, especially after being in vacuum. To make a mild mounting tape, sandwich double-sided tape between sticky parts of two Post-It notes so that the glued side of paper sheets is exposed. Cut off the unglued paper. To mount coverslips, attach a piece of this sandwich to the evaporator stage and attach coverslips. It is sufficient to attach just a corner or an edge of a coverslip to the paper. It is helpful to put marks on the paper to identify samples.

Platinum Shadowing

Source. Our system is set up to use platinum wire wrapped around tungsten wire as a source for shadowing. When voltage is applied, the tungsten wire heats up and the platinum melts and evaporates. Alternatively, platinum-carbon pellets can be used as a source. An advantage of pellets is that they produce finer grains.

Angle. Low angles from the source of platinum to the specimen stage provide high contrast, but reveal only the very top of the sample. High angles result in less contrast but allow for better visualization of the cell interior because of increased penetration of metal into deep hollows. We found a 45° angle to be most useful for whole mount cytoskeleton preparations, as it represents a reasonable compromise between contrast and penetration.

Thickness. Thicker coating reduces resolution but increases contrast and 3D range. In our experiments, a platinum layer thickness of 2.5–2.8 nm produces a fair balance between contrast and resolution. Thickness of the platinum layer can be monitored using a quartz crystal-based thickness monitor. If a thickness monitor is not available, approximate settings of the system may be established by a trial-and-error approach. In our system, 10 mg of platinum wire completely evaporated from a distance of 100 mm produced a layer of the required thickness.

Carbon Coating

Evaporate carbon at 90° with or without rotation to obtain a 2- to 3-nm-thick layer. The thickness of carbon is not very critical, as it is practically transparent to electrons. However, a layer thicker than 10 nm becomes visible and interferes with the formation of image. Too thin a carbon layer may be insufficient for stabilization and result in crumbling of replicas after the removal of coverslips.

2. Mounting of Replicas on Grids

Platinum-carbon replicas of the cytoskeleton are released from the coverslip with hydrofluoric acid. If cell areas that are going to be studied are thin and have low electron density, such as lamella in spread cultured cells (Fig. 4), removal of glass is sufficient. For thick and electron-dense cell regions, organic components can be depleted with a strong oxidative agent, e.g., household bleach. For correlative microscopy, it is easier to select the area of interest while the replica is still attached to the coverslip. After drying and metal coating, cells have good contrast and are visible even under the dissection microscope.

Solutions

1. *Hydrofluoric acid:* ~5% HF in water. Concentrated (49%) HF solution is supplied by the manufacturer in a plastic dispenser bottle. Work with HF in a fume hood, use plastic (not glass) dishes and pipettes, and wear gloves. Store in the fume hood. Prepare working solution in a 12-well dish (diameter 25 mm) before use. Drip several drops (~0.5–1.0 ml) of concentrated HF from the dispenser bottle into a well. Add distilled water almost to the top.
2. *0.01% Triton X-100:* Take 10 ml of distilled water and add 10 µl of 10% Triton X-100. Store at room temperature not longer than 1 month.

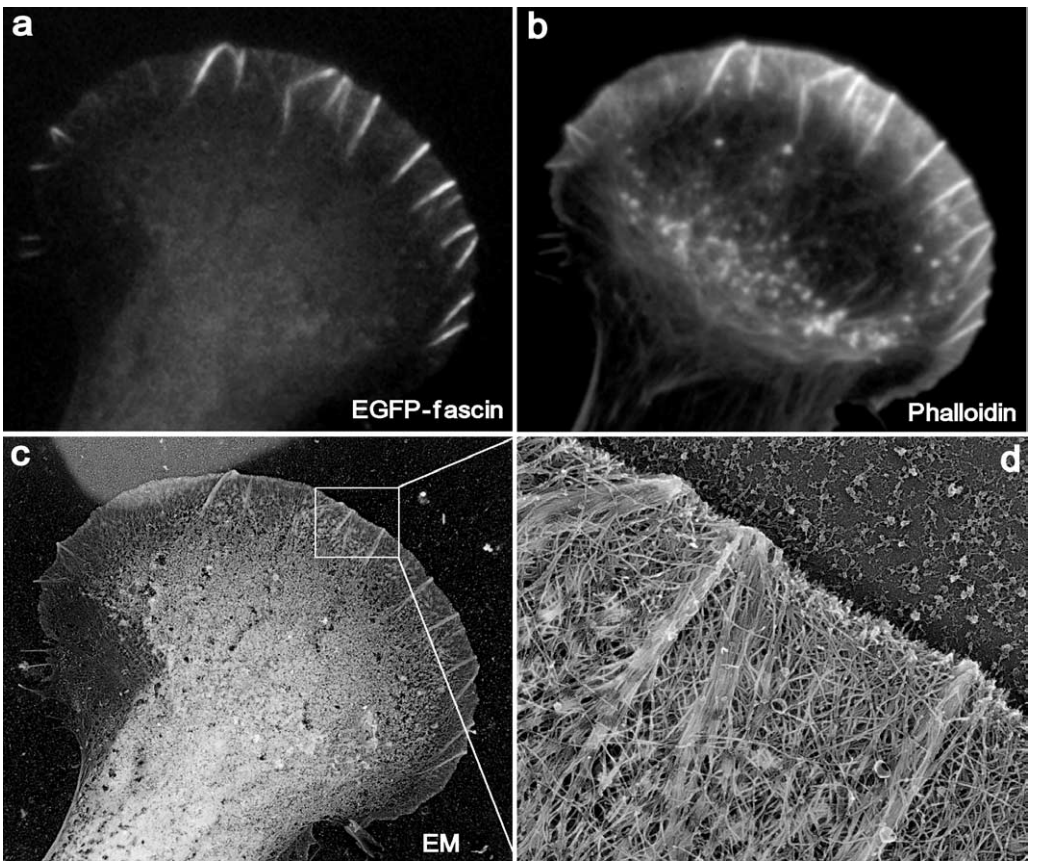

FIGURE 4 Correlative fluorescence and EM of mouse melanoma B16F1 cells. The cell shown was transiently transfected with EGFP-fascin (a) and, after extraction and fixation, stained with Texas red phalloidin (b). After EM processing, the same cell was identified at low magnification (c). Lighter background at the upper left corner is due to gold evaporation through a hole of the locator grid. (d) High-magnification view shows actin filament organization in the leading lamellipodium. Several microspikes within lamellipodium, which are enriched in fascin (see a), have actin filaments organized into tight bundles, whereas lamellipodium between microspikes, which is depleted in fascin, has actin filaments organized into the dendritic network.

3. *Clorox bleach (optional):* Dilute in distilled water 1:2 to 1:10 depending on the strength of bleach.

Steps

1. Using mild double-sided tape (see earlier discussion), immobilize a platinum-carbon-coated coverslip on the bottom of a wide petri dish with cell side up, leaving a region of interest unobstructed.

2. Under the dissection microscope, localize cells of interests using the gold pattern. Make cuts with any sharp tool (razor blade or needle) in the platinum-carbon layer around cells of interest. Continue the cuts up to the edges of the coverslip to facilitate release of the selected area from the rest of the replica.

3. Float a coverslip with cell side up onto the surface of the HF in a well. In minutes the coverslip falls down, leaving the replica floating. After separation of the coverslip, the replica falls apart along the introduced cuts. The pattern of the gold shadowing on the resulting pieces helps identify the desired replica fragments.

4. Fill another well with distilled water (~5 ml). Add ~2 µl of 0.01% Triton X-100. Using a platinum loop, transfer replica pieces onto the surface of water. Traces of detergent in the water prevent the replica from breaking apart, which usually happens because of a large difference in surface tension between HF and water. An overdose of detergent, however, can result in shrinkage and drowning of replicas. Wait 1 min or more.

5. Fill a well with distilled water. Transfer replica pieces onto the surface of pure distilled water. Wait 1 min or more. For electron-dense specimens, go through additional steps:

   a. Fill a well with diluted household bleach and transfer replica pieces onto its surface. Wait 2

to 20 min depending on the cell type and the strength of the bleach.

b. Fill another well with distilled water. Transfer replica pieces onto the surface of pure distilled water. Wait 1 min or more. Repeat the step once more.

Note: Depletion of organic material by bleach is not compatible with immunogold labelling, as it causes the degradation of antibody associated with colloidal gold particles and consequent elimination of gold label from replicas.

6. Mount replica pieces onto Formvar-coated EM grids with lower side of the replica to the Formar film. Use low mesh or single slot grids to reduce the chance of getting the region of interest onto a grid bar. Control under the dissection microscope is helpful for the targeted mounting of replicas on grids.

7. Examine samples in TEM. (Fig. 4) Present images in inverse contrast (as negatives) because it gives a more natural view of the structure, as if illuminated with scattered light.

IV. PITFALLS

1. *Cytoskeletal elements look distorted.* Most likely, extraction was not performed gently enough. Explore different extraction conditions comparing living and extracted cell images.

2. *Cytoskeletal elements look fragmented.* One possible reason is inadequate fixation. Check your reagents for fixation capacity. Another possibility is photodamage or phototoxicity during live cell imaging. Decrease light and/or exposure and close field diaphragm as much as possible to the area of interest during sequence acquisition.

3. *Cytoskeletal elements look flattened and fused with each other.* This is an artifact introduced by surface tension (Ris, 1985). To avoid this problem, always keep a layer of liquid over the specimens when they are transferred from one solution to another. The problem may also occur because of incomplete replacement of water to ethanol or ethanol to liquid CO_2 during dehydration and CPD. Any remaining traces of ethanol or water dry out below their critical points after CPD and ruin the structure. Another possible reason is high ambient humidity. Dried samples are highly hygroscopic. They may absorb moisture from air, which will subsequently dry below the critical point. Loading the evaporator is a step when samples are most susceptible to humidification, as it takes some time to get coverslips from the CPD holder and mount them onto the evaporator stage. Keep humidity in the room as low as possible. In our experience, it is sufficient to keep it under 50%. Also, prepare evaporator for coating in advance, before getting samples from the desiccator.

References

Lindroth, M., Bell, P. B., Jr., *et al*., (1992). Preservation and visualization of molecular structure in detergent-extracted whole mounts of cultured cells. *Microsc. Res. Tech.* **22**, 130–150.

Ris, H. (1985). The cytoplasmic filament system in critical point-dried whole mounts and plastic-embedded sections. *J. Cell Biol.* 100, 1474–1487.

Svitkina, T. M., and Borisy, G. G. (1998). Correlative light and electron microscopy of the cytoskeleton of cultured cells. *Methods Enzymol.* **298**, 570–592.

Svitkina, T. M., and Borisy, G. G. (1999). Arp2/3 complex and actin depolymerizing factor/cofilin in dendritic organization and treadmilling of actin filament array in lamellipodia. *J. Cell Biol.* **145**, 1009–1026.

Svitkina, T. M., Verkhovsky, A. B., *et al*., (1995). Improved procedures for electron microscopic visualization of the cytoskeleton of cultured cells. *J. Struct. Biol.* **115**, 290–303.

Svitkina, T. M., Verkhovsky, A. B., *et al*., (1997). Analysis of the actin-myosin II system in fish epidermal keratocytes: Mechanism of cell body translocation. *J. Cell Biol.* **139**, 397–415.

SECTION

10

Immunoelectron Microscopy

CHAPTER

29

Immunoelectron Microscopy with Lowicryl Resins

Arvid B. Maunsbach

I. INTRODUCTION

Lowicryl resins (Carlemalm *et al.*, 1982) are well suited for electron microscope immunocytochemistry of formaldehyde or formaldehyde/glutaraldehyde-fixed tissues. They provide both good ultrastructural preservation and preserve to a large extent tissue antigenicity. Embedding in acrylic resins is carried out at low temperature either by progressively lowering the temperature during dehydration and resin infiltration or by cryofixation followed by freeze substitution and UV polymerization at low temperature (Carlemalm *et al.*, 1985; Schwarz and Humbel, 1989; Sitte *et al.*, 1989). Thin Lowicryl sections can then be cut on an ultramicrotome at room temperature and labeled with the appropriate primary antibody, which can then be detected with a secondary antibody (or protein A) coupled to colloidal gold particles. A number of labeling principles and protocols have been developed and discussed (Griffiths, 1993; Larsson, 1988; Newman and Hobot, 1993; Roth, 1986; Schwarz and Humbel, 1989). The protocol given here represents a standard procedure we have applied in our laboratory for the localization of several different antigens at the ultrastructural level (Maunsbach and Afzelius, 1998).

Unstained sections of biological tissues show low contrast when examined in a transmission electron microscope. Almost invariably immunogold-labeled sections are therefore contrasted, or stained, by interaction with one or more solutions containing salts of heavy metals, such as uranyl acetate (Watson, 1958) and/or lead citrate (Reynolds, 1963). The staining is unspecific from a chemical point of view, but serves to enhance the contrast of cellular components in the microscope. In immunogold electron microscopy, section staining is important in order to determine the precise relationship between colloidal gold particles and tissue fine structure.

II. FREEZE SUBSTITUTION IN LOWICRYL HM20

A. Materials and Instrumentation

Liquid nitrogen
Lowicryl HM20 kit (Agar Scientific Ltd) containing HM20 resin (monomer E), HM20 cross-linker (D), HM20 initiator (C)
Water-free methanol (CH_3OH, Merck 106007)
Silica gel beads (Sigma S7651)
Sodium chloride (NaCl, Merck 106404)
Sodium dihydrogen phosphate monohydrate ($NaH_2PO_4 \cdot H_2O$, Merck 106346) Disodium hydrogen phosphate dihydrate ($Na_2HPO_4 \cdot 2H_2O$, Merck 106580)
Sucrose ($C_{12}H_{22}O_{11}$, BHD, Analar 102745c)
Uranyl acetate dihydrate [$(CH_3COO)_2UO_2 \cdot 2H_2O$, Polysciences 21477]
Fine forceps with cold-insulated shaft
Polyethylene capsules with pyramid shape and hinged lids for low-temperature embedding (BEEM capsules G360-1, Agar Scientific Ltd., Figs.1a and 1b)

Copyright 2006, Elsevier Science (USA).
All rights reserved.

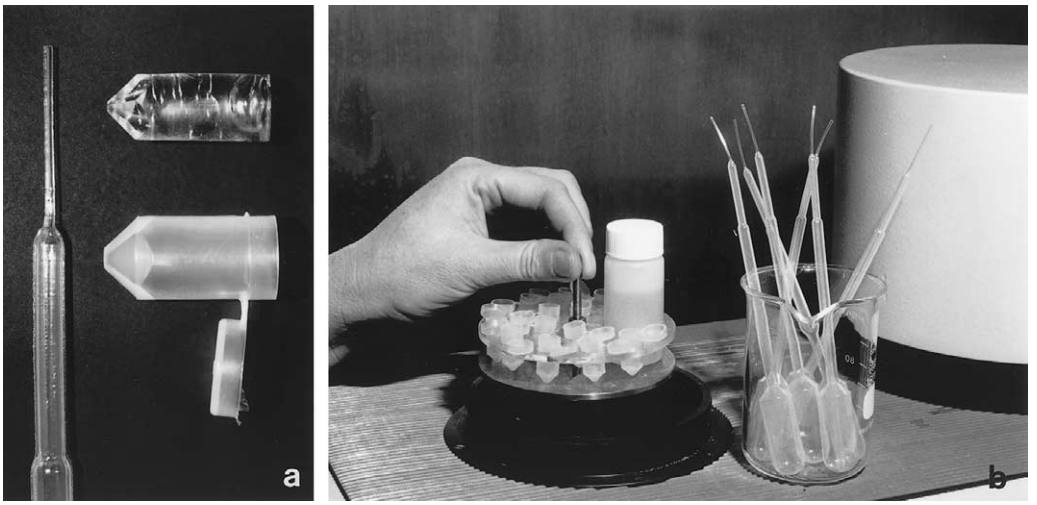

FIGURE 1 Freeze substitution in HM20. (a) Polyethylene Pasteur pipette with elongated tip (left), polyethylene capsule with hinged lid (lower right), and polymerized Lowicryl block after removal of capsule (upper right). (b) Holder with polyethylene capsules and vial for substitution fluid before being lowered into the Balzers FSU 010 freeze-substitution apparatus. To the right beaker with polyethylene Pasteur pipettes and to the far right part of a UV polymerization unit.

Disposable beaker for mixing resin
Polyethylene Pasteur pipettes with extended fine tips (Figs. 1a and 1b)
Freeze-substitution apparatus with temperature regulation between –85 and 0°C

Freeze-substitution unit (Leica EM AFS, Leica AG) or equivalent (e.g., home-made) freeze-substitution apparatus

UV lamp for polymerization with 350-nm UV light (if not built into the freeze-substitution apparatus)

B. Procedure for Freeze Substitution in Lowicryl HM20

Freeze substitution and Lowicryl HM20 embedding combine good preservation of cell ultrastructure and antigenicity (Figs. 2 and 4). For immunoelectron microscopy the tissue is usually fixed for short time with 4 or 8% paraformaldehyde or 4% paraformaldehyde plus 0.1% glutaraldehyde but is never postfixed in osmium tetroxide. The tissue blocks should not exceed 1.0 mm in any direction.

Solutions

Lowicryl HM20: To make about 20 g, gently mix 3.0 g cross-linker D and 17.0 g monomer E. Bubble dry nitrogen gas into the mixture for 5 min to exclude O_2, which inhibits Lowicryl polymerization. Add 0.1 g initiator C and mix gently until it is dissolved. Avoid making air bubbles.

Methanol: Dry the methanol with silica gel.

Methanol: Lowicryl HM20 mixtures in proportions 2 : 1 and 1 : 1

2.3 M sucrose in phosphate-buffered saline (PBS): To make 100 ml solution, weigh out 0.038 g sodium dihydrogen phosphate monohydrate, 0.128 g disodium hydrogen phosphate dihydrate, 0.877 g sodium chloride, and 78.7 g sucrose. Add water to about 95 ml. Use a magnetic stirrer until the sucrose is dissolved, or heat the solution in a microwave oven. Adjust pH if necessary to pH 7.2 and fill up with water to 100 ml.

0.5% uranyl acetate in methanol: To make 100 ml, dissolve 0.5 g uranyl acetate dihydrate in methanol to a total of 100 ml

Steps

1. Transfer the tissue directly from the aldehyde fixative to the buffered sucrose solution. Place the specimens in the sucrose for 2 h or overnight. Stir the solution occasionally to improve infiltration.

2. Cryofix the tissue in liquid nitrogen. Hold the specimen gently with the fine forceps provided with the cold-insulated handle. Remove excess sucrose solution. Move the forceps quickly into the liquid nitrogen and shake until bubbling stops. The specimen is either left temporarily for immediate processing or is placed in a tube for further storage in liquid nitrogen for weeks or months. Carefully follow the safety regulations when handling liquid nitrogen.

3. Transfer the frozen tissue very rapidly with a precooled forceps from the liquid nitrogen to the 0.5%

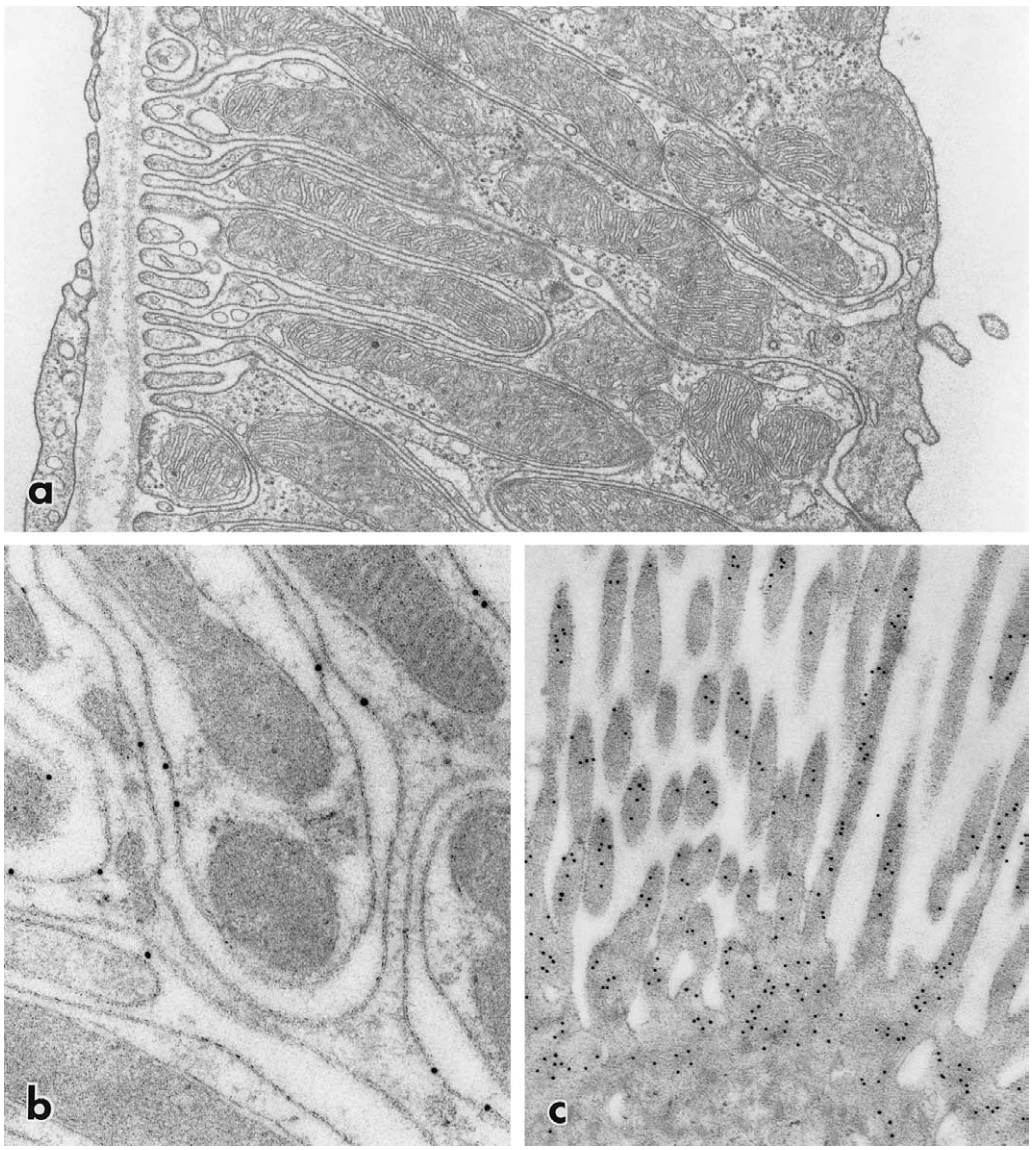

FIGURE 2 Electron micrographs of kidney cells following freeze substitution and embedding in Lowicryl HM20. (a) Thick ascending limb of the renal distal tubule perfusion fixed with 4% paraformaldehyde containing 0.4% picric acid. Cell fine structure is well preserved and cellular membranes stand out in good contrast. Magnification 30,000×. (b) Immunolocalization of Na,K-ATPase to basolateral membranes of distal tubule in rat kidney cortex. Perfusion fixation with 4% paraformaldehyde. The monoclonal antibody against the α subunit of Na,K-ATPase was detected with goat antimouse IgG on 10 nm colloidal gold. Note the precise association between basolateral membranes and gold particles. Magnification 80,000×. From Maunsbach (1992). (c) Apical part of proximal tubule cell in kidney perfusion fixed with 2% paraformaldehyde. Intracellular actin was immunolabeled with rabbit antiactin antibody, which was then detected with goat antirabbit IgG on 10 nm colloidal gold. Magnification 40,000×.

uranyl acetate/methanol solution, which is kept at –85 to 90°C in the capsules in the freeze-substitution unit. During this transfer great care must be taken not to warm the specimen. For this purpose the vessel with the liquid nitrogen must be placed immediately adjacent to the substitution unit.

4. Withdraw most of the substitution fluid from the capsules with a polyethylene Pasteur pipette. The diameter of the tip of the Pasteur pipette should be smaller than the size of the specimens, as the specimens are difficult to observe at this step and may otherwise be removed. Fill the capsules with temperature-equilibrated substitution fluid of the same composition as before and increase the temperature to –80°C for 24 h. Adjust the following rinsing and infiltration periods to suit regular working hours.

5. Rinse the specimens with one change of methanol at –80°C for about 20 h.

6. Rinse the specimens with one change of methanol at –70°C for 8 h.

7. Rinse the specimens three times with methanol at –45°C over a period of 20 h.

8. Infiltrate the specimens with a 2:1 mixture of methanol and Lowicryl HM20 at –45°C for 6 h.

9. Infiltrate the specimens with an 1:1 mixture of methanol and Lowicryl HM20 at –45°C for about 4 h.

10. Infiltrate the specimens with pure Lowicryl HM20 at –45°C for 8 h with three changes.

11. Infiltrate the specimens with pure Lowicryl HM20 at –45°C for 24 h.

12. Fill up the capsules completely with fresh Lowicryl HM20 and close the lids. Polymerize with indirect UV light at –45°C for 48 h.

13. Increase the temperature to 0°C and continue UV polymerization for 48 h. The specimens are now ready for conventional ultramicrotomy at room temperature.

C. Comments

1. Chemicals used during dehydration and embedding resins are toxic (mutagenic, allergenic, and, in some cases, perhaps carcinogenic) and should be handled with adequate safety precautions (Ringo *et al.*, 1982). Work in a well-ventilated hood and use gloves. Note that resins can penetrate most types of gloves within a short time.

2. Cryosectioning and freeze substitution followed by Lowicryl embedding are alternative procedures for immunoelectron microscopy. Immunolabeling of sections from freeze-substituted and Lowicryl embedded tissues usually provides a very high precision in probe localization (Figs. 2b, 2c, and 4). A major advantage is that Lowicryl blocks are stable and can be stored at 4 or –20°C and repeatedly resectioned and immunolabeled.

D. Pitfalls

1. It is necessary that the specimen is frozen ("cryofixed") without ice crystal formation, which will leave holes in the tissue. Tissue blocks should therefore be small and completely infiltrated with 2.3 *M* sucrose before freezing.

2. In order to avoid recrystallization of the tissue water during freeze substitution it is important that the temperature of the specimen does not increase when it is tranferred to the freeze-substitution unit or in connection with fluid changes. Fluids must be properly temperature equilibrated in the freeze-substitution unit before being added to the samples.

3. The size of the specimen for freeze substitution must be small to allow complete removal of water and of methanol. Remaining water or methanol will result in soft Lowicryl or holes in the tissues. Substitution times may require adjustment according to the tissue studied.

4. Capsules should be completely filled with Lowicryl and the lids closed to exclude oxygen during polymerization. Oxygen interferes with polymerization, which results in soft blocks.

III. IMMUNOLABELING OF LOWICRYL SECTIONS

A. Materials and Instrumentation

Disodium hydrogen phosphate dihydrate ($Na_2HPO_4 \cdot 2H_2O$, Merck 106580)
Sodium dihydrogen phosphate monohydrate ($NaH_2PO_4 \cdot H_2O$, Merck Cat. No. 1.06346)
Glycine ($C_2H_5NO_2$, Sigma G-7126)
Bovine serum albumin, BSA (fraction V, Sigma Cat. No. A 4503)
Skimmed milk powder (Merck 115363)
Gelatin (from cold water fish skin, Sigma Cat. No. G7765)
Polyethylenglycol 20,000
Goat antirabbit IgG (or other appropriate antibodies) conjugated to 10-nm (or, e.g., 5 nm) colloidal gold particles
Protein A conjugated to 10-nm colloidal gold particles (alternatively)
Uranyl acetate dihydrate [$(CH_3COO)_2UO_2 \cdot 2H_2O$, Polysciences 21477]
Trisodium citrate dihydrate [$(C_6H_5Na_3O_7 \cdot 2H_2O)$, Merck 106448]
Lead(II) nitrate [Pb $(NO_3)_2$, Merck 107398]
Sodium hydroxide (NaOH, Merck 106498)
Sodium azide (NaN_3, Merck 106688)
Sodium chloride (NaCl, Merck 106404)
Redistilled water
Parafilm (or dental wax)
Nickel grids (necessary for immunolabeling)
Fine forceps, antimagnetic
Disposable Pasteur pipettes
Filter paper, 0.2 µm
Magnetic stirrer

B. Procedures

Ultrathin sections of aldehyde fixed and Lowicryl HM20 or K4M-embedded tissue can be used reproducibly and conveniently for immunocytochemical detection of many antigens. Depending on the sensitivity of the antigen, the tissue is fixed either with

formaldehyde or mixtures of formaldehyde and glutaraldehyde (see article by Maunsbach). The Lowicryl-embedded tissue can be stored, preferably in the cold room, and resectioned repeatedly.

C. Solutions

a. *Rinsing solution*: phosphate-buffered saline (0.01 *M* sodium phosphate buffer containing 0.15 *M* sodium chloride) with 0.1% skimmed milk (or 1% BSA). Mix 0.7 ml 0.2 *M* $NaH_2PO_4 \cdot H_2O$ and 1.8 ml 0.2 *M* $Na_2HPO_4 \cdot 2H_2O$, 0.438 g NaCl. Adjust pH to 7.4 and fill up with redestilled H_2O to make 50 ml. Add 0.05 g milk powder (or 0.5 g BSA).

b. *Preincubation solution*: Rinsing solution with 0.05 *M* glycine. Add 0.375 g glycine per 100 ml rinsing solution.

c. *Solution for dilution of primary antibody*: Same as rinsing solution if skimmed milk is used. If BSA is used, the concentration should be 0.1%.

d. *Solution for dilution of gold-conjugated antibodies (or protein A)*: Same as solution for dilution of primary antibody but with the addition of 1.5 ml of 1% polyethyleneglycol and 0.555 g fish gelatine per 25 ml solution (to reduce aggregation of gold particles). The stability of solutions for preincubation, rinsing, and dilution of antibodies can be improved by adding 0.02 *M* sodium azide (NaN_3).

D. Steps

1. Place nickel grids with ultrathin sections of Lowricryl section side down on small drops (each 10–25 µl of the appropriate solutions). Place the drops on a piece of Parafilm (Fig. 3), and transfer the grids successively between drops. At each transfer most of the previous solution is removed by quickly touching the grid to a filter paper, but without allowing the grid to dry. Transfer the grid between the following drops.

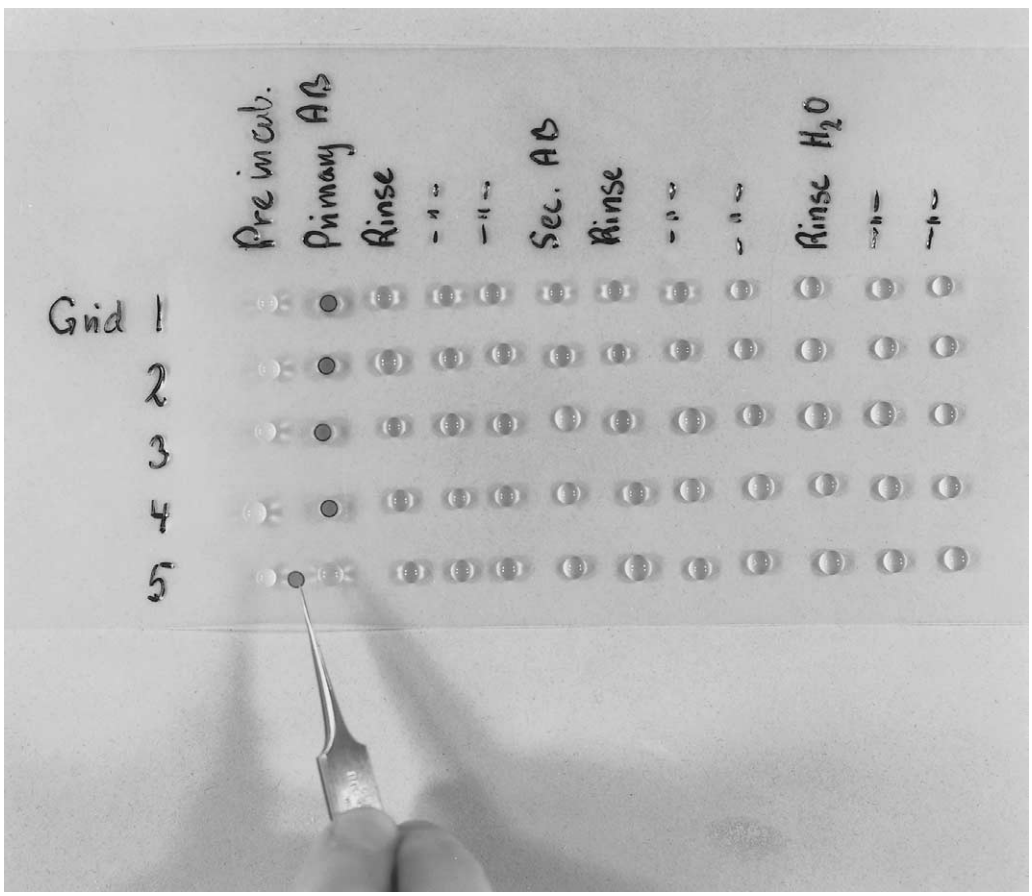

FIGURE 3 Immunolabeling of five grids on series of drops containing preincubation solution, rinsing solution, solution with primary antibodies (AB), rinsing solution, secondary antibody, and distilled water. The grids are transferred between the drops with a forceps. In practice, all drops are not placed at the Parafilm from the very beginning but are applied shortly before use.

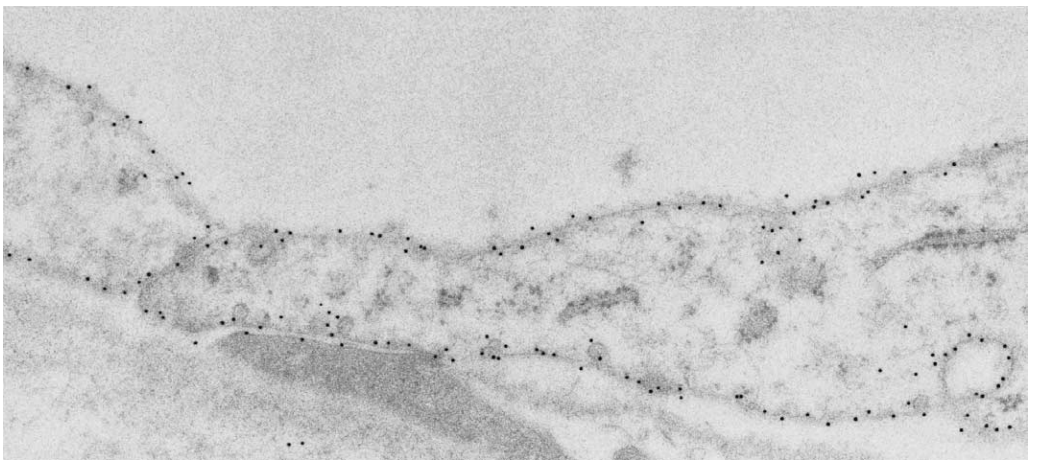

FIGURE 4 Cells in descending thin limb of inner medulla of human kidney labeled with polyclonal antibody against aquaporin-1 water channel. The tissue was fixed in paraformaldehyde and freeze substituted and embedded in Lowicryl HM20. The primary antibody was visualized with goat antirabbit IgG conjugated to 10-nm colloidal gold particles. Cells exhibit strong labeling of both apical and basal plasma membranes. Magnification 60,000×. From Maunsbach *et al.* (1997) with permission.

2. Preincubation solution for 15 min at room temperature.

3. Solution of primary antibody diluted 1:50–1:5000 depending on the characteristics of antigen and antibody. Incubate for 1 h at room temperature or at 4°C overnight in a moist chamber.

4. Rinsing solution three times, 5 min on each drop.

5. Secondary antibody (or protein A) conjugated to colloidal gold. Dilution 1:50–1:200, incubation time 1 h at room temperature.

6. Rinsing solution three times, 5 min on each drop.

7. Rinsing water (redestilled and filtered) 5 min on each of three drops.

8. Remove excess water with filter paper and air dry the grid.

9. Stain for 10 min on saturated and filtered uranyl acetate (see Section IV).

10. Rinse with 15–20 drops of redestilled water.

11. Dry the grid, which is now ready for examination in the electron microscope. Additional contrast can be obtained with lead citrate staining (see Section V).

E. Comments

Electron microscope immunocytochemistry requires careful control of the experimental conditions. As initial steps make sure that the antigen is present in the tissue by immunoblotting and that the antibody specifically and selectively recognizes the appropriate antigen. It is also advisable to apply immunofloures-cence and/or immunoperoxidase for overall localization of the antigen. Initial controls at the electron microscope level should include replacement of the primary antibody with buffer solution, with nonimmune serum, and, if possible, with preimmune serum from the same animal that produced the antibodies. Also, if at all available, the antibody should be absorbed with purified antigen before use (usually preabsorbed overnight in the cold room). Some common pitfalls or problems in electron microscope immunocytochemistry are listed next.

F. Pitfalls

1. Abscence of labeling or weak labeling may be due to destruction of antigen during fixation and/or embedding. Suggested remedies include (a) decrease concentration of fixative, (b) use formaldehyde alone instead of glutaraldehyde or glutaraldehyde/formaldehyde, (c) shorten fixation time, (d) use another type of Lowicryl, e.g., K4M, (e) use smaller gold particles (e.g., 5 nm; see Giberson and Demaree, 1994), (f) utilize different etching procedures (see Matsubara *et al.*, 1996; Maunsbach and Afzelius, 1998), (g) reduce the salt concentration in the solutions used for dilution of antibodies, and (h) turn to the alternative method of cryoultramicrotomy and labeling of cryosections. Make sure by Western blotting that the antigen exists in the tissue.

2. Abscence of labeling or weak labeling may also be due to no or low affinity of the antibody to the antigen, poor titer of the antibody, or the antibody is aged, has been stored improperly, or frozen and thawed repeatedly.

3. High backgound labeling may be due to insufficient rinsing of the grid during labeling or too high titer of the primary antibody or secondary antibody (or protein A).

4. High background staining may, in some cases, be prevented by increasing the sodium chloride concentration or the pH in the incubation solution for the primary antibody and/or the secondary gold conjugate. If the tissue contains high concentrations of free aldehyde groups following glutaraldeyde fixation, the sections should be exposed to 0.5 m*M* ammonium chloride before incubation.

5. Clustered colloidal gold particles may be observed if the primary antibody has aggregated or if the colloidal gold conjugate has aggregated and needs to be renewed.

IV. SECTION STAINING WITH URANYL ACETATE

Uranyl acetate staining (Watson, 1958) results in a uniform but fairly weak general staining of cellular components. There is a slight preference for increased contrast of DNA and RNA.

A. Materials

Uranyl acetate dihydrate [$(CH_3COO)_2UO_2 \cdot 2H_2O$, Polysciences 21477]
Trisodium citrate dihydrate [$(C_6H_5Na_3O_7 \cdot 2H_2O)$, Merck 106448]
Lead(II) nitrate [Pb $(NO_3)_2$, Merck 107398]
Sodium hydroxide (NaOH, Merck 106498)
Redistilled water
Parafilm (or dental wax)

B. Solution

Saturated solution of uranyl acetate: To make 100 ml, dissolve 7.69 g of uranyl acetate in 100 ml distilled water and stir for some hours. Store the solution at room temperature in the dark in a closed glass vial covered by aluminium foil.

C. Steps

1. Filter a suitable volume of stain solution through a 0.2-µm filter immediately before use.
2. Place a series of drops on the Parafilm with a clean Pasteur pipette. The number of drops should equal the number of grids to be stained (Fig. 5a).
3. Place the grids section side down on the drops with an interval of 1 min between each grid.
4. Leave the grids on the stain drops for 10 min.
5. Remove and rinse the grids in the same order they were placed on the staining solution. Lift the grid with a clean forceps and hold vertically. Jet slowly a stream of 15–20 drops of filtered water from a Pasteur pipette onto the grid (Fig. 5b).

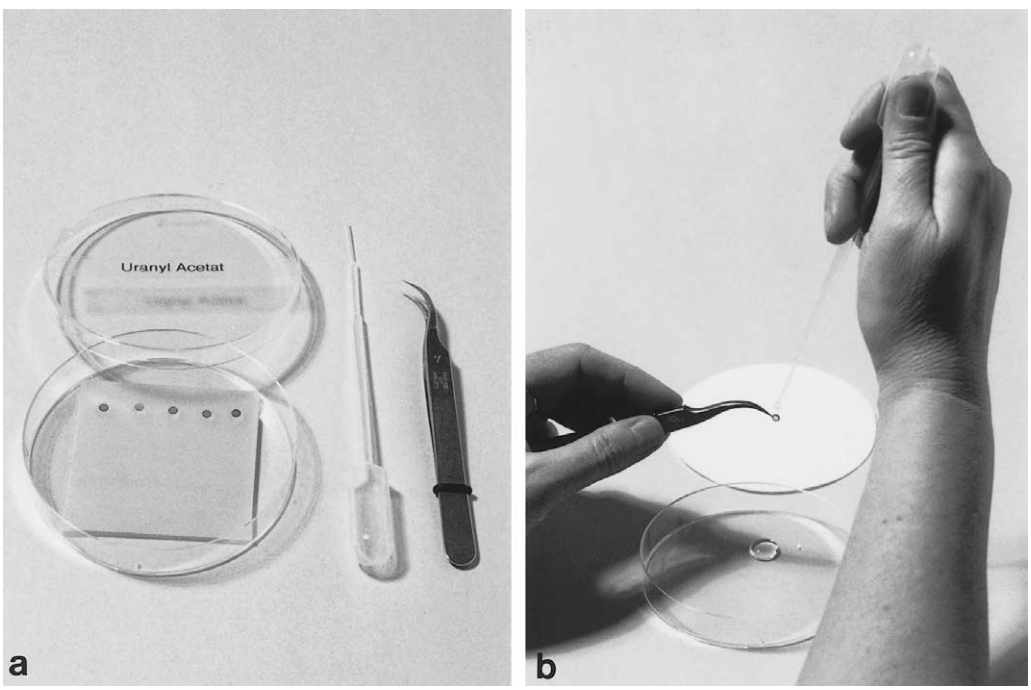

FIGURE 5 (a) Equipment for section staining with uranyl acetate (or lead citrate). With a clean Pasteur pipette, stain drops are placed on dental wax in a petri dish. (b) Rinsing of a stained grid with a stream of drops of redistilled water. Immediately afterward the edge of the grid is touched to filter paper to remove excess water.

6. Remove the last drop of water by touching the edge of the grid with a filter paper. Place a small piece of filter paper between the legs of the forceps to remove additional excess water.

7. Let the grid dry for 5 min while still clamped in the forceps.

V. SECTION STAINING WITH LEAD CITRATE

Lead staining (Reynolds, 1963) is used when a general survey of tissue ultrastructure is aimed at and gives a general increase in contrast of membranes and other tissue components.

A. Materials and Instrumentation

Trisodium citrate dihydrate [$(C_6H_5Na_3O_7{\cdot}2H_2O)$, Merck 106448]

Lead (II) nitrate [Pb $(NO_3)_2$, Merck 107398]

Sodium hydroxide (NaOH, Merck 106498)

Redistilled water

Parafilm (or dental wax)

B. Solution

Lead citrate solution: Boil about 50 ml redistilled water for 5 min in a beaker. Dissolve 1.33 g lead nitrate and 1.76 g sodium citrate in 40 ml of the boiled water. Stir the solution rapidly for 30 min with a magnetic stirrer or shake vigorously. The solution should become clear by adding 8.0 ml 1 *N* sodium hydroxide freshly prepared with redistilled water. Fill up to 50 ml with water. The solution should stand for 2 or 3 days before use. Store the solution at 4°C and use within 6–12 months.

C. Steps

1. Before use, filter 10 ml stain solution through filter paper into a 10-ml cylinder. Close the cylinder with a piece of Parafilm. Handle the cylinder carefully without shaking.

2. Take out the stain solution with a clean Pasteur pipette. Remove the solution from the middle of the cylinder to avoid precipitate.

3. To stain four grids, place four drops of stain on Parafilm. Do not stain more than four grids at a time, as a precipitate forms easily on the surface of the drops. (Surface precipitate can be minimized by placing NaOH tablets around the grids, but in practice we do not find this necessary.)

4. Immediately place the grids on the drops with an interval of half a minute.

5. Stain the sections for 2 min (range: 15 s to 20 min depending on desired contrast).

6. Remove the grids with intervals of half a minute with fine forceps. Hold the forceps with the grid vertically and squeeze gently from a Pasteur pipette 10–15 drops of redistilled water on the grid (Fig. 5b).

7. Touch the grid with filter paper and leave the grid to dry in the forceps with a small piece of filter paper between the legs of the forceps.

D. Pitfalls

1. Dirt may contaminate the sections unless all glassware, Parafilm, and pipettes are *meticulously clean* and all solutions filtered.

2. Excess rinsing of lead stain may gradually remove stain and may, in addition, make the staining more susceptible to beam damage in the electron microscope.

3. The surface of lead citrate drops rapidly acquires surface contamination due to interaction with carbon dioxide in the air. This will appear as contamination on the section. Therefore, drops must be placed on the Parafilm immediately before the grids are applied to surface of the drops.

E. Comments

The chemicals used for section staining are toxic and should be handled with adequate safety precautions. Staining should be performed in a well-ventilated hood, using gloves. The results of section staining depend in part on the preceding fixation of the tissue and on the characteristics of the embedding medium as well as the protocol of the staining process. Thus if uranyl acetete staining is carried out at 60°C instead of room temperature, contrast is greatly enhanced, which may reveal new tissue components but overstain others. Various instruments and procedures have been described for simultaneous staining of many grids, e.g., a full grid box. The author has never found these procedures helpful.

References

Carlemalm, E., Garavito, R. M., and Villiger, W. (1982). Resin development for electron microscopy and an analysis of embedding at low temperature. *J. Microsc* **126**, 123–143.

Carlemalm, E., Villiger, W., Hobot, J. A., Acetarin J.-D., and Kellenberger, E. (1985). Low temperature embedding with Lowicryl resins: Two new formulations and some applications. *J. Microsc.* **140**, 55–63.

Giberson, R. T., and Demaree, R. S., Jr. (1994). The influence of immunogold particle size on labeling density. *Microsc. Res. Tech.* **27**, 355–357.

Griffiths, G. (1993). "Fine Structure Immunocytochemistry." Springer-Verlag, Berlin.

Larsson, L-I. (1988). "Immunocytochemistry: Theory and Practice." CRC Press, Boca Raton, FL.

Matsubara, A., Laake, J. H., Davanger, S., Usami, S., and Ottersen, O. P. (1996). Organization of AMPA receptor subunits at a glutamate synapse: A quantitative immunogold analysis of hair cell synapses in the rat organ of corti. *J. Neurosci.* **16**, 4457–4467.

Maunsbach, A. B. (1992). Trends in tissue preparation for electron microscopy. *In "Electron Microscopy 92"* (A. Ríos, J. M. Arias, L. Megías-Megías, and A. López-Galindo, eds.), Vol. 1, pp. 3–8. University of Granada, Servicio de Publicaciones, Granada.

Maunsbach, A. B., and Afzelius, B. A. (1998). "Biomedical Electron Microscopy: Illustrated Methods and Interpretations." Academic Press, San Diego.

Maunsbach, A. B., Marples, D., Chin, E. Ning, G. Bondy, C., Agre, P., and Nielsen, S. (1997). Aquaporin-1 water channel expression in human kidney. *J. Am. Soc. Nephrol.* **8**, 1–14.

Newman, G. R., and Hobot, J. A. (1993). "Resin Microscopy and On-Section Immunocytochemistry." Springer-Verlag, Berlin.

Reynolds, E. S. (1963). The use of lead citrate at high pH as an electron-opaque stain in electron microscopy. *J. Cell Biol.* **17**, 208–212.

Ringo, D. L., Brennan, E. F., and Cota-Robles, E. H. (1982). Epoxy resins are mutagenic: Implications for electron microscopists. *J. Ultrastruct. Res.* **80**, 280–287.

Roth, J. (1986). Post-embedding cytochemistry with gold-labelled reagents: A review. *J. Microsc. (Oxford)* **143**, 125–137.

Schwarz, H., and Humbel, B. M. (1989). Influence of fixatives and embedding media on immunolabelling of freeze-substituted cells. *Scan. Microsc. Suppl.* **3**, 57–64.

Sitte, H., Neumann, K., and Edelmann, L. (1989). Cryosectioning according to Tokuyasu vs. rapid-freezing, freeze-substitution and resin embedding. *In "Immuno-gold Labeling in Cell Biology"* (A. J. Verkleij and J. L. M. Leunissen, eds.), pp. 63–93. CRC Press, Boca Raton, FL.

Watson, M. L. (1958). Staining of tissue sections for electron microscopy with heavy metals. *J. Biophys. Biochem. Cytol.* **4**, 475–478.

CHAPTER

30

Use of Ultrathin Cryo- and Plastic Sections for Immunocytochemistry

Norbert Roos, Paul Webster, and Gareth Griffiths

I. INTRODUCTION

The identification of cell surface and intracellular molecules for light and electron microscopic observations is an important technique for studying their location and function in the cell. A wide range of methods has therefore been developed to identify and localize molecules at the subcellular level. The term "immunocytochemistry" describes a set of methods that use molecules with specific binding ability to other molecules. The binding molecules, called "affinity markers," are diverse, but have in common the ability to specifically bind, and thus identify, other molecules. One special class of affinity markers that are widely used are antibodies. These are produced naturally by mammals and can be produced to bind to a large range of molecules, called antigens (e.g., a protein in the cell membrane) for indirect visualization. The antibodies are applied to specimens so that they will bind to its target molecules. For examination in an electron microscope, the antibody molecules are subsequently labelled with an electron-opaque marker, usually colloidal gold. However, for light microscopic examination, the use of fluorescent markers is recommended. As a prerequisite, these methods have to ensure the accessibility of the antigen to the antibody, preferably without compromising either the structure or the original localization of the target molecule. For electron microscopic examination, the specimen has to be thin (usually ultrathin sections of 50–100 nm), stained (heavy metal salts), dehydrated, and embedded in a supporting and stabilizing matrix.

Immunocytochemical methods can be divided into two classes: preembedding and postembedding methods. Preembedding methods are those in which the cell, or isolated organelle, is labelled before embedding and sectioning. While the outside layer of the cell/organelle may be accessible to antibodies, the labelling of intracellular structures must be preceded by a solvent or detergent permeabilization step. It is also possible to immunolabel purified small particles (e.g., viruses, coated vesicle) or cell fragments adsorbed onto the support film of a metal specimen grid. Although these are very useful methods for cytoskeletal elements (by definition, detergent/solvent insoluble), these approachs cannot be recommended as a general method for all antigens and are not considered further here (for a review, see Griffiths, 1993).

The term "postembedding" refers to techniques in which the material of interest (may it be tissues, cells, or purified organelles) is usually either frozen rapidly or fixed chemically, embedded in either a resin or a concentrated solution of cryoprotectant, and hardened by either polymerizing the resin or freezing the cryoprotected sample in order to be sectioned. Sections are subsequently labelled using specific antibodies and a visualization marker. There is now a general consensus that the labelling of sections is the best general approach to take for any immunocytochemical study (for more theoretical background, see Griffiths, 1993). The two most important advantages of postembedding over preembedding are (1) when the labelling is carried out on thin sections, the whole surface of the section has equal access to the reagents and (2) there is significantly less need to improve the accesibility of the reagents to the antigen by using a permeabilization protocol, which may destroy fine structural details or even remove or redistribute the antigen under study. This article discusses the practical aspects involved in the labelling of thin sections for electron microscopy.

Copyright 2006, Elsevier Science (USA).
All rights reserved.

Essentially all the reagents mentioned are widely available from all EM supply companies.

II. PROCEDURES

A. Conventional Preparation Procedures

For conventional electron microscopy preparation procedures, the cells or tissues are fixed chemically using aldehydes (e.g., glutaraldehyde and/or formaldehyde). This is usually followed by postfixating with osmium tetroxide, dehydrating in an organic solvent (ethanol or acetone), and subsequent embedding in a hydrophobic, epoxy resin such as Epon or Spurr. The resin is polymerized at elevated temperatures (60° to –70°C), and the cured, hardened blocks are sectioned at room temperature. The ultrathin sections are placed on metal support grids, stained using heavy metal salt solutions (uranyl acetate/lead citrate) and observed in the electron microscope. In general, because of the harsh treatment applied to the specimens, this approach is not useful for immunolabelling. However, there are exceptions to this statement. The most striking example of this involves an extensive and elegant series of studies by Ottersen and colleagues (1992) who performed immunolocalization experiments of amino acid neurotransmitters in brain tissue.

During the 1980s a new class of acrylic or methacrylate-based resins were developed for immunocytochemistry. The two key advantages of these resins over epoxy-based resins are that they are more hydrophilic and, in some cases, can be polymerized at low temperatures. There are two main "families" of these resins, namely Lowicryl resins and London resins (LR). In conjunction with the cryosectioning technique pioneered by Tokuyasu (1973, 1978), these resins have become widely and successfully applied for immunolabelling since the early 1990s. We will now point out the key practical features involved in using these two approaches.

B. Embedding in Acrylic Resins

London resins are perhaps the simplest to use, as in the case of LR white, the resin can be heat polymerized. Both LR white and LR gold are now widely used, and the manufacturers give detailed instructions on their use. A protocol for LR gold is as follows. In this example, infiltration and embedding are carried out at low temperature:

Solutions

1. *0.1 M phosphate-buffered saline (PBS) buffer, pH 7.4:* To make 1 liter, dissolve 2.25 g of $Na_2HPO_4 \cdot 2H_2O$, 0.257 g of $NaHPO4 \cdot H_2O$, and 8.767 g NaCl in 1000 ml distilled water
2. *0.5 M ammonium chloride:* To make 1 liter, dissolve 26.75 g of NH_4Cl in 1 liter PBS

Steps

1. Fix tissue pieces (less than 1 mm^3) with the fixative of your choice, e.g., 0.5% glutaraldehyde in phosphate buffer for 30 min to 2 h [note that for all immunocytochemical techniques the fixation step is critical [see Griffiths (1993) for discussion)].
2. Immerse in 0.5 *M* ammonium chloride in PBS (to quench free aldehyde groups) for 30 min.
3. Immerse in PBS for 15–60 min.
4. Immerse in 50% (vol) methanol at 0°C for 10 min.
5. Immerse in 80% (vol) methanol at –20°C or at 4°C for 60 min.
6. Immerse in 90% (vol) methanol at –20°C or at 4°C for 60 min.
7. Immerse in methanol and LR gold (1:1) at –20°C or at 4°C overnight.
8. Immerse in methanol and LR gold (1:2) at –20°C or at 4°C for 4 h.
9. Immerse in pure LR gold resin at –20°C or at 4°C for 2 h.
10. Immerse in pure LR gold resin + catalyst at –20°C or at 4°C for 2 h.
11. Immerse in pure LR gold resin + catalyst at –20°C or at 4°C overnight.
12. Immerse in pure LR gold resin + catalyst at –20°C or at 4°C and polymerize for 24 h.

LR white is similar but can be polymerized by heat (50°C), by a chemical accelerator at 4–20°C, or by UV light (see manufacturer's instructions). Heat polymerization in a microwave oven, where fully polymerized blocks are available in less than an hour, is also possible with LR white (McDonald, 1999). Polymerization using methods other than UV light enables specimens to be contrasted with osmium tetroxide. For impressive examples of combining LR white with the use of osmium tetroxide, see Tanaki and Yamashina (1994).

C. Progressive Lowering of Temperature (PLT) in Lowicryl Resins

The specimen is fixed chemically with aldehydes (postfixation with osmium tetroxide is omitted, as it can interfere with the polymerization process) and dehydrated with increasing concentrations of alcohol. During dehydration the temperature is lowered pro-

gressively to finally reach –25 to –35°C. Infiltration of the specimens with resin and subsequent polymerization can be performed at low temperatures, as Lowicryl resins have been designed to have an extremely low viscosity at low temperatures and can be polymerized using UV light instead of heat. The blocks can be sectioned at room temperature using standard equipment. The PLT method preserves antigenicity much better than conventional preparation methods and has been used extensively. A PLT regime is summarized here.

Steps

1. Use any of the standard aldehyde fixation procedures.
2. Immerse in 30% (vol) ethanol at 0°C for 30 min.
3. Immerse in 50% (vol) ethanol at –20°C for 60 min.
4. Immerse in 70% (vol) ethanol at –35°C (–50°C)[1] for 60 min.
5. Immerse in 95% (vol) ethanol at –35°C (–50°C to –70°C)[1] for 60 min.
6. Immerse in 100% (vol) ethanol at –35°C (–50 to –70°C)[1] for 60 min.
7. Immerse in 100% (vol) ethanol at –35°C (–50 to –70°C)[1] for 60 min.
8. Immerse in ethanol and resin (1:1) at –35°C (–50 to –70°C)[1] for 60 min.
9. Immerse in ethanol and resin (1:2) at –35°C (–50 to –70°C)[1] for 60 min.
10. Immerse in pure resin at –35°C (–50 to –70°C)[1] for 60 min.
11. Immerse in pure resin at –35°C (–50 to –70°C)[1] overnight.
12. Polymerize for 2 days at low temperature (–50 and –70°C, respectively)[1] with UV light.

The whole procedure can be performed with homemade equipment or, more reproducibly, using commercially available systems from Balzers or Leica microsystems Inc.

D. Cryopreparation Methods (See Fig 1)

1. Rapid Freezing

Chemical fixation of biological specimens is invariably prone to lead to the formation of artifacts. These artifacts can be avoided if biological structures are physically fixed by very rapid freezing. Rapid freezing is a prerequisite for obtaining a frozen specimen that is not destroyed by ice crystals, which would inevitably grow at too low cooling rates. Typically, biological specimens have to be cooled at a rate of 10^5 K/s in order to obtain vitrification, i.e., a state of ice in the cell that is amorphous, i.e., lacks ice crystals. Different freezing techniques have been developed to achieve this goal and the reader is referred to Robards and Sleyter (1985) and to Roos and Morgan (1989) for detailed descriptions of the available methods. However, to summarize, it is possible to freeze biological specimens rapidly with most of the available freezing techniques, provided that they are thin enough (virus suspensions, etc.). The only freezing method that allows bulk specimens to be vitrified is the high-pressure freezing technique (see Studer *et al.*, 1989; Dahl and Staehlin, 1989).

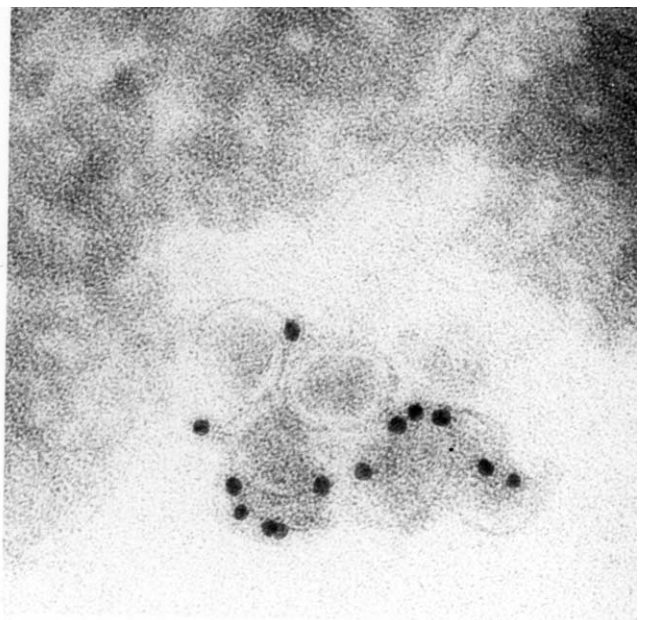

FIGURE 1 Cryoimmuno-EM of BHK-21 cells incubated with equine arteritis virus (EAV), Bucyrus strain. Cells were fixed, sectioned, and labelled for the EAV surface glycoprotein GP_5. Bar: 0.2 mm.

Courtesy of Dr. Ketil W. Pedersen, Department of Molecular Cell Biology, Biology Institute, University of Oslo.

2. Freeze Substitution

Bulk-vitrified specimens can be subjected to a dehydration regime called freeze substitution. In this procedure, the vitrified ice is slowly substituted by an organic solvent, preferably at low temperatures. The cold organic solvent is then subsequently replaced by a suitable resin that is kept at temperatures between –40 and –85°C, followed by polymerization with UV light at the same temperature. The resulting resin blocks can be sectioned and the sections labelled at room temperature. However, high-pressure freezing devices are not standard equipment for the average electron microscopy facility and one may have to

[1] for HM23 and K11M.

resort to a method that allows vitrification of the specimen at lower cooling rates by employing cryoprotectants, such as sucrose. Cryoprotectants used at reasonably high concentrations will prevent the formation of ice crystals in the specimen even at very low cooling, such as those achieved by immersion in liquid nitrogen. However, in order to allow the cryoprotectant to infiltrate the entire specimen, it has to be fixed chemically prior to infiltration. A freeze-substitution schedule for Lowicryl HM20 (van Genderen *et al*., 1991) is as follows.

Solution

2.3 M sucrose solution in PBS: To make 500 ml, dissolve 393.64 g of sucrose in PBS and adjust volume to 500 ml

Steps

1. Fix cell pellets and grow cells on filters or tissue (e.g., with 4% formaldehyde ± 0.1% glutaraldehyde in buffer) for 1 h. A recommended alternative is to add the fixative for 5–10 min to the culture medium at the culture temperature before switching to having the fix in a buffer.
2. Infiltrate the specimen with a cryoprotectant (e.g., 2.3 *M* sucrose) for 30–60 min depending on its size.
3. Cut specimen into small pieces (no more than 1 mm^3).
4. Mount specimen on specimen stubs and freeze in liquid nitrogen.
5. Transfer to methanol at –90°C supplemented with 0.5% uranyl acetate for 36 h.
6. Raise temperature to –45°C (at about 5°C/h).
7. Rinse several times with fresh methanol at –45°C.
8. Infiltrate with Lowicryl HM20 in the following series of Lowicryl/methanol mixtures: 1:1 for 2 h, 2:1 for 2 h, pure Lowicryl for 2 h, and than overnight.
9. Polymerize for 2 days at –45°C with UV light.
10. Section block at room temperature using a glass or preferably a diamond knife in an ultramicrotome.
11. Label with antibodies and gold (see later); all subsequent steps are done by floating the grids on drops as small as 5 µl.
12. Stain with 4% aqueous uranyl acetate for 10 min.
13. Rinse with distilled water.
14. Stain with lead citrate for 1–5 min.
15. Rinse in water, dry, and examine.

3. The Cryosectioning Technique (Tokuyasu Technique)

The thawed frozen section technique offers a number of advantages over most other methods for high-resolution immunolabelling. For more details, see Griffiths (1993).

1. It is potentially the most sensitive technique for immunolabelling, as initial aldehyde fixation is the only denaturation step for the antigen (freezing and thawing of the specimen do not seem to affect the antigenicity)
2. Because the sections are not embedded in resin, they offer the highest access of the antigen to the antibody relative to other techniques. Consequently, this approach is the most sensitive one for those antigens that are retained in the section; this is an important point, as many small soluble antigens may be very difficult to maintain in the sections.
3. The possibilities for staining/contrasting are greater than for any other method.
4. The entire procedure, including photographic documentation, can be performed in one working day.

As mentioned earlier, chemical fixation of the specimen prior to infiltration is a prerequisite. Usually a solution containing 4–8% paraformaldehyde in phosphate, HEPES, or PIPES buffer is used (pH between 6 and 8, determined by the buffer and the specimen to be fixed). The formaldehyde is often supplemented with 0.1–0.5% glutaraldehyde, which is a stronger cross-linker. Cryoprotected, vitrified biological specimens can be sectioned easily at low temperatures, provided the choice of cryoprotectant does not compromise the sectioning properties of the block. The most widely used cryoprotectant is sucrose. Employed at concentrations between 2.1 and 2.3 *M*, the blocks are usually easy to section. High concentrations of sucrose will give softer tissue blocks and will have to be sectioned at lower temperatures. For more difficult specimens (such as plant or insect tissues), an alternative cryoprotectant mixture developed by Tokuyasu consisting of 1.8 *M* sucrose and 20% (w/v) polyvinylpyrrolidone (PVP, MW 10,000) is recommended. Detailed descriptions of the cryosection method are available (Webster, 1999).

Solution

Sucrose/PVP infusion mixture: To make 100 ml, prepare a paste consisting of 20 g of PVP, 4 ml of 1.1 *M* Na_2CO_3 in a buffer such as 0.1 *M* phosphate (Na_2HPO_4) (total volume 20 ml), prepare 80 ml of 2.3 *M* sucrose in the same buffer, mix the paste and the sucrose solution thoroughly, cover the mixture and leave at room temperature overnight so that minute air bubbles can escape, and adjust pH to neutrality using 1 *M* NaOH (use pH indicator paper).

Infusion of small tissue blocks with sucrose solutions usually takes 15–60 min, whereas with

sucrose/PVP, at least 2 h are required. Overnight infiltration may offer more uniform infiltration of the cryoprotectant. Infiltrated specimens are cut to size and mounted on specimen stubs made of aluminium, silver, or copper and frozen by simply plunging them into liquid nitrogen. The stub is inserted into its position in the specimen arm of the cryomicrotome and the block is sectioned at temperatures in the range of −60 to −80°C for semithin sections or −80 to −120°C for ultrathin sections.

Sections are picked up using a wire loop (any pliable metal with a diameter of 1–2 mm) containing a drop of 2.3 *M* sucrose in PBS. Ideally, the sucrose is still fluid at the moment it makes contact with the section(s). The surface tension of the fluid will help stretch the compressed and wrinkly section(s). (*Note*: Stretching will not occur if picking up is done with an already frozen droplet, even if it is subsequently warmed up to room temperature.) Sections picked up in this way have one face exposed to the sucrose and the other face to the air. The latter will stick avidly to the surface of a formvar/carbon-coated EM specimen grid or a glass slide. One significant problem with pure sucrose pick up is that some parts of cells, notably the Golgi complex and endosomes, tend to overstretch during the picking up stage. In order to reduce the magnitude of this problem, Liu *et al*. (1996) developed the technique of picking up sections with a loop containing a 1:1 mixture of methyl cellulose (exactly the same solution used for embedding, see later) and 2.3 *M* sucrose. This is now the method of choice for picking up cryosections. One added advantage of retrieving sections with the sucrose/methyl cellulose mixture is that they can be stored, attached to specimen grids, and covered with dried sucrose/methyl cellulose for up to 6 months (Griffith and Postuma, 2002).

The sections are usually stained after labelling, embedded, and dried. Staining and embedding are achieved by exposing the sections to an inert organic polymer mixed with the stain, usually uranyl acetate. The most used polymer for embedding is methyl cellulose (polyvinyl alcohol and even resins have also been used for this purpose) containing 0.2–0.3% uranyl acetate.

Solution

0.2% methyl cellulose solution: Mix low-viscosity (25centipoise) methyl cellulose powder with cold triple-distilled water to make a 2% solution, leave refrigerated (methyl cellulose is more soluble at low temperatures) for 2–3 days, centrifuge the mixture at 100,000 *g* at 40°C for 1 h, store the solution in the fridge, where it will be stable for up to 6 weeks, and mix nine parts of the solution with one part of a 3% solution of uranyl acetate in water for contrasting/embedding

Use the following a labelling procedure for electron microscopy, in all cases, float the grids on drops (as little as 5 µl) on a strip of parafilm. The upper (non-section) side of the grids must be kept clean and dry, while the lower surface, with sections attached, should always be kept hydrated.

Steps

1. Collect grids by floating them on 1–5% fetal calf serum(FCS)/PBS on ice; wash in PBS once before going further. Note that many other reagents can be used to block nonspecific binding of antibodies such as 1% fish skin gelatin or 2% gelatin.
2. If the cells have been glutaraldehyde fixed, free aldehyde groups can be quenched in 0.02 *M* glycine in 5–10% FCS/PBS for 10 min; rinse twice in PBS for a total of 5 min.
3. Centrifuge antibody solution (1 min at 13,000 *g*), dilute in 1–5% FCS/PBS, and incubate sections for 15–60 min. Use the highest concentration of antibody that does not give background labelling over structures that do not contain the antigen.
4. Wash six times in PBS for a total of 15 min.
5. Incubate grids in protein A–gold for 20–30 min. Dilute protein A–gold in 1–5% FCS/PBS. The concentration is critical. Too high a concentration gives nonspecific binding.
6. Wash six times in PBS for a total of 25 min.
7. Wash four times in distilled water for a total of 5 min.
8. Incubate three times with 2% methyl cellulose solution (25cp) containing 0.1–0.4% uranyl acetate for 10–20 min (on ice!).
9. Pick the grid up with a 3-mm loop and remove excess fluid with filter paper.
10. Air dry the grid suspended in the loop.
11. The thickness of the methyl cellulose film determines the contrast and the extent of drying artefacts.
12. The grids can now be examined.

For double labelling, after step 6, float the grids on 1% glutaraldehyde in PBS for 5 min followed by many rinses in PBS (Slot *et al*., 1991). Repeat steps 2 to 6 using a different size of gold, followed by steps 7 to 12.

III. COLLOIDAL GOLD

Colloidal gold coupled to antibodies or other affinity markers is now the marker of choice for EM immunolabelling, as it is very electron opaque and

easily prepared reproducibly in a range of sizes. The gold particles can be conjugated to antibodies directly or to protein A. We prefer the latter, as we find it more stable and reproducible than IgG gold. However, a disadvantage of protein A is that it binds strongly only to certain species of IgG (rabbit, human, pig, and guinea pig always work; for a more detailed list, see Griffiths, 1993). When using a species of antibody that binds poorly (such as those from rat and mouse), an intermediate antibody step, such as a rabbit antimouse antibody, extends the usefulness of protein A gold. These reagents are now widely available from many commercial sources. For more details on the preparation of colloidal gold markers, see Griffiths (1993).

IV. PITFALLS

One common reason why EM methods are not applied more routinely is the amount of time and effort required to obtain a result. In recent years there have been many experiments using microwave ovens to aid in chemical fixation and embedding protocols. Although the effect of microwaves on biological specimens is still not fully understood, it is clear that routine embedding into epoxy resin or LR white is possible in less than 4 h (Giberson and Demaree, 1999).

1. There is no labelling. The first thing to consider is to try immunolabelling with a light microscopical approach (e.g., cryostat sections). If thick sections of lightly fixed specimens do not work (provided the secondary, visualizing antibodies are good), there is usually no point in continuing to the EM level. One exception to this statement is for small antigens that may be lost during the preparation for light microscopy. For these it is better to use an embedding approach, perhaps after freeze substitution. Provided one has a strong positive, specific signal at the LM level, a negative result at the EM level can be due to a number of reasons. In the case of plastic (e.g., Lowicryl) sections, a common reason is that the antibody has no access to the fixed antigen on the surface of the section. Usually, this is less of a problem with thawed cryosections. In the latter approach, fixation conditions can be reduced drastically (e.g., 5 min in 2% formaldehyde). While this will deleteriously affect the structure, it will help the investigator to decide if the problem is due to the fixation preventing access to the antigen. A second reason for a negative signal at the EM level, already alluded to, is that the antigen may have been washed away during the rinsing steps. This is a problem for small molecules, especially with the Tokuyasu approach. In this case one should crosslink the cells/tissues more severely (1–2% glutaraldehyde). For such antigens the resin approach is preferred. The third reason for lack of labelling is the quantitative aspect: the concentration of the antigens may be too low to detect. Note that the surface of a thin section provides a very small amount of antigen for the antibody when compared to, say, a whole cell at the immunofluorescent level. For more details, see Griffiths (1993).

2. There is too much labelling/"nonspecific" binding. Both the antibody and the gold may not have been diluted sufficiently. It is best to use a standardized gold reagent at its optimal concentration with a characterized primary antibody. If both are unknown, measure the OD_{520} of the diluted gold reagent (e.g., a 1:100 to 1:500 dilution). The commonly used range of final concentration gives an adsorbance of 0.1 at a 520-nm wavelength (generally 1:10 to 1:100 final concentration). The optimal concentration is the highest that does not give background labelling in the absence of a primary antibody. When the gold concentration has been standardized, combine this with a dilution series of the antibody and use the highest concentration that does not give background labelling. The definition of background is, of course, at the discretion of the investigator and assumes some knowledge of the antigen: a membrane protein, for example, would not be expected in the nucleoplasm. Background labelling can often be due to impurities in the antiserum. In this instance, the only solution is to purify the antibody, either by preparing an IgG fraction (e.g., ammonium sulfate precipitation) or by affinity purification. It should be noted that the latter approach often results in a significant, or even total, loss of the highest titre antibody molecules (they remain on the column during the elution procedure).

V. FINAL COMMENT

A positive signal in immuno-EM is only significant when independent proof is provided that the gold labelling one sees is really due to the antigen of interest. Such proof of specificity should be obtained by two different approaches (for more detail, see Griffiths 1993).

1. Immunochemical characterization to show that the antibody recognizes the antigen using an independent method such as immunoblotting or immunoprecipitation.

2. Biological proof of specificity. The best control here is to be able to correlate the labelling pattern with

structures known to contain or not contain the antigen. Any treatment that blocks or removes the antigen should eliminate the labelling.

References

Dahl, R., and Staehelin, L. A. (1989). *J. Electron Microsc. Tech.* **13**, 165–174.

Giberson, R. T., and Demaree, R. S., Jr. (1999). *Methods Mol. Biol.* **117**, 145–158.

Griffith, J. M., and Posthuma, G. (2002). *J. Histochem. Cytochem.* **50**, 57–62.

Griffiths, G. (1993). "Fine Structure Immunocytochemistry." Springer Verlag, Heidelberg.

Liou, W., Geuze, H. J., and Slot, J. W. (1996). *Histochem. Cell Biol.* **106**, 41–58.

McDonald, K. (1999). *Methods Mol. Biol.* **117**, 77–97.

Ottersen, O. P., Zhang, N., and Walberg, F. (1992). *Neuroscience* **46**, 519–534.

Robardo, A. W., and Sleytr, U. B. (1985). *In* "Practical Methods in EM" (A. M. Glauert, ed.), Vol. **10**, pp. 309–324 Elsevier, Amsterdam.

Roos, N., and Morgan, A. J. (1990). "Microscopy Handbooks of Royal Society" Oxford Univ. Press, Oxford.

Slot, J. W., Geuze, H. J., Gegengack, S., Leinhard, G. E., and James, D. E. (1991). *J. Cell Biol.* **113**, 123–136.

Studer, D., Michel, M., and M••ller, M. (1989). *Scan. Microsc.* **3**, 253–269.

Tamaki, H., and Yamashina, S. (1994). *J. Histochem. Cytochem.* **43**, 965–966.

Tokuyasu, K. T. (1973). *J. Cell Biol.* **57**, 551–565.

Tokuyasu, K .T. (1978). *J. Ultrastruct. Res.* **63**, 287–307.

van Genderen, I. L., van Meer, G., Slot, J. W., Geuze, H. J., and Voorhout, W. F. (1991). *J. Cell Biol.* **115**, 1009–1019.

Webster P. (1999). *Methods Mol Biol.* **117**, 49–76.

CHAPTER

31

Direct Immunogold Labeling of Components within Protein Complexes

Julie L. Hodgkinson and Walter Steffen

I. INTRODUCTION

Immunolabeling has long been applied to the study of localization and distribution of antigens within cells and tissues. Perhaps the most exciting recent development, however, is in the use of gold-conjugated antibody labeling in localizing the position of subcomponents in macromolecular complexes. As metal clusters are small and dense and can be specifically targeted to residues within molecular complexes, they can significantly enhance the structure–function information obtained from electron micrographs of macromolecular complexes. Colloidal gold can be prepared in sizes ranging from 1 nm to over 30 nm (e.g., Baschong *et al*., 1985; Slot and Geuze, 1985), allowing a simultaneous detection of several antigens within the same electron microscope preparation.

Gold particles can either be linked covalently to fortuitously placed reactive groups within, or added to, the protein complex under study or be conjugated with primary or secondary antibodies, which in turn bind to exposed epitopes on proteins, so-called indirect immunolabeling. When whole cells or ultrathin sections are labeled using an indirect immunogold labeling method, the distance between the colloidal gold and the epitope is normally below the level of resolution of these techniques. However, in terms of labeled protein complexes in a transmission electron microscope, the large distance between gold and antigen-binding site can be problematic in specifically localizing the epitope in question. The size of an antibody is about 15 nm, therefore the distance of a gold particle (centre of the particle) from the epitope will still be of the order of about 30 nm, even when a small gold particle such as 1 nm of gold is used. To identify a subunit within a complex of about 40 to 50 nm, such as cytoplasmic dynein, it is necessary to bring the gold particle much closer to the epitope. Use of a gold-conjugated primary antibody will bring the gold particle within a range of about 15 nm. Further improvement in resolution can be achieved when the colloidal gold is bound to an Fab fragment, obtained by a papain digest of IgGs (Mage, 1980).

This chapter article details our methods of preparing colloidal gold-conjugated primary antibodies (Fab fragments), which, in combination with a modified technique of negative staining, can be employed to identify subunits within protein complexes.

II. MATERIALS AND INSTRUMENTATION

1,2-Dichloroethane (VWR), bacitracin (Sigma, B0125), borax (Sigma, B3545), bovine serum albumin (BSA, Sigma, A7030), carbon rods (Agar, E416), Centricon-30 microconcentrators (Amicon), centrifuge rotor (Beckman, 80Ti), centrifuge tubes (Nalgene, 3118-0010), chloroform (VWR), column (MoBiTec, 2.5 ml), dimethylchlorosilane (Sigma, D6258), dithiothreitol (DTT, Sigma, D5545), EDTA (Sigma, E9884), filter paper (Whatman, 1001-150, 1004-150), forceps (Agar, T5268), Formvar (Agar, R1201), glass microscope slides (Agar, L4242), glycerol (Sigma, G6279), gold chloride (Sigma, G4022), grid storage boxes (Agar, G276A), grids (Taab Lab's), iodoacetamide (Sigma, I6125), lens tissue (EMS), magnetic stirrer (Agar, G3784), methanol (VWR), mica sheets (Agar, G250-1), Oak Ridge centrifuge tubes (Nalgene, 3118-0010), papain (Sigma, P4742), petri dishes (VWR, 402/0062/06, 02/0066/01), potassium

Copyright 2006, Elsevier Science (USA).
All rights reserved.

carbonate (Sigma, P5833), potassium chloride (Sigma, P9333), protein G (Sigma, P3296), protein G–Sephadex (Sigma, S1235), razor blades (Agar, T5016), Schott bottles (VWR, 215/0150/10), sodium azide (Sigma, S8032), sodium chloride (Sigma, S7653), sodium phosphate (Sigma, S8282, S7907), sodium thiocyanate (Sigma, S7757), microprobe sonicator (Jencons-PLS, Sonics Vibracell), staining jar (Agar, L4108), staining jars (Sigma, S6016), staining trough (VWR, 406/0230/10), ultracentrifuge (Beckman, LE80K), uranyl acetate (Agar, R1260A), and carbon evaporation unit (Edwards 306).

III. PROCEDURES

A. Preparation of Specimen Support for Transmission Electron Microscope

Ideally, very thin but stable support films are required for high-resolution transmission electron microscopy; however, this is problematic as very thin films are extremely fragile. It is for this reason that more robust holey films with an overlay of ultrathin carbon only over the holes are often used. The methodology is as follows.

1. Preparation of Holey Formvar Film

Solutions and Equipment (Materials)

1. 0.5% (w/v) Formvar in chloroform (freshly prepared)
2. 50-ml Schott bottle (wide neck)
3. 50% (w/v) glycerol in dH_2O
4. Forceps, self-closing
5. Glass staining trough spray-painted black of 7 cm depth and 12 cm width (or larger)
6. Grids, 300-mesh copper Maxataform HF35
7. Lens paper, lint free
8. Magnetic stirrer
9. Methanol
10. Microprobe sonicator
11. Microscope slides
12. Petri dishes, glass, 150 mm diameter
13. Razor blades
14. Staining jar (Coplin)
15. Whatman filter papers #1; #4, qualitative circles, 150 mm diameter

Steps

1. Freshly prepare 50 ml Formvar solution in a Schott bottle; stir to dissolve with magnetic stirrer for about 15–20 min.

2. Prepare fresh 50% glycerol solution and add 15–20 drops to dissolved Formvar; shake vigorously for 30 s. Sonicate for 2 min at full power using a microprobe sonicator. Probe should be placed one-third from bottom of solution in a 50-ml Schott bottle. The amount of glycerol and sonication time will vary depending on size and density of holes required. The bottle should feel warm after sonication.

3. Place Formvar–glycerol solution into a staining jar. Clean several microscope slides with lint-free lens tissue. Dip slides one at a time into the Formvar solution, remove rapidly and vertically to ensure an even film, stand on their ends on filter paper, and let dry completely. (*Note:* Prepare all of the slides at one time because the dispersion of glycerol solution is unstable and the droplets slowly coalesce.)

4. Test the film quality. As soon as a slide is dry, float off the film (see later), pick up a couple of grids (see step 6 for details), dry briefly, and check in EM for hole size, number, and distribution. The holes should be just larger than the photographic field at the desired working magnification.

5. Fill glass staining trough to the brim with clean dH_2O. Wipe surface with sheet of lint-free lens tissue.

6. Score edges of a slide with clean single-edged razor blade. Breath lightly onto the slide and then, with that side uppermost, carefully float off the film on to the water surface by slowly sliding the slide into the water at a 45° angle. Place grids on film, rough (dull) surface down using self-closing forceps. Cut a rectangular piece of #4 Whatman filter paper approximately 30% larger than the floated plastic film; slightly bend the ends up to use as handles. Pick grids and film up with filter paper rectangle by gently touching the paper horizontally to floating Formvar film. Place the strip of filter paper on more filter paper to dry. After the grids are dry, place filter paper/grids/Formvar on a bed of #1 filter paper saturated with methanol in a glass petri dish for 10 min. This "etching" procedure removes any glycerol/water droplets and dissolves any very thin plastic lying across the holes.

7. After the grids are dry, check a grid in the scope to ensure the spread and size of holes.

8. Place filter paper with grids in a glass petri dish and store in a refrigerator.

Comments and Pitfalls

Do not overload floating Formvar film with grids, as it will sink! As a rough guide, use no more than 25–30 grids per slide-sized piece of Formvar, neither should one place grids too close to the edge of the plastic. Reflected light from a lamp and/or a dark surface underneath the glass dish will help in observing films clearly. Because plastic films tend to be unsta-

ble in the electron beam, the holey Formvar can be substituted by holey carbon film to obtain more stable grids as follows. This is particularly important for high-resolution work.

2. Coating of Holey Formvar Grids with Thick Carbon for Additional Stability

Solutions and Equipment

1. 1,2-Dichloroethane
2. Carbon evaporation unit (Edwards 306)
3. Carbon rods, spectrographically pure
4. Grid storage box
5. Petri dishes, glass, 150 mm diameter

Steps

1. Place filter paper with grids in a carbon evaporator.
2. Coat grids heavily with carbon at a vacuum in the range 10^{-6} Torr.
3. Place filter paper/grids/Formvar/carbon on a bed of filter paper saturated with 1,2-dichloroethane in a glass petri dish for 2 h. This removes the Formvar, leaving the holey carbon. Remove and dry in a glass petri dish.
4. Store grids in a grid storage box. They are stable for several months.

3. Preparation of Ultrathin Carbon Support Films on Mica Sheets

Solutions and Equipment

1. Carbon evaporator unit
2. Carbon rods, spectrographically pure
3. Mica sheets, 75 × 25 mm
4. Petri dishes, plastic, 100 mm diameter

Steps

1. Freshly cleave mica sheets. Keep cleaved side clean; do not touch with fingers at any time!

2. In a carbon evaporator, expose mica sheets with new surface towards the carbon source. Coat mica sheets at a vacuum of 1×10^{-6} Torr or better with thin (about 10 nm) carbon film (*Note:* Gradual deposition over several evaporations produces stronger and better quality carbon film.) Avoid sparking during carbon deposition to ensure a smooth deposition.

3. Remove coated mica sheets from carbon evaporator, place in a plastic petri dish, and store in a refrigerator (careful, very delicate).

Comments and Pitfalls

From some mica brands, carbon may not float off easily. Cleave mica just before coating and do not expose to air for longer than absolutely necessary. Position a screw on the corner of the filter paper so that a shadow will fall on the paper when the carbon is evaporated. The area where the paper is shielded from the carbon source will appear light compared to the rest helping to judge thickness.

B. Digest of IgG with Papain (Fab)

The protocols to obtain Fab fragments vary depending on the type and isotype of antibody used. We have used the protocol described here successfully to generate Fab fragments from rabbit IgG and mouse IgG1.

Solutions and Equipment

1. 1 m*M* DTT
2. 100 m*M* EDTA
3. 1 *M* iodoacetamide (freshly prepared)
4. 5 mg/ml papain (can be stored as aliquots at –80°C)
5. Phosphate-buffered saline (PBS): 150 m*M* NaCl, 2.7 m*M* KCl, 50 m*M* phosphate, pH 7.5
6. Protein G–Sephadex column

Steps

1. Adjust antibody concentration to 1–2 mg/ml with PBS and add up to 2 m*M* EDTA and up to 1 m*M* DTT (depending on IgG type, use β-mercaptoethanol, DTT, or glycine as reducing agent).
2. Prepare a 5-mg/ml papain stock solution. Please note that some commercial papain does not dissolve readily and will therefore yield a much lower level of digestion.
3. Add papain to antibody solution; IgG : papain = 100 mg : 1 mg.
4. Incubate at 37°C for 30–60 min.
5. Stop reaction by adding up to 30 m*M* iodoacetamide and incubate in the dark on ice for 60 min.
6. Dialyze against PBS at 4°C.
7. Check efficiency of digest by SDS–PAGE (12% gel under reducing conditions).
8. Test antibody by immunochemistry.
9. Remove Fc from Fab via protein G or protein A column (use protocol according to manufacturer).

Comments and Pitfalls

In our view the most reliable method to generate Fab fragments is by using a papain digest; however, care should be taken when choosing the reduction medium and the source of papain as there can be a considerable variation in potency of the reaction. Other enzymes, which can be used to cleave antibodies, include ficin and pepsin (e.g., Mage, 1980; Marianai *et al.*, 1991). Please also note that protein A may not be used with all IgG isotypes and that some mouse IgG might bind to protein G via the Fab portion rather than the Fc.

C. Preparation of Colloidal Gold

Colloidal gold can be prepared easily in different sizes (e.g., Baschong and Wrigley, 1990; Slot and Geuze, 1985). We describe here our adaptation of the method by Baschong *et al*. (1985) to prepare 2–3 nm colloidal gold.

Solutions for Gold Preparation

1. 0.2 *M* K_2CO_3, 0.22 µm filtered
2. 1% (w/v) $HAuCl_4$ in dH_2O
3. 1.0 *M* NaSCN, 0.22 µm filtered
4. 200-ml siliconized Erlenmeyer flask

Steps [Modified According to Baschong et al. (1985)]

1. Siliconize an Erlenmeyer flask by rinsing it with a 5% solution of dimethylchlorosilane in chloroform in fume hood, rinse with water after evaporation of solvent in a fume hood, and bake at 180°C for 2 h.
2. Add 0.5 ml of 1% $HAuCl_4$ to 100 ml dH_2O in a siliconized Erlenmeyer flask followed by 0.75 ml of 0.2 *M* K_2CO_3 to gold solution while stirring.
3. Finally add 0.3 ml of 1 *M* NaSCN while stirring (note that the solution will become yellowish).
4. Leave solution in a dark place overnight and use the following day for binding to antibodies.

D. Binding of Gold to Antibody

In order to bind a single gold particle per IgG or Fab fragment it may be necessary to experiment in varying the protein colloidal gold ratio and/or adding varying amounts of an unspecific protein, e.g., BSA (Baschong and Wrigley, 1990) or bacitracin (Steffen *et al*., 1997). Newly developed gold probes from Nanoprobes (Stony Brook, NY), e.g., the 1.4 nm colloidal gold within an organic shell, allow the coupling of the gold probe covalently to an antibody.

Solutions for Gold Labeling of the Antibody

1. 10 mg/ml bacitracin
2. 10 mg/ml BSA
3. 10% (w/v) NaCl
4. 10% (w/v) NaN3 (kept in a dark bottle)
5. 10% (w/v) sucrose in PBS
6. 10X TBS: 100 m*M* Tris–HCl, 1.5 *M* NaCl, pH 7.4
7. 10-ml Oak Ridge centrifuge tubes
8. 2 m*M* borax
9. 5% dimethylchlorosilane in chloroform
10. Centricon-30 microconcentrator
11. Fume hood
10. PBS: 150 m*M* NaCl, 2.7 m*M* KCl, 10 m*M* phosphate, pH 7.5
11. Spectrophotometer
12. Ultracentrifuge, 80Ti rotor

Steps

1. Dialyse antibody into 2 m*M* borax or use Centricon microconcentrator for buffer exchange.
2. Adjust colloidal gold solution to pH 8.0.
3. Determine the minimum amount of antibody needed to stabilize the gold.
   a. Prepare a serial dilution of antibody from 100 to 5 µg IgG per 100 µl dH_2O.
   b. Add 0.5 ml colloidal gold solution and incubate for 2 min.
   c. Add 0.5 ml of 10% NaCl and incubate for 30 min.
   d. Measure the turbidity (formation of aggregates) using a spectrophotometer at $OD_{550\,nm}$. (An increase in turbidity will mark the minimal concentration to stabilize gold particles.)
4. Add antibody at determined minimal concentration (usually about 20 µg/ml) to colloidal gold solution while stirring and incubate on ice for 15 min.
5. Add 100 µg/ml bacitracin or BSA to cover the free surface of gold particles and incubate on ice for 60 min.
6. Add 1/10th of volume of 10X TBS and centrifuge through a 1-ml 10% sucrose cushion in a Beckman 80Ti rotor at 47,000 rpm (150,000 g_{ave}) for 30 min.
7. Aspirate supernatant and resuspend soft pellet in about 200 µl TBS containing 0.02% NaN_3 and store in a refrigerator.

Comments and Pitfalls

The 2- to 3-nm colloidal gold requires some time to develop. However, if the colloidal gold is stored for an extended period of time, it tends to form aggregates. We normally stabilise to colloidal gold with a protein solution, i.e., antibody, 12 to 24 h after initiation of the reduction of the gold solution.

E. Negative Staining of Immunogold-Labeled Protein Complexes

A hydrophilic carbon support film is critical in achieving uniform high-quality negative staining, but carbon films tend to become more hydrophobic over time when exposed to air. The carbon film can be exposed to ionised gas (glow discharge) to revitalize its hydrophilic property. In our method (see also Marchese *et al*., 1995), negative staining is carried out on a carbon surface that has never been exposed to air, thus maintaining the hydrophilic nature of the carbon. This is achieved by floating the carbon film first onto the protein solution and then onto uranyl acetate. An

example of an immunogold-labelled protein complex is illustrated in Fig. 1.

Solutions and Equipment

1. 1% (w/v) uranyl acetate in dH_2O (kept in the dark)
2. 1.5-ml Eppendorf reaction vials, painted black
3. Carbon-coated mica (see earlier discussion)
4. Forceps (several pairs of self-closing, fine-tipped forceps)
5. Grids with holey carbon film or holey Formvar film (see earlier discussion)
6. Single-edged razor blades
7. Small, adjustable angled lamp
8. Whatman filter paper #1

Steps

1. Paint the outside of a 1.5-ml Eppendorf reaction vial black.
2. Mix gold-conjugated primary antibody with isolated purified protein complex and incubate at room temperature for 10 min.
3. Dilute protein complex–antibody mixture to about 10 to 20 µg/ml and place about 250 µl of the mixture into the cap of a 1.5-ml Eppendorf reaction vial (Fig. 2, step 1).
4. Fill the reaction vial with freshly filtered (0.22-µm syringe filter) 1% uranyl acetate. Note that the meniscus of the staining solution should be slightly above the rim of the reaction vial (Fig. 2, step 1).
5. Reflect light from a lamp off the surface of the liquid at an angle of about ~45°.
6. Cut a thin carbon-coated mica sheet into about 3 × 5-mm pieces and score the carbon film with a clean single-edged razor blade about 2 mm from one side of the small mica sheet.
7. Using a pair of self-closing, fine-tipped forceps, partially float off the thin carbon film from the supporting mica sheet onto the surface of the protein solution (Fig. 2, step 2).
8. Withdraw the carbon film after 2–3 s and float the carbon film completely free of the mica onto the surface of the staining solution (Fig. 2, step 3).
9. Pick up the carbon film immediately with a 300-mesh grid coated with a holey Formvar or holey carbon film. [*Note:* Use a small adjustable angle light source to help visualise the thin carbon by reflection (Fig. 2, step 4)].
10. Remove excess uranyl solution by touching edge of grid with the edge of a torn filter paper (Fig. 2, step 5).
11. Let dry in a humid chamber (Fig. 2, step 6).

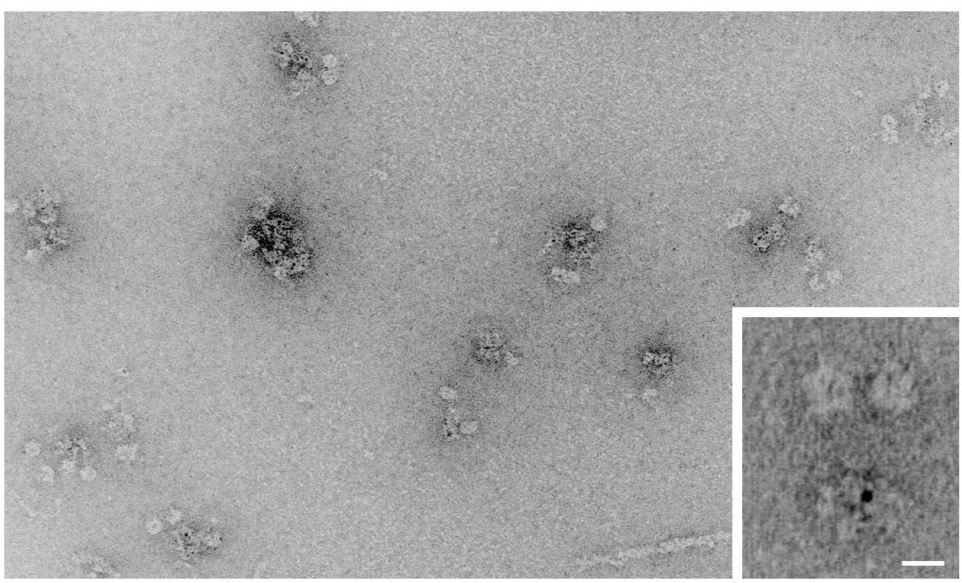

FIGURE 1 Immunogold labeling of cytoplasmic dynein. The image shows the formation of clusters caused by the antibody–gold complex. In this case the gold was stabilised primarily by the presence of antibodies. Cytoplasmic dynein with a single gold particle could be observed (insert), if gold probes were used, where the antibody was supplemented with a nonspecific protein during the antibody–gold complex formation. Magnification bar in insert 10 µm.

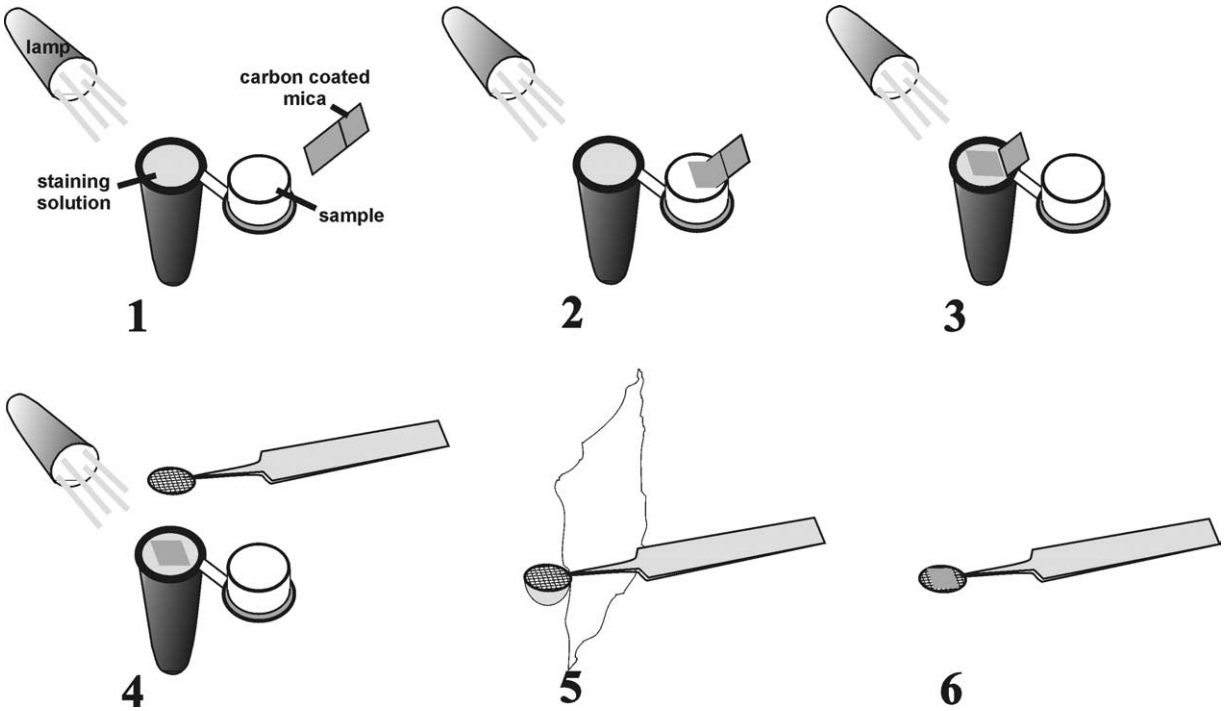

FIGURE 2 Diagram illustrating the procedure for negative staining of protein complexes. See text for details of the procedure.

IV. Outlook

Understanding the structural organization of a large protein complex is of increasing importance in our aim to understand their functional properties. Three-dimensional image reconstruction by single particle analysis has proven to be a useful tool to achieve this goal. A potential development in the use of immunogold-conjugated antibodies is in the high-resolution three-dimensional image reconstruction of macromolecular complexes, allowing for the specific localisation of functional epitopes within molecular complexes. Technological developments in the production and specificity of heavy metal clusters (Nanoprobes Inc.), and advances in transmission electron microscopy and image analysis have enabled for the orientation of actin subunits within actin filaments to be investigated (Steinmetz *et al*., 1998). Thus far such studies have only been carried out with gold particles directly (covalently) linked to the molecule of interest via incorporated His tags (Hainfeld *et al*., 1999) or fortuitously exposed, or added, cysteines (Zlotnick *et al*., 1997). In the case of antibodies, disulphide bonds can be employed to attach a gold particle at a specific site, thereby making single epitope labelling more reliable.

References

Baschong, W., Lucocq, J. J., and Roth, J. (1985). "Thiocyanate gold" small (2–3 nm) colloidal gold for affinity cytochemical labelling in electron microscopy. *Histochemistry* **83**, 409–411.

Baschong, W., and Wrigley, N. G. (1990). Small colloidal gold conjugated to Fab fragments or to immunoglobulin G as high-resolution labels for electron microscopy. *J. Electron Microsc. Technol.* **14**, 313–323.

Hainfeld, J. F., Liu W., Halsey, M. R., Freimuth, P., and Powell, R. D. (1999). Ni-NTA-gold clusters target his-tagged proteins. *J. Struct. Biol.* **127**, 185–198.

Mage, M. G. (1980). Preparation of Fab fragments from IgGs of different animal species. *Methods Enzymol.* **70**, 142–150.

Marchese-Ragona, S. P., Gagnon, C., White, D., Isles, M. B., and Johnson, K. A. (1995). High-resolution negative staining of the isolated dynein ATPase. *Methods Cell Biol.* **47**, 177–182.

Marinai, M., Camagna, M., Tarditi, L., and Seccamani, E. (1991). A new enzymatic method to obtain high-yield (Fab)2 suitable for clinical use from mouse IgG1. *Mol. Immunol.* **28**, 69–77.

Steffen, W., Hodgkinson, J. L., and Wiche, G. (1996). Immunogold-localisation of the intermediate chain within the protein complex of cytoplasmic dynein. *J. Struct. Biol.* **117**, 227–235.

Steinmetz, M. O., Stoffler, D., Muller, S. A., Jahn, W., Wolpensinger, B., Goldie, K. N., Engel, A., Faulstich, H., and Aebi, U. (1998). Evaluating atomic models of F-actin with an undecagold-tagged phalloidin derivative. *J. Mol. Biol.* **276**, 1–6.

Slot, J. W., and Geuze, H., J. (1985). A new method of preparing gold probes for multilabelling cytochemistry. *Eur. J. Cell Biol.* **38**, 87–93.

Zlotnick, A., Cheng, N., Stahl, S. J., Conway, J. F. Steven, A. C., and Wingfield, P. T. (1997). Localisation of the C-terminus of the assembly domain of hepatitis B virus capsid protein: Implications for morphogenesis and organisation of encapsidated RNA. *Proc. Natl. Acad. Sci. USA* **94**, 9556–9561.

PART

C

SCANNING PROBE AND SCANNING ELECTRON MICROSCOPY

SECTION

11

Scanning Probe and Scanning Electron Microscopy

CHAPTER

32

Atomic Force Microscopy in Biology

Dimitrios Fotiadis, Patrick L. T. M. Frederix, and Andreas Engel

I. INTRODUCTION

In the last decade the atomic force microscope (AFM) (Binnig *et al.*, 1986) has become a powerful tool in structural biology. The unique possibility of acquiring the topography of biological samples at high resolution under physiological conditions, i.e., in buffer solution, at room temperature, and under normal pressure, makes this instrument outstanding. The high signal-to-noise ratio of AFM topographs has not only allowed the observation of whole cells, chromosomes, nucleic acids, and proteins, but also the tracking of conformational changes of biomolecules during the exertion of their function (Engel *et al.*, 1999; Engel and Müller, 2000). Furthermore, time-lapse AFM imaging has enabled the monitoring of dynamic changes in the conformation, association, and functional state of individual proteins (Stolz *et al.*, 2000).

The principle of the AFM is relatively simple: A sharp tip mounted at the end of a flexible cantilever is raster scanned over a sample surface in a series of horizontal sweeps. The bending of the cantilever caused by the probe–sample interaction is detected by the deflection of a laser beam that is focused onto the end of the cantilever and reflected into an optical detector. This signal, termed deflection signal, is coupled to a servo system that moves the sample vertically to maintain the cantilever deflection at a constant value. The surface topography is then reconstructed from the vertical movement of the scanner. In this imaging mode, called contact mode, the probing tip always touches the surface with a constant force during scanning. An alternative and widely used imaging mode in biology is the tapping mode. Here, the AFM tip is oscillated rapidly in the vertical direction while scanning the sample. Oscillation of the tip reduces frictional forces, thereby minimizing artifactual deformation and displacement of the sample. Therefore, the tapping mode is used frequently to image the surface topography of weakly immobilized biomolecules, e.g., single proteins and fibrils. However, for imaging of biological membranes, the highest resolution so far obtained has been in contact mode.

This article focuses on the application of contact mode AFM to acquire subnanometer resolution structural information of membrane proteins from membrane specimens in liquid. Most of these proteins are fragile structures comparable to a submerged sponge. To prevent their damage by the scanning tip, soft cantilevers with spring constants of 0.01–0.1 N/m must be used, and scanning must be performed with minimal applied force to the tip (≤100 pN). An additional crucial factor for successful high-resolution imaging is the correct adjustment of the imaging buffer (Müller *et al.*, 1999). By optimizing these factors that minimize the force experienced by the sample, lateral resolutions down to 0.41 nm and vertical resolutions down to 0.10 nm have been achieved on biological membranes in solution (Stahlberg *et al.*, 2001). However, application of higher forces can be of advantage to perform precise and controlled "dissections" of biological samples by manipulation with the AFM tip (Fotiadis *et al.*, 2002).

In this article, contact mode AFM is illustrated using membranes that contain the heptahelical protein bacteriorhodopsin (BR). This 26-kDa integral protein acts as a light-driven proton pump in Haloarchaea (Oesterhelt and Stoeckenius, 1973). Photoisomerization of the chromophore from all-*trans* to 13-*cis* retinal initiates the unidirectional translocation of one proton across the cell membrane (reviewed by Oesterhelt *et al.*, 1992; Lanyi, 1997). This establishes an electrochemical

Copyright 2006, Elsevier Science (USA).
All rights reserved.

proton gradient across the membrane that can then be used for ATP synthesis and other energy-requiring processes in the cell. BR forms trimers and highly ordered two-dimensional (2D) trigonal crystal lattices (parameters: $a = b = 6.2\,\text{nm}$, $\gamma = 60°$) in the native membrane of the bacterium *Halobacterium salinarum*, these crystalline patches are termed purple membrane because of their color (Blaurock and Stoeckenius, 1971). The flatness of these crystalline membrane patches makes them very suitable for AFM. High-resolution three-dimensional structures of BR (Fig. 1) have been determined by electron and X-ray diffraction (for a review, see Cartailler and Luecke, 2003). In BR, the prosthetic group retinal (see Fig. 1; arrowhead) is bound covalently by a protonated Schiff base to K216 of helix G of the protein (the seven transmembrane α helices are generally denoted A to G). With the AFM it is the protruding domains, i.e., the termini and connecting loops between the helices, that are visualized, not the helices themselves that are embedded in the lipid bilayer. On the cytoplasmic side, the major protrusions of BR are the loop connecting the transmembrane α helices A and B and that connecting E and F (AB and EF loops; Fig. 1), of which the EF loop appears to be highly flexible (Müller *et al.*, 1995a). On the extracellular side the protruding B–C interhelical loop (BC loop; Fig. 1) forms a β hairpin and is fairly rigid.

The procedures described for BR in this article constitute a basis for sample preparation and application of AFM on other biological membranes.

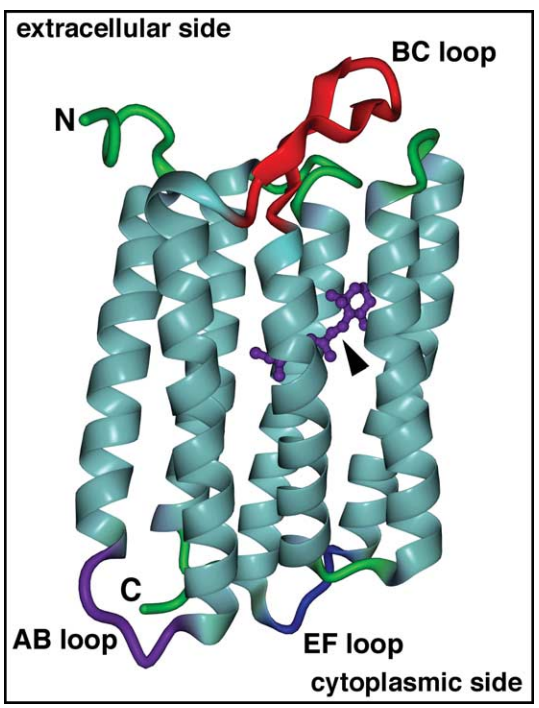

FIGURE 1 Bacteriorhodopsin with its retinal chromophore (arrowhead). The extracellular (top) and the cytoplasmic side (bottom) of BR with their prominent loops and termini are indicated. This illustration of BR was calculated using the coordinates of Kimura *et al.* (1997) and the visualization program DINO (http://www.dino3d.org/).

II. MATERIALS AND INSTRUMENTATION

A. Materials: Preparation of Mica Supports

Polished ferromagnetic stainless steel disks of 11 mm diameter (manufactured by the internal workshop services of the Biozentrum, Basel, Switzerland)
Teflon sheets of 0.25 mm thickness (Maag Technic AG, Birsfelden, Switzerland)
Mica sheets with a thickness between 0.3 and 0.6 mm (Mica House, 2A Pretoria Street, Calcutta 700 071, India)
"Punch and die" set from Precision Brand Products Inc. (2250 Curtiss Street, Downers Grove, IL 60515)
Ethanol [purity: >96% (v/v)]
Loctite 406 superglue (KVT König, Dietikon, Switzerland)
Araldite Rapid: Two-component epoxy glue from Ciba-Geigy, Basel, Switzerland
Scotch tape (3M AG, Rüschlikon, Switzerland)

B. Materials: Bacteriorhodopsin and Buffers

Sodium azide (NaN_3, Fluka Cat. No. 71289)
Tris [$H_2NC(CH_2OH)_3$, Merck Cat. No. 1.08382.2500]
Magnesium chloride hexahydrate ($MgCl_2{\cdot}6H_2O$, Fluka Cat. No. 63064)
Potassium chloride (KCl, Merck Cat. No. 1.04936.1000)
Purple membranes of *H. salinarum* (source: see Acknowledgments)
Stock suspension of purple membrane fragments: 0.25 mg/ml in double-distilled water containing 0.01% NaN_3 (stored at 4°C and protected from unnecessary light irradiation)

C. Instrumentation

A commercial multimode AFM equipped with a 120-µm scanner (j-scanner) and a liquid cell (Digital Instruments, Veeco Metrology Group, Santa Barbara, CA)
Oxide-sharpened Si_3N_4 micro cantilevers of 100 and 200 µm length, and nominal spring constants of 0.08

and 0.06 *N*/m from Olympus Optical Co. Ltd., Tokyo, Japan, and from Digital Instruments, Veeco Metrology Group, respectively.

III. PROCEDURES

A. Preparation of Mica Supports for Sample Immobilization

Steps

1. Punch Teflon disks of 0.5 in. and mica disks of 0.25 in. diameter using the "punch and die" set and a hammer.
2. Clean the steel and Teflon disks with ethanol and paper wipes.
3. Glue a Teflon disk centrally on a steel disk using the Loctite 406 superglue and allow the glue to dry.
4. Glue a mica disk centrally on the Teflon surface of the Teflon-steel disk with the Araldite two-component epoxy glue.
5. Let the supports dry overnight.

B. Preparing Bacteriorhodopsin for AFM Imaging

Solutions

1. *Adsorption buffer*: 20 m*M* Tris–HCl (pH 7.8), 150 m*M* KCl
2. *Imaging buffer for the extracellular side (ES-imaging buffer)*: 20 m*M* Tris–HCl (pH 7.8), 150 m*M* KCl, 25 m*M* $MgCl_2$
3. *Imaging buffer for the cytoplasmic side (CS-imaging buffer)*: 20 m*M* Tris–HCl (pH 7.8), 150 m*M* KCl

Steps

1. Dilute and mix 3 µl of purple membrane stock solution with 30 µl of adsorption buffer in an Eppendorf tube.

2. Cleave the mica by applying Scotch tape to the upper surface and then peeling off until a new smooth intact mica surface is exposed. This new surface is clean and molecularly flat, suitable for deposition of the specimen to be imaged.

3. Pipet 33 µl of the diluted purple membranes on the hydrophilic surface of the freshly cleaved mica support.

4. Allow the sample to adsorb for 15 to 30 min.

5. Wash away purple membrane fragments that are not firmly attached to the mica by removing approximately two-thirds of the fluid volume from the mica surface and readding the same volume of the desired imaging buffer. Repeat this washing procedure at least three times.

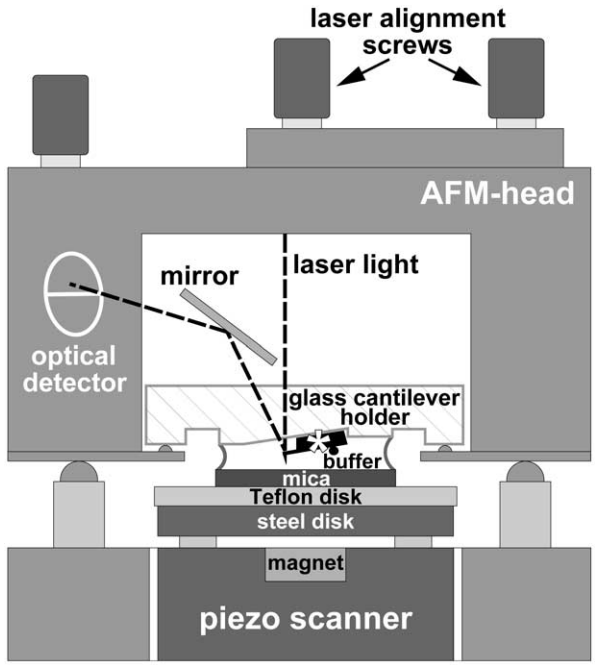

FIGURE 2 Schematic diagram of the atomic force microscope setup for imaging in liquid. The piezo scanner moves the sample in *xyz* directions under the fixed cantilever (marked by an asterisk).

6. Transport the specimen support and its associated fluid onto the piezo scanner of the AFM.

7. Place the AFM head with its mounted fluid cell and cantilever on the scanner (see Fig. 2).

8. Make sure that the space between the mica surface and the cantilever-fluid cell contains enough of the corresponding imaging buffer to avoid drying of the specimen during the imaging experiment. An experiment may last several hours.

9. Align the laser spot onto the cantilever and the reflecting beam into the photodiode with the appropriate laser alignment screws. *Caution*: It is very important not to put any reflective objects into the laser trajectory in order to avoid reflection of the laser light into your eyes! Additionally, wear appropriate protection glasses!

C. Operation of the AFM

All measurements are carried out under ambient pressure and at room temperature.

Steps

These steps assume basic knowledge of AFM operation.

1. Let the instrument equilibrate thermally.
2. Set the scan size to zero to prevent specimen deformation and contamination of the tip after engagement.
3. Initiate engagement process, i.e., permit the tip to approach the surface.
4. As soon as the tip is engaged, and prior to scanning the surface, set the operating point of the instrument to forces below 100 pN, i.e., minimal force.
5. Calibrate the deflection sensitivity of the cantilever using the force calibration menu of the control computer.
6. Start imaging and keep the forces during scanning as small as possible by correcting manually for thermal drift.
7. Optimize the feedback parameters of the system, i.e., the integral gain and the proportional gain, by increasing their values. If the feedback loop starts to oscillate, introducing noise, reduce these gains until the noise goes away.
8. Record two images of 512 by 512 pixels simultaneously at low magnification (frame size >1 µm), one showing the height signal in the trace direction and the other the deflection signal in the retrace direction. Set the scan speed to two to four lines per second. Crystalline structures are usually recognized more easily in the deflection signal image than in the height image.
9. Find and centre a suitable purple membrane fragment. Zoom in and set the scan speed to four to six lines per second. Record images of the height signals in both the trace and retrace directions at high magnification (frame size <1 µm). Comparison of the trace and the retrace images allows deformation of the sample in the fast scan direction to be detected. Such deformations can be minimized by working at minimal force. At such high magnifications, the scan range of the z piezo can be reduced to avoid limitation of the axial z resolution that might otherwise occur because of rounding errors during (16-bit) digitalisation of the analogue signal (AD conversion).

IV. COMMENTS

The following sections explain and help understand the features observed on the topographies acquired during the AFM experiment.

A. Morphology of Purple Membranes

Figure 3 shows a typical low-magnification topograph of purple membrane fragments adsorbed on mica. The diameter of the BR crystals varies between 0.5 and 1.5 µm. The number of adsorbed membrane fragments depends on the adsorption buffer and time and on the concentration of the purple membrane suspension deposited on the mica. It is advantageous not to adsorb membranes too densely on the mica surface; this decreases the probability to contaminate

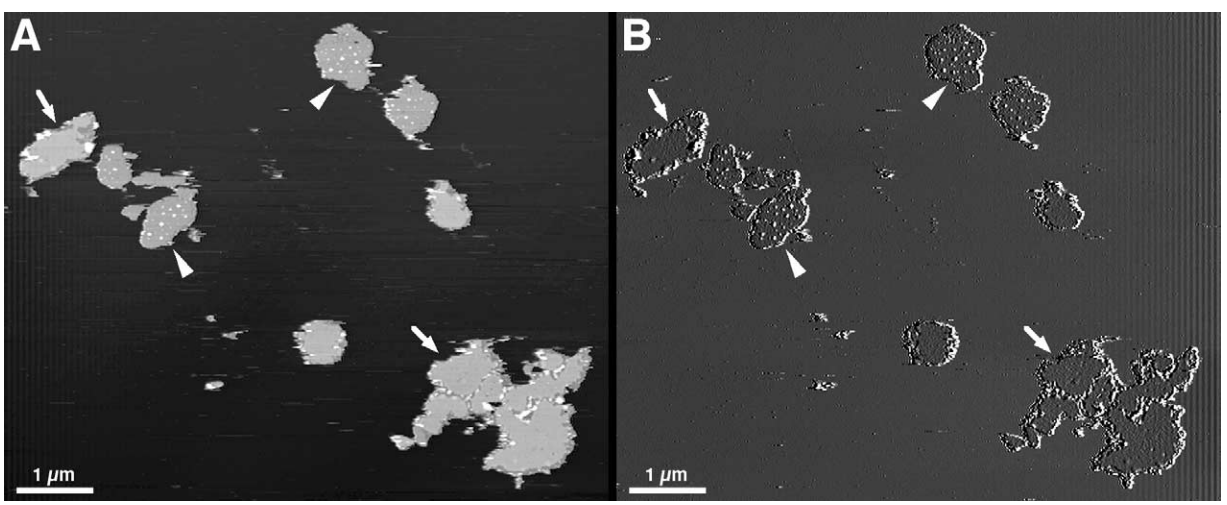

FIGURE 3 AFM images of purple membrane at low magnification: height (A) and deflection (B) signals recorded in trace and retrace directions, respectively. Membrane patches exposing the cytoplasmic side (arrowheads), which are decorated by small debris, can be distinguished from patches exposing the flat extracellular side (arrows). The membrane patches have a height of ~6 nm when imaged in CS-imaging buffer. Vertical brightness ranges: 12 nm (A) and 1 nm (B).

the AFM tip. Two different surfaces can be discerned: The extracellular side of purple membrane is fairly flat (Fig. 3; arrows), whereas the cytoplasmic side is characterized by protruding bumps of 10–30 nm in diameter (Fig. 3; arrowheads) (Müller *et al.*, 1995b, 1996). A feature that can be used to differentiate further between the two sides is the small difference in thickness seen when scanning in CS-imaging buffer. Purple membranes exposing the cytoplasmic side appear slightly thinner than those exposing the extracellular side. As described by Müller and Engel (1997), pH and electrolyte concentration affect the apparent height measured between the mica and the cytoplasmic or the extracellular side of the purple membrane. This results from different surface charge densities.

B. The Extracellular Surface of Purple Membrane

At high magnification, the appearance of the extracellular side of BR is characterized by protrusions extending 0.5 ± 0.1 nm out of the lipid bilayer (Fig. 4A and inset). The β hairpin in the loop connecting the transmembrane α helices B and C of BR constitutes the main portion of the observed protrusion.

C. Estimating the Resolution of AFM Topographs

The resolution of a micrograph containing a regular structure can be estimated from its power spectrum, i.e., its 2D Fourier transformation image. This was calculated from the topograph of the extracellular side of BR (Fig. 4A) and is displayed in Fig. 4B. Most software packages delivered with atomic force microscopes enable calculation of power spectra from recorded AFM topographs. Various public domain programs such as NIH image or ImageJ, both from the National Institutes of Health (Bethesda, MD), or SXM from the University of Liverpool (Liverpool, United Kingdom), have such algorithms implemented and can be downloaded for free (NIH image: http://rsb.info.nih.gov/nih-image/; ImageJ: http://rsb.info.nih.gov/ij/; and SXM: http://reg.ssci.liv.ac.uk/).

The larger the distance of the discernable spots from the origin in a power spectrum, the higher the resolution of the topograph. Here, spots extend beyond the 1-nm resolution limit (see broken circle in Fig. 4B). To calculate the resolution at a selected diffraction spot, Eq. (1) can be used. This equation is applicable to all lattice types, e.g., for trigonal, hexagonal, square, or orthorhombic lattices, which occur frequently in native

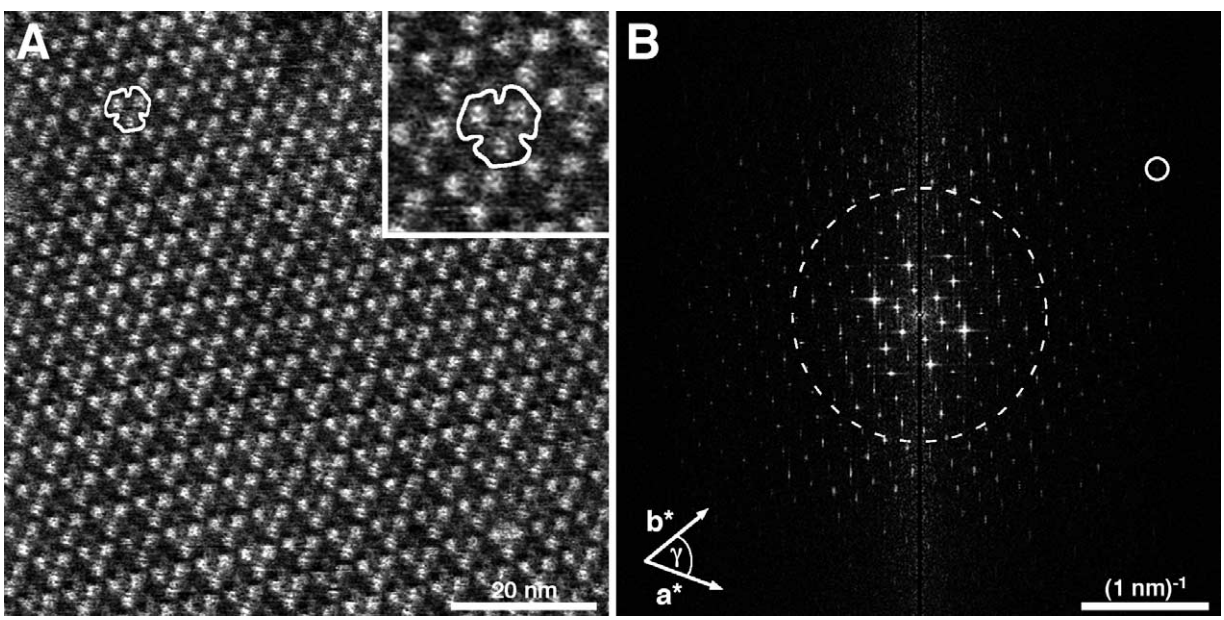

FIGURE 4 (A) The extracellular side of purple membrane at high magnification. For clarity, the area around the contoured BR trimer was enlarged and is displayed in the inset (frame size: 17 × 17 nm). (B) Power spectrum calculated by Fourier analysis from the image in A. The (3, 10) diffraction spot (small circle) is marked and represents a resolution of 0.46 nm. The broken circle represents the 1-nm resolution limit. Vertical brightness range: 0.8 nm (A and inset in A).

and reconstituted 2D crystals of membrane proteins (for further reading on crystallography, see Misell and Brown, 1987).

$$\delta = \frac{1}{|\vec{r}|} = \frac{\sin\gamma}{\sqrt{\frac{h^2}{a^2} + \frac{2 \cdot h \cdot k \cdot \cos\gamma}{a \cdot b} + \frac{k^2}{b^2}}} \quad (1)$$

where δ is resolution; $\vec{r}$ is vector from origin to the diffraction spot in Fourier space; a and b are basic lattice vectors in real space; γ is the angle between the basic lattice vectors; and h and k are Miller indices of the diffraction spot.

Example: The encircled spot (h, k) = (3, 10) in Fig. 4B corresponds to a lateral resolution of 0.46 nm assuming the lattice parameters of BR ($a = b = 6.2$ nm, $\gamma = 60°$).

D. The Cytoplasmic Surface of Purple Membranes

Imaging of the cytoplasmic surface of BR is force dependent because of the flexible EF loop (Müller *et al.*, 1995a). At minimal force (≤100 pN) applied by the AFM stylus (Fig. 5; area above the broken line and inset top left), the fully extended EF loops can be discerned as protrusions of 0.8 ± 0.2 nm height. These become less prominent or even disappear if the loading force is increased to ~200 pN (Fig. 5; area below the broken line and inset bottom left). At this force, the AB loops become visible with a height of 0.6 ± 0.1 nm above the lipid bilayer. The advantage of such force-induced conformational changes is that shorter loops otherwise covered by the bigger ones can be visualized.

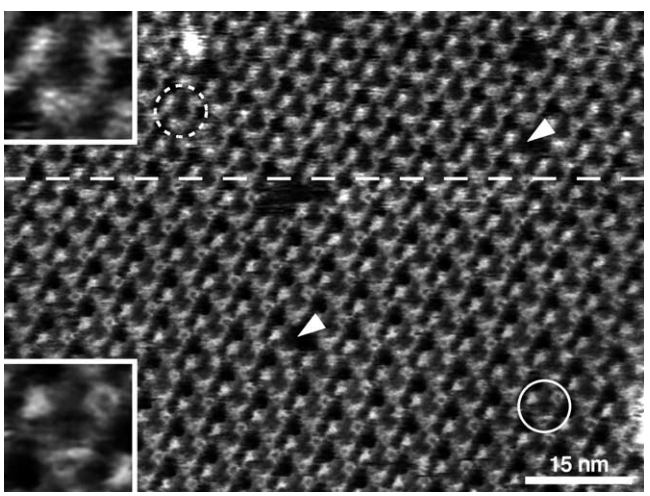

FIGURE 5 Force-dependent topography of the cytoplasmic surface of a purple membrane. The area above the broken line was recorded at minimal force applied to the AFM stylus (≤100 pN). At this force, the flexible EF loop is fully extended, whereas at a stylus force of ~200 pN (area below the broken line) the loop is pushed away by the scanning tip and is therefore almost not visible anymore. For clarity, areas (frame size: 7 × 7 nm) around the contoured trimers recorded at minimal force (broken circle; inset top left) and at a force of ~200 pN (solid circle; inset bottom left) are displayed enlarged as insets. Occasionally, defective BR trimers with a monomer missing can be found (arrowheads). Vertical brightness range: 1.2 nm.

V. PITFALLS

A. Damping of Vibrations

For high-resolution AFM imaging, a vibrationally and acoustically isolated setup of the microscope is crucial. Antivibration and damping tables or lead platforms suspended by bungee cords offer excellent vibration damping. Acoustic isolation of the AFM can be achieved efficiently by installing a vacuum bell jar around the microscope.

B. Adjustment of Buffer for High-Resolution AFM Imaging

Topographs of this membrane protein with a lateral resolution of 0.41 nm (Stahlberg *et al.*, 2001) can be recorded reproducibly with the AFM, provided the imaging buffer is adjusted correctly (Müller *et al.*, 1999) and the force applied to the tip is minimized. Under nonoptimal imaging conditions, even the smallest force that is adjustable by the instrument can be too high, leading to deformation of the biomolecules, e.g., concealing the EF-loop in BR (Fig. 5, lower portion). The effective interaction force acting between the AFM stylus and the specimen is determined by the force applied to the stylus, the electrostatic repulsion, and the van der Waals attraction between the two surfaces. By adjusting pH and ionic strength of the imaging buffer, van der Waals attraction and electrostatic repulsion between tip and sample can be balanced. The best imaging conditions are determined by recording and analyzing force–distance curves between tip and sample in different buffers. Conditions that yield force curves showing a small repulsion are ideal for high-resolution imaging. Under these conditions the tip is assumed to surf on a cushion of electrostatic repulsion, thereby minimizing the deformation experienced by the biomolecules. This screening method revealed the two slightly different imaging buffers for BR mentioned earlier, i.e., CS- and ES-imaging buffer. For further reading on this topic, see Müller *et al.* (1999), where buffer conditions for different biological samples are discussed.

C. Tip Effects and Artefacts

At this time, no commercial AFM tips are available with ideal point probes and perfect geometries in the subnanometer range. Therefore, tip effects and artefacts arising from the tip geometry are unavoidable and have to be considered when interpreting AFM topographies (for further reading on tip effects and artefacts, see Xu and Arnsdorf, 1994; Schwarz *et al.*, 1994). Tip effects occur when the probe does not have a single, small, and sharp interaction area with the sample. This leads to an AFM image that represents a convolution of the sample features with the tip shape. To be sure of having acquired the correct surface structure and not an artefact, the same surface topography of the object being investigated has to be reproduced several times using different tips from different batches. Tip artefacts can also be identified by changing the direction in which the AFM tip scans the sample (scan angle), as artefacts will rotate correspondingly (Xu and Arnsdorf, 1994). Ordered structures, e.g., mosaic 2D crystals, that are differently oriented with respect to the scan direction of the AFM tip, are also good indicators for tip artefacts. Ideally, the building blocks of the crystal, e.g., the BR trimer, should look the same in the differently oriented crystals. Finally, structures of samples that have been determined by other methods, e.g., the structure of BR by electron and X-ray crystallography, can be used to further compare and confirm AFM data.

Figure 6 displays topographs of the extracellular side of BR recorded with an artefact-free tip (Fig. 6A) together with images acquired with artefacteous tips (Figs. 6B–6D). Tentative explanations of the observed artefacts are omitted because the statements would be too speculative. We restrict ourselves to a comparison of artefacteous surfaces with the nonartefacteous one. Compared to Fig. 6A, the depression at the three-fold symmetry axis of the trimer in Fig. 6B is completely missing. The trimer seems to consist of a single plateau. The BR trimers in Fig. 6C have lost their trigonal shapes and resemble tetramers. In Fig. 6D the BR trimer is distorted, displaying a Y shape. The lipid areas that separate the neighbouring BR trimers cannot be resolved by the artefacteous tip, and instead ridges of constant height are seen (broken straight line).

VI. CONCLUDING REMARKS

This article presented procedures for sample preparation and AFM imaging of native 2D crystals of bacteriorhodopsin. The experience gained will enable the readers to perform similar AFM experiments with other biological membranes.

Acknowledgments

This work was supported by the Swiss National Research Foundation, the M. E. Müller Foundation, the Swiss National Center of Competence in Research (NCCR) "Structural Biology," and the NCCR "Nanoscale Science." The authors are indebted to Dr. Ansgar Philippsen for Fig. 1 and to Professors Dieter Oesterhelt (Max-Planck-Institut für Biochemie, Martinsried, Germany) and Georg Büldt (Forschungszentrum Jülich, Jülich, Germany) for kindly providing us with BR. The authors acknowledge Dr. David Shotton for constructive comments on the manuscript.

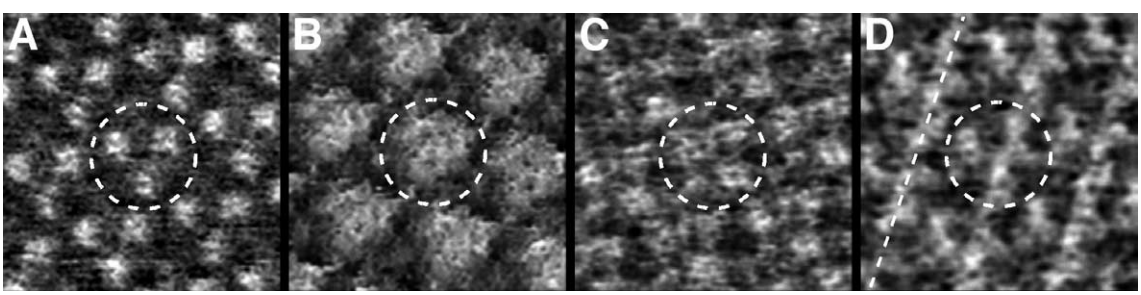

FIGURE 6 Tip-induced effects and artefacts on the extracellular surface of bacteriorhodopsin. (A) Artefact-free and (B–D) artefacteous topographies of BR. In B the characteristic central depression at the three-fold axis of the BR trimer is absent. The central trimer in C resembles a tetramer. In D the protrusions are not clearly separated, but connected along the broken line. In all images the central trimers are marked by broken circles. The frame sizes in A to D are 17 nm. The heights are 0.8 nm (A), 1.3 nm (B), 0.8 nm (C), and 0.8 nm (D).

References

Binnig, G., Quate, C. F., and Gerber, C. (1986). Atomic force microscope. *Phys. Rev. Lett.* **56**, 930–933.

Blaurock, A. E., and Stoeckenius, W. (1971). Structure of the purple membrane. *Nature New Biol.* **233**, 152–155.

Cartailler, J. P., and Luecke, H. (2003). X-ray crystallographic analysis of lipid-protein interactions in the bacteriorhodopsin purple membrane. *Annu. Rev. Biophys. Biomol. Struct.* **32**, 285–310.

Engel, A., Lyubchenko, Y., and Müller, D. J. (1999). Atomic force microscopy: A powerful tool to observe biomolecules at work. *Trends Cell Biol.* **9**, 77–80.

Engel, A., and Müller, D. J. (2000). Observing single biomolecules at work with the atomic force microscope. *Nature Struct. Biol.* **7**, 715–718.

Fotiadis, D., Scheuring, S., Müller, S. A., Engel, A., and Müller, D. J. (2002). Imaging and manipulation of biological structures with the AFM. *Micron* **33**, 385–397.

Kimura, Y., Vassylyev, D. G., Miyazawa, A., Kidera, A., Matsushima, M., Mitsuoka, K., Murata, K., Hirai, T., and Fujiyoshi, Y. (1997). Surface of bacteriorhodopsin revealed by high-resolution electron crystallography. *Nature* **389**, 206–211.

Lanyi, J. K. (1997). Mechanism of ion transport across membranes: Bacteriorhodopsin as a prototype for proton pumps. *J. Biol. Chem.* **272**, 31209–31212.

Misell, D. L., and Brown, E. B. (1987). "Electron Diffraction: An Introduction for Biologists." Elsevier Science, The Netherlands.

Müller, D. J., Büldt, G., and Engel, A. (1995a). Force-induced conformational change of bacteriorhodopsin. *J. Mol. Biol.* **249**, 239–243.

Müller, D. J., and Engel, A. (1997). The height of biomolecules measured with the atomic force microscope depends on electrostatic interactions. *Biophys. J.* **73**, 1633–1644.

Müller, D. J., Fotiadis, D., Scheuring, S., Müller, S. A., and Engel, A. (1999). Electrostatically balanced subnanometer imaging of biological specimens by atomic force microscope. *Biophys. J.* **76**, 1101–1111.

Müller, D. J., Schabert, F. A., Büldt, G., and Engel, A. (1995b). Imaging purple membranes in aqueous solutions at subnanometer resolution by atomic force microscopy. *Biophys. J.* **68**, 1681–1686.

Müller, D. J., Schoenenberger, C.-A., Büldt, G., and Engel, A. (1996). Immunoatomic force microscopy of purple membrane. *Biophys. J.* **70**, 1796–1802.

Oesterhelt, D., and Stoeckenius, W. (1973). Functions of a new photoreceptor membrane. *Proc. Natl Acad. Sci. USA* **70**, 2853–2857.

Oesterhelt, D., Tittor, J., and Bamberg, E. (1992). A unifying concept for ion translocation by retinal proteins. *J. Bioenerg. Biomembr.* **24**, 181–191.

Schwarz, U. D., Haefke, H., Reimann, P., and Güntherodt, H.-J. (1994). Tip artefacts in scanning force microscopy. *J. Microsc.* **173**, 183–197.

Stahlberg, H., Fotiadis, D., Scheuring, S., Rémigy, H., Braun, T., Mitsuoka, K., Fujiyoshi, Y., and Engel, A. (2001). Two-dimensional crystals: A powerful approach to assess structure, function and dynamics of membrane proteins. *FEBS Lett.* **504**, 166–172.

Stolz, M., Stoffler, D., Aebi, U., and Goldsbury, C. (2000). Monitoring biomolecular interactions by time-lapse atomic force microscopy. *J. Struct. Biol.* **131**, 171–180.

Xu, S., and Arnsdorf, M. F. (1994). Calibration of the scanning (atomic) force microscope with gold particles. *J. Microsc.* **173**, 199–210.

CHAPTER

33

Field Emission Scanning Electron Microscopy and Visualization of the Cell Interior

Terence Allen, Sandra Rutherford, Steve Murray, Siegfried Reipert, and Martin Goldberg

I. INTRODUCTION

Resolution in scanning electron microscopy (SEM) has improved dramatically in recent years so that for the majority of biological material, no significant differences exist in resolution between SEM and conventional transmission electron microscopy (TEM). High brightness sources (field emission) and novel final lens configurations have resulted in instrument resolutions of 0.5 to 1 nm, allowing direct, *in situ*, three-dimensional visualization of surface detail at molecular resolution. As all this technology relies on field emission sources of the electron beam, either by "cold" field emission or thermally assisted "Schottky" field emission, we refer to it as FESEM.

Surface imaging allows bulk samples to be examined without limitation of specimen thickness. Visualization of intracellular surfaces requires some means of access, such as isolation of cell fractions or macromolecules, or *in situ*, via fracture, or sectioning techniques. Cell-free systems, e.g., *in vitro* nuclear formation, allow biological interfaces such as developing nuclear envelopes to be imaged directly (Goldberg *et al*., 1992). True three-dimensional (3D) surface visualization can be achieved by tilting the specimen to make stereo pairs, and accurate surface measurements can be made from computerized 3D reconstructions. The surfaces can be characterized further by immunogold labeling, which can be unequivocally localized by the strong backscatter signal of the gold probes. For specimens that are thin enough to allow electron penetration, a scanning TEM (STEM) image can also be obtained readily and displayed simultaneously alongside the secondary electron image, producing complementary information from the transmitted beam/specimen interactions. The use of low accelerating voltages in FESEM has also been shown to be of advantage, reducing charging and penetration of the electron beam, but maintaining a high-resolution information content. High-pressure freezing, freeze substitution, and examination of cryohydrated specimens may all be used for FESEM (Muller and Hermann, 1990; Walther, 2003) but can be considered specialized and are not covered in this article, although we do describe the use of cryoultramicrotomy and cryoabrasion as techniques to access internal surfaces within the cell prior to conventional imaging by FESEM. Basically, we deal with techniques that rely on chemical preservation, followed by dehydration, critical point drying, and coating. Conventional SEM coating (up to 20 nm thickness) with sputtered gold completely obscures fine surface detail in HRSEM and must be replaced by high-resolution coating. We routinely coat with a 1- to 2-nm film of chromium or tungsten, which has a grain size of 0.3 to 0.5 nm (Apkarian *et al*., 1990).

II. MATERIALS AND INSTRUMENTATION

1. Glutaraldehyde (Agar Scientific)
2. Tannic acid (TAAB Laboratories)
3. TCH (Cat. No. T-2137. Sigma)

Copyright 2006, Elsevier Science (USA).
All rights reserved.

4. Osmium textroxide (Agar Scientific)
5. Uranyl acetate (Agar Scientific)
6. Molecular sieve (Merck Ltd.)
7. Arklone (trichlorotrifluoroethane) Taab Labs UK
8. HEPES (Sigma)
9. PIPES (Sigma)
10. Phosphate-buffered saline (PBS)
11. Tris–HCl
12. EDTA (Sigma)
13. Phenylmethylsulfonyl fluoride (PMSF, Sigma)
14. Percoll (Sigma)
15. Sorensen's phosphate buffer
16. Poly-L-lysine HBR, MW 150,000–300,000 (Cat. No. P-1399 Sigma)
17. Glass coverslips, 5–7 mm diameter
18. Silicon chips, $5 \times 5\,mm^2$ (Agar Scientific Ltd.)
19. Carbon-coated support grids
20. Fine forceps for handling
21. Microcentrifuge to spin suspended material onto coverslips
22. Microcentrifuge tubes, 1.5 ml, half-filled with polymerized EM resin, ideal for supporting coverslips, chips, and grids during specimen deposition by centrifugation
23 High-resolution scanning EM. Conventional "pinhole" final lens instruments with field emission sources will allow subcellular imaging, as will conventional transmission instruments with scanning attachments. To date, the highest resolution achieved has been in field emission instruments with the facility to position the specimen in, or very close to, the final lens. Recent technology has significantly improved the resolution of field emission instruments at lower accelerating voltages (1 kV), from around 4 to 1.5 nm, facilitating imaging without the need for metal coating. The microscope should also be equipped with a suitable high-resolution backscatter detector for immunogold labeling. The main suppliers for these instruments are Hitachi, Jeol, Philips, and Leo.
24. Critical-point drier, with high-purity CO_2 (<5 ppm water). Liquid CO_2 should be passed through a filter to remove water (Tousimis Research Corp., filter 8782).
25. Coating units. Oxygen, hydrocarbons, and water vapor all adversely affect the grain size of chromium or tantalum deposited by sputter coating (Apkarian *et al.*, 1990). We use an Edwards Auto 306 12-in. coating unit with cryopump, magnetron head, and suitable power source (Edwards High Vacuum International). Similar configurations using Denton HiVac and Balzers equipment with cold-trapped turbopumping have also been successful. Any system should use high-purity argon and have a shutter and a specimen table that tilts and rotates. Film thickness monitoring of coating deposition is an advantage. Several "benchtop" systems are currently on the market, many untested by the highest resolution. In our own very recent experience, the provision of a suitably performing coating system has often proved to be a limitation of the perceived performance of a newly acquired microscope, and suitable resources for a high-resolution coating system should be incorporated in any application for a field emission instrument. If possible, get in touch with an established group and get advice before committing to any particular coating system.

Pitfalls

It is crucial to visit manufacturers' demonstrations with the material that will be investigated to ascertain that suitable performance can be assured from the chosen equipment.

III. PROCEDURES

A. Exposing Surfaces within the Cell

1. Subcellular Fractionation

Organelles and macromolecules can be isolated by standard procedures, possibly requiring subsequent modifications in the light of HRSEM visualization, which are beyond the scope of this article. Basically, the specimens must be undamaged by osmotic shock, proteolysis, or unsuitable isolation buffers. They must also be clean. The surface of organelles should, for instance, be free of attached cytoskeletal remnants or cytoplasmic contamination. Where the specimens are available as purified macromolecules or viruses, they may be deposited on carbon-coated TEM grids in the conventional manner and viewed by HRSEM. In this situation, TEM negative staining will usually be replaced by fixation for SEM and air drying replaced by critical-point drying followed by chromium coating. If a STEM detector is available, the virus/macromolecule can be recognized as a transmitted "reference image" after this protocol and compared directly with the secondary electron (SEM) image. The thin coating of chromium applied for the secondary electron imaging does not interfere with the STEM imaging.

Adhering Sample to Support

Many cell components naturally adhere to glass coverslips, silicon chips, or carbon support film on grids. Glass coverslips may be a useful initial prepar-

ative substratum, as they can be checked in the phase-contrast microscope for the density and distribution of specimens and for the progression of various protocols such as detergent extraction of cytoplasm. Once the isolation protocol is established, coverslips should be replaced with silicon chips as specimen substrates, as silicon is a conductive substratum in contrast to glass, an insulator, which can generate problems with charging in the SEM. Tissue culture cells will grow in identical fashion on silicon as they do on glass or plastic, and isolated cytosol or organelles will also adhere naturally to silicon in the same way as they do to glass. If samples are fixed in suspension it may be necessary to coat the support with poly-L-lysine to facilitate adherence. Different samples may require slight modification, but the basic technique is as follows (Fig. 1).

Solution

Poly-L-lysine: Make a fresh 1-mg/ml solution of poly-L-lysine in sterile distilled water; use within 24 h.

Steps

1. Mark the surface of chip or coverslip with identification number using a diamond marker.
2. Place a 50-µl drop of poly-L-lysine on coverslip or chip; allow to stand for at least 60 min in a moist chamber to avoid drying. Rinse in sterile distilled water. The surface will retain its adhesive properties for up to 2 weeks in a refrigerator.
3. Place a 50-µl drop of suspended material (fixed and rinsed) on coverslip/chip. Allow to settle and attach at 4°C and unit gravity in a moist chamber (1 h to overnight). Alternatively, spin directly (see isolation of nuclei) onto silicon chip.
4. Allow bulk of drop to run off, put chip/coverslip back in fixative, and continue as for fresh tissue. Unfixed living samples (e.g., whole cells) may be distorted by poly-L-lysine. To spin down materials from suspension, use minicentrifuge tubes half-filled with polymerized EM resin to support the coverslip/silicon chip/grid.

2. *"In Situ" Exposure of Intracellular Surfaces*

Dry Fracture

This is a simple but extremely effective way of exposing internal surfaces in both tissues and cells. After fixation, dehydration, and critical-point drying,

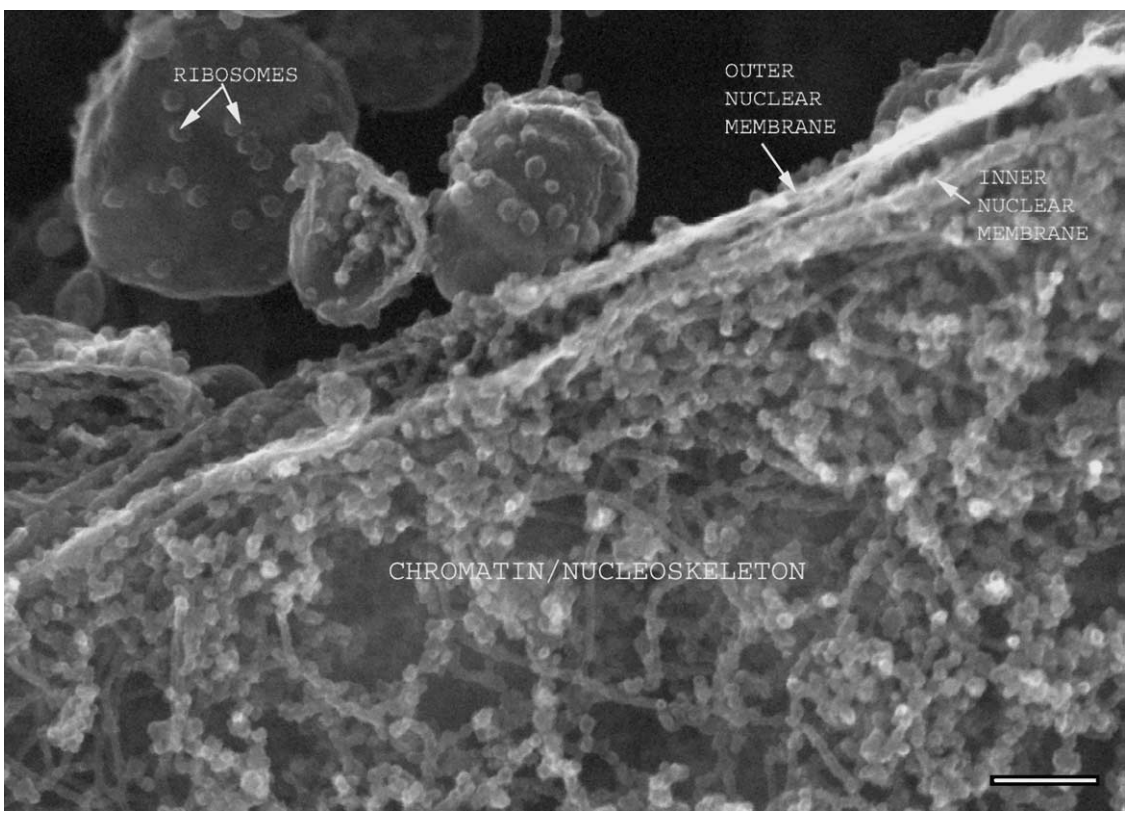

FIGURE 1 *Xenopus* nuclear assembly egg extract spun onto a silicon chip, fixed, frozen, and sandpapered while frozen showing a section through the edge of a nucleus where the two membranes of the nuclear envelope can be seen, as well as the chromatin and nucleoskeletal fibres on the nuclear interior. Bar: 125 nm.

merely gently press the surface of the specimen to a square of double-sided tape mounted to a second silicon chip and pull away without shearing, coat both chips as normal, and examine in the SEM. The fracture will remove material on the surface of the adhesive and leave fractured material "*in situ*." This technique may be enhanced by pretreatment with detergent (0.5% Triton X-100, 2–3 min for tissue culture cells), either alone or mixed with the primary fixative (2.0% paraformaldehyde and 0.1% glutaraldehyde), and subsequently refixed as described (Allen *et al*., 1998).

Resinless Sections

These methods involve sectioning of embedded specimens followed by exposure of internal surfaces by removal of the supporting material. This may vary among epoxy resins, various waxes, and even ice. Resins that require corrosive solvents for removal will tend to be prone to surface etching. A mixture of 50% propylene oxide and 50% sodium methoxide (dissolve 2 g NaOH pellets in 100 ml absolute methanol) will remove most resins.

3. Cryo Methods to Expose Internal Surfaces for FESEM

Surface imaging by FESEM may be achieved by isolating the cellular component of interest, such as mitochondria, but this approach does not allow access to the interior structure of such an organelle (see later). One way to expose such surfaces is to freeze the cells or tissue and cut cryo sections, which themselves can be viewed in the SEM, to "cryoplane" and expose the whole blockface in the SEM, or to "cryoabrade" the surface of the frozen sample and expose surface features in a different way. Samples are then thawed and processed for FESEM as normal. This gives a cross-sectional view but with much greater depth of information than in a resin-embedded thin section viewed in the TEM because the sections can be very thick, they are resin free, and there is a greater depth of focus. Information can also be gathered quite simply in 3D simply by taking stereo pairs, which also allows computerized 3D reconstruction and measurement of the surface. This method is also compatible with immunogold labelling (Fig. 2).

Cryomicrotomy is an adaptation of the widely used "Tokyasu" technique (Tokyasu, 1986, 89) for immuno-TEM.

Materials

Silicon chips
4% paraformaldehyde in PBS
2 *M* sucrose in PBS
Cryo stubs

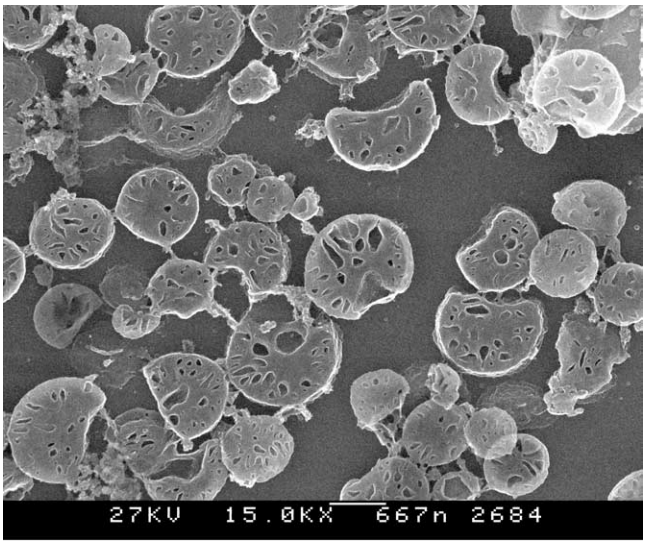

FIGURE 2 Low-power image of cryo-planed block face of a mitochondrial pellet where the internal cristae structure has been exposed. Scale bar: 667 nm.

Liquid nitrogen
Cryo ulramicrotome (e.g., Leica Ultracut R with FCS cryo attachment)

Steps

1. Fix samples (e.g., pellet of organelles) with 4% paraformaldehyde in PBS at room temperature for 30 min.
2. If possible, trim to a cube of about 1 mm^3.
3. Transfer to 2 *M* sucrose in PBS overnight at 4°C.
4. Mount sample on cryo stub for ultramicrotome and wick off excess sucrose.
5. Plunge into liquid nitrogen.
6. Mount into a cryo ultramicrotome, which has been precooled to –100°C.
7. Cut sections of 100–300 nm thickness.
8. As in the Tokyasu technique, pick up sections off the knife on a drop of sucrose suspended from a loop, where they thaw, and then touch the sucrose drop to a silicon chip where the sections adhere.
9. Place chip in PBS to wash off sucrose.
10. This can then be immunogold labeled, refixed, and processed for FESEM.

Pitfalls

These problems are associated with the Tokuyasu technique.

1. Poor infiltration of sample with sucrose leading to crumbly blocks.
2. Curling of sections.
3. Static.

4. Frosting.
5. Small sample size.

When processing the sample remaining on the pin for SEM, the specimen always detaches from the pin. This leaves a very small specimen that is easily lost during the dehydration and CPD steps. An additional problem is the attachment of the sample to a silicone chip after CPD. The sample is very fragile and it is not always easy to identify the "planed" side. Adhere the sample to the chip using a thin smear of silver dag. It is possible for the sample to flip over during this process. Also, because of the irregular shape of the sample, ensuring good contact and therefore a good earth path from specimen to chip can be tricky. It is easy to submerge the specimen in too much dag.

Cryo Abrasion

1. Centrifuge organelles onto a silicon chip.
2. Fix (e.g., 4% paraformaldehyde in PBS, room temperature for 30 min).
3. Transfer to 2 *M* sucrose in PBS for 2 h to overnight at 4°C.
4. Remove from sucrose and place on filter paper to dry the back of the chip.
5. Wick off most of the sucrose from the sample, leaving as thin a film as possible without drying.
6. Plunge into liquid nitrogen.
7. The sucrose step can be avoided if the sample can be frozen ultra-rapidly by plunging into liquid propane or ethane. The chip can then be held under liquid nitrogen or on a liquid nitrogen-cooled platform (such as the Leica EM CPC) while it is abraded with fine sandpaper (400–600 grade wet and dry abrasive as per automobile body and paintwork).
8. Thaw into fix and process for FESEM.

Specific Protocol for Mitochondrial Isolation and Exposure of Internal Structure by FESEM

Isolate mitochondria using the differential centrifugation method (Gottlieb *et al*., 2003). Harvest and place cells ($2.5–5 \times 10^8$) on ice for 15 min, centrifuge at 500 *g* for 5 min at 4°C, wash with ice-cold PBS, and subsequently wash with ice-cold mitochondrial isolation buffer (MIB) (200 m*M* mannitol, 70 m*M* sucrose, 1 m*M* EGTA, 10 m*M* HEPES, 0.5 mg/ml BSA; pH 7.4). Resuspend cells in ice-cold MIB and then homogenize in a syringe-driven cell disruptor. Spin the lysate at 800 *g* for 10 min at 4°C. Remove supernatants and spin at 10,000 *g* for 10 min at 4°C. Add fixative (3% glutaraldehyde) to the pellets and keep samples at 4°C for 1 h. Remove the fixative carefully and infiltrate the pellet with sucrose/PVP solution overnight (Tokuysau, 1989). During this process, leave the pellet undisturbed. Then carefully excise small (>1 mm^2) pieces of sample from the pellets and mount onto aluminium plunge freezing pins (Leica Microsystems, Milton Keynes). Mount the pins into a plunge freeze unit (Leica CPC) and freeze in liquid propane at a temperature of −182°C. Transfer the frozen specimen and pin under LN2 into a cryo ultramicrotome (Leica Ultracut S with FCS attachment). Using a diamond trimming knife (Diatome Cryotrim 45), trim several semithin sections (350 nm) from the sample in order to remove surface sucrose. Cut further semithin sections (350–400 nm) from the sample using a diamond cryo knife. Collect each section on a sucrose loop according to the "Tokuyasu" technique (Tokuyasu, 1986). Thaw the frozen sections onto 5-mm silicone chips and process for SEM as follows.

1. Transfer the chips with attached sections using a metal loop (2–3 mm diameter) and invert such that the chip is floated, section side down, in a plastic Petri dish (35-mm Falcon) containing double-distilled water.
2. Wash 3× over 15 min in order to rinse out the sucrose.
3. Fix by floating in 1% OsO4 in double-distilled water for 1 h.
4. Wash in double-distilled water 3× for 5 min each.
5. Then dehydrate the sections and critical point dry as described later.

Pitfalls

Aligning the cryo abrasive pad with the specimen is very tricky and must be done with care. It is very easy for the protruding abrasive shards of the wet and dry paper to embed themselves into the frozen block. Also, if the section advance is too great, the sample block can be literally ripped from the specimen pin. A few micrometres must be shaved off the sample face in order to ensure that all surface sucrose has been removed. This only leaves a few micrometres of well-frozen vitrified sample to work with. Once again, the sample size is very small and is easily damaged or lost in subsequent processing and mounting steps.

Identifying the abraded face can be tricky even under a stereomicroscope. The swirled pattern of the specimen pin that has been embossed into the underside of the sample can look very similar to the abraded face, leading to the specimen being mounted pin side up.

B. Fixation

Solutions

All fixatives are ideally made up just before use or at least the same day; both glutaraldehyde and

glutaraldehyde-tannic acid solutions should be filtered before use through a 0.22-µm filter. The 1% aqueous uranyl acetate should be stored in a brown bottle. Osmium tetroxide is made by breaking the glass ampoules in which the crystals are delivered, having previously washed them free of label and adhesive under the tap, in a fume cupboard. The ampoules plus crystals are dropped in the correct amount of buffer or distilled water where the osmium dissolves to give the appropriate final concentration. (*Note*: Osmium is extremely hazardous and appropriate precautions must be observed.) Thiocarbohydrazide or tannic acid solutions should also be made just prior to use (Allen *et al.*, 1988).

Pitfalls

Always use glutaraldehyde of EM-grade quality from a high stock concentration (50%) stored in a freezer. Low concentration stock solutions and storage in large bottles at room temperature will reduce the cross-linking properties of the glutaraldehyde.

Steps

1. Isolated Proteins and Nucleoproteins

1. Proteins and nucleoproteins on carbon support films on TEM grids may be floated on top of drops (25–50 µl) of the appropriate solutions spread on Parafilm.
2. Place in 1% glutaraldehyde in appropriate buffer for 10 min.
3. Wash in double-distilled water for 5 min.
4. Transfer to 1% uranyl acetate for 5 min.
5. Transfer to 100% ethanol for 1–2 min.
6. Air dry or critical point dry (see later).

2. Small and Easily Preserved Structures

Steps

1. Fix in 3% glutaraldehyde in Sorensen's phosphate buffer for 30 min.
2. Wash in Sorensen's for 5 min.
3. Postfix in 1% $Os0_4$ (in Sorensen's for 30 min).
4. Wash in double-distilled water for 5 min.
5. Dehydrate through ethanol series for 5 min each.
6. Place in Arklone for 5 min.
7. Critical point dry (see later).

3. Large and/or Fragile Structures (e.g., Whole Cells, Organelles, Cytoskeletal Preparations, Isolated Cells, or Nuclear Membranes)

Steps

1. Attach whole cells to specimen supports such as silicon chips and handle by changing the solutions in 35-mm-diameter petri dishes.
2. Fix in 2% glutaraldehyde, 0.2% tannic acid, and 0.1% HEPES, pH 7.4, for 10 min.
3. Wash in double-distilled water for 5 min.
4. Postfix in 0.1% $Os0_4$ in water for 10 min.
5. Wash in water for 5 min.
6. Stain with 1% aqueous uranyl acetate for 10 min.
7. Dehydrate through ethanol series and Arklone and critical point dry.

4. Isolation of Nuclei from Tissue Culture Cells

Steps

1. Take approximately 10 million tissue culture cells (usually from suspension culture), cool to 4°C, and pellet in a swing-out centrifuge (1000 *g* for 10 min).

2. Wash the pellet in PBS buffer and then resuspend in 8 ml ice-cold swelling/shearing buffer (50 m*M* Tris–HCl, pH 7.4, 5 m*M* MgCL, 1.3 m*M* EDTA, and 5 m*M* phenylmethylsulfonyl fluoride added shortly before use) in which nuclei are allowed to swell for 5 min.

3. Mechanically homogenize the cells using a plunger-type tissue grinder (e.g., Kontes Dounce), checking the number of strokes required for nuclear release by phase-contrast light microscopy (usually 10–20 strokes). Precool the plunger in ice prior to use. Alternatively, nuclei may be isolated by a single passage through a 26-G3/8 syringe needle (Microlance).

4. Prepare a Percoll gradient as follows: use a 13.5-ml Beckman centrifuge tube filled with 0.86 ml Percoll, density 1.130 g/ml, 2.74 ml 10 m*M* Tris–HCl (pH 7.4), and 0.40 ml 2.5 *M* sucrose. Add density marker beads to monitor gradient, red beads (1.12 g/ml) in Percoll containing 0.25 *M* sucrose, and yellow beads (1.049 g/ml) in Percoll containing 0.25 *M* sucrose. Spin for 30 min at 30,000 *g* at 4°C with a 60° angle head rotor; red beads will form a line 5 mm from the bottom of the tube, with the yellow beads a further 12 mm above.

5. Gently layer the homogenate on top of the gradient and spin for 10 min at 30,000 *g*, which generates two bands from the homogenate. Damaged nuclei and whole cells are found in the upper band 7 mm above the red beads, whereas the pure nuclear fraction is found 0.5 mm below the red beads. Remove this fraction and wash gently in 150 m*M* Tris–HCl (pH 7.4) for 5 min at 4°C.

6. Spin the isolated nuclei onto 5-mm poly-L-lysine-coated silicon slips. Spin the silicon chips in 1.5-ml Eppendorf tubes previously half-filled with polymerized resin. Overlay the Si chips with 0.5 ml of freshly isolated nuclear suspension and spin for 5 min at 1000 *g*.

7. Fix the whole chip (+nuclei) in 6% glutaraldehyde in 0.15 *M* Sorensen's buffer for 20 min, rinse

gently in buffer, and postfix in 1% osmium tetroxide in 0.15 *M* Sorensen's buffer for 1 h. Dehydrate, critical point dry, and coat with 3–4 nm of tantalum or chromium.

Pitfalls

1. Low yield of nuclei. Dounce tissue homogenizers are produced with different clearance distances between the polished tube and the pestle. Some homogenizers are designed just to disrupt tissues as a necessary step prior to homogenization of nonsuspension cells. Make sure that the clearance distance of the Dounce tissue homogenizer for the final release of the nuclei is small enough to disrupt whole cells. Some manufactures offer pestles with two different clearance distances to allow tissue disruption and release of the nuclei within one and the same tube. For certain cell types, making the buffer more hypotonic can help increase the yield of nuclei.

2. Enzymatic degradation of structures. It is good practice to ensure cooling for every preparation step prior to the fixation of nuclei on silicon chips. Moreover, the homogenate should be processed without delay. Therefore, preparation of the Percoll gradient before homogenization is recommended. To ensure a suitable ratio between biological material and buffer, a homogenizer with a sufficient capacity (for 8 ml) should be selected. Do not reduce the number of cells significantly to keep this ratio in a homogenizer with lower capacity, as this might cause problems with recognition of the nuclear layer after gradient centrifugation.

5. Preparation of in Vitro-Assembled Organelles for FESEM

Organelles, such as nuclei, endoplasmic reticulum (ER), and Golgi, can be assembled in cell-free extracts. Extracts made from frog eggs are a particularly powerful system for studying the assembly, dynamics, and functions of these organelles. Organelles can be isolated cleanly from the extract and their surfaces can be examined by FESEM. *In vitro*-assembled nuclei, as well as ER, can be prepared for FESEM as follows.

Solutions

1. *Membrane wash buffer (MWB)*: 250 m*M* sucrose, 50 m*M* KCl, 50 m*M* HEPES–NaOH (pH 8.0), 1 µg/ml aprototin, and 1 µg/ml leupeptin

2. *Fix buffer*: 150 m*M* sucrose, 80 m*M* PIPES–KOH (pH 6.8), 1 m*M* MgCL, 2% paraformaldehyde, and 0.25% glutaraldehyde

Steps

1. Prepare *Xenopus* egg extracts (Newmeyer and Wilson, 1991) and incubate extract with demembranated *Xenopus* sperm chromatin to assemble nuclei. ER and Golgi will also assemble in the same extract.

2. After the required time, remove a 4-µl extract, place in a 1.5-ml Eppendorf tube, and resuspend very gently in 1 ml of MWB. At this stage, centrifugation of *in vitro* nuclei and organelles onto 5-mm^2 silicon chips requires a simple modification of the 1.5-ml Eppendorf centrifuge tubes as follows. Remove lid from tube and cut tube with a sharp knife at a level where the cut end fits tightly into the lid, thus creating a "flat-bottomed" tube. Snap the cut end into the lid, having placed a silicon chip in the lid first.

3. Pipette the 1 ml of MWB containing the extract into the modified tube, spin in a swing-out rotor, inside a 10-ml centrifuge tube (with a single tissue as cushion), and spin for 10 min at 4°C or room temperature at 2000 *g*. Some leakage of the suspension at the joint between the cut end of the tube is not a problem at this point.

4. Pipette off most of the buffer, break open the tube, and remove the chip. Place the chip in 5 ml of fix buffer in a small petri dish for 10 min at room temperature.

5. Wash chip in 0.2 *M* cacodylate (pH 7.4), place in 1% OsO_4 in 0.2 *M* cacodylate for 10 min, wash twice in distilled water, and place in 1% aqueous uranyl acetate for 10 min (at room temperature) and then dehydrate, critical point dry, etc.

C. Critical-Point Drying

All traces of water should be removed from ethanol, Arklone, and CO_2. Let 100% ethanol and Arklone stand over molecular sieve for more than 24 h prior to use. High-purity liquid CO_2 (less than 5 ppm water) should be used and passed through a water filter as a precaution.

Steps

1. Exchange Arklone for CO_2.
2. Flush six times.
3. Leave in CO_2 for 30 min.
4. Flush six times.
5. Raise temperature to 40°C.
6. Release gas slowly (over about 15–20 min).
7. Transfer to coating unit as soon as possible.

Pitfalls

Critical-point-dried samples should be transferred immediately into the sputter coater to avoid rehydration, and coated samples are best viewed in the microscope directly. However, if it is known that the microscope cannot be accessed, it is better to pause

preparations after critical-point drying and store preparations under vacuum.

D. Sputter Coating

Steps

1. Pump specimen to at least 5×10^{-7} mbar.
2. Introduce high-purity argon to a pressure of 8×10^{-3} mbar.
3. Start specimen rotation (60 rpm).
4. Sputter at 50–100 mA current (voltage 450 V) and 60 rpm; specimen table should be tilted at 30°. Presputter onto the shutter for 20–60 s to remove the chromium oxide layer from the target.
5. Open shutter and deposit 2 nm chromium as indicated by a film thickness monitor (usually 20–30 s).
6. Examine in microscope as soon as possible, preferably within a day or two. Coatings are variable according to the specimen, but a general rule is that they deteriorate with time, usually over a few days to about 2 weeks.

E. Microscopy

Steps

1. A liquid nitrogen-cooled decontaminator (if present) should always be used; this is more likely to be fitted on an "in-lens" electron optical column configuration. Many recent field emission instruments are of conventional "pinhole configuration," but with very short working distances to optional decontamination devices.

2. Spot size and apertures should be as small as possible, consistent with a sufficient signal to visualize high resolution of specimen at photographic collection rates (e.g., 40-s scans).

3. An appropriate accelerating voltage must be selected. High-resolution scanning electron microscopes usually work in the range of 1–30 kV. Instrument resolution decreases with decreasing accelerating voltage; however, at high voltage there may be problems with charging and specimen penetration, leading to a nonspecific signal from below the specimen surface. At low voltage, penetration and charging are reduced, but so are resolution and signal. Signal is generated almost completely from the surface at 1.0 kV so there is no problem of a "bulk" signal from underlying structures. In general, we use high kilovolts for thin and conductive specimens and lower kilovolts for bulky or less conductive specimens; however, a wide range of kilovolts should be experimented with for each type of sample. The more recently produced field emission instruments have vastly improved low kilovolt performance, and specimens that have some inherent conductivity as a result of osmium fixation can be viewed uncoated at low kilovolts, without compromising signal and resolution.

F. Immunogold Labeling

The basics of specimen preparation for immunogold labeling are beyond the length limits for this article and are adequately covered elsewhere (see article by Roos *et al*. for additional information). For immunogold labeling for HRSEM, the following points are important.

1. Size of Probe

The choice of probe size is a compromise between sensitivity and subsequent detection. Very small gold probes (around 1 nm) have minimal steric hindrance and consequently label with maximum sensitivity. One-nanometer gold has been visualized by backscatter imaging in HRSEM (Hermann *et al*., 1991), but this is at the limits of resolution and is best increased in diameter *in situ* by silver or gold enhancement to a size at which it can be visualised more easily (around 5–10 nm). We have used both 5- and 10-nm gold as a good compromise between sensitivity and localization. Because most modern instruments will discriminate easily between 5- and 10-nm labeling, these can be used together successfully for double-labeling studies.

2. Coating

Using gold probes obviously prohibits gold coating for SEM. In the past, gold-labelled specimens have been coated with carbon, mainly to inhibit charging, but carbon produces a severely limited secondary electron signal and, consequently, little topographical information. We have found that a 1.5-nm chromium coating provides the ideal solution, retaining the full secondary electron-generated surface information, without compromising the detection of gold by backscattered electron detection (Allen and Goldberg, 1993).

In this situation, having found that "mixed" imaging of SE and BSE signals was not satisfactory, we have chosen to collect each signal separately (but simultaneously) and then to superimpose the gold BSE signal onto the secondary signal (retaining register) in Adobe Photoshop, often altering the colour to improve the appearance of label against the monochrome background. In modern instruments with good low kilovolt performance, uncoated or carbon-coated imaging will generate such a strong signal from gold probes that they are observed easily in secondary electron imaging.

IV. COMMENTS

Although field emission SEM has been available for some time, it is still a relatively new technique in cell biology. The procedures given here may need to be modified to optimize the preservation of some structures. Probably the most difficult step is exposing recognizable and undamaged intracellular surfaces. Isolation of organelles offers the possibilities of further characterization by other methods, but gives no "*in situ*" information and may involve extensive biochemical protocols. Resinless sections and dry fracture give *in situ* information, but only after some initial extraction of the cell. Freeze fracture, followed by frozen hydrated coating and visualization, may alleviate these problems but is limited by the plane of fracture, as the structure of interest may not be exposed. It is also technically difficult and expensive. Osmium etching results in spectacular images of intracellular membranes, but the uncertainty of what is removed makes interpretation difficult. Direct visualization of biological interfaces in cell-free systems (e.g., *in vitro* nuclear formation) is a particularly promising area (Goldberg *et al*., 1992, 1997). Considerable fresh structural information has also been demonstrated for nuclear pore complexes and associated structures (Ris, 1991; Goldberg and Allen, 1992, 1996; Kiseleva *et al*., 1996).

Acknowledgments

T. D. Allen, S. Rutherford, and S. Murray are supported by CRUK and M. W. Goldberg is supported by a Wellcome Lectureship. The mitochondrial pellets were supplied by Dr. E Gottlieb (Beatson Institute).

References

Allan, V. J., and Vale, K. (1994). Movement of membrane tubules along microtubules *in vitro*, *J. Cell. Sci.* **107**, 1885–1895.

Allen, T. D., and Goldberg, M. W. (1993). High resolution SEM in cell biology. *Trends Cell Biol* **3**, 203–208.

Allen, T. D., Jack, E. M., and Harrison, C. (1988). Three dimensional structure of human metaphase chromosomes determined by scanning electron microscopy. *In* "*Chromosomes and Chromatin*" (K. W. Adolph, ed.), Vol. 11, pp. 52–70. CRC Press, Boca Raton, FL.

Allen, T. D., Rutherford, S. A., Bennion, G. R., Wiese, C., Riepert, S., Kiseleva, E., and Goldberg, M. W. (1998). Three dimensional surface structure analysis of the nucleus. *Methods Cell Biol*. **53**, 125–138.

Apkarian, R. P., Gutekunst, M. I., and Joy, D. C. (1990). High resolution SEM study of enamel crystal morphology. *Electron Microsc. Tech*. **14**, 70–78.

Goldberg, M. W., and Allen, T. D. (1992). High resolution scanning electron microscopy of the nuclear envelope: Demonstration of a new regular, fibrous lattice attached to the baskets of the nucleoplasmic face of the nuclear pores. *J. Cell Biol*. **119**, 1429–1440.

Goldberg, M. W., and Allen, T. D. (1996). The nuclear pore complex and lamina: Three dimensional structures and interactions determined by field emission in lens scanning EM. *J. Mol Biol*. **257**, 848–865.

Goldberg, M. W., Blow, J. J., and Allen, T. D. (1992). The use of the field emission in-lens scanning electron microscope to study the steps of assembly of the nuclear envelope *in vitro*. *J. Struct. Biol*. **108**, 257–26.S.

Goldberg, M. W., Wiese, C., Allen, T. D., and Wilson, K. L. (1997). Dimples, pores, star rings and thin rings on growing nuclear envelopes: Evidence for structural intermediates in nuclear pore complex assembly. *J. Cell Sci*. **110**, 409–420.

Gottlieb, E., Armour, S. M., Harris, M. H., and Thompson, C. B. (2003). Mitochondrial membrane potential regulates matrix configuration and cytochrome c release during apoptosis. *Cell Death Differ*. **10**, 709–717.

Hermann, R., Schwartz, H., and Muller, M. (1991). High precision immunostaining electron microscopy using Fab fragments coupled to ultra-small colloidal gold. *J. Struct. Biol*. **107**, 38–47.

Kiseleva, E., Goldberg, M. W., Daneholt, B., and Allen, T. D. (1996). RNP export is mediated by structural reorganisation of the nuclear pore basket. *J. Mol. Biol*. **260**, 304–311.

Muller, M., and Hermann, H. (1990). Towards high resolution SEM of biological objects. *In* "*Proceedings 12th International Congress on Electron Microscopy*" (L. D. Peachy, D. R. Williams, eds.). Vol. 3, pp. 4–5. San Francisco Press, San Francisco.

Newmeyer, D. D., and Wilson, K. L. (1991). Egg extracts for nuclear import and nuclear assembly reactions. *In* "*Methods in Cell Biology*" (B. K. Kay, H. B. Peng, eds.), Vol. 36, pp. 608–635. Academic Press, San Diego.

Reipert, S., Reipert, B. M., and Allen, T. D. (1994). Preparation of isolated nuclei from K562 haemopoietic cell line for high resolution scanning electron microscopy. *Microsc. Res. Tech*. **29**, 54–61.

Ris, H. (1991). The three dimensional structure of the nuclear pore complex as seen by high voltage electron microscopy and high resolution low voltage scanning electron microscopy. *EMSA Bull*. **21**, 54–56.

Tokyasu, K. T. (1986). Application of cryomicrotomy to immunocytochemistry. *J. Microsc*. **143**, 139–149.

Tokuyasu, K. T. (1989). Use of poly(vinylpyrrolidone) and poly(vinyl alcohol) for cryoultramicrotomy. *Histochem. J*. **21**, 163–171.

Walther, P. (2003). Recent progress in freeze-fracturing of high pressure frozen samples. *J. Microsc*. **212**, 34–43.

PART

D

MICRODISSECTION

SECTION

12

Tissue and Chromosome Microdissection

CHAPTER

34

Laser Capture Microdissection

Virginia Espina and Lance Liotta

I. INTRODUCTION

Laser capture microdissection (LCM) is a technology for procuring pure cell populations from a heterogeneous tissue or cytological preparation under direct microscopic visualization. One of the most common problems encountered by the investigator involved in the proteomic or genetic analysis of tissue samples arises from the heterogeneous nature of the tissue and the need for a pure cell population for studies. There are often many cell populations in a single tissue. When working with malignant or premalignant tissues, the abnormal cells of interest may lie within, or very close to, areas of totally normal cells.

LCM enables the investigator to isolate single cells or multiple cells, representing specific malignant, premalignant, or normal tissues. The ability to analyze pure cell populations permits analysis of molecular events representative of the tissue at the time of sample procurement. Comparisons of molecular events at tissue interfaces may be analyzed in relation to the microtumor environment using LCM technology. The isolated cells may be assayed for DNA, RNA, or protein by any method with sufficient sensitivity.

A stained section of the heterogeneous tissue is mounted on a glass microscope slide and viewed under high magnification. The slide position is manipulated via a joystick, allowing visualization of the cells for microdissection. Cells of interest are directed under an infrared (IR) laser, mounted in the optical axis of the microscope. A thermoplastic film, placed in direct contact with the tissue section, is melted with a laser pulse. The molten polymer surrounds and embeds the cells in the vicinity of the laser pulse, forming a polymer–cell composite. When the film is lifted away from the tissue, the cells of interest are sheared from the tissue section and remain adhered to the polymer. Incorporation of an energy-absorbing dye into the thermoplastic film, coupled with the low energy of the IR laser, prevents damage to the cellular constituents. Extraction buffers are applied to the film for solubilization of DNA, RNA or protein contained in the captured cells (Fig. 1).

Automated LCM (AutoPix, Arcturus Bioscience, Mountain View, CA) combines the features of LCM, robotics, and imaging software to facilitate the visualization and microdissection of tissue. Quantitation of the laser spot size and percentage overlap of the laser pulses add a level of standardization to the microdissection technology. Cell recognition software enhances LCM technology for fluorescent immunostained tissues.

The AutoPix makes it possible for the operator to conduct "hands off" microdissection once the relevant cells are marked by the operator or are recognized by the computer image recognition software.

II. MATERIALS AND INSTRUMENTATION

A. Specimen

1. For protein analysis of microdissected tissue, use frozen tissue sections cut at 2–15 µm or cytospin preparations.
2. For RNA or DNA analysis of microdissected tissue, use frozen tissue sections cut at 2–15 µm, cytospin preparations, or ethanol or formalin-fixed paraffin-embedded tissue sections.

Copyright 2006, Elsevier Science (USA).
All rights reserved.

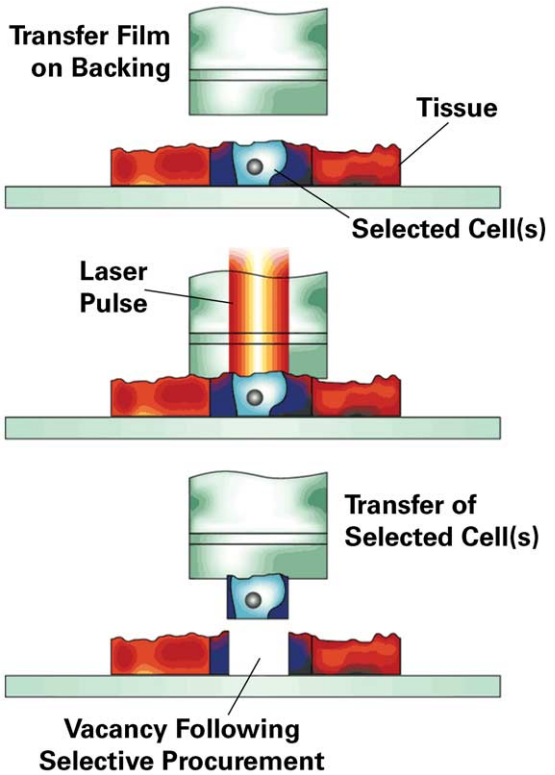

FIGURE 1 A polymer film is placed in direct contact with the tissue. A pulsed infrared laser melts the polymer, allowing the polymer to surround and embed the cells in the vicinity of the laser pulse. The polymer–cell composite is removed from the tissue section, resulting in microdissection of the cells.

3. Precleaned, uncoated glass microscope slides (Cat. No. G15978A, A. Daigger & Co.)
4. Hematoxylin and eosin (H&E) stain:
   a. Mayer's hematoxylin solution (Cat. No. MHS-128, Sigma Diagnostics)
   b. Hematoxylin is an inhalation and contact hazard. Wear gloves when handling.
   c. Eosin Y solution, alcoholic (Cat. No. HT1101-128, Sigma Diagnostics)
   d. Eosin Y is flammable. Store away from heat, sparks and open flames.
   e. Scott's tap water substitute blueing solution (Cat. No. CS410-4, Fisher Scientific)
5. Ethanol gradient: 70% (v/v in purified H_2O), 95%, and 100% ethanol
   a. Ethyl alcohol, absolute 200 proof for molecular biology (Cat. No. E702-3 Sigma-Aldrich Chemical Co.)
   b. Ethanol is flammable. Store away from heat, sparks and open flames. Do not ingest.
   c Contact hazard, wear gloves when handling.
   d. Purified water (type I reagent grade water)
6. Xylene or Sub-X xylene substitute xylene (Cat. No. 8671-10, Mallinckrodt Baker, Inc.;
   a. Sub-X Xylene substitute, (Cat. No. 03670, SurgiPath Medical Industries, Inc.)
   b. Xylene vapor is harmful or fatal, use with appropriate ventilation, and discard in appropriate hazardous waste container. Xylene and Sub-X xylene substitute are flammable; store and use away from heat, sparks, and open flame.
7. 500-µl microcentrifuge tubes (Safe-Lock Eppendorf tubes Cat. No. 22 36 361-1, Brinkmann Instruments; or GeneAmp 500-µl thin-walled PCR reaction tubes Cat. No. 9N801-0611, Perkin-Elmer Applied Biosystems)
8. 50-ml polypropylene tubes (Cat. No. 352070 Falcon Blue Max Becton-Dickinson and Co.)
9. Extraction buffer for constituent of interest
10. Tweezers or hemostat
11. 100-ml graduated cylinder

B. Instrumentation

1. PixCell II, IIe, or AutoPix laser capture microdissection system (PixCell IIe Cat. No. LCM1105 or AutoPix Cat. No. LCM1110, Arcturus Bioscience)
2. CapSure Macro LCM caps or HS CapSure LCM caps (CapSure Macro caps Cat. No. LCM0201; HS CapSure caps Cat. No. LCM0204, Arcturus Bioscience)
3. –80°C freezer
4. Vortex
5. 37–70°C oven
6. Microcentrifuge

III. PROCEDURE

A. Preparing Tissue Section

1. Prepare staining solution and ethanol gradient. Dispense approximately 50 ml each of Mayer's hematoxylin, eosin (optional for protein analysis), purified H_2O, and Scott's tap water into appropriately labeled covered containers, such as polypropylene Falcon tubes.
2. Dispense 50 ml of xylene or xylene substitute into a suitable labeled, covered container. Do not place xylene in polystrene containers, as xylene will dissolve the polystrene. Polypropylene tubes are recommended.
3. To prepare 70% ethanol, dispense 30 ml of purified H_2O into a 100-ml graduated cylinder. Add 70 ml of 200 proof ethyl alcohol. Mix well. Pour approximately 50 ml into two suitable labeled containers.

4. To prepare 95% ethanol, dispense 5 ml purified H_2O into a 100-ml graduated cylinder. Add 95 ml of 200 proof ethyl alcohol. Mix well. Pour approximately 50 ml into two suitable labeled containers.

5. Use tweezers or hemostats to dip slides in each solution for the indicated time. Blot slides on the short edge of the slide with an absorbent paper between each solution. Eosin is optional for staining tissue intended for protein analysis.

B. Protocol for Staining Frozen Tissue

a. 70% ethanol: 5 s
b. Purified water: 10 s
c. Mayer's hematoxylin: 15–30 s
d. Purified water: 10 s
e. Scott's tap water: 10 s
f. 70% ethanol: 10 s
g. Eosin-Y (optional): 3–10 s
h. 95% ethanol: 10 s
i. 95% ethanol: 10 s
j. 100% ethanol: 10 s
k. 100% ethanol: 1 min
l. Xylene or xylene substitute: 30–60 s

C. Protocol for Staining Paraffin-Embedded Tissue

a. Xylene: 5 min
b. Xylene: 5 min
c. 100% ethanol: 30 s
d. 95% ethanol: 30 s
e. 70% ethanol: 30 s
f. Purified water: 20 s
g. Mayer's hematoxylin: 15–30 s
h. Purified water: 20 s
i. Scott's tap water: 20 s
j. 70% ethanol: 20 s
k. Eosin-Y (optional): 3–10 s
l. 95% ethanol: 20 s
m. 95% ethanol: 20 s
n. 100% ethanol: 20 s
o. 100% ethanol: 1 min
p. Xylene or xylene substitute: 30–60 s

D. Conducting Microdissection

1. To begin operation of the PixCell II or IIe, turn on the power switches for:

PixCell II/IIe (switch is located at the right back of the microscope)
Controller (located on the back of the controller)
Video monitor (located on the lower front right) for PixCell II only
Computer (located on the front of the CPU)
Computer monitor (located on the front of the computer monitor)

There is no warm-up period required for the PixCell II/IIe. The instrument is ready for operation. The AutoPix requires a warm-up period of 1 h prior to use.

2. Load the CapSure cassette module with a CapSure cartridge.

a. Remove the CapSure cassette module from the platform.
b. Press in the locking pins on each end to hold the cassette in the load position.
c. Slide a CapSure cartridge onto the cassette until it stops. Two cartridges may be loaded onto the cassette module.
d. After the cartridges are loaded, pull the locking pins out to lock the cartridges in place. Load the cassette module onto the PixCell II/IIe.

3. Move the joystick into the vertical position to ensure proper positioning of the cap in relation to the capture zone.

4. Place the air dried microscope slide containing the prepared and stained specimen for microdissection on the stage. After the target area for dissection is in the viewing area, press the "vacuum" switch on the front of the controller to activate the vacuum and hold the slide in place during microdissection.

5. Slide the CapSure cassette backward or forward so that a cap is sitting at the "load" position. Swing the placement arm over the cap. While placing one hand over the weight to prevent jarring of the cap and improper seating, lift the placement arm and place the cap onto the slide.

6. Access the LCM software program by double clicking on the Arcturus software icon.

7. Enter your user name or select a name from the list. Click on "acquire data".

8. Enter a study name or select a study name from the list. Click on "select".

9. Enter the slide number and cap lot number. If desired, notes concerning the slide or study may be entered as "notes."

10. Click the checkbox for "stamp images with name, date, and time" if this information is to be imprinted on the images created during LCM. Click "continue." The live video screen displays the current image on the microscope. The images may be saved as you work.

Map image: lower power objective image of the general area to be microdissected
Before image: intact tissue prior to microdissection
After image: tissue after microdissection
Cap image: microdissected tissue only

11. Enable the laser by turning the key switch located on the front of the controller and then press the "laser enable" button. Pressing this button will activate the target beam when the placement arm is in the transfer position.
12. Verify that the laser is in focus.
    a. Select 7.5-µm spot size using the "spot size adjust" lever found on the left side of the microscope.
    b. Rotate the objectives of the microscope until the 10× objective is in use.
    c. Reduce the intensity of the light through the optics until the field viewed on the monitor is almost dark and the target beam is viewed easily.
    d. Using the "laser focus adjust" located just below the size adjustment lever, adjust the target beam until the beam reaches the point of sharpest intensity and most concentrated light with little or not "haloing." The laser should now be focused for any of the three laser sizes. Select the laser spot size suitable for the microdissection and cell size.
13. Press the red pendant button to fire a test laser pulse. Observe the spot as the laser is fired. Firing the laser pulse causes the polymer to melt or wet in the vicinity of the laser pulse. There should be a distinct clear circle surrounded by a dark ring. This dark ring is produced by a dye impregnated in the polymer film. The dye is concentrated around the edges of the melted polymer, permitting visualization of the melted polymer in the area of the laser pulse. This pattern indicates proper laser focusing, operation of the laser, and the performance of the CapSure film. The ring should be sharp in appearance. A "fuzzy" ring could indicate improper focusing of the laser.
14. Adjust the "power" and "duration" of the laser pulse with the up-and-down arrows on the front of the controller to obtain a wetted polymer spot with the same diameter as the selected laser size. Use the suggested ranges as a reference point. These settings can be adjusted up or down to customize the wetted polymer spot to the type and thickness of the tissue to be dissected. The suggested settings are as follow

Spot size	Power	Duration
7.5 µm	25 mW	3.0 ms
15 µm	30 mW	5.0 ms
30 µm	30 mW	8.0 ms

15. Single cell microdissection is possible by adjusting the power and duration settings such that a very narrow area of the polymer is melted with each laser pulse. Suggested settings for single cell microdissection are power 45 mW and duration 650 µs.
16. To perform the microdissection, locate the cells of interest. Using the target beam to guide the dissection, press the pendant switch for single shots. For a rapid fire of pulses, hold the pendent switch down. The frequency interval can be adjusted on the controller by selecting "repeat" and then selecting the desired time between laser pulses.
17. After the desired number of shots has been collected on a cap, remove the cap by lifting it off the slide using the placement arm. Lift and rotate the arm until the cap is over the "cap removal site." Lower the arm and then rotate the arm back toward the slide. The cap will remain sitting in place on the removal site. Remove the cap and blot the polymer surface using the LCM CapSure pad to remove any nonspecific tissue or debris that may have adhered to the surface (Fig. 2).
18. Insert the polymer end of the cap into the top of a 500-µl microcentrifuge tube. The sample is now ready for extraction of the desired components or to be frozen at –80°C for analysis at a later date.
19. Click the "done" button on the image toolbar. Another slide may be microdissected, another study initiated, or the program may be terminated.
20. Click "save images" to save the images on the C drive of the PC. The images may be copied to a PC-formatted, 100-mb zip disk as a .JPEG or .TIFF format after saving the image on the C drive.
21. Click on "save data."
22. After all dissections are completed, the PixCell II/IIe should be put in shutdown by first pressing the "laser enable" button to disable the laser. Turn off the power to the PixCell II/IIe, the controller, and the video monitor.

IV. COMMENTS

When using the 30-µm laser spot size, the operator can expect to collect on average five to six cells per laser pulse. Using this information, it is possible to estimate the number of cells captured based on the number of pulses fired during the collection of cells:

Number of pulses × 5 = total cells captured

V. PITFALLS

At least three classes of adhesive forces are acting on the selected cells during microdissection: (1) adhesion upward to the locally melted polymer, (2) adhesion laterally to the surrounding tissue elements, and

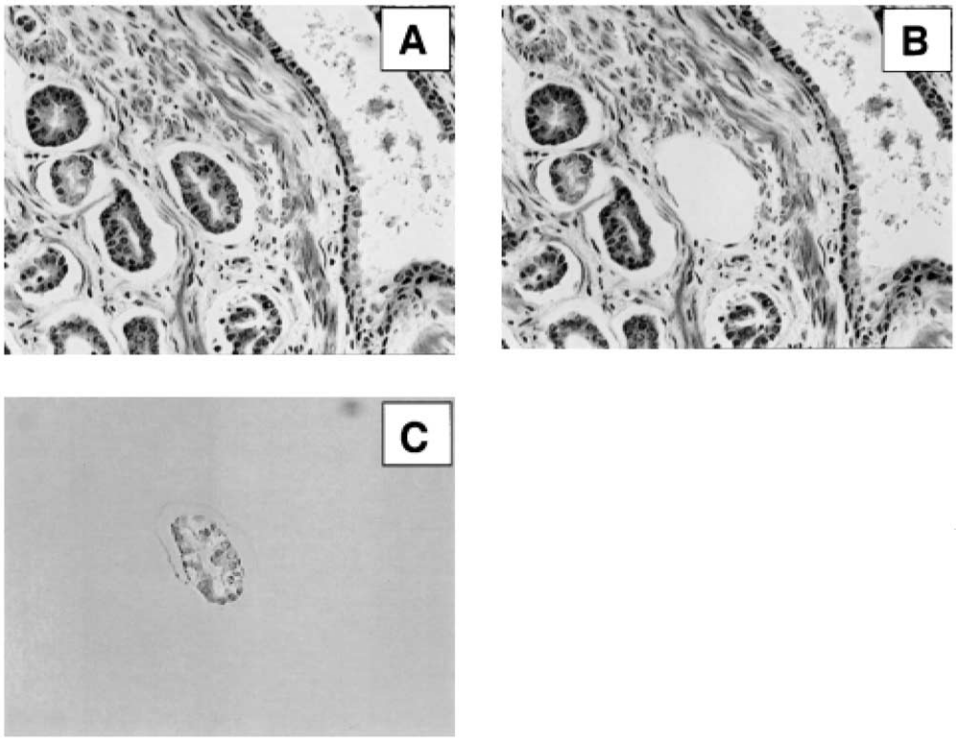

FIGURE 2 Laser capture microdissection of an individual gland in breast ductal carcinoma. (A) H&E stain of heterogeneous human breast tissue, (B) microdissection of the gland of interest, and (C) polymer–cell composite after transfer to film.

(3) adhesion downward to the glass slide. If adhesive forces #2 and #3 are too great, then microdissection may be incomplete. Lateral adhesive forces are largely a function of the extracellular matrix composition and tissue architecture. The operator does not have much control over lateral adhesive forces. However, slide coatings and treatments can markedly influence adhesion to the glass slide.

1. Maintaining upward adhesive forces:
   a. Tissue sections should be flat and free of folds and wrinkles. Unevenness can prevent proper seating of the polymer cap and limit effective cell capture.
   b. Incomplete deparaffinization of embedded tissues limits the amount of tissue transferred during microdissection. Deparaffinization times listed are minimal times and, if necessary, may be extended, allowing complete removal of the paraffin from the tissue section.
   c. Improper focusing of the laser may cause unsuccessful microdissection. The laser should be focused on the 7.5-μm spot size with the 10× objective. The laser should be focused at the beginning of each LCM session and whenever the slide type being used is changed or the cap is repositioned on the slide.
2. Limiting lateral adhesive forces: Tissue section thickness should be between 2 and 15 μm. Optimal microdissection is achieved with tissue sections cut at 5–8 μm.
3. Minimizing downward adhesive forces:
   a. Use plain, uncharged glass microscope slides for optimal microdissection. While some success has been achieved using poly-L-lysine, silanized, or charged slides with lung tissue, best results for the majority of tissues are obtained with plain glass slides.
   b. Preparation of frozen sections requires the slides to be frozen at −80°C or to proceed immediately with staining after placing the tissue section onto the slide. Never allow the tissue to dry on the slide. Drying the tissue on the slide makes LCM almost impossible and will denature the analyte molecules.
   c. Incomplete dehydration of the tissue section prior to LCM limits the operator's success in microdissection. The xylene rinse is essential for complete dehydration of the tissue on the slide. It is imperative that each staining proto-

col for LCM incorporates a thorough rinse in xylene or xylene substitute. If it is suspected that the slide is not completely dehydrated, allow it to sit in xylene for additional time.

References

Banks, R. E., Dunn, M. J., *et al*. (1999). The potential use of laser capture microdissection to selectively obtain distinct populations of cells for proteomic analysis. *Electrophoresis* **20**, 689–700.

Emmert-Buck, M. R., Chuaqui, R., *et al*. (1996). Laser capture microdissection. *Science* **274**(5289), 998–1001.

Fend, F., Emmert-Buck, M. R., *et al*. (1999). Immuno-LCM: Laser capture microdissection of immunostained frozen sections for mRNA analysis. *Am. J. Pathol*. **154**, 61–66.

Ornstein, D. K., Englert, C., *et al*. (2000). Characterization of intracellular prostate-specific antigen from laser capture microdissected benign and malignant prostatic epithelium. *Clin. Cancer Res*. **2**, 353–356.

Paweletz, C. P., Charboneau, L., *et al*. (2001). Reverse phase protein microarrays which capture disease progression show activation of pro-survival pathways at the cancer invasion front. *Oncogene*. **20**(16), 1981–1989.

Sgroi, D., Teng, S., *et al*. (1999). *In vivo* gene expression profile analysis. *Cancer Res*. **59**, 5656–5661.

Simone, N. L., Bonner, R. F., *et al*. (1998). Laser capture microdissection: Opening the microscopic frontier to molecular analysis. *Trends Genet*. **14**, 272–276.

Simone, N. L., Paweletz, C. P., *et al*. (2000). Laser Capture Microdissection: Beyond Functional Genomics to Proteomics. *Mole Diag*. **5**(4), 301–307.

CHAPTER

35

Chromosome Microdissection Using Conventional Methods

Nancy Wang, LiQiong Li, and Harindra R. Abeysinghe

I. INTRODUCTION

During cytogenetic analysis there are frequently complex chromosomal structural aberrations, which are unidentifiable by chromosome banding analysis. Fluorescence *in situ* hybridization (FISH) combined with G-banding analysis (Xu and Wang, 1994) has significantly improved the accuracy of chromosome identification. However, the efficacy of FISH analysis depends on the probes chosen, which in turn depend on the G-banding result. It is very difficult to choose the adequate probe(s) for FISH analysis when no clue is available from banding analysis. Therefore, FISH can serve as a tool for verification and confirmation. The recently developed multicolor or spectral karyotyping highly facilitates the identification of complex interchromosomal structural abnormalities. However, its application is limited to nonhomologous rearrangements and its efficacy depends on the size of the chromosome segment involved. Furthermore, it can identify the chromosomes involved but not the specific segment or breakpoints involved.

In contrast, the chromosome microdissection approach provides a straightforward method for identifying any chromosomal segment of unknown origin by dissecting the segment of interest and isolating, amplifying, fluorescence labeling, and reverse *in situ* hybridizing DNA to normal metaphase spreads (Ludecke *et al*., 1989; Bohlander *et al*., 1992; Carter *et al*., 1992; Meltzer *et al*., 1992; Ruano *et al*., 1992; Telenius *et al*., 1992; Guan *et al*., 1993; Zhang *et al*., 1993). Once the components of the aberrant chromosome are identified, conventional FISH with whole chromosome painting probes can be applied to define the relative position of the components in the marker chromosome. This micro-FISH approach has been applied successfully in the identification of ring chromosomes (Xu *et al*., 1995, 1998), homogeneous staining regions (Xu *et al*., 1996; Abeysinghe *et al*., 1999), and double minutes (Sen *et al*., 1994). Thus, micro-FISH can be used to identify not only the origin of the marker chromosome, but also the regions and breakpoints.

However, in the reverse FISH the specificity of the probe generated relies on the accurate recognition and dissection of the specific target chromosome/segment and on the precise extraction, amplification, and labeling of the DNA with minimum background contamination. The skills, procedures, and setup involved in micro-FISH are too complicated to be established in the routine clinical cytogenetic laboratory. This is the major limitation to the application of reverse FISH by chromosome microdissection. With a modified fixation procedure (Xu *et al*., 1995), however, specimens can be stored and shipped to experienced laboratories or diagnostic centers. In addition to its clinical application, chromosome microdissection can be used to generate band-specific probes (Guan *et al*., 1993) that can be used in establishing intrachromosomal spectral karyotyping. A combination of interchromosomal spectral karyotyping with intrachromosomal spectral banding analysis would be ideal for chromosome analysis in neoplasia.

II. MATERIALS AND INSTRUMENTATION

A. Materials

Methyl alcohol (Fisher Scientific, #MD3017-4)
Potassian chloride solution 0.075 *N* (Irvine Scientific, #9281)

Copyright 2006, Elsevier Science (USA).
All rights reserved.

Acetic acid, glacial ACS (Fisher Scientific, #A38-500)
Colcemid 10 µl/ml in HBSS (GIBCO, #15210-040)
Trypsin (1:250) (GIBCO, #27250-018)
KaryoMax Giemsa stain (Lab Chem Inc., #2C 14840-7)
Hank's balanced salt solution ×1; without $CaCl_2$ + Mg (Sigma, #119349)
Buffer tablets "GURR" (GIBCO, #10582-013)
Deionized distilled (dd) water
T7 DNA polymerase (Sequenase, Version 2.0, USB #70755Y)
Topoisomerase 1 (Promega, #M2851)
Biotin-16-dUTP (Boehringer Mannheim, #1093070)
Taq DNA polymerase (Applied Biosystems, #4311816)
Universal primer 5'-CCGACTCGAGNNNNNNNNAT GTGG-3' (Telenius *et al*., 1992)
15-ml sterile polystyrene tubes (Corning, #43005)
Microneedle (Sutter Instrument Co., #BR100-15)
Coverslips (VWR, 24 × 60 mm #48393-106)

B. Instrumentation

Incubator, 37°C
Inverted microscope (Nikon DIAPHOT-TMD)
9-in. Pasteur glass pipettes (VCR, #53283-915) and bulbs
Micromanipulators (Narashige, Models MM-88 and MO-302)
Micropipete puller (Narishige, Model PB-7)
Thermal cycler (MJ Research Inc., Model PTC-200)
Slide warmer (VWR)
Coplin jars (0.50-ml capacity)
Thin-walled microtubes (Laboratory Products Sales, #430)
Microcon YM-100 columns (Millipore, #42413)

III. PROCEDURES

A. Preparation of Cells for Microdissection

This procedure is modified from those of Wang and Federoff (1972) and Xu *et al*. (1994).

Solutions

1. *Colcemid metaphase arresting solution*: 10 µg/ml (Sigma D1925)
2. *Hypotonic solution*: Prepare daily by mixing 0.4% KCl (EM Science PX1405-1) (in dd H_2O) and 0.4% sodium citrate (EM Science PX0445-1) (in dd H_2O) in equal volume
3. *Fixation solution*: Prepare daily by mixing methanol (Mallinckrodt CAS 67-56-1) and glacial acetic acid (Fisher Scientific A38-500 CAS 64-19-7) in a ratio of 3:1 (v/v)
4. *Trypsin solution*: 0.625 g trypsin (1:250; GIBCO #27250-018) in 100 ml dd H_2O
5. *GURRS buffer solution*: Dissolve one GURRS buffer tablet (GIBCO 10582-013) in 1 liter dd H_2O, adjust pH to 6.8
6. *Giemsa staining solution*: 2–3 ml Giemsa (LabChem Inc. LC14840-7) in 50 ml GURRS buffer solution

Steps

1. Grow cells in cell culture medium supplemented with 10% fetal bovine serum at 37°C in a 6% CO_2 humidified incubator.
2. Prepare chromosome metaphase spreads from a proliferative cell population using colcemid (5–10 µl/ml) for metaphase arresting, hypotonic treatment followed by fixation for chromosome harvesting.
3. Harvest cells either *in situ* or in suspension and then drop on 24 × 60-mm #1.5 coverslips.
4. Perform Giemsa–trypsin–G-banding analysis (GTG) by standard procedure (Wang and Federoff, 1972) for identification of the target chromosome or chromosome segment for microdissection using an inverted microscope.

B. Chromosome Microdissection Combinded with FISH Analysis (Micro-FISH)

The procedure of micro-FISH is performed according to Guan *et al*. (1993) with modification (Xu *et al*., 1995).

Solutions

1. *0.625% banding trypsin*: Add 0.25 g trypsin (1:250) powder to 100 ml dd H_20, mix well, aliquot to 2.0 ml, and store at –20°C
2. *GURR buffer*: Reconstitute with ddH_20 (1 tablet/1 liter), adjust pH to 6.8
3. *Collection buffer (5 µl)*: 40 m*M* Tris–HCl, pH 7.5, 20 m*M* $MgCl_2$, 50 m*M* NaCl, 200 µ*M* of each dNTP, 1 unit Topo 1, and 5 pmol of universal primer
4. *PCR reaction mixture (50 µl)*: 10 m*M* Tris–HCl, pH 8.4, 2 m*M* $MgCl_2$, 50 m*M* KCl, 0.1 mg/ml gelatin, 200 µm of each dNTP, 50 pmol universal primer, and 2 units *Taq* DNA polymerase.
5. *T7 DNA polymerase working solution*: Dilute T7 DNA polymerase (13 U/µl) with dilution buffer to 1.5 U/µl.
6. *Labeling solution (50 µl)*: 100 m*M* Tris–HCl, pH 8.4, 2 m*M* $MgCl_2$, 50 m*M* dcl, 0.1 mg/ml gelatin, 200 µl 4 dNTP, 50 pmol universal primer, 20 µ*M* biotin-16-dUTP, and 2 units *Taq* DNA polymerase.
7. Whole chromosome painting probes obtained from commercial laboratories (Vysis)

1. Chromosome Microdissection and DNA Amplification

Steps

1. Prior to microdissection, fix cells in fixative solution by three washes.
2. Prepare metaphase spreads on 24 × 60-mm #1.5 coverslips and stain by GTG banding.
3. Make microneedles with the micropipette puller according to the manufacturer's manual and UV treat overnight to rule out background DNA contamination.
4. Perform microdissection on the target chromosome/segment, which is identified by its specific G-banding pattern, with glass microneedles (Fig. 1) controlled by a Narashige micromanipulator (Models MM-88 and MO-302) attached to an inverted microscope.
5. Transferr the dissected chromosome adherent to the microneedle to a 0.2-ml microcentrifuge tube containing 5 µl of collection buffer.
6. Cover the collection buffer with 45 µl of mineral oil and incubate at 37°C for 30 min, followed by heat soak at 94°C for 30 min.
7. Use a gene Amp PCR System 9600 (Perkin-Elmer Atus) for DNA amplification.
8. Perform an initial eight cycles of PCR (denaturation at 94°C for 1 min, anneling at 30°C for 2 min, and extension at 37°C for 2 min) by adding approximately 0.3 units of T7 DNA polymerase (Sequence Version 2.0, USB) at each cycle.
9. Add 50 µl of PCR reaction mixture to the tube.
10. Heat the reaction to 95°C for 3 min followed by 35 cycles at 94°C for 1 min, 56°C for 1 min, 72°C for 2 min, with a final extension at 72°C for 5 min.

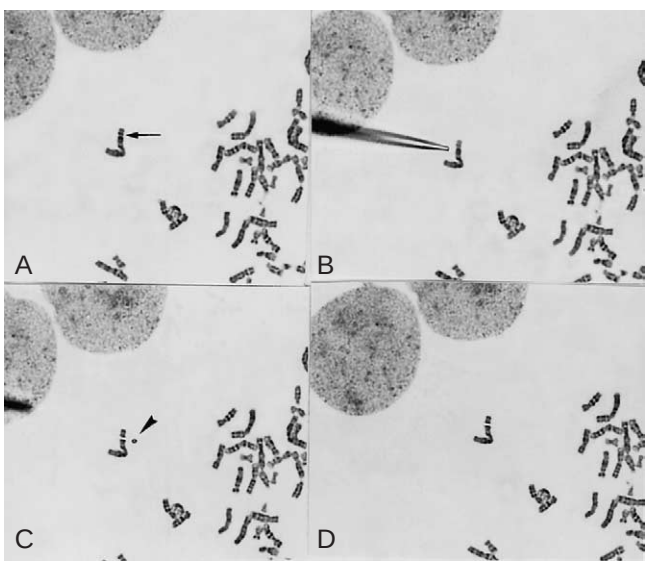

FIGURE 1 Microdissection procedure in progress. The glass needle is aligned using a micromanipulator and the chromosome band or region is dissected. The needle is then used to pick up the dissected piece (C) and transfer it into a collection tube.

2. Fluorescence Labeling of the PCR Product (Fig. 2)

Steps

1. Label a 2-µl aliquot of the PCR product for 16 cycles in a 50-µl secondary PCR with the same procedure

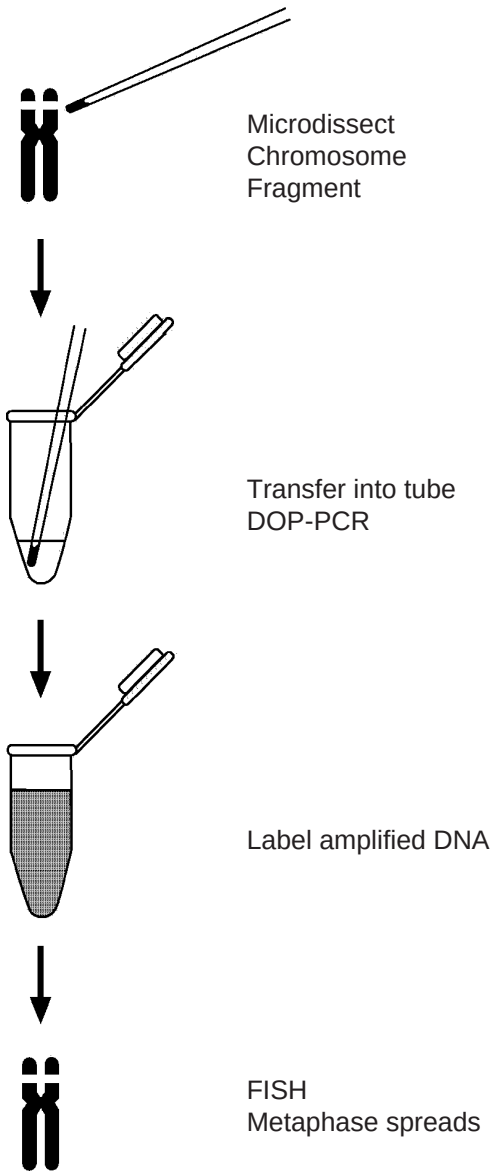

FIGURE 2 Diagram and flowchart of the micro-FISH procedure. Once the whole chromosome or segment is dissected, it is transferred into a collection tube and PCR amplified using random primers. An aliquot of this reaction is then reamplified by PCR with the addition of biotin/digoxigenin dUTP. The labeled PCR products are column purified for use as FISH probes.

as described earlier, except for the addition of 20 m*M* biotin-11-duTP (BMB).
2. Purify the labeled PCR products using a Centricon 100 (Amicon) filter.
3. Add 100 µg of the probe to a 10-µl hybridization mixture containing 55% formamide, 10% detran, 1 × SSC, and 5–10 µg COT-1 DNA (BCL).

3. Verification of the Specificity of the Dissected Chromsome/Segment

Steps

1. Grow the cells with the dissected chromosome/segment on 22 × 22-mm coverslips in 35 × 10-mm petri dishes.
2. Block the cells by treatment with colcemid (Gibco), 0.1 µg/ml for 1 h, hypotonically treated, fixed, and harvested using standard procedures.
3. G-band the chromosomes following trypsin treatment and stain with Giemsa stain.
4. After GTG-banding and karyotyping, destain slides with xylene, xylene/ethanol (1/1, v/v), and methanol/acetic acid (3/1, v/v), refix in 3.7% formaldhyde/phosphate-buffered saline (PBS), air dry, and reuse for FISH as described by Klever *et al*. (1991) using the biotin-labeled probe generated from the dissected chromosome/segment to verify the specificity of the probe.
5. Once the specificity of the probe is confirmed, the probe can be hybridized back to normal metaphase spreads to identify the origin of the dissected chromosome segment.

4. Identification of the Origin of the Dissected Chromosome/Segment(s)

Steps

1. Analyze normal metaphase spreads by GTG banding.
2. Apply FISH analysis with the probe specific for the dissected chromosome/segment to normal metaphase spreads after GTG-banding analysis using the procedure described in the previous section.
3. Combine the result obtained from GTG banding with that obtained from FISH analysis to identify the origin or components of the chromosome/segments dissected.

5. Forward FISH Analysis to Identify the Relative Position of the Components of the Dissected Chromosome

Steps

1. Apply FISH analysis with the commercially available whole chromosome painting probes specific for each of the chromosome components, which are identified by microdissection to the GTG-banded metaphase spreads containing the dissected chromosome.
2. Combining the G-banding and FISH results obtained from each probe determines the relative position of the components on the chromosome dissected.

References

Abeysinghe, H. R., Cedrone, E., Tyan, T., Xu, J., and Wang, N. (1999). Amplification of C-myc as the origin of the homogeneous staining region in ovarian carcinoma detected by micro-FISH. *Cancer Genet. Cytogenet.* **114**, 136–143.

Bohlander, S. K., Espinosa, R., III, LeBeau, M. M., Rowley, J. D., and Diaz, M. O. (1992). A method for the rapid sequence-independent amplification of microdissected chromosomal material. *Genomics* **13**, 1322–1324.

Carter, N. P., Ferguson-Smith, M. A., Perryman, M. T., Telenius, H., Pelmear, A. H., Leversha, M. A., Glancy, M. T., Wood, S. L., Cook, K., Dyson, H. M., Ferguson-Smith, M. E., and Willat, L. R. (1992). Reverse chromosome painting: A method for the rapid analysis of aberrant chromosomes in clinical cytogenetics. *J. Med. Genet.* **29**, 299–307.

Guan, X.-Y., Trent, J. M., and Meltzer, P. S. (1993). Generation of band specific painting probes from a single microdissection chromosome. *Hum. Mol. Genet.* **2**, 1117–11121.

Ludecke, H. J., Senger, G., Claussen, U., and Horsthemke, B. (1989). Cloning of defined regions of the human genome by microdissection of banded chromosomes and enzymatic amplification. *Nature (Lond)* **338**, 348–350.

Meltzer, P. S., Guan, X.-Y., Burgess, A., and Trent, J. M. (1992). Rapid generation of region specific probes by chromosome microdissection and their application. *Nature Genet.* **1**, 24–28.

Ruano, G., Pagliaro, E. M., Schwartz, T. P., Lamy, K., Messina, D., Gaensslen, R. E., and Lee, H. C. (1992). Heat soaked PCR: An efficient method for DNA amplification with applications to forensic analysis. *BioTech* **13**, 266–274.

Sen, S., Sen, P., Mulac-Jericevic, B., Zhou, H., Pirrotta, V., and Stass, S. (1994). Microdissected double-minute DNA detects variable patterns of chromosomal localization and multiple abundantly expressed transcripts in normal and leukemic cells. *Genomics* **19**, 542–551.

Telenius, H., Carter, N. P., Bebb, C. E., Nordenskjold, M., Ponder, B. A. J., and Tunnacliffe, A. (1992). Degenerate oligonucleotide-primed PCR: General amplification of target DNA by a single degenerate primer. *Genomics* **13**, 718–725.

Wang, H. C., and Federoff, S. (1972). Banding in human chromosomes treated with trypsin. *Nature New Biol.* **235**, 52–54.

Wang, N. (2002). Methodologies in cancer cytogenetics and molecular cytogenetics. *Am. J. Med. Genet.* **115**, 118–124.

Xu, J., Cedrone, E., Roberts, M., Wu, G., Gershagen, S., and Wang, N. (1995). The characterization of chromosomal rearrangements by a combined micro-FISH approach in a patient with myelodysplastic syndrome. *Cancer Genet. Cytogenet.* **83**, 105–110.

Xu, J., Tyan, T., Cedrone, E., Savaraj, N., and Wang, N. (1996). Detection of 11q13 amplification as the origin of a homogeneously staining region in small cell lung cancer by chromosome microdissection. *Genes Chromosomes Cancer* **17**, 172–178.

Xu, J., Fong, C. T., Cedrone, E., Sullivan, J., and Wang, N. (1998). Prenatal identification of de novo marker chromosomes using micro-FISH approach. *Clin. Genet.* **53**, 490–496.

Xu, J., and Wang, N. (1994). Identification of chromosomal structural alterations in human ovarian carcinoma cells using combined GTG-banding and repetitive fluorescence in situ hybridization (FISH). *Cancer Genet. Cytogenet.* **74**, 1–7.

Zhang, M., Meltzer, P., Jenkins, R., Guan, X.-Y., and Trent, J. M. (1993). Application of chromosome microdissection probes for elucidation of BCR-ABL fusion and variant Philadelphia chromosome translocations in chronic myelogenous leukemia. *Blood* **81**, 3365–3371.

CHAPTER

36

Micromanipulation of Chromosomes and the Mitotic Spindle Using Laser Microsurgery (Laser Scissors) and Laser-Induced Optical Forces (Laser Tweezers)

Michael W. Berns, Elliot Botvinick, Lih-huei Liaw, Chung-Ho Sun, and Jagesh Shah

I. INTRODUCTION

Individual chromosomes in living cells can be manipulated by optical scissors and optical tweezers. Early experiments (Berns *et al*., 1969) demonstrated that a low power-pulsed argon laser focused onto chromosomes of living mitotic salamander cells resulted in the production of a 0.5-μm lesion in the irradiated region of the chromosome. In these studies, the chromosomes were photosensitized with a low concentration of the vital dye acridine orange. Subsequent studies on salamander and rat kangaroo cells (PTK_2) indicated that the laser microbeam could be used to selectively inactivate the nucleolar genes (Berns, 1978). Using the 266-nm wavelength of a Nd:YAG laser, not only could the nucleolar genes be selectively deleted, causing a loss of nucleoli in the subsequent cell generation, but also a corresponding lack of one light-staining Giemsa band in the nucleolar organizer region of the chromosome could be demonstrated in cells descended from the single irradiated cell (Berns *et al*., 1979). With the further development of cloning techniques specific for single irradiated cells, cellular sublines with deleted ribosomal genes resulting from laser microbeam irradiation of the rDNA on the mitotic chromosome were established (Liang and Berns, 1983). In more recent studies it has been possible to use a picosecond laser to induce two-photon ablation of the ribosomal genes (Berns *et al*., 2000). These studies confirmed the earlier suggestion that short pulsed green lasers could be used to produce nonlinear multiphoton effects on cellular organelles (Calmettes and Berns, 1982). This nonlinear multiphoton effect was also demonstrated by Tilapur and Konig (2002) using a femtosecond laser to transiently disrupt the outer cell membrane.

In addition to the selective manipulation of chromosomes for both genetic studies and studies on chromosome movements during mitosis, pulsed lasers have been used to alter mitotic spindle structures such as centrosomes, microtubules, and chromosome kinetochores (see Berns *et al*., 1981). A major advance in subcellular irradiation occurred in 1997 when Khodjakov *et al*. (1997) described the use of green fluorescent protein (GFP) to light up microtubules and centrosomes in live cells so that these organelles could be selectively targeted. The advent of the use of GFP and its mutant constructs has become a major additive tool to laser microscopy because it permits visualization and targeting of a large number of cell structures and molecules in living cells that were not visualized and targeted easily with either conventional light or fluorescence microscopy.

In 1987, Ashkin and colleagues first used a tightly focused laser beam to generate optical trapping forces to move biological objects. The manipulation of chromosomes in living cells and in isolation buffer was reported by Berns *et al*. (1989). In this study, laser optical tropping force was applied to metaphase

Copyright 2006, Elsevier Science (USA).
All rights reserved.

chromosomes in order to study the generation of forces within the mitotic spindle. (Liang *et al*., 1991). The combination of laser cutting and laser tweezers was demonstrated by Wiegand-Steubing *et al*. (1991). The combined scissors and tweezers system was used for the fusion of two different mammalian cells and subsequently for chromosome cutting and trapping (Liang *et al*., 1993, 1994). Several good review articles on the use of laser ablation and laser traps should be consulted for a broader overview of this field and these technologies (Weber and Greulich, 1992; Berns *et al*., 1998; Schutze *et al*., 2002). Biologists now have a more complete set of optical tools to manipulate cells and their internal structures such as chromosomes and other structures involved in organelle movement.

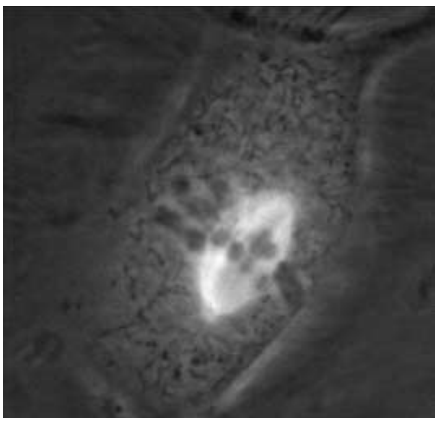

FIGURE 1 Dual-phase contrast and fluorescence image of a live PTK2 (rat kangaroo, *Potorous tridactylis*) cell in mitotic metaphase. The phase-dark chromosomes are aligned at the metaphase plate. Spindle microtubules contain the yellow fluorescent protein (YFP) variant of green fluorescent protein (GFP). Spindle microtubules can be seen attaching to the chromosomes and converging at each pole. See Fig. 7 for laser ablation of a microtubule bundle and transmission electron micrograph of the lesion in this cell.

II. MATERIALS AND INSTRUMENTATION

A. Cells

Rat kangaroo (*Potorous tridactylis*) kidney cells PTK_2 or PTK_1 are well suited for these studies because they have a low chromosome number (12–13) and they remain very flat throughout the entire cell cycle, allowing visualization of cytoplasmic and mitotic structures under phase, fluorescence, or DIC microscopy. The cells can be either standard lines available from the American Type Culture Collection (ATCC-CCL 167) or special sublines that have been transfected to express GFP or genetic variants of the GFP that absorb and emit wavelengths in other regions of the spectrum (Fig. 1).

B. Media, Chemical, and Supplies for Cell Culture

Modified Eagle's medium (Cat. No. 410-1500 ED), penicillin-G (Cat. No. 600-5140AG) 100 units/ml (working concentration for experiment, same as follows), streptomycin sulfate (Cat. No. 600-5140AG) 100 µg/ml, trypsin (Cat. No. 610-5050AJ) 0.25%, L-glutamine (Cat. No. 320-5030AJ) 2 m*M*, pancreatin (Cat. No. 610-5720AG), phenol red (Cat. No. 15-100-019), (phosphate-buffered saline) (PBS) without Ca^{2+} and Mg^{2+} (Cat. No. 310-4200), colcemid (Cat. No. 120-5210AD), and fetal bovine serum (Cat. No. 230-6140AJ) are from GIBCO. EDTA (Cat. No. 34103) and piperazine-*N*,*N*′-bis-2-ethane sulfonic acid monosodium monohydrate (PIPES) (Cat. No. 528132) are from Calbiochem. $CaCl_2$ (Cat. No. 07902) is from Sigma. Hexylene glycol (2-methyl-2,4-pentanediol) (Cat. No. 1134329) is from Eastman Chemical. Culture flasks T_{25} (Cat. No. 25106) and T_{150} (Cat. No. 25126) are from Corning. Centrifuge tubes, 15 ml (Cat. No. 2097) and 50 ml (Cat. No. 2098), are from Falcon. Hemacytometer "Bright Line" (Cat. No. B3180-2) is from Baxter. Centrifuge Dynac II is provided by Clay Adams.

C. Cell Culture Chambers

Chamber tops and bottoms, screws, sterile gaskets, sterile needles, and sterile syringes are components of the multipurpose culture chamber (see Fig. 2). For perfusion of cells with an exogenous agent during or immediately following laser exposure, the exit needle may be coupled to an empty receiving syringe or some other receptacle. The compounds and agents to be applied to the cells are in the injection syringe.

D. Lasers and Microscopy

The lasers and connecting optical system may be interfaced with either an upright or inverted microscope of any major microscope manufacturer. Historically, we have used Zeiss microscopes of various types (upright photomicroscope, inverted Axiomat, Universal M). The current system is built around an inverted Zeiss axiovert S100 microscope (Fig. 3). The mercury arc lamp was moved distally from the epi-illumination optics to accommodate a beam splitter (BS) to combine arc lamp illumination and the laser-trapping beam. A dual-view image module (not shown) and a Quantix

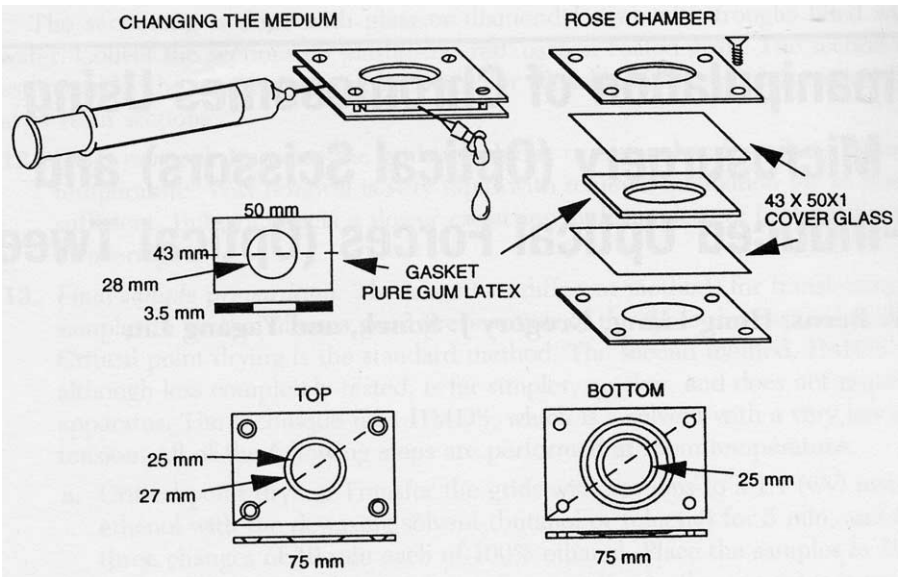

FIGURE 2 Multipurpose cell culture chamber with its component parts *(investigators may use any of a number of different cell chambers that are specifically adapted for their experiments).*

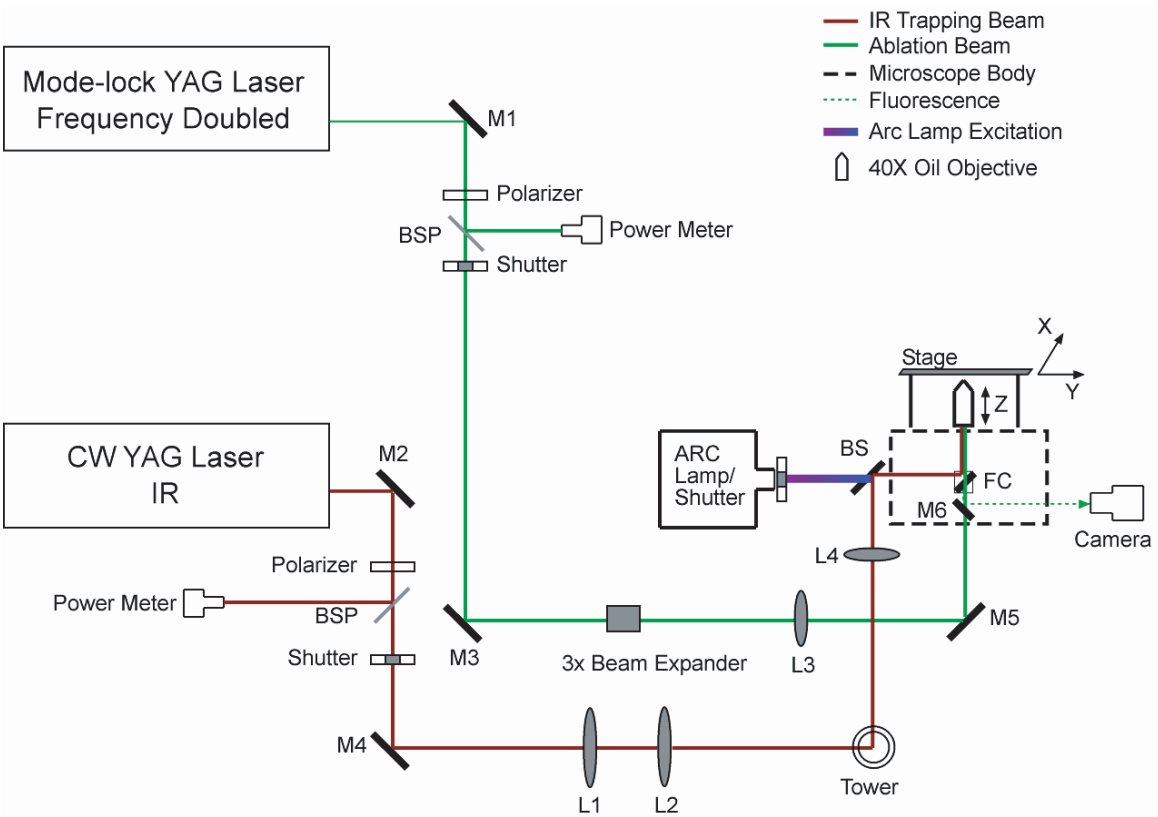

FIGURE 3 Schematic diagram of optical scissors and optical tweezers. M1–M6, mirrors; L1–L4, lenses; BSP, beam samplers; FC, filter cube; BS, beam splitter. Lasers from a variety of manufacturers may be used (see discussion in text). The YAG laser trapping beam can be divided into several beams that are reflected off of different motor-driven mirrors, resulting in multiple individually controlled trapping beams (Berns *et al.*, 1998).

Q-57 back-thinned, cooled CCD are mounted on a camera port of the microscope. Microscope risers (not shown) raise the microscope to access the underneath "Keller" port.

Two different laser systems are used for the cutting scissors beam. Both systems generate 532-nm green light by frequency doubling of the primary 1064-nm wavelength. One system is a Coherent Inc. mode-locked Antares Nd:YAG laser at a repetition rate of 76 MHz with a pulse duration of 100 ps (1064 nm) and 80 ps (532 nm). The other cutting system is a Spectra-Physics Inc. mode-locked Vanguard laser with a repetition rate of 76 MHz and a pulse duration of 10 ps at 532 nm.

Two different trapping lasers have been used: a Spectra-Physics Millenia IR continuous mode ND:YVO_4 laser at 1064 nm, with a maximum power of 10 W, and the primary 1064 wavelength of the pulsed Antares Nd:YAG laser operating at 76 MHz. The maximum power of the Antares laser is 18 W. For either laser, the actual power entering the microscope for the trapping experiments is 1–2 W, and the average power at the objective focal point in the sample is 10–300 mW. The high power of the primary output beam allows for splitting the beam into two beams (not shown in Fig. 3) so that multiple collinear trapping beams can be reflected off of precision motor-drive mirrors and directed into the microscope (Berns *et al*., 1998). This permits simultaneous application of forces on either different objects in the same microscope field or different points on the same object (Fig. 4). The 1064-nm wavelength has the beneficial properties of low water absorption and relatively good cell viability following exposure to the trap. Also, there is a particularly good cellular optical "window" for trapping at 800–820 nm and a lethal window at 740–750 nm (Vorobjev *et al*., 1993; Liang *et al*., 1996). Additionally, diode lasers are now available in useful wavelength ranges for optical trapping. They are more compact and less costly than the large YAG laser systems.

The cutting and trapping laser beams are sampled by partial reflection off a beam sampler (BSP) and monitored with a photodiode power meter. Power control is achieved with Glan polarizers in a motorized rotary mount. The two laser lines are shuttered individually with a minimum exposure time of 3 ms using a mechanical shutter. It should be mentioned that the lasers described earlier are just a few of many different types and models available from several different companies. Investigators may chose from a wide variety of different laser systems depending on individual investigator needs.

Two two-phase dual axis stepper motors operate the *x,y* microscope stage with several micrometer resolution. The stage is driven by a National Instruments stepper motor driver and a flex-motion PXI motion controller.

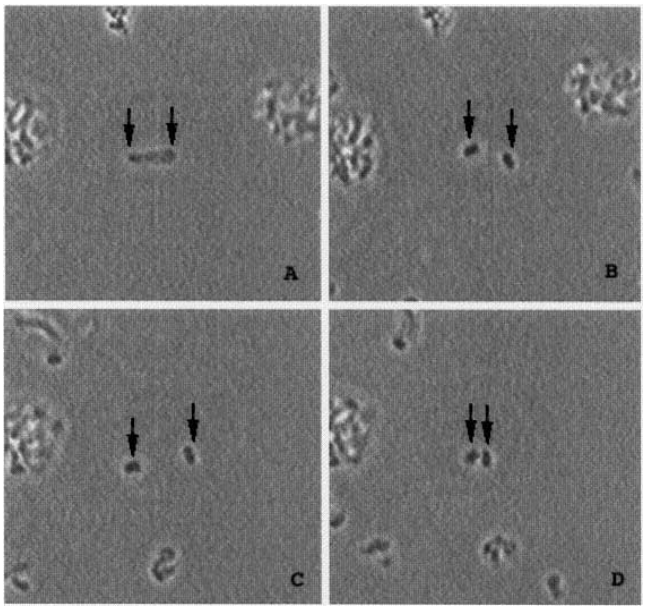

FIGURE 4 Model illustrating laser trapping and cutting of chromosomes in suspension. (A) A single chromosome is held in position using two different laser traps to hold each end of the chromome in the horizontal optical plane of the microscope field (arrows). (B) Two chromosome pieces immediately after being cut with the laser scissors beam; each piece is being held by a laser trap. (C) The two laser traps are used to move the two chromosome pieces apart. (D) The laser traps are used to move both chromosome pieces toward each other. Chromosome width is 2 µm.

1. Microscope and Microscope Modifications

1. A Zeiss Axiovert S100 inverted microscope with a motorized stepper motor stage (joystick controller) and motorized stepper motor for fine focus. A Ph3 Neofluar 40X, 1.3 NA or 63X, 1.4 NA oil immersion microscope objective lens is used.

2. Microscope risers (not shown) are used to lift the microscope 4.25 in. above the table for access to the underneath Keller port.

3. A RS-170 format CCD camera (SONY) for high-resolution, video frame rate imaging of the specimen is used. A Ropert Scientific Quantex Q-57 back-thinned and cooled CCD is used for low-light imaging of fluorescence.

4. An Optical Insight's dual view system is used for simultaneous imaging of two spectral bands on the Q-57 camera (not shown).

5. A modified epi-illumination light path is used whereby the arc lamp is removed from the Zeiss epi-illumination lens system and mounted 4 in. away. A

motorized shutter system (Vincent Associates) to shutter arc lamp illumination is used.

6. A short-pass dichroic BS centered at 1064 nm to combine the visible spectrum from the arc lamp with the IR trapping beam is used.

7. Customized fluorescent filter cubes (FC) with exciters and dichroic beam splitters designed to pass/reflect both the excitation band and a narrow band around the IR laser (centered at 1064 nm) are used.

2. *Laser Interfaces with Microscope*

1. Both the laser scissors and tweezers have their own variable attenuator to control laser power external to the main laser cavity. The attenuator, consisting of a glan laser linear polarizer (CVI Laser, LLC), is mounted in a stepper motor rotational mount (National Instruments) with motion driver and motion control hardware/software (National Instruments) to automate laser power contol.

2. Both laser lines pass through their own beam sampler (BSP) (CVI Laser, LLC), which reflects a small percentage of the attenuated laser beam toward a large area photodetector power meter (New Focus). The detector outputs a voltage proportional to the average power of the attenuated beam.

3. Both laser lines have a motorized shutter placed beyond the beam sampler and share a shutter driver with either RS-232 or TTL control (Vincent Associates). The IR shutter is controlled by a button on the joystick.

4. The 532-nm laser is expanded with a 3X beam expander (Newport) and is focused into the image plane of the Keller port with a f = 300-mm plano-convex lens, L3.

5. The 1064 laser is expanded with a custom-made 4X beam expander consisting of a f = 25.4-mm plano-convex lens, L1, and a f = 100-mm plano-convex lens, L2, which is mounted to allow axial displacement and thus control of divergence from a collimated beam for the purpose of focusing the laser relative to visible light in the microscope objective. The expanded beam is focused at the back focal plane of the Zeiss epifluorescent lens system, after reflection off of BS, with a f = 150-mm biconvex lens, L4.

6. An IR finder scope (FJW Optical Systems, Inc.) and an infrared sensor card (Coherent) are used for detecting and monitoring the IR laser. Some commercial home-use camcorders have a "night vision" mode, which will also visualize scatter of the beam. Please note that the finder scope or camcorder should never directly visualize the beam, only the scatter from optical elements.

7. A computer with appropriate software for recording images, controlling stepper motors, and controlling the shutters is used. A VCR or digital video recorder captures the RS-170 signal at video frame rates.

III. PROCEDURES

A. Preparation of PTK_2 Dividing Cells in Culture Chamber

Solution

0.125% viokase solution: To make 100 ml, dissolve 5 ml of pancreatin, 0.1 g of EDTA, and 0.25 ml of phenol red into 95 ml of PBS without Ca^{2+} and Mg^{2+}, adjust PH to 7.4.

Steps

1. Select a healthy, confluent or nearly confluent flask of cells.
2. Remove the old medium from the flask of cells using an unplugged sterile pipette attached to a vacuum flask.
3. Add 1.0 ml of viokase solution to the flask of cells.
4. Place the flask of cells with viokase in the 37°C incubator for 7–10 min. When the cells begin to lift free from the flask, rap the flask sharply two or three times to dislodge the cells completely.
5. Add 5 ml MEM to inactive the viokase and wash any adhering cells free.
6. Transfer the medium, viokase, and cell mixture to a sterile centrifuge tube.
7. Centrifuge the cell suspension for 4–5 min at 800–1000 rpm.
8. After centrifugation, carefully remove the stopper from the tube and very carefully aspirate the supernatant from the tube.
9. Resuspend the cell pellet in the drop remaining in the tube bottom.
10. Add 5 ml of MEM to the resuspended pellet and count a sample onto a hemocytometer. Count all four corners (i.e., four groups of 16 squares each), divide the result by 4, and multiply by 10^4. This gives the concentration of cells per milliliter of resuspended material.
11. Adjust the cell concentration to give 2.5–3.5 $\times$ 10^4 cells/ml and inject these into the chambers using a sterile syringe and 23-gauge needle (see Fig. 2)
12. Incubate the chambers (cell side down) at 37°C in a 5–7.5% CO_2 incubator. After 36–60 h, select chambers with dividing cells for experimentation.

B. Transfected Cell Lines

Generation of cell lines stably expressing fluorescent protein fusions of human α-tubulin were generated by amphotropic retroviral infection. The following procedures were used to generate two GFP mutants specific to our studies: yellow fluorescent protein (YFP) and cyan fluorescent protein (CFP). Investigators may use other methods to generate fluorescent genetic constructs specific to their needs

1. Excise the human α-tubulin cDNA fused at its N terminus to the enhanced yellow variant of green fluorescent protein (YFP) from a commercially available plasmid (Clontech) via an *Afe*I/*Mfe*I digest.
2. Ligate this fragment into the *Sna*BI/*Eco*RI sites of pBABEbsd, a retroviral vector based on pBABEpuro with a blasticidin resistance marker.
3. Generate the cyan version of the tubulin fusions (CFP-α-tubulin) by insertion of the α-tubulin cDNA into the CFP-C1 vector (Clontech) and then excise by *Afe*I/*Mfe*I and insert into pBABEpuro.
4. Cotransfect the retroviral plasmids containing the fluorescent protein–tubulin fusions into 293-GP cells (a human embryonic kidney cell line harbouring a portion of the murine Moloney leukemia virus genome) along with a VSV-G pseudotyping plasmid to generate amphotropic virus.
5. Forty-eight hours after transfection, collect, filter, and place the tissue culture supernatant into a subconfluent culture (30–40%) of PTK2 cells in 35-mm dishes.
6. Forty-eight hours after infection, split and replate cells in 10-cm dishes and subject to selection in 100 µg/ml puromycin (CFP-tubulin) or 10 µg/ml blasticidin (EYFP-tubulin) for 14 days.
7. Select high expressors (top 10%) by fluorescence-activated cell sorting (FACS).

C. Alignment of Laser Microbeam System

See Fig. 3 for a diagram of the system.

1. Aligning, Expanding, and Focusing the Trapping Beam

1. The key to bringing a laser into the microscope is to use the built-in light path of the microscope to define the optical axis outside of the microscope. With proper Köhler alignment and a 10X objective, close down the field aperature and insert a filter set with a deep red reflector. The narrow beam of light (from the halogen lamp of the microscope) emitting from the epi-illumination lens system will define the optical axis. Two iris diaphragms (not shown) are placed along the light path to define the optical path of the microscope. The laser is brought into the microscope so that it is centered within the same irises, thus aligning it with the optical axis.
2. The laser beam must be expanded to employ the full numerical aperture of the 40x NA1.3 objective lens. Mount lens L2 first and ensure that the beam is still aligned with the optical axis. Repeat procedure with lens L2, also ensuring that light emanating from L2 is collimated. Note that light emitting from the objective turret (with no objective in place) is not focused to infinity.
3. A third lens, L4, was added to the light path to collimate light through the objective turret. Remove the 40x objective and leave the turret empty. Position L4 until light from the turret is parallel, i.e., neither converging nor diverging.
4. Put a culture chamber with test sample under the microscope and bring into focus. Five- to 10-µm diameter beads (of polystyrene or other suitable material) make useful targets for fine-tuning the laser trap.
5. Slightly defocus the laser beam toward the specimen side. The bright spot of the laser beam will appear on the screen of the video monitor. Draw a cross with an erasable marker pen at the bright spot on the screen. The trap is now coincident with the cross hair on the monitor screen. Alternatively, a computer-generated cross hair can be positioned on the screen.
6. By mounting lens L2 in a *z*-translation mount, the relative focus between the image plane and the laser trap can be adjusted.

2. Alignment of Scissors Beam

1. As with the trapping beam, use the built-in light path of the microscope to define the optical axis outside of the microscope. With proper Köhler alignment and a 10X objective, close down the field aperture. Remove any fluorescent filter sets from the microscope stand so that light will exit the microscope via the underneath "Keller" port. The narrow beam of light (from the halogen lamp of the microscope) emitting from the Keller port will define the optical axis.
2. Two iris diaphragms (not shown in Fig. 2) are placed along the light path (at least 12–14 in. of separation between them). If the laser is brought into the microscope so that it is centered within the same irises, then the laser will be aligned and parallel to the optical axis of the microscope.
3. The laser beam must be expanded to employ the full numerical aperture (NA) of the 40 and 63X objective lenses. Place the 3X BS in the optical path using an adjustable mount and the irises to ensure that the laser beam is parallel and runs along the optical axis of the microscope.

4. Remove the 40x objective and leave the turret empty. Position L3 until light from the turret is parallel, i.e., neither converging nor diverging.

5. Put a culture chamber with a test sample under the microscope and bring it into focus.

6. Ensure that on the monitor the scissors beam coincides with the cross hair of the trapping beam. If not, carefully adjust L3 until it does. The laser scissors and tweezers are now aligned.

3. Microsurgery of Chromosomes and Cell Cloning[1]

1. After alignment of the laser microbeam, place a dried smear of red blood cells under the microscope objective and locate a monolayer region. The blood smear should be made on a cover glass, which may either be the bottom glass of a cell chamber (see Fig. 1) or be a cover glass that is simply mounted on a regular microscope slide with the red blood cell surface facing the slide so that the laser beam passes through the cover glass before contacting the red blood cell. Fire a burst of pulses of the laser beam on the red blood cell to produce a small hole (<1 μm) to verify that the cross hair on the TV screen is directly over the lesion. If the hole is too large, attenuate the laser output until a small threshold lesion of 0.25–0.5 μm is produced. For a high-quality single mode laser beam, this small threshold lesion spot represents the center of the laser beam Gaussian profile.

2. Remove the red blood cell slide and place the experimental sample under the microscope.

3. Select dividing cells that appear healthy. For PTK2 cells the cytoplasm should be free of vacuoles and the cells well flattened. The nuclear envelope and mitochondria should be clearly resolvable in interphase cells. In mitotic cells the chromosomes are dark when viewed under phase-contrast microscopy, and spindle micrtotubule bundles are clearly visible using fluorescence microscopy (Figs. 1 and 7).

4. The mitotic stage of dividing cells should be determined by the specific needs of the experiment.

5. Move the microscope stage so that the specific target site of the selected chromosome is under the cross hair on the monitor screen.

6. Fire the laser on the selected chromosome site. Gradually increase the laser power until a lesion appears. At the lesion-threshold energy density ($nJ/\mu m^2$), the lesion will appear as a small phase lightening at the point of laser focus. As the threshold energy density is surpassed, a phase-dark spot may appear in the center of the lesion, and at highest energy densities the chromosome can actually be cut into fragments (Fig. 4). Although the precise physical mechanisms of the laser ablation are not fully understood, it seems likely that multiphoton absorption and other nonlinear processes, such as plasma-induced cavitation bubbles and stress waves, are occurring in the laser focal volume (Vogel and Venugopalan, 2003).

7. Videotape the entire experiment or acquire images using a digital camera and a computer frame grabber. Record the image before and after irradiation. *In the case of genetic studies, the irradiated cell may be isolated and cloned into a viable population using either a laboratory-specific cloning procedure or a procedure similar to steps 8 to 12 (see Fig. 5).*

8. Under sterile conditions, remove nonirradiated cells from near the target cell using a micromanipulator.

9. Reseal the cell culture chamber.

10. Check the chamber at 12 h, and use the 532-nm laser beam to ablate cells migrating into the area of the cell being followed.

11. Monitor the proliferation of the target cell using the acquired images or simply by observation.

12. Collect descendent clonal cells by 0.125% viokase solution and then transfer into 1 well of a 12-well culture cluster containing normal medium.

13. Collect clonal cells with the 0.125% viokase solution until they are confluent and transfer them into a T_{25} culture flask.

14. When the proliferation of descendent clonal cells reaches a sufficient number they can be subjected to standard karyotypic and/or biochemical analysis. Additionally, selective regions may be cut from the chromosomes and subjected to polymerase chain reaction, gene cloning, and analysis (Shutze *et al*., 2002; He *et al*., 1997).

4. Optical Trapping of Chromosomes

1. Place a culture chamber under a microscope that contains either live dividing cells or chromosomes suspended in isolation buffer.

2. Select a specific chromosome under the microscope for experimentation.

3. In the case of a living cell, flat and large cells are especially good for micromanipulation. The selection of the mitotic stage depends on the specific goal of the experiment.

4. Locate the specific site of the selected chromosome at the cross hair on the monitor screen.

5. Open the shutter, allowing the trapping beam to enter the microscope. The trapping laser is focused at the prealigned site, which is located in the image plane of the microscope objective.

6. The chromosome near the focal point of the trapping beam will be drawn into the focal point.

[1] The cloning procedure just described is one that we have found useful. However, with recent developments in microfluidics and nanotechnology, these technologies may be used for cell isolation and cloning.

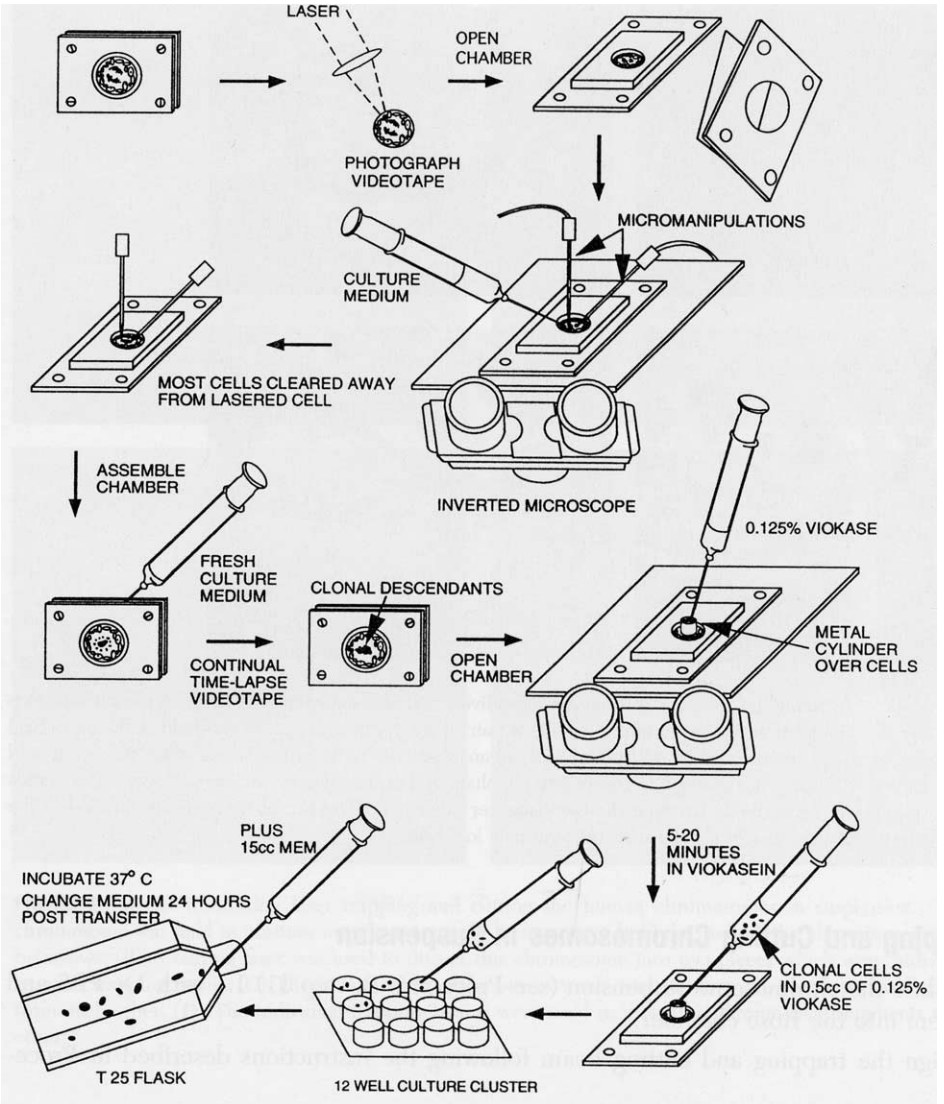

FIGURE 5 Diagram of the procedures for cloning single cells that have been irradiated at a specific chromosomal site. A variety of individualized procedures and technologies may be used depending on the investigator and laboratory needs.

7. Move the specimen stage at a speed less than 25 μm/s in the desired direction. The chromosome will be held at the trapping position. (Usually the sites on which the largest trapping force can be applied are at either ends of the chromosome.)

8. If the trapping force is not large enough to hold the chromosome, increase the power of the trapping beam by rotating the polarizer. (The trapping force is linearly proportional to the incident power of the trapping beam.)

9. Either videotape or digitally record the experiment. Individual digital should be acquired with the frame grabber. Record data before, during, and after manipulation by the optical trapping force.

10. The laser trap can be combined with the laser scissors. A chromosome can be held in the trap while the cutting (scissors) laser is used to cut it into fragments, each of which can be moved by laser traps (Fig. 4).

5. Irradiation of Mitotic Spindle

1. Because of low light levels from fluorescent structures, a sensitive digital camera is used for these experiments (Q-57 camera). Images are acquired using the computer frame grabber and are displayed on the computer monitor. Place a dried smear of red blood cells under the microscope objective and locate a monolayer region. Fire a series of pulses of the abla-

tion laser beam on the red blood cells to produce a small hole (<1 μm) to locate the laser focus while viewing on either the computer screen or the video monitor. Either mark cross hairs on the computer monitor to determine the focus location or note the pixel coordinates on the screen. A computer-generated cross hair may also be used to denote the point of laser focus.

2. Place a culture chamber under the microscope that contains either YFP or CFP microtubule-transfected cells.

3. Locate a cell in the desired stage of the cell cycle. This will depend on the nature of your experiment.

4. Move the stage to position the desired target under the cross hairs or onto the laser scissors pixel location.

5. Remove the fluorescent filter set by sliding the fluorescent slider to an empty position and push in the lever of the microscope stand to open the Keller port.

6. Open the shutter for a 3-ms pulse and immediately slide the appropriate filter set into place.

7. Acquire and save images before and after each ablation (Fig. 7)

6. Single Cell Serial Section Transmission Electron Microscopy

This is a very useful, but tedious, technique that allows precise ultrastructural definition of the nature and extent of laser damage at the sublight microscope level (Figs. 6 and 7). These methods may be adapted to individual investigator needs and vary between laboratories (Rattner and Berns, 1974; Liaw and Berns, 1981; Khodjakov *et al*., 1997).

1. Allow cells inside the culture chamber to become nearly confluent.

2. Insert one 23-gauge needle into the gasket on each side of the culture chamber; one for withdrawing culture medium and one for injecting Karnofsky fixative into the chamber. Bend the exit needle to approximately a 30° angle and attach a 5-ml syringe without a plunger. Attach the input needle to a 20-in.-length of i.d. 0.63-mm, o.d. 1.19-mm, silastic laboratory tubing (Fisher Scientific) coupled to a 10-ml syringe containing fixative. Attach a Nalgene polypropylene pinch clamp (Fisher Scientific) to the tubing between the syringe and the needle in order to prevent flow of any fixative into the chamber.

3. Photograph or digitally store at high and low magnification images of single cells selected for irradiation.

4. Perform the laser irradiation experiment.

5. Inject Karnofsky fixative into chamber immediately after irradiation.

6. Photograph/digitally store image of irradiated cell at high and low magnification.

7. While on the microscope stage, etch a 0.5-mm circle around the region containing the cell using a Carl Zeiss (Germany) diamond marking objective. This provides an etched circle that will be used for subsequent relocation of the irradiated cell. In addition, draw a 1- to 2-mm circle around this circle using either a wax pencil or a water-resistant felt-tip marking pen. This facilitates rapid location of the etched circle.

8. Wash the chamber (while still assembled) with saline.

9. Inject fresh Karnofsky fixative into the chamber.

10. After 30 min in fixative, remove the solution and inject the chambers with cacodylate buffer.

11. Place the chamber back under the microscope where the irradiated cell is relocated and digitally record under 63 and 10X magnification.

12. Change buffer, disassemble culture chamber, and put the bottom cover glass, which includes cells, diamond circle, and ink mark circle, in a petri dish with cells side up for embedding.

13. Postfix in 1% Os O_4, *en bloc* stain with uranyl acetate, dehydrate in ETOH, and embed in a 1- to 2-mm thin layer of Epon/Bed 812.

14. With a diamond marking pen, scribe a small circle on the plastic side matching the exact site of the diamond circle/ink circle on the cover glass.

15. Remove cover glass from plastic with cell by dipping the cover glass/plastic into liquid nitrogen. The differential contraction and expansion of the two materials result in the plastic containing the cells to separate cleanly from the glass.

16. From the nonscribed side of plastic, relocate the irradiated cell inside the new diamond pen scribed circle through the microscope and match with postfixation photographs. Make a smallest possible circle with the diamond marking objective around the cell. Make a square ink mark around the circle.

17. Cut out the piece of plastic along the square ink mark and glue onto a blank embedded plastic block with diamond circle side up.

18. Carefully trim the block face to include the irradiated cell. Take extra attention to align the knife and block face to get the perfect whole block face at first section as possible.

[2] A 3-ms shutter exposure of a 76-MHz laser allows 228,000 laser pulses onto the target. If experiments require single pulse exposure, either lasers operating a lower pulse repetition rate should be used (i.e., nanosecond pulse lasers operating at 10 Hz) or expensive pulse selection optoelectronics may be used.

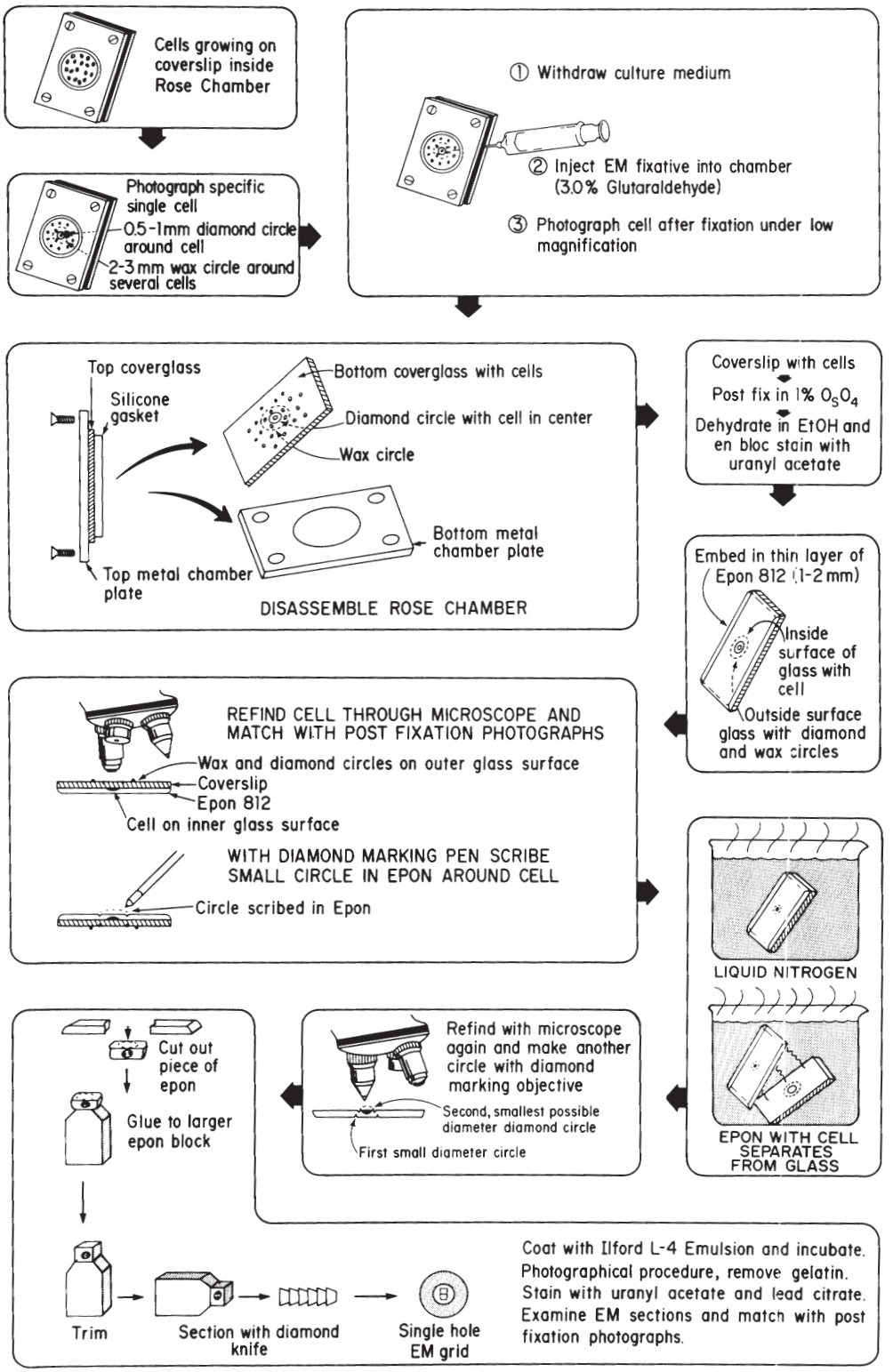

FIGURE 6 Diagram of the procedures used for single cell electron microscopy resulting in the recovery and observation of the laser-irradiated cell and organelle (see Fig. 7). This series of procedures was originally developed for EM autoradiography, thus the last step may not be needed in specific studies.

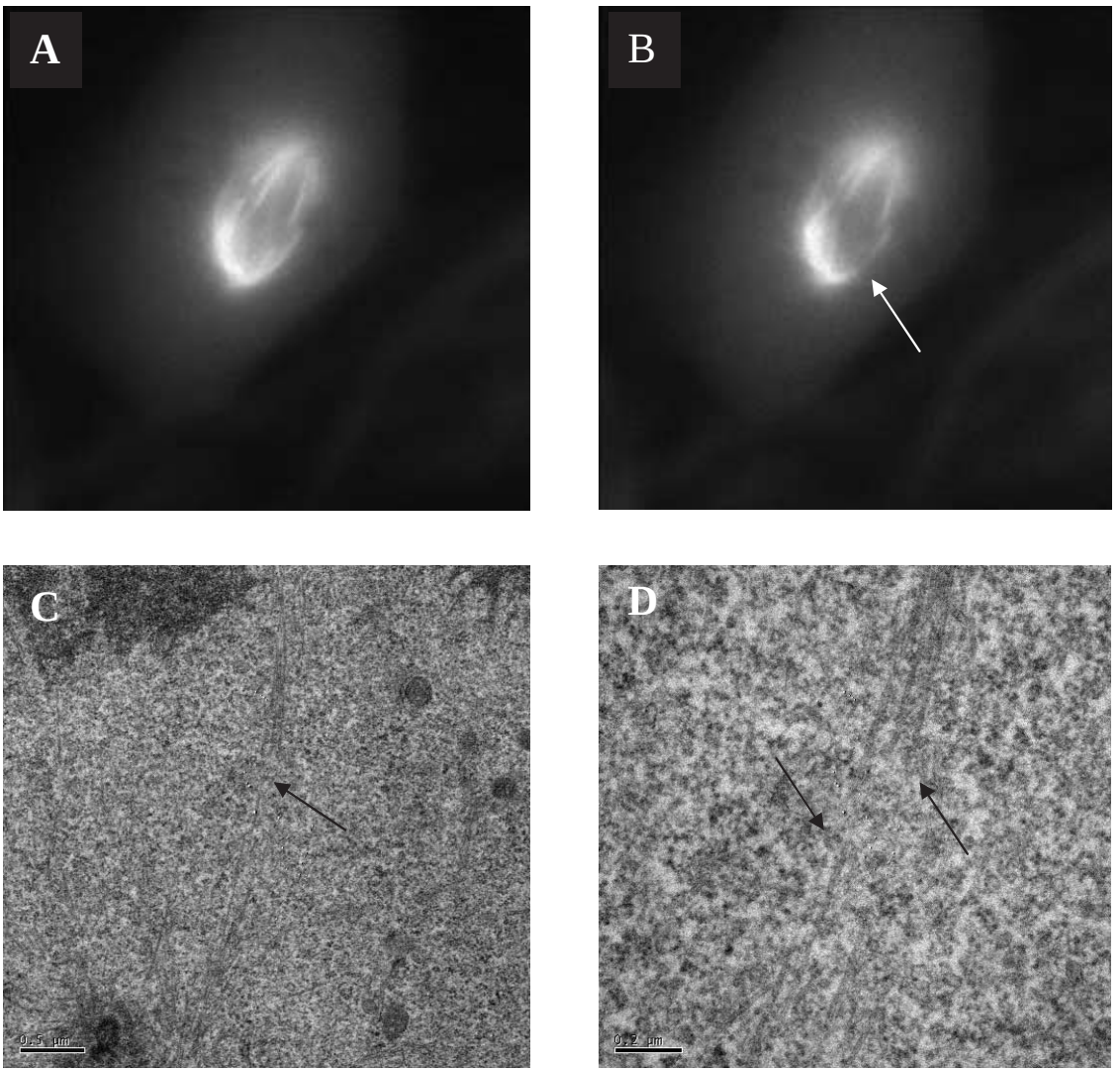

FIGURE 7 Fluorescent images of a PTK2 cell containing yellow fluorescent protein in the tubulin of metaphase microtubules. A microtubule bundle extending from the mitotic pole (centrosome region) to a single chromosome has been cut with the laser scissors, and the specific cut region has been imaged by electron microscopy. (A) Fluorescent microtubule spindle prior to laser exposure. (B) Microtubule bundle cut (arrow) using 0.5 nJ/pulse of the laser scissors; total energy needed to cut the bundle was 610 µJ/µm^2. (C) Low-magnification transmission electron micrograph (TEM) illustrating cut zone (arrow). (D) High-magnification TEM illustrating cleanly cut microtubule in the region corresponding to the loss of fluorescence following laser exposure (see image "B"). Note that individual microtubles that have been cut/ablated continue intact on either side of the ablation zone (arrows). Scale bar: 0.2 µm.

19. Serial section in 60 nm thick and place sections on 1 × 2-mm Formvar-coated slot EM grids in order. The linear ribbon of the sections will help keep sections and grids in perfect order. The slot grid will not obscure the specific cell.
20. Stain with uranyl acetate and lead citrate.
21. Examine sections through TEM. Match with postfixation images to find the irradiated cell/organelle.

IV. COMMENTS

The procedures described in this article, by in large have either been specifically developed for use in the authors laboratories or have been developed as a result of many years (1980–2004) of collaborations with investigators who have used the NIH LAMMP Biotechnology Resource at the Beckman Laser

Institute, Irvine, California. Thus, many of the procedures have evolved over the years and have been adapted to new technologies and to many different needs of the collaborating investigators. Also, as noted throughout this article, many of the precise methods can be modified and adapted further to specific needs of experimenters and laboratories. We would rather consider the procedures and techniques that we have described as *precise guidelines* as opposed to hard-and-fast protocols. Where possible, we have used very simplistic language so as to make execution and duplication of the procedures as simple as possible.

V. PITFALLS

1. Variation in laser output power can cause inconsistent experimental results. Turn on the lasers 30 min to 1 h before the experiment and continue to monitor the output power throughout the laser experiments. Laser power/energy may vary as much as 20–30% during the day and may be particularly affected by changes in environmental temperature, which subsequently can cause very small changes in intercavity mirror alignments. Temperature can also affect optical alignments on vibration tables and in the microscope. All of these changes can affect the amount of energy in the focused laser spot and therefore the results of the experiment. It is suggested that laser output power and energy in the microscope focal point be checked periodically as well as before and after the experiment.

2. Living cells will be damaged if exposed to the laser beam either for long periods of time or at too high irradiances. The average power <200 mW for the trapping beam and energy in the nJ – μJ/pulse in the focused spot for the scissors beam are recommended as exposure parameters. However, these are only rough guidelines, as the lasers now available have pulse durations in the femtosecond regime. The mechanisms of interaction of these short-pulse systems are not well understood.

3. Unwanted photo damage to cells should also be considered. Choose a laser with the appropriate wavelength to avoid regions of unwanted photon absorption. Also, limit the exposure of the cells to normal unfiltered microscope illumination as much as possible, as this light may also affect cell physiology, especially if a standard IR filter is not used in conjunction with normal microscope illumination. As a rule of thumb, use the minimal amount of illumination light necessary to generate a useable image. Where possible, use sensitive digital and analog detectors so as to minimize the amount of illumination light on the cells.

4. Microscope optics can be damaged if the laser beam is too intense. In order to prevent damage to the objective lens, do not adjust optical components (e.g., mirrors, beam splitters) while the objective is being exposed to the intense laser beam. The cement used to hold the small optical lenses in the objective absorbs laser light, creating thermal and/or stress wave damage to the lenses.

5. Laser exposure may produce eye injury and/or physical burns. Never view a laser beam directly or by specular reflection. Use laser safety glasses whenever possible. Be sure that the laser microscope has appropriate filtration or beam blocks so that the laser beam does not directly go through the oculars into the eyes. Where possible, enclose external beam paths and/or surround the optical table with appropriate laser safety curtains. There have been reported and unreported cases of retinal burns due to laser exposure. These have occurred when either aligning optics on the table surface or not blocking laser light from coming through the microscope ocular.

References

Ashkin, A., and Dziedzic, J. M. (1987). Optical trapping and manipulation of viruses and bacteria. *Science* **235**, 1517–1519.

Berns, M. W. (1978). The laser microbeam as a probe for chromatin structure and function. *Methods Cell Biol.* **18**, 277–294.

Berns, M. W., Aist, J. R., Wright, W. H., and Liang, H. (1992). Optical trapping in animal and plant cells using a tunable near-infrared titanium-sapphire laser. *Exp. Cell Res.* **198**, 375–378.

Berns, M. W., Chong, L. K., Hammer-Wilson, M., Miller, K., and Siemens, A. (1979). Genetic microsurgery by laser: Establishment of a clonal population of rat kangaroo cells (PTK_2) with a directed deficiency in a chromosomal nucleolar organizer. *Chromosoma* **73**, 1–8.

Berns, M. W., Olson, R. S., and Rounds, D. E. (1969). *In vitro* production of chromosomal lesion using an argon laser microbeam. *Nature* **221**, 74–75.

Berns, M. W, Tadir, Y., Liang, H., and Tromberg, B. (1998). Laser scissors and tweezers. *Methods Cell Biol.* **55**, 71–98.

Berns, M. W., Wang, Z., Dunn, A., Wallace, V., and Venugopalan, V. (2000). Gene inactivation by multiphoton targeted photochemistry. *Proc. Natl. Acad. Sci. USA* **17**, 9504–9507.

Berns, M. W., Wright, W. H., Tromberg, B. J., Profeta, G. A., Andrews, J. J., and Walter, R. J. (1989). Use of a laser-induced optical force trap to study chromosome movement on the mitotic spindle. *Proc. Natl. Acad. Sci. USA* **86**, 4539–4543.

Berns, M. W., Wright, W. H., and Wiegand-Steubing, R. (1991). Laser microbeam as a tool in cell biology. *Int. Rev. Cytol.* **129**, 1–44.

He, W. Y., Liu, Y., Smith, M., and Berns, M. W. (1997). Laser microdissection for generation of a human chromosome region specific library. *Microsc. Microanal.* **3**, 47–52.

Khojakov, A., Cole, R. W., and Rieder, C. L. (1997). A synergy of technologies: Combining laser microsurgery with green fluorescent protein tagging. *Cell Motil. Cytoskel.* **38**(4), 311–317.

Liang, H., and Berns, M. W. (1983). Establishment of nucleolar deficient sublines of PTK_2 (*Potorous tridactylis*) by ultraviolet laser microirradiation. *Exp. Cell Res.* **144**, 234–240.

Liang, H., Vu, K. T., Krishnan, P., Trang, T.C., Shin, D., Kimel, S., and Berns, M. W. (1996). Wavelength dependence of cell cloning efficiency after optical trapping. *Biophys. J.* **70**, 1529–1533.

Liang, H., Wright, W. H., Cheng, S., He, W., and Berns, M. W. (1993). Micromanipulation of chromosomes in PTK_2 cells using laser microsurgery (optical scalpel) in combination with laser induced optical force (optical tweezers). *Exp. Cell Res.* **204**, 110–120.

Liang, H., Wright, W. H., He, W., and Berns, M. W. (1991). Micromanipulation of mitotic chromosomes in PTK_2 cells using laser induced optical forces ("optical tweezers"). *Exp. Cell Res.* **197**, 21–35.

Liang, H., Wright, W. H., Rieder, C. L., Salmon, E. D., Profeta, G., Andrews, J., Liu, Y., Sonek, G. J., and Berns, M. W. (1994). Directed movement of chromosome arms and fragments in mitotic newt lung cells using optical scissors and tweezers. *Exp. Cell Res.* **213**, 308–312.

Liaw, L.-H. L., and Berns, M. W. (1981). Electron microscope autoradiography of serial sections of pre-selected single living cells. *J. Ultrastruct. Res.* **75**, 187–194.

Rattner, J. B., and Berns, M. W. (1974). Light and electron microscopy of laser microirradiated chromosomes. *J. Cell Biol.* **62**, 526–533.

Schutze, K., Becker, B., Bernsen, M., Bjoernsen, T., Brocksch, D., Bush, C., Clement-Sengewald, A., van Dijk, M. C. R. F., Friedman, G., Heckl, W., Lahr, G., Lindhal, P., Mayer, A., Nilsson, S., Scheidl, S. J., Stich, M., Stolz, W., Takemoto, M., Thalhammer, S., Vogt, T., and Burgemeister, R. (2002). Tissue microdissection. *In* (D. Bowtell and D. Sambrook, eds.) "DNA Microarrays." Cold Spring Harbor Laboratory Press, Cold Spring Harbor, NY.

Tilapur, U. K., and Konig, K. (2002). Targeted transfection by femtosecond laser. *Nature* (*Lond.*) **418**(6895), 290–291.

Vogel, A., and Venugopalan, V. (2003). Mechanisms of pulsed laser ablation of biological tissues. *Chem Rev.* **103**(2), 577–644.

Vorobjev, I. A., Liang, H., Wright, W. H., and Berns, M. W. (1993). Optical trapping for chromosome manipulation: A wavelength dependence of induced chromosome bridges. *Biophys. J.* **64**, 533–538.

Weber, G., and Greulich K. O. (1992). Manipulation of cells, organelles, and genomes by laser microbeam and optical trap. *Int. Rev. Cytol.* **133**, 1–41.

Wiegand-Steubing, R. A., Cheng, W. H., Wright, W. H., Numajiri, Y., and Berns, M. W. (1991). Laser induced cell fusion in combination with optical tweezers: The laser cell fusion trap. *Cytometry* **12**, 505–510.

PART

E

TISSUE ARRAYS

SECTION

13

Tissue Arrays

CHAPTER

37

Tissue Microarrays

Ronald Simon, Martina Mirlacher, and Guido Sauter

I. INTRODUCTION

Tissue microarray (TMA) technology significantly facilitates and accelerates *in situ* analysis of tissues (Bubendorf *et al*., 1999; Kononen *et al*., 1998) as it allows the simultaneous analysis of up to 1000 tissue samples on a single microscope glass slide. In this method, minute tissue cylinders (typical diameter: 0.6 mm) are removed from hundreds of different primary tumor blocks and subsequently brought into one empty "recipient" block. Paraffin-embedded tissues are optimal for TMA making, but frozen tissue samples can also be utilized (Simon and Sauter, 2002). Sections from such TMA blocks can be used for simultaneous *in situ* analysis of hundreds to thousands of tissue samples on the DNA, RNA, and protein level. The TMA technique has a number of distinct advantages as compared to the "sausage" block technique that has been suggested previously for analyzing multiple different tissues on one slide (Battifora, 1986). The regular arrangement of samples of identical shape and diameter on TMA sections greatly facilitates automated analysis and also orientation during manual analysis of staining. The cylindrical shape and the small diameter of the specimen taken out of the donor block maximize the number of samples that can be taken out of one donor block and minimize the tissue damage inferred to it. The latter is important for pathologists because they can give researchers access to their tissue material and at the same time retain their tissue blocks. Punched tissue blocks remain fully interpretable for all morphological and molecular analyses that may subsequently become necessary, provided that the number of punches is reasonably selected. Dozens of punches can be taken from one tumor without compromising interpretability (Bubendorf *et al*., 2001).

Virtually all tissues are suitable to be placed into a TMA. The range of TMA applications, therefore, is very broad. One of the most distinct advantages of TMAs is that one set of morphologically and clinically highly characterized tissues can be used for an almost unlimited number of studies. As of yet, TMAs have been used predominantly in cancer research. Most TMAs used in this field fall into one of three categories: prevalence, progression, and prognostic TMAs. Prevalence TMAs contain tumor samples lacking attached clinicopathological data. Despite this limitation, they are highly useful in determining the prevalence of a given alteration in tumor entities of interest. In the optimal case, such TMAs will contain tissue samples from various different tumor entities (multitumor TMAs) (Schraml *et al*., 1999). Progression TMAs allow for studies on molecular alterations in different stages of one particular tumor type (Bubendorf *et al*., 1999a,b; Kononen *et al*., 1998; Richter *et al*., 2000). Ideally, such a TMA would contain samples from normal tissues, precancerous lesions including carcinoma *in situ*, carcinomas of all different stages, and nodal and hematogenous metastases, as well as recurrences after initially successful treatment (Bubendorf *et al*., 1999a). Prognosis TMAs contain samples of tumors for which clinical follow-up data are available (Richter *et al*., 2000; Torhorst *et al*., 2001; Bremnes *et al*., 2002). Other TMA applications are obviously important but have not been largely exploited as of yet. For example, the normal expression pattern of gene products can optimally be tested on TMAs containing all kinds of normal tissues. Similarly, as for patient tissues, TMAs can be used for cell lines (Simon *et al*., 2002) and other

Copyright 2006, Elsevier Science (USA).
All rights reserved.

experimental tissues such as xenograft tumors or tissues from animal models.

II. TMA MANUFACTURING

Manufacturing TMAs is a four-step process, including sample collection, preparation of recipient blocks, construction of TMA blocks, and sectioning. Material requirements and the laboratory procedures for all of these steps are described separately.

A. Materials and Instrumentation

Sample Collection

Standard routine histology microscope for review of tissue sections
Colored pens to mark representative areas on stained slides, e.g., red for tumor, blue for normal, and black for premalignant lesions
Sufficient working space especially for large-scale projects that require extensive sorting of thousands of slides and blocks (For frozen tissue TMA making, sufficient empty freezer space is needed.)

B. Preparing Recipient Blocks

1. Paraffin-Embedded and Frozen Tissue

Slotted processing/embedding cassettes for routine histology (Electron Microscopy Sciences Inc., PA, e.g., EMS Cat. No. 70070)
Stainless-steel base molds for processing/embedding systems (Electron Microscopy Sciences Inc., e.g., EMS Cat. No. 62510-30)

2. Paraffin-Embedded Tissue Only

PEEL-A-WAY embedding paraffin pellets, melting point: 53–55°C (Polysciences Inc., PA, Cat. No. 19797)
Filter/filter paper (Schleicher & Schuell, Dassel, Germany; Faltenfilter diameter 185 mm, Cat. No. 311647)
Oven for paraffin melting

3. Frozen Tissue Only

OCT Tissue-Tek compound embedding medium (Sakura BV, The Netherlands; Cat. No. 4583)
Dry ice

C. TMA Block Making

1. Paraffin-Embedded and Frozen Tissue

Tissue arrayer (currently there are two commercial vendors for tissue arrayers: http://www.beecherinstruments.com; http://www.chemicon.com) and supplies (extra needles, block holder). Several groups have introduced inexpensive modifications to the existing commercially available manual non-automated arrayers, which improve performance markedly and facilitate frozen tissue arraying.
Premade empty recipient blocks (paraffin or frozen)
Illuminated magnifying lenses and supplies (e.g., Luxo U wave II/70, Cat. No. 27950, Luxo Inc., Switzerland) (optional)

2. Frozen Tissue Only

Dry ice to cool punching needles, tumor samples, and recipient block

D. TMA Block Sectioning

1. Paraffin-Embedded and Frozen Tissue

Boxes for slide storage
Refrigerator/freezer for slide storage

2. Paraffin-Embedded Tissue Only

Standard routine histology microtome and supplies (e.g., Leica SM2400, Leica Microsystems Inc., IL)
Sectioning Aid-System (Instrumedics Inc., NJ, Cat. No. PSA) containing ultraviolet curing lamp, adhesive-coated PSA slides, TPC solvent, TPC solvent can, hand roller, tape windows (optional)

3. Frozen Tissue Only

Standard routine histology cryostat and supplies (e.g., Microm, HM560, Walldorf, Germany)
CryoJane consumables: adhesive-coated slides (Instrumedics Inc., Cat. No. CS4x, tape windows, Cat. No. TW) (optional)

III. PROCEDURES

A. Sample Collection

Although a device is needed to manufacture TMAs, it must be understood that most of the work (approximately 95%) is traditional histology work. Therefore, the use of automated tissue arrayers cannot accelerate TMA production. This preparatory work is similar to what is needed for traditional studies involving "large" tissue sections. The major difference is the number of tissues involved, which can be an order of magnitude higher in TMA studies than in traditional projects. The different tasks related to sample collection include the following.

1. Exactly define the TMA to be made. Include normal tissues of the organ of interest and, if possible, of a selection of other organs as well.

2. Generate a list of potentially suited tissues.
3. Collect all slides from these tissues from the archive. In case of frozen tissues, representative slides of potential donor tissues may not be available and must be newly made.
4. One pathologist must review all sections from all candidate specimens to select the optimal slide. If possible, tissues (especially in the case of tumors) should be reclassified during this review process according to current classification schemes. Tissue areas suited for subsequent punching should be marked. It is advisable to prepare a freshly HE-stained section if the actual block surface is not well reflected on the available stained section. Different colors are recommended for marking different areas on one section (e.g., red for tumor, black for carcinoma *in situ*, blue for normal tissue).
5. Collect the required tissue blocks. These blocks and their corresponding marked slides must be matched and sorted together in the order of appearance on the TMA.
6. Define the structure (outline) of the TMA and compose a file that contains the identification numbers of the tissues together with their locations and real coordinates (as they need to be selected on the arraying device). As a distance between the individual samples, 0.2 mm is recommended for paraffin-embedded materials and 0.4 mm for frozen tissues if standard punching needles (diameter of 0.6 mm) are used. To facilitate navigation on the TMA, arranging the tissues in multiple sections (e.g., quadrants) is recommended. The distance between the quadrants may be 0.8 mm for paraffin-embedded materials and 1.0 mm for frozen tissues. For unequivocal identification of individual samples on TMA slides, it is important to avoid a fully symmetrical TMA structure. In our laboratory, capitalized letters define quadrants, whereas small letters and numbers define the coordinates within these quadrants. Examples of a TMA structure (outline) and data file containing the necessary information for making a TMA are given in Fig. 1 and Table I.

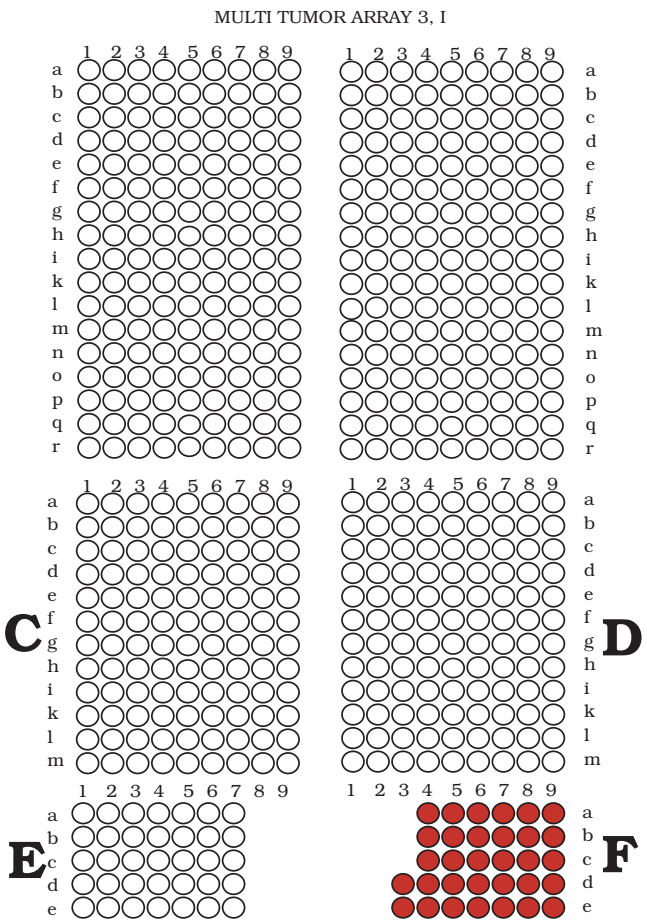

FIGURE 1 TMA outline example. The TMA has been divided into six subsections to facilitate navigation during microscopy. Dark gray spots represent a control subsection containing various normal tissues.

B. Preparing Recipient Blocks

1. Paraffin-Embedded Tissue

In contrast to normal paraffin blocks, tissue microarray blocks are cut at room temperature. Therefore, a special type of paraffin is needed with a melting temperature between 53 and 55°C ("Peel-A-Way" paraffin, see Section IIA).

1. Melt paraffin overnight at 60°C, filtrate, and pour in a stainless-steel mold.
2. Place a slotted plastic embedding cassette (as used in every histology laboratory) on top of the warm paraffin.
3. Cool down recipient paraffin blocks for 2 h at room temperature and for another 2 hr at 4°C. Remove blocks from the mold. It is important not to cool down the paraffin on a cooling plate because of the risk of block damage.
4. Quality check the recipient blocks to make sure that no air bubbles are included.

2. Frozen Tissue

Preparing recipient OCT blocks that are equally sized as paraffin recipient blocks ensures that the currently available tissue arrayers can be utilized for frozen TMA manufacturing.

1. Place OCT into a standard cryomold and cool down over dry ice to form recipient blocks.

TABLE I Simplified Example for a TMA Data File[a]

Tissue ID	Tissue type	Localization	Coordinates
1	Uterine cervix, pT2, G2, N0	A1a	0/0
2	Uterine cervix, pT3, G3, N1	A1b	800/0
3	Uterine cervix, pT1, G2, N0	A1c	1600/0
4	Uterine cervix, pT3, G3, N1	A1d	2400/0
5	Uterine cervix, pT3, G2, N0	A1e	3200/0
6	Uterine cervix, pT3, G3, N1	A1f	4000/0
7	Uterine cervix, pT1, G2, N0	A1g	4800/0
8	Uterine cervix, pT2, G2, N0	A1h	5600/0
9	Uterine cervix, pT3, G3, N1	A1i	6400/0
10	Uterine cervix, pT2, G2, N0	A1k	7200/0
11	Uterine cervix, pT3, G3, N1	A1l	8000/0
12	Uterine cervix, pT2, G2, N0	A1m	8800/0
13	Uterine cervix, pT1, G2, N0	A1n	9600/0
14	Uterine cervix, pT3, G3, N1	A1o	10400/0
15	Uterine cervix, pT2, G2, N0	A1p	11200/0
16	Uterine cervix, pT1, G2, N0	A1q	1200/0
17	Uterine cervix, pT1, G2, N0	A1r	12800/0
18	Uterine cervix, pT3, G3, N1	A2a	0/800
19	Uterine cervix, pT2, G2, N1	A2b	800/800
20	Uterine cervix, pT3, G2, N0	A2c	1600/800
21	Uterine cervix, pT1, G2, N0	A2d	2400/800
22	Uterine cervix, pT2, G2, N1	A2e	3200/800
23	Uterine cervix, pT1, G2, N0	A2f	4000/800
24	Uterine cervix, pT3, G2, N0	A2g	4800/800
25	Uterine cervix, pT3, G2, N0	A2h	5600/800
572	Prostate ca, hormone refractory	E7b	800/4800
573	Prostate ca, hormone refractory	E7c	1600/4800
574	Prostate ca, hormone refractory	E7d	2400/4800
575	Prostate ca, hormone refractory	E7e	3200/4800

[a] Coordinates refer to the punch positions selected on the arrayer device. Additional information, e.g., pathological or follow-up data, may be added.

2. Place an empty plastic biopsy embedding cassette on top of the freezing (but not yet completely frozen) OCT. This plastic cassette is subsequently filled with OCT.
3. After slight thawing, remove the completely frozen recipient block from the cryomold. Immediately place the recipient block on dry ice or in a freezer until used.

C. TMA Making

Only if all this preparatory work has been done can a tissue-arraying device be employed. Using these manually operated devices, excellent TMAs can be produced in the hands of a talented and experienced person. However, optimal arrays can be expected only after a significant training period, including several hundred, if not a few thousand, punches. A patient and enduring personality as well as keen eyesight are important prerequisites for operators of manual tissue arrayers. Early generation automated tissue arrayers are available but these devices are expensive, do not accelerate the TMA manufacturing process, and cannot be used for making frozen TMAs.

1. Paraffin-Embedded Tissue

The TMA manufacturing process consists of five steps that are repeated for each sample placed on the TMA.

1. Punch a hole into an empty recipient paraffin block.
2. Remove and discard the wax cylinder from the needle used for recipient block punching.
3. Remove a cylindrical sample from a donor paraffin block.
4. Place the cylindrical tissue sample in the premade hole in the recipient block.
5. Proceed to the new coordinates for the next tissue sample.

Exact positioning of the tip of the tissue cylinder at the level of the recipient block surface is crucial for the

quality and the yield of the TMA block. Placing the tissue too deeply into the recipient block results in empty spots in the first sections taken from the TMA block. Positioning the tissue cylinder not deep enough causes empty spots in the last sections taken from this TMA. However, a too superficial location of the tissue cylinder is less problematic than a too deep position, as protruding tissue elements can, to some extent, be leveled out after finishing the punching process. The use of a magnifying lens facilitates precise deposition of samples, especially for beginners.

As soon as all tissue elements are filled into the recipient block, the block is heated at 40° for 10 min. This improves adhesion between tissues and paraffin of the recipient block. Protruding tissue cylinders are then gently pressed deeper into the warmed TMA block using a glass slide.

2. Frozen Tissue

The recipient block must always be surrounded with dry ice to prevent melting. Make sure that the micrometer screws are not covered by ice. Malfunctions occur if the temperature of these elements gets too low. Continuously add more ice as melting occurs. The TMA manufacturing process consists of five steps that are repeated for each sample placed on the TMA.

1. Punch a hole into an empty recipient OTC array block.
2. Remove and discard frozen OTC from the needle.
3. Remove a cylindrical tissue sample (diameter 0.6 mm; height 4–5 mm) from frozen tissues. For this purpose, the same needle is used as previously for making a hole into the recipient array block. Switching to a larger needle is not needed. It is important to keep the tissue in the needle frozen during the procedure, e.g., by precooling the needle with a piece of dry ice before punching and while dispensing the tissue core into the recipient block. Use forceps for holding ice cubes for cooling needles.
4. Place the cylindrical tissue sample in the premade hole in the recipient OTC array block.
5. Proceed to the new coordinates for the next tissue sample.

Tissue arrayers that were initially designed for use on paraffin-embedded tissue can be utilized for frozen TMA making (Fejzo and Slamon, 2001). However, needles are at a higher risk of bending and breaking than in the case of paraffin-embedded tissues. Therefore, punching must be done slowly with minimal pressure to prevent needle damage. Despite this, frozen TMAs will become more irregular and distorted than TMAs from formalin-fixed material.

D. TMA Sectioning

Regular sections may be taken from frozen and paraffin-embedded TMA blocks using a standard microtome or cryostat. However, the more samples a TMA block contains, the more difficult regular cutting becomes. As a consequence, the number of slides of inadequate quality increases with the size of the TMA and, in turn, fewer sections from the TMA block can effectively be analyzed. Using a tape sectioning aid is therefore recommended.

The tape sectioning kit (Instrumedics) facilitates cutting and leads to highly regular nondistorted sections that are ideally suited for automated analysis. In addition, the tape system may prevent arrayed samples from floating off the slide if very harsh pretreatment methods are used. However, the sticky glued slides have the disadvantage of increased background signals between the tissue spots in some IHC analyses and of a slightly deteriorated morphology of some tissue samples because of small visible glue dots within the samples. The tissue samples themselves do not show increased nonspecific background in IHC. Use of the tape sectioning system is described next.

1. Paraffin-Embedded Tissues

1. Place an adhesive tape on top of the TMA block in the microtome immediately before cutting. Always use a hand roller in order to avoid bubbles.
2. Cut section (usually 5 µm). The tissue slice is now adhering to the tape.
3. Transfer the tissue slice on a special "glued" Instrumedics slide (use the hand roller for this purpose; stretching of the tissue in a water bath or on a heating plate is not necessary). It is important to store "glued" slides in darkness before usage. Adhering slide properties deteriorate rapidly under light exposure.
4. Expose the slide (tissue on the bottom) to UV light for 35 s in order to polymerize the glue on the slide and on the tape.
5. Dip the slides into TPC solution (Instrumedics) at room temperature for 5–10 s. The tape can then be removed gently from the glass slide. The tissue remains on the slide.
6. Air dry slides at room temperature.

2. Frozen Tissues

Slides, adhesive tape, and hand roller are optimally stored within the cryostat microtome. They can only be used if their temperature is identical to the temperature within the cryostat microtome.

1. Place a precooled adhesive tape on top of the TMA block in the cryostat microtome using a precooled hand roller immediately before cutting.

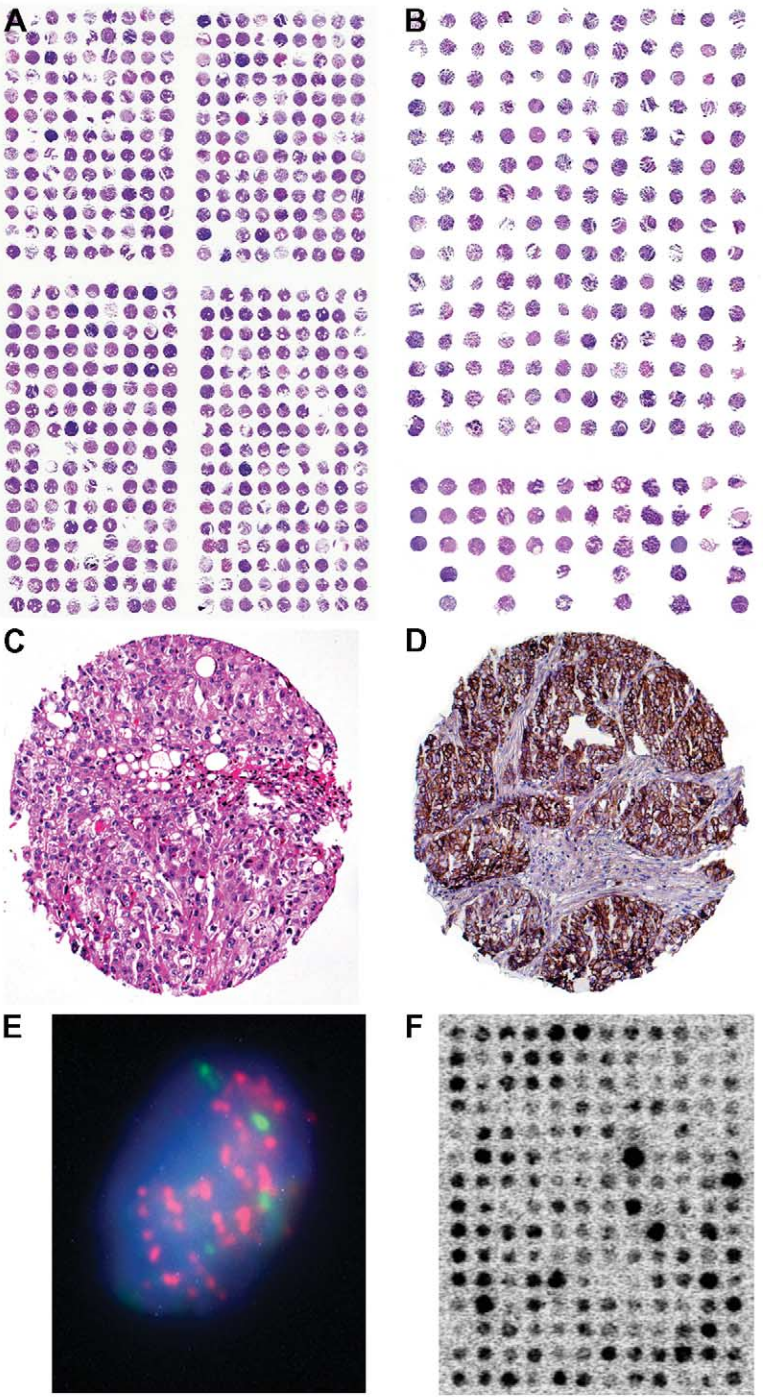

FIGURE 2 Examples of stained tissue sections. Hematoxylin and eosin (H&E)-stained sections of (A) a TMA from formalin-fixed, paraffin-embedded tissues containing 540 tissue spots and (B) a TMA from frozen tissue containing 228 tissue spots. Each tissue spot measures 0.6 mm in diameter. Missing samples result from the sectioning/staining process or indicate samples that are already exhausted. Note that the spot-to-spot distance is larger on the frozen TMA as compared to the paraffin TMA. (C) Magnification of a H&E-stained 0.6-mm tissue spot of a bladder carcinoma. (D) Immunohistochemistry against the EGFR protein in a pharynx cancer sample using the DAKO HercepTest. (E) FISH analysis of centromere 7 (green signals) and the EGFR gene (red spots) in cell nuclei (blue staining) of a tissue spot (630×). The high number of EGFR signals indicates gene amplification. (F) RNA *in situ* hybridization on a frozen TMA made from breast cancer tissues. A radioactively labeled oligonucleotide was used as a probe against mRNA of a lipoprotein-binding protein. The black staining intensity indicates the level of mRNA in each tissue spot.

TABLE II Troubleshooting

Problem	Possible cause	Paraffin embedded	Frozen
Missing tissue samples on first series of TMA sections taken from TMA blocks (same samples missing on all sections)	Tissue cores placed too deeply into the recipient block	As long as the TMA making is not completed, a too deeply placed tissue core can be removed using the thinner needle. Then another sample taken from the donor block can be used as a replacement	Removal of the too deeply positioned tissue is not recommended. Consider adding an additional sample of this tissue to the TMA block
Missing tissue samples on deeper sections taken from TMA blocks (same samples missing on all sections)	Tissue cores were not pushed into the recipient block deeply enough	Careful leveling out of the TMA block surface after finishing the punching process and placing the TMA block in an oven (10 min 40°C).	Careful leveling out of the TMA block surface after finishing the punching by gently pressing an empty glass slide on the surface (Do not use oven!)
	Tissue cores were too short	Check tissue blocks for presence of sufficient tumor material before final block selection	
Missing tissue samples on deeper sections taken of TMA blocks (different samples missing on different sections)	Samples float off the slide during harsh pretreatments	Use adhesive-coated slides	
	Samples come off the slide during the sectioning process	Avoid air bubbles between block and tape and between tape and adhesive-coated slide by using the hand roller. Slides and tapes may have irregular quality; it is important to check the material quality before use. Poor quality slides have inhomogeneous glue distribution	
Some tissues on the TMA section are very thin and partially destroyed	Tissue damage incurred during removal of the adhesive tape	Do not cut sections thinner than 5 µm. Exact timing of the tape removal process	Do not cut sections thinner than 10 µm
		Quality control of the unstained TMA slides under the microscope before use	Quality control of the unstained TMA slides under the microscope before use
Tissue on TMA section is not representative	Wrong area punched	Correct marking of areas on the HE-stained section that can be easily found on the block Careful selection of the marked area for punching	
Irregular distribution of samples on the TMA block	Needle is bent	Change needle	To some extent irregular sample arrangement must be accepted Changing the needle improves the regularity of the TMA Complete frozen TMA within 1 working day
Tissue cylinder cannot be removed from donor block	Needle is blunt	Change needle	Change needle
Paraffin cylinder cannot be removed from recipient block	Needle is blunt	Change needle	Change needle
Array block protrudes in the center ("hillock formation" in paraffin arrays)	Premade holes in the TMA recipient block are too short	Make deeper holes	
	Too small a distance between tissue cylinders	Select sufficiently large distance between different cylinders Careful leveling out of the TMA block surface after finishing the punching process and placing the TMA block in an oven (10 min 40°C).	
Paraffin recipient blocks crashes	Samples placed too closely to the border of the block	Select a distance of at least 3 mm between recipient block border and first tissue sample Use larger recipient blocks	
Tissue core cannot be placed into the recipient block	Paraffin: needles are not aligned properly	Align needles (see manual)	
	Frozen: tissue melts during the punching process		Carefully cool the needle before and during the punching process
Micrometer screw malfunction during arraying	Battery exhausted	Change battery	Change battery
	Frozen: Dry ice is covering micrometer screw		Remove dry ice from micrometer screw

2. Cut section (usually 10–12 µm). The tissue slide is now adhering to the tape.
3. Transfer the tissue slice on a special "glued" slide using a hand roller.
4. Put the slide on dry ice for 60 s.
5. Remove the tape gently (TPC solution is not required for removal of tape after ice pretreatment).
6. Immediately place slides into freezer (–70°C).

IV. COMMENTS

TMAs are suited for all types of *in situ* analysis methods, including immunohistochemistry, fluorescence *in situ* hybridization (FISH), and RNA *in situ* hybridization. All protocols that can be used on large sections will also work on TMAs. Extended deparaffinization is recommended, e.g., xylene exposure for 60–120 min. Examples of stained TMA sections are shown in Fig. 2. One of the most significant differences as compared to traditional large section studies is the high level of standardization that can be achieved in TMA experiments. All slides of one TMA study are usually incubated in one set of reagents, assuring absolutely identical concentrations, temperatures, and incubation times. Other minor variables that may have an impact on the outcome of *in situ* analyses such as the age of a slide (time between sectioning and use) or section thickness are also fully standardized if all tissues of one study are located on the same TMA section. As a result of this unprecedented standardization within each experiment, intralaboratory variations may occur if experiments are repeated under slightly different conditions. Significant differences that were observed after using TMA sections stored for different time spans may represent just one example of how minor variables can significantly affect the results of molecular *in situ* analyses (M. Mirlacher *et al*., unpublished observations, 2002).

V. TROUBLESHOOTING

For a description of problems, possible causes, and remedies, see Table II.

References

Battifora, H. (1986). The multitumor (sausage) tissue block: novel method for immunohistochemical antibody testing. *Lab. Invest.* **55**, 244–248.

Bremnes, R. M., Veve, R., Gabrielson, E., Hirsch, F. R., Baron, A., Bemis, L., Gemmill, R. M., Drabkin, H. A., and Franklin, W. A. (2002). High-throughput tissue microarray analysis used to evaluate biology and prognostic significance of the E-cadherin pathway in non-small-cell lung cancer. *J. Clin. Oncol.* **20**, 2417–2428.

Bubendorf, L., Kolmer, M., Kononen, J., Koivisto, P., Mousses, S., Chen, Y., Mahlamäki, E., Schraml, P., Moch, H., Willi, N., Elkahlhoun, A., Pretlow, T., Gasser, T., Mihatsch, M., Sauter, G., and Kallioniemi, O. (1999a). Molecular mechanisms of hormone therapy failure in human prostate cancer analyzed by a combination of cDNA and tissue microarrays. *J. Natl. Cancer Inst.* **91**, 1758–1764.

Bubendorf, L., Kononen, J., Koivisto, P., Schraml, P., Moch, H., Gasser, T., Willi, N., Mihatsch, M., Sauter, G., and Kallioniemi, O. (1999b). Survey of gene amplifications during prostate cancer progression by high-throughput fluorescence in situ hybridization on tissue microarrays. *Cancer Res.* **59**, 803–806.

Bubendorf, L., Nocito, A., Moch, H., and Sauter, G. (2001). Tissue microarray (TMA) technology: Miniaturized pathology archives for high-throughput in situ studies. *J. Pathol.* **195**, 72–79.

Fejzo, M. S., and Slamon, D. J. (2001). Frozen tumor tissue microarray technology for analysis of tumor RNA, DNA, and proteins. *Am. J. Pathol.* **159**, 1645–1650.

Kononen, J., Bubendorf, L., Kallioniemi, A., Bärlund, M., Schraml, P., Leighton, S., Torhorst, J., Mihatsch, M., Sauter, G., and Kallioniemi, O. (1998). Tissue microarrays for high-throughput molecular profiling of hundreds of specimens. *Nature Med.* **4**, 844–847.

Richter, J., Wagner, U., Kononen, J., Fijan, A., Bruderer, J., Schmid, U., Ackermann, D., Maurer, R., Alund, G., Knonagel, H., Rist, M., Wilber, K., Anabitarte, M., Hering, F., Hardmeier, T., Schonenberger, A., Flury, R., Jager, P., Luc Fehr, J., Schraml, P., Moch, H., Mihatsch, M. J., Gasser, T., Kallioniemi, O. P., and Sauter, G. (2000). High-throughput tissue microarray analysis of cyclin E gene amplification and overexpression in urinary bladder cancer. *Am. J. Pathol.* **157**, 787–794.

Schraml, P., Kononen, J., Bubendorf, L., Moch, H., Bissig, H., Nocito, A., Mihatsch, M. J., Kallioniemi, O. P., and Sauter, G. (1999). Tissue microarrays for gene amplification surveys in many different tumor types. *Clin. Cancer Res.* **5**, 1966–1975.

Simon, R., and Sauter, G. (2002). Tissue microarrays for miniaturized high-throughput molecular profiling of tumors. *Exp. Hematol.* **30**, 1365–1372.

Simon, R., Struckmann, K., Schraml, P., Wagner, U., Forster, T., Moch, H., Fijan, A., Bruderer, J., Wilber, K., Mihatsch, M. J., Gasser, T., and Sauter, G. (2002). Amplification pattern of 12q13-q15 genes (MDM2, CDK4, GLI) in urinary bladder cancer. *Oncogene* **21**, 2476–2483.

Torhorst, J., Bucher, C., Kononen, J., Haas, P., Schraml, P., Zuber, M., Köchli, O., Mross, F., Dieterich, H., Moch, H., Mihatsch, M., Kallioniemi, O., and Sauter, G. (2001). Tissue microarrays for rapid linking of molecular changes to clinical endpoints. *Am. J. Pathol.* **159**, 2249–2256.

PART

F

CYTOGENETICS AND *IN SITU* HYBRIDIZATION

SECTION

14

Cytogenetics

CHAPTER

38

Basic Cytogenetic Techniques: Culturing, Slide Making, and G Banding

Kim Smith

I. INTRODUCTION

During metaphase of the cell cycle, the condensed chromosomes align along the metaphase plate prior to chromatid separation and then move along the spindle fibres to the poles of the spindle. A spindle inhibitor, colchicine, can be added during metaphase, which disrupts the polymerisation of the spindle fibres, arresting the cell cycle at the stage when the chromosomes are fully condensed. It is possible to increase the number of metaphases by synchronising the cell cycle with a chemical blocking agent such as thymidine. The addition of excess thymidine results in the inhibition of DNA synthesis and the cells collecting in S phase. When the thymidine block is removed by washing the cells in fresh medium or by the addition of deoxycytidine, the synchronised cells progress to M phase and, by careful timing of the addition of colchicine and subsequent harvest, a large number of longer chromosomes in early metaphase can be collected.

In order to visualise the chromosomes, these cells are harvested with hypotonic and fixative stages. The hypotonic solution swells the cells, allowing the chromosomes to separate. The cells are fixed with glacial acetic acid/methanol, which removes water and hardens the cell membrane. The final fixed cell suspension is dropped onto a microscope slide where evaporation of the acetic acid/methanol fixative results in bursting of the cells and spreading of the metaphase chromosomes. Humidity plays a key role in the rate of evaporation of fixative and control of chromosome spreading, hence an optimal microenvironment is vital to the production of well-spread chromosomes (Fig. 1).

Routine G banding with trypsin gives each chromosome a distinct banded pattern that allows identification of discrete regions along each chromosome and the opportunity to screen for chromosomal imbalance of at least 3–5 Mb by standard microscopic analysis.

Diagnostic cytogenetic investigations are used routinely within the clinical setting to screen for chromosomal imbalance in a wide range of patients. These methods describe a synchronised suspension culture of blood and an unsynchronised adhesion culture of tissue.

II. MATERIALS AND INSTRUMENTATION

RPMI with 20 m*M* HEPES (52400-017), penicillin (10,000 U/ml)/streptomycin (10,000 µg/ml)/glutamine (29.2 mg/ml) (10378-016), trypsin 2.5% (15090-046), phytohaemagglutinin (10576-015), Hanks BSS (14180-046), and colcemid (15212-012) are from GIBCO. Hams F10 (N6013), thymidine (T9250), 2-deoxycytidine (D3897), colchicine (C9754), EDTA 0.02% (E8008), amphotericin B (A9528), and phosphate-buffered saline (PBS), pH 7.4 (P3813) are from Sigma. Heparin (101929) is from ICN. Ultroser G (15950-017) is from Biosepra. Fetal calf serum is from various sources, including Sigma, GIBCO, and Seralab. Methanol (101586B), glacial acetic acid (10001CU), KCl (101983K), Leishman's stain solution (350226N), buffer tablets, pH 6.8 (331992P), XAM mountant (361194V), and washed glass slides (406/0181/02) are from BDH. Difco trypsin (215320) is from Becton-Dickinson. Virkon (R330003/Q) is from Radleys. Tissue culture

Copyright 2006, Elsevier Science (USA).
All rights reserved.

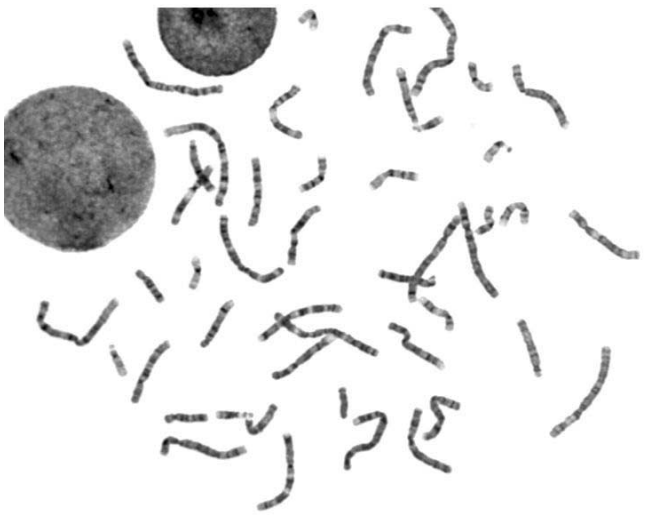

FIGURE 1 A metaphase from a synchronized blood culture. Courtesy of Lyndsey Connell, Oxford Cytogenetics Laboratory.

flasks (25 cm^2, Nunc 163371), blood culture tubes (Falcon 35-2027), 1-ml plastic pastettes (Alpha LW4010), sterile petri dishes (Sterilin 101R20), sterile scalpels (Swan Morton) and needed. Gas (5% CO_2/95% air) is required if a CO_2 incubator is not being used.

Equipment includes a class II laminar flow hood, incubator, centrifuge, inverted microscope, light microscope with phase 10 and 100× objectives, hot box oven, hot plate. Local humidity control can be helped by humidifiers, dehumidifiers, or controlled environment equipment.

III. PROCEDURES

A. Synchronised Cell Culture of Human T Lymphocytes

Blood should be collected into heparinised, ideally lithium heparin, tubes to prevent coagulation. Although whole blood is cultured, T lymphocytes are used routinely for blood cytogenetic investigations. As these cells are not spontaneously dividing, phytohaemagglutinin (PHA), a mitogen, must be added to transform the T lymphocytes and start cell division. PHA is only required during the first 24 h of cell culture and so is omitted from postsynchronisation release medium. Blood is routinely cultured for 72 h.

Solutions

1. *Phytohaemagglutinin* must be used within 2–3 weeks after rehydration.
2. *Phosphate-buffered saline pH 7.4*: Add one sachet to 1 litre distilled water
3. *Working stock solutions: Heparin* (1250 units/ml in distilled water), *thymidine* (10 mg/ml in PBSA), *2-deoxycytidine* (10 µg/ml in distilled water), and *colchicine* (250 µg/ml for blood in distilled water)
4. *Complete medium*: 100 ml RPMI, 20 ml fetal calf serum, 1 ml penicillin/streptomycin/glutamine, 0.2 ml heparin, and 2 ml phytohaemaglutinin
5. *Release medium*: 100 ml RPMI, 10 ml fetal calf serum, 2 ml penicillin/streptomycin/glutamine, and 2 ml deoxycytidine
6. *KCl hypotonic*: 0.056 M (4.2 g/litre)
7. *Fixative*: 3 : 1 methanol : glacial acetic acid

Steps

Day 1 Establishing Cultures

1. Dispense 5 ml of complete medium into a labelled sterile culture tube. Add 0.25 ml of blood with a sterile plastic pastette. Replace lid and invert to mix.
2. Place in a culture rack and incubate in a 37°C incubator. A culture rack with a slanted edge allows the tubes to lie at a 20–30° incline and increases the media/cell pellet surface area for improved exchange of gas and nutrients.

Day 3 Synchronisation. Add 0.2 ml thymidine to each culture in the late afternoon and reincubate for 17–18 h overnight.

Day 4 Synchronisation Release and Harvest

1. Centrifuge cultures at 1200 rpm for 5 min. Remove the supernatant from the culture tube, leaving approximately 1 cm depth of supernatant. Add 4 ml release medium and resuspend cells. Note time of release and reincubate.

2. Four hours after synchronisation release, add 0.1 ml colchicine per tube, invert culture tubes to mix, and reincubate cultures.

3. After 20 min incubation, centrifuge at 1200 rpm for 5 min. Remove supernatant, leaving approximately 0.5 ml in the tube. Resuspend cells and gently add 5 ml KCl hypotonic. Replace lid and invert the tube to ensure thorough mixing. Reincubate culture tubes for 5 min.

4. Centrifuge at 1200 rpm for 5 min. Remove supernatant. Resuspend cells thoroughly. Very gently, add 5 ml fixative (drop by drop at first and then more quickly) whilst continuously mixing the cell pellet either by flicking the tube or by mixing on a whirlimixer to prevent cell clumping. This stage is critical in producing clean preparations.

5. Centrifuge culture tubes at 1200 rpm for 5 min. Pour off supernatant. Resuspend cells thoroughly and

add 5 ml fixative. Centrifuge culture tubes again, resuspend cells, and add 5 ml fixative. If the cell suspension looks faintly brown, repeat centrifuging and fixing once more before slide making. The cells are ready for slide making or may be stored at –20°C.

B. Unsynchronised Cell Culture of Fibroblasts

Tissue viability is improved if the tissue sample is transported in transport medium supplied by the laboratory.

Solutions

1. *Working stock solutions: Heparin* (1250 units/ml), *amphotericin B* (0.25 mg/ml), and *colchicine* (500 µg/ml for tissues)
2. *Transport medium*: 100 ml Hams F10, 1 ml penicillin/streptomycin/glutamine, 0.2 ml heparin, and 1 ml amphotericin B
3. *Complete medium*: 100 ml Hams F10, 20 ml fetal calf serum, 1 ml penicillin/streptomycin/glutamine, 1 ml amphotericin B, and 2 ml Ultroser
4. *Trypsin/EDTA*: 10 ml of trypsin 2.5% added to 100 ml EDTA 0.02%
5. *KCl hypotonic*: 0.056 M (4.2 g/litre distilled water)
6. *Fixative*: 3 : 1 methanol : glacial acetic acid

Steps

Day 1 Establishing Cultures

1. Remove the tissue from the transport medium with a sterile pair of forceps and place in a sterile plastic petri dish. Using a sterile plastic pastette, add a few drops of medium to the tissue to prevent the sample from drying out. Mince the tissue finely with a sterile scalpel into ~0.5- to 1-mm^3 pieces.

2. Using a pastette, resuspend the minced tissue in a small volume (~0.25 ml) of medium and place on the growth surface of two labelled 25-cm^2 flasks. Ensure that the tissue pieces are as evenly spread as possible. Gently invert the flask so that tissue adheres to the surface in a minimal amount of medium. Add 5 ml of complete tissue medium to each flask by running the medium down the lower side of the inverted flasks. Gas (5% carbon dioxide/95% air) the flasks if using a standard non-CO_2 incubator, replace lids, and incubate at 37°C.

3. After several hours (or overnight if cultures are set up late in the day), carefully turn the flasks the right way up so medium now covers the tissue.

Days 6–8+ Processing and Harvesting of Cultures

1. Cultures are examined for the first time when they are 6–8 days old. Replace the medium with 5 ml of complete tissue medium. Gas (5% carbon dioxide/95% air) the flasks if using a standard non-CO_2 incubator, replace lids, and incubate at 37°C.

2. When sufficient cells have grown from the explants (covering one-half to two-thirds of the flask), the cells can be directly harvested or subcultured. Subcultured cells usually give a higher mitotic index.

Subculturing

1. Prewarm trypsin/EDTA to 37°C. Remove culture medium and gently rinse flask with ~1 ml of trypsin/EDTA. Add 0.5 ml of prewarmed trypsin/EDTA and reincubate for several minutes. Examine the flask under low magnification on an inverted microscope. The cells should appear either rounded up or floating in the medium. Tap the flask lightly two or three times to dislodge any remaining cells. Add 1 ml of medium and divide the cell suspension between two new labelled flasks.

2. Add 5 ml of complete medium to each flask, including the original, which can be retained as a backup. Gas (5% carbon dioxide/95% air) the flasks if using a standard non-CO_2 incubator, replace lids, and incubate at 37°C.

Harvesting of Cultures. Subcultured flasks are usually fed with 5 ml fresh medium the following day and harvested on the second day. The cells should be in logarithmic growth phase with a high mitotic activity.

1. Add 0.1 ml colchicine to each flask and reincubate for 2 h. Prewarm trypsin/EDTA to 37°C.

2. After 2 h, examine the cells under low magnification with an inverted microscope. A number of rounded, dividing cells should be present. Pour off the medium from the flask into a labelled centrifuge tube. Add 1 ml of trypsin/EDTA and rinse the flask, adding this to the centrifuge tube. Add 0.5–1 ml of trypsin/EDTA to each flask and incubate for 2–5 min. Tap the flask two or three times. Examine the flasks to check that cells are in suspension. Add 2 ml of culture medium to the flask and transfer all medium and cells to the centrifuge tube.

3. Centrifuge the tube at 1200 rpm for 7 min. Pour off the supernatant from the tube. Resuspend the pellet by flicking the tube. Add 5 ml KCl hypotonic solution to the tube and invert gently to mix. Centrifuge at 1200 rpm for 7 min. Pour off the hypotonic, resuspend the cell pellet, and gently and slowly add fixative whilst flicking the tube to prevent cell clumping. After approximately 0.5 ml has been added, top up more quickly to 5 ml. The cells are ready for slide making or may be stored at –20°C.

C. Slide Making

It is advisable to wipe the precleaned slide with a tissue soaked in either methanol or fixative immediately prior to slide making. Optimal conditions are 40–45% humidity in temperatures of 20–22°C.

Solution

Fixative solution: 3:1 methanol:glacial acetic acid

Steps

1. Centrifuge cell suspensions at 1200 rpm for 5 min. Pour off supernatant and resuspend the cell pellet by tapping the tube and add three drops of fixative.
2. Using a plastic pipette, place a single drop of cell suspension in the middle of a labelled slide from a height of 1 cm. The slide can be held flat, allowing the drop to spread as a circle or the slide can be held at 20–30° so that the drop runs down the length of the slide.
3. Add a single drop of fixative from the same height in the same manner when the area of cells becomes visible as a cloudy area and Newton's rings appear on the periphery. Allow the fixative to evaporate.
4. Check the cell density and metaphase spreading using a phase microscope.
5. If the slide has sufficient metaphases of an appropriate length, continue with slide making. If the cell density is too high, add a few more drops of fixative and check by making another slide. If the cell density is too low, add 5 ml fixative, centrifuge the suspension again, and repeat but add less fixative. Cell spreading can be altered by changing cell density, local humidity, or the rate of drying. Underspreading can be improved by breathing on the slide before adding the cell suspension, adding two drops of fixative to the cells on the slide, or placing the slide on a wet paper towel. Overspreading can be reduced by omitting the second drop of fixative, using cold fixative cooled in a freezer before use, or increasing local air flow and speed of drying.
6. Add 5 ml fixative to any remaining cell suspension and store at –20°C.
7. Age slides either overnight by putting in metal racks in a hot box oven at 70°C or for 1 h on a hot plate at 80°C or on the bench for several days.

D. G Banding

Solutions

1. *Hanks pretreatment solution*: 8 ml of Hanks BSS (10×) plus 40 ml of distilled water
2. *Phosphate-buffered saline pH 7.4*: Add one sachet of powder to 1 litre of distilled water
3. *Banding trypsin solution*: Rehydrate bottle of Difco trypsin with 10 ml of distilled autotoclaved water. Add 1 ml of trypsin solution to 40 ml PBSA.
4. *pH 6.8 buffer solution*: Add 1 tablet to 1 litre of distilled water
5. *Leishman's staining solution*: 40 ml, pH 6.8, buffer solution plus 8 ml Leishmans' stain

Steps

1. Place a test slide in the Hanks pretreatment solution for 3 min. Rinse the test slide in tap water for 5 s. Place the slide in the trypsin solution for 33 s (move slide gently in the solution). Whilst slide is in the trypsin solution, remove surface film from the stain by skimming with a piece of filter paper. Rinse slide in tap water. Place the slide in Leishman's staining solution for 2 min. Rinse slide in tap water. Blot carefully with filter paper and leave to dry or dry on a hot plate for a short time.
2. When dry, place three drops of XAM or similar mountant onto the slide along its length. Place a 22 × 50-mm coverslip onto the slide and blot gently to remove excess mountant.
3. Assess banding using the light microscope at 1000× magnification and adjust times for Hanks, trypsin, and stain as appropriate. If the chromosomes appear generally grey with indistinct banding, increase the Hanks pretreatment time. If the chromosomes are bloated and the chromatids appear to be separating, reduce trypsin time. If they appear generally dark with little banding, increase the trypsin time. Staining should be modified so there is a clear distinction between pale staining and dark staining regions of the chromosomes.

IV. COMMENTS

1. All culture work should be performed under the appropriate containment level (e.g., class 2 laminar flow cabinet).
2. All waste material from cell cultures should be decontaminated prior to disposal. Waste media and hypotonic can be decontaminated in 2% Virkon for a minimum of 10 min.
3. Fetal calf serum is variable in supporting good cell growth and should be batch tested prior to bulk purchase and use. It is advisable to combine smaller aliquots from two different batches or suppliers rather than a single volume from one supplier in preparing complete medium.

4. All complete culture media should be stored at 4°C and ideally used within 1 week of preparation.

5. Our laboratory routinely uses colchicine. Many laboratories use the less toxic colcemid, adding 0.1 ml of stock solution to 5 ml culture.

6. The methanol/glacial acetic acid fixative should be freshly made before harvesting and slide making.

7. Slides should be grease free to ensure optimal chromosome spreading. Precleaned slides may be purchased.

V. PITFALLS

If the first fixation stage of a blood culture results in a gelatinous cell suspension, add an equal volume of distilled water, mix, recentrifuge, and continue with protocol.

CHAPTER

39

A General and Reliable Method for Obtaining High-Yield Metaphasic Preparations from Adherent Cell Lines: Rapid Verification of Cell Chromosomal Content

Doris Cassio

I. INTRODUCTION

In vitro studies are becoming more and more frequent in numerous domains of cell biology. For such purposes, a great variety of cell lines have been established either from normal tissues or, more frequently, from tumours. Very few of these cells present a normal karyotype: they are generally hyperdiploid and often contain rearranged chromosomes. Moreover, depending on the length of time in culture and on the culture conditions, populations of these cell lines can change and drift. Therefore, some general culture rules have to be respected (Ian Freshney, 1987), and it is highly recommended to avoid working with cells maintained in culture for a large number of generations.

Because of possible drift, cell lines need to be followed and controlled, with one fundamental control being the stability of their chromosomal content. Unfortunately, such control is not systematic. Moreover, in the case of new cell lines, it is frequent that their phenotype is described in detail with little or no information on their karyotype. It should be noted that even if karyotyping methods have long been described in the literature (for the history of human cytogenetics, see Jeening Lawce and Brown, 1997), it is not always easy to obtain metaphasic preparations from some cell lines. We were confronted with such a situation for some hybrid lines, in particular polarized rat hepatoma–human fibroblast WIF clones (Cassio *et al*., 1991; Shanks *et al*., 1994). This article describes a new method for obtaining, at a high yield, metaphasic preparations from delicate cell lines. This method is easy and reliable and has been applied successfully by many people to more than 50 different cell lines from different species.

A. Principles of the Method

This method is a combination of the two methods described by Worton and Duff (1979), the suspension method generally used for nonadherent and adherent cells and the "*in situ*" method that has been specifically developped for adherent cells (Cox *et al*., 1974; Peakman *et al*., 1977). When we tried to prepare metaphases from the well-polarized hybrid cell line WIF-B (Shanks *et al*., 1994), we only succeeded with the "*in situ*" one. We performed many assays using the suspension method and they all failed: from two to three petri dishes containing 10^6 cells/dish in exponential phase, we obtained, at the best, a dozen metaphases (yield < 10^{-5}). In contrast, with the *in situ* method, the metaphase yield was very good and attained 1.5% of the total cell number (the maximal

Copyright 2006, Elsevier Science (USA).
All rights reserved.

expected value for cells with a generation time of 2.5 days).

In the suspension method, mitoses are detached (mechanically or by proteolysis), whereas in the *in situ* method, mitoses stay in place. As polarized WIF-B cells have a highly differentiated plasma membrane, organized in different domains, we hypothesized that mitotic cells from this line are very fragile and are lost during or after detachment (may be during centrifugation). Therefore, to isolate metaphases from this line, a new method was developped that avoids cell detachment, at least during the early steps. The first steps of this method (metaphase arrest, hypotonic swelling, and first fixation) are performed *in situ* and it is only after the first fixation that cells are detached.

B. Advantages of the Method

This method presents several advantages. First, it is applicable to every adherent cell line and does not depend on the adherent properties of the mitosis, as all mitoses (floating and adherent ones) are collected. Second, as with the *in situ* method, the yield in metaphases is very good (Fig. 1A) and therefore the metaphasic preparations are representative of the whole cell population. Third, this method requires fewer cells and is less wasteful in cells than the suspension method, an advantage for slow-growing cell lines where mitotic cells are rare or for cells where the results of karyotyping are required as soon as possible. Finally, as with the suspension method, the quality of the metaphase spreading is good (Fig. 1B) and can be adjusted, whereas with the *in situ* method, which allows only one attempt per culture, the spreading cannot be controlled and is very sensitive to cell overcrowding. Moreover, the chromosomes obtained by this new method are quite suitable for G banding, Giemsa 11 staining (Buys *et al.*, 1984) (Fig. 1C), and fluorescent *in situ* hybridization (FISH) (Fig. 1D).

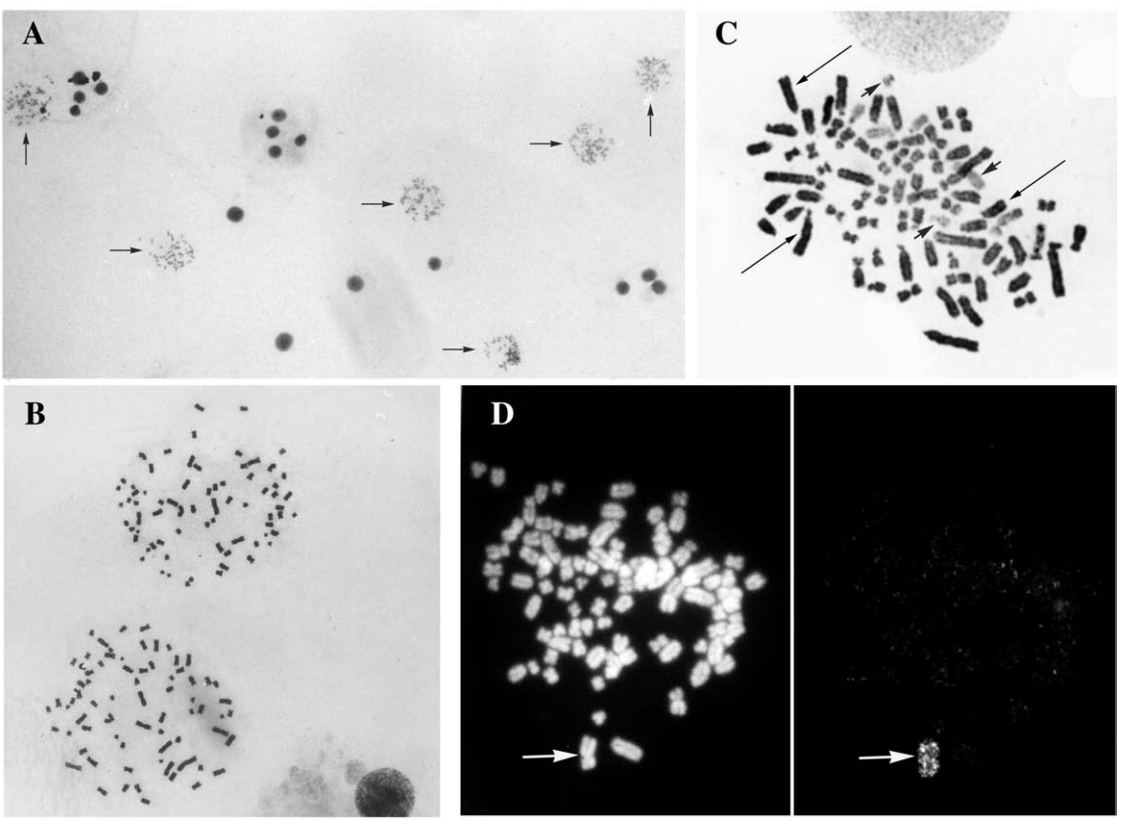

FIGURE 1 **Metaphases from HT29 and hybrid WIF lines.** (**A**) HT-29 cells at low magnification; metaphases were obtained at a high yield as attested by the presence of six metaphases (arrows) among some 30 cells. (**B**) HT-29 metaphases at a higher magnification to illustrate chromosome spreading. (**C**) Detection of human (pale staining, small arrows) and rat (dark staining, long arrows) chromosomes by Giemsa 11 staining in a metaphase of the human × rat hybrid WIF-B. (**D**) Detection by FISH (right) of one copy of the human chromosome 2 (arrow) in a WIF 12-E metaphase that was counterstained with propidium bromide to show all the chromosomes (left).

II. MATERIALS AND INSTRUMENTATION

Growth medium (available from local suppliers)
Colcemid (10 µg/ml; GIBCO, Cat. No. 2465)
Gurr buffer tablets, pH 6.8 (BDH, Cat. No. 33199)
Giemsa solution (Merck, Cat. No. 1.09204.0100)
10-cm tissue culture dishes (Falcon, Cat. No. 3003)
15-ml tubes (Falcon, Cat. No. 352099)
Precleaned, ground edge, microslides (ESCO, Cat. No. 2951R)
Glass jars

A low-speed centrifuge with a swinging-backet rotor for 15-ml tubes (as the IEC clinical centrifuge) is needed for harvesting cells, and a phase-contrast microscope is needed for examining cells and slides.

III. PROCEDURES

A. Cleaning and Frosting of Microscope Slides

Steps

1. Dip microscope slides in a jar containing 100 ml methanol plus two to three drops of concentrated HCl for 12–24 h.
2. Dry the slides one by one, place them in an appropriate jar, and freeze them at –20°C for at least 4 h and at the most 7 days.

B. Optimization of Growth

Step

Grow cells in 10-cm Petri dishes in appropriate medium so that cells will be in midexponential phase with many mitoses on the day of harvest. Renew the dishes with 10 ml of medium the day before the harvest.

C. Metaphase Arrest

Step

Add 0.2 ml of colcemid for 1 h at 37°C to the dish containing the maximal number of mitotic cells. The other dishes can be used later if necessary.

D. Hypotonic Swelling

Solutions

1. *Hypotonic solution (0.075 M KCl)*: add H_2O to 0.56 g KCl to make 100 ml
2. *Fixative*: Make **fresh** 3:1 methanol:glacial acetic acid; keep it at –20°C in an appropriate closed glass vessel and transfer to 4°C just before use.

Steps

1. Collect the culture medium of the Petri dish in a 15-ml tube and centrifuge at room temperature, at approximatively 1000 rpm (200 g) for 5 min, to collect the floating mitoses.
2. Immediately after starting centrifugation, add 5 ml of warm (37°C) hypotonic solution to the cells in the petri dish.
3. Incubate the cells in the hypotonic solution at 37°C.
4. As soon as the centrifuge stops, aspirate and discard the supernatant and add 1 ml of warm hypotonic solution to the pellet (depending on the cell line this pellet could be well visible or almost nonexistent). Resuspend the pellet rapidly by pipetting and add this suspension to the cells in the Petri dish, which now contain all the starting cells. Incubate at 37°C for a further 20–30 min.

Note: The swelling of the cells can be verified by examination under a microscope.

E. Fixation

Steps

1. Add very carefully to the petri dish 6 ml of cold (4°C) fixative with a **glass** pipette and place the dish on ice for 10 min.
2. Detach the cells from the dish with a **glass** Pasteur pipette by repeated pipetting. Depending on the cell line, this step could be very easy or more laborious. Control the detachment under the microscope. If the cells are very sticky, try gentle use of a cell scraper.
3. Transfer the cold cell suspension to a cold (4°C) 15-ml tube.
4. Centrifuge at approximatively 1000 rpm (200 g) for at least 5 min.
5. Remove all but about 0.2 ml of supernatant and resuspend gently by shaking cell pellet in this small volume (no pipetting). Add 1 ml of cold fixative slowly and then another 4 ml of cold fixative and leave on ice for at least 5 min.
6. Repeat steps 4 and 5 (with a smaller volume of fixative) twice; the fixative can be added more quickly on the last fixations. At this point preparations can be stored overnight at 4°C or slides can be made immediately.

F. Spreading and Air Drying

Spreading is done by air drying onto frozen slides.

Steps

1. Centrifuge the fixed cells at approximatively 1000 rpm (200 g) for at least 5 min.
2. Remove the supernatant and gently resuspend the pellet in about 0.5 ml of cold fixative (make fresh fixative if cells have been stored overnight).
3. Using a Pasteur pipette, drop two to three drops of the suspension at the top of a frozen slide inclined 20–30° from vertical. Let the drops run down the length of the slide as they spread. Wipe excess liquid from the underside of slide and let it dry at room temperature.
4. Check this first slide under phase contrast so that adjustments can be made on subsequent slides if cells are too crowded or if the spreading is poor.

G. COLORATION

As the present technique was developed to verify the cell chromosomal content, we use Giemsa "solid staining" (Worton and Duff, 1979), which gives uniform staining of the chromosomes and makes it easy to count them. However, other staining methods can be applied (Fig. 1).

Solutions

1. *Gurr buffer, pH 6.8*: Dissolve one Gurr buffer tablet, pH 6.8, in 1 liter H_2O
2. *5% Giemsa*: Add 5 ml of Giemsa to 95 ml of Gurr buffer (or 10 m*M* phosphate pH 6.8)

Steps

1. Dip the slides in 5% Giemsa at room temperature for 15 min.
2. Rinse twice with water and let dry at room temperature

IV. COMMENTS

Using this method, metaphasic preparations from of a panel of well-known and frequently used lines, including polarized lines (Caco-2, MDCK, HT-29) and hepatic ones, were isolated and analyzed (Table I).

TABLE I Chromosomal Content of a Panel of Cell Lines[a]

Cell line	Origin	Chromosome mean number[b] (range)	Published chromosome mean number[c] (range)
BW1-J	Hepatoma, mouse	64 (60–72)	64 (60–72)
Caco-2	Adenocarcinoma, colon, human	85 (78–98) 84 (67–102)	98 (91–107)
L (cl 1-D)	Connective tissue, mouse	51 (50–55)	51 (50–55)
Fao	Hepatoma, rat	51 (48–53)	52 (50–55)
HeLa	Epitheloid carcinoma, cervix, human	73 (68–79) 64 (61–68) 62 (43–83)	82 (70–86)
Hep G2	Hepatocellular carcinoma, human	52 (49–56) 50 (44–55)	55 (50–56)
HT-29	Adenocarcinoma, colon, human	71 (68–73)	70 (68–72)
MDCK	Normal kidney, canine	75 (68–82) 74 (68–77) 112 (80–144)	78 (65–89)
V79-4	Lung, chinese hamster	22 (22–23)	22 (20–23)
WI-38	Normal embryonic lung, human	46 (42–46)	46 (39–46)
WIF 12-E	Human fibroblast × rat hepatoma hybrid (WI-38 × Fao)	83 (79–86)	84 (79–92)

[a] Metaphases were prepared using the method described in this article.
[b] Mean and range obtained by analyzing at least 20 metaphases.
[c] According to the ATCC catalogue, Cassio and Weiss (1975) for BW1-J and Fao, Weiss and Green (1967) for cl 1-D, Knowles *et al*. (1980) for Hep G2, and Griffo *et al*. (1995) for WIF 12-E.

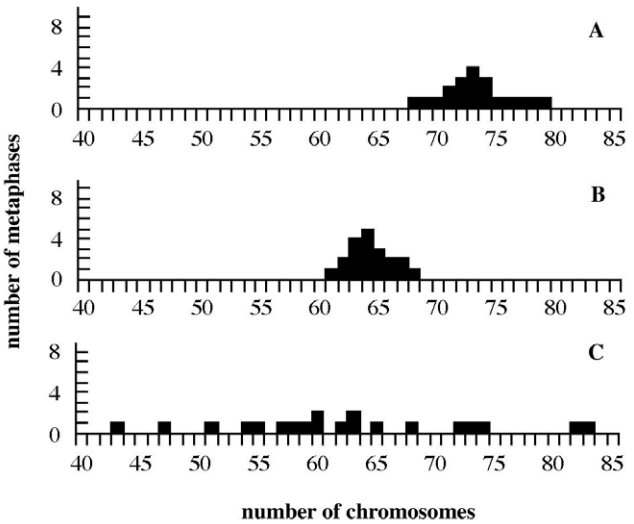

FIGURE 2 Chromosomal content of HeLa cells. Metaphases were prepared from HeLa cells (ATCC collection) cultured routinely in three different laboratories (A–C). The chromosomal content of each cell population is different, and in all cases the chromosome number is lower than expected (published mean chromosome number 82, range 70–86). Note the very heterogeneous karyotype of HeLa cells in C. These results show how cells of a same line can change and drift.

Some lines (BW1-J, cl 1-D, HT-29) displayed a chromosomal content similar or very near to that published previously, but the mean number of chromosomes, as the range, of other lines (Caco-2, HeLa) differed greatly from those published. Morever, in some cases, big differences were observed from the same line obtained from different laboratories. This was the case for HeLa cells (Fig. 2) and, to a lesser extent, for MDCK. In this latter case, one population over the three tested was very heterogeneous and greatly differed from the two others. Although both L and HeLa lines were established a long time ago (in 1940 and 1951, respectively) and thus cultured for a very large number of generations, the first line seems to be very stable, whereas the second one has considerable drift.

V. PITFALLS

1. Use only **glass** pipettes for adding the fixative and for detaching cells after the first fixation. Fluffy and fuzzy chromosomes are obtained using plastic pipettes.
2. Well-adherent cells can be detached by gentle pipetting at the end of the hypotonic shock before fixation.
3. The presence of a thin layer of cytoplasm embedding the chromosomes can be avoided by performing additional fixations and by improving the spreading (increase the distance between the drop and the slide and adjust the angle of the slide).

Acknowledgments

I thank C. Delagebeaudeuf for pushing me to develop this method, C. Hamon-Benais, and V. Bender for the illustrations, and L. Sperling for careful reading of the manuscript. This work was supported in part by the Curie Institute (PIC Signalisation Cellulaire Grant 914), CNRS, and INSERM (contrat Prisme 98-09).

References

Buys, C. H. C. M., Aanstoot, G. H., and Nienhaus, A. J. (1984). The Giemsa 11 technique for species-specific chromosome differentiation. *Histochemistry* **81**, 465–468.

Cassio, D., Hamon-Benais, C., Guerin, M., and Lecoq, O. (1991). Hybrid cell lines constitue a reservoir of polarized cells; isolation and study of highly differentiated hepatoma-derived hybrid cells able to form functional bile canaliculi *in vitro*. *J. Cell Biol*. **115**, 1397–1408.

Cassio, D., and Weiss, M. C. (1979). Expression of fetal and neonatal hepatic functions by mouse hepatoma-rat hepatoma hybrids. *Somat. Cell Genet*. **5**, 719–738.

Cox, D. M., Niewczas-Late, V., Riffel, M. I., and Hamerton, J. L. (1974). Chromosomal mosaicism in diagnostic amniotic fluid cell cultures. *Pediatr. Res*. **8,** 679–683.

Griffo, G., Hamon-Benais, C., Angrand, P. O., Fox, M., West, L., Lecoq, O., Povey, S., Cassio, D., and Weiss, M. C. (1993). HNF4 and HNF1, as well as a panel of hepatic functions are extinguished and reexpressed in parallel in chromosomally reduced rat hepatoma-human fibroblast hybrids. *J. Cell Biol*. **121**, 887–898.

Ian Freshney, R. I. (1987). Culture of animal cells. *In "A Manual of Basic Technique,"* 2nd Ed. A. R. Liss, New York.

Jennings Lawce, H., and Brown, M. G. (1997). Cytogenetics: An overwiew. *In "The AGT Cytogenetics Laboratory Manual"* (M. J. Barch, T. Knutsen, J. L. Spurbeck, eds.), 3rd Ed., pp. 19–50, Lippincott-Raven, Philadelphia.

Knowles, B., Howe, C. C., and Aden, D. P. (1980). Human hepatocellular carcinoma cell lines secrete the major plasma proteins and hepatitis B surface antigen. *Science* **209**, 497–499.

Peakman, D. C., Moreton, M. F., and Robinson, A. (1977). Prenatal diagnosis: Techniques used to help in ruling out maternal cell contamination. *J. Med. Genet*. **14**, 37–39.

Shanks, M. R., Cassio, D., Lecoq, O., and Hubbard A. L. (1994). An improved polarized rat hepatoma hybrid cell line. *J. Cell Sci*. **107**, 813–825.

Weiss, M. C., and Green, H. (1967). Human-mouse hybrid cell line containing partial complements of human chromosomes and functioning genes. *Proc. Nat Acad. Sci. USA* **58**, 1104–1111.

Worton, R. G., and Duff, C. (1979). Karyotyping. *Methods Enzymol*. **58**, 322–344.

Suggested Reading

Barch, M. J., Knutsen, T., and Spurbeck, J. L. (ed.) (1997). "The AGT Cytogenetics Laboratory Manual," 3rd Ed. Lippincott-Raven, Philadelphia.

SECTION

15

In Situ Hybridization

CHAPTER

40

Mapping Cloned DNA on Metaphase Chromosomes Using Fluorescence *in Situ* Hybridization

Margaret Leversha

I. INTRODUCTION

Fluorescence *in situ* hybridization (FISH) provides a quick means of placing almost any recombinant DNA clone onto a physical map. Clones can be mapped onto banded metaphase chromosomes for regional localization, to assign new markers to a chromosomal segment, to validate clones selected using previously assigned markers, or to characterize chromosomal rearrangements.

In genome mapping, unrecognized clone chimerism causes considerable problems with contig assembly and can result in much wasted effort when trying to extend or link contigs. For example, as many as 30–40% of YAC clones may contain coligated sequences from different genomic regions (Selleri *et al*., 1992). The shift to large-insert, single-copy plasmids such as PACs and BACs has substantially reduced the problem of clone chimerism. However, large-scale genome sequencing projects are revealing significant levels of regional homology that can confound mapping analyses at all levels (Cheung *et al*., 2001; Bailey *et al*., 2002). Preliminary FISH screening of clones is a simple and useful precaution.

DNA clones can also be ordered by FISH at increasing levels of resolution. Clones separated by 1–2 Mb can be ordered by pairwise, two-color FISH on metaphase chromosomes (Trask *et al*., 1991; Inazawa *et al*., 1994). Hybridization of sets of three clones to interphase nuclei provides mapping information down to about 50–100 kb (Lawrence *et al*., 1990; Trask *et al*., 1991), while the highest resolution is for overlapping clones on linear DNA molecules (Raap *et al*., 1996).

II. MATERIALS AND INSTRUMENTATION

DNase I (D-4527), DNA polymerase I (D-9380), bovine serum albumin (BSA, B-4287), dextran sulfate (D-8906), Denhardt's solution (D-2532), dithiothreitol (DTT, D-9779), SDS or sodium lauryl sulfate (L-4390), mouse antidigoxin FITC (F-3523), goat anti-mouse-FITC (F-0257), rabbit anti-mouse-FITC (F-7506), and DAPI (D-9542) are from Sigma. Deoxyribonucleotides (100 m*M* solutions of dATP, dCTP, dGTP, and dTTP) are from Amersham Biosciences (Cat. No. 27-2035-01). Human Cot-1 DNA (Cat. No. 15279011) is from Invitrogen. Formamide is from Fluka (Cat. No. 47670). Molecular biology grade mixed bed resin AG 501-X8 is from Bio-Rad (Cat. No. 143-6424). Biotin-16-dUTP (Cat. No. 1093070) and digoxigenin-11-dUTP (Cat. No. 1573152) are from Roche Diagnostics.

Berliner Glas microscope slides are from H. V. Skan Ltd., Solihull. Glass coverslips (No. 1–22 × 22 mm, 22 × 32 mm, 22 × 50 mm) and Nescofilm are from Fisher Scientific. Rubber cement can be obtained from art suppliers or from cycle shops (e.g., Halfords). Plastic syringes are from Becton-Dickinson, and 0.2-µm syringe filters are from Nalgene (Cat. No. 190-2520). Plastic slide boxes (50 slide capacity, Cat. No. 406028600), self-indicating silica gel (Cat. No.

Copyright 2006, Elsevier Science (USA).
All rights reserved.

300624V), Tween 20 (Cat. No. 66368 4B), glycerol (Cat. No. 101186M), 96% ethanol, and 99% ethanol are from BDH (VWR International).

Fine forceps suitable for handling slides and coverslips comfortably, without mishap (13 mm, Cat. No. E12), glass Coplin jars (Cat. No. E94), Hellendahl jars (Cat. No. E95), slide racks (Cat. No. E89.03, E89.055), and diamond marking pencils (Cat. No. E17) are from Raymond A. Lamb.

Cy3-streptavidin (Cat. No. PA43001) is from Amersham Biosciences. Texas red avidin DCS (Cat. No. A-2016), biotinylated antiavidin (Cat. No. BA-0300), and Vectashield (Cat. No. H-1000) are from Vector Laboratories Ltd. Filter paper discs, grade 4 (Cat. No. 1004 240), are from Whatman. Nonfat milk powder (e.g., Marvel) is widely available. Similarly, nail varnish from any inexpensive source should be adequate.

DNA concentrations are determined using a Hoefer TKO minifluorimeter. The slide drying bench (Cat. No. E18.1) is from Raymond A. Lamb. Also needed are at least two water baths (to be set at 37 and 65°C), a microcentrifuge for both 0.5- and 1.5-ml tubes, a 37°C oven, and facilities for performing agarose gel electrophoresis, as well as countup/countdown timers (e.g., Smiths), thermometers, micropipettes and sterile tips, domestic air-tight plastic freezer boxes, and lint-free tissues (Kimwipes). Incubation chambers are prepared using 245 × 245-mm^2 bioassay dishes (Nunc, Cat. No. 240835). Racks to accommodate a maximum of 16 slides are made by trimming four plastic 10-ml pipettes to fit and fixing them in place with rubber cement.

We use a Zeiss Axioskop epifluorescence microscope fitted with a 100-W mercury arc lamp, triple bandpass/dichroic filter blocks for both rhodamine (or Cy3) and Texas red (Chroma Technologies, sets 82000 and 83000), and a motorized excitation filter wheel (Ludl) and a Photometrics KAF1400 cooled CCD camera controlled by SmartCapture imaging software. Similar imaging systems can be obtained from Applied Imaging. SmartCapture software is supplied by Digital Scientific.

III. PROCEDURES

A. Probe Labeling

Solutions

1. *10× nick translation buffer*: 0.5 *M* Tris–HCl, pH 7.5, 0.1 *M* $MgSO_4$, 1 m*M* DTT, and 500 µg/ml BSA. To make 10 ml, mix 5 ml 1 *M* Tris–HCl (pH 7.5), 1 ml 1 *M* $MgSO_4$, 10 µl 1 *M* DTT, 500 µl 10 mg/ml BSA, and make up to 10 ml with sterile deionized water. Store 1-ml aliquots at –20°C.

2. *DNase I stock solution*: Resuspend 10,000 units in 1 ml 0.3 *M* NaCl and add 1 ml sterile glycerol. Store at –20°C.

3. *DNase I working solution*: To make 1 ml, mix 100 µl 10× nick translation buffer with 400 µl sterile deionized water and 500 µl sterile glycerol; then add 1 µl DNase I stock solution. Mix thoroughly and store at –20°C.

4. *0.5 mM dNTPs*: To make 1200 µl, mix 2 µl each of 100 m*M* dATP, dCTP, and dGTP and then add 1194 µl sterile deionized water. Store 50-µl aliquots at –20°C.

5. *1 mM biotin-16-dUTP or digoxigenin-11-dUTP*

6. *DNA polymerase I (10 units/µl)*

7. *0.5 M EDTA, pH 8.0*: To make 100 ml, mix 18.61 g EDTA in 80 ml deionized water, adjust to pH 8.0 with NaOH (the salt will not dissolve until near pH 8), and make up to volume with deionized water. Sterilize by autoclaving.

8. *1 M Tris–Cl, pH 7.4*: To make 100 ml, dissolve 12.11 g Tris base in 80 ml deionized water, adjust to pH 7.4 with HCl, and make up to volume with deionized water. Sterilize by autoclaving.

9. *3 M sodium acetate, pH 7.0*: To make 100 ml, dissolve 24.6 g sodium acetate (anhydrous) in 80 ml deionized water, adjust to pH 7.0 with glacial acetic acid, and make up to 100 ml with deionized water. Sterilize by autoclaving. Use small aliquots as working stock, replacing frequently.

10. *Absolute ethanol*: Store in a sterile 50-ml Falcon tube at –20°C.

11. *70% ethanol*: Store in a sterile 50-ml Falcon tube at –20°C.

12. *TE buffer (10 mM Tris–Cl, 1 mM EDTA)*: To make 100 ml, mix 1 ml of 1 *M* Tris–Cl, pH 7.4, and 0.2 ml of 0.5 *M* EDTA and make up to 100 ml with deionized water. This is best made prior to sterilizing the stock solutions of Tris and EDTA. Sterilize by autoclaving.

Steps

1. Prepare a water bath at 14°C. A robust polystyrene box (or ice bucket) with a lid is a suitable container (although some are not reliably water tight).

2. Place approximately 1 µg of each DNA sample to be labeled in 1.5-ml microfuge tubes and make up the volumes to 10 µl with sterile deionized water. Stand on ice.

3. Prepare 15 µl labeling master mix for each sample, allowing a little extra for dispensing. For 4 µg DNA, take 10 µl nick translation buffer, add 34 µl sterile deionized water, 7.5 µl dNTPs, 2.5 µl 1 m*M* biotin-16-

dUTP, 4 µl DNase I working solution, and 2 µl 10 U/µl DNA polymerase I. Mix thoroughly and pulse microfuge to collect all the solution in the base of the tube. Stand on ice.

4. Add 15 µl of master mix to each DNA sample and mix by pipetting several times.

5. Incubate the samples at 14°C for 40–60 min. The exact length of time must be determined for each new preparation of DNase I working solution.

6. Transfer the tubes to ice and add 2.5 µl 0.5*M* EDTA to each, mixing quickly with the pipette.

7. Add 2.5 µl 3*M* sodium acetate and 1 ml cold 100% ethanol to each tube. Mix by inversion.

8. Incubate at –20°C overnight.

9. Microfuge the tubes for 10 min at maximum speed. Remove the supernatants carefully so as not to disturb the visible pellets.

10. Carefully add 1 ml cold 70% ethanol to each tube. Microfuge again for 10 min. Carefully aspirate off the supernatant from the transparent pellets and air dry. Do not overdry.

11. Add 10 µl TE buffer to each tube and stand on ice for 15 min. Flick mix to resuspend.

12. Run 2-µl aliquots in a 1% agarose gel to assess the probe fragment length. A smear between 200 and 800 bp is satisfactory.

13. Store the probes at –20°C.

B. *In Situ* Hybridization

Solutions

1. *50% dextran sulfate*: To make 50 ml, weigh 25 g dextran sulfate into a graduated 100-ml pyrex bottle, add 20 ml deionized water, and heat in a 65°C water bath until dissolved. Make up to volume with deionized water and sterilize by autoclaving. Dispense 10-ml aliquots into sterile 50-ml Falcon tubes and store at –20°C.

2. *Deionized formamide*: Add 5 g Bio-Rad mixed bed resin AG 501-X8 to 100 ml formamide and stir in a fume hood for 60 min. Allow the beads to settle and decant the formamide. Store aliquots at –20°C.

3. *20× SSC (3 M NaCl, 0.3 M sodium citrate)*: To make 1 liter, dissolve 175.2 g sodium chloride and 88.2 g trisodium citrate in deionized water and make up to volume.

4. *10% SDS*: To make 50 ml, dissolve 5 g sodium dodecyl sulfate in 50 ml deionized water. Sterilize by filtering through a 0.2-µm filter.

5. *0.5 M Na_2HPO_4*: To make 100 ml, dissolve 7.098 g Na_2HPO_4 in deionized water and make up to volume. Sterilize working aliquots by filtration.

6. *0.5 M NaH_2PO_4*: To make 100 ml, dissolve 7.8 g $NaH_2PO_4.2H_2O$ in deionized water and make up to volume. Sterilize working aliquots by filtration.

7. *Hybridization buffer*: To make 50 ml, thaw a Falcon tube containing a 10-ml aliquot of 50% dextran sulfate, add 25 ml deionized formamide, 5 ml 20× SSC, 1 ml 50× Denhardt's solution, 4 ml 0.5*M* sodium phosphate buffer, pH 7.0 (2.308 ml Na_2HPO_4, 1.692 ml NaH_2PO_4), 0.5 ml 10% SDS, and 4.5 ml sterile deionized water. Mix very thoroughly by inversion, preferably on a rotator for 10 min. Dispense into 1-ml aliquots and store at –20°C. This should be stable for at least 1 year. Mix newly thawed aliquots thoroughly by vortexing.

8. *Cot-1 DNA*: Supplied at 1 mg/ml.

9. *70% formamide*: To make 100 ml, mix 70 ml formamide and 30 ml 2× SSC. Store at 4°C between uses and replace weekly. (Deionizing the formamide is not necessary.)

10. *70% ethanol in a Hellendahl jar*: Store at –20°C. Replace weekly.

11. *Ethanol series*: Hellendahl jars containing 70% ethanol (2×), 90% ethanol (2×), and 100% ethanol (1×).

12. *Coverslips*: 22 × 22-mm, 22 × 50-mm coverslips immersed in 100% ethanol in an air-tight plastic container.

Steps

1. Prepare a Coplin jar or Hellendahl jar containing 70% formamide. Place in a water bath and turn the temperature to 65°C. (The glass jars will not tolerate sudden temperature changes and should always be allowed to warm gradually.)

2. Set a second water bath to 37°C.

3. Prepare the probe hybridization mixes by adding 10 µl hybridization buffer to 0.5-ml microfuge tubes (dispensing will be aided by first warming the hybridization buffer). Stand the tubes on ice. Add 1 or 2 µl Cot-1 DNA to each tube, depending on whether one or two probes are to be added. Add 0.5 µl of biotinylated probe and/or 0.5 µl of another digoxigenin-labeled probe. Mix thoroughly by flicking the tubes and pulse microfuge the solutions to the bottom of the tubes.

4. Denature the probe mixes at 65°C for 10 min, ensuring that the tubes are fully sealed and not likely to take up water.

5. Transfer the probe mixes to the 37°C water bath to preanneal for at least 20 min (to several hours).

6. Check that the 70% formamide has reached 65°C using a thermometer reserved for the purpose.

7. Carefully immerse slides, paired back to back, into the 70% formamide at 5-s intervals. Start a count-up timer as the first pair of slides is immersed. Take

care to hold the slides clear of the steam from the water bath while preparing to place them in the formamide.

8. While the slides are denaturing, remove the Hellendahl jar of 70% ethanol from the freezer.

9. Denature the slides for 2 min. As the denaturation time elapses, remove the pairs of slides from the formamide and drain briefly against the inside of the jar. Immerse the slides, agitating briefly, in the cold 70% ethanol.

10. After 60 s in the cold 70% ethanol, transfer the slides with occasional agitation through an ethanol series at room temperature: 60 s each in successive jars of 70, 70, 90, 90, and 100% ethanol.

11. Separate the slide pairs and carefully wipe the backs of the slides dry. Air dry the slides standing in a rack on a slide-warming bench at 37–40°C.

12. Prepare the required number of 22 × 22-mm coverslips by removing them from the 100% ethanol and lightly polishing them dry with a lint-free tissue. Place the coverslips on a clean tissue on or by the slide-warming bench.

13. Place the dry slides flat on the slide-warming bench. Make sure that all are labeled and numbered clearly.

14. After the probes have preannealed at 37°C for at least 20 min, transfer the first hybridization mix to its target slide. As the volumes can be difficult to gauge accurately, set the micropipette for 12 µl and be careful to avoid bubbles when drawing up and discharging the mix onto the slide.

15. Using fine forceps, gently lower a clean coverslip over the mix. If bubbles are present, these can usually be disrupted by surface tension by allowing the hybridization mix to spread out under the upper half of the coverslip while the lower edge of the coverslip is still supported by the tip of the forceps. It is usually not worth trying to remove every last bubble as this may damage the chromosome preparations.

16. Repeat these steps for each remaining probe mix. If there are a large number to be processed, it may be preferable to station the slide bench next to the 37°C water bath and remove each mix from the water bath as required. Alternatively, the hybridization mixes can be placed on ice, but this can make the mixes more viscous and difficult to pipette.

17. Seal the edges of the coverslips with rubber cement. If the hybridization mix has not reached the edges of a coverslip because the coverslip cannot lie flat, it will be necessary to prevent the rubber cement from being drawn under the coverslip. If the coverslip cannot be flattened by gentle pressure over the high point, fill in the gap with extra hybridization buffer before sealing.

18. Place on a tray and hybridize overnight in a 37°C oven.

C. Visualization of Hybridization

Solutions

1. *50% formamide*: To make 200 ml, mix 100 ml formamide and 100 ml 2× SSC. Store at 4°C between uses and replace weekly.

2. *2× SSC*: To make 1 liter, take 100 ml 20× SSC and make up to volume with deionized water.

3. *4 × TNFM*: To make 1 liter, take 200 ml 20× SSC, add 700 ml deionized water, 500 µl Tween 20, and 50 g nonfat milk powder and mix vigorously, then make up to 1 liter with deionized water. Filter through several layers of Whatman No. 4 filter paper. (The solution should be a slightly translucent yellow-green color. If it remains cloudy try another brand of nonfat milk powder.)

4. *Immunochemical solutions*: Allow 100 µl per slide plus 50–100 µl excess. Protect from strong light.
   a. For biotinylated probes, make 2 aliquots of 4 µg/ml streptavidin-Cy3 and one aliquot of 4 µg/ml biotinylated antiavidin.
   b. For digoxigenin-labeled probes, make a 1:500 –1:1000 dilution of mouse antidigoxin-FITC and a 1:250 dilution of rabbit anti-mouse-FITC.
   c. For dual-color detection, use avidin-Texas red instead of streptavidin-Cy3. Combine the biotinylated antiavidin with the mouse antidigoxin-FITC, and the second avidin-Texas red with the rabbit anti-mouse-FITC.

5. *4 × T*: To make 200 ml, mix 40 ml 20× SSC, 160 ml deionized water, and 100 µl Tween 20.

6. *DAPI staining solution*: Prepare a Hellendahl jar with 75 ml of 2× SSC and 6 µl 1 mg/ml DAPI. Protect from light by wrapping in aluminium foil.

Steps

1. Place three Coplin jars or Hellendahl jars containing 2× SSC and two jars of 50% formamide into a water bath and warm to 42°C

2. Place a jar of 4 × TNFM to warm in a 37°C oven.

3. Prepare a humidified chamber by placing damp tissues in the bottom of an incubation dish and warm in a 37°C oven.

4. Prepare immunochemical solutions diluted in 4 × TNFM according to the haptens used. Stand at room temperature for 10 min and then microfuge for 10 min to pellet any protein complexes that might contribute to nonspecific background.

5. Remove the rubber cement from the slides using fine forceps and soak off the coverslips in the first jar of 2× SSC at 42°C, allowing approximately 5 min.

6. Transfer the slides to the first jar of 50% formamide for 5 min.

7. Repeat this incubation in the second jar of 50% formamide and then in each of the remaining jars of 2× SSC, agitating the slides briefly after each transfer.

8. Transfer the slides to the prewarmed jar of 4 × TNFM and incubate for 5–10 min at 37°C.

9. Remove the slides one by one from the 4 × TNFM and drain briefly, wipe the back, and blot excess liquid from the top and bottom edges. Place the slides on a rack in the prepared humidified chamber and apply 100 µl of the first immunochemical solution (streptavidin-Cy3 or mouse antidigoxin-FITC or avidin-Texas red). Overlay with a 25 × 50-mm strip of Nescofilm. *Note*: The slides must not dry out at any point during the procedure.

10. Incubate the slides at 37°C for 20–30 min.

11. Meanwhile, discard the three 2× SSC wash solutions and replace with 4 × TNFM, allowing the jars to warm to 42°C again.

12. Discard the Nescofilm strips, drain the slides, and rinse them in the three changes of 4 × TNFM at 42°C for 5 min each.

13. Repeat step 9 using the second antibody layer (biotinylated antiavidin, rabbit anti-mouse-FITC, or biotinylated antiavidin plus mouse antidigoxin-FITC).

14. Repeat steps 10–12.

15. Repeat step 9 using the final immunochemical layer (streptavidin-Cy3 or avidin-Texas red plus rabbit anti-mouse-FITC). If using only digoxigenin-labeled probes, proceed to step 17.

16. Repeat steps 10–12.

17. Wash twice in 4 × T at room temperature.

18. Stain the slides in DAPI for 2–3 min. Transfer the slides to a jar containing 2× SSC, rinse briefly, and pour off the 2× SSC (holding the slides in place with a gloved finger or forceps across the top of the jar). Rinse briefly with deionized water and pour off.

19. Dehydrate the slides by passing through an ethanol series, gently agitating 30–60 s in each of 70, 70, 90, 90, and 100% ethanol. Air dry.

20. Lightly polish 22 × 50-mm coverslips and lay them out on flat absorbant tissue. Apply 25–30 µl antifade solution to each coverslip.

21. Invert each slide over a coverslip, rest the bottom edge on the tissue, and gently lower until the slide touches the antifade droplet. Allow the coverslip to lift up to the slide before laying it flat. When the antifade has spread fully, gently blot any excess. Seal the edges of the coverslips with nail varnish. The slides can now be stored in the dark at 4°C for many weeks.

22. View the slides using an epifluorescence microscope equipped with the excitation and emission filters appropriate for the fluorochromes used.

IV. COMMENTS

A. Probe Labeling

Whole clone DNA preparations are usually the best material for nick translation. Bacterial clone DNA isolated by standard alkaline lysis should be satisfactory. Most matrix-binding protocols, as used by commercial kits, do not give very high yields for larger insert clones such as cosmids, PACs, or BACs (often only enough for one or two labeling reactions from 10 ml of bacterial culture) so be sure that sufficient DNA (of a concentration of at least 100 µg/ml) is obtained. Total yeast DNA gives good results for YACs, although the yeast genome may contribute excess ribosomal sequences that may not be fully suppressed during hybridization.

Different grades of DNase I have different levels of activity. New working solutions should be titrated to determine the best incubation time. A 50-µl reaction containing 2 µg DNA and 2 µl DNase I working solution in 1× nick translation buffer can be sampled at five intervals (e.g., at 20, 30, 40, 50, and 60 min) and the DNA fragments compared by electrophoresis. Even less expensive products, such as DN-25 (Sigma), are suitable for use after titration, allowing for the relative number of units per milligram of protein in the working solution. Enzyme activity is also affected by the amount of Ca^{2+} present in the reaction. Usually, sufficient Ca^{2+} is present in the original DNase I stock; however, higher grades of enzyme may need additional $CaCl_2$ to maintain active enzyme conformation during the nick translation reaction.

Approximately 70–80% of the original DNA is usually recovered after ethanol precipitation, giving a final probe concentration of 70–80 ng/µl. Probe concentrations can be verified by DNA fluorimetry if desired. Ethanol precipitation is not absolutely required for probe preparation and can be omitted after labeling repetitive DNA clones, such as chromosome-specific satellite DNAs, as these are routinely used at much lower hybridization concentrations (0.5–1 ng/µl) than "unique-sequence" clones (2.5–5 ng/µl). Ethanol precipitation enables the labeled probe to be concentrated so that it can be used without further precipitation prior to hybridization. This ensures more consistent results from one experiment to another.

Large insert clones can be mapped efficiently using direct labeling with fluorochrome-conjugated dUTPs. This avoids the time-consuming immunochemical detection steps described here, but may not be as effective in revealing smaller signals at secondary chromosomal sites.

B. Hybridization

The hybridization buffer can be dispensed more accurately after it is warmed to 65°C. The components may separate during freezing and the warmed solution should be mixed thoroughly before use. Probes will last several years if handled aseptically and stored at –20°C. They should be thawed and kept on ice when in use and returned to the freezer without delay (do not store in frost-free freezers). Routine metaphase mapping throughput can be increased by using pairs of biotin- and digoxigenin-labeled probes on two separate spots of metaphase cells on a single slide. The slide can be mounted in antifade under a single large coverslip.

C. Detection

The 4 × TNFM washes and the immunochemical incubations do not need to be performed at 37–42°C as the results are usually satisfactory at room temperature. However, it is preferable to protect the slides from bright light, and in a busy laboratory the slides can often be tucked away more safely and neatly by leaving them in an incubator or water bath.

If the clones to be mapped all localize to a small region, it may not always be possible to use a double-probe protocol as interpretation can be complicated by poor-quality probe. When performing dual-color analysis, it is easier to use fluorochromes that are spectrally well separated. Cy3 is a very stable, bright orange fluorochrome, but it can be difficult to use with FITC, as the Cy3 signals are often visible through FITC filters. This is a particular problem when imaging with black-and-white CCD cameras as strong Cy3 signals can be confused with FITC signals. Texas red is preferred for combinations with FITC (Fig. 1A).

The DAPI staining reveals a clear banding pattern, which permits chromosome identification, provided the slides are not overdenatured. If a digital image of the DAPI-stained metaphase is converted into a black-and-white inverted image, the chromosomes appear similar to a conventional G-banded metaphase (Fig. 1B).

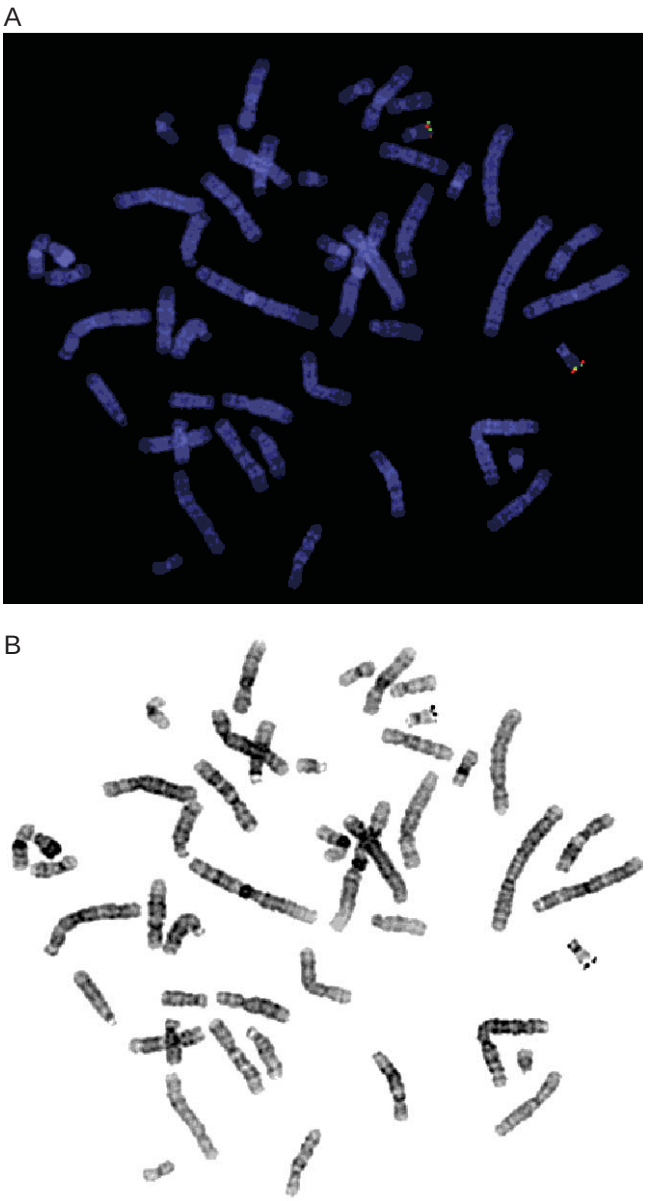

FIGURE 1 (A) Two-color hybridization of two cosmid clones mapping to chromosome 22. One cosmid was biotinylated and detected with avidin-Texas red (red) and the second cosmid was labeled with digoxigenin and visualized using FITC-conjugated antibodies (green). (B) Black-and-white inverted image of the metaphase shown in A. The chromosomes appear essentially G banded, although the 9qh region is dark in this example.

V. PITFALLS

1. If no signal is obtained, one possibility may be insufficient DNA. It is not unusual for spectrophotometric determinations of DNA concentration to be as much as 5–10 times higher than the real figure. Alternatively, the original DNA may have deteriorated. These problems are monitored easily by running approximately 100–200 ng of the original DNA next to the 2-µl aliquot of the precipitated nick-translated product in a standard 1% agarose gel. This will also reveal whether bacterial clones retain the expected size insert. When using labeled whole yeast DNA, it may be necessary to increase the amount of probe used per hybridization to ensure that there is sufficient YAC

probe present. Usually 80–100 ng of whole yeast probe will ensure clear YAC signals. Using additional amounts of probe may also assist the mapping of smaller insert clones.

Another major problem is poor hybridization efficiency because of poor-quality slide preparation. Probe accessibility is critical. Good-quality metaphase preparations, with well-spread chromosomes and a minimum of residual cytoplasm, are far more useful than any amount of protease pretreatment. RNase A digestion is not normally necessary at all.

It is always possible that the clone you are trying to map will never hybridize to your metaphase spreads. For example, human monochromosomal libraries made from material flow sorted from somatic cell hybrids may contain a small proportion of nonhuman clones. Try hybridizing a larger amount of probe (100–200 ng) without any Cot-1 DNA and no preannealing at 37°C. The abundant *Alu* short, interspersed repeat sequences are distributed throughout the human genome and should be present in most genomic clones. In the absence of preannealing, *Alu* signals should be distributed all over the chromosomes, concentrated in the G-light chromosome R bands.

It also appears that about 25–30% of cDNA clones cannot be localized by FISH (Korenberg *et al*., 1995). This may be due to the relatively short genomic extent of the target gene. Mapping cDNAs is a much more demanding process and every step must be rigorously optimized. Protease digestion around the chromosomal DNA may be useful here, but it must be carefully controlled to avoid loss of chromosome morphology (Fan *et al*., 1990). More sensitive detection systems, such as the use of tyramides, may also be useful (Raap *et al*., 1995).

2. If the cloned DNA does not cut well after nick translation, the large probe fragments will result in excessive background hybridization, which is seen as large, bright spots of signal all over the chromosomes and nuclei. Large spots of signal that appear to float above the spreads are nearly always indicative of excessive probe fragment length. Because DNase I digestion is affected by contaminants in the DNA, it may be necessary to repurify the sample before repeating nick translation. DNA that digests with restriction enzymes should be satisfactory. Try increasing the duration of the next nick translation reaction by at least 10 min. Check the concentration of your DNA also; the labeling reaction may have contained far too much DNA.

If the probe length is in the acceptable size range, it may be that one of the immunochemicals has deteriorated. These should always be kept in small aliquots and handled as aseptically as possible. Depending on the manufacturers' recommendations, it should be possible to store most reagents at –20°C, with a single working aliquot stored at 4°C. Avoid repeated freeze–thawing and, for this reason, do not store reagents in frost-free freezers. Using immunochemicals at too high a concentration can result in generalized nonspecific background over the slide. Similarly, precipitation of immunochemical complexes will occur if the slides are allowed to dry out during the detection procedure.

Certain clones may require increased amounts of Cot-1 DNA to suppress apparently nonspecific hybridization to other chromosomal regions. Another potential source of nonspecific background may be residual material in the fixed metaphase suspensions. This may be reduced by washing the cells in several changes of methanol/acetic acid fixative before preparing more slides. We routinely postfix slides in a Coplin jar of fixative, air dry, and then dehydrate through a fresh ethanol series before a final fixation in acetone.

Acknowledgment

My thanks to Dr. Nigel Carter for useful discussions over the manuscript.

References

BAC Resource Consortium (Cheung *et al*.) (2001). Integration of cytogenetic landmarks into the draft sequence of the human genome. *Nature* **409**, 953–958.

Bailey, J. A., Gu, Z., Clark, R. A., Reinert, K., Samonte, R. V., Schwartz, S., Adams, M. D., Myers, E., W., Li, P. W., and Eichler, E. E. (2002). Recent segmental duplications in the Human Genome. *Science* **297**, 1003–1007.

Fan, Y.-S., Davis, L. M., and Shows, T. B. (1990). Mapping small DNA sequences by fluorescence in situ hybridization directly on banded metaphase chromosomes. *Proc. Natl. Acad. Sci. USA* **87**, 6223–6227.

Inazawa, J., Ariyama, T., Tokino, T., Tanigami, A., Nakamura, Y., and Abe, T. (1994). High resolution ordering of DNA markers by multi-color fluorescent in situ hybridization of prophase chromosomes. *Cytogenet. Cell Genet*. **65**, 130–135.

Korenberg, J. R., Chen, X.-N., Adams, M. D., and Venter, J. C. (1995). Towards a cDNA map of the Human Genome. *Genomics* **29**, 364–370.

Lawrence, J. B., Singer, R. H., and McNeil, J. A. (1990). Interphase and metaphase resolution of different distances within the human dystrophin gene. *Science* **249**, 928–932.

Raap, A. K., Florijn, R. J., Blonden, L. A. J., Wiegant, J., Vaandrager, J.-W., Vrolijk, H., den Dunnen, J., Tanke, H. J., and van Ommen, G.-J. (1996). Fiber FISH as a DNA mapping tool. *Methods* **9**, 67–73.

Raap, A. K., van de Corput, M. P., Vervenne, R. A., van Gijlswijk, R. P., Tanke, H. J., and Wiegant, J. (1995). Ultra-sensitive FISH

using peroxidase-mediated deposition of biotin- or fluorochrome tyramides. *Hum. Mol. Genet*. **4**, 529–534.

Selleri, L., Eubanks, J. H., Giovannini, M., Hermanson, G., Romo, A., Djabali, M., Maurer, S., McElligott, D. L., Smith, M. W., and Evans, G. A. (1992). Detection and characterization of "chimeric" yeast artificial chromosome clones by fluorescent in situ suppression hybridization. *Genomics* **14**, 536–541.

Trask, B. J., Massa, H., Kenwrick, S., and Gitschier, J. (1991). Mapping of human chromosome Xq28 by two-color fluorescence in situ hybridization of DNA sequences to interphase cell nuclei. *Am. J. Hum. Genet*. **48**, 1–15.

Suggested Reading

Carter, N. P. (1996). Fluorescence in situ hybridization—state of the art. *Bioimaging* **4**, 41–51.

Lawrence, J. B. (1990). A fluorescence in situ hybridization approach for gene mapping and the study of nuclear organization. *In* "*Genome Analysis* (K. E. Davies and S. Tilghman, eds.), Vol. 1, pp. 1–38. Cold Spring Harbor Laboratory Press, Cold Spring Harden, NY.

Lichter, P., and Cremer, T. (1992). Chromosome analysis by non-isotopic in situ hybridization. *In* "*Human Cytogenetics: A Practical Approach*" (-D. E. Rooney and B. H. Czepulkowski, eds.), Vol. I., pp.157–192. Oxford Univ. Press, Oxford.

CHAPTER

41

Human Genome Project Resources for Breakpoint Mapping

Deborah C. Burford, Susan M. Gribble, and Elena Prigmore

I. INTRODUCTION

The announcement in April 2003 that the Human Genome Project was complete and was available publicly through intuitive genome browsers (e.g., see http://www.ensembl.org/Homo_sapiens/ and http://genome.ucsc.edu/cgi-bin/hgGateway) revolutionised experimental genome analysis. More precisely the study of chromosome rearrangements has been facilitated by the availability of easily accessible, ordered, fully sequenced tiling path clones covering the entire human genome. This resource enables chromosome breakpoints to be mapped more rapidly and with increased confidence.

Conventionally a chromosome rearrangement has been mapped by walking along a chromosome sequentially hybridising fluorescently labelled DNA clones (FISH) until the signal is no longer retained on one derivative chromosome but is seen on the reciprocal derivative chromosome. The genomic position of the breakpoint is then delineated by these two clones and the spanning clone can be found by FISHing clones at a higher resolution (McMullan *et al*., 2002). The genome annotation also now easily available on web browsers (e.g., http://vega.sanger.ac.uk/Homo_sapiens/) provides an additional level of information regarding the gene content of a genomic region of interest. Both known and predicted genes are detailed along with additional information, including repeat content, GC content, mouse homology, and many additional features. This information, together with the identification of breakpoint spanning clones linked directly to these databases, allows candidate genes involved in the phenotype of a patient to be identified readily.

Clones sequenced as part of the Human Genome Project are available readily to international researchers for minimal cost (e.g., BACPAC resources: http://bacpac.chori.org/, Invitrogen: http://clones.invitrogen.com/, and the Resources for Molecular Cytogenetics, University of Bari: http://www.biologia.uniba.it/rmc/). The sequence obtained from these clones is freely accessible (e.g., http://www.ncbi.nlm.nih.gov/genome/clone/, http://www.ensembl.org/Homo_sapiens/, and http://genome.ucsc.edu/cgi-bin/hgGateway).

The availability of such a comprehensive set of clones has not only greatly facilitated conventional approaches to breakpoint mapping studies but has also enabled the development of genome-wide, large insert clone DNA microarrays. The selection, DNA extraction, and labelling of clones for multiple sequential DNA clone *in situ* hybridisation experiments required to map breakpoints are often time-consuming processes. However, the clones can be used as ordered targets themselves for breakpoint mapping after gridded assembly on a DNA microarray (Fiegler *et al*., 2003a). DNA microarrays have been recently developed mostly with the aim of studying genome imbalance in tumour DNA samples (Solinas-Toldo *et al*., 1997). We have exploited this resource to study structural chromosome rearrangements, including rearrangements with no genomic imbalance. This type of analysis, termed array painting (Fiegler *et al*., 2003b), involves isolating derivative chromosomes away from other chromosome homologues by flow sorting (Carter, 1994) or microdissection prior to hybridisation onto the DNA microarrays.

The flow sorting strategy (see Fig. 1) enables large quantities of derivative chromosomes to be isolated before they are fluorescently labelled and hybridised

Copyright 2006, Elsevier Science (USA).
All rights reserved.

onto a target DNA microarray. Alternatively, smaller quantities (~500) of pure derivative chromosomes can be amplified using whole genome amplification. (WGA) procedures, such as DOP-PCR (Telenius *et al*., 1992; Fiegler *et al*., 2003a), Repli-G (Qiagen, 59043), or GenomiPhi (Amersham Biosciences, 25-6600-01) before they are fluorescently labelled and hybridised onto the array. Analysis of this type of hybridisation will then identify the components of each derivative chromosome according to the fluorescence intensities exhibited by the clones on the array (see Fig. 2).

The limit of array painting as a tool for mapping chromosome breakpoints is defined by the resolution of the clones gridded. At present we use a 1-Mb array to define the breakpoints to within a megabase (see Fig. 3) and then use conventional FISH methods (see article by Leversha) to refine the breakpoints and find the spanning clones. Clones that span the breakpoint show intermediate ratios on the array (see Fig. 2).

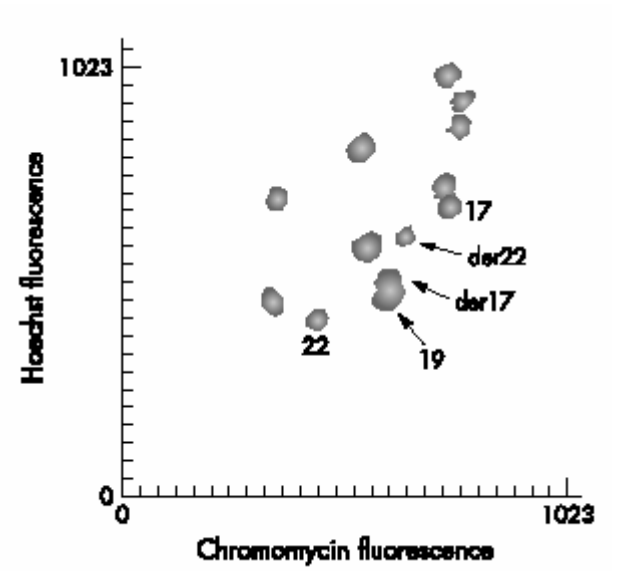

FIGURE 1 Partial flow karyotype of t(17;22)(q21.1;q12.2).

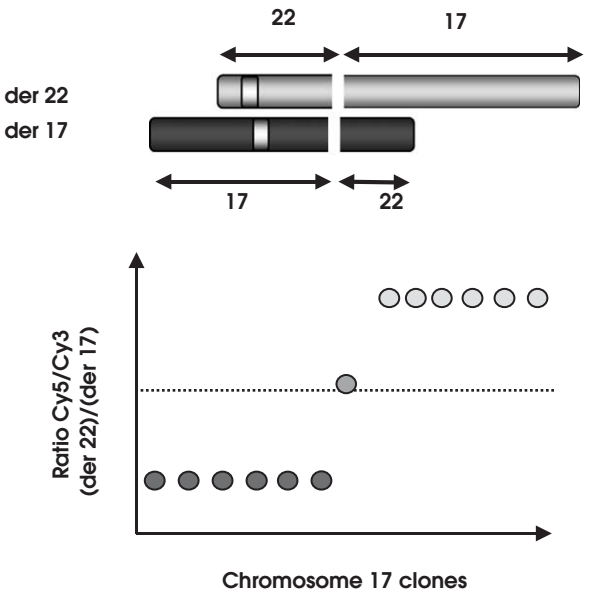

FIGURE 2 Basic principles of mapping translocation breakpoints by array painting.

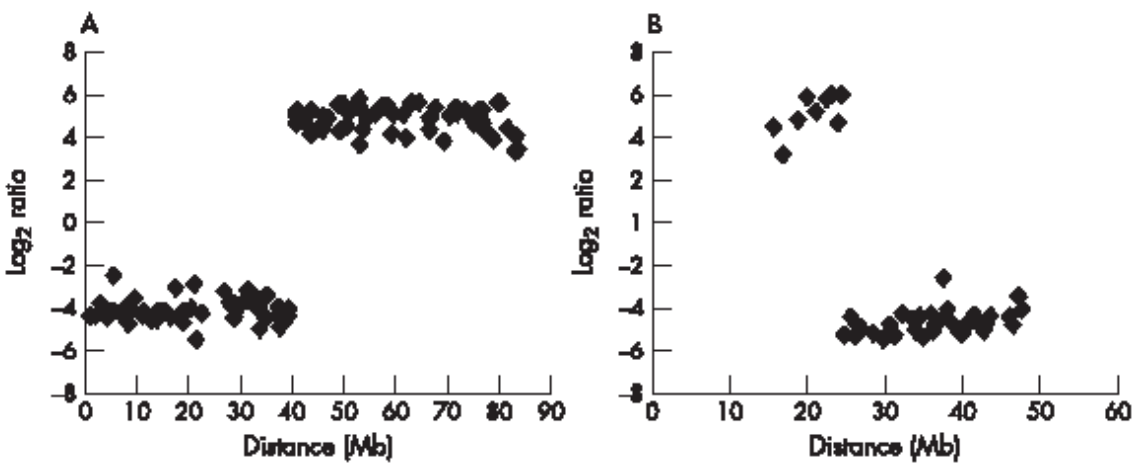

FIGURE 3 Array painting profiles for the derivative chromosomes of t(17;22): (A)1-Mb array chromosome 17 plot and (B)1-Mb array chromosome 22 plot.

Statistically, 1 in every 10 breakpoints will have spanning clones identified directly on the 1-Mb resolution array.

This technique has proven to be invaluable in the detailed study of chromosome rearrangements. When used in conjunction with array CGH, it can give an insight into rearrangements that might have been undetected by G-banding analysis. Increased array resolution, e.g., a tiling path array, in the study of simple chromosome rearrangements would identify spanning clones within a single experiment.

II. MATERIALS AND INSTRUMENTATION

A. Purification of Flow-Sorted DNA

N-Lauroylsarcosine sodium salt (Sigma, L5125)
Proteinase K (Invitrogen, 25530-015)
Phenylmethylsulfonyl fluoride (PMSF) (Sigma, P7626)
Pellet Paint nonfluorescent coprecipitant (Novagen, 70748)

B. Random Labeling of DNA for Array Painting

BioPrime DNA labeling kit (Invitrogen, 18094-011) contains 2.5× random primers solution, sterile water, Klenow fragment, and stop buffer
dNTPs (Amersham Biosciences, 27-2035-02)
Cyanine 3-dCTP (Perkin Elmer, NEL576001EA)
Cyanine 5-dCTP (Perkin Elmer, NEL577001EA)
Microspin G50 columns (Amersham Biosciences, 27-5330-01)

C. Array Hybridization

Herring sperm DNA (Sigma, D7290)
Human Cot-1 DNA (Roche, 1581074)
Deionised formamide for hybridisation buffer (Sigma, F9037)
Dextran sulphate sodium salt (Amersham Biosciences, 17-0340-02)
HPLC water (VWR International, 152736D)
Rubber cement (Weldtite, 02002)
Formamide (Sigma, 47670)
Yeast tRNA (Invitrogen, 15401-029)
Tween 20 (VWR International, 663684B)
Hellendahl jars (RA Lamb, E95)
Glass troughs (RA Lamb, E106 + E98)
Parafilm (Sigma, P7793)
Shake "n" stack hybridisation oven (Thermo Hybaid, HBMOJCT)

III. PROCEDURES

A. Purification of Flow-Sorted DNA

Solutions

1. *0.25 M EDTA/10% sodium lauroyl sarcosine*: For 10 ml, dissolve 1 g *N*-lauroylsarcosine in 5 ml filtered water and add 5 ml 0.5 *M* EDTA (pH 8.0). Store in 1 ml aliquots at 4°C.
2. *Proteinase K*: Resuspend 100 mg in 5 ml sterile water (final concentration of 20 mg/ml). Store 50 µl aliquots at –20°C. Do not freeze thaw.
3. *PMSF*: Resuspend 250 mg in 12.5 ml 96% ethanol (final concentration of 20 mg/ml). Store at 4°C up to a maximum of 6 months.
4. *5 M NaCl*: Dissolve 29.22 g NaCl (MW 58.44) in 100 ml sterile water. Autoclave and store at room temperature.
5. *Pellet Paint*: Store as 20 µl aliquots at –20°C. Avoid repeated freeze thawing. Working tube can be kept at 4°C.
6. *Absolute ethanol*: Store in a sterile 50 ml Falcon tube at –20°C.
7. *70% ethanol*: Store in a sterile 50 ml Falcon tube at –20°C.
8. *Sterile T1.0E (pH 8.0)*: For 100 ml, mix 1 ml 1 *M* Tris–HCl (pH 8.0), 1 ml 0.1 *M* EDTA (pH 8.0), and 98 ml water. Autoclave and store at room temperature.

Steps

Handle tubes containing flow-sorted material very gently!

Flow-sorted chromosomes come in batches of approximately 250,000 per 1.5 ml microfuge tube, sorted into chromosome sheath buffer [10 m*M* Tris–HCl (pH 8.0), 1 m*M* EDTA, 100 m*M* NaCl, 0.5 m*M* Na azide]. Sort 250,000 chromosomes into a volume of approximately 300 µl. Amounts of reagents will vary according to the quantity of sorted sample.

1. Add 30 µl 0.25 *M* EDTA/10% sodium lauroyl sarcosine and 3 µl proteinase K. Incubate overnight at 42°C.
2. Dilute stock PMSF to 4 mg/ml in 96% ethanol. Add 3.33 µl to sorted DNA tubes (40 µg/ml final). Incubate for 40 min at room temperature.
3. Add 13.44 µl 5 *M* NaCl (final 0.3 *M* including sheath buffer), 2 µl Pellet Paint, and 770 µl absolute ethanol. Mix gently by inversion. Precipitate overnight at –20°C or at –70°C for 30 min. (Tubes can be stored at this stage at –20°C if necessary.)
4. Pellet DNA in microfuge at full speed (11,000 *g*) at room temperature for 15 min. The hinge of the Eppendorf tube should face outwards so that the pellet is easily located.

5. Remove most of the supernatant with a P1000. Remove the remainder with P200, avoiding the pellet. Add 1 ml 70% ethanol without disturbing the pellet and then spin again for 7 min. Remove supernatant as before. Allow pellets to air dry (about 20 min).

6. Add 50 µl TE directly to the pellet to resuspend. DNA should separate from the wall of the tube immediately. Mix by *very* gentle flicking. Allow DNA to dissolve for at least 2 h.

B. Random Labeling of DNA for Array Palnting

Solutions

1. *2.5× random primer solution*: Found in BioPrime kit. Store at –20°C and use as supplied.
2. *Sterile water*: Found in BioPrime kit. Store at –20°C and use as supplied.
3. *10× dNTP mix*: To make 1 ml, mix 10 µl dCTP (1 m*M* final), 20 µl dATP (2 m*M* final), 20 µl dGTP (2 m*M* final), and 20 µl dTTP (2 m*M* final) in 930 µl TE buffer. Store 1 ml aliquots at –20°C.
4. *Cy3-dCTP*: Store as stock in the dark at –20°C.
5. *Cy5-dCTP*: Store as stock in the dark at –20°C.
6. *Klenow fragment*: Found in BioPrime kit. Store at –20°F and use as supplied.
7. *Stop buffer*: Found in BioPrime kit. Store at –20°C and use as supplied.

Tubes containing Cy dyes should be kept in the dark!

Steps

1. Labeling Reactions

1. To 50 µl resuspended chromosomes, add 60 µl 2.5× random primers solution and add 20.5 µl sterile water to make up to 130.5 µl.
2. Denature samples in a hot block for 10 min at 100°C and immediately cool on ice.
3. Add the following reagents on ice: 15 µl 10× dNTP mix, 1.5 µl Cy3- or Cy5-labelled dCTP, and 3 µl Klenow fragment. Mix thoroughly but gently.
4. Incubate the reaction at 37°C overnight.
5. Stop the reaction by adding 15 µl stop buffer.

2. Clean-up of Labeling Reactions

Use 3 columns per labelling reaction. Once the columns have been prepared, they must be used immediately to avoid the resin drying out.

Column Preparation

Steps

1. Resuspend the resin in the columns by gentle vortexing.
2. Loosen the cap one quarter turn and snap off the bottom closure.
3. Place the column in a 1.5 ml screw-capped tube.
4. Spin the columns for exactly 1 min at 735 *g*.

Sample Application

Steps

1. Place the columns in a new 1.5 ml tube and slowly apply 55 µl of the labelled sample to the centre of the angled surface of the resin bed, being careful not to disturb it. Do not allow any of the sample to flow around the side of the resin bed.
2. Spin the columns for 2 min at 735 *g*. Collect the purified samples in the support tube.
3. Discard the columns.
4. Combine the three samples.
5. Run 5 µl on a 1% agarose gel to check for correct labelling. Ideally, the fragments should range from 200 to 800 bp in size. Tubes containing the samples should be pink (Cy3) and blue (Cy5) in colour, indicating incorporation of the fluorescent dCTPs.

C. Array Hybridization

Solutions

1. *Human Cot-1 DNA*: Use as supplied (1 µg/ul). Store at –20°C.
2. *3 M NaAc pH 5.2*: For 200 ml, dissolve 49.2 g NaAc (anhydrous) in ~140 ml H_2O, pH to 5.2 with glacial acetic acid, make up to 200 ml, and then autoclave. Store at room temperature.
3. *Absolute ethanol*: Store in a sterile 50 ml Falcon tube at –20°C.
4. *Herring sperm DNA*: Use as supplied (10 mg/ml). Store at –20°C.
5. *40% formamide/2xSSC*: To make up 50 ml, mix 20 ml formamide, 5 ml 20 × SSC, and 25 ml sterile double distilled water (DDW). Store in a 50 ml Falcon at 4°C.
6. *Hybridisation buffer*: For 10 ml, mix 5 ml deionised formamide, 2 ml 50% dextran sulphate, 100 µl Tris, pH 7.4, 10 µl Tween 20, 1 ml 20 × SSC, and 1890 µl HPLC water.
7. *80% ethanol*: Store in a sterile 50 ml Falcon tube at –20°C.
8. *Yeast tRNA*: Make up to a final concentration of 100 µg/µl by dissolving in autoclaved water and store as 50-µl aliquots at –20°C.

9. *20% formamide/2xSSC*: To make up 50 ml, use 10 ml formamide, 5 ml 20 × SSC, and 35 ml DDW. Store in a 50 ml Falcon at 4°C.
10. *PBS/0.05% Tween 20*: Add 500 µl Tween 20 to 1 liter phosphate-buffered saline (PBS).
11. *50% formamide/2xSSC*: For 400 ml, mix 200 ml formamide, 40 ml 20xSSC, and 160 ml HPLC water. Incubate at 42°C prior to use.

1. Precipitation

Steps

1. Prepare 2 × 2 ml Eppendorfs.
2. Heat the herring sperm DNA on a 70°C hot block for 5 min before use.
3. To tube 1 add 180 µl Cy3-labelled DNA, 180 µl Cy5-labelled DNA, 135 µl human Cot-1 DNA, 55 µl 3*M* NaAc, pH 5.2, and 1400 µl 100% ice-cold ethanol.
4. To tube 2 add 80 µl herring sperm DNA, 135 µl human Cot-1 DNA, 23 µl 3*M* NaAc, pH 5.2, and 600 µl ice-cold 100% ethanol.
5. Mix the tubes gently and precipitate in the dark at –20°C overnight or at –70°C for 30 min.

2. Preparation of Slide

Steps

1. Place the slide over a dummy slide identifying the array area and apply a rubber cement ring closely around the grid using a small syringe, taking care not to go over the grid. Avoid thin threads of the cement going onto the array as you pull the syringe tip away.

2. After the first layer has dried, carefully apply a second layer over the first one.

3. Preparation of Humidity Chambers

Steps

1. In a fume hood, prepare a humidity chamber by pipetting a 40% formamide/2xSSC mix onto a Whatman paper strip until the paper is damp.

2. Leave the humidity chamber in the fume hood ready for use.

4. Prehybridization

Steps

1. Preheat the hybridisation buffer in a 70°C hot block.

2. Spin the precipitated DNAs for 15 min at 9500 *g*.

3. Remove the supernatant and add 500 µl 80% ice-cold ethanol.

4. Respin at 9500 *g* for 5 min.

5. Remove the supernatant with a P1000 and then a P200.

6. Respin at 9500 *g* for 1 min.

7. Remove any remaining supernatant with a P10 until the pellet is dry.

8. Resuspend the DNAs in 60 µl hybridisation buffer and 6 µl yeast tRNA (tube 1) and 140 µl hybridisation buffer (tube 2). This is best done by adding the hybridisation buffer and leaving the tube for 2–3 min in a 70°C hot block before resuspending the pellet using a displacement pipette. Ensure that the DNA is properly resuspended before continuing with the experiment. Denature the tube for 10 min at 70°C. Mix the sample after 5 min.

9. Pulse spin the tubes.

10. Place tube 1 into a 37°C hot block and incubate for 60 min in the dark.

11. Apply the contents of tube 2 onto the array grid and rock the slide to ensure even coverage within the well. Remove any air bubbles with a tip, but do not touch the grid. Work quickly to minimise drying of the slide.

12. Transfer the slide into the humidity chamber and place on the rocking table for 60 min shaking at 5 rpm.

5. Hybridization

Steps

1. Pulse spin tube 1.
2. Remove slide from humidity chamber.
3. Apply DNA onto the slide. Remove any air bubbles.
4. Rock the slide to mix the prehybridisation and hybridisation solutions and to ensure even coverage within the well.
5. Place the slide into a slide mailer humidified with 20% formamide/2xSSC.
6. Seal well with Parafilm and place into the hybridisation oven at 37°C.
7. Incubate with gentle rocking (5 rpm) for 48 h, turning the slide by 90° after 24 h.

6. Washing

Steps

1. Remove the slide from the incubator and increase the temperature of the hybridisation oven up to 42°C.
2. Remove the rubber cement.
3. Place the slide into a hellendahl jar containing PBS/0.05% Tween 20 to wash off excess hybridisation solution.
4. Transfer the slide into a glass trough and wash in PBS/0.05% Tween 20 for 10 min shaking at room temperature.
5. Transfer the slide into a preheated trough containing 50% formamide/2x SSC at 42°C. Incubate at 42°C with shaking for 30 min.

6. Transfer the slide into a trough of fresh PBS/0.05% Tween 20 and incubate at room temperature with shaking.
7. Transfer the slide into a metal rack and spin at 150 *g* for 5 min to dry.
8. Store the slide in a light-proof box at room temperature until ready to scan.

7. Scanning and Analysis

Our slides are scanned using an Axon 4000B scanner (Axon Instruments, Burlingame, CA) and the images are analysed by GenePix Pro 3.0 software (Axon Instruments, Burlingame, CA). Spots are defined using the automatic grid feature and adjusted manually where necessary. Fluorescence intensities of all spots are calculated after local background subtraction. The ratios of the intensities are then plotted in log 2 scale against the distance of the clones along the chromosomes from the p termini. Breakpoints are identified by a shift in ratio intensities typically from 4 log 2 to –4 log 2 (or vice versa), with a spanning clone showing an intermediate ratio close to 0 log 2.

IV. PITFALLS

Batches of Cot-1 DNA need to be tested before being used routinely in experiments. At present we order Cot-1 DNA from Roche (1581074) or Invitrogen (15279-011) and perform test hybridisations on the array using tumour cell line DNA with previously determined characteristic genomic copy number changes.

During array hybridisation, care must be taken to prevent the slides from drying out. Just before the hybridisation solution is added to the slide, some of the pre-hyb solution can be removed carefully with a pipette tip. However, this increases the chances of the slide drying out.

All gels used in this article are 1% agarose gels with ethidium bromide. It is advised that these gels are run before progression to the next step to check that each process has been performed successfully.

References

Carter, N. P. (1994). Bivariate chromosome analysis using a commercial flow cytometer. *Methods Mol. Biol.* **29**, 187–204.

Fiegler, H., Carr, P., Douglas, E. J., Burford, D. C., Hunt, S., Smith, J., Vetrie, D., Gorman, P., Tomlinson, I. P. M., and Carter, N. P. (2003a). DNA microarrays for comparative genomic hybridization based on DOP-PCR amplification of BAC and PAC clones. *Genes Chromosomes Cancer* **36**, 361–374.

Fiegler, H., Gribble, S. M., Burford, D. C., Carr, P., Prigmore, E., Porter, K. M., Clegg, S., Crolla, J. A., Dennis, N. R., Jacobs, P., and Carter, N. P. (2003b). Array painting: A method used for the rapid analysis of aberrant chromosomes using DNA microarrays. *J. Med. Genet.* **40**, 664–670.

McMullan, T. F. W., Crolla, J. A., Gregory, S. G., Carter, N. P., Cooper, R. A., Howell, G. R., and Robinson, D. O. (2002). A candidate gene for congenital bilateral isolated ptosis identified by molecular analysis of a de novo balanced translocation. *Hum. Genet.* **110**, 244–250.

Solinas-Toldo, S., Lampei, S., Stilgenbauer, S., Nickolenko, J., Benner, A., Döhner, H., Cremer, T., and Lichter, P. (1997). Matrix-based comparative genomic hybridization: Biochips to screen for genomic imbalances. *Genes Chromosomes Cancer* **20**, 399–407.

Telenius, H., Carter, N. P., Bebb, C. E., Nordenskjöld, M., Ponder, B. A. J., and Tunnacliffe, A. (1992). Degenerate oligonucleotide-primed PCR: General amplification of target DNA by a single degenerate primer. *Genomics* **13**, 718–725.

CHAPTER

42

Fine Mapping of Gene Ordering by Elongated Chromosome Methods

Thomas Haaf

I. INTRODUCTION

Fluorescence *in situ* hybridization (FISH) can be used to localize specific DNA sequences on metaphase chromosomes, interphase nuclei, and experimentally extended DNA or chromatin fibers. Depending on the hybridization target, FISH techniques show widely different levels of DNA resolution (Table I). They provide a rapid and accurate alternative to traditional molecular approaches for long-range physical mapping, including pulsed-field gel electrophoresis and radiation hybrid mapping. One important application has been the visual construction of contig maps of regions of interest, such as disease gene loci or chromosome breakpoints. Differential fluorescent probe labeling allows the ordering of multiple DNA sequences on the same chromosome. The DNA resolution of standard metaphase FISH is in the 1- to 3-Mb size range. Hybridization on less condensed interphase nuclei increases the resolution to around 100 kb. The average distance between two probe signals in the three-dimensional nuclear space correlates with physical distance up to 1–2 Mb. This allows one to determine the relative order and proximity of closely juxtaposed sequences, which cannot be resolved on metaphase chromosomes (Trask *et al*., 1989). Protocols for stretching out DNA in solution (Bensimon *et al*., 1994) or the chromatin of interphase nuclei (Parra and Windle, 1993; Haaf and Ward, 1994b; Heiskanen *et al*., 1994) have pushed the limits of resolution even further. Hybridization to experimentally extended DNA or chromatin fibers provides a mapping power in the order of 1–10 kb. The maximum distance possible for clone ordering may be up to several megabases; however, the average size of intact fibers is considerably smaller. Most fiber FISH techniques are informative over genomic distances from 100 to 500 kb.

Mechanically stretched or elongated chromosomes fill the resolution gap between metaphase FISH and fiber FISH, allowing the rapid and straightforward ordering and localization of clones along the length of an entire chromosome with a 100- to 200-kb resolution. Elongated chromosomes for high-resolution FISH are prepared by centrifuging colcemid-arrested metaphase spreads in hypotonic solution to microscope glass slides. The mechanical forces generated during cytocentrifugation result in mechanical stretching of chromosomes to 5 to 20 times their normal length due to their elastic consistency under moist conditions (Haaf and Ward, 1994a,b). Elongated chromosome FISH can be applied to large numbers of probes and provides a more than 10-fold increase in DNA resolution compared to standard metaphase mapping. This makes it possible to create 100-kb physical maps of a chromosome(s) or chromosome region(s) of interest in relatively short time (Laan *et al*., 1995, 1996).

Although various genome projects have provided very high-resolution physical maps of human and important animal genomes, FISH is still an exceptionally versatile mapping tool. For example, working with duplicated or repetitive sequences at the molecular level can be extremely tedious and, therefore, accurate mapping and sequencing of these regions remain tremendous tasks in the postgenomic era. In addition, FISH has important applications for mapping chromosome regions that have been deleted, amplified, and/or rearranged in human pathology or evolution. Of course, FISH techniques are useful not only for mapping the human genome. They can be

Copyright 2006, Elsevier Science (USA).
All rights reserved.

TABLE I DNA Targets and Resolution of Standard FISH Mapping Techniques

Target	DNA resolution	Upper limit of utility range	Major advantages/ disadvantages
Metaphase chromosome	1–3 Mb	Chromosome	Whole genome screening Chromosome banding Multicolor approaches (>3 colors)
Interphase nucleus	50–100 kb	1–2 Mb	Relatively simple and fast No chromosome identification No centromere–telomere orientation Statistical analysis required
Extended chromosomes	100–200 kb	Chromosome	Centromere–telomere orientation Nonuniform chromosome stretching Cytocentrifuge required
Chromatin/ DNA fibers	1–10 kb	500 kb–1 Mb	Many different, but usually relatively simple protocols for fiber preparation Nonuniform DNA/chromatin stretching Interpretation of hybridization signals often difficult
Molecular combing	1–10 kb	500 kb–1 Mb	DNA molecules aligned in a single direction and stretched homogeneously DNA combing apparatus and silanized coverslips required; technique is relatively complicated No simultaneous DNA–protein detection

adapted easily for the study of map-poor genomes from primitive vertebrates to humans.

II. MATERIALS AND INSTRUMENTATION

All reagents for elongated chromosome preparation are standard laboratory chemicals that can be obtained from many different suppliers, i.e., NaCl (Sigma-Aldrich, Cat.No. S7653), KCl (Sigma-Aldrich, Cat.No. P5405), Na_2HPO_4 (Sigma-Aldrich, Cat.No. S9638), KH_2HPO_4 (Sigma-Aldrich, Cat.No. P5655), HEPES dry powder (Sigma-Aldrich, Cat.No. H9897), glycerol 99.5% ACS reagent (Sigma-Aldrich, Cat.No. G7893), $CaCl_2{\cdot}2H_2O$ (Sigma-Aldrich, Cat.No. C3881), $MgCl_2{\cdot}6H_2O$ (Sigma-Aldrich, Cat.No. M0250), acetic acid (VWR, Cat.No. 1.00058.1000), methanol (VWR, Cat.No. 1.06008.1000), acetone (VWR, Cat.No. 1.59005.0500), Biocoll (Ficoll) separating solution (Biochrom, Cat.No 2 6115), and colcemid (Roche, Cat.No. 295892).

The cytocentrifuge (Cytospin 3) and the filter blots are from Thermo Shandon Inc.

III. PROCEDURES

A. Preparation of Elongated Chromosomes for FISH Mapping

The following protocol describes the preparation of elongated chromosomes from human lymphoblastoid or fibroblast cells (Haaf and Ward, 1994a,b). This technique can be adapted for other cell substrates, producing suitable targets for high-resolution FISH mapping.

Solutions

1. *Phosphate-buffered saline (PBS)*: 136 m*M* NaCl, 2 m*M* KCl, 10.6 m*M* Na_2HPO_4, and 1.5 m*M* KH_2PO_4, pH 7.3. To make 10× PBS stock solution, weigh 79.5 g NaCl, 1.5 g KCl, 15 g Na_2HPO_4, and 2 g KH_2PO_4. After dissolving in distilled water, complete to 1000 ml, pH, and autoclave. Store at room temperature. To make 1× PBS, dilute stock solution 1 : 10 with distilled water and use within 1 day.

2. *Hypotonic solution (for cell swelling)*: 10 m*M* HEPES, 30 m*M* glycerol, 1 m*M* $CaCl_2$, and 0.8 m*M* $MgCl_2$. To make 1000 ml, add 2.4 g HEPES, 2.2 ml anhydrous glycerol, 147 mg $CaCl_2{\cdot}2H_2O$, and 163 mg $MgCl_2{\cdot}6H_2O$. After dissolving, complete to 1000 ml with distilled water, pH, and filter if necessary. Store at 4°C and use within 1 week.

3. *Carnoy's fixative*: Mix one part acetic acid and three parts methanol. Store at –20°C and use within 1 day.

Steps

1. After harvesting a mitotically dividing cell culture(s), wash the cells one time in 1× PBS and resuspend the cell pellet in hypotonic solution to a concentration of 10^3 to 10^4 cells/ml. Incubate the cells at ambient temperature for 5–10 min.

2. Centrifuge 0.5-ml aliquots of this hypotonic cell suspension onto microscope slides at 1000 rpm for 4 min using a Shandon cytospin. Specifically, place the cell suspension in the cytobuckets of the centrifuge, the bases of which are formed by a filter blot and a glass slide (cleaned with ethanol). The whole structure is held together by a clip. During centrifugation the suspension fluid is absorbed by the filter blot and the cells become attached to the glass slide. After cytocentrifugation, the slide should carry a visible monolayer of cells in a designated area about 5 mm in diameter. Use a diamond pencil to mark the back of the slide to indicate the area on which the cells are sedimented.

3. Fix the slides for 30 min at –20°C in methanol and then overnight at –20°C in Carnoy's fixative. Air-dried slides stored at 4°C can be kept for months before use.

4. Select slides suitable for FISH mapping using a phase-contrast microscope at low magnification (10 to 20× lens without oil). A higher density of cells per slide results in poor chromosome stretching and cytoplasmic background ("dirt"). A lower density of cells results in disruption of metaphase spreads and individual chromosomes. Chromosomes extended to 5 to 20 times their normal length but still intact are most useful for high-resolution chromosome mapping. Good slides should contain 3–10 metaphase spreads with stretched chromosomes without broken arms. If less than half of the slides obtained after cytocentrifugation meet these criteria, the cell density in the hypotonic solution was either too high or too low.

5. Standard FISH protocols are used for mapping cloned DNA sequences such as cosmids, BACs, or YACs to acid-fixed elongated chromosomes (Haaf, 2000). Usually one probe is detected with a green fluorescent dye, a second probe with a red dye, and the chromosomes are counterstained in blue with DAPI (Figs. 1A and 1B). However, using modern FISH workstations for M-FISH or spectral karyotype analysis (SKY), many more DNA targets can be distinguished in different colors.

6. Determine the relative order of two hybridized clones that are <1 Mb apart on at least five elongated chromosomes. Because mechanically stretched chromosomes can be highly deformed, not all hybridized chromosome copies may be informative. If the order is not consistent on all five chromosomes, analyze five additional chromosome copies. In most cases, one slide should be sufficient for ordering probes that are 100–200 kb apart.

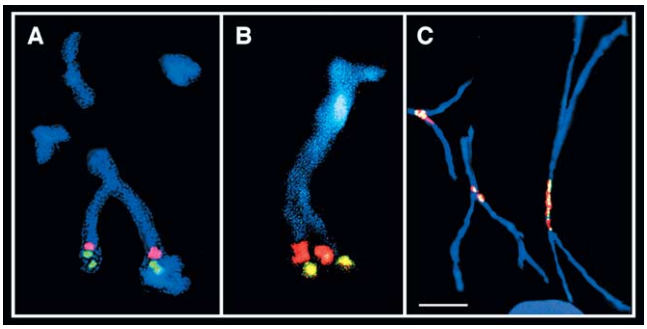

FIGURE 1 (A and B) Two-color FISH with two closely juxtaposed (<1 Mb) YACs from the 5q34-q35 region to chromosomes mechanically stretched to 5–10 times their normal length. (C) Colocalization of centromeric proteins (green) and α-satellite DNA (red) on chromosomes stretched to 10–20 times their normal length. Centromeric proteins were detected by indirect immunofluorescence staining with CREST antiserum and FITC-labeled antihuman IgG. α-satellite DNA was hybridized *in situ* with a digoxigenated human α-satellite cocktail probe and detected with rhodamine-conjugated antidigoxin antibody. Bar: 10 μm.

B. Preparation of Elongated Chromosomes for Combined Protein Immunofluorescence and FISH

The combined application of protein staining by immunofluorescent techniques and DNA staining by FISH provides a powerful tool for mapping chromosomal proteins to specific DNA sequences.

Steps

1. Harvest mitotic cells and centrifuge them onto slides as described earlier.

2. Fix the slides in methanol at –20°C for 30 min and then immerse in ice-cold acetone for a few seconds. After brief air drying, process the preparations for immunofluorescence staining. Because most protein antigens are not very stable, it is not recommened to store the slides before use.

3. Perform immunofluorescent staining of a protein of interest, i.e., as an example only, labeling of centromeric proteins (CENPs) by specific anti-CENP antibodies (Fig. 1C). Standard immunofluorescent protocols are used for incubation of the slides with primary and fluorescent-labeled secondary antibodies (Haaf, 1995). However, do not counterstain the preparations with DAPI.

4. Immediately after immunofluorescent staining, refix the preparations by incubating them in Carnoy's fixative overnight at –20°C and then hybridize them with a DNA probe(s) of interest.

IV. COMMENTS AND PITFALLS

1. The most suitable source of mitotic cells are long-term *in vitro* cell cultures such as EBV-transformed lymphoblasts, fibroblasts, or established cell lines. Usually, 10 µg/ml colcemid (Roche) is added to the culture medium 10–15 min before cell harvest to arrest cells in metaphase. Whole blood cultures cannot be used as a cell substrate because the erythrocytes are not destroyed by the hypotonic treatment required for elongated chromosome preparation. Therefore, it is necessary to separate white blood cells from red cells by density gradient centrifugation (in Biocoll/Ficoll separating solution) prior to short-term lymphocyte culturing.

2. Elongated chromosomes constitute a compromise between different demands. The mechanical stretching procedure inevitably impairs chromosome morphology. The chromosomes are deformed and cannot be banded; however, they provide a greater DNA resolution and allow the ordering of probes from the short-arm to the long-arm telomere. Usually, better chromosome morphology goes along with poor stretching and vice versa.

3. Chromosome elongation is not uniform over the entire length of a stretched chromosome and the same metaphase spread may contain both well-extended and poorly stretched chromosomes. Therefore it is very difficult to correlate the micrometer distance between two mapped loci or the relative distance from the short arm telomere (Flpter value) with physical distance in kilobases. Some regions, i.e., telomeres, which are usually attached to the surface of the glass slide, are more resistant to stretching than others.

4. Carnoy's fixation of immunofluorescent preparations and subsequent FISH do not grossly interfere with the fluorecent-labeled protein antigen–DNA complex. Although the intensity of the fluorescent protein signal is reduced to a certain extent, it is still visible after the relatively harsh *in situ* hybridization procedure. This allows one to analyze the results of protein immunofluorescence and DNA *in situ* hybridization simultaneously on the same elongated chromosomes.

References

Bensimon, A., Simon, A., Chiffaudel, A., Croquette, V., Heslot, F., and Bensimon, D. (1994). Alignment and sensitive detection of DNA by a moving interface. *Science* **265**, 2096–2098.

Haaf, T. (1995). Immunocytogenetic techniques. *In* "*Human Chromosomes. Principles and Techniques*" (R. S. Verma, A. Babu, eds.), pp. 232–270. McGraw-Hill, New York.

Haaf, T. (2000). Fluorescence in situ hybridization. *In* "*Encyclopedia of Analytical Chemistry*" (R. A. Meyers, ed.), Vol. 1, pp. 4984–5006. Wiley, Chichester.

Haaf, T., and Ward, D. C. (1994a). High resolution ordering of YAC contigs using extended chromatin and chromosomes. *Hum. Mol. Genet.* **3**, 629–633.

Haaf, T., and Ward, D. C. (1994b). Structural analysis of α-satellite DNA and centromere proteins using extended chromatin and chromosomes. *Hum. Mol. Genet.* **3**, 697–709.

Heiskanen, M., Karhu, R., Hellsten, E., Peltonen, L., Kallioniemi, O. P., and Palotie, A. (1994). High resolution mapping using fluorescence in situ hybridization to extended DNA fibers prepared from agarose-embedded cells. *BioTechniques* **17**, 928–933.

Laan, M., Kallioniemi, O. P., Hellsten, E., Alitalo, K., Peltonen, L., and Palotie, A. (1995). Mechanically streched chromosomes as targets for high-resolution FISH mapping. *Genome Res.* **5**, 13–20.

Laan, M., Isosomppi, J., Klockers, T., Peltonen, L., and Palotie, A. (1996). Utilization of FISH in positional cloning: an example on 13q22. *Genome Res.* **6**, 1002–1012.

Parra, I., and Windle, B. (1993). High resolution visual mapping of stretched DNA by fluorescent hybridization. *Nature Genet.* **5**, 17–21.

Trask, B., Pinkel, D., and van den Engh, G. (1989). The proximity of DNA sequences in interphase nuclei is correlated to genomic distances and permits ordering of cosmids spanning 250 kilobase pairs. *Genomics* **5**, 710–717.

CHAPTER

43

In Situ Hybridization Applicable to mRNA Species in Cultured Cells

Roeland W. Dirks

I. INTRODUCTION

RNA *in situ* hybridization (ISH) techniques allow the study of gene expression at the individual cell level in a histocytomorphological context. These techniques often involved the use of radioactive-labeled probes. However, because of resolution drawbacks limiting their applicability in the study of RNA distribution at (sub)cellular sites, these probes are replaced more frequently by hapten- or fluorophore-labeled ones. Nevertheless, radioactive ISH is still useful for detecting relatively low abundant RNA transcripts in tissue sections.

From the early 1980s, several nonisotopic-labeling methods have been developed that are most often based on the introduction of haptens (e.g., biotin and digoxigenin) or fluorochromes (e.g., fluorescein, rhodamine, coumarin, Cy3, and Cy5) that are conjugated to allyl or alkylamine-dUTP in DNA or RNA probes. Such probes provide a high spatial resolution and allow simultaneous detection of multiple RNA sequences (Dirks *et al*., 1991; Levsky *et al*., 2002) or RNA sequences together with proteins (Dirks, 1998; Snaar *et al*., 1999).

Direct ISH techniques, using fluorochrome-labeled probes, are used to detect relatively abundant mRNA species by conventional fluorescence microscopy. Using more advanced digital imaging microscopy, visualization of single RNA transcripts proved even possible when oligodeoxynucleotide probes were labeled with five fluorochromes per molecule and 10 oligonucleotide probes were hybridized to adjacent sequences on an RNA target (Femino *et al*., 1998).

Indirect ISH techniques, using haptenized probes, are often the method of choice because of their better sensitivity compared to direct fluorescence ISH approaches (Dirks *et al*., 1993). Furthermore, enhancement of ISH signals can be accomplished by applying multiple antibody layers or by the use of a tyramide-based detection method (Adams, 1992; Raap *et al*., 1995; van de Corput *et al*., 1998). Tyramide-based detection methods involve the use of an antihapten peroxidase-labeled antibody as a first antibody layer and a biotin, DNP, or fluorochrome tyramide that serves as a peroxidase substrate to generate and deposit many reporter molecules close to the hybridization site.

This article describes a protocol that allows sensitive detection of RNAs at cytoplasmic as well as at nuclear sites of cells that are grown or attached to microscopic slides.

II. MATERIALS AND INSTRUMENTATION

Dulbecco's modified Eagle medium without phenol red (DMEM, Cat. No. 1188-36), fetal bovine serum (FBS, Cat. No. 1050-64), l-glutamine (Cat. No. 2503-24), penicillin–streptomycin (Cat. No. 1514-22), and trypsin (Cat. No. 2509-28) are from Invitrogen Life Technologies. Salmon testes DNA (Cat. No. D-7656), dithiothreitol (DTT, Cat. No. D-0632), thimerosal (Cat. No. T-5125), polyvinylpyrrolidone (PVP, Cat. No. PVP-40), Tween 20 (Cat. No. P-1379), mouse monoclonal antidigoxin (Cat. No. D-8156), rabbit antimouse fluorescein isothiocyanate (FITC) (Cat. No. F-7506), Streptavidin-FITC (Cat. No. S-3762), and goat antirabbit FITC (Cat. No. F-9262) are from Sigma. Ficoll PM 400 (Cat. No. 1-30-0) is from Amersham Biosciences.

Copyright 2006, Elsevier Science (USA).
All rights reserved.

Bovine serum albumin fraction V (BSA, Cat. No. 44155) is from BDH. Formamide (Cat. No. 7042) and acetic acid (Cat. No. 6052) are from J. T. Baker. Amberlite MB1 ion exchanger (Cat. No. 40701) and 4,6,-diamidino-2-phenylindol 2HCl (DAPI, Cat. No. 18860) are from Serva. Acid-free formaldehyde (Cat. No. 3999) is from Merck. dATP (Cat. No. 1051 440), dCTP (Cat. No. 1051 458), dGTP (Cat. No. 1051 466), dTTP (Cat. No. 1051 482), DNase I (Cat. No. 104 158), digoxigenin-11-dUTP (Cat. No. 1093 088), sheep antidigoxigenin HRP (Cat. No. 1207 733), and blocking reagent (Cat. No. 1096 176) are from Roche. DNA polymerase I (Cat. No. M2051) is from Promega. Vectashield mounting medium is from Vector. Staining jars (100 ml) for object slides (Cat. No. L4110) are from Agar Aids Ltd. TSA fluorescein system (Cat. No. NEL701), TSA tetramethylrhodamine NEL702), TSA coumarin system (Cat. No. NEL703), and TSA biotin system (Cat. No. NEL700) are from NEN.

Fluorescence ISH results were examined with an epifluorescence microscope (DM, Leica) equipped with a 100-W mercury arc lamp and a triple excitation filter for red, green, and blue excitation (Omega). Digital images were captured with a cooled CCD camera (Photometrics).

III. PROCEDURES

A. Labeling of DNA by Nick Translation

Solutions

1. *Nick translation buffer (10x)*: 0.5 *M* Tris–HCl, pH 7.8, 50 m*M* $MgCl_2$, and 0.5 mg/ml BSA. To make 10 ml of the solution, add 5 ml of an autoclaved 1 *M* stock solution of Tris–HCl, pH 7.8, 0.5 ml of an autoclaved 1 *M* solution $MgCl_2$, and 5 mg of nuclease-free BSA and complete to 10 ml with autoclaved distilled water. Aliquot in 100-µl portions and store at –20°C.

2. *0.1 M DTT*: To make 10 ml, dissolve 150 mg of DTT in 10 ml of 0.01 *M* sodium acetate (pH 5.2). Filter the solution through a 0.2-µm filter, aliquot in 1-ml portions, and store at –20°C.

3. *Nucleotide mix*: 0.5 m*M* dATP, 0.5 m*M* dCTP, 0.5 m*M* dGTP, and 0.1 m*M* dTTP. To make 1 ml of the solution, add 5 µl each of 100 m*M* stock solutions dATP, dCTP, and dGTP and 1 µl of 100 m*M* stock solution dTTP. Complete to 1 ml with autoclaved distilled water and store at –20°C.

4. *1 mg/ml DNase I*: To make 1 ml, add 1 mg of DNase, 20 µl of a 1 *M* stock solution of Tris–HCl, pH 7.6, 50 µl of a stock solution of NaCl, 10 µl of a 100 m*M* stock solution of DTT, 0.1 mg of BSA, and 0.5 ml of glycerol. Complete to 1 ml with autoclaved distilled water and store at –20°C.

5. *10 mg/ml salmon testes DNA*: To make 10 ml, dissolve 100 mg DNA in 100 ml 0.3 *M* NaOH in TE, pH 7.8 (10 m*M* Tris–HCl, pH 7.8, 1 m*M* EDTA). Boil for 20 min at 100°C. Neutralize the solution by adding 5 ml of 2 *M* Tris–HCl, pH 7.5, 7.5 ml of 4 *M* HCl, and 12 ml of 2 *M* sodium acetate. Precipitate the DNA by adding 2 volumes of 100% –20°C ethanol and incubate for 1 h on ice. Centrifuge for 10 min at 2600 *g*, remove the ethanol, and dissolve the DNA pellet in 10 ml TE buffer.

6. *Deionized formamide*: To make 100 ml, add 5 g of ion exchanger to 100 ml formamide. Stir for 2 h and filter twice through Whatmann No. 1 filter paper. Aliquot in 1-ml portions and store at –20°C.

7. *20x SSC*: To make 1 liter, add 175.3 g NaCl and 88.24 g sodium citrate to distilled water. Adjust to pH 7.0 and complete to 1 liter. Autoclave the solution and store at room temperature.

8. *50X Denhardt's solution*: 1% PVP, 1% Ficoll (type 400), and 1% BSA. To make 500 ml of the solution, add 5 g Ficoll, 5 g PVP, 5 g BSA (fraction V), and distilled water to 500 ml. Sterilize the solution by filtration and store at –20°C.

Steps

1. Thaw the required stock solutions and keep them on ice. Prepare the labeling solution on ice and mix well. To make the labeling mixture, combine 26 µl autoclaved distilled water, 5 µl 10x nick translation buffer, 5 µl 100 m*M* DTT, 4 µl nucleotide mix, 2 µl digoxigenin-11-dUTP (0.25 m*M* stock solution), 1 µl probe DNA (1 µg, e.g., cDNA), 2 µl DNA polymerase I, and 5 µl of a 1 : 1000 DNase I dilution from a 1-mg/ml stock solution.

2. Place the labeling mixture for 2 h in a 16°C water bath.

3. Add 250 µl distilled water and precipitate the labeled probe by adding 30 µl of 3 *M* sodium acetate, pH 4.8, 5 µl salmon testes DNA, and 750 µl –20°C 100% ethanol. Mix well and place the solution on ice for 30 min.

4. Centrifuge for 30 min at 4°C in an Eppendorf centrifuge at maximum speed. Remove the ethanol completely and resuspend the pellet in 200 µl hybridization mixture to reach a probe concentration of 5 ng/µl. To make 10 ml hybridization mixture, combine 5 ml deionized formamide, 1 ml 20X SSC, 1 ml of 0.5 *M* sodium phosphate buffer, pH 7.0, 1 ml 50x Denhardt's solution, and 2 ml autoclaved distilled water. The probe mixture can be stored at 4°C for at least 1 year.

B. Culturing and Fixation of Cells

Solution

10x PBS (pH 7.2): Add 80 g NaCl, 2 g KCl, 15 g $Na_2HPO_4.2H_2O$, and 1.2 g KH_2PO_4 and adjust to 1 liter. Autoclave the solution and store at room temperature.

Steps

1. Trypsinize subconfluent cells that are grown in tissue culture flasks as a monolayer in DMEM supplemented with 10% FCS, 100 U of penicillin/ml, and 100 µg of streptomycin/ml and seed into petri dishes containing five microscopic object slides and 20 ml medium. Grow cells to subconfluency at 37°C in a humidified 5% CO_2 atmosphere.
2. Wash the object slides containing cells in PBS for 1 min at room temperature.
3. Fix the cells in PBS containing 3.7% formaldehyde, 5% acetic acid for 20 min at room temperature. To make 100 ml fixative, combine 75 ml distilled water, 10 ml 10x PBS, 10 ml formaldehyde (37% stock), and 5 ml acetic acid.
4. Wash the cells in PBS for 5 min at room temperature and transfer the object slides to a 100-ml staining jar.
5. Wash the cells in 70% ethanol and store the object slides in 70% ethanol at 4°C until use.

C. Pretreatment and Hybridization

Solution

0.1% pepsin: To make 100 ml, dissolve 0.1 g pepsin in distilled water, adjust pH to 2.0, and bring to 100 ml. Make this solution about 15 min before use and place in a 37°C water bath.

Steps

1. Wash the cells in PBS for 3 min at room temperature.
2. Incubate the cells in 0.1% pepsin solution for 2 min at 37°C.
3. Wash the cells in 70% ethanol for 30 s.
4. Wash twice in PBS for 30 s each.
5. Incubate in 1% formaldehyde in PBS for 5 min at room temperature.
6. Wash in PBS for 5 min and dehydrate the cells successively in 70, 90, and 100% ethanol for 3 min each.
7. Denature the probe dissolved in hybridization mixture for 5 min in an 80°C water bath.
8. Place the probe for 1 min on ice and spin down in a table centrifuge.
9. Apply 10 µl of the denatured probe mixture on the object slide and hybridize overnight at 37°C in a moist chamber, which consists of a 1-liter beaker covered with aluminium foil containing tissues moistened with 50% formamide/2x SSC, pH 7.0.

D. Posthybridization Washes

Solutions

1. *50% formamide/2x SSC wash solution*: To make 400 ml, add 200 ml formamide, 40 ml 20x SSC, and 160 ml distilled water and adjust the pH to 7.0.
2. *10x TBS*: To make 1 liter, dissolve 121.4 g Tris and 87.4 g NaCl in 800 ml distilled water. Adjust the pH to 7.4 with 6 *N* HCl and bring to a total volume of 1 liter.

Steps

1. Wash the slides in the 50% formamide/2x SSC solution at room temperature until the coverslips are released.
2. Transfer the slides to a new jar filled with 100 ml 50% formamide/2x SCC and wash for 10 min.
3. Wash the slides for 10 min each in 50% formamide/2x SSC at 42°C and in the same solution at room temperature.
4. Wash the slides in 2x SSC for 5 min at room temperature.
5. Wash the slides in 1x TBS for 5 min at room temperature.

E. Conventional Immunocytochemical Detection

Solution

Blocking solution: To make 100 ml, add 0.5 g blocking reagent and 100 µl thimerosal (to prevent bacterial growth). Complete to 100 ml with 1x TBS. Heat the mixture for 1 h at 60°C to dissolve the blocking reagent and aliquot in 10-ml portions. Store at –20°C.

Steps

1. Take a slide from the TBS solution and apply 100 µl blocking solution. Cover it with a 24 × 50-mm^2 coverslip and incubate for 30 min at 37°C in a moist chamber (1-liter beaker covered with aluminium foil containing tissue moistened with water).
2. Wash briefly with TBS to remove the coverslips.
3. Drain of as much of the TBS solution as possible and incubate the slides with mouse antidigoxigenin, diluted 1:500 in blocking solution under a coverslip for 45 min at 37°C in a moist chamber.
4. Remove the coverslips by a brief wash in TBS and wash the slides 3 × 5 min with TBS at room temperature.

5. Drain of as much of the washing solution as possible and incubate the slides with rabbit anti-mouse FITC diluted 1:500 in blocking solution as described in step 3.
6. Wash the slides as described in step 4.
7. Drain of as much of the washing solution as possible and incubate the slides with goat anti-rabbit FITC, diluted 1:500 in blocking solution, as described in step 3.
8. Wash the slides as described in step 4.
9. Dehydrate the slides for 3 min each in 70, 90, and 100% ethanol and air dry.
10. Apply 30 µl Vectashield containing 10 ng/µl DAPI (blue fluorescent DNA counterstain) on a slide and cover with a 24 × 50-mm^2 coverslip.
11. Examine the slides with a fluorescence microscope equipped with appropriate excitation and emission filters for FITC and DAPI fluorescence.

F. Tyramide Signal Amplification

Solution

10x TNT: To make 1 liter, dissolve 121.4 g Tris and 87.4 g NaCl in 800 ml distilled water. Ad 0.5 ml Tween 20. Mix thoroughly, adjust the pH to 7.4, and bring to a total volume of 1 liter.

Steps

1. Take slides from the TBS solution and apply 100 µl blocking solution. Cover with a coverslip and incubate for 30 min at 37°C in a moist chamber.
2. Wash briefly with TBS to remove coverslips.
3. Drain of as much of the washing solution as possible and incubate the slides with antidigoxigenin-HRP, diluted 1:500 in blocking solution, under a coverslip for 45 min at 37°C in a moist chamber.
4. Remove the coverslips by a brief wash in TNT and wash the slides 3 × 5 min with TNT at room temperature.
5. Drain of as much of the TNT solution as possible and apply 300 µl of a 1:50 dilution of a fluorescent (red, green, or blue) or biotin tyramide in 1x amplification diluent on each slide. Incubate the slides for approximately 10–30 min at room temperature without a coverslip.
6. Wash the slides 3 × 5 min with TNT at room temperature.
7. For detection of biotin tyramide, incubate the slides with steptavidin FITC diluted 1:1000 in blocking solution as described in step 3.
8. Wash the slides as described in step 4.
9. Dehydrate the slides in ethanol, air dry, and mount in Vectashield.

IV. COMMENTS

The protocol just described allows sensitive detection of specific mRNAs in a variety of cell types, including cultured cells, trypanosomes (Chaves *et al*., 1998), malaria parasites (Vervenne *et al*., 1994), and blood cells. The various steps in this protocol have been optimized for detecting RNA molecules in cultured mammalian cells by trial and error (Dirks *et al*., 1993) and may need some adjustments for specific applications. For example, if RNA FISH is applied at the electron microscopic level of resolution, sample preparation, fixation, and pretreatment conditions need to be adjusted (Macville *et al*., 1995,1996).

Compared to conventional immunocytochemical detection systems, the use of tyramide-based detection systems results in an at least a 10-fold increase in signal intensity (Raap *et al*., 1995). This is illustrated in Fig. 1, showing hybridization signals of human elongation factor (HEF) mRNA in HeLa cells and of IL-6 and G-CSF mRNA in human bladder carcinoma cells grown on microscope slides. If required, the localization properties of tyramides can be improved by the addition of dextran sulfate to the amplification diluent (Van Gijlswijk *et al*., 1996).

This hybridization protocol also allows bright-field microscopic visualization of hybridization signals when conjugates with peroxidase or alkaline phos-

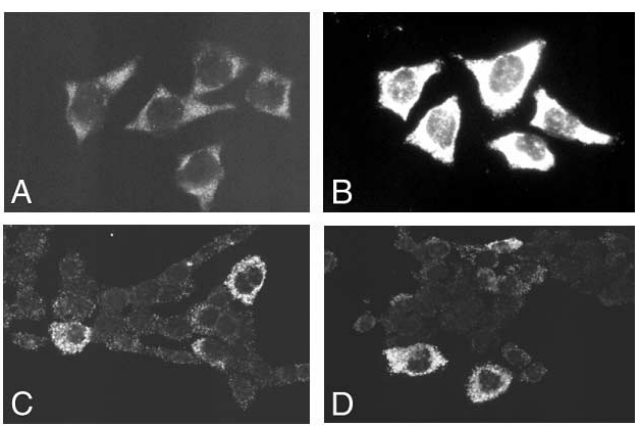

FIGURE 1 (**A**) Detection of HEF mRNA in HeLa cells using a digoxigenin-labeled DNA plasmid probe. The hybridized probe was visualized using a fluorescein-conjugated secondary antibody. (**B**) A hybridized HEF probe was visualized using a peroxidase-labeled antidigoxigenin antibody and fluorescein-tyramide. (**C**) Detection of IL-6 mRNA in 5637 bladder carcinoma cells using a cocktail of three HRP-labeled oligodeoxynucleotides and the TSA biotin system. (**D**) Detection of G-CSF mRNA in 5637 cells using a cocktail of three HRP-labeled oligodeoxynucleotides and the TSA biotin system (for details, see van de Corput *et al*., 1998).

phatase are used instead of fluorochrome antibody conjugates (Dirks *et al*., 1993).

As a positive control on the procedure, probes specific for housekeeping gene transcripts, like human elengation factor and actin mRNA, or for rRNA, such as 28S rRNA, can be used.

Finally, in order to study dynamic aspects of RNA localization, methods have been developed that allow hybridization of probes to RNAs and its subsequent visualization in living cells (Molenaar *et al*., 2001; Pederson, 2001).

V. PITFALLS

1. Probe labeling can be checked by performing a filter spot test. Spot 1 µl of a dilution series of the labeled probe on a nitrocellulose filter and incubate with sheep antidigoxigenin-alkaline phosphatase. After performing the NBT/BCIP reaction, a probe concentration of 5 to 1 pg/µl should be visible.

2. We noticed that it is important to use for the fixation of cells a good source of formaldehyde. Formaldehyde solutions of poor quality may lead to poor cell morphology, high levels of autofluorescence, or weak hybridization signals.

3. It is important to titrate the pepsin concentration and/or time of incubation in order to find a balance between morphology and signal intensity.

4. For optimal results it is sometimes necessary to denature the target mRNA. This is done just before hybridization, after applying the probe solution and coverslip on the slide, by placing the slide on an 80°C hot plate for 2 to 3 min.

5. The dilution and reaction time of labeled tyramides need to be optimized for each application. To diminish nonspecific background staining, the first antibody may be diluted further.

References

Adams, J. C. (1992). Biotin amplification of biotin and horseradish peroxidase signals in histochemical stains. *J. Histochem. Cytochem.* **40**, 1457–1463.

Chaves, I., Zomerdijk, J., Dirks-Mulder, A., Dirks, R. W., Raap, A. K., and Borst, P. (1998). Subnuclear localization of the active variant surface glycoprotein gene expression site in *Trypanosoma brucei*. *Proc. Natl. Acad. Sci. USA* **95**, 12328–12333.

Dirks, R. W. (1998). Combination DNA/RNA FISH and immunophenotyping. *In "Current Protocols in Cytometry"* (J. P. Robinson, Z. Darzynkiewics, P. N. Dean, A. Orfao, P. S. Rabinovitch, H. J. Tanke, and L. L. Wheeles, eds.), pp. 8.7.1–8.7.14. Wiley, New York.

Dirks, R. W., Van de Rijke, F. M., Fujishita, S., Van der Ploeg, M., and Raap, A. K. (1993). Methodologies for specific intron and exon RNA localization in cultured cells by haptenized and fluorochromized probes. *J. Cell Sci.* **104**, 1187–1197.

Dirks, R. W., Van Gijlswijk, R. P. M., Vooijs, M. A., Smit, A. B., Bogerd, J., Van Minnen, J, Raap, A. K., and Van der Ploeg, M. (1991). 3′-End fluorochromized and haptenized oligonucleotides as in situ hybridization probes for multiple, simultaneous RNA detection. *Exp. Cell Res.* **194**, 310–315.

Femino, A. M., Fay, F. S., Fogarty, K., and Singer, R. H. (1998). Visualization of single RNA transcripts in situ. *Science* **280**, 585–590.

Levsky, J. F., Shenoy, S. M., Pezo, R. C., and Singer, R. H. (2002). Single-cell gene expression profiling. *Science* **297**, 836–840.

Macville, M. V., Van Dorp, A. G., Dirks, R. W., Fransen, J. A., and Raap, A. K. (1996). Evaluation of pepsin treatment of electron microscopic RNA in situ hybridization on ultra-thin cryosections of cultured cells. *Histochem. Cell Biol.* **105**, 139–145.

Macville, M. V., Wiesmeijer, K. C., Dirks, R. W., Fransen, J. A., and Raap, A. K. (1995). Saponin pre-treatment in pre-embedding electron microscopic in situ hybridization for detection of specific RNA sequences in cultured cells: A methodological study. *J. Histochem. Cytochem.* **43**, 1005–1018.

Molenaar, C., Marras, S. A., Slats, J. C. M., Truffert, J.-C., Lemaitre, M., Raap, A. K., Dirks, R. W., and Tanke, H. J. (2001). Linear 2′ O-methyl RNA probes for the visualization of RNA in living cells. *Nucleic Acids Res.* **29**, e89.

Pederson, T. (2001). Fluorescent RNA cytochemistry: Tracking gene transcripts in living cells. *Nucleic Acids Res.* **29**, 1013–1016.

Raap, A. K., Van de Corput, M. P. C., Vervenne, R. A. W., Van Gijlswijk, R. P. M., Tanke, H. J., and Wiegant, J. (1995). Ultrasensitive FISH using peroxidase-mediated deposition of biotin- or fluorochrome tyramides. *Hum. Mol. Genet.* **4**, 529–534.

Snaar, S. P., Vincent, M., and Dirks R. W. (1999). RNA polymerase II localizes at sites of human cytomegalovirus immediate-early RNA synthesis and processing. *J. Histochem. Cytochem.* **47**, 245–254.

Van de Corput, M. P. C., Dirks, R. W., Van Gijlswijk, R. P. M., Van Binnendijk, E., Hattinger, C. M., De Paus, R. A., Landegent, J. E., and Raap, A. K. (1998). Sensitive mRNA detection by fluorescence in situ hybridization using horseradish peroxidase-labeled oligodeoxynucleotides and tyramide signal amplification. *J. Histochem. Cytochem.* **46**, 1249–1259.

Van Gijlswijk, R. P. M., Wiegant, J., Raap, A. K., and Tanke, H. J. (1996). Improved localization of fluorescent tyramides for fluorescence in situ hybridization using dextran sulphate and polyvinyl alcohol. *J. Histochem. Cytochem.* **44**, 389–392.

Vervenne, R. A. W., Dirks, R. W., Ramesar, J., Waters, A. P., and Janse, C. J. (1994). Differential expression in blood stages of the gene coding for the 21-kilodalton surface protein of ookinetes of *Plasmodium berghei* as detected by RNA in situ hybridization. *Mol. Biochem. Parasitol.* **68**, 259–266.

CHAPTER

44

In Situ Hybridization for Simultaneous Detection of DNA, RNA, and Protein

Noélia Custódio, Célia Carvalho, T. Carneiro, and Maria Carmo-Fonseca

I. INTRODUCTION

Fluorescence *in situ* hybridisation enables the detection of RNA and DNA in the cellular context, therefore allowing the study of gene expression at the single cell level. *In situ* hybridisation was described for the first time in 1969 in two independent studies (Gall and Pardue; 1969; John *et al*., 1969) that used radiolalelled probes and autoradiographic methods to detect abundant sequences. During the early eighties, nonisotopic probe-labelling methods were developed based on the introduction of haptens (such as biotin and digoxigenin) and fluorochrome-conjugated antibodies (for review, see Schwarzacher and Heslop-Harrison, 2000). The use of different probe labels and detection systems with multiple fluorochromes made possible the simultaneous detection of several target sequences in the same cell, including the detection of a specific gene and the corresponding pre-mRNA and/or mRNA (Custódio *et al*., 1999; Johnson *et al*., 2000; Xing *et al*., 1993, 1995). A combination of fluorescence *in situ* hybridisation with immunofluorescence further allows the simultaneous visualisation of genes, transcripts, and proteins.

A major problem when conjugating protocols to simultaneously detect DNA, RNA, and proteins is to achieve good preservation of the different targets throughout the procedure and, at the same time, make them accessible for the probes. This article describes protocols that have been optimised over the years for the simultaneous detection of DNA, RNA transcripts, and proteins involved in RNA metabolism in the nucleus of mammalian cultured cell lines.

II. MATERIALS AND INSTRUMENTATION

35 × 10-mm (P35) tissue culture dishes (Sarstedt, Cat. No. 83.1800)
10 × 10-mm glass coverslips
Tweezers (style #7, sharp, hooked, Sigma, Cat. No. T 4912)
Water bath (variable temperature)
Heat block
Incubator at 37°C
Moist chamber (plastic box with lid containing some wet tissues inside)
Vacuum pump
Milli-Q ultrapure or bidistilled water
dNTPset, 100 m*M* each dNTP (Qbiogene, Cat. No. NTACG100)
Digoxigenin-11-dUTP, alkali stable (Roche, Cat. No. 1093088)
Dinitrophenyl(DNP)-11-dUTP (Molecular Probes, Cat. No. C-7610)
Alexa Fluor 488-5-dUTP (Molecular Probes, Cat. No. C-11397)
Fluorescein-12-dUTP (Roche, Cat. No. 137 3242)
BIOTAQ DNA polymerase (BIOLINE, Cat. No. BIO-21040)
Oligonucleotide probes with amino-modified bases (MWG Biotech)
Cy3 monoreactive dye (Amersham Biosciences, Cat. No. PA23001)
Cy5 monoreactive dye (Amersham Biosciences, Cat. No. PA2500)
Alexa Fluor 488 oligonucleotide amine-labelling kit (Molecular Probes, Cat. No. A-20191)

Copyright 2006, Elsevier Science (USA).
All rights reserved.

Escherichia coli tRNA (Sigma, Cat. No. R-4251)
Herring sperm DNA (Sigma, Cat. No. D-6898)
Human COT-1 DNA (Invitrogen, Cat. No. 152 79 011)
Mouse COT-1 DNA (Invitrogen, Cat. No. 184 40 016)
Dextran sulfate (Sigma, Cat. No. D-8906)
Albumin, bovine (Sigma, Cat. No. A-2153)
Formamide, molecular biology grade (Calbiochem, Cat. No. 344206)
AG 501-X8(D) resin (Bio-Rad, Cat. No. 142–6225)
Poly-L-lysine, 0.01% solution (Sigma, P4832)
Ribonucleoside–vanadyl complexes, 200 m*M* (Sigma, Cat. No. R-3380)
Paraformaldehyde extra pure (Merck, Cat. No. 1.04005.1000)
Triton X-100 (Sigma, Cat. No. X-100)
Pepsin (Sigma, Cat. No. P-6887)
Gelatin from cold water fish skin (Sigma, Cat. No. G-7765)
Tween 20 (Sigma, Cat. No. P-9416)
Formamide p.a. (Merck, Cat. No. 1.09684)
Fluorescein-conjugated sheep antidigoxigenin (Roche, Cat. No. 1 333 062)
Alexa Fluor 488-conjugated goat antifluorescein (Molecular Probes, Cat. No. A-11090)
Cy3-conjugated mouse antidigoxin (Jackson ImmunoReseach Labs, Inc., Cat. No. 200-162-156)
Cy5-conjugated mouse antidigoxin (Jackson ImmunoReseach Labs, Inc., Cat. No. 200-172-156)
FITC-conjugated rabbit anti-DNP (Molecular Probes, Cat. No. A-6423)
Rabbit anti-DNP (Molecular Probes, Cat. No. A-6430)
Alexa Fluor 488-conjugated goat antirabbit (Molecular Probes, Cat. No. A-11034)
TRITC-conjugated donkey antirabbit (Jackson ImmunoReseach Labs, Inc., Cat. No. 711-025-152)
Other fluorochrome-conjugated secondary antibodies (Jackson ImmunoReseach Labs, Inc.)
Formaldehyde solution min. 37%, p.a. (Merck, Cat. No. 1.04003.1000)
Vectashield mounting medium (Vector, Cat. No. H-1000)
Microscopy glass slides
Nail polish

III. PROCEDURES

A. Labeling of Probes

There are several methods to label DNA probes. Choosing a specific method depends on the kind of probe to be labelled. For example, whole recombinant plasmids or purified inserts are easily labelled by nick translation, whereas it is more advantageous to label shorter DNA fragments (100–600 bp) by polymerase chain reaction (PCR). Oligonucleotides can be synthesised with amino-modified nucleotides (amino-allyl thymine) at specific positions in the sequence and labelled by conjugation with activated fluorophores.

1. Labelling of Probes by PCR

Solutions

1. *Sodium acetate 3 M, pH 5.5*. Weigh 40.81 g of $NaCH_3COOH$ to 100 ml of solution. Adjust the pH to 5.5 with acetic acid. Sterilise by autoclaving.
2. *10 mg/ml E.coli tRNA*. Dissolve 0.1 g of tRNA in 10 ml of sterile water. Aliquot and store at –20°C.

Steps

1. Make up the following PCR reaction:
   Sterile water to bring the final volume (including enzyme) to 50 µl
   5 µl 10 × PCR buffer (supplied with the enzyme)
   1.5 µl 50 m*M* $MgCl_2$ (the optimal concentration of $MgCl_2$ must be determined empirically; initially try 1.5 m*M*, taking into account that some PCR buffers already contain $MgCl_2$)
   1 µl 1 ng/µl template DNA
   2 µl primer mix, 10 µ*M* (10 pmol/µl) each
   1 µl 10 m*M* dATP
   1 µl 10 m*M* dCTP
   1 µl 10 m*M* dGTP
   3.75 µl 2 m*M* dTTP
   2.5 µl 1 m*M* dig-11-dUTP (or other modified nucleotide)
   2.5 units *Taq* DNA polymerase
   The ratio dTTP : modified nucleotide in the previous mixture is 3 : 1. This ratio is ideal for generating highly labelled probes necessary to detect target sequences present at a low copy number. To generate moderately labelled probes the ratio of dTTP : modified nucleotide in the PCR reaction should be increased.
2. Mix the reagents and centrifuge briefly to collect the mixture into the bottom of the tube.
3. Place the reaction in a termocycler and perform the PCR under the following conditions:
   Denaturation before the first cycle: 3 min at 95°C
   30 cycles of denaturation for 30 s at 95°C, annealing for 30 s at 60°C, and elongation for 1 min at 72°C
   Final elongation: 10 min at 72°C
   Cycling conditions will depend on the template and primers used. Other cycling conditions may be required to get optimal results.
4. Stop the reaction by chilling at 4°C. Run 5 µl of the reaction on an agarose gel and estimate the amount of product generated in the PCR reaction.

5. Add water to adjust the volume of the PCR reaction to 100 µl and purify the labelled probe by ethanol precipitation: add 5 µl of sodium acetate 3*M*, pH 5.5, 1 µl of 10 mg/ml *E.coli* tRNA (this will act as a carrier RNA to help precipitation), and 200 µl of cold 100% ethanol (–20°C).

6. Incubate for 15 min at –70°C or for 1 h at –20°C to allow precipitation of the labelled fragments.

7. Centrifuge at 13,000 rpm for 15 min at 4°C. Remove the supernatant and add 200 µl of cold 70%(v/v) ethanol. Centrifuge for 5 min in the same conditions.

8. Discard the supernatant completely and air dry the pellet. Dissolve the pellet in sterile water to achieve a concentration of probe of 10 ng/µl. Store at –20°C.

2. *Labelling of Modified Oligonucleotide Probes by Conjugation with Activated Fluorophores*

The oligonucleotide probes should be at least 40–50 nucleotides long to minimize the possibility of unspecific binding to nontarget cellular RNAs. When choosing the sequences, avoid regions that may form highly stable secondary structures or dimmerise. If more than one oligonucleotide is used in the same hybridisation, they all should have similar GC content. The oligonucleotides should be synthesised with four or five thymines in the sequence changed to amino-allyl thymine. The modified nucleotides should be at least 10 bases apart to prevent quenching (Long *et al*., 1995; Singer, 1998). The amino-modified thymine can then be coupled chemically to fluorophores as described.

Solutions

1. *Carbonate buffer*: 0.1*M* $NaHCO_3$, pH 8.8. Weigh 0.84 g of $NaHCO_3$ to 100 ml of solution. Adjust the pH with NaOH. Make aliquots and store at –20°C.
2. *Fluorophore solution*: Dissolve one vial of the activated fluorophore (Cy3 monoreactive dye, Cy5 monoreactive dye, or Alexa Fluor 488 from the oligonucleotide amine-labelling kit) in 30 µl of dimethyl sulfoxide. Store at –20°C.
3. *TE, pH 8.0 (10 mM Tris, 1 mM EDTA, pH 8.0)*: Add 1 ml of 1*M* Tris, pH 8.0, and 0.2 ml of 0.5*M* EDTA. Adjust the volume to 100 ml with water. Sterilise by autoclaving.

Steps

1. In a microtube, dilute 5 µg of the modified oligonucleotide (higher oligonucleotide concentration will decrease the yield of the labelling reaction) with carbonate buffer to a final volume of 35 µl (buffers containing primary amino groups, such as TRIS, should be avoided as they inhibit the conjugation reaction).

2. Add 15 µl of fluorophore solution and mix well by vortexing. Allow the labelling reaction to proceed for 24 h in the dark at room temperature.

3. Add sterile water to adjust the volume of the labelling reaction to 100 µl and purify the labelled oligonucleotide by two rounds of ethanol precipitation as follows. Add 10 µl of 3*M* sodium acetate, pH 5.5, 1 µl of 10 mg/ml *E.coli* tRNA, and 300 µl of cold 100% ethanol (–20°C). Incubate overnight at –20°C to allow precipitation of the labelled oligonucleotide probe.

4. Centrifuge at 13,000 rpm for 15 min at 4°C. Remove the supernatant and wash with 200 µl of cold 100% ethanol (do not use 70% ethanol as it will dissolve the precipitated oligonucleotide). Centrifuge for 5 min in the same conditions.

5. Remove the supernatant and dissolve the pellet in 100 µl of sterile water.

6. Reprecipitate by adding 10 µl of 3*M* sodium acetate, pH 5.5, and 300 µl of cold 100% ethanol and incubate for 4 h at –20°C.

7. Repeat step 4, then discard the supernatant completely, and air dry the pellet. Dissolve the labelled oligonucleotide in 100 µl of sterile water to achieve a final concentration of 50 ng/µl (assuming no losses during the procedure).

B. Preparation of Hybridization Mixture

Solutions

1. *20 × SSC (saline sodium citrate)*: 0.3*M* sodium citrate, 3*M* NaCl, pH 7.4. Weigh 88.24 g of sodium citrate and 175.32 g of NaCl for 1 liter of solution. Sterilise by autoclaving.

2. *50% dextran sulfate*: Dissolve 5 g of dextran sulfate in 4 ml of water. Adjust the volume to 10 ml and sterilise by autoclaving. Store at 4°C. Heat at 55°C and mix well before taking an aliquot.

3. *0.5M sodium phosphate buffer, pH 7.0*: 0.31*M* NaH_2PO_4 and 0.19*M* Na_2HPO_4. Weigh 1.84 g NaH_2PO_4 and 1.37 g Na_2HPO_4 for 50 ml of solution. Adjust the pH to 7.0 with 10*M* NaOH if necessary. Sterilise by autoclaving.

4. *10% bovine serum albumin (BSA)*: Dissolve 1 g of BSA in 7 ml of sterile water. Adjust the volume to 10 ml. Aliquot and store at –20°C.

5. *1 mg/ml sonicated herring sperm DNA (100–200 bp)*. Dissolve 0.1 g of herring sperm DNA in 10 ml of sterile water. Sonicate until the average fragment size is 100–200 bp (control the fragment size on agarose gel electrophoresis). Measure ODs at 260 nm to determine the concentration of the DNA and dilute to 1 mg/ml. Aliquot and store at –20°C.

6. *Deionized formamide*: Add 5 g of ion-exchange resine to 100 ml of molecular biology grade formamide. Stir for 3 h, wait for the resine to settle down, and filter through 0.22-µm or Whatmann No. 1. Aliquot and store at –20°C.

7. *50% formamide hybridization buffer*: 50% formamide, 2 × SSC, 10% dextran sulfate, and 50 m*M* sodium phosphate, pH 7.0. Add 5 ml of deionised formamide, 2 ml of 50% dextran sulfate, 1 ml of 20 × SSC, and 1 ml of 0.5 *M* sodium phosphate buffer, adjust the pH to 7.5 with 1 *N* HCl, and add sterile water to 10 ml. Mix well, aliquot, and store at –20°C.

8. *20% formamide hybridization buffer*: 20% formamide, 2 × SSC, 10% dextran sulfate, 0.2% BSA, and 1 µg/µl tRNA, pH 7.0. For 1 ml, add 200 µl of deionised formamide, 200 µl of 50% dextran sulfate, 100 µl of 20 × SSC, 20 µl of 10% BSA, 100 µl of 10 mg/ml tRNA, and 380 µl of sterile water. Mix well and store at 4°C.

1. PCR or Nick Translation-Labeled Probes

Long genomic cloned sequences can be used as probes, but they often contain repetitive sequences that can produce a high background due to cross-hybridization. To reduce this background, a suppressive hybridisation must be performed. In this case, an excess of unlabelled DNA enriched in repetitive sequences (e.g., COT-1 DNA and herring sperm DNA) is included in the hybridization mixture. For probes that do not contain repetitive sequences, a nonsuppressive hybridization is performed. In this case, tRNA is used as a carrier for probe precipitation.

Steps

1. For suppressive hybridization, add per hybridisation 10–100 ng of labelled probe, 5.6 µg of COT-1 DNA, and 2.4 µg of sonicated herring sperm DNA. For nonsuppressive hybridization, add 8 µg of *E.coli* tRNA to the labelled probe (the amount of probe in the hybridization must be determined empirically).

2. Precipitate by adding 0.05 volumes of 3 *M* sodium acetate, pH 5.0, and 2 volumes of cold ethanol (–20°C). Incubate for 15 min at –70°C or 1 h at –20°C.

3. Centrifuge at 13,000 rpm for 15 min at 4°C. Remove the supernatant and wash with cold 70%(v/v) ethanol. Centrifuge for 5 min in the same conditions.

4. Discard the supernatant completely and air dry the pellet. Dissolve the pellet in 50% formamide hybridization buffer (use 8 µl per hybridization) and store at –20°C. Note that before taking an aliquot of the hybridisation buffer this must be warmed up to 37°C and vortexed to homogenise all the components.

2. Oligonucleotide Probes

Prepare the hybridization mixture by diluting the labelled oligonucleotide in the 20% formamide hybridization buffer to the appropriate concentration (1–2 ng/µl of each oligonucleotide). If the oligonucleotide stock solution is too diluted, dry it in the Speed-Vac and then dissolve in the hybridization buffer.

C. Preparation of Cells

Solutions

1. *10× phosphate-buffered saline (PBS)*: 1.37 *M* NaCl, 26.8 m*M* KCl, 80.6 m*M* Na_2HPO_4, 14.7 m*M* KH_2PO_4. Weigh 80 g NaCl, 2 g KCl, 11.44 g Na_2HPO_4, and 2 g KH_2PO_4 for 1 liter of solution. Sterilise by autoclaving.

2. *7.4% paraformaldehyde (2 × PFA)*: Weigh 7.4 g of PFA into a glass flask, add water to 100 ml, and stir at 60°C for several hours with the flask closed. Add 100 µl of 1 *M* NaOH dropwise and keep stirring until the solution is completely clear (pH should be around 7.5). Let it cool down to room temperature and filter through a 0.22-µm filter. Store at –20°C in 5-ml aliquots. Thaw at 60°C and use within 1–2 days.

3. *3.7% formaldehyde in PBS*: Add 5 ml of 2 × PFA, 1 ml of 10 × PBS, and sterile water to 10 ml.

4. *3.7% formaldehyde/5% acetic acid/0.9% NaCl*: Add 5 ml of 2 × PFA, 0.5 ml of acetic acid, 0.3 ml 5 *M* NaCl, and sterile water to 10 ml.

5. *10% (w/v) Triton X-100*: Weigh 1 g of Triton X-100 and add sterile water to 10 ml. Dissolve by warming to 37°C and vortexing.

6. *0.5% Triton X-100 in PBS with 2 mM vanadyl–ribonucleoside complex*: Add 0.5 ml of 10% Triton X-100, 1 ml 10 × PBS, 100 µl of 200 m*M* vanadyl–ribonucleoside complex, and sterile water to 10 ml.

7. *0.01% (w/v) pepsin in 0.01 M HCl*. Prepare immediately before use with HCl at 37°C. Dissolve 5 mg of pepsin in 50 µl of 0.01 *M* HCl and then adjust the volume with 0.01 *M* HCl to 50 ml.

Steps

All the procedures are performed with cells attached on 10 × 10-mm glass coverslips placed in 35 × 10-mm tissue culture dishes. One dish can accommodate four of these coverslips, and 1 ml of solution is enough for each fixation, permeabilisation, and washing step.

1. Grow monolayer cells to subconfluent density directly on 10 × 10-mm coverslips and wash them in serum-free medium. Alternatively, wash suspension cells in serum-free medium and allow them to adhere

onto 10 × 10-mm poly-L-lysine-coated glass coverslips for 1 min at room temperature (approximately 2 × 10^5cells in 30 µl of medium per coverslip).

2. Fix and permeabilize the cells according to one of the following protocols.

   a. Fix with 3.7% formaldehyde in PBS for 10 min at room temperature, wash 3 × 5 min with PBS, permeabilise with 0.5% Triton X-100 in PBS with 2 m*M* vanadyl–ribonucleoside complex for 10 min, and wash again 3 × 5 min with PBS. **Proceed to protocols D, E, or F** (when conjugating more than one protocol, go sequentially from D to E to F).

   b. Fix with 4% formaldehyde, 5% acetic acid, and 0.9% NaCl for 20 min at room temperature, wash 4 × 5 min with PBS (include 2 m*M* vanadyl–ribonucleoside complex in the last wash), and leave in 70% ethanol at –20°C for at least 1 h. Before hybridization, rehydrate the cells in PBS and digest with 0.01% pepsin in 0.01 *M* HCl for 5 min at 37°C. Rinse with PBS and inactivate the protease by fixation with 3.7% formaldehyde in PBS for 5 min at room temperature. Wash 3 × 5 min with PBS and **proceed to protocol D or E** (cannot be used with protocol F).

Step 2b allows a better access of the probe to the target RNA sequences in the cell. Therefore, this protocol may be required when hybridizing with oligonucleotide probes that detect the splice junctions of mRNA. Note that monolayer cells may detach from the coverslip during treatment with pepsin.

D. Hybridization to RNA

Solutions

1. *20% (w/v) Tween 20*: Weigh 2 g of Tween 20 and add sterile water to 10 ml. Dissolve by warming to 37°C and vortexing.

2. *20% (w/v) gelatin from cold water skin fish*: Weigh 0.2 g of gelatin and add sterile water to 1 ml. Mix well, aliquot, and store at –20°C.

3. *50% formamide, 2 × SSC, 0.01% Tween 20, pH 7.0*: Add 5 ml of formamide, 1 ml of 20 × SSC, 5 µl of 20% Tween 20, and sterilile water to 10 ml. Adjust the pH to 7.0 with 1 *M* HCl (use deionised formamide and add 2 m*M* vanadyl–ribonucleoside complex for prehybridisation incubation and formamide p.a. in posthybridisation washes).

4. *20% formamide, 2 × SSC, 0.01% Tween 20, pH 7.0*: Add 2 ml of formamide, 1 ml of 20 × SSC, 5 µl of 20% Tween 20, and sterile water to 10 ml (use deionised formamide and add 2 m*M* vanadyl–ribonucleoside complex for prehybridization incubation and formamide p.a. in posthybridization washes).

5. *2 × SSC, 0.01% Tween 20*: Add 1 ml of 20 × SSC, 5 µl of 20% Tween 20, and water to 10 ml.

6. *4 × SSC, 0.1% Tween 20*: Add 100 ml 20 × SSC, 2.5 ml 20% Tween 20, and sterile water to 500 ml.

7. *4 × SSC, 0.1% Tween 20, 1% BSA, 0.2% gelatin*: To 1 ml add 200 µl 20 × SSC, 5 µl 20% Tween 20, 100 µl 10% BSA, 10 µl 20% gelatin, and 685 µl of sterile water.

Steps

1. Denature double-stranded DNA probes by heating the hybridization mixture at 75°C for 5 min (use 8 µl per coverslip). Place on ice for nonsupressive hybridization or at 37°C for 10 min for suppressive hybridization to allow preannealing of repetitive DNA sequences.

2. Incubate the cells in 50% formamide, 2 × SSC, 0.01% Tween 20, and 2 m*M* vanadyl–ribonucleoside complex for 5 min at 37°C (when hybridizing with oligonucleotides, use 20% formamide).

3. Aspirate the solution as much as possible, especially around the coverslip, without allowing the cells to dry. Place 8 µl of hybridisation mixture in the center of the coverslip and incubate at 37°C in a moist chamber for 3–16 h (1–3 h for oligonucleotides).

4. Perform posthybridisation washes at the desired stringency. The washes described here are just a guideline. For optimal results, the percentage of formamide, salt concentration, and temperature should be optimized for each probe. Wash sequentially as follows:

   Wash I: 3 × 5 min at 45°C with 50% formamide p.a., 2 × SSC, and 0.01% Tween 20

   Wash II: 3 × 5 min at 45°C with 2 × SSC and 0.01% Tween 20

   When hybridizing with oligonucleotides, the washes should be less stringent, e.g., wash at 37°C or at 42°C with only 20% formamide in wash I. Perform washes with all the solutions prewarmed at the desired temperature. This step can be performed either in an incubator or in a water bath with the dishes inside a floating metal platform.

5. Proceed to step 7 if the probe is labelled directly with a fluorescent dye and no amplification step is required. Alternatively, wash with 4 × SSC and 0.1% Tween 20 for 5 min at 37°C and proceed to step 6 for detection with the appropriate antibodies.

6. Aspirate the solution, place 5 µl of diluted antibody in the center of the coverslip, and incubate for 30 min at 37°C in a moist chamber. Following each incubation step wash 3 × 5 min with 4 × SSC and 0.1% Tween 20 at 37°C. For digoxigenin-labelled probes, use fluorescein-conjugated sheep antidigoxigenin (1/100) followed by Alexa Fluor 488-conjugated goat antifluo-

rescein (1/200) if an amplification step is required. Alternatively, use Cy3- or Cy5-conjugated mouse antidigoxin (1/250). For DNP-labelled probes, use FITC-conjugated rabbit anti-DNP or rabbit anti-DNP followed by Alexa Fluor 488-conjugated goat antirabbit or TRITC-conjugated donkey antirabbit. Dilute antibodies in 4 × SSC, 0.1% Tween 20, 1% BSA, and 0.2% gelatin.

7. Wash briefly in PBS, fix the signal with 3.7% PFA in PBS for 10 min at room temperature, and wash 3 × 5 min in PBS.

8. Proceed to **protocols E or F** or mount in a microscopy glass slide with Vectashield mounting medium and seal with nail polish.

E. Hybridization to DNA

Solutions

1. *70% formamide, 2 × SSC, 50 mM sodium phosphate, pH 7.0*: Add 7 ml of deionized formamide, 1 ml of 20 × SSC, 1 ml of 0.5 *M* sodium phosphate buffer, and sterile water to 10 ml. Adjust the pH to 7.0 with 1 *M* HCl.
2. *50% formamide, 2 × SSC, 50 mM sodium phosphate, pH 7.0*: Add 5 ml of deionized formamide, 1 ml of 20 × SSC, 1 ml of 0.5 *M* sodium phosphate buffer, and sterile water to 10 ml. Adjust the pH to 7.0 with 1 *M* HCl.

Steps

1. Denature the double-stranded DNA probes by heating the hybridization mixture at 75°C for 5 min (use 8 µl per coverslip). Place on ice for nonsupressive hybridization or at 37°C for 10 min for suppressive hybridization to allow preannealing of the repetitive DNA sequences.
2. Incubate the cells in 2 × SSC at 40°C for 5 min (this step is to prewarm the cells and avoid lowering the temperature in the denaturation step).
3. For denaturation, incubate at 73°C in 70% formamide, 2 × SSC, and 50 m*M* sodium phosphate, pH 7.0, for 3 min followed by 50% formamide, 2 × SSC, and 50 m*M* sodium phosphate, pH 7.0, for 1 min.
4. Aspirate the solution as fast as possible and place 8 µl of hybridization mixture in the center of the coverslip. Incubate for 16 h at 37°C in a moist chamber.
5. Perform posthybridization washes at the desired stringency. The washes described here are just a guideline. For optimal results, the percentage of formamide, salt concentration, and temperature should be optimized for each probe. Wash sequentially as follows:
   - Wash I: 3 × 5 min at 45°C with 50% formamide p.a., 2 × SSC, and 0.01% Tween 20
   - Wash II: 3 × 5 min at 45°C with 0.5 × SSC and 0.01% Tween 20
6. Proceed to step 8 if the probe is directly labelled with a fluorescent dye and no amplification step with antibodies is required. Alternatively, wash with 4 × SSC, 0.1% Tween 20 for 5 min at 37°C and proceed to step 7 for detection with the appropriate antibodies.
7. For detection of hybridization sites, follow step 6 of protocol D. When conjugating several protocols it is essential to avoid cross-reactivity between the antibodies used in the different protocols and to choose different fluorescent dyes for each detection.
8. Wash briefly in PBS, fix the signal with 3.7% PFA in PBS for 10 min at room temperature, and wash 3 × 5 min in PBS.
9. Proceed to **protocols F** or mount in a microscopy glass slide with Vectashield mounting medium and seal with nail polish.

F. Detection of Proteins by Indirect Immunofluorescence

Solutions

1. *PBS, 0.05% Tween 20*: To 500 ml add 50 ml 10 × PBS, 1.25 ml 20% Tween 20, and 450 ml of sterile water.
2. *PBS, 0.05% Tween 20, 0.2% gelatin*: Add 10 µl of 20% gelatin to 1 ml of PBS and 0.05% Tween 20.
3. *2% formaldehyde in PBS*: Prepare by adding 2.7 ml of formaldehyde solution at 37% to 50 ml of PBS.

Steps

1. Wash cells with PBS, 0.05% Tween 20 for 5 min.
2. Incubate with the primary antibody (diluted in PBS, 0.05% Tween 20, 0.2% gelatin) for 1 h at room temperature in a moist chamber.
3. Wash 3 × 5 min in PBS, 0.05% Tween 20 at room temperature.
4. Incubate with the appropriate secondary antibody (diluted in PBS, 0.05% Tween 20, 0.2% gelatin) for 30 min at room temperature in a moist chamber.
5. Wash 3 × 5 min in PBS, 0.05% Tween 20 at room temperature.
6. Wash briefly in PBS. Fix with 2% formaldehyde in PBS for 10 min.
7. Wash 3 × 5 min in PBS, mount in a microscopy glass slide with Vectashield mounting medium, and seal with nail polish.

For visualization of β-globin gene expression, see Fig. 1.

IV. COMMENTS

The methods described in this article can be used to detect RNA and DNA, RNA and protein, DNA and

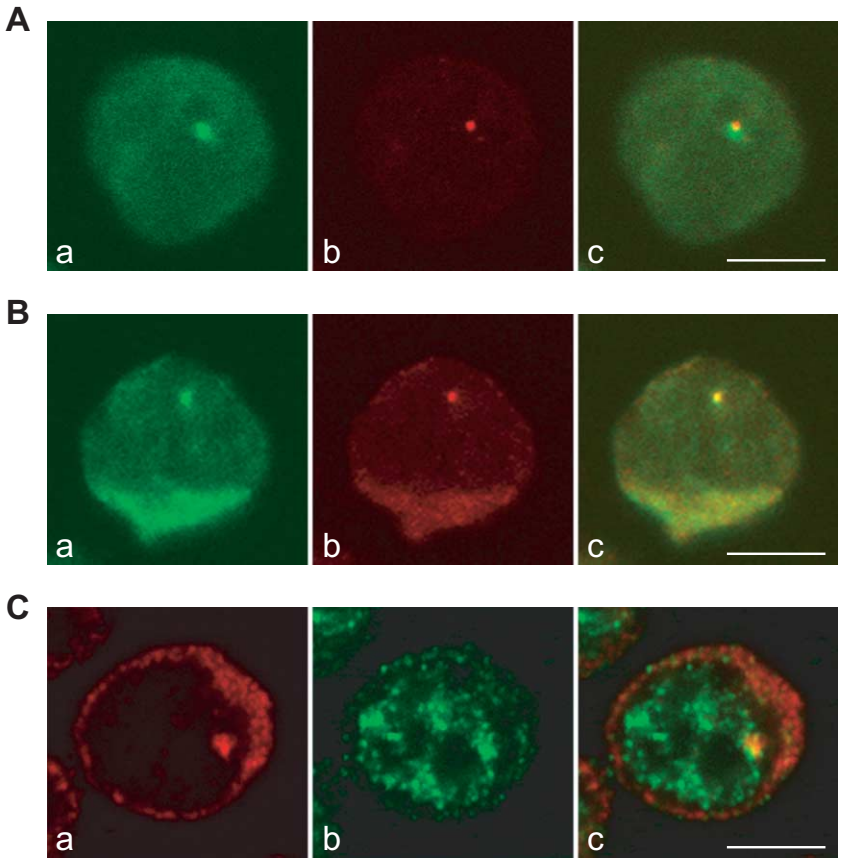

FIGURE 1 Visualization of β-globin gene expression at the single cell level. (A) Simultaneous detection of human β-globin RNA and DNA. Murine erythroleukaemia (MEL) cells were stably transfected with multiple copies of the human β-globin gene cloned in the micro-LCR expression vector (Collis *et al*., 1990; Custódio *et al*., 1999). After induction of β-globin gene expression, cells were fixed with formaldehyde/acetic acid, treated with pepsin, and hybridised with a probe complementary to the transcribed sequence of the gene, labeled with digoxigenin (a, signal detected with fluorescein). A bright fluorescent focus is detected in the nucleus. Following fixation of the RNA signal with formaldehyde, cells were denatured and hybridized with a probe that recognizes the micro-LCR, labelled with DNP (b, signal detected with Texas red). A fluorescent focus in the nucleus indicates the integration site of the transfected gene locus. Overlay of the green and red images in c shows colocalization of the two focal signals, indicating that the human β-globin RNA is detected in the nucleus at the site of transcription. (B) Simultaneous detection of human β-globin nascent transcripts and spliced mRNA. MEL cells expressing the human β-globin gene were fixed with formaldehyde/acetic acid, treated with pepsin, and hybridized sequentially to detect human β-globin nascent transcripts and spliced mRNA. The cells were first hybridized with a mixture of two splice junction oligonucleotide probes (SJ I/II probe complementary to the last 12 nucleotides of exon I and the first 12 nucleotides of exon II; SJ II/III complementary to the last and first 12 nucleotides of exons II and III, respectively) labeled with DNP (a, signal detected with fluorescein). Cells expressing the human β-globin gene for 4 days contain a fluorescent focus in the nucleus and additional cytoplasmic staining. Following fixation of the signal with formaldehyde, cells were incubated with a probe that hybridizes to the full-length human β-globin RNA, labeled with digoxigenin (b, signal detected with rhodamine). (c) A superimposition of the two images. The focal signals colocalize in the nucleus, indicating that splicing of β-globin pre-mRNA is taking place in close proximity to the site of transcription. (C) Simultaneous detection of human β-globin transcripts and an RNA processing factor. MEL cells expressing the human β-globin gene were fixed with formaldehyde, permeabilised with Triton, and hybridized with a probe that spans the transcribed sequence of the human β-globin gene (a, signal detected with Cy3). RNA is detected in the nucleus as a focus and in the cytoplasm. After fixation of the RNA signal with formaldehyde, cells were incubated with an antibody against the splicing coactivator SRm160 (rAb-SRm160; Blencowe *et al*., 1998) (b, signal detected with Alexa Fluor 488). SRm160 labels the nucleoplasm with a speckled pattern. Overlay of the two signals (c) shows colocalization of the nuclear RNA signal with a speckle of SRm160, indicating recruitment of this protein to the site of human β-globin RNA transcription and splicing. Bars: 5 μm.

protein, or RNA, DNA, and protein. In double RNA/DNA hybridization, hybridization to RNA is always performed first (without DNA denaturation, RNA is the only target for the probe). Then, the cellular DNA is denatured and hybridization to DNA is performed. The ideal probe for DNA detection should target nontranscribed regions of the genome and should not produce a signal if hybridised without prior denaturation of cellular DNA. The same probe, labelled with different reporters, can alternatively be used to simultaneously detect a DNA region and the corresponding transcripts. In this case, an RNase treatment must be introduced after the detection of the probe hybridized to RNA (Xing *et al*., 1995). An alkaline denaturation of DNA can also be performed instead of heat denaturation because it simultaneously degrades the cellular RNA (see Johnson *et al*., 2000). To minimise loss of the RNA signal during DNA denaturation, the probe hybridized to RNA should be detected with two layers of antibodies and fixed with formaldehyde. Direct labelling of the probe with fluorescent dyes without any step of signal amplification with antibodies is not recommended for this procedure. For multiple hybridisation and immunofluorescence experiments, different labels for the probes and fluorescent dyes coupled to antibodies must be combined. Particular attention should be taken to avoid cross-reactivity between antibodies used at different steps. For example, if a mouse antibody is used in detection of the RNA signal, antimouse immunoglobulin antibodies cannot be used either in the detection of the DNA signal or in immunofluorescence. When combining *in situ* hybridization with protein detection, the immunofluorescence is usually performed after the hybridization steps. This is especially important when conjugating RNA and protein detection because primary antibodies used for immunofluorescence are often contaminated with RNases, resulting in a significant decrease of the RNA signal. However, some epitopes are no longer recognised by the antibodies after incubation of the cells with formamide, especially after a denaturation step. In this case, immunofluorescence must be performed first and the signal fixed before hybridization. An important control to guarantee that the pattern of the antibody labelling is not changed by formamide is to stain cells using standard immunofluorescence conditions and to compare the pattern with the one obtained after RNA or DNA hybridization. The methods presented here were partly adapted from an original protocol reported by Zirbel *et al*., (1993). The pepsin treatment was introduced for the specific detection of splice junctions on nascent RNA transcripts in the nucleus (Wijgerde *et al*., 1995).

V. PITFALLS

Appropriate negative controls are essential to distinguish specific signals from fluorescent noise due to unspecific hybridization. For RNA hybridization the best control is to use cells that do not transcribe the target RNA. To overcome unspecific hybridisation, the stringency of the hybridization and posthybridization washes can be increased until no signal is obtained in the negative control cells, but without eliminating the signal in the cells that express the target RNA. If this is not possible, a new probe should be designed and tested in the same way. Control probes are also very important, especially when very small oligonucleotide probes are used. One example is splice junction probes. These probes are designed to hybridise with the last nucleotides of one exon and the first nucleotides of the following exon and to produce a stable hybrid only if the two halves of the probe hybridize. An appropriate control probe should be designed to exclude that only half of the probe is capable of producing a stable hybrid. Other negative controls for RNA hybridization include mock hybridization (no probe in the hybridization mixture) and RNase treatment before hybridization (0.1 mg/ml DNase-free RNase in 2 × SSC at 37°C for 1 h). Additional controls should be performed when using probes that contain plasmid sequences. Namely, the plasmid backbone (without insert) should be labelled and used as a probe. If this produces a signal (which happens frequently if the cells have been transfected with related plasmids), the insert should be isolated from the recombinant plasmid before labelling.

References

Blencowe, B. J., Issner, R., Nickerson, J. A., and Sharp, P. A. (1998). A coactivator of pre-mRNA splicing. *Genes Dev*. **12**, 996–1009.

Collis, P., Antoniou, M., and Grosveld, F. (1990). Definition of the minimal requirements within the β-globin gene and the dominant control region for high level expression. *EMBO J*. **9**, 233–240.

Custódio, N., Carmo-Fonseca, M., Geraghtly, F., Pereira, S. H., Grosveld, F., and Antoniou, M. (1999). Inefficient processing impairs release of RNA from the site of transcription. *EMBO J*. **18**, 2855–2866.

Gall, J. G., and Pardue, M. L. (1969). Formation and detection of RNA-DNA hybrid molecules in cytological preparations. *Proc. Natl. Acad. Sci. USA* **63**, 378–383.

Johnson, C., Primorac, D., McKinstry, M., McNeil, J., Rowe, D., and Lawrence, J. B. (2000). Tracking COL1A1 RNA in osteogenesis imperfecta splice-defective transcripts initiate transport from the gene but are retained within the SC35 domain. *J. Cell Biol*. **150**, 417–432.

Jonh, A., Birnstiel, M. L., and Jones, K. W. (1969). RNA-DNA hybrids at the cytological level. *Nature* **223**, 582–587.

Long, R. M., Elliott, D. J., Stutz, F., Roshbash, M., and Singer, R. H. (1995). Spatial consequences of defective processing of specific

yeast mRNAs revealed by fluorescent in situ hybridisation. *RNA* **1**, 1071–1078.

Schwarzacher, T., and Heslop-Harrison, P. (2000). "Practical in Situ Hybridisation." Bios Scientific, London.

Singer, R. H. (1998). Preparation of probes for in situ hybridisation. *In* "*The Singer Lab Online*": http://singerlab.aecom.yu.edu/protocols/insitu_probe_prep.htm.

Wijgerde, M., Grosveld, F., and Fraser, P. (1995). Transcription complex stability and chromatin dynamics *in vivo*. *Nature* **377**, 209–213.

Xing, Y., Johnson, C. V., Dobner, P. R., and Lawrence, J. B. (1993). Higher level organization of individual gene transcription and RNA splicing. *Science* **259**, 1326–1329.

Xing, Y., Johnson, C. V., Moen, P. T., McNeil, J. A., and Lawrence, J. B. (1995). Non-random gene organization: Structural arrangements of specific pre-mRNA transcription and splicing with SC-35 domains. *J. Cell Biol*. **131**, 1635–1647.

Zirbel, R. M., Mathieu, U. R., Kurz, A., Cremer, T., and Lichter, P. (1993). Evidence for a nuclear compartment of transcription and splicing located at chromosome domain boundaries. *Chrom. Res*. **1**, 93–106.

CHAPTER

45

Fluorescent Visualization of Genomic Structure and DNA Replication at the Single Molecule Level

Ronald Lebofsky and Aaron Bensimon

I. INTRODUCTION

DNA fibre fluorescent *in situ* hybridization (FFSH) techniques provide kilobase resolution for physical mapping, genomic structure, and/or DNA replication analysis at the single molecule level (Caburet *et al.*, 2002; Herrick and Bensimon, 1999). Objectives of DNA fibre preparation are similar for most techniques: (1) a high degree of stretching to obtain optimal resolution, (2) long fibres for long range studies, and (3) sufficient numbers of molecules to enable a population overview. DNA preparation by molecular combing constitutes an important advance in this area (Bensimon *et al.*, 1994). Molecules are stretched uniformly by a constant stretching force regardless of sequence content whereby 1 μm of stretched DNA represents 2 kb. Uniform stretching is important because the arduous task of calibrating each slide or areas within a slide with external controls is not required. Because the stretching force is one order of magnitude less than that needed to break the double helix, molecules that range between hundreds of base pairs to over one megabase are combed. The stretched DNA and molecule length provide a maximal resolution of 1–4 kb over megabase distances. In addition, DNA binding to slides used for molecular combing is very efficient. Tens of thousands of DNA molecules corresponding to between 30 and 100 mammalian genomes are combed per surface. Therefore, population data are obtainable without compromising the sensitivity of single molecule analysis. This article provides all the necessary protocols to set up molecular combing and to carry out physical mapping, genomic structure, and DNA replication studies using combed DNA as a substrate (Anglana *et al.*, 2003; Gad *et al.*, 2002; Herrick *et al.*, 2000; Maho *et al.*, 1999; Monier *et al.*, 1998; Pasero *et al.*, 2002).

II. MATERIALS AND INSTRUMENTATION

7-Octenyltrichlorosilane (539279), hydrogen peroxide solution 35 wt. % in water (H_2O_2) (349887), ammonium hydroxide solution (NH_4OH) (A6899), chloroform (C-5312), 5-bromo-2′-deoxyuridine (BrdU) BrdU (B-9285), 5-chloro-2′-deoxyuridine (CldU) (C-6891), 5-iodo-2′-deoxyuridine (IdU) (I-7125), EDTA (E-9884), sodium dodecyl sulfate (SDS) 10% solution (L-4522), 2-morpholinoethanesulfonic acid (MES) (M-2933), ethanol (EtOH) (E-7023), sodium hydroxide (NaOH) (S-8045), sodium acetate (NaAc) (71183), glacial acetic acid (45726), Hybri slips (Z36,590-4), trizma hydrochloride (Tris) (T-5941), sodium chloride solution (NaCl) 5 M (S-5150), Tween 20 (P-9416), and *N*-lauroylsarcosine sodium salt (L-9150) are from Sigma-Aldrich. The 22 × 22-mm cover glass (coverslip) (2865-22) is from Corning. Miscroscope slides (4951) are from Erie Scientific Company. Plug molds (1703706) are from Bio-Rad. Low melting temperature (LMT) Nusieve agarose (50081) is from Cambrex. Proteinase K (1.24568) is from Merck Biosciences. β agarase I and buffer (M0392S) are from New England Biolabs. Phosphate-buffered saline (PBS) 10× (PBS10X03), TE 1× (TE1X5000), deionized formamide

Copyright 2006, Elsevier Science (USA).
All rights reserved.

(FORMD003), dextran sulfate, sodium salt 50% (w/v) solution (DEXT5100), and SSC 20× (SSC20X02) are from Qbiogene. BioPrime DNA labelling kit (18094011) and human Cot-1 DNA (15279011) are from Invitrogen/Gibco-BRL. DIG High Prime (1585606), blocking reagent (1096176), FITC-conjugated sheep antidigoxigenin Fab fragments (1207741), antidigoxigenin-AP Fab fragments (1093274), antibiotin-AP Fab fragments (1426303), and dig-labelled control DNA (1585738) are from Roche. Herring sperm DNA (D1815) is from Promega. HybChamber mica (HYB-04) is from Genemachines. YOYO-1 iodide (Y3601), streptavidin, Alexa 350 conjugate (S11249), streptavidin, Alexa 488 conjugate (S32354), streptavidin, Alexa 594 conjugate (S32356), streptavidin, Alexa 750 conjugate (S21384), Alexa 350 goat antimouse IgG (A21049), Alexa 350 donkey antigoat IgG (A21081), Alexa 594 donkey antirat (A21209), Alexa 488 goat antimouse (A11029), Alexa 488 donkey antisheep (A11015), and SlowFade light antifade kit (S7461) are from Molecular Probes. Biotin-conjugated rabbit antistreptavidin (200-4695) and FITC-conjugated rabbit antidonkey (616-4202) are from Rockland. Mouse anti-BrdU (347580) and FITC-conjugated mouse anti-BrdU (347583) are from BD Biosciences. Rat anti-BrdU (ab6326) is from Novus Biologicals. Texas red-conjugated donkey antirat (712-075-153) is from Jackson. HybondN+ (82 mm), 50 discs (RPN82B) is from Amersham. Alkaline phosphatase substrate kit IV (SK-5400) is from Vector Laboratories.

The following can be purchased from a local laboratory equipment specialist: argon gas tank, oxygen gas tank, gas hydration device, UV lamp covered with quartz, 1000-µl glass syringe (Hamilton), water baths, rotating wheel, tissue culture incubator, hood for tissue culture, facilities for performing gel electrophoresis, plastic polypropylene jars for slides, tweezers, Kim Wipes, parafilm. Nail polish and Superglue can be bought from a local supermarket.

Teflon reservoirs with a 25 × 25 × 2-mm interior (approximately 1.3 ml volume), ceramic coverslip racks for 12 coverslips each, tubing with appropriate valves, and a treatment vessel for glass silanisation were all custom made at Institut Pasteur.

The combing machine, shown in Fig. 1, must have the following characteristics.

1. Coverslip holders that grip the silanised surface by an edge.
2. The capability to quickly descend the coverslip holders so that the coverslip is inserted into a combing reservoir.
3. The capability to lift the coverslip holders so that the coverslip is removed from the reservoir at a constant speed of 300 µm/s.

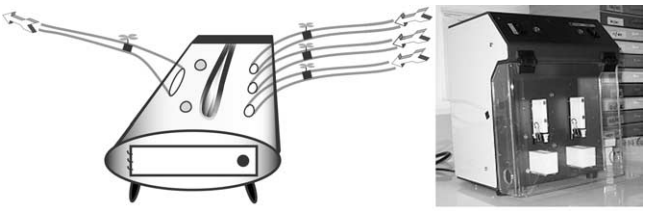

FIGURE 1 (A) The schematic of a glass treatment vessel shows all the required components: housing for a quartz-covered UV lamp, three tube entrances for pressurised gas flow, one tube exit, appropriate tubing and valves, entry ports along the roof of the vessel to inject silane via a syringe, and a door to introduce and remove racks of glass coverslips. (B) This combing machine, which can comb two coverslips at a time from two different reservoirs, is currently used at Institut Pasteur.

Fluorescent signals were examined with a Zeiss Axioplan 2 microscope equipped with a 75-W xenon arc lamp. Filter sets consisting of excitation, emission, and dichroic filters are from Omega Optical: XF03 for blue, XF100-2 for green, XF102-2 for red, and XF143-2 for infrared. Photos were taken using Smartcapture 2 software and a Photometrics HQ Coolsnap CCD camera. The optical capabilities of any other chosen hardware should be at least equal to the aforementioned system, as resolution and sensitivity must be optimal for single DNA molecule visualisation. An inverted microscope, a Zeiss Axiovert equipped with a xenon arc lamp and filters for green fluorescence, was used for DNA combing quality control. See Section IV,E for why this is used rather than an upright microscope.

III. PROCEDURES

A. Coverslip Silanisation for Molecular Combing

Solution

Pirana solution: Add 390 ml of NH_4OH and 360 ml of H_2O_2 immediately prior to each round of slide preparation.

Steps

1. Work in a fume hood.
2. Distribute seventy-two 22 × 22-mm coverslips into six ceramic racks.
3. To clean the surface, place racks with coverslips into the pirana solution and leave for 2 h.
4. Briefly rinse the coverslips three times with sterile ddH_2O.

5. Dry coverslips and racks with a stream of oxygen.
6. Place the racks in the treatment vessel.
7. Place one small aluminium pocket (holds less than 1 ml) next to each pair of ceramic racks.
8. Close the vessel, rendering it airtight.
9. Open the exit valve.
10. Fill the vessel with oxygen by (1) administering a flow of oxygen at a rate of 15 litre/min for 1 min, (2) applying an 8 litre/min flow for 5 min, and (3) reducing the flow to 0.160 litre/min. Keep this flow constant for the duration of the following step.
11. Cover the vessel with aluminium and turn on UV lamp for 1 h. UV converts oxygen to ozone, which helps cleanse the glass further.
12. Remove ozone by flushing vessel with a 2 litre/min flow of inert argon.
13. Apply an argon flow that is hydrated by 10% at a rate of 1 litre/min for 20 min.
14. Close all entry and exit valves. Allow hydration to continue for 10 min in the closed vessel.
15. Open the exit valve. Remove excess water vapour with a 0.9 litre/min flow of argon.
16. Using a syringe, inject 150 µl of 7-octenyltrichlorosilane into the vessel through the small ports by dispensing 50 µl into each aluminium pocket.
17. When finished, rinse the syringe three times with chloroform and then three times in 100% ethanol.
18. Shut off the argon flow and allow the pressure in the vessel to return to zero.
19. Close all valves. The silane will begin to vaporise naturally. Let this process occur overnight. This gas silanises the glass coverslips.
20. The following day, open the exit valve and rinse the vessel with an 8 litre/min argon flow for 5 min.
21. Open the vessel, remove the racks, and allow the slides to dry for 1 h at room temperature.
22. Store coverslips with aluminium wrapping in a dust-free environment.

B. Preparing High Molecular Weight DNA in Agarose Blocks

Solutions

1. *NaOH 30% (w/v)*: Dissolve 15 g of NaOH in 40 ml of ddH_2O. Bring the total volume to 50 ml.

2. *0.5 M EDTA, pH 8*: To make 1 litre, dissolve 186.12 g of EDTA in 900 ml of ddH_2O. Adjust the pH to 8 by adding NaOH 30% (w/v). Add ddH_2O for a final volume of 1 litre.

3. *1× PBS*: Add 900 ml of ddH_2O to 100 ml of 10× PBS to make 1 litre.

4. *1% LMT agarose*: Prepare 50 ml by adding 0.5 g to 50 ml of 1× PBS. Heat and mix to dissolve the agarose. Store at 4°C.

5. *10 mg/ml proteinase K stock*: Dissolve 500 mg of proteinase K in 50 ml of 0.5 *M* EDTA, pH 8. Make 1-ml aliquots and store at –20°C.

6. *Proteinase K digestion (PKD) solution*: *2 mg/ml proteinase K, 1% SDS, and 100 mM EDTA.* On the day of cell harvesting for DNA extraction, prepare 5 ml of PKD by adding a thawed 1-ml aliquot of proteinase K stock and 0.5 ml of 10% SDS to 3.5 ml of ddH_2O. Vortex. This is sufficient for 20 agarose blocks. Adjust the amount accordingly.

Steps

1. Prechill 50 ml of sterile 1× PBS in an ice bucket.
2. Turn on a 37°C water bath in the laboratory.
3. Melt LMT agarose in microwave and leave molten in 50°C water bath.
4. Preheat PKD solution at 50°C.
5. Cover bottom of plug molds with tape.
6. In tissue culture, harvest cells and collect pellet according to cell type and laboratory protocols.
7. Take off supernatant.
8. Resuspend cells in ice cold 1× PBS so that there are 250,000 cells/50 µl, i.e., for 2 million cells, resuspend in 400 µl of 1× PBS. Leave on ice until all samples have been resuspended in appropriate volumes.
9. Put cell suspension in 37°C water bath for 5 min.
10. Add an equal volume of 50°C molten LMT agarose and mix gently but thoroughly with a pipette.
11. Fill plug molds with cell/agarose mix (approximately 90 µl per plug).
12. Put the mold at 4°C for 20 min to allow blocks to solidify.
13. Eject plugs and add adequate amounts of the preheated PKD solution so that there is a minimum of 250 µl per block.
14. Leave overnight at 50°C to allow for deproteination of DNA.
15. The following day, remove the proteinase K digestion solution and replace it with 10 ml of 500 m*M* EDTA, pH 8.0. Blocks can be stored indefinitely at 4°C.

C. Labeling DNA for Replication Studies

Solutions

1. *1× PBS*: see Section III,B.

2. *10 mM CldU stock*: Dissolve 262.7 mg of CldU in 100 ml of 1× PBS. Make 2-ml aliquots and store indefinitely at –20°C.

3. *10 mM IdU stock*: Dissolve 354.1 mg of IdU in 100 ml of 1× PBS and store indefinitely at 4°C

4. *Media with 100 μM CldU/IdU (for adherent cell cultures)*: On the day of the experiment, prepare tissue culture tubes with a volume of media that corresponds to the size of the tissue culture flask. Add appropriate volume of CldU stock to make a 100 μ*M* final concentration, i.e., for a T75 flask, add 150 μl of CldU stock to 15 ml of media. Repeat with IdU. After addition, mix the media well and keep at 37°C in close proximity to the tissue culture hood.

1. Adherent Cell Cultures

Steps

1. Carry out steps 1–5 in Section III/B prior to the following.
2. Preheat a nucleotide-free media bottle in the same 37°C waterbath as media/CldU and media/IdU mixes.
3. Aspirate off media from the cell culture.
4. Add media/IdU mix and restore flask to 37°C incubator. Start a timer.
5. At t = 30 min, aspirate media/IdU and wash cells three times with warm nucleotide-free media as quickly as possible.
6. Add media/CldU mix and put the flask back in the 37°C incubator.
7. At t = 60 min, aspirate media/CldU mix.
8. Go step 6 in Section III,B and complete that protocol.

Suspension Cell Cultures

Steps

1. Carry out steps 1–5 in Section III/B prior to the following.
2. In a 37°C water bath with easy access to a tissue culture hood, warm a sufficient quantity of IdU and CldU to produce a 100 μ*M* final concentration of the cell culture volume, i.e., for a T75 containing 15 ml of cell suspension, warm 150 μl of IdU and CldU each.
3. To an exponentially dividing cell culture add warm IdU stock so that final concentration is 100 μ*M*.
4. Mix gently with a pipette and restore to 37°C incubator. Start the timer.
5. At t = 30 min, add warm CldU stock so that final concentration is 100 μ*M*.
6. Mix gently with a pipette and put back in 37°C incubator.
7. At t = 60 min, go step 6 in Section III,B and complete that protocol.

D. Putting DNA in Solution, Ready for Combing

Solutions

1. *NaOH 30% (w/v)*: see Section III,B.
2. *Combing buffer, 0.5 M MES, pH 5.5*: For 250 ml, dissolve 24.4 g of MES in 225 ml of sterile ddH_2O. Adjust the pH to 5.5 using NaOH 30% (w/v). Bring the final volume to 250 ml with sterile ddH_2O. Autoclave and store at room temperature.
3. *YOYO-1/TE mix*: On the day of the experiment, for each block to be prepared dilute 1 μl of YOYO-1 stock in 200 μl of TE. Scale according to how many agarose blocks are to be used. Keep in the dark at room temperature.
4. *10× β agarase buffer*: Included with β agarase enzyme

Steps

1. Remove one agarose block containing DNA from EDTA storage buffer and put in a 50-ml sterile tube (for DNA replication studies, see Section IV,E).
2. To remove residual proteinase K and SDS, wash five times in 50 ml TE on a rotating wheel.
3. Transfer agarose block to a sterile round-bottom 2-ml Eppendorf tube.
4. To stain DNA, add the YOYO-1/TE mix (200 μl) and leave sit at room temperature for 1 h in the dark.
5. Transfer block to sterile 15 ml and remove excess YOYO-1 by washing twice in 10 ml of TE on a rotating wheel protected from light.
6. Put the block in a new round-bottom 2-ml Eppendorf tube and add 200 μl of TE.
7. Heat the block at 69°C for 20 min to melt the LMT agarose.
8. Reduce temperature by putting the Eppendorf tube in a 42°C water bath for 10 min.
9. Warm the 10× β agarase buffer to 42°C during this period.
10. Add 30 μl of 10× β agarase buffer to the molten agarose/DNA mix, put back at 42°C, and wait for 5 min to allow the buffer to diffuse.
11. To digest agarose, add 1.5 μl of β agarase and incubate overnight at 42°C.
12. The following day, slowly add 900 μl of MES combing buffer to the DNA solution.
13. Put back in the 42°C water bath and allow the solution to mix for one 1 h.
14. Gently pour the DNA solution in a Teflon combing reservoir.
15. Add MES buffer so that the DNA solution nearly fills the reservoir.
16. Store DNA solution at room temperature in the dark for up to 1 month.

17. Once the DNA solution is in the reservoir, prevent evaporation when not combing by covering with Parafilm.
18. When finished with a DNA solution, empty and clean combing reservoir by boiling for 45 min in ddH_2O.

E. Molecular Combing

Steps

1. Place a silanised surface in the coverslip holder attached to the combing machine.
2. Let the machine lower the coverslip into the combing reservoir that contains the DNA to be combed.
3. Wait 5 min to allow DNA free ends to bind to the surface.
4. Release the ascent function of the combing machine to remove the coverslip. During removal, the meniscus moving along the hydrophobic surface is combing the DNA.
5. With an inverted microscope, visualise the YOYO-1 stained DNA as a combing quality check.
6. Bake the combed DNA at 65°C overnight with the surface untouched by the inverted microscope facing up.
7. Use Superglue to stick the coverslip to a slide and store at –20°C (see Fig. 2).

F. Labeling Probes with Biotin and/or Digoxigenin

1. Probe Labeling with Biotin-16-dUTP

Steps

1. All components are included in the BioPrime DNA labelling kit. Thaw components and keep on ice.
2. Add sterile ddH_2O to 500 ng of template DNA to a final volume of 24 µl.
3. Add 20 µl of 2.5× random primers and boil for 10 min to denature DNA.
4. Quickly place tubes on ice for 10 min.
5. Vortex and spin briefly.
6. Add 5 µl of 10× dNTPs (includes biotin-16-dUTP) and 1 µl of Klenow enzyme. Mix thoroughly with a pipette and spin to collect the reaction mix.

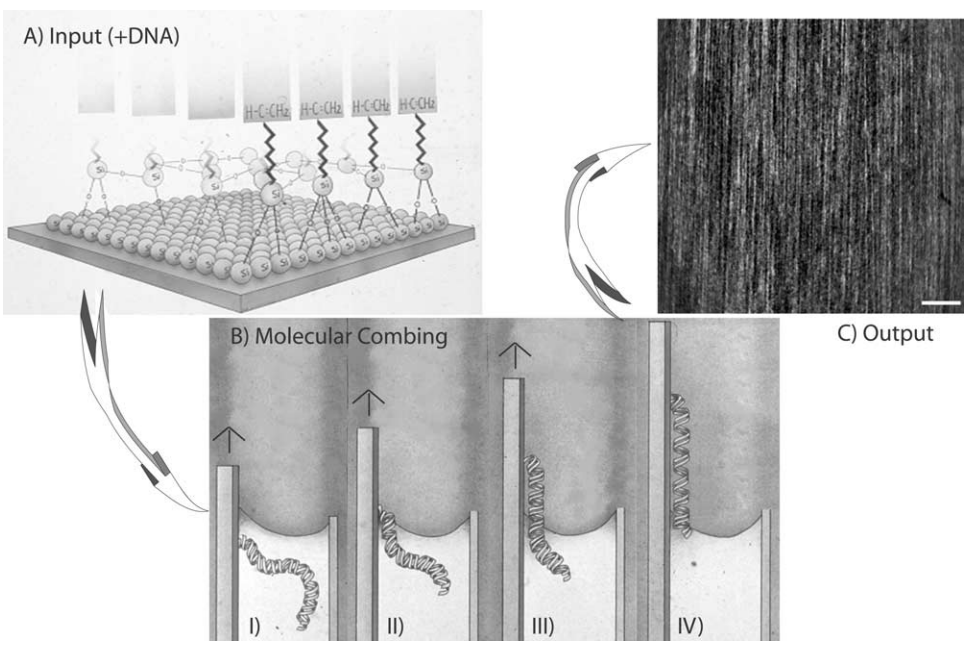

FIGURE 2 At the core of molecular combing is the silanised coverslip (A). An organic monolayer is covalently attached to inorganic glass via Si groups. At the terminal end of the carbon chains reside vinyl groups. It is a combination of the hydrophobic nature of the silanised glass and the terminal vinyl groups, which allow all the following processes of molecular combing to occur (B). DNA in solution attach to the coverslip by a free-end only (I). As the coverslip is removed from the reservoir, a meniscus is formed due to the interaction between the hydrophobic surface and the liquid DNA solution (II). This meniscus provides a constant force along the length of the DNA that yields evenly stretched molecules irrespective of sequence content (III). When the DNA is completely removed from the reservoir, it is immobilised in its stretched form (IV). The end product is a surface that is coated by stretched single DNA molecules (C). Bar: 20 µm.

7. Incubate at 37°C overnight. Once completed, store at –20°C.

2. Probe Labeling with Digoxigenin-11-dUTP

Steps

1. The Dig High Prime kit contains all the necessary components. Thaw components and keep on ice.
2. Add 1 µg of template DNA and sterile ddH_2O to a final volume of 16 µl.
3. Denature DNA by boiling for 10 min.
4. Chill on ice for a further 10 min.
5. Add 4 µl of Dig High Prime solution that contains random primers, dNTPs including digoxigenin-11-dUTP, and Klenow enzyme. Mix well with a pipette and spin quickly to collect the reaction mix.
6. Incubate at 37°C overnight. Once completed, store at –20°C.

G. Slide Preparation for Hybridization and/or Fluorescent Detection of DNA Replication

Solutions

1. *1× PBS*: See Section III,B. Keep at 4°C.
2. *1 M NaOH*: For 50 ml, dissolve 2 g of NaOH in 50 ml of sterile ddH_2O. Keep at room temperature and replace every 2 weeks.
3. *70, 90, and 100% ethanol (EtOH) dilution series*: Keep at –20°C

Steps

1. Remove slides to be used from –20°C and leave at room temperature for 1 h.
2. Place slides in 1 *M* NaOH for 30 min to denature combed DNA.
3. Rinse three times in 1× PBS from 4°C fridge and once for 3 min to neutralise the NaOH.
4. To help fix DNA, put slides through 70, 90, and 100% EtOH series for 5 min at each dilution.
5. Remove excess EtOH with a Kim Wipe and air dry at room temperature. Use slides immediately once dried (go to Section III,H step 11 or, if only detecting replication, proceed directly to fluorescent detection protocols and use Table No. 5 in Table I).

H. Hybridization and Posthybridization Washes

Solutions

1. *3 M NaAc, pH 5.2*: For 1 litre, add 246.1 g of NaAc to 800 ml of sterile ddH_2O and adjust pH to 5.2 using glacial acetic acid. Bring volume to 1 litre, autoclave, and store at room temperature.

TABLE I Probes, Labels, and Detection[a]

1. Dig and Biot probes and two replication labels: Four colour detection

Layers→	1	2	3	4
Dig (GR)	shαdigF	dαsh488		
Biot (IR)	SAV750	rbαSAVB	SAV750	
IdU (BL)			mαBrdU	gαm350
CldU (RD)			rαBrdU	dαrTR

2. Biot probes, two replication labels: Three colour detection

Layers→	1	2	3
Biot (GR)	SAV488	rbαSAVB	SAV488
IdU (BL)	mαBrdU	gαm350	dαg350
CldU (RD)	rαBrdU	dαrTR	

3. Dig and Biot probes, one replication label: Three colour detection

Layers→	1	2	3
Dig (GR)	shαdigF	dαsh488	
Biot (BL)	SAV350	rbαSAVB	SAV350
CldU (RD)	rαBrdU	dαrTR	

4. Dig and Biot probes: Two colour detection

Layers→	1	2	3
Dig (GR)	shαdigF	dαsh488	rbαdF
Biot (RD)	SAV594	rbαSAVB	SAV594

5. Two replication labels: Two colour detection

Layers→	1	2
IdU (GR)	mαBrdUF	gαm488
CldU (RD)	rαBrdU	dαr594

[a] Fluorophores or biotin conjugated to an antibody is represented by their symbol following the antibody abbreviation. Biot, biotin-labelled probe; Dig, digoxigenin-labelled probed; BL, blue; GR, green; RD, red; IR, infrared; α, anti; m, mouse; r, rat; rb, rabbit; g, goat; sh, sheep; d, donkey; SAV, streptavidin; 350, Alexafluor 350; 488, Alexafluor 488; 594, Alexafluor 594; 750, Alexafluor 750; TR, Texas red; F, FITC; and B, biotinylated.

2. *100% ethanol at –20°C*
3. *Hybridisation buffer: 50% formamide, 10% w/v dextran sulfate, 2XSSC, and 0.1% SDS.* To make 1 ml, add 500 µl of formamide, 200 µl of 50% dextran sulfate solution, 100 µl of 20× SSC, and 10 µl of 10% SDS solution to 190 µl sterile ddH_2O. Store at –20°C for up to one month.
4. *50% formamide/2× SSC*: For 1 litre, dilute 100 ml of 20× SSC in 400 ml sterile ddH_2O. To this add 500 ml of formamide. Solution can be stored in dark at 4°C for 1 month.

5. *2× SSC*: For 1 litre, add 100 ml of 20× SSC to 900 ml of sterile ddH_2O

Steps

1. Chill to 4°C a centrifuge for 1.5-ml Eppendorfs that can reach a speed of 15,000 rpm.
2. In a 1.5-ml Eppendorf add 1 µg of each probe, 5× the total probe amount of human 1× cot DNA, and 1 µl of herring sperm stock. Bring to a final volume of 50 µl with sterile ddH_2O. Vortex and centrifuge briefly.
3. To precipitate DNA, add 5 µl of 3 *M* NaAc, pH 5.2, and 150 µl of –20°C EtOH. Vortex and spin.
4. Put at –80°C for 30 min to complete precipitation.
5. Spin at 15,000 rpm in the 4°C chilled centrifuge for 30 min to pellet the DNA.
6. Remove the supernatant, not touching the white pellet, and air dry.
7. Once the pellet starts to turn translucent, add 25 µl of hybridisation buffer.
8. Vortex for 20 s to thoroughly mix. Spin briefly.
9. Place Eppendorf in boiling water for 5 min to denature DNA.
10. Immediately place in ice water for 10 min. Probes are ready for hybridisation.
11. Take slide from Section III,G step 5. Place probe/hybridisation mix on surface and cover with a Hybri-slip (light-weight plastic coverslip).
12. Place the slide in the HybChamber and add 50 µl of 2× SSC to the reservoir to prevent evaporation of the probe during incubation.
13. Close the HybChamber and incubate overnight at 42°C.
14. The following day remove 50% formamide/2× SSC from 4°C and leave at room temperature for 1 h.
15. Remove the slide from the HybChamber and carefully displace the Hybri-slip with tweezers.
16. In a fume hood, wash three times in 50% formamide/2× SSC 5 min each.
17. Wash three times in 2× SSC for 3 min each. Slides are ready for detection with fluorescent antibodies.

I. Detection with Fluorescent Antibodies

Solutions

1. *1× PBS*: See Section III,B and make 1 litre
2. *1× PBS 0.05% Tween 20*: For 1 litre, add 500 µl of Tween 20 to 1 litre of 1× PBS. Store at room temperature indefinitely.
3. *Detection buffer: Blocking reagent 1% (w/v) in 1× PBS 0.05% Tween 20*. For 100 ml, dissolve 1 g of blocking reagent in 100 ml 1× PBS 0.05% Tween 20 by heating and mixing alternatively. Autoclave and store 1-ml aliquots at –20°C.
4. *Antibody stocks*: All antibodies are prepared and stored according to the manufacturer's instructions. When received in powder format and where instructions are not indicated, dissolve antibodies in 1× PBS to give a concentration of 2 mg/ml. Store these diluted antibodies at –20°C in single-use aliquots.

Steps

The following steps are repeated for each layer (except for step 9 which ends the detection). Refer to Table 1 for antibodies used to detect replication and/or probes.

1. Immediately prior to use, thaw antibody aliquots, mix with a pipette, and spin briefly.
2. Dilute 1 µl of each antibody used for a layer in 25 µl of detection buffer. The only exception to this rule is mouse anti-BrdU (FITC), which is diluted 5:25.
3. Mix antibody mix with a pipette and spin briefly.
4. Place the antibody mix on the surface and cover with a glass coverslip.
5. Put in a humid chamber and leave at 37°C for 30 min. The only exception is the primary antibody layer to detect CldU and/or IdU, which is carried out at 37°C for 1 h.
6. Gently remove the coverslip by giving the slide a shake.
7. Wash slides three times in 1× PBS 5 min each.
8. Proceed to the next layer.
9. When finished washing the final layer, mount slides in Slowfade Light antifade mounting media and seal with nail polish (Fig. 3).

IV. COMMENTS AND PITFALLS

A. Coverslip Silanisation for Molecular Combing

1. DNA binding, a constant stretching force, the immobilisation of DNA, and its availability for further manipulation are all critically dependent on optimal glass silanisation. If the various cleaning steps (pirana, ozone) are not carried out properly, irregularities on the glass may cause poor silanisation. Furthermore, before putting the coverslips in the reaction vessel, slides must be completely dry, as wetness may also cause heterogeneous silanisation. When opening the ports for the syringe containing the silane, care must be taken to be as quick as possible, as contamination of the vessel by the surrounding air can affect the silanisation process.

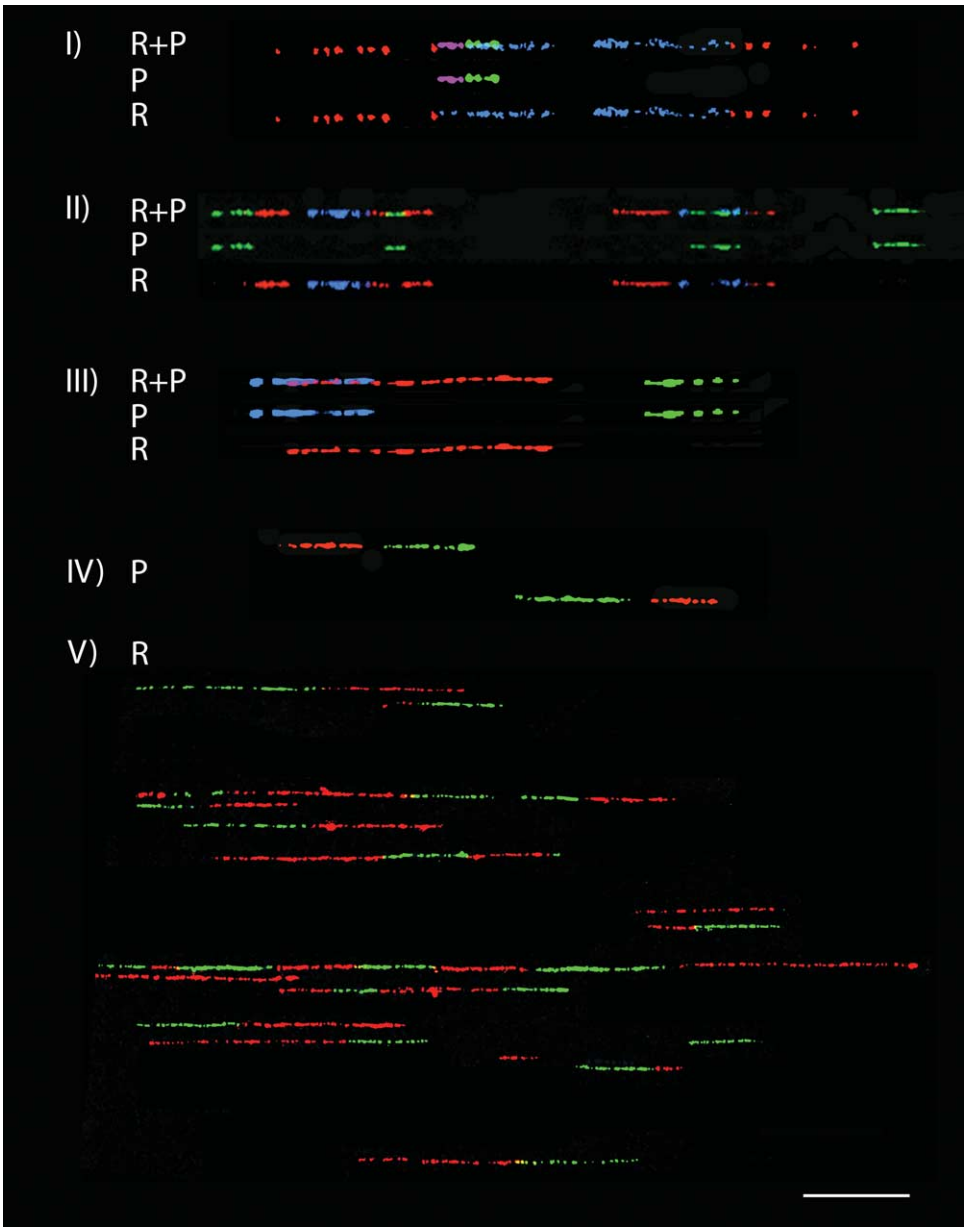

FIGURE 3 Results from all detection schemes. The first molecule in the triad found in I, II, and III are probes (P) and replication (R) together. This molecule has been decomposed digitally to provide probe and replication signals only (we have done this because looking at P + R together can be confusing). In IV, two probe sets on different molecules with different orientation are provided as they were found on the same field of view. A typical field of view with the 40× objective of DNA replication using the paradigm outlined in this article is shown (V). See Table I for details on what colours represent. Bar: 25 µm.

2. The materials used for coverslip preparation have been chosen because they are easy to clean and are chemically inert.

B. Preparing High Molecular Weight DNA in Agarose Blocks

1. The protocol given is for mammalian tissue culture cells only (for yeast, see Lengronne *et al.*, 2001).

2. In step 9, putting the cell suspension at 37°C for 5 min is required to raise the temperature sufficiently so that upon addition of molten agarose the agarose will not solidify before dispensing into blocks.

C. Labeling DNA for Replication Studies

1. Yeast DNA can be labelled by using a specific strain and some modified protocols (Lengronne *et al.*, 2001).

2. DNA replication protocols provided are for double labelling DNA from an asynchronous population of cells. Data obtainable from this type of labelling paradigm are origin position (when a region is localised using fluorescent hybridisation), interorigin distance, timing of firing of neighbouring origins, fork speed, and obstacles to fork progression (Anglana *et al.*, 2003). Time of labelling and synchronisation can be personalised according to needs.

3. It can be difficult to dissolve IdU and CldU in 1× PBS. The manufacturer recommends a basic solvent; however, addition of 1× PBS to cell culture when labelling cells is much less harsh to cells. Vortex and heat to 37°C to fully dissolve the nucleotides in 1× PBS.

4. When preparing for an experiment, only heat the correct amount of IdU and CldU to avoid degradation of the stock.

5. When mixing IdU and CldU with a suspension cell culture, mix well to evenly disperse the nucleotide. Do not mix with too much vigour so as not to break the cell–cell attachments with which many suspension cultures form and need to grow. In this way cells are not shocked during labelling and will proceed normally through S phase, providing robust DNA replication results.

6. It is important to be efficient when carrying out all steps after $t = 0$, as tardiness can affect the time of nucleotide incorporation and, therefore, how interpretable results are.

D. Putting DNA in Solution, Ready for Combing

1. Optimal DNA binding to the slides is achieved at pH 5.5 (Allemand *et al.*, 1997). Precision in combing buffer preparation is needed.

2. If sediment forms during MES preparation, filter the buffer using a sterile syringe and a 0.2-μ*m* filter. Store the MES combing solution at room temperature.

3. When preparing DNA with replication labels, protect from light whenever possible, i.e., wrap the tube in aluminium when washing out proteinase K and SDS. Labeled DNA is sensitive to light and omission of light protection can lead to shorter molecules.

4. Once the agarose has been melted, DNA is no longer protected from physical agitation. To attain the highest molecular weight DNA possible, avoid knocking the tube, handling it violently, or adding any solutions by a pipette quickly.

5. When adding the β agarase buffer or the β agarase itself, do not vortex or mix with a pipette as this will greatly shear the DNA. Allow the buffer and enzyme to naturally diffuse throughout the molten agarose/DNA mix.

6. It is critical that MES buffer is added as slowly as possible, as the currents generated are known to break DNA.

7. Teflon reservoirs are used because they do not absorb DNA and are easy to clean.

E. Molecular Combing

1. The combing machine needs to remove the coverslip at a constant rate of 300 μm/s. This speed generates the constant perpendicular force of the meniscus that aligns and stretches the DNA. Because it is not greater than the force needed to break the double helix, the combing process in itself is not responsible for short DNA molecules. Nonsterile materials at any step during DNA preparation and excessive physical agitation are the principal causes for DNA shearing. Avoid both whenever possible to attain the longest possible length of combed DNA.

2. When visualising the combed DNA under a microscope, an inverted microscope is preferred, as only one side is dirtied. The other side is preserved for use in hybridisation and fluorescent detection.

3. The density of combed DNA is a function of the concentration of the DNA solution. The 250,000 genomes that are used per combing solution yield approximately 100 genomes per 22 × 22-mm surface. This is an optimal combing density for physical mapping and genomic structure studies, as a maximum number of probes can be scored with one slide. For DNA replication studies, however, a lower combing density is required to minimise the occurrence of overlapping replication signals that can confuse results. This is achieved by starting with only one-third to one-half of an agarose block when preparing DNA. The approximately 100,000 genomes provide an optimal combing density for DNA replication studies corresponding to about 30 genomes per 22 × 22-mm surface.

4. Combing density can be increased slightly by repeatedly combing on the same slide and decreased by reducing the incubation time prior to removing the coverslip. However, more or less agarose blocks can equally be reprepared to suit the researcher's needs.

F. Labeling Probes with Biotin and/or Digoxigenin

1. Because maximal resolution on combed DNA is 1–4 kb, it is not recommended to use probes smaller than 4 kb. Aside from this, there are essentially no limits as to what is selected as a probe, i.e., PCR product, cosmid, BAC, and/or YAC.

2. Holes may appear in the hybridisation signal when repeats are covered with competitor Cot DNA

(included in the hybridisation mix). A 20% repeat content for the probe is acceptable and attempts should be made to not exceed this value.

3. To estimate probe concentration and to quickly determine whether random primed labelling worked, run an electrophoretic gel. Compare band intensity to control DNA ladders to estimate the concentration of DNA products. Reaction products should appear between a few hundred to a couple thousand base pairs. If bands appear near the size of the DNA template, the random primed labelling did not work.

4. Poor hybridisation signals can be due to a low amount of biotin and digoxigenin hapten incorporation during random primed labelling. To check for probe labelling, on a Hybond N+ membrane, spot 1 µl of a probe dilution series next to a similar dilution series of control biotin/digoxigenin DNA (biotin control DNA is included in the BioPrime kit). Incubate with sheep antibiotin/digoxigenin alkaline phosphatase. Use NBT/BCIP components in the alkaline phosphatase substrate kit IV to visualise spots. Probes are well labelled if the spot intensity is similar to that of the control DNA.

G. Slide Preparation for Hybridization and/or Fluorescent Detection of DNA Replication

1. When denaturating DNA on a slide and fixating DNA, fill a plastic polypropylene jar for slides with 50 ml of the corresponding solutions. These jars and this volume are used for any of the slide washings in all protocols listed in this article.

2. If carrying out hybridisation on combed DNA, probe and slide preparation should be timed so that they are both ready for use at the same time. To help ensure that this is achieved, step 5 in Section III,G should coincide with step 10 in Section III,H. If slides are initially put at room temperature and if both protocols proceed according to the times indicated this will happen. If there is a time difference in the two preparations, it is not recommended to shorten incubation or procedure times. If the probes are being prepared more quickly than the slides, they can be left at –80°C, centrifuged, and/or left sitting in the hybridisation buffer for longer times. If slide preparation is proceeding faster than expected, slides can be left at room temperature and/or fixed in EtOH for longer periods of time.

H. Hybridization and Posthybridization Washes

1. The advantage of including dextran sulfate in the hybridisation buffer is to increase the hybridisation efficiency of the probe. However, this additive can result in large fluorescent background spots that may obscure signals on the slide. The background level can vary from slide to slide and it is the decision of the researcher as to whether the noise is tolerable. An optional hybridisation buffer containing 50% formamide, 33% detection buffer, 10 m*M* NaCl, 0.5% SDS, and 0.5% *N*-lauroyl sarcosyl was developed to overcome this problem. Because there is no dextran sulfate, large fluorescent background spots are absent from the slide but hybridisation is less efficient. Proteins and higher concentrations of detergents are included to prevent nonspecific binding of the probe to the slide, thereby increasing its availability for hybridisation. This buffer has been used successfully and it is once again the researcher's decision as to whether this option is suitable.

2. The hybridisation temperature of 42°C is standard for hybridising probes on combed DNA. However, the temperature can be tailored to successfully hybridise various probes of different size and sequence content.

I. Detection with Fluorescent Antibodies

1. The antibodies have been chosen according to their specificity and sufficient signal brightness on single DNA molecules. Antibodies that have been added or substituted in the various schemes will improve the brightness of the signal. However, they are only compatible with the antibodies for a given detection scheme.

2. The green signal in all schemes has been designed to provide enough brightness so that it can be found using the oculars on the microscope. Use the FITC filter to find signals and then take pictures using the camera with the relevant filters to reveal all fluorophore signals.

3. The stringency of the washing buffer can be increased by washing with 2× SSC 0.05% Tween 20 instead of 1× PBS after each layer. This helps remove nonspecifically bound antibody and, therefore, reduces the background, although true signal intensity is also decreased slightly. If signals are considered not very bright, it is recommended to continue using 1× PBS for washes.

Acknowledgment

Ronald Lebofsky is supported by the Natural Sciences and Engineering Council of Canada.

References

Allemand, J.F., Bensimon, D., Jullien, L., Bensimon, A., and Croquette, V. (1997). pH-dependent specific binding and combing of DNA. *Biophys. J.* **73,** 2064–2070.

Anglana, M., Apiou, F., Bensimon, A., and Debatisse, M. (2003). Dynamics of DNA replication in mammalian somatic cells: nucleotide pool modulates origin choice and interorigin spacing. *Cell* **114,** 385–394.

Bensimon, A., Simon, A., Chiffaudel, A., Croquette, V., Heslot, F., and Bensimon, D. (1994). Alignment and sensitive detection of DNA by a moving interface. *Science* **265,** 2096–2098.

Caburet, S., Conti, C., and Bensimon, A. (2002). Combing the genome for genomic instability. *Trends Biotechnol.* **20,** 344–350.

Gad, S., Caux-Moncoutier, V., Pages-Berhouet, S., Gauthier-Villars, M., Coupier, I., Pujol, P., Frenay, M., Gilbert, B., Maugard, C., Bignon, Y.J., Chevrier, A., Rossi, A., Fricker, J.P., Nguyen, T.D., Demange, L., Aurias, A., Bensimon, A., and Stoppa-Lyonnet, D. (2002). Significant contribution of large BRCA1 gene rearrangements in 120 French breast and ovarian cancer families. *Oncogene* **21,** 6841–6847.

Herrick, J. and Bensimon, A. (1999). Imaging of single DNA molecule: applications to high-resolution genomic studies. *Chromosome Res.* **7,** 409–423.

Herrick, J., Stanislawski, P., Hyrien, O., and Bensimon, A. (2000). Replication fork density increases during DNA synthesis in X. laevis egg extracts. *J. Mol. Biol.* **300,** 1133–1142.

Lengronne, A., Pasero, P., Bensimon, A., and Schwob, E. (2001). Monitoring S phase progression globally and locally using BrdU incorporation in TK(+) yeast strains. *Nucleic Acids Res.* **29,** 1433–1442.

Maho, A., Bensimon, A., Vassart, G., and Parmentier, M. (1999). Mapping of the CCXCR1, CX3CR1, CCBP2, and CCR9 genes to the CCR cluster within the 3p21.3 region of the human genome. *Cytogenet. Cell Genet.* **87**, 265–268.

Michalet, X., Ekong, R., Fougerousse, F., Rousseaux, S., Schurra, C., Hornigold, N., van Slegtenhorst, M., Wolfe, J., Povey, S., Beckmann, J.S., and Bensimon, A. (1997). Dynamic molecular combing: stretching the whole human genome for high-resolution studies. *Science* **277,** 1518–1523.

Monier, K., Michalet, X., Lamartine, J., Schurra, C., Heitzmann, F., Yin, L., Cinti, R., Sylla, B.S., Creaven, M., Porta, G., Vourc'h, C., Robert-Nicoud, M., Bensimon, A., and Romeo, G. (1998). High-resolution mapping of the X-linked lymphoproliferative syndrome region by FISH on combed DNA. *Cytogenet. Cell. Genet.* **81,** 259–264.

Pasero, P., Bensimon, A., and Schwob, E. (2002). Single-molecule analysis reveals clustering and epigenetic regulation of replication origins at the yeast rDNA locus. *Genes Dev.* **16,** 2479–2484.

PART

G

GENOMICS

SECTION

16

Genomics

CHAPTER

46

Genomic DNA Microarray for Comparative Genomic Hybridization

Antoine M. Snijders, Richard Segraves, Stephanie Blackwood, Daniel Pinkel, and Donna G. Albertson

I. INTRODUCTION

DNA copy number aberrations are characteristic of many human cancers as well as developmental abnormalities. Array comparative genomic hybridization (CGH) can be used to quantitatively and precisely detect these DNA copy number aberrations (Solinas-Toldo *et al.*, 1997; Pinkel *et al.*, 1997). Bacterial artificial chromosome (BAC) clones have proven to yield sufficient signal intensity after hybridization to detect low-level DNA copy number aberrations as well as high-level amplifications (Snijders *et al.*, 2001). Also, when BAC clones are used that are mapped onto the sequence of the human genome, one can link aberrations directly onto the sequence.

However, because BAC clones are single copy vectors, their yield from a bacterial culture is relatively low, making it tedious to produce sufficient quantities of BAC DNA necessary to quantitatively detect DNA copy number aberrations. In addition, reliably depositing high molecular weight BAC DNA can be challenging due to the viscosity of the printing solution caused by the high concentration of the high molecular weight BAC DNA.

This article describes a polymerase chain reaction (PCR)-based method (Klein *et al.*, 1999) for producing large quantities of BAC DNA, which aims at maximizing the representation of each BAC (Snijders *et al.*, 2001). An overview of the procedure is shown in Fig. 1. In short, BAC DNA is cut with a frequently cutting restriction enzyme. Primers are ligated to the overhanging ends created by cleavage of the BAC DNA. A subsequent PCR is carried out to amplify the BAC DNA. Using only a fraction of the first PCR, a second PCR is performed, and this DNA product is made into spotting solution. This article also describes the DNA labeling and hybridization protocols used to obtain highly reproducible and quantitative data.

II. MATERIALS AND INSTRUMENTATION

A. Preparation of BAC DNA Spotting Solutions

10× One-Phor-All Buffer Plus [100 m*M* Tris–acetate (pH 7.5), 100 m*M* magnesium acetate and 500 m*M* potassium acetate] is from Amersham Pharmacia Biotech Inc. (Cat. No. 27-0901-02) and is stable at 4°C

*Mse*I restriction enzyme (50 U/µl) is from New England Biolabs (Cat. No. R0525M). Store at –20°C. Store on ice when in use return to –20°C as soon as possible.

20–500 ng of BAC DNA with minimal contamination from host DNA. A Qiagen plasmid minikit (Cat. No. 12125) can be used to purify BAC DNA by following a modification of the manufacturer's protocol (see Comment 1)

0.2-ml polypropylene PCR eight-tube strips with separate eight-cap strips (Cat. No. 1402-2700) and 96-well plate seal (Cat. No. 2920-0000) are from USA Scientific

Ultrapure agarose (Cat. No. 15510-027), ATP (10 m*M*) (Cat. No. 18330-019), T4 DNA ligase (5 U/µl) (Cat. No. 15524-041), dATP, dCTP, dGTP, and dTTP (100 m*M* each) (Cat. No. 10297-018) are from Invitrogen. Store ATP, T4 DNA ligase, and dNTPs at –20°C;

Copyright 2006, Elsevier Science (USA).
All rights reserved.

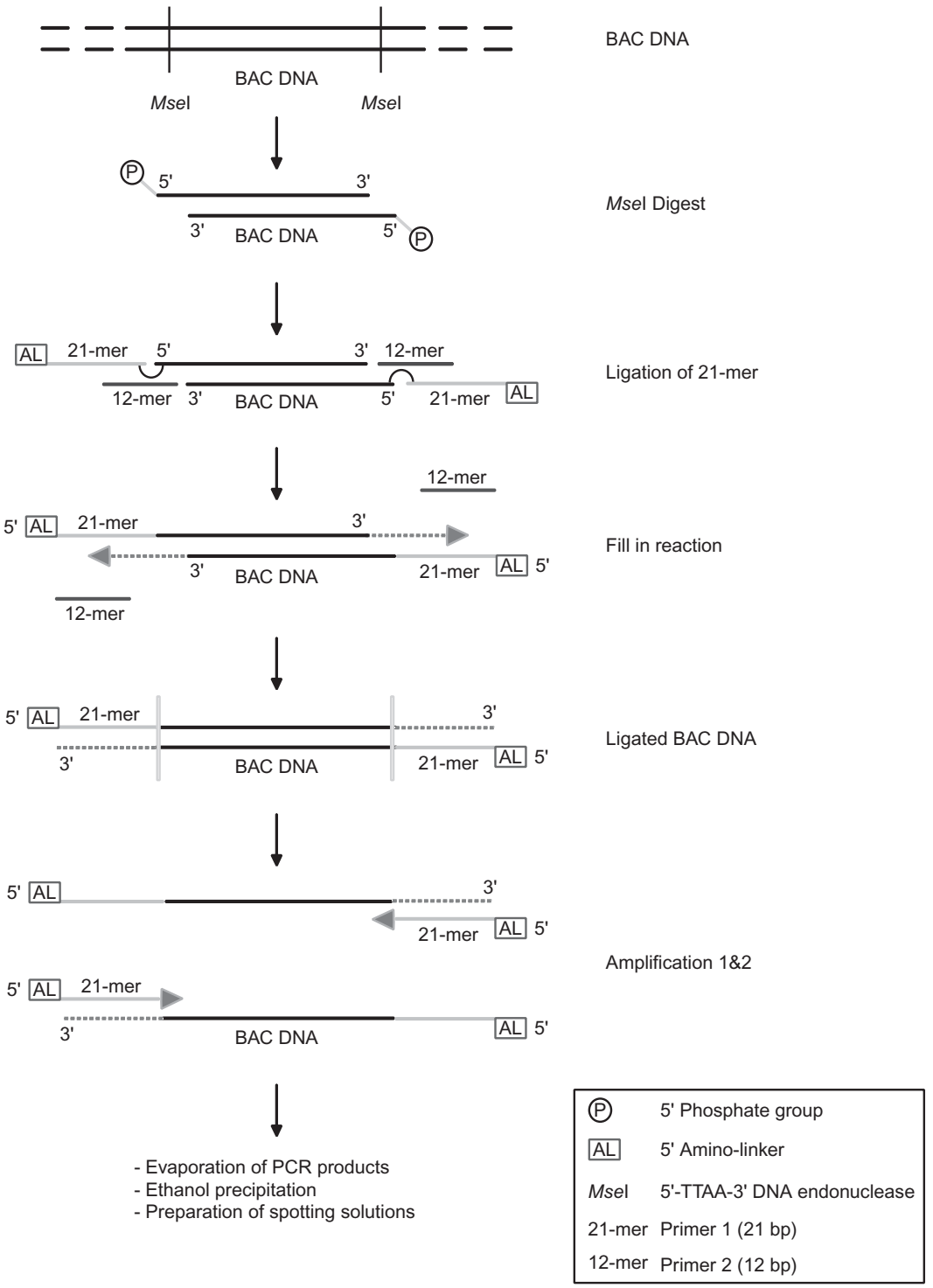

FIGURE 1 Overview of the ligation-mediated PCR procedure. BAC DNA is digested with the *Mse*I restriction enzyme, leaving a 5′-phosphorylated TA overhang. Primers are ligated to these overhangs. The 12-bp primer guides the amino linker containing the 21-bp primer to the overhang where the 21-bp primer is ligated by T4 DNA ligase. Because of the absence of a phosphate group at the 5′ end of the 12-bp primer, it will not get ligated to the BAC DNA. Primer 2 is melted off, after which DNA polymerase fills in the now single-stranded DNA overhang (as indicated with a dashed arrow). The now double-stranded, BAC DNA fragments are PCR amplified using a high-fidelity DNA polymerase; excess primer 2 from the ligation reaction will prime the reaction. A fraction of this ligation-mediated PCR is amplified in a second PCR reaction, which will be made into spotting solution.

when in use, keep the enzyme on ice. Return to –20°C as soon as possible.

Tris-base (Cat. No. BP152-500), Tris–Cl (Cat. No. BP152-1), boric acid (Cat. No. A74-1) and 1% ethidium bromide solution (1%) (Cat. No. BP1302-10) are from Fisher Scientific

Gel-loading solution (6×) (Cat. No. G7654; stable at 4°C), 3 *M* sodium acetate buffer solution (Cat. No. S7899), EDTA (Cat. No. E5134), and dimethyl sulfoxide (Cat. No. D8418) are from Sigma

φ X174 RF DNA/*Hae*III marker is from Promega (Cat. No. G1761)

Primer 1: 5′-AGT GGG ATT CCG CAT GCT AGT-3′ containing a 5′ amino linker (250 n*M* scale, HPLC purified) and primer 2: 5′-TAA CTA GCA TGC-3′ (100 n*M* scale, HPLC purified) are from IDT

Expand long template PCR system is from Roche (Cat. No. 1681842). Store at –20°C. Store on ice when in use; return to –20°C as soon as possible.

Reagent reservoirs with divider (Cat. No. 8095) and without divider (Cat. No. 8093) are from Matrix Technologies Corp.

10× *Taq* buffer II containing no $MgCl_2$, $MgCl_2$ (25 m*M*), and AmpliTaq Gold DNA polymerase (5 U/μl) are from PE Applied Biosystems (Cat. No. N8080245). Store at –20°C; when in use keep the enzyme on ice. Return to –20°C as soon as possible.

Ethyl alcohol (200 proof) is from Rossville Gold Shield Chemical Co.

Adjustable single channel pipettors are from Rainin (Cat. No. Gilson Pipetman P20, P200, P1000) and Eppendorf (Reference series 2000, Cat. No. 022470001)

Adjustable 8- or 12-channel multichannel pipettors are from Matrix Technologies (Cat. No. 6019, 0.5–12.5 μl; 6012, 5–250 μl; 6004, 15–1250 μl)

PCR machine capable of ramping at approximately 1.3°C/min is from PE Applied Biosystems (Model 9700, Cat. No. 4314878)

Electrophoresis power supplies (Cat. No. FBTIV816A) and UV transilluminator are from Fisher Scientific (Cat. No. FB-105)

Electrophoresis gel boxes are from USA Scientific (Cat. No. 3431-4000)

Fluorometer is from Bio-Rad (Versafluor, fluorometer, Cat. No. 170-2402)

Fan oven is from Techne (Model Hybridiser HB-1D)

Microwave is from General Electric

B. BAC Array-Based Comparative Genomic Hybridization

BioPrime DNA labeling systems (Cat. No. 18094011) [containing 2.5× random primers and Klenow fragments (40 U/μl)], dNTP solutions (100 m*M* each) (Cat. No. 10297-018), salmon sperm DNA (1 mg/ml) (Cat. No. 15632-011), and redistilled, ultrapure formamide (for preparation of hybridization mixture) (Cat. No. 15515-026) are from Invitrogen and stored at –20°C. Store Klenow fragments on ice when in use and return to –20°C as soon as possible.

Cy3 (Cat. No. PA53021)- and Cy5 (Cat. No. PA55021)-labeled dCTP (1 m*M*) are from Amersham Pharmacia Biotech Inc. Store at –20°C.

Tris base (Cat. No. BP152-500), dextran sulfate (Cat. No. BP1585-100), SDS (Cat. No. 5525-087), glycerol (Cat. No. BP229-1), formamide (for preparation of array wash solution) (Cat. No. F84-1), coverslips (24 × 50 mm) (Cat. No. 12531F), syringe (10 ml) (Cat. No. 14-823-28), monobasic monohydrate sodium phosphate (Cat. No. S369-500), dibasic heptahydrate sodium phosphate (Cat. No. S373-500), and microscope slides (Cat. No. 12-518-100B) are from Fisher Scientific.

Sephadex G-50 spin columns are from Amersham Pharmacia Biotech Inc. (Cat. No. 27-5330-01)

Human Cot-1 DNA is from Roche (Cat. No. 1581-074). Store at –20°C.

20× SSC (Cat. No. S6639), EDTA (Cat. No. E5134), DAPI stain (1 m*M*) (Cat. No. D9542) (store at –20°C), and 3 *M* sodium acetate buffer solution (Cat. No. S7899) are from Sigma

Ethyl alcohol (200 proof) is from Rossville Gold Shield Chemical Co.

Rubber cement is from Office Depot (Cat. No. 129791)

Silicone gasket (Press-to-Seal) is from PGC Scientific (Cat. No. 49698)

Binder clips are from OfficeMax (Cat. No. OM-211)

PBS (pH 7.4) lacking Ca^{2+} and Mg^{2+} is from the UCSF Cell Culture Facility (Cat. No. BG200). Store at 4°C.

Nonidet P-40 is from Fluka (Cat. No. 74385)

Slides for printing arrays (Corning GAP) are from VWR (Cat. No. 18888-302)

Adjustable single channel pipettors are from Rainin (Cat. No. Gilson Pipetman P20, P200, P1000)

UV Stratalinker 2400 is from Stratagene (Cat. No. 400676)

Rocking table (Cat. No. 40000-300) and 37°C incubator (Cat. No. 35824-756) are from VWR

Stereomicroscope is from Leica (Model MZ8)

III. PROCEDURES

Procedures for the preparation of spotting solutions are described in Sections III,A–III,E and are summarized in Fig. 2. Section III,F describes the labeling and hybridization procedure.

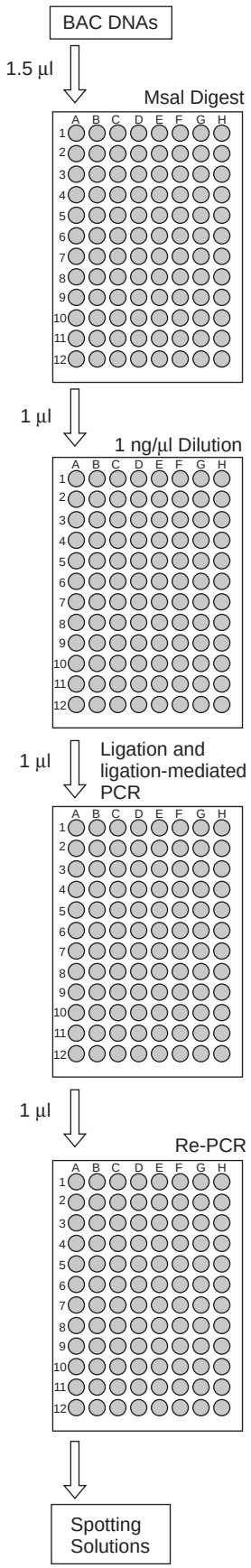

FIGURE 2 Flowchart of the ligation-mediated PCR procedure for 96 BAC clones. BAC DNA (1.5 µl) is digested. One microliter of each digest reaction is diluted to 1 ng/µl in H_2O. Note that due to varying BAC DNA concentrations, the amount of H_2O necessary to dilute 1 µl of digest reaction to 1 ng/µl can vary. A ligation and subsequent PCR reaction are performed using 1 µl (which equals 1 ng) of BAC DNA. A fraction (1 µl) of the ligation-mediated PCR is now reamplified in a second PCR reaction, which will be made into spotting solution.

A. Restriction Enzyme Digest of BAC DNA

The restriction enzyme digest is carried out in a 5-µl reaction volume containing 2.2× One-Phor-All Buffer Plus, 5 U *Mse*I restriction enzyme, and 20–500 ng BAC DNA.

Solutions

1. *Restriction enzyme buffer dilution:* Dilute the 10× One-Phor-All Buffer Plus to a final concentration of 0.8× in a final volume of 750 µl using sterile H_2O. Dispense 93 µl into each tube of an 8-tube strip. Leftover dilution can be stored at 4°C.
2. *Restriction enzyme diluion:* Dilute the *Mse*I restriction enzyme to a final concentration of 5 U/µl in a volume of 120 µl using 10× One-Phor-All Buffer Plus. Keep both the enzyme and the dilution on ice during this process. Return the enzyme to –20°C promptly after making the dilution and discard leftover dilution.
3. *TBE; electrophoresis buffer:* 0.089 *M* Tris–borate, 0.089 *M* boric acid, 0.008 *M* EDTA. To make 10 liters, dissolve 108 g Tris base, 55 g boric acid, and 40 ml 0.5 *M* EDTA (pH 8.0) in distilled H_2O. After dissolving, make up to 10 l with distilled H_2O. Store at room temperature.
4. *1% agarose solution:* Dissolve 1 g agarose per 100 ml of electrophoresis buffer. Mix and microwave until boiling and add ethidium bromide to a final concentration of 0.5 µg/ml.

Steps

1. Dispense 2.5 µl of the r*estriction enzyme buffer dilution* into each tube of twelve 8-tube PCR strips using a multichannel pipettor. Seal the tubes using a 96-well plate seal to prevent evaporation and possible contamination (see Comment 2).
2. Using a single channel pipettor (see Comment 3), add 1.5 µl BAC DNA (see Comment 1) to each tube. Only one 8-tube strip is handled at a time during this step. Keep the remaining eleven 8-tube strips covered using a 96-well plate seal. After adding the BAC DNA to each 8-tube strip, place the strip into a second 96-well plate rack and seal with a 96-well plate seal.

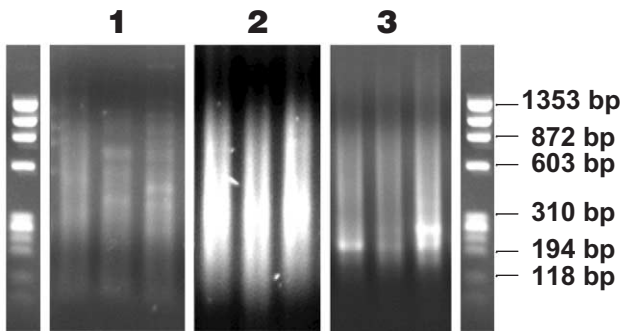

FIGURE 3 Agarose gel analysis of ligation-mediated PCR process. (1) Typical size range and DNA distribution of three *Mse*I digest reactions. (2) Three ligation-mediated PCR products. (3) Three Re-PCR reactions. All samples were run on a conventional 1% agarose gel containing 0.5 µg/µl ethidium bromide together with a φ X174 RF DNA/*Hae*III DNA marker, which has a size range from 72 to 1353 bp.

3. Dispense 1 µl of the *MSE*I *restriction enzyme dilution* into each tube using a single channel pipettor. Cap each 8-tube strip using an 8-cap strip and place on ice after adding the enzyme. The *restriction enzyme dilution* should stay on ice during this process.

4. Place the reaction into a PCR machine for an overnight incubation at 37°C, typically 12–16 h.

5. 1.75 µl of the digest reaction can be run on a conventional 1% agarose gel containing 0.5 µg/µl ethidium bromide along with a φ X174 RF DNA/*Hae*III marker to check fragment length. Sizes should range from 100 to 1500 bp (Fig. 3).

B. Ligation of Specific Primers to BAC DNA

The ligation reaction is carried out in a 10-µl reaction volume containing 5 µ*M* primer 1, 5 µ*M* primer 2, 0.5× One-Phor-All Buffer Plus, 1 m*M* ATP, 5 U T4 DNA ligase, and 1 ng digested BAC DNA.

Solutions

1. *TE:* 10 m*M* Tris–Cl (pH 7.4), 1 m*M* EDTA (pH 8.0). To make 100 ml, mix 1 ml 1 *M* Tris–Cl (pH 7.4) and 200 µl 0.5 *M* EDTA (pH 8.0) and make up to 100 ml with distilled H_2O. Autoclave to sterilize and store at room temperature.

2. *Primer 1*: 5′-AGT GGG ATT CCG CAT GCT AGT-3′ containing a 5′ amino linker. For stock solution, dissolve primer in TE (pH 7.4) to 500 µ*M*. For working solution, dilute stock solution to 100 µ*M* in distilled water. Store primer, stock solution, and working solution at –20°C.

3. *Primer 2*: 5′-TAA CTA GCA TGC-3′. For stock solution, dissolve primer in TE (pH 7.4) to 500 µ*M*. For working solution, dilute stock solution to 100 µ*M* in distilled water. Store primer, stock solution, and working solution at –20°C.

4. *Ligation solution*: Mix 56 µl primer 1, 56 µl primer 2, 56 µl One-Phor-All Buffer Plus, and 616 µl sterile water. Dispense 98 µl into each tube of an 8-tube strip. Store on ice.

5. *ATP solution*: Dispense ~62.5 µl of 10 m*M* ATP solution into each tube of an 8-tube strip. Cap with an 8-cap strip and keep on ice when in use. Store at 4°C.

Steps

1. Dilute 1 µl of each of the restriction digests to 1 ng/µl using sterile H_2O. Calculate the amount of sterile H_2O required to dilute 1 µl of each digest to a final DNA concentration of 1 ng/µl [e.g., if the BAC DNA concentration in the digest reaction is *X* ng/µl, the appropriate amount of sterile H_2O to add is (*X*-1) µl] (see Comment 4). Set up twelve new 8-tube strips: individually add the calculated amount of sterile H_2O to each new tube at the locations corresponding to the locations of each digest. Transfer 1 µl of each digest using a multichannel pipettor. Cover using a 96-well plate seal.

2. Dispense 7 µl of the *ligation solution* onto the bottom of twelve new 8-tube strips using a multichannel pipettor (see Comment 5). Seal the 8-tube strips using a 96-well plate seal.

3. Add 1 µl of the 1 ng/µl BAC DNA digest to the 7 µl *ligation solution* in each corresponding 8-tube strip (see Comment 6).

4. Place the twelve 8-tube strips into a PCR machine. Carry out the annealing reaction at 65°C for 1 min and then shift the temperature down to 15°C, with a ramp of ~1.3°C/min (in a Perkin-Elmer 9700 PCR machine this is a ramp rate of 5%).

5. As soon as the PCR machine reaches 15°C, promptly take out the tubes from the PCR machine and carefully open all 8-tube strips, including the 8-tube strip containing the ATP solution. Using a multichannel pipettor on the repeat pipetting mode, pick up 12.5 µl of 10 m*M ATP solution* and dispense 1 µl on the inside wall of each of the 96 tubes containing DNA. Gently tap the PCR rack so that the ATP slides into the DNA/primer solution. Seal with a 96-well plate seal. This procedure for adding the ATP reduces the probability of carryover contamination.

6. Using a single channel pipettor, dispense 1 µl of DNA T4 ligase enzyme (5 U) into each of the 96 tubes.

7. Place the reaction in a PCR machine for an overnight incubation at 15°C, typically 12–16 h.

C. Ligation-Mediated PCR

The ligation-mediated PCR is carried out in a reaction volume of 50 µl containing 0.6× 10×PCR buffer 1, 0.4 m*M* dNTP mixture, 3.5 U DNA polymerase mixture, and 10 µl ligation mixture (Section III,B).

Solutions

1. *10 mM dNTP solution*: For 250 µl, mix 25 µl of each of the nucleotide stock solutions (100 m*M* each) with 150 µl sterile H_2O. Keep on ice when in use, otherwise store at –20°C.
2. *PCR mix*: For 96 samples, mix 336 µl 10× PCR buffer 1, 224 µl *10 mM dNTP solution*, and 3920 µl sterile H_2O. Mix briefly by vortexing and place on ice.
3. *TBE; electrophoresis buffer:* 0.089 *M* Tris–borate, 0.089 *M* boric acid, 0.008 *M* EDTA. To make 10 liters, dissolve 108 g Tris base, 55 g boric acid, and 40 ml 0.5 *M* EDTA (pH 8.0) in distilled H_2O. After dissolving, complete to 10 liters with distilled H_2O. Store at room temperature.
4. *1% agarose solution:* Dissolve 1 g agarose in 100 ml TBE. Mix and microwave until the boiling point has been reached and then add ethidium bromide to a final concentration of 0.5 µg/ml.

Steps

1. Remove the ligations from the PCR machine. Pour the *PCR mix* into a reservoir. Uncap all 8-tube strips carefully. Using a multichannel pipettor on the repeat pipetting mode, pick up 205 µl of the diluted dNTP mixture and dispense 40 µl on the inside wall of five subsequent 8-tube PCR strips. Purge the remaining 5 µl PCR mixture back into the reservoir. Discard the pipette tips and repeat this process. For the last two remaining 8-tube strips, pick up 85 µl, while leaving the dispense volume at 40 µl. Dispense 40 µl on the inside wall of the two remaining 8-tube strips. Gently tap the PCR rack so that the diluted dNTP mixture slides into the DNA/primer solution. Seal with 8-tube strips.
2. Place PCR tubes in the PCR machine at 68°C for 4 min to melt off primer 2. After 4 min, take out the tubes and add 1 µl of DNA polymerase mixture (3.5 U/µl) to each tube individually using a single channel pipettor. Open one 8-tube strip at a time and close immediately after adding the enzyme mix and place on ice (see Comment 7).
3. Place the 8-tube strips in the PCR machine: 68°C for 3 min; 94°C for 40 s, 57°C for 30 s, 68°C for 1 min 15 s for 14 cycles, 94°C for 40 s, 57°C for 30 s, 68°C for 1 min 45 s for 34 cycles and 94°C for 40 s, 57°C for 30 s, and 68°C for 5 min for the last cycle, followed by incubation at 4°C (see Comment 8).
4. Run 3.5 µl of each PCR on a conventional 1% agarose gel containing 0.5 µg/ml ethidium bromide along with a φ X174 RF DNA/*Hae*III marker to check fragment length. Size of the PCR product should range from 70 to 2000 bp, with the highest concentration of product around 200 to 800 bp (Fig. 3) (see Comment 9).

D. Re-PCR of Ligation-Mediated PCR

Ligation-mediated PCR is used as a template in a Re-PCR reaction to generate DNA for spotting. Amplification is carried out in a 100-µl reaction containing 1× *Taq* buffer II, primer 1 (4 µ*M*), dNTP mixture (0.2 m*M*), $MgCl_2$ (5.5 m*M*), 2.5 U AmpliTaq Gold, and ligation-mediated PCR product (1 µl).

Solutions

1. *25 mM dNTP solution*: For 250 µl, mix 62.5 µl of each of the nucleotide stock solutions (100 m*M* each). Keep on ice when in use, otherwise store at –20°C.
2. *Primer 1*: 5′-AGT GGG ATT CCG CAT GCT AGT-3′ containing a 5′ amino linker. For stock solution, dissolve primer in TE (pH 7.4) to 500 µ*M*. For working solution, dilute stock solution to 100 µ*M* in distilled water. Store primer, stock solution, and working solution at –20°C.
3. *PCR mix*: For 96 samples, mix 1000 µl 10× *Taq* buffer II, 400 µl primer 1 (100 µ*M*), 80 µl dNTP solution (25 m*M*), 2200 µl $MgCl_2$ (25 m*M*), 50 µl AmpliTaq Gold (5 U/µl), and 6170 µl sterile H_2O. Mix briefly by vortexing and place on ice.
4. *TBE; electrophoresis buffer:* 0.089 *M* Tris–borate, 0.089 *M* boric acid, 0.008 *M* EDTA. To make 10 liters, dissolve 108 g Tris base, 55 g boric acid, and 40 ml 0.5 *M* EDTA (pH 8.0) in distilled H_2O. After dissolving, make up to 10 liters with distilled H_2O. Store at room temperature.
5. *1% agarose solution:* Dissolve 1 g agarose in 100 ml TBE. Mix and microwave until the boiling point has been reached and then add ethidium bromide to a final concentration of 0.5 µg/ml.

Steps

1. Pour the *PCR mix* into a reservoir. Using a multichannel pipettor, dispense 99 µl into each tube of twelve 8-tube strips. Seal using a 96-well plate seal.
2. Add 1 µl ligation-mediated PCR product to each corresponding 8-tube strip using a multichannel pipettor. Do this by unsealing one 8-tube strip of PCR mixture and one 8-tube strip containing the ligation-mediated PCR. Cap the 8-tube strip after adding the template and then cap the 8-tube strip containing the remaining ligation-mediated PCR. Move on to the next 8-tube strip.

3. Place the 8-tube strips, now containing 99 µl PCR mixture and 1 µl ligation-mediated PCR product, in a PCR machine: 95°C for 10 min; 45 cycles at 95°C for 30 s, 50°C for 30 s, 72°C for 2 min and a final extension at 72°C for 7 min, followed by an incubation at 4°C.

4. Run 4 µl of each reaction on a conventional 1% agarose gel containing 0.5 µg/ml ethidium bromide along with a φ X174 RF DNA/*Hae*III marker to check fragment length. Size of the PCR product should range from 200 to 1500 bp (Fig. 3) (see Comment 10).

E. Preparation of Spotting Solutions from Re-PCR Used for Array CGH

Steps

1. Dry down the Re-PCR products to a volume of approximately 50 µl by uncapping the 8-tube strips and placing the PCR rack face up in a hybridization oven set at 45°C (takes approximately 75 min). If you are using an oven in which the heat inlet is biased toward one side of the PCR rack, the rack should be rotated every 15 min to allow even evaporation. Reducing the volume of the Re-PCR is necessary to accommodate the ethanol and sodium acetate for DNA precipitation.

2. Precipitate the PCR products by adding 130 µl prechilled 100% ethanol and 5 µl 3*M* sodium acetate using a multichannel pipettor. Cap the 8-tube strips and invert the rack several times.

3. Chill the PCR rack at –20°C for 15 min.

4. Spin the plate at 1699 *g* for 90 min at 4°C.

5. Remove the supernatant carefully using a multichannel pipettor and add 100 µl 70% ethanol to the pellet using a multichannel pipettor and then recap the tubes.

6. Vortex each 8-tube strip until the pellets come loose. After vortexing all 8-tube strips, centrifuge rack at 1699 *g* for 45 min at 4°C.

7. Remove as much of the 70% ethanol as possible using a multichannel pipettor and dry the pellet at room temperature for approximately 90 min. The time depends on the amount of ethanol left on the pellet. Be careful not to overdry the pellets.

8. Add 15 µl of a 20% DMSO solution to the pellets using a multichannel pipettor. Handled only one 8-tube strip at a time at this stage. Cap the tubes and resuspend by flicking the bottom of the PCR tubes to loosen the pellet and briefly centrifuge.

9. Store the DNA solution at 4°C for an overnight (or longer) incubation. Use a multichannel pipettor to mix the solution until the pellet is completely in suspension. DNA solutions can be stored at 4°C (see Comment 11).

F. Random-Primed Labeling of Genomic DNA for Array CGH Analysis

Random-primed labeling is carried out in a 50-µl reaction volume containing 200–300 ng genomic DNA, 1× random primers, 40 U Klenow DNA polymerase, Cy3- or Cy5-labeled dCTP (40 µ*M*), and 1× dNTP mixture. The random-primed DNA product will typically range in size from 200 to 1500 bp, with the highest concentration around 400 bp.

Solutions

1. *Tris base*: For 1 liter of 1*M* Tris, dissolve 121.1 g Tris base in 800 ml of H_2O. Adjust the pH to 7.4 with concentrated HCl. Make up the volume to 1 liter with H_2O. Sterilize by autoclaving.

2. *EDTA*: For 1 liter 0.5*M* EDTA, add 186.1 g of disodium ethylenediaminetetraacetate·$2H_2O$ to 800 ml of H_2O. Stir vigorously and adjust the pH to 8.0 with NaOH. Sterilize by autoclaving.

3. *10× dNTP mixture*: 2 m*M* each of dATP, dTTP, and dGTP, 0.5 m*M* dCTP, 10 m*M* Tris base (pH 7.6), and 1 m*M* EDTA. For 200 µl 10× dNTP mixture, mix 4 µl each of 100 m*M* dATP, dGTP, and dTTP, 1 µl of 100 m*M* dCTP, 2 µl of 1*M* Tris, 0.4 µl of 0.5*M* EDTA, and 184.6 µl of dH_2O.

Steps

1. Mix ~200–300 ng of genomic DNA with 20 µl of 2.5× random primer solution and make up the volume to 42 µl with sterile H_2O.

2. Denature the DNA by heating the mixture at 99°C in a PCR machine for 10 min. Briefly centrifuge and place on ice.

3. Add 5 µl of the *10× dNTP mixture*, 2 µl of Cy3- or Cy5-labeled dCTP (1 m*M*), and 1 µl Klenow DNA polymerase (40 U/µl). Mix well, briefly centrifuge, and place tube in a PCR machine at 37°C for an overnight incubation.

4. Place the Sephadex G-50 column in a 1.5-ml tube and prespin the column at 730 *g* for 1 min.

5. Place the column in a clean 1.5-ml tube; apply the sample onto the column and spin at 730 *g* for 2 min to remove unincorporated nucleotides from the DNA mixture (see Comment 12).

G. Hybridization of Fluorescently Labeled Genomic DNA for Array CGH Analysis

Solutions

1. *Hybridization mixture*: Distribute 1 *g* of dextran sulfate (sodium salt, 500,000 MW) over the entire length of a 15-ml tube. While holding the tube horizontally, squirt in 5 ml of formamide. Close the tube

and shake vigorously for 30 s. Add 1 ml of 20× SSC and shake vigorously for 30 s. Dissolve overnight at room temperature. Add sterile H_2O to a final volume of 7 ml. The hybridization mixture should be stored in aliquots at –20°C.

2. *Formamide wash solution*: 50% formamide, 2× SSC in H_2O. For 50 ml, mix 25 ml formamide, 5 ml 20× SSC, and 20 ml H_2O, pH 7.0. Prepare fresh.

3. *PN buffer wash solution*: 0.1 *M* sodium phosphate, 0.1% Nonidet P-40, pH 8.0. Prepare 16 liters of 0.1 *M* Na_2HPO_4 and 0.1% Nonidet P-40, pH 9. While continuously measuring the pH, adjust the pH to 8.0 with 0.1 *M* NaH_2PO_4 and 0.1% Nonidet P-40 (approximately 1 liter). Make sure not to go below pH 8.0. Store at room temperature.

4. *DAPI solution*: 90% glycerol, 10% PBS, 1 µ*M* DAPI. For 1 ml, mix 900 µl glycerol, 100 µl PBS, and 1 µl (1 m*M*) DAPI. Vortex and store at –20°C.

Steps

1. Expose a printed array to 260,000 µJ of UV using a Stratalinker (see Comments 13 and 14).

2. Fill a 10-ml syringe with rubber cement and fit a 200-µl pipette tip on the syringe outlet. Apply a rubber cement ring around the array using a stereomicroscope to observe the area of the array. Air dry the rubber cement and apply a second thick layer of rubber cement on top of the first layer. Air dry the rubber cement.

3. Preparation of samples for hybridization to a ~12-mm square. Volumes should be increased for larger area arrays.
   a. Combine 50 µl labeled test genomic DNA, 50 µl labeled reference genomic DNA, and 35 µg (measured by fluorometry) of human Cot-1 DNA. Precipitate the DNA sample mixture with ethanol by adding 2.5 volumes of ice-cold 100% ethanol and 0.1 volumes of 3 *M* sodium acetate (pH 5.2). Mix the solution by inversion and collect the precipitate by centrifugation at 14,000 rpm for 30 min at 4°C.
   b. Carefully aspirate and discard the supernatant. Wipe excess liquid from the tube with a paper tissue, being careful not to disturb the pellet. Air dry the pellet for approximately 5–10 min. Dissolve the pellet in 5 µl sterile H_2O, 10 µl 20% SDS, and 35 µl hybridization mixture (see Comment 15).

4. Preparation of array blocking solution:
   a. Precipitate 50 µl of salmon sperm DNA (10 mg/ml) by adding 2.5 volumes of ice-cold ethanol and 0.1 volume of 3 *M* sodium acetate (pH 5.2). Mix the solution by inversion and collect the precipitate by centrifugation at 6400 rpm for 1–2 min.
   b. Carefully aspirate and discard the supernatant. Wipe excess liquid from the tube with a paper tissue, taking care not to disturb the pellet. Air dry the pellet for approximately 5–10 min. Dissolve the pellet in 5 µl sterile H_2O, 10 µl 20% SDS, and 35 µl hybridization mixture (see Comment 15).

5. Denature the DNA sample solution at 73°C for 10–15 min and incubate at 37°C for ~60 min.

6. Place a silicone gasket around the rubber cement and apply 50 µl of the salmon sperm DNA blocking solution to each array inside the rubber cement ring. Place a clean microscope slide on top to prevent evaporation (Fig. 4). Incubate at room temperature for 30 min.

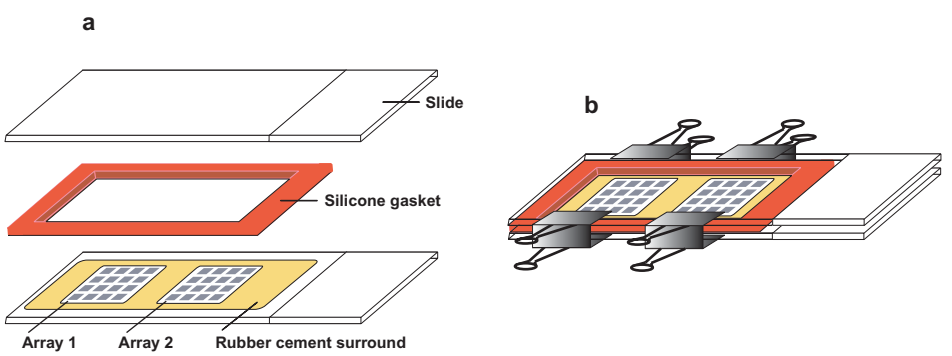

FIGURE 4 Array hybridization slide assembly. A ring of rubber cement is placed closely around each array. After applying the hybridization solution to each array, a silicon gasket is placed around the arrays, partly covering the rubber cement ring. A microscope slide is placed on top of the silicon gasket, and the whole slide assembly is clamped using binder clips. (a) Individual components of the slide assembly. (b) Complete slide assembly, including binder clips.

7. Carefully aspirate ~30–40 µl of salmon sperm hybridization mixture from the array and quickly apply the hybridization solution onto the array (see Comment 16).

8. Place a microscope slide on top of the gasket and clamp the assembly together (Fig. 4). Incubate the array for 1–2 nights at 37°C on a slowly rocking table.

9. Disassemble the slide assembly and rinse the hybridization solution from the slide under a stream of PN buffer.

10. Wash the slides in *formamide wash solution* (50% formamide, 2× SSC, pH 7) for 15 min at 45°C followed by a 15-min wash in *PN buffer wash solution* at room temperature.

11. Carefully remove the rubber cement with forceps while keeping the array moist with PN buffer.

12. If desired, arrays may be mounted in a *DAPI solution* to stain the array spots. Otherwise, rinse with sterile H_2O and allow to air dry.

13. Arrays are ready for imaging (see Comment 17).

IV. COMMENTS

1. BAC DNA is purified from 25-ml cultures using a modification of the Qiagen plasmid minipurification protocol. The volumes of buffers P1, P2, and P3 are increased from 0.3 to 1.5 ml. After adding buffer P3, incubate on ice for 10 min. Centrifuge at 4000 rpm for 45–60 min at 4°C. Filter the supernatant through a 35-µm nylon mesh (available from Small Parts Inc.) prior to loading onto Qiagen-tip 20 columns. Heat buffer QF to 65°C prior to adding it to the column. After elution, add 0.56 µl of isopropanol to the DNA, mix, and store at 4°C overnight. Mix and precipitate the DNA for 45 min at 14,000 rpm at 4°C. Air dry the pellet for 15–30 min. Then dissolve in 50 µl sterile H_2O. The BAC DNA concentration usually ranges from 20 to 400 ng/µl.

2. Roll back the plate seal of the 96-well plate (host plate) containing the digest buffer solution until the first 8-tube strip is exposed. Take out the first 8-tube strip and add BAC DNA to each tube. Place this 8-tube strip in a clean 96-well plate (recipient plate) and place a 96-well plate seal on top of the plate so that it covers the whole plate (one end of the plate seal will cover the 8-tube strip, the other end of the seal will stick to the 96-well plate). Go back to the host plate and roll back the plate seal until the next 8-tube strip becomes exposed. Take out the strip and add BAC DNA to each tube. Partially remove the 96-well plate seal of the recipient plate while leaving the first 8-tube strip covered. While holding the 96-well plate seal in one hand, place the next 8-tube strip in the recipient plate. Reseal the recipient plate and repeat this procedure until all 8-tube strips are done.

3. The use of a multichannel pipettor for pipetting small amounts (~1 µl) of enzyme has not been reliable. We found that by pipetting the enzymes *Mse*I, T4 DNA ligase, and the DNA polymerase mix separately using a single channel pipettor directly into the liquid in each tube has led to more reliable results. When the use of a multichannel pipettor is suggested, it is stated in the protocol.

4. To obtain accurate measurements of DNA concentration, a fluorometer should be used rather than a spectrophotometer.

5. Use a 12.5-µl multichannel pipettor to pick up 8 µl, dispense 7 µl, and throw away the remaining 1 µl and the pipette tips. The use of new pipette tips for each 8-tube strip is encouraged to ensure accuracy.

6. First carefully unseal the BAC DNA dilution plate and then, using a multichannel pipettor, pick up 1 µl of the first 8-tube strip. Unseal only the first 8-tube strip containing the primer solution, pick up the strip, and add the DNA directly into the 7-µl primer solution and cap both 8-tube strips after adding the DNA.

7. The 4-min incubation at 68°C will displace primer 2 (12-mer; T_m = ~40°C). It is essential to swiftly add the DNA polymerase mixture to each 8-tube strip, close the 8-tube strip with a 8-cap strip, and place the strip-tube on ice in order to prevent significant reannealing of primer 2. The subsequent 3-min incubation at 68°C will displace the reannealed primer 2 and extend the, now free, 3′ end of the digested BAC DNA. The process of taking twelve 8-tube strips out of the PCR machine, adding the enzyme mixture to each tube individually, placing the 8-tube strips on ice, and finally placing the 12 8-tube strips back into the PCR machine for amplification should take no longer than 10–15 min.

8. Depending on the type of PCR machine, cycle temperatures and times can be adjusted to obtain optimal results.

9. If a banding pattern appears in the smear, the ligation and/or ligation-mediated PCR has not been successful and should be repeated. All the products should have a smear ranging from 70 to 2000 bp. Any aberration from this smear, i.e., a small smear around 300–600 bp or a high molecular weight smear, is unacceptable and should therefore be discarded.

10. The Re-PCR will most likely have the highest concentration of product around 200–400 bp. The average PCR concentration should be 150 ng/µl as determined with a fluorometer.

11. The final concentration of the spotting solution should be approximately 0.8–1.3 µg/µl. After printing spotting solutions on a glass surface, the spots will

become nearly invisible due to the lack of salt in the spotting solutions. Breathing on the glass slide will make the arrays visible for a short period of time. Printed arrays should be left at room temperature for overnight to dry spots (see Comment 14).

12. The color of the DNA mixture is an indicator of the amount of labeled nucleotide incorporated during the labeling reaction.

13. Place the slide(s) in the Stratalinker, arrays facing up. The arrays should be given a fixed amount of *energy* (260,000 µJ) instead of the other available options the Stratalinker might have, such as *autocrosslink* or *time*. Overcross-linking the slide might result in a decrease in fluorescent hybridization signal (see Comment 14).

14. Depending on the type of slides used for arraying, the properties of the slide surface, as well as slide processing steps, may be different. Always follow manufacturers' recommended guidelines for handling slides. In this protocol the described slide processing steps were developed using, for example, Corning GAP slides.

15. Carefully pipette 5 µl sterile H_2O and 10 µl 20% SDS on the pellet. Incubate at room temperature for ~15 min. Add 35 µl of hybridization mixture while stirring the solution with the pipette tip. Do not dissolve the pellet by pipetting to prevent foam formation due to the presence of SDS.

16. Aspirate the salmon sperm DNA solution by tilting the array at approximately 45°, allowing the solution to slide to one side of the array. Aspirate approximately 30–40 µl of salmon sperm DNA solution using a 0.5- to 10-µl pipettor set at 10 µl. Discard each tip after aspirating salmon sperm DNA solution. Make sure the array does not dry out by swiftly removing the salmon sperm DNA solution and applying the sample solution. If more than one array is being hybridized on one slide, tilt the array at approximately 45°, aspirate 20 µl of salmon sperm DNA solution from array 1, aspirate 10 µl salmon sperm DNA solution from array 2, aspirate another 20 µl from array 1, and apply sample solution to array 1. Finally, aspirate 30 µl from array 2 and apply sample solution to array 2. Be careful not to generate bubbles when applying the sample solution to the array. This is to ensure that the microscope slide, which is placed on top of the silicone gasket (Fig. 4), does not touch the sample solution.

17. Images can be acquired using commercially available CCD or laser-scanning imaging systems (e.g., an Axon scanner 4000B). Image analysis and quantification can be done using commercially available image analysis programs (e.g., Genepix from Axon) or other programs, such as UCSF Spot (Jain *et al*., 2002).

References

Jain, A. N., Tokuyasu, T. A., Snijders, A. M., Segraves, R., Albertson, D. G., and Pinkel, D. (2002). Fully automatic quantification of microarray image data. *Genome Res*.

Klein, C. A., Schmidt-Kittle, O., Schardt, J. A., Pantel, K., Speicher, M. R., and Riethmuller, G. (1999). Comparative genomic hybridization, loss of heterozygosity, and DNA sequence analysis of individual cells. *Proc. Natl. Acad. Sci. USA* **96**, 4494–4499.

Pinkel, D., Segraves, R., Sudar, D., Clark, S., Poole, I., Kowbel, D., Collins, C., Kuo, W.-L., Chen, C., Zhai, Y., Dairkee, S. H., Ljung, B.-M., Gray, J. W., and Albertson, D. G. (1998). High resolution analysis of DNA copy number variation using comparative genomic hybridization to microarrays. *Nature Genet*. **20**, 207–211.

Snijders, A. M., Nowak, N., Segraves, R., Blackwood, S., Brown, N., Conroy, J., Hamilton, G., Hindle, A. K., Huey, B., Kimura, K., Law, S., Myambo, K., Palmer, J., Ylstra, B., Yue, J. P., Gray, J. W., Jain, A. N., Pinkel, D., and Albertson, D. G. (2001). Assembly of microarrays for genome-wide measurement of DNA copy number by CGH. *Nature Genet*. **29**, 263–264.

Solinas-Toldo, S., Lampel, S., Stilgenbauer, S., Nickolenko, J., Benner, A., Dohner, H., Cremer, T., and Lichter, P. (1997). Matrix-based comparative genomic hybridization: Biochips to screen for genomic imbalances. *Genes Chromosomes Cancer* **20**, 399–407.

CHAPTER

47

Genotyping of Single Nucleotide Polymorphisms by Minisequencing Using Tag Arrays

Lovisa Lovmar, Snaevar Sigurdsson, and Ann-Christine Syvänen

I. INTRODUCTION

An alteration of one nucleotide in a DNA sequence gives different phenotypic outcomes depending on its genomic location. Genomic nucleotide substitutions present in more than 1% of a population are denoted single nucleotide polymorphisms (SNPs). SNPs in protein-coding regions may alter the amino acid sequence of a protein, introduce stop codons, or produce new alternative splice sites in mRNA, thereby affecting the structure and function of the protein. SNPs located in the regulatory regions of a gene may alter binding sites for transcription factors and subsequently the expression level of the gene. The consequences of SNPs located in noncoding regions of the genome still remain largely unknown, but with the increasing interest in the function of noncoding RNA (Mattick and Gagen, 2001), their impact may soon become unravelled.

Following the completion of the draft sequence of the human genome (Lander *et al.*, 2001; Venter *et al.*, 2001), as well as of an increasing number of other genomes, the need for large-scale and high-throughput methods has increased. A promising and today widely used approach is the microarray format, which allows highly multiplex analysis of DNA, RNA, and proteins. This article describes the use of microarrays of immobilised oligonucleotides for SNP genotyping. Most SNP genotyping methods used today still depend on amplification of the region to be interrogated by the polymerase chain reaction (PCR) to provide the required sensitivity and specificity. Even though PCR was the technique that first enabled effective SNP genotyping, it is now the major factor limiting the high throughput of the methods due to the difficulties of designing robust multiplex PCR (Shuber *et al.*, 1995).

Significant advantages of performing assays in the microarray format are the reduced genotyping costs due to the simultaneous analysis of many SNPs in each sample and the small reaction volumes employed. Three major reaction principles are currently used for SNP genotyping on microarrays; hybridisation with allele-specific oligonucleotide probes, oligonucleotide ligation, and DNA polymerase-assisted primer extension (for a review on genotyping techniques, Syvanen, 2001). Due to their high specificity, the enzyme-assisted methods are gaining acceptance as the reaction principle of choice for multiplex SNP detection.

In the minisequencing reaction, a DNA polymerase is used to extend detection primers that anneal immediately adjacent and upstream of the sites of the SNPs. The primers are extended with differently labelled nucleotide analogues that are complementary to the nucleotides at the SNP sites. The method was initially devised with microtiter plates as the solid-phase support and has later been adapted to multiple assay formats (Syvanen, 1999), including microarrays with detection primers covalently attached to the microarray (Kurg *et al.*, 2000; Lindroos *et al.*, 2001; Pastinen *et al.*, 1997).

Copyright 2006, Elsevier Science (USA).
All rights reserved.

II. PRINCIPLE OF THE METHOD

A flexible alternative minisequencing system is based on generic oligonucleotides ("cTags") immobilised on the microarray instead of specific detection primers. Cyclic minisequencing reactions with fluorescently labelled dideoxynucleotides (ddNTPs) are performed in solution using detection primers with 5′ tag sequences complementary to one of the cTags included in the array. Each SNP is then interrogated by hybridizing the extended detection primers to their corresponding cTags with known locations in the array and the genotypes are deduced (Fig. 1A). The concept of using tagged PCR primers was first described for analysis of gene expression in yeast by PCR (Shoemaker *et al.*, 1996) and was later been applied to SNP genotyping by primer extension and capture on fluorescent microparticles (Cai *et al.*, 2000), high-density oligonucleotide arrays [Affymetrix, GenFlex arrays (Fan *et al.*, 2000)], and medium-density, custom-made oligonucleotide arrays in different formats (Hirschhorn *et al.*, 2000; Lindroos *et al.*, 2002).

The format presented here uses an "array of arrays" formed by a silicon rubber grid (Pastinen *et al.*, 2000) giving separate reaction chambers, each covering a subarray, that allow 80 samples to be analysed simultaneously for up to 200 SNPs on the same microscope slide (Fig. 1B). In contrast to the conventionally used format for mRNA expression, where a large number of genes are analysed in a relatively low number of samples, the "array of arrays" format allows for a large number of samples to be analysed simultaneously for an intermediate number of SNPs. The main steps of the assay are illustrated in Fig. 2.

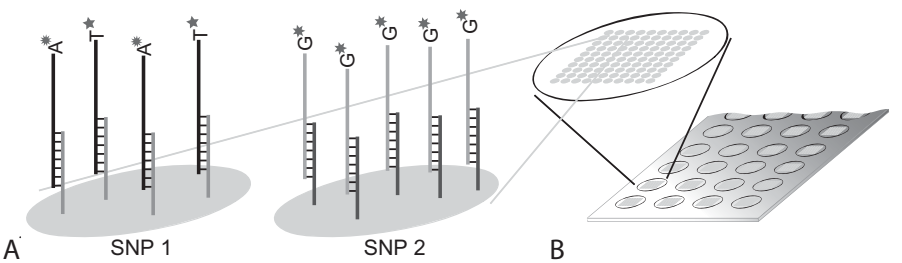

FIGURE 1 Schematic illustration of the microarray result for an individual that is heterozygote (A/T) for SNP 1 and homozygote (G/G) for SNP 2. The SNPs have been interrogated by hybridizing detection primers with 5′ tag sequences, extended with fluorescently labelled ddNTPs, to their complementary immobilised cTags (A). The format is an "array of arrays" with identical subarrays, allowing 80 samples to be analysed simultaneously for up to 200 SNPs on the same microscope slide (B).

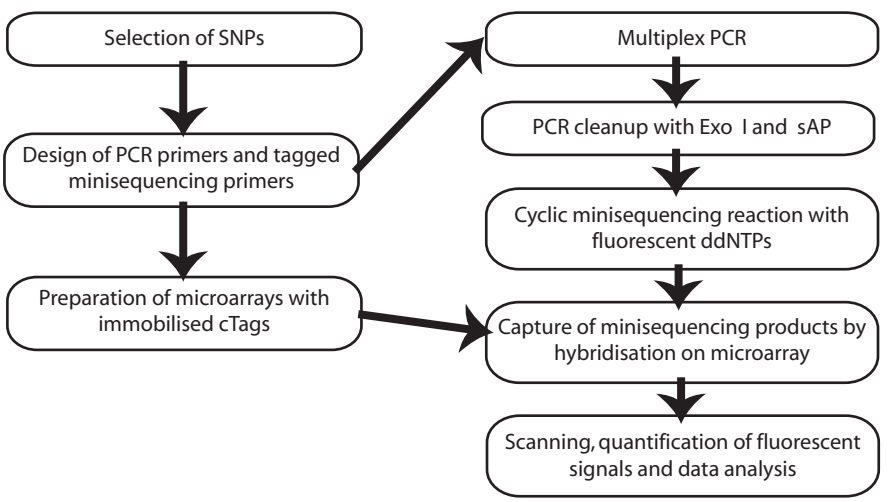

FIGURE 2 Steps of the procedure for genotyping of SNPs by minisequencing using tag arrays.

III. MATERIALS AND INSTRUMENTATION

The microarray slides are CodeLink-activated slides (reference number 25-6700-01) from Amersham Biosciences. The oligonucleotides are synthesized by Integrated DNA Technologies, and the tag sequences are obtained from Affymetrix. Elastosil (RT601) A (Cat.No. 60003804) and B (Cat.No. 60003815) are from Wacker-Chemie GmbH. In the multiplex PCR Ampli*Taq* Gold DNA polymerase, 5 U/µl, and GeneAmp 10× PCR gold buffer [100 m*M* Tris–HCl, pH 8.3, 500 m*M* KCl, 15 m*M* $MgCl_2$, and 0.01% (w/v gelatin)] (Part.No. N808-0245) from Applied Biosystems are used together with 10 m*M* dNTPs (Cat.No. 10297-018) from Invitrogen Life Technologies.

Exonuclease I (Ref.No. E70073Z), 10 U/µl, shrimp alkaline phosphatase (Ref.No. E70072Z), 1 U/µl, and ThermoSequenase (Ref.No. E79000Y), 32 U/µl, are from Amersham Biosciences. The fluorescent dideoxynucleotides used are Texas red-ddATP 85,000 $M^{-1}\,cm^{-1}$ (Prod.No. NEL 411), TAMRA-ddCTP 91,000 $M^{-1}\,cm^{-1}$ (Prod.No. NEL 473), R110-ddGTP 78,000 $M^{-1}\,cm^{-1}$ (Prod. No. NEL 495), and Cy5-ddUTP 250,000 $M^{-1}\,cm^{-1}$ (Prod. No. NEL 589), all from PerkinElmer Life Sciences. Reagents of the highest purity grade from various sources are used for preparation of buffers and other solutions.

A ProSys 5510A instrument from Cartesian Technologies Inc., with four Stealth Micro Spotting Pins (Cat.No. SMP3), from TeleChem International Inc., are used for microarray printing. A Tetrad programmable thermal controller from MJ Research is used for thermo cycling. For scanning of arrays, a ScanArray 5000 instrument from PerkinElmer Life Sciences is used. Additionally, a centrifuge, an incubation oven, a heat block at 42°C, and optimally a multichannel pipette and a pipetting robot are needed. For all instrumentation, other equivalent equipment could be used equally well.

IV. PROCEDURES

A. SNP Selection

SNPs can be identified either experimentally or in databases. Database searches may be aimed at genes of interest, candidate chromosomal regions, or randomly distributed SNPs with known allele frequencies (Table I).

Be aware that many of the SNPs are not validated and that the fraction of "real" SNPs in the databases is still unknown. Validation may be done in a particular population by analysing pooled DNA samples using quantitative minisequencing in microtiter plates or directly on the microarray as has been described (Lindroos *et al.*, 2002).

B. Primer Design

Design PCR primers flanking the SNPs of interest using available software. Primer 3, http://www.genome.wi.mit.edu/cgi-bin/primer/primer3_www.cgi, is freely available online or commercial software such as OLIGO: http://www.oligo.net/ can be purchased. The sequence of each PCR product should be "blasted" against the genome sequence (http://www.ncbi.nlm.nih.gov/BLAST/) and give a single hit only to the intended region.

Minisequencing primers anneal immediately adjacent and upstream of the SNP position. Minisequencing primers from both forward and reverse strands are helpful as internal controls for the genotyping results. Design the minisequencing primers to have a specific length of 18–22 bp and to have a common melting

TABLE I SNP Databases

Internet address	Comment[a]
http://www.ncbi.nlm.nih.gov/SNP/	The public SNP database, dbSNP, created and maintained by NCBI. Linked to additional resources within NCBI. Contains approximately 10 million human SNPs (5 million validated) as well as variations in several other genomes
http://snpper.chip.org/	Searches other databases such as dbSNP and the SNP consortium. Covers about 8 million SNPs (4.5 million validated) for which accurate positioning information is known
http://snp.cshl.org/	The SNP consortium is a public/private collaboration. Contains nearly 1.8 million SNPs
http://www.celeradiscoverysystem.com/	The Celera SNP reference database combines computed and validated variations in the human genome from work done at Celera and from public data sources. Contains a total of 4.1 million SNPs. Requires license to access

[a] The number of SNPs as of reported on Web pages January 2005.

temperature of 55–60°C to ensure specificity in the cyclic primer extension reaction. At the 5′ end of the primer add the tag sequences, complementary to the cTags, that will be spotted onto the microarray. The tags should be 20 bp long, have similar melting temperature, and not be complementary to either each other or the human genome. The Affymetrix GeneChip tag collection can be used as source for tag sequences. The complementary tag sequences (cTags) should have 15T residues as a spacer located 3′ of the specific sequence and a final 3′-amino group to enable covalent attachment of the cTags to the slides.

To avoid strong hairpin–loop structures, evaluate the final minisequencing primer, including the tag sequence, with primer design software that predicts secondary structures (mfold: http://www.bioinfo.rpi.edu/applications/mfold/old/dna/ or NetPrimer http://www.premierbiosoft.com/netprimer/netprimer.html). Secondary structures that involve the 3′ end of a primer may lead to misincorporation of nucleotides.

C. Microarray Preparation

Solutions

1. *2× print buffer:* 300 m*M* phosphate buffer, pH 8.5. Store at room temperature up to 1 month.
2. *Oligonucleotides:* Dissolve the cTags in 1× print buffer and dilute with dH_2O to a final concentration of 25 µ*M*. Store at –20°C but limit freeze–thaw cycles.
3. *1 M Tris–HCl, pH 9.0:* Dissolve 121.1 g Tris in 800 ml H_2O, adjust the pH to 9.0 with HCl, and adjust to a total volume of 1 litre.
4. *Blocking solution:* 50 m*M* ethanolamine, 100 m*M* Tris–HCl, pH 9.0, and 0.1% SDS. Prepare directly before use and preheat to 50°C. To make 500 ml, use 1.6 g ethanolamine, 50 ml 1 *M* Tris–HCl, 5 ml 10% SDS, and add water to 500 ml. Take care that the ethanolamine is highly corrosive and should be handled according to safety instructions.
5. *20×SSC:* 3 *M* NaCl and 300 m*M* sodium citrate, pH 7.0. Dissolve 175.3 g NaCl and 88.2 g sodium citrate in 800 ml H_2O. Adjust the pH to 7.0 with NaOH and adjust the volume to 1 litre. Autoclave and store at room temperature.
6. *10% SDS:* 10% (w/v) sodium dodecyl sulphate. Dissolve 100 g of SDS in 900 ml H_2O. Adjust the pH to 7.2 with HCl and adjust the volume to 1 litre. Store at room temperature.
7. *Washing solution:* 4×SSC and 0.1% SDS preheated to 50°C.

Prepare the arrays by contact printing the cTag oligonucleotides on CodeLink-activated slides (previously 3DLink slides). This may be done using a ProSys 5510A instrument with SMP3 pins that delivers 1 nl of the cTag solution to the slides as spots with a diameter of 125–150 µm and with a center-to-center distance of, for example, 200 µ*M*. For the possibility of using the "array of arrays" format, print spots in a subarray pattern of either a 384- or 96-well format (see Fig. 1). Mark the position of some subarrays on the back side of the slides using a diamond pen.

Postprocess the slides according to the instructions of the manufacturer. The following protocol for CodeLink-activated slides is given.

Steps

1. Prepare a saturated NaCl chamber with 75% relative humidity. In the bottom of a plastic container with an airtight lid, add as much solid NaCl to water as needed to form a 1-cm-deep slurry.
2. After printing, keep the arrays in the NaCl chamber between 4 and 72 h.
3. Deactivate the excess of amine-reactive groups by immersing the slides for 15 min in the blocking solution at 50°C.
4. Wash with dH_2O, washing solution at 50°C for 15–60 min, and dH_2O subsequently.
5. Spin dry the slides for 5 min at 900 rpm. Store the slides desiccated at 20°C until use.

A fluorescently labelled cTag may be included in the array as a spotting control. For each batch of printed slides it is useful to analyse a few subarrays by hybridisation as quality control of the spots. After deactivation of the slides, hybridize a 3′-fluorescently labelled oligonucleotide designed to hybridize to all cTags (5′-AAA AAA AAA ANN NNN NNN NN-3′) to some subarrays at 300 n*M* concentration in 6×SSC for 10 min with subsequent washing and scanning as described.

D. Preparation of Silicon Rubber Grid

Miniaturized silicon rubber (polydimethyl siloxan) reaction chambers are made using inverted microtiter plates with V-shaped wells as mould (Fig. 3).

Steps

1. Mix the two Elastosil RT 601 components in a 50-ml Falcon tube in a mass ratio of 9:1, i.e., 46.8 g of A and 5.2 g of B for 30 min (Elastosil RT625 may be used instead of RT601, thus giving a slightly softer silicon rubber).
2. Pour the mixture onto an inverted 384-well microtiter plate, leaving about 1–2 mm of the tip of the wells uncovered. Allow to harden overnight at room temperature.

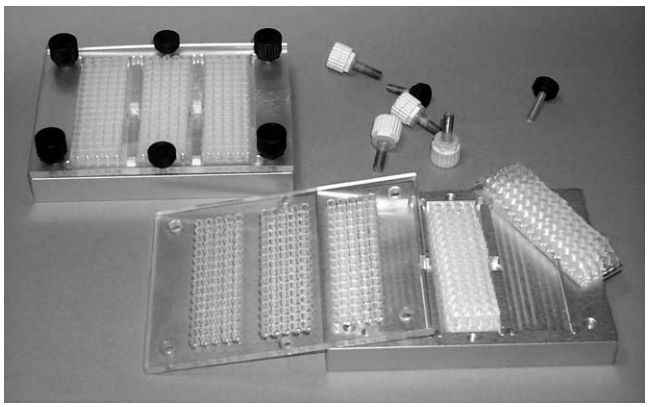

FIGURE 3 The arrayed slide is covered with a silicon rubber grid to give separate reaction chambers and is placed in a custom-made heat-conductive aluminium rack. A Plexiglas cover with a drilled hole through which the reaction chambers are accessed is tightly screwed on top the assembly, thus securing the silicon grid position during hybridisation.

3. Remove the silicon from the plate and use a scalpel to cut the silicon rubber into pieces of the size of microscope slides with the wells matching the printed subarrays.

The silicon is reusable, wash it with water and allow it to dry after each use.

E. Multiplex PCR

Primers for multiplex PCR should have as similar melting temperature and G/C content as possible. Different design programs, see earlier discussion, may be used to minimize primer–primer interactions. Complementary 3′ sequences in the primers can be avoided by designing primers with the same 3′ terminal nucleotides. Another possibility is the introduction of common tails on the 5′ ends of all PCR primers and subsequent amplification with one common primer for all the fragments at an elevated temperature (Brownie *et al*., 1997). An example of a protocol with the common tail approach that has been used for a 20-plex PCR reaction in 384-well format in our laboratory is given.

Primers with common tails for multiplex PCR should have 18–25 bp of specific sequence, have T_m 60–65°C, and give fragments about 100–200 bp long. On the 5′ end of both primers include a 26-bp-long common tail with T_m ~80°C (5′-GCG TAC TAG CGT ACC ACG TGT CGA CT-3′). In the PCR mixture use the tailed primers at 5 to 20 n*M* concentrations, depending on priming efficiency (trial and error), and use the primer complementary to the tail at 1 µ*M*. Amplify the genomic DNA using 1 ng/µl DNA, 0.04 U/µl Ampli*Taq* Gold DNA polymerase, and 200 µ*M* of dNTPs in 4 m*M* $MgCl_2$, 10 m*M* Tris–HCl, pH 8.3, 50 m*M* KCl, and 0.001% (w/v) gelatin and the primers as described earlier in a final volume of 10 µl. Amplify at 94°C for 5 min followed by four cycles of 94°C, 60°C and 72°C for 1 min each. Then do 35 cycles of 94°C for 1 min and 74°C for 2 minutes and finally do an extension at 72°C for 10 min. The success of the reactions may be verified on a 1% agarose gel for a subset of the samples.

TABLE II PCR Cleanup Reagents

Reagent (concentration)	Volume (µl)	Final concentration
PCR products	7	
$MgCl_2$ (50 m*M*)	1.5	7.1 m*M*
Tris–HCl, pH 9.5 (1 *M*)	0.5	0.05 *M*
ExoI (10 U/µl)	0.5	0.48 U/µl
sAP (1 U/µl)	1	0.10 U/µl
Total volume	10.5	

F. PCR Cleanup

Solutions

1. *$MgCl_2$ (50 mM):* To make a 1 *M* stock solution, dissolve 203.3 g $MgCl_3 \cdot 6H_2O$ in 800 ml of H_2O and adjust the volume to 1 litre. Autoclave and store at room temperature.
2. *Tris–HCl, pH 9.5:* Dissolve 121.1 g Tris in 800 ml H_2O, adjust the pH to 9.5 with HCl, and adjust to a total volume of 1 litre.
3. *Enzymes:* Keep the ExoI and sAP enzymes on ice during handling and store at –20°C.

Steps

1. For each sample, pool all multiplex PCR products.
2. Prepare a master mix of the PCR cleanup reagents (Table II).
3. To 7 µl of the pool, add 3.5 µl of the cleanup mixture to a total volume of 10.5 µl.
4. Incubate at 37°C for 30–60 min and inactivate the enzymes by heating to 95°C for 15 min.

Alkaline phosphatase (sAP) inactivates the remaining dNTPs and exonuclease I (ExoI) degrades the single-stranded PCR primers, thus limiting extension of them in the subsequent minisequencing reaction. Include negative PCR controls at this step.

G. Cyclic Minisequencing

Solutions

1. *Triton X-100 (0.5%, v/v):* Store at room temperature for up to 1 month.

2. *Tris–HCl, pH 9.5 (500 mM):* Dilute from 1 *M* Tris–HCl, pH 9.5.
3. *ThermoSequenase:* Keep on ice during handling, store at –20°C. Dilute the enzyme to required concentration directly prior to use.
4. *Fluorescent ddNTPs:* Keep light-protected aliquots in 4°C and store stock solutions at –20°C.

Steps

1. Prepare a master mix of the minisequencing reaction reagents (Table III).
2. After the cleanup step, add 4.5 µl of minisequencing reaction mixture to give a total volume of 15 µl.
3. Perform the minisequencing reaction using an initial 3 min at 95°C followed by 33 to 99 cycles of 20 s at 95°C and 20 s of 55°C in a thermocycler.

Additionally, an internal reaction control should be used. For that purpose, four synthesized single-stranded oligonucleotide templates differing only in one position mimicking the four possible alleles of a SNP are useful. Add the control template to the minisequencing reaction at a final concentration of 1.5 n*M*. A complementary-tagged minisequencing primer should be included with the other minisequencing primers and its cTag should be included in the array. Because fluorophores are light sensitive, protect all reaction mixtures containing fluorophores from light.

H. Capture by Hybridization

Solutions

1. *20×SSC:* See Section IV,C.
2. *Hybridisation control:* Oligonucleotide labelled with, for example, TAMRA, that hybridises to a corresponding cTag included in the array. Keep light-protected aliquots at 4°C and store stock solutions at –20°C.

TABLE III Minisequencing Reagents

Reagent (concentration)	Volume (µl)	Final concentration
PCR products after clean up	10.5	
Pool of tagged minisequencing primers (100 n*M* each)	0.75	5 n*M*
Fluorescently labelled ddNTPs[a] (5 µ*M*)	0.55	0.18 µ*M*
Triton X-100 (0.5%)	0.5	0.017%
Tris–HCl, pH 9.5 (500 m*M*)	0.5	17 m*M*
ThermoSequenase 1 U/µl	1	0.067 U/µl
H_2O	1.2	
Total volume	15	

[a] Texas red-ddATP, TAMRA-ddCTP, R110-ddGTP, and Cy5-ddUTP.

Steps

1. Position a silicon rubber grid over the arrayed slide with the aid of the diamond pen markings (see Fig. 3). Place the arrayed slides into the custom-made aluminium reaction rack and tighten the Plexiglas cover. Preheat the assembly on the side of a heat block to 42°C.
2. To the products from the minisequencing step, add 6.85 µl 20×SSC and 0.15 µl hybridisation control oligonucleotide at 45 n*M* concentration.
3. Transfer 20 µl of each sample to a separate reaction chamber on the microscope slide. A multichannel pipette is feasible for this step.
4. Hybridize for 2.5–3 h at 42°C in a humid environment accomplished, for example, by placing a wet tissue on the Plexiglas lid and cover it with plastic film and aluminium foil.

I. Washing

Solutions

1. *4×SSC:* Dilute from 20×SSC and store at room temperature
2. *2×SSC, 0.1% SDS:* Store at room temperature. Before use, preheat to 42°C.
3. *0.2×SSC:* Dilute from 20×SSC and store at room temperature.

Steps

1. After hybridization, take the slides from the reaction rack and rinse briefly with 4×SSC at 20–25°C.
2. Wash the slides twice for 5 min with 2×SSC and 0.1% SDS preheated to 42°C and twice for 1 min with 0.2×SSC at 20–25°C in 50-ml falcon tubes.
3. Finally, spin dry the slides for 5 min at 900 rpm and store them protected from light.

J. Scanning

If allowed by the scanner used, balance the signal intensity from each laser channel so that no signals are saturated and the signals from the four fluorophores are equally strong. Balancing is easy if a reaction control with signals from all four fluorophores is included on the array, as described earlier. An example of a scanning result is given in Fig. 4.

K. Data Analysis

A quantification program such as QuantArray handles the scanning images and quantitates the

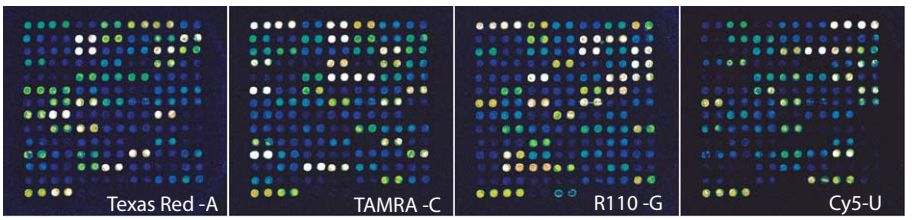

FIGURE 4 Scanning results for 45 SNPs in one subarray, i.e., one sample, after cyclic minisequencing with ddATP, ddCTP, ddGTP, and ddUTP labelled with Texas red, TAMRA, R110, and Cy5, respectively. Each cTag was spotted as horizontal duplicates, and both strands of all SNPs were analysed.

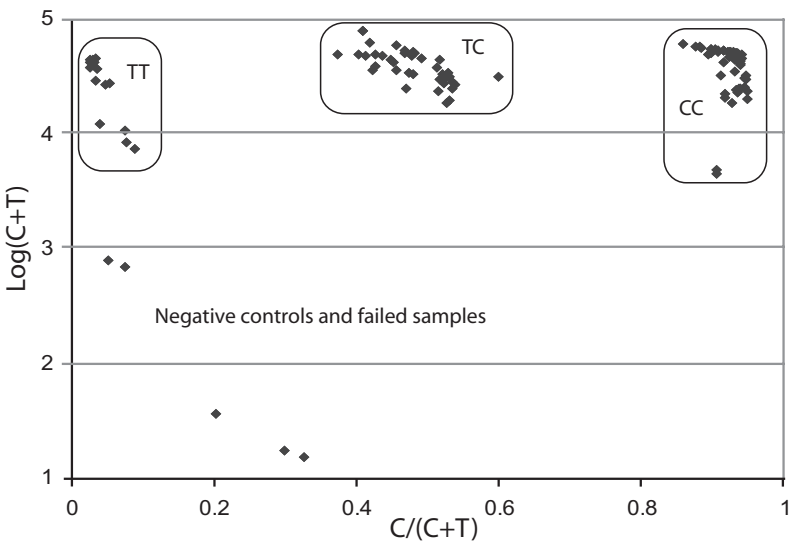

FIGURE 5 Scatter plot for one SNP with a C/T variation in 56 samples. The logarithm of the sum of the fluorescent signal from both alleles, C + T, on the *Y* axis has been plotted against the ratio, C/(C + T), on the *X* axis. The three distinct clusters represent the three different genotypes, whereas two negative controls and three failed samples fall outside the clusters.

signals from each spot. Raw data are collected as an Excel sheet. From the signals from each channel, subtract the background measured either around the spots or at negative control spots, i.e., spotted cTags without corresponding tagged primers. Assign the genotypes of the SNPs in each sample by calculating the ratios between the signals from one of the alleles and the sum of the signals from both the alleles: $\text{signal}_{\text{Allele 1}}/(\text{signal}_{\text{Allele 1}} + \text{signal}_{\text{Allele 2}})$. A scatter plot with this ratio on the *X* axis and the sum of the signals from both alleles on the *Y* axis is used for assigning the genotypes (Fig. 5). This scatter plot should give three distinct clusters with the homozygote samples clustering at each side and the heterozygotes in the middle. The ratios may vary between SNPs depending on the sequence surrounding it, the type of nucleotide incorporated, and the light intensity of the fluorophores.

V. PITFALLS

1. Hairpin and loop secondary structures in the primers can give rise to false signals. Some primers may occasionally fail to give signals, probably due to secondary structures either in the primer itself or in the PCR template.
2. Cy5-ddUTP can be used in higher concentrations than the other ddNTPs to compensate for its lower incorporation efficiency.
3. Insufficient amounts of the PCR products resulting in low signals may be compensated for by increasing the amount of cycles in the minisequencing step.
4. All solutions containing fluorophores are light sensitive and so are the slides after hybridization. To avoid bleaching, cover all reaction tubes and slides with aluminium foil.

5. Background problems can arise if the hybridisation chamber is not kept humid and the sample dries out on the slide.

6. If the Plexiglas cover is not tightened enough or if the silicon-rubber grid is damaged, leakage between reaction wells may occur. This can be controlled for by using differentially labelled hybridisation controls in adjacent reaction wells.

VI. COMMENTS

Depending on the available laboratory facilities or specific requirements of a project, this technique may be altered. Instead of multiplex PCR, single fragment PCR can be used with subsequent pooling of the amplified fragments, possibly after concentration using ethanol precipitation or spin dialysis. Different slides and attachment chemistries for the oligonucleotides have been tested, and new ones are continuously being developed (Lindroos *et al*., 2001). Depending on the number of SNPs to be interrogated, an inverted 96-well microtiter plate may be used as well for as silicon rubber mould to allow larger subarrays. When using the QuantArray program for signal analysing, the genotyping results can be visualised using the SNPSnapper software that has been custom made for this method (http://www.bioinfo.helsinki.fi/snpsnapper). Instead of using four differently labelled nucleotides in the same reaction, depending on the available microarray scanner, a single label or two labels may be used in four or two separate reactions, respectively (Liljedahl *et al*., 2003). It has been shown that the method described is quantitative and well suited to determine allele frequencies of SNPs in pooled DNA samples and is therefore a useful tool for rapid SNP validation (Lindroos *et al*., 2002).

References

Brownie, J., Shawcross, S., Theaker, J., Whitcombe, D., Ferrie, R., Newton, C., and Little, S. (1997). The elimination of primer-dimer accumulation in PCR. *Nucleic Acids Res.* **25**, 3235–3241.

Cai, H., White, P. S., Torney, D., Deshpande, A., Wang, Z., Marrone, B., and Nolan, J. P. (2000). Flow cytometry-based minisequencing: A new platform for high-throughput single-nucleotide polymorphism scoring. *Genomics* **66**, 135–143.

Fan, J. B., *et al.* (2000). Parallel genotyping of human SNPs using generic high-density oligonucleotide tag arrays. *Genome Res.* **10**, 853–860.

Hirschhorn, J. N., *et al.* (2000). SBE-TAGS: An array-based method for efficient single-nucleotide polymorphism genotyping. *Proc. Natl. Acad. Sci. USA* **97**, 12164–12169.

Kurg, A., Tonisson, N., Georgiou, I., Shumaker, J., Tollett, J., and Metspalu, A. (2000). Arrayed primer extension: Solid-phase four-color DNA resequencing and mutation detection technology. *Genet. Test.* **4**, 1–7.

Lander, E. S., *et al.* (2001). Initial sequencing and analysis of the human genome. *Nature* **409**, 860–921.

Liljedahl, U., *et al.* (2003). A microarray minisequencing system for pharmacogenetic profiling of antihypertensive drug response. *Pharmacogenetics* **13**, 7–17.

Lindroos, K., Liljedahl, U., Raitio, M., and Syvanen, A. C. (2001). Minisequencing on oligonucleotide microarrays: Comparison of immobilisation chemistries. *Nucleic Acids Res.* **29**, E69–69.

Lindroos, K., Sigurdsson, S., Johansson, K., Ronnblom, L., and Syvanen, A. C. (2002). Multiplex SNP genotyping in pooled DNA samples by a four-colour microarray system. *Nucleic Acids Res.* **30**, e70.

Mattick, J. S., and Gagen, M. J. (2001). The evolution of controlled multitasked gene networks: The role of introns and other noncoding RNAs in the development of complex organisms. *Mol. Biol. Evol.* **18**, 1611–1630.

Pastinen, T., Kurg, A., Metspalu, A., Peltonen, L., and Syvanen, A. C. (1997). Minisequencing: A specific tool for DNA analysis and diagnostics on oligonucleotide arrays. *Genome Res.* **7**, 606–614.

Pastinen, T., Raitio, M., Lindroos, K., Tainola, P., Peltonen, L., and Syvanen, A. C. (2000). A system for specific, high-throughput genotyping by allele-specific primer extension on microarrays. *Genome Res.* **10**, 1031–1042.

Shoemaker, D. D., Lashkari, D. A., Morris, D., Mittmann, M., and Davis, R. W. (1996). Quantitative phenotypic analysis of yeast deletion mutants using a highly parallel molecular bar-coding strategy. *Nature Genet.* **14**, 450–456.

Shuber, A. P., Grondin, V. J., and Klinger, K. W. (1995). A simplified procedure for developing multiplex PCRs. *Genome Res.* **5**, 488–493.

Syvanen, A. C. (1999). From gels to chips: "minisequencing" primer extension for analysis of point mutations and single nucleotide polymorphisms. *Hum. Mutat.* **13**, 1–10.

Syvanen, A. C. (2001). Accessing genetic variation: Genotyping single nucleotide polymorphisms. *Nature Rev. Genet.* **2**, 930–942.

Venter, J. C., *et al.* (2001). The sequence of the human genome. *Science* **291**, 1304–1351.

CHAPTER

48

Single Nucleotide Polymorphism Analysis by Matrix-Assisted Laser Desorption/Ionization Time-of-Flight Mass Spectrometry

Pamela Whittaker, Suzannah Bumpstead, Kate Downes, Jilur Ghori, and Panos Deloukas

I. INTRODUCTION

Modern humans as a species have a limited amount of genetic variation, most of which is attributable to common allelic variants. Any two haploid copies of the human genome differ at one site per kilobase on average (Sachidanandam *et al.*, 2001). Single nucleotide polymorphisms (SNPs) are the most abundant form of sequence variation, accounting for nearly 90% of all sequence variants in the human population. The remaining 10% consists of large and small insertions and deletions (indels). Simulation studies have estimated that there are between 10 and 15 million common (minor allele frequency greater or equal to 1%) SNPs in the human population (Kruglyak and Nickerson, 2001).

The identification and cataloguing of these common variants have been the objectives of the Human Genome Project (HGP; IHGSC, 2001). Systematic SNP discovery and mapping became feasible in the first instance with the availability of a draft sequence of the human genome (IHGSC, 2001). As a result, the International SNP Mapping Consortium reported a map of 1.42 million SNPs in 2001 (Sachidanandam *et al.*, 2001). With a finished reference sequence of the human genome now in hand (IHGSC, 2004), every identified variant can be mapped to a genomic location and correlated with genes and other functionally important sequences such as regulatory elements. Note that not all human sequence variants will have a unique map position in the genome due to the abundance of repeat elements such as LINEs and SINEs and extensive inter- and intrachromosomal segmental duplications (IHGSC, 2004). The presence of paralogous sequences, which are functionally important (e.g., gene families), throughout the genome further contributes to the complexity. Since 2001, systematic SNP discovery through both targeted and random genome-wide efforts has yielded over 7.2 million SNPs, which have unique map positions in the reference sequence and are available publicly (dbSNP; build 120). In addition to the publicly available SNP resources, a number of commercial entities have undertaken large-scale SNP discovery projects, most notably Celera and Perlgen.

A central goal of biomedical research is to identify and characterise the functional sequence variants with biochemical and phenotypic consequences. Although far from being complete, the existing collection of sequence variants already constitutes a rich genetic resource with the potential to accelerate discoveries in dissecting the molecular basis of common complex diseases and variable response to drugs as well as the study of population history. In this quest, SNPs have become the markers of choice due to their abundance and biallelic nature. The latter makes SNP typing amenable to both automation and high multiplexing. However, optimal use of SNPs as genetic markers requires knowledge of their distribution between and within populations. Furthermore, we need a better

Copyright 2006, Elsevier Science (USA).
All rights reserved.

understanding of the patterns of linkage disequilibrium (LD), which is the nonrandom association of SNP alleles, at a fine scale across the genome and in multiple populations. Studies have shown that by typing a sufficiently dense set of common SNPs (typically, minor allele frequency ≥5%) across a population sample (optimally above 50 unrelated individuals), one can construct a map in which most of the genome is represented as regions of high LD (Gabriel *et al*., 2002; Jeffreys *et al*., 2001; Ke *et al*., 2004; Patil *et al*., 2001). Note, however, that the degree and extent of LD are highly variable across the genome. Another important observation from these studies is that because the regions of high LD display a limited diversity of common haplotypes, it is possible to select a subset of the SNPs originally used to construct the map to capture (or tag) most or all of the information on common variation in the corresponding regions. These "haplotype tag SNPs" (htSNPs) (Johnson *et al*., 2001) could offer a three- to four-fold reduction in costs when conducting association studies.

Key to all studies of sequence variation is the availability of accurate, high-throughput, and inexpensive methods for assaying sequence variants. For the reasons described earlier, SNPs have become the markers of choice and in the last few years we have witnessed a true explosion in the number of techniques described in the literature for SNP typing. Broadly speaking though, there are four main reaction principles governing all SNP genotyping assays: hybridisation with allele-specific oligonucleotide (ASO) probes, oligonucleotide ligation (OLA), single nucleotide primer extension, and enzymatic cleavage (flap endonuclease; Invader assay). In contrast, there is an ever increasing choice of detection methods, such as fluorescence polarization, fluorescence resonance energy transfer (FRET), gel and capillary electrophoresis, matrix-assisted laser desorption/ionisation time-of-flight mass spectrometry (MALDI-TOF MS), denaturing high-performance liquid chromatography (DHPLC), DNA microarrays, and bead arrays (reviewed in Kristensen *et al*., 2001; Kwok, 2001; Mir and Southern, 2000; Syvänen, 2001).

Matrix-Assisted Laser Desorption / Ionisation Time-of-Flight Mass Spectrometry

Analysis of nucleic acids (>10 nucleotides long) by mass spectrometry became feasible with the introduction of ionization techniques, such as electrospray ionization (ESI) and matrix-assisted laser desorption / ionisation (Karas and Hillenkamp, 1988). Two key factors in terms of resolution and signal-to-noise ratio in the obtained mass spectra are sample preparation and the type of compound used to embed the sample, typically a small organic molecule that can crystalise (matrix). Introduction of the dried-droplet method for sample preparation (Nordhoff *et al*., 1992) and automated MALDI measurement (reviewed in Little *et al*., 1997) streamlined the use of MALDI-TOF MS in the analysis of DNA molecules. The principle of MALDI-TOF MS is shown in Fig. 1 (for a review, see Jurinke *et al*., 2004).

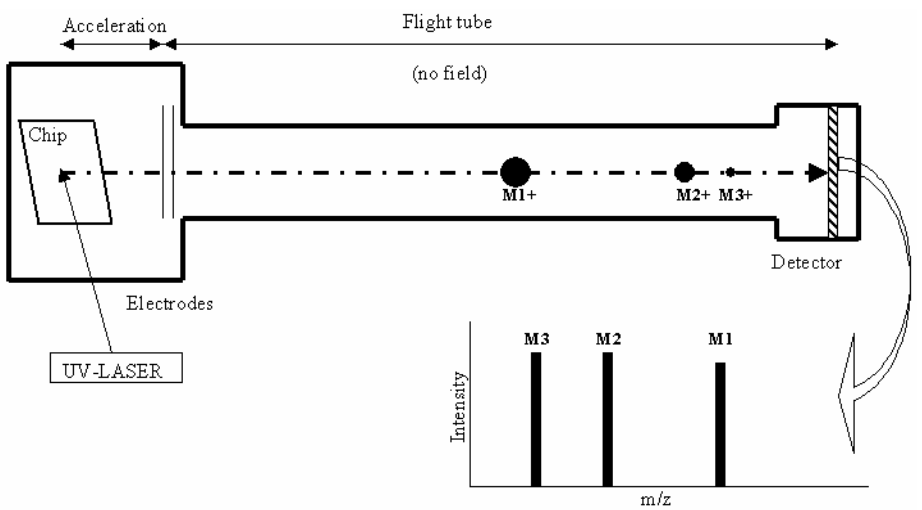

FIGURE 1 MALDI-TOF MS (modified from Pusch *et al*., 2001). Each spot on the chip consists of a matrix (e.g., 3-hydroxypicolinic acid) recrystallised in the presence of analyte. Firing UV laser pulses to a spot causes desorption and ionisation of matrix and analyte ions, which are accelerated prior to entering the flight tube by applying a potential. The time of flight of each ion is measured and converted into *m*/*z* (mass to charge ratio). The separation and detection of three positively, single-charged ions with different masses (M1, M2, and M3) are shown.

In SNP typing, MALDI-TOF MS has been coupled with assays based on primer extension. The two most common assays are the primer oligobase extension (PROBE; Fig. 2) (Brown *et al*., 1997) and the GOOD assay (Sauer *et al*., 2000)—for reviews, see Lechner *et al*. (2001) and Pusch *et al*. (2001). As a detection platform, MALDI-TOF MS has the rather unique feature, compared to other detection methods used in this field, of measuring an intrinsic property of the analyte, its mass. In addition, it requires only nanoliter quantities per sample. Among the commercially available platforms for SNP typing based on MALDI-TOF MS, the MassArray system (Sequenom, Inc.) has been widely used in many laboratories, including ours. The assay, homogeneous MassExtend, is based on PROBE and was developed to run as a homogeneous process with all steps performed in a single well. Up to 12 SNPs can be multiplexed per reaction, although four- to seven-plex reactions are currently the norm. The assay can be run manually or on a semiautomated platform for higher throughput.

II. MATERIALS AND INSTRUMENTATION

The MassArray system is from Sequenom, Inc. and is composed of a MassArray nanodispenser, a Brucker Biflex mass spectrometer, and a MultiMek. The system includes an ORACLE database and a suite of software tools for assay design (Spectrodesigner v.1.3.4) and real-time automated genotype calling (SpectroTyper v.2.0). Spectra acquisition occurs via the Brucker software installed on the mass spectrometer. The Roto-Shake Genie, 120 V, 60 Hz 0.5 amps is from Scientific Industries, Inc. (Cat. No. SI-1100). Thermocyclers, PTC-225 DNA Engine Tetrad with 384-well Alpha unit

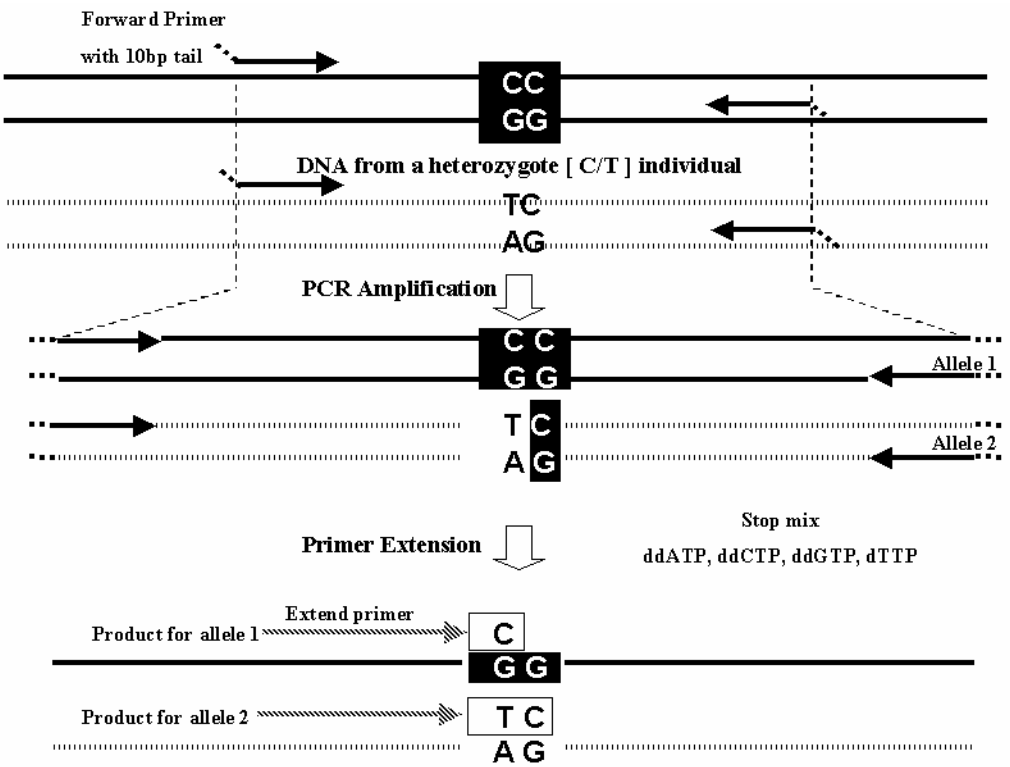

FIGURE 2 The PROBE assay for one SNP is shown. The assay works optimally with small amplicons 80–100 bp (specially in multiplex mode). Synthesizing the PCR primers with a universal 10-bp tail (not present in human DNA) increases their mass so that unused PCR primers do not interfere with product analysis. Post-PCR the unincorporated dNTPs are removed with shrimp alkaline phosphatase (not shown). Typically, the 3′ end of the extend primer is the base preceding the SNP. Multiplexing is achieved by varying the size of the extend primer used in each SNP assay, but the assays need to be compatible with the use of a single stop mix. In an optimal multiplex assay design, masses of all extend primers and possible extension products are chosen so that they differ by at least 30 Da from each other.

blocks, and Microseal "A" film (Cat. No. MSA-5001) are from MJ Research, Inc. The spectrofluorometer, the Cytofluor 4000 multiwell plate reader (any standard spectrofluorometer will work), optically clear microtitre plates (96-well cytoplate, Cat. No. CFCPN9610), and 10× polymerase chain reaction (PCR) buffer [10 m*M* Tris–HCl, 500 m*M* KCl, 15 m*M* $MgCl_2$, 0.01% (w/v) gelatine; Cat. No. N808-0189] are from Applied Biosystems. Multichannel electronic pipettors (Matrix Impact, 0.5–12.5 µl; Cat. No. 2009) are from Matrix. PCR primers (standard desalted oligonucleotides) and extend primers (reverse phase purified) are from Sigma-Genosys. The SpectroCLEAN kit (dimple 384-well plate; Cat. No. 11220), SpectroCHIP (384-well; Cat. No. 00601), SpectroCLEAN Resin (Cat. No. 10053), and 3-Oligo Calibrant mix (Cat. No. 00335) are from Sequenom, Inc. The PicoGreen dsDNA quantitation kit (Cat. No. P-7589) is from Molecular Probes. Titanium *Taq* polymerase (Cat. No. 8434-2) is from BD Biosciences—Clontech. Shrimp alkaline phosphatase 1 U/µl (Cat. No. 70092X), Thermosequanase DNA polymerase 32 U/µl (Cat. No. E 79000Z), ddNTPs (Cat. Nos. ddATP:27-2051, ddCTP:27-2061, ddGTP:27-2071, and ddTTP:27-2081), and dNTPs 100 m*M* (set of four: 27-2035-01) are from Amersham Biosciences (USB). Hotstart *Taq* DNA polymerase (Cat. No. 203203) is from Qiagen. THERMIPol DNA polymerase is from Solis Biodyne, Estonia. (no Cat No.). PCR 384-well microtitre plates (Thermo-Fast; Cat. No. TF-0384) are from ABgene. Source plates are from Bibby Sterilin (microtitre plates, 96-well V bottom, sterile; Cat. No. 612V96). HPLC grade H_2O (Cat. No. 152736D) and standard chemicals are from BDH.

Solutions

1. *TE buffer*: 10 m*M* Tris–HCl, 1 m*M* EDTA, pH75
2. *dNTP mix*: 5 m*M* each dNTP in H_2O
3. *DNA*: 1.75 ng/µl in T0.1E
4. *10x Thermosequenase buffer*: 260 m*M* Tris–HCl, pH 9.5, 65 m*M* $MgCl_2$
5. *Stop mix*: 500 µ*M* each appropriate ddNTP or dNTP in H_2O
6. *Extend primer mix*: 10 µ*M* each primer in H_2O

III. PROCEDURES

A. DNA Quantitation with PicoGreen

Accurate measurement of DNA concentration is not an important issue when genotyping individual samples by the homogeneous MassExtend protocol. In contrast, allele frequency estimation in pooled samples is completely dependent on the accurate measurement of DNA concentration in the samples used to form the pool. The following protocol is adapted from the PicoGreen dsDNA quantitation kit.

1. Dilute λ DNA standard solution to 5 ng/µl with TE buffer. In an optically clear microtitre plate, prepare the following dilutions of phage λ DNA in duplicate:

	1× TE	DNA Standard (µl)
Well 1	80	20
	84	16
	88	12
	92	8
	96	4
	98	2
	99	1
Well 8	100	0

2. Dilute each DNA sample to be measured with TE buffer to approximately 8 ng/µl (20 µl total) in duplicate. Aliquot 5 µl of each sample into two wells of the microtitre plate and add 95 µl of TE to each well (giving four wells per DNA in total).
3. Add 100 µl of 1× PicoGreen (kit solution diluted to 1× with TE) to each well with a multichannel pipette. Mix by spinning down plate at 4000 rpm (swing-out rotor) for 1 s. Note that this step needs to be executed as fast as possible.
4. Incubate plate in the dark (e.g., cover with aluminium foil) for 4 min.
5. Measure fluorescence in a standard spectrofluorometer: excitation: 480 nm and emission: 520 nm.
6. Subtract the fluorescence value of the blank from that of each sample. Use the λ dilutions (average value) to draw a standard curve of fluorescence versus DNA concentration.
7. Determine the DNA concentration of the samples from the standard curve. Compare duplicates for reproducibility.

B. SNP Genotyping with the Homogeneous MassExtend Protocol

The following protocol is a modification of the recommended protocol supplied by Sequenom, Inc. for use with the MassArray system. The experimental layout is based on a manual setup for typing 48 SNPs in four-plex reactions across a panel of 96 samples (95 DNAs and a negative control). The described setup includes dead volumes, whereas the volumes per single reaction are given in parentheses. Note that the procedure is amenable to many different formats in terms of SNPs vs samples vs level of multiplexing. For

example, assaying the same multiplex across 384 samples will require a single mix (see step 1) and adjustment of volumes accordingly. In addition, a number of standard robotic devices for liquid handling can be used to automate steps of the procedures.

1. SNP Selection and Assay Design

dbSNP is the main repository of publicly available SNP data and is maintained at the National Institute for Biotechnology Information (NCBI; http://www.ncbi.nlm.nih.gov/SNP) in the United States. dbSNP has three identifiers per SNP, namely the submitter SNP ID, the NCBI assay ID(ss) and the reference SNP ID(rs). Note that the same SNP can have more than one "ss" identifiers and hence it is recommended to always use the "rs" identifiers, which are unique. Typically, dbSNP will use the most recent and verified human genome sequence assembly, referred to as Golden Path or NCBI build, to obtain genome locations of all submitted SNPs. As the assembly of the human genome sequence is still evolving, it is possible that previously accessioned reference SNPs are either dropped (e.g., map to multiple locations) or two reference SNPs are merged to a new one with a different rs identifier. Although previous identifiers can be tracked, this remains an informatics challenge and should be monitored carefully in large-scale projects. Additional query tools such as dbSNP's "Entrez SNP" and the "EnsMart" of the Ensembl genome browser (http://www.ensembl.org/EnsMart/) allow the retrieval of SNPs with specified characteristics (e.g., experimentally verified, allele frequency cut off, coding, nonsynonymous, etc.) within a defined chromosomal region or gene. An additional source of validated SNP assays, allele frequencies, and, in the near future, common haplotypes and htSNPs is the international HapMap project (http://www.hapmap.org; International HapMap Consortium, 2003). Once SNPs have been selected and extracted from the database with 400 bp (minimum 120 bp) of flanking sequence either side of the SNP, it is recommended to perform a redundancy check with BLASTN. This is critical when dealing with large numbers of SNPs. Then, the sequences need to be parsed through a repeat masking programme such as RepeatMasker (http://repeatmasker.genome.washington.edu). Tag repeat sequences in lowercase to generate input SNP sequences for the SpectroDesigner v1.3.4 software. In general, the higher the number of SNP sequences in the input file, the higher the ability of SpectroDesigner to multiplex them successfully. For example, for 1000 of more SNPs and a four-plex level of multiplexing over 96% of SNPs get assays designed for. Optimal amplicon length is 80–100 bp but this is less critical when designing single-plex reactions. It is recommended to add a universal 10-bp tag to the PCR primers; this generates primers with masses outside the active window for analysis of the extended products (5–9 kDa). Note that newer versions of SpctroDesigner, e.g., v.2.0, support higher multiplexing, replexing of successful assays from different multiplexes, and assay design for triallelic SNPs and indels.

2. Marker and DNA Input Files

The output of SpectroDesigner lists the relationship of SNP assays in each multiplex, all designed primers and their masses, the appropriate Stop-Mixes (see step 5), and the masses of all expected products of primer extension. Read file into the MSPEC1 ORACLE database, which is the data repository of the MassArray system. In parallel, prepare a plate/sample input file and it into the database.

3. PCR Amplification of SNP loci (Four-plex Reactions)

1. Aliquot 2 µl of DNA (1.75 ng/µl) into each well of a 384-well PCR plate. For a panel of 96 samples, DNA1 is present in wells A1, A2, B1, and B2, DNA2 in wells A3, A4, B3, and B4, etc. To type 48 SNPs in four-plex reactions, prepare three plates. Centrifuge plates at 1000 rpm for 1 min. Prepare the following PCR mix:

1395.0 µl 10× PCR buffer (0.75 µl per reaction)
372.0 µl dNTP mix (0.2 µl per reaction)
18.6 µl H_2O (0.01 µl per reaction)
74.4 µl titanium *Taq* polymerase (0.04 µl per reaction)
1860.0 µl (1 µl per reaction)

Mix well and aliquot into 12 tubes (150 µl per tube). Label each tube according to a SNP multiplex and add 300 µl of the corresponding PCR primer mix (375 n*M* each primer; 2 µl per reaction). Use two 96-well source plates to aliquot the content of each tube (34 µl per well) across a plate row (i.e., tube 1 across A1–A12, tube 2 across B1–B12 . . . , tube 8 across H1–H12, tube 9 across A1'–A12', etc.; make a note of the exact order as it is needed in step 5).

2. We recommend placing a plastic template sheet colour coded according to the transfer pattern under the source and the PCR plate. Use a 12-channel pipette to transfer from the source to the PCR plates as follows: rows A–D and E–H of the first source plate and rows A'–D' of the second source plate will feed PCR plate 1, 2, and 3, respectively. Row A of the first source plate will feed positions 1, 3, 5, 7 . . . 23 in rows A, C, E, G, I, K, M, and O of PCR plate 1. Transfer 3 µl to each well (gently tap down plates and inspect that wells are filled uniformly). Seal plates with microseal mats (use a roller to ensure good and uniform adhesion of the

mat across the plate). Centrifuge plates at 1000 rpm for 1 min and place them on thermocyclers (for MJ Tetrads the programme parameters we use are: volume (µl) = 5 and heated lids: YES). Run PCR under the following conditions: 45 cycles each consisting of 20 s at 95°C, 30 s at 56°C, and 1 min at 72°C followed by one cycle for 3 min at 72°C followed by an indefinite cycle at 15°C (to prevent evaporation for overnight runs). Remove plates and spin down at 1000 rpm for 1 min.

4. Shrimp Alkaline Phosphatase Treatment

3. Prepare the following mix:

271.0 µl 10× Thermosequenase buffer (0.2 µl per reaction)
2032.5 µl H_2O (1.5 µl per reaction)
406.5 µl shrimp alkaline phosphatase (0.3 µl per reaction)
2710.0 µl (2 µl per reaction)

Aliquot 220 µl across a row of a 96-well plate. With a 12-channel pipette add 2 µl in each well of the reaction plates from step 2.

4. Seal each plate with a microseal mat and then centrifuge plates at 1000 rpm for 1 min. Incubate plates on a thermocycler under the following conditions: 20 min at 37°C followed by 5 min at 80°C followed by an indefinite cycle at 15°C. At this stage you can either seal and store plates at –20°C or proceed to the next step.

5. Oligobase Extention

5. Prepare the following mix:

479.0 µl 10× Thermosequenase buffer (0.2 µl per reaction)
914.9 µl H_2O (0.382 µl per reaction)
43.1 µl Thermosequenase (0.018 µl per reaction)
1437.0 µl (0.6 µl per reaction)

Label 12 tubes as in step 1 with the corresponding extend primer mix. Aliquot 114 µl of the aforementioned mix to each tube. To each tube add 95 and 171 µl of the appropriate extend primer mix (0.5 µl per reaction) and stop mix (0.9 µl per reaction), respectively. In the same order as in step 1 (i.e., match PCR to extend reactions), aliquot the content of each tube (26 µl per well) across a row of a 96-well source plate, referred to as extend source plates.

6. Aliquot the contents of the extend source plates into the reaction plates (from step 4) as described in step 2. Transfer 2 µl per well. Seal each plate with a microseal mat and then centrifuge plates at 1000 rpm for 1 min. Cycle plates under the following conditions: one cycle at 94°C for 2 min followed by 55 cycles each consisting of 5 s at 94°C, 5 s at 52°C, and 5 s at 72°C followed by an indefinite cycle at 15°C (to prevent evaporation for overnight runs). At this stage you can either seal and store plates at –20°C or proceed to the next step.

6. Desalting (Resin Step)

7. Add 16 µl of HPLC grade H_2O to each well of the reaction plates from step 6.

8. Use a spoon to apply resin onto a 384-well dimpled plate. Force the resin into the grooves of the dimpled plate using the spoon and the plastic scraper. Scrape off any excess resin and let the dimpled plate stand for 10–15 min at room temperature (resin becomes more compact as it dries out; timing will vary with each resin batch and needs testing).

9. Invert each 384-well reaction plate over a dimpled plate containing resin (allow time between plates if working alone). Align the wells of the two plates (it is easier to hold the two plates above eye level). Hold plates firmly and invert, ensuring no slippage. At this stage the resin should drop into the wells of the reaction plate—if you observe incomplete transfer, then tap the back of the dimple plate gently with a spoon.

10. Seal plates with "3 M scotch pad" adhesive sheets and put them in a plastic bag. Attach bag on the rotator using Velcro. Rotate for 10 min (typically, we set the rotator speed to 8).

11. Centrifuge plates for 4 min at 4000 rpm (maximum speed for centrifuge). At this stage samples are ready for spotting onto spectrochips.

7. Sample Spotting and Analysis by MALDI-TOF Mass Spectrometry

12. Spin the reaction plates from step 11 for 5 min at 4000 rpm.

13. Place plates into the holders of the SpectroPoint (spotting device) and an equal number of spectrochips on the black metal chip holder referred to as SCOUT plate (the Biflex mass spectrometer uses a SCOUT ion source). The spotting device should be operated according to the manufacturer's instructions. In brief, select the chip positions for the run in the "SCOUT plate" window. Click on the "Run" menu and enter the following settings:

Run type: Partial run
Spotting: Wet run
Transfer type: 384 to 384
Select "Main Spots"

Then click on the "Clean" menu and set "Clean cycles" to 1. Start the run. At the end of the run, add 3-oligo calibrant mix to each chip.

14. With tweezers, transfer the chips from the black SCOUT plate to the silver SCOUT plate by matching positions. We use a Biflex mass spectrometer, which runs both the original Bruker software and

Sequenom's SpectroTyper v.2.0 software (a switch box allows to change from one to the other). Note that newer instruments and software are available; follow the instructions provided by the manufacturer. In brief, select the Bruker software, open the mass spectrometer, and insert the loaded SCOUT plate. In the "Automatic probe introduction" window, click "Probe in." From the Auto X menu select "Teach Calib Posit" and look in the monitor if positions (A1 and P24 of chip 1) need adjusting. Switch to the SpectroTyper v.2.0 software, select the Plate Editor, and link the appropriate assay template(s) to the corresponding chip(s). Enter chip(s) into the queue (SpectroAcquire) and initiate the run.

8. Data Analysis

As spectra get acquired, genotype calling occurs in real time so that results are instantly available. Each call has an accompanying tag, namely conservative, moderate, aggressive, or bad spectra, which provides a measure of confidence of the underlying data (pick height, signal-to-noise ratio, etc.). Both conservative and moderate calls are of high quality, whereas aggressive calls may contain errors. Although it strongly depends on the marker assayed, there is a 2- to 10-fold increase in error rate in aggressive calls. Markers with more than 1–2% of aggressive calls are not robust. As a rule of thumb, data from SNPs with an overall call rate <70% should be excluded from further analysis. Robust assays yield a call rate of at least 80%. The software provides several tools to zoom into spectra and alter manually genotype calls.

IV. COMMENTS

One of the major issues relating to genotyping methods is the cost per genotype. Thermosequenase, which is used in the primer extension step in the aforementioned protocol, accounts for 20% of reagent costs per sample. We evaluated the THERMIPol DNA polymerase, which is 80-fold less expensive, as a one-to-one substitute for Thermosequenase (same buffer and cycling conditions). We found excellent concordance between the two enzymes, although we noted a slight drop in the average call rate: <1% with THERMIPol DNA polymerase.

For allele frequency estimation in pooled DNA samples (Ross *et al*., 2000; for review, see Jurinke *et al*.), we use the aforementioned protocol with the following modifications: PCR reactions contain 25 ng of DNA, 200 n*M* of each forward and reverse primer, and 0.04 U of HotStar *Taq* polymerase. Four aliquots per reaction are spotted on the Spectrochip. The laser of mass spectrometer is set to fire at five different areas of each matrix pad. Analysis requires MassARRAY quantitative gene analysis software. We conducted a statistical evaluation of the optimal design for association studies based on pooled DNA samples using this protocol (Downes *et al*., 2004).

V. PITFALLS

1. A problem encountered by all SNP typing methodologies that employ PCR amplification of the locus surrounding the variant to be assayed is allelic dropout. Typically, when screening nonvalidated SNPs we find that 2–3% of markers suffer from this problem. Appropriate controls during assay development, such as duplicate samples or DNAs from related individuals (families, trios), as well as analysis tests such as Hardy–Weinberg, should be applied to weed out nonrobust assays. Be cautious when calling a SNP monomorphic!

2. Although SpectroDesigner checks primers for self-complementarity, empirical data show that self-priming does occur, although with low frequency. Clearly, in the presence of a DNA template this type of reaction is suppressed. However, it is almost impossible without laborious side controls to know whether PCR amplification of a sample has occurred successfully for all the markers in a multiplex reaction. Typically, we test new assays against two positive and two negative controls prior to assaying a larger set of samples. In our experience, markers that trigger a reaction in both negative controls should be excluded (or redesign the assay).

TABLE I Relevant Masses in Da

	Deoxyribonucleotide				Dideoxyribonucleotide			
	dC	**dT**	**dA**	**dG**	**ddC**	**ddT**	**ddA**	**ddG**
ddC	16	31	40	56	0	15	24	40
ddT	1	16	25	41	15	0	9	25
ddA	8	7	16	32	24	9	0	16
ddG	24	9	0	16	40	25	16	0

Residue mass			
ddC	273	O	16
ddT	288	N	14
ddA	297	P	31
ddG	313	Fe	56
dC	289	*Na	23
dT	304	*K	39
dA	313		
dG	329		

3. DNA molecules are negatively charged due to their phosphate backbone, which in the presence of cations leads to adduct formation. For example, a sodium ion attached to an extended product will increase its mass by 23 Da (Table I). Typically, this will cause a split signal at the expected and the +23 Da mass positions. Adduct formation can lead to erroneous calling, especially at higher levels of multiplexing. Ensure that the desalting step is working, i.e., adjust rotation speed or increase incubation time.

References

Braun, A., Little, D. P., and Köster, H. (1997). Detecting CFTR gene mutations by using primer oligo base extension and mass spectrometry. *Clin. Chem*. **43**, 1151–1158.

Downes, K., Barratt, B. J., Akan, P., Bumpstead, S. J., Taylor, S. D., Clayton, D. G., and Deloukas, P. (2004). SNP allele frequency estimation in DNA pools and variance components analysis. *Biotechniques*, **36**, 840–845.

Gabriel, S. B., Schaffner, S. F., Nguyen, H., Moore, J. M., Roy, J., Blumenstiel, B., Higgins, J., DeFelice, M., Lochner, A., Faggart, M., Liu-Cordero, S. N., Rotimi, C., Adeyemo, A., Cooper, R., Ward, R., Lander, E. S., Daly, M. J., and Altshuler, D. (2002). The structure of haplotype blocks in the human genome. *Science* **296**, 2225–2229.

Jeffreys, A. J., Kauppi, L., and Neumann, R. (2001). Intensely punctate meiotic recombination in the class II region of the major histocompatibility complex. *Nature Genet*. **29**, 217–222.

Johnson, G. C., Esposito, L., Barratt, B. J., Smith, A. N., Heward, J., Di Genova, G., Ueda, H., Cordell, H. J., Eaves, I. A., Dudbridge, F., Twells, R. C., Payne, F., Hughes, W., Nutland, S., Stevens, H., Carr, P., Tuomilehto-Wolf, E., Tuomilehto, J., Gough, S. C., Clayton, D. G., and Todd J. A. (2001). Haplotype tagging for the identification of common disease genes. *Nature Genet*. **29**, 233–237.

Jurinke, C., Oeth, P., and van den Boom, D. (2004). MALDI-TOF mass spectrometry: A versatile tool for high-performance DNA analysis. *Mol. Biotechnol*. **26**, 147–164.

Karas, M., and Hillenkamp, F. (1988). Laser desorption ionization of proteins with molecular masses exceeding 10,000 daltons. *Anal. Chem*. **60**, 2299–2301.

Ke, X., Hunt, S., Tapper, W., Lawrence, R., Stavrides, G., Ghori, J., Whittaker, P., Collins, A., Morris, A. P., Bentley, D., Cardon, L. R., and Deloukas, P. (2004). The impact of SNP density on fine-scale patterns of linkage disequilibrium. *Hum. Mol. Genet*. **13**, 577–588.

Kristensen, V. N., Kelefiotis, D., Kristensen, T., and Borresen-Dale, A.-L. (2001). High-throughput methods for detection of genetic variation. *Biotechniques* **30**, 318–332.

Kruglyak, L., and Nickerson, D. A. (2001). Variation is the spice of life. *Nature Genet*. **27,** 234–236.

Kwok, P.-Y. (2001). Methods for genotyping single nucleotide polymorphisms. *Annu. Rev. Genomics Hum. Genet*. **2**, 235–258.

Lechner, D., Lathrop, M. G., and Gut, I. G. (2001). Large-scale genotyping by mass spectrometry: Experience, advances and obstacles. *Curr. Opin. Chem. Biol*. **6**, 31–38.

Little, D. P., Braun, A., O'Donnell, M. J., and Koster, H. (1997). Mass spectrometry from miniaturized arrays for full comparative DNA analysis. *Nature Med*. **3**, 1413–1416.

Mir, K. U., and Southern, E. M. (2000). Sequence variation in genes and genomic DNA: Methods for large-scale analysis. *Annu. Rev. Genomics Hum. Genet*. **1**, 329–360.

Nordhoff, E., Ingendoh, A., Cramer, R., Overberg, A., Stahl, B., Karas, M., Hillenkamp, F., and Crain, P. F. (1992). Matrix-assisted laser desorption/ionization mass spectrometry of nucleic acids with wavelengths in the ultraviolet and infrared. *Rapid Commun. Mass Spectrom*. **6**, 771–776.

Patil, N., Berno, A. J., Hinds, D. A., Barrett, W. A., Doshi, J. M., Hacker, C. R., Kautzer, C. R., Lee, D. H., Marjoribanks, C., McDonough, D. P., Nguyen, B. T., Norris, M. C., Sheehan, J. B., Shen, N., Stern, D., Stokowski, R. P., Thomas, D. J., Trulson, M. O., Vyas, K. R., Frazer, K. A., Fodor, S. P., and Cox, D. R. (2001). Blocks of limited haplotype diversity revealed by high-resolution scanning of human chromosome 21. *Science* **294**, 1719–1723.

Pusch, W., Wurmbach, J. H., Thiele, H., and Kostrzewa, M. (2002). MALDI-TOF mass spectrometry-based genotyping. *Pharmacogenomics* **3**, 537–548.

Ross, P., Hall, L., and Haff L. A. (2000). Quantitative approach to single-nucleotide polymorphism analysis using MALDI-TOF mass spectrometry. *Biotechniques* **29**, 620–626.

Sachidanandam, R., Weissman, D., Schmidt, S. C., Kakol, J. M., Stein, L. D., Marth, G., Sherry, S., Mullikin, J. C., Mortimore, B. J., Willey, D. L., Hunt, S. E., Cole, C. G., Coggill, P. C., Rice, C. M., Ning, Z., Rogers, J., Bentley, D. R., Kwok, PY., Mardis, E. R., Yeh, R. T., Schultz, B., Cook, L., Davenport, R., Dante, M., Fulton, L., Hillier, L., Waterston, R. H., McPherson, J. D., Gilman, B., Schaffner, S., Van Etten, W. J., Reich, D., Higgins, J., Daly, M. J., Blumenstiel, B., Baldwin, J., Stange-Thomann, N., Zody, M. C., Linton, L., Lander, E. S., and Altshuler, D. (2001). A map of human genome sequence variation containing 1.42 million single nucleotide polymorphisms. *Nature* **409**, 928–933.

Sauer, S., Lechner, D., Berlin, K., Lehrach, H., Escary, J. L., Fox, N., and Gut, I. G. (2000). A novel procedure for efficient genotyping of single nucleotide polymorphisms. *Nucleic Acids Res*. **28**, E13.

Syvänen, A.-C. (2001). Accessing genetic variation: Genotyping single nucleotide polymorphisms. *Nature Rev. Genet*. **2**, 930–942.

The International HapMap Consortium (2003). The International HapMap Project. *Nature* **426**, 7897–7896.

The International Human Genome Sequencing Consortium (2001). Initial sequencing of the human genome. *Nature* **409**, 860–921.

The International Human Genome Sequencing Consortium (2004). Finished sequence of the human genome. *Nature*, **431**, 931–945.

CHAPTER

49

Single Nucleotide Polymorphism Analysis by ZipCode-Tagged Microspheres

J. David Taylor, J. David Briley, David P. Yarnall, and Jingwen Chen

I. INTRODUCTION

With the completion of a representative human genomic sequence, emphasis is increasingly shifting toward rapid, cost-effective, high-throughput analysis of individual sequence variation. Although a portion of this variation occurs as nucleotide insertions and deletions, substitutions in the form of single nucleotide polymorphisms (SNPs) are the most common. The total number of SNPs in the human genome may exceed 10 million, if those occurring in only 1% of the population are included (Kruglyak and Nickerson, 2001). High-density analysis of SNPs may uncover a correlation between specific genotypic patterns and disease states (Irizarry, 2001).

Because of this potential payoff, much effort has been focused on the design of SNP analysis platforms and techniques (Syvanen, 2001). Microsphere-based platforms offer a high level of multiplexing capability and provide an "open" system in which reactions can be modified easily by combining different sets of reagent-bearing microspheres (Fulton *et al.*, 1997; Han *et al.*, 2001; Kettman *et al.*, 1998; Oliphant *et al.*, 2002). A plethora of genotyping techniques harness the ability of DNA polymerases to perform high-fidelity extension of a primer along a complementary template (Cai *et al.*, 2000; Chen *et al.*, 2000; Syvanen, 1999; Taylor *et al.*, 2001; Ye *et al.*, 2001).

The genotyping technique detailed here employs a bifunctional capture probe possessing a 3′ end complementary to the genomic target DNA and a 5′ end complementary to an oligonucleotide-covered microsphere. DNA polymerase extends the capture probe with a labeled dideoxynucleotide complementary to the polymorphic base. Reaction products are afterward sequestered onto microspheres and analyzed with a benchtop fluorimeter.

II. MATERIALS AND INSTRUMENTATION

N-(3-Dimethylaminopropyl)-N′-ethylcarbodiimide is from Pierce Biotechnology, Inc. (EDC, Cat. No. 22980). Tween 20 (Cat. No. P7949), 2-(*N*-morpholino)ethanesulfonic acid (MES, Cat. No. M2933), and 5 *M* NaCl (Cat. No. S5150) are from Sigma-Aldrich Corp. A 10% sodium dodecyl sulfate solution (SDS, Cat. No. 15553027), 20× SSC (Cat. No. 15557044), 1 *M* Tris-HCl, pH 8.0 (Cat. No. 15568025), 0.5 *M* EDTA (Cat. No. 15575020), and distilled water (Cat. No. 15230162) are from Invitrogen Corp. Unlabeled ddNTPs are ordered as a set of four separate 5 m*M* dideoxynucleotides from Amersham Biosciences Corp. (Cat. No. 27-2045-01), whereas unlabeled dNTPs are purchased as a blend of all four deoxynucleotides from Applied Biosystems (Cat. No. N808-0260). Biotin-11-ddATP (Cat. No. NEL548), biotin-11-ddCTP (Cat. No. NEL546), biotin-11-ddGTP (Cat. No. NEL549), and biotin-11-ddUTP (Cat. No. NEL547) are purchased as 1 m*M* solutions from Perkin-Elmer Life Sciences. Streptavidin, R-phycoerythrin conjugate (1 mg/ml) comes from Molecular Probes, Inc. (SA-PE, Cat. No. S-866).

Copyright 2006, Elsevier Science (USA).
All rights reserved.

AmpliTaq Gold DNA polymerase (Cat. No. 4311816) with accompanying GeneAmp 10× PCR Gold buffer and 25 m*M* $MgCl_2$ are from Applied Biosystems. Shrimp alkaline phosphatase (SAP, Cat. No. E70092Z), exonuclease I (Cat. No. E70073Z), and Thermo Sequenase DNA polymerase (Cat. No. E79000Y) with included 10× Thermo Sequenase reaction buffer are from Amersham Biosciences Corp.

Biotinylated and unmodified DNA oligonucleotides are synthesized by BioSource International. Amino-modified oligonucleotides are from Oligos Etc., Inc. Human genomic DNA from CEPH reference families is obtained from Coriell Cell Repositories.

The 96-well microtiter plates (Cat. No. AB-0800) and adhesive plate film (Cat. No. AB-0558) are from Marsh Bioproducts. A VWR Model 75D sonic water bath from VWR Scientific Products is used to sonicate microspheres. A Sorvall RT6000D tabletop centrifuge from Kendro Laboratory Products is used to spin microtiter plates. Sheath fluid (Cat. No. 40-50000), carboxylated microspheres (Cat. Nos. L100-C101-01 through L100-C200-01), and the Luminex 100 system are from Luminex Corporation. The RapidPlate 96/384 microplate pipetting workstation is from Zymark Corporation. The PTC-100 thermocyclers are from MJ Research.

III. PROCEDURES

A. Design and Preparation of Oligonucleotides

Steps

1. Design and synthesize forward and reverse PCR primers for amplification of each genomic polymorphism to be assayed. Primers should have a melting temperature (T_m) between 52 and 64°C. Designing all PCR primers to share a common T_m simplifies reaction setup and aids multiplex PCR strategies. Primer positions should be selected so that amplicons are as small as possible, ideally less than 100 bp, with the polymorphic base positioned centrally. Make 100 µ*M* stocks in distilled water.

2. Synthesize a complementary ZipCode (cZipCode) oligonucleotide for each microsphere type being used (up to 100 types). The sequences of a large set of compatible ZipCodes have been published (Iannone *et al.*, 2000). Oligonucleotides should have a 5′ amino group, followed by a 15 to 18-atom spacer. Good results are achieved with use of Uni-Link reagent (amino group plus 6-carbon spacer) followed by a 9-atom spacer. The spacer is followed by a 20 nucleotide tag sequence (LUC) common to all cZipCodes. Incorporation of this tag allows multiplexed quality assurance assays to be performed after microspheres are covalently coupled with oligonucleotides. The LUC tag is an arbitrarily selected portion of the luciferase reporter gene that does not share homology with human genomic targets. The LUC tag is followed by the 25 nucleotides complementary to the ZipCode. The T_m of the cZipCode, excluding the LUC tag, is between 61 and 66°C. The following cZipCode example has the LUC tag underlined: 5′—amino—15 carbon—CAG GCC AAG TAA CTT CTT CGC CGT ACC CTT CCG CTG GAG ATT TAC—3′. Make 1 m*M* stocks in distilled water.

3. Synthesize a biotinylated anti-LUC oligonucleotide with the sequence 5′—CGA AGA AGT TAC TTG GCC TG—3′. The 20mer is biotinylated at the 5′ end and has a T_m of 52°C. Make 10 µ*M* stocks in distilled water.

4. Design and synthesize a capture probe for each polymorphism to be assayed. Probes have a 25-nucleotide ZipCode at the 5′ end and a genomic target-specific 3′ end, terminating immediately before the polymorphic base. The T_m of the genomic target-specific portion should range between 51 and 56°C. The sequence of the positive control capture probe (step 5) serves as an example of these design rules. Make 100 µ*M* stocks in distilled water.

5. Synthesize a positive control capture probe with the sequence 5′—GTA AAT CTC CAG CGG AAG GGT ACG GAT CGG CGA TGC ACT TGG ATT—3′. The ZipCode (T_m = 61°C) is located at the 5′ end and the target-specific sequence (T_m = 52°C) is underlined. Make 10 µ*M* stocks in distilled water.

6. Synthesize a positive control target oligonucleotide with the degenerate sequence 5′—AAC CAG CGG GGC AAC CAA CNA ATC CAA GTG CAT CGC CGA T—3′. The sequence to which the positive control capture probe anneals is underlined. The incorporation of a fourfold degenerate base (N) allows use of a single positive control target, independent of the SNP allele being assayed. Make 10 µ*M* stocks in distilled water.

B. Covalent Coupling of Oligonucleotides to Carboxylated Microspheres

Solutions

1. *0.1 M MES, pH 4.0*: To make 50 ml, dissolve 0.976 g MES in 40 ml distilled water. Adjust pH to 4.0 and add distilled water up to 50 ml. Store at room temperature for months.

2. *30 mg/ml EDC*: Weigh 15 mg EDC directly into a microfuge tube, avoiding any clumps in the stock

bottle. Resuspend in 500 µl distilled water immediately before addition to microspheres. Solid EDC is highly hygroscopic and should be replaced each month. For large-scale couplings, always use a new bottle of EDC to minimize risk of failure in the coupling reaction. Do not prepare this solution in advance.

3. *0.1% SDS*: To make 50 ml, add 500 µl 10% SDS stock to 49.5 ml distilled water. Store at room temperature for months.

4. *0.02% Tween 20*: To make 50 ml, add 10 µl Tween 20 to 49.99 ml distilled water. Store at room temperature for months.

5. *1× TE, pH 8.0 (10 mM Tris–HCl, pH 8, 1 mM EDTA)*: To make 500 ml, combine 5 ml 1 M Tris–HCl, pH 8, 1 ml 0.5 *M* EDTA, pH 8, and 494 ml distilled water. Store at room temperature for months.

Steps

The following protocol has been used for coupling reactions of various sizes, ranging from 625,000 microspheres (50 µl of stock) to 100 million microspheres (8 ml of stock). The only reagent volume adjustment required with increasing microsphere number is a doubling of MES resuspension volumes to 100 µl (step 4) when more than 1 ml of microspheres is coupled.

1. Remove desiccant jar containing solid EDC from freezer and warm to room temperature before opening.
2. Pellet 1 ml of microspheres (12.5 million) by centrifugation in a benchtop microfuge for 5 min at full speed.
3. Carefully remove supernatant by pipette, leaving microsphere pellet completely dry.
4. Add 50 µl 0.1 *M* MES, pH 4.0, and resuspend microspheres.
5. Add 1.5 µl of the appropriate 1 m*M* amino-modified cZipCode oligonucleotide dissolved in distilled water.
6. Prepare a fresh 30-mg/ml solution of EDC in distilled water.
7. Immediately after solvation of the EDC, add 10 µl EDC solution to microspheres. Vortex and sonicate immediately.
8. Incubate at room temperature in the dark for 30 min. Vortex and sonicate every 10 min during this incubation step.
9. Repeat steps 6–8.
10. After the second 30-min incubation, add 800 µl 0.1% SDS, vortex, pellet microspheres, and remove supernatant.
11. Add 800 µl 0.02% Tween 20 to microspheres, vortex, pellet microspheres, and remove supernatant.
12. Resuspend microspheres in 1 ml 1× TE, pH 8.0, to make stocks of approximately 10,000 microspheres/µl. Keep individual microsphere types segregated until a quality control assay has been performed to assess coupling effectiveness for each microsphere.
13. Wrap tubes of microspheres in aluminum foil and store at 4°C.

C. Multiplexed Quality Control Assay for Newly Coupled Microspheres

Solutions

1. *Wash solution (1× SSC/0.02% Tween 20)*: To make 500 ml, combine 25 ml 20× SSC, 100 µl Tween 20, and 475 ml distilled water. Store at room temperature for months.
2. *Staining solution (8.33 µg/ml SA-PE)*: To make 50 ml, mix 417 µl SA-PE with 49.6 ml wash solution. Store wrapped in aluminum foil at 4°C for several months.

Steps

1. Mix together 1 µl of each microsphere type to be tested (up to a maximum of 20 microsphere types). Supplement with distilled water if final volume is less than 20 µl to create a final concentration of 500 microspheres of each type/µl.

2. If a previously tested microsphere is available that successfully passed the quality control assay and that is a different type from the multiplexed microspheres assembled in step 1, that microsphere can be used as an internal positive control. Dilute 1 µl of that microsphere with 19 µl of distilled water to create a solution of 500 microspheres/µl.

3. Combine in a single well of a 96-well plate the following: 2 µl of untested multiplexed microspheres (from step 1), 2 µl of a previously tested microsphere (from step 2), 2 µl 5 *M* NaCl, 0.5 µl of 10 µ*M* biotin-anti-LUC oligonucleotide for each microsphere type (maximum of 10.5 µl of oligonucleotide for 21 microsphere types), and distilled water up to 20 µl final volume.

4. Set up a second reaction that is similar to step 3, but omit the biotin-anti-LUC oligonucleotide. This reaction serves as a negative control.

5. Seal plate and incubate at 37°C for 1 h.

6. Add 120 µl wash solution to each well. Pellet microspheres by centrifuging plate at 2000 rpm for 5 min. Carefully remove supernatant.

7. Resuspend microspheres in 65 µl staining solution and incubate at room temperature in the dark for 30 min.

8. Place plate in LX100 and read 50 µl from each well. Successfully coupled microspheres will generally have mean fluorescent intensity (MFI) values of several thousand units. Microspheres with MFI values below 1000 should be recoupled.

D. Amplification of Genomic Targets and Amplicon Cleanup

Solutions

1. *1.3× PCR mix (261 µM dATP, 261 µM dCTP, 261 µM dGTP, 261 µM dTTP, 1.3× GeneAmp PCR Gold buffer (19.5 mM Tris–HCl, pH 8.0, 65 mM KCl), 3.91 mM $MgCl_2$)*: To make 1265 µl (enough for one 96-well plate), add 770 µl distilled water, 132 µl of 10 m*M* dNTP blend (2.5 m*M* of each dNTP), 198 µl 25 m*M* $MgCl_2$, and 165 µl GeneAmp 10× PCR Gold buffer. This solution can be made in large batches and stored in single-thaw aliquots at –20°C.

2. *PCR primer mix (1 µM each oligonucleotide primer)*: To make 330 µl (enough for one 96-well plate), combine 3.3 µl of each 100 µ*M* forward primer, 3.3 µl of each 100 µ*M* reverse primer, and dilute to 330 µl with distilled water. Carefully designed primer pairs that share a common T_m and that lack cross-complementarity may be multiplexed to robustly amplify up to 10 small amplicons simultaneously.

3. *PCR master mix (200 µM dATP, 200 µM dCTP, 200 µM dGTP, 200 µM dTTP, 3.0 mM $MgCl_2$, 1× GeneAmp PCR Gold buffer (15 mM Tris–HCl, pH 8.0, 50 mM KCl), 200 nM each PCR primer, 166.7 units/ml AmpliTaq Gold DNA polymerase)*: To make 1650 µl (enough for one 96-well plate), combine 1265 µl 1.3× PCR mix, 330 µl PCR primer mix, and 55 µl of 5 U/µl AmpliTaq Gold DNA polymerase. For best results, use master mix immediately.

4. *SAP/Exo digestion mix (1× GeneAmp PCR Gold buffer, 0.4 U/µl SAP, 0.8 U/µl exonuclease I)*: To make 550 µl (enough for one 96-well plate containing 15-µl PCR reaction volumes), combine 55 µl GeneAmp 10× PCR Gold buffer, 220 µl SAP, 44 µl exonuclease I, and 231 µl distilled water. For best results, prepare just prior to use.

Steps

1. Dispense 20 ng genomic DNA into each well of a 96-well plate. Heat to dryness by placing plates into a 55°C oven for 2 h. Dried plates may be safely stored at room temperature for up to 1 month.
2. Add 15 µl PCR master mix to each well of dried genomic DNA plate.
3. Seal plate and spin in centrifuge at 2000 rpm for 20 s.
4. Place plate in thermocycler and heat at 95°C for 10 min, followed by 40 cycles of 94°C for 30 s, 60°C for 30 s, and 72°C for 30 s, finishing with 5 min at 72°C and 4°C hold.
5. If multiplex PCR was not performed, combine equal volumes of all PCR amplicons generated across multiple plates into one common plate for multiplex cleanup. It is not necessary to combine the entire volume from the individual PCR reactions, but the total combined volume must be at least 15 µl per well.
6. For every 15 µl of PCR reaction volume per well, add 5 µl SAP/Exo digestion mix.
7. Mix thoroughly.
8. Incubate in thermocycler at 37°C for 30 min, followed by denaturation of enzymes at 80°C for 15 min and 4°C hold.
9. Plates may be safely stored at 4°C overnight or at –20°C for several days.

E. Polymerase Assay

Solutions

1. *20× positive control (250 nM positive control capture oligonucleotide, 250 nM positive control target oligonucleotide)*: To make 550 µl, mix 13.75 µl 10 µ*M* positive control capture oligonucleotide, 13.75 µl 10 µM positive control target oligonucleotide and 522.5 µl distilled water. Store at 4°C for up to 1 week or store frozen for several months, but avoid refreezing.

2. *20× capture probe multiplex (500 nM solution of each capture probe)*: To make 550 µl, combine 2.75 µl of each 100 µ*M* capture probe stock and add distilled water up to 550 µl. Store at 4°C for up to 1 week or store frozen for several months, but avoid refreezing.

3. *5× capture probe/positive control mix*: To make 2200 µl (typically enough for four 96-well plates of genotyping reactions), combine 550 µl of 20× positive control, 550 µl of 20× capture probe multiplex, and 1100 µl distilled water. Store at 4°C for up to 1 week or store frozen for several months, but avoid refreezing.

4. *1000× minus-A solution (1 mM ddCTP, 1 mM ddGTP, 1 mM ddTTP)*: To make 20 µl (enough for nine plates of reactions), combine 4 µl 5 m*M* ddCTP, 4 µl 5 m*M* ddGTP, 4 µl 5 m*M* ddTTP, and 8 µl distilled water. Store at 4°C for several days or store frozen for several months, but avoid multiple freeze–thaw cycles. Keep in mind that this solution is one specific example of the four solutions required to analyze all of the four possible alleles (A, C, G, and T). To assay an A/G biallelic SNP, you must also prepare a 1000× minus-G solution by substitution of 1 m*M* ddGTP with 1 m*M* ddATP.

5. *2.5× A mix (2.5× Thermo Sequenase reaction buffer, 2.5 µM ddCTP, 2.5 µM ddGTP, 2.5 µM ddTTP, 2.5 µM*

biotin-11-ddATP): To make 880 µl (enough for one 96-well plate of reactions), combine 220 µl 10× Thermo Sequenase buffer, 2.2 µl 1000× minus-A solution, 2.2 µl 1 m*M* biotin-11-ddATP, and 655.6 µl distilled water. Store at 4°C for several days or store frozen for several months, but avoid multiple freeze–thaw cycles. Keep in mind that this solution is one specific example of the four solutions required to analyze all of the four possible alleles (A, C, G, and T). To assay an A/G biallelic SNP, you must also prepare a 2.5× G mix by substitution of 2.5 µ*M* ddGTP with 2.5 µ*M* ddATP and replacement of 2.5 µ*M* biotin-11-ddATP with 2.5 µ*M* biotin-11-ddGTP.

6. *3× microsphere multiplex (100 microspheres of each type/µl, 1.5 M NaCl, 40 mM EDTA)*: To make 2200 µl (enough for two 96-well plates of reactions), combine 22 µl of each type of oligonucleotide-coupled microsphere (10,000/µl), 660 µl 5 *M* NaCl, 176 µl 0.5 *M* EDTA, and distilled water up to 2200 µl. If more than 62 microsphere types are being multiplexed, then the total volume will exceed 2.2 ml. In this case, combine all microsphere types, pellet the microspheres in a centrifuge, and carefully remove a sufficient volume of supernatant before the addition of NaCl and EDTA so that the final volume will equal 2200 µl. If protected from light by wrapping the tube in aluminum foil, this solution can be kept for over 1 year at 4°C.

7. *Wash solution*: See Section III,C, solution 1.

8. *Staining solution*: See Section III,C, Solution 2.

Steps

1. Retrieve plate of multiplexed, digested PCR amplicons from Section III,D, step 9. For every 20 µl of volume per well, add 10 µl of 5× capture probe/positive control mix.

2. From this plate containing PCR amplicons, capture probes and positive control, split out two allele-specific reaction plates by placing 12 µl/well into each of two 96-well plates.

3. Add 10 µl of Thermo Sequenase DNA polymerase to each 880-µl aliquot of 2.5× allele-specific mix. For example, add 10 µl Thermo Sequenase DNA polymerase to 880 µl 2.5× A mix and 10 µl Thermo Sequenase DNA polymerase to 880 µl 2.5× G mix.

4. Complete each allele-specific reaction plate by the addition of 8.1 µl/well of 2.5× A/enzyme mix to one plate and 8.1 µl/well of 2.5× G/enzyme mix to second plate. Each well contains a 20.1-µl reaction with 1× Thermo Sequenase reaction buffer, 1 µ*M* each of three unlabeled ddNTPs, 1 µ*M* of the fourth biotin-labeled ddNTP, multiplexed PCR products, multiplexed capture probes at 25 n*M* each, 12.5 n*M* positive control capture probe, 12.5 n*M* positive control target oligonucleotide, and 145 units/ml Thermo Sequenase DNA polymerase.

5. Seal plates, centrifuge briefly, and place into thermocyclers for a 2-min denaturation at 96°C, followed by 40 cycles of 94°C for 30 s, 55°C for 30 s, and 72°C for 30 s, finally holding at 25°C.

6. Remove plate sealers and add 10 µl/well of 3× microsphere multiplex to each plate. Mix well, reseal each plate, and place into thermocyclers. Incubate at 45°C for 1 h to sequester capture probes onto the microsphere surfaces.

7. Remove plate sealers and add 150 µl/well of wash solution. Centrifuge plates for 5 min at 2000 rpm to pellet microspheres. Carefully remove supernatant containing excess biotin-labeled ddNTPs using a RapidPlate 96/384 microplate pipetting workstation.

8. Resuspend each microsphere pellet in 65 µl of staining solution. Incubate at room temperature in the dark for 30 min.

9. Plates can be analyzed in the Luminex 100 system without further processing. Configure instrument settings to inject 50 µl of sample from each well and analyze at least 30 microspheres of each type per well (30 events).

IV. COMMENTS

Using the protocols described in this article, it is possible to routinely perform 50plex genotyping reactions, generating up to 4800 genotypes per pair of 96-well allele-specific plates.

V. PITFALLS

1. Failure to covalently couple oligonucleotides onto the carboxylated microspheres can frequently be traced to the EDC reagent. Dry EDC is a fine powder. Formation of clumps is a sign of water absorption and will result in poor coupling.

2. Another potential cause of failure in the coupling reaction is use of a poorly synthesized oligonucleotide. Always perform a small test coupling when a new oligonucleotide is synthesized. After an oligonucleotide has been demonstrated to couple effectively, freeze away small aliquots at –70°C for single-thaw use.

3. Microspheres can be photobleached by ambient laboratory light, causing them to lose their spectral identities. Because this is a cumulative process, long-term microsphere stocks, such as bulk carboxylated

microspheres and oligonucleotide-coupled stocks, should be rigorously protected by wrapping in aluminum foil. Coupling reactions in progress should always be placed inside a bench drawer or shaded under a sheet of aluminum foil. Likewise, polymerase reaction plates should not be left unprotected on the benchtop while waiting for availability of a centrifuge or Luminex 100.

4. Occasionally, a capture probe will consistently produce reaction products that display low signal strength or high backgrounds, resulting in poor signal-to-noise ratios. It is sometimes possible to correct this problem by redesigning the capture probe from the opposite genomic strand.

5. Effective removal of unincorporated biotinylated dideoxynucleotides during the wash step can be critical to maximize signal-to-noise ratios. This is especially true for SNPs with weaker signal strength. Remove the largest practical volume of supernatant from the microsphere pellet without risking disturbance of the pellet and resulting loss of microspheres.

References

Cai, H., White, P. S., Torney, D., Deshpande, A., Wang, Z., Marrone, B., and Nolan, J. P. (2000). Flow cytometry-based minisequencing: A new platform for high-throughput single-nucleotide polymorphism scoring. *Genomics* **66**, 135–143.

Chen, J., Iannone, M. A., Li, M., Taylor, J. D., Rivers, P., Nelsen, A. J., Slentz-Kesler, K. A., Roses, A., and Weiner, M. P. (2000). A microsphere-based assay for single nucleotide polymorphism analysis using single base chain extension. *Genome Res.* **10**, 549–557.

Fulton, R. J., McDade, R. L., Smith, P. L., Kienker, L. J., and Kettman, J. R. (1997). Advanced multiplexed analysis with the FlowMetrix system. *Clin. Chem.* **43**, 1749–1756.

Han, M., Gao, X., Su, J. Z., and Nie, S. (2001). Quantum-dot-tagged microbeads for multiplexed optical coding of biomolecules. *Nature* **19**, 631–635.

Iannone, M. A., Taylor, J. D., Chen, J., Li, M., Rivers, P., Slentz-Kesler, K. A., and Weiner, M. P. (2000). Multiplexed single nucleotide polymorphism genotyping by oligonucleotide ligation and flow cytometry. *Cytometry* **39**, 131–140.

Irizarry, K., Hu, G., Wong, M. L., Licinio, J., and Lee, C. J. (2001). Single nucleotide polymorphism identification in candidate gene systems of obesity. *Pharmacogenom. J.* **1**, 193–203.

Kettman, J. R., Davies, T., Chandler, D., Oliver, K. G., and Fulton, R. J. (1998). Classification and properties of 64 multiplexed microsphere sets. *Cytometry* **33**, 234–243.

Kruglyak, L., and Nickerson, D. A. (2001). Variation is the spice of life. *Nature Genet.* **27**, 234–236.

Oliphant, A., Barker, D. L., Stuelpnagel, J. R., and Chee, M. S. (2002). BeadArray technology: Enabling an accurate, cost-effective approach to high-throughput genotyping. *BioTechniques* **32**, S56–S61.

Syvanen, A. C. (1999). From gels to chips: "Minisequencing" primer extension for analysis of point mutations and single nucleotide polymorphisms. *Hum. Mutat.* **13**, 1–10.

Syvanen, A. C. (2001). Accessing genetic variation: Genotyping single nucleotide polymorphisms. *Nature Rev. Genet.* **2**, 930–942.

Taylor, J. D., Briley, D., Nguyen, Q., Long, K., Iannone, M. A., Li, M.-S., Ye, F., Afshari, A., Lai, E., Wagner, M., Chen, J., and Weiner, M. P. (2001). A flow cytometric platform for high throughput single nucleotide polymorphism analysis. *BioTechniques* **30**, 661–669.

Ye, F., Li, M., Taylor, J. D., Nguyen, Q., Colton, H. M., Casey, W. M., Wagner, M., Weiner, M. P., and Chen, J. (2001). Fluorescent microsphere-based readout technology for multiplexed human single nucleotide polymorphism analysis and bacterial identification. *Hum. Mutat.* **17**, 305–316.

CHAPTER

50

Polymerase Chain Reaction-Based Amplification Method of Retaining the Quantitative Difference between Two Complex Genomes

Gang Wang, Brendan D. Price, and G. Mike Makrigiorgos

I. INTRODUCTION

Technologies for analyzing gene expression and gene copy number changes are increasingly used in the detection, diagnosis, and therapy of cancer. The clinical outcome of various breast cancer therapies correlates closely with distinct mRNA expression profiles detected using DNA microarrays (Alizadeh *et al*., 2001; Perou *et al*., 1999; Ross and Perou, 2001; Sorlie *et al*., 2001; van't Veer *et al*., 2002). Array-based comparative genomic hybridization (array-CGH) can detect the amplification or deletion of candidate breast cancer genes as well as genomic instability within tumor cells (Albertson *et al*., 2000; Kallioniemi *et al*., 1992, 1994; Pinkel *et al*., 1998; Pollack *et al*., 1999). Subtractive hybridization methods, such as differential display or representational difference analysis, are also used for breast cancer gene discovery (Scheurle *et al*., 2000). Such genetic profiling–based diagnosis can potentially revolutionize the existing staging system and the management of early breast disease (Burki *et al*., 2000). However, analysis of genetic changes in tumors using these techniques requires "µgs" of pure tumor DNA (Klein *et al*., 1999; Lucito *et al*., 1998). Routine tumor biopsies often consist of inhomogeneous mixtures of stromal cells plus tumor cells with a wide range of genetic profiles (Rubin, 2002). Newer techniques, such as fine needle aspiration (FNA) and laser capture microdissection (LCM), allow for the removal of minute amounts of tissue from tumors (Rubin, 2002). LCM can isolate homogeneous populations of normal or tumor cells, potentially resolving tissue into single cells (Assersohn *et al*., 2002; Emmert-Buck *et al*., 1996). However, the yield of RNA/DNA from small cell numbers dictates that LCM must be coupled to a DNA amplification step, usually by use of the polymerase chain reaction (PCR) (Assersohn *et al*., 2002).

A major problem with PCR is that amplification occurs in a nonlinear manner and reproducibility is influenced by stray impurities (Heid, 1996). The exponential mode of DNA amplification and concentration-dependent PCR saturation are notorious for introduction of bias (Heid, 1996). As a result, when amplifying two complex DNA populations, the quantitative relationship between two genes after amplification is generally not the same as their relation prior to amplification. Real-time PCR strategies can retain the initial relation among alleles when a single gene is amplified from two sources (Celi *et al*., 1994). Further, methods exist to PCR amplify whole genomic DNA from as little as a single cell (Klein *et al*., 1999; Nelson *et al*., 1989; Zhang *et al*., 1992). However, the quantitative amplification of the entire population of DNA fragments ("alleles") from two different complex genomes is not possible using conventional PCR. Multiple strand displacement isothermal amplification (MDA) is an alternative to PCR that has shown promise in a number of investigations (Dean *et al*., 2002; Zhang *et al*., 1992). However, MDA requires long

Copyright 2006, Elsevier Science (USA).
All rights reserved.

DNA stretches to work effectively and therefore it is inefficient when formalin-fixed, archival genomic DNA is to be amplified (Lage *et al*., 2003) or when cDNA amplification for gene expression profiling on microarrays is required.

We have described balanced PCR (Makrigiorgos *et al*., 2002), a method that overcomes biases associated with PCR amplification of complex genomes and faithfully retains the difference among corresponding genes, or gene fragments over the entire sample. This approach, which can be applied to the amplification of both genomic DNA and cDNA, utilizes a simple principle (Fig. 1). Two distinct genomic DNA samples, a "target" sample and a "control" sample, are tagged with oligonucleotides (LN1, LN2) containing both a common (P1) and a unique DNA sequence (P2a, P2b). The genomic DNA samples are pooled and amplified in a single PCR tube using the common DNA tag, P1. By mixing the two genomes, PCR "loses" the ability to discriminate between the different alleles and the influence of impurities tends to cancel. The PCR-amplified pooled samples can subsequently be differentially labeled or separated using the DNA tag unique to each individual DNA sample. This balanced PCR approach has been validated with amplification of cDNA for gene expression profiling (Makrigiorgos *et al*., 2002) and genomic DNA for array CGH profiling (Wang *et al*., submitted for publication).

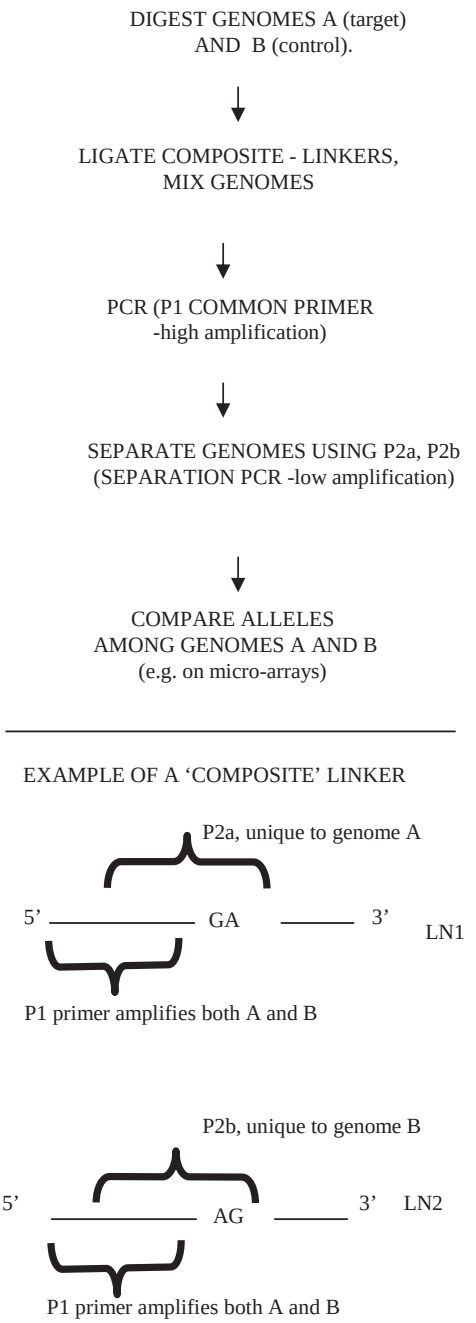

FIGURE 1 Outline of balanced PCR amplification of cDNA or genomic DNA. Reproduced with permission from Nature Publishing Group.

II. MATERIALS

*Nla*III (Cat. No. R0125S), *Dpn*II (Cat. No. R0543S), *Sau*3A (Cat. No. R0169S), and T4 DNA ligase (Cat. No. M0202T) are from New England Biolabs. Advantage 2 PCR kit (K1910-1) and TITANIUM *Taq* PCR kit (K1915-1) are from BD Biosciences. RNeasy minikit (Cat. No. 74104) and QIAquick PCR purification kit (Cat. No. 28104) are from Qiagen. The SuperScript double-stranded cDNA synthesis kit (Cat. No. 11917-020) is from Invitrogen. Picogreen dsDNA quantitation reagent (P-7581) is from Molecular Probes. Linkers are synthesized from Oligos Etc. PCR reactions are performed with a TechGene thermocycler (TECHNE).

III. PROCEDURES

A. Double-Strand cDNA Synthesis

The protocols recommended by the manufacturers were used to extract total RNA from breast or prostate cells (RNeasy minikit), to reverse transcribe to cDNA using Oligo(dT)$_{12–18}$ primers, and to synthesize double-stranded cDNA (SuperScript double-stranded cDNA synthesis kit).

B. Balanced PCR Protocol

This procedure is a modification of the one originally reported (Makrigiorgos *et al*., 2002) and can be

used for amplification of either cDNA or whole genomic DNA. The procedure has been tested with starting amounts of 1–10 ng total mRNA and with 1–10 ng of total genomic DNA extracted from target (e.g., tumor) and control (e.g., normal tissue) cells.

Steps

1. Digestion. The protocol described here employees either *Nla*III or *Dpn*II/*Sau*3A for double-stranded cDNA digestion. Mix 1 µl of 10 ng/µl cDNA from the target cells (e.g., tumor) or from the control cells (e.g., normal tissue) with 0.5 µl of 10× T4 DNA ligase buffer, 0.5 µl of 10 U/µl *Nla*III/*Dpn*II/*Sau*3A, and 3 µl of H_2O. Incubate this mixture at 37°C for 1 h.

2. Ligation. Add 0.5 µl of 10× ligase buffer, 0.3 µl of 2.8 µg/µl linker, and 3.7 µl H_2O into digestion solution. For digestion with *Nla*III, linker LN1 is used for control and LN2 for target cDNA (Table I). For digestion with *Dpn*II or *Sau*3A, linker LN1 and an equimolar amount LN1a are used for ligation to the control cDNA; and linker LN2 and an equimolar amount of LN2a are used for ligation to the target cDNA (Table II). Anneal the appropriate linkers to cDNA by serially decreasing temperature of the sample from 50 to 10°C at 5°C ramp in 5-min steps. Then add 0.5 µl of 2000 U/µl T4 DNA ligase and incubate at room temperature for 1 h.

3. Purification. Mix together cDNAs ligated to different linkers and purify the mixture with a QIAquick PCR purification kit. Purification is not needed if only a fraction of the ligation mixture (e.g., 10% of the total volume) is used in the subsequent coamplification PCR reaction.

4. Coamplification PCR. To 20 µl of purified-ligated DNA, add 5 µl of 10× Advantage 2 PCR buffer, 1 µl of 50× Advantage 2 polymerase mix, 1 µl of 50× dNTP mix (10 m*M* each), 1 µl of 10 µ*M* common primer P1, and 22 µl of H_2O. Perform PCR at 72°C for 8 min; 95°C for 1 min; 20 cycles of 95°C for 30 s; 72°C for 1 min; and then 72°C for 5 min. Purify the PCR product twice with QIAquick PCR purification kit and elute the DNA in 50 µl of H_2O. Quantify cDNA concentration with Picogreen. This procedure usually yields 2–3 µg cDNA from an original material of ~5 ng cDNA.

5. Separation. Mix 1 µl of 3 ng/µl DNA with 5 µl of 10× TITANIUM *Taq* PCR buffer, 1 µl of 50× TITANIUM *Taq* polymerase, 1 µl of 50× dNTP Mix (10 m*M* each), 5 µl of 4 µ*M* P2a for LN1-ligated cDNA or P2b for LN2-ligated cDNA, and 37 µl of H_2O. Separate and amplify cDNA at 95°C for 1 min; 10 cycles of 95°C for 30 s; 72°C for 1 min; and 72°C for 5 min. Each 10-cycle PCR reaction is expected to produce 1–1.5 µg cDNA. Scale the number of individual reactions as needed to produce the desired total amount of amplified cDNA.

TABLE I Sequences of Linkers and Primers Used in Conjunction with *Nla*III Digestion

		Sequences (5′–3′)
Linkers and primers	LN1	AACTGTGCTATCCGAGGGAAAGGACATG
	LN2	AACTGTGCTATCCGAGGGAAAGAGCATG
	P1	AGGCAACTGTGCTATCCGAGGGAA
	P2a	AACTGTGCTATCCGAGGGAAAGGA
	P2b	AACTGTGCTATCCGAGGGAAAGAG

TABLE II Sequences of Linkers and Primers Used in Conjunction with *Dpn*II or *Sau*3A Digestion

		Sequences (5′–3′)
Primers and linkers	LN1	AACTGTGCTATCCGAGGGAAAGGACATG
	LN1a	GATCCATGTCCT
	LN2	AACTGTGCTATCCGAGGGAAAGAGCATG
	LN2b	GATCCATGCTCT
	P1	AGGCAACTGTGCTATCCGAGGGAA
	P2a	AACTGTGCTATCCGAGGGAAAGGA
	P2b	AACTGTGCTATCCGAGGGAAAGAG

IV. EXAMPLES

Microarray Screening for Prostate and Lung cDNA before and after Balanced PCR

As an example of the balanced PCR to retain the difference among alleles between two cDNA populations, microarray studies of human prostate (representing the "target") and lung-derived cDNA (representing the "control") were employed. Digested cDNA was ligated to linkers and screened directly on the Affymetrix Genechip cancer microarrays following the procedure described earlier (Zhang *et al*., 2001). Next, prostate and lung cDNA samples were mixed 1:1 and amplified via balanced PCR for three consecutive PCR rounds of 20 cycles each. The samples were then separated using the procedure of Fig. 1 and screened on microarrays. The ratio of signal intensities after balanced PCR was plotted versus the same ratio prior to balanced PCR (Fig. 2A). The ratio of expression levels for the majority of genes remained relatively unchanged after balanced PCR, as indicated by the distribution of data in Fig. 2A ($R^2 = 0.92$). Next the experiment was repeated the "traditional" way, i.e., by PCR amplifying separately the prostate and lung cDNA samples and screening each on microarrays (Fig. 2B). Data indicate that, for a substantial fraction of genes,

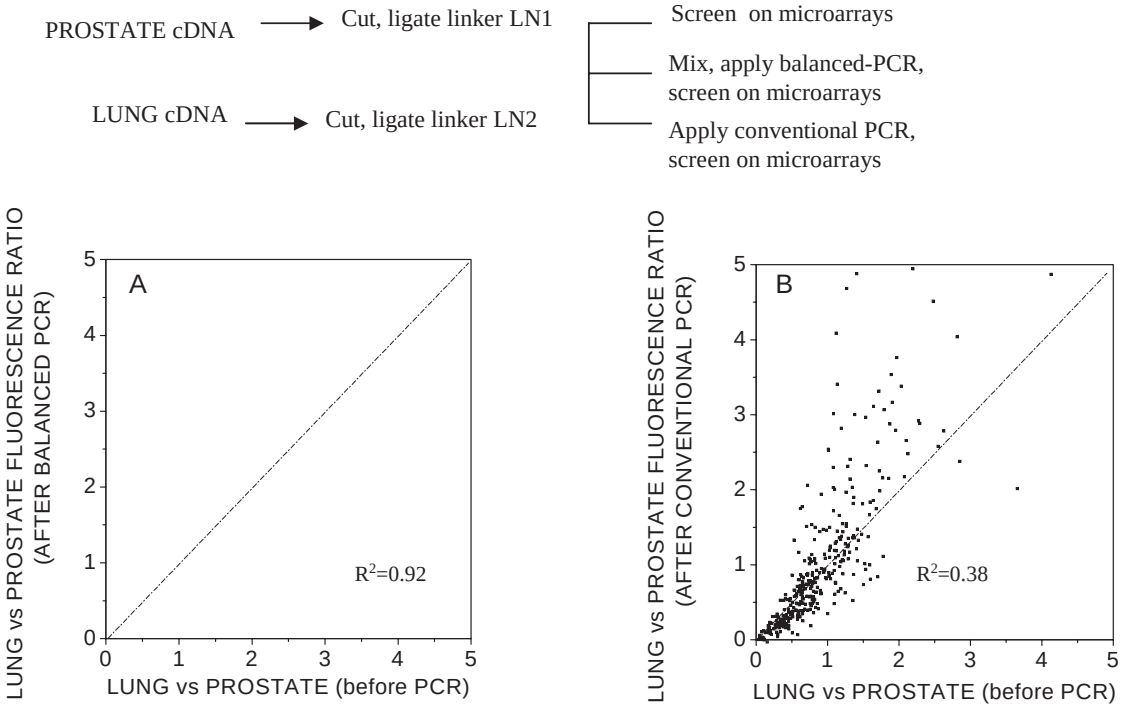

FIGURE 2 Comparison of relative expression of lung vs prostate tissue on microarrays before and after PCR amplification. (**A**) Amplification conducted using the current balanced PCR method. (**B**) Amplification conducted by performing conventional PCR, separately on lung and prostate cDNA samples.

the ratio of expression levels is substantially different from the original one, presumably due to PCR-introduced changes in the original relative expression levels among prostate and lung ($R^2 = 0.38$).

In Figs. 3A and 3B, the comparison between balanced PCR and conventional PCR is depicted for 30 genes that presented the highest upregulation in prostate versus lung. Most are widely known prostate—specific genes, such as the prostate-specific antigen (PSA), prostatic acid phosphatase, and prostatic kallikrein. Figure 3A indicates a good retention of the relative expression levels before and after balanced PCR for almost all these genes (correlation coefficient = 0.800). In contrast, Fig. 3B demonstrates that distortions are introduced if the samples are amplified separately, using conventional PCR, presumably due to a PCR-introduced change in the original relative expression levels among prostate and lung (correlation coefficient = 0.28). Genes important to prostate cancer development, such as PSA and prostatic acid phosphatase are overestimated by more than a factor of 10 when amplified via traditional PCR, but are quantitated correctly when amplified via balanced PCR prior to microarray screening. Of all 407 genes considered, the percentage of genes that had their relative signal change by more than 2-fold or by more than 1.3-fold after performing PCR amplification is depicted in Fig. 3C. Because the deviations observed using balanced PCR are less or equal to the microarray—related deviation [established by repeated application of a single sample on different arrays (Makrigiorgos *et al*., 2002)], it is concluded that balanced PCR introduced minimal distortion in the relative expression among prostate and lung (i.e., balanced PCR error < array error).

V. POTENTIAL PITFALLS USING BALANCED PCR

A. Efficiency of Enzymatic Treatments

A requirement for the success of balanced PCR is that treatment of target and control DNA is identical at all stages prior to mixing the samples. We conducted control studies and we included internal standards for digestion using *Sau*3A and ligation to derive the efficiency of digestion and ligation steps (Makrigiorgos *et al*., 2002). Both were found to be more than 95% efficient. However, if the enzymatic efficiency is reduced due to degradation of the enzyme stocks, impurities, or methylation sensitivity, bias may be introduced in

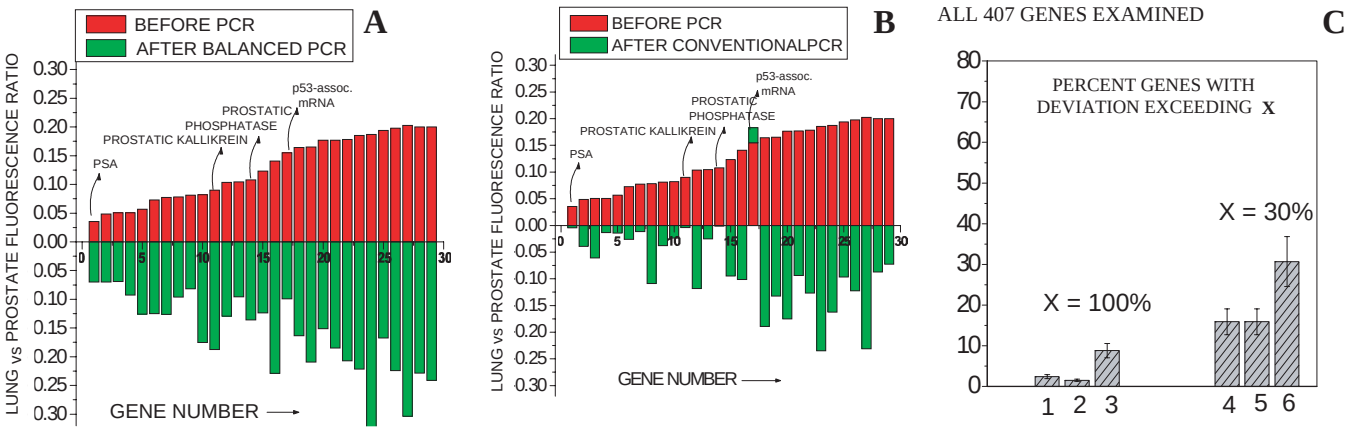

FIGURE 3 Comparison of relative expression of lung vs prostate specifically for the 30 genes highest upregulated in prostate vs lung. (**A**) Amplification conducted using the current balanced PCR method. (**B**) Amplification conducted by performing conventional PCR, separately on lung and prostate cDNA samples. (**C**) Fraction of genes whose relative expression among prostate and lung changes by more than 100% (**columns 1–3**) or 30% (**columns 4–6**) following PCR amplification. **Columns 1 and 4**, repeated application of the same sample on microarrays. **Columns 2 and 5**, amplification via balanced PCR. **Columns 3 and 6**, amplification via conventional PCR. Reproduced with permission from Nature Publishing Group.

the first step of the procedure. This can be avoided by using freshly obtained enzymes that are highly efficient and that are not sensitive to mammalian CpG methylation.

B. Post-PCR Separation

Another assumption is that the low cycle PCR used for reseparation of the two genomes following the common PCR step does not produce distortions among DNA samples. It is, in principle, possible that this PCR might itself produce some bias among alleles in the two populations. In practice, however, we have found that this 10 cycle separation PCR does not introduce significant distortion among alleles differing by at least 50-fold in initial concentration in any of the systems examined [plasmid, genomic DNA, cDNA (Makrigiorgos *et al*., 2002)]. However, it is not recommended to increase the separation PCR cycles to beyond 10.

C. The Effect of Mutations and Polymorphisms

Balanced PCR uses templates from enzyme-digested fragments. If mutations occur within the restriction sequences in the target or control cDNAs, then the enzyme will not digest at that position, but will act in the next available restriction sequence. As a result, certain gene fragments in the target genome will be different in size from their alleles in the control genome and PCR amplification may introduce bias if the fragment sizes are too different. Mutations that occur specifically at the restriction sites are not frequent. The most common form of mutations is single nucleotide polymorphisms (SNPs), which, between two given genomes, occur with a frequency of about 1:1000 bases. The chance that a four-base cutter enzyme used in balanced PCR encounters a SNP is roughly 4/1000 = 0.4%, and therefore it would affect only a small fraction of the sequences amplified. Because several SNPs are already tabulated in databases and more will become known in the near future, one can use computational methods to predict which restriction sites will be altered due to a SNP in order to anticipate potential PCR bias at these positions. If these sequences are vital, one may perform balanced PCR using a different restriction enzyme.

Acknowledgment

Funding for this work was provided in part by DOD Grant BC020504.

References

Albertson, D. G., Ylstra, B., Segraves, R., Collins, C., Dairkee, S. H., Kowbel, D., Kuo, W. L., Gray, J. W., and Pinkel, D. (2000). Quantitative mapping of amplicon structure by array CGH identifies CYP24 as a candidate oncogene. *Nature Genet.* **25**, 144–146.

Alizadeh, A. A., Ross, D. T., Perou, C. M., and van de Rijn, M. (2001). Towards a novel classification of human malignancies based on gene expression patterns. *J. Pathol.* **195**, 41–52.

Assersohn, L., Gangi, L., Zhao, Y., Dowsett, M., Simon, R., Powles, T. J., and Liu, E. T. (2002). The feasibility of using fine needle aspiration from primary breast cancers for cDNA microarray analyses. *Clin. Cancer Res.* **8**, 794–801.

Burki, N. G., Caduff, R., Walt, H., Moll, C., Pejovic, T., Haller, U., and Ward, D. C. (2000). Comparative genomic hybridization of fine needle aspirates from breast carcinomas. *Int. J. Cancer* **88**, 607–613.

Celi, F. S., Cohen, M. M., Antonarakis, S. E., Wertheimer, E., Roth, J., and Shuldiner, A. R. (1994). Determination of gene dosage by a quantitative adaptation of the polymerase chain reaction (gd-PCR): Rapid detection of deletions and duplications of gene sequences. *Genomics* **21**, 304–310.

Dean, F. B., Hosono, S., Fang, L., Wu, X., Faruqi, A. F., Bray-Ward, P., Sun, Z., Zong, Q., Du, Y., Du, J. Driscoll, M., Song, W., Kingsmore, S. F., Egholm, M., and Lasken, R. S. (2002). Comprehensive human genome amplification using multiple displacement amplification. *Proc. Natl. Acad. Sci. USA* **99**, 5261–5266.

Emmert-Buck, M. R., Bonner, R. F., Smith, P. D., Chuaqui, R. F., Zhuang, Z., Goldstein, S. R., Weiss, R. A., and Liotta, L. A. (1996). Laser capture microdissection. *Science* **274**, 998–1001.

Heid, C., Stevens, J., Livak, K., and Williams, P. (1996). *Real time quantitative PCR.* In "*Genome Methods: Genome Research*." Cold Spring Harbor Laboratory Press, Cold Spring Harbor, NY.

Kallioniemi, A., Kallioniemi, O. P., Piper, J., Tanner, M., Stokke, T., Chen, L., Smith, H. S., Pinkel, D., Gray, J. W., and Waldman, F. M., (1994). Detection and mapping of amplified DNA sequences in breast cancer by comparative genomic hybridization. *Proc. Natl. Acad. Sci. USA* **91**, 2156–2160.

Kallioniemi, A., Kallioniemi, O. P., Sudar, D., Rutovitz, D., Gray, J. W., Waldman, F., and Pinkel, D. (1992). Comparative genomic hybridization for molecular cytogenetic analysis of solid tumors. *Science* **258**, 818–821.

Klein, C. A., Schmidt-Kittler, O., Schardt, J. A., Pantel, K., Speicher, M. R., and Riethmuller, G. (1999). Comparative genomic hybridization, loss of heterozygosity, and DNA sequence analysis of single cells. *Proc. Natl. Acad. Sci. USA* **96**, 4494–4499.

Lage, J. M., Leamon, J. H., Pejovic, T., Hamann, S., Lacey, M., Dillon, D., Segraves, R., Vossbrinck, B., Gonzalez, A., Pinkel, D., Albertson, D. G., Costa, J., and Lizardi, P. M. (2003). Whole genome analysis of genetic alterations in small DNA samples using hyperbranched strand displacement amplification and array-CGH. *Genome Res.* **13**, 294–307.

Lucito, R., Nakimura, M., West, J. A., Han, Y., Chin, K., Jensen, K., McCombie, R., Gray, J. W., and Wigler, M. (1998). Genetic analysis using genomic representations. *Proc. Natl. Acad. Sci. USA* **95**, 4487–4492.

Makrigiorgos, G. M., Chakrabarti, S., Zhang, Y., Kaur, M., and Price, B. D. (2002). A PCR-based amplification method retaining the quantitative difference between two complex genomes. *Nature Biotechnol.* **20**, 936–939.

Nelson, D. L., Ledbetter, S. A., Corbo, L., Victoria, M. F., Ramirez-Solis, R., Webster, T. D., Ledbetter, D. H., and Caskey, C. T. (1989). Alu polymerase chain reaction: A method for rapid isolation of human-specific sequences from complex DNA sources. *Proc. Natl. Acad. Sci. USA* **86**, 6686–6690.

Perou, C. M., Jeffrey, S. S., van de Rijn, M., Rees, C. A., Eisen, M. B., Ross, D. T., Pergamenschikov, A., Williams, C. F., Zhu, S. X., Lee, J. C., Lashkari, D., Shalon, D., Brown, P. O., and Botstein, D. (1999). Distinctive gene expression patterns in human mammary epithelial cells and breast cancers. *Proc. Natl. Acad. Sci. USA* **96**, 9212–9217.

Pinkel, D., Segraves, R., Sudar, D., Clark, S., Poole, I., Kowbel, D., Collins, C., Kuo, W. L., Chen, C., Zhai, Y., Dairkee, S. H., Ljung, B. M., Gray, J. W., and Albertson, D. G. (1998). High resolution analysis of DNA copy number variation using comparative genomic hybridization to microarrays. *Nature Genet.* **20**, 207–211.

Pollack, J. R., Perou, C. M., Alizadeh, A. A., Eisen, M. B., Pergamenschikov, A., Williams, C. F., Jeffrey, S. S., Botstein, D., and Brown, P. O. (1999). Genome-wide analysis of DNA copy-number changes using cDNA microarrays. *Nature Genet.* **23**, 41–46.

Ross, D. T., and Perou, C. M. (2001). A comparison of gene expression signatures from breast tumors and breast tissue derived cell lines. *Dis. Mark.* **17**, 99–109.

Rubin, M. A. (2002). Understanding disease cell by cell. *Science* **296**, 1329–1330.

Scheurle, D., DeYoung, M. P., Binninger, D. M., Page, H., Jahanzeb, M., and Narayanan, R. (2000). Cancer gene discovery using digital differential display. *Cancer Res.* **60**, 4037–4043.

Sorlie, T., Perou, C. M., Tibshirani, R., Aas, T., Geisler, S., Johnsen, H., Hastie, T., Eisen, M. B., van de Rijn, M., Jeffrey, S. S., Thorsen, T., Quist, H., Matese, J. C., Brown, P. O., Botstein, D., Eystein Lonning, P., and Borresen-Dale, A. L. (2001). Gene expression patterns of breast carcinomas distinguish tumor subclasses with clinical implications. *Proc. Natl. Acad. Sci. USA* **98**, 10869–10874.

Telenius, H., Carter, N. P., Bebb, C. E., Nordenskjold, M., Ponder, B. A., and Tunnacliffe, A. (1992). Degenerate oligonucleotide-primed PCR: General amplification of target DNA by a single degenerate primer. *Genomics* **13**, 718–725.

van 't Veer, L. J., Dai, H., van de Vijver, M. J., He, Y. D., Hart, A. A., Mao, M., Peterse, H. L., van der Kooy, K., Marton, M. J., Witteveen, A. T., Schreiber, G. J., Kerkhoven, R. M., Roberts, C., Linsley, P. S., Bernards, R., and Friend, S. H. (2002). Gene expression profiling predicts clinical outcome of breast cancer. *Nature* **415**, 530–536.

Wang, G., Brennan, C., Rook, M., Wolfe, J., Leo, C., Chin, L., Pan, H., Liu, W., Price, B., and Makrigiorgos, G. M. (2004). Balanced-PCR amplification allows unbiased identification of genomic copy changes in minute cell and tissue samples. *Nucleic Acids Research*, **32,** e76.

Zhang, L., Cui, X., Schmitt, K., Hubert, R., Navidi, W., and Arnheim, N. (1992). Whole genome amplification from a single cell: Implications for genetic analysis. *Proc. Natl. Acad. Sci. USA* **89**, 5847–5851.

Zhang, Y., Price, B. D., Tetradis, S., Chakrabarti, S., Maulik, G., and Makrigiorgos, G. M. (2001). Reproducible and inexpensive probe preparation for oligonucleotide arrays. *Nucleic Acids Res.* **29**, E66–E66.

PART

H

TRANSGENIC, KNOCKOUTS, AND KNOCKDOWN METHODS

SECTION

17

Transgenic, Knockouts and Knockdown Methods

CHAPTER

51

Production of Transgenic Mice by Pronuclear Microinjection

Jon W. Gordon

I. INTRODUCTION

The technique for introducing generic material into the mouse germ line by pronuclear microinjection was first developed by Gordon *et al.* (1980). These animals, subsequently called "transgenic" (Gordon and Ruddle, 1981) to indicate the presence of foreign DNA within their genomes, frequently express the donor genes highly efficiently (Brinster *et al.*, 1981), with the tissue distribution of expression determined primarily by *cis*-acting promoter enhancer elements within or in the immediate vicinity of the genes themselves (Brinster *et al.*, 1981; reviewed by Palmiter and Brinster, 1986; Gordon, 1989). This technique has proven extremely important for basic investigations of gene regulation, creation of animal models of human disease (e.g., Stacey *et al.*, 1988), and genetic engineering of livestock (Hammer *et a.*, 1985; Gordon *et al.*, 1987). This technique has also been described in extensive detail in several other publications (Gordon and Ruddle, 1983).

II. MATERIALS AND INSTRUMENTATION

The following reagents are required for the production of transgenic mice. All stock numbers denote compounds from Sigma unless otherwise indicated: NaCl (Cat. No. S-9888), KCl (Cat. No. P-4504), KH_2PO_4 (Cat. No. P-5379), $MgSO_4 \cdot 7H_2O$ (Cat. No. M-1880), sodium lactate syrup (60%, Cat. No. L-1375), penicillin G (PEN-NA), streptomycin (Cat. No. S-6501), bovine serum albumin (BSA) (fraction V, Cat. No. A-8022), HEPES (Cat. No. H-3375), $CaCl_2$ (Cat. No. C-3881), sodium pyruvate (Cat. No. P-5280), hyaluronidase (Cat. No. H-3506), mineral oil (Cat. No. M-3516), propylene glycol (Cat. No. P-5280), NaOH (Cat. No. S-5881), concentrated HC1 (Fisher, Cat. No. A144-500), 100% ethanol (any supplier), Na pentobarbital (60 mg/ml, Fort Dodge, Cat. No. 1206-1E), pregnant mares' serum (Cat. No. G-4877), human chorionic gonadotropin (Cat. No. CG-10), and Fluorinert (3M, Cat. No. FC-77).

Equipment includes 35-mm tissue culture dishes (Falcon, Cat. No. 3001), 100-mm bacterial culture plates (Falcon, Cat. No. 1029), 10-ml pipette (Falcon, Cat. No. 7551), 5-ml pipette (Falcon, Cat. No. 7543), 15-ml sterile conical centrifuge tube (Falcon, Cat. No. 2097), 50-ml sterile conical centrifuge tube (Baxter, Cat. No. C3920-50), mounted 0.22-mm filter syringe (USA Scientific, Cat. No. F192), sterile filter apparatus (Nalgene, 100 ml, Cat. No. 120-0020; 250 ml, Cat. No. 116-0020; 500 ml, Cat. No. 450-0020), 9-in. Pasteur pipette (Kimble, Cat. No. 72050), depression slides (Fisher, Cat. No. 12-565A), surgical needles with cutting edge (Anchor, Cat. No. 1834-9), 4-0 silk (Ethicon, Cat. No. A-303), surgical iris scissors (Stroz, Cat. No. E-3404), No. 5 Dumont watchmaker's forceps (Fullam, Cat. No. 14040), hemostat (Fisher SCM 1004), microcapillary tubing for DNA injection (Cat. No. 1211L Omega Dot, Glass Co. of America), microcapillary tubing for making holding pipettes (Mertex, 100 × 0.5 mm i.d.), spinal needle for filling barrel of microcapillary tubing (Popper & Sons Quinke Babcock 26G), polyethylene tubing for connecting syringe to microneedle (Intramedic PE60, PE90, PE160, PE190), plastic tubing adaptor with Luer lock for PE tubing (Clay Adams A-1026, size B fits PE60 and PE90, size C fits PE160 and PE 190), vertical or horizontal pipette puller (e.g., David Kopf No. 700C), microforge (e.g.,

Copyright 2006, Elsevier Science (USA).
All rights reserved.

DeFonbrune MF-1), mechanical microinjector (e.g., Narishige M5-A), micromanipulation apparatus with phase-contrast optics, two micromanipulators, and dissecting microscope (e.g., Leitz or Narishige). When one micromanipulation device is chosen over another, the choice may dictate the use of supplies that are especially compatible with the equipment available. Also needed is a CO_2 incubator from a suitable supplier.

III. PROCEDURES

A. Preparation of Culture Media and Related Reagents

These procedures are from Gordon and Ruddle (1983) and Quinn *et al.* (1982).

Solutions

Weigh solids into a clear flask or appropriate sized disposable conical centrifuge tubes and add appropriate quantity of distilled H_2O (18 MO).

1. *10× stock solution A for M16 and M2 culture media:* Combine 5.534 g NaCl, 0.356 g KC1, 0.162 g KH_2PO_4, 0.293 g $MgSO_4 \cdot 7H_2O$, 4.439 g or 2.61 ml Na lactate (60% syrup), 1.0 g glucose, 0.060 g penicillin, and 0.05 streptomycin. Add distilled H_2O to 100 ml. If Na lactate syrup is weighed, use a small weighing boat and decant contents into flask, rinse boat two to three times with distilled H_2O, and decant rinse into flask. Solution can be stored for 3 months.
2. *10× stock solution B for M16 and M2 culture media:* Combine 2.101 g $NaHCO_3$ and 1.0 ml phenol red (0.5% solution). Add distilled H_2O to 100 ml. Can be stored for 2 weeks.
3. *100× stock solution C for M16 and M2 culture media:* 0.180 g Na pyruvate. Add distilled H_2O to 50 ml. Can be stored for 2 weeks.
4. *100× stock solution D for M16 and M2 culture media:* 0.252 g $CaCl_2 \cdot 2H_2O$. Add distilled H_2O to 10 ml. Solution can be stored for 3 months.
5. *10× stock solution E for M2 culture medium:* Weigh out 5.958 g HEPES (solid) and add 0.010 ml phenol red (0.5% solution). Add 50 ml distilled H_2O and then bring the pH to 7.4 with 5 *N* NaOH. Add distilled H_2O to 100 ml. Solution can be stored for 3 months.
6. *M16 medium from concentrated stocks:* To make 500 ml, combine 50 ml of stock A, 50 ml of stock B, 5 ml of stock C, 5 ml of stock D, and 390 ml of H_2O. Add 2 g BSA; dissolve without excessive frothing. Sterile filter into 50-ml sterile disposable conical centrifuge tubes.
7. *M2 medium from concentrated stocks:* To make 100 ml, combine 10.0 ml of stock A, 1.6 ml of stock B, 1.0 ml of stock C, 1.0 ml of stock D, 8.4 ml of stock E, and 78.0 ml of H_2O. Make up as for M16, but recheck pH prior to sterile filtration and adjust to 7.3–7.4 with concentrated NaOH if needed.
8. *M16 supplemented with hyaluronidase to remove cumulus cells:* Add hyaluronidase to a final concentration of 1–2 mg/ml to M2 or M16. Filter sterilize before use.
9. *Sodium pentobarbital anesthesia for surgery:* Mix 100% EtOH (10 ml), propylene glycol (20 ml), and water (70 ml) to produce 100 ml of diluent. Add sodium pentobarbital stock solution (60 mg/ml) to a final concentration of 6 mg/ml. Administer to mice at 60 mg/kg or 0.1 ml/10 g body weight.

B. Preparation of Holding Pipettes for Micromanipulation

Steps

1. Heat microcapillary tubing in a microburner and pull by hand to yield a shaft about 150 µm in outer diameter with a length of about 3 cm.
2. Place the pulled tubing on the microforge and break the shaft cleanly such that the shards of glass are protruding from the cylindrical end of the shaft.
3. Fire polish the aperture such that the diameter of the lumen is reduced to about 20–30 µm.
4. Bend the shaft to 90° in the microburner and bend the portion of the tubing that has not been heated 90° in the opposite direction, about 2 cm distant from the point at which the shaft was pulled.
5. About 2 cm further away from the tapered shaft, break the tubing with a diamond pen and fire polish the end to yield an "S-shaped" holding pipette. When used the pipette shaft will extend, parallel to the floor of the culture dish, into the microdrop for manipulation (Gordon and Ruddle, 1983). The tubing will then extend vertically up and over the edge of the tissue culture dish and attach to the instrument collar of the manipulator.

C. Preparation of Microneedles

Step

Microneedles are pulled from appropriate microcapillary tubing and used directly without further processing.

D. Micromanipulator Setup

Steps

1. The micromanipulation microscope should be equipped with interference optics and should be

inverted; 4× and 32× objectives, with 10× eyepieces, are recommended.
2. The instrument collar for the holding pipette should be connected via tubing to a microinjection device. The instrument collar for the microneedle may be connected to a 10-cc syringe.

E. Recovery and Microinjection of Embryos

Steps

1. Superovulate 10 immature female mice (5–6 weeks old) with 2.5 IU of pregnant mares' serum (Sigma Cat. No. G4877) between 12 noon and 1 PM.

2. Forty-eight hours later, administer 5 IU of human chorionic gonadotropin (Sigma Cat. No. CG-10) between 12 noon and 4 PM and place with fertile males to mate. At this time, place 15 mature, randomly cycling females with vasectomized males to generate pseudopregnant recipients.

3. The morning after mating, check immature and mature females for vaginal plugs indicative of mating. Retain those that have mated.

4. Between noon and 2 PM the same day, prepare five 35-mm tissue culture dishes, each with 2 ml of M16 medium, a depression slide with about 300 ml M16 containing hyaluronidase, and a 100-mm culture dish for micromanipulation containing a drop of M2 medium covered with mineral oil. This drop should be rectangular with dimensions of about 1 × 4 cm. Place the M16 and hyaluronidase in the incubator for equilibration, and the M2 microdrop can be placed directly on the microscope equipped for micromanipulation.

5. Between 1 and 2 PM, sacrifice the donor females and remove the oviducts, with ovaries and a small portion of the uterus still attached, to one of the dishes of M16. On the dissecting microscope, identify the distended portion of each oviduct and tear it open to release zygotes and associated cumulus cells. All oviducts should be done in the depression slide containing the hyaluronidase.

6. Place the depression slide in the incubator for 5 min. During this incubation, pull a microinjection needle on the pipette puller and place the base in DNA solution for filling. After the tip is filled, fill the shaft behind the DNA with fluorinert using a spinal needle.

7. Wash the denuded zygotes several times in M16 medium and select those with visible pronuclei and/or second polar bodies. Place these together in the M2 microdrop at one end of the drop.

8. Attach the holding pipette and microneedle to the instrument collars and lower them into the microdrop at the opposite end from the zygotes. Brush the microneedle tip against the holding pipette to break it slightly. This will help establish the flow of DNA. Raise the microtools off the floor of the dish and move the microscope stage to bring the zygotes into the field of vision. Lower the holding pipette and use suction to grasp one of the zygotes. Under high power, release and regrasp the zygote until a pronucleus is positioned for microinjection. Lower the microneedle until the tip is in the same focal plane as the pronuclear membrane. Insert the microneedle under the zona pellucida and apply forward pressure. If the microneedle aperture is open, the perivitelline space will swell slightly.

9. Insert the microneedle into the pronucleus and allow the flow of DNA to cause swelling of the pronucleus. Microinjection should not be considered successful unless this swelling is seen. After microinjection, immediately remove the microneedle from the zygote.

10. Raise the microtools off the floor of the dish and move the stage so as to carry the microinjected zygote, still attached to the holding pipette, to the opposite end of the microdrop. Release the zygote by applying positive pressure on the holding pipette. Allow the microinjected zygote to drift down to the floor of the dish and then move the stage so as to repeat the process on the next embryo. When all embryos are microinjected, remove them to a dish of M16 for about 1 h of culture.

F. Embryo Implantation

Steps

1. Load the surgical transfer pipette with medium, and bubble marker, more medium, and then 10–30 embryos.

2. Approach the ovary through a dorsal incision about 1 cm lateral to the midline, 1–2 cm below the costal margin. The ostium lies immediately adjacent to the ovary and the opening is always oriented toward the tail of the animal.

3. Open the ovarian bursa, avoiding trauma to large blood vessels. Identify the opening of the ostium and insert the surgical transfer pipette. To assure successful embryo transfer, the pipette should be advanced beyond the point of bursal attachment. Embryos are then expelled until the air bubble marker enters the oviductal lumen. Repeat this procedure on the opposite side if sufficient numbers of embryos are available.

4. Close the wound with a single suture through both the peritoneum and the skin. Pups born 19–21 days after transfer are then reared to weaning age and evaluated by polymerase chain reaction or Southern blotting for integration of the transgene.

G. Surgical Vasectomy of Males to Generate Pseudopregnant Recipient Females

Steps

1. Make a ventral midline incision about 1 cm in length above the position of the preputial gland, which is situated under the skin and can be appreciated as a bulging of the skin in the lower abdomen.
2. Squeeze the scrotal sac to force the testes to the incision location and expose the testes by grasping the associated fat pads with the forceps. Identify the vas deferens and lacerate it by blunt dissection.
3. Secure a lacerate loop of the vas deferens in the jaws of a hemostat, crush it, and tear it away.
4. Close the animal with a single suture through both the skin and the peritoneum. After about 1 week the animal can be used as a breeder.

IV. COMMENTS

Human chorionic gonadotrophin is now considered an anabolic steroid and, as such, requires a license for ordering as a controlled substance in the United States. Although M16 and M2 culture media are listed as being stable for only 2 weeks, we have found that they can be used for at least 2 months without diminution of success in transgenic mouse production. The reason for this is that embryos are maintained in these media for only a short time.

References

Brinster, R. L., Chen, H. Y., Trumbauer, M. E., Senear, A. W., Warren, R., and Palmiter, R. D. (1981). Somatic expression of herpes thymidine kinase in mice following injection of a fusion gene into eggs. *Cell* **27**, 223–231.

Gordon, J. W. (1989). Transgenic animals. *Int. Rev. Cytol.* **115**, 171–230.

Gordon, J. W., and Ruddle, F. H. (1983). Gene transfer into mouse embryos: Production of transgenic mice by pronuclear injection. *Methods Enzymol.* **101**, 411–433.

Gordon, J. W., Scangos, G. A., Plotkin, D. J., Barbosa, J. A., and Ruddle, F. H. (1980). Genetic transformation of mouse embryos by microinjection of purified DNA. *Proc. Natl. Acad. Sci. USA* **77**, 7380–7384.

Gordon, K., Lee, E., Vitale, J., Smith, A., Westphal, H., and Henninghausen, L. (1987). Production of human tissue plasminogen activator in transgenic mouse milk. *Biotechnology* **5**, 1183–1187.

Hammer, R. E., Pursel, V. G., Rexsroad, C. E., Jr., Wall, R. J., Roll, D. J., Ebert, K. M., Palmiter, R. D., and Brinster, R. L. (1985). Production of transgenic rabbits, sheep and pigs by microinjection. *Nature* **315**, 680–683.

Palmiter, R. D., and Brinster, R. L. (1986). Germ-line transformation of mice. *Annu. Rev. Genet.* **20**, 465–499.

Quinn, P., Barros, C., and Whittingham, D. G. (1982). Preservation of hamster oocytes to assay the fertilizing capacity of human spermatozoa. *J. Reprod. Fertil.* **66**, 161–168.

Stacey, A., Bateman, J., Choi, T., Mascara, T., Cole, W., and Jaenisch, R. (1988). Perinatal lethal osteogenesis imperfecta in transgenic mice bearing an engineered mutant pro-al(I) collagen gene. *Nature* **332**, 131–136.

CHAPTER

52

Gene Targeting by Homologous Recombination in Embryonic Stem Cells

Ahmed Mansouri

I. INTRODUCTION

Embryonic stem cells (ES) are derived from the inner cell mass of the mouse blastocyst and can be perpetuated in culture (Robertson, 1987). Chimeric embryos can be generated by injecting ES cells into blastocysts or by aggregating them with morulae. Adult mice develop normally from these embryos and ES cells contribute to all tissues, including the germline (Robertson, 1986; Gossler *et al.*, 1986). These unique characteristics allow the introduction of foreign DNA and the screening for rare integration events in ES cells, as well as ultimately the generation of ES cell-derived mouse strains. This strategy has been employed successfully for gene targeting by homologous recombination and has become a powerful tool in studying gene function. Using this procedure, designed mutations are introduced into particular genes and mouse lines carrying the mutated allele are generated (Capecchi, 1989). The use of site-specific recombination systems from the phage P1 (Cre recombinase and LoxP) and from *Saccharomyces cerevisiae* (Flp recombinase and FLP) has opened new avenues for a more sophisticated genetic engineering of mice (Utomo *et al.*, 1999).

II. MATERIALS AND INSTRUMENTATION

Dulbecco's modified Eagle's medium (DMEM, 4.5 g glucose/litre, Cat. No. 41965-039), glutanine (Cat. No. 25030-024), nonessential amino acids (Cat. No. 11140-035), sodium pyruvate (Cat. No. 11360-039), fetal calf serum (FCS, Cat. No. 10270106), geneticin (G418, Cat. No. 11811-064 for 10 g), trypsin/EDTA (Cat. No. 25300-054), and penicillin–streptomycin (Cat. No. 15140-122) are from In Vitrogen. Leukaemia inhibitory factor (LIF, Cat. No. ESG1107 LifESGROTM) is from Chemicon. EDTA (Cat. No. 8043) is from Roth, KCl (Cat. No. 0509) and Trizma base (Cat. No. 1414) are from Baker, NaCl (Cat. No. 1.0640.5000), KH_2PO_4 (Cat. No.1.12034), $Na_2HPO_4{\cdot}2H_2O$ (Cat. No. 6580.0500), and sodium dodecyl sulfate (SDS, Cat. No. 1.1.3760.1000) are from Merck, and D+glucose (Cat. No. G-5146), gelatine (Cat. No. G-1890), dimethyl sulfoxide (DMSO, Cat. No. D-8779), ganciclovir (Cat. No. G2536), mitomycin C (Cat. No. M-0503), and phenol red (Cat. No. P-5530) are from Sigma. Trypsin (Cat. No. L2103) is from Biochrom KG. Proteinase K (Cat. No. 1092766) is from Roche. Gene pulser and electroporation cuvettes (0.4 cm and 0.8 ml volume) are from Bio-Rad Laboratories GmbH and Endo free kit is from Qiagen.

Copyright 2006, Elsevier Science (USA).
All rights reserved.

Also needed are 13- to 15-day pregnant mice, sterile scissors and forceps, 50-ml sterilized gall beads (3-mm diameter), a stirring bar in a 500-ml Erlenmeyer flask, and 14.5-cm tissue culture dishes. The gene pulser and electroporation cuvettes are from Bio-Rad.

III. PROCEDURES

A. Preparation of Embryonic Fibroblasts

Solutions

1. *Phosphate-buffered saline (PBS):* To make 1 liter, add 8.0 g NaCl, 0.2 g KCl, 1.15 g $Na_2HPO_4 \cdot 2H_2O$, and 0.2 g KH_2PO_4 to distilled water, adjust pH to 7.2, and bring to a total volume of 1 liter. Sterilise by autoclaving and store at room temperature.
2. *Trypsin/EDTA:* For routine culture and for the preparation of embryonic fibroblasts from embryos, ready-to-use trypsin/EDTA from In Vitrogen can be used.
3. *Gelatine:* To make 1 liter, add 1 g to 1 liter of distilled water and autoclave. Mix after autoclaving and store at room temperature.
4. *Mitomycin C:* Resuspend 2 mg of mitomycin C in 2 ml of PBS and filter sterilise. Dilute with fibroblast medium to a concentration of 100 µg/ml (100 µl mitomycin C/10 ml medium) and store in 25-ml aliquots at –20°C. This is referred to as inactivation medium for fibroblasts. Thaw just before using. Use 10 ml for a 14.5-cm tissue culture dish.
5. *Medium for embryonic fibroblasts: [DMEM + 10% (v/v) FCS]:* To make 1 liter, add 100 ml of FCS (the serum is always heat inactivated at 56°C for 30 min before use for all media) to 900 ml of DMEM. Store at 4°C. When fresh embryonic fibroblasts are prepared from mouse embryos it is advisable to add antibiotics (penicillin/streptomycin). For routine tissue culture it is not necessary.
6. *Freezing medium (for fibroblasts and ES cells):* To make 10 ml of freezing medium, add 1 ml DMSO (cell culture grade) and 1 ml FCS to 8 ml of ES cell medium. After adding freezing medium, keep cells for 1 h at –20°C and tranfer to –70°C overnight before storing in liquid nitrogen.

Steps

1. Dissect ten 13- to 15-day embryos (we normally use NMRI or Balb/c mice) in PBS. Discard liver, head, and internal organs. Wash carcasses several times in PBS to remove blood.
2. Transfer carcasses to 5 ml of trypsin/EDTA and mince in small pieces.
3. Using a wide pipette, transfer the dissected embryo pieces to the Erlenmeyer flask containing the glass beads and add 50 ml of trypsin.
4. Incubate for 30 min at 37°C with gentle agitation on a magnet stirrer.
5. Using a pipette, remove the cell suspension from the flask and transfer to a sterile 50-ml tube. Leave the cell clumps in the flask.
6. Add 50 ml trypsin/EDTA to the remaining cell clumps in the flask and repeat step 4.
7. Spin down the cell suspension from step 5 at 1000 rpm for 10 min and resuspend pellet in embryonic fibroblast medium.
8. Remove the second cell suspension from the flask and treat as in step 7.
9. Pool cells from steps 7 and 8 and plate on 14.5-cm tissue culture dishes (about two embryos/dish).
10. Change medium after 24 h.
11. Once confluent (after 2 days), freeze cells by making five vials from each plate.
12. For routine culture, thaw one vial on an 8.5-cm plate. When confluent, passage the plate on 4 × 8.5-cm plates, which are again passaged (when confluent) on 4 × 14.5-cm plates. Treat the confluent 14.5-cm plates for 2.5 h with mitomycin C to inactivate the fibroblasts.

B. Inactivation of Fibroblasts

1. Thaw inactivation medium and warm to 37°C.
2. Change medium to inactivation medium (10 ml to each 14.5-cm plate) and place plates back into the incubator for 2.5 h.
3. Stop inactivation by washing the cells twice with 10 ml of PBS and add 20 ml of fresh medium to each plate.
4. Trypsinise cells and seed on gelatinised plates at a density of 8×10^4 cells/cm^2. Inactivated fibroblasts that are not needed can be frozen in liquid nitrogen and thawed when necessary. We normally freeze cells from one 14.5-cm dish in one vial.
5. To thaw inactivated feeder cells, warm vial quickly at 37°C, add 10 ml of feeder medium (mix well and take aliquot to determine cell density), and spin down for 5 min at 1000 rpm. After counting, reduce the number of the cells by 15% (taking into account dead cells during the freezing procedure) and plate as usual on gelatinised plates.
6. To gelatinise the plates, cover the surface with 0.1% gelatine for 15 min or longer at room temperature, remove before using, and leave plates to dry.

C. Routine Culture of Embryonic Stem Cells

ES cells should be cultured on a feeder layer of inactivated embryonic fibroblasts (Robertson, 1987) (typical morphology of ES cells is shown in Fig. 1). Embryonic fibroblasts should be used within a week when plated after inactivation. The ES cells should be split every second day (see later). To avoid differentiation, it is important that the ES cells are trypsinised to get a single cell suspension. Because totipotency in ES cells tends to be lost with passage number, it is advisable to subclone the cells after every 20 passages in order to recover the full potentiality. All ES cell lines are cultured in 15% serum except for R1 cells (provided by Dr. A. Nagy, Mount-Sinai Hospital in Toronto), which are cultured in 20% serum.

Solutions

1. *ES cell medium:* DMEM (4.5 g/litre glucose), 10^{-4} *M* β-mercaptoethanol, 2 m*M* glutamine, 1% of stock solution of nonessential amino acids, 1 m*M* Na pyruvate, 15% (v/v) FCS (tested batches), and 500 U/ml LIF. To make 500 ml, add 5 ml of glutamine, 5 ml of nonessential amino acids, 5 ml of sodium pyruvate, 5×10^5 units of LIF, and 0.5 ml of β-mercaptoethanol to DMEM. Adjust to 500 ml with DMEM and add 89 ml of FCS. Store at 4°C. This corresponds to 15% serum. If using RI-ES cells (provided by Dr. A. Nagy, Mount-Sinai Hospital in Toronto), use 100 ml of serum for a total volume of 500 ml medium.

2. *β-Mercaptoethanol stock*: To make 5 ml, add 35 µl of β-mercaptoethanol (14 *M*) to 5 ml of PBS, mix well, and filter sterilise. Store at 4°C in the dark (cover tube with aluminium foil) and use within 1 week.

3. *Saline/EDTA for dilution of trypsin:* To make 1 liter, add 0.2 g EDTA (disodium salt), 8.0 g NaCl, 0.2 g KCl, 1.15 g $Na_2HPO_4{\cdot}2H_2O$, and 0.2 g KH_2PO_4 to distilled water, check pH (7.2), bring to a total volume of 1 liter, and filter sterilise or autoclave. Store at room temperature.

4. *Trypsin/EDTA:* To make 1 liter, add 8.0 g NaCl, 0.40 g KCl, 0.10 g $Na_2HPO_4{\cdot}2H_2O$, 1.0 g glucose, 3.0 g Trizma base, 0.01 g phenol red, and 2.50 g trypsin (Difco 1:250) to distilled water, adjust pH to 7.6, bring to a total volume of 1 liter, filter sterilise, and store in aliquots at –20°C. Dilute this stock 1 : 4 in saline : EDTA for use as 0.05% trypsin/EDTA solution. Store at –20°C in 5- to 10-ml aliquots.

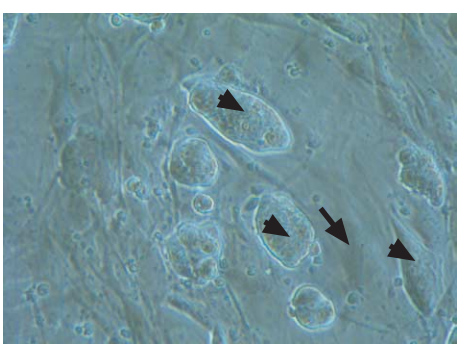

FIGURE 1 Typical morphology of ES cell colonies grown on embryonic fibroblasts. A black arrow indicates fibroblasts and arrowheads point to ES cells colonies.

Steps

1. On day 0, wash the confluent ES cells with PBS.
2. Add trypsin/EDTA (2,1, and 0.5 ml for a 8.5-, 6-, and 3.5-cm culture dish, respectively). Put back into the incubator for 5 min.
3. Using a plugged Pasteur pipette, pipette the cells up and down to get a single cell suspension.
4. Add an excess of medium to stop trypsinisation and mix well.
5. Spin down the cells at 1000 rpm for 5 min.
6. Remove the supernatant and resuspend the cells in new ES cell medium.
7. Split the cells one-fifth to one-eighth (depending on the growth rate, which can vary between serum batches and particular cell lines) on newly inactivated feeder plates.
8. On day 1, change medium.
9. On day 2, split cells on new feeder as in day 0.

D. Targeting Construct

The exogenous DNA fragment or so-called vector or targeting construct used for the targeting experiment consists of two domains of homology to the gene to be targeted: One on the 5′ end and the other on the 3′ end of the construct (Fig. 2). Between the 5′ end and 3′ end homologous parts, a neomycin resistance gene is introduced (1) as a selection marker to monitor the introduced DNA and (2) to interrupt the function of the gene analysed. The neomycin gene is therefore inserted into one exon or it may replace some of the coding sequences, which have to be deleted to abolish the function of the gene to be targeted. Two factors have been shown to influence the targeting efficiency: the size of the genomic fragment included into the construct (Deng and Capecchi, 1992) and the origin of the DNA (Riele *et al.*, 1992). Optimal targeting frequencies are often obtained with constructs, including more than 10 kb of homology. The length of DNA on each side of the *Neo* cassette should not be less than 1.5 kb. Increased targeting efficiencies have been observed when using isogenic DNA isolated from the 129SV

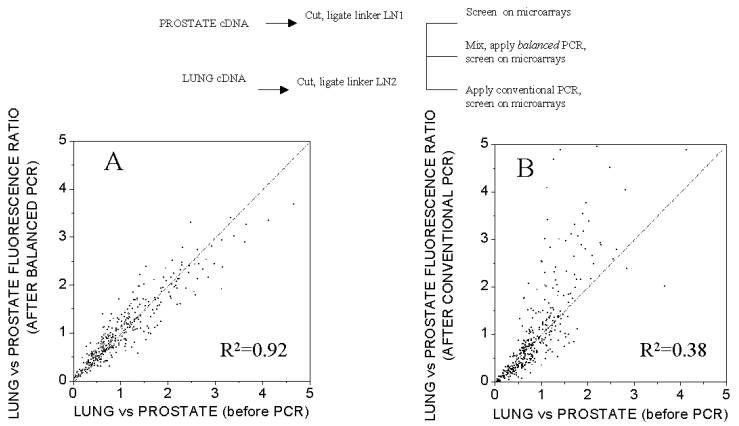

FIGURE 2 Targeting construct using the positive–negative selection procedure. Open boxes indicate exons. TK, HSV thymidine kinase genes; Neo, neomycin gene. Letters on the construct (A, B, C, and D) indicate restriction enzyme recognition sites. (a) Normal allele, (b) targeting construct, and (c) targeted allele. External probes for screening on the 5′ and 3′ ends are indicated by probe 1 and probe 2, respectively. The neo gene is flanked by LoxP sites (arrowheads) that can be recognised by the Cre recombinase. In this way the neo can be removed, if necessary.

genomic library, the mouse line from which most ES cell lines are derived.

The targeting frequency is variable depending on each particular locus. For some genes, the basic strategy described earlier gives an acceptable targeting frequency. However, for other loci, the frequency may be too low without enriching strategies. These strategies are designed to select against random integrations. Therefore, it is recommended to always design a construct using the positive–negative selection procedure (Mansour *et al.*, 1988). The herpes simplex thymidine kinase (TK) gene is added on either external side of the homologous parts of the basic *Neo*-containing construct (Fig. 2). A ubiquitous promoter, e.g., TK or PGK promoter (Soriano *et al.*, 1991), drives the TK. Selection with ganciclovir will kill all the cells that have retained the TK gene that are random integrations. The enrichment factor obtained is fivefold. The expression of the gene to be targeted can be followed by inserting β-galactosidase or green fluorescent protein (GFP) in front of *Neo* in the targeting construct. However, the targeting frequency in this case is lower in comparison to constructs containing only *Neo*.

The aforementioned strategy is already classical and now new methods are used. In fact, it turned out that the neo promoter/enhancer of the PGKneo may act on neighbouring genes and, hence, may interfere with the phenotype (Olson *et al.*, 1996). Therefore, taking advantage of the Cre recombinase of the phage P1, the neo can be removed after homologous recombination has occurred. DNA sequences flanked by LoxP sites (34 bp) that are in the same orientation are excised by the Cre recombinase. The Cre recombinase was shown to perform recombination at LoxP sites in ES cells (Sauer, 1999; Sauer and Henderson, 1990; Gu *et al.*, 1994) (Fig. 2).

In addition, the Cre recombinase opens the possibility of generating conditional knockouts. Specifically, in those cases, where gene targeting will result in a lethal or a phenotype with multiple defects, it is worth to generate a so-called floxed allele. The gene of interest will be modified according to the strategy shown in Fig. 3. Basically, a construct is generated, in which coding sequences are flanked by LoxP sites. One LoxP site is introduced in one intron using oligonucleotides. The second LoxP site is introduced in conjunction with the selection marker neo in another intron. We use the PGKneo that is flanked by FRT sites and carrying one LoxP site (Fig. 3). Flp recombinase from *S. cerevisiae* mediates site-specific deletion at directly repeated FRT sites. After successful homologous recombination into the locus of interest, the neo can be removed. Please check the targeted ES cells for the presence of the second LoxP site. This is practically achieved when mice are generated from targeted ES cells and mated to transgenic mice expressing Flp (Farley *et al.*, 2000). [These mice expressing Flp recombinase from the Rosa-26 locus are available at the Jackson Laboratory (http://tbase.jax.org/).]

Alternatively, a PGKneo that is flanked by two LoxP sites is used. Excision of the neo by Cre recombinase will result among other products into a floxed allele. However, to ensure that excision of the neo occurs, the neo cassette should also contain the TK gene. This will allow selection for excision of the neo after the first targeting experiment. To remove the neo, the targeted

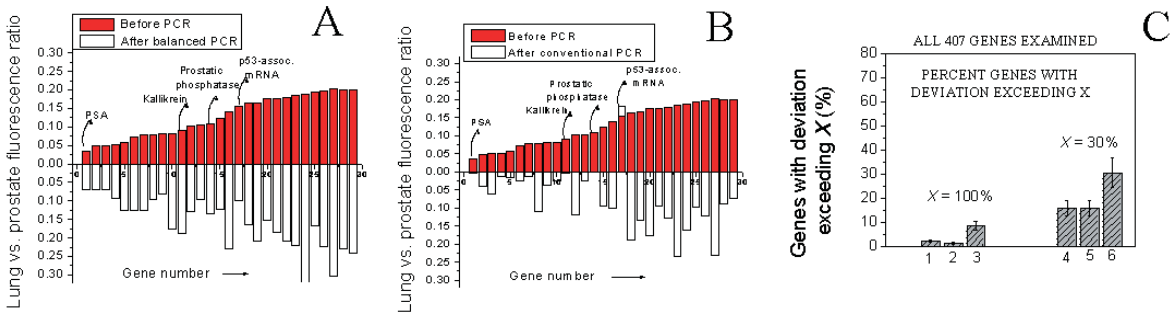

FIGURE 3 Currently used targeting construct to generate a conditional knockout. One LoxP site is inserted in front of the first exon, the neo gene that is flanked by FRT sites and carrying one LoxP site is introduced in one intron. After homologous recombination, targeted ES cells have to be checked for the presence of the second LoxP site. These targeted ES cells are used to generate chimeric mice and to derive a mouse line carrying the allele shown in C. Transgenic mice expressing Flp recombinase [e.g., under the Rosa26-locus; Farley *et al*., 2000; these mice are available at the Jackson Laboratory (http://tbase.jax.org/)] will be crossed to the mouse line carrying the genotype in C to excise the neo. Two LoxP sites will remain as shown in D, where the so-called floxed allele is indicated. Please do not forget to check if mice having both floxed alleles have a normal phenotype. (A) Normal allele; (B) targeting construct; (C) targeted allele in ES cells and mice; and (D) genomic structure of the floxed allele after excision of the neo by crossing to Flp-expressing mice. External probes at the 5'and 3' ends for screening are indicated by probes 1 and 2. Boxes indicated by E1 to E3 are exons. F, FLP site; L, LoxP site.

clones are subjected to a second electropration with a plasmid expressing Cre under the PGK promoter (Torres and Kühn, 1997). Ganciclovir selection will allow the specific removal of the LoxP sites flanking the neo. However, we think that it is more convenient to use the Flp strategy, as only one electroporation is required.

The construct should be linearised and introduced into ES cells by electroporation. DNA for electroporation should be prepared using the Qiagen endo free kit. The targeting vector should be linearised within the vector or outside the domain of homology (see Figs. 2 and 3) by the appropriate restriction enzyme. DNA is treated once with phenol/chloroform, precipitated, and resuspended in TE at 0.5 µg/µl. Check DNA integrity on agarose gel before electroporation.

E. Electroporation

Solutions

1. *G418:* Dissolve G418 (GIBCO) in PBS at a concentration of 250 mg/ml, filter sterilise, and store in small aliquots (1 ml) at –20°C. Thaw before use and add to the selection medium. G418 potency varies between batches and should be tested empirically with untransfected ES cells. The appropriate G418 concentration is usually between 200 and 350 µg/ml medium (100–175 µg active G418/ml medium). Ideally, control ES cells should die after 7 days and G418-resistant colonies will form by days 8 to 10, depending on the promoter driving neo expression.

2. *Ganciclovir:* Dissolve in distilled water at a concentration of 2 mg/ml. Dilute some aliquots to 2 m*M*, filter sterilise, and store at –20°C. The working concentration is 2 µ*M*.

Steps

See also Fig. 3

1. On day 0, split ES cells on a 8.5-cm feeder plate as described in Section III,C. Inactivate fresh feeder cells and prepare 8 × 8.5-cm feeder plates. The culture of the feeder for inactivation should be started 1 week before electroporation. The fibroblasts should be prepared from transgenic embryos carrying the Neo gene so that they are resistant to G418.
2. On day 1, change medium.
3. On day 2, change medium. Remove medium from the 8 × 8.5-cm feeder plates and add 6 ml of ES cell medium to each plate.
4. Four hours after changing medium, trypsinise the cells as described in Section III,C and add ES cell medium to 10 ml, mix well, and spin down for 5 min at 1000 rpm.
5. Aspirate the supernatant and resuspend the cells in 30 ml of PBS. Determine the cell number, which should be around 1.5×10^7 cells.
6. Spin down for 5 min at 1000 rpm.
7. Resuspend approximately 10^7 ES cells in 0.8 ml PBS containing 25 µg/ml of linearised DNA. Let suspension stand for 5 min at room temperature.
8. Pipette the cells up and down and transfer 0.8 ml of the suspension to one electroporation cuvette,

omitting air bubbles. Electroporate with one pulse of 500 µF and 250 V at room temperature. Let stand for 5 min at room temperature.

9. Using a plugged Pasteur pipette, transfer cells directly to ES medium (28 ml) and plate the cells on 7 × 8.5-cm feeder plates. Plate control ES cells (electroporated without DNA) at the same cell density.

10. Twenty-four hours after electroporation, change medium to selection medium with G418 or G418 with ganciclovir if using the PNS procedure.

11. Change medium every day.

12. At day 5 of selection, change selection medium in the PNS procedure to G418 only. Ganciclovir selection is only necessary for the first 4 days.

13. Eight days after selection, check control plate (there should be no ES cells left) and transfection plates for G418-resistant colonies. Big ES cell colonies (about 1000 cells) can be already picked. Do not let any colony get too large, as it would then differentiate.

F. Picking Clones

See also Fig. 4.

Steps

1. Using a microscope marker, make a circle under the desired clone.

2. Prepare a 96-well plate with 40 µl trypsin/EDTA in each well.

3. Under a dissecting microscope (in sterile hood), pick every marked clone individually and transfer to one well in the 96-well plate. We use a Gilson pipette and PCR 10-µl tip (FT 10 from SLG) to pick the colonies. Twelve to 24 cell clones can be handled in one step.

4. After the colonies are trypsinised (variable time), using a multichannel (12) pipette, transfer the 12–24 clones to a 24-well plate with fresh feeder layer (1 day old) and fresh ES cell medium (1 ml in each well). Mix well, replace in the incubator, and change medium every day. The transfer of clones from the 96-well plate to the 24-well plate is performed using only 6 channels of the pipette (leaving every second one empty). This permits the transfer of the contents of alternate wells from the 96-well plate to the 6-well plate.

5. Once the cells are confluent (3–5 days), they are trypsinised by adding 150 µl of trypsin/EDTA to each well and incubating for 5 min at 37°C.

6. Add 600 µl of ES cell medium to each well to stop trypsinisation, mix well, remove 400 µl from each well, transfer into a corresponding 24 well (for freezing), and add the remaining cells from the same clone to another 24 well (without feeder but the wells should

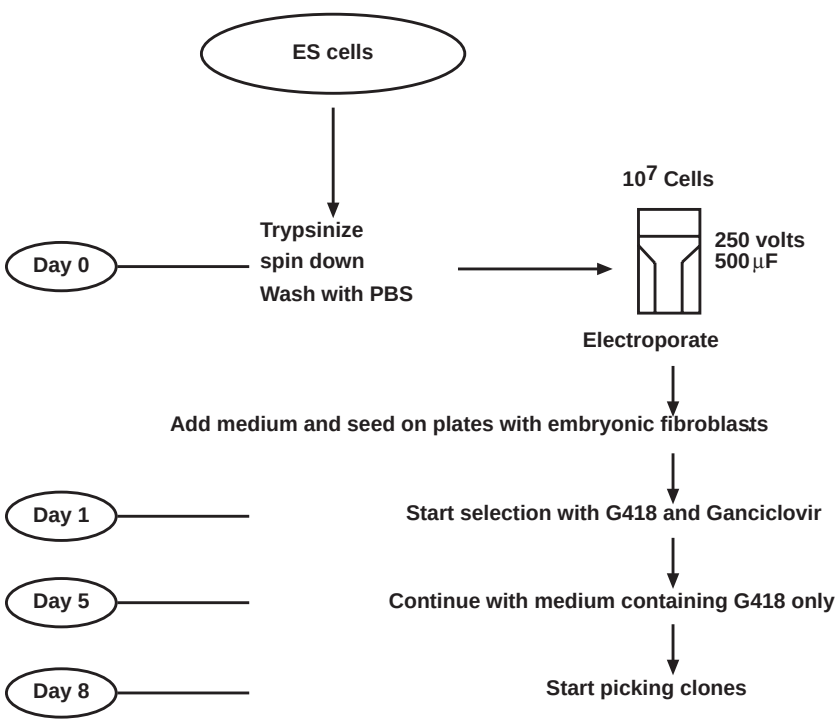

FIGURE 4 Scheme for the different steps of a standard electroporation.

be gelatinised) preequilibrated with 500 µl of ES medium.

7. When all wells are transferred, add 400 µl of 2× freezing medium to each well of the freezing plate. Mix to homogeneity, cover with a plastic bag and paper, and put into a Styrofoam box at –70°C. This is the master plate.
8. Proceed with all clones in this way.
9. The ES cells in the gelatinised plate will be used, when confluent, to prepare genomic DNA for screening (Fig. 5).

G. Analysis of Picked Clones by Southern Blot

Solutions

1. *Lysis buffer:* 100 m*M* Tris–HCl, pH 8.5, 5 m*M* EDTA, 0.2% SDS, 200 m*M* NaCl, and 100 µg/ml proteinase K
2. *Proteinase K stock solution*: 10 mg/ml H_2O
3. *TE*: 10 m*M* Tris–HCl, pH 8.0, and 1 m*M* EDTA (Laird *et al*., 1991)

The isolate clones should be checked individually to distinguish between random integrations and homologous recombination. We recommend genomic Southern analysis for this purpose. Genomic DNA is digested with an enzyme that will generate bands of different sizes from the wild type and the targeted allele and is probed with a genomic fragment not included in the targeting construct (see Fig. 2).

Steps

1. When cells in the gelatinised plates are confluent, remove medium and add 500 µl of lysis buffer to each well.
2. Leave overnight in the incubator at 37°C.
3. Transfer the DNA solution from each well to an Eppendorf tube and add 500 µl of lysis buffer to each well.
4. Spin down for 10 min and remove supernatant.
5. Add 500 µl 70% ethanol to wash pellet and spin down for 5 min.
6. Remove ethanol and dry pellet. Resuspend DNA in 50 µl 1/10 TE.
7. Use 15 µl from each sample for screening and digest with the appropriate restriction enzyme.

Positive clones will be expanded and rechecked. They can now be used to generate chimeras by

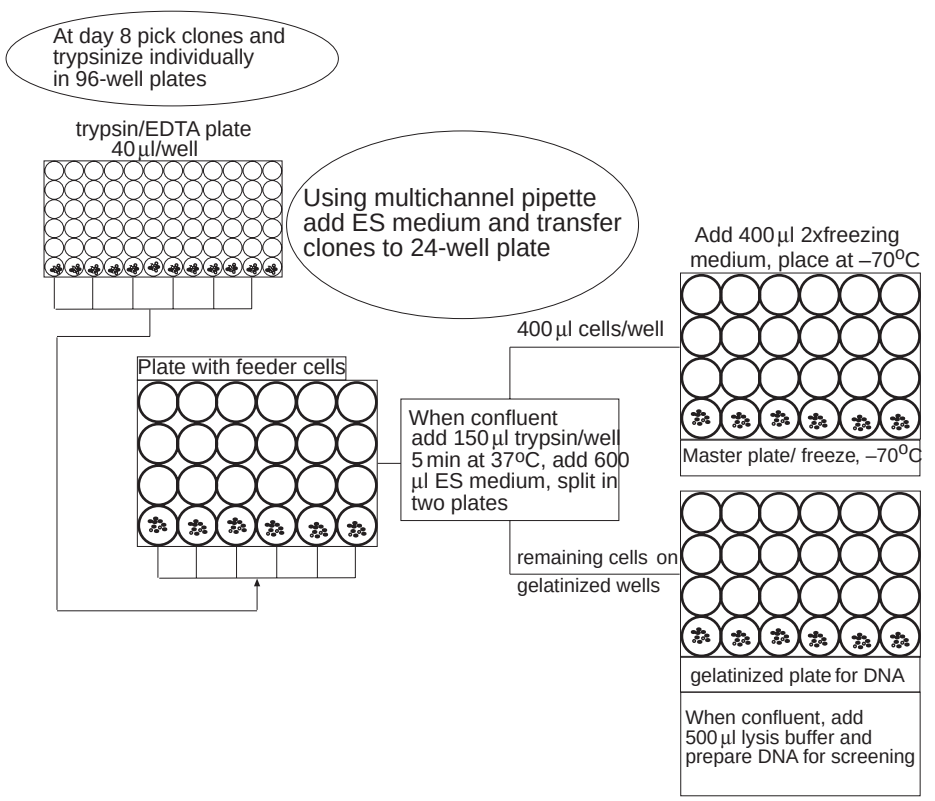

FIGURE 5 Scheme for picking clones and further handling until freezing. ES cell colonies are shown schematically as black dots in the 96 wells.

blastocyst injection or morula aggregation (Bradley, 1987).

H. Thawing Positive Clones from 24-Well Pates for Aggregation or Blastocyst Injection

Steps

1. Prepare 3.5-cm plates with an inactivated feeder layer.
2. The next day, prewarm ES cell medium at 37°C. Remove quickly the 24-well plate with the positive clones from the –70°C freezer and immediately add 1 ml of ES medium to the corresponding well. Pipette carefully up and down without taking the frozen cell into the pipette (it is just to go quickly with thawing). If there are several positive clones on the same plate, you can thaw them at the same time or put the 24-well plate back into the –70°C freezer after thawing one of them.
3. When thawed, transfer the cells to a Falcon tube (14 ml) and wash the well three to four times with ES medium. Add ES medium to adjust the total volume to 12 ml and spin down at 1000 rpm.
4. Plate the cells on a 3.5-cm plate and change the medium the next day.
5. When confluent, split cells and make frozen stocks. Check the clone by Southern blot before proceeding to aggregation or blastocyst injection.

I. Removing the neo Cassette from the Targeted Locus by the Cre Recombinase in ES Cells

In cases where the neomycin resistance gene has to be excised from the targeted locus, use PGK promoter-driven Cre to electroporate targeted ES cells.

Steps

1. Electroporate 10^7 targeted ES cells (Section III,E) with 25 µg of supercoiled Cre plasmid (we used PGK-Cre containing a nuclear localisation signal) and plate on one 14.5-cm dish containing inactivated feeder cells.
2. After 48 h trypsinise cells (see Section III,C) and plate 10^3 cells/8.5-cm dish with inactivated feeder cells. Make four plates and freeze the remaining cells. When colonies become visible and of reasonable size (it takes about 4 days), they should be picked and proceeded as described in Section III,F. We usually get about 10% positive clones.
3. Positive clones may be checked for their sensitivity to G418 by culturing one aliquot in a 96-well plate in ES medium containing G418.
4. Prepare DNA from positive clones and analyse by genomic Southern blot using appropriate probes.

IV. COMMENTS

It may happen that after the positive ES clones are thawed only few colonies are detected in the dish after a few days of culture. Do not subculture, just trypsinise the cells as usual and leave them in the same dish for another passage. In this way you can recover clones with few cells.

Plates are gelatinised in order to have an optimal attachment of the fibroblasts.

If the external probe for Southern blot contains repetitive sequences, use denatured mouse genomic DNA to block the repetitive elements. On the day of hybridisation, 1 ml of mouse tail genomic DNA (1 µg/µl) is heated at 95°C for 20 min (Eppendorf bench shaker). Keep on ice before use. Mix with the probe and denature for 5 min before adding to hybridisation mixture.

Each new batch of serum for ES cell culture should be tested before using. Therefore, several batches are tested. The following parameters have to be checked for each batch.

1. Plating efficiency. Trypsinise ES cells and plate about 1000 cells on a gelatinised 6-well plate. Make triplicates for each batch of serum. When colonies become apparent (about 5 to 6 days), fix with 4% PFA for 30 min and stain with giemsa. After drying, count colonies. The plating efficiency should be at least 20%. Do not forget to include your old batch of serum as a control.
2. Morphology of the cells and toxicity of the serum. Plate ES cells for normal culture on 6-well plates seeded with embryonic fibroblasts at different serum concentrations for each batch (15, 20, and 30%). Use duplicates. When ES cell become confluent, passage as usual. Check morphology of ES colonies for differentiation after each passage. Check also the difference in cell growth and death between 15 and 30%. It may show if a serum contains some toxic components. Passage the cells at least three times. We usually find that sera with the highest plating efficiency also have the best quality. Some companies offer already ES-tested serum for a higher cost, but this may not necessarily be the best one. When possible, always check serum at your own laboratory. A serum test takes about 3 to 4 weeks.

Acknowledgments

The author thanks Professor Peter Gruss for constant support and encouragement, Jens Krull and Sharif Mahsur for excellent technical assistance, and Anja Dietrich for critically reading the manuscript. This work is supported by the Max Planck Society.

References

Bradley, A. (1987). Production and analysis of chimeric mice. *In "Teratocarcinomas and Embryonic Stem Cells, a Practical Approach"* (E. J. Robertson, ed.), pp. 113–151. IRL Press Oxford, Washington.

Capecchi, M. R. (1989). The new mouse genetics: Altering the genome by gene targeting. *Trends Genet.* **5**, 70–76.

Deng, C., and Capecchi, M. R. (1992). Reexamination of gene targeting frequency as a function of the extent of homology between the targeting vector and the target locus. *Mol. Cell Biol.* **12**, 3365–3371.

Dymecki, S. M. (1996). Flp recombinase promotes site-specific DNA recombination in embryonic stem cells and transgenic mice. *Proc. Natl. Acad. Sci. USA* **93**, 6196–6196.

Farley, F. W., Soriano, P, Steffen, L. S., and Dymecki, S. M. (2000). Widespread recombinase expression using FLPeR (flipper) mice. *Genesis* **28**, 106–110.

Gossler, A., Doetschman, T., Korn, R., Serfling, E., and Kemler, R. (1986). Transgenesis by means of blastocyst-derived embryonic stem cell lines. *Proc. Natl. Acad. Sci. USA* **83**, 9065–9069.

Gu, H., Marth, J. D., Orban, P. C., Mossman, H., and Rajewski, K. (1994). Deletion of a DNA polymerase β gene segment in T cells using cell type-specific gene targeting. *Science* **265**, 103–106.

Laird, P. L., Zijderveld, A., Linders, K., Rudnicki, M., Jaenisch, R., and Berns, A. (1991). Simplified mammalian DNA isolation procedure. *Nucleic Acids Res.* **19**, 4293.

Mansour, S. L., Thomas, K. R., and Capecchi, M. R. (1995). Disruption of the protooncogene *int-2* in mouse embryo-derived stem cells: A general strategy for targeting mutations to non-selectable genes. *Nature* **336**, 348–352.

Olson, E. N., Arnold, H. H., Rigby, P. W. J., and Wol, B. J. (1996). Know you neighbors: Three phenotypes in null mutants of the myogenic bHLH gene MRF4. *Cell* **85**, 1–4.

Riele, H. R., Maandag, E. B., and Berns, A. (1992). Highly efficient gene targeting in embryonic stem cells through homologous recombination with isogenic DNA constructs. *Proc. Natl. Acad. Sci. USA* **89**, 5128–5132.

Robertson, E. J. (1986). Pluripotent stem cell lines as a route into the mouse germline. *Trends Genet.* **2**, 9–13.

Robertson, E. J. (1987). Embryo-derived stem cell lines. *In "Teratocarcinomas and Embryonic Stem Cells, a Practical Approach"* (E. J. Robertson, ed.), pp. 71–112. IRL Press Oxford, Washington.

Sauer, B. (1993). Manipulation of transgenes by site specific recombination: Use of *Cre* recombinase. *Methods Enzymol.* **225**, 890–900.

Sauer, B., and Henderson, N. (1990). Targeted insertion of exogenous DNA into the eukaryotic genome by the *Cre* recombinase. *New Biol.* **2**, 441–449.

Soriano, P., Montgomery, C., Geske, R., and Bradley, A. (1991). Targeted disruption of the c-src proto-oncogene leads to osteopetrosis in mice. *Cell* **64**, 693–702.

Torres, R. M., and Kühn, R. (eds.) (1997). "Laboratory Protocols for Conditional Targeting." Oxford Univ. Press, Oxford.

Utomo, A. R. H., Nikitin, A. Y., and Lee, W.-H. (1999). Temporal, spatial, and cell type-specific control of Cre-mediated DNA recombination in transgenic mice. *Nature Biotechnol.* **17**, 1091–1096.

CHAPTER

53

Conditional Knockouts: Cre-lox Systems

Daniel Metzger, Mei Li, Arup Kumar Indra, Michael Schuler, and Pierre Chambon

I. INTRODUCTION

Site-directed gene targeting in the mouse has led to marked advances in understanding the function played by gene products in mammalian development, as well as in adult homeostasis and pathophysiology. However, targeting a given mutation in the germ line has some inherent limitations, such as those created by embryonic lethality, occurrence of developmental aberrations, or compensatory effects by functionally redundant genes. In many instances, these limitations may preclude the determination of the function of a given gene product in a defined subset of cells, at a given time during the life of the animal, and therefore to discriminate between cell-autonomous and noncell-autonomous functions. Furthermore, germ line mutations are inadequate to generate mouse models of human diseases resulting from somatic mutations, such as most forms of cancer (Jonkers and Berns, 2002; Metzger and Chambon, 2001). To avoid these limitations, methods to achieve conditional gene targeting have been developed, based mainly on the properties of the bacteriophage P1 site-specific Cre recombinase. As the Cre recombinase efficiently and faithfully excises in animal cells a DNA segment flanked by two loxP sites (floxed DNA), spatially or temporally controlled somatic mutations can be obtained by controlling its expression with a cell-specific or an inducible promoter, respectively (Rajewsky *et al.*, 1996). However, these conditional gene targeting systems have themselves a number of limitations, as they are only either spatially or temporally controlled. Fortunately, two systems have been developed that allow the generation of somatic mutations in a defined gene, at a selected time of the life of the animal, and in a specific cell type. In one instance, the Cre/loxP system has been combined with tetracycline-dependent regulatory systems. Spatiotemporally controlled Cre recombinase expression was obtained by doxycycline (a tetracycline analog) administration to transgenic mice bearing two transgenes encoding (i) a tetracycline-controlled transactivator under the control of a tissue-specific promoter and (ii) the Cre recombinase under the control of a minimal promoter that contains the operator sites of the tet operon. However, the generation of mice harboring both transgenes and the two LoxP-flanked alleles of a given gene requires complex breedings, and further improvements are required to eliminate basal noninduced Cre expression (Branda and Dymecki, 2004; Lewandoski, 2001; Zhu *et al.*, 2002). In the second instance, a fusion between the Cre recombinase and a mutated steroid receptor ligand-binding domain results in ligand inducibility of the recombinase activity *in vivo* (Branda and Dymecki, 2004; Garcia and Mills, 2002; Metzger and Feil, 1999). Among these fusion proteins, Cre-ER^{T2} (obtained by fusing Cre to an estrogen-nonresponsive mutated ligand-binding domain of the human estrogen receptor ERα) is particularly effective. Cell-specific expression of Cre-ER^{T2} in transgenic mice allows efficient tamoxifen-dependent Cre-mediated recombination at loci flanked by LoxP sites, without background activity, thus generating spatiotemporally controlled targeted somatic mutations (Metzger *et al.*, 2003). We illustrate here the generation of such mutations in the mouse by describing strategies and techniques used to create temporally controlled somatic mutations in target genes of epidermal keratinocytes. In the epidermis, a dynamic stratified epithelium mainly composed of keratinocytes, the innermost basal cells, form a proliferative layer, from which keratinocytes periodically

Copyright 2006, Elsevier Science (USA).
All rights reserved.

withdraw from the cell cycle and commit to terminally differentiate, while migrating into the suprabasal layers (Fuchs, 1997). Terminally differentiated keratinocytes forming the cornified layer are lost daily from the surface of the skin and are replaced continuously by newly differentiating cells. Hair follicles that develop through a series of mesenchymal–epithelial interactions during embryogenesis are also dynamic structures that are mainly composed of keratinocytes and whose outer root sheath (ORS) is contiguous with the basal layer of the epidermis. Once formed, hair follicles periodically undergo cycles of regression, rest, and growth, through which old hairs are replaced by new ones (Hardy, 1992; Paus and Cotsarelis, 1999).

As an example we describe the selective ablation of the retinoid receptor RXRα in basal epidermal keratinocytes of adult mice.

II. MATERIALS AND INSTRUMENTATION

RXRαaf2(I) (Mascrez *et al*., 1998) and RXRα$^{L2/L2}$ mice (Li *et al*., 2001) can be obtained from Pr. P. Chambon (chambon@titus.u-strasbg.fr). RosaR26R (Soriano, 1999) can be requested from P. Soriano (psoriano@fhcrc.org).

Triton X-100 (Cat. No. T8787), KCl (Cat. No. 31248), dimethylformamide (Cat. No. D4551), glutaraldehyde (25%) (Cat. No. 49630), $MgCl_2$ (Cat. No. 63068), PBS (Dulbecco's phosphate-buffered saline) (Cat. No. D5652), potassium ferricyanide (Cat. No. 244023), potassium ferrocyanide (Cat. No. P3289), tamoxifen (Tam) (Cat. No. T5648), proteinase K (Cat. No. P6556), and *Taq* DNA polymerase (5 units/μl) (Cat. No. D4545) are from Sigma-Aldrich; Tris (Cat. No. GAUTRI00-66), SDS (20%) (Cat. No. GHYSDS02-07), NaCl (Cat. No. GAUNAC01-66), and stabilized phenol (Tris saturated; pH 7.5–8) (Cat. No. 018335) are from Eurobio. Chloroform (Cat. No. 438603) and formaldehyde [40% (w/v), Cat. No. 415661] are from Carlo ERBA. HCl (37%) (Cat. No. 100317), paraformaldehyde (Cat. No. 818715), and safranin (Cat. No. 115948) are from Merck. Cryomatrix (Frozen Embedding Resin) (Cat. No. 6769006) and Histosol plus (Cat. No. histol + I) are from Shandon Inc. dATP (100 m*M*) (Cat. No. 27-2050-03), dCTP (100 m*M*) (Cat. No. 27-2060-03), dGTP (100 m*M*) (Cat. No. 27-2070-03), and dTTP (100 m*M*) (Cat. No. 27-2080-03) are from Amersham. Diamidino-2-phenylindole dihydrochloride (DAPI) (Cat. No. 236276), and X-Gal (5-bromo-4-chloro-3-indolyl-β-D-galactopyranoside) (Cat. No. 745740) are from Roche Diagnostics. Dispase is from Invitrogen (Cat. No. 17105-041). Biotinylated mouse monoclonal 2CRE 2D8-1-2 antibody (Cat. No. MAB3120) and EDTA (Cat. No. EU0007B) are from Euromedex. CY3-conjugated streptavidin is from Jackson ImmunoResearch (Cat. No. 016-160-084). Vectashield mounting medium (Cat. No. H-1000) and normal goat serum (Cat. No. S-1000) are from Vector. Sunflower oil is from a grocery store.

Stericups (0.22 μm) are from Millipore (Cat. No. SCGPUOIRE). One-milliliter syringes (Cat. No. BS-01T) and 25-gauge needles (Cat. No. NN-2516R) are from Terumo. Histomolds 13×19 mm are from Leica (Cat. No. 14702218313).

The thermocycler (Gene Amp PCR system 9700) is from Perkin-Elmer Corporation. The cryostat (CM 3050S) and the fluorescent microscope (DM LB Type 307-072.057) are from Leica.

III. PROCEDURES

The following is an example of cell-specific temporally controlled somatic mutagenesis : excision of floxed genes in basal epidermal keratinocytes.

A. Establishment of Transgenic Mice Expressing Cre-ER^{T2} in Basal Epidermal Keratinocytes

1. Production of K14-Cre-ER^{T2} Transgenic Mice

To express Cre-ER^{T2} in epidermal basal keratinocytes, transgenic mice harboring Cre-ER^{T2} under the control of the keratin K14 (K14) regulatory sequences are established. To this end, a transgene encompassing the 2-kb human K14 promoter/enhancer, which is active in the dividing basal layer keratinocytes of the epidermis, the outer root sheath of hair follicles, and some other stratified squamous epithelia (e.g., oral and tongue epithelia) (Vassar *et al*., 1989), located upstream of the Cre-ER^{T2} encoding sequence (Fig. 1A), was injected into C57BL/6 × SJL zygotes (Li *et al*., 2000). The detailed description of the methods used to construct the transgene and to establish transgenic founder mice (F0) is not within the scope of this article (see Nagy *et al*., 2003; Sambrook and Russel, 2001).

2. Identification of K14-Cre-ER^{T2} Transgenic Founder Animals

Solutions

1. *Proteinase K stock solution at 10 mg/ml:* Dissolve 100 mg proteinase K in 10 ml distilled H_2O, and store as 0.5-ml aliquotes at –20°C.

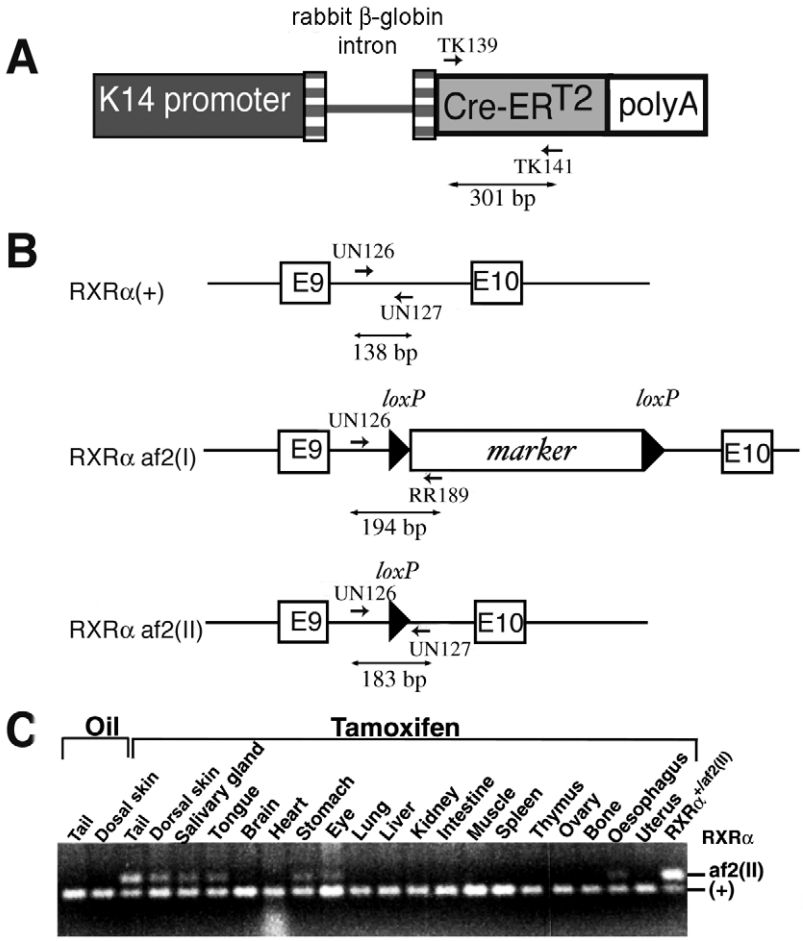

FIGURE 1 Characterization of the K14-Cre-ER^{T2} transgenic line. (A) Structure of the K14-Cre-ER^{T2} transgene. The human K14 promoter, the Cre-ER^{T2} coding sequence, and the simian virus 40 polyadenylation signal [poly (A)] are represented by black, grey, and open boxes, respectively. The rabbit β-globin intron and splice donor and acceptor sites are depicted by a line and hatched boxes, respectively. (B) Genomic structure of the RXRα WT, the RXRα af2(I) target allele, and the recombined RXRα af2(II) allele and the PCR strategies used to identify these RXRα alleles. (C) PCR detection of tamoxifen (Tam)-induced Cre-mediated DNA excision in mice. PCR was performed on DNA isolated from the indicated organs 1 day after oil- (vehicle) or Tam-treated K14-Cre-ER$^{T2\ (tg/0)}$/RXRα$^{+/af2(I)}$ mice, as well as from tail of RXRα$^{+/af2(II)}$ mice (last lane on the right), as indicated. Positions of the PCR products amplified from the WT RXRα allele (+) and the RXRα af2(II) allele are shown.

2. *Proteinase K digestion buffer*: 50 m*M* Tris (pH 8.0), 5 m*M* EDTA, 1% SDS; 0.2 *M* NaCl. To make 800 ml, assemble in the following order: 40 ml 1 *M* Tris–HCl (pH 8.0), 500 ml distilled water, 8 ml 0.5 *M* EDTA, 40 ml 20% SDS, 32 ml 5 *M* NaCl, and 180 ml distilled water. Store at room temperature.

3. *10× PCR buffer*: 500 m*M* KCl, 100 m*M* Tris–HCl, pH 8.8, 15 m*M* $MgCl_2$. To make 100 ml, add 50 ml 1 *M* KCl, 10 ml 1 M Tris–HCl (pH 8.8), and 1.5 ml 1 *M* $MgCl_2$ to 38.5 ml distilled water. Filter on a 0.22-µm stericup.

4. *Phenol/chloroform (1:1)*: Mix equal volume of stabilized phenol (Tris saturated, pH 7.5–8) and chloroform. Store at 4°C for a maximum of 2 weeks.

5. *dNTP mix (10 mM each)*: To make 1 ml, add 100 µl 100 m*M* dATP, 100 µl 100 m*M* dCTP, 100 µl 100 m*M* dGTP, and 100 µl 100 m*M* dTTP to 600 µl sterile distilled water. Store as 100-µl aliquots at –20°C.

6. *PCR Primers*: Oligonucleotides (1 µg/µl in H_2O) stored at –20°C.

For Cre PCR: TK139 (5′-ATTTGCCTGCATTACCG GTC-3′) and TK 141 (5′-ATCAACGTTTTCTTTTCG GA-3′).

Steps

1. Take a 0.5-cm tail biopsy from 2-week-old F0 mice and place them in a 1.5-ml microfuge tube.

2. To extract genomic DNA, add 250 µl proteinase K digestion buffer and 7.5 µl proteinase K stock solution (10 mg/ml) and incubate overnight at 55°C. Add an equal volume of phenol/chloroform (1:1), mix well, and microfuge at 15,000 *g* for 5 min at room temperature. Precipitate the supernatant with 500 µl ethanol (95%) and microfuge at 15,000 *g* for 5 min at room temperature. Wash the DNA pellet with 70% ethanol, air dry, and dissolve in 100 µl sterile distilled H_2O. DNA can be store at 4°C for weeks.

3. For genotyping, assemble in a 0.2-ml thermocycler tube 3 µl 10× PCR buffer, 0.6 µl dNTP (10 m*M* each), 0.06 µl 5′-primer (1 µg/µl) (TK 139), 0.06 µl 3′-primer (1 µg/µl) (TK 141), 0.2 µl *Taq* polymerase, 1 µl genomic DNA, and 20 µl H_2O. Place the tubes in a thermocycler and run the following procedure: 94°C, 5 min; 94°C, 20 s/55°C, 30 s/72°C, 5 s for 28 cycles; 72°C, 5–10 min.

4. Analyse the polymerase chain reaction (PCR) products on an ethidium bromide-stained 2.0% agarose gel (Feil *et al.*, 1996). A 301-bp product is indicative for the presence of the transgene (Fig. 1A; data not shown) and thus allows the identification of K14-Cre-ER^{T2} founder mice.

3. Identification of Founder Mice Transmitting the Transgene through the Germ Line

Transgenic founder mice are bred with C57BL/6 mice. Two week-old transgenic F1 offsprings are identified by genotyping (see Section III,A,2).

4. Identification of K14-Cre-ER^{T2} Transgenic Lines Exhibiting Tamoxifen-Dependent Cre Recombinase Activity in Basal Keratinocytes

a. Semiquantitative Analysis of Cre-ER^{T2}-Mediated LoxP-Flanked (Floxed) DNA Excision in Various Tissues. To analyse the recombinase activity of Cre-ER^{T2} transgenic mice in various organs, F1 K14-Cre-ER^{T2} mice are bred with mice bearing a floxed DNA segment within one of the two alleles of an autosomal gene, thus allowing identification of the WT and recombined alleles by PCR using a single primer pair. For that purpose, we use RXRα$^{+/af2(I)}$ mice (Mascrez *et al.*, 1998; see Fig. 1B).

Solution

Tamoxifen solution (1 mg/ml): Suspend 10 mg tamoxifen in 1 ml ethanol. Mix well by vortexing. Add 9 ml sunflower oil. Vortex for 2 min and sonicate for 30 min. Store as aliquots at –20°C for up to several months.

Steps

1. Breed F1 K14-Cre-ER^{T2} and RXRα$^{+/af2(I)}$ mice.

2. Genotype offsprings are as described in Section III,A,2. The PCR primers used to identify the RXRα af2(I) allele are UN126 (5′-CAAGGAGCCTC-CTTTCTCTA-3′) and RR189 (5′-AAGCGCAT-GCTCCAGACTGC-3′) (PCR product, 194 bp) (Fig. 1B).

3. Administer Tam to mice: Inject intraperitoneally 8-week-old K14-Cre-ER$^{T2(tg/0)}$/RXRα$^{+/af2(I)}$ mice daily with 100 µl Tam solution (0.1 mg) or oil (vehicle) for 5 days with a 1-ml syringe equipped with a 25-gauge needle (see also Comment 1).

4. Sacrifice Tam- and oil-treated mice by cervical dislocation 1 day after the last Tam injection and take organs/tissues (e.g., tail, brain, oesophagus, lung, heart, liver, tongue, salivary gland, intestine, kidney, thymus, eye, spleen, muscle, stomach, testis/ovary, and uterus).

5. Isolate genomic DNA from the various samples and analyze it by PCR as in Section III,A,2, except use UN126 (5′-CAAGGAGCCTCCTTTCTCTA-3′) and UN127 (5′-CCTGCTCTACCTGGTGACTT-3′) as PCR primers to amplify the 183-bp recombined RXRαaf2(I) allele [RXRαaf2(II)] and the 138-bp RXRα WT allele (see Figs. 1B and 1C).

K14-Cre-ER^{T2} lines exhibiting, after Tam treatment, efficient conversion of the RXRαaf2(I) allele into the RXRαaf2(II) allele in the dorsal skin and tail and no conversion in vehicle-treated (oil) control animals (Fig. 1C; data not shown) are selected for further analysis (see also Comment 2).

b. Characterization of Chimeric Cre Recombinase Expression Pattern in Skin of Selected K14-Cre-ER^{T2} Lines by Immunohistochemistry (IHC).

Solutions

1. *PBS (10×) solution*: Dissolve one bottle of PBS powder (95.5 g) in distilled H_2O and complete to 1 liter.

2. *PBS (1×) solution*: To make 1 liter, dilute 100 ml of 10 × PBS solution in 900 ml distilled water.

3. *Paraformaldehyde (8%)*: Dissolve 64 g paraformaldehyde in 500 ml distilled H_2O and add 8 ml of 1 *M* NaOH. Stir gently on a heating block (65°C) until the paraformaldehyde is dissolved. Add 80 ml 10 × PBS stock solution and allow the mixture to cool down to room temperature. Adjust the pH to 7.4 with 1 *M* HCl, and complete with H_2O to 800 ml. Filter the solution through a 0.22-µm stericup and store as 50-ml aliquots at –20°C. Avoid repeated freezing/thawing.

4. *Paraformaldehyde (2%)*: Dilute 50 ml paraformaldehyde (8%) fixation solution with PBS (1×) to a final volume of 200 ml.

5. *PBST solution: 0.1% (w/v) Triton X-100 in PBS*. To make 2 liters, add 200 ml 10 × PBS stock solution to 1500 ml distilled H_2O, 20 ml Triton X 100 [10% (w/v) in PBS], and complete to 2 liters with H_2O.

6. *5% normal goat serum/PBST*: Dilute normal goat serum in PBS to a final concentration of 5% (v/v). Aliquote and store at –20°C. Before use, add 40 µl Triton X-100 [10% (w/v) in PBS (1×)] to 4 ml 5% normal goat serum/PBS and keep on ice.

7. *DAPI (1 mg/ml) stock solution*: Dissolve 10 mg DAPI in 10 mg distilled water. Protect from light and store in aliquots (50 µl/tube) at –20°C.

8. *Vectashield containing DAPI (10µg/ml):* Add 10 µl DAPI (1-mg/ml stock solution) to 1 ml Vectashield. Mix well by vortexing for 1 min. Protect from light.

Steps

1. Administer Tam to K14-Cre-ER^{T2} mice as in Section III,A,4,a to induce Cre-ER^{T2} nuclear translocation (Brocard *et al*., 1997), thus facilitating Cre-ER^{T2} detection.
2. One day after the last Tam injection, take a tail biopsy from which bones are removed (or take shaved dorsal skin).
3. Place the samples into histomolds filled with Cryomatrix and freeze on dry ice. Store tissue blocks at –20°C until sectioning at 10 µm with a cryostat.
4. Perform Cre immunohistochemistry.
   a. Fix cryosections in paraformaldehyde (2%) for 5 min at room temperature.
   b. Wash with PBST (3 × 5 min) and then with PBS (5 min).
   c. Incubate for 30 min at room temperature in 5% normal goat serum/PBST.
   d. Incubate for 2 hr at room temperature or overnight at 4°C with the biotinylated mouse monoclonal 2CRE 2D8-1-2 antibody (1:1000 diluted in 5% normal goat serum/PBST).
   e. Wash slides with PBST (3 × 5 min) and with PBS (5 min).
   f. Incubate with CY3-conjugated streptavidine (1:400 diluted in PBS) for 1 h at room temperature.
   g. Wash with PBST (3 × 5 min) and with PBS (5 min).
   h. Mount the slides with Vectashield containing DAPI (10 µg/ml).
   i. Examine by fluorescent microscopy (excitation, 545 nm; emission 610 nm).

c. Characterization of Recombinase Activity at Cellular Level in K14-Cre-ER^{T2} Mice. Transgenic mice exhibiting Cre-ER^{T2} expression in most, if not all, basal keratinocytes are bred with transgenic lines that express a reporter gene such as LacZ, alkaline phosphatase (AP), or green fluorescent protein (GFP) after Cre-mediated floxed DNA excision. Note that the currently established Cre reporter lines (ACZL, RosaR26R, Z/AP, Z/EG, etc.) do not allow reporter gene expression in all cells/tissues of adult mice (Akagi *et al*., 1997; Brocard *et al*., 1997; Indra *et al*., 1999; Lobe *et al*., 1999; Novak *et al*., 2000; Soriano, 1999; Weber *et al*., 2001; unpublished results). Thus it is essential to breed the transgenic Cre-ER^{T2} lines to be analysed with appropriate reporter mice. For example, in epidermal keratinocytes, the ACZL (Akagi *et al*., 1997) is a good reporter line in suprabasal keratinocytes, but not in basal keratinocytes (Indra *et al*., 1999), whereas the RosaR26R (Soriano, 1999; hereafter called Rosa$^{fl/+}$) expresses LacZ in both basal and suprabasal cells after Cre-mediated recombination (Li *et al*., 2001).

Solutions

1. *LacZ fixation solution*: Prepare just before use and keep at 4°C. To make 50 ml, add 2.5 ml formaldehyde (40%) and 0.4 ml glutaraldehyde (25%) to 47.1 ml cold PBS (1×).
2. *Potassium ferricyanide (0.1 M)*: To make 100 ml, dissolve 3.29 g potassium ferricyanide in PBS and complete to 100 ml. Protect from light and store at 4°C.
3. *Potassium ferrocyanide (0.1 M)*: To make 100 ml, dissolve 4.22 g potassium ferricyanide in PBS (1×) and complete to 100 ml. Protect from light and store at 4°C.
4. *X-Gal (5-bromo-4-chloro-3-indolyl-β-D-galactopyranoside) stock solution*: Dissolve X-Gal in dimethylformamide at a final concentration of 40 mg/ml. Protect from light and store at –20°C.
5. *β-Galactosidase staining solution*: Prepare just before use. Add 2.5 ml potassium ferricyanide (0.1 *M*), 2.5 ml potassium ferrocyanide (0.1 *M*), 0.1 ml $MgCl_2$ (1 *M*), and 1.25 ml X-Gal stock solution (40 mg/ml) to 43.65 ml PBS (1×). Filter with a 0.22-µm stericup and protect from light.
6. *Safranin counterstaining solution [0.05% (w/v)]*: Dissolve 0.05 g Safranin in 100 ml distilled water and store at room temperature.

Steps

1. Breed K14-Cre-ER$^{T2(tg/0)}$ with Rosa$^{fl/+}$ mice.
2. Select K14-Cre-ER$^{T2(tg/0)}$/Rosa$^{fl/+}$ double transgenic offsprings by PCR genotyping as described in Section III,A,2. The primers used for genotyping the ROSA fl allele are VD23 (5′-CGCCGACGGCACGCT GATTG-3′) and VD24 (5′-GTTTCAATATTGGCTTC ATC-3′).
3. Inject 8- to 10-week-old K14-Cre-ER$^{T2(tg/0)}$/Rosa$^{fl/+}$ mice for 5 days with 0.1 mg Tam or oil as in Section III,A,4,a.
4. Take tail biopsies at days 5, 30, and 60 after Tam treatment.
5. Prepare 10-µm cryosections as in Section III,A,4,b.
6. β-Galactosidase staining of the section:

a. Incubate the slides with LacZ fixation solution at 4°C for 15 min.
b. Wash 3 × 5 min with PBS at room temperature.
c. Incubate in β-galactosidase staining solution overnight at 37°C (protect from light).
d. Wash 3 × 5 min with PBS at room temperature.
e. Rinse 2 × 30 s in distilled H_2O.
f. Safranin counterstaining (optional): after step e, immerse the slides in Safranin counterstaining solution for 1 min and rinse 2 × 30 s in distilled H_2O.
g. Dehydrate the slides in 90% ethanol for 30 s, in 100% ethanol for 30 s, in 100% ethanol for 2 min, and in Histosol plus 2 × 3 min.
h. Mount the slides.
i. Examine by light microscopy.

The absence of X-Gal staining in skin of untreated or vehicle treated K14-Cre-ER$^{T2(tg/0)}$/Rosa$^{fl/+}$ mice demonstrates that the recombinase activity of K14-Cre-ER$^{T2(tg/0)}$ mice is tightly controlled (Metzger *et al*., 2003).

Suprabasal cells are renewed in 5–10 days in mouse tail epidermis. As keratinocytes of the basal and suprabasal layers of the epidermis and of the outer root sheath of hair follicle are X-Gal stained 5 days after the beginning of Tam injection, recombination is induced rapidly by Tam. Furthermore, the X-Gal staining observed in most, if not all, keratinocytes of the epidermis and ORS of the hair follicle 30 and 60 days after Tam treatment shows that recombination is induced efficiently in epidermal stem cells of this K14-Cre-ER^{T2} transgenic line (see Metzger *et al*., 2003).

B. RXRα Ablation as Example of Conditional Somatic Mutagenesis of Target Genes in Epidermal Keratinocytes of Adult Mice

To determine the function of RXRα in epidermal keratinocytes of adult mice, RXRα is conditionally disrupted in basal keratinocytes of 8- to 10-week-old mice.

Solution

Dispase solution (4 mg/ml): Dissolve 40 mg dispase in 10 ml PBS (1×). Prepare just before use.

Steps

1. Establishment of K14-Cre-ER$^{T2(tg/0)}$/RXRα$^{L2/L2}$ and control mice.
   a. Breed floxed RXRα mice (RXRα$^{L2/L2}$) with K14-Cre-ER$^{T2(tg/0)}$ mice.
   b. Identify K14-Cre-ER$^{T2(tg/0)}$/RXRα$^{L2/+}$ offsprings by genotyping as described in Section III,A,2. Primers ZO243 (5′-TCCTTCACCAAGCACATCTG-3′) and ZO244 (5′-TGCAGCCCTCACAACTGTAT-3′) are used to identify RXRα L2 allele (701 bp) and (+) allele (669 bp) (Fig. 2A); the PCR program is 94°C, 5 min; 94°C, 10 s/56°C, 30 s/72°C 1 min for 32 cycles; 72°C 5–10 min.
   c. Breed K14-Cre-ER$^{T2(tg/0)}$/RXRα$^{L2/+}$ mice with RXRα$^{L2/L2}$ and identify K14-Cre-ER$^{T2(tg/0)}$/RXRα$^{L2/L2}$ offspring (pre-mutant mice), as well as K14-Cre-ER$^{T2(tg/0)}$/RXRα$^{L2/+}$ and K14-Cre-ER$^{T2(0/0)}$/RXRα$^{L2/L2}$ littermates (control mice) by genotyping as described earlier.

2. Administer oil or tamoxifen to 8- to 10-week-old sex- and age-matched K14-Cre-ER$^{T2(tg/0)}$/RXRα$^{L2/L2}$ and control littermates as in Section III,A,4.

3. Analyse the excision efficiency of the target gene in the tail epidermis 2 and 8 weeks after Tam/oil treatment.
   a. Take tail biopsies.
   b. Remove bones.
   c. Incubate samples in dispase (4 mg/ml in PBS) overnight at 4°C (or for 2 h at 37°C).
   d. Separate the dermis from the epidermis with forceps.
   e. Extract genomic DNA and analyse it by PCR as in Section III,A,2. Primers ZO243 (5′-TCCTTCACCAAGCACATCTG-3′) and UD196 (5′-TCACCTGGACTTGTCACCTAG-3′) are used to amplify the RXRαL$^-$ allele (426 bp, Fig. 2A).

The example shown in Fig. 2B demonstrates that RXRα L2 alleles were fully converted into RXRα L$^-$ alleles in the epidermis, but not in the dermis of Cre-ER^{T2} expressing mice, 2 weeks after Tam treatment, demonstrating the selectivity and efficiency of the K14-Cre-ER^{T2} transgene for mediating somatic ablation of RXRα in epidermal keratinocytes after Tam treatment (RXRα$^{ep-/-}$ mice). The absence of L2 to L$^-$ allele conversion in control mice expressing the K14-Cre-ER^{T2} transgene without Tam treatment shows that RXRα ablation is strictly dependent on Tam (Fig. 2B). Moreover, the presence of only RXRα L$^-$ alleles in K14-Cre-ER$^{T2(tg/0)}$/RXRα$^{L2/L2}$ mouse epidermis 8 weeks after Tam treatment indicates that RXRα was disrupted in most, if not all, epidermal stem cells (data not shown).

Efficient RXRα protein ablation in the interfollicular keratinocytes and outer root sheath of the hair follicle in Tam-treated K14-Cre-ER$^{T2(tg/0)}$/RXRα$^{L2/L2}$ mice can be verified by immunohistochemistry in skin biopsies using an antibody directed against RXRα, according to standard procedures (see Metzger *et al*., 2003).

The phenotypic analysis of mice in which a target gene is ablated in adult mouse skin can be investigated by macroscopic examination and histological analysis. For example, weekly examination of mutant and

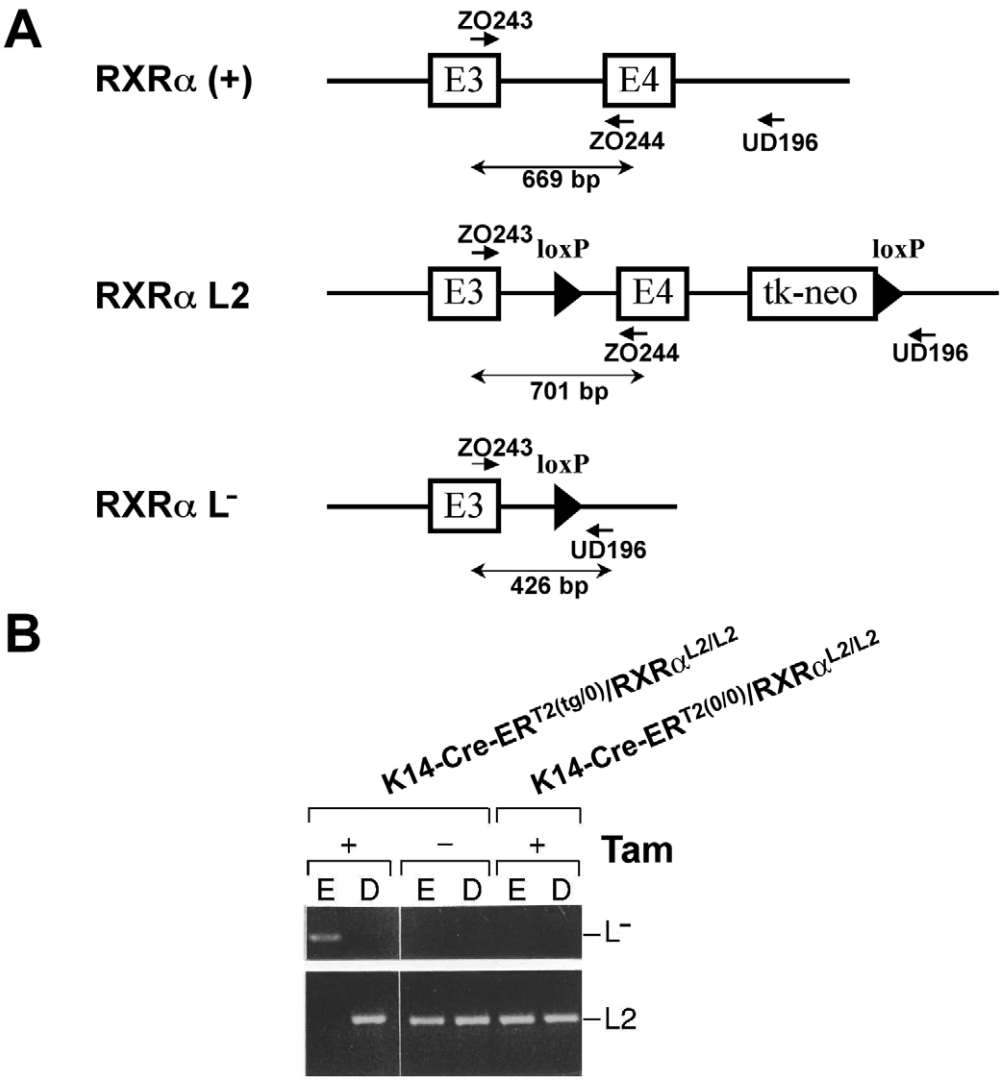

FIGURE 2 Temporally controlled RXRα ablation in epidermal keratinocytes. Schematic diagram of the RXRα WT (+) genomic locus, the floxed RXRα L2 allele, and the RXRα L⁻ allele obtained after tamoxifen (Tam)-induced Cre-mediated excision of exon 4. PCR primers to identify the RXRα +, L2, and L⁻ alleles are indicated. Arrowheads represent LoxP sites. (B) Efficiency of K14-Cre-ER^{T2}-mediated RXRα recombination in adult skin. L2 and L⁻ RXRα alleles were identified by PCR analysis of genomic DNA extracted from epidermis "E" or dermis "D" isolated from tail 2 weeks after administration of either Tam (+) or oil (vehicle; –) to K14-Cre-ER$^{T2(tg/0)}$/RXRα$^{L2/L2}$ and K14-Cre-ER$^{T2(0/0)}$/RXRα$^{L2/L2}$ mice, as indicated. PCR fragments corresponding to the RXRα L2 and L⁻ alleles are displayed.

control mice revealed hair loss in the ventral region of K14-Cre-ER$^{T2(tg/0)}$/RXRα$^{L2/L2}$ mice 6–7 weeks after Tam treatment, but not in oil-treated mice of the same genotype or in Tam-treated K14-Cre-ER$^{T2(tg/0)}$/RXRα$^{L2/+}$ mice. Twelve to 16 weeks after Tam treatment, large regions of ventral skin and smaller regions of dorsal skin of mutant animals were hairless. Cysts became visible under the skin surface, which enlarged and spread all over the body with time. With increasing age (>20 weeks), minor focal lesions appeared on hairless dorsal skin, on chins, and behind the ears. Histology of hairless skin showed disappearance of hair follicles and presence of utriculi and dermal cysts. Abnormal keratinocyte proliferation and differentiation were also observed, as well as inflammatory reactions (Li *et al.*, 2000; Metzger *et al.*, 2003).

IV. CONCLUSIONS

The K14-Cre-ER^{T2} mouse line generated and characterised according to the present procedure very

effectively allows Cre-mediated recombination of floxed DNA in basal epidermal keratinocytes upon low-dose Tam administration (0.1 mg for 5 days). As suprabasal keratinocytes are replaced continuously by basal cell-derived newly differentiated cells, the floxed DNA segment is deleted in all keratinocytes within 1 to 2 weeks. It is noteworthy that no background recombination was detected in the absence of Tam administration, which allows to tightly control the time at which the genetic modification is generated. Ablation of RXRα in adult mouse keratinocytes revealed important functions of this gene in epidermal keratinocyte proliferation and differentiation, hair cycling, and epidermal inflammation (Li *et al*., 2000). Importantly, selective induction of the recombinase activity of Cre-ER^{T2} proteins has been achieved in all mouse cell types as yet tested. We have established a number of mouse lines allowing temporally controlled somatic mutagenesis in various cell types and tissues, including adipocytes, hepatocytes, nervous system, male germ cells, skeletal myocytes, prostate epithelium (Imai *et al*., 2001a,b; Schuler *et al*., 2004; Weber *et al*., 2001, 2003; unpublished data). The only serious drawback resides in the availability of promoter-containing segments that allow the selective expression of the Cre-ER^{T2} transgene in all cells of a given cell-type, as using small promoter regions, no or mosaic transgenic expression is often observed. Flanking the transgene with insulator sequences or using large genomic promoter-containing segments, present in BACs or PACs, known to reduce gene silencing (Bell *et al*., 2001; Giraldo and Montoliu, 2001; Yang *et al*., 1997), appears to facilitate the establishment of potent Cre-ER^{T2} transgenic mice (unpublished data).

V. COMMENTS

1. The active form of tamoxifen, 4-hydroxytamoxifen, can also be administered, but as it is less soluble and more costly, but not more potent in the mouse, it is recommended to use tamoxifen, which is converted to 4-hydroxytamoxifen in the liver.

2. Recombination in the tongue, salivary gland, eye, stomach, and oesophagus is in agreement with the previously described promoter activity of the human K14 promoter (Vassar *et al*., 1989).

VI. PITFALL

Separate Tam-treated and untreated mice to avoid exposure of control mice to Tam.

Acknowledgments

We are grateful to P. Soriano for the generous gift of the RosaR26R mice. We thank present and past members of the laboratory who have contributed to developing the foregoing protocols, as well as E. Metzger and A. Van Es and the animal facility staff for animal care, the secretariat staff for typing, and the illustration staff for preparing the figures. This work was supported by funds from the Centre National de la Recherche Scientifique, the Institut National de la Santé et de la Recherche Médicale, the Collège de France, the Hôpital Universitaire de Strasbourg, the Association pour la Recherche sur le Cancer, the Fondation pour la Recherche Médicale, the Human Frontier Science Program, and the Ministère de l'Éducation Nationale de la Recherche et de la Technologie.

References

Akagi, K., Sandig, V., Vooijs, M., Van der Valk, M., Giovannini, M., Strauss, M., and Berns, A. (1997). Cre-mediated somatic site-specific recombination in mice. *Nucleic Acids Res*. **25**, 1766–1773.

Bell, A. C., West, A. G., and Felsenfeld, G. (2001). Insulators and boundaries: Versatile regulatory elements in the eukaryotic genome. *Science* **291**, 447–450.

Branda, C. S., and Dymecki, S. M. (2004). Talking about a revolution: The impact of site-specific recombinases on genetic analyses in mice. *Dev. Cell* **6**, 7–28.

Brocard, J., Warot, X., Wendling, O., Messaddeq, N., Vonesch, J. L., Chambon, P., and Metzger, D. (1997). Spatio-temporally controlled site-specific somatic mutagenesis in the mouse. *Proc. Natl. Acad. Sci. USA* **94**, 14559–14563.

Feil, R., Brocard, J., Mascrez, B., LeMeur, M., Metzger, D., and Chambon, P. (1996). Ligand-activated site-specific recombination in mice. *Proc. Natl. Acad. Sci. USA* **93**, 10887–10890.

Fuchs, E. (1997). Keith R. Porter Lecture, 1996. Of mice and men: Genetic disorders of the cytoskeleton. *Mol. Biol. Cell* **8**, 189–203.

Garcia, E. L., and Mills, A. A. (2002). Getting around lethality with inducible Cre-mediated excision. *Semin. Cell Dev. Biol*. **13**, 151–158.

Giraldo, P., and Montoliu, L. (2001). Size matters: Use of YACs, BACs and PACs in transgenic animals. *Transgen. Res*. **10**, 83–103.

Hardy, M. H. (1992). The secret life of the hair follicle. *Trends Genet*. **8**, 55–61.

Imai, T., Jiang, M., Chambon, P., and Metzger, D. (2001a). Impaired adipogenesis and lipolysis in the mouse upon selective ablation of the retinoid X receptor alpha mediated by a tamoxifen-inducible chimeric Cre recombinase (Cre-ER^{T2}) in adipocytes. *Proc. Natl. Acad. Sci. USA* **98**, 224–228.

Imai, T., Jiang, M., Kastner, P., Chambon, P., and Metzger, D. (2001b). Selective ablation of retinoid X receptor alpha in hepatocytes impairs their lifespan and regenerative capacity. *Proc. Natl. Acad. Sci. USA* **98**, 4581–4586.

Indra, A. K., Warot, X., Brocard, J., Bornert, J. M., Xiao, J. H., Chambon, P., and Metzger, D. (1999). Temporally-controlled site-specific mutagenesis in the basal layer of the epidermis: Comparison of the recombinase activity of the tamoxifen-inducible Cre-ER(T) and Cre-ER(T2) recombinases. *Nucleic Acids Res*. **27**, 4324–4327.

Jonkers, J., and Berns, A. (2002). Conditional mouse models of sporadic cancer. *Nature Rev. Cancer* **2**, 251–265.

Lewandoski, M. (2001). Conditional control of gene expression in the mouse. *Nature Rev. Genet* **2**, 743–755.

Li, M., Chiba, H., Warot, X., Messaddeq, N., Gérard, C., Chambon, P., and Metzger, D. (2001). RXR-alpha ablation in skin keratinocytes results in alopecia and epidermal alterations. *Development* **128**, 675–688.

Li, M., Indra, A. K., Warot, X., Brocard, J., Messaddeq, N., Kato, S., Metzger, D., and Chambon, P. (2000). Skin abnormalities generated by temporally controlled RXRalpha mutations in mouse epidermis. *Nature* **407**, 633–636.

Lobe, C. G., Koop, K. E., Kreppner, W., Lomeli, H., Gertsenstein, M., and Nagy, A. (1999). Z/AP, a double reporter for cre-mediated recombination. *Dev. Biol.* **208**, 281–292.

Mascrez, B., Mark, M., Dierich, A., Ghyselinck, N. B., Kastner, P., and Chambon, P. (1998). The RXRalpha ligand-dependent activation function 2 (AF-2) is important for mouse development. *Development* **125**, 4691–4707.

Metzger, D., and Chambon, P. (2001). Site- and time-specific gene targeting in the mouse. *Methods* **24**, 71–80.

Metzger, D., and Feil, R. (1999). Engineering the mouse genome by site-specific recombination. *Curr. Opin. Biotechnol* **10**, 470–476.

Metzger, D., Indra, A. K., Li, M., Chapellier, B., Calleja, C., Ghyselinck, N., and Chambon, P. (2003). Targeted conditional somatic mutagenesis in the mouse : Temporally-controlled knock out of retinoid receptors in epidermal keratinocytes. *Methods Enzymol.* **364**, 379–407.

Nagy, A., Gertsenstein, M., Vintersten, K., and Behringer, R. (2003). "Manipulating the Mouse Embryo: A Laboratory Manual." 3rd Ed. Cold Spring Harbor Laboratory Press, Cold Spring Harbor, NY.

Novak, A., Guo, C., Yang, W., Nagy, A., and Lobe, C. G. (2000). Z/EG, a double reporter mouse line that expresses enhanced green fluorescent protein upon Cre-mediated excision. *Genesis* **28**, 147–155.

Paus, R., and Cotsarelis, G. (1999). The biology of hair follicles. *N. Engl. J. Med.* **341**, 491–497.

Rajewsky, K., Gu, H., Kuhn, R., Betz, U. A., Muller, W., Roes, J., and Schwenk, F. (1996). Conditional gene targeting. *J. Clin. Invest.* **98**, 600–603.

Sambrook, J., and Russel, D. W. (2001). "Molecular Cloning: A Laboratory Manual." Cold Spring Harbor Laboratory Press, Cold Spring Harbor, NY.

Schuler, M., Dierich, A., Chambon, P., and Metzger, D. (2004). Efficient temporally-controlled targeted somatic mutagenesis in hepatocytes of the mouse. *Genesis*. **39**, 167–172.

Soriano, P. (1999). Generalized lacZ expression with the ROSA26 Cre reporter strain. *Nature Genet* **21**, 70–71.

Vassar, R., Rosenberg, M., Ross, S., Tyner, A., and Fuchs, E. (1989). Tissue-specific and differentiation-specific expression of a human K14 keratin gene in transgenic mice. *Proc. Natl. Acad. Sci. USA* **86**, 1563–1567.

Weber, P., Metzger, D., and Chambon, P. (2001). Temporally controlled targeted somatic mutagenesis in the mouse brain. *Eur. J. Neurosci.* **14**, 1777–1783.

Weber, P., Schuler, M., Gérard, C., Mark, M., Metzger, D., and Chambon, P. (2003). Temporally controlled site-specific mutagenesis in the germ cell lineage of the mouse testis. *Biol. Reprod.* **68**, 553–559.

Yang, X. W., Model, P., and Heintz, N. (1997). Homologous recombination based modification in Escherichia coli and germline transmission in transgenic mice of a bacterial artificial chromosome. *Nature Biotechnol.* **15**, 859–865.

Zhu, Z., Zheng, T., Lee, C. G., Homer, R. J., and Elias, J. A. (2002). Tetracycline-controlled transcriptional regulation systems: Advances and application in transgenic animal modeling. *Semin. Cell Dev. Biol.* **13**, 121–128.

CHAPTER

54

RNAi-Mediated Gene Silencing in Mammalian Cells

Derek M. Dykxhoorn

I. INTRODUCTION

RNA interference (RNAi) is the sequence-specific silencing of gene expression in response to double-stranded (ds)RNA. The term RNAi was first coined by Fire and colleagues (1998) when they discovered that the injection of long dsRNA into the nematode *Caenorhabditis elegans* led to the inhibition of gene expression by the targeted degradation of the homologous mRNA. These results were recapitulated *in vitro* by the silencing of gene expression due to the targeted cleavage of the homologous mRNA when long dsRNA was introduced into *Drosophila melanogaster* embryo extracts (Tuschl *et al*., 1999). Although these experiments demonstrated that the presence of long dsRNA initiates the process of RNAi, it has become increasingly clear that the sequence-specific effector molecules that mediate the targeted disruption of the mRNA are short RNA species. The long dsRNA introduced into *Drosophila* extracts was shown to be rapidly cleaved into ~22 nucleotide dsRNAs, termed short interfering (si) RNAs (Zamore *et al*., 2000). These siRNAs were shown to be sufficient to guide the degradation of the corresponding mRNA (Elbashir *et al*., 2001a). Similar short RNA species have been found in *C. elegans* and *Drosophila* embryos injected with long dsRNA, as well as in *Drosophila* Schneider 2 (S2) transfected with long dsRNA (Hammond *et al*., 2000; Parrish *et al*., 2000, Yang *et al*., 2000) (Fig. 1).

Biochemical and genetic studies have begun to provide the molecular details for how dsRNA can lead to the targeted disruption and silencing of gene expression. In the first step of the RNAi pathway, long dsRNA is cleaved into siRNAs. These siRNAs are 21–23 nucleotide dsRNA duplexes that have 5′-phosphate and 3′-hydroxyl groups. Importantly, siRNAs were shown to have symmetric 2–3 nucleotide 3′ overhangs reminiscent of an RNase III-like cleavage pattern. (Elbashir *et al*., 2001a). This knowledge led to the identification of the highly conserved Dicer family of RNase III enzymes as the mediator of the dsRNA cleavage (Bernstein *et al*., 2001). Upon formation, the siRNAs are unwound and one of the strands becomes incorporated into the multisubunit RNA-induced silencing complex (RISC). The strand that enters RISC appears to be determined by the thermodynamic stability of the 5′ end of the two strands, the strand with the lower thermodynamic stability predominating in RISC (Schwartz *et al*., 2003; Khvorova *et al*., 2003). The antisense strand of the siRNA guides the endonuclease activity of RISC to the homologous site on the cognate mRNA, resulting in the cleavage of the mRNA in the center of the siRNA–mRNA recognition site (reviewed in Dykxhoorn *et al*., 2003).

Although the introduction of long dsRNA has been effectively used for the silencing of gene expression in a variety of organisms (e.g., plants, *Drosophila*, and *C. elegans*), the application of this technology has been limited in vertebrate cells by the dsRNA-mediated induction of the sequence-nonspecific interferon response. The binding of long dsRNA leads to the activation of the dsRNA-dependent protein kinase (PKR). Once activated, PKR phosphorylates the α subunit of the translation initiation factor, EIF2α, leading to a general inhibition of translation and suppression of protein synthesis. In addition, long dsRNA activates 2′-5′ oligoadenylate synthase, leading to the conversion of ATP into 2′-5′ oligoadenylates [pppA(2′p5′A)n]. These oligoadenylates in turn activate RNase L, which leads to the nonsequence-specific cleavage of several RNA species, including ribosomal (r)RNA. This results

Copyright 2006, Elsevier Science (USA).
All rights reserved.

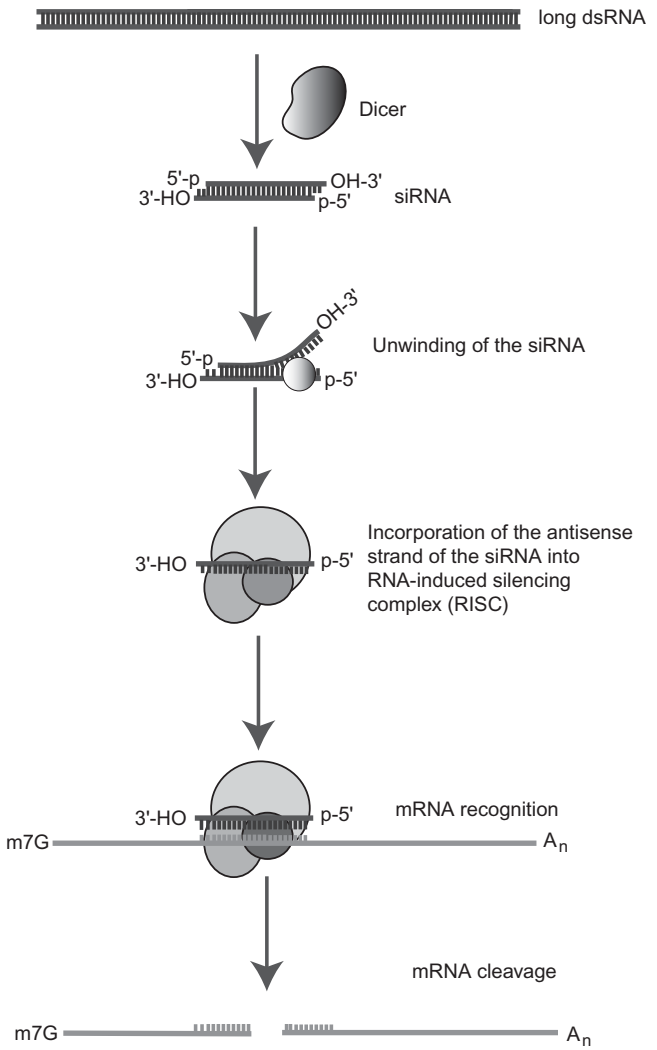

FIGURE 1 Schematic representation of the RNAi pathway. Long dsRNAs are cleaved by the RNase III-like enzyme Dicer into 21–23 nucleotide double-stranded short interfering (si)RNAs. The siRNAs are unwound into their single strands. The unwinding begins at the most thermodynamically unstable end of the siRNAs (Khvorova *et al.*, 2003; Schwarz *et al.*, 2003). Only one of the siRNA strands will predominate in the RNA-induced silencing complex (RISC). This choice appears to be based on the thermodynamic stability of the ends of the siRNA. The end of the siRNA that has the least stable binding at the 5′ end will preferentially enter RISC. The single strand of the siRNA incorporated into RISC will guide the protein–nucleic acid complex to the homologous site on the target mRNA. The mRNA is cleaved by the endonuclease activity of RISC.

in an inhibition of mRNA translation (Stark *et al.*, 1989). Activation of the interferon response can ultimately induce cells to undergo program cell death (apoptosis). However, the introduction dsRNA that is <30 nucleotides in length does not appear to induce the interferon pathway (Elbashir *et al.*, 2001b). Tuschl and colleagues demonstrated that the transfection of chemically synthesized siRNAs into mammalian cells effectively silenced gene expression without inducing the interferon response (Elbashir *et al.*, 2001b). This seminal discovery has led to the widespread use of RNAi for the targeted disruption of gene expression and the study of gene function, revolutioning the way reverse genetic experiments are performed in mammalian systems.

The demonstration that chemically or enzymatically synthesized siRNAs are capable of effectively silencing gene expression has led to the rapid development of RNAi-based technologies. These technologies have served to address two limitations inherent in the gene silencing by transfection of synthetic siRNAs, the transient nature of the silencing phenotype and the low efficiency of siRNA transfection in certain cell types, particularly primary cells. The transfection of siRNAs into rapidly dividing cells leads to a transient knockdown of the target gene. In rapidly growing cells (e.g., HeLa cells), the peak of silencing for most proteins occurs between 60 and 72 h posttransfection with a loss of silencing occurring approximately 5 days posttransfection (Dykxhoorn *et al.*, 2003). The decrease in the siRNA levels appears to correlate directly with the number of cell divisions, implying that it is a dilution of the siRNAs below a critical threshold level that leads to the loss of the silencing phenotype.

To increase the duration of silencing, DNA vector-based approaches have been developed that express siRNAs or precursors of siRNAs. The majority of these DNA-based RNAi systems rely on the expression of short RNA species from RNA polymerase III (pol III) promoters, particularly the U6 and H1 promoters. All of the elements required for efficient transcription from these promoters are located upstream of the transcription start site (+1), and the deletion of sequences downstream of the start site has no effect on the level of transcription (Paule and White, 2000). Although the U6 promoter has a requirement of a guanosine in the +1 position, the H1 promoter seems to have no such sequence constraints. Efficient termination of transcription is achieved in the absence of additional factors when the pol III encounters a simple run of four or more thymidine residues (Paule and White, 2000).

The siRNA expression constructs fall into two categories, those that express the individual strands of the siRNA in *trans* from tandem promoters and those that express sense and antisense strands in *cis* by expressing short hairpin (sh)RNAs that can be processed by dicer into active siRNAs. A number of groups have described the use of U6 promoters that express the sense and the antisense strands of a siRNA from separate transcription units (e.g., Lee *et al.*, 2002; Miyagishi and Taira, 2002). The strands will associate

in vivo to produce a functional siRNA. This mode of siRNA formation is completely independent of Dicer processing (Fig. 2).

The majority of siRNA-based expression systems have used pol III promoters to express hairpin RNA precursors that can be cleaved by Dicer to produce functional siRNAs. In addition to cleaving long dsRNA, Dicer has also been shown to process hairpin RNA, as demonstrated by the requirement of Dicer for the processing of the endogenous hairpin structures, e.g., the pre-let 7 micro(mi)RNA (Hutvagner and Zamore, 2002). Short hairpin RNA with fully complementary stems ranging between 19 and 29 nucleotides in length have been shown to produce active siRNAs when expressed from pol III promoters (e.g., Brummelkamp *et al*., 2002; Paddison *et al*., 2002). The expressed hairpin RNA serves as a substrate for Dicer cleavage producing siRNAs that can target mRNA cleavage by RISC.

These expression constructs have been cloned into a variety of vector systems, including plasmid, oncoretroviral, lentiviral, and adenoviral vectors, many of which are available commercially. The main advantage of the different vector systems is the ability to target different cell types and the ability to target cells that are refractory to the transfection of siRNAs (e.g., primary cells). Plasmids can be used to create cell lines that stably silence a particular gene of interest; however, the expression of siRNAs from plasmids requires the transfection of the plasmid into the cell type of interest. Like siRNAs, this approach is limited to cells that can be transfected easily. In contrast, the use of viral vectors greatly expands the range of cell types and cell lines that can be targeted for gene silencing, as these vectors rely on the infection of cells with the recombinant viral vectors, a process that is much more efficient than transfection. Although these vector systems facilitate transduction of cell types in different manners, the process of shRNA expression and the formation of active siRNAs is the same regardless of the vector system used.

The development of RNAi-based silencing approaches has made it possible to target virtually any gene of interest in an organism. This has opened up the potential to use RNAi-based technologies for large-scale genomic screens. This approach has been applied most successfully to *C. elegans* where RNAi-based approaches have been used to silence ~86% of the *C. elegans* genes (Kamath and Ahringer, 2003). Not only have RNAi-based gene silencing approaches been effective in gene function analysis, but these technologies also hold a great deal of potential as therapeutic

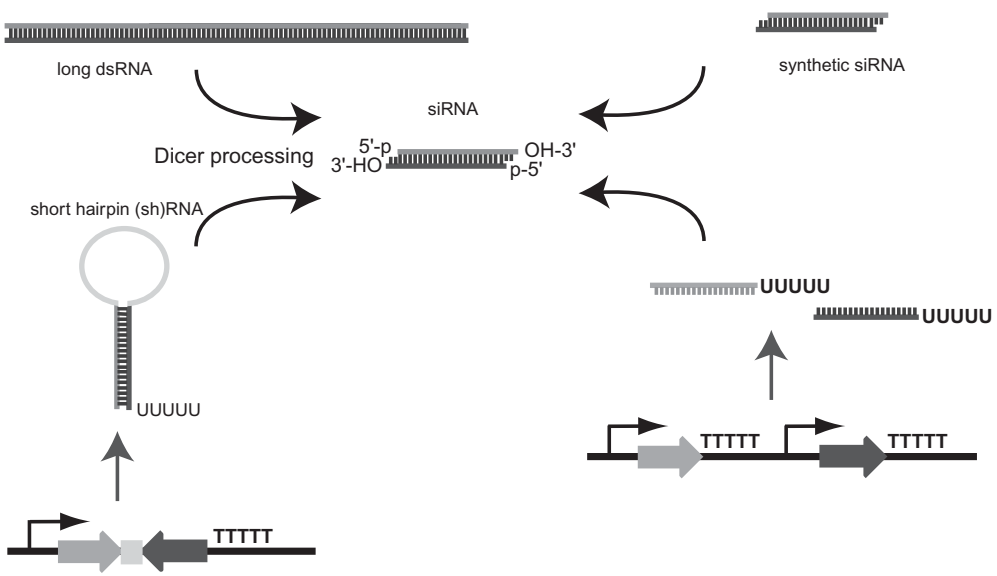

FIGURE 2 Strategies for siRNA formation. Long double-stranded RNAs and chemically synthesized siRNAs can be transfected directly into cells for a transient silencing phenotype. Unlike siRNAs, which can be unwound and incorporated into RISC, long dsRNA must be processed by Dicer to create active siRNAs. SiRNAs or siRNA precursors can be expressed from DNA vectors. The sense and antisense strands of the siRNA can be expressed from tandem pol III promoters. The strands can associate directly, forming an active siRNA. Alternatively, short hairpin RNAs can be expressed from pol III promoters. The shRNAs can be cleaved by Dicer to produce the active siRNAs. The RISC-mediated mRNA cleavage remains the same regardless of the method of siRNA production.

agents, such as the suppression of viral gene expression and replication (Novina *et al*., 2003).

II. MATERIALS AND INSTRUMENTATION

Oligofectamine (Cat. No. 12252-011), Lipofectamine 2000 (Cat. No. 12566-014), agarose (Cat. No. 15510-019), and bovine serum albumin (BSA, Cat. No. 15561-020) are from Invitrogen Corporation. Opti-MEM I reduced serum medium (Cat. No. 31985-062), Dulbecco's modified Eagle medium (DMEM, Cat. No. 11960-044), and fetal bovine serum (FBS, Cat. no. 10082-139) are from Gibco cell culture. *Apa*I (Cat. No. R0114S), *Eco*RI (Cat. No. R0101S), T4 DNA ligase (Cat. No. M0202S), and T4 DNA polymerase (Cat. No. M0203S) are from New England Biolabs. Nusieve GTG agarose (Cat. No. 50081) is from FMC. Phenol : chloroform : isoamyl alcohol (25 : 24 : 1) (Cat. No. 9730) is from Ambion. Chloroform (Cat. No. C2432), isoamyl alcohol (Cat. No. I9392), ammonium acetate (Cat. No. A1542), potassium acetate (Cat. No. P1190), magnesium acetate tetrahydrate (Cat. No. M2545), sodium acetate (Cat. No. S2889), sodium chloride (Cat. No. S7653), EDTA (Cat. No. E9884), glacial acetic acid (Cat. No. 45725), HEPES sodium salt (Cat. No. H7006), bromphenol blue (Cat. No. B0126), xylene cyanole FF (Cat. No. X4126), Ficoll 400 (Cat. No. F4375), ethidium bromide (Cat. No. E8751), ampicillin (Cat. No. A9518), and Tris borate–EDTA buffer (TBE, 5X concentrate, Cat. No. T6400) are from Sigma. Tris (Cat. No. 604200) and dNTP set, polymerase chain reaction (PCR) grade (Cat. No. 1969064), are from Roche. QIAquick gel extraction kit (Cat. No. 28704) is from Qiagen. One hundred percent ethanol (Cat. No. 111USP200) and 95% ethanol (Cat. No. 111000190) are from Pharmco products. Difco LB agar (Cat. No. 244510) is from BD Bioscience.

III. PROCEDURES

A. Designing effective siRNAs

siRNAs that target different regions of the same mRNA will differ markedly in the efficiency with which they silence gene expression. In order to achieve maximal levels of silencing, the choice of siRNAs is critical. Because mammalian RNAi is a cytoplasmic process, sequences corresponding to intronic regions should not be chosen. In addition, any regions of the mRNA that could potentially serve as binding sites for RNA-binding proteins should be avoided (e.g., the region surrounding the start codon and exon–exon boundaries). Traditionally, siRNAs were chosen that have an even representation and distribution of all the nucleotides within the antisense strand of the siRNA. Empirically, several sequence motifs have been consistently found to be associated with siRNAs that effectively silence gene expression, including $AAN_{19}TT$, $NAN_{19}NN$, $NARN_{17}YNN$, and $NANN_{17}YNN$ (where N = any nucleotide, R = a purine, and Y = a pyrimidine) (Martinez *et al*., 2002). Two groups have done an extensive analysis of the effect of different nucleotides and the entry of siRNA strands into RISC. They found that there were thermodynamic constraints upon the strands that governed the ability of one of the two strands to enter RISC and mediate effective silencing (Khvorova *et al*., 2003; Schwartz *et al*., 2003). In particular, the relative and absolute stabilities of the two 5′ ends of the siRNA strands determined which strand was capable of entering RISC, with the strand with the less thermodynamically stable 5′ end predominating in RISC and the other strand being destroyed.

It is always advisable to choose and test several different siRNAs against the same mRNA to determine the sequences that give the highest level of silencing. A BLAST search should be performed on all the selected sequences against sequence databases [e.g., EST or Unigene libraries from the National Center for Biotechnology Information (www.ncbi.nlm.gov)] to ensure that the siRNA sequence targets a single gene, thereby minimizing the chances of off-target effects. There are a number of Web sites that will predict potential siRNA sequences from a given mRNA sequence (see Table I).

B. Preparation of siRNA Strands

Solutions

1. *100% ethanol*
2. *95% ethanol*
3. *10 M ammonium acetate (pH 7.0)*: Dissolve 77.08 g ammonium acetate in distilled water, adjust pH to 7.0, and make up to 100 ml
4. *1 X annealing buffer (pH 7.4)*: 0.1 *M* potassium acetate, 2 m*M* magnesium acetate, 30 m*M* HEPES KOH (pH 7.4). Make a 1 *M* HEPES KOH solution by dissolving 238.3 g of HEPES in distilled water, adjust the pH to 7.4 by adding potassium hydroxide, and make up to 1 liter. Make 1 *M* potassium acetate and 1 *M* magnesium acetate as per Sambrook *et al*. (1989). For 10 ml of annealing buffer, add 0.3 ml 1 *M* HEPES KOH (pH 7.4), 1 ml 1 *M* potassium acetate, and 20 µl of 1 *M*

TABLE I Web Sites That Will Computationally Define Potential siRNAs against the mRNA Sequence of Choice

siRNA design site	Web address
Dharmacon siDesign center	http://www.dharmacon.com
Ambion siRNA converter	http://www.ambion.com/techlib/misc/siRNA_finder.html
Whitehead Institute of Biomedical Research at MIT	http://jura.wi.mit.edu/pubint/http://iona.wi.mit.edu/siRNAext/
Wadsworth Bioinformatics Center	http://sfold.wadsworth.org/sirna.pl
Molecula siRNA design service	http://www.molecula.com/new/siRNA_inquiry.html
GenScript siRNA target finder	http://www.genscript.com/ssl-bin/app/rnai
Qiagen siRNA design	http://www1.qiagen.com/siRNA

magnesium acetate; make up to 10 ml with distilled water.

Steps

Chemically synthesized siRNAs can be obtained from commercial RNA synthesis companies (see Table II). The siRNA strands are preferably synthesized using protected ribonucleoside phosphoramidites to increase their stability. If protected groups are used, siRNAs will require deprotection and desalting before use. For specific details regarding the preparation of siRNAs prior to their use in a gene-silencing experiment, see the protocols from the appropriate RNA synthesis company. These companies offer different synthesis options and degrees of purity.

1. siRNAs synthesized by Dharmacon Research (Boulder, CO) use the 2′-ACE protection chemistry. siRNAs are deprotected by resuspensing the lyophilized siRNA pellet in 400 µl of the 2′-deprotection buffer (100 m*M* TEMED-acetate, pH 3.8), mixing thoroughly by vortexing and incubating at 60°C for 45 min.
2. To desalt siRNAs, add 0.1 volume of 10 *M* ammonium acetate, pH 7.0 (40 µl), and 1500 µl of 100% ethanol to the deprotected siRNA solution and mix thoroughly by vortexing.
3. Incubate the siRNA solution at –20°C for 2 h.
4. Centrifuge the sample at 12,000 *g* for 30 min at 4°C to pellet the siRNA.
5. Carefully remove the supernatant without disturbing the pellet.
6. Wash the pellet by adding 200 µl of ice-cold 95% ethanol and centrifuging the sample at 12,000 *g* for 30 min.
7. Remove the supernatant and allow the pellet to completely dry in a Speed Vac.
8. Resuspend the pellet in water or in an appropriate buffer (e.g., 1 X annealing buffer).
9. Determine the concentration of the siRNA by UV spectroscopy.

TABLE II siRNA Synthesis Companies

siRNA synthesis companies	Address
Dharmacon Research, Inc.	Dharmacon, Inc. 2650 Crescent Drive, #100 Lafayette, CO 80026 USA www.dharmacon.com
Qiagen, Inc. (formerly Xeragon, Inc.)	Qiagen, Inc. 28159 Avenue Stanford Valencia, CA 91355 USA www.qiagen.com
Ambion, Inc.	Ambion, Inc. 2130 Woodward Austin, TX 78744 USA www.ambion.com
Proligo, Inc.	Proligo LLC 6200 Lookout Road Boulder, CO 80301 USA www.proligo.com
Sirna Therapeutics, Inc.	Sirna Therapeutics, Inc. 2950 Wilderness Place Boulder, CO 80301 USA www.sirna.com
Molecula Research Labs	13884 Park Center Road Herndon, VA 20171 USA www.molecula.com
EUROGENTEC	EUROGENTEC LIEGE Science Park Rue Bois Saint Jean 5 4102 SERAING BELGIUM www.eurogentec.be

C. Annealing siRNA Strands

Solutions

1. *0.5X TBE buffer*: For 1 liter, add 100 ml 5X TBE buffer and 900 ml distilled water
2. *10 mg/ml ethidium bromide*: Add 1 g of ethidium bromide to 100 ml of distilled water

Steps

1. Add equimolar amounts of the two siRNA strands to an Eppendorf tube. Typically, siRNA solutions that are between 20 and 100 µ*M* are used so the annealed siRNAs can be used directly in silencing experiments without further dilution.

2. Anneal the siRNA strands by heating to 95°C for 5 min. Slow cool the siRNA solution by reducing the temperature by 1°C every 30 s until 35°C and 1°C every minute until 5°C. This can be achieved with the use of a thermal cycler. Alternatively, the siRNA sample can be heated at 90°C for 1 min, followed by a 1-h incubation at 37°C. The duplexed siRNA should be stored at –20°C.

3. To test for complete annealing, single-stranded sense and antisense siRNAs and the annealed duplex siRNA can be run on a 4.0% Nusieve GTG agarose gel, stained with ethidium bromide, and visualized under UV light. Load 1 µl of a 20–100 µ*M* stock of each of the single strands and 0.5–1 µl of the duplex siRNA (20–100 µ*M* stock concentration) in 1× agarose gel loading buffer on a 4.0% Nusieve GTG agarose gel in 0.5× TBE buffer. The ethidium bromide can be added directly to the gel (0.5 µg/ml final concentration) when poured or the gel can be stained after electrophoresis by immersing the gel in 0.5X TBE containing ethidium bromide (0.5 µg/ml final concentration). The duplexed siRNAs should migrate more slowly in the gel than the single strands of the siRNA.

D. Parameters for the Efficient Transfection of siRNAs into Mammalian Cells

A variety of transfection reagents have been developed specifically for the transfection of siRNAs (see Table III). These different transfection reagents have been optimized for the transfection of different cell lines and have different protocols and requirements for optimal use. To achieve maximal levels of silencing, the transfection conditions for any particular cell line must be optimized. This includes optimizing the number of cells used in the transfection, the amount of siRNAs, and transfection reagent needed for optimal transfection. In addition the degree of silencing of any particular gene will be dependent on the abundance and half-life of that protein. Typically a knockdown phenotype can be seen between 24 and 72 h posttransfection; however, proteins with a longer half-life will only be decreased after extended periods of time. If the rate at which the siRNAs are diluted by the doubling of the cells is shorter than the half-life of the protein, it maybe necessary to retransfect the cells with the siRNAs. Alternatively, siRNAs can be expressed from a DNA vector to achieve a stable, long-lived silencing.

TABLE III Transfection Reagents Optimized for siRNA Transduction

Transfection reagent	Company
Oligofectamine Lipofectamine 2000	Invitrogen www.invitrogen.com
SiPORT lipid SiPORT amine	Ambion www.ambion.com
TransMessenger RNAiFECT	Qiagen www.qiagen.com
SiFECT	Promega www.promega.com
GeneEraser	Stratagene www.stratagene.com
TransIT-TKO	Mirus corporation www.genetransfer.com
iFECT	Molecula www.molecula.com

Although there are a variety of reagents available for siRNA transfection, we have predominately used Oligofectamine for the transfection of siRNAs into mammalian cells. In addition, Lipofectamine 2000 has been used effectively for the cotransfection of a plasmid and an siRNA. Oligofectamine is an excellent choice for the transfection of siRNAs due to the low level of toxicity that this lipid has on the cells; however, Oligofectamine is inefficient at transfecting plasmids. Unlike Oligofectamine, Lipofectamine 2000 is very effective at transfecting plasmids, but due to its toxicity to the cells, transfections should be performed on cells at higher cell densities and media containing the transfection media need to be removed 4 to 6 h after the start of the transfection and replaced with fresh media.

E. Transfection of siRNAs into Mammalian Cells with Oligofectamine

Solutions

1. *Oligofectamine*
2. *Dulbecco's modified Eagles media*
3. *Opti MEM I reduced serum medium*
4. Fetal bovine serum

Steps

1. Plate HeLa cells at 5×10^4 to 1×10^5 cells per well in a 6-well plate 16–24 h before the transfection. The cells should be plated in DMEM supplemented with 10% FBS but without antibiotics. For transfections with Lipofectamine 2000, plate the cells at a higher density (e.g., 4×10^5 cells/well) to combat some of its cytotoxic effects. Incubate the cells overnight at 37°C in a CO_2 incubator.
2. Prepare the siRNA–lipid complexes. For each well of the transfection:
   a. Add the annealed, double-stranded siRNA to serum-free, antibiotic-free DMEM or OptiMEM I reduced serum medium to give a final siRNA concentration of 10–100 pmol/transfection (100 pmol would be 1 µl of a 100 µ*M* siRNA solution in 1 ml final volume of the transfection reaction) in a 50-µl final volume. It is important to note that not all serum-free medium formulations [e.g., 293 SFM II (Invitrogen)] are compatible with cationic lipid transfection reagents and should be tested prior to use.
   b. Prepare the Oligofectamine by diluting 3 µl of Oligofectamine in serum-free, antibiotic-free DMEM or OptiMEM I reduced serum medium to a final volume of 50 µl. Mix the contents of the tube gently and let it incubate at room temperature for 5 to 10 min.
   c. Combine the diluted siRNA solution and the diluted Oligofectamine solution and mix gently. Incubate for 15–20 min at room temperature to allow for the siRNA–lipid complexes to form.
3. Remove growth media from the cells and wash once with serum-free, antibiotic-free DMEM. Add 900 µl of the serum-free, antibiotic-free medium on the cells. The transfection can be performed in OptiMEM I reduced serum medium without affecting the transfection efficiency. *Note*: If the health of the cells is compromised, transfection with Oligofectamine can be performed in the presence of serum.
4. Add 100 µl of the siRNA–lipid complexes to each well of the cells in serum-free medium and incubate the cells for 4 h at 37°C in a CO_2 incubator.
5. After the 4 h of incubation, add 1 ml of DMEM containing 20% serum to each well. For most cell types there is no need to remove the medium containing the siRNA–lipid complex due to the low degree of toxicity of Oligofectamine; however, the medium containing siRNA–lipid complexes can be removed and DMEM containing 10% serum can be add to the cells. Some cell types can be grown for extended periods of time in OptiMEM I reduced serum medium. For these cells, the siRNA–lipid complexes in OptiMEM can be grown for longer periods of time (e.g., overnight) without having to change the transfection medium.
6. Grown cells at 37°C in a CO_2 incubator until they are ready to be analyzed for the silencing phenotype. This is typically between 24 and 72 h posttransfection, but a time course experiment should be performed to determine the time of maximal gene silencing for each particular protein.

F. Cloning of shRNA into an U6 Promoter Containing Vector

Preparing Vectors That Have a Blunt end at the 5′ End

This protocol is for vectors that have an *Apa*I site directly at the start site of transcript on the U6 promoter (Fig. 3). The *Apa*I site (GGGCCC) is the first restriction site of the poly linker, with the first G of the recognition site being the +1 position of the transcript. Digesting with *Apa*I and creating a blunt end by treatment with T4 DNA polymerase will provide the necessary guanosine residue at the +1 position and will leave no additional residues at the 5′ end of the transcript. Vectors with this design include the pBS/U6 plasmid from Sui and colleagues (2002), which lacks a selectable marker but can be used in transient transfections and the pSHARP series of plasmids (available from the author), versions of which have hygromycin or zeocin selectable markers or dsRed fluorescent protein.

Solutions

1. *Phenol:chloroform:isoamyl alcohol (25:24:1)*
2. *Chloroform:isoamyl alcohol (24:1)*: For 25 ml, add 24 ml of chloroform and 1 ml of isoamyl alcohol
3. *3 M sodium acetate (pH 5.2)*: For 1 liter, dissolve 408.1 g of sodium acetate in distilled water, adjust the pH to 5.2 with glacial acetic acid, and bring the volume to 1 liter with distilled water
4. *100% ethanol*
5. *70% ethanol*: For 100 ml, combine 70 ml of 100% ethanol and 30 ml of distilled water
6. *0.5X TBE buffer*: For 1 liter, add 100 ml 5X TBE buffer and 900 ml distilled water
7. *10 mg/ml ethidium bromide*: Add 1 g of ethidium bromide to 100 ml of distilled water

Steps

1. Digest the vector with *Apa*I at 25°C for 1–3 h. Heat inactivate the enzyme by incubating the reaction at 75°C for 20 min.

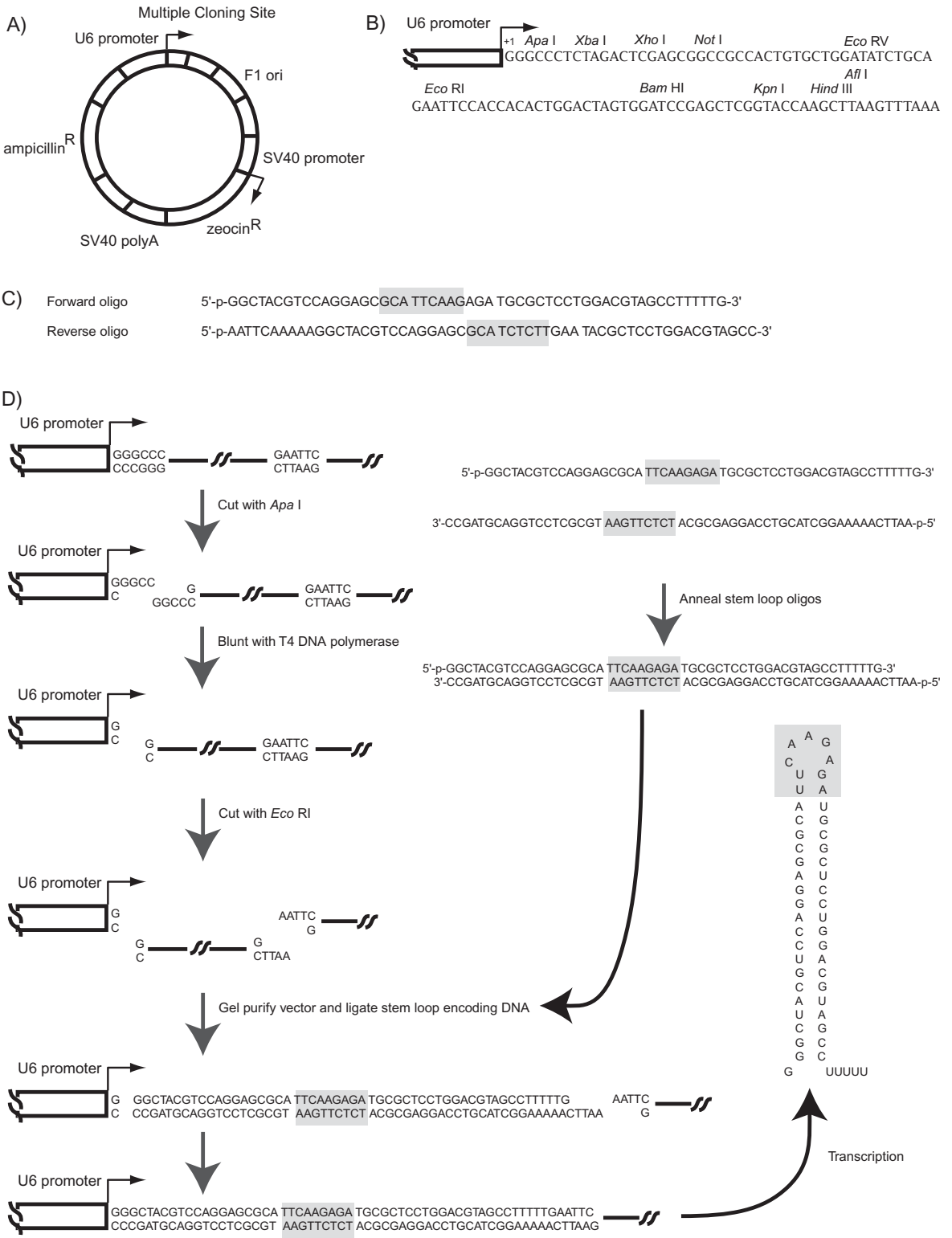
A)
Multiple Cloning Site
U6 promoter
F1 ori
ampicillin^R
SV40 promoter
zeocin^R
SV40 polyA
B)
U6 promoter
+1 Apa I Xba I Xho I Not I Eco RV
GGGCCCTCTAGACTCGAGCGGCCGCCACTGTGCTGGATATCTGCA
Afl I
Eco RI Bam HI Kpn I Hind III
GAATTCCACCACACTGGACTAGTGGATCCGAGCTCGGTACCAAGCTTAAGTTTAAA
C)
Forward oligo 5'-p-GGCTACGTCCAGGAGCGCA TTCAAGAGA TGCGCTCCTGGACGTAGCCTTTTTG-3'
Reverse oligo 5'-p-AATTCAAAAAGGCTACGTCCAGGAGCGCA TCTCTTGAA TACGCTCCTGGACGTAGCC-3'
D)
U6 promoter
GGGCCC CCCGGG GAATTC CTTAAG
Cut with Apa I
GGGCC C G GGCCC GAATTC CTTAAG
Blunt with T4 DNA polymerase
G C G C GAATTC CTTAAG
Cut with Eco RI
G C G C AATTC G CTTAA G
Gel purify vector and ligate stem loop encoding DNA
G C GGCTACGTCCAGGAGCGCA TTCAAGAGA TGCGCTCCTGGACGTAGCCTTTTTG AATTC
CCGATGCAGGTCCTCGCGT AAGTTCTCT ACGCGAGGACCTGCATCGGAAAAACTTAA G
GGGCTACGTCCAGGAGCGCA TTCAAGAGA TGCGCTCCTGGACGTAGCCTTTTTGAATTC
CCCGATGCAGGTCCTCGCGT AAGTTCTCT ACGCGAGGACCTGCATCGGAAAAACTTAAG
5'-p-GGCTACGTCCAGGAGCGCA TTCAAGAGA TGCGCTCCTGGACGTAGCCTTTTTG-3'
3'-CCGATGCAGGTCCTCGCGT AAGTTCTCT ACGCGAGGACCTGCATCGGAAAAACTTAA-p-5'
Anneal stem loop oligos
5'-p-GGCTACGTCCAGGAGCGCA TTCAAGAGA TGCGCTCCTGGACGTAGCCTTTTTG-3'
3'-CCGATGCAGGTCCTCGCGT AAGTTCTCT ACGCGAGGACCTGCATCGGAAAAACTTAA-p-5'
A A G C A U G A A U A C G C G C G A G G A C C C U G C A U C G G U U U U U
Transcription

◀ **FIGURE 3** Cloning of a short hairpin RNA expression cassette into a pol III promoter-based expression system. (A) Structure of the pSHARP-zeo plasmid. shRNAs are expressed from the U6 promoter. The plasmid also contains a zeocin resistance gene that allows for the selection of stable siRNA-expressing cell lines. (B) The multiple cloning site (MCS) of pSHARP vectors. The *Apa*I restriction site (GGGCĈC) has been cloned directly next to the U6 promoter. When the vector is cut with *Apa*I and blunted by T4 DNA polymerase, the first G of the *Apa*I recognition site forms the +1 G of the transcript. All of the sites listed are found uniquely in the MCS. (C) An example of oligo nucleotides that will be ligated together to form the DNA insert, which when expressed will produce the shRNA. This pair of oligo nucleotides encode for an shRNA that is active against the green fluorescent protein (GFP) (Stewart *et al*., 2003). The shRNA encodes a 19 nucleotide stem and a 9 nucleotide loop (TTCAAGAGA) (in the gray box) and a run of five thymidine residues for the termination of transcription (Brummelkamp *et al*., 2002). When the strands are annealed, they will form a blunt end at the 5′ end (relative to the forward oligo nucleotide) and the overhang of the *Eco*RI restriction site at the 3′ end. Each of the strands has been synthesized with a phosphate group at the 5′ end so the oligo nucleotide can be cloned directly into the vector after annealing. (D) Cloning strategy for the insertion of oligo nucleotides for the shRNA into the pSHARP vector. See the cloning protocol for cloning of shRNA into an U6 promoter-containing vector. The shRNA against GFP was produced by transcription from the U6 promoter. The shRNA is cleaved by Dicer, leading to the production of the active siRNA against GFP.

2. Purify the DNA. Add an equal volume of phenol:chloroform:isoamyl alcohol (25:24:1) to the DNA solution. Vortex the solution briefly (1 min) and centrifuge for 10 min at 12,000 *g* (~13,000 rpm in a microcentrifgue). Carefully remove the upper aqueous phase and place in a new tube.

3. Add an equal volume of chloroform:isoamyl alcohol (24:1), vortex briefly, and centrifuge for 10 min at 12,000 *g*. Remove the upper aqueous phase and place in a new tube.

4. Precipitate the DNA by adding 0.1 volume of 3 *M* sodium acetate (pH 5.2) and 2.5 volumes of 100% ethanol. Incubate at –20°C for 30 min. Centrifuge the sample at 12,000 *g* for 10 min at 4°C. Be careful to avoid the pelleted DNA and remove the supernatant.

5. Wash the DNA pellet by adding 200 µl of ice-cold 70% ethanol. Centrifuge the sample at 12,000 *g* for 10 min at 4°C. Remove the supernatant and air dry the pellet.

6. Blunt the *Apa*I site. Resuspend the DNA in distilled H_2O and add 0.1 volume of T4 DNA polymerase buffer, dNTP (100 µ*M* final concentration of each dNTP), and BSA (0.1 mg/ml final concentration). Add 5 units of T4 DNA polymerase/µg of DNA. Incubate at 37°C for 5 min. Heat inactivate by incubating at 75°C for 20 min. The 3′→5′ exonuclease activity of T4 DNA polymerase will chew back the 3′ overhang, which the 5′→3′ polymerase activity of T4 DNA polymerase will fill in, in the presence of excess dNTPs, leaving a blunt end on the vector and maintaining the +1 G residue.

7. Clean up the T4 DNA polymerase by repeating steps 2–5.

8. Digest the vector with *Eco*RI at 37°C for 1–3 h. Heat inactivate the enzyme by incubating at 75°C for 20 min.

9. Load the digested DNA on a 1.0% agarose gel made with 0.5 X TBE buffer. Add agarose gel loading buffer at 1 X final concentration to the DNA sample before loading on the gel.

10. To visualize the DNA, immerse the gel in 0.5 X TBE containing ethidium bromide to a final concentration of 0.5 µg/ml. Alternatively, the ethidium bromide can be incorporated into the agarose gel prior to pouring the gel (0.5 µg/ml final concentration). Visualize the DNA using UV light.

11. Purify the DNA from the gel. DNA embedded in the agarose is cut out of the gel and extracted from the agarose using the QIAquick DNA extraction kit (Qiagen).

Alternatively, some vectors have restriction enzyme sites that allow for cloning using sticky ends at both the 5′ and the 3′ ends of the inserted DNA oligo nucleotide. This would allow for cloning without the need for blunting one end by T4 DNA polymerase treatment after the first restriction endonuclease digestion. However, additional sequences would be present at the 5′ end of the resulting transcript.

G. Annealing the DNA Oligo Nucleotides

Solution

1. *STE buffer*: 10 m*M* Tris (pH 8.0), 50 m*M* NaCl, 1 m*M* EDTA. For 100 ml, add 1 ml 1 *M* Tris (pH 8.0), 5.0 ml 1 *M* NaCl, and 0.2 ml 0.5 *M* EDTA, making up to 100 ml with distilled water.

Steps

1. Resuspend the DNA oligo nucleotides in STE buffer at as high a concentration as possible (~1–10 OD_{260} units/100 µl).

2. Add equimolar amounts of each of the DNA oligo nucleotides to an Eppendorf tube.

3. Incubate the tube at 95°C for 10 min followed by a gradual cooling to room temperature. This can be

achieved by placing the samples in a heat block set to 95°C, incubating the sample for 10 min, and turning off the heating block and allowing it to cool to room temperature. The annealed oligo nucleotides can be stored at –20°C or used immediately for ligating into the prepared vector.

H. Ligating the Annealed DNA Oligo Nucleotides into the Prepared Vector

Solutions

1. *T4 DNA ligase*
2. *10X T4 DNA ligase buffer containing ATP*
3. *LB (Luria–Bertani) agar*: Dissolve 40 g of Difco LB agar and Miller powder in 1 liter of distilled water with heating. When fully dissolved, autoclave at 121°C for 15 min.
4. *Ampicillin*: Ampicillin can be prepared as a 50-mg/ml stock solution in distilled water and sterilized by filtration through a 0.22 µm filter. Store at –20°C.

Steps

1. Add the restriction enzyme digested and purified DNA vector and the annealed DNA oligo nucleotides at a molar ratio of 1:4 (vector:insert) using ~50–200 ng of vector DNA. Add T4 DNA ligase buffer containing ATP (1 m*M* final concentration) to a 1X final concentration. Add 1–2 µl of T4 DNA ligase (400 units/µl).
2. Incubate the ligation at 16°C for 16 h (overnight).
3. Transform the ligated DNA into chemically competent *Escherichia coli* cells (e.g., TOP 10 cells, Stratagene) and plate on LB agar medium supplemented with ampicillin (50 µg/ml final concentration).
4. Screen the individual clones by DNA sequencing to ensure that the DNA oligo nucleotide has been properly ligated into the vector.

I. Generation of Stable Silencing Cell Lines

Transfection of HeLa cells with the plasmid encoding the siRNA expression cassette using cationinc lipids (e.g., Lipofectamine 2000).

Solutions

1. *Lipofectamine 2000*
2. *Dulbecco's modified Eagles media*
3. *Opti MEM I reduced serum medium*
4. *Fetal bovine serum*

Steps

1. Prior to the transfection, it is important to perform a dosage curve to determine the best concentration of the antibiotic to use for the selection of stable siRNA expressing cell lines. This should be performed for every cell line that is going to be used and every drug that will be used.
2. The day before the transfection, plate HeLa cells at 4×10^5 cells/well in DMEM containing 10% fetal calf serum but without antibiotics. Incubate at 37°C in a CO_2 incubator. Plate an additional well that will not be transfected but will be treated with the antibiotic to control for the efficiency of drug selection.
3. Preparing the plasmid DNA–lipid complexes:
   a. Add 2–4 µg of plasmid DNA to serum-free, antibiotic-free DMEM or Opti-MEM I reduced serum medium (Invitrogen) in a 100 µl final volume. It is important to note that not all serum-free medium formulations [e.g., 293 SFM II (Invitrogen)] are compatible with cationic lipid transfection reagents and should be tested prior to use.
   b. Prepare the Lipofectamine 2000 by diluting 1–10 µl of Lipofectamine 2000 in serum-free, antibiotic-free DMEM or OptiMEM I reduced serum medium to a final volume of 100 µl. Mix the contents of the tube gently and let it incubate at room temperature for 5 min. To optimize the efficiency of transfection and minimize the cytotoxic effects of the Lipofectamine 2000, vary the ratio of DNA (µg):Lipofectamine 2000 between 1:0.5 and 1:5. To further reduce the likehood of cytotoxic effects, perform the transfection at high cell densities (~90% confluent for HeLa cells).
   c. Combine the diluted DNA solution and the diluted Lipofectamine 2000 solution and mix gently. Incubate for 15–20 min at room temperature to allow for the DNA–lipid complexes to form.
4. Remove growth media from the cells and wash with serum-free, antibiotic-free DMEM. Add 800 µl of serum-free, antibiotic-free medium or OptiMEM I reduced serum medium to the cells.
5. Add 200 µl of the DNA–lipid complexes to each well of the cells in serum-free medium or OptiMEM.
6. Incubate the cells for 4–5 h at 37°C in a CO_2 incubator. Due to the toxicity of Lipofectamine 2000, it is a good idea to monitor the health of the cells during the course of the transfection.
7. After 4–5 h of incubation, remove the transfection medium and wash the cells with DMEM containing 10% fetal calf serum. Add 2 ml of serum containing DMEM to the cells.
8. Incubate the cells at 37°C in a CO_2 incubator for 48 h posttransfection.

J. Selection of Stable siRNA Expressing Clones

Steps

1. Add the appropriate concentration of the antibiotic, as determined by the dosage curve, to each of the wells, including the control untransfected well. It may be necessary to split the cells prior to the addition of the antibiotic. In this case the cells can be directly split into medium that contains the antibiotic.

2. Grow the cells in the presence of the antibiotics, monitoring the effectiveness of the drug selection on the untransfected control cells. Continue to replace the medium containing the antibiotic on the cells every 2–3 days to ensure that appropriate levels of the antibiotic persist to maintain selection.

3. Single cell clones can be picked when all the cells in the control untransfected plate have died and visible colonies appear in the transfected plates. This can take 1 to 2 weeks after the start of selection. It is important to pick single colonies, as even with a very effective siRNA sequence, there will be a large degree of variability regarding the amount of silencing seen in different stable cell lines. The degree of silencing will be influenced by the site of plasmid integration and the number of plasmids integrated in any particular cell.

4. Single cell clones can be obtained by either directly picking isolated single colonies or by limited dilution and plating in 96-well plates at 0.3 cells/well.

K. Analysis of the Silencing Phenotype

Because siRNAs act by targeting homologous mRNA, the most direct measure of the efficiency of siRNAs is the analysis of mRNA levels. This can be achieved by Northern blot analysis or reverse transcriptase–polymerase chain reaction (RT-PCR) analysis. The analysis of the function of the silenced gene requires that there be a decrease in the level of the targeted protein and that this decrease has a recognizable phenotype. The protein levels in siRNA-treated cells can be assessed by Western blot analysis. This analysis requires that there be antibodies present against the target protein. The ultimate aim of the siRNA-mediated silencing would be to determine the phenotypic consequences of the decreased protein levels. This would require assays that are specific to the protein of interest.

IV. Comments

The most important aspects of a successful siRNA-based gene silencing experiment are the identification of siRNA sequences that effectively target the mRNA for degradation and the efficiency of transduction of the cell type of interest. If cell lines are used that are difficult to transfect, the lack of an observable silencing phenotype may be due to the limits of transfection and not the efficiency of the siRNA sequence. To standardize siRNA transfections, many companies sell siRNAs that are known to work effectively against a target gene. Once transfection conditions have been established that work for the control siRNAs, they can easily be carried over to testing the siRNAs of interest. Once an effective sequence has been identified, it can be used directly to transfect cells or it can be cloned into a DNA vector for stable gene silencing.

References

Bernstein, E., Caudy, A. A., Hammond, S. M., and Hannon, G. J. (2001). Role for a bidentate ribonuclease in the initiation step of RNA interference. *Nature* **409**, 363–366.

Brummelkamp, T. R., Bernards, R., and Agami, R. (2002). A system for stable expression of short interfering RNAs in mammalian cells. *Science* **296**, 550–553.

Dykxhoorn, D. M., Novina, C. D., and Sharp, P. A. (2003). Killing the messenger: Short RNAs that silence gene expression. *Nature Rev. Mol. Cell Biol.* **4**, 457–467.

Elbashir, S. M., Harborth, J., Lendeckel, W., Yalcin, A., Weber, K., and Tuschl, T. (2001a). Duplexes of 21-nucleotide RNAs mediate RNA interference in cultured mammalian cells. *Nature* **411**, 494–498.

Elbashir, S. M., Lendeckel, W., and Tuschl, T. (2001b). RNA interference is mediated by 21- and 22-nucleotide RNAs. *Genes Dev.* **15**, 188–200.

Fire, A., Xu, S., Montgomery, M. K., Kostas, S. A., Driver, S. E., and Mello, C. C. (1998). Potent and specific genetic interference by double-stranded RNA in *Caenorhabditis elegans*. *Nature* **391**, 806–811.

Hammond, S. M., Bernstein, E., Beach, D., and Hannon, G. J. (2000). An RNA-directed nuclease mediates post-transcriptional gene silencing in *Drosophila* cells. *Nature* **404**, 293–296.

Hutvagner, G., and Zamore, P. D. (2002). A microRNA in a multiple-turnover RNAi enzyme complex. *Science* **297**, 2056–2060.

Kamath, R. S., and Ahringer, J. (2003). Genome-wide RNAi screening in *Caenorhabditis elegans*. *Methods* **30**, 313–321.

Khvorova, A., Reynolds, A., and Jayasena, S. D. (2003). Functional siRNAs and miRNAs exhibit strand bias. *Cell* **115**, 209–216.

Lee, N. S., Dohjima, T., Bauer, G., Li, H., Li, M. J., Ehsani, A., Salvaterra, P., and Rossi, J. (2002). Expression of small interfering RNAs targeted against HIV-1 rev transcripts in human cells. *Nature Biotechnol.* **20**, 500–505.

Martinez, J., Patkaniowska, A., Urlaub, H., Luhrmann, R., and Tuschl, T. (2002). Single-stranded antisense siRNAs guide target RNA cleavage in RNAi. *Cell* **110**, 563–574.

Miyagishi, M., and Taira, K. (2002). U6 promoter-driven siRNAs with four uridine 3′ overhangs efficiently suppress targeted gene expression in mammalian cells. *Nature Biotechnol.* **20**, 497–500.

Novina, C. D., Murray, M. F., Dykxhoorn, D. M., Beresford, P. J., Riess, J., Lee, S. K., Collman, R. G., Lieberman, J., Shankar, P., and Sharp, P. A. (2002). siRNA-directed inhibition of HIV-1 infection. *Nature Med.* **8**, 681–686.

Paddison, P. J., Caudy, A. A., Bernstein, E., Hannon, G. J., and Conklin, D. S. (2002). Short hairpin RNAs (shRNAs) induce

sequence-specific silencing in mammalian cells. *Genes Dev.* **16**, 948–958.

Parrish, S., Fleenor, J., Xu, S., Mello, C., and Fire, A. (2000). Functional anatomy of a dsRNA trigger: Differential requirement for the two trigger strands in RNA interference. *Mol. Cell* **6**, 1077–1087.

Paule, M. R., and White, R. J. (2000). Survey and summary: Transcription by RNA polymerases I and III. *Nucleic Acids Res.* **28**, 1283–1298.

Sambrook, J., Fritsch, E. F., and Maniatis, T. M. (1989). "Molecular Cloning, a Laboratory Manual," 2nd Ed. Cold Spring Harbor Laboratory Press, Cold Spring Harbor, NY.

Schwarz, D. S., Hutvagner, G., Du, T., Xu, Z., Aronin, N., and Zamore, P. D. (2003). Asymmetry in the assembly of the RNAi enzyme complex. *Cell* **115**, 199–208.

Stark, G. R., Kerr, I. M., Williams, B. R., Silverman, R. H., and Schreiber, R. D. (1998). How cells respond to interferons. *Annu. Rev. Biochem.* **67**, 227–264.

Stewart, S. A., Dykxhoorn, D. M., Palliser, D., Mizuno, H., Yu, E. Y., An, D. S., Sabatini, D. M., Chen, I. S., Hahn, W. C., Sharp, P. A., Weinberg, R. A., and Novina, C. D. (2003). Lentivirus-delivered stable gene silencing by RNAi in primary cells. *RNA* **9**, 493–501.

Sui, G., Soohoo, C., Affar, el. B., Gay, F., Shi, Y., Forrester, W. C., and Shi, Y. (2002). A DNA vector-based RNAi technology to suppress gene expression in mammalian cells. *Proc. Natl. Acad. Sci. USA* **99**, 5515–5520.

Tuschl, T., Zamore, P. D., Lehmann, R., Bartel, D. P., and Sharp, P. A. (1999). Targeted mRNA degradation by double-stranded RNA *in vitro*. *Genes Dev*. **13**, 3191–3197.

Yang, D., Lu, H., and Erickson, J. W. (2000). Evidence that processed small dsRNAs may mediate sequence-specific mRNA degradation during RNAi in *Drosophila* embryos. *Curr. Biol.* **10**, 1191–1200.

Zamore, P. D., Tuschl, T., Sharp, P. A., and Bartel, D. P. (2000). RNAi: Double-stranded RNA directs the ATP-dependent cleavage of mRNA at 21 to 23 nucleotide intervals. *Cell* **101**, 25–33.

CHAPTER

55

Antisense Oligonucleotides

Erich Koller and Nicholas M. Dean

I. INTRODUCTION

Although the Human Genome Project revealed myriad gene sequences, the function of these new genes remains unknown. Few traditional approaches for studying gene function offer acceptable specificity in a time- and cost-effective manner. Therefore, progress has been slow in determining the function of these genes. Experimental approaches have become essential for determining the biological functions of cellular gene products. Antisense oligonucleotides (ASO) offer significant advantages over traditional methods in terms of specificity and versatility (Koller *et al*., 2000). ASOs validate the function of genes *in vitro* and *in vivo*. In addition, antisense oligonucleotides are developed as drugs with many products currently being tested in clinical trials (Monia *et al*., 2000).

ASOs are short stretches of synthetic, chemically modified nucleic acids that use Watson–Crick base pairing to specifically hybridize to mRNA sequences. For optimal activity, oligonucleotides must first be taken up by the cell or the targeted organ, and the targeted mRNA sequence must then be accessible to the oligonucleotide. *In vivo*, injected oligonucleotides are distributed mainly to the liver and kidneys before they become available to other tissues (Sands *et al*., 1994). *In vitro*, an uptake enhancer is generally, although not entirely, required. A large number of these are available. Antisense oligonucleotides inhibit protein expression by a variety of mechanisms. The best characterized mechanism involves RNase H-mediated cleavage of target mRNA. RNase H is an endonuclease that recognizes RNA–DNA duplexes and selectively cleaves the RNA strand (Dash *et al*., 1987; Kanaya and Ikehara, 1995). Several chemical modifications to antisense oligonucleotides that are designed to increase the affinity of oligonucleotides to RNA or enhance their nuclease resistance do not support RNase H-mediated cleavage (Baker *et al*., 1997). Therefore, additional mechanisms of action exist, including inhibition of translation, modulation of pre-mRNA splicing and modulation of poly(A) adenylation sites, steric blockage for ribosomal subunit attachment to mRNA at the 5′ cap site, and interference with proper mRNA splicing through antisense binding to splice donor or splice acceptor sites (Baker and Monia, 1999; Taylor *et al*., 1999).

Small interfering RNA has been used successfully to inhibit gene expression in mammalian cells. Comparison of siRNAs to RNase H-dependent oligonucleotides showed that they exhibit similar degrees of inhibition of gene expression (Vickers *et al*., 2002). This article focuses on RNase H-dependent oligonucleotides.

II. MATERIALS AND INSTRUMENTATION

Opti-MEM (Invitrogen, Cat. No. 31985070)
Lipofectin (Invitrogen, Cat. No. 18292011)
Oligofectamine (Invitrogen, Cat. No. 12252011)
Lipofectamine (Invitrogen, Cat. No. 18324012)
Cytofectin (Isis Pharmaceuticals, Inc.)
Ribogreen (Molecular Probes, Cat. No. R-11490)
Electroporator (BTX, T-820)
Real time RT-PCR machine (ABI PRISM, 7700 sequence detector)
Fugene 6 Roche (Biosciences, Cat. No. 1 814 443)
Superfect (Qiagen, Cat. No. 301305)

Copyright 2006, Elsevier Science (USA).
All rights reserved.

III. PROCEDURES

A. Oligonucleotide Design

Before ASOs are designed, the following questions need to be answered.

1. Is the sequence information for the gene of interest available? Sequence information for certain species can be limited.
2. Is the gene expressed in the targeted cells to be studied? A robust detection method will make it easier to test the effect of the ASO treatment.
3. Can these cells be transfected easily with ASOs (Table I)? Adherent cells are usually easier to transfect.
4. Are antibodies available to detect the protein?
5. What is the half-life of the protein to be inhibited? The treatment might not result in efficient target reduction if the half-life of the protein is longer than the half-life of the ASO. However, this is usually not a concern.
6. Is the mRNA accessible to a given ASO sequence? Inaccessibility is probably caused by the secondary structure of the mRNA or by proteins bound to mRNA. Therefore, several ASOs are generally designed to identify an oligonucleotide that displays robust inhibition of target expression. Generally, 5–10 different ASOs are evaluated to find a few sequences that are active in inhibiting RNA expression (Branch, 1998). The success rate varies from gene to gene target, but can be as high as 80%. The chance to see phenotypic changes increases with more potent oligonucleotides. These phenotypic effects have to be seen with more than one ASO to be specifically target related. Computer programs used for designing polymerase chain reaction (PCR) primers are useful in identifying potential antisense sequences. In addition to selecting sequences with a high T_m for target mRNA, these programs can be used to identify areas of oligonucleotide self-complementation that might interfere with antisense activity. A few other motifs should be avoided in antisense design. Four contiguous G residues generate ASOs that can prevent Watson–Crick hybridization (Wyatt *et al*., 1994). Furthermore, palindromes of six or more bases have been reported to induce interferon, and unmethylated CG can induce other immunostimulatory effects (Krieg *et al*., 1995; Monteith *et al*., 1997). Methylation of the 5′ position of the cytosine minimizes these effects.

B. Experimental Design

Using appropriate controls is crucial when performing experiments with ASOs. Oligonucleotides at high concentrations can be toxic for cells and complicate experimental interpretation Therefore, control ASOs should be included in your experiment. No single optimal control ASO exists, and we suggest evaluating multiple controls. These can be mismatched sequences, scrambled sequences (that have the same base composition but a different order of bases), or oligonucleotides in the sense orientation. They should have the same length and chemistry as the antisense oligonucleotide. A specific ASO should reduce target mRNA or protein in a dose-dependent manner. If you test oligonucleotides that utilize a non RNase H-dependent mechanism, you must measure protein reduction, as RNA levels might not be affected. In any case, always test the ability of the ASO to reduce target levels first before measuring any other phenotypic end points. Kinetic studies are necessary to determine when to perform phenotypic end point experiments. It is ideal to have more than one active ASO against a given target when phenotypic end points are measured to ensure specific effects. Some proteins with a long half-life time might require repeated transfections with the oligonucleotide before a decrease is observed.

C. Chemistry

Historical experiments with ASO utilized phosphodiester DNA with the disadvantage that it got metabolized rapidly (Thierry and Dritschilo, 1992). Since then, several chemical modifications have been introduced that increased nuclease resistance. Two such chemically modified oligonucleotides that are available commercially are phosphorothioate oligodeoxynucleotides and 2′-*O*-methyl oligonucleotides. Phosphorothioate oligodeoxynucleotides in which one of the nonbridging oxygen atoms in the nucleotide backbone is replaced with sulfur fully support RNase H activity and increase nuclease resistance dramatically (Akhtar *et al*., 1991; Campbell *et al*., 1990). Although binding affinity to mRNA is reduced, phosphorothioate ASOs are probably the most practical and effective choice for researchers performing antisense experiments. The addition of a methoxy group to the C2′ position of the sugar, in combination with a phosphorothioate backbone, provides further enhancement of nuclease resistance and increases the affinity of an oligomer for mRNA (Altmann *et al*., 1996). However, the 2′-*O*-methyl modification does not support RNase H-mediated cleavage of mRNA. If degradation of target mRNA is required as a mechanism of action, this modification must be incorporated into a gapped or chimeric structure with methyl modifications in the wings of the molecule and

oligodeoxynucleotides in the central portion (McKay *et al*., 1999).

D. Oligonucleotide Treatment

Transfection reagents, such us polycations, liposomes, peptides, and dendrimers, facilitate the uptake of oligonucleotides into cells (Kang *et al*., 1999). These reagents are more or less effective in adherent cells, but they generally do not work well for suspension cells. An alternative method for cells in suspension is electroporation. We have found that some primary cell types will effectively take up oligonucleotides in the absence of transfection reagents. However, higher ASO concentrations are required to achieve this uptake compared to transfections using transfection reagents. For example, in primary hepatocytes, efficient target reduction is achieved at 300 n*M* ASO.

Whatever method you use, each cell type must be optimized for transfection method and conditions. Table I will help in choosing the right experimental conditions. Because each method can lead to cell toxicity, it is important to normalize for cell number when target reduction is determined. In addition to observing apparent changes in phenotype under the microscope, it is useful to use ribogreen or some other method to ensure that the amount of RNA between treatment groups is comparable. For adherent cells, it is important that cells are spread and adhere to plastic. The delivery of oligonucleotides with cationic lipids is dependent on the interaction between the positively charged lipid and the negatively charged oligonucleotide.

1. Lipofectin

The cationic lipid called lipofectin is used frequently to transfect oligonucleotides into cells. Depending on cell type, a concentration range between 1 and 300 n*M* should be tested. Typically, IC_{50} values for target mRNA reduction range between 100 and 200 n*M*.

Solutions

1. *Opti-MEM*
2. *Lipofectin*
3. *Phosphate-buffered saline (PBS)*

Steps

1. Plate out cells the day before treatment so that they reach 60–80% confluency the next day. Plate 5000–15,000 cells/well for a 96-well plate or 0.4–1.4 × 10^6 cells/plate for a 100-mm plate.
2. The next day, gently wash plated cells with 5 ml sterile PBS (for 100-mm plate).
3. Aspirate off PBS and replace with Opti-MEM (GibcoBRL) containing 3 µl lipofectin/ml Opti-MEM per 100 n*M* oligo nucleotide used. *Note*: We do not use below 3 µl Lipofectin/ml Opti-MEM or above 15 µl Lipofectin/ml Opti-MEM (e.g., the same concentrations of lipid would be used for 50 and 100 n*M* treatments).
4. Incubate cells with oligo nucleotide/Lipofectin for 4–6 h at 37°C/5% CO_2.
5. Aspirate off oligo nucleotide/Lipofectin mixture and replace with complete growth media.
6. Harvest cells to analyze activity of oligonucleotides by method of choice (Northern blot, Western blot, RT-PCR, ribonucleotide protection assay or arrays).

2. Electroporation

Electroporation is used for cell lines that are not amenable to transfection with currently available transfection reagents, e.g., suspension cell lines (Bergan *et al*., 1993). Oligonucleotides that are neutral or partially charged, e.g., morpholinos, are not compatible with charged lipids either. Therefore, electroporation is the method of choice for suspension cells and transfection of neutral oligonucleotides into any cell type. Each cell line must be optimized for electroporation prior to experimental assays. The electric field strength (EFS) is defined as the voltage applied divided by the distance between the electrodes (V/cm). In general, as the EFS increases, the amount of DNA transfected is increased while cell viability decreases. The pulse length is determined by a number a variables, including buffer type, resistance, and capacitance (microfaradays), selection, and sample volume. Typically, a voltage titration is performed for each cell line (0–350 V, depending on cuvette) at constant capacitance and resistance and constant pulse length (6–9 ms) using a single pulse. It is very helpful to test the conditions with a highly expressed target using a well-characterized oligonucleotide. After determining the optimal voltage, it is recommended to do a dose–response curve with an ASO concentration between 1 and 20 µ*M*. Further optimization can be performed by adjusting the capacitance or pulse length. Typically, IC_{50} values for target mRNA reduction range between 1 and 10 µ*M*.

Steps

1. Resuspended cells (1 × 10^7 cells/ml) in 90 µl (1-mm cuvette) or 360 µl complete medium (2-mm cuvette).
2. Add cells to microcentrifuge tube containing 10 and 40 µl oligonucleotides, respectively.

TABLE I

Cell Name	Species	Cell type	Transfection method
Adherent tumor lines			
A549	hu	Lung	Lipofectin
C6	Rat	Glioma	Electroporation
EMT6	mu	Breast	Lipofectin
FAO	Rat	Hepatoma	Superfect
HCT116	hu	Colon	Cytofectin
HeLa	hu	Cervical	Lipofectin
HepG2	hu	Hepatocellular	Lipofectin
LNCap, PC3	hu	Prostate	Lipofectin
MCF7, MDA-MB-231	hu	Breast	Lipofectin
MiaPaCaII, Panc1	hu	Pancreas	Lipofectin
Shionogi	mu	Prostate	Lipofectamine
SW480	hu	Colon	Lipofectin
T24	hu	Bladder	Lipofectin
Lymphoma/leukemia			
BaF3 Pro-B cell	mu	Pro-B	Electroporation
Bcl-1	mu	B cell	Electroporation
Jurkat	hu	T cell	Electroporation
Monocyte/myeloid			
HL60	hu	Promyelocytic	Electroporation
THP1	hu	Monocyte	Electroporation
Immortalized			
undif. 3T3-L1	mu	Fibroblast	Lipofectin/cytofectin
Dif. 3T3-L1	mu	Adipocyte	Fugene 6, electroporation
A10	rat	Smooth muscle	Lipofectin
F11	rat	DRG	Lipofectin
L6	rat	Myotubes	lipofectin/superfect
NRK	rat	Kidney	Lipofectin
PC12	rat	Adrenal	Lipofectamine
Cos7	monkey	Kidney fibroblasts	Lipofectin/oliogfectamine
b.END	mu	Endothelial	Lipofectin/cytofectin
Chinese hamster ovary cells	Hamster	Ovary	Lipofectin
Primary			
Adult cardiac myocytes	Rat	Myocytes	Lipofectin
Neonatal cardiac myocytes	Rat	Myocytes	Fugene 6
Endothelial cells (HUVEC, HMVEC, HAEC)	hu	Endothelial	Lipofectin
Normal dermal fibroblasts	hu	Fibroblast	Lipofectin
Primary keratinocytes	hu	Keratinocytes	Lipofectin
Primary hepatocytes	mu, rat	Hepatocytes	Lipofectin
Aortic smooth muscle cells	Rat	Smooth muscle	Lipofectin
hu monocytes	hu	Monocyte	Cytofectin
hu macrophages	hu	Macrophages	Cytofectin
hu dendritic cells	hu	Dendritic	Cytofectin

3. Pipetted the cell oligonucleotide mix into the cuvette and electroporate immediately so that cells will not settle.
4. After electroporation, transfer the cell oligonucleotide mix into a 100-mm culture dish containing complete medium.
5. Incubate cells for 24 h until harvest for mRNA or protein. Protein reduction might require longer, depending on the half-life time of the protein of interest.

Acknowledgments

The authors thank Namir Sioufi for providing cell transfection protocols and Jon Bodnar for critical comments during the preparation of this manuscript.

References

Akhtar, S., Kole, R., and Juliano, R. L. (1991). Stability of antisense DNA oligodeoxynucleotide analogs in cellular extracts and sera. *Life Sci*. **49**, 1793–1801.

Altmann, K.-H., Dean, N. M., Fabbro, D., Freier, S. M., Geiger, T., Haner, R., Husken, D., Martin, P., Monia, B. P., Muller, M., *et al*. (1996). Second generation of antisense oligonucleotides: From nuclease resistance to biological efficacy in animals. *Chimia* **50**, 168–176.

Baker, B. F., Lot, S. S., Condon, T. P., Cheng-Flournoy, S., Lesnik, E. A., Sasmor, H. M., and Bennett, C. F. (1997). 2′-*O*-(2-Methoxy)ethyl-modified anti-intercellular adhesion molecule 1 (ICAM-1) oligonucleotides selectively increase the ICAM-1 mRNA level and inhibit formation of the ICAM-1 translation initiation complex in human umbilical vein endothelial cells. *J. Biol. Chem*. **272**, 1994–2000.

Baker, B. F., and Monia, B. P. (1999). Novel mechanisms for antisense-mediated regulation of gene expression. *Biochim. Biophys. Acta* **1489**, 3–18.

Bergan, R., Connell, Y., Fahmy, B., and Neckers, L. (1993). Electroporation enhances c-myc antisense oligodeoxynucleotide efficacy. *Nucleic Acids Res*. **21**, 3567–3573.

Branch, A. D. (1998). A good antisense molecule is hard to find. *Trends Biochem. Sci*. **23**, 45–50.

Campbell, J. M., Bacon, T. A., and Wickstrom, E. (1990). Oligodeoxynucleoside phosphorothioate stability in subcellular extracts, culture media, sera and cerebrospinal fluid. *J. Biochem. Biophys. Methods* **20**, 259–267.

Dash, P., Lotan, I., Knapp, M., Kandel, E. R., and Goelet, P. (1987). Selective elimination of mRNAs *in vivo*: Complementary oligodeoxynucleotides promote RNA degradation by an RNase H-like activity. *Proc. Natl. Acad. Sci. USA* **84**, 896–900.

Kanaya, S., and Ikehara, M. (1995). Functions and structures of ribonuclease H enzymes. *Subcell. Biochem*. **24**, 377–422.

Kang, S. H., Zirbes, E. L., and Kole, R. (1999). Delivery of antisense oligonucleotides and plasmid DNA with various carrier agents. *Antisense Nucleic Acid Drug Dev*. **9**, 497–505.

Koller, E., Gaarde, W. A., and Monia, B. P. (2000). Elucidating cell signaling mechanisms using antisense technology. *Trends Pharmacol. Sci*. **21**, 142–148.

Krieg, A. M., Yi, A. K., Matson, S., Waldschmidt, T. J., Bishop, G. A., Teasdale, R., Koretzky, G. A., and Klinman, D. M. (1995). CpG motifs in bacterial DNA trigger direct B-cell activation. *Nature* **374**, 546–549.

McKay, R. A., Miraglia, L. J., Cummins, L. L., Owens, S. R., Sasmor, H., and Dean, N. M. (1999). Characterization of a potent and specific class of antisense oligonucleotide inhibitor of human protein kinase C-alpha expression. *J. Biol. Chem*. **274**, 1715–1722.

Monia, B. P., Holmlund, J., and Dorr, F. A. (2000). Antisense approaches for the treatment of cancer. *Cancer Invest* **18**, 635–650.

Monteith, D. K., Henry, S. P., Howard, R. B., Flournoy, S., Levin, A. A., Bennett, C. F., and Crooke, S. T. (1997). Immune stimulation: A class effect of phosphorothioate oligodeoxynucleotides in rodents. *Anticancer Drug Des*. **12**, 421–432.

Sands, H., Cocuzza, A. J., Hobbs, F. W., Chidester, D., and Trainor, G. L. (1994). Biodistribution and metabolism of internally 3H-labeled oligonucleotides. I. Comparison of a phosphodiester and a phosphorothioate. *Mol. Pharmacol*. **45**, 932–943.

Taylor, J. K., Zhang, Q. Q., Wyatt, J. R., and Dean, N. M. (1999). Induction of endogenous Bcl-xS through the control of Bcl-x pre-mRNA splicing by antisense oligonucleotides. *Nature Biotechnol*. **17**, 1097–1100.

Thierry, A. R., and Dritschilo, A. (1992). Intracellular availability of unmodified, phosphorothioated and liposomally encapsulated oligodeoxynucleotides for antisense activity. *Nucleic Acids Res*. **20**, 5691–5698.

Vickers, T. A., Koo, S., Bennett, C. F., Crooke, S. T., Dean, N. M., and Baker, B. F. (2002). Efficient reduction of target RNA's by siRNA and RNase H dependent antisense agents: A comparative analysis. *J. Biol. Chem*. **23**, 23.

Wyatt, J. R., Vickers, T. A., Roberson, J. L., Buckheit, R. W., Jr., Klimkait, T., DeBaets, E., Davis, P. W., Rayner, B., Imbach, J. L., and Ecker, D. J. (1994). Combinatorially selected guanosine-quartet structure is a potent inhibitor of human immunodeficiency virus envelope-mediated cell fusion. *Proc. Natl. Acad. Sci. USA* **91**, 1356–1360.

CELL BIOLOGY

A LABORATORY HANDBOOK

Third Edition
Volume 4

Editor-in-chief
Julio E. Celis, Institute of Cancer Biology, *Danish Cancer Society, Copenhagen, Denmark*

Associate Editors
Nigel P. Carter, *The Sanger Center, Wellcome Trust, Cambridge, UK*
Kai Simons, *Max-Planck Institute of Molecular Cell Biology and Genetics, Dresden, Germany*
J. Victor Small, *Austrian Academy of Sciences, Salzburg, Austria*
Tony Hunter, *The Salk Institute, La Jolla, California, USA*
David M. Shotten, *University of Oxford, UK*

CELL BIOLOGY

A LABORATORY HANDBOOK

Third Edition
Volume 4

Edited by

Julio E. Celis
Institute of Cancer Biology, Danish Cancer Society,
Copenhagen, Denmark

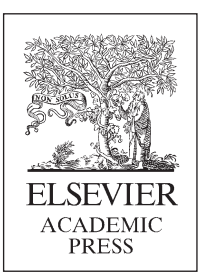

AMSTERDAM • BOSTON • HEIDELBERG • LONDON
NEW YORK • OXFORD • PARIS • SAN DIEGO
SAN FRANCISCO • SINGAPORE • SYDNEY • TOKYO

Elsevier Academic Press
30 Corporate Drive, Suite 400, Burlington, MA 01803, USA
525 B Street, Suite 1900, San Diego, California 92101-4495, USA
84 Theobald's Road, London WC1X 8RR, UK

This book is printed on acid-free paper.

Copyright © 2006, Elsevier Inc. All rights reserved.

No part of this publication may be reproduced or transmitted in any form or by any means, electronic or mechanical, including photocopy, recording, or any information storage and retrieval system, without permission in writing from the publisher.

Permissions may be sought directly from Elsevier's Science & Technology Rights Department in Oxford, UK: phone: (+44) 1865 843830, fax: (+44) 1865 853333, E-mail: permissions@elsevier.co.uk. You may also complete your request on-line via the Elsevier homepage (http://elsevier.com), by selecting "Customer Support" and then "Obtaining Permissions."

Library of Congress Cataloging-in-Publication Data
Application Submitted

British Library Cataloguing in Publication Data
A catalogue record for this book is available from the British Library

ISBN 13: 978-0-12-164734-6
ISBN 10: 0-12-164734-X
Set ISBN 13: 978-0-12-164730-8
Set ISBN 10: 0-12-164730-7

For all information on all Elsevier Academic Press publications visit our Web site at www.books.elsevier.com

Printed in China
05 06 07 08 09 10 9 8 7 6 5 4 3 2 1

Working together to grow
libraries in developing countries
www.elsevier.com | www.bookaid.org | www.sabre.org
ELSEVIER BOOK AID International Sabre Foundation

Contents of Volume 4

Contents of other Volumes

VOLUME 1

PART A. CELL AND TISSUE CULTURE: ASSOCIATED TECHNIQUES

Section 1. General Techniques

Section 2. Culture of Specific Cell Types: Stem Cells

Section 3. Culture of Specific Cell Types: Haemopoietic, Mesenchymal, and Epithelial

Section 7. Cell Separation Techniques

Section 8. Cell Cycle Analysis

Section 9. Cytotoxic and Cell Growth Assays

Section 10. Apoptosis

Section 11. Assays of Cell Transformation, Tumorigenesis, Invasion, and Wound Healing

PART E. TISSUE ARRAYS

Section 13. Tissue Arrays

PART F. CYTOGENETICS AND *IN SITU* HYBRIDIZATION

Section 14. Cytogenetics

Section 15. *In Situ* Hybridization

PART G. GENOMICS

Section 16. Genomics

PART H. TRANSGENIC, KNOCKOUTS, AND KNOCKDOWN METHODS

Section 17. Transgenic, Knockouts and Knockdown Methods

Contributors

Numbers in parenthesis indicate the volume (bold face) and page on which the authors' contribution begins.

Mads Aaboe (**4**: 83) Clinical Biochemical Department, Molecular Diagnostic Laboratory, Aarhus University Hospital, Skejby, Brendstrupgaardvej, Aarhus N, DK-8200, DENMARK

Tanja Aarvak (**1**: 239) Dynal Biotech ASA, PO Box 114, Smestad, N-0309, NORWAY

Harindra R. Abeysinghe (**3**: 345) Department of Pathology and Laboratory Medicine, University of Rochester School of Medicine, 601 Elmwood Ave., Rm 1-6337, Rochester, NY 14642

Ruedi Aebersold (**4**: 437) The Institute for Systems Biology, 1441 North 34th Street, Seattle, WA 98103-8904

Ueli Aebi (**3**: 233, 241) ME Muller Institute for Microscopy, Biozentrum, University of Basel, Klingelbergstr. 50/70, Basel, CH-4056, SWITZERLAND

Cheol-Hee Ahn (**4**: 29) School of Materials Science and Engineering, Seoul National University, Seoul, 151-744, SOUTH KOREA

Natalie G. Ahn (**4**: 443) Department of Chemistry & Biochemistry, University of Colorado, 215 UCB, Boulder, CO 80309

Ramiro Alberio (**4**: 45) School of Biosciences, University of Nottingham, Sutton Bonington, Loughborough, Leics, LE12 5RD, UNITED KINGDOM

Donna G. Albertson (**3**: 445) Cancer Research Institute, Department of Laboratory Medicine, The University of California, San Francisco, Box 0808, San Francisco, CA 94143-0808

Heiner Albiez (**1**: 291) Department of Biology II, Ludwig-Maximilians University of Munich, Munich, GERMANY

Terence Allen (**3**: 325) CRC Structural Cell Biology Group, Paterson Institute for Cancer Research, Christie Hospital NHS Trust, Wilmslow Road, Withington, Manchester, M20 4BX, UNITED KINGDOM

Noona Ambartsumian (**1**: 363) Department of Molecular Cancer Biology, Danish Cancer Society, Institute of Cancer Biology, Strandboulevarden 49, Copenhagen, DK-2100, DENMARK

Øystein Åmellem (**1**: 239) Immunosystems, Dynal Biotech ASA, PO Box 114, Smestad, N-0309, NORWAY

Patrick Amstutz (**1**: 497) Department of Biochemistry, University of Zürich, Winterthurerstr. 190, Zurich, CH-8057, SWITZERLAND

Jens S. Andersen (**4**: 427) Protein Interaction Laboratory, University of Southern Denmark—Odense, Campusvej 55, Odense M, DK-5230, DENMARK

Mads Hald Andersen (**1**: 97) Tumor Immunology Group, Institute of Cancer Biology, Danish Cancer Society, Strandboulevarden 49, Copenhagen, DK-2100, DENMARK

Helena Andersson (**4**: 63) Bioscience at Novum, Karolinska Institutet, Halsovagen 7-9, Huddinge, SE-141 57, SWEDEN

Peter W. Andrews (**1**: 183) Department of Biomedical Science, The University of Sheffield, Rm B2 238, Sheffield, S10 2TN, UNITED KINGDOM

Elsa Anes (**2**: 57) Faculdade de Farmacia, Universidade de Lisboa, Av. Forcas Armadas, Lisboa, 1649-019, PORTUGAL

James M. Angelastro (**1**: 171) Department of Pathology and Center for Neurobiology and Behavior, Columbia University College of Physicians

and Surgeons, 630 West 168th Street, New York, NY 10032

Sergey V. Anisimov (**4**: 103) Molecular Cardiology Unit, National Institute on Aging, NIH, 5600 Nathan Shock Drive, Baltimore, MD 21224

Celia Antonio (**2**: 379) Department of Biochemistry & Molecular Biophysics, College of Physicians & Surgeons, Columbia University, 701 W 168ST HHSC 724, New York, NY 69117

Shigehisa Aoki (**1**: 411) Department of Pathology & Biodefence, Faculty of Medicine, Saga University, Nebeshima 5-1-1, Saga, 849-8501, JAPAN

Ron D. Appel (**4**: 207) Swiss Institute of Bioinformatics, CMU, Rue Michel Servet 1, Geneva 4, CH-1211, SWITZERLAND

Rolf Apweiler (**4**: 469) EMBL Outstation, European Bioinformatics Institute, Wellcome Trust Genome Campus, Hinxton, Cambridge, CB10 1SD, UNITED KINGDOM

Nobukazu Araki (**2**: 147) Department of Histology and Cell Biology, School of Medicine, Kagawa University, Mki, Kagawa, 761-0793, JAPAN

Christopher M. Armstrong (**4**: 295) Dana Faber Cancer Institute, Harvard University, 44 Binney Street, Boston, MA 02115

Anthony J. Ashford (**2**: 155) Antibody Facility, Max Planck Institute of Molecullar Cell Biology and Genetics, Pfotenhauerstrsse 108, Dresden, D-01307, GERMANY

Daniel Axelrod (**3**: 19) Dept of Physics & Biophysics Research Division, University of Michigan, Ann Arbor, MI 48109-1055

Sheree Bailey (**1**: 475) Dept of Immunology, Allergy and Arthritis, Flinders Medical Centre and Flinders University, Bedford Park, Adelaide, SA, 5051, SOUTH AUSTRALIA

Nathalie Q. Balaban (**2**: 419) Department of Physics, The Hebrew University-Givat Ram, Racah Institute, Jerusalem, 91904, ISRAEL

William E. Balch (**2**: 209) Department of Cell and Molecular Biology, The Scripps Research Institute, 10550 North Torrey Pines Road, La Jolla, CA 92037

Debabrata Banerjee (**1**: 315) Department of Medicine, Cancer Institute of New Jersey, 195 Little Albany Street, New Brunswick, NJ 08903

Jiri Bartek (**4**: 253) Department of Cell Cycle and Cancer, Danish Cancer Society, Strandboulevarden 49, Copenhagen, DK-2100, DENMARK

Werner Baschong (**3**: 5) ME Muller Institute for Microscopy, Biozentrum, University of Basel, Klingelbergstrasse 50/70, Basel, CH-4056, SWITZERLAND

Philippe I. H. Bastiaens (**3**: 153) Cell Biology and Cell Biophysics Program, European Molecular Biology Laboratory, Meyerhofstrasse 1, Heidelberg, 69117, GERMANY

Jürgen C. Becker (**1**: 103) Department of Dermatology, University of Würzburg, Sanderring 2, Würzburg, 97070, GERMANY

Martin Béhé (**4**: 149) Department of Nuclear Medicine, Philipp's-University of Marburg, Baldingerstraße, Marburg/Lahn, D-35043, GERMANY

Thomas M. Behr (**4**: 149) Department of Nuclear Medicine, Philipp's-University of Marburg, Baldingerstraße, Marburg, D-35043, GERMANY

Stefanie Benesch (**2**: 399) Department of Cell Biology, Gesellschaft fur Biotechnoogische Forschung, Mascheroder Weg 1, Braunschweig, D-38124, GERMANY

Aaron Bensimon (**3**: 429) Laboratoire de Biophysique de l'ADN, Departement des Biotechnologies, Institut Pasteur, 25 rue du Dr. Roux, Paris Cedex 15, F-75724, FRANCE

John J. M. Bergeron (**2**: 41) Department of Anatomy and Cell Biology, Faculty of Medicine, McGill University, STRATHCONA Anatomy & Dentistry Building, Montreal, QC, H3A 2B2, CANADA

Michael W. Berns (**3**: 351) Beckman Laser Institute, University of California, Irvine, 1002 Health Sciences Road E, Irvine, CA 92697-1475

Joseph R. Bertino (**1**: 315) The Cancer Institute of New Jersey, 195 Little Albany Street, New Brunswick, NJ 08901

Paulo Bianco (**1**: 79) Dipartimento di Medicina Sperimentale e Patologia, Universita 'La Sapienza', Viale Regina Elena 324, Roma, I-00161, ITALY

Hans Kaspar Binz (**1**: 497) Department of Biochemistry, University of Zürich, Winterthurerstr. 190, Zürich, CH-8057, SWITZERLAND

R. Curtis Bird (**1**: 247) Department of Pathobiology, Auburn University, Auburn, Alabama 36849

Mina J. Bissell (**1**: 139) Life Sciences Division, Lawrence Berkeley National Laboratory, 1 Cyclotron Road, Bldg 83-101, Berkeley, CA 94720

Stephanie Blackwood (**3**: 445) Cancer Research Institute, University of California San Francisco, PO Box 0808, San Francisco, CA 94143-0808

Blagoy Blagoev (**4**: 427) Protein Interaction Laboratory, University of Southern Denmark—Odense, Campusvej 55, Odense M, DK-5230, DENMARK

Kenneth R. Boheler (**4**: 103) Laboratory of Cardiovascular Science, National Institute on Aging, NIH, 5600 Nathan Shock Drive, Baltimore, MD 21224-6825

Michelle A. Booden (**1**: 345) Lineberger Comprehensive Cancer Center, University of North Carolina at Chapel Hill, Chapel Hill, NC 27599-7295

Gary G. Borisy (**3**: 277) Department of Cell and Molecular Biology, Northwestern University Medical School, Chicago, IL 6011-3072

Elliot Botvinick (**3**: 351) Beckman Laser Institute, University of California, Irvine, 1002 Health Sciences Road, East, Irvine, CA 92697-1475

Gérard Bouchet (**4**: 207) Swiss Institute of Bioinformatics (SIB), CMU, rue Michel-Servet 1, Genève 4, CH-1211, SWITZERLAND

Rosemary Boyle (**4**: 437) The Institute for Systems Biology, 1441 North 34th St., Seattle, WA 98109

Susanne Brandfass (**1**: 563) Department of Biochemistry and Cell Biology, Max Planck Institute of Biophysical Chemistry, Am Faßberg 11, Gottingen, D-37077, GERMANY

Pascal Braun (**4**: 73) Department of Chemistry and Chemical Biology, Harvard University, 12 Oxford Street, Cambridge, MA 02138

Steven A. Braut (**4**: 121) Department of Anatomy and Structural Biology, Golding # 601, Albert Einstein College of Medicine of Yeshiva University, 1300 Morris Park Avenue, Bronx, NY 10461

Alvis Brazma (**4**: 95) EMBL Outstation—Hinxton, European Bioinformatics Institute, Wellcome Trust Genome Campus, Hinxton, Cambridge, CB10 1SD, UNITED KINGDOM

J. David Briley (**3**: 471) Department of Genomic Sciences, Glaxo Wellcome Research and Development, 5 Moore Drive, Research Triangle Park, NC 27709-3398

Simon Broad (**1**: 133) Keratinocyte Laboratory, London Research Institute, 44 Lincoln's Inn Fields, London, WC2A 3PX, UNITED KINGDOM

Nicholas H. Brown (**3**: 77) Wellcome Trust/Cancer Research UK Institute and Departmentt of Anatomy, University of Cambridge, Tennis Court Road, Cambridge, CB2 1QR, UNITED KINGDOM

Heather L. Brownell (**2**: 329, 341) Office of Technology Licensing and Industry Sponsored Research, Harvard Medical School, 25 Shattuck Street, Gordon Hall of Medicine, Room 414, Boston, MA 02115

Damien Brunner (**3**: 69) Cell Biology and Cell Biophysics Programme, European Molecular Biology Laboratory, Meyerhofstrasse 1, Heidelberg, D-69117, GERMANY

Suzannah Bumpstead (**3**: 463) Genotyping / Chr 20, The Wellcome Trust Sanger Institute, The Wellcome Trust Genome Campus, Hinxton, Cambridge, CB10 1SA, UNITED KINGDOM

Deborah C. Burford (**3**: 403) Wellcome Trust, Sanger Institute, The Wellcome Trust Genome Campus, Hinxton, Cambridge, CB10 1SA, UNITED KINGDOM

Gerald Burgstaller (**2**: 161) Department of Cell Biology, Institute of Molecular Biology, Austrian Academy of Sciences, Billrothstrasse 11, Salzburg, A-5020, AUSTRIA

Ian M. Caldicott (**1**: 157)

Angelique S. Camp (**1**: 457) Gene Therapy Centre, University of North Carolina at Chapel Hill, 7119 Thurston-Bowles (G44 Wilson Hall), Chapel Hill, NC 27599-7352

Keith H. S. Campbell (**4**: 45) School of Biosciences, Sutton Bonington, Loughborough, Leics, LE12 5RD, UNITED KINGDOM

Yihai Cao (**1**: 373) Microbiology & Tumor Biology Center, Karolinska Institute, Room: Skrivrum (G415), Box 280, Stockholm, SE-171 77, SWEDEN

Maria Carmo-Fonseca (**2**: 277, **3**: 419) Institute of Molecular Medicine, Faculty of Medicine, University of Lisbon, Av. Prof. Egas Moniz, Lisbon, 1649-028, PORTUGAL

T. Carneiro (**3**: 419) Faculty of Medicine, Institute of Molecular Medicine, University of Lisbon, Av. Prof. Egas Moniz, Lisboa, 1649-028, PORTUGAL

Nigel P. Carter (**2**: 133) The Wellcome Trust, Sanger Institute, The Wellcome Trust, Genome Campus, Hinxton, Cambridge, CB10 1SA, UNITED KINGDOM

Célia Carvalho (**3**: 419) Faculty of Medicine, Institute of Molecular Medicine, University of Lisbon, Av. Prof. Egas Moniz, Lisboa, 1649-028, PORTUGAL

Lucy A. Carver (**2**: 11) Cellular and Molecular Biology Program, Sidney Kimmel Cancer Center, 10835 Altman Row, San Diego, CA 92121

Doris Cassio (**1**: 231, **3**: 387) INSERM U-442: Signalisation cellulaire et calcium, Bat 443, Universite Paris-Sud, Street George Clemenceau Pack, 444, Orsay, Cedex, F-91405, FRANCE

Chris Catton (**3**: 207) Department of Zoology, University of Oxford, South Parks Road, Oxford, OX1 3PS, UNITED KINGDOM

Julio E. Celis (**1**: 527, **4**: 69, 165, 219, 243, 289) Danish Cancer Society, Institute of Cancer Biology and Danish Centre for Translational Breast Cancer Research, Strandboulevarden 49, Copenhagen O, DK-2100, DENMARK

Pierre Chambon (**3**: 501) Institut de Génétique et de Biologie Moléculaire et Cellulaire, 1 rue Laurent Fries, B.P.10142, Illkirch CEDEX, F-67404, FRANCE

Francis Ka-Ming Chan (**2**: 355) Department of Pathology, University of Massachusetts Medical School, Room S2-125, 55 Lake Avenue North, Worcester, MA 01655

Ming-Shien Chang (**3**: 87) Department of Physics, Duke University, 107 Physics Bldg, Durham, NC 27708-1000

Samit Chatterjee (**2**: 241) Margaret M. Dyson Vision Research Institute, Department of Ophthalmology, Weill Medical College of Cornell University, 1300 York Avenue, New York, NY 10021

Sandeep Chaudhary (**1**: 121) Veterans Affairs Medical Center, San Diego (V111G), 3350 La Jolla Village Drive, San Diego, CA 92161

Jingwen Chen (**3**: 471) Department of Genomic Sciences, Glaxo Wellcome Research and Development, 5 Moore Drive, Research Triangle Park, NC 27709

Yonglong Chen (**1**: 191) Institute for Biochemistry and Molecular Cell Biology, University of Goettingen, Justus-von-Liebig-Weg 11, Göttingen, D-37077, GERMANY

Yong Woo Cho (**4**: 29) Akina, Inc., Business & Technology Center, 1291 Cumberland Ave., #E130, West Lafayette, IN 47906

Juno Choe (**1**: 269) Institute for Systems Biology, 1441 N. 34th St, Seattle, WA 98103

Claus R. L. Christensen (**1**: 363) Department of Molecular Cancer Biology, Danish Cancer Society, Institute of Cancer Biology, Strandboulevarden 49, Copenhagen, DK-2100, DENMARK

Theodore Ciaraldi (**1**: 121) Veterans Affairs Medical Center, University of California, San Diego, 9500 Gilman Drive, La Jolla, CA 92093-9111

Aaron Ciechanover (**4**: 351) Center for Tumor and Vascular Biology, The Rappaport Faculty of Medicine and Research Institute, Technion-Israel Institute of Technology, POB 9649, Efron Street, Bat Galim, Haifa, 31096, ISRAEL

Mark S. F. Clarke (**2**: 233, **4**: 5) Department of Health and Human Performance, University of Houston, 3855 Holman Street, Garrison—Rm 104D, Houston, TX 77204-6015

Martin Clynes (**1**: 335) National Institute for Cellular Biotechnology, Dublin City University, Glasnevin, Dublin, 9, IRELAND

Philippe Collas (**1**: 207) Institute of Medical Biochemistry, University of Oslo, PO Box 1112 Blindern, Oslo, 0317, NORWAY

Kristen Correia (**4**: 35) Krumlauf Lab, Stowers Institute for Medical Research, 1000 East 50th Street, Kansas City, MO 64110

Pascale Cossart (**2**: 407) Unite des Interactions Bacteries-Cellules/Unité INSERM 604, Institut Pasteur, 28, rue du Docteur Roux, Paris Cedex 15, F-75724, FRANCE

Thomas Cremer (**1**: 291) Department of Biology II, Ludwig-Maximilians University of Munich, Munich, 80333, GERMANY

Robert A. Cross (**2**: 371) Molecular Motors Group, Marie Curie Research Institute, The Chart, Oxted, Surrey, RH8 0TE, UNITED KINGDOM

Matthew E. Cunningham (**1**: 171) Hospital for Special Surgery, New York Hospital, 520 E. 70th Street, New York, NY 10021

Noélia Custódio (**3**: 419) Faculty of Medicine, Institute of Molecular Medicine, University of Lisbon, Av. Prof. Egas Moniz, Lisboa, 1649-028, PORTUGAL

Zbigniew Darzynkiewwicz (**1**: 279) The Cancer Research Institute, New York Medical College, 19 Bradhurst Avenue, Hawthorne, NY 10532

Ilan Davis (**3**: 187) Wellcome Trust Centre for Cell Biology, Institute of Cell and Molecular Biology, The University of Edinburgh, Michael Swann Building, The King's Buildings, Mayfield Road, Edinburgh, EH9 3JR, SCOTLAND

Stephen C. De Rosa (**1**: 257) Vaccine Research Center, National Institutes of Health, 40 Convent Dr., Room 5610, Bethesda, MD 20892-3015

Nicholas M. Dean (**3**: 523) Functional Genomics, GeneTrove, GeneTrove (a division of Isis Isis Pharmaceuticals, Inc.), 2292 Faraday Avenue, Carlsbad, CA 92008

Anne Dell (**4**: 415) Department of Biological Sciences, Biochemistry Building, Imperial College of Science, Technology & Medicine, Biochemistry Building, London, SW7 2AY, UNITED KINGDOM

Panos Deloukas (**3**: 463) The Wellcome Trust, Sanger Institute, Hinxton, Cambridge, CB10 1SA, UNITED KINGDOM

Nicolas Demaurex (**3**: 163) Department of Cell Physiology and Metabolism, University of Geneva Medical Center, 1 Michel-Servet, Geneva, CH-1211, SWITZERLAND

Chris Denning (**4**: 45) Division of Animal Physiology, School of Biosciences, Institute of Genetics Room C15, University of Nottingham, Queens Medical Centre, Nottingham, NG7 2UH, UNITED KINGDOM

Ami Deora (**2**: 241) Margaret M. Dyson Vision Research Institute, Department of Ophthalmology, Weill Medical College of Cornell University, 1300 York Avenue, New York, NY 10021

Julien Depollier (**4**: 13) Centre de Recherche en Biochimie Macromoléculaire (UPR 1086), Centre National de la Recherche Scientifique (CNRS), 1919 Route de Mende, Montpellier Cedex 5, F-34293, FRANCE

Channing J. Der (**1**: 345) Department of Pharmacology, University of North Carolina at Chapel Hill, Lineberger Comprehensive Cancer Center, Chapel Hill, NC 27599

Bart Devreese (**4**: 259) Department of Biochemistry, Physiology and Microbiology, University of Ghent, K.L. Ledeganckstraat 35, Ghent, B-9000, BELGIUM

Alberto Diaspro (**3**: 201) Department of Physics, University of Genoa, Via Dodecaneso 33, Genoa, I-16146, ITALY

James Fred Dice (**4**: 345) Department Physiology, Tufts University School of Medicine, 136 Harrison Ave, Boston, MA 02111

Thomas J. Diefenbach (**4**: 307) Department of Physiology, Tufts University School of Medicine, 136 Harrison Avenue, Boston, MA 02111

Chris Dinant (**2**: 121) Biomolecular Sciences, UMIST, PO Box 88, Manchester, M60 1QD, UNITED KINGDOM

Da-Qiao Ding (**3**: 171) Structural Biology Section and CREST Research Project, Kansai Advanced Research Center, Communications Research Laboratory, 588-2 Iwaoka, Iwaoka-cho, Nishi-ku, Kobe, 651-2492, JAPAN

Gilles Divita (**4**: 13) Centre de Recherche en Biochimie Macromoléculaire (UPR 1086), Centre National de la Recherche Scientifique (CNRS), 1919 Route de Mende, Montpellier Cedex 5, F-34293, FRANCE

Eric P. Dixon (**1**: 483) TriPath Oncology, 4025 Stirrup Creek Drive, Suite 400, Durham, NC 27703

Bernhard Dobberstein (**2**: 215) Zentrum fur Molekulare Biologie, Universitat Heidelberg, Im Neuenheimer Feld 282, Heidelberg, D-69120, GERMANY

Lynda J. Donald (**4**: 457) Department of Chemistry, University of Manitoba, Room 531 Parker Building, Winnipeg, MB, R3T 2N2, CANADA

Wolfgang R. G. Dostmann (**2**: 299) Department of Pharmacology, University of Vermont, Health Science Research Facility 330, Burlington, VT 05405-0068

Adam Douglass (**3**: 129) Department of Cellular and Molecular Pharmacology, The University of California, San Francisco, School of Medicine, Medical Sciences Building, Room S1210, 513 Parnassus Avenue, San Francisco, CA 94143-0450

Kate Downes (**3**: 463) Genotyping / Chr 20, The Wellcome Trust, Sanger Institute, The Wellcome Trust Genome Campus, Hinxton, Cambridge, CB10 1SA, UNITED KINGDOM

Harry W. Duckworth (**4**: 457) Department of Chemistry, University of Manitoba, Room 531 Parker Building, Winnipeg, MB, R3T 2N2, CANADA

Derek M. Dykxhoorn (**3**: 511) CBR Institute for Biomedical Research, Harvard Medical School, 200 Longwood Ave, Boston, MA 02115

Lars Dyrskjøt (**4**: 83) Clinical Biochemical Department, Molecular Diagnostic Laboratory, Aarhus University Hospital, Skejby, Brendstrupgaardvej, Aarhus N, DK-8200, DENMARK

Christoph Eckerskorn (**4**: 157) Protein Analytics, Max Planck Institute for Biochemistry, Klopferspitz 18, Martinsried, D-82152, GERMANY

Glenn S. Edwards (**3**: 87) Department of Physics, Duke University, 221 FEL Bldg, Box 90305, Durham, NC 27708-0305

Andreas A. O. Eggert (**1**: 103) Department of Dermatology, Julius-Maximillians University, Josef-Schneider-Str. 2, Würzburg, 97080, GERMANY

Maria Ekström (**4**: 63) Bioscience at Novum, Karolinska Institutet, Huddinge, SE-141 57, SWEDEN

Andreas Engel (**3**: 317) Maurice E. Müller Institute for Microscopy at the Biozentrum, University of Basel, Klingelbergstrasse 70, Basel, CH-4056, SWITZERLAND

Anne-Marie Engel (**1**: 353) Bartholin Institutte, Bartholinsgade 2, Copenhagen K, DK-1356, DENMARK

José A. Enríquez (**2**: 69) Department of Biochemistry and Molecular and Cellular Biology, Universidad de Zaragoza, Miguel Servet, 177, Zaragoza, E-50013, SPAIN

Rachel Errington (**1**: 305) Department of Medical Biochemistry and Immunology, University of Wales College of Medicine, Heath Park, Cardiff, CF14 4XN, UNITED KINGDOM

Virginia Espina (**3**: 339) Microdissection Core Facility, Laboratory of Pathology, National Cancer Institute, 9000 Rockville Pike, Building 10, Room B1B53, Bethesda, MD 20892

H. Dariush Fahimi (**2**: 63) Department of Anatomy and Cell Biology II, University of Heidelberg, Im Neuenheimer Feld 307, Heidelberg, D-69120, GERMANY

Federico Federici (**3**: 201) Department of Physics, University of Genoa, Via Dodecaneso 33, Genoa, I-16146, ITALY

Daniel L. Feeback (**2**: 233, **4**: 5) Space and Life Sciences Directorate, NASA-Johnson Space Center, 3600 Bay Area Blvd, Houston, TX 77058

Patricio Fernández-Silva (**2**: 69) Dept of Biochemistry and Molecular and Cellular Biology, Univeridad de Zaragoza, Miguel Servet 177, Zaragoza, E-50013, SPAIN

Erika Fernández-Vizarra (**2**: 69) Dept of Biochemistry and Molecular and Cellulary Biology, Universidad de Zaragoza, Miguel Servet, 177, Zaragoza, E-50013, SPAIN

Patrick F. Finn (**4**: 345) Department of Physiology, Tufts University School of Medicine, 136 Harrison Ave, Boston, MA 02111

Kevin L. Firth (**2**: 329, **2**: 341) ASK Science Products Inc., 487 Victoria St, Kingston, Ontario, K7L 3Z8, CANADA

Raluca Flükiger-Gagescu (**2**: 27) Unitec—Office of Technology Transfer, University of Geneva and University of Geneva Hospitals, 24, Rue Général-Dufour, Geneva 4, CH-1211, SWITZERLAND

Leonard J. Foster (**4**: 363, 427) Protein Interaction Laboratory, University of Southern Denmark, Odense, Campusvej 55, Odense M, DK-5230, DENMARK

Dimitrios Fotiadis (**3**: 317) M. E. Müller Institute for Microscopy at the Biozentrum, University of Basel, Klingelbergstrasse 70, Basel, CH-4056, SWITZERLAND

Patrick L. T. M. Frederix (**3**: 317) M. E. Müller Institute for Microscopy at the Biozentrum, University of Basel, Klingelbergstrasse 70, Basel, CH-4056, SWITZERLAND

Marcus Frohme (**4**: 113) Functional Genome Analysis, German Cancer Research Center, Deutsches Krebsforschungszentrum, Im Neuenheimer Feld 580, Heidelberg, D-69120, GERMANY

Masanori Fujimoto (**4**: 197) Department of Biochemistry and Biomolecular Recognition, Yamaguchi University School of Medicine, 1-1-1, Minami-kogushi, Ube, Yamaguchi, 755-8505, JAPAN

Margarida Gama-Carvalho (**2**: 277) Faculty of Medicine, Institute of Molecular Medicine, University of Lisbon, AV. Prof. Egas Moniz, Lisbon, 1649-028, PORTUGAL

Henrik Garoff (**1**: 419, **4**: 63) Unit for Cell Biology, Center for Biotechnology. Karolinska Institute, Huddinge, SE-141 57, SWEDEN

Susan M. Gasser (**2**: 359) Friedrich Miescher Institute fr Biomedical Research, Maulbeerstrasse 66, Basel, CH-1211, SWITZERLAND

Kristine G. Gaustad (**1**: 207) Institute of Medical Biochemistry, University of Oslo, PO Box 1112 Blindern, Oslo, 0317, NORWAY

Benjamin Geiger (**2**: 419) Dept. of Molecular Cell Biology, Weizman Institute of Science, Wolfson Building, Rm 617, Rehovot, 76100, ISRAEL

Kris Gevaert (**4**: 379, **4**: 457) Dept. Medical Protein Research, Flanders Interuniversity Institute for Biotechnology, Faculty of Medicine and Health Sciences, Ghent University, Instituut Rommelaere—Blok D, Albert Baertsoenkaai 3, Gent, B-9000, BELGIUM

Jilur Ghori (**3**: 463) Genotyping / Chr 20, The Wellcome Trust, Sanger Institute, The Wellcome Trust, Genome Campus, Hinxton, Cambridge, CB10 1SA, UNITED KINGDOM

Alasdair J. Gibb (**1**: 395) Department of Pharmacology, University College London, Gower Street, London, WC1E GBT, UNITED KINGDOM

Mario Gimona (**1**: 557, **2**: 161, **4**: 145) Department of Cell Biology, Institute of Molecular Biology, Austrian Academy of Sciences, Billrothstrasse 11, Salzburg, A-5020, AUSTRIA

David A. Glesne (**1**: 165) Biosciences Division, Argonne National Laboratory, 9700 South Cass Avenue, Argonne, IL 60439-4844

Martin Goldberg (**3**: 325) Science Laboratories, University of Durham, South Road, Durham, DH1 3LE, UNITED KINGDOM

Kenneth N. Goldie (**3**: 267) Structural and Computational Biology Programme, EMBL, Meyerhofstrasse 1, Heidelberg, D-69117, GERMANY

Jon W. Gordon (**3**: 487) Geriatrics and Adult Development, Mount Sinai School of Medicine, One Gustave L. Levy Place, New York, NY 10029

Angelika Görg (**4**: 175) Fachgebiet Proteomik, Technische Universität München, Am Forum 2, Freising Weihenstephan, D-85350, GERMANY

Martin Gotthardt (**4**: 149) Department of Nuclear Medicine, Philipp's-University of Marburg, Baldingerstraße, Marburg/Lahn, D-35043, GERMANY

Frank L. Graham (**1**: 435) Department of Biology, McMaster University, Life Sciences Building, Room 430, Hamilton, Ontario, L8S 4K1, CANADA

Claude Granier (**1**: 519) UMR 5160, Faculté de Pharmacie, 15 Av. Charles Flahault, Montpellier Cedex 5, BP 14491, 34093, FRANCE

Lloyd A. Greene (**1**: 171) Department of Pathology and Center for Neurobiology and Behavior, Columbia University, College of Physicians and Surgeons, 630 W. 168th Street, New York, NY 10032

Susan M. Gribble (**3**: 403) Sanger Institute, The Wellcome Trust, The Wellcome Trust Genome Campus, Hinxton, Cambridge, CB10 1SA, UNITED KINGDOM

Gareth Griffiths (**2**: 57, **3**: 299) Department of Cell Biology, EMBL, Postfach 102209, Heidelberg, D-69117, GERMANY

Sergio Grinstein (**3**: 163) Cell Biology Program, Hospital for Sick Children, 555 University Avenue, Toronto, Ontario, M5G 1X8, CANADA

Pavel Gromov (**1**: 527, **4**: 69, 165, 243, 289) Institute of Cancer Biology and Danish Centre for Translational Breast Cancer Research, Danish Cancer Society, Strandboulevarden 49, Copenhagen, DK-2100, DENMARK

Irina Gromova (**4**: 219) Department of Medical Biochemistry and Danish Centre for Translational Breast Cancer Research, Danish Cancer Society, Strandboulevarden 49, Copenhagen, DK-2100, DENMARK

Dale F. Gruber (**1**: 33) Cell Culture Research and Development, GIBCO/Invitrogen Corporation, 3175 Staley Road, Grand Island, NY 14072

Markus Grubinger (**4**: 145) Institute of Physics and Biophysics, University of Salzburg, Hellbrunnerstr. 34, Salzburg, A-5020, AUSTRIA

Jean Gruenberg (**2**: 27, 201) Department of Biochemistry, University of Geneva, 30, quai Ernest Ansermet, Geneva 4, CH-1211, SWITZERLAND

Stephanie L. Gupton (**3**: 137) 10550 North Torrey Pines Road, CB 163, La Jolla, CA 92037

Cemal Gurkan (**2**: 209) Department of Cell and Molecular Biology, The Scripps Research Institute, 10550 North Torrey Pines Road, La Jolla, CA 92037

Martin Guttenberger (**4**: 131) Zentrum für Molekulariologie der Pflanzen, Universitat Tübingen, Entwicklungsgenetik, Auf der Morgenstelle 3, Tübingen, D-72076, GERMANY

Thomas Haaf (**3**: 409) Institute for Human Genetics, Johannes Gutenberg-Universität Mainz, 55101, Mainz, D-55131, GERMANY

Christine M. Hager-Braun (**1**: 511) Health and Human Services, NIH National Institute of Environmental Health Sciences, MD F0-04, PO Box 12233, Research Triangle Park, NC 27709

Anne-Mari Håkelien (**1**: 207) Institute of Medical Biochemistry, Institute of Medical Biochemistry, University of Oslo, PO Box 1112 Blindern, Oslo, 0317, NORWAY

Fiona C. Halliday (**1**: 395) GlaxoSmithKline, Greenford, Middlesex, UB6 OHE, UNITED KINGDOM

Gerald Hammond (**2**: 223) Molecular Neuropathobiology Laboratory, Cancer Reasearch UK London Research Institute, 44 Lincoln's Inn Fields, London, WC2A 3PX, UNITED KINGDOM

Klaus Hansen (**4**: 253)

Hironobu Harada (**1**: 367) Department of Neurosurgery, Ehime University School of Medicine, Shitsukawa, Toon-shi, Ehime, 791-0295, JAPAN

Robert J. Hay (**1**: 43, 49, 573) Viitro Enterprises Incorporated, 1113 Marsh Road, PO Box 328, Bealeton, VA 22712

Izumi Hayashi (**1**: 151) National Medical Center and Beckman Research Institute, Division of Neurosciences, City of Hope, 1500 E. Duarte Rd, Duarte, CA 91010-3000

Timothy A. Haystead (**4**: 265) Department of Pharmacology and Cancer Biology, Duke University Medical Center, Box 3813 Med Ctr, Durham, NC 27710

Rebecca Heald (**2**: 379) Molecular and Cell Biology Department, University of California, Berkeley, Berkeley, CA 94720-3200

Florence Hediger (**2**: 359) Department of Molecular Biology, University of Geneva, 30, Quai Ernest Ansermet, Geneva, CH-1211, SWITZERLAND

Rainer Heintzmann (**3**: 29) Randall Division of Cell and Molecular Biophysics, King's College London, Guy's Campus, London, SE1 1UL, UNITED KINGDOM

Frederic Heitz (**4**: 13) Centre de Recherche en Biochimie Macromoléculaire (UPR 1086), Centre National de la Recherche Scientifique (CNRS), 1919 Route de Mende, Montpellier Cedex 5, F-34293, FRANCE

Johannes W. Hell (**2**: 85) Department of Pharmacology, University of Iowa, 2152 Bowen Science Building, Iowa City, IA 52242

Kai Hell (**4**: 269) Adolf-Butenandt-Institut fur Physiologische Chemie, Lehrstuhl: Physiologische Chemie, Universitat Munchen, Butenandtstr. 5, Gebäude B, Munchen, D-81377, GERMANY

Robert R. Henry (**1**: 121) Veterans Affairs Medical Center, San Diego (V111G), 3350 La Jolla Village Drive, San Diego, CA 92161

Johan Hiding (**2**: 45) Göteborg University, Institute of Medical Biochemistry, PO Box 440, Göteborg, SE-403-50, SWEDEN

Yasushi Hiraoka (**3**: 171) Structural Biology Section and CREST Research Project, Kansai Advanced Research Center, Communications Research Laboratory, 588-2 Iwaoka, Iwaoka-cho, Nishi-ku, Kobe, 651-2492, JAPAN

Mary M. Hitt (**1**: 435) Department of Pathology & Molecular Medicine, McMaster University, 1200 Main Street West, Hamilton, Ontario, L8N 3Z5, CANADA

Julie Hodgkinson (**3**: 307) School of Crystallography, Birkbeck College, Unversity of London, Malet Street, London, WC1E 7HX, UNITED KINGDOM

Klaus P. Hoeflich (**2**: 307) Division of Molecular and Structural Biology, Ontario Cancer Institute, Department of Medical Biophysics, University of Toronto, 610 University Avenue, 7-707A, Toronto, Ontario, M5G 2M9, CANADA

Tracy L. Hoffman (**1**: 21) ATCC, P.O. Box 1549, Manassas, VA 20108

Jörg D. Hoheisel (**4**: 113) Functional Genome Analysis, German Cancer Research Center, Deutsches Krebsforschungszentrum, Im Neuenheimer Feld 580, Heidelberg, D-69120, GERMANY

Thomas Hollemann (**1**: 191) Institute for Biochemistry and Molecular Cell Biology, University of Goettingen, Justus-von-Liebig-Weg 11, Göttingen, D-37077, GERMANY

Caterina Holz (**4**: 57) PSF biotech AG, Huebnerweg 6, Berlin, D-14059, GERMANY

Akira Honda (**2**: 299) Department of Pharmacology, University of Vermont, Health Science Research Facility 330, Burlington, VT 05405-0068

Masanori Honsho (**2**: 5) Max Planck Institute of Molecular Cell Biology and Genetics, Pfotenhauerstrasse 108, Dresden, D-01307, GERMANY

Andrew N. Hoofnagle (**4**: 443) School of Medicine, University of Colorado Health Sciences Center, Denver, CO 80262

Eliezer Huberman (**1**: 165) Gene Expression and Function Group, Argonne National Laboratory, 9700 South Cass Avenue, Argonne, IL 60439-4844

M. Shane Hutson (**3**: 87) Department of Physics, Duke University, 107 Physics Bldg, Durham, NC 27708-1000

Andreas Hüttmann (**1**: 115) Abteilung für Hämatologie, Universitäkrankenhaus Essn, Hufelandstr. 55, Essen, 45122, GERMANY

Anthony A. Hyman (**2**: 155) Max Planck Institute of Molecular Cell Biology and Gene Technology, Pfotenhauerstrasse 108, Dresden, D-01307, GERMANY

Sherrif F. Ibrahim (**1**: 269) Institute for Systems Biology, 1441 N. 34th St, Seattle, WA 98103

Kazuo Ikeda (**1**: 151) National Medical Center and Beckman Research Institute, Division of Neurosciences, City of Hope, 1500 East Duarte Road, Duarte, CA 91010-3000

Elina Ikonen (**2**: 181) The LIPID Cell Biology Group, Department of Biochemistry, The Finnish National Public Health Institute, Mannerheimintie 166, Helsinki, FIN-00300, FINLAND

Pranvera Ikonomi (**1**: 49) Director, Cell Biology, American Type Culture Collection (ATCC), 10801 University Blvd., Manassas, VA 20110-2209

Mitsuhiko Ikura (**2**: 307) Division of Molecular and Structural Biology, Ontario Cancer Institute, Department of Medical Biophysics, University of Toronto, 610 University Avenue 7-707A, Toronto, Ontario, M5G 2M9, CANADA

Arup Kumar Indra (**3**: 501) Institut de Génétique et de Biologie Moléculaire et Cellulaire (IGBMC), 1 rue Laurent Fries, B.P.10142, Illkirch CEDEX, F-67404, FRANCE

Takayoshi Inoue (**4**: 35) National Institute for Neuroscience, 4-1-1 Ogawahigashi, Kodaira, Tokyo, 187-8502, JAPAN

Kumiko Ishii (**2**: 139) Supra-Biomolecular System Research Group, RIKEN (Institute of Physical and Chemical Research), 2-1, Hirosawa, Wako-shi, Saitama, 351-0198, JAPAN

Dean A. Jackson (**2**: 121) Department of Biomolecular Sciences, UMIST, PO Box 88, Manchester, M60 1QD, UNITED KINGDOM

Reinhard Jahn (**2**: 85) Department of Neurobiology, Max-Planck-Institut for Biophysical Chemistry, Am Faßberg 11, Gottingen, D-37077, GERMANY

Kim D. Janda (**1**: 491) Department of Chemistry, BCC-582, The Scripps Research Institute, 10550 N. Torrey Pines Road, La Jolla, CA 92037

Harry W. Jarrett (**4**: 335) Department of Biochemistry, University of Tennessee Health Sciences Center, Memphis, TN 38163

Daniel G. Jay (**4**: 307) Dept. Physiology, Tufts University School of Medicine, 136 Harrison Avenue, Boston, MA 02111

David W. Jayme (**1**: 33) Cell Culture Research and Development, GIBCO/Invitrogen Corporation, 3175 Staley Road, Grand Island, NY 14072

Ole Nørregaard Jensen (**4**: 409) Protein Research Group, Department of Biochemistry and Molecular Biology, University of Southern Denmark, Campusvej 55, Odense M, DK-5230, DENMARK

Jae Hyun Jeong (**4**: 29) Department of Chemical & Biomolecular Engineering, Center for Ultramicrochemical Process Systems, Korea Advanced Institute of Science and Technology, Daejeon, 305-701, SOUTH KOREA

Jeff A. Jones (**2**: 233) Space and Life Sciences Directorate, NASA-Johnson Space Center, TX 77058

Gloria Juan (**1**: 279) Research Pathology Division, Room S-830, Memorial Sloan-Kettering Cancer Center, 1275 York Avenue, New York, NY 10021

Melissa S. Jurica (**2**: 109) Molecular, Cell & Developmental Biology, Center for Molecular Biology of RNA, UC Santa Cruz, 1156 High Street, Santa Cruz, CA 95064

Eckhart Kämpgen (**1**: 103) Department of Dermatology, Friedrich Alexander University, Hartmannstr. 14, Erlangen, D-91052, GERMANY

Roger Karlsson (**2**: 165) Department of Cell Biology, The Wenner-Gren Institute, Stockholm University, Stockholm, S-10691, SWEDEN

Fredrik Kartberg (**2**: 45) Göteborg University, Institute of Medical Biochemistry, PO Box 440, Gothenburg, SE, 403-50, SWEDEN

Irina N. Kaverina (**3**: 111) Institute of Molecular Biotechnology, Austrian Academy of Sciences, Dr. Bohrgasse 3-5, Vienna, A-1030, AUSTRIA

Ralph H. Kehlenbach (**2**: 267) Hygiene-Institut-Abteilung Virologie, Universitat Heidelberg, Im Neuenheimer Feld 324, Heidelberg, D-69120, GERMANY

Daniel P. Kiehart (**3**: 87) Department of Biology, Duke University, B330g Levine Sci Bldg, Box 91000, Durham, NC 27708-1000

Katherine E. Kilpatrick (**1**: 483) Senior Research Investigator, TriPath Oncology, 4025 Stirrup Creek Drive, Suite 400, Durham, NC 27703

Jong-Duk Kim (**4**: 29) Department of Chemical & Biomolecular Engineering, Center for Ultramicrochemical Process Systems, Korea Advanced Institute of Science and Technology, Daejeon, 305-701, SOUTH KOREA

Maurice Kléber (**1**: 69) Institute of Cell Biology, Department of Biology, Swiss Federal Institute of Technology, ETH—Hönggerberg, Zurich, CH-8093, SWITZERLAND

Toshihide Kobayashi (**2**: 139) Supra-Biomolecular System Research Group, RIKEN (Institute of Physical and Chemical Research) Frontier Research System, 2-1, Hirosawa, Wako-shi, Saitama, 351-0198, JAPAN

Stefan Kochanek (**1**: 445) Division of Gene Therapy, University of Ulm, Helmholtz Str. 8/I, Ulm, D-89081, GERMANY

Anna Koffer (**2**: 223) Physiology Department, University College London, 21 University Street, London, WC1E 6JJ, UNITED KINGDOM

Antonius Koller (**4**: 383) Department of Cell Biology, Torrey Mesa Research Institute, 3115 Merryfield Row, San Diego, CA 92121

Erich Koller (**3**: 523) Functional Genomics, GeneTrove, Isis Pharmaceuticals, Inc., 2292 Faraday Ave., Carlsbad, CA 92008

Robert L. Kortum (**1**: 215) The Eppley Institute for Research in Cancer, The University of Nebraska Medical Center, 986805 Nebraska Medical Center, Omaha, NE 68198-6805

Irina Kratchmarova (**4**: 427) Protein Interaction Laboratory, University of Southern Denmark—Odense, Campusvej 55, Odense M, DK-5230, DENMARK

Geri E. Kreitzer (**2**: 189) Cell and Developmental Biology, Weill Medical College of Cornell University, LC-300, New York, NY 10021

Florian Kreppel (**1**: 445) Division of Gene Therapy, University of Ulm, Helmholtz Str. 8/I, Ulm, D-89081, GERMANY

Mogens Kruhøffer (**4**: 83) Molecular Diagnostic Laboratory, Clinical Biochemical Department, Aarhus University Hospital, Skejby, Brendstrupgaardvej, Aarhus N, DK-8200, DENMARK

Robb Krumlauf (**4**: 35) Stowers Institute for Medical Research, 1000 East 50th Street, Kansas City, MO 64110

Michael Kühl (**1**: 191) Development Biochemistry, University of Ulm, Albert-Einstein-Allee 11, Ulm, D-89081, GERMANY

Mark Kühnel (**2**: 57) Department of Cell Biology, EMBL, Postfach 102209, Heidelberg, D-69117, GERMANY

Anuj Kumar (**3**: 179) Dept. of Molecular, Cellular, and Developmental Biology and Life Sciences Institute, University of Michigan, 210 Washtenaw Avenue, Ann Arbor, MI 48109-2216

Thomas Küntziger (**1**: 207) Institute of Medical Biochemistry, Institute of Medical Biochemistry, University of Oslo, PO Box 1112 Blindern, Oslo, 0317, NORWAY

Yasuhiro Kuramitsu (**4**: 197) Department of Biochemistry and Biomolecular Recognition, Yamaguchi University School of Medicine, 1-1-1 Minami-kogushi, Ube, Yamaguchi, 755-8505, JAPAN

Sergei A. Kuznetsov (**1**: 79) Craniofacial and Skeletal Disease Branch, NIDCR, NIH, Department of Health and Human Services, 30 Convent Drive MSC 4320, Bethesda, MD 20892

Joshua Labaer (**4**: 73) Harvard Institute of Proteomics, 320 Charles Street, Boston, MA 02141-2023

Frank Lafont (**2**: 181) Department of Biochemistry, University of Geneva, 30, quai Ernest-Ansermet 1211, Geneva 4, CH-1211, SWITZERLAND

Yun Wah Lam (**2**: 103, 115) Wellcome Trust Biocentre, MSI/WTB Complex, University of Dundee, Dow Street, Dundee, DD1 5EH, UNITED KINGDOM

Angus I. Lamond (**2**: 103, 115) Wellcome Trust Biocentre, MSI/WTB Complex, University of Dundee, Dow Street, Dundee, DD1 5EH, UNITED KINGDOM

Lukas Landmann (**3**: 5) Institute for Anatomy (LL), Anatomisches Institut, University of Basel, Pestalozzistrasse 20, Basel, CH-4056, SWITZERLAND

Helga B. Landsverk (**1**: 207) Institute of Medical Biochemistry, Institute of Medical Biochemistry, University of Oslo, PO Box 1112 Blindern, Oslo, 0317, NORWAY

Christine Lang (**4**: 57) Department of Microbiology and Genetics, Berlin University of Technology, Gustav-Meyer-Allee 25, Berlin, D-13355, GERMANY

Paul LaPointe (**2**: 209) Department of Cell and Molecular Biology, The Scripps Research Institute, 10550 North Torrey Pines Road, La Jolla, CA 92037

Martin R. Larsen (**4**: 371) Department of Biochemistry and Molecular Biology, University of Southern Denmark, Campusvej 55, Odense M, DK-5230, DENMARK

Pamela L. Larsen (**1**: 157) Department of Cellular and Structural Biology, University of Texas Health Science Center at San Antonio, San Antonio, TX 78229-3900

Eugene Ngo-Lung Lau (**1**: 115) Leukaemia Foundation of Queensland Leukaemia Research Laboratories, Queensland Institute of Medical Research, Royal Brisbane Hospital Post Office, Brisbane, Queensland, Q4029, AUSTRALIA

Sabrina Laugesen (**4**: 371) Department of Biochemistry and Molecular Biology, University of Southern Denmark, Campusvej 55, Odense M, DK-5230, DENMARK

Daniel Laune (**1**: 519) Centre de Pharmacologie et Biotechnologie pour la Santé, CNRS UMR 5160, Faculté de Pharmacie, Avenue Charles Flahault, Montpellier Cedex 5, F-34093, FRANCE

Andre Le Bivic (**2**: 241) Groupe Morphogenese et Compartimentation Membranaire, UMR 6156, IBDM, Faculte des Sciences de Luminy, case 907, Marseille cedex 09, F-13288, FRANCE

Ronald Lebofsky (**3**: 429) Laboratoire de Biophysique de l'ADN, Departement des Biotechnologies, Institut Pasteur, 25 rue du Dr. Roux, Paris Cedex 15, F-75724, FRANCE

Chuan-PU Lee (**2**: 259) The Department of Biochemistry and Molecular Biology, Wayne State University School of Medicine, 4374 Scott Hall, 540 E. Canfield, Detroit, MI 48201

Eva Lee (**1**: 139) Life Sciences Division, Lawrence Berkeley National Laboratory, 1 Cyclotron Road, Bldg 83-101, Berkeley, CA 94720

Joon-Hee Lee (**4**: 45) School of Biosciences, University of Nottingham, Sutton Bonington, Loughborough, Leics, LE12 5RD, UNITED KINGDOM

Kwangmoon Lee (**1**: 215) The Eppley Institute for Research in Cancer, The University of Nebraska Medical Center, 986805 Nebraska Medical Center, Omaha, NE 68198-6805

Thomas Lee (**4**: 443) Dept of Chemistry and Biochemistry, Univ of Colorado, 215 UCB, Boulder, CO 80309-0215

Margaret Leversha (**3**: 395) Memorial Sloan Kettering Cancer Center, 1275 York Avenue, New York, NY 10021

Jeffrey M. Levsky (**4**: 121) Department of Anatomy and Structural Biology, Golding # 601, Albert Einstein College of Medicine of Yeshiva University, 1300 Morris Park Avenue, Bronx, NY 10461

Alexandre Lewalle (**3**: 37) Randall Centre, New Hunt's House, Guy's Campus, London, SE1 1UL, UNITED KINGDOM

Chung Leung Li (**1**: 115) Experimental Haematology Laboratory, Stem Cell Program, Institute of Zoology/Genomics Research Center, Academia Sinica, Nankang 115, Nankang, Taipei, 11529, R.O.C.

LiQiong Li (**3**: 345) Department of Pathology and Laboratory Medicine, University of Rochester School of Medicine, 601 Elmwood Ave., Rm 1-6337, Rochester, NY 14642

Mei Li (**3**: 501) Institut de Génétique et de Biologie Moléculaire et Cellulaire (IGBMC), 1 rue Laurent Fries, B.P.10142, Illkirch CEDEX, F-67404, FRANCE

Siming Li (**4**: 295) Dana Faber Cancer Institute, Harvard University, 44 Binney Street, Boston, MA 02115

Lih-huei Liaw (**3**: 351) Beckman Laser Institute, University of California, Irvine, 1002 Health Sciences Road E, Irvine, CA 92697-1475

Antonietta M. Lillo (**1**: 491) Department of Chemistry, BCC-582, The Scripps Research Institute, 10550 N. Torrey Pines Road, La Jolla, CA 92037

Uno Lindberg (**2**: 165) Department of Cell Biology, Stockholm University, The Wenner-Gren Institute, Stockhólm, S-10691, SWEDEN

Christian Linden (**1**: 103) Department of Virology, Julius-Maximillins University, Versbacher Str. 7, Würzburg, D-97080, GERMANY

Robert Lindner (**2**: 51) Department of Cell Biology in the Center of Anatomy, Hannover Medical School, Hannover, D-30625, GERMANY

Lance A. Liotta (**3**: 339) Chief, Laboratory of Pathology, National Cancer Institute Building 10, Room 2A33, 9000 Rockville Pike, Bethesda, MD 20892

Adam J. Liska (**4**: 399) Max Planck Institute of Molecular Cell Biology and Genetics, Pfotenhauerst 108, Dresden, D-01307, GERMANY

Hong Liu (**1**: 139) Life Sciences Division, Lawrence Berkeley National Laboratory, 1 Cyclotron Road, Bldg 83-101, Berkeley, CA 94720

Silvia Lommel (**2**: 399) Department of Cell Biology, German Research Center for Biotechnology (GBF), Mascheroder Weg 1, Braunschweig, D-38124, GERMANY

Giuseppe S. A. Longo-Sorbello (**1**: 315) Centro di Riferimento Oncologico, Ospedale "S. Vincenzo", Taormina, Contradra Sirinam, 08903, ITALY

Lovisa Lovmar (**3**: 455) Department of Medical Sciences, Uppsala University, Akademiska sjukhuset, Uppsala, SE-75185, SWEDEN

Eugene Lukanidin (**1**: 363) Department of Molecular Cancer Biology, Institute of Cancer Biology, Danish Cancer Society, Strandboulevarden 49, Copenhagen, DK-2100, DENMARK

Jiri Lukas (**4**: 253) Department of Cell Cycle and Cancer, Danish Cancer Society, Strandboulevarden 49, Copenhagen, DK-2100, DENMARK

Peter J. Macardle (**1**: 475) Department of Immunology, Allergy and Artritis, Flinders Medical Centre and Flinders University, Bedford Park, Adelaie, SA, 5051, SOUTH AUSTRALIA

Peder S. Madsen (**4**: 69) Institute of Medical Biochemistry, University of Aarhus, Ole Worms Alle, Building 170, Aarhus C, DK-8000, DENMARK

Nils E. Magnusson (**4**: 83) Clinical Biochemical Department, Molecular Diagnostic Laboratory, Aarhus University Hospital, Skejby, Brendstrupgaardvej, Aarhus N, DK-8200, DENMARK

Asami Makino (**2**: 139) Supra-Biomolecular System Research Group, RIKEN (Institute of Physical and Chemical Research) Frontier Research System, 2-1, Hirosawa, Wako-shi, Saitama, 351-0198, JAPAN

G. Mike Makrigiorgos (**3**: 477) Department of Radiation Oncology, Dana Farber-Brigham and Women's Cancer Center, 75 Francis Street, Level L2, Boston, MA 02215

Matthias Mann (**4**: 363, 427) Protein Interaction Laboratory, University of Southern Denmark, Odense, Campusvej 55, Odense M, DK-5230, DENMARK

Edward Manser (**4**: 285) Glaxo-IMCB Group, Institute of Molecular and Cell Biology, Singapore, 117609, SINGAPORE

Ahmed Mansouri (**3**: 491) Department of Molecular Cell Biology, Max-Planck-Institute of Biophysical Chemistry, Am Fassberg 11, Göttingen, D-37077, GERMANY

Alan D. Marmorstein (**2**: 241) Cole Eye Institute, Weill Medical College of Cornell Cleveland Clinic, 9500 Euclid Avenue, i31, Cleveland, OH 44195

Bruno Martoglio (**2**: 215) Institute of Biochemistry, ETH Zentrum, Building CHN, Room L32.3, Zurich, CH-8092, SWITZERLAND

Susanne E. Mason (**1**: 407) Department of Physiology, University of Maryland School of Medicine, 655 W. Baltimore St., Baltimore, MD 21201

Stephen J. Mather (**1**: 539) Dept of Nuclear Medicine, St Bartholomews Hospital, London, EC1A 7BE, UNITED KINGDOM

Arvid B. Maunsbach (**3**: 221, 289) Department of Cell Biology, Institute of Anatomy, Aarhus University, Aarhus, DK-8000, DENMARK

William Hayes McDonald (**4**: 391) Department of Cell Biology, The Scripps Research Institute, 10550 North Torrey Pines Rd, La Jolla, CA 92370

Kathleen M. McKenzie (**1**: 491) Department of Chemistry, BCC-582, The Scripps Research Institute, 10550 N. Torrey Pines Road, La Jolla, CA 92037

Alexander D. McLellan (**1**: 103) Department of Microbiology & Immunology, University of Otago, PO Box 56, 720 Cumberland St, Dunedin, NEW ZEALAND

Scott W. McPhee (**1**: 457) Department of Surgery, University of Medicine and Dentistry of New Jersey, Camden, NJ 08103

Jill Meisenhelder (**4**: 139) Molecular and Cell Biology Laboratory, The Salk Institute, 10010 North Torrey Pines Road, La Jolla, CA 92037

Paula Meleady (**1**: 13) National Institute for Cellular Biotechnology, Dublin City University, Glasnevin, Dublin, 9, IRELAND

Nicholas T. Mesires (**4**: 345) Department of Physiology, Tufts University School of Medicine, 136 Harrison Ave, Boston, MA 02111

Daniel Metzger (**3**: 501) Institut de Génétique et de Biologie Moléculaire et Cellulaire (IGBMC), Institut Clinique de la Souris (ICS), 1 rue Laurent Fries, B.P.10142, Illkirch CEDEX, F-67404, FRANCE

Martina Mirlacher (**3**: 369) Division of Molecular Pathology, Institue of Pathology, University of Basel, Schonbeinstrasse 40, Basel, CH-4031, SWITZERLAND

Suchareeta Mitra (**4**: 335) Department of Biochemistry, University of Tennessee Health Sciences Center, Memphis, TN 38163

Atsushi Miyawaki (**2**: 317) Laboratory for Cell Function and Dynamics, Advanced Technology Center, Brain Science Institute, Institute of Physical and Chemical Research (RIKEN), 2-1 Horosawa, Wako, Saitama, 351-0198, JAPAN

Dejana Mokranjac (**4**: 269) Adolf-Butenandt-Institut fur Physiologische Chemie, Lehrstuhl: Physiologische Chemie, Universitat Munchen, Butenandtstr. 5, Gebäude B, Munchen, D-81377, GERMANY

Peter L. Molloy (**4**: 325) CSIRO Molecular Science, PO Box 184, North Ryde, NSW, 1670, AUSTRALIA

Richard A. Moravec (**1**: 25) Promega Corporation, 2800 Woods Hollow Road, Madison, WI 53711-5399

José M. A. Moreira (**1**: 527) Institute of Cancer Biology and Danish Centre for Translational Breast Cancer Research, Danish Cancer Society, Strandboulevarden 49, Copenhagen O, DK-2100, DENMARK

May C. Morris (**4**: 13) Centre de Recherche en Biochimie Macromoléculaire (UPR 1086), Centre National de la Recherche Scientifique (CNRS), 1919 Route de Mende, Montpellier Cedex 5, F-34293, FRANCE

Robert A. Moxley (**4**: 335) Department of Biochemistry, University of Tennessee Health Sciences Center, Memphis, TN 38163

Anne Muesch (**2**: 189) Margaret M. Dyson Vision Research Institute, Department of Opthalmology, Weill Medical College of Cornell University, New York, NY 10021

Peggy Müller (**1**: 325) Zentrum für Angewandte Medizinische und Humanbiologische Forschung, Labor für Molekulare Hepatologie der Universitätsklinik und Polikinik für Innere Medizin I, Martin Luther University Halle-Wittenburg, Heinrich-Damerow-Street 1, Saale, Halle, D-06097, GERMANY

Steve Murray (**3**: 325) CRC Structural Cell Biology Group, Paterson Institute for Cancer Research, Christie Hospital NHS Trust, Wilmslow Road, Withington, Manchester, M20 4BX, UNITED KINGDOM

Connie Myers (**1**: 139) Life Sciences Division, Lawrence Berkeley National Laboratory, 1 Cyclotron Road, Bldg 83-101, Berkeley, CA 94720

Kazuyuki Nakamura (**4**: 197) Department of Biochemistry and Biomolecular Recognition, Yamaguchi University School of Medicine, 1-1-1 Minami-kogushi, Ube, Yamaguchi, 755-8505, JAPAN

Maithreyi Narasimha (**3**: 77) Wellcome Trust/Cancer Research UK Institute and Dept of Anatomyaraki, University of Cambridge, Tennis Court Road, Cambridge, CB2 1QR, UNITED KINGDOM

Dobrin Nedelkov (**4**: 279) Intrinsic Bioprobes, Inc., 625 S. Smith Road, Suite 22, Tempe, AZ 85281

Randall W. Nelson (**4**: 279) Intrinsic Bioprobes Inc., 625 S. Smith Road, Suite 22, Tempe, AZ 85281

Frank R. Neumann (**2**: 359) Department of Molecular Biology, University of Geneva, 30, Quai Ernest Ansermet, Geneva, CH-1211, SWITZERLAND

Walter Neupert (**4**: 269) Adolf-Butenandt-Institut fur Physiologische Chemie, Lehrstuhl: Physiologische Chemie, Universitat Munchen, Butenandtstr. 5, Gebäude B, Munchen, D-81377, GERMANY

Axl Alois Neurauter (**1**: 239) Immunosystem R & D, Dynal Biotech ASA, PO Box 114, Smestad, N-0309, NORWAY

Phillip Ng (**1**: 435) Dept of Molecular and Human Genetics, Baylor College of Medicine, One Baylor Plaza, Houston, TX 77030

Garth L. Nicolson (**1**: 359) The Institute for Molecular Medicine, 15162 Triton Lane, Huntington Beach, CA 92649-1041

Trine Nilsen (**4**: 275) Department of Biochemistry, Institute for Cancer Research, The Norwegian Radium Hospital, Montebello, Oslo, N-0310, NORWAY

Tommy Nilsson (**2**: 45) Göteborg University, Institute of Medical Biochemistry, PO Box, Göteborg, SE-403 50, SWEDEN

Lars Norderhaug (**1**: 239) Dynal Biotech ASA, PO Box 114, Smestad, N-0309, NORWAY

Robert O'Connor (**1**: 5, 13, 335) National Institute for Cellular Biotechnology, Dublin City University, Glasnevin, Dublin, 9, IRELAND

Lorraine O'Driscoll (**1**: 5, 335) National Institute for Cellular Biotechnology, Dublin City University, Glasnevin, Dublin, 9, IRELAND

Martin Offterdinger (**3**: 153) Cell Biology and Cell Biophysics Program, European Molecular Biology Laboratory, Meyerhofstrasse 1, Heidelberg, D-69117, GERMANY

Philip Oh (**2**: 11) Cellular and Molecular Biology Program, Sidney Kimmel Cancer Center, 10835 Altman Row, San Diego, CA 92121

Takanori Ohnishi (**1**: 367) Department of Neurosurgery, Ehime University School of Medicine, Shitsukawa, Toon-shi, Ehime, 791-0295, JAPAN

Sjur Olsnes (**4**: 19, 275) Department of Biochemistry, The Norwegian Radium Hospital, Montebello, Oslo, 0310, NORWAY

Shao-En Ong (**4**: 427) Protein Interaction Laboratory, University of Southern Denmark—Odense, Campusvej 55, Odense M, DK-5230, DENMARK

Akifumi Ootani (**1**: 411) Department of Internal Medicine, Faculty of Medicine, Saga University, Nebeshima 5-1-1, Saga, 849-8501, JAPAN

Valerio Orlando (**4**: 317) Dulbecco Telethon Institute, Institute of Genetics & Biophysics CNR, Via Pietro Castellino 111, Naples, I-80131, ITALY

Torben F. Ørntoft (**4**: 83) Clinical Biochemical Department, Molecular Diagnostic Laboratory, Aarhus University Hospital, Skejby, Brendstrupgaardvej 100, Aarhus N, DK-8200, DENMARK

Mary Osborn (**1**: 549, 563) Department of Biochemistry and Cell Biology, Max Planck Institute of Biophysical Chemistry, Am Faßberg 11, Gottingen, D-37077, GERMANY

Lawrence E. Ostrowski (**2**: 99) Cystic Fibrosis/Pulmonary Research and Treatment Centre, University of North Carolina at Chapel Hill, Thurston-Bowles Building, Chapel Hill, NC 27599-7248

Hendrik Otto (**2**: 253) Institut für Biochemie und Molekularbiologie, Universität Freiburg, Hermann-Herder-Str. 7, Freiburg, D-79104, GERMANY

Kerstin Otto (**1**: 103) Department of Dermatology, Julius-Maximillians University, Josef-Schneider-Str. 2, Würzburg, 97080, GERMANY

Michel M. Ouellette (**1**: 215) Department of Biochemistry and Molecular Biology, Eppley Institute for Research in Cancer, The University of Nebraska Medical Center, 986805 Nebraska Medical Center, Omaha, NE 68198-6805

Jacques Paiement (**2**: 41) Département de pathologie et biologie cellulaire, Université de Montréal, Case postale 6128, Succursale "Centre-Ville", Montreal, QC, H3C 3J7, CANADA

Patricia M. Palagi (**4**: 207) Swiss Institute of Bioinformatics, CMU, 1 Michel Servet, Geneva 4, CH-1211, SWITZERLAND

Kinam Park (**4**: 29) Department of Pharmaceutics and Biomedical Engineering, Purdue University School of Pharmacy, 575 Stadium Mall Drive, Room G22, West Lafayette, IN 47907-2091

Helen Parkinson (**4**: 95) EMBL Outstation—Hinxton, European Bioinformatics Institute, Wellcome Trust Genome Campus, Hinxton, Cambridge, CB10 1SD, UNITED KINGDOM

Richard M. Parton (**3**: 187) Wellcome Trust Centre for Cell Biology, Institute of Cell and Molecular Biology The University of Edinburgh, Michael Swann Building, The King's Buildings, Mayfield Road, Edinburgh, EH9 3JR, SCOTLAND

Bryce M. Paschal (**2**: 267) Center for Cell Signaling, University of Virginia, 1400 Jefferson Park Avenue, West Complex Room 7021, Charlottesville, VA 22908-0577

Wayne F. Patton (**4**: 225) Perkin-Elmer LAS, Building 100-1, 549 Albany Street, Boston, MA 02118

Staffan Paulie (**1**: 533) Mabtech AB, Box 1233, Nacha Strand, SE-131 28, SWEDEN

Rainer Pepperkok (**3**: 121) Cell Biology and Cell Biophysics Programme, European Molecular Biology Laboratory (EMBL), Meyerhofstrasse 1, Heidelberg, D-69117, GERMANY

Xomalin G. Peralta (**3**: 87) Department of Physics, Duke University, 107 Physics Bldg, Durham, NC 27708-1000

Martha Perez-Magallanes (**1**: 151) National Medical Center and Beckman Research Institute, Division of Neurosciences, City of Hope, 1500 E. Duarte Rd, Duarte, CA 91010

Stephen P. Perfetto (**1**: 257) Vaccine Research Center, National Institutes of Health, 40 Convent Dr., Room 5509, Bethesda, MD 20892-3015

Hedvig Perlmann (**1**: 533) Department of Immunology, Stockholm University, Biology Building F5, Top floor, Svante Arrhenius väg 16, Stockholm, SE-10691, SWEDEN

Peter Perlmann (**1**: 533) Department of Immunology, Stockholm University, Biology Building F5, Top floor, Svante Arrhenius väg 16, Stockholm, SE-10691, SWEDEN

Timothy W. Petersen (**1**: 269) Institute for Systems Biology, 1441 N. 34th St, Seattle, WA 98103

Patti Lynn Peterson (**2**: 259) Department of Neurology, Wayne State University School of Medicine, 5L26 Detroit Receiving Hospital, Detroit Medical Center, Detroit, MI 48201

Nisha Philip (**4**: 265) Department of Pharmacology and Cancer Biology, Duke University, Research Dr. LSRC Rm C115, Box 3813, Durham, NC 27710

Thomas Pieler (**1**: 191) Institute for Biochemistry and Molecular Cell Biology, University of Goettingen, Humboldtallee 23, Göttingen, D-37073, GERMANY

Daniel Pinkel (**3**: 445) Department of Laboratory Medicine, University of California San Francisco, Box 0808, San Francisco, CA 94143-0808

Javier Pizarro Cerdá (**2**: 407) Unite des Interactions Bacteries-Cellules/Unité INSERM 604, Institut Pasteur, 28, rue du Docteur Roux, Paris Cedex 15, F-75724, FRANCE

Andreas Plückthun (**1**: 497) Department of Biochemistry, University of Zürich, Winterthurerstrasse 190, Zürich, CH-8057, SWITZERLAND

Helen Plutner (**2**: 209) Department of Cell and Molecular Biology, The Scripps Research Institute, 10550 North Torrey Pines Road, La Jolla, CA 92037

Piotr Pozarowski (**1**: 279) Brander Cancer Research Institute, New York Medical College, Valhalla, NY 10595

Johanna Prast (**1**: 557) Institute of Molecular Biology, Austrian Academy of Sciences, Billrothstrasse 11, Salzburg, A-5020, AUSTRIA

Brendan D. Price (**3**: 477) Department of Radiation Oncology, Dana Farber-Brigham and Women's Cancer Center, 75 Francis Street, Level L2, Boston, MA 02215

Elena Prigmore (**3**: 403) Sanger Institute, The Wellcome Trust, The Wellcome Trust Genome Campus, Hinxton, Cambridge, CB10 1SA, UNITED KINGDOM

Gottfried Proess (**1**: 467) Eurogentec S.A., Liege Science Park, 4102 Seraing, B-, BELGIUM

David M. Prowse (**1**: 133) Centre for Cutaneous Research, Barts and The London Queen Mary's School of Medicine and Dentistry, Institute of Cell and Molecular Science, 2 Newark Street, Whitechapel London, WC2A 3PX, UNITED KINGDOM

Manuela Pruess (**4**: 469) EMBL outstation—Hinxton, European Bioinformatic Institute, Welcome Trust Genome Campus, Hinxton, Cambridge, CB10 1SD, UNITED KINGDOM

Eric Quéméneur (**4**: 235) Life Sciences Division, CEA Valrhô, BP 17171 Bagnols-sur-Cèze, F-30207, FRANCE

Leda Helen Raptis (**2**: 329, 341) Department of Microbiology and Immunology, Queen's University, Room 716 Botterell Hall, Kingston, Ontario, K7L3N6, CANADA

Anne-Marie Rasmussen (**1**: 239) Dynal Biotech ASA, PO Box 114, Smestad, N-0309, NORWAY

Andreas S. Reichert (**4**: 269) Department of Physiological Chemistry, University of Munich, Butenandtstr. 5, München, D-81377, GERMANY

Siegfreid Reipert (**3**: 325) Ordinariat II, Institute of Biochemistry and Molecular Biology, Vienna Biocenter, Dr. Bohr-Gasse 9, Vienna, A-1030, AUSTRIA

Guenter P. Resch (**3**: 267) Institute of Molecular Biology, Dr. Bohrgasse 3-5, Vienna, A-1030, AUSTRIA

Katheryn A. Resing (**4**: 443) Dept of Chemistry and Biochemistry, University of Colorado, 215 UCB, Boulder, CO 80309-0215

Donald L Riddle (**1**: 157) Division of Biological Sciences, University of Missouri, 311 Tucker Hall, Columbia, MO 65211

Mara Riminucci (**1**: 79) Department of Experimental Medicine, Universita' dell' Aquilla, Via Vetoio, Coppito II, L'Aquila, I-67100, ITALY

Terry L. Riss (**1**: 25) Promega Corporation, 2800 Woods Hollow Road, Madison, WI 53711-5399

Pamela Gehron Robey (**1**: 79) Craniofacial and Skeletal Disease Branch, NIDCR, NIH, Department of Health and Human Services 30 Convent Dr, MSC 4320, Bethesda, MD 20892-4320

Linda J. Robinson (**2**: 201)

Philippe Rocca-Serra (**4**: 95) EMBL Outstation—Hinxton, European Bioinformatics Institute, Wellcome Trust Genome Campus, Hinxton, Cambridge, CB10 1SD, UNITED KINGDOM

Alice Rodriguez (**3**: 87) Department of Biology, Duke University, Durham, NC 27708-1000

Enrique Rodriguez-Boulan (**2**: 189, 241) Margaret M Dyson Vision Research Institute, Department of Opthalmology, Weill Medical College of Cornell University, New York, NY 10021

Mario Roederer (**1**: 257) ImmunoTechnology Section and Flow Cytometry Core, Vaccine Research Center, National Institute for Allergy and Infectious Diseases, National Institutes of Health, 40 Convent Dr., Room 5509, Bethesda, MD 20892-3015

Peter Roepstorff (**4**: 371) Department of Biochemistry and Molecular Biology, University of Southern Denmark, Campusvej 55, Odense M, DK-5230, DENMARK

Manfred Rohde (**2**: 399) Department of Microbial Pathogenicity, Gesellschaft fur Biotechnoogische Forschung, Mascheroder Weg 1, Braunschweig, D-38124, GERMANY

Norbert Roos (**3**: 299) Electron Microscopical Unit for Biological Sciences, University of Oslo, Blindern, Oslo, 0316, NORWAY

Sabine Rospert (**2**: 253) Institut für Biochemie und Molekularbiologie, Universität Freiburg, Hermann-Herder-Str. 7, Freiburg, D-79104, GERMANY

Klemens Rottner (**3**: 111) Cytoskeleton Dynamics Group, German Research Centre for Biotechnology (GBF), Mascheroder Weg 1, Braunschweig, D-38124, GERMANY

Line Roy (**2**: 41) Department of Anatomy and Cell Biology, Faculty of Medicine, McGill University, STRATHCONA Anatomy & Dentistry Building, Montreal, QC, H3A 2B2, CANADA

Sandra Rutherford (**3**: 325) CRC Structural Cell Biology Group, Paterson Institute for Cancer Research, Christie Hospital NHS Trust, Wilmslow Road, Withington, Manchester, M20 4BX, UNITED KINGDOM

Beth Rycroft (**1**: 395) Department of Pharmacology, University College London, Gower Street, London, WC1E GBT, UNITED KINGDOM

Patrick Salmon (**1**: 425) Department of Genetics and Microbiology, Faculty of Medicine, University of Geneva, CMU-1 Rue Michel-Servet, Geneva 4, CH-1211, SWITZERLAND

Paul M. Salvaterra (**1**: 151) National Medical Center and Beckman Research Institute, Division of Neurosciences, City of Hope, 1500 E. Duarte Rd, Duarte, CA 91010-3000

R. Jude Samulski (**1**: 457) Gene Therapy Centre, Department of Pharmacology, University of North Carolina at Chapel Hill, 7119 Thurston Bowles, Chapel Hill, NC 27599-7352

Susanna-Assunta Sansone (**4**: 95) EMBL Outstation—Hinxton, European Bioinformatics Institute, Wellcome Trust Genome Campus, Hinxton, Cambridge, CB10 1SD, UNITED KINGDOM

Ugis Sarkan (**4**: 95) EMBL Outstation—Hinxton, European Bioinformatics Institute, Wellcome Trust Genome Campus, Hinxton, Cambridge, CB10 1SD, UNITED KINGDOM

Moritoshi Sato (**2**: 325) Department of Chemistry, School of Science, University of Tokyo, 7-3-1 Hongo, Bunkyo-Ku, Tokyo, 113-0033, JAPAN

Guido Sauter (**3**: 369) Institute of Pathology, University of Basel, Schonbeinstrasse 40, Basel, CH-4003, SWITZERLAND

Carolyn L. Sawyer (**2**: 299) Department of Pharmacology, University of Vermont, Health Science Research Facility 330, Burlington, VT 05405-0068

Guray Saydam (**1**: 315) Department of Medicine, Section of Hematology, Ege University Hospital, Bornova Izmir, 35100, TURKEY

Silvia Scaglione (**3**: 201) BIOLab, Department of Informatic, Systemistic and Telematic, University of Genoa, Viale Causa 13, Genoa, I-16145, ITALY

Lothar Schermelleh (**1**: 291, 301) Department of Biology II, Biocenter of the Ludwig-Maximilians University of Munich (LMU), Großhadernerstr. 2, Planegg-Martinsried, 82152, GERMANY

Gudrun Schiedner (**1**: 445) CEVEC Pharmaceuticals GmbH, Gottfried-Hagen-Straße 62, Köln, D-51105, GERMANY

David Schieltz (**4**: 383) Department of Cell Biology, Torrey Mesa Research Institute, 3115 Merryfield Row, San Diego, CA 92121

Jan E. Schnitzer (**2**: 11) Sidney Kimmel Cancer Center, 10835 Altman Row, San Diego, CA 92121

Morten Schou (**1**: 353) Bartholin Institute, Bartholinsgade 2, Copenhagen K, DK-1356, DENMARK

Sebastian Schuck (**2**: 5) Max Planck Institute of Molecular Cell Biology and Genetics, Pfotenhauerstrasse 108, Dresden, D-01307, GERMANY

Herwig Schüler (**2**: 165) Department of Cell Biology, The Wnner-Gren Institute, Stockholm University, Stockholm, S-10691, SWEDEN

Michael Schuler (**3**: 501) Institut de Génétique et de Biologie Moléculaire et Cellulaire (IGBMC), 1 rue Laurent Fries, B.P.10142, Illkirch CEDEX, F-67404, FRANCE

Ulrich S. Schwarz (**2**: 419) Theory Division, Max Planck Institute of Colloids and Interfaces, Potsdam, 14476, GERMANY

Antonio S. Sechi (**2**: 393) Institute for Biomedical Technology-Cell Biology, Universitaetsklinikum Aachen, RWTH, Pauwelsstrasse 30, Aachen, D-52057, GERMANY

Richard L. Segraves (**3**: 445) Comprehensive Cancer Center, University of California San Francisco, Box 0808, 2400 Sutter N-426, San Francisco, CA 94143-0808

James R. Sellers (**2**: 387) Cellular and Motility Section, Laboratory of Molecular Cardiology, National Heart, Lung and Blood Institute (NHLBI), National Institutes of Health, 10 Center Drive, MSC 1762, Bethesda, MD 20892-1762

Nicholas J. Severs (**3**: 249) Cardiac Medicine, National Heart and Lung Institute, Imperial College, Faculty of Medicine, Royal Brompton Hospital, Dovehouse Street, London, SW3 6LY, UNITED KINGDOM

Jagesh Shah (**3**: 351) Laboratory of Cell Biology, Ludwig Institute for Cancer Research, University of California, 9500 Gilman Drive, MC 0660, La Jolla, CA 92093-0660

Norman E. Sharpless (**1**: 223) The Lineberger Comprehensive Cancer Center, The University of North Carolina School of Medicine, Lineberger Cancer Center, CB# 7295, Chapel Hill, NC 27599-7295

Andrej Shevchenko (**4**: 399) Max Planck Institute for Molecular Cell Biology and Genetics, Pfotenhauerstrasse 108, Dresden, D-01307, GERMANY

David M. Shotton (**3**: 207, 249, 257) Department of Zoology, University of Oxford, South Parks Road, Oxford, OX1 3PS, UNITED KINGDOM

David I. Shreiber (**1**: 379) Department of Biomedical Engineering, Rutgers, the State University of New Jersey, 617 Bowser Road, Piscataway, NJ 08854-8014

Snaevar Sigurdsson (**3**: 455) Department of Medical Sciences, Uppsala University, Akademiska sjukhuset, Uppsala, SE-751 85, SWEDEN

Stephen Simkins (**1**: 483) TriPath Oncology, 4025 Stirrup Creek Drive, Suite 400, Durham, NC 27703

Ronald Simon (**3**: 369) Division of Molecular Pathology, Institute of Pathology, University of Basel, Schonbeinstrasse 40, Basel, CH-4031, SWITZERLAND

Kai Simons (**1**: 127, **2**: 5, 181) Max Planck Institute of Molecular Cell Biology and Genetics, Pfotenhauerstrasse 108, Dresden, D-01307, GERMANY

Jeremy C. Simpson (**3**: 121) Cell Biology and Cell Biophysics Programme, European Molecular Biology Laboratory (EMBL), Meyerhofstrasse 1, Heidelberg, D-69117, GERMANY

Robert H. Singer (**4**: 121) Department of Anatomy and Structural Biology, Golding # 601, Albert Einstein College of Medicine of Yeshiva University, 1300 Morris Park Avenue, Bronx, NY 10461

Mathilda Sjöberg (**1**: 419) Department of Biosciences at Novum, Karolinska Instituet, Huddinge, SE-141-57, SWEDEN

Camilla Skiple Skjerpen (**4**: 275) Department of Biochemistry, Institute for Cancer Research, The Norwegian Radium Hospital, Montebello, Oslo, N-0310, NORWAY

John Sleep (**3**: 37) Randall Division, Guy's Campus, New Hunt's House, London, SE1 1UL, UNITED KINGDOM

J. Victor Small (**1**: 557) Department of Cell Biology, Institute of Molecular Biology, Austrian Academy of Sciences, Billrothstrasse 11, Salzburg, A-5020, AUSTRIA

Joél Smet (**4**: 259) Department of Pediatrics and Medical Genetics, University Hospital, De Pintelaan 185, Ghent, B-9000, BELGIUM

Kim Smith (**3**: 381) Director of Cytogenetic Services, Oxford Radcliffe NHS Trust, Headington, Oxford, OX3 9DU, UNITED KINGDOM

Paul J. Smith (**1**: 305) Dept of Pathology, University of Wales College of Medicine, Heath Park, Cardiff, CF14 4XN, UNITED KINGDOM

Antoine M. Snijders (**3**: 445) Comprehensive Cancer Center, Cancer Research Institute, The University of California, San Francisco, Box 0808, 2340 Sutter Street N-, San Fransisco, CA 94143-0808

Michael Snyder (**3**: 179) Department of Molecular, Cellular and Developmental Biology, Yale University, P. O. Box 208103, Kline Biology Tower, 219 Prospect St., New Haven, CT 06520-8103

Irina Solovei (**1**: 291) Department of Biology II, Anthropology & Human Genetics, Ludwig-Maximilians University of Munich, Munich, GERMANY

Marion Sölter (**1**: 191) Institute for Biochemistry and Molecular Cell Biology, University of Goettingen, Justus-von-Liebig-Weg 11, Göttingen, D-37077, GERMANY

Lukas Sommer (**1**: 69) Institute of Cell Biology, Department of Biology, Swiss Federal Institute of Technology, ETH—Hönggerberg, Zurich, CH-8093, SWITZERLAND

Simon Sparks (**3**: 207) Department of Zoology, University of Oxford, South Parks Road, Oxford, OX1 3PS, UNITED KINGDOM

Kenneth G. Standing (**4**: 457) Department of Physics and Astronomy, University of Manitoba, 510 Allen Bldg, Winnipeg, MB, R3T 2N2, CANADA

Walter Steffen (**3**: 37, 307) Randall Division, Guy's Campus, New Hunt's House, London, SE1 1UL, UNITED KINGDOM

Theresia E. B. Stradal (**3**: 111) Department of Cell Biology, German Research Centre for Biotechnology (GBF), Mascheroder Weg 1, Braunschweig, D-38124, GERMANY

Per Thor Straten (**1**: 97) Tumor Immunology Group, Institute of Cancer Biology, Danish Cancer Society, Strandboulevarden 49, Copenhagen, DK-2100, DENMARK

Hajime Sugihara (**1**: 411) Department of Pathology & Biodefence, Faculty of Medicine, Saga University, Nebeshima 5-1-1, Saga, 849-8501, JAPAN

Chung-Ho Sun (**3**: 351) Beckman Laser Institute, University of California, Irvine, 1002 Health Sciences Road E, Irvine, CA 92697-1475

Mark Sutton-Smith (**4**: 415) Department of Biological Sciences, Imperial College of Science, Technology and Medicine, Biochemistry Building, London, SW7 2AY, UNITED KINGDOM

Tatyana M. Svitkina (**3**: 277) Department of Cell and Molecular Biology, Northwestern University Medical School, Chicago, IL 60611

Ann-Christine Syvänen (**3**: 455) Department of Medical Sciences, Uppsala University, Forskningsavd 2, ing 70, Uppsala, SE-751 85, SWEDEN

Masako Tada (**1**: 199) ReproCELL Incorporation, 1-1-1 Uchisaiwai-cho, Chiyoda-ku, Tokyo, 100-0011, JAPAN

Takashi Tada (**1**: 199) Stem Cell Engineering, Stem Cell Research Center, Institute for Frontier Medical Sciences, Kyoto University, 53 Kawahara-cho Shogoin, Sakyo-ku, Kyoto, 606-8507, JAPAN

Angela Taddei (**2**: 359) Department of Molecular Biology, University of Geneva, 30, Quai Ernest Ansermet, Geneva 4, CH-1211, SWITZERLAND

Tomohiko Taguchi (**2**: 33) Department of Cell Biology, Yale University School of Medicine, 333 Cedar Street, PO Box 208002, New Haven, CT 06520-8002

Kazusuke Takeo (**4**: 197) Department of Biochemistry and Biomolecular Recognition, Yamaguchi University School of Medicine, 1-1-1, Minami-kogushi, Ube, Yamaguchi, 755-8505, JAPAN

Nobuyuki Tanahashi (**2**: 91) Laboratory of Frontier Science, Core Technology and Research Center, The Tokyo Metropolitan Institute of Medical Sciences, 3-18-22 Honkomagome, Bunkyo-ku, Tokyo, 113-8613, JAPAN

Keiji Tanaka (**2**: 91) Laboratory of Frontier Science, Core Technology and Research Center, The Tokyo Metropolitan Institute of Medical Sciences, 3-18-22 Honkomagome, Bunkyo-ku, Tokyo, 133-8613, JAPAN

Chi Tang (**2**: 121) Dept of Biomolecular Sciences, UMIST, PO Box 88, Manchester, M60 1QD, UNITED KINGDOM

Kirill V. Tarasov (**4**: 103) Molecular Cardiology Unit, National Institute on Aging, NIH, 5600 Nathan Shock Drive, Baltimore, MD 21224

J. David Taylor (**3**: 471) Department of Genomic Sciences, Glaxo Wellcome Research and Development, 5 Moore Drive, Research Triangle Park, NC 27709-3398

Nancy Smyth Templeton (**4**: 25) Department of Molecular and Cellular Biology & the Center for Cell and Gene Therapy, Baylor College of Medicine, One Baylor Plaza, Alkek Bldg., Room N1010, Houston, TX 77030

Kenneth K. Teng (**1**: 171) Department of Medicine, Wiell Medical of Cornell University, 1300 York Ave., Rm-A663, New York, NY 10021

Patrick Terheyden (**1**: 103) Department of Dermatology, Julius-Maximillians University, Josef-Schneider-Str. 2, Würzburg, D-97080, GERMANY

Scott M. Thompson (**1**: 407) Department of Physiology, University of Maryland School of Medicine, 655 W. Baltimore St., Baltimore, MD 21201

John F. Timms (**4**: 189) Department of Biochemistry and Molecular Biology, Ludwig Institute of Cancer Research, Cruciform Building 1.1.09, Gower Street, London, WC1E 6BT, UNITED KINGDOM

Shuji Toda (**1**: 411) Department of Pathology & Biodefence, Faculty of Medicine, Saga University, Nebeshima 5-1-1, Saga, 849-8501, JAPAN

Yoichiro Tokutake (**3**: 87) Department of Physics, Duke University, 107 Physics Bldg, Durham, NC 27708-1000

Evi Tomai (**2**: 329) Department of Microbiology and Immunology, Queen's University, Room 716 Botterell Hall, Kingston, Ontario, K7L3N6, CANADA

Kenneth B. Tomer (**1**: 511) Mass Spectrometry, Laboratory of Structural Biology, National Institute of Environmental Health Sciences NIEH/NIH, 111 Alexander Drive, PO Box 12233, Research Triangle Park, NC 27709

Derek Toomre (**3**: 19) Department of Cell Biology, Yale University School of Medicine, SHM-C227/229, PO Box 208002, 333 Cedar Street, New Haven, CT 06520-8002

Sharon A. Tooze (**2**: 79) Secretory Pathways Laboratory, Cancer Research UK London Research Institute, 44 Lincoln's Inn Fields, London, WC2A 3PX, UNITED KINGDOM

David Tosh (**1**: 177) Centre for Regenerative Medicine, Department of Biology and Biochemistry, University of Bath, Claverton Down, Bath, BA2 7AY, UNITED KINGDOM

Yusuke Toyama (**3**: 87) Department of Physics, Duke University, 107 Physics Bldg, Box 90305, Durham, NC 27708-0305

Robert T. Tranquillo (**1**: 379) Department of Biomedical Engineering and Department of Chemical Engineering and Materials Science, University of Minnesota, Biomedical Engineering, 7-112 BSBE. 312 Church St SE, Minneapolis, MN 55455

Signe Trentemølle (**4**: 165) Institute of Cancer Biology and Danish Centre for Translational Breast Cancer Research, Danish Cancer Society,

Strandboulevarden 49, Copenhagen, DK-2100, DENMARK

Didier Trono (**1**: 425) Department of Genetics and Microbiology, Faculty of Medicine, University of Geneva, CMU-1 Rue Michel-Servet, Geneva 4, CH-1211, SWITZERLAND

Kevin Truong (**2**: 307) Division of Molecular and Structural Biology, Ontario Cancer Institute, Department of Medical Biophysics, University of Toronto, 610 University Avenue, 7-707A, Toronto, Ontario, M5G 2M9, CANADA

Jessica K. Tyler (**2**: 287) Department of Biochemistry and Molecular Genetics, University of Colorado Health Sciences Center at Fitzsimons, PO Box 6511, Aurora, CO 80045

Aylin S. Ulku (**1**: 345) Department of Pharmacology, University of North Carolina at Chapel Hill, Lineberger Comprehensive Cancer Center, Chapel Hill, NC 27599-7295

Yoshio Umezawa (**2**: 325) Department of Chemistry, The School of Science, University of Tokyo, 7-3-1 Hongo, Bunkyo-ku, Tokyo, 113-0033, JAPAN

Ronald Vale (**3**: 129) Department of Cellular and Molecular Pharmacology, The Howard Hughes Medical Institute, The University of California, San Francisco, N316, Genentech Hall, 1600 16th Street, San Francisco, CA 94107

Jozef Van Beeumen (**4**: 259) Department of Biochemistry, Physiology and Microbiology, University of Ghent, K.L. Ledeganckstraat 35, Ghent, B-9000, BELGIUM

Rudy N. A. van Coster (**4**: 259) Department of Pediatrics and Medical Genetics, University Hospital, University of Ghent, De Pintelaan 185, Ghent, B-9000, BELGIUM

Ger van den Engh (**1**: 269) Institute for Systems Biology, 1441 North 34th Street, Seattle, WA 98103-8904

Peter van der Geer (**4**: 139) Department of Chemistry and Biochemistry, University of California, San Diego, 9500 Gilman Dr., La Jolla, CA 92093-0601

Joël Vandekerckhovr (**4**: 379, 457) Department of Medical Protein Research, Flanders Interuniversity Institute for Biotechnology, KL Ledeganckstraat 35, Gent, B-9000, BELGIUM

Charles R. Vanderburg (**4**: 5) Department of Neurology, Massachusetts General Hospital, 114 Sixteenth Street, Charlestown, MA 02129

John Venable (**4**: 383) Department of Cell Biology, Scripps Research Institute, 10550 North Torrey Pines Road, La Jolla, CA 92037

Isabelle Vernos (**2**: 379) Cell Biology and Cell Biophysics Programme, European Molecular Biology Laboratory, Meyerhofstrasse 1, Heidelberg, D-69117, GERMANY

Peter J. Verveer (**3**: 153) Cell Biology and Cell Biophysics Program, European Molecular Biology Laboratory, Meyerhofstrasse 1, Heidelberg, D-69117, GERMANY

Marc Vidal (**4**: 295) Cancer Biology Department, Dana-Farber Cancer Institute, 44 Binney Street, Boston, MA 02115

Emmanuel Vignal (**2**: 427) Department Genie, Austrian Academy of Sciences, Billrothstrasse 11, Salzbourg–Autriche, A-520, 5020, AUSTRIA

Sylvie Villard (**1**: 519) Centre de Pharmacologie et Biotechnologie pour la Santé, CNRS—UMR 5094, Faculté de Pharmacie, Avenue Charles Flahault, Montpellier Cedex 5, F-34093, FRANCE

Hikka Virta (**1**: 127) Department of Cell Biology, European Molecular Biology Laboratory, Cell Biology Programme, Heidelberg, D-69012, GERMANY

Alfred Völkl (**2**: 63) Department of Anatomy and Cell Biology II, University of Heidelberg, Im Neuenheimer Feld 307, Heidelberg, D-69120, GERMANY

Sonja Voordijk (**4**: 207) Geneva Bioinformatics SA, Avenue de Champel 25, Geneva, CH-1211, SWITZERLAND

Adina Vultur (**2**: 329, 341) Department of Microbiology and Immunology, Queen's University, Room 716 Botterell Hall, Kingston, Ontario, K7L3N6, CANADA

Teruhiko Wakayama (**1**: 87) Center for Developmental Biology, RIKEN, 2-2-3 Minatojima-minamimachi, Kobe, 650-0047, JAPAN

Daniel Walther (**4**: 207) Swiss Institute of Bioinformatics (SIB), CMU, rue Michel-Servet 1, Genève 4, 1211, SWITZERLAND

Gang Wang (**3**: 477) Department of Radiation Oncology, Dana Farber-Brigham and Women's Cancer Center, 75 Francis Street, Level L2, Boston, MA 02215

Nancy Wang (**3**: 345) Department of Pathology and Laboratory Medicine, University of Rochester School of Medicine, 601 Elmwood Ave., Rm 1-6337, Rochester, NY 14642

Xiaodong Wang (**2**: 209) Department of Cell and Molecular Biology, The Scripps Research Institute, 10550 North Torrey Pines Road, La Jolla, CA 92037

Yanzhuang Wang (**2**: 33) Department of Cell Biology, Yale University School of Medicine, 333 Cedar Street, PO Box 208002, New Haven, CT 06520-8002

Yu-Li Wang (**3**: 107) Department of Physiology, University of Massachusetts Medical School, 377 Plantation St., Rm 327, Worcester, MA 01605

Graham Warren (**2**: 33) Department of Cell Biology, Yale University School of Medicine, 333 Cedar Street, PO Box 208002, New Haven, CT 06520-8002

Clare M. Waterman-Storer (**3**: 137) 10550 North Torrey Pines Road, CB 163, La Jolla, CA 92037

Jennifer C. Waters (**3**: 49) Department of Cell Biology, Department of Systems Biology, Harvard Medical School, 240 Longwood Ave, Boston, MA 02115

Fiona M. Watt (**1**: 133) Keratinocyte Laboratory, London Research Institute, 44 Lincoln's Inn Fields, London, WC2A 3PX, UNITED KINGDOM

Gerhard Weber (**4**: 157) Protein Analytics, Max Planck Institute for Biochemistry, Klopferspitz 18, Martinsried, D-82152, GERMANY

Peter J. A. Weber (**4**: 157) Proteomics Division, Tecan Munich GmbH, Feldkirchnerstr. 12a, Kirchheim, D-, 85551, GERMANY

Paul Webster (**3**: 299) Electron Microscopy Laboratory, House Ear Institute, 2100 West Third Street, Los Angeles, CA 90057

Jürgen Wehland (**2**: 399) Department of Cell Biology, Gesellschaft fur Biotechnoogische Forschung, Mascheroder Weg 1, Braunschweig, D-38124, GERMANY

Dieter G. Weiss (**3**: 57) Institute of Cell Biology and Biosystems Technology, Department of Biological Sciences, Universitat Rostock, Albert-Einstein-Str. 3, Rostock, D-18051, GERMANY

Walter Weiss (**4**: 175) Fachgebiet Proteomik, Technische Universität Muenchen, Am Forum 2, Freising Weihenstephan, D-85350, GERMANY

Adrienne R. Wells (**3**: 87) Department of Biology, Duke University, Durham, NC 27708-1000

Jørgen Wesche (**4**: 19) Department of Biochemistry, The Norwegian Radium Hospital, Montebello, Oslo, 0310, NORWAY

Pamela Whittaker (**3**: 463) Genotyping / Chr 20, The Wellcome Trust Sanger Institute, The Wellcome Trust Genome Campus, Hinxton, Cambridge, CB10 1SA, UNITED KINGDOM

John Wiemann (**3**: 87) Department of Biology, Duke University, B330g Levine Sci Bldg, Box 91000, Durham, NC 27708-1000

Sebastian Wiesner (**2**: 173) Dynamique du Cytosquelette, Laboratoire d'Enzymologie et Biochimie Structurales, UPR A 9063 CNRS, Building 34, Bat. 34, avenue de la Terrasse, Gif-sur-Yvette, F-91198, FRANCE

Ilona Wolff (**1**: 325) Prodekanat Forschung, Medizinnishce Fakultät, Martin Luther University Halle-Wittenburg, Magdeburger Str 8, Saale, Halle, D-06097, GERMANY

Ye Xiong (**2**: 259) The Department of Biochemistry and Molecular Biology, Wayne State University School of Medicine, 4374 Scott Hall, 540 E. Canfield, Detroit, MI 48201

David P. Yarnall (**3**: 471) Department of Metabolic Diseases, Glaxo Wellcome Inc, 5 Moore Drive, Research Triangle Park, NC 27709-3398

Hideki Yashirodas (**2**: 91) Laboratory of Frontier Science, Core Technology and Research Center, The Tokyo Metropolitan Institute of Medical Sciences, 3-18-22 Honkomagome, Bunkyo-ku, Tokyo, 133-8613, JAPAN

John R. Yates III (**4**: 383, 391) Department of Cell Biology, Scripps Research Institute, 10550 North Torrey Pines Road, La Jolla, CA 92037

Charles Yeaman (**2**: 189) Department of Cell and Developmental Biology, Weill Medical College of Cornell University, New York, NY 10021

Robin Young (**2**: 41) Département de pathologie et biologie cellulaire, Université de Montréal, Case postale 6128, Succursale "Centre-Ville", Montreal, QC, H3C 3J7, CANADA

Christian Zahnd (**1**: 497) Department of Biochemistry, Univerisity of Zürich, Winterthurerstr. 190, Zürich, CH-8057, SWITZERLAND

Zhuo-shen Zhao (**4**: 285) Glaxo-IMCB Group, Institute of Molecular and Cell Biology, Singapore, 117609, SINGAPORE

Huilin Zhou (**4**: 437) Department of Cellular and Molecular Medicine, Ludwig Institute for Cancer Research, University of California, San Diego, 9500 Gilman Drive, CMM-East, Rm 3050, La Jolla, CA 92093-0660

Timo Zimmermann (**3**: 69) Cell Biology and Cell Biophysics Programme, EMBL, Meyerhofstrasse 1, Heidelberg, D-69117, GERMANY

Chiara Zurzolo (**2**: 241) Department of Cell Biology and Infection, Pasteur Institute, 25,28 rue du Docteur Roux, Paris, 75015, FRANCE

Preface

Scientific progress often takes place when new technologies are developed, or when old procedures are improved. Today, more than ever, we are in need of complementary technology platforms to tackle complex biological problems, as we are rapidly moving from the analysis of single molecules to the study of multifaceted biological problems. The third edition of *Cell Biology: A Laboratory Handbook* brings together 236 articles covering novel techniques and procedures in cell and molecular biology, proteomics, genomics, and functional genomics. It contains 165 new articles, many of which were commissioned in response to the extraordinary feedback we received from the scientific community at large.

As in the case of the second edition, the *Handbook* has been divided in four volumes. The first volume covers tissue culture and associated techniques, viruses, antibodies, and immunohistochemistry. Volume 2 covers organelles and cellular structures as well as assays in cell biology. Volume 3 includes imaging techniques, electron microscopy, scanning probe and scanning electron microscopy, microdissection, tissue arrays, cytogenetics and in situ hybridization, genomics, transgenic, knockouts, and knockdown methods. The last volume includes transfer of macromolecules, expression systems, and gene expression profiling in addition to various proteomic technologies. Appendices include representative cultured cell lines and their characteristics, Internet resources in cell biology, and bioinformatic resources for in silico proteome analysis. The Handbook provides in a single source most of the classical and emerging technologies that are essential for research in the life sciences. Short of having an expert at your side, the protocols enable researchers at all stages of their career to embark on the study of biological problems using a variety of technologies and model systems. Techniques are presented in a friendly, step-by-step fashion, and gives useful tips as to potential pitfalls of the methodology.

I would like to extend my gratitude to the Associate Editors for their hard work, support, and vision in selecting new techniques. I would also like to thank the staff at Elsevier for their constant support and dedication to the project. Many people participated in the realization of the *Handbook* and I would like to thank in particular Lisa Tickner, Karen Dempsey, Angela Dooley, and Tari Paschall for coordinating and organizing the preparation of the volumes. My gratitude is also extended to all the authors for the time and energy they dedicated to the project.

Julio E. Celis
Editor

PART

A

TRANSFER OF MACROMOLECULES

SECTION

1

Proteins

CHAPTER

1

Impact-Mediated Cytoplasmic Loading of Macromolecules into Adherent Cells

Mark S. F. Clarke, Daniel L. Feeback, and Charles R. Vanderburg

I. INTRODUCTION

The advent of modern molecular biology, including the development of gene array technologies, has resulted in an explosion of information concerning the specific genes activated during normal cellular development, as well as those associated with a variety of pathological conditions. These techniques have provided a highly efficient, broad-based screening approach for those specific genes involved in regulating normal cellular physiology and identifying candidate genes directly associated with the etiology of specific disease states. However, this approach provides information at the transcriptional level only and does not necessarily indicate that the gene in question is in fact translated into a protein or whether posttranslational modification of the protein occurs.

The critical importance of posttranslational modification (i.e., phosphorylation, glycosylation, sialylation) to protein function has been recognized with regard to a number of proteins involved in a variety of important disease states. For example, altered glycosylation of the β-amyloid precursor protein results in an increase in the amount of β-amyloid peptide generated and hence secreted as insoluble extracellular amyloid deposits (Georgopoulou *et al.*, 2001; Walter *et al.*, 2001), a pathological hallmark of Alzheimer's disease. Abnormal phosphorylation of synapsin I has been linked to alterations in synaptic vesicle trafficking, leading to defective neurotransmission in Huntington's disease (Lievens *et al.*, 2002). Altered phosphorylation of the TAU protein involved in microtubule function has been linked to a number of neurodegenative diseases, such as Alzheimer's disease (Billingsley and Kincaid, 1997; Sanchez *et al.*, 2001). Aberrant sialylation of cell surface antigens has been detected in a number of different tumor cell types and has been linked to the acquisition of a neoplastic phenotype (Sell, 1990), whereas improper sialylation of sodium channels in cardiac tissue has been linked to heart failure (Ufret-Vincenty *et al.*, 2001; Fozzard and Kyle, 2002). In addition to the limitations associated with the total lack of information provided regarding posttranslational modification of the encoded protein, gene analysis cannot provide information on the role of protein–protein interactions within the cellular milieu. For example, a combination of gene and protein analysis may indicate that a particular protein is unregulated at both mRNA and protein levels, respectively. However, the presence of a regulatory protein(s) in the cellular milieu may result in this overexpression being of no physiological importance. For example, cytokine stimulation leading to an elicited cellular response is not only associated with the action of a particular cytokine at its specific receptor, but also with a cascade of downstream signal transduction events that are under the control of a variety of negative regulatory proteins (Carra *et al.*, 2000; Murphy *et al.*, 2000). Such protein–protein interactions underscore the complexity of the interplay between proteins in modulating cell function and are an excellent example of the limitations of gene analysis techniques in probing "cause-and-effect" relationships between gene expression and cellular response. It is the study of the interaction among gene expression, modified transcript splicing, and posttranslational modification on protein function as it impacts cellular/tissue phenotype, which is now the modern research field of proteomics.

One approach to overcoming the limitations of genetic analysis is to insert a protein of interest into a

Copyright 2006, Elsevier Science (USA).
All rights reserved.

cell and directly observe the effects on cell function. The direct "insertion" of a protein (in contrast to transfection of a genetic construct followed by protein expression) allows investigation of the functional role of the inserted molecule in determining cell phenotype in a fashion that also considers the role of protein–protein interactions in the cellular milieu. Insertion of individual or mixtures of purified proteins prepared in the ***native*** state also increases the possibility that any observed effects of the protein on cell phenotype/response are of true physiological relevance. As yet, such functional proteomic studies are limited by the availability of technologies that allow efficient insertion of native proteins directly into cells.

Microinjection (Bloom *et al*., 2003; Bubb *et al*., 2003), electroporation (Chow and Gawler, 1999; Ponsaerts *et al*., 2002), and lipid vesicle-mediated protein loading (Chen *et al*., 1993) all have been demonstrated to achieve protein insertion into cultured cells. Mechanical-based loading techniques such as biolistics (Maddelein *et al*., 2002), syringe loading (Clarke and McNeil, 1992), and scrape loading (McNeil *et al*., 1989) can also be used to load a variety of cell types with a range of proteins. However, apart from microinjection, which requires expensive equipment and skilled personnel to produce relatively few loaded cells, none of the aforementioned techniques have wide applicability to loading of either individual or mixtures of purified proteins into adherent primary cells in tissue culture. This article describes a technique, known as impact-mediated loading, that is capable of simultaneously loading a large number of adherent primary cells (>10,000 cells during a single procedure) with a variety of proteins at high efficiency. This approach is based on the production of transient plasma membrane wounds by particle impact with the cell membrane. We have used this technique previously in order to load dyes, antibodies, and plasmid constructs into the cytoplasm of a number of primary and established cell lines utilizing a crude, relatively uncontrolled experimental apparatus (Clarke *et al*., 1994). In addition, we have used a more refined version of this technique to study the effects of altered gravitational conditions on the membrane-wounding response of human primary myoblasts (Clarke *et al*., 2002). Based on observations made during these latter studies, we have developed a novel technology, known as the G-Loader (Fig. 1), which utilizes the effects of hypergravity at 200 *g* to enhance macromolecular loading into the cytoplasm of adherent cells via impact-mediated plasma membrane wounding (Clarke *et al*., 2001). The protocol described here specifically details the experimental approach used to load primary human skeletal myocytes with FITC-labeled IgG immunoglobulin as an example of the suitability of G-Loader technology for loading biologically active proteins into primary adherent cells.

II. MATERIALS AND INSTRUMENTATION

Dulbecco's modified Eagle's medium–F12 medium (X1 concentration) (DMEM/F12, Cat. No. 320-1885AG), bovine fetal calf serum (CS) (Cat. No. 200-6170AG), and penicillin–streptomycin solution (Cat. No. 600-5140AG) are obtained ready to use from Gibco BRL (Grand Island, NY). Alexa Fluor 488-labeled goat anti-mouse IgG (M_r 150,000 kDa) (Cat. No. A-11001) is obtained from Molecular Probes (Eugene, OR). Tissue culture flasks (T-75, T25, and 35-mm diameter plates) (Cat. Nos. 10-126-41, 10-126-26, and 25050-35) and sterile polypropylene conical centrifuge tubes (50 ml capacity) (Cat. No. 05-538-55A) are from Fisher Scientific (Pittsburgh, PA). The G-Loader technology and associated consumables are from Peilear Technologies (Houston, TX). Living cells loaded with fluorescently labeled IgG are examined utilizing an Zeiss Axiophot inverted microscope in order to view them in the 35-mm tissue culture plate directly.

III. PROCEDURES

A. Preparation of Tissue-Cultured Cells for Impact-Mediated Loading Using the G-Loader

Stock Solutions and Media Preparation

1. *Stock IgG solution*: Stock Alexa Fluor 488 goat anti-mouse IgG (2 mg/ml) can be stored at 4°C in the dark for up to a month or aliquoted and frozen in the dark at –80°C for storage up to a year. Prior to use on living cells, it is important to remove any preservative (e.g., sodium azide) from the immunoglobulin solution, as exposure of living cells to such contaminants can result in rapid cell death. Removal of such preservatives can be carried out using either a miniature dialysis device or buffer exchange using a 30,000 MW cutoff centrifugal miniature concentrator. One milliliter of stock IgG (2 mg/ml) solution should be dialyzed against a minimum of three changes of 100 ml of sterile DMEM/F12 medium over a period of 24 h prior to use. The total volume of dialyzed IgG solution should be adjusted to original volume prior to dialysis to maintain the overall IgG concentration. Buffer exchange using a centrifugal concentrator should

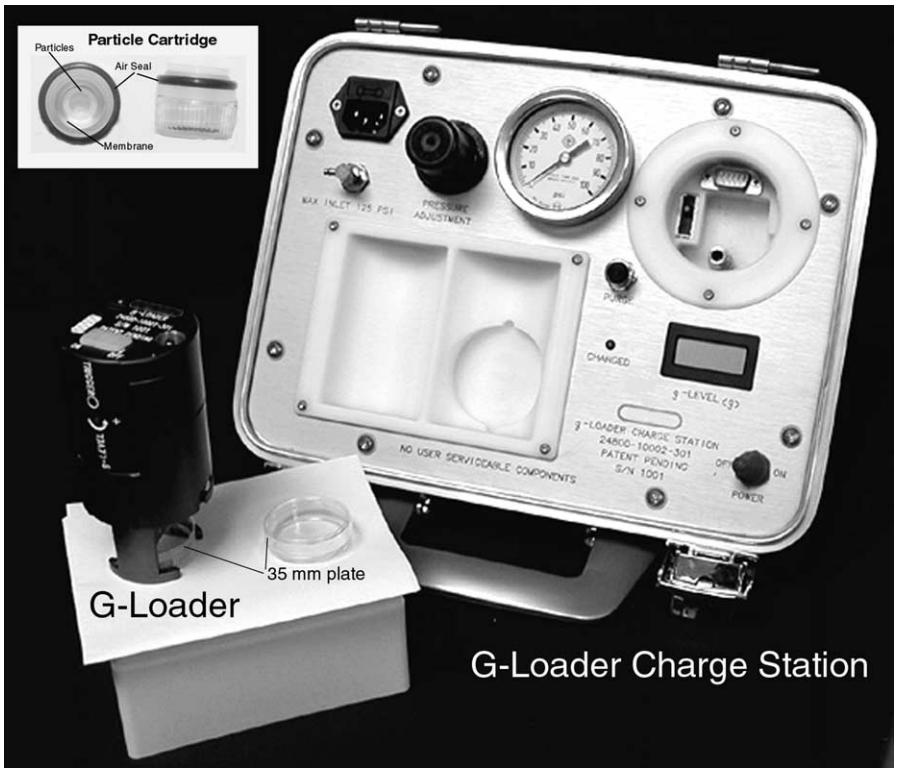

FIGURE 1 Impact-mediated loading apparatus known as the G-Loader. The G-Loader device itself is approximately 25 cm tall and 10 cm in diameter. A 35-mm tissue culture plate containing a monolayer of adherent cells is placed in the base of the G-Loader after being incubated with loading medium containing the macromolecule of interest. Prior to placing the cell sample into the G-Loader, a particle cartridge is inserted into the device consisting of a circular cartridge that supports a rupturable membrane on which is located a layer of 10-μm particles arranged in a specific pattern (see insert). In addition, the device has been charged with air to the required pressure and the on-board *g*-load accelerometer trigger has been set to the required *g* value using the G-Loader charging station (for benchtop operation there is a manual trigger button located on the side wall of the device). When the G-Loader is activated, either manually or by reaching a set *g* load, a metered volume of pressurized air is directed into the particle cartridge and the membrane ruptures and disperses particles into the airstream. The particles then impact the cell layer, inducing membrane wounding in a highly controllable and reproducible fashion.

involve a minimum of three complete exchanges of the original volume of stock IgG solution with serum-free DMEM/F12 medium.

2. *IgG loading solution*: Add 125 μl of stock IgG solution to 0.875 ml of serum-free DMEM/F12 to obtain final concentrations of 250 μg IgG/ml. Equilibrate this loading solution to the correct temperature and pH by incubating in a standard 5% CO_2 tissue culture incubator maintained at 37°C for a period of 30 min prior to loading cells with the IgG.

3. *10% FCS.DMEM/F12 tissue culture medium*: Add 5 ml of sterile penicillin/streptomycin solution and 50 ml of sterile fetal calf serum to 445 ml of sterile (X1) DMEM/F12 solution to obtain DMEM/F12 culture medium containing 10% FCS, 100 IU/ml penicillin, and 100 μg/ml streptomycin (10% FCS.DMEM). Store at 4°C for up to 21 days.

B. Culture of Human Primary Myoblasts

1. Obtain primary human myoblasts from the Clonetics Corporation (Walkersville, MD) and culture to confluence in T-75 (75 cm^2) culture flasks using 15 ml of 10% FCS.DMEM/F12 maintained at 37°C in a 5% CO_2 humidified atmosphere with subculture every fourth day.

2. The day prior to the loading procedure, trypsinize, collect by centrifugation, and resuspend cells in 5 ml of 10% FCS.DMEM/F12 as a single cell suspension. Determine the number of cells in the suspension using a hemacytometer and adjust cell density in the solution to 50,000 cells/ml using 10% FCS.DMEM/F12. Place 2 ml of this cell suspension into a 35-mm tissue culture plate and incubate cells overnight to allow formation of a monolayer. Under

these culture conditions the center of the 35-mm plate is between 60 and 80% confluent after 24 h of culture prior to loading.

3. Prior to loading, wash cells three times over a period of 5 min with warm, serum-free DMEM/F12 *containing no antibiotics* to remove any unattached cells and to wash away serum components that may interact with the IgG molecules being loaded.

C. Impact-Mediated Loading of IgG Using G-Loader Technology

1. Remove serum-free medium from the cell monolayer, replace with 400 µl of loading solution, and agitate the 35-mm plate gently so that the loading solution covers all of the culture surface. Agitate the loading solution for a minimum of 30 s to ensure that the dissolved macromolecule is in contact with the surface of the cells.

2. Remove the loading solution from the 35-mm plate by tilting the plate to one side and removing the loading solution with a 1-ml sterile pipette. *Note*: The loading solution can be reused on up to five additional 35-mm plates if used immediately after first centrifuging at 10,000 *g* for 1 min to remove any particulate/cellular material.

3. The cells are now ready to be loaded using the G-Loader technology. Place the 35-mm plate in the G-Loader and operate the firing mechanism in the tissue culture hood. Alternatively, the device and cells can be placed into the centrifuge and loading performed under hypergravity conditions (i.e., 200 *g*) (Fig. 1). In the case of human primary skeletal myoblasts and IgG loading, highly efficient cytoplasmic loading of IgG can be achieved without the need for the use of hypergravity conditions during impact-mediated loading.

4. Remove the 35-mm plate from the G-Loader and immediately place 2 ml of warm serum-free DMEM/F12 medium (without antibiotics) into the 35-mm plate to prevent drying of the cells. Gently wash the cell layer three times over 2 min with three changes of serum-free DMEM/F12 medium to remove both excess IgG and particles impacted with the cell surface.

5. Replace washing medium with 10% FCS.DME/F12 tissue culture medium and incubate for the required time period. After this time (0–24 h depending on the goal of the project), wash once with warm D-PBS (pH 7.2), replace with fresh D-PBS, and view the living cell monolayer by inverted fluorescent microscopy using UV excitation and emission at 488 nm.

IV. COMMENTS

This technology provides a highly efficient means of loading large macromolecules into living adherent cells with little or no disruption of the adherent monolayer. As can be seen in Fig. 2, there is little or no visually discernible damage to the cell monolayer 1 h after impact-mediated cytoplasmic loading of a 2×10^6-Da-sized fluorescent dextran. The protocol detailed here describes the procedure required to load fluorescently labeled IgG into cultured primary skeletal muscle cells (Fig. 3). In addition, this technique has been applied to a large number of different cell types and a wide variety of different macromolecules, including

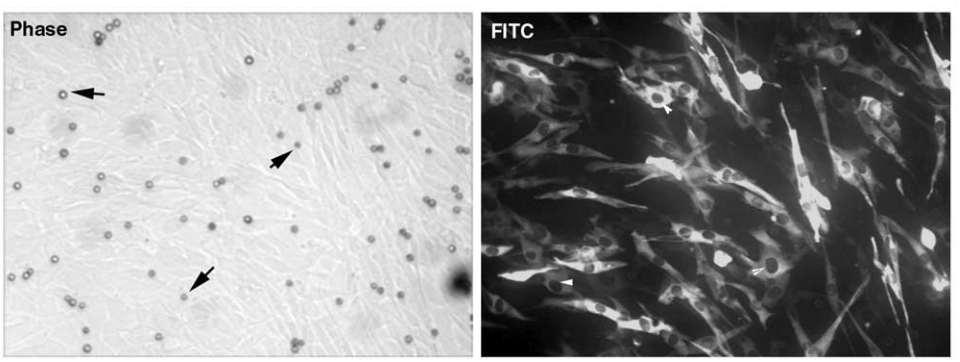

FIGURE 2 Paired phase-contrast and FITC-fluorescent micrographs of a Swiss 3T3 fibroblast monolayer 1 h after impact-mediated cytoplasmic loading of 2×10^6-Da fluorescent dextran (FDx). The monolayer was washed three times with warm serum-free DMEM to remove excess FDx (200 kDa) and to remove the majority of the particles (arrows). Note the clear exclusion of the 200-kDa dextran from the nuclear region of the cells (arrowheads) and little or no visual damage to the cell monolayer (left). Complete bead removal can be achieved by washing the monolayer multiple times with medium over a period of 4 h.

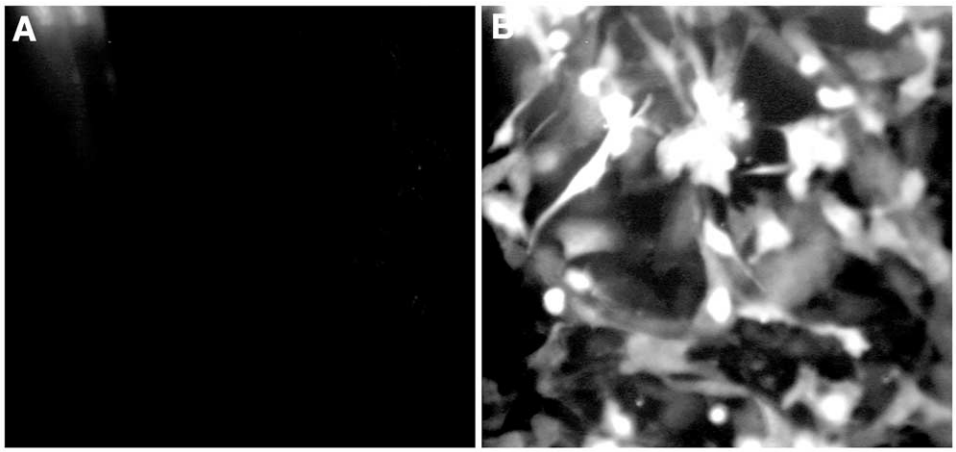

FIGURE 3 Fluorescent micrographs of (A) control and (B) Alexa Fluor 488 goat anti-mouse IgG-loaded primary human myoblasts. Control monolayers are treated in an identical fashion to loaded cells (including incubation with IgG loading solution) except that they are not subjected to impact-mediated loading. Micrographs were photographed under identical conditions immediately after loading and washing of monolayers. Note the somewhat "perturbed" appearance of the cells, an appearance that disappears after 20 to 60 min of additional culture in serum-containing medium (see Fig. 6).

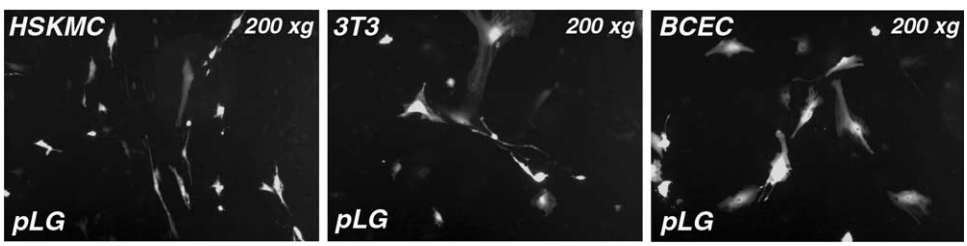

FIGURE 4 Fluorescent micrographs of primary human skeletal myoblasts (HSKMC), Swiss 3T3 cells (3T3), and primary bovine capillary endothelial cells (BCEC) 24 h after impact-mediated loading of a plasmid construct encoding for a green fluorescent protein, Lantern Green (pLG).

plasmid DNA constructs as a means of transfecting both primary and established cell lines (Fig. 4). Furthermore, this technique has the ability to simultaneously load two or more macromolecules directly into the cell cytoplasm of living cells, which are then localized to specific cellular compartments within the living cell based on size exclusion (Fig. 5). In addition, the use of hypergravity conditions during impact-mediated loading significantly increases the amount of fluorescently labeled IgG protein loaded into the cell cytoplasm (Fig. 6).

V. PITFALLS

The impact-mediated loading technology described here (i.e., The G-Loader) is a highly efficient means of simultaneously loading large numbers of living cells with large macromolecules. Under the conditions required for loading of macromolecules below 1×10^6 Da in size, the number of cells that are wounded, loaded, and survive the procedure is extremely high (approximately 70–80% of the starting population) (Fig. 1). One of the disadvantages of the technique described in this article for loading IgG is that not all cells in the 35-mm tissue culture dish are loaded. This is due to a limited particle impact area (approximately one-half of the culture area radiating from the center of the plate) generated by the device. This drawback can be overcome by growing cells only in the center region of the 35-mm plates utilizing a 20-mm-diameter cloning ring or plating cells on 20-mm-diameter glass coverslips located in the center of the 35-mm plates and removing the coverslips after loading. This approach yields a cell population in

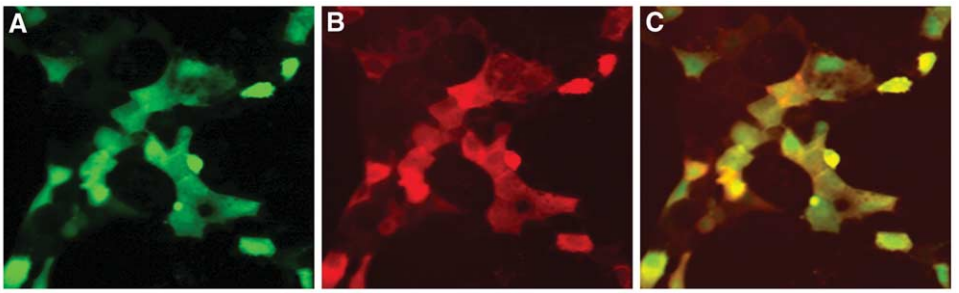

FIGURE 5 Matched fluorescent micrographs of NGF-differentiated PC-12 cells 20 min after impact-mediated loading of a mixture of fluorescently labeled dextrans. Two different-sized, different-colored dextran molecules (***green, FDx–10 kDa; red, TRITC–30 kDa***) were loaded simultaneously into monolayers of PC-12 cells using impact-mediated loading. Note exclusion of the larger dextran (red signal) from the nucleus of the cells (B), whereas the smaller dextran (green signal) is found in both the cytoplasm and the nucleus of the loaded cells (A). When a digital overlay of the images is generated, cells are colored predominantly orange in their cytoplasm (i.e., mixed red and green signal), whereas cell nuclei are green (C).

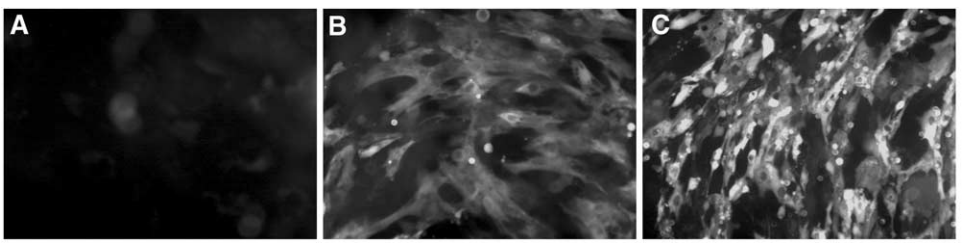

FIGURE 6 Fluorescent micrographs of Swiss 3T3 cell monolayers loaded cytoplasmically with Fluor 488 goat antimouse IgG employing impact-mediated loading at 1 *g* (B) and (C) 200 *g* in a benchtop centrifuge. Control cells (A) were exposed to IgG for the same period of time but were not impact loaded. Micrographs were taken at the same photographic conditions. Note the larger amount of IgG present in the cytoplasm of cells loaded at 200 *g* as compared to those loaded at 1 *g* and that IgG is excluded from the nuclear regions of the loaded cells.

which approximately 70–80% of the starting population is loaded. However, in those experiments where direct localization by microscopic techniques is utilized, the presence of unloaded cells in the region closest to the edge of the plate serves as an excellent internal negative control.

A second area of concern is the purity of the macromolecule that is being loaded. In initial experiments using commercially produced, fluorescently labeled IgG, IgM, and plant lectins, impact-mediated loading was observed at high efficiencies immediately after loading as determined by direct inspection of the cell layer by fluorescent microscopy. Subsequently, however, the majority of the cells died within 2 h of loading. After investigation, it was found that most commercially produced products had some form of preservative in the storage buffer that needed to be removed prior to contact with living cells during the loading procedure.

The G-Loader technology utilizes a combination of particle impact-induced membrane wounding and hypergravity conditions to load macromolecules directly into the cell cytoplasm. This technology appears to have utility for loading in a wide range of cell types, both established cell lines (e.g., COS, 3T3, C2C12 cells) and primary cell types (e.g., human myoblasts, bovine endothelial cells, chick corneal fibroblasts, rat gut epithelium), as well as multicellular microorganisms (e.g., hydra, nematodes, *Xenopus* ova). However, in order to achieve optimal loading efficiency, a mechanistic approach to determining impact pressure, macromolecular concentration in the loading solution, and whether or not hypergravity conditions are required for efficient loading is suggested. In addition, the nature of the macromolecule being loaded is also important. Those compounds that are highly charged or may interact with cell surface components may need longer contact with the

cells prior to loading, a higher loading solution concentration, or higher *g* load (i.e., 200 *g*) (Fig. 5) in order to achieve the most efficient cytoplasmic loading possible.

References

Billingsley, M. L., and Kincaid, R. L. (1997). Regulated phosphorylation and dephosphorylation of tau protein: Effects on microtubule interaction, intracellular trafficking and neurodegeneration. *Biochem. J.* **323**(Pt 3), 577–591.

Bloom, O., Evergren, E., Tomilin, N., Kjaerulff, O., Low, P., Brodin, L., Pieribone, V. A., Greengard, P., and Shupliakov, O. (2003). Colocalization of synapsin and actin during synaptic vesicle recycling. *J. Cell Biol.* **161**(4), 737–747.

Bubb, M. R., Yarmola, E. G., Gibson, B. G., and Southwick, F. S. (2003). Depolymerization of actin filaments by profilin: Effects of profilin on capping protein function. *J. Biol. Chem.* **278**(27), 24629–24635.

Carra, G., Gerosa, F., and Trinchieri, G. (2000). Biosynthesis and posttranslational regulation of human IL-12. *J. Immunol.* **164**(9), 4752–4761.

Chen, W., Carbone, F. R., and McCluskey, J. (1993). Electroporation and commercial liposomes efficiently deliver soluble protein into the MHC class I presentation pathway: Priming *in vitro* and *in vivo* for class I-restricted recognition of soluble antigen. *J. Immunol. Methods* **160**(1), 49–57.

Chow, A., and Gawler, D. (1999). Mapping the site of interaction between annexin VI and the p120GAP C2 domain. *FEBS Lett.* **460**(1), 166–172.

Clarke, M. S., and McNeil, P. L. (1992). Syringe loading introduces macromolecules into living mammalian cell cytosol. *J. Cell Sci.* **102**(Pt 3), 533–541.

Clarke, M. S., Vanderburg, C. R., and Feeback, D. L. (2002). The effect of acute microgravity on mechanically-induced membrane damage and membrane-membrane fusion events. *J. Gravit. Physiol.* **8**(2), 37–47.

Clarke, M. S., Vanderburg, C. R., Hay, E. D., and McNeil, P. L. (1994). Cytoplasmic loading of dyes, protein and plasmid DNA using an impact-mediated procedure. *Biotechniques* **17**(6), 1118–1125.

Clarke, M. S. F., Feeback, D. L., and Vanderburg, C. R. (2001). U.S. Patent Number **6,221,666.** "Method and apparatus for cytoplasmic loading using an impact-mediated procedure." USA.

Fozzard, H. A., and Kyle, J. W. (2002). Do defects in ion channel glycosylation set the stage for lethal cardiac arrhythmias? *Sci. STKE* **2002**(130), PE19.

Georgopoulou, N., McLaughlin, M., McFarlane, I., and Breen, K. C. (2001). The role of post-translational modification in beta-amyloid precursor protein processing. *Biochem. Soc. Symp.* **67**, 23–36.

Lievens, J. C., Woodman, B., Mahal, A., and Bates, G. P. (2002). Abnormal phosphorylation of synapsin I predicts a neuronal transmission impairment in the R6/2 Huntington's disease transgenic mice. *Mol. Cell Neurosci.* **20**(4), 638–648.

Maddelein, M. L., Dos Reis, S., Duvezin-Caubet, S., Coulary-Salin, B., and Saupe, S. J. (2002). Amyloid aggregates of the HET-s prion protein are infectious. *Proc. Natl. Acad. Sci. USA* **99**(11), 7402–7407.

McNeil, P. L., Muthukrishnan, L., Warder, E., and D'Amore, P. A. (1989). Growth factors are released by mechanically wounded endothelial cells. *J. Cell Biol.* **109**(2), 811–822.

Murphy, F. J., Hayes, M. P., and Burd, P. R. (2000). Disparate intracellular processing of human IL-12 preprotein subunits: Atypical processing of the P35 signal peptide. *J. Immunol.* **164**(2), 839–847.

Ponsaerts, P., Van den Bosch, G., Cools, N., Van Driessche, A., Nijs, G., Lenjou, M., Lardon, F., Van Broeckhoven, C., Van Bockstaele, D. R., Berneman, Z. N., and Van Tendeloo, V. F. (2002). Messenger RNA electroporation of human monocytes, followed by rapid *in vitro* differentiation, leads to highly stimulatory antigen-loaded mature dendritic cells. *J. Immunol.* **169**(4), 1669–1675.

Sanchez, M. P., Alvarez-Tallada, V., and Avila, J. (2001). The microtubule-associated protein tau in neurodegenerative diseases. *Rev. Neurol.* **33**(2), 169–177.

Sell, S. (1990). Cancer-associated carbohydrates identified by monoclonal antibodies. *Hum. Pathol.* **21**(10), 1003–1019.

Ufret-Vincenty, C. A., Baro, D. J., Lederer, W. J., Rockman, H. A., Quinones, L. E., and Santana, L. F. (2001). Role of sodium channel deglycosylation in the genesis of cardiac arrhythmias in heart failure. *J. Biol. Chem.* **276**(30), 28197–28203.

Walter, J., Fluhrer, R., Hartung, B., Willem, M., Kaether, C., Capell, A., Lammich, S., Multhaup, G., and Haass, C. (2001). Phosphorylation regulates intracellular trafficking of beta-secretase. *J. Biol. Chem.* **276**(18), 14634–14641.

CHAPTER

2

A Peptide Carrier for the Delivery of Biologically Active Proteins into Mammalian Cells: Application to the Delivery of Antibodies and Therapeutic Proteins

May C. Morris, Julien Depollier, Frederic Heitz, and Gilles Divita

I. INTRODUCTION

In order to circumvent the technological problems of gene delivery, an increasing interest is being taken in designing novel strategies to deliver full-length proteins into a large number of cells (Ford *et al*., 2001; Wadia and Dowdy, 2002). However, the development of peptide drugs and therapeutic proteins remains limited by the poor permeability and the selectivity of the cell membrane. Substantial progress has been made in the development of cell-penetrating peptide-based drug delivery systems that are able overcome both extracellular and intracellular limitations (Morris *et al*., 2000; Gariepy *et al*., 2001; Langel *et al*., 2002). A series of small protein domains, termed protein transduction domains (PTDs), have been shown to cross biological membranes efficiently, independently of transporters or specific receptors, and to promote the delivery of peptides and proteins into cells (for review see, Langel *et al*., 2002). The use of PTD-mediated transfection has proven that "protein therapy" can have a major impact on the future of therapies in a variety of viral diseases and cancers. TAT protein from immunodeficiency virus (HIV-1) (Schwarze *et al*., 1999; Schwarze and Dowdy, 2000), the third α helix of Antennapedia homeodomain (Derossi *et al*., 1994), VP22 protein from herpes simplex virus (Elliott and O'Hare, 1997), and transportan (Pooga *et al*., 2001), as well as polyarginine sequences (Futaki *et al*., 2000), have been used successfully to improve the delivery of covalently linked peptides or proteins into cells. However, PTDs display a certain number of limitations in that they all require cross-linking to the target peptide or protein. Moreover, protein transduction using the PTD-TAT-fusion protein system may require denaturation of the protein prior to delivery, introducing an additional delay between time of delivery and intracellular activation of the protein.

We have described a new strategy for the delivery of full-length proteins and peptides into mammalian cells based on a short amphipathic peptide carrier, Pep-1. This peptide carrier allows the delivery of several distinct proteins and peptides into different cell lines in a fully biologically active form, without the need for prior chemical covalent coupling or denaturation steps (Morris *et al*., 2001). Pep-1 is a 21 residue peptide (KETWWETWWTEWSQPKKKRKV) consisting of three domains with specific functions: a hydrophobic tryptophan-rich motif (KETWWETWWTEW), involved in the main interactions with macromolecules and required for efficient targeting to the cell membrane; a hydrophilic lysine-rich domain (KKKRKV) derived from the nuclear localization sequence (NLS) of simian virus 40 (SV-40) large T antigen, required to improve intracellular

Copyright 2006, Elsevier Science (USA).
All rights reserved.

delivery and solubility of the peptide vector; and a spacer domain (SQP), which improves the flexibility and the integrity of both hydrophobic and hydrophilic domains (Morris *et al*., 2001). Given that the mechanism through which Pep-1 delivers macromolecules does not involve the endosomal pathway, the degradation of macromolecules delivered is significantly limited and rapid dissociation of the Pep-1/macromolecule particle is favoured as soon as it has crossed the cell membrane. This peptide-based protein delivery strategy presents several advantages, including rapid delivery of proteins into cells with very high efficiency, stability in physiological buffers, lack of toxicity, and lack of sensitivity to serum. Pep-1 technology constitutes a powerful tool for basic research, and several studies have demonstrated that Pep-1 technology is extremely powerful for studying the role of proteins and for targeting specific protein/protein interactions *in vitro* as well as *in vivo* (Morris *et al*., 2001; Gallo *et al*., 2002; Wu *et al*., 2002, Pratt and Kurch, 2002, Aoshiba *et al*., 2003).

This article describes several protocols for the use of noncovalent Pep-1 technology for the delivery of biologically active proteins into mammalian cells *in vitro*.

II. MATERIALS AND INSTRUMENTATIONS

A. Products

β-Galactosidase is from the Chariot kit (Cat. No. 30025) or the β-galactosidase staining kit (Cat. No. 35001) from Active Motif (Carsbad-USA). Phosphate-buffered saline (PBS) (Cat. No. 14190-169), cell culture reagents Dulbecco's modified Eagle's medium (DMEM) (Cat. No. 41965-062), glutamine, and streptomycin/penicillin (Cat. No. 15140-130) are from Invitrogen Life Technologies (Carsbad, CA). Foetal bovine serum (FBS) is from PERBIO (Lot 3264EHJ, Cat. No. CH30160-03). Potassium ferricyanide (Cat. No. P3667), potassium ferrocyanide (Cat. No. P9387), magnesium chloride (Cat. No. M2670), 5-bromo-4-chloro-3-indolyl-β-D-galactopyranoside (X-gal; Cat. No. B4252), *N, N*-dimethylformamide (DMF) (Cat. No. D4551), formaldehyde (Cat. No. F8775), and glutaraldehyde (Cat. No. G5882) are from Sigma (St. Louis, MO).

B. Peptide Carrier Pep-1/Chariot

Pep-1 is 21 residue peptide KETWWETW WTEWSQPKKKRKV (molecular mass 2907 Da). The peptide is acetylated at it N terminus and carries a cysteamide group at its C terminus, both of which are essential for the stability of the peptide and the transduction mechanism (Morris *et al*., 2001). Pep-1 can be synthesized in house or obtained from commercial sources. Protocol for the synthesis and purification of Pep-1 and derivatives are described in Mery *et al*. (1993) and Morris *et al*. (1999, 2001). Also, Pep-1 is manufactured under the name of Chariot by Active Motif Inc. (Carlsbad, CA; http://www.activemotif.com, Cat. No. 30025). The protein transduction kit contains lyophilized Chariot and additional reagents required for the transduction protocol, including a positive transduction control (β-galactosidase Cat. No. 35001). All the protocols described for Pep-1 are directly transposable to Chariot.

III. PROCEDURES

A. Preparation of Pep-1/Protein or Pep-1/Peptide Complexes

This procedure is modified according to Morris *et al*. (2001).

Solutions

1. *Storage of Pep-1 powder*: Pep-1 is stable at least one year when stored at –20°C in a lyophilized form
2. *Stock solution of Pep-1*: Take the vial containing the peptide powder out of the freezer and equilibrate for 30 min at room temperature without opening the vial. This step is essential to limit hydration of the peptide powder. Resuspend the peptide at a concentration of 2 mg/ml (concentration: 0.68 m*M*) in water or in PBS buffer. Mix gently by tapping the tube or by vortexing at low speed for 20 s.
3. *Storage of the Pep-1 solution*: Because repeated freeze/thaw cycles can induce peptide aggregation, is recommended to aliquot the Pep-1 stock solution into tubes containing the amount you expect to use in a typical experiment prior to freezing. The Pep-1 stock solution is stable for about 2 months when stored at –20°C.

Steps

1. Dilute the amount of protein or peptide in 100 µl of PBS for each reaction. Use 0.5–1 µg of protein or 0.1–0.5 µg of peptide or low molecular weight protein per transduction reaction. The protein or peptide can be used at concentrations varying from 50 n*M* up

to 1 μ*M* or higher depending on the biological response expected.

2. For peptide or low molecular weight protein (<10 kDa) transduction, the Pep-1 solution must be diluted 1 : 10 in sterile H_2O (concentration: 68 μ*M*). At this stage, sonication of the peptide solution is recommended, to limit aggregation, for 5 min in a water bath sonicator. A probe sonicator can also be used: place the tube in water and sonicate for 1 min at an amplitude of 30%. In a tube dilute the appropriate volume of Pep-1 into 100 μl of sterile water or PBS for each reaction. For optimal transduction the molar ratio between Pep-1 and protein or peptide is generally 15 : 1 to 20 : 1.

3. Add 100 μl of diluted protein to 100 μl diluted Pep-1. Mix gently by tapping the tube. It is necessary to make the Pep-1/protein complex in a concentrated solution, which will be added to the cells and then be diluted to the final transduction volume (600 μl for 35-mm culture plate).

4. Incubate at 37°C for 30 min to allow the Pep-1/protein complex to form and then proceed immediately to the transduction experiments. At this stage, Pep-1/protein complexes should not be stored.

B. Protein Transduction Protocol for Adherent Cell Lines

The protocol is modified for 35-mm culture plates according to Morris *et al*. (2001). The amount of protein, Pep-1, transduction volume, and number of cells should be adjusted accordingly to the size of the culture plate used.

Steps

1. In a 6-well or a 35-mm tissue culture plate, seed 0.3×10^6 cells per well in 2 ml of complete growth medium. Incubate the cells at 37°C in a humidified atmosphere containing 5% CO_2 until the cells are 50–70% confluent. It is recommended to pass the cells the day before treatment for a better response following transduction.

2. Aspirate the medium from the cells to be transfected.

3. Wash the cells with PBS.

4. Overlay the cells with the 200 μl Pep-1/protein complex. Add 400 μl of serum-free medium to the overlay to achieve the final transduction volume of 600 μl for a 35-mm plate.

5. Incubate at 37°C in a humidified atmosphere containing 5% CO_2 for 1 h.

6. Add 1 ml of complete growth medium to the cells. Do not remove the Pep-1/protein complex. Then incubate at 37°C in a humidified atmosphere containing 5% CO_2 for 30 min to 24 h, depending on the cellular response expected. Peptides and proteins are fully released in the cells 1 and 2 h later, respectively.

7. Process the cells for observation or detection assays. Cells may be fixed or observed directly using live imaging technology.

8. For a 6-well plate, dilute Pep-1 into 600 μl of water or PBS and the protein into 600 μl of PBS. Mix the two solutions and then proceed as described in steps 1–7. For multiple transductions, do not use a mix that exceeds the volume required for six transductions per tube, as this may cause aggregation.

C. Protein Transduction Protocol for Suspension Cells

These conditions were optimized using several cell lines for the delivery of protein of size ranging from 5 to 100 kDa. However, efficient transduction may require optimization of Pep-1 concentration, cell numbers, and exposure time of cells to the Pep-1/protein complex.

Steps

1. The same number of cells recommended for seeding adherent cells is recommended for suspension cells (confluency between 50 and 70%). Culture cells in standard medium in 35-mm dishes or 6-well plates.

2. Form the Pep-1/protein or Pep-1/peptide complexes as described for adherent cells steps 1–4 in section III,A.

3. Collect the suspension cells by centrifugation at 400 *g* for 5 min. Remove the supernatant.

4. Wash the cells twice with PBS.

5. Centrifuge at 400 *g* for 5 min to pellet the cells. Remove the supernatant.

6. Solubilize the cell pellet in the Pep-1/protein or peptide complex solution (200 μl). Add serum-free medium to achieve a final transduction volume of 600 μl.

7. Incubate at 37°C in a humidified atmosphere containing 5% CO_2 for 1 h.

8. Add complete growth medium to the cells. Do not remove the Pep-1/protein or peptide complex. Continue to incubate at 37°C in a humidified atmosphere containing 5% CO_2 for 1 to 24 h depending on the expected cellular response. As described for adherent cells, peptides and proteins are fully released in the cells 1 and 2 h later, respectively.

9. Process the cells for observation or detection assays. Cells may be fixed or observed directly using live imaging spectroscopy.

D. Application: Transduction of β-Galactosidase as a Control Protein

Solutions

1. *Preparation of β-galactosidase*: β-Galactosidase is provided in a lyophilized form and stored at –20°C. Make a stock solution at 0.25 mg/ml in water. Aliquot into several tubes to avoid repeated freeze/thaw cycles, taking into account that 0.5–1.0 µg of β-galactosidase is used per transduction reaction on 35-mm plates. Store the stock solution at –20°C.

2. *Staining solution*: Prepare stock solutions in water. Mix 400 m*M* potassium ferricyanide (13.2 g for 100 ml), 400 m*M* potassium ferrocyanide (16.9 g for 100 ml), 200 m*M* of magnesium chloride (4.6 g for 10 ml), and 20 mg/ml X-Gal resuspended in DMF. Store solutions at –20°C in the dark. The staining solution should be prepared freshly: 250 µl of 400 m*M* potassium ferricyanide (4 m*M* final), 250 µl of 400 m*M* potassium ferrocyanide (4 m*M* final), 250 µl ml of 200 m*M* magnesium chloride (2 m*M* final), 1.25 ml X-Gal (20 mg/ml in DMF) (1 mg/ml final), and 23 ml of PBS.

3. *Fixation solution*: Prepare a 10-fold concentrated solution in PBS (10X) containing 20% formaldehyde and 2% glutaraldehyde. Store at 20°C.

1. Transduction Protocol

Steps

1. Dilute 6 µl of Pep-1 stock solution (0.68 m*M*) in 100 µl of sterile water.
2. Dilute 0.5 µg of β-Gal in 100 µl of PBS.
3. Add the Pep-1 solution to the β-Gal solution and mix gently
4. Incubate at 37°C for 30 min to allow the Pep-1/β-Gal complex to form.
5. Use the transduction protocol described in Section III,B (steps 1–7) for adherent cell lines and in Section III,C (steps 1–8) for suspension cell lines.

2. Staining Protocol

Steps

1. After 2 to 3 h, remove the growth medium from the transfected cells.
2. Rinse the cells three times with PBS.
3. Add fixing Solution. (Dilute the 10X stock in sterile water to make a 1X solution.) Incubate at room temperature for 5 min and rinse extensively with PBS.
4. Add a freshly made staining solution to the cells.
5. Incubate the cells at 37°C for 30 min to 2 h. Cells can be kept overnight at room temperature before analysis.
6. Analyze the percentage of cells transfected with β-galactosidase under a microscope.

E. Application: Delivery of Fluorescently Labelled Antibodies

Pep-1 strategy has been used for the delivery of antibodies into living cells. The protocol was optimized according to Morris *et al*. (2001) and to the Chariot guideline manual (www.activemotif.com).

Steps

1. Detection of fluorescently labelled antibodies in cells requires a large amount of antibody to be delivered. Depending on the sensitivity required to detect your antibody, it may be necessary to increase the amount of Pep-1 and antibody used. Using fluorescently labelled antibodies, concentrations in the final transduction volume of 0.1 µ*M* for antibody and 5 µ*M* for Pep-1 are recommended.
2. Incubate Pep-1 and antibody solution for 30 min at 37°C.
3. Overlay onto cultured cells for 1 to 3 h as described in Section III,C or III,D.
4. Extensively wash and observe cells by fluorescence microscopy. There is no need to fix the cells for observation.

IV. COMMENTS

A large variety of proteins, antibodies, and peptides have been successfully introduced into different cell lines using Pep-1/Chariot strategy and have been shown to retain their biological activity (Morris *et al*., 2001; Buster *et al*., 2002, Jurney *et al*., 2002; Gallo *et al*., 2002; Wu *et al*., 2002; Pratt and Kinch, 2002; Aoshiba *et al*., 2003). An update of published work using Chariot strategy is available on the Web site of Active Motif.

The advantages of the Pep-1 technology are directly associated with the mechanism through which this carrier promotes the delivery of proteins and peptides into cells.

a. The fact that Pep-1-mediated protein transduction is independent of the endosomal pathway significantly limits degradation and preserves the biological activity of the internalized protein for prolonged time periods.

b. An important property of Pep-1-based protein delivery is that it allows for the relatively rapid introduction of proteins into cells. That there is no need of covalent coupling for the formation of Pep-1/macromolecule particles favours rapid release of peptides or proteins into the cytoplasm as soon as the cell

membrane has been crossed. Then the final localization of the macromolecule is determined by its inherent intracellular targeting properties. Entry of Pep-1/macromolecule complexes into the cell occurs in a short time (10 min), and release of macromolecules varies from 1 to 3 h, depending on the nature of the protein and on its affinity for the target (Morris *et al*., 2001).

c. It is important that the process of complex formation between the Pep-1/protein was performed in the absence of serum to limit interactions with serum proteins. However, the transduction process itself is not affected by the presence of serum, which is a considerable advantage for most biological applications (Morris *et al*., 2001).

V. PITFALLS

1. Although this protocol was tested on several cells lines, conditions for efficient protein transduction should also be optimized for each cell line, including reagent concentration, cell number, and exposure time of cells to the Pep1/macromolecule complexes. β-Galactosidase should always be used as a positive control of transduction.

2. Low protein transduction efficiency may be associated with several parameters.

   a. For adherent cells, the optimal confluence is about 50–60%; a higher confluence (90%) reduces the transduction efficiency dramatically.

   b. Conditions for the formation of Pep-1/macromolecule complexes are critical and should be respected. Special attention should be paid to the recommended volumes, incubation times for the formation of Pep-1/macromolecule complexes, and time of exposure of these complexes to cells.

   c. ***Transduced macromolecules may be cytotoxic.*** Transfect the macromolecule at a lower concentration. Compare untransfected cells, cells incubated with Pep-1 alone, and cells with macromolecule alone. Transfect the β-galactosidase control protein.

3. Pep-1 interacts via hydrophobic and hydrophilic interactions. Each peptide or protein will have a different hydrophobicity pattern and may require a different amount of Pep-1. The association of Pep-1 with proteins depends on the structure and biophysical properties of both components of the complex, and thus complex formation may vary between different combinations of Pep-1 and macromolecules (Morris *et al*., 2001). The size of the protein or peptide may also affect the decaging procedure, and low efficiency may be observed for peptides shorter than 15 residues.

4. Diluting Pep-1 in dimethyl sulfoxide (DMSO) may improve the delivery of high molecular weight proteins and antibodies. Pep-1 should first be diluted in 60% DMSO and then combined with the antibody or protein dilution. The final concentration of DMSO should not exceed 20%. However, as this amount of DMSO may be toxic, it may need to be lowered for certain cell lines.

References

Aoshiba, K., Yokohori, N., and Nagai, A. (2003). Alveolar wall apoptosis causes lung destruction and amphysematous changes. *Am. J. Respir. Cell. Mol. Biol.* **28**, 555–562.

Buster, D., McNally, K., and McNally, F. J. (2002). Katanin inhibition prevents the redistribution of ã-tubulin at mitosis. *J. Cell Sci.* **115**, 1083–1092.

Derossi, D., Joliot, A. H., Chassaings, G., and Prochiantz, A. (1994). The third helix of the antennapedia homeodomain translocates through biological membranes. *J. Biol. Chem.* **269**, 10444–10450.

Elliott, G., and O'Hare, P. (1997). Intercellular trafficking and protein delivery by a Herpesvirus structural protein. *Cell* **88**, 223–233.

Ford, K. G., Souberbielle, B. E., Darling, D., and Farzaneh, F. (2001). Protein transduction: An alternative to genetic intervention? *Gene Ther.* **8**, 1–4.

Futaki, S., Suzuki, T., Ohashi, W., Yagami, T., Tanaka, S., Ueda, K., and Sugiura, Y. (2001). Arginine-rich peptides: An abundant source of membrane-permeable peptides having potential as carriers for intracellular protein delivery. *J. Biol. Chem.* **276**, 5836–5840.

Gallo, G., Yee, H. F., and Letourneau, P. C. (2002). Actin turnover is required to prevent axon retraction driven by endogenous actomyosin contractility. *J. Cell Biol.* **158**, 1219–1228.

Gariepy, J., and Kawamura, K. (2000). Vectorial delivery of macromolecules into cells using peptide-based vehicles. *Trends Biotechnol.* **19**, 21–26.

Langel, U. (2002). "*Cell Penetrating Peptides: Processes and Application*." CRC press, Pharmacology & Toxicology series.

Mery, J., Granier, C., Juin, M., and Brugidou, J. (1993). Disulfide linkage to polyacrylic resin for automated Fmoc peptide synthesis: Immunochemical applications of peptide resins and mercaptoamide peptides. *Int. J. Pept. Protein Res.* **42**, 44–52.

Morris, M. C., Chaloin, L., Heitz, F., and Divita, G. (2000). Translocating peptides and proteins and their use for gene delivery. *Curr. Opin. Biotechnol.* **11**, 461–466.

Morris, M. C., Chaloin, L., Mery, J., Heitz, F., and Divita G. (1999). A novel potent strategy for gene delivery using a single peptide vector as a carrier. *Nucleic Acids Res.* **27**, 3510–3517.

Morris, M. C., Depollier, J., Mery, J., Heitz, F., and Divita, G. (2001). A peptide carrier for the delivery of biologically active proteins into mammalian cells. *Nature Biotechnol.* **19**, 1173.

Pooga, M., Kut, C., Kihlmark, M., Hallbrink, M., Fernaeus, S., Raid, R., Land, T., Hallberg, E., Bartfai, T., and Langel, U. (2001). Cellular translocation of proteins by transportan. *FASEB J.* **8**, 1451.

Pratt, R. L., and Kinch, M. S. (2002). Activation of the EphA2 tyrosine kinase stimulates the MAP/ERK kinase signaling cascade. *Oncogene* **21**, 7690–7699.

Schwarze, S. R., and Dowdy, S. F. (2000). *In vivo* protein transduction: Intracellular delivery of biologically active proteins, compounds and DNA. *Trend Pharmacol. Sci.* **21**, 45–48.

Schwarze, S. R., Ho, A., Vocero-Akbani, A., and Dowdy, S. F. (1999). *In vivo* protein transduction: Delivery of a biologically active protein into the mouse. *Science* **285**, 1569–1572.

Wadia, J. S., and Dowdy, S. F. (2002). Protein transduction technology. *Curr. Opin. Biotechnol.* **13**, 52–56.

Wu, Y., Wood, M. D., Yi, T., and Katagiri, F. (2002). Direct delivery of bacterial avirulence proteins into resistant *Arabidopsis* protoplasts leads to hypersensitive cell death. *Plant J.* **33**, 130–137.

CHAPTER

3

Selective Permeabilization of the Cell-Surface Membrane by Streptolysin O

Jørgen Wesche and Sjur Olsnes

I. INTRODUCTION

Streptolysin O (SLO) is a bacterial exotoxin secreted by β-hemolytic streptococci. The toxin binds to cholesterol in the cell surface of mammalian cells where it oligomerises to form large pores in the plasma membrane (Bhakdi *et al*., 1985; Palmer *et al*., 1998). The pores can reach a diameter of 35 nm and allow the release of large proteins from the cytosol. Importantly, SLO binds to cholesterol on the plasma membrane at 4°C, while pore formation requires 37°C (Bhakdi *et al*., 1993). Thus, permeabilisation can be controlled easily by prebinding the toxin to cells at 4°C and then allowing permeabilisation to occur by incubating the cells at 37°C (Fig. 1).

SLO is used as a tool in cell biology to analyse the transport of toxins with intracellular targets (e.g., ricin and diphtheria toxin) and growth factors into the cytosol (Rapak *et al*., 1997; Wesche *et al*., 1999, 2000). In these experiments, labelled toxin or growth factor is added to intact cells and allowed to translocate into the cytosol before SLO is used to permeabilise the cells and allow the cytosolic proteins to leak out for analysis. In this way, only the protein that has reached the cytosol is obtained and not protein in intracellular membrane-bound compartments such as endosomes and the Golgi apparatus. This is very useful for studying the translocation of toxin mutants devoid of the enzymatic activity often used to assay translocation and for translocation of growth factors without defined cytosolic targets.

The toxin is also widely used in experiments involving semi-intact cells to follow cellular processes such as exocytosis and endocytosis. In these experiments, the plasma membrane is permeabilised selectively by SLO to release the cytosol without affecting intracellular membranes. Cytosol can then be added back either depleted for certain proteins or supplemented with antibodies or membrane-impermeable inhibitors and then cellular processes may be investigated under these conditions.

II. MATERIALS

Minimal essential medium with Earle's salts and without $NaHCO_3$ (Cat. No. 61100-087) is from GIBCO. HEPES (Cat. No. H-3375) and MESNA (2-mercaptoethanesulfonic acid sodium salt, Cat. No. M-1511) are from Sigma. SLO is from S. Bakhdi (for information on how to order SLO from Bhakdi's laboratory please consult http://www.mikrobiologie.medizin.uni-mainz.de/en/index.html). SLO can also be supplied by Sigma (Cat. No. S-5265).

III. PROCEDURES

A. Optimizing Permeabilisation

The concentration of toxin used to obtain optimal permeabilisation in the cells of interest must be determined experimentally. Increasing concentrations of the toxin should be tested for the optimal release of cytosolic components. An easy way to measure the degree of release is to measure the activity of the enzyme lactate dehydrogenase (LDH, 135 kDa). Commercial kits exist for the analysis of LDH activity (Sigma, Cat. No. TOX-7).

Copyright 2006, Elsevier Science (USA).
All rights reserved.

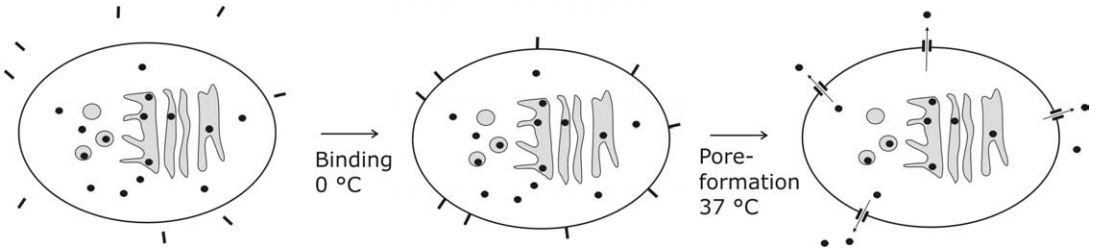

FIGURE 1 Selective permeabilisation using SLO. Radiolabelled ligand (black dots) may localise to intracellular membrane-bound compartments after endocytosis. Part of the ligand may also translocate to the cytosol. To discriminate between the different localisations, SLO is added (black lines) to selectively permeabilise the cell-surface membrane and allow the cytosolic proteins to leak out of the cell for analysis. SLO binds to the cell at 4°C, while insertion and pore formation require 37°C. Permeabilisation of the plasma membrane can therefore be controlled easily.

Solutions

1. *1 M MESNA*: To make 1 ml, dissolve 164.2 mg MESNA in 1 ml water
2. *HEPES medium*: Bicarbonate-free minimal essential medium with Earle's salts buffered with 20 m*M* HEPES to pH 7.4

Steps

1. Store SLO (~500 µg/ml) in aliquots at –80°C and thaw carefully on ice. To be active, SLO must be reduced by agents such as dithiothreitol or MESNA (MESNA is membrane impermeable and might be advantageous to avoid reduction of cellular components after addition of the toxin to cells).
2. Seed out cells growing in culture on tissue culture plates the day prior to the experiment. Before use, wash cells once in HEPES medium.
3. Dilute the toxin in HEPES medium to obtain the required concentrations (1–25 µg/ml) and add 10 m*M* MESNA to activate the toxin. After a 30-min incubation at 37°C with the reducing agent, add the toxin mixture to the cells and keep for 10 min at 4°C.
4. Remove nonbound toxin (and MESNA) by washing the cells once in HEPES medium.
5. Incubate the cells at 37°C for 10 min to allow permeabilisation to occur.
6. Transfer the cells to 4°C and keep for 30 min to let cytosolic proteins leak out into the medium.
7. The degree of permeabilisation can then be measured by analysing the release of the protein LDH into the medium. The optimal concentration of released LDH is normally between 60 and 80%. SLO concentrations that allow a higher release of LDH often affect intracellular membranes as well. To check if intracellular membranes have been affected, a Western blot analysis of organelle marker proteins may be used (Rapak *et al*., 1997). Ligands that are endocytosed by the cells, but not translocated to the cytosol (e.g., transferrin), can also be used to check if endosomes are affected by the treatment (Wesche *et al*., 2000).

B. Experiment

In the following experiment, translocation of the growth factor FGF-1 is used as an example of how SLO can be used to monitor translocation of an exogenously added protein to the cytosol.

Steps

1. Seed out NIH/3T3 cells on 6-wells tissue culture plates at a density of 2×10^5 cells per well. The next day, change the medium to medium containing 0.5% serum for starvation of the cells. After 24 h, add radiolabelled FGF-1 to the cells and incubate further for 6 h. Wash the cells once in HEPES medium and once in high salt/low pH medium (2 *M* NaCl, pH 4.0, in phosphate-buffered saline) to remove surface-bound FGF-1. (Pronase may also be used to remove surface-bound proteins.) Then wash the cells an additional time with HEPES medium.
2. Add SLO to the cells and keep for 10 min at 4°C.
3. Remove nonbound toxin by washing the cells in HEPES medium.
4. Incubate the cells at 37°C for 10 min to allow permeabilisation to occur.
5. Keep the cells at 4°C for 30 min to let cytosolic proteins leak out into the medium.
6. The content of the cytosol (released into the medium) can now be analysed by SDS–PAGE and fluorography (see Fig. 2). The remaining cell components can be lysed (1% Triton X-100 in HEPES buffer) and fractionated into a membrane and nuclear fraction by centrifugation (Fig. 2).

FGF-1 appears in the cytosol after 4 h and reaches a maximum after 6 h. FGF-1 is also found in the nuclear

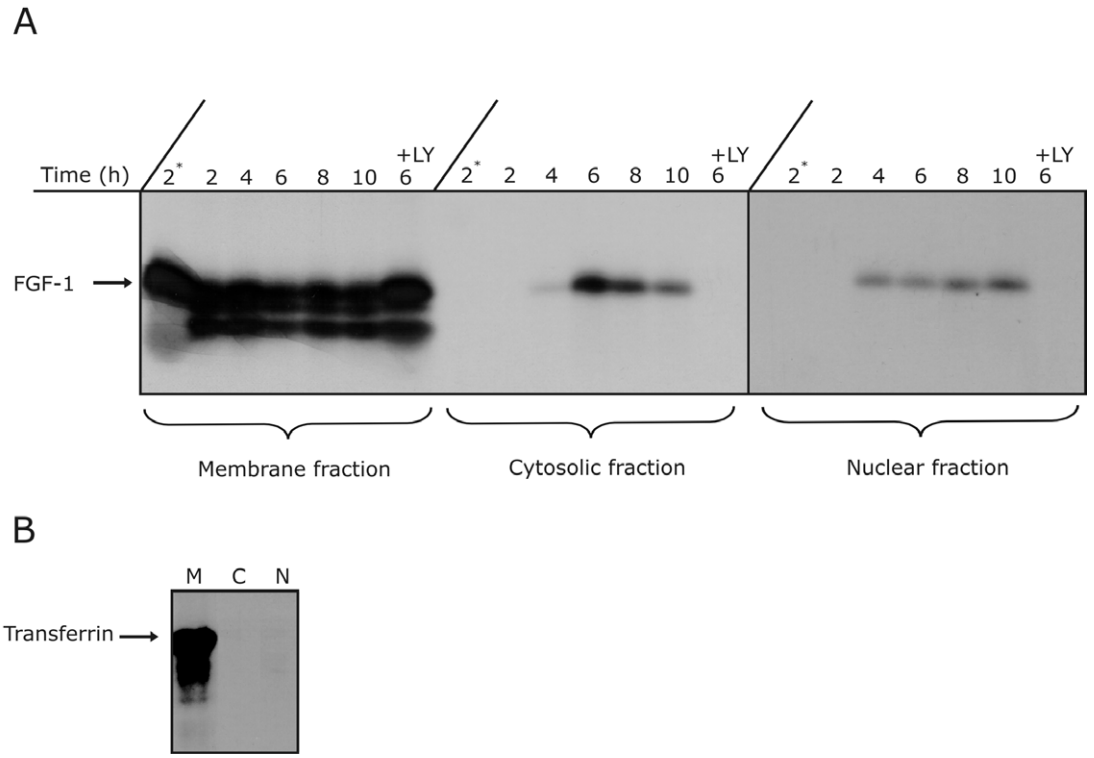

FIGURE 2 Transport of FGF-1 to the cytosol and the nucleus. Radiolabelled FGF-1 or transferrin was added to serum-starved NIH/3T3 cells and incubated for 6 h at 37°C. In lanes labelled +LY, the PI-3 kinase inhibitor LY294002 was added to block translocation to the cytosol and the nucleus. The time point labelled with an asterisk indicates that the incubation was performed at 4°C. The cells were then treated with SLO as described in the text. Cytosolic proteins were recovered from the medium and designated the cytosolic fraction. The remaining cell components were lysed with 1% Triton X-100 and fractionated into a nuclear fraction and a membrane fraction. FGF-1 was recovered from the different fractions by adsorption to heparin–Sepharose. The adsorbed material was analysed by SDS–PAGE and fluorography.

fraction. Transferrin that does not translocate to the cytosol or the nucleus is only found in the membrane fraction (Fig. 2).

IV. COMMENTS

The preparations of SLO vary a lot depending on the suppliers and there are also considerable batch variations. Each batch must therefore be tested for activity.

A mutant that does not require reduction has been constructed and has been reported to have the same activity as wild-type toxin (Pinkney *et al.*, 1989).

An alternative to SLO for plasma membrane permeabilisation is the mild nonionic detergent digitonin. As SLO, digitonin binds to cholesterol and therefore makes holes preferentially in the plasma membrane. A major difference, however, is that digitonin also permeabilises the cells at 4°C and is therefore more difficult to control.

Permeabilisation can also been done on cells in suspension by carefully centrifugating the cells between washes.

V. PITFALLS

SLO isolated from cultures of β-hemolytic streptococci may contain proteases that could cause cells growing on support to detach and may also attack intracellular proteins after permeabilisation (Bhakdi *et al.*, 1993).

Acknowledgment

J.W. is a fellow of the Norwegian Cancer Society.

References

Bhakdi, S., Tranum-Jensen, J., and Sziegoleit, A. (1985). Mechanism of membrane damage by streptolysin-O. *Infect. Immun.* **47**, 52–60.

Bhakdi, S., Weller, U., Walev, I., Martin, E., Jonas, D., and Palmer, M. (1993). A guide to the use of pore-forming toxins for controlled permeabilization of cell membranes. *Med. Microbiol. Immunol. (Berl)* **182**, 167–175.

Palmer, M., Harris, R., Freytag, C., Kehoe, M., Tranum-Jensen, J., and Bhakdi, S. (1998). Assembly mechanism of the oligomeric streptolysin O pore: The early membrane lesion is lined by a free edge of the lipid membrane and is extended gradually during oligomerization. *EMBO J.* **17**, 1598–1605.

Pinkney, M., Beachey, E., and Kehoe, M. (1989). The thiol-activated toxin streptolysin O does not require a thiol group for cytolytic activity. *Infect. Immun.* **57**, 2553–2558.

Rapak, A., Falnes, P. O., and Olsnes, S. (1997). Retrograde transport of mutant ricin to the endoplasmic reticulum with subsequent translocation to cytosol. *Proc. Natl. Acad. Sci. USA* **94**, 3783–3788.

Wesche, J., Rapak, A., and Olsnes, S. (1999). Dependence of ricin toxicity on translocation of the toxin A-chain from the endoplasmic reticulum to the cytosol. *J. Biol. Chem.* **274**, 34443–34449.

Wesche, J., Wiedlocha, A., Falnes, P. O., Choe, S., and Olsnes, S. (2000). Externally added aFGF mutants do not require extensive unfolding for transport to the cytosol and the nucleus in NIH/3T3 cells. *Biochemistry* **39**, 15091–15100.

SECTION

2

Genes

CHAPTER

4

New Cationic Liposomes for Gene Transfer

Nancy Smyth Templeton

I. INTRODUCTION

We developed improved liposomes that produce efficacy for the treatment of cancer (Ramesh *et al*., 2001; Shi *et al*., 2002; Tirone *et al*., 2001), cardiovascular diseases, and HIV-1 related diseases in small and large animal models. These liposomes condense nucleic acids, mixtures of nucleic acids and proteins, and viruses (Yotnda *et al*., 2002) on the interior of bilamellar invaginated vesicles (BIVs) produced by a novel extrusion procedure (Templeton *et al*., 1997). These nucleic acid : liposome complexes have extended half-life in the circulation, are stable in physiological concentrations of serum, have broad biodistribution, efficiently encapsulate various sizes of nucleic acids and other molecules, are targetable to specific organs and cell types, penetrate through tight barriers in several organs, are fusogenic with cell membranes, are optimized for nucleic acid : lipid ratio and colloidal suspension *in vivo*, can be size fractionated to produce a totally homogeneous population of complexes prior to injection, and can be administered repeatedly. We can add specific ligands either by ionic interactions or by covalent attachments to the surface of these nucleic acid–liposome complexes to accomplish targeted delivery to specific cell surface receptors. The ligands include monoclonal antibodies, Fab fragments, peptides, peptide mimetics, small molecules and drugs, proteins, and parts of proteins. In addition, the charge on the surface of these complexes can be modified in order to avoid uptake by nontarget cells using our novel technology called "reversible masking." We have also achieved high-dose systemic delivery of these complexes without toxicity *in vivo* by further purification of plasmid DNA. We have developed proprietary technologies for the detection and removal of contaminants found at high levels in clinical grade plasmid DNA preparations produced by several different companies. For instance, these DNA contaminants preclude high-dose delivery of complexes that may be required for the treatment of metastatic cancer. Our "Super Clean DNA" also provides for elevated levels of gene expression and prolonged transient expression *in vitro* and *in vivo*. Our complexes have been injected into mice, rats, rabbits, pigs, nonhuman primates, and humans. Currently, these complexes are injected intravenously into patients in clinical trials to treat lung cancer and will be used in upcoming trials to treat breast, pancreatic, head and neck cancers, hepatitis B and C, and restenosis. This article focuses on the production of these BIV liposomes and on mixing nucleic acid–liposome complexes. Because our processes are reproducible, we have standard operating procedures for the cGMP manufacture of these reagents that have been approved by the Food and Drug Administration for use in phase I/II clinical trials.

II. MATERIALS AND INSTRUMENTATION

The following materials are necessary: ethanol, paper towels, gloves, spatulas, 1-liter round-bottomed flask, cork ring to hold the round-bottomed flask, timer, small weigh boats, sterile 5% dextrose in water (D5W; Abbott Laboratories Inc. Part No. 1522-02), cGMP grade (Cat. No. 770890) or GLP grade (Cat. No. 890890) 18:1 dimethyldioctadecylammonium bromide (DOTAP) powder form (Avanti Polar Lipids), cGMP

Copyright 2006, Elsevier Science (USA).
All rights reserved.

grade synthetic cholesterol (Sigma Cat. No. C1231), ACS grade chloroform (Fisher Cat. No. C298-1), 0-grade argon gas, RBS pF detergent concentrate (Pierce Cat. No. 27960), sterile glass vials with screw tops, sterile 50-ml polypropylene conical tubes (Falcon Cat. No. 352098), sterile 15-ml polypropylene conical tubes (Falcon Cat. No. 352097), sterile polysulfone syringe filters 1.0 µm pore size 13 mm diameter (Whatman Cat. No. 6780-1310), sterile polysulfone syringe filters 0.45 µm pore size 13 mm diameter (Whatman Cat. No. 6780-1304), sterile ANOTOP syringe filters 0.2 µm pore size 10 mm diameter (Whatman Cat. No. 6809-1122), sterile ANOTOP syringe filters 0.1 µm pore size 10 mm diameter (Whatman Cat. No. 6809-1112), glass pipettes, sterile polystyrene pipettes, lens paper, parafilm, sterile 10-cc syringes (Becton Dickinson Cat. No. 309604), sterile water (Baxter Cat. No. 2F7114), sterile microfuge tubes, sterile pipette tips with no barriers, latex control particles (Beckman-Coulter Part No. 6602336), plastic cuvettes with caps (Beckman-Coulter Part No. 7800091), conductivity calibration standard (Beckman-Coulter Part No. 8301355), and EMPSL7 mobility standard (Beckman-Coulter Part No. 8304073).

The following instrumentation is necessary: Class II type A/B3 laminar flow biological safety cabinet (hood), vortex, analytical balance, rotary evaporator (Buchi Model R-114), vacuum aspirator (Brinkmann Model B-169), water baths, circulating water bath (Lauda Model E100), freeze dryer (Labconco Model Freezone 4.5), low-frequency sonicator (Lab-Line TansSonic Model 820/H), pipette aid, pipetmen, spectrophotometer (Beckman Model DU640B), spectrophotometer turbidity cell holder (Beckman Part No. 517151), UV silica-masked semimicrocell (Beckman Part No. 533041), submicron particle size analyzer with computer (Coulter Model N4 Plus), and zeta potential analyzer (Coulter Model Delsa 440SX).

III. PROCEDURES

A. Liposome Preparation

This procedure prepares 30 ml of BIV liposomes. The final yield is about 95%; therefore, approximately 28.5 ml of 5× stock liposomes is produced.

1. Clean all work surfaces and the hood with 70% ethanol.
2. Allow lipids, DOTAP, and synthetic cholesterol to come to room temperature.
3. Weigh 420 mg of DOTAP and place into a 1-liter round-bottomed flask.
4. Weigh 208 mg of synthetic cholesterol and place into the 1-liter round-bottomed flask.
5. Dissolve the lipids in 30 ml of chloroform.
6. Rotate on the rotary evaporator at 30°C for 30 min to make a thin film.
7. Dry the film in the flask under vacuum for 15 min.
8. Under the hood, add 30 ml of D5W to the film, cover with Parafilm, and make small holes in the Parafilm with a syringe needle.
9. Rotate the flask in a 50°C water bath for 45 min, rotating and swirling the flask until the film is in solution.
10. Place the flask in a 37°C water bath and continue to swirl for 10 min.
11. Cover the flask with more Parafilm (over the Parafilm with holes) and allow flask to sit overnight at room temperature.
12. The next day, remove the Parafilm with no holes and sonicate the flask at low frequency (35 kHz) for 5 min at 50°C.
13. Under the hood, place the contents from the flask into a sterile 50-ml tube and aliquot liposomes evenly into three sterile 15-ml tubes.
14. Place one 15-ml tube into a circulating water bath at 50°C (nearby the hood) for 10 min.
15. Under the hood, remove the plungers from four sterile 10-cc syringes and attach one of each pore size sterile filter (1.0, 0.45, 0.2, and 0.1 µm) to the syringes.
16. Under the hood, rapidly filter the liposomes through all four filters, starting with the largest pore size (1.0 µm) and ending with the smallest pore size (0.1 µm).
17. Under the hood, collect liposomes in a sterile 50-ml tube.
18. Repeat steps 14–16 for the remaining two 15-ml tubes and collect all liposomes in the same sterile 50-ml tube (listed in step 17) under the hood.
19. Under the hood, aliquot the liposomes into sterile glass tubes with screw caps, flush with argon or nitrogen gas through a 0.2-µm filter, and store at 4°C.
20. Rinse the round-bottomed flask with hot water, then with ethanol, and fill with 1× RBS and allow to sit overnight. The next day, rinse out the flask, then rinse with hot water, then with distilled water, and finally with ethanol. Seal the flask with Parafilm after it is dry.

B. Quality Assurance/Quality Control Testing for the Liposome Stock

1. Place 10 µl of liposomes into 190 µl of sterile water. Read the sample on the spectrophotometer at

OD_{400} using the turbidity holder and corresponding cuvette. The reading should be about 4.0, and the acceptable range is any reading lower than 4.5 OD_{400}.

2. Determine the size for the L100 and L200 standards using the particle size analyzer. If the standards are within range, proceed to assessing the liposome stock. Place 12 µl of liposomes into 4 ml of sterile water in the plastic cuvette. Determine the particle size, which should be about 200 nm, and the acceptable range is between 50 and 250 nm.

3. Access the mobility for the conductivity calibration standard and the mobility standard using the zeta potential analyzer. If the standard is within range, proceed to assessing the liposome stock. Place 120 µl of liposomes into 1880 µl of sterile water. Determine the zeta potential, which should be about 65 mV, and the acceptable range is between 50 and 80 mV.

4. Assays for residual chloroform in the liposome stock should not detect any chloroform. All sterility tests should show no observable growth or no contamination.

C. Complex Preparation

Using pipetmen and microfuge tubes, final volumes ranging from 50 to 1200 µl of complexes can be prepared.

1. Bring all reagents to room temperature.

2. Under the hood, dilute the 5× stock liposomes to 2× in D5W in a microfuge tube. For example, to mix a 300-µl final volume of complexes, dilute 60 µl of 5× stock liposomes in 90 µl of D5W.

3. Under the hood in a second microfuge tube, dilute the stock nucleic acid in D5W to 1 µg/ul. The volume of diluted nucleic acid must be identical to the volume of diluted stock liposomes in step 2. The final mixed complexes have a concentration of 0.5 µg of nucleic acid/ul. *Note*: The stock nucleic acid should be vortexed well prior to removing any aliquot for mixing complexes.

4. Under the hood, pipette the diluted nucleic acid into the diluted liposomes by rapid mixing at the surface of the liposomes. Rinse up and down about twice using the pipetman.

5. Read the sample (10 µl of the complexes in 190 µl of sterile water) on the spectrophotometer at OD_{400} using the turbidity holder and corresponding cuvette. The OD_{400} should be about 0.8, and the acceptable range is between 0.65 and 0.95 OD_{400}. If the complexes fall out of this range, then the amount of nucleic acid used for mixing must be adjusted. Specifically, if the OD_{400} is too low, then more nucleic acid must be used for mixing. If the OD_{400} is too high, then less nucleic acid must be used for mixing. If the nucleic acid is not adequately pure, then the appropriate OD_{400} of the complexes will not be obtained. *Note*: To avoid wasting material in order to establish the proper mixing conditions, we mix final volumes of complexes at 50 µl first before we begin large-scale mixing using new lots of nucleic acids.

6. When the proper mixing volumes have been established, more complexes can be mixed if needed following the steps given earlier. All complexes can be pooled after mixing, and the OD_{400} of the pooled complexes should be measured and should fall between 0.65 and 0.95 OD_{400}.

7. The particle size of the complexes can also be measured. Determine the size for the L300 and L500 standards using the particle size analyzer. If the standards are within range, proceed to assessing the complexes. Place 12 µl of complexes into 4 ml of sterile water in the plastic cuvette. Determine the particle size, which should be about 400 nm, and the acceptable range is between 200 and 500 nm.

8. Because the encapsulation of nucleic acids is spontaneous, the complexes can be administered after mixing. Complexes can also be stored in glass vials at 4°C and administered the following day.

IV. COMMENTS

The complexes can be administered and readministered into animals and humans by any delivery route. The dose and administration schedule will be determined by the specific nucleic acid therapeutic and disease model of the investigator and, therefore, must be optimized. Please also see Section V.

We have found that BIV DOTAP is best for transfection of cells in culture (Yotnda *et al*., 2002; N. S. Templeton, unpublished data). The same protocol is used to produce these liposomes; however, cholesterol is not added. Complexes made with BIV DOTAP are mixed using the procedure given earlier.

V. PITFALLS

1. Many investigators are not set up to produce liposomes in their laboratories. Therefore, the BIV liposomes and other custom services can be purchased from our nonviral core facility at the Baylor College of Medicine (contact Nancy Smyth Templeton at **NANCYT@bcm.tmc.edu** to place orders). The BIV DOTAP:Chol liposomes described here are also sold

by Qbiogene and are listed as the *In Vivo* GeneShuttle in their catalog.

2. Using the optimal liposomes for transfection is not necessarily enough to ensure success. Other reagents must be optimized, such as expression plasmid design (Lu *et al*., 2002) and plasmid DNA preparation (Templeton, 2002), for applications that use plasmid DNA.

References

Lu, H., Zhang, Y., Roberts, D. D., Osborne, C. K., and Templeton, N. S. (2002). Enhanced gene expression in breast cancer cells *in vitro* and tumors *in vivo*. *Mol. Ther.* **6**, 783–792.

Ramesh, R., Saeki, T., Templeton, N. S., Ji, L., Stephens, L. C., Ito, I., Wilson, D. R., Wu, Z., Branch, C. D., Minna, J. D., and Roth, J. A. (2001). Successful treatment of primary and disseminated human lung cancers by systemic delivery of tumor suppressor genes using an improved liposome vector. *Mol. Ther.* **3**, 337–350.

Shi, H. Y., Liang, R., Templeton, N. S., and Zhang, M. (2002). Inhibition of breast tumor progression by systemic delivery of the maspin gene in a syngeneic tumor model. *Mol. Ther.* **5**, 755–761.

Templeton, N. S. (2002). Liposomal delivery of nucleic acids *in vivo*. *DNA Cell Biol.* **21**, 857–867.

Templeton, N. S., Lasic, D. D., Frederik, P. M., Strey, H. H., Roberts, D. D., and Pavlakis, G. N. (1997). Improved DNA:liposome complexes for increased systemic delivery and gene expression. *Nature Biotech*. **15**, 647–652.

Tirone, T. A., Fagan, S. P., Templeton, N. S., Wang, X. P., and Brunicardi, F. C. (2001). Insulinoma induced hypoglycemic death in mice is prevented with beta cell specific gene therapy. *Ann. Surg*. **233**, 603–611.

Yotnda, P., Chen, D.-H., Chiu, W., Piedra, P. A., Davis, A., Templeton, N. S., and Brenner, M. K. (2002). Bilamellar cationic liposomes protect adenovectors from preexisting humoral immune responses. *Mol. Ther.* **5**, 233–241.

CHAPTER

5

Cationic Polymers for Gene Delivery: Formation of Polycation–DNA Complexes and *in vitro* Transfection

Yong Woo Cho, Jae Hyun Jeong, Cheol-Hee Ahn, Jong-Duk Kim, and Kinam Park

I. INTRODUCTION

Although nonviral gene delivery systems were first introduced with cationic lipids, cationic polymers (or polycations) have gained increasing attention in recent years as a nonviral vector for gene therapy due to their nonimmunogenicity and low acute toxicity. In both systems, DNA is incorporated into a complex by electrostatic interactions between anionic phosphate groups of DNA and cationic groups of lipids or polycations under physiological conditions. A large number of polycations have been studied as nonviral vectors, such as poly-L-lysine (Wu and Wu 1987), poly(ethylenimine) (Behr *et al*., 1999; Ahn *et al*., 2002), poly(amidoamine) dendrimers (Haensler and Szoka, 1993), poly(2-dimethylaminoethyl methacrylate) (Cherng *et al*., 1996), and chitosan (Lee *et al*., 1998). Cationic polymers have flexibility in designing a carrier with well-defined structural and chemical properties on a large scale as well as the ability to introduce functional moieties (e.g., targeting moieties). In general, the ability to vary and control the physicochemical properties in cationic lipid–based system is relatively limited. This article describes methods that are used commonly in characterizing polycation-based gene delivery systems in *in vitro* transfection, focusing on complex formation between polycations and DNA.

II. MATERIALS AND INSTRUMENTATION

HEPES (Cat. No. H4034), bicinchoninic acid (BCA) protein assay kit (Cat. No. BCA-1), fetal bovine serum (FBS, Cat. No. F3885), 100× penicillin–streptomycin (Cat. No. P0781), trypan blue (Cat. No. T0076), methylthiazoletetrazolium (MTT, Cat. No. M5655), and poly(L-aspartic acid) (Cat. No. P5387) are from Sigma (St. Louis, MO). Polyethylenimine (PEI, Cat. No. 40,872-7), glycerol (Cat. No. 19,161-2), and dimethyl sulfoxide (DMSO, Cat. No. 27,043-1) from Aldrich (Milwaukee, WI). Dulbecco's modified eagle's medium (DMEM, Cat. No. 12100-046) and 10× trypsin–EDTA (Cat. No. 15400-054) are from Gibco-BRL (Carlsbad, CA). Agarose (Cat. No. 161-3101), ethidium bromide (EtBr Cat. No. 161-0433), TBE (Tris/boric acid/EDTA, Cat. No. 161-0733), bromphenol blue (Cat. No. 161-0404), and xylene cyanole FF (Cat. No. 161-0423) are from Bio-Rad (Hercules, CA). The plasmid maxi kit (Cat. No. 12162) is from QIAgen (Valencia, CA). pSV-β-galactosidase (Cat. No. E1081), β-galactosidase enzyme assay system (Cat. No. E2000), pGL3 control containing the SV40 promoter-driven luciferase reporter gene (Cat. No. E1741), and Luciferase assay system (Cat. No. E1500) are from Promega (Madison, WI).

Copyright 2006, Elsevier Science (USA).
All rights reserved.

The spectrofluorometer (Spex FluoroMax-2) is from JY Horiba (Edison, NJ). The gel electrophoresis (Mini-PROTEAN 3 electrophoresis cell) system is from Bio-Rad. The microtiter plate reader (SOFTmax PRO) is from Molecular Device Corp. (Sunnyvale, CA). The luminometer (Lumat LB9507) is from Berthold Technologies (Oak Ridge, TN). The dynamic light scattering (90 plus) is from Brookhaven Instruments Corp. (Holtsville, NY).

III. PROCEDURES

A. Formation of Polycation/DNA Complexes (Polyplexes)

Solutions

1. *HEPES-buffered saline:* 15 m*M* HEPES, 150 m*M* NaCl, pH 7.4. To make 500 ml, add 1.787 g HEPES and 4.383 g NaCl to 480 ml water and adjust the pH to 7.4 with 1 *M* NaOH. Adjust the total volume to 500 ml with water. Sterilize the buffer by filtering through a filter with a 0.22-μm pore size.

2. *Plasmid stock solution:* Plasmid DNA (e.g., pSV-β-galactosidase or pGL3 control containing the SV40 promoter-driven luciferase reporter gene) is transformed into *Escherichia coli*. The transformed cells are grown in larger quantities (0.5–1.0 liter) of Luria and Bertan (LB) broth. The plasmid DNA is isolated using the plasmid maxi kit from QIAgen according to instructions of the manufacturer. The plasmid DNA is collected in HEPES-buffered saline and stored at 4°C. The purity is confirmed by 1% agarose gel electrophoresis, and DNA concentration can be measured by UV absorption at 260 nm.

3. *Polycation stock solution, 5 mg/ml in HEPES-buffered saline:* Dissolve 50 mg of a cationic polymer in 10 ml HEPES-buffered saline. Sterilize the polymer solution through a filter with a 0.22-μm pore size.

Steps

1. DNA: Dilute the plasmid DNA stock solution to a final concentration of 20 μg/ml in HEPES-buffered saline.

TABLE I Amount of Polyethylenimine (PEI) for Forming Polyplexes with Various N : P ratios[a]

N : P ratio	0.2	0.5	1.0	1.5	2.0	3.0	4.0	5.0	6.0
PEI (μl)[b]	0.10	0.26	0.52	0.77	1.03	1.55	2.06	2.58	3.10

[a] Twenty micrograms of DNA is used.
[b] PEI stock solution at 5 mg/ml in HEPES-buffered saline.

2. Cationic polymers: Make a series of dilutions in HEPES-buffered saline (see Table I). The N : P ratio is defined as the molar ratio of amino groups in polycations to phosphate groups in DNA.
3. Add polycation solutions to plasmid DNA solutions at different N : P ratios and vortex gently.
4. Incubate at room temperature for 30 min to allow complex formation.
5. Store at 4°C.

B. Analysis of Polycation/DNA Complexes

1. Ethidium Bromide Displacement Assay

The degree of DNA condensation by polycations can be determined by an EtBr displacement assay using a fluorometer (Wadhwa *et al*., 1995; Choi *et al*., 1998). Ethidium bromide intercalates between stacked base pairs of double-stranded DNA to give a significant increase of fluorescence intensity. Addition of a polycation causes a large drop in fluorescence intensity due to displacement of ethidium bromide molecules from DNA, which indicates the condensation of DNA to form complex particles.

Solutions

1. *Ethidium bromide at 10 mg/ml*: The stock solution should be stored in a bottle wrapped in aluminum foil at 4°C and in the dark.

2. *Plasmid DNA stock solution*: *(See solutions in Section III,A)*

3. *Stock solutions of polycations*: *(See solutions in Section III,A)*

Steps

1. The spectrofluorometer is operated with an excitation wavelength (λ_{ex}) of 510 nm and an emission wavelength (λ_{em}) of 590 nm. Use slit widths set at 10 nm and an integration time of 3 s. Perform all experiments in triplicate.
2. Dilute the DNA stock solution to a final concentration of 10 μg/ml, including 0.4 μg/ml EtBr in a test curvette (total volume of 2 ml).
3. Incubate the DNA solution for 15 min to ensure interactions between DNA and EtBr.
4. Measure the fluorescence and calibrate to 100%.
5. Measure the background fluorescence with EtBr alone and set to 0%.
6. Add aliquots of the polycation stock solution sequentially to the DNA solution at various N : P ratios, mix gently, and measure the fluorescence after each addition.
7. Plot the graph the relative fluorescence (%) *vs* N : P ratio.

8. Determine or compare the abilities of different polycations to condense DNA.

2. *Agarose Gel Retardation Assay*

The complex formation between polycations and DNA can be observed by a decrease of mobility of DNA in agarose gel electrophoresis (Ahn *et al*., 2002).

Solutions

1. *Ethidium bromide solution*: *See solutions in Section III,B*
2. *Loading buffer solution:* 0.25% (w/v) bromphenol blue, 0.25% (w/v) xylene cyanole FF, 5% glycerol
3. *Electrophoresis buffer solution*: The ionic strength and pH of the buffer can play major roles in complex stability. Standard electrophoresis buffers such as TBE (90 m*M* Tris–borate, 2 m*M* EDTA, pH 8.3) and TAE (40 m*M* Tris–acetate, 1 m*M* EDTA, pH 7.9) commonly prove satisfactory, but others such as TE (10 m*M* Tris, 1 m*M* EDTA) have been used.
4. *Dissociation buffer solution:* Dissolve 100 mg poly(L-aspartic acid) in 5 ml double distilled water.

Steps

1. Prepare polycation/DNA complexes at various N : P ratios in HEPES-buffered saline and incubate at room temperature for 30 min to allow the complexes to form properly.
2. Add aliquots of the polyplexes (20 µl) in Eppendorf tubes containing 2 µl gel-loading buffer and mix gently.
3. Load the complexes onto wells of the 0.8% agarose gel containing ethidium bromide (1 µg/ml). Also, apply the controls for free DNA and a free polycation to the gel.
4. Perform electrophoresis in 0.5× TBE buffer at 100 V until the bromphenol blue has migrated 5–7 cm through the gel.
5. Visualize and photograph the electrophoresed gel on an UV illuminator to show the location of DNA and complexes.
6. Incubate the gels in the dissociation buffer for 30 min to disturb polycation/DNA complexes and rephotograph the gel to show the presence of DNA dissociated from the polymer.

3. *Measurements of Particle Size*

Solutions

1. *Plasmid DNA stock solution in double-distilled water*: *See solutions in Section III,A*
2. *Stock solutions of polycations in double-distilled water*: *See solutions in Section III,A*

Steps

1. Turn on dynamic light-scattering equipped with a He–Ne laser at a scattering angle of 90°.
2. Set parameters for software. Set viscosity to 0.890 centipoise (cP), refractive index (RI) medium to 1.333 in water. However, if complexes are in 150 m*M* NaCl, set viscosity to 1.145 cP and RI medium to 1.340; if in HEPES, set viscosity to 1.546 cP and RI medium to 1.363. Set the temperature to 25°C for all the solutions.
3. Prepare 500-µl complexes at 20 µg/ml in test tubes and filter through a 0.45-µm filter. Cap the sample and allow it to equilibrate for 30 min before initiating measurements.
4. Calculate the particle size and size distribution using nonnegative least squares (NNLS) algorithms. When the difference between the measured and calculated baselines is less than 0.2%, accept the correlation function. If not, the concentration of complexes can be controlled to give a reasonable signal.
5. Measure the mean particle size, polydispersity factor using the Stokes–Einstein equation, and the cumulant method.

C. *In Vitro* Transfection

This procedure describes the *in vitro* transfection of 293T cells using cationic polymers, such as PEI and PLL, as a vector. The protocol can be used for all adherent cell types with slight modifications. For suspension type cells, cells need to be spun down before changing media.

Solutions

1. *HEPES-buffered saline*: *See solutions in Section III,A*
2. *Phosphate-buffered saline (PBS):* 137 m*M* NaCl, 2.7 m*M* KCl, 8.1 m*M* Na_2HPO_4, 1.47 m*M* KH_2PO_4, pH 7.4. To make 1 liter of 10× PBS, dissolve 80.06 g NaCl, 2.01 g KCl, 11.50 g of Na_2HPO_4, and 2.00 g KH_2PO_4 in 800 ml water. Adjust the pH to 7.4 with 1 *N* HCl. Adjust the total volume to 1 liter with water. To make 1 liter of 1× PBS, mix 100 ml 10× PBS (described earlier) with 900 ml of water. Sterilize the buffer through a filter with a 0.22-µm pore size.
3. *Tissue culture medium:* Tissue culture medium may vary, depending on the requirements of the cell line. Typically, Dulbecco's modified Eagle's medium (DMEM) supplemented with 10% fetal bovine serum, 100 units/ml penicillin–streptomycin, and 2 m*M* L-glutamine are used to maintain cell lines.
4. *Plasmid stock solution: See solutions in Section III,A*
5. *Stock solutions of polycations: See solutions in Section III,A*

6. *0.05% trypsin–0.02% EDTA solution (1×):* Add 10 ml of 10× trypsin–EDTA to 90 ml of PBS and store at 4°C

7. *0.5% trypan blue solution:* Dissolve 0.5 g trypan blue in 100 ml PBS and filtrate through a filtration paper to remove possible crystals. Store at –20°C

Steps

1. Passage 293T cells 3–4 days before the transfection experiment.
2. Detach the cells with trypsin–EDTA solution and determine the cell number and cell viability using trypan blue. Mix 50 µl cell suspension and 50 µl of 0.5% trypan blue solution. Bring the mixture into a counting chamber and count the number of uncolored (vital) and blue (dead) cells in a number of squares using a microscope. When more than 10 cells are counted per square, dilute the cell suspension and count again.
3. Seed cells in a 6-well tissue culture plate at a density of ~2×10^5 cells/well in 2 ml completed DMEM and incubate overnight at 37°C in a humidified atmosphere under 5% CO_2.
4. Prepare polycations/DNA complexes at various N : P ratios in HEPES-buffered saline and incubate for 20 min at room temperature (see steps in Section III,A).
5. Remove culture media from the cells and replace with 2 ml of serum-free DMEM.
6. Introduce 400 µl polyplexes to each well and incubate for 4 h at 37°C in an incubator.
7. Aspirate transfection media, replace with 2 ml of completed DMEM, and culture the cells in an incubator for 48 h at 37°C.
8. Evaluate the transfection efficiency.

D. Determination of Transfection Efficiency

1. β-*Galactosidase Activity*

The β-galactosidase activity in transfected cell lysates can be determined using the substrate *O*-nitrophenyl-β-D-galactopyranoside (ONPG).

Solutions

1. *Phosphate-buffered saline: See solutions in Section III,C*
2. β-*Galactosidase enzyme assay system with reporter lysis buffer (Promega) including reporter lysis buffer (5×), assay 2× buffer,* β-*galactosidase, 1 M sodium carbonate*

Steps

1. Remove growth media from the cells and wash twice with 2 ml PBS.
2. Add 200 µl of a lysis buffer to cover the cells and rock the 6-well plate slowly several times to ensure complete coverage of the cells.
3. Incubate at room temperature for 15 min.
4. Transfer the cell lysate to a microcentrifuge tube.
5. Centrifuge at top speed in a microcentrifuge for 2 min and transfer the supernatant to a fresh tube.
6. Pipette 50 µl of the cell lysates into wells of a 96-well plate.
7. Meanwhile, make a series of dilutions for the standard curve of β-galactosidase in 1× lysis buffer between 0 and 5.0×10^{-3} units. Prepare 50 µl of each β-galactosidase standard per well.
8. Add 50 µl of assay 2× buffer to each well of the 96-well plate and mix by pipetting.
9. Incubate at 37°C until faint yellow color has developed or the highest standard shows an absorbance of 2 or more.
10. Stop the reaction by adding 150 µl of 1 *M* sodium carbonate.
11. Measure the absorbance of the samples at 420 nm in a microtiter plate reader and calculate the β-galactosidase amount of a sample by comparing with the linear standard curve.
12. The β-galactosidase amount in each sample is normalized to milligrams of protein. Protein concentrations in cell lysates can be measured using a BCA protein assay kit according to instructions of the manufacturer.

2. Luciferase Activity

Solutions

1. *Phosphate-buffered saline: See solutions in Section III,C*
2. *Luciferase assay system (Promega) including a lysis buffer and luciferase assay reagent*

Steps

1. Remove growth media from the cells and wash twice with 2 ml PBS.
2. Add 200 µl of a lysis buffer to cover the cells and rock the 6-well plate slowly several times to ensure complete coverage of the cells.
3. Incubate at room temperature for 15 min.
4. Transfer the cell lysate to a microcentrifuge tube.
5. Centrifuge at top speed in a microcentrifuge for 2 min and transfer the supernatant to a fresh tube.
6. Dispense 20 µl of the supernatant into a luminometer tube.
7. Set the read time to 10 s (the read time can be varied).

8. Initiate reading by injecting 100 µl of Luciferase assay reagent into the tube.
9. Luciferase activity in each sample is normalized to milligrams of protein. Protein concentrations in cell lysates can be measured using a BCA protein assay kit according to instructions of the manufacturer.

E. *In Vitro* Cytotoxicity Assay

Cytotoxicity of polycation/DNA complexes can be evaluated by the MTT assay. The assay is based on the cleavage of the yellow tetrazolium salt, MTT, to form dark blue formazan crystals by active mitochondria dehydrogenases. This conversion only occurs in living cells.

Solutions

1. *MTT stock solution, 5 mg/ml in PBS*
2. *Tissue culture medium:* DMEM
3. *Polyplexes solution*

Steps

1. Seed cells in 24-well microplates at a density of ~4 $\times 10^4$ cells/well in 1 ml of completed DMEM and incubate overnight at 37°C in a humidified atmosphere under 5% CO_2.
2. Remove culture media from the cells and replace with 1 ml of serum-free DMEM.
3. Introduce 40 µl of polyplexes to each well and incubate for 4 h at 37°C in an incubator.
4. Aspirate transfection media, replace with 1 ml of completed DMEM, and culture cells in an incubator for 48 h at 37°C.
5. Remove old media and replace with new completed DMEM.
6. Add 50 µl of 5 mg/ml MTT solution to each well and incubate for 4 h at 37°C.
7. Remove MTT-containing media and add 750 µl of dime to each well and pipette up and down to dissolve formazan crystals formed by live cells.
8. Measure the absorbance at 570 nm using a microtiter plate reader
9. Calculate the absorbance percentage relative to that of untreated control cells.

IV. COMMENTS

Complex formation between polycations and DNA can be affected by several factors, such as the nature of the cation, the molecular weight of the polycation, the molecular architecture of the polycation, and the N : P ratio. Full complexation to form stable nanoparticles between 20 and 100 nm is necessary for effective transfection. Generally, shorter polycations need a higher N : P ratio to achieve full condensation.

V. PITFALLS

1. Large aggregates or precipitated materials can be observed in some cases. They lower the transfection efficiency and may cause toxic effects to cells. They may occur when the N : P ratio is too low or the pH of the transfection medium is too high. Generally, small cationic particles can be formed at the excess of positive groups of polycations compared with negative groups of DNA.

2. The size of polycation/DNA complexes may vary in different buffers mainly due to their different ionic strengths.

3. In some cases, complex particles may not be spherical. Particles with any extended structures may be ignored with light scattering, which leads to inaccurate results. Therefore, the morphology of complex particles must be checked using transmission electron microscopy or atomic force microscopy, as well as characterizing their size and distribution using light scattering.

4. Cell transfection can be performed in the absence or presence of serum. The effect of serum in the transfection medium will vary depending on the nature of polycations.

5. Cells of high passage number are transfected inefficiently.

References

Ahn, C.-H., Chae, S. Y., Bae, Y. H., and Kim, S. W. (2002). Biodegradable poly(ethylenimine) for plasmid DNA delivery. *J. Control. Release* **80**, 273–282.

Behr, J. P., Kichler, A., and Erbacher, P. (1999). Polyethylenimine: A family of potent polymers for nucleic acid delivery. *In "Nonviral Vectors for Gene Therapy"* (L. Huang, M.-C. Hung, and E. Wagner, eds.), pp. 192–207. Academic Press, New York.

Cherng, J.-Y., Wetering, P. V. D., Talsma, H., Crommelin, D. J. A., and Hennink, W. E. (1996). Effect of size and serum proteins on transfection efficiency of poly((2-dimethylamino)ethyl methacrylate)-plasmid nanoparticles. *Pharm. Res.* **13**, 1038–1042.

Choi, Y. H., Liu, F., Kim, J.-S., Choi, Y. K., Park, J. S., and Kim, S. W. (1998). Polyethylene glycol-grafted poly-L-lysine as polymeric gene carrier. *J. Control. Release* **54**, 39–48.

Haensler, J., and Szoka, F. C., Jr. (1993). Polyamidoamine cascade polymers mediate efficient transfection of cells in culture. *Bioconj. Chem.* **4**, 372–379.

Lee, K. Y., Kwon, I. C., Kim, Y.-H., Jo, W. H., and Jeong, S. Y. (1998). Preparation of chitosan self-aggregates as a gene delivery system. *J. Control. Release* **51**, 213–220.

Wadhwa, M. S., Knoell, D. L., Young, A. P., and Rice, K. G. (1995). Targeted gene delivery with a low molecular weight glycopeptide carrier. *Bioconj. Chem.* **6**, 283–291.

Wu, G. Y., and Wu, C. H. (1987). Receptor-mediated *in vitro* gene transformation by a soluble DNA carrier system. *J. Biol. Chem.* **262**, 4429–4432.

CHAPTER

6

Electroporation of Living Embryos

Takayoshi Inoue, Kristen Correia, and Robb Krumlauf

I. INTRODUCTION

Gene transfer by electroporation (EP) has been widely used to introduce exogenous molecules into both prokaryotic and eukaryotic cells. In the process of EP, transient pores at the cellular membrane are generated by electric shocks, allowing charged macromolecules such as DNAs, RNAs, and proteins to actively penetrate into cells by means of electrophoresis (Fig. 1A). Noncharged molecules can also be incorporated into cells by molecular diffusion. It was Japanese physicians who initially tried to perform gene therapy with EP *in vivo* (Okino and Mohri, 1987; Nishi *et al.*, 1996). However, the main difficulty in applying this approach to living tissues or organisms in the past was that the electric shocks often damaged cells and resulted in substantial cell death. A key breakthrough was the discovery that a rapid series of controlled square wave pulses (Fig. 1B) reduces the level of cell death dramatically. Using this modification, Muramatsu and colleagues (1997) reported the first remarkable results of EP-mediated gene transfer into developing chicken embryos. Based on these observation, chick embryologists around the world are now routinely utilizing this convenient technology perfected in Japan and it is also being applied to many other living tissues and organisms, including mammals (Momose *et al.*, 1999; Akamatsu *et al.*, 1999; Hass *et al.*, 2001; Reviewed in Itasaki *et al.*, 1999; Yasugi and Nakamura, 2000; Shwartz *et al.*, 2001; Inoue and Krumlauf, 2001; Osumi and Inoue, 2001; Takahahi *et al.*, 2002). As EP-mediated gene transfer is relatively nontoxic to cells and/or tissues and it is possible to precisely control the area selected for transfection (Fig. 1A), the method could further provide a powerful tool for human gene therapy. This article summarizes optimal conditions for EP-mediated gene transfer into chicken and mouse embryos, particularly with respect to situations for controlling the area of transfection.

II. PROCEDURES

A. EP-Mediated Gene Transfer in Chicken Embryos at the Early Primitive Streak Stage (HH stage 3+/5–)

Materials and Instrumentation

A variety of methods to efficiently target restricted regions in chicken embryos by EP have been described previously (Muramatsu *et al.*, 1997; Momose *et al.*, 1999; Itasaki *et al.*, 1999; Yasugi and Nakamura, 2000; Schwarts *et al.*, 2001). Above all, Momose *et al.* (1999) reported the microelectroporation method in which they can precisely target a confined region using the various positioning of a needle type and a wire type electrode. Here we introduce a modified protocol to facilitate EP into relatively young chicken embryos (stages HH 3+/5–). The following materials are required for this protocol.

Tape (3M scotch tape 1 in. width, 3M, USA); needle/spatula (#18-568, Miltex Instruments, USA); blunt scissors (#18-1478, Miltex Instruments, USA); transfer pipette (#232-205, Samco, USA); capillary tubes (#GC150F-10, Harvard Apparatus, USA); electrophoresis pipette tips (#23 35 165-6, Eppendorf, Germany); electroporator (CUY21, Bex Co. Ltd., Japan); electronic leads and 0.5-mm-diameter platinum wire electrode (Computech, USA); and forceps (#17-305X, Miltex, USA).

Copyright 2006, Elsevier Science (USA).
All rights reserved.

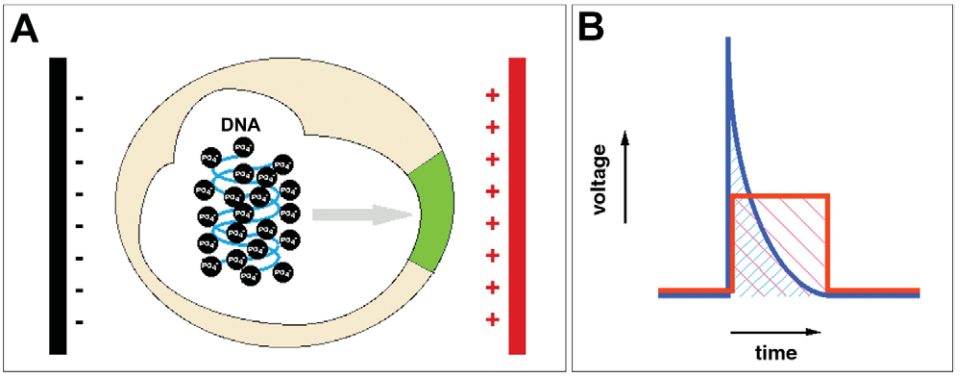

FIGURE 1 (A) The principle of electroporation (EP)-mediated gene transfer. As the DNA molecule includes negatively charged phosphate groups in its backbone (black circles), it naturally charges negative as a whole and will migrate toward the positive electrode (red) in the process of EP. As a result, a restricted area (green) can be targeted in the relevant tissue. (B) For living tissues or embryos, controlled square pulses (red) instead of canonical ones simply decay exponentially (blue) should be applied during EP. Note that the square pulse generates higher amount of energy at relatively lower voltages than the canonical one (the amount of energy is equal to the area with blue or red oblique).

Solutions

1. Plasmid DNA, Qiagen column purified and resuspended in sterile ddH_2O
2. 5% fast green (#EM-4510, VWR)
3. 10X phosphate-buffered saline (PBS): Add 8 g NaCl, 0.2 g KCl, 1.15 g Na_2HPO_4, and 0.2 g KH_2PO_4 to 100 ml of H_2O. Autoclave.

Steps

1. Preparing the DNA. On the day of EP, make 5 µl of solution containing 2 µg/µl plasmid DNA and 0.005% fast green in 1X PBS. It is possible to use two or more different plasmids (see comments later). Centrifuge the DNA solution for 30 s at 13,000 rpm to remove any particulates that might clog the capillary tip. Load 5 µl of the DNA solution into a pulled capillary tube using an electrophoresis pipette tip. Allow the DNA solution to reach the tip of the capillary tube and connect the capillary to a suction pipette.

2. Incubating the eggs. Incubate the eggs on their side until HH stage 3+/5–. This should be approximately 24 h in a humidified incubator at 35°C. Remove the eggs and set a timer for 2 h. Spray the top of the eggs with 70% ethanol and wipe off any debris. Put a piece of tape on the top of each egg, lengthwise. Adhere the tape to the eggshell, making sure that all creases are completely sealed to prevent leaking of egg white. The concave side of the spatula can be used to flatten the tape against the egg.

3. Opening the eggs. Set an egg horizontally on the egg holder. Use the point of the blunt scissors to put a hole in the top of the egg. Cut a long, 2 × 3-cm oval within the taped area of the egg, using short cuts to prevent cracking, leave the shell attached, and fold back. The embryo should be located in the center of the yolk. If the embryo is not at the center of the yolk, discard the egg. Remove any bubbles and 1–2 ml of thin egg white with a transfer pipette to lower the level of the embryo below the cut edge of the shell. Cover the embryo with a drop of thin egg white using the transfer pipette.

4. Staging the eggs. Place the egg under the microscope. Illuminate the egg from one side to view and stage the embryo (Hamburger and Hamilton 1951). Do **not** inject ink, as this will kill the embryo. Stage 3 embryos are round, whereas stage 4 to 5 embryos are pointed near the posterior end. The streak will be half the embryo length at stage 3 and three-quarters the embryo length at stage 4. At stage 5, the head process is visible anterior to the streak. If the embryo is abnormal in its development (if the shape is not symmetrical or if there is more than one streak), discard the egg. To optimize survival while electroporating the posterior mesoderm, choose embryos that are stage 4+/5–. To electroporate the most anterior mesoderm, such as head mesoderm and anterior somites, choose embryos that are stage 3+/4–.

5. Injecting DNA solution. To make a small hole in the vitelline membrane over the embryo, run the capillary tip over the membrane to create a small fold over the tip. Then lift the tip quickly, cutting a small hole in the fold. Insert the needle tip into the hole in the membrane and inject about 0.25 µl of DNA into the space

between the embryo and the membrane (Fig. 2A). Be careful not to scratch the surface of the embryo with the capillary tip. If the capillary tip becomes clogged, run the tip over the taped edge of the eggshell while expelling the DNA solution. After injection, the DNA should diffuse over the top of the embryo. If the yolk was injected, the DNA will be localized in a small area. If the DNA diffuses past the outside boundary of the embryo, then the DNA was injected on top of the vitelline membrane. In good injections, the primitive streak should be highlighted by the fast green tracer (Fig. 2A inset). Fast green can also highlight scratches in the surface of the embryo made by the capillary tip.

6. Performing electroporation. Set the electroporator to 7 V; 50 ms time length of the pulse (pON); 150 ms time length between pulses (pOFF); and three repetitions of pulses. Position the ends of the upper negative (black) and lower positive (red) wires parallel to one another and 4 mm apart (Fig. 2A). At about 20 mm from the ends, bend both wires up and back to help avoid contacting the eggshell when the electrode is positioned over the embryo. Dip electrode briefly in egg white. Pierce the yolk outside of the area opaca, about 25 mm posterior to the embryo with the forceps. Insert the lower wire and let the yolk settle back in place. Approximately 1 cm of the lower electrode should be contacting the egg white and yolk. Position the upper wire over the streak with the end at the node and the side covering the streak. Approximately 2 mm of the upper electrode should be contacting the surface of the egg white. This situation makes a radial electric field rather than a parallel one, enabling one to target a confined area giving rise to somites. While administering the pulses, small bubbles should form on the upper visible electrode tip. After administering the pulses, carefully remove the electrode and wipe it clean with a paper towel.

7. Reincubation of the egg. Replace the shell and tape up the window using two overlapping pieces of tape. Make sure that all creases are completely sealed to prevent leaking of egg white. Eggs should be returned to the incubator within 2 h of having been removed for maximum viability. After 24 h the electroporated DNA reporters should be expressed in the posterior somites and presomitic mesoderm if electroporated at stage 4+/5– (Figs. 2B–2E) and in the head mesoderm and anterior somites if electroporated at stage 3+/4– (Figs. 2F–2I).

Comments

1. **Promoters.** The expression plasmid pCA (see Section II,B) used in these experiments directs very strong and ubiquitous expression in most tissues of chick embryos. Other plasmids containing promoters

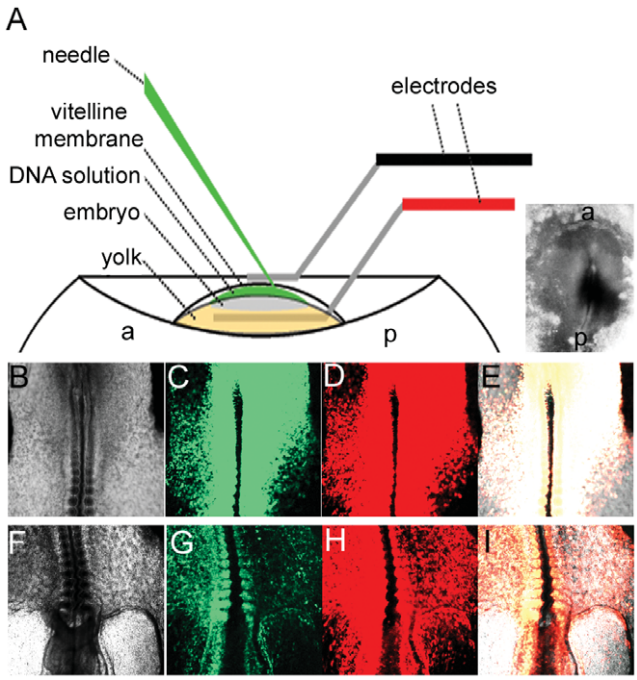

FIGURE 2 (A) Diagram of DNA injection and electroporation. To introduce the DNA solution, the tip of the injection needle is placed between the vitelline membrane and the embryo. To electroporate, the lower, red electrode is positioned within the yolk and the upper, black electrode is placed on top of the vitelline membrane overlying the embryo. The electrodes should be aligned with the anterior (a)/posterior (p) axis of the embryo as shown. (Inset) Stage 3+/4– chick embryo injected with DNA. Anterior is to the top. The DNA solution appears black, the embryo is gray, and the area opaca is white. The DNA solution collects within the streak and also diffuses over the surface of the embryo. (B–E) Stage 10 chick embryo electroporated at stage 4+/5– and incubated *in ovo*. Anterior is to the bottom. The plasmids pCA-dsRed express and pCA-GFP were combined at a concentration of 0.5 and 0.05 µg/µl, respectively. (B) Light microscope image of the posterior end of the embryo; anterior is to the bottom. (C) The CA promoter drives expression of GFP in all electroporated cells. GFP is expressed in somites, the presomitic mesoderm, and the lateral plate mesoderm. The neural tube of this embryo was not electroporated. (D) The same promoter drives expression of dsRED express in the same tissues. (E) Merged image of B, C, and D. Areas where strong GFP and dsRED expression overlap are yellow. (F–I) Stage 10 chick embryo electroporated at stage 3+/4– and incubated *in ovo*. Anterior is to the bottom. The plasmids pCA-dsRed express and cHoxb1 3′pGZ40-GFP were combined at a concentration of 0.25 and 0.75 µg/µl respectively. (F) Light microscope image of the head of the embryo; anterior is to the bottom. (G) The GFP protein driven by the Hoxb1 3′ enhancer is expressed strongly in somites and at a lower level in the head mesoderm. Its expression is driven by enhancers within region 3′ of chicken Hoxb1, which are linked to the chicken β-globin minimal promoter. (H) The dsRed express protein is driven by a ubiquitous promoter and marks the majority of electroporated cells. It is expressed in the head mesoderm, but not in the neural tube. Most embryos are also electroporated in the neural tube by this method, but this embryo clearly shows that expression in the mesoderm of this embryo is not due to the neural crest. (I) Merged image of F, G, and H. Areas where intense expression of both GFP and dsRed overlap are yellow.

that mediate widespread expression in chick embryos include pCAGGS (Niwa *et al*., 1991), MiwSV (Tomomura *et al*., 1990), pBK-CMV (Stratagene, USA), and pCS2 (Turner and Weintraub, 1994). For tissue-specific expression, a choice of unique enhancer sequences can be linked to the minimal β-globin promoter in pGZ40 (Itasaki *et al*., 1999).

2. **Stage and rate of survival.** The stage of the embryo at the time of EP affects the survival rate. At stage 3+, approximately 50–60% of embryos survive and develop normally. This mainly relates to a decrease in survival as a consequence of windowing of the egg and is not generally an affect of the EP itself. At stage 5–, approximately 80–90% of embryos develop normally.

3. **Multiple plasmids.** Depending on the strength of the promoters, it may be possible to use multiple plasmids. For example, a DNA concentration of 0.05 μg/μl is sufficient to visualize expression of pCA-GFP. Therefore, more DNA (2.45 μg/μl) from a plasmid with a weaker enhancer can be combined with the DNA of a stronger expressing plasmid. Mix both plasmids in the same tube before loading in the capillary tube for reproducibility. In the example shown, GFP is used as a positive control to determine how well the EP has worked (efficiency) and to determine what general area was electroporated.

Pitfalls

1. **Embryo drying.** A sign that the embryo is drying out during incubation is the presence of a hardened area of yolk adhering to the embryo. If the window is sealed well with tape and the embryos are still drying out, rotating the eggs at a 90° angle can help. This results in the uncut shell being positioned over the top of the embryo. Also, transient drying during embryo manipulation can affect the development of the embryo. Be sure to keep a drop of thin egg white on top of the embryo during the procedures.

2. **Positioning the electrode.** Inserting and removing the electrode can be difficult if the window is not large enough or if the embryo is oriented with its rostrocaudal axis along the short axis of the oval window. Keep the microscope on a low power so that the edge of the window can be seen. Rotate the top of the egg toward you so that the edge of the window is lower on the side facing the operator. If the bottom wire contacts the eggshell, pushing down may cause it to bend upward unexpectedly, poking into the embryo or narrowing the distance between the electrodes.

3. **Too much injectant.** If there is a large outpocketing of yolk sac, this is a sign that too much solution is being injected. If the opening of the capillary tip is too large, it will be difficult to inject the proper small volume of DNA solution. Too much fast green in the solution may also be toxic for embryos.

B. EP-Mediated Gene Transfer into Cultured Mouse Embryos

Materials and Instrumentation

For mouse whole embryo culture (WEC), we recommend a rotator bottle system with a continuous gas supply (from BTC engineering, UK, or Type10-0310 from Ikemoto Rika, Japan). The system allows mouse embryos at post-implantation stages (E7.0–E13.0) to develop normally for a few days *in vitro* culture. This time frame covers many of the dynamic events during mouse early organogenesis, permitting analysis of developmental processes over this period with EP (Fig. 3A). Embryo cultures may be initiated from E6.5, but it is hard to target a specific area with EP at this stage. Mouse embryos become more placenta dependent after E10.0 and the placenta does not grow well in the culture system. Hence it is very difficult to keep the *in vitro* embryo culture effective following this stage. To maintain embryos in good condition, the yolk sac and amnion must be opened to directly expose the embryo to culture media (Osumi and Inoue, 2001; Fig. 3L).

To obtain as many embryos as possible for EP, we use the CD-1/ICR mice strain (Charles River, USA). However, other mouse strains, including transgenic and/or mutant mice lines, are equally acceptable for the system. The morning when vaginal plugs are detected is designated as E0.5. Pregnant mice were sacrificed at the developmental stages of interest, as approved by the IACUC Review Committee for Animal Experimentation of the Stowers Institute for Medical Research.

An electroporator that can generate controlled square pulses is essential to EP of mouse embryos. We use CUY-21 (Bex Co. Ltd., Japan), which generates most stable pulses at lower voltages. For mouse experiments, other types of electroporators, such as the BTX-T820 (BTX, USA), are acceptable because relatively higher voltages compared with the chicken experiments are sufficient for efficient EP(see earlier discussion).

For mouse embryos, we used specially designed chamber type electrodes, where the distance between the electrodes is 2.5 cm (Fig. 3B). The electrodes and electric wires are now available commercially from TR Tech/Bex Co. Ltd., Japan. Electrodes made of platinum yield the best results because the metal is resistant to ionization during EP. For DNA injection, microcapillaries (#B100-58-10, Sutter Inc.) are pulled and the solutions are filled by suction with mouth pipette.

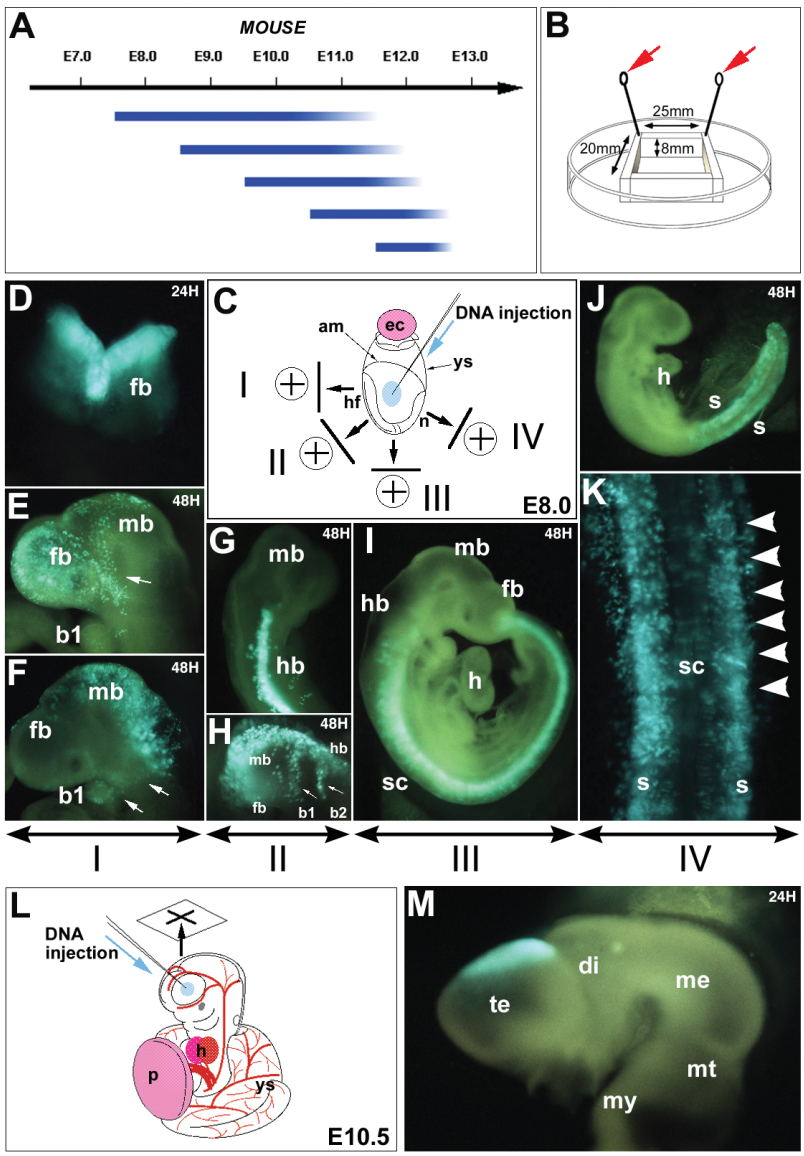

FIGURE 3 (A) Possible time schedules for mouse whole embryo culture after electroporarion (EP). The left edge of a blue bar indicates the start point of culture with EP, and the solid blue area represents the duration in which more than 75% of embryos can grow normally *in vitro*. (B) The electrode chamber designed for mouse embryos at any developmental stages. We made the chamber with silicone blocks on the 100-mm glass dish to be able to set two thin platinum plates (20 × 8 mm each) apart in a 25-mm distance. A lead wire is connected to each electrode and the end is bent to attach to the alligator clips from the electroporator (red arrows). (C) Schematic drawing of a mouse embryo at E8.0 ready for *in vitro* culture. DNA able to direct ubiquitous GFP expression (light blue oval) was microinjected into the amniotic cavity. By rotating the embryo in the electrode chamber filled with Tyrode's solution, various regions (I–IV) facing the positive (+) electrode were targeted by EP. (D–F) Results of EP in targeting region I of C. Embryos cultured *in vitro* for 24 or 48 h (24H/48H) showed a restricted pattern of GFP expression in anterior brain neuroepithelial cells. Neural crest cells emigrated from the forebrain, midbrain, and/or anterior hindbrain were also positive for GFP (white arrows in E and F). (G and H) Results of EP in targeting region II of C. Cells in the hindbrain and neural crest cells migrated out from the hindbrain to branchial arches (white arrows in H) harbored the exogenous GFP expression after 48 h of culture (48H). (I) Results of EP in targeting region III of C. The ventral part of the spinal cord strongly expressed GFP after 48 h of culture (48H). (J) Results of EP in targeting region IV of C. Pairs of posterior somite blocks express the exogenous GFP after 48 h of culture (48H) because cells just posterior to the node give rise to the somitic mesoderm. (K) A higher magnification of J. (L) Schematic drawing of a mouse embryo at E10.5 ready for *in vitro* culture. DNA able to direct GFP expression (light blue circle) was microinjected into the telencephalic vesicle, and the dorsal telencephalon was placed to face the positive (+) electrode in the electrode chamber. (M) After 24 h of culture (24H), strong GFP expression was found only in the dorsal part of the telencephalon. am, amnion; b, branchial arch, di, diencephalon; E, embryonic day; ec, ectoplacental cone; fb, forebrain; h, heart; hb, hindbrain; hf, head fold; mb, midbrain; me, mesencephalon; mt, metencephalon; my, myelencephalon; n, node; p, placenta; s, somite; sc, spinal cord; ys, yolk sac.

All embryo manipulations are performed under the binocular microscope ($MZ9_5$, Leica), and photographs are taken under a fluorescent microscope (MZ FLIII, Leica) fitted with a filter suitable for GFP.

The procedure described here is partly according to Akamatsu *et al*. (1999), Inoue *et al*. (2001), and Osumi and Inoue (2001).

Solutions

1. *Tyrode's solution, pH 7.4 (TS)*: Perform dissections and EP in TS to keep embryos in the best condition. Five liters of TS contains NaCl, 40.0 g; KCl, 1.0 g; $CaCl_2$, 1.0 g; $MgCl_2{\cdot}6H_2O$, 1.05 g; $NaH_2PO_4{\cdot}2H_2O$, 0.285 g; $NaHCO_3$, 5.0 g; and glucose, 5.0 g. To avoid possible precipitation of salts, we add these reagents in this order and sterilize by filtration. TS stored at 4°C should be prewarmed up to room temperature prior to use.

2. *Culture medium*: Prepare a 1 : 1 mixture of the rat serum and DMEM (#D5546, Sigma) containing L-glutamine and penicillin–streptomycin (100× solutions are available commercially from Gibco-BRL). The method used to collect rat serum was described previously (Hogan *et al*., 1994).

3. *DNA solutions*: Plasmid DNA solutions with high concentration (~5 μg/μl) are required for mouse EP protocol. The following experiments used the GFP expression vector driven by the cytomegalovirus enhancer and β-actin promoter (pCA-GFP; Inoue *et al*., 2001). After the Qiagen column and/or CsCl-based DNA purification, dissolve DNA into PBS (see earlier discussion) and add fast green (see earlier discussion) by 0.005% to be able to visualize the solution during the injection/EP processes.

Steps

1. Harvesting mouse embryos. Dissect the mouse embryos in the TS and preincubate them for more than 2 h in the culture system. Mice dissection procedures for WEC were described previously in details (Osumi and Inoue, 2001).

2. Preparations of electrode. Sterilize the electrode chamber briefly with 70% ethanol and then wash with TS three times.

3. Measure resistance. Transfer the embryo(s) from the culture bottle to the chamber and measure the resistance between electrodes. The resistance should be less than or equal to 120 Ω for optimal results. If not, add more TS to reduce the resistance.

4. Injection of DNA. DNA solutions may be injected into the region of interest while manually holding the embryo with forceps. For example, we inject DNA into the amniotic cavity for embryos at the 0–3 somite stages to direct ubiquitous GFP expression or into the lumen of the neural tube/brain ventricles at E9.0–12.0 to obtain region-specific expression in the nervous system (Figs. 3D–3I and 3M). A mouth pipette can control injections, and the volume of injectant may vary according to the developmental stages, but should be less than 0.5 μl.

5. Positioning embryos. Immediately after injection, center the embryo(s) in the chamber and arrange the embryo(s) so as to face the target region against the positive electrode (Figs. 3C and 3L). Negatively charged DNA molecules will migrate toward the positive electrode during EP. If a stable position cannot be obtained for the embryo(s), a block of agarose gel with a hollowed-out space can be used to hold them.

6. Electroporation. Send electric pulses. While the pON, pOFF, and the number of pulses can be fixed at 50 ms, 950 ms, and five repeats, respectively, the voltage should be changed depending on the embryonic stages. For optimal results we have found that application of 65 V for the 0–3 somite stage mouse embryos, 75 V for E9.5 mouse embryos, and 85 V for E10.5 mouse embryos with the 2.5-cm gap electrode chamber are best. For rat embryos, 1.1 times higher voltages are set than for mouse embryos (also see later for optimization of the EP parameters).

7. Embryo culture. Carefully transfer the embryo(s) into the fresh TS to get rid of any possible contamination of free radicals and/or ionized materials produced around the electrodes by EP. Then the embryo(s) can be put back into the WEC apparatus. The first evidence of exogenous gene expression can normally be detected after 6–8 h of EP, and 24–48 h culture is generally sufficient to see the maximum expression of reporter genes following the EP (Figs. 3D–3K and 3M).

8. Avoiding contamination. The chamber must be washed thoroughly with TS before trying the next round of EP. Repeat steps 3–7 until finishing up all embryos.

Comments

For efficient gene transfer, further optimization of the parameters of EP can be very helpful. The following are critical points in optimization.

i. Generally, a higher voltage is toxic for the cells, but it can yield better results. First try 25 V/cm with five pulses (pON 50 ms/pOFF 950 ms). This is a maximum voltage for any fragile tissues (e.g., early stage embryos).

ii. Keep in mind that the EP energy is proportional to total pulse length and square voltages. Doubling the

voltage results in the energy quadrupling, creating heat and damage to cells.

iii. The pulse length can be shortened to increase the voltage and the efficiency as well. For example, while a 2-ms pulse with 300 V generates exactly the same energy as a 50-ms pulse with 60 V, the former condition works much better than the latter condition with respect to the efficiency of gene transfer. It should be noted, however, that too high a voltage damages more cells. Hence this may not be effective for fragile early embryos and/or tissues.

iv. Time length between pulses (pOFF) can affect the EP efficiency. If the electroporator can control this parameter, shorter bursts are better, but it should not be too short to generate a continuous series of pulses.

A disadvantage of WEC is that the method is limited to events between E7.0 and 13.0, as it is difficult for the placenta to develop *in vitro*. However, there are established methods for *in utero* manipulations that could equally be applicable to EP, and several groups have indeed reported elegant results (Fukuchi-Shimogori and Grove, 2001; Saito and Nakatsuji, 2001). The ultrasound backscatter microscope has also been found to be effective at visualizing developing embryos and actually helps in perfecting the transfer genes *in utero* through EP (Takahashi *et al*., 2002). EP could further be extended to slice cultures of adult tissues or organ culture to investigate questions dealing with events after embryogenesis.

Pitfalls

We use highly concentrated DNA solutions for EP in mouse embryos because we found that solutions less than 1 μg/μl did not yield robust uniform patterns of expression. However, if mosaic expression is useful, then lower DNA concentration, as well as voltage, can be effective. It can be very difficult to load highly concentrated DNA into a capillary, but preheating of the solution for 10 min at 62°C can facilitate the process. Furthermore, the preheating process enhances the efficiency of EP, probably because DNA molecules in the solution stored at 4°C make aggregates, which could influence DNA transportation through cell membranes.

EP generates free radicals and/or ionized materials toxic enough to kill almost all of the cells around the electrodes. Therefore, the electrodes should not touch the embryo and/or tissues during EP and the length between electrodes should be set as distant as possible. It is hard to achieve normal growth of mouse embryo following EP at the somite stage between 4 and 9. The abnormality seen most frequently is a defect in the turning of embryos, so it is possible to examine other events during this period of development.

III. FUTURE PROSPECTIVE

Systems for EP-mediated gene transfer, as described here, are easily set up and EP is indeed an efficient way to evaluate gene function. Most current studies have utilized plasmid DNA. However, dyes, chemical reagents, antibodies, antisense morpholino oligonucleotides, double-strand RNAs, ribozymes, or bacterial artificial chromosomes could be mixed together in any combinations. These might be transferred into specific groups of cells or tissues for which there are not good cell culture models, as any charged macromolecules can be targeted using EP. Several research groups have actually reported excellent results of gene attenuation by dsRNA or morpholino oligonucleotides with EP (Takahashi *et al*., 2002; Mellitzer *et al*., 2002; Calegari *et al*., 2002). In the future, such broad accessibility should drastically change experimental designs in cell and developmental biology. EP will also offer a relatively high-throughput means of assaying or evaluating gene function and regulation, which must be important in light of the flood of information coming from the human genome project.

References

Akamatsu, W., Okano, H. J., Osumi, N., Inoue, T., Nakamura, S., Sakakibara, S., Miura, M., Matsuo, N., Darnell, R. B., and Okano, H. (1999). Mammalian ELAV-like neuronal RNA-binding proteins HuB and HuC promote neuronal development in both the central and the peripheral nervous systems. *Proc. Natl. Acad. Sci. USA* **96**, 9885–9890.

Calegari, F., Haubensak, W., Yang, D., Huttner, W. B., and Buchholz, F. (2002). Tissue-specific RNA interference in postimplantation mouse embryos with endoribonyclease-prepared hort interfering RNA. *Proc. Natl. Acad. Sci. USA* **99**, 14236–14240.

Fukuchi-Shimogori, T., and Grove, E. A. (2001). Neocortex patterning by the secreted signaling molecule FGF8. *Science* **294**, 1071–1074.

Haas, K., Sin, W. C., Javaherian, A., Li, Z., and Cline, H. T. (2001). Single-cell electroporation for gene transfer *in vivo*. *Neuron* **29**, 583–591.

Hamburger, V., and Hamilton, H. L. (1951). A series of normal stages in the development of the chick embryo. *J. Morph.* **88**, 49–92.

Hogan, B., Beddington, R., Costantini, F., and Lacy, E. (1994). Manipulating the Mouse Embryo, 2nd Ed. *Cold Spring Harbor Laboratory*, Cold Spring Harbor, NY.

Inoue, T., and Krumlauf, R. (2001). An impulse to the brain: Using *in vivo* electroporation. *Nature Neurosci.* **4**(**Suppl.**), 1156–1158.

Inoue, T., Tanaka, T., Takeichi, M., Chisaka, O., Nakamura, S., and Osumi, N. (2001). Role of cadherins in maintaining the compart-

ment boundary between the cortex and striatum during development. *Development* **128**, 561–569.

Itasaki, N., Bel-Vialar, S., and Krumlauf, R. (1999). "Shocking" developments in chick embryology: electroporation and *in ovo* gene expression. *Nature Cell Bio.* **1**, E203–E207.

Mellitzer, G., Hallonet, M., Chen, L., and Ang, S. (2002). Spatial and temporal 'knock down' of gene expression by electroporation of double-strand RNA and morpholinos into early postimplantation mouse embryos. *Mech. Dev.* **118**, 57–63.

Momose, T., Tonegawa, A., Takeuchi, J., Ogawa, H., Umesono, K., and Yasuda, K. (1999). Efficient targeting of gene expression in chick embryos by microelectroporation. *Dev. Growth Differ.* **41**, 335–344.

Muramatsu, T., Mizutani, Y., Ohmori, Y., and Okumura, J.-I. (1997). Comparison of three non-viral transfection methods for foreign gene expression in early chicken embryos *in ovo*. *Biochem. Biophys. Res. Commun.* **230**, 376–380.

Nishi, T., Yoshizato, K., Yamashiro, S., Takeshima, H., Sato, K., Hamada, K., Kitamura, I., Yoshimura, T., Saya, H., Karatsu, J., and Ushio, Y. (1996). High-efficiency *in vivo* gene transfer using intraarterial plasmid DNA injection following *in vivo* electroporation. *Cancer Res.* **56**, 1050–1055.

Niwa, H., Yamamura, K., and Miyazaki, J. (1991). Efficient selection for high-expression transfectants with a novel eukaryotic vector. *Gene* **108**, 193–199.

Okino, M., and Mohri, H. (1987). Effects of a high-voltage electrical impulse and an anticancer drug on *in vivo* growing tumors. *Jpn. J. Cancer Res.* **78**, 1319–1321.

Osumi, N., and Inoue, T. (2001). Gene transfer into cultured mammalian embryos by electroporation. *Methods* **24**, 35–42.

Saito, T., and Nakatsuji, N. (2001). Efficient gene transfer into the embryonic mouse brain using *in vivo* electroporation. *Dev. Biol.* **240**, 237–246.

Swartz, M., Eberhart, J., Mastick, G. S., and Krull, C. E. (2001). Sparking new frontiers: Using *in vivo* electroporation for genetic manipulations. *Dev. Biol.* **233**, 13–21.

Takahashi, M., Sato, K., Nomura, T., and Osumi, N. (2002). Manipulating gene expression by electroporation in the developing brain of mammalian embryos. *Differentiation* **70**, 155–162.

Tomomura, M., Kadomatsu, K., Nakamoto, M., Muramatsu, H., Kondoh, H., Imagawa, K., and Muramatsu, T. (1990). A retinoic acid responsive gene, MK, produces a secreted protein with heparin binding activity. *Biochem. Biophys. Res. Commun.* **171**, 603–609.

Turner, D. L., and Weintraub, H. (1994). Expression of achaete-scute homolog 3 in Xenopus embryos converts ectodermal cells to a neural fate. *Genes Dev.* **8**, 1434–1447.

Yasugi, S., and Nakamura, H. (2000). Gene transfer into chicken embryos as an effective system of analysis in developmental biology. *Dev. Growth Differ.* **42**, 195–197.

SECTION

3

Somatic Cell Nuclear Transfer

CHAPTER

7

Somatic Cell Nuclear Transplantation

Keith H. S. Campbell, Ramiro Alberio, Chris Denning, and Joon-Hee Lee

I. INTRODUCTION

The production of live offspring by nuclear transfer using a cultured cell population as nuclear donors was first reported in sheep (Campbell *et al.*, 1996). Since that time, offspring have been reported in a range of species, including sheep (Wilmut *et al.*, 1997), cattle (Cibelli *et al.*, 1998), mice (Wakayama *et al.*, 1998), pigs (Polejaeva *et al.*, 2000), cats (Shin *et al.*, 2002), rabbits (Chesne *et al.*, 2002), horses (Galli *et al.*, 2003), and rats (Zhou *et al.*, 2003), and from a variety of cell types derived from embryos, fetuses, juvenile, and adult animals (for review, see Campbell *et al.*, 2003). The ability to culture large numbers of cells *in vitro*, which can be used as successful nuclear donors, provides unique opportunities for the preservation and genetic modification of defined genomes. Primary cell populations have been used for the production of transgenic animals by gene addition (Schnieke *et al.*, 1997) and also by gene knockout (McCreath *et al.*, 2000; Denning *et al.*, 2001) and knockin strategies (McCreath *et al.*, 2000), producing animals for agricultural, medical, and research applications. Genotype preservation from both live (Wells *et al.*, 1998) and dead (Loi *et al.*, 2001) animals has been demonstrated. Many factors affect the development of embryos reconstructed by nuclear transfer (for review see, Campbell *et al.*, 2003). The methodology described here is based on the production of ovine embryos; with differences in timings, the methods are similar to those used in other species that have been produced by nuclear transfer.

II. MATERIALS AND INSTRUMENTATION

Embryo manipulations are carried out under a Leica MZ12.5 stereomicroscope and under a Leica DMIRBE inverted microscope fitted with differential interference contrast and epifluorescence. Both microscopes are fitted with Linkam M60 warmed stages. A MMO-202ND Narishige three-axis hanging joystick micromanipulator, one IM-5B Narishige injector for oocyte holding, and one Eppendorf Celltram Oil/Vario for cell transfer are fitted to the inverted microscope (Fig. 1A). The oocyte holding system is filled with Fuorinert FC77 (Sigma F-4758). Alternatively, the Narishige IM-9C injector can be used for oocyte holding. This system works properly with air.

Glass pipettes are prepared after pulling borosilicate capillaries (thin wall 1 mm o.d. × 0.8 mm i.d., Intrafil) on a P-97 Sutter Instruments Co. puller. For grinding the pipettes, the EG-400 (Narishige) micropipette grinder is used in conjunction with a microforge MF-830 (Narishige).

Cell fusion is performed with an Eppendorf multiporator fitted with a fusion chamber (electrodes 200 or 500 μm apart; Fig. 1B). For the fusion of somatic cells (15–18 μm) with a MII oocyte, a combination of an AC pulse and DC pulses give a fusion rate of more than 75% on sheep and cattle couplets.

Reagents are from Sigma unless specified. For isolation, culture, and assessment of donor cells, Glasgow MEM (G-5154), 200 m*M* glutamine (G-7513), 100 m*M* sodium pyruvate (S-8636), MEM nonessential amino

Copyright 2006, Elsevier Science (USA).
All rights reserved.

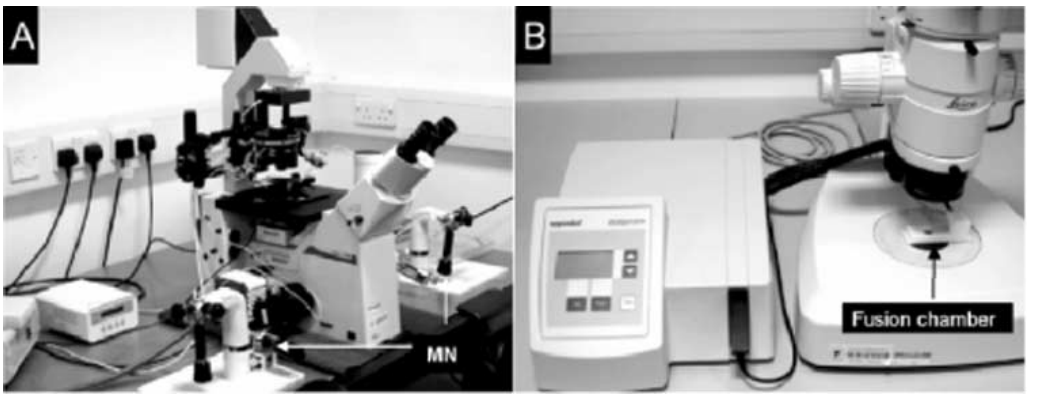

FIGURE 1 (A) Leica microscope fitted with Narishige micromanipulators (MN) for nuclear transplantation. (B) Eppendorf fusion machine with fusion chamber is used under a Leica MZ 12.5 stereomicroscope.

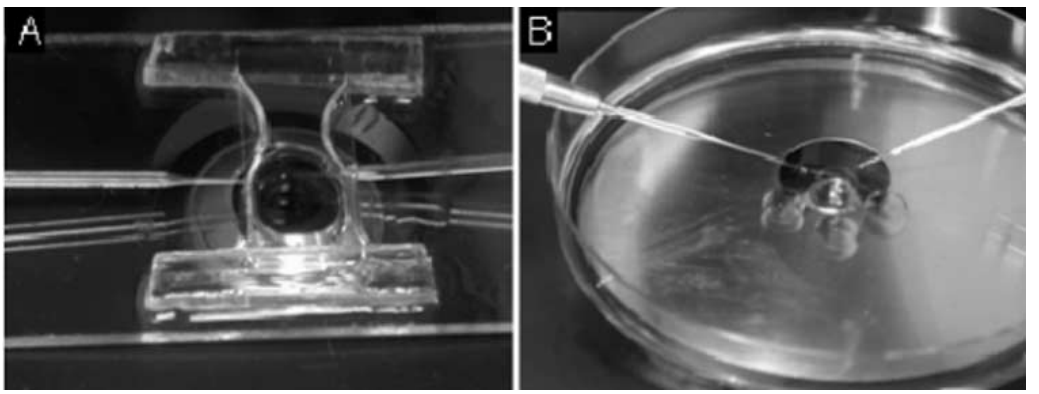

FIGURE 2 A micromanipulation chamber (A) or a plastic petri dish (B) can be used for micromanipulation.

acids (M-7145), trypsin (T-4044), Giemsa solution (G-3032), glycine (G-7126), phosphate-buffered saline (PBS) tablets (P-4417), gelatin (G-1890), trisodium citrate (C-3434), and dimethyl sulfoxide (DMSO) (D-5879) are used. Gentamycin (15750-037) is from Invitrogen/Gibco. Methanol (M/4000/17) and glacial acetic acid (A/0400/PB17) are from Fissons. Fetal calf serum (FCS) (SH-30088) is from HyClone. Vectashield mountant (H-1200) is from Vector Labs. Chamber slides (TKT-210-430L) are from Fisher Scientific. Monoclonal mouse antihuman Ki-67 antigen (clone MIB-1) (M-7240) and FITC-conjugated rabbit antimouse immunoglobulin (F-0261) are from Dako.

III. PROCEDURES

A. Preparation of Tools for Micromanipulation

Tools are prepared differently according to individual preferences relating to the position of the pipettes on the microscope. We will provide the technique used in our laboratory for performing NT with pipettes aligned horizontally to the oocyte (Fig. 2A), although it is also possible to conduct the manipulation at a 45°C angle (Fig. 2B).

1. Holding Pipette

Steps

1. Pull glass capillaries (GC10–100, Intrafil) by hand over a small flame to give a 100- to 150-μm diameter.
2. Mount capillaries with straight end onto the microforge and apply heat until the open tip is almost closed, ensuring an internal diameter of approximately 20 μm.

2. Enucleation Pipette

Steps

1. Pull glass capillaries using the microcapillary puller to give an initial taper, which reduces the diameter of the capillary to slightly greater than the diameter required, with the second taper being almost parallel.

2. Mount a drawn capillary on the microforge. Measure the diameter of the pipette using an eyepiece graticule and break at the required size, between 20 and 25 µm. The break is made by fusing the capillary onto a bead of glass, which is heated using the minimum temperature needed to stick the glass onto the capillary. The power is turned off and the capillary breaks by retraction of the cooled glass bead. Care should be taken to ensure that the capillary is not overheated, as this may cause distortion and thickening of the glass. The tip area must be straight so that it can be properly ground to a point.

3. Mount the pipette in the microforge at a 45° angle and ground it at medium speed ensuring a continuous water flow over the surface where the pipette is being ground.

4. Pipettes with thick walls can be made thin by dipping into 20% hydrofluoric acid for 30–60 s while continuously blowing air through (this prevents acid entering the inside of the pipette). If thin wall capillaries are used, there is no need for hydrofluoric acid dipping.

5. Wash with distilled water to remove acid.

6. Mount the pipette on the microforge with the tip hole in view. Heat the forge to the minimum temperature required to melt the glass bed. Touch the tip of the pipette against the glass bead and pull the tip of the pipette out to a sharp point.

3. Manipulation Chamber

Materials

1. Silicon vacuum grease (Beckman), coverlips, and plastic spacers of 2.5 cm.
2. Siliconized glass slides: Cover clean glass slides with Sigmacote (Sigma SL-2), drain, and let air dry.

Steps

1. Apply a line of wax 2 cm in length along both edges of the upper surface of a siliconized glass slide.
2. Apply silicon vacuum grease to both sides of two plexiglass spacers (2 cm), attach them parallel to the long axis of the slide, and press down firmly.
3. Pipette 60 µl of manipulation medium into the center of the chamber between the spacers. Place a clean coverslip (cleaned in 70% ethanol) on top of the spacers and push down firmly.
4. Turn the chamber upside down and fill with silicon oil until the drop of manipulation medium is enclosed in oil. This seals the ends, preventing evaporation of the manipulation medium.
5. Turn the chamber to the upright position.

B. Preparation of Equipment for Manipulation

Steps

1. Place a prepared manipulation chamber onto the stage of the microscope.
2. Put a small volume of manipulation medium into the holding pipette.
3. Attach the holding pipette to the left-hand side tool holder, ensuring that all air is removed from the hydraulic system.
4. Move the holding pipette into the manipulation chamber.
5. Coat the inside of the injection pipette with sigmacote by aspirating the solution through the pipette several times. Wash with water and mount onto the pipette holder.
6. Mount the pipette on the right side of the chamber and ensure that the system is free from air bubbles. A slight angle of approximately 5° from horizontal allows the pipette to pick up cells from the bottom of the chamber.

C. Enucleation of Oocytes

Solutions and Equipment

1. Manipulation chamber and microtools: *See Section III,A*
2. MII oocytes
3. *Hyaluronidase stock solution*: Dissolve hyaluronidase in PBS to give 750–1500 IU/mg (H-4272). Dispense into 1-ml (300 IU/ml) aliquots. Store at –20°C.
4. *Cytochalasin B (C-6762) stock solution*: 10 mg/ml in DMSO stored at –20°C
5. *Bisbenzimide (Hoechst 33342) stock solution*: 1 mg/ml in PBS. Prepare 10-µl aliquots and store at –20°C.

Steps

1. Select oocytes surrounded by at last three layers of cumulus cells.

2. Incubate the matured oocytes in a Falcon tube containing 400 µl of hyaluronidase (300 IU/ml) for 2 min at 37°C and then vortex for 4 min.

3. Wash denuded oocytes in modified HEPES-buffered SOF medium (supplemented with 4 mg/ml BSA) and return to maturation medium.

4. At regular intervals, place batches of 10–15 oocytes with extruded polar bodies into mHSOFaac/4 mg/ml BSA containing 50 µg/ml bisbenzimide (Hoechst 33342) and incubate for 15 min at 35°C on the heated stage.

5. After incubation, transfer each batch of treated oocytes to the manipulation chamber.

6. Using 20× magnification, pick up and attach a single oocyte to the holding pipette using negative pressure.

7. Change the magnification to 40× DIC and focus on the oocyte held by the pipette.

8. Bring the enucleation pipette into focus. Using the enucleation pipette, rotate the oocyte into a position where the polar body and the area of cytoplasm adjacent to it can be aspirated into the pipette (Fig. 3A).

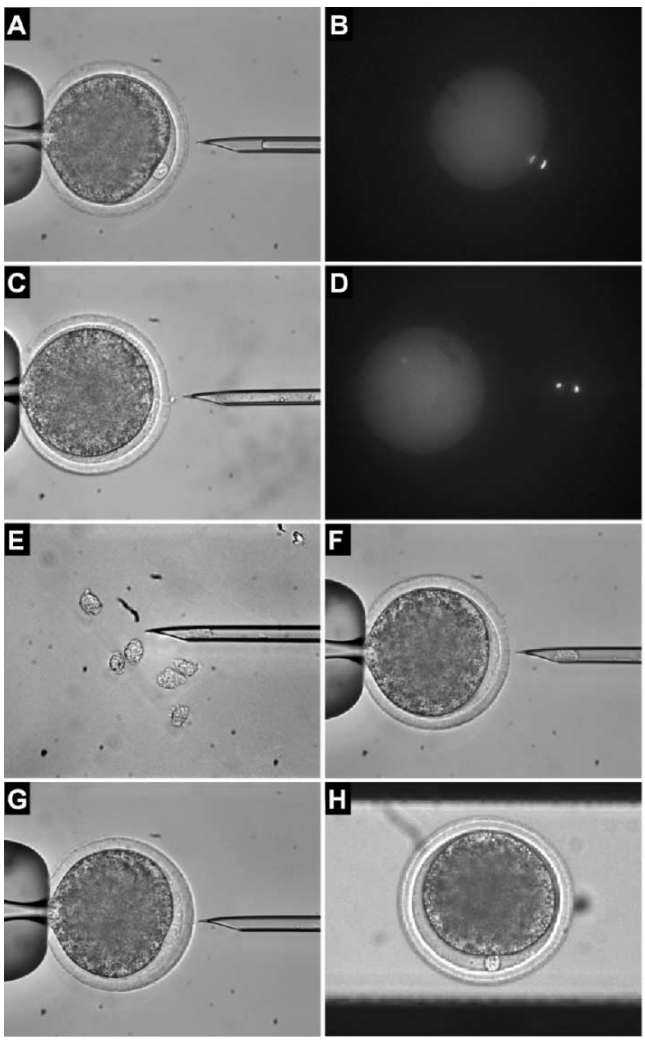

FIGURE 3 Oocyte enucleation and reconstruction of oocyte somatic cell couplets (A) holding the oocyte prior to enucleation (note position of the polar body). (B) Localisation of the polar body (PB) and metaphase plate (MP) by epifluorescence. (C) Enucleated oocyte (D) confirmed by epifluorescence (note PB and MP in the pipette). (E) Somatic cells in suspension. (F) Transfer into enucleated oocyte. (G) Cells after transfer should be in close contact with the oolema. (H) The couplet is positioned between the electrodes for fusion (note perpendicular orientation of the couplet to the electrodes).

9. Insert the enucleation pipette through the zona pelucida at a point opposite the holding pipette.

10. Manipulate the enucleation pipette into a position next to the polar body, apply a small amount of negative pressure, and aspirate the polar body and a small amount of cytoplasm from directly beneath it into the pipette (Fig. 3C).

11. Withdraw the pipette from the oocyte and remove the oocyte from the field of view.

12. Turn off the transmitted light source, change to UV illumination (blue light), and examine the aspirated karyoplast (while inside the pipette) for fluorescence using filter block UV-2A. If the metaphase has been removed, it will fluoresce with a blue color; the polar body will also be visible. The metaphase plate fluoresces with a lower intensity than the polar body (Figs. 3B and 3D).

13. Move the enucleated oocyte to the right-hand side of the chamber and discard the aspirated karyoplast form the pipette. If the enucleation was unsuccessful, it is possible to repeat the procedure a second time.

14. Remove completed batches of oocytes from the manipulation chamber and place into a microdrop or dish containing HEPES-SOF (4 mg/ml). Maintain at 37°C until the required number of oocytes have been enucleated.

D. Embryo Reconstruction

Solution and Equipment

1. Manipulation chamber and microtools
2. Cumulus-free enucleated MII oocytes
3. Serum-starved quiescent donor cells
4. *Calcium-free fusion medium*: 0.3 *M* manitol with addition 0.1 m*M* $MgSO_4$ in distilled H_2O with an osmolarity of 280 mOsm

Steps

1. Prepare a manipulation chamber, as for the enucleation procedure, containing HEPES-buffered SOF 4 mg/ml BSA.
2. Using a hand-drawn mouth pipette attached to aspirator tube (Sigma; A5177), place the nuclear donor cells into the upper left-hand corner of the chamber and a group of enucleated oocytes into the right hand corner of the chamber.
3. Pick up an enucleated oocyte with the holding pipette.
4. Move the holding pipette to the top.
5. Focus the microscope onto the bottom of the chamber.

6. Move the enucleation pipette to the chamber, maneuver it to the cells, and gently aspirate two to three suitable cells into the pipette (Fig. 3E).
7. Refocus on the enucleated oocyte and move the enucleation pipette until it is in focus.
8. Insert the enucleation pipette through the hole made previously in the zona pelucida. While holding the pipette against the cytoplasm, expel one donor cell into the perivitelline space (Fig. 3F). Ensure contact between the two cells of the couplet (Fig. 3G).
9. Transfer donor cells to groups of 10 oocytes. Upon completion of each batch, wash couplets in washing medium.
10. Place 100 µl of warm (35°C) fusion medium, spanning the electrodes, into the fusion chamber.
11. Pipette the reconstructed oocytes into the fusion medium but outside the electrodes and allow them to settle down for 15–30 s.
12. Using a hand-drawn capillary mouth pipette, place two to three couplets between the electrodes, moving them until the plane of contact between cytoplast and karyoplast is parallel to the electrodes. Precise orientation is necessary for fusion to occur (Fig. 3H).
13. Apply the fusion pulse, which consists of a 5-s AC pulse of 5 V/cm followed by one or two DC pulses of 35 V/cm for 30 µs (for electrodes 200 µm apart).
14. Remove the reconstructed oocytes from the chamber and wash each batch with washing medium.
15. Transfer them into a 50 µl drop of mSOFaaci/4 mg/ml BSA (Holm *et al.*, 1999). Incubate at 39°C for 15–20 min and then examine for cell fusion.
16. Refuse unfused couplets by two DC pulses of 35 V/cm for 30 µs.
17. Incubate fused couplets for 1 h in mSOFaaci and then activate.
18. Activate fused couplets in H-SOF plus 5 µ*M* calcium ionophore (A23187) for 5 min at 35°C and culture subsequently in mSOFaaci with 10 µg/ml of cycloheximide and 7.5 µg/ml cytochalasin B for 5 h.
19. Following activation, wash the reconstructed embryos and culture under oil in 50-µl droplets of mSOFaaci supplemented with 2%(v/v) BME, 1%(v/v) MEM, and 4 mg/ml BSA (fatty acids free) in a humidified atmosphere of 5% CO_2, 5% O_2, and 90% N_2 at 39°C.
20. At day 3 of culture, transfer cleaved embyos into mSOFaaci supplemented with 5% heat-inactivated FBS.
21. At days 7 to 8 transfer embryos surgically into naturally cycling, foster mother ewes, 7 days after estrus.

E. Isolation, Culture, and Preparation of Cells Used as Nuclear Donors

Solutions

1. *Culture medium:* To 500 ml of Glasgow MEM (GMEM) add 56 ml (10%) of FCS, 5.6 ml of L-glutamine, 5.6 ml of sodium pyruvate, and 5.6 ml of nonessential amino acids. Warm to 37°C before use.
2. *Low serum medium:* As in solution 1 but containing 0.5% FCS.
3. *Trypsin solution:* Aliquot and store at –20°C. Thaw and warm to 37°C before use.
4. *Gelatin solution*: Add 1 g of gelatin to 1000 ml Milli-Q water. Autoclave, allow to cool, and filter.
5. *Hypotonic solution:* Add 4 g of trisodium citrate to 1000 ml Milli-Q water. Filter sterilise.
6. *Karyotyping fixative:* Add 3 parts methanol to 1 part acetic acid.

Isolation of a Primary Culture

Steps

1. Add 20 ml of gelatin solution to a T175 flask. Place flask in tissue culture hood until cells have been prepared.
2. Remove the uterus from a 30- to 35-day-old pregnant ewe and immediately remove the fetus.
3. Eviscerate and decapitate the fetus and transfer the carcass to 10 ml PBS supplemented with 100 µg/ml gentamycin. Wash the carcass twice with 10 ml PBS–gentamycin.
4. Place the carcass in a 10-cm tissue culture dish and add 3 ml of trypsin solution. Use scissors to cut cubes of 1 mm. Incubate at 37°C for 10 min.
5. Add 10 ml of culture medium to the dissociating cells and transfer to a 15-ml tube.
6. Dissociate clumps by pipetting.
7. Stand tube for 1 min to allow larger clumps to settle.
8. Aspirate gelatin solution from T175 flask.
9. Avoiding the pelleted cells, transfer the cells in suspension to the gelatinised T175 flask.
10. Resuspend the remaining clumps in the tube in 10 ml culture medium. Repeat steps 6 and 7. Add the cell suspension to the same flask as before.
11. Discard the tube containing the remaining cell clumps.

12. Add culture medium to the T175 flask to a total volume of 50 ml.
13. Add gentamycin to a final concentration of 50 µg/ml and incubate cells for 24 h at 37°C in an atmosphere composed of 5% CO_2, 20% O_2, and 75% N_2.
14. Replace medium with fresh medium containing no antibiotic. Culture cells at 37°C.
15. Record time required for culture to reach confluence. Trypsinise, pellet, and cryopreserve aliquots of 1×10^6 cells in a mixture of 90% growth medium: 10% DMSO.
16. Subsequent passages and culture of cells do not require gelatinized flasks or antibiotics.

F. Preparation of Mitotic Spreads

Steps

1. Culture cells in a T25 flask to subconfluency.
2. Aspirate growth medium and wash once with warm (37°C) PBS.
3. Add 1 ml of trypsin solution. Incubate at 37°C and monitor the culture for detachment of cells.
4. When cells are detached, add 10 ml of culture medium.
5. Decant cells into a 15-ml tube and pellet at 300 *g* for 5 min.
6. Aspirate medium and resuspend cell pellet in 10 ml fresh growth medium.
7. Add 2 ml of the cell suspension and 8 ml of growth medium to a T25 flask.
8. Incubate for 24 h.
9. Trypsinise cells as described previously and resuspend in 10 ml culture medium.
10. Transfer the cell suspension to a 15-ml tube and pellet the cells at 300 *g* for 5 min.
11. To resuspend the cells, add 10 ml of hypotonic solution gradually while vortexing.
12. Incubate at room temperature for 15 min to allow cells to swell.
13. Pellet the cells at 300 *g* for 5 min. Discard supernatant.
14. Resuspend the cells by adding 6 ml of karytyoping fixative dropwise while vortexing.
15. Pellet the cells at 300 *g* for 5 min. Discard supernatant.
16. Repeat steps 13 and 14 twice more.
17. After the final spin, resuspend the pellet in 0.5 ml karytoping fixative.
18. Prepare spreads by dropping fixed cell suspension onto clean glass slide.
19. Air dry.
20. Stain with 3% Giemsa for 15 min at room temperature.

G. Induction and Assessment of Quiescence in Donor Cells

Solutions

1. *Fixative*: Prepare a 70% : 30% of mixture of methanol : 50 m*M* glycine. Store at –20°C. (Add 0.38 g glycine to 100 ml Milli-Q water.)
2. *Humidified chamber*: Place a sheet of filter paper into a 10-cm petri dish. Dampen with distilled water.
3. *PBS/1% FCS*: Add 1 ml of FCS to 100 ml sterile PBS
4. *1° antibody working solution*: Dilute Ki-67 antibody (clone MIB-1) 1:150 with PBS/1% FCS.
5. *2° antibody working solution*: Dilute FITC-conjugated rabbit antimouse antibody 1:20 with PBS/1% FCS.
6. Nail varnish.
7. Mountant (Vecta shield) containing 1 µg/ml DAPI.

Steps

1. Trypsinise an 80% confluent monolayer of donor cells and resuspend in growth medium.
2. Replate cells at one-fifteenth the original density in growth medium in 1-well glass chamber slides and continue to culture for 48 h.
3. Wash the monolayer three times with low serum medium and then continue culture in this medium.
4. Exit from the growth cycle; survival in the quiescent state must be established for each cell line. At the time of serum reduction and at 24-h intervals, process one slide for Ki-67 staining as detailed later.
5. Remove culture chamber and rubber gasket from one chamber slide.
6. Rinse in PBS at 4°C and fix in methanol: 50 m*M* glycine for 20 min at –20°C.
7. Wash in PBS.
8. Block in PBS/1% BSA for 30–45 min at room temperature.
9. Wash in PBS and transfer slide to humidified chamber.
10. Add 500 µl of 1° antibody solution to each slide. Incubate for 1 h at 37°C.
11. Wash three times with PBS/1% FCS.
12. Add 500 µl of 2° antibody solution. Incubate for 1 h at 37°C.
13. Wash three times with PBS/1% FCS.
14. Remove excess liquid. Add two drops of mounting and overlay with a coverslip. Seal edges with nail varnish.
15. Store at 4°C in darkness.
16. Examine using epifluorescence.

17. Record the percentage of Ki-67-positive nuclei. Ki-67 is a nuclear antigen expressed at all active stages of the cell cycle but absent in resting (G0 phase).

IV. PITFALLS

1. Ensure that enucleated oocytes are at MII at the time of enucleation. Oocytes that have activated spontaneously as a result of handling will resume meiosis; this will be visible as a third fluorescent area corresponding to the anaphase/telophase.

2. It is recommended to perform enucleation in early matured oocytes (17–19 h after onset of maturation) to guarantee close contact of the metaphase plate and the polar body. Metaphase plates from matured oocytes tend to move away from the polar body after they have reached the MII stage.

3. Avoid temperature oscillations during manipulation as these can cause spontaneous oocyte activation.

References

Campbell, K. H. S., and Alberio, R. (2003). Reprogramming the genome: role of the cell cycle. *Reprod. Suppl.* **61**, 477–494.

Campbell, K. H. S., McWhir, J., Ritchie, W. A., and Wilmut, I. (1996). Sheep cloned by nuclear transfer from a cultured cell line. *Nature* **380**, 64–66.

Chesne, P., Adenot, P. G., Viglietta, C., Baratte, M., Boulanger, L., and Renard, J. P. (2002). Cloned rabbits produced by nuclear transfer from adult somatic cells. *Nature Biotechnol.* **20**, 366–369.

Cibelli, J. B., Stice, S. L., Golueke, P. J., Kane, J. J., Jerry, J., Blackwell, C., Ponce, d. L. n., and Robl, J. M. (1998). Cloned transgenic calves produced from nonquiescent fetal fibroblasts. *Science* **280**, 1256–1258.

Denning, C., Burl, S., Ainslie, A., Bracken, J., Dinnyes, A., Fletcher, J., King, T., Ritchie, M., Ritchie, W. A., Rollo, M., de Sousa, P., Travers, A., Wilmut, I., and Clark, A. J. (2001). Deletion of the alpha(1,3)galactosyl transferase (GGTA1) gene and the prion protein (PrP) gene in sheep. *Nature Biotechnol.* **19**, 559–562.

Galli, C., Lagutina, I., Crotti, G., Colleoni, S., Turini, P., Ponderato, N., Duchi, R., and Lazzari, G. (2003). Pregnancy: A cloned horse born to its dam twin. *Nature* **424**, 635.

Holm, P., Booth, P. J., Schmidt, M. H., Greve, T., and Callesen, H. (1999). High bovine blastocyst development in a static *in vitro* production system using SOFaa medium supplemented with sodium citrate and myo-inositol with or without serum-proteins. *Theriogenology* **52**, 683–700.

Loi, P., Ptak, G., Barboni, B., Fulka, J., Jr., Cappai, P., and Clinton, M. (2001). Genetic rescue of an endangered mammal by cross-species nuclear transfer using post-mortem somatic cells. *Nature Biotechnol.* **19**, 962–964.

McCreath, K. J., Howcroft, J., Campbell, K. H. S., Colman, A., Schnieke, A. E., and Kind, A. J. (2000). Production of gene-targeted sheep by nuclear transfer from cultured somatic cells. *Nature* **405**, 1066–1069.

Polejaeva, I. A., Chen, S. H., Vaught, T. D., Page, R. L., Mullins, J., Ball, S., Dai, Y., Boone, J., Walker, S., Ayares, D. L., Colman, A., and Campbell, K. H. S. (2000). Cloned pigs produced by nuclear transfer from adult somatic cells. *Nature* **407**, 86–90.

Schnieke, A. E., Kind, A. J., Ritchie, W. A., Mycock, K., Scott, A. R., Ritchie, M., Wilmut, I., Colman, A., and Campbell, K. H. S. (1997). Human factor IX transgenic sheep produced by transfer of nuclei from transfected fetal fibroblasts. *Science* **278**, 2130–2133.

Shin, T., Kraemer, D., Pryor, J., Liu, L., Rugila, J., Howe, L., Buck, S., Murphy, K., Lyons, L., and Westhusin, M. (2002). Cell biology: A cat cloned by nuclear transplantation. *Nature* **415**, 859.

Wakayama, T., Perry, A. C., Zuccotti, M., Johnson, K. R., and Yanagimachi, R. (1998). Full-term development of mice from enucleated oocytes injected with cumulus cell nuclei. *Nature* **394**, 369–374.

Wells, D. N., Misica, P. M., Tervit, H. R., and Vivanco, W. H. (1998). Adult somatic cell nuclear transfer is used to preserve the last surviving cow of the Enderby Island cattle breed. *Reprod. Fertil. Dev.* **10**, 369–378.

Wilmut, I., Schnieke, A. E., McWhir, J., Kind, A. J., and Campbell, K. H. S. (1997) Viable offspring derived from fetal and adult mammalian cells. *Nature* **385**, 810–813.

Zhou, Q., Renard, J. P., Le Friec, G., Brochard, V., Beaujean, N., Cherifi, Y., Fraichard, A., and Cozzi, J. (2003). Generation of fertile cloned rats by regulating oocyte activation. *Science* **302**, 1179.

PART

B

EXPRESSION SYSTEMS

SECTION

4

Expression Systems

CHAPTER

8

Expression of cDNA in Yeast

Caterina Holz and Christine Lang

I. INTRODUCTION

The ability to express heterologous genes in yeast has become a powerful tool for many biological research techniques. Yeast combines the advantage of eukaryotic posttranslational modifications, such as phosphorylation, glycosylation, disulfide cross-linking, and subcellular targeting, with the expression of soluble proteins in large amounts. The yeast system is also very attractive as both the culture and the protocols for expression are easy to handle. The first species to be employed for the production of heterologous proteins was *Saccharomyces cerevisiae*. The host-vector systems for this organism are now well developed and a wealth of knowledge on its genetics and its physiology has been accumulated. This has led to its frequent use as a model eukaryote to understand the function and properties of many mammalian proteins in recent years (Romanos *et al*., 1992). Suitable *S. cerevisiae* host strains are available (or can be generated easily) that bear alterations to enhance protein production, such as the elimination of major proteases or the increase of transcription and expression level (Harashima, 1994). Both homologous and heterologous proteins may be produced in the cytoplasm or directed through the secretory pathway. The first approach, the intracellular expression of cDNAs by the yeast *S. cerevisiae*, is the focus of this article.

The most widely used expression vectors are *Escherichia coli*/yeast shuttle plasmids (Bonneaud *et al*., 1991) that are stabilized mitotically by autonomously replicating sequences (ARS/CEN region, 2-µm origin) or by integration into the yeast genome. Foreign genes, which are inserted in 2-µm-based plasmids, are maintained in high copy numbers; however, selection is required for growth and protein expression (Rose and Broach, 1990). This article describes the use of such an episomal expression plasmid that is easily introduced into yeast cells by lithium–acetate transformation into competent cells (Gietz *et al*., 1992) or by electroporation (Becker and Guarente, 1991).

Various strategies are available to induce the expression of the recombinant protein; the specific method chosen depends on the physiological characteristics of the yeast strain used. The use of inducible promoters is advisable when the product itself or its synthesis is deleterious to the cells or, as in cell biology studies, when the impact of the recombinant protein on cellular physiology is to be investigated. This article describes a method based on the expression vector pYEXTHS-BN (Holz *et al*., 2002), where the transcription of cDNAs is controlled by the Cu^{2+}-induced *CUP*1 promoter from the yeast metallothionein gene. This strong promoter is induced rapidly by copper sulfate (0.01 to 1 m*M*, depending on the copper resistance of the host strain) (Etcheverry, 1990; Ward *et al*., 1994). The cloned gene is fused to small antigenic epitopes. These epitope tags, the N-terminal His_6 tag (Porath, 1992) and the C-terminal StrepII tag (Schmidt *et al*., 1996), facilitate the subsequent immunological identification and purification of the gene product by two-step affinity chromatography. The intracellular double-tagged protein is released from the cells by disrupting the cell walls by enzymatic, chemical, or mechanical procedures as described here.

Copyright 2006, Elsevier Science (USA).
All rights reserved.

II. MATERIALS AND INSTRUMENTATION

The pYEXTHS-BN expression plasmid was constructed in the Protein Structure Factory laboratory (Berlin, Germany). The strain *S. cerevisiae* AH22*ura*3 (MATa, ura3Δ, leu2-23, 112, his4-519, can1) was provided by Berlin University of Technology, Department of Microbiology and Genetics (Germany). NaCl (Cat. No. 1.06404), $NH_4H_2PO_4$ (Cat. No. 1.01126), NH_4Cl (Cat. No. 1.01145), $Na_2HPO_4{\cdot}2H_2O$ (Cat. No. 1.06580), $NaH_2PO_4{\cdot}H_2O$ (Cat. No. 1.06346), $MgCl_2{\cdot}6H_2O$ (Cat. No. 1.05833), $CaCl_2{\cdot}H_2O$ (Cat. No. 1.02380), KH_2PO_4 (Cat. No. 1.04873), $MgSO_4{\cdot}7H_2O$ (Cat. No. 1.05886), sodium L-glutamate monohydrate (Cat. No. 1.06445), $ZnSO_4{\cdot}7H_2O$ (Cat. No. 1.08883), $FeSO_4{\cdot}7H_2O$ (Cat. No. 1.03965), $CuSO_4{\cdot}5H_2O$ (Cat. No. 1.02790), $MnCl_2{\cdot}4H_2O$ (Cat. No. 1.05927), $Na_2MoO_4{\cdot}2H_2O$ (Cat. No. 1.06521), nicotinic acid (Cat. No. 8.18714), L-histidine HCl (Cat. No. 1.04350), imidazole (Cat. No. 1.047169), isopropanol (Cat. No. 1.09634), 2-mercaptoethanol (Cat. No. 1.15433), glycine (Cat. No. 1.04169), and Tween 20 (Cat. No. 1.00731) are from Merck. *myo*-Inositol (Cat. No. 26310), pyridoxine (Cat. No. 33990), biotin (Cat. No. 15060), sucrose (Cat. No. 35580), dodecylsulfate-Na-salt (SDS) (Cat. No. 20783), Triton X-100 (Cat. No. 37240), and Ponceau S (Cat. No. 33429) are from Serva. Thiamine (Cat. No. T4625), calcium *d*-pantothenate (Cat. No. C8731), bovine serum albumin (BSA) (A-3912), phenylmethylsulfonyl-fluoride (PMSF) (Cat. No. 78830/Fluka), bromphenol blue (Cat. No. B-6131), EDTA sodium salt (Cat. No. E-5134), avidin (Cat. No. A-9275), and desthiobiotin (Cat. No. D-1411) are from Sigma. Tris base (Cat. No. 155004-038) is from Gibco/LifeTechnologies. Concentrated HCl (Cat. No. P074.1), glycerol (Cat. No. 3783.2), methanol (4627.2), milk powder (blotting grade) (Cat. No. T145.1), and glass beads (0.5 mm) (Cat. No. A553.1) are from Roth. Ni-NTA agarose (Cat. No. 30210), penta-His antibody (Cat. No. 34660), and polypropylene columns (1 ml, unpacked columns) (Cat. No. 34924) are from Qiagen. Rabbit antimouse IgG/HRP conjugate (Cat. No. P0260) is from Dako (Denmark), and Strep-Tactin HRP conjugate (Cat. No. 2-1502-001) and Strep-Tactin sepharose (50% suspension) (Cat. No. 2-1201-005) are from IBA GmbH (Göttingen, Germany). The ECL substrate western lightning chemiluminescence reagent plus (Cat. No. NEL 105) is from PerkinElmer Life Science, the polyvenylidene difluoride (PVDF) membrane (Cat. No. IPVH00010) is from Millipore, and the 3 MM chromatography paper (Cat. No. 3030-690) is from Whatman.

The incubator shaker (Innova 4430) is from New Brunswick Scientific. The centrifuge is from Heraeus Instruments (Megafuge 1.0R). The vortex (Vortex-2 genie, Model G-560) is from Scientific Industries Inc., the semidry blotter (Cat. No. 24200) is from H. Hölzel GmbH (Germany), and power supplies are from Bio-Rad (Power Pac 200/300). The imaging system (LAS-1000 luminescent image analyzer, Fujifilm) is from Raytest. The Thermomix Comfort (Cat. No. 5355000.011) is from Eppendorf. The micropipettes are from Gilson.

III. PROCEDURES

A. Copper-Inducible Expression of Proteins (Standard Scale)

The expression plasmid pYEXTHS-BN used here is a pYEXbx (Clontech) derivative, which was constructed to subclone cDNAs carrying a N-terminal *Bam*HI site and C-terminal *Not*I site overhang as polymerase chain reaction fragments (Holz *et al*., 2002). The expression of cDNAs is induced by adding $CuSO_4$. The strain *S. cerevisiae* AH22*ura*3 (Polakowski *et al*., 1998) is used as the expression strain. The plasmid DNA containing the cloned cDNA insert is transformed in *S. cerevisiae*, and the selected transformants are transferred to WMVIII medium for protein expression.

Solutions

1. *WM VIII medium*: See Table I
2. *0.5 M $CuSO_4$ stock*: Dissolve 6.2 g in 50 ml distilled water
3. *10× PBS stock*: 100 m*M* phosphate and 1.5 *M* NaCl. To make 2 liter, weigh 29.9 g of $Na_2HPO_4{\cdot}2H_2O$, 4.16 g of KH_2PO_4, and 175.32 g of NaCl and adjust to 2 liter with distilled water.
4. *1× PBS*: 8.4 m*M* Na_2HPO_4, 1.6 m*M* KH_2PO_4, and 150 m*M* NaCl. To make 500 ml, take 50 ml of 10× PBS and add distilled water to 500 ml.
5. *1 M Na_2HPO_4 stock*: To make 1 liter, weigh 177.99 g of $Na_2HPO_4{\cdot}2H_2O$ and bring up to 1 liter with distilled water
6. *1 M NaH_2PO_4 stock*: To make 1 liter, weigh 137.99 g of $NaH_2PO_4{\cdot}H_2O$ and top up to 1 liter with distilled water
7. *3 M NaCl*: To make 500 ml, weigh 87.66 g of NaCl and adjust to 500 ml with distilled water
8. *100 mM phenylmethylsulfonyl fluoride*: Dissolve 174 mg PMSF in 10 ml isopropanol. Divide the solution into 1-ml aliquots and store at –20°C.

TABLE I Components of WM VIII Protein Production Medium[a]

Ingredient	Amount
Component I: Autoclaved in 990 ml distilled water	
Sucrose	50 g
$NH_4H_2PO_4$	0.25 g
NH_4Cl	2.8 g
$MgCl_2 \cdot 6H_2O$	0.25 g
$CaCl_2 \cdot 2H_2O$	0.1 g
KH_2PO_4	2.0 g
$MgSO_4 \cdot 7H_2O$	0.55 g
myo-Inositol	0.075 g
Sodium L-glutamate monohydrate	10.0 g
Component II (microelements): Dissolved in 100 ml 10 m*M* EDTA, pH 8.0, and filter sterilized	
$ZnSO_4 \cdot 7H_2O$	43.7 mg
$FeSO_4 \cdot 7H_2O$	12.5 mg
$CuSO_4 \cdot 5H_2O$	2.5 mg
$MnCl_2 \cdot 4H_2O$	2.5 mg
$Na_2MoO_4 \cdot 2H_2O$	2.5 mg
Component III (vitamin stock solution): Dissolved in 200 ml H_2O, and filter sterilized	
Nicotinic acid (vitamin B)	0.5 g
Pyridoxine (vitamin B_6)	1.25 g
Thiamine (vitamin B_1)	0.5 g
Biotin	0.125 g
Calcium *d*-pantothenate	2.5 g
Component IV: Filter sterilized in 20 ml distilled water	
L-Histidine HCl	0.4 g

[a] Component I is mixed after autoclaving with 4 ml of component II, 4 ml of component III, and 2 ml of component IV. The pH will be approximately 6.

9. *Lysis buffer*: 100 m*M* NaPO4, pH 8.0, 300 m*M* NaC1, and 1% Triton X. To make 100 ml, add 9.3 ml of a 1 *M* stock solution of Na_2HPO_4, pH 8.0, 680 µl of a 1 *M* stock solution of NaH_2PO_4, 10 ml of a 3 *M* stock solution of NaCl, and 1 ml Triton X-100 (100%, Serva). Fill up to 100 ml with distilled water.

10. *1 M Tris–HCl (pH 6.8) stock*: Dissolve 121.1 g Tris base in 800 ml of H_2O. Adjust pH to 6.8 by adding concentrated HCl (about 80 ml), complete to 1 liter with distilled water, and sterilize by autoclaving.

11. *4× SDS PAGE sample buffer*: 0.2 *M* Tris–HCl, pH 6.8, 8% (w/v) SDS, 40% (v/v) glycerol, 5% (v/v) 2-mercaptoethanol, and 0.4% (w/v) bromphenol blue. To make 50 ml, add 10 ml of a 1 *M* stock of Tris–HCl, pH 6.8, 4 g of SDS, 20 ml of glycerol, 2.5 ml of β-mercaptoethanol, and 0.2 g bromphenol blue. Top up to 50 ml with distilled water.

Steps

1. Inoculate 20 ml WM VIII medium containing 40 mg/liter histidine in a 100-ml shake flask with a single colony of *S. cerevisiae* AH22*ura*3 bearing the pYEXbx derivative with target CDNA insert as preculture and grow overnight with shaking (200 rpm) at 28°C.

2. Inoculate 100 ml WM VIII medium containing 40 mg/liter histidine in a 500-ml shake flask with 1 ml from the preculture. Grow with shaking (200 rpm) at 28°C for 16–24 h to an OD_{600} of 7–10.

3. Induce the protein expression of the culture by adding 100 µl of a 0.5 *M* stock of $CuSO_4$ (0.5 m*M* final concentration) and incubate the culture with shaking for another 3–4 h at 28°C.

4. Collect an aliquot of 7–10 ml of the cell culture (corresponding to OD_{600} = 70) by centrifugation (10 min, 2500 *g*, 4°C).

5. Resuspend the cell pellet in 5 ml cold PBS. Repeat the spin and discard supernatant.

6. Freeze the washed cells in dry ice-ethanol or liquid nitrogen or store cell pellet at –70°C.

7. Thaw cells at room temperature and resuspend the cells in 300 µl ice-cold lysis buffer and add 3 µl of 100 m*M* stock solution of PMSF (1 m*M* final concentration).

8. Add 1 volume of sterile, acid-washed glass beads (0.5 mm) and disrupt the cells by seven cycles of 1 min full-speed vortexing/1 min cooling on ice.

9. Centrifuge the lysate for 15–20 min at 10,000 *g* at 4°C to remove cellular debris and transfer the supernatant to a fresh tube.

10. Take a 15-µl sample and add 5 µl 4× SDS–PAGE sample buffer, heat the sample at 95°C for 5 min, and store at –20°C for SDS–PAGE and Western blot analysis. *Note:* You cannot detect the recombinant target gene product directly from the total yeast protein after electrophoresis of proteins by staining the gel due to the low proportion of recombinant protein. This requires purifying the recombinant protein from crude extract or detecting the target protein by immunoblotting (Section III,D).

11. Proceed to protocols for purification (Sections III,B and III,C).

B. Affinity Purification of His_6-Tagged Proteins via Ni-NTA Agarose

Solutions

1. *1 M imidazole stock*: To make 100 ml, weigh 6.81 g of imidazole and complete to 100 ml with distilled water

2. *Wash buffer*: 50 m*M* $NaPO_4$, pH 8.0, 300 m*M* NaC1, and 5 m*M* imidazole. To prepare 500 ml, add 23.3 ml of a 1 *M* stock solution of Na_2HPO_4, pH 8.0, 1.7 ml of a 1 *M* stock solution of NaH_2PO_4, 50 ml of a

3 *M* stock solution of NaCl, and 2.5 ml of a 1 *M* stock solution of imidazole. Adjust pH to 8.0 with HCl and adjust volume to 500 ml with distilled water.

3. *Elution buffer*: 50 m*M* $NaPO_4$, pH 8.0, 300 m*M* NaCl, and 250 m*M* imidazole. To prepare 100 ml, add 4.66 ml of a 1 *M* stock solution of Na_2HPO_4, pH 8.0, 340 µl of a 1 *M* stock solution of NaH_2PO_4, 10 ml of a 3 *M* stock solution of NaCl, and 25 ml of a 1 *M* stock solution of imidazole. Adjust pH to 8.0 with HCl and adjust volume to 100 ml with distilled water.

Steps

1. Add 100 µl of a 50% slurry of Ni-NTA resin (100 µl resin has a capacity for 500 µg–1 mg His_6-tagged protein) to 300 µl cleared lysate that contains whole cell proteins (Section III,A, step 8) and mix gently by shaking for 60 min at 4°C.
2. Load the lysate Ni-NTA mixture into an unpacked column.
3. Collect the column flow through. Save flow through for SDS–PAGE analysis.
4. Wash three times with 400 µl wash buffer and collect wash fractions. Save wash fractions for SDS–PAGE analysis.
5. Elute the protein three times with 100 µl elution buffer. Collect the elution fractions and analyze by SDS–PAGE.

C. Affinity Purification via StrepTactin

The affinity purification is carried out according to Voss and Skerra (1997) with some modifications.

Solutions

1. *1 M Tris–HCl (pH 8.0) stock*: Dissolve 121.1 g Tris base in 800 ml of H_2O. Adjust pH to 8.0 by adding concentrated HCl (about 40 ml), top up to 1 liter with distilled water, and sterilize by autoclaving.
2. *250 mM EDTA stock*: Weigh 9.3 g of EDTA, top up to 100 ml with distilled water, and sterilize by autoclaving
3. *Buffer W*: 100 m*M* Tris–HCl, pH 8.0, 1 m*M* EDTA. To make 100 ml, take 10 ml of a 1 *M* stock solution of Tris–HCl, pH 8.0, and 400 µl of a 250 m*M* EDTA stock solution. Top up to 100 ml with distilled water.
4. *25 mM Desthiobiotin solution*: 25 m*M* Desthiobiotin and 100 m*M* Tris–HCl, pH 8.0. To make 100 ml, add 0.536 g Desthiobiotin, 10 ml of 1 *M* stock solution of Tris–HCl, pH 8.0, and top up to 100 ml with distilled water.
5. *Buffer E*: 100 m*M* Tris–HCl pH 8.0, 1 m*M* EDTA, and 2.5 m*M* Desthiobiotin. To make 100 ml, add 10 ml of a 1 *M* stock solution of Tris–HCl, pH 8.0, 400 µl of a 250 m*M* EDTA stock solution, and 10 ml of a 25 m*M* stock solution of Desthiobiotin. Adjust to 100 ml with distilled water.
6. *Avidin solution (2 mg/ml)*: Dissolve 5 mg avidin (65 units) in 2.5 ml buffer W.

Steps

1. Transfer 200 µl of 50% StrepTactin sepharose (IBA GmbH) into an unpacked column and wash twice with 600 µl buffer W.
2. Load 200 µl of the eluate from the Ni-NTA resin (Section III,B step 5) onto the equilibrated column to perform the second step of the two-step affinity chromatography purification or take 200 µl cleared lysate (Section III,A step 8), pretreat this lysate with 1 µl of avidin solution (2 mg/ml) to mask inhibiting biotinylated proteins for 30 min at 4°C, spin down the aggregates formed by centrifugation (15 min, 10,000 *g*, 4°C), and load the cleared supernatant onto the column.
3. Collect the column flow through. Save flow through for SDS–PAGE analysis.
4. Wash five times with 200 µl buffer W and collect wash fractions. Save wash fractions for SDS–PAGE analysis.
5. Elute protein with 5× 100 µl buffer E. Collect the elution fractions and analyze by SDS–PAGE.

D. Protein Analysis by Western Blot and Immunodetection with Anti-His Antibody or StrepTactin HRP Conjugate (Chemiluminescent Method)

The proteins are separated by 12.5% SDS–PAGE according to Laemmli (1970). Following electrophoresis, proteins in polyacrylamide gel are transferred to polyvinylidene difluoride (PVDF) membranes by semidry electroblotting as described later and characterized by immunodetection (Fig. 1).

Solutions

1. *Transfer buffer*: 25 m*M* Tris base, 192 m*M* glycine, and 10% methanol. To make 1 liter, weigh 3.03 g Tris base, 14.4 g glycine, add 100 ml methanol, and adjust to 1 liter with distilled water.
2. *PBST*: 8.4 m*M* Na_2HPO_4, 1.6 m*M* KH_2PO_4, 150 m*M* NaCl, and 0.1% (v/v) Tween 20. To make 1 liter, take 100 ml of 10× PBS, 1 ml Tween 20, and top up to 1 liter with distilled water.
3. *Blocking solution*: 2% (w/v) BSA in PBST. To make 100 ml, weigh 2 g of BSA and top up to 100 ml with PBST. Prepare fresh or keep at –20°C.
4. *Secondary antibody dilution buffer*: 5% (w/v) nonfat dried milk (milk powder) in PBST. To make

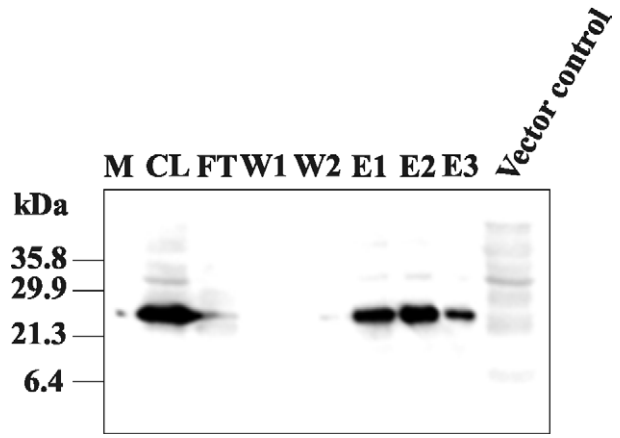

FIGURE 1 Expression and purification of the His_6/StrepII-tagged human G-substrate protein (21 kDa) from *S. cerevisiae* as an example. Cleared cell lysate (CL) was prepared and expressed protein purified via Ni-NTA. A clone carrying an empty expression vector was used as the negative control (vector control). The proteins were separated by SDS–PAGE and detected by immunoblotting with StrepTactin HRP conjugate. M, prestained Bio-Rad broad range marker; FT, flow through from Ni-NTA column; W1, wash fraction 1; W2, wash fraction 2; E1–E3, eluates 1–3.

100 ml, weigh 5 g of milk powder and top up to 100 ml with PBST.

Steps

1. Cut eight pieces of Whatman 3 MM paper and a piece of membrane to the same size as the gel. To avoid contamination, always handle the filter paper and membrane with gloves.
2. Wet the PVDF membrane in 100% methanol (or ethanol) for 15 s. Then transfer it to a container of distilled (or Milli-QR) water for 2 min.
3. Equilibrate the membrane for at least 5 min in the transfer buffer.
4. Soak the filter paper in transfer buffer.
5. Immerse the gel in the transfer buffer.
6. Place four sheets of filter paper in the center of the anode electrode plate (positive, usually red), avoiding air bubbles, and place the membrane on top of the filter paper.
7. Place the gel on top of the membrane and place four sheets of filter paper on top of the gel. Air bubbles can be removed by gently rolling a Pasteur pipette over each layer in the sandwich.
8. Place the cathode plate cover (negative, usually black) on the top of the assembled transfer stack.
9. Connect the anode and the cathode lead to their corresponding power supply outputs. Follow the manufacturer's instructions regarding current, voltage, and transfer times. The current density required is determined by the size of the gel: 1 mA/cm^2 is recommended (1-h transfer).
10. After transferring, mark the orientation of the membrane and the position of bands of the prestained protein standard. You can stain the blot to assess the quality of transfer with Ponceau-S red (reversible stain). Incubate membrane in staining solution (0.5% Ponceau S, 1% acetic acid) with gentle agitation for 2 min. The blot will be destained in distilled water or during the following immunological detection procedure.
11. Incubate the membrane for at least 1 h in blocking solution at room temperature. If using StrepTactin HRP conjugate for detection, subsequently pretreat the membrane in PBST containing 2 µg/ml avidin for 30 min to block biotinylated proteins.
12. Incubate with primary antibody (penta-His antibody, Qiagen) diluted at 1 : 1000/1 : 2000 or StrepTactin HRP conjugate diluted at 1 : 4000 in blocking solution at room temperature for 1 h. *Note:* Do not use dilution buffer containing milk powder for anti-His antibody. This will reduce sensitivity. Do not use milk powder for StrepTactin HRP conjugate either as it contains large amounts of cross-reacting biotin.
13. Wash membrane three times for 10 min each time in PBST at room temperature. When using StrepTactin HRP conjugate, proceed directly to step 16.
14. Incubate with secondary antibody solution for 1 h at room temperature. Either alkaline phosphatase or horseradish peroxidase (HRP)-conjugated antimouse IgG may be used. The rabbit antimouse IgG/HRP conjugate from DAKO yields good results. Dilute according to manufacturer's recommendations. Use 5% nonfat dried milk in PBST for incubation with the secondary antibody when using the chemiluminescent detection method.
15. Wash filter four times for 10 min each time in PBST at room temperature.
16. Perform detection reaction with AP or HRP chemiluminescence reagent and expose to X-ray film or detect by a luminescent imaging system according to the manufacturer's recommendations. Western lightning chemiluminescence reagent plus (PerkinElmer) yields good results.

References

Becker, D. M., and Guarente, L. (1991). High-efficiency transformation of yeast by electroporation. *Methods Enzymol.* **194**, 182–187.

Bonneaud, N., Ozier-Kalogeropoulos, O., Li, G. Y., Labouesse, M., Minvielle-Sebastia, L., and Lacroute, F. (1991). A family of low and high copy replicative, integrative and single-stranded *S. cerevisiae/E. coli* shuttle vectors. *Yeast* **7**, 609–615.

Etcheverry, T. (1990). Induced expression using yeast copper metallothionein promoter. *Methods Enzymol.* **185**, 319–329.

Gietz, D., St Jean, A., Woods, R. A., and Schiestl, R. H. (1992). Improved method for high efficiency transformation of intact yeast cells. *Nucleic Acids Res.* **20**, 1425.

Harashima, S. (1994). Heterologous protein production by yeast host-vector systems. *Bioprocess Technol.* **19**, 137–158.

Holz, C., Hesse, O., Bolotina, N., Stahl, U., and Lang, C. (2002). A micro-scale process for high-throughput expression of cDNAs in the yeast *Saccharomyces cerevisiae*. *Protein Expr Purif.* **25**, 372–378.

Laemmli, U. K. (1970). Cleavage of structural proteins during the assembly of the head of bacteriophage T4. *Nature* **227**, 680–685.

Polakowski, T., Stahl, U., and Lang, C. (1998). Overexpression of a cytosolic hydroxymethylglutaryl-CoA reductase leads to squalene accumulation in yeast. *Appl. Microbiol. Biotechnol.* **49**, 66–71.

Porath, J. (1992). Immobilized metal ion affinity chromatography. *Protein Expr. Purif.* **3**, 263–281.

Romanos, M. A., Scorer, C. A., and Clare, J. J. (1992). Foreign gene expression in yeast: A review. *Yeast.* **8**, 423–488.

Rose, A. B., and Broach, J. R. (1990). Propagation and expression of cloned genes in yeast: 2-micron circle-based vectors. *Methods Enzymol.* **185**, 234–279.

Schmidt, T. G., Koepke, J., Frank, R., and Skerra, A. (1996). Molecular interaction between the Strep-tag affinity peptide and its cognate target, streptavidin. *J. Mol. Biol.* **255**, 753–766.

Voss, S., and Skerra, A. (1997). Mutagenesis of a flexible loop in streptavidin leads to higher affinity for the Strep-tag II peptide and improved performance in recombinant protein purification. *Protein Eng.* **10**, 975–982.

Ward, A. C., Castelli, L. A., Macreadie, I. G., and Azad, A. A. (1994). Vectors for Cu(2+)-inducible production of glutathione S-transferase-fusion proteins for single-step purification from yeast. *Yeast* **10**, 441–449.

CHAPTER

9

Semliki Forest Virus Expression System

Maria Ekström, Henrik Garoff, and Helena Andersson

I. INTRODUCTION

The Semliki forest virus (SFV) is a positive-stranded RNA virus belonging to the alphaviruses (Schlesinger and Schlesinger, 1986). The SFV expression system is based on a cDNA copy of the viral genome. The cDNA has been cloned into an SP6-based transcription vector in such a way that exact copies of the alphavirus RNA genome can be transcribed *in vitro* (Liljeström and Garoff, 1991). In the SFV1 vector, genes coding for the viral structural proteins have been replaced with a polylinker region into which heterologous genes can be cloned. The recombinant plasmid then serves as a template for *in vitro* synthesis of recombinant RNA. When introduced into cells, the recombinant RNA self-replicates, as it codes for its own replicase, leading to high synthesis of the heterologous protein while competing out the host protein synthesis.

In the SFVC vector the viral capsid gene is retained and the heterologous gene is cloned directly downstream of the capsid gene by polymerase chain reaction (PCR) (Horton *et al*., 1989). Due to the presence of a translation-enhancing region in the capsid gene, the expression level reached using the SFVC vector is about 10 times higher than when using the SFV1 vector (Sjöberg *et al*., 1994).

The recombinant RNA can be either directly introduced into cells by electroporation or packaged *in vitro* by cotransfecting cells with the recombinant RNA and a packaging-deficient helper RNA (SFV/Helper 1 or SFV/Helper 2) encoding the structural proteins of SFV needed for the assembly of new virus particles (Liljeström and Garoff, 1991; Berglund *et al*., 1993). The virus stock obtained is then used to introduce the recombinant RNA into cells by way of infection. This article describes optimized protocols for the production of heterologous proteins in baby hamster kidney (BHK 21) cells using this system.

II. MATERIALS AND INSTRUMENTATION

Culture medium Glasgow MEM (BHK 21) (Cat. No. 21710), fetal bovine serum (FBS) (Cat. No. 10106), tryptose phosphate broth (Cat. No. 18050), 1 *M* HEPES (Cat. No. 15630), 200 m*M* L-glutamine (100×) (Cat. No. 25030), penicillin–streptomycin (Cat. No. 15140), trypsin–EDTA (10×) (Cat. No. 35400), phosphate-buffered saline (PBS) Dulbecco's without Ca^{2+} and Mg^{2+} (Cat. No. 14190), minimum essential medium (MEM) (Cat. No. 21090-022), bovine albumin fraction V solution 7.5% (BSA) (Cat. No. 15260-037), unlabeled methionine (Cat. No. 11086), and PBS Dulbecco's with Ca^{2+} and Mg^{2+} (Cat. No. 14040) are from Invitrogen. Corning/Life Sciences provided 75-cm^2 flasks (Cat. No. 3375), 15-ml centrifuge tubes (Cat. No. 430789), 50-ml centrifuge tubes (Cat. No. 430828), and 35-mm tissue culture plates (Cat. No. 430165). HEPES (Cat. No. 223778) and chymotrypsin (Cat. No. 1418467) are from Roche. Magnesium acetate (MgOAc) (Cat. No. 105819), sodium acetate (NaOAc) (Cat. No. 106268), potassium hydroxide (KOH) (Cat. No. 105033), TitriplexIII, EDTA (Cat. No. 108418), sodium dihydrogen phosphate monohydrate ($NaH_2PO_4 \cdot H_2O$) (Cat. No. 106346), disodium hydrogen phosphate dihydrate ($Na_2HPO_4 \cdot 2H_2O$) (Cat. No. 106580), sodium chloride (NaCl) (Cat. No. 106404), methanol (Cat. No. 106009), sodium hydroxide (NaOH) (Cat. No. 106469), glacial acetic acid (Cat. No. 100066), and isopropanol (Cat. No.

Copyright 2006, Elsevier Science (USA).
All rights reserved.

109634) are from Merck. Spermidine (Cat. No. S-2501), dithiothreitol (DTT) (Cat. No. D-9779), phenol : chloroform : isoamylalcohol (Cat. No. P-3803), diethyl pyrocarbonate (Cat. No. D-5758), bromphenol blue (Cat. No. B-6131), gelatin (Cat. No. G-9382), aprotinin (Cat. No. A-6279), phenylmethylsulfonyl fluoride (PMSF) (Cat. No. P-7626), methionine-free MEM (Cat. No. M-3911), and Ficoll 400 (Cat. No. F-4375) are from Sigma-Aldrich. Diguanosine triphosphate sodium (Cat. No. 27-4643-01), SP6 RNA polymerase (Cat. No. E2520Y), ATP (Cat. No. 27-2056-01), CTP (Cat. No. 27-2066-01), GTP (Cat. No. 27-2076-01), and UTP (Cat. No. 27-2086-01) are from Amersham Pharmacia Biotech. *SpeI* (Cat. No. R6591) and RNasin (Cat. No. N2511) are from Promega. Sea-plaque agarose (Cat. No. 50100) is from FMC Bio Products. Ether (Cat. No. 32203) and boric acid (Cat. No. 31146) are from Riedel-de-Haën. Xylene cyanol FF (Cat. No. 44306 2B) and Nonidet P-40 (NP-40) (Cat. No. 56009 2L) are from BDH Laboratory supplies. Electroporation cuvettes (Cat. No. ECU-104) are from EquiBio. The gene pulser is from Bio-Rad. Tris (Cat. No. 146861) is from Angus buffersbiochemicals. FluorSave Reagent (Cat. No. 345789) is from Calbiochem. Coverslips (18 × 18 mm) (Cat. No. 1.0) are from Menzel-Glaser. [^{35}S]Methionine (Cat. No. AG1094) is from Amersham Biosciences. BHK 21 cells C-13 (Cat. No. CRL 8544) are from American Type Culture Collection.

III. PROCEDURES

A. Preparation of mRNA *in vitro*

Solutions

1. *DEPC-H_2O*: To make 1 liter, add 1 ml of diethyl pyrocarbonate to distilled water and mix hard overnight at 37°C with a stirring magnet. Pour into RNase-free bottles and autoclave. Store at room temperature.
2. *3 M NaOAc, pH 6.0*: To make 10 ml, add 2.46 g of NaOAc, adjust pH with glacial acetic acid, and complete the volume with distilled water. Store at room temperature.
3. *1 M HEPES–KOH, pH 7.4, stock solution*: To make 10 ml, add 2.38 g of HEPES to DEPC-H_2O, adjust pH to 7.4 with 3 *M* KOH, and complete the volume to 10 ml with DEPC-H_2O. Store at 4°C.
4. *1 M MgOAc stock solution*: To make 10 ml, add 2.14 g of MgOAc to DEPC-H_2O. Store at 4°C.
5. *200 mM spermidine–HCl stock solution*: To make 3 ml, add 153 mg of spermidine to DEPC-H_2O. Store as aliquots at –20°C.
6. *10x SP6 buffer*: 400 m*M* HEPES–KOH, pH 7.4, 60 m*M* MgOAc, 20 m*M* spermidine–HCl. To make 10 ml, add 4 ml of 1 *M* HEPES–KOH, pH 7.4, stock solution, 600 µl of 1 *M* MgOAc stock solution, 1 ml of 200 m*M* spermidine–HCl stock solution, and complete the volume to 10 ml with DEPC-H_2O. Store as aliquots at –20°C.
7. *50 mM DTT*: To make 10 ml, add 77.1 mg of DTT to DEPC-H_2O. Store as aliquots at –20°C.
8. *rNTPmix*: 10 m*M* ATP, 10 m*M* CTP, 10 m*M* UTP, 5 m*M* GTP. To make 200 µl, add 20 µl of 100 m*M* ATP stock solution, 20 µl of 100 m*M* CTP stock solution, 20 µl of 100 m*M* UTP stock solution, 10 µl of 100 m*M* GTP stock solution, and complete the volume to 200 µl with DEPC-H_2O. Store as aliquots at –20°C.
9. *0.5 M EDTA, pH 8.0, stock solution*: To make 10 ml, add 1.86 g of Titriplex III to DEPC-H_2O, adjust pH to 8.0 with NaOH, and complete the volume to 10 ml with DEPC-H_2O. Store at room temperature.
10. *5x TD*: 20% Ficoll 400, 25 m*M* EDTA, pH 8.0, 0.05% bromphenol blue, 0.03% xylene cyanol. To make 10 ml, add 2 g of Ficoll 400, 0.5 ml of 0.5 *M* EDTA pH 8.0 stock solution, 5 mg of bromphenol blue, 3 mg of xylene cyanol, and complete the volume to 10 ml with DEPC-H_2O. Store as aliquots at –20°C.
11. *10x TBE*: To make 1 liter, add 60.55 g of Tris base, 30.9 g of boric acid, and 9.3 g of EDTA to distilled water. Store at room temperature.

Steps

1. Linearise 3 µg of plasmid DNA with 3 U *Spe*I at 37°C for 60 min in a total volume of 50 µl. Verify complete linearisation by gel electrophoresis.
2. Add H_2O to a final volume of 100 µl and add 10 µl 3 *M* sodium acetate, pH 6.0.
3. Add 100 µl phenol : chloroform : isoamylalcohol and mix.
4. Centrifuge at 16,000 *g* for 1 min at room temperature.
5. Transfer the water phase to a fresh tube.
6. Add 500 µl water saturated ether and mix.
7. Centrifuge at 16,000 *g* for 20 s at room temperature.
8. Remove the ether phase with a water jet pump.
9. Repeat steps 6–8.
10. Add 250 µl ethanol and incubate for 10 min at –70°C to precipitate the DNA. Centrifuge for 20 min at 12,000 *g* in a microcentrifuge at 4°C. Wash the pellet with 800 µl 75% ethanol. Centrifuge for 20 min at 12,000 *g*. Remove ethanol. Dry the pellet in a Speed Vac for 10 min or at room temperature for about 20 min. Resuspend the DNA pellet in 5 µl DEPC-H_2O.
11. Mix the following in a 1.5-ml tube at room temperature: 23 µl H_2O, 5 µl 10 × SP6 buffer, 5 µl 10 m*M*

diguanosine triphosphate sodium, 5 µl 50 m*M* DTT, and 5 µl rNTP mix. Centrifuge at 16,000 *g* for 10 s at room temperature to remove precipitates.Transfer to a fresh tube: 1.5 µl RNasin (50 units), 5 µl linearised DNA, and 60 U SP6 RNA polymerase

12. Incubate at 37°C for 1 h.
13. Take a 1-µl aliquot into 7 µl DEPC-H_2O, add 2 µl of 5 × TD loading buffer, and run the RNA mix on a 0.7% agarose TBE gel containing 0.02% ethidium bromide to check RNA production.
14. Freeze the rest of the RNA mix on dry ice and then transfer it to –70°C.

B. *In vivo* Packaging of Recombinant RNA into SFV Particles

Solution

BHK 21 medium: 500 ml of BHK medium G-MEM,
25 ml of fetal bovine serum,
50 ml of tryptose phosphate broth,
5 ml of 1 *M* HEPES,
5 ml of 200 m*M* glutamine, and
5 ml of 10,000 U/ml penicillin/10,000 µg/ml streptomycin.
Store at 4°C.

Steps

1. Grow BHK 21 cells in a 75-cm^2 bottle to late log phase in complete BHK medium.
2. Wash cells with 10 ml PBS (without Ca^{2+} and Mg^{2+}).
3. Wash cells with 2 ml of 1x trypsin–EDTA (0.5/0.2 mg/ml, respectively) in PBS (without Ca^{2+} and Mg^{2+}) and incubate the cells at 37°C for 10 min.
4. Add 2 ml of complete medium and pipette the solution back and forth to detach cells and to remove clumps, add 8 ml of complete BHK medium, and again pipette to remove aggregates.
5. Transfer cells to a 15-ml centrifuge tube and harvest cells by centrifugation for 5 min, 400 *g* at room temperature.
6. Resuspend cells in 5 ml of PBS (without Ca^{2+} and Mg^{2+}).
7. Harvest cells as in step 5.
8. Resuspend cells in 0.8 ml of PBS (without Ca^{2+} and Mg^{2+}).
9. Add 20 µl of SFV/Helper 1 or SFV/Helper 2 RNA and 20 µl of SFV recombinant RNA.
10. Transfer the mixture to a 0.4-cm electroporation cuvette.
11. Pulse twice at 850 V/25 µF. The time constant should show 0.4 after each pulse.
12. Transfer cells to 16 ml of complete BHK medium and rinse the cuvette with the same medium to collect all cells. Then transfer the medium to a 75-cm^2 bottle.
13. Incubate cells for 24 h at 37°C.
14. Clarify the growth medium by centrifugation in a 50-ml centrifuge tube at 1800 *g* 10 min, 4°C.
15. Aliquot into 1.5-ml Eppendorf tubes and freeze rapidly on dry ice pellets. Store at –70°C.

C. Titer Determination of Helper 1-Packaged Virus by Immunofluorescence

Solutions

1. *Supplemented MEM*: 500 ml of MEM, 5 ml of 1 *M* HEPES, 5 ml of 200 m*M* glutamine 5 ml of 10,000 U/ml penicillin/10,000 µg/ml streptomycin, and 14.1 ml of 7.5% BSA. Store at 4°C.
2. *2% PBS–gelatine stock solution*: To make 100 ml, add 2 g of gelatine to PBS. Autoclave. Store at room temperature.
3. *0.2% PBS–gelatine*: To make 100 ml, add 10 ml of 2% PBS–gelatine stock solution and complete the volume to 100 ml with PBS. Store at room temperature.

Steps

1. Grow BHK 21 cells on 18 × 18-mm glasscoverslips to about 80% confluency in complete BHK medium.
2. Pipette 50, 5, and 0.5 µl of recombinant virus stock to Eppendorf tubes and complete the volume to 500 µl with supplemented MEM (dilutions 1 : 10, 1 : 100, 1 : 1000).
3. Remove the medium and wash cells with 2 ml PBS (with Ca^{2+} and Mg^{2+}).
4. Add the total virus solution (500 µl) to the cells.
5. Incubate for 60 min at 37°C. Tilt the dishes every 20 min to ensure even distribution of virus particles.
6. Remove virus solution and add 3 ml complete BHK 21 medium and continue incubation for 5 h at 37°C.
7. Rinse coverslips twice with 2 ml PBS (with Ca^{2+} and Mg^{2+}). Fix cells in –20°C methanol for 6 min at –20°C.
8. Remove methanol and wash coverslips three times with 2 ml PBS.
9. Add 2 ml of 0.2% PBS–gelatine and incubate for 5 min at room temperature to block nonspecific binding.
10. Replace blocking buffer with the same containing primary antibody and incubate at room temperature for 30 min.
11. Wash cells twice with 2 ml of 0.2% PBS–gelatine and twice with 2 ml of PBS. Incubate for 5 min at

room temperature between each wash (total of 20 min).
12. Dilute secondary antibody in blocking buffer and incubate with cells at room temperature for 30 min.
13. Wash cells twice with 2 ml of 0.2% PBS–gelatine for 5 min and twice with 2 ml of PBS for 5 min.
14. Rinse coverslips in distilled water, dry, and mount in FluorSave reagent.
15. Count positive cells in a fluorescence microscope.

D. Titer Determination of Helper 2-Packaged Virus by Immunofluorescence

Solutions

1. *See solutions in Section III,C*
2. *10 mg/ml chymotrypsin A4 stock solution*: To make 1 ml, add 10 mg of chymotrypsin A4 to PBS with Ca^{2+} and Mg^{2+}. Store as aliquots at –20°C.

Steps

1. Grow BHK 21 cells on 18 × 18-mm glasscoverslips to about 80% confluency in complete BHK medium.
2. Activate virus stock by taking 55.5 µl virus stock solution and add 2.8 µl 10 mg/ml chymotrypsin and incubate for 30 min at room temperature.
3. Inactivate chymotrypsin by adding 29.1 µl aprotinin.
4. Pipette 78.7, 7.9, and 0.8 µl of activated virus to Eppendorf tubes and complete the volume to 500 µl with supplemented MEM (dilutions 1 : 10, 1 : 100, 1 : 1000).
5. Continue from step 3, Section III,C.

E. Metabolic Labeling of Infected Cells

Solutions

1. *Starvation medium*: 100 ml of methionine-free MEM, 1 ml of 200 m*M* glutamine, 1 ml of 1 *M* HEPES, and 1 ml of 10,000 U/ml penicillin/10,000 µg/ml streptomycin. Store at 4°C.
2. *15 mg/ml unlabelled methionine stock solution*: To make 100 ml, add 1.5 g of methionine to distilled water. Sterile filter. Store as aliquots at –20°C.
3. *Chase medium*: 500 ml of MEM, 5 ml of 200 m*M* glutamine, 5 ml of 1 *M* HEPES, and 5 ml of 10,000 U/ml penicillin/10,000 µg/ml streptomycin. Store at 4°C. Add 150 µg/ml of unlabelled methionine just before use from the stock solution.
4. *10% NP40 stock solution*: To make 100 ml, add 10 g of NP-40 to distilled water. Sterile filter. Store at room temperature.
5. *1 M Tris–HCl, pH 7.6, stock solution*: To make 100 ml, add 12.1 g of Tris and adjust pH with HCl. Complete the volume with distilled water. Autoclave. Store at 4°C.
6. *4 M NaCl stock solution*: To make 100 ml, add 23.4 g of NaCl to distilled water. Autoclave. Store at room temperature.
7. *0.2 M EDTA stock solution*: To make 100 ml, add 7.45 g of Titriplex III to distilled water and warm it to dissolve the EDTA. Sterile filter. Store at room temperature.
8. *10 mg/ml PMSF stock solution*: To make 1 ml, add 10 mg of PMSF to isopropanol. Store dark at room temperature. *Note:* Very toxic.
9. *1x lysis buffer*: 1% NP-40, 50 m*M* Tris–HCl, pH 7.6, 150 m*M* NaCl, 2 m*M* EDTA, 10 µg/ml PMSF. To make 100 ml, add 10 ml of 10% NP-40 stock solution, 5 ml of 1 *M* Tris–HCl, pH 7.6 stock solution, 3.75 ml of 4 *M* NaCl stock solution, 1 ml of 0.2 *M* EDTA stock solution, and complete the volume to 100 ml with distilled water. Store at 4°C. Add 10 µg/ml of PMSF just before use from the stock solution.

Steps

1. Grow BHK 21 cells to 80–100% confluency on a 35-mm tissue culture plate in complete BHK medium.
2. Dilute virus in supplemented MEM using a multiplicity of infection of 5.
3. Remove the medium and wash cells with 2 ml of PBS (with Ca^{2+} and Mg^{2+}).
4. Add 500 µl of the virus solution to the cells.
5. Incubate for 60 min at 37°C. Tilt every 20 min.
6. Remove virus solution and add 3 ml of complete BHK 21 medium and continue incubation for 6 h at 37°C.
7. Aspirate growth medium and wash cells twice with 2 ml of PBS (with Ca^{2+} and Mg^{2+}) prewarmed to 37°C.
8. Overlay cells with 2 ml of starvation medium prewarmed to 37°C and incubate plates at 37°C for 30 min.
9. Aspirate medium and replace with 500 µl of the same containing 100 µCi/ml of [^{35}S]methionine and incubate for appropriate pulse time at 37°C.
10. Aspirate pulse medium and wash cells twice with 2 ml of chase medium prewarmed to 37°C.
11. Overlay cells with 2 ml of chase medium and incubate for required chase time at 37°C.
12. Remove medium and wash cells with 2 ml of ice-cold PBS (with Ca^{2+} and Mg^{2+}).
13. Add 300 µl of ice-cold lysis buffer and incubate for 10 min on ice. Resuspend cells and transfer into an Eppendorf tube.

14. Centrifuge for 5 min at 3000 *g* at 4°C to pellet nuclei. Transfer supernatant to a fresh tube. Store at –70°C.
15. Assay for protein expression by SDS–PAGE and autoradiography.

F. Metabolic Labeling of Transfected Cells

Solutions

See solutions in Section III,E

Steps

See Section III,B, steps 1–8.

9. Add 20 µl of recombinant RNA.
10. Transfer the mixture to a 0.4-cm electroporation cuvette.
11. Pulse twice at 850 V/25 µF. The time constant should show 0.4 after each pulse.
12. Transfer cells to 16 ml of complete BHK medium, rinse the cuvette with the same medium to collect all cells, and transfer 3 ml to a 35-mm tissue culture plate.
13. Incubate cells for 7 h at 37°C.
14. Continue from step 7 Section III,E.

IV. COMMENTS

The cloning of recombinant DNA into the SFVC vector has been done by PCR (Horton *et al*., 1989). The capsid protein has autoproteolytic activity and will cleave itself from the heterologous protein, provided that the cleavage site is preserved (Melancon and Garoff, 1987). Systematic probing of tolerated amino acid residues round the cleavage site has not been done, but a proline residue in position +2 relative to the cleavage site will inhibit cleavage. Both signal sequence-bearing proteins, as well as myristoylated proteins, have been expressed from the SFVC vector and they are processed normally.

When using SFV/Helper 1 for the production of recombinant virus stocks, a replicative form of the SFV genome may form (Berglund *et al*., 1993). This probably occurs through recombination promoted by the viral replicase, switching from recombinant to helper RNA in the cotransfected cells (Weiss and Schlesinger, 1991). In nature, SFV can infect humans and care must therefore be taken when using SFV/Helper 1. According to the commission of the European Communities directive 95/30/EC, SFV is classified as a class 2 agent (Official Journal of the European Communities, No. L 155, 6. 7. 1995, pp. 41–42). A corresponding level of containment is recommended for work with SFV (workplace with restricted access, an observation window, and surfaces that are easy to clean).

Therefore, SFV/Helper 2 was designed for use in producing conditionally infectious particles (Berglund *et al*., 1993). These particles must be activated by chymotrypsin treatment. Using this helper, no replication-proficient virus has been found (Berglund *et al*., 1993).

SFV has a very broad host range and the recombinant virus stocks can therefore infect many kinds of eukaryotic cells. For transfecting cells using electroporation, the electroporation parameters must be optimized for every cell type. For BHK cells, as many as 10^8 to 10^9 infectious particles can be obtained when cotransfecting 10^7 cells with recombinant and SFV/Helper 2 RNA and incubating for 24 h.

V. PITFALLS

1. Avoid repeated freezing and thawing of the virus stock. This will reduce virus infectivity.
2. For use in electroporation, the cells should not have been passaged more than about 30 times.
3. When amplifying the vector, rearrangments of the DNA may occur. Therefore the vector should be checked thoroughly after amplification by different restriction enzyme digestions.

References

Berglund, P., Sjöberg, M., Garoff, H., Atkins, G. J., Sheahan, B. J., and Liljeström, P. (1993). Semliki Forest virus expression system: Production of conditionally infectious recombinant particles. *Bio/Technology* **11**, 916–920.

Horton, R. M., Hunt, H. D., Ho, S. N., Pullen, J. K., and Pease, L. R. (1989). Engineering hybrid genes without the use of restriction enzymes: Gene splicing by overlap extension. *Gene* **77**, 61–68.

Liljeström, P., and Garoff, H. (1991). A new generation of animal cell expression vectors based on the Semliki Forest virus replicon. *Bio/Technology* **9**, 1356–1361.

Melancon, P., and Garoff, H. (1987). Processing of the Semliki Forest virus structural polyprotein: Role of the capsid protease. *J. Virol.* **61**, 1301–1309.

Schlesinger, S., and Schlesinger, M. J. (eds.) (1986). "The Togaviridae and Flaviviridae." Plenum Press, New York.

Sjöberg, E. M., Suomalainen, M., and Garoff, H. (1994). A significantly improved Semliki Forest virus expression system based on translation enhancer segments from the viral capsid gene. *Bio/Technology* **12**, 1127–1131.

Weiss, B. G., and Schlesinger, S. (1991). Recombination between Sindbis virus RNAs. *J. Virol.* **65**, 4017–4025.

CHAPTER

10

Transient Expression of cDNAs in COS-1 Cells: Protein Analysis by Two-Dimensional Gel Electrophoresis

Pavel Gromov, Julio E. Celis, and Peder Madsen

I. INTRODUCTION

Transient and stable expression of exogenous cDNAs in eukaryotic cells provides a powerful approach for studying the corresponding gene products (see also related articles in this volume). Expression of a given protein is achieved by introducing an expression vector, harboring the cDNA of interest downstream an appropriate promoter, into eukaryotic cells. Several techniques are available for introducing DNA into eukaryotic cells (Ravid and Freshney, 1998; Thompson *et al*., 1999; Schenborn, 2000; Gromov and Celis, 2002): (i) electroporation (Chu *et al*., 1987; Shigekawa and Dower, 1988; Gehl, 2003), (ii) DEAE-dextran-mediated transfection (Sussman and Milman, 1984; Lopata *et al*., 1984; Schenborn and Goiffon, 2000a), (iii) calcium phosphate-mediated transfection (Wigler *et al*., 1978; Chen and Okayama, 1988; Schenborn and Goiffon, 2000b), and (iv) lipofection (Felgner *et al*., 1987; Whitt *et al*., 1990; Schenborn and Oler, 2000; Nicolazzi *et al*., 2003). All four techniques just mentioned can be used for transient transfection, although the method of choice usually depends on target cells, transfection efficiency, cytotoxity, cost, etc. Despite the relative high cost of liposome-mediated transfection, the method enjoys widespread use because of its reproducibility and high transfection rates.

This article describes a protocol for the effective transient transfection of COS-1 cells (Gluzman, 1981) using LipofectAMINE (Gibco, BRL) as a vehicle agent. The technique is carried out essentially according to the manufacturer's recommendation (Gibco, BRL) and is illustrated with the transient overexpression of three small GTP-binding proteins, arf, rab11, and p21-ras, using the pMT21 expression vector (Kaufman *et al*., 1991). The procedure offers an effective mean to produce considerable amounts of a given protein and, in addition, to faithfully reproduce some posttranslational modifications. In addition, the overexpressed protein can be used for antibody production as well as biochemical studies.

II. MATERIALS AND INSTRUMENTATION

A. Plasmid

Plasmid pMT21 (Kaufman *et al*., 1991) is used as an expression vector utilizing the adenovirus major late promoter for transcription initiation. The full-length cDNA of interest is subcloned into the pMT21 plasmid according to standard protocols (see, e.g., Sambrook *et al*., 1990).

B. COS-1 Cells

COS-1 monkey kidney cells (Gluzman, 1981) are grown in complete Dulbecco's modified Eagle's medium (DMEM) containing 10% fetal calf serum (FCS). General procedures for cultured cells are described in details elsewhere (see, e.g., Celis and Celis, 1997; see also article by Mcleady and O'Eonnor in volume 1).

Copyright 2006, Elsevier Science (USA).
All rights reserved.

C. Reagents

DMEM (Cat. No. 31966-021) is from GIBCO. Penicillin/streptomycin (Cat. No. A2213) are from Biocrom KG. FCS (Cat. No. 04-001-1A) is from Biological Industries. Tissue culture plates (24-well) (Cat. No. 662 160) are from Greiner. All other reagents and general tissue culture facilities are as described elsewhere (Celis and Celis, 1997).

III. PROCEDURES

The protocol has been slightly modified from the original guidelines provided by Gibco BRL Life Technology.

Solutions

1. *Complete Dulbecco's modified Eagle's medium*: Prepare as described by Celis and Celis (1997). To make 500 ml, mix 445 ml of DMEM medium, 5 ml of 10x stock penicillin/streptomycin, and 50 ml of FCS.
2. *Hank's buffered saline solution*: To make 1 liter, dissolve 0.4 g of KCl, 0.06 g of KH_2PO_4, 0.0621 g of $NaHPO_4{\cdot}2H_2O$, and 8 g of NaCl in 800 ml of distilled water. After dissolving, complete to 1 liter with distilled water.
3. *Lysis solution*: 9.8 *M* urea, 2% (w/v) Nonidet P-40 (NP-40), 2% ampholytes, pH 7–9, and 100 m*M* dithiothreitol. Prepare as described by Celis *et al*. in this volume.

Steps

The volumes given are for tranfections carried out in a single well of a 24-well tissue culture plate. For larger tissue culture dishes or multiwell labeling, adjust all amounts accordingly.

1. Seed COS-1 cells in a 24-well tissue culture plate (approximately 3×10^4 cells per well) in 0.3 ml of complete DMEM medium containing 10% of calf serum, 2 m*M* of glutamine, and antibiotics.

2. Grow the cells at 37°C in a humidified, 5% CO_2 incubator for approximately 24 h or until the cells reach about 80% confluence.

3. For each transfection (single well), prepare the following solutions in sterile plastic conical tubes.
   a. *DNA solution*: Prepare 20 µl of the pMT21 plasmid solution in DMEM medium lacking serum and antibiotics at a concentration of 0.01 mg/ml. Mix gently.
   b. *LipofectAMINE solution:* Add 1.5 µl of the commercial LipofectAMINE reagent stock solution (mix gently prior to use) to 20 µl of DMEM medium lacking serum and antibiotics. Mix gently.

4. To make the transfection mixture, combine the two solutions, mix gently, and incubate at room temperature for 30 min to allow DNA–liposome complexes to form.

5. In the meantime, wash COS-1 cells twice with 0.4 ml of serum-free DMEM medium.

6. For each transfection (single well), add 160 µl of serum-free DMEM medium to the tube containing the transfection mixture. Mix gently and overlay the diluted transfection mixture onto the washed cells.

7. Incubate the cells with DNA–liposome complexes for 8 h at 37°C in a humidified 5%, CO_2 incubator.

8. Following incubation, carefully aspirate the transfection mixture and replace it with 0.3 ml of complete DMEM solution. Incubate the cells for an additional 8–10 h.

9. Label the cells with [^{35}S]methionine for 14 h as described in the article by Celis *et al*. in this volume.

10. Aspirate the labeling medium from the plate and wash cells gently with 1 ml of Hank's buffered saline solution. Repeat the washing step once more. Carefully remove excess Hank's buffered saline solution from the plate. Aspirate as much of the solution as possible using an elongated Pasteur pipette.

11. Resuspend the cells in 40 µl of lysis solution and run two-dimensional (2D) gels as described in the article by Celis *et al*. or by Görg and Weiss in this volume. Alternatively, the cells can be harvested for Northern blotting or prepared for immunostaining.

12. Following 2D gel electrophoresis, dry the gels and subject them to autoradiography.

IV. COMMENTS

In average, about 15–30% transfection efficiency can be achieved as estimated by immunofluorescence. Transcription of the construct starts approximately 10 h after the addition of the transfection mixture to the cells as determined by Northen hybridization. Given the high pMT21 promoter activity, it is possible to harvest the cells for gene activity assays about 24 h after starting transfection. Transfection times may vary depending on the cell type and/or promoter activity.

Representative 2D gel autoradiographs (IEF) of [^{35}S]methionine-labeled proteins from transiently transfected COS-1 cells [ADP-ribosylation factor (Arf), rab11a, and p21-ras] are shown in Fig. 1. Arf is overexpressed as a single polypeptide, whereas the human rab11a and p21-ras constructs yield a set of spots that

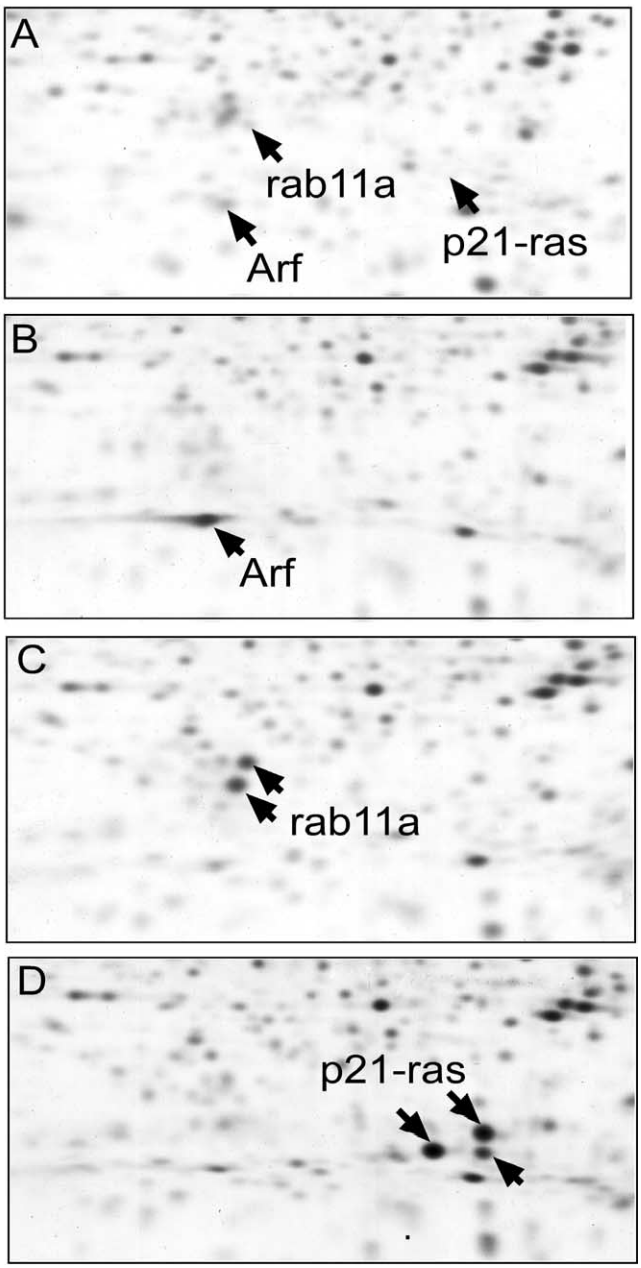

FIGURE 1 Two-dimensional gel (IEF) autoradiographs of [^{35}S]methionine-labeled proteins from COS-1 cells transfected transiently with pMT21 constructs: (A) control, nontransfected cells, (B) ADP-ribosylation factor (Arf), (C) rab11a, and (D) p21-ras.

reflect their posttranslational processing *via* geranylgeranylation and farnesylation, respectively. The COS-1 transfection system seems to reproduce a broad spectrum of posttranslational alterations of proteins and may represent an appropriate model system for the study of many posttranslational modifications.

To obtain significant amounts of the overexpressed protein, the protocol should be scaled up using six-well tissue culture plates. Resuspend the cells from one well in 60 µl of lysis solution, run 2D gels, and detect the overexpressed protein by Coomassie brilliant blue staining. Protein spots can then be electroeluted from the gel and used for immunization.

V. PITFALLS

1. Avoid growing the cells for more than 24 h prior to transfection. Always use the same conditions for cell culturing, as the transfection efficiency is sensitive to cell passage and confluence.
2. Avoid repeated freezing/defrosting of the plasmid DNA stock solution as it may induce one and double strain nicks in plasmid DNA, leading to linearization of supercoiled DNA. Linearized DNA is generally not as efficient a substrate for transient expression as supercoiled DNA. Aliquot the plasmid stock in several tubes (5–10 µl) and store at –70°C.
3. The LipofectAMINE commercial stock solution should be mixed gently before using.
4. Do not add antibacterial agents to transfection media.

References

Celis, J. E., and Celis, A. (1997). General procedures for tissue culture. *In* "*Cell Biology: A Laboratory Handbook*" (J. E. Celis, N. P. Carter, T. Hunter, K. Simons, D. M. Shotton, J. V. Small, eds.), pp. 5–16. Academic Press, San Diego.

Chen, C., and Okayama, H. (1988). Calcium phosphate-mediated gene transfer: A highly efficient system for stably transforming cells with plasmid DNA. *BioTechniques* **6**, 632–638.

Chu, G., Hayakawa, H., and Berg, P. (1987). Electroporation for the efficient transfection of mammalian cells with DNA. *Nucleic Acid Res*. **15**, 1311–1326.

Felgner, P. L., Gadek, T. R., Holm, M., Roman, R., Chan, H. W., Wenz, M., Northrop, J. P., Ringold, G. M., and Danielson, M. (1987). Lipofection: A highly efficient, lipid-mediated DNA/transfection procedure. *Proc. Natl. Acad. Sci. USA* **84**, 7413–7417.

Gehl J. (2003). Electroporation: Theory and methods, perspectives for drug delivery, gene therapy and research. *Acta Physiol. Scand*. **177**, 437–447.

Gluzman, Y. (1981). SV40-transformed semian cells support the replication of early SV40 mutants. *Cell* **23**, 175–182.

Gromov, P., and Celis, J. E. (2000). Gene transfer and expression in tissue culture cells. *In* "*Encyclopedia of Life Science*". Nature Publishing Group, London. http://www.els.net.

Kaufman, R. J., Davies, M. V., Wasley, L. C., and Michnik, D. (1991). Improved vectors for stable expression of foreign genes in mammalian cells by use of the untranslated leader sequence from EMC virus. *Nucleic Acid Res*. **19**, 4485–4490.

Lopata, M. A., Cleveland, D. W., and Sollner-Webb, B. (1984). High-level expression of a chloram-phenicol acetyltransferase gene by DEAE-dextran-mediated DNA transfection coupled with a dimethylsulfoxide or glycerol shock treatment. *Nucleic Acid Res*. **12**, 5707–5717.

Nicolazzi, C., Garinot, M., Mignet, N., Scherman, D., and Bessodes, M. (2003). Cationic lipids for transfection. *Curr. Med. Chem.* **10**, 1263–1277.

Ravid, K., and Freshney, I. (eds.) (1998). "*DNA Transfer to Cultured Cells*." Wiley-Liss, New York.

Sambrook, J., Fritsh, E. F., and Maniatis, T. (1990). "Molecular Cloning: A Laboratory Manual," 2nd Ed. Cold Spring Harbor Laboratory Press, Cold Spring Harbor, NY.

Schenborn, E. T. (2000). Transfection technologies. *Methods Mol. Biol.* **130**, 91–102.

Schenborn, E. T., and Goiffon, V. (2000a). DEAE-dextran transfection of mammalian cultured cells. *Methods Mol. Biol.* **130**, 147–153.

Schenborn, E. T., and Goiffon, V. (2000b). Calcium phosphate transfection of mammalian cultured cells. *Methods Mol. Biol.* **130**, 135–145.

Schenborn, E. T., and Oler, J. (2000). Liposome-mediated transfection of mammalian cells. *Methods Mol. Biol.* **130**, 155–164.

Shigekawa, K., and Dower, W. J. (1988). Electroporation of eukaryotes and prokaryotes: A general approach to the introduction of macromolecules into cells. *BioTechniques* **6**, 742–751.

Sussman, D. J., and Milman, G. (1984). Short-term, highly-efficiency expression of transfected DNA. *Mol. Cell Biol.* **4**, 1641–1643.

Whitt, M. A., Buonocore, L., Rose, J. K., Ciccarone, V., and Gebeyehu, G. (1990). TranfectACE reagent promotes transient transfection frequencies greater than 90%. *Focus* **13**, 8–12.

Wigler, M., Pellicer, A., Silverstein, S., and Axel, R. (1978). Biochemical transfer of single copy eukaryotic genes using total cellular DNA as donor. *Cell* **14**, 725–731.

CHAPTER

11

High-Throughput Purification of Proteins from *Escherichia coli*

Pascal Braun and Joshua LaBaer

I. INTRODUCTION

The preparation of purified protein provides a powerful tool enabling the study of the biophysical characteristics, structure, biochemistry, and functional activity of proteins. With the increased focus on proteomics approaches, there is a growing demand for high-throughput (HT) methods to study protein function. The recent development of protein microarrays and multiwell solution biochemistry enables the study of hundreds or more proteins at a time (Martzen *et al*., 1999; MacBeath and Schreiber, 2000; Zhu *et al*., 2001). These advances offer the possibility to help systematically analyze protein–protein interactions, delineate enzyme–substrate networks, and investigate the effects of posttranslational modifications and small molecules on protein interactions or activities (MacBeath, 2002; Zhu *et al*., 2001).

The use of these new technologies requires access to large numbers of purified proteins. The following protocols describe the expression and purification of proteins from *Escherichia coli* in an automatable 96-well format. The procedure has been shown to give yields in the range of 300 ng to 1 µg per 1 ml bacterial culture for ~50–80% of proteins up to 75 kDa (Braun *et al*., 2002).

II. MATERIALS AND INSTRUMENTATION

Refrigerated incubator shaker with adjustable temperature (20–37°C) with plate holders (alternatively, two standard incubator shakers: one in the cold room and one at room temperature will also work)
Collection plates (e.g., Corning costar # 3896)
96-deep well blocks 2.2 ml (Marsh Bioproducts, Cat. No. AB0600)
Gas-permeable seals (e.g., Abgene, Cat. No. AB-0718)
96-well filter plate 350 µl, GF/C (Whatman Unifilter, Cat. No. 7700-3301)
Eppendorf Thermoshaker R with 96-well plate holder (S534-41 and S534-46)
(Recommended): A 96-pin inoculator with pin length >2 in. that can reach the bottom of a 96-deep well block
Thermo Finnigen Multidrop 96 DW (MTX Labs, Cat. No. P97115)
Electronic 8-channel pipettes
96-well plate spectrophotometer
Centrifuge with plate holders (best is digital rpm indicator)
SDS–PAGE system that maximizes lane number to handle many samples (e.g., Bio-Rad criterion system—gels with 26 wells)
Aluminum sealing tape (Beckman Reorder# 538619)

III. PROCEDURES

The first step in high-throughput expression and purification of proteins is obtaining the corresponding protein expression constructs. The expression of proteins often requires that the gene sequences of interest be placed (1) under the control of a specific transcriptional promoter (regulated, strong/weak, etc.), (2) near specific translational signals (ribosome binding sites, etc.), (3) in association with a particular selectable marker (ampicillin, tetracycline, etc.) and, in many

Copyright 2006, Elsevier Science (USA).
All rights reserved.

cases (and nearly all conceivable HT screening scenarios), (4) linked at one or both ends to sequences encoding polypeptide tags to facilitate HT manipulations, such as purification (His_6, GST), detection (GFP), or functional readout (Gal4-AD) of the test proteins. The addition of peptide tags requires that the untranslated regions flanking the coding sequences be removed. Finally, the importance of ensuring that the expression clone sequences accurately reflect the natural gene sequence cannot be overemphasized. Even subtle changes in the amino acid sequences of proteins can have profound effects on protein function. The configuration of the clones should be determined in advance for each experiment and all of the clones should have the same configuration.

There is an increasing number of clone collections under construction or already available through both public and private sources that can provide useful starting material for protein expression experiments (Brizuela *et al*., 2001, 2002; Kikuchi *et al*., 2003; Reboul *et al*., 2003; Seki *et al*., 2002; Strausberg *et al*., 1999). Some of these clone collections contain full-length cDNAs, requiring that the user extract the coding sequences and place them into the appropriate vectors that support protein expression (Strausberg *et al*., 1999). Other clone collections have already configured the coding sequences into expression vectors, and their usefulness depends on whether the specific configuration suits the users needs (Martzen *et al*., 1999). The most flexible approach for protein expression utilizes recombinational cloning vectors, which enable the simultaneous and rapid transfer of the coding sequences into other plasmid vectors—in frame, without mutations (Hartley *et al*., 2000). These transfers occur in a single-step benchtop reaction that can be automated readily and nearly all vectors can be adapted (with a single fragment blunt ligation) to become recipient vectors. Thus clone collections that employ this approach can support a broad variety of experiments.

For bacterial transformation, several vendors provide competent cells in a 96-well format. The following protocol has been optimized for BL21pLys^S cells.

A. HT Protein Expression

Solutions

1. *TB media*: To prepare 1 liter of Terrific broth, mix 12 g Bacto-tryptone, 24 g yeast extract, and 4 ml glycerol and dissolve in 900 ml ddH_2O final volume. In a separate container, prepare a phosphate solution by mixing 2.31 g KH_2PO_4 with 12.54 g K_2HPO_4 and bring the final volume to 100 ml. Autoclave both solutions independently. Mix after solutions have cooled down.

2. *Ampicillin*: Dissolve 300 mg ampicillin in 3 ml H_2O. Store at –20°C. Make fresh weekly.

3. *Chloramphenicol*: Dissolve 340 mg chloramphenicol in 10 ml ethanol, store at –20°C.

4. *40% glucose*: Add 200 g L-glucose to 300 ml H_2O while stirring. Warm the solution to accelerate sugar dissolution. Once the glucose is in solution, bring the final volume to 500 ml to compensate for any evaporative loss. Filter sterilize and store at room temperature.

5. *1 M IPTG*: Dissolve 2.38 g IPTG in 10 ml H_2O. Aliquot and store at –80°C.

Steps

1. Aliquot 1 ml media into each well of a 96-deep well block. This is conveniently done using repetitive dispenser such as the Thermo Finnigen Multidrop. Alternatively, a repeat pipetting device (e.g., Eppendorf) can be used.

2. Inoculate cultures with bacteria containing the expression constructs. It is convenient to work with bacteria that are arranged in 96-well footprints. Dipping a sterilized 96-pin inoculation device into 96-well glycerol stocks and then softly pressing on agar will create such a footprint. After the colonies are grown, the same 96-pin device can be used to inoculate 96 O/N cultures simultaneously. Standard inoculation using sterile toothpicks will work, but careful attention must be paid to avoid mixing samples.

3. Grow cultures O/N at 37°C, 375 rpm for 14 h. Some experimentation with growth conditions may be necessary depending on the bacterial strain used. The cells should grow to early plateau, allowing slower growing colonies to catch up. However, avoid late plateau because different samples will reenter growth phase differentially. To avoid day-to-day variation, it is crucial to avoid growing the bacteria longer than 16 h.

4. Prepare a second culture block with 1.5 ml media containing appropriate antibiotics and 2% glucose.

5. After the O/N growth, check OD_{600} of the cultures using a 1:10 dilution. It is advisable to check the OD of the entire plate using a 96-well plate compatible spectrophotometer. However, when many blocks are processed in parallel or if only a standard spectrophotometer is available, sampling at least 24 wells of every plate to ensure even growth is acceptable. The overall variability should be <25%.

Bacteria settle quickly in the 96-well blocks. Whenever transferring bacteria, make sure that the O/N culture block is thoroughly mixed all the time. This can

be achieved by maintaining the culture block on a constantly rotating Eppendorf Thermoshaker.

6. Dilute the O/N cultures into the second block to achieve an average final OD_{600} = 0.1 Bacterial settling can also cause problems at this step. If possible, pipette all cultures simultaneously or mix the block with the O/N cultures constantly. Otherwise, the samples will get uneven starting densities.
7. Grow at 25°C until average OD_{600} of the culture is ~0.6 (~3.5 h).
8. Induce protein expression (with IPTG, etc.). We use IPTG at 1 m*M* final concentrations.
9. Express protein for 3 h at 25°C. We have found that cultures at 25°C grow more evenly and tend to have less protein degradation than at higher temperatures. Actual induction temperature and time may need adjustment depending on constructs and conditions.
10. *Optional:* Measure and record the OD_{600} of final culture while maintaining good mixing of the cultures.
11. *Optional:* Take an aliquot for Western blot analysis while maintaining good mixing of the cultures.
12. Harvest the cultures by centrifugation for 10–15 min, 4°C, 5000 *g*.
13. Decant media.
14. Freeze pellets to –20°C.

B. HT Protein Purification under Denaturing Conditions

Solutions

1. *Guanidine lysis buffer (GLB)*: 100 m*M* NaH_2PO_4, 10 m*M* Tris–HCl pH 8.0, 6 *M* guanidine hydrochloride, and 10 m*M* β-mercaptoethanol
2. *Ni-NTA matrix:* Ni-NTA can be obtained from Qiagen (Cat. No. 30210). Wash beads several times in GLB. After last wash, resuspend the beads in 10 volumes of GLB, forming a 10% slurry.
3. *Urea wash buffer (UWB):* 100 m*M* NaH_2PO_4, 10 m*M* Tris–HCl, and 8 *M* urea, adjust to pH 8.0
4. *Elution buffer (EB):* 100 m*M* NaH_2PO_4, 10 m*M* Tris–HCl, 8 *M* urea, and 500 m*M* imidazole, adjust to pH 8.0

Steps

1. Thaw the deep well block containing the bacterial pellets for 5–10 min at room temperature.
2. Pipette 100 µl GLB into each well. This step is conveniently done using a repeating device such as a Multidrop.
3. Resuspend pellets by shaking the plate on a Beckman Thermoshaker for 30–60 min at 750 rpm at room temperature. The use of a stationary-inverted 96-pin device will create enough turbulence to get a better resuspension (Fig. 1). This Swizzler improves lysis under both denaturing and nondenaturing conditions. If the goal is to recover functional protein by renaturation, the shaking speed should be reduced to 300 rpm after 5 min to minimize harmful oxidation of proteins.

FIGURE 1 A stationary-inverted 96-pin device.

4. Prepare two GF/C fiber plates.
   a. Filtration plate (to remove cell debris): Pipette 10 µl GLB into each well of the filtration plate.
   b. Binding plate (to capture the protein): Pipette 5 µl of 10% Ni-NTA slurry equilibrated in GLB buffer (0.5 µl bed volume) into the binding plate. Too much affinity matrix will increase nonspecific binding and lead to more impurities. Add 200 µl lysis buffer. Spin for 1.5 min at 16 *g*. Seal bottom with aluminum tape. Seal every well thoroughly!
5. Place the filtration plate on top of the binding plate, ensuring that well A1 is above well A1.
6. Transfer lysates from step 3 into filtration plate.
7. Spin the stacked plates at 2000 *g*, 2 min, 4°C.
8. Seal the top of the binding plate.
9. Rotate plate end over end for 45 min at room temperature.
10. Remove both seals. Remove the bottom seal first.

11. Spin at 50 *g* for 1.5 min into a waste vessel.
12. Wash the binding plate three times with UWB by adding 250 µl UWB followed by a 50 *g* spin for 90 s into a waste vessel at room temperature.
13. Place the binding plate on top of a 96-well collection plate.
14. Add 15 µl elution buffer to the binding plate.
15. Incubate at room temperature for 5 min.
16. Spin at 16 *g* for 1.5 min.
17. Repeat elution (steps 14–16) three more times (60 µl final volume).
18. After the final addition of elution buffer, spin once at 2000 *g* for 5 min. This hard spin will collect all remaining protein.

C. HT Protein Purification under Nondenaturing Conditions

Solutions

1. *10x phosphate-buffered saline (PBS):* Mix 80 g NaCl, 2.0 g KCl, 14.4 g Na_2PO_4, and 2.4 g KH_2PO_4 and dissolve in 900 ml ddH_2O. Adjust pH to 7.2 and bring volume to 1 liter.
2. *1x PBS:* Dilute 100 ml 10x PBS with 900 ml ddH_2O
3. *0.5 M EDTA, pH 8.0:* Dissolve 95 g EDTA in 450 ml ddH_2O. Start adjusting the pH with NaOH before the powder is dissolved to accelerate the dissolution process. Adjust pH to 8.0 and bring volume to 500 ml.
4. *DNase:* Dissolve 100 mg DNase (Sigma D-4527) in 10 ml H_2O. Aliquot in 0.5-ml aliquots and store at –80°C.
5. *Lysozyme:* Dissolve 300 mg lysozyme (enzyme grade) in 6 ml H_2O. Aliquot and store at –80°C.
6. *10% Triton X-100*: Slowly pipette 5 ml Triton X-100 in 45 ml H_2O. Rotate for a few hours or heat in a water bath until all flakes disappear. Store at room temperature.
7. *40x DNase buffer:* 900 m*M* $MgCl_2$, and 100 m*M* $MnCl_2$
8. *Wash buffer 1*: PBS, 2 m*M* EDTA; and 10% glycerol
9. *Wash buffer 2*: Tris–HCl, 100 m*M*, pH 8.0; NaCl, 500 m*M*; EDTA, 2 m*M*; 0.1% Triton X-100; and 10% glycerol
11. *Glutathione beads (Sigma G4510)*: Wash the beads three to six times in wash buffer 1 containing 5 m*M* dithiothreitol (DTT) (confirm the absence of ethanol smell) and store at 4°C
12. *Lysis buffer*: PBS, 2 m*M* EDTA; 10% glycerol; 5 m*M* DTT (*add fresh*), and protease Inhibitors (*add fresh*)
13. *Elution buffer*: Wash buffer 2 + 10 m*M* reduced glutathione. Verify and readjust the pH to 8.0, if necessary.
14. *Lysozyme mix*: Mix 64 µl lysozyme (50 µg/µl), 320 µl 10% Triton X-100, and 1016 µl lysis buffer. Pipette 8 × 150 µl into one column of a plate. From this reservoir, you can conveniently pipette the mix with an 8-channel pipette in step 4.
15. *DNase mix:* 80 µl DNase (10 mg/ml), 720 µl 40x DNase buffer, and 800 µl lysis buffer. Pipette 8 × 150 µl of this mix into 8 wells of one column of a plate. From this reservoir, one can conveniently pipette the mix with an 8-channel pipette in step 6.

Steps

1. Thaw the deep well block containing the bacterial pellets for 5–10 min at room temperature.
2. Pipette 100 µl lysis buffer into each well. This step is conveniently done using a repeating device such as a Multidrop.
3. Resuspend pellets by shaking the plate on a Beckman Thermoshaker for 30–60 min at 750 rpm, 4°C. The use of a stationary-inverted 96-pin device will create enough turbulence to improve resuspension (Fig. 1). This Swizzler improves lysis under both denaturing and nondenaturing conditions.
4. Add 10 µl lysozyme using an 8-channel pipetting device to transfer the mix from a column of wells of a 96-well plate.
5. Mix for 30 min at 300 rpm, 4°C. The lower speed reduces harmful oxidation of proteins. Preferably use a stationary 96-pin device to increase mixing.
6. Add 10 µl of DNase mix. An 8-channel electronic pipette is adequate.
7. Mix for 15 min at 300 rpm, 4°C.
8. Prepare two GF/C fiber plates.
   a. Filtration plate (to remove cell debris): Pipette 10 µl lysis buffer into each well of the filtration plate to wet the filters.
   b. Binding plate (to capture the protein): Pipette 50 µl of 50% slurry of GSH agarose beads in lysis buffer (25 µl bed volume) into the binding plate.
9. Add 200 µl lysis buffer.
10. Spin for 1.5 min at 16 *g*.
11. Seal bottom with aluminum tape. Seal every well thoroughly!
12. Place the filtration plate on top of the binding plate, making sure that well A1 is above well A1.
13. Transfer lysates from step 5 into filtration plate.
14. Spin the stacked plates at 2000 *g*, 2 min, 4°C.

15. Seal the top of the binding plate.

16. Rotate the sealed binding plate end over end for 45 min, 4°C.

17. Remove both seals. Remove the bottom seal first.

18. Spin at 16 *g* for 1.5 min into a waste vessel. Avoid higher speeds, which can dehydrate the matrix and denature the proteins, reducing yields and increasing nonspecific binding.

19. Wash the binding plate three times with wash buffer I by adding 250 µl wash buffer I followed by a 16 *g* spin for 90 s into a waste vessel at 4°C.

20. Wash the binding plate two times with wash buffer II by adding 250 µl wash buffer II followed by a 16 *g* spin for 90 s into a waste vessel at 4°C.

21. Place the binding plate on top of a 96-well collection plate.

22. Add 20 µl elution buffer to the binding plate.

23. Incubate at 4°C for 5 min.

24. Spin at 16 *g* for 1.5 min.

25. Repeat elution (steps 18–20) three more times (80 µl final volume).

26. After the final addition of elution buffer, spin once at 2000 *g* for 5 min. This hard spin will collect all remaining protein.

27. Analyze 10-µl eluate by SDS–PAGE and colloidal Coomassie blue staining

References

Braun, P., Hu, Y., Shen, B., Halleck, A., Koundinya, M., Harlow, E., and LaBaer, J. (2002). Proteome-scale purification of human proteins from bacteria. *Proc. Natl. Acad. Sci. USA* **99**, 2654–2659.

Brizuela, L., Braun, P., and LaBaer, J. (2001). FLEXGene repository: From sequenced genomes to gene repositories for high-throughput functional biology and proteomics. *Mol. Biochem. Parasitol.* **118**, 155–165.

Brizuela, L., Richardson, A., Marsischky, G., and Labaer, J. (2002). The FLEXGene repository: Exploiting the fruits of the genome projects by creating a needed resource to face the challenges of the post-genomic era. *Arch. Med. Res.* **33**, 318.

Hartley, J. L., Temple, G. F., and Brasch, M. A. (2000). DNA cloning using *in vitro* site-specific recombination. *Genome Res.* **10**, 1788–1795.

Kikuchi, S., Satoh, K., Nagata, T., Kawagashira, N., Doi, K., Kishimoto, N., Yazaki, J., Ishikawa, M., Yamada, H., Ooka, H., *et al*. (2003). Collection, mapping, and annotation of over 28,000 cDNA clones from japonica rice. *Science* **301**, 376–379.

MacBeath, G. (2002). Protein microarrays and proteomics. *Nature Genet* **32** (*Suppl*.), 526–532.

MacBeath, G., and Schreiber, S. L. (2000). Printing proteins as microarrays for high-throughput function determination. *Science* **289**, 1760–1763.

Martzen, M. R., McCraith, S. M., Spinelli, S. L., Torres, F. M., Fields, S., Grayhack, E. J., and Phizicky, E. M. (1999). A biochemical genomics approach for identifying genes by the activity of their products. *Science* **286**, 1153–1155.

Reboul, J., Vaglio, P., Rual, J. F., Lamesch, P., Martinez, M., Armstrong, C. M., Li, S., Jacotot, L., Bertin, N., Janky, R., *et al*. (2003). *C. elegans* ORFeome version 1.1: Experimental verification of the genome annotation and resource for proteome-scale protein expression. *Nature Genet* **34**, 35–41.

Seki, M., Narusaka, M., Kamiya, A., Ishida, J., Satou, M., Sakurai, T., Nakajima, M., Enju, A., Akiyama, K., Oono, Y., *et al*. (2002). Functional annotation of a full-length Arabidopsis cDNA collection. *Science* **296**, 141–145.

Strausberg, R. L., Feingold, E. A., Klausner, R. D., and Collins, F. S. (1999). The mammalian gene collection. *Science* **286**, 455–457.

Zhu, H., Bilgin, M., Bangham, R., Hall, D., Casamayor, A., Bertone, P., Lan, N., Jansen, R., Bidlingmaier, S., Houfek, T., *et al*. (2001). Global analysis of protein activities using proteome chips. *Science* **293**, 2101–2105.

PART

C

GENE EXPRESSION PROFILING

SECTION

5

Differential Gene Expression

CHAPTER

12

Microarrays for Gene Expression Profiling: Fabrication of Oligonucleotide Microarrays, Isolation of RNA, Fluorescent Labeling of cRNA, Hybridization, and Scanning

Mogens Kruhøffer, Nils E. Magnusson, Mads Aaboe, Lars Dyrskjøt, and Torben F. Ørntoft

I. INTRODUCTION

In less than a decade DNA microarray technology has become an indispensable part of functional genomics (Celis *et al.*, 2000). Functional gene expression studies provide insight into changes in the transcription profile resulting from disease, developmental processes, or physiological stimuli. DNA microarrays have especially demonstrated their great potential in human tumour classification and prediction (Thykjaer *et al.*, 2001; Dyrskjot *et al.*, 2003; van de Vijver *et al.*, 2002) but also within drug target discovery, drug action, and toxicity (for an overview and further references, see Heller *et al.*, 1999). Microarrays are not limited to any specific organism but its usefulness increases with increasing availability of sequence information.

A DNA microarray is an orderly arrangement of usually thousands of DNA spots typically less than 150 μm in diameter that provides a medium for hybridisation of labelled nucleic acids extracted from biological samples. The immobilised DNA samples on the array are called the probes and the sample that is labelled and hybridised to the probes is the target (Phimister, 1999). There are several steps in the design and implementation of a DNA microarray experiment and they require specialized robotics, imaging equipment, and software, which are all available commercially.

Since the first complete microarray protocols were published (Schena *et al.*, 1995; Shalon *et al.*, 1996), a wide variety of designs have developed that are mirrored in the numerous different DNA microarray protocols available. Common for them all are the four essential stages: (1) microarray fabrication, (2) target preparation, (3) hybridisation, and (4) data collection, normalisation, and bioinformatic analysis. In this chapter, protocols are outlined for the fabrication of oligonucleotide microarrays, preparation of amplified cRNA target, and the combination of these in the hybridisation procedure (Fig. 1).

For reviews of different aspects of the technology, please see Eisen and Brown (1999), Kricka (1998), Lemieux *et al.* (1998), Marshall and Hodgson (1998), and Schena and Davis (1999).

II. CHEMICALS

The following chemicals are from Sigma: sodium phosphate monobasic (Cat. No. S-0751), sodium phosphate dibasic (Cat. No. S-0876), Betaine monohydrate (Cat. No. B-2754), EDTA (Cat. No. E-5134), phenol (Cat. No. P-4557), $NaHCO_3$ (Cat. No. S-5761), $ZnCl_2$ (Cat.

Copyright 2006, Elsevier Science (USA).
All rights reserved.

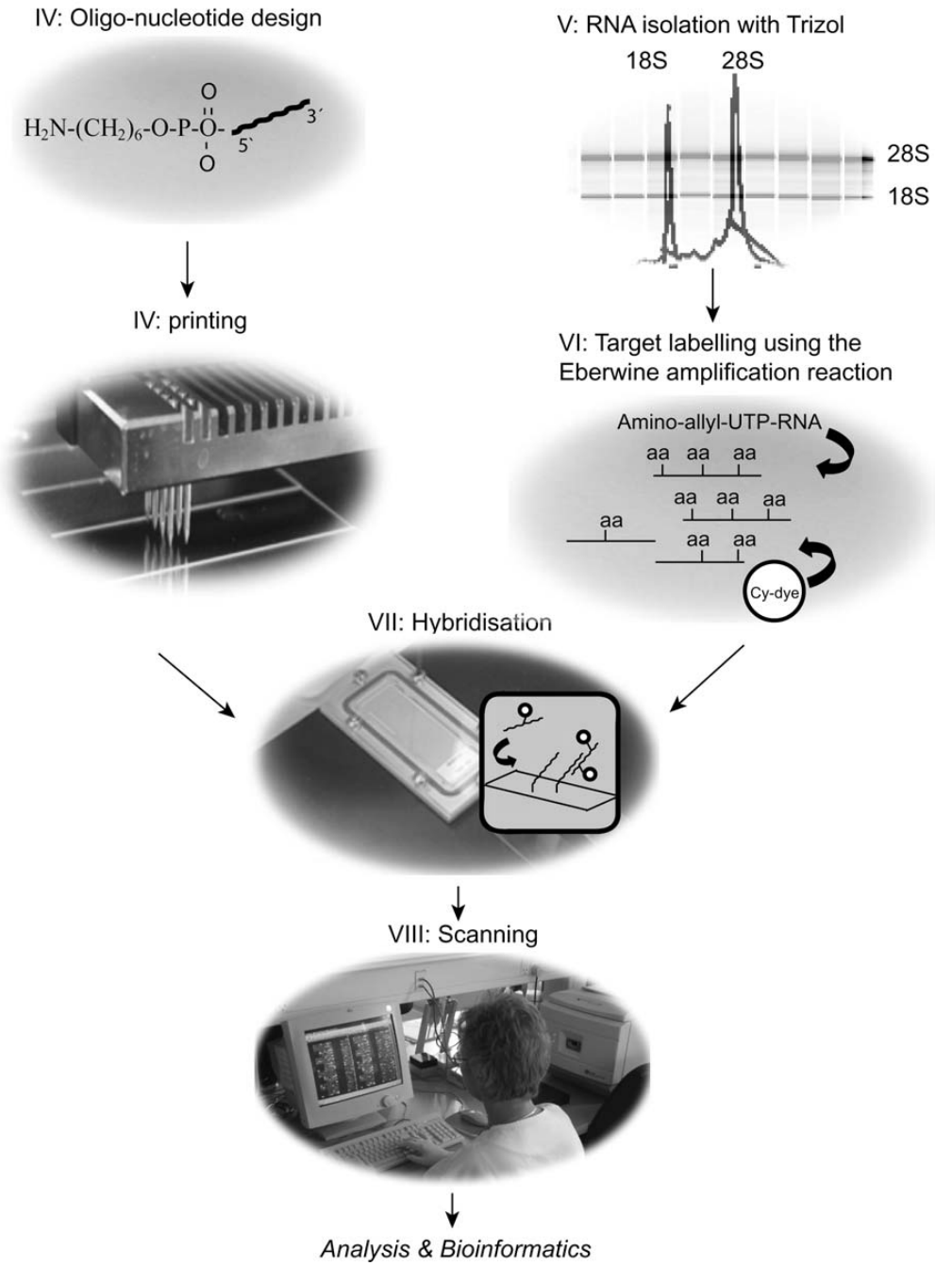

FIGURE 1 Flowchart of protocols outlined in this article for a complete microarray experiment where roman numbers refer to the relevant sections in the text. Upper left corner shows the two main fabrication steps of oligonucleotide microarrays: probe design and printing (Section IV). In the upper right corner, target preparation consisting of RNA isolation and labelling (Sections V and VI). In the middle, the combination of probes and target in the hybridisation reaction (Section VII) (Bottom) Data collection by scanning (Section VIII). Analysis and bioinformatics are beyond the scope of this chapter.

No. Z-4875), 7.5 *M* ammonium acetate (Cat. No. A-2706), 2-mercaptoethanol (Cat. No. M-3148), dimethyl sulfoxide (DMSO) (Cat. No. D-8779), 5-(3-aminoallyl)-2′-oxyuridine 5′-triphosphate (aa-UTP) 50 mg custom made (1-mg portions, Cat. No. A-5660), and Orange G (Cat. No. O-1625).

The following products are from Calbiochem: NaCl (Cat. No. 567441), Tris base (Cat. No. 648311), Tween 20 (Cat. No. 655204), sodium citrate (Cat. No. 567444), bovine serum albumin (Cat. No. 126575), SDS (Cat. No. 428023), formamide (Cat. No. 69189), and NaOH (Cat. No. 567530).

Glycerol (Cat. No. 818709), chloroform (Cat. No. 1.02445.1000), and isoamylalcohol (Cat. No. 748K 00555679) are from Merck. The tRNA is from Roche (Cat. No. 109495), and SeaKem GTG agarose (Cat. No. 50074) is from BMA products. Fish sperm DNA is from Serva (Cat. No. 18580.01), and ethidium bromide (Cat. No. U532813) is from Amersham Biosciences.

III. PREPARATION OF STOCK SOLUTIONS

1. *1 M Tris*: Add 121.1 g of Tris base in 800 ml of H_2O. Adjust the pH to 9.0 by adding 42 ml of concentrated HCl and bring the volume to 1 liter.
2. *TE* (*10 mM Tris–Cl, 1 mM EDTA*): To prepare 1 liter, mix 100 ml of 1 *M* Tris and 20 ml of 0.5 *M* EDTA and bring the volume to 1 liter.
3. *10 M NaCl*: Dissolve 399.7 g of NaCl in 800 ml of H_2O and bring the volume to 1 liter.
4. *0.5 M EDTA*: Add 186.1 g of EDTA·2 H_2O to 800 ml of H_2O. Stir on a magnetic stirrer. Adjust the pH to 8.0 with NaOH (~20 g of solid NaOH).
5. *20× SSC*: To make 1 liter, dissolve 175.3 g of NaCl and 88.2 g of sodium citrate in 800 ml of H_2O. Adjust the pH to 7.0 with a 10 *M* solution of NaOH and bring the volume to 1 liter.
6. *20× SSPE*: To make 1 liter, dissolve 175.3 g of NaCl and 27.6 g of $NaH_2PO_4{\cdot}H_2O$ and 7.4 g of EDTA in 800 ml of H_2O. Adjust the pH to 7.4 with a 10 *M* solution of NaOH and bring the volume to 1 liter.
7. *0.1 M carbonate buffer, pH 9.3*: To prepare 100 ml, dissolve 1.06 g of $NaHCO_3$ in 80 ml of H_2O. Adjust the pH with 10 *M* NaOH and bring the volume to 100 ml. Store frozen at –20°C in 1-ml aliqouts.
8. *10 M NaOH*: To prepare 1 liter, dissolve 40.0 g of NaOH in 800 ml of H_2O and adjust the volume to 1 liter.
9. *H_2O*: Molecular Biology Water (AccuGene, BMA products Cat. No. 51200), unless otherwise indicated in the text.

IV. FABRICATION OF OLIGONUCLEOTIDE MICROARRAYS

A. Introduction

Oligonucleotide microarrays are usually printed on slides with an activated surface that allows end-point attachment of 5′- or 3′-chemically modified DNA. The common theme is that the glass surface of the microarray slide is coated with active chemical groups, which facilitate the binding of end-modified DNA, typically amino modified. In this way, backbone binding is reduced and most of the immobilized DNA should be available for hybridisation. In the oligonucleotide microarray format, each gene is represented by one or more oligonucleotides that are designed solely on the basis of sequence information. This allows the user to design the probes avoiding cross-hybridisation with repetitive regions or regions that share similarity to other genes (Li and Stormo, 2001; Kane *et al*., 2000; Hudges *et al*., 2001). Oligonucleotide arrays have several advantages over cDNA microarrays. Gene-specific oligonucleotides can easily be designed and synthesised so there is no need for verification of bacterial clones and high-throughput production of polymerase chain reaction (PCR) products. In addition, oligonucleotide libraries covering large parts of the transcriptome are available from several companies.

B. Materials and Instrumentation

5′-modified 60-mer oligonucleotides dehydrated in a 96-well format are from DNA-Technology A/S, Denmark. CodeLink microarray slides are from Amersham Biosciences. The VersArray ChipWriter Pro System is from Bio-Rad Laboratories. The Biomek 2000 automated workstation is from Coultier Beckman inc. 384-well plates are from Genetix (Cat. No. x6003). The Array Designer 2.0 software is from Premier Biosoft International. The Hettich Rotina 35 R centrifuge is from Integrated Services TCP Inc. Humid chamber and container with rack are custom made at the Aarhus University workshop. Container and rack for blocking of 25 × 75-mm slides (Cat. No. 115067-0 and Cat. No. 115068-0) are from VWR international.

C. Procedures

1. Oligonucleotide Design

Several programs exist for oligonucleotide design. In Array Designer software, begin with the following criteria:

1. Length = 55–60
2. Distance from 3′ end < 999 bp
3. GC content 35–50%
4. $T_m = 75 \pm 5°C$
5. Hairpin $\Delta G_{max} = 3.0$ Kcal/mol
6. Self dimer $\Delta G_{max} = 6.0$ Kcal/mol
7. Maximum length of repeats ≤ 5 bp
8. Least cross-reactivity (Blast, http://www.ncbi.nlm.nih.gov/blast/)

If no probes are returned, reduce the stringency of one or more parameters in the software.

2. *Printing of Microarrays*

Solutions

1. 2× *printing buffer*: (300 m*M* sodium phosphate and 2 m*M* Betaine, pH 8.5. To prepare 100 ml, mix dissolve 0.41 g sodium phosphate monobasic, 3.785 g sodium phosphate dibasic, and 9 mg Betaine in 90 ml H_2O. Adjust pH to 8.5 using 1 *M* NaOH or 1 *M* HCl. Bring final volume to 100 ml with H_2O.
2. *Blocking Solution*: 0.1 *M* Tris, 50 m*M* ethanolamine, 0.1% SDS, pH 9.0. To prepare a 1-liter solution, dissolve 12.1 g Trizma base in 900 ml H_2O. Stir in 3.05 g ethanolamine and mix thoroughly. Adjust pH to 9.0 using 1 *M* NaOH or 1 *M* HCl. Bring final volume to 1 liter with H_2O. Add SDS to blocking solution to a final concentration of 0.1% prior to use.
3. *4× SSC, 0.1% SDS*

Steps

Steps 1–3 can be done manually or automated. We have implemented an automated workstation for all oligonucleotide dilutions and for preparation of source plates for printing.

1. Dissolve the 5′ amino-modified oligonucleotides in H_2O to a concentration of 120 µ*M*.
2. To prepare the source plate for printing, transfer 12.5 µl 2× spotting solution into each well of the source plate and then add 12.5 µl of 120 µ*M* oligonucleotide in a predetermined pattern. The final volume is 25 µl with an oligonucleotide concentration of 60 µ*M*.
3. Prepare the microarrayer for printing. This includes equilibrating to 30–35% relative humidity, design of a suitable program for printing, cleaning, and preconditioning of quilted pins. Clean the pins in 20% ethanol and dry them completely. Precondition the quill pins for 30 min to 1 h by printing on ordinary microscope slide with printing solution.
4. Place the slides and the source plate in the microarrayer and run the printing program.
5. Prepare a humid chamber by adding as much solid sodium chloride to H_2O as needed to form a 1-cm-deep slurry in the bottom of a plastic container with an airtight lid.
6. For DNA immobilisation, place slides in a humid chamber with approximately 75% relative humidity for 16–24 h at room temperature.
7. After immobilization, residual reactive groups are blocked. Place the slides in a rack (up to 20 slides) and submerge the slides in 300 ml blocking solution prewarmed to 50°C. Agitate gently for 15 min.
8. Discard the blocking solution and rinse the slides twice with H_2O at room temperature.
9. Wash the slides with 4× SSC, 0.1% SDS prewarmed to 50°C for 15 min with gentle agitation.
10. Rinse the slides twice by submerging in distilled water. This step removes residual salt and SDS.
11. Dry slides by centrifugation (800 rpm for 3 min).
12. Store the slides dark and desiccated until use.

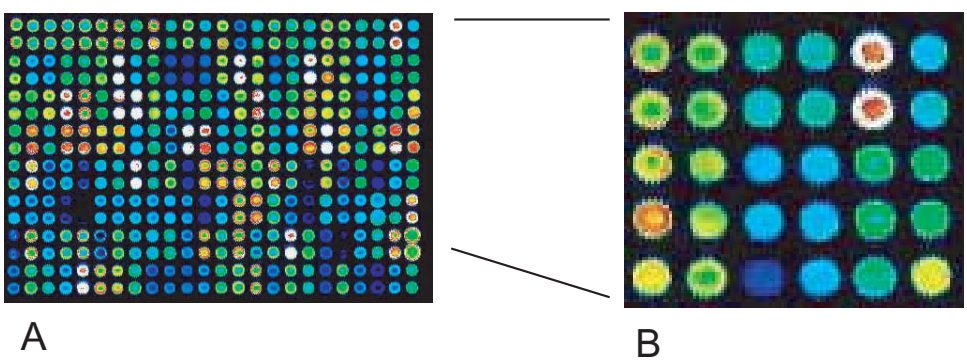

FIGURE 2 Control hybridisation of printed CodeLink slide for verification of spot presence and morphology. (A) Image of a slide with 5′ amine-modified oligonucleotides (60-mer) probes hybridised with a random 25-mer Cy5-labelled oligonucleotide and scanned at 633 nm with laser and PMT settings of 100 and 50%, respectively. (B) Magnified image.

3. *Quality Control of Printed Microarrays*

During printing of slides, one or more pins may be clogged for a longer or shorter period of time. This can result in abnormal or missing spots on a part of the microarray batch. We recommend performing quality control to evaluate printing errors and probe coupling efficiency for each 20th spotted slide in a batch (Fig. 2).

Solution

5′-Cy5-labelled 25-mer random oligonucleotide from DNA Technology A/S, DK

Steps

1. Dissolve the oligonucleotide in the hybridisation buffer (see Section VII) to a final Concentration of 5 µ*M*
2. Apply 25 µl of the hybridisation mix to the slide as described in Section VII and incubate for 30 min at room temperature.
3. Wash and dry the slide as described in Section VII.
4. Scan the slide with the 633-nm (Cy5) laser at a power setting of 100% and with the PMT setting at 50%.

V. ISOLATION OF TOTAL RNA WITH TRIZOL

A. Introduction

The quality of RNA for microarray experiments must be of high quality. It should be intact and contain no genomic DNA or enzyme inhibiting substances. Several extraction methods have been tested with a wide variety of biological samples. TRIzol has become our method of choice because it gives consistent, reliable results and is considerably less expensive than kit-based products. The outlined protocol is suitable for up to 100 mg of tissue, which should give you an abundant amount of total RNA compared to the 5 µg required per labelling reaction.

All materials should be RNase free and only handled using gloves. Keep a separate set of pipettes solely for RNA work. Glassware should be baked at 180°C for 6 h. The work area can be cleaned using RNase Zap to limit the risk of RNase contamination.

B. Materials and Instrumentation

RNAlater and RNase Zap are from Ambion. Lysing Matrix D (Cat. No. 6913-100) and Q-Bio gene are from Bio101 Systems. The Trizol reagent is from Invitrogen. Bio101 Fastprep, FP120, Savant Instruments Inc.

C. Procedures

Steps

1. After excision of a tissue sample, transfer it as fast as possible to a 1.5-ml microcentrifuge tube. Submerge the tube into a container with liquid nitrogen and then store in a –80°C freezer. Alternatively, add 5 (tissue) volumes of RNAlater and store at 25°C for a couple of days, at 4°C for up to a week, or at –20° or –80°C for long-time storage. Remove RNAlater before continuing with step 2.
2. Transfer the tissue to a lysing matrix placed on ice and add 1 ml TRIzol.
3. Place the matrix in the Fastprep homogeniser. Depending on how tenacious the tissue is, run the homogeniser one to three times for 25 s at 6.0 m/s^2. Cool the sample on ice between each treatment.
4. Spin the samples at 4°C for 10 min at max speed in microcentrifuge tubes or at 3000 *g* for 30 min in 15-ml conical tubes.
5. Transfer the homogenate to a microcentrifuge tube.
6. Add 0.2 ml of chloroform/isoamylalcohol (24:1) and shake vigorously for 15 s.
7. Incubate for 5 min on ice and then spin at max speed for 15 min at 4°C.
8. Transfer top (aqueous) layer to a new microcentrifuge tube, being careful not to pick up any of the white interphase layer (the lower phases may be saved for DNA and protein extractions).
9. If double extractions are needed, repeat steps 6–8, except that only 0.1 ml chloroform is added.
10. Precipitate RNA by adding 0.5 ml isopropanol, vortex, and leave on ice for 15 min.
11. Spin at max speed for 30 min at 4°C.
12. Pour off supernatant, add 1 ml cold 70% ethanol, and invert tube to loosen pellet.
13. Spin at max speed for 5 min at 4°C.
14. Pour off supernatant, spin briefly, and remove the remaining ethanol with a pipette.
15. Dry the pellet under a ventilated hood until the RNA is just dry.
16. Dissolve the RNA in 50 µl RNase-free H_2O by vortexing.
17. Measure the optical density at 260 and 280 nm to estimate the RNA concentration and purity. An OD_{260}/OD_{280} ratio of 2.0 indicates that the RNA is pure, but any value down to 1.7 is acceptable. The RNA concentration is calculated by the following equation: Concentration (µg/ml) = $OD_{260} \times 40 \times$ dilution factor. Verify RNA integrity by running 0.5 µg on a 1% agarose gel. The intensity of the 28S to 18S should have a ratio of approximately 2 : 1. Some species (e.g., drosophila) have 28S and 18S RNA that only move

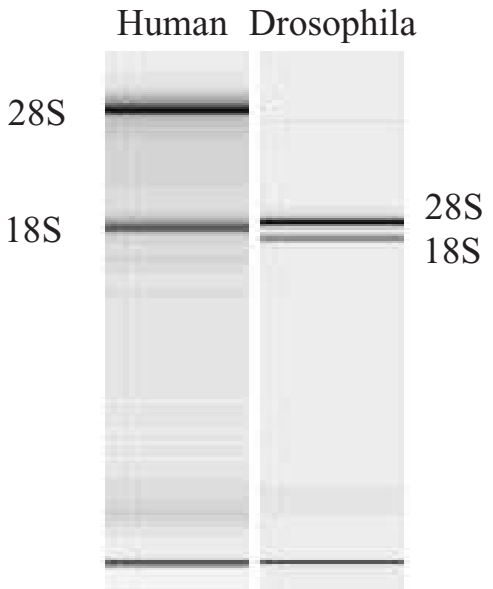

FIGURE 3 Total RNA from human and drosophila separated on a 4% Metaphor agarose gel for 90 min. High-quality RNA will have a 28S to 18S ratio of intensity of approximately 2 : 1.

with slightly different velocities (Fig. 3). In these cases, use a 4% Metaphor agarose gel (FMC Bio Products) and let it run for 90 min.

VI. SYNTHESIS OF LABELLED TARGET USING A MODIFIED EBERWINE AMPLIFICATION PROTOCOL

A. Introduction

We routinely use 5 µg of total RNA per labeling reaction using a modified Eberwine amplification protocol (Eberwine *et al*., 1992; 't Hoen *et al*., 2003) but any amount in the range of 200 ng–10 µg of total RNA will work fine. The procedures consist of several steps, starting with the conversion of messenger RNA into first strand cDNA through reverse transcription primed with a T7-tagged oligo(dT). Synthesis of the second-strand cDNA results in a T7-tagged double strand DNA that acts as template in the subsequent *in vitro* transcription (IVT). The incorporation of aminoallyl-UTP during IVT allows the conjugation of reactive-esterified flurophores to the cRNA. There are two clear advantages of this protocol compared to the synthesis of labelled cDNA by incorporation of fluorophore conjugated nucleotides during the reverse transcription: (1) a small amount of RNA down to 200 ng can be used instead of the otherwise recommended 20–50 µg and (2) there is no incorporation bias during incorporation of aminoallyl nucleotides as opposed to the incorporation of nucleotides coupled to two different sized Cy dyes.

B. Materials and Instrumentation

SuperScript double-stranded cDNA synthesis kit, Invitrogen; oligo$(dT)_{24}$-T7 reverse transcription primer with the sequence 5'-GGCCAGTGAATTGTAATAC GACTCACTATAGGGAGGCGGT_{24}), HPLC purified, DNA Technology, DK; gel electrophoresis equipment; PCR machine; MegaScript T7, Ambion; RNeasy kit, Qiagen; Cy dye PostLabelling reactive Dye Pack, Cat. No. RPN-5661, Amersham Biosciences.

C. Procedures

1. Preparation of Double-Stranded DNA

Solutions

1. *Hydrolysis buffer* (*1 ml*): 1 *M* NaOH, 2 m*M* EDTA Prepare by mixing 1 ml of 1 *M* NaOH and 4 µl of 0.5 *M* EDTA.
2. *Phenol* : *chloroform* : *isoamylalcohol solution* (*25* : *24* : *1*)
3. *7.5 M ammonium acetate*
4. *loading buffer* (*10 ml*): 0.4 ml of 50 mg/ml Orange G, 5 ml glycerol, and 4.6 ml H_2O

Steps

1. Mix total RNA (5 µg) with 100 pmol of oligo(dT)-T7 primer and add H_2O to a volume of 9.5 µl. Incubate the tube at 70°C for 10 min and immediately place on ice.

2. Thaw the following kit reagents on ice and then add to the RNA as follows: 2 µl H_2O, 4 µl 5× first strand buffer, 2 µl 0.1 *M* DTT, and 1 µl 10 m*M* dNTP. Mix gently and incubate at 37°C for 2 min before adding 1.5 µl SuperScript II. Mix gently by stirring with the pipette tip (final volume of 20 µl) and incubate at 42°C for 1 h.

3. Thaw the following reagents on ice and add 90 µl H_2O, 30 µl 5× second strand buffer, 3 µl 10 m*M* dNTP, 1 µl *E.coli* RNase H, 1 µl *E.coli* ligase, and 4 µl *E.coli* DNA polymerase I. Mix gently and incubate at 16°C for 2 h (at this point the reaction may be stored for later handling at –20°C).

4. Purify the cDNA product (total volume of 156.5 µl) by adding 156.5 µl phenol : chloroform : isoamylalcohol solution (25 : 24 : 1), mix carefully, and spin the tube for 10 min at max speed at 4°C.

5. Carefully transfer the water phase to a new tube.
6. Precipitate the cDNA by adding 80 µl of 7.5 *M* ammonium acetate, 400 µl 96% ethanol (–20°C), and mix carefully. Spin the tube for 30 min at max speed at 4°C.
7. Discard the supernatant and wash the DNA pellet with 200 µl of ice-cold 70% ethanol. Mix carefully and spin the tube for 10 min at max speed at 4°C.
8. Discard the ethanol and let the pellet air dry and then dissolve in 7 µl H_2O.
9. Check the quality of cDNA by gel electrophoresis by adding 3 µl loading buffer to 1 µl of cDNA and load it onto a 1% agarose gel (100 V for 25 min) (Fig. 4).

2. *Preparation of Aminoallyl-Labeled cRNA*

Place the RNA polymerase mix on ice, it is stored in glycerol and is not frozen at –20°C. Vortex the 10× reaction buffer and the ribonucleotide solutions (ATP, CTP, GTP, and UTP) until they are completely in solution. Once they are thawed, store the ribonucleotides on ice, but keep the reaction buffer at room temperature. Spin all reagents briefly before opening to prevent loss or contamination of material that may be present around the rim of the tube. The spermidine in the 10× reaction buffer can coprecipitate the template DNA if the reaction is assembled on ice. Add the 10× reaction buffer after the water and template DNA are already in the tube.

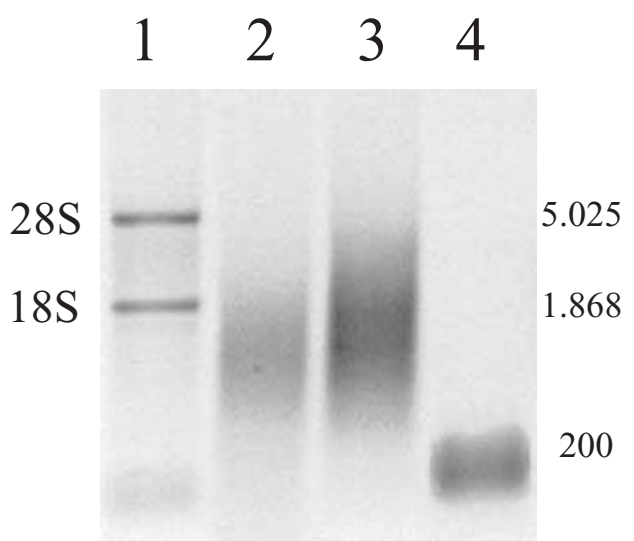

FIGURE 4 Control gel of products from the single steps in the probe preparation procedure. (1) Total RNA; (2) double-stranded cDNA will shown a smear with the highest intensity around 1500 bases; (3) cRNA from IVT should reflect the double-stranded cDNA in terms of size distribution; and (4) fragmented cRNA should be in a narrow range around 100 to 200 bases.

Solution

Prepare a 40 m*M* aminoallyl-UTP solution (stored at –80°C)

Steps

1. For each reaction (20 µl): 6 µl double-stranded cDNA, 1.1 µl H_2O, and 2 µl 10× reaction buffer. Mix and spin down. Keep the solution at room temperature.
2. Thaw the following reagents on ice and add 2 µl ATP, GTP, CTP (75 m*M*), 1.0 µl UTP (75 m*M*), 1.9 µl aa-UTP (40 m*M*) (the aa-UTP/UTP ratio is 1 : 1), and 2 µl of 10× RNA polymerase mix. Mix thoroughly by gently flicking the tube and then spin tube briefly to collect the reaction mixture at the bottom of the tube. Incubate at 37°C for 6 h or overnight.
3. Check the quality of aa-cRNA by gel electrophoresis: Add 3 µl loading buffer to 1 µl of aa-cRNA and load it onto a 1% agarose gel (100 V for 25 min).
4. Purify the aa-cRNA product using the RNeasy kit as follows: add 350 µl RLT buffer and 3.5 µl 2-mercaptoethanol. Mix and add 250 µl of 96% ethanol.
5. Transfer the sample to an RNeasy spin column and spin at max speed for 15 s.
6. Collect the run through and transfer it to the spin column again. Spin at max speed for 15 s.
7. Add 500 µl RPE and spin at max speed for 15 s.
8. Repeat step 7.
9. Transfer the spin column to a new tube and spin at max speed for 2 min to dry the filter in the column.
10. Elute the cRNA product with 50 µl H_2O. Place the column in a heating block (65°C) for 5 min.
11. Spin the column at the lowest possible speed for 1 min and continue at max speed for 1 min.
12. Repeat step 11.
13. Measure the absorbance at 260 and 280 nm (1 µl sample + 59 µl H_2O) and calculate the RNA concentration (1 OD = 40 µg/ml).
14. Aliquots (5 µg) of RNA may be stored at –80°C.

3. *cRNA Conjugation with Cy Dyes*

As the dyes are susceptible to photobleaching, all steps involving the labelled sample should be performed with as little light exposure as possible.

Solutions

1. *0.1 M carbonate buffer, pH 9.3*: To prepare 100 ml, dissolve 0.84 g of $NaHCO_3$ in 80 ml of H_2O. Adjust the pH with 10 *M* NaOH and bring the volume to 100 ml. Store frozen at –20°C in 1-ml aliqouts.
2. *1 M Tris (pH 9)*
3. *50 mM $ZnCl_2$*: To prepare 100 ml, dissolve 0.68 g of $ZnCl_2$ in 100 ml in H_2O. Store at room temperature.

4. *7.5 M ammonium acetate*
5. *70 and 96% ethanol*
6. *DMSO*

Steps

1. Speed-Vac 5 µg aa-cRNA to dryness. Resuspend in 4.5 µl 0.1 M carbonate buffer.
2. Add 9 µl DMSO to the Cy-dye vial and mix until the dye is completely dissolved. Add 4.5 µl of this mixture to the aa-cRNA solution.
3. Incubate at room temperature for 2.5 h.
4. To quench the remaining free Cy dyes, add 9 µl 1 *M* Tris (from –20°C) to the tube. Incubate at room temperature for 15 min.
5. Fragment the labelled RNA by adding 4.5 µl of 50 m*M* $ZnCl_2$ to the tube. It is important to mix the $ZnCl_2$ solution carefully before use. Incubate at 60°C for 30 min.
6. Precipitate the labelled RNA by first adding 2.25 µl of 7.5 M ammonium acetate to the tube. Then add 56.25 µl of 96% ethanol (4°C). Mix carefully.
7. Incubate at –20°C for 30 min or overnight.
8. Spin for 30 min at max speed (4°C).
9. Wash pellet with 70% ethanol (–20°C) and spin for 10 min at max speed (4°C).
10. Repeat step 9.
11. Remove the supernatant and dry the pellet for 5 min. This can be done in a Speed-Vac without heating.
12. Resolve the pellet in 60 µl H_2O and measure the absorbance at 260, 280, 550, and 650 nm.
13. Calculate the frequency of incorporation (FOI), which is the number of dye molecules per 1000 nucleotides. The optimal incorporation is 20–50 FOI.

FOI (dyes/1000 nucleotides): pmol dye × 340 per ng of cRNA

ng cRNA = $A_{260} \times 40 \times$ volume (µl)

pmol dye = **Cy3:** $A_{550} \times$ volume (µl)/0.15

Cy5: $A_{650} \times$ volume (µl)/0.25

VII. HYBRIDISATION

A. Introduction

The protocol outlined here is optimised for hybridisation of cRNA target to 60-mer oligonucleotide probes on CodeLink-activated slides. Other systems may benefit from different temperatures and hybridisation times and a different composition of the hybridisation buffer.

B. Materials and Instrumentation

Hybridisation chambers were custom made in John Kreitler's laboratory at Washington University School of Medicine (St. Louis, MO). LifterSlips are from Erie Scientific Company (Cat. No. 221x25-2-4635). The hybridisation oven is from Promega. The DNA 120 Speed-Vac is from Thermo Savant. The Plactronic rectangular hot plate (Cat. No. 6156100) is from J.P Selecta s.a.

C. Procedures

Solutions

1. The volume of hybridisation mix for one hybridisation (using LifterSlips) is 20 µl hybridisation buffer. To prepare 100 µl of hybridisation mix, combine 30 µl formamide [final concentration 30% formamide], 25 µl 20× SSC [final concentration 5× SSC], 1 µl 10% SDS [final concentration 0.1% SDS], 5 µl fish sperm DNA (0.66 mg/ml) [final concentration 0.033 mg/ml FS DNA], 5 µl tRNA (0.66 mg/ml tRNA) [final concentration 0.033 mg/ml tRNA], 10 µl 0.5% BSA [final concentration 0.05% BSA], and 24 µl H_2O. *Note: Formamide, SSC, and SDS should be filtered through a 0.22-µm syringe filter.*

2. *Nonstringent wash buffer* (*400 ml*): Mix 120 ml 20× SSPE, 0.2 ml 10% Tween 20, and 279.8 ml H_2O

3. *Stringent wash buffer* (*400 ml*): Mix 1.2 ml 20× SSPE and 398.8 ml H_2O

Steps

1. Combine 1 µg of each labelled cRNA (both Cy3 and Cy5, 1 : 1 ratio) and dry the combined target sample in a Speed-Vac for 30 min until the volume is only a few microliters (~2 µl). Avoid drying the sample completely.

2. Resuspend the sample in 20 µl hybridisation mix. Vortex slightly and incubate for 10 min at room temperature.

3. Place the slide and the LifterSlip on the heating plate (42°C) for a few minutes (array side up!). The LifterSlip should be cleaned with 96% ethanol and dried before use.

4. Denature the sample at 95°C for 2 min and let cool to 42°C in the prewarmed hybridisation oven until use.

5. Spin the sample for 5 min at 12,000 *g* and apply it onto the LifterSlip, avoiding air bubbles (Fig. 5A) and attach the slide (array side down!) to the liquid (Fig. 5B)—the LifterSlip should stick to the slide. Place the slide with the LifterSlip in the hybridisation chamber. To avoid drying out, add 70 µl 3× SSC to the reservoirs in the hybridisation chamber (Fig. 5C) and

FIGURE 5 Overview of the hybridisation procedure. (A) Applying the target sample to the LifterSlip. (B) Attaching the LifterSlip to the slide. (C) Humidifying the hybridisation chamber. See text for details.

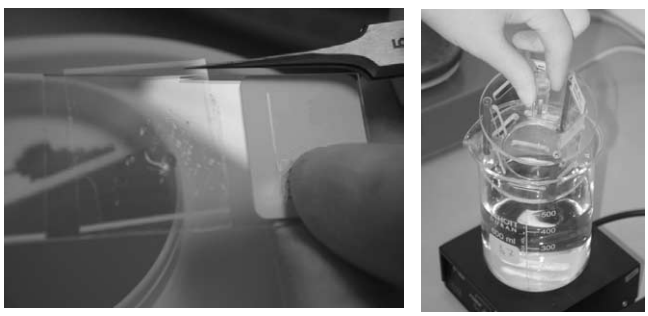

FIGURE 6 Overview of washing procedure. (A) Removing the LifterSlip from the slide. (B) Washing the slides. Slides have been placed in the rack.

make sure that the hybridisation chamber is closed tightly. Place it in the hybridisation oven at 42°C and incubate for 16 h. *These steps should be performed in a clean environment, as dust particles trapped within the hybridisation area will show on the scanning and hamper the results.*

Steps

1. Take out the hybridisation chamber with the slide from the hybridisation oven.
2. Remove the LifterSlip carefully with *a pair of tweezers* (Fig. 6A). Do not touch the array area. Try to remove it *vertically*, not horizontally.
3. Quickly transfer the slide into the slide rack and immediately submerge the slide rack into the nonstringent wash buffer (Fig. 6B). It is essential that the time used for these first steps (2–3) be minimised to ensure that the array area does not dry out.
4. Wash the slide for 30 s with gentle agitation in the nonstringent wash buffer.
5. Transfer the slide rack to the stringent wash buffer and wash for 10 s with gentle agitation.
6. Dry the slide by centrifugation (800 rpm for 3 min).

VIII. SCANNING

A. Introduction

Many different laser scanner and CCD camera imaging systems are available. This section outlines a few principles in the laser scanning imaging process, but it is recommended to read the manufactures instructions carefully for a detailed description.

B. Materials and Instrumentation

ScanArray 4000 laser scanner (Perkin Elmer)

Steps

After the slides have been dried they are ready to be scanned. For optimal fluorescence it is advisable to scan the slides immediately after they have been dried. If the slides cannot be scanned at this time, store them dark and desiccated.

1. Turn on the laser scanner and allow the 543-nm (Cy3) and 633-nm (Cy5) lasers to warm up. Set the desired parameters on the scanner, e.g., laser power and PMT gain and resolution. We recommend fixing the laser power at 100% and automatically adjust PMT settings. Otherwise, we recommend the following settings: 100% laser power and 55% PMT for the Cy5 fluorophore and 100% power and 70% PMT for the Cy3 fluorophore.
2. Select the area to be scanned. The (X, Y) values defining the position of the grid on the slide are set in the printing procedure.

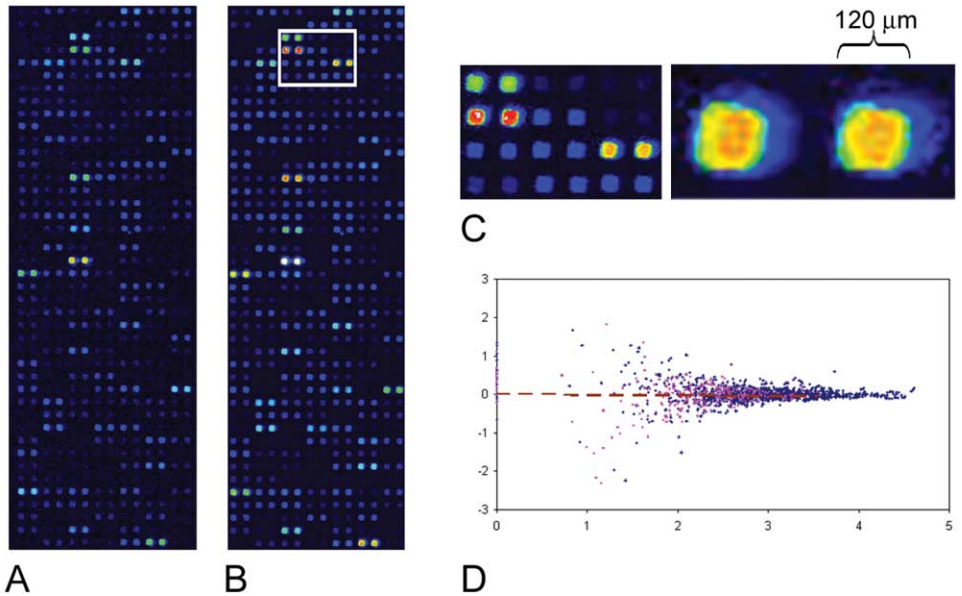

FIGURE 7 Two colour hybridisation. Scanned image of a Cy3- (A) and Cy5-labelled (B) cRNA hybridised overnight at 42°C. The same cRNA was labelled with the two dyes in order to measure the degree of variation between the two channels. (B) Enlarged view of spots. (C) MA plot of data generated from the two images. Data were normalised using a Lowess nonlinear normalisation and background corrected. The dotted line illustrates the regression line through the points. The correlation coefficient is 0.96 and indicates a low variation in a self versus self-hybridisation experiment.

3. Clean the backside of the slide to be scanned with a soft paper towel wetted with 96% ethanol. Allow the ethanol to evaporate.

4. Load the microarray (face up) into the scanner and scan the slide.

5. Save the Cy3 and Cy5 data images in an appropriate format for data analysis (Fig. 7).

IX. PITFALLS

1. Irregular spot morphology: Check the printing pins. Make sure that the temperature and humidity are kept constant when printing the slides.

2. The spotting solution should not contain aliphatic amino groups (e.g., Tris buffer) or nucleophiles (e.g., ethanolamine, lysine, and free ammonium), as these substances will compete for the active groups on the slide and inhibit the covalent coupling of the DNA to the slide. Detergents (e.g., Tween 20, SDS) should not be included in the printing solution, as they will decrease the binding efficiency on the CodeLink slides.

3. Uneven or high background after blocking: Make sure not to extend the time of blocking. Always use clean and freshly prepared solutions. Always clean glassware thoroughly after use.

4. Uneven or high background after hybridisation: Make sure that the target sample is washed properly after precipitation and does not contain free dye molecules. Be sure to use clean washing solutions and lab ware. Even trace amounts of dyes in lab ware may lead to increased background. Check that the labelling efficiency is in the desired range (20–50 dye molecules per 1000 nucleotides). Be sure the target has not dried out during incubation. If needed the sample volume may be increased.

5. Low signals after hybridisation: Check the labelling efficiency. Scan the slide again with increased laser power or PMT.

6. The spots are overlapping: Check that the relative humidity is below 35% during spotting.

References

Celis, J. E., Kruhøffer, M., Gromova, I., Frederiksen, C., Østergaard, M., Thykjaer, T., Gromov, P., Yu, Y., Pálsdóttir, H., Magnusson, N., and Ørntoft, T. F. (2000). Gene expression profiling: Monitoring transcription and translation products using DNA microarrays and proteomics. *FEBS Let.* **480**, 1–15.

Dyrskjot, L., Thykjaer, T., Kruhøffer, M., Jensen, J. L., Marcussen, N., Hamilton-Dutoit, S., Wolf, H., and Orntoft, T. F. (2003). Identify-

ing distinct classes of bladder carcinoma using microarrays. *Nature Genet*. **33**, 90–96.

Eberwine, J., Spencer, C., Miyashiro, K., Mackler, S., and Finnell, R. (1992). Complementary DNA synthesis in situ: Methods and applications. *Methods Enzymol*. **216**, 80–100.

Eisen, M. B., and Brown, P. O. (1999). DNA arrays for analysis of gene expression. *Methods Enzymol*. **303**, 179–205.

Hughes, T. R., Mao, M., Jones, A. R., Burchard, J., Marton, M. J., Shannon, K. W., Lefkowitz, S. M., Ziman, M., Schelter, J. M., Meyer, M. R., Kobayashi, S., Davis, C., Dai, H., He, Y. D., Stephaniants, S. B., Cavet, G., Walker, W. L., West, A., Coffey, E., Shoemaker, D. D., Stoughton, R., Blanchard, A. P., Friend, S. H., and Linsley, P. S. (2001). Expression profiling using microarrays fabricated by an ink-jet oligonucleotide synthesizer. *Nature Biotechnol*. **19**, 342 – 347.

Kane, M. D., Jatkoe, T. A., Stumpf, C. R., Lu, J., Thomas, J. D., and Madore, S. J. (2000). Assessment of the sensitivity and specificity of oligonucleotide (50mer) microarrays. *Nucleic Acids Res*. **28**, 4552–4557.

Kricka, L. (1998). Revolution on a square centimeter. *Nature Biotechnol*. **16**, 513.

Lemieux, B., Aharoni, A., and Schena, M. (1998). Overview of DNA chip technology. *Mol. Breed*. **4**, 277–289.

Li, F., and Stormo, G. D. (2001). Selection of optimal oligos for gene expression arrays, *Bioinformatics* **17**, 1067–1076.

Marshall, A., and Hodgson, J. (1998). DNA chips: An array of possibilities. *Nature Biotechnol*. **16**, 27–31.

Phimster, B. (1999). *Nature Genet*. **21** (Suppl.), 1.

Schena, M., and Davis, R. W. (1999). Genes, genomes and chips. *In* "*DNA Microarrays: A Practical Approach*" (M. Schena, ed.). Oxford Univ. Press, Oxford.

Schena, M., Heller, R. A., Theriault, T. P., Konrad, K., Lachenmeier, E., and Davis, R. W. (1998). Microarrays: Biotechnology's discovery platform for functional genomics. *Trends Biotechnol*. **16**, 301–306.

Schena, M., Shalon, D., Davis, R. W., and Brown, P. O. (1995). Quantitative monitoring of gene expression patterns with a complementary DNA microarray. *Science* **20**, 270, 467–470.

Shalon, D., Smith, S. J., and Brown, P. O. (1996). A DNA microarray system for analyzing complex DNA samples using two-color fluorescent probe hybridization. *Genome Res*. **6**, 639–645.

't Hoen, P. A., de Kort, F., van Ommen, G. J., and den Dunnen, J.T (2003). Fluorescent labelling of cRNA for microarray applications. *Nucleic Acids Res*. **31**, e20.

Thykjaer, T., Workman, C., Kruhøffer, M., Demtroder, K., Wolf, H., Andersen, L. D., Frederiksen, C. M., Knudsen, S., and Orntoft, T. F. (2001). Identification of gene expression patterns in superficial and invasive human bladder cancer. *Cancer Res*. **61**, 2492–2499.

CHAPTER

13

ArrayExpress: A Public Repository for Microarray Data

Helen Parkinson, Susanna-Assunta Sansone, Ugis Sarkans, Philippe Rocca-Serra, and Alvis Brazma

I. INTRODUCTION

ArrayExpress is a public repository for microarray data developed and maintained at the European Bioinformatics Institute. ArrayExpress has three major goals: (1) to serve as an archive for microarray data associated with scientific publications and other research, (2) to provide easy access to microarray data in a standard format for the research community, and (3) to facilitate the sharing of microarray designs and experimental protocols. ArrayExpress has been online since 2002 (Brazma *et al.*, 2003). ArrayExpress contains data from over 3400 hybridisations from 10 different organisms, including human and all major model organisms (as of January 2004). ArrayExpress accepts data from all microarray platforms and supports the following experiment types: gene expression experiments, CHG, and chromatin IP.

ArrayExpress supports two standards developed by the Microarray Gene Expression Data (MGED) Society (http://www.mged.org): minimum information about a microarray experiment (MIAME) (Brazma *et al.*, 2001), a content standard, and microarray expression data mark-up language (MAGE-ML), a format standard (Spellman *et al.*, 2002). MIAME specifies the minimum information that has to be provided about a microarray experiment to enable its unambiguous interpretation and potential reproducibility. According to MIAME conventions, a microarray *experiment* is defined as a set of related hybridisations (often related to a publication). To satisfy MIAME requirements, the description of the overall experiment structure-sample, hybridisation, array design, and protocol(s) used in the experiment, alongside raw and normalised data files-should be provided (Fig. 1). MIAME compliant data are loaded into ArrayExpress in MAGE-ML format and the ArrayExpress implementation is based on the MAGE-OM.

Since December 2002, many of the major scientific journals, including *The Lancet*, the *EMBO Journal* and journals from the *Nature* group require MIAME compliant data submissions to public repositories such as ArrayExpress and GEO (Edgar *et al.*, 2002). A third public repository, CIBEX, is currently under development at DDBJ, Japan. As a result of journal requirements, both the number of submissions and the amount of data in ArrayExpress are growing rapidly.

Data in ArrayExpress can be accessed via the Web interface at http://www.ebi.ac.uk/arrayexpress. Users requiring programmatic access should contact arrayexpress@ebi.ac.uk for advice.

ArrayExpress is organised into three sections: *arrays*, *protocols*, and *experiments*. Each experiment, array, and protocol in ArrayExpress is given a unique accession number (see Section III for format information). ArrayExpress provides a password-protected log-in service for private submissions—this option can be used for anonymous reviewing of microarray experiment-based publications or for submitters to access their data before release. When data are released, this facility is withdrawn.

This article describes how to submit and access data in ArrayExpress.

II. DATA SUBMISSION

Data can be submitted to ArrayExpress either online using the microarray experiment submission and annotation tool MIAMExpress (http://www.ebi.

Copyright 2006, Elsevier Science (USA).
All rights reserved.

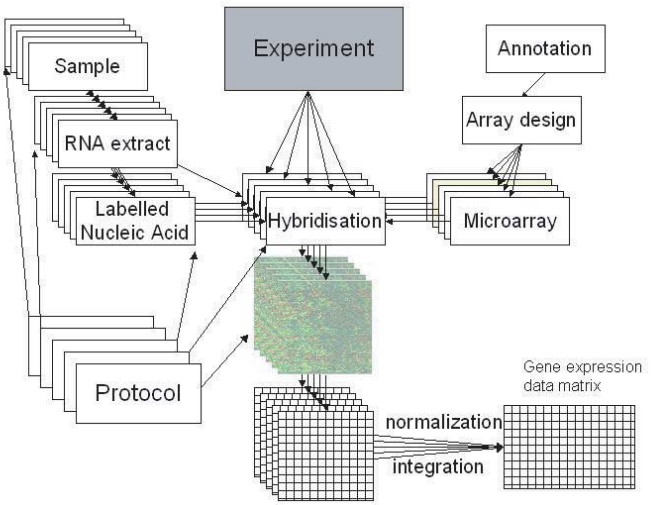

FIGURE 1 A schematic diagram of MIAME requirements showing relationships among the sections, including experiment structure, sample(s) description, hybridisation(s), array design(s), and protocols used.

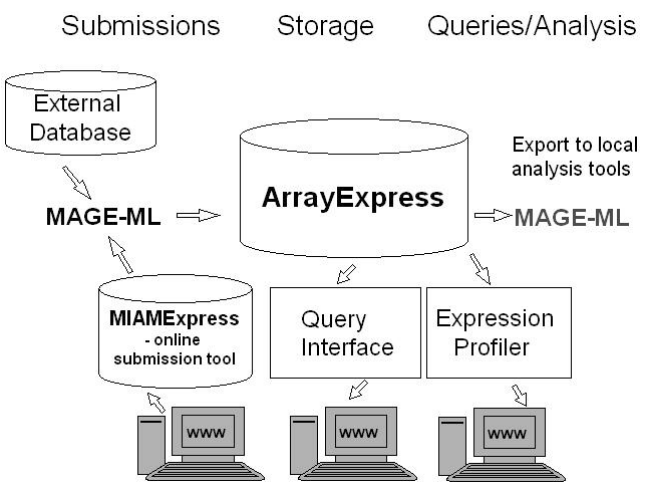

FIGURE 2 A schematic diagram of the ArrayExpress components, including data submission routes, data query, and data analysis.

ac.uk/miamexpress) or as a MAGE-ML-formatted file (Fig. 2). The second route is discussed briefly at the end of this section. The user opens an account, enters the experimental annotation, links the data files (normally stored on the user's local PC or file server accessible to the browser), and completes data submission. A typical submission of an experiment consisting of about 20 hybridisations will usually take 1 h (assuming that the submitter has read the basic instructions provided in the online help page). This section describes submission via MIAMExpress in detail.

To start a submission, users are required to create an account and provide contact details. They receive an email with their log-in details and can log-in again at any time whilst the submission is incomplete. A schematic diagram of a MIAMExpress submission is shown in Fig. 3. We suggest that users submit in the order: *arrays*, *protocols*, and *experiment(s)*. This is because the *arrays* and *protocols* are used within an *experiment* submission and observing this order speeds up the submission process. Users can try out MIAMExpress by clicking on the "Try me" option.

MIAMExpress is based on the MIAME checklist (Ball *et al.*, 2002) and the required fields appear as a series of text boxes, each of which has links to contextual help.

Whenever possible MIAMExpress uses drop-down lists of controlled vocabularies, helping the user select the appropriate term for the required field, and free text boxes are provided to add new terms. MIAMExpress is a generic tool, which is suitable for any species or domain, and is suitable for single and dual channel experiments and gene expression and CGH data submissions. MIAMExpress has been developed further for the toxicogenomics community (see Section II,C,6) and an Arabidopsis version is under development; both these versions have added domain-specific information and use specific vocabularies.

In MIAMExpress, as in MIAME, an *experiment* is defined as a group of related hybridizations. A completed submission consists of three parts: *arrays*, *protocols*, and *experiments*. The same *protocols* and *arrays* can be reused in many experiments, thereby making subsequent submissions quicker, especially if commercial arrays are used. MIAMExpress allows users to log back in to a submission at any time until it is completed. Once a submission is complete, data are exported from the MIAMExpress database (as MAGE-ML) and curated by the ArrayExpress curation team.

A. Arrays

Users need to submit details of the design of the array only if they are using a self-made array. The manufacturers normally provide details of commercial arrays. Users can check if their arrays are already present in the database using the "Browse existing arrays" link. If a particular commercial array is not present, the user should contact the ArrayExpress curation team (arrayexpress@ebi.ac.uk). ArrayExpress contains x commercial array designs from suppliers such as Agilent, Affymetrix, and Incyte and x user-supplied array designs, including many from academic facilities (figures from January 2004).

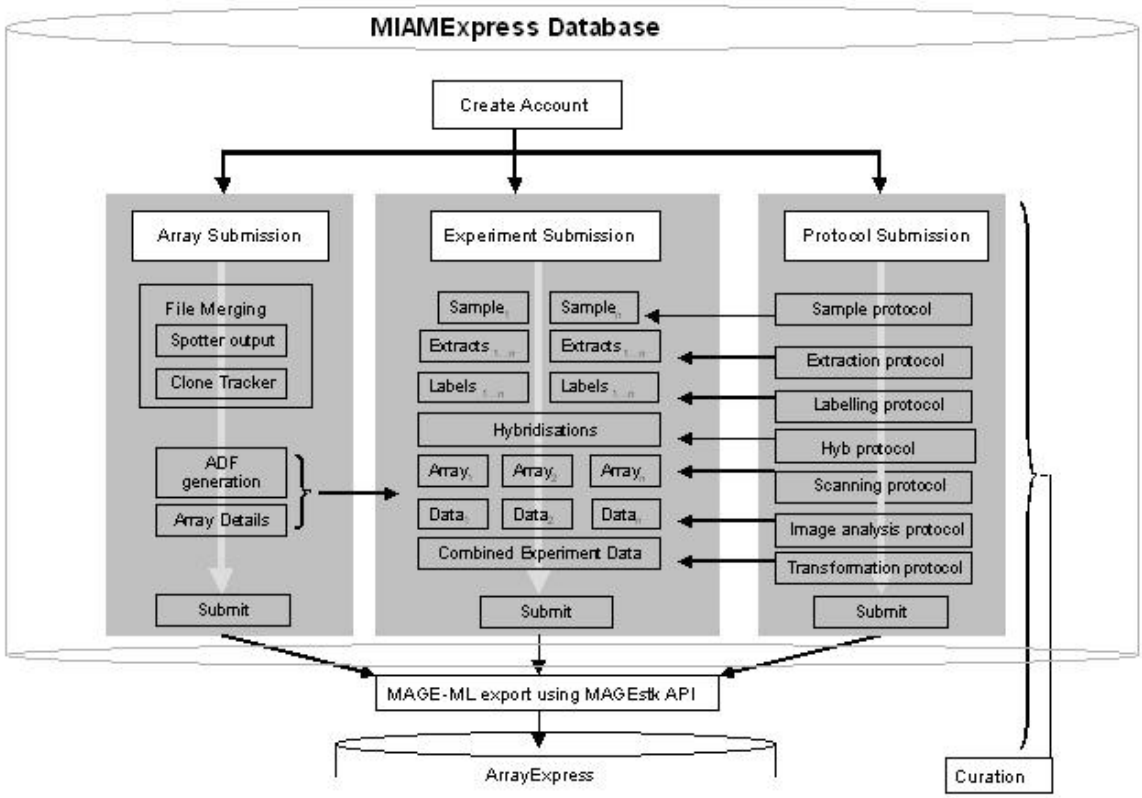

FIGURE 3 A schematic representation of the MIAMExpress submission process showing the branching tree structure of submissions.

Array designs are submitted in Array Design File (ADF) format; a simple tab delimited format, which is generated by merging a spotter output file and a clone tracker file. The ADF provides information layout (from the spotter output file) and the biological annotation for each spot (from the clone tracker file) in a single file. To allow users to access up-to-date annotation for their arrays, the ADF converter tool has been developed. It consists of a web form through which users submit a series of database identifiers, which describe the sequences on the array. These are submitted to EnsMart (Kasprzyk *et al.*, 2004), the output of the query is current sequence annotation (gene names, chromosomal location, and GO terms) in the form of database identifiers preformatted as an ADF-compatible file. Full help on the ADF is provided (http://www.ebi.ac.uk/miamexpress/help/adf/ADF_Help.htm) and the ArrayExpress curation team provides assistance in helping users generate ADF files for their arrays. MIAMExpress also allows submission of MIAME required information: species represented on the array, the surface/substrate type, a text description of the array, and finally the protocol used to manufacture the array. On submission of the array, users can use it immediately in an experiment submission and the ArrayExpress curation team will perform curation.

B. Protocols

All protocols (except those that relate to array design) are entered from a single protocol submission page. The different protocol types are sample growth, sample treatment, sample pooling, nucleic acid extraction, labelling, hybridisation, scanning, and data transformation (normalization). Different protocol types have different (MIAME) required parameters, e.g., when describing the labelling process, users must select which nucleic acid was labelled from a drop-down list of defined terms. Unchanged protocols can be reused in subsequent submissions.

C. Experiments

MIAMExpress employs a top-down annotation approach starting from the general information about the experiment, describing each sample and the extract(s) prepared from it, to a hybridisation(s)

process [linking labelled extract(s) to arrays], and the files (Fig. 3). Thus the user generates a branching tree structure as they enter information.

1. General Information

At the beginning of a submission, users are required to provide general information about the experiment, including a brief description and selecting an experiment design type and experimental factors from drop-down lists. For example, in an experiment where a sample is treated with a compound, the design type is "compound treatment" and factors could be the name of the compound. In cases where the supplied terms are not useful, users are encouraged to submit their own via the "other" text box present on all drop-downs. Information on publications and quality control methods can be provided. Users are asked to indicate the date for the experiment to be made public. Finally, in this section the total number of samples used in the experiment is provided and these are created for annotation. Samples can be added or deleted at any time during the submission process simply by returning to this experiment page and using the "Create" or "Delete" option.

2. Samples

Each sample is given a default name; we suggest that this is changed to one meaningful to the user. Species, sample type, and disease state information is supplied in boxes and the user decides which information is relevant for their experiment. This information can be copied across all samples for ease of submission. MIAME requires that sample-related protocols should be supplied and these are linked on this page. These can also be copied and pasted across multiple samples to limit the time needed for submission. It is also possible to navigate between samples by using the "Next" or "Previous" link; alternatively, these can be navigated by the list provided on the experiment page.

3. Extracts and Labelled Extracts

Each sample has one or more extracts—in single channel experiments usually there will be only one per sample. Users proceed from defining and describing a sample to creating a relationship between samples and extracts (Screenshot 1). Users define how many extracts they need and a drop-down list appears. Relevant samples are selected from this list. Pooling is supported as multiple samples can be linked to a single extract. For example, several organs from different mice may need to be pooled to provide sufficient nucleic acid for labelling. A "View/Edit" button opens the page for each extract. All extracts require an extraction protocol to be linked and where pooling is performed the pooling protocol can also be linked from this page. Protocol information can be propagated to all subsequent extracts, meaning users need only define this for the first sample. Users should complete all the extract annotation before proceeding to providing information about labelling.

Users are required to create labelled extracts for each extract. For a two-channel experiment with a dye swap, there will typically be two labelled extracts per extract: cy3 and cy5. For a single-channel system (like Affymetrix) the labelled extract-to-extract relationship is one to one. Once the labelled extracts are created, the labelling protocol is linked and this information can be propagated to all subsequent labelled extracts. The relationships among the samples, extracts, and labelled extracts are shown in Fig. 3.

4. Hybridizations

Hybridizations are created after the samples, extracts, and labeled extracts are annotated completely. If there are unannotated objects in the sample extract-labeled extract hierarchy (Fig. 3), an error page appears with hyperlinks to each object so they can be completed.

Users must select the number of hybridizations they want to create. Hybridizations can be added or deleted using the "Create" or "Delete" option. Each hybridization can be linked to the appropriate label by selecting them from a drop-down list. Array designs are selected from a list of the users own and publicly available designs.

5. Data Files

Data files are linked to hybridizations by uploading them from a local machine via a browse button. There is normally one raw and one normalized per hybridization. At least one data file per hybridization must be provided. MIAMExpress accepts data files in meta row, meta column data format, and block, row, and column data format (e.g., GenePix), which covers the majority of scanners. Full information and guidance on formatting cDNA and Affymetrix data files can be found in the contextual help (http://www.ebi.ac.uk/miamexpress/help/data_files.html). Relevant protocols must also be provided at this point (hybridization, scanning, normalization) and, as before, can be copied across all hybridizations after the first one has been annotated. Finally, a summary data file—the "Final Gene Expression Matrix" (FGEM)—may be provided. Typically this file will be generated from some transformation of the normalized data files and may be

averaged across replicates. For example, for a four-point time course experiment (0, 1, 2, 3), with two replicates per time point, the following data files may be submitted: eight raw data files (two per time point, one per hybridization), eight normalized files (two per time point, one per hybridization), and a FGEM file. Each column represents a single time point, where values have been averaged across the two replicates. Users can specify which hybridizations contributed to each column in the FGEM by providing the hybridization identifiers in the header row. Multiple quantitation types can also be provided in the same way. Rows in the FGEM typically correspond to genes and are matched with gene information provided in the ADF. On completion of submission, the experiment submission is locked; it can be released by curators, for example, to add additional information. The submission is exported from MIAMExpress in MAGE-ML format, an accession number is assigned, and it is loaded into ArrayExpress. All submissions are held confidential until the release date specified by the user.

6. Tox-MIAMExpress

Tox-MIAMExpress (http://www.ebi.ac.uk/toxmiamexpress/) is a specific version of the annotation and submission tool that links microarray data with biological end points (e.g., clinical observations, clinical chemistry, and histopathology evaluation) (Mattes *et al.*, 2004). While maintaining the general functionality of MIAMExpress, Tox-MIAMExpress provides the users with additional fields to describe toxicogenomics or pharmacogenomics specific details, such as treatment with a compound. Tox-MIAMExpress also allows submission of additional detail at the sample level. Users can provide the usual information on species and detail complex treatments such as compound/drug, dose, and delivery method. Details of blood/urine analysis commonly needed in toxicogenomics or pharmacogenomics experiments are provided via drop-down lists of terms and units. Pathological findings related to samples are entered onto a downloadable Excel spreadsheet (http://www.ebi.ac.uk/tox-miamexpress/pics/Pathology-Observation.xls). Protocols are linked to these sample treatments, in addition to the usual protocols required by MIAMExpress. Users provide information, including sample biometrics (e.g., body weight, organ weight), the target organ, and select nominal measurements, to describe any pathological changes of the organ (morphologies). This is then uploaded to Tox-MIAMExpress; the information is stored in the database and exported on completion of submission.

D. Direct MAGE-ML Submissions

Preparing MAGE-ML files is usually not a practical option for small laboratories. This direct submission route is used by laboratories with their own local microarray database systems or LIMS. In this case, a MAGE-ML export pipeline can be established from the source database directly to ArrayExpress. As of January 2004, MAGE-ML pipelines have been established from a number of local databases, including the Stanford Microarray Database (SMD) (Gollub 2003), TIGR microarray database (Saeed 2003), and German Genome Resource Centre (RZPD). Several microarray informatics tools, such as GeneSpring 6.1 (http://www.silicongenetics.com/), J-Express (http://www.ii.uib.no/~bjarted/jexpress/), and BioConductor (http://www.ebi.ac.uk/~ele/ext/submitter.html) are currently implementing MAGE-ML export and import. These developments will simplify data submission for many submitters and illustrate the utility of MAGE-ML as a data exchange format. Development of the pipeline from the SMD is described in an article available from the ArrayExpress Web site, which describes mapping a database to the MAGE-OM and implementing export using open source tools. If you wish to establish such a pipeline, please check the documentation on the ArrayExpress Web site (http://www.ebi.ac.uk/~ele/ext/submitter.html) or contact ArrayExpress at arraysubs@ebi.ac.uk for detailed advice.

III. ACCESSING DATA IN ARRAYEXPRESS

Querying data in ArrayExpress requires a web browser. Accession numbers in ArrayExpress are of the form E-XXXX-N, A-XXXX-N, or P-XXXX-N for experiments, array designs, and protocols respectively, where XXXX denotes an abbreviation of data source or data processing software and N is a number. For instance, an experiment submitted via a pipeline from the Stanford Microarray Database has accession numbers E-SMDB-N. All experiments submitted via MIAMExpress have accession numbers E-MEXP-N.

All routes to access and retrieve data from ArrayExpress consist of two basic steps.

1. Select the submission, i.e., experiment, array, or protocol, of interest by browsing or querying the database.
2. Explore the required information from the chosen submission and retrieve data.

Browsing or querying returns a brief description of the selected experiment, array, or protocol, which we will refer to as a *top-level* description. The top-level description consists of a brief summary of the submission and provides hyperlinks, which the users follow to explore data in detail or to perform specific tasks, such as retrieving raw or normalised data.

A. Retrieving the Top-Level Description

There are four ways to retrieve top-level descriptions.

1. Click on "View" experiments, arrays, or protocols.
2. Click on "Browse database."
3. Click on "Query database."
4. Click on "Log-in" (to access for submitters to non-public password-protected data).

The first two options are used to get an overview of the database. Query and log-in are described in detail in the following sections.

1. Query Database: Accessing Publicly Available Data

Clicking on "Query database" brings up the standard query interface page, which is organised into three separate sections: experiments, arrays, and protocols. The user is logged into the database as a "guest" by default and can only query public datasets. Experiments, arrays, or protocols can be retrieved quickly by their respective accession numbers or by their attributes, such as species, laboratory, or array type used in the experiment. For example, to retrieve all experiments from a single species *C. elegans*, select *Caenorhabiditis elegans* from the drop-down menu in the "organism" field of experiment menu and click on "query." This will retrieve all experiments that used samples of this species.

Combined queries are possible (for instance, by species and array type). If no query fields are completed, the query will retrieve all experiments, arrays, or protocols, respectively. Queries are case insensitive and wild cards are permitted. A query can be revised by going back to the query page (using the browser back button) and revising the selection criteria. For example, to retrieve all experiments involving human samples, you can select *Homo sapiens* from the drop-down list in the organism field and query for experiments. The user then can go back to the main query page and additionally choose *Affymetrix* from the array field to retrieve only experiments annotated as *Homo sapiens* and using Affymetrix arrays. If the query does not retrieve any results, this means that query criteria are too stringent and that there are no submissions in the database satisfying this particular combination of parameters. In this case the user should check the selected query parameters and relax them or use the browse options to explore data at a higher level.

2. Log-in: Accessing Password-Protected Data

Clicking on "Log-in" brings up the log-in page, where the user has to type in a user name and password. Passwords are only provided to the data submitter and authorised persons (with the permission of the submitter), such as journal editors and reviewers. Passwords are used to protect unreleased datasets until the specified release date. Once logged in, the query interface is identical to the query page described in Section IIIA.

B. Exploring the Experiment and Retrieving Data

Once an experiment, array, or protocol is selected, users can retrieve further details. For instance, experiments may contain raw and normalised data consisting of different quantitation types. The interface allows the user to select and export data from specific quantitation types from raw and/or normalised data. Users can also compare array designs or view protocols. This section describes data retrieval and exploration of experiments and protocols in detail.

Top-level information for experiments provides a brief free text description supplied by the submitter and an autogenerated experiment description, which indicates the number of samples and arrays used, hybridizations, and data files produced, as well as information on sample attributes, e.g., species. Hyperlinks help the user navigate to complete information on authors, laboratory, and type of experiment. By clicking on "Retrieve data," users retrieve a summary page of data associated with the particular experiment. The information is organized in two or more columns.

Column 1: Lists available data files and their type (raw or normalised). Raw data files are displayed first.
Column 2: List of quantitation types, with links to descriptions.
Column 3: List of sequence annotation, such as "Database accessions" and "Gene names" (only for arrays submitted after July 2003).

Any (or all) of the items in the columns can be exported to a tab-delimited data file. By clicking on "Export data," users can export the selected information and view them in tab-delimited format by clicking "View data matrix." The data matrix will appear in a new browser window and can be saved locally for future use. Alternatively, selected data can be imported

directly into Expression Profiler for analysis online (Vilo *et al.*, 2003).

Users can export data from several hybridisations/normalisations in a single file if the same array has been used, if data are about the same set of features (spots), reporters, or composite sequences (genes), and the same quantitation types are provided. In other cases, where, for example, only a subset of genes have expression values, data are exported as multiple files as the file will have different numbers of rows and/or columns.

C. Arrays

Users can query array designs by name, provider, and species. Details of the array layout and annotation are provided either as a spreadsheet (the ADF used to submit the array design through MIAMExpress) or as a simple tab-delimited file, both containing active hyperlinks to respective databases used for annotation. Both formats contain a single line for every feature (spot) on the array, except for Affymetrix arrays, where each line corresponds to a probe set due to the large number of rows in Affymetrix raw data files. Users can request complete Affymetrix data files by emailing arrayexpress@ebi.ac.uk and stating the accession number.

D. Protocols

When querying the protocols, users retrieve a list, including basic information (name, type, description) and protocol parameters.

IV. FUTURE PLANS

ArrayExpress repository can currently be queried by a number of parameters, including species, array design provider, and experiment type, as described earlier, returning a set of experiments, array designs, or protocols. However, querying the repository, users cannot retrieve, for example, all experiments where expression of a certain gene has been tested or the expression values of genes from a certain GO category and for samples treated under certain conditions.

To enable such granular queries, a data warehouse is under development. Users will be able to query parameters, including gene names, gene properties, ranges of expression values, and sample properties. The resulting query will return lists of genes, samples, or matrices of expression values (across many experiments). The database schema is very different from that of the ArrayExpress repository: whereas the repository has to be able to store all experimental details (MIAME and beyond) and import all well-formed MAGE-ML submissions, the main issue of the data warehouse is how well it can support queries of many different types.

The data warehouse will only contain a subset of the good quality experiments deposited in the database. Data from the repository to the data warehouse cannot be transferred automatically. It will require curation and selection of specific experimental properties important from the data mining perspective. For example, in the repository there is no distinction made among experiments on which measurements are the best estimates of gene expression levels and which specific sample properties (apart from experimental factors) are important from the data mining perspective.

A unique interface will allow users to query the repository and the data warehouse. Links from the data warehouse to the repository will be implemented to allow users to navigate from gene expression data to the experiment context.

Acknowledgments

The ArrayExpress design and software development is coordinated by Ugis Sarkans, with a major contribution from Gonzalo Garcia Lara. Mohammad Shojatalab coordinates MIAMExpress development, with major contributions from Niran Abeygunawardena and Sergio Contrino. The has been largely developed by the ArrayExpress curation team: Helen Parkinson, Ele Holloway, and Gaurab Mukherjee and Philippe Rocca-Serra and Susanna-Assunta Sansone. Susanna-Assunta Sansone developed the specification for Tox-MIAMExpress and implementation has been largely the work of Sergio Contrino. Helen Parkinson has coordinated the data curation and construction of MAGE-ML pipelines to ArrayExpress, with major contributions from Philippe Rocca-Serra, Ele Holloway, and the software development team. Anjan Sharma has developed a data management tool allowing curators to manage the growing number of data submissions. Ahmet Oezcimen is the ArrayExpress database administrator. Jaak Vilo, Misha Kapushesky, and Patrick Kemmeren developed expression Profiler. ArrayExpress is largely funded by the TEMBLOR grant from the European Commission, with contributions from International Life Sciences Institute, Health and Environmental Safety Institute (ILSI-HESI) and from CAGE grant from the European Commission. Incyte Genomics provided the initial funding. We also thank the MGED community, particularly Catherine

A. Ball, Gavin Sherlock, Pall Spellman, John Quackenbush, and Chris Stoeckert.

References

Ball, C. A., Sherlock, G., *et al*. (2002). Standards for microarray data. *Science* **298**(5593), 539.

Brazma, A., Hingamp, P., *et al*. (2001). Minimum information about a microarray experiment (MIAME)-toward standards for microarray data. *Nature Genet*. **29**(4), 365–371.

Brazma, A., Parkinson, H., *et al*. (2003). ArrayExpress: A public repository for microarray gene expression data at the EBI. *Nucleic Acids Res*. **31**(1), 68–71.

Edgar, R., Domrachev, M., and Lash, A. E. (2002) *Nucleic Acids Res*. **30**(1), 207–210.

Gollub, J., Ball, C. A., Binkley, G., Demeter, J., Finkelstein, D. B., Hebert, J. M., Hernandez-Boussard, T., Jin, H., Kaloper, M., Matese, J. C., Schroeder, M., Brown, P. O., Botstein, D., and Sherlock, G. (2003). The Stanford Microarray Database: Data access and quality assessment tools. *Nucleic Acids Res*. **31**(1), 94–96.

Kasprzyk, A., Keefe, D., Smedley, D., London, D., Spooner, W., Melsopp, C., Hammond, M., Rocca-Serra, P., Cox, T., and Birney, E., (2004). EnsMart: A generic system for fast and flexible access to biological data. *Genome Res*. **14**, 160–169.

Mattes, W. B., Sansone, S.-A., Bushel, P. R., and Waters, M. D., (2004). Database development in toxicogenomics: Issues and efforts. *Environ, Health Perspect, Toxicogenom*. **doi:10.1289/txg.6697**.

Saeed, A. I., Sharov, V., White, J., Li, J., Liang, W., Bhagabati, N., Braisted, J., Klapa, M., Currier, T., Thiagarajan, M., Sturn, A., Snuffin, M., Rezantsev, A., Popov, D., Ryltsov, A., Kostukovich, E., Borisovsky, I., Liu, Z., Vinsavich, A., Trush, V., and Quackenbush (2003). TM4: A free, open-source system for microarray data management and analysis. *Biotechniques* **34**(2), 374–378.

Spellman, P. T., Miller, M., *et al*. (2002). Design and implementation of microarray gene expression markup language (MAGE-ML). *Genome Biol*. **3**(9).

Vilo, J., Kapushesky, M., Kemmeren, P., Sarkans, U., and Brazma, A. (2003). "*Expression Profiler*." Springer-Verlag, New York.

CHAPTER

14

Serial Analysis of Gene Expression (SAGE): Detailed Protocol for Generating SAGE Catalogs of Mammalian Cell Transcriptomes

Sergey V. Anisimov, Kirill V. Tarasov, and Kenneth R. Boheler

I. INTRODUCTION

Serial analysis of gene expression (SAGE) is a sequencing-based technique that permits the simultaneous evaluation of thousands of transcripts in a single assay. SAGE relies on two major principles: (1) short DNA sequences are sufficient for identifying individual gene products and (2) concatenation (linking together) of short DNA sequences or tags increases the efficiency of identifying expressed mRNAs in a sequence-based assay. The transcript profile generated by SAGE currently relies on 14 to 21 base nucleotide sequences (SAGE tags) for gene identification (Velculescu, 1995; Saha, 2002). The technique generates large numbers of short tags, originating from the last (most 3′) unique location of a restriction enzyme recognition site in a cDNA generated from a single transcript. When the tags are sequenced, the technique can theoretically identify up to 4^{10} (1,048,576) unique transcripts; however, the newer LongSAGE method can distinguish 4^{17} different tags, a number sufficient to be virtually unique even within the whole genome.

II. MATERIALS AND INSTRUMENTATION

Kits: Messagemaker kit (Cat. No. 10298-016) and cDNA synthesis kit (Cat. No. 18267-013) are from Invitrogen. Deoxynucleotide triphosphates (dNTP) (Cat. No. US77100) are from Amersham.

Enzymes: T4 DNA Ligase (1 and 5 U/µl; Cat. Nos. 15224-017 and 15224-041) is from Invitrogen. Restriction enzymes *NlaIII* (Cat. No. 125S), *BsmFI* (Cat. No. 572S), *SphI* (Cat. No. 182S), and T4 polynucleotide kinase (PNK, Cat. No. 201S) with corresponding buffers are from New England Biolabs. DNA polymerase I Klenow fragment (Cat. No. M2201) is from Promega. AmpliTaq Gold polymerase (Cat. No. 4311814) is from Applied Biosystems.

DNA molecular weight markers: 25 bp (Cat. No. 10597-011), 100 bp (Cat. No. 15628-050), and 1 kb (Cat. No. 15615-016) are from Invitrogen.

Reagents: Dimethyl sulphoxide (DMSO, Cat. No. D2650), ammonium sulfate [$(NH_4)_2SO_4$, Cat. No. A5132], magnesium chloride ($MgCl_2$, Cat. No. M8266), potassium phosphate, monobasic (KH_2PO_4, Cat. No. P5379), potassium phosphate, dibasic (K_2HPO_4, Cat. No. P2222), sodium perchlorate ($NaClO_4$, Cat. No. S1513), and β-mercaptoethanol (Cat. No. M7522) are from Sigma. Agarose (Cat. No. 15510-027) is from Invitrogen, ATP (Cat. No. 27-1006.01) is from Amersham, and NaCl (Cat. No. 7581) is from Mallinckrodt.

Electrophoresis reagents: Polyacrylamide solutions (acrylamide : bisacrylamide, 19 : 1 (Cat. No. 161-0144) and 37.5:1 (Cat. No. 161-0148)), *N,N,N′,N′*-tetramethylenediamine (TEMED, Cat. No. 161-0800), and ammonium persulfate (Cat. No. 161-0700) are from Bio-Rad. TBE polyacrylamide precast gels (20%, Cat. No. EC6315) are from Novex.

Copyright 2006, Elsevier Science (USA).
All rights reserved.

Solutions: Ethylenediaminetetraacetic acid, disodium (Na_2EDTA, 0.5 *M*, pH 8.0, Cat. No. 3400-1003, Digene), phenol–chlorophorm–isoamyl alcohol mix (PC8, 25:24:1, pH 8.0, Cat. No. 0883, Amresco), isopropanol (Cat. No. 9084-01, J.T. Baker Inc.), and absolute ethanol (Cat. No. 201096, Warner-Graham Co.) are from commercial vendors. Tris/acetate/EDTA (TAE, 50×, Cat. No. 330-008-161), Tris–HCl (1 *M*, pH 7.5; Cat. No. 351-006-100; 1 *M*, pH 8.0 Cat. No. 351-007-100), sodium acetate ($C_2H_3NaO_2$, 3 *M*, pH 5.2, Cat. No. 351-035-060), NaCl (5 *M*, Cat. No. 351-036-100), and EDTA (0.25 *M*, pH 7.0, Cat. No. 118-090-060) are from Quality Biological. Diethylpyrocarbonate (DEPC, 0.1%)-treated water (Cat. 395-000), Tris/borate/EDTA buffer (TBE, 10×, pH 8.3, Cat. No. 336-000), and SOC media (Cat. No. 396-110) are from BioSource.

Other materials: Tryptone (Cat. No. 0123-17), yeast extract (Cat. No. 0127-01-7) and Bacto–agar (Cat. No. 0140-01) are from Difco. ElectroMAX DH10B cells (Cat. No. 18290-015), pZErO-1 (Cat. No. 2500-01), and zeocin (Cat. No. R250-01) are from Invitrogen. SYBR green I (Cat. No. S-7567) is from Molecular Probes, and glycogen (Cat. No. 901 393) is from Boehringer. Dynabeads M-280 (Cat. No. 112.05) are from Dynal.

Oligo-DNA linkers and primers are synthesized by Invitrogen. ***Linker 1A*** (gel purified): TTTGGATTTGCTGGTGCAGTACAACTAGGCTTAATAGGGACATG; ***linker 1B*** (gel purified): TCCCTATTAAGCCTAGTTGTACTGCACCAGCAAATCC[amino mod. C7]; ***linker 2A*** (gel purified): TTTCTGCTCGAATTCAAGCTTCTAACGATGTACGGGGACATG; ***linker 2B*** (gel purified): TCCCCGTACATCGTTAGAAGCTTGAATTCGAGCAG[amino mod. C7]; ***primer 1***: GGATTTGCTGGTGCAGTACA; ***primer 2***: CTGCTCGAATTCAAGCTTCT; ***5′-biotinylated oligo(dT)*** (gel purified): [biotin]T_{18}; ***M13 forward***: GTAAAACGACGGCCAGT; ***M13 reverse***: GGAAACAGCTATGACCATG.

Equipment: GeneAmp PCR systems 9600 and 9700 are from Perkin-Elmer. For polyacrylamide electrophoresis, use a protean II electrophoresis unit (Bio-Rad) or similar. For agarose electrophoresis, use Hoefer HE33 (Pharmacia) or similar. For precast polyacrylamide gels, use XCell II (Novex). Power supply: Power PAC 3000 (Bio-Rad) or similar. Electroporation is performed on Gene-Pulser II/Pulse Controller II system (Bio-Rad) in 0.2-cm cuvettes (Bio-Rad, Cat. No. 16086). The magnetic particle concentrator is of MPC-E type from Dynal; RT6000 centrifuge and H1000B rotor are from Sorvall.

Required standard laboratory equipment: Millipore H_2O system, bacterial incubator, orbital shaker, autoclave, imaging system with UV light, sequencer, and microfuge.

Plastics: SpinX microcentrifuge tubes (Cat. No. 8160) are from Costar, Hot Start 50 tubes (Cat. No. 6002) are from Molecular Bio Products, Nunc sterile 96-well plates with lids, U-shape (Cat. No. 81-6668-03) and SealPlates, sterile (Cat. No. 05-6125-12) are from PGC Scientific. Thermo-Fast 96-well detection plate Cat. No. AB-1100) and adhesive sealing sheets (Cat. No. AB-0558) are from Marsh Bioproducts. MicroAmp reaction tubes (Cat. No. 801-0580) and MicroAmp caps (Cat. No. 801-0535) are from Applied Biosystems.

Software: SAGE sequence analysis: SAGE 2000 V4.13 or better is recommended (available at http://www.sagenet.org); Database download: CuteFTP (GlobalSCAPE, Inc.), DOS to UNIX Text Converter (Streamline Solutions), WinRAR for Windows (any manufacturer); MS Access and MS Excel (Microsoft).

III. PROCEDURES

A. SAGE Protocol

This protocol is modified from those of Velculescu *et al.* (1995), Kenzelmann and Muhlemann (1999), and Anisimov *et al.* (2002). The whole protocol takes about 5–6 days, but this time will vary depending on the experience of the investigator.

Solutions

1. *2× binding and washing buffer (B + W):* 10 m*M* Tris–HCl (pH 7.5), 1 m*M* EDTA, 2.0 *M* NaCl. For 100 ml final, add 1 ml of 1 *M* Tris–HCl (pH 7.5), 1 ml 0.1 *M* EDTA, and 11.69 *g* of NaCl, adjust the volume with sterile H_2O, and store at room temperature.

2. *LoTE:* 3 m*M* Tris–HCl (pH 7.5), 0.2 m*M* EDTA (pH 7.5). For 50 ml final, add 150 µl 1 *M* stock solution of Tris–HCl and 100 µl 0.1 *M* stock solution of EDTA, adjust the volume with sterile H_2O, and store at 4°C

3. *10× PCR Buffer:* 166 m*M* $(NH_4)_2SO_4$, 670 m*M* Tris, pH 8.8, 67 m*M* $MgCl_2$, 100 m*M* β-mercaptoethanol. For 50 ml final, add 1.1 *g* of ammonium sulfate, 16.75 ml of Tris 2 *M* stock solution, 0.32 *g* of magnesium chloride, and 390 µl of β-mercaptoethanol, adjust the volume with sterile H_2O, distribute into 0.5-ml aliquots, and store at –20°C.

4. *Low salt LB agar plates with zeocin:* 1% tryptone, 0.5% yeast extract, 0.5% NaCl, 1.5% bacto-agar, 50 µg/ml zeocin. For 500 ml final, add 5 *g* of tryptone, 2.5 *g* of yeast extract, and 2.5 *g* of NaCl to 450 ml of dH_2O, stir, adjust pH of the solution to 7.5 with NaOH, add 7.5 *g* of Bacto-agar, and adjust the volume to 500 ml. Autoclave, cool to 55°C, add 250 µl of zeocin

100 µg/µl stock, and pour plates. Seal with Parafilm and foil and store at 4° for up to 1 month in the dark.

5. *TB medium base:* Add 12 *g* of tryptone, 24 *g* of yeast extract, 4 ml of glycerol to 900 ml dH_2O final volume and autoclave

6. *Phosphate buffer:* Add 2.3 *g* of KH_2PO_4 and 12.5 *g* of K_2HPO_4 to 100 ml dH_2O final volume and filter sterilize

7. *TB medium/zeocin:* For 1 liter, add 900 ml of TB medium base, 100 ml of phosphate buffer, and add 500 µl of zeocin (100 µg/µl). Store in dark room at 4° for up to 2 weeks.

8. *12% polyacrylamide solution:* For a 20 × 16 × 0.1-cm gel, add 29.4 ml of dH_2O, 13.1 ml of 40% PAAG mix (acrylamide : bisacrylamide, 19 : 1), 875 µl of 50× TAE, 438 µl of 10% ammonium persulfate, and 37.5 µl of TEMED

9. *8% polyacrylamide solution:* For a 20 × 16 × 0.1-cm gel, add 33.75 ml of dH_2O, 8.75 ml of 40% PAAG mix (Acrylamide : bisacrylamide, 37.5 : 1), 875 µl of 50× TAE, 438 µl of 10% ammonium persulfate, and 37.5 µl of TEMED

Preliminary and Routine Procedures

All incubations are performed in a water bath.

1. *Kinasing (phosphorylation) reaction for linkers:* In each of two Eppendorf tubes labeled "linker 1" and "linker 2," add 6 µl of LoTE, 2 µl of 10× kinase buffer, 2 µl of 10 m*M* ATP, and 1 µl of PNK (10 U/µl). Add 9 µl of linker 1B (350 ng/µl) to "linker 1" and 9 µl of linker 2B (350 ng/µl) to "linker 2". Incubate both tubes at 37°C for 30 min and then at 65°C for 10 min. Add 9 µl of linker 1A to "linker 1" and 9 µl of linker 2A to "linker 2." Incubate at 95°C for 2 min, transfer to 65°C for 10 min, then to 37°C for 10 min, and finally to room temperature for 20 min. Kinased linkers are stable at –20°C for up to a year.

2. *Control reaction for linkers:* Prepare four Eppendorf tubes marked as "1+," "1–," "2+," and "2–." Add 20 µl of LoTE, 8 µl of 5× ligation buffer, and 1 µl of kinased linker (linker 1 to tubes marked "1" and linker 2 to tubes marked "2") to each tube. Incubate all four tubes at 50°C for 2 min and then at room temperature for 15 min. Add 2 µl of T4 ligase (1 U/µl) to tubes marked "+" and 2 µl of LoTE to tubes marked "–" and incubate at 16°C for 2 h. Run 1 µl of each sample on 20% precast TBE polyacrylamide gel at 120 V for 3 h and stain with SYBR green I (20 µl/200 ml of 1× TBE buffer) for 15 min while shaking. Observe linkers on the gel under UV light. Only linkers dimerized with >70% efficiency (based on band fluorescence intensity) are acceptable.

3. *Prepare pZeRO-1:* To 4 µl of dH_2O, add 1 µl of restriction enzyme (RE) buffer 2, 2.5 µl of pZeRO-1 (1 µg/µl), 2.5 µl of *SphI* (5 U/µl), and incubate at 37°C for 25 min. Add 90 µl of TE (final concentration is 25 ng/µl) and heat inactivate enzyme at 68°C for 15 min. Quench on ice and use immediately. Linearized pZeRO-1 plasmid can be stored at –20°C, but its cloning efficiency decreases with time.

4. *Phenol–chloroform extraction:* Bring sample volume to 200 µl with LoTE and add an equal volume (200 µl) of PC8 and vortex. Separate the aqueous phase, which contains the DNA, from the organic phase by centrifugation in a microfuge at 7800 *g* for 2 min at room temperature. Transfer the aqueous phase into a fresh Eppendorf tube, while ensuring that no organic solution is included. Reextract if necessary.

5. *Ethanol (EtOH) precipitation:* DNA in aqueous solution can be precipitated by EtOH in the presence of sodium or ammonium acetate. Because of the small amount of DNA and small fragment sizes, glycogen is added as a career. For a 200-µl sample volume in LoTE, add 3 µl of glycogen (20 mg/ml), one-half volume 10 *M* ammonium acetate, and 2.2 volumes ice-cold (–20°C) 100% ethanol and vortex. Pellet the precipitated DNA by centrifugation in a microfuge at 15,300 *g* for 10 min. Remove the ethanol with care and always wash with 75% EtOH to remove any traces of salt. Centrifuge at 7800 *g* for 10 min, discard supernatant, dry the pellet, and resuspend in LoTE. In certain cases, an increased volume of ethanol or 10 min dry ice/ethanol incubation is required on the precipitation step, as indicated in the text.

6. *Isopropanol precipitation:* Bring sample volume to 450 µl with LoTE, add 3 µl of glycogen, 150 µl of 2 *M* sodium perchlorate and 330 µl of isopropanol. Vortex and spin at 15,300 *g* for 10 min at room temperature. Aspirate supernatant, dry the pellet, and resuspend in LoTE.

Steps

1. Prepare poly(A)$^+$ (mRNA) from total RNA with the Messagemaker kit according to the manufacturer's instructions (see Comment 1 and Pitfalls 1 and 2). A total quantity of 0.5–1.0 mg of total RNA gives the best mRNA yield and is convenient for handling.

2. Prepare cDNA from 5 µg of mRNA using a cDNA synthesis kit following the manufacturer's instructions. A 5′-biotinylated oligo$(dT)_{18}$ (500 ng/µl) is, however, suggested for first strand synthesis (see Comment 2). After the second strand reaction is terminated by the addition of 25 µl of 0.25 *M* Na_2EDTA (pH 7.5), extract cDNA sample with PC8, EtOH precipitate, and resuspend the pellet in 20 µl of LoTE.

3. To half the cDNA sample (10 µl), add 163 µl of LoTE, 2 µl of BSA (100×), and 5 µl of *Nla*III (anchoring enzyme, 10 U/µl) (see Pitfall 3). Incubate at 37°C for

1 h, extract with PC8, EtOH precipitate, and resuspend in 20 µl of LoTE. Use the second half of the cDNA sample as a backup.

4. Add 100 µl of resuspended M-280 streptavidin magnetic beads (Dynabeads) to two Eppendorf tubes marked "1" and "2". Use the magnetic particle concentrator to immobilize the beads and discard the storage buffer. Wash beads once with 200 µl 1×B+W buffer and discard the buffer. Add 100 µl of 2×B+W buffer, resuspend, and add 90 µl of dH_2O and 10 µl of cDNA digestion products to each Eppendorf tube. Incubate at room temperature in suspension for 15 min. Wash beads three times with 200 µl 1×B+W and then once with 200 µl LoTE, removing the wash each time after immobilizing the beads using the magnetic particle concentrator. Proceed immediately to step 5.

5. Resuspend the Dynabeads in 25 µl of LoTE and 8 µl of 5× ligase buffer. Add 5 µl of kinased linker 1 to the tube marked "1" and 5 µl of kinased linker 2 to the tube marked "2". Incubate both tubes at 50°C for 2 min and then at room temperature for 15 min. Add 2 µl of T4 ligase (high concentration, 5 U/µl) to each tube and incubate at 16°C for 2 h. Afterward, wash the beads four times with 200 µl 1×B+W and then two times with 1× RE buffer 4. Proceed immediately to step 6.

6. Resuspend the contents of tubes "1" and "2" in 84 µl of LoTE and then add 10 µl of 10× RE buffer 4, 2 µl of 100× BSA, and 2 µl of *Bsm*FI (2 U/µl, tagging enzyme). Incubate at 65°C for 1 h, mixing intermittently, immobilize Dynabeads using magnetic particle concentrator, and collect supernatants. Extract samples with PC8, EtOH precipitate, and resuspend pellets in 10-µl volumes of LoTE.

7. To each of these tagging enzyme digestion products, add 32.4 µl of dH_2O, 5 µl of 10× second strand buffer (from cDNA synthesis kit), 1 µl of 100× BSA, 1 µl of dNTPs (25 m*M*), and 0.6 µl of Klenow (5 U/µl) to fill in the 5′ DNA overhangs. Incubate at 37°C for 30 min, add 150 µl of LoTE, extract samples with PC8, and precipitate with a high concentration of EtOH [add 3 µl of glycogen, 100 µl of 10 *M* ammonium acetate, and 900 µl of ice cold (–20°C) 100% EtOH]. Vortex and pellet the precipitated DNA by centrifugation in a microfuge at 15,300 *g* for 10 min; remove the EtOH with care and wash with 75% EtOH. Centrifuge at 7800 *g* for 10 min, discard supernatant, and dry the pellets. Resuspend pellets in 6 µl of LoTE.

8. For ditag ligations, mix 2 µl of blunt-ended samples from the previous step, add 1.2 µl of 5× ligase buffer, and 0.8 µl of high concentration T4 ligase (5 U/µl). For negative control reactions, mix 2 µl volumes of blunt-ended samples from the previous step, 1.2 µl of 5× Ligase buffer, and 0.8 µl of dH_2O. Incubate at 16°C overnight, followed by the addition of 14 µl of LoTE. Proceed directly to PCR step.

9. Take 1-µl aliquots to make serial LoTE dilutions: 1/10, 1/25, 1/50, and 1/100 for ditag ligation reactions, 1/10 and 1/25 for negative control reactions, and one LoTE sample as an additional negative control. Prepare a PCR mix using 31.0 µl of sterile water, 1 µl of selected ligation reaction or control dilution, 5 µl of 10×PCR Gold buffer, 3 µl of $MgCl_2$ (25 m*M*), 3 µl of DMSO, 4 µl of dNTPs (25 m*M*), 1 µl each of primers (350 ng/µl each), and 1.0 µl of AmpliTaq Gold polymerase (5 U/µl). Use one strip (8 tubes) of MicroAmp reaction tubes for PCR. Cycling conditions (optimized for Gene Amp PCR system 9700) are as follows: 10 min at 95°C, followed by 28 cycles (30 s at 95°C, 1 min at 55°C, 1 min at 72°C), final extension at 72°C for 5 min, and a hold at 4°C.

10. Mix 20 µl of each PCR product with 4 µl of 6× loading buffer. Load the samples and 100-bp DNA ladder (one lane) to the wells of a 10-well 20% precast Novex TBE polyacrylamide gel. Use 1× TBE as a running buffer. Set voltage to 30 V until the entire sample has entered the gel and then increase the voltage to 120 V. Terminate the reaction when the bromphenol blue stain in the loading buffer migrates to the bottom of the gel. Stain gel with SYBR green I (20 µl/200 ml of 1× TBE buffer) for 15 min while shaking. Visualize by UV. Ligated ditags are located at ~102 bp. Another bright band is present at ~80 bp (linker–linker ligation), and the remaining bands are considerably less bright. The negative control reaction should lack the 102-bp band, and PCR with LoTE as a template (negative control) should not produce any bands (Fig. 1). The optimal dilution of the ditag ligation reaction products for large-scale PCR is considered based on 102-bp band brightness to background ratio and highest dilution ratio. Usually, 1/50–1/100 dilutions produce best results with comparatively low background and a large number of possible PCR reactions. If little or no ditags are visualized, the backup volume of blunt-ended cDNA tags (2 µl for each of the linkers) could be used to repeat steps 8–10 (without negative control); alternatively, backup cDNA could be used to repeat the protocol starting from step 3.

11. Once the conditions have been optimized, perform a large-scale PCR with a fresh LoTE dilution of the selected ditag ligation product as a template. Perform the reaction as described in step 10, except use a Thermo-Fast 96-well detection plate. Cover plate with adhesive sealing sheets and spin for 3 min at 600 *g* on a RT6000 centrifuge using a H1000B rotor (Sorvall) and adapters for 96-well plates. Run about 110–120 50-µl reactions in the GeneAmp 9700.

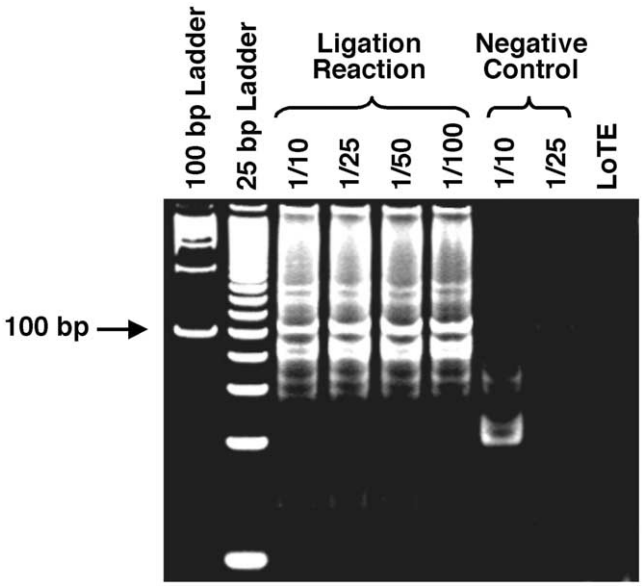

FIGURE 1 PCR amplification of ditags. PCR products of the serial LoTE dilution of ditag ligation reactions (1/10 to 1/100), negative control reaction (1/10 to 1/25), and LoTE-template reaction resolved on a 20% TBE polyacrylamide gel (Novex). Ditag ligation reaction products are represented by a major 102-bp band, whereas other bands represent products of linker–linker ligation (~80 bp) and unspecific products.

12. Combine the PCR products into 12 Eppendorf tubes (~450 µl in each), extract with PC8, EtOH precipitate (using 1 ml of absolute ethanol), and resuspend the pellets in 18 µl of LoTE (288 µl total). Add 57.6 µl of 6× loading buffer and load the entire volume into 8 wells of a 12% polyacrylamide gel (acrylamide : bisacrylamide, 19 : 1). Load a 100-bp DNA ladder to both end wells of the gel. Use 1× TAE as a running buffer. Electrophorese at 30 V until all the samples have fully entered the gel and then increase the voltage to 130 V. Terminate the reaction when bromphenol blue in the loading buffer migrates to the bottom of the gel. Stain gel with SYBR green I (20 µl/200 ml of 1× TAE buffer) for 15 min while shaking. Pierce the bottoms of eight 0.5-ml test tubes with a needle or surgical blade to form a hole with a diameter of about 0.8–1.0 mm and place them in 1.5-ml Eppendorf tubes. Visualize the gel by UV, and using a surgical blade, cut off the 102-bp bands and put the DNA into individual pierced tubes. Spin tubes at 15,300 *g* for 2 min at room temperature and then discard 0.5-ml tubes. Add 300 µl of LoTE to each Eppendorf and vortex. Incubate at 65°C for 15 min, mixing intermittently. Transfer the contents of each tube to individual SpinX tubes and spin at 15,300 *g* for 2 min at room temperature. Discard SpinX cartridges with a solid phase, EtOH precipitate the samples (aqueous phase) using 940 µl of absolute ethanol, and resuspend pellets in 14.8 µl volumes of LoTE (118.5 µl total).

13. Combine the entire contents into a one Eppendorf tube, add 15 µl of 10× RE buffer 4, 1.5 µl of 100× BSA, and 15 µl of *Nla*III (10 U/µl). Incubate at 37°C for 1 h and 15 min, extract sample with PC8, and add 50 µl of LoTE to bring the sample volume to 200 µl. EtOH precipitate on dry ice/ethanol bath [add 3 µl of glycogen (20 mg/ml), 67 µl of 10 *M* ammonium acetate and 733 µl of ice-cold (–20°C) 100% EtOH] and vortex. Place the sample in a dry ice/100% EtOH bath for 10 min. Pellet the precipitated DNA by centrifugation in a microfuge at 15,300 *g* for 15 min at 4°C. Remove the EtOH with care and wash with 75% EtOH. Centrifuge at 7800 *g* for 10 min at room temperature, discard supernatant, dry the pellet, and resuspend in 32 µl of LoTE (see Comments 3 and 4).

14. Add 6.4 µl of 6× loading buffer and load onto two wells of 12% polyacrylamide gel (acrylamide: bisacrylamide, 19:1). Two lanes are reserved for 100- and 25-bp DNA ladders. Run and stain the gel as described in step 12. Using a surgical blade, cut 24 to 26-bp bands from the gel (Fig.2) and place in individual bottom-pierced 0.5-ml tubes. Spin tubes at 15,300 *g* for 2 min at room temperature and then discard 0.5-ml tubes. Add 300 µl of LoTE to each Eppendorf and vortex. Incubate at 37°C for 15 min, mixing intermittently, transfer the contents of each Eppendorf tube to individual SpinX tubes, and spin at 15,300 *g* for 2 min at room temperature. Discard SpinX cartridges with a solid phase and distribute the aqueous contents to three Eppendorf tubes. EtOH precipitate on dry ice/ethanol bath (as described in step 13). Resuspend and combine the pellets in 7 µl of LoTE.

15. To the pooled purified ditags (7 µl total), add 2 µl of 5× ligation buffer and 1 µl of high concentration T4 ligase (5 U/µl). Ligate ditags to form concatemers by incubation at 16°C for 3 h (see Comment 5), add 90 µl of LoTE, and continue to incubate at 60°C for 5 min. Extract the sample with PC8, EtOH precipitate, and resuspend the pellet in 10 µl of LoTE.

16. Incubate the concatemers at 60°C for 5 min, add 190 µl of LoTE, extract with PC8, EtOH precipitate, and resuspend the pellet in 10 µl of dH_2O. Incubate at 60°C for 5 min and immediately load onto one well of an 8% polyacrylamide gel (acrylamide:bisacrylamide, 37.5:1) (see Comment 6). Employ the 100-bp DNA ladder and 1-kb DNA ladder as markers. Run and stain the gel as described in step 12. Using a surgical blade, cut and separate concatemers of 600–1100 ("light" cluster) and 1100–2500 bp ("heavy" cluster) (Fig.3) and place each into two labeled bottom-pierced 0.5-ml tubes. Spin at 15,300 *g* for 2 min at room

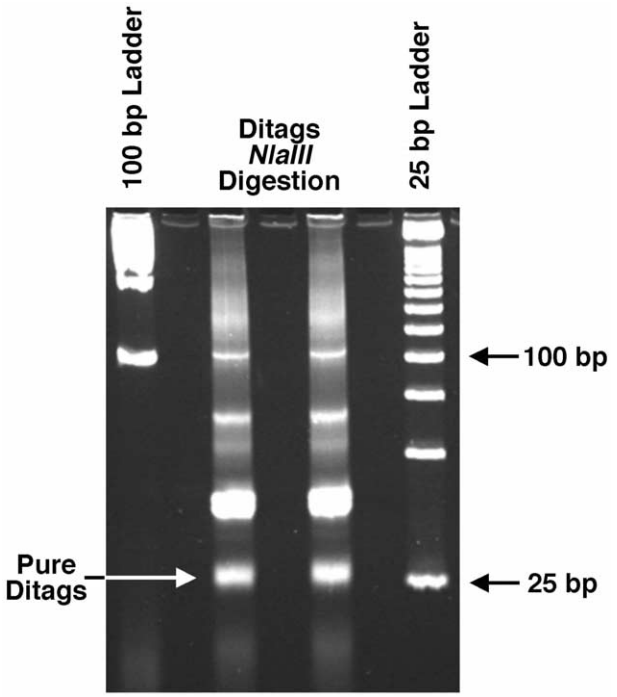

FIGURE 2 Pure ditags resolved on a 12% polyacrylamide gel. Bands represent (starting from the top) undigested linker–ditag–linker structures, products of incomplete anchoring enzyme digestion (one linker–ditag structures), pool of linkers, and pure ditags.

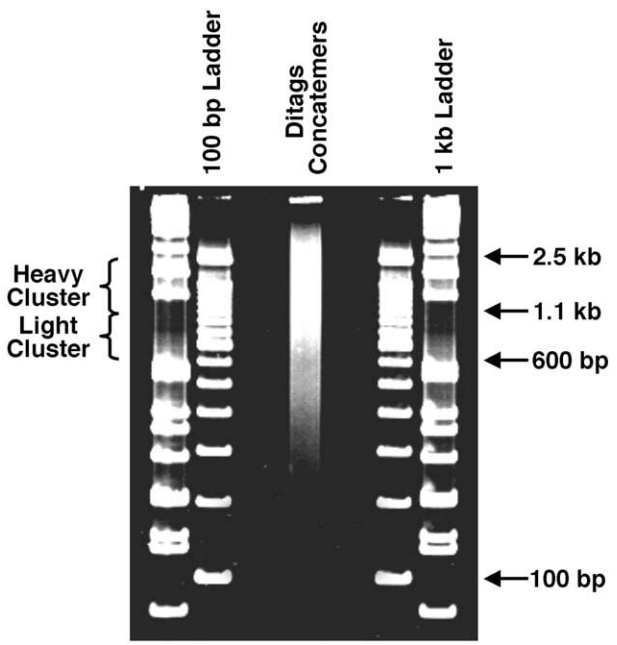

FIGURE 3 Ditag concatemers resolved on an 8% polyacrylamide gel using the "hot" variation of the original protocol (see Comment 6). Recommended "heavy" and "light" concatemer cluster sizes are 1100–2500 and 600–1100 bp, respectively.

temperature and discard 0.5-ml tubes. Add 300 µl of LoTE to each Eppendorf and vortex. Incubate at 65°C for 15 min, mixing intermittently. Transfer the contents of each Eppendorf tube to two SpinX tubes and spin at 15,300 *g* for 2 min at room temperature. Discard SpinX cartridges and transfer the aqueous phase from two SpinX tubes to one Eppendorf tube. EtOH precipitate using 933 µl of absolute ethanol and resuspend pellets in 5 µl total volume of LoTE for each "light" and "heavy" cluster of the sample.

17. To 5 µl of purified concatemers, add 2 µl of 5× ligase buffer, 1 µl of pZeRO-1 cut with *Sph*I (25 ng/µl), and 1 µl of T4 ligase (1 U/µl). Incubate at 16°C overnight, add 191 µl of LoTE to the samples, extract with PC8, EtOH precipitate, wash pellets three times with 70% ethanol, and resuspend pellets in 6 µl of LoTE. Use self-ligated pZeRO-1 vector as a negative control.

18. Electroporate bacteria with concatenated DNA by adding 2 µl of each sample to 40 µl of freshly thawed ElectroMAX DH10B cells on ice. Mix the contents gently by rotating a pipette tip in a test tube, rather than by trituration. On ice, transfer the mixture to the bottom of 0.2-cm electroporation cuvettes (avoiding bubbles) and electroporate: Voltage setting, 2.5 kV; capacitor, 25 µF; and resistance, 200 Ω. After the electric pulse, immediately transfer the cells to a 15-ml bacterial tube with 1 ml of prewarmed SOC media (no zeocin). Place in a bacterial shaker and incubate at 37°C for 40 min at 200 rpm.

19. Plate 80-µl aliquots of the cell/SOC solution onto 10-cm petri dishes with low salt LB agar plates supplemented with zeocin (50 ng/µl) (see Comment 7 and Pitfall 4). Incubate plates for about 20 h at 37°C.

20. Identify ~15–20 individual colonies from each "light" and "heavy" fraction to run a PCR control to determine cloning efficiency and the presence of concatemers in the clones (see Pitfall 5). For this purpose, prepare a 25-µl PCR reaction containing 18 µl of dH_2O, 2.5 µl of custom-made 10× PCR buffer (see *Solutions*), 1.5 µl of DMSO, 1.5 µl of dNTPs (25 m*M*), 0.5 µl of each M13 forward and reverse primer (both 350 ng/µl), and 0.1 µl of *Taq* polymerase (0.5 U), inoculated with a single bacterial colony picked with a sterile toothpick. Cycling conditions are: 2 min at 95°C, followed by 25 cycles (30 s at 95°C, 1 min 30 s at 56°C, 1 min 30 s at 70°C), final extension 70°C for 5 min, and hold at 4°C.

21. To the 5-µl aliquots of control PCR reactions, add 1 µl of 6× loading buffer and load onto an 1.2% agarose gel containing 1 µg/ml ethidium bromide and a 100-bp DNA ladder. Use 0.5× TBE as the running buffer, and electrophorese at 120 V. Estimate cloning

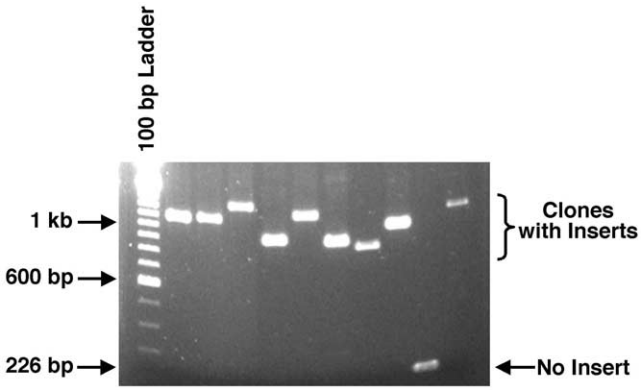

FIGURE 4 PCR control of cloning efficiency. A minor portion of the clones may lack inserts (PCR product will be of 226 bp size), whereas the majority should contain inserts with a size that varies as a function of concatemer length.

```
>FC16a06.seq                                              →
GATACACTACTATAGGGCGAATTGGGCCCTCTAGATGCATGTCTGTTTCT
GTTTATGTATTATCATGCAGACGGAAGGGCTTACTTAGCTCATGCCTGCT
CACGGCTCCACTTGGCCATGCAGGCCACACAGATCTCATTCTCATGGTTG
CTGAGAAGCCATAGCGGTCCATGGTGCTCCCACTATTGCAGAGGCCCATG
ATCCTGTGCTGTGGGGCTTGCCCATGATGGCAATTTCTGGACTCAGGGCA
TGTCTCAAACCCAATCAACATCAACATGTGGGCAAAGCCTTCCAAAGTCC
ATGTGTGGGTCTGGGGGCCATTGGGCATGTCTGACTTCCAGGGAGACCCA
GTCATGGTCTGGACGCGGGCTCCGGAGTTCATGGGAGACCCGCTTTTATT
ACTGTCCATGCTGCACTCCTGAGAACTGGGCACCCATGCTGCTGTAAAAC
TCACGGAATCCATGCTCCCTGCCCTAGTCTGTTCTGGCATGGCTGCCCTC
CCAACGGTGGTGCATGCTTACACGTCTCTGCCGCCTTCCCCATGCGCTGG
TTCCTCCTCAGCAACCATGTCCCTATTAAGGGCCTTCATCCCATGCCTAC
TAACCAGCAGGGATGGTCCATGGTGGCTCACTATGGAAGTCAGACATGTA
AGCTGTGAGCAACCAGCTCAGCATGGACGCGGAGCGTAACTAAGAGACAT
GGGTACAGGATAAAGCCGCGGCGCATGGGCAAGCCCCAGGAGTGGTGAGA
CATGTTGATTTTTTTGTTTTTTGCCTGCATGTTGATCCCCATCAT
```

FIGURE 5 Raw data file of the SAGE sequencing project. Correct concatemer structure with anchoring enzyme (*Nla*III) spacer (in bold) between 24- and 26-bp ditags. Arrow indicates the starting point of the insert.

efficiency by calculating the ratio of clones with inserts to the total number of clones amplified with PCR. Background clones without inserts will appear on the gel as 226-bp bands (Fig.4).

22. For those clones with inserts, add 180 µl of LoTE to the remaining PCR volume (20 µl), extract with PC8, add 250 µl of LoTE, and precipitate samples with isopropanol. Resuspend each pellet in 10 µl of LoTE.

23. For test sequencing, use forward and/or reverse M13 primers to ensure appropriate ditag formation. If inserts of the test clones demonstrate correct concatemer structure (Fig.5) and the cloning efficiency is satisfactory, the SAGE library should be sequenced until a sufficient number of tags (i.e., 40,000) can be identified. We recommend using a commercial vendor for sequencing (e.g., Agencourt Bioscience Corp.).

24. Many commercial sequencing services require libraries to be submitted as frozen glycerol stocks. For this, inoculate the wells of a 96-well plate containing 100 µl of TB/zeocin media with bacterial colonies using sterile toothpicks. We recommend that 1 well in each plate (H12) be filled with sterile LoTE to serve as a negative control for the sequencing reactions. Incubate plates for about 20 h at 37°C.

25. Copy the "master plates" by transferring 15 µl of the bacterial cultures to the corresponding wells of another set of 96-well plates containing 100 µl of TB/zeocin media. Stop further bacterial growth in the "master plates" by adding 40 µl of sterile 50% glycerol to the wells. Seal plates with adhesive SealPlate film and store at –80°C until the project is completed successfully.

26. Incubate the "copy plates" for about 18 h at 37°C. Stop the bacterial growth in the "copy plates" by adding 60 µl of sterile 50% glycerol to the wells. Seal plates with adhesive SealPlate film, freeze at –80°C, and ship for sequencing on dry ice (see Comment 8).

B. SAGE Analysis

This analysis protocol is based on the original SAGE 2000 software (Kinzler, 2000) and a separate SAGE analysis software protocol is available online from Invitrogen (I-SAGE kit; http://www.invitrogen.com/downloads/sagesoftware_man.pdf; Invitrogen Corp., 2001).

Steps

1. Database Creation

The aim is to create a complete, up-to-date data set to match with the SAGE tags generated in your library.

1. Download a current release of a GenBank database (e.g., rodent, primate) from the National Center of Biotechnology Information (NCBI) Web site using ftp software (e.g., CuteFTP) from ftp.ncbi.nlm.nih.gov/Genbank/.

2. Extract GenBank sequence files from the archives using WinRAR or comparable software.

3. Convert the GenBank sequence file format from UNIX to DOS using Streamline Solutions or other appropriate software. Raw sequence files should be marked with the suffix *.seq.

4. Open SAGE 2000 software. Go to "Database, Create" to generate a new database [suggested name should include species identification (e.g., Mm, mouse; Hs, human), nonredundant (NR) and/or EST affiliation, and numeric index of the dataset release].

Individual databases are recommended for NR and EST data sets. "Add Files" to the database using GenBank under "File Format" and in the cDNA mode under "Method."

2. SAGE Project Creation and Analysis

The aim is to create and analyze a gene expression profile based on SAGE library sequence data (SAGE catalog).

5. To create a new project, hit "Project/New Project" and use the following settings: anchoring enzyme, *Nla*III; tag length, 10 bp; and ditag length, 24 bp. Copy raw sequence files (see Comment 9) to a folder, where a new project has been created.

6. Extract SAGE tags from the sequences with the "Project/Add Tags" option. Reset "Stop position" constant to 2000 bp (this also depends on the sequencer type used for large-scale sequencing, producing reliable readings of various length). For preliminary analysis (preprocessing), we recommend performing the analysis on each individually selected file (i.e., select file, and hit "Analyze" until all the files have been analyzed). Record the output (i.e., number of "Good Tags" and "Duplicate Dimers") on a spreadsheet.

7. Once the preliminary analysis is complete, use spreadsheets to remove files associated with background clones (no SAGE tags detected) and clones that produced a minor number of "Good Tags" and/or "Duplicate Dimers" (≤4 tags or ≤2 duplicate dimers; tags derived from such clones may contain sequencing errors).

8. Create a new project as in step 5 and reanalyze sequence files that passed preprocessing criteria only, but this time use the "Auto Analyze" option.

9. We recommend that $(A)_{10}$ be excluded from the list of tags (accessible via "Analyze/Report/Exclude Tags Manager" path: hit "Add", type "1" and hit "OK"). An $(A)_{10}$ SAGE tag is generally uninformative, gives multiple matches to databases entries, and may originate from an anchoring enzyme recognition site located immediately before the poly(A) tail.

10. We recommend that the expression profile of your sequence data be created using the "Analyze/Report" path. For primary analysis, "Minimum tag count for report" should be reset to 1 (via "Settings/Minimum tag count for report" path) and "Options/Exclude Tags" checked. Using additional features, the expression profile (identified tags and absolute tag count) could be saved in MS Access database format (by having "Options/Save Output as MS Access File" option checked), and tags could be linked to selected SAGE database [by opening a selected database (see steps 1–4) and having "Options/Link to Database" option checked]. The latter permits direct matching of tags to the GenBank database. Also, more than one SAGE catalog can be analyzed simultaneously using the "All open projects" option.

11. The analysis of SAGE catalogs by linking them sequentially to NR and EST GenBank databases is recommended. To supplement GenBank data with UniGene data (which has a different structure) we recommend direct one-by-one online analysis via SAGEmap applet (http://www.ncbi.nlm.nih.gov/SAGE/) due to the notable presence of false positives in the "downloadable" "SAGEmap_tag_ug" data sets (available for human, mouse, rat, and a few other species at ftp://ftp.ncbi.nih.gov/pub/sage/map/).

12. For the comparison of multiple SAGE catalogs, we recommend MS Excel and MS Access statistical functions, not the SAGE 2000 function (accessible via "Analyze/Compare" path, with selected normalization value). MS Access files can be easily reformatted to MS Excel.

3. Outside Comparisons

The aim is to include publicly available SAGE data in the analysis. We encourage investigators to submit their SAGE data to the Gene Expression Omnibus (GEO) database.

13. Interlibrary comparisons among SAGE data are available via public databases, most importantly Entrez ProbeSet (http://www.ncbi.nlm.nih.gov/SAGE/index.cgi?cmd=libsearch). Individual SAGE catalogs of interest (use keywords such as "mouse," "cancer," and "brain") can be accessed and downloaded (using "Full table view" option). These are then converted from plain text to MS Excel table, tag abundance normalized to tags per million (tpm) value, and comparisons performed in convenient MS Excel or MS Access formats.

IV. COMMENTS

1. This protocol is optimized for "standard" SAGE using the *Nla*III/*Bsm*FI enzyme pair. Other anchoring and restriction enzymes could be used to generate longer tags (LongSAGE; Saha *et al.*, 2002) or to generate SAGE tags from genes lacking the *Nla*III recognition site (*Sau*3A is suggested and is recognized by SAGEmap; Lash *et al.*, 2000). Certain modifications of the SAGE protocol are also available for SAGE applications with a limited amount of starting material (microSAGE, Datson *et al.*, 1999; miniSAGE, Ye *et al.*, 2000; SAR-SAGE, Vilain *et al.*, 2003).

2. For cDNA synthesis, we recommend using α^{32}P dCTP labeling only to test the protocol and skip it

for the generation of most SAGE libraries. If used to calculate cDNA yield, isotope labeling allows tracing of the cDNA up to the tagging enzyme digestion step.

3. A modification of the ditag purification step, based on the employment of 5′-biotinylated linkers for PCR, followed by the magnetic separation of anchoring enzyme digestion products, has also been suggested (Powell, 1998). Although this modification shortens the ditag purification stage, it does not always result in good yields of ditags.

4. A few modifications of the original SAGE protocol are suggested to improve the yield of anchoring enzyme digestion of ditags (Angelastro *et al*., 2000; Damgaard Nielsen *et al*., 2003). We find that complete *Nla*III digestion is readily ensured by increasing the amount of enzyme, the overall reaction volume, and the digestion time (150 U, 150 µl, 1 h and 15 min, recommended).

5. Although concatenation time can vary from 45 min to overnight, which depends on the volume of ditags purified, we find that a 3-h concatenation produces good results.

6. A modification of the original SAGE protocol allows better resolution of concatemers in polyacrylamide gels, improving the overall yield of SAGE libraries (Kenzelmann and Muhlemann, 1999): 65°C, 15 min, chill on ice, 10 min; and then load onto the gel. We recommend using the "hot" variation of the same modification: 60°C, 5 min; PC8 extract; EtOH precipitate, 60°C, 5 min; and load immediately.

7. A X-Gal/IPTG blue/white selection can be employed to distinguish between bacterial colonies containing or lacking inserts (Angelastro *et al*., 2002) This technique is most useful when the number of bacteria without inserts is high.

8. With pZeRO-1, we recommend the M13 forward primer for sequencing. For clones originated from the "heavy" cluster of concatemers, an additional M13 reverse-primed sequence could be beneficial, yielding more tags from long inserts, but it leads to rapid accumulation of duplicate dimers due to the partial overlapping of sequences.

9. We recommend that each individual clone be designated by a nomenclature that contains a project script, plate number, and clone position in a 96-well plate. For example, file "EX15A08.seq" indicates association with experiment X, plate #15, well A8. All *.seq files generated in this manner represent individual SAGE library raw sequence files.

10. Other useful SAGE-related Web links:

SAGE home page: http://www.sagenet.org/

SAGEmap home page: http://www.ncbi.nlm.nih.gov/SAGE/

UniLib: http://www.ncbi.nlm.nih.gov/UniLib/index.cgi

SAGE Genie: http://cgap.nci.nih.gov/SAGE

GEO: http://www.ncbi.nlm.nih.gov/geo/

V. PITFALLS

1. The quality of the mRNA and the purity of oligo-DNA linkers and primers are of a great importance. We recommend the technique of Chirgwin *et al*. (1979) for the preparation of total RNA. Test linker kinasing efficiency before proceeding with the protocol.

2. Preciseness and RNase- or DNase-free conditions are important at most steps. Use DEPC-treated glassware and plasticware on the early steps of the work and aerosol barrier pipette tips throughout the whole experiment.

3. The commonly used anchoring enzyme *Nla*III has a half-life of only about 3 months at –20°C; therefore, use only fresh batches of enzyme for each SAGE project.

4. Zeocin is light sensitive and comparatively unstable. TB/zeocin media can be kept in the dark for up to 2 weeks. Low salt LB agar/zeocin plates should be protected from light immediately after pouring.

5. Cloning efficiency (ratio of clones with inserts to the total number of clones) is the major concern of researchers employing the SAGE method. Reasons for the appearance of background clones with the pZeRO-1/zeocin system are not completely clear. Suggested strategies rely on specific concatemer cluster sizes to achieve an acceptable range of cloning efficiency (i.e., >80%). While small concatemers routinely have high cloning efficiency, the number of SAGE tags extracted from each single clone is low. Extremely long concatemers (>2500 bp) have a tendency to circularize, preventing effective cloning. The suggested concatemer cluster sizes (600–1100 bp for "light" and 1100–2500 for "heavy") seem to have the best tag yield/clones sequenced ratio, allowing direct large-scale sequencing. In other cases, an additional PCR step or X-Gal/IPTG selection could be required to select clones with insert before sequencing.

References

Angelastro, J.M., Klimaschewski, L.P., and Vitolo, O.V. (2000). Improved NlaIII digestion of PAGE-purified 102 bp ditags by addition of a single purification step in both the SAGE and microSAGE protocols. *Nucleic Acids Res.* **15**, p.E62.

Angelastro, J.M., Ryu, E.J., Torocsik, B., Fiske, B.K., and Greene, L.A. (2002). Blue-white selection step enhances the yield of SAGE concatemers. *Biotechniques* **32**, 484–486.

Anisimov, S.V., Tarasov, K.V., Tweedie, D., Stern, M.D., Wobus, A.M., and Boheler, K.R. (2002). SAGE identification of gene transcripts with profiles unique to pluripotent mouse R1 embryonic stem cells. *Genomics* **79**, 169–176.

Chirgwin, J.M., Przybyla, A.E., MacDonald, R.J., and Rutter, W.J. (1979). Isolation of biologically active ribonucleic acid from sources enriched in ribonuclease. *Biochemistry* **18**, 5294–5299.

Damgaard Nielsen, M., Millichip, M., and Josefsen, K. (2003). High-performance liquid chromatography purification of 26-bp serial analysis of gene expression ditags results in higher yields, longer concatemers, and substantial time savings. *Anal. Biochemi.* **313**, 128–132.

Datson, N.A., van der Perk-de Jong, J., van den Berg, M.P., de Kloet, E.R., and Vreugdenhil, E. (1999). MicroSAGE: A modified procedure for serial analysis of gene expression in limited amounts of tissue. *Nucleic Acids Res.* **27**, 1300–1307.

Kenzelmann, M., and Muhlemann, K. (1999). Substantially enhanced cloning efficiency of SAGE (serial analysis of gene expression) by adding a heating step to the original protocol. *Nucleic Acids Res.* **27**, 917–918.

Lash, A.E., Tolstoshev, C.M., Wagner, L., Schuler, G.D., Strausberg, R.L., Riggins, G.J., and Altschul, S.F. (2000). SAGEmap: A public gene expression resource. *Genome Res.* **10**, 1051–1060.

Powell, J. (1998). Enhanced concatemer cloning-a modification to the SAGE (serial analysis of gene expression) technique. *Nucleic Acids Res.* **26**, 3445–3446.

Saha, S., Sparks, A.B., Rago, C., Akmaev, V., Wang, C.J., Vogelstein, B., Kinzler, K.W., and Velculescu, V.E. (2002). Using the transcriptome to annotate the genome. *Nature Biotechnol.* **20**, 508–512.

Ye, S.Q., Zhang, L.Q., Zheng, F., Virgil, D., and Kwiterovich, P.O. (2000). miniSAGE: Gene expression profiling using serial analysis of gene expression from 1 microg total RNA. *Anal. Biochem.* **287**, 144–152.

Velculescu, V.E., Zhang, L., Vogelstein, B., and Kinzler, K.W. (1995). Serial analysis of gene expression. *Science* **270**, 484–487.

Vilain, C., Libert, F., Venet, D., Costagliola, S., and Vassart, G. (2003). Small amplified RNA-SAGE: an alternative approach to study transcriptome from limiting amount of mRNA. *Nucleic Acids Res.* **31**, E24.

CHAPTER

15

Representational Difference Analysis: A Methodology to Study Differential Gene Expression

Marcus Frohme and Jörg D. Hoheisel

I. INTRODUCTION

Representational difference analysis (RDA) was originally developed for the identification of differences between two complex genomes (Lisitsyn *et al.*, 1993). Adapted slightly, cDNA-RDA was established by Hubank and Schatz in 1994. It aims at the detection of differentially expressed genes, comparing two sources of RNA, e.g., tumour and normal tissue, by means of a polymerase chain reaction (PCR)-coupled subtractive and kinetic enrichment procedure (Fig. 1). First, the two complex mRNA populations are reverse transcribed into cDNA. An initial digest with a restriction enzyme is followed by the addition of PCR adapters and subsequent amplification, thereby reducing the complexity of each sample. The resulting mixtures of gene fragments are named "representations" (Fig. 2). Differences in transcript levels in the tissues analysed are imaged in the representations by relative differences in the abundance of the respective cDNA fragments. In a subtractive hybridisation reaction with a strong kinetic component, one representation (#2)—named "driver"—serves as a competitor during the reannealing of the other (#1), which is called "tester" (Fig. 1). Due to an earlier change of adapters, only double-stranded tester molecules and therefore predominantly fragments unique to or overrepresented in the tester are exponentially amplified. The product is named "difference product" and may need further enrichment, acting as a tester in a subsequent round of RDA with an increased ratio of driver to tester, for example. Swapping the role of the two representations reverses the analysis mode, then identifying transcripts that are more abundant in representation #2 compared to #1.

cDNA-RDA has been proven to be a powerful tool for the identification of differentially expressed genes in many screens in both eukaryotic and prokaryotic systems. RDA is less prone to produce false positives than differential display and is easier to perform. The possibility of modifying the driver's composition, e.g., by spiking with certain fragments, offers an option of suppressing unwanted products. In comparison to microarray techniques, RDA has the advantage that there is no preselection in the set of analysed genes. Thus, unknown genes and unexpected splice variants are found. Moreover, difference products may serve as highly informative probe molecules on DNA arrays or be used as hybridisation samples. The protocols described here are similar to the originals of Hubank and Schatz (1994) but contain modifications found to be useful.

II. MATERIALS AND INSTRUMENTATION

Because the technique is very prone to pick up DNA contaminations, always use allocated (aliquots of) chemicals, buffers, plasticware, and so on and avoid common stocks. Take all precautions for RNA work but remember that DNA contaminations are a problem too that does not disappear by autoclaving. The preparation of most chemicals and buffers follows standard protocols using chemicals from various suppliers. However, always use high-quality grade products (p.a.

Copyright 2006, Elsevier Science (USA).
All rights reserved.

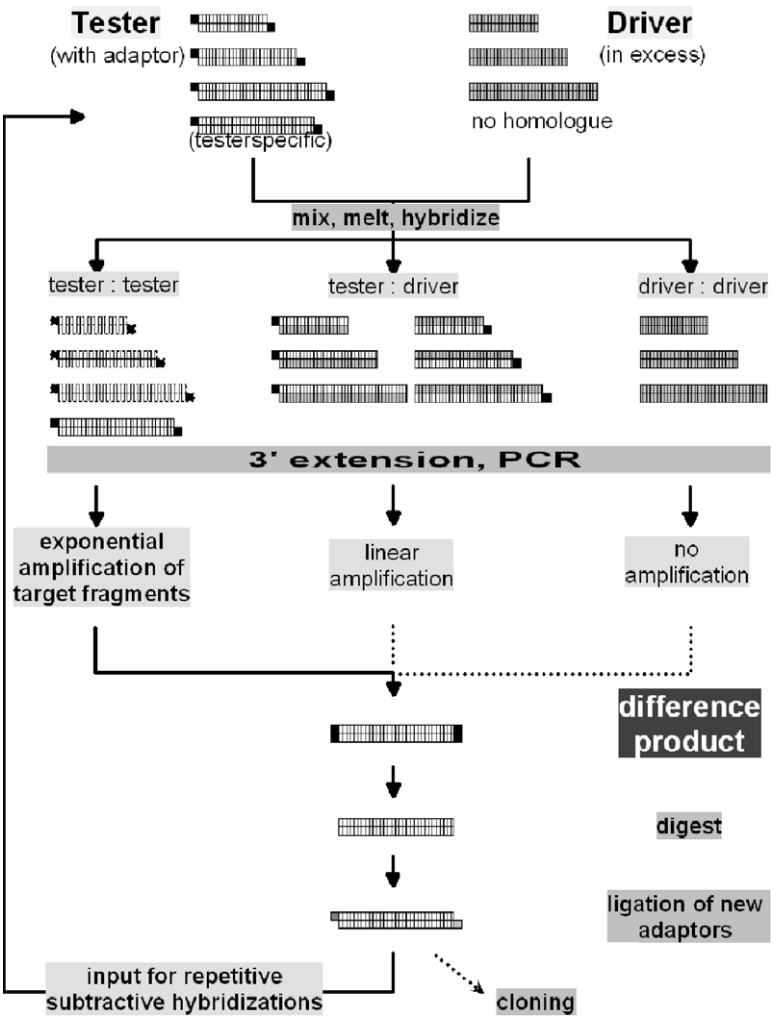

FIGURE 1 Schematic representation of the RDA procedure. Two cDNA populations are cut with a restriction enzyme. Subsequently, adapter molecules are added to the ends. The material is then PCR amplified to produce representations. The adapter of the tester sample is removed and replaced by a new molecule of different sequence (not shown). Tester and driver are mixed, denatured, and reannealed. During this process, the majority of tester molecules form duplexes with fitting driver molecules. Only fragments overrepresented in the tester or even lacking a homologue in the driver population will be amplified exponentially. The resulting difference product is either processed further or acts as a tester in another round of RDA.

or molecular biology grade) and prepare aliquots from freshly opened supplies.

Diethylpyrocarbonate (DEPC) is from Roth, Germany (Cat. No. K028.2), is diluted 1 : 1000 in water and autoclaved twice before being added to buffers. Low melting point (LMP) agarose is from Serva (Cat. No. 11408). The 50 × TAE stock solution for electrophoresis buffer consists of 2 *M* Tris–acetate (pH 8.2) and 50 m*M* EDTA. Various types of agarose are used for analytical gels as well as standard molecular weight markers with bands between 0.1 and 1 kb (100-bp ladders, pUC19/*Sau*IIIa digest, etc.); never use these markers on preparative tester gels, however. The ethidium bromide (Roth, Germany, Cat. No. 2218.1) stock solution (10 mg/ml) for gel staining is diluted 1 : 10,000 prior to use. Phenol/chloroform/isoamylalcohol (25 : 24 : 1) is equilibrated with Tris to a pH of 7.5 to 8.0 (Roth, Germany, Cat. No. UN2821); glycogen (1 µg/µl for molecular biology) is from Ambion (Cat. No. 9510); alternatively, linear acrylamide (Cat. No. 9520) may be used in precipitation.

Other chemicals are ethanol and 2-propanol (isopropanol); 1 *M* HCl for cleaning the gel chamber; 3 *M* sodium acetate (pH 5.3) (adjust pH with acetic acid, but use aliquots when checking the pH); 10 *M* ammonium acetate (sterile filter only, do not autoclave); 1 *M* Tris–HCl (pH 8.8) (8.5); 0.5 *M* EDTA stock (pH 8); TE: 10 m*M* Tris–HCl (pH 8.5); 1 m*M* EDTA; T1: 1 m*M* Tris–HCl (pH 8.5); T10: 10 m*M* Tris–HCl (pH 8.5); T50: 50 m*M* Tris–HCl (pH 8.8); 1 *M* $MgCl_2$; 1 *M* ammonium sulfate; 5x PCR buffer: 335 m*M* Tris–HCl (pH 8.8), 20 m*M* $MgCl_2$, 80 m*M* ammonium sulfate, 166 µg/ml

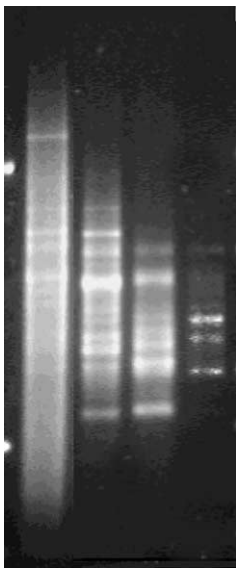

FIGURE 2 Difference products on an agarose gel. The four lanes of a 2.5% TAE agarose gel are shown. (Left to right) A tester representation and the three difference products resulting from iterative RDA are presented. The reduction in complexity is apparent. The white dots on the left margin indicate fragment sizes of 955 and 258 bp, respectively.

bovine serum albumm (BSA) (New England Biolabs, Cat. No. B9001S); nucleotides: dATP, dCTP, dGTP, and dTTP, each at 100 m*M* (Fermentas, Cat. No. R0181); dNTP mix containing 4 m*M* of each nucleotide; mineral oil (filtered) from Sigma (Cat. No. M 8662); alternatively, chill-out liquid wax from MJ Research is used; 10x ligase buffer: use buffer supplied with enzyme from New England Biolabs—if not available, prepare 500 m*M* Tris–HCl (pH 7.8), 100 m*M* $MgCl_2$, 100 m*M* dithiothreitot (DTT), 10 m*M* ATP—store frozen, mix vigorously before use; 300 m*M* EPPS (*N*-[2-hydroxyethyl]-piperazine-*N*′-[3-propanesulfonic acid] (pH 8.0) from Sigma (Cat. No. E-9502); 3x EE: 30 m*M* EPPS (pH 8.0), 3 m*M* EDTA; 5 *M* NaCl; yeast tRNA (Roche, Cat. No. 109495): set up as stock solution of 10 mg/ml; 0.5xTE/tRNA: mix tRNA stock with 1 volume TE; Qiaquick PCR purification kit (Cat. No. 28104); Qiaquick buffer QG (Cat. No. 19063); *Dpn*II: 10 U/µl from New England Biolabs (Cat. No. R0543L); T4 DNA ligase: 400 U/µl from New England Biolabs (Cat. No. M0202S) (if using ligase from another supplier, check the unit definition); mung bean nuclease: 10 U/µl from New England Biolabs (Cat. No. M0250S); *Taq* polymerase (5 U/µl) is purchased from different suppliers.

All oligonucleotides (final concentration 1 mg/ml) are purchased as HPLC-purified material.

R-Bam-12: d(GATCCTCGGTGA)

R-Bam-24: d(AGCACTCTCCAGCCTCTCACCGAG)

J-Bgl-12: d(GATCTGTTCATG)

J-Bgl-24: d(ACCGACGTCGACTATCCATGAACA)

N-Bgl-12: d(GATCTTCCCTCG)

N-Bgl-24: d(AGGCAACTGTGCTATCCGA GGGAA)

Reagents for fluorescence measurements include TNE buffer: 100 m*M* Tris–HCl (pH 7.4), 10 m*M* EDTA, 2 *M* NaCl; Hoechst-dye 33258 (BisBenzimide H33258; Sigma, Cat. No. B 2883); DNA standard: calf thymus DNA from Sigma (Cat. No. D 4764).

Plasticware should be resistant to phenol and chloroform and amicable to centrifugation at high speed. PCR plasticware is from ABgene: 96-well PCR plates with disposable covers; 8-well PCR strips with additional lid strips; and individual PCR tubes. Also 1.5 and 2-ml reaction tubes are required, as well as larger reaction vessels of up to 30 ml volume. For all pipetting steps, use filter tips in order to avoid contamination.

All technical equipment necessary is conventional and standard in molecular biology laboratories. However, it should be set aside for RDA experiments in order to avoid contamination. Required are the following: a minigel chamber and a power supply to run agarose gels at about 100 V; a set of pipettes; a small centrifuge for 2-ml reaction tubes; a centrifuge for spinning 30-ml tubes at 12,000 *g*; a UV transilluminator with camera; a vortex shaker; a timer; incubation blocks to keep reactions at precise temperatures between 37 and 100°C, preferably with a mixer function (e.g., Eppendorff Thermomixer comfort); a water bath or other equipment to keep reaction vessels at 14°C; and a refrigerator or cold room for storage. In principle, all incubation steps can be done in a thermocycler. The PCR machine should have a hot-lid function and hold 96-well plates (e.g., MJ Research PTC 200). For fluorescence measurements, we use a DyNAquant 200 device (Hoefer Scientific).

III. PROCEDURES

A. RNA Extraction and cDNA Synthesis

For RNA preparation, we recommend using a protocol that is well established for the particular biological system. Generally, our experiences with phenol/guanidinium-thiocyanate protocols (Trizol reagent from Invitrogen, Cat. No. 15596-026) are better than with column-based methods. In some experiments, we performed DNase treatments of total RNA preparations. However, we cannot generally recommend this because RNA degradation was observed several times. If required, however, use RQi RNase free DNase from Promega (Cat. No. M6101) with the

RNasin ribonuclease inhibitor (Cat. No. N2111) according to the supplier's recommendations. For mRNA isolation, magnetic beads are highly recommended (Dynal Dynabeads mRNA purification kit, Cat. No. 610.06). An estimation of the mRNA amount may be done by adsorption measurements. Make sure that the sample can be recovered from the cuvette.

Synthesis of double-stranded cDNA is preferably done following the protocol provided by Invitrogen with the Superscript double-stranded cDNA synthesis kit (Cat. No. 11917-010). Primer is $dT_{(15)}$ or $dT_{(13)}$ with an anchor of two random bases at the 5′ terminus. Radioactive label, used frequently for quantification and quality control, should only be added to an aliquot rather than to the whole cDNA preparation. The final yield of double-stranded cDNA should be similar to the initial amount of mRNA.

B. Generation of Representations; Preparation of Driver and Tester

1. For a digest, use 1–1.5 µg cDNA of good quality. If less than 1 µg is cleaved, the eventual number of cycling reactions may have to be increased.

2. Mix 10 µl 10x *Dpn*II buffer, 5 µl *Dpn*II, cDNA, and water to a total of 100 µl, incubate at 37°C for at least 2 h, inactivate the enzyme at 65°C for 10 min, and add 500 µl PB buffer of the Qiaquick kit.

3. Place a Qiaquick spin column in a collection tube (without lid), apply sample to column, and centrifuge 60 s to bind the cDNA. Discard the flow through and put the column back into the tube. To wash, add 750 µl of the supplied PE buffer, incubate 5 min, and spin for about 60 s. Discard flow through, put the column back into the tube, and spin for 1 min to remove residual buffer. Place column into fresh tube to elute the cDNA. Add 42 µl EB buffer to the centre of the membrane, incubate for 1 min, and spin for 1 min. Continue with the next step immediately.

4. Mix 8 µl *R-Bam-24*, 4 µl *R-Bam-12*, 6 µl 10x ligase buffer, and 39 µl of the Qiaquick column eluate. Place sample in a heating block of 50°C and let the block cool down for more than 1 h in a cold room until the block temperature is below 14°C. Place tube on ice and add 3 µl T4 DNA ligase for an overnight incubation at 14°C. Subsequently, dilute the ligation by the addition of 140 µl TE.

5. Prepare a PCR reaction to check whether digest and ligation worked. Mix 69 µl water, 20 µl 5x PCR buffer, 8.5 µl dNTP, 1 µl *R-Bam-24*, and 1 µl ligation product. Incubate at 72°C for 3 min to melt off the 12-mer oligomer and add 0.5 µl *Taq* polymerase. Incubate for 5 min at 72°C to fill in the ends. Cycle 20 times: 1 min at 95°C and 3 min at 72°C. Finally, keep the sample at 72°C for 10 min. Check 5 µl on a 2.5% gel. A DNA smear between 0.1 and 1 Kb should be visible.

It is highly recommended to perform a negative and a positive control. Both representations should have a similar yield in quality and quantity. If not, and especially if the input amount of cDNA is low, the cycle numbers have to be adjusted. Perform the PCR with additional cycles and remove 5 µl every second or third cycle during the 72°C incubation, starting at cycle 17. Check the products on a gel. With an increase in cycle number the faint DNA smear will grow in intensity, finally reaching a plateau. The plateau is characterised by a smear toward the slot or a shift of the product to smaller sizes—going along with a decrease in quality. Pick an optimal number of cycles for each representation, avoiding the plateau phase, but with a good yield. Both representations used in an RDA reaction must look similar on a gel.

6. Perform PCR for the production of more material, following the protocol established earlier. For a driver preparation, perform identical 100-µl reactions in all wells of a 96-well microtiter plate. Eight reactions are sufficient for preparing a tester, as less material is needed. Mix enzyme, reaction buffer, and DNA first before distributing the mix into the wells. Always include a negative control without DNA. For most analyses, reciprocal experiments are recommended: each cDNA serves as both driver and tester. In this case, a total of one 96-well plate worth of DNA is sufficient. After PCR, check a representative number of products on a 2.5% gel.

7. Combine the 96 driver reactions (or the 8 tester reactions) in one tube, add an equal volume of phenol/chloroform, and vortex vigorously. Spin briefly for phase separation and transfer the supernatant into a new tube. Warming the sample slightly may clear the phases if cloudy. Repeat the extraction, add one volume of chloroform, and vortex again. Spin and recover the supernatant. Do avoid the interphase. If necessary, repeat the extraction. Add 0.1 volume sodium acetate, 1 volume cold isopropanol, mix, and precipitate for 20 min at –20°C; longer incubation may result in salt precipitation. Spin for 15–30 min at high speed (>10,000 *g*). Remove the supernatant carefully and wash pellet with 70% ethanol. Spin again a few minutes, remove the ethanol, and dry the pellet (preferably at 37°C and not in a vacuum). Resuspend a driver in 200 µl T10 and a tester in 20 µl. Determine the concentration with a fluorometer.

8. ***For the preparation of a driver***, mix 300 µg DNA, 140 µl *Dpn*II buffer, 75 µl *Dpn*II, and water to a final volume of 1400 µl. Incubate at 37°C for 4 h and stop the reaction at 65°C for 15 min. Extract twice with phenol/chloroform and once with chloroform and precipitate with cold isopropanol as described earlier.

Resuspend the DNA in 200 µl T10 and determine its concentration. Dilute the digested driver to about 600 ng/µl and determine the concentration again before diluting the driver to precisely 500 ng/µl.

9. ***For the preparation of a tester***, mix 10 µg DNA, 10 µl *Dpn*II buffer, 5 µl *Dpn*II, and water to a final volume of 100 µl. Incubate at 37°C for 2 h, incubate at 65°C for 15 min, and add 500 µl PB buffer. Alternatively, take 10 µg *Dpn*II-digested driver (= 20 µl) and add 100 µl PB buffer. Purify the DNA with a Qiaquick spin column as described in Section III, B, **step 3**. Elute the DNA finally with 50 µl EB buffer.

10. Clean one minigel chamber for each tester; do not run different testers in one gel. Wash the chamber with detergent and rinse with water extensively; incubate all tools (combs, spacer, etc.) for 30 min in 1 *M* HCl and wash with plenty of water.

11. Load 10 µg tester DNA on a 1.3% LMP-agarose gel in TAE buffer without any other DNA (no marker!). Use only a small amount of loading buffer; even better, add glycerol (up to 10%) only and run bromphenol blue in a separate lane. Electrophoresis is at 100 V for a short time. The bromphenol blue should have migrated about 2 cm. Stain the gel in a fresh ethidium bromide solution (use once only). Check on a clean long wavelength UV transilluminator at low (preparative) intensity. There should be a smear of DNA and, directly below, a band from the adapter molecules. Cut out the smear portion (up to the slot), transfer with a clean scalpel to a tube, of which you know the weight, and determine the weight of the agarose plug.

12. For DNA extraction, use Qiaex spin colums with the Qiaex protocol. Melt the agarose plug at 50 to 55°C in three gel volumes QG buffer for 10 min. The buffer has a pH indicator. If the mixture is orange or purple, add sodium acetate (about 10 µl) until the colour turns yellow. Add one gel volume of isopropanol and mix. Place a Qiaquick spin column in a collection tube (without lid), apply the sample to the column, and centrifuge for 60 s to bind DNA. Proceed as in Section III, B, **step 3**. Elute the DNA with 30 µl EB buffer. Check the concentration fluorometrically.

13. Mix 1 µg purified tester DNA, 2 µl *J-Bgl-12*, 1 µl *J-Bgl-24*, 3 µl 10x ligase buffer, and water to a total reaction volume of 30 µl. Place in a heating block of 50°C and let it cool more than 1 h until the block temperature is below 14°C. Place the reaction on ice, add 1.5 µl T4 DNA ligase, and incubate overnight at 14°C. Dilute to approximately 10 ng/µl by addition of 70 µl T10 and finally incubate the tester at 50°C for 10 min.

14. Check the tester by performing PCR. Mix 69 µl water, 20 µl 5x PCR buffer, 8.5 µl dNTPs, 1 µl *J-Bgl-24*, and 1 µl tester. Incubate at 72°C for 3 min, add 0.5 µl *Taq* polymerase, and incubate at 72°C for 5 min. Cycle 25 times between 95°C for 1 min and 70°C for 3 min. Subsequently, incubate at 72°C for 10 min, cool down, and check 5 µl on a 2.5% agarose gel. The amplified tester should visually resemble the representation.

C. Subtractive Hybridisation and Generation of Difference Products

1. For the ***first subtractive hybridisation***, mix 80 µl digested driver (40 µg) with 40 µl tester (400 ng) (ratio 100 : 1) and incubate for 5 min at 95°C for denaturation. Extract once with 120 µl phenol/chloroform/isoamylalcohol and once with 120 µl chloroform. Add 30 µl ammonium acetate and 380 µl cold ethanol, mix, and precipitate at –70°C for 10 min. Spin at high speed for 15 min, remove supernatant carefully, wash with 70% ethanol, spin again, remove supernatant, and dry the pellet. Resuspend the DNA very thoroughly in 4 µl 3xEE by pipetting and vortexing or, preferably, by incubation in a heat mixer at 37°C for 10 min. Spin briefly, transfer into a new tube, and overlay with two drops of mineral oil (30–60 µl). Denature for 5 min at 98–100°C and mix immediately with 1 µl 5 *M* NaCl; penetration of the hot mineral oil with the pipette tip may be difficult. Place the reaction immediately at 67°C and incubate for 20 h.

2. Add 8 µl 0.5 × TE/tRNA and mix. Remove 8 µl mineral oil with same tip. Add 25 µl TE, mix thoroughly, and again remove some mineral oil using the very same tip. Add 362 µl TE, vortex, and place on ice for immediate use or store frozen.

3. Set up eight 100-µl PCR reactions for each experiment (and control). Mix 60 µl water, 20 µl 5x PCR buffer, 8.5 µl dNTPs, and 10 µl diluted hybridisation mix. Incubate at 72°C for 3 min, add 0.5 µl *Taq* polymerase, incubate at 72°C for 5 min, and add 1 µl *J-Bgl-24*. Pause the cycler at 72°C for all additions. Cycle 10 times between 95°C for 1 min and 70°C for 3 min. Then incubate at 72°C for 10 min and cool the sample.

4. Combine the eight reactions in a bigger tube and add 4 ml PB buffer. Place one Qiaquick spin column in a collection tube (without lid), apply 750 µl of sample, and centrifuge about 60 s. Discard the flow through and put the column back into the empty tube. Repeat this until the whole sample is loaded onto the column. Add 750 µl PE buffer, incubate for 5 min, and spin for about 60 s. Discard the flow through, put the column back into the tube, and spin for 1 min to remove residual buffer. Place column into a fresh tube. To elute DNA, add 42 µl T1, incubate for 1 min, and spin for 1 min.

5. Mix 14 µl water, 4 µl 10x mung bean nuclease buffer, 2 µl mung bean nuclease, 20 µl of the eluted DNA, and incubate at 30°C for 35 min. Stop the reaction by the addition of 160 µl T50 and an incubation at 98°C for 5 min. Chill on ice.

6. Set up a second PCR (two 100-µl reactions) on ice. Mix 60 µl water, 20 µl 5x PCR buffer, 8.5 µl dNTP, and 1 µl *J-Bgl-24*. On ice, add 10 µl of the DNA digested with mung bean nuclease. Incubate at 95°C for 1 min, cool to 80°C, add 0.5 µl *Taq* polymerase, and cycle 18 times between 95°C for 1 min and 70°C for 3 min. Incubate at 72°C for 10 min and cool on ice. Combine the two reactions and check 5 µl on a 2.5% gel. The crude product may still look similar to the representations but usually first discrete bands become visible.

7. Add 1 ml PB buffer and place the sample on a Qiaquick spin column in a collection tube. Apply 500 µl to column and centrifuge about 60 s. Discard flow through and put column back into the tube. Repeat the last two steps. Add 750 µl PE buffer, incubate for 5 min, and spin for about 60 s. Discard flow through, place column back into collection tube, and spin for 1 min to remove residual buffer. Place column into fresh tube (without lid). Add 85 µl buffer T1, incubate for 1 min, and spin for 1 min to elute DNA. Check DNA concentration fluorometrically. The product is ***difference product 1* (*DP1*)**.

8. To remove the adaptors, mix 10 µl *DpnII* buffer, 3 µl *Dpn*II, 5 µg DP1, and water up to 100 µl reaction volume. Incubate at 37°C for 2 h. Stop reaction at 65°C for 15 min, add 500 µl PB buffer, and continue as described in Section III, B, **step 3**.

9. For ligation of new adaptors, mix 6 µl 10x ligase buffer, 8 µl *N-Bgl-24*, 4 µl *N-Bgl-12*, 200 ng DNA, and water to a total volume of 60 µl. Place in a heating block and continue as described in Section III, B, **step 4**. Dilute ligation reaction to approximately 1.25 ng/µl by the addition of 100 µl T10. Stop reaction at 50°C for 10 min.

10. For a test PCR, set up a 100-µl reaction as described in Section III, B, **step 5**, but with *N-Bgl-24* and 25 cycles. The amplified product should look similar to DP1.

11. For the ***second subtractive hybridisation***, mix 80 µl digested driver (40 µg) with 40 µl diluted DP1 with *N-Bgl* adapter (50 ng) (ratio 800 : 1) and continue as described in Section III, C, **steps 1 and 2**.

12. For the first PCR after the second subtractive hybridisation, use *N-Bgl-24* primer and follow the protocol described in Section III, C, **steps 3 and 4**.

13. For mung bean nuclease digest, follow the protocol described in Section III, C, **step 6**.

14. For the second PCR, again use *N-Bgl-24* primer and follow the protocol described in Section III, C, **step 6**. On the gel, there should be less smear and more distinct bands.

15. To clean the PCR product, follow the protocol of Section III, C, **step 7**, resulting in ***difference product 2* (*DP2*)**.

16. To change the adapters, follow protocols in Section III, C, **step 8** and in Section III, B, **step 3**.

17. For ligation of new adapters (*J-Bgl*), follow the protocol of Section III, C, **step 9** using oligomers *J-Bgl-12* and *J-Bgl-24*. After an overnight ligation, dilute the reaction to 1 ng/µl by the addition of 140 µl TE and incubate at 50°C for 10 min. Dilute 2 µl of this with 778 µl T10 and add 20 µl (20 µg) yeast tRNA. The final DNA concentration is 2.5 pg/µl.

18. For a test PCR, follow the protocol in Section III, B, **step 14** using 1 µl (2.5 pg) DP2 with *J-Bgl* cassette as template. In a separate reaction, use 1 µl of digested DP2 as negative control. The amplified product should look similar to DP2.

19. For a ***third subtractive hybridisation***, mix 80 µl digested driver (40 µg) with 40 µl diluted DP2 with *J-Bgl* cassette (100 pg) (ratio 400,000 : 1) and continue as in Section III, C, **steps 1 and 2**.

20. Continue as in Section III, C, **steps 3 to 6**. For the second PCR, use 18 cycles instead of 29. If individual bands with no or little background smear appear, your ***difference product 3* (*DP3*)** is probably fine. If you want further enrichment, you may continue with a fourth RDA cycle using *N-Bgl* primers and a tester-to-driver ratio of 1 : 8,000,000 and/or competition with selected sequences. Start cloning the DNA fragments in the difference product either directly or after further purification.

D. Cloning and Analysis of Difference Products

Preferably the difference products are directly cloned into TA-cloning vectors (making use of the A overhang produced by the *Taq* polymerase), such as pGEM-T-Easy of Promega (Cat. No. A1360). A representative number of clones, determined according to the complexity of the band pattern on the gel, but at least eight times the number of visible bands), may be analysed by sequencing, restriction pattern analysis, hybridisation assays, and other procedures. Isolation and cloning of individual bands from the gel are also possible, but must be followed by analysis of several clones, as frequently there is more than one fragment. The latter process also selects against very rare fragments, which are present but insufficient in mass to be visible as a band.

RDA and arraying techniques are powerful tools for the identification of differential gene expression. Combining them can either produce microarrays that contain exclusively highly relevant probe molecules, focusing on the relevant information that can be gathered from hybridisation experiments, or simplify the analysis of global difference products. For the former, individual difference products of the second or third iterative RDA cycle are best suited, as they should represent differentially transcribed genes mainly and thus be very informative. Several libraries that result from

different difference analyses may be combined in one array. Initial arrays can be used for hybridising pools made of individual clones in order to identify repeatedly cloned fragments and thus reduce the redundancy. Validation of the RDA process is possible by a comparative hybridisation of the initially used cDNA or the driver and tester representations on such arrays (Chang *et al*., 1998; Welford *et al*., 1998; Frohme *et al*., 2000). Only fragments that originate from the respective difference products should give a signal in such an experiment. Furthermore RDA libraries may complement specific cDNA libraries used for arrays.

Another option is to use labelled difference products as targets for hybridisation on arrays. Because differential sequences are enriched already, differences in signal intensities will be more pronounced and therefore simpler to be detected, probably without the need for differential hybridisations using different dyes. Thus *in silico* analyses may become superfluous (Geng *et al*., 1998; Kim *et al*., 2001). More quantitative RDA-based analyses in connection with microarrays techniques were presented by Andersson and colleagues (2002, 2003).

IV. COMMENTS, PITFALLS, AND ALTERNATIVE PROTOCOLS

1. By increasing the initial cycle number, we could apply RDA to a few nanograms of original material, although with limited success. Also, this process may cause bias and will result in more false-positive fragments.

2. The starting material for RDA has to be selected carefully, not only because of the high demands in purity and quality, but also with respect of the experimental design. The result of a crude comparison of some tumour vs normal tissue may reflect the immune response rather than oncogenesis, for example.

3. Supplementing the driver with unwanted fragments, material from certain tissues or rDNA, for example, is a means to eliminate those in the difference products (Gress *et al*., 1997, Wada *et al*., 1997, Ushijima *et al*., 1997; Iwama *et al*., 1998, Bowler *et al*., 1999).

4. Frequently, DNA concentrations are estimated by comparing visually on an agarose gel the DNA of unknown concentration to a DNA of well-defined concentration. Because the representations and difference products are a smear with more or less distinct banding, this method is not very precise. Using adsorption measurement instead is obscured by the unused nucleotides and primers in the reaction mixture. By far the best results are obtained with fluorescence measurements.

5. Various publications suggest the use of other driver-to-tester ratios and longer hybridisation (Vician *et al*., 1997; Pastorian *et al*., 2000; Birkenmeyer *et al*., 2003). This may be helpful when the standard protocol fails. However, we found that alterations in ratios by a factor of up to fivefold did not remarkably alter the resulting difference products.

6. For most purposes, *Dpn*II is an appropriate restriction enzyme. Digestion of the PCR products may even be done directly in the amplification reaction after the addition of magnesium chloride (Vician *et al*., 1997). *Dpn*II could be replaced by *Sau*3A1 when a cDNA library cloned in recombinant bacteria is used as source material rather than RNA. A different representation of the cDNA or a bias toward longer fragments could be achieved with different enzymes (Edman *et al*., 1997; Morris *et al*., 1998; Pastorian *et al*., 2000; Felske, 2002). Note that the primer/adapter sequences have to be adapted then.

7. Several protocols describe omission of the digestion of single-stranded DNA with the mung bean nuclease (e.g., Welford *et al*., 1998). Instead it was suggested to dilute the first PCR product (Pastorian *et al*., 2000).

8. Extended use of nucleases (mung bean nuclease and exonuclease III) was reported (Kuvbachieva and Goffinet, 2002) to remove single-stranded DNA and unwanted (driver) duplexes prior to PCR. For this, thiodeoyxnucleotides were used to protect the tester hybrids from degradation.

9. Several authors describe improvements of RDA by alternative primers/adapters.

   a. It is reported that linear amplification of driver:tester heteroduplexes can be avoided by use of different primer/adaptors for generation of the driver and tester representations (Felske, 2002). Another protocol also uses different primers as well as a randomised amplification of the driver cDNA (Herblot *et al*., 1997).
   b. Additional primer pairs avoid repeated use of the original adapter/primer pair, thereby reducing the risk of carryover (Vician *et al*., 1997; Pastorian *et al*., 2000; Birkenmeyer *et al*., 2003).
   c. More selective PCR primers have been suggested (Birkenmeyer *et al*., 2003) to reduce the complexity of the representation. Nested primers (Michiels *et al*., 1998) might have a similar effect.

10. Spin columns used for the purification of PCR products may be replaced by Amicon or Centricon units (Vician *et al*., 1997) or by adapting RDA to solid-phase procedures (Odeberg *et al*., 2000). The latter makes use of representations generated with biotinylated primers. These can be removed after restriction cleavage with streptavidin-coated paramagnetic beads. In another protocol (Chu and Paul, 1998), driver–tester or driver–driver hybrids are removed by magnetic beads after subtractive hybridisation.

11. An initial melt-depletion procedure has been discussed (Hubank and Schatz, 1994). This process could make the resulting representations a better substrate for RDA. This modification uses denaturation followed by a short hybridization to let the more abundant DNA species reanneal before generation of the representations by PCR.

12. Changes in the relative composition of substrates during the RDA procedure were suspected to result in inefficient subtraction (Birkenmeyer *et al*., 2003). Using a driver, that has gone through a prior RDA subtraction procedure against itself should account for this problem.

13. In one publication (Luo *et al*., 1999), a conversion of tester–driver hybrids to driver only by another mung bean nuclease digest was suggested. This "differential subtraction chain" was reported to enhance RDA considerably.

14. The "phenol emulsion reassociation technique" was applied to improve the reassociation kinetics of the driver during subtractive hybridisation (Becker *et al*., 2001).

References

Andersson, T., Borang, S., Unneberg, P., Wirta, V., Thelin, A., Lundeberg, J., and Odeberg, J. (2003). Shotgun sequencing and microarray analysis of RDA transcripts. *Gene* **310**, 39–47.

Andersson, T., Unneberg, P., Nilsson, P., Odeberg, J., Quackenbush, J., and Lundeberg, J. (2002). Monitoring of representational difference analysis subtraction procedures by global microarrays. *Biotechniques* **32**, 1348–1358.

Becker, P., Hufnagle, W., Peters, G., and Herrmann, M. (2001). Detection of differential gene expression in biofilm-forming versus planktonic populations of *Staphylococcus aureus* using micro-representational-difference analysis. *Appl. Environ. Microbiol.* **67**, 2958–2965.

Birkenmeyer, L. G., Leary, T. P., Muerhoff, A. S., Dawson, G. J., Mushahwar, I. K., and Desai, S. M. (2003). Selectively primed adaptive driver RDA (SPAD-RDA): An improved method for subtractive hybridisation. *J. Med. Virol.* **71**, 150-159.

Bowler, L. D., Hubank, M., and Spratt, B. G. (1999). Representational difference analysis of cDNA for the detection of differential gene expression in bacteria: Development using a model of iron-regulated gene expression in *Neisseria meningitidis*. *Microbiology* **145**, 3529–3537.

Chang, D. D., Park, N. H., Denny, C. T., Nelson, S. F., and Pe, M. (1998). Characterization of transformation related genes in oral cancer cells. *Oncogene* **16**, 1921–1930.

Chu, C. C., and Paul, W. E. (1998). Expressed genes in interleukin-4 treated B cells identified by cDNA representational difference analysis. *Mol. Immunol.* **35**, 487–502.

Edman, C. F., Prigent, S. A., Schipper, A., and Feramisco, J. R. (1997). Identification of ErbB3-stimulated genes using modified representational difference analysis. *Biochem. J.* **323**, 113–118.

Felske, A. (2002). Streamlined representational difference analysis for comprehensive studies of numerous genomes. *J. Microbiol. Methods* **50**, 305–311.

Frohme, M., Scharm, B., Delius, H., Knecht, R., and Hoheisel, J. D. (2000). Use of representational difference analysis and cDNA arrays for transcriptional profiling of tumor tissue. *Ann. N. Y. Acad. Sci.* **910**, 85–105.

Geng, M., Wallrapp, C., Müller-Pillasch, F., Frohme, M., Hoheisel, J. D., and Gress, T. M. (1998). Isolation of differentially expressed genes by combining representational difference analysis (RDA) and cDNA library arrays. *Biotechniques* **25**, 434–438.

Gress, T. M., Wallrapp, C., Frohme, M., Müller-Pillasch, F., Lacher, U., Friess, H., Buchler, M., Adler, G., and Hoheisel, J. D. (1997). Identification of genes with specific expression in pancreatic cancer by cDNA representational difference analysis. *Genes Chrom. Cancer* **19**, 97–103.

Herblot, S., Vekris, A., Rouzaut, A., Najeme, F., de Miguel, C., Bezian, J. H., and Bonnet, J. (1997). Selection of down-regulated sequences along the monocytic differentiation of leukemic HL60 cells. *FEBS Lett.* **414**, 146–152.

Hubank, M., and Schatz, D. G. (1994). Abstract Identifying differences in mRNA expression by representational difference analysis of cDNA. *Nucleic Acids Res.* **22**, 5640–5648.

Iwama, A., Zhang, P., Darlington, G. J., McKercher, S. R., Maki, R., and Tenen, D. G. (1998). Use of RDA analysis of knockout mice to identify myeloid genes regulated *in vivo* by PU.1 and C/EBPalpha. *Nucleic Acids Res.* **26**, 3034–3043.

Kim, S., Zeller, K., Dang, C. V., Sandgren, E. P., and Lee, L. A. (2001). A strategy to identify differentially expressed genes using representational difference analysis and cDNA arrays. *Anal. Biochem.* **288**, 141–148.

Kuvbachieva, A. A., and Goffinet, A. M. (2002). A modification of representational difference analysis, with application to the cloning of a candidate in the reelin signalling pathway. *BMC Mol. Biol.* **3**, 6.

Lisitsyn, N., Lisitsyn, N., and Wigler, M. (1993). Cloning the differences between two complex genomes. *Science* **259**, 946–951.

Luo, J. H., Puc, J. A., Slosberg, E. D., Yao, Y., Bruce, J. N., Wright, T. C., Becich, M. J., and Parsons, R. (1999). Differential subtraction chain, a method for identifying differences in genomic DNA and mRNA. *Nucleic Acids Res.* **27**, e24.

Michiels, L., Van Leuven, F., van den Oord, J. J., De Wolf-Peeters, C., and Delabie, J. (1998). Representational difference analysis using minute quantities of DNA. *Nucleic Acids Res.* **26**, 3608–3610.

Morris, M. E., Viswanathan, N., Kuhlman, S., Davis, F. C., and Weitz, C. J. (1998). A screen for genes induced in the suprachiasmatic nucleus by light. *Science* **279**, 1544–1547.

Odeberg, J., Wood, T., Blucher, A., Rafter, J., Norstedt, G., and Lundeberg, J. (2000). A cDNA RDA protocol using solid-phase technology suited for analysis in small tissue samples. *Biomol. Eng.* **17**, 1–9.

Pastorian, K., Hawel, L., and Byus, C. V. (2000). Optimization of cDNA representational difference analysis for the identification of differentially expressed mRNAs. *Anal. Biochem.* **283**, 89–98.

Vician, L., Basconcillo, R., and Herschman, H. R. (1997). Abstract Identification of genes preferentially induced by nerve growth factor versus epidermal growth factor in PC12 pheochromocytoma cells by means of representational difference analysis. *J. Neurosci. Res.* **50**, 32–43.

Wada, J., Kumar, A., Ota, K., Wallner, E., Batlle, D. C., and Kanwar, Y. S. (1997). Representational difference analysis of cDNA of genes expressed in embryonic kidney. *Kidney Int.* **51**, 1629–1638.

Welford, S. M., Gregg, J., Chen, E., Garrison, D., Sorensen, P. H., Denny, C. T., and Nelson, S. F. (1998). Detection of differentially expressed genes in primary tumor tissues using representational differences analysis coupled to microarray hybridisation. *Nucleic Acids Res.* **26**, 3059–3065.

CHAPTER

16

Single Cell Gene Expression Profiling: Multiplexed Expression Fluorescence *in situ* Hybridization: Application to the Analysis of Cultured Cells

Jeffrey M. Levsky, Steven A. Braut, and Robert H. Singer

I. INTRODUCTION

Most current methods of measuring gene expression rely on averaging many cellular responses or artificial amplification steps to reach a detectable threshold of signal. In contradistinction, *in situ* assays circumvent these procedures to yield direct single cell expression information. Fluorescence *in situ* hybridization (FISH) is the gold standard for localization of nucleic acids (Fauth and Speicher, 2001; van der Ploeg, 2000). The introduction of amino-allyl-modified bases (Langer *et al.*, 1981) allowed the chemical synthesis of multiply labeled fluorescent oligomer hybridization probes (Femino *et al.*, 1998; Kislauskis *et al.*, 1993). This in turn allowed the application of multicolor/multispectral FISH (Nederlof *et al.*, 1990) to visualization of multiple RNA species simultaneously (Levsky *et al.*, 2002). With the introduction of visualization to gene expression assays we began to understand the complexity of behavior at the cell level, allowing reinvestigation of assumed consistencies of cell populations with single cell resolution (Elowitz *et al.*, 2002; Levsky *et al.*, 2002; Levsky and Singer, 2003).

II. MATERIALS AND INSTRUMENTATION

Oligomer probes are designed with OLIGO software from Molecular Biology Insights and synthesized on an Applied Biosystems automated DNA/RNA synthesizer (Model 394). Solid-support synthesis columns are from Applied Biosystems (dA, Cat. No. 400949; dC, Cat. No. 400950; dmf-dG, Cat. No. 401184; T, Cat. No. 400952). Phosphoramidites (dA, Cat. No. 10-1000-10; dC, Cat. No. 10-1010-10; dmf-dG, Cat. No. 10-1029-10; dT, Cat. No. 10-1030-10) and an amino-allyl-modified base for attachment of ester-conjugated fluorophores (C6-dT, Cat. No. 10-1039-05) are obtained from Glen Research. Oligonucleotide purification cartridges (OPC, Cat. No. 400771) and 2 *M* triethylamine acetate (TEAA, Cat. No. 400613) are from Applied Biosystems, and the anhydrous acetonitrile (Cat. No. 40-4050-50) is from Glen Research. Trifluoroacetic acid (TFA, Cat. No. BP618-500) is from Fisher, and triethylamine (TEA, Cat. No. T-0886) is from Sigma.

Fluorophores are from Amersham (Cy3, Cat. No. PA23001; Cy3.5, Cat. No. PA23501; Cy5, Cat. No. PA25001) and Molecular Probes (Oregon green 488,

Copyright 2006, Elsevier Science (USA).
All rights reserved.

Cat. No. O-6147; Alexa Fluor 488, Cat. No. A-10235 or A-20191). Sodium canbonate for labeling buffer (Cat. No. BP357-1), 25-ml pipettes for make-shift size-exclusion chromatography columns (Cat. No. 13-674-41E), and Pasteur pipettes (Cat. No. 13-678-20D) for filling the columns are from Fisher. Sephadex G-50 resin (Cat. No. 55897-100G) for purification is from Sigma. Columns are fashioned by removing the cotton from the top of one of these pipettes and using a portion of it to plug up the tip. Secure the "column" vertically to a ring stand and cap the tip with a 1.5-ml Eppendorf tube to prevent liquid loss. The vacuum concentrator system used is from Savant (Speed-Vac), and the UV spectrophotometer used for measurements of probe concentrations and labeling efficiencies is from Beckman (DU640).

Glass coverslips (Cat. No. 12-542B), glass slides (Cat. No. 12-518-103), 12 N HCl (Cat. No. A144-212), gelatin (Cat. No. G8-500), Parafilm (Cat. No. 13-374-12), forceps for coverslip manipulation (Cat. No. 08-953-E), and magnesium chloride (Cat. No. BP214-500) are from Fisher. The 20% paraformaldehyde for preparation of fixative (PFA, Cat. No. 15713) and coplin jars for washes (Cat. No. 72242-01) are from Electron Microscopy Sciences. 10× phosphate-buffered saline (PBS, Cat. No. 1 666 789), 20× sodium chloride/sodium citrate (SSC, Cat. No. 1 666 681), purified bovine serum albumin (BSA, Cat. No. 711 454), and *Escherichia coli* tRNA (Cat. No. 109 541) are from Roche. Triton X-100 (Cat. No. T-9284), formamide (Cat. No. F-4761), sheared salmon sperm DNA (ssDNA, Cat. No. D-7656), 4′,6-diamidino-2-phenylindole (DAPI, Cat. No. D-9564), and diethylpyrocarbonate (DEPC, Cat. No. D-5758) are from Sigma. The glass plates used for hybridization (Cat. No. 165-1824) are from Bio-Rad. The proLong Gold antifade reagent for mounting slides (Cat. No. P36934) is from Molecular Probes.

Upright fluorescence microscopes from Olympus are used to image multiple spectral signatures from the FISH specimens (Models AX70 and BX51) with a piezoelectric translator from Physik Instrumente (Cat. No. PZ54 E) to generate three-dimensional image stacks. Alternatively, microscopes featuring an internal harmonic drive may be used (e.g., BX61 from Olympus). Illumination is provided by a 100-W mercury arc lamp. Microscopes are outfitted with Olympus PlanApo 60x, 1.4 NA objectives and Chroma HiQ band-pass filters to separate fluorescence signals. Although other methods have been introduced to discern multiple fluorescence signals from chromosomes (Schrock *et al.*, 1996), they have not been applied successfully to detection of mRNA transcription sites. In Levsky (2002), we performed color coding of transcripts using the following filters from Chroma: DAPI (Cat. No. 31000), FITC (Cat. No. 41001), Cy3 (Cat. No. SP-102v1), Cy3.5 (Cat. No. SP-103v1), and Cy5 (Cat. No. 41008). High-resolution, low-noise fluorescence images are captured using charge-coupled device (CCD) cameras from Roper Scientific [Models CH-350(502) and CoolSNAP-HQ]. Acquisition and data manipulation are performed using IPLab software from Scanalytics. To ease data processing and avoid manual manipulations that introduce bias, we code our own filtering and data analysis software in the JAVA programming language using the Java development kit and advanced imaging library from Sun Microsystems.

III. PROCEDURES

A. Preparation of Fluorescent Oligomer Hybridization Probes

This procedure is according to Kislauskis (1993).

Solutions

1. *Diethylpyrocarbonate-treated distilled water (DDW)*: To make 1 liter, add 0.5 ml DEPC to 1 liter of distilled water. Shake or stir until DEPC is well distributed and then autoclave. Prepare enough of this to use in all other solutions.

2. *Labeling buffer (0.1 M Na_2CO_3, pH 9.0)*: To make 100 ml, weigh 1.06 g Na_2CO_3 and complete to 100 ml with DDW. Adjust pH to 9.0 by adding 10 *N* NaOH and store at 4°C.

3. *2 M TEAB stock*: To make 500 ml, take 138.3 ml (101 g) TEA and fill to 400 ml with DDW. Use dry ice to bubble in CO_2 until pH is below 8.0. Complete to 500 ml with DDW and store at 4°C. *Note*: *TEA is extremely hazardous so take care when handling. Use glassware instead of plasticware when measuring and transporting.*

4. *Filtration column running buffer (10 mM TEAB)*: To make 1 liter, take 5 ml of 2 *M* TEAB stock solution and complete to 1 liter with DDW. Store at 4°C.

5. *Filtration column running matrix*: To make approximately 200 ml, pour 200 ml of 10 m*M* TEAB into an Erlenmeyer flask. Add approximately 50 g of Sephadex G-50 and swirl to absorb the liquid. Suspension will settle. Store at 4°C. Prior to use, apply vacuum pressure to the flask to degas the suspension for at least 2 h before pouring matrix.

Steps

1. Having selected a gene of interest, choose four to five regions for probe fabrication, each 50 bases in length. Adjust search parameters within the OLIGO

software to receive best possible sequences for gene detection. Several considerations for probe design are:

i. Spanning different areas of the mRNA increases chances detection; intronic regions should be avoided.
ii. 50% GC content (or close to this) is optimal.
iii. Highly stable hairpins should be avoided.
iv. There must be enough well-spaced residues for substitution of modified bases. This depends on the modifier used. We space five modified thymidine residues at eight or more bases apart.
v. The sequences must not cross-react significantly with other mRNAs. Use BLAST to test this (see http://ncbi.nih.gov/blast).

2. Prepare the reversed antisense sequence of each designed oligonucleotide, substituting the modified bases appropriately.

3. Synthesize the oligonucleotides according to synthesizer specifications at a 0.2 µ*M* scale, specifying *TRITYL-ON*. Deprotect the crude products in a 65°C water bath for 1 h.

4. Aliquot the crude product into 200- to 300-µl portions and set one aside for immediate purification. Vacuum dry the remaining aliquots and then resuspend each pellet in 1.0 ml 10 m*M* TEAB plus 5 µl TEA. Store these at –80°C for future use. *Note*: *As the aliquots dry, the solutions become increasingly acidic and may cause detritylation of the oligonucleotides. To avoid this, add a drop of TEA to each tube periodically while drying them.*

5. Purify the remaining aliquot using the OPC according to recommended procedures (Applied Biosystems). Vacuum dry the final pure product and then resuspend in 100 µl DDW. Determine concentration of product using OD measurements at 260 nm.

6. Prepare a probe mixture with equal amounts of each oligonucleotide to obtain a final amount of 20 µg—either 4 or 5 µg of each oligonucleotide depending on how many were synthesized. Vacuum dry this mixture.

7. Resuspend the pellet in 10 µl labeling buffer and add it to the reaction vial containing approximately 1.0 mg of dye–ester conjugate. Alternatively, oligonucleotides can be labeled according to the manufacturer's specifications (Amersham or Molecular Probes). Vortex and leave at room temperature in the dark overnight.

8. Assemble a size-exclusion chromatography column by transferring 10 m*M* TEAB via a glass Pasteur pipette into the prepared 25-ml pipette/column until the liquid level is about a third of the way up. Add the G-50 suspension in the same manner and, as the matrix settles, remove the 1.5-ml tube "cap" to allow the matrix to settle above the cotton-plug stop, while permitting liquid to pass through. After the matrix has filled the pipette, pack it down with a continuous flow of TEAB for 10–15 min. This can be accomplished most easily using a siphoning system attached to the column.

9. Once the matrix has packed, remove the siphoning attachment and allow the buffer to run down to the level of the matrix, taking care not to let it run below. Add the 10 µl volume of probe/dye mixture to the column and wash the reaction vial with an additional 200–300 µl of fresh TEAB. Add the wash to the column and allow it to begin to run down into the matrix. When the dye product has been absorbed into the matrix, refill the column with buffer and reattach the siphoning system to provide continuous liquid flow.

10. As the labeled probe mixture runs down the column it will separate into two bands. The first, faster band will contain the desired pure product. Collect column eluates in 1.0-ml fractions to include this first band. Vacuum dry these fractions. Resuspend the selected fractions in DDW to achieve a total volume of 100 µl.

11. Measure OD of the final sample to determine final concentration and labeling efficiency for the product according to specifications of the dye manufacturers (Amersham, Molecular Probes). A final concentration of 40 ng/µl would indicate that all 20 µg of oligonucleotide initially labeled has been collected.

12. Labeled probe can be stored at 4°C or at –20°C for longer term storage.

B. Preparation of Cell Samples

Solutions

1. *Coverslips in 0.5% gelatin*: To make 200 ml, sterilize a box of coverslips by boiling in 0.1 *N* HCl for 20 min. Rinse and wash the coverslips in DDW several times. Weigh 1.0 g of gelatin and complete to 200 ml DDW. Stir and warm to dissolve completely. Transfer sterilized coverslips to gelatin solution and autoclave for 20 min. Store at 4°C.

2. *10× PBS stock*: To make 500 ml of DEPC-treated 10× PBS, take 500 ml 10× PBS and add 250 µl DEPC. Stir or shake to dissolve; autoclave.

3. *1 M $MgCl_2$ stock*: To make 100 ml, weigh 20.3 g $MgCl_2$ and complete to 100 ml with DDW.

4. *Washing solution (PBSM)*: To make 1 liter, take 100 ml 10× PBS stock, add 5 ml 1 *M* MgCl2 stock, and complete to 1 liter with DDW.

5. *Extractant (PBST)*: To make 1 liter, take 100 ml 10× PBS stock, add 5 ml Triton X-100, and complete to 1 liter with DDW. Stir gently to allow Triton to dissolve completely. *Note*: *This extractant has been used successfully to remove cytoplasm in cultured DLD-1 cells. The strength of the extractant must be optimized for each cell*

type to obtain optimal reduction of cytoplasmic background without damaging nuclei or loss of cells.

6. *Fixative (4% PFA)*: To make 50 ml, take one 10-ml vial of 20% paraformaldehyde stock, add 5 ml 10× PBS stock, and complete to 50 ml with DDW. Store at 4°C.

Steps

1. Grow cells under standard conditions and seed onto gelatinized coverslips in a petri dish. Cells are grown to empirically determined confluence such that they are sparse enough to facilitate automated separation of nuclei during image processing and dense enough to have significant amounts for analysis.
2. Any treatment steps, such as serum starvation and stimulation, can be performed at this point before fixation.
3. Wash the cells briefly with ice-cold PBSM.
4. Extract the cells for 60 s in PBST at room temperature.
5. Wash the cells twice briefly with ice-cold PBSM.
6. Fix the cells with the PFA fixative solution for 20 min at room temperature.
7. Wash the cells again twice briefly with ice-cold PBSM.
8. Fixed coverslips may be stored at 4°C in PBSM until use. *Note*: *Further extraction and background reduction can be obtained for some cell types by storage in 70% ethanol at 4°C. In some cases this can cause cells to detach from cover slips.*

C. Hybridization

This procedure is modified from Femino (1998) and Levsky (2002).

Solutions

1. *Washing solution (PBSM)*: To make 1 liter, take 100 ml 10× PBS stock, add 5 ml 1 *M* MgCl2 stock, and complete to 1 liter with DDW.
2. *Pre/posthybridization wash (50% formamide/2× SSC)*: To make 500 ml, take 250 ml formamide, add 50 ml 20× SSC stock, and complete to 500 ml with DDW.
3. *Probe competitor solution (ssDNA/tRNA)*: To make 100 µl of 10 mg/ml total concentration competitor, take 50 µl of 10 mg/ml sheared salmon sperm DNA and add 50 µl 10 mg/ml *E. coli* tRNA (prepared from solid by adding 10 mg to 1.0 ml DDW). Store at –20°C.
4. *Hybridization buffer*: To make 100 µl, take 60 µl DDW and add 20 µl BSA and 20 µl 20× SSC stock. Prepare fresh and hold on ice. *Note*: *This volume is sufficient for 10 hybridization reactions (10 coverslips).*
5. *Low-salt wash solution (2× SSC)*: To make 500 ml, take 50 ml 20× SSC stock and complete to 500 ml with DDW.
6. *Lower-salt wash solution (1855C):* To make 500 ml, take 25 ml 20× SSC stock and complete to 500 ml with DDW.
7. *Nuclear stain solution (DAPI)*: To make 1 liter, take 100 ml 10× PBS stock, add 50 µl 10 mg/ml DAPI stock (prepared from solid by adding 10 mg to 1.0 ml DDW), and complete to 1 liter with DDW. Shake or mix to dissolve DAPI completely and store at 4°C.
8. *Mounting medium*: Use the ProLong Gold antifade reagent according to manufacturer's specifications (Molecular Probes). About 25 µl of medium is needed per coverslip.

Steps

1. Test hybridization before color coding and multiple transcript detection. We start by using two bright dyes (Cy3 and Cy5) to show transcription sites. After this, assign each gene an arbitrary color code using combinations of dyes and test singly. Only after results are reproducible is multiplex detection performed.
2. Using forceps, place fixed coverslips vertically in a coplin jar, keeping note of which side has the cells on it. Rehydrate and wash the cells in PBSM for 10 min. *Note*: *All washes are at room temperature unless otherwise noted.*
3. Equilibrate the cells in prehybridization solution for 10 min.
4. Aliquot probe mixtures for gene(s) to be detected into tubes for each different combination of targets to be assayed. *Note*: *As a starting concentration, combine 20 ng of each probe for the 20 µl total final reaction volume. Optimal concentrations of the different probe mixtures are determined empirically by balancing the resultant colors detected upon imaging transcription sites.*
5. Add competitor solution to the probe mixture(s) in 100-fold excess. Vacuum dry this mixture, taking care not to overdry.
6. Resuspend the dry pellet in 10 µl formamide and place the tubes on a heating block at 85°C for 5–10 min and then place immediately on ice.
7. Add 10 µl of hybridization buffer to each tube, giving a final reaction volume of 20 µl.
8. Wrap a glass/plastic plate with Parafilm to allow enough working space for the amount of reactions you have. Dot each 20-µl reaction volume onto the plate, far enough apart such that coverslips can be placed over each volume without overlap.
9. Remove cover slips from prehybridization solution and blot off excess liquid. Place each coverslip—*cell side down*—on the hybridization mix already dotted onto the plate.

10. Wrap another layer of Parafilm over the plate and coverslips to seal the reactions. Press around the edges with a pen or similar instrument.

11. Incubate the plate at 37°C for 3 h, along with a sufficient amount of prehybridization solution to wash the coverslips twice after hybridization.

12. Remove the top layer of Parafilm and carefully lift the lower layer so that the coverslips can be easily removed without excessive manipulation. Place the coverslips back into coplin jars with the prewarmed wash, keeping track of the cell side, and incubate for 20 min at 37°C. Change and repeat this wash for another 20 min.

13. Remove ProLong Gold antifade reagent from –20°C and allow it to reach room temperature.

14. Change the solution with 2× SSC and incubate at room temperature for 10 min.

15. Change the solution with 1855C and incubate at room temperature for 10 min.

16. Change the solution with PBSM and incubate at room temperature for 10 min.

17. Counterstain nuclei by changing the solution with the prepared DAPI and incubating at room temperature for 1 min and then washing with PBSM.

18. Change the PBSM and keep at room temperature until ready to mount.

19. Mount each coverslip (cell side down) onto glass slides, using freshly prepared antifade mounting medium. Blot off excess liquid and store at –20°C.

D. Microscopy and Image Analysis

These procedures are from Levsky (2002).

Steps

1. Image stacks are acquired with high index oil immersion on a fluorescence microscope outfitted for optical sectioning. We use a step size of 0.5 μm to generate image volumes, as transcription site signals are bright and do not require more finely spaced planes on our setup. For future processing steps and for detecting less bright signals, closer optical sections may be needed. We use the 60× objective and additional magnification (when necessary) to yield digital images of roughly 100-nm per pixel resolution. The total magnification should be adjusted to yield similar resolution given the physical size of elements on the CCD camera used. High resolution enables morphometric processing of the signals.

2. Image volumes from different fluorescent channels are normalized by contrast enhancement to ensure interpretation is independent of relative intensity. This can be performed with commercial software, such as IPLab (Scanalytics), for the entire three-dimensional image stacks at one time to ensure that the sample is analyzed evenly. The "black value" for the enhancement should be set to the approximate extranuclear noise level for the sample, which can vary markedly. The "white value" should be slightly above the intensity for the center of the brightest signals, namely nuclear sites of transcription.

3. Digital signal enhancement can be approached by two methods: direct analysis of three-dimensional images or splitting the image into two-dimensional slices, slice-by-slice processing, and, finally, collation of data into a three-dimensional representation. Both approaches require similar filtering algorithms, but currently available implementations generally require decomposition into slices as they can only process two-dimensional images. Either way, the basic method of signal enhancement is simple convolution filtering using a kernel that approximates the size of the target signal. This implies that the kernel should be adjusted to approximate the size of empirically observed sites of transcription, as determined by the magnification used in image acquisition. The designed kernel should include surround penalty to decrease the chances of false-positive detection of larger areas of fluorescence noise (intrinsic or extrinsic to the sample). The center, or positively scored part of the kernel, should be large enough to ignore specular noise and camera defects, which can appear as highly intense single pixels.

4. Positive detection of sites of transcription depends on empiric selection of a threshold. If contrast enhancement (step 1) was performed correctly, this should allow a single color level to be used to distinguish between background levels and transcription site color codes in all fluorescence channels. This procedure may be performed using a segmentation algorithm for each color combination used for detection in the image, such that one singles out sites of each identity one at a time. Finding this tedious, we prefer to detect all suprathreshold signals and determine the color-coded identity at once by coding a simple algorithm. This procedure involves scanning the image pixel by pixel for suprathreshold signal, recording each putative signal, and marking off contiguous regions surrounding the signal such that they are not scored more than once. Location of the signal and intensity in all color bands (both point wise and with surrounding area) are recorded. The intensity values are compared with the threshold and identity of the site is assigned.

5. For visualization purposes, a pseudo-colored, flattened two-dimensional rendering is prepared. For a background, we prefer to use the middle Z slice of the nuclear counterstain image. Transcription site locations and identities (now arbitrarily pseudo-colored

and depicted with an artificial marker in the image) are shown. We have added a number adjoining the site to mark the Z section from which the center of the site was detected. This is necessary, as filtered and threshold-corrected data contain more than three colors of images and cannot be depicted unambiguously in red–green–blue color systems.

6. Nuclear bounds are generated by binarization and simple flood fill of the nuclear counterstain image. Binarization requires a single threshold to be chosen to distinguish between intranuclear and extranuclear; this can usually be done given appropriate exposure of the counterstain. Flood-fill algorithms will only work with discretely separated nuclei and must be modified significantly to interpret overlapping signals. Nuclei for which the flood-fill-defined area extends to the edge of the image plane should be ruled out for further analysis as their contents are incompletely imaged.

7. Joining the results of steps 4 and 5 now yields data of single cell gene expression profiles—a set of transcription sites for each nucleus analyzed. Each transcription site detected in a field is placed onto the flood-fill map and assigned a nucleus. Sets of nuclear data are exported for further statistical study.

IV. PITFALLS

1. The overlap of fluorophore colors should be considered carefully when designing a bar-coding scheme. Consideration of the strength of fluorophores, the separation between emission spectra, excitation characteristics of the lamp, and the filter sets to be used to discern signals is critical.

2. When assembling the G-50 column and loading sample do not let the liquid level run below the matrix. This will create cracks and bubbles, potentially disrupting complete band separation and adding to contamination of product with free dye.

3. Poorly labeled probes (<40%) can fail to detect transcription sites. To increase labeling efficiency, multiple serial labelings and purifications can be performed.

4. Probe mixtures that have a suspiciously high level of labeling (>80%) may contain free dye, which will increase background. Multiple purifications by G-50 column can be used to remedy this.

5. When placing the coverslips down onto the Parafilm-coated plates, care should be exercised to avoid bubbles occurring, thereby preventing total contact of the probe with the coverslip. Also take care not to touch or move the coverslips excessively once they are placed onto the Parafilm, as this may contribute to cell detachment and damage.

6. Some cell types have high inherent autofluorescence obscuring nuclear signals. Careful processing with adequate extraction can remedy this at times. Additional processing steps may be necessary for recalcitrant noise problems.

7. Transcript color codes in which the colors are balanced inadequately may "decay" such that the observed signal is misinterpreted as a different color code containing a subset of the original code. This is especially problematic under conditions of low transcript abundance and with less intense fluorophores (such as FITC derivatives). Color codes must be tuned carefully before multiplex detection.

References

Elowitz, M. B., Levine, A. J., Siggia, E. D., and Swain, P. S. (2002). Stochastic gene expression in a single cell. *Science* **297**, 1183–1186.

Fauth, C., and Speicher, M. R. (2001). Classifying by colors: FISH-based genome analysis. *Cytogenet Cell Genet* **93**, 1–10.

Femino, A. M., Fay, F. S., Fogarty, K., and Singer, R. H. (1998). Visualization of single RNA transcripts in situ. *Science* **280**, 585–590.

Kislauskis, E. H., Li, Z., Singer, R. H., and Taneja, K. L. (1993). Isoform-specific 3'-untranslated sequences sort alpha-cardiac and beta-cytoplasmic actin messenger RNAs to different cytoplasmic compartments. *J. Cell Biol.* **123**, 165–172.

Langer, P. R., Waldrop, A. A., and Ward, D. C. (1981). Enzymatic synthesis of biotin-labeled polynucleotides: Novel nucleic acid affinity probes. *Proc. Natl. Acad. Sci. USA* **78**, 6633–6637.

Levsky, J. M., Shenoy, S. M., Pezo, R. C., and Singer, R. H. (2002). Single-cell gene expression profiling. *Science* **297**, 836–840.

Levsky, J. M., and Singer, R. H. (2003). Gene expression and the myth of the average cell. *Trends Cell Biol.* **13**, 4–6.

Nederlof, P. M., van der Flier, S., Wiegant, J., Raap, A. K., Tanke, H. J., Ploem, J. S., and van der Ploeg, M. (1990). Multiple fluorescence in situ hybridization. *Cytometry* **11**, 126–131.

Schrock, E., du Manoir, S., Veldman, T., Schoell, B., Wienberg, J., Ferguson-Smith, M. A., Ning, Y., Ledbetter, D. H., Bar-Am, I., Soenksen, D., Garini, Y., and Ried, T. (1996). Multicolor spectral karyotyping of human chromosomes. *Science* **273**, 494–497.

van der Ploeg, M. (2000). Cytochemical nucleic acid research during the twentieth century. *Eur. J. Histochem.* **44**, 7–42.

PART

D

PROTEINS

SECTION

6

Protein Determination and Analysis

CHAPTER

17

Protein Determination

Martin Guttenberger

I. INTRODUCTION

The protein content of tissues or samples can serve a number of purposes: It can be a research topic of its own (e.g., in nutritional studies; Hoffmann *et al*., 2002), a loading control in gel electrophoresis (Ünlü *et al*., 1997), or a reference quantity in biochemical (e.g., yields in protein purification) or physiological (e.g., specific activities of enzyme preparations; Guttenberger *et al*., 1994) investigations. In addition, with the advent of proteomics, there is an increasing need for protein quantitation in complex sample buffers containing detergents and urea as potentially interfering compounds (Ünlü *et al*., 1997). In any case, care should be taken to obtain correct results. This article focuses on three techniques and outlines the specific pros and cons.

II. MATERIALS AND INSTRUMENTATION

The following reagents are from the indicated suppliers. All other reagents are of analytical grade (Merck):

A. Lowry Assay

From Lowry *et al*. (1951): Folin–Ciocalteu phenol reagent (Merck, Cat. No. 1.09001). A detergent-compatible modification of the Lowry assay is available as a kit (Bio-Rad 500-0116).

B. Bradford Assay

From Bradford (1976): Coomassie brilliant blue G-250 (Serva Blue G, Serva, Cat. No. 35050). The reagent for this assay is available commercially from Bio-Rad (Cat. No. 500-0006).

C. Neuhoff Assay (Dot-Blot Assay)

From Guttenberger *et al*. (1991) and Neuhoff *et al*. (1979): Ammonium sulfate for biochemical purposes (Merck, Cat. No. 1.01211), benzoxanthene yellow (Hoechst 2495, Merck Biosciences, Cat. No. 382057, available upon request), cellulose acetate membranes (Sartorius, Cat. No. SM 11200), glycine, and SDS (Serva, Cat. Nos. 23390 and 20763, respectively). Commercially available ammonium sulfate frequently contains substantial amounts of undefined UV-absorbing and fluorescing substances. These lead to more or less yellowish solutions. Use only colourless solutions to avoid possible interference in fluorometry.

Solutions are prepared from bidistilled water. Bovine serum albumin (BSA, fraction V, Roche, Cat. No. 735086) is used as a standard protein. Ninety-six-well, flat-bottomed polystyrene microtiter plates (Greiner, Cat. No. 655101) are used for the photometric tests.

III. PROCEDURES

With respect to convenience and speed, microplate reader assays are described where appropriate. These assays can be read easily in conventional instruments

Copyright 2006, Elsevier Science (USA).
All rights reserved.

by employing microcuvettes or by scaling up the volumes (fivefold).

The composition of the sample (extraction) buffer requires thought with respect to the avoidance of artifactual alterations of the protein and to the compatibility with the intended experimental procedures. The former requires strict control of adverse enzyme activities (especially proteases and phenol oxidases) and, in the case of plant tissues, of interactions with secondary metabolites. A convenient, semiquantitative assay for proteolytic activities allowing for the screening of suitable inhibitors was described by Gallagher *et al*. (1986). There is some uncertainty as to which assay gives the most reliable results in combination with extracts from plant tissues rich in phenolic substances. The influence of such substances can never be predicted. It is therefore imperative to minimize interaction of these substances with protein in the course of sample preparation. For a more detailed discussion of this problem, see Guttenberger *et al*. (1994).

A frequent source of ambiguity is the use of the term "soluble protein." Soluble as opposed to membrane-bound proteins stay in solution during centrifugation for 1 h at 105,000 *g* (Hjelmeland and Chrambach, 1984).

All assays described in this article quantitate protein relative to a standard protein. The choice of the standard protein can markedly influence the result. This requires special attention for proteins with a high content of certain amino acids (e.g., aromatic, acidic, or basic amino acids). For most accurate results, choose a standard protein with similar amino acid composition or, if not available, compare different assays and standard proteins. Alternatively, employ a modified Lowry procedure that allows for absolute quantitation of protein (Raghupathi and Diwan, 1994).

The most efficient way to prepare an exact dilution series of the standard protein employs a handheld dispenser (e.g., Eppendorf multipette). Typically a six-point series is pipetted according to Table I. In any case, avoid a concentration gradient of the sample buffer. Usually samples and standards may be kept at –20°C for a couple of weeks. For longer storage intervals, keep at –80°C.

TABLE I Pipetting Scheme for Preparation of a Standard Dilution Series[a]

Concentration	Blank	0.2×	0.4×	0.6×	0.8×	1.0×
Water	5	4	3	2	1	0
Standard protein (2×)	0	1	2	3	4	5
Buffer (2×)	5	5	5	5	5	5

[a] To prepare 1 ml of each concentration, 1 volume corresponds to 0.1 ml.

A. Lowry Assay

See Lowry *et al*. (1951).

Solutions

Note: For samples low in protein (0.02 mg ml^{-1} or less), prepare reagents A and B at double strength.

1. *Reagent A*: 2% (w/v) sodium carbonate (Na_2CO_3) in 0.10 *N* NaOH. To make 1 litre of reagent A (5000 determinations), dissolve 20 g Na_2CO_3 in 1 litre 0.10 *M* NaOH. Keep at room temperature in tightly closed screw-cap plastic bottles.
2. *Reagent B*: 0.5% $CuSO_4 \cdot 5H_2O$ in 1% sodium or potassium tartrate. To make 20 ml of reagent B, dissolve 0.1 g $CuSO_4 \cdot 5H_2O$ in 20 ml 1% tartrate (0.2 g sodium or potassium tartrate dissolved in 20 ml water). Keep at room temperature.
3. *Reagent C (alkaline copper solution)*: Mix 25 ml of reagent A and 0.5 ml of reagent B. Prepare fresh each day.
4. *Reagent D (Folin–Ciocalteu phenol reagent)*: Dilute with an equal volume of water just prior to use

Steps

1. Place 40 µl of sample (protein concentration 0.02–1 mg ml^{-1}) or blank into cavities of a microplate or into appropriate test tubes.
2. Add 200 µl of reagent C and mix. Allow to stand for at least 10 min.
3. Add 20 µl of reagent D and mix *immediately*. Allow to stand for 30 min or longer.
4. Read the samples in a microplate reader or any other photometer at 750 nm.

Modifications

1. The sample volume may be raised to 140 µl when samples are low in protein (0.02 mg ml^{-1} or less). In this case, employ double-strength reagent C.
2. If samples have been dissolved in 0.5 *M* NaOH (recommended for resolubilization of acid precipitates), omit NaOH from reagent A.

B. Bradford Assay

See Bradford (1976).

Solutions

1. *Protein reagent stock solution*: 0.05% (w/v) Coomassie brilliant blue G-250, 23.8% (v/v) ethanol, 42.5% (w/v) phosphoric acid. To make 200 ml of stock solution (5000 determinations), dissolve 0.1 g Serva

blue G in 50 ml 95% ethanol (denatured ethanol works as well), add 100 ml 85% phosphoric acid, and make up to 200 ml by adding water. The stock solution is available commercially (Bio-Rad). Keep at 4°C. The reagent contains phosphoric acid and ethanol or methanol. Handle with due care (especially when employing a dispenser)!

2. *Protein reagent*: Prepare from the stock solution by diluting in water (1 : 5). Filter immediately prior to use.

Steps

1. Place 4 µl of sample (protein concentration 0.1–1 mg ml^{-1}) or blank into cavities of a microplate or into appropriate test tubes.
2. Add 200 µl of protein reagent and mix. Allow to stand for at least 5 min.
3. Read the samples within 1 h in a microplate reader or any other photometer at 595 nm.

Modifications

1. For improved linearity and sensitivity, compute the ratio of the absorbances, 590 nm over 450 nm (Zor and Selinger, 1996).
2. Microassay: For diluted samples (less than 0.1 mg ml^{-1}), proceed as follows: Employ 200 µl of sample and add 50 µl of protein reagent stock.

C. Dot-Blot Assay

See Guttenberger *et al*. (1991). Do not change the chemistry of the membranes. Nitrocellulose will dissolve in the staining solution; PVDF membranes develop a strong background.

Solutions

1. *Benzoxanthene stock*: To prepare the stock solution add 1 ml of water to 0.5 g of the fluorescent dye (as supplied, weighing not necessary); keep at –20°C. The toxicity of benzoxanthene is not thoroughly studied, it might be mutagenic!

2. *Destaining solution*: Methanol/acetic acid (90/10, v/v). To make 1 litre, mix 100 ml acetic acid and 900 ml methanol.

3. *Staining solution*: To obtain 100 ml, dilute 80 µl benzoxanthene stock in 100 ml destaining solution. Be sure to pour the destaining solution onto the stock solution to prevent the latter from clotting. Keep staining and destaining solutions in tightly closed screw-cap bottles at 4°C in the dark. They are stable for months and can be used repeatedly. Take due care in handling the highly volatile solutions containing methanol!

4. *SDS stock*: To make 30 ml of 10% (w/v) SDS stock solution, dissolve 3 g SDS in approximately 20 ml of water, stir, and make up to 30 ml (allow some time for settling of foam). Keep at room temperature; it is stable for at least 1 year.

5. *Elution buffer*: 0.25 *M* glycine–sulfuric acid buffer (pH 3.6) and 0.02% (w/v) SDS. To prepare 1 litre, dissolve 18.8 g glycine in approximately 900 ml water and add 15 ml of 0.5 *M* sulfuric acid. Slight deviations from pH 3.6 are tolerable. Add 2 ml SDS stock and make up to 1 litre. Keep at room temperature; it is stable for months.

The following solutions are not needed for the standard protocol.

6. *Washing solution A*: Saturated ammonium sulfate, adjust to pH 7.0 with Tris. To make 1 litre, stir ammonium sulfate in warm water (do not heat excessively). Let the solution cool to room temperature overnight and titrate to pH 7.0 with a concentrated (approximately 2 *M*) solution of Tris (usually approximately 1 ml is required). Keep at room temperature. As ammonium sulfate tends to produce lumps in the storage bottle it might be easier to weigh the entire bottle, add some water, remove the resulting slurry, and weigh the empty bottle again. To produce a saturated solution (53.1%, w/v), dissolve 760 g ammonium sulfate in 1 litre water.

7. *Washing solution B*: Methanol/acetic acid/water (50/10/40, v/v). To make 1 litre, mix 100 ml acetic acid and 500 ml methanol; make up to 1 litre. Keep at 4°C.

8. *Drying solution*: 1-Butanol/methanol/acetic acid (60/30/10, v/v). To make 0.1 litre, mix 10 ml acetic acid, 30 ml methanol, and 60 ml butanol. Keep at 4°C; use up to six times.

Steps

The dot-blot assay is a versatile tool; its different modifications enable one to cope with almost every potentially interfering substance. In the following description the steps for all modifications are included.

1. Preparation of filter sheets (cellulose acetate membrane). *Handle the sheets with clean forceps and scissors, do not touch!* Cut one corner to aid in orientation during processing of the sheet. Mark the points of sample application (see later). Mount the membrane in such a way that the points of sample application are not supported (otherwise a loss of protein due to absorption through the membrane may be encountered). There are two different ways to achieve these requirements.

a. For routine assays it is recommended to mount the sheets in a special dot-blot apparatus (Fig. 1). Mark dot areas by piercing the sheets through small holes in the upper part of the device.

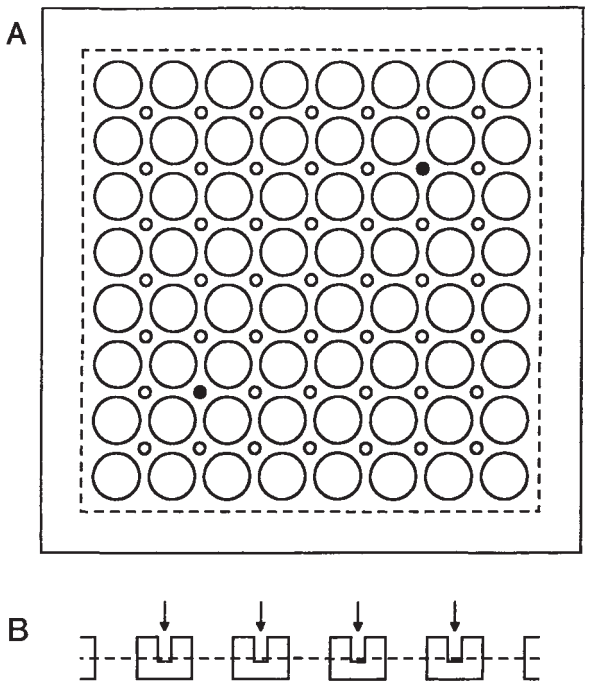

FIGURE 1 Dot-blot apparatus. (A) Top view. (B) Section along the diagonal. The apparatus has not been drawn to scale. Dashed lines indicate the position of the cellulose acetate membrane. Large circles correspond to the application points, small ones to the holes that are used for piercing the membrane (arrows in B), and solid small ones to the position of the pins that hold together the apparatus.

b. For occasional assays, mark the application points by impressing a grid (approximately 1-cm edge length) onto the filter surface (use a blunt blade and a clean support, preferably a glass plate covering a sheet of graph paper). Mount the sheets on a wire grating (preferably made from stainless steel, fixation by means of adhesive tape is recommended; cut off the taped areas prior to staining).

2. Apply samples (0.01–10 mg ml^{-1}) to the membrane sheets in aliquots of 2 µl (piston pipettes are highly recommended; well-rinsed capillary pipettes may be used instead). Leave to dry for a couple of minutes. Dilute samples may be assayed by applying samples repeatedly (let the sample dry prior to the next application).

3. Perform heat fixation. *Note*: *This step is imperative for samples containing SDS whereas it might prove deleterious to samples lacking SDS!* Bake the dot-blot membranes on a clean glass plate for 10 min at 120°C (oven or heating plate).

4. Remove interfering substances. *Note*: *This step is optional! Its use depends on the presence of potentially interfering substances (mainly carrier ampholytes, but also peptides and the buffer PIPES).* Remove interfering substances prior to protein staining by vigorous shaking in washing solution A (3 × 5 min), followed by gentle agitation in washing solution B (3 × 2 min).

5. Stain and destain. Perform staining (10 min) and destaining (5, 5, and 15 min) in closed trays (polyethylene food boxes work very well) on a laboratory shaker at ambient temperature. For the last destaining bath, employ fresh destaining solution; discard the first destaining bath. The incubation times given here represent the minimal time intervals needed. As long as the vessels are closed tightly, each of these steps may be delayed according to convenience (in case of the last destaining bath, rinse in fresh destaining solution before proceeding).

6. Dry the stained membrane sheets. To facilitate cutting dot areas from the sheets, the following drying step is recommended. Shake the membranes in drying solution for exactly 2 min, mount them between two clamps[1] (Fig. 2), and leave them to dry in a fume hood. The dried sheets may be stored in the dark for later analysis.

7. Elute. Prior to elution, cut the dots from the membrane sheet. Perform elution (45 min in 2 ml of elution buffer) in glass scintillation vials on a laboratory shaker at ambient temperature (bright illumination should be avoided). Dried sheets have to be rewetted in destaining solution prior to immersion in elution buffer. It is recommended to dispense the destaining solution (25 µl) and the elution buffer with appropriate repetitive devices (e.g., Eppendorf multipette and Brand dispensette, respectively).

8. Take readings in a fluorometer (e.g., Luminescence Spectrometer LS 50B; Perkin-Elmer; Beaconsfield, UK) at 425 (excitation) and 475 (emission) nm.

Modification

Skip elution and take readings directly from the wet membrane sheets (step 6) with a video documentation system (e.g., DIANA, Raytest GmbH, Straubenhardt, Germany; Hoffmann *et al*., 2002). Depending on the choice of filters, there might be considerable deviation from linearity.

IV. COMMENTS

With the exception of protein solutions, most stock solutions have a long shelf life. Discard any stock solu-

[1] Test for chemical resistance prior to first use: The edges of the clamp can be protected by a piece of silicon tubing cut open along one side.

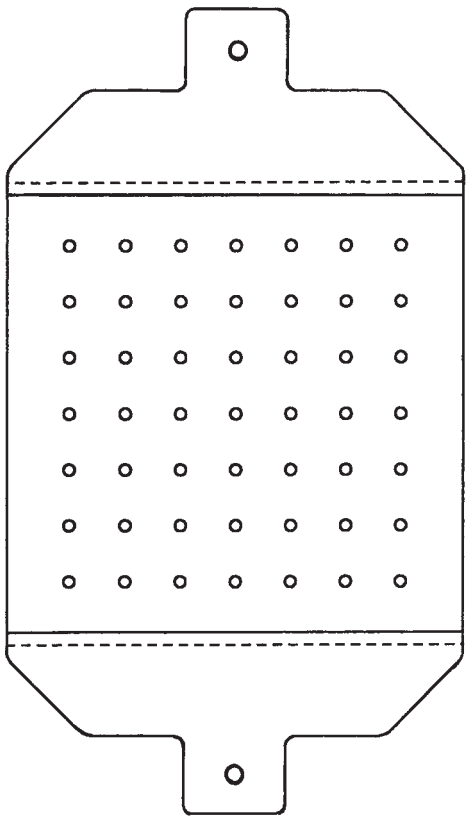

FIGURE 2 Membrane mounted for drying. Be sure to mount the drying membranes between two clamps of sufficient size to prevent distortion by uneven shrinkage. The weight of the lower clamp should keep the membrane spread evenly.

tion that changed its original appearance (e.g., got cloudy or discoloured).

Calculate standard curves according to the method of least squares. Appropriate algorithms are provided with scientific calculators and most spreadsheet programs for personal computers. It is better to compute standard curves employing single readings instead of means. Be aware of the basic assumptions made in regression analysis. For additional reading on the statistics of standard curves, compare Sokal and Rohlf (1995).

A. Lowry Assay

Pros: The Lowry assay exhibits the best accuracy with regard to absolute protein concentrations due to the chemical reaction with polypeptides. It is also useful for the quantitation of oligopeptides. This contrasts with the other two methods, which, as dye-binding assays, exhibit more variation depending on the different reactivity of the given proteins (standards as well as samples).

Cons: High sensitivity to potentially interfering substances; least shelf life of the reagents employed.

Recommendation: Employ where absolute protein contents are of interest.

B. Bradford Assay

Pros: The assay is widespread because of its ease of performance (only one stable reagent is needed, low sensitivity to potentially interfering substances, unsurpassed rapidity), its sensitivity, and its low cost.

Cons: High blank values, requires dual-wavelength readings for linearity, and possibly rather high deviations from absolute protein values (depending on the choice of standard protein).

Recommendation: Employ where relative protein contents are sufficient (in most cases such as electrophoresis) and where the assay shows no interference by sample constituents (compare Bradford, 1976).

C. Dot-Blot Assay

Pros: The dot-blot assay combines high sensitivity, an extended range of linearity (20 ng to 20 µg), and high tolerance to potentially interfering substances. The sample is not used up during assay. Hence, it may be reprobed[2] (Fig. 3) for immunological tests or detection of glycoproteins (Neuhoff *et al*., 1981).

Cons: More demanding and time-consuming than the other assays and rather expensive (chemicals and instrumentation).

Recommendation: Employ where (1) the other assays show interference, especially with complex sample buffers used in one-dimensional[3] and two-dimensional[4] electrophoresis; (2) the amount of sample is limited and/or reprobing of the dotted samples is desirable; or (3) the mere detection of protein in aliquots, e.g., from column chromatography, is needed (spot 0.2–2 µl onto membrane, process according to

[2] Sheets containing single dot areas can be marked conveniently by cutting the edges (Fig. 3, Neuhoff *et al*., 1979).

[3] Sample buffer according to Laemmli (1970): 62.5 m*M* Tris–HCl (pH 6.8), 2% (w/v) SDS, 10% (v/v) glycerol, 5% (v/v) 2-mercaptoethanol, and 0.001% (w/v) bromphenol blue. Range of the assay: 0.04 to 10 mg ml^{-1}, i.e., 80 ng to 20 µg in the test.

[4] Sample (lysis) buffer according to O'Farrell (1975): 9.5 *M* urea, 2% (w/v) Nonidet P-40, 5% (v/v) 2-mercaptoethanol, and 2% (w/v) carrier ampholytes. Standards are prepared by a stepwise dilution of the BSA stock solution in a modified sample buffer lacking carrier ampholytes. These are added from a doubly concentrated stock solution (4%, w/v) in sample buffer. Range of the assay: 0.02 to 8 mg ml^{-1}, i.e., 40 ng to 16 µg in the test.

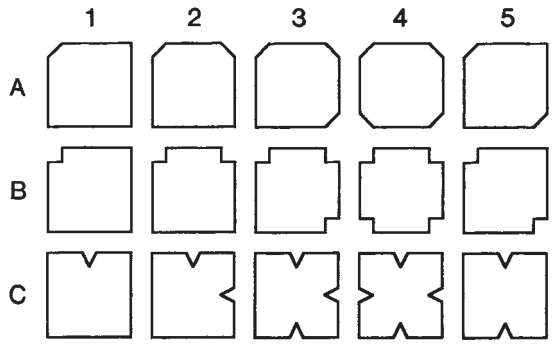

FIGURE 3 Useful incision patterns employed for marking membrane sheets prior to reprobing. Additional patterns may be generated by combination.

standard protocol, prevent evaporation by covering the destained membrane with a thin glass plate, view under UV light).

V. PITFALLS

1. Solutions containing protein exhibit an altered surface tension. Avoid foaming and pipette slowly and steadily.

2. Extraction or precipitation steps to eliminate interfering substances should be carefully controlled for complete recovery of protein (Lowry *et al.*, 1951). The more demanding dot-blot assay frequently is a good alternative because of a considerable gain of convenience and accuracy with respect to a simplified sample preparation.

3. Omission of known interfering buffer components from just those samples that are intended for protein determination is strongly discouraged as the solubility of proteins might be influenced (carrier ampholytes, e.g., enhance solubilization of membrane proteins in two-dimensional electrophoresis sample buffer; for references, see Guttenberger *et al.*, 1991).

4. In the case of photometers/fluorometers operating with filters (usually microplate readers), the correct wavelength may not be available. Instead, a similar wavelength may be employed [Lowry assay: 530–800 nm, Bradford assay: 540–620 nm, dot-blot assay: 366–450 nm (excitation), 450–520 nm (emission)]. In the case of fluorometry, allow for a sufficient wavelength interval between excitation and emission (consult the operating instructions of your instrument). Be aware that considerable deviations from the standard wavelengths will be at the expense of linearity and sensitivity.

5. In microplates it is important to achieve uniform menisci: Prick air bubbles with a thin wire and mix the plates on a gyratory shaker.

6. Analysis of dilute samples by application of larger sample volumes also increases the amount of potentially interfering substances. Include appropriate controls.

A. Lowry Assay

1. Many reagents used commonly in protein extraction interfere with this assay. The main groups of interfering substances are reductants (e.g., sulfhydryl compounds such as mercaptoethanol, reducing sugars such as glucose), chelating agents (e.g., EDTA), amine derivatives (many common buffering substances such as Tris), and detergents (e.g., Triton, SDS). A detailed list of interfering substances, along with remedies and tolerable limits, is provided by Petersen (1979).

2. Reagent D is not stable at a basic pH. Immediate mixing after the addition of reagent D is imperative. In microplates the use of a small plastic spatula is convenient for this purpose (change or rinse between samples).

3. The colour reaction takes about 80 min to come to completion. Prior to this, reading of samples over an extended period of time will give rise to experimental error (more than 20%; Kirazov *et al.*, 1993). Keep the reading interval to a minimum. Alternatively, both incubation steps can be cut to 3 min by raising the incubation temperature to 37°C (Shakir *et al.*, 1994). As the time to reach thermal equilibration will depend on the experimental setup, a test run in comparison to the original method is recommended.

B. Bradford Assay

1. The commonly used standard protein BSA is highly reactive in this dye-binding assay. As a consequence the protein content of the samples is underestimated. This systematic error does not matter in comparative analyses but brings about wrong absolute values. Bovine γ-globulin is a preferable standard.

2. The standard curves are not strictly linear in the original version of the assay. If the necessary equipment for the recommended dual-wavelength ratio is not available, do not extend the range of standard concentrations beyond one order of magnitude or do not calculate standard curves by means of linear regression.

3. Samples containing detergents (1% will interfere) must be diluted (if possible) or precipitated (compare Section V.2) prior to analysis.

4. The protein–dye complex is insoluble and will precipitate with time (Marshall and Williams, 1992). For highest accuracy, take readings within an interval between 5 and 20 min after addition of the reagent. With crude extracts (e.g., from mycelia of certain fungi), this interval may be considerably shorter—too short to take meaningful readings. In this case, alter the way of sample preparation or use another assay.

5. Plastic and glassware (especially quartz glass) tend to bind dye. Remove the resulting blue colour by one of the following procedures: (1) Rinse with glassware detergent (avoid strongly alkaline detergents with cuvettes; rinse thoroughly to remove detergent again), (2) rinse with ethanol or methanol, or (3) soak in 0.1 *M* HCl (takes several hours).

C. Dot-Blot Assay

1. Generally, it is imperative to prevent the membrane sheets from drying during one of the transfer steps (residual acetic acid will destroy the filter matrix).

2. In case of highly variable results, inspection of the stained filters (last destaining bath or dried) under UV illumination may be helpful: Background staining resulting from improper handling of the membranes will be visible (do not use UV-irradiated membranes for quantitative analyses).

3. After the washing procedure, thorough rinsing in washing solution B is imperative. Ammonium sulfate accumulating in the staining solution will interfere with the assay.

4. Although the dot-blot assay is extremely insensitive to potentially interfering substances, it is advisable to include appropriate controls (at least blank buffer and buffer plus standard).

5. In the case of buffers containing detergent plus carrier ampholytes, the storage conditions and the number of freeze–thaw cycles may prove important. Use fresh solutions or run appropriate controls.

6. If membrane sheets turn transparent upon drying, they have not been equilibrated properly in the drying solution (keep in time: 2 min) or the drying solution has been diluted by accumulation of destaining solution (do not reuse the drying solution too often).

References

Bradford, M. M. (1976). A rapid and sensitive method for the quantitation of microgram quantities of protein utilizing the principle of protein-dye binding. *Anal. Biochem.* **72**, 248–254.

Gallagher, S. R., Carroll, E. J., Jr., and Leonard, R. T. (1986). A sensitive diffusion plate assay for screening inhibitors of protease activity in plant cell fractions. *Plant Physiol.* **81**, 869–874.

Guttenberger, M., Neuhoff, V., and Hampp, R. (1991). A dot-blot assay for quantitation of nanogram amounts of protein in the presence of carrier ampholytes and other possibly interfering substances. *Anal. Biochem.* **196**, 99–103.

Guttenberger, M., Schaeffer, C., and Hampp, R. (1994). Kinetic and electrophoretic characterization of NADP dependent dehydrogenases from root tissues of Norway spruce (*Picea abies* [L.] Karst.) employing a rapid one-step extraction procedure. *Trees* **8**, 191–197.

Hjelmeland, L. M., and Chrambach, A. (1984). Solubilization of functional membrane proteins. *Methods Enzymol.* **104**, 305–318.

Hoffmann, E. M., Muetzel, S., and Becker, K. (2002). A modified dot-blot method of protein determination applied in the tannin-protein precipitation assay to facilitate the evaluation of tannin activity in animal feeds. *Br. J. Nutr.* **87**, 421–426.

Kirazov, L. P., Venkov, L. G., and Kirazov, E. P. (1993). Comparison of the Lowry and the Bradford protein assays as applied for protein estimation of membrane-containing fractions. *Anal. Biochem.* **208**, 44–48.

Laemmli, U. K. (1970). Cleavage of structural proteins during the assembly of the head of bacteriophage T4. *Nature* **227**, 680–685.

Lowry, O. H., Rosebrough, N. J., Farr, A. L., and Randall, R. J. (1951). Protein measurement with the Folin phenol reagent. *J. Biol. Chem.* **193**, 265–275.

Marshall, T., and Williams, K. M. (1992). Coomassie blue protein dye-binding assays measure formation of an insoluble protein-dye complex. *Anal. Biochem.* **204**, 107–109.

Neuhoff, V., Ewers, E., and Huether, G. (1981). Spot analysis for glycoprotein determination in the nanogram range. *Hoppe-Seyler's Z. Physiol. Chem.* **362**, 1427–1434.

Neuhoff, V., Philipp, K., Zimmer, H.-G., and Mesecke, S. (1979). A simple, versatile, sensitive and volume-independent method for quantitative protein determination which is independent of other external influences. *Hoppe-Seyler's Z. Physiol. Chem.* **360**, 1657–1670.

O'Farrell, P. H. (1975). High resolution two-dimensional electrophoresis of proteins. *J. Biol. Chem.* **250**, 4007–4021.

Peterson, G. L. (1979). Review of the Folin phenol protein quantitation method of Lowry, Rosebrough, Farr and Randall. *Anal. Biochem.* **100**, 201–220.

Raghupathi, R. N., and Diwan, A. M. (1994). A protocol for protein estimation that gives a nearly constant color yield with simple proteins and nullifies the effects of four known interfering agents: Microestimation of peptide groups. *Anal. Biochem.* **219**, 356–359.

Shakir, F. K., Audilet, D., Drake, A. J., III, and Shakir, K. M. M. (1994). A rapid protein determination by modification ot the Lowry procedure. *Anal. Biochem.* **216**, 232–233.

Sokal, R. R., and Rohlf, F. J. (1995). "Biometry." Freeman, New York.

Ünlü, M., Morgan, M. E., and Minden, J. S. (1997). Difference gel electrophoresis: A single gel method for detecting changes in protein extracts. *Electrophoresis* **18**, 2071–2077.

Zor, T., and Selinger, Z. (1996). Linearization of the Bradford protein assay increases its sensitivity: Theoretical and experimental studies. *Anal. Biochem.* **236**, 302–308.

CHAPTER

18

Phosphopeptide Mapping: A Basic Protocol

Jill Meisenhelder and Peter van der Geer

I. INTRODUCTION

Peptide mapping is a technique in which a radioactively labeled protein is digested with a sequence specific protease. The resulting peptides are separated in two dimensions on a thin-layer cellulose (TLC) plate by electrophoresis and chromatography. The peptides are visualized by autoradiography, giving rise to a peptide map.

Peptide maps of ^{35}S-labeled proteins are used most often to find out whether two polypeptides are related. Peptide maps of ^{32}P-labeled proteins are used to obtain information about the phosphorylation of the protein under investigation. Proteins can be labeled *in vivo* by incubating cells in the presence of [^{32}P]orthophosphate or by incubating them *in vitro* with an appropriate protein kinase in the presence of [γ-^{32}P]ATP. Proteins are usually separated from other contaminating proteins by SDS–PAGE and then subjected to phosphopeptide mapping or phosphoamino acid analysis.

II. MATERIALS AND INSTRUMENTATION

HTLE 7000 electrophoresis system (CBS Scientific, Del Mar, CA)

pH 1.9 electrophoresis buffer: 50 ml formic acid (88%, w/v), 156 ml glacial acetic acid, and 1794 ml deionized water

pH 3.5 electrophoresis buffer: 100 ml glacial acetic acid, 10 ml pyridine, and 1890 ml deionized water

pH 4.72 electrophoresis buffer: 100 ml *n*-butanol, 50 ml pyridine, 50 ml glacial acetic acid, and 1800 ml deionized water

pH 8.9 buffer: 20 g $(NH_4)_2CO_3$ and 2000 ml deionized water

Regular chromatography buffer: 785 ml *n*-butanol, 607 ml pyridine, 122 ml glacial acetic acid, and 486 ml deionized water

Phospho-chromatography buffer: 750 ml *n*-butanol, 500 ml pyridine, 150 ml glacial acetic acid, and 600 ml deionized water

Isobutyric acid buffer: 1250 ml isobutyric acid, 38 ml *n*-butanol, 96 ml pyridine, 58 ml glacial acetic acid, and 558 ml deionized water

Phosphoamino acid stocks: 1 mg/ml each in deionized water is stable for years at –20°C.

50 m*M* NH_4HCO_3 pH 7.3–7.6. Make up fresh; lower the pH by bubbling CO_2 through it if necessary. The pH of this buffer will drift overnight toward pH 8.0.

1.5-ml microfuge tubes with plastic pestles can be obtained from Kimble Kontes (Vineland, NJ). These pestles fit nicely into Sarstedt screw-cap microcentrifuge tubes.

RNase A is dissolved in deionized water at 1 mg/ml, boiled for 5 min, and stored at –20°C.

TPCK-treated trypsin (Worthington Lakewood, NJ) can be dissolved at 1 mg/ml in 1 m*M* HCl and is stable at –70°C for years.

III. PROCEDURES

A. Phosphopeptide Mapping

1. Separate the ^{32}P-labeled protein of interest from other contaminants by resolving the sample by

Copyright 2006, Elsevier Science (USA).
All rights reserved.

SDS–PAGE. Dry the gel onto Whatman 3MM paper, mark the paper backing around the gel with radioactive or fluorescent ink, and expose the gel to X-ray film. Line the gel up with the film using the markings on the paper backing and autorad, localize the protein of interest, and cut the protein band out of the gel with a clean, single edge razor or a surgical blade. Remove the paper backing from the gel slices by scraping gently with a razor blade.

2. Extract the protein from the gel by grinding the gel into small fragments. Place the gel slice(s) in a 1.7-ml screw-cap tube and hydrate briefly in 500 µl 50 m*M* NH_4HCO_3, pH 7.3–7.6. Grind the gel to small pieces using a fitted plastic, disposable pestle. Add 500 µl more NH_4HCO_3, 10 µl 10% SDS, and 10 µl βME, vortex, boil for 5 min, and extract for at least 4 h on an agitator at room temperature.

3. Spin down the gel bits by centrifugation in a microfuge for 5 min at 2000 rpm, transfer the supernatant to a new microfuge tube, and store at 4°C. This supernatant represents volume X(µl). Add (1300-X) µl more NH_4HCO_3 to the gel bits, vortex, and extract again for at least 4 h on an agitator at room temperature. Spin down the gel bits and combine this supernatant with the first extract.

4. Clear the (combined) extract by centrifugation. Spin 15 min at 15,000 rpm in a microfuge at room temperature. Transfer the supernatant to a new tube, leaving the final 20 µl behind to avoid transfer of particulate material. Repeat this step one or two more times. It is important that the final extract is free of any particulate materials (gel and paper bits).

5. Concentrate the protein by TCA precipitation. Add 20 µl RNase A (1 mg/ml) to the protein extract, mix, and incubate 20 min on ice. Add 250 µl ice-cold 100% TCA, mix, and incubate 1 h on ice. Spin 15 min at 15,000 rpm in a microfuge at 4°C and remove the supernatant. Add 0.5 ml 100% cold ethanol to the pellet, invert the tube, and spin 10 min at 15,000 rpm in a microfuge and remove the supernatant. Spin again briefly, remove residual ethanol, and briefly air dry the pellet.

6. To avoid the formation of oxidation-state isomers, oxidize the protein to completion by incubation in performic acid. Performic acid is formed by incubating 9 parts 98% formic acid with 1 part H_2O_2 for 30–60 min at room temperature and then cool on ice. Resuspend the TCA pellet in 50 µl cold performic acid, incubate for 1 h on ice, add 400 µl deionized water, freeze, and lyophilize.

7. In order to analyze the different phosphorylation sites, digest the protein with a sequence-specific protease. We routinely use trypsin because it works well on denatured protein and its specificity is well characterized. Resuspend the oxidized protein in 50 µl 50 m*M* NH_4HCO_3, pH 8.0. Add 10 µl 1 mg/ml TPCK-treated trypsin, vortex, and incubate for 4–16 h at 37°C. Add a second aliquot of trypsin, vortex, and incubate again for 4–16 h at 37°C.

8. Now subject the sample to several rounds of lyophilization to remove the ammonium bicarbonate. Add 400 µl deionized water to the sample, mix, and lyophilize. Repeat this procedure two to three times and then spin the final rinse for 5 min at 15,000 rpm in a microfuge and transfer the supernatant to a new tube and lyophilize.

The peptides are now ready for application onto a 20 × 20 TLC plate. Electrophoresis will be used for separation in the first dimension. Three different buffer systems are commonly used for electrophoresis (pH 1.9, pH 4.72, and pH 8.9). All three buffer systems should be tried to determine which will best separate the tryptic phosphopeptides of a particular protein.

9. Dissolve the final pellet in 5–10 µl of the electrophoresis buffer to be used; use deionized water instead of pH 8.9 buffer. Spot the peptide mix using a gel-loading tip fitted to an adjustable micropipette. Keep the sample on as small an area on the plate as possible by spotting the samples 0.3–0.5 µl at a time, drying the sample between spottings. Spot the sample 3 cm from the bottom of the plate and 5 cm from the left side for electrophoresis at pH 1.9 or 4.72 or 10 cm from the left hand side for electrophoresis at pH 8.9 (see Fig. 1a). Mark origins on the plate with a blunt, soft pencil. We like to spot 1 µl of marker dye mixture 2 cm from the top of the plate above the sample origin (dye origin first dimension, Fig. 1a). The mobilities of marker dyes can be used as standards when comparing different maps.

In our laboratories we use the HTLE 7000 electrophoresis system. This system should be connected to a power supply, cooling water, and an air line with a pressure regulator and should be set up according to the manufacturer's directions (Fig. 2).

10. Wet the TLC plate with electrophoresis buffer immediately before placing it onto the electrophoresis apparatus as described in Fig. 1. The plate should be damp with no puddles present. Shut off the air on the HTLE 7000, remove the securing pins, the neoprene pad, the Teflon insulator, and the upper polyethylene protector sheet and fold the electrophoresis wicks back over the buffer tanks. Wipe excess buffer from the upper and lower polyethylene protector sheets and place the TLC plate onto the lower polyethylene sheet. Fold the electrophoresis wicks so that they overlap ~1 cm onto the TLC plate. Reassemble the apparatus, insert the securing pins, and adjust the air pressure to

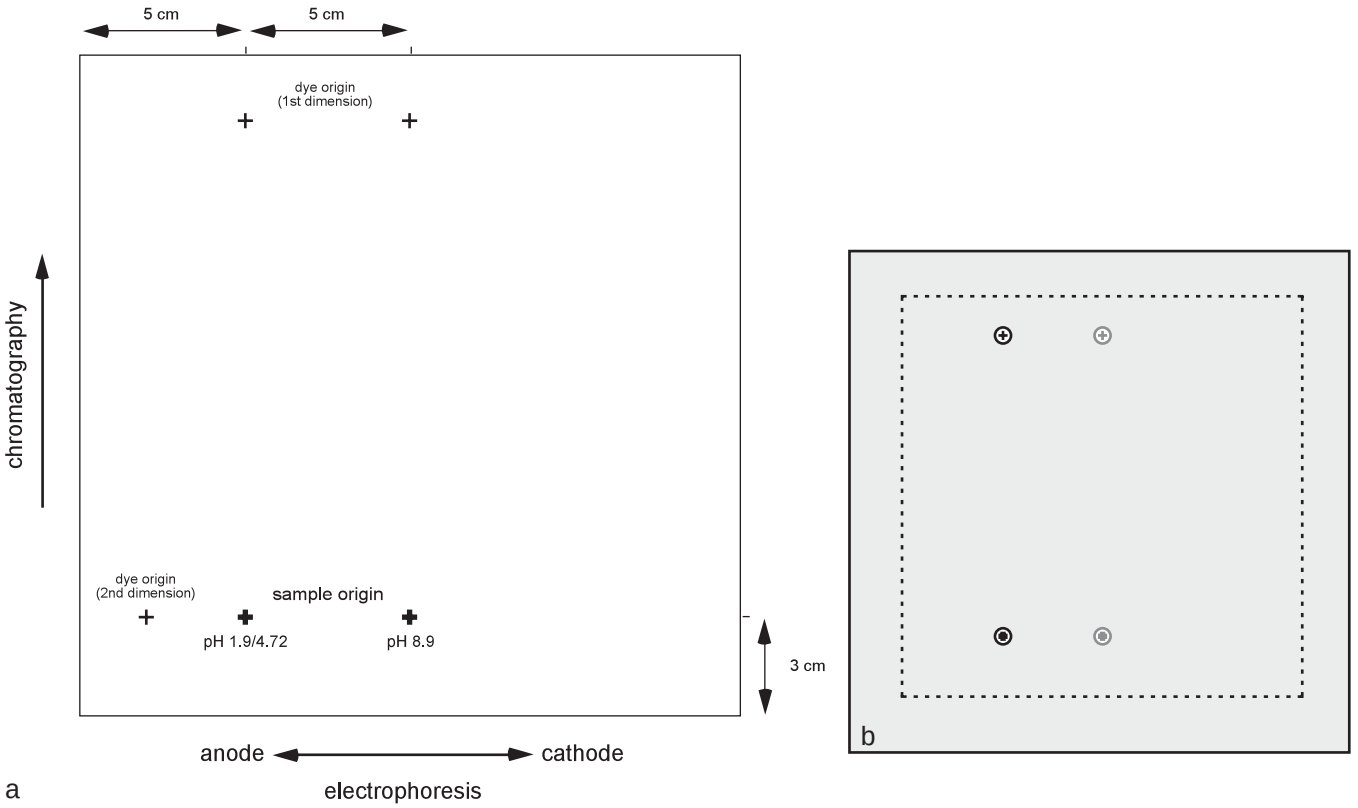

FIGURE 1 Applying the peptide mixture onto a TLC plate. (a) Phosphopeptide mixtures are usually separated by electrophoresis in the horizontal dimension and chromatography in the vertical dimension. The mixture is spotted 3 cm from the bottom of the plate and 5 cm from the left side for electrophoresis at pH 1.9 or pH 4.72 or in the center of the plate for electrophoresis at pH 8.9 (with the anode on the left and the cathode on the right after placing the plate on the HTLE 7000). We usually mark the sample and dye origin on the TLC plate with a soft blunt pencil. (b) Plates are wetted with electrophoresis buffer using a blotter composed of two layers of Whatman 3MM paper. Separate blotters are used for different electrophoresis buffers and each blotter can be used many times. A blotter contains two 1.5-cm-diameter holes that correspond to the sample and dye origin. The blotter is soaked in electrophoresis buffer and excess buffer is removed by blotting with a piece of 3MM paper. The blotter is then placed on the TLC plate so that the sample and dye origins are in the center of the two holes. The blotter is pushed onto the plate with the palm of the hand so that buffer is transferred from the blotter onto the plate. The edge of the holes is pushed onto the plate so that buffer moves from the blotter toward the center of the holes. This will concentrate the sample and dye on their origins. When the plate is completely wet, the blotter is removed and the plate is placed on the HTLE 7000. The electrophoresis apparatus is reassembled (Fig. 2) and electrophoresis is started.

10 lbs/in.^{2} Turn on the cooling water and switch on the high voltage power supply. We normally run maps for 20–30 min at 1000 V. When the run is finished, disassemble the apparatus and air dry the plate.

Running times and origins can be adjusted for individual proteins. We recommend increasing the running time rather than the voltage to get better separation of the peptides on the map.

11. Separate peptides in the vertical dimension by ascending chromatography. A plastic tank ($57 \times 23 \times 57$ cm) is available from CBS Scientific (Del Mar, CA 92014). These tanks can hold up to eight TLC plates. Tanks need to be equilibrated with chromatography buffer for at least 24 h before the run. Three different types of chromatography buffer are commonly used in our laboratories (regular chromatography, phospho-chromatography, and isobutyric acid buffers). We recommend trying the phospho-chromatography buffer first.

We like to spot 1.0 µl of marker dye in the right or left margin of the plate at the same level as the sample (dye origin second dimension, Fig. 1a). Place all plates in the tank at the same time, leaning them at the same angle; replace the lid and do not open the tank

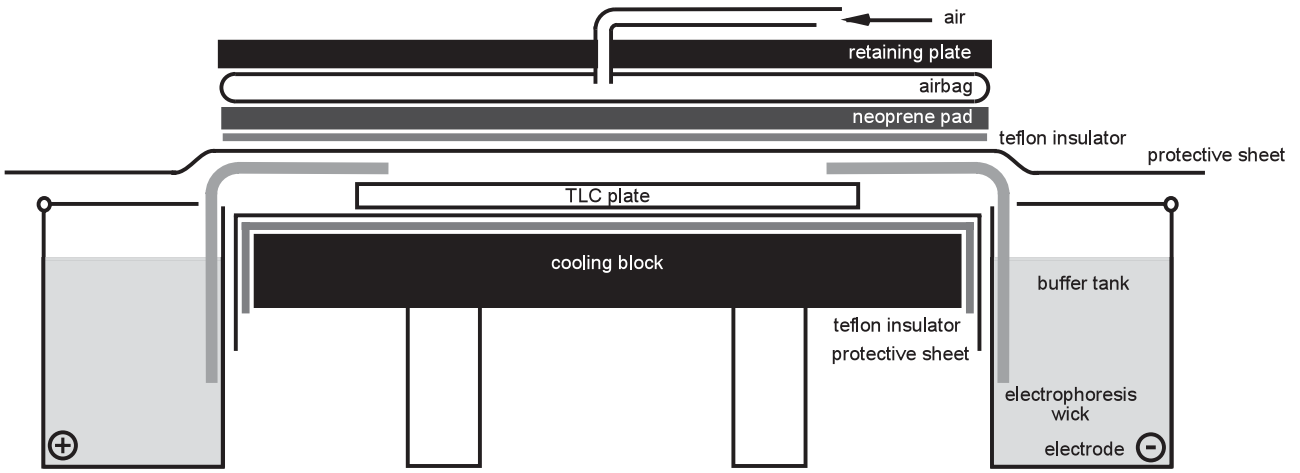

FIGURE 2 Setting up the HTLE 7000. Fill the buffer tanks with 600 ml freshly prepared electrophoresis buffer. Cover the cooling plate and fitted Teflon insulator with a polyethylene protector sheet that can be tucked between the cooling plate and the buffer tanks. Insert the wet electrophoresis wicks (14 × 20-cm double-layer Whatman 3 MM paper) into the buffer tanks and fold them over the cooling plate. Cover the cooling plate and electrophoresis wicks with the top polyethylene protector sheet, which should extend over the buffer tanks. Add the Teflon protector sheet, the neoprene pad, and close the cover. Insert the two pins to secure the cover before turning up the air pressure to 10 lbs/in.^{2} Immediately before starting electrophoresis, wet a plate as described in Fig. 1. Then turn off the air pressure, take out the pins, open the apparatus, and remove the neoprene pad, the Teflon protector, and the polyethylene sheet. Fold the electrophoresis wicks backward over the buffer tanks. Dry the bottom and top protector sheets with a Kimwipe, place the TLC plate on the apparatus, and fold the electrophoresis wicks over the cooling plate so that they overlap ~1 cm with the TLC plate. Place the polyethylene protector sheet on top of the TLC plate and reassemble the apparatus. Adjust the air pressure to 10 lbs/in.^{2}, turn on the cooling water, and start electrophoresis.

again while chromatography is in progress. The front advances more slowly as it climbs higher on the plate. Let chromatography proceed until the buffer front reaches 1–2 cm from the top of the plate. This can take from 8 to 16 h depending on the lot of cellulose plates, the ambient temperature, and the age of the buffer. At this point remove all plates from the tank and let them air dry. Mark the plates with fluorescent or radioactive ink and expose to X-ray film in the presence of an intensifier screen or to a PhosphorImager screen.

B. Phosphoamino Acid Analysis

1. To analyze the phosphoamino acid content of a phosphoprotein, the protein can be isolated exactly as described for phosphopeptide mapping (Section III,A, steps 1–6). Transfer a fraction of the sample resuspended in performic acid (step 6) to a screw-cap microfuge tube and lyophilize. If the entire sample is to be used for phosphoamino acid analysis, use the ethanol-washed TCA precipitate (step 5).

2. Hydrolyze the protein to liberate the individual phosphoamino acids. Dissolve the sample in 50 µl 6 *M* HCl and incubate for 1 h at 110°C.

3. Remove the hydrochloric acid by lyophilization.

4. Dissolve the amino acid mixture in 5–10 µl pH 1.9 buffer containing unlabeled phosphoamino acids as standards (70 µg/ml of each) by vortexing vigorously. Spin for 5 min at maximal speed in a microfuge to pellet particulate matter.

5. Spot the samples on a TLC plate as described for phosphopeptide mapping (step 9). Four samples can be analyzed simultaneously on a single TLC plate (Fig. 3a).

6. After all samples are spotted, wet the plate with pH 1.9 buffer using a blotter containing five holes that correspond to the four sample origins and a dye origin, as described for phosphopeptide mapping (step 10, Fig. 3b). Place the wetted plate immediately on the HTLE 7000 containing pH 1.9 buffer in the tanks and reassemble the apparatus. Resolve the samples in the first dimension by electrophoresis for 20 min at 1.5 kV (Fig. 3a, lower left) and air dry the plates.

7. Before running electrophoresis in the second dimension, wet the plate with pH 3.5 buffer containing ~0.1 m*M* EDTA using three rectangular blotters 10, 6, and 4 cm wide. Place blotters on the plate so that a ~1.5-cm strip of the plate containing the sample separated in the first dimension remains uncovered (Fig.

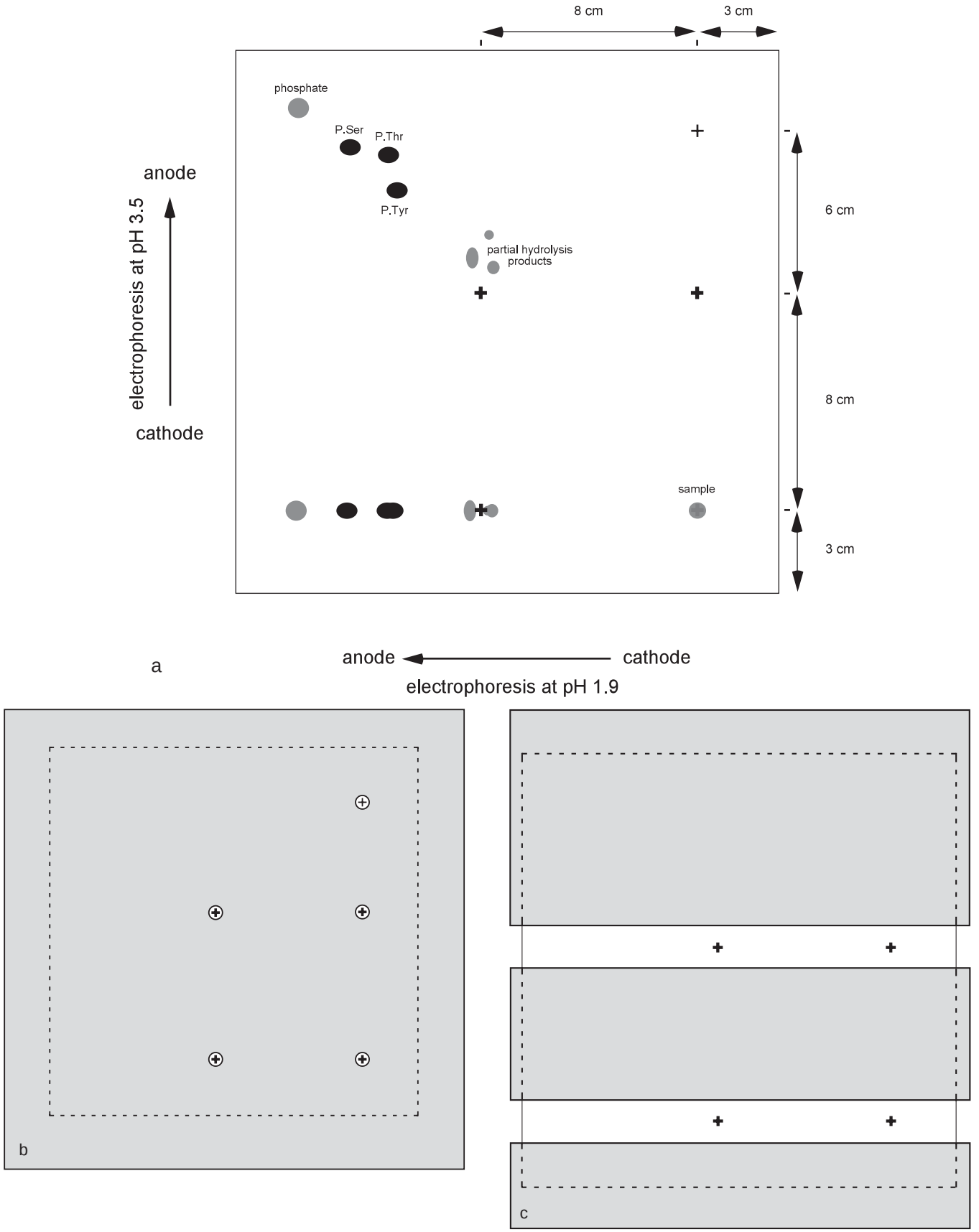

FIGURE 3 Separation of phosphoamino acids in two dimensions on a TLC plate. (a) Four samples can be separated on a single TLC plate at the same time. The four sample origins and an origin for marker dye are marked on the TLC plate with a blunt, soft pencil. Samples are first resolved in the horizontal dimension by electrophoresis at pH 1.9 (lower left quadrant). Subsequently the samples are resolved in the vertical dimension by electrophoresis at pH 3.5 (upper left quadrant). (b) After spotting the samples and marker dye, the plate is wetted with a blotter containing five holes, as shown. This will concentrate the samples and dye at their origins. (c) After electrophoresis in the first dimension, the plate is air dried. The plate is wetted with pH 3.5 buffer using three rectangular strips of Whatman 3M paper as blotters. Buffer will move from each strip as a horizontal line converging with the buffer from the adjacent strips, thereby concentrating the sample on this midpoint. When the plate is completely wet it is turned 90° counterclockwise and placed on the HTLE 7000 apparatus.

3c). By pressing the blotters onto the plate the buffer will migrate from the blotters and concentrate the samples on a line midway between the blotter edges (Fig. 3c). Turn the plate 90° counterclockwise to place it on the HTLE 7000. Reassemble the apparatus, now containing pH 3.5 buffer in the tanks, and carry out electrophoresis for 16 min at 1.3 kV (Fig. 3a, upper left). After separation in the second dimension, disassemble the apparatus and dry the plate.

8. To visualize the standard phosphoamino acids, spray the plate with 0.25% ninhydrin in acetone. Develop the ninhydrin stain by placing the plate for 5–15 min at 65°C.

9. Mark the plate around the edges with radioactive or fluorescent ink and expose it to X-ray film in the presence of an intensifier screen. After developing, align the X-ray film with the TLC plate using the radioactive or fluorescent markings. Phosphoamino acids are identified by comparing the mobility of the radioactive phosphoamino acids seen on the film with the mobility of the ninhydrin-stained phosphoamino acid standards.

IV. COMMENTS

Peptide maps provide information about the phosphorylation status of a protein. Only radioactively labeled peptides are visualized by autoradiography. In principle, every spot on the map represents a phosphorylation site; there are, however, exceptions (Boyle *et al*., 1991; Meisenhelder *et al*., 1999). Occasionally, two phosphorylation sites are close together and consequently are contained within a single peptide. If this is the case, a single spot may represent two phosphorylation sites. It is important to realize that single and doubly phosphorylated forms of a particular peptide will be resolved from each other because adding a phosphate group will add a negative charge to the peptide. It is also possible that as a consequence of partial digestion, multiple peptides/spots are generated that represent a single phosphorylation site.

We have described the basic protocol in which proteins are isolated from an SDS–PAGE gel before digestion with proteases. An alternative protocol exists in which proteins are transferred from the gel to a membrane. Membrane-bound proteins are then digested or hydrolyzed (Luo *et al*., 1990, 1991). Peptides and phosphoamino acids detach from the membrane and are analyzed as decribed here. A possible problem with this protocol is that not all peptides detach from the membrane, resulting in loss of information.

If the ultimate goal is to identify phosphorylation sites, then spots/peptides on the phosphopeptide map have to be matched to the amino acid sequence of the protein of interest. This is done best by making a list of possible peptides that can be generated by the protease used to cleave the protein. Now peptides can be eliminated from this list by gathering more information about the phosphopeptides of interest (Gould and Hunter, 1988; van der Geer and Hunter, 1990). The peptides can be isolated from the TLC plate and used to answer additional questions. What is the phosphoamino acid content of the peptide? Does it contain cleavage sites for other proteases? Which residue within the peptide is phosphorylated? Double-labeling experiments can be used to find out whether the peptide contains cysteine or methionine. Information obtained in these experiments can be used to eliminate candidate peptides from the list of possibilities until only one or two are left. The protein can also be analyzed using the peptide mapping program available at www.genestream.org; in this way some candidate peptides can be eliminated because their predicted mobility is substantially different from actual mobility on the map of the peptide in question. As verification of the identity of a phosphorylation site, the mutant protein in which the phosphorylation site has been changed to a nonphosphorylatable amino acid can be subjected to phosphopeptide mapping to confirm that the phosphorylation site of interest/spot(s) on the map has been eliminated.

REFERENCES

Boyle, W. J., van der Geer, P., and Hunter, T. (1991). Phosphopeptide mapping and phosphoamino acid analysis by two-dimensional separation on thin-layer cellulose plates. *Methods Enzymol.* **201**, 110–148.

Gould, K. L., and Hunter, T. (1988). Platelet-derived growth factor induces multisite phosphorylation of pp60c-src and increases its protein-tyrosine kinase activity. *Mol. Cell. Biol.* **8**, 3345–3356.

Luo, K., Hurley, T. R., and Sefton, B. M. (1990). Transfer of proteins to membranes facilitates both cyanogen bromide cleavage and two-dimensional proteolytic mapping. *Oncogene* **5**, 921–923.

Luo, K., Hurley, T. R., and Sefton, B. M. (1991). Cyanogen bromide cleavage and proteolytic peptide mapping of proteins immobilized to membranes. *Methods Enzymol.* 149–152.

Meisenhelder, J., Hunter, T., and van der Geer, P. (1999). Phosphopeptide mapping and identification of phosphorylation sites. *In* "*Current Protocols in Protein Science*", pp. 13.19.11–13.19.28. Wiley, New York.

van der Geer, P., and Hunter, T. (1990). Identification of tyrosine 706 in the kinase insert as the major colony-stimulated factor 1 (CSF-1)-stimulated autophosphorylation site in the CSF-1 receptor in a murine macrophage cell line. *Mol. Cell. Biol.* **10**, 2991–3002.

CHAPTER

19

Coupling of Fluorescent Tags to Proteins

Markus Grubinger and Mario Gimona

I. INTRODUCTION

Fluorescence microscopy in conjunction with fluorescent probes offers a powerful approach for gathering information about the localization of molecules in fixed and living cells. Fluorescent probes can be conjugated to proteins, nucleic acids, lipid analogs, antibodies, and ions. Microinjection of these conjugates, together with low light video or digital microscopy, can be used to study the organization and dynamics of specific molecules in live cells. The most widespread application for fluorescently labeled probes is that of secondary antibodies for immunofluorescence. Hence, most protocols for protein–dye conjugation are optimized for this special class of proteins. However, a large number of cytoskeletal proteins have been labeled successfully, particularly using thiol-reactive iodoacetamides and maleimides. Among them are actin, ADF, α-actinin, caldemon, calponin, desmin, kinesin, myosin, spectrin, tropomyosin, troponin, and tubulin. Likewise, the technique is useful for labeling extracellular matrix components such as fibronectin and collagen.

As a general rule, the attachment of a fluorescent label to a protein requires, in most cases, a compromise between optimal labeling efficiency and maximal preservation of protein function. This is explained easily by the pH optima at which some of the labeling reactions work best and the isoelectric points and solubility requirements of the protein of choice, which may often interfere. Because protein function should be regarded as the principal goal, lower labeling efficiencies should be accepted.

Overviews of the most commonly used commercial fluorescent dyes and their characteristics are given by Wang *et al*. (1982), DeBiasio *et al*. (1987), and Mason (1993). The "*Molecular Probes Handbook of Fluorescent Probes and Research Products*" by Haugland (2002) is also very informative.

Here is a short list of commonly used fluorescent dyes to label proteins through their thiol or amine groups:

1. **Thiol-reactive probes**: *Iodoacetamides*, e.g., iodoacetamide tetramethyl rhodamine (IAMTR), and *maleimides*, e.g., tetramethylrhodamine-5-maleimide.
2. **Amine-reactive probes**: *Isothiocyanates*, e.g., fluorescein isothiocyanate (FITC), *sulfonyl chlorides*, e.g., lissamine-rhodamine, and s*uccinimidyl esters*, e.g., 5′-carboxytetramethylrhodamine single isomer (5′-TAMRA-SE), 5′-carboxyfluorescein, (5′-FAM-SE), and Alexa 488 carboxylic acid succinimidyl ester dilithium salt.

All amine reactive probes will conjugate with aliphatic nonprotonated amines of proteins (or other amine-containing molecules). Consequently, the reaction has to take place in a slightly basic buffer to deprotonate the amine groups. For isothiocyanates and sulfonyl chlorides, 100–200 m*M* Na-bicarbonate at pH 9.0 or 50 m*M* sodium borate buffer at pH 8.5 are the most widely used conditions. Succinimidyl esters can be used at a pH range of 7.5–8.5; 100–200 m*M* Na-bicarbonate at pH 8.3 (no correction of pH needed) is ideal for this class of reagents. Alternatively, 50 m*M* phosphate buffer at pH 7.5 can be used. Avoid the use of amine-containing buffers such as Tris or glycine when coupling to reactive amine groups!

Copyright 2006, Elsevier Science (USA).
All rights reserved.

II. MATERIALS

Chemicals

NaCl	(M_r 58.44)	Merck, Cat. No.	1.06404
NaH_2PO_4	(M_r 156.01)	Merck, Cat. No.	1.06345
$NaHCO_3$	(M_r 84.01)	Merck, Cat. No.	1.06329
Na_2CO_3	(M_r 286.14)	Merck, Cat. No.	6391
Hydroxylamine	(M_r 69.49)	Sigma,	H-9876
Imidazole	(M_r 68.08)	Merck, Cat. No.	1.04716
$MgCl_2$	(M_r 203.30)	Merck, Cat. No.	5833
Sucrose	(M_r 342.39)	Fluka, Cat. No.	84-100

Prepacked Amersham Pharmacia PD-10 column (G-25) (Amersham Pharmacia Biotech, Cat. No. 17-0851-01; 30 prepacked columns per unit)

Column holders (any style; see Fig. 1A for a typical example)

Protein (1–5 mg/ml) in 100 m*M* Na-Bicarbonate, pH 8.3, or 10 m*M* phosphate buffer, pH 7.5–8.0

III. PROCEDURES

A. Coupling with Iodoacetamides

Solutions

1. *5′-IATMR (cysteine reactive):* Dissolve in dimethylformamide (DMF); final concentration 1 mg/ml

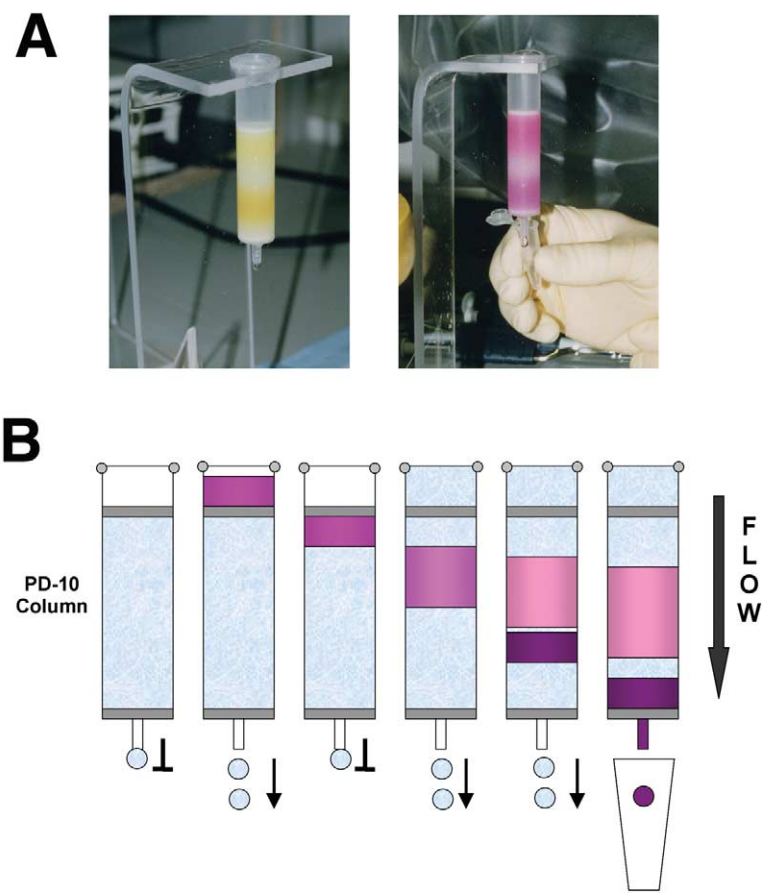

FIGURE 1 (A) Examples for the separation of labeled protein from free uncoupled dye on a PD-10 column. (Left) Alexa 488 maleimide-coupled calponin. (Right) Alexa 568 succinimidyl ester-coupled α-actinin. (B) Events of protein–dye separation using a PD-10 column (see Section VI,A).

2. *10× phosphate buffer 100 mM (NaH_2PO_4), pH 8.0:* Add 1.56 g to 100 ml water. Adjust pH with phosphoric acid
3. *Carbonate buffer 1 M ($NaHCO_3$/Na_2CO_3), pH 9.0*: Add 4.2 g $NaHCO_3$ and 14.3 g Na_2CO_3 to 100 ml distilled water
4. *NaCl stock 5 M (NaCl)*: Add 29.2 g to 100 ml distilled water

Steps

1. Dialyze the protein solution against 10 m*M* phosphate buffer, pH 8.0, overnight and measure volume.
2. Add 1/4 volume of 1 *M* carbonate buffer, pH 9.0, to the antibody or protein solution in a small glass vial embedded in ice in a medium-sized plastic or styrofoam beaker and add a small magnetic bar.
3. Stir gently on a magnetic stirrer (vigorous stirring will cause the protein to denature!).
4. Add the fluorophore in two to four aliquots in 10-min intervals (use 20–40 mg of dye/mg of antibody or protein). Let the coupling reaction proceed for a total of 60 min.
5. Load the coupled protein on a PD-10 column (1 × 10 cm) equilibrated in PBS or EDC buffer.
6. Collect the faster migrating band (dark red/violet) in a fresh sterile tube.
7. (Optional) Measure the coupling efficiency (F/P value; fluorophore to protein).

Estimation of Fluorophore/Protein Ratio

Molar concentrations of dye and protein are calculated and the ratio of these values is the molar dye/protein ratio. As an example, the molar extinction coefficient for 5′-IATR at 549 nm is 97,000 M^{-1} cm^{-1}. The ratio calculation is corrected for the absorbance at 280 nm (approximately 5% of the absorbance at 549 nm). A ratio of 2 : 1–5 : 1 is ideal.

B. Coupling with Succinimidyl Esters (SE)

Solutions

1. *200 mM Na-Bicarbonate, pH 8.3*: To make 100 ml, add 3.02 g to 100 ml distilled water
2. *1.5 M Hydroxylamine, pH 8.5*: Add 1.5 g to 5 ml of distilled water and adjust the pH to 8.5 with NaOH. Dilute 1 : 1 with distilled water prior to use.
3. *PBS, pH 7.4*: To make 1 litre, add 0.36 g NaH_2PO_4, 1.1 g Na_2HPO_4, and 9 g NaCl to 100 ml distilled water and adjust pH to 7.4 with HCl
4. *EDC buffer, pH 7.0*: 10 m*M* imidazole, 30 m*M* NaCl, 2 m*M* $MgCl_2$ (optional), and 4 m*M* NaN_3. To make 1 litre, add (from stocks) 10 ml imidazole (1 *M*), 6 ml NaCl (5 *M*), 2 ml $MgCl_2$ (1 *M*), and 1 ml NaN_3 (1 *M*).
5. 5′-Carboxytramethylrhodamine succinimidyl ester, single isomer or 5′-carboxyfluorescein succinimidyl ester, single isomer at 5 mg/ml in DMF.

Steps

1. Dialyze the antibody or protein solution against 100 m*M* Na-bicarbonate, pH 8.3, overnight and measure volume and concentration.
2. Place the protein (0.75–1.0 ml) solution in a small glass vial or Eppendorf tube embedded in ice in a medium-sized plastic or styrofoam beaker and add a small magnetic bar.
3. Stir gently on a magnetic stirrer (vigorous stirring will cause the protein to denature!).
4. Add 10–50 µl of the fluorophore (corresponds to about 0.1–0.25 mg of amine reactive dye). About one-third to one-fourth of the dye will conjugate to the protein.
5. Stop the reaction by adding 100 µl of freshly prepared 1.5 *M* hydroxylamine solution and incubate for 1 h at 4°C on ice.
6. Separate the conjugate from the unreacted fluorochrome and the hydroxylamine by gel filtration. Load the coupled protein on a PD-10 column equilibrated in PBS, pH 7.4, or EDC buffer.
7. Collect the faster migrating band in a fresh sterile tube (see Fig. 1).

IV. COMMENTS

1. The concentration of the protein solution should not be lower than 1 mg/ml (2–5 mg/ml is ideal).
2. Basic pH (carbonate buffer, pH 9.0) is necessary for obtaining satisfying coupling efficiency. Lower pH, however, may be necessary to stabilize the protein of interest but results in reduced coupling efficiency.
3. 5′-IATMR rhodamine is a specially purified rhodamine 5′-isomer. It should be dissolved in dimethylformamide (avoid dimethyl sulfoxide).
4. Add NaN_3 to the coupled proteins and store in small aliquots at –70°C.
5. Tris or other amine-containing buffer must be avoided.

V. PITFALLS

1. Aggregates, as well as under- and overlabelled proteins, are sources for artefacts.

2. 5′-IATMR, like other rhodamines, is extremely light sensitive and susceptible to repeated temperature changes. Aliquots should therefore be protected from light and stored at –70° C (for prolonged storage).

VI. PRACTICAL NOTES

A. Separation of Labeled Proteins from Uncoupled Free Dye by Gel Filtration Using a PD-10 Column

The scheme in Fig. 1B highlights the sequence of events during separation.

After the sealed bottom has been removed by a firm cut at the first rim (using a strong blade or a pair of scissors), the column is equilibrated with 5–7 volumes of buffer. *Note:* Due to the presence of a sinter layer atop the column bed, the columns will not run dry.

1. Equilibrate the column about 10 min before coupling is finished and let the flow come to a halt
2. Quickly add the protein–label mixture. *Note:* Due to the top sinter the gel bed cannot be damaged and the probe can be applied in a single flush. Avoid applying the sample dropwise as this will cause uneven penetration of the probe.
3. Let the probe enter the gel and wait until the flow has come to a halt.
4. Fill the top reservior with buffer and let the separation proceed.
5. In the last one-fourth of the column a three-phase separation should become visible featuring a bright zone separating the labeled protein (dark, fast migrating band) from the free dye (light, slower migrating band).
6. Collect the dark band containing only labeled protein. The dilution factor is about 1.5, so the entire peak fraction should fit into a single 1.5-ml Eppendorf tube.

B. Storage of Aliquots of Purified Conjugates by Liquid N_2 Infusion

As most fluorescently labeled protein probes will be used for microinjection, the storage of probes in small aliquots is required. In order to avoid hundreds of small tubes populating your freezer, the following storage method is recommended.

Add 1/10 volume of 0.6 g/ml sucrose (dissolved in the desired buffer) to the labeled protein and mix gently. Place a liquid N_2-resistant plastic beaker in a styrofoam box and fill the box and the beaker with liquid N_2. Pipette ***single*** drops of about 30–60 µl (using a 200-µl Gilson pipette and a yellow tip) directly onto the N_2 surface of the beaker. Avoid multiple drops on the surface as they will fuse and generate larger aggregates. The drop will float for about 10–20 s until the entire liquid is frozen and then sink rapidly to the bottom. Continue until the entire probe is at the bottom of the beaker. Prepare a labelled, prechilled 15-ml polycarbonate tube and gently maneuver the frozen drops into the tube and store at –70°C. Individual drops can be removed with a pair of tweezers and processed for microinjection.

References

Brantzaeg, P. (1973). Conjugates of immunoglobulin G with different fluorochromes. I. Characterization by anionic exchange chromatography. *Scand. J. Immunol. Suppl.* **2**, 273–290.

DeBiasio, R., Bright, G. R., Ernst, L. A., Waggoner, A. S., and Taylor, D. L. (1987). Five-parameter fluorescence imaging: Wound healing of living Swiss 3T3 cells. *J. Cell Biol.* **105**, 1613–1622.

Haugland, R. P. (2002). Handbook of Fluorescent Probes and Research Chemicals, 9th Ed. Molecular Probes Inc.

Mason, W. T. (1993). Fluorescent and Luminescent Probes for Biological Activity: A Practical Guide to Technology for Quantitative Real-Time Analysis. Academic Press, New York.

Wang, K., Feramisco, J. R., and Ash, J. F. (1982). Fluorescent localization of contractile proteins in tissue culture cells. *Methods Enzymol.* **85**, 514–562.

CHAPTER

20

Radioiodination of Proteins and Peptides

Martin Béhé, Martin Gotthardt, and Thomas M. Behr

I. INTRODUCTION

Radioiodination of biomolecules was established in 1948, when ^{131}I was the first radioisotope of iodine to be used for the labeling of a, at that time, polyclonal antikidney serum, performed and described by Pressmen and Keighley. The technical production of iodine-131 was pioneered in 1938 by Seaborg and Livingood. A variety of other iodine isotopes exist (Table I), from which ^{123}I, ^{125}I, and ^{131}I are the most widely used for the labeling of biomolecules for *in vitro* (i.e., radioimmunoassay) and *in vivo* (i.e., pharmacokinetic and metabolism) applications. ^{123}I, ^{125}I, and ^{131}I are γ emitters that can technically be detected easily, whereas ^{124}I emits positrons, which annihilate with an electron to produce two photons with an energy of 512 keV each. Due to this property, it can be used for positron emission tomography (PET). All these nuclides can be detected directly *in vitro* or *ex vivo* without a scintillation cocktail, whereas for *in vivo* imaging, the most suitable nuclides are ^{124}I for PET and ^{123}I (as well as, under certain conditions, ^{131}I) for single photon emission computer tomography (SPECT). ^{125}I is not suitable for *in vivo* imaging, due to its low energy of 35 keV, which is absorbed within a very short path length (a few millimeters, at best). However, this makes it very useful, together with the long half-life of 60 days for *ex vivo* (microautoradiography) and *in vitro* studies. ^{131}I decays by emitting photons with high energies (284, 364, and 637 keV) and electrons (0.6 and 0.8 MeV), the latter of which may cause substantial radiation exposure to tissues, rendering the isotope less optimal for its use in experiments. The main value of this isotope is its clinical application as a therapeutic nuclide in various therapies, including benign and malignant thyroid disorders or radioimmunotherapy.

All isotopes are available as NaI in neutral or basic solution, whereas ^{123}I, ^{125}I, and ^{131}I are commercially produced isotopes; ^{124}I can be delivered only by specialized cyclotron facilities. Because iodide (I^-) is a nonreactive form, it must be activated by an oxidizing agent to a reactive cationic species (I^+), which allows a spontaneous electrophilic substitution on aromatic rings with a good leaving group such as H^+ in p-kresol (tyrosine) or 4-methylimidazol (histidine) (Fig. 1). The iodination place is pH driven. The tyrosine moiety is labeled mainly at a pH around 7.5, whereas at a pH around 8.5, mainly the histidine is labeled, at a much lower yield though.

The tyrosine moiety can be labeled twice (Fig. 1). The second step, yielding di-iodinated tyrosyl moieties, occurs faster than the monoiodination reaction. Due to the stoichiometry of the reactants, in proteins, usually monoiodotyrosine residues prevail, whereas in peptides, di-iodinated tyrosyl moieties prevail at sufficiently high specific activities (Table II).

The possibility of rapid enzymatic deiodination of the mono- or di-iodinated tyrosine is a disadvantage. Two different kinds of iodination are known: (a) direct iodination as described earlier or (b) indirect iodination with the Bolton and Hunter reagents or similar via free amino groups.

II. MATERIALS AND INSTRUMENTS

Na^{125}I (Cat. No. IMS30) and ^{125}I Bolton and Hunter reagent (Cat. No. IM5861 or IM5862) are from

Copyright 2006, Elsevier Science (USA).
All rights reserved.

TABLE I Relevant Isotopes of Iodine

	$t_{½}$	γ energy (keV)	β energy (MeV)
^{123}I	13.1 h	159 (97.7%)	(Auger/conversion e$^-$)
^{124}I	4.17 days	603, 1691	β$^+$ 2.1
^{125}I	60.1 days	35 (100%)	(Auger/conversion e$^-$)
^{126}I	13.0 days	389, 688	β$^+$ 1.1; β$^-$ 0.9, 1.3
^{127}I	Stable		
^{129}I	1.59×10^7 year	40	β$^-$ 0.2
^{131}I	8.04 days	364 (83%) 637 (6.7%) 284 (6.9%)	β$^-$ 0.6, 0.8

TABLE II Iodine Molecules per mCi (or per MBq), as well as Antibody Molecules per mg of Protein

	$t_{½}$	N (mol)/mCi	N (molecules)/MBq
^{123}I	13.1 h	4.2×10^{-12}	1.1×10^{-13}
^{124}I	4.2 days	3.3×10^{-11}	9.1×10^{-13}
^{125}I	60.1 days	4.7×10^{-10}	1.3×10^{-11}
^{131}I	8.04 days	6.2×10^{-11}	1.7×10^{-12}
	N (mol)/mg		
IgG	6.7×10^{-9}		
$(Fab')_2$	1.0×10^{-8}		
Fab′	2.0×10^{-8}		

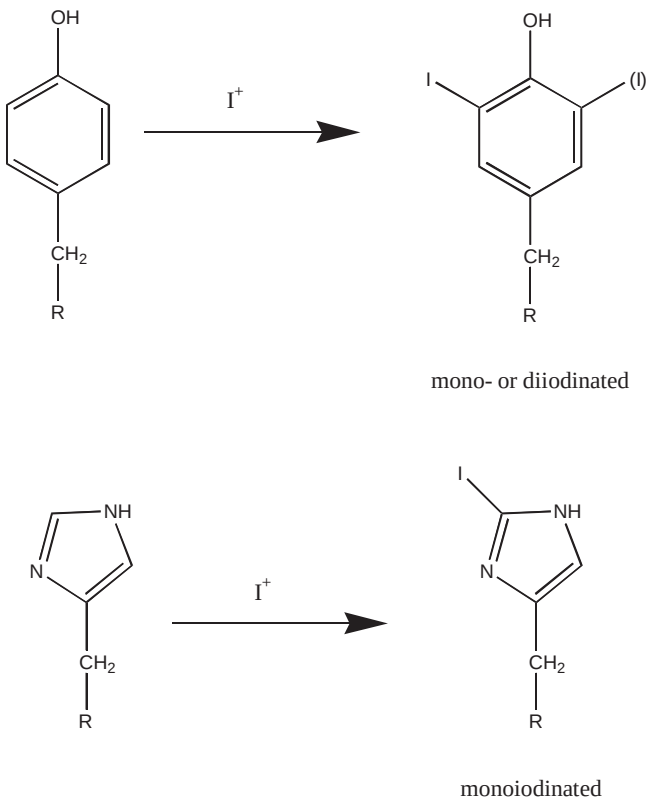

FIGURE 1 Schematic representation of the radioiodination procedure.

Amersham Bioscience. IM5862 is the di-iodo derivative used to achieve a higher specific activity. Na^{131}I (I-131-S) and Na^{123}I (I-123-S) are delivered by MDS Nordion. All radioisotopes of iodine are purchased in no carrier-added form. Iodo-Gen (T0656), chloramine-T (C9887), sodium metabisulfite (S1516), 3-(4-hydroxyphenyl) propionic acid, *N*-hydroxysuccinimide ester (H1256, Bolton–Hunter reagent), sodium acetate (S5636), chloroform (C5312), dichlormethane (32,026-0), phosphate-buffered saline (PBS) solution (P5119), sodium dihydrogen phosphate (S9638), disodium hydrogen phosphate (S9390), 1 *M* hydrochloric acid solution (H9892), boric acid (B0394), 1 *M* sodium hydroxide solution (S2770), 0.9% saline (8776), trifluoroacetic acid (T8506), HPLC water (27,073-3), and HPLC acetonitrile (57472-4) are from Sigma-Aldrich.

Tyr^3-octreotide and Exendin-3 are synthesized by Bachem. Minigastrin (G0267) is from Sigma-Aldrich.

Rituximab is a mouse–human chimeric anti-CD20 antibody (clone IDEC-C2B8, Mabthera), which is obtained commercially from Roche Pharma (via a pharmacy).

We use 1.5-ml tubes from Eppendorf (0030 120.086). The IB-F silical gel thin-layer strips (4463-02) are from Baker.

Radioactivity is measured with a Cobra II quantum automatic gamma counter from Perkin Elmer. HPLC is performed on a 535 pump and 545 UV/vis analyzer from Biotek with online flow radioactive analyzer 500TR from Perkin Elmer. PD-10 columns (17-0851-01) are from Amersham Bioscience. The HPLC protein column Bio-Silect SEC 250-5 (125-0476) is from Bio-Rad. The HPLC column is a CC 250/4.6 Nucleosil 120-5 C-18 (721712.46) from Marcherey-Nagel. The Speed-Vac Savant (SPD 101 B) is from Thermo Life Science connected with a MD4C vacuum pump (69 62 92) from Vacubrand.

III. PROCEDURES

A. Iodogen Radioiodination of an Antibody

Solutions

1. *Iodogene solution:* Dissolve 2.5 mg iodogene in 10 ml of chloroform or dichloromethane.

2. *0.05 M phosphate buffer, pH 7.4*: Prepare by dissolving 2.87 g Na_2HPO_4 and 0.66 g NaH_2PO_4 in 500 ml water (pH control must give a pH value of 7.4)
3. *0.1 M NaOH:* Dilute 1 *M* sodium hydroxide solution (S2770) 10 times

Steps

1. Add 200 µl of Iodogen solution (corresponding to 50 µg of Iodogen) to a 1.5-ml tube. Evaporate the chloroform or dichloromethane under gentle heating in a water bath (40–50°C) with constant and homogeneous rotation, plating the Iodogen homogeneously onto the inner surface of the vial. Batches of 20–30 vials can be produced simultaneously and stored for several months at –20°C.
2. Buffer 67 µg of the antibody Rituximab (1 mg of protein per 555–740 MBq (15–20 mCi) of ^{131}I, for molar ratios and other iodine isotopes, see Tables I and II) in 100 µl 0.05 *M* phosphate buffer, pH 7.4, and put into the Iodogen vial.
3. Add 37 MBq of ^{131}I in 5 µL 0.1 *M* NaOH to the reaction vial.
4. Stop the reaction after incubating for 30 min at room temperature by removing the reaction solution from the Iodogen vial to another 1.5-ml tube.
5. For quality control and purification, see special section.

B. Chloramine-T Radioiodination of Tyr^3-Octreotide

Solutions

1. *0.05 M sodium acetate buffer, pH 4.2:* Dissolve 410 mg of sodium acetate in 100 ml water. Adjust the pH to 4.2 by adding 1 *M* HCl.
2. *Tyr^3-octreotide solution:* Dissolve 5.3 mg tyr^3-octreotide in 10 ml 0.05 *M* sodium acetate buffer, pH 4.2
3. *0.05 M phosphate buffer:* Prepare 0.05 *M* phosphate buffer, pH 7.4, by dissolving 2.87 g Na_2HPO_4 and 0.66 g NaH_2PO_4 in 500 ml water (pH control must give a pH value of 7.4)
4. *Phosphate buffered saline (PBS)*
5. *Sodium meta-bisulfite:* Dissolve 20 mg sodium meta-bisulfite in 100 ml PBS
6. *Na^{125}I solution:* Available commercially

Steps

1. Add 3 µl of a 0.51 *M* tyr^3-octreotide solution in 0.05 *M* sodium acetate buffer, pH 4.2, to 20 µl of 0.05 *M* phosphate buffer, pH 7.4, into a 1.5-ml reaction tube.
2. Add 48 MBq of Na^{125}I solution in 2.8 µL 10^{-5} *M* NaOH.
3. Start the reaction by 1.6 µg chloramine-T in 20 µl 0.05 *M* phosphate buffer, pH 7.4.
4. Stop the reaction after incubating 1 min at room temperature by adding 20 µg sodium meta-bisulfite in 100 µl PBS.
5. For quality control and purification, see special section.

C. Production of ^{125}I-Labeled Bolton–Hunter Reagent

Radioiodination by the Bolton–Hunter procedure was performed essentially according to the original description (13).

Solutions

1. *PBS:* Available commercially
2. *Bolton–Hunter reagent solution:* Available commercially
3. *Chloramine-T solution:* Dissolve 2 mg of chloramine-T in 400 µl 0.25 *M* PBS, pH 7.4
4. *Sodium meta-bisulphite solution:* Solve 1.2 mg sodium meta-bisulphite in 600 µl 0.05 *M* PBS, pH 7.4

Steps

1. Add 37 MBq of Na^{125}I solution in 2.2 µl 10^{-5} *M* NaOH to 10 µl of Bolton–Hunter reagent solution in a 1.5-ml vial.
2. Add 40 µl of the chloramine-T solution to the reaction vial to start the reaction.
3. Stop the reaction after 10 s by the addition of the sodium meta-bisulphite solution.
4. After the addition of 200 µl dimethylformamide, extract the radioiodinated Bolton–Hunter reagent with two 500-µl portions of benzene.

D. Conjugation with the Bolton–Hunter Reagent

Solution

0.1 M sodium borate, pH 8.5: Dissolve 618 mg boric acid in 90 ml water. Adjust the pH with 1 *M* NaOH to pH 8.5 and make up volume to 100 ml with pure water.

Steps

1. Evaporate the solvent of the ^{125}I-labeled Bolton–Hunter reagent (from Section IIIC or commercially bought) in a hood under a gentle stream of dry nitrogen at room temperature.
2. Add 250 ng of minigastrin in 200 µl ice-cold borate buffer to the Bolton–Hunter tube.

3. Vortex the mixture for 2 h on ice.
4. Stop the reaction by removing the reaction solution from the reaction tube.
5. For quality control and purification, see special section.

E. Radioiodination of Exendin-3 on the Histidine Moiety

Solutions

1. *Iodogene solution:* Dissolve 2.5 mg in 10 ml of chloroform or dichloromethane.
2. *0.05 M Tris buffer, pH 8.5:* Dissolve 0.606 g of tris base (M_r 121.14) in approximately 90 ml of pure water. Titrate to pH 8.7 with 1 *M* HCl. Make up volume to 100 ml with pure water.

Steps

1. Add 200 µl of Iodogen solution (corresponding to 50 µg of Iodogen) to a 1.5-ml tube. Evaporate the chloroform or dichloromethane under gentle heating in a water bath (40–50°C) and constant and homogeneous rotation, plating the Iodogen homogeneously onto the inner surface of the vial. Batches of 20–30 vials can be produced simultaneously and stored for several months at –20°C.
2. Buffer 10 µg of exendin-3 in 100 µl 0.05 *M* tris buffer, pH 8.5, and put into the iodogen vial.
3. Add 37 MBq of ^{125}I in 2.2 µl 0.01 *M* NaOH to the reaction vial.
4. Stop the reaction after incubating 60 min at room temperature by removing the reaction solution from the Iodogen vial to another Eppendorf tube.
5. For quality control and purification, see special section.

F. Quality Control of Radioiodinated Antibody with Thin-Layer Chromatography

Solution

0.9% saline: Available commercially

Steps

1. Cover the floor of the chromatography tank with 0.9% saline to a depth of 5 mm.
2. Spot a droplet (approximately 1–5 µl) of the final product (radioiodinated antibody or protein) onto an ITLC silicagel IB-F flexible strip with a length of 10 cm at a distance of approximately 1 cm from the bottom.
3. After 20–30 s, place the strip into the chromatography tank.
4. Allow the strip to develop until the solvent front migrates to approximately 1 cm from the top of the strip. At this point, remove the strip from the tank and allow to dry.
5. Cut the strip in half.
6. Count its lower half, containing the radiolabeled protein, as well as its upper half, containing the unincorporated radionuclide ("free iodine"), in a γ counter.
7. Determine the amount of incorporated radioiodine as follows: Incorporated = 100% × (counts or activity of lower strip half)/(total counts or activity).

G. Quality Control and Purification of Radioiodinated Antibody with Low-Pressure PD-10 Coloumn (Fig. 2)

Solution

0.1 M phosphate buffer, pH 7.4: Dissolve 12 g of NaH_2PO_4 in approximately 900 ml of pure water. Titrate to pH 7.42 at the laboratory temperature of 20°C with monovalent strong base or acid as needed. Make up volume to 1000 ml with pure water.

Steps

1. Preequilibrate the PD-10 column with 40 ml phosphate buffer, pH 7.4
2. Apply 370 kBq (for purification: 37 MBq) of the final radiolabeled product onto the PD-10 column
3. Elute the PD-10 column with 20 ml of phosphate buffer, pH 7.4, collecting 0.5-ml fractions.
4. Count the activity in each fraction.
5. Purification: Combine the three samples of the first peak with the highest activity.

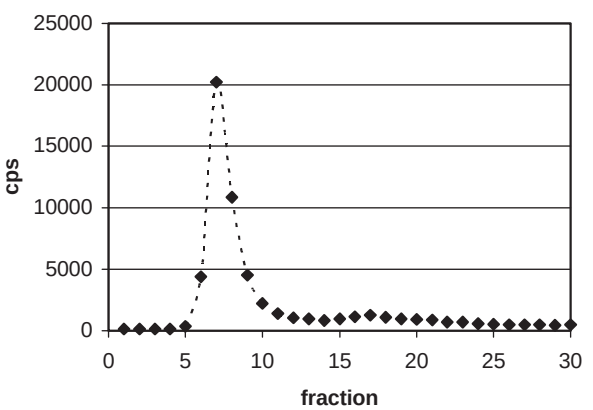

FIGURE 2 Typical elution profile of a radioiodinated monoclonal antibody (complete IgG) on a PD-10 column (Sephadex G-25 preequilibrated in a 15 × 50-mm polypropylene tube). The labeled IgG elutes in fractions 6–9, unbound iodine in fractions 15–22 (fraction size: 0.5 ml).

H. Quality Control and Purification of Radioiodinated Antibody with High-Pressure Liquid Chromatography (HPLC)

Solution

0.1 M phosphate buffer, pH 7.4: Dissolve 12 g of NaH_2PO_4 in approximately 900 ml of pure water. Titrate to pH 7.42 at the laboratory temperature of 20°C with monovalent strong base or acid as needed. Make up volume to 1000 ml with pure water.

Steps

1. Preequilibrate the size-exclusion HPLC column with 40 ml phosphate buffer, pH 7.4
2. Apply 37 kBq (for purification: 37 MBq or larger activities) of the final radiolabeled product onto the HPLC column.
3. Elute the substances with phosphate buffer, pH 7.4.
4. Collect the samples with a sample collector (purification or quality control) and measure with an online radioactivity detector (quality control).
5. Purification: Combine the three samples of the first peak with the highest activity.

I. Quality Control and Purification of Radioiodinated Peptides with HPLC

Solutions

1. *0.1% TFA:* Add 1 ml trifluoroacetic acid in 1 liter HPLC water.
2. *Acetonitrile HPLC:* Available commercially

Steps

1. First preequilibrate the C-18 HPLC column by starting an empty run (see Table III).
2. Apply 37 kBq (for purification: 37 MBq) of the final radiolabeled product onto the HPLC column.
3. Elute the substances with the gradient (Table III).

TABLE III Gradient for HPLC Quality Control and Purification for Radiolabelled Peptides

	Flow ml/min	0.1% TFA (%)	Acetonitrile (%)
0 min	1	95	5
5 min	1	95	5
20 min	1	45	55
25 min	1	45	55
40 min	1	0	100
45 min	1	0	100

4. Collect samples with a sample collector (purification or quality control) and measure on a γ counter or measure with an online radioactivity detector (quality control).
5. The acetonitrile can be evaporated on a Speed-Vac at a temperature of 60°C.
6. Purification: The radioionated peptide peak can be used for further experiments.

IV. PITFALLS

1. The iodination procedure must be performed within a hood because elementary iodine can be produced during synthesis, which is volatile.
2. The protein or peptide must be in the reaction vial before adding the radioiodine to avoid the formation of elementary iodine.
3. There must not be any additive proteins or substances with tyrosine-like structures in the solutions, as they would be radioiodinated too.
4. The solution with the iodinated protein or peptide should be adjusted to a protein content of about 2% with albumin after iodination to avoid unspecific deposition on the equipment.

V. COMMENTS

The described procedures can be changed easily between the isotopes and can be applied to proteins and their fragments or peptides without too much difficulty. The quality control part must be modified for any particular substance and can be applied to a purification procedure. The protocols can be transferred between the different iodine isotopes without major problems.

Immunoreactivity testing must be performed for antibodies and their fragments.

For the described Iodogen or chloramine-T radioiodination procedure, incorporation yields were between 60 and 90%, regardless of the antibody isotype or molecular form (IgG or fragments). After purification, the percentage of unbound radionuclide fell below 2% in all cases. Also, tyrosyl residues containing peptides were labeled successfully with yields between 60 and 85% using these procedures. With immunoconjugates, their molecular integrity was maintained at over 90% by using this Iodogen methodology, whereas chloramine-T iodination of $F(ab')_2$ fragments led to an up to 50% degradation to monovalent Fab' fragments. With peptides, oxidation of

methionine residues to their respective sulfoxide derivatives was only 15–30% with Iodogen, which stands in contrast to over 90% with the chloramine-T methodology. Finally, the tested immunoreactivities were above 85% in all cases (regardless of whether Iodogen or chloramine-T methodology was used).

Much higher variability in labeling yields was observed while using the Bolton–Hunter procedure (with incorporation yields between 20 and 55%). However, in accordance to the lack of contact to oxidants or reducing agents by using this procedure, no methionine oxidation was observed.

SECTION

7

Sample Fractionation for Proteomics

CHAPTER

21

Free-Flow Electrophoresis

Peter J. A. Weber, Gerhard Weber, and Christoph Eckerskorn

I. INTRODUCTION

Without prefractionation and enrichment, none of the existing techniques for the analysis of proteomes, such as two-dimensional electrophoresis (2-DE), or chromatographic methods, such as reversed-phase high-performance liquid chromatography (RP-HPLC), will be able to cope with the enormous complexity of biological samples and the extremely wide dynamic range of the protein concentrations. For example, this means that *low abundant proteins* are very likely to be hidden by highly expressed species.

Free-flow *isoelectric focusing* (Hannig, 1961; Krivankova and Bocek, 1998) of *protein mixtures* (Bernardo *et al*., 2000; Hoffmann *et al*., 2001; Maida *et al*., 2000; Weber and Bocek, 1996; Weber and Bocek, 1998) is one of the methods that fulfil the prerequisites to meet these *prefractionation* demands, i.e., to increase the amount of low abundant proteins and to dramatically reduce the complexity of protein mixtures. This is based on (1) the continuous operation principle, which allows the processing of large sample amounts; (2) the absence of any kind of gel or matrix that increases the recoveries of the proteins and makes this method highly compatible to virtually all kinds of follow-up analyses; and (3) the gentle procedure, which allows the fractionation of active enzymes and even protein complexes.

The power and resolution of free-flow isoelectric focusing are illustrated with the analysis of pig serum using a Pro Team *free-flow electrophoresis* (FFE) instrument. Detailed information about the instrument can be found in http://www.tecan.com. Please follow the "Proteomics" and "Fractionation" links.

II. MATERIALS AND INSTRUMENTATION

Pro Team HPMC (hydroxypropylmethylcellulose, Cat. No. 5170709) and Pro Team glycerol (Cat. No. 5170708), as well as the Pro Team FFE reagent basic kit (Cat. No. B132001) containing Prolyte 1, Prolyte 2, Prolyte 3, SPADNS (sulfanilic acid azochromotrop), and coloured pI markers, are from Tecan (Grödig, Austria). 1 *M* NaOH (Cat. No. 35256), 1 *M* H_2SO_4 (Cat. No. 35276), and petroleum benzene (Cat. No. 32248) are from Riedel-de Haën (Seelze, Germany). Urea (analytical grade, Cat. No. 24524) is from Serva (Heidelberg, Germany). Isopropanol (Cat. No. 9866.4) is from Karl Roth (Karlsruhe, Germany).

The Pro Team FFE apparatus is from Tecan (Grödig, Austria). It is equipped with seven 0.64-mm (i.d.) media tubes, one 1.42-mm (i.d.) counterflow tube, one 0.51-mm (i.d.) sample tube, a 0.4-mm spacer, and 0.65-mm filter paper strips. The water cooler IC006 ($P \geq 350$ W) is from Huber (Offenburg, Germany).

III. PROCEDURES

A. Preparation and Running of a Denaturing Free-Flow Isoelectric Focusing Experiment

Solutions

1. *Anode stabilisation media* (*inlet 1*): 14.5% (w/w) glycerol, 0.12% (w/w) HPMC, 100 m*M* H_2SO_4, and 8 *M* urea. To make 60 ml (~68.9 g), add 6.0 g of 1 *M* H_2SO_4, 14.0 g distilled water, 10.0 g 0.8% (w/w) HPMC, 10.0 g glycerol, and 28.9 g urea. Mix thor-

Copyright 2006, Elsevier Science (USA).
All rights reserved.

oughly by stirring. The solution should not be heated. Actual consumption: ~10 g/h.

2. *Separation media 1* (*inlet 2*): 14.5% (w/w) glycerol, 0.12% (w/w) HPMC, 11.6% (w/w) Prolyte 1, and 8 *M* urea. To make 60 ml (~68.9 g), add 8.0 g Prolyte 1, 12.0 g distilled water, 10.0 g 0.8% (w/w) HPMC, 10.0 g glycerol, and 28.9 g urea. Mix thoroughly by stirring. The solution should not be heated. Actual consumption: ~10 g/h.

3. *Separation media 2* (*inlet 3 + 4*): 14.5% (w/w) glycerol, 0.12% (w/w) HPMC, 19.4% (w/w) Prolyte 2, and 8 *M* urea. To make 120 ml (~137.8 g), add 26.7 g Prolyte 2, 13.3 g distilled water, 20.0 g 0.8% (w/w) HPMC, 20.0 g glycerol, and 57.8 g urea. Mix thoroughly by stirring. The solution should not be heated. Actual consumption: ~20 g/h.

4. *Separation media 3* (*inlet 5*): 14.5% (w/w) glycerol, 0.12% (w/w) HPMC, 14.5% (w/w) Prolyte 3, and 8 *M* urea. To make 60 ml (~68.9 g), add 10.0 g Prolyte 3, 10.0 g distilled water, 10.0 g 0.8% (w/w) HPMC, 10.0 g glycerol, and 28.9 g urea. Mix thoroughly by stirring. The solution should not be heated. Actual consumption: ~10 g/h.

5. *Cathode stabilisation media* (*inlet 6 + 7*): 14.5% (w/w) glycerol, 0.12% (w/w) HPMC, 100 m*M* NaOH, and 8 *M* urea. To make 120 ml (~137.8 g), add 12.0 g 1 *M* NaOH, 28.0 g distilled water, 20.0 g 0.8% (w/w) HPMC, 20.0 g glycerol, and 57.8 g urea. Mix thoroughly by stirring. The solution should not be heated. Actual consumption: ~20 g/h.

6. *Counterflow media* (*inlet 8*): 14.5% (w/w) glycerol, 0.12% (w/w) HPMC, and 8 *M* urea. To make 288 ml (~330.5 g), add 96.0 g distilled water, 48.0 g 0.8% (w/w) HPMC, 48.0 g glycerol, and 138.5 g urea. Mix thoroughly by stirring. The solution should not be heated. Actual consumption: ~46 g/h.

7. *Electrolyte anode circuit* (*+ve*): 100 m*M* H_2SO_4. To make 400 g, add 40.0 g 1 *M* H_2SO_4 and 360.0 g of distilled water. Mix thoroughly by stirring. Actual consumption: none, amount lasts for one working day.

8. *Electrolyte cathode circuit* (*–ve*): 100 m*M* NaOH. To make 400 g, add 40.0 g 1 *M* NaOH and 360.0 g of distilled water. Mix thoroughly by stirring. Actual consumption: none, amount lasts for one working day.

1. Disassembly, Cleaning, Reassembly, and Filling of the Instrument

Steps

1. Switch on the cooler first and set it to 10°C.

2. Attach the fractionation plate to the separation chamber front part via the magnetic holder and move the separation chamber to the vertical position.

3. Reduce the force of all separation chamber clamps (turn counterclockwise), open the clamps pairwise from the outside to the inside, and open the separation chamber by carefully pulling the front part.

4. Put the electrode membranes into a 1 : 1 mixture of glycerol : isopropanol and put the paper strips in distilled water.

5. Make sure that the sample tube is connected to the middle sample inlet and that the two other sample inlets are closed.

6. Clean the interior surfaces of the separation chamber with lint-free paper towels in the following order: distilled water—isopropanol—petroleum benzene—isopropanol—high-purity water. Use a separate paper towel for each cleaning operation.

7. Place the wet 0.4-mm spacer on the front plate of the separation chamber with even distance to the electrode seals. Take care that the separation media inlets do not get covered.

8. Place membranes on electrodes starting from the top to the bottom. The smooth side of the membrane should face towards the electrode seal. The membrane must not protrude over the electrode seal. Subsequently, place the paper strips congruently on the membranes in the same fashion.

9. Quickly move the separation chamber front part towards the back part, ensuring that the separation chamber front part is parallel with the back part. Then, close the middle pair of clamps simultaneously. Afterwards, close adjacent clamps pairwise. Finally, increase the clamping force pairwise starting from the centre by opening the pair of clamps, turning the clamps clockwise, and closing the clamps (the water drops underneath the spacer should get displaced, the membranes and filters should not be visible).

10. Place the fractionation plate on the fraction collector housing.

11. To fill the instrument with water, tilt the separation chamber 45° and turn the bubble trap in the filling position.

12. Place all media and counterflow tubes in a bottle with distilled water. Place the sample tube in an empty 2-ml reaction tube without tightening the screw.

13. Open the three-way stopcock on the counterflow tube in all directions and open the Luer lock closure on the cock. Place the upper counterflow tube outlet in the fractionation tray and the three-way stopcock in the bottle grid.

14. Close the media pump tube cassettes, start the pump (direction "IN") with a delivery rate of 50 rpm, and wait until the separation chamber is filled halfway. Reverse pumping direction and empty the separation chamber until the inlet areas of the spacer are reached and all air bubbles are gone. Reverse the pumping

direction again and fill the chamber bubble free until the counterflow reservoir is nearly full. Then reduce the pump speed to 20 rpm and fill the remaining part of the counterflow reservoir.

15. Fill the counterflow tube, including the bubble trap at maximum speed, reduce the flow rate to 20 rpm, and connect the Luer lock closure of the three-way stopcock. Finally, close the remaining opening of the three-way stopcock. The fractionation tubes will start dripping.

16. Tilt the chamber to the horizontal position and tap the fractionation plate on the fractionation collector housing. If a fractionation tube fails to deliver, connect a syringe to the corresponding fractionation tube and suck until liquid is coming out of the tube.

17. Dry the outside of the separation chamber and control for any kind of leakage.

18. Start the sample pump with 4 rpm (direction "IN") and tighten the adjusting screw until the tube starts to deliver. Subsequently, change the pumping direction until no air remains in the tube. Then stop the sample pump.

FIGURE 1 Stripe test to check the flow profile and the proper assembly of the Pro Team FFE instrument.

2. *Quality Control and Calibration of the Pumps*

Steps

1. To check the flow profile and the proper assembly of the instrument, dilute 500 µl of Pro Team SPADNS with 50 ml of distilled water. Then switch off the media pump, place the media tubes of inlets 2, 4, and 6 in the SPADNS solution, and leave the remaining media tubes of inlet 1, 3, 5, and 7 as well as the counterflow tube of inlet 8 in distilled water.

2. Run the media pump with 40 rpm (direction "IN") for at least 6 min: In the separation chamber, red and colourless stripes should appear that flow in parallel, with identical width, and sharp boundaries (see Fig. 1). The equivalent pattern should appear in a 96-well plate. If this is not the case, try to readjust the clamps and make sure that the sample pump screw is closed. Other reasons might be surface contamination of the separation chamber; incorrectly installed spacer, seals, paper strips, or membranes; and partially clogged or leaking media tubes.

3. To continue, switch off the media pump, return the media tubes of inlets 2, 4, and 6 to distilled water, and run the media pump at 40 rpm (direction "IN") to rinse the separation chamber for at least 6 min.

4. To calibrate the sample pump, fill a 2-ml reaction tube with approximately 1.5 ml of distilled water, weigh it accurately to a milligram, and immerse the sample tube into it.

5. Call up the dialogue "Calibrate sample pump" and follow the instructions.

6. Afterwards, weigh the reaction tube again and save the calibration.

7. To calibrate the media pump, fill an appropriate bottle with approximately 200 ml of distilled water, weigh it accurately to 10 mg, and immerse the media tubes (inlets 1–7 without counterflow tube 8) in the calibration solution.

8. Call up the dialogue "Calibrate media pump" and follow the instructions.

9. Afterwards, weigh the bottle again and save the calibration.

10. To fill the separation chamber with separation media, make sure that the media pump is switched off.

11. Immerse the liquid circuit tubes in the appropriate media (+ve: anode circuit, –ve: cathode circuit), close the safety cover of the electrode circuit bottles and the media pump, and turn on the electrode pump (flowing air bubbles in the electrode ducts indicate the proper function of the pump).

12. Immerse the media tubes into the corresponding separation media and the counterflow tube into the counterflow media.

13. Turn on the media pump with 20 rpm for 3 s (direction "OUT"). Tap the media bottles against the bottle grid. Reverse the direction of the media pump and rinse the separation chamber with 20 rpm for 15 min. Then adjust the rate of delivery to ~57 ml/h.

14. Set the voltage to 1200 V and the current to 50 mA, switch on the high voltage, and wait approximately 15 min until the current reached a stable minimum.

FIGURE 2 Performance test to check the functionality of the Pro Team FFE instrument. Red and the six yellow markers are separated according to their different pI values and mimic the actual separation of the proteins.

15. To check the performance of the instrument (Fig. 2), dilute the Pro Team pI markers 1 : 10 with separation media 2 and apply them via the middle sample inlet at a sample flow rate of 0.5 ml/h. As soon as coloured drops are visible at the fractionation tubes, wait 10 more minutes. Then collect the separated pI marker fractions in a 96-well plate by placing it on the drawer and moving it under the fractionation tubing outlets. You can avoid cross-contaminations during the collection by tapping the fractionation plate on the fractionation collector housing just before introducing and removing the drawer. The width of the red and the six yellow pI markers should be no more than 3–4 wells, otherwise the separation media have not been prepared properly or the separation chamber has not been assembled properly.

3. Fractionation of the Protein Sample by Free-Flow Isoelectric Focusing

Steps

1. Prepare the sample solution in accordance with the information mentioned in Section IV.

2. To avoid carryover when applying a new sample, make sure that the separation chamber and the sample tube get rinsed for 30 min (media pump direction "IN", ~57 ml/h; sample pump direction "OUT", 2 ml/h), that the voltage is on during this time, and that the current has reached its stable minimum.

3. Stop the sample pump, snip the end of the sample tube to create a tiny bubble at its end, immerse the tube into the sample vial, and turn on the sample pump (direction "IN") with a high flow rate until the bubble reaches the sample inlet. Then reduce the flow rate to ~1 ml/h.

4. As soon as the sample reaches the fractionation manifold (indicated by the red Pro Team SPADNS that you added to the sample), start collecting the sample fractions in a 96-well plate by placing it on the drawer and moving it under the fractionation tubing outlets. As soon as the red dye leaves the separation chamber you can stop the sample collection.

4. Shutting Down the Instrument

Steps

1. For active rinsing of the instrument you have to inactivate the instrument first, i.e., make sure that the high voltage is switched off as well as the media pump and the electrode pump.

2. Move the separation chamber to its horizontal position, place the counterflow tube, as well as the media tubes, in a bottle containing at least 1 liter of distilled water, and place the sample tube in an empty 2-ml reaction tube.

3. Operate the media pump for 30 min with 50 rpm (direction "IN") and the sample pump for 30 min with 4 rpm (direction "OUT").

4. To rinse the electrodes, remove the two "longer" electrode tubes signed with "+" or "–" from the electrode media and operate the electrode pump until the electrode ducts are almost free of electrode media. Then switch off the electrode pump. Remove the bottles with electrode media, place all four electrode tubes in a vessel containing approximately 500 ml of distilled water, and operate the electrode pump for approximately 10 min. Remove the two "longer" electrode tubes signed with "+" or "–" from the distilled water and operate the electrode pump until the electrode ducts are almost free of water. Finally, switch off electrode pump and remove the water vessel.

5. For passive rinsing of the instrument, exchange the 96-well plate drawer for a rinse tray with approximately 2 liters of distilled water. While operating the media pump (direction "IN"), dunk the fractionation plate into the rinse tray and stop the media pump. Place the counterflow and media tubes onto the bottle grid and remove the water vessel. Turn the bubble trap in the draining position. Tilt the chamber 45° upwards. Open every pair of clamps and relax clamping force for three complete revolutions (turn counterclockwise) and close it again. Remove the media pump safety cover and release the tube cassettes by pushing on the lower right side. Release the adjusting screw of the sample pump and place the sample tube on the bottle

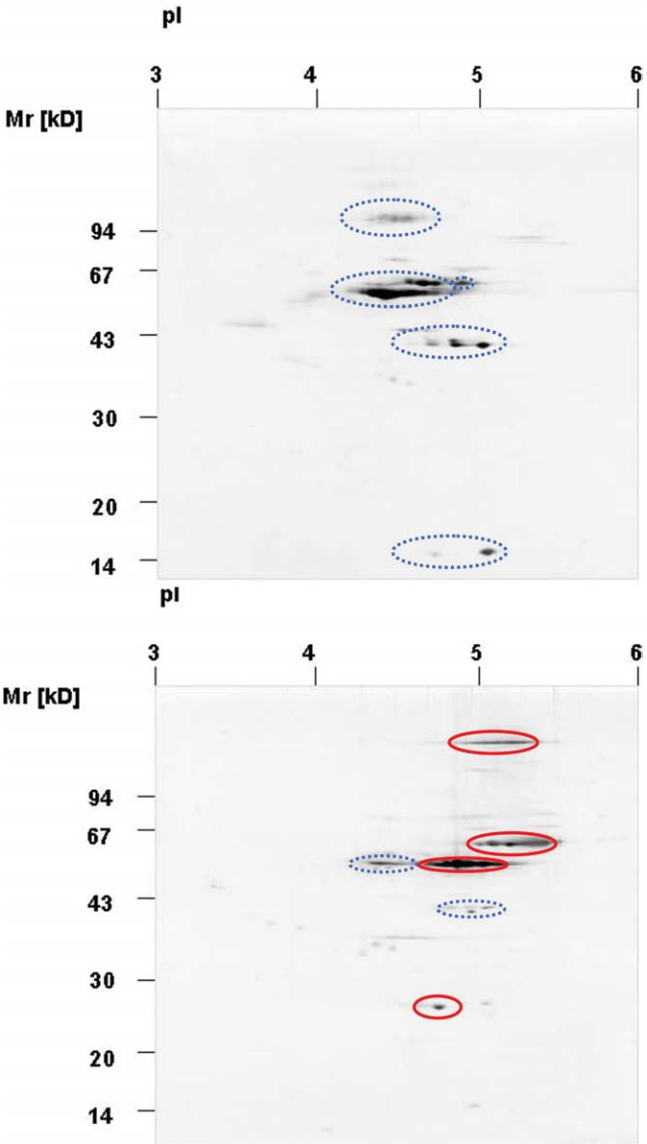

FIGURE 3 Silver-stained 2-DE analysis of two individual fractions of FFE–IEF-separated pig serum. Top: fraction 31; bottom: fraction 33. Coloured ellipses indicate the minor overlap of the two protein patterns.

grid. Finally, switch off the FFE and the cooler. If the FFE is used within the next 24 h it remains in this state. If the FFE is not used for a longer period of time, open the chamber on the next day. Rinse the spacer and filter paper with distilled water and store them dry. Store the membranes in glycerol : isopropanol (1 : 1).

B. Gel Examples

Figure 3 shows representative two-dimensional gels of individual FFE fractions after separation by IEF-FFE. For more information, the reader is encouraged to visit Tecan's Web site at http://www.tecan.com.

IV. PITFALLS

1. Use only high-purity water as well as chemicals of the highest grade available.
2. Never use acetone, powders (gloves!), silicon (latex gloves!), oil, grease, or adhesive in proximity of the separation chamber.
3. Air bubbles must not enter the separation chamber, as this would disturb the laminar flow profile and the resolution of the fractionation.
4. Make sure to prepare all solutions very carefully and to mix them thoroughly by stirring. The temperature of media should not exceed the working temperature by more than 15°C.
5. For optimal results, prepare the media freshly every day.
6. Prepare all solutions through weighing, as the high viscosity of glycerol and HPMC prevents accurate volumetric measurements.
7. Before fractionating a real sample, make sure to run two quality control experiments (see Figs. 1 and 2) to check the proper assembly and the functionality of the instrument.
8. The chemical and physical properties (density, conductivity, and viscosity) of the sample and the separation media should be similar, i.e., it is useful to dilute a concentrated sample with separation media.
9. To visualize the actual position of the colourless samples within the separation chamber, mix it with 1% of Pro Team SPADNS.
10. The total salt concentration in the sample should be less than 50 m*M*.
11. Turbid protein samples are an indication that protein precipitation has already occurred or that insoluble cell components are still present. You have to clarify turbid sample solutions by filtration or centrifugation before use.
12. You can add nonionic detergents such as CHAPS, octylglucoside, Triton X-100, and Triton X-114 (0.1–1%), as well as reducing agents such as dithiothreitol (up to 50 m*M*) or uncharged phosphines, to the samples to increase solubility.
13. Precipitation of proteins will appear as white lines in the separation chamber. You can tolerate precipitation as long as no immobile "islands" are formed. Otherwise you have to reduce the sample delivery rate or the concentration of the sample.

References

Bernardo, K., Krut, O., Wiegmann, K., Kreder, D., Micheli, M., Schafer, R., Sickman, A., Schmidt, W. E., Schroder, J. M., Meyer, H. E., Sandhoff, K., and Kroenke, M. (2000). Purification and characterization of a magnesium-dependent neutral sphingomyelinase from bovine brain. *J. Biol. Chem.* **275**, 7641–7647.

Hannig, K. (1961). Die trägerfreie kontinuierliche Elektrophorese und ihre Anwendung. *Fresenius Zeitschrift Anal. Chem.* **181**, 244–274.

Hoffmann, P., Ji, H., Moritz, R. L., Connolly, L. M., Frecklington, D. F., Layton, M. J., Eddes, J. S., and Simpson, R. J. (2001). Continuous free-flow electrophoresis separation of cytosolic proteins from the human colon carcinoma cell line LIM 1215: A non two-dimensional gel electrophoresis-based proteome analysis strategy. *Proteomics* **1**, 807–818.

Krivankova, L., and Bocek, P. (1998). Continuous free-flow electrophoresis. *Electrophoresis* **19**, 1064–1074.

Maida, R., Krieger, J., Gebauer, T., Lange, U., and Ziegelberger, G. (2000). Three pheromone-binding proteins in olfactory sensilla of the two silkmoth species *Antheraea polyphemus* and *Antheraea pernyi*. *Eur. J. Biochem.* **267**, 2899–2908.

Weber, G., and Bocek, P. (1996). Optimized continuous flow electrophoresis. *Electrophoresis* **17**, 1906–1910.

Weber, G., and Bocek, P. (1998). Recent developments in preparative free flow isoelectric focusing. *Electrophoresis* **19**, 1649–1653.

SECTION

8

Gel Electrophoresis

CHAPTER

22

Gel-Based Proteomics: High-Resolution Two-Dimensional Gel Electrophoresis of Proteins. Isoelectric Focusing and Nonequilibrium pH Gradient Electrophoresis

Julio E. Celis, Signe Trentemølle, and Pavel Gromov

I. INTRODUCTION

The sequencing of the human and other important genomes is only the beginning of the quest to understand the functionality of cells, tissues, and organs in both health and disease. Together with advances in bioinformatics, this development has paved the way to the revolution in biology and medicine that we are experiencing today. We are rapidly moving from the study of single molecules to the analysis of complex biological systems, and the current explosion of emerging technologies within proteomics and functional genomics (see other articles in this volume) promises to elicit major advances in medicine in the near future. In particular, proteomic technologies are expected to play a key role in the study and treatment of diseases as they provide invaluable resources to define and characterize regulatory and functional networks, investigate the precise molecular defect in diseased tissues and biological fluids, and for developing specific reagents to precisely pinpoint a particular disease or stage of a disease. For drug discovery, proteomics assist with powerful tools for identifying new clinically relevant drug targets and provide functional insight for drug development.

High-resolution two-dimensional (2D) polyacrylamide gel electrophoresis (PAGE), often referred as gel-based proteomics, multidimensional chromatography, and protein biochips in combination with mass spectrometry (McDonald and Yates, 2002; Yip and Lomas, 2002; Wu and McCoss, 2002 and references therein), are among the proteomic tools that are available for biomarker and drug target discovery. Considerable work is currently underway to explore applications of nongel-based proteomics in various areas of biology as this technology has much to offer.

2D PAGE is often considered the method of choice to separate complex protein mixtures present in cells, tissues, and fluids (Cash and Kroll, 2003; Ong and Pandey, 2001; Celis and Gromov, 1999). The technique separates proteins in terms of both their isoelectric points (pI) and molecular weights (M_r), and it is essentially a stepwise separation tool that combines isoelectric focusing and SDS–polyacrylamide gel electrophoresis. Using the current 2D PAGE technologies it is possible to (i) separate complex protein mixtures into their individual polypeptide components, (ii) compare the protein expression profiles of sample pairs (normal versus transformed cells, cells at different stages of growth or differentiation, etc.), and (iii) choose a condition of interest, e.g., the addition of a cytokine or a drug to a given cell type or tissue, and allow the cell or tissue to reveal the global protein behavioral response under conditions in which all of the detected proteins can be analyzed, both

Copyright 2006, Elsevier Science (USA).
All rights reserved.

qualitatively and quantitatively in relation to each other (Celis and Olsen, 1994). Protein profiles can be scanned and quantitated to search for protein differences (changes in the levels of preexisting proteins, induction of new products, coregulated polypeptides), and interesting targets or molecular signatures can be identified using additional proteomic technologies, such as mass spectrometry and Western blotting. Furthermore, by carrying out studies in a systematic manner, it is possible to store the information in comprehensive 2D PAGE databases that record how genes are regulated in health and disease (see, e.g., http://proteomics.cancer.dk; Celis *et al.*, 1995, 1998; Gromov *et al.*, 2002).

Today, 2D PAGE can be carried out using two separation modes in the first dimension: (i) conventional isoelectic focusing (IEF) gels and (ii) immobilised pH gradient (IPG) gels (see article by Görg and Weiss in this volume). In the first case, the pH gradient is generated and maintained by special amphoteric compounds, carrier ampholytes, that migrate and stack according to their pI when an electric field is applied. In contrast, IPGs are an integral part of the polyacrylamide matrix, a fact that is achieved by copolymerization of several nonamphoteric buffering species with various p*K* values (Immobilines), within the fibres of a gel (Bellqwist, 1982). This article presents protocols to resolve proteins based on conventional carrier ampholytes.

II. MATERIALS AND INSTRUMENTATION

Ampholines are from Pharmacia Biotech (pH 3.5–10, Cat. No. 80-1125-87; pH 7–9, Cat. No. 80-1125-94, and pH 8–9.5, Cat. No. 80-1125-95; the pH 8–9.5 ampholyte can be replaced by SERVALYT 9-11, Cat. No. 42909) and Serva (pH 5–7, Cat. No. 42905. Acrylamide (Cat. No. 161-0100), *N,N′*-methylenebisacrylamide (Cat. No. 161-0200), *N,N,N′N′*-tetramethylenediamine (TEMED, Cat. No. 161-0800), agarose (Cat. No. 162-0100), and ammonium persulfate (Cat. No. 161-0700) are from Bio-Rad. Dithiothreitol (DTT, Cat. No. D-0632) and bromphenol blue (Cat. No. B-6131) are from Sigma. Glycine (Cat. No. 808822) and urea (Cat. No. 821527) are from ICN Biomedical. Tris base (Cat. No.6483111) and Nonidet P-40 (NP-40, Cat. No. 492015) are from Calbiochem. SDS (Cat. No. 20763) is from Serva. Acrylamide (Cat. No. 10674) from Serva has also been used for the second dimension with essentially the same results. Filter-Count is from Packard (Cat. No. 6013149).

Dulbecco's modified Eagle medium (DMEM, Cat. No. 31966-021) is from GIBCO. Penicillin/streptomycin (Cat. No. A2213) are from Biocrom KG. Fetal calf serum (FCS, Cat. No. 04-001-1A) is from Biological Industries. The [^{35}S]methionine (Cat. No. SJ 204) and Amplify fluorographic reagent (Cat. No. NAMP100) are from Amersham. The 96-well plates (Cat. No. 655 180) and 50-ml culture flasks (Cat. No. 690 160) are from Greiner.

First-dimension glass tubes (14 cm in length and 2 mm inside diameter) are from Euro-GLAS. Prior to use they are washed with a solution containing 60 ml of alcohol and 40 ml of HCl. The glass tubes should be immersed in this solution for at least 30 min. Afterward they are washed thoroughly with glass-distilled water. Spacers are cut from 1-mm-thick polystyrene plates (Metzoplast SB/Hk). First- and second-dimension chambers, as well as the rack to hold the first dimension tubes, are homemade. X-ray films (X-OMAT UV; 18 × 24 cm, Cat. No. 524 9792) are from Kodak. The scalpels (Paragon No. 11) are from Paragon, and the long (Cat. No. V2A 1415 LL-10) and short (Cat. No. V2A 1406 LL-7) needles are from Acufirm. The aspiration pump (recirculates water) for drying gels is from Holm & Halby (HETO, Cat No. SUE 300Q).

Power supplies are from Pharmacia Biotech (EPS 500/400) or similar. The orbital shaker (Red Rotor PR70) is from Pharmacia.

III. PROCEDURES

A. Sample Preparation

1. Labeling of Cultured Cells with [^{35}S]Methionine Solutions

1. *Complete Dulbecco's modified Eagle's medium*: To make 500 ml, mix 445 ml of DMEM medium, 5 ml of 10× stock penicillin/streptomycin, and 50 ml of FCS.
2. *Methionine-free solution:* Supplement MEM lacking methionine with antibiotics (100 U/ml penicillin–100 µg/ml streptomycin) and 2% dialyzed (against 0.9% NaCl) fetal calf serum (FCS). Dispense in 1-ml aliquots and keep at –80°C.
3. *[^{35}S]Methionine (SJ 204, Amersham):* Aliquot in 100-µCi portions in sterile 1-ml cryotubes. Keep at –20°C. Freeze dry just before use.
4. *Labeling medium:* Add 0.1 ml of MEM lacking methionine to each ampoule containing 100 µCi of [^{35}S]methionine.

Steps

1. Grow the cells in complete DMEM and seed in a 96-well microtiter plate. Leave in a 37°C humidified, 5% CO_2 incubator until they reach the desired density (3000–4000 cells per well).
2. Freeze dry the [^{35}S]methionine and resuspend in labeling medium at a concentration of 1 mCi/ml. For one well, one needs 100 µCi of [^{35}S]methionine in 0.1 ml of labeling medium.
3. Remove the medium from the well with the aid of a sterile, drawn-out (under a flame) Pasteur pipette. Wash once with labeling medium. Add the labelling medium containing the radioactivity.
4. Wrap the plate in Saran wrap and place in the 37°C humidified, 5% CO_2 incubator for 16 h or shorter period (if necessary).
5. At the end of the labeling period, remove the medium with the aid of a drawn-out Pasteur pipette. Keep the medium if you want to analyze secreted or externalised proteins. Place the 96-well plate at an angle to facilitate removal of the liquid. Dispose of the radioactive medium according to the regulations enforced in your laboratory.
6. Resuspend the cells in 0.1 ml of O'Farrell's lysis solution. Pipette up and down (avoid foaming). Keep at –20°C until use.
7. Apply about 10^6 cpm to the first-dimension gels (IEF and NEPHGE) as described in Section III,B steps 6 and 7.

2. Labeling of Tissue Samples with [^{35}S]Methionine

1. Place the tissue sample on ice immediately after dissection and transport to the laboratory as fast as possible.
2. Remove clots and contaminating tissue with the aid of a scalpel. Rinse the piece two to three times in Hank's solution.
3. Mince the tissue sample in small specimens (about 1 mm^3) with the aid of a scalpel.
4. Place a tissue specimen in a 10-ml sterile plastic conical tube containing 0.2 ml of MEM lacking cold methionine and containing 2% dialyzed FCS and 200 µCi of [^{35}S]methionine and incubate for 16 h at 37°C in a humidified 5% CO_2 incubator.
5. Following incubation, carefully aspirate the medium and resuspend the tissue specimen in 0.2–0.3 ml of lysis solution. Homogenize using a small glass homogenizer.
6. Apply 20–50 µl to the first-dimension gels (IEF and/or NEPHGE) as described in Section III,B steps 6 and 7.

3. Preparation of Cell Extracts from Cultured Cells for Silver Staining

1. Plate cells in 50-ml culture flasks and grow until they reach 80% confluence.
2. Wash the monolayer three times with Hank's buffered saline. Carefully aspirate the fluid with the aid of an extended Pasteur pipette.
3. Add 0.6 ml of lysis solution. Rock at room temperature for a couple of min.
4. Aspirate and keep the extract at –20°C until use. Usually 20–30 µl of the sample can be applied to the first-dimension gel.

4. Preparation of Tissue Extracts for Silver Staining

1. Place the tissue sample on ice immediately after dissection and proceed further as described in Section III,A,2, steps 1–3.
2. Place four to six small tissue pieces in a glass homogenizer and add 1–2 ml of lysis solution. Homogenize at room temperature until the suspension clears up.
3. Keep at –20 °C until use. Usually 20–30 µl of the sample can be applied to the first-dimension gel.

B. Preparation and Running of First-Dimension Gels (IEF, NEPHGE)

This procedure is modified from those of O'Farrell (1975), O'Farrell *et al.* (1977), and Bravo (1984).

Solutions

1. *Lysis solution:* 9.8 *M* urea, 2% (w/v) NP-40, 2% ampholytes, pH 7–9, and 100 m*M* DTT. To make 50 ml, add 29.42 g of urea, 10 ml of a 10% stock solution of NP-40, 1 ml of ampholytes, pH 7–9, and 0.771 g of DTT. After dissolving, complete to 50 ml with distilled water. The solution should not be heated. Aliquot in 2-ml portions and keep at –20°C.

2. *Overlay solution:* 8 *M* urea, 1% ampholytes, pH 7–9, 5% (w/v) NP-40, and 100 m*M* DTT. To make 25 ml, add 12.012 g of urea, 0.25 ml of ampholytes, pH 7–9, 12.5 ml of a 10% stock solution of NP-40, and 0.386 g of DTT. After dissolving, complete to 25 ml with distilled water. The solution should not be heated. Aliquot in 2-ml portions and keep at –20°C.

3. *Equilibration solution:* 0.06 *M* Tris–HCl, pH 6.8, 2% SDS, 100 m*M* DTT, and 10% glycerol. To make 250 ml, add 15 ml of a 1 *M* stock solution of Tris–HCl, pH 6.8, 50 ml of a 10% stock solution of SDS, 3.857 g of DTT, and 28.73 ml of glycerol (87% concentration). After dissolving, complete to 250 ml with distilled water. Store at room temperature.

4. *Acrylamide solution:* 28.38% (w/v) acrylamide and 1.62% (w/v) *N,N′*-methylenebisacrylamide. To make 100 ml, add 28.38 g of acrylamide and 1.62 g of bisacrylamide. After dissolving, complete to 100 ml with distilled water. Filter if necessary. Store at 4°C and use within 3 to 4 weeks.

5. *NP-40:* 10% (w/v) NP-40 in H_2O. To make 100 ml, weigh 10 g of NP-40 and complete to 100 ml with distilled water. Dissolve carefully. Store at room temperature.

6. *Agarose solution:* 0.06 *M* Tris–HCl, pH 6.8, 2% SDS, 100 m*M* DTT, 10% glycerol, 1% agarose, and 0.002% bromphenol blue. To make 250 ml, add 15 ml of a 1 *M* stock solution of Tris–HCl, pH 6.8, 50 ml of a 10% stock solution of SDS, 3.857 g of DTT, 28.73 ml of glycerol (87% concentration), 2.5 g of agarose, and 2.5 ml of a 0.2% stock solution of bromphenol blue. Add distilled water and heat in a microwave oven. Complete to 250 ml with distilled water and aliquot in 20-ml portions while the solution is still warm. Keep at 4°C.

7. *1 M NaOH stock:* Weigh 4 g of NaOH and complete to 100 ml with distilled water. Keep at 4°C for no more than 2 weeks.

8. *1 M H_3PO_4 stock:* To make 100 ml, take 6.74 ml of H_3PO_4 (87%) and complete to 100 ml with distilled water. Keep at room temperature.

9. *20 mM NaOH:* To make 500 ml, take 10 ml of 1 *M* NaOH and complete to 500 ml with distilled water. Prepare fresh.

10. *10 mM H_3PO_4:* To make 500 ml, take 5 ml of 1 *M* H_3PO_4 and complete to 500 ml with distilled water. Prepare fresh.

Steps

1. Mark the glass tubes with a line (use Easy Marker from Engraver or a diamond-tipped pencil) 12.5 cm from the bottom (Fig. 1A, f). Seal the bottom end of the tube by wrapping with Parafilm and place it standing up in a rack (Fig. 1B).

2a. To make 12 first-dimensional IEF gels, use 4.12 g urea; 0.975 ml of acrylamide solution; 1.5 ml of 10% NP-40, 1.5 ml of H_2O; 0.30 ml of carrier ampholytes, pH range 5–7; 0.10 ml of carrier ampholytes, pH range 3.5–10; 15 µl of 10% ammonium persulfate; and 10 µl of TEMED.

2b. To make 12 first-dimensional NEPHGE gels, use 4.12 g urea; 0.975 ml of acrylamide solution; 1.5 ml of 10% NP-40; 1.69 ml of H_2O; 0.170 ml of carrier ampholytes, pH range 7–9; 0.020 ml of carrier ampholytes, pH range 9–11; 15 µl of 10% ammonium persulfate; and 10.5 µl of TEMED.

2c. Mix the urea, H_2O, acrylamide, NP-40, and ampholytes (kept at –20°C in 1-ml aliquots) in a tube containing a vacuum outlet (Fig. 1A, g). Swirl the solution gently until the urea is dissolved. The solution should not be heated. Add ammonium persulfate and TEMED, mix gently, and degas using a vacuum pump. Use a clean rubber stopper to control the vacuum.

3. Pour the solution into a 55-mm culture dish. Aspirate the liquid with a 10-ml syringe and add to the thin glass tubes (Fig. 1A, f) using a long needle (Fig. 1A, d). Insert the tip of the needle into the bottom of the tube and slowly fill to the mark to avoid air bubbles while moving up the needle (Fig. 1B).

4. Overlay the gel mix with 10 µl of glass-distilled water and leave to polymerise for 45 min. In the meantime, fill the lower chamber of the first dimension (Fig. 1C) with 250 ml of 10 m*M* H_3PO_4 (+; IEF gels) or 250 ml of 20 m*M* NaOH (–; NEPHGE gels).

5. Take the tubes from the rack and remove the Parafilm using a scalpel. Remove excess liquid from the upper part of the tube by shaking and dry using a thin strip of Whatman 3MM paper (Fig. 1A, c). Insert the tubes into the chamber, which holds up to 12 tubes (Fig. 1C). Tap the bottom of the tubes to remove trapped air bubbles.

6. Prerun IEF gels before adding the sample. First add 10 µl of lysis solution and then 10 µl of overlay solution. Use a Gilson microman pipette to apply the solutions. Fill the tubes as well as the upper chamger (–) with 20 m*M* NaOH. Prerun gels at room temperature for 15 min at 200 V, 30 min at 300 V, and 60 min at 400 V. After prerunning, disconnect the power supply and discard the upper and bottom solutions. Remove the tubes and wash the top of the gels with distilled water. Dry with a thin strip of Whatmann 3MM paper and apply the sample (up to 50 µl in lysis solution). Add 10 µl of overlay solution and fill the tubes with 20 m*M* NaOH. Fill the upper chamber with 20 m*M* NaOH (–) and the bottom one with 20 m*M* H_3PO_4. Run for 19 h at 400 V at room temperature.

7. NEPHGE gels are not prerun. Add the sample in lysis solution (up to 50 µl). Cover with 10 µl of overlay solution. Add 250 ml of 20 m*M* NaOH to the bottom champer (–) and fill the tubes and the upper chamber with 10 m*M* H_3PO_4 (+). Run the gels for 4.5 h at 400 V at room temperature.

8. Before stopping the run, add 3.5 ml of equilibration solution to 35-mm tissue culture dishes marked with the gel number in both the bottom part and the lid. Turn off the power supply and take the gels out with the aid of a syringe (Fig. 1A, h) filled with glass-distilled water. First, use a short needle (Fig. 1A, e) to loosen the gel at both ends of the tube. Then extrude the gel with the aid of pressure applied by a 20-ml syringe (Fig. 1D). Collect the gel in a sieve and place in the 35-mm culture dish containing the equilibration

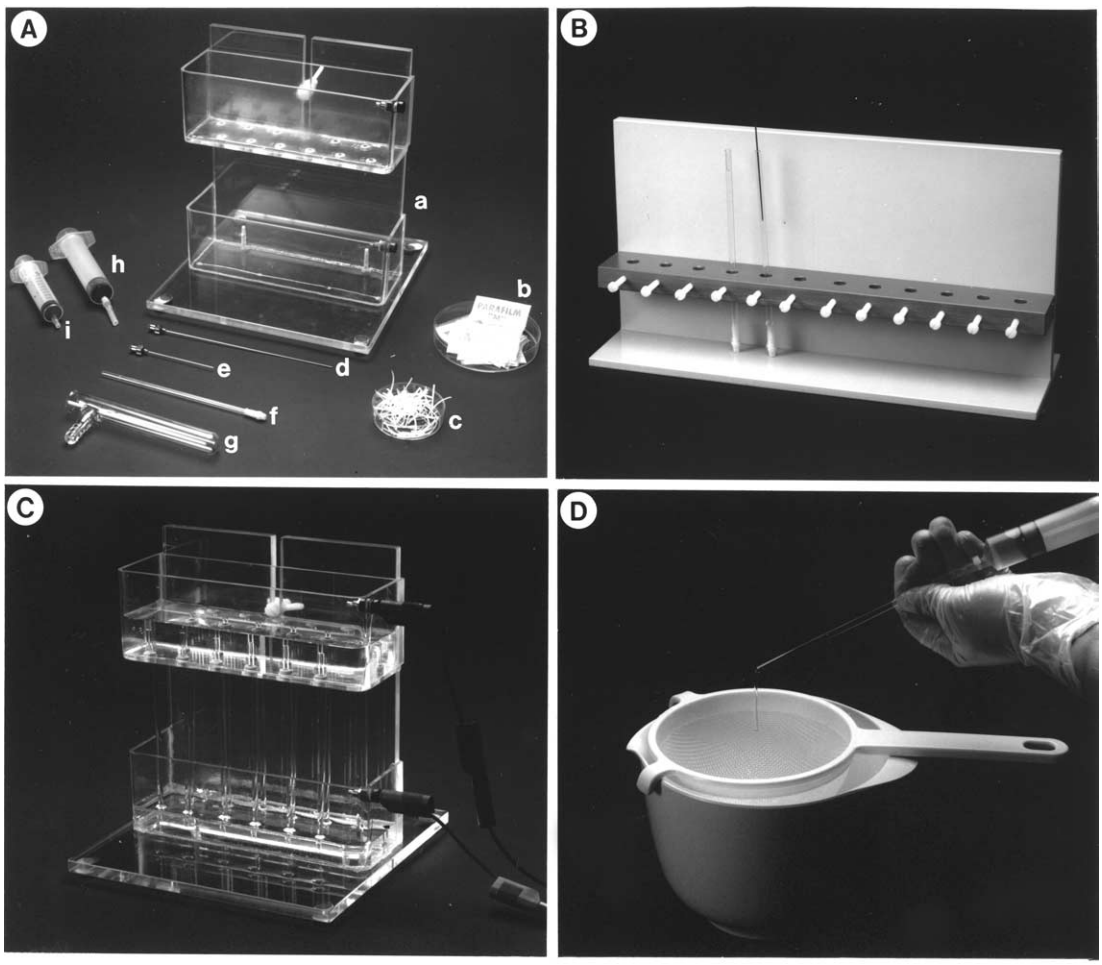

FIGURE 1 (A) First-dimension chamber and accessories for first-dimension. (a) First-dimension chamber, (b) Parafilm, (c) paper strips, (d) long needle for filling the tubes, (e) short needle for extruding the gel, (f) first-dimension tubes, (g) vacuum tube, (h) syringe connecting to a piece of rubber tubing, and (i) syringe. (B) Filling first-dimensional glass tubes with gel solution. (C) First-dimension chamber filled with tubes. (D) Extruding the first-dimension gel.

solution. Leave 2–5 min at room temperature and store at –20°C until use. Samples can be stored for at least 2 months under these conditions.

C. Second Dimension: SDS–Polyacrylamide (15%) Gel Electrophoresis

This procedure is performed essentially according to Laemmli (1970).

Solutions

1. *Solution A:* To make 500 ml, add 150 g of acrylamide and 0.75 g of bisacrylamide. After dissolving, complete to 500 ml with distilled water. Filter if necessary. Aliquot 100-ml portions and store at 4°C.
2. *Solution B:* To make 1 liter of 1.5 *M* Tris–HCl, pH 8.7, add 181.6 g of Tris base and titrate with HCl. Complete to 1 liter with distilled water. Aliquot 200-ml portions and store at 4°C.
3. *Solution C:* To make 1 liter of 1 *M* Tris–HCl, pH 6.8, add 121.1 g of Tris base and titrate with HCl. Complete to 1 liter with distilled water. Aliquot in 200-ml portions and store at 4°C.
4. *Solution D:* To make 100 ml, add 10 g of acrylamide and 0.5 g of bisacrylamide. Complete to 100 ml with distilled water. Filter if necessary. Aliquot in 200-ml portions and store at 4°C.
5. *10% SDS:* To make 1 liter, weigh 100 g of SDS and complete to 1 liter with distilled water. Filter if necessary. Store at room temperature.
6. *10% ammonium persulfate:* To make 10 ml, weigh 1 g of ammonium persulfate and complete to 10 ml with distilled water. This solution should be prepared just before use.

7. *Electrode buffer:* To make 1 liter of a 5× solution, add 30.3 g of Tris base, 144 g of glycine, and add 50 ml of 10% SDS solution. Complete to 1 liter with distilled water. Store at room temperature.

Steps

1. Store clean glass plates in dust-free boxes. One of the plates is 16.5 cm wide and 20 cm high and has a notch 2 cm deep and 13 cm wide. Cover the edges of the plate with a thin line of Vaseline. Use a plastic 10-ml syringe filled with vaseline and fitted with a Gilson tip (Fig. 2A). Place 1-mm-thick polystyrene spacers at the edges of the plate and cover with Vaseline (Fig. 2A). Place a small piece of paper without lines containing the gel number (written with pencil) at the corner of the plate (Fig. 2A).

2. Assemble the rectangular glass place 16.5 cm wide and 20 cm high together with the notched plate and spacers. Make sure that the vertical spacers are in contact with the horizontal one at the bottom. Hold the assembled plates together with the aid of fold-back clamps. Mark a line 2.5 cm from the top of the notched plate.

3. To make six 15% separation gels, mix the following solutions in a 250-ml filter flask containing a magnetic stirrer: solution A (acrylamide : bisacrylamide, 30 : 0.15), 75.0 ml; 10% SDS, 1.5 ml; solution B (1.5 *M* Tris–HCl, pH 8.8), 37.5 ml; H_2O, 35.22 ml; 10% ammonium persulfate, 750 µl; and TEMED, 30 µl.

4. Add ammonium persulfate and TEMED to the separation gel solution just before degassing using a vacuum pump. Pour the solution into the assembled plates until the marked line and overlay with distilled water. Leave the gels to polymerise for approximately 1 h.

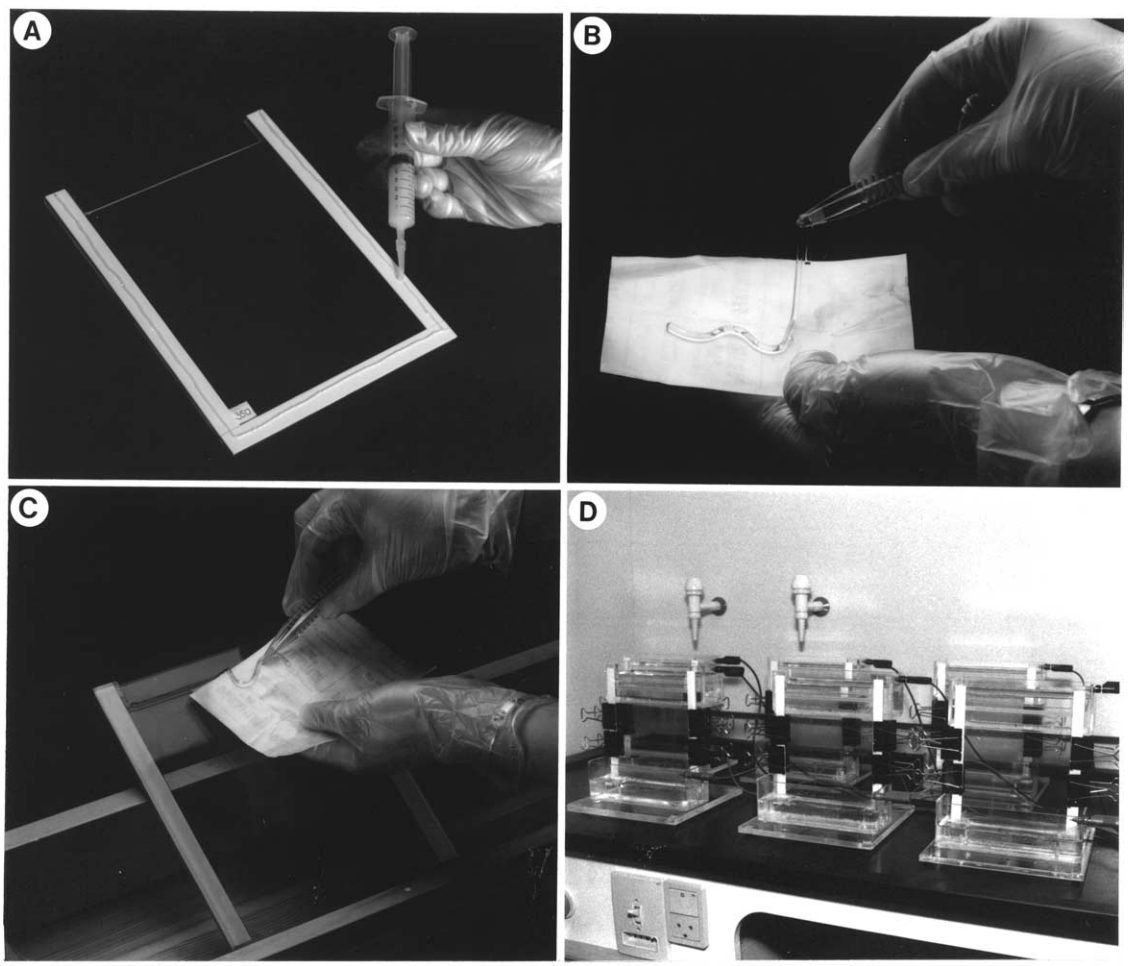

FIGURE 2 (A) Covering the spacers with Vaseline. (B) First-dimension gel prior to application to second-dimension gel. (C) Application of first-dimension gel to second-dimension gel. (D) Second-dimension chambers.

5. Remove excess liquid and dry the top of the gel with a strip of Whatman 3MM paper (2 × 9 cm).

6. To make 5% stacking solution for six gels, mix the following solutions: solution D (acrylamide : bisacrylamide, 10 : 0.5), 15.0 ml; 10% SDS, 0.3 ml; solution C (1.0 *M* Tris–HCl, pH 6.8), 3.6 ml; H_2O, 10.8 ml; 10% ammonium persulfate, 0.24 ml; and TEMED, 12 µl.

7. After degassing, add the stacking gel solution and insert a polystyrene spacer a few millimetres into the assembled plates. Keep in place with the aid of a fold-out clamp. Leave the gels to polymerise for approximately 1 h.

8. When the gel has polymerised, remove the top spacer and clean the top of the gel with a strip of Whatman 3MM paper. Remove the clamps as well as the horizontal spacer at the bottom with the aid of a spatula. Clean the space between the two glass plates using a thin spatula covered with tissue paper.

9. Lay the gels at an angle in order to facilitate application of the first dimension (Fig. 2C). Take out the culture dishes containing the first-dimension gels from the freezer 20 min before application. Once they are defrosted, melt the agarose solution in a microwave oven and immediately cover the top of the stacking gel with a small amount of agarose to fill the space left by the spacer.

10. Collect the first-dimension gel into a sieve (Fig. 1D) and place it on a piece of Parafilm (Fig. 2B). Place the gel carefully on top of the second dimension with the aid of plastic tweezers (Fig. 2C). Do not stretch the gel. Cover the gels with 2–3 ml of melted agarose. Eliminate air bubbles by pushing them out with the same pipette.

11. Clamp the gel plates to the electrophoresis chambers, which have been prefilled with 1× electrode buffer. Fill the upper chamber with enough electrode buffer to cover the agarose. Remove air bubbles at the bottom of the gel with electrode buffer using a 10-ml syringe joined to a bent needle.

12. Connect the electrodes (upper, –; lower, +) to the power supply. Run the gels at 10 mA for 4 h and at 3 mA overnight at room temperature (until the tracking dye has reached 1 cm from the bottom) (Fig. 2D). At the end of the run turn off the power supply, disassemble the plates, and remove the stacking gel with the aid of a scalpel. Process the separation gel for autoradiography, fluorography (see later), or for staining with either silver (see article by Gromova and Celis in this volume) or Coomassie brilliant blue. Gels can be used directly for blotting (see article by Celis *et al.* in Volume 1).

Figure 3 shows several representative autoradiographs and silver-stained gels of normal (Fig. 3A) and malignant tissues (Figs. 3B–3D) run under the conditions (IEF and NEPHGE) described in this article. For more information, the reader is encouraged to visit the group's Web site at http://proteomics.cancer.dk.

D. Other Procedures

1. Fluorography

This protocol is essentially from Amersham. The procedure increases the detection efficiency 1000-fold for ^{3}H and 15-fold for ^{35}S.

Solutions

1. *Fixation solution:* To make 1 liter, add 450 ml of methanol and 75 ml of acetic acid. Complete to 1 liter with distilled water.
2. *Amplify fluorographic reagent:* Available commercially from Amersham (Cat. No. NAMP100).

Steps

1. Place the gel in a rectangular glass pie dish (24 × 19 cm) and fix for 60 min at room temperature in fixative solution. Shake while fixing.
2. Place gel in 120 ml of amplifying fluorographic reagent and agitate for 30 min.
3. Dry gels.
4. Sensitize X-ray films by preflashing in the dark and expose the gels at –80°C in cassettes.

2. Quantitation of [^{35}S]Methionine-Labeled Protein Spots Excised from Two-Dimensional Gels

Steps

1. Localize protein spots with the aid of the X-ray film (Fig. 3). Before exposing, make four crosses at the corner of the gels using radioactive ink. Excise the proteins from dry gels using a scalpel.
2. Place gel pieces in counting vials containing 4 ml of Filter-Count, leave for 1 h, and count for 5 min in a scintillation counter.

IV. COMMENTS

Using the protocols described in this article, it is possible to resolve proteins having apparent molecular masses between 8.5 and 230 kDa and pI values from 4 to 12 (see also http://proteomics.cancer.dk). Autoradiographs can be quantitated using phosphorimaging autoradiography (BioRad; Amersham; Fuji). Several softwares for the analysing of 2D protein images are available. These include PDQUEST (BioRad), Z3 (Compugen), Phoretix (Nonlinear Dynamics), GelFox (Imaxia), ProteinMine (Scimagix), and Melanie, as well as several others. By carrying out

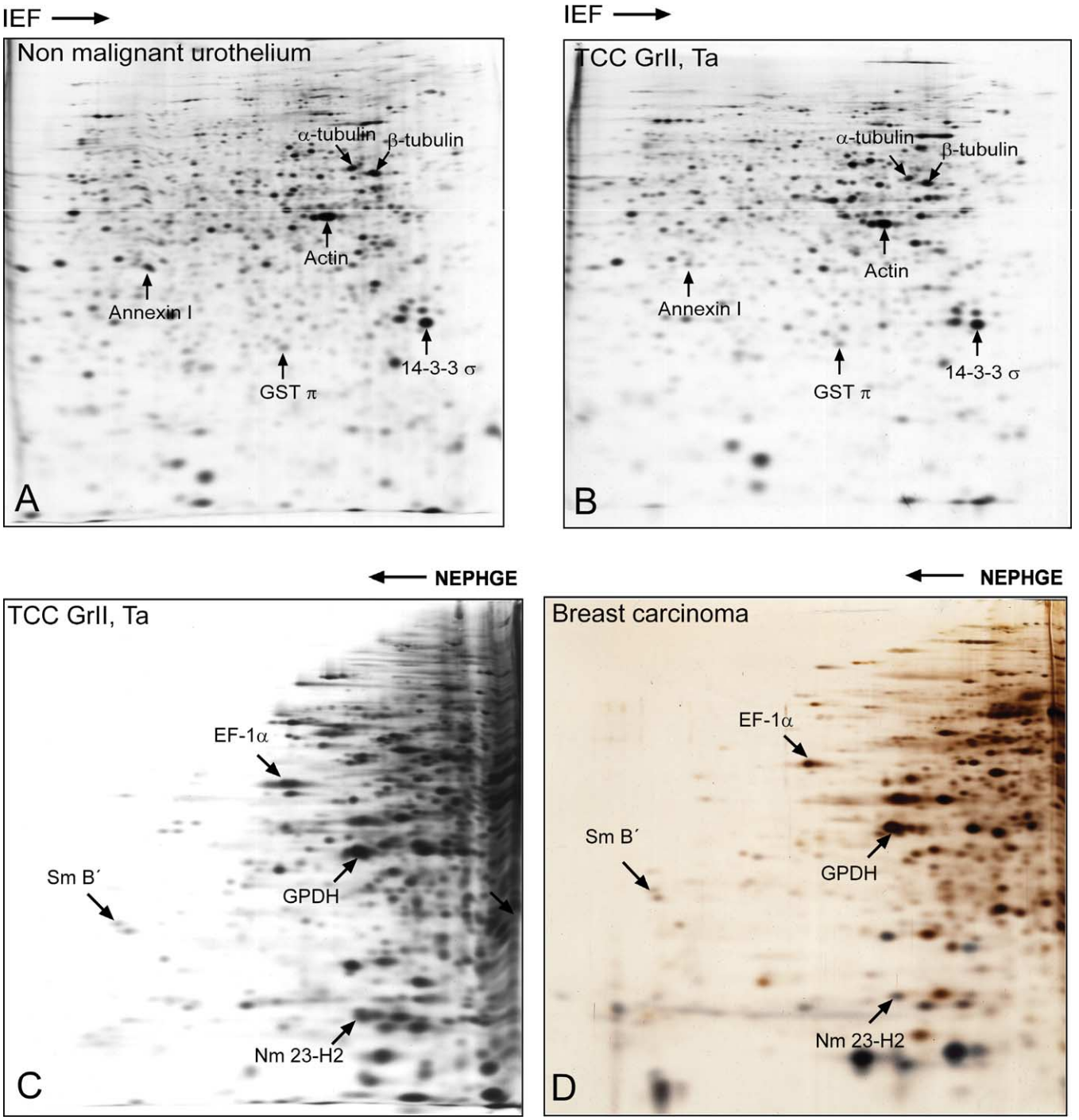

FIGURE 3 Two-dimensional patterns of whole protein extracts from human normal urothelium (A), a transitional cell carcinoma (B and C), and a breast tumor (D). Proteins were separated by 2D PAGE—IEF (A and B) and 2D PAGE—NEPHGE (C and D) and were visualized by autoradiography (A–C) and silver staining (D). The identity of a few proteins is indicated for reference.

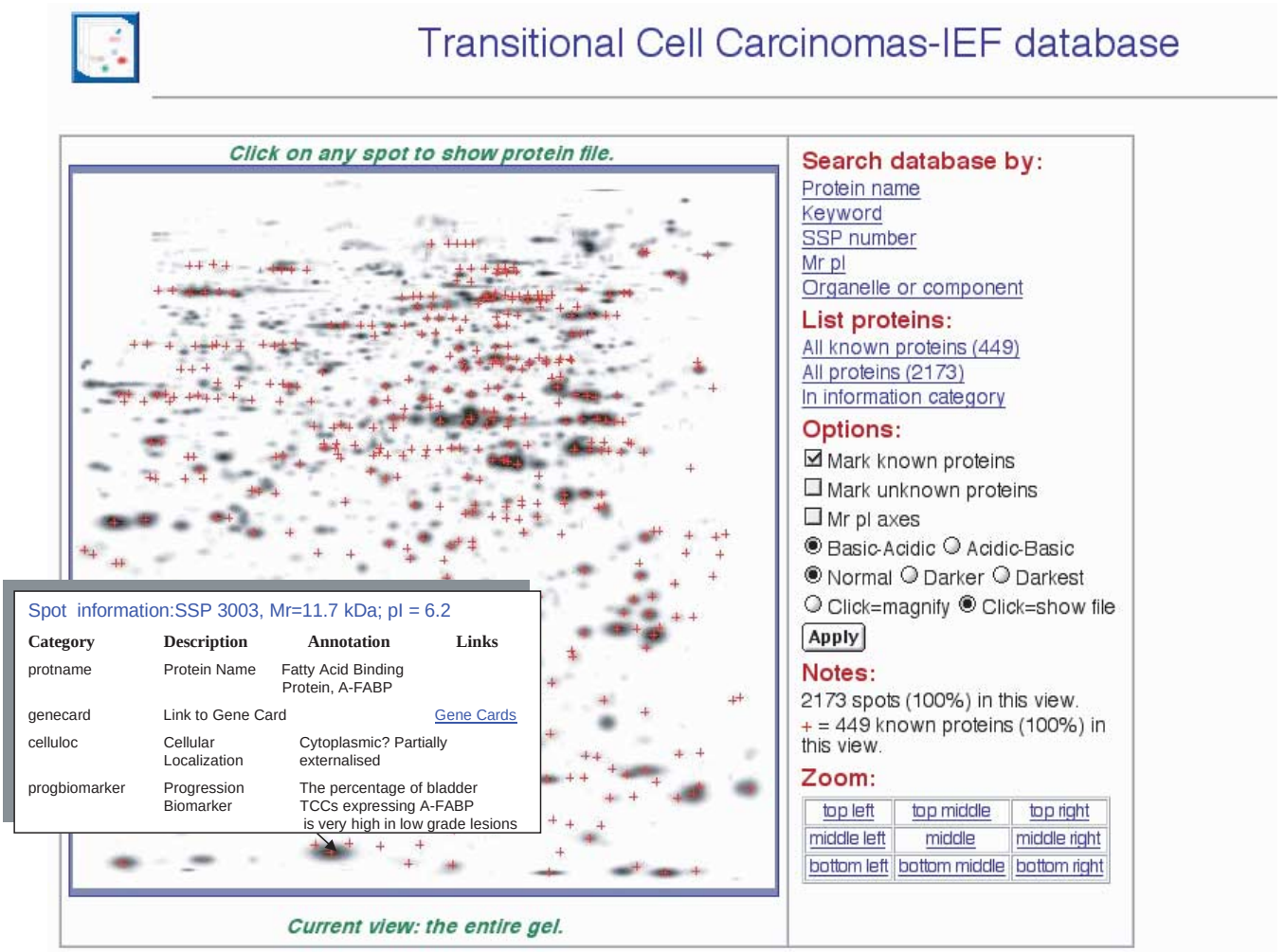

FIGURE 4 Master synthetic image of human bladder TCC proteins separated by IEF 2D PAGE as depicted in the Internet (http://proteomics.cancer.dk). Proteins flagged with a cross correspond to known proteins. By clicking on any spot, it is possible to open a file that contains protein information available in the database as well as links to other related Web sites. Only part of the file for A-FABP is shown.

systematic studies it is possible to store protein information in comprehensive 2D PAGE databases that record how genes are regulated in health and disease (see, e.g., http://proteomics.cancer.dk) (Fig. 4). As these databases achieve critical mass of data, they will become valuables sources of information for expediting the identification of signaling pathways and components that are affected in diseases (Celis *et al.*, 1991a,b, 1998; Gromov *et al.*, 2002).

V. PITFALLS

1. Do not heat the sample when dissolving in lysis solution or when defrosting.
2. For optimal results, titrate the ampholytes. Mix in various proportions, maintaining the final percentage fixed, and run first and second dimensions. Select the combination that gives the best separation (well-focused spots, no streaking, etc.). Store them at –20°C in 1- or 2-ml aliquots. Ampholytes can be stored for many years at –20°C.
3. Make sure that all glassware is washed properly. Rinse with glass-distilled water before drying.
4. The pH of the 1.5 *M* Tris–HCl, pH 8.8, solution should be checked carefully and regularly.
5. Use sterile, disposable pipettes to dispense the solutions. Do not allow other colleagues to use your solutions.

References

Anderson, N. L., and Anderson, N. G. (1978). Analytical technique for cell fractions. XXII. Two-dimensional analysis of serum and tissue proteins: Multiple gradient-slab gel electronporesis. *Anal. Biochem.* **85**, 341–354.

Bravo, R. (1984). Two-dimensional gel electrophoresis: A guide for the beginner. *In* "Two-Dimensional Gel Electrophoresis of Proteins: Methods and Applications" (J. E. Celis *et al.*, eds.), pp. 3–36. Academic Press, New York.

Celis, J. E. (ed.) (1996). Electrophoresis in cell biology. *Electrophoresis* **11**.

Celis, J. E., and Bravo, R. (eds.) (1984). "Two-Dimensional Gel Electrophoresis of Proteins: Methods and Applications." Academic Press, New York.

Celis, J. E., Gromov, P., Østergaard, M., Madsen, P., Honoré, B., Dejgaard, K., Olsen, E. Vorum, H., Kristensen, D. B., Gromova, I., Haunsø, A., Van Damme, J., Puype, M., Vandekerckhove, J., and Rasmussen, H. H. (1996). *FEBS Lett.* **398**, 129–134.

Celis, J. E., Leffers, H., Rasmussen, H. H., Madsen, P., Honore, B., Gesser, B., Dejgaard, K., Olsen, E., Ratz, G. P., Lauridsen, J. B., *et al.* (1991a). The master two-dimensional gel database of human AMA cell proteins: Towards linking protein and genome sequence and mapping information (update 1991). *Electrophoresis* **12**, 765–801.

Celis, J. E., Østergaard, M., Jensen, N. A., Gromova, I., Rasmussen, H. H., and Gromov, P. (1998). Human and mouse proteomic databases: Novel resources in the protein universe. *FEBS Lett.* **430**, 64–72.

Celis, J. E., Rasmussen, H. H., Leffers, H., Madsen, P., Honore, B., Gesser, B., Dejgaard, K., and Vandekerckhove, J. (1991b). Human cellular protein patterns and their link to genome DNA sequence data: Usefulness of two-dimensional gel electrophoresis and microsequencing. *FASEB J.* **5**, 2200–2208.

Celis, J. E., Rasmussen, H. H., Olsen, E., Gromov, P., Madsen, P., Leffers, H., Honoré, B., Dejgaard, K., Vorum, H., Kristensen, D. B., Østergaard, M., Haunsø, A., Jensen, N. A., Celis, A., Basse, B., Lauridsen, J. B., Ratz, G. P., Andersen, A. H., Walbum, E., Kjærgaard, I., Andersen, I., Puype, M., Van Damme, J., and Vandekerckhove, J. (1995). The human keratinocyte two-dimensional gel protein database (update 1995): Mapping components of signal transduction pathways. *Electrophoresis* **12**, 2217–2184.

Gromov. P., Østergaard, M., Gromova, I., and Celis, J. E. (2002). Human proteomic databases: A powerful resource for functional genomics in health and disease. *Prog. Biophys. Mol. Biol.* **80**, 3–22.

Klose, J. (1975). Protein mapping by combined isoelectric focusing and electrophoresis of mouse tissues: A novel approach to testing for induced point mutations in mammals. *Humangenetik* **26**, 231–243.

Laemmli, U. K. (1970). Cleavage of structural proteins during the assembly of the head of bacteriophage T4. *Nature (London)* **227**, 680–685.

Laskey, R. A., and Mills, A. D. (1975). Quantitative film detection of ^{3}H and ^{14}C in polyacrylamide gels by fluorography. *Eur. J. Biochem.* **56**, 335–341.

McDonald, W. H., and Yates, J. R., 3rd (2002). Shotgun proteomics and biomarker discovery. *Dis. Mark.* **18**, 99–105.

O'Farrell, P. H. (1975). High resolution two-dimensional electrophoresis of proteins. *J. Biol. Chem.* **250**, 4007–4021.

O'Farrell, P. Z., Goodman, H. M., and O'Farrell, P. H. (1977). High resolution two dimensional electrophoresis of basic as well as acidic proteins. *Cell* **12**, 1133–1142.

Ong, S. E., and Pandey, A. (2001) An evaluation of the use of two-dimensional gel electrophoresis in proteomics. *Biomol. Eng.* **18**, 195–205.

Wu, C. C., and McCoss, M. J. (2002). Shotgun proteomics: Tools for the analysis of complex biological systems. *Curr. Opin. Mol. Ther.* **4**, 242–250.

Yip, T. T., and Lomas, L. (2002). SELDI ProteinChip array in oncoproteomic research. *Cancer Res. Treatment* **1**, 273–274.

CHAPTER

23

High-Resolution Two-Dimensional Electrophoresis with Immobilized pH Gradients for Proteome Analysis

Angelika Görg and Walter Weiss

I. INTRODUCTION

Although promising progress has been made in the development of alternative protein separation techniques for proteome analysis, such as multidimensional chromatography–tandem mass spectrometry, there is still no generally applicable method that can replace two-dimensional gel electrophoresis (2D PAGE) in its ability to simultaneously separate and display thousands of proteins from complex biological samples. 2D PAGE separates proteins according to two independent parameters, i.e., isoelectric point (pI) in the first dimension and molecular mass (M_r) in the second dimension, by coupling isoelectric focusing (IEF) and sodium dodecyl sulfate polyacrylamide gel electrophoresis (SDS–PAGE). In comparison with the classical O'Farrell method (1975) of 2D PAGE based on the use of carrier ampholyte-generated pH gradients, 2D PAGE using immobilized pH gradients (IPG) in the first dimension (IPG-Dalt) (Görg *et al*., 1988) has proved to be extremely flexible with respect to the requirements of proteome analysis.

For proteome analysis it is essential to generate reproducible, high-resolution protein separations. Using the classical 2D PAGE approach of O'Farrell, it is, however, often difficult to obtain reproducible results even within a single laboratory, let alone between different laboratories. The problem of limited reproducibility is largely due to the synthetic carrier ampholytes (CA) used to generate the pH gradient required for IEF, for reasons such as batch-to-batch variability of CAs, pH gradient instability over time, cathodic drift etc. with resultant loss of alkaline proteins. These problems have been largely overcome by the development of immobilized pH gradients (IPG) (Bjellqvist *et al*., 1982) based on the use of the bifunctional Immobiline reagents, a series of 10 chemically well-defined acrylamide derivatives with the general structure CH_2=CH–CO–NH–R, where R contains either a carboxyl or an amino group. These form a series of buffers with different p*K* values between p*K* 1 and >12. Because the reactive end is copolymerized with the acrylamide matrix, extremely stable pH gradients are generated, allowing true steady-state IEF with increased reproducibility, as has been demonstrated in several interlaboratory comparisons (Corbett *et al*., 1994; Blomberg *et al*., 1995).

More than a decade ago, a basic protocol of IPG-Dalt was described by Görg *et al*. (1988), summarizing the critical parameters inherent to isoelectric focusing with IPGs and a number of experimental conditions that were not part of the classical 2D electrophoresis repertoire with CAs. In principle, this protocol is still valid today: The first dimension of IPG-Dalt, IEF, is performed in individual 3-mm-wide IPG gel strips cast on GelBond PAGfilm (either ready-made Immobiline DryStrips or laboratory made). Samples are applied either by cup loading or by in-gel rehydration. After IEF, the IPG strips are equilibrated with SDS buffer in the presence of urea, glycerol, dithiothreitol (DTT), and iodoacetamide and are applied onto horizontal or vertical SDS gels in the second dimension.

Copyright 2006, Elsevier Science (USA).
All rights reserved.

II. MATERIALS AND INSTRUMENTATION

Immobiline chemicals (Cat. Nos. 80125570–80125575), Pharmalyte pH 3–10 (Cat. No. 17-0456-01), Immobiline DryStrips pH 4–7, 3–10 and 3–10NL (Cat. Nos. 17-1233-01, 17-1234-01, and 17-1235-01), narrow-range Immobiline DryStrips covering the pH range between pH 3.5 and pH 6.7 (Cat. Nos. 17-6001-83–17-6001-87), ExcelGel SDS and buffer strips (Cat. No. 17-1236-01 and Cat. No. 80-1129-42), IEF electrode strips (Cat. No. 18-1004-40), CHAPS (Cat. No. 17-1314-01), acrylamide (Cat. No. 17-1302-01), *N*, *N*'-methylenebisacrylamide (Cat. No. 17-1304-01), TEMED (Cat. No. 17-1312-01), GelBond PAGfilm (Cat. No. 80-1129-37), and DryStrip cover fluid (Cat. No. 17-1335-01) are from Amersham Biosciences. Sodium dodecyl sulfate (SDS) (Cat. No. 20763), ammonium persulfate (Cat. No. 13375), glycine (Cat. No. 23390), kerosene (Cat. No. 26940), and ion exchanger (Serdolite MB-1, Cat. No. 40701) are from Serva. Trizma base (Cat. No. T-1503), DTT (Cat. No. D-0632), acrylamido buffers (p*K* 1.0, 10.3, and 12.0; Cat. No. 84885), thiourea (Cat. No. T8656), and iodoacetamide (Cat. No. I-6125) are from Sigma-Aldrich. Glycerol (Cat. No. 4093), urea (Cat. No. 84879), and a serine protease inhibitor (Pefabloc, Cat. No. 24839) are from VWR. Dimethylchlorosilane (Cat. No. 40140) is from Fluka. Water is deionized using the Milli-Q system of Millipore.

Apparatus for isoelectric focusing and horizontal SDS electrophoresis (Multiphor II, Cat. No. 18-1018-06), multiple vertical SDS electrophoresis (Ettan DALT Vertical System, Cat. No. 80-6466-46), thermostatic circulator (Multitemp III, Cat. No. 18-1102-78), power supply (Multidrive XL, Cat. No. 18-1013-68), IPGphor (Cat. No. 80-6469-88), IPGphor strip holders (Cat. No. 80-6416-68), cup-loading strip holders (Cat. No. 80-6459-43), IPG DryStrip reswelling tray (Cat. No. 80-6465-32), IPG DryStrip kit (Cat. No. 18-1004-30), and gradient gel kit (including glass plates with a 0.5-mm-thick U frame and gradient maker, Cat. No. 80-1013-74) are from Amersham Biosciences. Prior to use the glass plates are washed with a mild detergent, rinsed with deionized water, and air dried. If new glass plates are used, pipette 1–2 ml of dimethylchlorsilane (diluted 1 + 9 in trichlorethane) on the glass plate that bears the U frame and distribute it evenly with a fuzz-free filter paper. Let it dry for a few minutes, rinse again with water, and let it air dry. Repeat this procedure occasionally in order to prevent the gels from sticking to the glass plates.

III. PROCEDURES

A. Preparation of First-Dimensional IPG Gel Strips

Solutions

1. *Acrylamide/bisacrylamide solution (30% T, 3% C)*: 29.1% (w/v) acrylamide, 0.9% (w/v) *N*, *N*'-methylenebisacrylamide. To make 100 ml of the solution, dissolve 29.1 g of acrylamide and 0.9 g of bisacrylamide in deionized water and fill up to 100 ml. Add 1 g of Serdolite MB-1, stir for 10 min, and filter. This solution can be stored for 1 week at 4°C; however, for optimum results it is advisable to prepare it freshly the day you use it.

2. *Ammonium persulfate solution*: 40% (w/v) in deionized water. To prepare 1 ml of the solution, dissolve 0.4 g of ammonium persulfate in 1 ml of deionized water. This solution should be prepared freshly just before use.

3. *Solutions for casting immobiline gels*: To prepare 15 ml each of acidic and basic solutions, mix chemicals and reagent solutions as described in **Table I**. A huge selection of recipes for many types of narrow or broad pH gradient have been calculated (Righetti, 1990). Table I describes several of our favourate pH gradients for 2D electrophoresis.

Steps

IPG slab gels for 180-mm separation distance ($250 \times 180 \times 0.5\ mm^3$) are cast on GelBond PAGfilm. After polymerization, the IPG gels are washed extensively with deionized water, air dried, and stored frozen until used.

1. To assemble the polymerisation cassette, wet the plain glass plate (size $260 \times 200\ mm^2$) with a few drops of water. Place the Gelbond PAGfilm, hydrophilic side upward, on the wetted surface of the plain glass plate. The GelBond PAGfilm should overlap the upper edge of the glass plate for 1–2 mm to facilitate filling of the cassette. Expel excess water with a roller. Place the glass plate that bears the U frame (0.5 mm thick) on top of the Gelbond PAGfilm and clamp the cassette together (**Fig. 1A**). Put it in the refrigerator for 30 min.

2. To cast the IPG gel, pipette 12.0 ml of the acidic, dense solution into the mixing chamber of the gradient mixer. The outlet and connecting line between the mixing chamber and reservoir have to be closed! Add 7.5 µl of TEMED and 12 µl of ammonium persulfate and mix. Open the connecting line between the chambers for a second to release any air bubbles.

TABLE I Recipes for Casting Immobiline Gels with pH Gradients[a]

Linear pH gradient	pH 4–7		pH 4–9		pH 6–12		pH 4–12		pH 3–12	
	Acidic solution (pH 4)	Basic solution (pH 7)	Acidic solution (pH 4)	Basic solution (pH 9)	Acidic solution (pH 6)	Basic solution (pH 12)	Acidic solution (pH 4)	Basic solution (pH 12)	Acidic solution (pH 3)	Basic solution (pH 12)
Immobiline p*K* 1.0	—	—	—	—	—	—	—	—	1287 µl	—
Immobiline p*K* 3.6	578 l	302 µl	829 µl	147 µl	1367 µl	—	950 µl	—	306 µl	—
Immobiline p*K* 4.6	110 µl	738 µl	235 µl	424 µl	—	—	352 µl	74 µl	414 µl	—
Immobiline p*K* 6.2	450 µl	151 µl	232 µl	360 µl	188 µl	251 µl	319 µl	206 µl	558 µl	336 µl
Immobiline p*K* 7.0	—	269 µl	22 µl	296 µl	323 µl	125 µl	294 µl	103 µl	496 µl	168 µl
Immobiline p*K* 8.5	—	—	250 µl	71 µl	365 µl	84 µl	48 µl	522 µl	112 µl	699 µl
Immobiline p*K* 9.3	—	876 µl	221 µl	663 µl	497 µl	32 µl	52 µl	219 µl	84 µl	157 µl
Immobiline p*K* 10.0	—	—	—	—	50 µl	485 µl	41 µl	325 µl	25 µl	342 µl
Immobiline p*K* > 13	—	—	—	—	—	345 µl	—	531 µl	—	258 µl
Acrylamide/ bisacrylamide	2.0 ml	2.0 ml	2.0 ml	2.0 ml	2.25 ml	2.25 ml	2.5 ml	2.5 ml	2.25 ml	2.25 ml
deionized water	8.9 ml	10.7 ml	8.3 ml	11.1 ml	7.0 ml	10.5 ml	7.4 ml	10.5 ml	6.45 ml	10.8 ml
Glycerol (100%)	3.75 g	—	3.75 g	—	3.75 g	—	3.75 g	—	3.75 g	—
TEMED (100%)	10.0 µl	10.0 µl	10.0 µl	10.0 µl	10.0 µl	10.0 µl	10.0 µl	10.0 µl	10.0 µl	10.0 µl
Persulfate (40%)	15.0 µl	15.0 µl	15.0 µl	15.0 µl	15.0 µl	15.0 µl	15.0 µl	15.0 µl	15.0 µl	15.0 µl
Final volume	15.0 ml	15.0 ml	15.0 ml	15.0 ml	15.0 ml	15.0 ml	15.0 ml	15.0 ml	15.0 ml	15.0 ml

[a] For effective polymerization, acidic and basic solutions are adjusted to pH 7 with 4 *N* sodium hydroxide and 4 *N* acetic acid, respectively, before adding the poymerization catalysts (TEMED and ammonium persulfate).

3. Pipette 12.0 ml of the basic, light solution into the reservoir of the gradient mixer. Add 7.5 µl of TEMED and 12 µl of ammonium persulfate and mix with a spatula.

4. Switch on the magnetic stirrer at a reproducible and rapid rate; however, avoid excessive vortex. Remove the polymerisation cassette from the refrigerator and put it underneath the outlet of the gradient mixer. Open the valve connecting the chambers and, immediately afterwards, the pinchcock on the outlet tubing so that the gradient mixture is applied centrally into the cassette from a height of about 5 cm just by gravity flow. Formation of the gradient is completed in 2–3 min (**Fig. 1B**).

5. Keep the mold at room temperature for 15 min to allow adequate leveling of the density gradient. Then polymerize the gel for 1 h at 50°C in a heating cabinet.

6. After polymerization, wash the IPG gel for 1 h with 10-min changes of deionized water (500 ml each) in a glass tray on a rocking platform. Then equilibrate the gel in 2% (w/v) glycerol for 30 min and dry it overnight at room temperature, using a fan, in a dust-free cabinet. Afterward, protect the surface of the dry gel with a sheet of plastic film. The dried IPG gel can be stored in a sealed plastic bag at –20°C for at least several months without loss of function. Dried IPG gels in several pH ranges are also available commercially (Immobiline DryPlate).

7. For IEF in individual IPG gel strips, cut the dried IPG gels or the ready-made Immobiline DryPlates into 3-mm-wide strips with the help of a paper cutter (**Fig. 1C**). Alternatively, ready-cut IPG strips (Immobiline DryStrip) can also be used.

B. Running of First-Dimensional IPG Strips

The first dimension of IPG-Dalt, isoelectric focusing, is performed in individual 3-mm-wide IPG gel strips cast on GelBond PAGfilm. Instead of laboratory-made gels, ready-made gels (Immobiline DryStrip) can be used. Samples are applied either by in-gel rehydration or by cup loading after IPG strip rehydration (*see* **Table II and Fig. 2**). IPG-IEF can be simplified by using an integrated system, the IPGphor. This instrument features strip holders that provide rehydration of individual IPG strips with or without sample, optional separate sample cup loading, and subsequent IEF, all without handling the strip after it is placed in a ceramic strip holder.

Solutions

1. *Lysis solution*: 9.5 *M* urea, 2% (w/v) CHAPS, 2% (v/v) Pharmalyte pH 3–10, 1% (w/v) DTT. To prepare

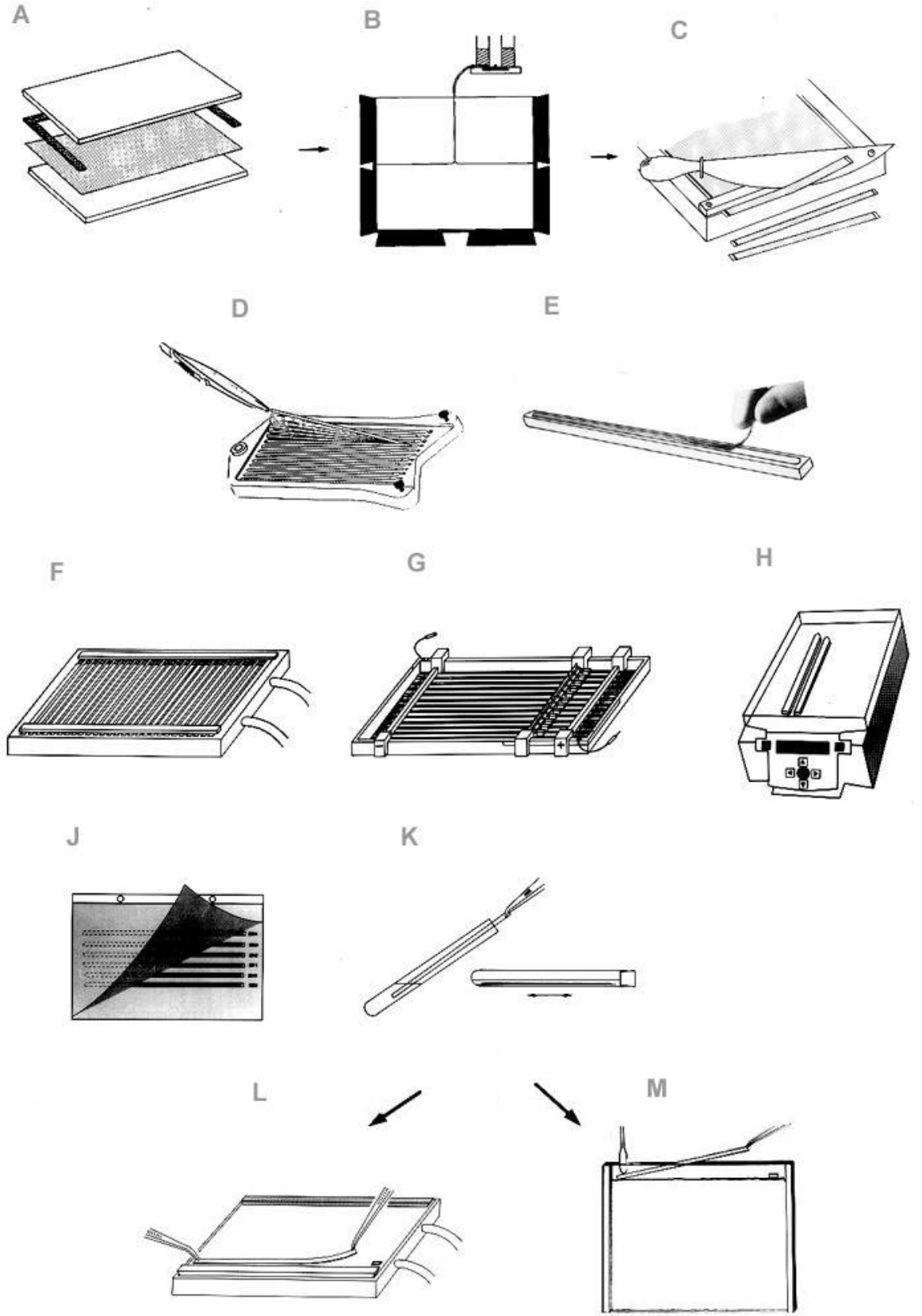

FIGURE 1 Procedure of IPG-Dalt (Görg *et al.*, 2000). (**A**) Assembly of the polymerisation cassette for the preparation of IPG and SDS gels on plastic backings (glass plates, GelBond PAGfilm and 0.5-mm-thick U frame). (**B**) Casting of IPG gels. (**C**) Cutting of washed and dried IPG slab gels (or IPG DryPlates) into individual IPG strips. (**D**) Rehydration of individual IPG strips in the IPG DryStrip reswelling tray. (**E**) Rehydration of individual IPG strips in the IPGphor strip holder. (**F**) IEF of individual IPG gel strips directly on the cooling plate of the IEF chamber. (**G**) IEF of individual IPG gel strips in the IPG DryStrip kit. (**H**) IEF of individual IPG gel strips on the IPGphor. (**J**) Storage of IPG strips after IEF. (**K**) Equilibration of IPG strips prior to SDS–PAGE. (**L**) Transfer of the equilibrated IPG strip onto onto the surface of a ready-made horizontal SDS gel along the cathodic buffer strip. (**M**) Loading of the equilibrated IPG strip onto onto the surface of a vertical SDS gel.

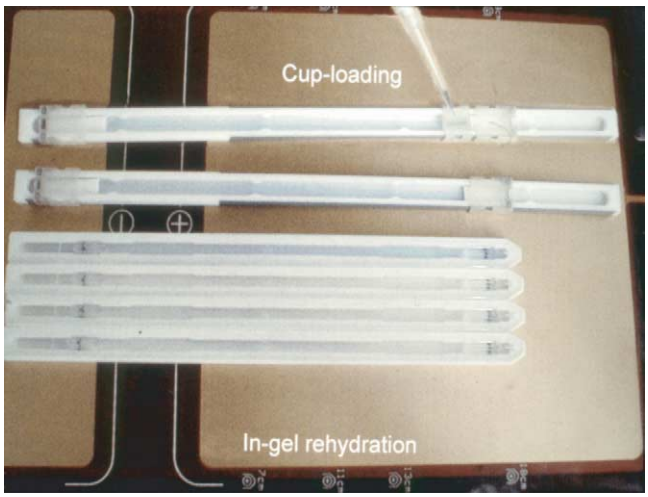

FIGURE 2 IPGphor: Sample application by in-gel rehydration and by cup loading.

TABLE II Sample Application

In-gel rehydration	Wide pH range IPGs between pH 3 and pH 12 (analytical and micropreparative runs)
Cup loading at the anode	Narrow pH range IPGs at the basic extreme (e.g., IPG 9–12)
Cup loading at the cathode	Narrow pH range IPGs at the acidic extreme (e.g., IPG 2.5–5)

50 ml of lysis solution, dissolve 30.0 g of urea in deionized water and make up to 50 ml. Add 0.5 g of Serdolite MB-1, stir for 10 min, and filter. Add 1.0 g of CHAPS, 0.5 g DTT, 1.0 ml of Pharmalyte pH 3–10, and 50 mg of Pefabloc to 48 ml of the urea solution.

2. *IPG strip rehydration solution*: 8 *M* urea, 0.5% (w/v) CHAPS, 15 m*M* DTT, 0.5% (v/v) Pharmalyte pH 3–10. To prepare 50 ml of the solution, dissolve 25.0 g of urea in deionized water and complete to 50 ml. Add 0.5 g of Serdolite MB-1, stir for 10 min, and filter. To 48 ml of this solution add 0.25 g of CHAPS, 0.25 ml Pharmalyte pH 3–10 (40% w/v), and 100 mg of DTT and complete to 50 ml with deionized water.

Notes

a. For solubilization of the more hydrophobic proteins, *thiourea/urea lysis solution* [2 *M* thiourea, 5–7 *M* urea, 2–4% (w/v) CHAPS, and/or sulfobetaine detergents, 1% DTT, 2% (v/v) carrier ampholytes] and *rehydration solution* consisting of a mixture of urea/thiourea [6 *M* urea, 2 *M* thiourea, 1% (w/v) CHAPS, 15 m*M* DTT, 0.5% (v/v) Pharmalyte pH 3–10] are recommended (Rabilloud *et al*., 1997).

b. Lysis solution and IPG strip rehydration solution should always be prepared freshly. Alternatively, small aliquots (1 ml) can be stored at –80°C. Lysis and rehydration solution thawn once should not be refrozen again. Never heat urea solutions above 37°C! Otherwise, protein carbamylation may occur.

c. It is important that the urea solution is deionized with an ion exchanger prior to adding the other chemicals because urea in aqueous solution exists in equilibrium with ammonium cyanate, which can react with the NH_3^+ of protein side chains (e.g., lysine) and introduce charge artifacts (= additional spots) on the 2D gel.

1. Rehydration of IPG DryStrips

Prior to IEF, the dried IPG strips must be rehydrated to their original thickness of 0.5 mm. IPG DryStrips are rehydrated either with sample already dissolved in rehydration buffer ("sample in-gel rehydration") or with rehydration buffer only, followed by sample application by "cup loading." Sample in-gel rehydration is generally not recommended for samples containing very high molecular weight, very alkaline, and/or very hydrophobic proteins, as these are taken up into the gel with difficulties only. In these cases, cup loading is preferred.

a. Rehydration of IPG DryStrips Using the IPG DryStrip Reswelling Tray

1. For *sample in-gel* rehydration (Rabilloud *et al*., 1994), directly solubilize a cell lysate or tissue sample (1–10 mg protein/ml) in an appropriate quantity of rehydration buffer. For 180-mm-long and 3-mm-wide IPG dry strips, pipette 350 µl of this solution into the grooves of the IPG DryStrip reswelling tray (**Fig. 1D**). For longer or shorter IPG strips, the rehydration volume has to be adjusted accordingly.

2. Remove the protective covers from the surface of the IPG DryStrips and apply the IPG strips, gel side down, into the grooves without trapping air bubbles. Then cover the IPG strip, which must still be moveable and not stick to the tray, with silicone oil (which prevents drying out during reswelling) or IPG cover fluid and rehydrate the strips overnight at approximately 20°C. Higher temperatures (>37°C) hold the risk of protein carbamylation, whereas lower temperatures (<10°C) should be avoided to prevent urea crystallization on the IPG gel.

3. For *cup loading*, rehydrate the IPG dry strips overnight in rehydration buffer in the reswelling tray as described earlier, however without sample.

b. Sample In-Gel Rehydration of IPG DryStrips Using IPGphor Strip Holders

1. Solubilize proteins in sample solubilization buffer and dilute the extract (protein concentration ≈10 mg/ml) with IPG strip rehydration solution (dilution: 1 + 1 for micropreparative runs, and 1 + 19 for analytical runs, respectively) to a final volume of 350–400 µl for 180-mm-long IPG strips.

2. Apply the required number of IPGphor strip holders (**Fig. 1E**) onto the cooling plate/electrode contact area of the IPGphor.

3. Pipette 350 µl of sample-containing rehydration solution (for 180-mm-long IPG strips) into the strip holder base. For shorter (e.g., 110 mm) IPG strips in shorter strip holders, use correspondingly less liquid.

4. Peel off the protective cover sheets from the IPG strip and slowly lower the IPG strip (gel side down) onto the rehydration solution. Avoid trapping air bubbles. The IPG strip must still be moveable and not stick to the tray. Cover the IPG strips with 1–2 ml of cover fluid and apply the plastic cover. Pressure blocks on the underside of the cover assure that the IPG strip keeps in good contact with the electrodes as the gel swells.

2. IEF on the Multiphor Flat-Bed Electrophoresis Apparatus

1. After IPG DryStrip rehydration, rinse the rehydrated IPG strips with distilled water for a few seconds and then blot them between two sheets of moist filter paper to remove excess rehydration buffer in order to avoid urea crystallization on the gel surface, which is held responsible for prolonged IEF and "empty" vertical lanes in the 2D pattern.

2. Apply up to 40 IPG strips (*rehydrated with or without sample solution*) side by side and 1–2 mm apart onto the surface of the kerosene-wetted cooling plate (**Fig. 1F**) of the horizontal flat-bed electrophoresis apparatus (e.g., Multiphor, Amersham Biosciences). It is of utmost importance that the acidic ends of the IPG gel strips face towards the anode.

3. Soak electrode paper strips (cut from 1-mm-thick filter paper, e.g., MN 440, Machery & Nagel) with deionized water, blot against filter paper to remove excess liquid, and place them on top of the aligned IPG gel strips at the cathodic and anodic ends. If samples have already been applied by sample in-gel rehydration, proceed as described in step 5).

4. In case of sample application by cup loading, apply the samples (20 µl; protein concentration 5–10 mg/ml) into silicon rubber frames (size: 2×5 mm^2) or special sample cups placed at either the anodic or the cathodic end of the IPG strips. (see **Fig. 1F**). For analytical purposes, load 50–100 µg of protein onto a single, 180-mm-long IPG gel strip. For micropreparative purposes, up to several milligrams of protein may be applied with the help of a special strip tray, the IPG DryStrip kit (**Fig. 1G**) (*see* **Notes**).

5. Position the electrodes and press them down on top of the IEF electrode paper strips. Place the lid on the electrofocusing chamber, connect the cables to the power supply, and start IEF. For maximal sample entry, the initial voltage should be limited to 150 V for 60 min and then increased progressively until 3500 V is attained. Current and power settings should be limited to 0.05 mA and 0.2 W per IPG strip, respectively. The optimum focusing temperature is 20°C (Görg *et al*., 1991). The time required for the run depends on several factors, including the type of sample, the amount of protein applied, the length of the IPG strips, and the pH gradient being used. Some typical running conditions are given in **Table III** (Görg *et al*., 2000).

6. After termination of IEF, the IPG strips can be used immediately for the second dimension. Alternatively, strips can be stored between two sheets of plastic film at –70°C for several months.

Notes

a. When basic IPG gradients are used for the first dimension (e.g., IPG 6–10), horizontal streaking can often be observed at the basic end of 2D protein profiles. This problem may be resolved by applying an extra electrode strip soaked in 20 m*M* DTT on the surface of the IPG strip alongside the cathodic electrode strip (Görg *et al*., 1995). This has the advantage that the DTT within the gel, which migrates towards the anode during IEF, is replenished by the DTT released from the strip at the cathode. Alternative approaches are (i) to use the noncharged reducing agent, tributyl phosphine, which does not migrate during IEF (Herbert, 1999), (ii) to substitute DTT in the rehydration buffer of the IPG strip by a disulfide such as hydroxyethyl disulfide (Olsson *et al*., 2002), or (iii) to apply high voltages (8000 V) for short running times (Wildgruber *et al*., 2002).

b. After sample entry, the filter papers beneath the anode and cathode should be replaced with fresh ones. This is because salt contaminants have quickly moved through the gel and have now collected in the electrode papers. For high salt and/or protein concentrations, it is recommended to change the filter paper strips several times. In case of IEF with very alkaline, narrow range IPGs, such as IPG 10–12, this procedure should be repeated once an hour.

c. For micropreparative IEF or for running very alkaline IPGs exceeding pH 10, a special strip tray (IPG DryStrip kit) is recommeded that has a frame that fits

TABLE III Running Conditions Using the Multiphor

Gel length	180 mm				
Temperature	20°C				
Current max.	0.05 mA per IPG strip				
Power max.	0.2 W per IPG strip				
Voltage max.	3500 V				
I. Analytical IEF					
Initial IEF					
Cup loading (20–50 µl)					
150 V, 1 h					
300 V, 1–3 h					
600 V, 1 h					
In-gel rehydration (350 µl)					
150 V, 1 h					
300 V, 1–3 h					
IEF to the steady state at 3500 V					
1–1.5 pH units		**4 pH units**		**7 pH units**	
e.g., IPG 5–6	24 h	IPG 4–8	10 h	IPG 3–10 L	6 h
e.g., IPG 4–5.5	20 h	IPG 6–10	10 h	IPG 3–10 NL	6 h
3 pH units		**5–6 pH units**		**8–9 pH units**	
IPG 4–7	12 h	IPG 4–9	8 h	IPG 3–12	6 h
IPG 6–9	12 h	IPG 6–12	8 h	IPG 4–12	8 h
II. Extended Separation Distances (240 mm)					
IEF to the steady state at 3500 V					
IPG 3–12	8 h				
IPG 4–12	12 h				
IPG 5–6	40 h				
III. Micropreparative IEF					
Initial IEF					
Cup loading (100 µl)					
50 V, 12–16 h					
300 V, 1 h					
In-gel rehydration (350 µl)					
50 V, 12–16 h					
300 V, 1 h					
IEF to the steady state at 3500 V					
Focusing time of analytical IEF plus approximately 50%					

[a] From Görg *et al*. (2000).

on the cooling plate of the Multiphor (**Fig. 1G**). This tray is equipped with a corrugated plastic plate that contains grooves allowing easy alignment of the IPG strips. In addition, the tray is fitted with bars carrying the electrodes and a bar with sample cups allowing application of samples at any desired point on the gel surface. The advantages are that the cups can handle a larger quantity of sample solution (100 µl can be applied at a time, but it is possible to apply a total of up to 200 µl portion by portion, onto a single IPG gel), and the frame allows one to cover the IPG strips with a layer of silicone oil that protects the gel from the effects of the atmosphere during IEF. In case of very basic pH gradients exceeding pH 10 (e.g., IPG 3–12, 4–12, 6–12, 9–12, 10–12) or narrow-range ("zoom" gels) pH gradients with 1.0 or 1.5 pH units with extended running time (>24 h), the IPG strips *must* be covered by a layer of silicone oil.

d. In case of cup loading, it is not recommended to apply proteins at (or proximate to) the pH area that corresponds with their pl in order to avoid that they are uncharged and poorly soluble and thus prone to precipitation at the sample application site.

e. The IEF run should be performed at 20°C, as at lower temperatures there is a risk of urea crystallization and at higher temperatures carbamylation might occur. Precise temperature control is also important because it has been found that alterations in the relative positions of some proteins on the final 2D patterns may happen (Görg, 1991).

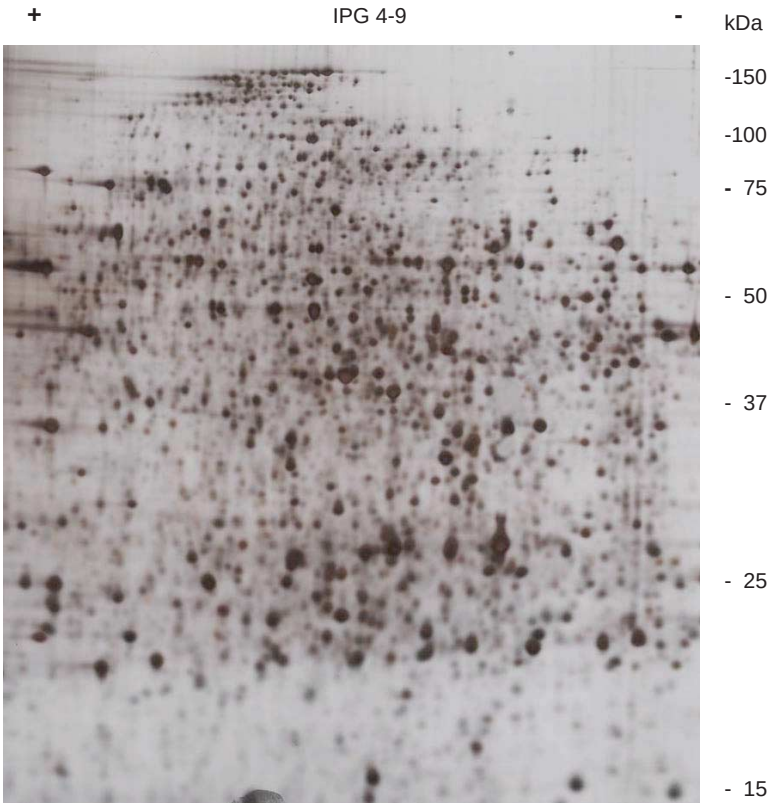

FIGURE 3 IPG-Dalt of mouse liver proteins. First dimension: IEF with IPG 4–9 run on the IPGphor. Separation distance: 24 cm. Sample application by cup loading near the anode. Second dimension: vertical SDS–PAGE, 13% T. Silver stain.

3. *IEF on the IPGphor*

Using the IPGphor, sample in-gel rehydration and IEF can be carried out automatically according to the programmed settings, preferably overnight. Alternatively, the IPGphor can also be used with a cup-loading procedure, which allows the application of quantities up to 100 µl. The instrument can accommodate up to 12 individual strip holders and incorporates Peltier cooling with precise temperature control and a programmable 8000-V power supply. The IPGphor saves about a day's worth of work by combining sample application and rehydration, as well as by starting the run at preprogrammed times, and by running the IEF at rather high voltages (Fig. 3).

a. IEF following In-Gel Rehydration of Sample

1. Apply the required number of strip holders onto the cooling plate/electrode contact area of the IPGphor. Pipette the appropriate amount of sample-containing rehydration solution into the strip holders, lower the IPG dry strips gel side down into the rehydration solution, and overlay with cover fluid (**Fig. 1E**).

2. Program the instrument (**Fig. 1H**) (desired rehydration time, volthours, voltage gradient). Apply low voltage (30–50 V) during IPG strip rehydration for improved entry of high M_r proteins into the polyacrylamide gel matrix (Görg *et al*., 1999, 2000).

3. After the IPG gel strips have been rehydrated (which requires 6 h at least, but typically overnight), IEF starts according to the programmed parameters (*see* **Table IV**).

4. After completion of IEF, store those IPG gel strips that are not used immediately for a second-dimension run between two sheets of plastic film at –70°C (**Fig. 1J**).

b. IEF after Sample Application by Cup Loading

When protein separation is performed in basic pH ranges, much better separations are obtained by applying sample *via* cup loading on separately rehydrated IPG strips than by sample in-gel rehydration. Sample cup loading is accomplished with a special cup-loading ("universal") IPGphor strip holder.

TABLE IV IPGphor Running Conditions[a]

Gel length	180 mm		
Temperature	20°C		
Current max.	0.05 mA per IPG strip		
Voltage max.	8000 V		
I. Analytical IEF			
Reswelling	30 V, 12–16 h		
Initial IEF:	200 V, 1 h		
	500 V, 1 h		
	1000 V, 1 h		
IEF to the steady state:	Gradient from 1000 to 8000 V within 30 min		
	8000 V to the steady state, depending on the pH used used		
1–1.5 pH units	**4 pH units**	**7 pH units**	
e.g., IPG 5–6 8 h	IPG 4–8 4 h	IPG 3–10 L	3 h
e.g., IPG 4–5.5 8 h		IPG 3–10 NL	3 h
3 pH units	**5–6 pH units**	**8–9 pH units**	
IPG 4–7 4 h	IPG 4–9 4 h	IPG 3–12	3 h
		IPG 4–12	3 h
II. Micropreparative IEF			
Reswelling	30 V, 12–16 h		
IEF to the steady state	Focusing time of analytical IEF + additional 50% (approximate)		

[a] From Görg *et al*. (2000).

1. Rehydrate IPG dry strips with rehydration buffer, without sample, in an IPG DryStrip reswelling tray (**Fig. 1D**) as described earlier for the Multiphor instrument.

2. Apply the required number of the cup-loading IPGphor strip holders onto the cooling plate/electrode contact area of the IPGphor instrument (**Fig. 1H**), and apply the rehydrated IPG gel strips into the cup-loading strip holders, gel side upwards and acidic ends facing towards the anode.

3. Moisten two filter paper electrode pads (size: 4 × 10 mm^2) with deionzed water, remove excess liquid by blotting with a filter paper, and apply the moistened filter paper pads at the anodic and cathodic ends of the IPG strip between the IPG gel and the electrodes. This is particularly important when analyzing samples containing high salt amounts.

4. Position the movable electrodes above the electrode filter paper pads and gently press the electrodes on the filter papers. Filter papers should be replaced after 2–3 h.

5. Position the movable sample cup near either the anode or the cathode and gently press the sample cup onto the surface of the IPG gel strip. Overlay the IPG strip with 5 ml of cover fluid (do not use silicone oil or kerosene!). If cover fluid leaks into the sample cup, rearrange the cup and remove the cover fluid from the cup with the help of tissue paper. Check again for leakage before pipetting the sample (20–100 µl) into the cup.

6. Program the instrument (desired volt hours, voltage gradient, temperature, etc.) and run IEF according to the settings recommended in **Table IV**.

Note

When IPG strips with separation distances <11 cm are used, voltage should be limited to 5000 V.

C. Second Dimension: Horizontal SDS Gel Electrophoresis

Solutions

1. *Tris–HCl buffer*: 1.5 *M* Tris–HCl, pH 8.8, 0.4% (w/v) SDS. To make 250 ml, dissolve 45.5 g of Trizma base and 1 g of SDS in about 200 ml of deionized water. Adjust the pH of the solution with 4 *N* HCl and fill up to 250 ml with deionized water. Add 25 mg of sodium azide and filter. The buffer can be stored at 4°C up to 2 weeks.

2. *Equilibration buffer*: 6 *M* urea, 30% (w/v) glycerol, 2% (w/v) SDS in 0.05 *M* Tris–HCl buffer, pH 8.8. To make 500 ml, add 180 g of urea, 150 g of glycerol, 10 g of SDS, and 16.7 ml of gel buffer. Dissolve in deionized water and fill up to 500 ml. The buffer can be stored at room temperature up to 2 weeks.

3. *Bromphenol blue solution*: 0.25% (w/v) of bromphenol blue in stacking gel buffer. To make 10 ml, dissolve 25 mg of bromphenol blue in 10 ml of gel buffer. Store at 4°C.

Steps

For the second dimension, an SDS pore gradient gel (0.5 mm thick on GelBond PAGfilm) is applied on the cooling plate of the horizontal electrophoresis unit. Then the equilibrated IPG gel strip is simply placed gel side down onto the surface of the SDS gel alongside the cathodic electrode buffer strip without any embedding procedure. Horizontal setups are particularly suited for the use of ready-made gels on film supports. This section describes the procedure for ready-made ExcelGels. For casting and running of laboratory-made horizontal SDS gels, *see* Görg and Weiss (2000).

1. Equilibration of IPG Gel Strips

The IPG gel strips are equilibrated twice, 15 min each (*see* **Table V**). During the second equilibration, 260 m*M* iodoacetamide is added to the equilibration buffer in order to remove excess DTT (responsible for the "point streaking" in silver-stained patterns) and to alkylate sulfhydryl groups for subsequent MALDI-MS.

1. Dissolve 100 mg of DTT in 10 ml of equilibration buffer (= equilibration buffer I). Take out the focused IPG gel strips from the freezer and place them into individual test tubes (200 mm long, 20 mm i.d.). Add 10 ml of equilibration buffer I and 50 µl of the bromphenol blue solution. Seal the test tubes with Parafilm, rock them for 15 min on a shaker (**Fig. 1K**), and then pour off the equilibration buffer.

TABLE V Equilibration of IPG Strips

Reagent	Purpose
50 m*M* Tris–HCl, pH 8.8	
+2% SDS	Improved protein transfer onto SDS gel
+6 *M* urea	Improved protein transfer onto SDS gel
+30% glycerol	Improved protein transfer onto SDS gel
+1% DTT	Complete reduction of disulphide bonds
+4.8% iodoacetamide	Removal of excess DTT (point streaking) Alkylation of SH groups for MALDI-MS

	DTT	Iodoacetamide
First step 15 min	+	–
Second step 15 min	–	+

2. Dissolve 480 mg of iodoacetamide in 10 ml of equilibration buffer (= equilibration buffer II). Add equilibration buffer II and 50 µl of bromophenol blue solution to the test tube as just described and equilibrate for another 15 min on a rocker.

3. After the second equilibration, place the IPG gel strip on a piece of moist filter paper to remove excess equilibration buffer. The strip should be turned up at one edge for a few minutes to drain off excess equilibration buffer.

2. Horizontal SDS–PAGE with Ready-Made Gels

Ready-made SDS gels (ExcelGel, 250 × 200 × 0.5 mm^3, on plastic backing; Amersham Biosciences) in combination with polyacrylamide buffer strips are used.

1. Equilibrate the IPG gel strips as described earlier (**Table V**).

2. While the strips are being equilibrated, begin the assembly of the SDS ExcelGel for the second dimension: Remove the ExcelGel from its foil package. Pipette 2–3 ml of kerosene on the cooling plate of the horizontal electrophoresis unit (15°C). Remove the protective cover from the top of the ExcelGel and place the gel on the cooling plate, with cut-off edge toward the anode. Avoid trapping air bubbles between the gel and the cooling block.

3. Peel back the protective foil of the cathodic SDS buffer strip. Wet your gloves with a few drops of deionized water and place the buffer strip on the cathodic end of the gel. Avoid trapping air bubbles between gel surface and buffer strip.

4. Repeat this procedure with the anodic buffer strip.

5. Place the equilibrated IPG gel strips gel side down on the surface of the ExcelGel, 2–3 mm apart from the cathodic buffer strip (**Fig. 1L**).

6. Press gently on top of the IPG gel strips with forceps to remove any trapped air bubbles.

7. Align the electrodes with the buffer strips and lower the electrode holder carefully onto the buffer strips.

8. Start SDS–PAGE at 100 V for about 60 min with a limit of 20 mA. When the bromphenol blue tracking dye has moved 4–5 mm from the IPG gel strip, interrupt the run, remove the IPG gel strip, and move the cathodic buffer strip forward so that it just covers the former contact area of the IPG gel strip. Readjust the electrodes and continue with electrophoresis at 800 V and 35 mA for about 180 min until the bromphenol blue dye front has reached the anodic buffer strip.

9. Proceed with protein staining with Coomassie blue, silver nitrate, or fluorescent dyes or with blotting.

D. Second Dimension: Multiple Vertical SDS–Polyacrylamide Gel Electrophoresis

First-dimension IEF and the equilibration step are performed as described previously, no matter whether the second dimension is run horizontally or vertically. After equilibration, the IPG gel strip is placed on top of the vertical SDS gel, with or without embedding in agarose.

Vertical SDS–PAGE is performed as described by Görg & Weiss (2000). A stacking gel is usually not necessary. For multiple runs, the Ettan DALT II (Amersham Biosciences) vertical electrophoresis apparatus is recommended because this system allows a large batch of SDS slab gels (up to 12) to be run under identical conditions. Ready-made gels on plastic backing are also available (Amersham Biosciences).

Solutions

1. *Gel buffer*: 1.5 *M* Tris–HCl, pH 8.6, 0.4% (w/v) SDS (Laemmli, 1970).

To make 500 ml, dissolve 90.85 g of Trizma base and 2.0 g of SDS in about 400 ml of deionized water. Adjust to pH 8.6 with 4 *N* HCl and fill up to 500 ml with deionized water. Add 50 mg of sodium azide and filter. The buffer can be stored at 4°C up to 2 weeks.

2. *Acrylamide/bisacrylamide solution (30.8% T, 2.6% C)*: 30% (w/v) acrylamide, 0.8% (w/v) methylenebisacrylamide in deionized water. To make 1000 ml, dissolve 300.0 g of acrylamide and 8.0 g of methylenebisacrylamide in deionized water and fill up to 1000 ml. Add 1 g of Serdolit MB-1, stir for 10 min, and filter. The solution can be stored up to 2 weeks in a refrigerator.

3. *Ammonium persulfate solution*: 10% (w/v) of ammonium persulfate in deionized water. To prepare 10 ml of the solution, dissolve 1.0 g of ammonium persulfate in 10 ml of deionized water. This solution should be prepared freshly just before use.

4. *Displacing solution*: 50% (v/v) glycerol in deionized water, 0.01% (w/v) bromphenol blue. To make 500 ml, mix 250 ml of glycerol (100%) with 250 ml of deionized water, add 50 mg of bromphenol blue, and stir for a few minutes.

5. *Overlay buffer*: Buffer-saturated 2-butanol. To make 30 ml, mix 20 ml of gel buffer with 30 ml of 2-butanol, wait for a few minutes, and pipette off the butanol layer.

6. *Electrode buffer*: To make 5 liter of electrode buffer stock solution, dissolve 58.0 g of Trizma base, 299.6 g of glycine, and 19.9 g of SDS in deionized water and complete to 5.0 liter.

7. *Equilibration buffer*: 6 *M* urea, 30% (w/v) glycerol, 2% (w/v) SDS in 0.05 *M* Tris–HCl buffer, pH 8.6. To make 500 ml, add 180 g of urea, 150 g of glycerol, 10 g of SDS, and 16.7 ml of gel buffer. Dissolve in deionized water and fill up to 500 ml. The buffer can be stored at room temperature up to 2 weeks.

8. *Agarose solution*: Suspend 0.5% (w/v) agarose in electrode buffer and melt it in a boiling water bath or in a microwave oven.

1. Casting of Vertical SDS Gels

Steps

1. The polymerisation cassettes (200×250 mm^2) are made in the shape of books consisting of two glass plates connected by a hinge strip with two 1.0-mm-thick spacers in between them.

2. Stack 14 cassettes vertically into the gel-casting box with the hinge strips to the right, interspersed with plastic sheets (e.g., 0.05-mm-thick polyester sheets).

3. Put the front plate of the casting box in place and screw on the nuts (hand tight).

4. Connect a polyethylene tube (*i.d.* 5 mm) to a funnel held in a ring stand at a level of about 30 cm above the top of the casting box. Place the other end of the tube in the grommet in the casting box side chamber.

5. Fill the side chamber with 100 ml of displacing solution.

6. Immediately before gel casting, add TEMED and ammonium persulfate solutions to the gel solution (**Table VI**). To cast the gels, pour the gel solution (about 830 ml) into the funnel. Avoid introduction of any air bubbles into the tube!

7. When pouring is complete, remove the tube from the side chamber grommet so that the level of the displacing solution in the side chamber falls.

8. Very carefully pipette about 1 ml of overlay buffer onto the top of each gel in order to obtain a smooth, flat gel top surface.

TABLE VI Recipes for Casting Vertical SDS Gels

	7.5% T 2.6% C	10% T 2.6% C	12.5% T 2.6% C	15% T 2.6% C
Acrylamide/ bisacrylamide (30.8%T, 2.6%C)	202 ml	270 ml	337 ml	404 ml
gel buffer	208 ml	208 ml	208 ml	208 ml
Glycerol (100%)	41 g	41 g	41 g	41 g
Deionized water	383 ml	315 ml	248 ml	181 ml
TEMED (100%)	42 µl	42 µl	42 µl	42 µl
Ammonium persulfate (10%)	6.0 ml	6.0 ml	6.0 ml	6.0 ml
Final volume	830 ml	830 ml	830 ml	830 ml

9. Allow the gels to polymerize for at least 3 h (better: overnight) at approximately 20°C.

10. Remove the front of the casting box and carefully unload the gel cassettes from the box using a razor blade to separate the cassettes. Remove the polyester sheets that had been placed between the individual cassettes.

11. Wash each cassette with water to remove any acrylamide adhered to the outer surface and drain excess liquid off the top surface. Discard unsatisfactory gels; in general the gels opposite to the front and rear plate of the gel casting box (due to the uneven thickness of these gels).

12. Gels not needed at the moment can be wrapped in plastic wrap and stored in a refrigerator (4°C) for 1–2 days.

2. Multiple Vertical SDS–PAGE Using Ettan Dalt II

Steps

1. Pour 1875 ml of electrode buffer stock solution and 5625 ml of deionized water in the lower electrophoresis buffer tank and turn on cooling (20°C).

2. Support the SDS gel cassettes in a vertical position to facilitate application of the first-dimension IPG gel strips.

3. Equilibrate the IPG gel strip as described earlier for horizontal SDS gels. Immerse it in SDS electrode buffer for a few seconds to facilitate insertion of the IPG strip between the two glass plates of the gel cassette.

4. Place the IPG gel strip on top of an SDS gel and overlay it with 2 ml of hot agarose solution (75°C). Carefully press the IPG strip with a spatula onto the surface of the SDS gel to achieve complete contact (**Fig. 1M**). If it is desired to coelectrophorese M_r marker proteins, soak a piece of filter paper (2×4 mm^2) with 5 µl of SDS marker proteins dissolved in electrophoresis buffer, let it dry (!), and apply it to the left or right of the IPG strip. Allow the agarose to solidify for at least 5 min and then place the slab gel into the electrophoresis apparatus (*see* later). Repeat this procedure for the remaining IPG strips. *Note*: Embedding in agarose is not absolutely necessary, but it ensures better contact between the IPG gel strip and the top of the SDS gel.

5. Wet the gel cassettes by dipping then into electrode buffer for a few seconds and then insert them in the electrophoresis apparatus. Pour 1250 ml of electrophoresis buffer stock solution and 1250 ml of deionized water in the upper electrophoresis tank, mix, and start SDS electrophoresis.

6. Run the SDS–PAGE gels with 50 mA (100 V maximum setting) for about 2 h. Then continue with 175 mA (200 V maximum setting) for about 16 h. *Note*: In contrast to the procedure of horizontal SDS–PAGE it is not necessary to remove the IPG gel strips from the surface of the vertical SDS gel once the proteins have migrated out of the IPG gel strip.

7. Terminate the run when the bromphenol blue tracking dye has migrated off the lower end of the gel.

8. Open the cassettes carefully with a plastic spatula. Use the spatula to separate the agarose overlay from the polyacrylamide gel. Peel the gel from the glass plate carefully, lifting it by the lower edge, and place it in a box of stain solution or transfer buffer, respectively. Then continue with protein staining or blotting.

IV. COMMENTS

Since the early 1990s, IPG-Dalt has constantly been refined to meet the requirements of proteome analysis. In particular, (i) the development of basic IPGs up to pH 12 has facilitated the analysis of very alkaline proteins (Görg *et al*., 1997, 1998, 1999; Wildgruber *et al*. 2002); (ii) the introduction of overlapping narrow-range IPGs to stretch the first dimension permits increased resolution (Δ pI = 0.01/cm) (Görg *et al*., 1988), as well as higher loading capacity for the analysis of less abundant proteins (Wildgruber *et al*., 2000); and (iii) the availability of ready-made IPG strips and integrated devices such as the IPGphor (Islam *et al*., 1998) have paved the way towards automation (Görg *et al*., 1999, 2000) (Fig. 4).

Using the protocols described in this article, it is possible to resolve proteins having apparent molecular masses between 10 and 200 kDa and pI values from 2.5 to 12. The protein-loading capacity for micropreparative runs is up to several milligrams of protein if narrow pH range IPGs (0.5–1 pH units wide) are used.

V. PITFALLS

1. Blot the rehydrated IPG gel strips to remove excess rehydration solution; as urea crystallization on the surface of the IPG gel strips might occur, which will disturb IEF patterns or prolong focusing time to reach the steady state.

2. Make sure that the orientation of the IPG gel strips on the cooling block of the IEF chamber is correct (acidic end towards anode). Check the temperature of the cooling block (20°C).

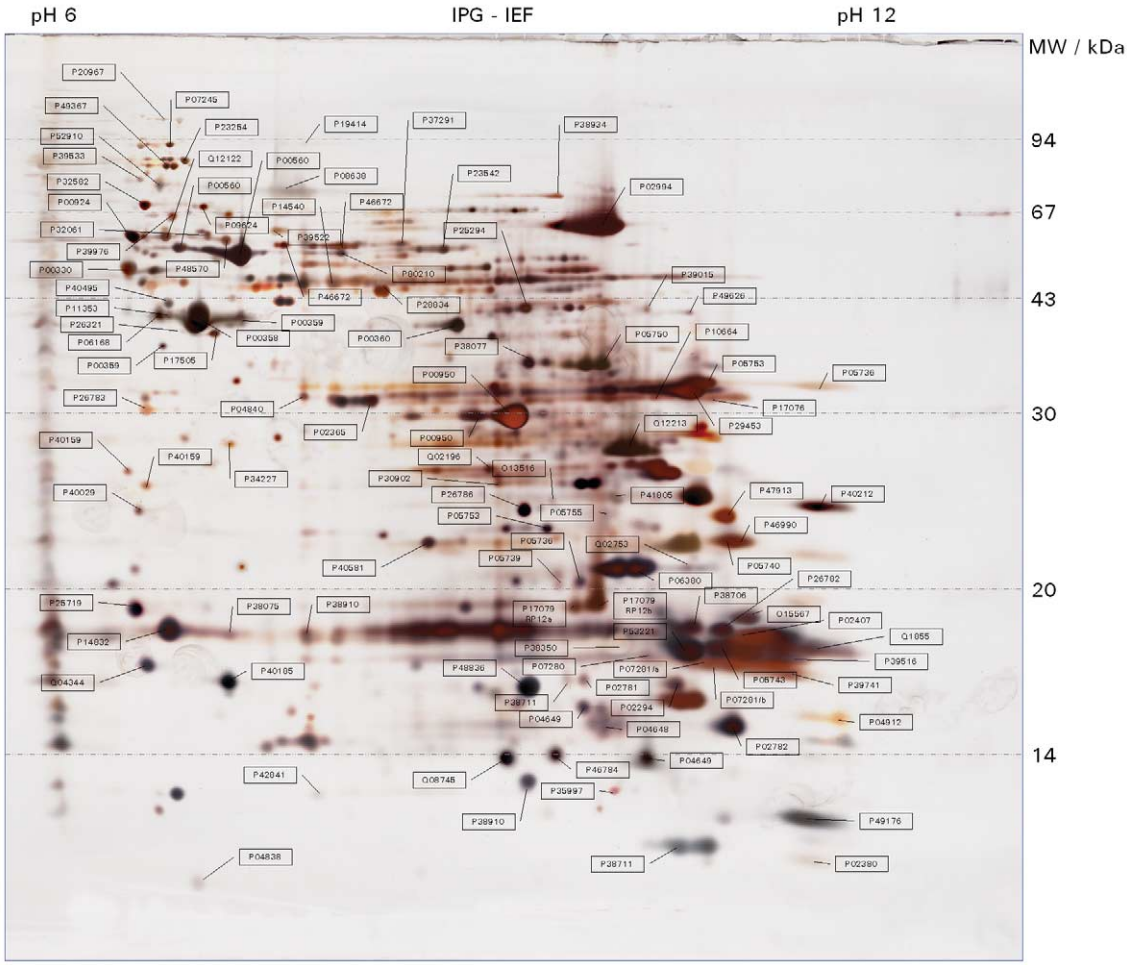

FIGURE 4 Web-based 2D reference map of alkaline *Saccharomyces cerevisiae* (strain FY1679) proteins showing 106 mapped and identified spots annotated by SWISS-PROT accession numbers. First dimension: IPG 6–12. Second dimension: SDS–PAGE, 15% T. Spot identification by MALDI-TOF-MS (Ettan z^2 MALDI-TOF, Amersham Biosciences) (with permission from Wildgruber *et al*., 2002) (http://www.wzw.tum.de/proteomik).

3. The sample solution should not be too concentrated to avoid protein precipitation at the sample application point. If you are in doubt, dilute the sample with lysis solution and apply a larger volume (>20 µl) instead.

4. For improved sample entry, start IEF at low voltage (150 V for 30 min, followed by 300 V for 60 min). Extend these times when the sample contains high amounts of salts or when large sample amounts (>50 µl) are applied *via* cup loading.

5. Sample in-gel rehydration: Use IPGphor and apply low voltage (30–50 V) during IPG strip rehydration for improved entry of high M_r proteins into the polyacrylamide gel matrix.

6. When analyzing samples containing high salt amounts, apply moistened filter paper pads at the anodic and cathodic ends of the IPG strip between the IPG gel surface and the electrodes and replace these filter papers with fresh ones after several hours.

7. Remove the IPG gel strip from the surface of the *horizontal* SDS–PAGE gel as soon as the bromphenol blue dye front has migrated 4–5 mm off the IPG gel strip. Then move the cathodic electrode wick (or buffer strip) forward so that it overlaps the area the IPG gel strip once covered.

References

Bjellqvist, B., Ek, K., Righetti, P. G., Gianazza, E., Görg, A., Westermeier, R., and Postel, W. (1982). Isoelectric focusing in immobilized pH gradients: Principle, methodology and some applications. *J. Biochem. Biophys. Methods* **6**, 317–339.

Blomberg, A., Blomberg, L., Norbeck, J., Fey, S., Mose Larsen, P., Larsen, M., Roepstorff, P., Degand, H., Boutry, M., Posch, A., and Görg, A. (1995). Interlaboratory reproducibility of yeast protein patterns analyzed by immobilized pH gradient two-dimensional gel electrophoresis. *Electrophoresis* **16**, 1935–1945.

Bossi, A., Righetti, P. G., Vecchio, G., and Severinsen, S. (1994). Focusing of alkaline proteases in pH 10–12 immobilized gradients. *Electrophoresis* **15**, 1535–1540.

Corbett, J. M., Dunn, M. J., Posch, A., and Gorg, A. (1994). Positional reproducibility of protein spots in two-dimensional polyacrylamide gel electrophoresis using immobilised pH gradient isoelectric focusing in the first dimension: An interlaboratory comparison. *Electrophoresis* **15**, 1205–1211.

Görg, A., Boguth, G., Obermaier, C., Posch, A., and Weiss, W. (1995). Two-dimensional polyacrylamide gel electrophoresis with immobilized pH gradients in the first dimension (IPG-Dalt): The state of the art and the controversy of vertical versus horizontal systems. *Electrophoresis* **16**, 1079–1086.

Görg, A., Boguth, G., Obermaier, C., and Weiss, W. (1998). Two-dimensional electrophoresis of proteins in an immobilized pH 4–12 gradient. *Electrophoresis* **19,** 1516–1519.

Görg, A., Obermaier, C., Boguth, G., Csordas, A., Diaz, J. J., and Madjar, J. J. (1997). Very alkaline immobilized pH gradients for two-dimensional electrophoresis of ribosomal and nuclear proteins. *Electrophoresis* **18,** 328–337.

Görg, A., Obermaier, C., Boguth, G., Harder, A., Scheibe, B., Wildgruber, R., and Weiss, W. (2000). The current state of two-dimensional electrophoresis with immobilized pH gradients. *Electrophoresis* **21**, 1037–1053.

Görg, A., Obermaier, C., Boguth, G., and Weiss, W. (1999). Recent developments in 2-D gel electrophoresis with immobilized pH gradients: Wide pH gradients up to pH 12, longer separation distances and simplified procedures. *Electrophoresis* **20,** 712–717.

Görg, A., Postel, W., Friedrich, C., Kuick, R., Strahler, J. R., and Hanash, S. M. (1991). *Electrophoresis* **12**, 653–658.

Görg, A., Postel, W., and Günther, S. (1988). The current state of two-dimensional electrophoresis with immobilized pH gradients. *Electrophoresis* **9**, 531–546.

Görg, A., and Weiss. (2000). 2D electrophoresis with immobilized pH gradients. *In "Proteome Research: Two Dimensional Electrophoresis and Identification Methods"* (T. Rabilloud, ed.), pp. 57–106. Springer, Berlin.

Herbert, B. (1999). Advances in protein solubilisation for two-dimensional electrophoresis. *Electrophoresis* **20**, 660–663.

Islam, R., Ko, C., and Landers, T. (1998). A new approach to rapid immobilised pH gradient IEF for 2-D electrophoresis. *Sci. Tools* **3**, 14–15.

Laemmli, U. K. (1970). Cleavage of structural proteins during the assembly of the head of bacteriophage T4. *Nature* **227**, 680–685.

O' Farrell, P. H. (1975). High resolution two-dimensional electrophoresis of proteins. *J. Biol. Chem.* **250**, 4007–4021.

O'Farrell, P. Z., Goodman, H. M., and O'Farrell, P. H. (1977). High resolution two-dimensional electrophoresis of basic as well as acidic proteins. *Cell* **12**, 1133–1142.

Olsson, I., Larsson, K., Palmgren, R., and Bjellqvist, B. (2002). Organic disulfides as a means to generate streak-free two-dimensional maps with narrow range IPG strips as first dimension. *Proteomics* **2**, 1630–1632.

Rabilloud, T., Adessi, C., Giraudel, A., and Lunardi, J. (1997). Improvement of the solubilization of proteins in two-dimensional electrophoresis with immobilized pH gradients. *Electrophoresis* **18**, 307–316.

Rabilloud, T., Valette, C., and Lawrence, J. J. (1994). Sample application by in-gel rehydration improves the resolution of two-dimensional electrophoresis with immobilized pH-gradients in the first dimension. *Electrophoresis* **15**, 1552–1558.

Righetti, P. G. (1990). "Immobilized pH Gradients: Theory and Methodology." *Elsevier*, Amsterdam.

Wildgruber, R., Harder, A., Obermaier, C., Boguth, G., Weiss, W., Larsen, P. M., Fey, S., and Görg, A. (2000). Towards higher resolution: Two-dimensional electrophoresis of *Saccharomyces cerevisiae* proteins using overlapping narrow immobilized pH gradients. *Electrophoresis* **21**, 2610–2616.

Wildgruber, R., Reil, G., Drews, O., Parlar, H., and Görg, A. (2002). Web-based two-dimensional database of *Saccharomyces cerevisiae* proteins using immobilized pH gradients from pH 6 to pH 12 and matrix-assisted laser desorption/ionization-time of flight mass spectrometry. *Proteomics* **2**, 727–732.

CHAPTER

24

Two-Dimensional Difference Gel Electrophoresis: Application for the Analysis of Differential Protein Expression in Multiple Biological Samples

John F. Timms

I. INTRODUCTION

Fluorescence two-dimensional difference gel electrophoresis (2D-DIGE) is a recently developed 2D gel-based proteomics technique that provides a sensitive, rapid, and quantitative analysis of differential protein expression between biological samples. Developed by Minden and co-workers (Unlu *et al*., 1997), the technique utilizes charge- and mass-matched chemical derivatives of spectrally distinct fluorescent cyanine dyes (Cy3 and Cy5), which are used to covalently label lysine residues in different samples prior to mixing and separation on the same 2D gel. Resolved, labelled proteins are then detected at appropriate excitation and emission wavelengths using a multiwavelength fluorescence detection device and the signals compared. As well as reducing the number of gels that need to be run, differential labelling and mixing mean that samples are subjected to the same handling procedures and microenvironments during 2D separation, raising the confidence with which protein changes can be detected and quantified. Because fluorescence detection also provides a superior linear dynamic range of detection and sensitivity to other methods (Patton, 2000), this technology is suited to the analysis of biological samples with their large dynamic ranges of protein abundance.

The 2D-DIGE methodology is now commercialized as the Ettan DIGE proteomics system (GE Healthcare), with a third dye (Cy2) introduced, allowing simultaneous analysis of three samples on a single gel. In expression profiling experiments, one dye is used to label an internal standard to be run on all gels against pairs of test samples labelled with the other two dyes. This allows the direct comparison of ratios of expression across multiple samples and gels, improving the ability to distinguish biological variation from gel-to-gel variation. Because the labelling strategy employed is compatible with downstream identification of gel spots by mass spectrometry (MS) (Tonge *et al*., 2001; Gharbi *et al*., 2002), 2D-DIGE is of particular use as a reproducible, high-throughput proteomic technology. This article describes the necessary materials and instrumentation, experimental design, and work flow for the preparation and labelling of samples for 2D-DIGE analysis. Image capture, analysis, and spot picking for MS identification are also described.

II. MATERIALS AND INSTRUMENTATION

The CyDye DIGE fluors *N*-hydroxysuccinimidyl (NHS) esters of Cy2 (Prod. Code RPK0272), Cy3 (Prod. No. RPK0273), and Cy5 (Prod. No. RPK0275) are from GE Healthcare. NHS-Cy3 and NHS-Cy5 are also synthesized in-house following the original published protocol (Unlu *et al*., 1997), with modifications

Copyright 2006, Elsevier Science (USA).
All rights reserved.

(unpublished data). Anhydrous 99.8% *N*,*N*-dimethylformamide (DMF, Cat No. 22,705-6) is from Aldrich, urea (Cat. No. U-0631), dithiothreitol (DTT, Cat. No. D-9163), thiourea (Cat. No. T-8656), and L-lysine (Cat. No. L-5626) are from Sigma. 1.5 *M* Tris solution, pH 8.8 (Prod. No. 20-79000-10), 1 *M* Tris solution, pH 6.8 (Prod. No. 20-7901-10), and 10× Tris–glycine SDS electrophoresis buffer (Prod. No. 20-64) are from Severn Biotech Ltd. Phosphate-buffered saline (PBS, Cat No. 14190-094) is from GIBCO. Nonidet P-40 (NP-40, Prod. No. 56009D2L), bromphenol blue (Prod. No. 200173J), methanol (Prod. No. 10158BG), and glacial acetic acid (Prod. No. 27013BV) are from VWR. 3-[(3-Cholamidopropyl)-dimethylammonio]-1-propanesulfonate (CHAPS, Cat No. B2006) and sodium dodecyl sulphate (SDS, Cat. No. B2008) are from Melford Laboratories Ltd. Coomassie protein assay reagent (Prod. No. 1856210) is from Pierce, S&S weighing papers (Cat. No. Z13411-2) are from Aldrich, and low-gelling temperature agarose (Cat. No. 05075) is from Fluka.

Ampholines (pH 3.5–10, Cat. No. 80-1125-87), Pharmalyte (pH 3–10, Cat. No. 17-0456-01), Immobiline DryStrip reswelling tray (Cat. No. 80-6465-32), Immobiline DryStrip IEF gels (IPG strips, Cat. No. 17-6002-45), Multiphor II electrophoresis unit (Cat. No. 18-1018-06), Ettan DALT low fluorescence glass plates (27 × 22 cm, Cat. No. 80-6475-58), Plus One Repel Silane (Cat. No. 17-1332-01), Plus One Bind Silane (Cat. No. 17-1330-01), reference markers (Cat. No. 18-1143-34), Ettan DALT 12-gel caster, separation unit, and power supply (Cat. Nos. 80-6467-22 and 80-6466-27), Typhoon 9400 imager (Cat. No. 60-0038-54), Ettan Spot Picker (Cat. No. 18-1145-28), and DeCyder differential analysis software (Cat. No. 56-3202-70) are from GE Healthcare. SYPRO Ruby protein gel stain (Cat. No. S-12000) is from Molecular Probes, and colloidal Coomassie brilliant blue G-250 tablets (CBB, Cat No. K26283182) are from Merck. The Immobilon-P polyvinylidene fluoride transfer membrane (PVDF, Cat. No. IPVH00010) is from Millipore.

III. PROCEDURES

A. Experimental Design

The following steps are guidelines for the design of 2D-DIGE expression profiling experiments. Several experiments are outlined to illustrate how samples can be fluorescently labelled and mixed for 2D gel separation and image analysis so that statistically meaningful data can be acquired. The throughput of the technique is, however, dependent upon the 2D gel running, image capture, and analysis capabilities of the laboratory. We routinely run 12-gel experiments providing accurate differential expression data for 24 samples, including an internal standard run on all gels for accurate spot matching and quantitation. The same gels are then poststained and proteins of interest are picked for MS identification. 2D-DIGE is applicable for the analysis of total cell lysates and complex protein mixtures from cultured cells, whole tissues, sorted or fractionated cells, whole organisms (*E. coli*, *S. pombe*, *C. elegans*, etc.), cellular subfractions (membrane, nuclear, cytoplasmic, etc.), or affinity-purified protein fractions.

Steps

1. Three spectrally distinct fluorescent CyDyes (Cy2, Cy3, and Cy5) can be used for differential labelling of protein samples. In the simplest expression profiling experiment, two individual samples are labelled with two different dyes, mixed, and resolved on a single 2D gel (see Section III,B). Because the same protein isoforms in each sample will comigrate, one can accurately measure differential expression as the ratio of the fluorescence intensities of comigrating spots. Thus, the problem of gel-to-gel variation is avoided. This type of single gel experiment is useful where only limited sample quantities are available, e.g., laser capture dissection-procured normal and cancer cells (Zhou *et al*., 2002).

2. To obtain statistically meaningful expression changes, at least triplicate samples should be labelled and analysed on separate gels. These may be biological replicates, e.g., three separately grown cell cultures or tissue from three individual animals, or may be experimental replicates, where three aliquots of the same sample are compared across different gels. Differential expression can then be taken as an average fold change (e.g., the average spot intensity ratio between differentially labelled spots matching across all three gels) with statistical confidence provided by applying a *t* test. Of note we have found considerable interanimal variation in liver lysates from mice (unpublished data), and it is therefore advisable to analyse samples from at least five individual animals for each treatment or condition to provide statistically meaningful data.

3. 2D-DIGE analysis is further improved by running a Cy-labelled internal standard on all gels against pairs of test samples, labelled with the other two CyDyes. This increases the ability to distinguish biological variation from gel-to-gel variation by increasing the confidence with which spots can be matched across gels and by allowing the direct comparison of expression ratios across samples. An equal

pool of all samples (including biological replicates) is best employed as an internal standard as it will contain proteins present in all samples. It is created simply by mixing and labelling equal amounts of protein from every sample and should provide sufficient material for the number of gels to be run. Equal amounts of standard and test samples are then resolved on each gel.

4. In an experiment comparing 100 µg of protein from cell A and cell B, lysates from triplicate cultures are prepared and protein concentrations determined (six samples). For simplicity, samples are adjusted to the same protein concentration by adding lysis buffer. Then 100 µg of each is labelled with Cy3 or Cy5 as shown in Table I. A pool consisting of a mixture of 50 µg of each of all the replicate samples (300 µg total) is labelled with Cy2. Following labelling, the samples are mixed appropriately for separation on three 2D gels as shown in Table I. This scheme controls for dye bias, although labelling combinations are interchangeable so long as each gel is loaded with samples labelled with distinct dyes. This experiment generates nine images for matching, cross-comparison, and statistical analysis in the biological variance analysis (BVA) module of DeCyder software.

5. For complex comparisons we recommend running 12 gels at once. This allows imaging within a day and fits with our downstream laboratory work flow. Although more gels can be run in an individual experiment, consistency may be compromised by running gels at different times or on different electrophoresis units, or may be impractical depending on man power, resources, and automation. Still, it is possible to compare 24 different samples in a single 12-gel 2D-DIGE experiment. For example, our laboratory was able to analyse lysates from two cell lines subjected to growth factor stimulation for four different time periods (8 conditions) using triplicate cultures (Gharbi *et al.*, 2002). The 24 lysates generated were labelled with Cy3 or Cy5 and run in pairs against the internal standard (a pool of all samples) labelled with Cy2. This generated 36 images for DeCyder BVA analysis, with an image acquisition time of ~8 h using a Typhoon 9400 imager.

TABLE I Example of Differential Labelling, Mixing, and Loading for Statistical Comparison of Protein Expression in Two Cell Lines Using 2D-DIGE

	Cy3	Cy5	Cy2
Gel 1	100 µg A, replicate 1	100 µg B, replicate 1	100 µg pool
Gel 2	100 µg B, replicate 2	100 µg A, replicate 2	100 µg pool
Gel 3	100 µg A, replicate 3	100 µg B, replicate 3	100 µg pool

B. Preparation of CyDye-Labelled Samples for 2D Electrophoresis

The following procedure can be applied for the preparation and labelling of multiple samples for 2D-DIGE comparative protein expression analysis. The procedure is based on the Ettan DIGE System (GE Healthcare), with some modifications. The protocol is designed to generate differentially labelled samples that are compatible with all systems for 2D gel electrophoretic separation. The principles and applications of 2D gel electrophoresis are discussed in more detail elsewhere in this volume. For brevity, the sample preparation is outlined for 24-cm pH 3–10 NL-immobilised pH gradient (IPG) gels. Accordingly, final volumes, protein loads, and IPG buffers may differ depending on the size and pH range of the first-dimension gels.

Solutions

1. *CyDyes (NHS-Cy2, -Cy3, -Cy5)*: From lyophilized powder (stored at –20°C), reconstitute to 1 m*M* stock by dissolving in the appropriate volume of anhydrous DMF. Keep stock solutions in the dark at –20°C; they are stable for up to 4 months.

2. *Lysis buffer*: 8 *M* urea, 2 *M* thiourea, 4% (w/v) CHAPS, 0.5% NP-40 (w/v), 10 m*M* Tris–HCl, pH 8.3. To make 100 ml, dissolve 48 g of urea and 15.2 g of thiourea in 50 ml of distilled H_2O. Add 4 g CHAPS, 0.5 g NP-40, and 0.67 ml of 1.5 *M* Tris, pH 8.8, solution. This should give a final pH of 8.3. Make up to final volume, aliquot, and store at –20°C. Do not heat.

3. *40% (w/v) CHAPS*: To make 50 ml, dissolve 20 g CHAPS in distilled H_2O and complete to 50 ml. Store at room temperature.

4. *10% (w/v) NP-40*: To make 50 ml, dilute 5 g of 100% NP-40 in distilled H_2O and complete to 50 ml. Store at room temperature.

5. *L-lysine solution*: 10 m*M* L-lysine in H_2O. Dissolve 9.1 mg in 5 ml distilled H_2O. Aliquot and store at –20°C.

6. *DTT solution*: 1.3 *M* DTT in H_2O. To make 10 ml, dissolve 2 g DTT in distilled H_2O and complete to 10 ml. Aliquot and store at –20°C. Do not heat.

7. *Ampholines/Pharmalyte mix*: Mix equal volumes of ampholines (pH 3.5–10) and Pharmalyte (pH 3–10). Store at 4°C. These broad pH range IPG buffers can be replaced with narrow range buffers depending on the first-dimension pH range.

8. *Bromphenol blue*: 0.2% (w/v) bromphenol blue in H_2O. To make 10 ml, weigh 20 mg bromphenol blue and complete to 10 ml with distilled H_2O. Filter and store at room temperature.

Steps

1. Wash cultured or fractionated cells, whole organisms, or tissues in PBS or, if possible, a low-salt buffer that does not compromise cellular integrity. Salts should be kept to a minimum so drain well. Subcellular or affinity-purified fractions should be prepared at high protein concentration (>2.5 mg/ml) in a low-salt buffer (<10 m*M*) or dialysed against a low-salt buffer.

2. Lyse cells in lysis buffer using appropriate physical disruption (sonnication, grinding, homogenisation, repeated passage through a 25-gauge needle). Do not let samples heat up. A volume of buffer should be used to give a final protein concentration of at least 1 mg/ml. For cellular fractions in a known volume of low-salt buffer and at >2.5 mg/ml, add urea, thiourea, 10% NP-40, 40% CHAPS, and 1.5 *M* Tris, pH 8.8, solution to give final concentrations of 8 *M* urea, 2 *M* thiourea, 4% (w/v) CHAPS, 0.5% (w/v) NP-40, and 10 m*M* Tris (same as lysis buffer). Rotate on a wheel at room temperature until reagents have dissolved. Because the volume is increased substantially upon reagent addition, amounts should be calculated for 2.5 times the original sample volume. Thus, for a 1-ml sample, add 1.2 g urea, 0.38 g thiourea, 250 µl 40% CHAPS, 125 µl 10% NP-40, 16.67 µl 1.5 *M* Tris, pH 8.8, and make to 2.5 ml with lysis buffer. Use weighing papers to avoid static during weighing. The final pH should be ~8.3, the optimum for NHS-CyDye labelling.

3. Determine protein concentrations using Pierce Coomassie protein assay reagent according to the manufacturer's instructions, using BSA in lysis buffer to generate a standard curve. It is recommended that at least four replicate assays are performed for each sample for accurate protein determination. Dilute concentrated samples with lysis buffer if necessary. For ease, samples should be adjusted to the same protein concentration at this point using lysis buffer.

4. Aliquot desired amount of sample into tubes for CyDye labelling. Typically we label 100 µg of protein in triplicate using a random combination of Cy3 and Cy5 across the sample set (See Experimental Design). Mix equal amounts of protein from each sample to create an internal standard. This is labelled with Cy2 and should provide enough material for the number of gels to be run (100 µg/gel).

5. Label samples by the addition of 4 pmol of the appropriate CyDye per microgram of protein (400 pmol/100 µg, equivalent to 4 µ*M* for a 1-mg/ml sample). CyDye stocks can be diluted with anhydrous DMF to avoid pipetting submicroliter volumes. Incubate samples on ice in the dark for 30 min. Note that protein lysates are viscous so ensure thorough mixing at all steps to avoid non-uniform labelling.

6. Quench reactions by adding a 20-fold molar excess of L-lysine. For 400 pmol CyDye, add 0.8 µl of 10 m*M* L-lysine solution. Incubate on ice in the dark for 10 min.

7. Mix Cy3- and Cy5-labelled samples appropriately and add a 100-µg aliquot of the Cy2-labelled pool (to give 300 µg total protein). Note that the final volume should be less than that required for reswelling of IPG strips (450 µl for 24-cm strips). This reswelling volume dictates the practical lower limit for sample protein concentrations.

8. Reduce samples by adding 1.3 *M* DTT to a final concentration of 65 m*M* (22 µl). Add carrier ampholines/Pharmalyte mix to a final concentration of 2% (v/v) (9 µl) and 1 µl of 0.2% bromphenol blue. Adjust volume to 450 µl with lysis buffer. Spin samples briefly.

9. Rehydrate Immobiline DryStrip pH 3–10 NL gels with samples overnight in the dark at room temperature in a reswelling tray according to the manufacturer's instructions (passive rehydration method). Other methods of sample loading (cup loading, rehydration under voltage) can also be applied depending on user preference.

10. Perform 2D electrophoresis following guidelines for the type of system employed, but see Section III,C for recommended modifications.

Comments

1. Primary amines and reducing agents should be avoided as they interfere with CyDye labelling. These include carrier ampholines/Pharmalytes and DTT, which are therefore added after labelling but prior to 2D-PAGE.

2. It is often necessary to use protease, kinase, and phosphatase inhibitors for the preparation of lysates and cellular fractions. We have found that aprotinin (17 µg/ml), pepstatin A (1 µg/ml), leupeptin (1 µg/ml), EDTA (1 m*M*), okadaic acid (1 µ*M*), fenvalerate (5 µ*M*), BpVphen (5 µ*M*), and sodium orthovanadate (2 m*M*), at the final concentrations shown, do not interfere with CyDye labelling.

3. The quantity of CyDye used for labelling is limiting in the reaction and only ~3% of protein molecules are labelled on an average of one lysine residue (minimal labelling). This minimal labelling approach maintains sample solubility and prevents heterogeneous labelling that would lead to vertical spot trains. However, because 436 Da (Cy2), 467 Da (Cy3), or 465 Da (Cy5) is added to the 3% of labelled molecules, a slight shift in migration is observed between

CyDye and poststained images (Gharbi *et al.*, 2002). This is more noticeable in the lower molecular weight range and necessitates poststaining with a general protein stain to attain accurate picking of the majority (97%) of unlabelled protein (see Section III,D).

C. Preparation of 2D Gels, Imaging, and Image Analysis

Isoelectric focusing and second-dimension polyacrylamide gel electrophoresis of CyDye-labelled samples can be performed on any system following the manufacturer's instructions. However, inclusion of the following steps is recommended for high sensitivity, reproducibility, accuracy in the determination of differential expression, and precise excision of protein features for MS identification. The steps are detailed for use with the Multiphor II IEF and Ettan DALT 12 PAGE separation systems for 24 × 20-cm 2D gels, but are generally applicable to other systems. All gel preparation and running steps should ideally be performed in a dedicated clean room to avoid contamination with particulates and nonsample proteins, such as skin and hair keratins. Image analysis and statistical analysis can be performed using various 2D gel analysis softwares (e.g., Melanie, Phoretix, ImageMaster), although DeCyder software is tailored specifically for use with the 2D-DIGE system and is relatively simple to use. Instructions for analysis using DeCyder software are found in the DeCyder software user manual.

Solutions

1. *Bind saline solution*: For twelve 24 × 20-cm plates, mix 16 µl of Plus One bind saline, 400 µl glacial acetic acid, 16 ml ethanol, and 3.6 ml distilled H_2O.

2. *Equilibration buffer*: 6 *M* urea, 30% (v/v) glycerol, 50 m*M* Tris–HCl, pH 6.8, 2% (w/v) SDS. To make 200 ml, dissolve 72 g urea in 100 ml distilled H_2O. Add 60 ml of 100% glycerol, 10 ml of 1 *M* Tris, pH 6.8, solution, and 4 g SDS. Dissolve all powders and adjust volume to 200 ml with distilled H_2O. Aliquot and store at –20°C.

3. *Agarose overlay*: 0.5% (w/v) low-melting point agarose in 1× SDS electrophoresis buffer. To make 200 ml, melt 1 g of agarose in 200 ml of 1× SDS electrophoresis buffer in a microwave on low heat. Add bromphenol blue solution to give a pale blue colour.

Steps

1. Prior to gel casting, treat low-fluorescence glass plates for gel bonding by applying 1.5 ml of fresh bind saline solution per plate and wiping over one surface with a lint-free tissue. Leave plates to dry for a minimum of 1 h. Note that only one plate in each set should be treated; treat the smaller, nonspacer "front plate" if using Ettan DALT 24-cm gel plates (Fig. 1A). Bonding allows easier handling of gels during scanning, protein staining, storage, and, importantly, automated spot excision.

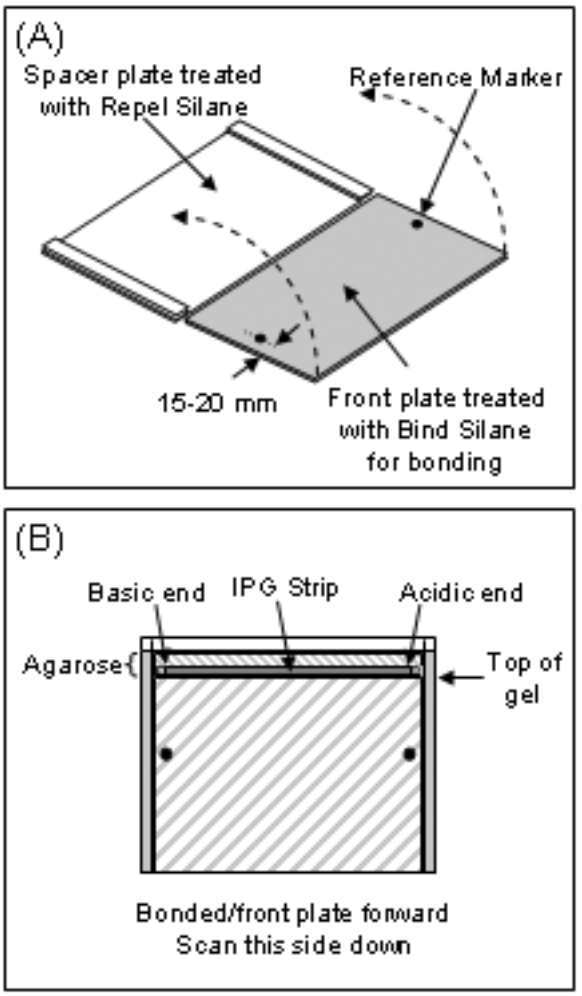

FIGURE 1 (A) Treatment of plates for bonding and reference marker positioning. (B) Casting and loading of second-dimension gels. Based on the Ettan DALT 24-cm strip format.

2. Treat the inner surface of clean and dry "spacer plates" with Repel Silane to ensure easy separation after running (Fig. 1A). Apply PlusOne Repel Silane solution to a lint-free tissue and wipe over the surface. Leave to dry for 10 min. Use in a well-ventilated area. Remove excess Repel Saline by wiping with a clean tissue, rinse with ethanol, then with distilled H_2O, and dry with a tissue.

3. Stick two reference markers to the bonded surface of the plates. These should be placed half-way

down the plates and 15–20 mm in from each edge (Fig. 1A). These markers are used as references for determining cutting coordinates for automated spot picking using the Ettan Spot Picker.

4. Assemble plates in casting chamber and cast gels according to the manufacturer's guidelines.

5. Perform IEF in the dark according to the manufacturer's guidelines.

6. Equilibrate strips for 15 min in equilibration buffer containing 65 m*M* DTT (reduction) and then 15 min in the same buffer containing 240 m*M* iodoacetamide. (alkylation).

7. Rinse strips in 1× SDS electrophoresis buffer and place onto the top of second-dimension gels in melted 0.5% agarose overlay, with the basic end of the strip towards the left hand side when the bonded plate is facing forward (Fig. 1B).

8. Run second-dimension gels until the dye front has completely run off to avoid fluorescence signals from bromphenol blue and free dye. For the Ettan DALT *twelve* system, this can be achieved by running 12% gels for 16 h at 2.2 W per gel.

9. Images are best acquired directly after the 2D run by scanning gels between their glass plates using a Typhoon 9400 imager or similar device. Ensure that both outer plate surfaces are clean and dry before scanning and that the bonded plate is the lower plate on the scanner bed. If the strip is placed correctly (Fig. 1B), the resulting image will not need to be rotated and give a consensus image with the acidic end to the left. Alternatively, gels can be scanned after fixing with the gel facing up from the bonded plate in the scanner, giving the same orientation of the image.

10. Perform an initial low-resolution scan (1000 µm) for one gel on the Cy2, Cy3, and Cy5 channels with the photomultiplier tube (PMT) voltages set low (e.g., 500 V). The optimal excitation/emission wavelengths for fluorescence detection using the Typhoon 9400 are 488/520 nm for Cy2, 532/580 nm for Cy3, and 633/680 nm for Cy5, although other instrumentation may vary slightly. An image is then built up by the scanner for each channel and is converted to grey-scale pixel values.

11. Using ImageQuant software for the Typhoon 9400, establish maximum pixel values in various user-defined, spot-rich regions of each image and adjust the PMT voltages for a second low-resolution scan to give similar maximum pixel values (within 10%) on each channel and without saturating the signal from the most intense peaks (i.e., <90,000 pixels). As a guide, increasing the PMT voltage by 30 V roughly doubles the pixel value. Repeat scans may be required until values are within 10% for the three channels. PMT voltages can be increased further to enhance the detection of low-intensity features, whilst producing tolerable saturation of only a few of the most abundant protein features.

12. Once set for the first gel, use the same PMT voltages for the whole set of gels scanning at 100-µm resolution. A 24 × 20-cm gel image takes ~10 min to acquire per channel and two gels are scanned simultaneously. Images are generated as .gel files, the same format as .tif files.

13. Crop overlayed images in ImageQuant and import into DeCyder Batch Analysis software for subsequent BVA analysis according to the DeCyder software user manual. Differential expression can also be detected visually using Adobe Photoshop by overlaying coloured images (made in the Channel Mixer) and merging using the "Multiply" option in "Layers" (Fig. 2D).

Comments

1. Low-fluorescence glass plates should be used to reduce background.

2. Bind Saline is extremely resistant to removal, and cleaned plates previously treated are still likely to bind acrylamide with subsequent use. For this reason, dedicated treated plates are marked with a diamond pen and reused in the same orientation for subsequent experiments. Bind and Repel saline should be reapplied for subsequent runs.

3. Plates with bonded gels are best cleaned by scraping with a sturdy straight-edged decorator's scraper in warm water with detergent. It is important to remove all gel material, as this produces a fluorescent signal in the Cy3 channel when dried.

4. CyDye-labelled, gel-separated proteins can also be visualized on membranes following electroblotting. The blotted PVDF membrane is scanned using the Typhoon Imager immediately after transfer, wet and face down under a low-fluorescence glass plate. These membranes are subsequently used for immunoblotting with specific antibodies, and the immunoblot signal is aligned directly with the CyDye signal. This alignment can be used for spot identification, validation of MS, or to identify post translationally modified proteins such as phosphoproteins. Note that gels must not be bonded and the plates used must never have been treated with bind saline.

D. Poststaining and Spot Excision

Bonded gels must be poststained to allow accurate picking (see earlier discussion). We have found that both Sypro Ruby and colloidal Coomassie brilliant blue (CBB) protein stains can be used in conjunction with CyDye labelling (Fig. 2). These general protein

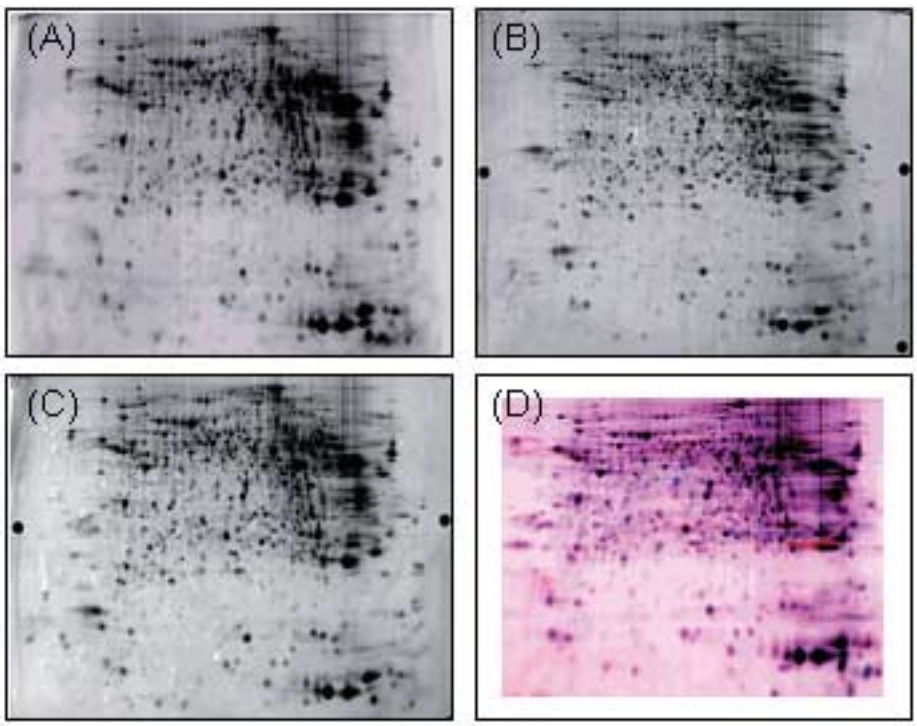

FIGURE 2 (A) Cy5 fluorescence image of 100 mg of mouse liver homogenate separated on a 24-cm pH 3–10 NL IPG strip and 12% PAGE gel. (B) SyproRuby poststained gel of 300 mg of mixed CyDye-labelled liver homogenate. (C) Colloidal CBB poststained gel of 300 mg of mixed CyDye-labelled liver homogenate. This is the same gel as shown in A. (D) Adobe Photoshop-generated Cy3/Cy5 coloured overlay of WT (red) and mutant (blue) mouse liver lysates showing differential expression.

staining methods are sensitive down to the low nanogram level and are reported to be compatible with downstream mass spectrometric identification of proteins (Scheler *et al*., 1998; Berggren *et al*., 2000; Lopez *et al*., 2000; Gharbi *et al*., 2002). MS-compatible silver staining (Shevchenko *et al*., 1996) is not recommended for bonded gels due to its insensitivity and variability from gel to gel.

Solutions

1. *Fixing solution*: 35% (v/v) methanol, 7.5% (v/v) acetic acid in distilled H_2O
2. *Colloidal CBB fixing solution*: For colloidal Coomassie brilliant blue staining, fix gels in 35% (v/v) ethanol, 2% (v/v) phosphoric acid in distilled H_2O
3. *Colloidal CBB staining solution*: 34% (v/v) methanol, 17% (w/v) ammonium sulphate, 3% (v/v) phosphoric acid in distilled H_2O

Steps

1. All gel staining steps should be performed in a dedicated clean room to avoid contamination.
2. After CyDye fluorescence scanning, remove spacer plate and immerse gels in fixing solution and incubate overnight with gentle shaking. Fixed and bonded gels can now be stored for many months at 4°C by sealing in plastic bags with 50 ml of 1% (v/v) acetic acid. The CyDye fluorescence signal is also detectable after several months of storage.
3. For poststaining with Sypro Ruby protein stain (Berggren *et al*., 2000), wash fixed gels for 10 min in distilled H_2O and incubate in Sypro Ruby stain for at least 3 h on a shaking platform in the dark. Pour off the stain and wash the gel in distilled H_2O or destain [10% (v/v) methanol, 6% (v/v) acetic acid] for three times 10 min. Drain and dry the outer surface of the glass plate and scan gel-side up in a Typhoon 9400 imager at the appropriate excitation/emission wavelength for the Sypro Ruby protein stain.
4. The colloidal CCB G-250 staining method has been modified from that of Neuhoff *et al*. (1988). Fix gels in colloidal CBB fixing solution for at least 3 h on a shaking platform. Wash three times for 30 min with distilled H_2O and incubate in CCB staining solution for 1 h. Add one crushed CCB tablet (25 mg) per 50 ml of staining solution (0.5 g/liter) and leave to stain for 2–3 days. No destaining step is required to visualise proteins. Stained gels can be imaged on a densitometer or

on the Typhoon scanner using the red laser and no emission filters.

5. Align poststained and CyDye gel images to identify spots of interest for cutting. Alignment and spot identification can be carried out by comparing images by eye or using Adobe Photoshop to overlay images. A shift in molecular weight between poststained and CyDye images should be apparent due to the increased mass of the dye-labelled fraction of proteins (Gharbi *et al*., 2002).

6. For automated spot picking, input and process poststained images in DeCyder software and create a pick list for the spots of interest by comparing with the results of the BVA analysis. To facilitate sample tracking and later data matching with MS results, the poststained image can be imported and matched within the current experimental BVA work space. This means that any spot picked according to the poststained image will have the same master spot number as in the BVA quantitative analysis. Define the positions of the two reference markers in DeCyder (left then right) and export the pick list coordinate file (.txt) to the spot picker controller.

7. Excise chosen spots from the poststained gel. In the case of visible colloidal CBB-stained gels, this can be done manually with a glass Pasteur pipette or gel-plug cutting pipette or on a robotic picker incorporating a "click-n-pick" format, such as the Ettan Spot Picker. The gel is best submerged under 1–2 mm of distilled water, and picking performed in a dedicated clean room.

8. For automated picking using an Ettan Spot Picker, open the imported pick list and align the instrument with the reference markers according to the manufacturer's instructions. Pick and collect spots in 96-well plates in 200 µl of water, drain, and store at –20°C prior to MS analysis. Sample preparation and protein identification by mass spectrometry are detailed elsewhere.

Comment

Harsh fixatives (e.g., >35% methanol) should not be used on bonded gels as they cause overshrinkage and cracking of gels.

References

Berggren, K., Chernokalskaya, E., Steinberg, T. H., Kemper, C., Lopez, M. F., Diwu, Z., Haugland, R. P., and Patton, W. F. (2000). Background-free, high sensitivity staining of proteins in one- and two-dimensional sodium dodecyl sulfate-polyacrylamide gels using a luminescent ruthenium complex. *Electrophoresis* **21**(12), 2509–2521.

Gharbi, S., Gaffney, P., Yang, A., Zvelebil, M. J., Cramer, R., Waterfield, M. D., and Timms, J. F. (2002). Evaluation of two-dimensional differential gel electrophoresis for proteomic expression analysis of a model breast cancer cell system. *Mol. Cell Proteomics* **1**(2), 91–98.

Lopez, M. F., Berggren, K., Chernokalskaya, E., Lazarev, A., Robinson, M., and Patton, W. F. (2000). A comparison of silver stain and SYPRO ruby protein gel stain with respect to protein detection in two-dimensional gels and identification by peptide mass profiling. *Electrophoresis* **21**(17), 3673–3683.

Neuhoff, V., Arold, N., Taube, D., and Ehrhardt, W. (1988). Improved staining of proteins in polyacrylamide gels including isoelectric focusing gels with clear background at nanogram sensitivity using Coomassie brilliant blue G-250 and R-250. *Electrophoresis* **9**(6), 255–262.

Patton, W. F. (2000). A thousand points of light: The application of fluorescence detection technologies to two-dimensional gel electrophoresis and proteomics. *Electrophoresis* **21**(6), 1123–1144.

Scheler, C., Lamer, S., Pan, Z., Li, X. P., Salnikow, J., and Jungblut, P. (1998). Peptide mass fingerprint sequence coverage from differently stained proteins on two-dimensional electrophoresis patterns by matrix assisted laser desorption/ionization-mass spectrometry (MALDI-MS). *Electrophoresis* **19**(6), 918–927.

Shevchenko, A., Wilm, M., Vorm, O., and Mann, M. (1996). Mass spectrometric sequencing of proteins silver-stained polyacrylamide gels. *Anal. Chem.* **68**(5), 850–858.

Tonge, R., Shaw, J., Middleton, B., Rowlinson, R., Rayner, S., Young, J., Pognan, F., Hawkins, E., Currie, I., and Davison, M. (2001). Validation and development of fluorescence two-dimensional differential gel electrophoresis proteomics technology. *Proteomics* **1**(3), 377–396.

Unlu, M., Morgan, M. E., and Minden, J. S. (1997). Difference gel electrophoresis: A single gel method for detecting changes in protein extracts. *Electrophoresis* **18**(11), 2071–2077.

Zhou, G., Li, H., DeCamp, D., Chen, S., Shu, H., Gong, Y., Flaig, M., Gillespie, J. W., Hu, N., Taylor, P. R., *et al.* (2002). 2D differential in-gel electrophoresis for the identification of esophageal scans cell cancer-specific protein markers. *Mol. Cell Proteomics* **1**(2), 117–124.

CHAPTER

25

Affinity Electrophoresis for Studies of Biospecific Interactions: High-Resolution Two-Dimensional Affinity Electrophoresis for Separation of Hapten-Specific Polyclonal Antibodies into Monoclonal Antibodies in Murine Blood Plasma

Kazuyuki Nakamura, Masanori Fujimoto, Yasuhiro Kuramitsu, and Kazusuke Takeo

I. INTRODUCTION

Affinity electrophoresis (AEP) was developed as a novel technique for separation of biomolecules by biospecific interactions with their ligands in an electric field (Nakamura, 1959). The techniques of rocket immunoelectrophoresis (Laurell, 1966) and crossed immunoelectrophoresis (Svenson and Axelsen, 1972) are based on the same principle. AEP has been applied not only for separation of a tiny amount of those biomolecules, but also for determination of dissociation constants (K_d) of those interactions (Takeo and Nakamura, 1972; Bog-Hansen, 1973; Horejsi and Kocourek, 1974; Caron *et al*., 1975; Takeo and Kabat, 1978; Nakamura *et al*., 1980; Shimura and Kasai, 1982) at different pH (Ek *et al*., 1980; Mimura *et al*., 1992) and temperatures for calculation of thermodynamic parameters (Tanaka *et al*., 1986; Kashiwagi *et al*., 1991).

Two-dimensional affinity electrophroesis (2DAEP), which was newly developed by a combination of isoelectric focusing (IEF) with AEP (Takeo *et al*., 1983), has been used for studies of the immune response *in vivo*. Hapten-specific polyclonal IgG antibodies, which were produced by immunization of rabbits and mice with the hapten of dinitrophenyl (DNP)- or fluorescein isothiocyanate (FITC)-conjugated protein carriers (Takeo *et al*., 1992; Nakamura *et al*., 1993), were separated into a large number of groups of IgG spots by 2DAEP, and each of the groups showed an identical affinity to the hapten but a different isoelectric point (p*I*) as in the case of monoclonal antibodies specific for the hapten. Diversification, affinity maturation, and subclass switching of the hapten-specific antibodies *in vivo* were evidenced in the course of immunization of a single mouse (Nakamura and Takeo, 1998). This article describes the procedures for 2DAEP used for separation of anti-DNP antibodies in murine blood plasma.

II. MATERIALS AND INSTRUMENTATIONS

Acrylamide (Cat. No. 00809-85), *N*, *N*′-methylenebisacrylamide (Bis) (Cat. No. 22402-02), and

Copyright 2006, Elsevier Science (USA).
All rights reserved.

N, *N*, *N'*, *N'*-tetramethylethylenediamine (TEMED) (Cat. No. 33401-72) are from Nacalai tesque (Kyoto, Japan). Carrier ampholytes, Parmalite pH 4–6.5 (Cat. No. 17-0452-01), Pharmalite pH 6.5–9 (Cat. No. 17-0454-01), and Pharmalite pH 5–8 (Cat. No. 17-0453-01) are from Amersham Biosciences (Little Chalfront, Buckinghamshire, UK). Chicken albumin (Cat. No. A-5503), dinitrofluorobenzene (DNFB)(Cat. No. D1529), dinitrophenyl glycine (Cat. No. 9504), β-alanine (Cat. No. A7752), L-lysine (Cat. No. L5501), human γ-globulins (HGG) (Cat. No. G4386), Tris (Cat. No. T6066), and 4-chloro-1-naphthol (Cat. No. C8890) are from Sigma (St.Louis, Mo). Sodium hydroxide (Cat. No. 28-2940), glycine (Cat. No. 12-1210-5), glycerol (Cat. No. 12-1120-5), urea (Cat. No. 32-0280-5), ammonium peroxodisulphate (APS) (Cat. No. 01-4910-2), potassium hydroxide (Cat. No. 24-4670-5), sucrose (Cat. No. 28-0010-5), methylene blue trihydrate (Cat. No. 19-3200-2), riboflavin (Cat. No. R4500), hydrochloric acid (Cat. No. 13-1700-5), sodium chloride(Cat. No. 28-2270-5), Tween 20 (Cat. No. 30-5450-5), and methanol (Cat. No. 19-2410-8) are from Sigma-Aldrich-Japan(Tokyo, Japan). L-Glutamic acid (Cat. No. 074-00505), hydrogen peroxide (Cat. No. 086-07445), and acetic acid (Cat. No. 012-00245) are from Wako (Osaka, Japan). POD-conjugated rabbit IgG fraction to goat IgG Fc (Cat. No. 55360) and goat antihuman γ-globulin antisera (Cat. No. 55074) are from ICN Pharmaceuticals, Inc. (Cappel Products). Other chemicals are of the highest available purity obtained from various sources.

A. Preparation of Antihapten Antisera

A BALB/c mouse (female, 2 months old) was immunized by an intraperitoneal injection of 50 μg of an antigen, hapten-conjugated protein carrier of DNP-conjugated chicken serum albumin (DNP-CSA) in an emulsion with an equal volume of Freund's complete adjuvant as the primary immunization. The second immunization was performed by an intraperitoneal injection of 50 μg of the antigen 2 weeks after the primary immunization and a boosting was made by an intraperitoneal injection of 100 μg of the antigen weeks after the second immunization. In the course of immunization, 150 μl of whole blood was taken by a puncture of the veniplex lining of an eyeball of a deeply anesthetized mouse every week. The blood was allowed to stand at 37°C for 2 h, and the blood clot was removed by centrifugation at 1000 *g* for 5 min to yield 70 μl of clear antisera. Antisera were stored at 4°C by adding 0.1% sodium azide and were submitted to 2DAEP.

B. Prepartion of Water-Soluble DNP-Conjugated Noncross-Linked Acrylamide–Allylamine Copolymer (DNP-PA) as an Affinity Ligand

Acrylamide monomer (40 g) and 4 g of allylamine were dissolved with 400 ml of distilled water in a 500-ml Erlenmeyer flask, followed by the addition of 0.8 ml of TEMED and 50 ml of 0.8% freshly prepared ammonium peroxodisulphate solution with gentle mixing. A small volume of distilled water was overlaid on top of the solution to shut off oxygen and was allow to stand overnight at 30°C. The solution was then extensively dialyzed against tap water for 3 days and distilled water with four changes a day for 2 days. Sodium bicarbonate (4.5 g) was added to the dialyzed solution, and 4.8 g of dinitrofluorobenzene in 15 ml of acetone was mixed by dropwise addition. The mixture was gently stirred overnight in the dark at 25°C using an evaporator without sucking.

The reaction mixture was then dialyzed against tap water for 5 days and distilled water with four changes a day for 2 days. The dialyzed solution was concentrated *in vacuo* until the DNP concentration reached 5–10 m*M* for storage at 4°C in the dark.

The concentration of DNP residue in DNP-conjugated noncross-linked acrylamide–allyamine copolymer (Fig. 1) was calculated from the absorbance at 360 nm in 0.1 *M* sodium hydroxide, using DNP-glycine as a standard (molar absorption at 360 nm was 17530 liter/mol/cm).

III. PROCEDURES

A. Preparation and Running of First-Dimension Gels (IEF)

Solutions

1. *Working solutions for capillary IEF polyacrylamide gels*: To make 6.0 ml of IEF gel solution, prepare the working solutions as shown in Table I
2. *Running buffer solution for anode*: To make 1 liter of 40 m*M* L-glutamic acid solution, dissolve 5.95 g of L-glutamic acid in distilled water and complete to 1 liter
3. *Running buffer solution for cathode*: To make 1 liter of 1 *M* NaOH, dissolve 40.0 g sodium hydroxide in distilled water and complete to 1 liter
4. *Sample solution*: To make 0.1 ml sample solution, mix 0.027 ml of antisera or purified antibodies with 0.055 ml of phosphate-buffered saline, pH 7.4 (PBS), and add 0.03 g of sucrose

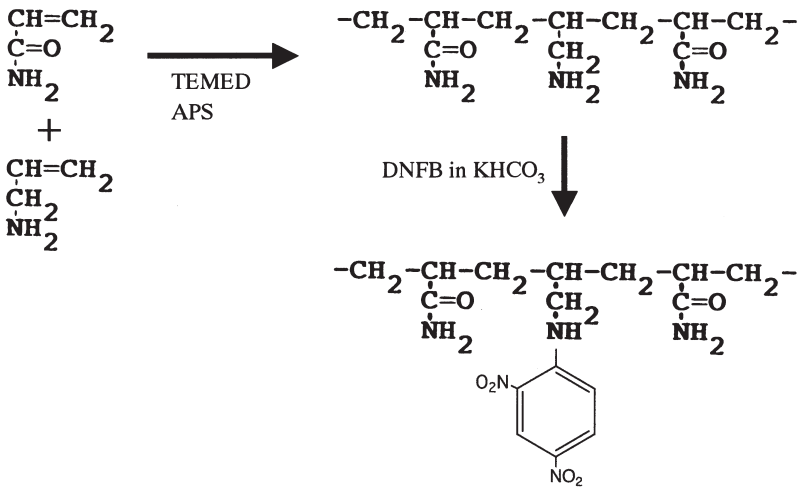

FIGURE 1 Preparation of water-soluble dinitrophenyl-conjugated noncross-linked acrylamide–allyamine copolymer (DNP-PA). TEMED, *N*, *N*, *N*′, *N*′-tetramethylethylenediamine; APS, ammonium peroxodisulphate; DNFB, dinitrofluorobenze.

TABLE I Preparation of Working Solutions for Capillary IEF Gels

Stock solutions and reagent	Volume and weight
Acrylamide solution	0.6 ml
Acrylamide 48.5 g	
Bis 1.5 g	
Dissolved in distilled water to 100 ml	
Carrier ampholyte	
Pharmalite	
pH 4–6.5	0.0094 ml
pH 6.5–9	0.0094 ml
pH 5–8	0.0094 ml
Glycerol solution	0.5 ml
Glycerol 40.0 g	
Dissolved in 100 ml distilled water	
L-Lysine solution	0.8 ml
L-Lysine 1.58 g	
Dissolved in distilled water to 100 ml	
Distilled water	0.98 ml
Urea	2.162 g
APS solution[a]	0.143 ml
Ammonium peroxodisulphate 0.21 g dissolved in distilled water to 10 ml	
TEMED	6 µl
Total volume	6.0 ml

[a] APS solution is prepared freshly before mixing with the deaerated acrylamide gel solution.

Steps

1. Mark the glass capillary (1.2 mm in inner diameter and 8.5 cm in height, Cat. No. 2-000-100, Drummond Scientific Co., Broomall, PA) at 7.5 cm from the bottom.
2. Prepare the gel solution by mixing 0.6 ml of the acrylamide solution, 0.094 ml of Pharmalite pH 4–6.5, 0.094 ml of Pharmalite pH 6.5–9, 0.188 ml of Pharmalite 5–8, 1.5 ml of 40% glycerol solution, 0.8 ml of L-lysine solution with 0.98 ml distilled water, and add 2.162 g of urea to yield 5.867 ml of gel solution. Deaerate the gel solution and mix with 0.143 ml of APS solution and 6 µl of TEMED well just before preparation of gels.
3. Pour two-thirds of the gel solution into a plastic cylindrical chamber (Fig. 2: 1.2 cm in inner diameter and 8.0 cm in height) and immerse the glass capillaries in the solution, avoiding the formation of air bubbles in the capillaries, which are tied with a rubber band.
4. Pour the residual solution into the chamber until the meniscus in the capillaries reaches the marker 7.5 cm from the bottom.
5. Stand the chamber at 25°C for 10 min and find a new surface of top of polyacrylamide gel, which is formed 0.6 mm beneath the original meniscus.
6. Remove the rubber band from the capillaries and seal the top of capillaries in the chamber with Parafilm tightly to avoid drying up during storage at 4°C. Use the capillary gels within 4 weeks.
7. Take the capillary from the chamber and wipe up gel crumbs clinging to the outer surface of the capillary.

8. Pour 10 µl of the sample solution onto the top of the capillary by a microsyringe and overlay the running buffer of 40 m*M* L-glutamic acid (for anode), filling up the capillary.

9. Insert the capillary into a hole of a cylindrical rubber connector and set the connector to the upper buffer reservoir (Fig. 2) tightly. After setting six capillaries and a thermometer with the rubber connector to the upper buffer reservoir (for anode) and avoid air bubbles on the bottom of gels with a small volume of the running buffer of 1 *M* NaOH for cathode.

10. Place the upper reservoir on the lower buffer reservoir (for cathode), which is filled with the running buffer of 1 *M* NaOH, and place the cooling device in the middle of the apparatus (Fig. 2, right).

11. Run the electrophoresis using a constant voltage power supply (Cat. No. 2197-010, Pharmacia LKB, Germany) with stepwise elevation of the voltage from 250 V for 15 min to 500 V for 15 min, 1000 V for 15 min, and 2000 V for 2 h and keep the temperature at 15°C using the cooling device.

12. Detach the capillaries from the apparatus and subject to second-dimension gels (AEP).

B. Preparation and Running Second-Dimension Gels (AEP)

Solutions

1. *Working solutions for AEP polyacrylamide gels*: To make 8.0 ml of the AEP gel solution, prepare the

TABLE II Preparation of Working Solutions for AEP Separating Gels[a]

Stock solution	Volume of working solution for a gel	
	Control gel	Affinity gel
Acrylamide solution Acrylamide 40.0 g Bis 1.067 g Dissolved in distilled water to 100 ml	1.0 ml	1.0 ml
Gel buffer solution 1 *M* KOH 48.0 ml Acetic acid 17.2 ml TEMED 4.0 ml Dissolved in distilled water to 100 ml	2.0 ml	2.0 ml
DNP-PA solution DNP-PA (at any concentration)	—	2.73 ml
Distilled water	2.73 ml	—
Sucrose solution Sucrose 40.0 g Dissolved in 100 ml distilled water	2.0 ml	2.0 ml
APS solution[b] Ammonium peroxodisulphate 0.21 g Dissolved in distilled water to 10 ml	0.27 ml	0.27 ml
Total volume	8.0 ml	8.0 ml

[a] Polyacrylamide gels are 5.13% in T, 2.59% in C, pH 4.3.
[b] APS solution is prepared freshly before mixing with the deaerated acrylamide gel solution.

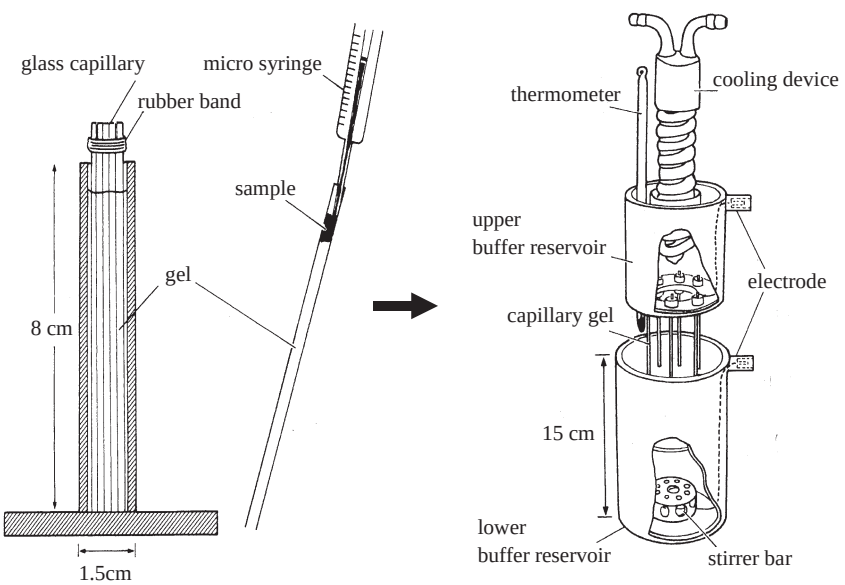

FIGURE 2 Preparation of capillary gels and apparatus for first-dimension isoelectric focusing (IEF).

TABLE III Preparation of Working Solutions for AEP Stacking Gel[a]

Stock solution	Volume of solution for four gels
Acrylamide solution	1.5 ml
Acrylamide	10.0 g
Bis	2.5 g
Dissolved in distilled water to 100 ml	
Gel buffer solution	1.5 ml
1 *M* KOH	48.0 ml
Acetic acid	2.87 ml
TEMED	0.46 ml
Dissolved in distilled water to 100 ml	
Sucrose solution	1.5 ml
Sucrose	40.0 g
Dissolved in 100 ml distilled water	
Distilled water	0.75 ml
Riboflavin solution[b]	0.75 ml
Riboflavin	4.0 mg
Dissolved in 100 ml distilled water	
Total volume	6.0 ml

[a] Polyacrylamide gels are 3.13% in T, 20.0% in C, pH 6.7.
[b] The solution should be prepared freshly or kept at 4°C in a brown bottle to use within a few weeks before mixing with the deaerated gel solution.

TABLE IV Preparation of Stacking Solution for AEP Gel

Stock solution	Volume of solution for four gels
Buffer solution	3.0 ml
1 *M* KOH	48.0 ml
Acetic acid	2.87 ml
Dissolved in distilled water to 100 ml	
Sucrose solution	1.5 ml
Sucrose	40.0 g
Dissolved in 100 ml distilled water	
Distilled water	3.7 ml
Methylene blue solution	3.8 ml
Methylene blue	50 mg
Dissolved in 100 ml distilled water	
Total volume	12.0 ml

working solutions as shown in Tables II and III for separating gel and stacking gel in Reisfeld's buffer system, respectively.

2. *Running buffer solution(Reisfeld, 1962)*: To make 500 ml of running buffer, pH 4.5, mix 100 ml of the stock solution (dissolve 31.2 g of β-alanine and 8.0 ml acetic acid with distilled water to make 1 liter) and 400 ml of distilled water. Check the pH before use.
3. *Stacking solution (Reisfeld, 1962)*: To make 12 ml of the stacking solution, prepare the working solutions as shown in Table IV. Check the pH before use.

Steps

All steps from 1 to 10 must be finished before the completion of the first-dimension IEF.

1. Mark the slab gel cassette (inner space; 100 mm in height, 85 mm in width, 1 mm in thickness, Cat. Nos. SE-400 and SE-401, Marysol, Tokyo, Japan) at 7.5 cm from the bottom and seal the bottom and both sides of the cassette.

2. Stand the cassette at 37°C in a dry incubator until gel preparation.

3. Prepare the AEP separating gel solution by mixing 1.0 ml of acrylamide solution, 2.0 ml of buffer solution, 2.73 ml of DNP-PA solution (substitute with 2.73 ml of distilled water for control gel solution), and 2.0 ml of 40% (w/v) sucrose solution to yield 7.73 ml of gel solution as shown in Table II.

4. Deaerate the gel solution and mix with 0.27 ml of APS solution well just before preparation of the gel.

5. Pour the gel solution into the cassette until the meniscus reaches the marker 7.5 cm from the bottom.

6. Overlay the DNP-PA solution of the same concentration as in the gel (substitute with distilled water for control gel) on top of the gel solution carefully with a syringe to avoid disturbances to the gel solution meniscus.

7. Stand the cassette at 37°C in a dry incubator to complete gelification within 30–40 min and find a new surface of gel beneath the solution.

8. Discard the residual solution on top of the gel and wash with 1 ml of the stacking gel solution, which has been prepared as in Table III, to remove residual DNP-PA on top of the gel. Shade the part cassette for the separating gel by wrapping with aluminum foil.

9. Place a comb in the cassette to prepare the stacking gel in 1 cm height on the top of the separating gel and pour the stacking gel solution, avoiding the formation of air bubbles.

10. Illuminate the stacking gel solution with a fluorescent lamp to complete gelification the stacking gel in 20–30 min.

11. Remove the comb from the cassette and find the stacking gel as shown in Fig. 3 (left). The narrow wells in both sides of the stacking gel are for marker proteins, if necessary.

12. Remove the seal of the bottom of the gel cassette and place two sets of the gel cassette onto the apparatus for AEP as shown in Fig. 3 (right), to fixing the cassette with clips.

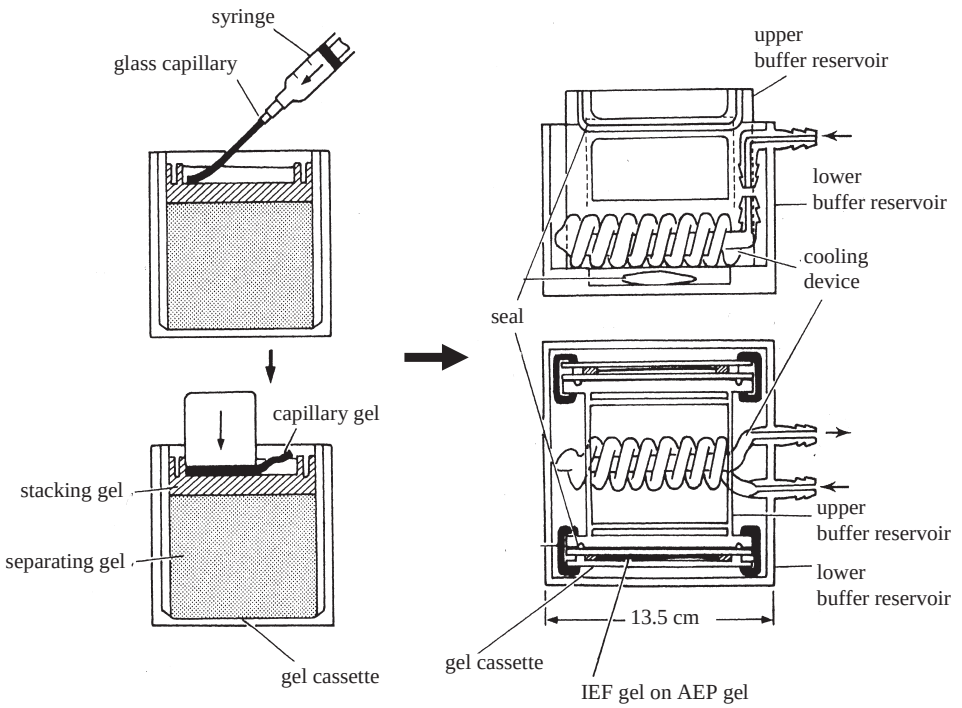

FIGURE 3 Preparation of affinity gels and apparatus for second-dimension affinity electrophoresis (AEP). The IEF capillary gel is put on top of the stacking gel of AEP tightly with a metal plate as indicated by the fine arrow (left). Water at the desired temperature circulates in the glass cooling device, which is connected to a thermostat apparatus.

13. Fill the lower buffer reservoir with the running buffer solution carefully, avoiding the formation of air bubbles at the bottom of the gel.

14. Fill the middle well of the stacking gel with the stacking, solution which has been prepared as described in Table IV.

15. Place the IEF capillary gel by pushing out from the glass capillary with an expeller of a syringe filled with the stacking solution as shown in Fig. 3 (left) and tightly fit on the top of the stacking gel.

16. Fill the upper buffer reservoir with the running buffer and run the electrophoresis at 50 V for 15 min and 80 V for 2.5 h until the methylene blue reaches the bottom of the separating gel.

17. Using a water circulating cooling device (Cat. No. LKB 2219-001, Pharmacia LKB, Germany) keep the temperature during electrophoresis at the desired temperature.

C. Immunoblotting

Solution

Blotting buffer solution: To make 4 liter of electrode buffer solution of 50 m*M* glycine, pH 2.5, mix 200 ml of 1 *M* glycine solution (dissolve 75.07 g of glycine with distilled water to 1 liter) with 100 ml of 1 *M* HCl solution and add distilled water to 4 liters.

Steps

Steps 1–4 must be completed before completion of the second electrophoresis of AEP.

1. Immerse two sheets of nitrocellulose (NC) membrane (Millipore, pore size 0.22 µm, 100 × 75 mm), four sheets of Whatman 3 MM filter paper (Cat. No. 3030917) in 100 × 80 mm, and two pieces of Scotch-Brite 3 M nylon sponge pad in 100 × 85 mm, into 1 liter of the blotting buffer solution and deaerate extensively with suction by an aspirator for 1 h.

2. Pour the deaerate blotting buffer into the buffer reservoir of the blotting apparatus with carbon electrodes (Fig. 4, left).

3. Immerse the cassette holder into 3 liters of the blotting buffer solution in a tray (32 × 23 × 6 cm).

4. Put a sheet of the Whatman 3 MM filter paper on a window of the cassette holder and lay the NC membrane on the filter paper to avoid leaving air bubbles between the sheets.

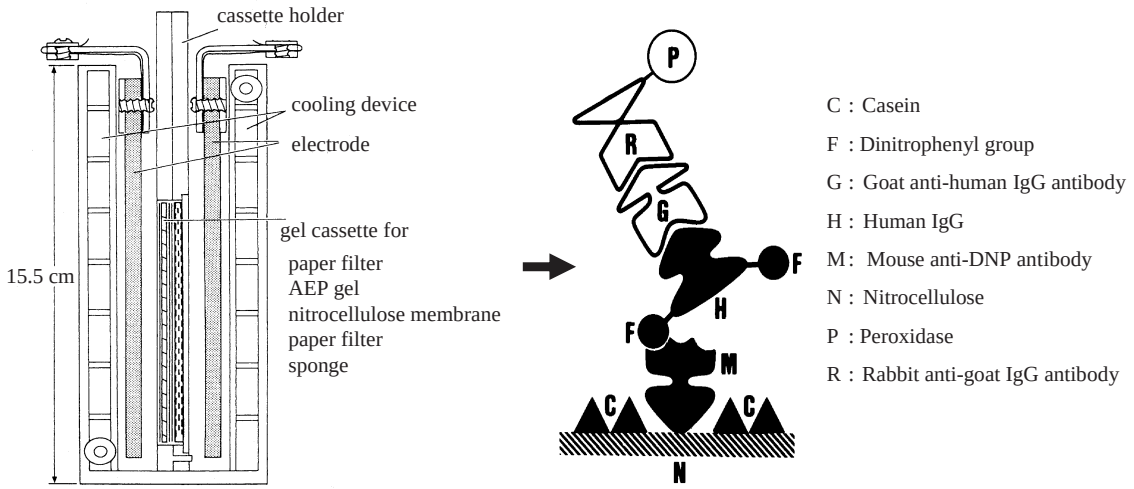

FIGURE 4 Blotting apparatus and a scheme for immunostaining of mouse anti-DNP antibodies on the NC membrane.

5. Remove the AEP gel cassette from the upper buffer reservoir (Fig. 3) immediately after the completion of AEP and leave the gel on the either side of the cassette plate.

6. Make a small hole with a metal punch (2 mm in diameter) at the corner of the bottom of the AEP gel on the anodic side of IEF.

7. Release the AEP gel from the cassette plate carefully using a rectangular metal spatular of (85 × 85 mm) and lay on the NC membrane carefully to avoid leaving air bubbles.

8. Overlay another sheet of the Whatman 3 MM filter paper on the AEP gel carefully and put on the sheet of nylon sponge pad.

9. Close the cassette holder and place the holder in the middle of the electrodes of the blotting apparatus as shown in Fig. 4.

10. Fill the buffer reservoir with the blotting buffer, if necessary, and run the electrophoresis at 5 V for 2 h.

11. Keep the temperature at 6°C using the cooling device.

12. After completion of blotting, remove the NC membrane from the AEP gel and immerse the NC membrane into Tris-buffered saline, pH 7.5 (TBS), to wash out the blotting buffer overnight at 4°C.

13. Start steps for immunostaining of mouse anti-DNP antibodies blotted on the NC membrane as shown in Table V.

14. Carry out all of the procedures for immunostaining in Tupperware (10 × 14 × 3 cm) at room temperature.

15. Take photographs of the patterns of the anti-DNP antibodies spots on the NC membrane as shown in Fig. 5 soon after immunostaining and store the NC membrane by wrapping with aluminum foil at 4°C if necessary.

IV. COMMENTS

Dissociation constants for interactions between each group of anti-DNP antibodies in mouse antisera and the DNP group can be determined using gels containing a series of different concentrations of DNP-PA for second-dimension AEP. The migration distance of an anti-DNP antibody is decreased by increasing the concentration of DNP-PA in the gel, and the dissociation constant (K_d) can be calculated by the equation $1/r = (1/R_o)[1 + (c/K_d)]$, where r is the relative migration distance of the antibody in the presence of DNP-PA, R_o is the relative migration distance of the antibody in the absence of DNP-PA, and c is the concentration of DNP-PA. To obtain reproducible results, the voltage of the electric field and the temperature of the gels should be kept constant during AEP.

TABLE V Procedure for Immunostaining of Anti-DNP Antibodies Blotted on NC Membrane[a]

No.	Step	Solution	Volume (ml) per NC membrane	Incubation time
1.	Washing	TBS[b]	100	Overnight
2.	Blocking	Skimmed milk[c]	20	1 h
3.	Washing	TBS	50	30 s
4.	Reaction with DNP–conjugate	DNP-conjugated HGG in 1% skimmed milk[d]	10	2 h
5.	Washing (repeat four times)	Tween-TBS[e]	50	10 min
6.	Reaction with anti-HGG antibody	Goat anti-HGG antisera in 1% skimmed milk[f]	10	2 h
7.	Washing (repeat four times)	Tween-TBS	50	10 min
8.	Reaction with POD-conjugated antibody	POD-conjugated rabbit antigoat IgG antibodies in 1% skimmed milk[g]	10	2 h
9.	Washing (repeat four times)	Tween-TBS	50	10 min
10.	Visualization	POD substrate solution[h]	20	5–15 min
11.	Washing (repeat four times)	Distilled water	50	5 min

[a] Carry out all steps of the procedure at room temperature with gentle shaking.

[b] Tris-buffered saline: dissolve 2 *M* Tris 50 ml, 1 *M* HCl 81 ml, and NaCl 43.5 g in distilled water to 5 liters.

[c] Dissolve 5 g of skimmed milk in 100 ml of TBS.

[d] Prepare DNP-conjugated human γ-globulin (HGG) (0.1 mg/ml) in 1% skimmed milk of TBS.

[e] Dissolve 50 mg of Tween 20 in 100 ml of TBS.

[f] Dissolve 0.08 ml of goat anti-HGG antisera in 1% skimmed milk of TBS.

[g] Dissolve 0.02 ml of peroxidase (POD)-conjugated rabbit antigoat IgG antibody solution in 1% skimmed milk of TBS.

[h] Dissolve 0.06 g of 4-chloro-1-naphthol in 20 ml of cold methanol and mix with 100 ml of TBS and 0.06 ml of 30% of hydrogen peroxide just before visualization.

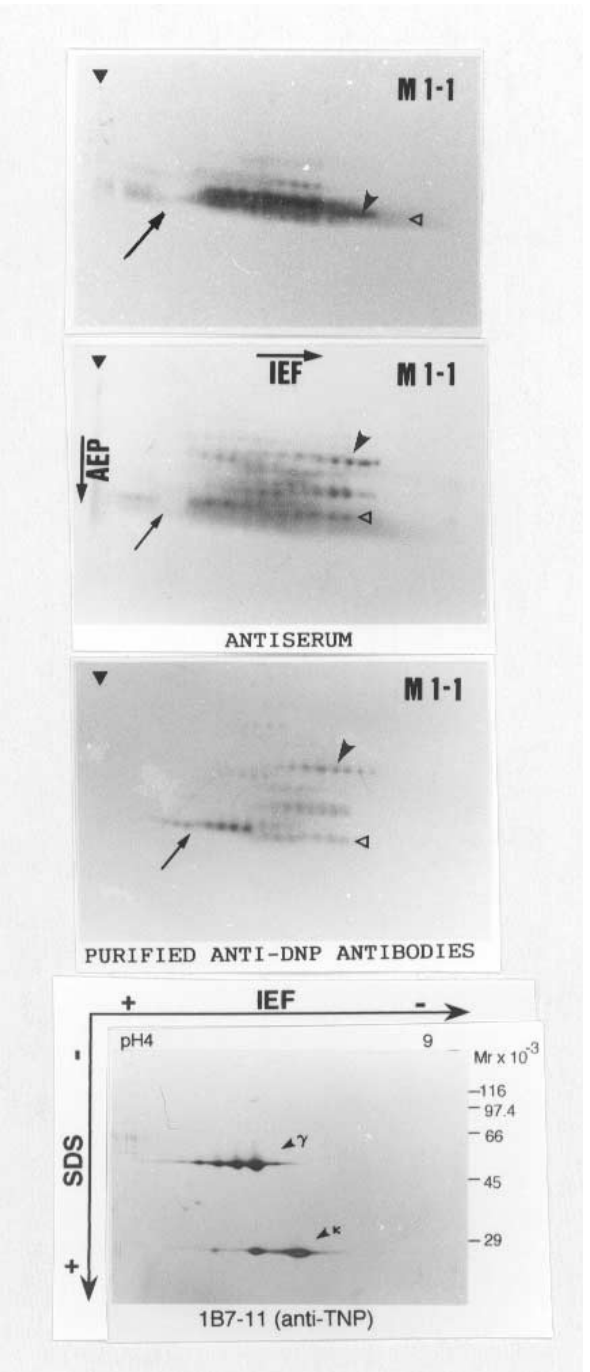

FIGURE 5 Separations of anti-DNP antibodies in mouse antisera by 2DAEP and of a mouse monoclonal antibody specific to the trinitrophenyl (TNP) group by 2DE. The 2DAEP patterns of anti-DNP antibodies in the absence of affinity ligand (a) and the presence of 0.1 m*M* DNP-PA (b) are shown. (c) The 2DAEP patterns of 2 μg of anti-DNP antibodies, which were purified from mouse antisera by affinity chromatography with DNP-conjugated lysine Sepharose in the presence of 0.1 m*M* DNP-PA. Arrows indicate the position of serum albumin which interferes with the blotting of anti-DNP antibodies on the NC membrane. Arrowheads indicate a group of IgG spots with an identical affinity to the ligand of DNP but different isoelectric points (pI), as in the case of the monoclonal antibody. (d) The 2DE patterns of the monoclonal antibody (IB7-11) specific to TNP separated by a combination of IEF and SDS–polyacrylamide gel electrophoresis. The γ and κ indicate the IgG heavy chain and light chain, respectively. Chains show the molecular heterogeneity with different pI values.

References

Bog-Hansen, T. C. (1973). *Anal. Biochem.* **56**, 480–488.
Caron, M., *et al*. (1975). *J. Chromatogr.* **103**, 160–165.
Ek, K., and Righetti, P. J. (1980). *Electrophoresis* **1**, 137–140.
Horejsi, V., and Kocourek, J. (1974). *Biochim. Biophys. Acta* **336**, 338–343.
Kashiwagi, S., *et al*. (1991). *Electrophoresis* **12**, 420–424.
Laurell, C.-B. (1966). *Anal. Biochem.* **15**, 45–52.
Mimura, Y., *et al*. (1992). *J. Chromatogr.* **597**, 345–350.
Nakamura, K., *et al*. (1980). *J. Chromatogr.* **192**, 351–362.
Nakamura, K., *et al*. (1993). *Electrophoresis* **14**, 81–87.
Nakamura, K., and Takeo, K. (1998). *J. Chromatogr. B.* **715**, 125–136.
Nakamura, S. (1966). "*Cross Electrophoresis*." Igaku Shoin, Tokyo and Elsevier, Amsterdam.
Nakamura, S., *et al*. (1959). *Nature (London)* **184**, 638–639.
Reisfeld, R. A., *et al*. (1962). *Nature* **195**, 281–283.
Shimura, K., and Kasai, K. (1982). *J. Biochem.* **92**, 1615–1622.
Svenson, P. J., and Axelson, N. H. (1972). *J. Immunol. Methods* **1**, 169–172.
Takeo, K. (1987). Affinity electrophoresis. *In* "*Advances in Electrophoresis*" (A. Chrambach, M.J. Dunn, and B. J. Radola, eds.), pp. 229–279. VCH, Weinheim.
Takeo, K., and Kabat, E. A. (1978). *J. Immunol.* **121**, 2305–2310.
Takeo, K., and Nakamura, S. (1972). *Arch. Biochem. Biophys.* **153**, 1–7.
Takeo, K., *et al*. (1983). *In* "*Electrophoresis 82*" (D. Stathakos, ed.), pp. 277–283. Walter de Gruyter, Berlin.
Takeo, K., *et al*. (1992). *J. Chromatogr.* **597**, 365–376.
Tanaka, T., *et al*. (1986). *Electrophoresis* **7**, 204–209.

CHAPTER

26

Image Analysis and Quantitation

Patricia M. Palagi, Daniel Walther, Gérard Bouchet, Sonja Voordijk, and Ron D. Appel

I. INTRODUCTION

Many proteomics studies involve comparisons of two-dimensional electrophoresis (**2-DE**) **gels** to identify protein expression changes between different samples. They need efficient **image analysis** software to automatically analyse gel images and extract pertinent biological data. The major steps in such analyses include detection of protein spots in the gels, finding corresponding spots among gels, computation of **protein expression** modifications, and statistical interpretation.

Currently, at least 10 different commercial software packages for the analysis of 2-DE gel images are available commercially. Some of them are descendents of the first generation of tools and software to analyse 2-DE gels, such as Gellab (Lemkin and Lipkin, 1981), THYCO (Anderson *et al.*, 1981), and Melanie (Appel *et al.*, 1997). Although each of these new systems has its own philosophy and approaches, most of them provide the basic operations and functionalities necessary to carry out a complete gel study. The objective of this article is to describe the main steps in a 2-DE gel analysis necessary to find out differently expressed proteins as performed with Melanie software version 4.

II. MATERIALS AND INSTRUMETATION

A. Software

The Melanie software (version 4) is developed at the Swiss Institute of Bioinformatics. It is commercialised under the name ImageMaster 2D Platinum by Amersham Biosciences in collaboration with GeneBio.[1] A demonstration version of the program and support documentation are freely available from GeneBio's Web site (www.genebio.com). Melanie Viewer, a reduced version of this software, can be freely downloaded from the ExPASy server (http://www.expasy.org).

To use the on-line manual and to access remote databases over the Internet with Melanie, Internet Explorer (Microsoft Corporation), Netscape Navigator (Netscape Communications Corporation), or Mozilla (The Mozilla Foundation) have to be installed on the computer.

B. Image Capture

Gel images may be produced with a large variety of image capture devices, ranging from flatbed document scanners, camera systems, densitometers, phosphor imagers, or fluorescence scanners. The default output format for most imaging equipment, and definitely the most appropriate one for further analysis by 2D software, is Tag Image File Format (TIFF, Aldus Corporation). This is the recommended format for use with Melanie, although the software can read some other file types.

The scanning resolution of the gel image is very important, as it influences the amount of visible details in the image. A low resolution corresponds to a large pixel size or a small number of pixels (or dots) per inch. When the image resolution is too low, the automatic spot detection becomes more difficult. However,

[1] Melanie 4 is currently also available from Bruker Daltonics integrated with their PROTEINEER spII spot picking robot.

Copyright 2006, Elsevier Science (USA).
All rights reserved.

when the scan resolution gets too high, the image file becomes very large, and this can slow down the gel analysis. A resolution of 100–200 μM (or about 250–150 dpi) is a good compromise.

The range of possible grey levels (intensity values) in a picture varies according to the image depth (number of bites used to represent a pixel). Images scanned with a higher image depth contain more information. In the case of an 8-bit image, for instance, one pixel has 256 possible grey values (0 to 255). A 16-bit image (65536 grey levels) may reveal subtler but often significant changes; however, it requires more memory. An image depth of at least 12 bits is judicious.

C. Computer Requirements

The Melanie software runs on any of the current Windows operating systems, i.e., 98/ME/NT/2000/XP.

The minimum recommended virtual memory is 256 MB, which is enough to open and process a large number of gels.

Melanie functions properly with a colour resolution of 8 bits (256 colours). However, to use its 3D View module, the colour resolution should be set to 24 bits (16.7 million grey values). It is also recommended to use a screen resolution of at least 1024 × 768 pixels.

III. PROCEDURES

A. Opening Gels and Setting up a Workspace

The investigation of six gels is explained step by step hereafter to describe the usual reasoning when carrying on a whole analysis of 2-DE gels. The examples and images shown in this article were generated with gels from a study of aortic smooth muscle cells from newborn (4-day-old) and aged (18-month-old) rats (Cremona *et al*., 1995). Each population has three gels and are called henceforth newborn and aged.

To start a new work session, import the gel images with the import function and, if necessary, choose a reduction factor. It is highly recommended to setup a workspace as soon as gels have been imported. It facilitates to organise the gel experiments and to work in a personalized environment. The workspace holds information on the relationships between gels such as their organisation into populations (classes) and their reference gel (the gel chosen to make the connection with the other gels). The workspace allows organising gels into projects that reflect the structure and design of the experimental studies facilitating the subsequent work.

i. Click on the Melanie *Workspace* icon in the toolbar to display the Melanie *Workspace* window and create a new workspace.
ii. Inside the workspace, create a new project with the name "*Aortic smooth muscle cells*." Select the newborn gels and add a new class to the project. The selected gels will immediately be allocated to the new class.
iii. Repeat the same procedure for aged gels.
iv. Choose the best representative gel among the six gels and set it as the reference gel.
v. Position the mouse cursor on the class names and right click to open the classes and make these settings active.

B. Viewing and Manipulating Gels

The following usual operation is to adjust the image contrast to improve its visualisation, i.e., to visually better differentiate the spots from the background. This kind of operation is often indicated because of differences between the images and the screen display depths. To adjust the gels contrast perform the following steps.

i. Select one or several gels and draw a region in these gels to get a preview of the contrast mapping modifications.
ii. Choose *View* → *Adjust Contrast* → *Current* from the menu.
iii. Select the gel for which you would like to display the histogram function by choosing it from the *Image* list.
iv. In the *Gel Display Settings* window, change the minimum and maximum grey levels by displacing the slider borders.
v. Click on OK to apply the visual changes to all selected gels.

In the case where many gels are opened simultaneously, their visible parts may become too small. Stacking gels, by displaying one gel on top of the others, thus creating a pile of gels, then becomes a good alternative to display and compare gels. To stack two or more gels, select them and drag them onto one of the display cells. The concept of stacking gels is very helpful to visually discover differences among gels and to add annotations. An example of stacked gels is given in Fig. 1.

A *Transparent* mode can also be used to visualise any similarities or differences between two gels by using a colour overlay of red and cyan. When the pixel colours

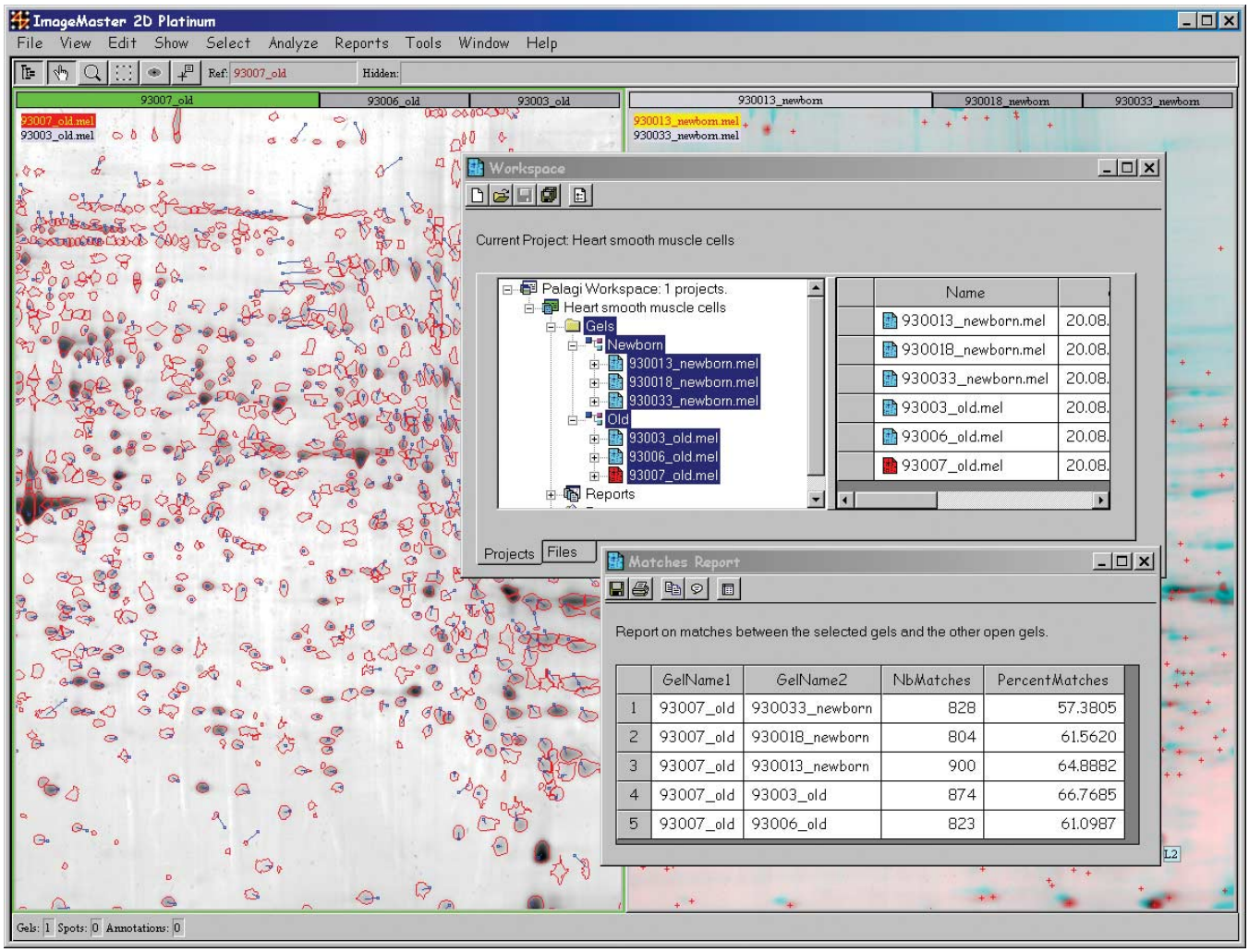

FIGURE 1 Spots are delimited by outlined shapes. Cell display at the left shows three gels in stacked mode. The paired spots in matched gels are linked by blue pair vectors. The Workspace window is displayed over the gels as well as a *Matches Report*.

of the two superimposed gels are added: overlapping spots appear as shades of grey, red and blue spots are present only in one of the gels, halos of red or blue around dark spots indicate that the protein is over- or underexpressed. This means that the fewer colours seen in the transparent mode, the more similar the gels are. To compare gels in the transparent mode:

i. Stack two or more gels.
ii. Select the stack reference.
iii. Choose *View* → *Stack* → *Show Transparent* from the menu.

Other useful functions are usually available at gel image analysis software. In case gels were scanned at the wrong orientation, they can be corrected with a rotate function. Cropping gels allows creating new gels with only defined regions. Scaling gels is particularly useful in the case of very large images where a reduction in size may significantly decrease time and memory required for the analysis. A calibration procedure can be very useful to compensate for image differences caused by variations in experimental conditions (e.g., protein loading, staining) and scanning properties (e.g., image depth).

C. Detecting and Quantifying Spots

The elementary component of a gel is the spot, a shape that can be detected automatically by a spot detection algorithm or adjusted manually by the user. It delimits a more or less tiny region in the gel where a protein or a mixture of proteins is present. Each spot

in a gel has an associated spot ID (a unique sequential number) automatically assigned to it when it is created. Moreover, a spot is automatically quantified, i.e., its optical density, area, and volume are computed. The spot detection algorithm of the Melanie software is optimised to identify a maximum number of proteins, while minimizing the number of artifacts detected. Three parameters have to be set to locate the spots automatically.

i. Smooth: it fixes the number of times the image is filtered before detecting spots, using a smooth-by-diffusion algorithm. The smooth parameter has to be optimised to detect all real spots and split as much as possible any overlapping spots.

ii. Min area: it eliminates spots that have an area smaller than a given threshold, eliminating dust particles that consist of a few very dark pixels (artifacts or noise).

iii. Saliency: it is based on the spot curvature and indicates how prominent a spot is. Real spots generally have high saliency values, whereas artifacts and background noise have small saliencies. Although the saliency is a very efficient quantity for filtering spots, it is also very dependent on the gels (e.g., gel resolution and image depth).

To detect spots automatically:

i. Select the gels from which spots will be detected.
ii. Draw a gel region with the *Region* tool on one or more selected gels in zones with representative spots.
iii. Choose *Edit* → *Spots* → *Auto-Detect* from the menu.
iv. The *Detect Spots* window appears on the screen, and spots in the active regions in selected gels are detected with the default parameters (Fig. 2).
v. Adjust the detection parameters if necessary. The default parameters are optimised to typical SDS–PAGE gels; however, refining the saliency parameter may be indicated. Each change in one of the spot detection parameters is immediately reflected in the selected region helping to choose the parameters. Using the cursor information window is very helpful to find optimal values for the spot filtering.
vi. Click on OK to detect all spots in the selected gels using the parameter values having been set. The spot shapes will be displayed over the gels.

Although it should be avoided to edit spots, they can be created, modified, merged, or deleted manually.

Once spots have been detected, the amount of protein present in each spot is computed automatically. Among the measured quantitative protein values, the most often used in analyses is the relative volume (%Vol). It is a normalized value that remains relatively independent of uninteresting variations between gels, particularly caused by varying experimental conditions. This measure takes into account variations due to protein loading and staining by considering the total volume over all the spots in the gel.

D. Annotating Spots and Pixels

Individual pixels and spots in a gel image may be indicated by annotations. In Melanie, annotations are active elements in the gel analyses and they can have several different purposes, e.g., be used to calibrate, align, and match gels or to be employed to mark spots with their proper information such as protein name, accession number, and so on. Annotations may also be used to mark spots with common characteristics, thus creating subsets. Annotations also offer the possibility to link and associate gel objects to external query engines or data sources of any format (text, html, spreadsheet, multimedia, 2-DE database entry) located locally or on the Internet.

An annotation is defined by its position on the gel (X and Y coordinates) and its set of labels. Each label belongs to a predefined or user-defined category. Among the available predefined annotation categories, some will be important for the explanations given in this chapter.

i. Ac: This category is provided to hold the accession number (AC) of the protein taken from a user-selected database, e.g., Swiss 2D-PAGE (Hoogland *et al*., 2000) or Swiss-Prot (Boeckmann *et al*., 2003), and can be the link to the remote database query engine of Melanie. When such a link is defined, a double click on a label of this category displays the corresponding protein entry in the chosen database with the selected browser software.

ii. Landmark: This is used to mark pixels or spots in the gels as reference points, for the operations of gel alignment or matching, and for the calculation of corresponding locations between gels. Two annotations are considered to refer to the same point in different gels when they hold identical labels.

To create an annotation:

i. Activate the *Annotation* tool.
ii. Double click on the pixel or spot in the gel where the annotation should be located.
iii. In the pop-up window, enter the name of a new category or choose one of the existing categories by clicking on its name.
iv. When a new category is created, the *Create Category* window will appear.

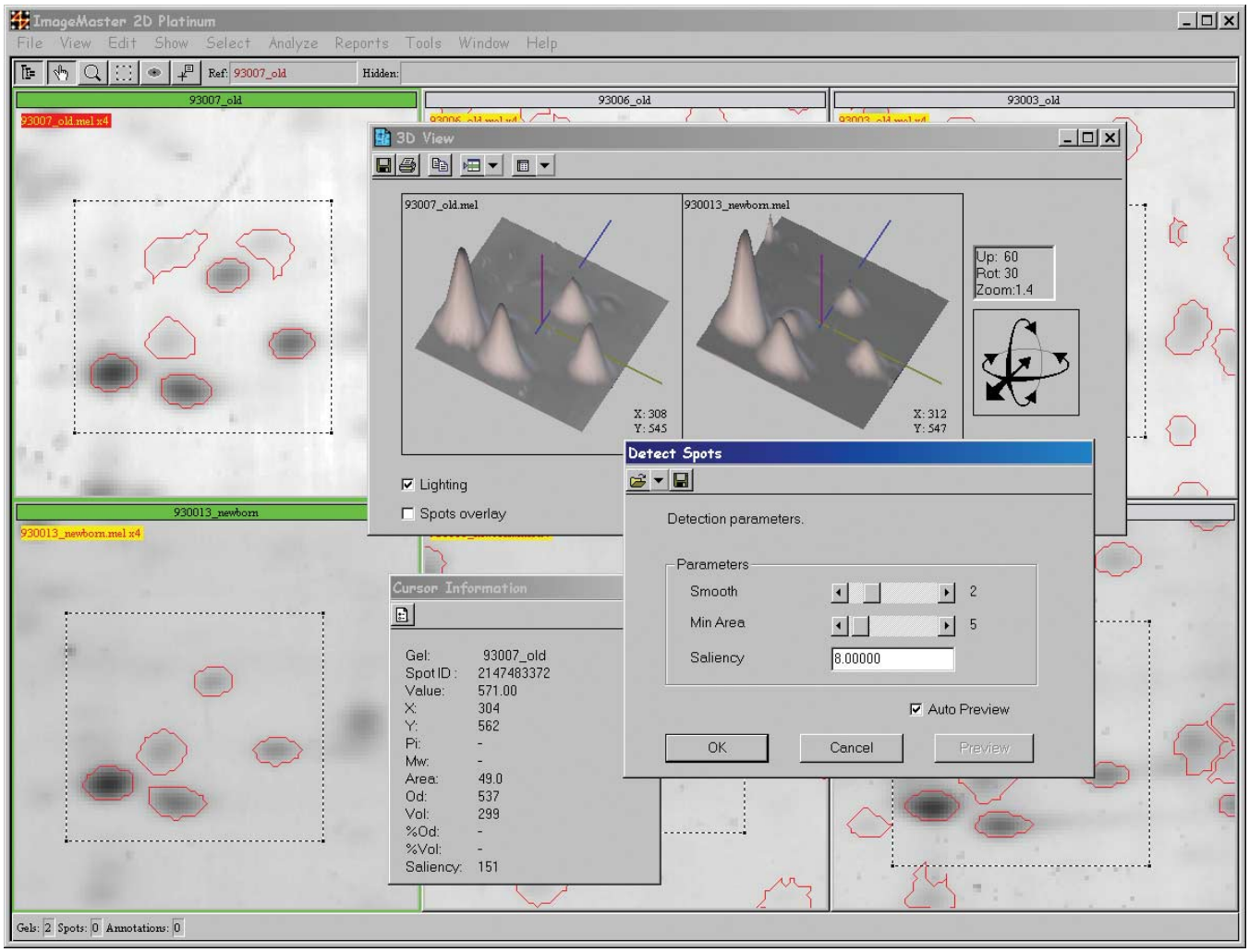

FIGURE 2 Three-dimensional view window details spot profiles of the selected regions on the gels. The cursor information window gives spot value information. Selected regions on the gels are updated in real time when adjusting spot detection parameters in the detect spots window.

v. Type the desired label in the next dialog box and click OK.
vi. The annotation is created and its label is displayed on the gel.

The predefined category *Set:* is used to mark spots with common properties by indicating that they belong to a set. The labels in such a category do not contain specific information. They only display the name of the set to which they belong.

To create a set:

i. Select one or many spots.

ii. Choose *Edit* → *Annotations* → *Add Labels* from the menu.

iii. In the pop-up window, click on the category called *Set:* and add a key word, which will be the name of the set. For instance, to mark spots that were found to be differently expressed and should be exported to a spot excision robot, the final category name might indicate *Set:ToPick*.

iv. A label containing the name of the set (e.g., *ToPick*) will be attached to the selected spots.

Figure 3 shows annotations of categories *Landmark*, *Set:Old*, *Set:Verified*, *Set:ToPick*, and *Comments*.

E. Matching Gels

After spots have been detected, and annotations of category *Landmark* have been possibly added to the gels, the next essential step is to match gel images, i.e., find the corresponding protein spots in different gels.

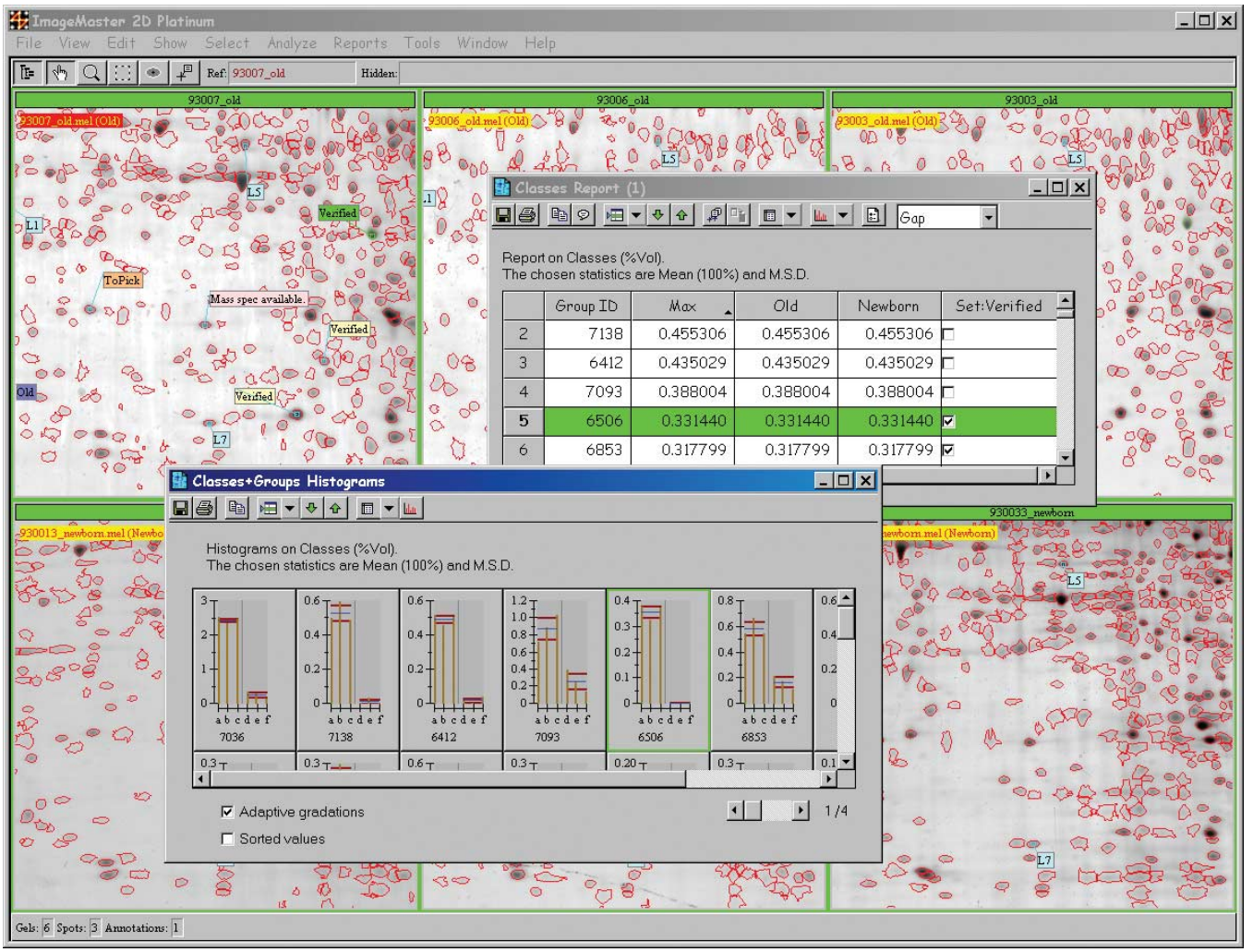

FIGURE 3 Annotations of numerous categories such as *Landmark*, *Set:ToPick*, *Set:Old*, and *Set:Verified* are displayed on the gels. Group 6506 has its histogram highlighted in the *Classes+Groups Histogram* window as well as in the *Classes Report* window.

A gel-matching algorithm compares two gel images to find *Pairs* of related spots, i.e., spots describing the same protein in both gels.

Matching two gels in Melanie means finding all the pairs between spots of the two gels. Matching several gels means picking out a *Reference gel* and then successively matching each gel with the reference gel. In this way, spots in all gels may be compared with spots in the reference gel.

All spots in selected gels that are paired with a given spot in the reference gel form a *Group*. A spot group is the basic element for analysing spot variations across gels and for producing reports and histograms, as well as for performing statistical and clustering analysis. Moreover, when several gels have been matched to a given reference gel, this reference gel provides a unique numbering scheme for spots across all gels. Indeed, each paired spot in a gel image may be associated to the corresponding Spot ID in the reference gel. The Spot ID in the reference gel is then called the *Group ID*.

To match two or more gels automatically:

i. Select the gels to be matched (including the match reference).
ii. Choose *Edit* → *Pairs* → *Auto-Match Gels* from the menu.
iii. Set the reference gel for matching in the pop-up dialog box, i.e., specify to what image the other gels should be matched and click *OK*.
iv. All selected gels are matched with the chosen reference gel.

When matching is completed, Melanie gives the total number of pairs found. In the example given in Fig. 1, gel *93007_old* is the reference gel and about 4200 pairs were found among this gel and the other 5. There are 840 pairs in average per gel as it can be seen on the *Matches Report* window.

F. Analysing and Reporting Data

There are numerous ways of finding variations in protein expression among gels with Melanie but only one of them is detailed in this article.

When populations of gels are known, e.g., when comparing gels of newborn-rat tissues against aged-rat tissue samples, the analysis is based on this classification. Consider that the classes are defined as described previously in Section IIIA. The next step is to find out which are the characteristic spots of each class, i.e., proteins that are expressed differently. The class spot values may be summarized by statistical and overlapping descriptors, such as mean, standard deviation, gap, ratio, and normalization. To investigate groups of spots according to these descriptors one possible way is to

i. Select the gels and then select the groups to be studied with *Select* → *Groups* → *All*.
ii. Choose *Analyze* → *Classes Report*.
iii. In the pop-up list, select the %Vol value type to be displayed.
iv. Accept the default statistics (mean 100% and mean-squared deviation 100%) in the subsequent dialog box.
v. Change the *Displayed value* at the top of the *Classes Report* window for *Ratio*, rank the report in descending order (by clicking on the column headers), and select the rows showing a ratio from the highest value until 2.
vi. Create a new report by choosing the *Report from selection* option in the *Classes Report* window.
vii. In the new window report, change the *Displayed value* for *Gap*. Rank the gap values in descending order. Select all rows from the Gap report and create a *Classes + Groups Histograms*.
viii. Use the created reports and the *Select on Gels* function on the reports to verify the pertinence of the given results. Use the green arrows on the report menu to select rows one by one.
ix. In the Gap report, create an annotation of category "Set" with name *Verified* and type Boolean. When results are reliable, select the field *Verified* in the Gap report (Fig. 3).
x. When finished, select all rows in the Gap report, refine the selection using the column "Verified" with value 1, and reselect the spots on the gels and on the displayed reports with the function "Select on gels + reports."

Melanie also proposes statistical tests to help investigate the significance of the resulting spot groups: two-sample *t* test, Mann–Whitney *U* test, and Kolmogorov–Smirnov test. The principle of those tests is to calculate the probability of observing data sampled from populations with different means by chance or by fact. In order to get the statistical test results:

i. Choose Analyze → Statistical Tests.
ii. In the pop-up list, select the %Vol value type.
iii. Choose one or more of the statistical tests among the two-sample *t* test, Mann–Whitney *U* test, and Kolmogorov–Smirnov test to be displayed.
iv. Sort, for example, the *t* test values in the report in descending order by clicking on the column header on the top of the *Statistical Tests Report* window.
v. Reselect the first 30 groups that have the highest two-sample *t* test value to concentrate the analysis on the most significant spot differences between classes.
vi. Click the *Classes + Groups Histograms* button at the top of the *Statistical Tests Report* window and then on each histogram to check up the obtained results.
vii. To obtain another view of the results, click the *Classes + Groups Histograms* button at the top of the *Classes Histograms* window and then on each histogram to check up the obtained results.
viii. Mark the resulting spots with labels from the "Set:" category and name *t* test.

Based on the explained procedures, groups composed of spots whose quantification values are unusual may be located. The detected variations can result from protein expression changes among gels or can be due to an inadequate detection or matching operation. Therefore, this analysis is not only useful for investigating extracted data, but also for controlling them.

Among the other Melanie functions to analyse gels, factor analysis and heuristic clustering are two options to check when gels correspond to experimentally known populations. These functions do not rely on any class attribution already set up; they blindly classify gels according to a global similarity and identify the characteristic spots of each population.

G. Integrating Data

Importing and exporting data to and from 2-DE analysis software are fundamental procedures. To

make data produced available for processing by other applications or to import information coming from external sources, Melanie uses the common XML format. The main interest of the XML format, besides being used directly by this software, is that external applications can easily extract necessary data.

Melanie exports all gel-related data into a single XML format file, which may include all available information on a set of gels, together with spots (shape, quantification, aligned coordinates), annotations, and pair information.

Spot coordinates can also be exported in XML format to spot excision robots. On the other hand, once the spots have been identified, by mass spectrometry analysis or Edman degradation, for example, the accession number of the identified proteins, as well as other identification data, may be imported from an XML file to annotate the gels

IV. COMMENTS

Working with many gels at a time may be a tiring task, especially when the images are of bad quality. Melanie 4.0 tools for controlling and automating gel analyses may make repetitive tasks less tedious.

The *History* guarantees a better control over the gel analysis study; the operations that have been performed during the current and preceding work sessions can be checked. The History operator consists of a list of actions that have been carried out on the open gels, the parameters, and the selection criteria used at the different steps.

To display a history window

i. Select the gels for which you would like to display the History.
ii. Choose *Edit* → *History* → *Show* from the menu.
iii. To insert a marker in the history, choose *Edit* → *History* → *Insert Marker* from the menu.
iv. To clear the list of actions, choose *Edit* → *History* → *Clear*.

The History function is directly related to the Script function. The *Script* operation enables the automation of parts of the analysis process. A script is a sequence of instructions that is carried out automatically by Melanie when it is run. It is a kind of program that may be encoded by the user without any programming knowledge, just by cutting and pasting some desired actions from the History to the Script. The easiest way to create a script is to

i. Carry out the desired sequence of operations on a set of gels.
ii. Display the *History* of these gels.
iii. Copy the required actions to a new script by selecting the actions and pressing the *New Script* icon in the History toolbar.

A *Script* window will then be displayed on the screen. It contains a list of action descriptors in the Script navigator (actions list), as well as a toolbar at the top of the window. The toolbar contains icons that correspond to standard functionalities, such as copy, paste, save, and print, which create and run the scripts.

In addition to *History* and *Script* operators, the Undo operator corrects mistakes and helps to better control the gel analysis processing. Any earlier state of an analysis may be selected in the action descriptor list of the Undo/Redo operator, which is a particular sequence of actions that can be cancelled any time. Through this multiple undo function, whole parts of the gel analysis may be recovered, avoiding errors.

V. PITFALLS

1. Spot editing: Quantitative protein data, especially the spot volume, are highly dependent on an optimal and reproducible definition of the spot borders and a correct splitting of partially overlapping spots. To guarantee reproducibility of quantitative work, it is highly recommended to create spots by using the automatic spot detection algorithm and to avoid manual editing as much as possible. At most, spots should be separated where necessary.

2. Be critical when matching gels: When the gels are very distorted or different, automatic matching may fail. The choice of landmarks or pairs is very important to obtain good matching results. During matching with Melanie version 4.0, landmarks essentially correct global deformations of gels. Therefore, it is recommended not to put landmarks on spots in locally distorted regions because this can worsen the matching results around such regions.

References

Anderson, N. L., Taylor, J., Scandora, A. E., Coulter, B. P., and Anderson, N. G. (1981). The TYCHO system for computer analysis of two-dimensional gel electrophoresis patterns. *Clin Chem.* **27**(11),1807–1820.

Appel, R. D., Hochstrasser, D. F., Roch, C., Funk, M., Muller, A. F., and Pellegrini, C. (1988). Automatic classification of two-dimensional gel electrophoresis pictures by heuristic clustering analysis: A step toward machine learning. *Electrophoresis* **9**,136–142.

Appel, R. D., Palagi, P. M., Walther, D., Vargas, J. R., Sanchez, J. C., Ravier, F., Pasquali, C., and Hochstrasser, D. F. (1997). MelanieII: A third generation software package for analysis of two-

dimensional electrophoresis images. I. Features and user interface. *Electrophoresis* **18**,2724–2734.

Boeckmann, B., Bairoch, A., Apweiler, R., Blatter, M.-C., Estreicher, A., Gasteiger, E., Martin, M. J., Michoud, K., O'Donovan, C., Phan, I., Pilbout, S., and Schneider, M. (2003). The SWISS-PROT protein knowledgebase and its supplement TrEMBL in 2003. *Nucleic Acids Res*. **31**,365–370.

Cremona, O., Muda, M., Appel, R. D., Frutiger, S., Hughes, G. J., Hochstrasser, D. F., Geinoz, A., and Gabbiani, G. (1995). Differential protein expression in aortic smooth muscle cells cultured from newborn and aged rats. *Exp. Cell Res*. **217**(2),280–287.

Hoogland, C., Sanchez, J.-C., Tonella, L., Binz, P.-A., Bairoch, A., Hochstrasser, D. F., and Appel, R. D. (2000). The 1999 SWISS-2DPAGE database update. *Nucleic Acids Res*. **28**,286–288.

Lemkin, P. F., and Lipkin, L. E. (1981). GELLAB: A computer system for 2D gel electrophoresis analysis. I. Segmentation of spots and system preliminaries. *Comput. Biomed. Res*. **14**(3),272–297.

SECTION

9

Detection of Proteins in Gels

CHAPTER

27

Protein Detection in Gels by Silver Staining: A Procedure Compatible with Mass Spectrometry

Irina Gromova and Julio E. Celis

I. INTRODUCTION

Silver staining is one of the procedures, in addition to Coomassie blue, R and G types, (Neuhoff *et al*., 1988) and fluorescent dyes (Steinberg *et al*., 1996; Patton, 2002; see also article by Patton in this volume), that are available for detecting proteins separated by gel electrophoresis. Switzer *et al*., (1979) introduced silver staining in 1979, a technique that today provides a very sensitive tool for protein visualization with a detection level down to the 0.3- to 10-ng level.

The basic mechanisms underlying silver staining of proteins in gels are relatively well understood. Basically, protein detection depends on the binding of silver ions to the amino acid side chains, primary the sulfhydril and carboxiyl groups of proteins (Switzer *et al*., 1979; Oakley *et al*., 1980; Merril *et al*., 1981, 1986), followed by reduction to free metallic silver (Rabilloud, 1990, 1999). The protein bands are visualized as spots where the reduction occurs and, as a result, the image of protein distribution within the gel is based on the difference in oxidation–reduction potential between the gel area occupied by the proteins and the free adjacent sites. A number of alterations in the silver-staining procedure can shift the oxidation–reduction equilibrium in a way that gel-separated proteins will be visualized as either positively or negatively stained bands (Merril *et al*., 1986).

Silver staining protocols can be divided into two general categories: (1) silver amine or alkaline methods and (2) silver nitrate or acidic methods (Merril, 1990). In general, the detection level using the various procedures is determined by how quickly the protein bands develop in relationship to the background (e.g., signal-to-noise ratio). The silver amine or alkaline methods usually have lower background and, as a result, are most sensitive but require extended procedures. Acidic protocols, however, are faster but slightly less sensitive. A comparative analysis of the sensitivity of a number of silver staining procedures has been published (Sorensen *et al*., 2002; Mortz *et al*., 2001). Clearly, each protocol has different advantages regarding timing, sensitivity, cost, and compatibility with other analytical methods, especially mass spectrometry (MS), a tool that is being used in combination with gel electrophoresis or chromatographic methods for rapid protein identification (see various articles in this volume). Until recently, most of the silver staining protocols used glutaraldehyde-based sensitizers in the fixing and sensitization step, thus introducing chemical modifications into proteins. The utilization of those chemicals causes the cross-linking of two lysine residues within protein chains, which affects MS analysis by hampering trypsin digestion and highly reduces protein extraction from the gel (Rabilloud, 1990).

Several modifications of the silver nitrate staining procedure have been developed for visualizing proteins that can be subsequently digested, recovered from the gel, and subjected to MS analysis (Shevchenko *et al*., 1996; Yan *et al*., 2000). This article describes a procedure that is slightly modified from these.

Copyright 2006, Elsevier Science (USA).
All rights reserved.

II. MATERIALS AND INSTRUMENTATION

Ultrapure water (>18 MΩ/cm resistance) for preparation of all buffers as well as during the washing steps is recommended. Use high-quality laboratory reagents that can be purchased from any chemical company.

III. PROCEDURE

To achieve the best results, i.e., high sensitivity and low background, it is very important to follow closely the incubation time throughout all steps as given in the protocol.

Solutions

1. *Fixation solution*: 50% ethanol (or methanol), 12% acetic acid, 0.05% formalin. To make 1 liter, add 120 ml of glacial acetic acid to 500 ml of 96% ethanol and 500 µl of 35% formaldehyde (commercial formalin is 35% formaldehyde). Complete to final volume with deionized water. Store at room temperature.
2. *Washing solution*: 20% ethanol (or methanol). To make 1 liter, add 200 ml 96% ethanol to 800 ml of deionized water. Store at room temperature.
3. *Sensitizing solution:* 0.02% (w/v) sodium thiosulfate ($Na_2S_2O_3$). To make 1 liter, add 200 mg of sodium thiosulfate anhydrate to a small volume of deionized water, mix well, and bring to the final volume of 1 liter.
4. *Staining solution*: 0.2% (w/v) silver nitrate ($AgNO_3$), 0.076% formalin. Prepare fresh. To make 1 liter, add 2 g of $AgNO_3$ to a small amount of deionized water. Add 760 µl of 35% formaldehyde. Dissolve and bring to final volume with deionized water. Precool the solution at 4°C before using.
5. *Developing solution*: 6% (w/v) sodium carbonate (Na_2CO_3), 0.0004% (w/v) sodium thiosulfate ($Na_2S_2O_3$), 0.05% formalin. To make 1 liter, add 60 g Na_2CO_3 to a small amount of deionized water and dissolve. Add 4 mg of sodium thiosulfate anhydrate to a small volume of deionized water and dissolve. Mix both solutions, add 500 µl of 35% formaldehyde, and bring to the final volume with water. Store at room temperature.
6. *Terminating solution*: 12% acetic acid. To make 1 liter, add 120 ml of glacial acetic acid to 500 ml of deionized water. Mix well and bring to the final volume with water. Store at room temperature.
7. *Drying solution*: 20% ethanol. To make 1 liter, add 200 ml of ethanol to 800 ml of deionized water. Mix well. Store at room temperature.

Steps

Use powder-free rubber gloves throughout the procedure. Wash the gloves with water during the staining procedure. The gel fixation and washing procedure can be carried in a staining try (polypropylene trays are recommended), but make sure that these are only used for silver staining. The size of the container has to be big enough to perform free movement of the gel during the shaking. For each step use sufficient volumes of the solutions to fully immerse the gels. Close the plastic trays or place the trays on top of each other to protect the gels from dust. Perform all steps at room temperature, one gel per tray, placed on a shaker at a very gentle speed. Do not touch the gel with bare hands or metal objects during handling. Plastic or Teflon bars (or ordinary glass pipettes) can be used to handle the gel. The staining procedure can be performed on any type of rotary shakers.

1. After electrophoresis, remove the gel from the cassette and place into a tray containing the appropriate volume of fixing solution. Soak the gel in this solution for approximately 2 h. Fixation will restrict protein movement from the gel matrix and will remove interfering ions and detergent from the gel. Fixation can also be done overnight. It may improve the sensitivity of the staining and decrease the background.
2. Discard the fixative solution and wash the gel in 20% ethanol for 20 min. Change the solution three times to remove remaining detergent ions as well as fixation acid from the gel.

Note: We recommend using 20% ethanol solution instead of deionized water to prevent swallowing of the gel. The size of the gel can be restored by incubating the gel in 20% ethanol for 20 min if water is used during the washing step

3. Discard the ethanol solution and add enough volume of the sensitizing solution. Incubate for 2 min with gentle rotation. It will increase the sensitivity and the contrast of the staining.
4. Discard the sensitizing solution and wash the gel twice, 1 min each time, in deionized water. Discard the water.
5. Add the cold silver staining solution and shake for 20 min to allow the silver ions to bind to proteins. ***Note***: Do not pour the staining solution directly on the gel as it may result in unequal background. Add the solution to the corner of the tray.
6. After staining is complete, pour off the staining solution and rinse the gel with a large volume of deionized water for 20–60 s to remove excess unbound silver ions. Repeat the washing once more. ***Note***:

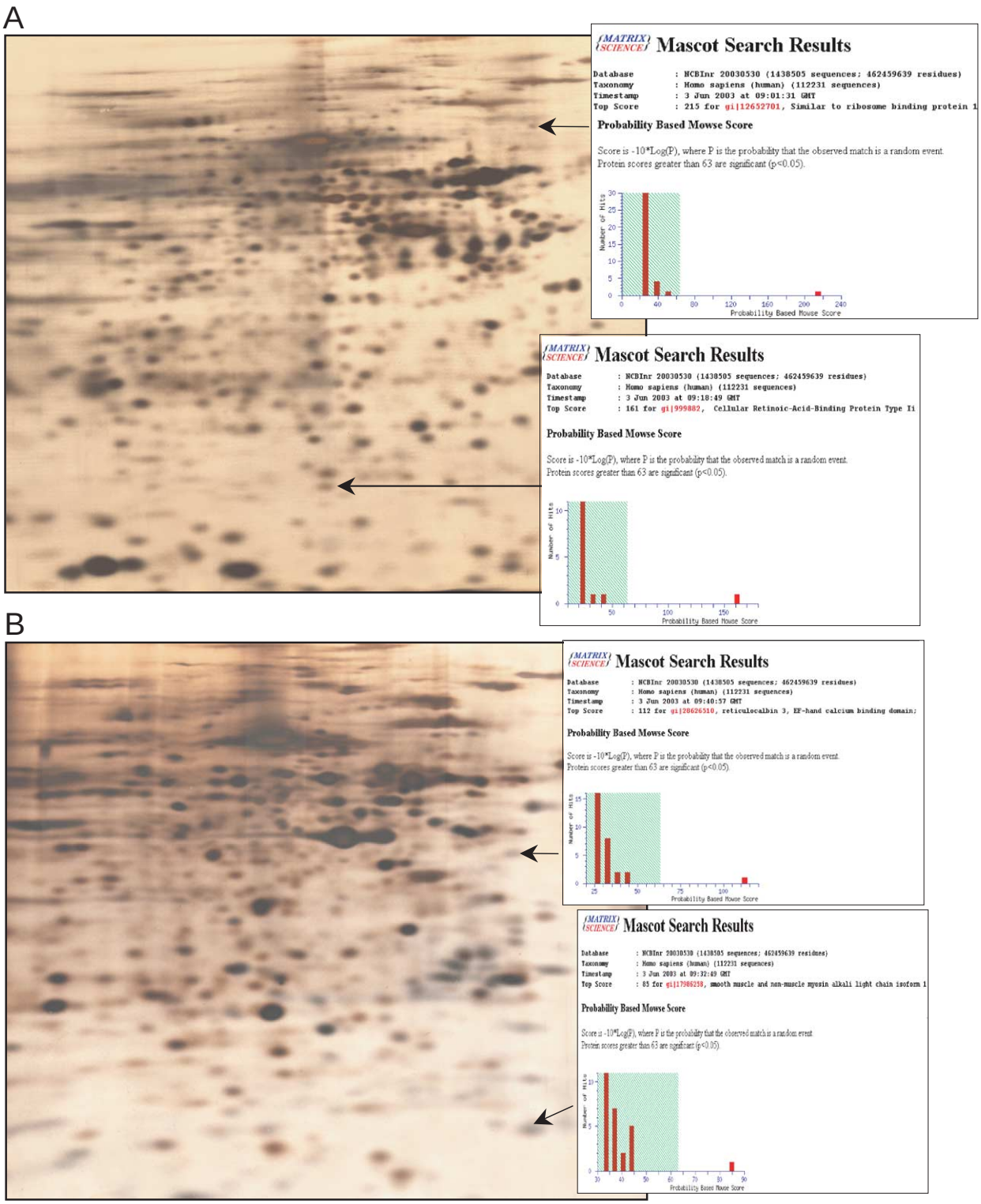

FIGURE 1 Gel image of normal human colon, location 7 (A), and human breast tumor biopsy (B) separated by two-dimensional gel IEF electrophoresis. Protein spots labeled on the gel images were identified by matrix-assisted laser desorption/ionization time-of-flight MS analysis. MS analysis of proteins resolved by gel electrophoresis utilizes extraction of the protein spot from the stained gel, followed by trypsin digestion, measurement, and database analysis (see also other articles in this volume).

Washing the gel for more than 1 min will remove silver ions from the gel, resulting in decreased sensitivity.

7. Rinse the gel shortly with the developing solution. Discard the solution.

8. Add new portion of the developing solution and develop the protein image by incubating the gel in 300 ml of developing solution for 2–5 min. The reaction can be stopped as soon as the desired intensity of the bands is reached.

9. Stop the reduction reaction by adding 50 ml of terminating solution directly to the gel while still immersed in the developing solution. Gently agitate the gel for 10 min. Development is stopped as soon as "bubbling" is over.

10. Moist gels can be kept in 12% acetic acid at 4°C in sealed plastic bags or placed in the drying solution for 2 h prior to vacuum drying.

Figure 1 shows silver-stained gels of whole protein extracts from a normal colon tissue biopsy and a breast tumor biopsy separated by two-dimensional gel electrophoresis as described by Celis *et al*., in this volume. Since the sensitivity of silver staining is in the same range as modern mass spectrometry, it makes this staining one of the most attractive techniques for protein visualization before MS analysis. Protein bands of various intensity can be excised from the gels and identified by MS analysis (see various articles in this volume).

IV. COMMENTS

When choosing the silver staining protocol it is necessary to remember that not all proteins are stained equally by this technique. Thus, several classes of highly negative charged proteins, including proteoglycans and mucins, which contain high levels of sulfated sugar residues, and some very acidic proteins are detected poorly by silver staining (Goldberg *et al*., 1997). Note that the linear dynamic range of the stain is restricted to approximately the 10-fold range, thus hampering the use of this method for quantitative protein expression analysis.

We replaced methanol for ethanol in all fixative solutions because of methanol toxicity. However, the use of ethanol in combination with acetic acid can result in the formation of ethyl acetate, which may interfere with protein identification by mass spectrometry. Several silver staining kits that offer improved sensitivity and that are compatibility with subsequent mass spectrometric analysis are available commercially, including: Silver Stain PlusOne, Amersham Pharmacia Biotech, Amersham, UK; and SilverQuest silver staining kit, Invitrogen, USA.

V. PITFALLS

1. To increase the sensitivity of the staining, use extended washing after fixation to remove all residual acid. This extra washing will reduce the background during development.

2. Development of the gel for a long period of time can decrease the yield of the peptides for subsequent mass spectrometric analysis. This is due to the fact that mainly unstained peptides from the inner part of the gel are eluted to the solutions following "in gel" tryptic digestion of the proteins.

3. Negative staining can be observed when an excess of protein is applied.

4. In some cases, artificial bands with a molecular mass of around 50–70 kDa, as well as streaking or yellow background, can be observed due to the presence of a high concentration of reducing agents such as 2-mercaptoethanol or dithiothreitol in the sample buffer.

5. It has been reported that the recovery of peptides from the gel for MS analysis could be increased by destaining of the silver-stained protein bands immediately after the staining procedure (Gharahdaghi *et al*., 1999).

References

Gharahdaghi, F., Weinberg, C. R., Meagher, D. A., Imai, B. S., and Mische, S. M. (1999). Mass spectrometric identification of proteins from silver-stained polyacrylamide gel: A method for the removal of silver ions to enhance sensitivity. *Electrophoresis* **20**, 601–605.

Goldberg, H. A., and Warner, K. J. (1997). The staining of acidic proteins on polyacrylamide gels: Enhanced sensitivity and stability of "Stains-all" staining in combination with silver nitrate. *Anal. Biochem*. **251**, 227–233.

Merril, C. R. (1990). Silver staining of proteins and DNA. *Nature* **343**, 779–780.

Merril, C. R., Dunau, M. L., and Goldman, D. (1981). A rapid sensitive silver stain for polypeptides in polyacrylamide gels. *Anal. Biochem*. **110**, 201–207.

Merril, C. R., and Pratt, M. E. (1986). A silver stain for the rapid quantitative detection of proteins or nucleic acids on membranes or thin layer plates. *Anal. Biochem*. **156**, 96–110.

Mortz, E., Krogh, T. N., Vorum, H., and Gorg, A. (2001). Improved silver staining protocols for high sensitivity protein identification using matrix-assisted laser desorption/ionization-time of flight analysis. *Proteomics* **1**, 1359–1363.

Neuhoff, V., Arold, N., Taube, D., and Ehrhardt, W. (1988). Improved staining of proteins in polyacrylamide gels including isoelectric focusing gels with clear background at nanogram

sensitivity using Coomassie brilliant blue G-250 and R-250. *Electrophoresis* **9**, 255–262.

Oakley, B. R., Kirsch, D. R., and Morris, N. R. (1980). A simplified ultrasensitive silver stain for detecting proteins in polyacrylamide gels. *Anal. Biochem.* **105**, 361–363.

Patton, W. F. (2002). Detection technologies in proteome analysis. *J. Chromatogr. B Anal. Technol. Biomed. Life Sci.* **771**, 3–31.

Rabilloud, T. (1990). Mechanisms of protein silver staining in polyacrylamide gels: A 10-year synthesis. *Electrophoresis* **10**, 785–794.

Rabilloud, T. (1999). Silver staining of 2-D electrophoresis gels. *Methods Mol Biol.* **112**, 297–305.

Shevchenko, A., Wilm, M., Vorm, O., and Mann, M. (1996). Mass spectrometric sequencing of proteins silver-stained polyacrylamide gels. *Anal. Chem.* **68**, 850–858.

Sorensen, B. K, Hojrup, P., Ostergard, E., Jorgensen, C. S., Enghild, J., Ryder, L. R., and Houen, G. (2002). Silver staining of proteins on electroblotting membranes and intensification of silver staining of proteins separated by polyacrylamide gel electrophoresis. *Anal. Biochem.* **304**, 33–41.

Steinberg, T. H., Jones, L. J., Haugland, R. P., and Singer, V. L. (1996). SYPRO orange and SYPRO red protein gel stains: One-step fluorescent staining of denaturing gels for detection of nanogram levels of protein. *Anal. Biochem.* **239**, 223–237.

Switzer, R. C., 3rd, Merril, C. R., and Shifrin, S. (1979). A highly sensitive silver stain for detecting proteins and peptides in polyacrylamide gels. *Anal. Biochem.* **98**, 231–237.

Yan, J. X., Wait, R., Berkelman, T., Harry, R. A., Westbrook, J. A., Wheeler, C. H., and Dunn, M. J. (2000). A modified silver staining protocol for visualization of proteins compatible with matrix-assisted laser desorption/ionization and electrospray ionization-mass spectrometry. *Electrophoresis* **17**, 3666–3672.

CHAPTER

28

Fluorescence Detection of Proteins in Gels Using SYPRO Dyes

Wayne F. Patton

I. INTRODUCTION

Operationally, fluorescent, noncovalent staining methods using SYPRO dyes resemble traditional, colorimetric staining procedures such as colloidal Coomassie blue dye staining. After electrophoresis, gels are incubated in a stain solution and proteins are visualized based upon differential dye binding to protein bands relative to the polyacrylamide gel matrix. Because proteins are not covalently modified with dye molecules and staining is performed postelectrophoretically, no alteration in the migration of proteins during electrophoresis occurs. These fluorescence-based staining methods are also highly compatible with downstream microchemical methods, such as Edman-based protein sequencing and peptide mass profiling by matrix-assisted laser desorption time-of-flight mass spectrometry (MALDI-TOF MS).

SYPRO Orange dye, SYPRO Red dye, and SYPRO Tangerine dye bind noncovalently to proteins in gels through interaction with SDS micelles (Steinberg *et al*., 1996a,b, 1997, 2000). These fluorophores are virtually nonfluorescent in aqueous solution, but they fluoresce in nonpolar solvents or when associated with SDS–protein complexes. Protein quantitation with fluorophores of this type is generally more reliable than that achieved with fluorophores that label primary amines alone (Patton, 2000). The dyes offer detection sensitivities comparable to those of colloidal Coomassie blue staining methods (Patton, 2000).

Because the staining properties of SYPRO Orange and SYPRO Red dyes are similar, the two protocols describing them have been grouped together in this article. SYPRO Orange protein gel stain is slightly brighter, whereas SYPRO Red protein gel stain has somewhat lower background fluorescence in gels. These dyes offer high sensitivity and rapid staining of SDS–polyacrylamide gels using a simple, one-step, 30- to 60-min staining procedure, with no destaining required (Steinberg *et al*., 1996a,b, 1997, 2000). Staining exhibits low protein-to-protein variability, high selectivity for proteins, and a broad linear detection range extending over three orders of magnitude. The 4- to 10-ng detection sensitivity of these SYPRO dyes is as high as rapid silver staining and colloidal Coomassie blue staining methods (Steinberg *et al*., 1996a,b, 1997, 2000; Patton, 2000, 2002). Both dyes are efficiently excited by UV and by visible illumination. Thus, stained gels can be viewed and photographed with a standard laboratory UV transilluminator, CCD camera, or any of a variety of laser scanners, in conjunction with the proper filters. SYPRO Orange stain (excitation/emission: ~470/569 nm) is preferable for argon ion or second-harmonic generation (SHG) laser-based instruments, and SYPRO Red stain (excitation/emission: ~547/631 nm) is preferable for green He-Ne or Nd : YAG lasers.

It is possible to stain SDS–PAGE gels during electrophoresis using the SYPRO stains in the running buffer; however, detection sensitivity in this case is four- to eight-fold poorer (Steinberg *et al*., 1996b). After electrophoresis, gels are briefly washed prior to visualizing proteins. In contrast to many silver staining and reverse staining methods, SYPRO dyes do not stain nucleic acids or bacterial lipopolysaccharides to a significant extent (Steinberg *et al*., 1996a,b, 1997, 2000). Gels may be completely destained in 30% aqueous methanol (Steinberg *et al*., 1996b). SYPRO Orange and Red protein gel stains are not suitable for staining proteins on blotting membrane or in

Copyright 2006, Elsevier Science (USA).
All rights reserved.

isoelectric focusing (IEF) gels and show reduced sensitivity when staining proteins in two-dimensional gels. Both SYPRO Orange and SYPRO Red stain require acetic acid, making them less suitable for applications involving electroblotting, electroelution, or measuring enzyme activity. While acetic acid may be omitted from the SYPRO Orange and SYPRO Red staining solutions, and proteins then recovered from gels, this yields substantially reduced sensitivity of detection and increased protein-to-protein variability in staining (Steinberg *et al*., 1996b, 2000).

SYPRO Tangerine protein gel stain is a versatile stain for detecting proteins separated by SDS–polyacrylamide gel electrophoresis (Steinberg *et al*., 2000). Like SYPRO Orange and SYPRO Red stains, it offers high sensitivity, a rapid and simple staining procedure, low protein-to-protein variability, high selectivity for proteins, and a broad linear range of detection. Staining is performed in a nonfixative solution that permits subsequent electroblotting, electroeleution, or detection of enzyme activity. Proteins stained without fixation can be used for further analysis by zymography (in-gel enzyme activity assay), provided SDS does not inactivate the protein of interest. Stained proteins can also be eluted easily from gels and used for further analysis. The stain is fully compatible with Edman-based sequencing and mass spectrometry (Steinberg *et al*., 2000). In addition, staining does not interfere with the transfer of proteins to blotting membranes, allowing visualization of proteins *before* proceeding with Western blotting or other blotting applications. Small regions of a gel or even individual bands can be excised before blotting. This enables one to use much smaller amounts of transfer membrane and immunodetection reagents. After transfer to membranes, proteins can be visualized using SYPRO Ruby protein blot stain. If protein fixation is preferred, the dye can be used with 7% acetic acid or 12.5% trichloroacetic acid (Steinberg *et al*., 2000). In this case, however, one should expect slightly higher background staining than with SYPRO Orange and SYPRO Red stains. SYPRO Tangerine protein gel stain is not suitable for staining proteins in IEF gels and shows only moderate sensitivity when staining proteins on two-dimensional gels.

SYPRO Ruby protein gel stain differs from the other SYPRO dyes that all bind through intercalation into SDS micelles (Berggren *et al*., 2000, 2002; Patton, 2000, 2002). Instead, this stain binds to proteins by a mechanism that is quite similar to Coomassie blue stain, via direct electrostatic interaction with basic amino acid residues (Patton, 2000). SYPRO Ruby dye readily stains glycoproteins, lipoproteins, calcium-binding proteins, fibrillar proteins, and other difficult-to-stain proteins. The dye is used in a simple staining procedure and is ideal for high-throughput gel staining. The stain is as sensitive as the best silver staining methods available and superior to them in terms of ease of use, linear dynamic range, and compatibility with downstream microchemical characterization techniques (Lopez *et al*., 2001; Nishihara and Champion, 2002; Gerner *et al*., 2002). SYPRO Ruby protein gel stain is an ultrasensitive dye for detecting proteins separated by SDS–polyacrylamide gels or two-dimensional gels (Berggren *et al*., 2000, 2002). The background fluorescence is low and the linear dynamic range of the stain extends over three orders of magnitude and shows low protein-to-protein variation. The stain is more sensitive than colloidal Coomassie blue dye and SYPRO Orange, Red, or Tangerine dyes and is comparable in sensitivity to the best available silver stains (Patton, 2000, 2002). The stain is ready to use and gels cannot overstain. Staining protocols are simple, although optimal staining incubation requires about 4 h, slower than times required for SYPRO Orange, SYPRO Red, and SYPRO Tangerine stains. Staining times are not critical though and staining can be performed overnight. SYPRO Ruby protein gel stain will not stain extraneous nucleic acids or lipopolysaccharides and is compatible with further downstream microchemical processing. SYPRO Ruby protein gel stain can be used with many types of gels, including two-dimensional gels, Tris–glycine SDS gels, Tris–tricine precast SDS gels, isoelectric focusing gels, and nondenaturing gels. SYPRO Ruby stain is also compatible with gels adhering to plastic backings, although the inherent blue fluorescence of the plastic must be removed with an appropriate emission filter. The stain does not interfere with subsequent analysis of proteins by Edman-based sequencing or mass spectrometry and the stain is especially well suited for peptide mass profiling using MALDI-TOF mass spectrometry (Berggren *et al*., 2000, 2001, 2002; Lopez *et al*., 2001). Stained gels can be visualized with a 300-nm UV transilluminator, various laser scanners, or other blue light-emitting sources. The dye maximally emits at about 610 nm. SYPRO Ruby protein gel stain has exceptional photostability, allowing long exposure times for maximum sensitivity.

This article presents protocols for staining proteins in SDS–polyacrylamide and two-dimensional gels using the different SYPRO dyes. The following protocols describe several steps following the preparation and running of SDS–polyacrylamide gels or two-dimensional gels. Some issues regarding further processing of proteins in the gels are also included. In general, gel electrophoresis should be performed according to standard procedures (Laemmli, 1970;

TABLE I

Protein stain	Excitation/ emission	Major applications	Features
SYPRO Ruby protein gel stain	280 nm, 450 nm /610 nm	Two-dimensional gels, IEF gels, one-dimensional (1D) SDS–PAGE	Highest sensitivity (1–2 ng/band; comparable to best silver staining methods), linear quantitation range over 3 orders of magnitude, compatible with fluorescence-based phosphoprotein and glycoprotein detection (multiplexed proteomics technology)
SYPRO Orange protein gel stain	300 nm, 470 nm /570 nm	1D SDS–PAGE	Good sensitivity (4–10 ng/band; comparable to colloidal Coomassie blue stain), linear quantitation range over 3 orders of magnitude
SYPRO Red protein gel stain	300 nm, 550 nm /630 nm	1D SDS–PAGE	Good sensitivity (4–10 ng/band; comparable to colloidal Coomassie blue stain), linear quantitation range over 3 orders of magnitude
SYPRO Tangerine protein gel stain	300 nm, 490 nm /640 nm	1D SDS–PAGE, staining before blotting, zymography, electroeleution	Good sensitivity (4–10 ng/band; comparable to colloidal Coomassie blue stain), linear quantitation range over 3 orders of magnitude, requires no alcohol or acid fixatives, ideal for protein elution from gels

O'Farrell, 1975). There are several important considerations to take into account when choosing effective and appropriate stains for an application. Table I outlines key features of the stains discussed in this article. Important notes regarding the protocols are included at the end of the article.

II. PROTOCOLS USING SYPRO ORANGE AND SYPRO RED PROTEIN GEL STAINS

A. Materials and Reagents

SYPRO Orange protein gel stain (Molecular Probes, Inc., Cat. No. S-6650, S-6651) and SYPRO Red protein gel stain (Molecular Probes, Inc., Cat. No. S-6653, S-6654) are provided as 5000× concentrated solutions in dimethyl sulfoxide (DMSO), either as a single vial containing 500 µl of stock solution or as a set of 10 vials, each containing 50 µl of stock solution. In each case, enough reagent is supplied to prepare a total of 2.5 liter of working stain solution, which is sufficient to stain ~50 polyacrylamide minigels. Before opening the vial, warm it to room temperature to avoid water condensation and subsequent precipitation. After thawing completely, briefly centrifuge the vial in a microcentrifuge to deposit the DMSO solution at the bottom of the vial. If particles of dye are present, redissolve them by briefly sonicating the tube or vortexing it vigorously after warming. Staining should be performed in plastic dishes (preferably polypropylene) (*see* Section V,B).

B. Gel Electrophoresis

1. SDS–PAGE

Prepare and run SDS–polyacrylamide gels according to standard protocols (Laemmli, 1970). Originally it was recommended to use 0.05% SDS in the running buffer instead of the usual 0.1% SDS. However, this recommendation was based upon separating molecular weight markers and would not be advisable for biological specimens containing hydrophobic proteins. The use of standard, 0.1% SDS in the running buffer decreases overall detection sensitivity only slightly and improves the resolution of protein bands in gels.

2. Two-Dimensional Gels

Neither SYPRO Orange nor SYPRO Red protein gel stain is recommended for high sensitivity detection of proteins in two-dimensional gels (See Table I). High-quality silver stains and SYPRO Ruby Protein Gel Stain offer better detection sensitivity.

C. Staining Protocol

1. Clean and thoroughly rinse the staining dishes before use. Residual detergent in staining dishes will compromise the detection of proteins.

2. Prepare the staining solution by diluting the stock SYPRO reagent 1 : 5000 in 7.5% (v/v) acetic acid and mixing vigorously. For 50 µl of stock, dilute into 250 ml acetic acid solution (*see* Section V).

3. Pour the staining solution into a small, clean plastic dish. For one or two standard-size minigels, use ~50 ml to 100 ml of staining solution; for larger gels, use 500 to 750 ml) (*see* Section V).

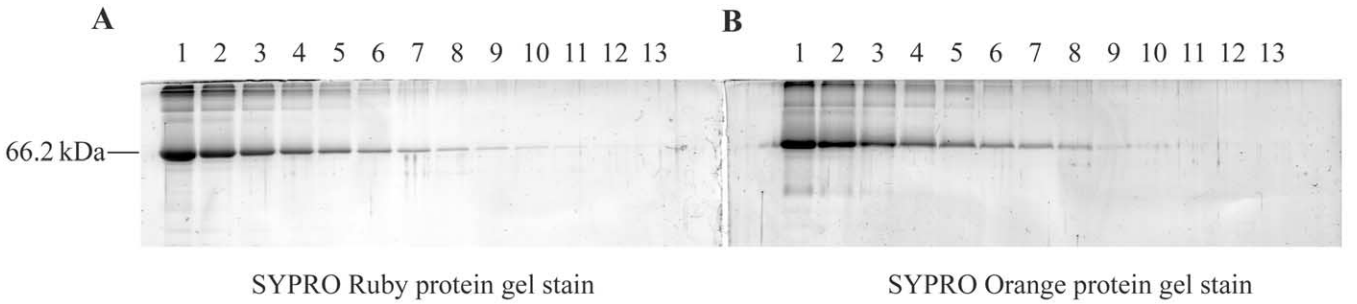

FIGURE 1 Comparison of detection sensitivity and brightness of SYPRO Orange protein gel stain and SYPRO Ruby protein gel stain using a laser-based gel-imaging system. Solution-quantified bovine serum albumin standard (Cat. No. P7656, Sigma Chemical Company, Saint Louis, MO) was applied to lanes of 10% SDS–polyacrylamide gels (1000–0.25 ng/lane) and separated by electrophoresis using standard procedures (Laemmli, 1970). Gels were then stained using either SYPRO Ruby protein gel stain or SYPRO Orange protein gel stain as described in the text. Subsequently, gels were imaged using a Fuji FLA 3000 laser-based gel scanner. Gels were scanned using the 473-nm second-harmonic generation (SHG) laser and 580-nm long-pass filter. (A) Gel stained with SYPRO Ruby protein gel stain and imaged using a laser-based gel scanner. (B) Gel stained with SYPRO Orange protein gel stain and imaged using a laser-based gel scanner. SYPRO Orange protein gel stain was capable of detecting 2 ng of bovine serum albumin while SYPRO Ruby protein gel stain was capable of detecting 0.5 ng of the protein. Figure courtesy of Ms. Courtenay Hart, Molecular Probes, Inc.

4. Place the gel into the staining solution. Protect the gel and staining solution from light at all times by covering the container with a lid or with aluminum foil.

5. Gently agitate the gel in stain solution at room temperature (50 rpm on an orbital shaker). Staining times range from 10 to 60 min, depending on the thickness and percentage of polyacrylamide in the gel. For 1-mm-thick 15% polyacrylamide gels, the signal is typically optimal at 40 to 60 min of staining. For standard SDS–PAGE minigels incubate for 40 to 60 min. Large gels sometimes require a preincubation in 7.5% acetic acid for 15 min prior to staining to reduce background fluorescence due to excess SDS in the gel.

6. Rinse briefly (<1 min) with 7.5% acetic acid to remove excess stain from the gel surface and to avoid accumulation of fluorescent dye on the surface of the transilluminator or gel scanner.

D. Viewing, Photographing, and Storing the Gel

View the stained gel on a standard 300-nm UV transilluminator (*see* Section V,E). Gels may be left in staining solution overnight without losing sensitivity. However, photographs should be taken as soon as possible after staining.

Gels may be photographed with a Polaroid or CCD camera. Use Polaroid 667 black-and-white print film and the SYPRO protein gel stain photographic filter (Molecular Probes, Inc., Cat. No. S-6656). Exposure times vary with the intensity of the illumination source; for an f stop of 4.5, use 2 to 5 s for SYPRO Orange stain and 3 to 8 s for SYPRO Red stain. CCD cameras and laser scanners provide high sensitivity detection; contact the manufacturer to determine the optimal filter sets (*see* Section V).

E. Destaining Gels

To destain gels, incubate overnight in 0.1% Tween 20. Alternatively, if thorough destaining is desired, incubate for prolonged periods in several changes of 7.5% acetic acid or 30% methanol.

III. PROTOCOL FOR SYPRO TANGERINE PROTEIN GEL STAIN

A. Materials and Reagents

SYPRO Tangerine protein gel stain (Molecular Probes, Inc., Cat. No. S-12010) is provided in a 500-µl unit size, as a 5000× concentrated solution in DMSO. One 500-µl unit size prepares a total of 2.5 liter of working stain solution, which is sufficient to stain ~50 polyacrylamide minigels. Before opening the vial, warm it to room temperature to avoid water condensation and subsequent precipitation. After thawing completely, briefly centrifuge the vial in a microcentrifuge to deposit the DMSO solution at the bottom of the vial. If particles of dye are present, redissolve them by briefly sonicating the tube or vortexing it vigorously after warming.

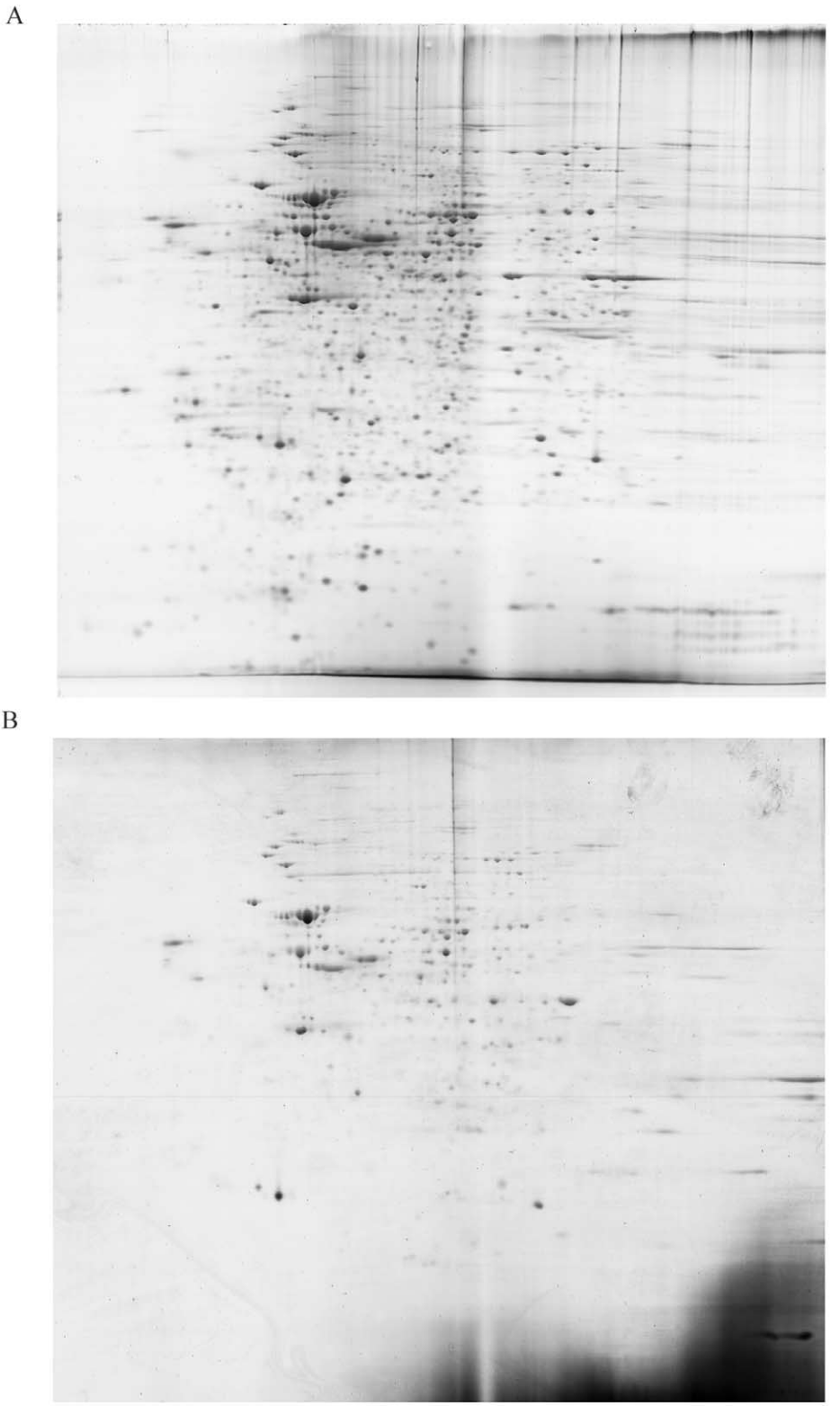

FIGURE 2 Comparison of the detection sensitivity of SYPRO Orange protein gel stain and SYPRO Ruby protein gel stain using a laser-based gel-imaging system. Jurkat cell extract (250 µg) was separated on a tube gel as a first dimension followed by 12.5% SDS–PAGE. Two-dimensional gels were stained with either SYPRO Ruby dye or SYPRO Orange dye overnight. Gels were destained for 2–3 h before imaging. (A) Gel stained with SYPRO Ruby protein gel stain. (B) Gel stained with SYPRO Orange protein gel stain. Figure courtesy of Dr. Birte Schulenberg.

1. Buffers

SYPRO Tangerine staining solution is prepared by diluting the stock reagent 1 : 5000 in one of a variety of buffers as described in the protocol. Staining should be performed in plastic dishes (preferably polypropylene) (*see* Section V,A).

2. SDS–PAGE

Prepare and run SDS–polyacrylamide gels according to standard protocols (Laemmli, 1970). The use of standard, 0.1% SDS in the running buffer is recommended to ensure complete solubilization of hydrophobic proteins.

3. 2-D Gels

SYPRO Tangerine gel stain is not recommended for high sensitivity detection of proteins in two-dimensional gels (See Table I). High-quality silver stains and SYPRO Ruby protein gel stain offer better detection sensitivity.

B. Staining Procedure

1. Clean and *thoroughly rinse* the staining dishes before use. Residual detergent in staining dishes will compromise the detection of proteins.

2. Prepare the staining solution by diluting the stock SYPRO Tangerine reagent 1 : 5000 in an appropriate buffer and mixing vigorously.

2a. If the proteins are to be used for electroelution, electroblotting, or zymography, dilute the stock solution into 50 m*M* phosphate, 150 m*M* NaCl, pH 7.0. For 50 µl of stock, dilute into 250 ml buffer. *Note: If no fixative is used before or during staining, some diffusion of the protein bands may occur, especially for smaller proteins.*

2b. Alternatively, use one of a wide range of buffers that are compatible with the stain. These include formate, pH 4.0; citrate, pH 4.5; acetate, pH 5.0; MES, pH 6.0; imidazole, pH 7.0; HEPES, pH 7.5; Tris acetate, pH 8.0; Tris–HCl, pH 8.5; Tris borate, 20 m*M* EDTA, pH 9.0; and bicarbonate, pH 10.0. Buffers should be prepared as 50–100 m*M* solutions containing 150 m*M* NaCl. The stock dye solution may also be diluted directly into 150 m*M* NaCl. For 50 µl of stock, dilute into 250 ml buffer.

2c. For fixative staining to minimize diffusion of the proteins, dilute the SYPRO Tangerine stock solution in 7.5% (v/v) acetic acid. For low percentage gels and for very small proteins, 10% acetic acid will result in better retention of the protein in the gel without compromising sensitivity (Steinberg *et al.*, 2000). However, note that acetic acid and other fixatives will interfere with the transfer of proteins to blotting membranes.

3. Pour the staining solution into a small plastic dish. For one or two standard-size minigels, use ~50 to 100 ml of staining solution; for larger gels, use 500 to 750 ml (*see* Section V,A).

4. Place the gel into the staining solution. Protect the gel and staining solution from light at all times by covering the container with a lid or with aluminum foil.

5. Gently agitate the gel in stain solution at room temperature (50 rpm on an orbital shaker). The staining times range from 10 to 60 min, depending on the thickness and percentage of polyacrylamide in the gel. For 1-mm–thick 15% polyacrylamide gels, the signal is typically optimal at 30 to 60 min of staining. For standard SDS–PAGE minigels prepared with 0.1% SDS in the running buffer, incubate for 30 to 60 min. Large gels, including large two-dimensional gels, sometimes require a preincubation in 7.5% acetic acid for 30 min prior to staining to reduce background fluorescence due to excess SDS in the gel. It is important to note, however, that acetic acid interferes with transfer to blots.

6. Use the following step if the proteins are to be transferred to a blot. After staining, incubate the gel in Western blotting buffer containing 0.1% SDS. The SDS is not absolutely required, but it helps in the transfer of some proteins to the blot.

C. Viewing, Photographing, and Storing the Gel

Detect the proteins in the stained gel using a standard 300-nm UV transilluminator, a blue-light transilluminator, 473-nm SHG laser, 488-nm argon ion, or 473-nm He–Ne laser-based imaging system (*see* Section V,E). Gels may be left in staining solution overnight without loss of sensitivity. However, photographs should be taken as soon as possible after staining. Gels may be documented by a Polaroid or CCD camera. Use Polaroid 667 black-and-white print film and the SYPRO protein gel stain photographic filter (Molecular Probes, Inc., Cat. No. S-6656). Exposure times vary with the intensity of the illumination source; for an f stop of 4.5, use a 2- to 5-s exposure time. CCD cameras and laser scanners provide high sensitivity; contact the manufacturer to determine the optimal filter sets (*see* Section V,F).

D. Destaining Gels

SYPRO Tangerine stain is readily destained by incubation in 7% acetic acid or 30% methanol.

E. Notes for SYPRO Tangerine protein gel stain

The SDS front at the bottom of the gel stains very heavily with SYPRO Tangerine stain. Unless the proteins that interest you are comigrating with the SDS front, it will be advantageous to run the SDS front off the gel. Colored stains and marker dyes, as well as commercially prestained protein markers, may interfere with SYPRO Tangerine dye staining and quench fluorescence.

IV. PROTOCOL FOR SYPRO RUBY PROTEIN GEL STAIN

A. Materials and Reagents

SYPRO Ruby protein gel stain (Molecular Probes, Inc., Cat. No. S-12000, S-12001, S-21900) is provided ready to use in 200 ml volume (will stain ~4 minigels), 1 liter volume (~20 minigels or 2–3 large-format gels), or 5 liter volume (~100 minigels or 10–15 large-format gels). Staining should be performed in plastic dishes (preferably polypropylene) (*see* Section V,B).

B. Protocol

Prepare and run SDS–PAGE or two-dimensional PAGE according to standard protocols (Laemmli, 1970; O'Farrell, 1975). Perform staining with SYPRO Ruby due using continuous, gentle agitation (e.g., on an orbital shaker at 50 rpm).

1. Clean and *thoroughly rinse* the staining dishes before use. Residual detergent in staining dishes will compromise the detection of proteins.
2. A range of fixatives have been validated for use with SYPRO Ruby protein gel stain, including 40% ethanol/10% acetic acid, 10% ethanol/7% acetic, acid 25% ethanol/12.5% trichloroacetic acid, and 10% ethanol/3% phosphoric acid. Harsher fixatives, such as 40% ethanol/10% acetic acid, are recommended as they retain proteins in gels better. Fix the gel in a plastic dish for 30 min. This step improves the sensitivity of the stain in two-dimensional gels, but is optional for one-dimensional SDS–PAGE gels.
3. Pour the staining solution into a small, clean plastic dish. For one or two standard-size minigels, use ~50 to 100 ml of staining solution; for larger gels, use 500 to 750 ml (*see* Section V,A).
4. Place the gel into the staining solution. Protect the gel and staining solution from light at all times by covering the container with a lid or with aluminum foil.
5. Gently agitate the gel in stain solution at room temperature (50 rpm on an orbital shaker). The staining times range from 90 min to 4 h, depending on the thickness and percentage of polyacrylamide in the gel. Specific staining can be seen in as little as 30 min. However, a minimum of 4 h of staining is required for maximum sensitivity and linearity. For convenience, gels may be left in the dye solution overnight or longer without overstaining.
6. *Optional.* After staining, rinse the gel in deionized water for 30–60 min to decrease background fluorescence. To better decrease background fluorescence the gel can be washed in a mixture of 10% methanol and 7% acetic acid for 30 min instead of water. The gel may be monitored periodically using UV illumination to determine the level of background fluorescence.

C. Viewing, Photographing, and Storing the Gel

View the stained gel on a standard 300-nm UV or a blue-light transilluminator (*see* Section V,E). Gels may also be visualized using various laser scanners: 473-nm (SHG) laser, 488-nm argon ion laser, and 532-nm (YAG) laser. Alternatively, use a xenon arc lamp, blue fluorescent light, or blue light-emitting diode (LED) source. Gels may be left in staining solution overnight without losing sensitivity. However, images should be acquired as soon as possible after staining. Gels may be imaged by a Polaroid or CCD camera. Use Polaroid 667 black-and-white print film and the SYPRO protein gel stain photographic filter (Molecular Probes, Inc., Cat. No. S-6656). Exposure times vary with the intensity of the illumination source; for an f stop of 4.5, try 1 s. CCD cameras and laser scanners provide high sensitivity; contact the manufacturer to determine the optimal filter sets (*see* Section V,F). To dry the stained gel for permanent storage, incubate the gel in a solution of 2% glycerol for 30 min. Dry the stained gel using a gel dryer. Note that proteins present at very low levels may no longer be detectable after gel drying.

V. NOTES

A. Staining

Minimal staining volumes for typical gel sizes:

50 ml for 8 cm × 10 cm × 0.75 mm gels (minigels)
330 ml for 16 cm × 20 cm × 1 mm gels
500 ml for 20 cm × 20 cm × 1 mm gels
or ~10 times the volume of the gel for other gel sizes

B. Staining Containers

Polypropylene dishes, such as Rubbermaid Servin' Savers, are the optimal containers for staining because the high-density plastic adsorbs only a minimal amount of the dye. Clean and rinse the staining containers well before use, as detergent will interfere with staining. Some rinse the containers with ethanol before use. For small gels, circular staining dishes provide the best fluid dynamics on orbital shakers, resulting in less dye aggregation and better staining. For large-format two-dimensional gels, polyvinyl chloride photographic staining trays, such as Photoquip Cesco-Lite 8 × 10-in. photographic trays (Genomic Solutions, Ann Arbor, MI), also work well. Another convenient staining option for large-format two-dimensional gels uses the Clearview three-drawer organizer (Sterilite, Cat. No. 1790, Townsend, MA). This polypropylene box provides a convenient format for staining three gels per unit and is available at many department stores. Glass dishes are not recommended as they have a tendency to bind dye.

C. Fixing Gels

For low percentage gels and for very small proteins, 10% acetic acid solution will result in better retention of the protein in the gel without compromising sensitivity. Acetic acid will interfere with transfer of the proteins to a blot. Therefore, for applications in which blotting will follow electrophoresis, use SYPRO Tangerine protein gel stain, which does not require acetic acid fixation.

D. Storing Gels

Always store gels in the dark to prevent photobleaching. When gels are stored in the staining solution, the signal decreases somewhat after several days; however, depending on the amount of protein in bands of interest, gels may retain a usable signal for many weeks. Gels may be dried between sheets of cellophane (BioRad Laboratories), although there is sometimes a slight decrease in sensitivity.

E. Viewing Gels

Viewing the Gel with UV Transillumination

Place the gel directly on the transilluminator; do not use plastic wraps or plastic backing. It is important to clean the surface of the transilluminator after each use with deionized water and a soft cloth (such as cheesecloth), as fluorescent dyes, such as SYPRO stains, will accumulate on the glass surface and cause a high background fluorescence.

The polyester backing on some precast gels is highly fluorescent. For maximum sensitivity using a UV transilluminator, the gel should be placed polyacrylamide side down and an emission filter, such as the SYPRO protein gel stain photographic filter (S-6656), used to screen out the blue fluorescence of the plastic. The use of a blue-light transilluminator or laser scanner will reduce the amount of fluorescence from the plastic backing so that the gel may be placed polyester side down.

Noticeable photobleaching can occur after several minutes of exposure to ultraviolet light. If a gel becomes photobleached, it can be restained by simply returning it to the staining solution.

F. Imaging Gels

Because of the low fluorescence, it is possible to take advantage of the integrating capability of photographic or CCD cameras and use long exposure times to increase the sensitivity, often making bands visible that are not visible to the eye. Images are best obtained by digitizing at about 1024 × 1024 pixels resolution with 12- or 16-bit gray scale levels per pixel. Contact the camera manufacturer for recommendations on filter sets. A CCD camera-based image analysis system can gather quantitative information that will allow comparison of fluorescence intensities between different bands or spots.

Acknowledgments

I gratefully acknowledge the many scientists who have contributed to the SYPRO dye development program over the years. These include Tom Steinberg, Kiera Berggren, Birte Schulenberg, Richard Haugland, Vicki Singer, Courtenay Hart, Brad Arnold, Nick Smith, Mary Nunally, and Laurie Jones. SYPRO is a registered trademark of Molecular Probes, Inc.

References

Berggren, K., Chernokalskaya, E., Lopez, M., Beechem, J., and Patton, W. (2001). Comparison of three different fluorescent visualization strategies for detection of *Escherichia coli* ATP synthase subunits after SDS-polyacrylamide gel electrophoresis. *Proteomics* **1**, 54–65.

Berggren, K., Chernokalskaya, E., Steinberg, T., Kemper, C., Lopez, M., Diwu, Z., Haugland, R., and Patton, W. (2000). Background-free, high-sensitivity staining of proteins in one- and two-dimensional sodium dodecyl sulfate-polyacrylamide gels using a luminescent ruthenium complex. *Electrophoresis* **21**, 2509–2521.

Berggren, K., Schulenberg, B., Lopez, M., Steinberg, T., Bogdanova, A., Smejkal, G., Wang, A., and Patton, W. (2002). An improved

formulation of SYPRO Ruby protein gel stain: Comparison with the original formulation and with a ruthenium II tris (bathophenanthroline disulfonate) formulation. *Proteomics* **2**, 486–498.

Gerner, C., Vejda, S., Gelbmann, D., Bayer, E., Gotzmann, J., Schulte-Hermann, R., and Mikulits, W. (2002). Concomitant determination of absolute values of cellular protein amounts, synthesis rates, and turnover rates by quantitative proteome profiling. *Mol. Cell Proteomics* **1**, 528–537.

Laemmli, U. (1970). Cleavage of structural proteins during the assembly of the head of bacteriophage T4. *Nature* **227**, 680–685.

Lopez, M., Berggren, K., Chernokalskaya, E., Lazarev, A., Robinson, M., and Patton, W. (2000). A comparison of silver stain and SYPRO Ruby protein gel stain with respect to protein detection in two-dimensional gels and identification by peptide mass profiling. *Electrophoresis* **21**, 3673–3683.

Nishihara, J., and Champion, K. (2002). Quantitative evaluation of proteins in one- and two-dimensional polyacrylamide gels using a fluorescent stain. *Electrophoresis* **23**, 2203–2215.

O'Farrell, P. (1975). High resolution two-dimensional electrophoresis of proteins. *J. Biol. Chem.* **250**, 4007–4021.

Patton, W. (2000). A thousand points of light; the application of fluorescence detection technologies to two-dimensional gel electrophoresis and proteomics. *Electrophoresis* **21**, 1123–1144.

Patton, W. (2002). Detection technologies in proteome analysis. *J. Chromatogr. B Biomed. Appl.* **771**, 3–31.

Patton, W., and Beechem, J. (2002). Rainbow's end: The quest for multiplexed fluorescence quantitative analysis in proteomics. *Curr. Opin. Chem. Biol.* **6**, 63–69.

Steinberg, T., Haugland, R., Singer V., and Jones, L. (1996a). Applications of SYPRO Orange and SYPRO Red protein gel stains. *Anal. Biochem.* **239**, 238–245.

Steinberg, T., Jones, L., Haugland, R., and Singer, V. (1996b). SYPRO Orange and SYPRO Red protein gel stains: One-step fluorescent staining of denaturing gels for detection of nanogram levels of protein. *Anal. Biochem.* **239**, 223–237.

Steinberg, T., Lauber, W., Berggren, K., Kemper, C., Yue, S., and Patton, W. (2000). Fluorescence detection of proteins in SDS-polyacrylamide gels using environmentally benign, non-fixative, saline solution. *Electrophoresis* **21**, 497–508.

Steinberg, T., Martin, K., Berggren, K., Kemper, C., Jones, L., Diwu, Z., Haugland, R., and Patton, W. (2001). Rapid and simple single nanogram detection of glycoproteins in polyacrylamide gels and on electroblots. *Proteomics* **1**, 841–855.

Steinberg, T., White, H., and Singer, V. (1997). Optimal filter combinations for photographing SYPRO Orange or SYPRO Red dye-stained gels. *Anal. Biochem.* **248**, 168–172.

CHAPTER

29

Autoradiography and Fluorography: Film-Based Techniques for Imaging Radioactivity in Flat Samples

Eric Quéméneur

I. INTRODUCTION

Autoradiography (ARG) is the photography-derived technique used to visualize the distribution of a compound labelled radioactively with either a β or γ emitting isotope in a biochemical sample. It has become a fundamental tool, particularly since slab gel electrophoresis has established as an inevitable techniques for separating and analysing complex mixtures of biomolecules. Any other flat samples such as blotting and dotting membranes, thin-layer chromatography plates, or microscopy slides are suitable. It is worth comparing ARG with numeric methods (phosphorimagers) that have popularised in many laboratories for 10 years. Indeed, films appear superior in terms of traceability and resolution. The resolution of a film depends on the size of metal grain in the photographic emulsion. A simple calculation shows that, assuming a grain diameter of 0.2 µm, a film displays a resolution of about 127,000 dpi compared to 600 dpi for a common laser printer. This resolution allows a possible magnification of up to 500-fold until the resolution of human eye (about 100 µm) is surpassed. In other terms, a 10×10-cm^2 autoradiographic picture is equivalent to a 25 million pixel digital image. Furthermore, an autoradiogram is exactly the same size as the sample, making it easy the precise location of a "hot spot" in a complex pattern.

Basically, autoradiographic techniques divide into two modes. The first one, direct ARG, is the direct exposure of film by β particles or γ rays emitted by the sample. In the second mode, the film is sensitized indirectly by the secondary light generated upon excitation of a "fluor" (fluorography) or a "phosphor" (indirect ARG with intensifying screen) by the radioactive emission. Autoradiography and fluorography look simple in appearence, but some fundamental notions should be known and kept in mind for obtaining sensitive, resolutive, and reproducible results. Among them, the notion that sensitivity and resolution are antagonistic concepts that cannot be matched simultaneously. Because of their path lengths, lower energy isotopes such as ^{3}H, ^{35}S, or ^{14}C have better resolution than higher ones such as ^{32}P or ^{125}I. This detection is not sensitive and indirect methods based on the emission of UV/blue photon promote sensitivity but decrease resolution (Fig. 1). Other important notions are discussed in Section IV.

II. MATERIALS AND INSTRUMENTATION

For catalog numbers of reagent, products, and equipment, see Table I. Dark room equipped with appropriate lighting systems: the red light could be a 7.5- to 15-W bulb covered with a red Kodak GBX-2 filter.

Labelling the corners of the sample to assist the accurate alignment of the sample to its autoradioradiogram is useful. Use either a nib and radioactive ink prepared by mixing 100 µl of Indian ink with a few microliters of the diluted radioisotope solution used in the experiment. Alternatively, a pen containing a

Copyright 2006, Elsevier Science (USA).
All rights reserved.

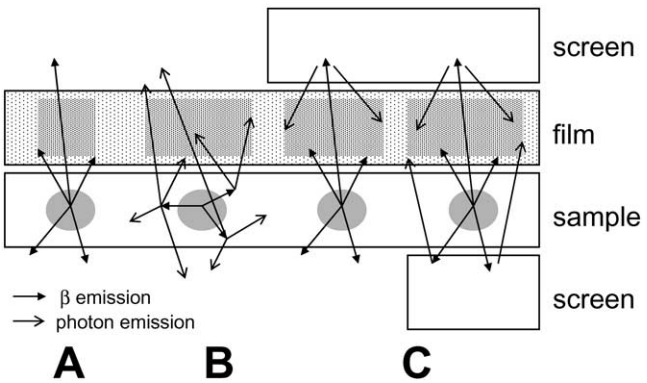

FIGURE 1 The underlying principle of the major detection methods and the way to assemble the various components in the cassette correctly. (A) Direct ARG; (B) fluorography; and (C) indirect ARG with either one or two intensifying screens. Note the variation in image size (resolution) depending on the nature and path of radiations.

phosphorescent ink or luminescent stickers can prove more convenient (e.g., Glogos II Autorad Markers, Stratagene).

Microscale standards (Amersham Biosciences) are convenient calibration strips for relative quantitation in all mode of detection. They are available for ^{3}H, ^{14}C, and ^{125}I with activity scales ranging from 3.74 to 4048 Bq/mg, from 3.7 to 31,890 Bq/g, and from 44 to 23,900 Bq/mg, respectively. For films and intensifying screens, see Table I for the appropriate choice.

II. PROCEDURES

Three procedures are reported here. The choice depends practically on the nature of the isotope (energy of emitted radiations) and on the yield of radi-

TABLE I Catalog Numbers of Reagents, Products, and Equipments Used

Darkroom safelight kit (Kodak, Cat. # 852 1429)
GBX-2 filter, 10 × 12 in. (Kodak, Cat. # 141 6940)
Pen with phosphorescent ink (Soquelec Cat. # R20105)
Glogos II Autorad Markers, 100 luminescent stickers (Stratagene, Cat. # 420 201)
Microscale standards
^{3}H microscales: 10 strips 0.111–4.07 kBq/mg + 10 strips 3.7–592 Bq/mg (Amersham Cat. # RPA510)
^{14}C microscales: 20 strips 1.15–32.7 kBq/g (Amersham Cat. # RPA504L)
^{14}C microscales: 20 strips 3.7–3700 Bq/g (Amersham Cat. # RPA511L)
^{125}I microscales: 20 strips 0.046–23.7 kBq/mg (Amersham Cat. # RPA523L)
Films
Hyperfilm MP, 20.3 × 25.4 cm, 75 sheets/box (Amersham, Cat. # RPN 1678K)
BioMax MS-2, 20.3 × 25.4 cm, 50 sheets/box (Kodak, Cat. # 837 7616)
BioMax MR-2, 20.3 × 25.4 cm, 50 sheets/box (Kodak, Cat. # 895 2855)
X-Omat AR-2, 20.3 × 25.4 cm, 50 sheets/box (Kodak, Cat. # 165 1579)
Cronex 10T, 10 × 12 in., 100 sheets/box (Agfa Medical, Cat. # LF5E3)
Intensifying screens
Hyperscreen, 20.3 × 25.4 cm (Amersham, Cat. # RPN 1669)
BioMax MS Screen, 20.3 × 25.4 cm (Kodak, Cat. # 851 8706)
TransScreen HE, 20.3 × 25.4 cm (Kodak, Cat. # 856 3959)
TransScreen LE, 20.3 × 25.4 cm (Kodak, Cat. # 162 2034)
Optex HighPlus (MCI Optonix, Cat. # 6102)
Cassettes
BioMax Cassette, 20.3 × 25.4 cm (Kodak Cat. # 820 9140)
Hypercassette, 20.3 × 25.4 cm (Amersham, Cat. # RPN 11649)

En^{3}Hance spray for fluorography, 2 oz. (NEN, Cat. # NEF 9700)
Enligthning rapid autoradiography enhancer, 1 liter (NEN)
Amplify fluorographic reagent, 1 liter (Amersham, Cat. # NAMP 100)
PPO (2,5-diphenyloxazole) scintillation grade, Sigma-Aldrich, Product # D210404
Cellulose paper Grade 3 MM Chr (thickness 0.34 mm), 20 × 25 cm, 100 sheets/box (Whatman, Cat. # 3030-866)
Cellulose paper grade 1 Chr (thickness 0.18 mm), 25 × 25 cm, 100 sheets/box (Whatman, Cat. # 3001-878)
Mineral oil, "Nujol" (Sigma-Aldrich, Cat. # M1180)
Orange-filtered preflash unit Sensitize (Amersham, Cat. # RPN 2051)
Kodak GBX developer, concentrate to make 3.8 liter (Kodak, Cat. # 190 0943)
Kodak GBX fixer, concentrate to make 3.8 liter (Kodak, Cat. # 190 2485)
Metal hanger for 20.3 × 25.4-cm films (Kodak, Cat. # 150 2764)

olabeling (amount of activity expected in a spot). A compromise has to be found between sensitivity and resolution. Table III might help in making the choice and in estimating the necessary exposure time.

A. Direct Autoradiography

This is the method of choice for high resolution whatever the isotope used, although it is rarely suitable for ^{3}H, ^{14}C, or ^{35}S under normal labelling conditions *in vivo*.

Steps

1. Protect the cassette from radioactivity by placing a Saran wrap or plastic sheet under the sample.

TABLE II Choosing the Right Combination of Films and Products

Priority	Method	Film	Screen
Speed, sensitivity	Indirect ARG *(high energy isotopes)*	Hyperfilm™ MP[a] BioMax™ MS[b]	Hyperscreen™[a] BioMax™ MS Screen[b]
	Fluorography *(low energy isotopes)*	X-Omat™ AR (XAR)[b] Super RX[c]	TranScreen™ HE[b] *(high energy isotopes)*
	Direct ARG *(high energy isotopes)*	Cronex 10T[d]	TranScreen LE[b] *(low energy isotopes)* Optex HighPlus[e]
Resolution	Direct ARG	BioMax™ MR[b] Hyperfilm™ 3H[a] Hyperfilm™ βmax[a]	

[a] Amersham;
[b] Eastman Kodak;
[c] Fuji;
[d] Agfa;
[e] MCI Optonix.

2. Put the sample in the cassette. Preferably, the sample should be dry. If not, cover it with Saran wrap in order to avoid sticking of the sample to the film. However, for a sample containing ^{3}H, it is important to remove any barrier such as Saran wrap or a cellophane sheet that may quench the emitted radiations.

3. If necessary, label distinctly two corners of the sample using the radioactive ink. This will help in the future superimposition of the gel and the film. Avoid moisture or glove powder on the surface of the sample.

4. In the dark room, place the film in close contact with the sample. When using single-coated films as recommended for ^{3}H (Fig. 2), the sensitive face of the film should face the sample (Fig. 1).

5. Close the cassette carefully and let it stand at room temperature for the necessary exposure time. Refer to Table II for an estimate of this exposure time. An overnight exposure would be sufficient for the detection of most ^{32}P-containing samples, whereas a 2- to 3-day exposure might be necessary for ^{35}S.

6. Remove the film from the cassette in the dark-room and process it according to the manufacturer's instructions or as described in Section III,E.

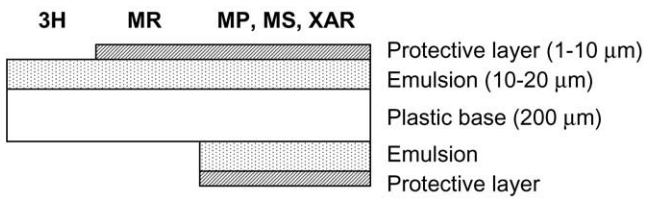

FIGURE 2 The structure of some commercially available films. The film types are ordered by increasing sensitivity but decreasing resolution. See Table II for film names and manufacturers.

TABLE III Choosing the Optimal Detection Method

Isotope	Radiation	E_{max} (MeV)	Path max in air	Minimal activity detected in 24 h in a 0.1-cm² band (in Bq)		
				Direct ARG	Fluorography	Indirect ARG
^{3}H	β^-	0.018	6 mm	15,000	15	inadequate
^{14}C, ^{35}S	β^-	0.156, 0.167	25 cm	10	400	inadequate
^{32}P	β^-	1.710	8 m	1	Inadequate	0.1
^{125}I	γ	0.035	>10 m	2.5	Inadequate	0.2
	X	0.027				
	Auger e^-	0.030				

B. Fluorography

Fluorography is particularly recommended for low-energy isotopes, when sensitivity is required and loss of resolution is acceptable. In pratice, it might be the only way to visualise ^{3}H-labeled compounds.

Solutions

Commercial reagents such as En^{3}Hance (NEN), Enligthning (NEN), or Amplify (Amersham) are efficient and convenient, but expensive.

Steps

1. Stain and destain the sample as usual, avoid TCA for fixing proteins and BET for staining nucleic acids because this would subsequently quench the fluorescence.
2. Work in a fume hood. Soak the sample in the scintillant reagent with gentle agitation for 1 h. The tray should contain enough reagent so that the sample is free floating and does not stick to the walls.
3. Discard the reagent and move to the 4°C cold room. Add slowly 500 ml cold 10% glycerol along the walls of the tray and shake slowly for 1 h. The low temperature prevents the fluor from diffusing out of the gel. The gel will turn white opaque after this step.
4. Put the sample on the top of a thick Whatman paper, cover it with a Saran wrap, and dry the ensemble under vacuum for 2 h at 60°C.
5. Let the sample reach the ambient temperature before putting it in the autoradiography cassette. In the dark room, prepare the cassette in the following order: gel/Saran/film. Exposure should be performed at –70/–80°C. For film processing, see Section III,E.

For seldom use of fluorography if the commercial reagent is not available in the laboratory, or if cost is a limiting factor, an efficient home-made reagent can be made: 20% 2,5-diphenyloxazole (PPO) in undiluted acetic acid (Skinner, 1983). The following procedure works well with most types of samples.

1. Soak sample in undiluted acetic acid for 5 min.
2. Impregnate with the reagent for 1.5 h with gentle agitation.
3. Soak in water for 30 min.
4. Dry and expose to film at –70°C.

C. Indirect Autoradiography with Intensifying Screens

The use of intensifying screens is not efficient for low-energy isotopes such as ^{3}H, ^{14}C, ^{33}P, or ^{35}S because the path of their β emission is too short to cross the film and reach the screen.

Steps

Steps 1–3 are the same as in Section III,A.

4. Place the film over the sample.
5. Place the screen over the film so that the matt white side (the side where the fluorescent material stands) faces the film. Note that the screen must have been kept in the dark for several hours before being introduced in the cassette in order to avoid a glow effect that would increase background on the film.
6. Close the cassette carefully and put it at –70/–80°C for the necessary exposure time (see Table III for estimation). By default, a 24-h exposure might be fine.

For transparent samples such as polyacrylamide gels, a second screen could be placed under the sample (white face up) to further increase sensitivity. Blots can be rendered translucent by impregnation with mineral oil (Rust, 1987). Kodak has introduced the TranScreen to solve the problem of the film attenuating the β particle before it reaches the screen. In our experience, with ^{3}H, the result has about twofold higher sensitivity compared to the conventional screen.

D. Film Preflashing

The preflashing of films increases their sensitivity for small amounts of radioactivity and expands the range for linear response. It is used only with photon-based detection (Sections III,B and III,C) and has no effect for direct autoradiography or for large amounts of radioactivity in short exposures. Preflashed films are only valid for a couple of days and must be stored at –70/–80°C if not used immediately.

Steps

1. In the dark room, install the orange-filtered flash, e.g., Sensitize (Amersham), at 50 cm above the film area.
2. Cut six film strips (just large enough to be processed) and cover them with a sheet of Whatman paper No. 1. Keep one of the strips in a closed cassette.
3. Make five consecutive flashes of 1 ms each while removing a strip between each in order to obtain a set of strips ranging from 1- to 5-ms exposure times.
4. Process the six strips and cut them to the format of a spectrophotometer cuvette holder (usually 1 × 4 cm).

5. Read absorbances at 545 nm on a spectrophotomer, plot the values of exposure time versus absorbance, and select the exposure time that gives an A_{545} in the range of 0.1–0.2.
6. In the dark room, select the film to be used for fluorography or with intensifying screens. Preflash it for the selected exposure time. The preflashed side of the film should face the sample when preparing the cassette (Fig. 1).

E. Processing of Films

Most laboratories dealing with a large number of autoradiograms have an automated processor. If this is the case, for optimal results with your sample, make sure that chemicals are fresh and the machine is regularly cleaned up. This article provides a method for the manual processing of films to those who are not equipped with such a machine or seldom use autoradiographic methods. Furthermore, some films are not protected by an antiscratch layer in order to maximize sensitivity to low-energy isotopes, e.g., Hyperfilms ^{3}H and βmax. They must be processed manually. The present method should work well in most cases, but it is obviously preferable to refer to the manufacturer's specific instructions.

Solutions

If only a single film or few films should be processed, prepare three trays or deep tanks for multiple processings containing the following solutions.

1. *Developer*: Kodak GBX developer
2. *Rinser*: Kodak GBX indicator stop or a large volume of tap water
3. *Fixer*: Kodak GBX fixer

Minimizing volumes is an environment-friendly attitude, but good results are obtained with generous volumes of fresh reagents. Collect carefully used solutions 1 and 3 in a dedicated can, which should then be evacuated as a toxic chemical waste.

Steps

1. In the dark room, open the cassette and remove the film. Gloves should not be damp or leave powder on the film. If the cassette comes from the –70°C freezer, let it reach the ambient temperature before opening.

2. Handle the film with suitable pliers or attach it to a metal hanger.

3. Immerse quickly in developer. Dislodge air bubbles by tapping the film against the tank wall. Then do not agitate during development, which will occur within 2–5 min depending on the temperature of the solution.

4. Remove film from the developer and transfer it to the rinser. Wash with continuous, moderate agitation for 30 s.

5. Place the film in the fixer for 10 min. Moderate agitation is recommended. The background should become uniformly transparent.

6. Wash in a large tank filled with running water for 5 min.

7. Hang the film on a line with a suitable clip attached to one corner and let it dry at room temperature in a dust-free area.

IV. COMMENTS

Whenever possible, blotting samples separated previously by electrophoresis from the gel matrix onto the surface of a nitrocellulose membrane should be performed. This has a minor impact on resolution but it improves tremendously the detection of all types of isotopes, particularly that of low-energy isotopes (Quéméneur, 1995). Films should be handled carefully when unpacking to avoid electrostatic artifacts that would print on the film.

V. PITFALLS

When working with high-energy isotopes such as ^{32}P or ^{125}I, do not stack cassettes during exposure because the path of the emission is sufficient to generate phantom images on the neighbouring film. In the same idea, do not store films too close to the working area. Film storage is extremely important for reproducible high-quality results. Ideal storage conditions are 10–20°C and 30–50% hygrometry. Avoid piling up film packages and use an upright position to diminish physical strains on the surface of the films.

The quality of the dark room and its equipment is critical. The inactinic safelight should be at a minimal distance of 1 m. The performance of the red filter decrease with time and it is reasonable to change it every 5 years.

References

Laskey, R. A. (1993). Efficient detection of biomolecules by autoradiography, fluorography or chemilumiscence, Review booklet #23, 2nd Ed.—Amersham Biosciences.

Laskey, R. A. (2002). Radioisotope detection using X-ray film. *In "Radioisotopes in Biology"* (R. J. Slater, ed.), 2nd Ed.", pp. 63–83. Oxford Univ. Press, Oxford.

Perng, G., Rulli, R. D., Wilson, D. L., and Perry, G. W. (1988). A comparison of fluorographic methods for the detection of 35S-labeled proteins in polyacrylamide gels. *Anal. Biochem.* **175**, 387–392.

Quéméneur, E., and Simonnet, F. (1995). Increased sensitivity of autoradiography and fluorography by membrane blotting. *Biotechniques* **18**, 100–103.

Rust, S., Kunke, H., and Assman, G. (1987). Mineral oil enhances the autoradiographic detection of ^{32}P-labeled nucleic acids bound to nitrocellulose membranes. *Anal. Biochem.* **163**, 196–199.

Skinner, M. K., and Griswold, M. D. (1983). Fluorographic detection of radioactivity in polyacrylamide gels with 2,5-diphenyloxazole in acetic acid and its comparison with existing procedures. *Biochem. J.* **209**, 281–284.

SECTION

10

Gel Profiling of Posttranslationally Modified Proteins

CHAPTER

30

Two-Dimensional Gel Profiling of Posttranslationally Modified Proteins by *in vivo* Isotope Labeling

Pavel Gromov and Julio E. Celis

I. INTRODUCTION

The repertoire of posttranslational modifications, which some cellular proteins may undergo after synthesis, falls into two main categories: chemical modifications and processing. Chemical modification involves the linkage of a chemical group to the terminal amino acid or carboxyl groups of the backbone or to reactive groups in the side chains of internal residues. Protein processing involves the proteolytic removal of the polypeptide segments from the premature protein chain. In some cases, both types of protein modifications are closely coupled. Such posttranslational modifications may alter the activity, life span, interactions, and/or cellular localization of proteins, depending on the nature of the modification(s). The most common chemical modifications include acetylation, methylation, phosphorylation, glycosylation, lipid-mediated modifications, and ADP-ribosylation, as well as several others (Mumby, 2001; Fu *et al*., 2002; Spiro, 2002; Corda *et al*., 2002; Sinensky, 2000; Cohen, 2000; Casey, 1995 and references therein). New multiplexing tools suitable for general protein detection, including posttranslational variants, have been employed in proteome analysis over the years and are reviewed by Patton (2002).

Each modification causes changes in the molecular weight and often in the charge of a protein, a fact that makes two-dimensional (2D) PAGE well suited for the detection of many posttranslational modifications in combination with mass spectrometry and/or Western immunoblotting if the epitope structure of the modified molecule is not altered by the modification (see article by Celis *et al*. in Volume 2). Several mass spectrometric approaches have been developed for the identification and analysis of various posttranslational modifications and have been reviewed by Abersold and Mann (2003) and by Sickmann *et al*. (2002).

In many cases, however, the identification and analysis of posttranslational modifications can be achieved by *in vivo* or *in vitro* labeling of the proteins with an appropriated isotope-labeled metabolite. Once the radiolabeled ligand is covalently attached to the protein, it can be readily detected on a gel or in a blot using autoradiography. This article describes protocols for 2D gel mapping of posttranslationally modified proteins as applied to the analysis of phosphorylated, glycosylated, and lipidated proteins (palmytoylated, myristoylated, farnesylated, and geranylgeranylated) from human keratinocytes and transformed human amnion cells (AMA).

II. MATERIALS AND INSTRUMENTATION

A. Transformed Human Amnion Cells

AMA cells are grown in complete Dulbecco's modified Eagle's medium (DMEM) containing 10% fetal calf serum (FCS). General procedures for culturing these cells are described in details elsewhere (Celis and Celis, 1997; see also article by Micleady and O'Commo in Volume 1).

Copyright 2006, Elsevier Science (USA).
All rights reserved.

B. Noncultured Human Keratinocytes

Noncultured unfractionated human epidermal keratinocytes are prepared from normal skin epidermis as described by Celis *et al*. (1995).

C. Reagents

DMEM (Cat. No. 31966-021) is from GIBCO. Penicillin/streptomycin (Cat. No. A2213) is from Biocrom KG. Dulbecco's modified Eagle's phosphate-deficient medium (Cat. No. 16-423-49) is from ICN. FCS (Cat. No. 04-001-1A) is obtained from Biological Industries. Tissue culture plates (24-well) (Cat. No. 662 160) are from Greiner. All other reagents and general tissue culture facilities are as described elsewhere (Celis and Celis, 1997). 2,5-Diphenyloxazole (PPO, Cat. No. D-4630) is from Sigma, and dimethylether (Cat. No. 823277) is from Merck. [^{35}S]Methionine (Cat. No. SJ 204), [^{32}P]orthophosphate (Cat. No. PBS 13A), [^{3}H]mannose (Cat. No. TRK364), [^{3}H]palmitic acid (Cat. No. TRK909), [^{3}H]myristic acid (Cat. No. TRK907), [^{3}H]farnesyl pyrophosphate (Cat. No. TRK917), and [^{3}H]geranylgeranyl pyrophosphate (Cat. No. TRK918) are from Amersham. Lovastatin is from Merck.

III. PROCEDURES

The protocols for metabolic labeling of posttranslationally modified proteins are illustrated using noncultured unfractionated human epidermal keratinocytes and AMA cells, but can be applied to other cultured cell lines. The volumes given in the following procedure are for labeling in a single well of a 24-well plastic culture plate. For larger tissue culture dishes or multiwell labeling, adjust all amounts accordingly.

A. Phosphorylation

Eukaryotic protein phosphorylation is a reversible covalent addition of phosphate to a protein molecule by means of formation of an ester bond between the phosphoryl group and serine, threonine, or tyrosine residues. Protein phosphorylation is one of the most common posttranslational modifications and is of crucial importance for many regulatory processes. Net phosphorylation is regulated by a complex cascade of protein kinases and phosphatases that catalyze phosphorylation and dephosphorylation reactions, respectively (Cohen, 2000 and references therein). While mass spectrometric methods have taken a leading role in the identification of phosphoproteins, protein radiolabeling with ^{32}P inorganic phosphate is still an effective and inexpensive method for the detection of the ^{32}P subproteome using 2D gels (Mason *et al*., 1998). This article presents a protocol for the detection of phosphorylated proteins that is based on the metabolic incorporation of [^{32}P]orthophosphate into cultured AMA cells and noncultured human keratinocytes, followed by 2D PAGE and autoradiography.

Solutions

1. *Complete Dulbecco's modified Eagle's medium*: To make 500 ml, mix 445 ml of DMEM medium, 5 ml of 10× stock penicillin/streptomycin, and 50 ml of FCS.
2. *Complete DMEM phosphate-free medium*: Prepare as described in the article by Celis and Celis (1997) using commercial DMEM phosphate-deficient medium.
3. *Hank's buffered saline solution*: To make 1 liter, dissolve 0.4 g of KCl, 0.06 g of KH_2PO_4, 0.0621 g of $NaHPO_4{\cdot}2H_2O$, and 8 g of NaCl in 800 ml of distilled water. After dissolving, complete to 1 liter with distilled water.
4. *Lysis solution*: 9.8 *M* urea, 2% (w/v) Nonidet P-40 (NP-40), 2% ampholytes, pH 7–9, and 100 m*M* dithiothreitol, (DTT). Prepare as described in the article by Celis *et al*. in this volume.
5. *[^{32}P]orthophosphate-labeling solution*: To prepare 0.25 ml, add 50 µl of commercial aqueous [^{32}P]orthophosphate solution (10 mCi/ml; HCl free) to 200 µl of complete DMEM phosphate-free medium.

Steps

1. Seed AMA cells in a 24-well tissue culture plate (approximately 3×10^4 cells per well) in 0.3 ml of complete DMEM medium containing 10% calf serum, 2 m*M* glutamine, and antibiotics.
2. Incubate the cells at 37°C in a humidified, 5% CO_2 incubator for approximately 24 h, or until the cells reach about 50% confluence.
3. Prior to labeling, aspirate the medium and wash twice with phosphate-free medium. Add 0.3 ml of phosphate-free medium and incubate the cells for 1 h.
4. Remove the phosphate-free medium and overlay with 0.25 ml of [^{32}P]orthophosphate-labeling solution (2 mCi/ml).
5. Incubate the cells at 37°C in a humidified, 5% CO_2 incubator for 8 h, or a shorter period if necessary.
6. Carefully remove the medium containing [^{32}P]orthophosphate from the plate and gently wash the cells twice with 1 ml of Hank's buffered

saline solution. Dispose of radioactive solutions according to the safety procedures enforced in your laboratory.
7. Repeat the washing twice more.
8. Carefully remove excess Hank's buffered saline solution from the plate using an elongated Pasteur pipette.
9. Resuspend the cells in 50 µl of lysis buffer and run 2D gels as described by Celis *et al*. and by Görg and Weiss in this volume.
10. Dry the gels and subject to phosphorimaging or to X-ray film autoradiography at –70°C using an amplifying screen.

Comments

Representative autoradiographs (IEF gel) of phosphoproteins from human keratinocytes and AMA cells labeled metabolically with [^{32}P]orthophosphate are shown in Fig. 1. To facilitate the identification of phosphorylated proteins, we recommend adding small amounts of [^{35}S]methionine-labeled proteins from the same cell type to the ^{32}P-labeled protein mixture. 2D gels can then be autoradiographed using two films placed on top of each other. The first film, which is placed in direct contact with the dried gel, visualizes both ^{35}S and ^{32}P isotopes, whereas the second one reveals only ^{32}P.

Identification of ^{32}P-labeled proteins can also be done in combination with 2D gel blot immunodetection. In this case, following 2D gel electrophoresis, the proteins are electroblotted to the nitrocellulose membrane and the blot is probed with the antibody of interest, e.g., against phosphotyrosine, prior or after autoradiography (see article by Celis *et al*. in Volume 1).

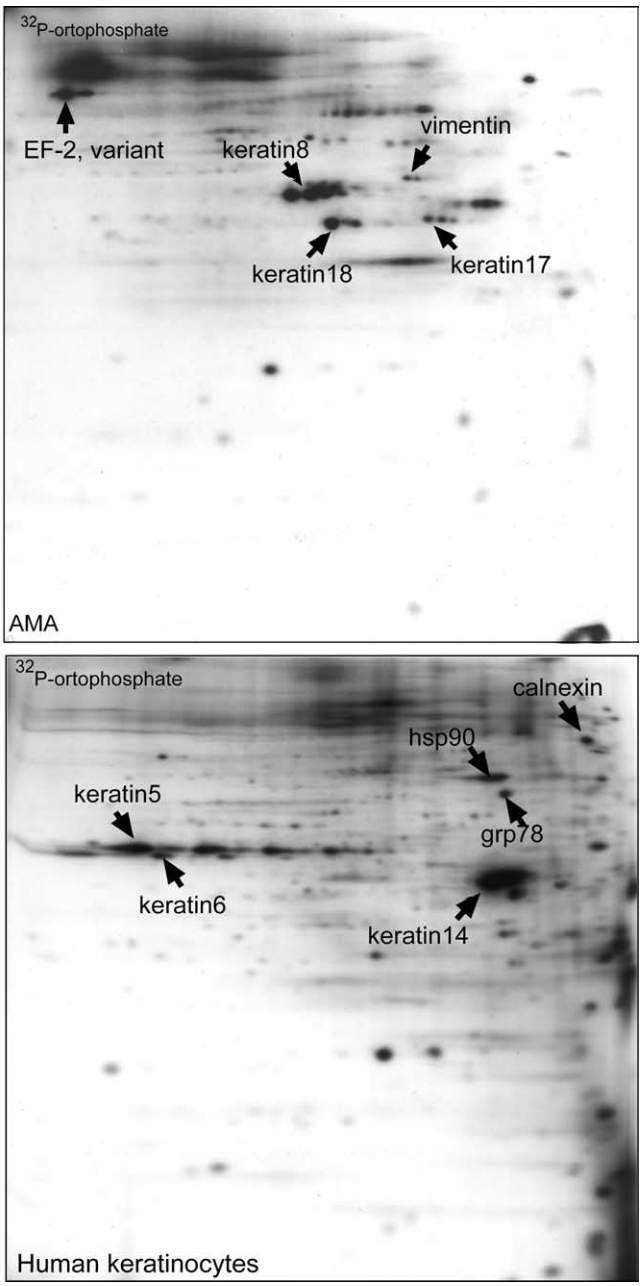

FIGURE 1 Two-dimensional (IEF) autoradiographs of whole protein extracts from AMA cells (top) and human keratinocytes (bottom) labeled with [^{32}P]orthophosphate. Several phosphoproteins are indicated as references.

B. Glycosylation

Protein glycosylation is perhaps one of the most abundant and structurally diverse types of posttranslational modification. Formation of the amino acid–sugar bond is a critical event in the biosynthesis of glycoproteins and leads to diverse biological functions (Spiro, 2002 and references therein). Glycoproteins can be detected by autoradiography after metabolic incorporation of ^{3}H or ^{14}C sugars into cultured cells or tissues (Chandra *et al*., 1998). The procedure for revealing glycosylated proteins described here is based on the metabolic incorporation of [^{3}H]mannose into cultured AMA cells, followed by 2D gel electrophoresis.

Solutions

1. *Complete Dulbecco's modified Eagle's medium*: Prepare as described in Section III,A.
2. *Hank's buffered saline solution*: Prepare as described in Section III,A.
3. *[^{3}H]Mannose–labeling solution*: 200 µCi/ml. Evaporate 50 µCi of commercial [^{3}H]mannose solution using a Speed–Vac centrifuge or by directing a gentle stream of nitrogen gas onto the surface of the solution (during this operation the temperature of

the solution should not exceed 30°C). Resuspend in 0.25 ml of complete DMEM medium.

4. *Lysis solution*: 9.8 *M* urea, 2% (w/v) NP-40, 2% ampholytes, pH 7–9, and 100 m*M* DTT. Prepare as described in Section III,A.
5. *Amplifying solution*: 7% of 2,5-diphenoloxazole (PPO) in dimethylether. To make 100 ml, weigh 7 g of PPO and complete to 100 ml with dimethylether. Store at –20°C in a hermetic glass vessel.

Steps

1. Plate and grow AMA cells in complete DMEM medium as described in steps 1 and 2 in Section III,A.
2. Aspirate the medium using an elongated Pasteur pipette and replace it with 0.25 ml of the [^{3}H]mannose-labeling solution.
3. Incubate the cells at 37°C in a humidified, 5% CO_2 incubator for 2 h.
4. Aspirate the labeling solution and wash the cells twice with Hank's buffered saline solution.
5. Carefully aspirate the excess of Hank's buffered saline solution using an elongated Pasteur pipette.
6. Resuspend the cells in 50 µl of lysis solution and run 2D gels as described by Celis *et al*. or by Görg and Weiss in this volume.
7. Following 2D gel electrophoresis, transfer the proteins onto a nitrocellulose membrane by electroblotting (see article by Celis *et al*. in Volume 1).
8. Dry the nitrocellulose blot overnight at room temperature.
9. Pour 100 ml of amplifying solution in a rectangular glass container.
10. Immerse the nitrocellulose blot into the amplifying solution for 1 s.
11. Place the nitrocellulose blot on the filter paper with the protein-bearing side facing upward and dry for 30 min.
12. Expose the dried nitrocellulose blot to an X-ray film for 1–7 days at –80°C.

Comments

A representative 2D gel (IEF) fluorograph of AMA cell proteins labeled with [^{3}H]mannose is shown in Fig. 2. Following exposure to an X-ray film, the membrane can be stained with amido black to aid in the identification of polypeptide spots. ^{3}H-labeled polypeptides can also be revealed by fluorography of dried gels stained with silver and saturated with the amplifying solution (Amersham; see also article by Celis *et al*. in this volume). However, ^{3}H fluorography from dried gels requires longer exposure times as compared to fluorography using nitrocellulose blots. To facilitate protein identification, we recommend adding a concentrated, unlabeled AMA protein extract to the ^{3}H-labeled protein sample prior to 2D gel electrophoresis.

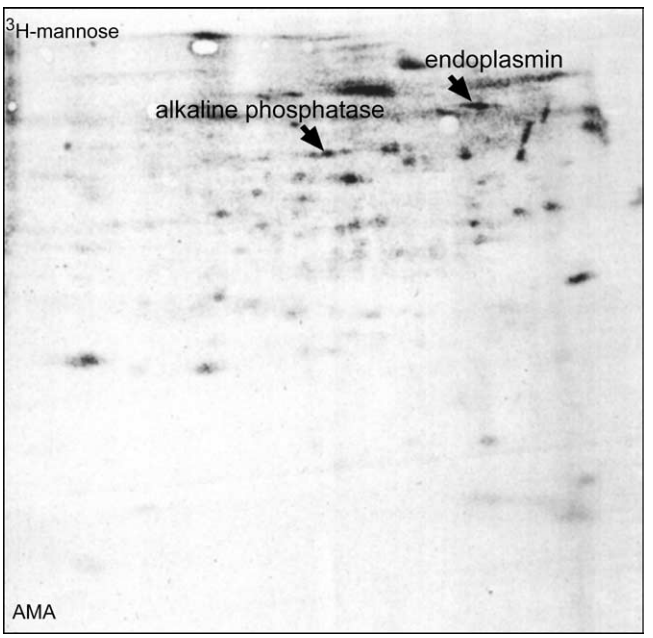

FIGURE 2 Two-dimensional (IEF) fluorograph of whole protein extracts from AMA cells labeled with [^{3}H]mannose. Several glycoproteins are indicated as references.

C. Palmitoylation and Myristoylation

Protein lipidation involves co- or posttranslational modification by specific lipids. For most lipid-modified proteins, attached lipids appear to direct or enhance the interaction with both membrane lipids and other proteins, resulting in their specific membrane localization (Casey, 1995). Lipid modified proteins are classified based on the identity of the attached lipid. Palmitoylation and myristoylation are the result of the cotranslational addition of the saturated 16-carbon fatty acid palmitate or 14-carbon fatty acid myristate, respectively, to a glycine residue at the N or C terminus of the protein. The procedure for revealing lipidated proteins described here is based on the metabolic incorporation of either [^{3}H]palmitate or [^{3}H]myristate into cultured AMA cells, followed by 2D gel electrophoresis.

Solutions

1. *Complete Dulbecco's modified Eagle's medium*: Prepare as described in Section III,A.
2. *Hank's buffered saline solution*: Prepare as described in Section III,A.

3. *[^{3}H]Palmitic acid–labeling solution*: 200 µCi/ml. Evaporate 50 µCi of commercial [^{3}H]palmitic acid solution (supplied in ethanol) using a Speed–Vac centrifuge or by directing a gentle stream of nitrogen gas onto the surface of the solution (during this operation the temperature of the solution should not exceed 30°C). Resuspend the label in 0.25 ml of complete DMEM medium.

4. *[^{3}H]Myristic acid–labeling solution*: Prepare as described earlier for [^{3}H]palmitic acid solution

5. *Lysis solution*: 9.8 *M* urea, 2% (w/v) NP-40, 2% ampholytes, pH 7–9, and 100 m*M* DTT. Prepare as described in Section III,A.

6. *Amplifying solution*: 7% of PPO in dimethylether. Prepare as described in Section III,B.

Steps

Grow, label, and handle AMA cells as described in Section III,B.

Comments

Representative 2D gel blot fluorographs, with IEF in the first dimension, of [^{3}H]palmitoylated (Fig. 3A) and [^{3}H]myristoylated (Fig. 3B) proteins from cultured AMA cells are shown in Fig 3. Spots indicated with arrowheads are labeled with both fatty acids.

D. Isoprenylation: Farnesylation and Geranylgeranylation

Posttranslational modifications of protein with isoprenoids play important roles in targeting a number of proteins to the plasma membrane, as well as in protein–protein interactions, and membrane-associated protein traffic (Sinensky, 2000 and references therein). Protein isoprenylation consists in the covalent attachment of 15-carbon isoprenoid farnesyl or 20-carbon isoprenoid geranylgeranyl via a stable thioether bond to a cysteine residue located in the C-terminal "CAAX," "CC," or "CXC" boxes (Clarke, 1992; Cox and Der, 1992). The method for detecting isoprenylated proteins is based on the specific inhibition of endogenous mevalonate (prenoid precursor) synthesis by lovastatin, followed by metabolic labeling of isoprenylated proteins *in vivo* with either [^{3}H]farnesyl- or [^{3}H]geranylgeranyl pyrophosphate. The protocol described here follows closely those of Danesi *et al*. (1995) and Gromov *et al*. (1996).

Solutions

1. *Complete Dulbecco's modified Eagle's medium*: Prepare as described in Section III,A.

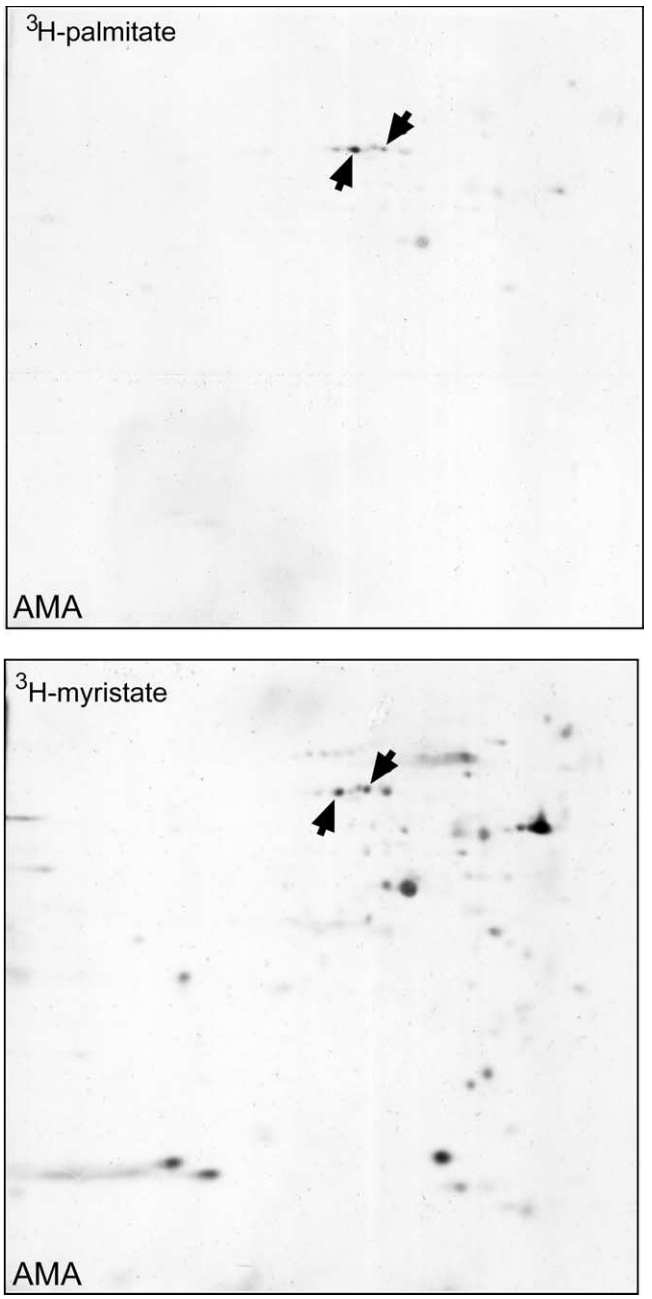

FIGURE 3 Two-dimensional (IEF) fluorographs of whole protein extracts from AMA cells labeled with [^{3}H]palmitic acid and [^{3}H]myristic acid. Proteins indicated with closed arrowheads incorporated both lipids.

2. *Hank's buffered saline solution*: Prepare as described in Section III,A.

3. *10 mM lovastatin*

4. *[^{3}H]Farnesyl-PP labeling solution*: 50 µCi/ml. Evaporate 12.5 µCi of commercial [^{3}H]farnesyl-PP solution using a Speed–Vac centrifuge or by directing

a gentle stream of nitrogen gas onto the surface of the solution (during this operation the temperature of the solution should not exceed 30°C). Resuspend in 0.25 ml of complete DMEM medium and add 0.5 ml of 10 m*M* lovastatin.

5. *[^{3}H]Geranylgeranyl-PP labeling solution*: Prepare as described previously for [^{3}H]farnesyl-PP

6. *Lysis solution*: 9.8 *M* urea, 2% (w/v) NP-40, 2% ampholytes, pH 7–9, and 100 m*M* DTT. Prepare as described in Section III,A.

7. *Amplifying solution*: 7% of PPO in dimethylether. Prepare as described in Section III,B.

Steps

1. Plate and grow AMA cells in complete DMEM medium until they reach about 80% confluence as desribed in steps 1 and 2 of Section III,A.
2. Aspirate the medium from the plate and replace it with 0.25 ml of fresh, complete DMEM medium. Add 1.25 µl of 10 m*M* lovastatin (final concentration is 50 µ*M*).
3. Incubate the cells at 37°C in a humidified, 5% CO_2 incubator for 6 h.
4. Following incubation, remove the medium and replace it with 50 µCi/ml of either [^{3}H]farnesyl- or [^{3}H]geranylgeranyl-PP labeling solutions.
5. Incubate the cells at 37°C in humidified, 5% CO_2 incubator for 16 h.
6. Remove the labeling medium and rinse the cells twice with 0.5 ml of Hank's buffered saline solution.
7. Proceed as described in Section III,B, steps 5–12.

Comments

Lovastatin induces growth inhibition and apoptosis, especially at high concentration and after prolonged treatment (Perez-Sala and Mollinedo, 1994; Patterson *et al*., 1994). Therefore, when labeling other cell types, it may be necessary to lower its concentration. Also, the efficiency of labeling may differ between cell types due to possible differences in the uptake of the isoprenoids.

Some isoprenylated proteins can be modified by both farnesyl and geranylgeranyl (Gromov *et al*., 1996). Representative ^{3}H fluorographs of AMA proteins labeled with [^{3}H]farnesyl- or [^{3}H]geranylgeranyl-PP are shown in Figs. 4A and 4B, respectively.

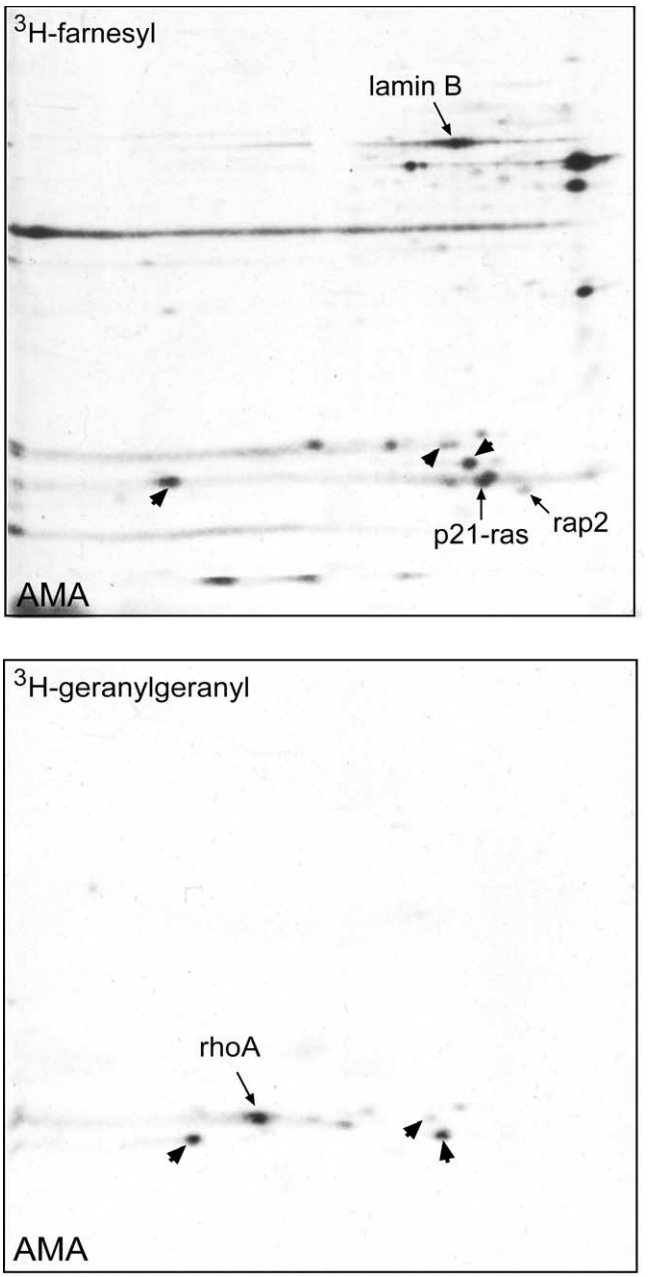

FIGURE 4 Two-dimensional (IEF) fluorographs of whole protein extracts proteins from AMA cells labeled with [^{3}H]farnesyl-PP (top) and [^{3}H]geranylgeranyl-PP (bottom). Several prenylated proteins are indicated with arrows. Proteins labeled with both isoprenoids are indicated with closed arrowheads.

IV. PITFALLS

1. Use as short a labeling time as possible in order to reduce the effect of secondary labeling.
2. Proteins that carry the same posttranslational modification may require different labeling times due to differences in protein metabolism.
3. Do not immerse the nitrocellulose filter into the amplifying solution longer than 1 s as the dimethylether destroys the membrane.

References

Aebersold, R., and Mann, M. (2003). Mass spectrometry-based proteomics. *Nature* **422**, 198–207.

Casey, P. J. (1995). Protein lipidation in cell signaling. *Science* **268**, 221–225.

Celis, A., and Celis, J. E. (1997). General procedures for tissue culture. *In "Cell Biology: A Laboratory Handbook"* (J. E. Celis, N. Carter, T. Hunter, D. Shotton, K. Simons, J. V. Small, eds.), Vol. 1, pp 5–16. Academic Press, San Diego.

Celis, J. E., Rasmussen, H. H., Gromov, P., Olsen, E., Madsen, P., Leffers, H., Honoré, B., Dejgaard, K., Vorum, H., Kristenesen, D. B., Øsregaard, M., Haunsø, A., Jensen, N. A., Celis, A., Basse, B., Lauridsen, J. B., Ratz, G. P., Andersen, A. H., Walbum, E., Kjærgaard, I., Andersen, I., Puype, M., Damme, J. V., and Vandekerckhove, J. (1995). The human keratinocyte two-dimensional gel protein database (update 1995): Mapping components of signal transdauction pathways. *Electrophoresis* **16**, 2177–2240.

Chandra, N., Spiro, M., and Spiro, J. (1998). Identification of a glycoprotein from rat liver mitochondrial inner membrane and demonstration of its origin in the endoplasmic reticulum. *J. Biol. Chem.* **273**, 19715–19721.

Clarke, S. (1992). Protein isoprenylation and methylation at carboxy-terminal cystein residues. *Annu. Rev. Biochem.* **61**, 355–386.

Cohen, P. (2000). The regulation of protein function by multisite phosphorylation: A 25 year update. *Trends Biochem. Sci.* **25**, 596–601.

Cox, A. D., and Der, C. J. (1992). Protein prenylation: More than just glue? *Curr. Opin. Cell Biol.* **4**, 1008–1016.

Danesi, R., Mc Lellan, C. A., and Myers, C. E. (1995). Specific labeling of isoprenylated proteins: Application to study inhibitors of the post-translational farnesylation and geranylgeranylation. *Biochem. Biophys. Res. Commun.* **206**, 637–643.

Fu, M., Wang, C., Wang, J., Zafonte, B. T., Lisanti, M. P., and Pestell, R. G. (2002). Acetylation in hormone signaling and the cell cycle. *Cytokine Growth Factor Rev.* **13**, 259–276.

Gromov, P., and Celis, J. E. (1996). Identification of isoprenyl modified proteins metabolically labeled with [^{3}H]farnesyl- and [^{3}H]geranylgeranyl-pyrophosphate. *Electrophoresis* **17**, 1728–1733.

Mason, G. G., Murray, R. Z., Pappin, D., and Rivett, A. J. (1998). Phosphorylation of the ATPase subunits of the 26S proteasome. *FEBS Lett.* **430**, 269–274.

Mumby, M. (2002). A new role for protein methylation: Switching partners the phosphatase ball. *Sci. STKE* **79**, PE1.

Patterson, S. D., Grossman, J. S., D'Andrea, P., and Latter, G. I. (1994). Reduced numatrin/B23/nucleosphosmin labeling in apoptotic jurcat T lymphoblasts. *J. Biol. Chem.* **270**, 9429–9436.

Patton, W. F. (2002). Detection technologies in proteome analysis. *J. Chromatogr. B* **771**, 3–31.

Perez-Sala, D., and Mollinedo, F. (1994). Inhibition of isoprenoid biosynthesis induces apoptosis in human promyelocytic HL-60 cells. *Biochem. Biophys. Res. Commun.* **199**, 1209–1215.

Sickmann, A., Mreyen, M., and Meyer, H. E. (2002). Identification of modified proteins by mass spectrometry. *IUBMB Life* **54**, 51–57.

Sinensky, M. (2000). Recent advances in the study of prenylated proteins. *Biochim. Biophys. Acta* **1484**, 93–106.

Spiro, R. G. (2002). Protein glycosylation: Nature, distribution, enzymatic formation, and disease implications of glycopeptide bonds. *Glycobiology* **12**, 43R–56R.

SECTION

11

Protein/Protein and Protein/Small Molecule Interactions

CHAPTER

31

Immunoprecipitation of Proteins under Nondenaturing Conditions

Jiri Lukas, Jiri Bartek, and Klaus Hansen

I. INTRODUCTION

Immunoprecipitation of native proteins has proven to be a powerful and widely used approach in addressing questions related to the nature of a single protein or protein complexes existing under different biological conditions. A number of characteristics can be revealed using this method: (1) what is the relative molecular weight of the protein under study, (2) does it contain any posttranslational modifications, such as phosphorylation, acetylation, and glycosylation, (3) is the protein part of a larger multiprotein complex, (4) does it interact with nucleic acids or other ligands, and (5) does the level of the protein change upon growth factor stimulation, during progression through the different phases of the cell cycle, or during the transition between active proliferation and differentiation?

Combined with the recent improvements of protein microsequencing techniques and mass spectrometry, immunoprecipitation also gives the researcher an option to obtain sequence information from unknown proteins identified through coimmnunoprecipitation and thereby collect data on multiprotein complexes. Very recently, several papers have described high-throughput analysis of multiprotein complexes in yeast using the mass spectrometry approach in a technique called high-throughput mass spectrometric protein complex identification (HMS-PCI) (Ho *et al.*, 2002) and tandem-affinity purification (TAP) and mass spectrometry (Puig *et al.*, 2001; Gavin *et al.*, 2002). The future will surely bring this kind of screening technique into focus, as it can, compared to conventional two-hybrid screens (which detect only those binary interactions not influenced by posttranslational modifications), detect interactions that require protein modifications.

A critical prerequisite for successful analysis of immunoprecipitated native proteins is the quality of the primary antigen-specific antibodies. For the most straightforward interpretation of results, such a reagent should form specific immunocomplexes with the antigen in its native form without dissociating other associated proteins. In this context, one obvious possibility is to express the protein under investigation as an epitope-tagged protein from an exogenous promoter or even from an endogenous promoter (when possible), which gives the chance to immunoprecipitate the protein using specific antibodies against the tag epitope, such as Myc, Flag, and His. These tags can even be combined. Various strategies in how to obtain such reagents are described elsewhere (Harlow and Lane, 1988; Erica Golemis, 2002). This article shares experiences gained with immunoprecipitation under native conditions that have been obtained during studies of various proteins involved in cell cycle regulation (Lukas *et al.*, 1995; Hansen *et al.*, 2001). We provide a detailed description of an optimized immunoprecipitation protocol that could serve as a basis for isolating native proteins and protein complexes from mammalian cells.

II. MATERIALS AND INSTRUMENTATION

The following chemicals are from Sigma-Aldrich (see catalogue numbers in parentheses). HEPES (H-7523), NaCl (S-3014), EDTA (E-5134), EGTA (E-4378), glycerol (G-5516), Tween 20 (P-1379), Triton X-100 (X-

Copyright 2006, Elsevier Science (USA).
All rights reserved.

100), IGEPAL CA-630 (I7771), sodium dodecyl sulfate, SDS (L-4509), dithiothreitol, DTT (D-9779), β-glycerophosphate (G-6251), sodium fluoride, NaF (S-1504), sodium orthovanadate, Na_3-VO_4 (S-6508), leupeptine (hemisulfate salt, L-2884), aprotinin (A-1153), phenylmethylsulfonyl fluoride, PMSF (P-7626), bromphenol blue (B-7021), and myelin basic protein, MBP (M1891). Histone H1 is from Roche (223549).

Protein G–Sepharose 4 fast flow (17-0618-01) and protein A–Sepharose 4 fast flow (17-0974-01) are from Pharmacia Biotech.

Safe-Lock 1.5-ml polypropylene tubes are from Eppendorf (0030 123.328), and 15-ml conical polypropylene tubes are from Corning (430791). Cell scrapers (179693), 92-mm tissue culture dishes (150350), and 80-cm^2 tissue culture flasks (153732) are from Nunc. Protein concentration is measured by the Bio-Rad protein assay kit from Bio-Rad (500-0006).

III. PROCEDURES

Stock Solutions

1. *1 M HEPES, pH 7.5*: To make 1 liter, dissolve 238.3 g of HEPES in 800 ml of distilled water, adjust the pH to 7.5 with 10 *N* NaOH, and complete the volume to 1 liter. Sterilize by autoclaving; store at room temperature.

2. *1 M Tris, pH 7.5*: To make 1 liter, dissolve 121.1 g of Trizma base in 800 ml of distilled water (room temperature). Adjust the pH to 7.5 by concentrated HCl and fill up to 1 liter with distilled water. Autoclave and store at room temperature.

3. *5 M NaCl*: Disolve 292.2 g of NaCl in 800 ml of distilled water. Adjust the volume to 1 liter, autoclave, and store at room temperature.

4. *0.5 M EDTA*: To make 100 ml, add 18.6 g EDTA to 80 ml of distilled water. Stir vigorously on a magnetic stirrer. Adjust the pH to 8.0 with concentrated HCl and let the powder dissolve completely (the disodium salt of EDTA will not go into solution until the pH of the solution reaches approximately 8.0 by the addition of HCl). Adjust the final volume to 100 ml, autoclave, and store at room temperature.

5. *0.5 M EGTA*: To make 100 ml, add 19.0 g of EGTA to 80 ml distilled water. Stir and adjust the pH to 8.0 with HCl (see EDTA preparation). Adjust the volume to 100 ml, autoclave, and store at room temperature.

6. *1 M DTT (100× stock)*: Dissolve 5 g of DTT in 32 ml of distilled water. Sterilize by filtration (do not autoclave!), dispense into 1-ml aliquots, and store at –20°C.

7. *1 M β-glycerophosphate (100× stock)*: To make 100 ml, dissolve 21.6 g of β-glycerophosphate in 80 ml of distilled water. Adjust the volume 100 ml, autoclave, and store at room temperature.

8. *0.5 M NaF (500× stock)*: To make 100 ml, dissolve 2.1 g of NaF in a total amount of 100 ml of distilled water. Autoclave and store a room temperature.

9. *0.1 M Na_3VO_4 (100× stock)*: Dissolve 200 mg of Na_3VO_4 in 10.8 ml of distilled water, sterilize by filtration, dispense in multiple (100 µl) aliquots, and freeze at –20°C. Once recovered from the freezer, use the batch instantly and only once. Do not refreeze repeatedly.

10. *10 mg/ml leupeptin (1000× stock)*: Dissolve 25 mg of leupeptin in 2.5 ml of precooled distilled water, dispense into 0.5-ml aliquots, and freeze at –20°C.

11. *2 mg/ml aprotinin (1000× stock)*: Dissolve 10 mg of aprotinin in 5 ml of distilled water, dispense into 0.5-ml aliquots, and freeze at –20°C. Do not refreeze repeatedly; once recovered, store the batch for a maximum of 1–2 weeks at 4°C.

12. *0.1 M PMSF (1000× stock)*: To make 10 ml, dissolve 174 mg of PMSF in pure isopropanol (store at 4°C) (PMSF is highly unstable in aqueous solutions).

13. *2× Laemmli SDS sample buffer*: 100 m*M* Tris–HCl, pH 6.8, 200 m*M* DTT, 4% SDS, 20% glucerol, and approximately 0.2% bromphenol blue. To make 10 ml, mix 1 ml of Tris–HCl, pH 6.8, 2 ml of 1 *M* DTT, 4 ml of 10% SDS, 2 ml glycerol, and 1 ml of distilled water. Add traces of bromphenol blue powder to obtain the desired blue color and mix well. Divide into 0.5- to 1-ml aliquots and freeze at –20°C.

Buffers

A number of different lysis buffers have been described in the literature to effectively extract native proteins from mammalian cells. The following sections offer three different protein extraction buffers that have been used repeatedly and successfully in cell cycle studies for the evaluation of protein–protein interactions and for functional assays such as measuring *in vitro* kinase activity of the immunoprecipitated protein complexes.

1. *Lysis buffer 1 (Matsushime et al., 1994)*: 50 m*M* HEPES, pH 7.5, 150 m*M* NaCl, 1 m*M* EDTA, 2.5 m*M* EGTA, 10% (v/v) glycerol, and 0.1% Tween 20. To make 1 liter of 1× basic stock solution, add 50 ml of 1 *M* HEPES, pH 7.5, 30 ml of 5 *M* NaCl, 2 ml 0.5 *M* EDTA, 5 ml of 0.5 *M* EGTA, 100 ml glycerol, and 1 ml Tween 20 into 812 ml of distilled water. Stir well on a magnetic stirrer and store at 4°C. Immediately prior to use, add DTT (1 : 1000 from a 1 *M* stock); phosphatase inhibitors: NaF (1 : 500 from a 0.5 *M* stock),

β-glycerophosphate (1 : 100 from a 1 *M* stock), and Na_3VO_4 (1 : 1000 from 0.1 *M* stock); and protease inhibitors: leupeptin (1 : 1000 from a 10-mg/ml stock), aprotinin (1 : 1000 from a 2-mg/ml stock), and PMSF (1 : 1000 from a 0.1 *M* stock). Keep on ice throughout the whole procedure.

2. *Lysis buffer 2 (Jenkins and Xiong, 1996)*: 50 m*M* Tris–HCl, pH 7.5, 150 m*M* NaCl, and 0.5% (v/v) IGEPAL CA-630. To make 1 liter of 1× basic stock, add 50 ml of 1 *M* Tris–HCl, pH 7.5, 30 ml of 5 *M* NaCl, and 5 ml IGEPAL CA-630 into 915 ml of distilled water. Store at 4°C. Immediately prior to use, add DTT, phosphatase inhibitors, and protease inhibitors as described for buffer 1.

3. *Lysis buffer 3 (Pagano et al., 1993)*: 50 m*M* Tris, pH 7.5, 250 m*M* NaCl, 5 m*M* EDTA, and 0.1% (v/v) Triton X-100. To make 1 liter of 1× basic stock, add 50 ml of 1 *M* Tris–HCl, pH 7.5, 50 ml of 5 *M* NaCl, 10 ml of 0.5 M EDTA, and 1 ml Triton X-100 into 889 ml of distilled water. Store at 4°C. Immediately prior to use, add DTT, phophastase inhibitors, and protease inhibitors as described for buffer 1.

4. *Kinase assay buffer*: 20 m*M* HEPES, pH 7.2, 1 m*M* DTT, 10 m*M* $MgCl_2$, 10 m*M* $MnCl_2$, 2.5 m*M* EGTA, 1 m*M* NaF, 0.2 m*M* sodium orthovanadate, 2.5 μg/ml leupeptin, and 2 μg/ml aprotinin; should be prepared fresh from stock solutions upon use.

A. Cell Lysis

For all three lysis buffers, highly effective extraction of native proteins can be achieved by the following protocol.

Steps

1. Wash the cell monolayer twice with ice-cold phosphate-buffered saline (PBS) using 10 ml of PBS per washing step for a surface corresponding to a 92-mm diameter tissue culture dish or to a 80-cm^2 tissue culture flask.

2. Add 2.5 ml of ice-cold PBS and dislodge the cells with a cell scraper. Transfer the cell suspension into a prechilled 15-ml polypropylene test tube and repeat the same procedure with another 2.5 ml in order to recover the cells quantitatively. Spin for 5 min in a precooled (4°C) centrifuge (1000 *g*), discard the supernatant, wash the pellet briefly with 5 ml of cold PBS, and spin again. The cell pellet is now ready for lysis or, for many assays, can be frozen quickly by dipping the tube into liquid nitrogen and stored at –80°C until use.

3. Lyse the cells by adding 3–5 pellet volumes of ice-cold lysis buffer, vortex vigorously (4°C) for 10 s, and keep on ice for an additional 30 min. Throughout this period, resuspend the cells by brief vortexing every 5–10 min (4°C).

In the case of buffer 1, efficient lysis has been reported (Matsushime *et al*., 1994) that involves resuspension of the cell pellet in lysis buffer and subsequent brief sonication on ice. We have successfully reproduced this procedure in our laboratory using a Branson sonifier 250 (2 × 10-s pulses at output level position 6).

In several cases it can be advantageous to avoid the scraping of cells into PBS and to perform a more instant lysis procedure based on adding lysis buffer directly to the cell monolayer (200 μl per surface corresponding to a 92-mm diameter tissue culture dish; see previous discussion for further specifications) that has been washed previously three times with ice-cold PBS. Distribute the lysis buffer on the cell monolayer (after draining off PBS) and collect the lysate with a cell scraper. Transfer the cell lysate into a prechilled 1.5-ml Eppendorf tube. Incubate the lysate on ice for an additional 30 min with occasional brief vortexing (4°C) in order to obtain an efficient protein extraction.

4. Centrifuge the protein extract in a microfuge cooled down to 4°C for 15 min at 20,000 *g* to pellet cell debris. Transfer the cleared extract to a clean test tube prechilled on ice and measure the total amount of extracted protein (in our laboratory, we use the Bio-Rad protein assay system and exactly follow the manufacturer´s protocol with the protein standards supplied with the kit).

B. Preclearing

Preequilibrate the protein A(G)–Sepharose beads supplied by the manufacturer by three successive rounds of resuspension in 10× bead volume of lysis buffer and gentle pelleting by brief (10 s) spinning in a microfuge. To eliminate nonspecific contaminants that can potentially associate with the beads, mix the cell lysate [up to 2 mg of total protein in total volume of 1 ml per tube with 50 μl of preeqiulibrated protein A(G)–Sepharose (in a 50% slurry)] and rotate in the cold room for 30 min. Pellet the beads by a 5-min centrifugation in a precooled microfuge (20,000 *g*) and carefully transfer the supernatant into a clean prechilled Eppendorf tube, leaving the beads behind. The protein extract is now ready for immunoprecipitation with specific antibodies. To improve the preclearing step, one can use general nonspecific control IgG (precoupled to proteinA/G-Sepharose) from the same species as the specific antibody used for the final immunoprecipitation. It is an advantage to use chemically cross-linked control IgG (Harlow and Lane, 1988).

C. Immunoprecipitation

Steps

1. To presaturate protein A(G)–Sepharose beads with antibodies, aliquot 10–20 µl of beads (50% slurry), preequlibrated with the chosen lysis buffer, into Eppendorf tubes containing 0.5 ml of lysis buffer. Add the desired antibodies in saturating amounts. The amount of antibody varies significantly depending on the titer and source of a particular batch and should be determined beforehand. As a rough guide, we recommend starting with 1 µg of purified immunoglobulin, 1–2 µl of mouse ascites, 100–200 µl of hybridoma supernatant, or 2–4 µl of crude rabbit antiserum per 10 µl of beads (note that protein A–Sepharose is particularly suitable for all antibodies of rabbit origin and for mouse IgG2 subclasses. For other subclasses of mouse immunoglobulins, use protein G–Sepharose in order to achieve high-affinity binding). Rotate slowly for 1 h in the cold room and then wash the beads three times in 2 ml of lysis buffer [to pellet the beads between the washing steps, centrifuge briefly in a cooled microfuge (5000 *g*)].

2. Add the protein extract to a 10- to 20-µl aliquot (50% slurry) of beads precoated with the desired antibody and adjust the volume with the lysis buffer to 0.5–1 ml. The total amount of protein input in each sample depends very much on the type of assay and the relative abundance of the protein under study. Thus for sensitive functional assays, such as measuring *in vitro* kinase activity, as little as 50 µg of total protein could be sufficient, but the usual input ranges between 200 µg and 2 mg of total extracted proteins. Close the tubes and rotate end over end in the cold room for 90 min up to 2–3 h (it is not recommended to immunoprecipitate overnight, as this will increase the risk of proteolysis and dephosphorylation of proteins, even in the presence of diverse inhibitors).

3. Pellet the beads for 10 s in a cooled microfuge (5000 *g*) and wash four times by resuspending the beads in 1 ml of of lysis buffer. Gently invert the tubes several times between each washing step.

4. After the last wash, aspirate the lysis buffer above the beads carefully (we recommend using a blunt-ended 25-gauge needle connected to a vacuum pump). For kinase reactions, continue to step 5, for other immunoprecipitations, continue to step 6.

5. For kinase reactions, wash the beads twice in 1 ml of kinase assay buffer and remove excess liquid above the beads. Start the kinase reaction by adding kinase assay buffer including the appropriate protein substrate (from 1–2 µg per reaction) and ATP. The amount of nonlabeled ATP to be added to the reaction depends on the kinase under study but should normally be in the range of 15–200 µ*M* (final concentration). Furthermore, it is convenient to include [□^{32}P]-ATP (1–10 µCi per reaction; >3000 Ci/mmol) in order to be able to quantitate the incorporation of phosphate in the target substrate by exposure on X-ray film or a PhosphorImager screen. The kinase reaction should take place at 30°C for 10–30 min (should be optimized for the kinase under investigation). Reactions are terminated by the addition of 2× LSB containing 5 m*M* EDTA and heating for 5 min at 95°C. In cases where a phosphospecific antibody has been developed, it is possible to omit the isotope and instead perform immunoblotting after electrophoresis.

6. For one-dimensional SDS-PAGE analysis, resuspend the beads in 30 µl of 2× Laemmli SDS sample buffer and heat the samples on a heating block (95°C) for 4–5 min. Finally, centrifuge the tubes in a microfuge for 1 min at room temperature and load the samples directly on the gel by use of thin gel-loading tips.

In case the size of the protein of interest is close to 50 or 25 kDa, which also corresponds to the size of the heavy and light chains of immunoglobulins used for the immunoprecipitation, it can be an advantage to use chemically cross-linked antibodies as described by Harlow and Lane (1988). Because the cross-linking of antibodies preferentially takes place between the heavy chain and protein A/G, it is recommended to elute the immunoprecipitated proteins using Laemmli sample buffer without DTT or other reducing agent and, after heating at 95°C for 4–5 min, transfer the eluted material to a clean tube, avoiding beads, and thereafter add a similar volume of Laemmli sample buffer containing the appropiate amount of DTT or other reducing agent and then heat to 95°C again in order to reduce disulfide bonds in the immunoprecipitated proteins. The sample is now ready to load on the gel as described earlier. By using this two-step elution procedure, you can almost completely avoid disturbing signals from heavy and light chains upon Western blotting or staining of the gel.

Figure 1 shows an example of an immunoprecipitation of the cyclin-dependent kinase 4 (Cdk4) from primary mouse fibroblasts in complex with its associated subunits: D-type cyclins and Cdk inhibitors. Figure 2A shows an example of *in vitro* kinase assays using specific antibodies against three different kinase complexes in immunoprecipitation: Erk1 and Erk2 combined, cyclin D/Cdk4(6), and cyclin E/Cdk2. Three different substrates were used in the *in vitro* kinase reaction, which also included [□^{32}P]-ATP. The right-hand side of Fig. 2A shows the effect of the

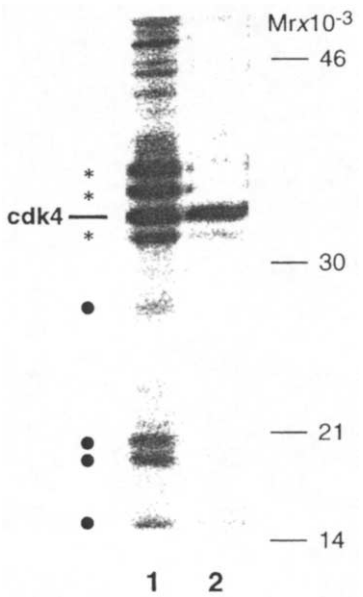

FIGURE 1 Primary mouse embryonic fibroblasts were labeled with [^{35}S]methionine, lysed in buffer 1, and immunoprecipitated with rabbit polyclonal antibody against the Cdk2 C-terminal peptide (kindly provided by Dr. M. Pagano). Lane 1 shows a labeled Cdk4 protein coprecipitated along with the associated subunits: D-type cyclins (marked by asterisks) and Cdk inhibitors (marked by closed circles). The parallel reaction in lane 2 was subsequently heated and incubated with SDS in order to dissociate specific protein–protein interactions and was reimmunoprecipitated with the same antibody.

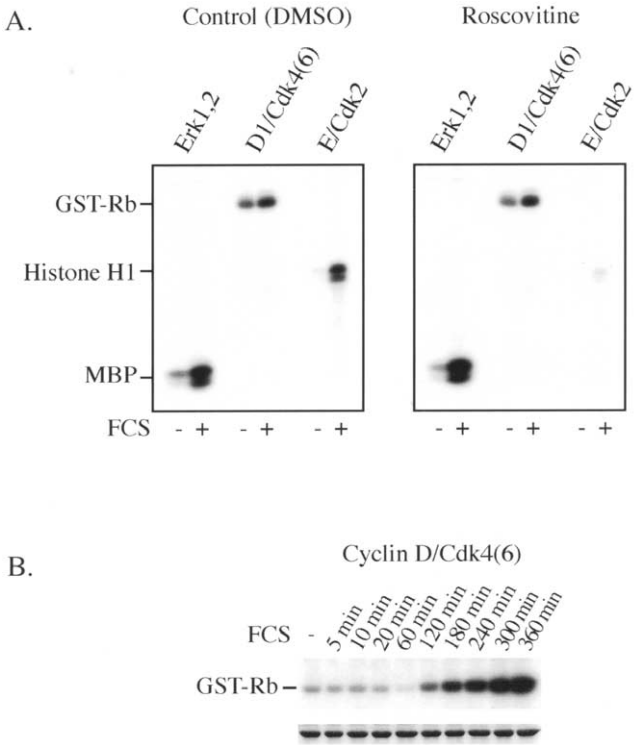

FIGURE 2 Human glioblastoma cells (T98G) were starved (0.1% FCS) for 48 h before readdition of serum (10%). After 5 min a lysate was prepared for measuring Erk1 and Erk2 activation; at 6 h a lysate was made to measure cyclin D/Cdk4(6) activation; and at 12 h a lysate was made in order to measure cyclin E/Cdk2 activation. The following antibodies were used: Santa Cruz antibodies against Erk1 (Santa-Cruz SC-093) and Erk2 (Santa-Cruz SC-154) were mixed; DCS 6 mouse monoclonal antibody to cyclin D1 was used to immunoprecipitate cyclin D1/Cdk4(6) complexes; and the mouse monoclonal antibody to cyclin E, HE172, was used to immunoprecipitate cyclin E/Cdk2 complexes. In the *in vitro* kinase reactions, myelin basic protein (MBP) was used as a substrate for Erks, whereas the GST-Rb fusion protein was used as a substrate for Cdk4(6) and histone H1 as a substrate for Cdk2. The kinase reactions in A were performed in the absence (DMSO control) or presence of the Cdk2 inhibitor roscovitine (5 μM final concentration).

Cdk2-specific inhibitor roscovitine when included in the final kinase reaction. Figure 2B shows a time course of activation of cyclin D/Cdk4(6) after the release of serum-starved T98G cells (a human glioblastoma cell line). It is obvious that the activity of the complex increases with time after release as cells progress through G1 and approach the G1/S phase transition. The bottom part of Fig. 2B indicates that the loading on the gel was equal for all samples by staining for the substrate GST-Rb.

References

Gavin, A. C., *et al*. (2002). Functional organization of the yeast proteome by systematic analysis of protein complexes. *Nature* **415**, 141–147.

Golemis, E. (2002). "Protein–Protein Interactions." Cold Spring Harbor Laboratory Press, Cold Spring Harbor, NY.

Hansen, K., Farkas, T., Lukas, J., Holm, K., Rönnstrand, L., and Bartek, J. (2001). Phosphorylation-dependent and -independent functions of p130 cooperate to evoke a sustained G1 block. *EMBO J.* **20**, 422–432.

Harlow, E., and Lane, D. (1988). "Antibodies: A Laboratory Manual." Cold Spring Harbor Laboratory Press, Cold Spring Harbor, NY.

Ho, Y., *et al*. (2002). Systematic identification of protein complexes in *Saccharomyces cerevisiae* by mass spectrometry. *Nature* **415**, 180–183.

Jenkins, C. W., and Xiong, Y. (1996). Immunoprecipitation and immunoblotting in cell cycle studies. *In* "*Cell Cycle Materials and Methods*" (M. Pagano, ed.), pp. 250–264. Springer Lab Manual.

Lukas, J., Bartkova, J., Rohde, M., Strauss, M., and Bartek, J. (1995). Cyclin D1 is dispensable for G1 control in retinoblastoma gene-deficient cell independently of cdk4 activity. *Mol. Cell. Biol.* **15**, 2600–2611.

Matsushime, H., Quelle, D. E., Shurtleff, S. A., Shibuya, M., and Sherr, C. J. (1994). D-type cyclin-dependent kinase activity in mamalian cells. *Mol. Cell. Biol.* **14**, 2066–2076.

Pagano, M., Pepperkok, R., Lukas, J., Baldin, V., Ansorge, W., Bartek, J., and Draetta, G. (1993). Regulation of the cell cycle by the cdk2 protein kinase in cultured human fibroblasts. *J. Cell Biol.* **121**, 101–111.

Puig, O., Caspary, F., Rigaut, G., Rutz, B., Bouveret, E., Bragado-Nilsson, E., Wilm, M., and Seraphin, B. (2001). The tandem affinity purification (TAP) method: A general procedure of protein complex purification. *Methods* **24**(3), 218–229.

Xiong, Y., Hannon, G., Zhang, H., Casso, D., Kobayashi, R., and Beach, D. (1993). p21 is a universal inhibitor of the cyclin kinases. *Nature* **366**, 701–704.

CHAPTER

32

Nondenaturing Polyacrylamide Gel Electrophoresis as a Method for Studying Protein Interactions: Applications in the Analysis of Mitochondrial Oxidative Phosphorylation Complexes

Joél Smet, Bart Devreese, Jozef Van Beeumen, and Rudy N. A. Van Coster

I. INTRODUCTION

Under native PAGE conditions, polypeptides retain their higher order structure, enzymatic activity, and interaction with other polypeptides. The migration of proteins depends on many factors, including size, shape, and native charge. The resolution of nondenaturing electrophoresis is generally not as high as that of SDS–PAGE, but the technique is useful when the native structure or enzymatic activity of a protein must be preserved following electrophoresis. One straightforward approach to native electrophoresis is to omit the sodiumdodecylsulfate (SDS) and the reducing agent dithiothreitol (DTT) from the standard Laemmli SDS protocol (Amersham Bioscience Web site: http://www4.amershambioscience.com). The separation of water-soluble proteins using the Laemmli system can simply be done by replacing SDS with Triton X. The published methods can be devided into two classes: (i) relying on the own charge of the protein to determine the anodic or cathodic migration at a given pH and (ii) using charged, mild detergents to induce a charge shift so that all proteins binding the detergent migrate in the same direction. The methods for native electrophoresis of membrane proteins, however, suffer from many drawbacks. Any new method designed to separate them must include a charge shift method. Two components were introduced for that purpose: Coomassie blue G for the separation of multiprotein complexes ("blue native PAGE") and taurodeoxycholate for the separation of lower molecular mass proteins ("native PAGE") (Schägger and von Jagow, 1991).

The blue native PAGE technique is particularly useful for the characterization of mitochondrial oxidative phosphorylation (OXPHOS) enzymes. Combining this separation technique with histochemical staining makes it possible to quantify mitochondrial enzymes *in situ* (Zerbetto *et al.*, 1997). It allows to evaluate the enzymatic activities of the complexes I, II, IV, and V in heart and skeletal muscle, liver and cultured skin fibroblasts and to detect deficiencies. Also, the amount of protein in the complexes I, II, III, IV, and V can be evaluated using silver or Coomassie staining. Often the complexes are even visible in the gel without additional staining. When the background is high, immunoblotting has to be used to visualise the amount of complex proteins (Van Coster *et al.*, 2001).

Combining blue native PAGE with SDS–PAGE reveals a two-dimensional pattern showing the individual subunits of the five OXPHOS multienzyme complexes. The implementation of mass spectrometric techniques, e.g., mass fingerprinting and mass spectrometric sequence analysis, allows the unambiguous

Copyright 2006, Elsevier Science (USA).
All rights reserved.

identification of the individual subunits (Devreese *et al*., 2002).

II. MATERIALS AND INSTRUMENTATION

Tris–HCl (Cat. No. T1378), sucrose (Cat. No. S0389), glycerol (Cat. No. G6279), phenylmethylsulfonyl fluoride (PMSF, Cat. No. S0389), dimethyl sulfoxide (DMSO, Cat. No. D5879), Tricine (Cat. No. T0377), aminocaproic acid (Cat. No. A7824), bis–Tris (Cat. No. 9754), dodecyl β-D-maltoside (Cat. No. D4641), nitro blue tetrazolium (NBT, Cat. No. N6876), phenazinemethosulfate (PMS, Cat. No. P9625), succinic acid (Cat. No. S2378), 3,3′-diaminobenzidine (DAB, Cat. No. D8001), catalase (Cat. No. C9322), cytochrome c (Cat. No. C7752), magnesium sulfate (Cat. No. M7506), lead(II) nitrate (Cat. No. L7281), adenosinetriphosphate (ATP, Cat. No. A5394), Tween 20 (Cat. No. P1379), and the Gelbond film (Cat. No. E0389) are from Sigma. Serva Blue G (Cat. No. 35050) is from Serva. Acrylamide (Cat. No. 161-0101), *N*,*N*′-methylenebisacrylamide (bisacrylamide, Cat. No. 161-0201), ammonium persulfate (APS, Cat. No. 161-0700), *N*,*N*,*N*′,*N*-tetramethylenediamine (TEMED, Cat. No. 161-0800), the gel-staining Coomassie Bio-Safe solution (Cat. No. 161-0787), the blotting grade blocker (Cat. No. 170-6404), the gel-drying solution (Cat. No.161-0752), and the transparent membranes (Cat. No. 165-0963) are from Bio-Rad. SDS (Cat. No. 44215) is from BDH Laboratories. Nicotinamide adenine dinucleotide, reduced form (NADH, Cat. No. 107735), is from Roche. The silver stain kit GelCode SilverSNAP (Cat. No. 24602) and the Bradford reagent for protein determination (Cat. No. ZZ23238) are from Pierce. Whatman paper (Cat. No. 3030672) is from VWR. PVDF immunoblot membranes (Cat. RPN2020F), ECL films (Cat. No. RPN 3103K), the secondary IgG HRP-linked whole AB to mouse (Cat. No. NA931), and the ECL plus kit (Cat. No. RPN2132) are from Amersham Biosciences. The different primary antibodies against OXPHOS subunits are from Molecular Probes (http://www.probes.com). The homogeniser Model L42 is from Schwaben Präsizion Nordlingen. The glass/glass dual tube tissue homogenisers of different volumes are from Kontes, distributed by Helma Benelux. The air-driven ultracentrifuge airfuge (Cat. No. 340401) and the microcentrifuge tubes (Cat. No. 344718) are from Analis. Minigels (gel size 8.3 × 7.3 cm) are run on a Mini-Protean three electrophoresis cell (Cat. No. 165-3302). All parts, such as glass plates, combs, casting stand, spacers, electrode assembly, tank lid with power cables, and power supply (Model 200/2.0), are from Bio-Rad. The Mini Trans-Blot cell (Cat. No. 170-3930) and the Hydrotech gel-drying system (Model 583, Cat. No. 165-1745) equipped with a Hydrotech vacuum pump (Cat. No. 165-1782) are from Bio-Rad. The hot plate (Präzitherm, type PZ 28-2 T), the Inolab pH level 1 pH meter, and the orbital shaker (a GFL model 3006) are from VWR. Pipettes (P1000, P100, and P25) are from Hamilton. The Sharp JX-330 scanner is from Amersham Biosciences.

III. PROCEDURES

A. Isolation of Mitochondria from Tissues and Cultured Fibroblasts

This procedure is performed according to Scholte *et al*. (1992). In order to isolate a sufficient amount of mitochondria, at least 100 mg (wet weight) of tissue (muscle, heart, liver) is needed. Starting from cultured fibroblasts, after harvesting, a pellet volume of 100 µl (approximately three T75 Falcon flasks) is needed.

B. Solubilization of Mitochondria

Solutions

1. *Protease inhibitor solution*: 1 mM PMSF in DMSO. Prepare a 25-ml solution by dissolving 4.3 mg PMSF into 25 ml DMSO, aliquot in 1-ml portions, and store at –20°C.
2. *Solution A*: 750 m*M* aminocaproic acid, 50 m*M* Bis–Tris, and 20 µ*M* PMSF. To make 25 ml, dissolve 2.46 g aminocaproic acid and 0.26 g Bis–Tris and add 20 µl of 1 m*M* PMSF in DMSO solution; adjust pH to 7.4 and adjust volume to 25 ml. Divide into single-use aliquots of 1 ml and store at –20°C. Samples can be stored under these conditions up to 3 months.
3. *Solution B*: Laurylmaltoside 10%. Dissolve 0.5 g in 5 ml distilled water, divide into single-use aliquots of 150 µl, and store at –20°C. Samples can be stored under these conditions maximally for 3 months.

Steps

1. Place the mitochondrial pellets (stored at –80°C) on ice.
2. Add a mixture of 96 µl solution A and 12 µl solution B equivalent to a mitochondrial pellet resulting from approximately. 100 mg of tissue or a fibroblast pellet of 100 µl.
3. Dissolve the pellet by pipetting up and down and by vortexing the tube strongly.
4. Pipette the solubilized material into a microcentrifuge tube (max 200 µl/tube).
5. Centrifugate in the airfuge at 100,000 g for 15 min.

6. Pipette the clear supernatant containing the oxidative phosphorylation enzyme complexes into an Eppendorf tube; avoid pipetting material from the pellet, which is discarded.
7. Use 5 µl of the solution to determine the protein content according to the Bradford (1970) method.
8. Store at –80°C if the supernatant cannot be submitted to electrophoresis within 2 h after preparation.

C. First-Dimension BN-Polyacrylamide Gel Electrophoresis

This is a procedure according to Schägger (1995).

Solutions

1. *Cathodal buffer (colorless)*: 50 m*M* tricine, 15 m*M* bis–Tris. To make 1 liter, dissolve 9.0 g tricine and 3.1 g bis–Tris in distilled water, adjust pH to 7.0 and complete to 1 liter with distilled water. Store for a maximum of 2 months at 4°C.

2. *Cathodal buffer (colored)*: Colorless buffer + 0.02% Serva Blue G. Add 0.2 g Serva Blue G to 1 liter of colorless cathodal buffer.

3. *Anodal buffer (5× concentrated)*: 250 m*M* bis–Tris. To make 1 liter, dissolve 52 g bis–Tris in distilled water, adjust pH to 7.0, and complete to 1 liter. Dilute prior to use 1/5 with distilled water. Store for 2 months maximum at 4°C.

4. *Acrylamide/bisacrylamide mixture (49.5% T, 3% C)*: To make a 250-ml solution, add 3.13 g bisacrylamide to 250 ml of the 40% solution from the supplier. Devide into 10-ml aliquots, which are stored at –20°C for 3 months maximum.

5. *Gel buffer (3× concentrated)*: 1.5 *M* aminocaproic acid and 150 mM bis–Tris. To make 100 ml, dissolve 19.7 g aminocaproic acid and 3.1 g bis–Tris, adjust pH to 7.0, and complete to 100 ml with distilled water. Divide into 10-ml aliquots, which are stored at –20°C for 3 months maximum.

6. *10% ammonium persulfate solution*: To make 10 ml, dissolve 1 g APS in 10 ml distilled water and divide into 1-ml aliquots, which are stored at –20°C for 3 months maximum. Use within 24 h.

7. *Sample loading buffer*: 5% Serva Blue G and 750 m*M* aminocaproic acid. Prepare a solution of 1 ml by dissolving 50 mg Serva Blue G and 98 mg aminocaproic acid in a final volume of 1 ml distilled water. Divide into single-use 100 µl aliquots and store them for 3 months maximum.

Steps

1. Assemble the Mini-Protean gel apparatus according to the manual of the supplier. Gel dimensions are 8.0 × 7.3 × 0.1 cm.

TABLE I

Reagents	5% T	13% T	Stacking gel 4% T
A–B mixture (49.5% T–3% C)	0.8 ml	1.7 ml	0.4 ml
Gel buffer (3×)	2.1 ml	1.8 ml	1.5 ml
Glycerol	—	0.9 ml	—
AD	3.4 ml	1.0 ml	2.6 ml
Total volume	**6.3 ml**	**5.4 ml**	**4.5 ml**
APS (10%)	35 µl	18 µl	36 µl
TEMED	3.5 µl	1.8 µl	3.6 µl

2. Prepare a 5% and 13% T gel solution in order to make a 5–13% resolving gel gradient (see Table I).
3. Finally add the APS and TEMED to the 5 and 13% solutions and vortex both solutions.
4. Pipette 2× 100 µl of the 5% solution into the 13% solution and vortex.
5. Pipette 2× 100 µl between the glass plates at the left and right side of both gels.
6. Repeat steps 4 and 5 until you reach a level of approximately 1 cm under the comb.
7. Overlay with water and leave to polymerize. After a minimum of 1 h, place at 4°C overnight.
8. Prepare the 4% stacking gel solution.
9. Remove the water using Whatman paper and pour the solution on top of the resolving gel. Insert the comb (e.g., 10-well comb) and let polymerize for 45 min.
10. Poor the cold (<10°C) colored cathodal buffer between the two glass plates at a level 0.5 cm below the bottom of the sample wells.
11. Add 5 µl of sample loading buffer to 100 µl of the solubilized mitochondrial sample, which is kept on ice, and vortex.
12. Load the calculated volume (depending of the amount of protein) of the sample into the sample wells (20–100 µg of protein/lane). Two lanes are needed if you want to evaluate the activities by activity staining (see Section III,F).
13. Completely fill the space between the glass plates with colored cathodal buffer.
14. Place the gel assembly into the anodal buffer tank and poor the anodal buffer into the tank up to a level above the bottom end of the glass plates.
15. Cool the apparatus to 4°C and connect the electrodes to the power supply.
16. Run the gels at 75 V for 1 h.
17. Replace the colored cathodal buffer by the colorless buffer without rinsing the cathodal buffer chamber and run the gels at 200 V until the Serva Blue tracking dye has run off the gel completely

(approximately 3 h). The gels can be used immediately for protein staining (see Section III,D), immunoblotting (see Section III,E), activity staining (see Section III,F), or can be stored for several months at –80°C.

D. Protein Staining

1. *Coomassie Staining*

Steps

1. Fix the gels in a 50/40/10 mixture of distilled water/methanol/acetic acid by shaking on an orbital shaker for 30 min.
2. Stain the gels by transferring them into the Bio-Safe Coomassie staining solution and place them on the shaker for 60 min.
3. Destain the gels by transferring them in a tray filled with distilled water and put on the shaker for 60 min, refresh, and continue destaining on the shaker overnight.
4. Put the gels in a drying solution for 30 min.
5. The gels then can be dried on Whatman paper or between two transparent membranes according to the manufacturer's protocols. Normally a 2-h drying time at 80°C is sufficient (Fig. 1).

2. *Silver Staining*

Steps

1. Fix the gels in 50 ml of a 50/40/10 mixture of distilled water/methanol/acetic acid by shaking on an orbital shaker for 30 min.
2. Wash the gels twice for 5 min with 50 ml 10% ethanol solution and twice for 5 min with distilled water.
3. Stain the gels with 50 ml of a 50/1 mixture of the staining/enhancing solution for 30 min.
4. Rinse with distilled water for 1 min.
5. Transfer the gels into 50 ml of a 50/1 mixture of developer/enhancer solution for 2 to 5 min.
6. When the bands are clearly visible, stop the development by placing the gels in 50 ml of a 5% acetic acid solution.
7. Dry the gels on Whatman paper or between two transparent membranes according to the manufacturer's protocols. Normally a 2-h drying time at 80°C is sufficient (Fig. 1).

E. Immunoblotting

Solutions

1. *Towbin blotting buffer* (Towbin *et al.*, 1979): 10× concentrate (0.25 *M* Tris and 1.92 *M* glycine, pH 8.5).

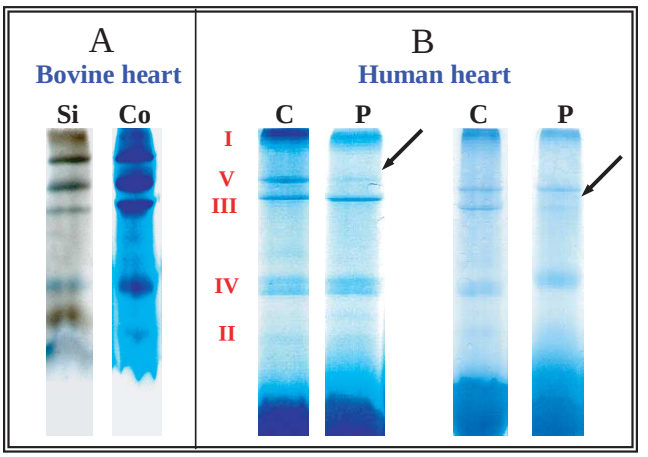

FIGURE 1 (Left) Complex proteins are visualized using protein staining (silver and Coomassie). (Right) Complex proteins are visible prior to any protein staining. Arrows mark complexes with low amounts of protein.

To make 1 liter (10×), dissolve 30.3 g Tris and 144 g glycine in distilled water, complete to 1 liter.

2. *Phosphate-saline buffer*: 10× concentrate (0.8 *M* Na_2HPO_4, 0.2 *M* NaH_2PO_4, 1 *M* NaCl). To make 250 m1 (10×), dissolve 28.4 g Na_2HPO_4, 6.9 g NaH_2PO_4, and 14.5 g NaCl, complete to 250 ml with distilled water.

3. *Washing buffer (0.1% Tween 20)*: Dilute 100 ml 10× phosphate-saline buffer with 900 ml distilled water and add 1 ml Tween 20, adjust pH to 7.5.

4. *Blocking reagent*: 5% blocking reagent in washing buffer. To make 100 ml solution, dissolve 5 g blocking reagent in a final volume of 100 ml washing buffer.

5. *Primary antibody dilution*: Make a dilution of the primary OXPHOS antibodies into the blocking solution. Minimally, 20 ml is needed for incubation of the two membranes. When using the ECLplus system, a concentration of 1 µg/20 ml primary antibody is, in most cases, sufficient to detect even very low amounts of protein.

6. *Secondary antibody dilution*: Make a 1/2000 dilution of the secondary HRP antibody: 10 µl of antibody solution in 20 ml blocking solution.

7. *ECLplus detection reagent*: Place reagents A and B at room temperature for 1 h. Just prior to the detection procedure, mix reagents A and B in a 40 : 1 ratio. For two membranes, 4 ml of solution A and 100 µl of solution B are needed. Keep away from light.

Steps

1. Cut the PVDF membranes and Whatman papers (two per gel) in a size such that they completely cover the gel.

2. Dip the PVDF membranes briefly into 100% methanol and incubate them, together with the Whatman papers and the sponges, for 30 min in the Towbin blotting buffer.
3. Fill the blotting cassette with sponge–paper–gel–membrane–paper–sponge (in this order) and close the cassette. Make sure no air bubbles are trapped between the gel and the membrane.
4. Place the cassette into the holder, with the membrane facing the cathode. Insert the ice box and fill the blotting chamber with 600 ml Towbin blotting buffer.
5. Connect the electrodes and run for 1 h at 100 V.
6. Remove the membranes from the cassette, dip them briefly into methanol, and place them in 20 ml washing buffer for 30 min.
7. Incubate the membranes in 20 ml blocking solution for at least 1 h on the orbital shaker.
8. Remove the blocking solution, add 20 ml of the primary antibody solution, and incubate on the orbital shaker for a minimum of 1 h.
9. Remove the primary antibody solution and wash the membranes at least three times for 5 min with 30 ml of washing buffer on the shaker.
10. Add 20 ml of the 1/2000 dilution of the secondary HRP antibody and incubate using the orbital shaker for at least 1 h.
11. Remove the secondary antibody solution and wash the membranes at least three times for 5 min with 30 ml of washing buffer.
12. Place the membrane, protein side facing up, in a tray and add the detection reagent on the whole surface of the membrane using a pipette. Let react for 5 min. Take the membranes with a forceps, let excess reagent drip off, and fix the membranes between two sheets of transparent membrane in a film cassette.
13. Place an ECL hyperfilm on the membrane for several time intervals in order to obtain the best signal-to-noise result on the film (Fig. 2).
14. After detection, wash the membranes three times for 5 min with 30 ml of washing buffer on the shaker; these can then be stored in a sealed plastic bag for several months at –20°C.

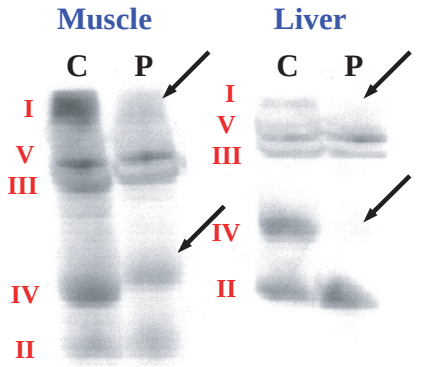

FIGURE 2 Immunoblotting of OXPHOS complexes using one specific antibody to one subunit of each complex and ECLplus detection. Arrows mark low CRM of the complex in patient lanes (P) as compared to controls (C).

F. In-Gel Activity Staining

This is the procedure according to Zerbetto *et al.* (1997), with certain modifications.

Staining Solutions

1. *Complex I (10×)*: 2 m*M* Tris–HCl, pH 7.4, 0.1 mg/ml NADH, and 2.5 mg/ml NBT. To make 25 ml of a 10× solution, dissolve 6.0 mg Tris–HCl, 2.5 mg NADH, and 62.5 mg NBT in distilled water. Adjust pH to 7.4, complete to 25 ml, and divide into 3-ml single-use aliquots, which are kept at –80°C.

2. *Complex II*: 4.5 m*M* EDTA, 10 m*M* KCN, 0.2 m*M* PMS, 84 m*M* succinic acid, and 10 m*M* NBT in a 1.5 m*M* phosphate buffer, pH 7.4. Prepare 0.1 *M* phosphate buffer, pH 7.4, by mixing a 100-ml solution of 1.36 g KH_2PO_4 and a 100-ml solution of 1.74 g K_2HPO_4. Prepare a 1.5 m*M* buffer solution by adding 98.5 ml distilled water to 1.5 ml 0.1 *M* buffer. To make 25 ml solution, dissolve 33 mg EDTA, 16 mg KCN, 1.5 mg PMS, 0.56 g succinic acid, and 200 mg NBT in the 0.1 *M* phosphate buffer, adjust pH to 7.4, complete to 25 ml, and divide into 3-ml single-use aliquots, which are kept at –80°C.

3. *Complex IV*: 5 mg DAB dissolved in 9 ml phosphate buffer (0.05 *M*, pH 7.4), 1 ml catalase (20 µg/ml), 10 mg cytochrome c, and 750 mg sucrose. Prepare a 0.05 *M* phosphate buffer by adding 13.5 ml distilled water to 13.5 ml 0.1 *M* phosphate buffer (see complex II). Dissolve 2 mg catalase in 100 ml distilled water. To make 30 ml solution, dissolve 15 mg DAB, 30 mg cytochrome c, and 2.25 g sucrose, add 3 ml of the catalase solution, complete to 27 ml with 0.05 *M* phosphate buffer, adjust pH to 7.4, and divide into 5-ml single-use aliquots, which are kept at –80°C.

4. *Complex V*: 35 m*M* Tris–HCl, 270 m*M* glycine, 14 m*M* $MgSO_4$, 0.2% $Pb(NO_3)_2$, and 8 m*M* ATP, pH 7.8. To make 25 ml solution, dissolve 0.11 g Tris–HCl, 0.51 g glycine, 42 mg $MgSO_4$, 50 mg $Pb(NO_3)_2$, and 0.11 g ATP, adjust pH to 7.8, complete to 25 ml, adjust pH to 7.4, and divide into 3-ml single-use aliquots, which are kept at –80°C.

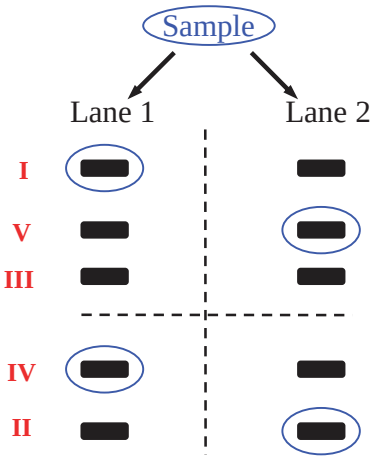

FIGURE 3 Schematic drawing of the five OXPHOS complexes and cutting of the gel.

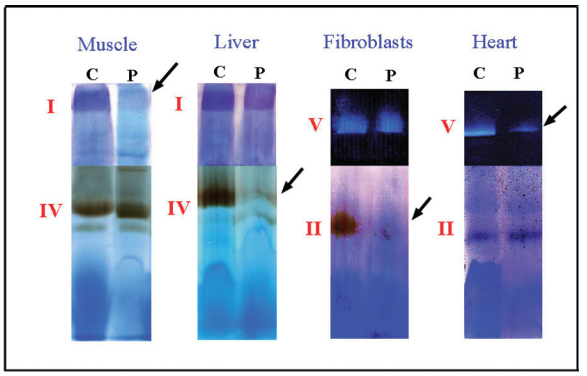

FIGURE 4 Activity staining of OXPHOS complexes in different tissues. Arrows mark deficient complexes in patients (P) in comparison with controls (C).

Steps

1. Thaw the staining solutions. Prepare a 1/10 dilution of the 10× complex I staining solution by adding 9 ml distilled water to 1 ml of the (10×) solution. Pour approximately 1 ml of each staining solution for one gel into the four staining trays (one tray/complex) (dimensions: e.g., 8 × 15 cm).

2. The gels were kept at –80°C, first thaw the gel quickly by immersing the plate in a water bath. Divide the gel as shown in Fig. 3. Using a sharp scalpel knife, divide the gels into four parts (dotted lines). The upper part of the first lane is used for complex I staining and the lower part for complex IV staining. The upper part of the second lane is used for complex V staining and the lower part for complex II staining.

3. Place the gels into the appropriate staining solutions. Cover with the rest of the staining solution and place on a hot plate at 37°C.

4. Keep the gels humid by adding 1 ml of an isotonic saline solution (0.87 g NaCl per 100 ml distilled water) at regular time intervals.

5. The bands of complexes I and II reach their maximum intensity after 3–4 h and the bands of complexes IV and V after 4–6 h.

6. Thereafter, fix the gels for 15 min in 50 ml of a mixture of 50% methanol and 10% acetic acid, except gels stained for complex V, which are rinsed with distilled water.

7. Place the gels between two Gelbond films and scan in transmission mode using a JX-330 scanner. To evaluate the white complex V band, scan the gel in the reflection mode using a black background. Staining for complex I results in a dark blue/purple band, and staining of Complex V gives a white band, both visible in the upper part of the gel. In the lower part of the gel, staining for complex IV results in a brown band and complex II staining results in a dark purple band. (Fig. 4)

8. The gels then can be dryed on Whatman paper or between two transparent membranes according to the manufacturers protocols. Normally 2 h of drying time at 80°C is sufficient.

References

Bradford, M. M. (1970). *Anal. Biochem.* **74**, 248–254.

Devreese, B., Vanrobaeys, F., Smet, J., Van Beeumen, J., and Van Coster, R. (2002) Mass spectrometric identification of mitochondrial oxidative phosphorylation subunits separated by two-dimensional blue-native polyacrylamide gel electrophoresis. *Electrophoresis* **23**(15), 2525–2533.

Schägger, H. (1995). Quantification of oxidative phosphorylation enzymes after blue native electrophoresis and two-dimensional resolution: Normal complex I protein amounts in Parkinson's disease conflict with reduced catalytic activities. *Electrophoresis* **16**(5), 763–770.

Schägger, H., and von Jagow, G. (1991). Blue native electrophoresis for isolation of membrane protein complexes in enzymatically active form. *Anal. Biochem.* **199**(2), 223–231.

Scholte, H. R., Ross, J. D., Blow, W., Boonman, A. M., van Diggelen, O. P., Hall, C. L., Huijmans, J. G., Luyt-Houwen, I. E., Kleijer, W. J., de Klerk, J. B., *et al.* (1992). Assessment of deficiencies of fatty acyl-CoA dehydrogenases in fibroblasts, muscle and liver. *J. Inherit. Metab. Dis.* **15**(3), 347–352.

Towbin, H., *et al.* (1979). *Proc. Natl. Acad. Sci. USA* **76**, 4350.

Van Coster, R., Smet, J., George, E., De Meirleir, L., Seneca, S., Van Hove, J., Sebire, G., Verhelst, H., De Bleecker, J., Van Vlem, B., Verloo, P., and Leroy, J. (2001). Blue native polyacrylamide gel electrophoresis: A powerful tool in diagnosis of oxidative phosphorylation defects. *Pediatr. Res.* **50**(5), 658–665.

Zerbetto, E., Vergani, L., and Dabbeni-Sala, F. (1997). Quantification of muscle mitochondrial oxidative phosphorylation enzymes via histochemical staining of blue native polyacrylamide gels. *Electrophoresis* **18**(11), 2059–2064.

CHAPTER

33

Affinity Purification with Natural Immobilized Ligands

Nisha Philip and Timothy A. Haystead

I. INTRODUCTION

This article discusses affinity chromatography-based techniques to study protein interaction between other proteins or small ligands. The first procedure involves the use of toxin microcystin LR (MC-LR) conjugated to a biotin or Sepharose matrix to biochemically examine phosphatase–protein interactions. MC linked to biotin has the advantage of using mild conditions to elute bound proteins and also the holoenzyme components remain intact. Using this technique we identified various PP-1-binding proteins, including regulatory subunits from different tissues (Campos *et al*., 1996).

The second method, termed proteome mining, is employed to discover protein targets of drugs. A natural ligand, immobilized in an orientation that favors binding with its protein interactors, is used to capture a subproteome. We have, in the past, used the ligand ATP to isolate the purine-binding proteome, which includes various protein and nonprotein kinases, dehydrogenases, heat shock proteins, and other ATP using enzymes (Haystead *et al*., 1993, 1994; Davies *et al*., 1994; Shellman *et al*., 1999).This process first involves the application of saturating amounts of tissue or cell extract to the matrix. Once the ATP-binding proteome is captured, various drugs are applied to the column. If the drug can compete with the natural ligand, the protein is eluted. Proteins are resolved by 1DE and identified by mass spectrometry. In our laboratory, this technique was used successfully to identify targets of antimalarials in the human purine-binding proteome (Graves *et al*., 2002).

This method can be modified to identify protein–protein interactions in the purine-binding proteome. Once the ATP-binding proteome is captured on the resin, specific inhibitors to the protein of interest can be used to elute it and its interactors. The proteins are resolved by 1DE and identified by mass spectrometry.

II. MATERIALS AND INSTRUMENTATION

Microcystin-LR is from Alexis biochemicals (Cat. No. 350-012-M001). Ethanol is from Aaper alcohol, and dimethyl sulfoxide (DMSO) is from Mallinckrodt (Cat. No. 5507-04). Cysteamine hydrochloride (Cat. No. M6500), sodium hydroxide (Cat. No. 93065), acetonitrile (Cat. No. A998), glacial acetic acid (Cat. No. A6283), sodium bicarbonate (Cat. No. S6014), Tris-hydrochloric acid (Cat. No. T6066), EDTA (Cat. No. E5134), EGTA (Cat. No. E4378), dithiothreitol (Cat. No. D9779), Triton X-100 (Cat. No. T9284), sodium chloride (Cat. No. S9625), and magnesium chloride (Cat. No. M0250) are from Sigma. Trifluroacetic acid (Cat. No. 9470-01) is from J. T. Baker. The protease inhibitors leupeptin (Cat. No. 1017101), phenylmethylsulfonyl fluoride (PMSF, Cat. No. 0837091), aprotonin (Cat. No. 0236624), and pepstatin (Cat. No. 0253286) are from Roche. EZ-Link sulpho-NHS-biotin (Cat. No. 21217) and avidin Sepharose (Cat. No. 20347) are from Pierce. NP-40 (Cat. No. 492015) is from Calbiochem.

III. PROCEDURES

A. Synthesis of Microcystin Biotin

This procedure is modified from that of Campos (1996).

Copyright 2006, Elsevier Science (USA).
All rights reserved.

Solutions

1. *5 M NaOH stock*: Weigh 20 g NaOH and complete to 100 ml with Millipore water. Store at room temperature
2. *0.1 M $NaHCO_3$*: Add 8.14 g $NaHCO_3$ to 100 ml Millipore water
3. *Buffer A*: 25 m*M* Tris, pH 7.5, 1.5 m*M* EGTA, 4 m*M* EDTA, 1 m*M* DTT plus protease inhibitors (4 µg/ml leupeptin, 0.1 m*M* PMSF, 0.1 µg/ml aprotonin, and 0.1 µg/ml pepstatin)
4. *Buffer B*: Buffer A with 0.5% Triton X-100
5. *Buffer C*: Buffer A with 0.6 *M* NaCl and 0.5% Triton X-100

Steps

1. Dissolve 3 mg microcystin-LR in 90 µl ethanol and mix with 150 µl water, 200 µl DMSO, 100 µl cysteamine hydrochloride solution, and 67 µl 5 *M* NaOH (add NaOH last).
2. All components need to be degassed with nitrogen before mixing.
3. Incubate reaction at 50°C for 60 min.
4. Cool solution on ice.
5. Mix in an equal volume of glacial acetic acid (617 µl).
6. Dilute sample to 6 ml with 0.1% TFA.
7. Reduce pH to 1.5 by dropwise addition of TFA (18–20 µl).
8. Apply to C18 Sep Pak resin that has already been equilibrated in 0.1% TFA.
9. Wash with 0.1% TFA in 10% acetonitrile.
10. Elute with 10 ml of 0.1% TFA in 100% acetonitrile.
11. Dry by evaporating the solution at 45°C in a Speed-Vac.
12. Dissolve MC-AET in 200 µl methanol. Make up volume to 900 µl by adding 0.1 *M* $NaHCO_3$ (pH 8.3).
13. Dissolve 50 mg NHS-LC-biotin in DMSO.
14. Set up reaction MC-AET dissolved in methanol and NHS-LC-biotin dissolved in DMSO and rotate for 1 h at 37°C.
15. Apply to C18 Sep Pak resin equilibrated in 0.1% TFA.
16. Wash with 0.1% TFA in 10% acetonitrile.
17. Elute with 10 ml of 0.1% TFA in 100% acetonitrile.
18. Dry by evaporating at 45°C in a Speed-Vac.
19. Dissolve in 200 µl ethanol and store at –20°C.

B. Affinity Purification of PP-1 and PP-2A Holoenzymes

Steps

1. Powder frozen tissue (muscle, bladder, or liver) in liquid nitrogen.
2. Weigh 30 g wet weight of tissue and homogenize in 10 ml buffer A. Centrifuge at 15,000 *g* for 90 min at 4°C.
3. Keep the supernatant aside. Homogenize the pellet in 25 ml buffer B.
4. Recentrifuge at 15,000 *g* for 10 min at 4°C.
5. Decant supernatant off and homogenize pellet in buffer C. Incubate the homogenate for 30 min at 4°C and add equal volume of buffer C.
6. Centrifuge at 15,000 *g* for 30 min.
7. Dialyze the supernatant against 20 volumes of buffer A for 6 h.
8. Both cytosolic and particulate fractions are used for further analysis.
9. Preclear the endogenous biotinylated proteins in the lysate by passing over avidin–Sepharose (2 × 5-cm column) equilibrated in buffer A.
10. Wash avidin–Sepharose with 10 volumes of buffer A.
11. Mix the precleared lysate with 10 µ*M* MC-biotin and apply to the washed avidin–Sepharose.
12. Wash the column extensively with buffer A containing 1 *M* NaCl followed by buffer A.
13. Elute bound proteins with buffer A containing 1 m*M* biotin.
14. Analyze the column fractions by SDS–PAGE and silver staining (Fig. 1).

C. Proteome Mining

This technique has been modified from Haystead (1993) and Graves (2002).

Solutions

1. *Lysis buffer*: 25 m*M* Tris–HCl, pH 7.5, 60 m*M* MgCl2, 60 m*M* NaCl, 1 m*M* DTT, 0.2% NP-40, and protease inhibitors (4 µg/ml leupeptin, 0.1 m*M* PMSF, 0.1 µg/ml aprotonin, and 0.1 µg/ml pepstatin).
2. *Buffer A*: 25 m*M* Tris–HCl, pH 7.5, 60 m*M* MgCl2, 60 m*M* NaCl, 1 m*M* DTT
3. *Buffer B*: Buffer A + 0.5 *M* NaCl

Steps

1. Homogenize 10 g of tissue in 40 ml of lysis buffer until mixture turns frothy.
2. Spin lysate in ultracentrifuge at 100,000 *g* for 1 h at 4°C.
3. Filter the supernatant over glass wool and also through a 0.2-µm filter.
4. Wash ATP–Sepharose resin in 50 ml low salt buffer to yield a bed volume of 1 ml.
5. Combine the supernatant with the ATP–Sepharose and rotate for 30 min at room temperature.

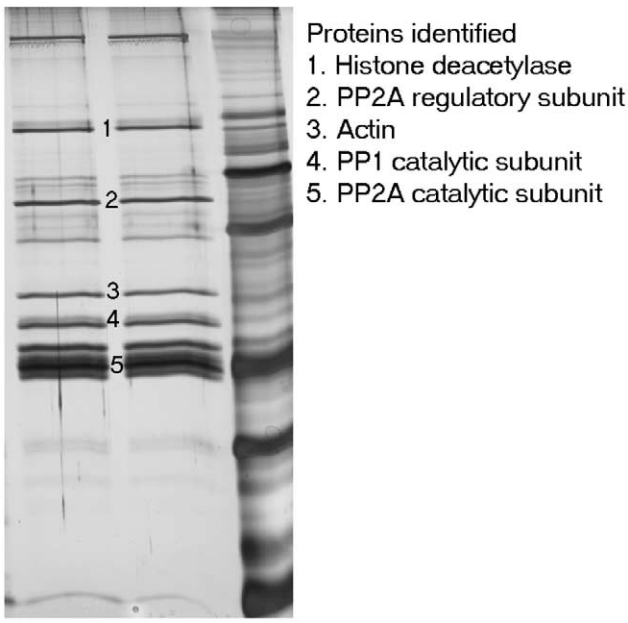

FIGURE 1 Microcystin–biotin eluate of rabbit muscle lysate.

6. Wash with 50 ml of buffer B followed by 50 ml buffer A.
7. Combine resin with 100 µ*M* drug (e.g., staurosporine) in buffer A at pH 7.5 and rotate for 15 min at room temperature.
8. Collect the eluate and resolve by SDS–PAGE and silver staining.
9. Identify eluted proteins by mass spectrometry (Fig. 2).

IV. COMMENTS

To identify binding partners of proteins bound to the ATP resin, the column is subjected to milder wash conditions; 250 m*M* NaCl washes are performed in these cases.

V. PITFALLS

1. Wash buffers need to be cold (4°C) to minimize degradation of proteins.

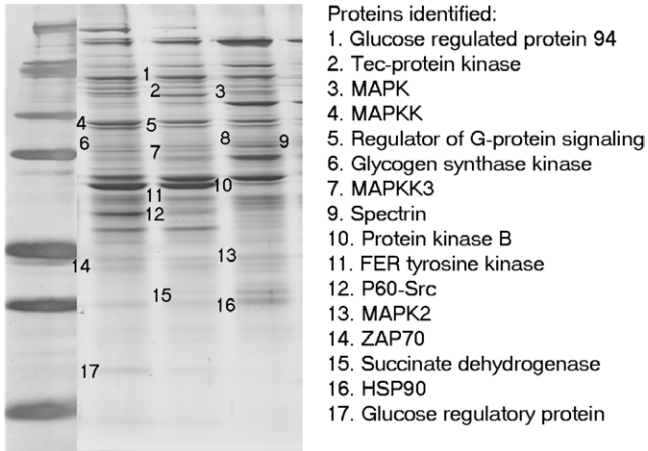

FIGURE 2 Staurosporine elution profile of ATP resin charged with human placenta.

2. MC-biotin has to be prepared fresh and is not reusable as it is lost during elution.
3. Its important to know solubility conditions of the drugs used to elute proteins off the resin, e.g., stuarosporine elutions are performed at room temperature, as the inhibitor precipitates at low temperatures.

References

Campos, M., Fadden, P., *et al*. (1996). Identification of protein phosphatase-1-binding proteins by microcystin-biotin affinity chromatography. *J. Biol. Chem*. **271**(45), 28478–28484.

Davies, S. P., Hawley, S. A., *et al*. (1994). Purification of the AMP-activated protein kinase on ATP-gamma-sepharose and analysis of its subunit structure. *Eur. J. Biochem*. **223**(2), 351–357.

Graves, P. R., Kwiek, J. J., *et al*. (2002). Discovery of novel targets of quinoline drugs in the human purine binding proteome. *Mol. Pharmacol*. **62**(6), 1364–1372.

Haystead, C. M., Gregory, P., *et al*. (1993). Gamma-phosphate-linked ATP-sepharose for the affinity purification of protein kinases: Rapid purification to homogeneity of skeletal muscle mitogen-activated protein kinase kinase. *Eur. J. Biochem*. **214**(2), 459–467.

Haystead, T. A., Haystead, C. M., *et al*. (1994). Phosphorylation of PHAS-I by mitogen-activated protein (MAP) kinase: Identification of a site phosphorylated by MAP kinase *in vitro* and in response to insulin in rat adipocytes. *J. Biol. Chem*. **269**(37), 23185–23191.

Shellman, Y. G., Svee, E., *et al*. (1999). Identification and characterization of individual cyclin-dependent kinase complexes from *Saccharomyces cerevisiae*. *Yeast* **15**(4), 295–309.

CHAPTER

34

Analysis of Protein–Protein Interactions by Chemical Cross-Linking

Andreas S. Reichert, Dejana Mokranjac, Walter Neupert, and Kai Hell

I. INTRODUCTION

Protein–protein interactions can be studied by a variety of approaches. Frequently employed methods include copurification and coimmunoprecipitation of protein complexes. For studying molecular interactions *in vivo*, yeast two-hybrid assays (Toby and Golemis, 2001) and fluorescence-based approaches using fluorescence resonance energy transfer and bioluminescence resonance energy transfer have been developed (reviewed in Boute *et al.*, 2002; Lippincott-Schwartz *et al.*, 2001). A rather versatile method capable of detecting even weak and transient interactions is chemical cross-linking. The basis of this technique is to covalently link closely apposed proteins or protein domains by chemical cross-linkers. A large number of cross-linkers are available that differ in their selectivity of reactive groups, spacer arm length, bi- or trifunctionality, membrane permeability, solubility, cleavability, use of iodination, and the presence of affinity tags such as biotin (Pierce Biotechnology, Inc. provides a list of a wide choice of available reagents). In order to select a suitable cross-linker, these characterisitics have to be considered. Chemical properties of the protein, such as the presence of functional groups and its chemical environment, have to be taken into account. Most importantly, cross-links between two proteins can only be established when suitable side chains are present in the right distance and are accessible. Therefore, the characterization of protein–protein interactions by chemical cross-linking often requires empirical testing of a variety of different cross-linkers and reaction conditions. Photoreactive derivates can be used independent of the presence of functional side chains in the proteins to be cross-linked; these can be incorporated co- or posttranslationally (reviewed in Brunner, 1996).

Another important issue is to identify an unknown protein that was cross-linked to the protein of interest. When a known protein is suspected to be cross-linked, several approaches can be employed. One possibility is to check whether the cross-link can be immunoprecipitated by using an antibody against the partner protein in question. Another way is to perform the cross-linking experiment in a mutant background that either lacks the candidate protein or contains a variant that can be distinguished from the endogenous protein (e.g., by the presence of a protein tag or by a variation of its apparent size). For identification of unknown binding partners, it is advisable to enrich the cross-link by affinity chromatography and subsequently identify the protein, e.g., by mass spectrometry (reviewed in Farmer and Caprioli, 1998). In that respect, one may consider the use of proteins that contain an affinity tag (e.g., GST or $His_{6–10}$) or to use biotinylated and/or cleavable cross-linkers.

In the following example the interaction of a mitochondrially targeted precursor protein with components of the mitochondrial inner membrane translocase complex TIM23 is investigated by chemical cross-linking. To this end, the precursor protein $pb_2\Delta19(167)DHFR_{K5}$ (Schneider *et al.*, 1994) is radiolabelled upon translation *in vitro* and incubated with isolated energized mitochondria from *Neurospora crassa* (for a review about mitochondrial import, refer to Neupert, 1997). The precursor protein is arrested during the *in vitro* import reaction at a certain stage spanning both the outer and the inner membrane. Such a trapping step is often necessary to increase the specificity and yield of the cross-linking reaction. After addition of the homobifunctional,

Copyright 2006, Elsevier Science (USA).
All rights reserved.

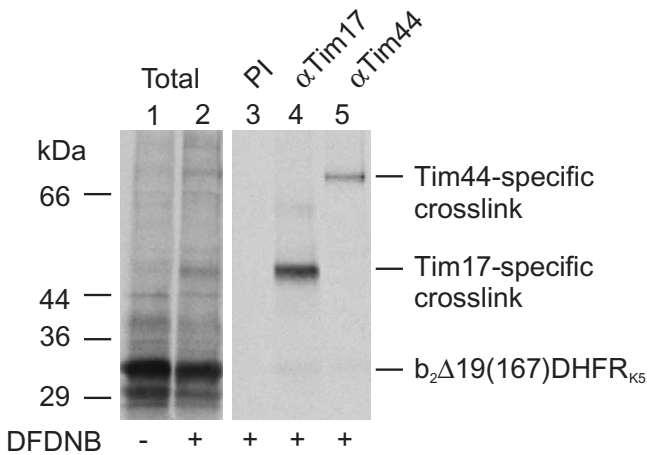

FIGURE. 1 Cross-linking of arrested b2Δ19(167)$DHFR_{K5}$ to Tim17 and Tim44. Radiolabelled b2Δ19(167)$DHFR_{K5}$ was arrested during import into isolated mitochondria from *Neurospora crassa*. After import, a portion (1/12) of mitochondria were mock treated in the absence of the cross-linker DFDNB (lane 1). The rest was subjected to cross-linking with 200 µ*M* DFDNB for 30 min on ice and another portion (1/12) of the sample was withdrawn (lane 2). Mitochondria were reisolated and used for SDS–PAGE directly (lanes 1 and 2). For immunoprecipitation of cross-linked species, the remaining portion (10/12) of the sample was lysed, split in three aliquots, and incubated with preimmune serum (lane 3) and antibodies raised against Tim17 (lane 4) or Tim44 (lane 5). Immunoprecipitates were harvested and subjected to SDS–PAGE and autoradiography. Exposure times for lanes 1 and 2 were approximately 10 times shorter than for lanes 3 to 5.

noncleavable, amine-specific cross-linker 1.5-difluoro-2,4-dinitrobenzere (DFDNB) cross-links can be detected by SDS–PAGE and autoradiography (Fig. 1). In order to identify to which of the known proteins of the TIM23 complex the precursor was cross-linked, the samples were immunoprecipited using antibodies against Tim17 and Tim44, subunits of the TIM23 complex.

II. MATERIALS AND INSTRUMENTATION

NADPH (Cat. No. 1045), NADH (Cat. No. 1051), and HEPES (Cat. No. 1009) are from Gerbu, Germany. Methotrexate (MTX, Cat. No. A6770), sorbitol (Cat. No. S-1876), and glycerol (Cat. No. G-7757) are from Sigma-Aldrich. KCl (Cat. No. 104936), Mg/acetate · $4H_2O$ (Cat. No. 105819), KH_2PO_4 (Cat. No. 104873), $Na_2EDTA \cdot 2H_2O$ (Titriplex, Cat. No. 108418), glycine (Cat. No. 104201), $MnCl_2 \cdot 4H_2O$ (Cat. No. 105927), KOH (Cat. No. 105033), Tris (Cat. No. 108382), NaCl (Cat. No. 106404), $NaH_2PO_4 \cdot H_2O$ (Cat. No. 106349), Triton X-100 (Cat. No. 108603), dimethyl sulfoxide (DMSO, Cat. No. 102952), ethanol (Cat. No. 100983), and NaOH (Cat. No. 106467) are all from Merck KG, Germany. Sodium dodecyl sulfate (SDS, Cat. No. 20760), bromphenol blue (15375), and phenylmethyl sulforyl fluoride (PMSF, Cat. No. 32395) are from Serva, Germany. ATP · $3H_2O$ (Cat. No. 635316) and protein A–Sepharose CL-4B (Cat. No. 170963) are from Roche, Switzerland, and Amersham Biosciences, Sweden, respectively. DFDNB (Cat. No. 21525) is from Pierce Biotechnology, Inc.

III. PROCEDURES

A. Arrest of a Radiolabelled Precursor Protein as a Translocation Intermediate

Solutions

1. *0.1 mM methotrexate (MTX)*: First make a 10 m*M* stock solution by dissolving 4.54 mg in 1 ml DMSO. Store at –20°C. Dilute the stock solution 100-fold with distilled water to 0.1 m*M* MTX prior to use.
2. *100 mM NADPH*: Dissolve 8.87 mg in 100 µl distilled water. Make fresh each time.
3. *200 mM ATP*: Dissolve 60.5 mg ATP in 500 µl distilled water and adjust with 10 *M* KOH to pH 7. Make aliquots and store at –20°C.
4. *200 mM NADH*: Dissolve 14.2 mg NADH in 100 µl distilled water. Make fresh each time.
5. *2× import buffer*: Dissolve 2.38 g HEPES, 18.2 g sorbitol, 1.19 g KCl, 0.43 g Mg acetate · $4H_2O$, 54.4 mg KH_2PO_4, 186.12 mg $Na_2EDTA \cdot 2H_2O$, and 99 mg $MnCl_2 \cdot 4H_2O$ in 90 ml distilled water. Adjust pH to 7.2 with KOH and fill up with distilled water to 100 ml. Store at –20°C and thaw each time before use.

Steps

1. The precursor protein was synthesized in the presence of [^{35}S]methionine using reticulocyte lysate from Promega, USA, according to the manufacturer's instructions. Preincubate 50 µl of the obtained lysate containing the radiolabelled precursor protein with 0.5 µl of methotrexate (0.1 m*M*) and 1.25 µl of 100 m*M* NADPH for 10 min at 25°C.
2. Mix 600 µl 2× import buffer with 24 µl methotrexate (MTX, 0.1 m*M*), 60 µl NADPH (100 m*M*), 24 µl ATP (200 m*M*), 30 µl NADH (200 m*M*), and 390 µl distilled H_2O thoroughly. Add 60 µl mitochondria (10 mg/ml) freshly prepared from *N. crassa* (Sebald *et al.*, 1979), 12 µl of pretreated lysate, and mix gently.
3. Incubate for 15 min at 25°C. Stop the import reaction by placing the sample on ice.

B. Cross-Linking

Solutions

1. *20 mM DFDNB*: Dissolve 2.04 mg in 500 µl DMSO. Make fresh immediately before use.
2. *1 M glycine, pH 8.0*: Dissolve 7.51 g in 90 ml distilled water, adjust with KOH to pH 8.0, and fill up to a total volume of 100 ml with distilled water. Store at –20°C.
3. *SHKCl*: Dissolve 10.93 g sorbitol, 476 mg HEPES, and 596 mg KCl in 90 ml distilled water, adjust with KOH to pH 7.2, and fill up to 100 ml with distilled water. Store at 4°C.
4. *Laemmli buffer (without β-mercaptoethanol)*: Dissolve 1 g SDS, 5 ml glycerol, and 0.36 g Tris in 40 ml of distilled water. Adjust to pH 6.8 with HCl, add 4 mg bromphenol blue, and fill up to 50 ml with distilled water. Store at room temperature.

Steps

1. Split the import reaction into a 100-µl aliquot and an 1100-µl aliquot, representing 50 and 550 µg mitochondrial protein, respectively.
2. Add 1 µl DMSO to the 50-µg aliquot for mock treatment (total, no cross-link reagent) and 11 µl DFDNB (20 m*M* stock in DMSO) to the latter aliquot.
3. Incubate the samples for 30 min on ice.
4. Stop the cross-linking reaction by the addition of 1 *M* glycine, pH 8.0, to a final concentration of 0.1 *M* and incubate 10 min on ice.
5. Remove a 100-µl aliquot from the sample containing the DFDNB (total, plus cross-link reagent). The rest of the sample (1000-µl aliquot) can be used for identification of the cross-linked protein. As an example, see Section IIIC. Centrifuge the samples (totals, plus and minus cross-link reagent) for 10 min at 21,000 g at 4°C to reisolate mitochondria. Wash samples once carefully with 1 ml SHKCl and centrifuge again as described earlier.
6. Remove the supernatant and resuspend the pellet in 25 µl Laemmli buffer.
7. Resolve mitochondrial proteins and cross-linked products by SDS–PAGE. The radiolabelled cross-linked products can be visualized by autoradiography.

C. Identification of the Cross-Linked Product by Immunoprecipitation

Solutions

1. *1 M NaPi buffer, pH 8.0*: Dissolve 13.8 g $NaH_2PO_4 \cdot H_2O$ in 90 ml distilled water. Adjust pH to 8.0 with NaOH and fill up with distilled water to 100 ml. Store at 4°C.
2. *1 M NaCl*: Dissolve 58.44 g NaCl in 1 liter distilled water. Store at room temperature.
3. *10% (w/v) SDS*: Dissolve 10 g SDS in distilled water and bring to a final volume of 100 ml. Store at room temperature.
4. *20% (w/v) Triton X-100*: Dissolve 10 g Triton X-100 in distilled water and bring to a final volume of 50 ml. Store light protected at room temperature.
5. *TBS buffer*: Dissolve 1.21 g Tris and 9 g NaCl in 950 ml distilled water. Adjust pH to 7.4 with HCl and fill up with distilled water to 1 liter.
6. *SHKCl*: See solutions in Section IIIB.
7. *0.2 M PMSF*: Dissolve 34.8 mg PMSF in 1 ml ethanol. Prepare fresh each time.
8. *SDS lysis buffer*: Mix 20 µl 1 *M* NaPi buffer, pH 8.0, 100 µl 1 *M* NaCl, 100 µl 10% (w/v) SDS, and 775 µl distilled water. Finally add 5 µl 0.2 *M* PMSF.
9. *IP buffer*: Add 0.5 ml 20% (w/v) Triton X-100 to 50 ml TBS buffer.

Steps

1. For three immunoprecipitation reactions, take 75 µl protein A–Sepharose CL-4B (PAS) beads and wash three times with 1.5 ml TBS buffer.
2. Take 25 µl of PAS beads in 500 µl TBS buffer per reaction and add affinity-purified antibodies (approximately 10 µg of IgGs) against Tim17 or Tim44, or preimmune serum, respectively.
3. Incubate for at least 30 min at 4°C under gentle shaking.
4. Before immunoprecipitation, wash the PAS beads with the bound antibodies twice with 1 ml TBS and once with 500 µl IP buffer.
5. Take the 1000-µl aliquot from the cross-link reaction (Section IIIB, step 5) for immunoprecipitation and centrifuge for 10 min at 21,000 *g* at 4°C.
6. Wash isolated mitochondria with 1 ml SHKCl and centrifuge again as in step 5.
7. Lyse mitochondria by resuspension in 50 µl SDS lysis buffer and shake gently for 15 min at room temperature.
8. Dilute with Triton X-100-containing IP buffer to 1 ml.
9. Centrifuge the sample for 30 min at 125,000 *g* in a TLA45 rotor at 2°C to remove nonsolubilized and aggregated material.
10. Take the supernatant and add equal amounts to PAS beads coupled to antibodies against Tim17, Tim44, or preimmune serum, respectively (see earlier). Fill up to 1 ml with IP buffer.
11. Rotate supernatant for 2 h at 4°C.
12. Wash PAS beads twice with 1 ml IP buffer and once with 1 ml TBS.

13. Elute bound material by adding 40 µl Laemmli buffer. Keep sample for 3 min at 95°C and remove eluate from the PAS beads.

14. Analyze the precipitated material by SDS–PAGE and autoradiography.

IV. COMMENTS

One limitation of this technique is that the amounts of cross-linked as related to noncross-linked protein species are normally less than 1% in case of transient interactions but can exceed 10% with stable interactions. Therefore, it is common to halt a biological process at a defined step to increase the cross-linking yield. In the example given earlier, the precursor protein is arrested at a stage, where it spans the outer and the inner mitochondrial membrane via the translocation machineries. Complete import into mitochondria is inhibited by the C-terminal DHFR domain of the precursor protein, which is stably folded due to the presence of the substrate analogue methotrexate and the cosubstrate NADPH. Translocation intermediates can also be generated by depletion of matrix ATP or depletion of membrane potential. Import at low temperature prolongs the time of interaction. Another strategy could be to use mutants, which still have the potential to transport the precursor to a certain intermediate stage but not further.

DFDNB is a homobifunctional aryl halide-containing cross-linker, which contains two reactive fluorine atoms and reacts with amines. It should be noted that DFDNB is not completely specific for amine groups, but can also react with amino acids containing thiol, phenolate, and imidazolyl groups. Commonly used compounds to cross-link amines are the family of *N*-hydroxysuccinimide esters (NHS esters). NHS esters react with deprotonated primary amines present at the N terminus of proteins or in the side chain of lysine residues within proteins. It is important that the cross-linking reaction is performed under alkaline conditions within the pH range of 7.5 to 9 to reduce the protonation of the amine groups.

Cross-link efficiencies between interacting proteins are not predictable. Therefore, cross-link conditions have to be optimised for each protein–protein interaction. In addition to the test of various cross-linkers (e.g., BMH, DSG, DSG, EDC, MBS, and SPDP) with different reactivities and spacer lengths, the concentration of the cross-linker can be titrated and the temperature and reaction time can be modified. We normally test cross-linkers at 12°C, room temperature, or on ice in a concentration range of 0.05 to 1 m*M*.

It is also possible to introduce additional functional groups within the protein to facilitate the cross-link reaction. In the example, additional lysines were added in a position within the precursor protein, where they were likely to be in close contact to the translocation components.

V. PITFALLS

1. As stated earlier, DFDNB and NHS esters react with primary amines. Buffers containing primary amines such as Tris cannot be used as reaction buffers. They would react with the cross-linking reagent and quench the cross-linking reaction. Indeed, Tris at pH 7.5–8 is used as a quenching reagent similar to glycine. In addition, the reaction buffers should not contain high amounts of unspecific proteins, such as bovine serum albumine, whose lysines would compete for the cross-linker. When using thiol-specific reagents, reducing agents such as dithiothreitol or β-mercaptoethanol have to be omitted. For example, some [^{35}S]methionine preparations contain β-mercaptoethanol for stabilisation. These should not be used for labelling of proteins *in vitro* if the obtained lysate is directly used for a cross-linking reaction with a thiol-specific cross-linker.

2. Hydrolysis of most cross-linking reagents occurs quite rapidly. Therefore the cross-linkers have to be kept dry during storage to prevent hydrolysis. It is recommended to store the cross-linker under nitrogen once the vial is opened. As this is not always practicable, we store them in an exsiccator. To protect the cross-linker against condensing water, make sure that the vial is equilibrated to room temperature before opening.

3. In an immunoprecipition experiment the detection of cross-linked products can be complicated by the coelution of IgG chains. Under reducing conditions the light and heavy chains of IgGs are separated and have apparent molecular masses of approximately 25 and 50–60 kDa, respectively. In contrast, under nonreducing conditions, when light and heavy chains are not separated, the IgGs have a molecular mass of larger than 150 kDa. This has to be considered when a cross-linked protein is in the respective size range.

References

Boute, N., Jockers, R., and Issad, T. (2002). The use of resonance energy transfer in high-throughput screening: BRET versus FRET. *Trends Pharmacol. Sci.* **23**, 351–354.

Brunner, J. (1996). Use of photocrosslinkers in cell biology. *Trends Cell Biol.* **6**, 154–157.

Farmer, T. B., and Caprioli, R. M. (1998). Determination of protein-protein interactions by matrix-assisted laser desorption/ionization mass spectrometry. *J. Mass Spectrom.* **33**, 697–704.

Lippincott-Schwartz, J., Snapp, E., and Kenworthy, A. (2001). Studying protein dynamics in living cells. *Nature Rev. Mol. Cell Biol.* **2**, 444–456.

Neupert, W. (1997). Protein import into mitochondria. *Annu. Rev. Biochem.* **66**, 863–917.

Schneider, H. C., Berthold, J., Bauer, M. F., Dietmeier, K., Guiard, B., Brunner, M., and Neupert, W. (1994). Mitochondrial Hsp70/MIM44 complex facilitates protein import. *Nature* **371**, 768–774.

Sebald, W., Neupert, W., and Weiss, H. (1979). Preparation of *Neurospora crassa* mitochondria. *Methods Enzymol.* **55**, 144–148.

Toby, G. G., and Golemis, E. A. (2001). Using the yeast interaction trap and other two-hybrid-based approaches to study protein-protein interactions. *Methods* **24**, 201–217.

CHAPTER

35

Peroxisomal Targeting as a Tool to Assess Protein–Protein Interactions

Trine Nilsen, Camilla Skiple Skjerpen, and Sjur Olsnes

I. INTRODUCTION

Assessing protein–protein interactions is essential in order to elucidate the molecular mechanisms of the cell. Several methods have been developed to identify, monitor, or confirm such interactions, but they all suffer from limitations, such as being purely *in vitro* methods, not adaptable for mammalian systems, or laborious to implement. By exploiting the peroxisomal targeting machinery it is possible to assay for protein–protein interactions in living mammalian cells in a simple and affordable way. Two peroxisomal targeting signals (PTSs) have been described where PTS-1 consists of a C-terminal tripeptide (typically Ser-Lys-Leu) and PTS-2 of an N-terminal nonapeptide (Gould *et al.*, 1989; Swinkels *et al.*, 1991). Protein oligomers can be imported into the lumen of peroxisomes and, as a consequence, proteins lacking a PTS can be imported in a "piggyback fashion" (McNew and Goodman, 1994; Titorenko *et al.*, 2002).

This specific feature is exploited in the protein–protein interaction assay described here. Initially the protein of interest is targeted to the peroxisomes by adding PTS-1 to its extreme C terminus. This targeting is confirmed by colocalising the expressed PTS-tagged protein with the peroxisomal marker catalase (Fig. 1). After confirming peroxisomal targeting, cells are cotransfected with the PTS-tagged protein and a potential interacting partner lacking a PTS. Following coexpression and binding of the two overexpressed proteins in the cytosol, interacting partners can be colocalised in the peroxisomal lumen. Such colocalisation indicates that the two proteins in question bind to each other *in vivo* (Skjerpen *et al.*, 2002).

II. MATERIALS AND INSTRUMENTATION

NH_4Cl (Cat. No. 11145-1), $NaH_2PO_4 \cdot H_2O$ (Cat. No. 17157-1), $Na_2HPO_4 \cdot 12H_2O$ (Cat. No 16579-1), NaCl (Cat. No. 16404-1), and glycerol (Cat. No. 14094-1) are from VWR International.

Tris–HCl (Cat. No. T-1503), digitonin (Cat. No. D-1407), and Triton X-100 (Cat. No. T-9284) are from Sigma. The FuGENE 6 transfection reagent (Cat. No. 1 815 091) is from Roche Molecular Biochemicals, and paraformaldehyde (Cat. No. 762 40) is from Fluka Chemika. Mowiol (Cat. No. 475904) is from Calbiochem. The confocal microscope used for collecting images is a Leica TCS NT from Wezlar, Germany, and the software used for image processing is Adobe Photoshop 5.0 (Mountain View, CA).

III. PROCEDURES

A. Plasmid Preparation

Steps

1. Clone the cDNAs encoding the proteins to be analysed into plasmid vectors suitable for transient transfection.
2. Purify the plasmid DNA. Anion-exchange chromatography, using disposable columns such as Qiagen, is recommended in order to produce high-quality DNA.

Copyright 2006, Elsevier Science (USA).
All rights reserved.

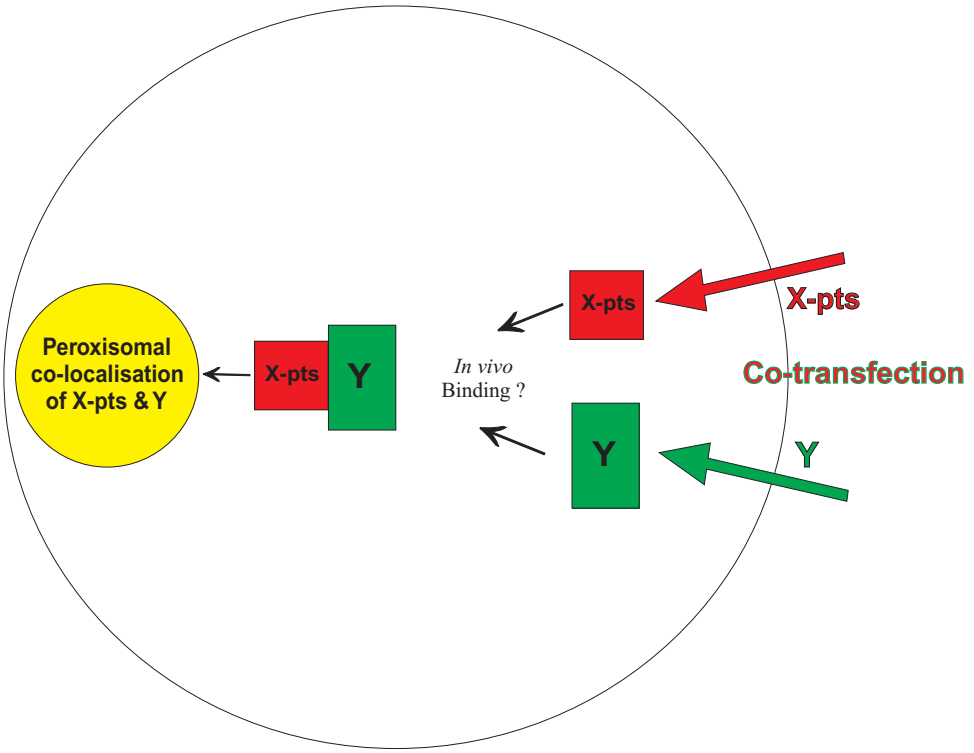

FIGURE 1 Peroxisomal colocalisation of two interacting proteins, X and Y. Protein X (red) is targeted to the peroxisomes by the addition of a peroxisomal-targeting sequence (PTS). X-pts and its potential interacting partner, Y (green), are then cotransfected into cells. If there is an *in vivo* interaction between X-pts and Y in the cytosol, Y can be cotransported into the peroxisomes after the binding takes place in a "piggyback" fashion. In this case the two proteins will colocalise in the peroxisomes as seen when merging the immunofluorescent images of X-pts (red) and Y (green), which will yield yellow-coloured peroxisomes.

B. Cotransfection and Confocal Microscopy Analysis

Solutions

1. *Phosphate-buffered saline (PBS)*: To make 1 litre, dissolve 0.16 g $NaH_2PO_4 \cdot H_2O$, 1.98 g $Na_2HPO_4 \cdot 12H_2O$, and 8.1 g NaCl in water

2. *40 µg/ml digitonin*: To make a stock solution of 400 µg/ml, dissolve 16 mg digitonin in 40 ml PBS. Sterile filter and store in aliquots at –20°C. Dilute 1 : 10 to get a working concentration of 40 µg/ml.

3. *3% paraformaldehyde*: To make 150 ml of 3% paraformaldehyde, heat 90 ml H_2O to 60°C and add 4.50 g paraformaldehyde. Stir for 3 h in a sterile hood and make sure not to overheat the solution. Add 2 *N* NaOH drop wise until the solution is clear. Add 50 ml 3× PBS (to make 250 ml 3×PBS, dissolve 0.12 g $Na_2HPO_4 \cdot 12H_2O$, 1.49 g $Na_2HPO_4 \cdot 12H_2O$, and 6.08 g NaCl in water, no pH adjustment) and adjust the pH to 7.2 with HCl. Add water until the total volume is 150 ml. Filter the solution and store aliquots at –20°C.

4. *50 mM NH_4Cl*: Make a 0.5 *M* stock solution by dissolving 4.01 g NH_4Cl in 150 ml PBS. Store at room temperature and dilute 1 : 10 to obtain a working solution of 50 m*M*.

5. *0.1% Triton X-100*: To make a stock solution of 10%, add 1 ml Triton X-100 to 9 ml H_2O. Sterile filter and store the aliquots at –20°C. Dilute 1 : 100 to get a working solution of 0.1%.

6. *Mowiol*: Add 6.7 g 87% glycerol and 2.4 g Mowiol to 6 ml H_2O and 12 ml 0.2 *M* Tris–HCl, pH 8.5. Mix for 10 min at 50°C. Centrifuge the solution for 15 min at 5000 rpm in a Sorvall RC5C centrifuge. Sterile filter and store the aliquots at –20°C.

Steps

1. Plate cells on glass coverslips in a plastic dish (typically ~2×10^5 cells/3.5-cm^2 well, depending on cell type) and incubate overnight at 37°C.

2. Cotransfect the cells with approximately 0.5–1.0 µg DNA of each construct by conventional methods for transient transfection, such as the FuGENE 6 transfection reagent. Allow expression for 20–24 h at 37°C.

3. All the following steps are performed at room temperature. Wash the cells in PBS for 5 min on the bench.

4. Incubate with digitonin dissolved in PBS (20–40 µg/ml, depending on cell density and cells type) for 10 min and wash the cells carefully in PBS for 5 min.

5. Fix the cells in 3% paraformaldehyde in PBS for 20–50 min at room temperature or at 4°C overnight.

6. Quench the autofluorescence with 50 m*M* NH_4Cl in PBS for 10 min.

7. Incubate the cells in 0.1% Triton X-100 in PBS for 5 min.

8. Block unspecific antibody binding sites with 5% FCS in PBS for 20 min.

9. Incubate the cells with primary antibodies. Place the coverslips with cells facing down for 20 min on a piece of Parafilm where 15 µl of the primary antibody solution has been placed. Ensure that catalase detection is included to be able to confirm peroxisomal targeting of the complex.

10. Transfer the coverslips back to the plastic dish and wash three times in PBS for 5 min.

11. Incubate with secondary antibodies as described in step 9.

12. Wash twice for 5 min in PBS.

13. Rinse the coverslips briefly in water and mount on a clean glass slide with Mowiol.

14. Collect separate immunofluorescence images of the two proteins and catalase in cotransfected cells using a confocal microscope.

15. Process the images using suitable software such as Adobe Photoshop 5.0. Merge images representing the PTS-tagged protein and catalase to confirm peroxisomal targeting in the relevant cell. Then merge the image of the protein lacking a PTS with either catalase or its potential interacting partner to analyse for colocalisation.

IV. COMMENTS

The immunofluorescent protocol described here is designed specifically to visualise the peroxisomes

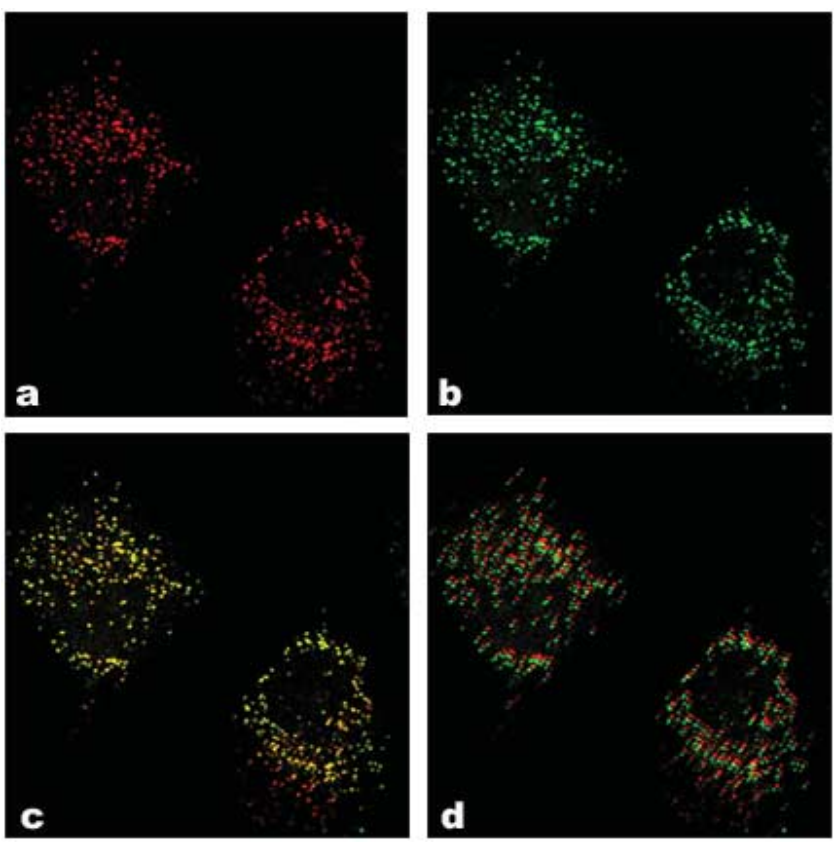

FIGURE 2 Askew imaging ensures detection of protein colocalisation specificity in merged images. (A) Confocal image representing protein X-pts. (B) Confocal image representing protein Y. (C) Merged confocal image of A and B. (D) Confocal image merged askew.

against a low background of cytosolic material. Digitonin is a cholesterol-specific detergent and will therefore leave noncholesterol-containing compartments such as the peroxisomes intact. Because the plasma membrane contains a substantial amount of cholesterol, the cytosolic material can be depleted from the cell by digitonin treatment prior to fixation. The antibodies used in immunoflourescence are given access to the organelle lumen by Triton X-100 treatment.

V. PITFALLS

1. Before initiating cloning, ensure that detection of both expressed proteins by immunofluorescence will be feasible. If no antibodies suitable for immunofluorescence microscopy are available, tags such as Myc or green fluorescence protein should be added to the construct. Adding an autofluorescent marker to at least one of the proteins will facilitate the immunofluorescent procedure as it requires triple staining.

2. It is recommended to use cell lines that are tranfected easily, as this assay is dependent on cotransfection. In principle, any transfectable cell line can be used depending on the purpose of the study.

3. Some cells lines, such as COS-1 cells, are more susceptible to digitonin treatment than others and tend to loosen from the coverslip. In such cases it is recommended to decrease the digitonin concentration.

4. If one or both of the proteins in question are associated with intracellular membranes, it may be difficult, if not impossible, to redirect these proteins to the peroxisomes. A solution to this problem can be to delete the protein domain responsible for the attachment and use the truncated soluble form in this assay. Such an approach has been successful in the detection of protein–protein interaction studies (Nilsen *et al*., 2004).

5. It may be difficult to determine whether the colocalisation between two proteins is specific, especially if the confocal images have a high background. In order to ensure specificity, merge the two images askew by the approximate diameter of one peroxisome in the relevant image. Using Adobe Photoshop 5.0, select and copy an image approximately one peroxisomal diameter smaller on two sides of the rectangle than the full size image. Then merge it onto its corresponding image of the interacting protein. The two images will now be askew, as merging is centered automatically. When merging a red (X-pts) and a green (Y) image askew, yellow-stained peroxisomes as observed in conventional merged images will appear as red and green (Fig. 2).

Acknowledgment

T.N and C.S.S are fellows of the Norwegian Cancer Society.

References

Gould, S. J., Keller, G. A., Hosken, N., Wilkinson, J., and Subramani, S. (1989). A conserved tripeptide sorts proteins to peroxisomes. *J. Cell Biol.* **108**, 1657–1664.

McNew, J. A., and Goodman, J. M. (1994). An oligomeric protein is imported into peroxisomes in vivo. *J. Cell Biol.* **127**, 1245–1257.

Nilsen, T., Skjerpen, C. S., and Olsnes, S. (2004). Peroxisomal targeting as a tool to assay protein-protein interactions into living cell. *J. Biol. Chem.* **279**, 4794–4801.

Skjerpen, C. S., Nilsen, T., Wesche, J., and Olsnes, S. (2002). Binding of FGF-1 variants to protein kinase CK2 correlates with mitogenicity. *EMBO J.* **21**, 4058–4069.

Swinkels, B. W., Gould, S. J., Bodnar, A. G., Rachubinski, R. A., and Subramani, S. (1991). A novel, cleavable peroxisomal targeting signal at the amino-terminus of the rat 3-ketoacyl-CoA thiolase. *EMBO J.* **10**, 3255–3262.

Titorenko,V. I., Nicaud, J. M., Wang, H., Chan, H., and Rachubinski, R. A. (2002). Acyl-CoA oxidase is imported as a heteropentameric, cofactor-containing complex into peroxisomes of *Yarrowia lipolytica*. *J. Cell Biol.* **156**, 481–494.

CHAPTER

36

Biomolecular Interaction Analysis Mass Spectrometry

Dobrin Nedelkov and Randall W. Nelson

I. INTRODUCTION

Biomolecular interaction analysis mass spectrometry (BIA/MS) is multidimensional methodology for functional and structural protein analysis (Krone *et al*., 1997; Nelson *et al*., 1997a,b, 2000a,b). In essence, BIA/MS represents a synergy of two individual technologies: surface plasmon resonance (SPR) sensing and matrix-assisted laser desorption/ionization time-of-flight (MALDI-TOF) mass spectrometry. SPR is employed for quantification, whereas MS is utilized to delineate the structural features of the analyzed proteins. Proteins are affinity captured and quantified from solution via ligands covalently attached on the SPR sensor surface. Because the SPR detection is nondestructive, proteins retrieved on the SPR sensing surface can be further analyzed via mass spectrometry, either directly from the sensor/chip surface (as described in most of the publications from our laboratory) or separately, following elution and microrecovery (Gilligan *et al*., 2002; Nelson *et al*., 1999; Sonksen *et al*., 1998, 2001). The combination of SPR with MS overcomes the limitation of nondiscriminatory SPR detection and allows for elucidation of nonspecific binding (NSB) of other biomolecules to the surface-immobilized biomolecules (or to the underivatized sensor surface itself), binding of protein fragments, protein variants (existing due to posttranslational modifications and point mutations), and complexed (with other molecules) proteins. The BIA/MS approach has been utilized for isolation, detection, and identification of epitope-tagged proteins (Nelson *et al*., 1999), detection of food pathogens (Nedelkov *et al*., 2000), analysis of human urine protein biomarkers (Nedelkov and Nelson, 2001a), delineation of *in vivo* assembled multiprotein complexes (Nedelkov and Nelson, 2001c; Nedelkov *et al*., 2003), and screening for protein functionalities (Nedelkov and Nelson, 2003). Detection of attomole amounts of proteins from complex biological mixtures is possible via the combined SPR-MS approach (Nedelkov and Nelson, 2000a). The modus operandi of the BIA/MS approach is illustrated via the analysis of apolipoproteins A-I and A-II (apoA-I and apoA-II) from human plasma sample.

II. MATERIALS AND INSTRUMENTATION

Biacore X Biosensor (Biacore AB, Uppsala, Sweden) is utilized for the protein affinity retrieval and SPR analysis. Ligands (e.g., antibodies) are immobilized on the carboxymethyldextran surface of a CM5 research grade sensor chip (Biacore AB, Cat. No. BR. 1000-14) using amine-coupling kit chemicals (Biacore AB, Cat. No. BR-1000-50).

A chip cutter with a circular heated cutter head (made in our laboratory) is used for excising a chip/plastic mount of a defined circular shape that fits into an appropriately configured MALDI mass spectrometer target (Nedelkov and Nelson, 2000b).

The MALDI matrix is applied to the chip via an aerosol-spraying device (also developed in our laboratory). The device consists of an aspirating/sheath gas needle (~30-μm orifice), backed by ~30 psi of compressed air (Nedelkov and Nelson, 2000b). The air/matrix solution ratio can be adjusted to produce a fine mist of matrix solution that is aimed at the entire surface of the cutout chip. The matrix of choice is α-cyano-4-hydroxycinnamic acid (ACCA, Aldrich,

Copyright 2006, Elsevier Science (USA).
All rights reserved.

Milwaukee, WI, Cat. No. 47,687-0), which is further processed by powder-flash recrystallization from a low-heat-saturated acetone solution of the original stock.

MALDI-TOF mass spectrometry analysis from the chip surface is performed on a custom-made MALDI-TOF mass spectrometer (Intrinsic Bioprobes, Inc.). The instrument consists of a linear translation stage/ion source capable of precise targeting of each of the flow cells under a focused laser spot. Ions generated during a 4-ns laser pulse (357 nm, nitrogen) are accelerated to a potential of 30 kV over a single-stage ion extraction source distance of ~2 cm before entering a 1.5-m field-free drift region. The ion signals are detected using a two-stage hybrid (channel plate/discrete dynode) electron multiplier. Time-of-flight spectra are produced by signal averaging of individual spectra from 50 to 100 laser pulses (using a 500-MHz; 500-Ms/s digital transient recorder). Custom software is used in acquisition and analysis of mass spectra. All spectra are obtained in the positive ion mode.

III. PROCEDURES

A. SPR Analysis and Protein Affinity Retrieval

Ligands, Solutions, and Buffers

1. *Ligands*: When using antibodies (or other proteins) as ligands, dilute the original stock solutions with 10 m*M* acetate buffer, pH 5.0, to a final ligand concentration of 0.01–0.1 mg/mL.

2. *Buffers and solutions*: Ultrapure, molecular biology grade, sterile water (American Bioanalytical, Natick, MA, Cat. No. 7732-18-5) is used for solution making. HBS-EP [0.01 *M* HEPES, pH 7.4, 0.15 *M* NaCl, 0.005% (v/v) polysorbate 20, 3 m*M* EDTA] is typically used as a running buffer in the SPR biosensor. From the amine-coupling kit, make 400 m*M* solution of EDC [*N*-ethyl-*N*′-(dimethylaminopropyl)carbodiimide] in the ultrapure water, 100 m*M* solution of *N*-hydroxy-succinimide (NHS), and use the 1 *M* ethanolamine (pH 8.5) solution as supplied. Make 60 m*M* HCl for ligand surface regeneration.

Steps

1. Remove a new CM5 sensor chip from its packaging, take out the chip from the plastic housing cassette, wash it with five 200-µl aliquots of water, dry, and put the chip back in the cassette.

2. Insert the chip into the Biosensor (via the dock command), prime, set the flow rate at 5 µl/min, and let it equilibrate with the HBS-EP running buffer at 5 µl/min for 10–20 min.

3. Set the flow to a single flow cell and start the amine-coupling surface preparation procedure from the Biosensor software. Mix 35 µl of the EDC solution and 35 µl of the NHS solution in a small vial, and inject 35 µl of the mixture over the flow cell surface to activate the carboxyl groups of the dextran matrix.

4. After the surface activation injection has ended, inject 70 µl of the antibody solution. Monitor the SPR response for a sharp increase that will indicate binding of the antibody to the chip surface.

5. Inject 35 µl of the ethanolamine solution to block free (unreacted) esters.

6. Inject 20 µl of the HCl solution to release any noncovalently attached antibody.

7. Measure the SPR response (in resonance units, RU) at the end of the EDC/NHS injection and subtract it from the final SPR response measured after the HCl injection to yield an accurate estimate on the total amount of antibody immobilized on the surface of the flow cell. Because 1 RU equates to 1 pg of proteinacious material per 1 mm^2 of the flow cell surface (the FC dimensions are 0.5 × 2 mm), a response of ~15,000 RUs at the end of the injection, indicating the immobilization of ~100 fmol antibody ($MW_{antibody}$ ~ 150,000, 1 RU = 1 pg protein), is generally satisfactory.

8. Repeat steps 2–6 for immobilization of the other antibody in the second flow cell. Alternatively, leave the second flow cell underivatized and use as control.

9. Switch the flow to both flow cells, and let the antibody surface equilibrate with the running buffer for 10–20 min.

10. Inject a 50-µl aliquot of sample (e.g., plasma sample diluted appropriately) and record the SPR response at the end of the injection.

11. Stop the flow of the buffer (set the flow rate at 0 µl/min) and quickly remove (undock) the chip from the biosensor.

12. Wash the chip with three 200-µl aliquots of ultrapure water and dry it under a stream of nitrogen.

B. MALDI-TOF Mass Spectrometry Analysis of Chips

Solution

Make a fresh solution of the MALDI matrix [aqueous solution of ACCA in 33% (v/v) acetonitrile and 0.4% (v/v) trifluoroacetic acid]

Steps

1. Place a piece of transparent tape on the glass side of the chip so that it covers both the glass chip itself and the surrounding plastic support area.

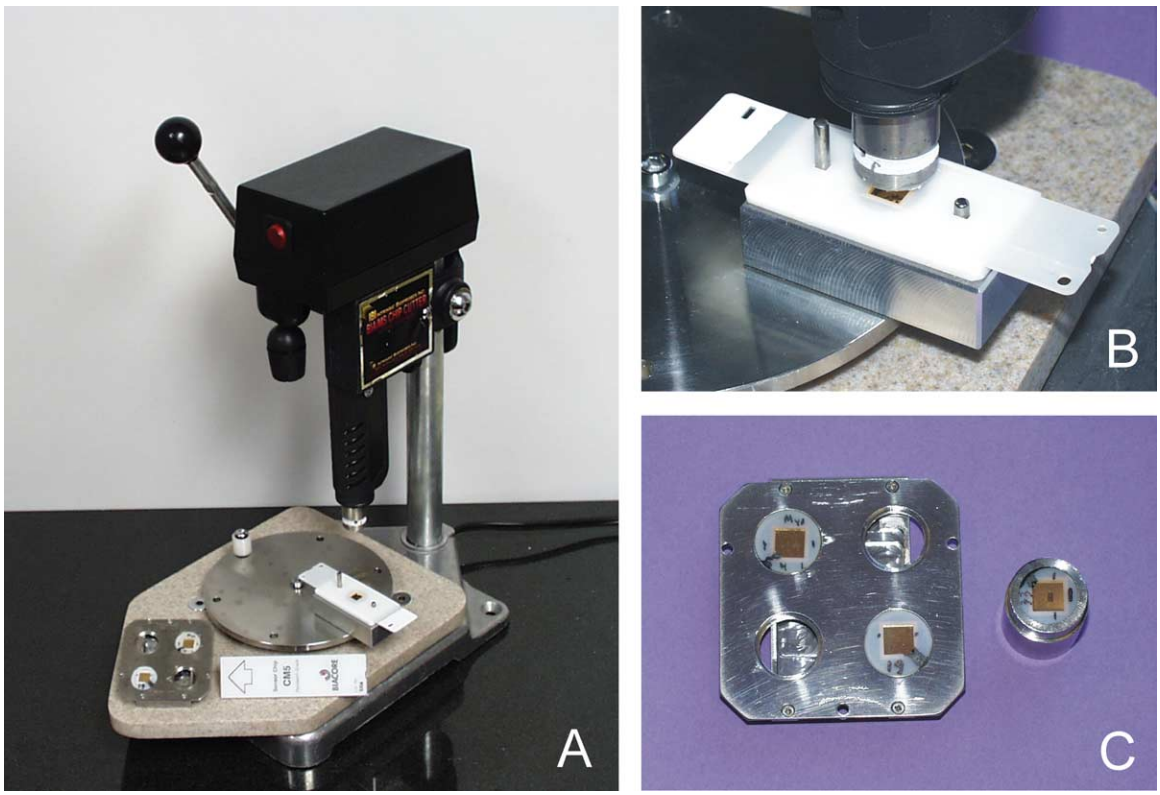

FIGURE 1. (A and B) IBI's chip cutter device. (C) The cutout chip fits into appropriately configured MALDI targets.

2. Warm up the chip cutter and place the chip in the positioning holder, with the active side facing down (**Fig. 1A**). Rotate the holder to position the chip underneath the heater head (**Fig. 1B**) and gently push down the circular heated head onto the chip. After few seconds, release back the cutter head, rotate the holder, and remove the chip.

3. To separate the round chip/support piece from the rest of the plastic support, gently press on one side of the circle cutout.

4. Remove the tape from the back of the chip cutout and position the chip on a flat surface in a chemical hood, with the active side facing up.

5. Fill in the solution holder on the sprayer device with matrix solution and adjust appropriately the air-to-matrix solution ratio on a test surface. Then, position the device ~5 cm from the chip surface and, in one swift motion, spray the matrix evenly over the entire chip surface (**Fig. 2A**). The matrix mist should moisten, but not completely wet the chip surface (i.e., the tiny matrix droplets should stay as individual drops on the surface and not be connected into one large liquid drop). The matrix droplets will desorb the proteins from their respective capturing affinity ligand and, upon rapid drying, the matrix/protein mixture will be redeposited on the same area from where the proteins were captured originally in the SPR analysis (**Figs. 2B and 2C**). To prevent fast initial evaporation, cover briefly (for 10–20 s) the chip with a small cap and then let it go to dryness.

6. Place a double-stick tape on the back of the chip and place the chip in the MALDI target so that it is firmly positioned and attached in the probe holder (**Fig. 1C**). Carefully insert the probe into the mass spectrometer. Target each flow cell individually with the laser and acquire mass spectra.

7. Following the MS analysis, chips can be stored shortly at room temperature for further analysis and reevaluation. After a week or so, the quality of mass spectra obtained from the stored chips deteriorates significantly.

D. Example

As an example of concerted BIA/MS analysis, we show the investigation of two human apolipoproteins from human plasma. Antibodies to apolipoprotein A-I (Cat. No. 11A-G2B, 1 mg/ml) and apolipoprotein

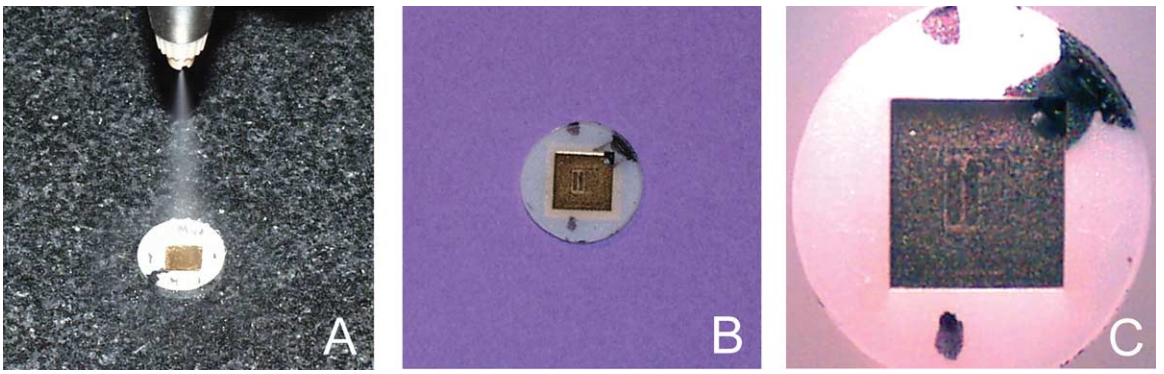

FIGURE 2. (A) Post-SPR spraying of the chip with MALDI matrix. (B and C) Dried-out protein/matrix mix chip surface showing the preserved spatial resolution between the two flow cells.

A-II (Cat. No. 12A-G1B, 1 mg/ml) were purchased from Academy Biomedical (Houston, TX). Human blood was obtained from a single subject recruited within Intrinsic Bioprobes Inc. (IBI), following a procedure approved by the IBI's Institutional Review Board (IRB), and after signing of an informed consent form. Human blood (45 µl) was drawn under sterile conditions from a lancet-punctured finger with a heparinized microcolumn (Drummond Scientific Co., Broomall, PA), mixed with 200 µl of HEPES-buffered saline (HBS-EP) buffer [0.01 *M* HEPES, pH 7.4, 0.15 *M* NaCl, 0.005% (v/v) polysorbate 20, 3 m*M* EDTA], and centrifuged for 30 s (at 7000 rpm, 2500 *g*) to pellet red blood cells. The supernatant (plasma) was further diluted 10-fold with HBS-EP buffer to yield plasma sample diluted 100-fold.

Figure 3a shows the immobilization of anti-apoA-I and anti-apoA-II in flow cell 1 (FC1) and flow cell 2 (FC2), respectively. The SPR responses indicate immobilization of ~100 fmol of antibody in each flow cell. **Figure 3b** shows a sensorgram resulting from the injection of a 50-µl aliquot of the 100-fold diluted plasma over both flow cells in series. Responses of ~500 RUs are indicated in both flow cells. **Figures 3c and 3d** show mass spectra obtained from the surfaces of the two flow cells following plasma sample injection. The mass spectrum obtained from FC1 contains multiply charged ions from apoA-I, in line with the immobilized antibody specificity. Two minor signals due to apoC-I and apoC-I' are also seen and can be attributed to nonspecific binding to the carboxymethyldextran surface (Nedelkov and Nelson, 2001b). The spectrum obtained from the surface of FC2 contains multiply charged signals from apoA-II. Three major peaks are observed for each charge state: (1) cysteinylated form of apoA-II (cys-apoA-II, MW 8827) (apoA-II contains a single cysteine residue, which is cysteinylated readily *in vivo*), (2) cys-apoA-II missing one terminal glutamine residue [cys-apoA-II (-Gln), MW 8699] (both the C and the N apoA-II termini residues are glutamines), and (3) an apoA-II missing one terminal Gln residue [apoA-II (-Gln), MW 8580]. The native apoA-II (MW 8708) signal is most likely concealed in the mass spectrum by the strong cys-apoA-II (-Gln) peak. The apoA-II homodimer was barely observed in the spectrum (region not shown). Similar results were obtained in another study using a different approach to apolipoprotein extraction and affinity retrieval (Niederkofler *et al*., 2003).

IV. COMMENTS

Protein modifications (at the native MW level) can be assessed rapidly via BIA/MS, as shown in the apoA-II example. Similarly, protein complexes can be delineated by the observance of signals from the constituent complex components in the MS analysis, and SPR detection can be utilized to monitor specific protein–protein interactions.

V. PITFALLS

1. Contrary to typical kinetic SPR analysis, it is recommended that high ligand densities are utilized in the initial stage of BIA/MS so that ample amounts of analyte are captured for subsequent MALDI-TOF MS analysis.
2. Lower flow rates (promoting mass transfer effects) should also be utilized to increase the binding of the analyte to the immobilized ligands. At high flow

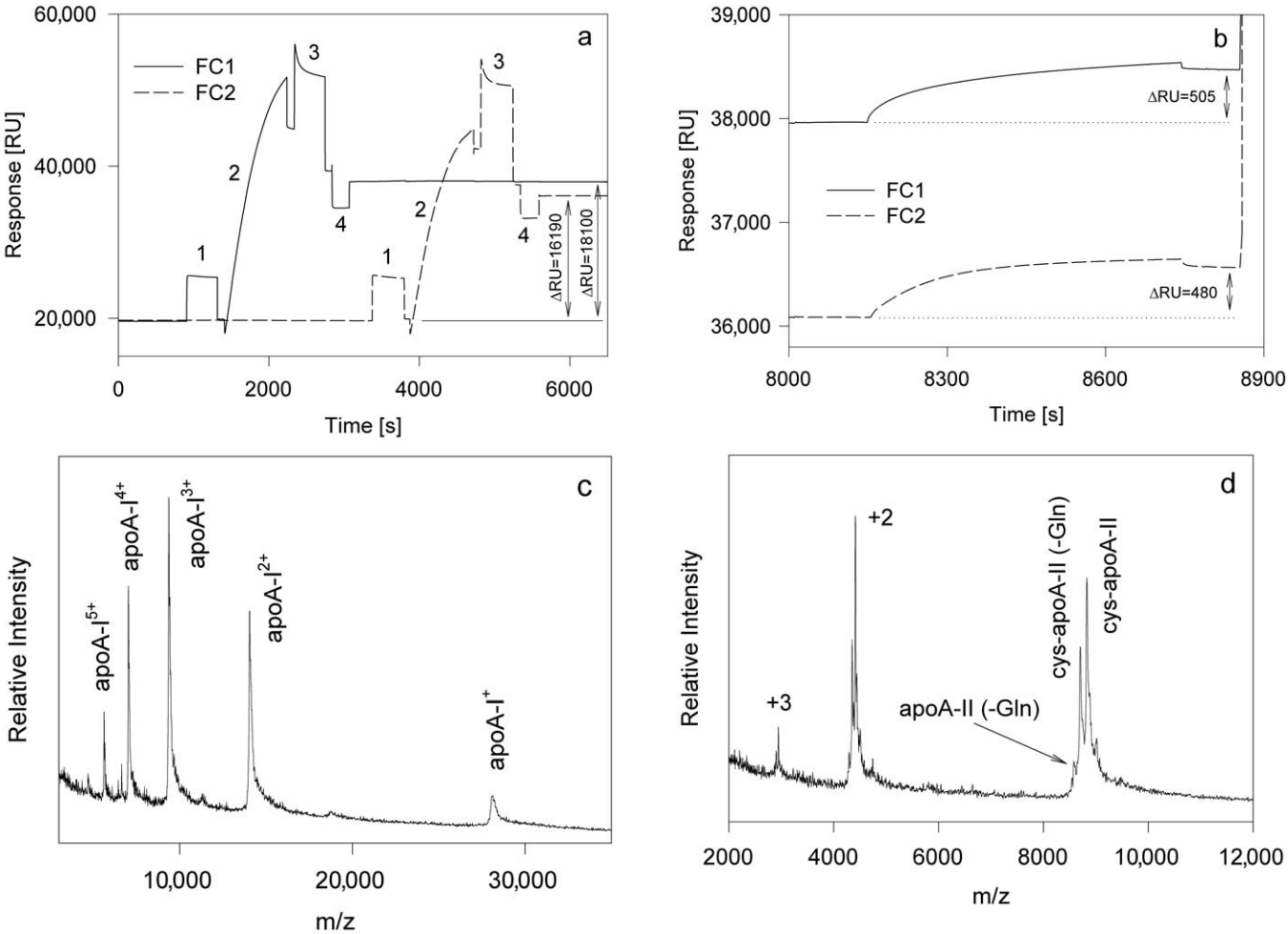

FIGURE 3. **(a)** SPR sensorgrams showing the immobilization of anti-apoA-I and apoA-II antibodies in FC1 and FC2, respectively, via (1) EDC/NHS surface activation, (2) antibody injection, (3) ethanolamine blocking, and (4) HCl for noncovalently attached antibody stripping. **(b)** SPR sensorgram showing the injection of 50 µl of 100-fold diluted human plasma over both flow cells. **(c)** Mass spectrum taken from surface FC1 showing the presence of multiply charged apoA-I ions. **(d)** Mass spectrum taken from the surface of FC2 showing the presence of multiple forms of apoA-II.

rates (60–100 µl/min) low-concentration analytes will not be captured in amounts permissible to downstream MS analysis.

3. Following sample analysis, the chip should be removed promptly from the biosensor to avoid losses of the captured proteins (especially when the interaction system under study exhibits fast dissociation phase). When possible, the undocking should be executed from within the root control software of the biosensor (OS9). For the same reasons, lengthy postcapture washes of the chip should be avoided.

4. Generally, higher quality mass spectra are obtained with ACCA for proteins smaller than ~25 kDa, whereas sinapic acid yields better results for higher molecular mass (>25 kDa) proteins. For the BIA/MS, however, ACCA is superior in that it is a better energy-absorbing matrix and, consequently, requires less laser power. Lower laser power means that more spectra can be obtained from a single spot and the fast burning through the matrix/sample layer is avoided. Generally, the appearance and the intensity of the multicharged ion analyte signals obtained with ACCA are better indicators of the presence and the mass of the on-chip retained analyte during the BIA/MS analysis.

5. Reapplication of more matrix (following initial application and MS analysis) does not yield better signals and generally results in a decreased signal-to-noise ratio.

References

Gilligan, J. J., Schuck, P., and Yergey, A. L. (2002). Mass spectrometry after capture and small-volume elution of analyte from a surface plasmon resonance biosensor. *Anal. Chem*. **74**, 2041–2047.

Krone, J. R., Nelson, R. W., Dogruel, D., Williams, P., and Granzow, R. (1997). BIA/MS: Interfacing biomolecular interaction analysis with mass spectrometry. *Anal. Biochem*. **244**, 124–132.

Nedelkov, D., and Nelson, R. W. (2000a). Exploring the limit of detection in biomolecular interaction analysis mass spectrometry (BIA/MS): Detection of attomole amounts of native proteins present in complex biological mixtures. *Anal. Chim. Acta* **423**, 1–7.

Nedelkov, D., and Nelson, R. W. (2000b). Practical considerations in BIA/MS: Optimizing the biosensor-mass spectrometry interface. *J. Mol. Recogn*. **13**, 140–145.

Nedelkov, D., and Nelson, R. W. (2001a). Analysis of human urine protein biomarkers via biomolecular interaction analysis mass spectrometry. *Am. J. Kidney Dis*. **38**, 481–487.

Nedelkov, D., and Nelson, R. W. (2001b). Analysis of native proteins from biological fluids by biomolecular interaction analysis mass spectrometry (BIA/MS): Exploring the limit of detection, identification of non-specific binding and detection of multi-protein complexes. *Biosens. Bioelectron*. **16**, 1071–1078.

Nedelkov, D., and Nelson, R. W. (2001c). Delineation of *in vivo* assembled multiprotein complexes via biomolecular interaction analysis mass spectrometry. *Proteomics* **1**, 1441–1446.

Nedelkov, D., and Nelson, R. W. (2003). Delineating protein-protein interactions via biomolecular interaction analysis-mass spectrometry. *J. Mol. Recogn*. **16**, 9–14.

Nedelkov, D., Nelson, R. W., Kiernan, U. A., Niederkofler, E. E., and Tubbs, K. A. (2003). Detection of bound and free IGF-1 and IGF-2 in human plasma via biomolecular interaction analysis mass spectrometry. *FEBS Lett*. **536**, 130–134.

Nedelkov, D., Rasooly, A., and Nelson, R. W. (2000). Multitoxin biosensor-mass spectrometry analysis: A new approach for rapid, real-time, sensitive analysis of Staphylococcal toxins in food. *Int. J. Food Microbiol*. **60**, 1–13.

Nelson, R. W., Jarvik, J. W., Taillon, B. E., and Tubbs, K. A. (1999). BIA/MS of epitope-tagged peptides directly from *E. coli* lysate: Multiplex detection and protein identification at low-femtomole to subfemtomole levels. *Anal. Chem*. **71**, 2858–2865.

Nelson, R. W., Krone, J. R., and Jansson, O. (1997a). Surface plasmon resonance biomolecular interaction analysis mass spectrometry. 1. Chip-based analysis. *Anal. Chem*. **69**, 4363–4368.

Nelson, R. W., Krone, J. R., and Jansson, O. (1997b). Surface plasmon resonance biomolecular interaction analysis mass spectrometry. 2. Fiber optic-based analysis. *Anal. Chem*. **69**, 4369–4374.

Nelson, R. W., Nedelkov, D., and Tubbs, K. A. (2000a). Biomolecular interaction analysis mass spectrometry: BIA/MS can detect and characterize proteins in complex biological fluids at the low- to subfemtomole level. *Anal. Chem*. **72**, 404A–411A.

Nelson, R. W., Nedelkov, D., and Tubbs, K. A. (2000b). Biosensor chip mass spectrometry: A chip-based proteomics approach. *Electrophoresis* **21**, 1155–1163.

Niederkofler, E. E., Tubbs, K. A., Kiernan, U. A., Nedelkov, D., and Nelson, R. W. (2003). Novel mass spectrometric immunoassays for the rapid structural characterization of plasma apolipoproteins. *J. Lipid Res*. **44**, 630–639.

Sonksen, C. P., Nordhoff, E., Jansson, O., Malmqvist, M., and Roepstorff, P. (1998). Combining MALDI mass spectrometry and biomolecular interaction analysis using a biomolecular interaction analysis instrument. *Anal. Chem*. **70**, 2731–2736.

Sonksen, C. P., Roepstorff, P., Markgren, P. O., Danielson, U. H., Hamalainen, M. D., and Jansson, O. (2001). Capture and analysis of low molecular weight ligands by surface plasmon resonance combined with mass spectrometry. *Eur. J. Mass Spectrom*. **7**, 385–391.

CHAPTER

37

Blot Overlays with ^{32}P-Labeled GST-Ras Fusion Proteins: Application to Mapping Protein–Protein Interaction Sites

Zhuo-shen Zhao and Edward Manser

I. INTRODUCTION

A well-characterized system includes ligand–receptor interactions, cell adhesion events, antigen recognition, and virus–host recognition: inside the cell the formation of multiple protein complexes during the assembly of cytoskeletal elements and interplay of proteins in signal transduction pathways are some of the best studied. In recent years, a number of popular techniques have evolved to analyze protein–protein interactions. Among these, immunoprecipitation, yeast two-hybrid analysis (Bartel and Fields, 1995; Fields and Song, 1989) and Western overlay assays are the most commonly used.

Protein overlays allow the researcher to visualize protein interactions on a blot and only require that the target be in the correct conformation for binding following SDS electrophoresis and transfer to a solid-phase membrane. The primary challenge is to produce a sensitive protein "probe" by recombinant techniques. This article describes the generation and use of such a probe for overlay binding in which the small GTP-binding protein Ras is used as an acceptor domain that can be labeled rapidly with [γ-^{32}P]GTP. In brief, target proteins of interest are first separated by SDS–polyacrylamide electrophoresis and are immobilized on a PVDF membrane. A radiolabeled Ras fusion protein is incubated with this membrane and, after a suitable time, the blot is processed to detect specific interaction (Fig. 1) as first described (Zhao *et al*., 2000a). This assay can be used to identify specific binding partners in a complex mixture of proteins or for examining interactions between two proteins to determine a target site. In some cases where protein solubility is a problem, SDS–PAGE is the only route of protein isolation, as immunoprecipitation can only tolerate mild detergents. When protein expression in yeast is toxic, the protein overlay technique provides a useful adjunct to two-hybrid methods. A key advantage of protein overlays is their flexibility. Proteins expressed by a variety of means can be subject to SDS electrophoresis and overlay: total cell extracts, relatively pure recombinant proteins, or even conjugated peptides can be used as targets. Finally, proteins or peptides can be synthesized with specific posttranslational modifications or subsequently modified (e.g., by phosphorylation) and then assessed for changes to the protein–protein interaction in a quantitative manner.

II. MATERIALS AND INSTRUMENTATION

pGEX-2TK vector and glutathione–Sepharose 4B beads are from Amersham Pharmacia Biotech (Piscataway, NJ; Cat. Nos. 27-4587-01 and 17-0756-01,). [γ-^{32}P]GTP (~6000 Ci/mmol) is from NEN Life Science Products (Boston, MA, Cat. No. BLU/NEG/

Copyright 2006, Elsevier Science (USA).
All rights reserved.

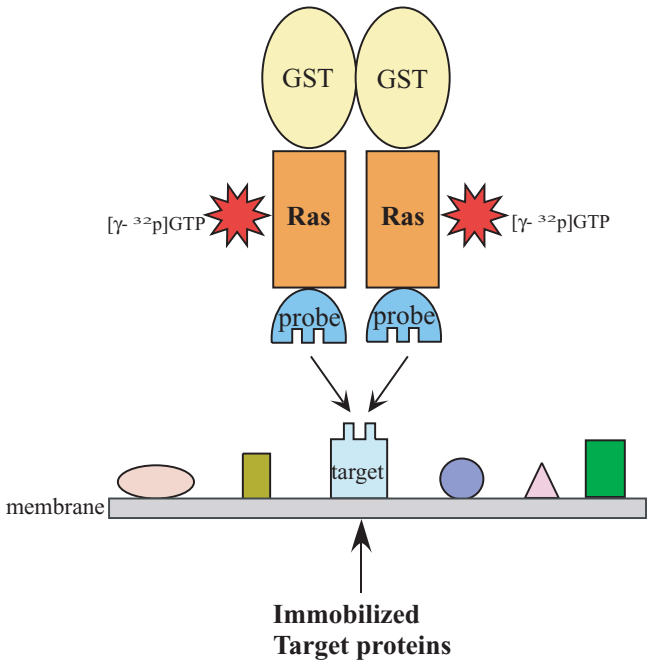

FIGURE 1 A schematic diagram showing the Ras overlay assay. The GST–Ras–probe fusion protein forms a dimer through the GST tag (in light yellow), which further stabilizes the probe–target interaction. The GTPase-deficient Ras mutant (in orange) allows high-affinity radiolabelled GTP (in red) binding.

004Z). The PVDF membrane is from Perkin Elmer NEN (Cat. No. NEF1002). Acrylamide/bisacrylamide is from Genomic Solutions Inc. (Ann Arbor, MI, Cat. No. 80-0084), Ammonium persulfate and *N,N,N′,N′*-tetramethylenediamine (TEMED) are from Bio-Rad (Cat. No. 161-0700 and Cat. No. 161-0800, respectively). Glycine (Cat. No. G-7126) and Trizma base (Cat. No. T-1503) are from Sigma, and SDS (Cat. No. 44215HN) is from BDH. Mini-PROTEAN II module including gel casts, glass plates, spacers (1.5 mm thickness), combs, and running tank are from Bio-Rad (Cat. No. 165-2944).

III. PROCEDURES

A. Construction of Expression Vector for Probe Labeling

The cDNA fragment encoding GTPase-deficient mutant H-Ras^{G12V} residues 1–185 was amplified by polymerase chain reaction (PCR) with forward primer: 5′ gaagatctatgacggaatataagctggtgg 3′ and reverse primer: 5′ gggaattcggggatcccttgcagctcatgcagccggg 3′. The PCR product was digested with *Bgl*II (introduced by forward primer) and *Eco*RI (introduced by reverse primer) and ligated to a *Bam*HI- and *Eco*RI-linearized pGEX-4T-1 vector. The resulting vector pGEX-Ras allows us to express a given cDNA downstream of the multiple cloning sites as a GST-Ras^{G12V} fusion protein with the cDNA product C-terminal to the other two domains. The fusion protein is labeled with [γ-^{32}P]GTP via the Ras GTP-binding module.

B. Purification of GST-Ras-Probe Fusion Protein for Labeling

Solutions

1. *Bacteria lysis buffer*: 50 m*M* Tris (pH 8.0), 0.5% (w/v) Triton X-100, 0.5 m*M* $MgCl_2$, and 133 m*M* NaCl. This solution can be kept at 4°C for at least 6 months. Add 1 mg/ml lysozyme, 0.5 m*M* phenylmethylsulforyl fluoride, 5 m*M* dithiothreitol (DTT) and 1 tablet of Roche's complete protease inhibitor cocktail (Cat. No. 1697498) freshly before use.
2. *Washing buffer*: Phosphate-buffered saline (PBS) with 0.1% (w/v) Triton-X 100
3. *Elution buffer*: 50 m*M* Tris–Cl (pH 8.5), 10% (v/v) glycerol in PBS. Add freshly glutathione (reduced form) to 1.5 mg/ml and DTT to 5 m*M* before use.
4. *Bradford solution*: Dilute 1 : 5 of Bio-Rad protein assay solution (Cat. No. 500-0002)

Steps

1. Subclone the cDNA fragment encoding protein to be used as a probe to the pGEX-Ras vector in frame with the GST-Ras^{G12V} cassette. Transform the resultant plasmid into *Escherichia coli* BL21 strain (from Stratagene, Cat. No. 200133) and plate on a LB agar plate containing 100 µg/ml ampicillin. Incubate the transformation plate at 37°C overnight.

2. Inoculate five colonies into a 1-liter flask containing 400 ml of LB broth with 100 µg/ml ampicillin. Grow the culture in a 37°C incubator with shaking for approximately 4 h until the absorbance of $OD_{600\ nm}$ reaches ~ 1.0.

3. Induce protein expression by adding IPTG to a final concentration of 0.25 mg/ml (4 ml of a 25-mg/ml stock per 400-ml culture flask). Incubate with shaking for 4 h at room temperature.

4. Collect cells by centrifugation (Sorvall RC 5C and GS3 rotor) at 6000 rpm for 10 min and decant the supernatant. The pellet can be processed immediately or be stored at –80°C for future use.

5. Resuspend the cell pellet completely in 40 ml of ice-cold bacteria cell lysis buffer and keep the cell suspension on ice for 5 min.

6. Sonicate the cell suspension (3 × 20 s), allowing 20 s for cooling between each ultrasonic burst of the

XL sonicator (Heat System-Ultrasonics Inc., Farmingdale, NY). During sonication, keep the suspension on ice and avoid foaming.

7. Remove cell debris by centrifugation for 30 min at 40,000 rpm, 4°C using a Ti50.2 rotor (Beckman).

8. Load 400 µl of glutathione–Sepharose 4B into a Poly-Prep chromatography column (Bio-Rad Cat. No. 731-1550). Wash the column twice with 10 ml of washing buffer.

9. Pass the centrifuge cleared supernatant through the glutathione–Sepharose 4B column. Wash the column two times with 10 ml of ice-cold washing buffer.

10. Elute the GST fusion protein in stepwise elution buffer containing reduced glutathione in 200-µl fractions.

11. Determine the protein concentration using the Bradford assay and aliquot and store in aliquots of 1 mg/ml at –80°C.

C. Labeling Fusion Protein Probe with [γ-^{32}P]GTP

Solution

Nucleotide exchange buffer (2×): 100 m*M* NaCl, 50 m*M* HEPES (pH 7.3), 10 m*M* EDTA, 1 mg/ml bovine serum albumin (BSA), and 0.1% (w/v) Triton X-100. Filter the buffer through a 0.2-µm syringe filter (Sartorius, Cat. No. 11107-25-N) and store in aliquots at –20°C.

Step

Add 10 µg of GST-Ras^{G12V}-probe fusion protein into a 1.5-ml Eppendorf tube containing 25 µl of 2× exchange buffer and 5 µCi of [γ-^{32}P]GTP. Make up the volume to 50 µl. Incubate the reaction at room temperature for 5 min and return to ice until use.

D. Preparation and Transfer of Proteins to Membrane

Solution

Semidry transfer buffer: Per 1 liter, add 6 g Trizma base (Sigma, Cat. No. T1503), 3 g glycine, and 10% (v/v) methanol in distilled water

Steps

1. Separate protein samples containing target proteins on a SDS–PAGE gel and blot onto a PVDF membrane using a Bio-Rad semidry blotter.
2. Stain the membrane with 0.05% Coomassie blue R250 for 1 min and destain with 40% methanol and 10% acetic acid until protein bands on the membrane are clear.
3. Record the image of protein bands on the membrane with a digital camera or a scanner for reference purpose.
4. Block the membrane with 5% skimmed milk at least 1 h before probing.

E. Overlay and Autoradiography

Solutions

1. *Binding buffer (2×)*: 100 m*M* HEPES, pH 7.3, 200 m*M* NaCl, 10 m*M* $MgCl_2$, 1 µg/µl BSA, and 0.1% Triton X-100. Filter the buffer through a 0.2-µm syringe filter and store at –20°C.
2. *Washing buffer (1×)*: Phosphate buffer saline containing 10 m*M* HEPES (pH 7.3), 5 m*M* $MgCl_2$, and 0.05% Triton X-100 (keep at 4°C)

Steps

1. Transfer the blocked membrane to a 50-ml BD Falcon high-clarity polypropylene conical centrifuge tubes (Cat. No. 352070) and rinse the membrane once with 1× binding buffer. Check that there are no air bubbles between the membrane and the wall of the tube. Dilute the radioactive labeled probe in 4 ml of 1× binding buffer and transfer into the tube containing the membrane: incubate for 2 h on a standard clinical spiral mixer behind a radioactive shield (at 4°C or room temperature).

2. Decant the probe carefully into a radioactive waste container and wash the membrane three times (5 min each) with ice-cold washing buffer. Blot residual liquid with Whatman 3MM filter paper, wrap it with Saran warp, and either expose to Hyperfilm MP (Amersham Biosciences, Cat. No. RPN6K) or a PhosphorImager screen at –20°C for 30 min. For optimal signals, additional exposures may be required. We illustrate the use of this technique to map the PIX-binding site within GIT1 (Fig. 2). In the absence of a specific interaction, we do not observe "background binding." Note that although GST is a dimer in solution, there is no signal when overlaid onto GST immobilized on the target membrane.

IV. COMMENTS

The protein-labeling method described in this article has a number of advantages over others: (a) the process is rapid, it takes ~5 min to label a probe; (b) the only reagent required is [γ-^{32}P]GTP; (c) over 60% labeling efficiency is obtained easily; the free probe does not need to be removed; (d) less waste is generated, a

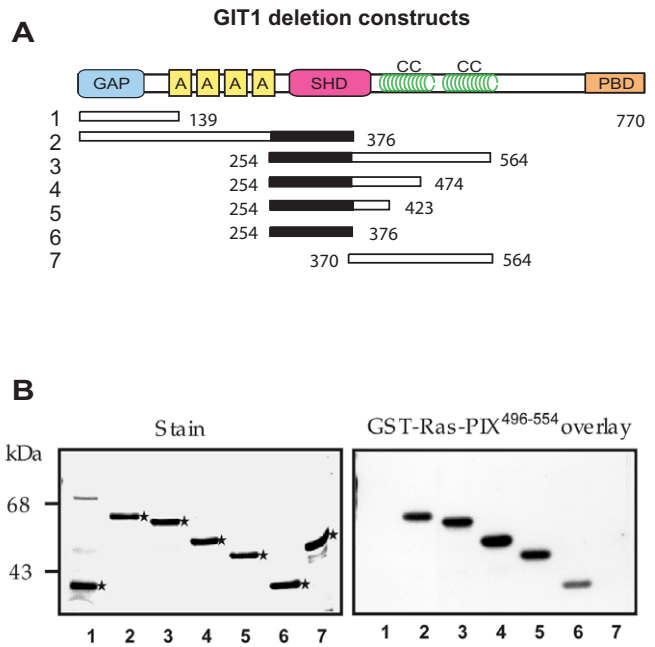

FIGURE 2 Mapping the PIX-binding domain on GIT1 by the overlay assay. (A) Schematic diagram showing the domain structure of GIT1 and deletion constructs used in the overlay assay to determine the PIX-binding region. (B) An overlay assay using the GIT1-binding sequence in PIX as a probe. GST fusion proteins (0.5 μg) of each GIT1 deletion construct shown in A were separated on SDS–PAGE and transferred onto a PVDF membrane. Proteins on the membrane were stained with Coomassie blue (left) and overlaid with [γ-^{32}P]GTP-labeled GST–Ras–PIX$^{496–554}$ (right). The minimal PIX-binding region determined by this assay corresponds to the SHD (Spa2 homologous domain) (lane 6). PAK and GIT1 can simultaneously bind PIX at its N-terminal and C-terminal, respectively, and form a PAK–PIX–GIT1 trimeric complex. This complex, through interaction with its effectors, plays an important role in regulating cell focal adhesion dynamics and cell motility.

single 5-min step with no additional processing compared to other radiolabeling methods such as phosphorylation of chemical modification; (e) as fusion proteins can be stored at –80°C for many years in aliquots, labeling is reproducible and does not rely on the quality of any other biological; and (f) use of the ^{32}P radioisotope provides very high sensitivity. We have used this method to characterize interactions between PAK, PIX, and GIT1 in detail (Zhao *et al.*, 2000b). In some instances, the sensitivity is such that protein partners can be visualized directly in total cell or tissue lysates. The GST moiety mediates probe dimerization, which in fact provides a stabilization of probe binding (in the same manner as bivalent antibodies), which increases sensitivity of the overlay assay.

V. PITFALLS

1. Use recently purchased radioactive [γ-^{32}P]GTP for best sensitivity.
2. Seal the Falcon tube with Parafilm to prevent any leakage of the radioactive probe.
3. Make sure that the incubation tube is level: because the Falcon tube lid is wider than the tube, one option is to use another Falcon tube cut across the body about 2 cm from the lid and insert the end of probe tube into this.

References

Bartel, P. L., and Fields, S. (1995). Analyzing protein-protein interactions using two-hybrid system. *Methods Enzymol.* **254**, 241–263.

Fields, S., and Song, O. (1989). A novel genetic system to detect protein-protein interactions. *Nature* **340**, 245–246.

Zhao, Z. S., Manser, E., and Lim, L. (2000a). Interaction between PAK and nck: A template for Nck targets and role of PAK autophosphorylation. *Mol. Cell. Biol.* **20**, 3906–3917.

Zhao, Z. S., Manser, E., Loo, T. H., and Lim, L. (2000b). Coupling of PAK-interacting exchange factor PIX to GIT1 promotes focal complex disassembly. *Mol. Cell. Biol.* **20**, 6354–6363.

CHAPTER

38

Ligand Blot Overlay Assay: Detection of Ca^{+2}- and Small GTP-Binding Proteins

Pavel Gromov and Julio E. Celis

I. INTRODUCTION

Protein-targeting interactions play a central role in most biological processes. Their detection and analysis *in vitro* can provide important information on specificity, affinity, and structure/function relationships that are realized *via* these interactions. Protein blot overlay assays, also known as "Western–Western," "Far–Western," "ligand," or "affinity" blotting, are powerful techniques for detecting and analyzing proteins or protein motifs involved in cellular-targeting processes (Clegg *et al.*, 1998 and references therein).

These methods are based on the principle that proteins, or protein fragments resolved by electrophoresis and transferred to an immobilizing matrix such as nitrocellulose or a nylon membrane, can react with putative binding ligands. This article describes protocols for identifying Ca^{+2}- and GTP-binding proteins using whole cellular protein extracts from noncultured human psoriatic keratinocytes and COS-1 cells.

II. MATERIALS AND INSTRUMENTATION

A. ^{45}Ca Overlay Assay

Imidasole (Cat. No. I-0250) is from Sigma, $MgCl_2 \cdot 6H_2O$ (Cat. No. 105832) is from Merk. $^{45}CaCl_2$ (Cat. No. CES3) is from Amersham. Nitrocellulose membrane sheets (Hybond C, Cat. No. RPN. 203C) are from Amersham. X-ray films (X-Omat UV, 18 × 24 cm, Cat. No. 524 9792) are from Kodak.

B. α-^{32}GTP Overlay Assay

Tween 20 (Cat. No. 822 184) and $MgCl_2 \cdot 6H_2O$(Cat. No. 105832) are from Merk. Dithiothreitol (DTT, Cat. No. D-0632) and ATP (Cat. No. A-2383) are from Sigma. Tris base (Cat. No. 648311) is from Calbiochem. [α-^{32}P]GTP (10 mCi/ml, Cat. No. PB 10201) and nitrocellulose membranes (Hybond C, Cat. No. RPN. 203C) are from Amersham. X-ray films (X-Omat UV, 18 × 24 cm, Cat. No. 524 9792) are from Kodak. All other reagents and materials are as described elsewhere (Celis and Celis, 1997).

III. PROCEDURES

The protocol for blot overlay detection of Ca^{+2}- and GTP-binding proteins is exemplified using whole cellular protein extracts from noncultured human psoriatic keratinocytes and COS-1 cells, but can be applied to a variety of other cultured cells, tissue samples, and biological fluids.

A. ^{45}Ca Overlay Assay

Calcium ion is a universal intracellular signal that acts as a important second messenger for many cellular processes and whose effect is modulated by specific calcium-binding proteins (Berridge *et al.*, 1998). According to well-conserved structural elements, these proteins can be grouped into different families, including annexins, C2 domain proteins, and EF-hand proteins (Celio *et al.*, 1996; Maki *et al.*, 2002;

Copyright 2006, Elsevier Science (USA).
All rights reserved.

Heizmann *et al*., 2002). The calcium overlay assay (Maruyama *et al*., 1984) as described here is essentially a specific application of a general metal ion-binding assay (Aoki *et al*., 1986) and is widely used for studying various calcium-binding proteins (Son *et al*., 1993), including those containing EF hands (Hoffmann *et al*., 1993). Proteins are separated by means of one (1D)- or two-dimensional (2D) gel electrophoresis (see article by Celis *et al*. and article by Görg and Weiss in this volume), transferred to a nitrocellulose membrane, and overlaid with radioactive ^{45}Ca. Calcium-binding proteins are detected by autoradiography or phosphorimaging.

Solutions

The volumes given in the protocol are for 2D gel nitrocellulose blots (14 × 16 cm). The volumes for 1D gel blots (0.6 × 16 cm) are given in parentheses.

1. *Washing buffer*: 60 m*M* KCl, 5 m*M* $MgCl_2$, and 10 m*M* imidazole–HCl, pH 6.8. Prepare stock solutions in glass-distilled water. To make 1 liter of 3 *M* KCl, dissolve 223.6 g in 700 ml of water and bring to 1 liter. To make 1 liter of 1 *M* $MgCl_2$, dissolve 203.1 g in 700 ml of water and bring to 1 liter. Just before use, prepare 40 ml of the 1 *M* imidazole solution by dissolving 2.72 g of imidazole in 20 ml of distilled water and adjust to pH 6.8 with HCl. Complete to 40 ml with distilled water. To make 500 ml (20 ml) of washing buffer, enough for one 14 × 16-cm (0.6 × 14-cm) membrane, combine the following: 10 ml (0.4 ml) of 3 *M* KCl, 2.5 ml (0.1 ml) of 1 *M* $MgCl_2$, 5 ml (0.2 ml) of 1 *M* imidazole, and complete to 500 ml (20 ml) with distilled water.
2. *Probing buffer*: Add 15 µl (2 µl) of $^{45}CaCl_2$ to 15 ml (2 ml) of washing buffer (final concentration of 1 µCi/ml)
3. *Aqueous ethanol*: Prepare 150 ml (5 ml) of 67% aqueous ethanol per membrane. Add 50 ml (1.67 ml) of distilled water to 100 ml (3.33 ml) of 96% ethanol.

Steps

1. Work with radioactivity according to the safety procedures enforced in your laboratory.
2. Transfer proteins from the gels to the nitrocellulose membrane as described in the article by Celis *et al*. in Volume 1.
3. Place the nitrocellulose sheet in a rectangular glass container (19 × 24 cm) containing 100 ml of washing buffer. Wear gloves when handling the membrane. The nitrocellulose sheet should be placed with the protein-bearing side facing upward. Rinse the nitrocellulose sheet twice with washing buffer.
4. Remove the membrane from the blotting chambers and wash briefly with the blotting buffer. The membrane can be dried and stored in a plastic bag at room temperature until further use.
5. Soak the membrane in 150 ml (2 ml) of washing buffer and shake gently for 20 min.
6. Remove the washing buffer and add 150 ml (2 ml) of fresh washing buffer. Shake gently for 20 min.
7. Repeat step 6.
8. Place the membrane or strip in a plastic bag and add 15 ml (2 ml) of probing buffer. Seal the bag and incubate for 10 min with gentle agitation. Alternatively, incubate the membrane in an appropriate rectangular glass or plastic container containing 150 ml (2 ml) of probing buffer. The incubation can be extended up to 1 h without adverse effects. Handle radioactive material with care.
9. Transfer the membrane to an appropriate glass or plastic container and add 150 ml (2 ml) of aqueous ethanol. Shake for 5 min with gentle agitation. Dispose of the radioactive solutions according to the safety procedure in your laboratory.
10. Carefully remove the nitrocellulose sheet or strip from the container using plastic tweezers and air dry for at least 4 h at room temperature.
11. Expose the dried membrane to X-ray film for 1 h to 3 days at room temperature. The membrane can be stained with amido black after autoradiography to facilitate protein identification.

Figure 1 shows an isoelectric focusing two-dimensional gel of total protein extracts from psoriatic keratinocytes transferred to nitrocellulose membrane and probed with $^{45}CaCl_2$.

Comments

No significant differences in calcium binding are observed when using membranes that had been dried before probing or membranes that had been used directly after blotting.

To decrease nonspecific binding, competing metal ions such as Mg^{+2} may be added in steps 5–8 to a final concentration of 10 m*M*.

The use of a rotating roller system (see Fig. 1 in the article by Celis *et al*. in Volume 1) for incubation of nitrocellulose membranes facilitates the handling of the membrane, reduces considerably the volume of reagents used, and provides even detection of the calcium-binding proteins.

Pitfalls

1. Use a fresh imidazole solution.
2. Do not dry the membrane between pieces of filter paper as it leads to severe background problems.

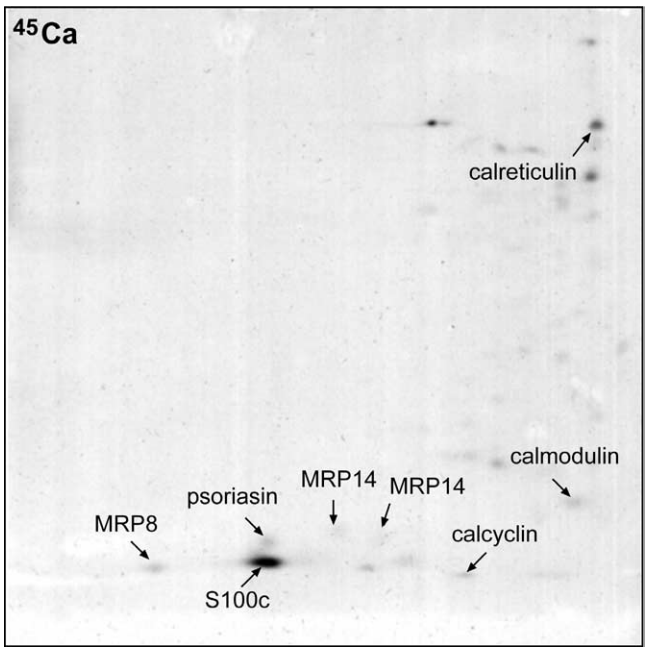

FIGURE 1 Calcium-binding proteins expressed by psoriatic keratinocytes. Autoradiograph of a $^{45}Ca^{2+}$ blot overlay of a 2D gel of whole protein extracts from noncultured, psoriatic keratinocytes.

B. α-^{32}GTP Overlay Assay

Small GTP-binding proteins constitute a rapidly increasing family of monomeric regulatory switches that have been adopted to control various cellular activities. These include proliferation and differentiation (Ras), protein transport and secretion (Rab), cytoskeletal (Rho), and nuclear assembly (Ran) (Manser, 2002; Dasso 2002; Pruitt and Der, 2001; Jaffe and Hall 2002). Unlike oligomeric G proteins, which are composed of α, β, and γ subunits, these proteins are able to bind GTP specifically when separated by SDS–PAGE and blotted onto nitrocellulose or nylon membranes. The blot overlay nucleotide-binding assay allows detection of small GTP-binding proteins in polypeptide mixture separated by one or 2D PAGE. The protocol presented here follows closely those described by McGrath *et al.* (1984), Doucet and Tuana (1991), and Gromov and Celis (1994).

Solutions

The volumes given are for nitrocellulose blot sheets of 14 × 16 cm in size.

1. *10% Tween 20*: To make 50 ml, weigh 5 g of Tween 20 and complete to 50 ml with distilled H_2O. Mix carefully. Store at room temperature.

2. *100 mM ATP*: To make 1 ml, add 55.1 mg of ATP and complete to 1 ml with distilled water. Aliquot in 100-µl portions and store at –20°C.

3. *0.1 M $MgCl_2$*: To make 50 ml, weigh 0.102 g of $MgCl_2 \cdot 6H_2O$ and complete to 50 ml with distilled water. Store at 4°C.

4. *Washing buffer*: 50 m*M* Tris–HCl, pH 7.6, 10 µ*M* $MgCl_2$, and 0.3% Tween 20. To make 1 liter, add 6.055 g of Tris base to 800 ml of distilled H_2O and titrate with HCl. Add 30 ml of a 10% stock solution of Tween 20 and 100 ml of a 0.1 *M* stock solution of $MgCl_2$. After dissolving, complete to 1 liter with distilled H_2O and store at 4°C.

5. *ATP overlay buffer*: 50 m*M* Tris–HCl, pH 7.6, 10 µ*M* $MgCl_2$, 0.3% Tween 20, 100 m*M* DTT, and 100 µ*M* ATP. To make 100 ml, dissolve 1.54 g DTT in 90 ml of washing buffer and add 100 µl of a 0.1 *M* stock solution of ATP. After dissolving, complete to 100 ml with washing buffer and store at 4°C.

6. *Binding buffer*: 50 m*M* Tris–HCl, pH 7.6, 10 µ*M* $MgCl_2$, 0.3% Tween 20, 100 m*M* DTT, 100 µ*M* ATP, and 1 n*M* [α-^{32}P]GTP [1 µCi [α-^{32}P]GTP/ml]. To make 100 ml, add 10 µl of a 10-mCi/ml solution of [α-^{32}P]GTP to the ATP overlay buffer. Prepare directly in the binding container prior to use (see step 4).

Steps

1. Transfer proteins from the gels to the nitrocellulose membrane as described in the article by Celis *et al.* in volume 1.
2. Place the nitrocellulose sheet in a rectangular glass container (19 × 24 cm) containing 100 ml of washing buffer. Wear gloves when handling the membrane. The nitrocellulose sheet should be placed with the protein-bearing side facing upward. Rinse the nitrocellulose sheet twice with washing buffer.
3. Remove the washing buffer from the container and fill it with 50 ml of ATP overlay buffer. Place the container on an orbital shaker and incubate for 10 min with gentle agitation at room temperature.
4. Remove the blotting container from the orbital shaker platform and add 10 µl of a 10-mCi/ml solution of [α-^{32}P]GTP. Incubate with gentle agitation for 60 min at room temperature. Handle radioactive material with care.
5. Remove the binding buffer from the container and fill it with 50 ml of washing buffer. Soak the nitrocellulose sheet for 10 min at room temperature. Dispose of radioactive solutions according to the safety regulations in your laboratory.
6. Repeat the washing procedure twice at room temperature (10 min per wash). Use as much washing buffer as possible.

7. Carefully remove the nitrocellulose sheet from the container using plastic tweezers and air dry for at least 4 h at room temperature.
8. Place the air-dried nitrocellulose sheet into a cassette for autoradiography (12–72 h at –80°C) using an X-ray film and an intensifying screen.

Comments

The use of a rotating roller system for incubating the membranes is recommended.

DTT (100 m*M* final concentration in steps 3 and 4) enhances the GTP-binding ability of small GTP-binding proteins. This improves considerably the signal-to-noise ratio as well as the sensitivity of the procedure (Gromov and Celis, 1994).

To reduce background, we recommend ATP as an effective competitor for nonspecific binding of GTP to the nitrocellulose. Alternatively, use bovine serum albumin (0.3% final concentration) in the overlay and binding buffer as recommended by McGrath *et al.* (1984) and Doucet and Tuana (1991).

Bound [α-^{32}P]GTP can be removed from the nitrocellulose blot without detectable loss of proteins by incubating the membrane in a solution containing 50 m*M* Tris–HCl, pH 7.4, and 1% SDS for 30 min at room temperature. The blot can be then reprobed with [α-^{32}P]GTP. In this case do not dry the membrane after probing and perform autoradiography, keeping the membrane in the plastic bag.

To facilitate the identification of [α-^{32}P]GTP-binding proteins on whole protein extracts separated by 2D gel electrophoresis, we recommend adding a small amount of [^{35}S]methionine-labeled proteins from an appropriate source (e.g., keratinocytes) to the protein mixture prior to electrophoresis. Following the [α-^{32}P]GTP-binding overlay assay, the nitrocellulose blot is subjected to autoradiography using two films placed on top each other. The first film, which is placed in direct contact with the blot, visualizes both ^{35}S and ^{32}P isotopes, while the second one reveals only ^{32}P. The positions of detected spots may be compared with those in the master keratinocyte database (http://proteomics.cancer.dk). Using the protocol described here, it is possible to detect many small GTP-binding proteins in various cell types and tissues. Representative 2D autoradiographs of [α-^{32}P]GTP-binding proteins from COS-1 cells that transiently express ADP-ribosylation factor, rab11a, and p21-ras are shown in Fig 2 (see also article by Gromov *et al.* in this volume).

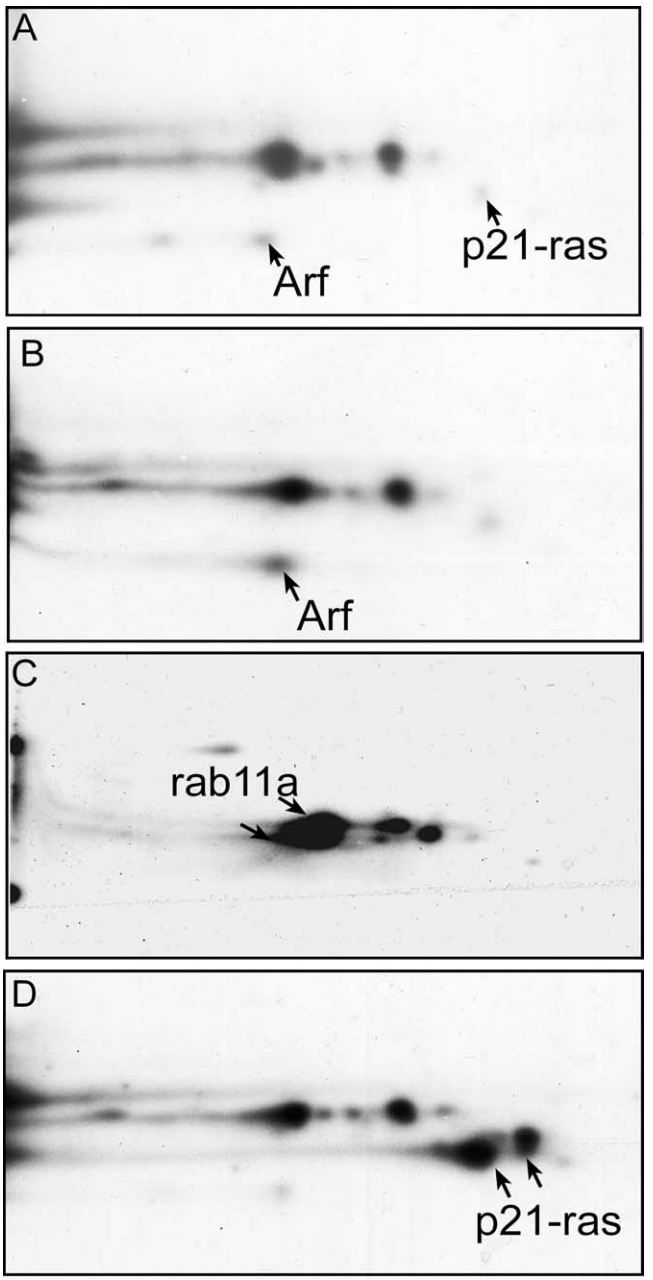

FIGURE 2 Two-dimensional blot autoradiographs of [α-^{32}P]GTP-binding proteins from COS-1 cells that transiently express several small GTP-binding proteins. (A) Control, nontransfected cells, (B) ADP-ribosylation factor (Arf), (C) rab11a, and (D) p21-ras (see also article by Gromov *et al.* in this volume).

Pitfalls

1. Do not dry the nitrocellulose membrane after protein transfer as it substantially reduces the efficiency of GTP binding.

2. Make sure that the solution covers the whole nitrocellulose sheet surface during agitation. Avoid scratching or tearing of the nitrocellulose membrane during manipulation.

3. Use high-grade ATP. Small traces of cold GTP, which may contaminate commercial ATP, decrease the efficiency of [α-^{32}P]GTP binding.

References

Aoki, Y., Kunimoto, M., Shibata, Y. Y., and Suzuki, K. T. (1986). Detection of metallothionein on nitrocellulose membrane using Western blotting technique and its application to identification of cadmium-binding proteins. *Anal. Biochem*. **157**, 117–122.

Berridge, M. J., Bootman, M. D., and Lipp, P. (1998). Calcium—a life and death signal. *Nature* **395**, 645–648

Celio, M., Pauls, T., and Schwaller, B. (1996). "*Guidebook to the Calcium-Binding Proteins*", pp. 1–238. Oxford Univ. Press., Oxford.

Celis, A., and Celis, J. E. (1997). General procedures for tissue culture. *In* "*Cell Biology: A Laboratory Handbook*" (J. E. Celis, N. Carter, T. Hunter, D. Shotton, K. Simons, and J. V. Small eds.), Vol. 1, pp 5–16. Academic Press.

Clegg, R. A. (ed.) (1998). Protein targeting protocols. *In* "*Methods in Molecular Biology*," Vol. 88. Humana Press, Totowa, NJ.

Dasso, M. (2002). The Ran GTPase: Theme and variations. *Curr. Biol*. **12**, R502–R508.

Daucet, J.-P., and Tuana, B. S. (1991). Identification of low molecular weight GTP-binding proteins and their sites of interaction insubcellular fractions from skeletal muscle. *J. Biol. Chem*. **266**, 17613–17620.

Gromov, P. S., and Celis, J. E. (1994). Some small GTP-binding proteins are strongly downregulated in SV40 transformed human keratinocytes. *Electrophoreis* **15**, 474–481.

Hoffmann, H. J., Olsen, E., Etzerodt, M., Madsen, P., Thogersen, H.-G., Kruse, T., and Celis, J. E. (1994). Psoriasin binds calcium and is differentially regulated with respect to other members of the S100 protein family. *J. Invest. Dermatol*. **103**, 370–375.

Jaffe, A. B., and Hall, A. (2002). Rho GTPases in transformation and metastasis. *Adv. Cancer Res*. **84**, 57–80.

Heizmann, C. W., Fritz, G., and Schafer, B. W. (2002). S100 proteins: Structure, functions and pathology. *Front Biosci*. **7**, 1356–1368.

Maki, M,, Kitaura, Y., Satoh, H., Ohkouchi, S., and Shibata, H. (2002). Structures, functions and molecular evolution of the penta-EF-hand Ca2+-binding proteins. *Biochim. Biophys. Acta* **1600**, 51–60.

Manser, E. (2002). Small GTPases take the stage. *Dev. Cell* **3**, 323–328.

Maruyama, K., Mikawa, T., and Ebashi, S. (1984). Detection of calcium-binding proteins by ^{45}Ca autoradiography on nitrocellulose membrane after sodium dodecyl sulfate gel electrophoesis. *J. Biochem*. **95**, 511–519.

McGrath, J. P., Capon, D. J., Goeddel, D. V., and Levinson, A. D. (1984). Comparative biochemical properties of normal and activated human ras p21 protein. *Nature* **310**, 644–649.

Pruitt, K., and Der, C. J. (2001). Ras and Rho regulation of the cell cycle and oncogenesis. *Cancer Lett*. **171**, 1–10.

Son, M., Gunderson, R. E., and Nelson, D. L. (1993). A 2nd member of the novel Ca^{2+}-dependent protein-kinase family from paramecium-tetraurelia; purification and characterization. *J. Biol. Chem*. **268**, 5840–5948.

CHAPTER

39

Modular Scale Yeast Two-Hybrid Screening

Christopher M. Armstrong, Siming Li, and Marc Vidal

I. INTRODUCTION

The observation that most transcription factors can be separated into a DNA-binding domain (DB) and a transcriptional activation domain (AD) led to the development of the yeast two-hybrid (Y2H) system as an *in vivo* screen or selection to identify and characterize protein interactions (Fields and Song, 1989). Using the Y2H, one can identify potentially interacting proteins (X–Y heterodimers or X–X homodimers) by generating two different hybrid proteins: one with protein X fused to DB and the other with protein Y fused to AD (see Fig. 1). If protein X and Y interact, the AD can be brought to the promoter by DB-X and thereby activate the gene driven by that promoter (usually a selectable or screenable marker). By fusing a library to the AD (Fields and Song, 1989) and, in some special cases, to DB (Du *et al.*, 1996), it is possible to screen for proteins and identify potential interactors.

Two-hybrid screens have been used quite successfully by scientists interested in identifying potential interacting partners to their protein of interest. While this one gene at a time approach has been fruitful, the ease of use of Y2H has allowed it to be scaled up to perform screens on more of a proteome scale (Ito *et al.*, 2000; Uetz *et al.*, 2000; Walhout *et al.*, 2000). While whole genome two-hybrids may be beyond the scope or interest of most laboratories, medium size screens (on the level of 20 to 50 genes) can be done easily by one or a few scientists (Davy *et al.*, 2001; Drees *et al.*, 2001; Boulton *et al.*, 2002). Screens of this size allow scientists to approach problems on a more modular scale, i.e., studying most of the genes involved in a process rather than a few at a time (Hartwell *et al.*, 1999), thereby addressing more global questions than traditional single gene approaches allow.

While the Y2H is quite powerful, it is important to remember that genes identified in a Y2H screen are only potential interactors and further experiments are necessary to validate the relevance of the interactions. Techniques such as GST-pulldowns or immunoprecipitations can help confirm that the interaction exists, while analysis of expression patterns and phenotypes can help establish the functional relevance of the predicted interactions. The power of the Y2H is its ability to act as a starting point for the identification of interacting proteins.

Many variations of the method exist, but the fundamentals are the same for all of them. Here we use the strains and vectors described in Vidal *et al.* (1996), but the protocols work just as well with other strains so long as you take into account any changes in selectable markers and reporter assays that may be an issue. The strain used is MaV203, which has three screening markers: *GAL1::lacZ*, *SPAL10::URA3*, and *GAL1::HIS3* (Vidal *et al.*, 1996). Initial screening uses the *HIS3* marker to identify potential positives. Secondary screening is then done with other markers to test the strength of the interactions. The techniques here are derived in part from the techniques described in Walhout and Vidal (2001), but have been streamlined to make it possible to work with many baits in parallel.

Copyright 2006, Elsevier Science (USA).
All rights reserved.

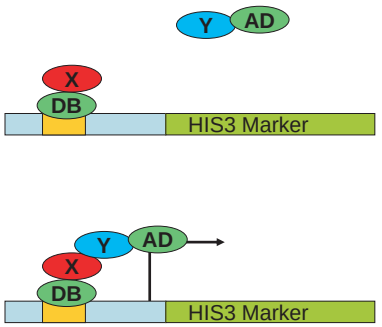

FIGURE 1 Two-hybrid interactions. (Top) Two fusion proteins are created, DB-X and AD-Y. If protein X fails to interact with protein Y, then the activation domain will not be brought to the promoter and the marker gene (in this case HIS3) will fail to activate. (Bottom) Protein X and protein Y interact successfully, bringing the activation domain to the promoter and activating the marker gene successfully.

II. MATERIALS AND INSTRUMENTATION

Bacto agar is obtained from Labscientific (Cat. No. A466). Bactopeptone (Cat. No. DF0118170), yeast extract (Cat. No. DF0127-17-9), ammonium sulfate (Cat. No. A702-500), *N,N*-dimethylformamide (Cat. No. D119-1), 3-mm glass beads (Cat. No. 11-312A), and 125-mm Whatman filter papers (Cat. No. 09-868C) are from Fisher Scientific. 3-Amino-1,2,4-triazole (3-AT, Cat. No. A-8056), salmon testes DNA (Cat. No. D9156), glucose (Cat. No. G8270), polyethylene glycol MW 3350 (Cat. No. P-4338), lithium acetate (Cat. No. L-4158), 5-bromo-4-chloro-3-indolyl-β-D-galactopyranoside (X-Gal, Cat. No. B-4252), 2-mercaptoethanol (Cat. No. M-3148), yeast synthetic drop-out medium amino acid supplement (without histidine, leucine, tryptophan, and uracil) (Cat. No. Y-2001), tryptophan (Cat. No. T-0254), uracil (Cat. No. U-0750), and histidine (Cat. No. H-6034) are from Sigma. 5-Fluoroorotic acid (5FOA, Cat. No. 1555) is from BioVectra. Zymolyase-20T (Cat. No. 120491) is from Seikagaku. Airpore tape sheets (Cat. No. 19571) are from Qiagen. Nitrocellulose filters (Cat. No. WP4HY13750) are from Osmonics. Eight-and-a-half-inch replica velvets (#2008) and 6-in. replica blocks (#4006) can be obtained from Cora Styles Needles 'N Blocks (www.corastyles.com).

MaV203 yeast strain (MATα, leu2-3,112, trp-901, his3Δ200, ade2-1, gal4Δ, gal80Δ, SPAL10::URA3, GAL1::lacZ, GAL1::HIS3-@LYS2, can1^R, cyh2^R) can be obtained from Invitrogen as part of the ProQuest two-hybrid system with Gateway Technology (Cat. No. 10835–031) or directly from the Vidal laboratory (http://vidal.dfci.harvard.edu/).

III. PROCEDURES

A. Preparation of Yeast Culture Plates and Medium

1. *YPD liquid media*: Add 10 g of yeast extract and 20 g of Bactopeptone to 1 liter of dH_2O and autoclave. Add 50 ml of 40% glucose before use.
2. *20 mM uracil*: Dissolve 1.21 g of uracil in 500 ml of ddH_2O. Filter to sterilize. Note that it may be necessary to heat the water to get the uracil into solution.
3. *100 mM histidine*: Dissolve 7.76 g of histidine in 500 ml of ddH_2O. Filter to sterilize and wrap the bottle in foil.
4. *40 mM tryptophan*: Dissolve 4.08 g of tryptophan in 500 ml of ddH_2O. Filter to sterilize and wrap the bottle in foil and keep at 4°.
5. *Synthetic complete (SC) liquid medium*: To prepare a liter of SC medium, add 1.4 g of yeast synthetic drop-out medium amino acid supplement, 1.7 g of yeast nitrogen base, and 5 g of ammonium sulfate into 925 ml of water. Adjust the pH with 10 *N* NaOH to a final pH of 5.9. Autoclave media to sterilize. Add 50 ml 40% glucose before use. This media is -Leu, -Trp, -Ura, -His. To supplement with a missing amino acid/nucleotide, add 8 ml of the appropriate solution (e.g., to make SC-Leu-Trp, add 8 ml of 20 m*M* uracil and 8 ml of 100 m*M* histidine).
6. *Synthetic complete (SC) agar plates*: To prepare a liter of SC plates (ten to twelve 15-cm petri dishes), add 1.4 g of yeast synthetic drop-out medium amino acid supplement, 1.7 g of yeast nitrogen base, and 5 g of ammonium sulfate into 425 ml of water. Adjust pH to 5.9 with 10 *N* NaOH. At the same time, in a separate flask, add 20 g of bacto agar into 500 ml of water. Autoclave both agar and SC solutions. After autoclaving, mix the flasks. Cool to 55°C in a water bath. Add 50 ml of 40% glucose and 8 ml of the appropriate amino acid solution before pouring.
7. *SC-Leu plates*: Prepare 1 liter of SC/agar and add 8 ml of 20 m*M* uracil, 8 ml of 100 m*M* histidine, and 8 ml of 40 m*M* tryptophan before pouring. Pour into ten to twelve 15-cm petri plates.
8. *SC-Leu-Trp plates*: Prepare 1 liter of SC/agar and add 8 ml of 20 m*M* uracil and 8 ml of 100 m*M* histidine before pouring. Pour into ten to twelve 15-cm petri plates.
9. *SC-Leu-Trp-His+3-AT plates (3-AT plates)*: Prepare 1 liter of SC/agar and add 8 ml of 20 m*M* uracil and 1.18 g of 3-AT powder before pouring (this makes 20 m*M* 3-AT plates). Pour into ten to twelve 15-cm petri plates.
10. *SC-Leu-Trp+5-FOA plates (5-FOA plates)*: Prepare 1 liter of SC/agar and add 8 ml of 20 m*M* uracil and 8

ml of 100 m*M* histidine before pouring. Add 2 g of 5-FOA powder and stir to dissolve. It will take a while for 5-FOA to go into solution. Pour into ten to twelve 15-cm petri plates.

11. *YPD plates*: Add 10 g of yeast extract and 20 g of Bactopeptone to 500 ml of dH_2O. At the same time, in a separate flask, add 20 g of bacto agar to 500 ml of dH_2O. Autoclave both flasks and mix afterward. Cool to 55°C in a water bath. Add 50 ml of 40% glucose and pour into ten to twelve 15-cm petri plates.

B. Preparation of DB-ORF Bait Strains

Any cloning strategy can be used to generate DB-ORF fusion vectors. The Gateway recombination method (Walhout *et al.*, 2000) is useful for the cloning of large numbers of DB-ORF baits. For the strains and plasmids that we describe, the DB plasmid has a *LEU2* marker and the AD plasmid has a *TRP1* marker, but other variations of the two-hybrid system use other markers. It is important to make sure that the selective plates you use match the markers of the vectors you are using. After obtaining the constructs, the next step is to introduce them into the two-hybrid strain (MaV203 in this method). Several transformation protocols that are optimized for the scale of the transformation to be performed are given throughout the article, but any yeast transformation protocol should work. The following protocol is optimized for transforming large numbers of baits in a 96-well plate.

Solutions

1. *1 M lithium acetate stock solution*: Add 51 g of lithium acetate into 500 ml of ddH_2O. Autoclave to sterilize.

2. *10× TE stock solution*: 100 m*M* Tris–HCl (pH 7.5), 10 m*M* EDTA, autoclave

3. *50% PEG stock solution*: Dissolve 125 g of polyethylene glycol in warm ddH_2O and finalize to 250 ml. Sterilize by filtration (the PEG solution is very viscous and takes a long time to filter).

4. *TE/LiAc*: To make 50 ml, add 5 ml of 10× TE and 5 ml of 1 *M* LiAc into 40 ml of sterile ddH_2O

5. *TE/LiAc/PEG*: To make 50 ml, add 5 ml of 10× TE and 5 ml of 1 *M* LiAc into 40 ml of 50% PEG

6. *Boiled ssDNA*: Boil the 10 mg/ml of salmon testes DNA for 5 to 10 min and chill on ice before transformation

Steps

1. Start an overnight culture of MaV203 yeast by scratching a small clump of cells from a patch into at least 0.5 ml of media for each bait you plan to transform (a minimum of 5 ml of media should be used).

2. The next day, take 0.5 ml of the overnight culture for each transformation.

3. Spin down the cells at 2000 rpm for 5 min.

4. Wash the cells by adding 0.25 ml of ddH_2O for each transformation.

5. Spin down the cells and wash in 100 µl of TE/LiAc for each transformation.

6. Spin down the cells and resuspend the cell pellet in 20 µl of TE/LiAc for each transformation.

7. Add 2 µl of boiled ssDNA for each tansformation.

8. Aliquot 22 µl of yeast into the wells a 96-well plate.

9. Add 50–100 ng of the appropriate DB-ORF DNA to each well. A transformation without DB-ORF DNA serves as a negative control.

10. Add 100 µl of TE/LiAc/PEG to each well and mix by pippetting.

11. Incubate the plates at 30°C for 30 min.

12. Heat shock at 42°C for 15 min.

13. Spin down and remove the TE/LiAc/PEG solution with a multichannel pipette.

14. Add 120 µl of ddH_20 to each well, but be careful not to resuspend the cells. Remove 105 µl of ddH_20 from each well and resuspend the cells in the remaining 15 µl of liquid.

15. Using a multichannel pipette, spot 6–7 µl onto two 15-cm SC-Leu plates. You should be able to spot all 96 wells onto a 15-cm plate (see Fig. 2). The second plate is to have a copy in case spots run together or one plate is contaminated. You can spot onto additional plates if necessary.

16. Incubate for 2 to 3 days at 30°C.

17. Plates can be stored at 4°C for up to 2 months. Fifteen percent glycerol stocks can also be created and stored at –80°C indefinitely.

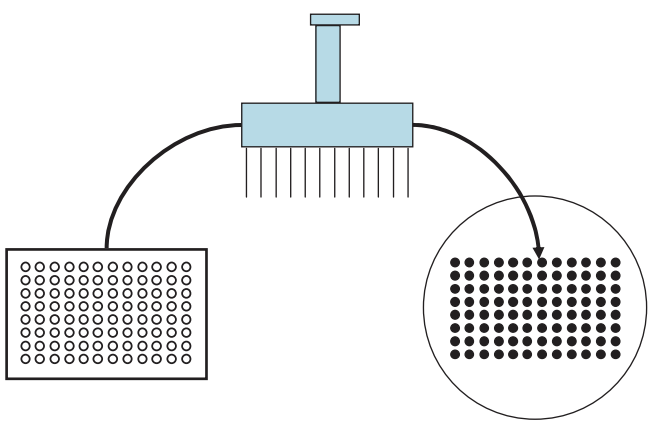

FIGURE 2 Spotting a 96-well plate onto a 15-cm agar plate. If a 12-tip multichannel pipette is used, all 8 rows of a 96-well plate can fit easily onto an agar plate as diagrammed.

C. Introduction of cDNA Libraries

Once the bait strains have been created, an AD-cDNA library needs to be transformed into the yeast. Typically, for most cDNA libraries, at least 10^6 independent clones need to be screened to get good coverage of a library, thereby requiring a high efficiency transformation procedure. If a large number of baits are being screened or if you are using a normalized ORFeome library (Reboul *et al.*, 2003), it may be preferable to screen as few as 2×10^5 colonies. While more potential interactions will be identified if you screen more colonies, screening a smaller number can still identify many interesting interactions and will allow you to screen a larger number of baits as well. We give protocols for both large and small numbers of colonies to be screened. Positives are screened for their ability to activate the *HIS3* marker. In MaV203, *HIS3* has a low level of activity, leading to moderate growth on SC-His media. To overcome this, the medium is supplemented with 3-AT, an inhibitor of *HIS3*, to reduce the background growth (Durfee *et al.*, 1993).

Solutions and Media

See transformation solutions in Section IIIB. SC-Leu liquid media, SC-Leu-Trp plates, and SC-Leu-Trp-His + 3-AT plates (referred to as 3-AT plates from here on) are needed.

Protocol 1. Introduction of AD Library into Y2H Strain (30 Plate Scale)

Steps

1. Grow the DB-ORF baits in 3 ml of SC-Leu yeast liquid media at 30°C for approximately 24 h.
2. Resuspend the cells well by vortexing and inoculate 80–100 µl in 250 ml of YPD and incubate at 30°C for 15 to 18 h until the OD_{600} reaches 0.3 to 0.6. *Note*: It may be necessary to vary the amount of cells added and the time of incubation for the cells to be ready at the right time.
3. Harvest the cells by centrifuging for 5 min at 1800 rpm.
4. Wash the cell pellet in 50 ml of ddH_2O.
5. Wash the cells in 10 ml of TE/LiAc.
6. Resuspend the cells in $5 \times OD_{600}$ ml of TE/LiAc (e.g., if the $OD_{600} = 0.5$, then add 2.5 ml of TE/LiAc).
7. Transfer 1.6 ml of resuspended cells into a 15-ml Falcon tube and add 160 µl of boiled ssDNA and 20–30 µg of cDNA library.
8. Add TE/LiAc/PEG to final volume of 9 ml. Mix by inverting several times and aliquot at 1 ml into 1.5-ml Eppendorfs.
9. Incubate at 30°C for 30 min to 1 h.
10. Heat shock at 42°C for 15 min.
11. Transfer the cells into a 15-ml Falcon tube and spin down at 1800 rpm for 5 min.
12. Remove the supernatant and resuspend the cells in 9 ml of sterile ddH_2O.
13. Take 10 µl and add to 10 ml of ddH_2O to create a 1 : 1000 dilution.
14. To about thirty 15-cm 3-AT plates, add approximately twenty-five 3-mm glass beads. Plate 300 µl of cells from step 12 on each 15-cm 3-AT plate. Spread the cells evenly by shaking the plates with glass beads. Remove beads when done. The beads can be washed, autoclaved, and reused.
15. To measure transformation efficiency, plate 300 µl of the 1 : 1000 diluted cells on a SC–Leu-Trp plates. Count the colonies 2 to 3 days after plating.
16. Incubate the 3-AT plates for 4 to 5 days at 30°C and take to Section III,D.

Protocol 2. Introduction of AD Library in Y2H Strain (Three Plate Scale)

Steps

1. Grow the DB-ORF baits in 3 ml of SC-Leu yeast medium at 30°C for approximately 24 h.
2. Resuspend the cells well by vortexing and inoculate 10–15 µl in 35 ml of YPD and incubate for 15 to 18 h at 30°C until the OD_{600} reach 0.3 to 0.6. This can be done in 50-ml Falcon tubes. *Note*: It may be necessary to vary the amount of cells added and the time of incubation for the cells to be ready at the right time.
3. Harvest the cells by centrifuging for 5 min at 1800 rpm.
4. Wash the cell pellet in 1.5 ml of ddH_2O by vortexing and transfer to a 2.0-ml Eppendorf.
5. Spin at highest speed for 5 s in a microcentrifuge.
6. Wash the cells in 1 ml TE/LiAc and spin again.
7. Resuspend the cells in 275 µl of TE/LiAc.
8. Add 30 µl of boiled ssDNA and 3–5 µg of the normalized AD-library.
9. Add 1.5 ml TE/LiAc/PEG and mix by inverting several times.
10. Incubate at 30°C for 30 min to 1 h.
11. Heat shock at 42°C for 15 min.
12. Spin down the cells.
13. Remove the supernatant and resuspend the cells in 900 µl of sterile ddH_2O.
14. Take 10 µl and add to 10 ml of ddH_2O to create a 1 : 1000 dilution
15. To three 15-cm 3-AT plates, add approximately twenty-five 3-mm glass beads. Plate 300 µl of cells from step 12 on each 15-cm 3-AT plate. Spread the cells evenly by shaking the plates with glass beads. Remove beads when done. The beads can be washed, autoclaved, and reused.

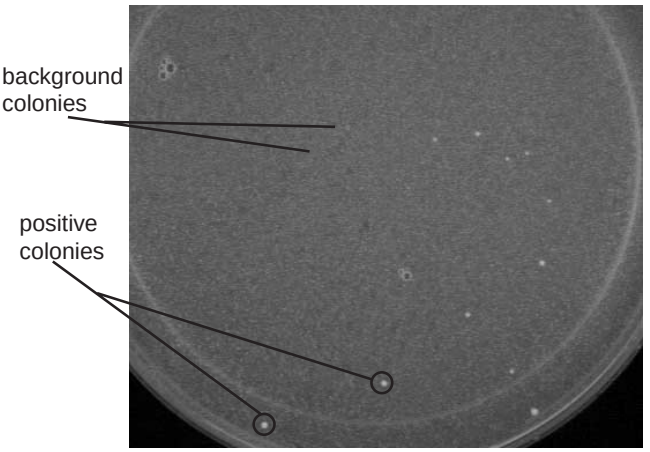

FIGURE 3 An example of a 3-AT screening plate before colonies have been picked. Two of the colonies that are likely two-hybrid positives have been circled.

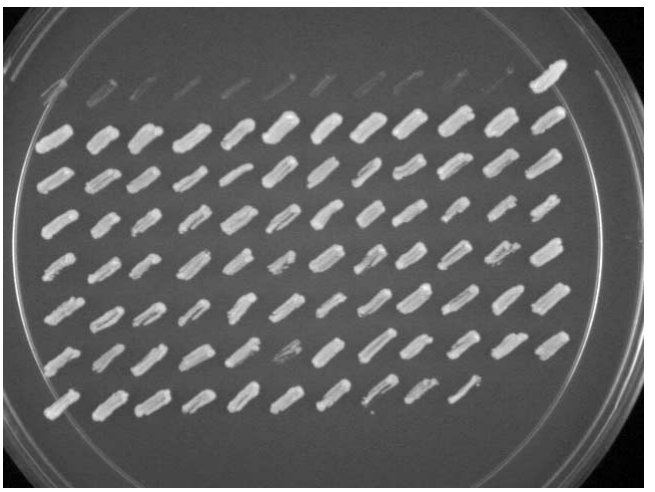

FIGURE 4 An example of positive colonies that have been picked and patched onto a 3-AT plate. By patching them in the same pattern and dimensions as a 96-well plate, it makes it easier to manipulate the samples at later stages.

16. Calculate the transformation efficiency by plating 300 µl of 1 : 1000 diluted cells on SC-Leu-Trp plates.

D. Isolation of Two-Hybrid Positives

After 4 to 5 days of growth, colonies with interacting proteins should have grown enough to isolate them. At times it is difficult to differentiate a true positive from a large background colony, but later in Section III,E you can use the phenotypic assays to help differentiate them. Colonies are initially grown on 3-AT plates after picking to allow true positives to outgrow any background cells that might have been picked up accidentally.

Solutions

1. SC-Leu-Trp-His + 3-AT plates
2. SC-Leu-Trp liquid media

Steps

1. Get the plates from Section II,C. See Fig. 3 for an example of what a screening plate might look like (with positive colonies growing in a field of background colonies).
2. Use a toothpick to pick colonies that grow above the background. Patch the colony in a small streak onto a 15-cm 3-AT plate. Typically we divide the plate into 96 sectors that correspond to a 96-well plate so that the positives can be stored and manipulated in a 96-well format in the future (see Fig. 4). If you only have a small number of positives you will not fill up a plate, but if you have many baits and a large number of positives then you could fill up many plates with potential positive clones.
3. Incubate the plates at 30°C for 2 to 3 days.
4. When the patches have grown up, use a multichannel pipette with tips to scrape a small clump of cells into 120 µl of SC–Leu-Trp medium in U-bottom 96-well plates (see Fig. 5). Seal the plates with airpore tape.
5. Incubate the plates at 30°C for 2 days before making a 15% glycerol stock.
6. Take the remaining culture to Section III,E for phenotypic assays.

E. Phenotypic Assays

Picking positive colonies is only the first step in identifying potential interacting proteins. It is frequently difficult to determine which of the colonies are true positives and which are merely large growing background colonies. It is important to retest the potential positives and see if they are able to activate expression of a variety of different two-hybrid reporters. We generally look for colonies that are able to activate at least two of the three two-hybrid reporters. It is also important to include at least one positive and one negative control on the plates. A good negative control would be the empty AD and DB vectors, whereas a strong positive control would be the full-length Gal4 transcription factor. For a description of a larger set of two-hybrid controls, see Walhout and Vidal (2001).

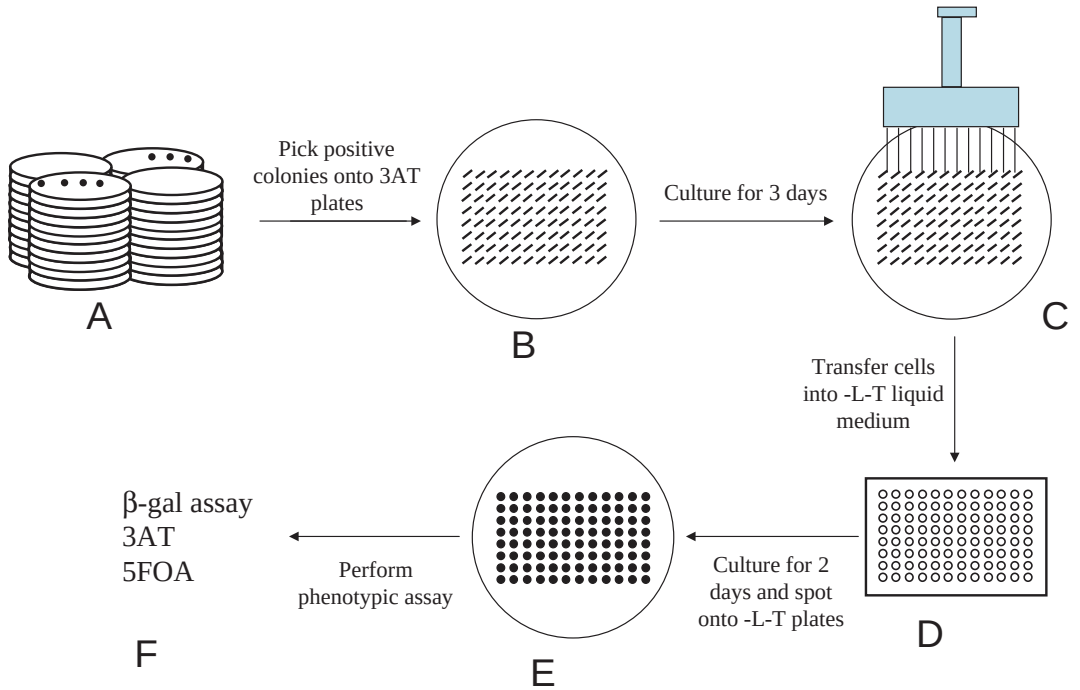

FIGURE 5 Diagram of picking positives. First gather the library transformation screening plates (A) and pick the positives onto a fresh 3-AT plate (B). After 3 days of growth, use a multichannel pipette with tips (C) to transfer the positives to liquid SC-Leu-Trp in a 96-well plate (D). After 2 days of growth, spot the cells onto a SC-Leu-Trp plate (E) and use to replica plate for the phenotypic assays (F).

Solutions and Materials

You need SC-Leu-Trp plates, 3-AT plates, 5-FOA plates, and YPD plates. Note that 5-FOA selects against URA3-positive strains, i.e., positive interactors will not grow on 5-FOA. You also need circular nitrocellulose filters.

Steps

1. Get the 96-well plates from Section III,D. Spot 5 µl of culture onto a SC-Leu-Trp plate. Grow at 30°C for 1 to 2 days.

2. You will use three different plates to assay the three two-hybrid reporters: YPD for lacZ, 3-AT for HIS3, and 5-FOA for URA3. The 5-FOA and 3-AT plates can be used as is, but the YPD plate needs a nitrocellulose filter placed on it prior to replica plating. This is necessary to remove the yeast from the YPD plate and perform the β-Gal filter lift assay (see Section III,F). If there are bubbles between the filter and the agar or if the filter is misaligned, use forceps to move the filter or remove the bubble.

3. Using replica velvets and a replica block, replica plate the yeast from the SC–Leu-Trp growth plate to the YPD/filter, 3-AT, and 5-FOA plates. Use the same velvet for each of the assay plates; there should be enough yeast on it for all three plates.

4. Replica clean the 3-AT and 5-FOA plates as follows. Use a clean velvet to remove excess yeast from the 3-AT plate (press firmly but not harshly). Repeat with a clean velvet until there is no longer any visible sign of yeast on the plate. Then repeat one more time (we typically clean with four velvets). Repeat the procedure with the 5-FOA plate. Replica cleaning is necessary to decrease the background growth and to ensure that you start out with comparable amounts of cells in each spot; it is not necessary to perform on the YPD/filter plates.

5. Culture all three assay plates at 30°C. After 1 day the YPD plate should have large spots of yeast on the filter. Take the YPD plate to Section III,F to perform β-Gal filter lift assays.

6. Examine 3-AT and 5-FOA plate. If the negative control shows growth after 1 day, replica clean again.

7. When the controls on the 3-AT and 5-FOA plates have grown to the appropriate levels (it normally takes 2 days for 5-FOA and 3 days for 3-AT), remove plates

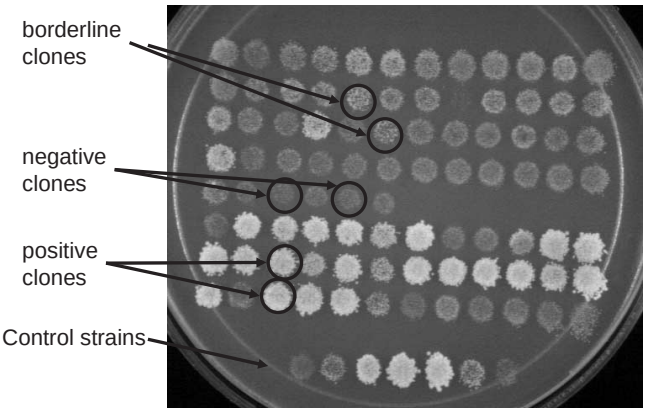

FIGURE 6 An example of a 3-AT assay plate. The bottom seven patches are a range of controls. A range of strengths of interactions can be seen by the strength of growth on the spots. Clones that are indicative of positive and negative interactions have been circled as well as a couple of clones that are on the border between being positive and negative.

and score the results. (See Fig. 6 for an example of what a 3-AT assay plate can look like.)

8. Score the 3-AT and 5-FOA plates along with the β-Gal filters from Section III,F. Any strain that passes at least two of the three tests is considered positive. Consolidate all of the positives into fresh 96-well plates.

9. Grow plates for 2 days and make glycerol stocks of the strains.

F. β-Gal Filter Lift Assay

Solutions

1. *Z buffer*: To make a liter, add 16.1 g $Na_2HPO_4{\cdot}7H_2O$, 5.5 g $NaH_2PO_4{\cdot}H_2O$, 0.75 g KCl, and 0.246 g $MgSO_4{\cdot}7H_2O$. Autoclave to sterilize.
2. *4% X-Gal*: Dissolve 40 mg in 1 ml of *N,N*-dimethylformamide. Store at –20°C wrapped with foil.
3. β-*Gal solution*: For each plate, prepare 5 ml of Z buffer with 120 µl of 4% X-Gal and 13 µl of 2-mercaptoethanol. Make fresh each time.

Steps

1. Retrieve the YPD/filter plates from Section III,E.

2. Make up the β-Gal solution according to the number of plates that are needed to assay.

3. For each for each plate to be assayed, get one empty 15-cm petri plate. Put two pieces of Whatman filter paper in the plate. Add 5 ml of β-Gal solution to each plate. Let the paper soak up the solution and make sure there are no bubbles under the Whatman paper.

4. Remove the nitrocellulose filter from the YPD (with yeast on the filter) and place in liquid nitrogen for at least 30 s. This lyses the cells.

5. Remove the filter from liquid nitrogen and allow it to thaw in air (this should take ~30 s). Once the filter is flexible again, place in a petri plate with β-Gal solution-soaked Whatman paper. Use forceps to remove any bubbles that may be under the filter.

6. Put the β-Gal assay plates at 37°C overnight. The next day you can read the results with positives being blue; the stronger the positive, the stronger the blue.

7. Remove the Whatman filter paper. The filters can be stored dry for at least 6 months.

G. Yeast PCR to Identify Preys

Once you have identified the clones that pass the phenotypic assays, it is necessary to isolate prey DNA from the yeast clones and identify them by sequencing. Prey DNA can be obtained by polymerase chain reaction (PCR) using the universal primers on the vector (typically we make primers to the activation domain sequence and the termination sequence; the primer sequences that we use are listed later).

Solutions and Media

1. SC-Leu-Trp plates, YPD plates
2. Lysis solution: To make 1 ml, add 2.5 mg zymolyase to 0.1 *M* sodium phosphate buffer (pH7.4). The solution can be stored at –20°C.

Primer sequences: Activation domain –CGCGTTTG GAATCACTACAGGG

Termination sequence –GGA GAC TTG ACC AAA CCT CTG GCG

Steps

1. Spot 5 µl of the positives from the 96-well plate culture or the glycerol stocks made in Section III,E, steps 8 and 9 onto a SC-Leu-Trp plate. Culture at 30°C for 1 day.

2. Replica plate to YPD. Culture at 30°C for 1 day.

3. Add 15 µl of lysis solution to each well in a 96-well PCR plate.

4. Using a multichannel pipette, scrape some of the yeast cells off the YPD plate (one row at a time as in Section III,D, step 4) and resuspend into the 15-µl lysis solution.

5. Put the yeast at 37°C for 5 min then at 95°C for 5 min (this can be done in a PCR machine).

6. Set up the PCR plate using a final volume of 50 µl for each reaction.

7. Make a 1 : 10 dilution of the yeast lysis from step 5. Add 5 µl to the PCR plate.

8. Perform PCR using 5-min extension times to make sure that the large ORF inserts are isolated.

9. The PCR products can be sent out for sequencing after confirming it works. Note that most PCR products need to be purified from the primers to be sequenced properly. We use the Millipore MultiScreen PCR plates (Fisher, Cat. No. MANU-030-10) to purify PCR products.

H. Retest by Gap Repair

Sometimes a positive isolate will occur not because the two proteins interact, but through a spontaneous self-activation mutation that makes the growth independent of the two plasmids. This makes it important to isolate the AD-ORF from the strain and retest it in the bait strain. The easiest way to do this is by gap repair (Orr-Weaver *et al*., 1983). This involves introducing into yeast both a vector cut at the insert sites and the insert itself. If there is some homology between the insert and the cut vector, the yeast will repair it by ligating the insert into the vector.

The protocol is essentially the same as the method listed in Section III,B with a few exceptions.

Step 1. Instead of starting a culture with untransformed MaV203 at the beginning, start a culture with MaV203 transformed with the DB-ORF of interest.

Step 9. Instead of using DB-ORF DNA, use 25 ng of linearized AD plasmid DNA and 2.5 µl of the PCR product from Section III,G. The AD plasmid should be cut in the linker region between the AD sequence and the termination sequence (in our plasmids, we use *Sma*I) as that way the PCR product can have homology to the AD sequence and the termination sequence and gap repair can be efficient.

Step 15. Select on -Leu, -Trp plates instead of -Leu.

Step 17. Perform phenotypic assays as in Section III,E, skipping step 1 and only using the 3-AT and β-Gal assays.

IV. COMMENT

Notes on High-Throughput Two Hybrid

The simplicity of two-hybrid screening allows for the screening of large numbers of baits of interest at a time. This allows a scientist to study a greater number of genes, but it requires the researcher to be more organized from the start. Here are several points to remember when screening large numbers.

1. Work in 96-well formats from the beginning. This will allow you to transform all the baits that you want to study in 1 day.
2. When transforming the bait strains with the library, it is still necessary to do each transformation individually, but you can do six or more in a day.
3. When picking the colonies, try to patch them on a 96-well grid so that it will be easier to transfer your positives to 96-well plates in the future.
4. Try to keep track of data such as gene names and strength of interactions in the phenotypic assay in a spreadsheet such as Microsoft Excel. This can allow you to monitor your positives easily and keep track of which ones pass all the phenotypic tests.

The strength of the two-hybrid system is its ease of use. It can identify many potential interactors and maybe even bring interaction networks to light. It is ultimately, however, a first-pass prediction of interactions and should be thought of as a jumping off point to other more detailed studies.

References

Boulton, S. J., Gartner, A., *et al.* (2002). Combined functional genomic maps of the *C. elegans* DNA damage response. *Science* **295**(5552), 127–131.

Davy, A., Bello, P., *et al.* (2001). A protein-protein interaction map of the *Caenorhabditis elegans* 26S proteasome. *EMBO Rep.* **2**(9), 821–828.

Drees, B. L., Sundin, B., *et al.* (2001). A protein interaction map for cell polarity development. *J. Cell Biol.* **154**(3), 549–571.

Du, W., Vidal, M., *et al.* (1996). RBF, a novel RB-related gene that regulates E2F activity and interacts with cyclin E in Drosophila. *Genes Dev.* **10**(10), 1206–1218.

Durfee, T., Becherer, K., *et al.* (1993). The retinoblastoma protein associates with the protein phosphatase type 1 catalytic subunit. *Genes Dev.* **7**(4), 555–569.

Fields, S., and Song, O. (1989). A novel genetic system to detect protein-protein interactions. *Nature* **340**(6230), 245–246.

Hartwell, L. H., Hopfield, J. J. *et al.* (1999). From molecular to modular cell biology. *Nature* **402**(6761 Suppl.), C47–C52.

Ito, T., Tashiro, K., *et al.* (2000). Toward a protein-protein interaction map of the budding yeast: A comprehensive system to examine two-hybrid interactions in all possible combinations between the yeast proteins. *Proc. Natl. Acad. Sci. USA* **97**(3), 1143–1147.

Orr-Weaver, T. L., Szostak, J. W., *et al.* (1983). Genetic applications of yeast transformation with linear and gapped plasmids. *Methods Enzymol.* **101**, 228–245.

Reboul, J., Vaglio, P., *et al.* (2003). *C. elegans* ORFeome version 1.1: Experimental verification of the genome annotation and resource for proteome-scale protein expression. *Nature Genet.* **34**(1), 35–41.

Uetz, P., Giot, L., *et al.* (2000). A comprehensive analysis of protein-protein interactions in *Saccharomyces cerevisiae*. *Nature* **403**(6770), 601–603.

Vidal, M., Brachmann, R., *et al*. (1996). Reverse two-hybrid and one-hybrid systems to detect dissociation of protein-protein and DNA-protein interactions. *Proc. Natl. Acad. Sci. USA* **93**(19), 10315–10320.

Walhout, A. J., Sordella, R., *et al*. (2000). Protein interaction mapping in *C. elegans* using proteins involved in vulval development. *Science* **287**(5450): 116–122.

Walhout, A. J., Temple, G. F., *et al*. (2000). GATEWAY recombinational cloning: Application to the cloning of large numbers of open reading frames or ORFeomes. *Methods Enzymol* **328**, 575–592.

Walhout, A. J., and Vidal, M. (2001). High-throughput yeast two-hybrid assays for large-scale protein interaction mapping. *Methods* **24**(3), 297–306.

SECTION

12

Functional Proteomics

CHAPTER

40

Chromophore-Assisted Laser Inactivation of Proteins by Antibodies Labeled with Malachite Green

Thomas J. Diefenbach and Daniel G. Jay

I. INTRODUCTION

Chromophore-assisted laser inactivation (CALI) permits direct inactivation of proteins within cells or tissues with high spatial and temporal resolution. CALI converts nonfunction-blocking antibodies into function-blocking antibodies through the use of covalently linked chromophores, such as malachite green isothiocyanate (MGITC) and fluorescein isothiocyanate (FITC). Cells or tissues loaded with labelled antibody are exposed to laser light, which results in the generation of free radicals that locally damage the protein to which the antibody is attached. Using free-radical quenchers, the inactivation mechanism for MG-mediated CALI was found to be dependent on hydroxyl radical generation, with the hydroxyl radicals so generated having a half-maximal radius of inactivation of 15 Å (Jay, 1988; Liao *et al*., 1994; Linden *et al*., 1992). In the case of FITC-mediated CALI (FALI) (Beck *et al*., 2002), singlet oxygen is the reactive species, and evidence suggests a half-maximal inactivation radius of ~40 Å (Beck *et al*., 2002). Thus, the specificity of CALI and the process of photoactivation make possible a protein knockdown strategy with high spatial and temporal control. Protein function can be perturbed directly during precise periods of development without concerns accompanying the use of molecular genetic approaches, such as lethality or compensation. In addition, CALI can be performed on two scales: CALI and micro-CALI. CALI employs a laser to produce a 2-mm-diameter laser spot useful for irradiation of tissue samples, culture dishes, or microtiter wells. Micro-CALI uses a less powerful laser linked to an inverted microscope. By focussing laser light through an objective lens, spot sizes 2–100 μm in diameter are attainable. Micro-CALI can therefore be used to target individual cells or subdomains within cells. Furthermore, the utility of CALI has been expanded to include targeting of EGFP–protein constructs (Rajfur *et al*., 2002), RNA sequences (Grate and Wilson, 1999), and the use of a membrane-permeable fluorescein derivative that targets recombinant protein sequences (Adams *et al*., 2002; Marek and Davis, 2002). For recent, comprehensive reviews of the utility of CALI, see Buchstaller and Jay (2000) and Rubenwolf *et al*. (2002). For application-specific use of CALI, consult Beermann and Jay (1994).

II. MATERIALS AND INSTRUMENTATION

A. Micro-CALI

For micro-CALI, a nitrogen laser (Model VSL-337ND-S, Laser Science, Inc., Franklin, MA; 75 kW peak power; Model 337201-00 for a 110-V circuit) is used in conjunction with a DUO-220 visible tunable dye laser module (Laser Science, Inc.; Model 337220-00 for a 110-V circuit). A more compact, less powerful (30 kW peak power) alternative is the VSL-337 nitrogen laser (Laser Science, Inc.; Model 337000-00 for 110 V) with DYE-120 (Laser Science, Inc.; Model 337120) visible tunable dye laser module. For CALI using

Copyright 2006, Elsevier Science (USA).
All rights reserved.

malachite green, DCM dye [4(dicyanomethylene)-2-methyl-6-(*p*-diethylaminostyryl)-4H-pyran](Laser Science, Inc., Cat. No. 337999 PBD) is used to generate 630 nm light (the peak excitation wavelength of malachite green is 620 nm). The dye resides in a cuvette in the dye laser module. Dyes are also available for fluorescein and GFP excitation wavelengths. The laser light is routed through the rear port of a Nikon Diaphot 200-inverted microscope or similar type of microscope (i.e., Zeiss Axiovert) (Fig. 1).

The rear microscope port has attached to it a Nikon TE dual mercury lamp house adapter (Micro Video Instruments Inc.), to which the 100-W mercury arc lamp is mounted opposite the laser input. The lamp house adapter permits rapid switching between fluorescence and laser illumination using a rotating mirror. The equivalent attachment for the Zeiss Axiovert is the dual-mirror lamp housing attachment (Cat. No. 447230, Carl Zeiss MicroImaging, Inc.). The laser light is directed through a dichroic mirror that reflects wavelengths greater than 600 nm (e.g., Cat. No. 590DCLP, Chroma Technology Corp.) mounted in a Nikon epifluorescence filter cube. Thus, no excitation or barrier filters are required. The 590DRSP dichroic reflects greater than 90% of 620-nm laser light. The laser light then passes through an objective lens, which should be the highest numerical aperture (NA) possible at either 20, 40, 60, or 100× magnification. If the NA is too low, insufficient light will reach the specimen plane. Examples of suitable objective lenses include a Nikon Plan Apo 40× 0.95NA DMPh3 (a phase-contrast objective lens) and a Nikon Plan Apo 60× 1.4NA oil objective lens or equivalent. Low fluorescence immersion oil is important for micro-CALI to prevent light scattering. A recommended oil is Cargille type DF (Cat. No. 04108A-AB, Structure Probe, Inc., 120 ml) and is suited for inverted microscope use only (it has higher viscosity than oil for upright microscopes). The laser light then passes through No. 1.5 coverslips (Cat. No. 12-541B, Fisher Scientific Company, 22 × 22 mm), which are optimized for most microscope objectives that are standardized for use with coverslips of 0.17 mm thickness. Laser light intensity can be measured at the specimen plane using a light meter (see later). Because malachite green is strictly a chromophore, there is no fluorescence emission to observe during micro-CALI. However, the laser light itself is in the visible spectrum and may partially obscure the center of the image field. To block this light, a low-pass filter that transmits wavelengths below 620 nm can be

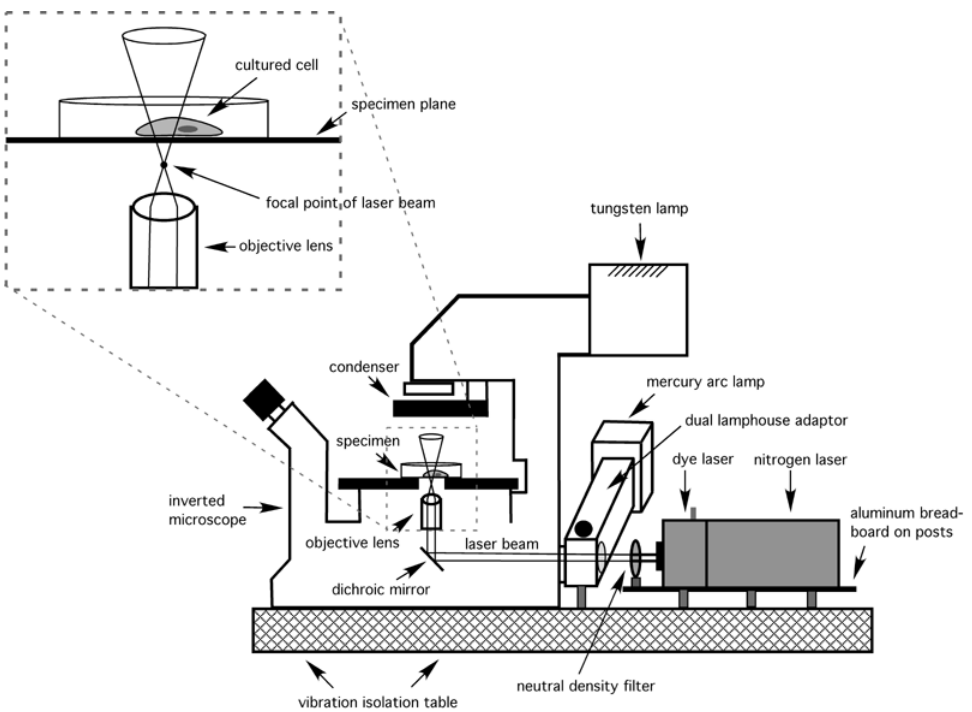

FIGURE 1 A schematic of micro-CALI configuration. Light from a nitrogen dye laser is directed to the rear port of an inverted epifluorescence microscope. An expanded view of the dotted square illustrates that the focal point of the laser beam should be above the specimen plane so that the specimen is exposed to the divergent portion of the beam.

placed in the filter cube or port leading to a CCD digital camera (custom filter from Chroma Technology Corp.). The laser itself is mounted on a solid 300 × 600-mm aluminum breadboard (Cat. No. M-SA-12 and other mounting hardware from Newport Corp.) that stands on six aluminum posts (Cat. No. TPS1, 2, or 3 metric posts, Newport Corp.) held in place with sliding base clamps (Cat. No. SB-TPS, Newport Corp.). To maintain alignment of the laser with the microscope optics, it is important that the laser and microscope be stationed on a breadboard (Cat. No. MIG-33-2-ML or higher quality, Newport Corp.) mounted onto a vibration isolation table (any model from Newport). A neutral density filter set is used to reduce the laser light intensity (and to some extent laser spot size) without altering the wavelength. A set of five filters—0.2, 0.3, 0.5, 0.6, and 1.0—are recommended and can be used singly or in combination (Cat. No. 22000A UV ND, Chroma Technology Corp.). The neutral density filters are mounted on a breadboard between the laser and the microscope using an optical mount (P100-AC "Performa" performance optical mount with 1-in. aperture, Newport). Opticians refer to percentage transmission (the reciprocal of which is percentage absorbance and therefore the percentage reduction of light transmitted). A neutral density filter of ND 0.2 = 63% transmission (37% reduction), ND 0.3 = 50% (50% reduction), ND 0.5 = 32% (68% reduction), ND 0.6 = 25% (75% reduction), and ND 1.0 = 10% (90% reduction). When placed in series, the reduction in light intensity is additive. Without neutral density filters or an objective lens, the light measured at the specimen plane with the VSL-337ND-S laser with dye module is approximately 60 µJ average energy at 30 Hz (3 ns pulse duration), down from the 300-µJ output without the dye module. A recommended laser light meter is the Orion PE with PE10 head (2 µJ–10 mJ sensitivity) from Ophir Optronics Ltd. To align the laser, the center of the laser light birefringence pattern should be at the center of the primary reflecting mirror. The microscope can then be positioned so that the laser light is seen exiting the objective lens. To visualize and confirm laser output and alignment at the specimen plane, irradiate a spot of ink (blue ink for 630 nm light, red ink for 488 nm light) on a glass coverslip at the specimen plane (Fig. 2A) using the desired objective lens.

The ink will absorb the laser light, creating a hole in the ink and delineating the margins of the laser spot. This spot can be imaged digitally on a computer and used as an overlay. Alternatively, a stage micrometer can be used to reference the position of the spot. It is good practice to fire the laser about 10 times to confirm the boundaries of the hole (Fig. 2B) as some burn-in can occur (spot area increases), especially if the laser is

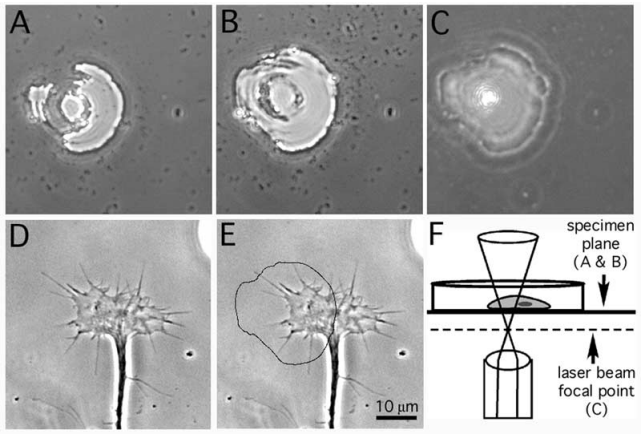

FIGURE 2 (A) Using a 40× objective lens, the shape and position of the laser beam can be determined by irradiating a glass coverslip marked with blue ink. Blue ink absorbs the 630-nm light and burns away the ink, leaving a bright spot. (B) After 10 laser pulses, more ink has been burned away, leaving a slightly larger spot. After about 10 pulses, the spot does not change significantly. (C) By focussing the objective lens below the level of the ink (or from the viewer's perspective, above the specimen plane), the focal point (and therefore the centre) of the laser beam can be located in relation to the spot in the ink. (D) A growing tip of an axon, the growth cone, from a neuron isolated from dorsal root ganglion of embryonic chick. The microspikes, or filopodia, are clearly seen emanating from the growth cone. (E) The perimeter of the laser spot from B is superimposed onto the growth cone (black line) showing how the spot can be used to irradiate a small portion of a cellular structure (scale bar: 10 µm).

not aligned perpendicular to the specimen plane. Depending on the distance between the laser and the objective lens, the focal point of the laser light will likely fall above or below the specimen plane (Fig. 2C). It is important that the focal point of the laser is *not* at the specimen plane as this will cause thermal damage (and even chipping of the glass coverslip) on account of the very high power density of coherent laser light at a focal point (Fig. 2F). It is also important to check manufacturer's specifications of the objective lens used to ensure that the lens coatings can withstand laser light (specifically, peak laser power) without degrading. The duration of continuous irradiation for a single CALI treatment should not exceed 5 min as periods greater than this may cause quenching of the chromophore. To minimize nonspecific effects of long-term laser illumination, periods of irradiation could be interspersed with 5-min rest periods. Because the size of the laser spot is typically 10–20 µm in diameter (although with lower power objectives it can be over 100 µm in diameter), micro-CALI can be used to inactivate proteins in single cells or small regions of cells. For example, we have used micro-CALI to examine the

function of distinct myosins (Diefenbach *et al*., 2002) in the growing tips of nerve cell axons (Figs. 2D and 2E), which are typically 10 μm in diameter.

B. CALI

To avoid stray or direct laser light entering the eyes, approved safety goggles are imperative for use with class IV lasers, in addition to following recommended safety precautions of the laser manufacturer. This includes using light-absorbing material (black cloth or tinted plexiglass) as a shield to prevent reflection of stray laser light. For CALI, a tunable neodymium : yttrium–aluminum–garnet (Nd : YAG) laser (Quanta Ray Model GCR-11, Spectra Physics) is used to pump a custom-fabricated dye laser using the DCM dye as for micro-CALI. Alternatively, a tunable Surelite OPO (optical parametric oscillator) Nd : YAG laser (Continuum Scientific Service) is also suitable (Fig. 3).

The laser output is 630 nm for MGITC (488 nm for FITC), 10 Hz, 6 ns pulse width, and 15 mJ peak energy per pulse. A beam splitter (glass slide) can be used to take a fraction (i.e., 1/6th) of the light and direct it at a 90° angle to a laser light meter (Model JD500 or EM400, Molectron Detector, Inc.). The light is then directed vertically through a right-angle prism and focussed using a 25-mm-diameter plano-convex lens (Cat. No. SPX016AR.14, Newport Corporation) to a 2-mm diameter spot (typically the spot is a flat oval, 2 mm on the short axis and 4 mm on the long axis). Spot size and shape can be recorded, viewed on preexposed photographic paper (600 film, Polaroid Corp.), and altered using an adjustable miniature diaphram (Cat. No. MH-2P, Newport Corporation) placed between the output of the dye laser and the 1/6th beam splitter. To test laser effectiveness at the specimen plane, control *in vitro* experiments are necessary to establish suitable irradiation times. However, for most applications, the duration of irradiation for a single treatment is typically 2 min and no longer than 5 min. For irradiation of FITC-labelled antibodies, a source of incoherent light can also be used. For example, a 300-W slide projector with a 488-nm narrow band-pass filter has been employed to illuminate microtiter plates (Beck *et al*., 2002).

Although cost effective, the system has to be configured to ensure uniform illumination over the entire sample, and adequate precautions should be taken to prevent thermal damage, such as cooling of the sample during irradiation or increasing the distance of the sample from the light source.

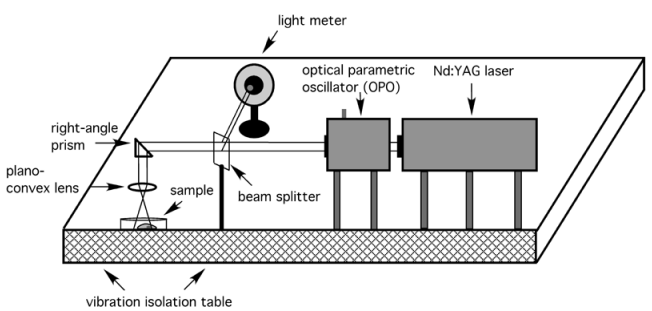

FIGURE 3 A schematic of macro-CALI configuration. An Nd : YAG laser feeds light into an optical parametric oscillator that tunes the wavelength to 630 nm. Light energy is measured from a meter that receives a fraction of the light internally reflected from a beam splitter (glass slide). The light is reflected down to the vibration isolation table surface using a right-angle prism and is focussed to the desired spot size using a plano-convex lens.

III. PROCEDURES

A. Antibody Labelling

Antibody labelling involves covalently binding malachite green isothiocyanate (Fig. 4; Cat. No. M-689, Molecular Probes, Inc.) or fluorescein isothiocyanate (Cat. No. F-143, Molecular Probes, Inc.) to nonfunction-blocking, polyclonal or monoclonal IgG antibodies, Fab fragments, or recombinant single chain variable fragments (scFvs).

Solutions

1. *Phosphate-buffered saline (PBS) buffer*: 15 liters of 0.1 *M* PBS buffer
2. *Hank's balanced salt solution*: Ca^{2+}/Mg^{2+} free, 15 ml (HBSS, Gibco, Cat. No. 24020117, Invitrogen Corporation)
3. *10 mg/ml MGITC*: Weigh 10 mg and resuspend in 1 ml dimethyl sulfoxide (DMSO) in a 1.5-ml centrifuge tube

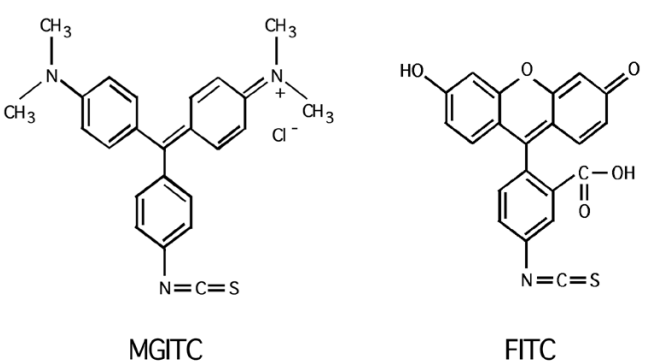

FIGURE 4 Chemical structure of malachite green isothiocyanate (MGITC) and fluorescein isothiocyanate (FITC).

4. *Bovine serum albumin (BSA)*: 5 mg/ml (500 µl; weigh 5 mg and resuspend in 1 ml PBS) for blocking the membrane of the concentrating tube and 20 mg/ml (weigh 20 mg and resuspend in 1 ml PBS) to combine with the antibody solution
5. *Antibody solution*: Typically 100 to 200 µg in physiological solution suited to the target cells (i.e., Hank's balanced salt solution without Ca^{2+}/Mg^{2+})
6. *0.5 M $NaHCO_3$ stock*: To make 100 ml, take 4.2 g of $NaHCO_3$ and dissolve in less than 100 ml of distilled, deionized water. Add 1 *M* NaOH dropwise to bring the pH to 9.5 and bring the volume up to 100 ml with water

Steps

1. Dialyze antibodies (10,000 molecular weight cutoff) against PBS buffer (pH 7.4) overnight at 4°C.

2. Antibodies can be concentrated by centrifugation (see step 10).

3. Prepare MGITC as a 10-mg/ml solution in DMSO. Because MGITC is very hygroscopic, it should be prepared fresh from powder and kept in a sealed tube just prior to labelling.

4. Add an equal (1 : 1) amount of BSA (Cat. No. B2518, Sigma-Aldrich Corporation) to the antibody solution as a stabilizing reagent.

5. Add a 10-fold molar excess of MGITC to the antibody solution to yield an optimal labelling ratio of 5 MGITC : 1 antibody molecule (or 1 MGITC : 1 Fab or scFv). Typically, between 100 and 200 µg of antibody is labelled at a time. The volume of antibody should be between 20 and 500 µl, as too large a volume of reaction mixture will reduce labelling reaction efficiency.

6. Add 500 µl of 0.5 *M* $NaHCO_3$ (pH 9.5) to the antibody solution.

7. Add MGITC to the antibody solution in a stepwise fashion, which favors the labelling reaction over the hydrolysis reaction. Divide the total volume of antibody into three equal aliquots. Add the first aliquot and mix gently for 5 min, followed by the second aliquot for another 5 min, and incubate the third aliquot for 15 min. A rocker (Cat. No. 14-512-28, Lab-Line Maxi Rotator, Fisher Scientific Company) is used to gently mix the reaction mixture during incubation.

8. The free MGITC label in solution is an emerald green color. As the labelling reaction proceeds (hydroxylation at the central carbon of the triarylmethane of amino groups, forming a thioester), the color changes to a deep sea-blue color. The hydrolysis product is purple and forms an insoluble precipitate.

9. After incubation, centrifuge the mixture at high speed (6400 rpm) on a minicentrifuge (Cat. No. EF4241A, Costar WX4241A, Daigger Laboratory Supplies) for 30 s to precipitate any hydrolyzed dye.

10. Separate unbound MGITC and buffer salts from the reaction mixture using a prepacked, 5-cc Sephadex G25 gel filtration column (PD-10, Cat. No. 17-0851-01, Amersham Biosciences Corporation) using a medium suitable for cell loading as an eluant, such as HBSS (Cat. No. 24020117, GIBCO, Invitrogen Corporation) with or without calcium and magnesium.

11. Usually 1–1.5 ml of eluant is collected. Depending on the initial concentration, concentrate the antibody solution to 1.0 mg/ml in Centricon tubes (30,000 MW cutoff; preblocked with 5 mg/ml BSA) using a centrifuge (Sorval RC-5, or equivalent) at 4200 rpm and 20°C. The eluant should be kept above 15°C to avoid precipitation of residual, free MGITC, which is toxic to cells.

12. Once concentrated, determine the molar labelling ratio by measuring the optical density of a diluted sample of the solution at 620 nm based on a molar aborptivity of MGITC of 150,000 $M^{-1}cm^{-1}$ and dividing the concentration of dye by the original concentration of the mixture as follows:

$$\text{MGITC to protein ratio} = [\text{MGITC}]/[\text{IgG protein}]$$

$$[\text{MGITC}] = [(\text{optical density @ } 620\,\text{nm}) \times \text{dilution factor of sample}]/150{,}000\,M^{-1}\text{cm}^{-1}$$

$$[\text{IgG protein}] = [(\text{mass of antibodies/molecular weight of IgG}) + (\text{mass of BSA/molecular weight of BSA})]/\text{total volume of labelled antibody recovered from column}$$

The molecular weight of IgG is approximately 150,000 and for BSA it is 66,000.

13. Aliquot the concentrated antibody solution, quick freeze on dry ice, and store at –80°C, which will keep it viable for up to 6 months, after which time some of the dye dissociates from the antibody.

B. Antibody Loading

Steps

1. It is advisable to centrifuge the aliquots of MGITC-labelled antibody prior to cell loading to precipitate and thus separate any free dye from the labelled antibody solution. Free MGITC is toxic to cells, whereas bound MGITC is not.

2. Using the supernatant collected, perform loading as per the following suggestions. Labelled antibodies raised against extracellular or cell surface proteins can be applied directly to cells in culture or injected into tissue *in vivo*. For intracellular protein targets, MGITC-labelled antibodies can be loaded using trituration (Borasio *et al*., 1989; see article by Clarke *et al*.), microinjection, lipofection, or electroporation. Generally, the cell type dictates the type of loading permissible, with

neurons requiring microinjection or trituration, and nonneuronal cells being more tolerant of lipofection or electroporation. Cells sensitive to increases in intracellular calcium (i.e., neurons) can be loaded and washed in calcium/magnesium-free HBSS. To confirm loading, cells can be coloaded with either nonimmune FITC-IgG (i.e., Cat. No. F6397, Sigma) or FITC-dextran (Cat. No. D-7168, Molecular Probes). Because free, unbound dye in the MGITC–antibody solution is toxic, loading should not take any longer than 5 min to minimize the exposure of cells to the antibody solution.

3. For trituration loading, treat cells with 0.25% trypsin (Sigma) in HBSS for 15 to 30 min at 37°C, although this step will depend on cell type.

4. Wash cells in HBSS or Ca^{2+}/Mg^{2+}-free HBSS.

5. Remove most of the HBSS and add the MGITC-labelled antibody solution (50 µl or less). Cells are trituration loaded by gently but rapidly passing the cells through either a P200 pipetteman tip about 50 times or through a fire-polished (tip diameter 0.5 mm or less) glass pipette about 5–10 times. It is important that bubbles are not formed during trituration, as exposure of cells to air will reduce their viability.

6. Wash cells immediately after loading via centrifugation at low rpm (30 s at 1400 *g* on a Costar WX4241A minicentrifuge, Cat. No. EF4241A, Daigger Laboratory Supplies) to remove the antibody solution and gently resuspend in HBSS or Ca^{2+}/Mg^{2+}-free HBSS.

7. Wash cells again in HBSS and resuspend in cell culture medium prior to plating.

8. To confirm loading, use epifluorescence microscopy to locate cells that contain FITC-dextran or FITC-IgG as the loading marker. If cell viability is a concern, viability can be determined using the trypan blue dye exclusion test (de Costa *et al*., 1999). The half-life of MGITC-labelled antibodies in loaded cells will depend on the cell type. Six hundred and twenty-nanometer laser light penetration can be up to 5 mm; however, this depth will be highly dependent on tissue type, with shorter wavelengths penetrating less. To confirm effectiveness of CALI or penetration of laser light in previously loaded tissues *in vivo*, laser irradiation followed by immunohistochemistry of the target protein can be used to demonstrate loss of antigenicity through CALI-induced damage of the target protein (Sakuri *et al*., 2002).

IV. COMMENTS

Control Experiments for CALI

To establish a specific effect of CALI on a protein target, the following control experiments can be performed.

1. Cells that have not been loaded with antibody are exposed to laser light (no antibody, laser control) to exclude an effect of laser light alone.

2. Cells are loaded with preimmune MGITC-labelled IgG and exposed to laser light (IgG control) as an antibody specificity control and MG-labelled antibody control.

3. Cells are loaded with MG-labelled specific antibody without exposure to laser light (MG–antibody, no laser control) as a control for the non-function-blocking nature of the antibody and an MG toxicity control.

4. As a control for nonspecific free radical damage of neighboring proteins during CALI, cells can be loaded with an MG-labelled Fab fragment derived from an anti-Fc antibody (MG–anti-Fc). By directing this MG–anti-Fc against the unlabelled primary antibody, the MG is effectively positioned ~100 Å away from the antibody-binding site (Sakuri *et al*., 2002). Because the half-maximal radius for inactivation by MG is 15 Å (Liao *et al*., 1994), the additional distance from the antigenic site should yield no significant effect with laser irradiation.

5. *In vitro* CALI of an isolated protein preparation using an assay of protein function can be used to demonstrate loss of protein function that complements results of CALI from cell-based assays.

6. An assay of β-galactosidase function can be used as a positive control for CALI (Liao *et al*., 1994).

V. PITFALLS

1. The utility of CALI is determined in part by the retention of damaged protein in the cell region irradiated. Diffusion of unirradiated protein, degradation of damaged protein, or synthesis of new protein will determine the half-life of the effect of CALI in cells and tissues. Retention of labelled antibody will also determine the utility of CALI and will be cell type specific. For proteins subjected to CALI thus far, the effectiveness of CALI has been observed typically up to 10–15 h after loading (Diamond *et al*., 1993; Sakurai *et al*., 2002), while over 15 h after loading there can be considerable reduction in effectiveness (Sakurai *et al*., 2002).

2. An important consideration in the efficiency of CALI is the specificity of the antibody. The antibody may be highly specific for its intended epitope, sufficiently abundant inside or outside the cell, and optimally labelled with MGITC or FITC, but may still not have an effect on protein function if it binds to a site on the protein that is not essential for the biological function being tested. Polyclonal antibodies that rec-

ognize a greater number of epitopes on a single protein can partially circumvent this limitation, as could the use of more than one monoclonal antibody. In addition, addressing protein function at the level of more than one epitope can be helpful in elucidating the function of distinct protein domains.

3. Abundance of the native protein should be considered when determining the effectiveness of CALI. Because CALI is a knockdown strategy employing a limited number of antibodies per cell, typically less than 100% of the protein targeted is inactivated in an entire cell. Thus, it is technically difficult to inactivate a highly abundant intracellular protein, such as actin. Despite this limitation, most proteins will occupy a small percentage of the total protein in a given cell type, and antibodies targeted against extracellular domains of integral membrane proteins would not be so limited.

4. There are a number of considerations when selecting MGITC or FITC for applications utilizing CALI. First, FITC requires a 488-nm excitation wavelength of light. This wavelength has higher energy and is absorbed more readily by cells and tissues, which necessitates brief illumination periods with laser light, and cell viability tests with longer illumination periods using incandescent light. MGITC requires a longer excitation wavelength (620 nm), which not only has lower energy, but is also a wavelength not significantly absorbed by biological material. Second, FITC has been reported to be 50 times more efficient than MGITC in *in vitro* assays (Surrey *et al*., 1998). The half-maximal radius of inactivation of FITC (~40 Å; Beck *et al*., 2002) is 2.7 times greater than that of MGITC (15 Å). However, the inactivation radius of FITC is still half the average distance between proteins in a cell (80 Å; Linden *et al*., 1992). Therefore, although there is a greater chance of nonspecific effects of FITC-induced radical generation on neighboring proteins, appropriate control experiments can be used to rule out such effects. Third, unlike *in vitro* assays, cell-based assays contend with the scavenging of free radicals by endogenous scavengers. Ascorbate and glutathione scavenge hydroxyl radicals, and ergothioneine and carotenoids scavenge singlet oxygen (Chaudiere and Ferrari-Iliou, 1999). The relative abundance of these scavengers will determine the lifetime, and therefore the radius, of generated free radicals. Furthermore, scavenging ability is dependent on the antioxidant capacity of the cell (Beiswanger *et al*., 1995), with proliferating or tumorigenic cells in general displaying a greater capacity to deal with oxidative stress (for review, see Das, 2002). Fourth, oxidative damage resulting from irradiation of MGITC (hydroxyl radical) or FITC (singlet oxygen) occurs through distinct mechanisms. For the hydroxyl radical, hydroxylation of aromatic amino acids likely occurs through an addition reaction to form a hydroxycyclohexadienyl radical on the aromatic ring, which is then oxidized to form a phenol (Halliwell and Gutteridge, 1989). Singlet oxygen likely reacts with tryptophan, histidine, methionine, and cysteine. In general, the reactions are very complicated and can proceed through several mechanisms, yielding distinct decomposition products (Halliwell and Gutteridge, 1989). Finally, hydroxyl radical and singlet oxygen differ in their ability to react with amino acids. The second order rate constant (from Halliwell and Gutteridge, 1989) for the reaction of histidine with singlet oxygen is 30 times less ($10^8\ M^{-1}\ s^{-1}$) than the reaction with hydroxyl radical ($3 \times 10^9\ M^{-1}\ s^{-1}$), 300 times less for methionine (OH′ = $5.1 \times 10^9\ M^{-1}\ s^{-1}$, singlet oxygen = $1.7 \times 10^7\ M^{-1}\ s^{-1}$), and 283 times less for tryptophan (OH′ = $8.5 \times 10^9\ M^{-1}\ s^{-1}$, singlet oxygen = $3 \times 10^7\ M^{-1}\ s^{-1}$). Thus, singlet oxygen shows much less reactivity than hydroxyl radical to amino acids targeted by either radical, and the presence of endogenous scavengers may amplify these differences. In short, comparison of results of *in vitro*-based CALI assays and cell-based CALI assays, or of experiments using MGITC or FITC, should keep in mind the differences inherent to these applications.

References

Adams, S. R., Campbell, R. E., Gross, L. A., Martin, B. R., Walkup, G. K., Yao, Y., Llopis, J., and Tsien, R. Y. (2002). New biarsenical ligands and tetracysteine motifs for protein labelling *in vitro* and *in vivo*: Synthesis and biological applications. *J. Am. Chem. Soc.* **124**, 6063–6076.

Beck, S., Sakurai, T., Eustace, B. K., Beste, G., Schier, R., Rudert, F., and Jay, D. G. (2002). Fluorophore-assisted light inactivation: A high-throughput tool for direct target validation of proteins. *Proteomics* **2**, 247–255.

Beermann, A. E., and Jay, D. G. (1994). Chromophore-assisted laser inactivation of cellular proteins. *Methods Cell Biol.* **44**, 715–732.

Beiswanger, C. M., Diegmann, M. H., Novak, R. F., Philbert, M. A., Graessle, T. L., Reuhl, K. R., and Lowndes, H. E. (1995). Developmental changes in the cellular distribution of glutathione and glutathione S-transferases in the murine nervous system. *Neurotoxicology* **16**, 425–440.

Buchstaller, A., and Jay, D. G. (2000). Micro-scale chromophore-assisted laser inactivation of nerve growth cone proteins. *Microsc. Res. Tech.* **48**, 97–106.

Chaudiere, J., and Ferrari-Iliou, R. (1999). Intracellular antioxidants: From chemical to biochemical mechanisms. *Food Chem. Toxicol.* **37**, 949–962.

da Costa, A. O., de Assis, M. C., Marques Ede, A., and Plotkowski, M. C. (1999). Comparative analysis of three methods to assess viability of mammalian cells in culture. *Biocell* **23**, 65–72.

Das, U. N. (2002). A radical approach to cancer. *Med. Sci. Monit.* **8**(4), RA79–RA92.

Diamond, P., Mallavarapu, A., Schnipper, J., Booth, J., Park, L., O'Connor. T. P., and Jay, D. G. (1993). Fasciclin I and II have distinct roles in the development of grasshopper pioneer neurons. *Neuron* **11**, 409–421.

Diefenbach, T. J., Latham, V. M., Yimlamai, D., Liu, C. A., Herman, I. M., and Jay, D. G. (2002). Myosin 1c and myosin IIB serve opposing roles in lamellipodial dynamics of the neuronal growth cone. *J. Cell. Biol.* **158**, 1207–1217.

Grate, D., and Wilson, C. (1999). Laser-mediated, site-specific inactivation of RNA transcripts. *Proc. Natl. Acad. Sci. USA* **96**, 6131–6136.

Halliwell, B., and Gutteridge, J. M. C. (1989). "Free Radicals in Biology and Medicine," 2nd Ed. Clarendon Press, Oxford.

Jay, D. G. (1988). Selective destruction of protein function by chromophore-assisted laser inactivation. *Proc. Natl. Acad. Sci. USA* **85**, 5454–5458.

Liao, J. C., Roider, J., and Jay, D. G. (1994). Chromophore-assisted laser inactivation of proteins is mediated by the photogeneration of free radicals. *Proc. Natl. Acad. Sci. USA* **91**, 2659–2663.

Linden, K. G., Liao, J. C., and Jay, D. G. (1992). Spatial specificity of chromophore-assisted laser inactivation of protein function. *Biophys. J.* **61**, 956–962.

Marek, K. W., and Davis, G. W. (2002). Transgenically encoded protein photoinactivation (FlAsH-FALI): Acute inactivation of synaptotagmin I. *Neuron* **36**, 805–813.

Rajfur, Z., Roy, P., Otey, C., Romer, L., and Jacobson, K. (2002). Dissecting the link between stress fibres and focal adhesions by CALI with EGFP fusion proteins. *Nature Cell Biol.* **4**, 286–293.

Rubenwolf, S., Niewohner, J., Meyer, E., Petit-Frere, C., Rudert, F., Hoffmann, P. R., and Ilag, L. L. (2002). Functional proteomics using chromophore-assisted laser inactivation. *Proteomics* **2**, 241–246.

Sakurai, T., Wong, E., Drescher, U., Tanaka, H., and Jay, D. G. (2002). Ephrin-A5 restricts topographically specific arborization in the chick retinotectal projection *in vivo*. *Proc. Natl. Acad. Sci. USA* **99**, 10795–10800.

Surrey, T., Elowitz, M. B., Wolf, P. E., Yang, F., Nedelec, F., Shokat, K., and Leibler, S. (1998). Chromophore-assisted light inactivation and self-organization of microtubules and motors. *Proc. Natl. Acad. Sci. USA* **95**, 4293–4298.

SECTION

13

Protein/DNA Interactions

CHAPTER

41

Chromatin Immunoprecipitation (ChIP)

Valerio Orlando

I. INTRODUCTION

Current notion of chromatin *in vivo* tends to include any component, DNA, RNA, histone and non-histone proteins that by interacting with defined chromosomal regions contribute to gene specific, as well as global aspects of gene regulation and in general all DNA-dependent processes that take place inside the nucleus of eukaryotic cells.

Chromatin immunoprecipitation (ChIP) is a deductive *in vivo* method that allows the investigation of any chromatin component in its natural context (Orlando, 2000). By this method, living cells are fixed with formaldehyde and fragmented chromatin is subjected to immunoprecipitation. After reversal of crosslinks, specific genomic fractions obtained by immunopurification can be analyzed by semiquantitave methods like conventional PCR, real-time PCR and Southern hybridization. This method can be used to analyze the *in vivo* distribution of any factor and relate this to the activity of a particular gene or locus. Recent applications of the ChIP technology have also allowed the investigation of binding profiles of specific families of factors and core chromatin modifications on a genome wide scale. The completion of several genome projects and the development of microchips containing whole genome sequence arrays, in combination with the ChIP technology (ChIP on CHIP) has been giving a tremendous impulse to our understanding of genome biology.

II. MATERIALS AND INSTRUMENTATION

Tissue culture media: Serum free2 insect cell culture medium, (Hyclone HYQ-SFX, SH30278.02), Penicillin/Streptomycin 100 mg/ml (EuroClone ECB3001D)

Chemicals: Boric acid (BDH, 20185.291); CsCl, Biotechnology grade (EuroClone EMR 016001), 100% Ethanol (Merck); Ethylendiamine tetraacetic acid Sodium salt (Na-EDTA, Serva, 11278), Ethylene Glycol-bis (β-aminoethyl ether)-N,N,N′,N′-tetraacetic acid (EGTA, Calbiochem, 324626), Formaldehyde 37% solution (Sigma F1268), Hepes (Serva, 25245), Glycerol (J. T. Baker, 7044), Glycine (Serva 23390), Glycogen (New England Biolabs); LiCl (Serva, 28053), NaCl (J. T. Baker 1764), Na-acetate 3-hydrate (BDH, 10235 5P); (Phenol/Chloroform saturated with 100 mM Tris-HCl pH 8 (EuroClone, EMR 187100); Sodium Dodecyl Sulphate (SDS) (BDH 444464T), Tris (hydroxymethyl)methylamine (BDH 443866G)

Detergents: Nonidet P40 (NP40, Euroclone 181250), Triton X-100 (TX-100, Serva 37240), Na-deoxycholate Sodium-salt (Serva, 18330), Sarkosyl (N-Lauroyl-Sarkosine, Sigma L-9150)

Enzymes: Proteinase K (stock 20 mg/ml New England Biolabs); RNase DNase free (stock 10 mg/ml New England Biolabs); Taq Polymerase: EuroTaq (EuroClone, EME010001).

Copyright 2006, Elsevier Science (USA).
All rights reserved.

Glass beads (150–212 microns, acid washed, Sigma G-1145); Dialysis tubes (1/4 in., GIBCO, 15961)

Tubes (0.45 mm); Capillary tubes (50 µl Corning 7099S-50).

Instrumentation: Lab top centrifuge (Eppendorf 5415 R); Ultracentrifuge (Beckman L7-65); Rotor: Beckman SW55; Sonifier (Branson 250 or Misonix 200) equipped with a microtip (diam.: 0.2 cm) Refractometer (Horizon 2000); Peristaltic pump (Watson Marlow "Dirrel" 4661); Power supplies, (Pharmacia EPS200); Rotor wheel (FALC F200); Gel Doc 2000 (BIORAD); PCR (MJ PT200); Analytical balance (Sartorius).

III. PROCEDURES

The following protocol was readapted for *Drosophila* tissue culture cells from the one described for mammalian cells by Peggy Farnham and collegues (Weinmann *et al*., 2002).

Solutions:

1. Fixing solution: 11% Formaldehyde (from a 37% stock equilibrated with methanol), 100 mM NaCl, 1 mM Na-EDTA, 0.5 mM EGTA, 50 mM HEPES pH 8.0. To make 100 ml, 29.7 ml of 37% formaldehyde, 2 ml of a 5 M stock solution of NaCl, 1 ml of a 100 mM stock solution of Na-EDTA, 500 µl of a 0.1 M stock of EGTA and 5 ml of a stock solution of 1 M HEPES pH 8.

2. Phosphate Buffer Saline (PBS) pH 7.4

3. 2. Cell lysis buffer: 10 mM PIPES pH 8, 85 mM KCl, 0.5% NP40, proteinase inhibitors. To make 100 ml, 2 ml of a 0.5 M stock solution of HEPES pH8, 2.83 ml of a 3 M stock solution of KCl, 5 ml of a 10% NP40 stock solution and proteinase inhibitors

4. Nuclei lysis buffer: 50 mM Tris-HCl pH 8, 10 mM EDTA, 0.8% SDS, proteinase inhibitors. To make 100 ml, 5 ml of a 1 M stock solution of Tris-HCl pH8, 2 ml of a 0.5 M stock solution of Na-EDTA pH8, 0.4 ml of a 20% stock solution of SDS and protinase inhibitors.

5. 14. Dilution Buffer: 10 mM Tris-HCl pH 8, 0.5 mM EGTA, 1% Triton X-100, 140 mM NaCl, proteinase inhibitors. To make 100 ml, 1 ml of a 1 M stock solution of Tris-HCl pH8, 0.5 ml of a stock solution of EGTA, 10 ml of 10% Triton X-100 and proteinase inhibitors.

Steps

1. Grow 100 ml *Drosophila* Schneider SL-2 tissue culture cells (25°C, in serum free-medium, Hyclone, 100 U/ml penicillin, 100 µg/ml streptomycin) in cell culture bottles to a density of 3–6 × 10^6 per ml. See Section III, step 1.

2. Pour fixing solution (1/10th of volume of cells, 11 ml) directly into the flask and gently mix. Leave at 4°C for decided fixation time. Fixation time ranges between 5 min up to 1 hr and has to be adjusted empirically by checking the immunoprecipitation efficiency.

1. Stop HCHO fixation by adding solid glycine to 125 mM and mix well. Pellet cells into a 50 ml Falcon tubes (2000 rpm, 5 min., Hereaus Minifuge or eq.) and wash once with cold PBS.
2. Take up cell pellet into 15 ml of cell lysis buffer and leave on ice for 10 minutes. Spin down cells and take up pellet into 2 ml of nuclei lysis buffer, transfer 15 ml Falcon tubes and leave on ice for 10 minutes.

3. Add ca. 0.5 ml glass beads (100–212 microns, acid-washed). Store on ice.

4. Sonicate each aliquot, 3–6 × 30 sec. in 1 min intervals (output near microtip limit), using a high power sonicator (e.g. Branson 250 or Misonix XL). Each tube is cooled in a beaker with an ice/water mix. The sonicator-tip should be immersed roughly 1/4. Avoid foaming.

5. Transfer the suspension into 2 × 1.5 ml Eppendorf tubes (leaving most of the glass beads in the old tube) and spin for 10 min. at mix.-speed in a tabletop centrifuge in the cold room. Transfer supernatants to a 15 ml Falcon tube and add dilution buffer up to 8 ml. Rotate at 4°C for 10 min. on a wheel. Take an aliquot of 50 µl for DNA-analysis (Procedure B). Of the rest prepare aliquots of 1 ml and store at –80°C ore use the chromatin directly for immunoprecipitation (Procedure C).

B. Reversal of Crosslinks

In order to estimate the average size of the DNA and trace it along the gradient, remove about 1/10 vol (50 µl) of each fraction to a microfuge tube containing 50 µl and proceed for DNA purification (reversal of crosslinks). The same procedure (except for gel analysis) is performed after chromatin immunoprecipitation, before PCR analysis (Section III C, steps 6–7).

Solutions

1. TE: 10 mM Tris pH 8, 1 mM EDTA. To make 100 ml, 1 ml of a 1 M stock solution of Tris-HCl pH8, 200 µl of a 0.5 M stock solution of Na-EDTA pH8.

2. 20% SDS, Phenol/Chloroform, Chloroform, Na-acetate pH 5.2.

3. TBE 1× (agarose gel running buffer); to make 1 L of 5× TBE, add to 800 ml of autoclaved distilled water

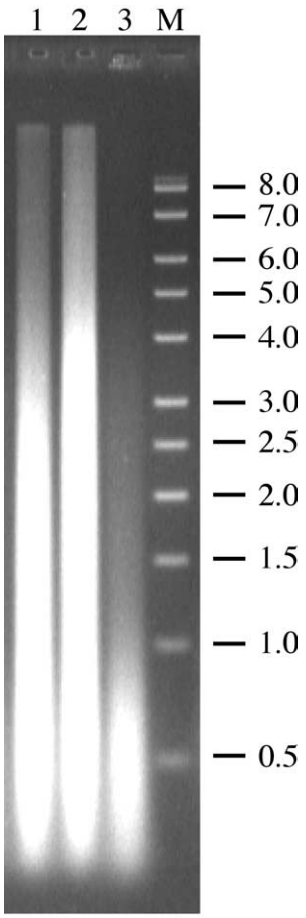

FIGURE 1. Determination of chromatin DNA average size after sonication. An aliquot of decrosslinked, purified *Drosophila* SL2 tissue culture cell chromatin DNA was analyzed on a 0.8% agarose gel. A comparison between samples sonicated with or without glass beads is shown. The presence of glass beads ensures a highly efficient and reproducible chromatin DNA shearing. Lane 1: 1% formaldehyde, 10 min crosslinking, no Glass beads. Lane 2: 1% formaldehyde, 20 min crosslink, no Glass beads; Lane 3: 1% formaldehyde, 10 min crosslinking, Glass beads (150–212 microns, acid washed, Sigma G-1145). Similar results were obtained with Drosophila embryos as well as with several mammalian tissue culture cells. Note that a considerable variability can be observed among various preparations depending on crosslinking conditions, sonicator device and operator.

27 g of Tris-HCl, 13.75 g of Boric acid, 10 ml of a 0.5 M stock solution of Na-EDTA. Fill up to 1 L with autoclaved distilled water.

4. 6× DNA loading buffer (Promega, DV 4371).

Steps

1. Add 50 µl of TE and incubate tubes overnight at 65°C.

2. Add Proteinase K (Sigma) to 500 µg/ml and SDS to 0.5%. Incubate at 50°C for ca. 3 h. Extract once with phenol-chloroform and once with chloroform. Precipitate chromatin DNA in the presence 0.3 M Na-acetate pH 5.2 with three volumes of ethanol.

3. Spin 30 min wash in 70% ethanol. During centrifugation pour a 0.8% agarose gel.

4. Take up pellets in 10 µl of TE. Add RNase A to 10 µg/ml and incubate 30 min at 37°C. Add 2 µl of 6× loading buffer (Promega). Load and run the gel in 1× TBE 10–15 cm.

5. Stain gel by 0.5 µg/ml ethidium bromide. Take a picture with a GelDoc apparatus (Biorad) or Polaroid film.

C. Immunoprecipitation

Prior to immunoprecipitation of fixed chromatin it is absolutely necessary to test the antibody to check its compatibility with crosslinked material and certain detergents. Normally, "ChIP quality" of the antibody maybe anticipated by its performance in immunohistochemistry, as the crosslinking agent is often the same. (formaldehyde or para-formaldehyde). Pilot immunoprecipitation experiments using protein extracts or a purified antigen may be performed to check compatibility with certain detergents. The conditions described below work well, especially for rabbit polyclonal antibodies and are considered to be very stringent. Noteworthy, due to the growing interest for histone modifications, and the intrinsic problems of immuno-responsiveness, particular care should be taken in the choice of the commercially available antisera (Perez-Burgos *et al*., 2003). Particularly for the analysis of histone modifications, the use of non-crosslinked chromatin immuno-precipitation approaches (N-ChIP) and specific immuno-reagents that would recognize non-fixed epitopes, may be considered as a highly valuable alternative to X-ChIP (O'Neill and Turner, 2003).

Solutions

1. RIPA buffer (10 mM Tris-HCl pH 8, 1 mM EDTA pH 8.0, 0.5 mM EGTA, 1% Triton X-100, 0.1% Na-Deoxycholate, 0.1% SDS, 140 mM NaCl, 1 mM PMSF). To make 100 ml, 1 ml of a stock solution of 1 M Tris-HCl, pH 8, 200 µl of a stock solution of 0.5 M Na-EDTA, 0.5 ml of a 0.1 M EGTA stock solution, 10 ml of a 10% Triton X100 stock solution, 1 ml of 10% stock solution of Na-Deoxycholate, 0.5 ml of a 20% SDS stock solution.

6. LiCl-buffer (0.25 M LiCl, 0.5% NP 40, 0.5% Na-Deoxycholate, 1 mM Na-EDTA, 10 mM Tris-HCl, pH 8). To make 100 ml, 5 ml of a 5 M stock solution of LiCl, 5 ml of a 10% stock solution of NP40, 5 ml of a 10% stock solution of Na-Deoxycholate, 1 ml of Tris-HCl pH8 and 200 µl of EDTA.

7. TE (1 mM Na-EDTA, 10 mM Tris-HCl, pH 8), To make 100 ml, 1 ml of a stock solution of 1 M Tris-HCl pH 8, 200 µl of a stock solution of 0.5 M Na-EDTA.

8. Protein A Sepharose beads CL4B (PAS) (Sigma, P 3391) or Protein A/G-PLUS Agarose (Santa Cruz Biotechnology, sc 2003).

Steps

1. Swell PAS by adding 1 vol of RIPA buffer to 1 vol (e.g. 200 µl) of PAS. Rotate on a wheel for 10–20 min at RT. Spin for 5 sec in Eppendorf centrifuge. Take up supernatant and re-suspend PAS in 1 vol of RIPA.

2. Adjust one aliquot (500 µl) of purified chromatin to immunoprecipitation conditions (RIPA buffer). To make a 800-µl suspension add sequentially: 80 µl of a 10% stock solution of Triton X-100, 8 µl of a 10% stock solution of Na-Deoxycholate, 4 µl of 20% stock solution of SDS, 22.4 µl of 5 M stock solution of NaCl, 4 µl a 0.1 M stock solution of EGTA.

3. As a preclearing step, add 20 µl of 50% PAS previously swollen and equilibrated in RIPA (step 1). Incubate for 1–2 hour at 4°C for pre-clearing and spin for 5 minutes in a tabletop centrifuge (14,000 rpm, 4°C).

4. Transfer supernatant to a new tube and add the appropriate amount of antibody (usually dilutions of 1 : 100, 1 : 500). Do not overload with antibody: this will result in higher non-specific immunoprecipitation. The same amount of precleared chromatin is used as negative control, without the addition of antibody (mock-control). Incubate the samples overnight at 4°C on a wheel.

5. Spin samples 10 min. in a tabletop centrifuge (14,000 rpm, 4°C). Transfer supernatants to 1.5 ml new tubes. Add 20 µl of the 50% PAS suspension. After incubation for further 2–4 hours wash the PAS-pellet 5 times with 600 µl of RIPA buffer, 1× with 600 µl LiCl-buffer and 1× with 600 µl TE (pH 8). Always pellet the beads with short spins (15″ max speed) with a tabletop centrifuge. At the end, take up PAS pellet in 100 µl of TE.

6. Add 1 µg of RNAse (DNAse-free), incubate at 37°C for 30 min. Incubate samples overnight at 65°C.

7. Next day adjust samples to 0.5% SDS and 0.5 mg/ml proteinase K and incubate for 3 more hours at 50°C. Phenol-Chloroform extract the samples. Back-extract the phenol phase by adding an equal volume of TE (pH 8). Combine the aqueous phases and chloroform extract. Precipitate DNA by adding Glycogen to 100 µg/ml as carrier, 1/10 volume of 3 M sodium acetate pH 5.2 and 3 volumes of 100% ethanol. Incubate at –20°C for some hours up to overnight. Spin down DNA and wash pellet in 70% ethanol, air dry briefly and re-suspend the precipitated DNA in 15–50 µl of TE (depends on initial input material) and store at 4°C (do not freeze) for PCR analysis (Section V).

IV. PURIFICATION OF *IN VIVO* FIXED CHROMATIN FROM DROSOPHILA SL2 (OR MAMMALIAN) TISSUE CULTURE CELLS VIA CSCL GRADIENT

This procedure was described in Solomon and Varshavsky, 1988 and readapted by Orlando and Paro, 1993). Its application is now limited to particular cases in which insoluble macromolecular complexes may interfere with immunoprecipitation efficiency (Schwartz et al., 2005)

Solutions

5. Fixing solution: 11% Formaldehyde (from a 37% stock equilibrated with methanol), 100 mM NaCl 1 mM Na-EDTA, 0.5 mM EGTA, 50 mM HEPES pH 8.0. To make 100 ml, 29.7 ml of 37% formaldehyde, 2 ml of a 5 M stock solution of NaCl, 1 ml of a 100 mM stock solution of Na-EDTA, 500 µl of a 0.1 M stock of EGTA and 5 ml of a stock solution of 1 M HEPES pH 8.

6. Phosphate Buffer Saline (PBS) pH 7.4

7. Wash solution A: 10 mM Tris-HCl pH 8.0, 10 mM Na-EDTA pH 8.0, 0.5 mM EGTA pH 8.0, 0.25% Triton X100. To make 200 ml, 2 ml of a stock solution of 1 M Tris-HCl pH 8, 8 ml of a stock solution of 0.5 M Na-EDTA, 1 µl of a 0.1 M EGTA stock solution, 5 ml of a 10% Triton X100 stock solution.

8. Wash solution B: 10 mM Tris-HCl pH 8.0, 1 mM Na-EDTA pH 8.0, 0.5 mM EGTA pH 8.0, 200 mM NaCl, 0.01% Triton X100. To make 200 ml, 2 ml of a stock solution of 1 M Tris-HCl pH 8, 400 µl of a stock solution of 0.5 M Na-EDTA, 1 ml of a 0.1 M EGTA stock solution, 8 ml of a 5 M NaCl stock solution.

9. Wash solution C: 10 mM Tris-HCl pH 8.0, 1 mM Na-EDTA pH 8.0, 0.5 mM EGTA pH 8.0. To make 200 ml, 2 ml of a stock solution of 1 M Tris-HCl pH 8, 400 µl of a stock solution of 0.5 M Na-EDTA, 1 ml of a 0.1 M EGTA stock solution.

Steps

1. Grow cells at a convenient density ($3–6 \times 10^6$ for *Drosophila* SL2 cells or similar for mammalian cells). The criterion to calculate the amount of cells to be grown is that one needs at least 20–30 microgram DNA per immunoprecipitation. If one assumes that the DNA content of a diploid Drosophila cell nucleus is 0.4 pg, then 1×10^9 cells would contain about 0.4 mg of total DNA. The *Drosophila* genome is ten times less

complex than mammalian genome. Thus, if mammalian cells are to be used, the initial cell input may be changed accordingly, though depending on the antigen and efficiency of immunoprecipitation this may also be unnecessary.

2. Add 1/10 vol/vol of fixing solution to obtain a final concentration of 1% formaldehyde. Fixation time ranges between 5 min up to 1 hour and has to be adjusted empirically.

3. Stop fixation by adding Glycine powder to a final concentration of 0.125 M. Solubilize glycine by gentle shaking.

4. Pellet cells in 50 ml Falcon tubes spun at 700 xg for 5 min.

5. Take up pellets in 15 ml PBS and repeat centrifugation as in step 4.

6. Take up pellets in 15 ml Solution A and gently shake or rotate for 10 min.

7. Centrifuge as in step 4.

8. Take up pellets in 15 ml of Solution B and procede as in steps 6–7.

9. Take up pellet in 5 ml of solution C.

10. Add approximately 1/3 vol/vol of acid-washed glass beads.

11. Sonicate sample (chilled on ice) by 3–5 × 30 sec bursts. Let the tubes rest on ice for approximately 1 min between each burst.

12. Add 250 µl of 10% Sarkosyl (0.5% final concentration).

13. Transfer suspension in 1.5 ml Eppendorf tubes and let rotate on a wheel for 20 min.

14. Spin debris for 5 min in Eppendorf centrifuge at maximum speed. Take up supernatant and transfer to new tubes.

B. Chromatin Purification by Isopycnic Centrifugation

Solutions

3. Dialysis buffer (TEE): 10 mM Tris pH 8, 1 mM EDTA, 0.1 mM EGTA, 5% glycerol. To make 1 L, 10 ml of a 1 M stock solution of Tris-HCl pH 8, 2 ml of a 0.5 M stock solution of Na-EDTA, 5 ml of a 0.1 M stock solution of EGTA.

4. TE: 10 mM Tris pH 8, 1 mM EDTA. To make 100 ml, 1 ml of a 1 M stock solution of Tris-HCl pH8, 200 µl of a 0.5 M stock solution of Na-EDTA pH8.

Steps

1. Add 2.84 g (0.568 g per ml of cell lysate) of CsCl powder to cell lysate (approximately 4 ml) in 15 ml Falcon tube. Mix gently until the salt has dissolved. Adjust volume to 5 ml with buffer TEE supplemented with 0.5% Sarkosyl. Final density should be 1.42 g/cm^3.

2. Check density with a refractometer or by weighing the suspension on a analytical balance.

3. Transfer the solution into a 5 ml polyallomere Beckman tube (for Beckman SW55 rotor). Spin at 40,000 rpm (Beckman L7-65 ultracentrifuge, SW55 rotor) at 22°C for at least 24 hours.

4. Elute 10 × 50 µl fractions per gradient with a peristaltic pump at about 1 ml/min with tubings of 0.045 inches internal diameter (#1 bottom—#10 top). Alternatively, carefully pipette from the top layer of the gradient 10 × 500 µl aliquots with a Gilson pipette. Check the density profile of fractions with a Refractometer or by weighing each fraction on an analytical balance. The peak-fraction of crosslinked chromatin should have a density of 1.39 g/cm^3. Routinely, chromatin is found at gradient fractions spanning density values between 1.350 and 1.450 g/cm^3.

5. Dialyse fractions in dialysis bags against 300 volumes (approx. 1.5 L) of dialysis buffer. After 2 h, change the buffer and continue dialysis overnight.

For chromatin-IPs, fractions that contain the crosslinked chromatin (usually fractions 3–4) are pooled and re-aliquoted in 500 µl aliquots. Chromatin suspension can be either directly processed for immunoprecipitation of stored at –80°C (stable for several months).

V. ANALYSIS OF IMMUNOPRECIPITATED CHROMATIN AND BINDING SITES IDENTIFICATION

A. PCR analysis

When the sequence of the target region of the protein of interest is known, the immunopurified DNA can be directly used as template for a semi-quantitative PCR using primer pairs that span the putative binding sites. In this case amplification is obtained if protein binding occurs, otherwise no amplification will be obtained. Primer pairs (melting temperature 64–68°C, around 25 bp) amplifying 400–500 bp fragments in the target region of interest are designed with the appropriate software, e.g., Proligo®, www.proligo.com). For each primer pair the optimal magnesium concentration (1–2 mM $MgCl_2$) has to be assayed with 200 ng of total genomic DNA from SL-2 culture cells.

Perform PCR in 25–40 µl reactions with the immunoprecipitated material and the genomic control

with the optimal magnesium concentration for each primer pair using 1–3 µl of the immunoprecipitated DNA (in 1× reaction buffer, 0,25 mM NTPs, 1 µM primer, 0,5 U Taq polymerase). PCR scheme: 1. 94°C, 3 min, 1×, 2. 94°C, 1 min, 60–65°C, 1 min, 72°C, 1 min, 28×; 3. 94°C, 1 min, 60–65°C, 1 min, 72°C, 7 min; 1×.

For individual primer pairs the annealing temperature and number of cycles may have to be adjusted until no signal is detected for the mock-ip DNA, but the amplification on the genomic template is not altered. Signals obtained with the antibody-ip DNA under these conditions are considered as significant. After the amplification add gel loading buffer and separate half of the reaction on a 1.5% agarose gel and visualize amplified DNA with ethidium bromide.

In order to allow decisions whether the protein of interest or its enzymatic products are significantly presenta a given site in the genome, the measurement of target DNA in the ChIP fraction is analyzed by PCR.

The enrichment for a given ChIP product is function of the relative amount of selected PCR product detected and it should always be higher than the control IP product. This can be measured by quantifying each of the PCR band products by conventional software (e.g., ImageQuant®, or QuantityONE®). The intensities of resolved bands are quantified and plotted in a diagram as percentage of the total input, the total of chromatin DNA used for the immunoprecipitation. In order to have an internal control, it is convenient to have on the same gel serial dilutions of the input. In some cases, a useful control is to include in the analysis promoter sequences of another genes that are likely not to contain the same factors.

When possible, RealTime PCR methodology should be used. The two methods do not differ in terms of "biological significance" of the data produced; RealTime PCR is way less time consuming as it measures the amount of PCR product present in the reaction at a given time point (in particular during the exponential phase) and also gives a direct graphic representation of the measurements as compared to control reactions and input DNA standards.

In all cases, it is imperative to compare ChIP results obtained in functionally distinct contexts, e.g., the same ip performed on the same regulatory region in two different transcription states of the same gene.

Finally, it has to be emphasized that, when comparing ChIP results between different antisera, as each antibody would work different, the ChIP method per se cannot be considered quantitative. This is due to the different precipitation efficiencies of the diverse antisera, thus it is not possible to compare signal intensities from one immunoprecipitation to another when analyzing the same PCR amplification product obtained with different antisera. Thus, conclusions or comparisons regarding the amounts of the various proteins present in the same region are not feasible.

Current models in gene regulation favor a highly dynamic organization of the eukaryotic nucleus (Osborne *et al*., 2004). Thus, the intensities obtained from the quantification of the PCR-amplified immunopurified DNA, may not be considered as an indication for the amount of protein or number of molecules bound to a certain region, but rather as a rate of turnover, a measure for the presence of the molecules of a protein at a certain region at the timepoint of fixation. High intensities would correspond to proteins (or their enzymatic product) present at a genomic region in most of the cells at the timepoint of fixation and *viceversa*. However, the on/off rate of regulatory factors and multienzymatic complexes from DNA *in vivo* is in the order of milliseconds. That leads to the conclusion that ChIP enrichments simply testify the mean/event situation represented by million cells at the time of fixation and applied to one ideal cells. Indeed, as ChIP technology works in the range of minutes, the ultimate limit of this technology if talking about single cell reality, may remain the resolution and determination of which factor would be actually present on a particular sequence at the exact time when a given event is taking place.

VI. SINGLE LOCUS UP TO GENOME WIDE ANALYSIS OF CHIP DNA

There are further ways to analyze of immunoprecipitated chromatin. ChIP anaylysis can be performed over a large genomic region or entire chromosomes, by using the immunoprecipitated DNA as a probe in a Southern analysis. This approach has been successfully used in *Drosophila* (Orlando and Paro, 1993; Orlando *et al*., 1997; Strutt *et al*., 1997; Orlando *et al*., 1998).

An extension of this is the ChIP on CHIP approach, in which the ChIP probe is used to hybridize a genomic microchip. This approach appears to be a highly powerful way to gain insights on direct targets and genome wide distribution of any chromosome associated regulatory protein factor. Details about these applications can be found in the web sites of the Rick Young and Peggy Farnham laboratories (see below and Ren *et al*., 2000; Lee *et al*., 2002; Weinmann *et al*., 2002; Cawley *et al*., 2004). There procedures will not be described here as working protocols.

Amplification of Immunoprecipitated DNA

This procedure can be used to amplify ChIP DNA for both Southern analysis and ChIP on CHIP experiments in *Drosophila* or mammalian cells. Due to the heterogeneity of the immunoprecipitated chromatin DNA, a linker modified DNA PCR strategy is carried out (Strutt *et al*., 1997; Orlando *et al*., 1998). The adapter is prepared as follows: two oligonucleotides, a 24-mer of sequence 5′AGAAGCTTGAATTCGAGCAGTCAG, and a 20-mer of sequence 5′CTGCTCGAATTCAA GCTTCT, are synthesized. Only the 24-mer should be 5′ phosphorylated. Equimolar amounts of the two oligonucleotides are mixed and allowed to anneal. Immunopurified-chromatin DNA (approx. 1 ng) is resuspended in 9 µl ligase buffer (12.5 mM $MgCl_2$, 25 mM DTT, 1.25 mM ATP, 50 mM Tris-HCl, pH 7.6) containing 0.1 µM final concentration of linker. Ligation is carried out by the addition of 4U of T4 DNA ligase (Boehringer) incubation at 4°C for 24 hr. Pilot experiments with digested or sonicated genomic DNA should be performed in advance to test all reagents. To this aim, a fixed amount of ChIP DNA (ranging between 0.1 to 10 ng of DNA) should be tested with various concentrations of linkers (0.1 to 10 micromolar).

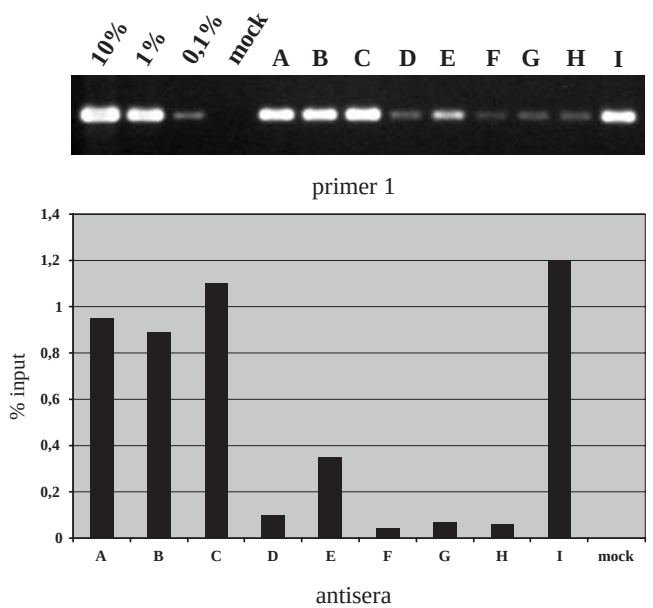

FIGURE 2 An example for the analysis of protein presence at a specific site using X-ChIP. A gel resulting from precipitations of chromatin with various antibodies (A–I) is shown on top. PCR reactions with 10, 1 and 0.1% of the input DNA are loaded to determine the linear range of amplification. Below the gel, a quantitative analysis of ethidium bromide-stained bands is shown. Values on the *y* axis represent the amount of immunoprecipitated DNA as a percentage of the input.

The ligated mixture is directly used as a template in a 100 µl PCR reaction using Taq I polymerase and 1× corresponding buffer. The primer used is the 20-mer oligonucleotide described above added to a final concentration of 1 µM. Amplifications is performed using one cycle of 94°C, 2 min; 35 cycles of 94°C, 1 min, 55°C, 1 min, 72°C, 1 min; 1 cycle of 94°C, 1 min, 55°C, 1 min, 72°C, 10 min.

After PCR, PCR products should be analyzed on a 1.2% agarose gel. Linkers are designed in a way that they can be eliminated by HindIII digestion. ChIP DNA is then purified through a PCR purification kit (Qiagen).

Southern analysis and DNA binding sites mapping

When the immunopurified DNA is used a probe, prior to radiolabeling the amplified DNA is freed from linkers. After PCR samples are extracted once with pheno-chloroform and once with chloroform-isoamylalcohol, and ethanol precipitated. Linkers are removed by digesting the DNA with HindIII and separated by gel filtration (Chroma-spinTE100, Clontech or QiaQuick PCR purification kit (Qiagen)). An aliquot with linkers may be saved to be used as reservoir.

DNA probes are routinely labeled by oligonucleotide random-primed DNA synthesis with α (^{32}P)-dCTP (Specific activity 3000 Ci/mmol, Amersham).

The hybridization procedure is the one described by Church and Gilbert (1984) with nylon membranes (Gene Screen Plus) preferably baked at 80°C for 2 hr. Briefly, prehybridization is done for 3 hr at 65°C in 7% SDS, 1 mM EDTA, 1% BSA, 0.5 M Na_2HPO_4 (pH 7.2), heat-denatured DNA directly added to prehybridization solution. Filters are washed at 65°C once in 5% SDS, 1 mM Na-EDTA, 0.5% BSA, 40 mM Na_2HPO_4 for 10 min and at least 4 times for 5 min in the same buffer but containing 1% SDS. This protocol seems to guarantee practically no background. This allows, when necessary, the use of higher quantities of probe (up to 50–100 ng/ml) in order to partially compensate for dilution due to its peculiar complexity.

For a more sensitive and quantitative analysis of the hybridization signals a Phosphorimager is used.

PhosphorImager analysis

The identification of a binding site *in vivo* is based on the analysis of the enrichment of specific genomic regions obtained by ChIP. Therefore, determining the baseline as background value above which a given fragment is "elected" as an *in vivo* binding site is crucial. To this aim Southern analysis results are carefully processed by PhosphorImager analysis.

While analyzing Southern hybridization results, specific criteria have to be followed. In particular, the intensity of a hybridization signal is proportional to M_r, and the resulting values should be normalized with respect to M_r.

The amount of signal is given in arbitrary units by the ImageQuant® software or equivalent (e.g., QuantityOne® by Biorad), as a result of the integration of a selected area on the screen corresponding to the band. The absolute value is obtained by dividing the quantitation value by the kb of the fragment. The choice of the Mr set as a reference may reflect the average size of the chromatin fragments (0.5–1 kb). The relative intensity value will be calculated by subtraction of the "background" value obtained from the hybridization and quantification of the corresponding signal on the same fragment obtained by using a mock DNA probe (control/non-enriched). The mock IP probe should hybridize approximately uniformly to all fragments (dependent on M_r).

It has to be mentioned that repetitive elements are always strongly enriched in immunoprecipitations and therefore hybridize strongly to all immunoprecipitated DNA probes. These elements can be identified by their strong hybridisation obtained when genomic DNA is to be used as a probe.

Finally, all relative values of individual genomic restriction fragments may be aligned and plotted against the genomic region of interest, representing the distribution *in vivo* of the protein of interest.

CONCLUSION

In general, ChIP should not be considered as a confirmatory technique. Conversely, ChIP should be used as diagnostic method challenging the *in vivo* distribution of proteins in chromosomes. As more and more novel mechanisms and genetic pathways controlling gene expression are being discovered, several surprises coming from ChIP studies can be anticipated. Moreover, the completion of genome projects and the construction of high resolution genomic microarrays combined with ChIP (ChIP on CHIP) provide unique tools for genome wide target gene identification, epigenetic landscaping and genetic network decoding. However, before embarking on a ChIP-trip, clear cut functional experiments should be planned to help to validate any anticipated result and in most cases try learn directly from chromosomes, what we do not know yet.

References

Cawley, S., Bekiranov, S., Ng, H., Kapranov, P., Sekinger, E. A., Kampa, D., Piccolboni, A., Sementchenko, V., Cheng, J., Williams, A. J., Wheeler, R., Wong, B., Drenkow, J., Yamanaka, M., Patel, S., Brubaker, S., Tammana, S., Helt, G., Struhl, K., and Gingeras, T. R. (2004). Unbiased Mapping of Transcription Factor Binding Sites along Human Chromosomes 21 and 22 Points to Widespread Regulation of Noncoding RNAs. *Cell* **116**, 499–509.

Church, M. G., and Gilbert, W. (1984). Genomic sequencing. *Proc. Natl. Acad. Scie. USA* **81**, 1991–1995.

Lee, T. I., Rinaldi, N. J., Robert, F., Odom, D. T., Bar-Joseph, Z., Gerber, G. K., Hannett, N. M., Harbison, C. R., Thompson, C. M., Simon I., Zeitlinger J., Jennings, E. G., Murray, H. L., Gordon, D. B., Ren, B., Wyrick, J. J., Tagne, J., Volkert T. L., Fraenkel, E., Gifford, D. K., and Yong, R. A. (2002). Transcriptional Regulatory Networks in *Saccharomyces cerevisiae*. *Science* **298**, 799–804.

O'Neill, L. P., and Turner, B. M. (2003). Immunoprecipitation of native chromatin: N-ChIP. *Methods* **31**, 76–82.

Orlando, V., and Paro, R. (1993). Mapping Polycomb represseddomains in the bithorax complex using *in vivo* formaldehyde cross-linked chromatin. *Cell* **75**, 1187–1198.

Orlando, V., Strutt, H., and Paro, R. (1997). Analysis of chromatin structure by *in vivo* formaldehyde cross-linking. *Methods* **11**, 205–214.

Orlando V., Jane, E., Chinwalla, V., Harte, P. J., and Paro R. (1998). Binding of Trithorax and Polycomb proteins to the bithorax complex: dynamic changes during early embryogenesis. *EMBO J.* **17**, 5141–5150.

Orlando, V. (2000). Mapping chromosomal proteins *in vivo* by formaldehyde crosslinked-chromatin immunoprecipitation. *Trends Biochem Scie.* **25**, 99–104.

Osborne, C. S., Chakalova, L., Brown, K. E., Carter, D., Horton, A., Debrand, E., Goyenechea, B., Mitchell, J. A., Lopes, S., Reik, W., Fraser, P. (2004). Active genes dynamically colocalize to shared sites of ongoing transcription. *Nat. Genet.*, **36**, 1065–1071.

Perez-Burgos, L., Peters, A., Opravil, S., Kauer, M., Mechtler, K., and Jenuwein, T. (2003). Generation and characterization of methyllysine histone antibodies. *Methods in Enzymology* **376**, 234–254.

Ren, B., Robert, F., Wyrick, J. J., Aparcio, O., Jennings, E. G., Simon, I., Zeitlinger, J., Schreiber, J., Hannett, N., Kanin, E., Volkert, T. L., Wilson, C. J., Bell, S. P., and Young, R. A. (2000). Genome-wide location and function of DNA binding proteins. *Science* **22**, 2306–2309.

Schwartz, Y. B., Kahn, T. G., and Pirrotta, V. (2005). Characteristic low density and shear sensitivity of cross-linked chromatin containing polycomb complexes. *Mol. Cell. Biol.* **25**, 432–439.

Solomon, M. J., Larsen, P. L., and Varshavsky, A. (1987). Mapping protein-DNA interactions *in vivo* with formaldehyde: evidence that histone H4 is retained at a highly transcribed gene. *Cell* **37**, 937–947.

Weinmann, A. S., Yan, P. S., Oberley, M. J., Huang, T. H., and Farnham, P. J. (2002). Isolating human transcription factor targets by coupling chromatin immunoprecipitation and CpG island microarray analysis. *Genes Dev.* **16**, 235–244.

C H A P T E R

42

Gel Mobility Shift Assay

Peter L. Molloy

I. INTRODUCTION

Because they are conceptually simple and also relatively straightforward to perform practically, gel mobility shift assays (otherwise known as gel retardation or electrophoretic mobility shift assays) have become one of the most widely used techniques in molecular and cell biology. They provide a key point of entry for identification of protein–DNA interactions important for regulation of gene expression. The discussion in this article focuses on DNA-binding proteins in relation to transcriptional control, but similar principles apply to the use of gel mobility shift assays to study protein/DNA interactions in other processes (replication, recombination, and repair), as well as proteins involved in RNA metabolism. The assay relies on the increased molecular size and decreased charge : mass ratio of a protein–DNA complex compared to free DNA and the observation that many protein–DNA complexes are stable through electrophoresis. Specific protein–DNA complexes can therefore be readily distinguished from free DNA by their slower mobility during electrophoresis. The use of labelled DNA probes in gel mobility shift assays enables visualisation of the specific complexes even in complex protein mixtures. The format of the assays allows both characterisation of DNA sequence requirements for protein binding and characterisation or identification of the proteins involved in complex formation, linking back to the cellular regulatory networks controlling gene expression.

II. MATERIALS AND INSTRUMENTATION

Electrophoresis requires a power supply capable of supplying approximately 30 mA at 200 to 300 V. Conditions described are for a vertical gel apparatus with 20 × 20-cm plates and 0.75- to 1-mm spacers. Conditions can be scaled down for a minigel apparatus, e.g., Bio-Rad 8 × 7.3 cm.

General chemicals should all be analytical reagent grade. Solutions for DNA-binding reactions should be prepared using nuclease-free water and reagents. HEPES (Cat. No. H4034), Nonidet P-40 (identical to Igepal CA-630, Cat. No. I8896), and dithiothreitol (DTT, Cat. No. D5545) can be purchased from Sigma Chemical Co. Nonspecific competitor polynucleotides, poly(dI-dC) · poly(dI-dC), poly(dG-dC) · poly(dG-dC), and poly(dA-dT) · poly(dA-dT) are available from Amersham Biosciences, (Cat. Nos. 27-7880-02, 27-7910-02, and 27-7870-02, respectively). Nuclease-free bovine serum albumin (BSA) can be purchased from Promega. Restriction enzymes, Klenow fragment of DNA polymerase 1, T4 polynucleotide kinase, and premixed acry-lamide solutions are available from a number of suppliers.

Radioactive nucleotides [α-^{32}P]dATP or dCTP (>3000 Ci/mmol, 10 mCi/ml) and [γ-^{32}P]ATP (>3000 Ci/mmol, 10 mCi/ml) can be purchased from Amersham Biosciences. Reagents for nonradioactive labelling of DNA probes are also available, e.g., digoxygenin-labelling kit from Roche Applied Science and chemiluminescent kit from Pierce. Direct post-

Copyright 2006, Elsevier Science (USA).
All rights reserved.

electrophoresis staining for DNA and protein components of complexes using sensitive dyes are now also possible (Jing *et al.*, 2002)

Nuclear extracts and related reagents, including specific oligonucleotide sets, are available from Promega, and a kit for nuclear extract preparation can be purchased Pierce. A wide range of antibodies targeted to transcription factors and other DNA-inding proteins is available from Santa Cruz Biotechnology, Inc. and also Chemicon; both catalogues indicate which antibodies are suitable for "supershifting." A range of individual protease inhibitors and prepared cocktails are available from Roche Applied Science and Calbiochem.

III. PROCEDURES

A. Preparation of Probes and Competitor DNAs

Procedures described in this article utilise ^{32}P-labelled probes that have traditionally been used in gel shift assays to allow ready visualisation and potential quantification by autoradiography or phosphorimaging. It is important to use proper shielding (e.g., Perspex screens) to limit exposure to ^{32}P radiation. There are also a number of nonradioactive methods available for visualisation of complexes, including fluorescent probes and biotinylated or digoxygenin-labelled probes. Nonradioactively labelled probes have advantages in safety and length of storage but also have disadvantages, such as the greater number of handling steps needed for visualisation, sensitivity levels, and linearity of signals. Probes are normally prepared by either restriction enzyme digestion and labelling or by labelling of oligonucleotides.

1. Restriction Digestion

Labelling of restriction digests of 1 to 2 µg of plasmid DNA should provide sufficient DNA probe to perform 50 to 100 binding reactions (for a 3-kb plasmid, 2 µg yields about 1 pmol of fragments). To minimise the effect of nonspecific binding to the probe and the number of potential binding sites, restriction fragments should be relatively short (ideally less than 100 bp). If possible, it is best to have binding sites located centrally within the fragment; because affinity is often enhanced by nonspecific interaction of proteins with DNA surrounding their specific binding site, a fragment length of at least 30 to 40 bp is advisable. Restriction enzymes that leave 5′ overhangs are most convenient as they can readily be filled in and radiolabelled using the Klenow fragment of DNA polymerase I and an appropriate [α-^{32}P]dNTP in the presence of other unlabelled deoxynucleotides.

For end labelling, we digest 2 µg of plasmid DNA in a 20-µl reaction in the recommended enzyme buffer. To this is added 20 µCi of suitable ^{32}P-labeled deoxynucleotide for end labelling along with the other three unlabelled dNTPs to a concentration of 100 µ*M* each and 1 unit of Klenow fragment of DNA polymerase I. After a 15-min incubation at room temperature, the fourth unlabelled dNTP is added to 100 µ*M* and incubation is continued for 5 min. Chasing the reaction with the unlabelled nucleotide is important, as single-stranded ends can provide avid binding sites for some proteins.

For optimal gel shift results it is important to gel purify restriction fragment probes. Depending on their size, probes can be separated on 5 to 10% acrylamide gels. For digests of 1–2 ug of DNA, load digest in a 2.5-cm-wide well on a 1-mm-thick gel in TBE buffer and electrophorese at 10 V/cm until the bromphenol blue dye is near the bottom of the gel. For probes 50 bp or less, we routinely run gels and elute small DNA fragments in the cold room. This avoids DNA melting, as single-strand DNAs can produce artefactual results. After the gel apparatus is dismantled, leaving the gel on one of the glass plates, it is covered with plastic wrap and exposed to X-ray film for 2 to 5 min, marking the film for alignment with the gel. The position of the labelled band is identified from the autoradiograph, and the gel slice is excised with a scalpel blade. Fragments can be recovered by elution overnight on a rocking platform or shaker. Depending on its concentration, DNA probes may be used directly or ethanol precipitated and resuspended in TE buffer. Storage of radiolabelled fragments in 0.5 m*M* DTT or 1 m*M* β-mercaptoethanol is recommended to limit radiolytic breakdown.

Unlabelled competitor DNA fragments are prepared similarly except that the quantity of DNA is increased to 5 µg, restriction digestion is done in 50 µl, and all four deoxynucleoside triphosphates are added for end filling. A thicker, 2-mm gel should be used and the gel stained lightly with ethidium bromide (soaking in 0.5 µg/ml solution for 5 to 10 min) for fragment visualisation and isolation. The unlabelled competitor needs to be concentrated by ethanol precipitation.

2. Oligonucleotide Probes

Once a target region for protein binding within a gene regulatory region is identified, oligonucleotide probes provide a powerful way to characterise DNA sequences responsible for DNA–protein complex formation. Sets of mutations within the putative binding site can be prepared and assayed readily and

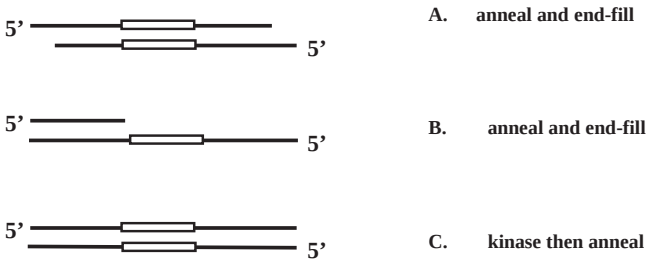

FIGURE 1 Preparation of oligonucleotide probes. Three methods as described in the text for preparation of oligonucleotide probes are shown. The boxed region indicates sequences required for protein–DNA binding. (A and B) Oligonucleotides are extended from 3′ ends to flush-ended double-stranded oligonucleotides. (C) Fully two complementary oligonucleotides are annealed after kinase labelling.

binding and migration of complexes can be compared with complexes formed on binding sites for well-characterised proteins. Probes may be prepared by end filling using deoxynucleoside triphosphates (A and B in Fig. 1) or by kinasing one or both strands. For methods A and C, two complementary 25–30 base oligonucleotides must be prepared for each sequence to be studied. For method B, a single 12-base primer adjacent to the binding sequence to be studied can be used to prime on separate oligonucleotides containing variants of the target sequence.

a. End-Filling Reactions. Mix 2 pmol of each oligonucleotide (for method A) or 2 pmol of the long oligonucleotide and 10 pmol of primer for method B in 10 µl of medium salt restriction enzyme buffer, warm to 60°C, and allow to cool slowly to room temperature. Adjust the reaction volume to 20 µl with additional 10× restriction enzyme buffer, 20 µCi of ^{32}P-labeled deoxynucleotide, the other three unlabelled dNTPs to a concentration of 100 µ*M*, and 1 unit of Klenow fragment of DNA polymerase I. Incubation and chase with unlabelled dNTP are as for labelling restriction fragments.

b. Kinase Reactions. Incubate oligonucleotides for 30 min at 37°C in 20 µl final volume reactions containing 2 pmol of oligonucleotide, 2 µL of 10× kinase buffer, 3 µl (30 µCi) of [γ-^{32}P]ATP, and 1 µl of polynucleotide kinase. After kinasing one or both complementary oligonucleotides, mix 20-µl reactions containing 2 pmol of each and add 5 µl of 100 m*M* $MgCl_2$. Heat the mix to 60°C and allow oligonucleotides to anneal by cooling slowly to room temperature.

After labelling by either method, load reactions on a 10% acrylamide/0.5% bisacrylamide gel run at 4°C in TBE buffer and purify fragments as described earlier. Gel purification is essential to remove any single-stranded oligonucleotide.

B. Protein–DNA-Binding Reactions

1. Protein Source

Nucleic acid-binding proteins used in gel shift assays may be either purified proteins (endogenous or expressed recombinant proteins) or contained in relatively crude cellular or nuclear extracts. *In vitro* expression in coupled transcription/translation extracts is a convenient way to produce proteins if the gene has been cloned. For many studies, nuclear extracts from cells or tissues in which a gene is expressed provide the starting point for the identification of transcription factors relevant to the expression of a gene. The nuclear extract preparation is based on the principle that elevated levels of salt release specific DNA-binding proteins from chromatin; it is critical that the salt level remains below that which will begin to dissociate histones that bind DNA strongly and non-specifically and interfere with gel shift assays. Preparation of nuclear extracts is usually based on the method of Dignam *et al*. (1984), which is applicable to quantities of 10^8 to 10^9 cells in culture. After isolation of a crude nuclear fraction, proteins are extracted in 0.42 *M* NaCl and the extract is dialysed against buffer containing 0.1 *M* KCl. A number of variations of the method have been published that allow for extract preparation from tissue sources (Gorski *et al*., 1986; Fei *et al*., 1995) or rapid miniextract preparation from small numbers of cultured cells (e.g., Schreiber *et al*., 1989). The rapid ammonium sulfate nuclear extract protocol of Slomiany *et al*. (2000) provides a convenient approach for the isolation of high activity extracts from a range of starting sources. When preparing extracts from tissue sources, it is especially important to minimise proteolytic degradation. Early methods included the serine protease inhibitor phenylmethylsulfonyl fluoride, but use of an inhibitor cocktail is recommended to obtain extracts of maximal activity and to avoid potential confusion caused by probes binding to different proportions of intact proteins and proteolytic fragments in extracts from different tissues or cell types.

2. Reaction Setup and Parameters

For each protein–DNA interaction studied it is necessary to optimise the binding conditions. For nuclear extracts and a range of binding proteins, the standard conditions shown in Table I provide a good starting point. Because the amount of a specific protein in an extract and the amount of nonspecific DNA-binding

TABLE I Protein–DNA-Binding Reaction Conditions with Nuclear Extracts

Component[a]	Standard conditions	Range/alternates
HEPES (pH to 7.9 with 2 *M* KOH)	12 m*M*	Tris–HCl pH range 6.5–8.5
KCl	60 m*M*	0–200 m*M* sodium or ammonium salts
EDTA	0.6 m*M*	0.1 m*M* EGTA for selective inhibition of Ca-dependent proteases
Glycerol	12%	0–12%
Dithiothreitol (DTT)	1.2 m*M*	0 to 5 m*M*. *Note*: Binding of some proteins is redox sensitive, whereas for others binding may be enhanced by higher levels of DTT
NP40	0.1%	Up to 2% Tween or Triton X-100 as alternates
poly(dI-dC) : poly(dI-dC).	1 µg/20 µl Rn.	200 ng to 4 µg; other synthetic DNA polymers or mixed sequence DNA such as calf thymus or *E. coli*
Nuclease-free BSA	10 µg/20 µl Rn	Up to 20 µg
$MgCl_2$		Up to 10 m*M*
Labelled DNA probe	10 fmol	
Temperature	30°C	0–37°C
Time	30 min	5–30 min
Protease inhibitors		Use as required. Cocktail of inhibitors or individual inhibitors: AEBSF (Pefabloc), leupeptin, aprotinin, calpain inhibitors I and II, soybean trypsin inhibitor, chymostatin, pepstatin

[a] HEPES, KCl, EDTA, glycerol, and DTT are all contained within binding buffer A, which comprises 20 m*M* HEPES, pH 7.9, 100 m*M* KCl, 1 m*M* EDTA, 2 m*M* DTT, and 20% glycerol. Prepare by dissolving the HEPES base, KCl, and EDTA and adjusting the pH to 7.9 using 2 *M* KOH. Add glycerol and adjust the volume prior to autoclaving. Buffer without DTT can be stored at room temperature. Buffer with DTT should be stored in aliquots at –20°C.

proteins will vary widely, it is important to initially survey a range of protein and nonspecific DNA competitor concentrations to identify levels that allow clear distinction of the protein–DNA complexes.

A setup for a typical exploratory experiment is shown in Table II. Reactions should be set up on ice in 1.5- or 0.5-ml microfuge tubes, first adding all components except the nuclear extract and DNA probe. For nuclear protein extracts, a wide range of protein concentrations, e.g., from 2 to 20 µg in a 20-µl reaction, should be assayed. A typical nuclear extract contains 2 to 4 µg of protein per microliter. Levels of purified proteins need to be titrated to determine optimal levels. It can be preferable to add the nuclear extract prior to the probe if the extract contains significant levels of avid, nonspecific DNA-binding proteins, but in practice the order of addition does not normally make a significant difference. The important point is that the protein and DNA probe should not come into contact until the final mixing step. Binding reactions are typically incubated at 30°C for 30 min. Binding buffer (4 µl) containing bromphenol blue dye is added to aid in gel loading. Provided the binding buffer contains >5% glycerol, there is no need for addition of a density reagent. At this early stage it is also a good idea to test the separation of complexes on different gel systems (see later), as the buffer type and ionic strength can significantly affect separation and band quality.

The exploratory conditions of Table II were applied to the binding site for an ets-related protein (GGAA core sequence) found in the N-ras gene promoter (Fig. 2). The amount of specific complex formed increases with increasing levels of nuclear extract, but at higher levels of extract, a significant fraction of the labelled probe is trapped in the well. A clear signal with minimal background is achieved with 0.5 to 1 µl of nuclear extract and 1 µg of poly(dI-dC) competitor. Replacement of poly(dI-dC) with either poly(dA-dT) or poly(dG-dC) reveals the presence of additional complexes, indicating the value of testing alternate nonspecific competitor DNAs.

Table I indicates a range of possible variations of binding conditions, and the effect of reaction conditions on complex formation should be explored systematically.

TABLE II Exploration of Binding Conditions

Reaction #	1	2	3	4	5	6	7	8	9	10	11	12
Nuclear extract[a]	0	1	2	4	8	12	4	4	4	4	4	4
Binding buffer A[b]	12	11	10	8	4	0	8	8	8	8	8	8
BSA, 10 mg/ml	1	1	1	1	1	1	1	1	1	1	1	1
poly(dI-dC) : poly(dI-dC), 2 mg/ml[c]	1	1	1	1	1	1	0.5	1.5	2	1	1 dAT[e]	1 dGC[e]
NP-40, 2%	1	1	1	1	1	1	1	1	1	1	1	1
$MgCl_2$, 100 mM[d]										1		
H_2O	3	3	3	3	3	3	3.5	2.5	2	2		
DNA probe (10 fmol)	2	2	2	2	2	2	2	2	2	2	2	2

[a] Conditions based on nuclear extract being dialysed against binding buffer A.
[b] Composition of buffer is in footnote to Table I.
[c] Polynucleotides are dissolved in 10 m*M* Tris–HCl, 0.1 m*M* EDTA, pH 8, and stored in aliquots at –20°C.
[d] $MgCl_2$ should be prepared from fresh solid using sterile, nuclease-free water and filter sterilised.
[e] dAT = poly(dA-dT) · poly(dA-dT)poly and dGC = (dG-dC) · poly(dG-dC), both prepared as in footnote c.

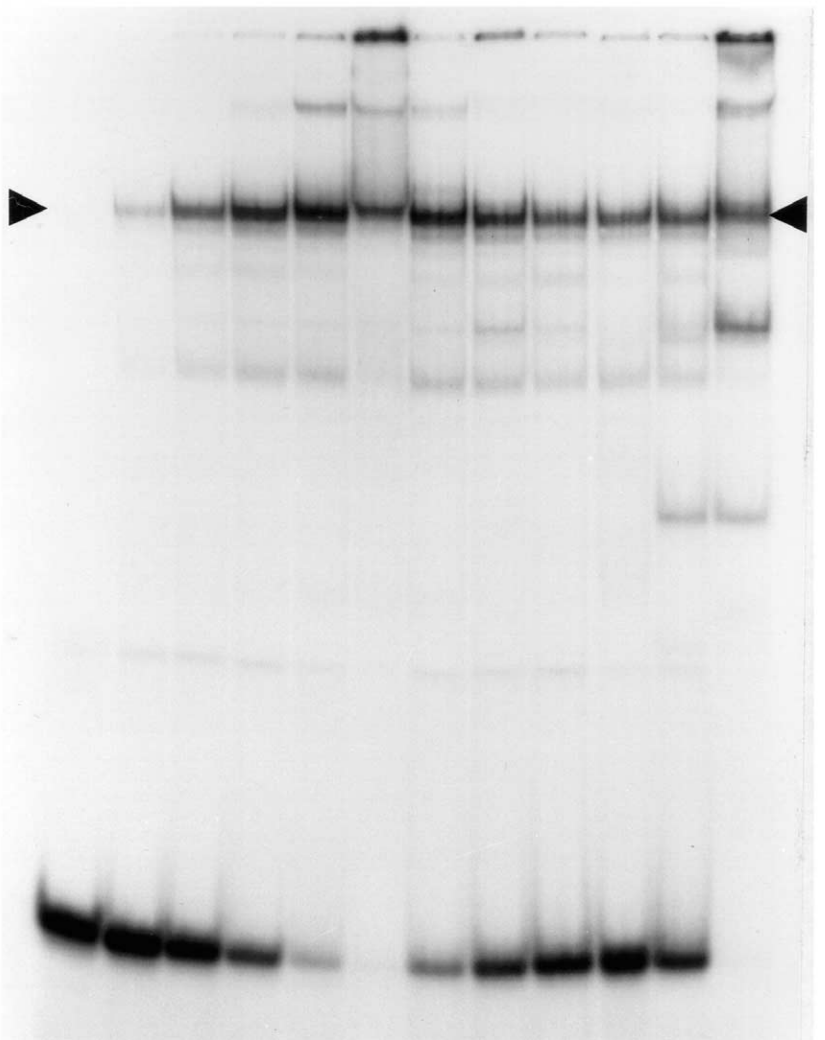

	1	2	3	4	5	6	7	8	9	10	11	12
Nuc. extract (µl)	0	0.2	0.5	1.0	2.0	4.0	1.0	1.0	1.0	1.0	1.0	1.0
poly dI-dC (µg)	1.0	1.0	1.0	1.0	1.0	1.0	0.5	1.5	2.0	1.0		
poly dX-dY, 1µg											dA-dT	dG.dC
$MgCl_2$, 5 mM	-	-	-	-	-	-	-	-	-	+	-	-

FIGURE 2 Analysis of protein–DNA-binding conditions. Binding reactions were set up using a 50 bp fragment containing a binding site for an ets-related protein. Reaction components were as in Tables I and II; the variation in specific components is indicated in the table beneath the gel lanes. Free and bound complexes were separated on a 5% acrylamide gel(30:1 acrylamide: bisacrylamide) run in TNAE buffer. The major specific complex is indicated by the arrow.

a. Time and Temperature. While reactions are often incubated for 30 min, all that is necessary is sufficient time for complex formation to have reached equilibrium, which can often be as short as 5–10 min. Binding reactions are done most commonly at 30°C or room temperature. Lower temperatures sometimes improve binding, e.g., Sp1 binds better at 20°C than at 30°C. Lower temperatures and/or shorter times of incubation can also limit the effect of phosphatases that may be present in some extracts (critical if the active form of a protein is phosphorylated or if probe 5′ is end labelled) (Laniel and Guerin, 1998). Similar considerations apply to the inhibition of nucleases if divalent ions are present in the binding reaction. A characteristic downward smearing of the unbound DNA band is indicative of nuclease activity.

b. Ionic Strength. The relative level of formation of specific and nonspecific complexes is influenced significantly by the concentration of monovalent cation; increased salt concentrations can favour the formation of specific complexes. Most nonspecific protein–DNA interactions are principally ionic and the strength of interaction declines as the salt concentration is increased. For sequence-specific complexes, key interactions involve hydrogen bonding and hydrophobic interactions between bases and amino acids, although the interaction between positively charged amino acids and the phosphate backbone still makes an important contribution to overall affinity. When working with crude protein extracts, salt concentrations in the range of 50 to 100 m*M* are generally optimal, but individual complexes can sometimes be differentiated by their stability at concentrations up to 200 m*M*. Particularly for purified proteins, when the issue of nonspecific binding by other proteins is not an issue, use of a lower or no added monovalent ion can improve binding affinity.

c. Divalent Ions. While many protein–DNA complexes form in the absence of divalent ions, it is advisable to always evaluate binding in both the presence and the absence of Mg^{2+}, as sometimes binding properties can be affected significantly. An illustrative example is binding of the helix–loop–helix protein USF. In the presence of Mg^{2+}, the rates of both association and dissociation and equilibrium binding are affected significantly and even the sequence specificity of binding is altered (Chodosh *et al*., 1986; Bendall and Molloy, 1994). In some cases, a specific metal ion can be necessary for DNA binding and as well as inclusion of the metal ion in the binding reaction it may be necessary to omit EDTA from the electrophoresis buffer (Anderson *et al*., 1990). Examples are the metal response element-binding factor that requires Cd^{2+} and Zn finger proteins, which require low levels of Zn^{2+} for proper protein folding.

d. Nonionic Detergents and BSA. The addition of a nonionic detergent and a carrier protein such as NP-40 and BSA helps minimise protein aggregation and generally results in less smearing of bands and less trapping of the DNA probe in the wells. This is beneficial when working with crude nuclear extracts or to minimise protein denaturation and sticking to tube walls when working with highly purified proteins

e. Nonspecific Competitor DNA. All DNA-binding proteins will bind to a certain extent to both the specific probe and nonspecific competitor DNA. The purpose of the nonspecific competitor is to bind as much of the nonspecific DNA-binding proteins in an extract with minimal binding of the specific protein being studied. Synthetic copolymers have become the preferred choice for competing nonspecific DNA binding because they are less likely to be able to bind efficiently with sequence-specific DNA-binding proteins. Natural, mixed sequence competitor DNAs such as *Escherichia coli* or salmon sperm DNA can also prove to be very effective. However, competitors that have similarity to the binding site of the protein(s) being studied have the potential to interfere significantly with specific binding. For example, poly(dA-dT) would be a poor choice of competitor for studying binding of the TATA-binding protein.

C. Specificity of Protein–DNA Complex Formation: Characteristics of Target DNA Site

Gel retardation assays can be used effectively both to establish that formation of a complex is dependent on specific DNA-sequences and to define the sequence characteristics of the DNA binding site. This can be achieved through a combination of DNA-binding assays using probes of different sequence and competition experiments using unlabelled competitor DNAs.

1. Competitor DNA

Competition assays are based on the principle that the amount of a sequence-specific complex formed on a labelled probe will be reduced in proportion to the amount of competitor DNA if the competitor DNA has specificity for the same sequence. In contrast, if the competitor lacks the specific binding site the additional DNA will compete generally for binding of proteins in the reaction and will add to the overall level of nonspecific competitor DNA. Competitor DNAs may

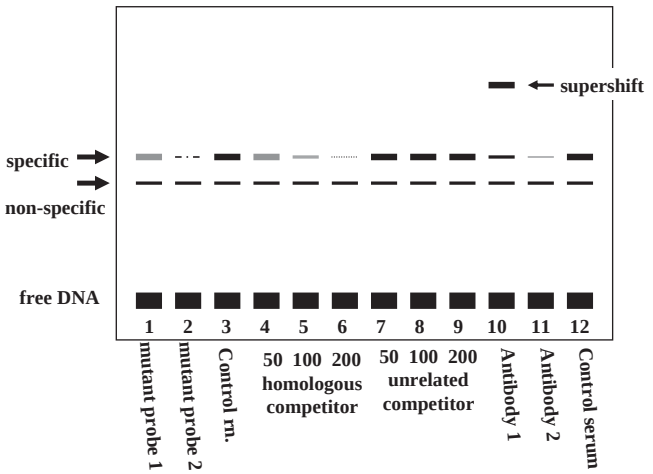

FIGURE 3 Gel mobility shift schematic. The control binding reaction that produces a specific as well as a nonspecific complex is shown in track 3. Reactions are identical to that of track 3 except for a single factor as indicated below each track. Tracks 3 to 12 all contain the same labelled DNA probe. Tracks 1 and 2 contain labelled mutant probes of different binding affinity. In tracks 4 to 6, competitor unlabelled DNA identical in sequence to the probe has been added at 10-, 50-, and 200-fold excess. In tracks 7–9 an unrelated competitor DNA of the same length as the labelled probe has been added at 10-, 50-, and 200-fold excess. In track 10, an antibody that specifically binds the protein in the specific complex without disrupting the DNA-binding interaction has been added. In track 11, antiserum that binds the protein in the specific complex and disrupts complex formation has been preincubated in the reaction prior to probe addition. In track 12, nonimmune control serum has been added.

be either restriction fragments or oligonucleotides (see earlier discussion for preparation), but for comparison between competitors it is important to use DNAs of equivalent size as affinity can increase significantly with increasing fragment size, particularly with oligonucleotides of about 20 bp. Competitor DNAs should minimally include a DNA fragment identical to the probe and a control of equivalent length but unrelated sequence (Fig. 3, tracks 4–9). Competitors with specific mutations can be used to identify or confirm the location of bases important for binding; this approach can be extended to a series of mutants to provide a detailed analysis of the relative importance of different bases to binding affinity. If binding of a known protein is suspected, competition with a DNA fragment that contains a known high-affinity binding site surrounded by unrelated DNA can provide good supporting evidence.

For competition assays the level of DNA-binding protein should not be saturating on the labelled probe; binding of 20 to 30% of the labelled probe in the absence of competitor is a good starting point. It is reasonable to use up to 1 pmol of competitor in a 20-ul reaction, allowing, for example, 10-, 50-, and 200-fold ratios if 5 fmol of probe is included in the reaction. For proper comparison of relative binding affinities the probe and competitor should be added together. It is important to remember, especially with impure protein preparations, that binding kinetics are not simple and that the final level of binding seen depends not just on the specific binding parameters of the protein with its specific DNA target, but also the binding of the protein to both specific and nonspecific competitor DNAs and to other proteins in the reaction, as well of the binding of the DNA probe to other proteins.

2. *Direct Analysis of Binding to Probes of Different Sequences*

Complementary to the aforementioned competitor approach, DNA fragments of different sequence can be used as labelled probes. Probes covering sequence variants in the same way as for competitor analysis can be run in parallel. Formation of complexes with equivalent migration in the gel provides evidence that both sequences can bind the same protein (Fig. 3, tracks 1–3). This approach is well suited to analysis of series of mutations within a fragment and identification of bases critical for binding. An approach that allows relative binding affinities to be estimated is to include a reference-labelled DNA probe of different size in binding reactions; if probe lengths are sufficiently different, it can be feasible to separate complexes formed on the separate probes and quantify binding in relation to the reference probe (Bendall and Molloy, 1994). The principle of reacting proteins with sequence variants can be extended to incubating proteins with populations of oligonucleotides containing segments of random sequence DNA. Complexes can be isolated from gels and successive rounds of PCR and gel retardation used to isolate enriched populations of DNA-binding sites (Oliphant *et al*., 1989). For studies of a limited number of base positions, bound populations can be studied by direct sequencing (Luo *et al*., 1997)

D. Characterisation of DNA-Binding Proteins

Gel retardation assays can provide an entry point for identification and characterisation of proteins regulating gene expression. Antibodies to a wide range of characterised transcription factors are available and can be used to determine if a specific protein is contained in a complex (see Fig. 3). If an antibody binds to or near the DNA-binding domain it may disrupt complex formation, reducing the amount of

complex formed (track 11). Conversely, if the target epitope is distant from the DNA-binding domain, antibody binding will not be disrupted and formation of a ternary DNA–protein–antibody complex will produce a supershifted complex of lower mobility (track 10).

In many instances the nature of the binding sequence provides a guide to possible binding proteins. Comparison can then be made of the migration of protein complexes formed on the sequence under study and known high affinity sites for the candidate protein. Protease clipping can be further used to confirm the equivalence of complexes formed on the two target DNA sequences (e.g., Watt and Molloy, 1993). For many proteins, cDNA clones can be used to express candidate proteins and binding and complex migration compared between nuclear extracts and expressed proteins and between complexes formed by the expressed proteins on known binding sites and the sequence being analysed.

For complexes where the protein involved is unknown, gel retardation can be used to determine the molecular weight of a protein. This can be done indirectly through plotting mobility vs gel concentration (Orchard and May, 1993) or by cross-linking protein DNA complexes and subsequent electrophoresis on SDS–polyacrylamide gels (Miyamoto *et al*., 1995). With the advent of increasingly sensitive proteomic technology, the direct identification of proteins using mass spectrometry has become feasible (see Woo *et al*., 2002).

E. Kinetic Analysis

For purified proteins, gel retardation assays provide a convenient approach to the determination of association and dissociation rates and equilibrium-binding constants of protein–DNA complexes (Meisterernst *et al*., 1988; Chodosh *et al*., 1986). Accurate data can be obtained if the distribution between complex and free DNA and protein is not altered during gel loading and running. Bain and Ackers (1998) have described a cryogenic gel system where the rapid quenching of reactions by transfer to –40°C and electrophoresis at this temperature results in almost complete stabilisation of species distribution. As well as its application in kinetic analysis, this gel system may allow visualisation of complexes that are present in solution but are not stable under conditions normally used in gel retardation experiments. With crude nuclear or cell extracts, the number of competing reactions for binding of proteins and DNA means that it is difficult to obtain good kinetic data (for discussion, see Cann, 1989), although measurement of dissociation rates is possible.

F. Gel Preparation and Running

1. Gel Matrix

Acrylamide : bisacrylamide gels with acrylamide concentration 5% and ratios to cross-linker of 30 : 1 to 80 : 1 are used most commonly. Concentrations can be adjusted readily to provide the best resolution for individual complexes. Agarose gels can also be used in gel retardation assays; they can be useful for separation of large complexes such as nucleosomes or when using large DNA fragments as probes. With gel additives, agarose can also provide similar resolution to acrylamide gels (Chandrasekhar *et al*., 1998)

2. Electrophoresis Conditions

Gel retardation assays rely on the continued association of protein–DNA complexes during electrophoresis. To minimise dissociation of complexes, it is best to conduct electrophoresis at 4°C (in a cold room or refrigerated cabinet) and in low ionic strength buffers. Commonly used buffers and electrophoretic conditions are provided in Table III. Because buffer conditions can differentially affect the migration and/or stability of complexes, it is valuable to test the different systems and choose the one that proves best for the complexes being studied.

Complex dissociation is minimised in the low salt TNAE buffer, but its low buffering capacity means that the running buffer needs to be recirculated. The higher

TABLE III Electrophoresis Buffers and Conditions

Buffer	Components	Running conditions
TNAE	6.7 m*M* Tris–HCl, pH 7.9 3.3 m*M* sodium acetate 1 m*M* Na_2EDTA Adjust the pH of a 50× stock buffer to 7.9	Gel 5% acrylamide, 40 : 1 acrylamide : bisacrylamide Prerun at 10–15 V/cm for at least 30 min. Gel run at 10–15 V/cm for 2–3 h
TG	50 m*M* Tris base 380 m*M* glycine 1.67 m*M* Na_2EDTA Prepare a ×5 stock solution	Gel 5% acrylamide, 30 : 1 or 80 : 1 acrylamide : bisacrylamide. Prerun at 10 V/cm for at least 30 min. Gel run at 15 V/cm for 2–3 h
TBE	89 m*M* Tris base 89 m*M* boric acid 2 m*M* EDTA, pH 8.3 Prepare a 5× stock solution	Gel 5% acrylamide, 40 : 1 or 30 : 1 acrylamide : bisacrylamide, prepared and run in either $\frac{1}{2}$× or $\frac{1}{4}$× TBE Prerun at 10–15 V/cm for at least 30 min. Gel run at 10–15 V/cm for 2–3 h

salt buffers are more convenient in that they do not require recirculation and background nonspecific binding to the probe can be reduced. However, not all complexes are stable in the higher salt buffers. For convenience, electrophoresis at room temperature should also be tested, taking care to lower the voltage to about two-thirds that used in the cold in order to prevent the gel from overheating.

References

Anderson, R. D., Taplitz, S. J., Oberbauer, A. M., Calame, K. L., and Herschman, H. R. (1990). Metal-dependent binding of a nuclear factor to the rat metallothionein-I promoter. *Nucleic Acids Res.* **18**, 6049–6055.

Bain, D. L., and Ackers, G. K. (1998). A quantitative cryogenic gel-shift technique for analysis of protein-DNA binding. *Anal. Biochem.* **258**, 240–245.

Bendall, A. J., and Molloy, P. L., (1994). Base preferences for binding by the bHLH-Zip protein USF: Effects of MgCl2 on specificity and comparison with binding of Myc family members. *Nucleic Acids Res.* **22**, 2801–2810.

Cann, J. R. (1989). Phenomenological theory of gel electrophoresis of protein-nucleic acid complexes. *J. Biol. Chem.* **264**, 17032–17040.

Chandrasekhar, S., Soubar, W. W., and Abcouwer, S. F. (1998). Use of modified agarose gel electrophoresis to resolve protein-DNA complexes for electrophoretic mobility shift assay. *Biotechniques* **24**, 217–218.

Chodosh, L. A., Carthew, R. W., and Sharp, P. A. (1986). A single polypeptide possesses the binding and transcrption activities of the adenovirus major late transcription factor. *Mol. Cell. Biol.* **6**, 4723–4733.

Dignam, J. D., Lebowitz, R. M., and Roeder, R. G. (1983). Accurate transcription initiation by RNA polymerase II in a soluble extract from isolated mammalian nuclei. *Nucleic Acids Res.* **11**, 1475–1489.

Fei, Y., Matragoon, S., and Liou, G. I. (1995). Simple and efficient method for the preparation of nuclear extracts. *Biotechniques* **18**, 984–987.

Gorski, K., Carneiro, M., and Schibler, U. (1986). Tissue-specific *in vitro* transcription from the mouse albumin promoter. *Cell* **47**, 767–776.

Jing, D., Agnew, J., Patton, W. F., Hendrickson, J., and Beechem, J. M. (2003) A sensitive two-color electrophoretic mobility shift assay for detecting both nucleic acids and proteins in gels. *Proteomics* **3**, 1172–1180.

Laniel, M.-A., and Guerin, S. L. (1998). Improving sensitivity of the electrophoretic mobility shift assay by restricting tissue phosphatase activities. *Biotechniques* **24**, 964–969.

Luo, B., Perry, D. J., Zhang, L., Kharat, I., Basic, M., and Fagan, J. B. (1997). Mapping sequence specific DNA-protein interactions: A versatile quantitative method and its application to transcription factor XF1. *J Mol. Biol.* **266**, 479–492.

Meisterernst, M., Gander, I., Rogge, L., and Winnacker, E.-L. (1988). A quantitative analysis of nuclear factor I/DNA interactions. *Nucleic Acids Res.* **16**, 4419–4435.

Miyamoto, S., Cauley, K., and Verma, I. M. (1995). Ultraviolet cross-linking of DNA binding proteins. *Methods Enzymol.* **254**, 632–641.

Oliphant, A. R., Brandl, C. J., and Struhl, K. (1989). Defining the sequence-specificity of DNA-binding proteins by selecting binding sites from random-sequence oligonucleotides: Analysis of yeast GCN4 protein. *Mol. Cell. Biol.* **9**, 2944–2949.

Orchard, K., and May, G. E. (1993). An EMSA-based method for determining the molecular weight of a protein-DNA complex. *Nucleic Acids Res.* **21**, 3335–3336

Schreiber, E., Matthias, P., Muller, M. M., and Schaffner, W. (1989). Rapid detection of octamer binding proteins with 'mini-extracts' prepared from a small number of cells. *Nucleic Acids Res.* **17**, 6419

Slomiany, B. A., Kelly, M. M., and Kurtz, D. T. (2000). Extraction of nuclear proteins with increased DNA binding activity. *Biotechniques* **28**, 938–942

Watt, F., and Molloy, P. L. (1993). Specific cleavage of transcription factors by the thiol protease, m-calpain. *Nucleic Acids Res.* **21**, 5092–5100.

Woo, A. J., Dods, J. D., Susanto, E., Ulgiati, D., and Abraham, L. J. (2002). A proteomics approach for the identification of DNA binding activities observed in the electrophoretic mobility shift assay. *Mol. Cell. Proteomics* **1**, 472–478.

CHAPTER

43

DNA Affinity Chromatography of Transcription Factors: The Oligonucleotide Trapping Approach

Suchareeta Mitra, Robert A. Moxley, and Harry W. Jarrett

I. INTRODUCTION

The purification of transcription factors is a complex topic. A brief search of genetic databases reveals over 10,000 transcription factor entries. Of these, several hundred have now been purified. Typically these purifications have involved some form of DNA affinity chromatography. Most recent purifications use specific, double-stranded oligonucleotide sequences attached covalently to a suitable chromatographic support. This topic has been reviewed elsewhere (Gadgil *et al*., 2000).

We described a variant of this technique called oligonucleotide trapping (Gadgil and Jarrett, 2002), depicted in Fig. 1. A column ('the trap") is prepared with the single-stranded oligonucleotide ACACACA CAC attached to CNBr-activated Sepharose through an aminoalkyl linker. Another DNA ("the probe") is prepared, which has a double-stranded region containing the element bound by a transcription factor and additionally has a GTGTGTGTGT single-stranded tail. The probe is mixed with a cell extract containing a transcription factor to be purified along with salt and various competitors and surfactants, which improve selectivity. The mixture is then applied to the trapping column and, after washing thoroughly, the column can be eluted either using high salt concentrations or using low salt and elevated temperatures.

The method has several advantages. The same "trap" column can be used with a variety of probes to purify different transcription factors and other DNA-binding proteins. The probe can be 5′ end labeled to test new trap columns and, during protein purification, to follow the efficiency of column trapping of the protein–DNA complex. The labeled probe can be used directly in an electrophoretic mobility shift assay (EMSA) to follow transcription factor binding, to measure the amount of transcription factor present in various cell fractions, and to assess the effect of various competitors, detergents, and so on on this binding. The trapping method also has much higher capacity for transcription factors than traditional, covalent DNA affinity chromatography. This is because virtually all of the probe DNA is active and productively binds the transcription factor while much of covalently coupled DNA is usually inactive or inaccessible for binding (Gadgil and Jarrett, 2002; Massom and Jarrett, 1992). This article describes the current oligonucleotide trapping method practiced in our laboratory.

II. MATERIALS AND INSTRUMENTATION

CNBr-activated Sepharose (C-9142), heparin (H-3393), *N,N,N′,N′*-tetramethylethylenediamine (T-9281), polydeoxyinosinic-deoxycytidylic acid [poly(dI), dC, P-4929], and igepal CA-630 (I-3021) are from Sigma. Acrylamide (161-0101) and *N,N′*-methylene-bisacrylamide (161-0201) are from Bio-Rad. Oligonucleotides are purchased from Integrated DNA Technologies (IDT), but other suppliers have also been used with good results. For oligonucleotides that will be coupled covalently to Sepharose (e.g.,

Copyright 2006, Elsevier Science (USA).
All rights reserved.

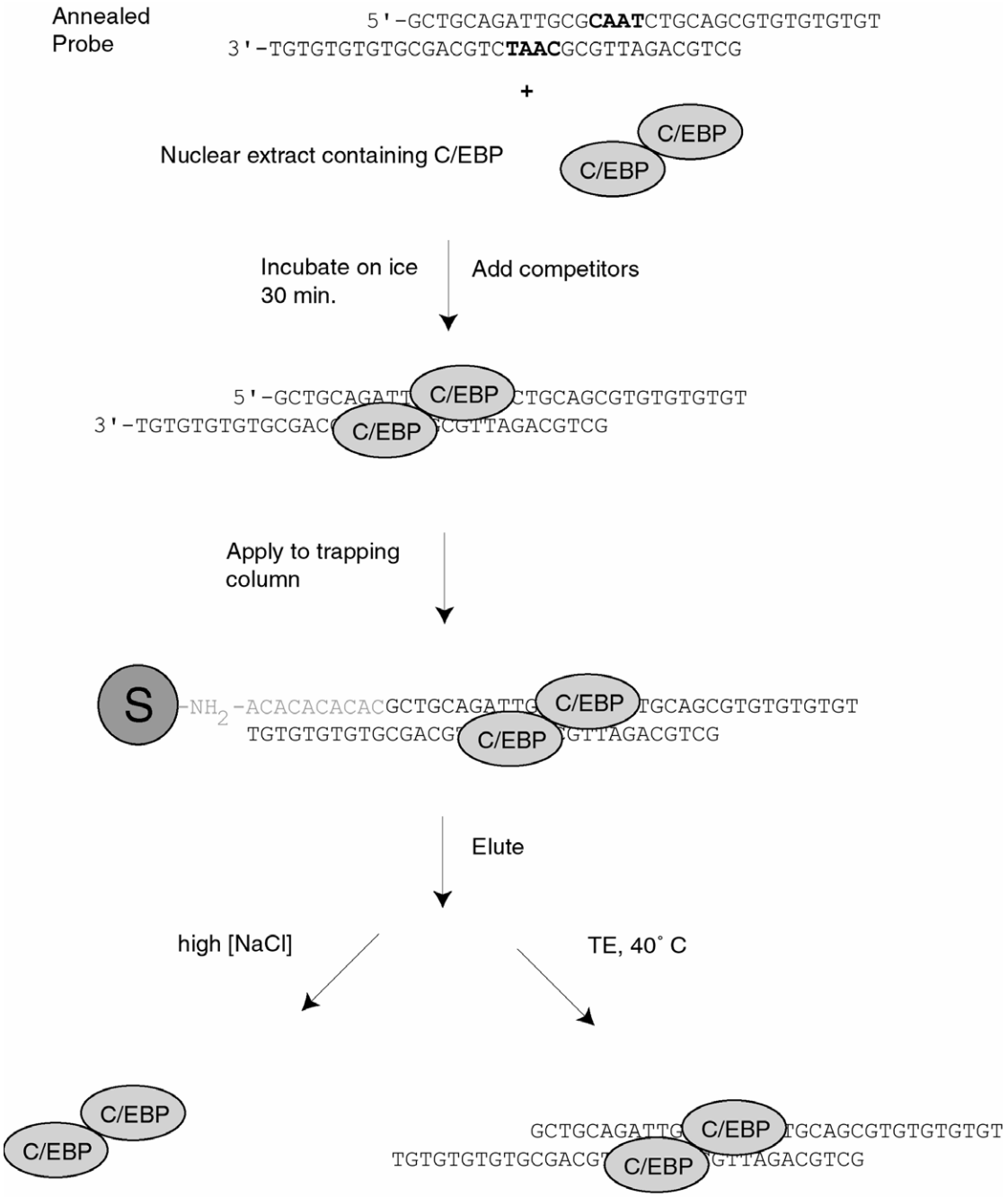

FIGURE 1 Oligonucleotide-trapping purification of the CAAT enhancer-binding protein (C/EBP) is shown schematically.

ACACACACAC), the "5′ Amino Modifier C6" is added on the last (5′) cycle. We have also used the Applied Biosystems Aminolink II reagent for this purpose and it also works well. We purchase unpurified oligonucleotides at the 1-µmol scale which have "trityl off" and are deblocked.

Chromatography is either by simply using gravity flow with a fraction collector or using a Bio-Rad Biologic LP Chromatograph (Cat. No. 731-8300). Electrophoresis is with the Bio-Rad Mini-Protean II apparatus (Cat. No. 165-2944) and the PowerPac 200 power supply (Cat. No. 165-5050).

III. PROCEDURES

A. Preparation of Oligonucleotides

Solutions

1. *0.5 M EDTA*: 15 g Na_4EDTA, 3.2 g Na_2EDTA, 81 ml distilled water; autoclave for 45 min
2. *1 M Tris, pH 7.5*: 60.6 g Tris base, 31.25 ml fresh 37% HCl, 441 ml distilled water, 0.5 ml 0.5 *M* EDTA. Check the pH of a 1 : 10 dilution. Autoclave for 1 h.
3. *TE*: 10 m*M* Tris, 1 m*M* EDTA, pH 7.5. To make 100 ml, add 1 ml 1 *M* Tris, pH 7.5, 0.2 ml 0.5 *M* EDTA, and sterile distilled water to complete 100 ml.
4. *3 M sodium acetate*: For 100 ml, add 40.8 g sodium acetate trihydrate, 5 ml glacial acetic acid, 0.2 ml 0.5 *M* EDTA, and 66 ml H_2O. Autoclave for 45 min.
5. *70% ethanol*: For 100 ml, mix 70 ml absolute ethanol with 30 ml distilled water. Keep in a –20°C freezer and use while cold.

Steps

1. Dissolve a dried, unpurified oligonucleotide (1 µmol) in 300 µl of TE, 30 µl 3 *M* sodium acetate, and add 1 ml of absolute ethanol for oligonucleotides longer than 12-mers and 1.32 ml ethanol for those between 6- and 11-mers.

2. Place the mixture in a –85°C freezer for 1 h and then centrifuge at 4°C at 16,000 *g* for 12 min. Aspirate the supernatant carefully away.

3. Wash the pellet with 500 µl 70% ethanol (80% is used for shorter oligonucleotides), centrifuge again, and discard the supernatant.

4. Dry the oligonucleotide for 5 min in a Speed-Vac SC110 (Savant) at room temperature. Oligonucleotides purified by this simple ethanol precipitation are used for all our DNA-affinity chromatography experiments and we have found them to be of adequate purity. For long-term storage, the oligonucleotides are either left dry or dissolved in 500 µl TE, adjusted to 1 m*M* using their absorption at 260 nm (we use an Excel spreadsheet we configured to calculate molar absorptivities based upon a sequence; a similar calculator is available on the internet at http://www.basic.nwu.edu/biotools/oligocalc.html), and stored at –20°C. If stored in TE, oligonucleotides must be again precipitated and washed with ethanol prior to coupling, as Tris interferes with coupling.

B. Preparing the ACACACACAC-Sepharose Column

Solutions

1. *Coupling buffer*: 0.1 *M* $NaHCO_3$, pH 8.3, 0.5 *M* NaCl. To prepare 1 liter, dissolve 8.40 g $NaHCO_3$ in 800 ml distilled water, adjust the pH to 8.3 with HCl, add 29.22 g NaCl, and complete to 1 liter. Keep in a 4°C refrigerator and put on ice an hour before use.

2. *1 mM HCl*: 43 µl of concentrated (11.6 *M*) HCl in a total volume of 500 ml distilled water. Keep in a 4°C refrigerator and put on ice an hour before use.

3. *Blocking buffer*: 0.1 *M* Tris, pH 8.0, 0.5 *M* NaCl. For 1 liter, dissolve 12.1 g Tris base in 800 ml distilled water, adjust to pH 8 with HCl, add 29.22 g NaCl, and complete to 1 liter. Store at 4°C.

4. *1 M* NaN_3: Dissolve 6.50 g sodium azide to a total volume of 100 ml with distilled water.

5. *TE/azide*: 10 m*M* Tris, 1 m*M* EDTA, 10 m*M* NaN_3, pH 7.5. To make 100 ml, add 1 ml 1 *M* Tris, pH 7.5, 0.2 ml 0.5 *M* EDTA, 1 ml 1 *M* NaN_3, and sterile distilled water to complete 100 ml.

Steps

1. Dissolve the dried, ethanol-precipitated 5′-[amino modifier C6]-ACACACACAC oligonucleotide, 200 nmol, in 2 ml coupling buffer, transfer to a 15-ml polypropylene screw-cap tube (Sarstedt # 62.554.002), and keep on ice.

2. Suspend 1.2 g CNBr-preactivated Sepharose in 100 ml ice-cold 1 m*M* HCl, cover with Parafilm, and invert occasionally while keeping in an ice-water slurry for 15 min.

3. Filter on a coarse sintered glass funnel (Pyrex brand, available from Fisher #36060-150C) and wash with an additional 100 ml ice-cold 1 m*M* HCl. Filter under vacuum until the filtered cake of resin just begins to form cracks and immediately scrape the Sepharose into the DNA-coupling buffer solution and mix with a vortex mixer.

4. The slurry should be watery enough to mix easily; if not, add an additional milliliters of coupling buffer. Mix the slurry in a cold room (4°C) overnight on a tube rotator (Cole Parmer Roto-Torque A-07637-00) at low speed just sufficient to keep the resin from settling.

5. The next day, filter the resin again, and wash five times with 5-ml portions of blocking buffer. Determine the absorption at 260 nm of the combined washes and measure their volume (typically 25–30 ml) either

gravimetrically or volumetrically. The amount of coupling is determined by difference using

$$\%\ \text{coupling} = 100\% - \frac{A_{260} \times \text{volume (ml)}}{200 \times 10^{-9} \times 111,250 \times 10}$$
$$= 100 - \frac{A_{260} \times \text{volume (ml)}}{0.2225}$$

where 111,250 $M^{-1}cm^{-1}$ is the calculated molar absorptivity of CACACACACA. For example, if the total washes were 30 ml, the absorbance would be 0.742 if none couples. If the washes actually have $A_{260} = 0.186$, the equation calculates 75% coupling. To convert this to nanomoles DNA per milliliter Sepharose, the 1.2-g preactivated Sepharose yields 3.5 ml/g or about 4.2 ml DNA–Sepharose. Thus 75% coupling would give 0.75 × 200 nmol/4.2 ml = 36 nmol DNA/ml Sepharose.

6. Leaue the resin as a watery slurry in blocking buffer with mixing overnight in the cold room (4°C) and then put in TE/azide (10 m*M* Tris, pH 7.5, 1 m*M* EDTA, 10 m*M* NaN_3) and store at 4°C. We store resins in graduated 15-ml polypropylene tubes as 50% settled resin/50% liquid mixtures for a year or more with no loss of activity.

7. Then pack the $(AC)_5$-Sepharose into a 1-ml syringe column (Bio-Rad Poly-Prep empty columns, Cat. No. 731-1550 or Alltech Extract-Clean, Cat. No. 211101). This is done simply by adding 1 ml of the well-mixed 50% slurry to the column and allowing it to drain and overlaying with fresh buffer. We usually place an extra column frit on top of the 0.5-ml packed support bed to prevent disturbing it and keep the column in TE/azide when not in use. Assuming 75% coupling as described earlier, this column should bind 18 nmol of probe.

Pitfalls

There are essentially three kinds of failure we have observed as we help others do trapping.

1. Tris cannot be present during DNA coupling to CNBr-activated Sepharose. It can be removed effectively from DNA stored in TE by careful ethanol precipitation.

2. After hydration in 1 m*M* HCl and filtration, care must be taken not to introduce air into the Sepharose. Filter only until cracks begin to appear in the filtrate and stop, leaving a moist cake. Once air is introduced, the Sepharose particles will float, making column packing difficult or impossible.

3. Columns should usually only be used when EDTA is present. DNases all require divalent cations and, in the absence of EDTA, can destroy columns. In some cases, using divalent cations is unavoidable though and this will lessen column lifetime.

C. Preparing the Probe

The oligonucleotides, usually one for each strand, are obtained commercially and separately ethanol precipitated as described in Section III,A. In the case of C/EBP, an internally symmetric sequence [i.e., $EP24(TG)_5$] was used (Gadgil and Jarrett, 2002), requiring a single oligonucleotide. Probes are usually stored at –20°C as 1 m*M* solutions in TE. A portion of either strand can be labeled using the 5′ polynucleotide kinase reaction and [γ-^{32}P]ATP (Sambrook *et al*., 1989). In our laboratory, 5′ end labeling is performed with oligonucleotide in excess over ATP. Just prior to use, probe strands are annealed by diluting to 10–100 μ*M* in TE0.1 (10 m*M* Tris, pH 7.5, 1 m*M* EDTA, 0.1 *M* NaCl) and heating to 95°C for 5 min followed by a linear decrease to 4°C at 1 h in a thermocycler. They can also be annealed by boiling 50 ml water in a 100-ml beaker, removing it from the heat, and adding the sealed tube containing the DNA. After allowing the beaker to cool for 30 min, the tube is removed to an ice bath. In the case of $EP24(TG)_5$, after annealing we have

5′-GCTGCAGATTGCG**CAAT**CTGCAGCGTGT
GTGTGT-3′
3′-TGTGTGTGTGCGACGTC**TAAC**GCGTTAG
ACGTCG-5′

When first using a new probe or trap, we generally test the apparatus by 5′ end labeling the probe (about 10,000 counts per minute of ^{32}P in 1–2 nmol DNA is sufficient) and applying it to the trap column in TE0.1 at 4°C. If all of the ^{32}P is attached to the DNA (i.e., proper care was taken to remove any excess [γ-^{32}P]ATP used for labeling) and if the trap column has sufficient capacity (e.g., 18 nmol in the example given for 75% coupling), greater than 95% of the counts should be retained by the trapping column. The column is then placed in a 37°C water bath and eluted with TE. All of the bound counts should elute. This test can also be included during purification itself, i.e., the 5′ end-labeled probe can be used during purification to monitor column performance.

D. Preparing the Cell Extract

Most transcription factors are in the nucleus and are prepared from nuclear extracts. However, for a new transcription factor, this is not at all certain and should be ascertained. C/EBP is found in the nucleus of rat liver. In this case, a nuclear extract prepared by the method of Gorski *et al*. (1986) was used as the starting

point. Other methods for preparing nuclear extracts can also be used. Other fractions should also be checked for activity, however, to be certain of localization and to follow the success of the preparation. In working with other transcription factors, we have found that extracting the nucleus with 0.36 *M* $(NH_4)SO_4$ as in the usual method (Gorski *et al*., 1986) did not effectively release the transcription factor and higher salt, i.e., 0.6 *M* $(NH_4)SO_4$, was required. Therefore, monitoring each fraction as cells are fractionated and perhaps altering the fractionation procedure to accommodate the protein of interest are usually worthwhile.

Monitoring is accomplished by preparing serial dilutions of each cell fraction and adding these to an electrophoretic gel shift assay (EMSA). This is usually a qualitative analysis. For example, we typically use three-fold serial dilutions and note for each fraction (cytosol, nuclear extract) the dilution that gave an approximate 50% of the maximal shift obtained. This 50% shift is thus a rough unit of activity. Where the bulk of activity resides is determined from the dilution required for 50% shift and accounting for the volume of each fraction.

Alternatively, several kits are available for preparing nuclear extracts (i.e., the ones from Panomics, Inc., Cat. No. AY2002 or Active Motif, Cat. No. 40010) and nuclear extracts already prepared from a variety of cell lines are available commercially (see Active Motif's catalogue). While these may not be suitable in all cases, they can certainly save time when applicable.

For C/EBP, the rat liver nuclear extracts prepared (Gadgil and Jarrett, 2002) are dialyzed into 25 m*M* HEPES, pH 7.6, 40 m*M* KCI, 0.1 m*M* EDTA, I m*M* dithiothreitol, and 10% glycerol, adjusted to 5 mg/ml protein, and stored in 0.2-ml aliquots at –85°C.

E. Electrophoretic Mobility Shift Assay

Here we describe the complete assay in use in our laboratory, including directions for preparing the gel. Alternatively, we have also used 4–12% Bio-Rad Tris/glycine ready gels (with 0.25× TBE as the running buffer) with good results.

Solutions

1. *5× TBE*: To make 1 liter, dissolve 30.03 g Tris base, 15.25 g boric acid, 10 ml *0.5 M* EDTA, and add distilled water to 1000 ml and store at room temperature
2. *5 M NaCl*: Combine 29.2 g NaCl, 89 ml distilled water, and 0.1 ml 0.5 *M* EDTA. Autoclave for 45 min and store at room temperature.
3. *5× incubation buffer (for 8 ml)*: Combine 400 µl I *M* Tris–Cl (pH 7.5), 80 µl 0.5 *M* EDTA (pH 8.0), 320 µl 5 *M* NaCl, 1.6 ml glycerol, and 3.2 µl β-mercaptoethanol. Add distilled water to 8 ml and store at 4°C for up to 1 week.
4. *Acrylamide*: Combine 29 g acrylamide, 1 g *N,N'*-methylene-bisacrylamide, and distilled water to a total of 100 ml. Store at 4°C for up to 1 month.
5. *10% ammonium persulfate*: Weigh 0.1 g ammonium persulfate and add 1 ml distilled water. Discard after 1 day.
6. *N,N,N',N'-Tetramethylethylenediamine (TEMED)*
7. *1 µg/µl dI.dC*: Dissolve 1 mg polydeoxyinosinic–deoxycytidylic acid in 1 ml TE
8. *10× TE0.1*: For 1 liter, combine 12.1 g Tris base, 20 ml 0.5 *M* EDTA, and 800 ml distilled water. Titrate to pH 7.5 with HCl, dissolve 58.44 g NaCl, and complete to 1000 ml with distilled water.
9. *TE0.4*: For 100 ml, mix 10 ml 10× TE.1, 6 ml 5 *M* NaCl, and complete to 100 ml
10. *TE1.2*: For 100 ml, mix 10 ml 10× TE.1, 22 ml 5 *M* NaCl, and complete to 100 ml. Store solutions 8–10 at room temperature.

1. Gel Preparation

Steps

1. Prepare the gel (5% acrylamide) in an 16 × 100-mm test tube by combining 7.7 ml distilled water, 0.5 ml 5× TBE, 1.7 ml acrylamide, 0.1 ml 10% ammonium persulfate, and 20 µl TEMED.
2. Mix well and quickly pour into the assembled plates and place the comb of a Bio-Rad protein II minigel apparatus.
3. Let the gel polymerize.
4. Fill the gel tank with 0.25× TBE (15 ml 5× TBE completed to 300 ml with distilled water). Remove the comb, wash, and fill the wells with 0.25× TBE.
5. For some transcription factors, preelectrophorese the gel for 30 min at 100 V.

2. Mobility Assay

Steps

1. In a microtube, combine 5 µl 5× incubation buffer, I µl 1 µg/µl poly(dI-dC), 1–5 µg transcription factor or nuclear extact, 20,000 cpm ^{32}P-labeled annealed oligonucleotides, and distilled water for 25 µl total.
2. Mix gently and incubate at room temperature for 20 min.
3. Add 2 µl of bromphenol blue (0.1% in distilled water) to each sample and mix gently.
4. Load 20–25 µl onto gel.
5. Run gel at 150 V for 1 h until the dye front is ~1 mm from bottom.

6. Dry gel overnight or place in a water-tight Zip-Lock bag.
7. Expose film overnight at –85°C using an intensifying screen or use a Phosphorimager.

F. Oligonucleotide Trapping

By adding different dilutions of nuclear extract to a gel shift, performed using a known amount of DNA, usually a total shift of the DNA can be obtained. By observing what dilution was just sufficient to give a total shift (or, better, use densitometry to determine what gives a 50% shift), the approximate concentration of the DNA-binding activity can be obtained. This method should be applied to a new transcription factor to estimate its concentration. We have experience with only a small number of transcription factors, but the highest concentration we have found of a transcription factor in a nuclear extract is about 40 fmol/µl (40 n*M*). This number may not be meaningful to all transcription factor/nuclear extract combinations but does provide a starting point for estimation. If a nuclear extract is diluted 10-fold into TE0.1 and an annealed probe is added to give a concentration of 40 n*M* or greater, the DNA should be in 10-fold or greater excess over the transcription factor. At this very low concentration of DNA, very little nonspecific binding should occur and yet all of the transcription factor should be bound. To test if the conditions are correct, EMSA can be performed under the conditions of chromatography to test whether binding is complete. Thus, if the nuclear extract is diluted 10-fold into TE0.1 and increasing amounts of 5′-end-labeled DNA probe are added (from 0.1 to 1000 n*M*) and the mixture is applied to EMSA, all of the DNA should be shifted at the lower concentrations but eventually a point will be reached where all of the DNA is not shifted because it is now in excess. An excess of about 10-fold is appropriate.

We also use a similar approach to determine which competitors and detergents we can use during trapping. We have found that heparin [an inhibitor of double-stranded DNA binding (Gadgil and Jarrett, 1999)], in concentrations as high as 4 mg/ml, and $(dT)_{18}$ (a competitor of single-stranded DNA binding), as high as 20 µ*M*, have little effect on the DNA binding of many transcription factors but can diminish nonspecific binding greatly. However, we have found some transcription factors, notably some members of the E2F family, do not bind DNA even when very small amounts of heparin are used (unpublished data). Poly(dI,dC) at 0.05 mg/ml can greatly diminish nonspecific binding greatly. Similarly, we find that 0.1% igepal, Triton, or Tween detergents do not adversely affect most gel shifts but we have found exceptions. We usually test various concentrations of each of these reagents in an EMSA experiment before using them in chromatography.

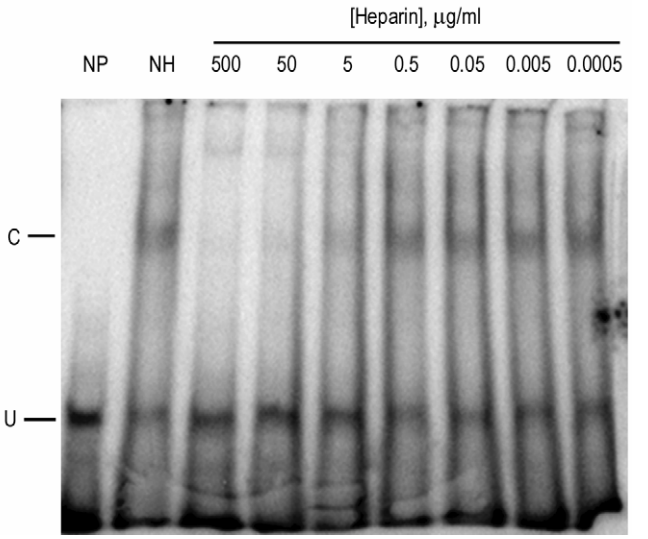

FIGURE 2 Electrophoretic mobility shift assay (EMSA) of C/EBP in the presence of heparin. EMSA was performed as in Section III,E in the presence of the heparin concentrations shown. NP, no protein added showing the position of the unshifted (U) oligonucleotide. NH, no heparin added to the complete assay mixture showing the position of the shifted complex (C).

Such an experiment to determine the concentration of heparin to use in the purification of rat liver C/EBP is shown in Fig. 2. Concentrations of heparin of 0.5 µg/ml or less have no effect on the gel shift observed and 0.5 µg/ml would then be chosen tentatively for use in trapping. The same experiment is then performed with each component to be tested (detergents, dIdC, etc.) to find the highest concentration that can be used safely. As a last test, a mixture containing all the components is then tested to ascertain that there is no synergism between the reagents that could affect DNA binding adversely.

Trapping is then performed using this tested combination. What follows is a set of conditions that work well for rat liver C/EBP.

Steps

1. Combine 1 ml 10X TE0.1, 1 µl 5 mg/ml heparin (0.5 µg/ml final), 90 µl 1 m*M* $(dT)_{18}$ (9 µ*M* final), 0.5 ml 1 mg/ml dI,dC (50 µg/ml final), and distilled water to complete 8 ml. Cool on ice 30 min.
2. Add 1 ml rat liver nuclear extract and mix gently. Add 20 µl 100 µ*M* annealed EP24GT trapping oligonucleotide (final is 200 n*M* strand, 100 n*M* duplex) and mix gently. Incubate on ice for 30 min.

3. Chromatography. All operations take place in a 4°C cold room. All solutions are kept on ice. Apply the trapping mixture to the 0.5 ml $(AC)_5$-Sepharose column at about 0.3 ml/min.

4. Wash the column with 20 ml TE0.4. Elute the column by either of two procedures (see Fig. 1)

5a. High salt: Elute the column with 10 ml TE1.2 (10 m*M* Tris, pH 7.5, 1 m*M* EDTA, 1.2 *M* NaCl).

5b. Temperature: Place the column in a 37°C water bath and elute with 10 ml 37°C TE (no salt).

6. Column fractions are then assayed by EMSA. In either case, the conditions for EMSA are not ideal. For high salt elution, the salt can interfere with electrophoresis and DNA binding; therefore, only 1–2 µl can be added safely to the 25-µl gel-shift mixture. For temperature, the protein–DNA complex elutes and the DNA acts as a "cold competitor" in EMSA and diminishes the amount of shift observed. However, in either case, a gel shift is observed sufficiently to identify the active fractions. Our experience has been that temperature elution gives somewhat higher purity than salt elution (Gadgil and Jarrett, 2002).

G. Other Applications

We have extended the trapping method in two directions. We have developed a CNBr-activated HPLC silica (Jurado *et al*., 2002) and produced $(AC)_5$-silica. This allows trapping to be performed using the much higher mass transfer characteristics of 7-µm, 300-Å pore silica. Second, we have extended the method to restriction enzymes and used catalytic means for elution. An example of this technique is shown in Fig. 3. In this case, the trapping oligonucleotide is

Ecogt 5′-GCATGC**GAATTC**GCATGTGTGTGTGT
3′-CGTACG**CTTAAG**CGTA

which of course binds to the *Eco*RI restriction endonuclease. This oligonucleotide was used to trap *EcoR*I from a crude bacterial (*E. coli* strain RY13) extract (400 µl) in the presence of EDTA. *Eco*RI binds DNA in the absence of Mg^{2+} (presence of EDTA) but is catalytically inactive (Jurado *et al*., 2000). Once bound to the column and washed thoroughly, the enzyme was eluted catalytically by adding Mg^{2+} (50 m*M*) to the column buffer. The enzyme binds Mg^{2+}, digests the column DNA, and elutes. It is detected in Fig. 3 by its characteristic digestion of λ phage DNA (in fractions 11–23).

Once columns are eluted catalytically, the DNA is converted to product (in this case, digested DNA) and are no longer useful for affinity chromatography. However, by using the trapping approach, the digested DNA is simply removed (by washing with 37°C TE or 70°C water) to return to $(AC)_5$-silica and then the EcoGT DNA is replaced (i.e., trapped) for the next purification. This strategy allows DNA, rather than columns, to become a consumable reagent in the catalytic chromatography of enzymes such as endonucleases.

IV. CONCLUSIONS

Trapping has proven to be a useful technique for the purification of transcription factors. It allows the protein–DNA complex to form in solution at low concentrations and under conditions that can be tested beforehand using the EMSA assay with the same DNA.

It has now been extended to DNases and can probably also be applied to DNA or RNA polymerases and to DNA repair enzymes, although we have not yet done so.

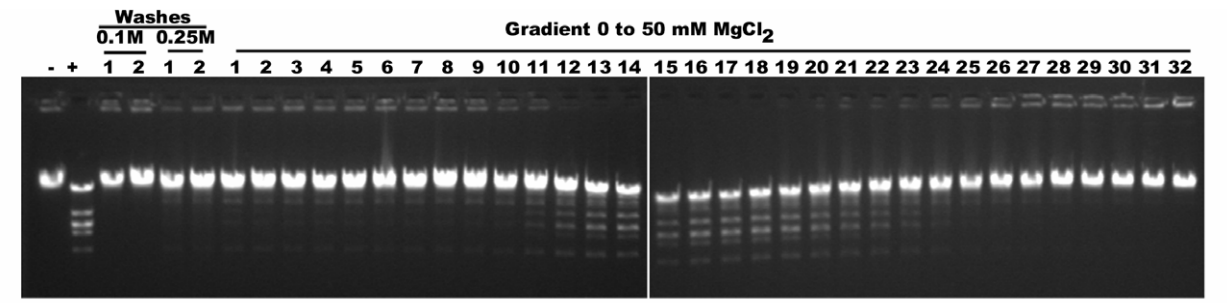

FIGURE 3 Catalytic chromatography of *Eco*RI using the trapping approach on a 4.6 × 50-mm $(AC)_5$-silica column. Fractions were assayed as described previously (Jurado *et al*., 2000) by digestion of λ phage. A minus sign shows control reaction without *Eco*RI, and a plus sign shows digestion with pure *Eco*RI. After loading 0.4 ml of the RY13 extract, the column was washed with 10 ml of a buffer containing 1 m*M* EDTA and 0.1 *M* KCl and then with 0.25 *M*. Following washing, the column was eluted with a linear gradient to 50 m*M* $MgCl_2$. The chromatography conditions are described in more detail elsewhere (Jurado *et al*., 2000).

Acknowledgment

This work was supported by the National Institutes of Health (GM43609).

References

Gadgil, H., and Jarrett, H. W. (1999). Heparin elution of transcription factors from DNA-Sepharose columns. *J. Chromatogr. A* **848**, 131–138.

Gadgil, H., and Jarrett, H. W. (2002). An oligonucleotide trapping method for purification of transcription factors. *J. Chromatogr. A* **966**, 99–110.

Gadgil, H., Jurado, L. A., and Jarrett, H. W. (2000). DNA affinity chromatography of transcription factors. *Anal. Biochem.* **290**, 147–178.

Gorski, K., Carneiro, M., and Schibler, U. (1986). Tissue-specific *in vitro* transcription from the mouse albumin promoter. *Cell* **47**, 767–776.

Jurado, L. A., Drummond, J. T., and Jarrett, H. W. (2000). Catalytic chromatography. *Anal. Biochem.* **282**, 39–45.

Jurado, L. A., Mosley, J., and Jarrett, H. W. (2002). Cyanogen bromide activation and coupling of ligands to diol-containing silica for high performance affinity chromatography: Optimization of conditions. *J. Chromatogr. A* **971**, 95–104.

Massom, L. R., and Jarrett, H. W. (1992). High-performance affinity chromatography of DNA. II. Porosity effects. *J. Chromatogr. A* **600**, 221–228.

Sambrook, J., Fritsch, E. F., and Maniatis, T. (1989). "Molecular Cloning, a Laboratory Manual," 2nd Ed. Cold Spring Harbor Laboratory Press, Cold Spring Harbor, NY.

SECTION

14

Protein Degradation

CHAPTER

44

Protein Degradation Methods: Chaperone-Mediated Autophagy

Patrick F. Finn, Nicholas T. Mesires, and James Fred Dice

I. INTRODUCTION

Proteins can be degraded within lysosomes by several different pathways (Dice, 2000). Chaperone-mediated autophagy (CMA) is a lysosomal pathway of proteolysis that degrades 30% of cytosolic proteins during nutritional deprivation. Substrates for this pathway of proteolysis have targeting sequences biochemically related to the pentapeptide KFERQ (Dice, 1990). Molecular chaperones, such as the constitutively expressed heat shock 70-kDa protein (hsc70), along with cochaperones (Agarraberes and Dice, 2001), bind to substrate proteins and may unfold them, which is a necessary prerequisite to import (Salvador *et al.*, 2000). A molecular chaperone in the lysosomal lumen (lyhsc70) is required for import of the substrate protein (Agarraberes *et al.*, 1997) and for optimal membrane insertion of the receptor for this proteolytic pathway, lysosome-associated membrane protein 2a (lamp 2a) (Cuervo and Dice, 2000).

Another lysosomal pathway of proteolysis, macroautophagy, is induced in rat liver for the first day of starvation, but macroautophagy declines to basal levels by the second day (Dice, 2000). CMA is only activated slightly during the first day of starvation but is activated greatly during longer starvation times (Cuervo *et al.*, 1995). This pattern suggests that the relatively nonselective macroautophagy provides amino acids during short starvation times but that the substrate selective CMA is used for prolonged starvation. Presumably, the substrates for CMA are dispensable under these conditions.

Primary human fibroblasts in culture stimulate macroautophagy when they become confluent. Withdrawal of serum growth factors from confluent fibroblasts activates CMA (Chiang and Dice, 1988). However, not all cells in culture behave in this orderly manner. For example, hepatocytes and kidney tubule cells may simultaneously activate macroautophagy and CMA in response to withdrawal of growth factors.

We have reproduced CMA using isolated lysosomes and defined components, such as molecular chaperones, ATP, and an ATP-regenerating system (Chiang *et al.*, 1989; Cuervo *et al.*, 2000; Terlecky and Dice, 1993). We have used lysosomes isolated from rat liver or from a variety of cultured cells in such assays. Others have used yeast vacuole preparations to study CMA (Horst *et al.*, 1999). It is with these *in vitro* preparations that many molecular details of CMA have been established.

II. MATERIALS AND INSTRUMENTATION

There are no special materials or instrumentation required to reproduce CMA *in vitro*. Standard laboratory equipment, including a low-speed centrifuge, an ultracentrifuge, a scintillation counter, a fluorimeter, and materials for sodium dodecylsulfate polyacrylamide electrophoresis (SDS–PAGE), are all that are needed. We give specific sources for materials that we use, but except when stated in Section IV, this does not imply that products from other venders are inferior.

III. PROCEDURES

A. Cell Culture

In order to obtain enough lysosomes for experimentation, you should grow cells on several 500-cm^2

Copyright 2006, Elsevier Science (USA).
All rights reserved.

diameter plates (Corning Science Products, Acton, MA 01720, #431110). The cell culture conditions for IMR-90 fibroblasts (Coriell Institute for Medical Research, Camden, NJ 08103) are as follows: high glucose Dulbecco's modified Eagle's medium (DMEM) (Sigma Chemical Company, St. Louis, MO 63178, #D5648), 10% newborn calf serum (NCS; Atlanta Biologicals, Norcross, GA 30093, #S11250), and 1% penicillin/streptomycin with fungicide (GIBCO/Invitrogen, Rockville, MD 20849, #15240-062) grown at 37°C in 5% CO_2. Once the cells reach confluence, cells can be trypsinized (GIBCO/Invitrogen, Rockville, MD 20849, #25300-054) and replated following standard cell culture procedures.

B. Harvesting Cells

The procedures for isolating lysosomes are shown schematically in Fig. 1. Once the cells are ready to harvest, usually at confluence, media can be removed from the plate using a vacuum flask and Pasteur pipette. The cells should then be washed twice with cold (4°C) phosphate-buffered saline (PBS; 720 m*M* Na_2HPO_4/28 m*M* NaH_2PO_4/26 m*M* NaCl, pH 7.2). Next, add 1 ml of PBS to the plate and gently rock the plate to ensure that cells are covered with PBS. Collect the cells by scraping the monolayer with a rubber policeman. Repeat with other 500-cm^2 plates of cells and add the collected cells to an ice-cold 15-ml corex

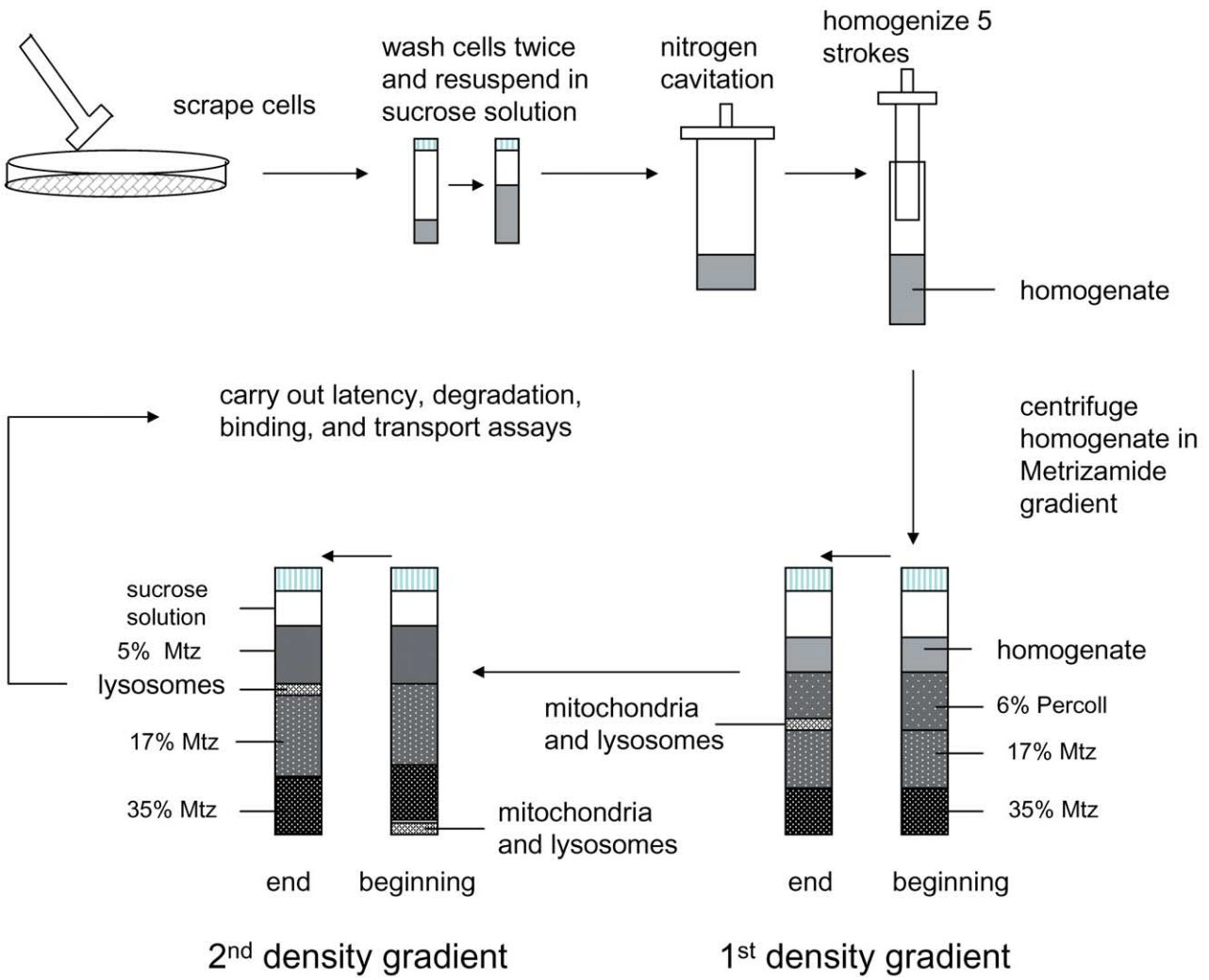

FIGURE 1 Preparation of lysosomes from cultured cells. Procedures are as described in the text.

tube (VWR, Marlboro, MA 01752, #8441-15; see Comment 1). Centrifuge the cells at 500 *g* for 5 min at 4°C and discard the supernatant. Gently resuspend the pellet in 2 ml 0.25 *M* sucrose (Sigma, #S-9378), pH 7.2 (sucrose solution), centrifuge again, and discard the supernatant.

C. Preparation of Lysosomes

Resuspend the pelleted cells in 1 ml of sucrose solution and place them into a nitrogen cavitation chamber (Kontes Glass Company, Vineland, NJ 08360, #08363-1502). Attach the cavitation chamber to a nitrogen tank and equilibrate the cavitation chamber to 30 pounds per square inch over a period of 1 min and cavitate for an additional 5 min. We have shown that this cavitation pressure and time are optimal for IMR-90 fibroblasts, human embryo kidney (HEK 293), and Chinese hamster ovary (CHO) cells. For other cell types you should optimize the pressure and time to achieve maximal cell disruption with minimal lysosomal disruption. To increase lysosomal yield, homogenize with five strokes of a loose-fitting Teflon pestle (Thomas Scientific, Swedesboro, NJ 08085, #AA22). Transfer the homogenate back to the corex tubes and centrifuge at 2500 *g* for 15 min at 4°C to separate nuclei from the cytoplasm.

While you perform this centrifugation you should pour the first density gradient. In a Beckman centrifuge tube (Beckman Instruments, Fullerton, CA 92634, #344059) pipet 2 ml of 35% metrizamide (Mtz; Accurate Chemical and Scientific Corporation, Westbury, NY 11590, #AN-6300KG) in sucrose solution (see Comment 2). Next layer 2 ml of 17% Mtz in sucrose solution, followed by 3 ml of 6% Percoll (Amersham Biosciences Corporation, Piscataway, NJ 08855, #17-0891-01) in sucrose solution. Layer the postnuclear supernatant on top of the gradient. This gradient should be centrifuged in a swinging bucket rotor such as the Beckman SW40.1 using a Beckman L8-M or equivalent ultracentrifuge at 69,000 *g* for 35 min at 4°C with the rate of acceleration and deceleration set to 7. The band of interest containing lysosomes and mitochondria will migrate at the 17% Mtz/6% Percoll interface. Aspirate and discard the upper bands and collect 1.2 ml of the lysosomal/mitochondria band. Add the 1.2 ml of lysosomes/mitochondria to 0.875 ml of 80% Mtz resulting in a 35% Mtz solution into another Beckman centrifuge tube. This will be the bottom portion of the second gradient. Keep this tube on ice while pouring the gradient. Place the tube into a larger tube or beaker containing ice at the bottom. Next, layer 2 ml of 17% Mtz in sucrose solution followed by 2 ml of 5% Mtz in sucrose solution. Fill the centrifuge tube to the top with sucrose solution, place the tube in the swinging bucket, and centrifuge using the same settings as the previous gradient. The pure lysosomal fraction will float to the 17% Mtz/5% Mtz interface (Storrie and Madden, 1990). Collect the lysosomes in 0.8–1.2 ml. These lysosomes can be used directly for transport, latency, or binding and uptake assays.

For SDS–PAGE or to separate lysosomal membrane from the matrix, further centrifugation is necessary to concentrate the lysosomes or to separate the Mtz from lysosomes. Take the lysosomal fraction from the second gradient and divide it into two polycarbonate ultracentrifuge tubes (Beckman Instruments, Spinco Division, Palo Alto, CA 94304, #343778). Dilute in 4 volumes of sucrose solution and centrifuge at 100,000 *g* for 45 min. You will notice a small pellet of lysosomes at the bottom of the tube. This pellet can be resuspended in SDS–PAGE buffer, boiled for 5 min, and subjected to SDS–PAGE. In order to separate membrane from matrix the pellet should be resuspended in 0.1 ml of water. Freeze and thaw the lysosomal resuspension five times and then centrifuge at 150,000 *g* for 30 min. The pellet from this centrifugation is the lysosomal membrane and the supernatant is the matrix fraction. The supernatant can be removed with a pipette and the pellet resuspended in the same hypotonic buffer. The membrane and matrix can then be subject to SDS–PAGE or other analytical methods.

D. Lysosomal Enzyme Latency Assay

The latency assay is necessary to determine the percentage of broken lysosomes after isolation. The latency assay is conducted using a 96-well 0.22-µm filter plate (available from Millipore, Bedford, MA 01730, #MAGVN2210) along with a 96-well plate. The first step is to wet the desired wells of the filter plate with distilled water for 5 min at room temperature. Shake the water out of the plate and then block the wells with 20 mg/ml of bovine serum albumin (BSA) in water. Next, filter the blocking solution with a vacuum manifold (Millipore, Bedford, MA 01730, #MAVM0960R). Add 42.5 µl of 10 m*M* MOPS solution [3-(*N*-morpholino)propanesulfonic acid]/0.25 *M* sucrose, pH 7.2 (USB Corporation, Cleveland, OH 44128, #19256), per well and 7.5 µl of lysosomes directly from the gradient. Apply the vacuum for 30 s or until all the solution is filtered. Take the flow through and assay for β-hexosaminidase as described below. For total β-hexosaminidase activity, add 7.5 µl

of lysosomes and 42.5 µl of MOPS solution. These samples can also be stored at –20°C until assaying.

For the β-hexosaminidase assay, prepare glass test tubes with the flow through from the filter plate in MOPS solution, leaving one tube as a blank. Next, add 0.2 ml of reaction mixture [10 ml acetate buffer, 10 ml β-hexosaminidase substrate solution, 0.5 ml Triton X-100, 19.5 ml of water (see Comment 3)]. Incubate at 37°C for 45 min. Stop the assay by adding 0.5 ml of 0.5 *M* glycine/0.5 *M* Na_2CO_3. Measure the fluorescence using a fluorimeter with an excitation of 364 nm and an emission of 448 nm with the slit set at 3 nm. Calculate the percentage of broken lysosomes using the formula: fluorescence of filtrate/fluorescence of total lysosomes ×100. Generally, lysosomes preparations are considered successful if less then 5% of lysosomes are broken. Lysosome preparations with greater than 10% breakage should not be used.

E. Reductive Methylation of CMA Substrate Proteins

Glyceraldhyde-3-phosphate dehydrogenase (GAPDH; Sigma, #G-2267) and ribonuclease A (RNase A; Worthington Chemical Company, Lakewood, NJ 08701, #LS003433) are the most commonly used substrate proteins to study the transport of proteins into isolated lysosomes during CMA due to their commercial availability, as well as the ability to label them by reductive methylation without denaturing the proteins (see Comment 4). Labeling reactions are typically done using 250 µCi of [^{14}C]formaldehyde (Perkin-Elmer Life Sciences, Boston, MA 02118, #NEC-039H) and 1 mg of either GAPDH or RNase A.

Before the labeling reaction is performed, prepare disposable G-50 Sephadex (Sigma, #G-50-80) columns in 1-ml syringes that have had the plungers removed and the tips plugged with glass fiber. Place empty columns into glass tubes, fill the columns with resin to the 1-ml mark on the syringe barrel, and allow to drain. Draining is facilitated by centrifugation at 300 *g* for 2 min (see Comment 5). Next, equilibrate columns with 5 ml of 10 m*M* MOPS (pH, 7.2) and centrifuge at 300 *g* for 1 min. Prepare six columns for the labeling reaction (see Comment 6).

Equilbrate GAPDH or RNase A (1 mg) into MOPS buffer by adding 100 µl of a 10-mg/ml solution to one of the prepared G-50 Sephadex columns. The flow through containing the protein equilibrated in MOPS buffer will be used in the subsequent labeling reaction. Add 50 µl of a 5-µCi/µl solution (250 µCi total) of [^{14}C]formaldehyde to the equilibrated protein solution followed by 50 µl of a 9-mg/ml solution of NaCNBr (Sigma, #AS-8638) and incubate the reaction at 25°C for 1 h. During this incubation, block the remaining G-50 Sephadex columns to prevent nonspecific binding by adding 2 ml of 10 mg/ml BSA followed by centrifugation as described earlier. Equilibrate the columns with another 5 ml of MOPS buffer. After incubation, add 75 µl of the labeling reaction to 3 of the blocked columns, place in clean glass tubes, and centrifuge for 2 min. Flow through from the centrifugation step contains the labeled protein, which is then collected and pooled from the three columns. Unreacted [^{14}C]formaldehyde remains in the column. To determine labeling efficiency, place 2 µl of the protein flow through into 98 µl of MOPS buffer and determine acid-soluble and insoluble radioactivity as described later. The labeled protein solution should be diluted 1 : 50 in MOPS buffer before use for transport assays.

F. Protein Transport and Degradation Assay

CMA substrate proteins are transported across the lysosomal membrane and are degraded by hydrolases present in the lysosomal lumen. Transport of [^{14}C]GAPDH into isolated lysosomes can be quantified by an increase in acid-soluble radioactivity as it is degraded into amino acids and small peptides. Data are expressed as the percentage of total radioactivity that is converted to acid-soluble radioactivity during the incubation period.

Use 10 to 40 µl of the lysosomal fraction from the second Mtz gradient in a total reaction volume of 100 µl of 0.25 *M* sucrose, 10 m*M* MOPS, pH 7.2, and 5 m*M* dithiothreitol. Add 10 µl of a 1 : 50 dilution of [^{14}C]GAPDH stock solution to lysosomes and allow transport and degradation to proceed for 90 min at 25°C. To stop the transport assay, filter the reaction mixture using Millipore multiscreen assay filter plates (96-well format, 0.22-µm pore size) and a vacuum manifold. Filters should be wetted and blocked as described in Section III,D. The acid-insoluble protein is then precipitated from the filtrate using trichloroacetic acid (TCA) as outlined below.

To precipitate acid-insoluble radioactivity, add 100 µl of 20% TCA to the filtrate followed by 10 µl of 20 mg/ml BSA as carrier protein. Incubate for 1 h to overnight at 4°C. Separate precipitated proteins by centrifugation at 13,000 *g* for 10 min. Remove the resulting supernatant, which contains acid-soluble radioactivity, from the pellet, which contains acid-insoluble radioactivity. Wash the pellets with an additional 100 µl of 20% TCA and, after centrifugation, pool the supernatants. Solubilize the pellets with 100 µl of 1 *N* NaOH followed by neutralization with 8.3 µl of 12 *N* HCl. Count radioactivity in the pooled acid-soluble fraction as well as the solubilized and neutral-

ized acid-insoluble fraction by scintillation counting. The percentage protein degraded is acid-soluble radioactivity/acid-soluble + acid-insoluble radioactivity × 100. CMA activity is stimulated by the inclusion of hsc70, ATP, and an ATP-regenerating system (Chiang *et al.*, 1989, Terlecky and Dice, 1993).

G. Protein Binding and Transport Assay

Substrates of CMA specifically bind to lamp2a in the lysosomal membrane (Cuervo and Dice, 1996). Chymostatin-treated lysosomes do not significantly degrade proteins that are transported into the lysosomal lumen. To measure the amount of binding and transport of CMA substrate proteins by isolated lysosomes, treat 198 µl of lysosomes from the second Mtz gradients with 2 µl of a 10 m*M* chymostatin (Sigma, #C-7268) stock dissolved in dimethyl sulfoxide for 10 min on ice. After chymostatin treatment, dilute the lysosomes three-fold in 10 m*M* MOPS/0.25 sucrose, pH 7.2, buffer for a final chymostatin concentration of 33 µ*M*. Use 100 µl of diluted lysosomes for the binding/transport assay. Add 20 µg of nonradioactive GAPDH or RNase A to chymostatin-treated lysosomes and incubate the reaction for 20 min at 37°C. Treat one replicate of each with 2.5 µl of a 2-mg/ml stock of proteinase K (Sigma, #P6556) and incubate on ice for 15 min. Inhibit proteinase K by the addition of 10 µl of a 24 m*M* 4-(2-aminoethyl)-benzene sulfonyl fluoride (Sigma, #A8456) stock solution dissolved in dimethyl sulfoxide. Collect lysosomes by centrifugation at 100,000 *g* for 30 min. Resuspend the pelleted lysosomes in SDS–PAGE sample buffer and separate the proteins by SDS–PAGE. Alternatively, you may collect lysosomes by filtration as described earlier followed by punching and boiling the filters in electrophoresis sample buffer. The binding and uptake of CMA substrates are then assessed via immunoblotting using anti-GAPDH (Biodesign International, Saco, ME 04072, #H86504M) or anti-RNase A antibodies (Rockland Immunochemicals, Gilbertsville, PA 19525, #200-4188). Substrate that is susceptible to proteinase K cleavage is bound to the surface of lysosomes. Sunstrate that is not susceptible to proteinase K is in the lysosomal matrix. You may substitute [^{14}C]GAPDH or [^{14}C]RNase A in the aforementioned assay to provide a quantitative measure of substrate binding and uptake into isolated lysosomes.

IV. COMMENTS

1. Throughout the entire lysosomal preparation the samples should be kept on ice. Failure to keep the samples on ice will significantly decrease lysosomal recovery and increase the percentage of lysosomes that are broken.

2. An 80% Mtz stock solution (w/v) should be made several days prior to the lysosomal preparation. Dissolve the Mtz very slowly in sucrose solution using a stir bar and stir plate mixer. Generally, making 120 ml will take 8 h. Once the Mtz stock solution is made it should be divided into 40-ml aliquots and frozen in disposable 50 ml conical tubes wrapped with aluminum foil at –20°C.

3. Make the β-hexosaminidase reaction mixture using the following reagents: 0.4 *M* sodium acetate (Sigma, #S-8628), pH 4.4, 10% Triton X-100 (Sigma, #X-100), and β-hexosaminidase substrate solution (4 m*M* 4-methylumbelliferyl-*N*-acetyl-β-D-glucosaminide (Sigma, #M-2133) in water. Sonicate to dissolve and, for immediate use, keep at 37°C. For storage, keep at –20°C wrapped with aluminum foil.

4. Some preparations of RNase A from Sigma Chemical Company contain trace amounts of RNase B. RNase A preparations from Worthington Chemical Company should be used.

5. The Sepadex-50 compacts by approximately one-third with this centrifugation.

6. Extra G-50 Sephadex columns in addition to the four required are prepared in case some columns have bubbles in the resin layer. Bubbles will impede the flow of fluid through the column and may affect recovery of labeled protein and should not be used.

V. PITFALLS

It is crucial that the lysosomal preparation contain few broken lysosomes. In our experience, preparations with <5% broken lysosomes give reproducible results. Preparations with >10% broken lysosomes should be discarded. Results using preparations of lysosomes with breakage between 5 and 10% should be regarded with suspicion.

References

Agarraberes, F. A., and Dice, J. F. (2001). A molecular chaperone complex at the lysosomal membrane is required for protein translocation. *J. Cell Sci.* **114**, 2491–2499.

Agarraberes, F. A., Terlecky, S. R., and Dice, J. F. (1997). An intralysosomal hsp70 is required for a selective pathway of lysosomal protein degradation. *J. Cell Biol.* **137**, 825–834.

Chiang, H.-L., and Dice, J. F. (1988). Peptide sequences that target proteins for enhanced degradation during serum withdrawal. *J. Biol. Chem.* **263**, 6797–6805.

Chiang, H.-L., Terlecky, S. R., Plant, C. P., and Dice, J. F. (1989). A role for a 70-kilodalton heat shock protein in lysosomal degradation of intracellular proteins. *Science* **246**, 382–385.

Cuervo, A. M., and Dice, J. F. (1996). A receptor for the selective uptake and degradation of proteins by lysosomes. *Science* **273**, 501–503.

Cuervo, A. M., and Dice, J. F. (2000). Regulation of lamp2a levels in the lysosomal membrane. *Traffic* **1**, 570–583.

Cuervo, A. M., Gomes, A. V., Barnes, J. A., and Dice, J. F. (2000). Selective degradation of annexins by chaperone-mediated autophagy. *J. Biol. Chem.* **275**, 33329–33335.

Cuervo, A. M., Knecht, E., Terlecky, S. R., and Dice, J. F. (1995). Activation of a selective pathway of lysosomal proteolysis in rat liver by prolonged starvation. *Am. J. Physiol.* **269**, C1200–C1208.

Dice, J. F. (1990). Peptide sequences that target cytosolic proteins for lysosomal proteolysis. *Trends Biochem. Sci.* **15**, 305–309.

Dice, J. F. (2000). "*Lysosomal Pathways of Protein Degradation*." Landes Bioscience, Austin, TX.

Horst, M., Knecht, E., and Schu, P. (1999). Import into and degradation of cytosolic proteins by isolated yeast vacuoles. *Mol. Biol. Cell* **10**, 2879–2889.

Storrie, B., and E. A. Madden (1990). Isolation of subcellular organelles. *Methods Enzymol.* **182**, 203–225.

Terlecky, S. R., and Dice, J. F. (1993). Polypeptide import and degradation by isolated lysosomes. *J. Biol. Chem.* **268**, 23490–23495.

CHAPTER

45

Methods in Protein Ubiquitination

Aaron Ciechanover

I. INTRODUCTION

Degradation of a protein via the ubiquitin-proteasome (UPS) pathway involves two discrete and successive steps: **(a)** tagging of the substrate by covalent attachment of multiple ubiquitin molecules and **(b)** degradation of the tagged protein by the 26S proteasome complex with release of free and reusable ubiquitin. This last process is mediated by ubiquitin recycling enzymes (isopeptidases; deubiquitinating enzymes; DUBs)(for a scheme of the UPS, see Fig. 1).

Conjugation of ubiquitin, a highly conserved 76 residue polypeptide, to the protein substrate proceeds via a three-step cascade mechanism. Initially, the ubiquitin-activating enzyme, E1, activates ubiquitin in an ATP-requiring reaction to generate a high-energy thiol ester intermediate, E1-S~ubiquitin. One of several E2 enzymes (ubiquitin-carrier proteins or **ub**iquitin-**c**onjugating enzymes, UBCs) transfers the activated ubiquitin from E1 via an additional high-energy thiol ester intermediate, E2-S~ubiquitin, to the substrate that is specifically bound to a member of the ubiquitin-protein ligase family, E3. There are several families of E3 enzymes. Members of the RING finger-containing E3s, the largest family of E3s, catalyze direct transfer of the activated ubiquitin from E2 to the E3-bound substrate. For HECT (**H**omologous to the **E**6-AP **C T**erminus) domain E3s, the ubiquitin is transferred from the E2 to an active site Cys residue on the E3 to generate a third high-energy thiol ester intermediate, ubiquitin-S~E3, prior to its transfer to the ligase-bound substrate.

E3s catalyze the last step in the conjugation process: covalent attachment of ubiquitin to the substrate. Ubiquitin is generally transferred to an ε-NH_2 group of an internal lysine residue in the substrate to generate a covalent isopeptide bond. In some cases however, ubiquitin is conjugated to the N-terminal amino group of the substrate. By successively adding activated ubiquitin moieties to internal lysine residues on the previously conjugated ubiquitin molecule, a polyubiquitin chain is synthesized. The chain is recognized by the downstream 26S proteasome complex. Thus, E3s play a key role in the ubiquitin-mediated proteolytic cascade, as they serve as the specific substrate-recognition elements of the system. Approximately 1,000 different E3s have been identified in the human genome based on specific, commonly shared structural motifs. A single modification by ubiquitin or by ubiquitin-like proteins (UBLs), such as the Small Ubiquitin MOdifier (SUMO) or NEDD8, serves other, nonproteolytic purposes, such as routing cellular proteins to subcellular destinations or to the lysosome/vacule for degradation. UBLs are also conjugated via their C-terminal residue to an internal lysine residue in the acceptor protein. The specific enzymes that catalyze modification by ubiquitin-like proteins are somewhat different from those involved in conjugation of ubiquitin, although they utilize a similar mechanism. SUMO, for example, is conjugated by a heterodimeric E1, Aosl•Uba2, and the E2-conjugating enzyme Ubc9. Although Ubc9 can recognize the SUMOylation motif and transfer SUMO to certain substrates, for other proteins, specific E3 enzymes have been described (for reviews on poly- and oligoubiquitination and on UBLs, see Pickart, 2001; Weissman, 2001; Glickman and Cicchanover, 2002; Schwartz and Hochstrasser, 2003; Hicke and Dunn, 2003; Huang *et al.*, 2004).

Degradation of the polyubiquitinated substrates is carried out by the 26S proteasome that does not

Copyright 2006, Elsevier Science (USA).
All rights reserved.

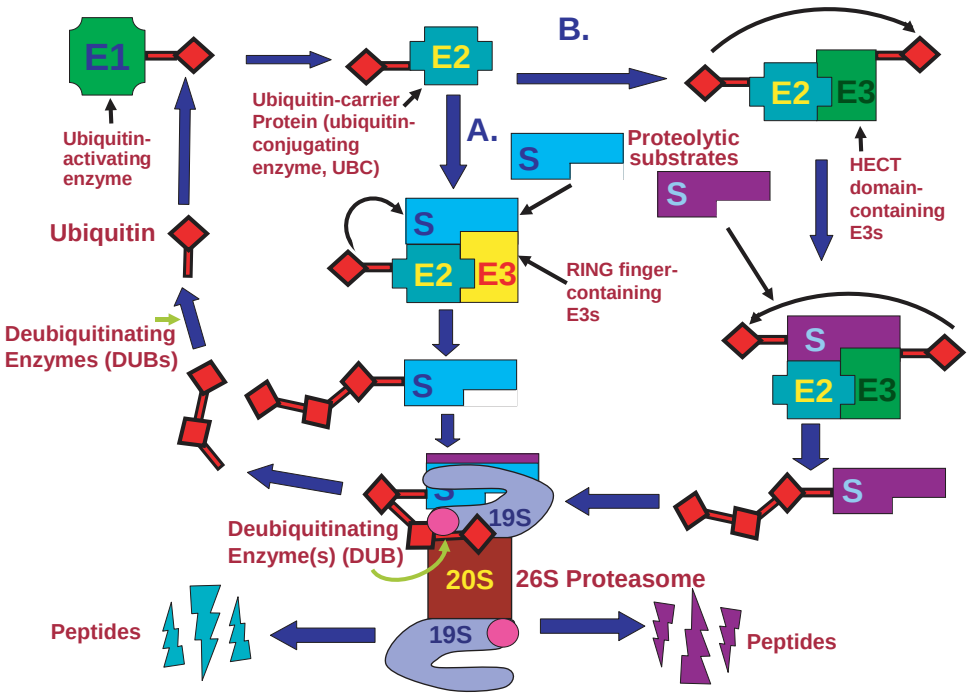

FIGURE 1 Ubiquitin is first activated to a high-energy intermediate by E1. It is then transferred to a member of the E2 family of enzymes. From E2 it can be transferred directly to the substrate (S; light blue) that is bound specifically to a member of the ubiquitin ligase family of proteins, E3. This occurs when the E3 belongs to the RING finger family of ligases (A). In the case of an HECT domain-containing ligase (B), the activated ubiquitin is transferred first to the E3 before it is conjugated to the E3-bound substrate (S; dark purple). Additional ubiquitin moieties are added successively to the previously conjugated moiety to generate a polyubiquitin chain. The polyubiquitinated substrate binds to the 26S proteasome complex (constituted of 19S and 20S subcomplexes): the substrate is degraded to short peptides, and free and reusable ubiquitin is released via the activity of deubiquitinating enzymes. These enzymes are both proteasomal and soluble.

recognize, in the vast majority of cases, nonmodified substrates. The proteasome is a multicatalytic protease that degrades polyubiquitinated proteins to short peptides. It is composed of two subcomplexes: a 20S core particle (CP) that carries the catalytic activity and a regulatory 19S regulatory particle (RP). The 20S CP is a barrel-shaped structure composed of four stacked rings, two identical outer α rings, and two identical inner β rings. The eukaryotic α and β rings are composed each of seven distinct subunits, giving the 20S complex the general structure of $\alpha_{1\text{-}7}\beta_{1\text{-}7}\beta_{1\text{-}7}\alpha_{1\text{-}7}$. The catalytic sites are localized to some of the β subunits. Each extremity of the 20S barrel can be capped by a 19S RP. One important function of the 19S RP is to recognize ubiquitinated proteins and other potential substrates of the proteasome. A ubiquitin-binding subunit of the 19S RP has indeed been identified; however, its biological function and mode of action have remained enigmatic. A second function of the 19S RP is to open an orifice in the α ring that will allow entry of the substrate into the proteolytic chamber. Also, because a folded protein would not be able to fit through the narrow proteasomal channel, it is assumed that the 19S particle unfolds substrates and inserts them into the 20S CP. Both the channel opening function and the unfolding of the substrate require metabolic energy, and indeed, the 19S RP contains six different ATPase subunits. Following degradation of the substrate, short peptides derived from the substrate are released, as well as reusable ubiquitin. These peptides are further degraded into free amino acids by cytosolic amino- and carboxypeptidases. A small fraction of the peptides is transported across the ER membrane, binds to the MHC class I complex, and is carried to the cell surface to be presented to cytotoxic T cells. In case the peptides are derived from a "nonself" antigen, the T cell lyses the presenting cell. Proteasomal degradation is not always complete. In some cases, the proteasome processes the ubiquitinated substrate in a limited manner, releasing a truncated product. In the case of the NF-κB transcriptional regulator, an active subunit (p50 or p52) is thus released

from a longer inactive precursor (p105 or p100). For reviews on the proteasome, see Zwickl *et al.* (2002), Gröll and Huber (2003), Adams (2003), and Glickman and Adir (2004).

A major, yet unresolved problem is how the UPS achieves its high specificity and selectivity toward its innumerable substrates. Why are certain proteins extremely stable in the cell, whereas others are extremely short-lived? Why are certain proteins degraded only at a particular time point during the cell cycle or only following specific extracellular stimuli, yet they are stable under most other conditions? It appears that specificity of the ubiquitin system is determined by two distinct and unrelated groups of proteins: (i) E3s and (ii) modifying enzymes and ancillary proteins. Within the ubiquitin system, substrates must be recognized and bind to a specific E3 as a prerequisite to their ubiquitination. In most cases, however, the substrates are not recognized in a constitutive manner and they must undergo a posttranslational modification such as specific phosphorylation or oxidation that renders them susceptible for recognition. In some other cases the target proteins are not recognized directly by the E3, and their recognition depends on association with ancillary proteins such as molecular chaperones that act as recognition elements in *trans* and serve as a link to the appropriate ligase. Other proteins, such as certain transcription factors, have to dissociate from the specific DNA sequence to which they bind in order to be recognized by the system. Stability of yet other proteins depends on oligomerization. Thus, in addition to E3s, modifying enzymes, such as kinases, ancillary proteins, or DNA sequences to which substrates bind, also play an important role in the recognition process. In some instances, it is the E3 that must be switched on by undergoing posttranslational modification in order to yield an active form that recognizes the target substrate.

II. MATERIALS AND INSTRUMENTATION

ATP (adenosine-5′-triphosphate disodium salt)(Sigma A-7699)
ATP-γ-S (adenosine-5′-[γ-thio]triphosphate tetralithium salt)(Sigma A-1388)
Chloramine-T (Sigma C-9887)
Creatine phosphokinase (CPK; from rabbit muscle) (Sigma C-3755)
Creatine phosphate (CP; phosphocreatine, disodium salt) (Sigma P-7936)
Cultured cells (HeLa, 293, Cos; E1 WT and its mutant cells—CHO-E36 and CHO-ts20) for preparation of cell extract and for pulse–chase labeling and immunoprecipitation experiments
Cycloheximide (Sigma C-1988)
2-Deoxyglucose (2-DOG; Sigma D-6134)
Diethylaminoethyl cellulose (DEAE; DE52; Whatman 4057-050)
2,4-Dinitrophenol (DNP; Aldrich D198501)
1,4-Dithiothreitol (DTT)(Sigma D-8255)
Dulbecco's modified Eagle medium (DMEM) with high glucose, L-glutamine, and sodium pyruvate (GIBCO 11995-065)
DMEM with high glucose, without L-glutamine, sodium pyruvate, and L-methionine (Biological Industries, Beit Ha'emek, Israel 01-054-1)
Epoxomicin (BIOMOL International L.P. PI-127)
N-Ethylmaleimide (NEM; Sigma E-1271)
Foetal bovine serum (certified, heat inactivated; US)(GIBCO 10082-147)
Foetal calf serum, dialyzed (Biological Industries, Beit Ha'emek, Israel 04-011-1)
Anti-HA antibody (Roche; clone 3F10; 1867423)
HEPES buffer (Sigma H-4034)
Hexokinase (~1,500 units/ml as ammonium sulfate slurry, Roche 1426362)
6 × Anti-His antibody (Qiagen; RGS; 34610)
[^{125}I]Na (350–600 mCi/ml; Amersham Biosciences IMS 300)
clasto-Lactacystin β-lactone (BIOMOL International L.P. PI-108)
Z-Leu-Leu-Leu-H (MG132; BIOMOL International L.P. PI-102)
L-[^{35}S]methionine (>1000 Ci/mmol; *in vitro* translation grade; Amersham biosciences SJ1515)
L-[^{35}S]methionine (×1000 Ci/mmol; cell labeling grade; Amersham biosciences SJ1015)
Methylated ubiquitin (MeUb; BIOMOL International L.P. UW8555)
Anti-Myc antibody (Roche; clone 9E10; 1667149)
New Zealand white rabbits (preferably females) of ~2 kg body weight (2-3 months old; for preparation of reticulocyte lysate)
Phenylhydrazine-HCl (Sigma P-6926)
Ribonuclease inhibitor (recombinant RNasin; Promega N2511)
Salts (KCl, NaCl, $MgCl_2$, NaF, NaN_3, ammonium sulfate, NaPi, KPi) (various suppliers; of highest analytical grade)
Sodium bisulfite (sodium metabisulfite; Sigma S-9000)
Translation-transcription kit (rabbit reticulocyte lysate based; L4600, L4610, or L4950, dependent on the RNA polymerase promoter in the vector, SP6, T3 or T7, respectively; TNT; Promega)

Translation-transcription kit (wheat germ extract based; L4120, L4130, or L4140, dependent on the RNA polymerase promoter in the vector, T3, SP6, or T7, respectively; TNT; Promega)
Trichloroacetic acid (TCA; 100% solution; Sigma T-0699)
Tris buffer (Trizma base; Tris base; THAM; Trometamol; 2-Amino-2-(hydroxymethyl)-1,3-propanediol; Sigma T-1378)
Ubiquitin (Sigma U-6253)
Ubiquitin (His-tagged; BIOMOL International L.P. UW8610)
Ubiquitin aldehyde (UbAl; BIOMOL International L.P. UW8450)
Ubiquitin, antibody (BIOMOL International L.P. PW8810)
Water (nuclease free; Promega P1193)
Dialysis tubing (SnakeSkin, Pierce, 68100)
Desalting column (PD-10, Amersham Biosciences 17-0851-01)
Nitrogen cavitation bomb (Parr Instrument Company)

III. PROCEDURES

A. Preparation of Cell Extracts for Monitoring Conjugation and Degradation

To conjugate or degrade a protein substrate *in vitro*, one has to utilize the appropriate cell extract. Rabbit reticulocyte lysate contains the enzymes required for degradation of most proteins and can be therefore used in most cases. Reticulocytes have several advantages. They contain a relatively small number of proteins and do not have lysosomes from which proteases can leak during preparation of the extract. Unlike cultured cells lysate, one can obtain reticulocyte lysate in a relatively large amount. Also, the lack of requirement for tissue culture media and sera makes this lysate significantly less expansive then its nucleated cultured cells counterpart. All these attributes make this lysate an ideal extract in which one can test conjugation and proteolysis of the studied protein. For monitoring conjugation and degradation of labeled proteins in the crude extract, it is not necessary to deplete ATP from the cells prior to the preparation of the extract. This will be necessary, however, in order to reconstitute the cell-free proteolytic system and to monitor dependence of the proteolytic process on the addition of exogenous ubiquitin. It will also be necessary in order to monitor conjugation of labeled or tagged ubiquitin to different substrates. Depletion of ATP from cells leads to deubiquitination of most proteins. Once such an ATP-depleted lysate is fractionated over the anion-exchange resin diethylaminoehtyl (DEAE)-cellulose, ubiquitin is eluted in the unadsorbed, flow-through material (fraction I) that also contains several E2 enzymes. Fraction II, the high salt eluate, contains E1, the remaining E2s, all the E3s, and the 26S proteasome.

1. Preparation of Reticulocyte Lysate

Steps

1. Inject rabbits subcutaneously with 10 mg/kg of phenylhydrazine (freshly dissolved in phosphate-buffered saline, PBS) on days 1, 2,4, and 6.
2. Bleed the rabbits from the ear artery or vein or from the heart (following anaesthesia) on day 8. Induction of reticulocytosis is dramatic, and more then 90% of the circulating red blood cells are reticulocytes as determined by methylene blue or brilliant cresyl blue staining.
3. Wash the cells three times with ice-cold PBS and, using a Pasteur pipette, aspirate carefully the thin layer of white blood cells ("buffy coat") that overlays the pelleted red blood cells.
4. Lyse the cells in 1.6 volumes (of pelleted cells volume) of ice-cold $H_2O \times 2$ (double distilled water) containing 1 m*M* DTT (diluted from 1 *M* solution).
5. Centrifuge at 80,000 *g* for 1 h at 4°C to remove particulate material.
6. Collect the supernatant and freeze in aliquots at –70°C.
7. To deplete ATP, wash cells twice in PBS and resuspend in 1 volume of Krebs Ringer phosphate buffer (120 m*M* NaCl, 4.8 m*M* KCl, 1 m*M* $CaCl_2$, 1.2 m*M* $MgSO_4$, and 16.5 m*M* NaPi, pH 7.4) containing 20 m*M* 2-deoxyglucose and 0.2 m*M* 2,4-dinitrophenol. Following incubation accompanied by gentle shaking for 90 min at 37°C, wash cells twice in PBS, lyse, and centrifuge as described previously.

2. Preparation of Extract from Cultured Cells

All procedures are carried out at 4°C.

Steps

1. Wash cells three times in HEPES (20 m*M* pH 7.5)-saline buffer and resuspend to a concentration of 10^7–10^8/ml in 20 m*M* HEPES, pH 7.5, that contains also 1 m*M* DTT.
2. Cavitate cells in a high-pressure nitrogen chamber. For HeLa cells, the best conditions are 1000 psi for 30 min. However, these conditions may vary among different cell species. For example, it may be necessary to repeat the pressure cycle twice. Make sure that most of the cells are disrupted by visualizing the suspension in a light microscope before and after cavitation. Following disruption, one should observe intact nuclei (that are not broken) and cell debris.

3. Centrifuge the homogenate successively at 3,000 g and 10,000 g for 15 min each time and then at 80,000 g for 60 min. Collect and freeze the supernatant at –70°C.

4. To deplete ATP, wash cells twice in HEPES-saline buffer and resuspend in Krebs Ringer phosphate buffer (to a density of 10^7 cells/ml) in the presence of 2-deoxyglucose, 2,4-dinitrophenol (as described earlier), 20 m*M* NaF, and 10 m*M* of NaN_3. Following incubation for 60 min at 37°C, wash cells twice in HEPES-saline, resuspend in HEPES-DTT, lyse, and centrifuge as described earlier.

B. Fractionation of Cell Extract to Fraction I and Fraction II

As described earlier, fractionation of the lysate into fraction I and fraction II separates ubiquitin from many of the other components of the system, thus enabling one to monitor the dependence of conjugation and degradation upon the addition of exogenous ubiquitin and certain E2 enzymes. To fractionate the lysate, ATP-depleted lysate is resolved on a DEAE-cellulose column. In the ATP-depleted lysate, all the ubiquitin is free: it was released from conjugates by isopeptidases during incubation in the presence of the glycolysis and respiration inhibitors. In the absence of ATP, reconjugation cannot occur. Under these conditions, ubiquitin is resolved in fraction I, and fraction II is dependent for its conjugating and proteolytic activities upon the addition of exogenous ubiquitin. In cell extracts from which ATP was not depleted, the ubiquitin that is still conjugated to endogenous protein substrates will adsorb to the anion-exchange resin DEAE (via the protein substrate moiety) and will elute in fraction II. During incubation, the bound ubiquitin will be released by the activity of isopeptidases and will be available for conjugation to other proteins, including the test substrate examined. Therefore, it will be difficult to demonstrate ubiquitin-dependent conjugation and degradation in fraction II that is prepared from an extract from which ATP was not depleted. In addition, the bound ubiquitin fraction, when released, will dilute any added labeled or tagged ubiquitin, thus decreasing the detectable signal in the biosynthesized ubiquitin adducts.

All procedures are carried out at 4°C.

Steps

1. Swell the DEAE resin in 0.3 *M* KPi, pH 7.0, for several hours. Use enough resin to adsorb all the proteins in the extract that can be bound. As a rule, use 0.6 resin volume per volume of reticulocyte lysate, or 1 ml resin/~5 mg protein of nucleated cell extract [in principle, one can use also a chromatographic system such as the AKTÄ FPLC (Amersham Biosciences) with a Mono Q column, although for resolution of large quantities, the DEAE resin procedure is advantageous].

2. Load the resin onto a column and wash with 10 column volumes of a buffer containing 5 m*M* KPi, pH 7.0, and 1 m*M* DTT (buffer A).

3. Load the extract. Once all the material is loaded, elute fraction I with buffer A. When resolving reticulocyte lysate, collect only the dark red fraction. When resolving mucleated cell extract, collect only the fractions with the highest absorption at 280 nm. Freeze fraction in aliquots at –70°C.

4. Wash the column extensively with a buffer containing 20 m*M* KCl in buffer A. When resolving reticulocyte lysate, make sure all the hemoglobin is eluted. When resolving nucleated cell extract, wash until the absorbency at 280 returns to baseline.

5. Elute fraction II with 2.5 column volumes of a buffer containing 20 m*M* Tris–HCl, pH 7.2, 1 m*M* DTT, and 1 *M* KCl.

6. Add to the eluted fraction II ammonium sulfate to saturation (~70 g/li solution) and swirl on ice for 30 min.

7. Centrifuge at 15,000 rpm for 15 min.

8. Resuspend pellet in 0.2–0.3 of the volume of the original extract in a buffer containing 20 m*M* Tris–HCl, pH 7.2, and 1 m*M* DTT. At times, it will be difficult to dissolve all the proteins. This is not essential. They will be dissolved during dialysis.

9. Dialyze against two changes of a large volume of a buffer containing 20 m*M* Tris–HCl, pH 7.2, and 1 m*M* DTT. Dialysis should be carried out on ice. Remove particulate material by centrifugation at 15,000 rpm for 15 min. Freeze in aliquots at –70°C.

C. Labeling of Proteolytic Substrates

In most cases, monitoring the conjugation and/or degradation of a specific protein requires its labeling. The fate of the protein can also be followed via Western blot analysis using specific antibodies directed against the test protein [Western blot analysis will not be described here; however,the conjugation and degradation assays for labeled proteins (described later) can be applied in an almost identical manner for unlabeled proteins, using immune detection]. Two methods of labeling have proven to be useful: iodination and biosynthetic incorporation of [^{35}S]methionine. Iodination is utilized mostly when a purified recombinant/commercial protein is available. The main advantage of the method is the high specific radioactivity that can be attained. The disadvantage of the method is that one needs a pure protein. Also, during iodination, unless it is carried out using the Bolton–

Hunter reagent, the protein can be damaged from the chloramine T used to oxidize the iodide. In addition, during storage, the labeled substrate may be subjected to radiochemical damage. A different method of labeling utilizes incorporation of ^{35}S-labeled methionine to a protein that is synthesized in a cell-free system from its corresponding cDNA/mRNA. The generated protein is native; however, the specific activity obtained is relatively low. Also, the labeled protein is contained in the crude extract in which it is synthesized and it is not pure. This extract contains, among other proteins, enzymes of the ubiquitin system that may interfere in the reconstitution of a cell-free system from purified components.

Despite these shortcomings, metabolic labeling of proteins is the most frequently used procedure to label them and follow their fate *in vitro*. To label proteins biosynthetically, one can first synthesize the mRNA on the cDNA template, using the appropriate RNA polymerase. Following digestion of the cDNA, the extracted mRNA can be translated *in vitro* in reticulocyte or wheat germ extracts. Alternatively, one can use a coupled transcription–translation cell-free extract that synthesizes the mRNA and translates it simultaneously. Such systems are available commercially (TNT; Promega). An even more advanced system (Quick TNT; Promega) contains all the necessary components for biosynthesis, except for the template cDNA and the labeling amino acid. Biosynthesis is carried out basically according to the manufacturer's instructions. In principle, it is preferable to use wheat germ extract. This extract lacks many, although not all, of the mammalian E3 enzymes. Therefore, in most cases, a protein synthesized in this extract can be used in experiments in which a cell-free system is reconstituted from purified enzymes and, in particular, when the role of a specific E3 is tested. A protein synthesized in reticulocyte lysate may be "contaminated" in many cases with its cognate E2 and/or E3 enzyme(s). This enzyme(s), which is being carried to the reconstituted system, may interfere with the examination of the role of an exogenously added E2 and/or E3 in the conjugation/degradation of the translated protein. However, at times, one must use the reticulocyte lysate, as the translation efficiency in the wheat germ extract is extremely low. In that case, the "contaminating" E2 or E3 in the reticulocyte lysate can be inactivated, if necessary, by NEM (10-min incubation at room temperature in a final concentration of 10 m*M* of freshly prepared solution). Because E1, all known E2s, and some of the E3s (HECT domain-containing) have an essential –SH group, the alkylating agent inactivates them. The NEM is then neutralized by the addition of DTT (final concentration of 7.5 m*M*). It should be noted that this procedure can also denature/inactivate the substrate. Alternatively, the labeled substrate can be immunoprecipitated immobilized from the translation mixture, and the system can be reconstituted using the isolated protein. In most cases, however, the substrate can still be utilized and reproduces faithfully the behavior of the native substrate. The cDNA template coding for the test protein should be driven by one of the following RNA polymerase promoters: SP6, T7, or T3.

Radioiodination of Proteins

Steps

1. Add the following reagents in the following order to 1.5-ml microcentrifuge (Eppendorf) tube. The volume of the reaction mixture can vary from 20 to 100 µl.
   a. NaPi, pH 7.5, final concentration of 100 m*M*
   b. Protein substrate, 10–500 µg
   c. Unlabeled NaI, 50 nmol (use a stock solution of 10 m*M* in H_2O)
   d. Radiolabeled $Na^{125}I$, 0.1–2.0 mCi
   e. Chloramine-T solution (10 mg/ml in 10 m*M* NaPi, pH 7.4, freshly dissolved), 10–50 µg
2. Mix once (vortex) and incubate for 1–2 min at room temperature.
3. Add 20–100 µg Na-metabisulfite solution (20 mg/ml in 10 m*M* NaPi, pH 7.4, freshly dissolved) and mix. Add two-fold the amount of the added chlovamine T.
4. To remove unreacted radioactive iodine, resolve the mixture over a desalting column (PD10) equilibrated with 10 m*M* Tris–HCl, pH 7.6, and 150 m*M* NaCl. Collect fractions (in a fraction collector or manually) of ~10% of column volume each.The radioactive protein is typically eluted in fraction 4 (void volume of the column, which is ~35% of the total volume of the column). To keep a relatively small elution volume, it is recommended not to follow the one step elution procedure suggeted by the manufacturer.
5. Store in aliquots at –18°C.

When monitoring conjugation, the *in vitro*-translated substrate can be used without further processing. This is also true in many cases when the degradation of the labeled substrate is followed by monitoring its disappearance in PhosphorImager-analyzed SDS–PA electrophoresed gels. However, as the degradation of certain proteins is not always efficient, it may be difficult to follow with accuracy the disappearance of 10–30% of a labeled protein band in a gel. In this case it will be necessary to monitor the release of radioactive material into a TCA-soluble fraction. For such preparations, in order to decrease background, the excess of unincorporated labeled methionine (or iodine) in the preparation of the trans-

lated protein must be first removed. This can be achieved via chromatography over DEAE exactly as described earlier for fractionation of lysate into resin-unadsorbed (fraction I) and adsorbed fractions (fraction II). The vast majority of the labeled proteins will resolve in fraction II, whereas the labeled amino acid (or iodine) will be eluted in fraction I. If the labeled protein is eluted in fraction I, changing the pH may lead to its adsorption. Alternatively, extensive dialysis of the labeled protein against a solution of 20 m*M* Tris–HCl, pH 7.6, 150 m*M* NaCl that also contains 1 m*M* of unlabeled methionine (or No. I) will also remove efficiently the labeling amino acid.

D. Conjugation of Proteolytic Substrates *in vitro*

To demonstrate that the degradation of a certain protein proceeds in a ubiquitin-dependent manner, it is essential to demonstrate the intermediates in the process, ubiquitin–protein adducts. Typically, incubation of the labeled protein in a complete cell extract supplemented with ubiquitin and in the presence of ATP will lead to the formation of high molecular mass adducts that can be detected following resolution of the mixture in SDS–PAGE. To increase the amount of the adducts generated, one can use two approaches, independently or simultaneously. The nonhydrolyzable ATP analog, adenosine-5′-*O*-(3-thiotriphosphate), ATP-γ-S, can be used instead of ATP (Johnston and Cohen 1991). The ubiquitin-activating enzyme, E1, can catalyze activation of ubiquitin in the presence of the analog, as it utilizes the α–β high energy bond of the nucleotide that is cleavable also in the analog. In contrast, assembly and activity of the 26S proteasome complex require the β–γ bond, which cannot be cleaved in the analog. Caution should be exercised, however, when utilizing the ATP analog. Often, phosphorylation of the target protein is required in order for the ubiquitin ligase to recognize it (for example, see Yaron *et al.*,1997). In these cases, the analog cannot substitute for the hydrolyzable native nucleotide, ATP. An additional approach to increase the amount of generated conjugates in a cell-free system is to use ubiquitin aldehyde (UbAl), a specific inhibitor of certain ubiquitin C-terminal hydrolases, isopeptidases (Hershko and Rose, 1987).

Steps

1. Add the following reagents to a 0.5-ml microcentrifuge (Eppendorf) tube. The volume of the reaction mixture can vary from 10.0 to 50.0 µl. Addition of all the reagents should be carried out on ice:

a. 50 m*M* Tris–HCl, pH 7.6 (1 *M* stock solution)
b. 5 m*M* $MgCl_2$ (1 *M* stock solution)
c. 2 m*M* DTT (1 *M* stock solution)
d. 5.0–30 µl of reticulocyte lysate or 50–200 µg of complete mucleated cell extract protein
e. 2.5–10 µg ubiquitin (10 mg/ml stock solution in H_2O)
f. 0.5–2.0 µg UbAl (1 mg/ml stock solution in H_2O)
g. ATP and ATP-regenerating system [0.5 m*M* ATP (0.1 *M* stock solution), 10 m*M* CP (0.5 *M* stock solution), and 2.5–10 µg CPK (10 mg/ml stock solution in 10 m*M* Tris, pH 7.2) or 2 m*M* ATP-γ-S (0.1 *M* stock solution)]
h. For depletion of endogenous ATP, the system should contain instead of ATP and the regenerating system 10 m*M* 2-DOG (1 *M* stock solution) and 0.2–1.0 unit hexokinase (ammonium sulfate slurry; centrifuge an aliquot of the slurry and resuspend to the same volume in 20 m*M* Tris–HCl buffer, pH 7.6. Dilute in the same buffer. Stock solution in the buffer can be stored at 4°C for at least 4 weeks)
i. For the substrate, use either a labeled protein (25,000–100,000 cpm) or an unlabeled substrate in an amount that is sufficient for detection by Western blot analysis (100–2000 ng)

Typically we prepare three reaction mixtures: (i) one that contains Tris, $MgCl_2$, DTT, ubiquitin, and UbAl, (ii) one that contains ATP, CP, and CPK, and (iii) one that contains 2-DOG and hexokinase.

2. Incubate the mixture for 30 min at 37°C and resolve via SDS–PAGE (7.5–10% acrylamide).

3. Detect high molecular mass conjugates by PhosphorImager analysis (labeled proteins) or via enhanced chemiluminescence (ECL) following Western blot (for unlabeled substrates) using a specific primary antibody against the test protein and a secondary tagged antibody.

There are several ways to demonstrate that the high molecular mass adducts generated are indeed ubiquitin conjugates of the test protein.

a. It is expected that the adducts will not be generated in an ATP-depleted system.

b. Generation of conjugates of the specific substrate should be inhibited reversibly by the addition of increasing amount of MeUb (Hershko and Heller, 1985). This reductively methylated derivative of ubiquitin lacks free amino groups and therefore cannot generate polyubiquitin chains. It serves therefore as a chain terminator in the polyubiquitination reaction, and consequently as an inhibitor in this reaction.

c. Adducts can be precipitated from the reaction mixture with an antibody directed against the test protein and, following SDS–PAGE, can be further detected with an antiubiquitin antibody. Alternatively, the reaction can be carried out in the presence of His-, HA-, or Myc-tagged ubiquitin (His-tagged ubiquitin is

available commercially; HA- and Myc-tagged ubiquitins or the bacterial expression cDNA clones that code for them can be obtained from different researchers), and the immunoprecipitate can be detected with an antibody against the appropriate tag.

d. A cell-free system can be reconstituted from purified or isolated components of the ubiquitin system and the formation of conjugates can be followed, dependent upon the addition of these components. Instead of adding a complete cell extract, it is possible to add fraction II (50–200 μg; derived from ATP-depleted cells) and free or tagged ubiquitin (2.5–10 μg: same amount as added to supplement the complete extract; see earlier discussion). Because fraction II is devoid of ubiquitin, the formation of conjugates that is dependent upon the addition of exogenous ubiquitin will strongly suggest that the high molecular mass derivatives generated slurring the reaction are indeed ubiquitin adducts of the test substrate. Because not all E2 enzymes are present in fraction II, it may be necessary, at times, to add to the reconstituted system purified UbcH5a, b, or c, UbcH7, or UbcH8 (~0.5–2.0 μg; available from BIOMOL International L.P.). In most cases, one of the UbcH5 (typically b or c) enzymes will be able to reconstitute activity and support conjugation.

E. Degradation of Proteolytic Substrates *in Vitro*

With several exceptions, cell-free systems for monitoring the degradation of proteolytic substrates are similar to those used for monitoring their conjugation. In the proteolytic assays however, unlike in the conjugation assays, ATP (and not ATP-γ-S) must be used, as activity of the 26S proteasome complex is dependent upon cleavage of the high-energy β–γ bond (see earlier discussion). ATP is added along with ATP-regenerating system as described earlier. Also, UbAl is not added. Following incubation for 2–3 h at 37°C, the reaction mixture is resolved via SDS–PAGE and disappearance of the substrate can be monitored either via PhosphorImager analysis (in case the protein substrate is radioactively labeled) or via Western blot analysis (in case of unlabeled substrate). Control reactions are complete mixtures that have been incubated on ice and/or mixtures that were incubated at 37°C in the absence of ATP. At times, degradation efficiency is low and it is difficult to follow the reduction in the amount of a protein band in gel analysis. In these cases, it is necessary to monitor the appearance of radioactivity in the TCA-soluble fraction. Here, only a radioactive substrate can be used. In moA cases, radioiodinated proteins can be used directly. At times, excess unincorporated iodine must be removed. *In vitro*-translated proteins must first undergo DEAE fractionation or extensive dialysis in order to remove excess unincorporated labeled methionine (see earlier discussion). At the end of the incubation, a carrier protein (10–25 μl of 100 mg/ml solution of BSA) is added, followed by the addition of 0.5 ml of ice-cold TCA (20%). Following mixing, the reaction is incubated on ice for 10 min and centrifuged (5 min at 15,000 *g*). The supernatant is collected and the radioactivity is determined in either a β-scintillation counter (for methionine) or a γ-counter (for iodine-labeled substrates). Again, control reactions are complete mixtures that have been incubated on ice and/or mixtures that were incubated at 37°C in the absence of ATP.

F. Involvement of Ubiquitin System in Degradation of Proteins *in vivo*: Effect of Specific Proteasomal Inhibitors and Inactivation of E1 on Stability of Proteins in Intact Cells

All the known proteolytic substrates of the ubiquitin system are degraded, following generation of the polyubiquitin chain, by the 26S proteasome. The opposite notion, that all substrates of the 26S proteasome must be ubiquitinated prior to their recognition by the enzyme, is true in all but one established case, that of ornithine decarboxylase (ODC) (Murakami *et al*., 1992). This enzyme is degraded by the 26S complex without prior ubiquitination. A noncovalent association with a specific binding protein, antizyme, renders ODC susceptible to degradation. The core catalytic subunit of the 26S enzyme is the 20S proteasome complex and inhibition of this complex inhibits all proteolytic activities of the 26S proteasome. To test whether a certain protein is degraded by the proteasome, it is possible to inhibit the enzyme, both *in vitro* and *in vivo*. Inhibition of the proteasome in a cell-free system requires higher concentrations of the inhibitor (two- to five-fold) compared to the concentrations required to inhibit it in cultured cells. Also, as noted earlier, for accumulation of ubiquitin adducts in cell-free systems, it is possible to inhibit the proteasome by using ATP-γ-S, the nonhydrolyzable ATP analog (see earlier discussion). Stabilization of a protein following inhibition of the proteasome is a strong indication that the protein is indeed degraded by this enzyme. Furthermore, inhibition of the 20S proteasome may lead to accumulation of ubiquitin adducts of the test protein that cannot be detected under conditions of rapid degradation when the proteasome is active. Detection of such intermediates serves as strong support for the notion that the protein is degraded by the 26S proteasome complex following its tagging by ubiquitin. The

adducts can be detected by probing the specific immunoprecipitate that was resolved via SDS–PAGE and blotted onto the membrane with an anti-ubiquitin antibody. Alternatively, to increase the sensitivity of the signal, the cells can be transfected with a cDNA coding for HA-, His-, or Myc-tagged ubiquitin, and the immunoprecipitate can be detected with the appropriate anti-tag antibody.

Determination of Stability (Half-Life; $t_{1/2}$) of a Protein in Cells; Effect of Proteasome Inhibitors

Steps

1. Wash cells (in case the fate of a naturally occurring protein is monitored; or transfected cells in case a cDNA coding for a specific protein was transfected to them) twice in a methionine-free medium at 4°C.
2. Add methionine-free medium that contains dialyzed serum (serum is added in the concentration used for growing the cells).
3. Incubate for 30 min (to remove endogenous methionine), remove the medium (by aspiration for adherent cells and following centrifugation at 800 *g* for 10 min for cells in suspension), and add fresh methionine-free medium with dialyzed serum. To save on labeled methionine, for adherent cells add medium to barely cover the cells (1–1.5 ml to a 60-mm dish). For cells in suspension, resuspend cells to 2×10^6/ml.
4. Add labeled methionine (50–250 μCi/ml) and continue the incubation for 1 h (pulse).
5. Add the inhibitor to the experimental dishes. Lactacystin or its lactone inhibitor (which penetrates cells better) or epoxomicin should be added to a final concentration of 5–20 μ*M*, whereas MG132 should be added to a final concentration of 20–50 μ*M*. The inhibitor should be added for 0.5 h (the last 30 min of the labeling period).
6. Remove the labeling medium.
7. Add ice-cold complete medium that contains, in addition to the inhibitor, also 2 m*M* of unlabeled methionine, and wash the cells twice. The complete medium should contain also 10% untreated complete FLS.
8. Add prewarmed complete medium (that contains the inhbitior and 2 m*M* of unlabeled methionine) and continue the incubation for the desired time periods (chase).
9. Withdraw samples at various time points and monitor degradation/stabilization of the target protein by immunoprecipitation, SDS–PAGE, and PhosphorImaging analysis. High molecular mass conjugates of the labeled protein should be precipitated by a specific antibody directed against the target protein under study. To avoid proteolysis of the conjugates by ubiquitin C-terminal hydrolases, it is recommended to dissolve the cells in a detergent-containing lysis buffer at 100°C. Also, the buffer should contain 10 m*M* NEM to inhibit ubiquitin hydrolases. The NEM can be later neutralized by DTT (7.5 mμ) or β-mercaptoethenol (15 mμ).

Instead of using pulse–chase labeling and immunoprecipitation, one can use cycloheximide (20–100 μg/ml diluted from 20 to 100 mg/ml freshly water-dissolved solution) to stop protein synthesis and follow its degradation via Western blot analysis. The advantage of this approach is that it does not necessitate the use of radioactive material and immunoprecipitation, and one can load a whole cell extract onto the gel. Utilization of the proteasome inhibitors in this system is similar to that described previously for the pulse–chase labeling approach. The disadvantage of the method is the potential interference of the drug in the proteolytic process. Thus, if cycloheximide inhibits the synthesis of a short-lived ubiquitin ligase, E3, involved in the process, the test protein can be stabilized or further destabilized, dependent on the role of the ligase in its degradation.

A complementary approach to the utilization of proteasome inhibitors, stabilization of the protein and accumulation of ubiquitin adducts, is the use of cells that harbor a temperature-sensitive mutation in the ubiquitin-activating enzyme E1, the first enzyme in the ubiquitin proteolytic cascade. At the nonpermissive temperature, the cells fail to conjugate the target proteins, which are consequently stabilized. Such cells can be, for example, the CHO-E36 (WT) and CHO-ts20 (E1 ts mutant) (used, for example, in Aviel *et al.*, 2000). The experimental approach used with these cells can be either pulse–chase labeling and immunoprecipitation or a cycloheximide chase.

Acknowledgments

Research in the laboratory of A.C. is supported by grants from Prostate Cancer Foundation (PCF) Israel—Centers of Excellence Program, the Israel Science Foundation founded by the Israeli Academy of Sciences and Humanities—Centers of Excellence Program, and the Foundation for Promotion of Research in the Technion. A.C. is an Israel Cancer Research Fund (ICRF) Professor. Infrastructural equipment was purchased with support of the Wolfson Charitable Fund Center of Excellence for studies on *Turnover of Cellular Proteins and its Implications to Human Diseases*.

References

Adams, J. (2003). The proteasome: Structure, function, and role in the cell. *Cancer Treat. Rev.* **29** (Suppl. 1), 3–9.

Aviel, S., Winberg, G., Massucci, M., and Ciechanover, A. (2000). Degradation of the Epstein–Barr virus latent membrane protein 1 (LMP1) by the ubiquitin-proteasome pathway: Targeting via ubiquitination of the N-terminal residue. *J. Biol Chem*. **275**, 23491–23499.

Glickman, M. H., and Adir, N. (2004). The proteasome and the delicate balance between destruction and rescue. *PLoS Biol*. **2**, E13.

Glickman, M. H., and Ciechanover, A. (2002). The ubiquitin proteasome pathway: Destruction for the sake of construction. *Physiol. Rev.* **82**, 373–428.

Gröll, M., and Huber, R. (2003). Substrate access and processing by the 20S proteasome core particle. *Int. J. Biochem. Cell Biol*. **35**, 606–616.

Hershko, A., and Heller, H. (1985). Occurrence of a polyubiquitin structure in ubiquitin-protein conjugates. *Biochem. Biophys. Res. Commun*. **128**, 1079–1086.

Hershko, A., and Rose, I. A. (1987). Ubiquitin-aldehyde: A general inhibitor of ubiquitin-recycling processes. *Proc. Natl. Acad. Sci. USA* **84**, 1829–1833.

Hicke, L., and Dunn, R. (2003). Regulation of membrane protein transport by ubiquitin and ubiquitin-binding proteins. *Annu. Rev. Cell Dev. Bio*. **19**, 141–172.

Huang, D. T., Walden, H., Duda, D., and Schulman, B. A. (2004). Ubiquitin-like protein activation. *Oncogene* **23**, 1958–1971.

Johnston, N. L., and Cohen, R. E. (1991). Uncoupling ubiquitin-protein conjugation from ubiquitin-dependent proteolysis by use of β, γ-nonhydrolyzable ATP analogues. *Biochemistry* **30**, 7514–7522.

Murakami, Y., Matsufuji, S., Kameji, T., Hayashi, S.-I., Igarashi, K., Tamura, T., Tanaka, K., and Ichihara, A. (1992). Ornithine decarboxylase is degraded by the 26S proteasome without ubiquitination. *Nature* **380**, 597–599.

Pickart, C. M. (2001). Mechanisms of ubiquitination. *Annu. Rev. Biochem*. **70**, 503–533.

Schwartz, D. C., and Hochstrasser, M. (2003). A superfamily of protein tags: Ubiquitin, SUMO and related modifiers. *Trends Biochem. Sci*. **28**, 321–328.

Weissman, A. M. (2001). Themes and variations on ubiquitylation. *Nature Rev. Cell Mol. Biol*. **2**, 169–179.

Yaron, A., Gonen, H., Alkalay, I., Hatzubai, A., Jung, S., Beyth, S., Mercurio, F., Manning, A. M., Ciechanover, A., and Ben-Neriah, Y. (1997). Inhibition of NF-κB cellular function via specific targeting of the IκBα-ubiquitin ligase. *EMBO J*. **16,** 6486–6494.

Zwickl, P., Seemüller, E., Kapelari, B., and Baumeister W. (2001). The proteasome: A supramolecular assembly designed for controlled proteolysis. *Adv. Protein Chem*. 59, 187–222.

SECTION

15

Mass Spectrometry: Protein Identification and Interactions

CHAPTER

46

Protein Identification and Sequencing by Mass Spectrometry

Leonard J. Foster and Matthias Mann

I. INTRODUCTION

In the postgenomic world, research priorities are shifting toward understanding the function of gene products, and proteomics is the term given to large-scale determination of gene product function, starting with where and when the products are expressed. The underlying technology required for mass spectrometry-based proteomic experiments is very young and still undergoing rapid development in both hardware and software areas (Aebersold and Goodlett, 2001; Aebersold and Mann, 2003; Mann *et al*., 2001; Washburn *et al*., 2002). The most powerful and most popular method for elucidating the protein composition of highly complex samples is proteolytic digestion of the proteins to peptides followed by single- or multidimensional high-pressure liquid chromatography (HPLC or LC) with on-line coupling to electrospray ionization tandem mass spectrometry (MS/MS) to generate peptide fragmentation spectra . These fragments are then compared to theoretical fragments predicted from amino acid sequence databases to arrive and protein identifications. We prefer quadrupole time-of-flight hybrid mass spectrometers, sacrificing the ease of use of ion trap-type spectrometers for higher resolution data. This article describes the general procedures used in our laboratory for sequencing and identifying proteins from highly complex samples. Because this is not a literature review, the reference list is not comprehensive and does not necessarily refer to the original description of a given technique.

II. MATERIALS AND INSTRUMENTATION

Urea (Cat. No. U5128), thiourea (Cat. No. T8656), dithiothreitol (DTT, Cat. No. D9163), absolute ethanol (EtOH, Cat. No. E7023), iodoacetamide (Cat. No. I1149), and heptafluorobutyric acid (HFBA, Cat. No. H7133) are from Sigma. LysC is from Wako (Osaka, Japan, Cat. No. 12502543). Sequencing-grade porcine trypsin (Cat. No. V511C) is from Promega, acetonitrile (Cat. No. 34881) is from Riedel-da Haën, methanol (Cat. No. M/4056/17) is from Fisher, and acetic acid (Cat. No. 6052) is from J. T. Baker. All water used here is "MilliQ"-quality distilled, deionized water. The following consumables are all obtained from the indicated sources: C18 Empore extraction disks (3M, Cat. No. 2215), P200 pipette tips (Gilson but any laboratory plastics supplier will suffice), 22-gauge flat-tip syringes (Hamilton, Cat. No. 90134), LC columns (New Objective, FS 360-100-8-N-20-C15), and 50- and 20-µm-inner-diameter fused silica capillary tubing (Polymicro Technologies LLC, Cat. Nos. 020375 and 050375). Vydac prototype 3-µm C18 beads (Cat. No. 218MSB3) are a kind gift from Grace Vydac (Hesperia, CA). The helium pressure cells used in our laboratory are custom made by a local metal workshop, but similar instruments can be purchased from Brechbühler AG (http://home.flash.net/~massevo). The HPLC system used in these protocols is the Agilent 1100 Series with 0.2- to 20-µl/min flow rate. The hybrid quadrupole TOF mass spectrometer is

Copyright 2006, Elsevier Science (USA).
All rights reserved.

from MDS Sciex and Applied Biosystems. All peptide fragmentation data are searched against the appropriate databases using a dual processor LinuxOS Mascot search engine (Matrix Science).

III. PROCEDURES

A. Sample Preparation

1. In-Solution Digestion

In-solution digestion can be used where the protein sample contains no detergent and is relatively simple (i.e., <300 proteins).

Solutions

1. *8 M urea*: 8 *M* urea in 10 m*M* HEPES, pH 8.0. To make 10 ml, dissolve 4.80 g urea and 23.8 mg HEPES in 10 ml water. Adjust pH with NaOH. Store at room temperature.
2. *6 M urea/2 M thiourea*: 6 *M* urea, 2 *M* thiourea in 10 m*M* HEPES, pH 8.0. To make 10 ml, dissolve 3.60 g urea, 23.8 mg HEPES, and 1.52 g thiourea in water. Adjust pH as necessary with NaOH. Solutions of thiourea often contain insoluble particles so it is a good idea to centrifuge this sample at 5000 *g* for 10 min to clarify it. Store at 4°C.
3. *8 M guanidine*: 8 *M* guanidine HCl, pH 1.5. To make 10 ml, dissolve 7.65 g guanidine HCl in water. Adjust pH with HCl.
4. *Digestion buffer*: 50 m*M* NH_4HCO_3. To make 10 ml, dissolve 40 mg NH_4HCO_3 in 10 ml water. Store at room temperature.
5. *Iodoacetamide stock solution*: 0.5 µg/µl iodoacetamide in digestion buffer. To make 10 ml, dissolve 5 mg iodoacetamide in 10 ml digestion buffer. Separate into 100-µl aliquots and store at –20°C.
6. *DTT stock solution*: 0.5 µg/µl DTT in water. To make 10 ml, dissolve 5 mg DTT in 10 ml water and store at –20°C.
7. *LysC stock solution*: 0.5 µg/µl. To make 1 ml, dilute 0.5 µg in 1 ml digestion buffer. Separate into small aliquots and store at –20°C.

Steps

1. Solubilize the protein pellet (either precipitated from solution or a centrifuge pellet from a subcellular fractionation) in 8 *M* urea, 6 *M* urea/2 *M* thiourea or 8 *M* guanidine. Selection of the particular denaturant will be sample specific, but urea/thiourea works best for membrane proteins. Keep the volume as small as possible.
2. Add 1 µg DTT/50 µg sample protein and incubate for 30 min at room temperature. If material is limiting, then the protein mass needs only to be roughly estimated.
3. Add 5 µg iodoacetamide/50 µg sample protein and incubate for 20 min at room temperature.
4. Add 1 µg LysC/50 µg sample protein and incubate for 3 h or overnight, at room temperature.
5. Dilute sample with 4 volumes digestion buffer, add 1 µg trypsin/50 µg sample protein, and incubate overnight at room temperature. Digested peptides may be stored at –20°C indefinitely.

2. In Gel Digestion

This procedure is as described by Shevchenko *et al*., (1996). Single-dimension SDS–PAGE can be used to reduce sample complexity but sample recovery is likely much less than in-solution digestions and so should only be used for complex (>300 proteins) samples where sample amount is not limited.

Solutions

1. *Digestion buffer*: 50 m*M* NH_4HCO_3. To make 10 ml, dissolve 40 mg NH_4HCO_3 in 10 ml water. Store at room temperature.
2. *NH_4HCO_3/EtOH*: 50% digestion buffer/50% EtOH. Combine equal volumes of digestion buffer and neat ethanol. Store at room temperature.
3. Trypsin solution: Dilute trypsin stock solution to 12.5 ng/µl with digestion buffer. Prepare *immediately* prior to use to minimize autocatalysis.
4. *Iodoacetamide*: 55 m*M* iodoacetamide in digestion buffer. To make 1 ml, dissolve 10.2 mg iodoacetamide in 1 ml digestion buffer. Prepare fresh.
5. *DTT*: 10 m*M* DTT in water. To make 1 ml, dilute 10 µl of a 1 *M* DTT solution in 990 µl water and store at –20°C.
6. *Extraction solution*: 3% trifluoroacetic acid (TFA), 30% acetonitrile. To make 1 ml, dilute 300 µl acetonitrile and 30 µl TFA in 670 µl water.

Steps

1. Excise individual stained gel bands and/or molecular weight ranges and place gel pieces in clean 1.5-ml microfuge tubes.
2. Chop each gel piece into smaller pieces approximately 1 mm per side using a scalpel.
3. Wash the gel pieces twice with NH_4HCO_3/EtOH for 20 min each at room temperature. Discard the supernatant each time. For each of the steps described here, enough solution should be used to cover the gel pieces.
4. Dehydrate the gel pieces by incubating for 10 min in absolute EtOH. Discard solution afterward.
5. Reduce the proteins by incubating for 45 min in DTT at 56°C. Discard solution afterward.

6. Block free sulphydryl groups by incubating for 30 min in iodoacetamide at room temperature. Discard solution afterward.

7. Wash gel pieces once with digestion buffer for 20 min at room temperature. Discard supernatant afterward.

8. Dehydrate pieces as in step 4.

9. Wash gel pieces once as in step 7.

10. Dehydrate gel pieces twice as in step 4.

11. Remove remaining ethanol from gel pieces by vacuum centrifugation.

12. Digest proteins with trypsin overnight at 37°C. Add enough trypsin solution to cover the dehydrated gel pieces. When the gel has swelled as much as possible (~20 min), remove excess trypsin solution and cover gels in digestion buffer.

13. Add 2 µl TFA to the digestion, quickly finger vortex the solution, and separate the liquid from the gel pieces, storing the liquid in a clean microfuge tube.

14. Extract the gel pieces by adding extraction solution to cover the gel. Shake the mixture vigorously for 5 min at room temperature. Remove the liquid and combine with that from step 13.

15. Dehydrate gel pieces in acetonitrile for 10 min at room temperature. Combine supernatant from this step with that from steps 13 and 14.

3. Desalting, Filtering, and Concentration

This procedure is identical to that described by Rappsilber *et al.* (2003).

Solutions

1. *Sample buffer*: 1% TFA, 5% acetonitrile. To prepare 1 ml, dilute 10 µl TFA and 50 µl acetonitrile in 940 µl water.
2. *Buffer B*: 0.02% HFBA, 0.5% acetic acid, 80% acetonitrile in water. To make 500 ml, combine 400 ml acetonitrile, 2.5 ml acetic acid, and 50 µl HFBA and top to 500 ml with water.

Steps

1. Prepare as many desalting columns as necessary by punching out small disks of C18 Empore filter using a 22-gauge flat-tipped syringe and ejecting the disks into P200 pipette tips. Ensure that the disk is securely wedged in the bottom of the tip.

2. Condition a column by forcing 5 µl of methanol through the Empore disk with a syringe fitted to the end of the pipette tip.

3. Remove any remaining organic solvent in the column by forcing 5 µl of sample buffer through.

4. Prepare the peptide sample for binding to reverse-phase material. For in-solution digestions, dilute the sample 3× with buffer A and pH the resulting solution to <2.5 with acetic acid. For in-gel digestions, dry down the extracted peptides in a vacuum centrifuge, resuspend in 100 µl sample buffer, and pH the resulting solution to <2.5 with acetic acid.

5. Force the acidified peptide sample through the C18 column.

6. Wash the column with 10 µl of sample buffer.

7. Elute the peptides from the C18 material using 5 µl buffer B. Elute directly into a microfuge tube.

B. LC/MS/MS

1. Column Preparation

This procedure is identical to that described by Rappsilber *et al.* (2003).

Solutions

1. *Matrix slurry*: Place a few cubic millimeters of dry Vydac matrix, a small magnetic stirbar, and 300 µl methanol in a 1.5-ml flat-bottomed sample vial.
2. *Buffer B as described earlier.*
3. *Buffer A*: 0.5% acetic acid, 0.02% HFBA. To make 500 ml, dilute 2.5 ml acetic acid and 50 µl HFBA in 500 ml water.

Steps

1. Insert the vial of matrix slurry in the helium pressure cell and position of the cell on a magnetic stir plate. Ensure that the plate is capable of rotating the bar inside the vial.

2. Insert an empty fused silica column into the pressure cell and tighten the seal. The back end of the column should rest in the matrix slurry but high enough that it is not bumped by the rotating stirbar.

3. Apply 30 to 50 bar helium to the system. The beads should be visible collecting in the column tip.

4. Allow the packing to proceed until the desired column length is achieved. Usually we use columns of between 7 and 10 cm in length.

5. Slowly release the pressure from the system. The column should remain tightly packed. If the packing separates, then it usually indicates that the tip of the column is blocked in some manner. Columns can be emptied by reversing the column orientation in the pressure cell and forcing methanol through the column backward.

6. Before loading any peptides onto the column, wash any methanol from the matrix by forcing buffer A through the column for 5 min using the pressure cell with 50 bar helium. At this pressure the flow rate should be 0.3 to 0.5 µl/min.

7. Column resolution can be checked using the mass spectrometer as a readout by analyzing a known amount (we use 100 fmol) of trypsin-digested bovine serum albumin. In a 20-min linear gradient from 5 to 80% buffer B, peptides should elute in approximately 20 s (width at half-maximum).

2. *Liquid Chromatography*

This procedure is similar to that described by Rappsilber *et al.* (2002) and Foster *et al.* (2003) with some modifications. For a comprehensive review of more advanced LC plumping, see Rappsilber *et al.* (2003).

Solutions

Buffer B and sample buffer as described earlier.

Steps

1. Remove all liquid from the desalted peptide sample by vacuum centrifugation.
2. Resuspend the peptide sample in 3 µl sample buffer. Alternatively, if only a small fraction of the desalted sample is to be analyzed, then instead of evaporating and resuspending, it can be directly diluted sufficiently with sample buffer to reduce the acetonitrile content to <5%. The high organic solvent content here will prevent peptides from binding to the reverse-phase matrix.
3. Measure the output rate of the HPLC pump required to achieve a flow rate through the column of 200 nl/min. Volumes this low can be measured by collecting the flow through in a graduated glass capillary.
4. Load the peptide sample onto the analytical column prepared earlier using the pressure cell again. Place the microfuge tube containing the sample in the cell, insert the analytical column, tighten the seal, and apply 50 bar pressure. Semiaccurate volumes can be loaded in this way by simply measuring the volume of liquid collecting at the column tip.
5. During sample loading, prepare the HPLC plumping (Fig. 1) and gradient program (Fig. 2). The HPLC system should be situated as close to the mass spectrometer orifice as possible (50 cm separating the two allows enough working space).
6. Flush the HPLC plumbing for 5 min with 7% buffer B in buffer A to remove air bubbles from the system.
7. Reset the flow to 0.00 µl/min and insert the analytical column containing the sample peptides into the plumbing system (Fig. 1).

3. *Acquiring Mass Spectra*

This procedure is similar to that described previously (Blagoev *et al.*, 2003; Foster *et al.*, 2003; Rappsilber *et al.*, 2002).

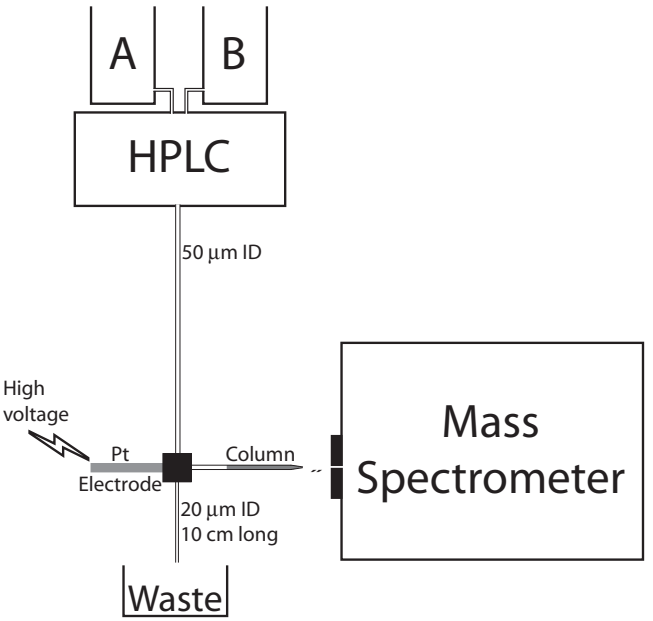

FIGURE 1 Simplest HPLC plumbing arrangement. The HPLC pump forces a mixture of buffers A and B out of the pump at a high flow rate. This high flow rate is then split, with most of the volume going through 20-µm capillary tubing (to provide back pressure) to a waste collection vessel and the remaining flow (200 nl/min) being forced through the analytical column. Electrospray voltage (1800 V) is applied to a platinum (Pt) electrode in the fourth port of the splitter, spraying the sample into the spectrometer for analysis.

Steps

1. Calibrate the mass spectrometer using a calibration standard containing at least two ions of known masses spanning the mass region to be measured.
2. Set up an acquisition method for the LC/MS experiment. Typically the method should be approximately 30 min longer than the HPLC elution program to allow time for the gradient delay and setup (see Fig. 2a for a typical elution gradient profile). Current mass spectrometers work by performing a few short experiments that are repeated over and over for the entire length of the LC run. Each cycle typically involves one survey scan (MS, see Fig. 2b for an example) from which the software chooses between two and four of the most intense peptides for product ion scans (called an MS–MS scan or fragmentation scan, see Fig. 2c) before starting the cycle again. The cycle length and scan times are defined by the user and should be adjusted to get sufficient sampling across an LC peak. For instance, if peptides elute from the LC column in 10 s and a cycle time of 15 s was in use, then it would be possible for a peptide to elute from the column and never be recorded by a survey scan (and thus never be

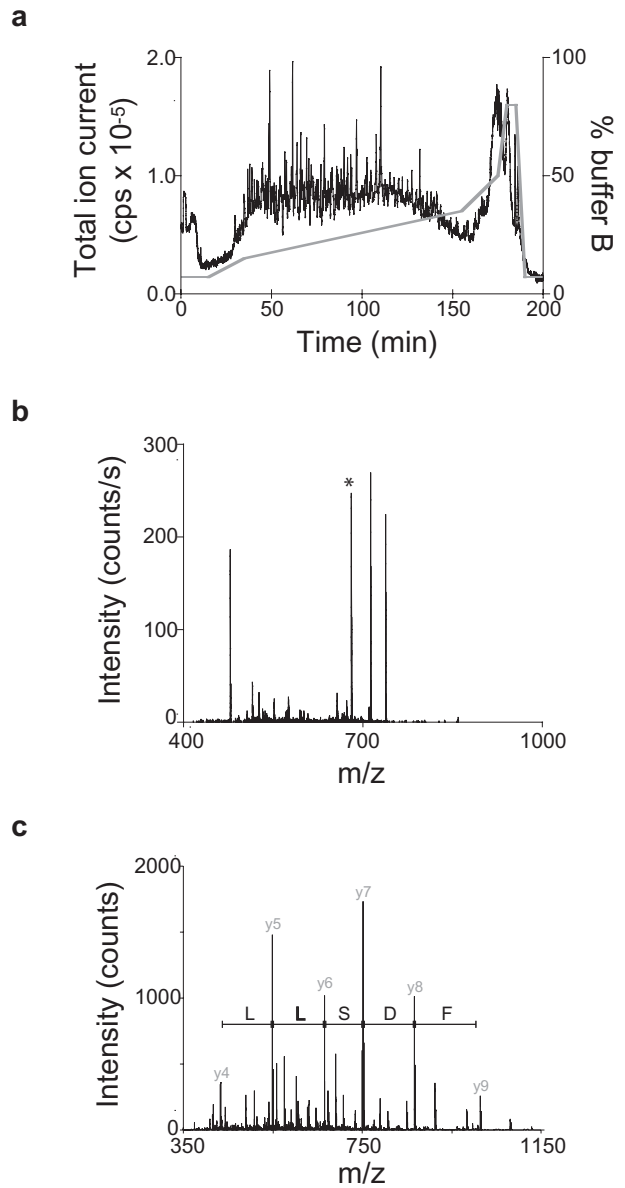

FIGURE 2 Sample LC, MS, and MS/MS traces. (a) Typical elution profile of a reversed-phase HPLC program and the associated total ion chromatogram registered by the mass spectrometer detector. Most of the peptides will elute from the analytical column between 15 and 35% B and so the majority of analysis time is spent in this range. (b) A typical survey or MS scan. Multiply charged ions such as the one indicated by an asterisk (*) detected in this spectra would then be selected for subsequent fragmentation. (c) A typical fragmentation or MS-MS scan. The Y-ions used to identify this peptide are labeled.

chosen for sequencing). The other major factor in deciding cycle times is sensitivity. The scan times should be long enough such that sufficient ion statistics are obtained for confident identifications. Cycle times are largely dependent on the duty cycle and the sensitivity of the mass spectrometer. For the QSTAR Pulsars in use in our laboratory, the following settings are typical: one 1.0-s MS time-of-flight (TOF) experiment followed by three or four 1.5-s information-dependent MS/MS TOF experiments, only multiply charged ions selected for sequencing, 3 min and 0.9 Da exclusion windows, enhancement around 700 Da, MS and MS/MS scan windows of 400 to 1200 Da, 35 counts/s IDA threshold, 1800 to 2000 V spray voltage.

3. Position the analytical column in front of the orifice plate and use the tuning mode of the mass spectrometer software to adjust the column position for maximum sensitivity.

4. Start the HPLC pump to the predetermined flow rate (see Section III,B,2) using a mix of 5% B in A.

5. Add a sample to the acquisition queue that calls the method described in step 2.

6. Start this sample and open the file to check that the detector is receiving a stable signal.

7. Start the elution program on the HPLC described in Section III,B,2.

C. Protein Identification

1. Mascot Searching

There are a number of commercial products for searching measured fragmentation spectra against theoretical spectra predicted from sequence databases. We use the Mascot search engine in our laboratory.

Steps

1. Mascot cannot interpret raw mass spectra itself and must by given a peak list to work with. Different mass spectrometer manufacturers use different software to do this but the output is all generally similar. For spectra acquired with ABI Analyst, fragmentation spectra are processed from the LC/MS file using the IDA Processor supplied with Analyst. If the mass spectrometer is tuned properly, then the default settings in IDA Processor are a good starting point for optimal extraction.

2. Use Mascot to search the peak list file against the protein sequence database of interest with. Standard settings for Mascot v1.8 are shown in Fig. 3. We typically search any human samples against the IPI database (to download, go to http://srs.ebi.ac.uk/srs6bin/cgi-bin/wgetz?-page+LibInfo+-id+1hEHl1KZ36s+-lib+IPI) rather than NCBI due to the high redundancy of the latter. The UniProt database from the creators of IPI and with financial backing from NIH will likely replace all general databases as the library of choice for such searches.

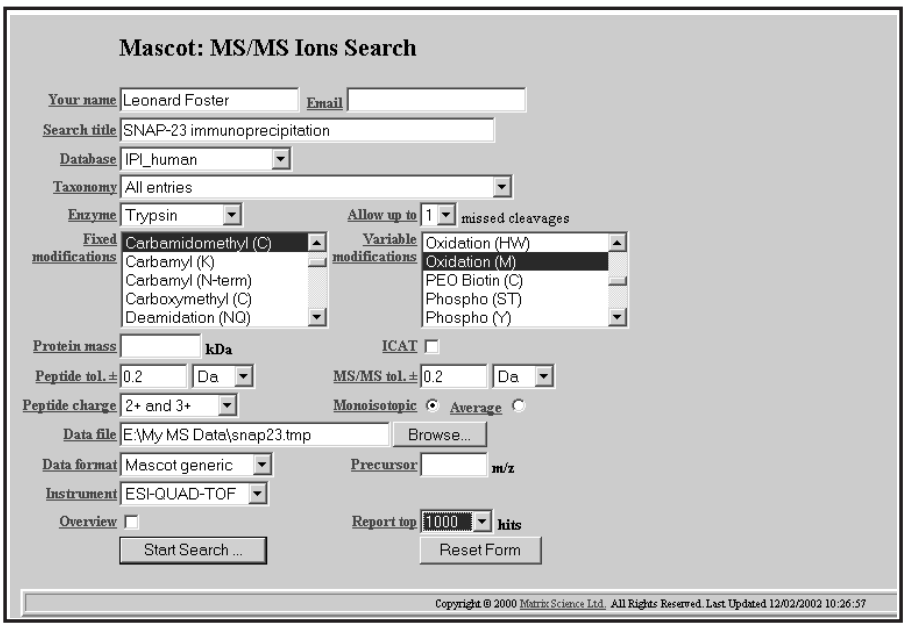

FIGURE 3 Typical parameters for a Mascot search.

2. *Understanding Mascot Output, Confirming Identifications, and Internal Calibration*

Steps

1. Peptides are coded in Mascot according to the rules listed in Table I. Only checked queries should be further considered for positive identifications. Thus, any protein with no checked queries can and should be immediately discarded from the "hit list", as their identifications were based on spectra who fit different peptides more closely.

2. With the remaining queries some guidelines can be established to minimize time-consuming manual verification. Depending on the database searched and the conditions used for the search, the significance level in Mascot scores will shift. With the conditions specified in Fig. 3 we typically accept any protein with a single IonsScore <45 or two IonsScores < 30 with no further verification.

3. Any remaining proteins in the list should be verified manually by direct examination of the fragmentation spectra of the peptides used for the identification. For a quadrupole-TOF hybrid instrument, we look for a Y-ion series of at least three fragments and a Mascot score that is distinct from all other matches to that spectra. Many additional sequence-specific factors can be considered but are beyond the scope of this article (Rappsilber *et al.*, 2003).

4. While certain types of mass spectrometers have inherently high mass accuracy, spectra obtained from these instruments can often be improved even further.

Table I Coding Scheme for Queries (Peptides) in Mascot

Coding method	Meaning
Bold type	First use of spectra in the output list
Light type	Subsequent use of spectra
Red type	Highest-scoring match of spectra
Black type	Less than the highest-scoring match of spectra
Checked query	Highest-scoring use of spectra

By simply calculating the mass errors for each identified peptide (the difference between the measured mass and the calculated mass for the amino acid sequence), a regression correction can be calculated that, when applied back against the whole data set, can greatly improve the mass accuracy. Using the highest-scoring peptides from a Mascot search, we have obtained mass accuracies <10 ppm, representing up to 10-fold improvements over the raw data. While there will always be outliers, peptides with a mass deviation larger than twice the average mass deviation should be inspected carefully.

IV. COMMENTS

A. Keratin

There are, of course, many biological studies where the identification of keratins by mass spectrometry

would be interesting (i.e., studies of intermediate filaments), but the vast majority of keratin identifications are unwanted. Fortunately, keratin contamination does not have to be accepted as a *fait d'accompli*, as careful sample handling can severely reduce and sometimes eliminate keratins altogether.

1. Check all solutions before use—with any sign of precipitates, or "floaties," new solutions should be prepared.
2. Use Milli-Q-quality water for everything.
3. Work in a laminar flow hood where possible. Remember that flow hoods are *not* fume hoods, however, so do not use large volumes of volatile or hazardous chemicals in them.
4. *Never* bring the sample into contact with anything that may have been touched by fingers or had dust fall on it. Implicit in this is to keep unused sample tubes and pipette tips in covered containers.
5. When working with solutions, take care not to pass anything over the top of the open container, as particles may fall off. Beyond this, always enter a container with a pipettor or forceps with the container tilted so that any dust that might fall does not end up in the container.

B. Gloves

We have not yet resolved the gloves/no gloves issue in our laboratory. While they certainly help prevent flakes of skin from falling off our hands, they may increase static charges on sample tubes, thereby attracting air-borne particles. Regardless, by following the general rules described earlier, any additional benefits of gloves seem to be minimal, as those who use them in our laboratory generally see no more or less keratin contamination than those who do not.

V. PITFALLS

While much of the sample handling and data acquisition can be automated fairly easily, there is currently no commercially available software designed to handle the enormous volumes of data that this procedure is capable of generating. For single experiments the manual verification of spectra assignments and data compilation is a relatively simple task but one that grows exponentially more complex with each additional set of results added to the data set. Interpretation and analysis are additionally hampered by the lack of standards in the field for what constitutes an "identified protein." It is hoped that open source or public domain packages will become available soon to make these processes more efficient, transparent, and comparable between groups.

An additional pitfall is the observation that two analyses of the same sample will often not give identical lists of protein components. This is not due to the database search software but rather to the data the software has available. For unknown reasons the mass spectrometer does not choose the same set of peptides for sequencing in duplicate runs, even under identical conditions using the very simplest samples (i.e., purified bovine serum albumin). Proteins that are abundant enough to have three or four (or more) peptides selected for sequencing will likely be found in parallel analyses, but in complexity-limited samples where a large fraction of identifications are based on single peptides, an investigator should not expect to identify the same proteins in a second analysis. To get around this problem, we typically analyze a single sample multiple times and/or attempt to fractionate the sample prior to reversed-phase HPLC (either at protein or peptide levels).

References

Aebersold, R., and Goodlett, D. R. (2001). Mass spectrometry in proteomics. *Chem. Rev.* **101**, 269–295.

Aebersold, R., and Mann, M. (2003). Mass spectrometry-based proteomics. *Neture* **422**(6928), 198–207.

Blagoev, B., Kratchmarova, I., Ong, S. E., Nielsen, M., Foster, L. J., and Mann, M. (2003). A proteomics strategy to elucidate functional protein-protein interactions applied to EGF signaling. *Nature Biotechnol.* **21**.

Foster, L. J., de Hoog, C. L., and Mann, M. (2003). Unbiased quantitative proteomic analysis of lipid rafts reveals high specificity for signalling factors. Submitted for publication.

Mann, M., Hendrickson, R. C., and Pandey, A. (2001). Analysis of proteins and proteomes by mass spectrometry. *Annu. Rev. Biochem.* **70**, 437–473.

Rappsilber, J., Andersen, J. S., Ishihama, Y., Ong, S. E., Foster, L. J., and Mann, M. (2003). A recipe collection for the identification of peptides in complex mixtures. *Sci. STKE*.

Rappsilber, J., Ishihama, Y., and Mann, M. (2003). Stage (STop And Go Extraction) tips for MALDO, nanoelectrospray, and LC/MS sample pre-treatment in proteomics. *Anal. Chem.* **I75**, 663–670.

Rappsilber, J., Ryder, U., Lamond, A. I., and Mann, M. (2002). Large-scale proteomic analysis of the human spliceosome. *Genome Res.* **12**, 1231–1245.

Shevchenko, A., Wilm, M., Vorm, O., and Mann, M. (1996). Mass spectrometric sequencing of proteins silver-stained polyacrylamide gels. *Anal. Chem.* **68**, 850–858.

Washburn, M. P., Ulaszek, R., Deciu, C., Schieltz, D. M., and Yates, J. R., 3rd (2002). Analysis of quantitative proteomic data generated via multidimensional protein identification technology. *Anal. Chem.* **74**, 1650–1657.

CHAPTER

47

Proteome Specific Sample Preparation Methods for Matrix-Assisted Laser Desorption/Ionization Mass Spectrometry

Martin R. Larsen, Sabrina Laugesen, and Peter Roepstorff

I. INTRODUCTION

Early in the beginning of the 1990s a number of groups demonstrated that it was possible to identify proteins in databases based on peptide mass maps obtained by mass spectrometric (MS) analysis of peptides derived by specific enzymatic proteolysis of a given protein (Henzel *et al.*, 1993; Mann *et al.*, 1993; Pappin *et al.*, 1993; James *et al.*, 1993). Shortly after that, the field of proteomics started to expand concurrent with the development of more sensitive mass spectrometers so that even very low amounts of gel-separated proteins could be identified. Presently, most mass spectrometers routinely allow analysis of peptides or proteins in the low femtomole level.

With the development of sensitive mass spectrometers, the real limitation for the analysis of complex and contaminated peptide and protein mixtures is sample preparation prior to mass spectrometric analysis. Therefore, major efforts have been invested into developing new methods for sample preparation prior to MS.

In the traditional sample preparation method for matrix-assisted laser desorption/ionization (MALDI) MS, the analyte and matrix solutions are mixed directly on the MALDI target, referred to as the dried droplet method (Karas and Hillenkamp, 1988; Hillenkamp *et al.* 1991). Alternatively, the matrix and analyte solutions can be mixed in a test tube prior to application onto the target. The tolerance of this method toward nonvolatile contaminants is limited to the efficiency of the crystallization process and to sample washing postmatrix crystallization. Additionally, it has been reported that the matrix solution conditions (especially the solvent) have a large influence on the quality of the MALDI-MS analysis (Cohen and Chait, 1996). With the introduction of the fast evaporation or thin-layer method (Vorm *et al.*, 1994), an increase in sensitivity and resolution was obtained. Here, the matrix is dissolved in a highly volatile organic solvent, which is applied onto the target to create a thin homogeneous layer of matrix crystals. The analyte solution is placed on top of the film and dried at ambient temperature followed by rinsing, resulting in decreased alkali metal adduct formation and a concomitant increase in signal intensity and sensitivity. The fast evaporation method was further developed with the inclusion of nitrocellulose (NC) in the matrix (Jensen *et al.*, 1996; Kussmann *et al.*, 1997). The presence of NC reduced the intensity of the alkali metal ion adducts, presumably because it binds the alkali metal ions very strongly, thereby preventing them from entering the gas phase. A noteworthy improvement in sample preparation for both MALDI-MS and electrospray ionization (ESI) MS came with the introduction of custom-made disposable microcolumns as a fast cleanup step prior to MS, first introduced by Wilm and Mann (1996). They used a pulled capillary needle in which they packed a small volume of reversed-phase

Copyright 2006, Elsevier Science (USA).
All rights reserved.

chromatographic material. The analyte molecules were eluted directly into a nano-ESI capillary needle by centrifugation prior to mass analysis. Later, this sample preparation was simplified by using Eppendorf GELoader tips packed with chromatographic material or prepacked microcolumns (e.g., ZipTips, Millipore) (Gobom *et al*., 1997, Kussmann *et al*., 1997; Erdjument-Bromage *et al*., 1998). Elution of the analyte from the microcolumns with matrix solution was later demonstrated to be a very efficient sample preparation method for MALDI (Gobom *et al*., 1999). The use of microcolumns allows upconcentration and desalting of highly diluted samples prior to MS analysis, resulting in an increase in the sensitivity and of the overall quality of the mass spectra. In addition, significantly higher sequence coverage from peptide mass maps is observed, which is important not only for unambiguous protein identification, but especially for complete characterization of posttranslational modifications in proteomics.

This article reports a number of protocols currently used in our laboratory for MALDI-MS sample preparation optimised for proteomic research, i.e., high sensitivity, high tolerance towards low molecular weight contaminants, and high sequence coverage. We focus mainly on sample preparation methods involving sample cleanup using microcolumn technology, as traditional methods such as the dried droplet and the fast evaporation method have been described extensively in Roepstorff *et al*. (1998).

II. MATERIALS AND INSTRUMENTATION

The GELoader pipette tips are from Eppendorf (Hamburg, Germany). The chromatographic column materials, Poros R2 and Poros Oligo R3, are from PerSeptive Biosystems (Framingham, MA). α-Cyano-4-hydroxycinnamic acid (4HCCA) and activated charcoal (C-5510) are from Sigma (St. Louis, MO). 2,5-Dihydroxybenzoic acid (DHB) and 2-hydroxy-5-methoxybenzoic acid (HMB) are from Aldrich. Acetonitrile, formic acid (FA), and trifluoroacetic acid (TFA) are all analytical grade and obtained from different manufacturers. Disposable syringe (1 ml) are from BD Plastipak. The water is from a Milli-Q system (Millipore, Bedford, MA).

MALDI mass spectra are recorded on a Bruker Reflex III mass spectrometer (384 sample plate inlet), a Perseptive Voyager STR mass spectrometer, or a TOF-Spec 2E (Micromass, Manchester, UK). All are equipped with delayed extraction.

III. PROCEDURES

A. Preparation of Matrix Solutions

1. Matrix Solutions Containing 4HCCA

a. *4HCCA (I)*: Dissolve 10–20 mg 4HCCA in 1 ml 70% acetonitrile/0.1% TFA
b. *4HCCA (II)*: Dissolve 10–20 mg 4HCCA in 1 ml acetone/water (99/liter, v/v)

2. Matrix Solutions Containing 2,4,6-THAP

THAP: Dissolve 10 mg 2,4,6-THAP in 0.5 ml acetonitrile/water (70/30, v/v)

3. Matrix Solutions Containing DHB

DHB: Dissolve 20 mg DHB in 0.5 ml acetonitrile/water (50/50, v/v)

4. Mixed Matrix Solutions

a. *4HCCA/DHB*: Dissolve 20 mg 4HCCA in 1 ml acetonitrile/5% FA (70 : 30, v/v). Dissolve 20 mg DHB in 1 ml acetonitrile/0.1% TFA (70 : 30, v/v). The two solutions are then combined in a 1 : 1 volume ratio
b. *DHB/HMB (super DHB)*: Dissolve 9 mg DHB and 1 mg HMB in 0.5 ml acetonitrile/water (20/80, v/v)

B. Sample Preparation for MALDI-MS Analysis

1. Traditional Dried Droplet Method

The dried droplet method originally introduced by Karas and Hillenkamp (1988) is the oldest sample preparation method and is, in many applications, still the preferred one for MALDI-MS. It is surprisingly simple, it provides good results for different types of samples, and it can tolerate moderate concentrations of low molecular weight contaminants. This matrix preparation method is used preferentially in proteomics for high throughput automated peptide mass mapping of proteins present in relative high abundance. The following matrices are traditionally used with this method: 4HCCA (I), THAP, and DHB.

Steps

1. Mix equal volumes of analyte and matrix solutions and, if appropriate, 0.1% TFA or 2% FA on the sample support.
2. Let the sample dry at ambient temperature. Alternatively, evaporation of the solvent can be assisted by a stream of inert gas.
3. If the matrix solution is 4HCCA or THAP, then the matrix crystals can be washed by depositing 10 µl

of 0.1% TFA on top of the dried preparation and then removing it carefully with a piece of paper tissue.

Note: A common problem with the dried droplet method is the accumulation of analyte/matrix crystals in the periphery of the sample surface, especially in the presence of low molecular weight contaminants. For DHB, the analytes tend to associate with the big crystals that form at the periphery of the sample surface, whereas salts are found predominantly in the smaller crystals formed in the centre of the sample surface. This is the reason why it is often necessary to search for "sweet" spots on the sample surface. Inclusion of acid in the first step increases tolerance towards low molecular weight contaminants and helps in the crystallization process.

2. *Mixed Matrix Dried Droplet Method*

The use of matrix mixtures was reported in the 1990s by Karas and coworkers (Tsarbopoulos *et al.*, 1994). They described a matrix mixture consisting of DHB and HMB (super DHB), which was used predominantly for the analysis of glycosylated proteins. Mixed matrices presumably combine the different properties of the individual matrices to a property superior to the individual matrices. Our group developed a mixed matrix solution consisting of 4HCCA and DHB, which has proven to be very useful in analysis of low amounts of peptides and proteins (Laugesen and Roepstorff, 2003). Here the hydrophilic matrix (DHB) forms crystals in the outer edge of the spot, whereas the hydrophobic 4HCCA matrix forms crystals in the centre of the spot. An increased tolerance towards salts is observed, presumably because the peptides cocrystalize with matrix in the centre, whereas the salt molecules are upconcentrated in the hydrophilic DHB edge. An example of the performance of the 4HCCA/DHB matrix compared to traditional dried droplet using only one of the matrices is shown in Fig. 1.

Steps

1. Mix the two matrix solutions in a small Eppendorf tube in a proper ratio (typically 1 : 1) and vortex intensively.

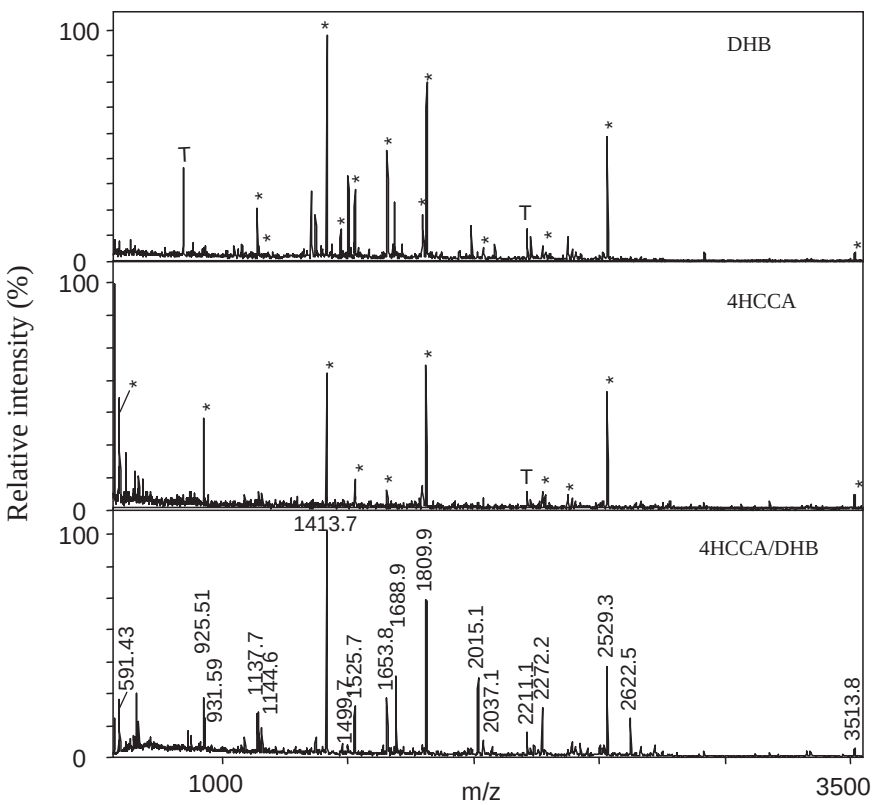

FIGURE 1 MALDI-MS peptide mass maps of peptides derived by tryptic digestion of a silver-stained spot obtained from 2D-PAGE of proteins extracted from barley grain. Spectra were obtained with DHB, CHCA, and the matrix mixture preparations. Asterisks indicate signals matching protein z-type serpin from barley. Commonly observed trypsin autodigest signals are indicated by T.

2. Mix an equal volume of analyte, matrix mix solution, and, if appropriate, 0.1% TFA or 2% formic acid on the sample support.
3. Let the solution dry at ambient temperature.

Note: These matrix preparations are not washable, as DHB is soluble in water/0.1% TFA solution. Desorption with the laser is performed in the centre of the preparation.

3. Fast Evaporation Thin-Layer/Sandwich Method

The fast evaporation method is used less frequently in proteome analysis nowadays. However, several laboratories prepare a layer of matrix prior to spotting sample and matrix on top. The method is especially useful to ensure even crystallization when anchor chip targets are used.

Steps

1. Place a small droplet (0.5 µl) of the matrix solution [4HCCA (II)] onto the MALDI target so that it spreads out. Evaporation of the solvent results in a homogeneous layer of matrix crystals.
2. Apply 0.5 µl 2% FA or 0.1% TFA, 0.5 µl analyte solution, and 0.5 µl 4HCCA (I) on top of the thin matrix layer. The addition of FA or TFA solution is not necessary if the analyte solution is already acidified.
3. Let the solution dry at ambient temperature.
4. The matrix crystals can be washed as described earlier.

Note: The fast evaporation methods are used exclusively with 4HCCA and THAP as matrices.

4. Micropurification Method

The dominating sample preparation method used for proteomics in our laboratory and many other laboratories involves the use of microcolumns, either homemade GELoader tip (Eppendorf) columns or prepacked microcolumns (e.g., ZipTips, Millipore). This sample preparation method is compatible with 4HCCA, DHB, HMB, and the DHB/4HCCA mixture.

This section describes the use of GELoader tip microcolumns and refers to the manufacturer's protocol for the ZipTips.

Steps

1. Make a partially constricted GELoader pipette tip by squeezing the narrow end. The two most common ways to generate a partially constricted GELoader pipette tip are illustrated in Fig. 2. Put the narrow end of a GELoader tip flat on a hard surface. Then roll a 1.5-ml microfuge tube over the final 1 mm of the tip. Alternatively, fix the narrow end of the GELoader tip using a flat-surface forceps and twist the tip to close the end.

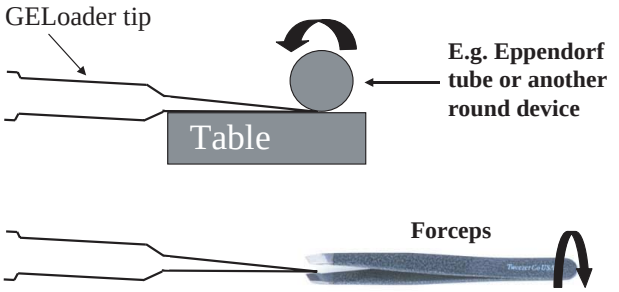

FIGURE 2 Preparation of a constricted GELoader tip can be performed in a number of different ways. One way is to roll a 1.5-ml Eppendorf tube over the narrow end of the tip with gentle pressure to squeeze the approximately last 0.5 mm of the tip flat (top). The other strategy is to use a forceps to twist the last 1 mm of the tip (bottom).

2. Prepare a slurry of 100–200 µl chromatographic material, e.g., Poros R2, Oligo R3, or Graphite powder, in 70% acetonitrile (approximately 1.5 mg/100 µl).
3. Load 20 µl 70% acetonitrile in the top of the constricted GELoader tip followed by approximately 0.5 µl of the chromatographic material slurry. Use a 1-ml syringe fitted to the diameter of the GELoader tip via a disposable pipette tip to press the liquid down gently, thereby generating a small column at the end of the constricted tip. Push tall liquid out of the column before performing the next step.
4. Apply 20 µl of 2% FA or 0.1% TFA to the top of the column. Press approximately 10 µl through the column for equilibration. Leave the remaining 10 µl on top of the column bed.
5. Mix the analyte with the remaining acid solution and use gentle air pressure to press the liquid through the column. Leave approximately 3 µl of solvent on top of the column. Do not dry the column in this step!
6. Apple 10–20 µl of 2% FA or 0.1% TFA on top of the remaining solution and use air pressure to wash the column. In this step, all liquid should be pushed out of the column.
7. Elute the peptides with 0.5 µl matrix solution directly onto the MALDI MS target. The eluent should be spotted in several small droplets on the target for a further concentration. Most peptides are only present in the two first droplets, but some may come later depending on the size and hydrophobicity. As an alternative the peptides can be eluted with increasing concentrations of organic solvent and applied by the dried droplet method.
8. Depending on the size of the column and the abundance/concentration of the analyte molecules that have been loaded, the column can be reused from

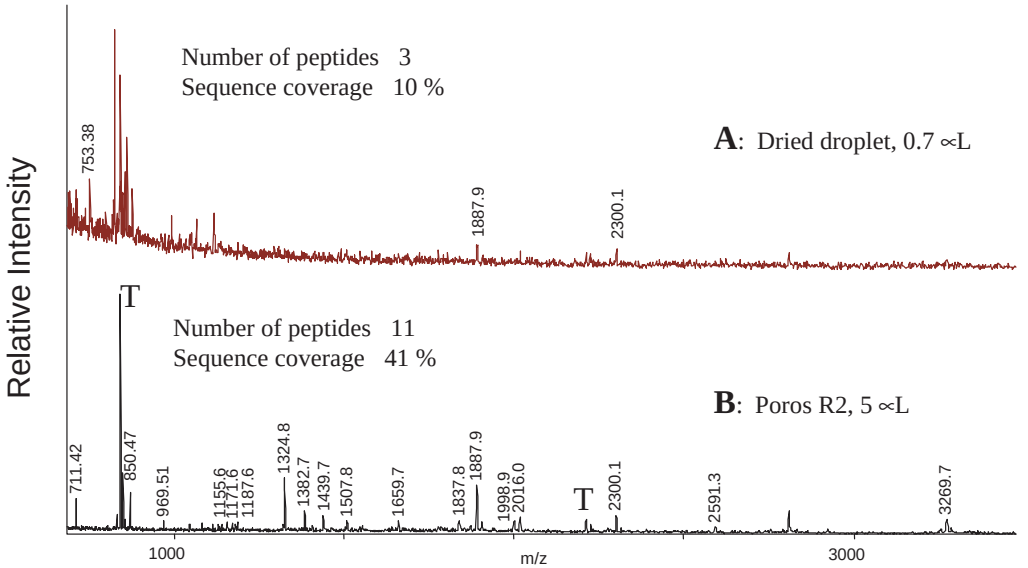

FIGURE 3 MALDI-MS peptide mass maps of peptides derived by tryptic digestion of a protein from a 2D gel of a membrane preparation from *Pseudomonas aeruginosa* (hypothetical protein, NC_002516). (A) Spectrum obtained using the dried droplet method with 0.7 µl peptide solution. Three peptides were detected covering 10% of the protein. The protein could not be identified using this peptide mass map. (B) Spectrum obtained after desalting and concentration of 5 µl peptide solution using a Poros R2 GELoader tip microcolumn. Eleven peptides were detected, and the protein could be identified easily with 41% sequence coverage. T indicates peptides originating from tryptic autodigestion.

2 to 10 times after extensive washing with 70–100% acetonitrile.

Notes: Using microcolumns, the low molecular weight contaminants can be removed easily from the analyte molecules and diluted samples are concentrated readily with a resulting increase in sensitivity and sequence coverage. An example is shown in Fig. 3. Several types of reversed-phase material can be used for column packing. Poros R2 and Poros Oligo R3 have proven excellent in our hands. Graphite powder has been used as an alternative to reversed-phase material, giving superior recovery of hydrophilic peptides and higher sequence coverage (Larsen *et al.*, 2002). Examples of the use of Poros R2 and graphite column materials in proteome analysis are given in Fig. 4.

The same procedure as described for GELoader tip microcolumns can be used with commercially available ZipTip microcolumns, resulting in increased sensitivity compared to the protocol described by the manufacturer.

The performance of the homemade microcolumn is superior to that of the commercially available ZipTips, especially for analysis of very low abundant proteins from 2D gels. An example of the performance of Poros R2 versus ZipTip C_{18} is shown in Fig. 5.

C. Column Material for GELoader Tip Microcolumns Used in Proteomics

The most common chromatographic material used for microcolumns in proteomics is reversed-phase material. However, other kind of materials can be applied with success.

i. Poros R2 and Oligo R3 are the main reversed-phase material used in proteomics to desalt and concentrate peptides prior to mass spectrometry. Poros R2 is designed for the general separation of proteins, peptides, and nucleic acids. The binding strength is similar to low carbon-loading C8 or C18 supports. The Oligo R3 medium is designed for hydrophilic peptides and nucleic acids and is similar to high carbon-loading C18 supports.

ii. Graphite powder can be used as an alternative to RP material as a peptide cleanup medium, especially for small hydrophilic peptides or phosphopeptides (Chin and Papac, 1999; Larsen *et al.*, 2002). However, it also works very well for all other peptides if they are eluted with the 4HCCA matrix (Larsen *et al.*, 2002). Alternatively, it can be used to desalt and concentrate carbohydrates prior to mass spectrometric analysis.

iii. Anion (e.g., Poros HQ) and cation (e.g., Poros S) exchange columns are used less frequently for protein

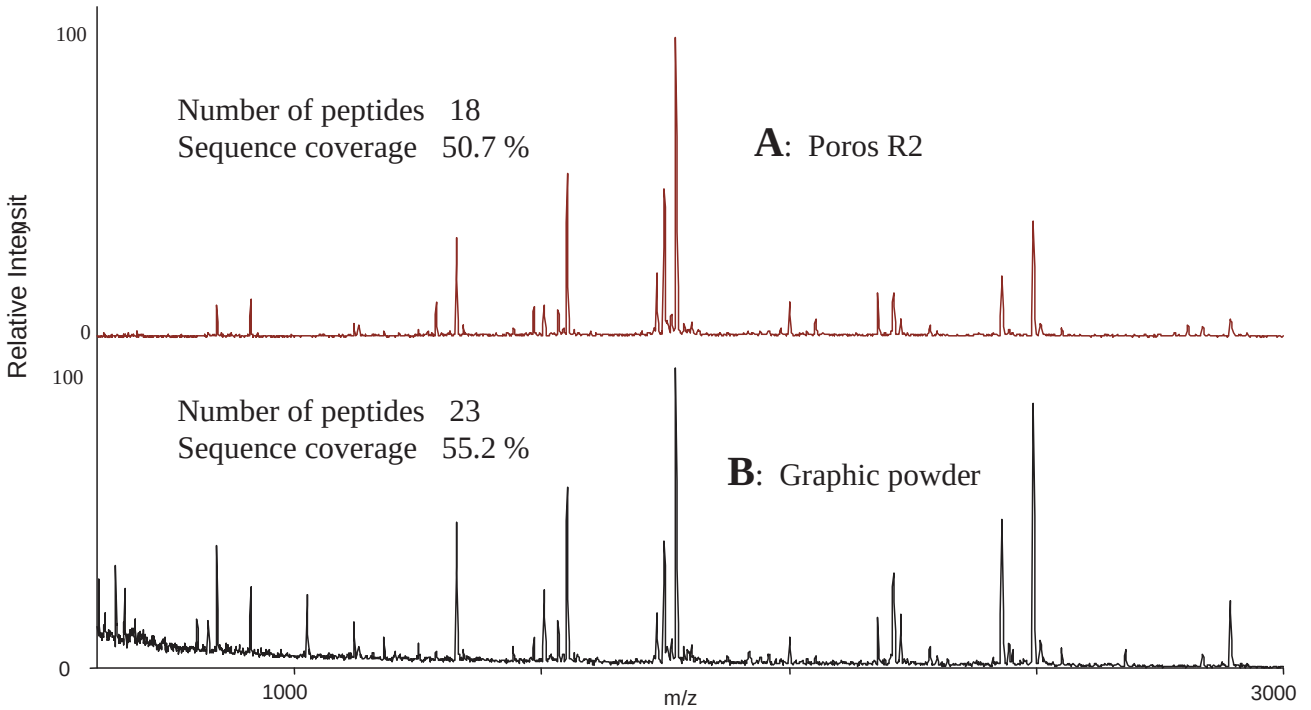

FIGURE 4 MALDI-MS peptide mass maps of peptides derived by tryptic digestion of a protein from a 2D gel of a membrane preparation from *Pseudomonas aeruginosa* (probable porin, NC_002516). An aliquot of the peptide solution was desalted and concentrated using a Poros R2 and a graphite powder GELoader tip microcolumn, respectively. (A) Spectrum obtained from the Poros R2 column. A total of 18 peptides could be assigned to the sequence of the probable porin covering 50.7% of the sequence. (B) Spectrum obtained from the graphite powder column. Twenty-three peptides covering 55.2% of the sequence could be assigned.

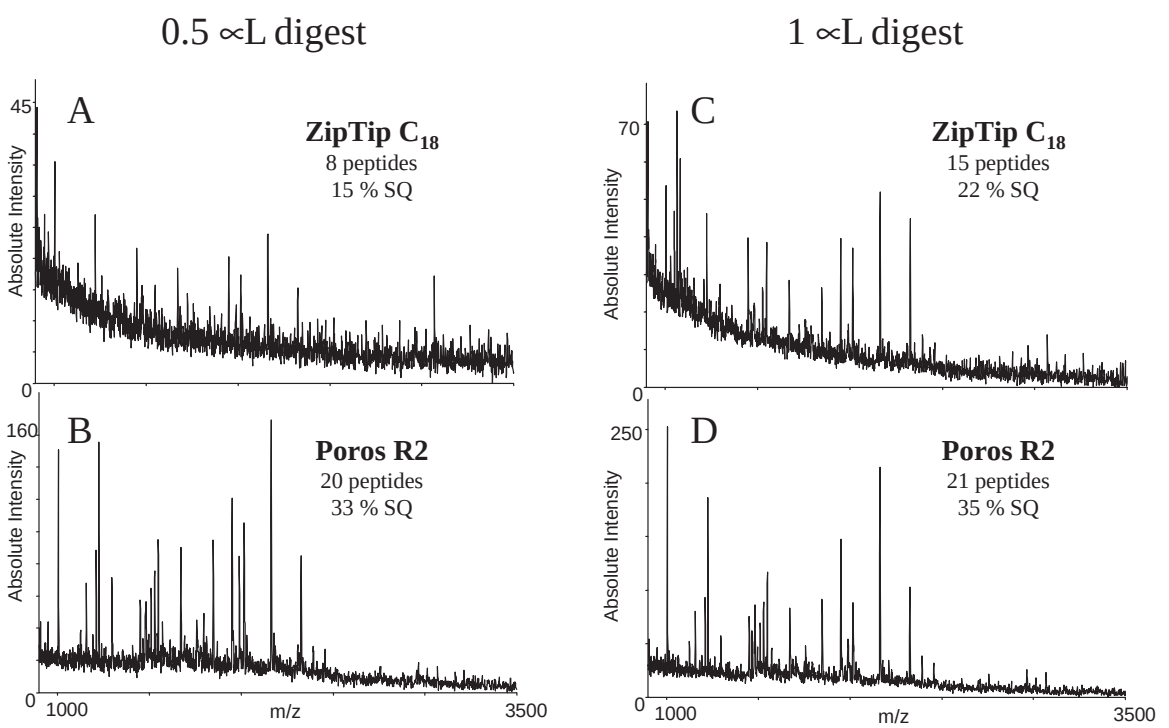

FIGURE 5 Comparison of GELoader tip microcolumns with the commercially available ZipTip C_{18}. A weak Coomassie-stained spot on a 2D gel of a membrane preparation from *Pseudomonas aeruginosa* [Fe(III)-pyochelin receptor precursor, NP_252911] was submitted to in-gel digestion using trypsin in a total volume of 20 µl buffer. Aliquots (0.5 and 1 µl) were desalted and concentrated on the two different microcolumns. Spectra obtained from the ZipTip C_{18} microcolumn purification of 0.5- and 1-µl aliquots are shown in A and C, respectively. Spectra obtained from the GELoader tip microcolumn purification of 0.5- and 1-µl aliquots are shown in B and D, respectively. As judged from the intensity of the peptide signals (absolute intensities), GELoader tip microcolumns are between 5 and 10 times more sensitive than the commercially available ZipTip columns.

identification purposes in proteomics but can be advantageous for specific purposes, such as the isolation of specific peptides when the goal is full characterization of proteins. Protocols for the use of these types of column materials are available from the resin manufacturer's home page (www.applied biosystems.com).

Note: Many other types of column material can be packed into the small GELoader tip microcolumns, including immobilized metal affinity material, immobilized enzymes, and immobilized DNA/RNA.

D. Selection of Sample Preparation Method in Proteomics

The choice of matrix and sample preparation method for MALDI-MS analysis of peptides in proteome analysis is very dependent on the amount and complexity of the sample to be analysed. In general, peptides derived by proteolytic digestion of proteins visible by Coomassie blue require less sensitive sample preparation methods than proteins visible by more sensitive staining procedures, such as silver staining or fluorescent staining (e.g., Sypro Ruby). For the first category of peptides, a standard dried droplet or sandwich method is fast and straightforward and results in detection of sufficient peptides for ambiguous protein identification. In addition, these methods are automated easily and therefore suitable for high-throughput proteomics. For a lower amount of starting material, the dried droplet or sandwich methods will not provide enough peptide signals due to suppression effects by low molecular weight contaminants or simply because the sample is too diluted. In such cases, desalting and concentration using microcolumns will be needed. As judged from the intensity of the peptides in the example shown in Fig. 5, the homemade GELoader tip microcolumns are 5–10 times more sensitive than commercially available tips. However, commercially available microcolumns are easy to handle and are compatible with several different liquid-handling robots, making them suitable for high-throughput proteomics. The combined use of different matrices and several types of microcolumns may be needed if the goal is to obtain the highest possible sequence coverage. This is relevant for observation of posttranslationally modified peptides and for determination of the processing sites when the proteins are truncated.

E. Final Comments

The sample preparation procedures are under constant development and may also vary according to the individual experimentalist. Therefore, this article should merely serve as a source of inspiration. It must, however, be kept in mind that the quality of all solvents and chemicals is of paramount importance for success. Therefore, all new batches of solvents and chemicals must be checked with a standard protein digest before being used. In addition, we always aliquot the solvents immediately after positive testing, as any solvent will be contaminated after opening the bottle a few times in the laboratory.

References

Chin, E. T., and Papac, D. I. (1999). The use of a porous graphitic carbon column for desalting hydrophilic peptides prior to matrix-assisted laser desorption/ionization time-of-flight mass spectrometry. *Anal. Biochem.* **273**(2), 179–185.

Cohen, S. L., and Chait, B. T. (1996). Influence of matrix solution conditions on the MALDI-MS analysis of peptides and proteins. *Anal. Chem.* **68**(1), 31–37.

Erdjument-Bromage, H., Lui, M., Lacomis, L., Grewal, A., Annan, R. S., McNulty, D. E., Carr, S. A., and Tempst, P. (1998). Examination of micro-tip reversed-phase liquid chromatographic extraction of peptide pools for mass spectrometric analysis. *J. Chromatogr. A* **826**(2), 167–181.

Gobom, J., Nordhoff, E., Ekman, R., and Roepstorff, P. (1997). Rapid micro-scale proteolysis of proteins for MALDI-MS peptide mapping using immobilized trypsin. *Int. J. Mass Spectrom. Ion Proc.* **169/170**, 153–163.

Gobom, J., Nordhoff, E., Mirgorodskaya, E., Ekman, R., and Roepstorff, P. (1999). Sample purification and preparation technique based on nano-scale reversed-phase columns for the sensitive analysis of complex peptide mixtures by matrix-assisted laser desorption/ionization mass spectrometry. *J. Mass Spectrom.* **34**, 105–116.

Henzel, W. J., Billeci, T. M., Stults, J. T., and Wong, S. C. (1993). Identifying proteins from two-dimensional gels by molecular mass searching of peptide fragments in protein sequence databases. *Proc. Natl. Acad. Sci. USA* **90**, 5011–5015

Hillenkamp, F., Karas, M., Beavis, R. C., and Chait, B. T. (1991). Matrix-assisted laser desorption/ionization mass spectrometry of biopolymers. *Anal. Chem.* **63**(24), 1193A–1203A.

James, P., Quadroni, M., Carafoli, E., and Gonnet, G. (1993). Protein identification by mass profile fingerprinting. *Biochem. Biophys. Res. Commun.* **195**, 58–64

Jensen, O. N., Podtelejnikov, A., and Mann, M. (1996). Delayed extraction improves specificity in database searches by matrix-assisted laser desorption/ionization peptide maps. *Rapid Commun. Mass Spectrom.* **10**(11), 1371–1378.

Karas, M., and Hillenkamp, F. (1988). Laser desorption ionization of proteins with molecular masses exceeding 10,000 daltons. *Anal. Chem.* **60**, 2299–2301.

Kussmann, M., Nordhoff, E., Nielsen, H. R., Haebel, S., Larsen, M. R., Jacobsen, L., Jensen, C., Gobom, J., Mirgorodskaya, E., Kristensen, A. K., Palm, L., and Roepstorff, P. (1997). MALDI-MS sample preparation techniques designed for various peptide and protein analytes. *J. Mass Spectrom.* **32**, 593–601.

Larsen, M. R., Cordwell, S. J., and Roepstorff, P. (2002). Graphite powder as an alternative or supplement to reversed-phase material for desalting and concentration of peptide mixtures prior to matrix-assisted laser desorption/ionization mass spectrometry. *Proteomics* **2**, 1277–1287.

Laugesen, S., and Roepstorff, P. (2003). Combination of Two Matrices Results in Improved Performance of MALDI MS for Peptide Mass Mapping and Protein Analysis. *J. Am. Soc. Mass. Spectrom.* **14**: 992–1002.

Mann, M., Højrup, P., and Roepstorff, P. (1993). Use of mass spectrometric molecular weight information to identify proteins in sequence databases. *Biol. Mass Spectrom.* **22**, 338–345.

Pappin, D. J. C., Højrup, P., and Bleasby, A. J. (1993). Rapid identification of proteins by peptide-mass finger printing. *Curr. Biol.* **3**, 327–332.

Roepstorff, P., Larsen, M. R., Rahbek-Nielsen, H., and Nordhoff, E. (1998). Sample preparation methods for matrix assisted laser desorption/ionization mass spectrometry of peptides, proteins and nucleic acids. *In "Cell Biology: A Laboratory Handbook,"* 2rd Ed. Vol. 4, pp. 556–565.

Tsarbopoulos, A., Karas, M., Strupat, K., Pramanik, B. N., Nagabhushan, T. L., and Hillenkamp, F. (1994). Comparative mapping of recombinant proteins and glycoproteins by plasma desorption and matrix-assisted laser desorption/ionization mass spectrometry. *Anal. Chem.* **66**(13), 2062–2070.

Vorm, O., Roepstorff, P., and Mann, M. (1994). Matrix, surfaces made by fast evaporation yield improved resolution and very high sensitivity in MALDI TOF. *Anal. Chem.* **66**, 3281–3287.

Wilm, M., and Mann, M. (1996). Analytical properties of the nanoelectrospray ion source. *Anal. Chem.* **68**(1), 1–8.

CHAPTER

48

In-Gel Digestion of Protein Spots for Mass Spectrometry

Kris Gevaert and Joël Vandekerckhove

I. INTRODUCTION

Modern techniques for studying complex protein mixtures utilize two main analytical techniques: (a) one- or two-dimensional polyacrylamide gel electrophoresis (1D or 2D PAGE) for dividing the protein mixture into its individual components and (b) accurate mass spectrometry (MS) for identifying these proteins. Different gel-staining procedures are available for visualizing gel-separated proteins, of which most are compatible with further MS analysis. Different types of Coomassie brilliant blue staining (Bennett and Scott, 1971; Wilson, 1983) and silver-staining procedures (Merril *et al*., 1979) are by far the most used visualisation protocols prior to mass spectrometric analysis. Proteins spots of interest, e.g., protein spots of which the staining intensity (thus concentration) and/or the position (modification status) differs between two compared samples, are excised from the gel and cleaved into peptides after protease addition. The generated peptide mixture elutes out of the gel passively and is analyzed by a variety of chromatographic and mass spectrometric methods (e.g., reviewed by Aebersold and Mann, 2003).

Frequently, trypsin is used to generate peptides, cleaving at the carboxy-terminal side of lysine and arginine, generating peptides of an average size of about 10 amino acids. For most proteins, this leads to a sufficient number of analyzable peptides and thus to unambiguous identification. This article describes a standard protocol for *in-gel* tryptic protein digestion leading to MS-based protein identification and characterization.

II. MATERIALS AND INSTRUMENTATION

A Sentry ionizing air blower (product number 4003143) is from Simco, Deerlijk, Belgium. Singly wrapped sterile stainless steel scalpels (product number 10.295.10MN) are from BCB Ltd., Cardiff, UK. Singly wrapped Eppendorf Biopur Safe-Lock micro test tubes (product number 0030 121.589) are from VWR International Belgium, Leuven, Belgium. Water (product number 4218) and acetonitrile (product number 9017) used to prepare the different buffers are of the best quality available and are both from Malinckrodt Baker B.V., Deventer, The Netherlands. Sequencing grade modified trypsin (product number V5111) is from Promega Benelux BV, Leiden, The Netherlands. Ammonium hydrogen carbonate (product number A-6141) is from Sigma-Aldrich Corp., St. Louis, MO. Recombinant, proteomics grade trypsin from *Pichia pastoris* (product number 3 357 228) can be obtained from Roche Diagnostics GmbH, Penzberg, Germany. Peptide synthesizer graded trifluoroacetic acid (product number PTS6045) is from Rathburn Chemicals Ltd., Walkerburn, Scotland, UK.

III. PROCEDURE

In-Gel Digestion of Proteins Separated in Polyacrylamide Gels

The following procedure is derived from a general procedure that has been described previously (Rosenfeld *et al*., 1992), but to which important

Copyright 2006, Elsevier Science (USA).
All rights reserved.

modifications are added. Generally, this approach can be used to digest proteins *in gel* independent from the procedure that was used to visualize them, although care must be taken, as some silver-staining protocols use amino acid cross-linkers that render most of the proteins inaccessible for the employed protease. In the following procedure, trypsin is used to digest the protein into peptides. In principle, every available protease can be used as long as the final buffer conditions (pH, additives, etc.) are met.

Solutions

1. *Wash solution*: Prior to *in-gel* digestion, excised gel pieces containing the proteins are washed extensively with an aqueous acetonitrile solution (1/1, v/v) of the highest purity available. This solution is preferentially freshly prepared in small volumes (e.g., 10 ml).

2. *Digestion buffer*: This buffer must always be freshly prepared and consists of 50 m*M* ammonium bicarbonate dissolved in water of the highest purity available. The pH of this buffer does not need any adjustment and will be around 7.8.

Steps

1. Following Coomassie or silver staining, wash the polyacrylamide gels in water to remove excess substances, derived from the electrophoresis and staining procedure, from the gel matrix. Repeat this washing step at least three times (for 30 min each), each time using fresh volumes of water.

2. Then transfer the gel to a clean container and keep moist during the excision of protein spots. Immediately prior to gel spot excision, open the container and blow a stream of ionized air over it. This air stream almost completely eliminates charging of plastic material by static electricity by neutralising the surface of the working area. When a neutralizing air stream is not used, dust particles will be attracted to the gel container, the polyacrylamide gel, gloves, scalpel, and microtest tubes.

3. Excise protein spots using a sterile scalpel or a hollow stainless steel needle, and excise only the heart of the protein spot (i.e., the most intensely coloured gel area). Using the scalpel blade or a clean forceps, transfer each individual protein spot to a Biopur microtest tube. Prior to excising the next protein spot, wash the scalpel (and the forceps) extensively with methanol to remove small gel particles that may stick to it and thus cross-contaminate other protein spots.

4. Cover each protein spot with wash solution and incubate for 15 min at room temperature. During this wash step, gel pieces will shrink and buffer components (and Coomassie) are efficiently extracted from the gel.

5. Centrifuge the tubes briefly, remove the wash solution, and submerge the gel pieces for a second time in this solution for 15 min at room temperature.

6. Following a second centrifugation step, remove the wash solution and transfer the tubes to a centrifugal vacuum concentrator in which the gel pieces are dried to complete dryness (this takes about 10 min).

7. Rehydrate the dried gel pieces with 10 µl (corresponding to 0.1 µg) of a freshly prepared 0.001% (w/v) trypsin solution in 50 m*M* ammonium bicarbonate (pH 7.8) for 10 min at room temperature, after which excess trypsin solution is removed.

8. Subsequently submerge the rehydrated gel pieces in 50 m*M* ammonium bicarbonate buffer (pH 7.8); depending up the size of the excised gel pieces, between 50 and 100 µl of buffer must be added.

9. Close the tubes and place into a thermostatically controlled incubator, and tryptic digestion proceeds overnight at 37°C.

10. Terminate protein digestion by adding 10 µl of 10% (v/v) trifluoroacetic acid (TFA).

11. Following a brief centrifugation step, remove and transfer the supernatant containing the peptide mixture to a new tube, which is frozen at –20°C until further analysis (e.g., by mass spectrometric techniques).

IV. COMMENTS

1. It has been shown that the removal of metallic silver from silver-stained proteins by oxidation with hydrogen peroxide prior to *in-gel* digestion not only increases the overall sensitivity of MS-based protein identification, but also augments the coverage of the sequence of the analyzed protein (Sumner *et al*., 2002). One of the side effects is that methionines and carbamidomethylated cysteines will be (at least partly) oxidized to their sulfoxide derivatives (Gevaert *et al*., 2002). This will increase the complexity of the generated peptide mixtures in two ways: (a) all peptides containing methionine and/or cysteine will be present as couples (oxidized and nonoxidized forms) and (b) neutral losses of the side chains of the oxidized amino acids give rise to satellite peaks (Steen and Mann, 2001), which may cause problems during MALDI-MS analysis. In contrast, this added complexity might help in identifying proteins, as peptides containing rare amino acids (methionine and cysteine) can be recognized in the peptide mass maps and verify the database findings of search algorithms.

2. When analyzing Coomassie-stained protein spots by MALDI-MS-based peptide mass fingerprint-

ing (reviewed by Cottrell, 1994), it is important to remove as much of the noncovalently bound Coomassie molecules as possible during the washing steps (steps 4, 5, and 6 of the procedure). Coomassie molecules ionize rather efficiently in MALDI mode and thereby suppress ionization of peptide molecules. Even more severe, in some cases, Coomassie ions will saturate the detector of the mass spectrometer, making it less sensitive for peptide ions striking it. Furthermore, these Coomassie ions disturb the lower mass section of the peptide mass maps, possibly masking some important small peptide ions.

3. The accuracy of protein identification largely depends on the total number of peptides that are available for analysis. Proteins that have many hydrophobic patches are sometimes difficult to digest, as either the protease has limited access to the chain of the protein or the liberated peptides are too hydrophobic and thus do not elute well out of the gel pieces. For such proteins, the efficiency of protein digestion is improved by adding detergents or chaotropes that partly unfold the protein in the gel, thereby exposing more cleavage sites. Unfortunately, the choice of such additional components is rather limited, as many of them block the action of the protease or interfere with further reversed-phase high-performance liquid chromatographic (RP-HPLC) analysis or with mass spectrometric analyses. One detergent that has proven to be particularly useful for the digestion of membrane proteins is octyl-β-glucopyranoside (van Montfort *et al*., 2002). This detergent increases the recovery of hydrophobic peptides following digestion and does not interfere with subsequent MS analysis. From our experience, we have found that, especially when working with trypsin, fairly high concentrations of urea (up to 4 *M*) in the protein digestion buffer can be tolerated without any severe effect on the activity of the protease. Urea notably increases the total coverage of the analyzed protein and thus simplifies protein identification by mass spectrometry. The main drawback when using urea is carbamylation of free amino groups by ammonium cyanate present in urea solution, which, in addition to making less sites available for tryptic cleavage, makes the peptide mixtures more complex.

4. Particularly when employing MALDI-MS for protein identification, it is important to remove any substances that might interfere with the matrix crystallization and the ionization processes. Such substances include salts, buffering substances, chaotropes, and detergents. Several procedures have been described (Gevaert *et al*., 1997) and are compatible with the *in-gel* digestion procedure described here.

5. Recombinant trypsin made in the yeast *Pichia pastoris* has been made available commercially. The main advantage of this protease over other commercially available proteases is the complete absence of nontryptic proteolytic activity. Other types of proteases, although treated with specific inhibitors of commonly copurifying proteases, still lead to nontryptic peptides, which complicate peptide mass maps and make unambiguous protein identification more complex. For example, the most prominent contamination found in trypsin isolated from mammalian organs is chymotrypsin. Because chymotrypsin cleaves at the C-terminal side of five different amino acids, upon prolonged incubation of protein substrates with "chymotrypsin-contaminated" trypsin, this leads to very complex peptide mass maps.

6. Transient or permanent modifications of amino acid side chain are molecular switches to control the activity of a great number of proteins/enzymes. Mass spectrometric analysis is the sole technology available for the in-depth analysis of the vastness of modifications that occur *in vivo*. However, when digesting a gel-separated protein with only one enzyme, too few ionisable peptides will be generated so as to cover the complete sequence of the analyzed protein and thus many possible modifications may escape analysis. Therefore, it is advantageous to use multiple enzymes either in sequence or together in order to generate many protein fragments and thus cover as much of the protein sequence as possible. Combinations of site-specific and unspecific proteases have been used for that purpose (e.g., MacCoss *et al*., 2002).

V. PITFALLS

1. One of the major pitfalls encountered frequently is contamination of protein spots with human epidermal keratins. During *in-gel* protein digestion, keratins that are present digest as well and will give a characteristic and easily recognizable pattern of peptide masses in the mass maps obtained (Parker *et al*., 1998). To our experience, it is very important to wear clean gloves during all steps of the procedure, i.e., when mounting and handling polyacrylamide gels, when excising stained proteins out of the gel, and when handling the test tubes containing these spots prior to digestion. Next to this, the staining procedures are preferentially kept as short as possible and in the smallest volume possible, as it has been shown that a long exposure of gels to air increases the risk for keratin contamination (Sinha *et al*., 2001). In our laboratory, we minimize this problem by working in a

laminar air flow hood during the excision of protein spots and during preparation of the protein digests. Furthermore, the gels and the test tubes are constantly in a flow of neutralizing air by which electrostatic charging of plastic surface, which attracts dust particles (and thus keratins), is reduced.

2. Because it is very difficult to estimate the amount of protein present in a gel, in some cases too much protease will be added. Although many of the proteases that are available commercially are so-called "proteomics grade", during typical incubation times, they give rise to autodigestion products. These peptides can, in some cases, be used as internal standards, by which the peptide mass will be determined more accurately (e.g., Li *et al*., 1997) or, when overrepresented, suppress ionization of peptides from the analyzed proteins, thus hampering protein identification.

Acknowledgment

K.G. is a Postdoctoral Fellow of the Fund for Scientific Research—Flanders (Belgium) (F.W.O.-Vlaanderen).

References

Aebersold, R., and Mann, M. (2003). Mass spectrometry-based proteomics. *Nature* **422**, 198–207.

Bennett, J., and Scott, K. J. (1971). Quantitative staining of fraction I protein in polyacrylamide gels using Coomassie brillant blue. *Anal. Biochem.* **43**, 173–182.

Cottrell, J. S. (1994). Protein identification by peptide mass fingerprinting. *Pept. Res.* **7**, 115–124.

Gevaert, K., Demol, H., Puype, M., Broekaert, D., De Boeck, S., Houthaeve, T., and Vandekerckhove, J. (1997). Peptides adsorbed on reverse-phase chromatographic beads as targets for femtomole sequencing by post-source decay matrix assisted laser desorption ionization-reflectron time of flight mass spectrometry (MALDI-RETOF-MS). *Electrophoresis* **18**, 2950–2960.

Gevaert, K., Van Damme, J., Goethals, M., Thomas, G. R., Hoorelbeke, B., Demol, H., Martens, L., Puype, M., Staes, A., and Vandekerckhove, J. (2002). Chromatographic isolation of methionine-containing peptides for gel-free proteome analysis: Identification of more than 800 *Escherichia coli* proteins. *Mol. Cell. Proteomics* **1**, 896–903.

Li, G., Waltham, M., Anderson, N. L., Unsworth, E., Treston, A., and Weinstein, J. N. (1997). Rapid mass spectrometric identification of proteins from two-dimensional polyacrylamide gels after in gel proteolytic digestion. *Electrophoresis* **18**, 391–402.

MacCoss, M. J., McDonald, W. H., Saraf, A., Sadygov, R., Clark, J. M., Tasto, J. J., Gould, K. L., Wolters, D., Washburn, M., Weiss, A., Clark, J. I., and Yates, J. R., 3rd (2002). Shotgun identification of protein modifications from protein complexes and lens tissue. *Proc. Natl. Acad. Sci. USA* **99**, 7900–7905.

Merril, C. R., Switzer, R. C., and Van Keuren, M. L. (1979). Trace polypeptides in cellular extracts and human body fluids detected by two-dimensional electrophoresis and a highly sensitive silver stain. *Proc. Natl. Acad. Sci. USA* **76**, 4335–4339.

Parker, K. C., Garrels, J. I., Hines, W., Butler, E. M., McKee, A. H., Patterson, D., and Martin, S. (1998). Identification of yeast proteins from two-dimensional gels: Working out spot cross-contamination. *Electrophoresis* **19**, 1920–1932.

Rosenfeld, J., Capdevielle, J., Guillemot, J. C., and Ferrara, P. (1992). In-gel digestion of proteins for internal sequence analysis after one- or two-dimensional gel electrophoresis. *Anal. Biochem.* **203**, 173–179.

Sinha, P., Poland, J., Schnölzer, M., and Rabilloud, T. (2001). A new silver staining apparatus and procedure for matrix-assisted laser desorption/ionization-time of flight analysis of proteins after two-dimensional electrophoresis. *Proteomics* **1**, 835–840.

Steen, H., and Mann, M. (2001). Similarity between condensed phase and gas phase chemistry: Fragmentation of peptides containing oxidized cysteine residues and its implications for proteomics. *J. Am. Soc. Mass Spectrom.* **12**, 228–232.

Sumner, L. W., Wolf-Sumner, B., White, S. P., and Asirvatham, V. S. (2002). Silver stain removal using H_2O_2 for enhanced peptide mass mapping by matrix-assisted laser desorption/ionization time-of-flight mass spectrometry. *Rapid Commun. Mass Spectrom.* **16**, 160–168.

van Montfort, B. A., Canas, B., Duurkens, R., Godovac-Zimmermann, J., and Robillard, G. T. (2002). Improved in-gel approaches to generate peptide maps of integral membrane proteins with matrix-assisted laser desorption/ionization time-of-flight mass spectrometry. *J. Mass Spectrom.* **37**, 322–330.

Wilson, C. M. (1983). Staining of proteins on gels: Comparisons of dyes and procedures. *Methods Enzymol.* **91**, 236–247.

CHAPTER

49

Peptide Sequencing by Tandem Mass Spectrometry

John R. Yates, III, David Schieltz, Antonius Koller, and John Venable

I. INTRODUCTION

Microcolumn reversed-phase HPLC electrospray ionization tandem mass spectrometry (ESI-MS/MS) is a rapid and sensitive technique for the analysis of complex mixtures of peptides (Hunt *et al*., 1986; Griffin *et al*., 1991). This technique can be used to determine the amino acid sequence of unknown peptides, to verify the structure of proteins, and to determine post-translational modifications. In particular, the strength of this approach is the analysis of peptides in complicated mixtures. Two approaches for sequence analysis of peptides are described: low flow rate infusion (microelectrospray ionization) and reversed-phase microcapillary liquid chromatography tandem mass spectrometry (Gale and Smith, 1993; Emmett and Caprioli, 1994; Andren *et al*., 1994; Wilm and Mann, 1994; Davis *et al*., 1995). Algorithms have been developed to help interpret tandem mass spectra to derive a sequence *de novo* and an example of their use is illustrated.

II. MATERIALS AND INSTRUMENTATION

Solvents are from Fisher Scientific (Springfield, NJ): J. T. Baker, 2-propanol 9095-02, acetonitrile OPTIMA A996-4, J. T. Baker, acetic acid 6903-05. Fused silica capillaries are from Polymicro Technologies (Tucson, AZ): 375 µm o.d. × 20 µm i.d., TSP375020, 365 µm o.d. × 100 µm i.d., TSP200100. Reversed-phase chromatographic supports are from Zorbax Eclipse XDB. The column packing device is homemade and is shown in Fig. 1. The microelectrospray platform was built in the The Scripps Research Institutes instrument shop (Fig. 2). The XYZ manipulator is from Newport Corp. (Irvine, CA). MT-XYZ and the high voltage connector suitable for the ThermoFinnigan electrospray voltage are from Lemo USA (www.lemo.com) (San Jose, CA; P/N 4-89626). A P-2000 laser puller is from Sutter Instruments (Novato, CA).

The electrospray ionization tandem mass spectrometers, LCQ and Q-TOF mass spectrometers, are from ThermoFinnigan (San Jose, CA) and Waters (Milford, MA), respectively. Pumps for HPLC and HP1100 are from Agilent (Palo Alto, CA). DeNovoX is provided with the BioWorks software from ThermoFinnigan.

III. PROCEDURES

A. Preparation of Microcolumns for Reversed-Phase HPLC

Solutions

1. *HPLC solvent A*: To make 1 liter, add 5 ml of formic acid to 995 ml of distilled and deionized water
2. *HPLC solvent B*: To make 1 liter, add 5 ml of formic acid to a solution of 200 ml of distilled and deionized water and 795 ml of acetonitrile

Steps

1. Construct microcapillary columns according to Gatlin *et al*. Rinse 50-cm piece of fused silica capillary (365 µm o.d. × 100 µm i.d.) with 2-propanol and dry. Remove the polyimide coating with a low temperature flame in the middle of the capillary. Position the

Copyright 2006, Elsevier Science (USA).
All rights reserved.

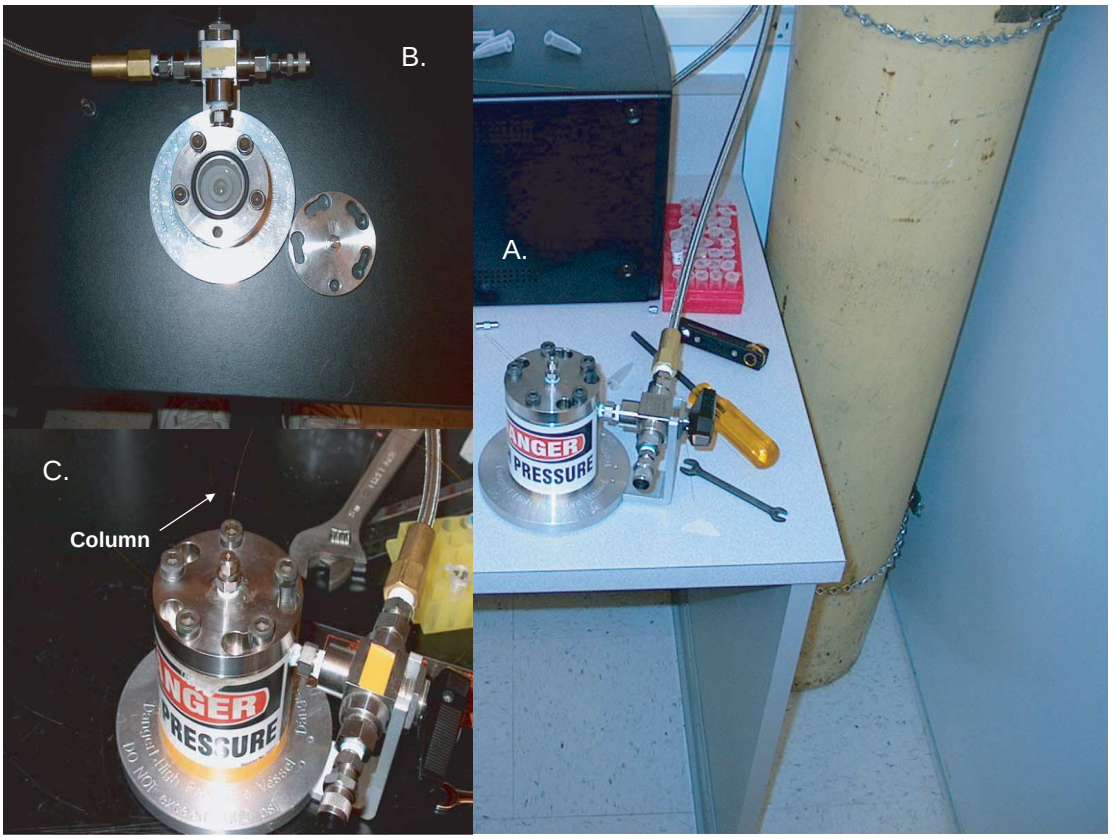

FIGURE 1 Pneumatic device for packing capillary columns and loading samples. A: Device is shown connected to gas line. B: Device is shown with the top removed showing the inside. A slot can be seen where an eppendorf tube can be inserted for either column packing or sample loading. C: Pneumatic device with a fused silica capillary column.

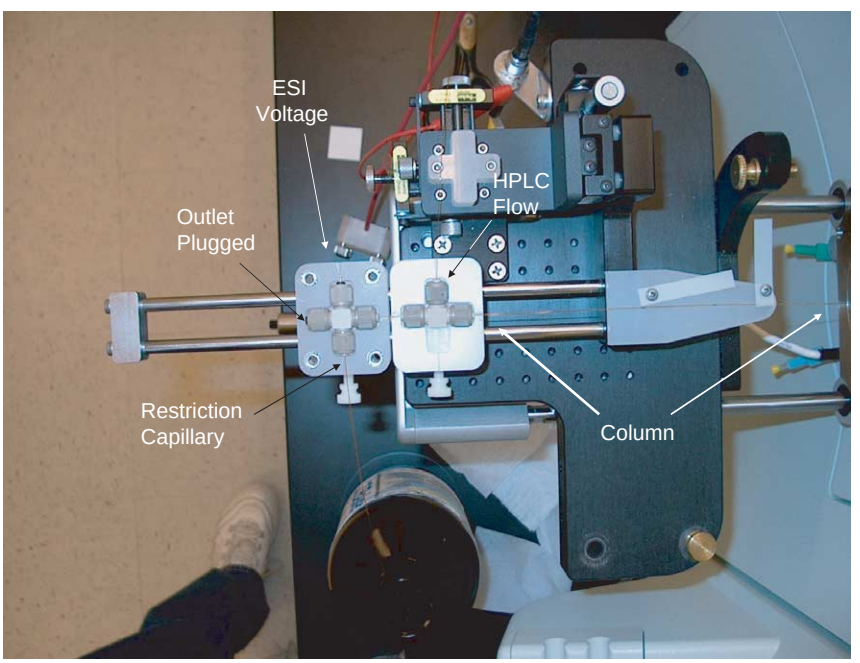

FIGURE 2 Microelectrospray stage for capillary liquid chromatography. HPLC solvent is initially split using a peak microTee to another microTee. This microTee contains a gold electrode for application of the ESI voltage and a restriction capillary to create back pressure and direct flow to waste.

capillary on a laser puller and pull to create two columns each with tips containing 5-µm openings. The settings on the laser puller for 365 × 100-µm i.d. capillary are heat 270, filament 0, velocity 30, delay 128, and pull 0. Repeat this program three times before the capillary is pulled. This program produces a 5-µm tip, although the exact program may depend on mirror alignment and capillary positioning. *Caution*: Conditions to pull a capillary may vary from puller to puller.

2. The packing device is depicted in Fig. 1A. Insert the blunt end of the column into the swagelock fitting in the top of the packing device. To pack the column, fill a polypropylene Eppendorf centrifuge tube (1.5 ml) with ~100 µg of packing material and 1 ml of methanol and sonicate briefly to suspend the material and minimize aggregation. Place the solution in a high-pressure packing device (Fig. 1B), insert the column, and place the end of the column in the solution (Fig. 1C). Use helium gas at a pressure of ~500 psi to drive the packing material into the column. Continue packing until the material fills a length of the capillary corresponding to 10–20 cm. Allow the pressure to slowly drop to zero. Condition the column by rinsing with 100% solvent B and slowly reducing the percentage of solvent B until it reaches initial HPLC conditions (100% solvent A). Use a linear gradient of 100% solvent A to 20% solvent A over 30 min to finish conditioning the column.

3. Configuration for microcolumn HPLC is shown in Fig. 2 and 3.

Gradient:	linear, 30–60 min, 0 to 100% (80 : 20 acetonitrile: 0.5% acetic acid)
Flow:	100 µl/min, flow split to final flow rate 200–300 nl/min
Columns:	100 µm i.d. × 20–25 cm, Phenomonex AQUA, 5-µm particles

B. Low Flow Rate Infusion Tandem Mass Spectrometry of Peptides

Media and Solutions

1. *1 : 1 0.5% acetic acid/ methanol*: To make 100 ml, add 2.5 ml of glacial acetic acid to 47.5 ml of distilled and deionized water and add 50 ml of HPLC grade methanol. Store in closed container at room temperature.

Steps

1. To accomplish low flow rate infusion, create a liquid metal junction. Valco fitting (P/N MU1XCTI), titanium is preferred because it is a biologically inert material. The fused silica capillary is 375 µm o.d. ×20 µm i.d.

2. To infuse a sample, connect an entrance line of fused silica capillary to a syringe pump or to a device to pneumatically drive the liquid at a flow rate of 10–200 nl/min. Strip a fused silica microelectrospray needle (4 cm of 375 µm o.d. × 20 µm i.d.) of its polyimide coating near the exit and then connect to the Valco fitting. Place a voltage (900–2000 V) on the fitting to transfer the potential to the liquid and form the electrospray. Place the exit end of the electrospray needle close (0.1–0.5 mm) to the entrance of the heated capillary.

3. The advantage of low flow rate infusion is that a small volume of sample can be infused over a long time period (5–30 min). This allows time to record a mass spectrum and then to begin acquiring tandem mass spectra of ions observed in the mass spectrum. Low flow rate infusion works quite well for reasonably uncomplicated peptide mixtures. Complicated peptide mixtures, such as those derived from proteolytic digestion of large proteins or mixtures of proteins, can suffer from ion suppression. The tandem mass spectrum shown in Fig. 4 was acquired through infusion and subjected to *de novo* sequence analysis as discussed later.

C. Analysis of Peptides by Microcolumn Liquid Chromatography Microelectrospray Ion Trap Mass Spectrometry (LCQ)

Steps

1. Insert the packed 10- to 20-cm column into an Upchurch PEEK tee. Insert the blunt end of the column into the tee and direct the solvent from the HPLC into one of the other arms of the tee. Insert a length of fused silica into the remaining arm of the tee and connect to a second Upchurch PEEK tee. Insert into one of the arms a gold wire so that a length of the wire protrudes approximately 1–2 cm (Fig. 2). Attach the electrospray voltage to the gold wire. In the remaining arm of the tee, insert a length of fused silica 365 × 5 µm. The fused silica tubing is used to create a restriction to the HPLC flow to force 100–300 nl/min through the microcolumn and this solvent is directed to waste. The microelectrospray source connected to an ion trap mass spectrometer is depicted in Fig. 2.

Electrospray voltage: –1800–2000 V

2. An aliquot of sample is injected to record the molecular weight of the peptides.

Scan mass range:	400–1500 amu
Electron multiplier voltage:	1000 V

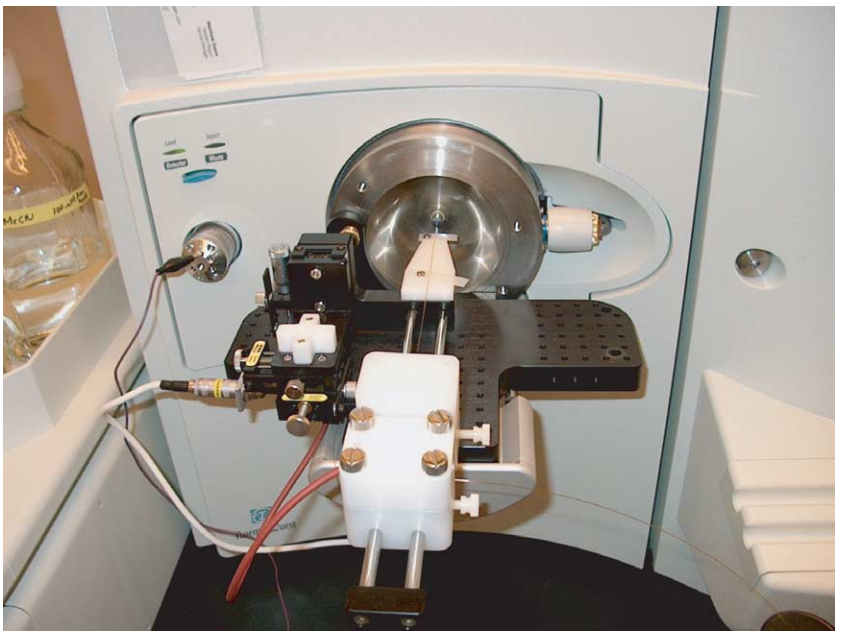

FIGURE 3 Microelectrospray source is shown connected to the mass spectrometer. The column is aligned with the opening in the heated capillary using the XYZ manipulator.

3. Sequence analysis of peptides is performed during a second HPLC analysis by selecting the precursor ion with a 3 u Full Width at Half Height (FWHH) wide notch and exciting the ions within the ion trap to induce fragmentation. Collision energies are on the order of 35 eV. The fragment ions are then scanned out of the ion trap to an electron multiplier set at 1000 V.

4. Alternatively, the LCQ mass spectrometer can automatically acquire tandem mass spectra over the course of an LC analysis. The analysis incorporates a unit mass resolution scan to find the most abundant ion above a preset ion abundance threshold. This ion is isolated and a high mass resolution scan is acquired. By resolving the isotopic peaks of the isolated ion, the charge state can be determined. For example, if the m/z distance between the isotope peaks is 1, then the charge state is +1. If the m/z distance is 0.5, then the charge state is +2. The LCQ can resolve a +4 charge state up to an m/z value of 1500. The tandem mass spectrum for Glu-fibrinopeptide is shown in Fig. 4.

IV. Comments

Under low-energy, multiple collision conditions, peptides fragment primarily at the amide bonds, producing sequence-specific fragmentation patterns. When fragment ions are produced the charge can be retained on the N terminus of the fragment of the ion to form ions of type b. If the charge is retained on the C-terminal fragment, the ion is of type y. There is no easy method to distinguish a b-ion from a y-ion without derivatization of the peptide. The mass spectrum shown in Fig. 6 was obtained by a ThermoFinnigan LCQ Deca ion trap mass spectrometer. A hallmark of this instrument is the ability to automatically acquire tandem mass spectra. After a mass spectrum is obtained, the data system identifies the most abundant ion and then acquires a tandem mass spectra in the next scan.

To demonstrate the sequencing process, the MS/MS spectrum for the peptide shown in Fig. 4 is interpreted. The process is demonstrated on a tandem mass spectrum acquired on an LCQ ion trap mass spectrometer. The process is identical to the one followed for triple quadrupole mass spectrometers as described in Yates *et al*. (1994) and McCormack *et al*. (1994). The mass spectrum is produced by collisional activation of a doubly charged ion, $(M + 2H)^{2+}$, at m/z 786.10. The protonated molecular weight of this peptide is calculated by multiplying the m/z value by 2 and subtracting the weight of one proton to give a value of 1571.2 (average mass). Subtraction of the highest mass fragment ion, m/z 1396.2 (1571.2 – 1396.2 = 175.0), from the $(M + H)+$ value yields a mass of 175. The mass fits C-terminal Arg. If this peptide was created through trypsin digestion, then this is a good assignment. Subtraction of the ion at 1396.2 from the next highest ion, 1285.4, yields a mass difference of 110.8, which does not correspond

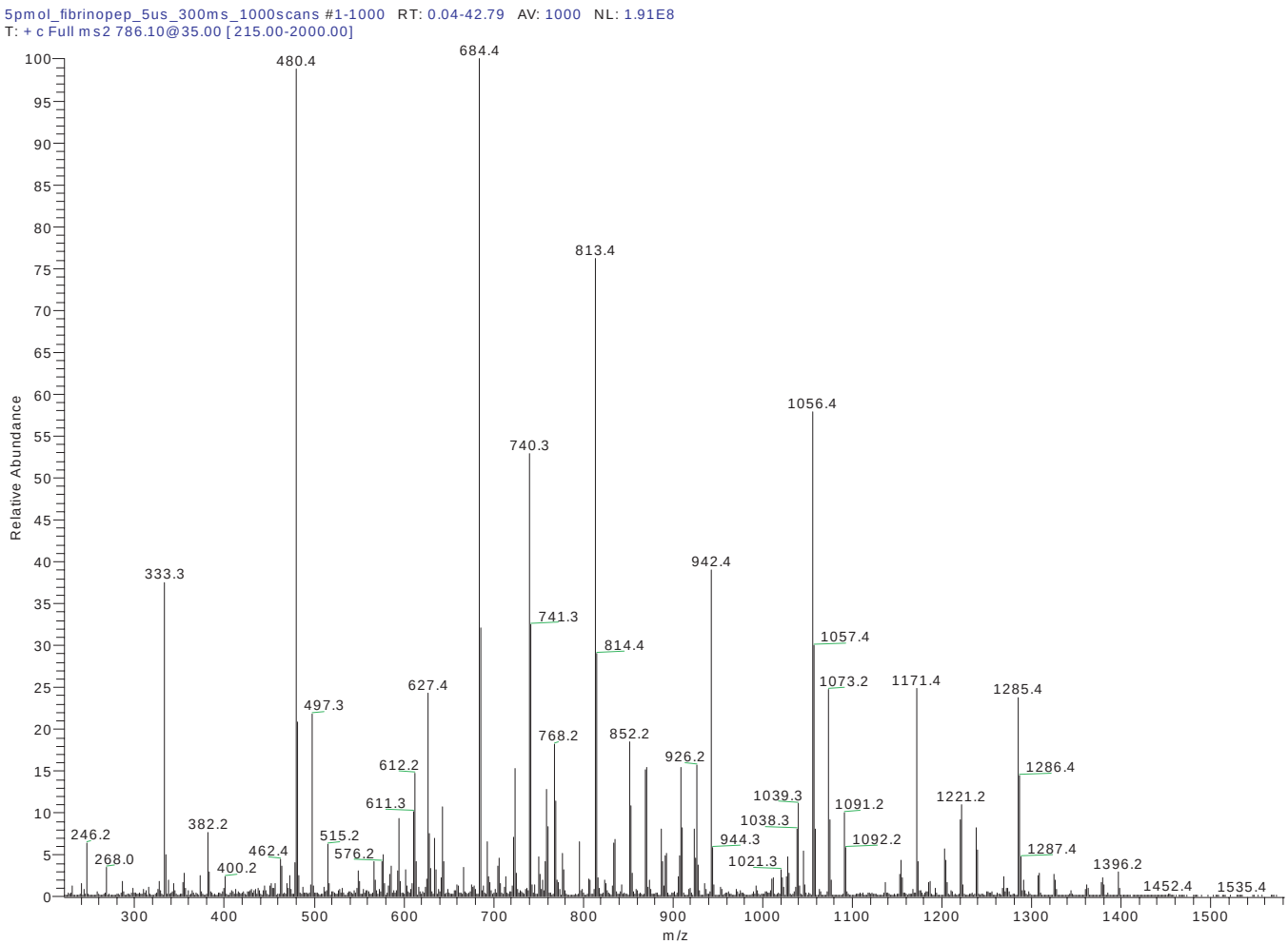

FIGURE 4 A tandem mass spectrum of the doubly charged ion, (M+2H)+2 786.10, of Glu-Fibrinopeptide.

to a mass for one of the common amino acids. This situation strongly suggests the ion at 1285.4 is of a different type. Assuming the ion at 1285.4 is of type y and that y-ions tend to predominate in tandem mass spectra of doubly charged peptide ions created through trypsin digestion, then it would be worthwhile to start from this point in the spectrum. A window can be set for where the next ion should reside in the spectrum using a range between a mass of 57 (Gly) and 186 (Trp). This window assumes no modifications to amino acids that would be larger then Trp. The next ion that fits the aforementioned criteria is 1171.4, which corresponds to a mass of 114 or Asn. The difference between the next ion at 1056.4 and 1171.4 is 115 for Asp and then the difference between this ion and 942.4 is 114. Thus far a sequence of Asn–Asp–Asn has been determined. The next abundant ion in the spectrum is 813.4, which nets a difference of 129 or Glu. An abundant ion is observed at 740.3, which yields a difference of 73. This value does not correspond to the weight of a common amino acid and thus can be temporarily discounted. Proceeding to the next ion to determine if a mass difference exists with the ion at 813.4 that provides a better fit, the ion at 684.4 is tried. This ion produces a mass difference of 129 and we now have a sequence of Asn–Asp–Asn–Glu–Glu. The next set of ions are less abundant and the largest of this group 627.4 gives a mass difference of 57 corresponding to Gly. If the other ions are tried, none produce as close a fit with an amino acid residue mass. The next two ions are rather obvious at 480.4 and 333.3. These ions yield a sequence of Phe–Phe. Two ions remain in the low end of the mass spectrum but only 246.2 produces a good fit and the amino acid Ser is obtained. The sequence now corresponds to Asn–Asp–Asn–Glu–Glu–Gly–Phe–Phe–Ser. By using the presumption the ion series used to interpret the sequence was of type y, this sequence corresponds to

the N-terminal sequence of the peptide. We know the C-terminal residue of the peptide is Arg so a calculation of the difference between 175 and 246.2 produces a mass of 71 and thus Ala. Completion of the sequence will require closer scrutiny of ions at the ends of the spectrum. At the high mass end of the spectrum between ions at 1285.4 and 1396.2 there are several ions. The ion at 1384.6 is 99 Da from the ion at 1285.4 and could be a Val residue. The corresponding ion at 286 is present at the low *m/z* end of the spectrum, confirming this residue as the likely sequence. The difference between 1384.6 and 1571.2 is 186.6. This corresponds to a Trp residue or a combination of two or more amino acids. Several combinations of amino acids will fit this mass: Glu–Gly, Asp–Ala, or Ser–Val. There is insufficient information in the spectrum to differentiate these possible sequences. The Ser–Val sequence can be eliminated by converting the peptide to its methyl ester as neither Ser nor Val should convert to a methyl ester with a *resulting* mass increase of 14 Da. The final sequence for the peptide derived from this spectrum is [EG,DA,SV]NDNEEGFFSAR.

De Novo Sequencing Algorithm

Results from two different *de novo* sequencing algorithms are shown in Fig. 5 and 6. The DeNovoX program automatically determines a complete or partial amino acid sequence of an unknown peptide by interpreting its MS/MS spectra. It is capable of identifying peptides with posttranslational modifications, mutations, or single amino acid deletion in the peptide. The probability-based program, which is optimized for data collected with the ThermoFinnigan LCQ ion trap instrument, takes data files that contain the *m/z* values and intensities of ions in MS/MS

FIGURE 5 Interpretation output from the DeNovoX program on the tandem mass spectrum shown in Figure 4.

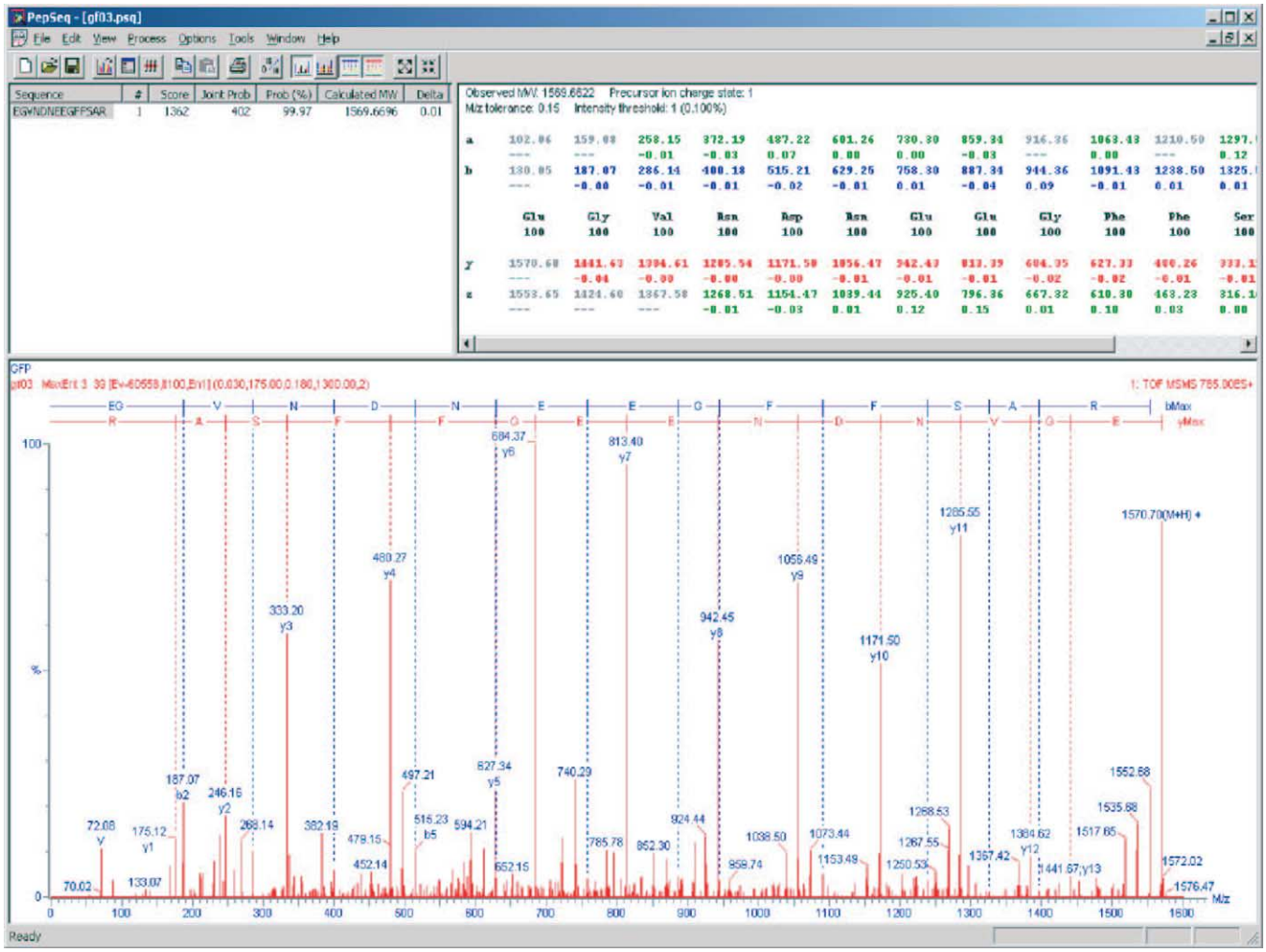

FIGURE 6 Interpretation output of the MassSeq program using a tandem mass spectrum acquired on a Q-TOF mass spectrometer (data not shown).

spectra together with the information on the respective parent ion mass and charge state as input. The data files are processed by the DeNovoX program in a fully automated mode. The program takes into account over 25 different factors relevant to *de novo* peptide sequencing. Amino acid tables that specify the amino acids considered for the search can be selected by the user and can include all major post-translational modifications. All other parameters are set by default in the program, including the mass tolerance of 0.8 Da for fragment ions. A list of suggested sequence tags and completed sequences with respective probability values are included in the output of the program, in addition to assigned spectra. The sequence interpretation with the highest probability is WVNDNEEGFFSAR and is shown in Fig. 5. The correct sequence is EGNDNEEGFFSAR. Clearly the first two amino acid residues are incorrect for reasons similar to those encountered in the manual interpretation. Ion trap tandem mass spectra are often lacking the necessary sequences to definitively identify the N-terminal amino acid residues. These sequences can then be used for further database searches (e.g., BLAST search).

Peptide tandem mass spectrometry data obtained by Q-TOF mass spectrometers can be sequenced using the MassSeq program from MicroMass. *De novo* sequencing is performed by using the MaxEnt 3/MassSeq programs in the Waters-Micromass Masslynx 3.5 software package. The raw tandem mass spectrum is first processed with the Massive Inference algorithm (MaxEnt 3) (Jaynes, 1957; Skilling, 1989), which produces a spectrum where any higher charge state ion is collapsed into a single charge state and the isotopic

distribution of each peak is folded into the lowest mass member (^{12}C isotope). Interpretation of the processed spectrum is performed by the MassSeq program, which generated candidate sequences based on the molecular mass of the peptide. Because the total number of possible sequences is very large, a terminated Markov Chain Monte Carlo algorithm is employed to generate a smaller, yet representative set of sequences. Predicted spectra are generated from each of the candidate sequences using probabilistic fragmentation and then each are compared to the MaxEnt 3 processed spectrum. The final result is a list of sequences, which are scored based on their probability of a correct match to the MaxEnt 3 spectrum. Within each resulting peptide sequence, each amino acid is assigned a probability as to how likely the residue is correct assigned to that position in the sequence. Therefore, this method provides the ability to sequencing peptides *de novo* and have information on the degree of likelihood that the sequence is correct. Q-TOF spectra often contain more information about the sequence and the complete sequence can often be inferred. Interpretation of a tandem mass spectrum of Glu-fibrinopeptide is shown in Fig. 6. Both algorithms produce a nearly complete sequence.

V. PITFALLS

1. Results from sequencing should be checked by derivatizing the peptide to ensure that the appropriate mass shift is observed. One derivatization method consists of forming the peptide methyl ester by adding 2 *N* methanolic HCl to the dry peptide. A second tandem mass spectrum can be acquired for the derivatized peptide to determine if the fragment ions also shift by the correct mass increment.

2. Distilled and deionized water must be used in the HPLC solvents to avoid the production of sodium or potassium adducts.

References

Andren, P. E., Emmett, M. R., and Caprioli, R. M. (1994). Micro-electrospray—zeptomole-attomole per microliter sensitivity for peptides. *J. Am. Soc. Mass Spectrom.* **5**, 867–869.

Davis, M. T., Stahl, D. C., Hefta, S. A., and Lee T. D. (1995). A microscale electrospray interface for online, capillary liquid-chromatography tandem mass-spectrometry of complex peptide mixtures. *Anal. Chem.* **67**, 4549–4556.

Emmett, M. R., and Caprioli, R. M. (1994). Micro-electrospray mass spectrometry: Ultra-high-sensivity analysis of peptides and proteins. *J. Am. Soc. Mass Spectrom.* **5**, 605–613.

Gale, D. C., and Smith, R. D. (1993). Small volume and low flow rate electrospray ionization mass spectrometry of aqueous samples. *Rapid Commun. Mass Spectrom.* **7**, 1017–1021.

Gatlin, C. L., Kleemann, G. R., Hays, L. G., Link, A. J. & Yates, J. R. (1998). Protein identification at the low femtomole level from silver-stained gels using a new fritless electrospray interface for liquid chromatography-microspray and nanospray masss spectrometry. *Anal Biochem* **263**, 93–101.

Griffin, P. R., Coffman, J. A., Hood, L. E., and Yates, J. R. III (1991). Structural analysis of proteins by HPLC-MS and HPLC-MS/MS using electrospray ionization on a triple quadrupole mass spectrometer. *Int. J. Mass Spectrom. Ion Proc.* **111,** 131–149.

Hunt, D. F., Yates, J. R. III, Shabanowitz, J., Winston, S., and Hauer, C. R. (1986). Protein sequencing by tandem mass spectrometry. *Proc. Natl. Acad. Sci. USA* **84**, 620–623.

Jaynes, E. T. (1957). Information theory and statistical mechanics, I. *Phys. Rev.* **106**, 620–630.

Kennedy, R. T., and Jorgenson, J. W. (1989). Preparation and evaluation of packed capillary liquid chromatography columns with inner diameters from 20 to 50 μm. *Anal. Chem.* **56**, 1128–1135.

McCormack, A. L., Eng, J. K., and Yates, J. R. III (1994). Peptide sequence analysis on quadrupole mass spectrometers. *Methods* **6**, 274–283.

Skilling, J. (1989). *In* "Maximum Entropy and Bayesian Methods" (J. Skilling, ed.), p. 45. Kluwer Academic, Dordrecht.

Wilm, M. S., and Mann, M. (1994). Electrospray and taylor-cone theory, doles beam of macromolecules at last. *In. J. Mass Spectrom. Ion Proc.* **136**, 167–180.

Yates, J. R. III, McCormack, A. L., Hayden, J., and Davey, M. (1994). Sequencing peptides derived from the class II major histocompatibility complex by tandem mass spectrometry. *In* "Cell Biology: A Laboratory Handbook" (J. E. Celis, ed.), pp. 380–388. Academic Press, San Diego.

CHAPTER

50

Direct Database Searching Using Tandem Mass Spectra of Peptides

John R. Yates III and William Hayes McDonald

I. INTRODUCTION

Whole genome sequencing has provided a sequence infrastructure to the enormous benefit of mass spectrometry and protein biochemistry. The ability to match tandem mass spectra to sequences in protein or nucleotide databases allows accurate and high throughput identification of peptides and proteins (Eng *et al*., 1994; Yates *et al*., 1995a,b, 1996). Furthermore, this data analysis capability, when combined with automated acquisition of tandem mass spectra, allows direct analysis and identification of proteins in mixtures. Applications of this procedure to rapidly survey the identities of proteins in protein complexes, subcellular compartments, cells, or tissues are made possible because of the combination of tandem mass spectrometry and database searching (McCormack *et al*., 1995; Link *et al*., 1997, 1999; Washburn *et al*., 2001; Florens *et al*., 2002). The method allows both automated and accurate searches of protein and nucleotide databases, as well as the use of spectra of posttranslationally modified peptides. Modifications such as phosphorylation, methylation, and acetylation can be identified through the analysis of digested protein complexes (Cheeseman *et al*., 2002; MacCoss *et al*., 2002). A detailed description of the manner in which tandem mass spectra are processed and then used to search databases is described.

II. MATERIALS AND INSTRUMENTATION

Tandem mass spectra of peptides were obtained by electrospray ionization tandem mass spectrometry (Finnigan MAT, San Jose, CA) as described previously (Gatlin *et al*., 1998; Verma *et al*., 2000; Washburn *et al*., 2001).

Several computer algorithms now exist to search tandem mass spectra through sequence databases. Information about these programs can be accessed through the following URLs: http://www.matrixscience.com, http://prospector.ucsf.edu, http://pepsea.protana.com, http://fields.scripps.edu/sequest, and http://www.proteometrics.com. This article discusses the use of SEQUEST, as we have the most experience with this program. SEQUEST searches were performed on a PC Linux computing cluster described elsewhere using a parallelized version of the SEQUEST algorithm (Sadygov, 2002). Methods for data reduction, preliminary scoring, and cross-correlation analysis used in the computer algorithm have been described in detail elsewhere (Eng *et al*., 1994; Yates *et al*., 1995a,b). Search results are analyzed with the program DTAselect (Tabb *et al*., 2002). Information on how to obtain the DTAselect program can be found at http://www.sequest.org. This program can accommodate output from the

Copyright 2006, Elsevier Science (USA).
All rights reserved.

SEQUEST and Mascot search programs. Databases can be obtained over the Internet using anonymous ftp to the National Center for Biotechnology Information (NCBI) (ftp://ncbi.nlm.nih.gov). Databases such as the GenBank database of nucleotide sequences, the NRP (nonredundant protein) database, and dbEST—the collection of expressed sequence tag sequences—can be obtained from the NCBI site. The complete *Saccharomyces cerevisiae* sequence can be obtained from Stanford Genomic Resources (http://genome-www.stanford.edu).

III. PROCEDURES

A. Method for Database Search with Tandem Mass Spectra

Steps

1. Convert raw, binary data from an MS/MS file to ASCII in the following format:

```
1734.9    2
 110.3    49422.8
 112.3    32433.3
 112.9    65452.1
   :        :
```

The first line in the file contains (M + H)+ and charge state information. Conversion of binary data is accomplished automatically by SEQUEST with data files from ThermoFinnigan mass spectrometers. Most mass spectrometers can convert proprietary data file formats to a form that can be used by the database search programs or the search programs can read the formats directly. The next task calculates the molecular weight of the peptide based on its precursor *m*/*z* value. This calculation is accomplished with the program *2to3*, which identifies the charge state of the precursor ion by identifying related fragment ion pairs (Sadygov *et al*., 2002). Fragment ion pairs sum to the molecular weight of the peptide and by initially assuming that the precursor ion is doubly charged and checking that related fragment ion pairs exist in the spectrum will verify this assumption. A molecular weight based on a +3 charge state is then calculated and the existence of fragment ion pairs. The correct molecular weight will produce a much larger number of related ion pairs. This program is designed to use nominal resolution spectra where the charge state based on isotope spread cannot be calculated. If the spectrum does not contain a minimum amount of fragmentation information to identify the charge state, then that spectrum is not used for database searching.

2. For SEQUEST searches, search parameters can be set in the param.h header file. This includes the database to be searched, whether it is a nucleotide or protein database, and whether to perform calculations using average or monoisotopic masses. The set of sequence ions (types b and y) to be considered can also be selected as well as the relative abundance values to be used during the theoretical reconstruction of tandem mass spectra. The masses of amino acids to consider for modified peptides can be input. The mass tolerance for the peptide (M + H)+ can be set as well. Enzyme or chemical cleavage specificity can be entered from the following list: no enzyme, trypsin, chymotrypsin, clostripain, cyanogen bromide, iodoso benzoate, proline endopeptidase, *Staphylococcus aureus* V8 protease, lysine endoproteinase, arginine endoproteinase, AspN-endoproteinase, and elastase.

3. The tandem mass spectrometry data file is then processed in two ways. First the precursor ion is removed and the remaining ions are normalized. This process is not required when analyzing ion trap mass spectra. All but the top 200 most abundant ions are then removed from the search file. This processed spectrum is used to search the database. To perform the cross-correlation analysis described later, a second file from the tandem mass spectrum is created. The spectrum is divided into 10 equal regions and within each region the ions are normalized to the most abundant ion. The molecular weight of the peptide in the tandem mass spectrum is calculated directly from the precursor ion.

4. A search of the database involves scanning each entry to find linear combinations of amino acids, proceeding from the N to the C terminus, that are within some tolerance of the mass of the peptide represented by the tandem mass spectrum. Sequence selection can also be guided by the cleavage specificity of the protease used to create the peptide, including consideration of incompletely digested peptides from either side of the primary sites, or it can be performed with no assumptions about how the peptide was created. If a nucleotide database is searched, the nucleotide sequences are translated "on the fly" to protein sequences in 6-reading frames (Yates *et al*., 1995b). Chemical modifications can be considered by changing the amino acid mass used to calculate the masses of the peptides. The modified amino acid is then considered at every occurrence in the sequence (Yates *et al*., 1995a,b).

5. Once an amino acid sequence is within the defined mass tolerance, a preliminary evaluation is performed (Eng *et al*., 1994). First, the number (n_i) of predicted fragment ions that match ions observed in the spectrum within the fragment ion mass tolerance and their abundances (i_m) are summed. If an ion series is continuous, i.e., if consecutive sequence ions are

present, then a component of the score, β, is incremented. A sequence that matches a continuous set of ions is weighted more heavily then one that matches a few sequence ions randomly. If an immonium ion is present in the spectrum (not usually the case with Ion Trap MS/MS data), then the associated amino acid must be present in the sequence under consideration or an additional component of the score, ρ, is increased or decreased correspondingly. The total number of predicted sequence ions is also noted (n_t). A score is calculated for each amino acid sequence by using the following relationship in Eq. (1),

$$\mathrm{Sp} = \left(\sum \mathrm{im}\right) * \mathrm{ni} * (1+\beta) * (1+\rho) / \mathrm{n_x}. \qquad (1)$$

6. Each of the top 500 scoring sequences are subjected to a cross-correlation analysis. This is performed by reconstructing a model tandem mass spectrum for each of the amino acid sequences in the list of 500 and comparing each one to the processed experimental tandem mass spectrum (step 2) by using a cross-correlation function. The cross-correlation function is a very sensitive signal processing method used to compare the coherence of two signals (Owens, 1992). This is performed, in effect, by translating one signal across another. If two signals are the same or very similar, the correlation function should maximize when there is no offset between the signals. A cross correlation score is computed for each of the 500 amino acid sequences.

7. Cross-correlation values are normalized by dividing the XCorr value by the autocorrelation of the experimental tandem mass spectrum. The formula used to calculate a normalized cross-correlation value is shown by Eq. (2). By normalizing correlation scores for tandem mass spectra of +1, +2, and +3 ions, the scores are roughly equivalent and a statistical confidence for each sequence assignment can be assessed (MacCoss *et al*., 2002).

$$XCorr = \frac{Corr(Exp, Theo)}{\sqrt{Corr(Exp, Exp) * Corr(Theo, Theo)}} \qquad (2)$$

B. Data Assembly and Filtering

Steps

1. For very large analyses, such as multidimensional liquid chromatography experiments (MudPIT), extremely large data sets can be produced. A program, DTASelect, is used to assemble, filter, and display the results from search (Tabb *et al*., 2002). The program is especially suited for the analysis of data produced in multidimensional liquid chromatography separations together. DTASelect can be used with output from SEQUEST or Mascot searches. Figure 1 shows output from DTASelect from a multidimensional analysis of the *S. cerevisiae* proteasome. In the first column, the probability the match is correct is shown. The closer the value is to 1 the higher the probability the match is correct. This entry in the table is linked to the tandem mass spectrum and a representation of the quality of the sequences is fit to the spectrum. How well other sequences fit to the spectrum can be viewed from this page as well. Each of the predicted b- and y-ions are aligned with matching fragment ions in the spectrum. Mass differences between predicted fragment ions and fragments ions observed in the spectrum are shown in the upper right hand side of the page. At the bottom of the figures are check boxes to indicate the validation status of the fit of the spectrum to the sequence (Fig. 2). Access to individual search data allows the inspection of search results to look for sequence similarity between sequences.

2. In the second and third columns marked XCorr and DeltaCn, respectively, are scores for the tandem mass spectrum's match to the sequence. The values under XCorr are obtained from the cross-correlation analysis and are normalized as described earlier. The larger the value, the closer the fit between the experimental tandem mass spectrum and the model tandem mass spectrum constructed from the sequence. The DeltaCn value is the difference between the normalized XCorr values for the first and second search results. The larger DeltaCn is the more dissimilar the first and second answers will be.

3. The fourth and fifth columns show the (M + H)+ value calculated from the precursor ion chosen for MS/MS and the (M + H)+ value calculated from the sequence, respectively.

4. Columns SpR, SpScore, and Ion% show the rank of the peptide match based on the preliminary score, the preliminary score and the percentage of ions matched between the experimental spectrum, and sequence ions predicted from the sequence. Generally, short peptides produce an SpR that is less than one. The correct result usually matches a large percentage of ions, Ion%, between those predicted and those observed. Larger peptides can result in a low percentage of ion matches because of the limited mass range of the ion trap mass spectrometer.

5. In the last column the matched sequence is shown. The actual matching sequence is preceded and terminated by a period. Amino acid residues before the preceding period and after the terminating period are shown to illustrate the enzymatic cleavage sites.

6. Peptide matches are grouped by gene locus, and information pertaining to the protein is shown in the header. From left to right the information shown in the header describes the validation status of peptides matched to that protein, the locus name for the gene,

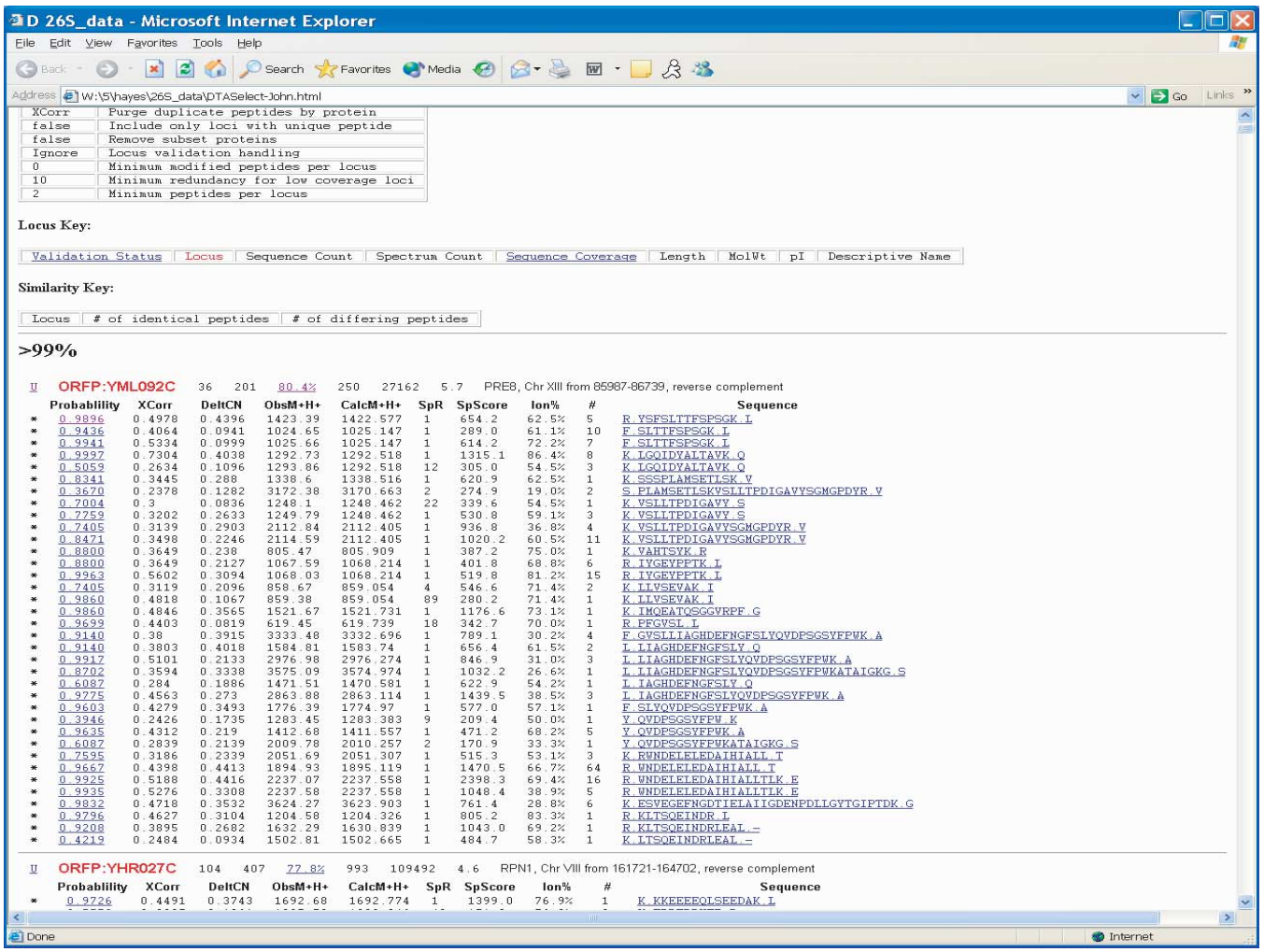

FIGURE 1 DTASelect output for analysis of the *S. cerevisiae* proteasome.

the number of peptides identified, the spectrum count indicating the total number of spectra matched (redundant spectra are included), percentage sequence coverage, which is linked to a visual display of coverage and overlap (Fig. 3), protein length, molecular weight, pI, and the descriptive name for the protein.

IV. COMMENTS

SEQUEST software can provide highly accurate protein identifications. The highly specific information represented in a tandem mass spectrum allows proteins present in mixtures to be identified, as each tandem mass spectrum is a specific address to a protein in the same manner that an amino acid sequence can be highly specific for a protein. Generally, several or more spectra are obtained for each protein, but a protein can be identified on the basis of one tandem mass spectrum if the following criteria are met: the amino acid sequence represented by the tandem mass spectrum is at least seven amino acids in length, the tandem mass spectrum contains a sufficient number of sequence ions to allow validation of the identified sequence, and the amino acid sequence is unique to a single protein within the organism from which the protein was derived.

When evaluating a match between a spectrum and a sequence, several scores should be considered. The greater the probability value, the more statistically significant the match will be. These probability scores are based on empirical measures. The DTASelect program does retain search results with lower probabilities as their significance may increase if many higher scoring spectra match to the same protein. The normalized

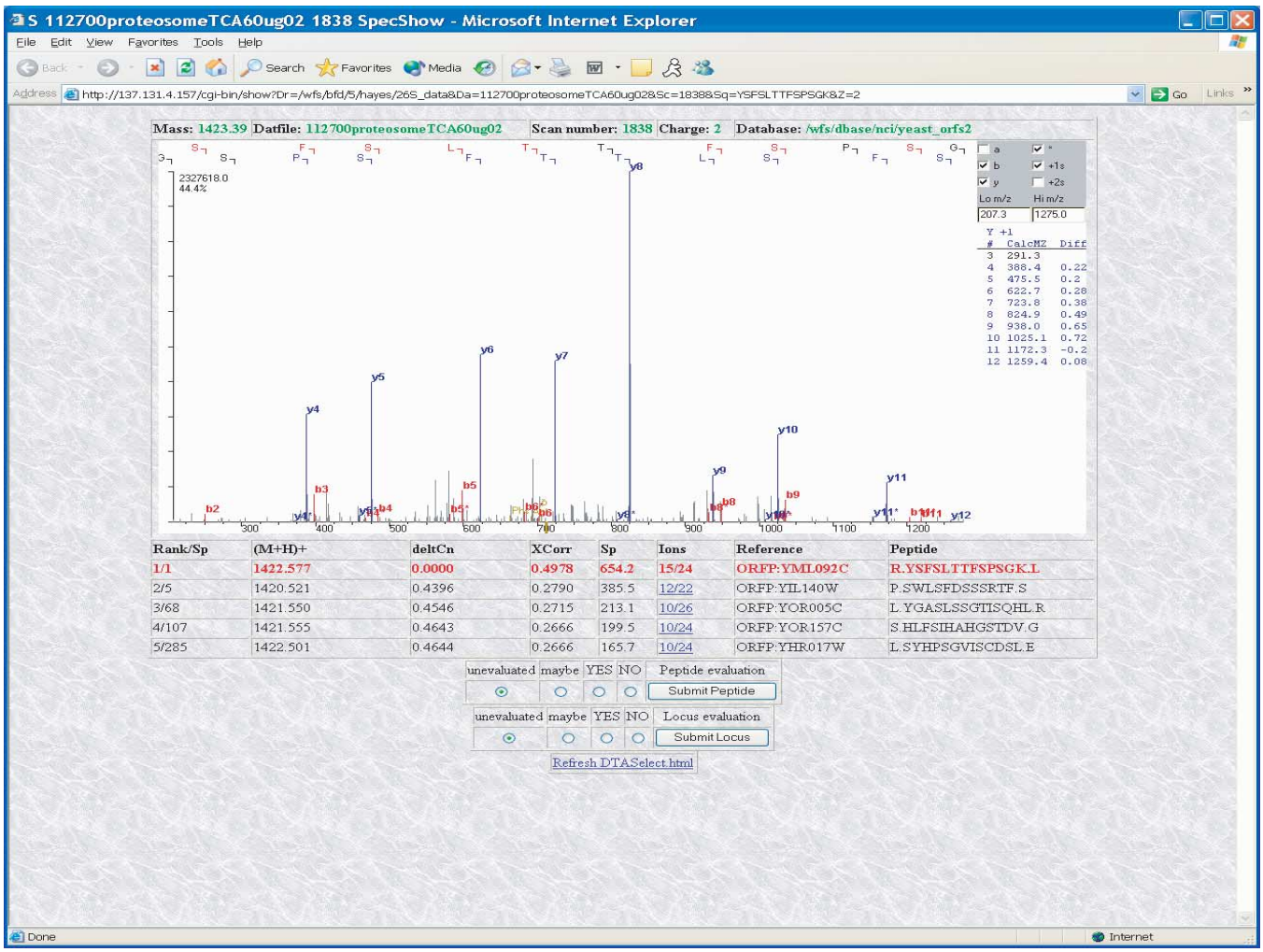

FIGURE 2 Following the link from the probability value displayed in the first column (Fig. 1), information for individual searches of tandem mass spectra can be found. This is useful to determine if a close score is the result of identifying two closely related sequences. The tandem mass spectrum is shown as well as the match to the sequence.

cross-correlation value provides a mathematical evaluation of how close the experimental MS/MS fits to a model derived from the sequence. The limitations of this method relate to the ability to model a sequence as a spectrum and the predictability of peptide fragmentation. The DeltaCn value reflects how well the spectrum matches the model spectrum in comparison to background matches from the database. The XCorr value is an inherent property of the spectrum and changes as a function of spectral quality, whereas DeltaCn changes as a function of spectral quality and database size (e.g., background). Thus these two values provide a good quantitative measure of the match quality.

SEQUEST is ideal for creating a high-throughput, automated system for the identification of proteins from two-dimensional gels. By combining an autosampler with an HPLC protein, digests can be automatically injected and separated and tandem mass spectra automatically acquired. Tandem mass spectra can be acquired through an instrument control program on the ThermoFinnigan LCQ series mass spectrometer allowing unattended acquisition. Proteins present in mixtures can also be identified through the acquisition of tandem mass spectra and matching spectra to their respective proteins. Database sequence errors can be tolerated by the adjustment of parameters such as the ion series and mass tolerance to be used in a search. Database searching using tandem mass spectra enables "shotgun proteomics" or the analysis of digested protein mixtures. Unlike a 2 Dimensional Gel Electrophoresis analysis, it is only after a database search

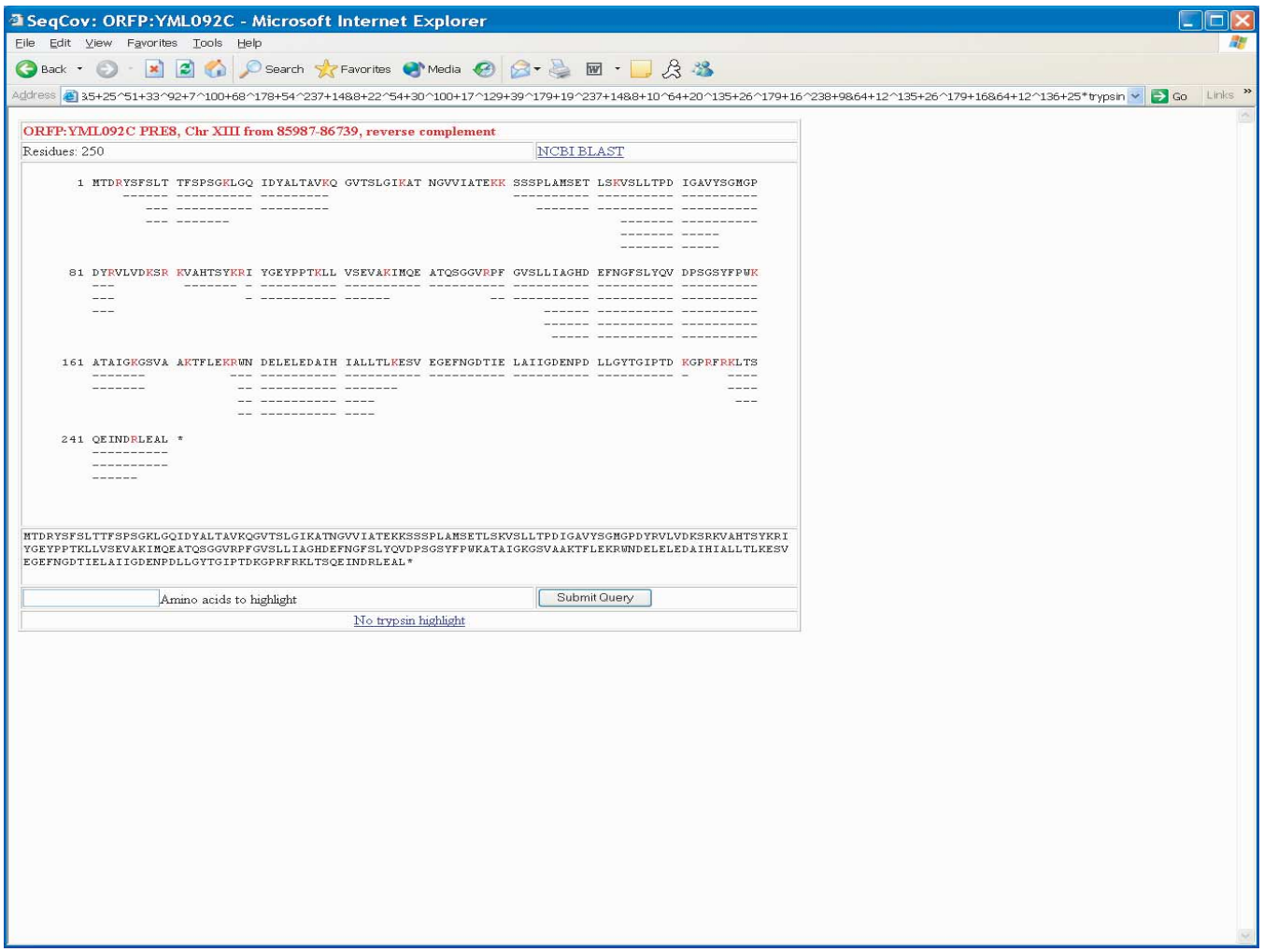

FIGURE 3 Following the link from the percentage in the locus header, sequence coverage of the protein can be observed. This figure shows regions of the protein where peptides were identified. This information is useful when a search of modification is desired. Regions lacking sequence coverage could represent sites of modification, areas that were difficult to digest, or areas where digestion yields too many short peptides. By using the input box at the bottom of the page, specific amino acid residues can be highlighted. Sites of K and R in the sequence are shown.

can relationships among spectra be determined. For relatively simple protein mixtures, combining the "shotgun proteomics" method with multidimensional liquid chromatography can yield reasonably good protein sequence coverage.

V. PITFALLS

1. All tandem mass spectra should be validated against the sequence matched in the database.
2. SEQUEST will match a tandem mass spectrum to a similar, mass conserved sequence if the correct sequence is not present in the database.
3. SEQUEST can match tandem mass spectra with a relatively poor signal-to-noise ratio to the correct sequence, but the spectrum should be of sufficient quality for validation or the match should be considered tentative.

References

Cheeseman, I. M., Anderson, S., *et al*. (2002). Phospho-regulation of kinetochore-microtubule attachments by the *Aurora kinase* Ipl1p. *Cell* **111**(2), 163–172.

Eng, J. K., McCormack, A. L., *et al*. (1994). An approach to correlate tandem mass spectral data of peptides with amino acid sequences in a protein database. *J. Am. Soc. Mass Spectrom.* **5**, 976–989.

Florens, L., Washburn, M. P., *et al*. (2002). A proteomic view of the *Plasmodium falciparum* life cycle. *Nature* **419**(6906), 520–526.

Gatlin, C. L., Kleemann, G. R., *et al*. (1998). Protein identification at the low femtomole level from silver-stained gels using a new fritless electrospray interface for liquid chromatography-microspray and nanospray mass spectrometry. *Anal Biochem* **263**(1), 93–101.

Link, A. J., Carmack, E., *et al*. (1997). A strategy for the identification of proteins localized to subcellular spaces: Application to *E. coli* periplasmic proteins. *Int. J. Mass Spectrom. Ion Proc.* **160**, 303–316.

Link, A. J., Eng, J., *et al*. (1999). Direct analysis of protein complexes using mass spectrometry. *Nature Biotechnol*. **17**(7), 676–682.

MacCoss, M. J., McDonald, W. H., *et al*. (2002). Shotgun identification of protein modifications from protein complexes and lens tissue. *Proc. Natl. Acad. Sci. USA* **99**(12), 7900–7905.

MacCoss, M. J., Wu, C. C., *et al*. (2002). Probability-based validation of protein identifications using a modified SEQUEST algorithm. *Anal. Chem.* **74**(21), 5593–5599.

McCormack, A. L., Eng, J. K., *et al*. (1995). Microcolumn liquid chromatography-electropray ionization tandem mass spectrometry. *Biochem. Biotech. Appli. Electrospray Ionization Mass Spectrom.* **619**, 207–225.

Owens, K. G. (1992). Application of correlation analysis techniques to mass spectral data. *Appl. Spectrosc. Rev.* **27**(1), 1–49.

Sadygov, R. G., Eng, J., Durr, E., Saraf, A., McDonald, H., MacCoss, M. J., and Yates, J. R. III (2002). Code developments to improve the efficiency of automated MS/MS spectra interpretation. *J. Proteome Res.* **2**, 211–215.

Tabb, D. L., McDonald, H. W., Yates, J. R., III (2002). DTASelect and Contrast: Tools for aseembling and comparing protein identifications from shotgun proteomics. *J. Proteome Res.* **1**(1), 21–36.

Verma, R., Chen, S., *et al*. (2000). Proteasomal proteomics: Identification of nucleotide-sensitive proteasome-interacting proteins by mass spectrometric analysis of affinity-purified proteasomes. *Mol. Biol. Cell* **11**(10), 3425–3439.

Washburn, M. P., Wolters, D., *et al*. (2001). Large-scale analysis of the yeast proteome by multidimensional protein identification technology. *Nature Biotechnol*. **19**(3), 242–247.

Yates, J. R., 3rd, Eng, J. K., *et al*. (1995a). Mining genomes: Correlating tandem mass spectra of modified and unmodified peptides to sequences in nucleotide databases. *Anal. Chem.* **67**(18), 3202–3210.

Yates, J. R., 3rd, Eng, J. K., *et al*. (1995b). Method to correlate tandem mass spectra of modified peptides to amino acid sequences in the protein database. *Anal. Chem.* **67**(8), 1426–1436.

Yates, J. R., 3rd, McCormack, A. L., *et al*. (1996). Mining genomes with MS. *Anal. Chem*. **68**(17), 534A–540A.

CHAPTER

51

Identification of Proteins from Organisms with Unsequenced Genomes by Tandem Mass Spectrometry and Sequence-Similarity Database Searching Tools

Adam J. Liska and Andrej Shevchenko

I. INTRODUCTION

The analysis of proteomes by mass spectrometric methods that correlate peptide fragments from proteins with database entries *in silico* has been dependent on the sequencing of genomes. Mass spectrometry and database sequences have enabled the analysis of the human, mouse, and *Arabidopsis* proteomes, among others. Due to the high homology between living organisms at the molecular level, it is possible to use the available protein sequences accumulated in databases from a range of organisms as a reference for the identification of proteins from organisms with unsequenced genomes by sequence-similarity database searching. As research continues in organisms such as *Xenopus*, maize, cow, and others with limited database sequence resources, sequence-similarity searching is a powerful method for protein identification. This article focuses on MS BLAST (Shevchenko *et al.*, 2001) and MultiTag (Sunyaev *et al.*, 2003) as bioinformatic methods for the identification of proteins by the interpretation of tandem mass spectra of peptides and sequence-similarity searching.

II. MATERIALS AND INSTRUMENTATION

In analyses where MS BLAST is utilized for protein identification, tandem mass spectra of peptides can be acquired with any ionization source and mass spectrometer that enables *de novo* sequence prediction: nanoelectrospray, LC/MS/MS, o-MALDI (MALDI quadrupole TOF), MALDI TOF-TOF, QqTOF, triple quad, PSD MALDI-TOF, and ion trap. Alternatively, in analyses where MultiTag is applied, tandem mass spectra of peptides can be acquired with any ionization source and tandem mass spectrometer that enables the creation of peptide sequence tags (Mann and Wilm, 1994): nanoelectrospray, LC/MS/MS, QqTOF, triple quad, or other novel system.

Software for *de novo* sequence prediction from tandem mass spectra is often included in the software packages associated with mass spectrometers: BioMultiview, BioAnalyst (both are from MDS Sciex, Canada), BioMassLynx (Micromass Ltd, UK), BioTools (Bruker Daltonics, Germany), and DeNovoX (ThermoFinnigan). The Lutefisk program (Johnson and Taylor, 2000) can be acquired from http://www.

Copyright 2006, Elsevier Science (USA).
All rights reserved.

hairyfatguy.com/Sherpa/. BioAnalyst with the ProBlast processing script can generate a complete MS BLAST query automatically from multiple-spectra files acquired by nanoelectrospray or LC/MS/MS (Nimkar and Loo, 2002). A web browser such as Internet Explorer or Netscape is also required to gain access to the MS BLAST web interface located at http://dove.embl-heidelberg.de/Blast2/msblast.html. An independent BLAST computer (Paracel BlastMachine system) may also be purchased and installed for rapid and private MS BLAST operation.

Sequence tags that contain a few confidently designated amino acid residues and mass values that lock the short sequence stretch into the length of the peptide can often be generated from tandem mass spectra with the software packages associated with mass spectrometers. Microsoft Excel or an alternative spreadsheet program is required for compiling of search results before submission to MultiTag. BioAnalyst software has an associated processing script that produces a list of database search results from a generated list of sequence tags to accelerate spectra processing with MultiTag.

III. PROCEDURES

A. Identification of Proteins by MS BLAST Database Searching

1. MS BLAST is a specialized BLAST-based tool for the identification of proteins by sequence-similarity searching that utilizes peptide sequences produced by the interpretation of tandem mass spectra (Shevchenko *et al*., 2001). The algorithm and principles of BLAST sequence-similarity searching are reported in detail elsewhere (Altschul *et al*., 1997). A useful list of BLAST servers accessible on the web is provided in Gaeta (2000).

2. Peptide sequences are generated from the interpretation of tandem mass spectra from the analysis of a single in-gel or in-solution digest of an unknown protein, edited and assembled into a query list for the MS BLAST search. If tandem mass spectra were interpreted by *de novo* sequencing software, disregard relative scores and use the entire list of candidate sequences (or some 50–100 top scoring sequence proposals per fragmented peptide precursor) (Fig. 1). Automated interpretation of tandem mass spectra often requires adjustment of parameters that affect the quality of predicted sequences. It is therefore advisable to test the settings in advance using digests of standard proteins and to adjust them if necessary. Note that the settings may depend on a charge state of the fragmented precursor ion. Use only the standard single-letter symbols for amino acid residues. If the software introduces special symbols for modified amino acid residues, replace them with standard symbols.

3. When interpreting MS/MS spectra manually, try making the longest possible sequence stretches, although their accuracy may be compromised. For example, it is usually difficult to interpret unambiguously fragment ion series at the low m/z range because of abundant peaks of chemical noise and numerous fragment ions from other series. In this case, it is better to include many complete (albeit low confidence) sequence proposals into the query rather than using a single (although accurate) three or four amino acid sequence stretch deduced from a noise-free high m/z segment of the spectrum.

4. Gaps and ambiguities in peptide sequences can occur due to the fragmentary nature of tandem mass spectra of peptides. Some *de novo* sequencing programs may suggest a gap in the peptide sequence that can be filled with various isobaric combinations of amino acid residues. For example,

$$\text{DTPS[...]HYNAR, } [...] = [\text{S, V}] \text{ or } [\text{D, A}]$$

If one or two combinations were suggested, include all variants into a searching string:

-DTPSSVHYNAR-DTPSVSHYNAR-
DTPSDAHYNAR-DTPSADHYNAR-

If more combinations were possible, the symbol X can be used instead to fill the gap. Zero score is assigned to X symbol in PAM30MS scoring matrix and therefore it matches weakly any amino acid residue:

-DTPSXXHYNAR-

Note that MS BLAST is sensitive to the number of amino acid residues that are filling the gap. If the gap could be filled by a combination of two and three amino acid residues, consider both options in the query

-DTPSXXHYNAR-DTPSXXXHYNAR-

5. Isobaric amino acids need to be altered in the MS BLAST query. L stands for Leu (L) and Ile (I). Z stands for Gln (Q) and Lys (K), if undistinguishable in the spectrum. Use Q or K if the amino acid residue can be determined. The query string needs to be further altered for cleavage site specificity. If the proposed sequence is complete, a putative trypsin cleavage site symbol B is added prior to the peptide sequence:

...-BDTPSVDHYNAR-

It is often difficult to determine two amino acid residues located at the N terminus of the peptide. In this case, present them as

...-BXXPSVDHYNAR-...

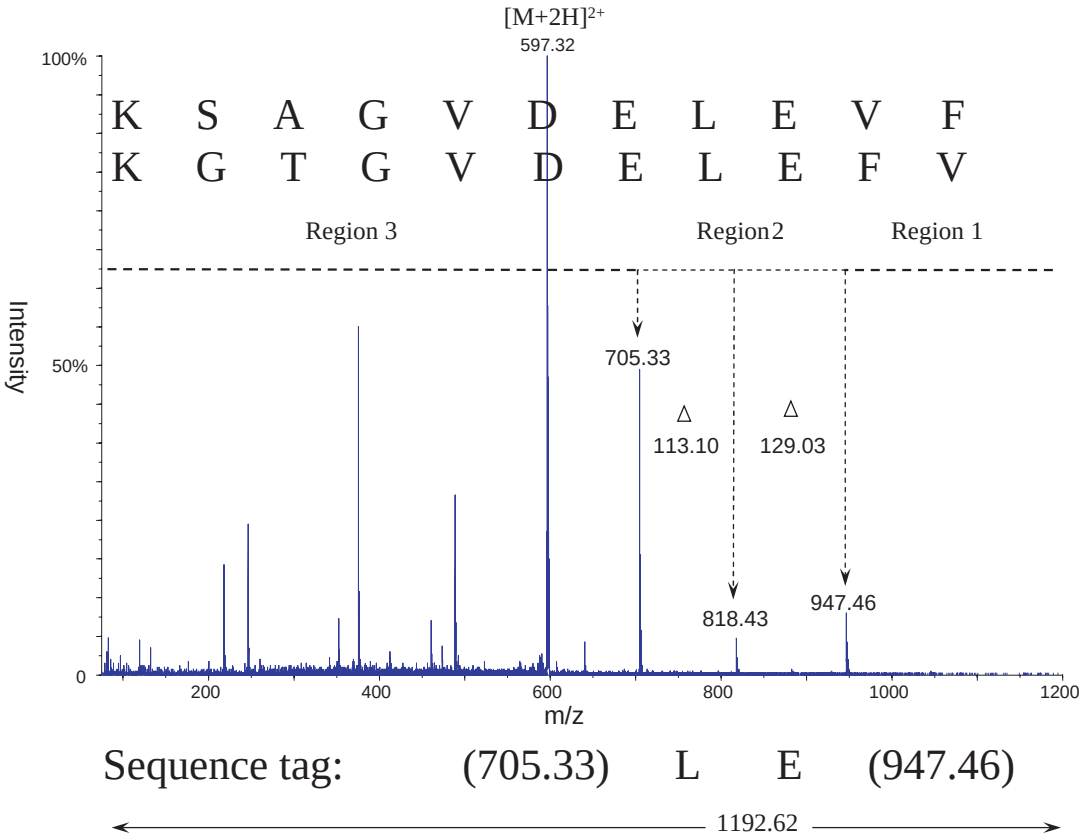

FIGURE 1 A spectrum with *de novo*-predicted amino acid sequences and a manually constructed sequence tag. Multiple candidate peptide sequences can be generated from a single spectrum for MS BLAST analysis, whereas MultiTag requires one sequence tag per spectrum.

MS BLAST will then consider BXX residues in possible sequence alignments.

6. The regular BLAST search must be altered in options and settings for an MS BLAST query:

NOGAP is absolutely essential, it turns off gapped alignment method so that only high-scoring pairs (HSPs) with no internal gaps are reported.

SPAN1 is absolutely essential, it identifies and fetches the best matching peptide sequence among similar peptide sequences in the query. Therefore the query may contain multiple partially redundant variants of the same peptide sequence without affecting the total score of the protein hit.

HSPMAX 100 limits the total number of reported HSPs to 100. Set it to a higher number (e.g., 200) if a large query is submitted and a complete list of protein hits (including low confidence hits) is required in the output.

SORT_BY_TOTALSCORE places the hits with multiple high scoring pairs to the top of the list. Note that the total score is not displayed, but can be calculated, if necessary, by adding up scores of individual HSPs.

EXPECT: It is usually sufficient to set EXPECT at 100. Searching with higher EXPECT (as, 1000) will report many short low-scoring HSPs, thus increasing the sequence coverage by matching more fragmented peptides to the protein sequence. Note that low scoring HSPs do not increase statistical confidence of protein identification. The EXPECT setting also does not affect the scores of retrieved HSPs.

MATRIX: PAM30MS is a specifically modified scoring matrix. It is not used for conventional BLAST searching.

PROGRAM: blast2p.

DATABASE: nrdb95 are default settings of the MS BLAST interface.

FILTER: Filtering is set to "none" default. However, if the sequence query contains many repeating stretches (as . . . EQEQEQ . . .), filtering should be set to "default."

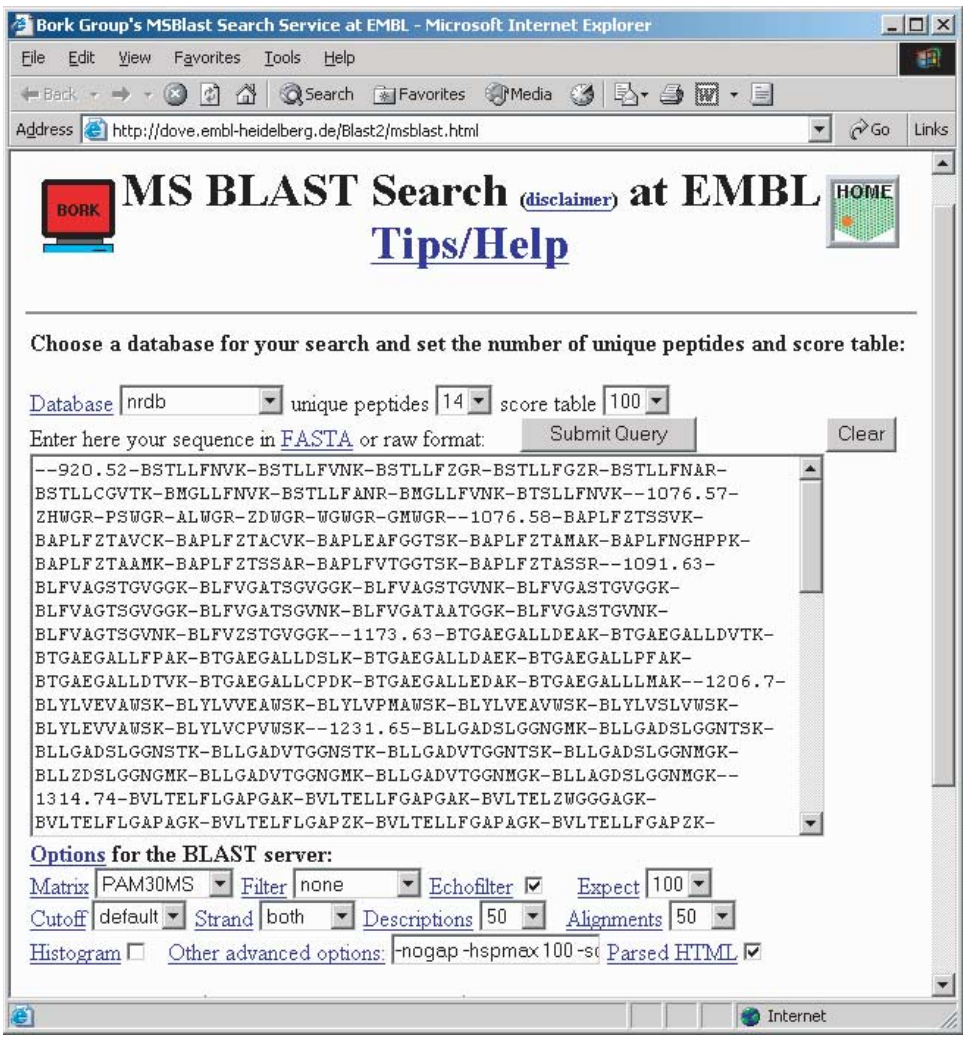

FIGURE 2 The MS BLAST web interface. A generated query is pasted in the input window, the number of tandem mass spectra from which sequences were derived is input in "unique peptides," and all other settings are set automatically according to MS BLAST parameters.

At the EMBL web interface, all parameters are preset and only the number of fragmented peptides and query sequences need to be input.

7. Space all candidate sequence proposals obtained from MS/MS spectra with a "–" (minus) symbol and merge them into a single text string that can be pasted directly into the query window at the MS BLAST web interface (Fig. 2). The query may contain space symbols, hard returns, numbers, and so on, as the server ignores them. For example, it is convenient to keep masses of precursor ions in the query, as it makes retrospective analysis of data much easier. Statistical evaluation is a very important element of MS BLAST protocol, as the query typically comprises many incorrect and partially redundant peptide sequences. Note that the statistics of conventional BLAST searching are not applicable and therefore ignore reported E-values and P-values. Thresholds of statistical significance of MS BLAST hits were estimated in a computational experiment and scoring thresholds were set conditionally on the number of reported HSPs and the size of the database searched. Experimental MS BLAST hits are evaluated based on the number of fragmented precursors (this value is entered in the search parameters), and confident hits appear in red, borderline hits in green, and random matches in black at the web interface cited earlier (Fig. 3).

8. MS BLAST can, in principle, be used to search protein, EST, and genomic databases. The EMBL site only supports protein BLAST searching due to available computational capacity. A script can be written to retrieve specific genomic sequences that lie within the

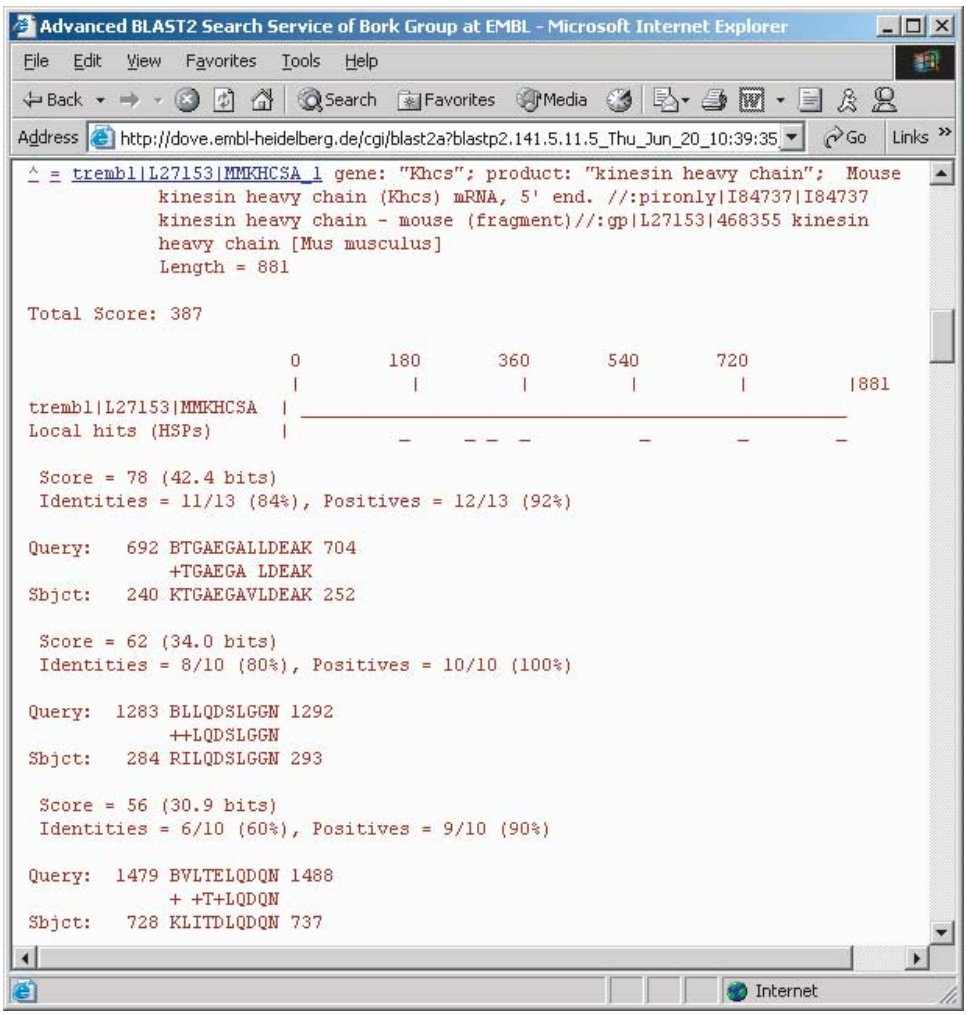

FIGURE 3 A section of the MS BLAST output where three of seven matched peptides to one database entry are shown. A list of matching database entries with the highest significance match at the top of the list is generated. Significant hits are color coded for easy data interpretation.

aligned peptides from a ***tblastn*** search against specific genomic databases. This search enables the use of unannotated genomic sequences and makes it possible to identify novel genes in large genomes. However, in both EST and genomic searches, different scoring schemes would need to be developed and installed locally. To set up a local BLAST searching engine, WU-BLAST 2.0 can be acquired from http://blast.wustl.edu/.

B. Identification of Proteins by MultiTag Database Searching

1. MultiTag is a software program that sorts compiled results from database searches with partial and complete sequence tags and calculates the significance of matches that align multiple sequence tags (for a complete description, see Sunyaev *et al.*, 2003). MultiTag is based on error-tolerant searching with multiple partial sequence tags. This technique enables the correlation of search results from multiple searches with sequence tags representative of numerous spectra and gauges the significance of those matches.

2. Sequence tags should be generated manually from tandem mass spectra acquired in the analysis of a single in-gel or in-solution digest of an unknown protein or proteins. Some mass spectrometer software enables the automatic prediction of sequence tags; however, for best results it is advisable to make sequence tags by manual interpretation or gauge the accuracy of the automatic prediction software with a standard protein prior to the analysis of unknown samples. One sequence tag per spectrum should be made using prominent Y-ions, usually larger

than the multiply charged precursor. Sequence tags made with two to four amino acids each from multiple MS/MS spectra should be compiled in a text file list that includes the tag followed by the parent mass.

(360.20)FLL(733.44)918.64

(561.27)LA(745.40)935.48

(866.41)DEA(1181.52)1422.59

3. Each sequence tag is used to search a protein database, and the results from four searches are compiled in a spreadsheet. For the most specific results, mass tolerances should be narrow, taking into consideration the best accuracy of the mass spectrometer employed. The database is first searched using the complete sequence tag:

(866.41)DEA(1181.52)

This search will only find proteins that contain peptides with exactly these amino acids, spaced with exact amino acids residues that give mass combinations to make up the gaps to the peptide's termini. The second search allows for one error within the amino acid representation itself:

(866.41)D?A(1181.52)

The third search allows for errors between the analyzed peptide and the database at the C terminus of the peptide (searching with regions 1 and 2 only):

DEA(1181.52)

The fourth search allows for errors between the analyzed peptide and the database at the N terminus of the peptide (searching with regions 2 and 3 only):

(866.41)DEA

In the first column of the results table, the parent mass should be followed by an "NC", "E", "N", or "C" for sequence tag search results from complete, one-error, regions 1 and 2 (N-terminal match), and regions 2 and 3 (C-terminal match), respectively. The second, third, fourth, fifth, and six columns should include the amino acid sequence of the peptide matched, the molecular weight of the protein the tag matched, the accession number of the entry, the name of the protein, and the species name, respectively (Fig. 4). Compile the search results in a spreadsheet from all searches with the sequence tags generated, and save results as a text file.

4. Submit the search results table to MultiTag. Designate the mass tolerance used for searching (in daltons), input the approximate number of entries in the database searched, input the list of tags used to generate search results, and compute significance. Results will be sorted, with the database entry containing the most unlikely correlation event at the top of the list, and probabilities are calculated (Fig. 5). Results can be evaluated based on the number of sequence tags matched, E-values and P-values [count (predicted)]. E-values lower than 1×10^{-3} and P-values lower than 1×10^{-4} can be considered significant matches. Final E-values are highly dependent on the number of tags submitted for database searching; more tags will tend to diminish the significance of the alignment of multiple tags to one database entry. Reported P-values are less affected by the number sequence tags in the query. P-values reflect an approximation of the probability that the tags that are aligned will match randomly to an entry in a database of a specific size and at a specific mass accuracy, while neglecting the query size (number of sequence tags). Low P-values (but with higher E-values) are good indicators of alignments having borderline significance that need further manual evaluation to conclude a confident identification. Three partial sequence tags are normally specific enough to identify one entry in a database of 1,000,000 entries, at a mass accuracy of 0.1 Da.

IV. COMMENTS

It is not known in advance if the sequence of the analyzed protein is already present in a database. Therefore, conventional database-searching routines based on stringent matching of peptide sequences should be applied first (Mann and Wilm, 1994; Perkin *et al*., 1999). Only if the protein is unknown and no convincing cross-species matches can be obtained is it recommended to proceed with *de novo* interpretation of tandem mass spectra and sequence-similarity searching.

The success of MS BLAST and MultiTag identification depends on the size of a query and the corresponding database, the number of peptides aligned, the quality of peptide sequences or sequence tags, and the sequence similarity between the protein of interest and its homologues available in a database. On average, candidate sequences determined for five tryptic peptides should be submitted to MS BLAST or MultiTag searching to identify the protein by matching to a homologous sequence. With 10 sequences submitted and aligned, MS BLAST can identify 50% of homologues containing 50% sequence similarity, and MultiTag can identify 50% of homologues at 70% sequence similarity. However, because MultiTag can utilize less

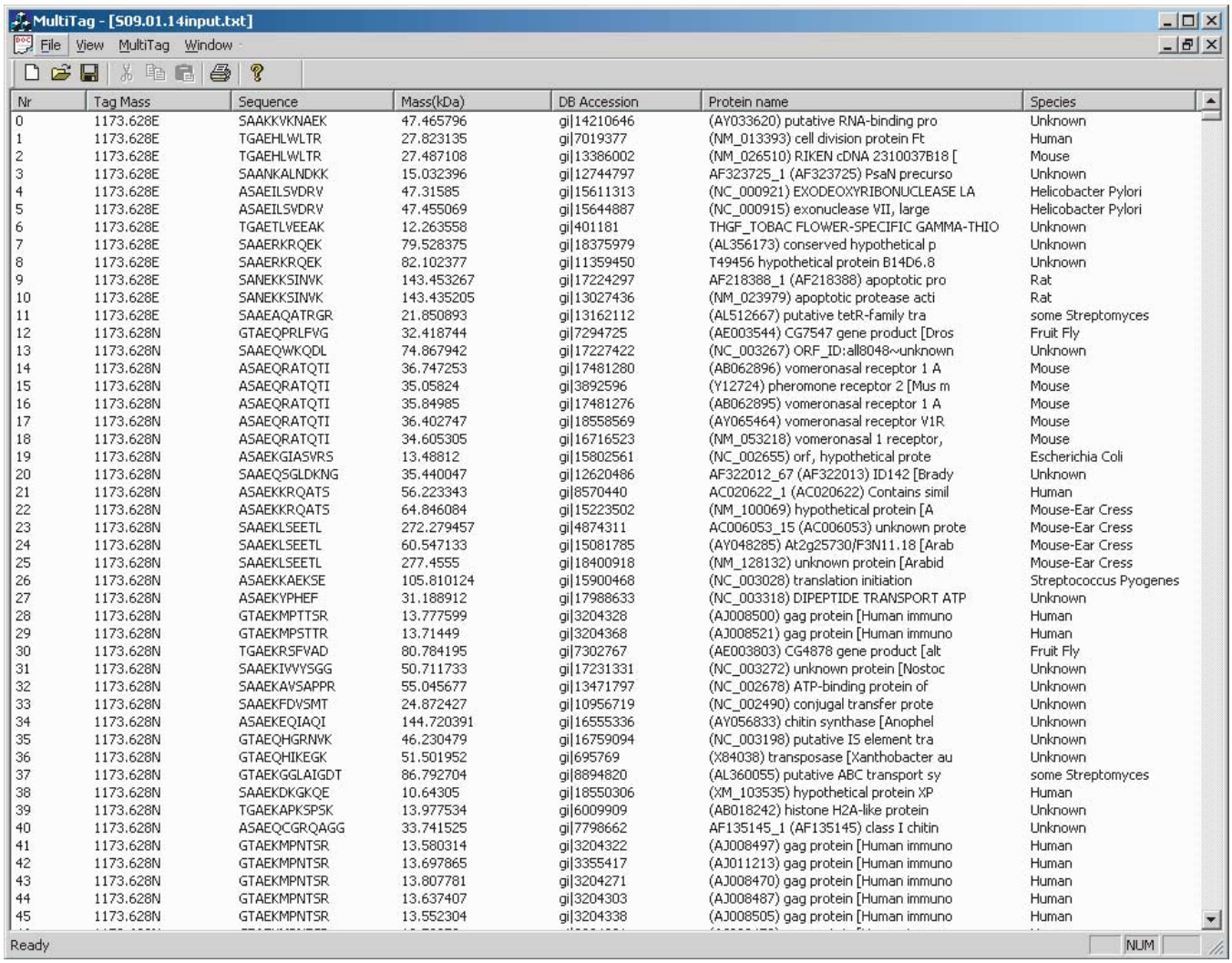

MultiTag - [S09.01.14input.txt]

File View MultiTag Window

Nr	Tag Mass	Sequence	Mass(kDa)	DB Accession	Protein name	Species
0	1173.628E	SAAKKVKNAEK	47.465796	gi|14210646	(AY033620) putative RNA-binding pro	Unknown
1	1173.628E	TGAEHLWLTR	27.823135	gi|7019377	(NM_013393) cell division protein Ft	Human
2	1173.628E	TGAEHLWLTR	27.487108	gi|13386002	(NM_026510) RIKEN cDNA 2310037B18 [	Mouse
3	1173.628E	SAANKALNDKK	15.032396	gi|12744797	AF323725_1 (AF323725) PsaN precurso	Unknown
4	1173.628E	ASAEILSVDRV	47.31585	gi|15611313	(NC_000921) EXODEOXYRIBONUCLEASE LA	Helicobacter Pylori
5	1173.628E	ASAEILSVDRV	47.455069	gi|15644887	(NC_000915) exonuclease VII, large	Helicobacter Pylori
6	1173.628E	TGAETLVEEAK	12.263558	gi|401181	THGF_TOBAC FLOWER-SPECIFIC GAMMA-THIO	Unknown
7	1173.628E	SAAERKRQEK	79.528375	gi|18375979	(AL356173) conserved hypothetical p	Unknown
8	1173.628E	SAAERKRQEK	82.102377	gi|11359450	T49456 hypothetical protein B14D6.8	Unknown
9	1173.628E	SANEKKSINVK	143.453267	gi|17224297	AF218388_1 (AF218388) apoptotic pro	Rat
10	1173.628E	SANEKKSINVK	143.435205	gi|13027436	(NM_023979) apoptotic protease acti	Rat
11	1173.628E	SAAEAQATRGR	21.850893	gi|13162112	(AL512667) putative tetR-family tra	some Streptomyces
12	1173.628N	GTAEQPRLFVG	32.418744	gi|7294725	(AE003544) CG7547 gene product [Dros	Fruit Fly
13	1173.628N	SAAEQWKQDL	74.867942	gi|17227422	(NC_003267) ORF_ID:all8048~unknown	Unknown
14	1173.628N	ASAEQRATQTI	36.747253	gi|17481280	(AB062896) vomeronasal receptor 1 A	Mouse
15	1173.628N	ASAEQRATQTI	35.05824	gi|3892596	(Y12724) pheromone receptor 2 [Mus m	Mouse
16	1173.628N	ASAEQRATQTI	35.84985	gi|17481276	(AB062895) vomeronasal receptor 1 A	Mouse
17	1173.628N	ASAEQRATQTI	36.402747	gi|18558569	(AY065464) vomeronasal receptor V1R	Mouse
18	1173.628N	ASAEQRATQTI	34.605305	gi|16716523	(NM_053218) vomeronasal 1 receptor,	Mouse
19	1173.628N	ASAEKGIASVRS	13.48812	gi|15802561	(NC_002655) orf, hypothetical prote	Escherichia Coli
20	1173.628N	SAAEQSGLDKNG	35.440047	gi|12620486	AF322012_67 (AF322013) ID142 [Brady	Unknown
21	1173.628N	ASAEKKRQATS	56.223343	gi|8570440	AC020622_1 (AC020622) Contains simil	Human
22	1173.628N	ASAEKKRQATS	64.846084	gi|15223502	(NM_100069) hypothetical protein [A	Mouse-Ear Cress
23	1173.628N	SAAEKLSEETL	272.279457	gi|4874311	AC006053_15 (AC006053) unknown prote	Mouse-Ear Cress
24	1173.628N	SAAEKLSEETL	60.547133	gi|15081785	(AY048285) At2g25730/F3N11.18 [Arab	Mouse-Ear Cress
25	1173.628N	SAAEKLSEETL	277.4555	gi|18400918	(NM_128132) unknown protein [Arabid	Mouse-Ear Cress
26	1173.628N	ASAEKKAEKSE	105.810124	gi|15900468	(NC_003028) translation initiation	Streptococcus Pyogenes
27	1173.628N	ASAEKYPHEF	31.188912	gi|17988633	(NC_003318) DIPEPTIDE TRANSPORT ATP	Unknown
28	1173.628N	GTAEKMPTTSR	13.777599	gi|3204328	(AJ008500) gag protein [Human immuno	Human
29	1173.628N	GTAEKMPSTTR	13.71449	gi|3204368	(AJ008521) gag protein [Human immuno	Human
30	1173.628N	TGAEKRSFVAD	80.784195	gi|7302767	(AE003803) CG4878 gene product [alt	Fruit Fly
31	1173.628N	SAAEKIVVYSGG	50.711733	gi|17231331	(NC_003272) unknown protein [Nostoc	Unknown
32	1173.628N	SAAEKAVSAPPR	55.045677	gi|13471797	(NC_002678) ATP-binding protein of	Unknown
33	1173.628N	SAAEKFDVSMT	24.872427	gi|10956719	(NC_002490) conjugal transfer prote	Unknown
34	1173.628N	ASAEKEQIAQI	144.720391	gi|16555336	(AY056833) chitin synthase [Anophel	Unknown
35	1173.628N	GTAEQHGRNVK	46.230479	gi|16759094	(NC_003198) putative IS element tra	Unknown
36	1173.628N	GTAEQHIKEGK	51.501952	gi|695769	(X84038) transposase [Xanthobacter au	Unknown
37	1173.628N	GTAEKGGLAIGDT	86.792704	gi|8894820	(AL360055) putative ABC transport sy	some Streptomyces
38	1173.628N	SAAEKDKGKQE	10.64305	gi|18550306	(XM_103535) hypothetical protein XP	Human
39	1173.628N	TGAEKAPKSPSK	13.977534	gi|6009909	(AB018242) histone H2A-like protein	Unknown
40	1173.628N	ASAEQCGRQAGG	33.741525	gi|7798662	AF135145_1 (AF135145) class I chitin	Unknown
41	1173.628N	GTAEKMPNTSR	13.580314	gi|3204322	(AJ008497) gag protein [Human immuno	Human
42	1173.628N	GTAEKMPNTSR	13.697865	gi|3355417	(AJ011213) gag protein [Human immuno	Human
43	1173.628N	GTAEKMPNTSR	13.807781	gi|3204271	(AJ008470) gag protein [Human immuno	Human
44	1173.628N	GTAEKMPNTSR	13.637407	gi|3204303	(AJ008487) gag protein [Human immuno	Human
45	1173.628N	GTAEKMPNTSR	13.552304	gi|3204338	(AJ008505) gag protein [Human immuno	Human

Ready NUM

FIGURE 4 Compiled and formatted search results from sequence tag searching are input in the MultiTag software via opening a text-formatted results file.

intense and noisy spectra, it can outperform MS BLAST in many cases (for a more thorough discussion on homologue identification specificity, see Sunyaev *et al.*, 2003).

Both MS BLAST and MultiTag can identify proteins present in mixtures. Usually two or three components per sample can be identified easily. The sensitivity of both methods is determined primarily on the quality of the *de novo* sequences or sequence tags.

V. PITFALLS

1. Poor sample preparation can frequently deteriorate the quality of tandem mass spectra of peptides. The digestion of proteins with trypsin or other proteases should be carried out with chemicals of the highest degree of purity available. Plasticware (pipette tips, gloves, dishes, etc.) may acquire a static charge and attract dust, thus leading to contamination of samples with human and sheep (wool) keratin during in-gel or liquid digestion. Any polymeric detergents (Tween, Triton) should not be used for cleaning the laboratory materials.

2. When generating *de novo* sequences or sequence tags, if the software automatically extrapolates the parent mass from the precursor isotope cluster in the MS/MS spectra or the proceeding survey scan in a LC/MS/MS run, it is advisable to manually calculate this value, as software may determine the parent mass incorrectly by designating an incorrect charge state or ^{12}C monoisotopic peak of the parent ion isotope cluster, thus disabling correct *de novo* sequence prediction and sequence tag prediction.

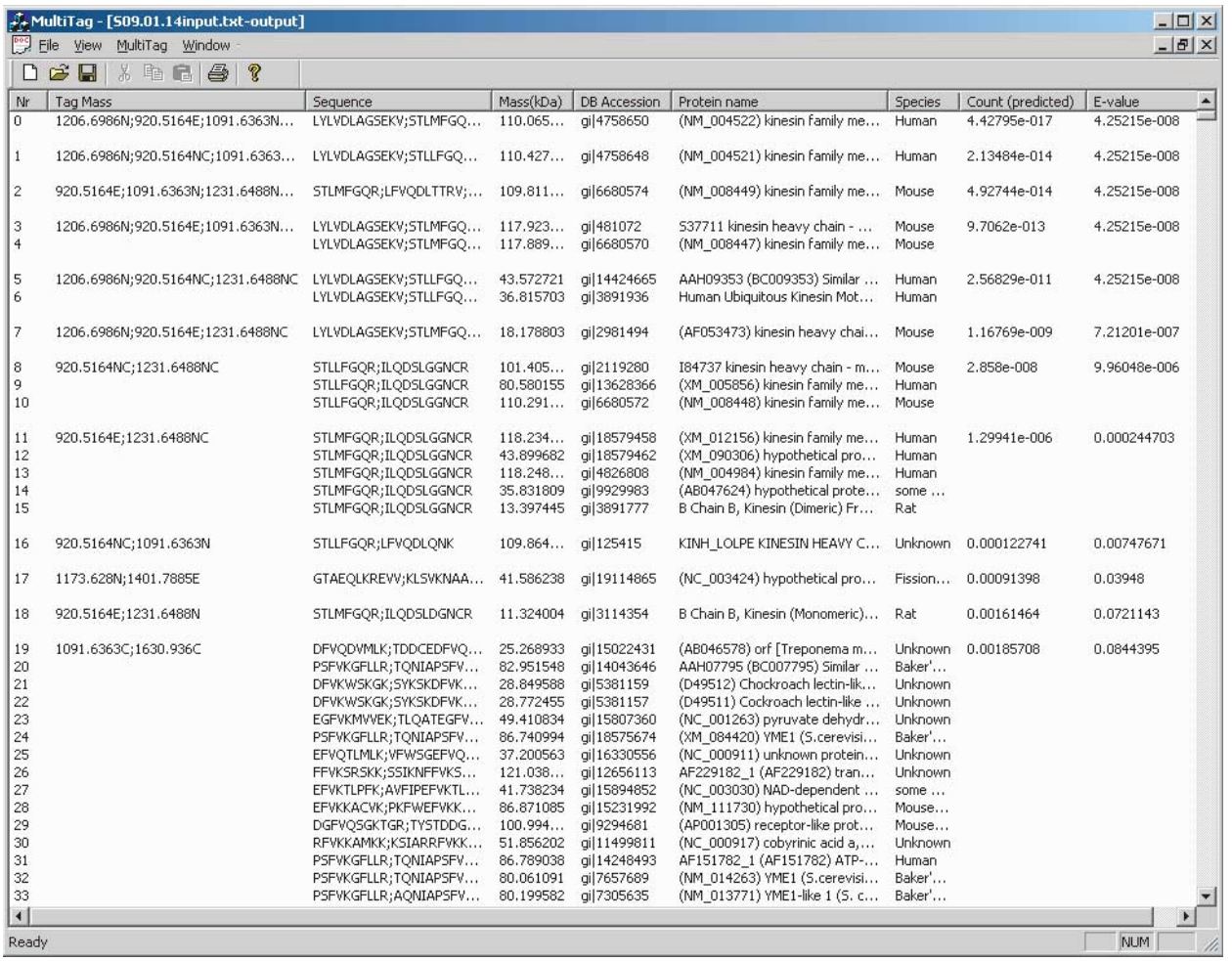

Nr	Tag Mass	Sequence	Mass(kDa)	DB Accession	Protein name	Species	Count (predicted)	E-value
0	1206.6986N;920.5164E;1091.6363N...	LYLVDLAGSEKV;STLMFGQ...	110.065...	gi|4758650	(NM_004522) kinesin family me...	Human	4.42795e-017	4.25215e-008
1	1206.6986N;920.5164NC;1091.6363...	LYLVDLAGSEKV;STLLFGQ...	110.427...	gi|4758648	(NM_004521) kinesin family me...	Human	2.13484e-014	4.25215e-008
2	920.5164E;1091.6363N;1231.6488N...	STLMFGQR;LFVQDLTTRV;...	109.811...	gi|6680574	(NM_008449) kinesin family me...	Mouse	4.92744e-014	4.25215e-008
3	1206.6986N;920.5164E;1091.6363N...	LYLVDLAGSEKV;STLMFGQ...	117.923...	gi|481072	S37711 kinesin heavy chain - ...	Mouse	9.7062e-013	4.25215e-008
4		LYLVDLAGSEKV;STLMFGQ...	117.889...	gi|6680570	(NM_008447) kinesin family me...	Mouse		
5	1206.6986N;920.5164NC;1231.6488NC	LYLVDLAGSEKV;STLLFGQ...	43.572721	gi|14424665	AAH09353 (BC009353) Similar ...	Human	2.56829e-011	4.25215e-008
6		LYLVDLAGSEKV;STLLFGQ...	36.815703	gi|3891936	Human Ubiquitous Kinesin Mot...	Human		
7	1206.6986N;920.5164E;1231.6488NC	LYLVDLAGSEKV;STLMFGQ...	18.178803	gi|2981494	(AF053473) kinesin heavy chai...	Mouse	1.16769e-009	7.21201e-007
8	920.5164NC;1231.6488NC	STLLFGQR;ILQDSLGGNCR	101.405...	gi|2119280	I84737 kinesin heavy chain - m...	Mouse	2.858e-008	9.96048e-006
9		STLLFGQR;ILQDSLGGNCR	80.580155	gi|13628366	(XM_005856) kinesin family me...	Human		
10		STLLFGQR;ILQDSLGGNCR	110.291...	gi|6680572	(NM_008448) kinesin family me...	Mouse		
11	920.5164E;1231.6488NC	STLMFGQR;ILQDSLGGNCR	118.234...	gi|18579458	(XM_012156) kinesin family me...	Human	1.29941e-006	0.000244703
12		STLMFGQR;ILQDSLGGNCR	43.899682	gi|18579462	(XM_090306) hypothetical pro...	Human		
13		STLMFGQR;ILQDSLGGNCR	118.248...	gi|4826808	(NM_004984) kinesin family me...	Human		
14		STLMFGQR;ILQDSLGGNCR	35.831809	gi|9929983	(AB047624) hypothetical prote...	some ...		
15		STLMFGQR;ILQDSLGGNCR	13.397445	gi|3891777	B Chain B, Kinesin (Dimeric) Fr...	Rat		
16	920.5164NC;1091.6363N	STLLFGQR;LFVQDLQNK	109.864...	gi|125415	KINH_LOLPE KINESIN HEAVY C...	Unknown	0.000122741	0.00747671
17	1173.628N;1401.7885E	GTAEQLKREVV;KLSVKNAA...	41.586238	gi|19114865	(NC_003424) hypothetical pro...	Fission...	0.00091398	0.03948
18	920.5164E;1231.6488N	STLMFGQR;ILQDSLDGNCR	11.324004	gi|3114354	B Chain B, Kinesin (Monomeric)...	Rat	0.00161464	0.0721143
19	1091.6363C;1630.936C	DFVQDVMLK;TDDCEDFVQ...	25.268933	gi|15022431	(AB046578) orf [Treponema m...	Unknown	0.00185708	0.0844395
20		PSFVKGFLLR;TQNIAPSFV...	82.951548	gi|14043646	AAH07795 (BC007795) Similar ...	Baker'...		
21		DFVKWSKGK;SYKSKDFVK...	28.849588	gi|5381159	(D49512) Chockroach lectin-lik...	Unknown		
22		DFVKWSKGK;SYKSKDFVK...	28.772455	gi|5381157	(D49511) Cockroach lectin-like ...	Unknown		
23		EGFVKMVVEK;TLQATEGFV...	49.410834	gi|15807360	(NC_001263) pyruvate dehydr...	Unknown		
24		PSFVKGFLLR;TQNIAPSFV...	86.740994	gi|18575674	(XM_084420) YME1 (S.cerevisi...	Baker'...		
25		EFVQTLMLK;VFWSGEFVQ...	37.200563	gi|16330556	(NC_000911) unknown protein...	Unknown		
26		FFVKSRSKK;SSIKNFFVKS...	121.038...	gi|12656113	AF229182_1 (AF229182) tran...	Unknown		
27		EFVKTLPFK;AVFIPEFVKTL...	41.738234	gi|15894852	(NC_003030) NAD-dependent ...	some ...		
28		EFVKKACVK;PKFWEFVKK...	86.871085	gi|15231992	(NM_111730) hypothetical pro...	Mouse...		
29		DGFVQSGKTGR;TYSTDDG...	100.994...	gi|9294681	(AP001305) receptor-like prot...	Mouse...		
30		RFVKKAMKK;KSIARRFVKK...	51.856202	gi|11499811	(NC_000917) cobyrinic acid a,...	Unknown		
31		PSFVKGFLLR;TQNIAPSFV...	86.789038	gi|14248493	AF151782_1 (AF151782) ATP-...	Human		
32		PSFVKGFLLR;TQNIAPSFV...	80.061091	gi|7657689	(NM_014263) YME1 (S.cerevisi...	Baker'...		
33		PSFVKGFLLR;AQNIAPSFV...	80.199582	gi|7305635	(NM_013771) YME1-like 1 (S. c...	Baker'...		

FIGURE 5 A section of MultiTag output. Margins may be adjusted to see the full list of tags matched, as well as full peptide sequences aligned, names, and so on. Results may be saved as text files to be viewed in an appropriate spreadsheet application.

3. MultiTag is laborious. Without scripted sequence tag database searching and processing of search results, manual data processing can demand extended effort; however, in cases where conventional methods fail to identify analyzed proteins, positive identifications are of a high value to cell biological studies.

4. Poor queries tend to obscure protein identification by both MS BLAST and MultiTag. It is best to submit fewer higher quality sequences than numerous lower quality sequences to MS BLAST. MS BLAST is particularly susceptible to low-complexity glycine- and proline-rich sequences generated incorrectly by *de novo* software. These low-complexity sequences tend to mask correct alignments. MultiTag functions best with sequence tags containing multiple (2–4) amino acids that have a low prevalence, such as tryptophan (W) or methionine (M), whereas common amino acids such as leucine (L) in the tag tend to be of less significance and are likely to produce more false positives. Sequence tags generated from larger peptides also have more significance in a database search than those generated from smaller peptides.

References

Altschul, S. F., Madden, T. L., Schaffer, A. A., Zhang, J., Zhang, Z., Miller, W., and Lipman, D. J. (1997). Gapped BLAST and PSI-BLAST: A new generation of protein database search programs. *Nucleic Acids Res*. **25**, 3389–3402.

Gaeta, B. A. (2000). BLAST on the Web. *Biotechniques* **28**, 436–440.

Johnson, R. S., and Taylor, J. A. (2000). Searching sequence databases via de novo peptide sequencing by tandem mass spectrometry. *Methods Mol. Biol*. **146**, 41–61.

Mann, M., and Wilm, M. (1994). Error-tolerant identification of peptides in sequence databases by peptide sequence tags. *Anal. Chem.* **66**, 4390–4399.

Nimkar, S., and Loo, J. A. (2002). Orlando FL. Application of a new algorithm for automated database searching of MS sequence data to identify proteins. Abstract 334.

Perkins, D. N., Pappin, D. J., Creasy, D. M., and Cottrell, J. S. (1999). Probability-based protein identification by searching sequence databases using mass spectrometry data. *Electrophoresis* **20**, 3551–3567.

Shevchenko, A., Sunyaev, S., Loboda, A., Bork, P., Ens, W., and Standing, K. G. (2001). Charting the proteomes of organisms with unsequenced genomes by MALDI-quadrupole time-of-flight mass spectrometry and BLAST homology searching. *Anal. Chem.* **73**, 1917–1926.

Sunyaev, S., Liska, A., Golod, A., Shevchenko, A., and Shevchenko, A. (2003). MultiTag: Multiple error-tolerant sequence tag search for the sequence-similarity identification of proteins by mass spectrometry. Submitted for publication.

CHAPTER

52

Identification of Protein Phosphorylation Sites by Mass Spectrometry

Rhys C. Roberts and Ole N. Jensen

I. INTRODUCTION

Tight regulation of cellular proteins is a prerequisite for viable cell function. Cells require various mechanisms whereby intracellular pathways can be activated and inactivated in a reversible manner depending on the prevailing environment at a particular moment in time. Reversible phosphorylation of proteins is one such mechanism. The importance of phosphorylation is exemplified by the finding that at least 2% of the human genome encodes proteins with predicted kinase domains (Lander *et al.*, 2001). Furthermore, other workers predict that approximately a third of all proteins expressed in vertebrates can be phosphorylated at some point in their lifetime (Hunter, 1998).

Many phosphoproteins have been identified through incorporation of radioactively labelled ATP (usually [γ-^{32}P]ATP) either in cells or following incubation with specific kinases *in vitro*. Once identified, the significance of phosphorylation can then be addressed. In eukaryotes, phosphorylation occurs predominantly on serine, threonine, and tyrosine residues. Ideally, the specific phosphorylated residue should be pinpointed in order to gain further important insights into the consequences of the addition and removal of a phosphate group.

Identifying specific phosphorylated residues can be fraught with difficulties. Most strategies, as stated previously, have used radioactively labelled ATP to phosphorylate the protein of interest. The purified phosphorylated protein can then be cleaved using specific chemical or enzymatic processes (e.g., CNBr or trypsin) before separation of the peptides by an appropriate method (e.g., SDS–PAGE, HPLC, or thin-layer chromatography). The radioactively labelled peptide, which should contain the phosphorylated residue, is detected, isolated, and the sequence determined, usually by Edman degredation (Moyers *et al.*, 1995). In addition, phosphoamino acid analysis can be used to determine the nature of the phosphorylated residue (Sefton, 1995). This approach relies on a high degree of protein phosphorylation with radiolabelled phosphate. Handling large amounts of radiolabelled ^{32}P is clearly a potential hazard and, in practice, the efficiency of protein phosphorylation can vary significantly from case to case. Furthermore, the amount of protein required for identification using this approach means that only those proteins available in significant quantities, with high incorporation of radiolabelled phosphate, are feasible for phosphorylation site identification. Because phosphorylated residues are not detected by conventional Edman sequencing, many sites are determined indirectly. In many cases, subsequent mutational analysis is used to support the identification of the putative phosphorylation site.

Following many developments and improvements in biological mass spectrometry, unambiguous identification of specific phosphorylation sites is possible without the use of radioactive isotopes (Larsen *et al.*, 2001; Stensballe *et al.*, 2001). The main principle behind phosphorylation site identification by mass spectrometry is the fact that the mass of a specific residue increases by 80 Da upon phosphorylation. Therefore, by accurately measuring the masses of a mixture of peptides from a phosphorylated protein (whose

Copyright 2006, Elsevier Science (USA).
All rights reserved.

sequence is known) following specific enzymatic or chemical cleavage, potentially phosphorylated species with a mass shift of 80 Da can be observed. Phosphorylation can be confirmed by dephosphorylating the peptide mix with alkaline phosphatase and observing the disappearance of the 80-Da peptide signal. The specific site of phosphorylation can then be determined by tandem mass spectrometry using, for example, a quadrupole time-of-flight (TOF) mass spectrometer.

To maximise the yield of phosphorylated peptides, techniques such as Fe^{3+}-IMAC (immobilised metal affinity chromatography) micropurification can be used prior to analysis by mass spectrometry. This technique is based on the relative affinity of Fe^{3+} for phosphorylated residues. By using this method, it is possible to identify specific phosphorylation sites in proteins phosphorylated to a low degree.

This article describes a stepwise approach for the identification of phosphorylation sites by mass spectrometry. First, phosphopeptide enrichment by Fe^{3+}-IMAC micropurification is described. This is followed by a method to confirm phosphorylation by using alkaline phosphatase to dephosphorylate the peptide mixture already analysed on a MALDI-TOF mass spectrometer. Finally, unambiguous determination of a phosphorylation site using nanoelectrospray ionisation and tandem mass spectrometry is described.

II. MATERIALS AND INSTRUMENTATION

Milli-Q H_2O (Millipore) is used throughout this method. Formic acid, acetic acid, trifluoroacetic acid, methanol and trifluoroacetic acid (TFA), and acetonitrile (all HPLC grade) are from Sigma. Ethylenediaminetetraacetic acid (EDTA), NaCl, and $FeCl_3$ are from Sigma. Ni^{2+}-NTA (nitrilotriacetic acid)-silica (16–24 µm particle size) is supplied by Qiagen, and OligoR3 reverse-phase resin is from PE biosystems. 2,5-Dihydroxybenzoic acid (DHB) is supplied by Sigma. Calf intestinal alkaline phosphatase is from Roche (0108138). GELoader tips (1–10 µl) from Eppendorf (0030 001.222) are used for making micropurification columns.

MALDI time-of-flight analysis of peptides is performed using a REFLEX II time-of-flight mass spectrometer with delayed extraction (Bruker-Daltonics). The samples are ionised with a nitrogen laser (λ = 337 nm) and data acquired in the positive ion mode. "moverz" (Proteometrics Ltd.) is used to analyse the spectra obtained.

Electrospray mass spectrometry is performed on a Q-TOF hybrid mass spectrometer fitted with a nano-ESI Z-spray interface (Micromass). Nanoelectrospray needles (gold/pallidum precoated borosilicate glass) are from MDS Protana, Odense Denmark. The instrument is used in positive ion mode with the following typical settings: needle 700–1000 V; cone 55 V; collision gas (Argon) pressure 5.5–6.0 $\times$ 10^{-5} atm; collision energy 4–34 eV. Commonly, the nanoelectrospray flow rate would be in the order of 15–50 nl/min. Selected ions are subject to collision-induced dissociation (CID) with argon gas, and fragment ions are detected by the orthogonal time-of-flight analyser. Resulting data are analysed using the MassLynx software supplied by Micromass.

III. PROCEDURES

A. Phosphopeptide Enrichment by Fe^{3+} IMAC Micropurification

Following separation and purification of the protein of interest (e.g., by SDS–PAGE, reverse-phase HPLC), the phosphorylated protein is cleaved into a peptide fragment either by enzymatic digest or by chemical cleavage. For separation by SDS-PAGE followed by in-gel digestion of a protein with trypsin, followed by the extraction of peptides, see article by Gevaert and Vandekerckhove.

1. Preparation of Fe^{3+}-NTA

Steps

1. Resuspend 15 mg Ni^{2+}-NTA silica in 200 µl H_2O in a 1.5-ml microcentrifuge tube.
2. Pellet the resin in a benchtop centrifuge and remove the supernatant. Wash the resin with 200 µl H_2O.
3. Incubate the resin with 50 m*M* EDTA in 1 *M* NaCl for 2 min at room temperature. Centrifuge and discard the supernatant. Repeat once.
4. Wash once with 200 µl H_2O and twice with 200 µl 100 m*M* acetic acid.
5. Incubate resin with 400 µl 50 m*M* $FeCl_3$: 50 m*M* acetic acid for 5 min at room temperature, mixing gently. Pellet the resin and discard the supernatant. Repeat once.
6. Wash with 200 µl 100 m*M* acetic acid and once with 200 µl 3 : 1 100 m*M* acetic acid : 100% acetonitrile. Wash again with 200 µl 100 m*M* acetic acid.
7. Resuspend the resin in 100 µl 100 m*M* acetic acid. The resin is now ready for use and can be stored at 4°C for 3–4 weeks.

2. *Preparation of Microcolumn*

Steps

1. Take a 1- to 10-µl GELoader tip (Eppendorf) and gently twist the tip end with fingers and thumb. Care must be taken to make the tip outflow sufficiently narrow in order to pack the resin, whilst avoiding complete occlusion.
2. Add 10 µl of the prepared Fe^{3+}-NTA resin to the microcolumn and pack into the tip using a 10 ml syringe for pressure. The column should measure 20–25 mm in height.
3. The Fe^{3+}-NTA IMAC microcolumn is now ready for use.

3. *Purification of Phosphopeptides by Fe^{3+}-IMAC*

Steps

1. Dilute the peptide mixture with 30x excess 100 m*M* acetic acid (e.g., from a Coomassie-stained band resuspended in a final volume of 20 µl, take 1–2 µl and dilute in 60 µl of 100 m*M* acetic acid).
2. Add the resuspended petide mixture to the Fe^{3+}-NTA IMAC microcolumn and load very slowly using the 10-ml syringe for pressure. For optimum binding of phosphopeptides, this step should take 15–20 min.
3. Wash the column sequentially with 20 µl 100 m*M* acetic acid, 20 µl 3 : 1 100 m*M* acetic acid : 100% acetonitrile, and 20 µl 100 m*M* acetic acid.
4. Elute the bound phosphopeptides with 2× 5 µl H_2O, pH 10.5 (NH_3). To concentrate the peptides prior to analysis, the eluted peptides can be applied directly into 60 µl of 5% formic acid in a preequilibrated OligoR3 microcolumn. Prepare the microcolumn in a similar manner to the Fe^{3+}-IMAC microcolumn but using OligoR3 reversed-phase resin (PE Biosystems) in 5% formic acid and forming a column height of 2–3 mm.
5. Wash the bound peptides with 20 µl 5% formic acid.
6. Elute the peptides directly onto the MALDI target with 1 µl of DHB [DHB (Sigma) 20 µg/µl in 70% acetonitrile/0.1% TFA]. Allow the eluate to crystalise before analysis by MALDI mass spectrometry (Fig. 1).

4. *Analysis of Purified Phosphopeptides by MALDI*

Steps

1. Measure the masses of the purified peptides by MALDI mass spectrometry as described previously (see article by Roepstorff *et al*.).
2. Identify peptide peaks corresponding to predicted peptide masses +80 Da. Candidate phosphopeptides are identified in this way and by also looking for phosphorylated partially digested peptides. In addition, the presence of a metastable ion, corresponding to a phosphopeptide which has undergone β elimination (detected ~98 Da lower than the predicted phosphorylated peptide), is highly suggestive of a phosphorylated species.

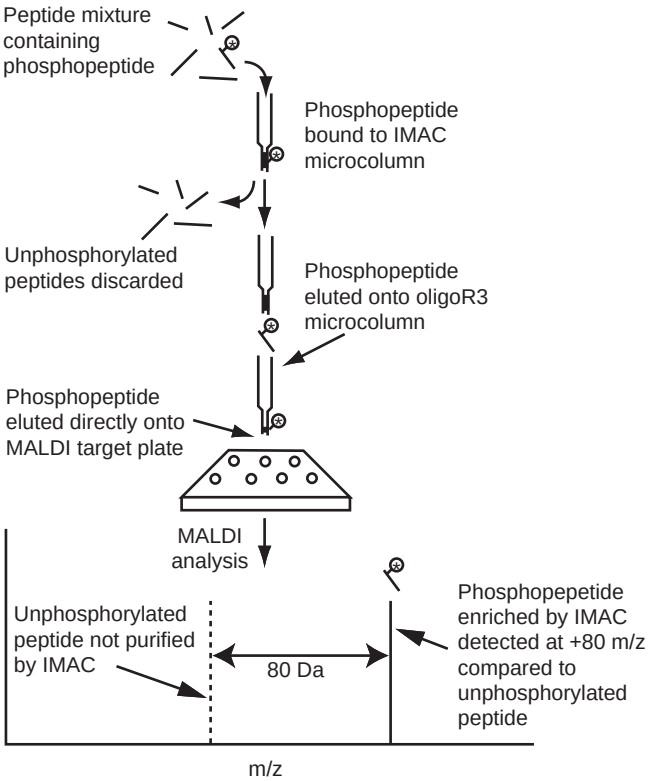

FIGURE 1 Schematic diagram illustrating the method of selective purification of phosphopeptides by Fe^{3+}-IMAC followed by analysis by MALDI mass spectrometry. A mixture of peptides is applied to the IMAC microcolumn and the phosphorylated peptide (labelled with asterisks) is selectively purified prior to desalting and concentrating using an OligoR3 microcolumn. The peptides are eluted directly onto the MALDI target for analysis by MALDI mass spectrometry. The phosphorylated peptide corresponds to a signal seen at 80 Da with respect to its unphosphorylated counterpart.

B. Confirmation of Phosphorylation Using Alkaline Phosphatase

1. Remove the MALDI target from the mass spectrometer.
2. Resuspend the crystallised peptides in 0.5 µl 70% acetonitrile in 100 m*M* NH_4HCO_3.
3. Transfer to a new OligoR3 microcolumn containing 20 µl dephosphorylation mixture (19 µl 100 m*M* NH_4Cl with 1 unit alkaline phosphatase).
4. Seal the column with Parafilm and incubate at 37°C for 1 h.

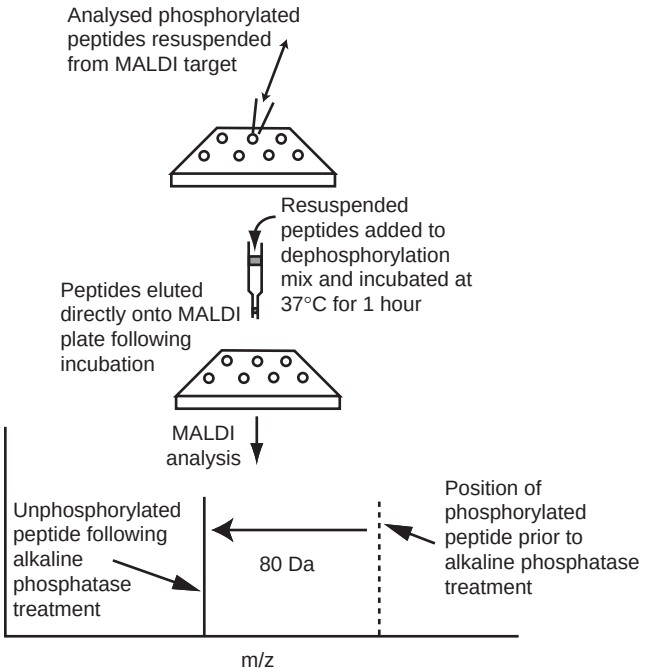

FIGURE 2 Schematic diagram illustrating the use of alkaline phosphatase to confirms that a candidate phosphopeptide is phosphorylated. Following initial MALDI analysis, the crystallised peptides are resuspended and added to a dephosphorylation mixture containing alkaline phosphatase. The mixture is present in a preequilibrated OligoR3 microcolumn. Following incubation for 1 h at 37°C, the peptides are purified and desalted on the microcolumn and eluted directly onto the MALDI target plate for further analysis. The disappearance of the signal corresponding to the phosphopeptide and the appearance of a signal 80 Da smaller confirm that the peptide of interest is indeed phosphorylated.

5. Acidify the enzyme mixture by adding 20 µl 5% formic acid and purify the peptides using the OligoR3 microcolumn as described earlier.
6. Elute the peptides using DHB onto the MALDI target and analyse as before.
7. Peaks corresponding to dephosphorylated peptides should now be seen, confirming that these peptides are indeed phosphorylated (Fig. 2).

C. Identification of Specific Phosphorylation Sites by Tandem Mass Spectrometry Using Nanoelectrospray Ionisation

Once candidate phosphopeptides are detected by IMAC and MALDI mass spectrometry, the precise residue should be identified. This can be achieved by selecting and sequencing the phosphopeptide using a nanoelectrospray quadrupole time-of-flight mass spectrometer. Sample preparation is vital to ensure successful analysis.

For analysis by nanoelectrospray, 5x the amount of peptide mixture is typically required, which will need to be determined on an individual basis. To minimise nonspecificc binding of phosphopeptides to the Fe^{3+}-IMAC microcolumn, three to four microcolumns are used simultaneously, and the bound peptides are concentrated on a single OligoR3 column prior to analysis.

Steps

1. Apply the phosphopeptide mixture to three to four Fe^{3+}-IMAC microcolumns simultaneously and wash as described in Section III,A.
2. Elute the peptides onto a single OligoR3 microcolumn and wash with 5% formic acid.
3. Elute the peptides directly into a nanospray needle with 1 µl 50% methanol : 1% formic acid.
4. Analyse the peptide mixture on the quadrupole time-of-flight mass spectrometer and select the relevant candidate phosphopeptides for further analysis.
5. Sequence the phosphopeptide by collision-induced dissociation.
6. The phosphorylated residue can be identified by observing a mass difference equalling the mass of an amino acid +80 Da between two sequential ions (Fig. 3) or by observing a series of dephosphorylated ions resulting from β elimination (with masses corresponding to 98 Da lower than the predicted phosphorylated ion or 18 Da lower than the nonphosphorylated counterpart). By careful analysis of data obtained, the phosphorylated residue can be deduced.

IV. COMMENTS AND PITFALLS

A. Sample Preparation

The importance of sample preparation cannot be overemphasised. Often, the proportion of the protein sample that is phosphorylated is very low. Therefore, without meticulous sample handling from protein purification to analysing peptides, the chances of success diminish rapidly. Many potential problems have been described previously when analysing peptides by mass spectrometry, such as contamination with exogenous proteins (e.g., keratin) and inadequate desalting prior to ionisation (a particular problem with electrospray ionisation). To maximise the success rate for identifying phosphorylation sites, these factors must be optimised.

Purification of phosphopeptides by Fe^{3+}-IMAC is a method to select and concentrate the phosphorylated species prior to analysis by mass spectrometry. It is an

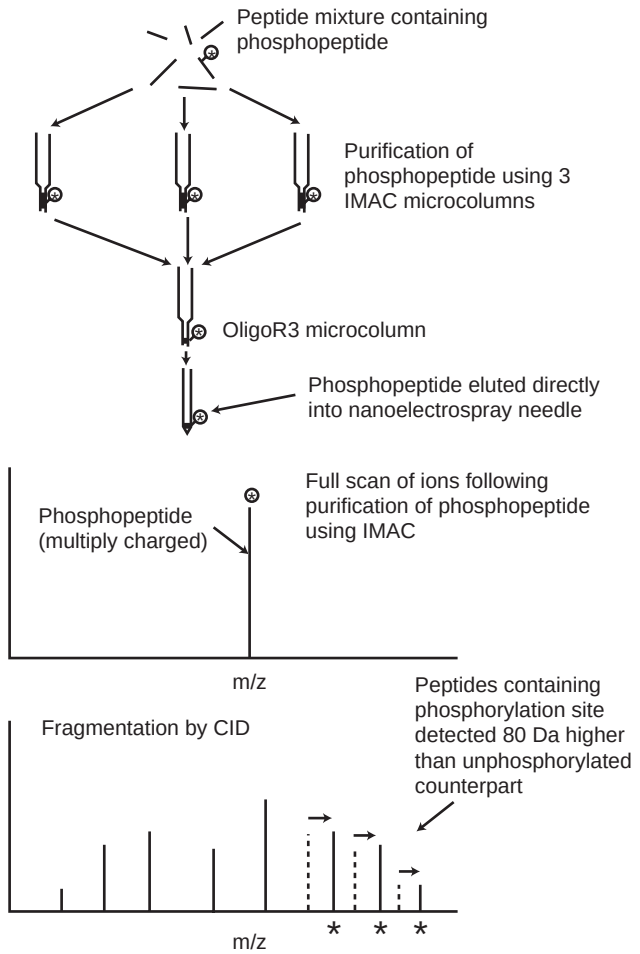

FIGURE 3 Schematic diagram illustrating the identification of specific sites of phosphorylation by IMAC micropurification and nanospray tandem mass spectrometry. The phosphopeptide is purified by using Fe^{3+}-IMAC microcolumns in parallel, prior to concentration and desalting on a single OligoR3 column. Once the multiply charged ion corresponding to the phosphopeptide is identified, the ion is fragmented by collision-induced dissociation (CID) with the production of specific fragment ions. The specific site of phosphorylation can be determined by careful analysis of this spectrum, looking particularly for phosphorylated and nonphosphorylated ions. In this simple schematic, a complete y-ion series is shown from a hypothetical nine residue phosphopeptide. The four largest y-ions are detected 80 Da higher than the predicted masses for the unphosphorylated peptide (indicated with dashed lines). This confirms that the fourth residue from the C-terminal is the site of phosphorylation. Further confirmation can be obtained by analysing the b-ion series and identifying the corresponding confirmatory ions.

extremely effective technique to assist in the identification of phosphorylation sites. However, this technique can yield a very high background of nonspecific binding if a number of key points are not followed closely. First, it is important to ensure that the peptide sample is well diluted. Second, the sample should be applied to the resin for at least 10 min, if not longer, with the minimum amount of back pressure applied from the syringe. Both these steps reduce the amount of nonspecific binding to the Fe^{3+}-IMAC microcolumn and facilitate successful outcomes.

Because the phosphorylated peptide might exist in a small quantity, it is sometimes worth purifying three to four aliquots of peptide sample on separate Fe^{3+}-IMAC microcolumns. The phosphopeptides can then be eluted onto a single OligoR3 microcolumn. This last step concentrates the peptides prior to analysis and also desalts the sample effectively, ensuring optimal analysis by mass spectrometry.

B. The Phosphoprotein

In addition to the amount of phosphorylation of an individual protein, specific factors relating to the phosphoprotein itself may determine the ease to which a phosphorylation site is identified. For example, the molecular mass of the peptide containing the phosphorylation site should ideally be between 500 and 4000 Da. Peptides with masses outside this range are very difficult to analyse using the methods described in this chapter. Trypsin is usually the enzyme of choice for producing measurable peptides. However, other enzymes, such as chymotrypsin, Lys-C, or Arg-N, may be required to isolate a phosphopeptide in the detectable range. Chemical cleavage with CNBr can also be used. A rare difficulty arises when a nonphosphorylated peptide has the same molecular weight as the phosphopeptide of interest.

In many cases, phosphorylation sites are flanked by polar residues. Generally, peptides containing polar residues are ionised more efficiently than their nonpolar counterparts. However, occasionally, a hydrophobic sequence surrounding the phosphorylation site may decrease the efficiency of ionisation, resulting in low detection rates. In addition, some peptides prove difficult to sequence by CID and this problem is exacerbated when the amount of phosphorylated peptide is small.

With respect to Fe^{3+}-IMAC micropurification, a particular difficulty arises when a protein contains a number of acidic repeats. The acidic residues, glutamate and aspartate, have signficant affinities to Fe^{3+} and hence may result in a high background when analysed.

A further obstacle when attempting to pinpoint sites of phosphorylation occurs when the specific phosphate group is lost upon ionisation. Although this property can lead to difficulty in identifying the phosphorylated species, the same property can be used to identify a specific site. If the phosphate group is lost through β elimination, a signal can be seen correspon-

ding to 98 Da less than the predicted phosphopeptide. Conversely, in some cases, the intact phosphorylated peptide remains undetected while its degraded product becomes the principal ion seen on analysis.

C. Ionisation and Analysis

As discussed earlier, a balance is required when analysing a phosphopeptide mixture to ensure efficient ionisation on the one hand whilst also protecting the phosphate group. At lower energies, the phosphopeptide will not be seen, whilst if the energy of ionisation is too high, the labile phosphate group will be lost. The optimal settings and conditions may need to be determined for different phosphoproteins. We have found that DHB is the matrix of choice for the analysis of most phosphopeptides.

An interesting phenomenon relating to phosphopeptides is the "suppression effect." This is a term describing the low detection of phosphorylated peptides when ionised in the presence of their nonphosphorylated counterparts. Fe^{3+}-IMAC is used to discard the nonphosphorylated species and can result in a phosphoprotein signal that was not detectable before micropurification.

This article describes sequencing using a quadruplole time-of flight mass spectrometer. It is possible to obtain very high resolution data using these instruments. However, these mass spectrometers are less sensitive than their MALDI-TOF counterparts and, in practice, approximately 5x as much sample is required for sequence analysis by electrospray ionisation. In addition, the Q-TOF is less tolerant than a MALDI-TOF mass spectrometer to salt and samples should always be desalted thoroughly before analysis. We routinely micropurify all our peptide samples on self-made reverse-phase microcolumns prior to both MALDI and electrospray ionisation to ensure optimal results at all times.

References

Hunter, T. (1998). The Croonian Lecture 1997. The phosphorylation of proteins on tyrosine: Its role in cell growth and disease. *Philos. Trans. R. Soc. Lond. B. Biol. Sci.* **353**, 583–605.

Lander, E. S., Linton, L. M., Birren, B., Nusbaum, C., Zody, M. C., Baldwin, J., Devon, K., Dewar, K., Doyle, M., FitzHugh, W., Funke, R., Gage, D., Harris, K., Heaford, A., Howland, J., Kann, L., Lehoczky, J., LeVine, R., McEwan, P., McKernan, K., Meldrim, J., Mesirov, J. P., Miranda, C., Morris, W., Naylor, J., Raymond, C., Rosetti, M., Santos, R., Sheridan, A., Sougnez, C., Stange-Thomann, N., Stojanovic, N., Subramanian, A., Wyman, D., Rogers, J., Sulston, J., Ainscough, R., Beck, S., Bentley, D., Burton, J., Clee, C., Carter, N., Coulson, A., Deadman, R., Deloukas, P., Dunham, A., Dunham, I., Durbin, R., French, L., Grafham, D., Gregory, S., Hubbard, T., Humphray, S., Hunt, A., Jones, M., Lloyd, C., McMurray, A., Matthews, L., Mercer, S., Milne, S., Mullikin, J. C., Mungall, A., Plumb, R., Ross, M., Shownkeen, R., Sims, S., Waterston, R. H., Wilson, R. K., Hillier, L. W., McPherson, J. D., Marra, M. A., Mardis, E. R., Fulton, L. A., Chinwalla, A. T., Pepin, K. H., Gish, W. R., Chissoe, S. L., Wendl, M. C., Delehaunty, K. D., Miner, T. L., Delehaunty, A., Kramer, J. B., Cook, L. L., Fulton, R. S., Johnson, D. L., Minx, P. J., Clifton, S. W., Hawkins, T., Branscomb, E., Predki, P., Richardson, P., Wenning, S., Slezak, T., Doggett, N., Cheng, J. F., Olsen, A., Lucas, S., Elkin, C., Uberbacher, E., Frazier, M., *et al.*, (2001). Initial sequencing and analysis of the human genome. *Nature* **409**, 860–921.

Larsen, M. R., Sorensen, G. L., Fey, S. J., Larsen, P. M., and Roepstorff, P. (2001). Phospho-proteomics: Evaluation of the use of enzymatic de-phosphorylation and differential mass spectrometric peptide mass mapping for site specific phosphorylation assignment in proteins separated by gel electrophoresis. *Proteomics* **1**, 223–238.

Moyers, J. S., Linder, M. E., Shannon, J. D., and Parsons, S. J. (1995). Identification of the in vitro phosphorylation sites on Gs alpha mediated by pp60c-src. *Biochem. J.* **305**, 411–417.

Sefton, B. M. (1995). Phosphoamino acid analysis, *In "Current Protocols in Protein Science"* (J. E. Coligan, B. M. Dunn, D. W. Speicher, and P. T. Wingfield, Eds.), pp. 13.3.1–13.3.8. Wiley, New York.

Stensballe, A., Andersen, S., and Jensen, O. N. (2001). Characterization of phosphoproteins from electrophoretic gels by nanoscale Fe(III) affinity chromatography with off-line mass spectrometry analysis. *Proteomics* **1**, 207-222.

CHAPTER

53

Analysis of Carbohydrates/ Glycoproteins by Mass Spectrometry

Mark Sutton-Smith and Anne Dell

I. INTRODUCTION

Electron impact mass spectrometry (EI-MS) has been employed in carbohydrate analysis since the early 1960s and is still used for defining sugar compositions and for linkage analysis (Albersheim *et al.*, 1967). The introduction of fast atom bombardment-mass spectrometry (FAB-MS) at the beginning of the 1980s (Morris, 1980; Barber *et al.*, 1981; Dell *et al.*, 1983) revolutionised the structure determination of a very wide range of carbohydrate-containing biopolymers (Fukuda *et al.*, 1985; Laferte *et al.*, 1987; Dell *et al.*, 1990; McConville *et al.*, 1990). A decade later, electrospray ionisation (ES-MS) (Fenn *et al.*, 1990) and matrix-assisted laser desorption ionisation (MALDI-MS) technologies (Karas and Hillenkamp, 1988; Karas *et al.*, 1989) expanded the range of glycobiological structural problems amenable to mass spectrometry because of their higher sensitivity and applicability to much larger molecules (Lopez *et al.*, 1997). The lessons learnt from FAB-MS investigations in the 1980s (Fukuda *et al.*, 1984, 1985; Dell, 1987) have turned out to be equally applicable to ES-MS and MALDI-MS. Notably, it has been found that although native samples are amenable to MS analysis, it is often desirable to prepare derivatives prior to analysis. As a general rule, derivatisation vastly improves sensitivity and derivatised glycans yield fragment ions much more reliably than their native counterparts. Permethylation is the most important type of derivatisation employed in carbohydrate MS.

Broadly speaking, MS can be exploited in two general ways in the analysis of carbohydrates and glycoproteins.

i. Detailed characterisation of purified individual glycopolymers or mixtures of glycopolymers. This usually requires acquisition of MS data from both intact material and chemical, and enzymatic digests. Case studies that exemplify strategies applicable to a range of glycopolymers are described elsewhere (Sasaki, *et al.*, 1987; Dell *et al.*, 1995).

ii. Glycomics analyses that involve screening of cell and tissue extracts for their overall glycan content. Examples of such strategies are given elsewhere (Sutton-Smith, *et al.*, 2000; Manzi, *et al.*, 2000) and at the NIH Functional Glycomics Consortium Web site http://web.mit.edu/glycomics/consortium.

This article documents protocols for isolating, derivatising, and digesting glycans and glycopeptides in preparation for MS analysis. The emphasis is on glycoprotein analysis, but many of the methodologies are also applicable to other glycopolymers, such as glycolipids and polysaccharides. Also documented are procedures for high-sensitivity MS and MS/MS analyses of glycans and glycopeptides. The generic strategy is outlined below and in Fig. 1.

1. Preparation of biological matrix for analysis
2. Purification of glycoprotein(s)
3. Reduction/carboxymethylation
4. Tryptic digestion or, in some instances, cynanogen bromide degradation
5. *N*-Glycosidase F digestion
6. Separation of *N*-glycans from peptides/*O*-glycopeptides
7. Reductive elimination of *O*-glycans from *O*-glycopeptides
8. Dowex purification of *O*-glycans
9. Permethylation of *N*- and *O*-glycans
10. MALDI-TOF MS profiling of *N*- and *O*-glycans

Copyright 2006, Elsevier Science (USA).
All rights reserved.

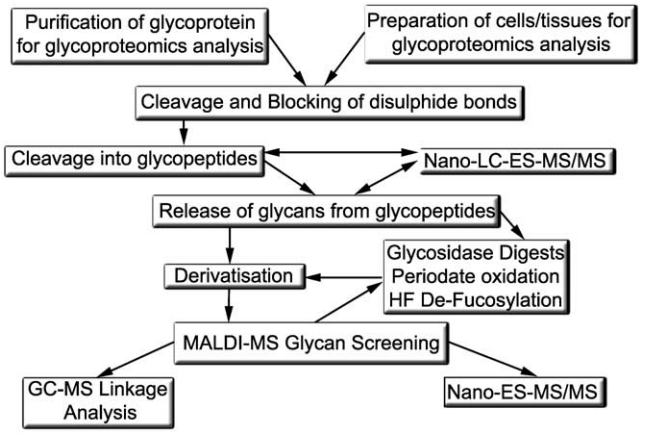

FIGURE 1 Glycomics strategy for screening mammalian cells, tissues, and glycoproteins.

11. ES-MS/MS on key selected peaks observed in the MALDI profile

The initial steps for glycoproteome analysis of mammalian biological matrices, such as cells, biological fluids, tissues, and organs, involve homogenisation and sample cleanup by dialysis. For screening glycans in mammalian tissues, 100–400 mg of tissue is sufficient for a series of MS analyses, including glycan profiling, sequential exoglycosidase digestions, specific chemical degradations, linkage analyses, and MS/MS studies. As a rough guide, high-quality mapping data can be obtained from 10% of a typical extract from a single mouse kidney. For specific glycoproteins, initial steps usually involve some form of immunoprecipatation or affinity chromatography with, or without liquid chromatography purification or electrophoresis.

Once initial steps have been performed, the disulphide bridges are split by reduction and blocked by carboxymethylation. This allows the glycoproteins to be efficiently cleaved by trypsin, or another protease (or by cyanogen bromide if enzymatic digestion is problematical due to poor solubility in the digestion buffer). Once the glycopeptides are generated, these can be purified by reversed-phase chromatography (e.g., Sep-Pak or MicroTrap purification), or be analysed directly by nano-ES-LC/MS/MS before, or after *N*-glycosidase F digestion. Alternatively, the glycopeptides are digested with *N*-glycosidase F and separated into *N*-glycan and *O*-glycopeptide fractions, with the latter being subject to reductive elimination. The released *N*- and *O*-glycans are permethylated and analysed by MALDI and nano-ES-MS/MS. To complement the screening experiments, GC-MS linkage analysis and sugar analysis are performed to provide details of the linkages and the sugar compositions in the sample. In detailed studies the released glycans are often treated with chemical and/or enzymatic reagents to further characterize ambiguous glycan assignments, but this is outside the scope of this article. Initial assignments of relevant signals in MALDI-MS spectra are based on compositions that take into account biosynthetic considerations.

II. MATERIALS AND INSTRUMENTATION

Ammonium acetate (Cat. No. 100134T), ammonium hydrogen carbonate (Ambic, Cat. No. 103025E), hydrochloric acid (HCl, Cat. No. 101254H), and ion-exchanger Dowex 50 W-X8 (H+ form, Cat No. 105221) are from VWR. High-quality solvents: acetonitrile (UPS, ultra purity solvent, Cat. No. H050), dimethyl sulfoxide (DMSO) (Hi Dry, anhydrous solvent, D4281), methanol (UPS, ultra purity solvent, Cat No. H411), and propan-1-ol (SPS, super purity solvent, H624) are from Romil. Acetic acid (SpS, super purity reagent, Cat. No. H014), ammonia solution (SpS, super purity reagent, Cat No. H058), and sodium hydroxide are also from Romil. Acetic anhydride (Cat. No.4295) and methyl iodide (Cat. No. 0347) are from Lancaster. Acetyl chloride (Cat. No. 23,957-7), ammonium formate (Cat. No. F-2004), adrenocorticotropic hormone fragment (ACTH)1–17 (Cat. No. A-2407), ACTH fragment 18–39 (Cat. No. A-0673), ACTH fragment 7–38 (Cat. No. A-1527), ACTH fragment 1–39 (Cat. No. A-0423), angiotensin I (Cat. No. A9650), bradykinin (B-4764), calcium hydride lumps, +4 mesh (Cat. No. 213322), cyanogen bromide (Cat. No. 16774), 2,5-dihydroxybenzoic acid (Cat. No. G-5254), dithiothreitol (DTT, Cleland's reagent, Cat. No. D-5545), ethelyene glycol (Cat. No. 10,246-8), EDTA (Cat. No. 43,178-8), formic acid (Cat No. 94318), hexanes (Cat. No. 15,617-5), hydrogen chloride gas (Cat. No. 29,542-6), hydrofluoric acid 48% (HF, Cat. No. 33,926-1), iodoacetic acid (IAA, Cat. No. I-4386), insulin (bovine pancreas, Cat. No. I-5500), leucine enkephalin (Cat. No. L-9133), exo-β-mannosidase (*Helix pomatia*, Cat. No. M9400), neurotensin (Cat. No. N-6383), sodium acetate (Cat. No. 24,124-5), sodium m-periodate (Cat. No. S-1878), sodium borodeuteride ($NaBH_4$ Cat. No. 20,559-1), potassium borohydride (KBH_4 Cat. No. 438472), sodium chloride (Cat. No. 20,443-9), sodium dodecyl sulfate (SDS, Cat. No. 436143), Tris(hydroxymethyl)aminomethane (Tris, Cat. No. 154563) and trypsin (bovine pancreas, TPCK-treated, T-1426) are from Sigma-Aldrich. 3-((3-Cholamidopropyl)dimethyl-ammonio)-1-propane

sulfonate (CHAPS, Cat. No. 810126) and *N*-glycosidase F (*Escherichea coli*, Cat. No. 1365177) are from Roche Diagnostics. Exo-β-galactosidase (bovine testes, Cat. No. EG02), exo-β-*N*-acetylhexosaminidase (*Streptomyces pneumoniae*, Cat. No. E-GL01), exo-α-mannosidase (jack bean, Cat. No. E-AM01), exo-neuraminidase (*Clostridium perfringes*, Cat. No.), and exo-neuraminidase (*Streptococcus pneumoniae*, Cat, No. E-S007) are from Qa-Bio. Endo-β-galactosidase (*Escherichia freundii*, 100455) is from Seikagaku corporation. Tri-sil "Z" derivatizing agent (Cat. No. 49230) and Snakeskin Pleated dialysis tubing (Cat. No. 68700) are from Perbio Science UK Ltd. Ultra pure water is generated from an Analytical Purite Neptune ultrapure water purification system from Purite Ltd.

Homogenisation of cells and tissues is achieved with a compact electric CAT homogeniser (×*120*)-fitted *T6.1* dispersion shaft from Ingenieurburo CAT. Sonications of cells are achieved by a VC 130 PB (130 W) Vibra-Cell ultrasonic processor within a sound-abating enclosure from Sonics & Materials Inc. Screw-cap style Pyrex disposable culture tubes (Cat. No. 99449-13, 7.5 ml) capped with disposable phenolic lids (Cat. No. 99999-13) and plasticware are from Corning. Caps are lined with Teflon inserts (Cat. No. 0402) from Owens Polyscience Ltd. Sep-Pak Classic C_{18} cartridges (Cat. No. WAT051910) are from Waters Ltd. Medium NanoES capillaries (Cat. No. ES387) for the Micromass Q-Tof are from Proxeon Biosytems. The Hamilton syringe (Cat. No. 002520) is from SGE. MicroTrap peptide cartridges (Cat. No. 004/25108/02) and the Manual Trap Holder kit (Cat. No. 004/25111/01) are from Michrom BioResources, Inc.

III. PROCEDURES

A. Preparation of Homogenates/Cell Lystates

Wear suitable protective clothing, including safety glasses, and work in a fume hood when preparing all solutions and performing various steps of the protocols.

Solutions

1. *Solution A:* 80% (v/v) methanol in H_2O. To make 25 ml, add 5 ml of ultrapure water to 20 ml methanol to make a 80% (v/v) methanol solution.
2. *Solution B:* 33.33% ultrapure water, 33.33% formic, and 33.33% methanol. To make 30 ml, add 10 ml of formic acid and 10 ml of methanol to 10 ml of ultrapure water.
3. *Dilute acetic acid:* To make a 5% acetic acid solution, add 25 ml of acetic acid and complete to 500 ml with ultrapure water. Store at room temperature.
4. *Dialysis buffer:* 50 m*M* Ambic buffer. To make 4.5 liters, add 17.6 g of Ambic and complete with 4.5 liters of water. Adjust to pH 7.5 with dilute acetic acid. Prepare fresh on day of use.
5. *10% SDS:* To make 100 ml, add 10 g of SDS and complete with 100 ml of ultrapure water. Store at room temperature.
6. *Homogenisation buffer:* 0.5% SDS (w/v) in 50 m*M* Tris. To make 50 ml, add 0.3029 g of Tris and complete to 50 ml with ultrapure water. Adjust the pH to 7.4 with dilute acetic acid. Withdraw 2.5 ml of the solution and add 2.5 ml of 10% SDS.
7. *Cell lysis buffer:* 25 m*M* Tris, 150 m*M* NaCl, 5 m*M* EDTA, and 1% CHAPS at pH 7.4. To make 50 ml, add 0.1514 g of Tris, 0.4383 g NaCl, 0.5 g CHAPS, and 0.0731 g EDTA. After dissolving in a small volume of ultrapure water, complete to 50 ml and adjust to pH 7.4 with dilute acetic acid.

1. Homogenisation

Steps

1. Immerse the tip of the dispersion shaft into solution A; activate the drive motor at a low to intermediate setting for 60 s.
2. Examine the tip and carefully remove any residual debris with a 3-mm hypodermic needle. Avoid scratching the dispersion shaft.
3. Put the dispersion shaft in solution B and sonicate in a sonicator bath for 10 min.
4. Repeat step 1 with fresh homogenisation buffer to clean the dispersion shaft.
5. Add 2–3 ml of ice-cold homogenisation buffer to the sample.
6. Homogenise on ice for 10 s. Repeat two or three times, pausing for 15 s between each homogenisation step.
7. Transfer the homogenate to high-quality dialysis tubing and seal.
8. Place the sample into cool dialysis buffer and dialyse at 4°C. Change the buffer regularly with fresh buffer over a period of 48 h.
9. Lyophilise the sample in a clean screw-capped glass culture tube covered with perforated Parafilm.

2. Sonication of Cells

Steps

1. Immerse the probe of the sonicator into solution A; activate the ultrasonic processor in continuous mode at 20 A for 10 s. Sonicate the probe again with ultrapure water and then the cell lysis buffer.

2. Add enough ice-cold cell lysis buffer (1–2 ml) to completely suspend the cell pellet.
3. Sonicate on ice in continuous mode at 40 A for 10 s. Repeat two or three times, pausing for 15 s between each sonication.
4. Transfer the homogenate to high-quality dialysis tubing and seal.
5. Place the sample into cool dialysis buffer and dialyse at 4°C. Change the buffer regularly with fresh buffer over a period of 48 h.
6. Lyophilise the sample in a clean screw-capped glass culture tube covered with perforated Parafilm.

B. Cleavage and Blocking of Disulphide Bridges

Wear suitable protective clothing, including safety glasses, and work in a fume hood when preparing all solutions and performing various steps of the protocols.

Solutions

1. *Tris buffer:* 0.6 *M* Tris. To make 50 ml, weigh 3.63 g of Tris and complete to 50 ml with ultrapure water. Adjust to pH 8.5 with acetic acid. Degas by passing a slow stream of nitrogen (oxygen free) through the solution via a Pasteur pipette.
2. *Dilute acetic acid:* To make a 5% acetic acid solution, add 25 ml of acetic acid and complete to 500 ml with ultrapure water. Store at room temperature.
3. *Dialysis buffer:* 50 m*M* Ambic buffer. To make 4.5 liters, add 17.6 g of Ambic and complete with 4.5 liters of water. Adjust to pH 8.5 with dilute acetic acid. Prepare fresh on day of use.

1. Reduction and Carboxymethylation of Homogenates/Cell Lysates

Steps

1. Weigh 10 mg of DTT and dissolve in 5 ml of degassed Tris buffer to make a 2-mg/ml DTT solution.
2. Add 0.5 ml of the DTT solution to the sample.
3. Incubate for 60 min at 37°C and then centrifuge.
4. Weigh 60 mg of IAA and dissolve in 1 ml of degassed Tris buffer.
5. Add 0.5 ml of fresh IAA solution to the sample.
6. Incubate in the dark at room temperature for 90 min.
7. Transfer the homogenate to high-quality dialysis tubing and seal.
8. Place the sample into cool dialysis buffer and dialyse at 4°C. Change the buffer regularly with fresh buffer over a period of 48 h.
9. Lyophilise the sample in a clean screw-capped glass culture tube covered with perforated Parafilm.

2. Reduction and Carboxymethylation of Glycoproteins

Steps

1. Weigh out 1 mg of DTT and add 1 ml of Tris buffer to make a 1 µg/µl DTT solution.
2. Predict the number disulphide bridges in the glycoprotein if the disulphide bridges have not been mapped previously, i.e., (No. of cysteines ÷ 2).
3. Add enough Tris buffer (~200 µl) to completely dissolve sample and add the appropriate volume of DTT to the sample by using the following equation: Volume of DTT (L) = (No. of disulphide bridges) × (No. of moles of glycoprotein) × (4 × 154.3).
4. Incubate for 60 min at 37°C and then centrifuge.
5. Weigh out 1 mg of IAA and add 1 ml of Tris buffer to make a 1 µg/µl IAA solution.
6. Add the appropriate volume of IAA to the sample using the following equation: Volume of IAA (L) = (No. of moles of DTT in sample) × (5 × 186.0).
7. Incubate in the dark at room temperature for 90 min.
8. Transfer the homogenate to high-quality dialysis tubing and seal.
9. Place the sample into cool dialysis buffer and dialyse at 4°C. Change the buffer regularly with fresh buffer over a period of 48 h.
10. Lyophilise the sample in a clean screw-capped glass culture tube covered with perforated Parafilm.

C. Cleavage into Glycopeptides

Wear suitable protective clothing, including safety glasses, and work in a fume hood when preparing all solutions and performing various steps of the protocols.

Solutions

1. *Dilute acetic acid:* To make a 5% acetic acid solution, add 25 ml of acetic acid and complete to 500 ml with ultrapure water. Store at room temperature.
2. *Ambic buffer:* To make 50 ml, weigh 0.1977 g of ammonium hydrogen carbonate and complete with 50 ml ultrapure water. Adjust to pH 8.4 with ammonia solution. Prepare fresh on day of use.
3. *20 and 40% Propan-1-ol:* To make 50 ml of each solution, add 10 ml and 20 ml of propan-1-ol to separate clean glass bottles, and complete to 50 ml with ultrapure water. Prepare fresh on day of use.

1. Tryptic Digestion of Homogenates/Cell Lysates

Steps

1. Weigh out 1 mg of trypsin and add 1 ml of Ambic buffer to make a 1 µg/µl trypsin solution.
2. Add sufficient solution (300–600 µl) to completely cover the sample.
3. Incubate at 37°C for 14 h and then centrifuge.
4. Terminate the reaction by dispensing 2 drops of acetic acid with a Pasteur pipette.
5. Attach a 10-ml glass syringe to a Sep-Pak C_{18} cartridge and condition by eluting successively with methanol (5 ml), 5% acetic acid (5 ml), propan-1-ol (5 ml), and 5% acetic acid (3×5 ml).
6. Load the sample onto a cartridge.
7. Elute stepwise with 5% acetic acid (20 ml), 20% propan-1-ol solution (4 ml), 40% propan-1-ol solution (4 ml), and 100% propan-1-ol (4 ml). Collect all the fractions apart from the 5% acetic acid fraction (hydrophilic contaminants).
8. Reduce the volume with a Speed-Vac and lyophilise the sample in a clean screw-capped glass culture tube covered with perforated Parafilm.

2. Tryptic Digestion of Glycoproteins

Steps

1. Weigh out 1 mg of trypsin and add 1 ml of Ambic buffer to make a 1 µg/µl trypsin solution.
2. Estimate the approximate amount of glycoprotein.
3. Add sufficient solution (100–200 µl) to completely cover the sample, incubate at 37°C for 5 h and then centrifuge.
4. Dispense 3 drops of acetic acid from a Pasteur pipette to terminate the reaction.

3. Cyanogen Bromide Cleavage of Glycoproteins

Wear suitable protective clothing, including safety glasses, and work in a fume hood due to the toxic cyanogen bromide.

Steps

1. Add 700 µl of formic acid to 300 µl of water in an Eppendorf to make a 70% formic acid solution.
2. Add 8–10 good quality white cyanogen bromide crystals to the Eppendorf.
3. Vortex the mixture until the crystals dissolve completely.
4. Ensure that the glycoprotein sample is dry. Dissolve the sample in minimum amount of the cyanogen bromide solution, typically 100–200 µl.
5. Incubate at room temperature for 14-20 h.
6. Terminate the reaction by adding 4 volumes of ultrapure water.
7. Reduce the volume with a Savant Speed-Vac and lyophilise the sample in a clean screw-capped glass culture tube covered with perforated Parafilm.

D. Cleavage of Glycans From Glycopeptides

Wear suitable protective clothing, including safety glasses, and work in a fume hood when preparing all solutions and performing various steps of the protocols.

Solutions

1. *Dilute acetic acid:* To make a 5% acetic acid solution, add 25 ml of acetic acid and complete to 500 ml with ultrapure water. Store at room temperature.
2. *Ambic buffer:* To make 50 ml, weigh 0.1977 g of ammonium hydrogen carbonate and complete with 50 ml ultrapure water. Adjust to pH 8.4 with ammonia solution. Prepare fresh on day of use.
3. *20 and 40% propan-1-ol:* To make 50 ml of each solution, add 10 ml and 20 ml of propan-1-ol to separate clean glass bottles and complete to 50 ml with ultrapure water. Prepare fresh on day of use.
4. *0.1 M KOH:* To make 100 ml, weigh 0.56 g of KOH and complete to 100 ml with ultrapure water. Store at room temperature.
5. *Dowex solution:* To prepare 100 g of Dowex beads, add 100 g of Dowex beads and complete with 100 ml of 4 *M* HCl and decant. Repeat this twice more and then wash beads by adding, agitating, and decanting with ultrapure water until the pH does not change (usually 10–15 times). Wash the beads three times with 150 ml of dilute acetic acid and leave the beads immersed in dilute acetic acid. The treated beads can be kept equilibrated in this state for many months at room temperature.
6. *10% methanolic acetic acid:* To make 25 ml, add 2.5 ml of acetic acid and complete to 25 ml with methanol. Prepare fresh on day of use.

1. N-Glycosidase F Digest

Steps

1. Dissolve the 20% and 40% Sep-Pak fractions of the tryptic digest each in 150 µl of Ambic buffer and combine.
2. Add 5 U of *N*-glycosidase F, incubate at 37°C for 20–24 h, and then centrifuge.
3. Lyophilise the sample.
4. Separate *N*-glycans from the mixture using the Sep-Pak C_{18} propanol-1-ol / 5% acetic acid system.

2. Separation of N-Glycans from Peptides/O-Glycopeptides by Sep-Pak C_{18} Purification

Steps

1. Attach a 10-ml glass syringe to a Sep-Pak C_{18} cartridge and condition by eluting successively with methanol (5 ml), 5% acetic acid (5 ml), propan-1-ol (5 ml), and 5% acetic acid (3×5 ml).
2. Load the sample on to a cartridge.
3. Elute stepwise with 5% acetic acid (5 ml), 20% propan-1-ol solution (4 ml), 40% propan-1-ol solution (4 ml), and 100% propan-1-ol (4 ml). Collect all fractions.
4. Reduce the volume with a Speed-Vac and lyophilise the sample in a clean screw-capped glass culture tube covered with perforated Parafilm.
5. Permethylate the 5% acetic acid fraction (the *N*-glycan fraction).
6. Perform reductive elimination on the 20% propan-1-ol fraction.

3. Reductive Elimination

Steps

1. Add 54–55 mg of KBH_4 to 1 ml of 0.1 *M* KOH.
2. Add 400 µl of the $NaBH_4$ solution to the sample in a Teflon-lined screw-capped culture tube.
3. Incubate at 45°C overnight for 20–24 h and then centrifuge.
4. Terminate the reaction by adding 5 drops of acetic acid from a Pasteur pipette until fizzing stops.
5. Assemble the desalting column by packing a Pasteur pipette fitted with a piece of silicone tubing at its tapered end (to control the flow) with Dowex beads.
6. Elute the desalting column with 15 ml of acetic acid.
7. Load the sample onto the top of the desalting column.
8. Elute with 5% acetic acid and collect 5 ml in a glass culture tube.
9. Reduce the volume on a Savant Speed-Vac and lyophilise.
10. Remove excess borate by coevaporating with 10% methanolic acetic acid (4 × 0.5 ml) under a stream of nitrogen at room temperature. Repeat twice more.

E. Derivatisation of Glycans and Sep-Pak Cleanup

Wear suitable protective clothing, including safety glasses, and work in a fume hood when preparing all solutions and performing various steps of the protocols.

Solutions

1. *Anhydrous DMSO solution:* To make 400 ml, using a steel spatula carefully place good sized calcium hydride lumps into a clean 500-ml round-bottomed Quick-fit flask. Avoid putting powder into the flask. Add 400 ml of DMSO and stand overnight or longer until all powder has settled to the bottom. Keep the stopper tight and replace immediately each time after the DMSO has been dispensed. This DMSO stock solution may be kept as a stock solution at room temperature.
2. *15, 35, 50, 75% Acetonitrile solutions:* To make 100 ml of each solution, add 15, 35, 50, and 75 ml of acetonitrile to separate clean glass bottles and complete them to 100 ml with ultrapure water. Store at room temperature.

1. NaOH Permethylation

Wear suitable protective clothing, including safety glasses, and work in a fume hood due to the caustic NaOH and toxic methyl iodide.

Steps

1. Place 5 pellets of NaOH in a dry mortar and add 3 ml of anhydrous DMSO to the pellets.
2. Grind the NaOH pellets with a pestle to form a slurry. This should be done fairly swiftly to avoid excessive absorption of moisture from the atmosphere. Ensure the sample to be permethylated is completely dry.
3. Add 0.5–1 ml of the slurry to the sample and then add 0.2–0.5 ml of methyl iodide (or deuteromethyl iodide).
4. Vortex the sample and agitate the reaction mixture on an automatic shaker for 10 min at room temperature.
5. Quench the reaction by slow dropwise additions of ultrapure water (~1 ml) with constant shaking to lessen the effects of the highly exothermic reaction.
6. Add 1–2 ml of chloroform and make up to 5 ml with ultrapure water.
7. Mix thoroughly and allow the mixture to settle into two layers. Remove and discard the upper aqueous layer.
8. Wash the lower chloroform layer several times with ultrapure water.
9. Dry down the chloroform layer under a gentle stream of nitrogen.
10. Purify the mixture by Sep-Pak C_{18} purification.

2. Purification of Permethylated Samples by Sep-Pak C_{18} Purification

Steps

1. Condition the Sep-Pak cartridge by eluting successively with methanol (5 ml), ultrapure water (5 ml), acetonitrile (5 ml) and ultrapure water (3 × 5 ml).
2. Dissolve the sample in 1 : 1 methanol : ultrapure water (200 µl).
3. Load it onto the Sep-Pak cartridge.
4. Elute stepwise with 5 ml of ultrapure water and 3 ml each of 15, 35, 50, and 75% aqueous acetonitrile. Collect the fractions in culture tubes.
5. Reduce the volume by Savant Speed-Vac and lyophilise.

F. Useful Glycan Degradation Procedures

Wear suitable protective clothing, including safety glasses, and work in a fume hood when preparing all solutions and performing various steps of the protocols.

Solutions

1. *50 mM ammonium acetate:* To make 50 ml, add 0.1927 g of ammonium acetate and complete with 50 ml of ultrapure water. Adjust the pH to optimum range of the glycosidase.
2. *50 mM ammonium formate:* To make 50 ml, add 0.1577 g of ammonium formate and complete with 50 ml of ultrapure water. Adjust the pH to the optimum range of the glycosidase.

1. Hydrofluoric Acid 2-, 3-, and 4-Linked Fucose Removal

Wear suitable protective clothing, including safety glasses, and work in a fume hood due to toxic HF.

Steps

1. Add 50 µl of 48% HF to sample using a plastic micropipette tip. Ensure the sample is in a clean Eppendorf and is completely dry before adding the HF.
2. Incubate the sample on ice at 4°C for 20 h.
3. Terminate the reaction by drying under a gentle stream of nitrogen.
4. Dissolve the sample in 5% acetic acid and transfer to a screw-capped glass culture tube for subsequent glycosidase digestion or permethylation.

2. Mild Periodate Oxidation for O-Glycan Core Definition

Steps

1. Add 100 µl of 2–20 m*M* sodium m-periodate in ammonium acetate buffer (100 m*M*, pH 6.5) and incubate in the dark at 0°C for 20 h.
2. Quench the reaction by adding 2–3 µl of ethylene glycol.
3. Stand at room temperature for 1 h and then lyophilise.
4. Incubate the sample with 400 µl of $NaBH_4$ in 2 *M* NH_4OH (10 mg/ml) for 2 h.
5. Terminate the reaction by adding a few drops of acetic acid dispensed from a Pasteur pipette until fizzing stops.
6. Assemble the desalting column by packing a Pasteur pipette fitted with a piece of silicone tubing at its tapered end (to control the flow) with Dowex beads.
7. Elute the desalting column with 15 ml of acetic acid.
8. Load the sample onto the top of the desalting column.
9. Elute with 5% acetic acid and collect 5 ml in a glass culture tube.
10. Reduce the volume on a Savant Speed-Vac and lyophilise.
11. Remove excess borates by coevaporating with 10% methanolic acetic acid (4 × 0.5 ml) under a stream of nitrogen at room temperature. Repeat twice more.

3. Exo-glycosidase Digestion

Perform glycosidase digestions on released or partially digested glycans.

Steps

1. Add up to 1 nmol of the glycan in an Eppendorf or a screw-capped glass culture tube.
2. Adjust the pH of ammonium acetate to the pH optimum of the glycosidase and then add 50 µl to the sample. Suitable pH values are as follows: α-mannosidase (jack bean, pH 5), β-mannosidase (*Helix pomatia*, pH 4.6), β-galactosidase (bovine testes, pH 4), neuraminidase (*Clostridium perfringes,* pH 6), neuraminidase (*Streptococcus pneumoniae*, pH 6), and endo-β-galactosidase (*Bacteroides fragilis*, pH 5.8).
3. Add enough glycosidase to digest the sample. As a rough guide use the following amounts: α-mannosidase (jack bean, 20 mU), β-mannosidase (*H. pomatia*, 10 mU), β-galactosidase (bovine testes, 20 mU), neuraminidase (*C. perfringes,* 60 mU),

neuraminidase (*S. pneumoniae*, 10 mU), and endo-β-galactosidase (*B. fragilis*, 50 mU).
4. Incubate at 37°C for 20 h and then centrifuge.
5. Add a second aliquot and incubate at 37°C for a further 12 h.
6. Lyophilise the sample in a clean screw-capped glass culture tube covered with perforated Parafilm.
7. Remove an appropriate aliquot and permethylate for subsequent analysis by MALDI-MS. *NB*: for β-*N*-acetylhexosaminidase (*S. pneumoniae* 80 mU, pH 5), use ammonium formate

G. Defining Linkages and Sugar Compositions

Wear suitable protective clothing, including safety glasses, and work in a fume hood when preparing all solutions and performing various steps of the protocols.

Solutions

1. *2.0 M TFA:* Add 200 µl TFA to 1.1 ml of water. Prepare fresh on day of use.
2. *2.0 M NH_4OH:* Add 200 µl NH_3 to 1.62 ml of water. Prepare fresh on day of use.
3. *10% methanolic acetic acid:* To make 25 ml, add 2.5 ml of acetic acid and complete to 25 ml with methanol. Prepare fresh on day of use.
4. *Methanolic HCl:* To make a 1.0 *M* solution, add dropwise 100 µl of acetyl chloride to 1.3 ml of ice-cold methanol with constant shaking between each addition. Prepare fresh on day of use. Alternatively, for a rapid way of preparing a solution of approximately 1.0 *M* concentration, connect a Pasteur pipette to tubing attached to a cylinder of HCl gas and bubble the gas into 1 ml of methanol at room temperature until the bottom of the glass tube is hot to the touch.

1. Linkage Analysis of Permethylated Glycans

Steps

1. Add 200 µl of 2 *M* TFA to the permethylated sample and incubate at 121°C for 2 h.
2. Allow to cool, centrifuge, and dry under nitrogen.
3. Weigh out 10–20 mg $NaBD_4$ and add the appropriate volume of 2.0 *M* NH_4OH to make a 10-mg/ml solution.
4. Add 200 µl of the reducing reagent to the hydrolysates and stand at room temperature for 2 h.
5. Add 5 drops of acetic acid dropwise with a Pasteur pipette until fizzing stops and dry under nitrogen. It is not necessary to wait for complete dryness before proceeding to the next step.
6. Add 1 ml of 10% acetic acid in methanol and evaporate the solution under nitrogen until dry. Repeat twice more.
7. Add 200 µl acetic anhydride and incubate at 100°C for 1 h. Dry down under a stream of nitrogen.
8. Add 1 ml of chloroform and wash with ultrapure water.
9. Vortex the mixture and allow the two layers to separate. Discard the upper water layer.
10. Repeat two more times and dry under nitrogen. The resulting partially methylated alditol acetates (PMAA) can now be dissolved in a small volume of hexanes and analysed by GC-MS.

2. TMS Sugar Analysis

Steps

1. Add 200 µl of the methanolic–HCl reagent to the underivatised sample in a Teflon-lined screw-capped glass culture tube.
2. Incubate overnight (14–16 h) at 80°C and centrifuge.
3. Remove the reagent by blowing down under a stream of nitrogen.
4. Add the following reagents sequentially with thorough mixing in between: 500 µl of methanol, 10 µl (one drop from Pasteur pipette) of pyridine, and 50 µl of acetic anhydride.
5. Stand at room temperature for 15 min and remove the reagent by blowing down under a stream of nitrogen.
6. Break a 1-ml Tri-sil Z ampoule and add 100–200 µl of the TMS derivatisation reagent to the sample.
7. Stand at room temperature for about 15 min and dry down under a gentle stream of nitrogen.
8. Add a small squirt of hexane (~500 µl) and dry down again.
9. Add 1 ml of hexanes, mix thoroughly, and centrifuge at 3000 rpm for about 5–10 min.
10. Transfer the clear hexane supernatant to a new tube.

H. Mass Spectrometry

Solutions

1. *1% TFA solution:* To make 100 ml, add 1 ml of TFA to 99 ml of ultrapure water. Store at room temperature.
2. *0.1% TFA solution:* To make 100 ml, add 100 µl of TFA to 99.9 ml of ultrapure water. Store at room temperature.

3. *30% and 60% acetonitrile TFA solutions:* To make 50 ml of each solution, add 15 ml and 30 ml of acetonitrile to clean glass bottles and complete to 50 ml with 0.1% TFA to make 30 and 60% acetonitrile solutions.

I. Gas Chromotography–Mass Spectrometry

Analyse derivatised monosaccharide mixtures on a PerkinElmer's Clarus 500 gas chromograph / mass spectrometer (GC-MS) fitted with a RTX-5 column (30 × 0.32 mm internal diameter, Restek Corp.). Dry down the hexanes and redissolve the derivatives in ~50 µl of hexanes. Samples may be injected directly onto the column or by the autosampler. For PMAA analysis, the oven is held at 90°C for 1 min and subsequently ramped to 290°C at a rate of 8°C/min, held at 290°C for 5 min and finally to 300°C at a rate of 10°C/min. For standards, various synthetic glycans can be permethylated and taken through the linkage protocol to generate retention information for various linkages. As a rough guide, the elution times are ordered as follows: terminal fucose, terminal hexoses, linked hexoses, terminal *N*-acetylhexosamines, and finally linked *N*-acetylhexosamines. Note that sialic acids are not observed in this analysis. For TMS derivatives the oven is held at 90°C for 1 min and subsequently ramped to 140°C at a rate of 8°C/min, then to 200°C at a rate of 5°C/min, and finally to 300°C at a rate of 10°C/min. For TMS derivatives, arabitol is used as an internal standard to track the reproducibility of retention times and for quantitative information. Monosaccharide standards usually include 1 nmol/µl solutions of arabitol, fucose, glucose, galactose, mannose, GlcNAc, GalNAc, and NeuAc.

J. Matrix-Assisted Laser Desorption Ionisation Mass Spectrometry

MALDI MS is generally performed in positive reflectron mode using a Perspective Biosystems Voyager-DE STR MALDI workstation equipped with delayed extraction technology. Data acquisition is performed using Voyager 5 Instrument Control Software, and data processing by Data Explorer MS processing software. Calibration is performed by external calibration of a mixture of leucine, enkephalin, bradykinin, bradykinin (fragment 1–8), angiotensin I, neurotensin, adrenocorticotropic hormone fragment (ACTH) 1–17, ACTH fragment 18–39, ACTH fragment 7–38, ACTH fragment 1–39, and insulin. Typical mass ranges are as follows: permethylated *N*-glycans in the range of *m*/*z* 1000-7000, and permethylated *O*-glycans in the range of *m*/*z* 500–4000. Permethylated glycans are usually in the 35%, 50%, and 75% fractions. The relevant fractions for *N*- and *O*-glycan studies are the 5% acetic acid fraction (*N*-glycans) and the 20% propan-1-ol fraction (*O*-glycopeptides) obtained after N-glycosidase.

1. MALDI Sample Preparation of Derivatised Glycans

Steps

1. Weigh 10 mg of DHB in an Eppendorf.
2. Add 200 µl of water and 800 µl methanol to the DHB
3. Vortex the matrix solution until the DHB completely dissolves.
4. Dissolve the derivatised glycans in a small volume of methanol ~5–10 µl.
5. Mix a 1-µl aliquot of the derivatised glycans with 1 µl or the fresh DHB solution.
6. Spot 1 µl of the sample matrix mixture on a clean stainless steel target and allow it to dry under vacuum. Perform MALDI-TOF experiments.

2. MALDI Sample Preparation of Peptides and Glycopeptides

If the sample has not been purified by Sep-Pak, perform steps 1–4, otherwise go to step 5.

Steps

1. Assemble a manual Microtrap Holder with a clean MicroTrap peptide cartridge.
2. Condition the cartridge by eluting successively with acetonitrile (5 × 20 µl) and then 0.1% TFA (8 × 20 µl).
3. Load the sample onto the column and then elute with 0.1% TFA (20 µl × 5) without collection.
4. Elute stepwise with 20 µl each of 30% and 60% acetonitrile in 0.1% TFA. Collect the fractions in Eppendorfs.
5. Weigh 10 mg of α-cyanocinnamic acid in an Eppendorf.
6. Add 1 ml of 30% acetonitrile in 0.3% TFA to the α-cyanocinnamic a acid and mix.
7. Dissolve the sample in an appropriate volume of 0.1% TFA to make a picomole per microliter solution if the sample is dry.
8. Mix a 1-µl aliquot of the peptides with 1 µl fresh α-cyanocinnamic acid solution.
9. Spot 1 µl of the sample matrix mixture on a clean stainless steel target and allow it to dry under vacuum. Perform MALDI-TOF experiments.

K. Nanoflow Electrospray Ionisation

Nano-ES MS and nano-ES MS/MS data are acquired using positive ion mode of a quadrupole

orthogonal acceleration time-of-flight, Q-Tof 1, mass spectrometer (Waters Ltd, UK) fitted with a Z-spray atmospheric ion source. In MS mode the quadrupole is used in RF-only mode and transmits about two decades in mass to the TOF. In MS/MS the quadrupole is in resolving mode, allowing selection of precursors for collision in the hexapole gas cell. A voltage of 1.5 kV is applied to the NanoES capillary tip, generating a nanoflow in the range of 10–30 nl/min. Argon and nitrogen are used as the collision and bathing gases, respectively. Collision gas pressure is maintained at 10^{-4} mbar, and collision energies up to 90eV are used for large glycopeptides, but do not usually exceed 50 eV for most peptides. As a rough guide, collision energies for doubly charged peptides range from <18 eV for m/z values of <500 to collision energies >35 eV for species with m/z values >1200. Collision energies are usually varied between 40 and 70 eV for permethylated glycans. Data are acquired and processed using Masslynx 4 software (Waters Ltd., UK). The instrument is calibrated with a 0.1 to 1 pmol/µl solution [Glu^1]-fibrinopeptide B in methanol / 5% (v/v) aqueous acetic acid [1 : 3, (v/v)]. Experiments may also be performed in a similar fashion on other quadrupole orthogonal acceleration time-of-flight instruments, such as the QSTAR Pulsar I mass spectrometer (AB/MDS Sciex, Toronto, Canada) fitted with a nanoelectrospray ion source (MDS Proteomics, Odense, Denmark) controlled by Analyst QS software.

1. ES Sample Preparation of Derivatised Glycans

Steps

1. Dissolve derivatised glycans in a suitable volume of methanol (~10 µl).
2. Withdraw a few microliters of the sample into a clean Hamilton syringe and inject into a nano-ES capillary.
3. Open the tip of the needle and load into the nano-ES interface of the mass spectrometer. Perform MS and MS/MS experiments.

2. ES Sample Preparation of Glycopeptides

If the sample has not been purified by Sep-Pak, perform steps 1–4, otherwise go to step 5.

Steps

1. Assemble a manual Microtrap Holder with a clean MicroTrap peptide cartridge.
2. Condition the cartridge by eluting successively with acetonitrile (5 × 20 µl) and then 0.1% TFA (8 × 20 µl).
3. Load the sample onto the column and then elute with 0.1% TFA (20 µl × 5) without collection.
4. Elute stepwise with 20 µl each of 30% and 60% acetonitrile in 0.1% TFA. Collect the fractions in Eppendorfs.
5. Withdraw a few microliters of the sample into a clean syringe and inject into a nano-ES capillary.
6. Open the tip of the needle and load into the nano-ES interface of the mass spectrometer. Perform MS and MS/MS experiments.

L. Nano-LCMS/MS Q-Star Hybrid MS/MS

Complex tryptic digests are analysed by nano-LC-MS/MS using a reversed-phase nano-HPLC system (Dionex, Sunnyvale) connected to a quadrupole TOF mass spectrometer (QSTAR Pulsar I, MDS Sciex, Canada). The digests are separated by a binary nano-HPLC gradient generated by an Ultimate pump fitted with a Famos autosampler and a Switchos microcolumn-switching module (LC Packings, Amsterdam, Netherlands). An analytical C18 nanocapillary (75 µm i.d. × 15 cm, PepMap) and a micro precolumn C18 cartridge (300 µm i.d. × 1 mm) are employed for on-line peptide separation. Digests are injected onto the precolumn by a Famos autosampler with volumes from volumes typically ranging from 0.5 to 5 µl. The digests are first loaded onto the precolumn and eluted with 0.1% formic acid in water (HPLC grade, Purite) for 2–4 min. The sample is then transferred onto an analytical C18 nanocapillary HPLC column and eluted at a flow rate of 150–200 nl/min using the following gradient: 0–5 min 99% A, 5–10 min 99–90% A, 10–70 min 90–60% A, 70–71 min 60–50% A, 71–75 min 50–5% A, 75–85 min 5% A, 85–86 min 5–95% A, 86-90 min and 95% A. Solvent A = 0.05% (v/v) formic acid in 95 : 5 (v/v) water:acetonitrile; solvent B = 0.04% formic acid in 95 : 5 (v/v) acetonitrile:water. Data acquisition was performed using Analyst QS software with an automatic information-dependent acquisition (IDA) function. Similar experiments may also be performed on other quadrupole orthogonal acceleration time-of-flight instruments such as the MicroMass Q-ToF MS (Waters Ltd., UK) fitted with a CapLC system (Waters Ltd., UK) or with the same nano-HPLC system (Dionex, Sunnyvale) described earlier.

IV. COMMENTS

The protocols outlined in this article are suitable for profiling the major *N*- and *O*-glycan populations on a wide range of mammalian cells, fluids, tissues, and organs. In addition, these methodologies are used rou-

tinely to complement detailed studies of specific biologically active glycopolymers.

V. PITFALLS

1. Use ion-free ultrapure water at all times for washing plasticware and glassware. Always use ion-free ultrapure water to prepare solutions.
2. Clean all glassware thoroughly before use with water before drying in a 90°C oven. Do not use detergents to clean glassware.
3. Use screw-capped disposable Pyrex culture tubes with caps that have Teflon inserts as much as possible, i.e., incubations, reactions, and drying steps.
4. Use prepierced Parafilm (American National Can) to cover glass culture tubes during vacuum centrifugation and lyophilisation to minimise potential cross contamination.
5. Where possible, use glassware rather than plasticware in all steps apart from steps involving HF, as HF reacts with glass, e.g. use sterile nonplugged Pasteur pipettes to dispense solutions >0.2 ml and use sterile glass micropipettes to dispense solutions < 0.2 ml except for HF transfers.
6. Prior to reduction/carboxymethylation, take appropriate measures to ensure that extracts or samples are as free as possible of detergents and involatile salts.
7. TMS derivatives are volatile so do not leave for extended periods under nitrogen.
8. For detergent solutions, add the detergents after adjusting the pH in order to prevent precipitation.
9. When using gloves, wear the powder-free type.
10. For bulky tissues, it is advisable to split the sample, as large amounts of material can be difficult to process. As a rough guide, a mouse kidney should be split into two, whereas a mouse small intestine should be split into at least four samples.

References

Albersheim, P., Nevins, D. J., English, P. D., and Karr, A. (1967). A method for the analysis of sugars in plant cell wall polysaccharides by gas-liquid chromatography. *Carbohydr. Res*. **5**, 340–345.

Barber, M., Bordoli, R. S., Sedgwick, R. D., and Tyler, A. N. (1981). Fast atom bombardment of solids (F.A.B): A new ion source for mass spectrometry. *J. Chem. Soc. Chem. Commun*. **7**, 325–327.

Dell, A. (1987). F.A.B.: Mass spectrometry of carbohydrates. *Adv. Carbohydr. Chem. Biochem*. **45**, 19–72.

Dell, A., Azadi, P., Tiller, P., Thomas-Oates, J., Jennings, H. J., Beurret, M., and Michon, F. (1990). Analysis of oligosaccharides epitopes of meningococcal lipopolysaccharides by fast-atom-bombardment mass spectrometry. *Carbohydr. Res*. **200**, 59–76.

Dell, A., Morris, H. R., Easton, R. L., Panico, M., Patankar, M., Oehniger, S., Koistinen, H., Seppala, M., and Clark, C. F. (1995). Structure analysis of the oligosaccharides derived from glycodelin, a human glycoprotein with potent immunosuppressive and contraceptive activities. *J. Biol. Chem*. **270**, 24116–24124.

Dell, A., Morris, H. R., Egge, H., von Nicolai, and Strecker, G. (1983). Fast-atom-bombardment mass spectrometry for carbohydrate structure determination. *Carbohyr. Res*. **115**, 41–52.

Fenn, J. B., Mann, M., Meng, C. K., Wong, S. K., and Whitehouse, C. M (1990). Electrospray ionization-principles and practice. *Mass Spectrom. Rev*. **9**, 37–70.

Fukuda, M., Bothner, B., Ramsamooj, P., Dell, A., Tiller, P. R., Varki, A., and Klock, J. C. (1985). Structures of sialylated fucosyl polylactoaminioglycans isolated from chronic myelogenous leukemia cells. *J. Biol. Chem*. **260**, 12957–12967.

Fukuda, M., Dell, A., and Fukuda, M. N. (1984). Structure of fetal lactosaminoglycan. The carbohydrate moiety of band 3 isolated from human umbilical cord erythrocytes. *J. Biol. Chem*. **259**, 4782–4791.

Karas, M., and Hillenkamp, F. (1988). Laser desorption ionization of proteins with molecular masses exceeding 10,000 daltons. *Anal. Biochem*. **191**, 332–336.

Karas, M., Igendoh, A., Bahr, U., and Hillenkamp, F. (1989). Ultraviolet-laser desorption ionization mass-spectrometry of femtomolar amounts of large proteins. *Biomed. Environ. Mass Spectrom*. **18**, 841–843.

Laferte, S., Fukuda, M. N., Fukuda, M., Dell, A. and Dennis J. W. (1987). Glycosphingolipids of lectin-resistant mutants of the highly metastatic mouse tumour cell line, MDAY-D2. *Cancer Res*. **47**, 150–159.

Lopez, M., Coddeville, B., Langridge, Plancke, Y., Sautierre, P., Chaabihi, H., Chirat, F., Harduin-Lepers, A., Cerutti, M., Verbert, A., and Delannoy, P. (1997). Microheterogeneity of the oligosaccharides carried by the recombinant bovine lactoferrin expressed in *Mamestra brassicae* cells. *Glycobiology* **7**, 635–651.

Manzi, A. E, Norgard-Sumnicht, K., Argade, S., Marth, J. D., van Halbeek, H., and Varki, A. (2000). Exploring the glycans repertoire of genetically modified mice by isolation and profiling of the major glycan classes and nano-NMR analysos of glycans mixtures. *Glycobiology* **10**, 669–689.

McConville, M. J., Homans, S. W., Thomas-Oates, J. E., Dell, A., and Bacic, A. (1990). Structures of the glycoinositolphospholipids from *Leishmania major*: A family of novel galactofuranose-containing glycolipids. *J. Biol. Chem*. **265**, 7285–7294.

Morris, H. R. (1980). Biomolecular structure determination by mass spectrometry. *Nature* **286**, 447–452.

Saski, H., Bothner, B., Dell, A., and Fukuda (1987). Carbohydrate structure of erythropoietin exopressed in Chinese hamster ovary cells by a human erythropoietin cDNA. *J. Biol. Chem*. **262**, 12059–12076.

Sutton-Smith, M., Morris, H. R., and Dell, A. (2000). A rapid mass spectrometric strategy suitable for the investigation of glycan alterations in knockout mice. *Tetrahedron-Asymmetry* **11**, 363–369.

CHAPTER

54

Stable Isotope Labeling by Amino Acids in Cell Culture for Quantitative Proteomics

Shao-En Ong, Blagoy Blagoev, Irina Kratchmarova, Leonard J. Foster, Jens S. Andersen, and Matthias Mann

I. INTRODUCTION

Analysis by combined liquid chromatographic separation and mass spectrometry (LC-MS) is rapidly becoming the most popular and effective approach for large-scale protein identification (Aebersold and Mann, 2003; Yates, 2000) (see also article by Foster and Mann). The increasing sensitivity and the development of better protein/peptide separation methods will surely extend the catalogues of proteins emerging from proteomics projects. However, the significance of such data is further amplified if such identifications are coupled with quantitative abundance information. Indeed, it has been argued that almost all proteomics experiments should soon be converted to a quantitative format as qualitative lists of proteins may not be sufficient in the future (Aebersold and Mann, 2003).

Quantitative methods in mass spectrometry (MS) rely largely on the principle of stable isotope labelling (SIL). Differential incorporation of stable isotopic nuclei (^{2}H, ^{13}C, ^{15}N, ^{18}O) allows the "light" and a "heavy" form of the same peptide to be resolved in the mass spectrometer due to their mass difference. The ratio of signal intensities of the two peptides measures peptide abundance and, correspondingly, the relative abundance of the two proteins.

The main strategies for stable isotope incorporation can be broadly classified into two groups: "postharvest" incorporation and metabolic incorporation. The prototypical example of the former approach is the "isotope-coded affinity tag" (ICAT) reagent described in 1999 (Gygi *et al.*, 1999). In this approach, biotinylated tags are differentially mass encoded with stable isotopes (either 0 or 8 deuteriums) and bear a chemical moiety targeted at cysteine sulphydryl groups. The protein samples to be compared are derivatised separately with the two forms of ICAT, digested, and purified over an avidin column to enrich ICAT-labelled peptides for subsequent mass spectrometric analyses. Several other variations on this chemical derivatisation theme have been applied since then (Goodlett *et al.*, 2001; Regnier *et al.*, 2002; Olsen *et al.*, 2004).

Metabolic incorporation of stable isotopes for MS quantitation of proteins was first introduced in 1998 for bacteria (Langen *et al.*, 2000) and in 1999 in yeast (Oda *et al.*, 1999). These first reports relied on growing simpler organisms on ^{15}N-enriched media. The growth of mammalian cells in ^{15}N-enriched media has also been described (Conrads *et al.*, 2001) but is largely untenable for most cell culture protocols due to the lack of a source of ^{15}N-enriched serum. In our laboratory, we have developed a method (SILAC) for stable isotope labelling by amino acids specifically suited for mammalian cell culture (Ong *et al.*, 2002). Independently, other groups have also described similar experiments for use in yeast (Jiang and English, 2002) and in mammalian systems (Zhu *et al.*, 2002).

The name SILAC (for stable isotope labelling by amino acids in cell culture) is apt as it accurately describes the mode in which the stable isotope labels are delivered, and the acronym is an extension

Copyright 2006, Elsevier Science (USA).
All rights reserved.

of SIL already popularised from the small molecule field and in NMR. Rather than introducing the mass differential in all nitrogen atoms as in ^{15}N labelling, the SILAC method relies on stable isotope containing amino acids. This makes the incorporation of stable isotopes sequence dependent and inherently predictable. Furthermore, by introducing the stable isotope label in the form of amino acids in growth media, the label is effectively "encoded" into each newly synthesized protein. This differs significantly from chemical derivatisation methods that target specific amino acid residues. For instance, a limitation of the ICAT approach is that not all proteins contain cysteine. Often, SILAC labelling is more practical, as beyond preparation of labelling media, there are no chemical modifications required to "encode" proteins with quantitative information. Indeed, the chemical derivatisations required in postharvest labelling methods are not usually compatible with high-sensitivity MS measurements.

Importantly, SILAC provides investigators with two cell populations, grown in parallel and thus identical save for the fact that the proteins from each individual population are distinguishable by MS. The "encoded" cells can be mixed at harvest and can be subjected to any biophysical separation or protein purification directly. This contrasts with postharvest labelling approaches that require separate processing of protein samples until the label has been incorporated. Derivatisation methods that incorporate the label at the peptide level (i.e., after proteins have been processed enzymatically) demand that these purification steps and protein digestion steps be done individually, thus significantly compromising the accuracy of quantitation.

This article describes the study of C2C12 muscle differentiation with SILAC as an example. One set of cells are kept at the myoblast stage whilst the other set is induced to differentiate into myotubes (Ong *et al.*, 2002). Cells from both samples are mixed 1 to 1 and lysed. Proteins extracted from the mixture are then analysed by standard MS techniques (Fig. 1). Many muscle-specific proteins, such as myosin, were found to be highly upregulated whilst other proteins, such as histones, were found at similar levels in both samples. This illustrates the ability of the SILAC approach to accurately measure changes in protein expression during a cell differentiation experiment.

Another intrinsic benefit of "coded" cell populations is apparent when SILAC is coupled to standard

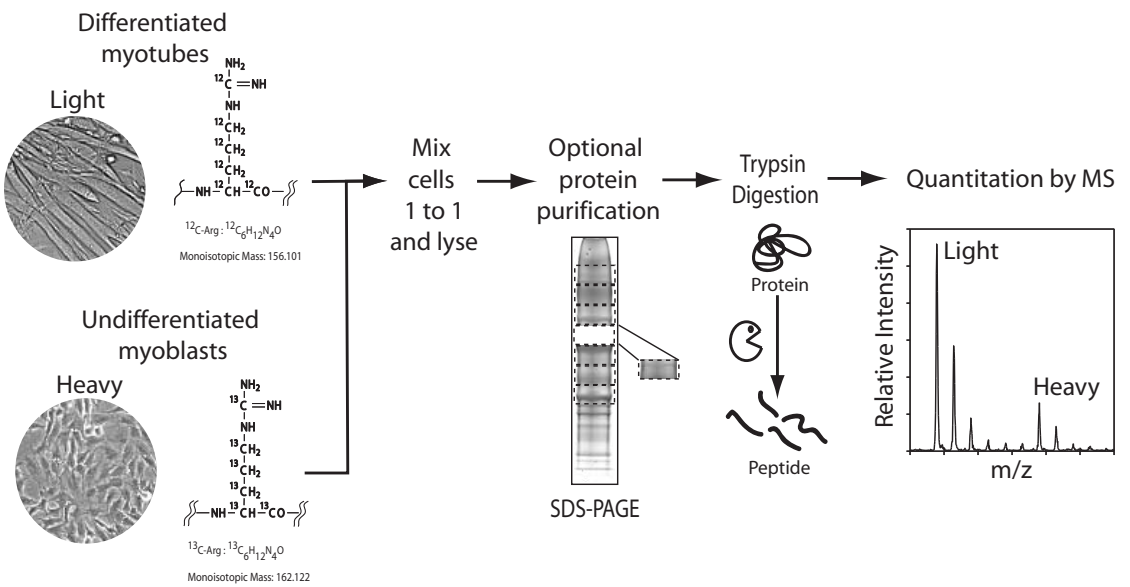

FIGURE 1 An overview of a quantitative study of C2C12 muscle differentiation with SILAC. Myoblasts are grown to confluence separately in "light" and "heavy" media. Myoblasts in "light" $^{12}C_6$-Arg media are induced to differentiate to form myotubes by reducing serum concentration to 2% dialysed FBS. Myoblasts in $^{13}C_6$-Arg are left undifferentiated. Cells are harvested and mixed 1 to 1 after protein concentration determination. Nuclei and cytoplasmic fractions from mixed cells are obtained. Proteins were separated on a SDS–PAGE gel, and gel slices were excised and digested with trypsin. Peptides were extracted from gel slices and analysed by LC-MS. The ratio of relative intensities of the "light" over the "heavy" peak cluster gives the fold increase in relative abundance of the protein during muscle differentiation.

biochemical purifications of proteins with antibodies or bait proteins (Fig. 2). Pull-down experiments and subsequent MS identification have been used for large-scale analysis of protein complexes and protein–protein interactions (Gavin *et al*., 2002; Ho *et al*., 2002). The exquisite sensitivity of mass spectrometers generates large lists of identified proteins that are purportedly true binders to the bait. Although informative, it is not always easy to judge if a particular protein identified in this way is a real interaction partner or a nonspecific "background" interaction with the antibody/bait. This necessitates time-consuming and often difficult follow-up experiments to validate one's findings. Such uncertainty can be appropriately addressed with the following approach that combines SILAC with affinity purifications.

SILAC-labelled cells are used to generate separate pools of proteins or protein complexes that are distinct to an affinity bait. Cells may be differentially treated with a drug or growth factor; alternatively, cells may express the wild-type or mutant form of a component of a protein complex. Proteins from both states can be mixed in equal proportions and then purified together over the affinity bait. In this manner, peptides from proteins specific to the differential treatment will give a large differential ratio whilst background, nonspecific interactions with the bait will be close to the 1-to-1 ratio of mixing.

In one example, $^{13}C_6$-Arg-labelled cells were stimulated briefly with EGF alongside untreated, unlabelled cells. Cells were lysed and equal amounts of protein from each sample were combined for subsequent affinity purification with the SH2 domain from Grb2 as a bait (Blagoev *et al*., 2003). As the SH2 domain of Grb2 binds to phosphorylated tyrosines on the EGF receptor upon stimulation, we observed specific enrichment of the phosphorylated EGF receptor along with its associated proteins. Direct interaction partners exhibited a large (> fivefold) enrichment of one peptide form versus the other and were easily distinguished from background-binding proteins, which showed a 1-to-1 ratio (see Fig. 1). This discrimination between specific interaction partners and background binding is extremely powerful and addresses many of the inadequacies of previous approaches.

Using three different forms of arginine with SILAC makes it possible to functionally encode three cellular states in a single experiment. We have used $^{13}C_6$-Arg, $^{13}C_6{}^{15}N_4$-Arg in addition to normal arginine to label all arginine-containing peptides in the proteome (Blagoev *et al*., 2004). This is especially useful in cases where various time intervals of drug treatment are examined or where multiple cellular conditions are presented to an affinity bait. Using immunoprecipitation as an example, applying the "two-state" approach with only two distinct quantitative labels would require two separate pull downs followed by separate MS identifications and quantitative analyses. With triple encoding, this is reduced to a single experiment with a shared affinity purification step.

Like other methods of labelling that rely on metabolic incorporation of stable isotopes, SILAC can only be used with live cells. In dynamic studies of protein abundance in live cells (Pratt *et al*., 2002), SILAC has obvious advantages over chemical methods. Clearly the two approaches (metabolic incorporation and postharvest derivatisation) are complementary, each with their accompanying strengths and limitations.

Stable isotopes for quantitative measurements in proteomics are becoming increasingly important, as MS has grown to become a cornerstone technology in this field. The sensitivity and high mass accuracy of mass spectrometric readouts will likely mean that these tools will become indispensable in the life science field for years to come.

II. MATERIALS AND INSTRUMENTATION

Dialysed foetal bovine serum (FBS) (Cat. No. 12480-026), L-glutamine (Cat. No. 25030-024), penicillin/streptomycin (Cat. No. 15070-063), custom-synthesised media—Dulbecco's modified Eagle medium (like Cat. No. 21969 but without amino acids) and RPMI 1640 (like Cat. No. 61870 but without amino acids) are from Invitrogen. MEM Eagle's deficient with Earle's salts and L-glutamine, without L-leucine, L-lysine, L-methionine (Cat No. M7270), L-arginine (Cat. No. A-6969), L-leucine (Cat No. L-8912), L-lysine (Cat. No. L-9037), and all remaining unlabelled L-amino acids were from Sigma. L-$^{13}C_6$-Arginine (Cat. No. CLM-2265) and L-$^{13}C_6$-lysine (CLM-2247) are from Cambridge Isotope Labs. Leucine-5,5,5-d3 (Cat. No. 48,682-5) is from Sigma-Isotec. All water is "Milli-Q" quality distilled, deionised water.

Sequencing-grade porcine trypsin (Cat. No. V511C) is from Promega. Dithiothreitol (DTT, Cat. No. D-9163) and iodoacetamide (Cat No. I-1149) are from Sigma. The HPLC system used in LC-MS analyses is the Agilent 1100. The hybrid quadrupole time-of-flight mass spectrometer is supplied by MDS-SCIEX-Applied Biosystems. The search engine for protein and peptide identification from LC-MS data is the Mascot search program from Matrix Science.

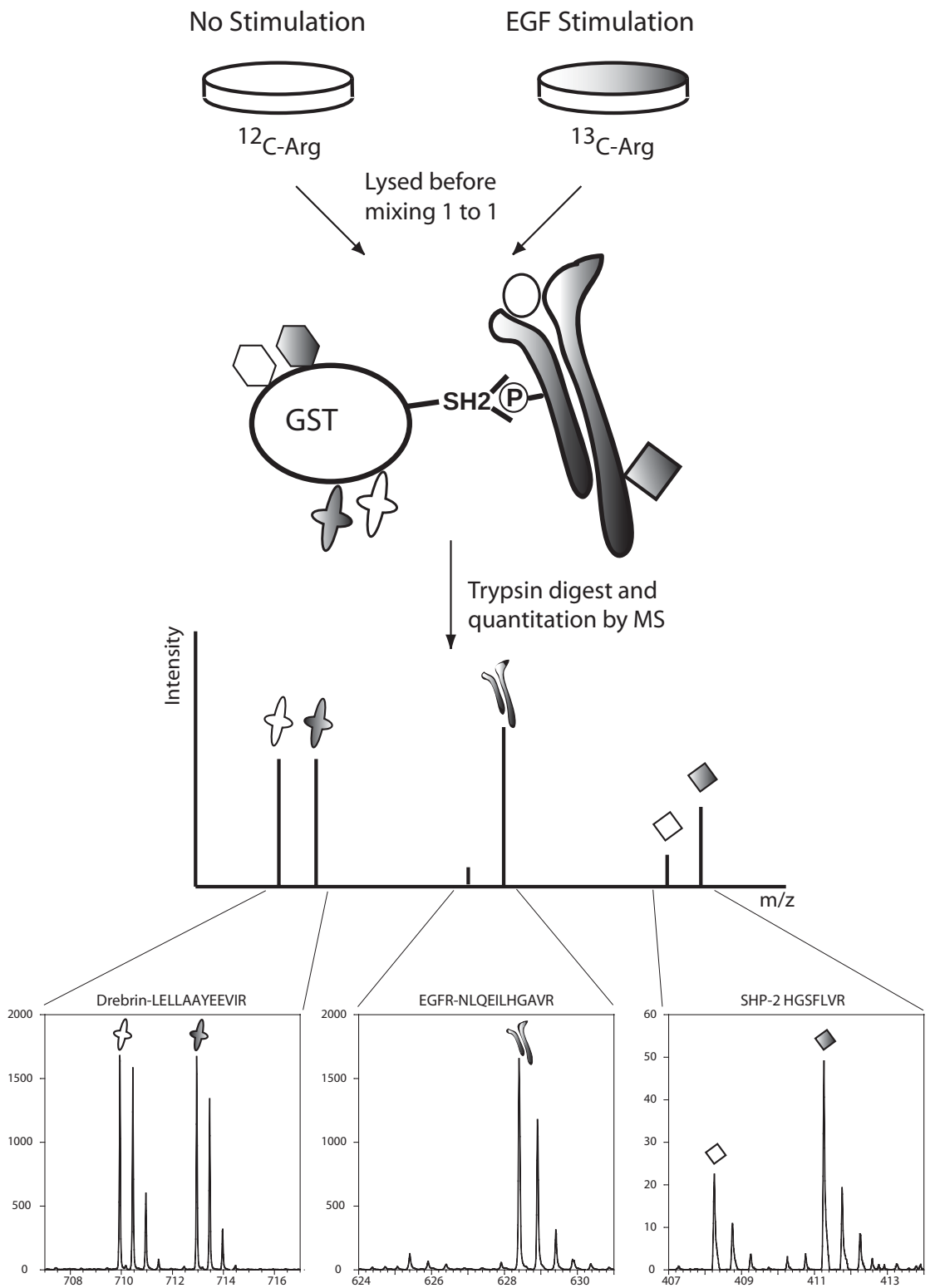

FIGURE 2 SILAC discriminates between true interaction partners in affinity purifications—posttranslational modification-dependent enrichment of epidermal growth factor receptor (EGFR) and associated proteins by binding to GST-SH2(Grb2) upon EGF stimulation. Two cell populations are differentially labelled with ^{13}C-Arg-SILAC. After treatment of "heavy" cells with EGF, lysates from both cell populations are mixed 1 to 1 and incubated with GST-SH2(Grb2). Proteins that interact specifically with the bait in conjunction with EGF stimulation will exhibit a large differential ratio in their peptide ratios. In contrast, nonspecific interactions with GST beads will bind equally from both cell populations with ratios similar to the original mixing ratio. Drebrin, an actin-binding protein, shows up with a peptide ratio of 1 (left spectrum), indicating that it was not pulled down by specific interaction with the bait. Quantitation of EGFR (middle spectrum) and Shp-2 (right spectrum) peptides gives enrichment ratios of >10 and 2.5, respectively, strongly indicative that they were affinity purified by the bait in response to EGF treatment.

III. PROCEDURES

A. Labelling Media Preparation

Cell culture media can be prepared exactly according to the experimenter's specifications to suit any particular cell type (refer to Volume 1 for cell culture techniques). The only requirement is that the labelling AA of choice is substituted with an isotopically "heavy" form to distinguish it from unlabeled, "light" media. We have applied SILAC extensively in a variety of cell types in human and rodent systems and with an assortment of stable isotope nuclei-containing amino acids and found that cell growth, nutrient use, and general morphology are similar to cells grown in standard cell culture media.

Media preparations depleted in certain amino acids are available in powdered form. We have previously used MEM with Earle's salts deficient in lysine, methionine, and leucine (powdered media). Presently, we obtain standard media formulations (DMEM and RPMI) deficient in specific amino acids as custom-synthesised products from Invitrogen. A primary concern may be the availability of certain types of dialysed serum (horse, calf), even though most cell culture media companies routinely supply dialysed FBS. A limitation of the use of dialysed serum is the potential loss of low molecular mass (below 10 kDa) components, which may be important for cell growth, through the dialysis process but the importance of using dialysed serum cannot be overstated. It is absolutely necessary to avoid the contribution of unlabelled AAs in labelling media and is critical for accurate quantitation (Ong *et al*., 2002).

The choice of a labelling amino acids for use in SILAC is likewise important. Common amino acids such as leucine (70% of all tryptic peptides contains at least one leucine residue—human IPI database, EBI) are preferable, generating several quantitatable peptides per protein. Alternatively, an enzymatic digest with trypsin for mass spectrometric analysis produces peptides with lysine or arginine at the C-terminal of the peptide. Labelling with arginine or lysine therefore results in incorporation of a single labelled residue in half of the tryptic peptides. If both AAs are used in SILAC, essentially all tryptic peptides would be labelled and quantitatable—a critical advantage in the quantitation of posttranslational modifications.

Essential amino acids are an obvious first choice in SILAC experiments. However, not all cell lines are capable of *de novo* synthesis of nonessential amino acids such as arginine and the empirical evaluation of a particular amino acid may well be worthwhile.

The use of $^{13}C_6$-arginine (where all ^{12}C atoms are substituted with ^{13}C) in SILAC is particularly desirable because of the suitable mass differential encoded, as well as the coelution of peptide pairs (Zhang and Regnier, 2002)(see later). ^{13}C-containing amino acids cost more in comparison to deuterated amino acids. By testing cell lines with growth media containing less arginine or lysine, we find that significantly reducing the amount of these amino acids does not adversely affect the growth of cells. Because both control and experimental cell populations are grown on identical media compositions (other than the form of the labelling AA), the reduction of a particular amino acid concentration does not compromise the validity of the experiment. However, it is important to test each separate cell line for the nutritional requirements for a particular amino acid. For example, a cell line may begin to synthesize arginine *de novo* when the arginine concentration is reduced by a third whilst others (e.g., HeLa) only begin to do so at one-tenth the normal arginine concentration (DMEM media). Reducing the levels of labelled amino acids may be cost effective and, in some cases (see later), even necessary.

Separately, we find that arginine is metabolically converted to proline in certain cell lines when supplied at concentrations described in standard media formulations. This observation was made as peptides containing [^{13}C]-proline were detected in MS analyses in the samples from human adenocarcinoma (HeLa) cells but not in a mouse fibroblast cell line (NIH 3T3). This proline conversion was undetectable when one-fifth of the original arginine concentration was used with HeLa cells.

As an example, this article describes the preparation of DMEM (a common media preparation for many commonly used cell types) for use with SILAC and arginine labelling (Ong *et al*., 2003), but we reiterate that the general approach is directly applicable to one's custom media preparations (Ong *et al*., 2004). An additional resource for SILAC information is available on our laboratory's Web page at http://www.cebi.sdu.dk/silac.html.

Solutions

1. *Base media preparation*: The formulation of labelling media should be prepared according to the needs of the cell lines used. Labelling media should only be distinct in the form of labelling amino acid used. A base media should be prepared in the same manner right up to the final addition of normal or labelling amino acid. The custom media formulations we purchase only require the addition of the labelling amino acid, dialysed serum (10% FBS), penicillin (50 units/ml), streptomycin (50 µg/ml), and glutamine (2 m*M* final) before use.

2. *Preparation of amino acid stock solutions*: Concentrated stock solutions of amino acids are dissolved in phosphate-buffered saline and filter sterilized with a 0.22-µm filter. These stocks should be prepared at as high a concentration as possible to minimise the dilution of other media components, e.g., arginine and lysine are prepared as 1000× (84 and 146 mg/ml, respectively) stocks. With labelled amino acids, it may be necessary to prepare unfiltered stock solutions and to filter media only after addition of the labelled amino acid in order to avoid losses due to filtration.

3. *Dialysed serum*: We use dialysed serum obtained from a commercial source. It is also possible to dialyse existing serum stocks in order to employ lower molecular weight cutoff dialysis filters and/or to reduce costs but it can be difficult to maintain consistency and to avoid contamination.

Steps

1. Work in a sterile environment. To two separate lots of base media, add the appropriate amount of arginine (either normal L-arginine to give "normal" media or L-$^{13}C_6$-arginine to give "labelling" media) to make up a full complement of amino acids, according to the manufacturer's specifications. Filter media through a 0.22-µm filter if unfiltered amino acid stocks are used.
2. Add antibiotics and glutamine as required along with 10% (v/v) dialysed serum to media containing the full complement of amino acids. Media are now ready for use and can be stored at 4°C like standard cell culture media.

B. Incorporation of Labelled AA in Growing Cells

Cells growing in normal cell culture media (in our example, murine C2C12 myoblasts) are passaged into dishes containing either normal or labelling media. C2C12 cells are allowed to undergo at least five cell doublings in SILAC media to ensure full incorporation of the labelled amino acid (Fig. 3). After five cell doublings, only a minimal amount of the original unlabelled AA should exist in the entire protein population—a theoretical maximum of $(1/2)^5$ or 3.125% could remain. In actuality, the cells would incorporate the label much sooner through normal protein turnover and in addition to novel synthesis. Furthermore, during cultivation to obtain sufficient cell numbers for the intended experiment, continual passages will result in faster incorporation of the label (Fig. 3). When working with a new cell line or if certain experimental parameters have been changed (i.e., a different lot of dialysed serum is used), it is best to assay the state of incorporation by obtaining a protein sample for MS analysis before beginning the experiment. Ideally, small aliquots of unmixed cells from each condition should be saved from each experiment in order to check for incorporation state. MS analysis of proteins from the labelled lysates will reveal if the unlabelled amino acid is present in the protein sample. A correction factor for the protein ratios may be applied if necessary or the experiment can be repeated with cells after a longer period of adaptation.

Steps

1. From a dish of cells grown in standard cell culture media, passage cells into two separate lots, one containing the unlabelled "light" SILAC media and the other with labelled "heavy" SILAC media.
2. Grow cells in respective labelling media for a minimum of five cell doublings. If working with immortalised cells, passage the cells to deplete the cell populations of normal amino acid and to increase rate of incorporation of label.
3. Perform differential treatment of cell populations, i.e., differentiation protocol, and drug treatment protocol, and growth factor treatment.

C. Cell Harvesting and Protein Purification

Steps (Assuming SILAC-Labelled Cells Have Been Treated Differentially)

1. Harvest cells from the tissue culture dish as in normal protocols. Save a small aliquot of unmixed cell populations to check levels of incorporation of the labelled AA if necessary.
2. Mix the two cell populations in a specific ratio (e.g., 1 to 1). This should be based on cell number (measured with a haemocytometer or Coulter counter) or protein concentration (determined by the Bradford method or the equivalent). In some instances and with sufficient sample, a combination of several experiments with different mixing ratios may be advantageous to expand the dynamic range of quantitation.
3. Optional protein purification steps may be included at this point. Examples include subcellular fractionation, gel filtration, immunoprecipitations, and one- or two-dimensional gel electrophoresis.
4. Digest proteins with a protease with high cleavage specificity, e.g., trypsin. With ^{13}C-Arg SILAC,

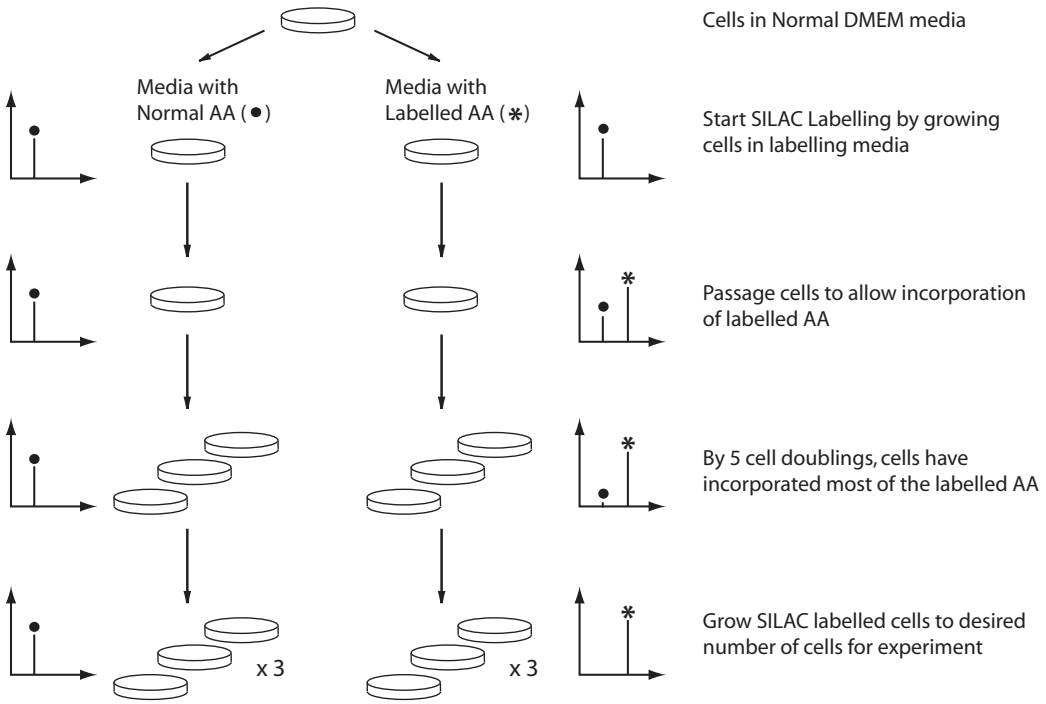

FIGURE 3 SILAC cell labelling and incorporation of labelled amino acid with continual passage of cells. Cells in standard DMEM supplemented with normal FBS, antibiotics, and glutamine are passaged into two separate dishes containing either isotopically "light" or "heavy" media. X–Y plots illustrate the presence of "light" and "heavy" peak clusters for a quantitatable peptide pair. The filled dot (•) indicates the peptide containing a normal amino acid, whilst asterisks (*) mark the peptide bearing the labelled, isotopically heavy amino acid. Cells grown in "heavy" media incorporate the labelled amino acid rapidly, as seen by the presence of the characteristic peptide pair even after the first passage. The intensity of the normal amino acid-containing peptide diminishes over time and, after sufficient cell doublings and passages, only the fully labelled peptide is detectable.

approximately half of the tryptic peptides contain arginine as the C-terminal amino acid and are quantitatable. Analyse samples with MS.

D. Analysis and Quantitation of SILAC Samples by Mass Spectrometry

A main benefit of SILAC is the option to mix cells prior to any further treatment of the sample. It is therefore possible to perform a subcellular fractionation to obtain organelles such as the nuclei without having to worry about introducing quantitative errors by way of differential treatment of samples. The downstream processing of protein samples for mass spectrometric analyses are similarly straightforward. Reduction, alkylation, and enzymatic digestion of protein samples (as described in Shevchenko *et al*., 1996) (see article by Foster and Mann) are performed on the same sample. Biases that may arise through labelling efficiency and enzymatic cleavage are thus avoided.

Mass spectrometric analyses can be performed with any of the standard MS instruments, but best results are obtained with a high mass accuracy, high-resolution instrument to resolve the natural isotope clusters of peptides. In our laboratory, we use the combination of nano-flow capillary liquid chromatography for the separation of complex peptide mixtures with subsequent detection and identification by a hybrid quadrupole time-of-flight mass spectrometer (QSTAR PULSAR—ABI).

In a typical LC-MS experiment, peptides eluting from the reversed-phase column are ionised and electrosprayed directly into the mass spectrometer. The mass spectrometer first obtains a survey MS scan where the entire mass range is analysed. From the survey scan, suitable peptides (of charge state $z = 2$, 3, or 4) can be selected for fragmentation in the collision cell in the MS/MS mode. The fragmentation of peptides in MS/MS spectra produces characteristic fragments, which give sequence-specific information for subsequent protein identification (Aebersold and Goodlett, 2001; Mann *et al*., 2001). This acquisition cycle, comprising of a survey scan followed by several MS/MS scans, is repeated throughout the LC-MS run. Ion intensities of monoisotopic peaks from each survey scan MS are used to quantitate peptide pairs. The ratios obtained from peptides used to identify a particular protein can then be averaged to give the relative ratio of protein abundance. Different laboratories approach MS analyses in subtly different ways depending on available instrumentation; we present here some guiding principles for quantitative analyses that should be applicable to anyone working in this field.

Guidelines

1. In quantitative LC-MS, a balance has to be struck between the goal of peptide identification (MS/MS sequencing events) and accurate quantitation (MS survey scans across eluting peaks). If the instrument is configured to perform a MS survey scan (taking 1 s) followed by four MS/MS spectra (each 1.5 s), the machine spends only one-seventh of the total run time acquiring the MS spectrum from which peptide ratios are acquired. Therefore, it is important that sufficient data points are collected (at least nine points for a Gaussian curve) to accurately plot the ion intensities across the eluting peptide peak.

2. In all cases where quantitation is performed, one should check that no unrelated peak clusters overlap the peptides in question. This is especially important where adequate protein/peptide separation steps do not precede MS analyses. Quantitation should be based on distinct peptide signals, and best results are obtained from peptides with a minimum signal-to-noise (S/N) ratio of 10.

3. The selection of a suitable amino acid and the mass shift that will be incorporated by the stable isotopes is important. A common amino acid such as leucine is present in about 70% of unique tryptic peptides in the human proteome and is thus a good choice as a labelling amino acid. We also favour arginine and lysine, as enzymatic cleavage with trypsin generates peptides with these amino acids at C termini. The mass shift generated from the labelling should ideally be large enough (4 Da or greater) to avoid overlapping of isotope clusters (Fig. 4A). If peptide isotope clusters overlap, calculation of the isotopic envelope of each peptide based on sequence composition can still provide accurate quantitation data.

4. Care should be taken when quantitating different proteins that have regions of sequence identity (a protein family for, e.g., the histones), as some peptides can be shared across several proteins. Quantitation based on a shared peptide may not accurately reflect the quantitation of any single protein, but might instead be an average across multiple proteins. Quantitation is best based on peptides unique to the protein of interest.

5. Many labelling reagents make use of deuterium (^{2}H) instead of ^{15}N and ^{13}C. There is a tendency for peptides labelled with deuterated reagents to elute earlier than the corresponding unlabelled peptide in reversed-phase chromatography due to isotope effects. As peptide quantitation is obtained from the MS survey scan at various time points across the elution of a peptide (Fig. 4B, left), accurate determination of the peptide ratio is possible at each sampling point of the MS. More data points are required with partially resolved peaks in order to accurately plot each eluting peptide peak (Fig. 4B, right) and quantitation should be based on peak area of the extracted ion chromatogram or a sampling of MS spectra over the retention times of the peptide pair. Although generally more expensive, using ^{13}C-substituted amino acids in SILAC helps reduce errors in quantitation caused by separation of the peptide pair. It also simplifies the process of quantitation, as the peptide ratio can be obtained from each MS scan directly. Having said that, it is very straightforward to obtain good quantitation data from deuterated reagents by simply being aware of the potential pitfalls.

6. Adequate ion statistics for quantitation peaks. Regardless of the type of mass spectrometer used to acquire quantitative data, it is imperative that mass spectra acquired should comprise enough data collection events in order to accurately describe the peptide peaks. For peptide identification, this requirement may not be as critical, but it should be apparent that accurate quantitation is only achievable where sufficient data points can be averaged. In cases where highly differential peptide ratios are observed, one of the peaks may not be detectable above noise. Here, it may be sufficient to assign the smaller peak at the level of noise and describe a lower limit of the peptide ratio rather than to give some arbitrary (and most likely incorrect) value to the smaller peak.

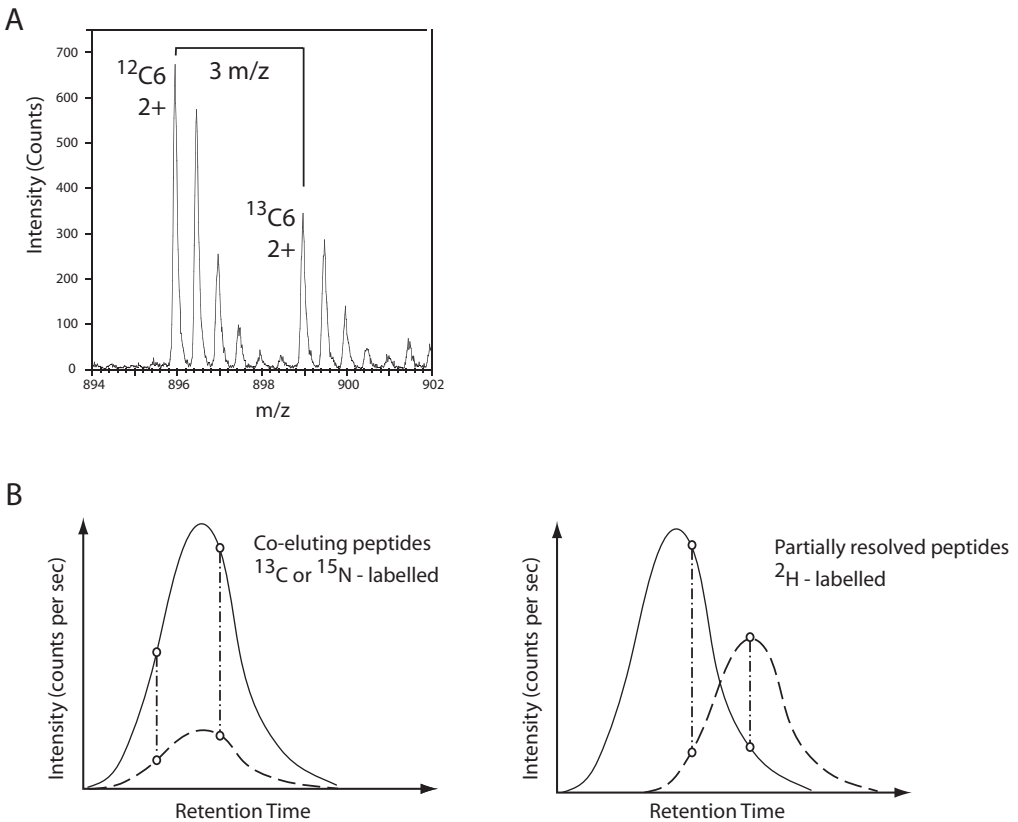

FIGURE 4 Peptide quantitation in MS. (A) A doubly charged SILAC-$^{13}C_6$-arginine-labelled peptide pair in the MS survey scan (acquisition time of 1 s) with 3 *m/z* separation between the "light" and the "heavy" peak. There is clear separation between peak clusters and unrelated peaks are absent. If peptides elute from the reversed-phase column over a period of 40 s, about 7 to 15 (depends on MS acquisition parameters) of these MS spectra may be acquired by the mass spectrometer. Each of these spectra give peak ratios, which are averaged to give a peptide ratio and standard deviation. (B) An example of coeluting peptides in an LC-MS run (left) and noncoeluting peptides (right). The peaks are extracted ion chromatograms (XICs) that monitor a particular mass range over time (see text for discussion on the adequate MS acquisition events to accurately describe a peak). Vertical dotted lines are examples of two individual MS acquisition events across the eluting peak. From the coeluting pair (left), it is apparent that similar ratios will be obtained regardless of the point when the peak is sampled. However, the partially resolved peaks (right) show inverse peptide ratios at the two time points indicated.

References

Aebersold, R., and Goodlett, D. R. (2001). Mass spectrometry in proteomics. *Chem Rev.* **101**(2), 269–295.

Aebersold, R., and Mann, M. (2003). Mass spectrometry-based proteomics. *Nature* **422**(6928). 198–207.

Blagoev, B., Kratchmarova, I., Ong, S. E., Nielsen, M., Foster, L. J., and Mann, M. (2003). A proteomics strategy to elucidate functional protein-protein interactions applied to EGF signaling. *Nature Biotechnol.* **21**(3), 315–318.

Blagoev, B., Ong, S.E., Kratchmarova, I., and Mann, M. (2004). Temporal analysis of phosphotyrosine-dependent signaling networks by quantitative proteomics. *Nat Biotechnol.* **22**(9), 1139–45.

Conrads, T. P., Alving, K., Veenstra, T. D., Belov, M. E., Anderson, G. A., Anderson, D. J., Lipton, M. S., Pasa-Tolic, L., Udseth, H. R., Chrisler, W. B., Thrall, B. D., and Smith, R. D. (2001). Quantitative analysis of bacterial and mammalian proteomes using a combination of cysteine affinity tags and 15N-metabolic labeling. *Anal. Chem.* **73**(9), 2132–2139.

Gavin, A. C., Bosche, M., Krause, R., Grandi, P., Marzioch, M., Bauer, A., Schultz, J., Rick, J. M., Michon, A. M., Cruciat, C. M., Remor, M., Hofert, C., Schelder, M., Brajenovic, M., Ruffner, H., Merino, A., Klein, K., Hudak, M., Dickson, D., Rudi, T., Gnau, V., Bauch, A., Bastuck, S., Huhse, B., Leutwein, C., Heurtier, M. A., Copley, R. R., Edelmann, A., Querfurth, E., Rybin, V., Drewes, G., Raida, M., Bouwmeester, T., Bork, P., Seraphin, B., Kuster, B., Neubauer, G., and Superti-Furga, G. (2002). Functional organization of the yeast proteome by systematic analysis of protein complexes. *Nature* **415**(6868), 141–147.

Goodlett, D. R., Keller, A., Watts, J. D., Newitt, R., Yi, E. C., Purvine, S., Eng, J. K., von Haller, P., Aebersold, R., and Kolker, E. (2001). Differential stable isotope labeling of peptides for quantitation and de novo sequence derivation. *Rapid Commun. Mass Spectrom.* **15**(14), 1214–1221.

Gygi, S. P., Rist, B., Gerber, S. A., Turecek, F., Gelb, M. H., and Aebersold, R. (1999). Quantitative analysis of complex protein mixtures using isotope-coded affinity tags. *Nature Biotechnol.* **17**(10), 994–999.

Ho, Y., Gruhler, A., Heilbut, A., Bader, G. D., Moore, L., Adams, S. L., Millar, A., Taylor, P., Bennett, K., Boutilier, K., Yang, L., Wolting, C., Donaldson, I., Schandorff, S., Shewnarane, J., Vo, M., Taggart, J., Goudreault, M., Muskat, B., Alfarano, C., Dewar, D., Lin, Z., Michalickova, K., Willems, A. R., Sassi, H., Nielsen, P. A., Rasmussen, K. J., Andersen, J. R., Johansen, L. E., Hansen, L. H., Jespersen, H., Podtelejnikov, A., Nielsen, E., Crawford, J., Poulsen, V., Sorensen, B. D., Matthiesen, J., Hendrickson, R. C., Gleeson, F., Pawson, T., Moran, M. F., Durocher, D., Mann, M., Hogue, C. W., Figeys, D., and Tyers, M. (2002). Systematic identification of protein complexes in *Saccharomyces cerevisiae* by mass spectrometry. *Nature* **415**(6868), 180–183.

Jiang, H., and English, A. M. (2002). Quantitative analysis of the yeast proteome by incorporation of isotopically labeled leucine. *J. Proteome Res.* **1**(4), 345–350.

Langen, H., Takacs, B., Evers, S., Berndt, P., Lahm, H. W., Wipf, B., Gray, C., and Fountoulakis, M. (2000). Two-dimensional map of the proteome of *Haemophilus influenzae*. *Electrophoresis 21*(2), 411–429.

Mann, M., Hendrickson, R. C., and Pandey, A. (2001). Analysis of proteins and proteomes by mass spectrometry. *Annu. Rev. Biochem.* **70**, 437–473.

Oda, Y., Huang, K., Cross, F. R., Cowburn, D., and Chait, B. T. (1999). Accurate quantitation of protein expression and site-specific phosphorylation. *Proc. Natl. Acad. Sci. USA* **96**(12), 6591–6596.

Olsen, J. V., Andersen, J. R., Nielsen, P. A., Nielsen, M. L., Figeys, D., Mann, M., and Wisniewski, J. R. (2004). HysTag–a novel proteomic quantification tool applied to differential display analysis of membrane proteins from distinct areas of mouse brain. *Mol Cell Proteomics.* **3**(1), 82–92.

Ong, S. E., Mittler, G., and Mann, M. (2004). Identifying and quantifying in vivo methylation sites by heavy methyl SILAC. *Nat. Methods.* **1**, 119–126.

Ong, S. E., Blagoev, B., Kratchmarova, I., Kristensen, D. B., Steen, H., Pandey, A., and Mann, M. (2002). Stable isotope labeling by amino acids in cell culture, SILAC, as a simple and accurate approach to expression proteomics. *Mol. Cell Proteomics* **1**(5), 376–386.

Ong, S. E., Kratchmarova, I., and Mann, M. (2003). Properties of 13C-substituted arginine in stable isotope labeling by amino acids in cell culture (SILAC). *J. Proteome Res.* **2**(2), 173–181.

Pratt, J. M., Petty, J., Riba-Garcia, I., Robertson, D. H., Gaskell, S. J., Oliver, S. G., and Beynon, R. J. (2002). Dynamics of protein turnover, a missing dimension in proteomics. *Mol. Cell Proteomics* **1**(8), 579–591.

Regnier, F. E., Riggs, L., Zhang, R., Xiong, L., Liu, P., Chakraborty, A., Seeley, E., Sioma, C., and Thompson, R. A. (2002). Comparative proteomics based on stable isotope labeling and affinity selection. *J. Mass Spectrom.* **37**(2), 133–145.

Shevchenko, A., Wilm, M., Vorm, O., and Mann, M. (1996). Mass spectrometric sequencing of proteins silver-stained polyacrylamide gels. *Anal. Chem.* **68**(5), 850–858.

Yates, J. R., 3rd (2000). Mass spectrometry: From genomics to proteomics. *Trends Genet.* **16**(1), 5–8.

Zhang, R., and Regnier, F. E. (2002). Minimizing resolution of isotopically coded peptides in comparative proteomics. *J. Proteome Res.* **1**(2), 139–147.

Zhu, H., Pan, S., Gu, S., Bradbury, E. M., and Chen, X. (2002). Amino acid residue specific stable isotope labeling for quantitative proteomics. *Rapid Commun Mass Spectrom.* **16**(22), 2115–2123.

CHAPTER

55

Site-Specific, Stable Isotope Labeling of Cysteinyl Peptides in Complex Peptide Mixtures

Huilin Zhou, Rosemary Boyle, and Ruedi Aebersold

I. INTRODUCTION

Relative quantification of proteins from different samples by mass spectrometry (MS) is based on the stable isotope dilution approach (Gygi *et al*., 1999; Han *et al*., 2001; Smolka *et al*., 2002; Zhou *et al*., 2002). Proteins or peptides are labeled with chemically identical tags that differ in mass due to a stable isotope content. In a typical experiment, proteins (or peptides derived from proteolytic digestion of proteins) from one sample are labeled with an isotopically heavy mass tag, whereas the light isotope tag is used to label the sample to be compared. The isotopically labeled peptides are combined, purified or separated into fractions, and analyzed by mass spectrometry, which measures the mass and ion abundance of peptides. Because isotopically heavy and light forms of a peptide of the same amino acid sequence are chemically identical, they generate responses with identical sensitivity from the mass spectrometer and are readily distinguished based on their mass differences. Therefore the measured ion abundance ratio between heavy- and light-labeled peptides by the mass spectrometer is the actual abundance ratio of this peptide from two different samples. In this way, the relative abundance of peptides, and thus proteins, in two different samples can be determined accurately. Quantitative and comparative analysis of protein abundance from different samples has many applications, including large-scale protein expression profiling from different cell states to identify proteins that are unique in one cell condition, not the other, or comparative analysis of protein complexes derived from different cell states to reveal their compositional differences. In this case, conventional protein purification techniques would be used to enrich the protein complexes of interest. Many cell biological processes are carried out by large, multisubunits protein complexes. It would be an essential step to identify their protein components and dynamic changes in protein compositions under a different cell context. Comparative protein analysis by mass spectrometry would be a powerful tool toward this goal.

This article describes a method for site-specific stable isotope labeling of cysteinyl peptides in complex peptide mixtures via a solid-phase capture and release process, and the concomitant isolation of the labeled peptides (Zhou *et al*., 2002). The recovered, tagged peptides were analyzed by microcapillary liquid chromatography and tandem mass spectrometry (μLC-MS/MS) to determine their sequences and relative abundance.

II. MATERIALS AND INSTRUMENTATION

1. Amino propyl glass beads, 200–400 mesh, pore size 170 Å (Sigma, St. Louis, MO., G4518)
2. Organic solvents: anhydrous dimethylformamide (DMF, Aldrich, 22705-6) and dichloromethane (DCM, Aldrich, 220997-1L)
3. 1-Hydroxybenzotriazole (HOBt) (Nova Biochem, Laufelfingen, Switzerland, 01-62-0008)

Copyright 2006, Elsevier Science (USA).
All rights reserved.

4. Fmoc-protected amino acids: Fmoc-aminoethyl photolinker (Nova Biochem, 01-60-0042) and Fmoc-γ-amino butyric acid (Fmoc-GABA) (Nova Biochem, 04-12-1088)
5. Diisopropyl carbodiimide (DIC) (Aldrich, D12540-7)
6. Acetic anhydride (Aldrich, 24284-5)
7. Pyridine (Aldrich, 36057-0)
8. Piperidine (Aldrich, 104094)
9. D6-γ-aminobutyric acid (d6-GABA) (Isotec, Inc., 82-222-02-7)
10. Fmoc-*N*-hydroxysuccinimide (Fmoc-Osu) (Nova Biochem, 01-63-0001)
11. Diisopropyl ethyl amine (DIPEA) (Aldrich, D12580-6)
12. Iodoacetic anhydride (Aldrich, 28426-2)
13. Micro Bio-Spin columns (Bio-Rad Labs, Hercules, CA, 732-6204)
14. Blak-Ray long-wave UV lamp (100 W, VWR Scientific, Inc., 36595-020)
15. Tri(caboxyl ethyl)phosphine (TCEP) (Pierce, 20490)
16. Trypsin, sequencing grade (Promega, V5111)

Stable isotope-labeled peptides can be analyzed by all types of mass spectrometry instrumentation, including electrospray ionization (ESI) and matrix-assisted laser desorption ionization (MALDI)-based techniques. We typically use liquid chromatography (LC) and ESI-tandem mass spectrometry to analyze complex peptide mixtures. A tandem mass spectrometer allows identification of peptide sequences as well as their relative ion abundance of the isotopically related peptides in the same experiment. The Finnigan LCQ ion-trap instrument is used in combination with the Hewlett-Packard HP1100 series HPLC system.

III. PROCEDURES

A. Synthesis of Solid-Phase Isotope-Labeling Reagents

A schematic diagram of the chemical structure of the solid-phase reagent is shown in Fig. 1. Synthesis of solid-phase reagents is based on a method that has been published previously (Holmes and Jones, 1995). For synthesis of beads with a heavy isotope, Fmoc-d6-GABA was prepared from d6-GABA and Fmoc-OSu, as described in Section III,B because the Fmoc-protected, deuterated amino acid is not available commercially. The methods described involve standard peptide chemistry, making it possible to use other amino acids with isotopically heavy or light forms.

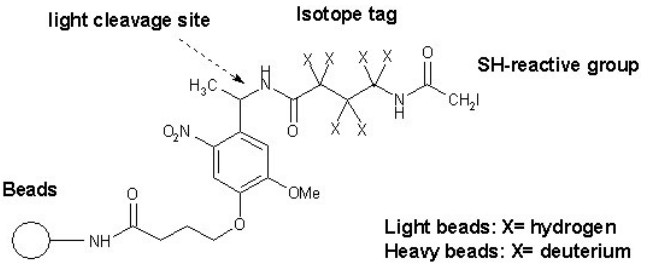

FIGURE 1 A schematic diagram of the solid-phase isotope-tagging reagent showing the chemical structure. The aminopropyl glass bead is first coated by a photocleavable linker molecule. Peripheral to the photocleavable linker, an amino acid, γ-aminobutyric acid, is used as an isotope-encoding mass tag that can be either nondeuterated (d0) or deuterated (d6). Following the isotope mass tag, an iodoacetyl group is used as a SH-reactive group to capture cysteinyl peptides. Following capture, photocleaving will lead to the recovery of cysteinyl peptides with the isotope tags attached to their cysteine residues.

Steps

1. Load 100 mg of aminopropyl glass beads in an empty Bio-Rad column or other column of suitable size. Wash beads once with 1 column volume of anhydrous DMF.
2. Form amino acid ester: Dissolve 120 µmol each of HoBt and Fmoc-aminoethyl photolinker in 0.8 ml of dry DMF completely. Add to this solution 120 µmol of DIC for 30 min. (Keep light-sensitive reagents from direct room light.)
3. Add the amino acid ester to the beads, mixing the beads by pipetting a few strokes. Incubate for 90 min.
4. Wash beads with 3 column volumes of DMF and 2 column volumes of dry dichloromethane. Always remove excess solvent between washes by applying a little pressure (squeeze a Pasteur pipettor bulb or apply house vacuum).
5. Block: Prepare a 1-ml mixture of 20% acetic anhydride, 30% pyridine, and 50% dichloromethane. Add this mixture to the beads for 30 min to block residual free amines on the beads.
6. Wash beads with 2 column volumes of dichloromethane and 3 column volumes of DMF. Remove excess DMF.
7. Deprotect: Prepare 3 ml of 20% (v/v) piperidine/DMF solution. Add 1 ml to the beads and incubate for 30 min. Collect all of the 1-ml flow through containing Fmoc released from the photolinker. Calculate the capacity of the beads by measuring the absorbance of the released Fmoc. Use 20% piperidine/DMF solution as a blank solution and measure absorbance at 290 nm (A_{290}) of the 1/100 dilution (by 20% piperdine/DMF) of the flow through. The A_{290} should be between

0.6 and 0.8. Calculate capacity according to the formula: [A_{290} × dilution factor × flow through volume (ml)]/[1.65 × weight of beads (mg)] = capacity (mmol/g).

8. Wash beads with 5 column volumes of dry DMF.

9. Repeat steps 2 to 8 with Fmoc-d0-GABA or its heavy form. The calculated capacity for GABA should be close to that for the photolinker.

10. Attach iodoacetyl group to the beads (Zhou *et al.*, 2001): Dissolve 120 µmol of iodoacetic anhydride in 0.8 ml dry DMF and add to the beads. Immediately add 132 µmol of diisopropyl ethyl amine (DIPEA) to the beads and mix well by pipetting a few strokes. Let it incubate for 90 min.

11. Wash the beads with 5 column volumes of DMF and excess methanol; dry the beads in a Speed-Vac (covered in foil). The beads can be stored in the dark at room temperature or in the refrigerator indefinitely.

B. Synthesis of Fmoc-Protected Amino Acid

The following procedure permits custom synthesis of Fmoc-protected amino acid for attachment to solid phase as described previously.

Steps

1. Dissolve 600 µmol d6-GABA in 3 ml 9% sodium carbonate in water in a vial under stirring.

2. Dissolve 900 µmol Fmoc-OSu in 3 ml DMF. Add to d6-GABA solution in one proportion. Continue to stir for 30 min at room temperature.

3. Divide the sample into six 1.5-ml Eppendorf tubes and dry out DMF under reduced pressure in a Speed-Vac.

4. Add 1 ml H_2O to dissolve the white powder as much as possible. Spin down and collect the supernatant. Repeat the water wash. Combine all of the supernatant, adding water until the final volume is 15 ml. Discard insoluble material.

5. Add 600 µl concentrated HCl to the supernatant very slowly. The solution should become cloudy immediately with foam due to carbon dioxide and precipitation of reagent. Check by pH paper that the final pH is approximately 2.

6. Extract Fmoc-d6-GABA: Add 4 ml or more ethyl acetate to the acidified aqueous solution, wait for phase separation, and collect the ethyl acetate phase that contains Fmoc-d6-GABA. Repeat this extraction procedure three times and combine the extracts.

7. Wash the ethyl acetate extract once with 3 ml 0.1% HCl in H_2O and once more with 3 ml of water. Dry the extract completely in a Speed-Vac. The dried sample can be used directly with the assumption of >90% yield.

C. Preparation of Protein Digest

For labeling with SH-specific solid-phase reagents, it is advantageous to label peptides instead of proteins because proteins may possess tertiary structures that render some cysteine residues inaccessible to the solid-phase reagent. Protein digestion can be performed with any commercially available and suitable protease. Trypsin is used most frequently. For example, proteins in 100 µl 0.2 *M* Tris, pH, 8.0, can be digested by 1/50 (w/w) trypsin at 37°C overnight.

D. Capture and Release of Isotope-Labeled Peptides

Keep light-sensitive beads out of direct light as much as possible. Brief exposure to room light should not significantly affect the performance of the reagents.

1. Reduce protein digest with 5 m*M* TCEP for 30 min at room temperature. Because TCEP is quite acidic, it is essential that there is sufficient buffering capacity; 200 m*M* Tris, pH, 8.0, in the buffer should be sufficient to maintain the pH. TCEP is usually prepared as a 250 m*M* solution in water and kept at –20°C prior to use. We found that the TCEP stock solution is stable for many months at –20°C.

2. Weigh 5 mg each of isotopically light and heavy beads into tubes that are covered with foil to protect against light.

3. Add reduced protein digests to the beads (or the beads to the protein digest) and shake immediately for 15 min on a vortex mixer at a speed such that the beads should be suspended in the solution, not settled in the bottom of the tube. Efficient mixing of the beads with peptides is important for binding to occur.

4. After 15 min of binding, quench the labeling reaction with 2 µl β-mercaptoethanol for 1–2 min. The solid-phase isotope-labeling reagent should have excess capacity compared to the cysteinyl peptides. The addition of β-mercaptoethanol will block any remaining iodoacetyl group on the beads and prevent any possible side reactions to occur.

5. Combine the beads by loading onto a foil-wrapped Bio-Spin column, rinsing with water and methanol to transfer all beads. (Retain the flow through of each labeling reaction separately for analysis of noncysteine-containing peptides if so desired.) Wash with

   a. 2 × 1 ml 2 *M* NaCl
   b. 2 × 1 ml 0.1% TFA

c. 2 × 1 ml 80% ACN/0.1% TFA
d. 2 × 1 ml MeOH
e. 2 × 1 ml 28% NH_4OH : MeOH (1 : 9 v/v)
f. 2 × 1 ml MeOH
g. 2 × 1 ml water

6. Seal bottom of Bio-Spin column with a cap. Suspend beads in 200 µl 20 m*M* Tris/1 m*M* EDTA, pH 8, and 4 µl β-mercaptoethanol with a magnetic stirrer on a stir plate.

7. Expose beads to UV light for 2 h and then collect the supernatant through the Bio-Spin column.

8. Wash the remaining beads with 5 × 100 µl 80% ACN/0.4% acetic acid, combining with the previous supernatant.

9. Reduce the sample volume in Speed-Vac to approximately 200 µl. Check that the pH is acidic.

E. Sample Cleanup and Mass Spectrometric Analysis

Although the labeled peptides appear to be highly pure, free from side reactions of the peptides themselves, we have observed side products other than peptides following photocleaving of the beads. These residual products are likely to be impurities generated during synthesis of the solid-phase reagent. Because these products interfere with MS analysis of peptide samples, it is necessary to remove them prior to MS analysis. Additionally, we have observed that these side products are not positively charged under acidic pH, whereas peptides are positively charged due to protonation of basic residues such as the N terminus, histidine, lysine, and arginine. We therefore devised a strategy using cation-exchange chromatography to remove adducts from peptides. A disposable mixed cation-exchange (MCX) cartridge can be used.

Steps

1. Load sample onto MCX column (30-mg beads).
2. Wash with 3 column volumes of 0.1% TFA in water.
3. Wash with 3 column volumes of 80% ACN/0.1% TFA in water.
4. Wash by 1 column volume of water to prevent salt formation.
5. Elute in 500 µl of elution solvent consisting of 1 volume of ammonia solution (28% NH_4OH stock) and 9 volume of methanol.
6. Dry out ammonia and methanol in a Speed-Vac and resuspend the sample in 10 µl water for MS analysis.

There are several advantages to this solid-phase approach for isotopic labeling of peptides. First, isolation of cysteine-containing peptides and stable isotope incorporation are achieved in a single step. Therefore, the solid-phase method is rather simple. Second, the covalent attachment of peptides to a solid phase allows for the use of stringent wash conditions to remove noncovalently associated molecules. Third, this procedure is unaffected by the presence of proteolytic enzymes, such as trypsin, or strong denaturants or detergents, such as urea or SDS. There is no need for additional steps for their removal prior to peptide capture by the solid-phase beads and it is easy to remove them by washing. Fourth, the standard solid-phase peptide chemistry involved in the coupling process enables the use of a range of natural or unnatural amino acids in place of the d0/d6-GABA to function as the isotopic mass tag. This allows for synthesis of beads with a range of mass tags for analysis of multiple samples (i.e., more than two) in a single experiment if desired.

F. An Example of Protein Quantitation

We show an example of protein quantitation by this approach (see Table I). Three proteins—glyceraldehyde 3-phosphate dehydrogenase from rabbit, bovine lactoalbumin, and ovalbumin from chicken—were prepared in different amounts and labeled by the solid-phase isotope-tagging reagents. Following light cleavage, the recovered peptides were analyzed by mass spectrometry, and the isotopically labeled peptides were identified and quantified as described (Gygi *et al.*, 1999; Han *et al.*, 2001; Eng *et al.*, 1994). The agreement with expected values was generally within 20% and, for any given protein, consistent ratios were observed. Additional application of this method can be found elsewhere (Zhou *et al.*, 2002).

IV. NOTES

1. The amine capacity of the aminopropyl glass beads should be measured, despite the value quoted by the manufacturer. Other derivatized beads may be used in place of the glass beads if desired, provided that they have good swelling properties under aqueous condition. Clearly, the use of the newly synthesized reagents should be tested with standard cysteinyl peptides.

2. During synthesis of the Fmoc-protected amino acid, it is important to acidify the sample very slowly and to shake well. This should alleviate foaming due to the release of carbon dioxide following the change of pH. Also, one could use more ethyl acetate than pre-

TABLE I Quantitation of Protein Mixture by Solid-Phase Isotope Tagging and MS

Gene name	Cys-containing peptides found	Observed ratio (light/heavy)	Expected ratio (light/heavy)
G3P_rabit	VPTPNVSVVDLTC*R	4.6	4.0
	IVSNASC*TTNC*LAPLAK	4.3	
LCA_bovin	DDQNPHSSNIC*NISC*DK	1.8	2.0
	FLDDDLTDDIMC*VK	1.9	
	LDQWLC*EK	2.1	
	ALC*SEK	2.0	
	C*EVFR	1.9	
Oval_chick	YPILPEYLQC*VK	1.0	1.0
	LPGFGDSIEAQC*GTSVNVHSSLR	0.9	
	ADHPFLFC*IK	1.1	

[a] Isotopically labeled cysteine residues are marked by asterisks.

scribed in order to achieve better phase separation during the extraction step.

3. For protein digestion by trypsin, proteins can be denatured by boiling for a few minutes if the protein concentration is not so high as to cause precipitation. In the current protocol, proteins are not reduced prior to digestion; however, it is possible that one could reduce proteins prior to digestion.

4. TCEP is quite acidic and the optimal pH for solid-phase capture of cysteinyl peptides is 8.0. Therefore, it is essential that there is sufficient buffering capacity, such as 200 m*M* Tris at pH 8.0. In this case, the pH of the solution would be not strongly affected by the addition of 5 m*M* TCEP.

5. It is necessary to quench the capturing reaction after 15 min by mercaptoethanol or other excess SH-containing reagent because histidine side chains or other nucleophilic functional groups could suffer potential side reactions with the iodoacetyl group on the solid-phase beads. The protocol for washing beads following the quenching reaction can be altered by individual investigators, as we found that solid-phase-captured peptides are stable to a variety of washing conditions.

6. The UV light can be filtered through a copper sulfate solution that passes light of 300 to 400 nm. Although we used a long-wave UV lamp, the cleaving reaction can be accelerated by using a more powerful mercury arc lamp according to Holmes and Jones (1995).

7. When small amounts of peptides are expected, it is particularly important to remove labeling contaminants.

8. The use of β-mercaptoethanol in the photocleaving buffer prevents methionine oxidation.

9. Although very stringent washing steps were used to remove nonspecifically associated molecules from the solid phase after capturing, they may not be entirely necessary for all applications. The readers are encouraged to test different washing conditions for their own applications.

10. Some of the materials used here were published previously (Zhou et al., 2002).

References

Eng, J., McCormack, A.L., and Yates, J.R., 3rd (1994). An approach to correlate tandem mass spectral data of peptides with amino acid sequences in a protein database. *J. Am. Soc. Mass Spectrom.* **5**, 976–989.

Gygi, S.P., *et al*. (1999). Quantitative analysis of complex protein mixtures using isotope-coded affinity tags. *Nature Biotechnol.* **17**, 994–999.

Han, D., Eng, J., Zhou, H., and Aebersold, R. (2001). Quantitative profiling of differentiation induced membrane associated proteins using isotope coded affinity tags and mass spectrometry. *Nature Biotechnol.* **19**, 946–951.

Holmes, C.P., and Jones, D.G. (1995). Reagents for combinatorial organic synthesis: Development of a new o-nitrobenzyl photolabile linker for solid phase synthesis. *J. Org. Chem.* **60**, 2318–2319.

Smolka, M., Zhou, H., and Aebersold, R. (2002). Quantitative protein profiling using two-dimensional gel electrophoresis, isotope-coded affinity tag labeling, and mass spectrometry. *Mol. Cell Proteomics* **1**, 19–29.

Zhou, H., Boyle, R., and Aebersold, R. (2002). Quantitative protein analysis by solid phase isotope tagging and mass spectrometry. *In "Protein-Protein Interactions"* (H. Fu, ed.), Humana Press, New Jersey.

Zhou, H., Ranish, J.A., Watts, J.D., and Aebersold, R. (2002). Quantitative proteome analysis by solid-phase isotope tagging and mass spectrometry. *Nature Biotechnol.* **5**, 512–515.

Zhou, H., Watts, J.D., and Aebersold, R. (2001). A systematic approach to the analysis of protein phosphorylation. *Nature Biotechnol.* **19**, 375–378.

CHAPTER

56

Protein Hydrogen Exchange Measured by Electrospray Ionization Mass Spectrometry

Thomas Lee, Andrew N. Hoofnagle, Katheryn A. Resing, and Natalie G. Ahn

I. INTRODUCTION

Hydrogen exchange-mass spectrometry (HX-MS) is a technique that measures the rate of exchange between protons on macromolecules and isotopically labeled water. It is commonly applied to the exchange of protein backbone amide hydrogens with deuterium oxide, where each exchange event leads to a mass increase of 1 Da, which can be monitored by mass spectrometry. The measurement can be used to obtain information about aspects of solution structure, protein folding, and conformational mobility (Chowdhury *et al*., 1990; Zhang and Smith, 1993; Johnson and Walsh, 1994; Resing and Ahn, 1998; Hoofnagle *et al*., 2001) and can also be used to analyze protein solvent accessibility and ligand-binding sites (Neubert *et al*., 1997; Mandell *et al*., 1998; Andersen *et al*., 2001). Both electrospray ionization (ESI) and matrix-assisted laser desorption ionization (MALDI) methods can be used for HX-MS (Chowdhury *et al*., 1990; Mandell *et al*., 1998), although each ionization method has its own advantages (discussed by Hoofnagle *et al*., 2003). This article outlines a practical protocol for hydrogen exchange measurements on proteins using ESI-MS, which provides high protein sequence coverage and low back-exchange, thus improving the sensitivity of HX-MS for monitoring changes in solvent accessibility and conformational mobility.

II. MATERIALS AND INSTRUMENTATION

Pepsin (Cat. No. P6887), succinic acid (Cat. No. S5047), sodium citrate (Cat. No. S4641), and deuterium oxide (Cat. No. 15188-2) are from Sigma-Aldrich, trifluoroacetic acid (Cat. No. 28904) is from Pierce, and HPLC grade water (Cat. No. 26830-0025) and HPLC grade acetonitrile (Cat. No. 32573-0025) are from Fisher. Capillary HPLC columns (10–15 cm × 500 µm i.d.) are constructed from fused silica tubing (320 µm i.d. for outlet, 500 µm i.d. for inlet, Cat. No. TSP320450, TSP530700, respectively, Polymicro Technologies), assembled with epoxy glue (Cat. No. 302 part A, 302 part B, Epoxy Technology), and hand packed with reversed-phase POROS 20 R1 resin (Cat. No. 1-1028-02, Applied Biosystems Inc.) as described by Resing and Ahn (1997). Modifications to the previously described HPLC system added polyetheretherketone (PEEK) loading loops for sample injection (1 ml) and solvent precooling (2 ml) from Upchurch (Cat. No. 1820, 1821) and a PEEK HPLC injector apparatus from Rheodyne (Cat. No. 9010). Hamilton syringes are from SGE (50 µl, 250 µl, 1 ml, Cat. No. 004312, 006312, 008105, respectively), sample tubes and caps are from Bio-Rad (Cat. No. 223-9391, 223-9393), and screw cap tubes are from CLP (Cat. No. 3463). A stainless steel pan and an ice bucket serving, respectively, as ice bath

Copyright 2006, Elsevier Science (USA).
All rights reserved.

and dry ice/ethanol/water bath are from Fisher Scientific (Cat. No. 13-361A, 11-676).

For data collection we obtain excellent results with a quadrupole time-of-flight (TOF) mass spectrometer (QStar Pulsar, Applied Biosystems Inc.) with standard electrospray source and AnalystQS software, interfaced with any HPLC capable of delivering a steady flow rate of 10–40 µl/min (e.g., Agilent Model 1100 capillary HPLC system or Eldex MicroPro HPLC-2g). Incubations are carried out in a circulating water bath (Cat. No. 13271-036, VWR). Useful for data reduction are software for nonlinear least squares (e.g., Datafit 7.1, Oakdale Engineering Inc.) and spreadsheet analyses (e.g., Microsoft Excel).

III. PROCEDURES

A. HX-MS Data Collection

The basic protocol involves timed incubations of protein in 90% (v/v) D_2O at neutral pH, which allows in-exchange of deuterons for protons within timescales ranging from seconds to hours. At the end of each incubation, the in-exchange reaction is quenched by rapidly lowering pH and temperature. Pepsin is added in amounts that enable rapid protein digestion (1–5 min), and the resulting peptides are separated by reversed-phase HPLC coupled to LC/MS. In order to minimize back-exchange of deuterium for water, all steps following the quench are carried out at 0°C. Applications of this protocol have been reported by Resing *et al*. (1998, 1999) and Hoofnagle *et al*. (2001).

Solutions

1. D_2O (99.9% atom D), stored at room temperature.
2. *Pepsin solution*: Dissolve lyophilized pepsin in HPLC grade water to 2 mg/ml and store in 50-µl aliquots at –80°C. Each day, thaw a new aliquot, dilute to 0.5 mg/ml in HPLC grade water, clarify by centrifugation for 20 min × 12,000 rpm, and store on ice.
3. *Citrate/succinate solution*: 25 m*M* sodium citrate + 25 m*M* sodium succinate is titrated with HCl to pH 2.40, filtered through a 0.22-µm membrane, and stored on ice.
4. *HPLC buffers*: Make buffer A [0.05% trifluoroacetic acid (TFA) in HPLC grade water] and buffer B [0.05% TFA in 100% (v/v) HPLC grade acetonitrile] fresh daily.
5. *Step gradient solutions*: Mix buffers A and B in appropriate ratios to yield solutions of 5, 7.5,10, 12.5, 15, 17.5, 20, 22.5, 25, 30, 35, 40, and 50% (v/v) acetonitrile, 0.05% TFA. Prepare 2-ml aliquots of each in screw-cap vials and store on ice.
6. *HPLC grade water*: ~100 ml for washing the sample loop, stored on ice.
7. *Protein sample*: Ideally > 90% pure at ~10 µ*M* stored long term at –80°C in 50-µl aliquots. Thaw new aliquots each day, clarify by centrifugation for 20 min × 12,000 rpm, and store on ice.
8. *Dry ice bath*: Add dry ice to ethanol : water (23 : 77) in an ice bucket to form a slurry at –10°C. This is used to quickly lower sample temperature after the in-exchange reaction.

Steps

1. A recommended configuration is shown in Fig. 1. Place a 2-ml PEEK loop between pump and injector to facilitate solvent cooling. Immerse this, the PEEK injector, a 1-ml sample loop, and the reversed-phase column at 0°C in an ice/water slurry. Run the HPLC pump isocratically in buffer A at 40 µl/min and equilibrate the reversed-phase column in this solution. Maintain protein sample, citrate/succinate, step gradient solutions, and HPLC water on ice and maintain D_2O at room temperature.
2. Equilibrate D_2O in a water bath at 10°C. *Note*: Performing the in-exchange reaction at 10°C reduces exchange rates to levels measurable in the dead time of the experiment (~5 s).
3. Aliquot 10 µl protein (~100 pmol) to a sample tube and equilibrate in the 10°C water bath for 30 s.
4. Initiate the in-exchange reaction by transferring 90 µl D_2O to protein. Incubate protein + D_2O at 10°C for varying times (e.g., 5–18,000 s). *Note*: In order to minimize sample heating in these and subsequent steps, use P200 pipettors attached to tips that have been prechilled by storing the pipettor + tip in a 15-ml tube on ice.
5. After incubation, remove the sample tube from the water bath to the –10°C dry ice bath and begin timing the postincubation period at t = 00:00 (min:sec). Incubate the sample in the –10°C bath briefly enough to cool rapidly to 0°C but not long enough to freeze the solution.
6. At t = 00:05, add 90 µl citrate/succinate solution to the sample tube and gently mix by tapping the tube against the walls of the dry ice bath.
7. At t = 00:20, remove the sample tube to ice. Immediately add 10 µl × 0.5 mg/ml pepsin to the sample and mix gently.
8. Between t = 00:20 and t = 00:40, load the 200-µl volume into the sample loop using a 250-µl Hamilton syringe, prechilled on ice and insulated by wrapping the syringe barrel with Parafilm to 0.5 cm thickness in order to minimize heat transfer from handling.
9. At t = 01:20, inject the digest onto the column, running isocratically in buffer A at 40 µl/min.

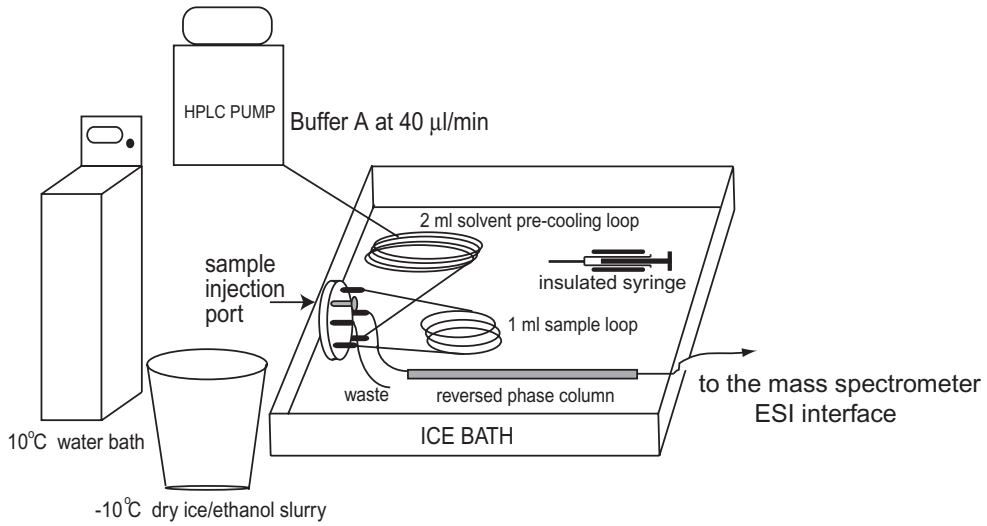

FIGURE 1 Experimental setup for hydrogen exchange-mass spectrometry. The reversed-phase column, injector, 2-ml solvent precooling loop, 1-ml injection loop, and Hamilton syringes wrapped with Parafilm are immersed in ice to minimize back-exchange during chromatography. The HPLC pump washes the column with buffer A (0.05% TFA in water) at a flow rate of 40 µl/min. Before buffer A reaches the injector apparatus, it is cooled to 0°C as it passes through the 2-ml solvent precooling loop. The protein sample, citrate/succinate solution, pepsin, and step gradients are stored separately on ice. The water bath is set at the desired temperature (e.g., 10°C) for in-exchange reactions, and a –10 C° bath (dry ice/23% ethanol/77% water) for quenching the in-exchange reaction is prepared.

10. At t = 06:20, switch the injector back to the load position and allow the column to desalt at 40 µl/min. While the column is washing, rinse the sample loop with ≥2 ml cold water and then load a step gradient into the sample loop by injecting 40 µl of buffer B followed successively with 17.5-µl aliquots of 50, 40, 35, 30, 25, 22.5, 20, 17.5, 15, 12.5, 10, 7.5, and 5% (v/v) acetonitrile, 0.05% TFA. Forming the HPLC gradient in the sample loop minimizes the dead time of the gradient.

11. Configure the mass spectrometer computer for data collection. At t = 12:00, attach the column to the electrospray source.

12. At t = 12:20, start data collection on the mass spectrometer. Immediately set the HPLC flow rate to 20 µl.

13. At t = 13:20, inject the gradient onto the column. Peptide elution is usually complete within 10 min.

B. Data Analysis

Peptic peptides are identified by LC/MS/MS sequencing, run under conditions outlined in steps 1–13, except without D_2O. An example of peptide identification by MS/MS and data reduction is presented by Resing *et al*. (1999). The following discussion of HX data analysis specifies the AnalystQS software available with the ABI QStar Pulsar for analysis of quadrupole TOF data (WIFF files). Other programs with equivalent features can be substituted.

1. Calculation of Weighted Average Mass

Steps

a. Open the data file with AnalystQS and open the "extract ion" dialog box.
b. Enter the mass/charge (m/z) for an ion and view the extract ion chromatogram (XIC). Select the scan range corresponding to the extract ion and view the mass spectrum. Smooth the spectrum three times and then adjust the threshold to view the m/z values of all isotopic peaks.
c. List the m/z and signal intensities of each isotopic peak for each ion. Save data in a text file, generating separate text files for each peptide at each time point.
d. Open text files with a spreadsheet program (e.g., Microsoft Excel). List the m/z and signal intensity in the first and second columns, respectively. The weighted average mass for each ion of each peptide ($M_{t,wa}$) is then calculated by Eq. (1):

$$M_{t,wa} = \left(\left[\sum(m/z \times \text{intensity})\Big/ \sum(\text{intensity})\right] \times z\right) - z \quad (1)$$

where $\Sigma(m/z \times \text{intensity})$ is the mass/charge of each isotopic form (column 1) multiplied by its corre-

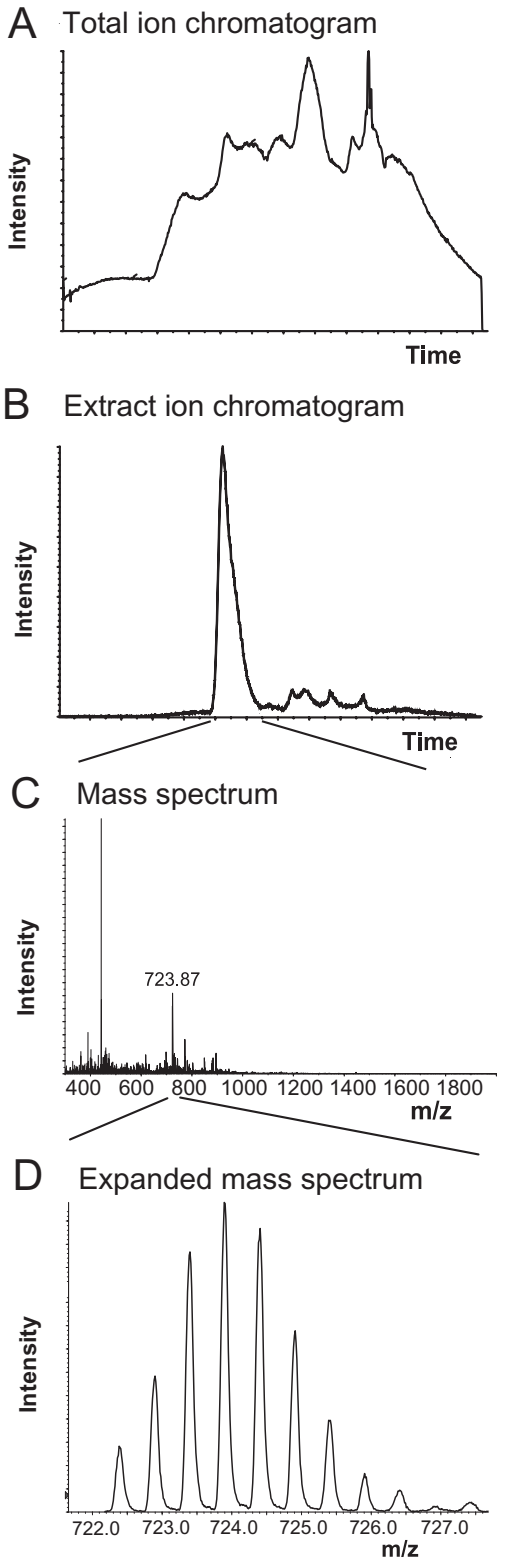

FIGURE 2 Processing mass spectra for a peptide (EETARFQPGYRS, undeuterated MH_2^{+2} =721.2). (A) Total ion chromatogram showing the data set from a single time point. (B) Extract ion chromatogram identifying the subset of ions with *m/z* between 721.0 and 723.0 showing maximal peak intensity between 5 and 6 min. (C) Mass spectrum displaying all ions eluting between 5 and 6 min. (D) Expanded spectrum of ions between *m/z* 721.0 and 726.0, where isotopic peaks are separated by 0.5 Da for MH_2^{+2} ions. Each peak is labeled, and the *m/z* values and intensities are imported in text file format into a spreadsheet for calculating weighted average mass.

sponding signal intensity (column 2) and summed over all observed isotopic forms for the ion, and Σ(intensity) is the sum of intensities for all isotopic forms (Fg. 2).

2. *Correction for Artifactual In-Exchange*

Artifactual in-exchange occurs after quenching the in-exchange and is facilitated by the partial denaturation of protein in acidic solution. This correction requires measuring the weighted average mass at t = 0 (M_0), which is measured by reversing the order of adding citrate/succinate and D_2O in place of steps 4–6 in Section III,A.

The peptide mass corrected for artifactual in-exchange can be calculated by Eqs. (2) and (3):

$$M_{t,\mathrm{corr(IE)}} = (M_{t,\mathrm{wa}} - LM_{\infty,90})/(1-L) \quad (2)$$

$$L = (M_0 - M_{\mathrm{calc}})/(M_{\infty,90} - M_{\mathrm{calc}}) \quad (3)$$

where $M_{t,\mathrm{corr(IE)}}$ is the corrected peptide mass at time t, $M_{t,\mathrm{wa}}$ is the observed weighted average mass at time t, L is the fraction of artifactual in-exchange at t = 0, M_0 is the observed peptide mass at t = 0, M_{calc} is the theoretical average mass of the peptide, and $M_{\infty,90}$ is the theoretical mass of the peptide with complete deuterium exchange at backbone amide hydrogens (for incubation in 90% D_2O). ($M_{\infty,90} - M_{\mathrm{calc}}$) is equal to the total number of nonproline amide residues in the peptide (total number of nonproline residues, minus one), multiplied by 0.9.

3. *Back-Exchange Correction*

Deuterons at backbone amides will slowly back-exchange to hydrogen during HPLC separation in water. We have used three different methods for estimating the fractional back-exchange for each peptide in the sample and have observed similar results with each.

Use the following steps for direct measurement of back-exchange.

Steps

1. Dilute the protein sample (500 pmol in 50 µl) with 50 µl H_2O. Add 90 µl citrate/succinate solution and digest with 10 µl pepsin as in steps 6 and 7 in Section III,A. Load peptides onto the column and desalt. Inject 30 µl of 40% acetonitrile, 0.05% TFA

onto the column, and collect all peptides into one tube.

2. Lyophilize the peptides, dissolve them in 30 µl of the buffer used to prepare the protein sample, add 270 µl D_2O, and heat to 90°C for 90 min in order to completely deuterate the peptides.

3. Cool the sample on ice and load 300 µl volume into the sample loop. Inject the peptide onto the column after 1 min of incubation in the sample loop as in steps 8 and 9 in Section III,A and proceed with steps 10–13. Measure the weighted average mass of each peptide (Section III,B).

4. Fractional back-exchange can be calculated for each ion using Eq. (4):

$$\mathrm{BE} = (M_0 - M_{\mathrm{BE}})/(M_{\infty,90} - M_{\mathrm{calc}}) \tag{4}$$

where BE is the fractional back-exchange of the peptide and M_{BE} is the observed mass of the peptide in the back-exchange experiment.

The following equation calculating the fractional back-exchange was derived empirically by Resing *et al*. (1999):

$$\mathrm{BE} = L \times (\%\mathrm{H_2O}/\%\mathrm{D_2O}) + [(\text{peptide elution time from HPLC in min} + 6\,\text{min}) \times 0.01/\text{min}] \tag{5}$$

where L is the fraction of artifactual in-exchange at t = 0 from Eq.(3) and ($\%H_2O/\%D_2O$) is the ratio of H_2O to D_2O during proteolysis (Section III,A, step 7; e.g., 0.55/0.45 for initial incubation with 90% D_2O). The calculation is based on an observed back-exchange of approximately 1% for each minute the peptide is on the column prior to elution.

The exchange rates for amide backbone hydrogens have been measured empirically, accounting for inductive and steric blocking effects within different primary sequences (Bai *et al*., 1993). This study presents tables and equation that can be used to calculate predicted back-exchange rates at 0°C. The program HXPep (Zhang *et al*., 1997), written by Dr. Zhongqi Zhang (Amgen Inc., Thousand Oaks, CA), calculates exchange rates using the derivation of Bai *et al*. (1993) and can be used to calculate back-exchange rates by entering the peptide sequence, choosing "NH/D_2O" exchange, "oligo" peptide size, "low salt," "pH/pD read of 2.400," "0°C," and "C-terminal considered." For each backbone amide hydrogen,

$$\mathrm{BE_{amide}} = k_{\mathrm{HXPep}} \times (\text{elution time} + \text{wash time}) \tag{6}$$

where BE_{amide} is the average back-exchange for each backbone amide hydrogen and k_{HXPep} is the rate of exchange calculated for the amide hydrogen by HXPep. For the entire peptide, fractional back-exchange may be calculated as

$$\mathrm{BE} = \sum(\mathrm{BE_{amide}})/(M_{\infty,90} - M_{\mathrm{calc}}) \tag{7}$$

where $\Sigma(BE_{amide})$ equals the sum of BE_{amide} calculated from Eqn.(6) for every amide hydrogen in the peptide.

After estimating fractional back-exchange using any of the aforementionial methods, the weighted average mass of each ion is corrected by Eq.(8):

$$M_{\mathrm{t,corr(BE)}} = M_{\mathrm{calc}} + (M_{\mathrm{t,corr(IE)}} - M_{\mathrm{calc}})/(1 - \mathrm{BE}) \tag{8}$$

where $M_{t,corr(BE)}$ is the peptide mass at time t after exchange in 90% D_2O, corrected for artifactual in-exchange and back-exchange.

C. Curve Fitting

Following correction for artifactual in-exchange and back-exchange, data may be fit using nonlinear least squares to a sum of exponentials (Resing *et al*., 1999; Hoofnagle *et al*., 2003). Further discussion and details on curve fitting and modeling are described by Resing and Ahn (1998) and Resing *et al*., (1999).

The time courses are modeled by a sum of exponentials in which each amide hydrogen exchanges with deuterium at a given rate. While in theory each amide backbone hydrogen is represented by a separate rate constant, in practice, exchange rates are averaged into fast (>1 min^{-1}), intermediate (0.1–1.0 min^{-1}) and slow rates (0.002–0.1 min^{-1}), and time courses can be fit with one, two, or three exponential terms:

$$Y = N - Ae^{-k_1 t} - Be^{-k_2 t} - Ce^{-k_3 t} \tag{9}$$

where Y is the observed weighted average mass corrected for back-exchange and artifactual in-exchange [i.e., $M_{t,corr(BE)}$], A, B, and C correspond to the number of amides (multiplied by 0.9), respectively, exchanging with average rate constants k_1, k_2, and k_3, and N is the peptide mass after maximal in-exchange of deuterium (=M_{calc} + A + B + C).

Some backbone amides are nonexchanging over the experimental time period and cannot be fit to this equation. For instance, in the protein kinase ERK2, 44% of backbone amides show no exchange after the longest time point of 5 h (rate constant < 0.002 min^{-1}) (Hoofnagle *et al*., 2001). The number of amides in this nonexchanging group (NE) can be estimated by subtracting the number of exchanging amides (A + B + C) from the total number of backbone amides in the peptide, excluding proline residues.

Steps

1. Start the DataFit program with a new project using one independent variable.

2. Enter time (minutes) and $M_{t,corr(BE)}$ in columns 1 and 2, respectively.
3. Under the Solve menu, select "Define User Model" and then select "New."
4. Enter the equation describing the sum of up to three exponentials under Model Definition:

$$\text{"Y} = n - a*\text{Exp}(-d*x) - b*\text{Exp}(-e*x) - c*\text{Exp}(-f*x)\text{"}$$

5. Similarly, enter equations describing the sum of two and one exponentials.
6. For each equation, provide initial guesses of parameter values for nonlinear least squares. Test several different initial guesses, which should converge to the same fit.
7. Select Regression under the Solve menu to fit data to the three user-defined models.
8. Record parameter values and standard errors (Fig. 3), choosing the equation fit with lowest variance.

IV. PITFALLS

1. The buffer conditions for the exchange reaction should be optimized to minimize protein denaturation. Salt and buffer concentrations should be low as possible to minimize buffer/salt-catalyzed hydrogen exchange. We have found that 5 m*M* sodium phosphate, pH 7.0, 50 m*M* sodium chloride in the exchange reaction produces minimal back-exchange. The sample pH should be identical between experimental conditions in order to minimize effects on hydrogens that exchange via EX2 mechanism, where observed exchange rates vary with pH of the solution (Clarke and Itzhaki, 1998). Higher buffer concentrations may be used when varying solutes that influence pH, e.g., see Andersen *et al*. (1998).

2. The duration of pepsin digestion and the amount of protease should be optimized to generate the greatest number of peptides in the size range of 8–15 amino acids, which yields optimal resolution for exchange measurements. Peptides should be short enough to enable mass resolution, but long enough to bind the HPLC column and provide some sequence overlap.

3. The acetonitrile concentrations in the step gradient solutions should be varied to optimize peptide resolution from reversed-phase chromatography. Peptide elution should be spread throughout the gradient, while eluting all peptides within 10 min of gradient injection.

4. In order to avoid instrument bias and variations in data collection, randomize the time points and

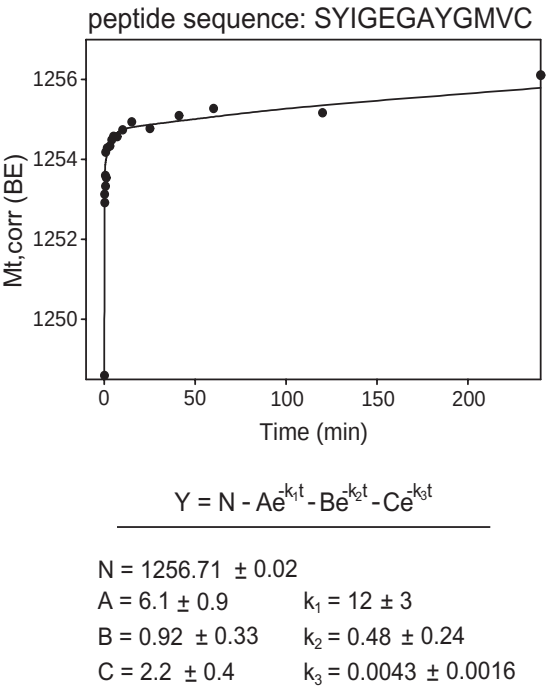

FIGURE 3 Curve fitting and modeling. Weighted average masses corrected for artifactual in-exchange and back-exchange [$M_{t,corr(BE)}$] are plotted vs incubation time with D_2O. Time courses are fit to a sum of exponentials by nonlinear least squares. Nonlinear least-square parameters and their standard errors obtained include k_1, k_2, and k_3 (rate constants, min^{-1}), A, B, C (0.9 × number of amides exchanging with apparent rate constants k_1, k_2, and k_3, respectively), and $N = M_{calc} + 0.9(A + B + C)$.

samples during data collection. Perform instrument calibration and measure the $t = 0$ experiment each day.

5. The quality of curve fitting varies with the data quality and the number of time points. Typically, at least 20 data points between 5 s and 3 h are required for curve fitting with modest standard errors. In addition, because the distribution of time points affects curve fitting, best results are achieved by including more time points during the transition between fast and intermediate exchange rates (0–30 min for most peptides) than during the times close to maximal in-exchange.

6. In optimizing the acquisition method for the ABI QStar qTOF mass spectrometer, the orifice voltage, the pulse frequency, and the declustering potential (DP) were optimized to reduce fragmentation at the orifice and to obtain the best signal at minimal peptide sample. Parameters in our acquisition method are: Mass range is 300–2000 amu; accumulation time is 1 s; duration is 50 min; cycles are 3000; delay time is 0 s; cycle time is 1 s; pulser frequency is 7 kHz; pulse 1 duration is 13 µs; pause between mass range is 5 ms;

ionspray voltage is 5200 V; declustering potential is 40 V; and declustering potential 2 is 20 V.

References

Andersen, M. D., Shaffer, J., Jennings, P. A., and Adams, J. A. (2001). Structural characterization of protein kinase A as a function of nucleotide binding: Hydrogen-deuterium exchange studies using matrix-assisted laser desorption ionization-time of flight mass spectrometry detection. *J. Biol. Chem.* **276**, 14204–14211.

Bai, Y., Milne, J. S., Mayne, L., and Englander, S. W. (1993). Primary structure effects on peptide group hydrogen exchange. *Proteins*, **17**, 75–86.

Barksdale, A. D., and Rosenberg, A. (1982). Acquisition and interpretation of hydrogen exchange data from peptides, polymers, and proteins. *Methods Biochem. Anal.* **28**, 1–113.

Chowdhury, S. K., Katta, V., and Chait, B. T. (1990). Probing conformational changes in proteins by mass spectrometry. *J. Am. Chem. Soc.* **112**. 9012–9013.

Clarke, J., and Itzhaki, L. S. (1998). Hydrogen exchange and protein folding. *Curr. Opin. Struct. Biol.* **8**, 112–118.

Hoofnagle, A. N., Resing, K. A., and Ahn, N. G. (2003). Protein analysis by hydrogen exchange and mass spectrometry. *Annu. Rev. Biophys. Biomol. Struct.* **32**, 1–25.

Hoofnagle, A. N., Resing, K. A., Goldsmith, E. J., and Ahn, N. G. (2001). Changes in conformational mobility upon activation of extracellular regulated protein kinase-2 as detected by hydrogen exchange. *Proc. Natl. Acad. Sci. USA* **98**, 956–961.

Johnson, R. S., and Walsh, K. A. (1994). Mass spectrometric measurement of protein amide hydrogen-exchange rates of apomyoglobin and holo-myoglobin. *Protein Sci.* **3**, 2411–2418.

Mandell, J. G., Falick, A. M., and Komives, E. A. (1998). Identification of protein-protein interfaces by decreased amide proton solvent accessibility. *Proc. Natl. Acad. Sci. USA* **95**, 14705–14710.

Neubert, T. A., Walsh, K. A., Hurley, J. B., and Johnson, R. S. (1997). Monitoring calcium-induced conformational changes in recoverin by electrospray mass spectrometry. *Protein Sci.* **6**, 843–850.

Resing, K. A., and Ahn, N. G (1998). Deuterium exchange mass spectrometry as a probe of protein kinase activation: Analysis of wild-type and constitutively active mutants of MAP kinase kinase-1. *Biochemistry* **37**, 463–475.

Resing, K. A., Hoofnagle, A. N., and Ahn, N. G. (1999). Modeling deuterium exchange behavior of ERK2 using pepsin mapping to probe secondary structure. *J. Am. Soc. Mass. Spectrom.* **10**, 685–702.

Zhang, Z. Q., and Smith, D. L. (1993). Determination of amide hydrogen-exchange by mass spectrometry: A new tool for protein structure elucidation. *Protein Sci.* **2**, 522–531.

CHAPTER

57

Nongel-Based Proteomics: Selective Reversed-Phase Chromatographic Isolation of Methionine-Containing Peptides from Complex Peptide Mixtures

Kris Gevaert and Joël Vandekerckhove

I. INTRODUCTION

Contemporary gel-free or nongel proteome analytical techniques are used increasingly as alternatives to highly resolving two-dimensional polyacrylamide gel electrophoresis (2D PAGE) for the analysis of complex protein mixtures. Some of the limitations of 2D PAGE (e.g., its bias to mainly visualize well-soluble, abundant proteins) can be overcome by these novel techniques, explaining their increasing success. A variety of procedures have been described and definitely the most interesting ones are those in which peptides, constituting the original proteins, are analyzed (e.g., Gygi *et al.*, 1999; Geng *et al.*, 2000; Washburn *et al.*, 2001; Zhou *et al.*, 2001). In these techniques, we can distinguish three general steps. First, the protein mixture is digested in solution using a highly specific protease. Second, the generated peptide mixture or an (affinity/covalently) isolated subset of it is separated by a liquid chromatographic step(s) (LC) and analyzed by automated tandem mass spectrometry (MS/MS). Third, the obtained peptide fragmentation spectra are fed into database-searching algorithms and linked to peptide and protein amino acid sequences stored in databases. We have described a technique for reversed-phase (RP) HPLC-based isolation of representative peptides of a proteome (peptides containing rare amino acids that are well distributed over a given proteome) (Gevaert *et al.*, 2002). Because this technique has a number of similarities to the previously described diagonal electrophoresis (Brown and Hartley, 1966) and diagonal chromatography (Cruickshank *et al.*, 1974) methods, we call this technique COmbined FRActional DIagonal Chromatography or COFRADIC. The core technology of COFRADIC is a chromatographic shift, evoked by a chemical or enzymatic reaction, of representative peptides between two identical separations steps. This article describes the different steps involved in the COFRADIC-based isolation of methionine-containing peptides as their sulfoxide derivatives using currently available RP-HPLC instrumentation.

II. MATERIALS AND INSTRUMENTATION

HPLC-graded water (product number 4218) and acetonitrile (product number 9017) used to prepare the HPLC solvents are of the best quality available and are from Malinckrodt Baker B.V., Deventer, The Netherlands. Peptide synthesizer graded trifluoroacetic acid (product number PTS6045) is from Rathburn Chemicals Ltd. (Walkerburn, Scotland, UK). The RP column used for separations is a 2.1 i.d. × 150-mm ZORBAX 300SB-C18 column (product number 883750-902) and

Copyright 2006, Elsevier Science (USA).
All rights reserved.

is from Agilent Technologies (Waldbronn, Germany). The hydrogen peroxide stock solution [30% (w/w), product number 21,676-3] is from Aldrich Chemical Co., Inc. (Milwaukee, WI).

The HPLC system used to sort the methionine peptides is an Agilent 1100 series capillary LC system, equipped with an Agilent 1100 series capillary pump, thermostatted microwell-plate sampler, thermostatted column compartment, variable wavelength detector, and a thermostatted fraction collector. The system runs under the control of a 3D Agilent ChemStation.

III. PROCEDURES

Chromatographic Isolation of Methionine-Containing Peptides

This procedure describes the isolation of methionine-containing peptides using a porous silica-based C18 RP-HPLC column with an internal diameter of 2.1 mm and a length of 15 cm. When using other brands or types of reversed-phase columns, clearly the amount of material used for the isolation of methionine-peptides, the solvent flow rate, the collection scheme for the primary fractions, and the evoked retention time shifts should be checked and, if necessary, adapted.

Solutions

1. *HPLC solvents:* For the chromatographic sorting of methionine-peptides, HPLC solvent A consists of 0.1% (v/v) trifluoroacetic acid (TFA) in water and solvent B contains 70% (v/v) acetonitrile and 0.1% (v/v) TFA in water. At least 1 litre of each solvent is made so that during the isolation procedure, the same HPLC solvents can be used, thereby increasing the overall reproducibility of the COFRADIC procedure for the isolation of methionine-peptides. These HPLC solvents should be thoroughly degassed prior to use.

2. *Oxidation solution:* The oxidation solution must be freshly prepared prior to the chromatographic isolation of methionine-peptides (secondary runs, see later) and consists of 3% (v/v) of H_2O_2 and 1% (v/v) TFA in water.

Steps

1. Typically, load a total of 1 to 10 nmol of a digested protein mixture, such as a cell lysate, onto a 2.1 i.d. × 150-mm C18 RP column. Following injection, equilibrate the column for 10 min with solvent A. Then, create a binary solvent gradient to 100% of solvent B over a time span of 100 min at a constant flow rate of 80 µl/min. This HPLC separation is referred to as the primary run.

2. During this primary run, peptide fraction collection starts from 40 min on (corresponding to an acetonitrile concentration of 21%) and, in total, 48 primary fractions of 1 min (or 80 µl) are collected in the wells of a microtitreplate (see Fig. 1A).

3. Using this setup, pool primary fractions, which are separated by 12 min, (Table I) and dry to complete dryness in a centrifugal vacuum concentrator. Prior to the methionine-oxidation reaction and the secondary runs, redissolve these pooled peptide fractions in 70 µl of 1% (v/v) TFA in water.

4. The methionine oxidation reaction is done by transferring 14 µl of the freshly made oxidation solution to the vial containing the pooled peptides. The reaction proceeds for 30 min at a 30°C, after which the sample must be immediately injected onto the RP-HPLC column.

5. Separated the oxidized peptides on the same column as the one used for the primary separation and under identical chromatographic conditions. In the experimental setup described here, methionine-sulfoxide containing peptides typically elute in a time frame 3 to 8 min before the elution of the unmodified, methionine-free peptides, which elute in the same interval as during the primary run (see Fig. 1B). Thus, during these secondary runs, the shifted methionine-sulfoxide peptides can be time-based collected in a distinct number of subfractions in a microtitreplate (see Table I).

6. The sorted peptides are analysed most conveniently by a mass spectrometer. For LC-MS/MS experiments using an electrospray ionisation (ESI)-based mass spectrometer, multiple secondary fractions obtained during one secondary run may be pooled, dried to complete dryness, and redissolved in an appropriate solvent for further analysis. Alternatively, matrix-assisted laser desorption ionisation (MALDI)-based analysis combined with collision-induced dissociation can be used for peptide identification. In this case, peptide fractions are not pooled in order to keep the complexity of the samples as low as possible, but are dried and redissolved in a small volume of MALDI matrix solution and finally loaded on a MALDI target for further analysis.

7. Finally, convert the information in the obtained peptide fragmentation spectra to peak lists in which the masses of the observed peptide fragment ions and their relative or absolute intensities are saved. These peak lists are then used to identify the corresponding peptides using commercially available database search engines such as MASCOT (Perkins *et al.*, 1999).

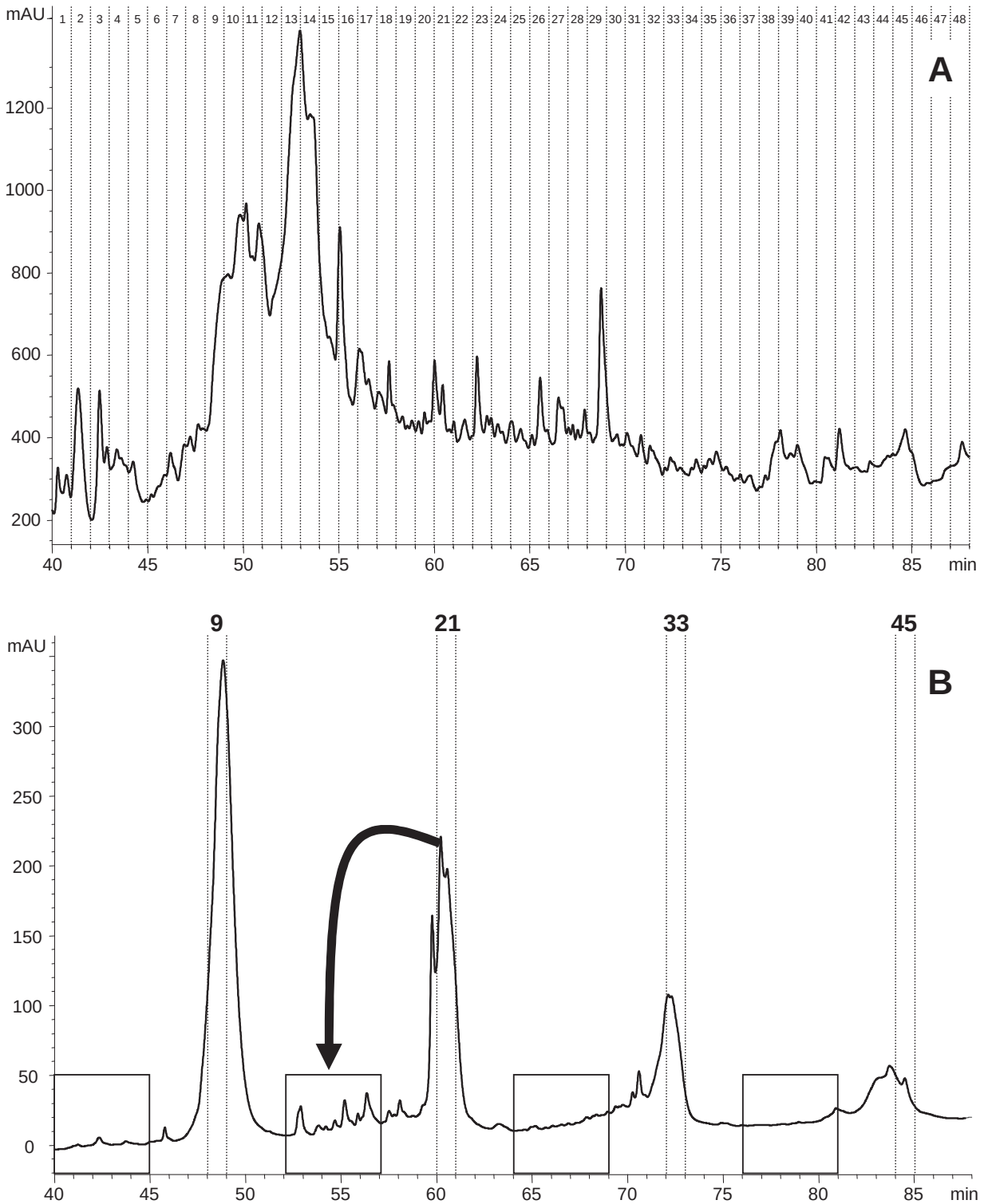

FIGURE 1 (A) UV absorption chromatogram (214 nm) of a reversed-phase HPLC separation of a tryptic digest of a human sputum sample. Peptides are fractionated in 48 distinct fractions. (B) Prior to the isolation of methionine-peptides, four fractions (in this case, fractions 9, 21, 33, and 45) are combined and oxidized to their methionine-sulfoxide counterparts. When rerun on the same column and under identical chromatographic conditions, the oxidized peptides shift out of this primary collection interval (an 8- to 3-min hydrophilic shift) and can be specifically collected (shaded boxes) for further LC-MS/MS analysis.

TABLE I Primary and Secondary RP-HPLC Fraction Collection Scheme for the Isolation of Methionine-Peptides[a]

Secondary run	Primary fractions				Elution of primary fractions				Elution of methionine-sulfoxide peptides			
A	12	24	36	48	51–52	63–64	75–76	87–88	43–48	55–60	67–72	79–84
B	11	23	35	47	50–51	62–63	74–75	86–87	42–47	54–59	66–71	78–83
C	10	22	34	46	49–50	61–62	73–74	85–86	41–46	53–58	65–70	77–82
D	9	21	33	45	48–49	60–61	72–73	84–85	40–45	52–57	64–69	76–81
E	8	20	32	44	47–48	59–60	71–72	83–84	39–44	51–56	63–68	75–80
F	7	19	31	43	46–47	58–59	70–71	82–83	38–43	50–55	62–67	74–79
G	6	18	30	42	45–46	57–58	69–70	81–82	37–42	49–54	61–66	73–78
H	5	17	29	41	44–45	56–57	68–69	80–81	36–41	48–53	60–65	72–77
I	4	16	28	40	43–44	55–56	67–68	79–80	35–40	47–52	59–64	71–76
J	3	15	27	39	42–43	54–55	66–67	78–79	34–39	46–51	58–63	70–75
K	2	14	26	38	41–42	53–54	65–66	77–78	33–38	45–50	57–62	69–74
L	1	13	25	37	40–41	52–53	64–65	76–77	32–37	44–49	56–61	68–73

[a] The pooling scheme of primary RP-HPLC fractions and the time interval (given in minutes) during which they elute from the column during the primary run are indicated. The collection of methionine-sulfoxide peptides during 12 consecutive secondary runs (A–L) is indicated in the last column (given in minutes). These peptides generally elute in a time interval of 5 min starting 8 min prior to the elution of their respective primary fractions. Primary and secondary fraction collection time intervals corresponding to a particular primary fraction are indicated by an identical colour code.

IV. COMMENTS

Using mass spectrometric analysis, the presence of a methionine-sulfoxide side chain in sorted peptides can be recognized easily by the unstable behaviour of the methionine-sulfoxide side chain. In both MALDI- and ESI-based experiments, the facile loss of methane sulfenic acid (64 amu) has been observed (Lagerwerf *et al*., 1996). Furthermore, we have noticed that, especially in the postsource decay (PSD) mode (Spengler *et al*., 1992), peptides baring methionine-sulfoxide residues tend to fragment preferentially at this residue, thereby only a small amount of vibration energy is left for fragmentation of the peptide backbone. Generally, we noticed that MALDI-PSD spectra obtained from peptides containing a methionine-sulfoxide residue are very difficult to interpret, as only a small number of sequence-specific fragment ions (due to fragmentation of peptide bonds) are observed. However, we have not observed a similar behaviour for these type of peptides when analyzed by ESI-MS/MS, meaning that LC-MS/MS can be used routinely to analyze sorted methionine-sulfoxide peptides by fragmentation.

One of the interesting features of COFRADIC is the fact that during secondary runs, methionine-sulfoxide peptides elute in a five times larger time interval compared to the primary run (see Table I, last column). This means that the sorted peptides are delivered in a much less condensed manner for analysis by LC-MS/MS, thus implying that more peptides will be finally analyzed, resulting in a higher coverage of the analyzed proteome.

The aforementioned method for the isolation of methionine-peptides as their sulfoxide derivatives can be highly automated using existing HPLC equipment such as automated injectors and fraction collectors. It should be clear that, in theory, every type of peptide that contains an amino acid that can be specifically altered using chemicals and/or enzymes can be sorted using the COFRADIC technology. For example, similar strategies can be used for selective isolation of cysteine-containing peptides, phosphorylated peptides, and peptides spanning the amino-terminal part of the protein.

V. PITFALLS

1. Do not incubate methionine-peptides for more than 30 min in 0.5% H_2O_2, as this leads to over-oxidation, resulting in the formation of methionine-sulfones. The hydrophilic shift evoked by this sulfone is smaller as compared to the one evoked by the sulfoxide and may thus interfere with the isolation procedure.

2. Likewise, following the oxidation reaction, the altered peptides must be injected immediately onto the reversed-phase column. We have noticed that storing the peptides in the oxidation solvent, even just for a couple of hours, in the freezer leads to almost complete oxidation of methionine to the sulfone derivative, oxi-

dation of cysteine to cystic acid, and almost complete destruction of tryptophane residues.

3. It is important to keep the chromatographic conditions for the primary run and the secondary run as similar as possible. This means that the same HPLC solvents should be used and that the column compartment should be controlled thermostatically.

Acknowledgments

K.G. is a Postdoctoral Fellow of the Fund for Scientific Research - Flanders (Belgium) (F.W.O. - Vlaanderen). The project was further supported by the GBOU-research initiative of the Flanders Institute of Science and Technology (IWT).

References

Brown, J. R., and Hartley, B. S. (1966). Location of disulphide bridges by diagonal paper electrophoresis: The disulphide bridges of bovine chymotrypsinogen. *Biochem. J.* **101**, 214–228.

Cruickshank, W. H., Malchy, B. L., and Kaplan, H. (1974). Diagonal chromatography for the selective purification of tyrosyl peptides. *Can. J. Biochem.* **52**, 1013–1017.

Geng, M., Ji, J., and Regnier, F. E. (2000). Signature-peptide approach to detecting proteins in complex mixtures. *J. Chromatogr. A* **870**, 295–313.

Gevaert, K., Van Damme, J., Goethals, M., Thomas, G. R., Hoorelbeke, B., Demol, H., Martens, L., Puype, M., Staes A., and Vandekerckhove, J. (2002). Chromatographic isolation of methionine-containing peptides for gel-free proteome analysis: Identification of more than 800 *Escherichia coli* proteins. *Mol. Cell. Proteomics* **1**, 896–903.

Gygi, S. P., Rist, B., Gerber, S. A., Turecek, F., Gelb, M. H., and Aebersold, R. (1999). Quantitative analysis of complex protein mixtures using isotope-coded affinity tags. *Nature Biotechnol.* **17**, 994–999.

Lagerwerf, F. M., van de Weert, M., Heerma, W., and Haverkamp, J. (1996). Identification of oxidized methionine in peptides. *Rapid Commun. Mass Spectrom.* **10**, 1905–1910.

Perkins, D. N., Pappin, D. J., Creasy, D. M., and Cottrell, J. S. (1999). Probability-based protein identification by searching sequence databases using mass spectrometry data. *Electrophoresis* **20**, 3551–3567.

Spengler, B., Kirsch, D., Kaufmann, R., and Jaeger, E. (1992). Peptide sequencing by matrix-assisted laser-desorption mass spectrometry. *Rapid Commun. Mass Spectrom.* **6**, 105–108.

Washburn, M. P., Wolters, D., and Yates, J. R., III (2001). Large-scale analysis of the yeast proteome by multidimensional protein identification technology. *Nature Biotechnol.* **19**, 242–248.

Zhou, H., Watts, J. D., and Aebersold, R. (2001). A systematic approach to the analysis of protein phosphorylation. *Nature Biotechnol.* **19**, 375–378.

CHAPTER

58

Mass Spectrometry in Noncovalent Protein Interactions and Protein Assemblies

Lynda J. Donald, Harry W. Duckworth, and Kenneth G. Standing

I. INTRODUCTION

Mass spectrometry (MS) has emerged as an important tool in the study of proteins and their interactions over the past several years (Daniel *et al.*, 2002; Robinson, 2002). Electrospray (ESI) provides a gentle ionization method that does not disrupt the weak bonds found in noncovalent complexes, and the adoption of nanospray technology (Wilm and Mann, 1996) has allowed the concentration of the buffer to be varied over a large range. Moreover, the use of time-of-flight (TOF) spectrometers for this purpose (first by Tang *et al.*, 1994) has removed previous limitations on the *m*/*z* values that can be examined, particularly after such instruments have been modified in order to study larger and larger assemblies (Chernushevich *et al.*, 1999; Rostom and Robinson, 1999; Rostom *et al.*, 2000; Van Berkel *et al.*, 2000).

Because the mass spectrum shows all the components present in a sample, information may be acquired on quantity, stoichiometry, and equilibria. Problems in the method arise from the limited selection of suitable buffers, interference from inorganic ions (especially Na^+ and K^+), and difficulties inherent in maintaining an uncooperative protein in solution under conditions required for the mass spectrometry.

II. MATERIALS

Ammonium acetate (99.999% Cat. No. 37,233-1), dithiothreitol (99%, Cat. No. 45,777-9), and 1,1,1-trichloroethane (Cat. No. 40,287-7) are from Aldrich. Ammonium bicarbonate is Fisher certified grade (Cat. No. A643). Dimethylchlorosilane is from Pierce (Cat. No. 83410). Methyl alcohol is from Mallinckrodt (Cat. No. 3041). Acetic acid (99+%) (Cat. No. A6283), formic acid (ACS reagent) (Cat. No. F4636), and substance P (Cat. No. S2136) are from Sigma. Dialysis membranes for waterbugs are from Spectra/Por (Cat. No. 132 128 for 50 K MWCO; 132 113 for 8 K MWCO; 132 703 for 12–14 K MWCO). For salt removal from ligands, we use Spectra/Por Dispodialyser MWCO 500, 1 ml capacity (Cat. No. 135 504). Centricon ultrafiltration units are from Amicon Bioseparations (Millipore) (YM10 is Cat. No. 4205; YM30 is Cat. No. 4208; YM50 is Cat. No. 4224). All plasticware is from Fisher Scientific: LDPE drop dispensing bottles (Fisher Cat. No. 03-006), 100-ml beakers (Nalgene Cat. No. 1201-0100), and syringe filters SFCA, 0.2 µm, 25 mm (Nalgene Cat. No. 190-2520). Microcentrifuge tubes, 0.6-ml flat top (Fisher Cat. No. 05-407-16) and 1.5 ml (Fisher Cat. No. 05-406-16), are used for waterbug construction. The 10-ml sterile syringes are latex free with Luer-lok from Becton-Dickinson (Cat. No. 309604). Nanospray capillaries are from Protana (types S and N), and New Objective PicoTip (type Econo12). GELoader tips are from Eppendorf (Cat. No. 22 35 165-6).

Some samples are prepared in a Sorvall RC-5B refrigerated centrifuge with a Sorvall SS34 rotor. Water from a reverse osmosis supply is run through a Barnstead NANOpure II system set at 17.0 MΩ/cm. All buffers are prepared with this grade of water.

Copyright 2006, Elsevier Science (USA).
All rights reserved.

III. INSTRUMENTATION

Mass spectrometry measures the ratio of the mass (m) to the charge (z) of an ion. Because many commercial instruments have a limited m/z range (usually <4000 for quadrupole mass filters), ions with large m/z values, such as those from buffered proteins, cannot be measured. Consequently, most intact protein and protein–ligand complexes require the "unlimited" m/z range found in TOF mass analyzers, and orthogonal ion injection (Verentchikov *et al*., 1994) enabled the use of such instruments with ESI sources. Tang *et al*. (1994) pioneered the measurement of noncovalent complexes by ESI-TOF MS. More recently, we have added a heated metal capillary to provide another stage of pumping and desolvation and a new section containing a small RF quadrupole to provide collisional cooling of the ions (Krutchinsky *et al*., 1998). A schematic diagram of the main elements of the instrument is shown in Fig. 1.

Some of the results reported here were obtained with a conventional electrospray ion source. In this device, solution is delivered to the sharpened tip of a stainless steel needle by a syringe pump. Alternatively, we use a glass nanospray source, which requires less sample, at lower concentration, and is tolerant of high concentrations of buffer. A potential difference of 3–3.5 kV (1 kV for nanospray) between the tip of the needle and the inlet of a heated metal capillary starts the ionization process. A counterflow of hot nitrogen gas helps with desolvation. We usually use nitrogen as this "curtain" gas, but sometimes use SF_6, especially for very large complexes, because it is considerably more efficient than nitrogen both in removing adducts and in dissociating complexes.

Expansion of the ion mixture into the next region produces a supersonic jet. Normally we apply a declustering voltage to the focusing electrode. Up to 300 V potential difference for nitrogen (or 400 V for SF_6, due to its superior insulating properties) can be maintained between the focusing electrode and the

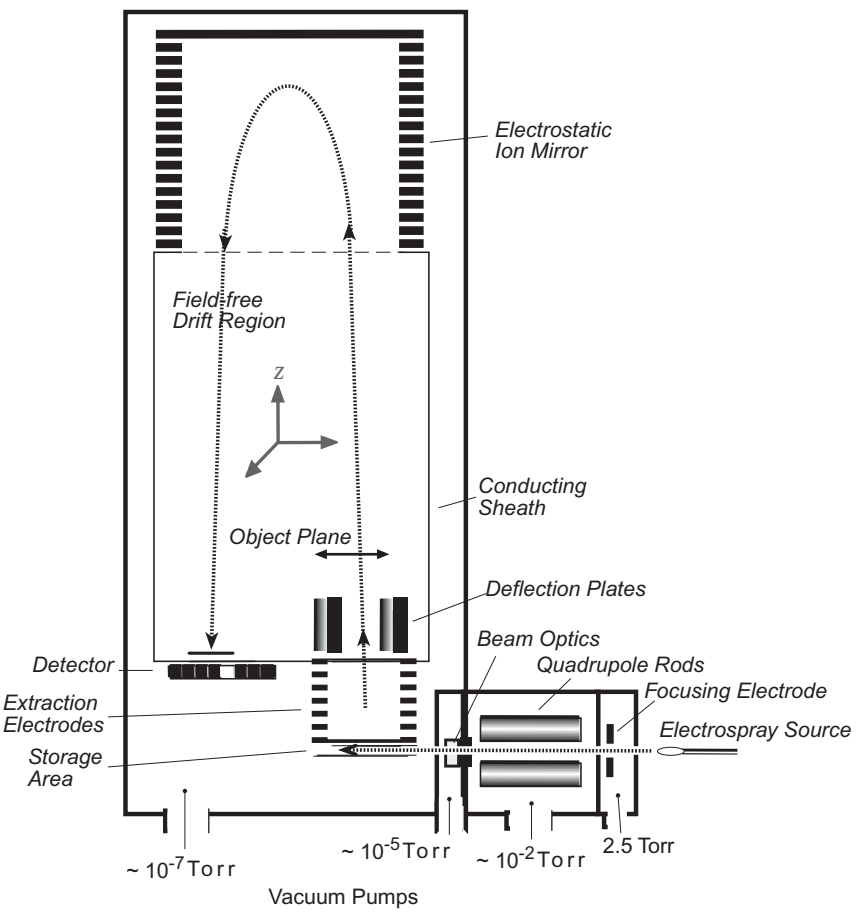

FIGURE 1 Schematic diagram of an electrospray ionization time-of-flight mass spectrometer. The ion path is indicated by the dotted line. A more detailed description can be found in Chernushevich *et al*. (1999).

flat aperture plate further downstream; the voltage is determined empirically for each protein or complex. A small opening in the plate connects this region to the second pumping stage where the ions oscillate in the two-dimensional potential well produced by the RF quadrupole and are cooled to near-thermal energies by collisions with the ambient gas (Krutchinsky *et al*., 1998). After passing through the quadrupole, the ion beam is focused and directed into the storage region of the modulator, entering perpendicular to the TOF axis at an energy <10 eV. After a group of ions has filled the storage region, it is accelerated along the TOF axis by applying a pulse to the extraction electrodes, which also starts the TOF measurement. The time of flight is recorded for each ion using TOFMA, an in-house software program that is also used for data analysis.

IV. PROCEDURES

A. Finding the Correct Conditions for the Protein

Our successes have come from the two commercially available volatile buffers, ammonium acetate and ammonium bicarbonate, but it is possible to have a small amount of nonvolatile material present in the sample (often unintentionally). Na^+ and K^+ are the worst contaminants, but buffer components such as glucose, glycerol, polyethylene glycol, and detergents are best avoided.

Using the preparative buffer of the protein as a guide, choose ammonium acetate for pH < 7 or ammonium bicarbonate for pH > 7. The pH can be adjusted with ammonium hydroxide or acetic acid. However, these solutions do change pH over time, and it is best to prepare the samples and then acquire spectra as soon as practicable. Choose a concentration that is close to the ionic strength of the preparative buffer and prepare the protein at a high concentration so that both it and the buffer can be diluted during the experiment. Dithiothreitol can be added to limit oxidation. If possible, the exact protein concentration should be determined from the known molar extinction coefficient and measurement of UV absorbance of an aliquot.

In our instrument, the declustering voltage, Vc, is an important component of the successful spectrum. At the "right" voltage, there is a perfect balance between maximum desolvation needed for high resolution and the collisionally induced dissociation of the intact complex. In practice, it is always wise to take spectra at several voltages because each will provide different kinds of information.

B. Desalting with "Waterbugs"

This procedure is modified from Orr *et al*. (1995). It is an efficient method of salt exchange and can also be used to assess the suitability of different buffer conditions.

1. Preparation of Apparatus

Steps

1. Prepare 2% sialysation solution by adding 10 ml of dimethyldichlorosilane to 500 ml of 1,1,1-trichloroethane. Mix carefully, working in a fume hood.
2. Cut the rim and the attached lid from microcentrifuge tubes using a razor or scalpel. It is very important that the cut edge is smooth or it will puncture the dialysis tubing.
3. Wash the lids with methanol and allow them to air dry.
4. Wearing gloves, transfer the lids to a clean beaker containing sialysation solution. Agitate carefully and decant off the solution.
5. Wash the lids in running tap water and then rinse several times with nanopure water.
6. Tip onto a fresh tissue, cover with a second tissue, and allow to air dry.
7. Minimize handling the waterbugs by using clean forceps for transfer. They should be stored in a covered container, such as a plastic petri dish, to avoid dust contamination.

2. Sample Introduction

Steps

1. Wash hands thoroughly. Do *not* use hand cream. It is much easier to do this without gloves; only step 6 *requires* that no gloves be worn. Hand cream components and the powder used in gloves can all cause adducts in the mass spectrum.
2. Prepare a clean, salt-free work surface.
3. For volumes of 10–50 µl, use the lids from 0.6-ml microcentrifuge tubes. For volumes up to 200 µl, use lids from 1.5-ml microcentrifuge tubes.
4. Prepare and chill the appropriate buffer, using plastic beakers kept specifically for this purpose.
5. Choose dialysis tubing with the appropriate MWCO and cut into squares of about 1.5-cm sides. Immerse them in nanopure water for about 10 min.
6. Rub the dialysis tubing squares between ungloved thumb and finger to separate the two layers. (This should be done in advance of setup if gloves are required for sample handling.)
7. Place a lid assembly on the clean work surface. Using an accurate pipettor, transfer a measured

volume of pure protein into the lid of the former microcentrifuge tube.

8. Place a single layer of dialysis tubing over the sample. Hold it in place with the rim of the microcentrifuge tube and carefully press down around the edge. Check the profile carefully in good light to make sure the dialysis membrane is intact. If not, remove the rim, discard the dialysis membrane tubing, and try again.

9. Place the waterbug onto the surface of the buffer, membrane side down. Gentle stirring is optional. Do this at 4°C, especially if the protein is unstable.

10. After at least 4 h, remove the waterbug using clean tongs. Working quickly, invert several times and then transfer to a fresh container of buffer. After a further 4–6 h (or overnight), repeat into a third plastic container of fresh buffer. If using 1-liter beakers, and less than 1 ml total sample, then three changes are sufficient. If using smaller containers in order to use less buffer, then increase the number of buffer changes to five or six.

3. Recovery of Sample

Steps

Set a pipettor at the expected recovery volume. Puncture the dialysis membrane with the tip of the pipettor and withdraw the sample. Put into a clean microcentrifuge tube. If the volume recovered is less than expected, there may be some residue on the underside of the dialysis membrane. Measure the concentration using an aliquot of the recovered sample. The method used will depend on the protein and may require most of the sample.

If the sample has precipitated, add acetic acid by puncturing the dialysis membrane with the end of the pipette tip and then inject the acid, adjust the volume, and remove the solubilized protein. Normally 5 µl of acetic acid is adequate for 100 µl of sample prepared in 5 m*M* buffer. Formic acid may also be used. This sample can be analysed for mass determination.

C. Desalting by Ultrafiltration

The following is based on the Centricon user guide (Millipore Corp., 2001) that comes with the centrifugal filter devices. Any refrigerated centrifuge may be used, provided it has a fixed-angle rotor, adaptors for 17 × 100-mm tubes, and is capable of running at 1000–7600 *g*. This requires much less buffer than the waterbug method, but it is more laborious and some proteins may come out of solution when they are concentrated too much.

Steps

1. Prepare and chill the appropriate buffer. The 99.999% ammonium acetate can be used directly. For ammonium bicarbonate buffer, make 100 ml at the desired concentration and then force through a 0.2-µm filter into a plastic container, such as a drop dispensing bottle, which has never been used for anything else.

2. Select a filtration device with a MWCO that will hold back the protein. Assemble the device and rinse the sample reservoir with buffer.

3. Add protein solution to the sample reservoir and fill it with buffer. Centrifuge for an appropriate length of time. Normally, it takes 15–30 min in a Centricon 30 or 50 to reduce the volume to about 100 µl, depending on the concentration of the sample. Buffer components such as glycerol and glucose will slow down the process, and it is best to try and omit these at some earlier stage in the purification. If the retentate vial is attached to the Centricon unit, it may not fit in a closed rotor. We normally use the vial and do not close the rotor.

4. When the volume has been decreased to about 100 µl, add more buffer, put the retentate vial back onto the unit, invert gently several times, and then recentrifuge.

5. Repeat the fill and spin at least six times. The residual salt concentration should be *at least* three orders of magnitude less than that of the protein.

D. Final Preparation of the Protein(s) or Complex

Calibrate the instrument by electrospray using a 10^{-5} *M* solution of substance P in 50% methanol, 2% acetic acid. Other calibrants can be substituted.

For electrospray, dilute the protein to 5–20 µ*M* in 5 m*M* buffer. Load into the electrospray needle by back pressure on the syringe pump. Adjust the needle in the holder and turn on the spray voltage to about 3 kV. Adjust the declustering voltage until a clear spectrum appears. Adjust the position of the end of the needle and the voltages until a cone is formed at the end. Collect spectra at various voltages.

For nanospray, cut the capillary to ~3 cm. Using a GELloader tip on a 1- to 10-µl pipettor set at 2.5 µl, rinse the inside of the capillary with an aliquot of the buffer used for the protein preparation. Discard this and reload the tip with sample. Assemble the capillary in its holder and attach to the mass spectrometer. If using a Protana capillary, brush it against the front cone of the instrument to break off the end. (New Objective capillaries are open already.) Establish some

back pressure to the assembly to force the sample to the orifice. Gradually turn up the nozzle voltage to 1 kV and adjust the declustering voltage until a clear spectrum emerges. Often the first burst of ions is badly contaminated by salts so it is best to be patient.

V. SPECIFIC EXAMPLES

A. A Small DNA-Binding Protein

The *Escherichia coli trp* apo-repressor protein TrpR is a dimer in the high salt buffer conditions used for nuclear magnetic resonance and X-ray crystallographic measurements (Zhang *et al*., 1987; Zhao *et al*., 1993). The pure enzyme is stable when lyophilized in elution buffer (10 m*M* $NaPO_4$ pH 7.6, 0.1 m*M* EDTA, 0.45 *M* NaCl). For our first experiments (Potier *et al*., 1998), an aliquot of protein was dissolved in water and dialysed in "waterbugs" against 10-ml aliquots of 10 m*M* ammonium acetate. Just before mass analysis by electrospray ionization, samples were diluted to 10 µ*M* protein in 5 m*M* ammonium acetate. As shown in Fig. 2A, the spectrum was complex, with two charge envelopes for the monomer, centred at the 7^+ and 10^+ ions, and good evidence for dimer, trimer, and perhaps higher order aggregates, all of which indicate a partially unfolded or denatured protein. If specific DNA was added to the protein before dialysis, a new ion envelope appeared that corresponded to a complex of one dsDNA and two protein monomers (Potier *et al*., 1998), in keeping with results from other analytical methods.

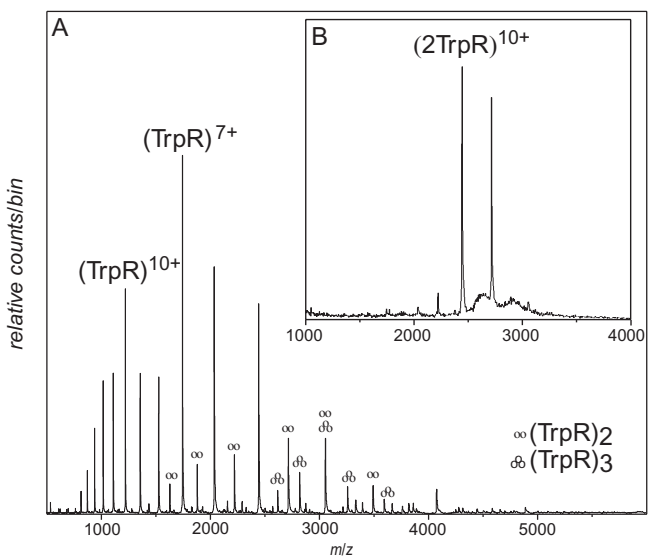

FIGURE 2 Spectra of *E. coli trp* apo-represor protein. (A) A 10 µ*M* protein prepared in 10 m*M* NH_4OAc by "waterbug" dialysis (8000 MWCO membrane) diluted to 5 m*M* just before electrospray. Nitrogen curtain gas with an 80-V declustering voltage. (B) A 2 µ*M* protein transferred into 500 m*M* NH_4OAc using a Centricon 10, diluted to 250 m*M*, and analysed by nanospray in a Protana type S capillary. Nitrogen curtain gas with a 100-V declustering voltage.

More recently, the development of nanospray ionization has expanded the limits of buffer concentration. If the same TrpR protein is prepared in the same way, but with 500 m*M* ammonium acetate, the spectrum is completely different (Fig. 2B), with one compact ion envelope of four ions, a spectrum typical of that of a properly folded protein. Deconvolution of these data gives a mass of 24452 Da, as expected for a dimer. Other DNA-binding proteins have shown the same sorts of buffer dependence (Donald *et al*., 2001; Kapur *et al*., 2002), where a very high concentration of buffer is required to maintain the protein in a native state, yet the DNA–protein complexes are relatively more stable at lower buffer concentrations.

B. A Large Allosterically Regulated Protein

Citrate synthase is a key enzyme for the entry of two-carbon units into the citric acid cycle and is essential in the biosynthesis of amino acids related to glutamate. Although many organisms have a homodimeric citrate synthase, that of *E. coli* crystallizes as a hexamer (Nguyen *et al*., 2001). This protein cannot be frozen and is most stable when stored at high concentration in buffer (20 m*M* Tris–Cl, pH 7.8, 1 m*M* EDTA, 50 m*M* KCl) and is best desalted with a 50 K MWCO Centricon unit and kept at high concentration until just before mass analysis. When the protein was desalted using 20 m*M* ammonium bicarbonate and diluted so that the final buffer concentration was 5 m*M*, the electrospray spectrum was similar to that shown in Fig. 3A. There are three distinct charge envelopes, representing ions from a dimer (96 kDa), a tetramer (192 kDa), and a hexamer (288 kDa). Increasing the concentration of protein changed the spectrum to one with no tetramer and a preponderance of hexamer ions (Ayed *et al*., 1998; Krutchinsky *et al*., 2000). Addition of the allosteric inhibitor NADH (also desalted into ammonium bicarbonate) also changed the spectrum, providing data that were used to calculate equilibrium constants. These agreed well enough with results from sedimentation equilibrium measurements, considering that the latter depend on averages, whereas a mass spectrum shows all the components in the mixture. If the protein is desalted into 100 m*M* ammonium bicarbonate and analysed by nanospray, then the response of the enzyme to salts can be ascertained (Fig. 3) because NH_4^+, like K^+, is an activator of

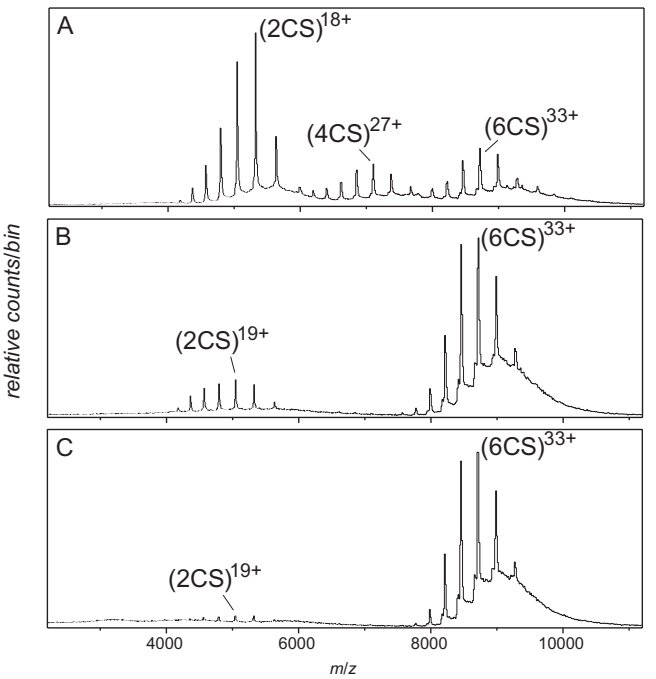

FIGURE 3 Spectra of *E. coli* citrate synthase. Samples were transferred into 100 m*M* NH_4HCO_3 using a Centricon 50, diluted to 10 μ*M* protein, and analysed by nanospray ionization from a New Objective PicoTip. For all spectra, the curtain gas was SF_6 and the declustering voltage was 200 V. (A) 5 m*M* NH_4HCO_3 showing three charge envelopes for dimer (2CS), tetramer (4CS), and hexamer (6CS); (B) 20 m*M* NH_4HCO_3; and (C) 100 m*M* NH_4HCO_3.

citrate synthase (Faloona and Srere, 1969; Stokell *et al*., 2003). In this case, changing only the concentration of buffer causes a change in the spectrum from one where ions from dimers are the most abundant, at 5 m*M* buffer, to one where ions from hexamers are the most abundant, at 100 m*M* buffer.

C. A Large Very Stable Enzyme with a Haem Residue at Its Active Site

Haem-containing bacterial catalase–peroxidases are large bifunctional enzymes that degrade hydrogen peroxide as part of their oxidative defense system. Haem is an essential component of the active site; mass spectrometry measurements have revealed heterogeneity of haem composition in the tetrameric *E. coli* enzyme HPI (Hiller *et al*., 2000). However, the comparable enzyme from *Burkholderia pseudomallei*, KatG, is a dimer of 160 kDa (Carpena *et al*., 2003; Donald *et al*., 2003) and it seemed reasonable to expect two haems in the folded protein. This enzyme is so stable it can be kept frozen in 5 m*M* ammonium acetate and it remains a dimer even with very high declustering voltage in the mass spectrometer. However, the ion envelope changes shape as the declustering voltage is increased (Fig. 4), with a concomitant increase of a singly charged ion at *m*/z 616. The deconvolutions show clearly a loss in mass from the dimer, in two steps of ≈ 600 Da. The high declustering voltage required to dissociate this complex gives an indication of its stability, and the single protein ion seen at lower voltage suggests that the stable form of the enzyme has one haem per subunit. Using a modified commercial instrument, Robinson's group has done similar experiments to fragment the 804-kDa GroEL chaperonin assembly (Rostom and Robinson, 1999) and to dissect intact ribosomes (Rostom *et al*., 2000).

Acknowledgments

We thank James McNabb and Victor Spicer for their invaluable technical assistance. The pure proteins were supplied by Cheryl Arrowsmith, Peter Loewen, Gillian Sadler, David Stokell, and Jack Switala. This research was funded by grants from the Natural Sciences and Engineering Research Council of Canada (to HWD and KGS), the Canadian Institute of Health Research (to HWD, P. Hultin, and G. Brayer), and the U.S. National Institutes of Health (GM 59240 to KGS).

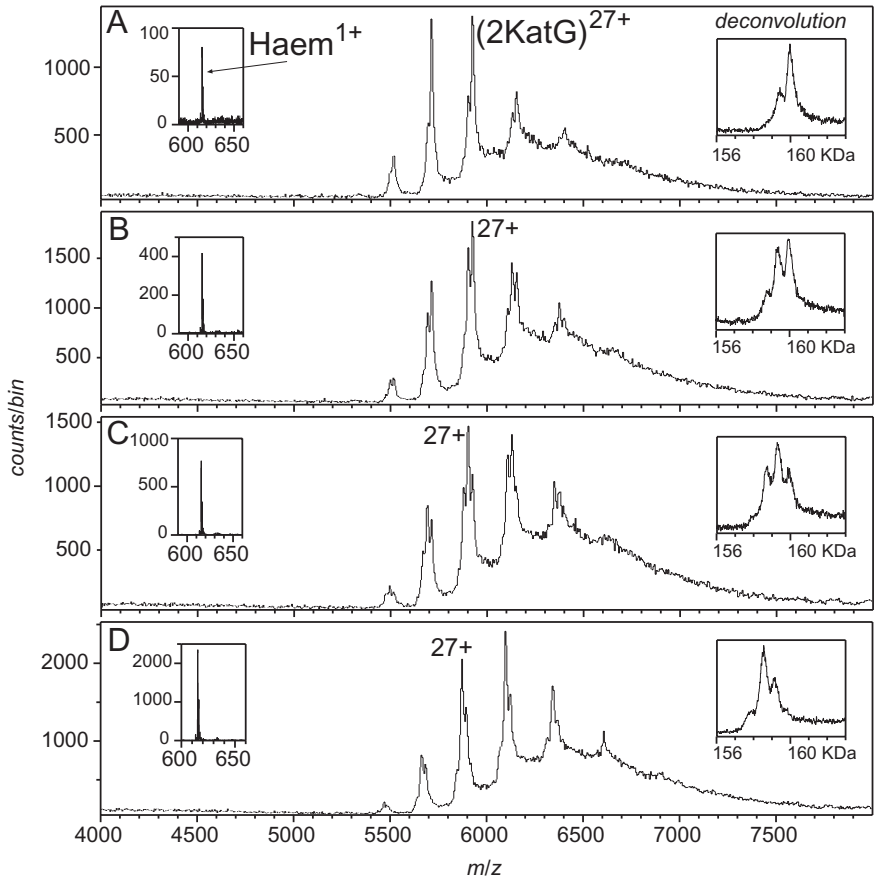

FIGURE 4 Spectra of the *B. pseudomallei* KatG protein prepared in 5 m*M* NH_4OAc using "traditional" dialysis and analysed by electrospray at 10 μ*M* protein. The curtain gas was SF_6, and the declustering voltage was varied in order to dissociate the haem from the complex. (A) 150 V, (B) 200 V, (C) 250 V, and (D) 300 V.

References

Ayed, A., Krutchinsky, A. N., Ens, W., Standing, K. G., and Duckworth, H. W. (1998). Quantitative evaluation of protein-protein and ligand-protein equilibria of a large allosteric enzyme by electrospray ionization time-of-flight mass spectrometry. *Rapid Commun. Mass Spectrom.* **12**, 339–344.

Carpena, X., Loprasert, S., Mongkolsuk, S., Switala, J., Loewen, P. C., and Fita, I. (2003). Catalase-peroxidase KatG of *Burkholderia pseudomallei* at 1.7 Å resolution. *J. Mol. Biol.* **327**, 475–489.

Chapman, J. R. (ed.) (2000). Protein and peptide analysis: New mass spectrometric applications. *In* "*Methods in Molecular Biology*," Vol. 146. Human Press, Totawa, NJ.

Chernushevich, I. V., Ens, W., and Standing, K. G. (1999). Orthogonal-injection TOFMS for analysing biomolecules. *Anal. Chem.* **71**, 452A–461A.

Daniel, J. M., Friess, S., Rajagopalan, S., Wendt, S., and Zenobi, R. (2002). Quantitative determination of noncovalent binding interactions using soft ionization mass spectrometry. *Int. J. Mass Spectrom.* **216**, 1–27.

Donald, L. J., Hosfield, D. J., Cuvelier, S. L., Ens, W., Standing, K. G., and Duckworth, H. W. (2001). Mass spectrometric study of the *Escherichia coli* repressor proteins, IclR and GclR, and their complexes with DNA. *Protein Sci.* **10**, 1370–1380.

Donald, L. J., Krokhin, O. V., Duckworth, H. W., Wiseman, B., Deemagarn, T., Singh, R., Switala, J., Carpena X., Fita, I., and Loewen, P. C. (2004). Characterization of the catalase-peroxidase KatG from *Burkholderia pseudomallei* by mass spectrometry. *J. Biol. Chem.*

Faloona, G. R., and Srere, P. A. (1969). *Escherichia coli* citrate synthase: Purification and the effect of potassium on some properties. *Biochemistry* **8**, 4497–4503.

Golemis, E. (ed.) (2002). "Protein-Protein Interactions: A Molecular Cloning Manual." Cold Spring Harbor Press, Cold Spring Harbor, NY.

Hiller, A., Peters, B., Pauls, R., Loboda, A., Zhang, H., Mauk, A. G., and Loewen, P. C. (2000). Modulation of the activities of catalase-peroxidase HPI of *Escherichia coli* by site-directed mutagenesis. *Biochemistry* **39**, 5868–5875.

Kapur, A., Beck, J. L., Brown, S. E., Dixon, N. E., and Sheil, M. M. (2002). Use of electrospray ionization mass spectrometry to study binding interactions between a replication terminator protein and DNA. *Protein Sci.* **11**, 147–157.

Krutchinsky, A. N., Ayed, A., Donald, L. J., Ens, W., Duckworth, H. W., and Standing, K. G. (2000). Studies of noncovalent

complexes in an electrospray ionization/time-of-flight mass spectrometer. *Methods Mol. Biol.* **146**, 239–249.

Krutchinsky, A. N., Chernushevich, I. V., Spicer, V. L., Ens, W., and Standing, K. G. (1998). A collisional damping interface for an electrospray ionization time-of-flight mass spectrometer. *J. Am. Soc. Mass Spectrom.* **9**, 569–579.

Millipore Corporation (2001). Centricon centrifugal filter devices. User Guide.

Nguyen, N. T., Maurus, R., Stokell, D. J., Ayed, A., Duckworth, H. W., and Brayer, G. D. (2001). Comparative analysis of folding and substrate binding sites between regulated hexameric type II citrate synthases and unregulated dimeric type I enzymes. *Biochemistry* **40**, 13177–13187.

Orr, A., Ivanova, V. S., and Bonner, W. M. (1995). "Waterbug" dialysis. *Biotechniques* **19**, 204–206.

Potier, N., Donald, L. J., Chernushevich, I., Ayed, A., Ens, W., Arrowsmith, C. H., Standing, K. G., and Duckworth, H. W. (1998). Study of a noncovalent *trp* repressor: DNA operator complex by electrospray ionization time-of-flight mass spectrometry. *Protein Sci.* **7**, 1388–1395.

Robinson, C. V. (2002). Characterization of multiprotein complexes by mass spectrometry. *In* "*Protein-Protein Interactions: A Molecular Cloning Manual*" (E. Golemis, ed.), pp. 227–240. Cold Spring Harbor Press, Cold Spring Harbor, NY.

Rostom, A. A., Fucini, P., Benjamin, D. R., Juenemann, R., Nierhaus, K. H., Hartl, U., Dobson, C. M., and Robinson, C. V. (2000). Detection and selective dissociation of intact ribosomes in a mass spectrometer. *Proc. Natl. Acad. Sci. USA* **97**, 5185–5190.

Rostom, A. A., and Robinson, C. V. (1999). Detection of the intact GroEL chaperonin assembly by mass spectrometry. *J. Am. Chem. Soc.* **121**, 4718–4719.

Stokell, D. J., Donald, L. J., Maurus, R., Nguyen, N. T., Sadler, G., Choudhary, K., Hultin, P. G., Brayer, G. D., and Duckworth, H. W. (2004). Probing the roles of key residues in the unique allosteric NADH binding site of Type II citrate synthase of *E. coli*. *J. Biol. Chem.*

Tang, X. J., Brewer, C. F., Saha, S., Chernushevich, I., Ens, W., and Standing, K. G. (1994). Investigation of protein-protein noncovalent interactions in soybean agglutinin by electrospray ionization time-of-flight mass spectrometry. *Rapid Commun. Mass Spectrom.* **8**, 750–754.

VanBerkel, W. J. H., Vandenheuvel, R. H. H., Versluis, C., and Heck, A. J. R. (2000). Detection of intact megaDalton protein assemblies of vanillyl-alcohol oxidase by mass spectrometry. *Protein Sci.* **9**, 435–439.

Verentchikov, A. N., Ens, W., and Standing, K. G. (1994). Reflecting time-of-flight mass spectrometer with an electrospray ion source and orthogonal extraction. *Anal. Chem.* **66**, 126–133.

Wilm, M., and Mann, M. (1996). Analytical properties of the nanoelectrospray ion source. *Anal. Chem.* **68**, 1–8.

Zhang, R. G., Joachimiak, A., Lawson, C. L., Schevitz, R. W., Otwinowski, Z., and Sigler, P. B. (1987). The crystal structure of *trp* aporepressor at 1.8 Å shows how binding of tryptophan enhances DNA affinity. *Nature* **327**, 591–596.

Zhao, D., Arrowsmith, C. H., and Jardetzky, O. (1993). Refined solution structures of the *Escherichia coli trp* holo- and aporepressor. *J. Mol. Biol.* **229**, 735–746.

PART

E

APPENDIX

SECTION

16

Appendix

CHAPTER

59

Bioinformatic Resources for *in Silico* Proteome Analysis

Manuela Pruess and Rolf Apweiler

I. INTRODUCTION

In the last years, the continual advancement in sequencing technology and proteome research has led to the massive rise of numbers of protein sequences from a wide range of species, representing a new challenge in the field of bioinformatics. Structure determination is also proceeding at an increasingly rapid rate, and all these data need to be stored in comprehensive specialised databases. These databases deal with nucleic acid sequences, protein sequences, and protein tertiary structures, respectively. Moreover, the sequences need to be assembled and analysed to represent a solid basis for further comparisons and investigations. Especially databases about model organisms such as *Mus musculus*, *Drosophila melanogaster*, *Caenorhabditis elegans*, *Arabidopsis thaliana*, or *Brachydanio rerio* (zebrafish) are of great interest.

To get as much information out of data as possible and to make use of the combination of different resources are two of the current challenges. An important instrument is the *in silico* analysis of proteomes. The term "proteome" is used to describe the protein equivalent of the genome. Most of the predicted protein sequences lack a documented functional characterisation. The task is to provide statistical and comparative analysis and structural and other information for these sequences as an essential step toward the integrated analysis of organisms at the gene, transcript, protein, and functional levels. Whole proteomes, as they are becoming more and more available, represent an important source for meaningful comparisons between species. To fully exploit the potential of this vast quantity of data, tools for *in silico* proteome analysis are necessary. There are genome and proteome analysis sites available, which benefit from the information stored in different databases and make use of different protein analysis tools to provide computational analysis of whole proteomes. Other proteomic tools focus on similarity searches, structure analysis and prediction, detection of specific regions, alignments, data mining, two-dimensional PAGE analysis, or protein modelling, respectively.

This article is dedicated to the description of some important sources for proteome analysis such as sequence databases and analysis tools. It aims at enabling the researcher to take advantage of all the different data sources available for optimal evaluation of sequences and structures.

II. RESOURCES AND THEIR USE

Biomolecular databases are, in combination with database search tools and tools for the computational analysis of the data, invaluable resources for biological and medical research. Their importance is ever increasing, especially as much data are no longer published in conventional publications, but are only available from databases. (All databases mentioned in the following, as well as their URLs, are listed in Table I.)

A. Sequence Databases

Sequence databases are comprehensive sources of information on nucleotide and protein sequences.

1. Nucleotide Sequence Databases

Nucleotide sequence databases store data on nucleic acid sequences submitted by genome sequenc-

Copyright 2006, Elsevier Science (USA).
All rights reserved.

TABLE I All Databases and Resources Important for the Analysis of Proteins and Proteomes Mentioned in the Text

Resource	Database (short name)	URL
Nucleotide sequence databases	DDBJ	http://www.ddbj.nig.ac.jp
	EMBL Bank	http://www.ebi.ac.uk/embl/
	GenBank	http://www.ncbi.nlm.nih.gov
Protein sequence databases	CluSTr	http://www.ebi.ac.uk/clustr
	PIR	http://pir.georgetown.edu
	Swiss-Prot	http://www.ebi.ac.uk/swissprot/, http://www.expasy.org/
	TrEMBL	http://www.ebi.ac.uk/trembl/
Protein tertiary structure databases	CATH	http://www.biochem.ucl.ac.uk/bsm/cath
	CCDC	http://www.ccdc.cam.ac.uk/
	DSSP	http://www.sander.ebi.ac.uk/dssp/
	FSSP	http://www.ebi.ac.uk/dali/fssp/
	HSSP	http://www.sander.ebi.ac.uk/hssp/
	PDB	http://www.rcsb.org/pdb/, http://www.ebi.ac.uk/msd/
	SCOP	http://scop.mrc-lmb.cam.ac.uk/scop/
Genome analysis databases	COG	http://www.ncbi.nlm.nih.gov/COG/
	Ensembl	http://www.ensembl.org/
	KEGG	http://www.genome.ad.jp/kegg/
	RefSeq	http://www.ncbi.nlm.nih.gov/LocusLink/refseq.html
	WIT	http://wit.mcs.anl.gov/WIT2/
Proteome analysis databases and tools	ExPASy	http://www.expasy.org
	Proteome Analysis DB	http://www.ebi.ac.uk/proteome
	InterPro	http://www.ebi.ac.uk/interpro
	IPI	http://www.ebi.ac.uk/IPI
	SRS	http://srs.ebi.ac.uk/
	SWISS-2DPAGE	http://www.expasy.ch/ch2d/

ing projects and individual researchers. Nucleotide sequence data are collected, organised, and distributed by the International Nucleotide Sequence Database Collaboration (Stoesser *et al*., 2001), which is a joint effort of the nucleotide sequence databases EMBL-Bank (maintained at the European Bioinformatics Institute, Hinxton, UK), the DNA Data Bank of Japan (maintained at the National Institute of Genetics, Mishima, Japan), and GenBank (maintained at the National Center for Biotechnology Information, Bethesda, MD). Nucleotide sequence databases are data repositories, accepting nucleic acid sequence data from the community and making it freely available. The databases strive for completeness, with the aim of recording and making available every publicly known nucleic acid sequence. EMBL-Bank, GenBank, and DDBJ automatically update each other every 24 h with new or updated sequences. Since their conception in the 1980s, nucleic acid sequence databases have experienced constant exponential growth. There is a tremendous increase of sequence data due to technological advances. At the time of writing, the DDBJ/EMBL/GenBank Nucleotide Sequence Database contains more than 79 billion nucleotides in more than 46 million individual entries and is doubling their size every year. Today, electronic bulk submissions from the major sequencing centers overshadow all other input and it is not uncommon to add in 1 day more than 30,000 new entries to the archives.

2. Protein Sequence Databases

Protein sequence databases store information on proteins. Here it has to be distinguished between universal databases covering proteins from all species and specialised data collections storing information about specific families or groups of proteins or about the proteins of a specific organism. Two categories of universal protein sequence databases can be discerned: simple archives of sequence data and annotated databases where additional information has been added to the sequence record. Especially the latter are of interest for the needs of proteome analysis.

PIR, the Protein Information Resource (Wu *et al*., 2002), has been the first protein sequence database, which was established in 1984 by the National Biomedical Research Foundation (NBRF) as a successor of the original NBRF Protein Sequence Database. Since 1988 it has been maintained by PIR-International, a collaboration among Georgetown University/NBRF, the Munich Information Center for Protein Sequences (MIPS), and the Japan International Protein Information Database (JIPID). The PIR release 80.00 (Dec-2004) contains 283,416 entries. It presents sequences from a wide range of species.

The PIR stopped this database's activities in 2004. The existing staff that worked at Georgetown University/NBRF on the maintenance of PIR started during 2002 to collaborate with the groups in charge of Swiss-Prot and TrEMBL (see later) and is now contributing to the maintenance of these databases.

Swiss-Prot (Bairoch and Apweiler, 2000) is an annotated protein sequence database established in 1986 and maintained since 1988 collaboratively by the Swiss Institute of Bioinformatics (SIB) and the EMBL Outstation—The European Bioinformatics Institute (EBI). It strives to provide a high level of annotation, such as the description of the function of a protein, its domain structure, posttranslational modifications, and variants, with a minimal level of redundancy. More than 60 biomolecular databases, such as the EMBL/GenBank/DDBJ international nucleotide sequence database, the PDB tertiary structure database (Bhat *et al*., 2001), or PubMed, are cross-referenced to provide a high level of integration. The links sum up to more than 4,000,000 individual links in total. Swiss-Prot contains data that originate from a wide variety of biological organisms. Release 45.5 (Jan-2005) contains a total of 167,089 annotated sequence entries from 8,811 different species; 11,777 of them are human sequences. The annotation of the human sequences is part of the HPI project, the human proteomics initiative (O'Donovan *et al*., 2001), which aims at the annotation of all known human proteins, their mammalian orthologues, polymorphisms at the protein sequence level, and posttranslational modifications and at providing tight links to structural information and clustering and classification of all known vertebrate proteins.

TrEMBL (Translation of EMBL nucleotide sequence database) (Bairoch and Apweiler, 2000) is a computer-annotated supplement to Swiss-Prot, created in 1996 with the aim to make new sequences available as quickly as possible. It consists of entries in Swiss-Prot format derived from the translation of all coding sequences (CDSs) in the EMBL Nucleotide Sequence Database, except the CDSs already included in Swiss-Prot. TrEMBL release 28.5 (Jan-2005) contains 1,560,235 entries, which should be eventually incorporated into Swiss-Prot. Before the manual annotation step, automated annotation (Kretschmann *et al*., 2001) is applied to TrEMBL entries to accelerate the annotation process.

SP_TR_NRDB (or abbreviated SPTR or SWALL) is a database created to overcome the problem of the lack of comprehensiveness of single sequence databases: it comprises both the weekly updated Swiss-Prot work release and the weekly updated TrEMBL work release. The CluSTr (Clusters of Swiss-Prot and TrEMBL proteins) database (Kriventseva *et al*., 2001) is a specialised database, which offers an automatic classification of Swiss-Prot and TrEMBL proteins into groups of related proteins. The clustering is based on a hierarchical single-linkage clustering of all pairwise comparisons between protein sequences, yielding a hierarchical organisation of clusters.

3. Protein Structure Databases

The number of known protein structures is increasing very rapidly and these are available through PDB, the Protein Data Bank. PDB represents the single worldwide repository for the processing and distribution of three-dimensional biological macromolecular structure data, gained by techniques of X-ray crystal structure determination, nuclear magnetic resonancy, cryoelectron microscopy, and theoretical modeling.

In addition, there are also a number of derived databases, which enable comparative studies of three-dimensional structures as well as to gain insight on the relationships among sequence, secondary structure elements, and three-dimensional structure. DSSP (Dictionary of Secondary Structure in Proteins; Kabsch and Sander, 1983) contains the derived information on the secondary structure and solvent accessibility for the protein structures stored in PDB. HSSP (Homology-derived Secondary Structure of Proteins; Dodge *et al*., 1998) is a database of alignments of the sequences of proteins with known structure with all their close homologues. FSSP (Families of Structurally Similar Proteins; Holm and Sander, 1996) is a database of structural alignments of proteins. It is based on an all-against-all comparison of the structures stored in PDB. Each database entry contains structural alignments of significantly similar proteins but excludes proteins with high sequence similarity, as these are usually structurally very similar.

The SCOP (Structural Classification of Proteins) database (Lo Conte *et al*., 2002) has been created by manual inspection and abetted by a battery of automated methods. This resource aims to provide a detailed and comprehensive description of the

structural and evolutionary relationships between all proteins whose structure is known. As such, it provides a broad survey of all known protein folds and detailed information about the close relatives of any particular protein.

Another database that attempts to classify protein structures in the PDB is the CATH database (Pearl *et al*., 2001), a hierarchical domain classification of protein structures in the PDB. There are four major levels in this hierarchy: class, architecture, topology (fold family), and homologous superfamily.

B. Genome Analysis Databases

There are a number of databases that address some aspects of genome comparisons. The Kyoto Encyclopedia of Genes and Genomes (KEGG; Kanehisa *et al*., 2002) is a knowledge base for systematic analysis of gene functions, linking genomic information with higher order functional information. The WIT project (Overbeek *et al*., 2000) attempts to produce metabolic reconstructions for sequenced (or partially sequenced) genomes. A metabolic reconstruction is described as a model of the metabolism of the organism derived from sequence, biochemical, and phenotypic data. KEGG and WIT mainly address regulation and metabolic pathways, although the KEGG scheme is being extended to include a number of nonmetabolism-related functions. The Clusters of Orthologous Groups of proteins (COGs; Tatusov *et al*., 2001) provide a phylogenetic classification of proteins encoded in complete genomes. COGs group together related proteins with similar but sometimes nonidentical functions.

Ensembl (Hubbard *et al*., 2002) is a project to develop a software system that produces and maintains automatic annotation on metazoan genomes. By presenting up-to-date assembled sequence data and automatic analysis of the genomes, it represents an important resource for the interpretation of metazoan genome data.

Functional annotation of genomes is also provided in the framework of the NCBI Reference Sequence project (RefSeq; Pruitt and Maglott, 2001), which creates reference sequence sets for the naturally occurring molecules of the central dogma, from chromosomes to mRNAs to proteins. Toward this goal, intermediate larger genomic regions are also produced.

C. Proteome Analysis Databases and Tools

Tools and databases for proteome analysis provide algorithmic analysis and information about protein sequences and structures derived from comprehensive protein databases. It is sometimes difficult to distinguish between "database" and "tool," as databases providing precomputed data and search algorithms can both offer a high functionality towards protein analysis.

1. Proteome Analysis Databases

The classic proteomics databases are those of two dimensional gel electrophoresis gels and their analysis is like the SWISS-2DPAGE database (Hoogland *et al*., 2000) and the human keratinocyte two-dimensional gel protein database from the universities of Aarhus and Ghent. Such databases allow interesting insights into the proteome of a given cell under given experimental conditions. Analysis of the protein spots on a gel by mass spectrometry has enabled the identification of many proteins on such gels, although the majority of proteins are usually still unidentified.

An additional way to gain insights into the variety of proteins produced by an organism is the bioinformatics exploitation of genome sequences. Genome sequencing is proceeding at an increasingly rapid rate, which leads to an equally rapid increase in predicted protein sequences entering the protein sequence databases. Most of these predicted protein sequences are without a documented functional role. The challenge is to bridge the gap until functional data have been gathered through experimental research by providing computational analysis as an essential step towards the integrated analysis of organisms at the gene, transcript, protein, and functional levels. Proteome analysis databases have been set up to provide comprehensive statistical and comparative analyses of the predicted proteomes of fully sequenced organisms.

The Proteome Analysis Database (Apweiler *et al*., 2001b) has the general aim of integrating information from a variety of sources that will together facilitate the classification of proteins in complete proteome sets. The proteome sets are built from the Swiss-Prot and TrEMBL protein sequence databases that provide reliable, well-annotated data as the basis for the analysis. Proteome analysis data are available for all the completely sequenced organisms present in Swiss-Prot and TrEMBL, spanning archaea, bacteria, and eukaryotes. In the proteome analysis effort, the InterPro (Apweiler *et al*., 2001a) and CluSTr resources have been used. Links to structural information databases such as PDB, HSSP, and SCOP are provided for individual proteins from each of the proteomes. A functional classification using gene ontology (GO; Ashburner *et al*., 2000) is also available. The Proteome Analysis Database provides a broad view of the proteome data classified according to signatures describing particular sequence motifs or sequence similarities

and, at the same time, affords the option of examining various specific details, such as structure or functional classification. It currently (as of January 2005) contains statistical and analytical data for more than 210 complete proteomes.

The International Protein Index (IPI) provides a top-level guide to the main databases that describe the human and mouse proteome, namely Swiss-Prot, TrEMBL, RefSeq, and EnsEMBL. IPI maintains a database of cross-references between the primary data sources with the aim of providing a minimally redundant yet maximally complete set of human proteins (one sequence per transcript).

2. *Proteome Analysis Tools*

Traditional proteomics tools, such as those accessible from the EBI's SRS server or from the ExPASy server represent a variety of possibilities to analyse proteins. They help identify and characterise proteins, convert DNA sequences into amino acid sequences, and perform similarity searches, pattern and profile searches, posttranslational modification prediction, primary structure analysis, secondary and tertiary structure prediction, detection of transmembrane regions, alignments, and biological text analysis. Moreover, software is available for two-dimensional PAGE analysis, automated knowledge-based protein modelling, and structure display and analysis.

The analysis of whole proteomes represents an even bigger challenge. Large and comprehensive databases and knowledge bases are developed and used that provide large sets of precomputed data. To gather this comprehensive data, a vast amount of underlying information is necessary. The Proteome Analysis Database, mentioned earlier, uses annotated information about proteins from the Swiss-Prot/TrEMBL database and automated protein classifications from InterPro, CluSTr, HSSP, TMHMM (Sonnhammer *et al*., 1998), and SignalP (Nielsen *et al*., 1999). An example of data available for a single organism is shown in Fig. 1. Precomputation permits comparisons of whole proteomes of completely sequenced organisms with those of others. Users of the database can perform their own interactive proteome comparisons between any combinations of organisms in the database. Moreover, structural features of individual proteomes, such as protein length distribution, amino acid composition, and the affiliation of the different proteins to protein families, can be requested. Users are also able to run FASTA similarity searches (Fasta3) of their own sequence against a complete proteome or a set of complete proteomes. It is possible to download a proteome set or a list of InterPro matches for a given organism, to see the current status of all complete proteomes in Swiss-Prot and TrEMBL, and to download GO annotation for the human proteome.

Organism : *Drosophila melanogaster*

Drosophila melanogaster, the fruit fly, is one of the most valuable organisms in biological research and has been studied for many years.
The whole genome of *D. melanogaster* was sequenced in collaboration between Celera Genomics, the Berkeley Drosophila Genome Project (BDGP) and the European Drosophila Genome Project (EDGP).

Statistical analysis of the *D. melanogaster* proteome is presented in the table below:

InterPro [help]	CluSTr [help]	Structure [help]	InterPro comparative analysis [help]
General statistics (proteins with InterPro hits) Top 30 hits Top 200 hits 15 most common families 15 most common domains 15 most common repeats Top 30 proteins with the highest occurrence of different InterPro hits	General statistics List of singletons 30 biggest clusters Clusters without InterPro links Clusters without HSSP links	Protein length distribution *Primary* Amino acid composition *Secondary* Proteins with HSSP links *Tertiary* Proteins with PDB links	*Proteome comparisons* *vs. A. thaliana, C. elegans, H. sapiens and S. cerevisiae* *Top 30 hits* *vs. A. thaliana, C. elegans, H. sapiens and S. cerevisiae* *Top 200 hits* *vs. A. thaliana, C. elegans, H. sapiens and S. cerevisiae* *15 most common families* *vs. A. thaliana, C. elegans, H. sapiens and S. cerevisiae* *15 most common repeats* *vs. A. thaliana, C. elegans, H. sapiens and S. cerevisiae*

FIGURE 1 Top-level statistical analysis page for the *Drosophila melanogaster* proteome, taken from the Proteome Analysis database.

III. COMMENTS

The last years have seen a tremendous increase in genomic data, particularly in the amount of data contributing to the understanding of the molecular basis of genetic diseases. Every week new discoveries are made that link genetic diseases to defects in specific genes. The Swiss-Prot and TrEMBL databases are in response to these developments gradually enhanced by the addition of a number of features that are specifically intended for researchers working on human genetic diseases and polymorphisms. The latter are of importance as they represent the basis for differences between individuals, which are of particular interest for research on topics such as disease susceptibility and differences in response to drug treatment. The comprehensive capturing of such data in sequence databases is fundamental for proteome analysis tools, such as the proteome analysis database, which combines information about different proteins of a given organism to comprehensive information about a complete proteome. A proteome can be regarded as a whole new unit, analysable according to different points of view (such as distribution of domains and protein families, and secondary and tertiary structure of proteins), and makes it comparable to other proteomes. To use proteomics data in areas such as healthcare and drug development, the characteristics of proteomes of entire species have to be understood before differentiation between individuals can be surveyed.

IV. PITFALLS

The number of proteome analysis tools and databases is increasing and most of them are providing high-quality resources of computational analysis and annotation. However, the user should not forget that *in silico* tools and databases have, like wet lab technologies, their very own pitfalls. The material in databases and the output of tools are trustworthy, but only to a certain point, just as the results of wet lab experiments. It is important to emphasise again that most sequence data today come from large-scale sequencing efforts and lack experimental functional characterisation. Many sequencing centres still annotate the predicted coding sequences just based on automated high-level sequence similarity searches against protein sequence databases. However, this methodology has several drawbacks.

i. Because many proteins are multifunctional, the assignment of a single function, which is still common in genome projects, results in loss of information and outright errors.
ii. Because the best hit in pairwise sequence similarity searches is frequently a hypothetical protein or poorly annotated or has simply a different function, the propagation of wrong annotation is widespread.
iii. There is no coverage of position-specific annotation such as active sites.
iv. The annotation is not updated constantly and is thus outdated quickly.

It is also worth mentioning that a single sentence describing some predicted properties of an unknown protein should not be regarded as full annotation, but rather more as an attempt to characterise a protein. Full annotation means the combination of extracting experimentally verified information from the literature with sequence analysis to add as much reliable and up-to-date information as possible about properties such as the function(s) of the protein, domains and sites, catalytic activity, cofactors, regulation, induction, subcellular location, quaternary structure, diseases associated with deficiencies in the protein, tissue specificity of a protein, developmental stages in which the protein is expressed, pathways and processes in which the protein may be involved, and similarities to other proteins.

The Swiss-Prot knowledge base strives to provide extensive annotation as defined previously. However, annotation to such a high quality requires careful and detailed analysis of every sequence and of the scientific literature. This is the rate-limiting step in the production of Swiss-Prot and only a relatively small portion of the whole sequence data submitted to the sequence databases can be annotated to such a high standard and gets incorporated into Swiss-Prot.

Users of bioinformatics tools and databases should in no way feel discouraged in using these important resources, but they should bear in mind the potential pitfalls, check all data carefully, and not blindly rely on data. We also stress that all databases appreciate suggestions for improvements and the reporting of errors, which allow data custodians to improve their resources.

References

Apweiler, R., Attwood, T. K., Bairoch, A., Bateman, A., Birney, E., Biswas, M., Bucher, P., Cerutti L., Corpet F., Croning M. D., Durbin R., Falquet L., Fleischmann W., Gouzy J., Hermjakob, H., Hulo, N., Jonassen, I., Kahn, D., Kanapin, A., Karavidopoulou, Y., Lopez, R., Marx, B., Mulder, N. J., Oinn, T. M., Pagni, M., Servant, F., Sigrist, C. J., and Zdobnov, E. M. (2001a). The

InterPro database, an integrated documentation resource for protein families, domains and functional sites. *Nucleic Acids Res*. **29**, 37–40.

Apweiler, R., Biswas, M., Fleischmann, W., Kanapin, A., Karavidopoulou, Y., Kersey, P., Kriventseva, E. V., Mittard, V., Mulder, N., Phan, I., and Zdobnov, E. (2001b). Proteome Analysis Database: Online application of InterPro and CluSTr for the functional classification of proteins in whole genomes. *Nucleic Acids Res*. **29**, 44–48.

Ashburner, M., Ball, C. A., Blake, J. A., Botstein, D., Butler, H., Cherry, J. M., Davis, A. P., Dolinski, K., Dwight, S. S., Eppig, J. T., Harris, M. A., Hill, D. P., Issel-Tarver, L., Kasarskis, A., Lewis, S., Matese, J. C., Richardson, J. E., Ringwald, M., Rubin, G. M., and Sherlock, G. (2000). Gene ontology: Tool for the unification of biology. The Gene Ontology Consortium. *Nature Genet*. **25**, 25–29.

Bairoch, A., and Apweiler, R. (2000). The Swiss-Prot protein sequence database and its supplement TrEMBL in 2000. *Nucleic Acids Res*. **28**, 45–48.

Bhat, T. N., Bourne, P., Feng, Z., Gilliland, G., Jain, S., Ravichandran, V., Schneider, B., Schneider, K., Thanki, N., Weissig, H., Westbrook, J., and Berman, H. M. (2001). The PDB data uniformity project. *Nucleic Acids. Res*. **29**, 214–218.

Dodge, C., Schneider, R., and Sander, C. (1998). The HSSP database of protein structure-sequence alignments and family profiles. *Nucleic Acids Res*. **26**, 313–315.

Holm, L., and Sander, C. (1996). The FSSP database: Fold classification based on structure-structure alignment of proteins. *Nucleic Acids Res*. **24**, 206–209.

Hoogland, C., Sanchez, J.-C., Tonella, L., Binz, P.-A., Bairoch, A., Hochstrasser, D. F., and Appel, R. D. (2000). The 1999 SWISS-2DPAGE database update. *Nucleic Acids Res*. **28**, 286–288.

Hubbard, T., Barker, D., Birney, E., Cameron, G., Chen, Y., Clark, L., Cox, T., Cuff, J., Curwen, V., Down, T., Durbin, R., Eyras, E., Gilbert, J., Hammond, M., Huminiecki, L., Kasprzyk, A., Lehvaslaiho, H., Lijnzaad, P., Melsopp, C., Mongin, E., Pettett, R., Pocock, M., Potter, S., Rust, A., Schmidt, E., Searle, S., Slater, G., Smith, J., Spooner, W., Stabenau, A., Stalker, J., Stupka, E., Ureta-Vidal, A., Vastrik, I., and Clamp, M. (2002). The Ensembl genome database project. *Nucleic Acids Res*. **30**, 38–41.

Kabsch, W., and Sander, C. (1983). Dictionary of protein secondary structure: Pattern recognition of hydrogen-bonded and geometrical features. *Biopolymers* **22**, 2577–2637.

Kanehisa, M., Goto, S., Kawashima, S., and Nakaya, A. (2002). The KEGG databases at GenomeNet. *Nucleic Acids Res*. **30**, 42–46.

Kretschmann, E., Fleischmann, W., and Apweiler, R. (2001). Automatic rule generation for protein annotation with the C4.5 data mining algorith applied on Swiss-Prot. *Bioinformatics* **17**, 920–926.

Kriventseva, E. V., Fleischmann, W., Zdobnov, E. M., and Apweiler, R. (2001). CluSTr: A database of clusters of Swiss-Prot+TrEMBL proteins. *Nucleic Acids Res*. **29**, 33–36.

Lo Conte, L., Brenner, S. E., Hubbard, T. J. P., Chothia, C., and Murzin, A. G. (2002). SCOP database in 2002: Refinements accommodate structural genomics. *Nucleic Acids Res*. **30**, 264–267.

Nielsen, H., Brunak, S., and von Heijne, G. (1999). Machine learning approaches for the prediction of signal peptides and other protein sorting signals. *Protein Eng*. **12**, 3–9.

O'Donovan, C., Apweiler, R., and Bairoch, A. (2001). The human proteomics initiative (HPI). *Trends Biotechnol*. **19**, 178–181.

Overbeek, R., Larsen, N., Pusch, G. D., D'Souza, M., Selkov, E.Jr., Kyrpides, N., Fonstein, M., Maltsev, N., and Selkov, E. (2000). WIT: Integrated system for high-throughput genome sequence analysis and metabolic reconstruction. *Nucleic Acids Res*. **28**, 123–125.

Pearl, F. M. G., Martin, N., Bray, J. E., Buchan, D. W. A., Harrison, A. P., Lee, D., Reeves, G. A., Shepherd, A. J., Sillitoe, I., Todd, A. E., Thornton, J. M., and Orengo, C. A. (2001). A rapid classification protocol for the CATH Domain Database to support structural genomics. *Nucleic Acids Res*. **29**, 223–227.

Pruitt, K. D., and Maglott, D. R. (2001). RefSeq and LocusLink: NCBI gene-centered resources. *Nucleic Acids Res*. **29**, 137–140.

Sonnhammer, E. L. L., von Heijne, G., and Krogh, A. (1998). A hidden Markov model for predicting transmembrane helices in protein sequences. *In "Proc. of Sixth Int. Conf. on Intelligent Systems for Molecular Biology"* (J. Glasgow, T. Littlejohn, F. Major, R. Lathrop, D. Sankoff, and C. Sensen, eds.), pp. 175–182. AAAI Press, Menlo Park, CA.

Stoesser, G., Baker, W., van den Broek, S., Camon, E., Garcia-Pastor, M., Kanz, C., Kulikova, T., Lombard, V., Lopez, R., Parkinson, H., Redaschi, N., Sterk, P., Stoehr, P., and Tuli, M. A. (2001). The EMBL nucleotide sequence database. *Nucleic Acids Res*. **29**, 17–21.

Tatusov, R. L., Natale, D. A., Garkavtsev, I. V., Tatusova, T. A., Shankavaram, U. T., Rao, B. S., Kiryutin, B., Galperin, M. Y., Fedorova, N. D., and Koonin, E. V. (2001). The COG database: New developments in phylogenetic classification of proteins from complete genomes. *Nucleic Acids Res*. **29**, 22–28.

Wu, C. H., Huang, H., Arminski, L., Castro-Alvear, J., Chen, Y., Hu, Z.-Z., Ledley, R. S., Lewis, K. C., Mewes, H.-W., Orcutt, B. C., Suzek, B. E., Tsugita, A., Vinayaka, C. R., Yeh, L.-S., Zhang J., and Barker, W. C. (2002). The Protein Information Resource: An integrated public resource of functional annotation of proteins. *Nucleic Acids Res*. **30**, 35–37.

List of Suppliers

3M AG
Rüschlikon, Switzerland
http://www.3m.com/

AAPER Alcohol
PO Box 339
Shelbyville, KY 40066-0339
USA
TEL 800-456-1017
FAX 502-633-0685

AB
SE-75184 Uppsala
Sweden
TEL 46-018 6121900
FAX 46-018 6121920
http://www.amershambiosciences.com

Abbott Laboratories
100 Abbott Park Road
Abbott Park, IL 60064
http://abbott.com

Abgene
ABgene House
Blenheim Road, Epsom KT19 9AP
UK

Abgene, Inc.
565 Blossom Road
Rochester, NY 14610
USA
TEL 585-654-4800
FAX 585-654-4810

Academy Bioanalytical
1417 Kress Street, Houston
TX 77020
USA

Accurate Chemical and Scientific Corporation
300 Shames Drive
Westbury, NY 11590
http://www.accuratechemical.com

Active Motif
1914 Palomar Oaks Way
Suite 150
Carlsbad California 92008
USA
TEL 877 222 9543
TEL 760 431 1263
FAX 760 431 1351
http://www.activemotif.com

Acufirm
Landsteinerstr 2
Dreieich, D-63303
Germany
TEL +49 6103 9833
FAX +49 6103 983470
E-MAIL ernstkratz@acufirm.de

Affinity Bioreagents
14818 West 6th Avenue
Suite 10A
Golden, Colorado 80401
USA

Copyright 2006, Elsevier Science (USA).
All rights reserved.

Affymetrix, Inc.
3380 Central Expressway
Santa Clara, CA 95051
USA
TEL +1-888-362-2447
FAX 408-731-5441
http://www.affymetrix.com

African Reptile Park
30 Easson Rd.
Steenberg 7945
Capetown, South Africa

Agar Scientific Limited
66A Cambridge Road
Stansted Essex, CM24 8DA
England
TEL (+44) 1279 813519
FAX +44 279 815106
http://www.agarscientific.com

Agfa Medical
Agfa-Gevaert Headquarters
Septestraat, 27
2640 Morstel
(Belgium)
http://www.agfa.com/healthcare

Agilent Technologies
395 Page Mill Rd.
P.O. Box #10395
Palo Alto, CA 94303
USA
TEL 800-227-9770
TEL 302-993-5304
FAX 302-633-8901
http://www.agilent.com

AID, Autoimmun Diagnostika GmbH
Ebinger Strasse 4
D-72479 Strassberg
Germany
TEL +49-7434-9364-0
FAX +49-7434-9364-40
http://www.elispot.com

Air Products Europe
Hersham Place
Molesley Road
Walton-on-Thames, Surrey KT12 4RZ
UK
TEL (+44) 1932 249200
FAX (+44) 1932 24 9565

Alcon Laboratories Inc.
6201 S. Freeway
Fort Worth, Texas
USA
http://www.alconlabs.com/

Aldrich Chemical Co., Inc.
1001 West St. Paul Avenue
Milwaukee, WI 53233
USA
TEL 414-273-3850
FAX 414-273-4979

Alexis Biochemicals
6181 Cornerstone Court East
Suite 103
San Diego, CA 92121
TEL 858-658-0065
TEL 800-900-0065

Alfa Aesar Johnson Matthey
Postbox 11 07 65
D-76057 Karlsruhe
Germany
TEL (+49) 721 84007 280
http://www.alfa-chemcat.com

Alltech Associates, Inc.
2051 Waukegan Rd.
Deerfield, IL 60015

Alpha Laboratories, Division of Eurofins Scientific, Inc.
1365 Redwood Way
Petaluma—CA 94954
TEL 1-800-92-ALPHA
TEL 707-792-7300
FAX 707-792-7309
http://www.alphalabs.com/index.html

Alpha Laboratories Ltd.
40 Parham Drive
Eastleigh Hampshire SO50 4NU
UK
TEL +44 (0) 23 8048 3000
FAX +44 (0) 23 8064 3701
E-MAIL info@alphalabs.co.uk

Ambion Inc.
2130 Woodward St.
Austin, Texas 78744
USA
http://www.ambion.com

American Bioanalytical
15 Eire Dr.
Natick, MA 01760-1329
USA
TEL (800)443-0600
E-MAIL info@americanbio.com
http://www.americanbio.com/contact.asp

American Type Culture Collection (ATCC)
12301 Parklawn Drive
Rockville, Maryland 20852
USA
TEL (301)-881-2600
FAX (301)-770-1848

American Type Culture Collection (ATCC)
P.O. Box 1549
Manassas, VA 20108
TEL 1 703 365 2700
FAX 1 703 365 2750
http://www.atcc.org/

Amersham Biosciences
800 Centential Avenue
PO Box 1327
Picataway, NJ 08855-1327
USA
TEL 732-457-8000
FAX 732-457-0557
http://www.amershambiosciences.com

Amersham Biosciences
Munzinger Str. 9
D-79111 Freiburg
Germany
TEL +49 761 451 90
FAX +49 761 4519 159
http://www.amershambiosciences.com

Amersham Biosciences Corp.
800 Centennial Ave
Piscataway, NJ 08855
USA
TEL 1-732-457-8000
FAX 1-732-457-0557
TEL 1-800-526-3593
FAX 1-877-295-8102
http://www4.amershambiosciences.com

Amersham Biosciences Europe GmbH,
Branch office Benelux
Bergrand 230
4707 AT Rosendaal,
The Netherlands
http://www.amershambiosciences.com

Amersham Biosciences Europe GmbH
Zweigniederlassung Österreich
Wurzbachgasse 18, A-1152 Wien
AUSTRIA
TEL +43 1 57 606 16 13
FAX +43 1 57 606 16 14
E-MAIL cust.servde@amersham.com
http://www1.amershambiosciences.com

Amersham Biosciences UK Ltd.
International Trading Divison,
Pollards Wood
Nightingales Lane
Chalfont St Giles
Buckinghamshire, HP8 4SP
England
TEL +44 1494 49 8163
FAX +44 1494 49 8235
http://www.amershambiosciences.com

Amersham Pharmacia Biotech
AB
SE-75184 Uppsala
Sweden
TEL 46-018 6121900
FAX 46-018 6121920
http://www.amershambiosciences.com

Amersham Pharmacia Biotech
500 Morgan Blvd.
Baie d'Urfe, PQ H9X 3V1
Canada
TEL 1-800-463-5800

Amersham Pharmacia Biotech
P.O. Box 1327
Piscataway, NJ 08855-1327
TEL 1-800-526-3593
http://www.amershambiosciences.com

Amicon
Millipore
290 Concord Rd.
Billerica, MA 01821
USA
http://www.millipore.com

Amicon Bioseparations (Division of Millipore Corporation)
Amicon Ltd.
Upper Mill
Stonehouse, Glos. GL10 2BJ
UK
TEL +44 (0)1453825181
FAX +44 (0)1453826686

Amimed BioConcept
Innovationszentrum Nordwestschweiz
Gewerbestrasse 14
Postfach 427 CH—4123 Allschwil 1
Switzerland
TEL +41 61 486 80 80
FAX +41 61 486 80 00
E-MAIL info@bioconcept.ch
http://www.bioconcept.com

Amresco/Electra Box Diagnostica AB
Box 2035
Tyreso 2, 13502
Sweden
TEL 46-8-712-3000
FAX 46-8-712-6509

AMRESCO Inc.
30175 Solon Industrial Parkway
Solon, Ohio 44139
TEL (Local): 440-349-1313
TEL 800-366-1313
FAX 440-349-1182
E-MAIL info@amresco-inc.com

Anachemia Chemicals Inc.
3 Lincoln Blvd.
Rouses Point, NY 12979
TEL 800-323-1414
http://www.anachemiachemicals.com

Analis
rue Dewez 14
5000 Namur
TEL ++32 (0)81 25 50 50
FAX ++32 (0)81 23 07 79

Angus Buffers and Biochemicals
2236 Liberty Drive
Niagara falls, New York
USA
TEL 1-800-648-6689

Antec International Ltd.
Chilton Industrial Estate
Sudbury, Suffolk C010 2KD
UK

Apex Microtechnology Corporation
5980 N. Shannon Road
Tucson, AZ 85741-5230
USA
TEL (+01) 520 690-8600
FAX (+01) 520 888-3329
E-MAIL sales@apexmicrotech.com
http://eportal.apexmicrotech.com

Apodan A/S
Lergravsvej 63
Copenhagen, Denmark

Applied Biosystems
850 Lincoln Centre Drive
Foster City, CA 94404
TEL 800-327-3002
TEL +1-650-638-5800
FAX +1-650-638-5884
http://www.appliedbiosystems.com/

Applied Precision, LLC
1040 12th Avenue Northwest
Issaquah, Washington 98027
USA
TEL 425.557.1000
FAX 425.557.1055

AR42J-B13 cells: Professor I Kojima
Department of Cell Biology
Gunma University
Maebashi, Gumma 3718512
Japan

Arcturus Engineering, Inc.
400 Logue Ave.
Mountain View, CA 94043
TEL 888-446-7911
http://www.arctur.com

Asahi Techno Glass
3-7-2 Nihonbashi-honcho
Chuo-ku, Tokyo 103-0023
Japan
TEL 81-3-5625-2751
http://www.atgc.co.jp

Assistent Glasware
Karl Hecht KG
Stettener Str. 22-24
97647 Sondheim, Germany
http://www.hecht-assistent.de

Atlanta Biologicals
1425 Oakbrook Drive
Norcross, GA 30093

Atto Bioscience
15010 Broschart Road
Rockville, MD 20850

Austral Biologicals
125 Ryan Industrial Ct.
Suite 207
San Ramon, CA 94583

Avanti Polar Lipids, Inc.
700 Inductrial Park Drive
Alabaster, AL 35007
TEL 1-800-227-0651
TEL 205-663-2494
FAX 1-800-229-1004
FAX 205-663-0756
http://www.avantilipids.com

Aventis Behring
PO Box 1230.
35002 Marburg
Germany

Avestin Europe GmbH
Weinheimer Str. 64b
D68309 Mannheim
Germany
Axis-Shield PoC AS
Marstrandgata 6
PO Box 6863
Rodeløkka, 0504 Oslo
Norway
TEL +47 22 04 20 00
FAX +47 22 04 20 10
http://www.axis-shield-poc.com

Axon Instruments, Inc.
3280 Whipple Road
Union City, CA 94587
USA
TEL +1 510-675-6200
FAX +1 510-675-6300
http://www.axon.com/

Bachem AG
Hauptstrasse 144
4416 Bubendorf, 19406
Switzerland
TEL +41 61 935 2323
FAX +41 61 935 2325
http://www.bachem.com/

Bachem Bioscience Inc.
3700 Horizon
Drive King of Prussia, PA
TEL +1 800 634 3183
FAX +1 610 239 0800

Bachem, California
3132 Kashiwa Street
Torrance, CA 90505
USA

Bacto Laboratories Pty Lt
Falcon Labware
PO Box 295
Liverpool, NSW 2170
Australia
TEL +61 (0)2 9602 5499
FAX +61 (0)2 9601 8293
E-MAIL info@bacto.com.au
http://www.bacto.com.au

Baker Company
PO Box Drawer E
Sanford, ME 04073
USA
TEL 207-324-8773
FAX 207-324-3869
E-MAIL bakerco@bakerco.com
http://www.bakerco.com

BAL-TEC
Föhrenweg 16
FL-9496 Balzers
Principality of Liechtenstein
TEL +423-388-1212
FAX +423-388-1260
http://www.bal-tec.com/

Bal-TEC AG
Postfach 75
FL-9496 Balzers
Fürstentum Liechtenstein
TEL +41 75 388 5611
FAX +41 75 388 5660

Barnstead International
2555 Kerper Blvd.
PO Box 797
Dubuque, IA 52001-1478
TEL 800-446-6060
FAX 563-589-0516

Baxter Scientific Products
1750 Stone Ridge Dr.
Stone Mountain, GA 30083
USA
TEL 404-270-9645
FAX 800-964-5227

B. Braun Biotech International
Schwarzenberger Weg 73-79
D-34212 Melsungen
Germany
http://www.bbraunbiotech.com

B. Braun Medical AG
Seesatz CH-6203
Sempach-Station
Switzerland
TEL +41 848 83 00 44
FAX +41 800 83 00 43
E-MAIL info.bbmch@bbraun.com
http://www.bbraun.com

BCB Ltd.
Moorland Rd
Cardiff, CF24 2YL
UK
TEL (029) 2046 4464
FAX (029) 2048 1100
http://www.bcb.ltd.uk

BD Biosciences
1-2900 Argentia Road
Mississauga, ON L5N 7X9
Canada
TEL 1-888-259-0187

BD Biosciences
133 Venture Ct.
Lexington, KY 40511-2624

BD Biosciences
2350 Qume Drive
San Jose, CA 95131-1807

BD Biosciences
Two Oak Park Drive
Bedford, MA 01730
USA (Becton, Dickinson and Company)
Tullastrasse 8-12
69126 Heidelberg
Germany
http://www.bdbiosciences.com

BD Biosciences (and Pharmingen)
European Office
Customer Service
Erembodegem—Dorp 86, 9320 Erembodegem
Belgium
TEL +32 53720211
FAX +32 53720450
E-MAIL bdb@europe.bd.com
http://www.bdbiosciences.com

BD Biosciences/Clontech
1020 East Meadow Circle
Palo Alto, CA 94303-4230
TEL (+44) 01865 781688
FAX (+44) 01867 781 627

BD Biosciences Discovery Labware
Two Oak Park Drive
Bedford, MA 01730
USA

BD Biosciences GmbH
Postfach 10 16 29
D-69008 Heidelberg
Germany

BD Biosciences—Immunocytometry Systems
2350 Qume Drive
San Jose, California, 95131-1807
TEL 1 877.232.8995
FAX 1 408.954.2347
E-MAIL facservice@bdis.com
http://www.bd.com

BD Biosciences Pharmingen
10975 Torreyana Road
San Diego, CA 92121
TEL 858-812-8800
FAX 858-812-8888
Toll Free: 877-232-8995
E-MAIL info@pharmingen.com
http://www.bdbiosciences.com.

BD Biosciences—Transduction Laboratories
133 Venture Ct.
Lexington, KY 40511-2624
TEL 859-259-1550
FAX 859-259-1413
TEL 0-227-4063
E-MAIL tlbinfo@translab.com
http://www.bdbiosciences.com

BD Clontech
1020 East Meadow Curcle
Palo Alto, CA 94303

BDH
Merck House
Poole, Dorset, BH15 1TD
England
http://www.bdh.com

BDH, Inc.
350 Evans Avenue
Toronto, Ontario, M8Z 1K5
Canada
TEL 416-255-8521
http://www.bdhinc.com

BDH Chemicals
Broomroad
Poole, Dorset BH12 4NN
England
TEL +44 202 666856
FAX +44 202 660444

BDH Laboratories
Roche Diagnostics GmbH
Roche Applied Science
Sandhofer Straße 116
D-68305 Mannheim
http://www.roche-applied-science.com

BD Pharmingen
10975 Torreyana Road
San Diego, CA, 92121

BD Plastikpak
1 Becton Drive
Franklin Lakes, NJ 07417
USA
http://www.bd.com

Beckman Coulter AB
Archimedesvägen 7
Box 11156
S-16111 Bromma
TEL 46 8 564 859 00
FAX 46 8 564 859 01

Beckman-Coulter
6755 Mississauga Road
Suite 600
Mississauga
Ontario, Canada L5N 7Y2
TEL 800-387-6799
http://www.beckmancoulter.com

Beckman Coulter (U.K.) Limited
Oakley Court
Kingsmead Business Park
London Road
High Wycombe, Buckinghamshire HP11 1JU
England
TEL 44 (0) 1494 441181
FAX 44 (0) 1494 463843
http://www.beckmancoulter.com/

Beckman Coulter, Inc.
4300 N. Harbor Boulevard
P.O. Box 3100
Fullerton, CA 92834-3100
USA
TEL +1 (800) 742-2345
FAX +1 (714) 773-8283
http://www.beckman.com

Beckman Coulter GmbH
Frankfurter Ring 115
80807, München
Germany
TEL 49 89 35870226
FAX 49 89 35870490

Beckman Coulter Inc.
11800 SW 147th Avenue
Miami, FL 33196
http://www.beckmancoulter.com

Beckman Instruments, Inc.
2500 Harbor Boulevard
Box 3100, Fullerton
California, 92634-3100
USA
TEL 800-742-2345
FAX 800-643-4366
http://www.beckman.com

Beckman Instruments Inc.
Spinco Division
P.O. Box 10200
Palo Alto, California 94304
USA
TEL 800-551-1150
TEL 415-859-1694
FAX 800-643-4366

Becton, Dickinson and Company
1 Becton Drive
Franklin Lakes, NJ 07417
TEL 201.847.6800
http://www.bd.com/

Becton Dickinson Biosciences—Transduction Laboratories
133 Venture Ct.
Lexington, KY 40511-2624
TEL 859-259-1550
FAX 859-259-1413
TEL 800-227-4063
E-MAIL tlbinfo@translab.com
http://www.bdbiosciences.com

Becton Dickinson Biosciences
2350 Qume Drive
San Jose, CA 95131-1807
USA
TEL +1 800 223-8226
TEL 877.232.8995
FAX +1 408 954-2347
http://www.bdbiosciences.com

Becton Dickinson GmbH
Tullastr. 8-12
69126 Heidelberg
Germany

Becton Dickinson Labware
Two Oak Park
Bedford, MA 01370
TEL 1-800-343-2035
(Outside the USA, 617-275-0004)
FAX 617-275-0043

Becton Dickinson UK Ltd.
Between Towns Road
Cowley, Oxford, Oxfordshire, OX4 3LY
TEL 01865 748844
FAX 01865 781635
E-MAIL bduk customerservice@europe.bd.com

Bellco Glass, Inc.
340 Edrudo Road
P.O. Box B
Vineland, New Jersey, 08360
USA
TEL 800-257-7043
FAX 609-691-3247
E-MAIL cservice@bellcoglass.com
http://www.bellcoglass.com

Berthold Technologies
99 Midway Lane
Oak Ridge, TN 37831
USA
http://www.berthnoldtech.com

BFI Optilas, Germany
Assar-Gabrielsson-Strasse 1
D-63128 Dietzenbach
Germany,—Calbiochem
http://www.calbiochem.com

Biacore AB
Rapsgaten 7
SE-754 50 Uppsala
Sweden

Bibby Sterilin
distributed via Appleton Woods Ltd Lindon House
Heeley Road
Selly Oak, Birmingham
West Midlands, B29 6EN
UK

Billups-Rothenberg, Inc.
PO Box 977
Del Mar, CA 92014-0977
TEL 1 877 755-3309 (Toll free in U.S.)
TEL 1 858 535-0545 (International)
FAX 1 858 535-0546
E-MAIL bri@brincubator.com
http://www.brincubator.com

Biochrom AG
Leonorenstraße 2-6 D-12247
Berlin Germany
TEL +49 30 7799 06-0
FAX +49 30 771 0012
http://www.biochrom.com

Biochrom Ltd
Cambridge Science Park
Milton Road, Cambridge, CB4 0FJ
UK
TEL +44 (0)1223 423723
FAX +44 (0)1223 420164
http://www.biochrom.co.uk/contact.htm

BioComp Instruments Inc.
650 Churchill Row
Fredericton, NB E3B 1P6
Canada
TEL 506-453-4812
FAX 506-453-3583
TEL 800-561-4221
E-MAIL dhc@unb.ca
http://www.biocompinsruments.com

BioConcept
Innovationszentrum Nordwestschweiz Gewerbestrasse
14 Postfach 427 CH—4123 Allschwil 1
Switzerland
TEL +41 61 486 80 80
FAX +41 61 486 80 00
E-MAIL info@bioconcept.ch
http://www.bioconcept.com

Biocrom KG
Leonorenstr. 2-6
D-12247 Berlin
Germany
TEL +49-30-77 99 06 0
FAX +49-30-77 10 01 2
E-MAIL info@biochrom.de
http://www.biochrom.de

Biodesign Inc. of New York
P.O. BOX 1050
CarmelL, NY 10512
TEL 845-454-6610
FAX 845-454-6077
E-MAIL service@biodesignofny.com
http://www.biodesignofny.com/ny.com

Biodesign International
60 Industrial Park Road
Saco, Maine 04072
USA

Bioline USA Inc.
PMB 311, 28 South Main Street
Randolph, MA 02368-4800
USA
TEL 781 830 0360
FAX 781 830 0205

Bioline GmbH
Im Biotechnologiepark
TGZ 2, D-14943 Luckenwalde
Germany
TEL +49 (0) 3371 68 12 29
FAX +49 (0) 3371 68 12 44
E-MAIL info@bioline.com
http://www.bioline.com/n_distribut2.htm
http://bioline.com

Bioline Ltd.
16 The Edge Business Centre
Humber Road, London NW2 6EW
UK
TEL +44 (0) 20 8830 5300
FAX +44 (0) 20 8452 2822

Biological Indstries Ltd.
Kibbutz Beit Haemek
25115 Israel
TEL 972-(0)4-996-0595
FAX 972-(0)4-996-8896
E-MAIL info@bioind.com
http://www.bioind.com/

Bio-Logic—Science Instruments SA
1, rue de l'Europe
F-38640—CLAIX
France
TEL +33 476 98 68 31
FAX +33 476 98 69 09

BIOLOG Life Science Institute
Forschungslabor und Biochemica-Vertrieb GmbH
Flughafendamm 9a
P.O. Box 107125
D-28071 Bremen
Federal Republic of Germany
http://www.biolog.de

Biomedical Resources International, Inc.
100 Fountain Street Framingham
MA 01702

Biomol Feinchemikalien, Waidmannstr
35, D 22769 Hamburg

Bioresearch Information
4300 N. Harbor Boulevard
P.O. Box 3100
Fullerton, CA 92834-3100
USA
TEL 1-800-742-2345
FAX 1-800-643-4366
http://www.beckmancoulter.com/

BIOMOL Research Laboratories, Inc.
5120 Butler Pike
Plymouth Meeting, PA 19462-1202
N-ethylmaleimide (NEM; Sigma E-1271)
TEL 1-800-942-0430
TEL 610-941-0430
FAX 610-941-9252
http://www.roche.de/

Bioptechs Inc.
3560 Beck Rd.
Butler, PA 16002
TEL 877-LIVE-CELL (5483-2355)
Direct 724-282-7145
FAX 724-282-0745
http://www.bioptechs.com

Bio-Rad Cell Science Division
Bio-Rad House
Maylands Avenue
Hemel Hempstead, Hertfordshire HP2 7TD
England
TEL 1-(800) 4 BIORAD
TEL 1-(800) 424 6723

Bio-Rad Laboratories
2000 Alfred Nobel Drive
Hercules, CA 94547
USA
TEL (800) 424-6723
TEL (510) 741-1000
FAX (510) 741-5800
FAX (800) 879-2289
E-MAIL lsg.orders.us@bio-rad.com
http://www.bio-rad.com

Bio-Rad Laboratories GmbH
Heidemannstrasse 164
D-80939 München
Postfach 45 01 33
D-80901 München
Germany
FAX 49 (89) 31884-100
http://www.bio-rad.de

Bio-Rad Laboratories S.A.
López de Hoyos
245-247
28043 Madrid, Spain
http://www.bio-rad.com

Biosciences AB
SE-751 84 Uppsala
Sweden

BioSource International
542 Flynn Road
Camarillo, CA 93102
USA

BioSource International
Distributed by Medicorp Inc.
5800 Royalmount
Montreal, PQ H4P 1K5
Canada
TEL 1-877-733-1900

Biostatus Limited
56 Charnwood Road
Shepshed, Leicestershire
LE12 9NP
UK
TEL 07957 575402
FAX 01509 651061
E-MAIL enquiry@biostatus.co.uk
http://www.biostatus.co.uk

Bio-Tek Instruments, Inc.
Highland Park
P.O. Box 998
Winooski, Vermont 05404-0998, USA
TEL (888) 451-5171
TEL (802) 655-4740
FAX (802) 655-7941
http://www.biotek.com/

BioVectra
160 Christian Street
Oxford, Connecticut 06478, USA
http://www.biovectra.com/

BioWhittaker (Clonetics)
8830 Biggsford Road
Wallcersville, MD 21793

BioWhittaker/Cambrex
One Meadowlands Plaza
East Rutherford, NJ 07073
USA

Biozym
31840 Hessisch Oldendorf
Germany

Bitplane AG
Badenerstrasse 682
CH-8048 Zürich
Switzerland
http://www.bitplane.com

BMG Labtechnologies Inc.
2415 Presidential Drive
Bldg 204, Suite 118
Durham, North Carolina 27703
http://www.bioresearchonline.com

BOC-Edwards
Manor Royal
Crawley, Sussex, RH10 2LW
UK
TEL +44 (0)1293528844
FAX +44 (0)1293533453

BOCHEM
Industriestraße 3
35781 Weilburg
Germany
http://www.bochem.de/

Boehringer Mannheim Gmbh—now Roche Diagnostics
Sandhofer Strasse 116
D-68305 Mannheim
Germany
http://www.roche.de/

Boehringer Manheim—now Roche Diagnostics
201 Boulevard Armand Frappier
Laval PQ H7V 4A2
Canada
TEL 1-800-263-5887
Boehringer Mannheim
9115 Hague Rd
P.O. Box 50414
Indianapolis, IN 46250

Boule (Corning Costar)
Nordic Denmark
Egensvej 25
DK-2770 Kastrup
Denmark

Boule Nordic AB
Box 1080
141 22 Huddinge
Sweden
http://www.boule.se/nordic/

Brain Research Laboratories
Waban PO Box 88
Newton, MA 02468
USA
http://www.brainresearchlab.com

Brand, Germany
11 Bokum Rd.
Essex, CT 06426
http://www.brandtech.com/

Brand GmbH+Co KG
Otto Schott Str. 25
D-97877 Wertheim
Germany
FAX 49 (9342) 808-236
http://www.brand.de

Branson Korea Co., LTD.
8th floor, Dongil Techno Town, #823
Kwanyang-2dong
Dongan-gu, Anyang-si, Kyonggi-do
Korea
TEL (82 31)422-0631
FAX (82 31)422-9572
E-MAIL buc@branson.co.kr

Braun Biotech Int.
34212 Melsungen
Germany
http://www.bbraunbiotech.com

Brechbühler AG
Steinwiesenstrasse 3
8952 Schlieren
Switzerland
TEL +41 1 732 31 31
FAX +41 1 730 61 41
E-MAIL info@sciex.com

Brinkmann Instruments, Inc.
One Cantiague Road
PO Box 1019
Westbury, NY 11590
USA
TEL 800-645-3050
http://www.brinkmann.com/

Bristol-Myers Squibb Canada, Inc.
2365 Cote-de-Liesse
Saint-Laurent, Quebec, H4N 2M7
Canada
TEL 800-267-0005
http://www.bms.com

Brookhaven Instruments Corporation
750 Blue Point Road
Holtsville, NY 11742-1896
USA
http://www.bic.com

Bruker
40 Manning Road
Manning Park
Billerica, MA 01821
http://www.bdal.com/

Brunschwig AG
PO-Kasten CH-4009 Basel
Switzerland
TEL +41 61 308 91 11
FAX +41 61 308 91 19
E-MAIL info@brunschwig-ch.com
http://www.brunschwig-ch.com

BTC engineering
12 Shirley Close
Milton, Cambridge CB4 4BG
UK

BTX
11199 Sorrento Valley Road
San Diego, CA 92121-1334
USA

BTX Instrument Division
Harvard Apparatus, Inc.
84 October Hill Road
Holliston, MA 01746-1388
http://www.btxonline.com

Caenorhabditis Genetics Center
250 Biological Sciences Center
University of Minnesota
1445 Gourtner Ave.
St. Paul, MN 55108
Cairn Research Ltd.
Graveney Road
Faversham, Kent, ME13 8UP
UK
TEL +44 (0)1795 590140
FAX +44 (0)1795 594510
http://www.cairn-research.co.uk

CalBiochem
10394 Pacific Center Court
San Diego, California 92121
USA
Mailing Address:
P.O. Box 12087
La Jolla, California 92039-2087, USA
TEL 1 800 854-3417
TEL 1 858 450-9600
FAX 1 800 776-0999
FAX 1 858 453-3552
E-MAIL orders@calbiochem.com
http://www.calbiochem.com

Caltag
1849 Bayshore Blvd. #200
Burlingame, CA 94010
TEL 650.652.0468
TEL 800.874.4007
FAX 650.652.9030
E-MAIL caltag@caltag.com
http://www.caltag.com

Cambrex (former BioWhittaker Inc.)
8830 Biggs Ford Rd.
Walkersville, MD 21793
USA
TEL +1 800/638-8174
FAX +1 301/845-8338
E-MAIL cs@biowhittaker.com
http://www.cambrex.com/default.asp

Cambridge Bioscience
24-25, Newmarket Road
Cambridge CB5 8LA
UK
TEL (+44) 1223 316855
FAX (+44) 1223 360732

Cambridge Isotope Laboratories
50 Frontage Road
Andover, MA 01810-5413
USA
http://www.isotope.com

Carlo Erba Reagenti
Chaussée du Vexin
27106 Val de Reuil
France
http://www.carloerbareagenti.com

Carl Roth GmbH & Co.
Schoemperlenstrasse 1-5
D-76185 Karlsruhe
Germany
E-MAIL info@carlroth.de
http://www.Carl-Roth.de

Carlson Scientific Inc.
514 S. Third Street
Peotone, IL 60468

Carl Zeiss
Carl-Zeiss-Str. 22
73447 Oberkochen
Germany
http://www.zeiss.com

Carl Zeiss France SAS
60, route de Satrouville
78230 Le Pecq
France
TEL +33 1 34802000
FAX +33 1 34802001
http://www.zeiss.com

Carl Zeiss Ltd.
PO Box 78
Woodfield Road
Welwyn Garden City
Herts, AL7 1LU
UK
TEL 01707 871300
FAX 01707 871289
http://www.zeiss.co.uk

Carl Zeiss MicroImaging, Inc.
One Zeiss Drive
Thornwood, NY 10594
USA
TEL 1-800-233-2343
FAX 1-914-681-7446
E-MAIL micro@zeiss.com
http://www.zeiss.com/micro/

Cartesian Technologies Europe, Ltd.
8 Blackstone Road
Huntingdon, Cambridgeshire
PE296EF, UK
TEL +44 (0) 1480 426700
FAX +44 (0) 1480 426767
http://www.cartesiantech.com/

CBS Scientific
420 South Cedros
Solana Beach, CA 92075

Cellgro, Mediatech, Inc.
13884 Park Center Rd.
Herndon, VA 20171
TEL 800-235-5476
http://www.cellgro.com

Cell Signaling Technology
166B Cummings Center
Beverly, MA 01915
Cell Systems Biotech GmbH
53562 St. Katharinen
Germany

Charles River Laboratories, Inc.
251 Ballardvale Street
Wilmington, MA 01887-1000
http://www.criver.com

Chemicon International
28820 Single Oak Drive
Temecula, CA 92590
USA

Chemicon International
Fischbacher Weg 3A
D-65719 Hofheim

CHIMERx,
6143 North 60th Street
Milwaukee WI 53218

Chiron B.V.
4560 Horton Street
Emeryville, CA 94608
USA
TEL +1 (510) 655-8730
FAX +1 (510) 655-9910
http://www.chiron.com/chironglobal.html

Chroma Technology
Chroma Technology Inc Business Office
74 Cotton Mill Hill
Brattleboro, VT 05302
USA
TEL 1-800-824-7662
TEL 1-802-428-2500
FAX 1-802-428-2525
http://www.chroma.com/

Chroma Technology Corp.
10 Imtec Lane
PO Box 489
Rockingham, VT 05101
USA
2TEL 1-802-257-1800
FAX 1-802-257-9400
E-MAIL info@chroma.com
http://www.chroma.com/index.cfm

Chromatographic Specialities
300 Laurier Blvd.
Brockville, Ontario, K6V 5W1
Canada
TEL 613-342-4678
FAX 613-342-1144
http://www.chromspec.com

Clarkson Chromatorgaphy products Inc
213 Main Street
Sout Williamsport PA 17701
USA

Clay Adams
Div. of Becton Dickinson
Diagnostic Instr. Sys.
383 Hillen Rd.
Towson, MD 21204
USA
TEL 800-638-8656

Clontech
21 Between Towns Road
Cowley, OX4 3LY Oxford
UK

Clontech
1020 East Meadow Circle
Palo Alto, CA 94303-4230
USA
http://www.corning.com/lifesciences

Cocalico Biologicals, Inc.
494 Stevens Road
P.O. Box 265
Reamstown, PA 17567
TEL 717-336-1990

Coherent (U.K.) Ltd.
28 St Thomas
The Cambridgeshire Business Park
Ely, CB7 4EX
UK
TEL 011 44 1353 658833
FAX 011 44 1353 659107
E-MAIL coherent-ltd@cohr.com

Cohesion Technologies, Inc.
2500 Faber Place
Palo Alto, CA 94303
TEL 650-320-5500
FAX 650-320-5511
E-MAIL admin@cohesiontech.com

Cole-Parmer
625 East Bunker Court
Vernon Hills
Illinois 60061-1844
USA
TEL 800-323-4340
FAX 847-247-2929

Color your Enzyme, Inc.
Dr. R. Bowers
Queen's University
Kingston, Ontario, K7L 3N6
Canada
TEL (613)533-6000 ext. 75005

CompuCyte Corporation
12 Emily Street
Cambridge MA 021139
TEL 800-840-1303
TEL 617-492-1300
E-MAIL salesinfo@compucyte.com

Computech
1701 Iron Street
Kansas City, MO 64116
USA

Continental Lab Products
5648 Copley Drive
San Diego, CA92111 USA
Continuum Scientific Service
3150 Central Expressway
Santa Clara, CA 95051-0816
USA
TEL 1-800-532-1064
TEL 1-408-727-3240
FAX 1-408-727-3550
E-MAIL Continuum@ceoi.com
http://www.continuumlasers.com/mainswf.html

Cora Styles Needles 'N Blocks
105 Cypress Point
Hendersonville, NC 28739
USA
http://www.corastyles.com/

Coriell Cell Repositories
403 Haddon Avenue
Camden, NJ 08103
USA

Corning, NY
14831, Sutter Instrument Co
40 Leveroni Court
Novato, CA 94949
Distributed by VWR/Canlab.
8567 Chemin Dalton
Ville Mont-Royal
PQ H4T 1V5
Canada
TEL (514)344-3525
http://www.corning.com

Corning (Life Science) Inc.
P.O. Box 5000
Corning, New York 14830
USA
TEL 800-492-1110
TEL 978-635-2200
FAX 978-635-2476
E-MAIL CLSCustServ@corning.com
http://catalog.corning.com/Lifesciences/

Corning B.V.
Life Sciences
Koolhovenlaan 12
1119 NE Schiphol-Rijk
The Netherlands
TEL 31 (0) 20-659-6051
FAX 31 (0) 20-659-7673
http://www.corning.com

Corning Costar Corporation
One Alewife Center
Cambridge, MA 02140
USA
TEL 617-868-6200
FAX 617-868-2076

Corning Incorporated Life Sciences
45 Nagog Park
Acton, MA 01720
USA
TEL 978-635-2200
TEL 800-492-1110
FAX 978-635-2476
E-MAIL clswebmail@corning.com
http://www.corning.com

Corning Science Products Corning Costar
Am Kuemmerling 21-25
55294 Bodenheim
Germany
TEL ++49 6135 9215-0
FAX ++49 6135 5148
http://www.corning.com/lifesciences
Coulter
http://www.beckmancoulter.com/

Covance Research Products
P.O. Box 7200
Denver, PA 17517

CPG Inc.
3 Borinski Road
Lincoln Park, NJ 07035
USA
TEL (201) 305-8181
FAX (201) 305-0884

Crescent Chemical Company, Inc.
1324 Motor Parkway
Islandia, NY 11749
USA
FAX 1 (631) 348-0913
http://www.creschem.com

CVI Laser Corp.
361 Lindbergh Ave.
Livermore, CA 94550
USA
TEL 510-449-1064
FAX 510-294-7747

Cytoskeleton, Inc.
1650 Fillmore Street
Suite #240
Denver, CO 80206
USA

DACO Corporation
Carpinteria, CA
TEL 800-235-5763
http://www.dakousa.com

Daigger Laboratory Supplies
620 Lakeview Parkway
Vernon Hills, IL 60061
TEL 1-800-621-7193
FAX 1-800-320-7200
E-MAIL daigger@daigger.com
http://www.daigger.com/

DAKO
DakoCytomation Denmark A/S
Produktionsvej 42
DK-2600 Glostrup
Denmark

Dako Cytomation
6392 Via Real
Carpinteria, CA 93013
TEL 805-566-6655
TEL 800-235-5743/800-424-0021
FAX 805-566-6688

DakoCytomation GmbH
Hamburger Strasse 181
D-22083 Hamburg
Germany
E-MAIL info@dakocytomation.de
http://www.dakocytomation.com

DAKO Danmark A/S
Productionsvej 42
DK-2600 Glostrup
Denmark
TEL 45 44 85 95 00
FAX 45 44 85 84 29
E-MAIL contact@dakocytomation.com
http://www.dako.com

Dako UK Ltd.
Denmark House
Angel Drove
Ely CB7 4ET
England

DELTA Acoustics & Vibrations
Building 356
Akademivej
DK-2800 Lyngby
Danemark
2TEL ++45-45-931211
FAX ++45-45-931990
E-MAIL dh@delta.dk

Denley Instruments
Thermo Life Sciences International (UK) Ltd.
Unit 5 The Ringway Centre
Edison Road
Basingstoke, RG21 6YH , Hampshire
UK
TEL +44 (0)1256 817282
FAX +44 (0)1256 817292
http://www.thermo-lifesciences.co.uk

Deville Scientific Inc.
P.O. Box 4588
Metuchen, NJ, 08840

Dianova
20148 Hamburg, Germany

Diatec.com AS
Gaustadalleen 21
0349 Oslo
Norway
TEL +47 22 95 86 25
FAX +47 22 95 86 49
E-MAIL diatec@diatec.com
http://www.diatec.com

DIFCO BD
1 Becton Drive
Franklin Lakes, NJ 07417
USA
TEL 201.847.6800

Difco (Voigt Global Distribution LLC)
P.O. Box 412762
Kansas City, MO 64141-2762
USA
http://www.vgdusa.com/DIFCO.htm

Digital Instruments
Veeco Metrology Group
Santa Barbara, CA
USA
http://www.veeco.com/

Digital Scientific Limited
Sheraton House
Castle Park, Cambridge CB3 0AX
UK
TEL +44 (0) 1223 329993
FAX +44 (0) 1223 460178
E-MAIL digitalscientific.co.uk

Digitial Equipment Corp.
PO Box 9501
Merrimack, NH
USA
TEL 800-344-4825
TEL 800-234-2298
http://www.dec.com

Dionex Corporation
1228 Titan Way
P.O. Box 3603
Sunnyvale, CA 94085-3603

DOJINDO Laboratories
2025-5 Tabaru
Mashiki-machi, Kamimashiki-gun
Kumamoto, 861-2202
Japan
TEL (+81) 96-286-1515
FAX (+81) 96-286-1525
E-MAIL info@dojindo.co.jp
http://www.dojindo.com

Dounce
Wheaton Science Products An Alcan Packaging Company
1501 N.10th Street
Millville, NJ 08332-2093
USA
TEL 800-225-1437
FAX 856-825-1368
TEL 1 856-825-1100
FAX 1 856-825-4568

Dow Corning Corporation
PO Box 994
Midland, MI 48686-0994, USA
http://www.dowcorning.com

Dow Corning STI, Inc.
Walnut Site
20832 Currier Road
Walnut CA 91789
USA
TEL +1 909 595 6331
FAX +1 909 595 1946

Drummond Scientific Co.
500 Parkway
Box 700
Broomall, PA, 19008
USA

Dumont, via Fine Sciene Tools
http://www.finescience.com/fst/misc/dumont.html

DuPont NEN
549 Albany Street
Boston, MA 02118

Dupont NEN Research Products—now PerkinElmer Canada Inc.
501 Rowntree Dairy Road, Unit #6
Woodbridge, ON L4L 8H1
Canada
TEL 1-800-561-4646

Duxford Cambridge
CB2 4PZ
England

Dynal Biotech
Deutsche Dynal
Bramfelder Chaussee 41
Postbox 710190
D 22177 Hamburg
Germany

Dynal Biotech ASA
PO Box 114
Smestad, 0309 Oslo
Norway
TEL +47 22 06 10 00
FAX +47 22 50 70 15
E-MAIL dynal@dynalbiotech.com
http://www.dynalbiotech.com

DYNEX Technologies, A Capital Genomix Company
14340 Sullyfield Circle Chantilly
Virginia 20151-1683
USA
TEL 703-631-7800
TEL 800-288-2354
FAX 703-631-7816

Eastman Chemical Co.
Laboratory & Research Products
1001 Lee Road
Rochester, NY 14652-3512
USA
TEL 800-225-5352
FAX 800-879-4979

Eastman Kodak Co.
Scientific Imaging Systems
343 State St.
Rochester, NY 14652
TEL 203-786-5657
TEL 877-SIS-HELP
FAX 203-786-5656
E-MAIL sis-info@kodak.com
http://www.kodak.com/go/scientific

EBioscience
6042 Cornerstone Court
Suite B-D
San Diego, CA 92121
USA

ECACC, CAMR
Salisbury
Wiltshire, SP4 OJG
UK

EDWARDS
Manor Royal
Crawley, West Sussex, RH10 9LW
UK
http://www.edwards.boc.com/

Eldex Laboratories, Inc.
30 Executive Court
Napa, CA 94558-6278
USA

Electron Microscopy Sciences
1560 Industry Road
P.O. Box 550
Hatfield, PA 19440
USA
TEL 1-215-412-8400
FAX 1-215-412-8450
http://www.emsdiasum.com/ems/

Electron Microscopy Sciences
P.O. Box 251
321 Morris Road
Fort Washington, PA 19034
TEL 215/646-1566
FAX 215/646-8931
E-MAIL SGKCCK@aol.com
http://www.emsdiasum.comm/home.html

EMBL Workshop
EMBL Heidelberg
Meyerhofstrasse 1
D-69117 Heidelberg
Germany
TEL +49 6221 3870
FAX +49 6221 387306
http://www.embl-heidelberg.de/

EMD Biosciences, Inc.
CALBIOCHEM®
10394 Pacific Center Court
San Diego, California 92121
USA

EMD Biosciences, Inc.
P.O. Box 12087
La Jolla, CA 92039-2087
USA
TEL 858 450 9600
FAX 858 453 3552
http://www.emdbiosciences.com/html/EMD/intl_sales_office.html
http://www.emdbiosciences.com/html/CBC/home.html

EMD Biosciences Inc.
10394 Pacific Centre Court
San Diego California 92121
USA
TEL 1-800-854-3417

E. Merck
Postfach 4119
D-6100 Darmstadt 1
BRD
TEL +49 6151 700
FAX +49 6151 72 2000

EM Science
480 S. Democrat Road
Gibbstown, NJ 08027
TEL 800-222-0342

Endecotts Limited
9 Lombard Road
London, SW19 3TZ
England
TEL +44 (0) 20 8542 8121
FAX +44 (0) 20 8543 6629
E-MAIL sales@endecotts.com Bellingham

Epoxy Technology
14 Fortune Drive
Billerica, MA01821
USA

Eppendorf
Barkhausenweg 1
22339 Hamburg
Germany
TEL ++49 40 53 8010
FAX ++49 40 53 801-556
http://www.eppendorf.com/en/splash.php

Eppendorf France
Parc des Grillons
60, Route de Sartrouville
78230 Le Pecq, France
TEL +33 1 30 15 67 40
FAX +33 1 30 15 67 45
http://www.eppendorf.com/france

Eppendorf Vertrieb Deutschland GmbH
Peter-Henlein-Strasse 2
D-50389 Wesseling-Berzdorf
Germany

EquiBio
Action Court, Ashford Road
Ashford, Middlesex, TW 151XB-UK
TEL 44-1784-425000
FAX 44-1784-248085

Erie Scientific Company
20 Post Road
Portsmouth, NH 03801
USA
E-MAIL eriesci.com

ESCO
1 South Point Dr.
Lake Forest California 92630
TEL 949-330-3602

Essex Pharma
PO Box 83 03 47
81737 München
Germany

Ethicon Incorporated
Somerville
New Jersey 08876-0151
USA
TEL 1-800-4-ETHICON

Euroclone
Via Figino 20/22
20016 Pero (Milano)
ITALY

Euromedex
24 rue des Tuileries
BP 74684 SOUFFELWEYERSHEIM
67458 MUNDOLSHEIM CEDEX
FRANCE
TEL +33 3 88 18 07 27
FAX +33 3 88 18 07 28

EXFO Burleigh Products Group Inc.
7647 Main St. Fishers
Victor, NY 14564-8909
USA
TEL +1 585 924-9355
FAX +1 585 924-9072
E-MAIL info@burleigh.com

Falcon
Becton Dickinson Labware
2 Bridgewater Lane
Lincoln Park, NJ 07035

Falcon
2350 Qume Drive
San Jose, CA 95131-1807
USA
TEL (800) 223-8226
TEL (877) 232-8995
FAX (408) 954-2347
http://www.bdbiosciences.com/discovery_labware/

Falls Church Store
260 W. Broad Street
Falls Church, Virginia, 22046
TEL 1-888-STOCKS6 (1.888.786.2576)
TEL 1.703.579.4209
FAX 1.703.995.4422
E-MAIL Scripophily.com
http://www.scripophily.net/millabinc1.html

Fermentas
BWI Commerce Park
7520 Connelley Drive
Suite A
Hanover, MD 21076
TEL (800) 340-9026
FAX (800) 472-8322
http://www.fermentas.com/

FERMENTAS UAB
V.Graiciuno 8
Vilnius 2028, Lithuania

F. Hoffmann-La Roche Ltd.
Diagnostics Division
Grenzacherstrasse 124
CH-4070 Basel
Switzerland
TEL 41-61-6881111
FAX 41-61-6919391

F. Hoffmann-La Roche Ltd
Group Headquarters
Grenzacherstrasse 124
CH-4070 Basel, Switzerland
TEL +41-61-688 1111
FAX +41-61-691 9391
E-MAIL Pharma (Rx) Webmaster (non-US residents)
http://www.roche.com

Roche Consumer Health
Wurmisweg, CH-4303 Kaiseraugst
Switzerland
TEL +41-61-688 1111
FAX +41-61-691 9391
E-MAIL Consumer Health Webmaster
http://www.roche.com/home.html

Fine Science Tools GmbH
Fahrtgasse 7-13
D-69117 Heidelberg
Germany
TEL +49 62 21 90 50 50
FAX +49 62 21 60 00 01
E-MAIL europe@finescience.com
http://www.finescience.com

Fischer Chemicals
Bishop Meadows Road
Loughborough, Leicestershire LE110RG
UK
TEL (+44) 01509 231166
FAX (+44) 01509 555111

Fisher Scientific AG
Wilstrasse 57
CH-5610 Wohlen
Switzerland
TEL 41-56-618-41-11
FAX 41-56-618-41-41
E-MAIL info@ch.fishersci.com

Fisher
Becton, Dickson
1 Becton Drive
Franklin Lakes, NJ 07417
USA
http://www.bd.com/

Fisher Bioblock Scientific
Bd Sébastien Brant
BP 50111, 67403 Illkirch Cedex
France
TEL +33 (0)3 88 67 14 14
Fax +33 (0)3 88 67 11 68
http://www.bioblock.com/

Fisher Laboratory Equipment Division
600 Business Center Drive
Pittsburgh, PA 15205
USA
TEL 1-800-926-0505
FAX 1-412-490-7286
http://www.fishersci.com

Fisher Scientific
2000 Park Lane Dr.
Pittsburgh, PA 15275-9943
USA
TEL 800-766-7000
TEL 201-467-6400
FAX 800-926-1166
FAX 201-379-7415
http://www.fishersci.com

Fisher Scientific
2761 Walnut Avene
Tustin, CA 92780
TEL 714-669-4600
TEL (800) 766-7000

Fisher Scientific
3970 John's Creek St.
Ste 500
Suwanee, GA 30024

Fisher Scientific
9999 Veteran's Memorial Dr.
Houston TX 77038
TEL 1-800-766-7000
https://www1.fishersci.com/index.jsp

Fisher Scientific
Customer Service Centre
112 Colonnade Rd.
Nepean, ON, K2E 7L6
Canada
TEL 800-234-7437
http://www.fishersci.ca

FISHER Scientific
Pittsburg, PA
TEL 1-800-766-7000 (USA)

Fisher Scientific
P.O. Box 14989
St. Louis, MO 63178 USA

Fisher Scientific International, Inc.
1200 Denison St.
Unionville, Ontario L3R 8G6
Canada
TEL 416-479-8700
http://www.fisherscientific.com

Fisher Scientific International, Inc.
Liberty Lane
Hampton, NH 03842
TEL (603) 926-5911
FAX (603) 929-2379
E-MAIL webmaster@nh.fishersci.com
http://www.fishersci.com

FJW Optical System, Inc.
629 S.Vermont St.
Palatine, IL 60067-6949
USA
TEL 708-358-2500
FAX 708-358-2533

Fluka
Chemie GmbH
CH-9471, Buchs
Germany

Fluka
Industriestrasse 25
9471 Buchs, Switzerland
TEL ++41(0)81 755 25 11
FAX ++41(0)81 755 28 15
E-MAIL Fluka@sial.com
http://www.sigmaaldrich.com/

FMC BioProducts
191 Thomaston Street
Rockland, ME 04841
USA
TEL 800 341 1574
TEL 207 594 3400
FAX 800 362 5552, 207 594 3491

FMC Corporation
1735 Market Street
Philadelphia, PA 19103
USA
TEL 215-299-6000
FAX 215-299-5998

Fresenius
Else-Kröner-Str. 1
61352 Bad Homburg
Germany

GATAN
5933 Coronado Lane
Pleasanton, CA 94588
USA
http://www.gatan.com/

GE Bayer Silicones
Bergen op Zoom
The Netherlands

Gemini Bio-Products
1301 East Beamer Street
Woodland, CA 95776
TEL 1.800.543.6464
TEL 1.530.668.3636
FAX 1.530.668.3630
http://www.gembio.com

GeneMachines
935 Washington Street
San Carlos, California 94070
USA
E-MAIL genemachines.com

General Mills Inc.
800 Derr Street
Vallejo, CA 94590, USA
http://www.generalmills.com

Geneva Bioinformatics (GeneBio) S.A.
25 Avenue de Champel
CH- 1206 Geneva
Switzerland
TEL +41 22 702 99 00
FAX +41 22 702 99 99
E-MAIL info@genebio.com
http://www.genebio.com/

GERBU Biochemicals GmbH
Am Kirchwald 6
69251 Gaiberg
Germany
http://www.gerbu.de/

Geron Corp.
230 Constitution Drive
Menlo Park, CA 94025
USA
TEL 1-650-473-7700
http://www.geron.com

GIBCO
9800 Medical Cnt Dr.
P.O. Box 6482
Rockville, Maryland

GIBCO
Distributed by Invitrogen Canada Inc.
2270 Industrial St.
Burlington, ON L7P 1A1
Canada
TEL 1-800-263-6236

GIBCO
Invitrogen Ltd
3 Fountain Drive
Inchinnan Business Park , Paisley
UK
TEL 0141 814 6100
FAX 0141 814 6260
http://www.invitrogen.com

GIBCO
P.O. Box 880
Langley, OK 74350-0880
TEL 918-782-4000
FAX 918-782-4002
E-MAIL gibco@worldnet.att.net

GIBCO-BRL
Invitrogen Corporation
1600 Faraday Avenue
PO Box 6482
Carlsbad, California 92008
TEL (760) 603-7200
TEL 800-955-6288
FAX (760) 602-6500
E-MAIL tech_service@invitrogen.com
http://www.gibcobrl.co

GIBCO BRL
Life Technologies
9800 Medical Center Drive
Rockville, MD, 20849

GIBCO BRL Div. of Invitrogen
64271 P.O. Box 9418
Gaithersburg MD 20898
TEL +1-301-840-8000
FAX +1-301-670-8539
http://www.gibcobrl.com

GIBCO BRL / Life Technologies GmbH
Technologiepark Karlsruhe
Emmy-Noether-Strasse 10
D-76131 Karlsruhe
E-MAIL eurocustom@lifetech.com
http://www.lifetech.com

GIBCO Invitrogen Sarl
BP 96
95613 Cergy Pontoise Cedex
France
TEL +33 1 34 32 31 00
FAX +33 1 30 37 50 07
http://www.invitrogen.com

GIBCO Laboratories
3175 Staley Road
Grand Island, NY 14072
TEL (800) 828-6686

GIBCO products from Invitrogen
PO box 3326
4800 DH Breda
The Netherlands
http://www.invitrogen.com/

Gilson, Inc.
3000 W. Beltline Hwy.
P.O. Box 620027
Middleton, WI 53562-0027
USA
TEL 608-836-1551
TEL 800-445-7661
FAX 608-831-4451
http://www.gilson.com/

Glaswarenfabrik Karl Hecht KG
97647 Sondheim
Germany
http://www.hecht-assistent.de/

Glen Research
22825 Davis Drive
Sterling, VA 20164
USA
TEL 1-703-437-6191
FAX 1-703-435-9774
http://www.glenresearch.com/

GLW GmbH
Hüberstrasse 19
D-97084 Würzburg
Germany

Goldschmidt UK Ltd., TEGO House
Chippenham Drive
Kingston, Milton Keynes
Bucks MK10 OAF
UK

Goodfellow Cambridge Ltd.
Ermine Business Park
Huntingdon, Cambridgeshire, PE29 6WR
lUK

Goudoh-Shusei
Tokyo, Japan
http://www.godo.jp

Grace Vydac (Hesperia, CA, USA)
Western US Grace Vydac Representative
Peter R. Krinsky, Western Region Sales Manager
Anaheim, CA
TEL 1-714-518-3353
FAX 1-714-518-3356
E-MAIL pete.krinsky@grace.com

GRATICULES Ltd.
17-19 Morley Road
Tonbridge, Kent TN9 1RN
UK

Greiner-Bio One
Maybachstrasse 2
72636 Frickenhausen
Germany
FAX 49 (7022) 948-514
http://www.greiner-bio-one.com/

Greiner Bio-One Inc.
1205 Sarah Street
Longwood, FL 32750
USA
TEL 407-333-2800
TEL 800-884-4703
FAX 407-333-3001
E-MAIL info@greinerbiooneinc.com
http://www.greinerbioone.com

Hamamatsu
325-6, Sunayama-cho
Hamamatsu City, Shizuoka Pref. 430-8587
Japan
TEL (+81) 53-452-2141
FAX (+81) 53-456-7889
E-MAIL webmaster@hq.hpk.co.jp
http://www.hamamatsu.com

Hamamatsu Photonics
360 Foothill Rd.
Bridgewater, NJ 08807
TEL 908-231-0960
TEL 1-800-524-0504
FAX 908-231-1218
http://www.hamamatsu.com

Hamamatsu Photonics Deutschland GmbH
Arzbergerstr 10
D-82211 Herrsching am Ammersee
Germany

Hamilton Deutschland GmbH
Fraunhoferstr 17
D-82152 Martinsried
Germany
TEL +49-(0)89-5526-49-0
FAX +49-(0)89-5526-49-10

Hansatech Instruments Ltd.
Narborough Road
Pentney
King's Lynn, Norfolk PE32 1JL
England
http://www.hansatech-instruments.com

Harco (Harlow Chemical Company Ltd)
Central Road
Templefields, Harolow, CM20 2BH
Essex
http://www.harlowchem.com

Harlan Bioproducts for Science
P.O. Box 29176
Indianapolis, IN
TEL 1-800-972-4362
FAX 1-317-357-9000
http://www.hbps.com

Harlan Sera Labs Ltd.
Dodgeford Lane
Loughborough
Leicestershire, LE12 9TE
England
TEL 01530 222123
FAX 01530 224970
E-MAIL hslcsd@harlanuk.co.uk
http://www.harlanseralab.co.uk//home.html

Harvard Apparatus, Inc.
84 October Hill Road
Holliston, MA 01746
TEL 508-893-8999
TEL 800-272-2775
FAX 508-429-5732
http://www.harvardapparatus.com

Harvard Apparatus ltd.
Fircroft Way
Edenbridge , Kent TN8 6HE
U.K.
TEL +44 (0)1732 864001
FAX +44 (0)1732 863356

Headway Research, Inc.
3713 Forest Lane
Garland, TX 75042-6928
USA
TEL (972) 272-5431
FAX (972) 272-7817

Henogen SA
Site de Seneffe
14, rue de la Marlette
7180 Seneffe
Belgium

Heraeus
Heraeus Holding GmbH
Heraeusstraße 12-14
D-63450 Hanau

Heraeus Centrifuges, by Kendro Laboratory Products
275 Aiken Road
Asheville, NC 28804

Heraeus Instruments/, Kendro Laboratory Products GmbH
Robert-Bosch-Strasse 1
D-63505 Langenselbold
Germany
E-MAIL info@kendro.com
http://www.heraeus-instruments.de

Heraeus S.A.
Manuel Tovar
24, 28034 Madrid
Spain
http://www.sorvall.com

Hettich Zentrifugen
Andreas Hettich GmbH & Co.KG
Gartenstr 100
D-78532 Tuttlingen
TEL +49 7461 705 0
FAX +40 7461 705 125
E-MAIL info@hettichLab.com
http://www.HettichLab.com

Hewlett-Packard
http://www.hewlettpackard.com/
H. Hölzel Laborgeräte GmbH
Bahnhofstraße 23
D-85457 Wörth / Hörlkofen
Germany
E-MAIL info@hoelzel-gmbh.de
http://www.hoelzel-gmbh.de

Hitachi
Tokyo, Japan
http://www.hitachi.com

Hoefer Scientific Instruments
654 Minnesota Street
San Francisco CA 94107
USA

Hoffmann-La Roche AG
Emil-Barell-Str. 1
79639 Grenzach-Wyhlen
Germany

Hoffmann-La Roche Inc.
340 Kingsland Street
Nutley, NJ 07110
USA
TEL +1-973-235 5000
FAX +1-973-235 7605
http://www.rocheusa.com

Hoffmann-La Roche Ltd
Diagnostics Division
Grenzacherstrasse 124
CH-4070 Basel
Switzerland
TEL +41-61-688 1111
FAX +41-61-691 9391
http://www.roche.com

Holm & Halby
Vallensbækvej 35
DK-2605 Brønby
Denmark
TEL +45 43 26 94 00
E-MAIL info@holm-halby.dk
http://www.holm-halby.dk/

Houm AS
PO box 83 Grefsen
TEL +47 22 09 40 00
FAX +47 22 09 40 40
E-MAIL firmapost@houm.no
http://www.houm.no

Huber Kältemaschinenbau GmbH
Werner-von-Siemens-Strasse 1
77656 Offenburg
Germany

HV Skan Ltd.
425-433 Stratford Road
Shirley, Solihull, B90 4AE (Road Map)
West Midlands
TEL 0121 733 3003
FAX 0121 733 1030
http://www.skan.co.ukFisher Scientific

HyClone
925 West 1800 South
Logan, UT 84321 USA
TEL 1-800-492-5663
http://www.HyClone.com

Hydro Systems
PO Box 12137
Research Triangle Park, NC 27709
USA

IBA GmbH
Rudolf-Wissell-Str. 28
D-37079 Goettingen
Germany
E-MAIL info@iba-go.com
http://www.iba-go.com

ICN (now MP Biomedicals)
Biomedica GmbH, Medizinprodukte GmbH & Co. KG
Divischgasse 4, 1210 Wien
AUSTRIA
TEL +43 1 291 0754
FAX +43 1 291 0771
E-MAIL sales@biomedica@bmgrp.at
http://www.biomedica.co.at, www2.icnbiomed.com

ICN Biomedicals, Inc.
1263 South Chillicothe Road
Aurora OH 44202-8064
USA
http://www.icnbiomed.com/

ICN Biomedicals, Inc.
15 Morgan Street
Irvine, California 92618-2005
USA
TEL 800-854-0530
TEL 714-545-0113
FAX 800-334-6999
FAX 714-557-4872
http://www.icnbiomed.com/

ICN Biomedicals Inc.
3300 Hyland Ave.
Costa Mesa, CA 92626
TEL 714-545-0100
TEL 800-854-0530
FAX 800-334-6999
E-MAIL sales@icnbiomed.com
hhttp://www.icnbiomed.com

IDT
1710 Commercial Park
Coralville, IA 52241
TEL 800-328-2661
http://www.idtdna.com/

IKA Works, Inc.
2635 Northchase
PKWY SE Wilmington, NC 28405
USA
TEL 910-452-7059
TEL 800-733-3037
E-MAIL usa@ika.com

Ikemoto Rika
3-25-11, Hongo
Bunkyo-ku, Tokyo 113-8680
JAPAN
http://www.ikemoto.co.jp

ImageJ
Rasband, W., National Institute of Health (NIH)
Bethesda, Maryland
USA
http://rsb.info.nih.gov/ij

Industrial and Scientific
The Grip
Hadstock Road
Linton, Cambridge CB1 6NR
UK
TEL (+44) 01223 891953
FAX (+44) 01223 894223

Ingenieurburo CAT
M. Zipperer GmbH
79219, Staufen
Germany

Innomed-Konsult AB
Box 6141
S-102 33 Stockholm
Sweden
http://www.innomed.se/

Instrumedics, Inc.
61 South State Street
Hackensack, NJ 07601
USA
TEL 800-237-2772
TEL 201-343-1313
FAX 201-487-4884
E-MAIL info@instrumedics.com
http://www.instrumedics.com

Integrated DNA Technologies
1710 Commercial Park
Coralville, IA 52241
USA
TEL +1-800-328-2661
FAX 319-626-8444
http://www.idtdna.com

Intelligent Imaging Innovations, Inc.
820 16th Street
Suite 850
Denver, CO 80202

Interferon Sciences Inc.
783 Jersey Avenue
New Brunswick NJ 08901-3660
USA
http://www.interferonsciences.com/

INTERGEN Company
Two Manhattanville Road
Purchase, New York 10577
USA
TEL 1-800-431-4505

Intervet Germany
Feldstr. 1a
D 85716 Unterschleissheim

Intracel
Unit 4
Station Road
Shepreth. Royston, Herts. SG8 6PZ
http://www.intracel.co.uk/

Intrinsic Bioprobes, Inc.
625 S. Smith Rd.
Suite 22
Tempe, AZ 85284
USA

Invitrogen
1600 Faraday Avenue
Carlsbad, CA 92008
TEL (760) 603-7200
FAX (760) 602-6500
http://www.invitrogen.com

Invitrogen
9800 Medical Center Drive
P.O. Box 6482
Rockville, MD 20849-6482
USA
TEL +1-301-610-8709
FAX +1-301-610-8724
http://www.invitrogen.com

Invitrogen AG
Elisabethenstrasse 3
Postfach 533
CH-4019 Basel
Switzerland

Invitrogen Corporation
Thistedgade 6
stuen, 2630 Taastrup
Denmark
http://www.invitrogen.com

Invitrogen Canada, Inc.
2270 Industrial St.
Burlington, Ontario, L7P 1A1
Canada
TEL 800-263-6236
FAX 800-387-1007
http://www.invitrogen.com

Invitrogen GmbH
Technologiepark Karlsruhe
Emmy-Noether Strasse 10
76131 Karlsruhe
Gebührenfreie Bestellungen
TEL 0800 083 09 02
FAX 0800 083 34 35
Technical Information: Euro Tech-LineSM—0800 181 54 50
E-MAIL eurotech@invitrogen.com

Invitrogen S.A.
Edificio Océano
Parque Mas Blau
C/ Garrotxa 10-12
08820 Prat de Llobregat (Barcelona)
Spain
http://www.invitrogen.com

Irvine Scientific
2511 Daimle Street
Santa Ana, CA 92705
TEL (800) 437-5706

ISCO
PO Box 5347
Lincoln NE 68505, USA
TEL (402) 464-0231

ITC Biotechnologies (Clontech)
Tullastr. 4
D 69126 Heidelberg

IWAKI
Asahi Technoglass Corporation
7-2 Nihonbashi-Honcho3-chome
Chuo-ku, Tokyo 103-0023
Japan

IWAKI, Scitech Division
Asahi Techno Glass
1-50-1 Gyouda
Funabasi, Chiba
Japan

Jackson
P.O. Box 9
872 West Baltimore Pike
West Grove, PA 19390, USA
TEL 1-800-FOR-JAXN (367-5296)
TEL 610-869-4024
FAX 610-869-0171
http://www.jacksonimmuno.com/

The Jackson Laboratory
600 Main Street
Bar Harbor
Maine 04609
USA
TEL 207-288-6000
TEL 207-288-6051
http://www.jax.org/

Jackson Immuno Research Labs Incorporated,
Stratech Scientific Ltd
61-63 Dudley Street
Luton, Bedfordshire LU2 0NPK4
UK
TEL (+44) 01582 529000
FAX (+44) 01582 481895
Jasco International Co. Ltd.
4-21 Sennin-cho 2-chome
Hachioji, Tokyo 193-0835
Japan
TEL 81-426-66-1322
FAX 81-426-65-6512

Jencons (Scientific) Ltd.
Cherrycourt Way
Stanbridge Road
Leighton Buzzard, Bedfordshire LU7 4UA
UK
TEL (+44) 1525 372010
FAX (+44) 1525 379547

Jencons Scientific Inc.
800 Bursca Drive
Suite 801
Bridgeville, PA 15017
TEL 800-846-9959
TEL 412-257-8861
FAX 412-257-8809
E-MAIL info@jencons.com

JRH Biosciences, Inc.
13804 W. 107th Street
Lenexa, KS
TEL 1-800-255-6032
FAX 1-913-469-5584
http://www.jrhbio.com/

JRH Biosciences Ltd.
Smeaton Road
West Portway
Andover, Hampshire SP10 3LF
UK
http://www.jrhbio.com/

J.T. Baker
Mallinckrodt Baker B.V.
Teugseweg 20
P.O. Box 1
7400 AA, Deventer
The Netherlands
TEL 31-570-687500
FAX 31-570-687574
E-MAIL service.nl@mkg.com
http://www.jtbaker.com

JT Baker
Mallinckrodt Baker, and Inc.
222 Red School Lane
Phillipsburg NJ 08865
USA

JY Horiba
3880 Park Avenue
Edison, NJ 08820-3012
USA
http://www.jobinyvon.com

KEBO
Fagerstagatan 18A
SE-163 94 Stockholm
Sweden
http://www.kebolab.se/

Kendro Laboratory Products
31 Pecks Lane
Newtown, CT 06470-2337 USA
Kimble / Kontes
Vineland, New Jersey
USA
TEL (888) 546-2531 Extension 1
TEL (856) 692-3600 Extension 1
FAX (856) 794-9762
E-MAIL cs@kimkon.com

KIBBUTZ BEIT HAEMEK
25115 ISRAEL
TEL 972-(0)4-996-0595
FAX 972-(0)4-996-8896
E-MAIL info@bioind.com
http://www.bioind.com/

Kinetic Imaging Limited
2 Brunel Road
Croft Business Park
Bromborough, Wirral, Merseyside CH62 3NY
TEL 0151 343 0060
FAX 0151 343 1524
http://www.kineticimaging.com

Kodak
Distributed by VWR/Canlab.
8567 Chemin Dalton
Ville Mont-Royal, PQ H4T 1V5
Canada
TEL (514)344-3525

Kodak Laboratory Chemicals
Building 70
Eastman Kodak Company
343 State St., Rochester, NY
TEL 1-800-225-5352
FAX 1-800-225-5352

Kodak Scientific Imaging Systems
Eastman Kodak Company, 4
Science Park, New Haven, CT 06511
USA
www.kodak.com/US/en/health/scientific

Kojair Tech Oy
Tellollisuusitie 3
35700 Vilpulla, Finland
http://www.kojair.com

Kontes Glass Company
1022 Spruce Street
Vineland, NJ 08360

KVT König
Dietikon, Switzerland
http://www.kvt.ch/

Labassco
Aminogatan 30
431 53 Mölndal
Sweden
TEL +46-31-730 70 00
FAX +46-31-706 30 30

Lab Chem Inc.
200 William Pitt Way
Pittsburgh, PA 15238
Labconco Corporation
8811 Prospect Avenue
Kansas City, Missouri 64132-2696
TEL (800) 821-5525
TEL (816) 333-8811
FAX (816) 363-0130
http://www.labconco.com

Labcor Products Inc.
7309 Governors Way
Frederick, MD, 21704
USA

Lab-Line Instruments, Inc.
15th and Bloomingdale Avenues
Melrose Park, IL 60160

Laboratoires EUROBIO
avenue de Scandinavie 7
91953 Les Ulis Cedex B
France
TEL +33(0)1 69 07 94 77
FAX +33(0)1 69 07 95 34
http://www.eurobio.fr/

Laboratory Products Sales
1655 Buffalo Rd.
Rochester, NY 14624

Laborel
Caspar Stormsvei 2
Postboks 109 Alnabru
0614 Oslo
TEL +47 23 05 19 30
FAX +47 23 05 19 31
E-MAIL laborel@laborel.no
http://www.laborel.no

Labscientific
114 West Mt. Pleasant Avenue
Livingston, New Jersey 07039
USA
http://www.labscientific.com/

Lancaster Synthesis Ltd.
Newgate, White Lund
Morecambe, Lancashire LA3 3DY

Laser Science, Inc.
8E Forge Parkway
Franklin, MA 02038
USA
TEL 1-508-553-2353
FAX 1-508-553-2355
E-MAIL Via the website
http://www.laserscience.com/index.html

LC Laboratories
165 New Boston Street
Woburn, MA 01801

Leica
111 Deer Lake Road
Deerfield, IL 60015 USA
Leica Microsystems
www.light-microscopy.com

Leica Microsystems AG
Ernst-Leitz-Strasse 17-37
Wetzlar, 35578
Germany
http://www.leica-microsystems.com

Leica Microsystems Inc.
2345 Waukegan Road
60015 Bannockburn
TEL +1 800 248 0123
Fax +1 847 405 0164
http://www.leica-microsystems.com

Leica Mikrosysteme Vertrieb GmbH
Lilienthalstrasse 39-45
Bensheim, D-64625
Germany
TEL +49 6251 136 0
FAX +49 6251 136 155
http://www.leica-microsystems.com

Leysop Ltd.
18 Repton Court
Repton Close
Basildon, Essex, SS13 1LN
England
FAX (+44) 1268 522111
E-MAIL sales@leysop.com
http://www.leysop.co.uk

Life Imaging Services, LIS
CH-4153 Reinach BL
Switzerland
http://www.lis.ch

Life Science Headquarters
549 Albany Street
Boston, Massachusetts 02118
USA

Life Science Research
2000 Alfred Nobel Drive
Hercules, California 94547
USA
TEL 1-800-424-6723
FAX 510-741-5800
E-MAIL lsg.orders.us@bio-rad.com
http://www.bio-rad.com

Life Science Products Inc.
P.O. Box 1150
Frederick, CO 80530
USA
TEL 1-800-245-5774
http://www.e-LSPI.com

Life Technologies
76344 Eggenstein-Leopoldshafen
Contact Invitrogen Corp.
1600 Faraday Ave.
Carlsbad, CA 92008, USA
TEL 1-800-955-6288
http://www.invitrogen.com

Life Technologies, Inc.
P.O. Box 68
Grand Island, NY 14072-0068
USA
TEL 800-828-6686
FAX 800-331-2286

Life Technologies, Inc.
P.O. Box 6009
Gaithersburg, MD 20884-9980

LKB-Wallac
PerkinElmer Analytical Instruments
Chalfont Rd.
Seer Green
Beaconsfield, Bucks HP9 2FX
UK
TEL +44 (0)1494 874515
FAX +44 (0)1494 679335
http://uk.instruments.perkinelmer.com

Lochhamer Schlag 19
D—82166 Gräfelfing
Germany
TEL 49 89 895 662 0
FAX 49 89 895 662 101
http://www.till-photonics.de/home_e.htm

Ludl Electronic Products Ltd.
171 Brady Avenue
Hawthorne, NY 10532
USA

Luminex Corporation
12212 Technology Blvd.
Austin, TX 78727
USA

Luxo Corporation
200 Clearbrook Road
Elmsford, NY 10523
TEL 914-345-0067
FAX 914-345-0068

Luxo Schweiz GmbH
Oberebenestrasse 67
CH—5620 Bremgarten AG
TEL +41 56 633 88 28
FAX +41 56 633 99 04
http://www.luxo.com/

Maag Technic AG
Birsfelden
Switzerland
http://www.maagtechnic.ch/

MABTECH
Gamla Värmdöv. 2
SE-131 37 Nacka
Sweden

Mallinckrodt
675 McDonnell Blvd.
Hazelwood, MO 63042
USA

Mallinckrodt Baker
Im Leuschnerpark 4
D-64347 Griesheim
Germany

Mallinckrodt Baker, Inc.
222 Red School Lane
Phillipsburg NJ 08865
USA
TEL 908-859-2151
TEL 1-800-582-2537 (within U.S.)
FAX 908-859-6905
http://www.jtbaker.com/

Mallinckrodt Baker B.V.
Teugseweg 20
P.O. Box 1
7400 AA, Deventer
The Netherlands
TEL 31-570-687500
FAX 31-570-687574
E-MAIL service.nl@mkg.com

Mallinckrodt Laboratory Chemicals
A Division of Mallinckrodt Baker, Inc.
222 Red School Lane
Phillipsburg, NJ 08865
TEL (800) 582-2537
TEL (908) 859-2151 (outside U.S.)
FAX (908) 859-6905
E-MAIL infombi@mkg.com
http://www.mallchem.com/prodlit/prod_lit.asp

Marcherey-Nagel GmbH
Postfach 10 13 52
D-52313 Duren
Germany
TEL +49 (0) 2421-9690
FAX +44 (0) 2421-969 199
http://www.macherey-nagel.com/

Marienfeld Laboratory Glassware
Paul Marienfeld GmbH & Co. KG
Am Wöllerspfad 4
97922 Lauda-Königshofen
Germany
TEL +49 (0) 9343 6272-0
FAX +49 (0) 9343 6272-25
E-MAIL info@marienfeld-superior.com
http://www.marienfeld-superior.com

Marysol
Tokyo, Japan

Matrix
Lower Meadow Road
Brooke Park
Handforth, Wilmslow, Cheshire, SK9 3LP
UK

Matrix Science Ltd.
8 Wyndham Place
London W1H 1PP
UK
http://www.matrixscience.com

Matrix Technologies Corp
22 Friars Drive
Hudson, NH 03051
USA
TEL (866) 229 9770
http://www.matrixtechcorp.com

Matsunami Glass Ind., Ltd.
2-1-10 Yasaka-cho
Kishiwada City, Osaka 596-0049
Japan
TEL 81-724-33-1163
FAX 81-0724-36-2265

MatTek Corp.
200 Homer Ave.
Ashland, MA 01721
USA
TEL (508) 881-6771
FAX (508) 879-1532
E-MAIL information@mattek.com
http://www.mattek.com

Max F. Keller GmbH
Elsteinstrasse 14a
D-68169 Mannheim
Postfach 121036
TEL 0621 / 3227932
TEL 0621 / 3227927

MCI Optonix
Division of USR Optonix, Inc.
P.O. Box 509
Cedar Knolls, NJ 07927
USA
http://www.mcio.com

McMaster
http://www.mcmaster.com/

MDS, Inc.
100 International Blvd.
Toronto, Ontario, M9W6J6
TEL 416-675-4530
FAX 416-675-0688
http://www.mdsintl.com

MDS Nordion
447 March Road
Ottawa, ON K2K 1X8
Canada
TEL +1 613 592 2790
FAX +1 613 592 6937
http://www.mds.nordion.com/

MDS Sciex
71 Four Valley Drive
Concord, ON L4K 4V8
Canada
http://www.sciex.com

Medinor
Nils Hansens vei 4
Postboks 94 Bryn
0611 Oslo
Norway

Melford Laboratories Ltd.
Bildeston Rd.
Chelsworth
Ipswich, Suffolk, IP7 7LE
UK
TEL (+44) 1449 741178
FAX (+44) 1449 741217

Melles Griot
051 Palomar Airport Rd. #200,
Carlsbad, CA 92009
2TEL (760) 268-5131
TEL (800) 835-2626
FAX (760) 804-0049
E-MAIL sales@irvine.mellesgriot.com
http://www.mellesgriot.com

Melles Griot Ltd.
1 Saint Thomas Place
Cambridgeshire Business Park
Angel Drove, Ely, CB7 4EX
Cambridgeshire
TEL 01353 654500
FAX 01353 654555
http://www.mellesgriot.com

MENZEL-GLAZER
Gerhard Menzel
Glasbearbeitungswerk
Gmbh & Co. KG
Saarbrückener Str. 248
D-38116 Braunschweig
Germany
TEL 0531/59008-0
FAX 0531/509799

Merck
Frankfurter Str. 250
64293 Darmstadt
Germany
TEL +49 6151 72-3000
FAX +49 6151 72-3333
FAX +49 6151 72 7495
E-MAIL catalog@merck.de, AR@merck.de
http://www.merck.de

Merck & Co., Inc.
One Merck Drive
P.O. Box 100
Whitehouse Station, NJ 08889-0100
USA
TEL 908-423-1000

Merck Biosciences
Boulevard Industrial Park
Padge Road
Beeston, Nottingham NG9 2JR
UK
http://www. merckbiosciences.co.uk

Merck Biosciences GmbH (formerly Calbiochem-Novabiochem GmbH)
Ober der Roth 4
D-65796 Bad Soden
Germany
FAX 49 (6196) 62361
http://www.calbiochem.com

Merck Biosciences Ltd.*
Boulevard Industrial Park
Padge Road
Beeston, Nottingham, NG9 2JR
UK
TEL 0115 943 0840
FAX 0115 943 0951
http://www.merckbiosciences.co.uk/html/CNUK/account_managers.htm

Merck Eurolab
10, rue de la Durance
B.P. 36
67023 Strasbourg Cedex 1
France
TEL +33 3 88 65 80 20
FAX +33 3 88 39 74 41
http://www.merckeurolab.fr

Merck KGaA
D-64271 Darmstadt
Germany
TEL (49)-6151-72-0
FAX (49)-6151-72-2000
E-MAIL catalog@merck.de
http://www.merck.de

Merck Ltd.
Laboratory Supplies
Merck House
Seldown, Poole, Dorset, BH15 1TD, UK
TEL 44-1202-669700
FAX 44-1202-665599
E-MAIL stella.taylor@merck-ltd.co.uk
http://www.merck-ltd.co.uk

Merck Schuchardt OHG
Eduard-Buchner-Str. 14-20
85662 Hohenbrunn
Germany
TEL +49 8102 802-0
FAX +49 8102 802-175
http://www.schuchardt.de

Merck/VWR International GmbH
Hilpertstr. 20a
D-64295 Darmstadt
Germany
E-MAIL darmstadt@de.vwr.com
http://www.vwr.com

Mica House
2A Pretoria Street
Calcutta 700 071
India

Michrom BioResources
1945 Industrial Drive
Auburn, CA 95603

Microbix Biosystems, Inc.
341 Bering Avenue
Toronto, Ontario, M8Z 3A8
Canada
TEL 416-234-1624
FAX 416-234-1626
http://www.microbix.com

MICROM International GmbH
Robert-Bosch-Str. 49
D-69190 Walldorf
TEL +49 6227-836 0
FAX +49 6227-836 111
http://www.microm.de

Micro Video Instruments Inc.
11 Robbie Road
P.O. Box 518
Avon, MA 02322
USA
TEL 1-508-580-0080
FAX 1-508-580-8623
E-MAIL Via the website
http://www.mvi-inc.com/home.htm

Milian SA
Route du Vélodrome 35
CH-1228 Plan-les-Ouates, Geneva
Switzerland
http://www.milian.com

Millipore
290 Concord Rd.
Billerica, MA 01821
USA
TEL 1-978-715-4321
http://www.millipore.com

Millipore AG
Chriesbaumstrasse 6
CH-8604 Volketswil
Switzerland
TEL +41 848 645 645
FAX +41 848 645 644
http://www.millipore.com

Miltenyi Biotech GmbH
Friedrich-Ebert-Str. 68
51429 Bergisch-Gladbach
Germany

Miltex instruments
http://www.ssrsurgical.com

MJ Research, Inc.
5350 Capital Court, #102
Reno, NV 89502
USA
http://www.mjr.com/

MJ RESEARCH, INC.
590 Lincoln Street
Waltham, MA 02451
TEL (617) 923-8000
TEL (888) 735-8437
FAX (617) 923-8080
E-MAIL info@mjr.com
http://www.mjr.com

MJ Research Inc.
149 Grove St.
Watertown, MA 02172

MoBiTec
Wagenstieg 5 D-37077
Göttingen
TEL (+49) 551-371062
FAX (+49) 551-34987

MoBiTec GmbH
Lotzestrasse 22a
37083 Göttingen, Germany
http://www.mobitec.de

Molectron Detector, Inc.
7470 SW Bridgeport Road
Portland, OR 97224
USA
TEL 1-800-366-4340
FAX 1-503-620-8964
E-MAIL info@molectron.com
http://www.molectron.com/index.asp

Molecular Biology Insights
8685 US Highway 24
Cascade, CO 80809-1333
USA
TEL 1-800-747-4362
TEL 1-719-684-7988
FAX 1-719-684-7989
http://www.oligo.net/

Molecular BioProducts, Inc.
9880 Mesa Rim Road
San Diego, CA 92121-2979
USA

Molecular Devices Corporation
1311 Orleans Avenue
Sunnyvale CA 94089-1136
USA
TEL +1-408-747-1700
TEL 800-635-5577
FAX +1-408-747-3601
http://www.moleculardevices.com

Molecular Devices Ltd.
135 Wharfedale Road
Winnersh Triangle
Winnersh, Wokingham RG41 5RB
England

Molecular Dynamics
928 East Arques Avenue
Sunnyvale, CA 94068
USA
TEL 1-800-333-5703
http://www.mdyn.com

Molecular Probes
29851 Willow Creek Road
PO Box 22010
Eugene, OR 97402-0469
USA
TEL 1-800-438-2209
FAX 1-800-438-0228
http://www.probes.com/

Molecular Probes
PoortGebouw
Rijnsburgerweg 10
2333 AA Leiden
The Netherlands
TEL +31 71 52 36 850
FAX +31 71 52 33 419
http://www.probes.nl

Molecular Probes Europe BV
Poortgebouw
Rijnsburgerweg 10
2333 AA Leiden
The Netherlands
TEL +31-71-5233378
FAX +31-71-5233419
http://www.probes.com/

Moss, Inc.
P.O. Box 189
Pasadena, Maryland 21123-0189
USA
TEL +1-800-932-6677
FAX +1-410-768-3971
http://www.mosssubstrates.com

Motion Analysis Corporation
3617 Westwind Blvd.
Santa Rosa, California 95403
TEL 707.579.6500
FAX 707.526.0629
http://www.motionanalysis.com

mouse models of human cancer consortium (MMHCC)
http://web.ncifcrf.gov/researchresources/mmhcc/

MP Biomedicals Corporate Headquarters
15 Morgan
Irvine, CA 92618-2005
TEL 800.633.1352
E-MAIL sales@mpbio.com

MSD Sharp & Dohme GmbH
Lindenplatz 1
D-85540 Haar
Germany

MTX Labs, Inc.
8456 Tyco Road
Building D
Vienna, Virginia 22182
USA
TEL 01.703.821.1045
TEL 1.800.848.6474
FAX 01.703.821.1046
Tech Support 703.821.3948
E-MAIL Info@mtxlsi.com

MWG Biotech (Headquarters)
Anzinger Str. 7a
D-85560 Ebersberg
Germany
TEL +49-08092-8289-0
FAX +49-08092-21084
E-MAIL info@mwgdna.com
http://www.mwg-biotech.com/

Nacalai tesque
498 Higashitamaya-cho
Nijo Karasuma, Nakagyo-ku Kyoto 6040855
Japan
TEL +81-75-251-1723
FAX +81-75-251-1762
E-MAIL info.intl@nacalai.co.jp

Nakagyo-ku
Kyoto 604-0855
Japan
TEL 81-75-211-2516
FAX 81-75-231-2455

Nalge (Europe) Limited
Unit 1a, Thorn Business Park
Hereford HR2 6JS
UK
TEL +44 (0) 1432 263933
FAX +44 (0) 1432 376567

Nalge (Europe) Ltd.
Foxwood Court
Rotherwas, Hereford HR2 6JQ
UK
TEL +44-01432-263933
FAX +44-01432-351923

Nalgene
TEL 1-800-625-4327
FAX 585-586-8987
E-MAIL nnitech@nalgenunc.com
http://www.nalgenunc.com/

Nalge Nunc Internacional
75 Panorama Creek Drive
P.O. Box 20365
Rochester, NY 14602-0365
USA
TEL 1-800-625-4327
FAX 585-586-8987
E-MAIL nnics@nalgenunc.com
http://www.nalgenunc.com

Nanoprobes
95 Horse Block Road
Yaphank, NY 11980-9710
USA

Narashige
27-9 Minamikarasuyama 4-chome
Setagaya-Ku, Tokyo
Japan
TEL 81-3-3308-8233
FAX 81-3-3308-2005
E-MAIL sales@narishige.co.jp
http://www.narishige.co.jp/products/electro/index2.htm

Narishige International LTD
Unit 7, Willow Business Park
Willow Way, London SE26 4QP
UK
http://www.narishige.co.jp/niusa/index.htm

Narishige International USA, INC.
1710 Hempstead Turnpike
East Meadow, NY 11554
USA
TEL 516-794-8000
TEL 1-800-445-7914 (within the USA)
FAX 516-794-0066
E-MAIL narishige-usa@pb.net
http://www.narishige.co.jp/niusa/index.htm

NASCO—Fort Atkinson
901 Janesville Avenue
P.O. Box 901
Fort Atkinson, WI 53538-0901
TEL 1-800-558-9595
FAX 920-563-8296
http://www.nascofa.com/prod/Home

National Diagnostics U.S.A.
305 Patton Drive
Atlanta, Georgia 30336
USA
http://www.nationaldiagnostics.com

National Instruments Corporation
11500 N Mopac Expwy
Austin, TX 78759-3504
TEL (+01) 512-683-0100
FAX (+01) 512-683-8411
http://www.ni.com

National Scientific Co.
205 East Paletown Road
Quakertown, PA 18951
USA
TEL 215-536-2577
FAX 215-536-5811

NBS Biologicals Ltd.
14 Tower Square
Hungtingdon, Cambs PE29 7TD
England
http://www.nbsbio.co.uk

NEN
PerkinElmer, European Headquarters
Via Tiepolo, 24
20052 Monza
Italy
http://it.Instruments.perkinelmer.com

NEN (New England Nuclear)
Now part of Perkin Elmer Life and Analytical Sciences, Inc.
549 Albany Street
Boston MA 02118-2512 (USA)
las.perkinelmer.com/content/corporate/about/nenlifescience.html

NeoLab
Rischerstr. 7
69123 Heidelberg

NeoLab MIGGE Laborbedarf-Vetriebs GmbH
Rischerstr. 7
D-69123 Heidelberg
Postbox 10 40 80
Germany
TEL (0)-62 21/84 42-0 switchboard
FAX (0)-62 21/84 42 33
neoLab (0)-62 21/83 32 26 MIGGE
E-MAIL info@neolab.deTEL
http://www.neolab.de

Neomarkers
47790 Westinghouse Drive
Fremont, California 94539
USA

Nerliens
Postboks 2955
Tøyen, 0608 Oslo
Norway
TEL +47 22 66 65 00
FAX +47 22 66 65 01
E-MAIL info@nmas.no
http://www.vwrsp.com

New Brunswick Scientific Co., Inc.
P.O. Box 4005
44 Talmadge Road
Edison, New Jersey 08818-4005
TEL +1 (732) 287-1200
TEL +1 (800) 631-5417
FAX +1 (732) 287-4222
E-MAIL bioinfo@nbsc.com
http://www.nbsc.com/

NEW ENGLAND BIOLABS
32 Tozer Road
Beverly, MA 01915-5599
2TEL (978) 927- 5054
TEL (USA Orders) 1-800-632-5227
http://www.neb.com

New England Nuclear
Contact PerkinElmer Life and Analytical Sciences Inc.
549 Albany Street
Boston, MA 02118
USA
TEL 1-800-762-4000
http://las.perkinelmer.com/

New Focus Corporate Offices
2584 Junction Avenue
San Jose, CA 95134
USA
TEL 1-866-NUFOCUS (USA and Canada only)
TEL (408) 919-1500
E-MAIL contact@newfocus.com

New Objective, Inc.
2 Constitution Way
Woburn, MA 01801-1023
USA
TEL (888) 220-2998 U.S.
TEL (781) 933-9560
FAX (781) 933-9564
E-MAIL sales@newobjective.com

Newport Corp.
1791 Deere Ave.
Irvine, CA 92714
USA
TEL 800-222-6440
FAX 714-963-2015
E-MAIL uk@newport.com 253-1680
http://www.newport.com/

Newport Scientific
8246-E Sandy Court
Jessup, Maryland 20794
http://www.newport.com

Nihon Pharmaceutical
Higashicanda 1-9-8
Chiyoda Tokyo 101-0031
Japan
TEL 03-3864-8411
FAX 03-3864-8837

NIKON
1300 Walt Whitman Road
Melville, NY 11747
http://www.nikonusa.com

Nikon DIAPHOT-TMD
Fuji Bldg. 2-3, 3-chrom
Marunouchi Chiyoda-Ku, Tokyo 157
Japan

Nipa Laboratories Inc.
Llantwit Fadre
Pontypridd, Mid Glamorgan CF38 2SN
UK
TEL (+44) 1443 205311
FAX (+44) 1443 207746

Nissui Pharmaceutical Co.
Tokyo, Japan
http://www.nissui-pharm.co.jp
Nitta Gelatin Co. Ltd.
Osaka, Japan
http://www.nitta-gelatin.co.jp

NORTON PERFORMANCE PLASTICS CORP.
Akron, Ohio 44305
USA
http://www.tygon.com/

Nova Biochem
Laufelfingen, Switzerland
http://www.emdbiosciences.com/html/NBC/home.html

Novagen
Merck Biosciences Ltd.
Boulevard Industrial Park
Padge Road
Beeston, Nottingham, NG9 2JR
UK
TEL 0800 622935
FAX 0115 943 0951
E-MAIL customer.service@merckbiosciences.co.uk

Novocastra Laboratories Ltd
Balliol Business Park West
Benton Lane, Newcastle upon Tyne, NE12 8EW
UK
TEL +44 (0) 191 215 0567
FAX +44 (0) 191 215 1152

Novo Nordisk
NOVO NORDISK A/S
NOVO ALLE, DK 2880 BAGSVAERD
DENMARK

Novus Biologicals, Inc.
PO Box 802
Littleton, CO, 80160
USA
E-MAIL novus-biological.com

NuAire, Inc.
2100 Fernbrook Lane
Plymouth, MN 55447
USA
http://www.nuaire.com

NUNC
75 Panorama Creek Drive
Rochester, NY 14625
USA
http://www.nalgenunc.com/

Nunc A/S
Box 280
Kamstrup, DK 4000
Roskilde
Denmark
TEL +45-42359065
http://www.nunc.nalgenunc.com

Nunclon
Nunc Gmbh & Co. KG
Postfach 120543
D-65083 Wiesbaden
TEL +49 6111 86740
FAX +49 6111 867474
E-MAIL nunc@nunc.de
http://www.nunc.de

N.V. Mettler-Toledo S.A.
Leuvensesteenweg 384
1932 Zaventem
Belgium
TEL +32 2 334 02 11
FAX +32 2 334 03 34
http://www.mt.com

Oakdale Engineering, Inc.
23 Tomey Road
Oakdale, PA 15071
USA

Office Depot Corporate Support Center
2200 Old Germantown Road
Delray Beach, FL 33445
TEL 1-800-463-3768
http://www.officedepot.com/

Office Max
http://www.officemax.com

Oligos Etc. Inc.
PO Box 727
9775 SW Commerce Circle C-6
Wilsonville, OR 97070

Olympus America
Olympus America Inc.
2 Corporate Center Drive
Melville, NY 11747
USA
TEL 1-800-645-8160
http://www.olympusamerica.com/seg_section/seg_home.asp

Olympus Optical Co., Ltd.
Tokyo, Japan
http://www.olympus-global.com/

Omega Optical, Inc.
210 Main Street
Brattleboro, VT 05301
USA
TEL (802) 254-2690
TEL (866) 488-1064
FAX (802) 254-3937
http://www.omegafilters.com

Once/Millpledge Veterinary
Whinleys Estate
Clarborough
Redford, Knotts, DN229A
UK

Oncogene Science from Cedarlane Laboratories Ltd.
5516-8th Line
R.R.2
Hornby, ON L0P 1E0
Canada
TEL 1-800-268-5058

Ophir Optronics Inc.
9 Electronics Avenue
Danvers Industrial Park
Danvers, MA, USA 01923
TEL 1-800-383-0814
FAX 1-978-774-8202
E-MAIL sales@ophiropt.com
http://www.ophiropt.com/

Optical Insights, LLC
1807 Second Street
Suite #100
Santa Fe, NM 87505
2TEL 505-955-1585
International: 001-505-955-1585
http://www.optical-insights.com

Oriel
150 Long Beach Blvd.
Stratford, CT 06615
USA
2TEL (203) 377-8282
FAX (203) 378-2457
http://www.oriel.com

Osmonics
G.A. Murdock Inc.
1200 Division Ave. S.
P.O. Box 465
Madison, SD 57042, USA
http://www.gamurdock.com/gam/out/BRANDS/Osmonics.htm

Osram
Hellabrunner Straße 1
81543 München
Germany

Oswel Research Products Ltd.
Unit 2
Winchester Hill Commercial Park
Winchester Hill
Romsey, Hampshire SO51 7UT
England
OVA Production
Farmer: Pär-Erik Wejåker Sörgården, Morgongåva
Sweden

Owens polyscience Ltd.
34 Chester Road
Macclesfield, Cheshire, SK11 8DG

Oxoid Limited
Wade Road
Basingstoke, Hampshire, RG24 8PW
UK
http://www.oxoid.com

Oxoid Ltd.
Wade Road
Basingstoke RG24 OPW
England

PAA Laboratories
1 Technine
Guard Avenue
Houndstone Business Park
Yeovil Somerset BA22 8YE
UK
TEL ++44 193 541-1418

PAA Laboratories GmbH
Haidmannweg 9
A-4061 Pasching
Austria
TEL 43 7229 64865
FAX 43 7229 64866

Packard, see PerkinElmer Life and Analytical Sciences, Inc.
549 Albany Street
Boston, MA 02118-2512
USA
TEL (+1) 203-925-4602
FAX 203-944-4902
E-MAIL productinfo@perkinelmer.com
http://www.perkinelmer.com

Packard Instruments Co. Inc.
2200 Warrenville rd.
Downers Grove, Illinois 60515
USA
TEL (1) 312-969-6000

Pall Corporation
Europa House
Havant Street
Portsmouth, Hampshire, PO1 3PD
UK
TEL +44 (0) 23 9230 3303
FAX +44 (0) 23 9230 2509
http://www.pall.com/

Panasonic
Matsushita Electric Corporation of America
One Panasonic Way
Secaucus, NJ 07094
http://www.panasonic.com

Panreac química S.A.
Riera de Sant Cugat, 1
E-08110 Montcada i Reixac (Barcelona)
Spain
http://www.panreac.es

Parale Mitsui
Bldg., 8
Higashida-cho
Kawasaki-ku, Kawasaki, Kanagawa, 210-0005
Japan
http://www.nikon.com

Parr Instrument Company
211 53rd Street
Moline, Illinois 61265-9984
TEL 1-800-872-7720
TEL (309) 762-7716
FAX (309) 762-9453

Partec AG
Sonnenweg 7
CH-4144 Arlesheim
Switzerland
TEL 061 72 77 55

PE Applied Biosystems
850 Lincoln Centre Drive
Foster City, CA 94404
USA
TEL 800.327.3002
TEL 650.638.5800
http://www.appliedbiosystems.com

Pelco International
P.O. Box 492477
Redding, CA 96049-2477
U.S.A.
TEL 530-243-2200
TEL 800-237-3526 (Canada)
FAX 530-243-3761
E-MAIL sales@pelcoint.com
http://www.pelcoint.com/

PeproTech EC Ltd.
PeproTech House
29 Margravine Road
London W6 8LL
UK
TEL (0)20 7610 3055
TEL (0)20 7610 3062
FAX (0)20 7610 3430

Perbio GmbH
Adenauerallee 113
53113 Bonn
Germany
TEL 49 228 9125650
FAX 49 228 9125651

Perbio-Science
Knutpunkten 34
SE-252 78 Helsingborg
Sweden
TEL +46 42 26 90 90
FAX +46 42 26 90 98
http://www.perbio.com

Perbio Science (Branch Office)
Industriezone III
Industrielaan 27
B-9320 Erembodegem-Aalst
BELGIUM
TEL +32 53 83 44 04
FAX +32 53 83 76 38
http://www.piercenet.com

Perbio Science UK Ltd.
Century House
High Street
Tattenhall, Cheshire CH3 9RJ

Perkin Elmer
204 Cambridge Science Park
Cambridge CB4 0GZ
UK

PerkinElmer
45 William Street
Wellesley, MA 02481-4078
USA

PerkinElmer Instruments GmbH
Ferdinand-Porsche-Ring 17
63110 Rodgau-Jügesheim
FAX 49 (01803) 929526
http://www.perkin-elmer.de

PerkinElmer Life & Analytical Sciences, Inc.
(New England Nuclear Lifesciences)
549 Albany Street
Boston, MA 02118-2512
TEL 1-800-762-4000
TEL 203-925-4602
FAX 1-203-944-4902
E-MAIL productinfo@perkinelmer.com
http://www.perkinelmer.com/nenlifescience.asp

PerSeptive
850 Lincoln Centre Drive
Foster City, CA 94404
http://www.appliedbiosystems.com/

Perseptive Biosystems
500 Old Connecticut Path
Framingham, MA 01701
USA
TEL 800-899-5858
FAX 508-383-7851

PGC Scientific
7311 Governors Way
Frederick, MD 21704
USA
TEL (301) 620-7777
http://www.pgcsci.com/

Pharmacia
Am Wolfsmantel 46
D-91058 Erlangen
Germany

Pharmacia & Upjohn Pty LtD
15 Brodie Hall Dve
Bentley WA 6102
Australia
http://www.pharmacia.com

Pharmacia Fine Chemicals
Amersham Biosciences Corp.
800 Centennial Ave
P.O. Box 1327
Piscataway, NJ 08855
USA
http://www5.amershambiosciences.com

Pharmingen
1-6800 Kitimat Road
Mississauga ON, L5N 5M1
Canada
TEL 1-888-259-0187

Phillip Harris Scientific
618 Western Avenue
Park Royal, London W3 0TE
UK
TEL (+44) 181 992 5555
FAX (+44) 181 993 8020

Phoenix Flow Systems
11575 Sorrento Valley Road
San Diego, CA, 92121
TEL 1-800-886-FLOW (3569)
TEL (619) 453-5095
FAX (619) 259-5268
http://www.phnxflow.com

Photometrics Roper Scientific
3440 E. Britannia Drive
Suite 100
Tucson, Arizona 85706
Roper Scientific Benelux
Ir. D.S. Tuijnmanweg 10
Triple P Building, 4131 PN Vianen
The Netherlands
http://www.photomet.com

Photometrics Roper Scientific
3440 East Britannia Drive
Tucson, AZ 85706
USA
http://photomet.com

Photon Technology International, Inc.
1009 Lenox Drive
Lawrenceville, NJ 08648
http://www.pti-nj.com

Physik Instrumente (PI) GmbH & Co. KG
Auf der Roemerstrasse
D-76228 Karlsruhe/Palmbach
Germany
TEL (+49) 721 4846-0
FAX (+49) 721 4846-100
E-MAIL info@pi.ws
http://www.pi.ws

Physik Instrumente GmbH
Auf der Romerstrase 1
Karlsruhe null, D76228
GERMANY
TEL 49-7243-604-100
FAX 49-7243-604-145
http://www.physikinstrumente.com/

Pierce
P.O. Box 117
3747 N. Meridian Road
Rockford, IL 61105
USA
TEL +1-800-842-5007
TEL 815-968-8148
FAX 1-800-842-5007
E-MAIL cs@piercenet.com
http://www.piercenet.com

Pierce Chemical Company
Perbio Science UK Ltd.
Century House
High Street
Tattenhall, Cheshire CH3 9RJ
UK
TEL +44 (0)1829 771 744
FAX +44 (0)1829 771 644
http://www.piercenet.com

Polaroid Corporation
Corporate Headquarters
1265 Main Street—
Bldg. W3
Waltham, MA 02451
USA
TEL 1-800-343-5000
http://www.polaroid.com/us/index.jsp

Polymicro Technologies, LLC
18019 N. 25th Avenue
Phoenix, AZ 85023-1200
TEL 602-375-4100
FAX 602-375-4110

Polysciences, Inc.
400 Valley Rd.
Warrington, PA 18976-2522
TEL 800/523-2575
FAX 800/343-3291
E-MAIL info@polysciences.com

PolysciencesEurope
GmbHHandelsstr. 3
D-69214 Eppelheim
Germany
TEL (49)6221-765767
FAX (49)6221-764620
E-MAIL info@polysciences.de
http://www.polysciences.com/shop/

Precision Brand Products Inc.
Downers Grove, IL
USA
http://www.precisionbrand.com

Prime Tech
635 Nakamukaihara Tsuchiura-shi
Ibaraki 300-0841
JAPAN
TEL +81-29-830-4517
FAX +81-29-830-4515
E-MAIL pmm@primetech-jp.com
http://www.primetech-jp.com/english/newproduct.htm

Princeton Research Instruments, Inc.
42 Cherry Valley Road
Princeton, NJ 08542
USA

Princeton Scientific Instruments, Inc.
7 Deer Park Drive
Monmouth Junction, New Jersey 08852
USA
TEL +1 732 274 0774
FAX +1 732 274 0775
http://www.prinsci.com/

PROBES
Molecular Probes Europe BV
Poortgebouw, Rijnsburgerweg 10
2333 AA Leiden
The Netherlands
TEL +31-71-5233378
FAX +31-71-5233419
http://www.probes.com

Progen Biotechnik GmbH
Maaßstrasse 30
69123 Heidelberg
Germany
TEL 49 6221 8278-13
FAX 49 6221 8278-23

ProImmune Limited
Oxford BioBusiness Centre
Littlemore Park
Littlemore, Oxford OX4 4SS
UK
TEL +44 1865 405 128
FAX +44 1865 405 123
E-MAIL enquiries@proimmune.com
http://www.proimmune.co.uk

Promega Benelux BV.
Kenauweg 34
PO Box 391
2300 AJ Leiden
THE NETHERLANDS
TEL (31) 71 5324244
FAX (31) 71 5324907

Promega Corporation
2800 Woods Hollow Road
Madison, WI 53711
USA
TEL 606-274-4330
TEL 800-356-9526
FAX 608-277-2601
http://www.promega.com

Promega—from Fisher Scientific
112 Colonnade Road
Nepean ON K2E 7L6
Canada
TEL 1-800-234-7437

Promega GmbH
Schildkrötstr. 15
D-68199 Mannheim
Germany

Promega Ltd.
Delta House
Enterprise Road
Chilworth Research Centre, Southampton
England

Proxeon Bioseparations
Staermosegaardsvej 6
DK 5230 Odense M
Denmark

Purite Ltd.
Bandet Way
Thame, Oxon OX9 3SJ

QA Bio.
240 Eaton Road
San Mateo, CA 94402
USA

Qbiogene, Inc.
2251 Rutherford Road
Carlsbad, CA 92008
USA
TEL 800-424-6101
FAX 760-918-9313
E-MAIL orders@qbiogene.com
http://qbiogene.com

Qbiogene, Europe offices
Parc d'Innovation
BP 50067
67402 ILLKIRCH CEDEX
France
TEL +33 3 88 67 54 25
FAX +33 3 88 67 19 45
E-MAIL eurorders@qbiogene.com
http://qbiogene.com/about/distributors

QIAGEN
28159 Avenue Stanford
Valencia, CA 91355
TEL 800-426-8157
FAX (800) 718-2056
http://www.qiagen.com

QIAGEN
QIAGEN HOUSE
Fleming Way
Crawley West Sussex RH10 9NQ
UK

QIAGEN AG
Auf dem Wolf 39
CH-4052 Basel
Switzerland

QIAGEN GmbH
Max-Volmer-Str 4
40724 Hilden
Germany
http://www.qiagen.com/

QIAGEN Inc.
28159 Avenue Stanford
Valencia, CA 91355
TEL 800-426-8157
TEL 800-DNA-PREP
TEL (800-362-7737)
FAX 800-718-2056

Quantel SA
17, Avenue de l'Atlantique
Z.A. de Courtaboeuf
BP 23-91941 Les Ulis Cedex
France
TEL 33 (1) 69 29 17 00
FAX 33 (1) 69 29 17 29

Quantronix Corp.
45 Adams Ave.
Hauppauge, NY 11788
USA
TEL 800-235-5953

Queen's University Core Facility
Ms. Sook Shin
Queen's University Kingston, ON K7L 3N6
Canada
TEL (613)533-6837

R&D Systems Europe
Abington Science Park
Abington, OX14 3NB
UK
http://www.RnDSystems.com

R&D Systems Inc.
614 McKinley Place N.E.
Minneapolis, MN 55413
TEL 1 800 349 74 75
TEL 1 612 379 29 56
FAX 1 612 656 44 00
E-MAIL info@rndsystems.com
http://www.rndsystems.com

Rainin
7500 Edgewater Dr.
Oakland, CA 94621
TEL (510)564-1600
http://www.rainin.com

RA Lamb
Units 4 & 5 Parkview Industrial Estate
Alder Close
Lottbridge Drove
Eastbourne, East Sussex, BN23 6QE
UK
TEL 01323 737000
FAX 01323 733000
E-MAIL sales@ralamb.com

Rathburn Chemicals Ltd.
Walkerburn, Scotland
EH43 6AU
TEL (44) (0)1 896 870 651
FAX (44) (0)1 896 870 633

Raymond A Lamb LLC.
7304 Vanclaybon Drive
Apex, NC 27502
USA
TEL 919387-1237
FAX 919-387-1736
E-MAIL sales@ralamb.com

Raytest GmbH
Benzstr. 4
D 75339 Straubenhardt
Germany
E-MAIL info@raytest.de
http://www.raytest.de

Reichert Division der Leica Aktiengesellschaft
Hernalser Hauptstr. 219
Postfach 95
A-1171 Vienna
Austria
TEL +43 1 4616 410
FAX +43 1 46 0326

Research Products International Corp.
410 N. Business Center Drive
Mount Prospect, IL 60056-2190
TEL 800 323 9814
http://www.rpicorp.com

Rheodyne LP
PO box 1909
Rohnert Park, CA 94927-1909
USA

Riedel-de-Haen
Sigma-Aldrich Laborchemikalien GmbH
P.O. Box 100262
30918 Seelze
Germany
TEL +49 5137 82 38 0
FAX +49 5137 82 38 0
E-MAIL Riedel@sial.com
http://www.sigma-aldrich.com

Roche
Basel, Switzerland
F. Hoffmann-La Roche Ltd
Group Headquarters
Grenzacherstrasse 124
CH-4070 Basel
Switzerland
TEL +41-61-688 1111
FAX +41-61-691 9391
http://www.roche.com/

Roche (F. Hoffmann-La Roche Ltd)
Diagnostics Division
Grenzacherstrasse 124
CH-4070 Basel
Switzerland
TEL 41-61-688-1111
FAX 41-61-691-9391
http://www.roche.com/

Roche Applied Science
9115 Hague Road
P.O. Box 50414
Indianapolis, IN 46250-0414, USA
TEL (800) 428-5433
FAX (800) 428-2883
http://www.roche-applied-science.com

Roche Diagnostics
Sandhoferstrasse 116
68305 Mannheim
Germany
FAX 49 (621) 759-4083
http://www.roche-diagnostics.com

Roche Diagnostic Corporation
9115 Hague Road
PO Box 50457
Indianapolis, IN 46256
USA
TEL 1-800-428-5433
http://www.roche-diagnostic.com

Roche Diagnostics, S.L.
Molecular Biochemicals
Copérnico, 60
08006 Barcelona
Spain
http://biochem.roche.com

Roche Diagnostics Corporation
201 Boulevard Armand Frappier
Laval, Quebec, H7V 4A2
Canada
TEL 800-363-5887
FAX 800-667-7050
http://www.biochem.roche.com

Roche Diagnostics Ltd.
Bell Lane, Lewes
East Sussex BN7 1LG

Roche Diagnostics Nederland B.V.
Postbus 1007
300 BA Almere
The Netherlands

Roche Molecular Biochemicals
Roche Norge
Division Diagnostics
Pb 6610 Etterstad, N-0607 Oslo
Norway

Roche Pharma (Schweiz) AG
Schönmattstrasse 2
CH-4153 Reinach BL
Switzerland
TEL +41-61-715 4111
FAX +41-61-715 4112
http://www.roche.com/

Roche Products Ltd
40 Broadwater Road
Welwyn Garden City
Hertfordshire, AL7 3AY

Rockland Immunochemicals
P. O. Box 316
Gilbertsville, PA 19525
http://rockland-inc.com

Romil Ltd.
The Source
Convent Drive
Ultra-pure waterbeach, Cambridge GB-CB59QT

Roper Scientific
3660 Quakerbridge Road
Trenton, NJ 08619
USA
TEL 609-587-9797
FAX 609-587-1970
sold by Visitron (CH and Germany) or Universal Imaging (UK)
http://www.roperscientific.com

Roper Whitney of Rockford, Inc.
2833 Huffman Blvd.
Rockford, IL 61103
USA
http://66.165.84.245/index2.asp

Rossville
Gold Shield Chemical Company
Hayward, CA 94545

RZPD (German Resource Centre for Genome Research GmbH)
Heubnerweg 6
D-14059 Berlin
Germany

Sakura Finetek Europe B.V.
Energieweg 1
3640 AB Mijdrecht
PO Box 80
The Netherlands
TEL +297 280 666
FAX +297 280 373
http://www.bayer.nl

Samco
1050 Arroyo Ave.
San Fernando, CA 91340-1822
USA

Santa Cruz Biotechnology, Inc.
2145 Delaware Ave.
Santa Cruz, CA 95060
TEL 831-457-3800
TEL 800-457-3801
FAX 831-457-3801
E-MAIL scbt@scbt.com
http://www.scbt.com

SARSTEDT AG & Co.
Rommelsdorfer Straße
Postfach 1220
51582 Nümbrecht
Germany
TEL +49 2293 305 0
FAX +49 2293 305 122
E-MAIL info@sarstedt.com
http://www.sarstedt.com

Sarstedt, Inc.
PO Box 468
Newton, NC 28658

SARSTEDT Inc.
6373 Des Grandes Prairies
Montreal PQ H1P 1A5
Canada
TEL 1-888-727-7833

Sartorius Corp.
131 Heartland Blvd.
Edgewood, NY 11717
USA
FAX 1 (631) 254-4253
http://www.sartoriuscorp.com

Sartorius GmbH
Weender Landstr. 94-108
D-37075 Göttingen
Germany
FAX 49 (551) 308-289
http://www.sartorius.de

Savant (now a division of Thermo Electron Corporation)
Thermo Electron Corporate Headquarters
81 Wyman Street
Waltham, MA 02454-9046
USA
TEL 1-877- 843-7668
FAX 1-781-622-1207
http://www.thermo.com/

Scanalytics, Inc.
8550 Lee Highway
Suite 400
Fairfax, VA 22031 USA
TEL 1-703-208-2230
FAX 1-703-208-1960
http://www.scanalytics.com/

Scharlau Chimie S.A.
Ctra. de Polinyà a Sentmenat
Km. 8, 2
08181 Sentmenat (Barcelona)
Spain
http://www.sharlau.com

Schering-Plough Co., Ltd.
Osaka, Japan
http://www.schering-plough.co.jp

Schleicher & Schuell
Hahnestrasse 3
D-37586 Dassel
Germany
TEL ++49 5561 791 463
FAX ++49 5561 791 583
http://www.schleicher-schuell.com/icm11be.nsf/(html)/FramesetBioScience

Schleicher & Schuell Bioscience Inc.
10 Optical Avenue
Keene, NH 03431

Schleicher & Schuell GmbH
Grimsehlstr. 23
37574 Einbeck
Germany
http://www.schleicher-schuell.com/

Schott Glasware
Bacto Laboratories Pty Ltd
PO Box 295
Liverpool, NSW, Australia 2170
TEL +61 (0)2 9602 5499
FAX +61 (0)2 9601 82
http://www.bacto.com.au

Scientific Industries, Inc.
70 Orville Dr.
Bohemia, NY 11716
USA
http://www.scientificindustries.com

Scientific Laboratory Supplies
Unit 27
Wilford Industrial Estate
Ruddington Lane
Wilford, Nottingham NG11 7EP
UK
TEL (+44) 115 9821111
FAX (+44) 115 9825275

Scios Nova Inc.
820 West Maude Avenue
Sunnyvale, California 94086
USA
http://www.sciosinc.com/

Scripophily.com
P.O. Box 223795
Chantilly, Virginia, 20153

Sefar America Inc.
http://www.sefaramerica.com

SEIKAGAKU
124 Bernard Saint Jean Dr.
East Falmouth, MA 02536-4445
USA
http://www.acciusa.com/seikagaku/index.asp

SEIKAGAKU
Seikagaku Corporation
1-5 Nihonbashi-honcho
2-chome, Chuo-ku, Tokyo 103-0023
Japan
TEL (81)-3-3270-0966
FAX (81)-3-3270-0538

Sequenom Inc.
3595 John Hopkins Court
San Diego, CA 92121-1331

Sera Laboratories International Ltd.
Unit A 1 horsted
Haywards Heath, RH17 7BA (Road Map) West Sussex
TEL 01722 790000
http://www.sli-ltd.com

Serologicals Corp.
5655 Spalding Drive
Norcross, GA 30092
USA
TEL 1-679-728-2000
http://www.serologicals.com

Serotec
22 Bankside
Station Approach
Kidlington, Oxford, OX5 1JE

Serva
AL-Labortechnik
Friedmühle 430 A
A—3300 Amstetten
Austria
TEL +43 7472 234 233
FAX +43 7472 234 234
http://www.serva.de

Serva Electrophoresis GmbH
Carl-Benz-Str. 7
D-69115 Heidelberg
P.O.B. 10 52 60
Germany
TEL +49 (0) 6221 13840-0
FAX +49 (0) 6221 13840-10
E-MAIL info@serva.de
http://www.serva.de

Severn Biotech Ltd.
Unit 2
Park Lane
Stourport Rd
Kidderminster, Worcestershire, DY11 6TJ
UK

SGE, Inc.
2007 Kramer Lane
Austin, TX 78758
USA

Shimadzu America/ Shimadzu Scientific Instruments, Inc.
7102 Riverwood Drive
Columbia, MD 21046, USA
TEL (410) 381-1227/ 800-477-1227
FAX (410) 381-1222
http://www.ssi.shimadzu.com

Shinjuku Monolith
3-1 Nishi-Shinjuku 2-chome
Shinjuku-ku, Tokyo 163-0914
Japan

Shipley
Corporate and Manufacturing Headquarters
455 Forest Street
Marlborough, MA 01752
TEL 508 481-7950
TEL 800 832-6200
FAX 508 485-9113

Siegfried (USA), Inc.
33 Industrial Park Road
Pennsville, NJ 08070
TEL +1 856 678 3601
FAX +1 856 678 4008
E-MAIL info@siegfried-usa.com

Siegfried Ltd.
Untere Bruehlstrasse 4
CH-4800 Zofingen
Switzerland
TEL +41 62 746 1111
FAX +41 62 746 1103
http://www.siegfried.ch/

Sierra BioSource Inc.
260 Cochrane Circle
Ste E
Morgan Hill, CA 9503

Sigma Aldrich Denmark A/S
Vejlegaardsvej 65B
DK-2665
Vallensbaek Strand
http://www.sigmaaldrich.com

Sigma Aldrich
P.O. Box 14508
St. Louis, MO 63178
http://www.sigma-aldrich.com

SIGMA-ALDRICH Handels GmbH
Favoritner Gewerbering 10
1100 Wien
Austria
TEL +43 1 605 81 10
FAX +43 1 605 81 20
E-MAIL sigma@sigma.co at
http://www.sigmaaldrich.com

Sigma-Aldrich Sweden AB
Stockholm, Sweden
http://www.sigmaaldrich.com/

Sigma-Aldrich
3050 Spruce St.
St. Louis, MO 63103
TEL 314-771-5750
TEL 800-325-3010
TEL 314-771-5765
FAX 800-325-5052
FAX 314-771-5757
E-MAIL custserv@sial.com
http://www.sigma-aldrich.com

Sigma-Aldrich
Norway A/S
Tevlingveien 23
1081 Oslo

Sigma-Aldrich Canada Ltd.
2149 Winston Park Dr.
Oakville, Ontario, L6H 6J8
TEL 800-565-1400
www.sial.com

SIGMA-Aldrich Chemie GmbH
Eschenstr. 5
D-82024 Taufkirchen
Germany
TEL 49 89 65131103
FAX 49 89 65131144
E-MAIL DECustsv@eurnotes.sial.com
http://www.sigma-aldrich.com

Sigma-Aldrich Chimie S.ar.l.
L'Isle d'Abeau Chesnes
B.P. 701
38297 Saint Quentin
Fallavier Cedex, France
TEL 08 00 21 14 08
FAX 08 00 03 10 52
http://www.sigma-aldrich.com

Sigma-Aldrich Co. Ltd.
Fancy Road
Poole, Dorset, BH12 4QH
UK
TEL +44 (0)1202733114
FAX +44 (0)1202715460

Sigma-Aldrich Company Ltd.
The Old Brickyard
New Rd
Gillingham, Dorset SP8 4XT
UK
TEL +44 (0) 1747 833000, 0800 717181
FAX 0800 378785
http://www.sigmaaldrich.com

Sigma-Aldrich Denmark A/S
Vejlegårdsvej 65B
2665 Vallensbæk Strand
Denmark

Sigma Aldrich Germany
Eschenstr. 5
D 82024 Taufkirchen
Germany

Sigma-Aldrich Japan
Tokyo, Japan
E-MAIL sia1jpts@sial.com
http://www.wako-chem.co.jp

Sigma Aldrich Química S.A.
Ronda de Poniente 3
2ª planta
Apartado de Correos 278
Tres Cantos (Madrid)
Spain
http://www.sigmaaldrich.com

Sigma Biosciences
Fancy Road
Poole, Dorset BH17 7NH
UK
TEL (+44) 1202 733114
FAX (+44) 1202 715460

Sigma-Isotec
3858 Benner Rd.
Miamisburg, OH 45342
USA
http://www.isotec.com

Silicon Graphics
1600 Amphitheatre Parkway
Mountain View, CA 94043

Simco Nederland B.V.
Aalsvoort 74
7241 MB Lochem
TEL +31 (0)573 288333
FAX +31 (0)573 257319
E-MAIL info@antistatic.nl

SIS Chemicals
Linden House1
The Square
Pennington, Lymington, Hampshire S0418GN
UK

Skatron Instruments
P.O. Box 8
3401 Lier
Norway
TEL 47-3285-4250
FAX 47-328-54204

Small Parts, Inc.
13980 N.W. 58th Court
P.O. Box 4650
Miami Lakes, FL 33014-0650
http://www.smallparts.com/

Solamere Technology Group
1427 Perry Ave
Salt Lake City, UT 84103
USA

Solis Biodyne
Pikk 14
51013 Tartu
Estonia

Solon Manufacturing Mompany
Meriden Cooper Corporation
PO Box 692
Meriden CT 06450
TEL (203) 237-8448
FAX (203) 238-1314

Sonics & Material Inc.
53 Church Hill Road
Newtown, CT 06470-1614
USA

Soquelec Ltd.
5757 Cavendish Blvd.
Suite 540
Montreal, Quebec W4H 2W8
(Canada)
http://www.soquelec.com

Sorvall
Kendro Laboratory Products GmbH
Wiegelestraße 4
A-1230 Wien
AUSTRIA
TEL +43 1 801 40-0
FAX +43 1 801 40 40
E-MAIL info.at@kendro.spx.com
http://www.sorvall.com

Specialty media
580 Marshall Street
Phillipsburg, NJ 08865
USA
TEL 888-209-8870
TEL 908-213-6555
FAX 908-387-1670
E-MAIL questions@cmt-inc.net
http:///www.specialitymedia.com

Spectra Physics
1335 Terra Bella Avenue
Post Office Box 7013
Mountain View, CA 94039
USA
TEL 650-961-2550
FAX 650-968-5215
E-MAIL service@splasers.com
http://www.spectraphysics.com/

Spectrum Europe B.V. Europe
P.O. Box 3262
NL-4800 DG Breda
The Nederlands
TEL +31 76 5719 419
FAX +31 76 5719 772
http://www.spectrapor.com

Spherotech, Inc.
1840 Industrial Dr.
Suite 270
Libertyville, IL 60048-9467
TEL (800) 368-0822
TEL (847) 680-8922
FAX (847) 680 8927

Stanford Photonics
1032 Elwell Court
Suite 104
Palo Alto, CA 94303
http://www.stanfordphotonics.com/

Stratagene
11011 N. Torrey Pines Road
La Jolla, CA 92037
USA
TEL 1-858-535-5400
http://www.stratagene.com

Stratagene
1834 State Highway 71 West
Cedar Creek, TX 78612
TEL (800) 424-5444
FAX (512) 321-3128
http://www.stratagene.com

Strathmann
Habichthorst 30
22459 Hamburg
Germany

Structure Probe, Inc.
569 East Gay Street
West Chester, PA 19380
USA
TEL 1-800-242-4774
TEL 1-610-436-5400
FAX 1-610-436-5755
E-MAIL spi3spi@2spi.com
http://www.2spi.com/spihome.html

Sumalsa (Suministros de material y aparatos de laboratorio S.A.)
Obispo Tajón
18 bajo
50005 Zaragoza
Spain
http://www.thermospectronic.com

Sun Microsystems, Inc.
4150 Network Circle
Santa Clara, CA 95054
USA
TEL 1-800-555-9786
TEL 1-650-960-1300
http://www.sun.com/

Surgipath Medical Industries, Inc.
5205 Rt. 12
Richmond, IL 60071
USA
TEL 800-225-3035
http://www.surgipath.com/

SÜSS MicroTec Lithography GmbH
Schleissheimer Str. 90
D-85748 Garching / Munich
Germany
TEL (+49) [0] (89) 32007-0
FAX (+49) [0] (89) 32007-162

Sutter Instrument Company
51 Digital Drive
Novato, CA 94949
USA
TEL 415.883.0128
FAX 415.883.0572
E-MAIL info@sutter.com
http://www.sutter.com

Swiss Institute of Bioinformatics
Biozentrum—Basel University
Klingelbergstrasse 50-70
4056 Basel
Switzerland
TEL +41 61 267 2042
FAX +41 61 267 2024
E-MAIL admin@isb-sib.ch
http://www.expasy.org/

Taab Laboratories Equipment Ltd.
3 Minerva House
Calleva Ind Park
Aldermaston, Reading, Berks, RG7 4QW
England
TEL +44 (0)1734817775
FAX +44 (0)1734817881

Taconic M&B
Bomholtvej 10
P.O. Box 1079
DK-8680 Ry
Denmark

TaKaRa
Takara Biomedical Group
TAKARA SHUZO CO., LTD.
Seta 3-4-1, Otsu, Shiga 520-2193
Japan

Tecan Austria GmbH
Untersbergstr. 1a
5082 Grödig
Austria

Techne
3 Terri Lane
Suite 10
Burlington, N.J. 08016
TEL 800-225-9243
http://www.techneusa.com

Technologiepark
Emmy-Noether Strasse 10
76131 Karlsruhe
Germany

Technical Video
PO Box 693
Woods Hole MA 02543
USA
TEL 508-563-6377
FAX 508 563-6265

Ted Pella, Inc.
P.O. Box 492477
Redding, CA 96049
TEL 800-237-3526

TeleChem International, Inc.
ArrayIt Division
524 E. Weddell Drive
Suite #3
Sunnyvale, CA 94089, USA
TEL +1-408-744-1331
FAX +1-408-744-1711
http://arrayit.com/

Termo Spectronic (Europe, Middle East and Africa)
Mercers Row
Cambridge CB5 8HY
U.K.

Terumo Neolus
44-1,2 chome
Hatagaya, Shibuya-ku, Tokyo,
Japan
Terumo Neolus, Benelux Sales Division
Researchpark Zone 2
Haasrode Interleuvenlaan 40 B-3001 Leuven
Belgium
TEL 32-16-38-14-02
FAX 32-16-38-15-55
http://www.terumo.co.jp

Tetko Inc.
P.O. Box 346
Lancaster, NY 14086
USA
http://tetko.com/

The MathWorks, Inc.
3 Apple Hill Drive
Natick, MA 01760-2098
USA
TEL 508-647-7000
FAX 508-647-7001

Therma Electron Corporation (formerly Forma Scientific)
Headquarters: Informatics and Services
18 Commerce Way
Woburn, MA 01801-1086
United States
TEL +1 781 933 4689 (866 INFOLAB)
FAX +1 781 933 6322
http://www.forma.com/

Thermo Electron Corp.
Via Fisher Scientific Canada
Customer Service Centre
112 Colonnade Rd
Nepean, ON, K2E 7L6
TEL 800-234-7437
http://www.thermo.com

Thermo Electron Informatics (former Thermo LabSystem)
St. Georges Court
Hanover Business Park
Altrincham, Cheshire, WA14 5TP
UK
TEL +44 161 942 3000
FAX +44 161 942 3001
http://www.thermo.com/com/cda/home/1,1089,,00.html

Thermo Electron Molecular Biology
Sample Preparation
Molecular Biology
450 Fortune Blvd
Milford, MA 01757
USA
TEL +1 508 482 7000
http://www.thermo.com

ThermoFinnigan
355 River Oaks Parkway
San Jose, CA 95134
USA
TEL 408-965-6000

Thermo Hybaid
Contact Thermo Electron Corporation
81 Wyman Street
Waltham, MA 02454
USA
TEL1-877-843-7668
http://www.thermo.com/

Thermo Labsystems Oy
Ratastie 2
P.O.Box 100
Vantaa, 01620
Finland
TEL +358-9-329100
FAX +358-9-32910500
http://www.thermo.com

Thermo Life Sciences—UK
Unit 5
The Ringway Centre
Edison Rd, Basingstoke RG21 6YH
UK
TEL 01256 817282
FAX 01256 817292
http://www.thermo.com/

Thermo Savant / Thermo EC
100 Colin Drive
Holbrook, NY 11741-4306
USA
http://www.thermo.com

Thermo Shandon, Inc.
171 Industry Dr.
Pittsburgh, PA 15275
USA
TEL 412-788-1133
TEL 800-547-7429
FAX 412-788-1138
E-MAIL thermoshandon@thermoshandon.com
http://www.thermoshandon.com

Thomas Scientific
P.O. Box 99
Swedesboro, NJ 08085
U.S.A
TEL 800-345-2100
FAX 856-467-3087
http://www.thomassci.com/contact/index.jsp

Thompson B&SH Co. Ltd.
8148 Ch. Devonshire
Montreal, QC
TEL 514-739-1971

T.I.L.L. Photonics GmbH
Lochhamer Schlag 19
D-82166 Gräfelfing
Germany
http://www.till-photonics.com

Treff
Treff AG
Taastrasse 16
CH-9113 Degersheim

TR Tech/Bex Co. Ltd.
2-22-3-104
Sengoku, Bunkyo-ku, Tokyo 112-0011
JAPAN

Turner BioSystem
845 W. Maude Avenue
Sunnyvale, CA, 94085

UCSF Cell Culture Facility
Box 0528
San Francisco CA 94143
http://www.ccf.ucsf.edu/

Uniblitz by Vincent Associates
803 Linden Avenue
Rochester, NY 14625
USA

United Chemical Technologies, Inc.
2731 Bartram Road
Bristol, PA 19007-6893
TEL (215) 781-9255
TEL 800-541-0559
FAX (215) 785-1226

United States Biochemical Corp.
P.O. Box 22400
Cleveland OH 44122
USA
TEL +1-216-765-5000
FAX +1-216-464-5075

Universal Imaging Corp.
502 Brandywine Parkway
West Chester, PA 19380
USA
TEL 610-344-9410
FAX 610-344-9515
http://www.universal-imaging.com/

Universal Imaging Corporation Limited
PO Box 1192
43 High Street Marlow
Buckinghamshire SL7 1GB
UK
TEL +44 1628 890858
FAX +44 1628 898381
http://www.image1.com

Upchurch Scientific
P.O. Box 1529
619 Oak Street
Oak Harbor, WA 98277
USA
TEL 800-426-0191
FAX 800-359-3460
Upjohn
7171 Portage Rd
Kalamazoo, MI 49001-0199

Upstate Biotechnology, Inc.
10 Old Barn Road
Lake Placid NY 12946
http://www.upstatebiotech.com/.

USA Scientific, Inc.
PO Box 3565
Ocala, FL 34478-3565
TEL 1-800-LAB-TIPS (522-8477)
TEL 352-237-6288
http://www.usascientific.com

USB Corp.
26111 Miles Road
Cleveland, OH 44128
USA
TEL 800 321 9322
FAX 216 464 5075

VACUUBRAND GMBH + CO KG
Postfach 1664
D-97866 Wertheim
Alfred-Zippe-Str. 4
D-97877 Wertheim
TEL +49 (0) 9342 / 808-0
FAX +49 (0) 9342 / 59880
http://www.vacuubrand.de/

Valco Instruments Co. Inc.
P.O. Box 55603
Houston, TX 77255
USA
TEL 800-227-9770
TEL 800-367-8424
FAX 713-688-8106

Valeant Pharmaceuticals (previously ICN)
Valeant Plaza
3300 Hyland Avenue
Costa Mesa, CA 92626
USA
TEL 1.800.548.5100
TEL 1.714.545.0100
FAX 1.714.556.0131
http://www.valeant.com

Vector Laboratories
16 Wulfric Square
Bretton, Peterborough, Cambridgeshire PE3 8RF
England
http://www.vectorlabs.com/

Vector Laboratories
3390 South Service Road
Burlington ON L7N 3J5
Canada
TEL 1-888-629-2121

Vector Laboratories, Inc.
30 Ingold Road
Burlingame, CA 94010
USA
TEL 800 227 6666
TEL 415-697-3600
FAX 415-697-0339
http://www.vectorlabs.com

Vedco Inc.
http://www.vedco.com

Vel, Merck-Belgolabo
Haasrode Researchpark Zone 3
Geldenaaksebaan 464
B-3001 Leuven
Belgium
TEL +32 16 385 011
http://www.vel.be

Verity Software House
PO Box 247
Topsham, ME 04086
E-MAIL verity@vsh.com
http://www.vsh.com

Video Scope International, Ltd.
105 Executive Drive
Dulles, Virginia 20166-9558
TEL (703) 437-5534
FAX (703) 742-8947
E-MAIL info@videoscopeintl.com

VidraFoc S.A.
Badajoz, 50
08005 Barcelona
Spain
http://www.vidrafoc.com

VisiTech International Ltd.
Unit 92 Silverbriar
Sunderland Enterprise Park (East), Sunderland, SR5 2TQ
UK

Visitron Systems GmbH
Gutenbergstrasse 9
D-82178 Puchheim
Germany
http://visitron.de

VWR
3745 Bayshore Blvd.
Brisbane CA 94005
TEL 1-800-932-5000
http://www.vwr.com

VWR
50 D'Angello Road
Marlboro, MA 01752

VWR
P.O. Box 5015
Bristol, CT 06011

VWR International
1310 Goshen Pkwy
West Chester, PA 19380
TEL 800-932-5000
TEL (610) 431-1700
FAX (610)431-9174
http://www.vwrsp.com

VWR International
2360 Argentia Road
Mississauga, Ontario L5N 5Z7
Canada
TEL 800-932-5000
TEL 905-813-7377
FAX 800-668-6348
http://www.vwrsp.com

VWR International, Inc.
10105 Carroll Canyon Road
San Diego, CA 92131
TEL 858-695-7600

VWR International AS
PO Box 45
Kalbakken, (Kakkelovnskroken, 1), 0901 Oslo
Norway
TEL +47 02290
FAX +47 22 90 00 40
E-MAIL info@no.vwr.com
http://www.vwrsp.com

VWR International GmbH (formerly Merck)
Hilpertstrasse 20a
64295 Darmstadt
Germany

VWR International Holding GmbH
Branch Office Belgium
Woluwedal 28, B-1932
Zaventem
TEL 00322-7115858
FAX 00322-7115920
http://www.vwr.com

VWR International Limited
Hunter Blvd
Magna Park
Luttereworth, Leicestershire LE17 4XN
UK
TEL 0800 223344
FAX (+44) 01202 665599

VWR International Ltd
Merck House
Poole, Dorset, BH15 1TD
England
TEL 01202 660444
FAX 01202 666856
http://www.bdh.com

VWR Scientific
USA
VWR International
1310 Goshen Parkway
West Chester, PA 19380
USA
http://www.vwr.com

VWR Scientific Corporation
P.O. Box 1002
600C Corporate Court
South Plainfield, NJ 07080
USA

VWR Scientific Products
133 South Center
Suite 700
Morrisville, NC 27560
USA

Wacker-Chemie GmbH
Hauptverwaltung
Hanns-Seidel-Platz 4
81737 München
GERMANY
TEL +49 (0)89 6279-01
FAX +49 (0)89 6279-1770
http://www.wacker.com

Wako Pure Chemicals Industries, Ltd.
1-2,Doshomachi 3-Chome
Chuo-ku, Osaka 540-8605
Japan

Wako Chemicals USA, Inc.
1600 Bellwood Road
Richmond, VA 23237-1326
TEL 804-271-7677
FAX 804-271-7791
TEL 877-714-1924

Waring Laboratory
314 Ella T. Grasso Ave.
Torrington, CT 06790
TEL 1-800-4WARING
TEL (1-800-492-7464)
E-MAIL waring@conair.com

Warner Instrument Corp.
1125 Dixwell Ave.
Hamden, CT06514
USA

Waters Ltd UK
730-740 Centennial Court
Centennial Park
Elstree, Hertsfordshire, WD6 3SZ

Waters/Micromass
34 Maple Street
Milford, MA. 01757
http://www.micromass.se

Watkins and Doncaster
PO Box 5
Cranbrook, Kent TN18 5E2
UK

WeldtiteProducts Ltd.
Harrier Road
Barton-on-Humber, DN18 SRP
UK
TEL 01652 660000
http://www.weldtite.co.uk

Western Region
Sci. Pro. Div.
39899 Balentine Dr. #325
Newark, CA 94560
USA
TEL 800-222-7740

Whatman, Inc.
401 West Morgan Road
Ann Arbor, MI 48108
USA
http://www.whatman.com

Whatman Inc.
9 Bridewell Place
Clifton, NJ 07014
TEL 800-441-6555

Whatman International Ltd.
Whatman House
St Leonard's Road
20/20 Maidstone
Kent, ME16 0LS
UK
TEL +44 (0) 1622 676670
FAX +44 (0) 1622 677011
http://www.whatman.com

Wheaton Science Products
An Alcan Packaging Company
1501 N. 10th Street
Millville, NJ 08332-2093
USA
TEL 800-225-1437
FAX 856-825-1368
TEL 1 856-825-1100
FAX 1 856-825-4568

Wolfram Research (Mathematica)
http://www.wolfram.com/

World Precision Instruments
Astonbury Farm Business Centre
Aston, Stevenage. SG2 7EG.
TEL +44 (0)1438 880025
FAX +44 (0)1438 880026
E-MAIL wpiuk@wpi-europe.com

World Precision Instruments, Inc.
175 Sarasota Center Boulevard
Sarasota, Florida 34240
USA
TEL (941) 371-1003
FAX (941) 377-5428
http://www.wpiinc.com/

Worthington Biochemical Corporation
Pharmacia Biotech Inc.
800 Centennial Ave.
P.O. Box 1327
Piscataway, NJ 08855-1327
USA
TEL 1 800-445-9603 (Canada and the US)
TEL 1 732-942-1660 (International)
E-MAIL Corporate Webmaster@roche.com
http://www.worthington-biochem.com

Wyeth: Fort Dodge Animal Health
http://www.wyeth.com

XENOTEK Engineering (Steve Novotny)
525 North 27th Street
Belleville, IL 62226
USA
TEL 618-235-9110
TEL 800-260-5656
FAX 618-235-9167
FAX 800-859-0898

Yamato Scientific Co. Ltd.
1-6 Honcho 2-Chome
Nihonbashi Chuo-ku
Tokyo103
Japan
TEL +81-3-3231-1124
FAX +81-3-3231-1144
E-MAIL english-website@yamato-net.co.jp
http://www.yamato-net.co.jp

Zeiss
Carl Zeiss Promenade 10
07745 Jena
Germany

Zimmer, Inc.
P.O. Box 708
1800 West Center Street
Warsaw, IN 46581-0708

Zymed Laboratories, Inc.
52 South Linden Avenue, Suite 3
South San Francisco, CA 94080
USA
TEL 800 874 4494
TEL 1 415 871 4494
FAX 1 415 871 4499
http://www.zymed.com/

Index

Copyright 2006, Elsevier Science (USA).
All rights reserved.

B

C

D

E

F

G

H

I

J

K

L

M

N

O

P

Q

R

S

T

W

X

Y

Z